ANGEWANDTE CHEMIE
International Edition in English
Volume 32 · Number 1
January 1993
Pages 1–130

Marine Metabolites and Metal Ion Chelation: The Facts and the Fantasies

By Joseph P. Michael and Gerald Pattenden*

The marine environment is a seemingly inexhaustible treasury of organisms whose secondary metabolites bear witness to the lavishness and inventiveness with which nature is able to manipulate molecular architecture. But to what purpose are these diverse and often grotesque compounds produced? This review is founded on the premise that some of them may be involved in the uptake and transport of metal ions present in the aquatic milieu. Many metabolites produced by terrestrial organisms are known to act as ionophores, but the case for similar behavior by their marine counterparts is far hazier. Notwithstanding the relative abundance of certain metal ions in the oceans, and of metabolite structures possessing features that should facilitate the chelation of metal ions, few attempts to establish a connection between these two phenomena have been reported. We have whittled down the voluminous literature of natural products derived from marine sources to expose a core of observations and speculations germane to our premise. These facts and fantasies are evaluated in this review. A mere handful of metal-containing complexes has actually been isolated; furthermore, attempts to prepare such complexes in vitro are rare, and spectroscopic evidence for metal–metabolite interactions, whether in vivo or in vitro, is not common. Only with the vanadium-sequestering tunichromes does a logical (but by no means complete) picture begin to emerge. In several other cases, the plausibility of metal chelation, though mooted by authors, remains unsupported by experimental evidence. However, continuing efforts to obtain structural, and particularly conformational, information on the metabolites by means of X-ray crystallography, nuclear magnetic resonance spectroscopy, and molecular mechanics calculations would seem to provide the key to a rational approach to this neglected topic. On the basis of recent studies dealing with such structural aspects, we present a selection of candidate compounds, some of which are the targets of our own synthetic attentions, whose potential for binding to metal cations merits further research.

1. Introduction

To the chemist familiar with terrestrial secondary metabolites having structures that tend to conform to securely established biogenetic postulates, many natural products from marine sources must seem quite freakish. Unexpected and bizarre molecular architecture, unusual functional groups, stereochemical quirks—these all challenge one's perception of nature as a machinist working to cunning but time-honored patterns. Yet why should marine metabolism mimic terrestrial metabolism? Indeed, a recent review lists several cogent reasons why we should expect significant differences in the biosynthetic pathways that operate on land and in the

[*] Prof. G. Pattenden, Prof. J. P. Michael
Department of Chemistry, The University
GB-Nottingham NG7 2RD (UK)

 © VCH Verlagsgesellschaft mbH, W-6940 Weinheim, 1993 0570-0833/93/0101-0001 $ 10.00+.25/0

sea.[1] For example, the marine environment, though teeming with life forms, is a biosynthetically bleak one. The oceans may be comparatively rich in carbon, buffered as they are to pH 8.2–8.5 with carbonate and bicarbonate, but few organisms other than algae can exploit this carbon source photosynthetically. Other customary nutrients such as amino acids and sugars occur only at the parts-per-billion level; and nitrogen, available principally as the ammonium or nitrate ion, tends to be a limiting nutrient. It comes as no surprise, therefore, that metabolites of marine plants and animals may be formed very slowly, and in only trace amounts. The metabolites that the organisms are capable of manufacturing despite these handicaps are thus all the more awesome in their variety.

On the other hand, the oceans, while inhomogeneous, contain substantial quantities of dissolved inorganic salts; indeed the salinity may reach levels as high as 40%.[2] Chloride, bromide, bicarbonate, and sulphate ions account for the larger part of the anionic species. Common metal cations, e.g. sodium, potassium, magnesium, and calcium, reach concentrations above 10^{-3} M, while most other metal ions, including important trace elements such as vanadium, manganese, iron, cobalt, copper, zinc, and molybdenum, occur in concentrations below 10^{-6} M. Some consequences of the ionic constituents, such as the occurrence of chloro and bromo groups in certain marine metabolites, are therefore readily comprehended. Altogether more subtle, however, is the effect of the metal ions. Their interaction with marine organisms in the external milieu (uptake and accumulation) has been reviewed,[3] and is not at issue here. Furthermore, the indisputable physiological role of certain metals in the intracellular medium, a phenomenon of immense biochemical importance,[4] is also not an issue. For us as chemists, the most intriguing feature is the possible relationship between metal ions and the secondary metabolites. Many marine natural products seem to have structural features that make them ideal for interacting with metals, for example, polar functional groups in potentially chelating arrangements, macrocyclic cavities and geometries apparently tailor-made for wrapping around metal ions. Yet the grounds for supposing that such interactions really exist are by and large so tenuous that few researchers who publish in the field of marine natural products venture so much as a sentence on likely roles for metal ions in either the chemistry or the biochemistry of these compounds.

Can marine metabolites sequester and transport metal ions in vivo? Do metal ions provide a convenient template for biological assembly of the metabolites? Could metal–ligand complexation play a part in the pronounced biological activity of many of the compounds? Might in vitro studies of interactions still provide revealing results even if mutual in vivo effects prove elusive? These are some of the perhaps ingenuous but nonetheless provocative questions that provided the inspiration for this review. We entered this arena as practising synthetic organic chemists, interested in two specific families of structurally novel and biologically important marine metabolites: 1) the ulapualide group of trisoxazole-containing macrolides, for example **82**, found in nudibranchs (sea slugs) and sponges (see Section 7.6),[5] and 2) the thiazole/dihydrothiazole/dihydrooxazole-containing lissoclinamide family of cyclic peptides (**76**–**78**), produced by tunicates (sea squirts) of the genus *Lissoclinum* (see Section 7.5).[6] In our research, and in this review, we have explored an intuitive hypothesis of congruence between metals and marine metabolites. Structural analogies with well-explored terrestrial metabolites, especially polyether antibiotics and siderophores, for which the phenomenon has often been convincingly documented,[7] led us to hope that we could uncover similar information for their marine counterparts.

We began by first compiling a short-list of potentially ligating species from the thousands of known marine metabo-

Gerald Pattenden is Sir Jesse Boot Professor of Organic Chemistry at the University of Nottingham. He recieved his PhD from Queen Mary College, London University, in 1966, and in the same year he was appointed to a lectureship at University College, Cardiff. In 1972 he moved to Nottingham and was made Professor in 1980. His research concentrated on total synthesis of natural products and the discovery and design of new synthetic methods in Organic Chemistry. He has recently initiated studies of molecular recognition and metal transport phenomena with natural macroheterocycles, cyclic peptides, and siderophores.

Born and educated in South Africa, Jo Michael received his PhD degree in 1975 from the University of the Witwatersrand, Johannesburg. He spent two years as a post-doctoral research fellow with Dr Ian Fleming at Cambridge University before returning to his alma mater as a lecturer in 1978. He is currently Associate Professor in the Department of Chemistry. His interests in the synthesis of natural products and in synthetic methodology have taken him on sabbatical leave to the University of California, Berkeley, where he collaborated with Professor Paul A Bartlett (1984), and more recently to the University of Nottingham (1991–92).

lites described in the literature.[8] We excluded those examples in which the metal ion is present merely as a counterion for anionic residues such as carboxylate and sulfate. The more than 300 publications dealing with the compounds on our short-list were then scrutinized for even the slightest comment relating to interactions between the marine metabolites and metals, or to structural studies that might have a bearing on the topic. A slim core of facts emerged, accompanied by an equally insubstantial collection of fantasies that a handful of authors had been brave enough to voice. Our interpretation of our readings reflects the perspectives of two somewhat naive organic chemists who sense that an opportunity for significant research is being overlooked. We air these impressions in the hope that researchers in the field may find in them the incentives to start remedying what we perceive as a deficiency in contemporary chemistry.

2. The Isolation of Complexes of Marine Metabolites with Metals

The least disputable evidence for the interaction of marine metabolites with metals must come, of course, from the direct isolation of metal-containing complexes. Such complexes, other than the ubiquitous magnesium-containing chlorophylls *a* and *b*, are rare indeed. The new chlorophyll c_3 (**1**), from the alga *Emiliana huxleyi*,[9] is hardly a startling addition to the catalog. Far more exciting is tunichlorin (**2**), a nickel-containing blue-green pigment from the tunicate *Trididemnum solidum*.[10] The function of the nickel, which can be replaced under laboratory conditions by copper(II), is as yet unknown. A cautionary note must be sounded, however: metal-containing porphyrinoid pigments from marine sources may be the exception rather than the rule, since the number of related compounds isolated in metal-free form is significantly large. In addition to the well-known pigment bonellin (**3**), associated with defence and larval masculinization of the echurian worm *Bonellia viridis*,[11] recent isolations of metal-free tetrapyrrole marine metabolites include

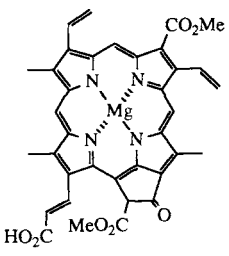

1

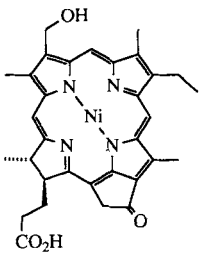

2

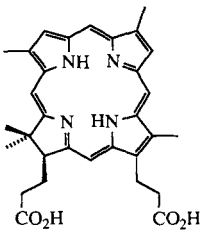

3

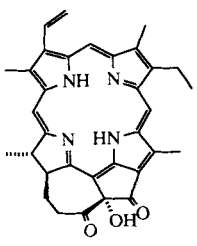

4

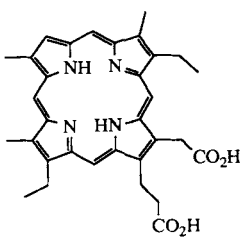

5

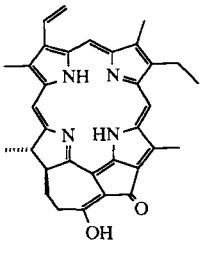

6

chlorophyllone-A (**4**) from the mollusc *Ruditapes philippinarum*,[12] corallistin A (**5**) from the demosponge *Corallistes* sp.,[13] and cyclopheophorbide enol (**6**) from the sponge *Darwinella oxeata*.[14] These compounds are certainly capable of forming metal complexes; as long ago as 1939, zinc, copper, and iron complexes of bonellin were prepared,[15] and more recently a zinc complex of corallistin A has been characterized.[13]

The unusual guanidine alkaloid clathridine **7** has been isolated together with its 2:1 zinc complex from the sponge *Clathrina clathrus*.[16] The latter compound is a genuine

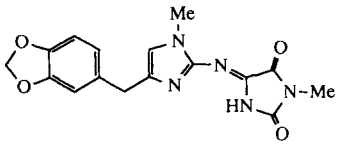

7

metabolite. The solid-state structure, determined by X-ray crystallography,[17] shows a distorted tetrahedral arrangement of the ligands around the metal (Fig. 1[18]). Zinc is an

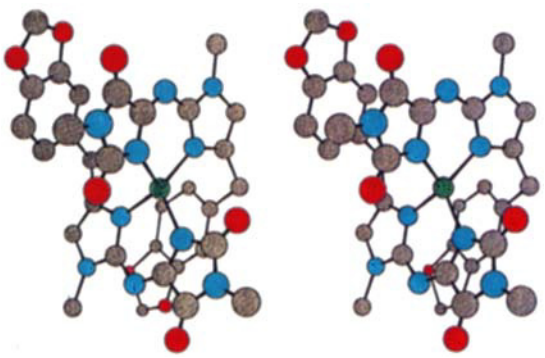

Fig. 1. Stereoscopic view of the crystallographically determined structure of the zinc complex of clathridine **7**. The metal is shown in green.

extremely important constituent of metalloenzymes, but its function in the clathridine chelate is unclear. The structure of clathridine is by no means unique; a small family of similar alkaloids, including naamidines A–D (**8**), and isonaamidines A and B (**9**),[19] pyronaamidine (**10**),[20] and corallistine (**11**),[21] has now been isolated from a variety of sponges. Is it possible that they, too, are coordinated to metals in nature, and that these complexes have so far escaped detection?

The most interesting examples of metal-containing marine natural products are provided by the aplasmomycins, for example aplasmomycin A (**12a**), boron-containing antibacterial metabolites from the cultured marine microorganism *Streptomyces griseus*.[22] Boron can hardly be regarded as a metal, but its encapsulation in the macrocyclic cavity of the aplasmomycins as tetracoordinate borate confers the same sort of rigidity on the structure that a chelated metal ion would. Has this factor a bearing on the observation[23] that deboroaplasmomycin A is devoid of biological activity? A further dimension comes from the fact that the negatively charged borate–macrocycle complex necessitates ion pairing with a monovalent cation. As isolated, the aplasmomycins

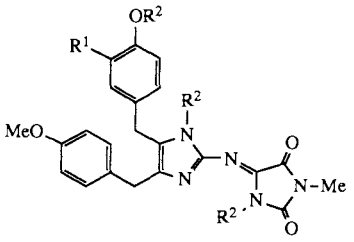

8 R^1 = H, OH ; R^2 = H, Me

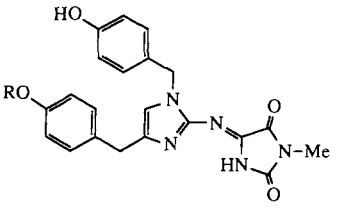

9 R = H, Me

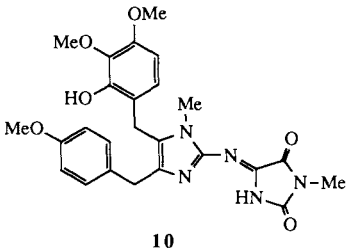

10

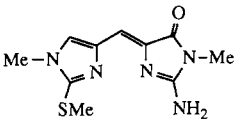

11

are sodium salts,[23, 24] but the initial X-ray structural studies on aplasmomycin A were on the silver salt.[25] The metal cation turned out to be located in the macrocyclic cavity, five-coordinated to two of the oxygens of the borate, two OH groups, and water (Fig. 2a). Even more noteworthy are some recent structural studies on the sodium salt of aplasmomycin C (**12c**), various conformers and polymorphs of which were separated and examined by single-crystal diffraction methods.[26] The cation was located within the cavity as expected, but the different conformers (Fig. 2b, c) were stabilized by either six- or four-coordination of sodium! The ability of aplasmomycins to envelop metal cations is thus in no doubt. In fact, one of the few semiquantitative studies of metal affinity for marine metabolites[23] shows that all three aplasmomycins bind alkali metal cations according to the trend Rb > K > Cs ~ Na > Li. There was no demonstrable affinity for Mg or Ca dications. Aplasmomycins A (**12a**) and B (**12b**) were able to transport K^+ ions across a bulk phase; deboroaplasmomycin A and the more heavily derivatized aplasmomycin C were not.

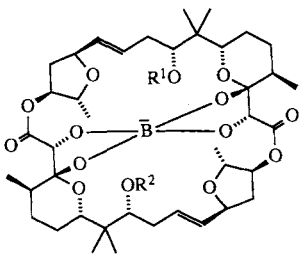

12a $R^1 = R^2 = H$
12b R^1 = Ac, R^2 = H
12c $R^1 = R^2$ = Ac

Finally, two peptidic isolated of marine animals, neither of which has been fully characterized, are worthy of mention here. The violet Fe^{3+}-binding pigment adenochrome, from the branchial heart of *Octopus vulgaris*, has been known for most of this century, and was the first known non-porphyrin iron-chelating metabolite from the animal kingdom. The last attempt to unravel its structure, published in 1979,[27] was based on analysis of the iron-free analogue, also a natural

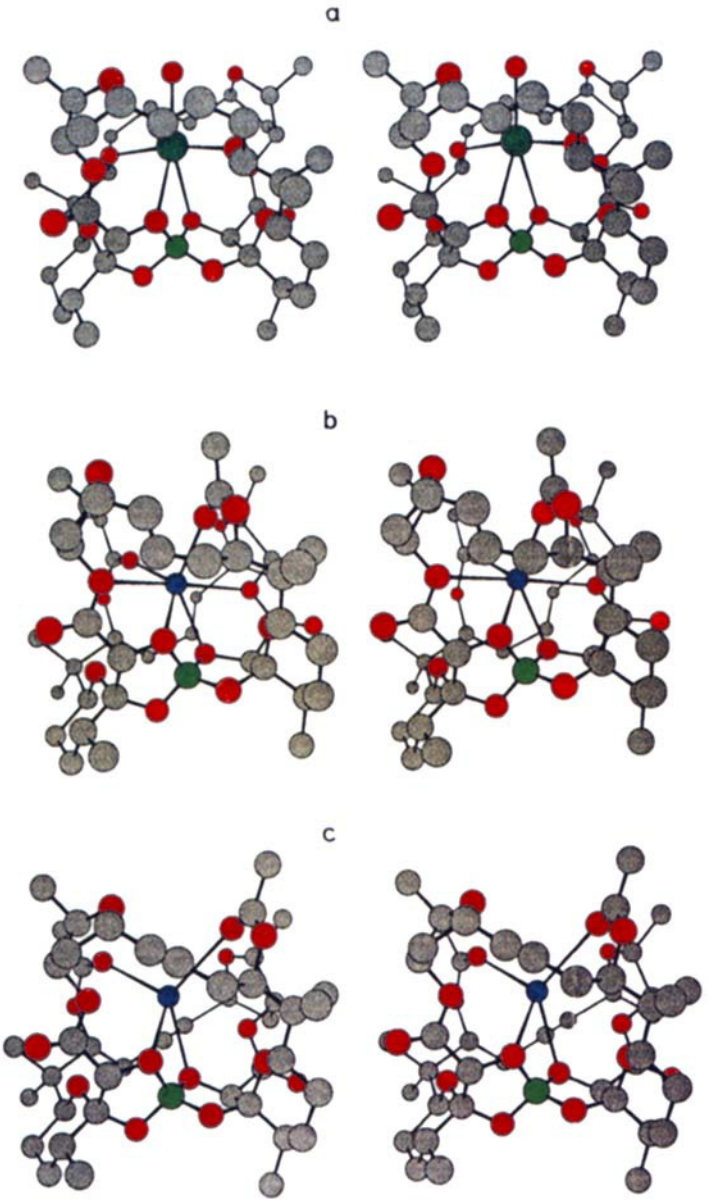

Fig. 2. Stereoscopic views of the X-ray crystal structures of a) the silver complex of aplasmomycin A **12a**; b) aplasmomycin C (**12c**) with six-coordinate sodium; and c) aplasmomycin C with four-coordinate sodium. Boron is shown in light green, silver in dark green, and sodium in dark blue. Hydrogen-bonded chloroform molecules forming part of the crystal lattice have been omitted from b), and only one of two atropisomeric molecules in the asymmetric unit is shown in c).

product. This was shown to be a mixture of several closely related peptides constructed from glycine and the novel DOPA-derived amino acids **13**–**15**, called adenochromines (DOPA = 3-(3,4-dihydroxyphenyl)alanine). The pigment could be reconstituted as a blue precipitate from desferriadenochrome and iron(III) chloride at pH 4.5. In view of intense current interest in the metal-binding properties of naturally occurring catechols (see **16** and **17** in Section 3), it is important that the structure of adenochrome components be solved and their biological function probed. Also worthy of further investigation are the geodiastatins A and B, which are silicon-containing chromoproteins from the sponge *Geodia mesotriaena*, a rare example of an animal that deposits a silica rather than a limestone skeleton.[28] Do these

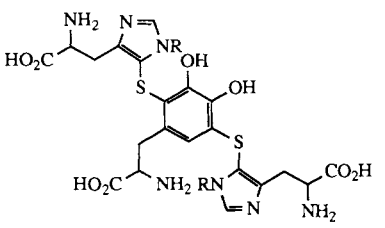

13

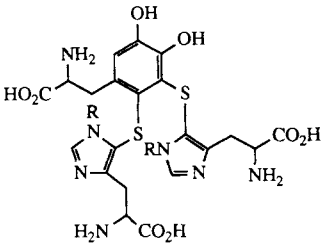

14

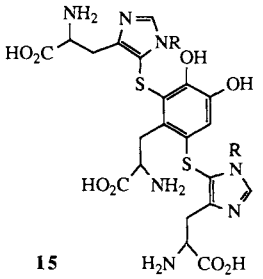

15

metabolites play a role in the formation of these siliceous structures and the protection of the sponge surface from predators?

3. Lessons from the Tunichromes

The saga of the tunichromes, air-sensitive yellow pigments present in specialized blood cells of sea squirts (tunicates), has been summarized in a recent review[29] that tellingly illustrates the frustrating uncertainties clouding the issue of the importance and function of metal–metabolite association in vivo. It has been known for decades that sea squirts are capable of assimilating metals such as vanadium, manganese, iron, niobium, and tantalum from sea water, often concentrating them to an extraordinary degree.[30] *Ascidia nigra*, for instance, is a vanadium-sequestering tunicate having intracellular levels of the metal as high as 0.15 M, ten million times the level in sea water, while a related species, *A. ceratodes*, can concentrate the element to an incredible 1 M.[31] About 90% of the vanadium is in the air-sensitive V^{III} state and the remainder is V^{IV}, observations all the more startling in the light of the element's presence as stable V^{V}-containing vanadates in the oceans. If the reduced form of vanadium is stabilized as a simple hydrated complex in the organism, it would require an acidic intracellular environment corresponding to about 0.01 M sulfuric acid, since insoluble V_2O_3 would precipitate above pH 3. Evidence for such an extraordinary milieu is not lacking, but the current view is that acidic "compartments" in cells, though credible, can be responsible for the stabilization of only a small fraction of the V^{III}. Far more compelling evidence exists for the presence in tunicate blood cells of endogenous organic ligands that can stabilize the reduced form of the metal by chelation. This is where the tunichromes come into the story.

Early studies with an unpurified "tunichrome" pigment showed that it behaved as a powerful reducing agent towards V^{V} and Fe^{III}. These observations spearheaded protracted research efforts to isolate the pure constituents of the pigment. After considerable experimental heartache, the inordinately unstable tunichromes, which decompose by oxidation, hydrolysis, and polymerization, were isolated by some unusual chromatographic procedures and then characterized by chemical and spectroscopic methods.[31] A more recent functional group protection–deprotection strategy has made the individual compounds somewhat more accessible.[32] To date, five tunichromes have been identified: An-1 (**16a**), An-2 (**16b**), and An-3 (**16c**) from *Ascidia nigra*; Mm-1 (**17a**) and Mm-2 (**17b**) from the iron-sequestering tunicate *Molgula manhattensis*. The compounds are hydroquinoid peptides that incorporate DOPA and hydroxy-DOPA units. The catechol and pyrogallol components of these compounds are, in principle, splendid chelating partners for Fe^{II}, Fe^{III}, V^{III}, and $V^{IV}O$, for which complex constants for the parent ligands are of the order of 10^{10} to 10^{28}. The auguries for tunichrome–metal binding are thus promising. What, then, are the facts?

The evidence collected to date, almost all qualitative, is that tunichromes An-1, An-2, and An-3 (**16**) react with V^{IV} and V^{V} to produce insoluble green or green-black polynuclear complexes with a binding stoichiometry of 2:1–3:1. Some spectroscopic data (UV and ESR) have been recorded on the complexes, but the heterogeneous nature of the species clearly frustrates the kinds of studies that one would dearly love to see. The formation of precipitates is in itself interesting, however, since vanadium is often associated with the formation of granules or intracellular membranes in blood cells. Another approach to the problem, the attempted isolation of an intact vanadium–tunichrome complex from ascidian blood, was largely unsuccessful; nevertheless, a green fraction, designated An-C, was isolated. While it has up to now eluded purification and characterization, it contains about 1% vanadium and has the spectroscopic hallmarks of an An–V complex. There might well be greater promise for qualitative studies with Mm-1 (**17a**), which appears to form soluble chelates with V^{III}, V^{IV}, and Fe^{II}. Recent syntheses[33] of An-1 (**16a**), Mm-1 (**17a**), and Mm-2 (**17b**) should ensure that in future sufficient quantities of these labile compounds will be available to extend our understanding of their fascinating bioinorganic chemistry.

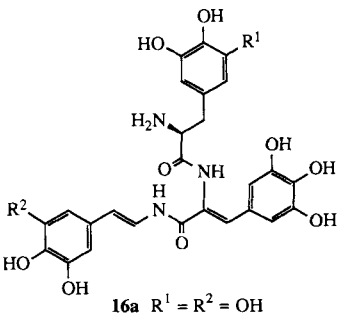

16a $R^1 = R^2 = OH$
16b $R^1 = H, R^2 = OH$
16c $R^1 = R^2 = H$

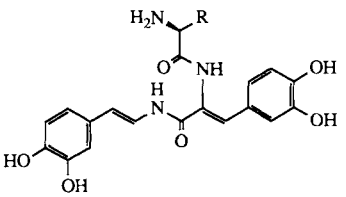

17a R = H
17b R = *i*Bu

It is very important to highlight a caveat that the principal researchers of tunichrome stress repeatedly: despite the attractions of the tunichrome–metal hypothesis, there is in fact no direct definitive evidence linking *any* marine metabolite, let alone tunichrome, to metal ion assimilation in tunicates. The indirect evidence, however, is extremely alluring. For

example, spectroscopic signals similar to those obtained for reconstituted tunichrome–vanadium complexes have been detected in the signet ring cells.[31] Analytical data on ascidian blood are also intriguing. An important assay for free (that is, unoxidized and uncomplexed) tunichrome, by acetylation and HPLC analysis, has shown that the dried blood of *A. nigra* contains about 0.3–0.4 μmol of free tunichrome per mg. The level of vanadium is about 0.16 μmol per mg. Furthermore, cell sorting of fluorescence-activated intact cells showed which of the several types of blood cells held most of the free tunichrome and which the vanadium, thereby providing the first unambiguous demonstration of the coexistence of tunichrome and vanadium in the same intracellular compartments.[34] The two species are admirably matched to constitute a redox couple, the biological implications of which, persuasively outlined in two reviews,[29, 35] now surely enters the realm of fantasy. For instance, the mechanistic key for regulating vanadium influx into vanadium-containing cells (vanadocytes) may well be provided by excess tunichrome, which undergoes concomitant oxidation. The quinoid products of tunichrome oxidation, effectively also styrenes by virtue of unsaturation in the peptide backbone, plausibly can undergo polymerization and crosslinking to protein and cellulose, in the process perhaps generating the tough "tunic" that is so characteristic a feature of the animals. Furthermore, now that an earlier proposal that vandium might serve to transport oxygen in the blood is clearly untenable, an alternative hypothesis[35] postulates a role for the redox couple in anaerobic respiration. By ascribing to the metallic species the same sort of electron-scavenger function that molecular oxygen would normally fulfill, it is surmized that tunicates should be able to survive the periods of oxygen deprivation that may occur in their customary habitat.

The tunichrome story should provide useful analogies for exploring the chemistry of other DOPA-derived metabolites, for instance the long-unresolved problem of adenochrome's structure or the biological function of clionamide (**18**)[36] and the celenamides (**19**),[37] unstable metabolites of the burrowing sponge *Cliona celata*. Celenamide D (**20**), in particular, bears a remarkable similarity to the An-tunichromes (**16**), in its peptide backbone and the styrene-like disposition of its catechol and pyrogallol units, while compounds **18** and **19** have 6-bromotryptophan replacing a DOPA unit. A single fantasy concerning this group of compounds has found its way into print: the phenolic portion of **18** might well function as a chelating agent for calcium, since *Cliona celata* is often found boring into the calcium carbonate shells of other marine animals.[36] The recently described halocyamines **21** and **22**[38] from the ascidian *Halocynthia roretzi* are more distant relatives of the tunichromes, in which both 6-bromotryptophan and histidine join DOPA as formal constituents, but similar considerations might underlie a potentially exciting coordination chemistry.

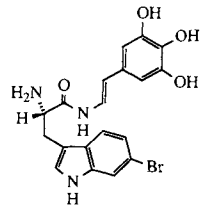

18

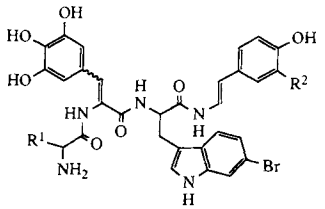

19 $R^1 = i\text{Bu}, i\text{Pr}$; $R^2 = \text{H}, \text{OH}$

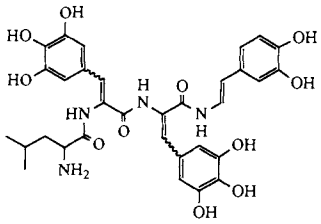

20

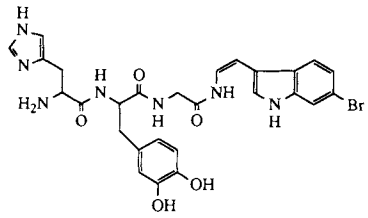

21

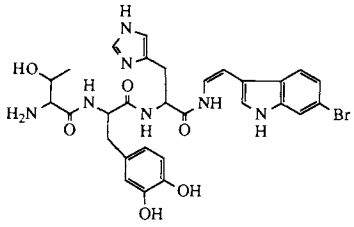

22

4. "Obvious" Ligands

For the overwhelming majority of marine natural products there is no evidence whatsoever for interaction with metal ions in vivo. In the quest for such interactions under laboratory conditions, the informed chemist can be expected to follow the leads provided by classical coordination chemistry, which teaches us to associate good metal-chelating properties with certain structural features. A case in point is the 1,3-diketone unit, celebrated for its ability to form stable complexes with many metal ions by way of its enol tautomer. Metabolites possessing this structural unit are thus "obvious" contenders in the coordination stakes. However, the scarcity of examples based on such clear-cut analogies is noteworthy; even qualitative evidence, such as colorimetric tests for metal complexation, is uncommon. For the simple dinoflagellate metabolite **23**, for instance, the evidence for interaction with metals was a spot test, reported in a simple phrase stating that the compound was "strongly ferric chloride positive", on which was built a minor fantasy concerning the potential of the compound as an excellent trace-metal chelator.[39] Even with a more complex natural product such as the acyl tetramic acid discodermide (**24**) from the sponge

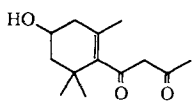

23

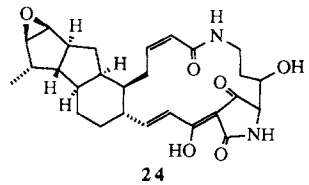

24

Discodermia dissoluta,[40] complexation studies were confined to the observation of an orange-red coloration with iron(III) chloride and the formation of a greenish-yellow complex with copper(III) acetate; both features were used as supporting evidence for the enolized 1,3,5-tricarbonyl grouping.

Yet the lure of the "obvious" can be dangerous for the unwary. A cautionary tale is tucked away in the literature pertaining to a group of condensed polycyclic alkaloids found in certain tunicates. In attempts to elucidate the structure of 2-bromoleptoclinidinone, an antileukemic metabolite isolated from *Lissoclinides* sp., the range of likely structures was narrowed down to several candidates, including **25a** and **26**, on the basis of long-range NMR coupling data.[41] Structure **25a**, which incorporates a 1,10-phenanthroline substructure, was ruled out partly because the alkaloid failed to give a red complex with the iron(II) ion, a simple colorimetric test that is usually very sensitive to this tricyclic ligand. The correct structure was later shown, in fact, to be **25a**;[42] for whatever reason, the intuitively expected interaction with the metal ion was not manifested. This is not an isolated observation: related alkaloids such as ascididemin **25b**,[43] eilatin **27**,[44] and calliactine[45] also failed to give complexes with Fe^{II}. (The structure of calliactine, incidentally, is still unsolved, but formerly discarded structures based on 1,10-phenanthroline should now be reconsidered.) In point of fact, the ability to form complexes depends very much on the metal used. Eilatin (**27**) associates with Ni^{II}, as evidenced by shifts in its UV spectrum on the addition of salts of the metal.[44] To come full circle, 2-bromoleptoclinidinone (**25a**) has recently been converted into an octahedral Ru^{II} complex that can intercalate into double-stranded DNA and serve as the initial site for photochemical cleavage.[46] The message

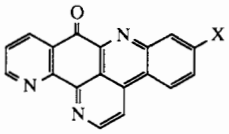

25a X = Br
25b X = H

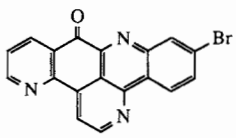

26

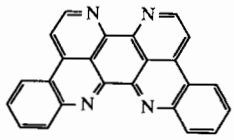

27

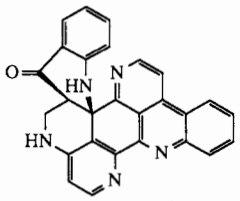

28

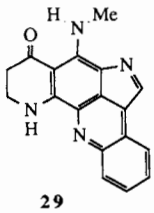

29

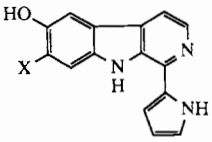

30 X = H, Br

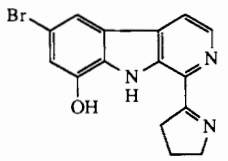

31

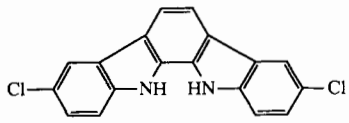

32

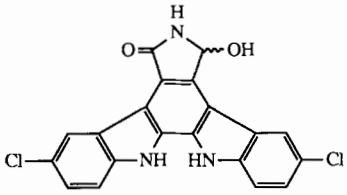

33

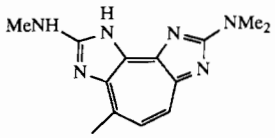

34

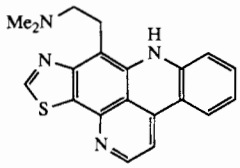

35

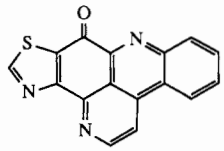

36

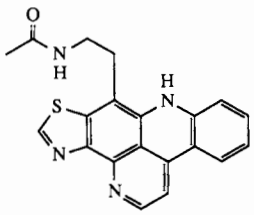

37

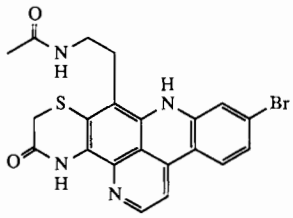

38

of the story is that the mere expectation of metal–metabolite interaction is not enough; the acute researcher needs to probe relationships between ligand structure and metal selectivity as well. A small group of marine alkaloids having 2,2′-linked azacyclic rings would thus appear to contain interesting candidates for chelation studies, since not only are the nitrogen atoms suitably placed for bidentate coordination to metal ions, but subtle electronic influences and spatial effects arising from small structural differences in the rest of the polycyclic skeletons should guarantee a measure of selectivity. Compounds deserving attention include other 1,10-phenanthrolines or reduced analogues such as eudistone B (**28**),[47] and plakinidine A (**29**),[48] several β-carbolines bearing pyrrol-2-yl or dihydropyrrol-2-yl substituents at C1 such as the eudistomins **30**[49] and eudistomidin A (**31**),[50] indolo[2,3-*a*]carbazoles like tjipanazoles D (**32**) and J (**33**),[51] bisimidazoles like paragracine (**34**) and related alkaloids,[52] and finally an interesting group of alkaloids in which one of the pyridine rings of the phenanthroline system is replaced by thiazole or 1,4-thiazine as in nordercitin (**35**)[53] and kuanoniamines A (**36**) and D (**37**),[54] and shermilamine A (**38**).[55]

Perhaps the most important examples of "obvious" ligands are hydroxamates and catechols, which have the potential to bind and transport iron(III) ions. Natural siderophores have profound biological significance,[56] since they can assimilate iron from a variety of sources and transport it across membranes to sites where it is needed for functions such as respiration. Few siderophores have been isolated from marine sources, however. One of them is bisucaberin (**39**), a 22-membered hydroxamate-based macrocycle from the bacterium *Alteromonas haloplanktis*.[57, 58] Its ability to sensitize tumor cells to macrophage-mediated cytolysis was suspected to arise from its trapping of iron within the cells, thereby

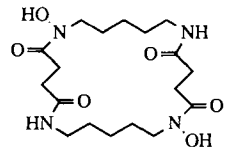

39

preventing the metal from participating in mitochondrial respiration.[57] The evidence stemmed from the failure of a preformed bisucaberin complex to stimulate tumor lysis. The bisucaberin–iron complex could be formed as a red water-soluble species with iron(III) chloride. So far there have been no quantitative studies on the bisucaberin–metal interaction, but researchers who have synthesized the metabolite report that they are currently measuring binding constants with Fe^{III} and Cu^{II}.[59]

Despite the profusion of phenolic natural products from marine sources, very few are proven siderophores. Anguibactin (**40**), a somewhat exotic metabolite possessing catechol, hydroxamate, imidazole, and thiazoline units, was isolated[60] from the virulent fish pathogen *Vibrio anguillarum* 775. The full structure was deduced only after crystallographic investigation of a derivative.[61] The compound has

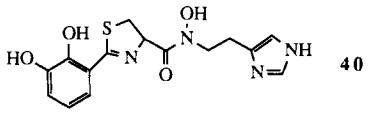

40

such an affinity for the iron(III) (but not iron(II)) ion that the microorganism source had to be cultured in an iron-starved medium, and the metabolite purified with deionized chromatographic materials.[60, 61] The bonus was that anguibactin (**40**) could easily be assayed spectrophotometrically with iron(III) perchlorate. Indeed, metal chelation was exploited as an aid in structure elucidation: evidence for the catechol unit was deduced from colorimetric tests with Fe^{III}, and from characteristic features in the IR, UV/VIS, and resonance Raman spectra of the complex.[60] As a token of the compound's high affinity for iron(III) ions, a complex was prepared in solution by ligand exchange with the (ethylenediaminetetraacetate)iron complex. Electrophoretic mobility showed that the binding with Fe^{III} had displaced three protons, and FAB mass spectrometry provided evidence for a 1:1 complex by showing an ion for $[M + Fe + 2H]^+$. The most conclusive evidence for anguibactin's ability to function as a ligand, however, has so far been revealed only as a note added in proof:[61] the racemic metabolite and Ga^{III} form a crystalline 1:1 complex, the structure of which has been elucidated by single-crystal X-ray diffraction. The ligand coordinates to the metal through the deprotonated imidazole ring, the hydroxy group of hydroxamate, the nitrogen atom of the thiazoline ring, and the catechol unit's *ortho*-hydroxy group.

Conspicuously rare in the foregoing pages are examples of a ligand type that has become a modern classic: the macrocycle. There is no dearth of macrocyclic marine metabolites containing suitable donor atoms for chelation; aspirant ionophores, which include macrolides, macrolactams, cyclic peptides, and polyethers, flaunt structural features that should make a coordination chemist drool. It is surprising, therefore, that the metal-binding properties of so few of these have been examined, and that even their potential for coordination has largely been passed over without comment. Apart from the comparatively predictable porphyrins and the more interesting aplasmomycins (**12**) and bisucaberin (**39**), ionophore activity has been reported only for the sarains (**41**),[62] sponge alkaloids in which the macrocycle can scarcely be regarded as a donor of "obvious" type. These alkaloids are effective phase-transfer catalysts, facilitating the esterification of potassium acetate with benzyl chloride almost as well as [18]crown-6 does.

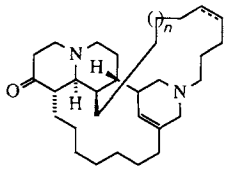

41, $n = 1, 2$

Opportunities for substantial research effort are clearly being missed with macrocyclic marine natural products in general. However, this is an appropriate moment at which to stress a fundamental feature that needs to be properly evaluated before one embarks on wild speculations. For effective ligand function, it is essential that likely donor atoms or groups be directed towards a focal position at which a metal ion can be located. Structural features such as the folding of the molecular backbone, the directionality of polar functional groups, intramolecular separations, and (for macrocyclic substances) approximate cavity size and shape, are all fundamental to the proper understanding of metal complexation. The three-dimensional shapes of the molecules are thus critically important factors in the quest for metal–metabolite interaction, and a knowledge of molecular conformation can prevent the waste of time and effort. Since genuine examples of metal–metabolite interactions involving compounds of marine origin are exceedingly rare, researchers keen to take up the challenge presented by the phenomenon should be guided not only by the gross structural features of the candidate ligands but also by any available conformational data. It is also important to realize that the most highly populated conformer may not actually be suitable for complexation; molecular reorganization may be necessary to get the donor atoms into appropriate orientations for metal chalation. A great deal of the remaining material in this review will be concerned with speculations constructed on the basis of conformational data from a variety of sources.

5. Chelation and Spectroscopy

Spectroscopic methods figure prominently in the coordination chemist's examination of both qualitative and quantitative aspects of metal–ligand interactions.[63] These methods are generally sensitive, seldom requiring large quantities of materials, and therefore suited to the study of compounds that may be available in only limited amounts, as most

marine metabolites are. It is consequently most surprising that despite the inevitable use of spectroscopic techniques for elucidating the structures of marine natural products, applications in studying interactions with metal ions have almost never been considered. The sole examples we have come across reporting the use of optical spectroscopies (IR, UV, and Raman) were pointed out in previous sections of this review.

Fast-atom bombardment (FAB) mass spectrometry has frequently been used as an indicator for metal ion interaction with marine metabolites. Molecular ions of low intensity can be enhanced by complexation with metal cations sputtered from solution by fast atom impact, because fragmentation of the resulting $[M + \text{metal}]^+$ species is often suppressed. Alkali metal iodides are commonly used with complex natural products, although Ag^+ and Tl^+ have also found application.[64] It is doubtful, however, whether the technique necessarily indicates the sort of chelation effect that we are discussing in this review. Association of species in the gas phase is intrinsically unlikely to be a good analogy for interactions (if any) in the solution phase or in the solid state, and will in any case seldom be a reliable guide to the site-specificity of metal binding unless a metal-enhanced fragment ion is present as well. Those who have applied the method in studying marine metabolites have never looked for effects other than the obvious one of molecular ion enhancement. Some researchers have even pointed out the dangers of interpretating the interaction: for example bryostatins 1–3 (see Section 7.1) were observed to complex strongly with Ag^+ in the FAB mass spectrum, but, as acknowledged in a footnote, complexation with the diene side chain might be the factor responsible for the association.[65] The interested reader may care to draw his or her own conclusions about the nature of the metal–metabolite interaction for the following marine natural products: bengamides (for example, **42** with Na^+);[66] various bryostatins (**52** with Li^+, Na^+, K^+, Cs^+, or Ag^+);[65,67] discodermins (**43** with Na^+);[68] iejimalides (**44** with K^+);[69] janolusimide (**45** with Na^+);[70] laulimide and isolaulimide (**46** and **47** with K^+ or Cs^+);[71] neristatin 1 (**54** with Li^+);[72] oscillariolide (**48** with Na^+);[73] and patellazole C (**49** with K^+).[74]

The almost total neglect of NMR methods for detecting metal–metabolite interactions is all the more disappointing in view of the prominence of one- and two-dimensional NMR methods in the elucidation of the structures of marine natural products. As far as we are able to determine, only two publications, both very recent, report such metal complexation. A study of the conformation in solution of okadaic acid (**50a**), isolated for the dinoflagellate *Prorocentrum lima* as an unspecified "metal complex", revealed diagnostically useful, though minor, chemical shift differences between the free and the complexed metabolite.[75] Far more significant, however, and perhaps the most important in vitro study on the complexation of the marine natural product to date, is the thorough series of investigations on jasplakinolide[76] (**51**, also known as jaspamide[77]), a sponge metabolite of considerable interest because of its anthelminthic, insecticidal, ichthyotoxic, cytotoxic, and antifungal properties.

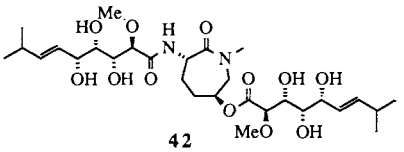

42

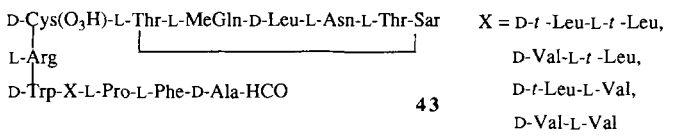

43

X = D-*t*-Leu-L-*t*-Leu, D-Val-L-*t*-Leu, D-*t*-Leu-L-Val, D-Val-L-Val

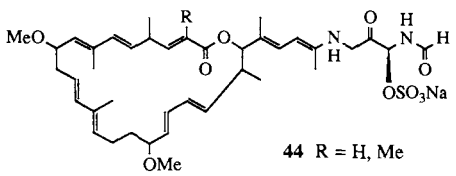

44 R = H, Me

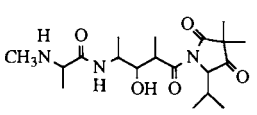

45

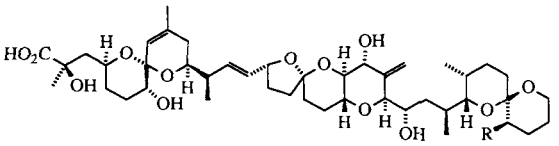

50a R = H
50b R = Me

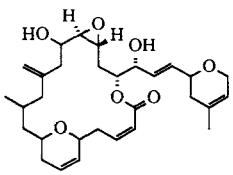

46

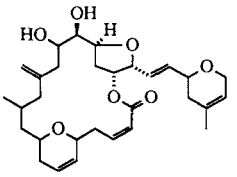

47

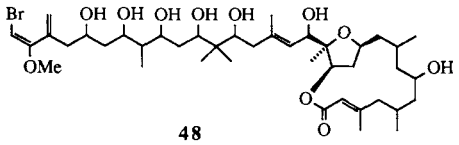

48

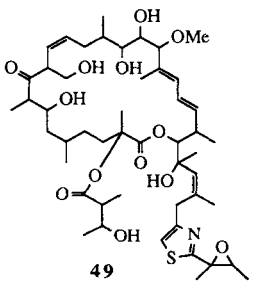

49

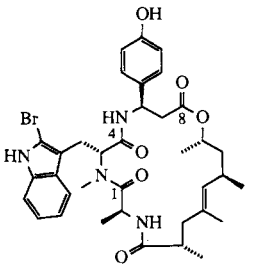

51

Compound **51** was the first mixed macrocyclic polyketide–depsipeptide to be isolated from a marine organism. In an extension of a comprehensive investigation of conformational effects in solution,[78] the titration of the macrolide with various alkali metal salts ($LiClO_4$, LiBr, NaSCN, KSCN; in CD_3CN) was monitored by ^1H and ^{13}C NMR spectroscopy.[79] Significant differences in the chemical shifts

were found only with lithium as cation. Moreover, the signals most affected suggested that only the carbonyl oxygen atoms at C1, C4, and C8 were involved in forming a 1:1 chelate. The values of the observed proton coupling constants at the endpoint of the titration suggested a conformation for the macrocycle corresponding to just one of two

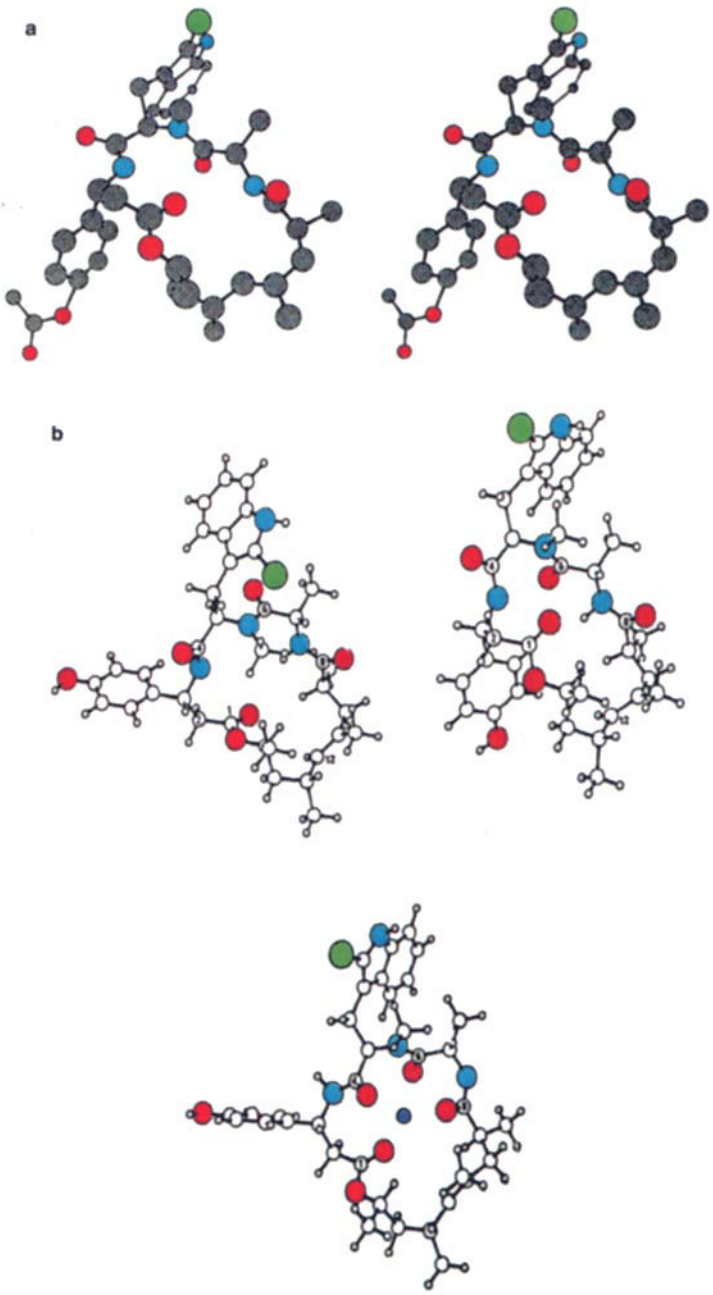

Fig. 3. a) Stereoscopic view of the X-ray crystal structure of the acetate of jasplakinolide **51**. b) Top: structures derived from molecular mechanics calculations for the two major conformers, $1g^+$ and $1g^-$, of jasplakinolide. Bottom: corresponding structure for the lithium complex of jasplakinolide. (Adapted and reprinted with permission from ref. [79].)

major conformations deduced from a similar interpretation of J values for the uncomplexed ligand and also from constrained minimization and dynamics calculations (Fig. 3).[78] A weak binding constant of about 60 M^{-1} and a ΔG value of -10 kJ/mol^{-1} were calculated. These are the only quantitative data we have uncovered that relate to metal-binding to marine natural products!

The jasplakinolide studies break new ground for a further reason: they contain the only example of the molecular modeling of a marine metabolite in the presence of metal ions. When the interactions of sodium and lithium cations with likely backbone conformations of the macrocycle were modeled with a constant dielectric term similar to the dielectric constant of acetonitrile, the conformation most suited to metal binding proved to be essentially the same as that deduced from the NMR studies (Fig. 3b). Calculated coupling constants agreed well with experimentally determined ones. The computed metal–ligand affinity was reasonable only for lithium, which lay in the plane of the macrocycle at an acceptable bonding distance of about 2.0–2.1 Å from the same three carbonyl groups that were indicated in the spectroscopic study, and considerably further from other donor sites. A footnote contains the intriguing mention of a higher order (2:1?) jasplakinolide–LiBr complex that precipitated from solution.

At this point it is perhaps appropriate to highlight the importance of NMR methods in studying molecular conformation in solution. The difficulties of extracting this information, however, can be immense. The Karplus equation (and its many successors) quantifying the relationship between vicinal coupling constants ($^3J_{H,H}$ in particular) and dihedral angles allows one, in principle, to construct, albeit piecemeal, a three-dimensional model of a given molecule as long as certain provisos are borne in mind. Firstly, if conformers interconvert at rates equal to or faster than the timescale of the NMR experiment, observed J values may translate into misleading torsional relationships. Secondly, because of the nature of the terms in the Karplus equation, a given coupling constant will, more often than not, correspond to several alternative values of the dihedral angle. It may thus not be possible to fit the data to a unique conformation. It is not surprising, therefore, that detailed conformational analyses of complicated marine natural products are rather rare. One must also bear in mind that the most abundant conformation in solution will not necessarily be the best for embracing a metal cation. In the more speculative sections of this review that follow, NMR conformational studies that might have implications for metal–metabolite interaction will be presented alongside studies that employ crystallographic and computational techniques.

6. Crystallographic and Computational Signposts for Chelation

X-Ray crystallography is a powerful and much-used tool in the structural elucidation of uncomplexed marine metabolites, often providing the only unambiguous evidence for structural features, stereochemistry, and even absolute configuration. By contrast, diffraction studies involving metal complexes of marine metabolites are woefully few (see the previously described aplasmomycins (**12**) and the zinc complex of clathridine **7**), especially when compared with the ever-growing number of similar studies on metal complexes of terrestrial natural products. However, a significant bonus

of crystallographic methods is that topological information, generally difficult to obtain by other means, can be extracted relatively easily. Admittedly, electrostatic forces, hydrogen bonds, and packing considerations may all conspire to produce a solid-state conformation that might be misleading for studies of complexation equilibria and kinetics in solution. On the other hand, crystallographic data should be seen as a signpost: not an infallible guide to the complexation phenomenon, but a useful aid to those of us seeking direction. It is regrettable that the accumulation of X-ray diffraction data relating to marine metabolites is still a largely untapped resource, since as long as one has access to atomic coordinates (e.g., from the Cambridge Structural Database, see reference [18]), the manipulation of data is relatively straightforward. As will be indicated in subsequent sections, several authors have explicitly extracted conformational information from their crystallographic data, and a few have even gone as far as expressing tentative opinions on implications for the binding of cations by marine metabolites.

Molecular mechanics calculations, once securely in the domain of theoretical chemists, have now become a tool that is widely available to all chemists, thanks largely to the commercial availablility of computer software packages in varying degrees of sophistication. At their best, they offer the average user comparatively painless access to a variety of alternative methods of modeling structures, computing energy minima, and obtaining information (including graphical information) on molecular topology. It is possible to be too naive in using these methods, however, and one needs to be aware of their inherent limitations. The force fields themselves may be designed for specific molecular types; the parameters contained therein, though representing workable averages, are invariably subjective to some extent (they can usually be modified, at one's peril); parameters for unusual bond types or atoms in unusual environments may simply not be present; and the time taken to perform calculations may vary considerably according to the available equipment. The time can often be shortened if one commences from atomic coordinates derived from sources such as X-ray crystallographic data, but unless well versed in the methods, one might compute a local energy minimum that is biased towards the starting coordinates. The best packages will have a conformational search option allowing the location of all stable conformations within a specified energy range as well as the global energy minimum. This can be especially important for predicting suitable conformations for metal chelation, as the lowest energy conformation need not have an appropriate geometry for metal binding. One must also realize that the species modeled is generally an isolated molecule, the conformation of which may not be typical of the state of affairs in a molecular ensemble present in solution. Molecular dynamics calculations, which can simulate a solvent environment, are preferable in many cases, but require much more computer time. In the light of these problems it is little wonder that very few marine metabolites have been modeled by computational methods. Modeling of metal–metabolite interactions is, in consequence, unknown with this group of natural products, except for jasplakinolide,[78] as previously mentioned. A major contributory factor to this unsatisfactory state of affairs is the paucity of properly parametrized data for metal ions.[80]

7. Hypotheses and Hunches

In the absence of other information relating to metal complexes of marine natural products, conformational studies by spectroscopic, crystallographic, and computational methods should be seen as providing useful grounds on which to base hypotheses. The subjective manipulation of conformational data thus provides a necessary bridge between the worlds of fact and fantasy. In the following section, we cross over into the realm of fantasy, highlighting published speculations that have been based on conformational premises. We also present additional examples of candidate structures that we consider to be worthy of the attention of interested chemists.

7.1. The Bryostatins

The growing family of bryostatins (**52**–**54**), macrolides from the marine bryozoan *Bugula neritina*, is of considerable interest because of the antineoplastic, cytostatic, and immunomodulatory activity of certain members. To date, bryostatins 1–15 have been reported, and several related compounds have also been described.[65,67] Most are characterized by the "bryopyran" core **55**, a 20-membered tetraoxamacrolide in which three of the four oxygen atoms are constituents of tetrahydropyran rings and the fourth is in the acyloxy group of the lactone. The best studied and most

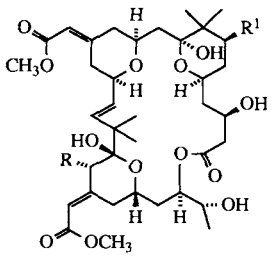

52 R= H, OH, $OCOR^2$
R^1= OH, $OCOR^3$

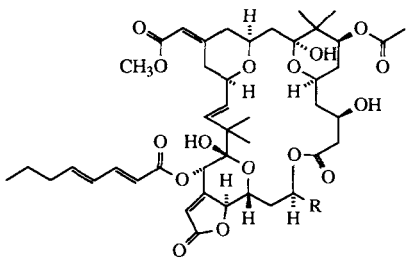

53 R= CH(OH)Me, COMe

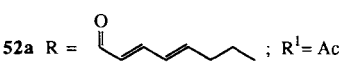

52a R = ; R^1= Ac

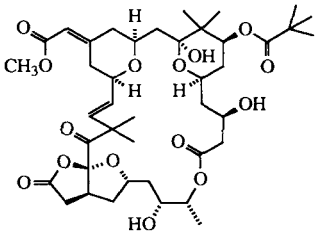

54

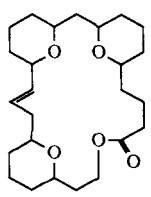

55

abundant compound, bryostatin 1 (**52a**) has been the subject of much spectroscopic and biological study, and an X-ray crystallographic investigation at low temperature has revealed its full structure (Fig. 4).[81] The authors of this study

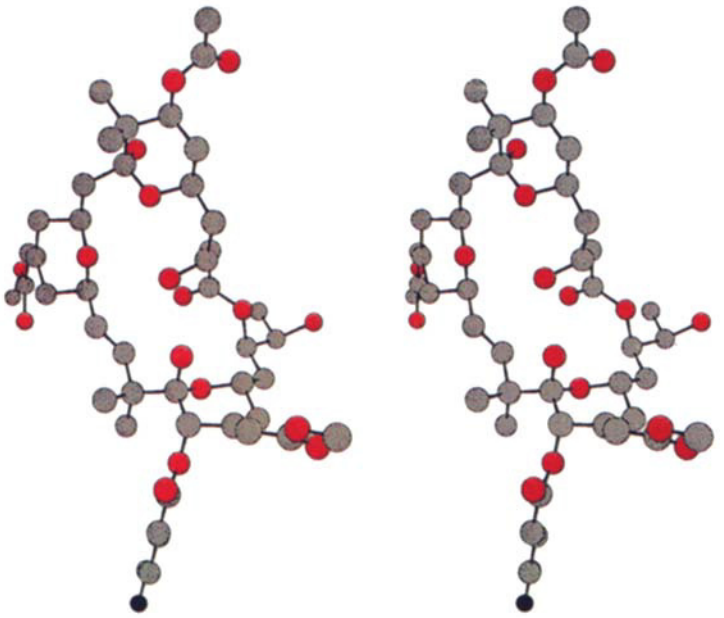

Fig. 4. Stereoscopic view of one of two molecules in the asymmetric unit of bryostatin 1 (**52a**). The disordered alkyl side chain is represented by the black circle.

highlighted the "scoop shape" of the molecule in the solid state, pointing out the location of the tetrahydropyran oxygen atoms, the carbonyl group of the lactone, and two other hydroxy groups on the interior surface of the oxygen-rich cavity. These are the bare facts. The minor fantasy derived therefrom is typical of the bland and inoffensive statement that one encounters in the literature of potential marine ionophores: "The size and shape of this cavity and the arrangement of oxygen atoms suggest that the molecule may have cation-binding capabilities, similar to the polyether antibiotics."[81] The lipid chain, it was felt, might swing over the cavity and seal one side. A later publication developed the theme, adding a speculation relating to some biological explorations: "The bryostatins may prove to be important ionophores for altering membrane permeability."[82] In these few tentative words and the previously mentioned FAB-MS results resides the *entire case* for bryostatins as metal chelators, at least as presented in the chemical literature. Now that an improved isolation procedure has ensured the availability of gram quantities of bryostatin 1 for important clinical purposes,[83] it is to be hoped that material can be spared for enterprising workers to take up the challenge of its coordination chemistry.

7.2. Other Macrolides and Polyethers

The scoop shape, an attractive vehicle for encapsulating a cation, is not limited to macrocycles. X-ray structure analysis has shown that the sponge metabolite acanthifolicin (**56**), a linear polyether containing spirofused tetrahydrofuran and tetrahydropyran rings, forms a cavity of diameter 5–7 Å, which is held in place by a hydrogen bond (Fig. 5a).[84]

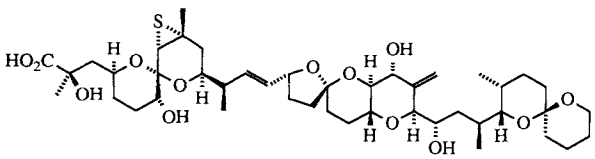

56

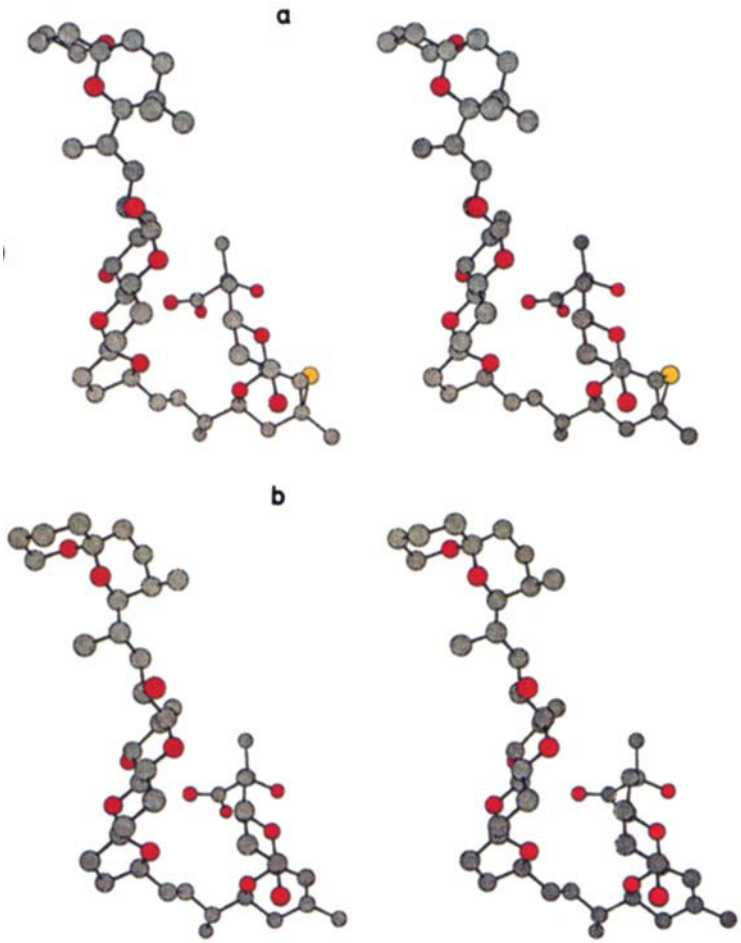

Fig. 5. Stereoscopic views of the X-ray crystal structures of a) acanthifolicin (**56**) and b) a derivative of okadaic acid **50a**. The *o*-bromobenzyl ester group of the latter has been omitted for clarity.

Ten oxygen atoms cluster around this cavity, seven of them within 4 Å of a central point. "A situation quite suitable for complexation of a cation" was the sole comment on this highly suggestive arrangement. The X-ray crystal structure (Fig. 5b) of the closely related dinoflagellate product okadaic acid (**50a**), determined for the *o*-bromobenzyl ester,[85] is similar to that of acanthifolicin (**56**), but the conformation and its implications have passed without comment. The previously mentioned NMR study of okadaic acid's solution conformation,[75] incidentally, correlated well with the solid-state conformation. Some relatives of okadaic acid, the dinophysistoxins **50b**, are thought to be produced by dinoflagellates ingested by edible molluscs that then cause severe diarrhoea on human consumption;[86] it would be fascinating to explore a possible connection between toxicity and ionophore activity.

Linear, bridged, and spirocyclic tetrahydrofuran and tetrahydropyran units are components of several other marine metabolites whose structures have been disclosed by X-ray diffraction techniques. The macrolide ring of pectenotoxin 1

(**57**), another diarrhetic shellfish toxin produced by a dinoflagellate present in the digestive gland of scallops, is a "large oxygen-rich cavity ... grossly similar to the cavities found in the polyether ionophores from terrestrial microorganisms".[86] Most of the polyether macrolides produced by sponges of the genus *Theonella* have slipped by without comments relevant to our present purpose, other than in the case of the antifungal and cytotoxic compounds swinholide A (**58a**). Initially formulated as a 22-membered macrolide,[87]

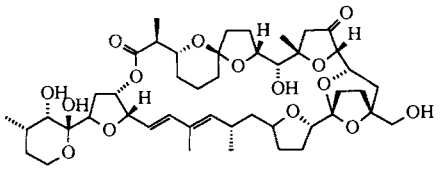

57

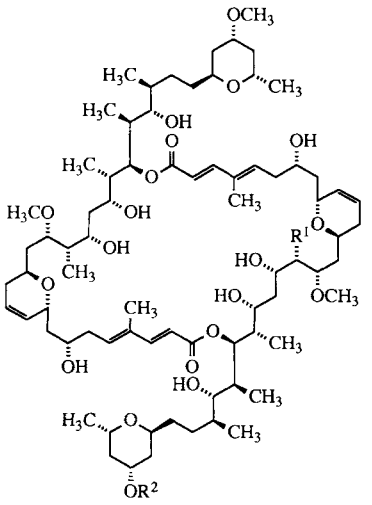

58a $R^1=R^2=Me$
58b $R^1=H$, $R^2=Me$
58c $R^1=Me$, $R^2=H$

it was later shown by FAB-MS to have twice the expected molecular mass.[88] X-ray crystallography on a diketoester derivative[89,90] subsequently revealed a 44-membered macrodiolide having a twisted saddle shape with turns at the dihydropyran rings, and slightly distorted from the expected C_2 symmetry. This derivative structure was extrapolated to the parent metabolite,[90] for which the authors deduced a conformation in which "oxygen atoms ... are all directed into the interior of the ring structure". The argument was taken no further; perhaps nothing more than imagination makes us sensitive to the reverberations of this unadorned statement and the published stereoscopic views of the molecule (Fig. 6). The relatives of swinholide A (**58a**) are numerous: swinholides B (**58b**) and C (**58c**),[91] isoswinholide A (**59**),[91] bistheonellides A, B, and C (**60**)[92,93] (the first of which has also been named as misakinolide A[94]), and isobistheonellide A (**61**)[93] are all macrodiolide isomers or lower homologues of swinholide A that might reasonably be expected to behave towards metal ions in a related fashion. Norhalichondrin A (**62**), an antitumor agent from the sponge *Halichondria okadai*, appears to be the only other complex polyether marine metabolite to have been the subject of crystallographic investigation,[95] but in this case the comparative rigidity imposed by the arrays of fused tetrahydrofuran and tetrahydropyran rings makes the macrocycle an unpromising receptacle for metal ions.

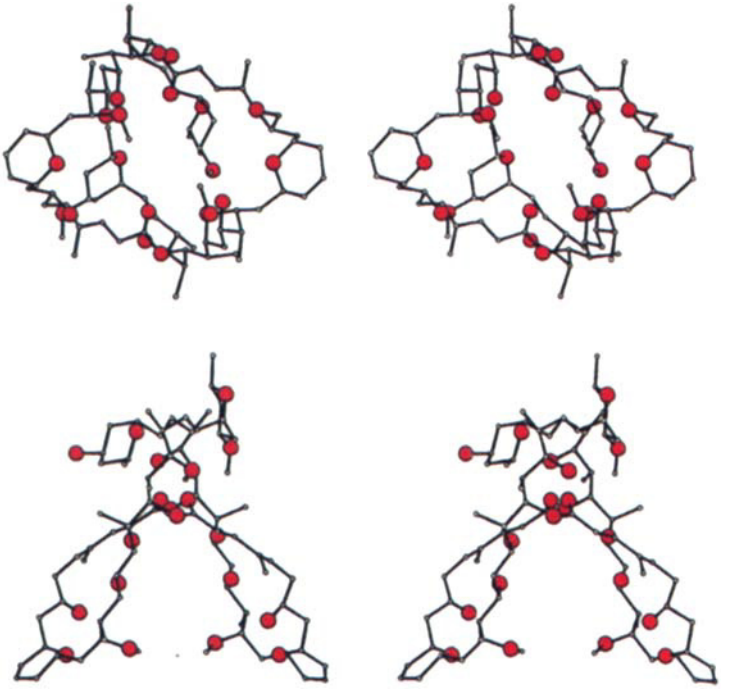

Fig. 6. Stereoscopic views of a possible molecular conformation for swinholide A (**58a**), viewed aloing the pseudo-C_2 symmetry axis of the molecule (top), and perpendicular to this axis (bottom). (Adapted and reprinted with permission from ref. [90].)

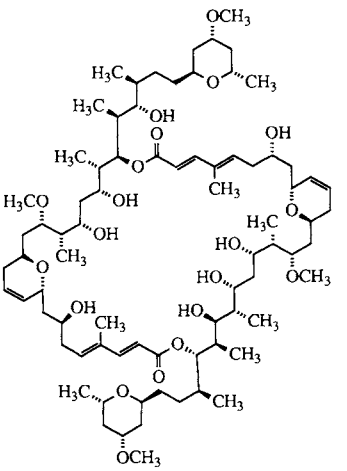

59

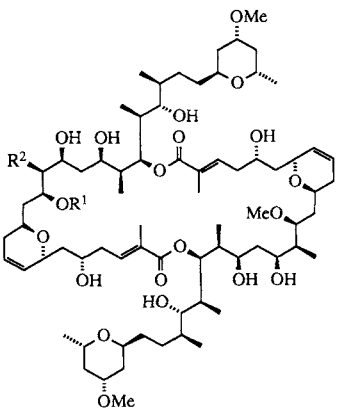

60 $R^1 = R^2 = H$, Me

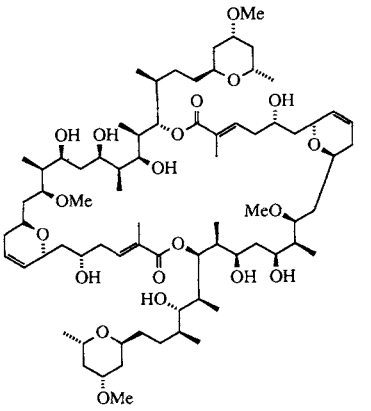

61

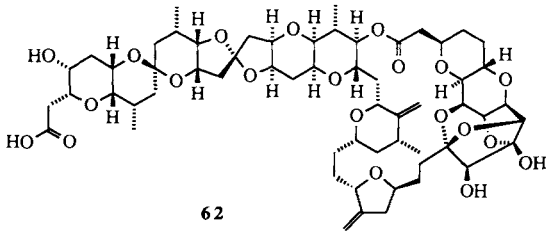

62

Solid-state conformations revealed by diffraction methods may prove a less useful guide when molecules are floppy, since steric effects and electrostatic repulsions may promote accessible conformations remote from those needed for a comparatively ordered metal-centered chelate. Thus, while several polyethers from red algae of the genus *Laurencia* have been studied by crystallography, the disposition of the donor oxygen atoms in the resulting solid-state structures is not suitable for multidentate interaction with cations unless substantial molecular reorganization occurs. The potential ability of compounds like chilenones A (**63**)[96] and B (**64**),[97] thyrsiferol (**65a**),[98,99] and venustratriol (**65b**)[99] to wrap themselves around metal ions is not apparent from the published structural models. Teurilene (**66**),[100] an elegantly symmetrical linear tristetrahydrofuran, though tantalizingly reminiscent of a cleaved crown ether, would also need flexing of its solid-state conformation to enfold a cation. There is not even a hint of a possible ionophoric role in any of the publications dealing with these compounds.

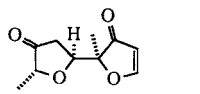

63

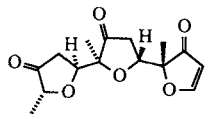

64

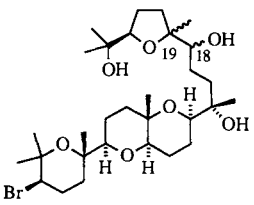

65a 18β-OH, 19β-Me
65b 18α-OH, 19α-Me

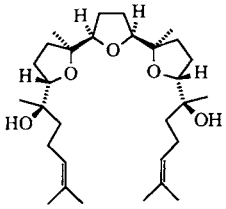

66

7.3. The Didemnins

Caribbean tunicates of the genus *Trididemnum* are the source of a small family of cyclic peptides called the didemnins, which are powerful antitumor and antiviral agents.[101] Didemnins A (**67a**), B (**67b**), and C (**67c**) in particular have been the subjects of numerous structural, synthetic, and biological studies.[11a,102] Furthermore, conformations of didemnins A and B in solution have been elucidated by NMR methods,[103,104] and rationalized further with the aid of restrained molecular dynamics calculations.[104] The structure of **67b**, the most potent metabolite of the group, has also been determined crystallographically.[105] The spectroscopic, crystallographic, and calculational approaches agree substantially on the conformation adopted by the essentially rigid macrocyclic ring. Minor differences (and alternative conformations) tend to arise from variations in the orientation of side-chain substituents rather than the basic ring structure. However, the commentary provided by the authors on the crystallographic analysis introduces, for the first time in this review, a note of genuine doubt about the feasibility of interaction with cations. The conformation of the cyclic moiety, it is pointed out, "resembles the cavity formation of many large polypeptides that form complexes". It is a "twisted figure 8", stabilized by a transannular hydrogen bond. A closer look at the oxygen atoms shows that "most of them are pointed away from the interior of the cavity" (see Fig. 7). What significance does one attach to this

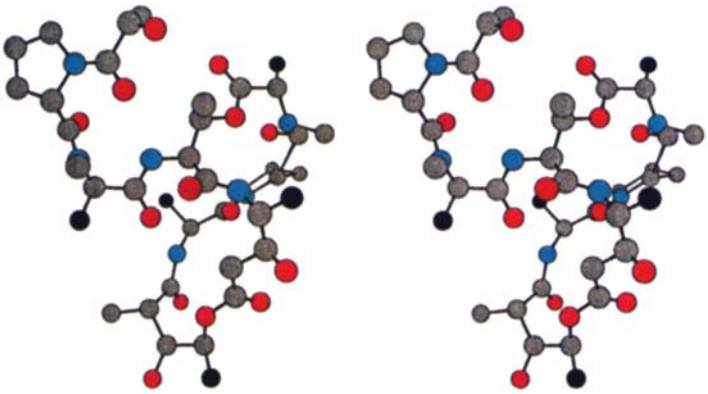

Fig. 7. Stereoscopic view of the crystallographically determined structure of the backbone of didemnin B (**67b**). Various side chains, omitted for clarity, are represented by the black circles.

observation? An isolated study in the biological literature has demonstrated that didemnins A and B fail to complex or transport sodium and potassium cations.[106] The temptation to link this observation and the conformational findings

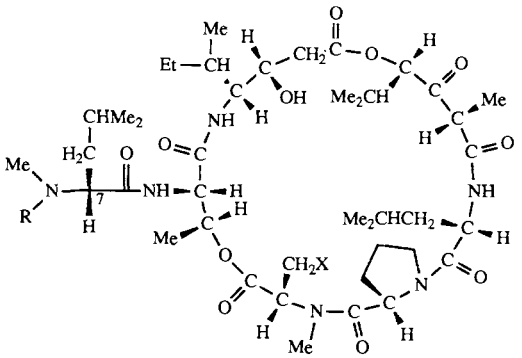

X = 4-OMeC$_6$H$_4$

67a R = H

67b R = MeCHOHC(=O)–N<

67c R = MeCHOHC(=O)–

is irresistible; the likely connection is indeed explicitly mentioned in the crystallographic study. To our knowledge, these results, considered in combination, constitute the only serious evidence *against* a metal–metabolite association to be found in the whole canon of researches dealing with marine natural products. It is interesting that while a synthetic analogue of didemnin B (**67b**) with a methyl-L-leucine substituent replacing the natural methyl-D-leucine at position 7 has considerably reduced biological activity, NMR and molecular dynamics calculations on the major conformer showed only minor differences in conformation for the macrocyclic backbone compared with **67b**.[107]

7.4. The Dolastatins

The dolastatins, for example **68**–**73**,[108] form a heterogeneous group of potent antineoplastic and cytostatic peptides isolated from the sea hare *Dolabella auricularia*, though the primary source may be a dietary cyanobacterium. Of the fifteen numbered dolastatins, seven have been fully or partially characterized,[101] sometimes only after intense efforts that have included the total synthesis of alternative structures. The only link between these compounds is their name and their source; otherwise, points of structural similarity are few. Some are linear and some cyclic, and all contain unusual components that include highly modified amino acid residues, lactone units, polyketide fragments, and thiazole rings. Furthermore, none of these compounds has been characterized crystallographically, and the literature contains no speculations whatsoever on possible ionophoric roles. Unpromising subjects for metal complexation though these compounds appear to be, an important conformational study affords a glimmer of hope. The cyclic, thiazole-containing metabolite, dolastatin 3 (**68**), the most intensively investigated member of the group, has been synthesized and thoroughly characterized by NMR in $CDCl_3$ and $(CD_3)_2SO$ solution.[109] Circular dichroism measurements have indicated conformational homogeneity in solution, a fact confirmed by the detection of just one conformer by NMR. A self-consistent set of torsion angles was deduced from J values, and the resulting conformation was refined further by means of force-field calculations. The final model (Fig. 8) shows a saddle-shaped macrocycle with turning points between the two thiazole units and at the center of the loop centered on leucine. An intriguing observation, not explored further, was that all but one of the N–H bonds point into the middle of the ring. This is the sort of orientation that should

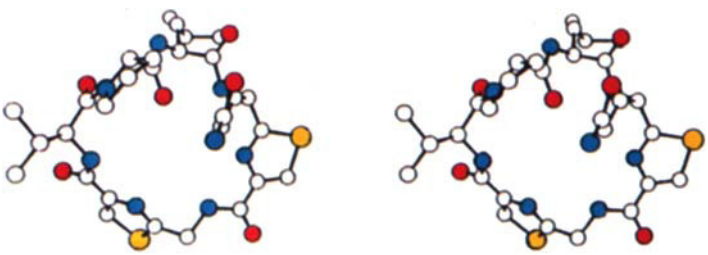

Fig. 8. Stereoscopic view of the probable conformation of dolastatin 3 (**68**) in solution, as determined from NMR data and force-field calculations. (Adapted and reprinted with permission from ref. [109].)

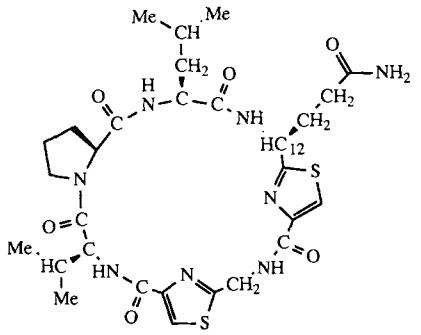

68

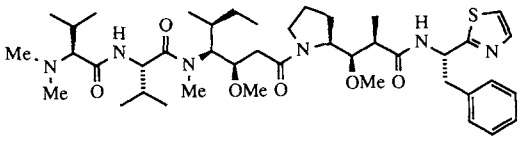

69

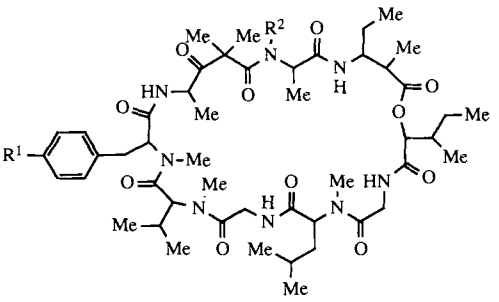

70a R^1 = OMe, R^2 = H
70b R^1 = H, R^2 = Me

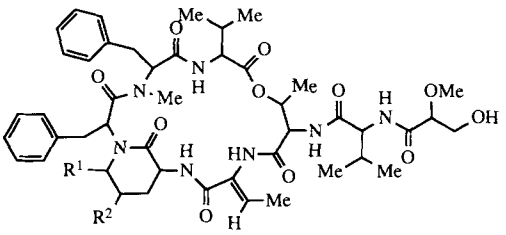

71a R^1 = OH, R^2 = H
71b R^1-R^2 = $\Delta^{14,15}$

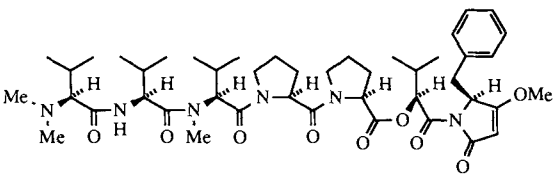

72

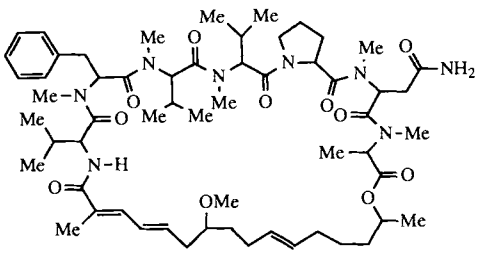

73

facilitate metal ion encapsulation. An analogous study on a biologically inactive synthetic diastereomer of dolastatin 3, differing only in absolute configuration at position 12 (12*R* rather than 12*S*), showed the only major conformational difference of the macrocycle to be the orientation of the (Gln)Thz unit.[110]

It should be pointed out that other marine organisms also produce natural products related to some of the dolastatins. The blue-green alga *Lyngbya majuscula*, responsible for an irritating condition known as "contact dermatitis" or "swimmer's itch", produces cyclic peptides, majusculamide C (**74a**) and 57-normajusculamide C (**74b**),[111] that differ in minor structural details from dolastatins 11 (**70a**) and 12 (**70b**). Any investigation of the metal-binding properties of the structurally diverse dolastatins should thus also give attention to similar metabolites from other sources.

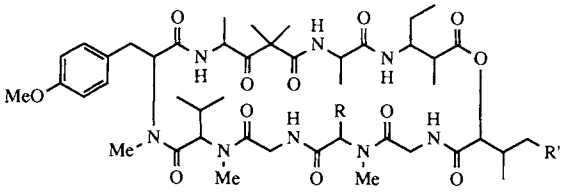

74a R = CH(Me)CH_2Me, R' = Me
74b R = CH(Me)CH_2Me, R' = H

7.5. *Lissoclinum* Peptides

Tunicates of the genus *Lissoclinum* produce several different classes of natural products, perhaps in cooperation with algal symbionts.[101] The best investigated animal is *L. patella*, the metabolites of which differ with geographical location. The largest group of compounds consits of a range of cyclic hepta- and octapeptides distinguished by the presence of thiazole (or dihydrothiazole) and dihydrooxazole rings in the macrocyclic periphery. This rather closely allied group of cytotoxins comprises ascidiacyclamide (**75a**),[112] lissoclinamides 1–8 (**76b–g**, **77**),[113–117] patellamides A–D (**75b–e**),[116,118] ulicyclamide (**76a**),[113,119] ulithiacyclamide (**75f**),[119,120] and ulithiacyclamide B (**78**),[121] as well as a number of related compounds in which the dihydrooxazole ring has been opened.[114] Spectroscopic methods have played a crucial role in the assignment of these structures, and abundant conformational data from NMR studies are available in consequence. Several X-ray crystallographic structure determinations also provide a good basis for speculations derived from conformational considerations.

There are interesting topological similarities between ulithiacyclamide (**75f**) and ascidiacyclamide (**75a**). Peptide **75f**,[119,120,122] the most potent cytotoxin in the group, has been the subject of a detailed conformational study by NMR spectroscopy. The data was used as input for energy minimization calculations,[123] which revealed an unambiguous dependence of the conformation on solvent. In a relatively nonpolar medium ($CDCl_3$ or C_6D_6), the molecule is saddle-shaped, has twofold symmetry, and a radius of curvature of about 3.4 Å. The disulfide bond is an integral stabilizing element in the structure, forming a 'strap' across the slightly

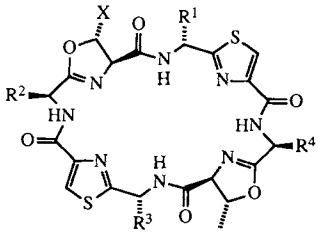

	X	R^1	R^2	R^3	R^4
75a	Me	D-Val	L-Ile	D-Val	L-Ile
75b	H	D-Val	L-Ile	D-Val	L-Ile
75c	Me	D-Ala	L-Leu	D-Phe	L-Ile
75d	Me	D-Ala	L-Val	D-Phe	L-Ile
75e	Me	D-Ala	L-Ile	D-Phe	L-Ile
75f	Me	D-Leu	L-$^1/_2$Cys	D-Leu	L-$^1/_2$Cys

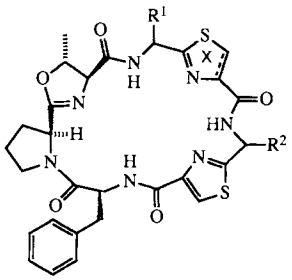

	X	R^1	R^2
76a ulicyclamide	thiazole	β-L-Ile	α-D-Ala
76b lissoclinamide 1	thiazole	β-L-Val	α-D-Ile
76c lissoclinamide 2	dihydrothiazole	α-D-Ile	α-D-Ala
76d lissoclinamide 3	dihydrothiazole	α-D-Ile	β-L-Ala
76e lissoclinamide 4	dihydrothiazole	α-D-Val	β-L-Phe
76f lissoclinamide 5	thiazole	α-D-Val	β-L-Phe
76g lissoclinamide 6	dihydrothiazole	α-D-Val	α-D-Phe

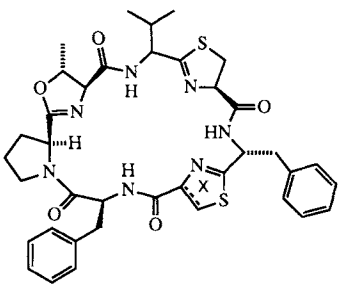

77a lissoclinamide 7 X = dihydrothiazole
77b lissoclinamide 8 X = thiazole

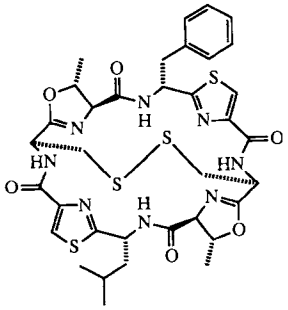

78

convex surface of the cavity, which is an approximate rectangle of dimensions 6 by 8 Å (Fig. 9). All four N–H bonds

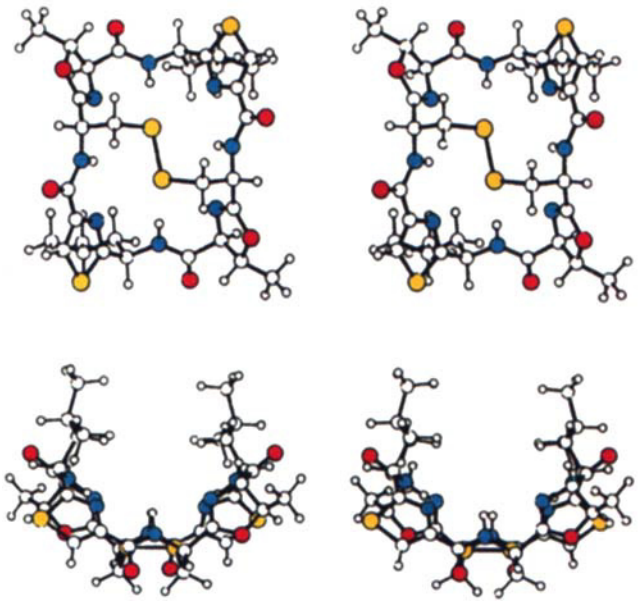

Fig. 9. Stereoscopic view of a likely conformation of ulithiacyclamide (**75f**) in chloroform solution, as viewed alog the C_2 axis (top), and perpendicular to this axis (bottom). (Adapted and reprinted with permission from ref. [123].)

point into the cavity, as do the nitrogen atoms of the azole units. The saddle shape is maintained in $(CD_3)_2SO$ solution, but the cavity is shallower and wider and the N–H bonds adjacent to the thiazole rings point away from the cavity. The molecular topology revealed in a crystallographical study of **75a**[124, 125] is remarkably similar to the nonpolar conformation of **75f**: the macrocyclic backbone is saddle-shaped with the heterocycles at the corners, and cylindrically curved (radius approximately 4 Å) about a line between the isoleucine units. The roughly rectangular cavity measures about 7.5 by 6.1 Å. Most importantly for our purposes, the N–H bonds and nitrogen lone pairs are directed towards the interior of the molecule (Fig. 10). The hollows are not empty, but occupied by benzene molecules of crystallization. Thoughts of metal chelation obviously occurred to the authors, who commented:[125] "There is no direct evidence of the interaction of these peptides with metal ions." However,

Fig. 10. Stereoscopic view of X-ray crystal structure of ascidiacyclamide (**75a**) showing encapsulation of a molecule of benzene. A second highly disordered benzene molecule has been omitted for clarity.

an intriguing suggestion about possible interactions with biomolecules was put forward on the basis of differential scanning calorimetric results obtained with a model phospholipid and nucleic acid. A conformational study of **75a** by NMR methods gave results essentially in agreement with the solid-state conformation.[125]

A comparison of coupling constants for patellamides B (**75c**) and D (**75e**)[115] suggested a structural analogy with ascidiacyclamide (**75a**), and it was postulated that these two metabolites should thus also have N–H bonds and nitrogen lone pairs pointing into the cavity, "orientations ideal for chelation to metal ions". However, an X-ray crystallographic study of **75e**[116] has shown that the solid-state conformation is quite different from that of **75a**. The molecule is severely folded into a "twisted figure 8" that deviates significantly from its potential twofold symmetry. Four transannular NH···O hydrogen bonds hold the molecule in the observed conformation. Most interestingly, an unexpected new feature emerges: the thiazole rings are aligned nearly parallel; the distance between them is a remarkably small 4.1 Å (Fig. 11). This evidence for transannular π stacking,

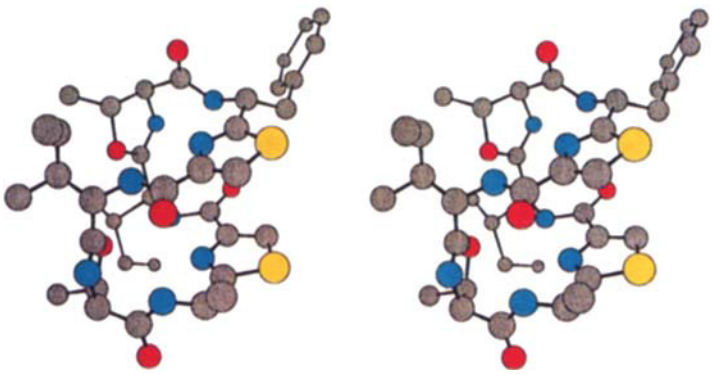

Fig. 11. Stereoscopic view of the X-ray crystal structure of patellamide D (**75e**).

unique for a marine metabolite, might well have implications for an electron-transport function for the compound in nature, as befits a charge-transfer complex, though this is not mentioned by the authors. Could it also possibly indicate interaction with metal ions by π coordination—even sandwiching—rather than by simple chelation? As a tailpiece to this interesting study, energy minimizations were performed on the structure revealed by crystallography and on a different conformation constrained to fit the ascidiacyclamide saddle. The former was calculated to be about 10 kcal mol^{-1} more stable than the latter.

Patellin 2 (**79**), a dihydrothiazole-containing cyclic hexapeptide, is strucutrally quite distinct from the compounds in the previous group.[126] Any hypothesis relating to interaction with metal ions would have to take into account a number of conformational ambiguities that have shown up in both solution and solid-state studies. For instance, *cis*/*trans* isomerization about the Val-Pro bond was responsible for a temperature- and solvent-dependent doubling up of NMR signals, the *trans* conformer dominating in polar solvents. The rotational barrier, calculated by minimization of dynamics data, was a comparatively modest 21 kcal mol^{-1}.

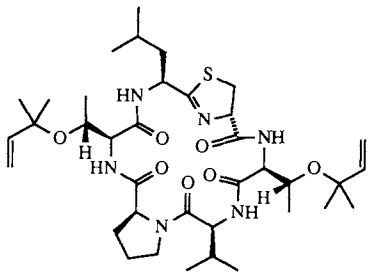

79

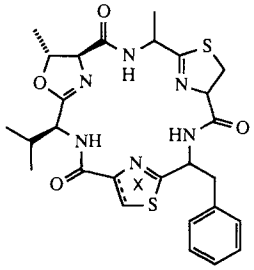

80a X = dihydrothiazole
80b X = thiazole

The *trans*-amide conformer occurred in the crystallographically determined structure (Fig. 12), but the dihydrothiazole ring was disordered, and had to be modeled with two conformations. Molecular mechanics calculations also located two distinct minima, corresponding to forms in which the torsion angles approximate those found in the solid-state structure. From the viewpoint of potential cation binding, the most significant feature of the crystallographic study is that all the nonpolar residues lie on one face of the somewhat bowed ring, while the dihydrothiazole and most of the carbonyl groups lie on the other, slightly concave, face.

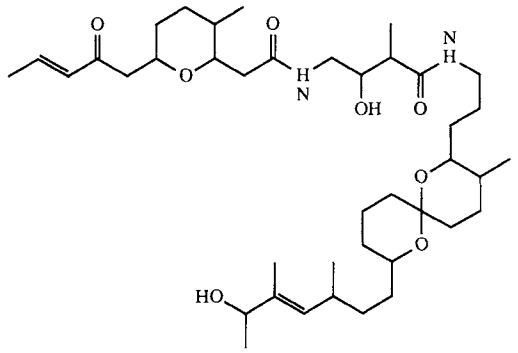

81

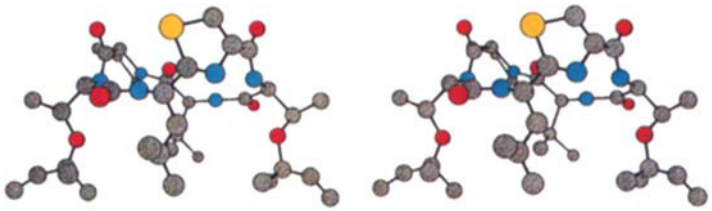

Fig. 12. Stereoscopic view of the X-ray crystal structure of patellin-2 (**79**).

A different tunicate, *Lissoclinum bistratum*, produces a further two cyclic hexapeptides, bistratamides A (**80a**) and B (**80b**), containing a dihydrooxazole ring and either two dihydrothiazole rings or one thiazole and one dihydrothiazole ring.[127] Conformational analysis of bistratamide B by NMR gave two alternative sets of dihedral angles. The larger angles corresponded to a conformation in which all nitrogen atoms pointed towards the center of the ring, the smaller to a conformation in which only the heterocyclic nitrogens do. Both might conceivably be suitable for metal attachment. The same animal also produces[127] two exceedingly potent cytotoxins of quite different constitution, bistratene A (**81**, also known as bistramide A[128]) and its acetate, bistratene B, which, as peptide derivatives having additional oxygen functionalities, should also function as ionophores.

7.6. Oxazole Metabolites

Amongst the most fascinating macrolides from marine sources are a number of compounds in which three contiguous oxazole rings, linked between positions 2 and 4, form part of the macrocyclic ring. They also possess a functionalized lipid-like side chain that terminates in an *N*-methyl-*N*-

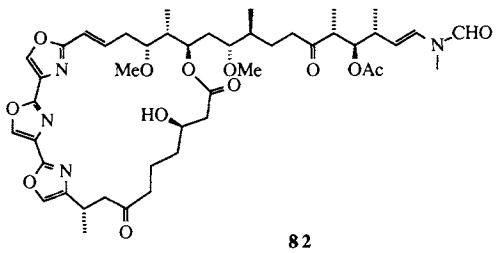

82

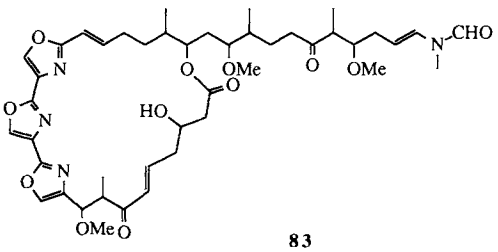

83

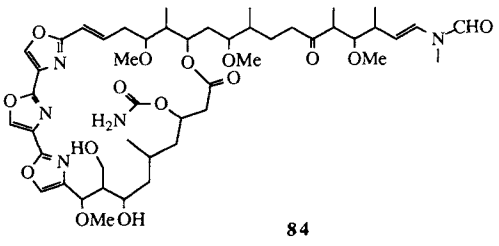

84

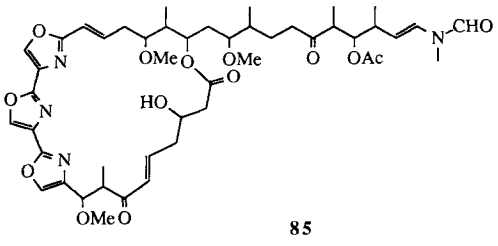

85

alkenylformamide group. These compounds, though forming a structurally homogeneous set, come from two distinct classes of marine organism: nudibranchs (principally *Hexabranchus sanguineus*), and sponges (including *Halichondria* sp. and *Mycale* sp.). The sponges might possibly form part of the diet of the animals. The nudibranch metabolites were isolated from the egg masses, which in their natural environment are remarkable for remaining untouched by predators. In fact, this unusual property provided the initial incentive for searching for deterrent chemical principles in the egg masses. The metabolites of interest from both nudibranches and sponge sources include, amongst others, ulapualide A (**82**),[129] halichondramide (**83**),[130] kabiramide A (**84**),[131] and mycalolide A (**85**).[132] Although gross structural features for these compounds are secure, their relative stereochemistry has not been established. In the absence of crystallographic information, the resolution of these problems will probably have to await total synthesis. However, the structures are so patently plausible as ligands for metal chelation that our research group in Nottingham has been enticed into carrying out a molecular mechanics study on 'dummy' metal-chelated ulapualide A (**82**) using varying combinations of its oxygen and nitrogen atoms as ligating sites. Perhaps somewhat whimsically, by using the chelated models shown in **86** and **87**, this study has permitted us to predict the relative stereochemistry shown in formula **82** for ulapualide A. This is more significant than it may appear at first sight, since the stereochemistry revealed for the polyol side chain in **82** correlates with the corresponding chiral centers in scytophycin B (**88**), a related metabolite whose structure has been secured by X-ray measurements.[133] We now look forward to the outcome of the synthetic endeavors with these fascinating and unusual trisoxazole-containing macrolides.[134]

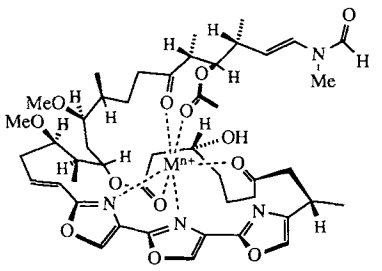

86

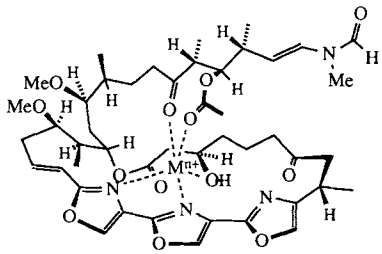

87

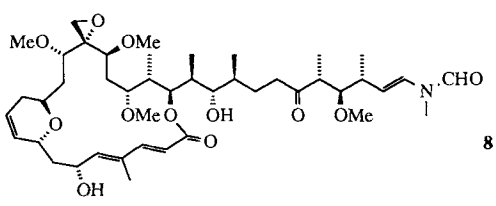

88

We also draw attention to several marine bisoxazoles that merit consideration as potential ligands: bengazoles A (**89**) and B (**90**) from a sponge of the family Jaspidae;[135] hennoxazoles, for example **91**, from the sponge *Polyfibrospongia* sp.;[136] and diazonamides A (**92a**) and B (**92b**), unique macrobicyclic bisoxazoles from the ascidian *Diazona chinensis*.[137] The macrocyclic cavities of **92** may lack sufficient functionality for holding cations, but an X-ray structure determination of a acetal/amide derivative of **92b** has shown that the oxazole rings are twisted at 29° to each other, which places both nitrogen atoms orientated away from the cavity but in principle still able to cooperate as a bidentate ligand.

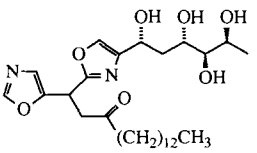

89

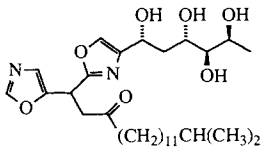

90

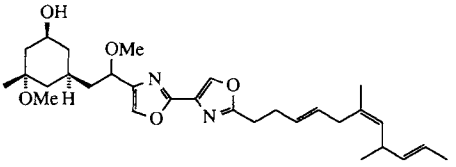

91

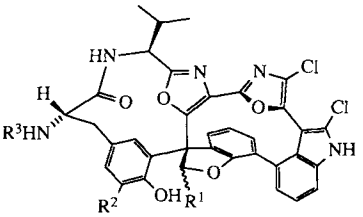

92a R^1 = OH, R^2 = H, R^3 = $COCH(NH_2)CH(CH_3)_2$
92b R^1 = OH, R^2 = Br, R^3 = H

7.7. Bastadins

Many sponge metabolites derived from bromotyrosine moieties[101] are characterized by the presence of free oxime groups, which should encourage chelation by metal ions. For our purposes the most interesting are the bastadins (e.g., **93**–**95**), antimicrobial compounds in which four bromotyrosine-derived segments are linked into chains or, further, into macrocycles by amide and ether bonds.[138, 139] Crystal structures have been obtained[139] of bastadin-4 (**95a**) as the trispyridine solvate, and of the tetramethyl ether of bastadin-5 (**95b**) (Fig. 13). Of the latter the authors remarked that "there appeared to be a sizable 'hole' inside the macrocyclic ring, which might accommodate small mono- or divalent metal cations". Though the hole was partially blocked by one of the methoxyimino protecting groups, the hope was expressed that "one or more of the unmethylated natural products could behave as an ionophore". The conformation of the elongated rectangular ring in **95a** is probably atypical, since hydrogen bonding to the solvent of crystallization on the outside of the macrocyclic cavity is likely to distort the structure.

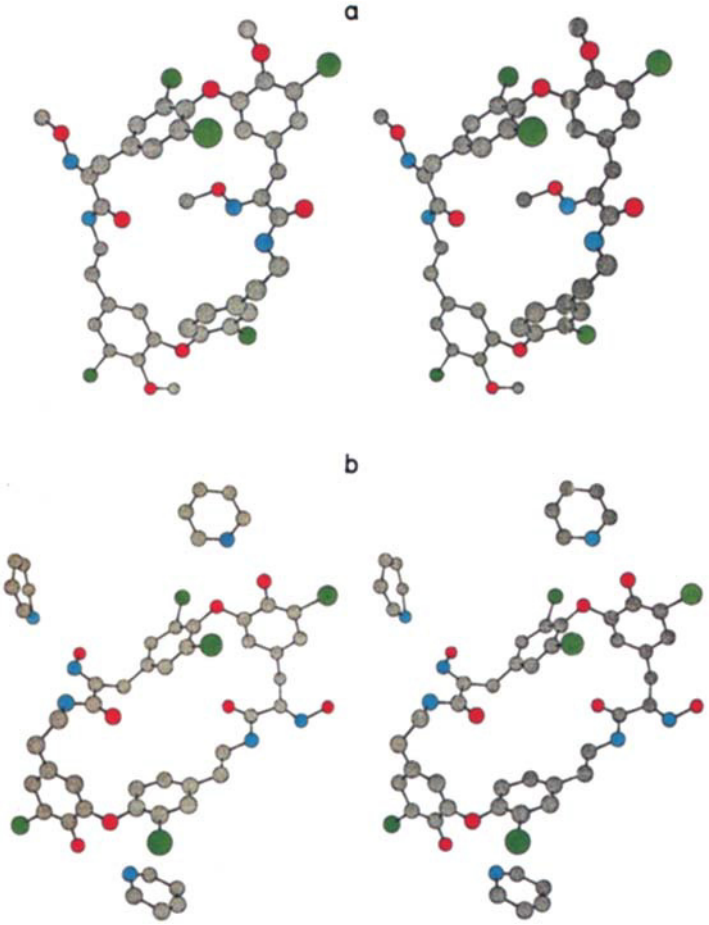

Fig. 13. Stereoscopic views of the X-ray crystal structures of a) the tetramethyl ether derivative of bastadin-5 **95b**; and b) the pyridine solvate of bastadin-4 **95a**.

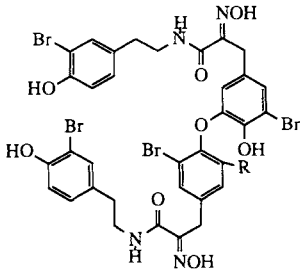

93 R = H, Br

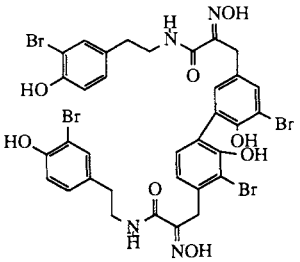

94

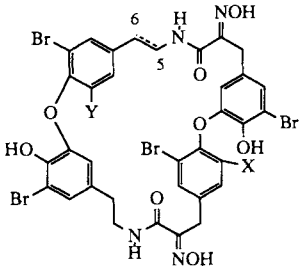

95a C5-C6 = CH=CH, X = Br, Y = H
95b C5-C6 = CH_2-CH_2, X = Br, Y = H

8. Summary and Outlook

The preceding pages present the case for potential and known interactions of marine natural products with metal ions. The progression has been from solid facts to nebulous fantasies. So tenuous does the link become in the end that additional natural product examples would have to be chosen on no better grounds that the aesthetic appeal of their structures (or intuitive guesswork, which might amount to the same thing). Many other marine polyethers, macrolides, cyclic peptides, alkaloids, and the like no doubt deserve a mention, but the reader whose interest has been quickened by our survey will be at least as able as we are to compile a short-list of personal favorites for further attention.

What are the major problems in undertaking metal-chelation studies of marine matabolites? The limiting factor is often the availability of materials. Marine organisms are seldom prodigal in the production of secondary metabolites. The fact that sub-centrigram quantities of componds are routinely isolated and analyzed is a tribute both to the painstaking efforts of dedicated researchers and to the sensitivity of modern analytical and spectroscopic techniques. The scaling up of isolation procedures (assuming that the source organism is sufficiently prolific for large-scale collection) poses enormous logistic problems. Worthy of highlighting in this regard is the recent extraction of 18 g of pure bryostatin 1 (**52a**) from 28000 pounds of damp *Bugula neritina*, processed in 15 batches over 10 months.[83] Many organisms can, of course, be grown in culture, though we are some way off from large-scale microbiological production of desirable metabolites at will. Bioengineering of suitable genetic material for the controlled production of important products is also not practicable at this stage. As we see it, organic synthesis will continue to serve as the most important alternative source of interesting metabolites well into the next century. Far from being a passé discipline, the art of organic synthesis plays a more vital role than ever before in ensuring access to valuable compounds that are otherwise nearly impossible to come by. However, we should be disingenuous if we failed to acknowledge the frequently inefficient and uneconomical nature of synthetic processes. The fearsome structural complexity of many marine natural products, while certain to succumb to persistent and imaginative assault by creative synthesists, will always militate against rapid and plentiful access. In the short term, dreams of studying metal chelation will probably remain unfulfilled for many important marine metabolites. Another problem arises from the still incompletely characterized, stereochemical features of many interesting compounds. Obviously, the task of the synthetic chemist is impeded by imprecise definition of the target. However, stereoselective routes to some of the alternative structures can, and do, result in analogues that in themselves are worthy of study. The synthesis of model compounds, too, is not to be despised, because the first tentative phase of chelation studies on them may provide valuable indications of the behavior of the natural metabolites.

Significantly, most new marine natural products have been isolated after biological screening of crude plant and animal extracts for desirable activity. Whether the biological activity involves metal chelation has seldom been discussed, and we are not qualified to pass comment. The questions we posed in the introduction concerning possible in vivo relationships between metabolites and metal ions have scarcely been illuminated by the facts we have managed to uncover.

We must make it clear that the biological and medical literature has, in general, not been examined in the compilation of this review; important references to the phenomenon under consideration may well be lurking in this unexplored body of information.

What sort of studies might we wish to see in the future? Firstly, simple qualitative evidence for metal–metabolite interaction should be relatively easy to obtain, and should provide a broad foundation for more detailed investigations. Spectroscopic changes on the addition of metal ions to solutions of natural products are certainly within the ambit of virtually all researchers. The preparation and isolation of characterizable complexes would be even more convincing. Because conformational aspects of the interaction are important to study, it is imperative to add to the catalogue of crystallographic structures of metal complexes of marine natural products. In terms of physical properties, the lack of thermodynamic data on the binding and stability of metal–metabolite complexes is a serious omission that could be remedied. Studies on the kinetics of complexation would follow naturally once the thermodynamic aspects are clarified. Finally, molecular mechanics studies, which have the advantage of not even requiring the isolated compound, must assume a greater importance once reliable parameters for metal ions become more widely available.

It is understandable but unfortunate that few daydreams on the topic of metal–metabolite interaction have appeared in print. The natural caution of authors, and the conservatism of many referees and editors who excise speculative statements, no doubt play a part in suppressing the fantasies that may excite less timorous researchers into action. By throwing the spotlight on a topic that has hitherto lain dormant in the dark recesses of the literature, we hope that we have focused attention on the latent possibilities that await exploration.

9. Addendum

The following material, published after the completion of the manuscript, casts more light on some of the major issues addressed in this review.

1. The vanadium-sequestering tunicate *Phallusia mammillata* is the source of three new tunichromes, Pm-1 (the major metabolite), Pm-2, and Pm-3 (**96a–c**).[140] The compounds lack one of the double bonds of the An-tunichromes **16** (Section 3), and it may be significant that **16** appeared as artifacts when the Pm-tunichromes were purified by chromatography on silica gel rather than on the polystyrene phases recommended in this later paper (80–90% recovery of compounds). A highly relevant point is that ^{13}C CP-MAS NMR spectra of lyophilized blood cells of *P. mammillata* corresponded closely with the solution spectra of Pm-1: the native tunichrome is thus present in the blood cells as free pigment and not as a vanadium-bound species. Semiquantitative comparison of tunichrome content with sulfate and vanadium content has revealed approximately equivalent amounts of sulfate in the morula cells and vanadium (aquasulfatovanadium complex?) in blood cells. A new mechanism for the uptake, reduction, and concentration of vanadium has been proposed, the reduction stage being mediated by a

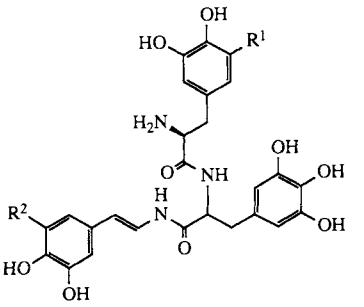

96a $R^1 = R^2 = OH$
96b $R^1 = H, R^2 = OH$
96c $R^1 = OH, R^2 = H$

tripeptide sulfoconjugate that itself undergoes oxidative decarboxylation to give the observed styrylamide residue of the tunichromes.

2. Faulkner et al. have shown that the structures proposed for the dercitamine family of alkaloids (nordercitin (**35**), Section 4) are incorrect.[141] The positions of nitrogen and sulfur in the thiazole must be interchanged; the compounds are, in fact, members of the same series as the kuanoniamines. More importantly, however, these researchers have used NMR and fluorescence measurements to show that kuanoniamine D (**37**) forms ML_2 complexes with divalent metal cations such as Co^{2+}, Cu^{2+}, Fe^{2+}, and Zn^{2+}. Stability constants for the binding of **37** to $CoCl_2$ and $Cu(OAc)_2$ were determined from fluorescence studies to be $2.5 \times 10^{10}\ M^{-2}$ and $1.3 \times 10^{10}\ M^{-2}$, respectively.

3. The zinc complex of clathridine **7** has been isolated from another sponge, *Leucetta microrhaphis*.[142]

J. P. M. wishes to thank the University of the Witwatersrand, Johannesburg, and the Foundation for Research Development, Pretoria, for financing his sabbatical leave at the University of Nottingham.

Received: March 13, 1992 [A 890 IE]
German version: *Angew. Chem.* **1993**, *105*, 1

[1] M. J. Garson, *Nat. Prod. Rep.* **1989**, *6*, 143–170.
[2] J. P. Riley, R. Chester, *Introduction to Marine Chemistry*, Academic Press, London, **1971**.
[3] K. Kustin, G. C. McLeod, *Top. Curr. Chem.* **1977**, *69*, 1–37.
[4] K. Kustin, G. C. McLeod, T. R. Gilbert, Le B. R. Briggs, 4th, *Struct. Bonding (Berlin)* **1983**, *53*, 139–160.
[5] D. W. Knight, G. Pattenden, D. E. Rippon, *Synlett* **1990**, *1*, 36–37; M. J. Kiefel, J. Maddock, G. Pattenden, *Tetrahedron Lett.* **1992**, *33*, 3227–3290.
[6] M. North, G. Pattenden, *Tetrahedron* **1990**, *46*, 8267–8290; G. Pattenden, *J. Heterocycl. Chem.* **1992**, *29*, 607–618.
[7] For leading references see: W. Wierenga in *The Total Synthesis of Natural Products, Vol. 4* (Ed.: J. ApSimon), Wiley-Interscience, New York, **1981**, pp. 263–351; J. W. Westley, *Polyether Antibiotics. Naturally Occurring Ionophores*, Dekker, New York, **1982**; *Iron, Siderophores, and Plant Diseases* (Ed.: T. R. Swinburne), Plenum, New York, **1986**; M. Dobler, *Ionophores and their Structures*, Wiley-Interscience, New York, **1981**; S. H. Laurie in *Comprehensive Coordination Chemistry, Vol. 2* (Ed.: G. Wilkinson), Pergamon, Oxford, **1987**, pp. 959–988.
[8] For comprehensive summaries, see: D. J. Faulkner, *Nat. Prod. Rep.* **1992**, *9*, and earlier annual summaries in this series.
[9] C. J. R. Fookes, S. W. Jeffrey, *J. Chem. Soc. Chem. Commun.* **1989**, 1827–1828.
[10] K. L. Rinehart, V. Kishore, K. C. Bible, R. Sakai, D. W. Sullins, K.-M. Li, *J. Nat. Prod.* **1988**, *51*, 1–21.
[11] L. Agius, J. A. Ballantine, V. Ferrito, V. Jaccarini, P. Murray-Rust, A. Pelter, A. F. Psaila, P. J. Schembri, *Pure Appl. Chem.* **1979**, *51*, 1847–1864; J. A. Ballantine, A. F. Psaila, A. Pelter, P. Murray-Rust, V. Ferrito, P. J. Schembri, V. Jaccarini, *J. Chem. Soc. Perkin Trans. 1* **1980**, 1080–1089.
[12] K. Sakata, K. Yamamoto, H. Ishikawa, A. Yagi, H. Etoh, K. Ina, *Tetrahedron Lett.* **1990**, *31*, 1165–1168.

[88] M. Kobayashi, J. Tanaka, T. Katori, M. Matsuura, I. Kitagawa, *Tetrahedron Lett.* **1989**, *30*, 2963–2966.
[89] I. Kitagawa, M. Kobayashi, T. Katori, M. Yamashita, J. Tanaka, M. Doi, T. Ishida, *J. Am. Chem. Soc.* **1990**, *112*, 3710–3712; M. Kobayashi, J. Tanaka, T. Katori, M. Matsuura, M. Yamashita, I. Kitagawa, *Chem. Pharm. Bull.* **1990**, *38*, 2409–2418.
[90] M. Doi, T. Ishida, M. Kobayashi, I. Kitagawa, *J. Org. Chem.* **1991**, *56*, 3629–3632.
[91] M. Kobayashi, J. Tanaka, T. Katori, I. Kitagawa, *Chem. Pharm. Bull.* **1990**, *38*, 2960–2966.
[92] Y. Kato, N. Fusetani, S. Matsunaga, K. Hashimoto, R. Sakai, T. Higa, Y. Kashman, *Tetrahedron Lett.* **1987**,*28*, 6225–6228.
[93] J. Kobayashi, S. Tsukamoto, A. Tanabe, T. Sasaki, M. Ishibashi, *J. Chem. Soc. Perkin Trans. 1* **1991**, 2379–2383.
[94] J. Tanaka, T. Higa, M. Kobayashi, I. Kitagawa, *Chem. Pharm. Bull.* **1990**, *38*, 2967–2970.
[95] D. Uemura, K. Takahashi, T. Yamamoto, C. Katayama, J. Tanaka, Y. Okumura, Y. Hirata, *J. Am. Chem. Soc.* **1985**, *107*, 4796–4798; Y. Hirata, D. Uemura, *Pure Appl. Chem.* **1986**, *58*, 701–710.
[96] A. San-Martin, J. Rovirosa, O. Muñoz, M. H. M. Chen, R. D. Gunerat-ne, J. Clardy, *Tetrahedron Lett.* **1983**, *24*, 4063–4066.
[97] A. San-Martin, J. Rovirosa, C. Xu, H. S. M. Lu, J. Clardy, *Tetrahedron Lett.* **1987**, *28*, 6013–6014.
[98] J. W. Blunt, M. P. Hartshorn, T. J. McLennan, M. H. G. Munro, W. T. Robinson, S. C. Yorke, *Tetrahedron Lett.* **1978**, 69–72.
[99] S. Sakemi, T. Higa, C. W. Jefford, G. Bernardinelli, *Tetrahedron Lett.* **1986**, *27*, 4287–4290.
[100] T. Suzuki, M. Suzuki, A. Furusaki, T. Matsumoto, A. Kato, Y. Imanaka, E. Kurosawa, *Tetrahedron Lett.* **1985**, *26*, 1329–1332.
[101] C. M. Ireland, T. F. Molinski, D. M. Roll, T. M. Zabriskie, T. C. McKee, J. C. Swersey, M. P. Foster in *Bioorganic Marine Chemistry, Vol 3*, (Ed.: P. J. Scheuer), Springer-Verlag, Berlin, **1989**, pp. 1–46.
[102] K. L. Rinehart, Jr., J. B. Gloer, R. G. Hughes, Jr., H. E. Renis, J. P. McGovren, E. B. Swynenberg, D. A. Stringfellow, S. L. Kuentzel, L. H. Li, *Science* **1981**, *212*, 933–935.
[103] B. Banaigs, G. Jeanty, C. Francisco, P. Jouin, J. Poncet, A. Heitz, A. Cave, J. C. Prome, M. Wahl, F. Lafargue, *Tetrahedron* **1989**, *45*, 181–190.
[104] H. Kessler, M. Will, J. Antel, H. Beck, G. M. Sheldrick, *Helv. Chim. Acta* **1989**, *72*, 530–555.
[105] M. B. Hossain, D. van der Helm, J. Antel, G. M. Sheldrick, S. K. Sandu-ja, A. J. Weinheimer, *Proc. Natl. Acad. Sci. USA* **1988**, *85*, 4118–4122.
[106] L. H. Li, L. G. Timmins, T. L. Wallace, W. C. Krueger, M. D. Prairie, W. B. Im, *Cancer Lett.* **1984**, *23*, 279–288.
[107] H. Kessler, S. Mronga, M. Will, U. Schmidt, *Helv. Chim. Acta* **1990**, *73*, 25–47.
[108] G. R. Pettit, Y. Kamano, C. L. Herald, C. Dufresne, R. B. Bates, J. M. Schmidt, R. L. Cerny, H. Kizu, *J. Org. Chem.* **1990**, *55*, 2989–2990, and references therein.
[109] C. W. Holzapfel, W. J. van Zyl, M. Roos, *Tetrahedron* **1990**, *46*, 649–660.
[110] M. W. Bredenkamp, C. W. Holzapfel, W. J. van Zyl, *Liebigs Ann. Chem.* **1990**, 871–875.
[111] D. C. Carter, R. E. Moore, J. S. Mynderse, W. P. Niemczura, J. S. Todd, *J. Org. Chem.* **1984**, *49*, 236–241; J. S. Mynderse, A. H. Hunt, R. E. Moore, *J. Nat. Prod.* **1988**, *51*, 1299–1301.
[112] Y. Hamamoto, M. Endo, M. Nakagawa, T. Nakanishi, K. Mizukawa, *J. Chem. Soc. Chem. Commun.* **1983**, 323–324; Y. Hamada, S. Kato, T. Shioiri, *Tetrahedron Lett.* **1985**, *26*, 3223–3226.
[113] J. M. Wasylyk, J. E. Biskupiak, C. E. Costello, C. M. Ireland, *J. Org. Chem.* **1983**, *48*, 4445–4449.
[114] D. F. Sesin, p. J. Gaskell, C. M. Ireland, *Bull. Soc. Chim. Belg.* **1986**, *95*, 853–867.
[115] B. M. Degnan, C. J. Hawkins, M. F. Lavin, E. J. McCaffrey, D. L. Parry, A. L. van den Brenk, D. J. Watters, *J. Med. Chem.* **1989**, *32*, 1349–1354.
[116] F. J. Schmitz, M. B. Ksebati, J. S. Chang, J. L. Wang, M. B. Hossain, D. van der Helm, M. H. Engel, A. Serban, J. A. Silfer, *J. Org. Chem.* **1989**, *54*, 3463–3472.
[117] C. J. Hawkins, M. F. Lavin, K. A. Marshall, A. L. van den Brenk, D. J. Watters, *J. Med. Chem.* **1990**, *33*, 1634–1638.
[118] C. M. Ireland, A. R. Durso, Jr., R. A. Newman, M. P. Hacker, *J. Org. Chem.* **1982**, *47*, 1807–1811.
[119] C. Ireland, P. J. Scheuer, *J. Am. Chem. Soc.* **1980**, *102*, 5688–5692.
[120] U. Schmidt, D. Wetter, *Tetrahedron Lett.* **1986**, *27*, 3495–3496.
[121] D. E. Williams, R. E. Moore, V. J. Paul, *J. Nat. Prod.* **1989**, *52*, 732–739.
[122] S. Kato, Y. Hamada, T. Shioiri, *Tetrahedron Lett.* **1986**, *27*, 2653–2656.
[123] T. Ishida, H. Ohishi, M. Inoue, M. Kamigauchi, M. Sugiura, N. Takao, S. Kato, Y. Hamada, T. Shioiri, *J. Org. Chem.* **1989**, *54*, 5337–5343.
[124] T. Ishida, M. Inoue, Y. Hamada, S. Kato, T. Shioiri, *J. Chem. Soc. Chem. Commun.* **1987**, 370–371.
[125] T. Ishida, M. Tanaka, M. Nabae, M. Inoue, S. Kato, Y. Hamada, T. Shioiri, *J. Org. Chem.* **1988**, *53*, 107–112.
[126] T. M. Zabriskie, M. P. Foster, T. J. Stout, J. Clardy, C. M. Ireland, *J. Am. Chem. Soc.* **1990**, *112*, 8080–8084.
[127] B. M. Degnan, C. J. Hawkins, M. F. Lavin, E. J. McCaffrey, D. L. Parry, D. J. Watters, *J. Med. Chem.* **1989**, *32*, 1354–1359.
[128] D. Gouiffès, S. Moreau, N. Helbecque, J. L. Bernier, J. P. Hénichart, Y. Barbin, D. Laurent, J.-F. Verbist, *Tetrahedron* **1988**, *44*, 451–459; M. P. Foster, C. L. Mayne, R. Dunkel, R. J. Pugmire, D. M. Grant, J.-M. Kornprobst, J.-F. Verbist, J.-F. Biard, C. M. Ireland, *J. Am. Chem. Soc.* **1992**, *114*, 1110–1111.
[129] J. A. Roesener, P. J. Scheuer, *J. Am. Chem. Soc.* **1986**, *108*, 846–847.
[130] M. R. Kernan, D. J. Faulkner, *Tetrahedron Lett.* **1987**, *28*, 2809–2812; M. R. Kernan, T. F. Molinski, D. J. Faulkner, *J. Org. Chem.* **1988**, *53*, 5014–5020.
[131] S. Matsunaga, N. Fusetani, K. Hashimoto, K. Koseki, M. Noma, *J. Am. Chem. Soc.* **1986**, *108*, 847–849; S. Matsunaga, N. Fusetani, K. Hashimoto, K. Koseki, M. Noma, H. Noguchi, U. Sankawa, *J. Org. Chem.* **1989**, *54*, 1360–1363.
[132] N. Fusetani, K. Yasumuro, S. Matsunaga, K. Hashimoto, *Tetrahedron Lett.* **1989**, *30*, 2809–2812; N. Fusetani, T. Sugawara, S. Matsunaga, H. Hirota, *J. Org. Chem.* **1991**, *56*, 4971–4974.
[133] M. Ishibashi, R. E. Moore, G. M. L. Patterson, C. Xu, J. Clardy, *J. Org. Chem.* **1986**, *51*, 5300–5306.
[134] Professor D. J. Faulkner has kindly let us know of his quantitative results, now being prepared for publication, on the binding of model trisoxazoles that we synthesized and dihydrohalichondramide to various metal cations. This seems to be the first deliberately devised chelation study of the kind that we are advocating in this review.
[135] M. Adamczeski, E.Quiñoá, P. Crews, *J. Am. Chem. Soc.* **1988**, *110*, 1598–1602.
[136] T. Ichiba, W. Y. Yoshida, P. J. Scheuer, T. Higa, D. G. Gravalos, *J. Am. Chem. Soc.* **1991**, *113*, 3173–3174.
[137] N. Lindquist, W. Fenical, G. D. Van Duyne, J. Clardy, *J. Am. Chem. Soc.* **1991**, *113*, 2303–2304.
[138] R. Kazlauskas, R. O. Lidgard, P. T. Murphy, R. J. Wells, *Tetrahedron Lett.* **1980**, *21*, 2277–2280; S. Miao, R. J. Andersen, T. M. Allen, *J. Nat. Prod.* **1990**, *53*, 1441–1446; E. O. Pordesimo, F. J. Schmitz, *J. Org. Chem.* **1990**, *55*, 4704–4709.
[139] R. Kazlauskas, R. O. Lidgard, P. T. Murphy, R. J. Wells, J. F. Blount, *Aust. J. Chem.* **1981**, *34*, 765–786.
[140] E. Bayer, G. Schiefer, D. Waidelich, S. Scippa, M. de Vicentiis, *Angew. Chem.* **1992**, *104*, 102; *Angew. Chem. Int. Ed. Engl.* **1992**, *31*, 52–54.
[141] G. P. Gunawardana, F. E. Koehn, A. Y. Lee, J. Clardy, H. He, D. J. Faulkner, *J. Org. Chem.* **1992**, *57*, 1523–1526.
[142] H. He, D. J. Faulkner, A. Y. Lee, J. Clardy, *J. Org. Chem.* **1992**, *57*, 2176–2178.

Mercury, a Structural Building Block and Source of Localized Reactivity in Extended Metal–Metal Bonded Systems

By Lutz H. Gade*

Transition metal–mercury complexes were among the first compounds of study for the concept of direct metal–metal bonding which was established more than three decades ago. Since then, a large number of such systems have been synthesized and studied. The fact that mercury is readily attached to a large variety of main group or transition metals has stimulated its use as a general building block in the systematic synthesis of mixed-metal clusters. The past decade has witnessed a rapid expansion of bimetallic cluster chemistry in which species containing mercury have played a prominent role, and which has led to the discovery of many unprecedented cluster structures and reactions. In particular, the ability of mercury to form multicenter metal–metal bonds with polynuclear cluster fragments has substantially extended its coordination chemistry which was thus far dominated by simple linear structural arrangements. Although certain structural motifs are found to be common to many of the transition metal–mercury clusters investigated to date and thus enable a relatively systematic synthetic approach, the multitude of surprising discoveries has kept the interest in the chemistry of the element itself alive. The recent discovery of the redox and photochemical reactivity of some of these systems has opened up an exciting and promising area of cluster research. Its significance for the synthetic methodology lies in the fact that the increasing redox activity of molecular carbonyl clusters on going to higher nuclearities appears to set a limit on the size of metal frameworks attainable by the standard preparative methods. On the other hand, their potential use as photochromes or redox mediaters in coupled electron-transfer reactions provides an additional stimulus for future studies in this field.

1. Introduction

Nowadays, the study of the properties of clusters is a vast and highly structured area of research, which draws its experimental and theoretical methods and techniques from virtually every scientific discipline.[1] A special class of systems studied in this field is that of molecular cluster complexes, in particular, polynuclear metal carbonyl clusters and their derivatives.[2] These have received considerable attention with regard to both their structural chemistry and reactivity. The ever growing number of high-nuclearity clusters containing up to a few dozen metal atoms has led to an increased interest in their chemical and physicochemical properties.[3, 4] While the fascinating structures of many of these molecules are well established by X-ray crystallography, our knowledge of their chemical transformations is rather limited. This is largely due to the delicate energy balance between the metal–metal and metal–ligand bond relationships of the species formed in the cluster aggregation, a situation which prohibits the selective and localized manipulation of their ligand shells or metal frameworks. Most standard synthetic approaches (e.g., thermally or chemically induced ligand substitutions or additions), which have successfully served in the chemistry of low-nuclearity systems, lead if performed on large clusters to more or less complete breakdown of the metal framework. Alternatively, complex cascades of cluster degradation and aggregation reactions generate products that are structurally unrelated to the initial substrate. These standard techniques are therefore of limited value for the development of a general synthetic strategy and have fuelled the widespread perception of the "hit-and-run" nature of cluster synthesis.

On the other hand, mixed-metal frameworks containing metal atoms or cluster subunits with significantly different electronic properties offer the potential to direct chemical changes towards the interfaces between these components. This anticipated reactive behavior originates from the introduction of metal–metal bond polarity in the framework. The idea itself is reminiscent of the synthetic strategies employed in organic chemistry for the construction of complicated functionalized hydrocarbons that are based on the exploitation of specifically introduced bond polarities (e.g. the generation of nucleophilic or electrophilic centers of reactivity) for the regio- or even stereoselective formation or cleavage of C–C bonds.

The potential of mercury to form heterobimetallic complexes with transition metal complex fragments was recognized long before the direct metal–metal bonding between transition metals became a generally accepted concept in inorganic chemistry. Compounds containing mercury atoms directly bonded to a complex fragment have long since entered standard textbooks of inorganic chemistry.[5] The fact that the metal is readily attached to a large variety of other main group or transition metals has made it an attractive candidate for a "universal glue" in the systematic synthesis of high-nuclearity clusters. This may involve the addition of Hg–ligand fragments to cluster frameworks or the incorporation of naked Hg atoms or aggregates into an extended framework.

The past decade has witnessed a rapid expansion of the chemistry of bimetallic clusters containing mercury, such that it now rivals that of gold, its precious neighbor in the

[*] Dr. L. H. Gade
University Chemical Laboratory
Lensfield Road, GB-Cambridge CB21EW (UK)
New address:
Institut für Anorganische Chemie der Universität
Am Hubland, D-W-8700 Würzburg (FRG)

periodic table. This has entailed the discovery of many unprecedented cluster structures and reactions. The ability of mercury to form multicenter metal–metal bonds, and thus bridge metal–metal edges, or cap triangular faces of cluster cores, has substantially extended the coordination chemistry of the element, which was peviously dominated by linear structural arrangements in its molecular species. Developments in this area that have generated a multitude of new data therefore warrant a reassessment of the structural chemistry of mercury. This is one of the aims of this article; the other is to provide a critical survey of the progress made in the development of generalized synthetic concepts in the chemistry of high-nuclearity mixed-metal clusters.

2. Historical Milestones in the Chemistry of Molecular Transition Metal–Mercury Compounds

The publication by Hock and Stuhlmann in 1928 "*Über die Einwirkung von Quecksilbersalzen auf Eisenpentacarbonyl*" must be regarded as the birth of transition metal–mercury complex chemistry.[6] In this and a series of subsequent papers[7] they reported the results of reactivity studies of $[Fe(CO)_5]$ towards mercuric salts, and the characterization of the products obtained from these reactions (Scheme 1). They provided the archetypal examples for

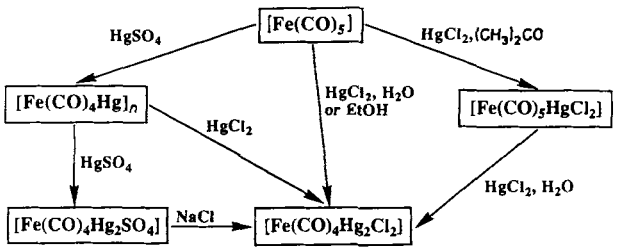

Scheme 1. The reactions of $[Fe(CO)_5]$ with Hg salts reported by Hock and Stuhlmann.

much of the chemistry reported in this area in later years. Reacting $[Fe(CO)_5]$ with one equivalent of $HgCl_2$ while cooling the reaction mixture yielded the product $[Fe(CO)_5(HgCl_2)]$, a Lewis acid–base adduct of the mercuric salt with the carbonyl complex. Nowadays several structurally characterized examples for this kind of complex confirm the authors' interpretation of their results, which at the time were based solely on a complete elemental analysis. In the presence of an excess of $HgCl_2$, the reaction went further to the dimercurated complex $[Fe(CO)_4Hg_2Cl_2]$. While this formulation was correct, its structure remained obscure. The fact that this complex could also be obtained by the reaction of the oligomeric $[Fe(CO)_4Hg]_n$ with $HgCl_2$ led to its original formulation as $[Fe(CO)_4Hg(HgCl_2)]$, that is, an $HgCl_2$ adduct of the iron carbonyl derivative $[Fe(CO)_4Hg]$. The latter was first isolated from the reaction of $[Fe(CO)_5]$ with an aqueous solution of $HgSO_4$. The structure of this completely insoluble material remained speculative and for a long time was thought to be polymeric.[8] More recently the crystal structure of the analogous Cd compound has been reported, and this shows the species to be a cyclic tetramer,[9] a geometry which may therefore also be assumed for $[Fe(CO)_4Hg]_n$.

While the work on iron carbonyl derivatives was conducted with the specific aim of exploring the chemical reactivity of $[Fe(CO)_5]$ towards mercury(II) salts, the next mercury–carbonyl complex to be reported was a by-product of research aimed in a totally different direction. In an early example of bioinorganic chemistry, Schubert studied the interaction of a Co^{II}–cysteine complex with carbon monoxide.[10] Instead of the desired mixed carbonyl-cysteine complex he observed the disproportionation of the complex, which yielded $[Co^{III}(cys)_3]^{3-}$ (cys = $[SCH_2CH(NH_2)Co_2]^{2-}$) and $[Co(CO)_4]^-$. The latter component could not be isolated, but on reaction with $HgCl_2$ a novel compound precipitated, which was correctly formulated as $[\{(CO)_4Co\}_2Hg]$. This work was followed up by Hieber et al. who developed several high-yield syntheses for this complex and its Zn and Cd analogues.[11] At the same time Hein and Pobloth reported the synthesis of the first carbonyl–organomercury compound $[Fe(CO)_4(HgCH_3)_2]$, as well as a detailed investigation of the thermal symmetrization (dismutation) to $[Fe(CO)_4Hg]_n$ and $[(CH_3)_2Hg]$ [Eq. (a)].[12] Equilibria of this

$$[Fe(CO)_4(HgCH_3)_2] \rightleftharpoons 1/n[Fe(CO)_4Hg]_n + [(CH_3)_2Hg] \quad (a)$$

kind were later found to dominate the chemistry of this class of mercury compounds and play an equally important role in the reactions of transition metal clusters containing mercury.

By the mid-1940s, the most important synthetic routes leading to these mixed-metal compounds had been well established. However, the molecular structures of most of the products remained poorly understood. Both the Fe–Hg and

Lutz H. Gade was born in 1963 in Bonn and raised in Johannesburg (South Africa). From 1983–1988 he studied chemistry at Bonn University and at the Technical University Munich, where he wrote his diploma thesis under F. H. Köhler. Thereafter he took up short-term employment in the pharmaceutical industry. He worked on his Ph.D. from 1989–1991 with Jack Lewis at Cambridge University, and since 1991 has been a Liebig fellow at Würzburg University. His research interests include polar metal–metal bonds in polynuclear coordination compounds, the coordination chemistry of early transition metals, and the photochemistry of organometallic compounds.

Co–Hg compounds were generally regarded as salts of the carbonyl metalates, a notion which was irreconcilable with the absence of any saltlike behavior. This confusion about their molecular structures seems to have temporarily inhibited further development of transition metal–mercury chemistry until about 1960. Within this period, the concepts of chemical bonding, particularly with regard to polynuclear transition metal compounds, developed rapidly. This fundamentally changed the inorganic chemist's approach to the theoretical understanding of such compounds. The crucial step in this "revolution" was the report of the crystal structure analysis of $[Fe_2(CO)_9]$ by Powell and Ewens in 1939, which led the authors to invoke a metal–metal bond between the two Fe centers.[13] This view was immediately endorsed by Pauling,[14] but initially met with fierce opposition from other researchers.[15] However, the amount of experimental data supporting the presence of covalent metal–metal bonds and the solution they offered to many problems arising from the apparently contradictory experimental results obtained earlier, along with the application of new physicochemical methods for the characterization of polynuclear compounds, won wide acceptance for this new concept.[16] Apart from the polynuclear metal carbonyls and low-valent halides of the early transition metals, the Hg-containing compounds discussed above, as well as the mercurous ion Hg_2^{2+} were prime targets for reinvestigation within this conceptual framework.

From 1960 onwards there was a rapid succession of publications on new syntheses and properties of transition metal–mercury complexes, beginning with the report of the Co–Hg vibrational band in the Raman spectrum of $[\{(CO)_4Co\}_2Hg]$.[17] Nyholm and Vrieze synthesized the complexes $[(Ph_3As)_3RhCl_2(HgCl)]$[18] and $[(Ph_3P)_2Ir(CO)Cl_2(HgCl)]$,[19] and Stiddard et al. prepared the septacoordinate complex $[W(CO)_3(bipy)(HgCl)_2]$.[20] At the same time the *cis* geometry of the two Fe–Hg bonds in $[Fe(CO)_4(HgCl)_2]$[21] was derived from its IR spectrum and confirmed by X-ray crystallography a few years later.[22]

Up to the late 1970s, an enormous amount of work concerning various aspects to Hg–transition metal bonding was published. This has been comprehensively reviewed by Hsieh and Mays[23] and later by Burlitch.[24] The latest development in this area is the application of Hg reagents in the synthesis of mixed-metal carbonyl clusters initiated by the work of Rosenberg et al. in 1980. This area will be highlighted in this article.

3. Structural Principles Determining the Buildup of Molecular Clusters Containing Isolated Hg Atoms or Hg_n Subclusters

3.1. Building Chains, Rings, and Cages with Mononuclear Transition Metal Complex Fragments

The preferred linear coordination of the mercury atoms involved in two-center two-electron (2c2e) bonding to a transition metal sets relatively narrow limits on the possible types of cluster structures incorporating mercury. On the other hand, it makes their analysis, at least superficially, straightforward and lends a certain predictability to their geometries. These will be mainly governed by the functionality of the transition metal complex fragments, that is, the number of M–Hg bonds (M, M′ = transition metal complex fragment) a single fragment can form as well as the relative configuration of the Hg groups coordinated to the transition metal. Three possible structural types have been observed so far:[25, 26]

a) simple trimetallic complexes of the type M-Hg-M′ for monofunctional fragments M and M′;

b) chain and ring structures $(\text{-Hg-M-})_n$ requiring difunctionality of M;

c) three-dimensional cluster structures for trifunctional complex fragments.

The chemistry of the first type of compounds M-Hg-M′ has been reviewed elsewhere and is not within the scope of the article.[23, 24] A representative example would be $[\{Cp(CO)_3Mo\}_2Hg]$, a compound which has been studied extensively with regard to its physicochemical properties as well as its reactivity.[27]

Structurally characterized examples of open, metallic-chain structures containing more than one mercury unit linking only mononuclear complex fragments have not been reported to date. The only such species identified so far involve triangular cluster units.[28] However, mercury atoms have generally proved to be ideal "linkers" in metal chain structures, as was first observed in $[\{(Ph_3GeHg)(Ph_3Ge)CpNi\}_2Hg]$, which was isolated from the reaction of $[Cp_2Ni]$ with $[(Ph_3Ge)_2Hg]$ (Scheme 2a).[29] A heptametallic chain structure containing Fe, Hg, and Sn atoms was obtained and structurally characterized from the symmetrization of $[(CO)_3CpMoHgFe(CO)_4SnCl_2Fe(CO)_4]^-$ (Scheme 2b, [Eq. (b)]).[30]

$$2[Et_4N][(CO)_3CpMoHgFe(CO)_4SnCl_2Fe(CO)_4] \rightleftharpoons [Et_4N]_2[\{Fe(CO)_4SnCl_2Fe(CO)_4\}_2Hg] + [\{(CO)_3CpMo\}_2Hg] \quad (b)$$

In this compound, the Hg and Sn atoms are coordinated in a *cis* arrangement to the central $[Fe(CO)_4]$ units, and therefore generate a folded-chain structure. The *cis* coordination of two Hg atoms to the transition metal complex

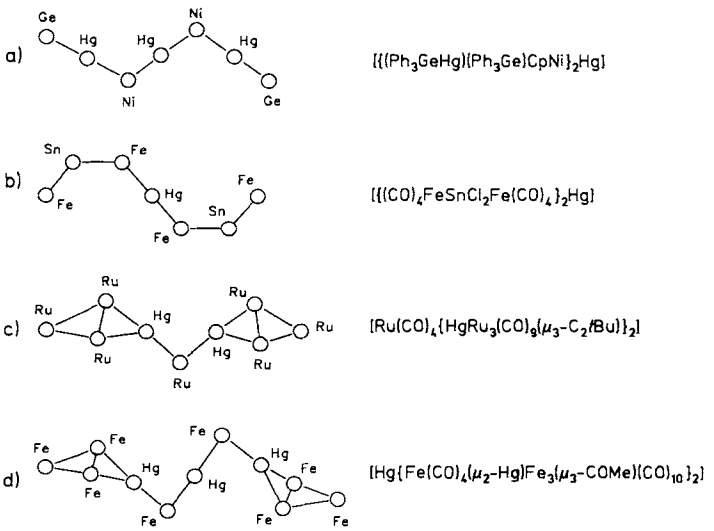

Scheme 2. Examples of metal chain structures containing mercury atoms as linking units.

fragments may also lead to the formation of closed-ring structures, as was proposed for $[Fe(CO)_4Hg]_n$ ($n = 4$) in the previous section.

The structure of such a cyclic mercury compound was substantiated by replacing the $[Fe(CO)_4]$ complex fragment by its isolobal analogue $[(MeCp)Mn(CO)_2]$; thus Gäde and Weiss obtained the tetrameric complex $[\{(MeCp)Mn(CO)_2Hg\}_4]$ by reacting $K[(MeCp)Mn(CO)_2GeH_3]$ with $HgCl_2$ (Fig. 1).[31] This fascinating compound, along with its

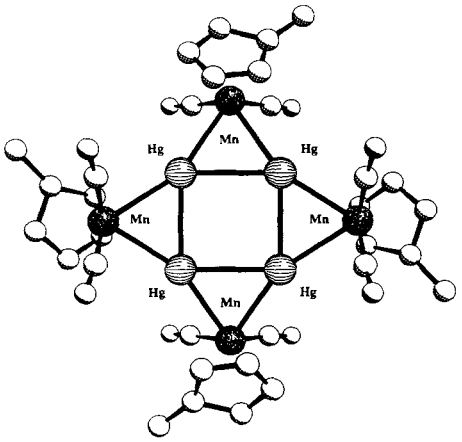

Fig. 1. The molecular structure of $[\{(MeCp)Mn(CO)_2Hg\}_4]$.

Re analogue,[32] remains the only structurally characterized example of its kind to date. In contrast to the $(FeCd)_4$ ring which is distorted by the coordination of acetone molecules to two of the Cd atoms, the $(MnHg)_4$ cluster has a highly symmetrical metal core, in which there are very short distances between the Hg atoms (2.89 Å). This structural feature, along with the nonlinearity of the Mn-Hg-Mn subunits, suggests a significant degree of secondary bonding interaction between the Hg centers. In this complex the mercury atoms may be assigned a formal oxidation state of II and thus possess closed 5d valence shells, which should imply a repulsive interaction between the Hg atoms for the Hg–Hg distances found. However, Hoffmann and other theoreticians have shown that in such compounds with closed-shells, an admixture of s and p wave functions into the molecular orbitals primarily composed of d functions partially converts bonding and antibonding interactions into more bonding and nonbonding ones, respectively.[33] This disruption of the closed d valence shells in heavy atoms has also been invoked for the explanation of the ubiquitous d^{10}–d^{10} attraction in Au^I compounds.[34] To summarize, in polymetallic compounds containing two or more mercury atoms in close proximity, there may be attractive secondary bonding interactions between the Hg atoms in addition to the primary σ-type bonding to the transition metal centers.

A remarkable cluster geometry is found for the metathesis product of $[HOs_3(CO)_{11}]^-$ with Hg^{II} salts. In contrast to the Ru analogue which fragments under the same reaction conditions (see Section 3.5), condensation and subsequent deprotonation occurs, yielding the dodecanuclear, extremely photolabile, "raft" cluster $[\{Os_3(CO)_{11}Hg\}_3]$ (Fig. 2).[35] The $Os(CO)_3$ vertex of each $Os_3(CO)_{11}$ triangle is therefore the difunctional metal complex fragment. In addition to the

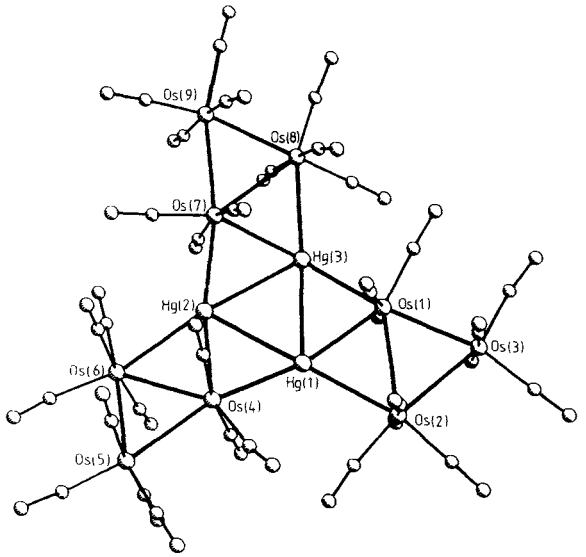

Fig. 2. The structure of the Os–Hg cluster $[\{Os_3(CO)_{11}Hg\}_3]$.

Os–Hg bonds (d(Os–Hg) = 2.71–2.76 Å) in the central Os_3 macrotriangular structure, there are donor/acceptor interactions between an $Os(CO)_4$ vertex and each mercury atom (d(Os–Hg) = 2.98–3.05 Å). The fact that the Hg–Hg distances in the central Hg_3 triangle are significantly greater than those in the Hg_4 square of $[\{(MeCp)Mn(CO)_2Hg\}_4]$ is attributed by King to the *trans* influence of these Os–Hg dative bonds.[26]

Transition metal–mercury compounds containing trifunctional metal complex fragments may form three-dimensional cluster structures ("cages"), as found in $[Hg_6Rh_4(PMe_3)_{12}]$ (Fig. 3 top)[36] and $[Hg_9Co_6(CO)_{18}]$ (Fig. 3 bottom).[37] As King has pointed out,[26] these clusters contain mercury polyhedra within transition metal macropolyhedra, the number of Hg atoms being equal to the number of edges in the respective macropolyhedron. For the macropolyhedra whose vertices have a connectivity of 3 this would constitute a series of clusters with the general formula $[\{Hg_3(ML_3)_2\}_{n+1}]$ ($n = 1,2,3,\ldots$). Thus, $[Hg_6Rh_4(PMe_3)_{12}]$ is the first member of this series containing a mercury octahedron inside a rhodium macrotetrahedron, while $[Hg_9Co_6(CO)_{18}]$ is built up from a tricapped trigonal prism of nine Hg atoms inside a cobalt trigonal macroprism of six Co atoms. The cobalt compound has an interesting chemistry in solution: fragmentation to $[(XHg)_3Co(CO)_3]$ occurs on reaction with HgX_2 (X = I, Cl, O_2CCF_3), a process which can be reversed for $[(ClHg)_3Co(CO)_3]$ upon addition of PPh_3. The Hg_9Co_6 cluster may therefore be seen as the (three-dimensional!) symmetrization product of the trimercurated Co complex.

More recently Strähle and Wurst have reported the synthesis and structure of the Pt–Hg cluster $[Hg_6Pt_4(dippb)_4]$ (dippb = 1,4-bis(diisopropylphosphinobutane)), which has a similar metal framework to $[Hg_6Rh_4(PMe_3)_{12}]$.[38] In contrast to the rhodium cluster, which has a skeletal electron count of 132 and thus conforms to the effective atomic number (EAN) rule, the Pt–Hg cluster lacks four skeletal electrons, and metal–metal bonding within the system is explained by invoking the presence of two three-center two-electron (Pt-Hg-Pt) bonds. The presence of the three-

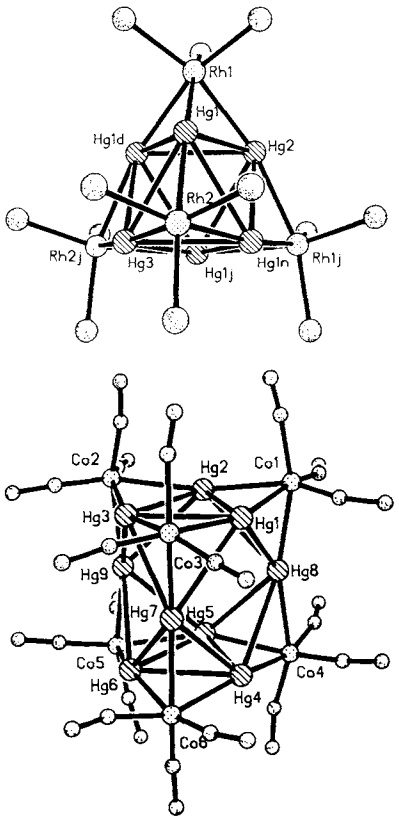

Fig. 3. The molecular structures of $[Hg_6Rh_4(PMe_3)_{12}]$ (top) and $[Hg_9Co_6(CO)_{18}]$ (bottom).

center two-electron (3c2e) bonds is thought to be reflected in the local distortion within the Hg_6Pt_4 macrotetrahedron found in the solid-state structure.

A unique Mo_4Hg_4 metallacubane forms the central unit of $[\{CpMo(CO)_3HgMo\}_4]$ obtained by Ziegler et al. as a by-product of the reaction of $[CpMo(CO)_3]^-$ (generated in situ by reduction of $[CpMo(CO)_3]_2$ with Na/Hg) with 2-butenylchloride.[39] Both the naked molybdenum and mercury atoms within the cube have an unusual coordination environment, and in spite of numerous attempts to synthesize further compounds of this type by varying the metals, it remains the only example of its kind to date.

3.2. The Structural Environment of the Linking Hg Atom in Mixed-Metal Clusters

The basic structural motif in transition metal–mercury compounds is the linear M-Hg-M' unit, as was discussed in Section 3.1 for mononuclear transition metal complex fragments, and its metal–mercury bonding can be described as 2c2e bonding of an sp-hybridized Hg atom. However, for a mercury atom linking cluster fragments there is the additional possibility of primary metal–metal bonding through multicenter bonds. The most frequently encountered structural arrays **A**–**E** observed in mixed-metal Hg clusters are summarized in Scheme 3.

In the substructures **A**–**E** the metal–mercury bonding may be viewed simplistically as arising from the bonding interaction of an Hg 6sp hybrid orbital with a frontier orbital of suitable (σ!) symmetry of the metal fragment. Such a bonding situation would electronically allow unhindered internal rotation of the molecule around an axis through the mercury atom and the midpoint of the bridged M–M vectors or capped M_3 triangles. The variation of the dihedral angle between the M_2Hg and M'_2Hg planes in compounds of type **C** is therefore most probably a consequence of steric interactions between the sets of ligands on the two bridged cluster fragments (see Section 3.3). Examples of structural types **A**–**E** have been synthesized and structurally characterized over the past decade and many aspects of the M–Hg bonding in these compounds has been studied in detail. Since structures of type **A** have already been discussed in Section 3.1, the next two sections will focus on types **B** and **C** as well as **D** and **E**.

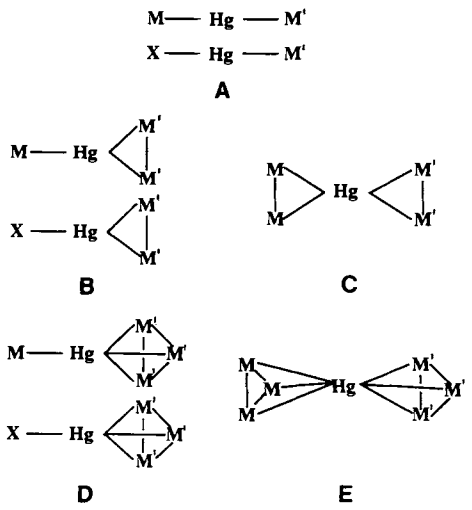

Scheme 3. The principal structural environments of a linking Hg atom in metal clusters. M, M' = cluster fragment.

3.3. Clusters with Hg Atoms in Edge-Bridging Positions (Type B and C)

The systematic application of the synthetic techniques developed for Hg-bound mononuclear complexes to cluster chemistry was pioneered by Rosenberg et al. who synthesized the first metal cluster in which an HgX fragment occupies an edge-bridging position (type **B**).[40] The preparation of $[Ru_3(\mu_3\text{-}C_2t\text{Bu})(CO)_9(HgX)]$ (X = Br, I) could be achieved either by reaction of a phenylmercury halide with the hydrido cluster $[Ru_3(\mu_3\text{-}C_2t\text{Bu})(CO)_9H]$ or metathetical condensation of the deprotonated anion with HgX_2 (X = Br, I) (Fig. 4 top). Essentially the same coordination geometry of the mercury atom is obtained if the halide is replaced by a mononuclear organometallic fragment, as in $[M_3(\mu_3\text{-}C_2t\text{Bu})(CO)_9(Hg\text{-}m)]$ (m = $CpRu(CO)_2$, $CpFe(CO)_2$ for M = Ru; m = $(CO)_4Co$, $CpMo(CO)_3$ for M = Os), although these clusters are monomeric in the crystal.[41, 42]

The XHg-bridged clusters themselves may be employed as Hg fragments in further cluster buildup, as was again first achieved in Rosenberg's group with the synthesis of $[\{Ru_3(\mu_3\text{-}C_2t\text{Bu})(CO)_9\}_2Hg]$ (Fig. 4 bottom).[43] As in the case of the simple bridged species, the bonding in this cluster can be described in terms of the interaction of Hg 6sp orbitals with suitable cluster fragment orbitals. The wide variation of the dihedral angle ($\measuredangle_{dih}$) between the M_2Hg and the

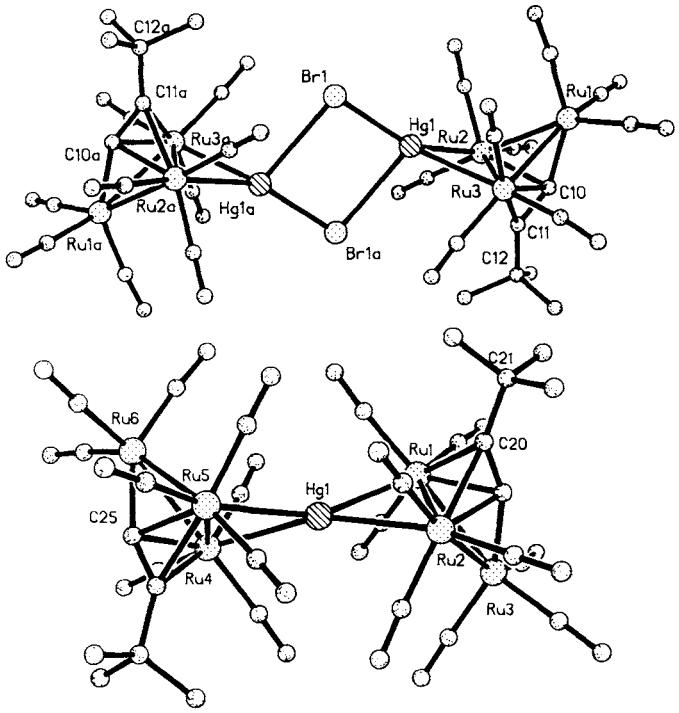

Fig. 4. The solid-state structures of $[Ru_3(\mu_3\text{-}C_2t\text{Bu})(CO)_9(HgBr)]$ (top) and $[\{Ru_3(\mu_3\text{-}C_2t\text{Bu})(CO)_9\}_2Hg]$ (bottom).

M'_2Hg planes in compounds of this type is to be interpreted as a manifestation of the system's steric constaints and is consistent with the simple bonding model assumed here (Table 1).[41-49] The linking of triangular clusters through transition metal–mercury chains of the kind encountered in Section 3.1 may be understood as an extension of the building principles discussed so far. In the simplest reported example, $[cis\text{-}Ru(CO)_4\{HgRu_3(CO)_9(\mu_3\text{-}C_2t\text{Bu})\}_2]$,[61] the two Ru_3 triangles are connected through a $RuHg_2$ bridge (Scheme 2c), whereas the linking unit in $[Hg\{Fe(CO)_4(\mu\text{-}Hg)Fe_3(\mu_3\text{-}COCH_3)(CO)_{10}\}_2]$ is an Hg_3Fe_2 zigzag chain (see Scheme 2d).[28]

Table 1. Transition metal cluster containing μ_4-linking Hg atoms.

Compound	$\measuredangle_{dih}$ [a]	ref.
$[\{(\mu\text{-}C_2t\text{Bu})Ru_3(CO)_9\}_2Hg]$	44.6	43
$[\{(\mu\text{-}H)(\mu_3\text{-}S)Os_3(CO)_9\}_2Hg]$	65.0	41
$[\{Cp(\mu_3\text{-}COCH_3)Fe_2Co(CO)_7\}_2Hg]$	46.2	44
$[\{Cp(\mu_3\text{-}COCH_3)Fe_2Rh(CO)_7\}_2Hg]$	71.9	44
$[\{(\mu_3\text{-}COCH_3)Ru_3(CO)_{10}\}_2Hg]$	45.5	28
$[\{Ru_6C(CO)_{16}\}_2Hg]^{2-}$	73.7	46
$[\{(\mu_3\text{-ampy})Ru_3(CO)_9\}_2Hg]$ [b]	35.8	47
$[\{(CH_3CN)_3Ni_3(dppm)\}_2Hg]$ [c]	9.7	48
$[\{Os_{10}C(CO)_{24}\}_2Hg]^{2-}$	38.4	49

[a] $\measuredangle_{dih}$ = torsion angle. [b] ampy = 2-aminopyridine. [c] dppm = bis(diphenylphosphino)methane.

A characteristic feature of the behavior of these systems in solution is the high degree of fluxionality of the cluster fragments linked through the Hg bridge. This fluxional behavior can be observed on the NMR timescale and includes both the rotation of the molecules around the internal axis through the Hg atom and the midpoints of the bridged M–M vectors as well as the migration of the Hg fragment around the edge of the M_3 triangles. In view of the importance of this intramolecular dynamic behavior for the properties of virtually all Hg-containing clusters in solution, this topic will be discussed in detail in Section 4.

The method of metathetical condensation (or, as normally called in cluster chemistry, redox condensation) of anionic clusters with Hg^{II} salts has been successfully applied in the selective buildup of high-nuclearity clusters with a mercury atom in a type **B** or **C** environment, such as $[Os_5(CO)_{15}(HgX)]^-$ (X = Cl, CF_3),[50] $[\{Ru_6C(CO)_{16}\}_2Hg]^{2-}$,[46] and in particular, $[\{Os_{10}C(CO)_{24}\}_2Hg]^{2-}$,[49] the largest reported species of its kind (Fig. 5). On going to anionic clusters of higher nuclearity, the choice of the appropriate mercury salt gains in importance, due to the weaker nucleophilicity of the polynuclear metal carbonyl fragment as well as its propensity to follow competing reaction pathways leading to the partial degradation or rearrangement of the metal framework structures (Section 5). The use of $[Hg(O_3SCF_3)_2]$ instead of the more conventional halides has proved to be crucial in the selective synthesis of these compounds.[51]

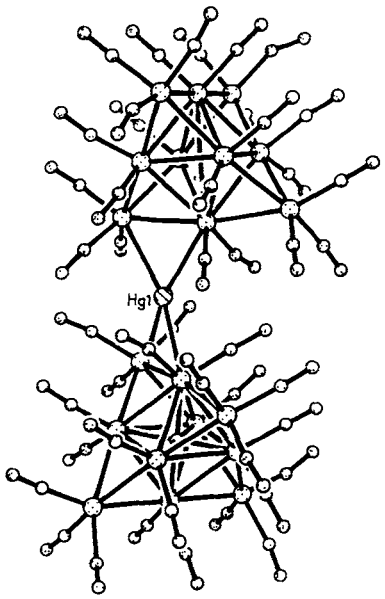

Fig. 5. The molecular structure of the dianion $[\{Os_{10}C(CO)_{24}\}_2Hg]^{2-}$.

3.4. Clusters with Hg Atoms in Face-Capping Positions (Type D und E)

The first example of a d^{10}-metal complex fragment capping a triangular face of a cluster was reported by Lauher and Wald in 1981 for $[FeCo_3(CO)_{12}(AuPPh_3)]$ in the successful attempt to demonstrate the isolobal relationship between $[R_3PAu]$ and [H].[52] The complex fragments [R–Hg] are isoelectronic (and isolobal) with [L–Au] and should therefore exhibit a similar structural chemistry. This was realized by Braunstein et al. who synthesized and structurally characterized $[RuCo_3(CO)_{12}(Hg\text{-}m)]$ (m = $Co(CO)_4$, $Mo(CO)_3Cp$) (Type **D**)[53] and the μ_6-Hg-linked cluster $[\{RuCo_3(CO)_{12}\}_2Hg]$ (Type **E**).[54]

Detailed comparative studies of the structural changes in the $[RuCo_3(CO)_{12}]^-$ unit on capping the Co_3 triangle with various d^{10} complex fragments such as $(Ph_3P)Cu$, $(Ph_3P)Au$, and R–Hg, revealed that while the overall geometry is similar for all these systems, specific geometrical distortions in the $RuCo_3$ tetrahedron seem to depend on the capping metal complex fragment.[55, 56] This has shown that while these isolobal fragments should formally lead to similar structures, their influence on the electronic (and thus geometrical) structure of the principal cluster core differs significantly. The influence of different electrophilic metal capping groups as well as steric effects on the core geometry of a cluster has been reported by Shriver et al. They studied the effect of [H] and [L–M] groups (M = Cu, Au, Hg) on the equilibrium between the tetrahedral and butterfly structures in $[Fe_4(CO)_{13}]^{2-}$ (Scheme 4).[57, 58] While $[Fe_4(CO)_{13}(AuPEt_3)]^-$ and $[Fe_4(CO)_{13}(HgCH_3)]^-$ have a lower butterfly/tetrahedron ratio in solution than was found for the protonated compound $[HFe_4(CO)_{13}]^-$, the introduction of a sterically demanding complex fragment such as $\{Mo(CO)_3Cp\}$ at the mercury atom favors the butterfly structure in which the mercury atom bridges the "hinge" in a type **B** fashion.

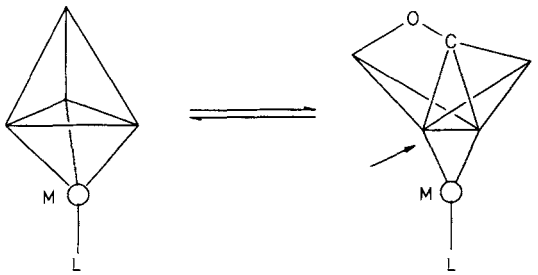

Scheme 4. The equilibrium between the tetrahedral and butterfly structures of metalated derivatives of $[Fe_4(CO)_{13}]^{2-}$; M = Hg, Au, Cu, L = ligand. The arrow indicates the hinge position in the butterfly structure.

The addition of capping Hg units to cluster cores has recently been reported for hexa- and heptanuclear clusters, for examples $[Os_6(CO)_{18}(HgY)]^-$ (Y = Cl, Br, CF_3),[50] $[Ir_6(CO)_{15}(HgCl)]^-$,[59a] (Fig. 6) and $[Re_7C(CO)_{21}(HgY)]^{2-}$ (Y = Cl, Br, CN, Ph, CH_3).[59b] The structures of the Re_7 clusters, however, could not be confirmed by X-ray structure analysis. The largest structurally characterized clusters with Hg atoms in a μ_3 position are yet again derived from $[Os_{10}C(CO)_{24}]^{2-}$: $[Os_{10}C(CO)_{24}(HgBr)]^-$ and $[Os_{10}C(CO)_{24}(HgCF_3)]^-$ (Fig. 7).[49, 60] While the (HgBr) cluster is thermally unstable with respect to symmetrization and cluster degradation, the introduction of the strongly electron-withdrawing CF_3 group significantly stabilizes the $(HgCF_3)$ cluster with respect to subsequent conversions.

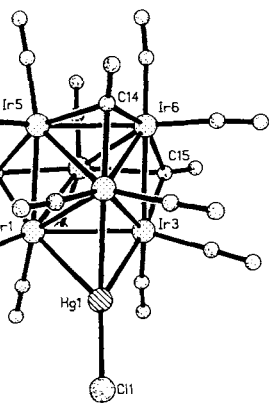

Fig. 6. Mercury in a μ_3-capping position: the structure of $[Ir_6(CO)_{15}(HgCl)]^-$.

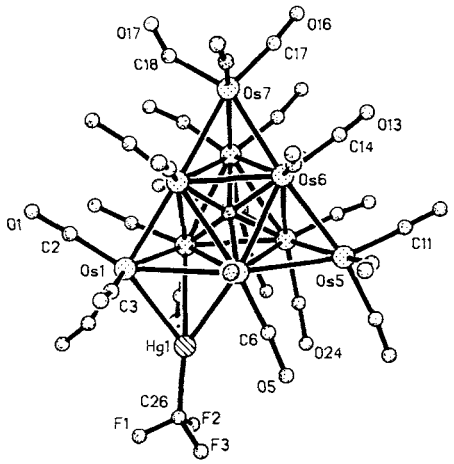

Fig. 7. The solid-state structure of $[Os_{10}C(CO)_{24}(HgCF_3)]^-$.

3.5. The Oxidative Addition of Hg^{II} Salts to Clusters: Fragmentation, Core Rearrangement, or Subsequent Demercuration

Oxidative addition reactions play an important role in the synthesis of di- and trinuclear transition metal–mercury bonded systems but have not found wide application in cluster chemistry. The main reason is the nonspecific degradation of the cluster metal cores, which normally accompanies this reaction. For example, on reacting $[HRu_3(CO)_{11}]^-$ with HgI_2, successive degradation of the triangular Ru cluster occurs, ultimately leading to $[Ru(CO)_4Hg]_n$, the ruthenium analogue of the well-known iron carbonyl derivative.[61] On the other hand, a μ_3-bridging ligand may sufficiently stabilize the Ru_3 framework to allow simple metathetical condensation, such as that leading to $[Ru_3(\mu_3\text{-}C_2tBu)(CO)_9(HgI)]$.[40]

Oxidative addition to a cluster core invariably leads to the fission of metal–metal bonds. Stable products are generated only if the metal framework of the cluster is structurally reinforced so as to accommodate the necessary rearrangement. This consideration provided the basis for Saharan's investigations into the reactivity of the neutral cluster $[Ru_5C(CO)_{15}]$ towards Hg^{II} salts.[50] The square-pyramidal carbido cluster has been known to undergo rearrangement to a more open, bridged wingtip, butterfly structure on oxidative addition of various reagents (Fig. 8 top).[62] Addition of $HgCl_2$ to the cluster led to the formation of the bridged butterfly structure with an HgCl fragment in a μ_2 position across the two Ru atoms on the hinge (Fig. 8 bottom). In the solid state, the cluster is dimeric with an Hg_2Cl_2 unit linking the two Ru_5 cluster fragments. A similar, though monomer-

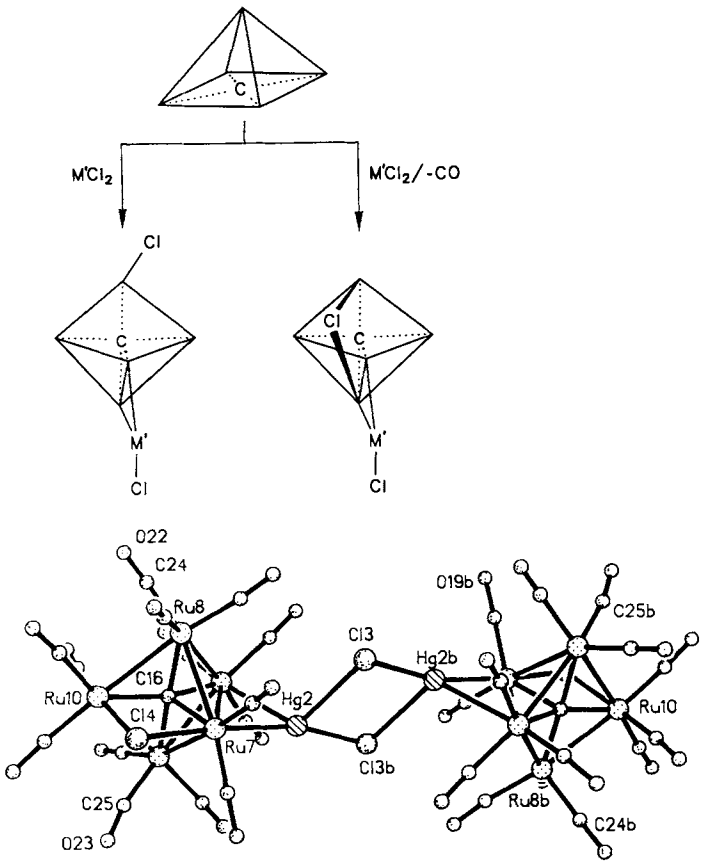

Fig. 8. Top: the oxidative addition of $M'X_2$ (M' = transition metal, X = halide) to the core of $[M_5C(CO)_{15}]$ (M = Ru, Os) and its subsequent rearrangement from a square pyramid to a wingtip-bridged butterfly structure. Bottom: the structure of $[\{Ru_5C(CO)_{15}Cl(HgCl)\}_2]$ as determined by X-ray crystallography.

ic, structure has been estabilished for the product of the reaction with $[F_3CHg(O_2CCF_3)]$.[63]

An oxidative addition is most probably the first reaction step in the formation of a range of osmium clusters isolated from the reaction of $[Os_6(CO)_{18}]$ with $[Hg(O_2CCF_3)_2]$.[64] The only product containing mercury which was characterized is the dimercury pentaosmium cluster $[HOs_5Hg_2(CO)_{15}(O_2CCF_3)_3]$, which consists of a bridged tetrahedral Os_5 core, to which two μ_2-$Hg(O_2CCF_3)$ units are attached (Fig. 9). The third trifluoroacetate ligand is coordinated to

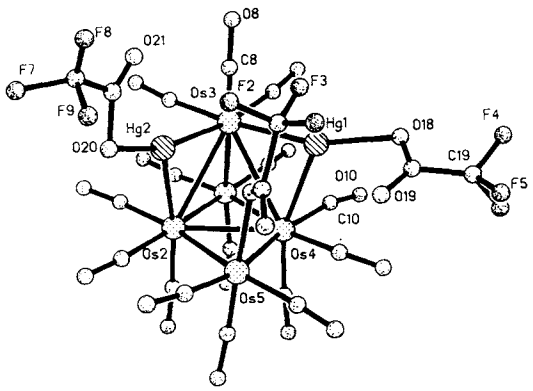

Fig. 9. The molecular structure of $[HOs_5Hg_2(CO)_{15}(O_2CCF_3)_3]$, a model for the oxidative addition of Hg salts to clusters containing metal atoms in tetrahedrally capping positions.

the bridging Os atom in close proximity to the two adjacent Hg groups. The osmium core is derived from the capped trigonal-bipyramidal structure of $[Os_6(CO)_{18}]$ by removal of the cap and opening up of the trigonal bipyramid. It may be regarded as a model for an intermediate in the partial degradation of $[M_{10}C(CO)_{24}]^{2-}$ by $[Hg(O_2CCF_3)_2]$ to yield $[M_{18}Hg_3C_2(CO)_{42}]^{2-}$ (M = Ru, Os). This reaction will be discussed in more detail in Section 5.

3.6. "Tinkering" with Platinum Clusters

Triangular platinum carbonyl clusters and their derivatives are ideal building blocks for the construction of high-nuclearity clusters. This concept has been dubbed by Hoffmann's group as the "tinkertoy approach".[65] The experimental foundation was laid by Chini's group in the

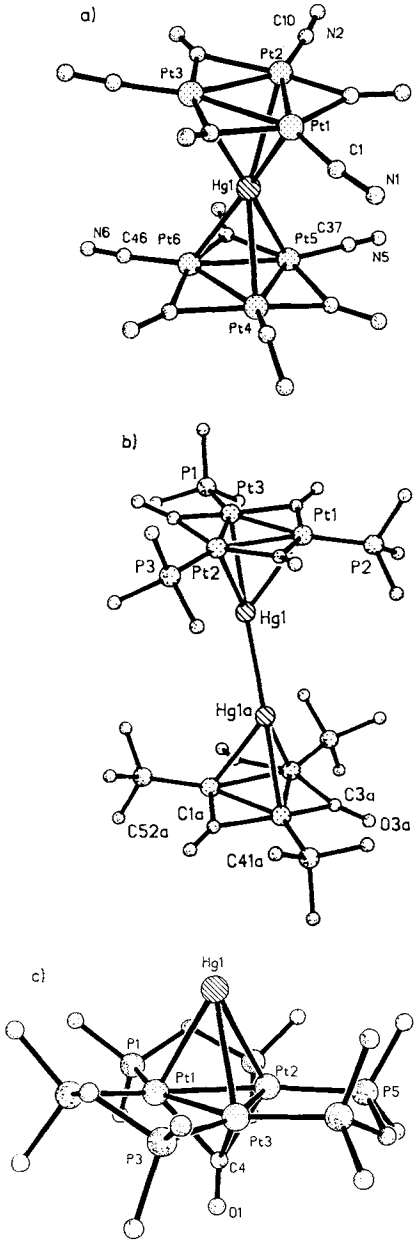

Fig. 10. The molecular structure of $[Hg\{Pt_3[(2,6\text{-}Me_2C_6H_3NC)_6\}_2]$ (a), $[Hg_2\{Pt_3(CO)_3(PPhiPr)_2)_3\}_2]$ (b), and $[Hg\{Pt(\mu_3\text{-}CO)(dppm)_3\}]$ (c).

1970s, who characterized a whole series of platinum clusters $[Pt_3(\mu_2\text{-}CO)_3(CO)_3]_n$ ($n = 2-6, 10$.) containing stacked $[Pt_3(CO)_6]$ units.[3a] By reacting the derivatives of the Pt_3 clusters containing 42 CVEs (*c*luster *v*alence *e*lectron) with metallic mercury, it has been possible to intercalate Hg_n fragments ($n = 1$, 2) between the platinum Pt_3 disks in a sandwich-type fashion.

Three varieties of this structural type have been found to date: $[Hg\{Pt_3(2,6\text{-}Me_2C_6H_3NC)_6\}_2]$, in which a mercury atom is intercalated between two Pt_3 triangles (Fig. 10a);[66] $[Hg_2\{Pt_3(CO)_3(PPhiPr_2)_3\}_2]$, which contains a dimercury fragment almost linearly linking two parallel Pt cluster units (Fig. 10b);[67] and $[HgPt_3(CO)(dppm)_3]$ (dppm = bis(diphenylphosphino)methane), which has a mercury atom capping a single Pt_3 fragment (Fig. 10c).[68]

The first of these compounds was obtained by Yamamoto et al. on reduction of dichloro-bis(2,6-xylylisocyanide)-platinum(II) with sodium amalgam, a process which has been studied in some detail with electrochemical techniques.[69] It is thought that a two-electron reduction generates—via a series of postulated intermediates—the unsaturated fragment $[Pt(2,6\text{-}Me_2C_6H_3NC)_2]$, which trimerizes and reacts with the mercury present in the reaction medium (either from the amalgam or the Hg pool electrode used in the investigations) to generate the Pt_6Hg cluster. ESCA (*e*lectron *s*pectroscopy for *c*hemical *a*nalysis) studies of the compound suggest that the system is most appropriately described by the interaction of a neutral Hg atom with two 42 CVE Pt clusters.[70] This electronic situation has also been assumed in an EHMO (extended Hückel molecular orbital) fragment orbital analysis of the Hg–Pt bonding in the system (Fig. 11).[65, 71] This is dominated by the interaction of the filled 6s orbital of the mercury atom with two a_1' orbitals of the $(Pt_3)_2$ fragment. The degree of stabilization of the bound

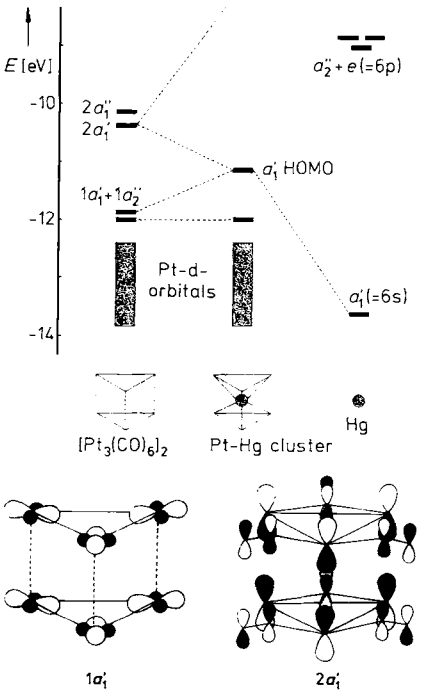

Fig. 11. Top: simplified diagram of the interaction between $[Pt_3(CO)_6]_2$ and the 6s orbital of Hg (adapted from ref. [65]). Bottom: the $1a_1'$- and $2a_1'$ frontier orbitals of the Pt cluster fragment, drawn separately for clarity.

mercury atom appears to depend primarily on the energy of the $2a_1'$ LUMO of the $(Pt_3)_2$ unit, which mixes into the $1a_1'$ HOMO of the cluster, and is primarily of ligand π^* character. The Pt–Hg bonding should therefore be enhanced by π-acceptor ligands such as isocyanides coordinated to the Pt complex fragments. From the point of view of its reactivity, the cluster was found to be a useful precursor for the (L_2Pt) fragment in the synthesis of a (L_2Pt)-bridged diplatinum A-frame complex.[72]

The dimercury cluster $[Hg_2\{Pt_3(CO)_3(PPhiPr_2)_3\}_2]$ was synthesized simply by exposing a solution of the triplatinum cluster to metallic mercury.[67] The two triangular $[Pt_3(CO)_3(PPhiPr_2)_3]$ units are each capped by a mercury atom and then joined through what the authors call a Hg–Hg interaction in the solid state (see Fig. 10b). The mercury–mercury distance of 3.225 Å suggests that this interaction is at best weak, and there seems to be no direct evidence for the dimeric structure in solution.

That monomeric units with a capping Hg atom are feasible entities has recently been shown by Puddephatt et al., who prepared $[HgPt_3(CO)_3(dppm)_3]^{2+}$ and $[Hg_2Pt_3(CO)_3(dppm)_3]^{2+}$.[68] The monomercury complex has been characterized by a single-crystal X-ray structure analysis (Fig. 10c). An EHMO analysis of the compound indicated a very small stabilization energy for the mercury bound to the Pt core, a result which is experimentally reflected in the facile displacement of the Hg by weak nucleophiles such as CO.

Both these compounds are examples for clusters containing unligated Hg atoms on the surface of their metal frameworks. Other examples for the formal addition of a naked Hg atom to a cluster framework are the mixed-metal systems $[Pt\{AuPPh_3\}_8Hg_2]^{2+}$[73] and $[Ni_8Hg(PPh)_6(PPh_3)_4]$,[74] in which the mercury is screened by neighboring ligands.

3.7. Mercury Subclusters within Larger Metal Arrays

A characteristic feature of mercury chemistry is the formation of compounds with Hg–Hg bonds in solids, coordination compounds, amalgams, and in subunits of mixed-metal high-nuclearity clusters. The location of several mercury atoms at very close proximity in large clusters is a fairly recent discovery, and the chemical consequences of the emergence of a domain structure within the metal core are only beginning to be understood (see Section 6). We will therefore at first briefly recapitulate the structural chemistry of Hg_n units not bound to other metal complex fragments, and discuss the mercury substructures in the light of these results.

The existence of the dimercury(I) Hg_2^{2+} ion is an equally intriguing and puzzling fact of heavy metal chemistry, and has given rise to countless theoretical and experimental investigations over the past two centuries.[75, 76] The stability of the dimer made mercury a promising element for the formation of further subvalent metal ions. The syntheses of these poly-mercury cations were developed primarily in Gillespie's group and culminated in the characterization of $Hg_{3-\delta}(AsF_6)$ ($0 < \delta < 0.15$), a compound with a unique solid-state structure containing AsF_6^- anions and infinite cationic Hg_n chains, whose lattice parameters are mutually incommensurate.[77] As for the simplest member of this series, the Hg_3^{2+} ion, the metal–metal bonding in this species is

predominatly of σ_{6s} character. The preference of a linear arrangement of the Hg atoms over, for example, a conceivable triangular geometry can be easily rationalized in terms of a simple MO scheme which only involves the 6s orbitals (Scheme 5).[78] For the dication a linear geometry will clearly

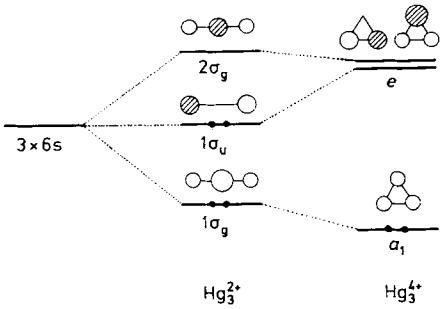

Scheme 5. A qualitative MO scheme for a linear and a triangular $[\{M(ns)\}_3]^{y+}$ ($y = 2, 4$) system.

be preferred since the population of antibonding orbitals is thus avoided. On the other hand, a tetracationic species Hg_3^{4+} would adopt a triangular arrangement due to the decreased energy of the bonding σ orbital for this configuration. This is indeed observed for the formal Hg_3^{4+} clusters in the mineral terlinguaite, $Hg_4Cl_2O_2$,[79] and the trinuclear coordination complex $[Hg_3(dppm)_3(SO_4)_2]$ (Fig. 12).[80]

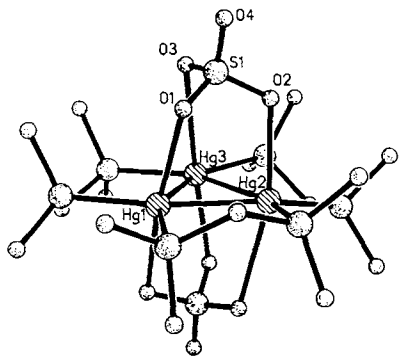

Fig. 12. Structure of the trimercury cluster $[Hg_3(dppm)_3(SO_4)_2]$.

In addition to these multinuclear cationic clusters, the structures of anionic Hg_n clusters in alkali metal amalgams have recently received considerable attention due to the work of Deiseroth et al., who developed a new preparative technique for the synthesis and isolation of crystalline phases of varying composition.[81] The most spectacular result has been the discovery of Hg_8 cubes along with Hg_4 square-planar clusters in $Rb_{15}Hg_{16}$.[82] The Hg-Hg-Hg angles of approximately 90° found for these clusters indicate the predominance of σ_{6p} type bonding between the Hg atoms. The bonding electrons are provided by the alkali metals, which are formulated as monocations.

In view of the tendency of mercury in various oxidation states between +1 and −1 to form aggregates with metal–metal bonds, it might be anticipated that Hg subclusters should be readily incorporated into larger cluster frameworks, as has been found for gold, the neighbor of mercury in the periodic table.[83, 84] However, thus far there are only a few examples of transition metal–mercury clusters which qualify for this category. The cage structures of the type $[Hg_3(ML_3)_2]_{n+1}$ ($n = 1, 2, \ldots$) mentioned in Section 3.1 appear to be constructed around Hg_n subunits. However, the large intramolecular Hg–Hg distances found in their solid-state structures (d(Hg–Hg) > 3.0 Å) and, consequently, weak bonding interactions between the mercury atoms make such an interpretation questionable.

A series of high-nuclearity Ru–Hg and Os–Hg clusters derived from $[M_{10}C(CO)_{24}]^{2-}$ (M = Ru, Os) may be interpreted along the lines of the concept of metal domains referred to in the heading of this subsection. This is justified not only on the basis of their structural data, but also in the light of their chemical behavior with respect to transformations involving their metal cores.

The formation of a trinuclear Hg subunit within the framework of a large carbonyl cluster was the unexpected result of the reaction of $[Ru_{10}C(CO)_{24}]^{2-}$ with $Hg(O_2CCF_3)_2$, which yielded the cluster dianion $[Ru_{18}Hg_3C_2(CO)_{42}]^{2-}$.[85] The subsequent reinvestigation of the corresponding reaction with the osmium analogue led to the isola-

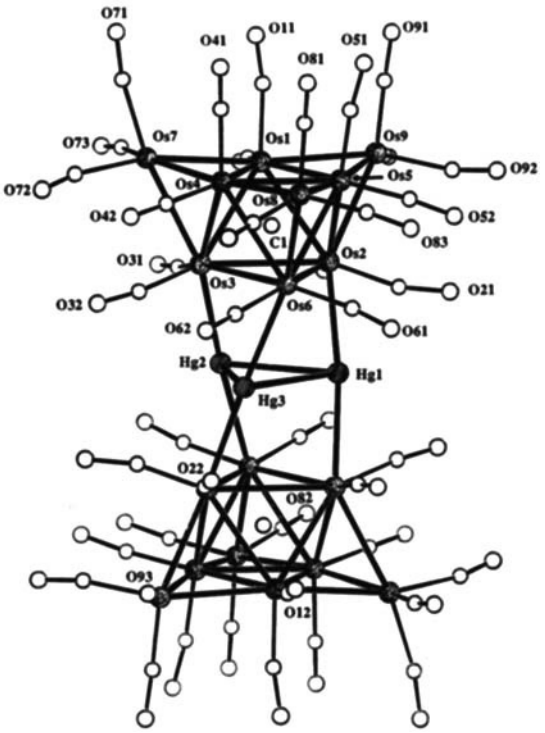

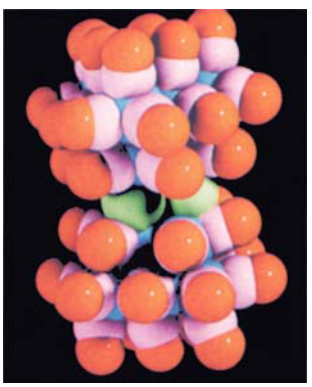

Fig. 13. Top: plot of the molecular structure of $[Os_{18}Hg_3C_2(CO)_{42}]^{2-}$. Bottom: computed space-filling model (CHEM-RAY) of the cluster, showing the exposed situation of the central Hg_3 unit. Red spheres = O, pink = C, green = Hg, blue = Os.

tion and characterization of $[Os_{18}Hg_3C_2(CO)_{42}]^{2-}$ (Fig. 13 top).[49] Both compounds contain the Hg_3 subcluster sandwiched between two tricapped octahedral $[M_9C(CO)_{21}]$ units, which are derived from the framework of the tetracapped, octahedral starting materials, $[M_{10}C(CO)_{24}]^{2-}$, by removal of a capping $Os(CO)_3$ vertex. Although the ligand-free central Hg_3 unit of the cluster is shielded very little by the neighboring carbonyl groups, as seen in the space-filling model (Fig. 13 bottom), the compound is surprisingly stable with respect to nucleophilic attack. The osmium cluster, in particular, has been the object of extensive studies into the reactivity at the interfaces between the different metal domains within these so far unique mixed-metal clusters.[86-89] The reversible photochemical and redox extrusion and reinsertion of mercury atoms has yielded the complete series $[Os_{18}Hg_xC_2(CO)_{42}]^{y-}$ ($x = 1-3$, $y = 1-4$). While the bonding interaction between the Hg atoms in the Hg_3 species is thought to be rather weak (d(Hg–Hg) = 2.927 Å), the significant shortening of the Hg–Hg distance in its photolysis product $[Os_{18}Hg_2C_2(CO)_{42}]^{2-}$ (2.745 Å; Fig. 14) is indicative of a significant degree of bonding between both Hg atoms. Its electronic nature remains poorly understood because the simple electron counting rules and the concept of formal oxidation states of individual metal atoms, used so successfully in the analysis of metal–metal bonded systems, break down for mixed-metal clusters of this size.

To exemplify this, let us consider $[Os_{18}Hg_2C_2(CO)_{42}]^{2-}$ (Fig. 14). Assuming that the polyhedral skeletal electron pair theory is applicable to the two nonaosmium moieties $[Os_9C(CO)_{21}]$, which require an electron count of 122 and thus a formally tetraanionic charge,[90] we are faced with the unreasonable oxidation state of III for the mercury atoms. If this extreme, but in simpler cases useful, approach does not hold, how then is the structure of the dimercury fragment embedded in the osmium core to be analyzed? The answer to this problem is most likely related to the fact that large metal clusters may accommodate a whole range of oxidation states (and therefore a certain degree of electron deficiency) without the accompanying bond breaking or formation associated with redox processes in low-nuclearity species. In other words, the bonding within the metal core of such systems cannot be reduced to a mere series of localized interactions.

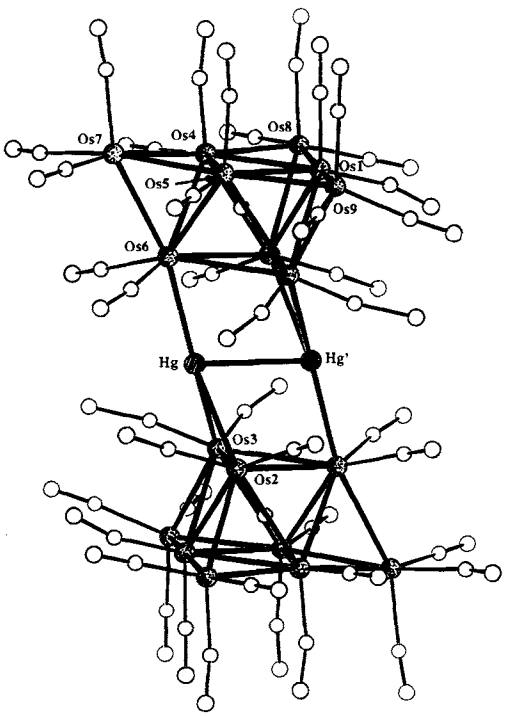

Fig. 14. Molecular structure of the photolysis product, the dianion $[Os_{18}Hg_2C_2(CO)_{42}]^{2-}$.

4. Mercury as a Ligand? The Dynamic Properties of Mercury-Containing Carbonyl Clusters

Mercury as a ligand?[91] This may seem rather paradoxical in view of the approach chosen so far, which has considered Hg-containing units in clusters as an intergral part of their metal frameworks. Nevertheless, this is a fairly common approach whenever the transition metal atom to which the mercury atom is bonded is in the focus of interest rather than the metal–metal bonding itself. To a certain extent this was the case in some of the early work. Thus Nyholm and Vrieze deduced a spectrochemical ligand-field sequence for various Hg–Y groups coordinated to $[(Ph_2MeAs)_2X_2Rh]$ complex fragments,[18b, 19b] and Lewis and Wild related the frequency of the υ(CO) bands in the infrared spectra of $[Fe(CO)_4(HgY)_2]$ to the group electronegativity of the mercury units.[21b]

If there is a property of Hg fragments in clusters that justifies their comparison to other ligands coordinated to the respective principal metal core, it is the dynamic behavior observed in solution. The plots of the molecular structures shown here may convey the impression of rigid metal cores embedded in their equally static ligand shells. While in many cases this is an adequate view of the molecules packed in a single crystal, spectroscopic studies performed on their solutions have revealed the existence of dynamic processes effecting the permutation of nuclear positions in these systems. For transition metal carbonyl clusters containing Group Ib or IIb metal complex fragments in their framework core, fluxionality[92] involving these subunits has been widely observed.[83] This typical behavior may be exemplified by the results obtained for two types of clusters. Type **I** are triangular M_3 clusters, which are linked by a μ_4-Hg bridge, and type **II** are the mercurated derivatives of $[Os_{10}C(CO)_{24}]^{2-}$.

Systematic variable temperature NMR studies of clusters of the type $[\{M_3\}_2Hg]$ (**I**), as discussed in Section 3.3, have been carried out in the groups of Rosenberg[41, 93] and Farrugia.[28, 44] The observed fluxionality may be essentially broken down into two elementary processes (Fig. 15), the rotation around an internal axis through the Hg atom and

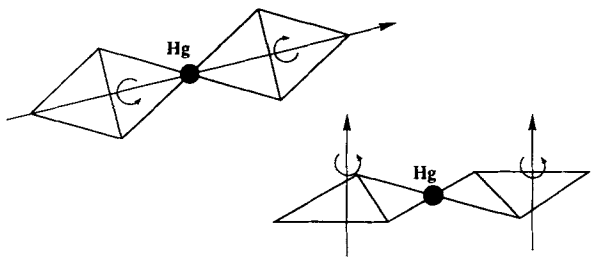

Fig. 15. The two elementary processes which are proposed to account for the dynamic behavior of a series of $[\{M_3\}_2Hg]$ clusters in solution.

the midpoints of the bridged M–M vectors, and at least the partial migration of the Hg complex fragment around the M_3 triangles. The remarkable conclusion drawn from these studies is that a μ_2-Hg moiety has about the same mobility on these clusters as a μ_2-hydrido ligand.[41]

The interpretation of the ^{13}C NMR spectra obtained for $[Os_{10}C(CO)_{24}(HgY)]^-$ (Y = Cl, Br, I, CF_3, $Mo(CO)_3Cp$) (**IIa**) and $[\{Os_{10}C(CO)_{24}\}_2Hg]^{2-}$ (**IIb**) has been slightly more involved.[94] At the high-temperature limit of (**IIa**) the exchange between all positions on the tetrahedral Os_{10} core is a fast process resulting in the effective T_d symmetry of the compound. On cooling the samples, an intermediate dynamic regime is reached in which the chemical exchange of the Hg–Y fragment is restricted to a rotation around a single vertex of the tetrahedron (Fig. 16). Only for the

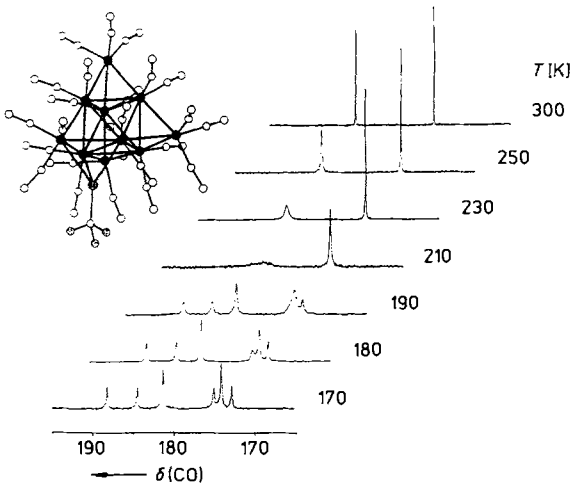

Fig. 16. Variable low-temperature ^{13}C NMR spectra of $[Os_{10}C(CO)_{24}(HgCF_3)]^-$.

$[\{Os_{10}C(CO)_{24}\}_2Hg]^{2-}$ cluster with a linking Hg has it been possible to freeze out the static metal core structure. On heating samples of this compound, a rapid migration of the Hg "linker" around a single vertex in both Os_{10} subclusters is observed, a motion which implies a fast rotation of the two halves relative to each other, as is depicted in Figure 17.

A comparison of the variable-temperature NMR spectra recorded for the Hg–Y-capped Os_{10} clusters with that of the monohydrido species $[HOs_{10}C(CO)_{24}]^-$ has revealed that in these Hg compounds the mobility of the Hg–Y fragment even exceeds that of the isolobal hydrido ligand.[95] Thus, in

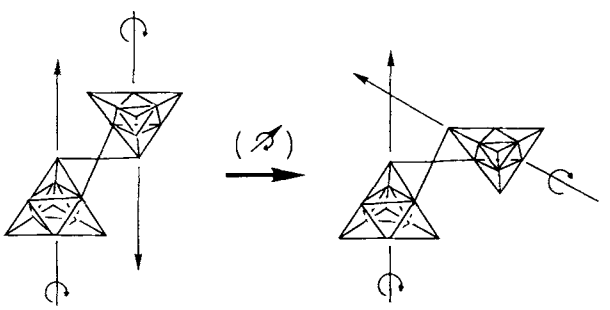

Fig. 17. The proposed intramolecular motion of the Os_{10} cluster fragments in $[\{Os_{10}C(CO)_{24}\}_2Hg]^{2-}$ relative to the Hg bridge, to explain the high-temperature ^{13}C NMR spectral patterns (from ref. [94]).

this context the Hg group displays a behavior that is otherwise typical of ligands in clusters.

5. Characteristics of the Chemical Reactivity of the Hg Complex Fragment Attached to Cluster Cores

Redistributions, that is, symmetrizations or asymmetrizations, of the kind introduced in Section 2 dominate the chemical reactivity of Hg fragments attached to both low- and high-nuclearity metal frameworks [Eq. (c)]. The rela-

$$2\,[M_m(CO)_n(HgY)] \rightleftharpoons [\{M_m(CO)_n\}_2Hg] + HgY_2 \qquad (c)$$

tive stability of the asymmetric over the symmetric components in these equilibria depends on the properties of both the cluster fragment $[M_m(CO)_n]$ (for instance its charge) and the ligand Y coordinated to the mercury center. It has been found that an increased electronegativity of Y stabilizes the asymmetric product M_m-Hg-Y. Another criterion is the strength of the Hg–Y bond. While the factors determining the redistribution reactions of Hg-linked mononuclear complexes have been known for a long time, these studies now include systems with μ_2-Hg-bridged $[M_m(CO)_n]$ units (Scheme 6).

$$2\,[Mn_2(\mu\text{-}HgY)(\mu\text{-}PPh_2)(CO)_8] \rightleftharpoons [\{Mn_2(\mu\text{-}PPh_2)(CO)_8\}_2Hg] + HgY_2$$

$$2\,[Fe_2(CO)_8(\mu\text{-}Hg\text{-}M)]^- \rightleftharpoons [\{Fe_2(CO)_8\}_2Hg]^{2-} + M_2Hg$$

$$2\,[Fe_2(CO)_7(\mu\text{-}PPh_2)(\mu\text{-}Hg\text{-}M)] \rightleftharpoons [\{Fe_2(CO)_7(\mu\text{-}PPh_2)\}_2Hg] + M_2Hg$$

$$2\,[Ru_3(CO)_9(\mu_3\text{-}C_2\,t\text{Bu})(\mu\text{-}HgX)] \rightleftharpoons [\{Ru_3(CO)_9(\mu_3\text{-}C_2\,t\text{Bu})\}_2Hg] + HgX_2$$

Y = Ph, Cl, CN X = Br, I

M = $Mo(CO)_3Cp$, $W(CO)_3Cp$, $Mn(CO)_5$, $Co(CO)_4$, $Fe(CO)_2Cp$

Scheme 6. Redistribution equilibria of transition metal–mercury compounds containing μ_2-Hg fragments.

For $[Mn(\mu\text{-}HgY)(\mu\text{-}PPh_2)(CO)_8]$ it was found, that while the phenyl derivative (i.e., Y = Ph) symmetrized immediately under the reaction conditions of its synthesis, the equilibrium for the more electronegative chloride (Y = Cl) was almost completely on the side of the asymmetric reactant.[96] On the other hand, the negative charge on $[Fe_2(CO)_8(\mu_2\text{-}Hg\text{-}m)]^-$ appears to stabilize the asymmetric species, while in the case of the neutral μ_2-PPh_2-bridged complex immediate symmetrization occurs.[97] The greater bond energy of the Hg–Br bond in $HgBr_2$ is thought to be the reason for the more strongly favored symmetrization of the bromomercury–ruthenium cluster $[Ru_3(CO)_9(\mu_3\text{-}C_2t\text{Bu})(HgBr)]$ in comparison to its iodo analogue.[43b] Thus, to suppress the symmetrization of an asymmetric transition metal–mercury cluster the ligand Y coordinated to the mercury atom should be a highly electronegative fragment as well as a bad leaving group.

The ideal ligand at the Hg atom in this respect is probably the CF_3 group, which effectively stabilizes the monomer-

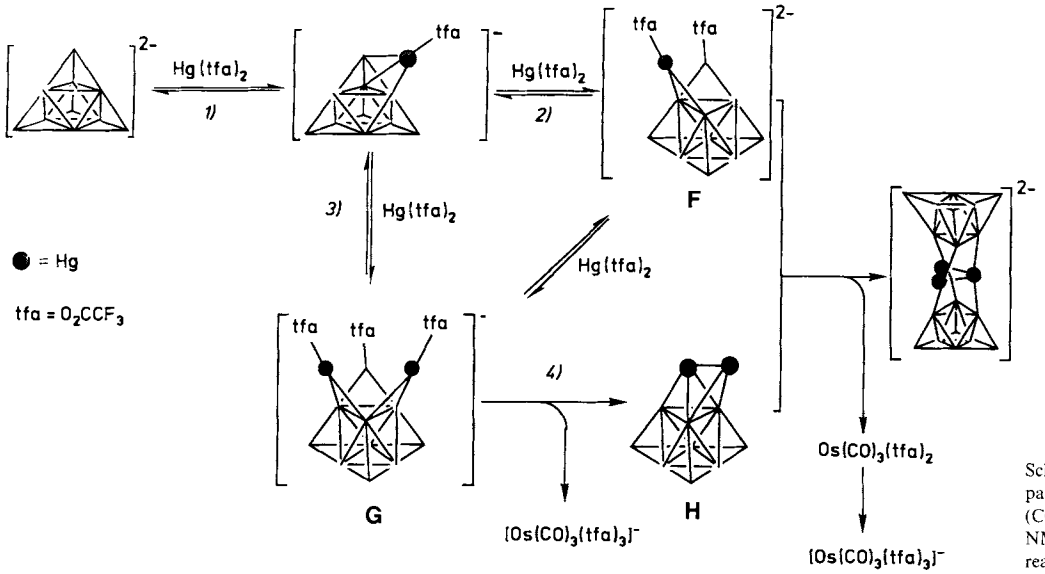

Scheme 7. A proposed mechanistic pathway leading to $[Os_{18}Hg_3C_2(CO)_{42}]^{2-}$ based on IR and ^{13}C NMR spectroscopic studies of the reaction mixture.

cury-capped or -bridged cluster even in cases where a whole range of other ligands have failed. This has been shown in the synthesis of $[Os_{10}C(CO)_{24}(HgCF_3)]^-$ and $[Os_{10}H_4(CO)_{24}(HgCF_3)]^-$, the only thermally stable Hg-capped derivatives of the decanuclear parent cluster dianions.[49, 60] The effective blocking of one coordination site at the mercury atom has therefore enabled the characterization of model compounds for the proposed primary intermediate in the more complicated reaction cascades that result from the treatment of the parent cluster dianions $[Os_{10}Z(CO)_{24}]^{2-}$ ($Z = H_4$, C) with Hg^{II} salts.

While the Hg–Y bond is the focus of the discussion of the redistribution chemistry of mercury bound by transition metals, its effect on the principal cluster core may open up additional reaction pathways. The effect an electrophilic attack of a cationic Hg fragment may have on the subsequent conversions of the cluster has been pointed out in Section 3.5 in the discussion of the oxidative addition reactions of Hg salts. The attached Hg fragment activates (i.e. polarizes) the metal framework towards an attack by nucleophiles, such as the displaced anion of the mercury salt or the oxidative addition of a second HgY_2 molecule. Another conceivable secondary reaction is the rearrangement of the ligand Y in the Hg–Y group bound to a neighboring metal center in the cluster. This is expected to be particularly facilitated for labile, potentially bidentate anions such as carboxylates, which may explain their efficiency in cluster degradation reactions, for example $[Os_6(CO)_{18}]$ with $Hg(O_2CCF_3)_2$ (see Section 3.5).[64]

One of the most thoroughly studied reactions, in which these considerations play a role, is the conversion of $[Os_{10}C(CO)_{24}]^{2-}$ to $[Os_{18}Hg_3C_2(CO)_{24}]^{2-}$ with $Hg(O_2CCF_3)_2$. IR and ^{13}C NMR spectroscopic investigations of this reaction as well as the knowledge of the results reviewed in Section 3.5 have led to the proposal of a mechanistic model for this multiple-step transformation (Scheme 7).[51] This comprises the three fundamental reaction types cited above: electrophilic addition of the $Hg–Y^+$ fragment to the cluster (step 1), nucleophilic attack of the displaced anion of the Hg salt on the polarized metal core (steps 2 and 3), and internal rearrangement of the Hg-bound ligands (step 4) yielding the proposed intermediate (**H**) as well as the isolated second reaction product $[Os(CO)_3(O_2CCF_3)_3]^-$. Condensation of (**F**) and (**H**) leads to the final reaction product. The proposed intermediate (**G**) is adequately modeled by $[HOs_5Hg_2(CO)_{15}(O_2CCF_3)_3]$, the only structurally characterized Hg-containing degradation product of $[Os_6(CO)_{18}]$ with $Hg(O_2CCF_3)_2$ (see Section 3.5).

A frequently observed secondary reaction of electrophilic mercurations, which also defines the limits of the synthetic approach discussed in this and the previous section, is the thermal demercuration of the cluster. Anionic carbonyl clusters that have low oxidation potentials are simply oxidized by the attacking Hg reagent with the concomitant precipitation of metallic mercury. The increasing redox activity of clusters on going to high nuclearities has so far prohibited the synthesis of transition metal–mercury clusters containing significantly more than twenty metal atoms. This is illustrated by the completely different behavior of the tetrahydridodecaosmium cluster $[Os_{10}H_4(CO)_{24}]^{2-}$ towards Hg^{II} salts in comparison to its carbido analogue.[60] While the carbido cluster may be regarded as the ideal substrate for redox condensation reactions with Hg electrophiles, $[Os_{10}H_4(CO)_{24}]^{2-}$ is readily oxidized to the radical monoanion by most mercury salts. The same applies to even larger osmium cluster dianions such as $[Os_{17}(CO)_{36}]^{2-}$[98] and $[Os_{20}(CO)_{40}]^{2-}$.[99] These species are known to have a high density of reversibly coupled redox states, a situation which has so far inhibited their use in cluster condensation reactions.[100] The competition between redox reactions and redox condensation reactions is thus an important factor to be considered in cluster synthesis!

6. The Redox and Photochemistry of the Transition Metal–Mercury Bond: Site-Specific Core Manipulation in High-Nuclearity Clusters

The photosensitivity of carbonyl complexes with one or more Hg units bound to the transition metal atoms was

noticed and reported in the early studies on these compounds. Ever since Schubert warned that $[\{Co(CO)_4\}_2Hg]$ had to be manipulated and stored under exclusion of light to avoid photoinduced precipitation of metallic mercury,[10] this characteristic reactivity of a whole range of similar species has only been of interest with regard to the protective measures necessary for their synthesis. It was not until 1988 that the first systematic photochemical investigation of the reaction (d) was reported by Vogler and Kunkeley.[101] The

$$[\{(CO)_4Co\}_2Hg] \overset{h\nu}{\rightleftharpoons} [Co_2(CO)_8] + Hg \qquad (d)$$

fragmentation may be understood as being triggered by a metal-to-metal charge transfer (MMCT) transition from the primarily cobalt-centered HOMO to a low-lying primarily mercury-centered unoccupied orbital. This transition effectively amounts to a photochemically driven intramolecular redox reaction, a point of view which is of great heuristic value in the study of high-nuclearity mixed-metal clusters.

The main reason for the paucity of systematic photochemical studies of this kind is probably the lack of interest that the chemical transformations associated with the Hg extrusion have created so far. In addition, the frequently encountered thermal instability of the primary photochemical products may be another aspect which has discouraged the development of this area. The situation should be somewhat different for mixed-metal clusters for which photochemical reactions of this kind might open up new routes to synthetic targets unattainable by the standard preparative techniques.

The example par excellence for these conceptual considerations is the octadecaosmium–trimercury cluster $[Os_{18}Hg_3C_2(CO)_{42}]^{2-}$. Its photochemical behavior may well herald a range of comparable metal core manipulations in other mixed-metal clusters. The structure (see Fig. 13) with its clearcut borderlines between the osmium and mercury subunits appeared predestined for core transformations following a photoinduced Hg-extrusion step. Indeed, on irradiation of the deep purple solutions of its $[(Ph_3P)_2N]^+$ salt, a single mercury atom is ejected generating the dimercury species $[Os_{18}Hg_2C_2(CO)_{42}]^{2-}$, which if stirred in the dark in the presence of the precipitated Hg metal, reincorporates an Hg atom to regenerate the starting material completely. Since the Hg-extrusion and Hg-reinsertion steps are accompanied by a change in color of the solution studied, the $Os_{18}Hg_3$-cluster dianion is an example of a photochromic system. The same behavior was found for the corresponding monoanionic species, which are reversibly generated from the dianions by a one-electron oxidation. The tri- and dimercury clusters $[Os_{18}Hg_3C_2(CO)_{42}]^{n-}$ and $[Os_{18}Hg_2C_2(CO)_{42}]^{n-}$ ($n = 1, 2$) are therefore linked by a reversible photochemical and redox cycle as depicted in Scheme 8. The low quantum yields of the two photochemical reactions of approximately 0.5% are probably a consequence of the large number of nonreactive deactivation pathways in these systems.[86, 87, 102]

It was pointed out that the MMCT transition, which induces the loss of one mercury atom, may be viewed as an intramolecular redox reaction in which the population of an Os–Hg/Hg–Hg antibonding orbital leads to the destabilization of the central Hg_3 unit. If this simplistic view holds, the population of the same antibonding orbital from an external electron source, that is reduction of the cluster, should lead

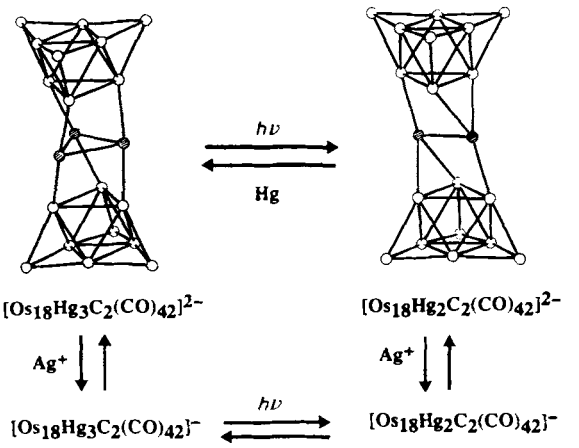

Scheme 8. The reversible photochemical and redox cycle linking $[Os_{18}Hg_3C_2(CO)_{42}]^{n-}$ and $[Os_{18}Hg_2C_2(CO)_{42}]^{n-}$; $n = 1,2$.

to essentially the same structural transformation. This consideration was the starting point of a rich redox chemistry and electrochemistry of the osmium–mercury clusters as summarized in Scheme 9. Particularly notable is the struc-

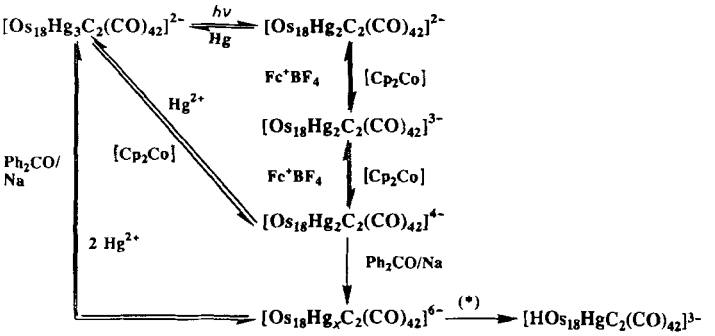

Scheme 9. The network of reversible photochemical redox transformations of $[Os_{18}Hg_mC_2(CO)_{42}]^{n-}$ ($n = 1-3$, $m = 2-6$). Fc = ferrocene; (*) = workup.

tural relationship between the electron deficient cluster which has fewer electrons than required by the Wade–Mingos rules, $[Os_{18}Hg_2C_2(CO)_{42}]^{2-}$, and the corresponding "electron-precise" tetraanion $[Os_{18}Hg_2C_2(CO)_{42}]^{4-}$ (Fig. 18, see Section 3.7).[88] While the dianion has a distorted core geometry with an Hg–Hg distance of 2.745 Å, the tetraanion shows a significant straightening of the metal core and increase of the Hg–Hg bond length to 2.827 Å. The ejection of a second Hg atom was feasible with a strong reducing agent such as Na/Ph_2CO or $Na/C_{10}H_8$, yielding μ_6-Hg linked clusters in various oxidation states, of which the protonated species $[HOs_{18}HgC_2(CO)_{42}]^{3-}$ has been structurally characterized by X-ray crystallography.[89]

The reductive extrusion of Hg atoms from compounds with metal–mercury bonds is a well established route to mononuclear anionic metal carbonyls, the Hg-bonded species functioning as stable precursors to these materials. A prominent example is the formation of $[Co(CO)_4]^-$ by reduction of $[\{(CO)_4Co\}_2Hg]$ with Na/Hg.[103] On the other hand, the oxidative cleavage of Hg–transition metal bonds is a less well understood process. Reactions of this type may proceed along complex multistep pathways as has been shown recently in a study of the redox chemistry of

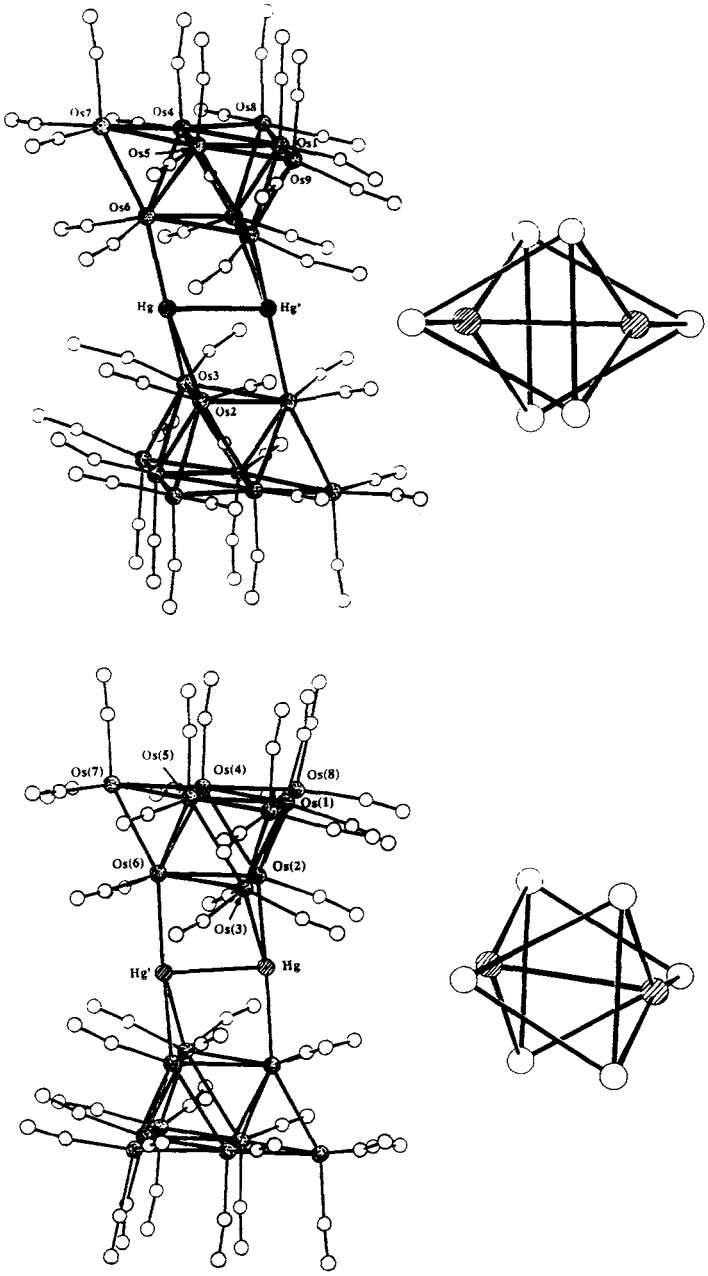

Fig. 18. Left: comparison of the molecular structures of $[Os_{18}Hg_2C_2(CO)_{42}]^{2-}$ (top) and $[Os_{18}Hg_2C_2(CO)_{42}]^{4-}$ (bottom). Right: the structural changes accompanying the two-electron reduction on viewing the molecule along an axis perpendicular to the Os_3 triangles adjacent to the dimercury unit.

$[\{CpMo(CO)_2(PPh_3)\}_2Hg]$.[104] The oxidation of high-nuclearity clusters in the presence of mercury metal may be even more complicated. Chemical and electrochemical oxidation of $[Os_{10}C(CO)_{24}]^{2-}$ in the presence of Hg leads to cluster aggregation, although neither the possible reaction pathways nor the exact nature of the products have been established beyond doubt.[105]

7. Conclusion and Outlook

The wealth of data accumulated over the past decade has impressively demonstrated the potential of mercury reagents in the construction of metal cluster frameworks. While certain structural motifs are found to be common to many of the systems known so far, which enables a relatively systematic synthetic approach to mercury–transition metal clusters, surprises have been plentiful and have kept the interest in the chemistry of the element itself alive.

The step into the regime of high-nuclearity species has only recently been made and has yielded unprecedented structures and reactive transformations. One of the lessons learnt in the investigation of such systems is a consequence of the large variety of potential reactive interactions with mercury salts. To avoid complicated product mixtures arising from redistribution reactions, subsequent demercurations, partial cluster degradation, etc., it is necessary to focus as much attention on the solution properties of the Hg reagent as on the cluster itself. The most important properties of mercury compounds in this respect are their solubility in polar aprotic solvents, the degree of dissociation of the relevant salt in these media, and the strength of the Hg–ligand bond in comparison to the Hg–metal bonds to be formed. Through careful control of these properties, by choice of the appropriate reagent, it should be possible to generate certain cluster types selectively, and in this area considerable progress is to be expected in the near future. In other words, transition metal–mercury cluster chemistry should be viewed as being rooted as much in the chemistry of the element Hg as in mixed-metal cluster chemistry.

The systematic application of photo- and electrochemical techniques to large mixed-metal clusters with their preformed breakage points or "sticky ends" is an exciting and promising area of cluster research.[106] This is so particularly since the increased redox activity of molecular carbonyl clusters on going to higher nuclearities appears to set a limit to the size of metal frameworks attainable by the standard preparative methods. Few examples that fall into this category have been studied to date, and it is therefore too early to draw general conclusions about their reactivity. However, in the same way as mercury has played a prominent role at various stages in the development of organotransition metal chemistry and the concept of direct bonding between metal atoms in molecular structures (Section 2), it may open up new entries into the buildup of extended metal–metal bonded systems.

The author would like to thank particularly Prof. Lord Lewis (Cambridge) and Prof Brian Johnson (Edinburgh) for introducing him to the fascinating field of high-nuclearity cluster chemistry and inspiring the writing of this article; likewise Dr. Phil Bailey (Munich) for his stimulating proposals or vehement opposition to some of the thoughts expressed here. Prof. Mary McPartlin (London), Prof. Alistair Lees (Binghamton), Prof. Joe Lauher (Stony Brook) as well as Dr. Paul Raithby, Dr. Martin Mays, and Dr. Catherine Housecroft (Cambridge) have pointed out many important aspects of the chemistry of Hg–transition metal clusters, and they as well as Prof. J. Strähle (Tübingen) communicated experimental data prior to publication. I am grateful to Dr. Paul Raithby for his help with the production of the figures and to Prof. Helmut Werner (Würzburg) for providing the facilities for the writing of this review. The author's own contributions to the area were financially supported by the British Council, the Kurt Hahn Trust, the Studienstiftung des deutschen Volkes as well as ICI PLC.

Received: July 24, 1992 [A 888 IE]
German version: *Angew. Chem.* **1993**, *105*, 25

[1] For monographs and reviews covering the more general aspects of this field see for example: a) *Transition Metal Clusters* (Ed.: B. F. G. Johnson), Wiley, New York, **1980**; b) D. M. P. Mingos, D. Wales: *Introduction to Cluster Chemistry*, Oxford, **1990**; c) D. M. P. Mingos, T. Slee, L. Zhenyang, *Chem. Rev.* **1990**, *90*, 383; d) *Metal Clusters* (Ed.: M. Moskovits), Wiley, New York, **1986**; e) *Metal Clusters in Catalysis* (Eds.: B. C. Gates, L. Guczi, H. Knözinger), Elsevier, Amsterdam, **1986**; f) *The Chemistry of Metal Cluster Complexes* (Eds.: D. F. Shriver, H. D. Kaesz, R. D. Adams), VCH, Weinheim; **1990**.

[2] For early reviews see for instance: a) P. Chini, G. Longoni, V. G. Albano, *Adv. Organomet. Chem.* **1976**, *14*, 285; b) E. Band, E. L. Muetterties, *Chem. Rev.* **1978**, *78*, 639; c) E. L. Muetterties, *Angew. Chem.* **1978**, *90*, 577; *Angew. Chem. Int. Ed. Engl.* **1978**, *17*, 545; d) E. L. Muetterties, T. N. Rodin, E. Band, C. F. Brucker, W. R. Pretzer, *Chem. Rev.* **1979**, *79*, 91; e) B. F. G. Johnson, J. Lewis, *Adv. Inorg. Chem. Radiochem.* **1981**, *24*, 225. Molecular cluster chemistry has been traditionally divided into the areas of low- and high-nuclearity species with a borderline which is somewhat arbitrarily drawn at the metal atom number six. Reviews published since 1985 covering various aspects of low-nuclearity cluster chemistry include: f) W. L. Gladfelter, *Adv. Organomet. Chem.* **1985**, *24*, 41; g) P. R. Raithby, M. J. Rosales, *Adv. Inorg. Chem. Radiochem.* **1985**, *29*, 170; h) R. D. Adams, I. T. Horvath, *Prog. Inorg. Chem.* **1985**, *33*, 127; i) A. J. Deeming, *Adv. Organomet. Chem.* **1986**, *26*, 1; j) E. Sappa, A. Tiripicchio, A. J. Carty, T. E. Toogood, *Prog. Inorg. Chem.* **1987**, *35*, 437; k) D. F. Shriver, M. J. Sailor, *Acc. Chem. Res.* **1988**, *21*, 374; l) R. D. Adams, *Chem. Rev.* **1989**, *89*, 1703. The chemistry and structures of high-nuclearity clusters has been reviewed in: m) M. D. Vargas, J. N. Nicholls, *Adv. Inorg. Chem. Radiochem.* **1986**, *30*, 123; n) G. Schmid, *Struct. Bonding (Berlin)* **1985**, *62*, 51.

[3] Representative examples may be found in: a) P. Chini, *J. Organomet. Chem.* **1980**, *200*, 37; b) S. Martinengo, A. Sironi, P. Chini, *J. Am. Chem. Soc.* **1978**, *100*, 7076; c) G. Ciani, A. Magni, A. Sironi, S. Martinengo, *J. Chem. Soc. Chem. Commun.* **1981**, 1280; d) S. Martinengo, G. Ciani, A. Sironi, *J. Am. Chem. Soc.* **1980**, *102*, 7564; e) A. Ceriotti, D. Dermartin, G. Longoni, M. Manassero, M. Marchioni, G. Piva, M. Sansoni, *Angew. Chem.* **1985**, *97*, 708; *Angew. Chem. Int. Ed. Engl.* **1985**, *24*, 697; f) A. Ceriotti, A. Fait, G. Longoni, G. Piro, F. Demartin, M. Manassero, N. Masciocchi, M. Sansoni, *J. Am. Chem. Soc.* **1986**, *108*, 891; g) D. Fenske, J. Ohmer, J. Hachgenei, *Angew. Chem.* **1985**, *97*, 993; *Angew. Chem. Int. Ed. Engl.* **1985**, *24*, 993; h) E. G. Mednikov, N. K. Eremenkov, Y. L. Slovokhotov, Y. T. Struchkov, *J. Chem. Soc. Chem. Commun.* **1987**, 218; i) B. K. Teo, M. C. Hong, H. Zhang, D. B. Huang, *Angew. Chem.* **1987**, *99*, 943; *Angew. Chem. Int. Ed. Engl.* **1987**, *26*, 897; j) B. K. Teo, M. C. Hong, H. Zhang, D. B. Huang, X. Shi, *J. Chem. Soc. Chem. Commun.* **1988**, 204; k) D. Fenske, H. Krautscheid, *Angew. Chem.* **1990**, *102*, 799; *Angew. Chem. Int. Ed. Engl.* **1990**, *29*, 796; l) D. Fenske, H. Krautscheid, S. Balter, *ibid.* **1990**, *102*, 1513 and **1990**, *29*, 1452; m) A. Fumagalli, S. Martinengo, G. Ciani, N. Masciocchi, A. Sironi, *Inorg. Chem.* **1992**, *31*, 336.

[4] Examples of systems which represent the intermediate regime between molecular species and metal colloids have been reported and studied in: a) G. Schmid, R. Pfeil, R. Boese, F. Bandermann, S. Meyer, G. H. M. Calis, J. W. A. van der Velden, *Chem. Ber.* **1981**, *114*, 3634; G. Schmid, N. Klein, *Angew. Chem.* **1986**, *98*, 910; *Angew. Chem. Int. Ed. Engl.* **1986**, *25*, 922; c) G. Schmid, *Polyhedron* **1988**, *7*, 2321; d) J. P. Fackler, C. J. McNeal, R. E. P. Winpenny, L. H. Pignolet, *J. Am. Chem. Soc.* **1989**, *111*, 6434; e) J. O. Malm, J. O. Bovin, A. Petford-Long, D. J. Smith, G. Schmid, N. Klein, *Angew. Chem.* **1988**, *100*, 580; *Angew. Chem. Int. Ed. Engl.* **1988**, *27*, 555; f) G. Schmid, B. Morun, J. O. Malm, *ibid.* **1989**, *101*, 772 and **1989**, *28*, 778; g) M. N. Vorgaftik, V. P. Zarogodnokov, I. P. Stolzarov, I. I. Moiseev, V. I. Likholobov, D. I. Kochubey, A. L. Chuvilin, V. I. Zaikowski, K. I. Zamaraev, G. I. Timofeeva, *J. Chem. Soc. Chem. Commun.* **1985**, 937.

[5] See for example: F. A. Cotton, G. Wilkinson, *Advanced Inorganic Chemistry*, 5th ed., Wiley, New York, **1988**, p. 614.

[6] H. Hock, H. Stuhlmann, *Ber.* **1928**, *61*, 2097. This paper reports one of the first *systematic* investigations into the reactivity of metal carbonyls. The authors apparently wanted to avoid a competitive situation with W. Hieber and remark at the end: "*.....wir bitten, uns das Gebiet noch für einige Zeit zu überlassen.*" In exchange they offer not to continue working in an area harvested by the group in Heidelberg. For an account of their research activities at the time see: W. Hieber, *Adv. Organomet. Chem.* **1970**, *8*, 1.

[7] H. Hock, H. Stuhlmann, *Ber.* **1929**, *62*, 413; *ibid.* 2691.

[8] See for example: A. F. Wells, *Structural Inorganic Chemistry*, 3rd ed., Oxford University Press, Oxford, **1962**, p. 734.

[9] R. D. Ernst, T. J. Marks, J. A. Ibers, *J. Am. Chem. Soc.* **1977**, *99*, 2090.

[10] M. P. Schubert, *J. Am. Chem. Soc.* **1933**, *55*, 4563.

[11] a) W. Hieber, H. Schulen, *Z. Anorg. Allg. Chem.* **1937**, *232*, 17; b) *ibid.* **1939**, *243*, 151; c) W. Hieber, U. Teller, *ibid.* **1942**, *249*, 43.

[12] a) F. Hein, H. Pobloth, *Z. Anorg. Allg. Chem.* **1941**, *248*, 84; b) F. Hein, E. Heuser, *ibid.* **1942**, *249*, 293.

[13] H. M. Powell, R. V. G. Ewens, *J. Chem. Soc.* **1939**, 286.

[14] L. Pauling, *The Nature of the Chemical Bond*, 2nd ed., Oxford University Press, London, **1940**, p. 254.

[15] K. A. Jensen and R. W. Asmussen suggested a nonmetal–metal bonded structure represented by two formally zwitterionic resonance structures, *Z. Anorg. Chem.* **1944**, *252*, 234. In a reply to this proposal Ewens pointed out that this was nothing else but assuming a covalent bond without actually saying so, *Nature* **1948**, *161*, 530.

[16] For example, a correct structure for $[\{(CO)_4Co\}_2Hg]$ including two Co–Hg bonds is proposed in: J. W. Cable, R. K. Sheline, *Chem. Rev.* **1956**, *56*, 1.

[17] H. Stammreich, K. Kawai, O. Sala, P. Krummholz, *J. Chem. Phys.* **1961**, *35*, 2175.

[18] a) R. S. Nyholm, K. Vrieze, *Proc. Chem. Soc. London* **1963**, 138; b) *J. Chem. Soc.* **1956**, 5331.

[19] a) R. S. Nyholm, K. Vrieze, *Chem. Ind. London* **1964**, 318; b) *J. Chem. Soc.* **1965**, 5335.

[20] M. C. Ganorkar, M. H. B. Stiddard, *J. Chem. Soc. Chem. Commun.* **1965**, 22. This preparation was repeated a few years later by Lewis et al. who characterized the compound as the oxidative elimination product $[W(CO)_3(bipy)Cl(HgCl)]$ (K. Edgar, B. F. G. Johnson, J. Lewis, S. B. Wild, *J. Chem. Soc (A)* **1968**, 2851). Since both groups report analytical data consistent with their respective formulations this remains one of the mysteries of mercury chemistry. However, in the light of the reactions of a series of closely related compounds, the formulation put forward by Lewis appears to be correct.

[21] a) D. M. Adams, D. J. Cook, R. D. W. Kemmit, *Nature* **1965**, *205*, 590; b) J. Lewis, S. B. Wild, *J. Chem. Soc. A* **1966**, 69.

[22] H. W. Baird, L. F. Dahl, *J. Organomet. Chem.* **1967**, *7*, 503.

[23] A. T. T. Hsieh, M. J. Mays in *MTP Int. Rev. Sci. Inorg. Chem. Ser. One*, **1972**, *6*, 43.

[24] J. M. Burlitch in *Comprehensive Organometallic Chemistry, Vol. 6* (Eds.: G. Wilkinson, F. G. A. Stone, E. W. Abel), Pergamon, Oxford, **1982**, p. 983.

[25] In this section some aspects of King's conceptual approach for the analysis of Hg cluster structures are being used [26].

[26] R. B. King, *Polyhedron* **1988**, *7*, 1813.

[27] M. J. Albright, M. D. Glick, J. P. Oliver, *J. Organomet. Chem.* **1978**, *161*, 221, and references therein.

[28] A. Bianchini, L. J. Farrugia, *Organometallics* **1992**, *11*, 540.

[29] L. N. Zakharov, Y. T. Struchkov, S. N. Titova, V. T. Bychkov, G. A. Domrachev, G. A. Razumaev, *Cryst. Struct. Commun.* **1980**, *9*, 549. The cadmium analogue could be obtained by a similar reaction and has also been structurally characterized, S. N. Titova, V. T. Bychkov, G. A. Domrachev, Y. T. Razumaev, Y. T. Struchkov, L. N. Zakharov, *J. Organomet. Chem.* **1980**, *187*, 167.

[30] M. Ferrer, A. Perales, O. Rossel, M. Seco, *J. Chem. Soc. Chem. Commun.* **1990**, 1447.

[31] W. Gäde, W. Weiss, *Angew. Chem.* **1981**, *93*, 796; *Angew. Chem. Int. Ed. Engl.* **1981**, *20*, 803.

[32] N. E. Kolobova, Z. Valueva, E. I. Kazimirchuk, V. G. Adrianov, Y. T. Struchkov, *Izv. Akad. Nauk. SSSR Ser. Khim.* **1984**, 920.

[33] See for example: A. Dedieu, R. Hoffmann, *J. Am. Chem. Soc.* **1978**, *100*, 2074 and references therein.

[34] a) Y. Jiang, S. Alvarez, R. Hoffmann, *Inorg. Chem.* **1985**, *24*, 729. The importance of the relativistic contraction of s and p orbitals in heavy metal chemistry has been pointed out by Rösch, Schmidbaur et al. in: N. Rösch, A. Görling, D. E. Ellis, H. Schmidbaur, *Angew. Chem.* **1989**, *101*, 1410; *Angew. Chem. Int. Ed. Engl.* **1989**, *28*, 1357.

[35] M. Fajardo, H. D. Holden, B. F. G. Johnson, J. Lewis, P. R. Raithby, *J. Chem. Soc. Chem. Commun.* **1984**, 24.

[36] a) J. M. Ragosta, J. M. Burlitch, *J. Chem.Soc. Chem. Commun.* **1985**, 1187; b) *Organometallics* **1986**, *5*, 1517; c) *ibid.* **1988**, *7*, 1469.

[37] R. A. Jones, F. M. Real, G. Wilkinson, A. M. R. Galas, M. B. Hursthouse, *J. Chem. Soc. Dalton Trans.* **1981**, 126.

[38] J. Strähle, K. Wurst, *Z. Anorg. Allg. Chem.* **1991**, *595*, 239.

[39] a) J. Deutscher, S. Fadel, M. L. Ziegler, *Angew. Chem.* **1977**, *89*, 746; *Angew. Chem. Int. Ed. Engl.* **1977**, *16*, 704; b) *Chem. Ber.* **1979**, *112*, 2413.

[40] R. Fahmy, K. King, E. Rosenberg, A. Tiripicchio, M. Tiripicchio-Camellini, *J. Am. Chem. Soc.* **1980**, *102*, 3626.

[41] E. Rosenberg, K. I. Hardcastle, M. W. Day, R. Gobeto, S. Hajela, R. Muftikian, *Organometallics* **1991**, *10*, 203.

[42] In contrast to these species which were specifically prepared by metathesis reactions, the first compound exhibiting this kind of Hg metal bonding ever to be reported was $[Ge\{Co_2(CO)_7\}\{Co_2(CO)_6[HgCO(CO)_4]\}]^-$. This was a minor product (yield ca. 5%) in the nonspecific synthesis of a variety of Co–Ge clusters, D. N. Duffy, K. M. Mackay, B. K. Nicholson, W. T. Robinson, *J. Chem. Soc. Dalton Trans.* **1981**, 381.

[43] S. Ermer, K. King, K. I. Hardcastle, E. Rosenberg, A. M. M. Lanfredi, A. Tiripicchio, M. Tiripicchio-Camellini, *Inorg. Chem.* **1983**, *22*, 1339.

[44] L. J. Farrugia, *J. Chem. Soc. Chem. Commun.* **1987**, 147.

[45] M. P. Gomez-Sal, B. F. G. Johnson, J. Lewis, P. R. Raithby, S. N. A. B. Syed-Mustaffa, *J. Organomet. Chem.* **1984**, *272*, C21.

[46] B. F. G. Johnson, W. L. Kwik, J. Lewis, P. R. Raithby, V. P. Saharan *J. Chem. Soc. Dalton Trans.* **1991**, 1037.

[47] P. L. Andren, J. A. Cabeza, A. Llamazares, V. Riera, C. Bois, Y. Jeannin, *J. Organomet. Chem.* **1991**, *420*, 431.
[48] J. Gong, J. Huang, P. E. Fanwick, C. P. Kubiak, *Angew. Chem.* **1990**, *102*, 407; *Angew. Chem. Int. Ed. Engl.* **1990**, *29*, 396.
[49] L. H. Gade, B. F. G. Johnson, J. Lewis, M. McPartlin, H. R. Powell, *J. Chem. Soc. Chem. Commun.* **1990**, 110.
[50] V. P. Saharan, Ph.D. Thesis, Cambridge University, **1991**.
[51] L. H. Gade, Ph.D. Thesis, Cambridge University, **1991**.
[52] J. W. Lauher, K. Wald, *J. Am. Chem. Soc.* **1981**, *103*, 7648.
[53] a) P. Braunstein, J. Rosé, A. Tiripichio, M. Tiripicchio-Camellini, *J. Chem. Soc. Chem. Commun.* **1984**, 391; b) *J. Chem. Soc. Dalton Trans.* **1992**, 911.
[54] P. Braunstein, J. Rosé, A. Tiripicchio, M. Tiripicchio-Camellini, *Angew. Chem.* **1985**, *97*, 761; *Angew. Chem. Int. Ed. Engl.* **1985**, *24*, 767.
[55] P. Braunstein, J. Rosé, A. Dedieu, Y. Dusansoy, J. P. Mangeot, A. Tiripicchio, M. Tiripichio-Camellini, *J. Chem. Soc. Dalton Trans.* **1986**, 225.
[56] R. Bender, P. Braunstein, C. de Meric de Bellefon, *Polyhedron* **1988**, *7*, 2271.
[57] a) C. P. Horwitz, E. M. Holt, C. P. Brook, D. F. Shriver, *J. Am. Chem. Soc.* **1985**, *107*, 8136; b) C. P. Horwitz, D. F. Shriver, *ibid.* **1985**, *107*, 8147.
[58] J. Wang, M. Sabat, C. P. Horwitz, D. F. Shriver, *Inorg. Chem.* **1988**, *27*, 552.
[59] a) R. Della Pergola, F. Demartin, L. Garlaschelli, M. Manassero, S. Martinengo, N. Masciocchi, M. Sansoni, *Organometallics* **1991**, *10*, 2239; b) T. J. Henly, J. R. Shapley, *ibid.* **1989**, *8*, 2729.
[60] L. H. Gade, B. F. G. Johnson, J. Lewis, M. McPartlin, H. R. Powell, *J. Chem. Soc. Dalton Trans.* **1992**, 921.
[61] E. Rosenberg, D. Ryckmann, I. N. Hsu, G. W. Gellert, *Inorg. Chem.* **1986**, *25*, 194.
[62] B. F. G. Johnson, J. Lewis, J. N. Nicholls, J. Puga, K. H. Whitmire, *J. Chem. Soc. Dalton Trans.* **1983**, 783.
[63] V. P. Saharan, Cambridge University, personal communication.
[64] a) M. P. Diebold, S. R. Drake, B. F. G. Johnson, J. Lewis, M. McPartlin, H. R. Powell, *J. Chem. Soc. Chem. Commun.* **1988**, 1358; b) M. P. Diebold, B. F. G. Johnson, J. Lewis, V. P. Saharan, M. McPartlin, H. R. Powell, *J. Organomet. Chem.* **1991**,*405*, C25.
[65] D. J. Underwood, R. Hoffmann, K. Tatsumi, A. Nakamura, Y. Yamamoto, *J. Am. Chem. Soc.* **1985**, *107*, 5968.
[66] Y. Yamamoto, H. Yamazahi, T. Sakurai, *J. Am. Chem. Soc.* **1982**, *104*, 2329.
[67] A. Albinati, A. Moor, P. S. Pregosin, L. M. Venanzi, *J. Am. Chem. Soc.* **1982**, *104*, 7672.
[68] a) G. Schoettel, J. J. Vittal, R. J. Puddephatt, *J. Am. Chem. Soc.* **1990**, *112*, 6400. More recently Pt_3 clusters capped on *both* sides by HgX units have been reported: b) A. Albinati, K.-H. Dahmen, F. Demartin, J. M. Forward, C. J. Longley, D. M. P. Mingos, L. M. Venanzi, *Inorg. Chem.* **1992**, *31*, 2223.
[69] Y. Yamamoto, K. Takahashi, K. Matsuda, H. Yamazaki, *J. Chem. Soc. Dalton Trans.* **1987**, 1833.
[70] Y. Yamamoto, H. Yamazaki, *J. Chem. Soc. Dalton Trans.* **1989**, 2161.
[71] Theoretical studies of related M_3 systems have been published by: a) C. Mealli, *J. Am. Chem. Soc.* **1985**, *107*, 2245; b) D. I. Gilmour, D. M. P. Mingos, *J. Organomet. Chem.* **1986**, *302*, 127.
[72] Y. Yamamoto, K. Takahashi, H. Yamazaki, *J. Am. Chem. Soc.* **1986**, *108*, 2458.
[73] a) R. P. F. Kanters, J. J. Bour, P. P. J. Schlebos, J. J. Steggerda, *J. Chem. Soc. Chem. Commun.* **1988**, 1634; b) J. J. Bour, W. van den Berg, P. P. J. Schlebos, R. P. F. Kanters, M. F. J. Schoondergang, W. P. Bosman, J. M. M. Smits, P. T. Beurskens, P. van der Sluis, *Inorg. Chem.* **1990**, *29*, 2971.
[74] D. Fenske, J. Magull, *Z. Naturforsch. B* **1990**, *45*, 121.
[75] The dispute over the correct chemical formulation of mercurous chloride involved some of the most famous chemists of the 19th century: a) E. Mitscherlich, *Annalen* **1834**, *12*, 137 (the measurements on mercurous chloride are quoted on p. 166); b) H. S. Deville, L. Troost, *ibid.* **1858**, *105*, 213; c) R.Rieth, *Ber.* **1870**, *3*, 666; d) E. Erlenmeyer, *Annalen*, **1864**, *131*, 124; e) A. W. Williamson, *J. Chem. Soc.* **1864**, *42*, 211; f) W. Harris, V. Meyer, *Ber.* **1894**, *27*, 1482. The matter could only be regarded as settled after the extensive thermodynamic and electrochemical studies published by Ogg in 1898: g) A. Ogg, *Z. Phys. Chem. Stöchiom. Verwandtschaftsl.* **1898**, *27*, 285. The existence of a covalent metal–metal bond was conclusively proved by Woodward in 1934 who found a ν(Hg–Hg) band (169 cm^{-1}) in the Raman spectrum of an aqueous solution of $Hg_2(NO_3)_2$: h) L. A. Woodward, *Philos. Mag.* **1934**, *18*, 823.
[76] A qualitative theoretical understanding of the properties of Hg_2^{2+} has only been possible since the performance of computers allowed relativistic quantum mechanical calculations of systems containing heavy atoms: a) T. Ziegler, J. G. Snijders, E. J. Baerends, *J. Chem. Phys.* **1981**, *74*, 1271; b) R. P. Neisler, K. S. Pitzer, *J. Phys. Chem.* **1987**, *91*, 1084.
[77] a) G. Torsi, G. Mamantov, *Inorg. Nucl. Chem. Lett.* **1970**, *6*, 843; b) C. G. Davies, P. A. W. Dean, R. J. Gillespie, P. K. Ummat, *J. Chem. Soc. Chem. Commun.* **1971**, 782; c) R. J. Gillespie, J. Passmore, *Acc. Chem. Res.* **1971**, *4*, 413; d) B. D. Cutforth, R. J. Gillespie, P. R. Ireland, *J. Chem. Soc. Chem. Commun.* **1973**, 723; e) I. D. Brown, B. D.Cutforth, C. G. Davies, R. J. Gillespie, P. R. Ireland, J. E. Vekris, *Can. J. Chem.* **1974**, *52*, 791; f) A. J. Schultz, J. M. Williams, N. D. Miro, A. G. MacDiarmid, A. J. Heeger, *Inorg. Chem.* **1978**, *17*, 646. Review: I. D. Brown, W. R. Datars, R. J. Gillespie in *Extended Linear Chain Compounds, Vol. 3* (Ed.: J. S. Miller), Plenum, New York, **1983**, p. 1.
[78] See for instance: T. A. Albright, J. K. Burdett, M. H. Whangbo *Orbital Interactions in Chemistry*, Wiley, New York, **1985**.
[79] a) K. Brodersen, G. Göbel, G. Liehr, *Z. Anorg. Allg. Chem.* **1989**, *575*, 145. The structure of terlinguaite had originally been determined by: b) S. Scavnicar, *Acta Crystallogr.* **1956**, *9*, 956.
[80] B. Hämmerle, E. P. Müller, D. L. Wilkinson, G. Müller, P. Peringer, *J. Chem. Soc. Chem. Commun.* **1989**, 1527.
[81] a) H. J. Deiseroth, A. Strunk, W. Bauhofer, *Z. Anorg. Allg. Chem.* **1988**, *558*, 128; b) H. J. Deiseroth, A. Strunk, *Angew. Chem.* **1987**, *99*, 701; *Angew. Chem. Int. Ed. Engl.* **1987**, *26*, 687.
[82] H. J. Deiseroth, A. Strunk, *Angew. Chem.* **1989**, *101*, 1286; *Angew. Chem. Int. Ed. Engl.* **1989**, *28*, 1251.
[83] The results of NMR studies performed on clusters containing Group Ib metals are reviewed in: I. D. Salter, *Adv. Organomet. Chem.* **1989**, *29*, 249.
[84] A particularly interesting example taken from the chemistry of transition metal-gold clusters is the series $[Pt(AuPPh_3)_n]^{m+}$: a) R. P. F. Kanters, P. P. J. Schlebos, J. J. Bour, W. P. Bosman, H. J. Behm, J. J. Steggerda, *Inorg. Chem.* **1988**, *27*, 4034.
[85] a) P. J. Bailey, B. F. G. Johnson, J. Lewis, M. McPartlin, H. R. Powell, *J. Chem. Soc. Chem. Commun.* **1989**, 1513; b) P. J. Bailey, M. J. Duer, B. F. G. Johnson, J. Lewis, G. Conole, M. McPartlin, H. R. Powell, C. E. Anson, *J. Organomet. Chem.* **1990**, *383*, 441.
[86] E. Charalambous, L. H. Gade, B. F. G. Johnson, T. Kotch, A. J. Lees, J. Lewis, M. McPartlin, *Angew. Chem.* **1990**, *102*, 1772; *Angew. Chem. Int. Ed. Engl.* **1990**, *29*, 1137.
[87] L. H. Gade, B. F. G. Johnson, J. Lewis, M. McPartlin, T. Kotch, A. J. Lees, *J. Am. Chem. Soc.* **1991**, *113*, 8698.
[88] L. H. Gade, B. F. G. Johnson, J. Lewis, M. McPartlin, *J. Chem. Soc. Dalton Trans.* **1992**, 3249.
[89] L. H. Gade, B. F. G. Johnson, J. Lewis, M. McPartlin, unpublished results, **1990/1991**.
[90] a) K. Wade in *Transition Metal Clusters* (Ed.: B. F. G. Johnson), Wiley, New York, **1980**; b) D. M. P. Mingos, *Acc. Chem. Res.* **1984**, *17*, 311; M. McPartlin, *Polyhedron* **1984**, *3*, 1279.
[91] A separate chapter by P. A. W. Dean on mercury as a ligand in coordination compounds has appeared in *Comprehensive Coordination Chemistry, Vol. 2* (Eds.: G. Wilkinson, R. D. Gillard, J. A. McCleverty), Pergamon, Oxford, **1987**, p. 1.
[92] The original definiton of "fluxionality" as put forward by Doering and Roth was strictly limited to the interconversion between *equivalent* molecular configurations, such as for example those of bullvalene, but did not include isomerizations: W. von E. Doering, W. Roth, *Angew. Chem.* **1963**, *75*, 27; *Angew. Chem. Int. Ed. Engl.* **1963**, *2*, 15. However, in cluster chemistry this term is normally not used with these restrictions and does, for instance, include reversible isomerization processes. See for example: E. L. Muetterties, E. Band, *Chem. Rev.* **1978**, *78*, 639.
[93] S. Hajela, B. M. Novak, E. Rosenberg, *Organometallics* **1989**, *8*, 468.
[94] L. H. Gade, B. F. G. Johnson, J. Lewis, *J. Chem. Soc. Dalton Trans.* **1992**, 933.
[95] P. J. Bailey, L. H. Gade, B. F. G. Johnson, J. Lewis, *Chem. Ber.* **1992**, *125*, 2019.
[96] J. A. Iggo, M. J. Mays, *J. Chem. Soc. Dalton Trans.* **1984**, 643.
[97] R. Reina, O. Rossell, M. Seco, *J. Organomet. Chem.* **1990**, *398*, 285.
[98] E. Charalambous, L. H. Gade, B. F. G. Johnson, J. Lewis, M. McPartlin, H. R. Powell, *J. Chem. Commun.* **1990**, 688.
[99] A. J. Amoroso, L. H. Gade, B. F. G. Johnson, J. Lewis, P. R. Raithby, W. T. Wong, *Angew. Chem.* **1991**, *103*, 103; *Angew. Chem. Int. Ed. Engl.* **1991**, *30*, 107.
[100] D. Coughlin, L. H. Gade, B. F. G. Johnson, J. Lewis, unpublished results, **1991**.
[101] A. Vogler, H. Kunkeley, *J. Organomet. Chem.* **1988**, *355*, 1.
[102] B. F. G. Johnson, L. H. Gade, J. Lewis, W. T. Wong, *Mater. Chem. Phys.* **1991**, *29*, 85.
[103] *Organometallic Syntheses Vol. 1* (Eds.: J. J. Eisch, R. B. King), Academic Press, New York, **1965**, p. 101.
[104] C. C. Lin, p. L. Gibson, *Inorg. Chem.* **1992**, *31*, 167.
[105] S. R. Drake, M. H. Barley, B. F. G. Johnson, J. Lewis, *Organometallics* **1988**, *7*, 806.
[106] For reviews covering various aspects of the electrochemistry of clusters, see: a) P. Lemoine, *Coord. Chem.* **1988**, *83*, 169; b) W. E. Geiger, *Prog. Inorg. Chem.* **1985**, *33*, 275; c) S. R. Drake, *Polyhedron* **1990**, *9*, 455.

Colloidal Semiconductor Q-Particles: Chemistry in the Transition Region Between Solid State and Molecules

By Horst Weller*

In semiconductor particles of nanometer size, a gradual transition from solid-state to molecular structure occurs as the particle size decreases. Consequently, a splitting of the energy bands into discrete, quantized levels occurs. Particles that exhibit these quantization effects are often called "Q-particles" or, generally, quantized material. The optical, electronic and catalytic properties of Q-particles drastically differ from those of the corresponding macrocrystalline substance. The band gap, a substance-specific quantity in macrocrystalline materials, increases by several electron volts in Q-particles with decreasing particle size. In Q-particles there are approximately as many molecules on the surface as in the interior of the particle. Therefore, the nature of the surface as well as the particle size is also largely responsible for the physico-chemical properties of the particle. Q-particles of many materials can be prepared in the form of colloidal solutions or embedded in porous matrices and are stable over a long period of time. In sandwich colloids, in which Q-particles of different materials are coupled, as well as in porous semiconductor electrodes containing Q-particles in the pores, very efficient primary charge separation is observed. As a result, sandwich colloids have greatly enhanced photocatalytic activity relative to the individual particles, while electrodes modified with Q-particles show high photocurrents. This article deals with the size quantization effect, the synthesis and characterization of Q-particles, as well as with the spectroscopic, electrochemical, and electron-miroscopic investigation of these particles.

1. Introduction: The World of Neglected Dimensions

In 1915, Ostwald[1] entitled his famous book on colloid chemistry "The World of Neglected Dimensions", implying that this was a science in its own right. This opinion is certainly correct as the physical and chemical properties of colloids largely depend on their size and shape, two parameters that are of only secondary importance in classical chemistry.

In spite of the tremendous development in colloid chemistry in the subsequent decades, the world of extremely small particles with sizes in the nanometer range was neglected for a long time. As Ostwald stated, it concerns a size range in which a continuous transition occurs from condensed materials to molecular structures.

Only recently has research in many fields of chemistry and physics commenced providing a basis for nanometer technology, such as, for example, the synthesis of ligand-stabilized clusters,[2, 3] the spectroscopic examination of clusters in the gas phase,[4] the examination of ceramics and metals having crystalline regions of only a few nanometers in size,[5] attempts to miniaturize semiconductor structures into the nanometer region (quantum wells, quantum wires, quantum dots),[6] and the study of the photochemistry and optical and catalytic properties of metal and semiconductor particles with sizes in the nanometer range, both in solution and in thin layers (see [5–9] and references therein). Of special interest are those properties that differ greatly from those of the corresponding macrocrystalline material.

The size quantization effects in colloidal semiconductors, the subject of this article, has led to great interest in these systems. The charge carriers generated by light absorption, which are free to move in a macrocrystalline material, "feel" the particle walls in nanometer large particles. As a result of this situation, described in quantum mechanics as a particle-in-a-box, the band gap increases the smaller the particles become. The onset of the absorption of light and the position of the fluorescence bands are shifted to shorter wavelengths. This can be clearly seen in Figure 1 from the color of the cadmium phosphide powders. Cadmium phosphide is a semiconductor which has a band gap of only 0.5 eV in the macrocrystalline state and is consequently black (bottom left). The powders were prepared by the careful drying of colloidal solutions under vacuum. The powders can be redissoved in water. The average particle size decreases in the opposite direction to the arrows, the color of the material changes to brown (about 30 Å particles) through red, orange, yellow to white (about 15 Å), and the band gap increases to 4 eV.

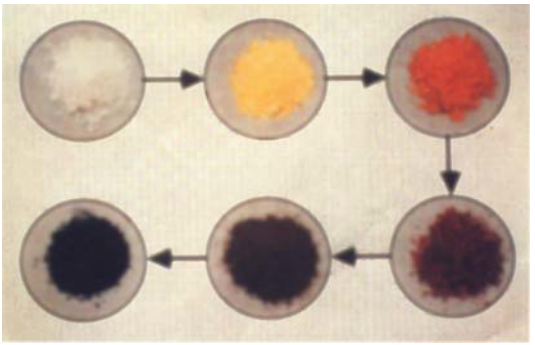

Fig. 1. Q-Cd_3P_2 powder. The particle size increases in the direction of the arrows. The size quantization effect can be clearly seen from the color of the particles.

[*] Dr. H. Weller
Hahn-Meitner-Institut, Abteilung Photochemie
Glienicker Strasse 100, 1000 Berlin 39 (FRG)

Work on colloidal semiconductors started at the beginning of the 1980s with the aim of splitting water photocatalytically.[10, 11] The basic idea of these experiments was to reduce the water to hydrogen by means of the light-induced conduction-band electrons and to oxidize it to oxygen by the holes. Hydrogen production with high quantum yields was achieved when electron donors, such as amines, alcohols or sulfur containing substances were added to the solution.[12, 13] The simultaneous production of hydrogen and oxygen was, however, not achieved. All the photoreactions of colloidal semiconductors described to date for the production of hydrogen in the presence of a donor have been exothermic and are only catalyzed by light. In other words, the end products, hydrogen and oxidized donor, have a lower energy content than the starting materials. There is therefore no point in using these systems for solar energy conversion.

As well as the reports on the attempts to split water, there are also many papers[14] on the use of semiconductor particles in the photocatalytic synthesis of organic compounds and in the photocatalytic destruction of halogenated hydrocarbons. These will not be discussed further here.

Surface boundary processes, such as photocatalytic reactions on semiconductors, are not largely understood even today. One problem arising during the examination of surface processes on macroscopic samples is the very small ratio of the surface to the bulk material. Very sensitive and complicated measurements must be used to separate surface from bulk properties. This problem is readily overcome when colloidal systems in the nanometer range are used. The dispersity (the ratio of surface to bulk) is so big in such particles that a similar number of atoms are located on the surface as in the crystal lattice structure of the bulk. Also, because the particles are so small, the colloidal solutions are completely transparent, so established stationary and time-resolved optical spectroscopy methods, as used in homogeneous systems, can be employed to study the reaction processes.

The main subject of this article is the influence of the particle size and surface properties on the energies of the electronic levels and on the reactivity and kinetics of the charge carriers in Q-particles. The chemical and photochemical aspects of Q-particles will be especially discussed. In another report,[15] more emphasis will be placed on the physical properties of these particles and properties relevant to materials science.

After an initial brief description of the energy levels in macrocrystalline semiconductors, the results of a few theoretical models of the size quantization effect will be discussed and compared to experimentally obtained data. The present state of the preparation and characterizaton of small particles will be described by means of examples in a further section. This will be followed by a section in which methods will be presented which enable mainly monodisperse samples with uniform surface characteristics to be obtained. The effect of surface modifications on the photochemical properties will be dealt with in Section 5 by using fluorescence measurements and photocorrosion experiments as a basis for discussion. The last part of this article considers the examination of charge separation in sandwich colloids (particles in which two different semiconductor materials are coupled) and in semiconductor layers (where the small particles are deposited on a very rough polycrystalline electrode). In particular, ultrafast electron transfer reactions that result in a higher photocatalytic activity in sandwich colloids and in increased photocurrents in the modified layers will be discussed.

2. From Semiconductor to Molecules

2.1. The Energy Levels of a Semiconductor

The semiconductor properties observed in many inorganic substances are not properties of individual molecules or atoms but are a result of the arrangement of the constitutive elements in an ordered crystal lattice. The overlapping of the atomic orbitals in the crystal leads to the formation of a continuum of the position-independent electronic energy levels, the energy bands. A typical energy scheme of a semiconductor is shown in Figure 2. The valence band in an undoped semiconductor is completely filled at 0 K, whereas the conduction band is empty. The energy differene between the valence and conduction band is called the band gap. An electron can be excited from the valence band into the conduction band by the absorption of a quantum of light. A positive charge (a hole) remains in the valence band. The electron and hole can move independantly of one another in the crystal, which results in electrical conductivity. The electron and hole also experience coulombic forces and can form a Wannier exciton, a state that is very similar to a hydrogen atom. In molecular terminology an exciton would be called the first excited state. However, from solid state physics one knows that, because of the interaction of the electron and

Horst Weller, born in 1954 in Siegen, Westphalia, began to study chemistry at the University of Göttingen in 1974. He obtained his PhD in 1982 at the Max Planck Institute for Biophysical Chemistry under the supervision of his namesake A. Weller. Since 1983 he has been employed as a scientist in the group of A. Henglein at the Hahn–Meitner Institute in Berlin where he became deputy leader of the photochemistry department in 1989. In 1991 he received the Bodenstein Prize of the German Bunsengesellschaft and in 1992 completed his habilitation and became a lecturer in Physical Chemistry at the Technical University of Berlin. His sphere of work concentrates on small particle research.

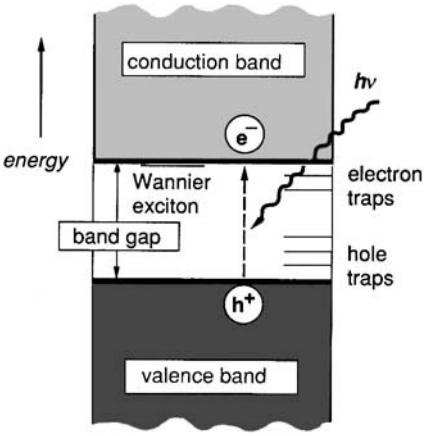

Fig. 2. Energy scheme of a semiconductor.

hole with the core levels of the atoms in the crystal, the masses of the electrons and holes must be replaced by the so-called effective masses (m*). This is the ratio of the masses of the electrons and holes in a semiconductor to the masses of the electrons in vacuum. As the effective masses are usually small and, additionally, because the crystal with its electrons screens the charge carriers in the exciton (expressed by the high frequency dielectric constant), the binding energy of the exciton is small and its radius large. For example, the binding energy of the excitons in CdS is only 0.05 eV and its radius approximately 25 Å (for comparison, the binding energy of a hydrogen atom is 13.51 eV and its radius 0.53 Å). The small binding energy results in the very rapid dissociation of the excitons into free charge carriers at room temperature. Usually, excitons are observed by their sharp absorption and emision lines in optical spectra only at temperatures close to absolute zero.

Beside bands and excitonic energy levels, semiconductors contain traps for electrons and holes. These are interstitial atoms, impurities, dislocations, and defects. Traps are frequently located on the surface as a result of the disturbed bonding forces there. The charge carriers can recombine from traps, either radiatively or nonradiatively, or undergo transfer to electron donors or acceptors. They can also recombine from the bands and excitonic state. The traps in nanometer large particles are found mainly on the surface as a result of the large surface to bulk ratio.

2.2. The Size Quantization Effect

In the case of nanometer large particles, the unusual situation exists that the particle size is the same as or actually smaller than the size of the excitons in macrocrystalline material. The electron–hole pair can only "fit" into such a particle when the charge carriers assume a state of higher kinetic energy. In solid state terminology this results in the energy bands splitting into discrete quantized levels and the "band gap" increasing with decreasing particle size. Particles that show this size quantization effect are frequently called Q-particles or quantum dots. Whether one can speak of bands or excitons at all in this situation is a purely semantic question. On one hand, the electron and hole, because of their increased kinetic energy, move practically freely within the particle, a situation similar to that in the energy bands. On the other hand they experience a coulombic attraction, which is why this state is frequently called "excitonic" (I shall use this terminology in this article). When one comes into a size range of 1–2 nm, in which each particle consists of a few dozen molecules, it is better to talk about molecular orbitals. From the difficulties experienced in the terminology, one can already see that the properties of such particles lie between those of the solid state and their molecules.

The shift of the electronic levels with decreasing particle size, easily seen in Figure 1 from the color of the particles, can also be seen in Figure 3 which shows the absorption spectra of three CdS samples of different particle size. The

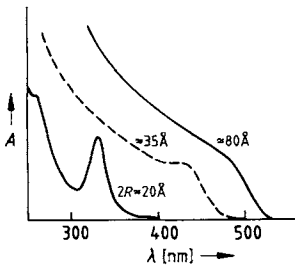

Fig. 3. Absorption spectra of three colloidal CdS solutions containing CdS particles of different size.

spectra are labeled with the appropriate average particle diameters (80 Å, 35 Å, and 20 Å). Macrocrystalline CdS has an absorption edge at approximately 515 nm, which is close to the beginning of absorption of the 80 Å particles. As well as a strong blue shift of the absorption edge, a clear maximum is formed near the start of absorption with decreasing particle size. This maximum is assigned to the optical transition of the first excitonic state.

Many model calculations concerning the size quantization effect have been published in the past few years.[16–32] The majority of these calculations start from the macroscopic solid state and determine the increase of the band gap with decreasing particle size on the basis of a particle-in-a-box assumption. The differences in the models lie in the complexity of the calculation and the boundary conditions. Efros et al.[16] described the first calculation. They used spherical, infinite potential wells and ignored the coulombic interaction between the charge carriers. Brus et al.[18, 19] developed the energy levels of the first excited state by considering the coulombic interactions and polarization terms. They showed[18] that the coulombic interaction could not be ignored. In some papers[21, 22] the coulombic interaction was introduced into the wave functions of the electron and hole as a perturbation parameter. Like the increase in the energy of the first excited state, the splitting of the bands into discrete excitonic levels is a direct consequence of the size quantization effect. Weller et al.[22] made a quantum mechanical calculation of the energy values of higher excited states as a function of particle size for the first time. The expansion of the quantum mechanical models by including Hylleraas functions, which led to very exact results for the description of the helium atom,[35] brought no significant improvements in the calculation of the first excited state in Q-particles. Similar results were described recently.[23, 24, 28] However, comparison of the experimental results with different calcu-

lations[21, 33] showed that, as suggested by Brus,[17] it is necessary to include finite barrier heights in the description of the experimental results (see below). The most universal particle-in-a-box calculation has recently been presented by Nosaka.[30] In this calculation the barrier height and effective masses (m^*) of the charge carriers of any semiconductor can be introduced into an analytical formula and the first excited state calculated as a function of particle size. All the previously presented calculations assume the validity of the effective mass approximation. The appropriate values for the effective masses as well as the high frequency dielectric constants are taken from macrocrystalline solids, which results in the greatest uncertainty of these calculations.

On the basis of work by Burdett,[34] Wang[26] described the first molecular orbital calculations (tight binding) for Q-particles for PbS, while Lippens et al.[29] did the same for CdS and ZnS. These calculations are not better per se than the particle-in-a-box calculations. Although they avoid the problem of the effective mass approximation, they do not include the altered bonding forces of the surface atoms as compared to the bulk atoms.

The first pseudopotential calculations have recently been presented by Rama Krischna and Friesner,[31] as well as by Einevoll.[32] In the former paper even the different crystal structures and particle shapes are considered.

The results of some calculations and their comparison with experimental values will be shown in the next section. The wavelength of the excitonic absorption (shoulder on maximum in the spectra) is shown in Figure 4 as a function of the particle size for different CdS samples. In this case

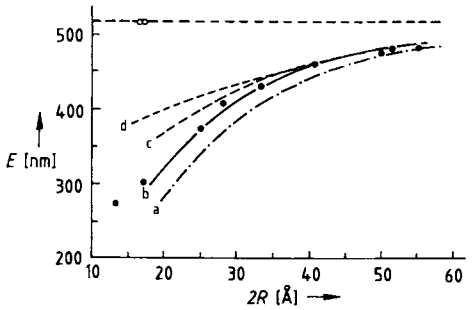

Fig. 4. Energy (converted to light wavelength) of the first excitonic transition in CdS particles as a function of the particle size; —oo—: energy in the macrocrystal. The curves a–d show the results of different quantum mechanical calculations (see text). •: values determined with the electron microscope.

the size was determined exclusively by electron microscopy.[21, 33, 36, 37] Other authors[27, 38] calculated the average particle size from the line width in X-ray powder diffractograms using the Scherrer formula.[39] This method usually gives smaller particle sizes than electron microscopy for the same optical absorption. This discrepancy probably arises because in X-ray diffraction measurements the particle size does not determine the line width directly. Instead the width depends on the size of the crystalline regions within a particle. This leads to false results when the particles are not perfectly crystalline (as the ones shown in the lower part of Figure 5).

Figure 4 shows the results of different calculations in curves a–d. Good agreement with the experimental values is obtained with curve b (particle-in-a-box with finite barrier height[21]) and, with some restrictions, with curve c (tight-binding calculation[29]). Curve a (infinite potential well[18]) and curve d (pseudopotential calculation[31]), on the other hand, show large deviations from the experimental points. (Rama Krishna and Freiser[31] obtain good agreement for their calculated values with the values obtained from X-ray measurements.[27])

Similar results to CdS are obtained when the experimental values are compared with the calculations for PbS[26, 30] and ZnO.[40] Also in these cases the particle-in-a-box calculation with finite barrier heights and the tight-binding (PbS) calculation agree quite well with the experimental values.

In spite of certain deviations the relatively good agreement of the theoretical models with the experimental results is astonishing, especially as the models start from very different assumptions and questionable simplifications must be introduced in the calculations.

Because of the large percentage of surface in Q-particles, the question of the effect of surface characteristics and the chemical environment of the particle on the optical absorption arises. Recently the absorption behavior of approximately 40 Å diameter CdS particles stabilized by sulfonic acid has been examined.[41] These colloids were dried and redissolved in organic solvents of very different polarity (between *n*-hexane and *n*-propanol) without any significant change occurring in the absorption spectra. In this work the subsequent exchange of the stabilizer, 4-dodecylbenzenesulfonic acid, by polyphosphate, polysilicate, and thiols was also described. Again only minor changes were registered in the absorption spectra.

3. Preparation and Characterization of Small Particles

Most of the research on Q-particles has been performed on colloidal samples of CdS, CdSe, and PbS. Reports on the synthesis of other Q-particles include ZnS, ZnO, TiO_2, AgI, AgBr, HgI_2, PbSe, ZnTe, CdTe, In_2S_3, In_2Se_3, Cd_3P_2, Cd_3As_2,[7–9, 14, 42] and recently also GaAs.[43, 44] The sulfides, selenides, tellurides, and phosphides are usually prepared by precipitation by H_2S, H_2Se, H_2Te, or PH_3, or their alkali metal salts from a solution containing the metal ion. Either AsH_3 or $As(CH_3)_3$ is used for the preparation of the arsenides. The oxides are prepared, for example, by the hydrolysis of the alkoxy compounds. Stable colloidal solutions are obtained by the addition of stabilizers (tensides, organic or inorganic polymers).

A much used method for the preparation of Q-particles is precipitation in the presence of sodium polyphosphate as stabilizer (average chain length about 15 PO_3^- units). Polyphosphate is well suited for the stabilization of nanometer large particles, because the chain is strongly bound by metal ions onto the particle surface. It causes electrostatic repulsion between particles because of its charge, and also keeps them apart sterically because of its chain length. Other frequently used stabilizers for the chalkogenides are thiols. In the following, the preparation of Q-CdS with different particles sizes will be described as an example.

In an aqueous solution cadmium ions are complexed with polyphosphate chains (PP^{2n-}) [Eq. (1)].

$$n\,Cd^{2+} + PP^{2n-} \rightleftharpoons Cd_nPP \quad (1)$$

From the concentration ratio of Cd^{2+} to PP^{2n-} (approximately one Cd^{2+} ion per two to six PO_3^- units) and the absolute concentration (of the order of 10^{-4} M), conditions are chosen under which most of the Cd^{2+} ions are bound to the polyphosphate. After the addition of H_2S, seed formation occurs by the reaction of the sulfide with free Cd^{2+} ions [Eq. (2)].

$$m\,Cd^{2+} + m\,S^{2-} \rightleftharpoons (CdS)_m \quad (2)$$

The formation of the seeds is accelerated by high pH values because of the dissociation equilibrium of H_2S [Eq. (3)].

$$H_2S \rightleftharpoons 2H^+ + S^{2-} \quad (3)$$

The growth of the seeds occurs either because the Cd^{2+} ions are liberated in the equilibrium described in (1) and CdS grows on the seeds (growth from a supersaturated solution [Eq. (5)], or by the process of Ostwald ripening whereby larger seeds grow at the expense of smaller ones [Eq. (4) and (5)].

$$(CdS)_n \longrightarrow (CdS)_{n-1} + Cd^{2+} + S^{2-} \quad (4)$$

$$Cd^{2+} + S^{2-} + (CdS)_m \longrightarrow (CdS)_{m+1}\ (m > n) \quad (5)$$

A requirement for the preparation of especially small particles is rapid formation of crystal seeds but slow growth of these seeds. This can be realized by keeping the pH slightly alkaline during the preparation and when an excess of Cd^{2+} ions is present.[20] Also, vigorous shaking is necessary to ensure thorough mixing. Very good, reproducible mixing can also be realized when two chromatography pumps are used.[45] The resulting colloid contains particles of between 13 Å and 20 Å. Figure 5a shows an electron microscope photograph of a sample containing 13 Å particles. In the lower part of the figure a single particle is shown. The lattice planes of cubic CdS (zinc blende structure) can be seen even with these very small particles.

The main difference in the preparation of the larger particles in samples b and c lies in the relative amounts of Cd^{2+} and S^{2-} ions; the preparation occurs under stoichiometric conditions, that is, more H_2S is used than in a. The seed formation also occurs under slightly alkaline conditions, but during the precipitation the pH drops to about 4 as a consequence of the released protons.[33] Under these conditions the growth of the particles by the reactions (4) and (5) is accelerated. The growth can be stopped by increasing the pH once more to between 9 and 10. Sample b was kept at pH 4 for about 10 minutes and sample c for a few hours. The particles in sample c are, therefore, bigger than in sample b. Even larger particles are obtained when the precipitation occurs under weakly acidic conditions. The ratio of the rate of seed formation to particle growth is displaced in the direction of growth. Sample d from Figure 5 (average size of 250 Å) was prepared under such conditions. The electron microscope photographs of individual particles from these samples are shown in the lower part of Figure 5. The crystal lattice planes with distances typical for a zinc blende structure can be clearly seen. The particles shown, which are typical for each sample, have a perfect crystal structure.

It is still unknown why nearly all the existing methods for the preparation of colloidal CdS particles with nanometer dimensions result in the cubic zinc blende structure, whereas macrocrystalline CdS nearly always has the hexagonal wurzite structure. Hexagonal Q-CdS particles are only formed during the cathodic deposition from a dimethyl sulfoxide solution of sulfur containing Cd^{2+} ions.[46]

For very small CdS particles less than 20 Å across, it has been observed that when the stabilizer is polyphosphate the growth does not occur continuously but that certain particle sizes are preferred.[20, 63] This behavior is known from clusters in the gas phase. The occurrence of such "magic numbers" was first observed by Weller et al.[20] There are two reasons why particles with preferred agglomeration numbers

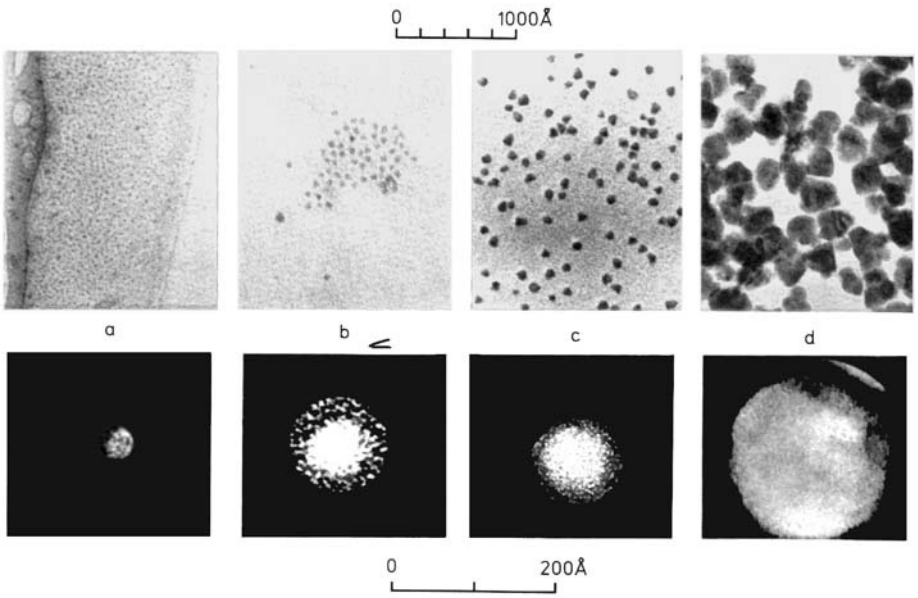

Fig. 5. Electron microscope photographs of polyphosphate-stabilized CdS particles of different sizes (a–d). Single particles of each sample at higher magnification are shown in the lower part of the figure.

can be formed: certain structures are thermodynamically especially stable, or the growth of the initially formed, smallest particles with agglomeration number k occurs not by Ostwald ripening but by the combination of the particles. The particles so formed would then have agglomeration numbers of $2k$, $3k$, and so on. Which of the two mechanisms is operative with CdS is unclear, as well as the exact "magic numbers".

In many laboratories attempts to synthesize and characterize defined semiconductor clusters are in progress.[2, 3] The largest CdS cluster with a defined structure has the formula $Cd_{10}S_4(C_6H_5S)_{16}^{4-}$ and is pyramidal.[47] This cluster does not show an excitonic absorption band. Dance[47] suggested that the next larger, especially stable cluster would have the structure $Cd_{20}S_{13}(C_6H_5S)_{22}^{8-}$. Wang and Herron[42] have recently claimed that they have synthesized this cluster but have not yet been able to isolate it.

In the past few years further methods for the preparation of semiconductor particles have been developed. Just a few are listed here: preparation in inverse micelles,[48-50] vesicles,[51] Langmuir–Blodgett films,[52] glasses,[53-55] polymer films,[56, 57] clay minerals,[54] zeolites,[54, 58] and on porous TiO_2 layers.[59, 60]

The basic idea behind many of these preparative methods, that of controlling the particle size by the size of the reaction space (e.g. in micelles or zeolites), is, in principle, an attractive idea. These methods are doomed, however, because the individual reaction steps of the seed formation, the growth, and stabiliztion of the small particles are not well enough understood and hence, cannot be sufficiently controlled. Generally, the preparation of stable colloidal samples of Q-particles is a very empirical field. Beause of the complexity of the individual coupled reaction steps, minimal variations in the preparative conditions can lead to very different results. I therefore recommend that an interested reader who would like to prepare Q-particles in his own laboratory (which is neither difficult nor time-consuming) follow exactly the recipes given in the original literature.

4. On the Road to Monodispersity

4.1. Size Fractionation

Many of the interesting properties of Q-particles can only be observed when the examined samples are nearly monodisperse. Thus, a separation of the bands into discrete excitonic levels, as predicted by theory, (see Section 2.2), should only be observed in nearly monodisperse samples. Also, the very pronounced nonlinear optical properties that should be observed in Q-particles require narrow size distributions.[42]

Recently, methods for the size fractionation of colloidal samples have been developed. The best results have been obtained by size exclusion chromatography and gel electrophoresis, methods that have for a long time been successfully applied in biochemistry and polymer science.[37, 61-63]

In size exclusion chromatography, the colloidal solution of the semiconductor particles forms the mobile phase which flows through a stationary phase consisting of porous SiO_2 spheres. Small particles penetrate deeper into the pores than the bigger ones. The elution time for the smaller particles is, therefore, longer than for the larger ones. Hence, the elution time is a measure of the particle size. The exact relation between the particle radius (R) and the retention time (t_r) is given by Equation (6),[63, 64] where k_1 and k_2 are experimental constants.

$$k_1 + k_2 \lg R = t_r \tag{6}$$

Conventional low-pressure column chromatography and high-pressure gel chromatography (HPGC) have both been successfully applied for the size fractionation of Q-particles. HPGC can also be used as a very convenient method for the determination of the average particle size as well as the size distribution, after the calibration of analytical columns.[63]

In the case of gel electrophoresis, the particles are introduced on to the top of a column containing weakly crosslinked polyacrylamide. The upper and lower ends of the column are dipped into buffer solution. After the establishment of an electrical field the particles move through the gel as a result of their surface charge. Two parameters, the charge on the particle and its size, determine their rate of movement and, thus, their separation. The bigger the charge and the smaller the diameter, the faster the particles move through the gel. When using polyacrylamide gels the particle size has the greater effect (molecular sieve effect).[65] When the leading particle front has moved approximately two thirds through the gel, the gel is cut into thin slices and the particles dissolved out of the slices. The gel residues are filtered from the resulting colloidal solution with membrane filters, and the soluble impurities removed by washing with dilute sodium hydroxide in an ultrafiltration apparatus.

Very monodisperse samples, with a standard deviation from the average size of about 7–8%, are obtained by using both HPGC and gel electrophoresis. Without size fractionation, the best preparation methods result in about two times larger standard deviations.

4.2. Discrete Optical Transitions in Samples with Narrow Size Distributions

Figure 6 shows the absorption spectra of a CdS sample after separation by electrophoresis at room temperature and at 77 K. The particle size was 55 ± 4 Å. The second derivative spectra are shown in the lower part of the figure. A 1:1

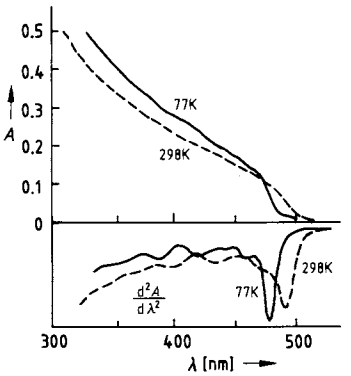

Fig. 6. Upper part: Absorption spectra of a Q-CdS sample separated by gel electrophoresis, at 298 K (broken) and 77 K (solid line). The particle size is 55 ± 4 Å. Lower part: The second derivative spectra.

ethanol/methanol mixture containing about 2% of water, which forms an optically transparent glass at low temperatures, was used as the solvent.

The absorption spectrum at room temperature has a steep increase in absorption at about 500 nm with several weak shoulders at shorter wavelengths. At 77 K the spectrum is shifted to shorter wavelengths, and the shoulders are better visible. Both these observations result from the decreased coupling of the electron with the optical (LO) phonons. The structure of the spectra can be seen more clearly from the second derivative spectra. The position of the minima in the second derivative gives a good approximation of the position of the shoulders of the absorption spectra. These shoulders arise from transitions to discrete higher excitonic levels. The structuration can only be observed after gel electrophoretic separation. The starting material with a wide size distribution (about 20% standard deviation from the average size) has an unstructured spectrum, since the line widening due to inhomogeneities is so big that it covers the discrete optical transitions in the spectrum. Koch obtained similar results[66] for the simulated absorption spectra of Q-particles.

In order to prove the existence of discrete optical transitions in samples with somewhat worse size distributions, Brus applied the technique of optical hole burning and fluorescence excitation spectroscopy (both at 15 K).[9] In the second technique the fluorescence with the longest wavelength resulting from the largest particles was observed while varying the excitation wavelength. The smaller particles in the sample had, therefore, no influence on the resulting excitation spectrum.

The energetic positions of the first five excitonic transitions can be obtained from the derivative absorption spectra of Q-CdS samples fractionated by gel electrophoresis (as in Fig. 6). Figure 7 shows the energies of the first five excitonic transitions in Q-CdS as a function of the particle size.[36] All the transitions move to higher energy with decreasing particle size and the energy difference between the transitions becomes ever larger.

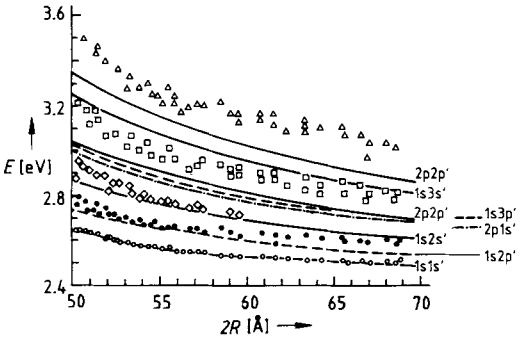

Fig. 7. Energy of the first five excitonic transitions in Q-CdS as a function of particle size. The points are taken from the absorption spectra of CdS samples separated by gel electrophoresis.

The curves resulting from a particle-in-a-box calculation (according to ref. [22]) are also shown. These curves were calculated from the product of the wave functions of the electron and hole in the indicated quantum states (the prime gives the state of the positive hole). Two different sets of curves are shown. In the first set the states have a total magnetic moment of $L = 0$ (solid lines: 1s1s', 1s2s', 2p2p', 1s3s', 2p3p'), and in the second $L = 1$ (broken lines: 1s2p', 2p1s', 1s3p'). To what extent these transitions are allowed is difficult to know: the classical selection rules for atoms are certainly not strictly valid.

The comparison between the experimentally determined points and the calculated curves is not very satisfactory. Only the curves for 1s1s' and 1s2p' agree with the experimental points in the examined size range. Definite deviations can be seen for the higher transitions. The reason for this is probably some of the simplifications used in the calculations. These are mainly the use of an infinite barrier height, the assumption that the effective masses approximation is also valid for higher states, and the use of the hexagonal CdS solid state values for the effective masses, as well as the dielectric constants[67] for Q-particles with cubic structure.

To explain the experimental data on the electronic states of Q-particles, new efforts in the area of theoretical physics and chemistry are necessary.

5. Fluorescence, Photochemical Reactivity, and Surface Modification of Q-Particles

The wave functions of the exciton fill the whole volume of the Q-particles. Already at the moment of their formation the electrons and holes have a large probability that they will be resident on the surface of the particle. Diffusion processes of the charge carriers from the interior of the particle to the surface or to the traps, which are of importance in macrocrystalline semiconductors, are therefore of no significance in Q-particles. Consequently, the time for the charge carriers to be caught in the traps is very short. Measurements of the two-photon ionization of Q-ZnS and Q-CdS[68,69], as well as measurements by Bawendi et al.,[70] have shown that the time required to trap at least one of the two charge carriers lies in the range of 100 femtoseconds or shorter. All chemical reactions and recombination processes are thus very dependent on the surface traps. The recombination of the charge carriers can be easily measured by stationary or time-resolved fluorescence spectroscopy, which is therefore a convenient method for the study of changes of the particle surface, for example, by the exchange of the solvent and stabilizer in already prepared colloidal CdS.[41] As already described in Section 2.2, the absorption spectra of the CdS remain practically constant. On the other hand, very great differences in the fluorescence spectra result, both in the intensity as well as in the spectral distribution.

5.1. Blocking of the Traps on the Particle Surface

An impressive example of how the fluorescence properties can be altered by surface reactions is the modification of the surface of Q-CdS particles with $Cd(OH)_2$.[33] After preparation from equimolar amounts of the ions, the CdS solution is slightly acidic and exhibits the typical weak red fluorescene of colloidal CdS with a quantum yield of the order of 10^{-4}. After increasing the pH to 11 and adding Cd^{2+} ions in excess, the fluorescence quantum yield increases to about 0.2. The absorption and fluorescence spectrum of such an fluo-

rescence-activated colloid is shown in Figure 8. The sharp excitonic fluorescence band near the beginning of the absorption can be clearly seen. When the spectrum is magnified 40 times weak red fluorescence at the same spectral position as before activation, originating from the recombination of trapped charge carriers, can be seen. Before the activation the intensity of this band is about ten times smaller.

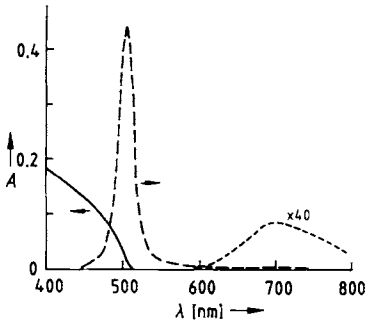

Fig. 8. Absorption and fluorescence spectrum of a fluorescence-activated, colloidal CdS sample (2×10^{-4} M solution). The long-wavelength fluorescence is magnified 40 times.

The centers for the otherwise dominant radiationless recombination are mostly blocked by the fluorescence activation. Pulse radiolytic measurements by Kumar et al. show that these radiationless recombination centers arise from trapped holes.[71] These are S^- or HS^- radicals on the surface of the particles, which are also responsible for the photocorrosion.[72] It is probable that the fluorescence activation chemically involves first the deprotonation of the HS^- groups followed by the binding of the excess Cd^{2+} ions on the deprotonated surface sulfide groups. The free valencies of the surface sulfide groups present in the nonactivated colloid are saturated with Cd^{2+} ions and the hole traps are, therefore, blocked. As the activation occurs in alkaline media, $Cd(OH)_2$ should also be present on the particle surface, as well as polyphosphate.

Henglein, in one of the first papers about colloidal CdS particles, described similar results for fluorscence activation obtained by the addition of Cd^{2+} ions to a SiO_2-stabilized CdS colloid,[73] as did Dannhauser et al. by the addition of amines to Q-Cd_3As_2,[48] Wang et al. by the treatment of Q-CdS in Nafion films with ammonia,[74] and Kortan et al. by the precipitation deposition of ZnS on CdSe.[75]

The exact fluorescence mechanism in Q-prticles is very complex. From careful and comprehensive examinations by different groups[76-78] of the excitonic fluorescence, it can be said that at least one of the charge carriers involved in the recombination process is trapped in very shallow traps. O'Neil et al.[76] and Eychmüller et al.[77] assume that the electrons are at first trapped and that, after thermally returning to the conduction band, they recombine with free holes. On the other hand, Bawendi et al.[78] postulate a model in which there is a strong resonance between free holes and holes in shallow traps.

The fluorescence, which is strongly red shifted from the absorption, is usually assigned to the recombination of trapped holes. The fluorescence decay (as well as that of excitonic fluorescence) follows a multiexponential decay law, and decay times of up to the microsecond range are observed.[77] An analysis of the decay kinetics, which are mainly determined by the depth of the traps and the distance between the charge carriers located in the traps, is very complicated and results in physically unreliable conclusions.[76]

To understand the photocatalytic properties of Q-particles it is very important to know, at least approximately, the depth of the electron and hole traps. In this connection, the discussion at present centers around whether the electrons are trapped in flat traps and the holes in deep ones or vice versa.[77, 78] The latest fluorescence quenching experiments with electron acceptors with different redox potentials show that the electron traps lie energetically only slightly under the edge of the conduction band in CdS Q-particles.[79]

5.2. Photostability of Fluorescence-Activated CdS Particles

The modification of the surface of CdS particles with cadmium hydroxide leads not only to the drastic changes in the fluorescence behavior already described, but also to an enormous increase in the stability of the particles towards photocorrosion.[33] The optical absorption of CdS particles at $\lambda = 400$ nm as a function of irradiation time (irradiation wavelength 366 nm) is shown in Figure 9. With a nonactivated colloid the absorption decreases by a factor of 2 within three minutes. The CdS dissolves with the formation of Cd^{2+} and SO_4^{2-} ions [Eq. (7)].

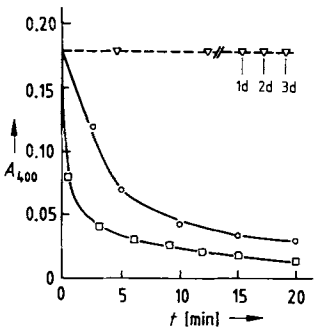

Fig. 9. Photochemical decomposition of colloidal CdS (2×10^{-4} M). Solid line: without (○) and with (□) a 1×10^{-4} M solution of Tl^+ ions. Broken line: fluorescence-activated CdS.

$$CdS \xrightarrow[O_2]{h\nu} Cd^{2+} + SO_4^{2-} \quad (7)$$

The first step in this process is again the formation of S^- or HS radicals which subsequently react with oxygen.[72] The quantum yield for this process is 0.001 decomposed CdS molecules per absorbed photon. The rate of decomposition can be increased by the addition of Tl^+ ions, an effective scavenger of the photoinduced electrons in CdS colloids (see also ref. [73]). For comparison, no decomposition occurs in a fluorescence-activated colloid even after three days of irradiation. From the measured photon flux it can be easily calculated that after this time each CdS particle has absorbed 1.7×10^8 photons (every molecule 1.7×10^5). Rhodamine B,

one of the most frequently used laser dyes, would have decomposed 20% under the same irradiation conditions.

The extraordinary photostability of surface-modified CdS colloids arises from the fact that the first stage of this corrosion, namely the formation of HS and/or S^- radicals by the reaction of the positive hole on the surface, is largely repressed after the reaction of Cd^{2+} ions with the surface sulfur groups. In addition, the layer of $Cd(OH)_2$ and polyphosphate could prevent the attack by oxygen on the trapped holes.

5.3. Formation of New Traps on the Particle Surface

An elegant method to alter the traps on the particle surface is the partial precipitation of the particle into a more insoluble compound. So, for example, the addition of Ag^+ [80] or Hg^{2+} ions to a CdS colloid results in the production of a few molecules or larger aggregates (depending on the amounts added) of Ag_2S or HgS directly on the particle surface [Eq. (8)].

$$(CdS)_n + m\,Hg^{2+} \longrightarrow [(CdS)_{n-m}(HgS)_m] + m\,Cd^{2+} \quad (8)$$

Under these conditions a homogeneous mixed crystal does not result. HgS and Ag_2S are semiconductors whose band gaps lie within the band gap of CdS, as can be easily seen from Figure 10. As a consequence, the photogenerated elec-

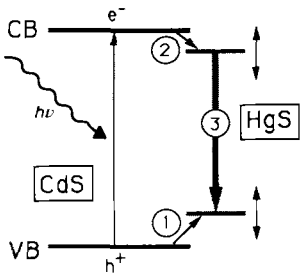

Fig. 10. Energy scheme of CdS particles with HgS (or Ag_2S) regions on the surface. CB: conduction band edge, VB: valence band edge.

trons and holes in the CdS are transferred to the HgS or Ag_2S regions in the modified particles. This can clearly be seen from the fluorescence of the particles. Figure 11 shows the fluorescence spectra of CdS samples prepared in the same manner as the fluorescence-activated colloids in Section 5.1 but to which small amounts of Hg^{2+} ions were added. Apart from the excitonic CdS fluorescence band, a broad band can be seen at longer wavelengths, which results from the recombination of the charge carriers in the HgS part of particles (step 3 in Fig. 10). The HgS areas on the CdS particles grow with more added Hg^{2+} ions and the fluorescence maximum is shifted to longer wavelengths. This can be understood in terms of the size quantization effect and results from the variable positions of the band edges in Figure 10. Time-resolved fluorescene measurements and fluorescence-quenching experiments with CdS–HgS colloids show that practically immediately after the excitation of the CdS the holes are transferred to the HgS (step 1 in Fig. 10), whereas the electrons require about 100 ps for this process (step 2, Fig. 10).[81]

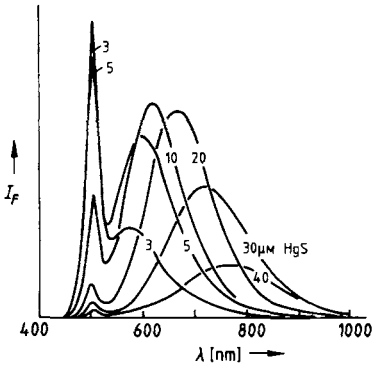

Fig. 11. Fluorescence spectra of a CdS sample (2×10^{-4} M) after the addition of different amounts of Hg^{2+} ions.

The modification of the CdS particle surface with HgS is evident from the color of the fluorescence. Figure 12 shows the fluorescence of five samples with different quantities of HgS. The turquoise blue/green fluorescence arises from pure fluorescence-activated CdS. In the other samples the quantity of HgS and therefore the size of the HgS regions increases from the sample with the yellow/green to that with the red fluorescence.

Fig. 12. Fluorescence of CdS colloids with small areas of HgS. The size of the HgS areas increases from left to right.

6. Sandwich Colloids

In the examples given in the previous section the applied term "surface modifiation" is certainly no longer correct, especially for the samples with higher amounts of HgS. One should really speak here of two strongly coupled Q-particles of different materials. During the past years such sandwich colloids have been examined in many laboratories.[80–88] Of special interest are those systems in which, because of the coupling of two particles, efficient charge separation results.[83, 84] The energy scheme of such a sandwich colloid is shown in Figure 13. Excitation with visible light occurs in the particle with the smaller band gap (CdS or Cd_3P_2) and results in the formation of electron–hole pairs. The TiO_2 or ZnO particles have a larger band gap and an energetically lower lying conduction band. Consequently, the electrons excited by light are transferred from the CdS (or Cd_3P_2) particles to the TiO_2 (or ZnO) particles, whereas the holes remain in the CdS (or Cd_3P_2). Such sandwich colloids are prepared by mixing two separately prepared colloidal solu-

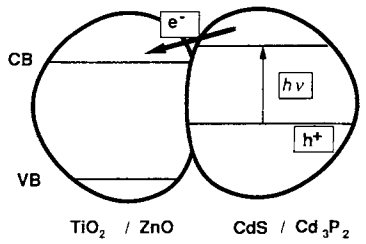

Fig. 13. Schematic representation of a sandwich colloid. CB: conduction band edge, VB: valence band edge.

tions. The trick is that a small quantity of a weakly acidic, concentrated solution of positively charged TiO_2 (or ZnO) particles is added under vigorous stirring to a dilute, alkaline solution of negatively charged CdS (or Cd_3P_2) particles. The solution must remain alkaline. Under such conditions a coagulation of the positively and negatively charged particles begins but is stopped when the original positive charge on the oxide particles becomes negative in the alkaline medium. With this method transparent colloidal solutions can be prepared in which every CdS (or Cd_3P_2) particle is coupled with at least one TiO_2 (or ZnO) particle. The formation of the sandwich colloids can be followed especially well by fluorescence-quenching experiments. Figure 14 shows the excitonic fluorescence intensity of fluorescence-activated CdS particles as a function of the added amount of TiO_2. When the

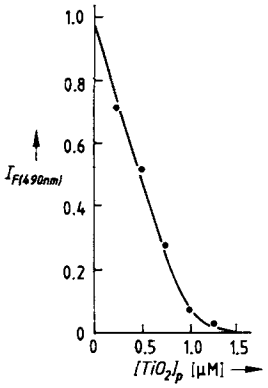

Fig. 14. Intensity of the excitonic CdS fluorescence as a function of the quantity of added TiO_2 (given as particle concentration). The particle concentration of CdS was 0.2 μM.

particle concentration reaches 0.6 μM TiO_2, the fluorescence has dropped to 1/e of the original value. Under these conditions there are about three TiO_2 particles for every CdS particle present in the solution. With these concentrations and a CdS fluorescence decay time of 10 ns the fluorescence quenching cannot arise from the diffusion of the TiO_2 particles to the CdS particles followed by an electron transfer in the encounter complex. The diffusion process is at least five orders of magnitude too slow to compete with the fluorescence decay. Sandwich colloids in which a fast electron transfer can occur from CdS to TiO_2 must be formed. In order to gain some information about the rate of these processes, the decay time for the Cd_3P_2 fluorescence in Cd_3P_2–TiO_2 sandwich colloids was measured and amounted to less than one picosecond (for comparison: in Cd_3P_2 colloids without TiO_2 it was a few 100 ns).[88]

This extremely fast and efficient primary charge separation results in the CdS–TiO_2 sandwich colloids exhibiting a much higher photocatalytic activity than the individual colloids.[83] Methyl viologen (MV^{2+}) is reduced to the blue MV^+ radical by irradiating CdS with visible light in the presence of methanol as a hole scavenger. From the known extinction coefficient of MV^+ ($\varepsilon_{605nm} = 11000\ M^{-1}cm^{-1}$) and the measured photon flux, a quantum yield for the reduction of MV^{2+} of $\Phi = 0.13$ is obtained when fluorescence-activated CdS is used. As shown in Figure 15, after the addition of TiO_2 (i.e., after the formation of sandwich colloids) the quantum yield increases drastically. The quantum yield approaches 1 when the TiO_2 particle concentration is higher than 1.5 μM. Evidently, in this concentration range all the CdS particles are coupled with at least one TiO_2 particle. As expected, the increase in the quantum yield (Fig. 15) follows the decrease in the fluorescene intensity in Figure 14.

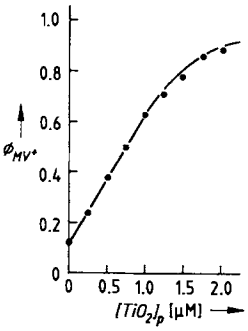

Fig. 15. Quantum yield of MV^+ formation by irradiation of a fluorescence activated CdS as a function of the added quantity of TiO_2 (particle concentration as in Fig. 14). Irradiation wavelength: 436 nm; the solution contained 0.1 M methanol as hole scavenger.

In sandwich colloids of CdS (or Cd_3P_2) with ZnO, the transferred electron in the ZnO can be substantiated by spectroscopy.[84] In this case a stored electron leads (as incidentally also with CdS particles) to bleaching of the optical absorption near the band edge.[40, 89, 90] This effect, which forms the basis of the nonlinear optical behavior of Q-particles, is considered in another report.[15]

Gopidas et al. have reported electron microscope photographs of sandwich colloids.[86] However, it is never clear whether the particles were already coupled in solution or whether the coupling resulted when the sample was dried for the microscope.

7. Q-Particles in Modified Semiconductor Layers

In order to utilize the fascinating properties of Q-particles for typical semiconductor applications the particles must be in electrical contact.

Recently, Hodes reported that when CdSe is electrochemically deposited on electrically conducting glass, agglomerated Q-particles are formed and not a compact film.[46, 91, 92] Such electrodes in photoelectrochemical cells exhibit photocurrents arising from the Q-particles. In order to absorb significant quantities of incident light, ten to twenty coatings of the Q-particles must be deposited one over the other, and thus the released electrons must be transported over many particles to the back contact. Energy is lost with every jump of the electrons from one particle to another, so the photocurrents and voltage attainable with such systems are relatively low.

This problem can be overcome by depositing the Q-particles on a very porous TiO_2 electrode, to which the electrons are transferred after light absorption.[59, 60, 93] Less than a monolayer of particles is necessary for practically all the incident light to be absorbed, because of the large surface area of the electrodes. For several years such porous TiO_2 electrodes have been used with great success by Grätzel et al. as substrate electrodes for dye sensitization.[94–97]

An electron microscope picture of such a TiO_2 electrode shows clearly the raw surface (Fig. 16). The surface is

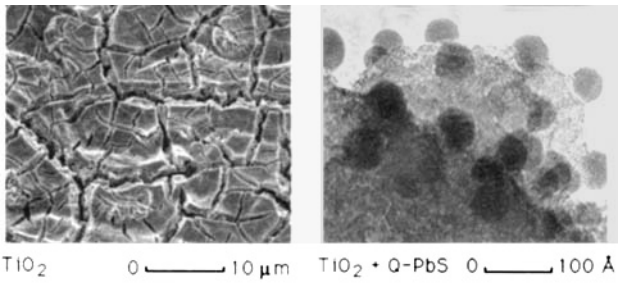

Fig. 16. Electron microscope photographs of a porous TiO_2 electrode. In the right hand photograph at greater magnification, the Q-PbS particles can be seen.

400 times larger than the geometric area of the electrode as determined by BET (BET = Brunauer, Emmett, Teller) measurements. The thickness of the TiO_2 layer was about 20 µm. The electrode, after the deposition of Q-PbS, is shown at a higher magnification on the right hand side of Figure 16. It can be clearly seen that individual particles, approximately 60 Å big, are stuck on to the crystalline background of TiO_2. The characteristic reflections of cubic PbS (galena) are found adjacent to the anatase reflections of TiO_2 in X-ray diffraction diagrams of such electrodes.[93]

The procedure for depositig the particles is very simple. The porous electrode is dipped into a concentrated solution of a cadmium (or lead) salt. It is washed with water and subsequently dipped into a Na_2S solution. The metal ions adsorbed on the oxidic surface react with the initial formation of CdS (or PbS) particles of approximately 30 Å. When this submergence procedure is repeated (each cycle forms one coating), new CdS (or PbS) is formed mainly on the small particles formed during the first coating. Hence, the particle size increases with the number of coatings.

This can be easily seen from the optical reflection spectra of a TiO_2 electrode after different numbers of coatings (Fig. 17). The absorption of the particles is shifted to longer wavelengths with increasing number of coatings, as a result of the size quantization effect. The average particle size increases from 34 to 104 Å. The simultaneous increase over the whole absorption spectrum results from the increased quantity of PbS deposited on the electrode.

The corresponding photocurrent spectra are shown in Figure 18. The photocurrent yield (number of electrons detected in the exterior current circuit per number of photons arriving at the electrode) is shown as a function of the incident light wavelength. As in the reflection spectra, the red shift can be seen with increasing particle size. The quantum yield attains values of 70%. If we compensate for the reflection losses, this implies that the primary electron transfer from the Q-

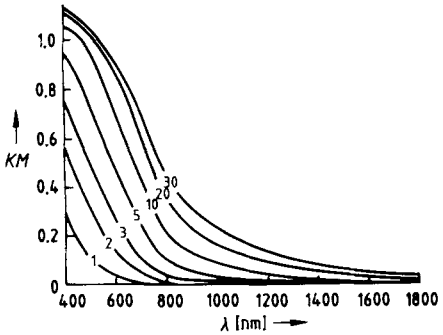

Fig. 17. Spectra of the diffuse reflections of a TiO_2 electrode after different numbers of coatings (number given for on each curve) of PbS. The Kubelka Munk values [98], which correspond to optical densities in transparent systems, are shown on the ordinate. The particles grow with increasing number of coatings from 34 to 39, 42, 50, 71, 82, and 104 Å.

particles into the TiO_2 layer must occur with a quantum efficiency of almost 1. This is in agreement with the very high rate of electron transfer observed in sandwich colloids.[86, 88]

It can be seen from the photocurrent spectra in Figure 18 that the photocurrent quantum yield decreases when the particle sizes reach 50 Å or more. The reason for this lies in the

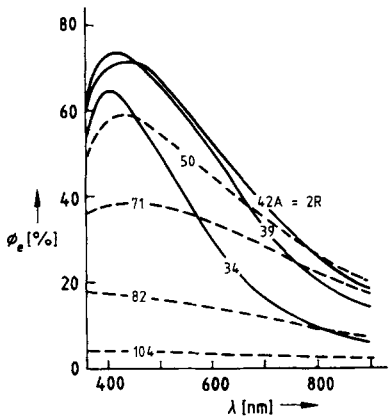

Fig. 18. Photocurrent spectra of porous titanium dioxide electrodes with different size Q-PbS particles. The electrochemical cell was purged with nitrogen and contained a solution of 0.1 M Na_2S and 1 M KCl as electrolyte, a Pt counter electrode, and a Ag/AgCl reference electrode. The measurements occurred under potentiostatic conditions.

relative positions of the bands of PbS and TiO_2. The energy of the conduction band edge of macrocrystalline PbS lies below that of TiO_2; a sensitization is thus impossible. Only by increasing the energy level of the PbS conduction band as a result of the size quantization effect is electron transfer possible. The critical size of PbS particles above which no efficient electron transfer occurs, lies between 40 and 50 Å (corresponding to a band gap of about 1.3 eV).[60, 93]

At present the biggest obstacle for potential applications is the stability of the electrodes. In the case of electrodes sensitized with Q-CdS, the photocurrent decreases to about half the original value after a few months and for those sensitized with PbS already after a few days. It remains to be seen if surface modification or embedding in pure solid state systems can overcome these problems.

8. Conclusions and Prospects

Q-Particles represent a novel state of matter in chemistry and materials science. The chemical and physical properties of the particles can be greatly varied by changing the particle size without changing the chemical composition. In the areas of catalysis, electronics, and optics, a wide variety of applications are conceivable. Also, it is much easier to prepare Q-particles in gram quantities than cluster compounds in the gas phase. Developments in preparation are moving in the direction of soluble powders of Q-particles with narrow size distributions, enabling Q-particles to be handled more like "normal" chemicals.

Surface processes on Q-particles can be very readily examined because of the very large surface to volume ratios. In solution or in transparent solid matrices the methods of optical spectroscopy, either stationary or time-resolved, can be easily employed, which is not the case in a molecular beam or on single-crystal surfaces. It is therefore conceivable that molecular beam and surface physics on the one hand, and Q-particle colloid chemistry on the other, will increasingly supplement one another in the examination of nanometer large clusters or particles and in surface science.

In the area of "nanostructuration" new physical and chemical properties can be expected from the combination of different materials each a few nanometers big. Here also colloid chemistry offers an interesting alternative to the gas-phase processes usually used in materials science.

By embedding the Q-particles in porous semiconductor electrodes the possibility of utilizing the fascinating electronic properties of the particles for optoelectronic and photovoltaic applications can be attempted for the first time. As in the whole of this research area, however, one is at the very beginning and in the phase of fundamental research.

Finally it should be said that similar effects to those that occur when going from molecules to compact materials can also be observed in the case of colloid metals.[7, 8, 99, 100]

Received: May 14, 1992 [A 887 IE]
German version: *Angew. Chem.* **1993**, *105*, 43
Translated by Dr. I. Popovic, and L. Katsikas, Belgrade.

[1] Wo. Ostwald, *Die Welt der vernachlässigten Dimensionen*, Steinkopf, Dresden, **1915**.
[2] D. Fenske, J. Ohmer, J. Hachgenei, K. Merzweiler, *Angew. Chem.* **1988**, *100*, 1300; *Angew. Chem. Int. Ed. Engl.* **1988**, *27*, 1277.
[3] J.-F. You, G. C. Papaefthymiou, R. H. Holm, *J. Am. Chem. Soc.* **1992**, *114*, 2697.
[4] M. M. Kappes, *Chem. Rev.* **1988**, *88*, 369.
[5] H. Gleiter, *Phys. Bl.* **1991**, *47*, 753.
[6] Special Section in *Science* **1991**, *254*, 1300.
[7] A. Henglein, *Top. Curr. Chem.* **1988**, *143*, 113, and references therein.
[8] A. Henglein, *Chem. Rev.* **1989**, *89*, 1861, and references therein.
[9] L. E. Brus, *Appl. Phys. A.* **1991**, *53*, 465, and references therein.
[10] J. R. Darwent, G. Porter, *J. Chem. Soc. Chem. Commun.* **1981**, 145.
[11] J. R. Darwent, *J. Chem. Soc. Faraday Trans. 2* **1981**, *77*, 1703.
[12] K. Kalyanasundaram, M. Grätzel, E. Pelizetti, *Coord. Chem. Rev.* **1986**, *69*, 57.
[13] A. Bard, *Ber. Bunsenges. Phys. Chem.* **1988**, *92*, 1187.
[14] D. W. Bahnemann in *Photochemical Conversion and Storage of Solar Energy* Eds.: E. Pelizzetti, M. Schiavello), Kluver, Dordrecht, **1991**, p. 251, and references therein.
[15] H. Weller, *Adv. Mater.* **1993**, *5*, 88–95.
[16] A. L. Efros, A. L. Efros, *Sov. Phys. Semicond. (Engl. Transl.)* **1982**, *16*, 772.
[17] L. E. Brus, *J. Chem. Phys.* **1983**, *79*, 5566.
[18] L. E. Brus, *J. Chem. Phys.* **1984**, *80*, 4403.
[19] R. Rossetti, J. L. Ellison, J. M. Gibson, L. E. Brus, *J. Chem. Phys.* **1984**, *80*, 4464.
[20] A. Fojtik, H. Weller, U. Koch, A. Henglein, *Ber. Bunsenges. Phys. Chem.* **1984**, *88*, 969.
[21] H. Weller, H. M. Schmidt, U. Koch, A. Fojtik, S. Baral, A. Henglein, W. Kunath, K. Weiss, E. Diemann, *Chem. Phys. Lett.* **1986**, *124*, 557.
[22] H. M. Schmidt, H. Weller, *Chem. Phys. Lett.* **1986**, *129*, 615.
[23] Y. Kayanuma, *Solid State Commun.* **1986**, *59*, 405.
[24] S. V. Nair, S. Sinha, K. C. Rustagi, *Phys. Rev. B: Condens. Matter* **1987**, *35*, 4098.
[25] T. Rajh, M. W. Peterson, J. A. Turner, A. J. Nozik, *J. Electroanal. Chem. Interfacial Electrochem.* **1987**, *228*, 55.
[26] Y. Wang, A. Suna, W. Mahler, R. Kasowski, *J. Chem. Phys.* **1987**, *87*, 7315.
[27] Y. Wang, N. Herron, *Phys. Rev. B: Condens. Matter* **1990**, *42*, 7253.
[28] Y. Kayanuna, *Phys. Rev. B: Condens. Matter* **1988**, *38*, 9797.
[29] P. E. Lippens, M. Lanoo, *Phys. Rev. B: Condens. Matter* **1989**, *39*, 10935.
[30] Y. Nosaka, *J. Phys. Chem.* **1991**, *95*, 5054.
[31] M. V. Rama Krishna, R. A. Friesner, *J. Chem. Phys.* **1991**, *95*, 8309.
[32] G. T. Einevoll, *Phys. Rev. B: Condens. Matter* **1992**, *45*, 3410.
[33] L. Spanhel, M. Haase, H. Weller, A. Henglein, *J. Am. Chem. Soc.* **1987**, *109*, 5649.
[34] J. K. Burdett, *Prog. Solid State Chem.* **1984**, *15*, 173.
[35] E. A. Hylleraas, *Z. Phys.* **1930**, *65*, 209.
[36] L. Katsikas, A. Eychmüller, M. Giersig, H. Weller, *Chem. Phys. Lett.* **1990**, *172*, 201.
[37] A. Eychmüller, L. Katsikas, H. Weller, *Langmuir* **1989**, *6*, 1605.
[38] M. G. Bawendi, A. R. Kortan, M. L. Steigerwald, L. E. Brus, *J. Chem. Phys.* **1989**, *91*, 7282.
[39] S. F. Bertram in *Handbook of X-ray* (Ed.: E. F. Kaelbe), McGraw-Hill, New York, **1967**, p. 17–19.
[40] M. Haase, H. Weller, A. Henglein, *J. Phys. Chem.* **1988**, *92*, 482.
[41] U. Resch, A. Eychmüller, M. Haase, H. Weller, *Langmuir*, **1992**, *8*, 2215.
[42] Y. Wang, N. Herron, *J. Phys. Chem.* **1991**, *95*, 525, and references therein.
[43] M. A. Olshavsky, A. N. Goldstein, A. P. Alivisatos, *J. Am. Chem. Soc.* **1990**, *112*, 9438.
[44] H. Ushida, C. J. Curtis, A. J. Nozik, *J. Phys. Chem.* **1991**, *95*, 5382.
[45] C.-H. Fischer, M. Giersig, *Langmuir* **1992**, *8*, 1475.
[46] G. Hodes, *Isr. J. Chem.*, in press.
[47] I. G. Dance, A. Choy, M. L. Scudder, *J. Am. Chem. Soc.* **1984**, *106*, 6285.
[48] T. Dannhauser, M. O'Neil, K. Johansson, D. Whitten, G. McLendon, *J. Phys. Chem.* **1986**, *90*, 6074.
[49] P. Lianos, J. K. Thomas, *Chem. Phys. Lett.* **1986**, *125*, 299.
[50] M. L. Steigerwald, A. P. Alivisatos, J. M. Gibson, T. D. Harris, R. Kortan, A. J. Muller, A. M. Thayer, T. M. Duncan, D. C. Douglass, L. E. Brus, *J. Am. Chem. Soc.* **1988**, *110*, 3046.
[51] H. J. Watzke, J. H. Fendler, *J. Am. Chem. Soc.* **1987**, *91*, 854.
[52] E. S. Smotkin, L. Chongmok, A. J. Bard, A. Campion, M. A. Fox, T. E. Mallouk, S. E. Webber, J. M. White, *Chem. Phys. Lett.* **1988**, *152*, 265.
[53] A. I. Ekimov, A. L. Efros, A. A. Onuschenko, *Solid State Commun.* **1985**, *56*, 921.
[54] R. D. Stramel, T. Nakamura, J. K. Thomas, *J. Chem. Soc. Faraday Trans. 1* **1988**, *84*, 1287.
[55] T. Raijh, M. I. Vucemilovic, N. M. Dimetrievic, O. I. Micic, A. Nozik, *Chem. Phys. Lett.* **1988**, *143*, 305.
[56] Y. Wang, A. Suna, M. Mahler, R. Kasowski, *J. Phys. Chem.* **1987**, *87*, 7315.
[57] W. Mahler, *Inorg. Chem.* **1988**, *27*, 435.
[58] Y. Wang, N. Herron, *J. Phys. Chem.* **1987**, *91*, 257.
[59] R. Vogel, K. Pohl, H. Weller, *Chem. Phys. Lett.* **1990**, *174*, 241.
[60] H. Weller, *Ber. Bunsenges. Phys. Chem.* **1991**, *95*, 1361.
[61] C.-H. Fischer, H. Weller, A. Fojtik, C. Lume-Pereira, E. Janata, A. Henglein, *Ber. Bunsensges. Phys. Chem.* **1986**, *90*, 46.
[62] C.-H. Fischer, J. Lilie, H. Weller, L. Katsikas, A. Henglein, *Ber. Bunsenges. Phys. Chem.* **1989**, *93*, 61.
[63] C. H. Fischer, H. Weller, L. Katsikas, A. Henglein, *Langmuir* **1989**, *5*, 429.
[64] H. Determann, *Gelchromatographie*, Springer, Berlin **1967**, p. 115.
[65] H. R. Maurer, *Disc Electrophoresis and Related Techniques of Polyacrylamide Gel Electrophoresis*, 2nd ed., de Gruyter, Berlin, **1971**, p. 20.
[66] S. W. Koch, *Phys. Bl.* **1990**, *46*, 167.
[67] *Landolt – Börnstein, Zahlenwerte und Funktionen aus Naturwissenschaft und Technik, Vol. III-17b*, Springer, Berlin, **1982**, p. 170.
[68] N. P. Ernsting, M. Kaschke, H. Weller, L. Katsikas, *J. Opt. Soc. Am. B: Opt. Phys.* **1990**, *7*, 1630.
[69] M. Kaschke, N. P. Ernsting, H. Weller, U. Müller, *Chem. Phys. Lett.* **1990**, *168*, 543.
[70] M. G. Bawendi, W. L. Wilson, L. Rothberg, P. J. Carroll, T. M. Jedju, M. L. Steigerwald, L. E. Brus, *Phys. Rev. Lett.* **1990**, *65*, 1623.
[71] A. Kumar, E. Janata, A. Henglein, *J. Phys. Chem.* **1988**, *92*, 2587.
[72] S. Baral, A. Fojtik, H. Weller, A. Henglein, *J. Am. Chem. Soc.* **1988**, *108*, 375.
[73] A. Henglein, *Ber. Bunsenges. Phys. Chem.* **1982**, *86*, 301.
[74] Y. Wang, A. Suna, J. McHugh, E. Helinski, P. A. Lucas, R. D. Johnson, *J. Chem. Phys.* **1990**, *92*, 6927.

[75] A. R. Kortan, R. Hull, R. L. Opila, M. G. Bawendi, M. L. Steigerwald, P. J. Caroll, L. E. Brus, *J. Am. Chem. Soc.* **1990**, *112*, 1327.
[76] M. O'Neil, J. Marahn, G. McLendon, *J. Phys. Chem.* **1990**, *94*, 4356.
[77] A. Eychmüller, A. Hässelbarth, L. Katsikas, H. Weller, *Ber. Bunsenges. Phys. Chem.* **1991**, *95*, 79, and references therein.
[78] M. G. Bawendi, P. J. Carroll, W. L. Wilson, L. E. Brus, *J. Chem. Phys.* **1992**, *96*, 946.
[79] A. Hässelbarth, A. Eychmüller, H. Weller, *Chem. Phys. Lett.*, in press.
[80] L. Spanhel, H. Weller, A. Fojtik, A. Henglein, *Ber. Bunsenges. Phys. Chem.* **1987**, *91*, 88.
[81] A. Eychmüller, A. Hässelbarth, H. Weller, *J. Lumin.* **1992**, *53*, 113; A. Hässelbarth, A. Eychmüller, R. Eichberger, M. Giersig, H. Weller, *J. Phys. Chem.*, in press.
[82] H. Weller, U. Koch, M. Gutierrez, A. Henglein, *Ber. Bunsenges. Phys. Chem.* **1984**, *88*, 649.
[83] L. Spanhel, H. Weller, A. Henglein, *J. Am. Chem. Soc.* **1987**, *109*, 6632.
[84] L. Spanhel, A. Henglein, H. Weller, *Ber. Bunsenges. Phys. Chem.* **1987**, *91*, 1359.
[85] A. Henglein, M. Gutierrez, H. Weller, A. Fojtik, J. Jirkovsky, *Ber. Bunsenges. Phys. Chem.* **1989**, *93*, 593.
[86] K. R. Gopidas, M. Bohorquez, P. V. Kamat, *J. Phys. Chem.* **1990**, *94*, 6435.
[87] P. V. Kamat, *J. Am. Chem. Soc.* **1991**, *113*, 9705.
[88] R. Kietzmann, F. Willig, H. Weller, R. Vogel, D. N. Nath, R. Eichberger, P. Liska, J. Lehnert, *Mol. Cryst. Liq. Cryst.* **1991**, *194*, 169.
[89] U. Koch, A. Fojtik, H. Weller, A. Henglein, *Chem. Phys. Lett.* **1985**, *122*, 507.
[90] D. W. Bahnemann, C. Kormann, R. Hoffmann, *J. Phys. Chem.* **1987**, *91*, 3789.
[91] G. Hodes, A. Albu-Yaron, *Proc. Electrochem. Soc.* **1988**, *88*, 298.
[92] G. Hodes, T. Engelhard, A. Albu-Yaron, A. Pettford-Long, *Mater. Res. Soc. Symp. Proc.* **1990**, *164*, 81.
[93] R. Vogel, P. Hoyer, H. Weller, unpublished.
[94] N. Vlachopoulos, P. Liska, J. Augustynski, M. Grätzel, *J. Am. Chem. Soc.* **1988**, *110*, 1216.
[95] O. Enea, J. Moser, M. Grätzel, *J. Electroanal. Chem. Interfacial Electrochem.* **1989**, *259*, 59.
[96] B. O'Regan, J. Moser, M. Anderson, M. Grätzel, *J. Phys. Chem.* **1990**, *94*, 8720.
[97] B. O'Regan, M. Grätzel, *Nature* **1991**, *353*, 737.
[98] F. Wilkinson, G. Kelly in *Handbook of Organic Photochemistry, Vol. 1* (Ed.: J. C. Scaiano), CRC-Press, Boca Raton, Fl, USA, **1989**, p. 293.
[99] A. Henglein, P. Mulvaney, T. Linnert, *Farad. Discuss. Chem. Soc.* **1991**, *92*, 31.
[100] A. Henglein, *Labor 2000* **1992**, 110.

Transmembrane Signaling of T Lymphocytes by Ligand-Induced Receptor Complex Assembly

By Klaus Eichmann*

T lymphocytes (T cells) are the central cell type initiating all immune responses. They are able to recognize other cells in the body that have been invaded by foreign living or nonliving matter. In such cells, foreign peptides generated by intracellular breakdown are complexed with molecules of the major histocompatibility complex (MHC) specially designed for peptide binding. Peptide-loaded MHC molecules appear on the surface of these cells and alert the immune system. The molecular complex which T cells use for recognition of peptide-loaded MHC molecules is among the most sophisticated and versatile receptor systems in biology. It consists of specific and nonspecific transmembrane components which assemble to a functional signal transduction unit as the result of ligand binding. Correct assembly leads to activation and relocation of enzymes including membrane-associated, tyrosin-specific protein kinases and phosphatases. Transmembrane signaling in T cells depends on the correct assembly and cooperation among multiple molecular components. This may be related to a multitude of different cellular responses of T cells at different stages of differentiation, all elicited through the T cell receptor complex.

1. Introduction

A major task of the immune system is to protect the vertebrate macroorganism against a myriad of microorganisms. To this end, the immune system is able to generate a series of effector cells and molecules appropriate to the elimination of most microbial invaders. These include antibodies for the neutralization of extracellular infectious agents, various cells and molecules with cytolytic properties mainly to eliminate cells harboring infectious agents or tumor cells, molecular systems for the stimulation of phagocytic cells with antimicrobial principles such as the generation of reactive nitrogen or oxygen intermediates, etc. The diversity of effector systems is a direct corollary to the heterogeneity of infectious agents. Nevertheless all immune responses are initiated by the same basic events, which are summarized in a highly simplified schematic drawing in Scheme 1: Upon entering the body, an antigen is first encountered by macrophages, cells with a "sticky" surface which are present in the blood stream as well as in all tissues. Macrophages as well as a few other cell types are able to engulf the antigen then destroy the engulfed material by the phagolysosomal pathway. This is the end of most microorganisms which are thus eliminated in a nonspecific manner without involving the components of the specific immune system. However, a number of infectious agents including viruses, bacteria, and parasites are more or less resistent to destruction by this mechanism. Nevertheless some of their antigens are processed by macrophages, in other words, proteins are broken down into peptides, which are complexed with the gene products of the major histocompatibility complex (MHC) and presented on the cell surface.[1] Two classes of MHC molecules are responsible for two distinct processing pathways: Proteins derived from phagocytized extracellular antigens are processed in such a way that their peptides are presented with MHC class II molecules. In contrast, peptides derived from proteins which were synthetized within the cell, for example by viruses, are presented with MHC class I molecules.[1] Peptides presented with MHC molecules are recognized by T lymphocytes, which as a corollary to the two types of processing pathways and MHC molecules can be categorized in two distinct subsets, CD4 T cells and CD8 T cells.[2] CD4 T cells have a recognition system for peptides presented by MHC class II and are therefore activated mainly by extracellular infectious agents. Activated CD4 cells produce cytokines involved in the recruitment of inflammatory cells and in the activation ("helper cells") of B lymphocytes that produce antibodies. CD8 T cells have a recognition system for peptides presented by MHC class I molecules; as a consequence, they are activated mainly by intracellular infectious agents.[3] Activated CD8 cells are cytotoxic ("killer cells") and able to destroy cells harboring infectious agents.

As indicated in Scheme 1, the activation of lymphocytes by antigens is a highly integrated process of cellular cooperation involving direct interactions between cells as well as intercell communication by soluble mediators (lymphokines). In addition to CD8 and CD4 T cells, macrophages and B lymphocytes are activated in this process. The major task of activated macrophages is eliminating intracellular pathogens, the major task of activated B cells is secreting antibodies. An attempt to give a full account of all known cellular and molecular events which constitute an immune response would be beyond the scope of this review.[*] Rather, I will restrict myself to describing the multimolecular membrane complex that mediates recognition by and activation of CD4 and CD8 T cells.

2. The Ontogeny of T Lymphocytes

The stem cells for all hemopoetic (blood-cell producing) cells of vertebrates are found during embryonic development

[*] Prof. Dr. K. Eichmann
Max-Planck-Institut für Immunbiologie
Postfach 11 69, D-W-7800 Freiburg (FRG)

[*] Editorial note: Overviews of this and related topics are provided by good biochemistry and immunology textbooks, for example, D. Voet, J. G. Voet, *Biochemistry*, Wiley, New York, **1990**; J. Klein, *Immunology*, Blackwell Scientific, Oxford, **1990**.

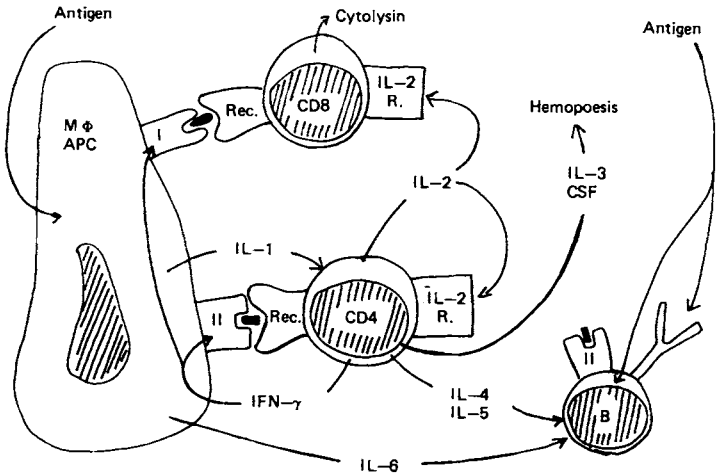

Scheme 1. A very simplified schematic representation of cell types, receptor molecules, soluble mediators, and reaction pathways in a specific immune response. Abbreviations: MΦ = macrophage, APC = antigen-presenting cell, I/II = class I and class II molecules of the major histocompatibility complex, CD8/CD4 = T cells belonging to CD8 and CD4 subsets, Rec. = MHC/antigen-specific αβCD3 T cell receptor, IFN-γ = interferon-γ, IL = interleukin, IL-2R = interleukin-2 receptor, CSF = colony stimulating factor, B = B lymphocyte. This review focuses on the events in the molecular recognition that takes place between CD4 and CD8 T cells and macrophages.

mainly in the yolk sak, during fetal life mainly in the liver, and during adult life in the bone marrow.[4] These stem cells become committed to producing distinct types of cells including T cells, B cells, macrophage-granulocyte cells, etc. Precursor cells committed to T cell lineage leave their tissue of origin and seek the thymus, an epithelial organ that has developed from the fifth pharyngeal pouch and is the primary site for the generation of mature T lymphocytes and the selection of T cell receptors (TCRs) that distinguish "self" from "non-self".[5, 6] Mature T lymphocytes leave the thymus and repopulate the peripheral lymphoid organs as naive, resting, peripheral T cells. Maturation of T lymphocytes is first observed in fetal life, peaks at adolescence, continues throughout adult life, and decreases then with age. Mature naive T lymphocytes die in the periphery within days to weeks unless they encounter and are activated by antigen-presenting cells (APCs) presenting a suitable peptide on their MHC molecules. The MHC/peptide complex is registered by the specific T cell recognition system. Activated T cells divide several times, giving rise to clones of effector cells which, after elimination of the antigen, return to the resting state and become long-lived memory T cells, all having the same recognition system. Memory T cells can be reactivated by the same MHC/peptide combination any time later, giving rise to a new effector and memory cell population with the same specificity.[7]

Thus, during its lifetime, a clone of T lymphocytes comprises T cells with the same recognition system in quite distinct stages of differentiation. Recognition of the MHC/peptide complex leads to quite distinct cellular responses at each differentiation stage. In the thymus, recognition of the MHC/peptide complex (both "self") results in one of two responses: Thymic T cells with efficient recognition (high affinity?) are actively deleted to ensure tolerance of "self", a phenomenon termed negative selection. In contrast, positive selection induces other thymic T cells to mature and is generated by yet poorly understood (low affinity?) means of recognition of the MHC/peptide complex.[5] Positively selected T cells repopulate the periphery, and their receptors recognize self MHC molecules loaded with foreign peptides that were not present during thymic selection. Cells that were neither positively nor negatively selected, that is, those that do not recognize self MHC, also die within the thymus. Recognition of the MHC/peptide complex is again required for activation of naive peripheral T cells to generate clones of functionally competent effector cells. Activated effector cells use their recognition system once again to synthesize and excrete effector molecules. Memory cells are reactivated by their recognition system to develop into secondary effector and memory cells. Taken together, a number of distinct cellular responses are induced through the specific recognition system of T cells, a phenomenon unique to T lymphocytes and worthy of a detailed molecular analysis.

3. The Molecules Involved in T Cell Recognition

In this review the nature and properties of the recognition complex on T lymphocytes will be discussed, with particular emphasis on how its members interact with each other and regulate each other's function. This requires some degree of knowledge on their structure, which I will describe only briefly; the interested reader is referred to many excellent review articles in this field.[8–13] Moreover, an understanding of T cell recognition is not possible without a brief discussion of the physiological ligand, the MHC/peptide complexes on APC. This subject is discussed further in more detailed reviews.[1, 8]

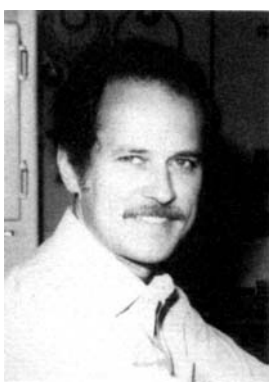

Klaus Eichmann was born in 1939 in Kassel, Germany. He studied medicine from 1959 to 1965 at the Universities of Marburg and Munich and received his doctorate in 1966 in Marburg. He then spent three years at the Rockefeller University in New York in the department led by Prof. Richard M. Krause, first as a research associate and later as an assistant professor. Upon his return to Germany, he became a group leader at the Institut für Genetik at the University of Cologne and later department head at the Deutsche Krebsforschungszentrum in Heidelberg. Since 1981 he has been Director of the Max-Planck-Institut für Immunbiologie in Freiburg and a member of the Max-Planck-Gesellschaft. Since the mid-1980s his research group has been studying the molecular processes on the T cell membrane that lead to signal transduction and activation.

3.1. MHC Molecules and Peptide Presentation

The MHC is a gene complex which is highly conserved in all vertebrate species studied.[14] It contains several types of genes which are more or less closely related to immune functions. For the present purpose it suffices to discuss two types of MHC genes, the class I and class II genes, both occurring in several different functional copies per haploid genome (haplotype).[15] Their most unusual property is an unusual degree of polymorphism, resulting in the practical consequence that each individual haplotype represents a unique combination of alleles, and no two phenotypes are identical. This fact accounts for most of the problems connected with tissue transplantation.[14, 15]

The proteins encoded by MHC class I and class II genes belong to the immunoglobulin (Ig) superfamily, whose common unit is the Ig-like domain consisting of approximately 110 amino acids folded in two parallel layers of three to four antiparallel strands of β sheet, connected by a disulfide bond.[16] MHC class I proteins consist of three domains in tandem; the amino-terminal domains (α1 and α2) are atypical in that they form α-helical regions sitting on a single monolayer of a β sheet (Fig. 1). The α-helical portions of the α1 and α2 domains are arranged in parallel forming a groove between them whose bottom is provided by the combined β sheets of both domains. The α3 domain is typically Ig-like and is attached to the cell surface by a transmembrane region followed by a cytoplasmic tail. Noncovalently attached to the α3 domain is the non-MHC encoded β2 microglobulin (β2M), a single Ig domain structure.[8] The MHC class II proteins are heterodimers; each chain consists of an N-terminal atypical domain (α1 and β1) followed by a typical Ig domain (α2 and β2) and transmembrane and cytoplasmic regions. The α1 and β1 domains together form a structure similar to that described above for the α1 and α2 domains of MHC class I (Fig. 1).

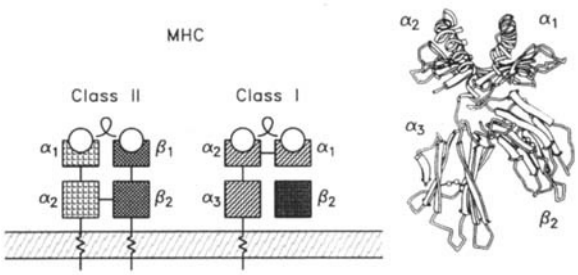

Fig. 1. Schematic representation of MHC class II and class I molecules and the three-dimensional crystal structure of a human MHC class I molecule. The typical Ig domains are represented by squares. The α-helical regions of the atypical domains are indicated by open circles. The position of the peptide in the cleft between the α-helical regions is indicated; in the crystal structure the cleft between the α-helical regions is empty. The crystal structure does not include the transmembrane portion, since the protein used for crystallization was obtained by papain digestion of MHC class I molecules from cell surfaces (cf. [1, 8]).

The grooves of both types of MHC molecules are receptacles for peptides with eight to ten amino acids for MHC class I and somewhat longer for MHC class II.[17, 18] Several algorithms have been developed to predict peptide sequences that fit into MHC grooves, but to date none is entirely reliable.[1] Most data suggest that the MHC fit is determined by no more than one or two amino acid positions at one or both ends of the peptide, whereas the rest of the sequence may vary widely.[17–20][*] Hence, a single MHC molecule can bind and present many different peptides. There is no indication that any difference is made at this stage between self and foreign peptides. However, due to selection of T cell receptors in the thymus (thymic selection), only foreign peptides alert the T cell system to the presence of foreign invaders within the antigen-presenting cell.

3.2. The T Cell Receptor

The T cell receptor (TCR) also termed $\alpha\beta$ CD3 complex, consists of seven transmembrane polypeptides (Fig. 2). Two

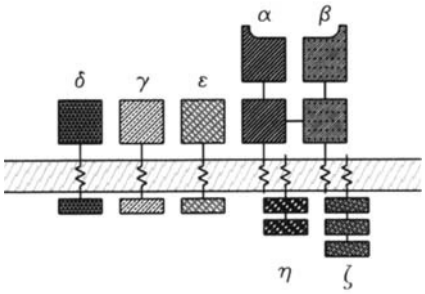

Fig. 2. Schematic representation of the components of the $\alpha\beta$ CD3 T cell receptor. The α and β chains form disulfide-linked heterodimers. The distal domains of both chains contain the binding sites for MHC peptide complexes. These two chains as well as the γ, δ, and ε chains belong to the Ig superfamily. η and ζ chains consist predominantly of cytoplasmic regions. Ig domains are indicated by squares, domains containing intracellular signal sequences, by rectangles. The ζ chain occurs as a homodimer or as a heterodimer with η. The exact composition of the CD3 complex is unknown, and there is no three-dimensional information on any of its components.

of these, the α and β chains, form a heterodimer that shows molecular diversity similar to antibody molecules and confers specific recognition properties to the TCR and to the T cells expressing it.[21, 22] Similar to antibody-producing B cells, T cells rearrange the genes for the α and β chains from a number of V (variable), D (diversifying), J (joining), and C (constant) gene segments in such a way that a very large number of different α and β chains are made. Yet one T cell expresses only a single pair ($\alpha\beta$) with one defined combining site structure. This pair of rearranged receptor genes is transmitted to all progeny of a T cell, accounting for the fact that all members of a clone of T cells have the same recognition specificity. The gene structure of the T cell receptor and its rearrangement have been described in detail.[8, 13] Both α and β chains have two extracellular Ig domains; the distal domains carry the variable portions and form the combining site for the MHC/peptide complex, the proximal domains are invariant. The α and β chains are linked by a disulfide bridge and anchored in the cell membrane by transmembrane regions with very short cytoplasmic tails. There is no information to date on the three-dimensional structure of TCR $\alpha\beta$ heterodimers.

[*] Editorial note: New insights on MHC/peptide complexes from X-ray crystal structures were reported recently: D. H. Fremont, M. Matsumura, E. Stura, P. A. Peterson, I. A. Wilson, *Science* **1992**, *257*, 919; M. Matsumura, D. H. Fremont, P. A. Peterson, I. A. Wilson, *ibid.* **1992**, *257*, 927; see also M. Barinagu, *ibid.* **1992**, *257*, 880.

The five additional polypeptides of the CD3 complex (γ, δ, ε, η, ζ) are noncovalently associated with αβ. They have larger cytoplasmic regions and are strongly suspected to play a role in transmembrane signaling. The η and ζ subunits have extracellular portions consisting of only nine amino acids but have large intracellular tails carrying characteristic sequence motifs which are suspected to play a role in coupling the CD3 complex to intracellular protein tyrosine kinases.[23-25] They occur as ζ–ζ homodimers and ζ–η heterodimers. The η and ζ subunits are highly homologous to one another and to the γ chain of the high-affinity IgE receptor (FcεRI);[26] together they form a new protein family of signal transducers with apparently similar function. The γ, δ, and ε subunits have extracellular Ig domains and are expressed as noncovalently associated δε and γε pairs.[27-29] Because of their relationship to the Ig superfamily[30] these chains have been suspected to be involved in coupling the CD3 complex to other surface receptors (see below). Their cytoplasmic parts contain sequence motifs similar to those which characterize the η and ζ subunits, but with fewer repeats.[31]

3.3. The Accessory Molecules CD4 and CD8

These molecules were first known as *markers* by which the two major subsets of T cells, helper and killer T cells, can be distinguished by using appropriate monoclonal antibodies.[2, 32, 33] The molecules became of interest with the discovery that, without exception, CD4 T cells carry αβ TCR that recognizes MHC class II and CD8 T cells carry αβ TCR that recognizes MHC class I.[2] Since in principle there is no differences between the αβ TCR of the two types of cells, it became clear that CD4 and CD8 themselves are involved as receptors in MHC recognition.

Both CD4 and CD8 are members of the Ig superfamily.[11, 12, 34, 35] CD4 is a monomeric transmembrane polypeptide with four extracellular Ig-like domains (Fig. 3). In a crystallographic study on a fragment comprising the two distal domains, both were shown to be tightly and rigidly connected by a continuous strand of a β sheet.[36, 37] CD8 is a disulfide-linked heterodimer of α and β chains, each carrying a single Ig-like domain which is linked by a hinge region to its transmembrane part (Fig. 3). There is no information on the three-dimensional structure of CD8,[*] but functional considerations suggest that the Ig domains of the α and β chains of CD8 are at the same distance from the cell surface as the most distal domain of CD4. The hinge regions of both chains must thus have highly extended linear structures. The cytoplasmic tails of both CD4 and of the α chain of CD8 are associated with the cytoplasmic protein tyrosine kinase $p56^{lck}$ (lck).[38-40]

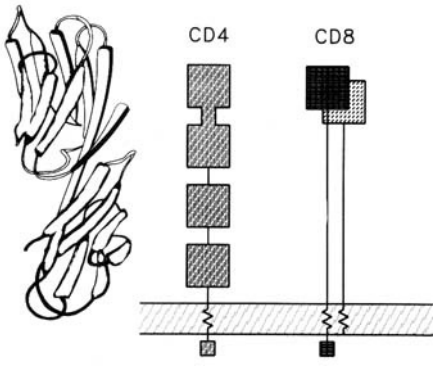

Fig. 3. Schematic representation of the accessory molecules CD4 and CD8. Ig-like domains are indicated by patterned squares. The crystal structure of a fragment corresponding to the two distal Ig domains of CD4 is shown on the left (cf. ref. [36, 37]). The rigid connection of the two domains by a β strand suggests that they form a functional unit. The two Ig domains of CD8 (α and β) may form a similar structure as the two distal domains of CD4 as an alternative to the configuration shown. The cytoplasmic tails of CD4 and of the CD8 α chain contain a sequence which serves as contact site for $p56^{lck}$.

When overexpressed in COS cells,[**] CD4 mediates adhesion to cells expressing MHC class II,[41] and the CD8 α chain mediates adhesion to cells expressing MHC class I.[42, 43] The binding site of CD4 for MHC class II has been broadly defined by mutagenesis experiments; it extends across one side of the two distal Ig domains and overlaps with the smaller and more concise region involved in HIV-GP120 binding.[44, 45] The binding site of MHC class II for CD4 is unknown but is expected to reside within nonpolymorphic regions, that is, in the α2 and/or β2 domains.

The binding site of CD8 for MHC class I has been shown by mutagenesis experiments to involve the Ig domain of the α chain.[46] The binding site for CD8 on MHC class I has been mapped by mutagenesis experiments and by the study of natural variants to a defined region within the α3 domain, also a conserved portion of the molecule.[43, 47-49]

3.4. Molecules Involved in Tyrosine Phosphorylation

3.4.1. Tyrosine Kinases

T cell receptors appear to activate two signal transduction pathways.[50] One involves phospholipase Cγ1 (PLCγ1) which cleaves phosphatidyl inositol into inositol phosphates and diacylglycerol, resulting in a rise in intracellular Ca^{2+} levels, on the one hand, and in activation of protein kinase C on the other. This leads to the phosphorylation of serin in numerous components including the CD3γ chain[51] and to rapid activation of secondary messengers such as p21 ras and c-raf kinase.[52, 53] It is not known how the CD3 complex is coupled to PLCγ1 or to further messenger systems that reach the cell nucleus.[50] The second perhaps more relevant signal transduction pathway appears to involve tyrosine phosphorylation of several substrates including CD3ζ and PLCγ1.[54-56] None of the CD3 subunits possess intrinsic protein tyrosine kinase (PTK) activity but cytoplasmic PTKs appear to be associated with components of CD3 as well as with CD4 and CD8: fyn[50] and lck,[38-40] both members of the src family. Little is known about fyn, except that it can be coprecipitated with the CD3 complex; lck forms a coimmunoprecipitate with both CD4 and CD8.[38-40] It binds to a distinct cystein-rich sequence in their cytoplasmic tails, as shown by deletional and mutational analyses.[57-59] lck was first described as a tyrosine kinase that was overexpressed in a lymphocytic leukemia.[38] Whereas the carboxyl terminal

[*] The crystal structure of a CD8α homodimer was in the meantime reported: D. J. Kahy, R. Axel, W. A. Hendrickson, *Cell*, **1992**, *68*, 1145.

[**] COS cells: Denotation for one of the cell lines derived from the established simian kidney cell line CV1 by treatment of the cells with a mutant of the simian virus SV40.

part of the molecule is highly homologous to members of the src family, unique features of the amino terminus include the binding motif for CD4/CD8 and the myristilation site that mediates association with the inner face of the T cell membrane (Fig. 4). Two tyrosine residues, 394 and 505, appear to regulate lck activity: phosphorylation of Tyr 394 enhances lck activity, whereas phosphorylation of Tyr 505 results in loss of kinase activity. Indeed, mutation of Tyr 505 to phenylalanine converts lck to a constitutively active form.[60]

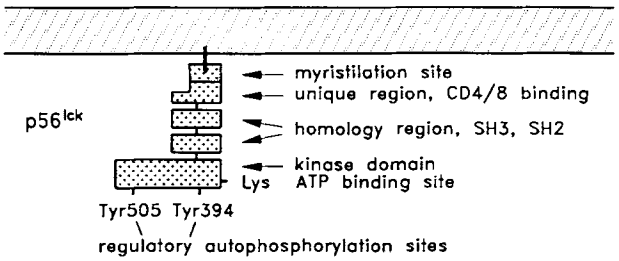

Fig. 4. Schematic representation of $p56^{lck}$ pointing out the typical structural properties of all members of the src tyrosin kinase family (taken from ref. [60]). The CD4/CD8 binding region is unique to $p56^{lck}$. Homologous regions SH3 and SH2 may interact with components of the cytoskeleton. Autophosphorylation of the regulatory tyrosine residues has been suggested to alter the angle of attachment of the kinase domain to the rest of the molecule, thereby regulating kinase activity [60].

3.4.2. CD45, a Tyrosine Phosphatase

Originally termed "leucocyte common antigen", CD45 is expressed on all cells of hemopoetic origin.[61] It consists of an extracellular domain, a transmembrane region, and a cytoplasmic tail with two tyrosine phosphatase domains in tandem (Fig. 5).[62, 63] Isolated CD45 has tyrosine-specific phosphatase activity.[63]

The extracellular domain of CD45 is of special interest because it occurs in multiple molecular versions due to differential RNA splicing.[61] This part of the molecule is encoded by seven exons, three of which, termed A, B, and C, may be differentially spliced, accounting for a total of eight possible isoforms[64] (Fig. 5). The complete molecule containing exons A, B, and C is expressed on all white blood cells.[61] In contrast, the incomplete versions are expressed in a restricted fashion (CD45R) and mark T cells at distinct stages of differentiation: naive peripheral T cells express incomplete isoforms containing one or two of the three variable exons mostly including A (CD45RA) or B (CD45RB), whereas memory T cells express a short version lacking all three exons (CD45RO).[64-76] The latter form may also be expressed on immature thymocytes.[68, 69]

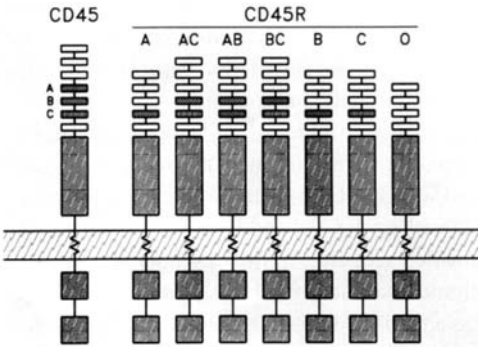

Fig. 5. Schematic representation of the complete CD45 molecule (left) and the family of splicing isoforms. The isoforms containing exon A (CD45RA) and B (CD45RB) can be distinguished from complete CD45 and from CD45RO by monoclonal antibodies. Not all possible isoforms have been clearly demonstrated to be expressed on T cells. The molecule does not belong to the Ig superfamily. The intracellular portion has been shown by structural and functional analyses to be a protein tyrosine phosphatase (see ref. [61]).

The expression of different versions of the CD45 extracellular domain at defined stages of T cell differentiation strongly suggests that CD45 plays a regulatory role in recognition-related signal transduction. It is likely that the various isoforms interact with other cell surface molecules either on the same or on a different cell. For example, low molecular weight isoforms on memory T cells have been shown to associate with components of the CD3 complex or with CD4,[77, 78] whereas high molecular weight isoforms seem to behave independently of the TCR in the membrane of naive T cells.[77]

The PTK lck can act as a substrate of CD45.[79, 80] This was studied in crosslinking experiments[80] and in transfected cell lines expressing lck with CD4 or CD8 in the presence and absence of CD45.[79] The degree of autophosphorylation of lck upon surface crosslinking of CD4/CD8 was reduced in the presence of CD45. Moreover, crosslinking of CD45 to CD4/CD8 led to dephosphorylation of lck. In these experiments, dephosphorylation of lck was accompanied by an increase in kinase activity of lck, suggesting that CD45 regulates lck activity through dephosphorylation of Tyr 394. Antibodies to CD45 had inhibitory or stimulatory effects on several cellular functions.[81-84]

4. Experimental Approaches to Studying T Cell Activation Molecules

Two genetic methods are being used to assess the functional role of T cell activation molecules. The first involves the selection of loss variants of T cell lines or clones growing in vitro and/or their transfection with the appropriate normal or mutated genes to reexpress molecules under study. This approach is restricted to T cells growing in vitro, which are by definition activated T cells, that is, they are at a late stage of differentiation. The second method is the study of genetically manipulated mice in which relevant genes are introduced as transgenes or are inactivated by homologous recombination in embryonic stem cells. Transgenic expression or deletion ("knockout") of the molecules discussed in this review mostly leads to perturbation of the maturation of T cells in the thymus; this restricts the information of this approach to the early stages of T cell development. Naive peripheral T cells are per definition resting and thus cannot be continually cultured in vitro. Nevertheless, this cell type must be the primary target of studies on T cell activation. These studies, therefore, often utilize primary T cells recovered ex vivo from blood or lymphoid organs which are analyzed in short-term culture. Since this type of experiment does not allow genetic manipulation of clonal cells, results are often not as unambigious. In contrast, the interpretation of results from genetic experiment is limited by the fact that

the studies apply to the very early and very late stages of T cell differentiation.

4.1. Transmembrane Signaling of Resting Peripheral T Lymphocytes

In this section the molecular events at the membrane of naive peripheral T cells during T cell activation will be described. This is only the beginning of a complicated cascade of molecular processes extending through the cytoplasm into the nucleus, eventually resulting in the induction of gene transcription. Restricting myself to the initial steps, I refer the reader to a competent recent review[50] of the intracellular events following activation.

Physiological T cell activation involves the interaction of a T cell with an antigen-presenting cell (APC) and includes the specific recognition by the αβ heterodimer on the T cell membrane of the MHC molecule presenting a peptide on the APC. The interaction between two cells is difficult to study on the molecular level. Attempts to reduce the complexity include using truncated soluble receptor molecules, an approach which has thus far not been fully successful. Alternatively, ligands on the surface of the APC have been replaced by soluble reagents such as mitogenic lectins or antibodies. Lectins have proven useful to some extent, but their ligand specificity is often broad and undefined. Monoclonal antibodies (mAbs) of defined specificity for individual T cell surface molecules have been successfully used in these studies, and some key experiments will be discussed here.

4.1.1. The Importance of Crosslinking

Addition of a mAb to any component of the αβ CD3 complex to a culture of peripheral lymphocytes from blood or spleen leads to the activation of the T cells in the culture. Various parameters can be used to monitor this T cell activation such as increase in cell size, mobilization of Ca^{2+}, activation of several enzymes, transcription of genes for lymphokines and lymphokine receptors, cell division etc.[85–88] mAbs to a handful of other T cell surface components also can cause activation, but the significance of this observation is not clear.[89] I will restrict this discussion to signaling events involving the αβ CD3 complex that reflect T cell activation by a specific antigenic challenge.

Activation of T cells by anti-TCR mAbs requires the presence of non-T cells having Fc receptors, for example macrophages. After depletion of Fc receptor positive cells from the culture, anti-TCR mAb is unable to activate T cells. However, T cells depleted of Fc receptor positive cells can be activated efficiently by anti-TCR mAb coupled to a solid-phase carrier.[88, 90, 91] This demonstrates that individual ligation (or even dimerization) of the TCR is insufficient to activate a T cell. Cell surface aggregation of the TCR is required for successful transmembrane signaling.

4.1.2. The Role of CD4 and CD8 in Resting T Cells

Soluble mAbs to CD4 and CD8 inhibit the activation of the corresponding T cell regardless of whether the activation is induced by APC, lectins, or anti-TCR mABs bound to a solid support.[90, 92–99] Since the latter two activation protocols do not involve MHC molecules as ligands for CD4 or CD8, inhibition by anti-CD8/4 mAbs could not be due to blocking of MHC binding. This has raised a long discussion on the possibility that the accessory molecules are receptors of negative or inactivating signals to T cells. Although this is still maintained by some investigators,[100] negative signaling is in my opinion excluded by the following findings: The efficiency of the activation of T cells by crosslinking the TCR by anti-TCR mAbs is enhanced by at least two orders of magnitude when antibodies to CD8/CD4 are included, that is when the TCR is coaggregated with CD8/CD4.[90, 92, 93, 101–105] When heterozygous T cells expressing two different CD8 alleles were used, activation was achieved by coaggregation of only one of the CD8 alleles to the TCR. This activation could be inhibited by antibodies to the coaggregated CD8 allele but not by antibodies to the free CD8 allele.[92] This experiment shows that inhibition of T cell activation by anti-CD8/4 mAbs occurs by blocking of the association of the accessory molecule with the TCR. Aggregation of the TCR alone—by whatever ligand—induces a sufficient degree of association with CD4/CD8 for low-level activation to occur, which is blocked by anti-CD4/CD8 mAbs. The spontaneous association due to TCR crosslinking is greatly enhanced when the accessory molecule is forcefully coaggregated with the TCR, either experimentally by solid-phase antibodies, or physiologically by MHC molecules on APC, to which both the TCR and the accessory molecule bind at the same time. This model predicts that the accessory molecules must have two combining regions, one for the MHC molecule on the APC and the other for the TCR on the same T cell (see next section).

It is generally accepted that the close proximity between the TCR and CD4/CD8 required in the activation of resting T cells is related to the necessity of relocating the protein tyrosine kinase (PTK) lck next to the CD3 complex. As mentioned in Section 3.4.1., lck is associated with CD8/CD4 on the inner face of the T cell membrane. Moreover, CD3 phosphorylation and TCR-CD4 association is induced in parallel by the same antibodies.[100] The sole purpose of the formation of the TCR–CD4/CD8 complex may thus be to achieve tyrosine phosphorylation of the CD3 ζ chain.

4.1.3. Relationship between CD4/CD8 and the T Cell Receptor in the Resting State

The studies of transmembrane signaling in resting peripheral T cells described in the previous section suggest the formation of a complex between the TCR and CD4/CD8. This opens the question on the configuration of both molecular components in the resting state itself. The simplest assumption would be that the two components on the T cell membrane are completely independent and that proximity between the two is induced only upon binding with the appropriate ligand (Fig. 6 top). Some experimental evidence has been reported in favor of this model.[106–109] However, a number of previous indirect experiments have suggested that some form of association exists continually.[110–113] This has been confirmed recently by direct immunoprecipita-

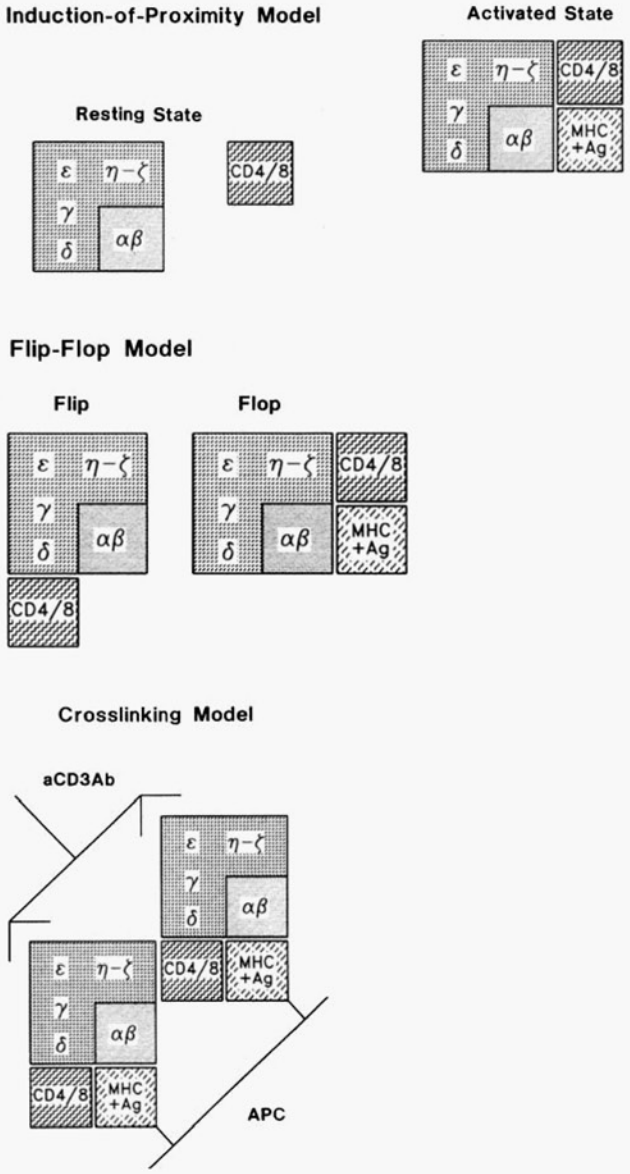

Fig. 6. Three models for complex assembly between αβ CD3, the accessory molecules CD4/CD8, and the MHC/peptide complex during T cell activation. Top: The "induction-of-proximity" model predicts that the accessory molecules and αβ CD3 on the T cell membrane are independent of each other in the absence of the MHC/peptide complex. Mutual binding of both components to the MHC/peptide complex induces proximity between CD4/CD8 and αβ CD3 on the outer cell surface, as a consequence leading to proximity between lck and cytoplasmic tails of CD3 components on the inner face of the T cell membrane. Middle: The "flip-flop" model takes the association of the accessory molecules CD4/CD8 with the CD3 δ chain on resting T cells into account. It predicts two different configurations of the complex, one in which the association between CD4/CD8 and CD3 δ maintains the resting state, and another in which MHC-binding induces the flipover of CD4/CD8 to CD3 ζ, thus leading to ζ chain phosphorylation and T cell activation. Bottom: The "crosslinking model" does not require alterations within the complex during activation. It can explain activation of T cells by MHC on APC as well as by antiCD3 antibody-mediated crosslinking. However, it is possible that antibody-induced T cell activation occurs according to the crosslinking model, whereas T cell activation by MHC/peptide binding occurs according to the flip-flop model.

tion experiments, which clearly demonstrate that CD4/CD8 are associated with the CD3 δ chain on resting T cells.[114] Virtually every CD3 δ is associated with an accessory molecule. In contrast, after activation this association is no longer found. This suggests that the TCR–CD4/CD8 complex is highly dynamic and oscillates between several different conformations, each relating to a functional status of the T cell.

4.1.4. Models for the Formation of the Activation Complex

A Flip-Flop Model

In the resting state (flip state), CD4/CD8 is associated with the CD3 δ chain.[114] For activation, lck must be relocated next to the CD3 ζ chain. It is thus possible that CD4/CD8 flips over from CD3 δ to CD3 ζ (flop state), carrying lck along (Fig. 6 middle). In this model, lck would be kept at a distance from CD3 ζ in the resting state, thus preventing an accidental encounter followed by activation, unless the proper MHC peptide complex induces the flop state. This model requires the induction of conformational changes within at least one member of the complex.

A Crosslinking Model

This mechanism may indeed coexist with a flip-flop mechanism. It simply proposes that aggregation of the complex which exists in the resting state may result in accidental proximity between CD3 ζ and CD4/CD8-lck, which induces activation (Fig. 6 bottom). In contrast to the flip-flop model, there is no mechanism that prevents accidental activation in this model. There is also no requirement for conformational changes.

Figure 7 shows a currently accepted schematic representation of a possible configuration of the activation complex during transmembrane signaling. It is obvious that this is a

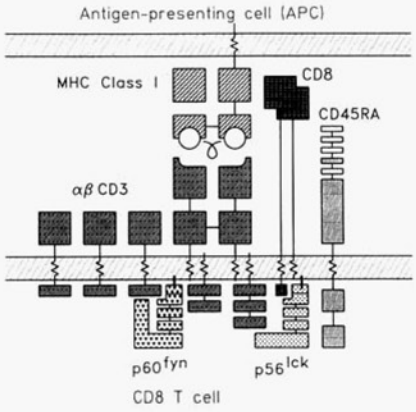

Fig. 7. Possible configuration of the T cell recognition complex during activation. The precise molecular association of $p60^{fyn}$ with components of the CD3 complex is unknown. The molecules interacting with CD45 or CD45R isoforms are also unknown. A similar picture may be drawn for MHC class II and CD4.

minimal model. There is insufficient information on CD45, for example, to make reasonable predictions on its involvement in the activation complex. More sophisticated techniques must be developed to elucidate multimolecular functional complexes within cellular membranes.

4.2. Transmembrane Signaling in Activated T Cells

Upon further encounter with the antigen-presenting cells (APCs), activated T cells respond either with or without the induction of transcriptional activity. For example, the induction of the release of cytolytic molecules from activated $CD8^+$ cytotoxic T cells (CTL) requires no transcription. In

contrast, production of cytokines by activated $CD4^+$ or $CD8^+$ T cells in most cases requires induction of transcription of the corresponding genes. Tissue culture lines or hybridomas representing most types of activated T cells have been established, so that their study have most successfully employed a genetic approach. In the first place, transfection of the genes for the α and β chains of individual TCR into hybridomas have established that the $\alpha\beta$ heterodimer of the CD3 complex alone is responsible for the specificity of a T cell to a certain MHC/peptide complex.[21, 22] Nevertheless, these experiments also revealed that the recognition process itself was inefficient without the proper accessory molecule: TCRs recognizing MHC class I molecules required CD8,[115–118] whereas TCRs recognizing MHC class II molecules required CD4 for optimal recognition;[119] the improper heterologous accessory molecules also had some improving effect.[119–123] These experiments formed the basis for the hypothesis on the affinity-enhancing role of accessory molecules: The binding of both the TCR and the accessory molecule to the same MHC target efficiently enhanced a per se low-affinity TCR–MHC interaction; much less enhancement was observed when the accessory molecule bound to a different MHC molecule on the APC.

More ambigious results were obtained when the signaling role of accessory molecules was assessed in activated T cells. One type of experiment employed transfection of the genes deleted of their cytoplasmic tail, in other words their products were not able to associate with lck. These truncated accessory molecules nevertheless enhanced activation by APC, albeit less efficiently than the complete accessory molecules.[124–127] Another type of experiment employed CD8-deficient variants of CTL and their CD8 transfectants. Whereas the activation of these cells by APCs was essentially dependent on CD8, their activation by anti-TCR mAbs was fully maintained in CD8 loss variants, both for transcriptional and nontranscriptional responses.[117, 118, 128] Together, these results suggest that activated T cells are to some degree independent of the transmembrane signaling function of the accessory molecules. This is brought out in situations in which the TCR is engaged with a high-affinity ligand, for example anti-TCR mAb. These interpretations are also in line with previous observations on single activated $CD8^+$ and $CD4^+$ T cell lines and clones which cannot be inhibited by anti-CD8/4 mAb.[129–131] Variants selected from T cell clones for low expression of CD4 have been shown to be even more sensitive to activation by APC than the cells expressing CD4 at a normal level.[132] Experiments using hybridoma cells transfected with CD3 $\gamma\delta\varepsilon$ without functional CD3 ζ have revealed efficient induction of transcriptional responses, also suggesting a partial independence of activated T cells of the CD4/CD8–lck–CD3 ζ signaling pathway. It was proposed that the CD3 $\gamma\delta\varepsilon$ components provide an alternative transmembrane signaling route.[31] It is possible that this pathway is relatively inactive in naive T cells and takes over in activated T cells.

4.3. The Bifunctional Nature of Accessory Molecules

The activation of resting naive T cells depends primarily on transmembrane signaling by TCR–CD4/CD8 association. In contrast, transmembrane signaling in activated T cells is partly independent of CD4/CD8. Nevertheless, most activated T cells depend on CD4/CD8 for MHC/peptide recognition, undoubtedly through their MHC-binding function. This situation was utilized in a recent study in which, using monoclonal anti-CD8 mAbs, epitopes related to the binding of MHC to CD8 could be distinguished from epitopes related to TCR association.[133] The study showed that distinct regions on the CD8 molecule are involved in either function. Moreover, both functions involved epitopes on the α and the β chain of CD8. Whereas the MHC-binding region is undoubtedly associated with the V domain of the α and perhaps also the β chain, there is no structural information as yet on the location of the TCR-binding region. Logically this region should be somewhere between the V region and the cell surface, that is, within the hinge region of CD8 (Fig. 7).

5. The Recognition Complex in Thymic Selection

Thymic selection requires the intact thymus either in vivo or in organ culture. It has therefore not been possible to analyze events inducing selection of T cell receptors in the thymus at the level of single cells, not to speak of single molecules. Biochemical signaling pathways leading to positive and negative selection responses have thus, with some exception,[134] not been studied conclusively to date. Nevertheless, highly sophisticated experimental protocols, utilizing transgenic mice or mice in which individual genes have been deleted, have allowed the functional roles of several members of the T cells recognition complex in thymic selection to be assessed.

The role of the TCR $\alpha\beta$ heterodimer was studied in mice transgenic for rearranged α and β genes isolated from individual CD8 or CD4 T cell clones with known MHC/peptide recognition.[5, 6] Encounter of the TCR $\alpha\beta$ heterodimer with the homologous MHC/peptide complex during the development of T cells in the thymus induced deletion by apoptotic cell death, thus preventing self-reactive cells to emerge from the thymus. If the T cells failed to encounter the correct MHC molecule in the thymus they did not mature. Successful maturation and generation of mature T cells leaving the thymus depends on the presence of the correct MHC molecule during thymic development. These results proved that the TCR $\alpha\beta$ heterodimer was instrumental in thymic selection: Encounter with the self-MHC/self-peptide complex induces a deletional response, encounter of self MHC alone induces a maturational response, failure to encounter a fitting structure results in developmental arrest.

T cells carrying transgenes for a TCR with MHC class I recognition emerge from the thymus only as $CD8^+$ cells, whereas T cells carrying transgenes for a TCR with MHC class II recognition emerge from the thymus only as $CD4^+$ cells. These results suggest that only those T cells in which the specificity of the $\alpha\beta$ TCR correlates to the accessory molecule are allowed to become positively selected and mature. This has been shown to be the result of an instructional process which occurs at the stage at which immature T cells in the thymus express both CD4 and CD8 and which ends with the shutdown of the expression of the noncorresponding accessory molecule.[135, 136] A reasonable assumption is

that thymocytes are positively selected when the αβ TCR and the accessory molecule bind to the same MHC molecule.[137] Mice carrying mutated transgenic MHC molecules that are unable to bind CD8 or CD4 can neither positively nor negatively select T cells that recognize such MHC molecules.[138] Thus, some form of cooperation between the TCR and the accessory molecules appears to be required for both positive and negative selection. The differences between transmembrane signaling events leading to positive and negative selection responses are the subject of current intense investigation. These experiments with transgenic mice have been recently complemented by research with mouse strains in which the corresponding genes are deleted. As expected, mice that fail to express MHC class I[139] or class II[140] molecules fail to develop CD8 and CD4 T cells, respectively. In addition, mice that fail to express CD8 or CD4 molecules fail to develop T cells whose TCRs recognize MHC class I and class II molecules, respectively.[141]

Taken together, there is little doubt that the same recognition system that allows for T cell activation in the periphery is also involved in thymic selection. Nevertheless, the responses elicited in thymocytes differ distinctly from those in peripheral T cells. These differences may result from the way in which the recognition complex is assembled or which individual members of the complex are coupled to second and subsequent messenger systems in the cytoplasm. There is little doubt that the T cell recognition complex is one of the most sophisticated and versatile signaling structures in biology.

6. Conclusion

T lymphocytes are capable of recognizing other cells containing foreign living or nonliving matter (antigen presenting cells, APCs). These foreign structures are broken down within the APC, and resulting peptides are complexed with newly synthesized MHC molecules which are then exposed on the cell membrane. Complexes of MHC molecules with foreign peptides are recognized and bound by a recognition complex composed of specific and nonspecific components on the T cell membrane. As a consequence of recognition and binding, specific and nonspecific members of the recognition complex assemble in the T cell membrane in such a way that transmembrane signaling results, most likely through relocation and activation of membrane-associated protein tyrosine kinases and phosphatases and tyrosine phosphorylation/dephosphorylation. The cellular responses elicited by this complex are diverse and differ according to the stage of T cell development and differentiation. Factors determining the nature of the response may reside in the numerous ways of complex assembly or in differential coupling to intracellular messengers.

Further analyses leading to a more detailed understanding of the T cell activation complex would be highly desirable, both for the development of better theoretical models and for applications in medicine. Methods could be designed for medical interference with immune disorders such as autoimmune diseases, allergies, and immunodeficiencies. This would require new technologies for the analysis of complexes of macromolecules as they exist in cell membranes, including their dynamic changes. In the past, immunology has greatly benefitted from basic analytical technology developed in many other scientific disciplines, including chemistry. The task of developing methods for the analysis of macromolecular complexes and their dynamics may provide a new challenge for chemists, particularly protein and membrane chemists. Such an effort, if successful, would result in a much deeper insight than is presently possible into functional events at cell membranes, including transmembrane signaling of T lymphocytes.

Received: April 27, 1992 [A 889 IE]
German version: *Angew. Chem.* **1993**, *105*, 56

[1] J. B. Rothbard, M. L. Gefter, *Annu. Rev. Immunol.* **1991**, *9*, 527.
[2] S. L. Swain, *Immunol. Rev.* **1983**, *74*, 129.
[3] G. Möller (Ed.), *Immunol. Rev.* **1987**, *98*.
[4] G. Möller (Ed.), *Immunol. Rev.* **1988**, *104*.
[5] H. A. von Boehmer, *Annu. Rev. Immunol.* **1988**, *6*, 309.
[6] B. J. Fowlkes, D. M. Pardoll, *Adv. Immunol.* **1989**, *44*, 207.
[7] G. Möller (Ed.), *Immunol. Rev.* **1986**, *91*.
[8] M. M. Davis, P. J. Bjorkman, *Nature* **1988**, *334*, 395.
[9] J. D. Ashwell, R. D. Klausner, *Annu. Rev. Immunol.* **1990**, *8*, 139.
[10] B. E. Bierer, B. P. Sleckman, S. E. Ratnofsky, S. J. Burakoff, *Annu. Rev. Immunol.* **1989**, *7*, 579.
[11] J. R. Parnes, *Adv. Immunol.* **1989**, *44*, 265.
[12] D. R. Littman, *Annu. Rev. Immunol.* **1987**, *5*, 561.
[13] P. Marrack, J. Kappler, *Adv. Immunol.* **1986**, *38*, 1.
[14] G. Möller (Ed.), *Immunol. Rev.* **1990**, *113*.
[15] *Molecular Evolution of the Major Histocompatibility Complex* (Eds.: J. Klein, D. Klein), (*NATO ASI Ser. H: Cell Biol.* **1991**, *59*).
[16] A. F. Williams, A. N. Barclay, *Annu. Rev. Immunol.* **1988**, *6*, 381.
[17] O. Rötzsche, K. Falk, *Immunol. Today* **1991**, *12*, 447.
[18] T. S. Jardetzky, W. S. Lane, R. A. Robinson, D. R. Madden, D. C. Wiley, *Nature* **1991**, *353*, 326.
[19] G. M. Van Bleek, G. G. Nathensen, *Nature* **1990**, *348*, 213.
[20] O. Rötzsche, K. Falk, K. Deres, H. Schild, H. Narda, J. Metzger, G. Jung, H. G. Rammensee, *Nature* **1990**, *348*, 252.
[21] Z. Dembic, W. Haas, S. Weiss, J. McCubrey, H. Kiefer, H. von Boehmer, M. Steinmetz, *Nature* **1986**, *320*, 232.
[22] T. Saito, A. Weiss, J. Miller, M. A. Norcross, R. N. Germain, *Nature* **1987**, *325*, 125.
[23] A. M. Weissman, M. Baniyash, D. Hou, L. E. Samelson, W. H. Burgess, R. D. Klausner, *Science* **1988**, *239*, 1018.
[24] Y. J. Jin, L. K. Clayton, F. D. Howard, S. Koyasu, M. Sieh, R. Steinbrich, G. E. Tarr, E. L. Reinherz, *Proc. Natl. Acad. Sci. USA* **1990**, *87*, 3319.
[25] M. Reth, *Nature* **1989**, *338*, 383.
[26] H. Küster, H. Thompson, J. P. Kinet, *J. Biol. Chem.* **1990**, *265*, 6448.
[27] F. Koning, W. L. Maloy, J. E. Coligan, *Eur. J. Immunol.* **1990**, *20*, 299.
[28] R. S. Blumberg, S. Ley, J. Sancho, N. Lonberg, E. Lacy, F. McDermott, V. Schad, J. L. Greenstein, C. Terhorst, *Proc. Natl. Acad. Sci. USA* **1990**, *87*, 7220.
[29] A. de la Hera, U. Müller, C. Olsson, S. Isaaz, A. Tunnacliffe, *J. Exp. Med.* **1991**, *173*, 7.
[30] D. P. Gold, H. Clevers, B. Alarcon, S. Dunlap, J. Novotny, A. Williams, C. Terhorst, *Proc. Natl. Acad. Sci.* USA **1987**, *84*, 7649.
[31] A. M. K. Wegener, F. Klournier, A. Noevelar, T. Broker, F. Luton, B. Malissen, *Cell* **1992**, *68*, 83.
[32] H. Cantor, E. A. Boyse, *J. Exp. Med.* **1975**, *141*, 1376.
[33] D. P. Dialynas, D. B. Wilde, P. Marrack, A. Pierres, K. A. Wall, W. L. Havran, G. K. Otten, M. R. Loken, M. Pierres, J. Kappler, F. W. Fitch, *Immunol. Rev.* **1983**, *74*, 29.
[34] P. J. Maddon, D. R. Littman, M. Godfrey, D. E. Maddon, L. Chess, R. Axel, *Cell* **1985**, *42*, 93.
[35] P. J. Maddon, S. M. Molineaux, D. E. Maddon, K. A. Zimmerman, M. Godfrey, F. W. Alt, L. Chess, R. Axel, *Proc. Natl. Acad. Sci.* **1987**, *84*, 9155.
[36] J. Wang, Y. Yan, T. P. J. Garrett, J. Liu, D. W. Rodgers, R. L. Garlick, G. E. Tarr, Y. Husain, E. L. Reinherz, S. C. Harrison, *Nature* **1990**, *348*, 411.
[37] S.-E. Ryu, P. D. Kwong, A. Truneh, T. G. Porter, J. Arthos, M. Rosenberg, X. Dai, N.-H. Xuong, R. Axel, R. W. Sweet, W. A. Hendriekson, *Nature* **1990**, *348*, 419.
[38] J. D. Marth, E. G. Peet, E. G. Krebs, R. M. Perlmutter, *Cell* **1985**, *43*, 393.
[39] C. E. Rudd, J. M. Trevillyan, J. V. Dasgupta, L. L. Wong, S. F. Schlossman, *Proc. Natl. Acad. Sci. USA* **1988**, *85*, 5190.
[40] A. Veillette, M. A. Bookman, E. M. Horak, J. B. Bolen, *Cell* **1988**, *55*, 301.
[41] C. Doyle, J. L. Strominger, *Nature* **1987**, *330*, 256.
[42] A. M. Norment, R. D. Salter, P. Parham, V. H. Engelhard, D. R. Littman, *Nature* **1988**, *336*, 79.
[43] R. D. Salter, A. M. Norment, B. P. Chen, C. Clayberger, A. M. Krensky, D. R. Littman, P. Parham, *Nature* **1989**, *338*, 1.
[44] D. Lamarre, A. Ashkenazi, S. Fleury, D. H. Smith, R. P. Sekaly, D. J. Capon, *Science* **1989**, *245*, 743.

[45] L. K. Clayton, M. Sieh, D. A. Pious, E. L. Reinherz, *Nature* **1989**, *339*, 548.
[46] S. K. Sanders, R. O. Fox, P. Kavathas, *J. Exp. Med.* **1991**, *174*, 371.
[47] J. M. Connolly, T. H. Hansen, A. L. Ingold, T. A. Potter, *Proc. Natl. Acad. Sci. USA* **1990**, *87*, 2137.
[48] T. A. Potter, T. V. Rajan, R. F. Dick II, J. A. Bluestone, *Nature* **1989**, *337*, 73.
[49] R. D. Salter, R. J. Benjamin, P. K. Wesley, S. E. Buxton, T. P. J. Garrett, C. Clayberger, A. M. Krensky, A. M. Norment, D. R. Littman, P. Parham, *Nature* **1990**, *345*, 41.
[50] R. D. Klausner, L. E. Samelson, *Cell* **1991**, *64*, 875.
[51] D. A. Cantrell, A. A. Davies, M. J. Crumpton, *Proc. Natl. Acad. Sci. USA* **1985**, *82*, 8158.
[52] J. Downward, J. D. Graves, P. H. Warne, S. Rayter, D. A. Cantrell, *Nature* **1990**, *348*, 719.
[53] J. N. Siegel, R. D. Klausner, U. R. Rapp, L. E. Samelson, *J. Biol. Chem.* **1990**, *265*, 18472.
[54] L. E. Samelson, M. D. Patel, A. M. Weissman, J. B. Harford, R. D. Klausner, *Cell* **1986**, *46*, 1083.
[55] D. J. Park, H. W. Rho, S. G. Rhee, *Proc. Natl. Acad. Sci. USA* **1991**, *88*, 5453.
[56] A. Weiss, G. Koretsky, R. Schatzman, T. Kadlecek, *Proc. Natl. Acad. Sci. USA* **1991**, *88*, 5484.
[57] A. S. Shaw, K. E. Amrein, C. Hammond, D. F. Stern, B. M. Sefton, J. K. Rose, *Cell* **1989**, *59*, 627.
[58] A. S. Shaw, J. Chalupny, J. A. Whitney, C. Hammond, K. E. Amrein, P. Kavathas, B. M. Sefton, J. K. Rose, *Mol. Cell. Biol.* **1990**, *10*, 1853.
[59] J. M. Turner, M. H. Brodsky, B. A. Irving, S. D. Levin, R. M. Perlmutter, D. R. Littman, *Cell* **1990**, *60*, 755.
[60] A. Veillette, N. Abraham, L. Caron, D. Davidson, *Semin. Immunol.* **1991**, *3*, 143.
[61] M. L. Thomas, *Annu. Rev. Immunol.* **1989**, *9*, 339.
[62] H. Charbonneau, N. K. Tonks, K. A. Walsh, E. H. Fisher, *Proc. Natl. Acad. Sci. USA* **1988**, *85*, 7182.
[63] N. K. Tonks, H. Charbonneau, C. D. Diltz, E. H. Fischer, K. A. Walsh, *Biochemistry* **1989**, *27*, 8695.
[64] L. Lefrancois, M. L. Thomas, M. J. Bevan, I. S. Trowbridge, *J. Exp. Med.* **1986**, *163*, 1337.
[65] E. B. Bell, S. M. Sparshott, *Nature* **1990**, *348*, 163.
[66] M. L. Birkeland, P. Johnson, I. S. Trowbridge, E. Pure, *Proc. Natl. Acad. Sci. USA* **1989**, *86*, 6734
[67] K. Bottomly, M. Luqman, L. Greenbaum, S. Carding, J. West, T. Pasqualini, D. Murphy, *Eur. J. Immunol.* **1989**, *19*, 617.
[68] C. Janossy, M. Bofill, D. Rowe, J. Muir, P. C. L. Beverley, *Immunology* **1989**, *66*, 517.
[69] D. A. Law, L. L. Spruyt, D. J. Paterson, A. F. Williams, *Eur. J. Immunol.* **1989**, *19*, 2289.
[70] M. Luqman, P. Johnson, I. Trowbridge, K. Bottomly, *Eur. J. Immunol.* **1990**, *20*, 17.
[71] M. Merkenschlager, P. C. L. Beverley, *Int. Immunol.* **1989**, *1*, 449.
[72] M. Merkenschlager, H. Ikeda, D. Wilkinson, P. C. L. Beverley, J. Trowsdale, A. G. Fisher, D. M. Altman, *Eur. J. Immunol.* **1991**, *21*, 79.
[73] F. Powrie, D. Mason, *J. Exp. Med.* **1989**, *169*, 653.
[74] F. Powrie, D. Mason, *Cur. Top. Microbiol. Immunol.* **1990**, *159*, 81.
[75] D. M. Rothstein, A. Yamada, S. F. Schlossman, C. Morimoto, *J. Immunol.* **1991**, *146*, 1175.
[76] M. Sanders, M. W. Makgoba, S. Shaw, *Immunol. Today* **1988**, *9*, 195.
[77] U. Dianzani, M. Luqman, J. Rojo, J. Yagi, J. L. Baron, A. Woods, C. A. Janeway, Jr., K. Bottomly, *Eur. J. Immunol.* **1990**, *20*, 2249.
[78] C. Volarevic, M. Burns, J. J. Sussman, J. D. Ashwell, *Proc. Natl. Acad. Sci. USA* **1990**, *87*, 7085.
[79] H. L. Ostergaard, I. S. Trowbridge, *J. Exp. Med.* **1990**, *172*, 347.
[80] J. A. Ledbetter, G. L. Schieven, F. M. Uckun, J. B. Imboden, *J. Immunol.* **1991**, *146*, 1577.
[81] J. A. Ledbetter, N. K.Tonks, E. H. Fischer, E. A. Clark, *Proc. Natl. Acad. Sci. USA* **1988**, *85*, 8628.
[82] J. Marvel, G. Poirier, E. Lightstone, *Eur. J. Immunol.* **1989**, *19*, 2005.
[83] G. Pawelec, H. J. Buhring, C. Muller, *Cell. Immunol.* **1990**, *127*, 514.
[84] T. C. R. Prickett, D. N. J. Hart, *Immunology* **1990**, *68*, 250.
[85] S. C. Meuer, R. E. Hussey, D. A. Cantrell, J. C. Hodgdon, S. F. Schlossman, K. A. Smith, E. L. Reinherz, *Proc. Natl. Acad. Sci. USA* **1984**, *81*, 1509.
[86] A. Weiss, J. Imboden, D. Shoback, J. Stobo, *Proc. Natl. Acad. Sci. USA* **1984**, *81*, 4169.
[87] A. Weiss, J. Imboden, K. Hardy, B. Manger, C. Terhorst, J. Stobo, *Annu. Rev. Immunol.* **1986**, *4*, 593.
[88] I. N. Crispe, M. J. Bevan, U. D. Staerz, *Nature* **1985**, *317*, 627.
[89] G. Möller (Ed.), *Immunol. Rev.* **1989**, *111*.
[90] K. Eichmann, N. W. Boyce, R. Schmidt-Ullrich, J. I. Jönsson, *Immunol. Rev.* **1989**, *109*, 39.
[91] C. A. Janeway, U. Dianzani, P. Portoles, S. Rath, E. P. Reich, J. Rojo, J. Yagi, and D. B. L. P. 6. Murphy, *Cold Spring Harbor Symp. Quant. Biol.* **1989**, *54*, 657.
[92] J. I. Jönsson, N. W. Boyce, K. Eichmann, *Eur. J. Immunol.* **1989**, *19*, 253.
[93] N. W. Boyce, J. I. Jönsson, F. Emmrich, K. Eichmann, *J. Immunol.* **1988**, *141*, 2882.
[94] M. Bekoff, T. Kakiuchi, H. M. Grey, *J. Immunol.* **1985**, *134*, 1337.
[95] C. A. Janeway, Jr., *Nature* **1988**, *335*, 208.
[96] P. Wassmer, C. Chan, L. Lodgeberg, E. M. Shevach, *J. Immunol.* **1985**, *135*, 2237.
[97] P. M. Rosoff, S. J. Burakoff, J. L. Greenstein, *Cell* **1987**, *49*, 845.
[98] J. P. Tite, A. Sloan, C. A. Janeway Jr., *J. Mol. Cell. Immunol.* **1986**, *2*, 179.
[99] I. Bank, L. Chess, *J. Exp. Med.* **1985**, *162*, 1294.
[100] U. Dianzani, A. Shaw, B. K. Al-Ramadi, R. T. Kubo, C. A. Janeway, Jr. *J. Immunol.* **1992**, *148*, 678.
[101] F. Emmrich, U. Strittmatter, K. Eichmann, *Proc. Natl. Acad. Sci. USA* **1986**, *83*, 8298.
[102] F. Emmrich, L. Kanz, K. Eichmann, *Eur. J. Immunol.* **1987**, *17*, 643.
[103] F. Emmrich, P. Rieber, R. Kurrle, K. Eichmann, *Eur. J. Immunol.* **1988**, *18*, 645.
[104] K. Eichmann, J. I. Jönsson, I. Falk, F. Emmrich, *Eur. J. Immunol.* **1987**, *17*, 643.
[105] P. Anderson, M. Blue, C. Morimoto, S. F. Schlossman, *J. Immunol.* **1987**, *139*, 678.
[106] A. Kupfer, S. J. Singer, C. A. Janeway Jr., S. L. Swain, *Proc. Natl. Acad. Sci. USA* **1987**, *84*, 5888.
[107] A. Kupfer, S. J. Singer, *Proc. Natl. Acad. Sci. USA* **1988**, *85*, 8216.
[108] A. Kupfer, S. J. Singer, *J. Exp. Med.* **1989**, *170*, 1697.
[109] R. S. Mittler, S. J. Goldman, G. L. Spitalny, S. J. Burakoff, *Proc. Natl. Acad. Sci. USA* **1989**, *86*, 8531.
[110] J. M. Rojo, C. A. Janeway, Jr., *J. Immunol.* **1988**, *140*, 1081.
[111] J. M. Rojo, K. Saizawa, C. A. Janeway, Jr., *Proc. Natl. Acad. Sci. USA* **1989**, *86*, 3311.
[112] K. Saizawa, J. Rojo, C. A. Janeway, Jr., *Nature* **1987**, *328*, 260.
[113] P. Anderson, M. L. Blue, S. F. Schlossman, *J. Immunol.* **1988**, *140*, 1732.
[114] S. Suzuki, J. Kupsch, K. Eichmann, K. M. Saizawa, *Eur. J. Immunol.* **1992**, *22*, 2475.
[115] Z. Dembic, W. Haas, R. Zamoyska, J. R. Parnes, M. Steinmetz, H. von Boehmer, *Nature* **1987**, *326*, 510.
[116] J. Gabert, C. Langler, R. Zamoyska, J. R. Parnes, A. M. Schmidt-Verhulst, B. Malissen, *Cell* **1987**, *50*, 545.
[117] R. Schmidt-Ullrich, K. Eichmann, *Int. Immunol.* **1990**, *2*, 247.
[118] D. Lj. Jankovic, D. Woodland, I. Melchers, H. U. Weltzien, R. T. Kubo, K. Eichmann, *J. Exp. Med.* **1986**, *163*, 1459.
[119] J. L. Greenstein, J. Kappler, P. Marrack, S. J. Burakoff, *J. Exp. Med.* **1984**, *159*, 1213.
[120] J. L. Greenstein, B. Malissen, S. J. Burakoff, *J. Exp. Med.* **1985**, *162*, 369.
[121] W. G. Ballhausen, A. B. Reske-Kunz, B. Tourvieille, P. S. Ohashi, J. R. Parnes, T. W. Mak, *J. Exp. Med.* **1988**, *167*, 1493.
[122] B. Jones, P. A. Khavari, P. J. Conrad, C. A. Janeway, Jr., *J. Immunol.* **1987**, *139*, 380.
[123] P. Aparicio, J. A. Lopez de Castro, *Hum. Immunol.* **1989**, *24*, 295.
[124] M. C. Miceli, P. von Hoegen, J. R. Parnes, *Proc. Natl. Acad. Sci. USA* **1990**, *88*, 2623.
[125] M. C. Miceli, J. R. Parnes, *Semin. Immunol.* **1991**, *3*, 133.
[126] N. Glaichenhaus, N. Shastri, D. R. Littman, J. M. Turner, *Cell* **1991**, *64*, 511.
[127] N. J. Chalupny, J. A. Ledbetter, P. Kavathas, *EMBO J.* **1991**, *10*, 1201.
[128] A. Reimann, A. Ehrfeld, J. Kupsch, B. Maier, K. M. Saizawa, B. Clinchy, K. Eichmann, *Immunol. Lett.* **1991**, *30*, 149.
[129] R. Shimonkevitz, B. Luescher, J. C. Cerottini, H. R. MacDonald, *J. Immunol.* **1985**, *135*, 892.
[130] J. L. Maryanski, P. Pala, J. C. Cerottini, H. R. MacDonald, *Eur. J. Immunol.* **1988**, *18*, 1863.
[131] P. Marrack, R. Endres, R. Shimonkevitz, A. Zlotnik, D. Dialynas, F. W. Fitch, J. Kappler, *J. Exp. Med.* **1983**, *158*, 1077.
[132] M. K. Saizawa, E. Hug, S. Haque, P. Portholes, S. Suzuki, K. Eichmann, *J. Immunol.* **1992**, *148*, 702.
[133] K. Eichmann, A. Ehrfeld, I. Falk, H. Goebel, J. Kupsch, A. Reimann, A. Zgaga-Griesz, K. M. Saizawa, P. Yachelini, K. Tomonari, *J. Immunol.* **1991**, *147*, 2075.
[134] T. H. Finkel, R. T. Kubo, J. C. Cambier, *Immunol. Today* **1991**, *12*, 79.
[135] P. Borgulya, H. Kishi, U. Muller, J. Kirberg, H. von Boehmer, *EMBO J.* **1991**, *10*, 913.
[136] E. A. Robey, B. J. Fowlkes, J. W. Gordon, D. Kioussis, H. von Boehmer, F. Ramsdell, R. Axel, *Cell* **1991**, *64*, 99.
[137] P. Yachelini, I. Falk, and K. Eichmann, *J. Immunol.* **1990**, *145*, 1382.
[138] A. L. Ingold, C. Landel, C. Knoll, G. A. Evans, T. A. Potter, *Nature* **1991**, *352*, 721.
[139] M. Zijlstra, N. E. Simister, J. M. Loring, D. H. Raulet, R. Jaenisch, *Nature* **1990**, *344*, 742.
[140] D. Cosgrove, D. Gray, A. Dierich, J. Kaufman, M. Lemeur, C. Benoist, D. Mathis, *Nature* **1992**, in press.
[141] W. P. Fungleung, M. W. Schilham, A. Rahemtulla, T. M. Kundig, M. Vollenweider, J. Potter, W. van Ewijk, T. W. Mak, *Cell* **1991**, *65*, 443.

X-ray Structure Analysis of FeMo Nitrogenase—Is the Problem of N_2 Fixation Solved?

By *Dieter Sellmann**

Metalloenzymes rank among the most active and efficient catalysts, and the elucidation of the structure–function relationships in these metalloenzymes not only presents a fascinating challenge for research, but also can potentially show ways to new industrial catalysts with previously unattainable activity. Many of these metalloenzymes, for example, ferredoxins, hydrogenases, nitrate reductases, and last but not least nitrogenases,[1] contain transition metals in sulfur-dominated coordination spheres in their active centers. Nitrogenase research recently took a big step forwards: in the summer of last year the scientific community was galvanized by reports describing the X-ray crystal structure analysis of crystalline nitrogenase, which for the first time led to a concrete model for the active centers of iron–molybdenum nitrogenase.[2]

Like photosynthesis, enzymatic N_2 fixation is one of the fundamental synthetic processes of nature. It is catalyzed by nitrogenases, which catalyze the reduction of the usually inert N_2 molecule to ammonia. The nitrogenases known today can be classified according to the metals they contain as FeMo, FeV, and FeFe nitrogenases. The nitrogenases that have been most thoroughly studied are the FeMo nitrogenases, and for a long time molybdenum was considered an essential metal for nitrogenases.[1b] The discovery of FeV nitrogenases, however, showed that the role of molybdenum possibly can be fulfilled by other metals,[3a, b] and the isolation of nitrogenases containing exclusively iron finally ended the belief that two different metals are necessary for the activation and reduction of N_2.[3c]

The FeMo nitrogenases consist of two proteins, the Fe protein and the FeMo protein, which can be purified separately. The Fe protein ($M_r \approx 60000$) is a dimer of two identical subunits, which are bridged by one $[Fe_4S_4]$ cluster. It functions as a *specific* one-electron donor for the FeMo protein, and as yet no other protein or reducing agent has been able to assume the function of the Fe protein. The FeMo protein is a $\alpha_2\beta_2$ tetramer with $M_r \approx 220000$, containing two Mo centers, 32 ± 3 Fe centers, and 32 ± 3 S^{2-} units (Fig. 1).

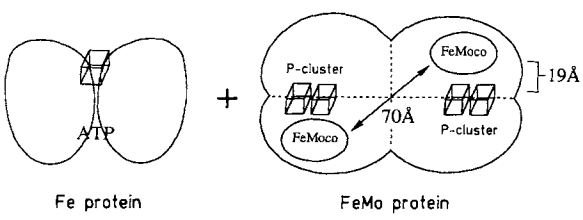

Fig. 1. Schematic representation of FeMo nitrogenase. Fe and FeMo protein form the complete enzyme. The spatial arrangement of the metal–sulfur clusters and a proposal for the binding site of the adenosine triphosphate (ATP) in the Fe protein result from the X-ray structure analyses of the two proteins according to [2] and [8]. Cube = Fe_4S_4; FeMoco = FeMo cofactor.

[*] Prof. Dr. D. Sellmann
Institut für Anorganische Chemie der Universität
Egerlandstrasse 1, D-W-8520 Erlangen (FRG)

Only the combined effect of the Fe *and* the FeMo protein in the presence of a reducing agent such as $Na_2S_2O_4$ makes possible the reduction of N_2. As Equation (a) shows, during this process 2 mol H^+ ions are always reduced to give H_2,

$$N_2 + 8\,H^+ + 8\,e^-\ (\text{e.g. from } Na_2S_2O_4) + 16\,\text{MgATP} \xrightarrow{N_2\text{-ase}} 2\,NH_3 + H_2 + 16\,\text{MgADP} + 16\,PO_4^{3-} \quad (a)$$

and 16 mol magnesium adenosine triphosphate (MgATP) are required. The role of the MgATP is not yet understood. The reduction potential of $Na_2S_2O_4$ alone would be sufficient for the reduction of N_2 to NH_3, which thermodynamically requires $E^0 = -280$ mV at pH 7. In this respect, the hydrolysis of MgATP is a waste of energy.[4]

The FeMo protein contains the FeMo cofactors; these are the active centers at which bonding, activation, and reduction of the N_2 molecule occur. The interest was focussed on these cofactors, since a solution to the "nitrogenase problem" was expected from the elucidation of the composition and structure of these cofactors. The separation of the cofactors from the protein was achieved for the first time in 1977.[5] They have a surprisingly low molecular mass of $M_r \approx 1500$, and were characterized as clusters with the composition [1 Mo; 6–8 Fe; 8–9 S^{2-}; 1 homocitrate]. Hence it followed that two such FeMo cofactors must be present in the FeMo protein, although the data, 6–8 Fe and 8–9 S^{2-}, show that the exact composition could not be determined unambiguously. Only in 1988 was it finally confirmed that homocitrate is an endogenous ligand of the FeMo cofactor and essential for their biosynthesis.[6a] The structure of the isolated cofactor remains unknown to the present day despite many efforts. Despite its relatively small molecular mass it could not be obtained in a crystalline form, such that an X-ray structure analysis was impossible. Spectroscopic investigations such as EXAFS (*e*xtended *X*-ray *a*bsorption *f*ine *s*tructure) provided accurate MoS, MoO/MoN, and FeS distances, however, they did not allow conclusive proposals for the structure. The numerous model complexes, whose syntheses was initiated by the determination of the composition of the cofactor, all showed deviating Mo:Fe:S^{2-} ratios.[6b]

In the same way, the structure of the other [FeS] centers in the FeMo protein remained unresolved. Extrusion experiments yielded evidence that these [FeS] centers contain $[Fe_4S_4]$ units,[7] their spectroscopic properties, however, differed so clearly from those of other $[Fe_4S_4]$ proteins that they were only described as "unusual P clusters".

For the first time, light was shed upon this darkness by the X-ray structure analysis of crystalline FeMo protein whose results were published in 1990 by J. T. Bolin et al.[8] (Fig. 1). They showed that the two FeMo cofactors are located approximately 70 Å apart in two different subunits of the protein. At a distance of approximately 19 Å from the FeMo cofactors, one "P cluster" each is situated, which, according

to the analytically determined metal content of the FeMo protein, must consist of approximately 8 Fe and 8 S^{2-} groups. Thus, the long-discussed hypothesis that the two Mo centers of the FeMo protein jointly participate in the activation of the N_2 molecule was invalidated. An ellipsoid form of the FeMo cofactors could also be deduced from the electron densities, due to the low resolution (5 Å), however, the arrangement of the individual atoms in these cofactors remained open to question.

For this arrangement, D. C. Rees et al. have now proposed a model.[2b] This model is based on the X-ray structure analyses of three crystal forms of the FeMo protein, which was isolated from *Azobacter vinelandii* and *Clostridium pasteurianum*. Even this X-ray structure analysis with the best resolution achieved so far (2.7 Å; $R = 0.20$) does not allow the identification of single atoms in the [MS] clusters. However, the combination of electron densities determined by experiment, with peptide sequences established by biochemistry, the results of mutagenesis studies, EXAFS, and other spectroscopic results, the composition of the isolated FeMo cofactor determined by chemical analysis, and X-ray structural data of model complexes has resulted in such a convincing picture of the FeMo cofactors and P clusters that the solution of the nitrogenase structure has probably reached a preliminary end for the present. The proposed structure of these clusters is depicted in Figure 2.

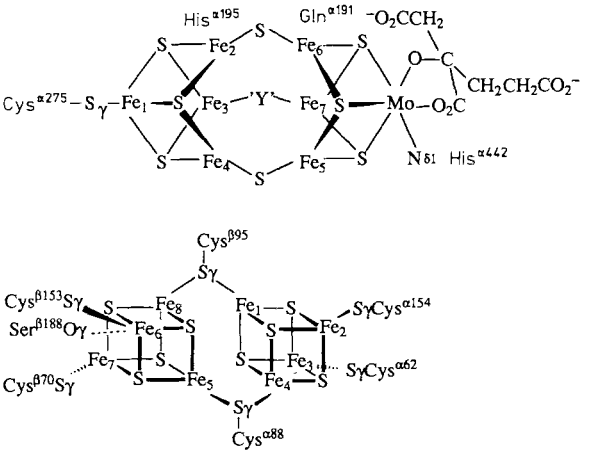

Fig. 2. Structure of the FeMo cofactors (top) and of the unusual P clusters in the FeMo protein of nitrogenase (bottom) (according to [2]). Distances in the FeMo cofactor [Å]: Fe1–Mo = 7.5, Fe2–Fe6 = 2.8, Fe2–Fe5 ≈ 3.8, Fe–S ≈ 2.3, Mo–S ≈ 2.4

The FeMo cofactor consists of $[Fe_4S_3]$ and $[Fe_3MoS_3]$ cubane fragments, which are linked by two S^{2-} and one "Y" bridge. The nature of the Y bridge could not yet be determined unambiguously; it has a lower electron density than the two S^{2-} bridges, and possibly is a NH or O donor. The cluster is bound to the cysteine α275 residue and the histidine α442 side group of the protein at the Fe1 and the Mo atom, respectively. The coordination sphere of the hexacoordinated molybdenum is completed by homocitrate. Two other side chains of the protein, histidine α195 and glycine α191, are approximately 5 Å away from Fe2 and Fe6, respectively, and do not appear to directly bind to the metals. (Cysteine α275, histidine α442, histidine α195, and glycine α191 are conserved in all known FeMo protein sequences, additionally, mutagenesis studies have showed that cysteine α275 and histidine α195 are necessary for the binding of the FeMo cofactor to the FeMo protein.) With the exception of the tetrahedrally coordinated Fe 1, in a remarkable way all the other six Fe atoms are surrounded by only three donors resulting in a coordination geometry which is approximately trigonal planar.

The P clusters contain $[Fe_4S_4]$ cubane units; this had been concluded previously from extrusion experiments.[7] The close bridging of two such clusters via thiolate residues of the protein (cysteine β95 and cysteine α88) as well as the pentacoordination of the Fe6 atom may be responsible for the fact that the spectroscopic properties of the $[Fe_4S_4]$ units in the P clusters so distinctly differ from those of typical $[Fe_4S_4]$ proteins.

The structure of the FeMo cofactor proposed now by Rees et al. explains for the first time and in a plausible way most of the previous analytical, spectroscopic, and chemical findings.[6b] Due to the threefold linkage of the two cubane fragments by S^{2-} and "Y" bridges, it differs significantly from all complexes, which had been proposed previously as structural models. Figure 3 shows a selection of such complexes.[9] These compounds are called structural—in contrast to functional—models because they contain the essential components of the cofactor (Fe, Mo, S^{2-}), but do not show any reactivity towards N_2.

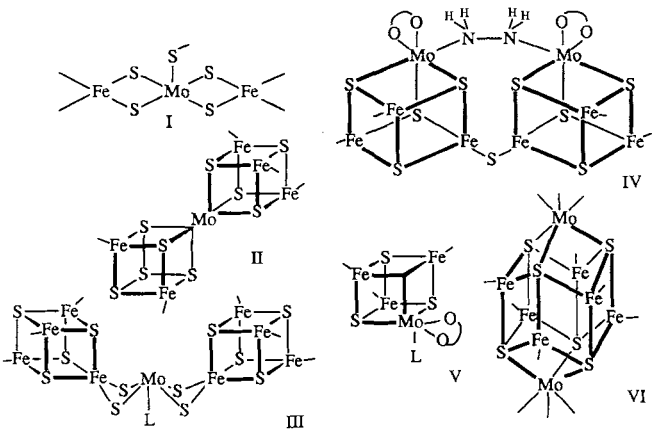

Fig. 3. Previously proposed structural models for the FeMo cofactor [9a]: linear model I, double cubane models II, III, and IV, monocubane model V, prismane model VI. Only the cores of IV [9b], V [9c], and VI [9d] could so far be characterized in isolable complexes by X-ray structure analysis.

The bonding of the FeMo cofactor to the protein by cysteine and histidine only, and the absence of protein-bound bridging ligands within the cluster explain why the cofactor can be extracted from the protein as an intact entity. The cofactor, in a first approximation, contains five magnetically inequivalent kinds of Fe [(Fe 1, Fe 3, Fe 7, (Fe 2 + Fe 4), and (Fe 5 + Fe 6)], which were detected by ENDOR (*e*lectron *n*uclear double *r*esonance) studies with ^{57}Fe.[6b] The distances within the cofactor agree with those obtained from Fe and Mo EXAFS studies. The structure also explains why the cofactor in the protein-bound state is resistant to water, whereas it is decomposed by water with a half life of approximately 2 h in the isolated state. The coordinatively unsatu-

rated Fe atoms in trigonal-planar environments can be expected to allow a facile attack of H_2O, and a subsequent hydrolytic cleavage of the [Fe-S-Mo] bridges.

Is the problem of N_2 fixation now solved, and is the further quest for other model compounds a waste of time? Apart from the fact that important details of the N_2 fixation such as the interaction between the Fe protein and the FeMo protein, the flux of electrons from the reducing agent via the Fe protein to the MoFe protein and from there to the cofactor, or the role of the MgATP for the reduction according to Equation (a) remain as unsolved as before, also the question which directly interests the chemist is still unanswered. At which site on the FeMo cofactor does the N_2 molecule attack to become coordinated, activated, and reduced? All these questions are concerned with the problem of how nitrogenase functions. In answering these questions one is only at the beginning, one can now proceed, however, on structurally safer grounds.

At which site on the FeMo cofactor could the N_2 molecule bind? This question particularly stimulates the imagination of the chemist. One proposal is that the N_2 molecule coordinates side-on to the two Fe atoms, which are linked to one another by the as yet unidentified Y bridge (Fig. 4a).[10a]

In the same manner one can speculate that the N_2 molecule binds end-on between these two Fe atoms, whereby the cluster "breathes" (Fig. 4b). The two [FeSFe] bridges between the cubane fragments should be flexible and thus guarantee variable distances between the Fe atoms (linked via the Y bridge). End-on coordination of the N_2 molecule to two metals has been established for many binuclear N_2 complexes.[10b] In both cases the formation of N–H···X bridges between the reduction intermediates diazene and hydrazine, and the protein environment could facilitate the reduction of N_2.[10c] Finally it has to be discussed whether the N_2 molecule completely slips into the cagelike center of the cofactor and binds to six Fe centers (Fig. 4c). However, if this is so, how can the reduction of other, sometimes considerably larger nitrogenase substrates such as ethylisocyanide be explained? And also the reduction of numerous other nitrogenase substrates, starting from H^+ via C_2H_2 to azide and cyanide, [10d] still remains to be explained.

Beyond all that one has to take into account that the FeMo protein characterized by X-ray structure analysis was in the "resting state" (no substrate binding). What happens to the cofactor in the "turnover state" of the enzyme? It is almost certain that the embedding protein changes its conformation when going from the resting state to the turnover state, as is also the case for hemoglobin. Do side chains move so close to the Fe centers, that these become four or fivefold coordinated and can only thus bind the N_2 molecule?

And what about the Mo atom which for many years was propagated as the binding site for the N_2 molecule? It seems to play no role anymore in the present discussions between the experts. The Mo atom in the resting state of the enzyme probably has the oxidation state + IV, [6b] appears to be coordinatively saturated, and is thus indeed not predestined for the binding of N_2. However, there is a difference between the results of the X-ray structure analysis and the EXAFS studies. The EXAFS studies indicate an $[S_4O_2]$ donor set for the molybdenum in the protein, but an $[S_3O_3]$ or $[S_3O_2N]$ set for the molybdenum in the isolated FeMo cofactor,[6b] as is

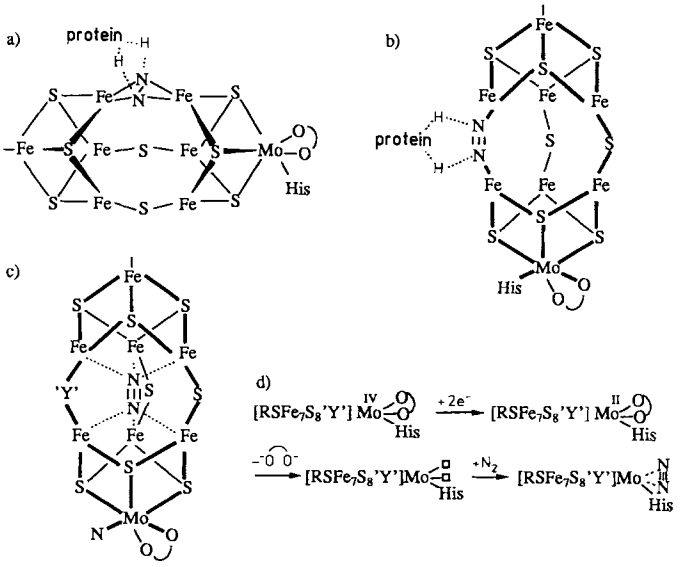

Fig. 4. Proposals for the bonding of N_2 to the FeMo cofactor. a) Side-on and b) end-on coordination of N_2 at the two Fe centers, which are linked by the Y bridge. The H atoms indicate H bonds to the protein, which stabilize the potential intermediates diazene and hydrazine in the course of N_2 reduction. c) Coordination of N_2 within the cage. d) Proposal for a reaction sequence when N_2 coordinates to the Mo center of the cofactor.

shown in the model in Figure 2 (top). (The EXAFS investigations allow no differentiation between N and O donors.) It has recently been proven that at least CO, which is isoelectronic to N_2, can coordinate to $[Mo^{IV}S_4]$ centers.[10e] What happens if, in the turnover state, the $[Fe_7S_9]$ unit of the cofactor serves as electron relay only? Then, after electron transfer to the molybdenum, the hard Mo^{IV} could become a soft Mo center, for example, of the oxidation state + II. Consequently, the hard homocitrate ligand could dissociate, the Mo center would gain free coordination sites for the binding of N_2, and the N_2 reduction could begin (Fig. 4d).

There are thus still many questions, which may be answered—if perhaps not conclusively, then at least approximately—by studies with model compounds. These model compounds must be oriented on the cluster shown in Figure 2 (top), and this will provide a challenge for synthetic chemists. If compounds can be obtained with the characteristic features of the FeMo cofactor, it should also be possible to use them for those cross-linking experiments with apoproteins, which so far could be carried out with the isolated FeMo cofactor only. Also attempts to crystallize the natural FeMo cofactor are now by no means redundant. On the contrary, they have become even more urgent in order to finally confirm the present model of the FeMo centers of nitrogenase by an X-ray structure analysis of the low molecular weight isolated FeMo cofactor.

What can be derived from all these results for the development and synthesis of new catalysts? It is difficult to envisage a compound such as the FeMo cofactor as catalyst for an ammonia synthesis which can compete with the Haber–Bosch process. This cofactor needs numerous auxiliaries—protein environments, specific reduction proteins, MgATP etc.—in order to display its activity. To sum up: here too nature could be the teacher, not in the sense that details, but rather principles of construction should be adhered to. One

of these principles appears to be: in order to catalyze the most difficult reactions under the mildest conditions, use catalysts which consist of transition metals and sulfur ligands. And this is to quote Fontane[11]—a wide field.[12]

German version: *Angew. Chem.* **1993**, *105*, 67

[1] a) *Iron-Sulfur Proteins* (Ed.: G. Spiro), Wiley, New York, **1982**; b) *Molybdenum Enzymes* (Ed.: G. Spiro), Wiley, New York, **1985**.

[2] a) M. M. Georgiadis, H. Komiya, P. Chakrabarti, D. Woo, J. J. Kornuc, D. C. Rees, *Science* **1992**, *257*, 1653; b) Jongsun Kim, D. C. Rees, *ibid.* **1992**, *257*, 1677.

[3] a) P. E. Bishop, D. M. L. Jarlenski, D. R. Hetherington, *Proc. Natl. Acad. Sci. USA* **1980**, *77*, 7342; b) P. E. Bishop, *Trends Biol. Sci.* **1986**, *11*, 225; c) J. R. Chisnell, R. Premakumar, P. E. Bishop, *J. Bacteriol.* **1988**, *170*, 27.

[4] *Nitrogen Fixation: Achievements and Objectives. Proc. 8th Int. Congr. Nitrogen Fixation* (Eds.: P. M. Grashoff, L. E. Roth, G. Stacey, W. E. Newton), Chapman and Hall, New York, **1990**.

[5] V. K. Shah, W. J. Brill, *Proc. Natl. Acad. Sci USA* **1977**, *74*, 3249.

[6] a) T. R. Hoover, J. Imperial, P. W. Ludden, V. K. Shah, *J. Bacteriol.* **1988**, *170*, 1978; b) An excellent summary of the FeMoco research: B. K. Burgess, *Chem. Rev.* **1990**, *90*, 1377.

[7] A. Müller, K. Knüttel, E. Krickemayer, A. Hildebrand, M. Bögge, K. Schneider, A. Armatage, *Naturwissenschaften* **1991**, *78*, 460, and references therein.

[8] J. T. Bolin, A. E. Ronco, L. E. Mortenson, T. V. Morgan, M. Williamson, N.-H. Xuong in [4], pp. 117–124.

[9] a) B. A. Averill, *Struct. Bond. (Berlin)* **1983**, *53*, 59; b) D. Coucouvanis, *Acc. Chem. Res.* **1991**, *24*, 1; c) S. Ciurli, R. H. Holm, *Inorg. Chem.* **1989**, *28*, 1685.

[10] a) W. H. Orme-Johson, *Science* **1992**, *257*, 1639; b) F. Bottomley in *A Treatise on Dinitrogen Fixation* (Eds.: R. W. F. Hardy, F. Bottomley, R. C. Burns), Wiley, New York, **1979**, pp. 109–169; c) D. Sellmann, W. Soglowek, F. Knoch, M. Moll, *Angew. Chem.* **1989**, *101*, 1244; *Angew. Chem. Int. Ed. Engl.* **1989**, *28*, 1271; d) R. W. F. Hardy in [10b], p. 515; e) D. Sellmann, F. Grasser, F. Knoch, M. Moll, *Angew. Chem.* **1991**, *103*, 1346; *Angew. Chem. Int. Ed. Engl.* **1991**, *30*, 1311.

[11] Theodor Fontane (1819–1898) was a respected German writer.

[12] Note added in proof (Dec. 12, 1992): Recently an article has been published describing the tertiary and quaternary structures of the MoFe protein from *Azobacter vinelandii*, based on a 2.7 Å resolution X-ray crystallographic analysis; J. Kin, D. C. Rees, *Nature* **1992**, *360*, 553.

Tellurium—An Interesting Bonding Partner for Transition Metals: New Results from Molecular Chemistry

By *Ulrich Siemeling**

In transition metal chemistry, ligands containing oxygen and sulfur are extremely important; the abundant complex chemistry of oxo, sulfido, alkoxido, and thiolato ligands, to name only the simplest, has consequently been well-studied. Considerably less is known about the complex chemistry of the heavier elements of Group 16, selenium and tellurium.[1] The molecular chemistry of transition metal–tellurium compounds, in particular, is for many an area bordering inorganic and organometallic chemistry, which rarely attracts attention, and when, only because of a chemical oddity, such as the tellurocarbonyl complex **1** synthesized by Roper et al.[2]

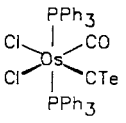

1

However, recently this has changed. The great interest in II/VI semiconductors has helped transition metal–tellurium chemistry to take off: defined precursor compounds for these materials[3] make possible a whole range of different preparations, including particularly interesting high-tech variations such as nanoclusters[4] and thin layers.[5]

In 1987 Steigerwald et al. showed that phenyltellurolates of cadmium and mercury gave the corresponding semiconducting metal tellurides in a polycrystalline form on heating to typically 120–200 °C.[6] This thermolysis reaction basically known for a long time for transition metal chalcogenates[7] occurs according to Scheme 1.

$$[M(TeR)_2]_n \xrightarrow[\Delta]{} (MTe)_n + n\ TeR_2$$

Scheme 1. M = Cd, Hg; R = Ph.

In the meantime, a growing interest in tellurolate chemistry has been observed. Bochmann et al.[8] and Arnold et al.[9] described, at the same time and independently from one another, tellurolysis as preparatively the most important method for the synthesis of transition metal tellurolates. The starting materials for this method, the tellurols R'TeH **2**, are generally photo- and especially thermolabile (Scheme 2). These compounds can, however, be isolated as solids with suitable choice of the group R'. Whereas the crystalline tellurophenols **2a–c** described by Bochmann et al. decompose above approximately −30 °C, the tellurol **2d** prepared by Arnold et al. survives undamaged with exclusion of light even at much higher temperatures: it melts at 130 °C without decomposition!

The cadmium tellurolate **3a** was prepared starting from **2a** (ArTeH). Subsequent heating of **3a** in mesitylene afforded cadmium telluride as expected; analoguously, the corre-

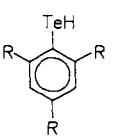

2a – c

2d

Scheme 2. a: R = Me, b: R = *i*Pr, c: R = *t*Bu.

[*] Dr. U. Siemeling
Fakultät für Chemie der Universität
Universitätsstrasse, D-W-4800 Bielefeld 1 (FRG)

 © VCH Verlagsgesellschaft mbH, W-6940 Weinheim, 1993 0570-0833/93/0101-0067 $ 10.00+.25/0

sponding homoleptic zinc tellurolate **3b** is formed by the tellurolysis of diethyl zinc or bis(trimethylsilyl)amide zinc with **2d**.

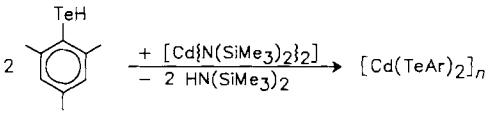

2a **3a**

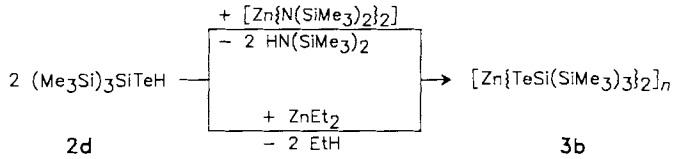

2d **3b**

The tellurolates of the early transition metals, which were previously extremely rare, for example **3c,d**, are easily accessible starting from **2d**.[10] According to X-ray crystal structure analyses, the homoleptic tellurolates **3c** and **3d** are both

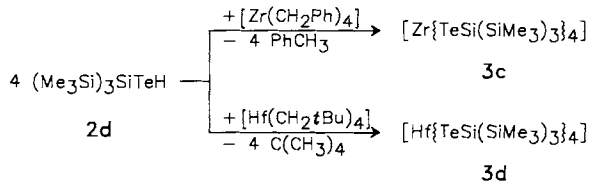

monomeric, in contrast to **3a** and **3b**, and are therefore clearly Lewis acidic. The reaction of **3c,d** with the chelating phosphane 1,2-bis(dimethylphosphino)ethane (dmpe) leads to the octahedrally coordinated adducts **4a** and **4b**, respectively, which each react with an additional equivalent of dmpe, accompanied by the loss of $Te[Si(SiMe_3)_3]_2$, to give the very interesting compounds **5a** and **5b** (Scheme 3).

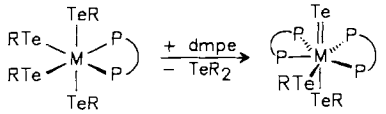

4a – b **5a – b**

Scheme 3. R = $Si(SiMe_3)_3$; a: M = Zr; b: M = Hf.

These complexes are stabilized intermediates (and can therefore be isolated) in the decomposition of metal tellurolates to the corresponding metal tellurides (cf. Scheme 1). At the same time they belong to a class of compounds, namely the terminal tellurido complexes, for which only one year ago not one example existed in transition metal chemistry.

The first complex of this kind, **7**, was synthesized by Rabinovich and Parkin by the reaction of the tungsten compound **6** (itself already remarkable) with elemental tellurium.[11] Also Gibson et al. have reported the preparation of a terminal tellurido complex **9**, which was synthesized from **8** by a similar method.[12] That the synthesis of terminal tellurido complexes was imminent in the last few months is supported by the fact that the compounds **5a,b**, and **9** were introduced at the same time, namely, at this year's Gordon Research Conference on organometallic chemistry.

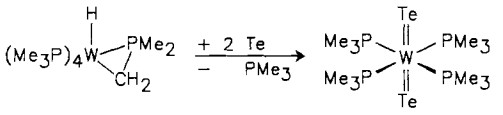

6 **7**

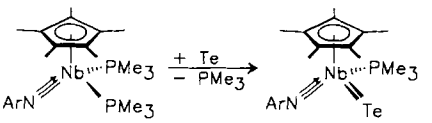

8 **9**

In a time when transition metal compounds, which contain multiple-bonded main group elements or main group complex fragments are intensely researched,[13] these compounds presented here are without doubt highly attractive, and it will be interesting to see how transition metal–tellurium chemistry develops in the future.

German version: *Angew. Chem.* **1993**, *105*, 70

[1] a) F. Berry in *Comprehensive Coordination Chemistry, Vol. 2* (Eds.: G. Wilkinson, R. D. Gillard, J. A. McCleverty), Pergamon, Oxford, **1987**, pp. 661–674; b) M. A. Ansari, J. A. Ibers, *Coord. Chem. Rev.* **1990**, *100*, 223–266; c) N. A. Compton, R. J. Errington, N. C. Norman, *Adv. Organomet. Chem.* **1990**, *31*, 91–182.

[2] G. R. Clark, K. Marsden, W. R. Roper, L. J. Wright, *J. Am. Chem. Soc.* **1980**, *102*, 1206–1207.

[3] P. O'Brian, *Chemtronis* **1991**, *5*, 61–70.

[4] M. L. Steigerwald, L. E. Brus, *Acc. Chem. Res.* **1990**, *23*, 183–188.

[5] K. Ploog, *Angew. Chem.* **1988**, *100*, 611–639; *Angew. Chem. Int. Ed. Engl.* **1988**, *27*, 593–621.

[6] M. L. Steigerwald, C. R. Sprinkle, *J. Am. Chem. Soc.* **1987**, *109*, 7200–7201.

[7] Compare with, for example, the previously reported thermal decomposition of di(1-phenylethylselenolato)mercury to mercury selenide (D. S. Margolis, R. W. Pittman, *J. Chem. Soc.* **1957**, 799–805); for the formation of ZnS and CdS by thermolysis of the homoleptic thiolato complexes of the type $[M(SMe)_2]_n$ (M = Zn, Cd) see: K. Osakada, T. Yamamoto, *J. Chem. Soc. Chem. Commun.* **1987**, 1117–1118.

[8] M. Bochmann, A. P. Coleman, K. J. Webb, M. B. Hursthouse, M. Mazid, *Angew. Chem.* **1991**, *103*, 975–976; *Angew. Chem. Int. Ed. Engl.* **1991**, *30*, 973–974.

[9] B. O. Dabbousi, P. J. Bonasia, J. Arnold, *J. Am. Chem. Soc.* **1991**, *113*, 3186–3188.

[10] V. Christou, J. Arnold, *J. Am. Chem. Soc.* **1992**, *114*, 6240–6242.

[11] D. Rabinovich, G. Parkin, *J. Am. Chem. Soc.* **1991**, *113*, 9421–9422.

[12] U. Siemeling, V. C. Gibson, *J. Chem. Soc. Chem. Commun.*, **1992**, 1670–1671.

[13] a) W. A. Herrmann, *Angew. Chem.* **1986**, *98*, 57–77; *Angew. Chem. Int. Ed. Engl.* **1986**, *26*, 56–76; b) W. A. Nugent, J. M. Mayer, *Metal-Ligand Multiple Bonds*, Wiley, New York, **1988**.

Communications may be submitted in English *or* in German. Further details regarding the submission of communications can be found in the "Notice to Authors" reproduced in the January issue of the journal. Copies thereof may be obtained from the editorial office upon request.

Multicomponent Self-Assembly: Spontaneous Formation of a Cylindrical Complex from Five Ligands and Six Metal Ions**

By *Paul Baxter*, *Jean-Marie Lehn*,* *André DeCian*, and *Jean Fischer*

Self-assembly consists of the spontaneous generation of a well-defined, discrete supramolecular architecture from a given set of components under specific conditions. Such processes require the design of "programmed" supramolecular systems that rely on the information stored in the components and on the interaction algorithm that operates through molecular recognition events.[1, 2] Depending on the nature of the molecules involved, the self-assembly can be organic or inorganic. In the assembly of supermolecules from metal ions and ligands, the latter must contain the steric program that is "read" by the metal ions following the algorithm represented by their coordination geometry. The self-assembly of a given superstructure involves three stages: *recognition* between the components, correct *orientation* so as to allow growth, and *termination* of the process leading to a discrete, finite supramolecular species.[1-3]

The formation of double-helical metal complexes, the helicates,[3-6] results from the self-organization of oligobipyridine (bpy) strands and Cu^+ or Ag^+ ions that possess tetrahedral coordination geometry.[3-5] The interaction of appropriately substituted oligo-bpy strands or related ligands with metal ions prefering octahedral coordination may yield triple-helical complexes.[7, 8] Closed inorganic structures have been obtained, for instance, from the self-assembly of Ni^{2+}[9a] or Cu^{2+}[9b] ions and bis-β-diketone type ligands, of four Pt^{II} metal complex fragments and four 4,4'-bpy groups,[10] and of four Cu^+ ions and four bispyridylpyridazine ligands.[11]

The self-assembly of the helicates and related structures involves just one type of ligand and metal ion. Further progress in the understanding and the control of the self-assembly and self-organization of inorganic (as well as of purely organic) superstructures requires the conception of systems capable of spontaneously generating well-defined inorganic complexes from a larger set of components, comprising at least two types of ligands and/or metal ions. The design and choice of these components must fulfill criteria at all three levels of molecular programming and information input that determine the output of the desired final species—recognition, orientation, and termination.

We report here on two such multiligand, multimetal, self-assembly processes involving two types of ligands and several Cu^+ ions: the generation of a cylindrical complex **1** and the related component species **2** (Scheme 1). The formation of a capped complex will be described elsewhere.[12]

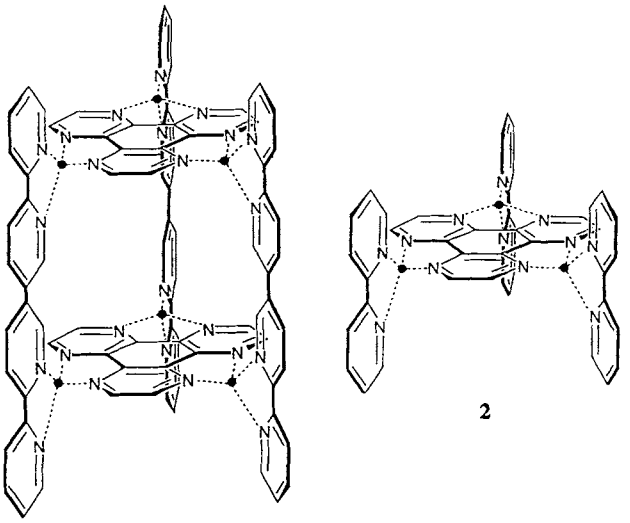

2

Scheme 1. Schematic representation of the structures of **1** and **2**. Phenyl and methyl substituents are omitted for clarity. ● = Cu.

Hexaazatriphenylene (HAT) and its derivatives are ligands with three metal coordination sites, which yield, for instance, a trinuclear complex by complexation of three $[Ru(bpy)_2]^{2+}$ units.[13, 14] It appeared that a similar complex might be formed with three $[Cu(bpy)]^+$ units or related groups.

Hexaphenylhexaazatriphenylene Ph_6-HAT **3** was synthesized by condensation of benzil with hexaaminobenzene,[15, 16] which was obtained by reduction of 1,3,5-triamino-2,4,6-trinitrobenzene with sodium in liquid ammonia.[16, 17] When 3 equiv dimethyl-bpy **4** and 1 equiv **3** in CH_2Cl_2 were treated with $[Cu(CH_3CN)_4]BF_4$ in CH_3CN, the reaction mixture showed first the reddish color ($\lambda_{max} = 457$ nm, $\varepsilon = 6550\ M^{-1}cm^{-1}$) characteristic of bis-bpy Cu^I complexes (for $Cu^I(\mathbf{4})_2]^+$: $\lambda_{max} = 454$ nm, $\varepsilon = 6700\ M^{-1}cm^{-1}$[18]). After 1.5 equiv $[Cu(CH_3CN)_4]BF_4$ the solution turned brown and after the addition of 2.5 equiv, intensely purple ($\lambda_{max} = 568$ nm, $\varepsilon = 15\,700\ M^{-1}cm^{-1}$; shoulder at 700 nm, $\varepsilon = 6570\ M^{-1}cm^{-1}$), an unusual color for a Cu^I complex. These observations may be interpreted as follows: initially the $[Cu(\mathbf{4})_2]^+$ complex is formed exclusively until at 1.5 equiv the free ligand **4** is consumed. Upon further addition of $[Cu(CH_3CN)_4]BF_4$, the weaker ligand Ph_6-HAT **3** (whose pyrazine-type N atoms are poorer binding sites than the bpy N atoms) participates; the $[Cu(bpy)_2]^+$ species opens up and $[Cu(bpy)]^+$ units bind to the coordination sites of ligand **3**. Finally at 3 equiv $[Cu(CH_3CN)_4]BF_4$, a single

[*] Prof. Dr. J.-M. Lehn, Dr. P. Baxter
Laboratoire de Chimie Supramoléculaire
Institut Le Bel, Université Louis Pasteur
4, rue Blaise Pascal, F-67000 Strasbourg (France)
Dr. A. DeCian, Prof. Dr. J. Fischer
Laboratoire de Cristallochimie et de Chimie Structurale
Institut Le Bel, Université Louis Pasteur
4, rue Blaise Pascal, F-67000 Strasbourg (France)

[**] This work was supported by the Centre National de la Recherche Scientifique (URA 422 and URA 424). P. B. thanks the Royal Society for a one-year postdoctoral fellowship. We thank Prof. G. Wipff and E. Engler, Strasbourg, for the computer-generated representations.

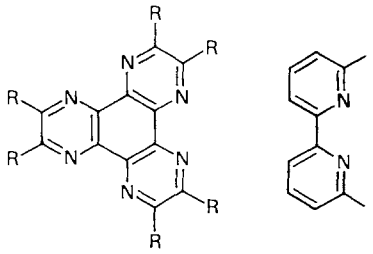

3 R =

4

species is present, the trinuclear circular complex **2** (as the **2**-$(BF_4)_3$ salt).

This proposed sequence is supported by mass spectrometry performed on the solutions containing different amounts of the Cu^I salt, which reveals the formation of $[Cu(\mathbf{4})_2]BF_4$ and $[Cu_3(\mathbf{3})(\mathbf{4})_3](BF_4)_3$.[19] The ^1H NMR spectrum of the **2**-$(BF_4)_3$ in CD_2Cl_2 also corresponds to the postulated structure.

Treatment of **3** itself with 3 equiv $[Cu(CH_3CN)_4]BF_4$ in CH_3CN also afforded an orange-red solution which may correspond to the formation of branched oligomeric and polymeric Cu^I complexes. This would amount to the spontaneous growth through self-assembly of coordination compounds resembling dendrimer-[20] and arborol-type[21] structures. Such a process may allow an entry into the self-assembly of oligomeric and polymeric coordination architectures from branching multinucleating ligands and suitable metal ions.[22]

The results above were taken as sufficient evidence for the generation of complex **2**. They also suggested that it might be possible to achieve the self-assembly of a cylindrical, cagelike structure **1** if **4** were replaced by ligand **5**, in which two bpy subunits are linked in the 5,5′ positions. The quaterpyridine (qpy) **5** was synthesized as follows: lithiation of **6** with BuLi followed by treatment with $SnMe_3Cl$ (1.2 equiv) gave **7** (63%; b.p. 200–205 °C). The regioselective monolithiation of 2,5-dibromopyridine at position 5 with 1 equiv *n*BuLi and subsequent treatment with $CuCl_2$ (0.5 equiv) was followed by oxidative dimerization with O_2 to provide **8** (30%; m.p. 248–249.5 °C). Finally reaction of **8** with 2 equiv **7** in the presence of $[Pd(PPh_3)_4]$ gave **5** (68%; m.p. 249.5–250 °C).

During the slow addition of a solution of $[Cu(MeCN)_4]BF_4$ (6 equiv in CH_3CN) to a stirred mixture of **3** (2 equiv) and **5** (3 equiv) in CH_2Cl_2 under argon, the color of the reaction mixture changed from initially reddish brown through dark brown to finally deep purple. The suspension of **5** went into solution, and after about 20 h of stirring the solvent was evaporated under vacuum leaving a dark-purple, air-stable, solid. This was redissolved in CH_3NO_2, filtered, and benzene was added dropwise to the filtrate. The solid was removed by filtration and then dried under vacuum at room temperature to give deep-purple, microcystalline powder in quantitative yield (λ_{max} = 546 nm, ε = 27 600 $M^{-1}cm^{-1}$; 699 nm, ε = 13 500 $M^{-1}cm^{-1}$; CH_2Cl_2).

The ^1H NMR spectrum, the FAB (fast atom bombardment) mass spectrum, and the microanalytical data agree with the formulation of this compound as $[Cu_6(\mathbf{3})_2(\mathbf{5})_3](BF_4)_6$, that is, **1**-$(BF_4)_6$. This complex was found to be markedly more stable than the trinuclear complex **2**; repeated recrystallizations of the latter, for example, from CH_2Cl_2/hexane invariably resulted in some decomposition, whereas the hexanuclear complex **1** was stable under the same conditions; **1** also underwent slow oxidation upon exposure to air for several months. The ^1H (500 MHz) and ^{13}C (50.3 MHz) NMR spectra of **1**-$(BF_4)_6$ indicate that all three qpy ligands as well as the two Ph_6-HAT ligands are equivalent in solution on the NMR timescale.

The construction of complex **1** was confirmed by its X-ray crystal structure determination (Fig. 1).[23] It is indeed an

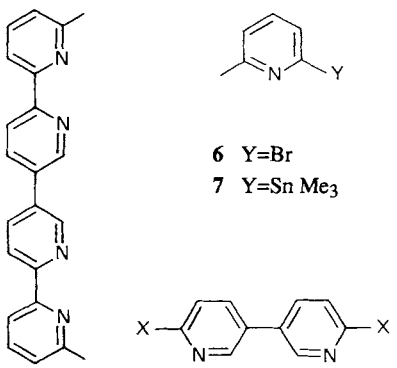

5

6 Y=Br
7 Y=Sn Me$_3$

8 X=Br

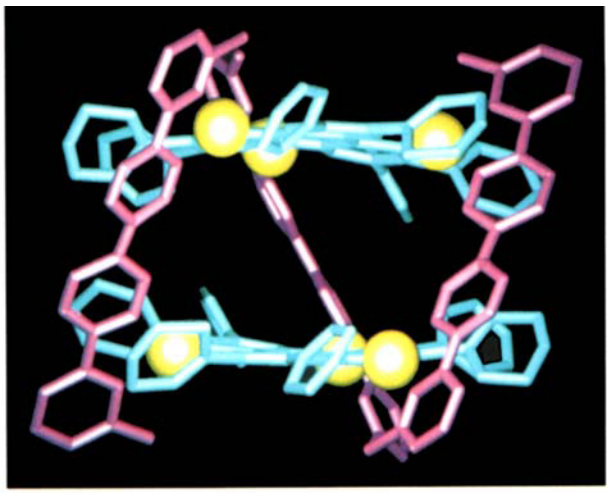

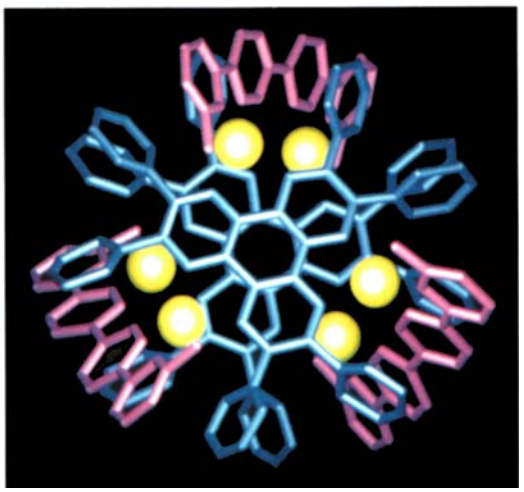

Fig. 1. Model of the crystal structure of the self-assembled cylindrical inorganic complex **1**. Top: Side view. Bottom: View along the vertical axis.

inorganic cagelike compound resulting from the self-assembly of two flat circular HAT ligands **3** that form the top and bottom, three bridging quaterpyridine groups **5**, and six Cu^{I} ions that hold the five organic components together.

Complex **1** possesses a C_2 axis passing through the middle of the central C–C bond of one of the qpy units; this distorsion from the threefold symmetry may be due to crystal packing. The top and bottom HAT units are close to planar (maximum deviation from mean plane 0.19 Å) and almost parallel to each other (13.3° angle between the normals to their mean planes); they are not eclipsed as shown in Scheme 1, but rotated with respect to each other by about 27° (Fig. 1 bottom). Every bpy group in the three qpy units is approximately planar (maximum deviation of 0.32 Å), and the two bpy groups of the two equivalent qpy groups are twisted with respect to each other by an angle of 36°; those of the qpy located on the binary axis are twisted by 25°. The vertical qpy bridges are inclined by an angle of 66° with respect to the axis passing through the center of the two HAT units. The Cu^{+} sites are distorted from tetrahedral coordination, with a dihedral angle of 72° between the N-Cu-N planes corresponding to the bpy and HAT units. The three Cu^{+} ions lie in the HAT plane and form approximately an equilateral triangle with a mean edge length of 6.85 Å. The planes of the phenyl rings form a 60° angle with the plane of the respective HAT unit. The overall twist of the structure results in a triple-helical shape of the complex. Bond lengths and angles do not show any peculiarity.

Complex **1** has a cylindrical internal cavity with a height of 7.4 Å (mean distance between the HAT planes) and a radius of about 5.5 Å (based on the nitrogen atoms of the three qpy groups). Taking the van der Waals radii into account the cylindrical void has a height of approximately 4 Å and a radius of 4 Å; one may envisage binding substrate molecules in this cavity, in particular flat, aromatic units of suitable dimensions. Thus **1** would be a self-assembled molecular receptor for appropriate substrate species.[*]

An investigation into the precise structural requirements of the ligands **3** and **5** which control the self-assembly of the cage complex **1** is in progress. We are also working on the extension of the process described here to related ligands.

The formation of structure **1** demonstrates the remarkable self-organization of a closed inorganic architecture by the spontaneous and correct assembly of altogether eleven particles consisting of two types of ligands and one type of metal ion. The operation of this instructed supramolecular system fulfills the three levels of molecular programming and of information input: recognition, orientation, and termination.

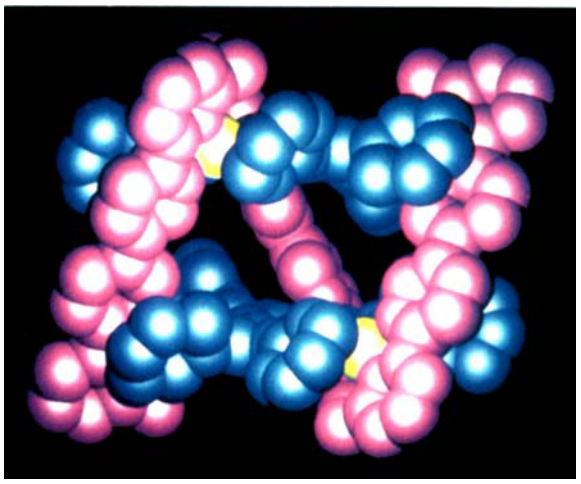

Fig. 2. CPK representation of **1**. The side view corresponds to Figure 1 top.

[*] If a suitable substrate were to be spontaneously and selectively included into **1** in the course of the self-assembly, this would represent an assembly of twelve (!) partners into an elective community (EC), a very timely process.

Received: October 14, 1992 [Z 5624 IE]
German version: *Angew. Chem.* **1993**, *105*, 92

[1] J.-M. Lehn, *Angew. Chem.* **1990**, *102*, 1347; *Angew. Chem. Int. Ed. Engl.* **1990**, *29*, 1304.
[2] J.-M. Lehn in *Perspectives in Coordination Chemistry* (Eds.: A. F. Williams, C. Floriani, A. E. Merbach), Verlag Helvetica Chimica Acta, Basel and VCH, Weinheim, **1992**, p. 447.
[3] A. Pfeil, J.-M. Lehn, *J. Chem. Soc. Chem. Commun.* **1992**, 838.
[4] J.-M. Lehn, A. Rigault, J. Siegel, J. Harrowfield, B. Chevrier, D. Moras, *Proc. Natl. Acad. Sci. USA* **1987**, *27*, 2565; J.-M. Lehn, A. Rigault, *Angew. Chem.* **1988**, *100*, 1121, *Angew. Chem. Int. Ed. Engl.* **1988**, *27*, 1095.
[5] T. M. Garrett, U. Koert, J.-M. Lehn, A. Rigault, D. Meyer, J. Fischer, *J. Chem. Soc. Chem. Commun.* **1990**, 557.
[6] See also: E. C. Constable, R. Chotalia, *J. Chem. Soc. Chem. Commun.* **1992**, 64, and references cited therein.
[7] R. Krämer, J.-M. Lehn, unpublished results.
[8] A. F. Williams, C. Piguet, G. Bernardinelli, *Angew. Chem.* **1991**, *103*, 1530; *Angew. Chem. Int. Ed. Engl.* **1991**, *30*, 1490.
[9] a) R. Köhler, R. Kirmse, R. Richter, J. Sieler, E. Hoyer, *Z. Anorg. Allg. Chem.* **1986**, *537*, 133; b) J. R. Bradbury, J. L. Hampton, D. P. Martone, A. W. Maverick, *Inorg. Chem.* **1989**, *28*, 2392.
[10] M. Fujita, J. Yazaki, K. Ogura, *J. Am. Chem. Soc.* **1990**, *112*, 5645.
[11] M.-T. Youinou, N. Rahmouni, J. Fischer, J. A. Osborn, *Angew. Chem.* **1992**, *104*, 771; *Angew. Chem. Int. Ed. Engl.* **1992**, *31*, 733.
[12] R. Krämer, J.-M. Lehn, unpublished results.
[13] R. Nasielski-Hinkens, M. Benedek-Vamos, D. Maetens, J. Nasielski, *J. Organomet. Chem.* **1981**, *217*, 179.
[14] A. Masschelein, A. Kirsch-De Mesmaeker, C. Verhoeven, R. Nasielski-Hinkens, *Inorg. Chim. Acta* **1987**, *129*, L13.
[15] B. Kohne, K. Praefcke, *Liebigs Ann. Chem.* **1985**, 522.
[16] J. Nasielski, C. Moucheron, D. Verhoeven, R. Nasielski-Hinkens, *Tetrahedron Lett.* **1990**, *31*, 2573.
[17] D. Z. Rodgers, *J. Org. Chem.* **1986**, *51*, 3904.
[18] J. R. Hall, M. R. Litzow, R. A. Plowman, *Anal. Chem.* **1963**, *35*, 2124; E. Müller, C. Piguet, G. Bernardinelli, A. F. Williams, *Inorg. Chem.* **1988**, *27*, 849.
[19] FAB and electrospray mass spectrometry have been used to identify the complexes formed in solution from various ligands and metal ions; such data give direct information on complexation equilibria: P. Baxter, A. Van Dorsselaer, R. Krämer, J.-M. Lehn, A. Marquis-Rigault, unpublished results.
[20] D. A. Tomalia, A. M. Naylor, W. A. Goddard III, *Angew. Chem.* **1990**, *102*, 119; *Angew. Chem. Int. Ed. Engl.* **1990**, *29*, 138; C. J. Hawker, J. M. J. Fréchet, *J. Am. Chem. Soc.* **1990**, *112*, 7638.
[21] G. R. Newkome, Z.-q. Yao, G. R. Baker, V. K. Gupta, P. S. Russo, M. J. Saunders, *J. Am. Chem. Soc.* **1986**, *108*, 849; G. R. Newkome, G. R. Baker, M. J. Saunders, P. S. Russo, V. K. Gupta, Z.-q. Yao, J. E. Miller, K. Bouillion, *J. Chem. Soc., Chem. Commun.* **1986**, 752.
[22] For the stepwise synthesis of branched multinuclear complexes see: G. Denti, S. Campagna, S. Serroni, M. Cianio, V. Balzani, *J. Am. Chem. Soc.* **1992**, *114*, 2944, and references therein. See also: S. Serroni, G. Denti, S. Campagna, A. Juris, M. Ciano, V. Balzani, *Angew. Chem.* **1992**, *104*, 1540; *Angew. Chem. Int. Ed. Engl.* **1992**, *31*, Nr. 11.
[23] a) Crystal data: Suitable single crystal of **1**-$(BF_4)_4F_2 \cdot 4C_2H_2Cl_4 \cdot 5H_2O$ were obtained by slow diffusion of pentane into a solution of **1**-$(BF_4)_6$ in 1,1,2,2-tetrachloroethane (initially cooled in air to liquid N_2 temperature) at room temperature. A single crystal was cut out from a cluster of crystals and mounted on a rotation-free goniometer head (Philips PW1100/16 automatic diffractometer). $M = 4104.9$, monoclinic, space group $C2/c$, $a = 33.978(10)$, $b = 30.141(9)$, $c = 20.840(6)$ Å, $V = 19846.8$ Å^3, $\varrho_{calcd} = 1.374$, $Z = 4$, $\mu(Cu_{K\alpha}) = 33.755$ cm^{-1} (graphite monochromator). A total of 9377 reflections were collected at −100 °C; the temperature was held constant with a gas flow device of our own construction. For all calculations the Enraf-Nonius Mole/VAX package [23b] was used, with the exception of data reduction program which was our own. The raw step-scan data were converted to intensities by the Lehmann–Larsen method [23c]. The intensities of three reflections measured every hour during the entire data collection period showed a decay of 46%; therefore a second data collection was started using two crystals. With the first one, data with $3° < \theta < 35°$ were collected, with the second remaining data. For each crystal, a linear decay of 16% was corrected. After application of separate Lorentz, polarization, and absorption corrections, the latter based on psi scans, the scale between the two sets was determined from 120 common reflections using a least-squares procedure. The structure was solved using MULTAN [23d]. After refinement of the heavy atoms, the hydrogen

atoms of the core were introduced in structure factor calculations by their computed coordinates (C–H = 0.95 Å) and isotropic temperature factors such as $B(H) = 1.3$ Beqv(C) Å^2, but not refined. The overall temperature factor of the structure is high (5.4 Å^2) indicating some disorder and low diffraction power, therefore the accuracy obtained is lower than normally expected. Full least-squares refinements; $\sigma^2(F^2) = \sigma^2_{counts} + (pI)^2$. $R(F) = 0.103$, $Rw(F) = 0.147$. The scattering factor coefficients and anomalous dispersion coefficients come from ref. [23c]. b) B. A. Frenz, *The Enraf-Nonius CAD4-SDP* in *Computing in Crystallography*, (Eds.: H. Schenk, R. Olthof-Hazekamp, H. Van Koningveld, G. C. Bassi), Delft University Press, **1978**, pp. 64–71; c) M. S. Lehmann, F. K. Larsen, *Acta Crystallogr. Sect. A* **1974**, *30*, 580; d) G. Germain, P. Main, M. M. Woolfson, *ibid. B* **1970**, *26*, 274; *ibid. A* **1971**, *27*, 368; e) D. T. Cromer, J. T. Waber, *International Tables for X-Ray Crystallography, Vol. IV*, The Kynoch Press, Birmingham, **1974**, Tables 2.2 b and 2.3.1; f) further details of the crystal structure investigation are available on request from the Director of the Cambridge Crystallographic Data Centre, University Chemical Laboratory, Lensfield Road, GB-Cambridge, CB2 1EW (UK), on quoting the full journal citation.

Cavities for Binding Two Metal Atoms: A Novel Pentanuclear Copper(I) Complex with an Anionic, Pentadentate Aryl Ligand with Two *ortho*-Chelating Diamine Substituents**

By *G. Marc Kapteijn, Ingrid C. M. Wehman-Ooyevaar, David M. Grove, Wilberth J. J. Smeets, Anthony L. Spek*, and *Gerard van Koten**

The design and use of multidentate ligands is of great interest in organometallic chemistry.[1] We are studying the construction of cavities formed by organic ligands, in which a metal ion is bound by a metal–carbon σ bond and the metal center is coordinatively saturated as a result of additional intramolecular coordination of heteroatoms present in the surface enclosing the cavity. A simple representative of this class of ligands is the anionic aryldiamine ncn which coordinates through the two N and one C atoms and exhibits

$[2,6\text{-}(CH_2NMe_2)_2C_6H_3]^-$ ncn

versatile bonding modes ranging from monodentate (σ-C) and bidentate (C,N) to tridentate (*mer*- or *fac*-N,C,N),[2] depending on the metal (structure **A** in Scheme 1). Interestingly, several examples are known in which ncn formally binds two metal atoms by either a two-electron three-center (2e-3c) bond, whereby C_{ipso} bridges two metal atoms, as in **1**[3] and **2**,[4] or by a (2e + 2e)-3c bond, whereby C_{ipso} bridges two unlike metal atoms as in **3** (structure **B** in Scheme 1).[5] The structures of **1** and **2** in the solid state and in solution

$[Li_2(ncn)_2]$ **1** $[Cu_4Br_2(ncn)_2]$ **2**

$[TaCl_2(\mu\text{-ncn})(\mu\text{-C-}t\text{Bu})(ZnCl)]$ **3**

[*] Prof. Dr. G. van Koten, G. M. Kapteijn, I. C. M. Wehman-Ooyevaar, Dr. D. M. Grove
Debye Research Institute
Department of Metal-Mediated Synthesis
University of Utrecht
Padualaan 8, NL-3584 CH Utrecht (The Netherlands)
W. J. J. Smeets, Dr. A. L. Spek
Bijvoet Centre for Biomolecular Research
Laboratory for Crystal and Structural Chemistry
University of Utrecht

[**] This research was supported by Shell Research B.V. (G. M. K., I. C. M. W-O.) and also in part (W. J. J. S., A. L. S.) by the Netherlands Foundation for Chemical Research (S. O. N.) with financial aid from the Netherlands Organization for Scientific Research (N. W. O.).

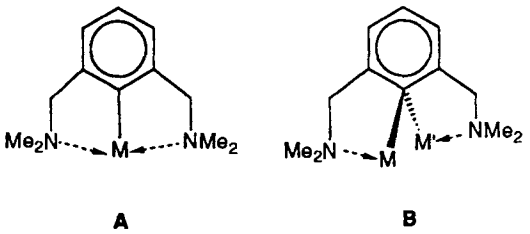

A B

Scheme 1. Bonding modes of ncn. In structures of type A ncn may function as a two-, four-, or six-electron donor ligand.

clearly show that completion of the Li and Cu coordination spheres requires formation of larger aggregates. In the case of **1** this is achieved by dimerization; in the case of **2** by linkage of two Cu(ncn) units with two CuBr units. We have now expanded the simple cavity of ncn by replacing one methyl group of each NMe_2 unit by $CH_2CH_2NMe_2$ to form a potentially pentacoordinate, anionic N,N,C,N,N ligand **4**. We report here on our investigation of the bonding properties of **4** to copper(I) centers, specifically on an arylcopper copper bromide compound in which aryldicopper cations are stabilized by intramolecular coordination and a $CuBr_3$ dianion.

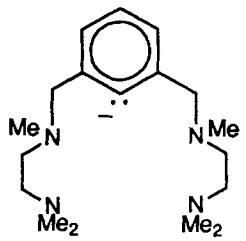

4

The precursor to **4**, compound **5**, was synthesized from the reaction of 1 equivalent of $2,6\text{-}(CH_2Br)_2C_6H_3Br$ with 2 equivalents of $HN(Me)CH_2CH_2NMe_2$ in the presence of NEt_3 as a base.[6] Treatment of **5** with two equivalents of

$2,6\text{-}[CH_2N(Me)CH_2CH_2NMe_2]_2C_6H_3Br$ **5**

n-butyllithium afforded the lithium salt of **4** which was isolated as the unique adduct **6** of aryllithium and lithiumbromide.[6] When **6** was treated with two equivalents of CuBr in benzene a novel type of pentanuclear Cu^I complex **7** was

$[Li_2Br(\mathbf{4})]$ **6** $[Cu_5Br_3(\mathbf{4})_2]$ **7**

isolated in 73% yield.[7] In the X-ray crystal structure of **7** the monoclinic unit cell contains two molecules of **7** and two molecules of diethyl ether. **7** is a pentanuclear Cu^I complex most readily described as two cationic organocopper moieties $[Cu_2(\mathbf{4})]^+$ linked by a $CuBr_3^{2-}$ dianion (Fig. 1).[8] The two aryl ligands **4** bridge a pair of Cu atoms (Cu2, Cu3 or Cu4, Cu5) at the anionic C_{ipso} center, the Cu-C_{ipso}-Cu angles are very acute (Cu2-C1-Cu3 73.8(2); Cu4-C19-Cu5 73.6(2)°). In combination with the short Cu ··· Cu distances (Cu ··· Cu 2.456(1) Å) and the four similar Cu–C distances (Cu–C 2.049(6) Å) these geometric parameters are indicative

of a 2e-3c Cu_2C_{ipso} bond (for a discussion of this bonding see ref. [9]).

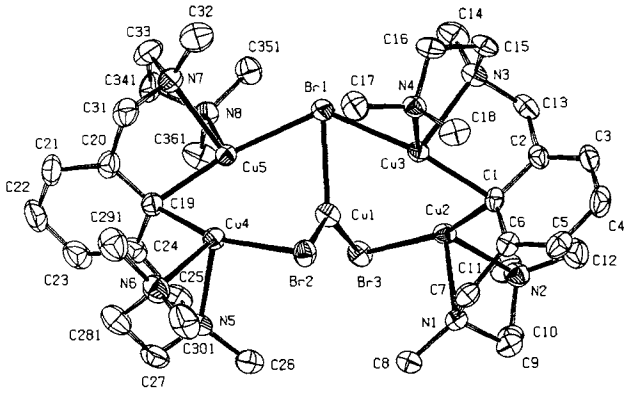

Fig. 1. Crystal structure of **7** (ORTEP, thermal ellipsoids at 30% probability). Only one of the configurations giving rise to the disorder is shown. Selected distances [Å] and angles [°]: Cu1-Br1 2.459(1), Cu1-Br2 2.389(2), Cu1-Br3 2.398(2), Cu2-C1 2.020(6), Cu3-C1 2.076(6), Cu4-C19 2.038(7), Cu5-C19 2.062(6), Cu2-Br3 2.448(1), Cu2-N1 2.288(6), Cu2-N2 2.316(6), Cu2···Cu3 2.458(1), Cu4···Cu5 2.454(1), Cu1···Cu (mean) 2.77(8); Br1-Cu1-Br2 114.97(6), Br1-Cu1-Br3 109.48(5), Br2-Cu1-Br3 135.47(5), Cu2-C1-Cu3 73.8(2), Cu4-C19-Cu5 73.6(2), Cu3-Br1-Cu5 130.35(4).

In each $[Cu_2(\mathbf{4})]^+$ unit the two copper atoms are held in a polyamine cavity and the C_{ipso} bridged Cu atoms are tetracoordinate through $Cu-N_2$ chelate coordination of the $N(Me)CH_2CH_2NMe_2$ substituents and an additional interaction with a Br atom of the central $CuBr_3^{2-}$ unit. The Cu–N distances (2.203(6)–2.334(6) Å) fall in the range for Cu–$N(sp^3)$ bond lengths observed in *ortho*-chelated organocopper compounds.[10] The central Cu atom (Cu1) is bonded to all three Br atoms and has a distorted trigonal geometry in which the Cu–Br bond lengths are 2.389(2)–2.459(1) Å and the Br–Cu–Br angles are 114.97(6) (Br1-Cu1-Br2), 109.48(5) (Br1-Cu1-Br3), and 135.47(5)° (Br2-Cu1-Br3). To our knowledge only three complexes characterized by X-ray crystallography have been reported to contain a $CuBr_3^{2-}$ ion and these all concern the free dianion which has substantially shorter Cu–Br bond lengths than **7** (typically 2.37 to 2.39 Å).[11] The Br atoms in **7** have additional interactions with the $[Cu_2(\mathbf{4})]^+$ ions; Br1 with both cations (bonds to Cu3 and Cu5) and Br2 and Br3 each to one cation (bonds to Cu4 and Cu2, respectively). We believe the correct way to view complex **7** is as a pentanuclear Cu^I aggregate $[\{Cu_2(\mathbf{4})^+\}_2(CuBr_3^{2-})]$ in which the central dianionic unit bridges the two cationic units. The formation of aggregates is normal in organocopper chemistry, and it has been argued that these may be thought of as assemblies of either neutral RCu, CuX, CuSR, CuH, RLi units or anionic R_2Cu^-, R_2Li^- units, depending on the solution equilibria. However, the combination of Cu_2R^+ units and a $CuBr_3^{2-}$ unit present in **7** is without precedent in copper chemistry. ^1H and ^{13}C NMR studies have shown that the structure of **7** in solution is similar to that in the solid state, but fluxional processes are operative and still under investigation.

These results in Cu^I chemistry show that the monoanionic pentadentate ligand **4** is capable of binding two metal atoms in a unique manner. In **7** the Cu_2C_{ipso} bond can be considered as arising from the interaction of a Cu^+ ion with a neutral 2e-2c Cu–C_{ipso} bond at C_{ipso}, and the whole is then stabilized by appropriate chelate coordination. It is this idea that we are currently exploring for the synthesis of polynuclear organometallic species in which the coordination of a C_{ipso}–$(M_{n+1})^{n+}$ unit with a relatively stable metal–carbon bond is completed by additional inter- and intramolecular coordination. In this way the cavity formed by a polyamine encloses metal atoms so that they are close to each other, while leaving one side open for binding of either anions or small neutral molecules.

Experimental Procedure

7: To a suspension of CuBr (0.55 g, 3.83 mmol) in benzene (15 mL) was added a solution of **6** (0.77 g, 1.92 mmol) in benzene (15 mL). After 1 h of stirring the yellow solution was evaporated to dryness and the residue dissolved in diethyl ether. After 2d at −20 °C yellow crystals were isolated; 0.82 g, yield 73%.

Received: September 3, 1992 [Z 5553 IE]
German version: *Angew. Chem.* **1993**, *105*, 88

[1] a) G. R. Newkome, F. R. Fronczek, W. A. Deutsch, T. Kawato, D. K. Kohli, W. E. Puckett, B. D. Olivier, G. Chiari, *J. Am. Chem. Soc.* **1981**, *103*, 3423; b) J. R. Briggs, A. G. Constable, W. S. McDonald, B. L. Shaw, *J. Chem. Soc. Dalton Trans.* **1982**, 1225; c) M. D. Fryzuk, P. A. MacNeil, *Organometallics* **1983**, *2*, 682; d) H. Rimml, L. M. Venanzi, *J. Organomet. Chem.* **1984**, *260*, C52.

[2] D. M. Grove, G. van Koten, H. J. C. Ubbels, *Organometallics* **1982**, *1*, 1366; H. C. L. Abbenhuis, D. M. Grove, P. van der Sluis, A. L. Spek, G. van Koten, *Recl. Trav. Chim. Pays-Bas* **1990**, *109*, 446; P. L. Alsters, H. J. Teunissen, J. Boersma, G. van Koten, *ibid.* **1990**, *109*, 487; P. L. Alsters, J. Boersma, G. van Koten, *Tetrahedron Lett.* **1991**, *32*, 675; G. van Koten, *Pure Appl. Chem.* **1989**, *61*, 1681.

[3] E. Wehman, C. J. M. Erkamp, D. M. Knotter, J. T. B. H. Jastrzebski, C. H. Stam, G. van Koten, *Organometallics* **1989**, *8*, 94.

[4] W. J. J. Smeets, A. L. Spek, A. H. H. van der Zeijden, G. van Koten, *Recl. Trav. Chim. Pays-Bas* **1988**, *107*, 431.

[5] H. C. L. Abbenhuis, N. Feiken, H. F. Haarman, D. M. Grove, E. Horn, H. Kooijman, A. L. Spek, G. van Koten, *Angew. Chem.* **1991**, *103*, 1046; *Angew. Chem. Int. Ed. Engl.* **1991**, *30*, 996.

[6] I. C. M. Wehman-Ooyevaar, G. M. Kapteijn, D. M. Grove, A. L. Spek, G. van Koten, *J. Organomet. Chem.* submitted. This paper describes the synthesis, properties, and X-ray crystal structure of **6**. Compound **6** is the first example of a monomeric organolithium compound containing one additional equivalent of lithium bromide.

[7] **7**: ^1H NMR (200.13 MHz, C_6D_6, 24 °C): δ = 6.9–6.8 (m, 3, Ar-*H*), 2.75 (brs, NCH_3), 2.2 (brm, CH_2-CH_2), 1.9 (brs, $N(CH_3)_2$), Ar-CH_2-N protons not observed. ^{13}C NMR (50.32 MHz, C_6D_6, 24 °C): δ = 151.7 (Ar-C2 and 6), 128.4 (Ar-C4), 127.1 (Ar-C3 and 5), 69.4 (Ar-CH_2-N), 59.2 (-CH_2-), 52.4 (br, -CH_2-), 47.6 (-$N(CH_3)_2$), 46.4 (NCH_3), C_{ipso} not observed.

[8] Crystal data for **7**: $C_{36}H_{66}Br_3Cu_5N_8 \cdot C_4H_{10}O$, M_r = 1242.54, brownish plate-shaped crystals (0.86 × 0.43 × 0.08 mm), monoclinic, space group $P2_1$, with a = 11.132(1), b = 14.969(1), c = 15.232(2) Å, β = 90.33(1)°, V = 2537.9(4) Å^3, Z = 2, $\rho_{calcd.}$ = 1.626 g cm^{-3}, $F(000)$ = 1260, $\mu(Mo_{K\alpha})$ = 44.5 cm^{-1}, 6055 independent reflections ($1.34 < \theta < 27.5$ °; $\omega/2\theta$ scan; T = 295 K) were measured on an Enraf–Nonius CAD-4T/rotating anode diffractometer using graphite-monochromated $Mo_{K\alpha}$ radiation (λ = 0.71073 Å). Data were corrected for Lorentz-polarization effects, linear decay (19.5%) of the intensity control reflections, and absorption (DIFABS; correction range 0.759–1.237). The structure was solved by Patterson (SHELXS86) and difference Fourier techniques. Six carbon atoms [C28, C29, C30, C34, C35, and C36] were found disordered over two positions (52:48 ratio). Hydrogen atoms were introduced at calculated positions and refined riding on their carrier atoms [C–H = 0.98 Å]. All non-hydrogen atoms were refined with anisotropic thermal parameters, convergence was reached at R = 0.0312, wR = 0.0326, $w = 1/[\sigma^2(F) + 0.000343F^2]$ for 4322 reflections with $I > 2.5\sigma(I)$ and 577 parameters. The absolute structure was checked by refinement with opposite anomalous dispersion factors ($-if''$) resulting in R = 0.0362, wR = 0.0408. A final difference Fourier map shows no residual density outside −0.36 and 0.43 e A^{-3}. Further details of the crystal structure investigation are available on request from the Director of the Cambridge Crystallographic Data Centre, University Chemical Laboratory, Lensfield Road, GB-Cambridge CB2 1EW (UK), on quoting the full journal citation.

[9] G. van Koten, J. G. Noltes, *Comprehensive Organometallic Chemistry, Vol. 2* (Eds.: G. Wilkinson, F. G. A. Stone, E. W. Abel), Pergamon Press, Oxford, **1982**, Chapter 14.

[10] G. van Koten, *J. Organomet. Chem.* **1990**, *400*, 283.

[11] S. Jagner, G. Helgesson, *Adv. Inorg. Chem.* **1991**, *37*, 10, and references therein.

 © VCH Verlagsgesellschaft mbH, W-6940 Weinheim, 1993 0570-0833/93/0101-0073 $ 10.00+.25/0

Detection of Trimethylenemethane by IR Spectroscopy: The Result of an Unexpected Photoisomerization of Methylenecyclopropane in a Halogen-Doped Xe Matrix**

By *Günther Maier,* Hans Peter Reisenauer, Klaus Lanz, Ralf Tross, Dorothée Jürgen, B. Andes Hess, Jr.*, and *Lawrence J. Schaad*

Dedicated to Professor Rudolf Hoppe on the occasion of his 70th birthday

Cyclobutadiene (**1**) and trimethylenemethane (**2**) are the parent molecules of two fundamentally different families of conjugated hydrocarbons. Cyclobutadiene is the first member of the series of cyclic conjugated hydrocarbons (Kekulé compounds); trimethylenemethane, of the non-Kekulé hydrocarbons.[1]

1 **2**

Following simple Hückel theory, in **1** and **2** four π electrons are distributed over four C atoms, and one electron is placed in each of the two degenerate nonbonding molecular orbitals. Accordingly, both the square form of **1** (D_{4h}) and **2** (D_{3h}) should have triplet ground states. This is indeed true for **2** but not for **1**. The distinct arrangements of the individual centers account for this difference.[2]

During our studies of cyclobutadiene[3] we wondered even years ago[4] if matrix-isolation spectroscopy would be a good tool for the study of trimethylenemethane. Compound **2** was first prepared in 1966 by Dowd[5a] by irradiation of 4-methylenedihydropyrazole **3** in an organic matrix at −185 °C, and its existence was proven by ESR spectroscopy. Despite great efforts[6] our current understanding of **2** is still quite limited. The only certainty is that the irradiation of suitable precursors, for example **3**, **4**, or **7** (γ radiation), gives rise to triplet **2** in such low concentrations that it can be detected only with ESR spectroscopy.[5, 7] Species **2** is capable of existence at temperatures up to −150 °C.[5a] We report here for the first time the IR spectrum of **2**.

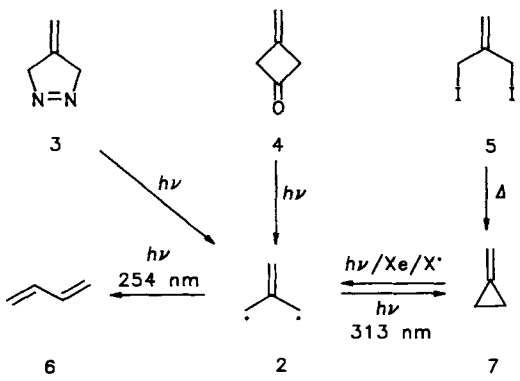

Our previous attempts[4] at isolating **2** in an argon matrix gave the following results: After irradiation (313 nm) of **3** in argon at 10 K a well-resolved ESR spectrum of **2** could be recorded, but in the IR spectrum only the bands of methylenecyclopropane **7** were recognizable.[8] When **3** was subjected to flash pyrolysis (400–600 °C) and the fragments were then isolated in argon at 10 K, **2** could not be detected even by ESR spectroscopy. The IR spectrum again showed only the bands of **7**. Diiodide **5**[9] was inert to irradiation (Ar, 10 K, 254 nm), and the combination of flash pyrolysis (500–800 °C)/matrix isolation[10] again provided exclusively **7**.

Despite these disappointing results we recently reopened our investigations, and our efforts have been rewarded: When ketone **4** was irradiated (Ar, 10 K, 300 nm) the ESR spectrum of **2** was observed. In the IR spectrum besides the bands of **7**, two miniscule absorptions are seen at 758 and 500 cm^{-1}[11] with an intensity ratio of roughly 4:1. These correspond to the two most intense bands in the predicted IR spectrum of **2**[12, 13] (Fig. 1).

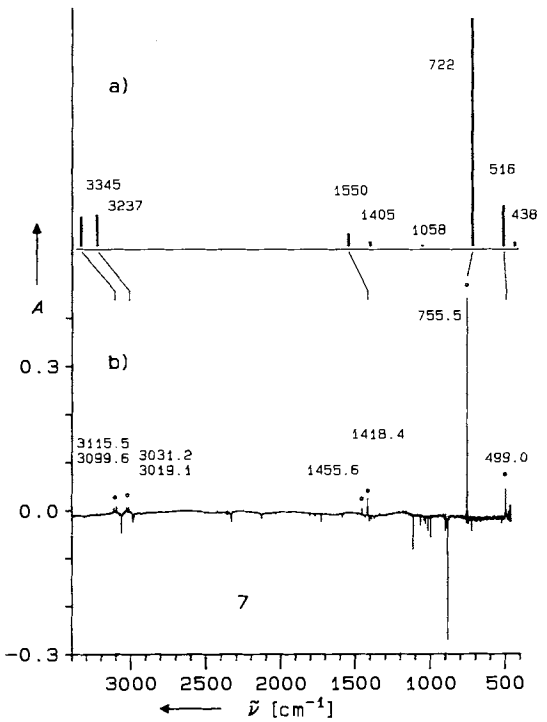

Fig. 1. IR spectrum of **2**: a) calculated (ab initio UMP2/6-31G*), b) measured (Xe matrix, 12 K, difference of the spectra after irradiation of **7**/Br_2 with light with a wavelength of 254 nm followed by irradiation with light with a wavelength of 313 nm). The bands with negative values of A arise from compound **7**.

Even more importantly, we found that these same bands (756, 499 cm^{-1}) arose when **5** was subjected to flash pyrolysis at 600 °C with xenon, the product mixture condensed at 10 K, and the matrix finally irradiated (254 nm). This observation was initially confusing, since **5** and methylenecyclopropane **7** formed in the thermolysis are photostable in xenon when irradiated separately. We conducted a long list of experiments to solve this mystery. The results: a) The source of **2** in these reactions is not **5** but **7**. b) The photoconversion **7** → **2** takes place in a xenon or a xenon/argon matrix (limiting ratio 1:4), but not in a pure argon matrix. c) Halo-

[*] Prof. Dr. G. Maier, Dr. H. P. Reisenauer, Dr. K. Lanz, Dipl.-Chem. R. Tross, Dipl.-Chem. D. Jürgen
Institut für Organische Chemie der Universität
Heinrich-Buff-Ring 58, D-W-6300 Giessen (FRG)
Prof. B. A. Hess, Jr., Prof. L. J. Schaad
Department of Chemistry, Vanderbilt Univerity
Nashville, TN 37235 (USA)

[**] Small Rings, Part 75. This research was supported by the Fonds der Chemischen Industrie. – Part 74: G. Maier, A. Schick, I. Bauer, R. Boese, M. Nussbaumer, *Chem. Ber.* **1992**, *125*, 2111–2117.

gen atoms (I$^{\bullet}$, Br$^{\bullet}$, or Cl$^{\bullet}$) must be present in the irradiation. d) The same IR spectrum is recorded regardless of which halogen is used.

Based on these results we devised two methods for the production of **2**. The halogen, that is, bromine or iodine, is pyrolyzed with xenon at 750 °C. The halogen atoms that arise are frozen onto a window cooled to 10 K along with a gaseous mixture of **7**/xenon, which is introduced separately. A Hg low-pressure lamp (254 nm) is then used for the irradiation. The formation of **2** by this procedure is faster and more effective than by the direct irradiation of halogen molecules (Cl_2, Br_2, or I_2) in a xenon matrix in the presence of **7**.

The identification of trimethylenemethane (**2**) formed in the xenon matrix is based primarily on the comparison of the measured with the calculated (ab initio UMP2/6-31G*; Table 1) IR spectrum (Fig. 1). Because of the D_{3h} symmetry

Table 1. Calculated vibrational spectrum of **2**; symmetry of the vibrations, wavenumbers in cm^{-1}, intensity in $km\,mol^{-1}$.

Sym.	$\tilde{\nu}$	Int.	Sym.	$\tilde{\nu}$	Int.
E'	438	1.58	E'	1058	0.02
A_1''	492		E'	1405	2.00
E''	498		E'	1550	6.78
A_2''	516	23.39	A_1'	1572	
E''	687		E'	3237	18.00
A_2''	722	133.72	A_1'	3243	
A_1'	982		A_2'	3342	
A_2'	992		E'	3345	16.88

of **2**, only 14 of the 24 fundamental vibrations are IR active and should result in 8 IR bands ($6E'$, $2A_2''$; calculated spectrum Fig. 1 top). The five most intense bands correlate well with the observed bands. The two strongest absorptions are assigned to the out-of-plane deformations (A_2'') of the hydrogen atoms (756 cm^{-1}) and C atoms of the framework (499 cm^{-1}) according to the calculations. The asymmetric C–C stretching frequency (E') calculated at 1550 cm^{-1} may correlate to the band observed at 1418 cm^{-1}. The IR band registered at 1456 cm^{-1} does not have an equivalent in the calculated spectrum and probably results from a combination vibration. Two weak "doublets" are observed in the region typical for C–H stretching frequencies; these correlate well with the two calculated E' type IR absorptions at 3345 and 3237 cm^{-1}. Matrix effects probably cause the splitting of these bands.

Besides the IR spectrum discussed, the typical ESR spectrum of **2** should also be measureable. This was achieved only with difficulty, as only very broad signals can be obtained in xenon matrices. A series of experiments with ketone **4** as the precursor and various argon/xenon ratios showed that the ESR bands were less resolved with an increasing proportion of xenon in the matrix.

A chemical structural proof of trimethylenemethane was found in the isomerization of **2** back to **7** upon irradiation (313 nm). This photoreaction is evident in the difference spectrum (Fig. 1 bottom). The bands of the product **7** appear as negative peaks, those of the starting material **2** as positive peaks. Light with a wavelength of 254 nm transforms **2** into *s-trans*-butadiene (**6**). Because of this photolability, a certain stationary concentration of **2** cannot be exceeded (maximum 25%[14]).

How does one explain the photoexcitation of **7**, a compound that does not absorb in the UV range? We assume that the photochemically or thermally generated halogen atoms X$^{\bullet}$ form exciplexes with xenon when irradiated, which then immediately relax to form the triatomic charge-transfer complexes **9**.[15] The exciplexes can be detected by UV absorption spectroscopy (Xe/I$^{\bullet}$: $\lambda_{max} = 280$ nm, Xe/Br$^{\bullet}$: $\lambda_{max} = 310$ nm, Xe/Cl$^{\bullet}$: $\lambda_{max} = 354$ nm), **9** with emission spectroscopy ($\mathbf{9} \rightarrow Xe + Xe + X^{\bullet} + h\nu$).[15] We presume that the energy stored in **9** is transferred to **7** across a long distance (ratio 7:Xe and X$^{\bullet}$:Xe < 1:1000). Exactly how the energy is relayed and how the ring cleavage of **7** is induced remains open. In any case the energy stored in **9** (50–

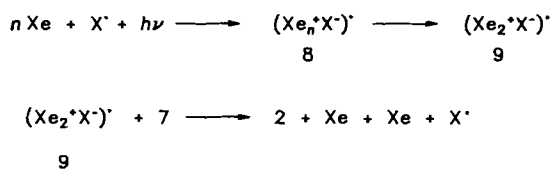

75 kcal mol^{-1}) is enough for the conversion of **7** into the excited singlet state of **2**,[16, 17] which then undergoes intersystem crossing to the triplet ground state. At 10 K the kinetic energy is too low to allow the back reaction to **7**, once **2** is formed.

If this description is true, irradiation in the presence of halogen atoms may be a fundamentally new method for the generation of highly reactive species in a xenon matrix. This could be applied to cases for which the previous methods (matrix photolysis of absorbing starting materials or the combination flash pyrolysis/matrix isolation) cannot be applied.

Received: September 19, 1992 [Z 5582 IE]
German version: *Angew. Chem.* **1993**, *105*, 119

[1] M. J. S. Dewar, *The Molecular Orbital Theory of Organic Molecules*, McGraw-Hill, New York, **1969**, p. 232–236.
[2] W. T. Borden, E. R. Davidson, *J. Am. Chem. Soc.* **1977**, *99*, 4587–4594.
[3] Review: G. Maier, *Angew. Chem.* **1988**, *100*, 317–341; *Angew. Chem. Int. Ed. Engl.* **1988**, *27*, 309–332, and references therein
[4] K. Lanz, *Diplomarbeit*, Universität Giessen, **1981**. See also footnote 14 in [10].
[5] a) P. Dowd, *J. Am. Chem. Soc.* **1966**, *88*, 2587–2589; b) P. Dowd, K. Sachdev, *ibid.* **1967**, *89*, 715–716; c) P. Dowd, A. Gold, K. Sachdev, *ibid.* **1968**, *90*, 2715–2716; d) R. J. Baseman, D. W. Pratt, M. Chow, P. Dowd, *ibid.* **1976**, *98*, 5726–5727; e) P. Dowd, M. Chow, *ibid.* **1977**, *99*, 6438–6440; f) P. Dowd, M. Chow, *Tetrahedron* **1982**, *38*, 799–807.
[6] Reviews: a) P. Dowd, *Acc. Chem. Res.* **1972**, *5*, 242–248; b) J. A. Berson, *ibid.* **1978**, *11*, 446–453; c) W. T. Borden, E. R. Davidson, *ibid.* **1981**, *14*, 69–76; d) J. A. Berson, *Capturable Diradicals of the Trimethylenemethane Series* in *Diradicals* (Ed.: W. T. Borden), John Wiley, New York, **1982**, pp. 151–194; e) D. A. Dougherty, *Acc. Chem. Res.* **1991**, *24*, 88–94.
[7] a) K. Takeda, H. Yoshida, K. Hayashi, S. Okamura, *Bull. Inst. Chem. Res. Kyoto Univ.* **1967**, *45*, 55–62; b) T. Yamaguchi, M. Irie, H. Yoshida, *Chem. Lett.* **1973**, 975–978; c) H. Yoshida, O. Edlund, *Chem. Phys. Lett.* **1976**, *42*, 107–110; d) O. Claesson, A. Lund, T. Gillbro, T. Ichikawa, O. Edlund, H. Yoshida, *J. Chem. Phys.* **1980**, *72*, 1463–1470.
[8] Cf. the same result from the matrix irradiation of **4**: A. Krantz, cited in footnote 14 in [5e].
[9] P. S. Skell, R. G. Doerr, *J. Am. Chem. Soc.* **1967**, *89*, 4688–4692.
[10] In analogy to the generation of allyl radical from allyl iodide: G. Maier, H. P. Reisenauer, B. Rohde, K. Dehnicke, *Chem. Ber.* **1983**, *116*, 732–740.
[11] Spectrometer: Bruker FT-IR IFS-85; these bands could not be found with the grating instrument we had used previously [4].
[12] 757 and 511 cm^{-1} (DZP/SCF; corrected): C. P. Blahous III, Y. Xie, H. F. Schaefer III, *J. Chem. Phys.* **1990**, *92*, 1174–1179; these authors also refer to the importance of the matrix IR spectrum of **2**.
[13] Our first calculation (November 1987; UHF/6-31G*) gave values of 731 and 523 cm^{-1}. The most recent data (UMP2/6-31G*) are listed in Table 1. We also calculated the spectra anticipated for the isotopomers of **2**. Current efforts are directed toward the experimental determination of these spectra.
[14] The yield given is based on the calculated band intensities of **2** (UMP2/6-31G*) and **7** (MP2/6-31G*).

 © VCH Verlagsgesellschaft mbH, W-6940 Weinheim, 1993 0570-0833/93/0101-0075 $ 10.00+.25/0

[15] a) M. E. Fajardo, V. A. Apkarian, *J. Chem. Phys.* **1986**, *85*, 5660–5681; *ibid.* **1988**, *89*, 4102–4123; *ibid.* **1988**, *89*, 4124–4136. The absorption spectra we measured correspond to the reported excitation spectra of the initially formed exciplexes **8**. The same is true of the emission spectra of the triatomic species **9**; b) I. Last, T. F. George, *J. Chem. Phys.* **1987**, 86, 3787–3794; I. Last, T. F. George, M. E. Fayardo, V. A. Apkarian, *ibid.* **1987**, *87*, 5917–5927.

[16] Triplet **2** is 27.5 kcal mol^{-1} higher in energy than **7**; singlet **2** is 15.3 kcal mol^{-1} higher in energy than triplet **2**: R. Janoschek, *Chem. Unserer Zeit* **1991**, *25*, 59–66; R. Janoschek, University of Graz, private communication.

[17] A single-electron transfer (SET) mechanism for the ring opening of **7** cannot be assumed. The energy for the irradiation is not enough to ionize **7** (IP = 9.57 eV; K. B. Wiberg, G. B. Ellison, J. J. Wendoloski, C. R. Brundle, N. A. Kuebler, *J. Am. Chem. Soc.* **1976**, *98*, 7179–7187).

Didodecylsexithiophene—A Model Compound for the Formation and Characterization of Charge Carriers in Conjugated Chains**

By *Peter Bäuerle,* Uwe Segelbacher, Kai-Uwe Gaudl, Dieter Huttenlocher,* and *Michael Mehring*

Oligothiophenes are among the best investigated model compounds for electrically conducting polymers.[1] The excellent properties, which in some respects surpass those of the related polymers,[2] are attained by stepwise chemical assembly leading to compounds with well-defined structures and controlled chain and conjugation length. The stability of the oligothiophenes in both their neutral and oxidized forms allows the precise characterization of the electronic structure and the charge carrier responsible for the conductivity along the conjugated chains.[3] The characterization of oligothiophenes in solution, in which the cooperative interactions characteristic of the solid state are eliminated, is more difficult because of their inherent reactivity in the oxidized state ($n \leq 5$) and their poor solubility with increasing chain length ($n \geq 6$). However, when the reactive terminal positions[4] are blocked or solubilizing alkyl groups are introduced to the oligomer,[5] the precise characterization of the oligomers in solution is possible.

In this context we have synthesized 3‴″-4′-didodecyl-2,2′:5′,2″:5″,2‴:5‴,2⁗:5⁗,2⁗′-sexithiophene (**1**), whose alkyl substituents in contrast to the compounds in previous studies are fixed at defined positions, and whose structure is established unambiguously by NMR spectroscopy and X-ray structure analysis.[6, 7] Sexithiophene **1** is the first compound of this type that can be oxidized to form a stable dication and also reduced to form a stable dianion. We report here on the preparation and characterization of the

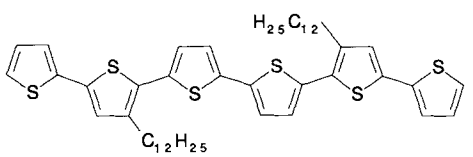

1

[*] Dr. P. Bäuerle, Dr. K.-U. Gaudl
Institut für Organische Chemie und Isotopenforschung der Universität
Pfaffenwaldring 55, D-W-7000 Stuttgart 80 (FRG)
Dipl.-Phys. U. Segelbacher, Dipl.-Phys. D. Huttenlocher,
Prof. M. Mehring
2. Physikalisches Institut der Universität
Pfaffenwaldring 57, D-W-7000 Stuttgart 80 (FRG)

[**] Thiophenes, Part 9. This research was supported by the Deutsche Forschungsgemeinschaft (SFB 329) and the Bundesminister für Forschung und Technologie (TK 0325). We thank Dr. A. Grupp and Dr. S. Sariciftci for helpful discussions. – Part 8 [6].

redox states of **1**; a dimerization of the radical cation $\mathbf{1}^{\bullet+}$ to $(\mathbf{1})_2^{2+}$ was also observed.

Controlled electrochemical and chemical oxidation (with iron trichloride), and reduction (with potassium) led to the different redox states of **1**, which were characterized by cyclic voltammetry, and absorption (Table 1) and ESR spectroscopy. The cyclic voltammogram exhibits two reversible waves in the oxidation part ($E_1^\circ = 0.34$ V and $E_2^\circ = 0.54$ V[8]) which correspond to a one-electron transfer in each step leading to the radical cation $\mathbf{1}^{\bullet+}$ and the dication $\mathbf{1}^{2+}$, respectively (Fig. 1). The first oxidation potential of **1** is close to that of polythiophene ($E^\circ = 0.30$ V[9]), which shows only one extremely broad redox wave because of the chain-length distribution in the polymer. Since the alkyl side chains improve the solubility, the reduction of **1** could also be examined. Two further reversible one-electron transfer steps were evident in the reduction cycle of the cyclic voltammogram ($E_3^\circ = -2.27$ V and $E_4^\circ = -2.40$ V) providing the radical anion $\mathbf{1}^{\bullet-}$ and the dianion $\mathbf{1}^{2-}$ (Fig. 1).

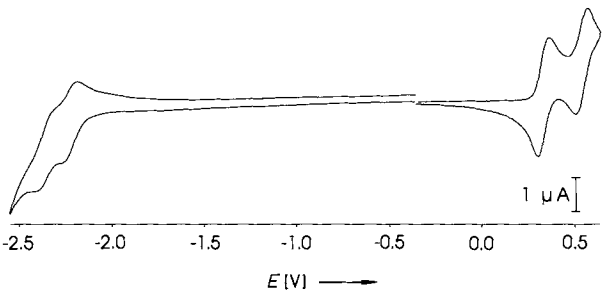

Fig. 1. Cyclic voltammogram of **1** recorded with a scan rate of 100 mVs^{-1}. The oxidation was measured in dichloromethane, the reduction in THF. The potentials are referenced to ferrocene (Fc)/Fc$^+$.

The stability of all the redox states allowed their characterization by absorption spectroscopy. In comparison to the unsubstituted sexithiophene **2** ($\lambda_{max} = 432$ nm, $E = 2.87$ eV),[3] the neutral dialkylsexithiophene **1** absorbs as expected at a somewhat shorter wavelength ($\lambda_{max} = 416$ nm, $E = 2.97$ eV), due to the steric interaction of the alkyl chains with the conjugated π system. This interaction is also reflected in the crystal structure of **1** by the twisting of the relevant thiophene rings by 10.8°.[7] Two bands are observed in the absorption spectrum of cation radical $\mathbf{1}^{\bullet+}$, each with shoulders [sh] at higher energies ($E = 0.87$, 1.14[sh], 1.60, 1.81[sh] eV) (Fig. 2 top); the structure and position of these bands are almost identical to those of $\mathbf{2}^{+}$ [3] (Table 1), indicating that the conjugated system becomes more planar during the transition from **1** to $\mathbf{1}^{\bullet+}$. Variable-temperature measurements show that the absorption spectrum changes with decreasing temperature; only two of the transitions ($E = 1.60$ and 0.87 eV) can be attributed to $\mathbf{1}^{\bullet+}$. These tran-

Table 1. Physical properties of the various redox states of **1** in comparison to **2** (values in parentheses from ref. [3]).

	1	$\mathbf{1}^+$	$(\mathbf{1})_2^{2+}$	$\mathbf{1}^{2+}$	$\mathbf{1}^-$	$\mathbf{1}^{2-}$
E° [V] [a]		0.34		0.54	−2.27	−2.40
E_1 [eV] [b]	2.97 (2.87)	1.60 (1.59)	1.81 (1.81 [c])	1.47 (1.36)	1.58	1.36
E_2 [eV] [b]		0.87 (0.84)	1.12 (0.98 [c])	1.31 (1.24)	0.72	1.20

[a] Redox potentials determined by cyclic voltammetry measured vs. Fc/Fc$^+$. [b] Transition energies determined from absorptions spectra. [c] These transitions were previously assigned [3] to the monocation $\mathbf{2}^{\bullet+}$.

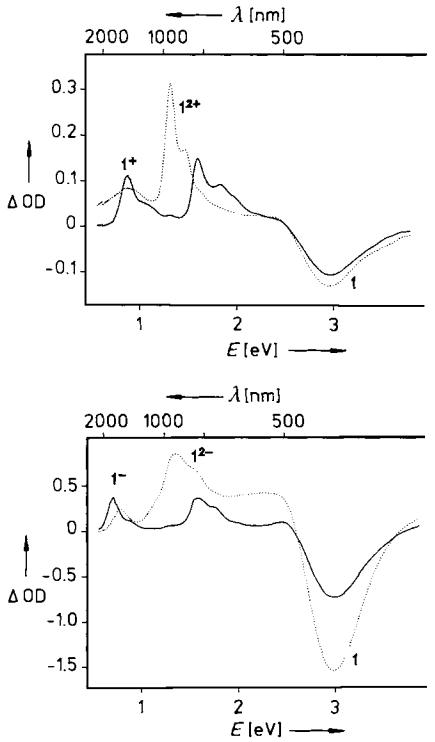

Fig. 2. Top: Difference absorption spectra of cation radical $\mathbf{1}^{\bullet+}$ (–) and dication $\mathbf{1}^{2+}$ (···) (vs. **1**) generated by chemical oxidation of **1** in dichloromethane with iron trichloride. Bottom: Difference absorption spectra of anion radical $\mathbf{1}^{\bullet-}$ (--) and dianion $\mathbf{1}^{2-}$ (···) (vs. **1**) obtained by reduction of **1** in THF with elemental potassium. OD = optical density.

sitions almost disappear at lower temperatures, whereas the bands at $E = 1.81$ and 1.14 eV become more pronounced (Fig. 3). This observation can be easily explained by the re

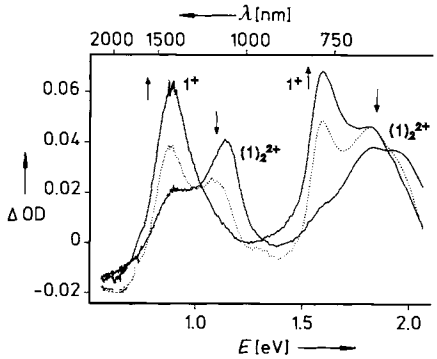

Fig. 3. Temperature-dependent absorption spectra of the dimer equilibrium $\mathbf{1}^{\bullet+} \rightleftharpoons (\mathbf{1})_2^{2+}$ starting at 244 K(--↓), 274 (···), and 294 K (–↑).

versible equilibrium between monocation $\mathbf{1}^{\bullet+}$ and a dimeric radical cation $(\mathbf{1})_2^{2+}$. Stable dimers of this type, also called pimers, have been described for other large aromatic cations of porphyrins,[10] phthalocyanines,[11], perylenes,[12] and viologens.[13] In every case the formation of the π dimer is accompanied by a blue-shift of the absorption band(s) of the monocation and the simultaneous emergence of a long-wavelength charge-transfer transition.[14] The π dimerization of cation radicals is also discussed in the context of the formation of conducting radical ion salts.[15]

At higher concentrations the dimerization of $\mathbf{1}^{\bullet+}$ to $(\mathbf{1})_2^{2+}$ is favored. ESR measurements also prove that spin pairing occurs as the temperature is lowered, causing the intensity of the ESR signal of $\mathbf{1}^{\bullet+}$ to decrease. Based on the temperature-dependence of the equilibrium constant, a value for the dimerization enthalpy, $\Delta H = -21$ kcal mol^{-1}, was found and determined from the intensity of the ESR signals. Although known for many years, the dimerization process has been neglected in the discussion of the properties of conducting polymers. The first report of the dimerization of a terthiophene cation radical was published only recently. In that case the dimerization tendency ($\Delta H = -10$ kcal mol^{-1}) is only half the value found for $(\mathbf{1})_2^{2+}$, correspoonding to the size of the molecule.[16] The variable-temperature studies of a series of oligothiophenes (trimer to pentamer) with combined in situ UV/VIS/NIR and ESR spectroscopy clearly demonstrates the dependence of the dimerization of the cation radicals on the chain length.[17]

Further oxidation of $\mathbf{1}^{\bullet+}$ leads to dication $\mathbf{1}^{2+}$, whose absorption spectrum exhibits a band with two maxima ($E = 1.47$ and 1.31 eV) (Fig. 2 top). In comparison to the absorptions of $\mathbf{2}^{2+}$ these bands are again shifted to higher energies. In this case, measurements at various temperatures do not show changes in the absorption spectrum, and an equilibrium with the dimer can thus be ruled out.

Successive chemical reductions of **1** provide monoanion $\mathbf{1}^{\bullet-}$ and dianion $\mathbf{1}^{2-}$. The π–π^* transitions of the anions are generally shifted to lower energies in comparison to those of the cations $\mathbf{1}^{\bullet+}$ and $\mathbf{1}^{2+}$ (Table 1). The absorption spectrum of anion radical $\mathbf{1}^{\bullet-}$ shows a band with fine structure and a maximum at $\lambda_{max} = 781$ nm ($E = 1.59$ eV). An absorption at unusually low energy in the near-IR regime is found ($\lambda_{max} = 1725$ nm, $E = 0.72$ eV; Fig. 2 bottom), which is very similar to that observed for the anion radicals of oligo-*p*-phenylenevinylenes.[18] The ESR spectrum of $\mathbf{1}^-$ proves its paramagnetic nature. In analogy to $\mathbf{1}^{2+}$, $\mathbf{1}^{2-}$ has an absorption band at $\lambda_{max} = 912$ nm ($E = 1.35$ eV; Fig. 2 bottom). Although dimerizations of anion radicals are known,[19] none is observed for the anionic species of **1**.

ESR measurements conducted for the unequivocal identification of the paramagnetic radical ions $\mathbf{1}^{\bullet+}$ and $\mathbf{1}^{\bullet-}$ also allowed the determination of the spin density distributions. The *g*-factors ($g = 2.0023$ and 2.0046, respectively) are in agreement with those of the radical ions of unsubstituted oligothiophenes[20] and doped poly(3-methylthiophene).[21] The *g*-factor of $\mathbf{1}^{\bullet-}$ is substantially greater than that of $\mathbf{1}^{\bullet+}$, indicating that the orbitals of the sulfur atoms are significantly involved in the SOMO of $\mathbf{1}^{\bullet-}$. In contrast, the electronic structure of cation radical $\mathbf{1}^{\bullet+}$ more closely resembles that of a *cis*-polyene system due to the limited involvement of the sulfur atoms in the SOMO. A preliminary determination and assignment of the spin densities was possible by simulation of the ESR spectra and accompanying calculations.[22] The spin density distributions obtained are represented in Figure 4. Besides the expected localization of spin density at the terminal α C atoms, it is worth noting that in both paramagnetic species the largest hyperfine coupling constants and the highest spin densities are localized on β carbon atoms. This is in agreement with the fact that in the course of the oxidative polymerization of heterocycles such as thiophenes and pyrroles even at short chain lengths incorrect linkages and cross-couplings occur due to α,β-couplings and β,β-couplings, respectively, which interfere and interrupt the conjugated chain. Similar charge distributions were calculated for pyrrole oligomers.[23]

The enhanced stability and solubility of **1** allow the precise characterization of the electronic structure of the different redox states. The temperature-dependent formation of the diamagnetic dimeric cation radical $(\mathbf{1})_2^{2+}$ in solution pro-

 © VCH Verlagsgesellschaft mbH, W-6940 Weinheim, 1993 0570-0833/93/0101-0077 $ 10.00+.25/0

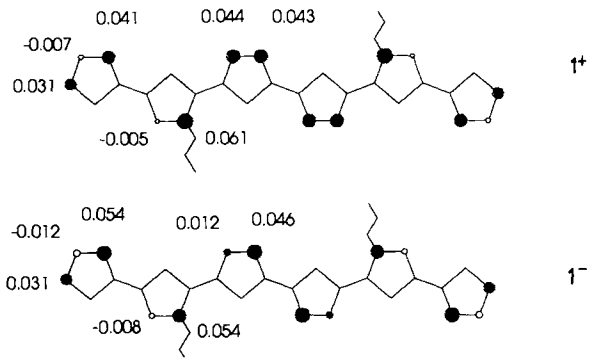

Fig. 4 The experimentally determined spin-density distribution of cation radical $\mathbf{1}^{\bullet+}$ (top) and anion radical $\mathbf{1}^{\bullet-}$ (bottom). The radii of the circles are proportional to the spin density; unfilled circles represent negative spin densities.

vides a new alternative to the description of the doping behavior of polythiophenes and conducting polymers in general. Thus, the formation of corresponding dimeric species complementary to polarons and bipolarons, can now be considered as the first mechanistic step during doping. This fact easily explains the observation that the ESR activity of polarons in conducting polymers[21] and cation radicals in longer oligomers[5a] is detected only at unexpectedly low levels of doping, in the first case, or not at all, in the second. Nevertheless, the findings described here do not necessarily disagree with the existence of polaronic and bipolaronic bands in highly doped conjugated polymers. In addition, the anionic redox states of **1** are the first models for negatively charged defects in thiophene chains. The n-doping of polythiophene is possible otherwise only under extreme conditions.[24]

Received: August 31, 1992 [Z 5547 IE]
German version: *Angew. Chem.* **1993**, *105*, 125

[1] Z. Xu, D. Fichou, G. Horowitz, F. Garnier, *J. Electroanal. Chem.* **1989**, *267*, 339–342; C. vanPham, A. Burckhardt, R. Shabana, D. D. Cunningham, H. B. Mark, Jr., H. Zimmer, *Phosphorous Sulfur Silicon Relat. Elem.* **1989**, *46*, 153–168; F. Martinez, R. Voelkel, D. Naegele, H. Naarmann, *Mol. Cryst. Liq. Cryst.* **1989**, *167*, 227–232; J. Nakayama, T. Konishi, M. Hoshino, *Heterocycles* **1988**, *27*, 1731–1754; H. Nakahara, J. Nakayama, M. Hoshino, K. Fukuda, *Thin Solid Films* **1988**, *160*, 87–97; D. D. Cunningham, L. Laguren-Davidson, H. B. Mark, Jr., C. vanPham, H. Zimmer, *J. Chem. Soc. Chem. Commun.* **1987**, 1021–1023; J. Nakayama, T. Konishi, S. Murabayashi, M. Hoshino, *Heterocycles* **1987**, *26*, 1793–1796.
[2] B. Xu, G. Horowitz, D. Fichou, F. Garnier, *Adv. Mater.* **1990**, *2*, 592–594.
[3] D. Fichou, G. Horowitz, B. Xu, F. Garnier, *Synth. Met.* **1990**, *39*, 243–260.
[4] P. Bäuerle, *Adv. Mater.* **1992**, *4*, 102–107.
[5] a) A. Yassar, D. Delabouglise, M. Hmyene, B. Nessak, G. Horowitz, F. Garnier, *Adv. Mater.* **1992**, *4*, 490–494; b) D. Delabouglise, M. Hmyene, G. Horowitz, A. Yassar, F. Garnier, *ibid.* **1992**, *4*, 107–110; c) W. ten Hoeve, H. Wynberg, E. E. Havinga, E. W. Meijer, *J. Am. Chem. Soc.* **1991**, *113*, 5887–5889; d) E. E. Havinga, I. Rotte, E. W. Meijer, W. ten Hoeve, H. Wynberg, *Synth. Met.* **1991**, *41*, 473–478; e) D. M. deLeeuw, *ibid.*, in press (Proc. Int. Conf. Synth. Met. Göteborg, **1992**).
[6] P. Bäuerle, F. Pfau, H. Schlupp, F. Würthner, K.-U. Gaudl, M. Balparda Caro, P. Fischer, *J. Chem. Soc. Perkin Trans 2*, in press.
[7] P. Bäuerle, K.-U. Gaudl, F. Pfau, S. Henkel, unpublished results. In the X-ray structures of sexithiophene **1** and the related precursor 3′-dodecyl-2,2′:5′,2″-terthiophene both have the same torsion angle with a value of 10.8 and 11.0°, respectively, for the thiophene rings which are sterically hindered by the alkyl side chains. In the case of **1** not all of the bond lengths and angles have yet been obtained with satisfactory precision because of the small size of the crystals examined and the resulting weak reflections. For this reason the X-ray structure is not discussed further here.
[8] Oxidations of **1** were measured in dichloromethane, reductions in tetrahydrofuran at a concentration of 5×10^{-4} mol L^{-1} with tetrabutylammonium hexafluorophosphate (0.1 M) as the supporting electrolyte. The working electrode was a platinum disk 1 mm in diameter, the counterelectrode a platinum wire, and the reference electrode a Ag/AgCl electrode which was calibrated with ferrocene after each measurement.
[9] We measured the oxidation potential of polythiophene under identical conditions.
[10] J. Fuhrhop, P. Wasser, D. Riesner, D. Mauzerall, *J. Am. Chem. Soc.* **1972**, *94*, 7996–8001.
[11] E. Ough, Z. Gasyna, M. J. Stillman, *Inorg. Chem.* **1991**, *30*, 2301–2310.
[12] K. Kimura, T. Yamazaki, S. Katsumata, *J. Phys. Chem.* **1971**, *75*, 1768–1774.
[13] W. Geuder, S. Hünig, A. Sachy, *Tetrahedron* **1986**, *42*, 1665–1677.
[14] Since the absorption bands of the dimer $(\mathbf{1})_2^{2+}$ are blue-shifted relative to those of $\mathbf{1}^{\bullet+}$, we suspect that another charge-transfer absorption exists in the near-IR region ($E < 0.6$ eV), which cannot be observed because of the solvent absorptions in this region.
[15] V. Enkelmann, B. S. Morra, C. Kröhnke, G. Wegner, J. Heinze, *Chem. Phys.* **1982**, *66*, 303–313.
[16] M. G. Hill, K. R. Mann, L. L. Miller, J.-F. Penneau, *J. Am. Chem. Soc.* **1992**, *114*, 2728–2730.
[17] U. Segelbacher, P. Bäuerle, D. Huttenlocher, A. Grupp, M. Mehring, unpublished results.
[18] R. Schenk, H. Gregorius, K. Müllen, *Adv. Mater.* **1991**, *3*, 492–493.
[19] R. H. Boyd, W. D. Phillips, *J. Chem. Phys.* **1965**, *43*, 2927–2929.
[20] A. Alberti, L. Favoretto, G. Seconi, *J. Chem. Soc. Perkin. Trans. 2*, **1990**, 931–935.
[21] M. Schärli, H. Kiess, G. Harbeke, W. Berlinger, K. W. Blazey, K. A. Müller, *Springer Ser. Solid State Sci.* **1988**, *76*, 277–280.
[22] Since ENDOR measurements were not possible and selectively deuterated compounds not available, the spin-density distribution and hyperfine coupling constants were calculated with an INDO program (M. Plato, E. Tränkle, W. Lubitz, F. Lendzian, K. Möbius, *Chem. Phys.* **1986**, *107*, 185–196). Assignment of the fitted hyperfine values was possible by comparison to those obtained by theoretical calculations. A detailed presentation of the ESR results will be published in due course (D. Huttenlocher, A. Grupp, P. Bäuerle, M. Mehring, unpublished results).
[23] R. J. Waltman, J. Bargon, *Tetrahedron*, **1984**, *40*, 3963–3970.
[24] M. Aizawa, S. Watanabe, H. Shinohara, H. Shirakawa, *J. Chem. Soc. Chem. Commun.* **1985**, 264–265.

Reaction of Buckminsterfullerene with *ortho*-Quinodimethane: a New Access to Stable C_{60} Derivatives**

By *Pavel Belik, Andreas Gügel, Jochen Spickermann*, and *Klaus Müllen**

The fullerene synthesis reported by Krätschmer et al. in 1990,[1] the discovery of fascinating material properties of fullerenes and their derivatives,[2] and the development of efficient processes to separate fullerene mixtures[3] have led to a burgeoning number of publications on this class of material in the last two years. These papers are primarily concerned with the physico-chemical aspects of fullerenes and less with their functionalization.[4] This one-sidedness has the following causes: 1) C_{60} is an exceptionally stable molecule that adds most reaction partners reversibly only,[5] 2) fullerene and fullerene adducts are only slightly soluble, 3) the determination of the structure of fullerene adducts is extremely complex because of the large number of possible products and isomers, and 4) high-performance chromatographic methods are necessary to separate the fullerene adducts. Nevertheless, there are already some papers which report successful syntheses and isolations of fullerene derivatives.[6] Here we present a new access to stable C_{60} derivatives.

For addition to the electron-poor "superalkene" C_{60} (**1**), which easily adds radicals, *o*-quinodimethane[7] seemed particularly suitable. It can be prepared in situ containing differ-

[*] Prof. Dr. K. Müllen, Dipl.-Chem. P. Belik, Dipl.-Chem. A. Gügel, J. Spickermann
Max-Planck-Institut für Polymerforschung
Ackermannweg 10, D-W-6500 Mainz (FRG)

[**] We thank Dipl.-Chem. U. Koch for preparing the structural formulas. This work was supported by the Bundesministerium für Forschung und Technologie (project 13 N 6076).

ent functional groups[8] and forms very reactive dienes that can form [4 + 2] cycloadducts even with the least reactive dienophiles.

A simple method to generate *o*-quinodimethane is the iodine-induced 1,4-elimination at 1,2-bis(bromomethyl)-benzene, which is usually performed in dimethylformamide (DMF).[9] Because C_{60} (**1**) is almost insoluble in DMF, the synthesis must be transferred to toluene through the phase transfer catalyst, [18]crown-6. C_{60} (**1**) reacts with 1 equivalent of 1,2-bis(bromomethyl)benzene, 2.2 equivalents of KI, and 8.1 equivalents of [18]crown-6 within 6 h in boiling toluene to form the monoadduct **2** (88%, based on converted C_{60}) and the bisadduct **3** (7%). Unchanged C_{60} (37.8% based on employed amount of C_{60}) was recovered (Scheme 1).

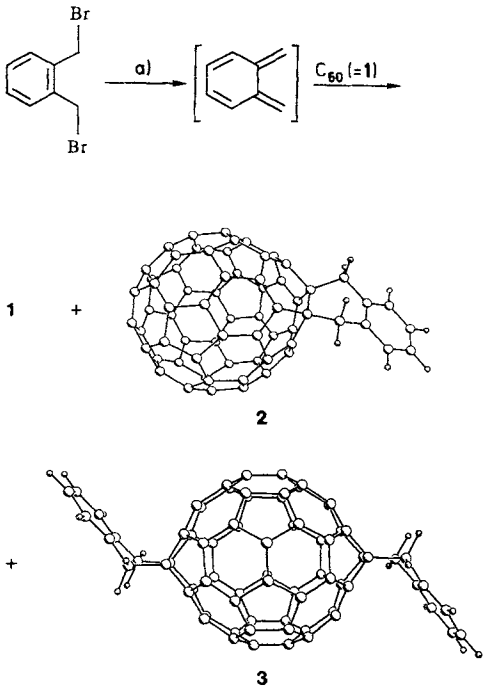

Scheme 1. Reaction of C_{60} with *o*-quinodimethane (for **3** only one of the possible isomers is given) [15]. a) KI, [18]crown-6, toluene, reflux.

The separation of **1**, **2**, and **3** was achieved by gel permeation chromatography (GPC) on polystyrene gel with toluene as eluent[10] (Fig. 1). Since the products are sufficiently soluble in toluene (solubility of the monoadduct: about 30 mg mL^{-1}), 10 gram amounts of crude product can be separated on a 20 × 600 mm column per day.[3]

The reversibility of addition reactions has often proved to be the central problem in C_{60} chemistry.[5] The elugram of the crude product, as well as the mass spectrum of fractions 1 and 2,[11] show that adducts **2** and **3** do not fragment during the reaction or in the mass spectrometer. The monoadduct sublimes above about 400°C without decomposition. Only traces of a trisadduct can be detected.

NMR spectroscopy yields important information about structure. Addition at a double bond between two annelated six-membered rings is proved by the number of ^{13}C NMR signals in the region for aromatic carbon atoms. Seventeen such signals indicate a C_{2v} symmetry for the molecule (a result of rapid ring inversion of the cyclohexene unit). Addition at a double bond between a five- and a six-membered ring would lower the symmetry because of the absence of a

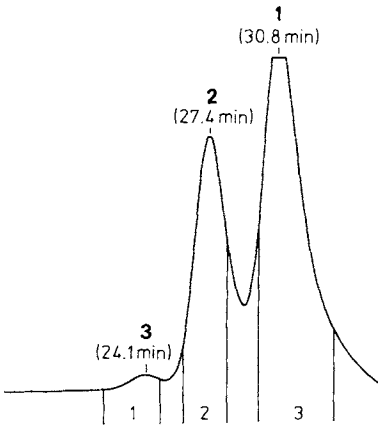

Fig. 1. Separation of **1**, **2**, and **3**, indicating cuts for fractions 1, 2, and 3. Column: 20 × 600 mm; stationary phase: Shodex K-2001 polystyrene gel, 5 μm, 50 Å; mobile phase: 5 mL min^{-1} toluene; detection: UV at 340 nm; injection of 1 mL of toluene solution.

mirror plane. The ^{13}C chemical shift (δ = 66.09) for the two C_{60} carbon atoms that participated in the addition, as well as the number of signals in the region for aromatic carbon atoms, rule out a 1,6-substituted [10]annulene[12] as structural unit, since 18 signals would be expected. The ring inversion of the cyclohexene ring is slow on the NMR time scale at room temperature. This is easy to recognize by the splitting of the signals for the methylene protons.

This synthesis is a valuable addition to preparative fullerene chemistry because of its selectivity and the high stability of the adducts. Its versatility was tested through an analogous reaction of C_{60} with bis-*o*-quinodimethane (Scheme 2). The bisadduct of this reaction was isolated by

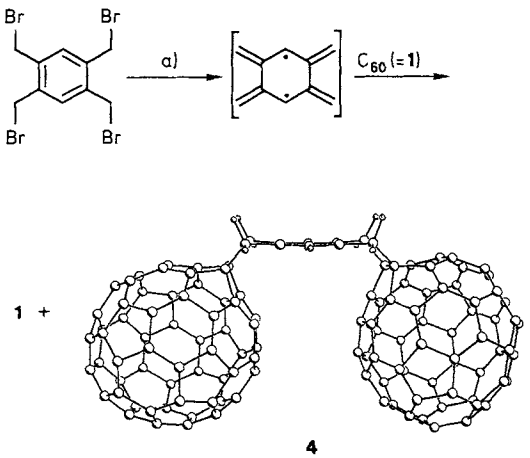

Scheme 2. Reaction of C_{60} with bis(*o*-quinodimethane) (for **4** only the *cis* isomer is represented) [15]. a) KI, [18]crown-6, toluene, reflux.

GPC and characterized by ^{1}H NMR spectroscopy and mass spectrometry. Typical for compound **4**, a dumbbell-shaped molecule, is a distinctly lower solubility than C_{60} and a slightly longer elution time on the GPC column (all the compounds we studied thus far eluted before C_{60}). This makes the isolation of larger amounts of **4** considerably more difficult.

We are now trying to prepare adducts that are suitable for polymerization, for example by transformation with *o*-quinodimethanes functionalized with carboxyl and hydroxyl groups.

Experimental Procedure

Preparation: C_{60} (**1**, 100 mg, 0.139 mmol) [13], 1,2-bis(bromomethyl)benzene (37 mg, 0.139 mmol), KI (50 mg, 0.3 mmol), and [18]crown-6 (300 mg, 1.13 mmol) in toluene (50 mL) were heated under reflux under an inert atmosphere (argon) in the dark for 6 h. The solution became dark brown. The reaction mixture was allowed to cool to room temperature, washed with NaOH (5%) and then H_2O, and evaporated to dryness under vacuum. The brown solid was taken up in toluene (10 mL), and the solution filtered through a 0.25 μm Teflon membrane filter. After the chromatographic separation described next, methanol was added to fraction 2 to precipitate the brown solid, which was dried for 4 h at 100 °C and 10^{-2} Torr.

Chromatography [3,14]: Elution pump: Master pump M 305 with pump head 25SC; injection pump M 306 with pump head 25SC. Detector: UV detector M 115 with 0.3 μL flow-through cell (light path 0.1 mm). Fraction collector: 201 C. Column: 20 × 600 mm filled with polystyrene gel (5 μm, 50 Å). Amount injected: 1 mL of the toluene solution. Mobile phase: toluene, 5 mL min^{-1}.

Fraction 1: **3** (7%, based on converted C_{60}); MS(FD): *m/z* 822 ([*M* of **2**−2H]$^+$, 8%), 824 (M^+ of **2**, 7%), 928 (M^+, 100%), 944 ([*M* + O]$^+$, 9%), 1032 (M^+ of trisadduct, 4%); UV/VIS (CH_3Cl): unstructured.

Fraction 2: **2** (88%, based on converted C_{60}); MS(FD): *m/z* 824([*M*]$^+$, 100%), 840 ([M^+ + O]$^+$, 2%), 928 (M^+ of **3**, 2%); UV/VIS (CH_3Cl): similar to C_{60}, but less structured; ^{1}H NMR (500 MHz, $C_2Cl_4D_2$, 28 °C): δ = 4.46 (d broadened, 2 H; CH_2); 4.82 (d broadened, 2 H; CH_2); 7.57–7.59, 7.69–7.71 (m, AA'BB' system of the arene); measurement at 125 °C: δ = 4.70 (s, 4 H; CH_2); ^{13}C NMR (125 MHz, $C_2Cl_4D_2$, 80 °C, *J*-modulated spin echo for ^{13}C): δ = 45.28 (benzyl-C); 66.09 (aliphat. quaternary C_{60} C atoms); 128.02, 128.09 (H-subst. aromat. C atoms), 135.76, 138.21, 140.20, 141.66, 142.13, 142.30, 142.62, 143.17, 144.78, 145.42, 145.49, 145.51, 145.85, 146.30, 146.52, 147.76, 156.93 (17 arene signals).

Fraction 3: **1** (37.8%, based on initial C_{60}).
4: ^{1}H NMR (500 MHz, CS_2, 28 °C): δ = 4.79 (d broadened, 4H; CH_2); 5.27 (d broadened, 4 H; CH_2); 8.18 (s, 2H; arene).

Received: September 12, 1992 [Z 5569 IE]
German version: *Angew. Chem.* **1993**, *105*, 95

[1] W. Krätschmer, L. D. Lamb, K. Fostiropolous, D. R. Huffman, *Nature* **1990**, *347*, 354.
[2] See for example R. C. Haddon, *Acc. Chem. Res.* **1992**, *25*, 127–134; P. W. Stephens, D. Cox, J. W. Lauher, L. Mihaly, J. B. Wiley, P. Allemand, A. Hirsch, K. Holczer, Q. Li, J. D. Thompson, F. Wudl, *Nature* **1992**, *355*, 331–332; Y. Wang, L. Cheng, *J. Phys. Chem.* **1992**, *96*, 1530–1532.
[3] A. Gügel, M. Becker, D. Hammel, L. Mindach, J. Räder, T. Simon, M. Wagner, K. Müllen, *Angew. Chem.* **1992**, *104*, 666–667; *Angew. Chem. Int. Ed. Engl.* **1992**, *31*, 644–645; M. S. Meier, J. P. Selegue, *J. Org. Chem.* **1992**, *57*, 1924–1926.
[4] Of the 334 papers published between 1.5.1992 and 25.8.1992, only 13 were concerned with functionalization of fullerenes; see for example T. Suzuki, Q. Li, K. C. Khemani, F. Wudl, *J. Am. Chem. Soc.* **1992**, *114*, 7300–7301.
[5] In our experience, compounds like allylmagnesium bromide, phenyllithium, diphenylisobenzofuran, or tetraphenylcyclopentadienone add reversibly to C_{60}, and the retroreactions for some start in solution at room temperature already. However, extensive fragmentation and retroreactions of the adducts are always observed in the mass spectrometer under FD or FAB conditions.
[6] For example: J. M. Hawkins, A. Meyer, T. A. Lewis, S. Loren, F. J. Hollander, *Science* **1991**, *252*, 312–313; T. Suzuki, Q. Li, K. Khemani, F. Wudl, Ö. Almarson, *ibid.* **1991**, *254*, 1186–1188; A. Hirsch, A. Soi, H. R. Karfunkel, *Angew. Chem.* **1992**, *104*, 808–810; *Angew. Chem. Int. Ed. Engl.* **1992**, *31*, 766–768.
[7] J. J. McCullough, *Acc. Chem. Res.* **1980**, *13*, 270–276; J. L. Charlton, M. M. Alauddin, *Tetrahedron* **1987**, *43*, 2873–2889.
[8] See for example P. G. Sammes, *Tetrahedron* **1976**, *32*, 405–422; K. P. C. Vollhardt, *Angew. Chem.* **1984**, *96*, 525–541; *Angew. Chem. Int. Ed. Engl.* **1984**, *23*, 539–556; W. Oppolzer, D. A. Roberts, T. G. C. Bird, *Helv. Chim. Acta* **1979**, *62*, 2017–2021; W. Oppolzer, D. A. Roberts, *ibid.* **1980**, *63*, 1703–1705; R. Gray, C. G. Harruff, J. Krymowski, J. Peterson, V. Boekelheide, *J. Am. Chem. Soc.* **1978**, *100*, 2892–2893; Y. Tamura, A. Wada, M. Sasho, Y. Kita, *Tetrahedron Lett.* **1981**, *22*, 4283–4286; T. Tuschka, K. Naito, B. Rickborn, *J. Org. Chem.* **1983**, *48*, 70–76; Y. Ito, M. Nakatsuka, T. Saegusa, *J. Am. Chem. Soc.* **1980**, *102*, 863–865; Shin-ichi Inaba, R. M. Wehmeyer, M. W. Forkner, R. D. Rieke, *J. Org. Chem.* **1988**, *53*, 339–344.
[9] M. P. Cava, D. R. Napier, *J. Am. Chem. Soc.* **1957**, *79*, 1701–1705; M. P. Cava, A. A. Deana, K. J. Muth, *ibid.* **1959**, *81*, 6458–6460.
[10] The factors causing the separation are unknown. A mechanism based purely on size considerations can be excluded, because the difference in size of the products is too small and the retention times too long. Similarly good separations are also obtained with other C_{60} addition products.
[11] The FD mass spectra were recorded on a ZAB 2-SE FPD (VG instruments). The sample was placed on the emitter wire dissolved in CS_2.
[12] E. Vogel, *Pure Appl. Chem.* **1982**, *54*, 1015–1039.
[13] The C_{60} purified by chromatography over polystyrene (see ref. [3]) still contains toluene after drying at 80 mbar and 80 °C (according to TGA measurements, 3 equiv). Drying for 24 h in an oil-pump vacuum at 200 °C removes the toluene completely. The C_{60} free of toluene was used for further reaction.
[14] Pumps, detector, and fraction collector from the company Gilson (Abimed Analysen-Technik GmbH, Langenfeld); column from Showadenko.
[15] The structures were optimized with the force-field program MOMO (H. Beck, M. Dyrbusch, E. Egert, MOMO, version 1.0, University of Frankfurt, **1991**), and the cartesian coordinates transferred to XP for manipulation (XP-Interactive Molecular Graphics, Version 4.1, Siemens Analytical X-Ray Inst. Inc., **1990**).

Photosensitized Oxygenation of an Acyl Furan: Isolation of the First Furan Dioxetane by Rearrangement of its Endoperoxide and Selected Chemical Transformations**

By *Waldemar Adam,* Michael Ahrweiler,* and *Markus Sauter*

Recently we reported the novel thermal rearrangement of benzofuran dioxetanes to the 1-oxaspiro[2,5]octadienone derivative,[1] which are formed in addition to the usually expected dioxetane cleavage products [Eq. (a)]. Analogous

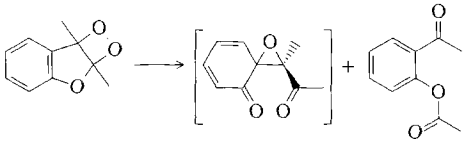

(a)

cis-diacyl-substituted epoxides have been observed for the thermolysis of furan endoperoxides,[2, 3] but the mechanistic details of this isomerization still need to be convincingly defined. We suspected that furan dioxetanes are immediate precursors to such *cis*-diacyloxiranes, which constitute photooxygenation products of furans.[2b] Indeed, the isomerization of a furan endoperoxide to its dioxetane has been followed by spectroscopy,[2d] but the subsequent rearrangement to the epoxide not mentioned. In Scheme 1 we present the first example of such a sequence of transformations in the photooxygenation of the acyl furan **1**. Remarkable is the fact that the furan dioxetane **3** is sufficiently persistent (actually less labile than its endoperoxide **2**) to permit isolation and full characterization.

2,3,6,6-Tetramethyl-4,5,6,7-tetrahydrobenzo[*b*]furan-4-one (**1**), prepared according to the literature,[4] gave with singlet oxygen at −35 °C the endoperoxide **2** in quantitative yield (Scheme 1, step a). The endoperoxide **2** rearranged in solution at −20 °C within two days (step b) and instantly on silica gel (step c) into the dioxetane **3**. The spectroscopic data in Table 1 and iodometric titration support the structural assignment of the peroxides **2** and **3**. At elevated temperature (step d), the endoperoxide **2** decomposed directly into the dioxetane cleavage product **4** and the spiroepoxide **5** in a ratio of 42:58. Under the same conditions (step d), the dioxetane **3** gave the expected cleavage product **4** and the spiroepoxide **5** in ratio of 40:60. Most surprising was the quan-

[*] Prof. Dr. W. Adam, Dipl.-Chem. M. Ahrweiler, Dipl.-Chem. M. Sauter
Institut für Organische Chemie der Universität
Am Hubland, D-W-8700 Würzburg (FRG)

[**] This work was supported by the Deutsche Forschungsgemeinschaft (SFB-172: "Molekulare Mechanismen kanzerogener Primärveränderungen") and the Fonds der Chemischen Industrie.

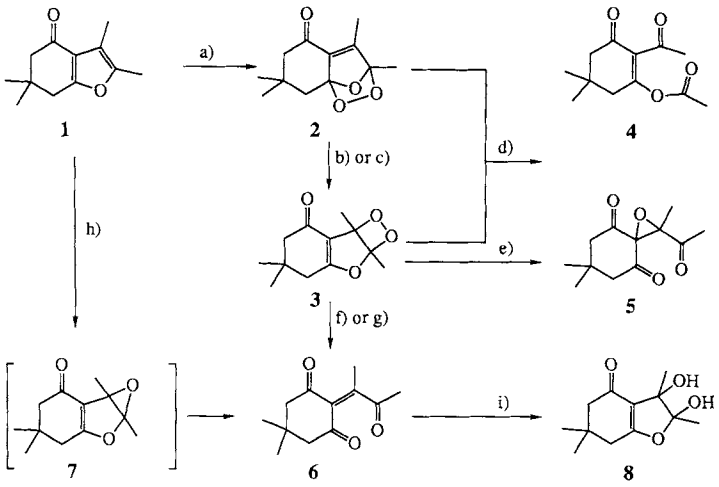

Scheme 1. a) O_2, tetraphenylporphyrin (TPP), *hv*, CH_2Cl_2, −35 °C, 1.5 h, ca. 100%; b) $CDCl_3$, −20 °C, 48 h, ca. 75%; c) silica gel, pentane, −40 °C, 74%; d) $CDCl_3$, 20 °C, 12 h, ca. 85%, **4**:**5** = 40:60; e) 1 mol% Et_4NBr_4, $CDCl_3$, 0 °C, 4 h, > 95% **5**; f) Ph_2S, CD_2Cl_2, −100 °C, 1 min, > 95%; g) PPh_3, $CDCl_3$, −80 °C, > 95%; h) [D_6]dimethyldioxirane, [D_6]acetone, −40 °C, 1.5 h, > 95%; i) 1.1 equiv H_2O, [D_6]acetone, −20 °C, 1 h, > 90%.

titative rearrangement (step e) of the dioxetane **3** to the spiroepoxide **5** with catalytic amounts (1 mol%) of Et_4NBr. A control experiment revealed that the endoperoxide **2** was stable towards Et_4NBr under these conditions. The structure of the unusual spiroepoxide **5** was assigned on the basis of spectroscopic data and elemental analysis. Characteristic are the epoxide ^{13}C resonances at $\delta = 73.1$ and 73.9 (Table 1).

Deoxygenation of the dioxetane **3** by Ph_2S (step f) or Ph_3P (step g) gave the enedione **6** quantitatively. Not even traces of the expected epoxide **7** could be detected by ^1H or ^{13}C NMR monitoring of the deoxygenation product mixture at temperatures as low as −100 °C. No persistent furan epoxides are known to date;[5] for example, epoxidation of furanes by *meta*-chloroperoxobenzoic acid[6a] and dimethyldioxirane[6b] afforded enediones quantitatively as oxidation products.

Table 1. Physical and spectroscopic data of **2**–**6** and **8** [a].

2: Colorless oil; ^1H NMR [b]: $\delta = 1.05$, 1.06 (s, 6 H), 1.76 (s, 3 H), 2.15 (s, 2 H), 2.23 (s, 3 H), 2.30 (s, 2H); ^{13}C NMR [c]: $\delta = 10.7$ (q), 11.4 (q), 28.6 (q), 28.9 (q), 32.3 (s), 35.9 (t), 53.6 (t), 112.5 (s) [d], 132.0 (s), 152.8 (s), 194.9 (s).

3: Yellow prisms, m.p. 63–64 °C (CH_2Cl_2/pentane); ^1H NMR [b]: $\delta = 1.08$, 1.19 (s, 6 H), 1.76 (s, 3 H), 1.86 (s, 3 H), AB system ($\delta_A = 2.22$, $\delta_B = 2.38$, $J = 13.0$ Hz, 2 H), AB system ($\delta_A = 2.40$, $\delta_B = 2.60$, $J = 20.0$ Hz, 2 H); ^{13}C NMR [c]: $\delta = 16.9$ (q), 17.3 (q), 28.2 (q), 28.9 (q), 33.8 (s), 37.6 (t), 51.3 (t), 94.1 (s), 116.0 (s), 119.8 (s), 181.5 (s) 194.0 (s); IR (CCl_4): ν[cm^{-1}] = 2970, 2870, 1670, 1625, 1465, 1385, 1300, 1230, 1150.

4: ^1H NMR [e]: $\delta = 1.20$ (s, 6 H, CH_3), 2.02 (s, 2 H), 2.15 (s, 2 H), 2.23 (s, 3 H, CH_3), 2.47 (s, 3 H, CH_3); ^{13}C NMR [f]: $\delta = 21.2$ (q), 26.9 (q), 27.7 (q), 32.5 (s), 43.1 (t), 51.3 (t), 129.9 (s), 165.8 (s), 167.4 (s), 194.5 (s), 196.8 (s).

5: Colorless oil; ^1H NMR [e]: $\delta = 0.93$ (s, 3 H), 1.04 (s, 3 H), 1.33 (s, 3 H), 2.24 (s, 3 H), 2.62 (m, 4 H); ^{13}C NMR [f]: $\delta = 13.4$ (q), 26.9 (q), 27.7 (q), 30.3 (q), 31.2 (s), 54.8 (t) 55.1 (t), 73.1 (s), 73.9 (s), 199.5 (s), 200.4 (s), 205.1 (s); IR (CCl_4): ν[cm^{-1}] = 2980, 2960, 1750, 1740, 1510, 1420, 1380, 1130.

6: Colorless powder, m.p. 135–137 °C (acetone); ^1H NMR [e]: $\delta = 1.10$ (s, 6 H), 2.33 (s, 3 H), 2.36 (s, 3 H), 2.52 (s, 2 H), 2.59 (s, 2 H); ^{13}C NMR [f]: $\delta = 19.9$ (q), 27.5 (q), 28.3 (q), 30.2 (s), 52.2 (t), 54.1 (t), 129.0 (s), 167.1 (s), 197.6 (s), 198.7 (s), 205.2 (s); IR (CCl_4): ν[cm^{-1}] = 2980, 1705, 1670, 1610, 1365, 1240.

8: ^1H NMR [b]: $\delta = 1.07$ (s, 6 H, CH_3), 1.42 (s, 3 H, CH_3), 1.49 (s, 3 H, CH_3) 2.18 (s, 2 H), 2.24 (s, 2 H); ^{13}C NMR [c]: $\delta = 20.2$ (q), 20.6 (q), 27.6 (q), 33.3 (s), 37.6 (t), 51.4 (t), 76.2 (s), 103.5 (s), 131.7 (s), 177.1 (s), 194.7 (s).

[a] For all new compounds consistent elemental analyses were obtained except for **2**, **4** and **8**, which were too labile for purification; the purity of the peroxides **2** and **3** was > 98% as determined by iodometry. [b] 200 MHz, −20 °C. [c] 50 MHz, −20 °C. [d] Two carbons with identical resonances, established by the inverse gated technique. [e] 250 MHz, 20 °C. [f] 100 MHz, 20 °C.

It appeared to us important, therefore, to attempt the direct epoxidation of the tetrahydrobenzofuran **1**. Indeed, treatment with [D_6]dimethyldioxirane in an NMR tube at −40 °C (step h) resulted in the enedione **6** quantitatively. Unfortunately, the tetrahydrobenzofuran **1** was not sufficiently reactive towards this dioxirane to conduct the epoxidation below −40 °C; however, in view of our deoxygenation results for dioxetane **3** (steps f and g), the expected furan epoxide **7** probably rearranges to the enedione **6** already at −100 °C.

When enedione **6** was treated with water (step i), the labile diol **8** was obtained essentially quantitatively. The ^{13}C NMR signals at $\delta = 76.2$ and 103.5 for the tertiary alcohol and the acetal carbons are in the expected region; these results cast doubt on the existence of the recently proposed epoxide **9**, for which a nearly identical chemical shift is obtained.[5a] Within 4 h at −20 °C or upon warming to room temperature, the diol **8** decomposed completely to a complex mixture. The lability of diol **8** precluded attempts to purify it by low-temperature chromatography (silica gel, −30 °C).

Thus, we succeeded in isolating and fully characterizing the first furan dioxetane through thermal or silica gel catalyzed isomerization of its furan endoperoxide. The subsequent rearrangement of the furan dioxetane to the corresponding spiroepoxide seems to be quite general and was hitherto not recognized. It occurs selectively on treatment with catalytic amounts of Et_4NBr, an unprecedented process in dioxetane chemistry. The mechanism of this novel Br^--catalyzed rearrangement of furan dioxetanes to *cis*-diacyloxirane apparently involves a S_N2 attack on the dioxetane peroxide bond.[7]

Received: August 22, 1992 [Z 5527 IE]
German version: *Angew. Chem.* **1993**, *105*, 104

[1] W. Adam, L. Hadjiarapoglou, T. Mosandl, C. R. Saha-Möller, D. Wild, *J. Am. Chem. Soc.* **1991**, *113*, 8005–8011.

[2] a) H. H. Wasserman, A. Lieberles, *J. Am. Chem. Soc.* **1960**, *82*, 2086; b) J. P. LeRoux, J. J. Basselier, *C.R. Acad. Sci. Paris Sect. C* **1970**, *271*, 461–462; c) M. R. Iesce, F. Cermola, M. C. Graziano, G. Cimminiello, R. Scarpati, *J. Chem. Soc. Perkin Trans. 1* **1992**, 1855–1858, and references cited therein; d) M. R. Iesce, M. C. Graziano, F. Cermola, R. Scarpati, *J. Chem. Soc. Chem. Commun.* **1991**, 1061–1062.

[3] a) K. Gollnick, A. Griesbeck, *Tetrahedron* **1985**, *41*, 2057–2068; b) E. L. Clennan, *ibid.* **1991**, *47*, 1343–1382.

[4] E. Bisagni, R. Royer, *Bull. Soc. Chim. Fr.* **1962**, 925–932.

[5] S. Oishi, S. D. Nelson, *J. Org. Chem.* **1992**, *57*, 2744–2747. In this paper the furan epoxide **9a** is proposed on the basis of ^{13}C NMR spectroscopic data; however, not only are the reaction conditions rather unusual for the formation of such labile epoxides, and contrary to our experience with the more persistent benzofuran epoxides **10a** [1], but the reported data are more consistent with the structure of the diol **9b**. This becomes evident if the spectroscopic data of the epoxide-diol pairs is compared with that of **10a**,**b** [1] and **11a**,**b** [6c]. Presumably diol **9b** results from the hydrolysis of the enedione, the rearrangement product of the epoxide **9a**, because it is difficult to prepare anhydrous solutions of dimethyldioxirane in acetone.

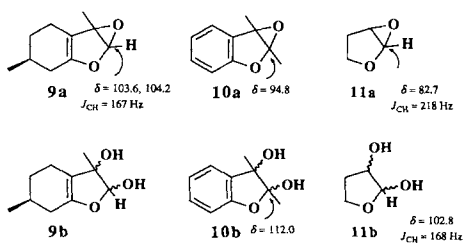

[6] a) P. W. Jennings, *J. Org. Chem.* **1989**, *53*, 5186–5188; b) B. M. Adger, C. Barrett, J. Brenan, M. Anthony, M. C. Kervey, R. W. Murray, *J. Chem. Soc. Chem. Commun.* **1991**, 1553–1554; c) S. W. Baertschi, K. D. Raney, M. P. Stone, T. M. Harris, *J. Am. Chem. Soc.* **1988**, *110*, 7929–7931.

[7] W. Adam, M. Heil, *J. Am. Chem. Soc.* **1992**, *114*, 5591–5598.

$[(Me_3Sn^{IV})_2Mo^{VI}O_4]$: An Organometallic Quasi-AB_2 System with a Layered Structure**

By *Ulrich Behrens, Abdul K. Brimah, Kenan Yünlü,* and *R. Dieter Fischer**

Organometallic esters, for example of the type $[(R_3E^{IV}O)_2Cr^{VI}O_2]$ (R = alkyl, aryl; E = Si, Ge, Sn, Pb), are found relatively often in patent literature; however, up to now hardly any basic research has been conducted on the compound class $[(R_3E^{IV})_2M^{VI}O_4]$ (M = Cr, Mo, W).[1] So far, only one compound (R = Ph, E = Si, M = Cr[2]) has been characterized by X-ray diffraction, while the higher homologues with M = Mo and W have remained unknown.

Through our work on novel three-dimensional coordination polymers of the general composition $[(R_3E)_nM(\mu\text{-}X)_m]_\infty$ (X is e.g. CN, SCN, O[3]), we have found that compounds of the type $[(R_3E)_2MO_4]$ (**1**) with E = Sn and Pb; M = Mo and W, but not Cr, are accessible by precipitation from aqueous solution [Eq.(a)].

$$2\,R_3ECl + Na_2[MO_4] \xrightarrow[(Me_2CO)]{H_2O} [(R_3E)_2MO_4]\downarrow + 2\,NaCl \qquad (a)$$

1a, R = Me, E = Sn, M = Mo
1b, R = Me, E = Pb, M = Mo
1c, R = Me, E = Sn, M = W

In contrast to the chemically more labile, yellow Cr homologues,[1] the colorless molybdates and tungstates **1**[4] are sparingly soluble in H_2O (pH range 3–10) and stable up to 350 °C. So far we have only obtained optimal single crystals of **1a** as an unexpected by-product during attempts to crystallize coordination polymers **2**[5] in air [Eq.(b)][24].

$$4\,Me_3SnCl + K_4[Mo(CN)_8]\cdot 2\,H_2O \xrightarrow[(O_2)]{H_2O} \underset{\mathbf{2}}{[(Me_3Sn)_4Mo(CN)_8]_\infty} + 4\,KCl \quad (+\,\mathbf{1a}) \qquad (b)$$

The less abundant, colorless crystals of **1a** grew, nevertheless, faster than the yellow crystals of **2** from the initially saturated, clear solution of the starting materials. Formation of **1a** from Me_3SnCl and $K_4[Mo^{IV}(CN)_8]\cdot 2H_2O$ did not occur when air was strictly excluded; the question concerning the true origin of the $[Mo^{VI}O_4]^{2-}$ ions still needs to be addressed.[6, 7, 17] The identity of product obtained according to Equations (a) and (b), **1a**, was confirmed by the good correlation of the experimental Debye–Scherrer photograph of **1a** from reaction (a) with the powder diagram calculated[8] from single-crystal data of **1a** from reaction (b).

Although the structural framework of **1a** (Fig. 1) contains tetrahedral MoO_4 and trigonal-bipyramidal (tbp) Me_3SnO_2 units (with shared O atoms),[9] principally conceivable *three*-dimensional networks (e.g. of the cristobalite type[10]) are not formed. The actual, relatively compact,[11] *layered* structure resembles that of the genuine AB_2 system HgI_2 (red modification[12]). Replacement of the Hg atoms with Mo atoms and of the iodide bridges with the practically linear {O–Sn–O} bridges would provide **1a**. Layers result from the interlinkage of quasi-linear strands (Scheme 1) parallel to the *a* and *b* axes. Only van der Waals forces may be acting between adjacent layers with the sequence ABCDA···. The uniform Mo–O distance of 1.770(8) Å corresponds roughly to those observed in $K_2[MoO_4]$ and $[MoO_3(tren)]$ (tren = diethylenetriamine[13]). The ν and δ (Mo–O) vibrational frequencies are weakly shifted in comparison to those of the "free" $[MoO_4]^{2-}$ ions.[14] The uniform Sn–O distance of 2.268(9) Å in **1a** correlates well with the corresponding distances in the tbp-configured R_3SnO_2 building unit of the polymeric esters $[(R_3Sn)_2CO_3]_\infty$ (R = Me, Et, *i*Bu[16]).

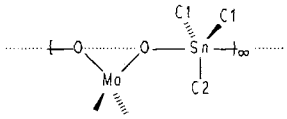

Scheme 1.

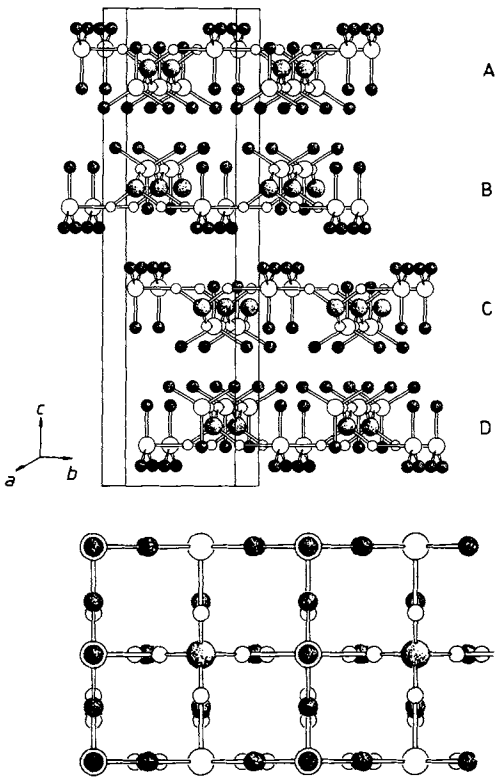

Fig. 1. Top: The layered structure and unit cell of **1a** (SCHAKAL plot: H atoms are omitted). Open circles: large, Sn; small, O; dotted circles: large, Mo; small, C. Bond lengths [Å]: Sn–O, 2.268(9), Mo–O, 1.770(8), Sn–C1, 2.095(18), Sn–C2, 2.147(18); bond angles [°]: O-Mo-O', 107.4(5), 110.5(3), O-Sn-O', 179.8(4), Mo-O-Sn, 143.6(4), O-Sn-C1, 90.0(1), O-Sn-C2, 90.1(2). Bottom: The framework of **1a** as viewed along the *c* axis.

The Pb homologue of **1a**, $[(Me_3Pb)_2MoO_4]$ (**1b**), which can even be crystallized according to Equation (a) (but not (b)[17]), is isostructural with **1a**. The poorer quality of the single crystal of **1b** and its strong X-ray absorption led, however, to less satisfactory results for the structure analysis.[18] $[(Me_3Sn)_2WO_4]$ (**1c**) is also isostructural with **1a** according to its X-ray powder diagram. Corresponding "alloyed" polymers with variable Mo/W or Mo/Cr content (and E = Sn) are also accessible by Equation (a). The CP-MAS ^{13}C solid-state NMR spectra of both **1a** and **1b** show only *one* symmetric signal between + 20 and −40 °C, despite the fact that there are two nonequivalent methyl C atoms in the asymmetric unit.[19] Obviously the Me_3Sn groups rotate "freely" about the O-Sn-O axes on the NMR timescale.[20]

[*] Prof. Dr. R. D. Fischer, Prof. Dr. U. Behrens, Dr. A. K. Brimah, Dr. K. Yünlü
Institut für Anorganische und Angewandte Chemie der Universität
Martin-Luther-King-Platz 6, D-W-2000 Hamburg 13 (FRG)

[**] This work was supported by the Deutsche Forschungsgemeinschaft and the Fonds der Chemischen Industrie. We thank T. M. Soliman (deceased), K. Saliminia, and J.-U. Schütze for carrying out certain experiments.

Because of their polymeric layered structures, **1a** and **1b** differ fundamentally from the monomeric molecular compounds $[(Ph_3SiO)_2CrO_2]$[2] and $[(Me_3SiO)_2SO_2]$.[21] In contrast, the anionic sublattice $[(Et_3Sn^{IV})_2Cu^{I}(CN)_4^-]_\infty$ in the new host–guest system $[(nBu_4N)(Et_3Sn)_2Cu(CN)_4]_\infty$ [22] has a noncubic, *three*-dimensional framework comprised of bent [-Cu-CN-Sn-NC-]$_\infty$ chains. The new polymers **1** appear destined to open the way to genuine intercalation compounds; on the other hand, it cannot be ruled out that the incorporation of appropriately sized guest molecules may occasionally result in the formation of, for example, cristobalite-like *three*-dimensional host systems. Attempts to incorporate cobaltocene into **1a** according to Equation (c)[23] (with $0 < n \leq 1$) showed that even under relatively mild conditions light-brown to gray products form slowly from the colorless starting material **1a**; the IR spectra of the products show metallocene absorption bands in addition to the otherwise unchanged vibrational spectra of the starting material.

$$[(Me_3Sn^{IV})_2Mo^{VI}O_4] + n[Cp_2Co^{II}] \rightarrow [(Cp_2Co^{III})_n(Me_3Sn^{IV})_2Mo^{V}_nMo^{VI}_{1-n}O_4] \quad (c)$$

Experimental Procedure

Typical preparation of **1**, R = Me, M = Mo: A saturated aqueous solution of 1.2 g (5 mmol) $Na_2[MoO_4]\cdot 2H_2O$ was added dropwise with stirring to a saturated aqueous solution of 1.0 g (5 mmol) Me_3SnCl. The air-stable, colorless precipitate which occurred spontaneously was filtered, washed on the frit thoroughly with H_2O, and dried at 100 °C in a drying oven. Yield: 1.0 g (80%). Decomposition temp.: 360 °C (discolored to ocher-yellow). The organotin compounds with R ≠ Me which are less soluble in H_2O were fully dissolved by adding some acetone.

Received: September 4, 1992 [Z 5556 IE]
German version: *Angew. Chem.* **1993**, *105*, 117

[1] J. Holecek, R. Wagener, *Main Group Met. Chem.* **1988**, *11*, 91.
[2] a) B. Stensland, P. Kierkegaard, *Acta Chem. Scand.* **1970**, *24*, 211. b) Furthermore, the structure of the three-dimensional polymer $[(Me_3Sn)_3CrO_4(OH)]$ is also known: A. M. Domingos, G. M. Sheldrick, *J. Chem. Soc. Dalton Trans.* **1974**, 477.
[3] See: U. Behrens, A. K. Brimah, T. M. Soliman, R. D. Fischer, D. C. Apperley, N. A. Davies, R. K. Harris, *Organometallics*, **1992**, *11*, 1718, and references therein.
[4] The corresponding molybdates with R = Me, Et, *n*Pr, *n*Bu, and Ph and the tungstates with R = Me, Et, and *n*Pr were prepared (from the appropriate R_3SnCl and $Na_2[MO_4]\cdot 2H_2O$) and characterized by IR spectroscopy and elemental analysis (each gave the correct analytical values!).
[5] K. Yünlü, S. Dülsen, R. D. Fischer, unpublished results, **1984**.
[6] $K_4[Mo(CN)_8]\cdot 2H_2O$ was obtained by reductive cyanization of $Na_2[MoO_4]$ (cf. G. Bauer, *Handbuch der Präparativen Anorganischen Chemie*, Enke, Stuttgart, **1991**, p. 1551); the material did not have any significant IR or Raman bands in the range where the very strong ν(Mo–O) absorption of MoO_4^{2-} is found [24].
[7] Upon exposure to light the yellow $[Mo^{IV}(CN)_8]^{4-}$ hydrolyzes to the red $[Mo^{IV}O_2(CN)_4]^{4-}$ (cf. J. T. Hoard, T. A. Hamor, M. D. Glick, *J. Am. Chem. Soc.* **1968**, *90*, 3177), but neither this anion nor its blue protonated product $[Mo^{IV}O(OH)(CN)_4]^{3-}$ react spontaneously with O_2 (but with CO_2); cf. P. R. Robinson, E. O. Schlemper, R. K. Murmann, *Inorg. Chem.* **1975**, *14*, 2035.
[8] Calculation program PULVERIX; we thank Dr. H. Viebrock for performing the calculation.
[9] X-ray structural analysis of **1a** (M_r = 487.52): Tetragonal, space group $I4(1)/amd$ (No. 141); $a = b = 7.390(2)$, $c = 25.936(5)$ Å, $V = 1416.5(6)$ Å^3; $Z = 4$; $\varrho_{calcd} = 2.286$ g cm^{-3}; crystal size $0.2 \times 0.3 \times 0.8$ mm; Syntex $P2_1$ four-circle diffractometer, 2θ range: 4.5–55.0°, 478 symmetry-independent reflections of which 311 with $F > 4\sigma(F)$ were utilized for the refinement (SHELXTL PLUS); 23 refined parameters, $R = 0.038$, $R_w = 0.039$ (after absorption correction with DIFABS). Further details of the crystal structure investigation may be obtained from the Fachinformationszentrum Karlsruhe, Gesellschaft für wissenschaftlich-technische Information mbH, D-W-7514 Eggenstein-Leopoldshafen 2 (FRG) on quoting the depository number CSD-56682, the names of the authors, and the journal citation.
[10] One cubic cristobalite-like three-dimensional polymer with adamantane-like cavities (half filled) is, for example, $[(NMe_4^+)Cu^{I}Zn^{II}(CN)_4]_\infty$, see: B. F. Hoskins, R. J. Robson, *J. Am. Chem. Soc.* **1990**, *112*, 1546; cf. also: T. Kitazawa, S. Nishikiori, A. Yamagishi, R. Kuroda, T. Iwamoto, *J. Chem. Soc. Chem. Commun.* **1992**, 413; Furthermore, the three-dimensional polymer $[CoHg(SCN)_4]_\infty$ has a "diamondlike" structure; cf.: J. W. Jefferey, K. M. Rose, *Acta Crystallogr. Sect. B* **1968**, *24*, 653.
[11] Formula volume, V_f, as determined by X-ray diffraction (calcd from: $V_f = 0.602\, V_f/Z = M_r/\varrho_{calc}$): 220 Å^3; calculated for a hypothetical cristobalite-like three-dimensional polymer: 480 Å^3.
[12] G. A. Jeffrey, M. Vlasse, *Inorg. Chem.* **1967**, *6*, 396; see also H. Krebs, *Grundzüge der Anorganischen Kristallchemie*, Enke, Stuttgart, **1968**, p. 230 and U. Müller, *Anorganische Strukturchemie*, Teubner, Stuttgart, **1991**, p. 248.
[13] a) B.M. Gatehouse, P. Leverett, *J. Chem. Soc.* **A 1969**, 849; $(Mo-O)_{av} = 1.76 \pm 0.01$ Å; b) F. A. Cotton, R. C. Elder, *Inorg. Chem.* **1964**, *3*, 397; $(Mo-O)_{av}$: 1.737 Å, see also [15].
[14] Despite the local D_{2d} symmetry of each $Mo(OSn)_4$ fragment, the observed vibrational spectrum of the MoO_4 unit follows the selection rules for T_d symmetry: $K_2[MoO_4]$ ($\tilde{\nu}$ in cm^{-1}), IR 318, *841*; Raman 318, *841*, 897 [15]. **1a**, IR *860*; Raman 310, 348, *867*, 918 (ν(Mo–O) in italics).
[15] F. Gonzalez-Vilchez, W. R. Griffith, *J. Chem. Soc. Dalton Trans.* **1972**, 1416.
[16] R = Me, *i*Bu (Sn-O 2.248–2.272 Å) J. Kümmerlein, A. Sebald, H. Reuter, *J. Organomet. Chem.* **1992**, *427*, 309, R = Et (Sn-O 2.27 Å) A. K. Brimah, M. Kapphahn, R. D. Fischer, unpublished results.
[17] Even when a diluted $Me_3PbCl/K_4[Mo(CN)_8]$ solution (4:1) was kept under N_2, only dark undefinable products precipitated (see also refs.[6,7]).
[18] *a*: 7.634(9) Å, *c*: 25.922(32) Å, essentially the same atomic coordinates as for **1a**; Mo–O 1.85(4) Å, Pb–O 2.35(5) Å; $R = 0.1058$, $R_w = 0.0889$ (despite absorption correction with DIFABS) for $w^{-1} = \sigma^2 F$. No data were deposited.
[19] Only a sharp singlet and a weaker satellite doublet were observed for both. $\delta(^{13}C)/^1J(^{13}C, ^{119}Sn)$ or $^1J(^{13}C, ^{209}Pb)$ [ppm/Hz]: **1a**, 3.8/488; **1b**, 20.6/350. We thank Dr. M. Kapphahn (Hamburg) for performing the CP-MAS NMR investigation.
[20] See also: D. C. Apperley, N. A. Davies, R. K. Harris, S. Eller, P. Schwarz, R. D. Fischer, *J. Chem. Soc. Chem. Commun.* **1992**, 740.
[21] Cf. L. H. Sommer, G. T. Kerr, F. C. Whitmore, *J. Am. Chem. Soc.* **1948**, *70*, 445.
[22] A. K. Brimah, U. Behrens, R. D. Fischer, unpublished results.
[23] For a most recent example of $Mo^{VI} \rightarrow Mo^{V}$ reduction with $[Cp_2Co]$ see: Z. Xiao, C. G. Young, J. H. Enemark, A. G. Wedd, *J. Am. Chem. Soc.* **1992**, *114*, 9194
[24] Note added in proof (Dec. 15, 1992): Experiments with analytically pure $K_4[Mo(CN)_8]\cdot 2H_2O$ prepared from MoO_3 [6] (ν(Mo–O) IR and Raman bands are completely absent) did not afford any **1a**.

A Diastereoselective Synthesis of β-(*N*-Acylamino)aldehydes by Rearrangement of *O*-Vinyl-*N*,*O*-Acetals**

By *Herbert Frauenrath,* Thomas Arenz, Gerhard Raabe,* and *Martin Zorn*

Dedicated to Professor Hermann Stetter on the occasion of his 75th birthday

Chiral carbonyl compounds with a nitrogen-containing substitutent in the β position are important building blocks or intermediates in the synthesis of pharmaceuticals such as β-lactams. The stereoselective construction usually required is achieved by the Mannich reaction, the conjugated addition of amines to α,β-unsaturated carbonyl compounds, and the addition of enolates or allyl metal compounds to imines.[1–6] These methods, however, do not allow access to a great number of target structures. We report here on a new synthe-

[*] Prof. Dr. H. Frauenrath, Dipl.-Chem. T. Arenz, Dr. G. Rabbe, Dipl.-Chem. M. Zorn
Institut für Organische Chemie der Technischen Hochschule
Professor-Pirlet-Strasse 1, D-W-5100 Aachen (FRG)

[**] This research was supported by the Deutsche Forschungsgemeinschaft.

Table 1. Synthesis of compounds **1**–**3**[a].

Cmpd. **1**-**3**	R	R^2	R^3	Yield [%] **1**	Yield [%] [b] **2**	*cis*:*trans* [b]	Yield [%] [c] **3**	*de*	Mol % TMSOTf
a	CH_3	CH_3	$C(CH_3)_3$	93	90 (88)	18:82 (89:11)	67 (70)	>96	100
b	C_6H_5	CH_3	$C(CH_3)_3$	82	88 (90)	28:72 (45:55)	48 (62)	88	50
c	$C(CH_3)_3$	CH_3	$C(CH_3)_3$	68	65	27:73	53 (58)	>96	50
d	CH_3	CH_3	$CH(CH_3)_2$	66	93 (88)	40:60 (83:17)	67 (80)	70	60
e	C_6H_5	CH_3	$CH(CH_3)_2$	86	95 (88)	32:68 (82:18)	62 (75)	58	30

[a] All new compounds gave correct elemental analyses and suitable IR spectra (for ^1H NMR and ^{13}C NMR spectroscopic data of **3a** see Table 2). [b] Reaction temperature 70 °C; data in parentheses from reaction at 0 °C. [c] Data in parentheses: yields determined by NMR spectroscopy.

sis of chiral β-(*N*-acylamino)aldehydes which proceeds with high *syn* selectivity and requires few steps.

In recent work on the acid-catalyzed rearrangement of *N*,*O*-acetals **2** we showed that *N*,*N*-dialkyl *O*-allyl-*N*,*O*-acetals **1** (R^1,R^2 = alkyl) form aminomethylbutadienes even under the conditions for the isomerization of **1**; the Mannich products **3** are most likely the intermediates.[7] In contrast, *N*,*N*-diacylated *N*,*O*-acetals **2** (R^1,R^2 = RCO) do not undergo acid-catalyzed rearrangement.[8] Thus, monoacylated compounds **2** (R^1 = RCO, R^2 = alkyl) should be suitable starting materials with intermediate reactivity for the stereoselective synthesis of β-(*N*-acylamino)aldehydes.

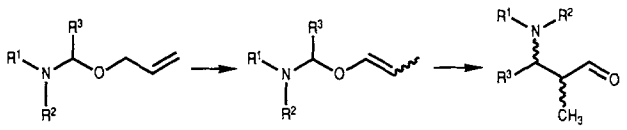

1 **2** **3**

Compounds **1a**–**e** (Table 1) were prepared in a one-pot reaction by acylation of Schiff bases **4** followed by alcoholysis with allyl alcohol according to the procedure of Böhme et al.[9] Compounds **1a**–**e** were isomerized to **2a**–**e** with ruthenium hydrides generated in situ from $[RuCl_2(PPh_3)_3]$ and $NaBH_4$.[10] We observed here that in the isomerization the configuration of the double bond could be influenced by temperature (Table 1). This indicates that the catalyst induces a further *cis*–*trans* isomerization.

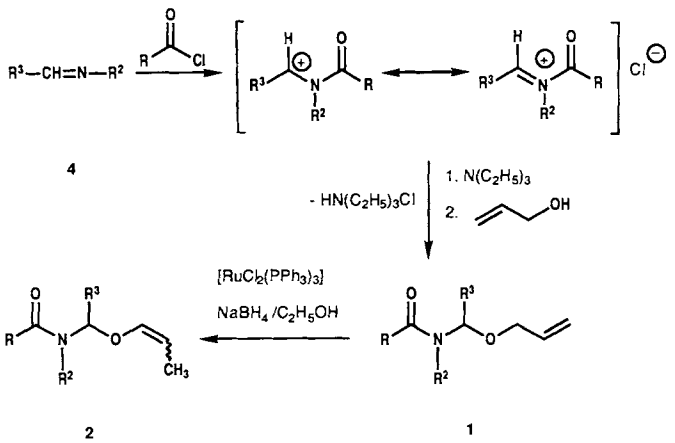

4

2 **1**

In the rearrangements of **2a**–**c** in the presence of trimethylsilyl trifluoromethanesulfonate TMSOTf, β-(*N*-acylamino)aldehydes **3a**–**c** were formed in 48–67% yield with high diastereoselectivity (Table 1).[11]

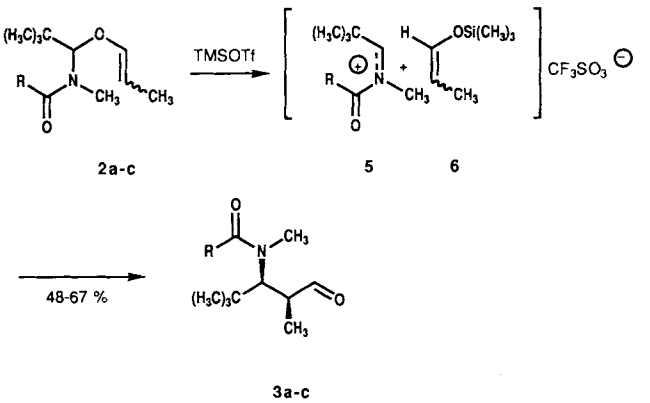

2a-c **5** **6**

3a-c

The relative configurations of the stereocenters formed were determined by X-ray structure analysis; compounds **3a** and **3b** are *syn* configurated (Fig. 1).[12]

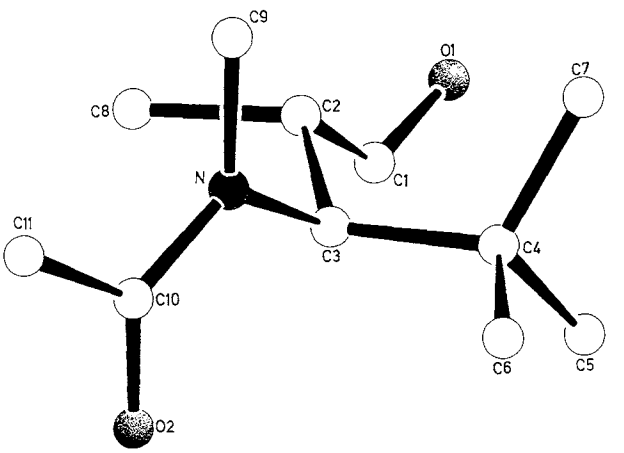

Fig. 1. Crystal structure of *syn*-**3a** (Schakal plot)[16].

The rearrangements of **2d** and **2e**, *N*,*O*-acetals of enolizable aldehydes, proceed analogously to the rearrangements of **2a**–**c** and give *syn*/*anti* mixtures of **3d** and **3e**, respectively (Table 1). Compounds **3d**,**e** were assigned to the *syn* and *anti* series, respectively, by comparison of their NMR data with that of **3a**,**b** (Table 2). In the *E* form of **3a**,**b** the protons β to the carbonyl groups and the protons of the acyl group showed large NOEs. The NMR spectra of freshly prepared solutions of **3a**, whose amide bond was proven by X-ray

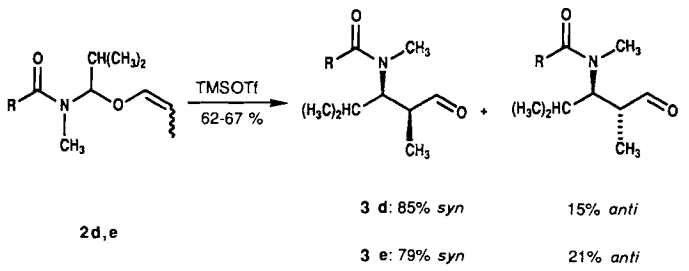

Table 2. Physical data of **3a**.

3a: B.p. 74–75 °C/0.04 Torr, m.p. 55 °C. ^{1}H NMR (500 MHz, $CDCl_3$): δ = 0.96 (s, 9H; $C(CH_3)_3$, *Z*), 0.97 (d, *J* = 6.7 Hz, 3H; $CHCH_3$, *Z*), 0.98 (s, 9H; $C(CH_3)_3$, *E*), 1.00 (d, *J* = 6.7 Hz, 3H; $CHCH_3$, *E*), 2.13 (s, 3H; H_3CC=O, *Z*), 2.21 (s, 3H; H_3CC=O, *E*), 2.65–2.78 (br, m, 1H; *CH*CHO, *Z*), 2.86–2.97 (m, 1H; *CH*CHO, *E*), 2.81 (s, 3H; NCH_3, *E*), 2.90 (s, 3H; NCH_3, *E*), 3.86 (d, *J* = 10 Hz, 1H; NCH, *E*), 4.94 (br d, *J* = 11 Hz, 1H; NCH, *Z*), 9.56 (d, *J* = 5 Hz, 1H; CHO, *Z*), 9.71 (d, *J* = 7 Hz, 1H; CHO, *E*); ^{13}C NMR (125 MHz, $CDCl_3$): δ = 12.8 ($CHCH_3$, *Z*), 13.1 ($CHCH_3$, *E*), 21.9 (H_3CC=O, *Z*), 22.4 (H_3CC=O, *E*), 28.4 ($C(CH_3)_3$, *Z*), 28.7 ($C(CH_3)_3$, *E*), 31.0 (NCH_3, *Z*), 33.2 (NCH_3, *E*), 35.8 ($C(CH_3)_3$, *Z*), 36.6 ($C(CH_3)_3$, *E*), 46.7 (CHCHO, *E*,*Z*), 59.0 (br, NCH, *Z*), 65.4 (N-CH, *E*), 171.6 (C=O, *E*), 171.9 (C=O, *Z*), 201.4 (CHO, *E*), 202.4 (CHO, *Z*)

structure analysis to have a *Z* configuration, showed almost exclusively the *Z* form. With time, however, the rotamers attained equilibrium, at which the *E* rotamer is the minor form.

In contrast to the rearrangement of *O*-vinyl-*O*,*O*-acetals, the diastereoselectivity of the formation of **3** does not depend on the configuration of the double bond in **2**. For example, both 40:60 and 83:17 mixtures of *cis*/*trans* **2d** yielded **3d** with the same *syn*/*anti* ratio of 85:15. Pure *cis* **2b** (prepared by isomerization of **1a** with $KOC(CH_3)_3$/DMSO, 37% yield) provided the *syn* diastereomer **3b** with the same selectivity (*de* = 88%) as that obtained from 28:72 mixture of *cis* and *trans* **2b**. We presume that the rearrangement **2** → **3** proceeds intermolecularly; the mechanism is currently under investigation.

Experimental Procedure

To a solution of 30 mmol of **2** in 15 mL of CH_2Cl_2 at 0 °C under nitrogen was added dropwise the appropriate amount (Table 1) of TMSOTf. The reaction mixture was stirred for 24 h at 0 °C then poured into a cooled, saturated solution of K_2CO_3. The organic phase was removed and the aqueous phase extracted with CH_2Cl_2 (3 × 15 mL). The combined organic layers were dried over $MgSO_4$. After the solvent was removed, products **3** were isolated by distillation under reduced pressure or by recrystallization (ether/pentane = 3/1) (Table 2).

Received: September 2, 1992 [Z 5551 IE]
German version: *Angew. Chem.* **1993**, *105*, 74

[1] D. Seebach, C. Betschart, M. Schiess, *Helv. Chim. Acta* **1984**, *67*, 1593.
[2] H. Kunz, W. Pfrengle, *Angew. Chem.* **1989**, *101*, 1041; *Angew. Chem. Int. Ed. Engl.* **1989**, *28*, 1067.
[3] E. G. Nolan, A. Alloco, M. Broody, A. Zuppa, *Tetrahedron Lett.* **1991**, *32*, 73.
[4] B. de Lange, F. van Bolhuis, B. L. Feringa, *Tetrahedron* **1989**, *45*, 6799.
[5] M. J. Brown, *Heterocycles* **1989**, *29*, 2225.
[6] D. J. Hart, D.-C. Ha, *Chem. Rev.* **1989**, *89*, 1447.
[7] T. Arenz, H. Frauenrath, *Angew. Chem.* **1990**, *102*, 929; *Angew. Chem. Int. Ed. Engl.* **1990**, *29*, 932.
[8] H. Frauenrath, H. Tönnießen, unpublished.
[9] H. Böhme, K. Hartke, *Chem. Ber.* **1963**, *96*, 600.
[10] H. Frauenrath, J. Runsink, *J. Org. Chem.* **1987**, *52*, 2709.
[11] Compounds **3** were obtained as racemates. For simplification, only one enantiomer of each is shown in the schemes.
[12] **3a**: Suitable single crystals were obtained from a pentane solution at 0 °C. Monoclinic, space group $P2_1/n$, (no. 14), a = 7.9891(6), b = 15.5901(6), c = 10.8412(7) Å, β = 111.349(3)°, V = 1257.6 Å^3, M_r = 199.3, Z = 4, $F(000)$ = 440, ρ_{calc} = 1.053 g cm^{-3}, μ = 5.75 cm^{-1}. Enraf-Nonius four-circle diffractometer, $\Omega/2\theta$-scans, 20 °C, $Cu_{K\alpha}$ radiation, (λ = 1.54179 Å, graphite monochromator), 2390 independent reflections ($\pm h + k + l$), of which 1903 were observed ($I > 2\sigma(I)$), R_m = 0.014), $\sin\theta/\lambda_{max}$ = 0.621 for solution and refinement. All hydrogen-atom positions located, 128 parameters in the last refinement, R = 0.066 (R_w = 0.079), residual electron density 0.2 e Å^{-3}. – **3b**: Suitable single crystals were obtained from a pentane solution at 0 °C. Monoclinic, space group $P2_1/n$, (no. 14), a = 7.218(2), b = 14.904(3), c = 14.536(3) Å, β = 93.171(8)°, V = 1561.4 Å^3, M_r = 261.37, Z = 4, $F(000)$ = 568, ρ_{calc} = 1.112 g cm^{-3}, μ = 0.78 cm^{-1}. Enraf-Nonius four-circle diffractometer, $\Omega/2\theta$-scans, 20 °C, $Mo_{K\alpha}$ radiation, (λ = 0.71069 Å, graphite monochromator), 4714 independent reflections ($\pm h + k + l$), of which 1690 were observed ($I > 2\sigma(I)$), R_m = 0.011) and used in the refinement, $\sin\theta/\lambda_{max}$ = 0.616 the solution and refinement. The positions of the hydrogen atoms of the *tert*-butyl group were calculated, the others could be located, 173 parameters in the last refinement, R = 0.065 (R_w = 0.048), residual electron density 0.3 e Å^{-3}. Both structures were solved by direct methods (GENSIN[13], GENTAN[14]) with the XTAL3.0 program package[15]. Further details of the crystal structure investigation may be obtained from the Fachinformationszentrum Karlsruhe, Gesellschaft für wissenschaftlich-technische Information mbH, D-W-7514 Eggenstein-Leopoldshafen 2 (FRG) on quoting the depository number CSD-56487, the names of the authors, and the journal.
[13] *"GENSIN", V. Subramanian, S. R. Hall XTAL3.0 Reference Manual* (Eds.: S. R. Hall, J. M. Stewart), Universities of Western Australia and Maryland, **1990**.
[14] *"GENTAN", S. R. Hall XTAL3.0 Reference Manual* (Eds.: S. R. Hall, J. M. Stewart), Universities of Western Australia and Maryland, **1990**.
[15] *XTAL3.0 Reference Manual* (Eds.: S. R. Hall, J. M. Stewart), Universities of Western Australia and Maryland, **1990**.
[16] E. Keller, *Chem. Unserer Zeit* **1986**, *20*, 178.

New Half-Sandwich Polysulfidorhenium Complexes

By *Max Herberhold*,* *Guo-Xin Jin*, and *Wolfgang Milius*

Many oligo- and polysulfido complexes have been synthesized during the last two decades.[1, 2] From this work it became apparent that rhenium complexes with sulfur-rich coordination spheres—similar to the molybdenum and tungsten complexes[3, 4] previously studied in more detail—could be interesting structure-chemical models for metal sulfide catalysts, for example, for hydrodesulfurization.[5] Thus, in the mononuclear Re^V ion $[ReS(S_4)_2]^-$, the monosulfido ligand is the apex and the two tetrasulfido chelate ligands are the base of a tetragonal pyramid.[5, 6] In the binuclear Re^V ion $[Re_2(S)_2(S_3)_2(S_4)_2]^{2-}$, a tetrasulfido chelate ring is coordinated to each Re atom; the formal Re–Re double bond (2.636 Å) is spanned by two monosulfido and two trisulfido bridges.[7] The highly symmetrical, tetranuclear Re^{IV} ion $[Re_4S_4(S_3)_6]^{2-}$ consists of a distorted $Re_4(\mu_3\text{-}S)_4$ cube, whose six faces are bridged with S_3 units.[6, 8] Complexes of the type $[Re_4(\mu_3\text{-}S)_4(S_3)_n(S_4)_{6-n}]^{4-}$ are also known,[9] containing both S_3 and S_4 bridges between the Re^{IV} centers.

The structural diversity of the complexes is reduced if part of the coordination sphere is blocked by the voluminous Cp* ligand (Cp* = C_5Me_5). In the following, the first two Cp*Re complexes are described, which contain exclusively sulfido ligands in the remainder of the coordination sphere.[10]

Starting from $[Cp^*Re(O)Cl_2]$ (**1**)[11, 12] two products (**2** and **3**) can be obtained by the reaction with Na_2S_4 in THF. An equimolar ratio of **1** and Na_2S_4 gives almost only the

[*] Prof. Dr. M. Herberhold, Dr. G.-X. Jin,[+] Dr. W. Milius
Laboratorium für Anorganische Chemie der Universität
Postfach 10 12 51, D-W-8580 Bayreuth (FRG)
[+] Permanent address:
Institute for Coordination Chemistry
University of Nanjing (People's Republic of China)

 © VCH Verlagsgesellschaft mbH, W-6940 Weinheim, 1993 0570-0833/93/0101-0085 $ 10.00+.25/0

black oxo complex **2**, which had been previously prepared from **1** and $[Cp_2TiS_5]$ as the source of sulfur.[13] With increasing excess of Na_2S_4, mixtures of **2** and **3** are obtained with a rising share of **3**. The green complex **3** is formed almost quantitatively if an excess of a solution of $(NH_4)_2S_x$ ($x \approx 10$) in methanol is added. Desulfurization of **3** with triphenylphosphane leads to the black binuclear complex **4**.

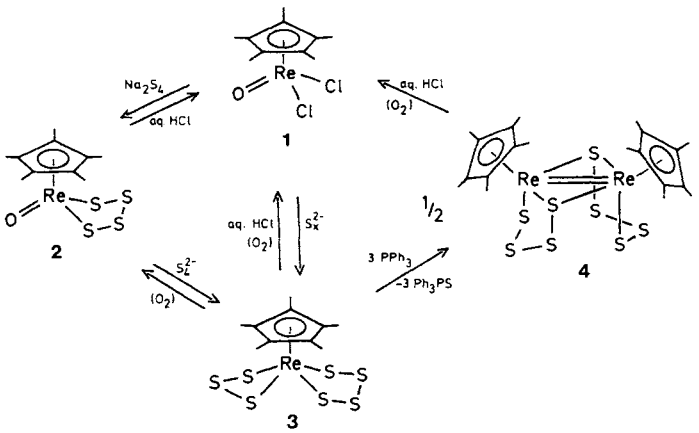

X-ray structure analyses were carried out for complexes **3** and **4** (Figs 1 and 2, respectively).[25] In the mononuclear complex **3** Re^V is the center of a tetragonal pyramid; complex **3**, like **1** and **2**, is a 16-electron complex. The Re–S distances to the S_3^{2-} chelate ligands (2.301(2), 2.336(3) Å) are significantly shorter than those to the S_4^{2-} chelate ring (2.350(2), 2.395(3) Å), but still longer than those in **2** (2.244(2) and 2.264(1) Å).[13] The Cp* ring is unsymmetrically π-coordinated (Re–C distances 2.257(9)–2.443(8) Å), however, this is not unusual for mononuclear Cp*Re complexes with unsymmetrical tripodal structure.[11, 14–16]

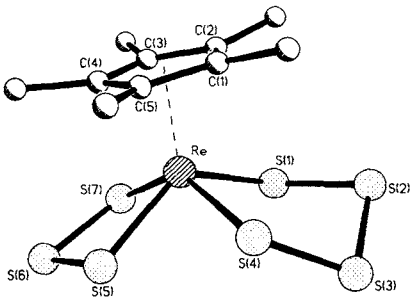

Fig. 1. Crystal structure of **3**. Selected distances [Å] and angles [°]: Re-S(1) 2.350(2), Re-S(4) 2.395(3), Re-S(5) 2.301(2), Re-S(7), 2.336(3), Re-Cp* (center) 1.993, Re-C(1) 2.406(7), Re-C(2) 2.443(8), Re-C(3) 2.330(9), Re-C(4) 2.257(9), Re-C(5) 2.276(8), S(1)-S(2) 2.090(4), S(2)-S(3) 2.010(4), S(3)-S(4) 2.083(4); S(5)-S(6) 2.042(4); S(6)-S(7) 2.054(3); S(1)-Re-S(4) 89.6(1), S(5)-Re-S(7) 75.6(1), S(1)-Re-S(7) 82.7(1); S(4)-Re-S(5) 76.5(1).

The binuclear Re^{III} complex **4** contains two S_4^{2-} chelate ligands, which are arranged so that one S atom of each ligand bridges the Re atoms (Fig. 2). In contrast to the oligosulfido chelate ligands in **2** and **3**, which are formally two-electron ligands, the S_4^{2-} ligands in **4** function as four-electron ligands. The Re–Re distance (2.618(1) Å) lies in the range for a double bond (2.38–2.65 Å);[17] thus **4** is formally an 18-electron complex. The cisoid arrangement of the two S_4^{2-} ligands in **4** causes the sulfur atoms S2 and S8 as well as S4 and S6 to approach each other to a distance of 3.369 and 3.438 Å, respectively. The corresponding rhodium compound $[Cp_2^*Rh_2S_8]$[18] is less symmetrical.

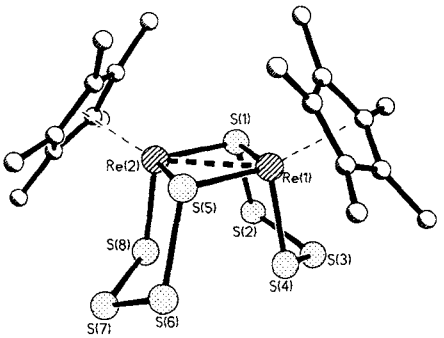

Fig. 2. Crystal structure of **4**. Selected distances [Å] and angles [°]: Re(1)-S(1) 2.283(3), Re(1)-S(4) 2.294(3), Re(1)-S(5) 2.290(2); Re(2)-S(1) 2.291(2), Re(2)-S(5) 2.266(3), Re(2)-S(8) 2.287(3); Re(1)-Re(2) 2.618(1); Re(1)-Cp* (center) 1.961, Re(2)-Cp* (center) 1.958, S(1)-S(2) 2.315(4), S(2)-S(3) 2.022(5), S(3)-S(4) 2.080(4), S(5)-S(6) 2.302(4), S(6)-S(7) 2.027(4), S(7)-S(8) 2.082(4); S(1)-Re(1)-S(5) 109.7(1), S(1)-Re(2)-S(5) 110.3(1), Re(1)-S(1)-Re(2) 69.9(1), Re(1)-S(5)-Re(2) 70.2(1).

Surprisingly, there are clear differences between the structures of **4** and the formally analogous 18-electron complex $[Re_2(CO)_6(\mu\text{-}S_4)_2]^{2-}$ (**5**), formed by the action of sulfur on $[Re(CO)_5]^-$.[19] Both complex **4** with approximate C_2 symmetry and complex **5** with C_i symmetry have a planar Re_2S_2

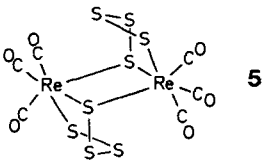

5

center, but only in **4** exists a binding Re–Re interaction (Re=Re 2.618(1) Å in **4**, Re···Re 4.07 Å in **5**). Consequently only **5** has acute angles at the rhenium atoms (73.7(3)°).

The simultaneous coordination of a S_3^{2-} and a S_4^{2-} chelate ligand in **3** is remarkable; indications for the formation of $[Cp^*Re(S_4)_2]$ have so far not been found. Complexes with S_7^{2-} chelate ligands such as $[(PMe_3)_3M(S_7)]$ (M = Ru, Os)[20] and $[(S_7)_2Bi(\mu\text{-}S_6)Bi(S_7)_2]^{4-}$[21] are known, but are rare. The selenium analogues of the complexes **2**, **4**[22] and **5**[23] were also characterized by X-ray crystallography; they are isostructural with the corresponding sulfur complexes.

Experimental Procedure

3: A green solution of **1** (0.18 g, 0.44 mmol) [11,12] in THF (80 mL) was treated with a solution of $(NH_4)_2S_x$ ($x \approx 10$) in MeOH [24] and stirred for 4 h. After removal of the solvent, the green residue was purified by chromatography on silica gel (Merck, Kieselgel 60). S_8 was eluted with toluene/pentane (2:1), and **3** was eluted with CH_2Cl_2. Recrystallization from $CHCl_3$/hexane at −25 °C gave dark green crystals of **3** (0.23 g, 95.8%, m.p. 194 °C). IR (CsI): $\tilde{\nu}$[cm^{-1}] = 499 (μ – S_3); ^{1}H NMR ($CDCl_3$): δ = 1.90 (s, C_5Me_5); ^{13}C NMR ($CDCl_3$): δ = 11.3 ($C_5\mathit{Me}_5$), 104.4 (C_5Me_5); EI-MS (70 eV): m/z = 546 (M^+, 4%), 514 (M^+ – S, 3%), 482 (M^+ – 2S, 70%), 450 (M^+ – 3S, 14%), 418 (M^+ – 4S, 100%).

4: A solution of **3** (0.15 g, 0.27 mmol) and PPh_3 (0.29 g, 1.10 mmol) in $CHCl_3$ or CH_2Cl_2 (ca. 30 mL) was stirred for 10 h. Upon chromatography on silica gel

Ph_3PS was eluted with CH_2Cl_2, followed by **4** with CH_2Cl_2/THF (5:1). Compound **4** was slowly crystallized from CH_2Cl_2 (black prisms, 0.03 g, 24.5%, m.p. 225 C). ^1H NMR ($CDCl_3$): $\delta = 2.02$ (s, C_5Me_5); ^{13}C NMR ($CDCl_3$): $\delta = 11.5$ ($C_5\mathit{Me}_5$), 100.6 (C_5Me_5); EI-MS (70 eV): $m/z = 836$ ($M^+ - 2S$, 7%), 804 ($M^+ - 3S$, 9%), 772 ($M^+ - 4S$, 100%), 740 ($M^+ - 5S$, 30%), 708 ($M^+ - 6S$, 28%).

Received: September 8, 1992 [Z 5561 IE]
German version: *Angew. Chem.* **1993**, *105*, 127

[1] Reviews: a) M. Draganjac, T. B. Rauchfuss, *Angew. Chem.* **1985**, *97*, 745; *Angew. Chem. Int. Ed. Engl.* **1985**, *24*, 742; b) A. Müller, E. Diemann, *Adv. Inorg. Chem.* **1987**, *31*, 89; c) J. W. Kolis, *Coord. Chem. Rev.* **1990**, *105*, 195.
[2] J. Wachter, *J. Coord. Chem.* **1987**, *15*, 219; *Angew. Chem.* **1989**, *101*, 1645; *Angew. Chem. Int. Ed. Engl.* **1989**, *28*, 1613.
[3] A. Müller, *Polyhedron* **1986**, *5*, 323; M. A. Harmer, T. A. Halbert, W.-H. Pan, C. L. Coyle, S. A. Cohen, E. I. Stiefel, *ibid.* **1986**, *5*, 341; D. Coucouvanis, A. Hadjkyriacou, M. Draganjac, M. G. Kanatzidis, O. Ileperuma, *ibid.* **1986**, *5*, 349.
[4] M. Herberhold, G.-X. Jin, A. Müller, M. Penk, *Z. Naturforsch. B* **1991**, *46*, 25.
[5] F. A. Cotton, P. A. Kibala, M. Matusz, *Polyhedron* **1988**, *7*, 83.
[6] A. Müller, E. Krickemeyer, H. Bögge, *Z. Anorg. Allg. Chem.* **1987**, *554*, 61.
[7] A. Müller, E. Krickemeyer, V. Wittneben, H. Bögge, M. Lemke, *Angew. Chem.* **1991**, *103*, 1501; *Angew. Chem. Int. Ed. Engl.* **1991**, *30*, 1512.
[8] A. Müller, E. Krickemeyer, H. Bögge, *Angew. Chem.* **1986**, *98*, 258; *Angew. Chem. Int. Ed. Engl.* **1986**, *25*, 272.
[9] A. Müller, unpublished, cited from [1 b].
[10] [Cp*ReS_3] is unknown and the existence of [$Cp^*_2Re_2S_4$] has not been proven unequivocally.
[11] W. A. Herrmann, U. Küsthardt, M. Flöel, J. Kulpe, E. Herdtweck, E. Voss, *J. Organomet. Chem.* **1986**, *314*, 151.
[12] W. A. Herrmann, M. Flöel, J. Kulpe, J. K. Felixberger, E. Herdtweck, *J. Organomet. Chem.* **1988**, *355*, 297.
[13] J. Kulpe, E. Herdtweck, G. Weichselbaumer, W. A. Herrmann, *J. Organomet. Chem.* **1988**, *348*, 369.
[14] W. A. Herrmann, E. Herdtweck, M. Flöel, J. Kulpe, U. Küsthardt, J. Okuda, *Polyhedron* **1987**, *6*, 1165.
[15] M. Herberhold, B. Schmidkonz, M. L. Ziegler, O. Serhadle, *Z. Naturforsch. B* **1987**, *42*, 739.
[16] W. A. Herrmann, G. Weichselbaumer, R. A. Paciello, R. A. Fischer, E. Herdtweck, J. Okuda, D. W. Marz, *Organometallics* **1990**, *9*, 489.
[17] W. A. Herrmann, R. Serrano, A. Schäfer, U. Küsthardt, *J. Organomet. Chem.* **1984**, *272*, 55.
[18] H. Brunner, N. Janietz, W. Meier, B. Nuber, J. Wachter, M. L. Ziegler, *Angew. Chem.* **1988**, *100*, 717; *Angew. Chem. Int. Ed. Engl.* **1988**, *27*, 708.
[19] T. S. A. Hor, B. Wagner, W. Beck, *Organometallics* **1990**, *9*, 2183.
[20] J. Gotzig, A. L. Rheingold, H. Werner, *Angew. Chem.* **1984**, *96*, 813; *Angew. Chem. Int. Ed. Engl.* **1984**, *23*, 814.
[21] A. Müller, M. Zimmermann, H. Bögge, *Angew. Chem.* **1986**, *98*, 259; *Angew. Chem. Int. Ed. Engl.* **1986**, *25*, 273.
[22] M. Herberhold, G.-X. Jin, W. Milius, unpublished.
[23] S. C. O'Neal, W. T. Pennington, J. W. Kolis, *Can. J. Chem.* **1989**, *67*, 1980.
[24] M. Herberhold, G.-X. Jin, W. Kremnitz, A. L. Rheingold, B. S. Haggerty, *Z. Naturforsch. B* **1991**, *46*, 500.
[25] Data for the crystal structure analyses of $C_{10}H_{15}S_7Re$ (**3**) and $C_{20}H_{30}S_8Re_2$ (**4**): diffractometer: Siemens P4 ($Mo_{K\alpha}$, $\lambda = 0.71073$ Å, graphite monochromator). **3**: monoclinic; $P2_1/n$, $a = 7.177(2)$, $b = 14.238(3)$, $c = 15.878(3)$ Å, $\beta = 95.35(3)°$, $Z = 4$, dark red platelets, dimensions $0.20 \times 0.20 \times 0.015$ mm. Measured range: $3° \le 2\theta \le 55°$; measured octants *hkl* and *hkl̄*; T = 295 K; measured reflections: 4935; independent reflections: 3574, of which observed ($F \ge 3\sigma(F)$): 2767; empirical absorption correction (ψ scan), minimum/maximum transmission factors: 0.2698/0.7718 ($\mu_{Mo} = 84.06$ cm^{-1}); structure solution with direct methods (SHELXTL PLUS); number of refined parameters: 164; $R = 0.043$; $wR = 0.028$ ($w^{-1} = \sigma^2(F)$); maximum/minimum residual electron density: 1.76/−1.25 eÅ^{-3}. **4**: monoclinic; $P2_1/n$, $a = 8.946(2)$, $b = 14.230(3)$, $c = 20.874(4)$ Å, $\beta = 90.23(3)°$, $Z = 4$, black, prismatic crystals, dimensions $0.15 \times 0.15 \times 0.20$ mm. Measured range: $3° \le 2\theta \le 50°$; measured octants *hkl* and *hkl̄*; T = 295 K; measured reflections: 6384; independent reflections: 4675, of which observed ($F \ge 0\sigma(F)$): 4675; absorption correction with DIFABS (N. Walker, D. Stuart, *Acta Crystallogr. Sect. A* **1983**, *39*, 158) ($\mu_{Mo} = 108.3$ cm^{-1}); structure solution with direct methods (SHELXTL PLUS); number of refined parameters: 271; $R = 0.054$, $wR = 0.034$ ($w^{-1} = \sigma^2(F)$); maximum/minimum residual electron density: 1.90/−1.62 eÅ^{-3}. Further details of the crystal structure investigation may be obtained from the Fachinformationszentrum Karlsruhe, Gesellschaft für wissenschaftlich-technische Information mbH, D-W-7514 Eggenstein-Leopoldshafen 2 (FRG) on quoting the depository number CSD-56683, the names of the authors, and the journal citation.

$[(\eta^5\text{-}CH_3C_5H_4)Mn(CO)(dppfe)]$: Two Isomers Distinguished by their Characteristic CO Stretching Frequencies, which Differ Only in Rotation of the Methylcyclopentadienyl Ligand: Evidence for an Intramolecular M–CO ··· H–C Interaction

By *Satoru Onaka,* Hiroyuki Furuta*, and *Shigeru Takagi*

The importance of C–H ··· O interactions in determining the molecular and solid-state properties of organic compounds is well known.[1–4] Hirota and Nishio recently reported that the intramolecular interaction of C–H groups with π-electron system is another important factor for the conformation of organic molecules.[5, 6] For organometallic compounds, however, we know of few papers that have suggested a C–H ··· OC–M interaction in the form of either a C–H ··· O hydrogen bond or an interaction between C–H and the π system of CO,[7] although there are a significant number of compounds in which a particular conformation is supposed to be induced by intramolecular C–H ··· OC–M interactions. Here we report a serendipitious example in which such a C–H ··· OC–M interaction is responsible for one of the conformations of a carbonyl (methylcyclopentadienyl)manganese derivative.

$[(\eta^5\text{-}CH_3C_5H_4)Mn(CO)\{[\eta^5\text{-}C_5H_4P(C_6H_5)_2]_2Fe\}]$ **1**

When we allowed crystals of the title compound **1**[8, 9] to grow from CH_2Cl_2/hexane, we found that **1** crystallizes in two different crystal forms with slightly different colors, an orange-yellow isomer (**1a**) and an orange-red isomer (**1b**). The two isomers were obtained in approximately 1:1 ratio and separated under a microscope with a needle. The orange-yellow isomer **1a** (Nujol mull) exhibits a strong ν(CO) band at 1835 m^{-1}, while the orange-red isomer **1b** (Nujol mull) exhibits a strong ν(CO) peak at 1810 cm^{-1}. The molecular structures for **1a** and **1b** are shown in Figure 1, projec-

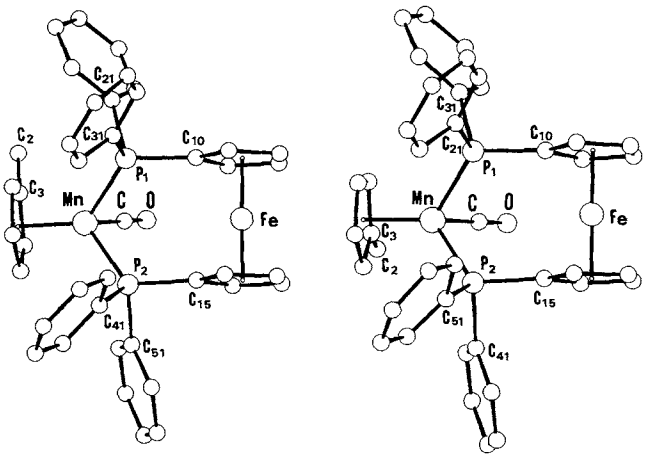

Fig. 1. Left: Crystal structure of **1a**. Selected bond lengths [Å]: Mn-P1 2.2274(9), Mn-P2 2.2096(8), Mn-C 1.741(3), C-O 1.172(4), C2-C3 1.502(5), Mn-C3 2.161(3), Mn-C4 2.125(4), Mn-C5 2.124(4), Mn-C6 2.156(3), Mn-C7 2.160(3). Right: Crystal structure of **1b**. Selected bond lengths [Å]: Mn-P1 2.216(2), Mn-P2 2.208(2), Mn-C 1.754(7), C-O 1.169(9), C2-C3 1.50(1), Mn-C3 2.151(8), Mn-C4 2.151(8), Mn-C5 2.154(9), Mn-C6 2.147(9), Mn-C7 2.128(8).

[*] Prof. Dr. S. Onaka, H. Furuta, Dr. S. Takagi
Department of Chemistry, Nagoya Institute of Technology
Gokiso-cho, Showa-ku, Nagoya 466 (Japan)

[**] dppfe = 1,1′-bis(diphenylphosphino)ferrocene.

 © VCH Verlagsgesellschaft mbH, W-6940 Weinheim, 1993 0570-0833/93/0101-0087 $ 10.00+.25/0

tions of the $(\eta^5\text{-}CH_3C_5H_4)Mn(CO)P_2$ unit for these molecules along the axis through the manganese atom and the center of the methylcyclopentadiene ring in Figure 2, and a side view of this group in **1b** in Figure 3.[10] Isomer **1a** has a

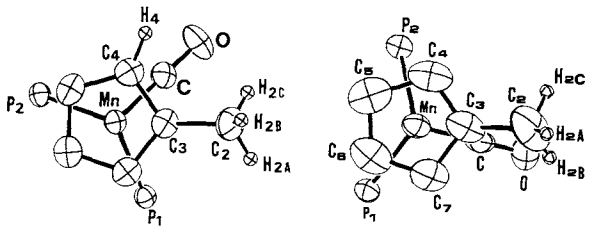

Fig. 2. Conformations of **1a** (left) and **1b** (right) in the crystal. Selected bond lengths [Å]: $C\cdots H_{2C}$ 3.06(3), $O\cdots H_{2C}$ 3.22(3), $O\cdots H4$ 3.18(3) (**1a**) and $C\cdots H_{2B}$ 2.75(9), $O\cdots H_{2B}$ 2.78(9) (**1b**).

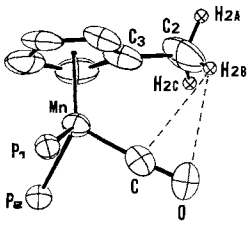

Fig. 3. Side view of the $(\eta^5\text{-}CH_3C_5H_4)Mn(CO)P_2$ unit in **1b**.

staggered conformation, while isomer **1b** is found in an eclipsed conformation.[10, 11] The distances between the CO group and the closest hydrogen atoms of the methyl substituent in **1b** are $H_{2B}\cdots C = 2.75(9)$ Å and $H_{2B}\cdots O = 2.78(9)$ Å, whereas the corresponding distance in **1a** is much longer, $H_{2C}\cdots C = 3.06(3)$ Å. The methyl hydrogen atom H_{2B} in **1b** is almost equidistant from the C and the O atoms of the CO group, consistent with the interaction of H_{2B} with the π electrons of the C≡O bond (the distance between H_{2B} and the midpoint of the C≡O bond is 2.70(9) Å). The Mn-C-O group is bent slightly toward the methyl group (∢ Mn-C-O in **1b** is 175.3(6)°). The contacts between the Cl atoms of the solvent molecule, (CH_2Cl_2) and **1** are greater than 3.0 Å in these crystals. Thus, it is unlikely that the solvent molecules and/or crystal packing forces induce the eclipsed conformation and overcome the repulsive forces normally associated.[11] Rather, the eclipsed conformation is favored over the staggered because of the C-H···OC interaction. The π-electron density of the CO group should be reduced by this largely electrostatic interaction, thus accounting for the significantly lower CO stretching frequency for the eclipsed isomer.

It is worthwhile to compare these results to those obtained for $[In\{CpMo(CO)_3\}_3]$ by Norman et al.[7] Here the canting of the CO groups in each $CpMo(CO)_3$ unit may arise from the interaction between one of the C–H bonds in the C_5H_5 group of the adjacent $CpMo(CO)_3$ unit with the CO group concerned. The C–H···CO distances reported (2.52–2.72 Å) are somewhat shorter than the range in **1b** (2.75–2.78 Å) and consistent with a similar type of interaction. However, this report lacks spectral evidence to verify the proposed interaction.

Figure 4 shows a typical IR spectrum ($\tilde{\nu}_{CO}$ region) of compounds **1** in $CHCl_3$; **1a** and **1b** afford the same $\tilde{\nu}_{CO}$ spectrum. The spectrum shows an asymmetric absorption band, which

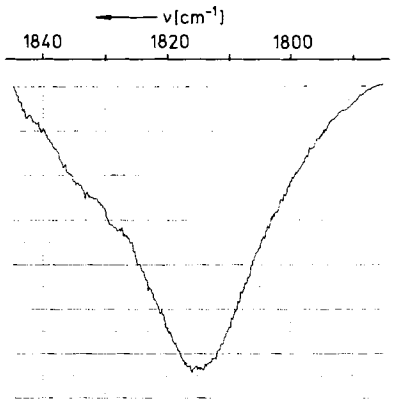

Fig. 4. IR spectrum of **1b** in $CHCl_3$ solution (ν_{CO} region).

is apparently composed of at least two bands, one around 1830 cm^{-1} and one at 1815 cm^{-1}. The former peak should arise from the staggered isomer and the latter peak from the eclipsed isomer. The existence of two conformers in solution was also demonstrated previously by temperature-dependent ^1H NMR spectroscopy.[8] Thus, the C–H···OC–M interaction is effective not only for solids but also for solutions.

Intramolecular C–H···OC–M interactions should not be overlooked in organometallic compounds when conformations of a molecule in the solid state and/or in solution or that of a reactive intermediate are analyzed. Similar interactions are quite likely to occur in the surface processes between the adsorped CO and alkanes on the catalyst.

Received June 16, 1992
Revised: September 28, 1992 [Z 5406 IE]
German version: *Angew. Chem.* **1993**, *105*, 105

[1] G. R. Desiraju, C. V. K. M. Sharma, *J. Chem. Soc. Chem. Commun.* **1991**, 1239.
[2] R. Taylor, O. Kennard, *J. Am. Chem. Soc.* **1982**, *104*, 5063.
[3] J. A. R. P. Sharma, G. R. Desiraju, *Acc. Chem. Res.* **1982**, *19*, 222.
[4] D. R. Desiraju, *Acc. Chem. Res.* **1991**, *24*, 290.
[5] a) M. Nishio, M. Hirota, *Tetrahedron* **1989**, *45*, 7201; b) M. Hirota, M. Nishio, *Kagaku (Kyoto)* **1991**, *46*, 592.
[6] a) K. Sakakibara, M. Hirota, *Chem. Lett.* **1989**, 921; b) S. Araki, K. Sakakibara, M. Hirota, M. Nishio, S. Tsuzuki, K. Tanabe, *Tetrahedron Lett.* **1991**, *32*, 6587.
[7] L. M. Clarkson, W. Clegg, D. C. R. Hockless, N. C. Norman, T. B. Marder, *J. Chem. Soc. Dalton Trans.* **1991**, 2229.
[8] S. Onaka, *Bull. Chem. Soc. Jpn.* **1986**, *59*, 2359.
[9] S. Onaka, T. Moriya, S. Takagi, A. Mizuno, H. Furuta, *Bull. Chem. Soc. Jpn.* **1992**, *65*, 1415.
[10] **1a**: $C_{41}H_{35}OFeMnP_2 \cdot CH_2Cl_2$, $M = 801.3$, triclinic, $a = 10.937(6)$, $b = 14.671(4)$, $c = 10.930(2)$ Å; $\alpha = 94.63(2)$, $\beta = 91.35(3)$, $\gamma = 100.03(3)°$, $V = 1723(1)$ Å^3, space group $P\bar{1}$, $Z = 2$, $\mu(Mo_{K\alpha}) = 10.9$ cm^{-1}, $\rho_{calcd} = 1.54$ $g\,cm^{-3}$, 5948 reflections ($|F_0| > 4\sigma(|F_0|)$), $R = 0.044$ ($R_w = 0.028$). **1b**: $C_{41}H_{35}OFeMnP_2 \cdot CH_2Cl_2$, $M = 801.3$, monoclinic, $a = 18.836(3)$, $b = 20.341(3)$, $c = 9.655(2)$ Å, $\beta = 91.02(2)°$, $V = 3699(1)$ Å^3, space group $P2_1/n$, $Z = 4$, $\mu(Mo_{K\alpha}) = 10.2$ cm^{-1}, $\rho_{calcd} = 1.44$ $g\,cm^{-3}$, 3234 reflections ($|F_0| > 4\sigma(|F_0|)$), $R = 0.053$ ($R_w = 0.049$). The independent reflections ($3° < 2\theta < 55°$ for **1a**; $3° < 2\theta < 45°$ for **1b**) were measured on a MAC MXC^3 diffractometer using $Mo_{K\alpha}$ radiation with $\omega - 2\theta$ scans. The structures were solved by direct methods (MULTAN 78), and all non-hydrogen atoms were refined anisotropically. The positions of all hydrogen atoms were determined from the difference Fourier map and were refined isotropically. The structural refinements were made by full-matrix least-squares method on a SUN SPARC2 workstation. Further details of the crystal structure investigation are available on request from the Director of the Cambridge Crystallographic Data Center, University Chemical Laboratory, Lensfield Road, GB-Cambridge CB21EW (UK), on quoting the full journal citation.
[11] It was shown previously that when compound **1** is recrystallized from $CHCl_3$/hexane, orange-red crystals (**1c**) are obtained, which contain chloroform as a solvent of crystallization [8,9]. These crystals are isomorphous with those of **1b**, and the isomer present is isostructural with that in **1b** and has the same CO stretching frequency ($\tilde{\nu}(CO) = 1810$ cm^{-1}).

Synthesis of the Tris(9-fluorenylidene)cyclopropane Dianion and Related Dianions: [3]Radialenes with Novel Electronic Properties**

By *Masahiko Iyoda,* Hiroyuki Kurata, Masaji Oda, Chiaki Okubo*, and *Kichisuke Nishimoto**

Dedicated to Professor Emanuel Vogel on the occasion of his 65th birthday

According to Hückel MO theory for cyclic polyenes, five-membered rings act as electron acceptors, while three-membered rings act as electron donors. Thus, the cyclopropenium resonance structure (**1a**) with three anionic cyclopentadienyl units can be expected to contribute to the stabilization of the dianion $\mathbf{1}^{2-}$ derived from **1**. We recently reported the synthesis of tris(9-fluorenylidene)cyclopropane (**2**)[1,2] and bis(9-fluorenylidene)-9′-xanthenylidenecyclopropane (**3**).[2] Since the [3]radialene **2** shows remarkably positive reduction potentials by cyclic voltammetry, the resonance structure **2a** can be expected to contribute considerably to the stabilization of the dianion $\mathbf{2}^{2-}$.[1]

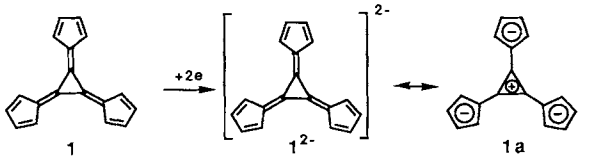

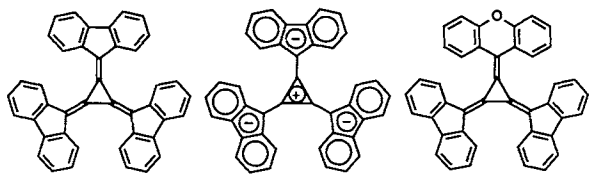

We now describe the preparation and spectroscopic characterization of the stable dianions $\mathbf{2}^{2-}$ and $\mathbf{3}^{2-}$, together with the dianions of bis(9-fluorenylidene)ethene (**4**)[3] and 9,9′-bifluorenylidene (**5**),[4] as well as the novel electronic properties of the [3]radialenes **2** and **3** and their dianions in their ground and excited states.[5]

The sodium salts of the dianions $\mathbf{2}^{2-}$–$\mathbf{5}^{2-}$ were prepared by reduction of **2**–**5** with sodium in THF. Qualitative electronic spectra of the salts could be measured satisfactorily with degassed solutions; however, no ^{1}H and ^{13}C NMR spectra of the sodium salts of the dianions $\mathbf{2}^{2-}$–$\mathbf{4}^{2-}$ could be obtained because of their extremely poor solubility in THF. Therefore, a series of lithium salts were prepared by reduction of the corresponding hydrocarbons with lithium in [D$_8$]THF. The dianions $\mathbf{2}^{2-}$–$\mathbf{5}^{2-}$ with lithium counterions are very stable and moderately soluble in THF. They can be stored at room temperature in NMR tubes for a year without any detectable decomposition.

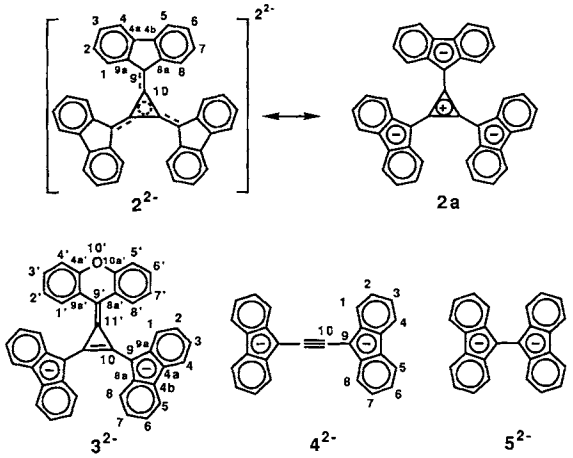

The ^{1}H and ^{13}C NMR data for the dianions $\mathbf{2}^{2-}$ and $\mathbf{3}^{2-}$ as well as the neutral compound **2** are summarized in Table 1.[6] The ^{1}H and ^{13}C NMR spectra of the dianions $\mathbf{4}^{2-}$ and $\mathbf{5}^{2-}$ are similar and reveal the formation of charged diatropic species. In the case of the dianion of **4**, the contribution of the resonance structure shown as $\mathbf{4}^{2-}$ is dominant. Thus, the ^{13}C NMR resonance signals of the sp hybridized carbon atoms (C10) were observed at high field (δ = 111.64) owing to their increased acetylenic character.

Table 1. ^{1}H and ^{13}C NMR data [a] of **2** and the dianions $\mathbf{2}^{2-}$ and $\mathbf{3}^{2-}$.

2: ^{1}H NMR (400 MHz): δ = 7.88 (d, ^3J(H,H) = 7.3 Hz, H-1,8), 7.42 (t, ^3J(H,H) = 7.3 Hz, H-2,7), 7.28 (d, ^3J(H,H) = 7.3 Hz, H-4,5), 7.22 (t, ^3J(H,H) = 7.3 Hz, H-3,6); ^{13}C NMR (100 MHz): δ = 140.84 (C-8a, 9a), 138.44 (*C*-4a,4b), 126.88 (*C*-3,6), 128.76 (C-2,7), 128.33 (C-4,5), 124.45 (C-10), 120.39 (C-1,8), 118.11 (C-9)

Li_2-**2**: ^{1}H NMR (400 MHz): δ = 8.24 (d, ^3J(H,H) = 7.5 Hz, H-1,8), 7.84 (d, ^3J(H,H) = 7.1 Hz, H-4,5), 6.67 (t, ^3J(H,H) = 7.0 Hz, H-2,7), 6.62 (t, ^3J(H,H) = 7.0 Hz, H-3,6); ^{13}C NMR (100 MHz): δ = 141.07 (C-8a,9a), 129.31 (C-4a,4b), 126.07 (C-10), 121.41 (C-2), 121.03 (C-1), 118.53 (C-4), 114.46 (C-3), 89.59 (C-9)

Li_2-**3**: ^{1}H NMR (400 MHz): δ = 8.00 (d, ^3J(H,H) = 7.9 Hz, H-1,8), 7.79 (d, ^3J(H,H) = 7.5 Hz, H-4,5), 7.37 (dd, ^3J(H,H) = 7.8, ^4J(H,H) = 1.5 Hz, H-4′,5′), 6.62 (t, ^3J(H,H) = 7.3 Hz, H-2,7), 6.55 (t, ^3J(H,H) = 7.1 Hz, H-3,6), 6.02 (dd, ^3J(H,H) = 7.7, ^4J(H,H) = 1.5 Hz, H-1′,8′), 5.92 (dt, ^3J(H,H) = 7.4, ^4J(H,H) = 1.5 Hz, H-2′,7′), 5.83 (dt, ^3J(H,H) = 7.4, ^4J(H,H) = 1.5 Hz, H-3′,6′); ^{13}C NMR (100 MHz): δ = 151.17 (C-4a′, 10a′), 140.79 (C-8a,9a), 134.88 (C-8a′,9a′), 128.37 (C-4a,4b), 123.45 (C-10), 123.15 (C-2′,7′), 123.07 (C-1′,8′), 120.79 (C-2,7), 120.68 (C-1,8), 119.18 (C-11′), 118.33 (C-4,5), 117.03 (C-3′,6′), 113.76 (C-3,6), 112.76 (C-4′,5′), 89.91 (C-9), 75.30 (C-9′)

[a] In [D$_8$]THF.

The ^{1}H and ^{13}C NMR data of the dianion $\mathbf{2}^{2-}$ reflect its highly symmetrical structure. Since the ^{1}H NMR signals of $\mathbf{2}^{2-}$ at δ = 6.6–8.2 are temperature independent in the range −80 to +30 °C, $\mathbf{2}^{2-}$ exists most probably in a stable, symmetric conformation with twisted bonds between the cyclopropane and fluorenylidene units (twist angle is calculated to be 30° by geometric optimization with the AM-1 program). The ^{13}C NMR chemical shifts of the fluorenylidene carbon

[*] Prof. Dr. M. Iyoda
Department of Chemistry, Faculty of Science
Tokyo Metropolitan University
Hachioji, Tokyo 192-03 (Japan)
H. Kurata, Prof. Dr. M. Oda
Department of Chemistry, Faculty of Science
Osaka University
Toyonaka, Osaka 560 (Japan)
Prof. Dr. K. Nishimoto, C. Okubo
Department of Chemistry, Faculty of Science
Osaka City University
Sumiyoshi-ku, Osaka 558 (Japan)

[**] This work was supported by the Ciba-Geigy Foundation (Japan) for the Promotion of Science and by Grant-in-Aid for Scientific Research no. 63540396 from the Japanese Ministry of Education, Science, and Culture.

atoms C9 and the cyclopropane carbon atoms C10 of 2^{2-} were observed at very high and very low fields, respectively. The ^{1}H NMR spectrum of 3^{2-} is temperature dependent, as expected from the unsymmetrical charge density in the fluorene units. Thus, the spectrum at room temperature shows sets of signals for two four-spin systems, one of which is assigned to the fluorene unit and the other to the xanthene unit. However, the spectrum at $-25\,^{\circ}C$ gave very broad signals, and the spectra at lower temperatures ($< -50\,^{\circ}C$) showed well-resolved, complex sets of signals corresponding to three four-spin systems, two for the unsymmetrical fluorene unit and one for the symmetrical xanthene unit. The activation energy $\Delta G^{\neq}$ of the rotation of the fluorene units in 3^{2-} was estimated to be 12.0 kcal mol^{-1} ($-50\,^{\circ}C$).

The electronic spectra of Na_2-**2** and Na_2-**3** show a marked hypsochromic shift (150–250 nm) compared with the neutral compounds **2** and **3**. Thus, blue solutions of **2** and **3** change to red on reduction with sodium.[8] In contrast, the electronic spectra of Na_2-**4** show a remarkable bathochromic shift (300–400 nm).[8] Therefore, electronic properties of [3]radialene dianions are obviously different from those of other dianions.

In order to estimate the charge distribution in **2**–**5** and 2^{2-}–5^{2-}, MO calculations were carried out on these molecules.[9] A relatively good correlation between the calculated charge densities of **2**–**5** and 2^{2-}–5^{2-} and their ^{13}C NMR data can be derived, although ^{13}C chemical shifts are sometimes affected by other factors such as bond orders, ring current, hybridization, and steric effects.

As shown in Table 2, the calculated charge densities of **2** and 2^{2-} reflect the novel electronic properties of the [3]radialene system. The neutral **2** in the ground state (S_0) shows a marked charge separation, and positive charges at the central cyclopropane carbon atoms C10. Interestingly, these calculated positive charges in 2^{2-} remain almost unchanged in the ground state, in spite of the increase of negative charge density in the three fluorene units when **2** is converted into 2^{2-}. The distance between the carbon atoms C9 and C10 in **2** is 1.385 (observed)[10] and 1.382 Å (calculated) and in 2^{2-} 1.428 Å (calculated). Therefore, the symmetric resonance structure **2a** with charge separation makes a relatively large contribution to the stabilization of 2^{2-}.

Table 2. Calculated charge densities of **2** and 2^{2-} in the ground state (S_0) and the excited states (S_1).

Compound	Charge density [a]
2 (S_0)	+ 0.031 (1,8); + 0.012 (2,7); + 0.014 (3,6); + 0.039 (4,5); − 0.070 (4a,4b); − 0.073 (8a,9a); − 0.099 (9); + 0.192 (10)
2 (S_1)	+ 0.042 (1,8); + 0.007 (2,7); + 0.021 (3,6); + 0.047 (4,5); − 0.082 (4a,4b); − 0.074 (8a,9a); − 0.118 (9); + 0.294 (10)
2^{2-} (S_0)	− 0.030 (1,8); − 0.054 (2,7); − 0.093 (3,6); − 0.031 (4,5); − 0.073 (4a,4b); − 0.023 (8a,9a); − 0.205 (9); + 0.146 (10)
2^{2-} (S_1)	− 0.012 (1,8); − 0.075 (2,7); − 0.071 (3,6); − 0.038 (4,5); − 0.063 (4a,4b); − 0.034 (8a,9a); − 0.081 (9); + 0.002 (10)

[a] Numbers of the appropriate C atoms in parentheses.

In the excited state S_1, the calculated positive charges at the C10 carbon atoms are considerably higher in **2**. This charge transfer causes a bathochromic shift and the deep blue color of **2** in solution. The amount of charge transfer from the three-membered ring to the fluorenyl groups in **2** are calculated to be 0.58 electron for the ground state and 0.88 for the excited state. On the other hand, the calculated positive charges on the C10 carbon atoms in 2^{2-} are apparently smaller than in **2** (back charge transfer). This effect causes a hypsochromic shift and the deep red color of 2^{2-} in solution. The amount of back charge transfer from the fluorenyl groups to the three-membered ring is calculated to be 0.56 for the ground state and 0.99 for the excited state. From analogous calculations similar electronic properties can be expected for the ground and excited states of **3** and 3^{2-}.

Received: September 5, 1992 [Z 5559 IE]
German version: *Angew. Chem.* **1993**, *105*, 97

[1] M. Iyoda, H. Otani, M. Oda, *Angew. Chem.* **1988**, *100*, 1131; *Angew. Chem. Int. Ed. Engl.* **1988**, *27*, 1080.
[2] M. Iyoda, A. Mizusuna, H. Kurata, M. Oda, *J. Chem. Soc. Chem. Commun.* **1989**, 1690.
[3] J. M. Edinger, A. R. Day, *J. Org. Chem.* **1971**, *36*, 240.
[4] Y. Cohen, J. Klein, M. Rabinovitz, *J. Chem. Soc. Chem. Commun.* **1986**, 1071; R. H. Cox, *J. Magn. Reson.* **1970**, *3*, 223.
[5] For a recent review of radialenes see: H. Hopf, G. Maas, *Angew. Chem.* **1992**, *104*, 953; *Angew. Chem. Int. Ed. Engl.* **1992**, *31*, 931.
[6] The dianionic nature of 2^{2-}–5^{2-} was deduced from the correlation of ^{1}H and ^{13}C NMR data with charge densities [7], quenching experiments, and comparison with reported values [4].
[7] G. Fraenkel, R. E. Carter, A. MacLean, J. H. Richards, *J. Am. Chem. Soc.* **1960**, *82*, 5846; R. Schaeffer, W. G. Schneider, *Can. J. Chem.* **1963**, *41*, 966; H. Spiesecke, W. G. Schneider, *Tetrahedron Lett.* **1961**, *468*; D. A. Forsyth, G. A. Olah, *J. Am. Chem. Soc.* **1976**, *98*, 4086.
[8] The absorption maxima and ε values (calculated on the assumption of quantitative formation of the dianions): Na_2-**2**: UV/VIS (THF): λ_{max} [nm] (log ε) = 533 (sh, 4.01), 480 (4.57), 445 (sh, 4.38), 356 (4.22), 303 (sh, 4.75) 269 (4.97), 259 (4.97); Na_2-**3**: UV/VIS (THF): λ_{max} [nm] (log ε) = 534 (3.21), 455 (4.58), 448 (4.56), 394 (sh, 4.03), 330 (sh, 3.98), 305 (sh, 4.29), 280 (4.54), 254 (4.46); Na_2-**4**: UV/VIS (THF): λ_{max} [nm] (log ε) 827 (4.28), 742 (4.00), 624 (sh, 4.04), 567 (4.56), 486 (sh, 3.80), 410 (4.03), 382 (4.01), 293 (4.61).
[9] The calculations were performed according to the PPP method (π-electron approximation) with a new gamma (two-electron repulsion integral) and variable β technique: K. Nishimoto, L. S. Forster, *Theor. Chim. Acta* **1965**, *3*, 407; K. Nishimoto, *2nd Int. Symp. Chem. Functional Dyes*, Kobe, **1992**, p. 40; *Proc. Chem. Functional Dyes '92*, Plenum, New York, **1993**, 2A-1. New gamma is proposed for the calculation of the electronic spectra of dyes. The calculated electronic spectra of [3]radialenes agree with the experimental ones.
[10] M. Iyoda, N. Ueno, M. Oda, unpublished results.

Two Modifications of a Cyclopentadienylthallium(I) Complex Linking the Chemistry of the Cp and Arene Complexes of Main Group Elements**

By *Walter Frank*,* *Dietmar Kuhn*, *Stefan Müller-Becker*, and *Abbas Razavi*

The interactions between main group metals and aromatic π-systems have been studied primarily with cyclopentadienyl compounds; in the last few years, however, arene complexes have also received much attention.[1, 2] Are mixed π-arene-π-Cp complexes (Cp = cyclopentadienyl) also capable of existence? Coordinatively unsaturated monomeric units such as CpTl, CpSnCl, and $CpSbCl_2$ should be able to bind arenes. These building blocks are accessible only when their competing aggregation producing oligomers or polymers with bridging Cp or halide ligands is prohibited. The sole report

[*] Prof. Dr. W. Frank, Dipl.-Chem. D. Kuhn, Dr. S. Müller-Becker
Fachbereich Chemie der Universität
Erwin-Schrödinger-Strasse, D-W-6750 Kaiserslautern (FRG)
Dr. A. Razavi
Fina-Research
B-6520 Feluy (Belgium)

[**] Heavy Metal π-Complexes, Part 7. This research was supported by the Fonds der Chemischen Industrie and the Forschungsfonds des Landes Rheinland-Pfalz. – Part 6: W. Frank, *J. Organomet. Chem.* **1991**, *406*, 331.

of the addition of such a compound to arenes described the reactions of the extremely thermolabile pentachlorocyclopentadienylthallium,[3] but closer examination of the bonding relationships in the adducts was not possible. In studies of (dimethylphenylsilyl)- and (benzyldimethylsilyl)-tetramethylcyclopentadienylthallium with NMR spectroscopy, the $^{203,205}Tl-^{13}C$ and $^{203,205}Tl-^{1}H$ couplings for the arene–carbon and arene–hydrogen interactions, respectively, were interpreted as indicative of an intramolecular Tl–arene interaction in solution.[4] By using the 9-(1-cyclopentadienyl-1-methylethyl)fluorenyl ligand **1**, we have succeeded in synthesizing two modifications of the Tl^{I} complex **3**, whose solid-state structures show each thallium atom to be coordinated to three aromatic systems.

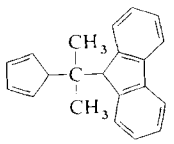

1

We prepared **3** by the metathesis of the lithium derivative **2**[5] and thallium(I) chloride [Eq.(a)] and by the direct metalation of **1**-H with thallium ethoxide [Eq.(b)].[5] Method (a) provided modification **3a**, while (b) yielded modification **3b**. Single crystals of both modifications were examined by X-ray diffraction.

$$\underset{\mathbf{2}}{[C_{13}H_9C(CH_3)_2C_5H_4]Li} + TlCl \xrightarrow[LiCl]{\text{hexane}} \underset{\mathbf{3a}}{[C_{13}H_9C(CH_3)_2C_5H_4]Tl\text{-}I} \quad (a)$$

$$\underset{\mathbf{1}}{C_{13}H_9C(CH_3)_2C_5H_5} + TlOC_2H_5 \xrightarrow[C_2H_5OH]{C_6H_5CH_3} \underset{\mathbf{3b}}{[C_{13}H_9C(CH_3)_2C_5H_4]Tl\text{-}II} \quad (b)$$

The primary interaction in both modifications is a slightly distorted η^5 Tl–Cp coordination (Fig. 1) which takes up most of the binding potential of the thallium atoms according to the analysis of the Tl–C distances. In addition, two secondary contacts between thallium and the aromatic systems in both structures lead to the formation of chains (**3a**) or layers (**3b**) of coordination polymers (Fig. 2). The structure of **3a** is reminiscent of the zigzag chain arrangement found for many Tl–Cp derivatives with bridging Cp ligands.[7] In this case, however, the Cp bridge is very unsymmetrical. The coordination sphere of the Tl atoms is completed by an "intramolecular", η^3-like π-arene contact to the fluorenyl system perpendicular to the direction of the chain. No bridging Cp ligands are found in **3b**. The two layer-forming contacts here are of the Tl–arene type (η^2- and η^3-like). For the η^2-like variation a comparison to the η^5-Cp complexes having additional intramolecular η^2-Cp coordination[8] is instructive. The metal–arene distances indicate that the strength of the metal–arene interactions in both modifications lies in the middle of the known spectrum.[9] Nonclassical Tl–Tl interactions[10] can be discounted in both modifications because of the observed distances.

Both **3a** and **3b** are readily soluble in aromatic solvents. Solutions in the same solvent show the same properties. Complex **3** is monomeric in benzene, and its ^1H NMR spectrum is temperature-dependent: at low temperatures the spectrum is in accord with the atomic arrangement shown in Figure 1 (left) (point group symmetry C_1). As the temperature is increased a dynamic intramolecular process raises the observed symmetry of the molecule (C_s), and finally the

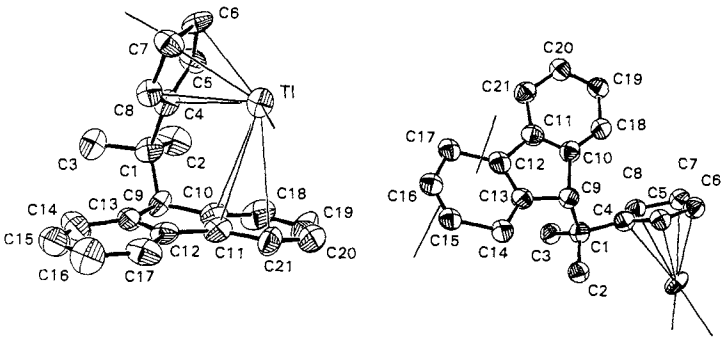

Fig. 1. Quasi-molecular units of **3a** (left) and **3b** (right). The thermal ellipsoids are drawn at the 50% level; hydrogen atoms are omitted for clarity; the directions of the subsequent linkages in the solid state are indicated. Selected distances [pm] in **3a**: Tl-C4 296.4(9), Tl-C5 295.0(8), Tl-C6 280.0(9), Tl-C7 273(1), Tl-C8 286(1), Tl-C10 350.5(8), Tl-C11 337.4(8), Tl-C21 349.2(9), Tl-C20 373(1), Tl-C19 390(1), Tl-C18 380.3(9); in **3b**: Tl-C4 284(2), Tl-C5 281(2), Tl-C6 271(2), Tl-C7 272(2), Tl-C8 275(2). The distances and angles in the $C_{21}H_{19}$ ligands have the anticipated values.

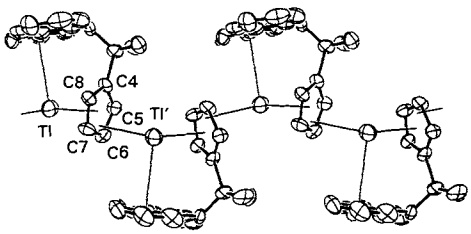

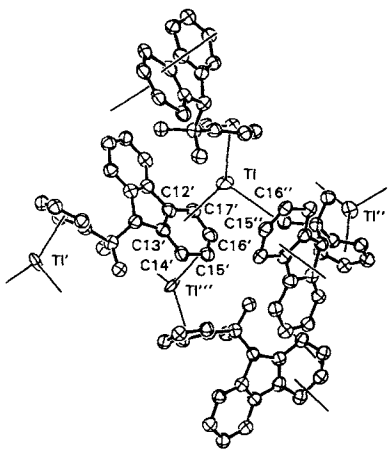

Fig. 2. The linkage of the quasi-molecular units in the crystal; a section of a polymeric chain of **3a** (top; ': 0.5−x, −0.5 + y, 0.5 + z) and of the three-dimensional network of **3b** (bottom; the four quasi-molecular units were chosen so that the complete surroundings of one Tl atom and one (fluorenyl)isopropyl-Cp fragment are visible for each compound; ': 0.5 − x, 1.5 + y, 1.5 + z, '': − x, 1 − y, 0.5 + z). Distances [pm] relevant for the linkage in **3a**: Tl-C4' 361.9(9), Tl-C5' 342(1), Tl-C6' 313(1), Tl-C7' 312.3(9), Tl-C8' 340.2(8), E(= plane)1(C4-C8)-Tl 256(1), E2(C4'-C8')-Tl 306(1), E3(C10, C11, C18-C21)-Tl 329(1); in **3b**: Tl-C12' 336(2), Tl-C13' 367(2), Tl-C14' 388(2), Tl-C15' 375(2), Tl-C16' 357(2), Tl-C17' 346(2), Tl-C15'' 345(2), Tl-C16'' 341(2), E1(C4–C8)-Tl 250(2), E2(C12'-C17')-Tl 326(2), E3(C12''-C17'')-Tl 336(2).

$^{203,205}Tl$ couplings collapse indicating metal–ligand dissociation.

In the mass spectrum (electron impact) the highest mass observed is that of the M^+ peak. The fragmentation patterns indicate that the Tl atoms do not bind exclusively to Cp in the fragmentation; fragments in which thallium is bound to

the fluorenyl system are also evident and are possibly an indication of the considerable strength of the intramolecular Tl–arene interaction in the gas phase.

Experimental Procedure

3a: A suspension of **2** (0.28 g, 1.0 mmol)[5] and TlCl (0.24 g, 1.0 mmol) in hexane (15 mL) was stirred for 24 h at room temperature. The clear, yellowish solution was filtered away from a brown precipitate. The filtrate was concentrated under high vacuum giving a solid or oily residue which was then taken up in benzene (4 mL) and stored at room temperature. Within 24 h colorless crystals of **3a** (0.220, 46%) had formed, which melt at 123 °C (decomp) and are soluble in benzene and other arenes, minimally soluble in dichloromethane, and insoluble in hexane. Correct elemental analysis. MS (EI, 70 eV): *m/z* 476 ($M^{\oplus}$, 3%), 370 ($M^{\oplus} - C_8H_{10}$, 10), 311 ($M^{\oplus} - C_{13}H_9$, 14), 205 ($Tl^{\oplus}$, 60), 165 ($C_{13}H_9^{\oplus}$, 100), 106 ($C_8H_{10}^{\oplus}$, 9), 91 ($C_7H_7^{\oplus}$, 14); molecular mass (cryoscopic, C_6H_6) 465.

3b: A solution of **1** (0.27 g, 1.0 mmol)[5] in toluene (20 mL) was added dropwise to a solution of thallium ethoxide (0.25 g, 1.0 mmol) in toluene (20 mL) at 0 °C over 1 h. The reaction mixture was then stirred for 24 h at approximately 60 °C to give a pale yellow solution above an oily sediment. When the solution was concentrated colorless crystals of **3b** formed which were washed with hexane (0.40 g, 85%). In several experiments the crystallization lasted days. The elongated crystals, readily soluble in aromatic solvents and insoluble in hexane, have an apparently metastable melting point of 97 °C (second heating 105–107 °C). Correct elemental analysis.

3a, b: ^{1}H NMR (400 MHz, [D$_8$]toluene, 193 K, TMS, all signals broad): δ = 0.66 (s, 3H; CH_3), 1.48 (s, 3H; CH_3), 4.17 (s, 1H; CH), 5.62, 5.83, 5.99, 6.74 (m, 4H; C_5H_4), 7.11–7.66 (m, 8H; arom. H); ^{1}H NMR (400 MHz, [D$_6$]toluene, 298 K, TMS): δ = 0.88 (s, 6H; $C(CH_3)_2$), 3.88 (s, 1H; CH), 5.72, 5.93 (m, 4H, J(H,Tl) ca. 28 and 21 Hz; C_5H_4), 6.80–7.33 (m, 8H; arom. H); ^{13}C{^{1}H} NMR (100.6 MHz, [D$_6$]benzene, 300 K): δ = 23.0 (C2, C3), 39.2 (C1), 60.8 (C9), 105.3 (br. s), 107.5 (C5, C8 and C6, C7), 119.7, 120.3 (br. s) (C17, C21 and C14, C18), 125.9, 126.0 (C15, C19 and C16, C20), 127.1 (br. s) (C4), 142.9, 147.0 (C10, C13 and C11, C12).

Received: July 29, 1992 [Z 5489 IE]
German version: *Angew. Chem.* **1993**, *105*, 102

[1] P. Jutzi, *Adv. Organomet. Chem.* **1986**, *26*, 217.
[2] H. Schmidbaur, *Angew. Chem.* **1985**, *97*, 893; *Angew. Chem. Int. Ed. Engl.* **1985**, *24*, 893; H. Schmidbaur, T. Probst, B. Huber, O. Steigelmann, G. Müller, *Organometallics* **1989**, *8*, 1567.
[3] G. Wulfsberg, R. West, *J. Am. Chem. Soc.* **1972**, *94*, 6069.
[4] H. Schumann, H. Kuchl, A. Dietrich, L. Esser, *Chem. Ber.* **1990**, *123*, 1811.
[5] J. A. Ewen, R. L. Jones, A. Razavi, J. D. Ferrara, *J. Am. Chem. Soc.* **1988**, *110*, 6255.
[6] **3**: $C_{21}H_{19}Tl$, M_r = 475.78; **3a**: a = 1132.3(8), b = 949.2(4), c = 1539.4(6) pm, β = 96.89(8)°, Z = 4, space group $P2_1/n$, four-circle diffractometer, $Mo_{K\alpha}$ radiation, 2117 independent reflections with $F > 2\sigma(F_0)$, empirical absorption correction, 207 refined parameters, R = 0.053, R_w = 0.039; **3b**: a = 1689.2(4), b = 971.4(6), c = 998.8(4) pm, Z = 4, space group $Pna2_1$, four-circle diffractometer, $Mo_{K\alpha}$ radiation, 1043 independent reflections with $F > 2\sigma(F_0)$, empirical absorption correction, 200 refined parameters, R = 0.052, R_w = 0.036, polarity: η = 0.80(9). Further details of the crystal structure investigations may be obtained from the Fachinformationszentrum Karlsruhe, Gesellschaft für wissenschaftlich-technische Information mbH, D-W-7514 Eggenstein-Leopoldshafen 2 (FRG), on quoting the depository number CSD-56746, the names of the authors, and the journal citation.
[7] a) E. Frasson, F. Menegus, C. Panattoni, *Nature* **1963**, *199*, 1087; b) M. B. Freedman, L. G. Sneddon, J. C. Huffman, *J. Am. Chem. Soc.* **1977**, *99*, 5194; c) H. Werner, H. Otto, H. J. Kraus, *J. Organomet. Chem.* **1986**, *328*, C57; d) S. Harvey, C. L. Raston, B. W. Skelton, A. H. White, M. F. Lappert, G. Srivastava, *ibid.* **1987**, *328*, C1; e) D. M. Schubert, M. A. Bandman, W. S. Rees, C. B. Knobler, P. Lu, W. Nam, M. F. Hawthorne, *Organometallics* **1990**, *9*, 7; f) P. Jutzi, J. Schnittger, M. B. Hursthouse, *Chem. Ber.* **1991**, *124*, 1693.
[8] F. X. Kohl, R. Dickbreder, P. Jutzi, G. Müller, B. Huber, *Chem. Ber.* **1989**, *122*, 871.
[9] a) H. Schmidbaur, W. Bublak, J. Riede, G. Müller, *Angew. Chem.* **1985**, *97*, 402; *Angew. Chem. Int. Ed. Engl.* **1985**, *24*, 414; b) J. Beck, J. Strähle, *Z. Naturforsch. Sect. B* **1986**, *41*, 1381; c) M. D. Noirot, O. P. Anderson, S. H. Strauss, *Inorg. Chem.* **1987**, *26*, 2216; d) H. Schmidbaur, W. Bublak, B. Huber, J. Hofmann, G. Müller, *Chem. Ber.* **1989**, *122*, 265.
[10] C. Janiak, R. Hoffmann, *J. Am. Chem. Soc.* **1990**, *112*, 5924.

Functional Modeling of CO Dehydrogenase: Catalytic Reduction of Methylviologen by CO/H_2O with an N, O, S-Ligated Nickel Catalyst**

By *Zheng Lu,* Corbet White, Arnold L. Rheingold,* and *Robert H. Crabtree**

An important class of CO dehydrogenases,[1] of which that from *Clostridium thermoaceticum* (*Ct*) is the best characterized, catalyzes reaction (a), the reduction of the electron acceptor methylviologen (MV^{2+}) with CO. Essential to the

$$CO + H_2O + 2\,MV^{2+} \rightleftharpoons CO_2 + 2\,MV^{\bullet+} + 2H^+ \qquad (a)$$

enzyme is nickel, which is believed to be the site of CO binding.[2] Of the two Ni centers, one is close to and probably linked to a Fe_4S_4 cluster. CO reduces the Ni^{II} form of the protein to an EPR-active Ni^{I} form. The EPR signal for this form (g = 2.028 and 2.074) shows coupling to ^{61}Ni, ^{57}Fe, and ^{13}C (of the CO) in the isotopically labeled protein, indicating that the unpaired electron resides on the Ni, CO carbon, and Fe atoms. EXAFS data suggests the presence of a N- (or O-) and S-donor coordination sphere around Ni.[3] We have therefore been looking for Ni complexes with an N,O,S ligand environment which show catalytic activity in CO dehydrogenase (CODH) reactions. Active catalysts must bind the substrate to the metal, yet thiolato ligands tend to reduce the number of open sites and catalytic activity by forming μ-SR bridges. Thioamides are more convenient S-donors than thiolates, because they seem to be less apt to form such bridges, yet they bind in the iminothiolate ($R_2N^+{=}C{-}S^-$) form.[4]

We found that the new complex [{Ni(tmtss)}$_2$] (**1a**)

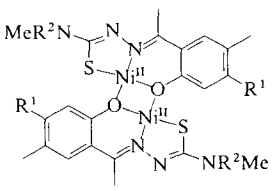

1a, R^1 = Me, R^2 = H
1b, R^1 = H, R^2 = Me

(tmtssH_2 = 2′-hydroxy-4′,5′-dimethylacetophenone-4-methylthiosemicarbazone) catalyzes the CODH reaction shown in Equation (a) with MV^{2+} as the electron acceptor. The unusual O-bridged structure **1** was assigned on the basis of a crystal structure[5] (Fig. 1) of the closely related species **1b**, which is a less active catalyst but crystallizes well.

The $MV^{\bullet+}$ formed in Eq. (a) was detected by its characteristic dark blue color (λ_{max} = 610 nm). The protons released were detected from the change in the pH of the medium during the reaction. Finally, the CO_2 formed was precipitated as $CaCO_3$ after passing the gas mixture through aqueous $Ca(OH)_2$. When the reaction was conducted with CO/$H_2{}^{18}O$/MV^{2+}/**1a**, the ν_4 and ν_5 bands (CO_3^{2-}) of the $CaCO_3$ precipitated were shifted from 872 and 710 cm^{-1} to 863 and 664 cm^{-1} resulting from ^{18}O–^{16}O substitution of the carbonate. The complex is selective for CO and does not give $MV^{\bullet+}$ with RNC or H_2. Recrystallization of **1a** caused no

[*] Z. Lu, Prof. Dr. R. H. Crabtree
Chemistry Department, Yale
225 Prospect Street, New Haven, CT 06511-8118 (USA)
C. White, Prof. Dr. A. L. Rheingold
Chemistry Department, University of Delaware

[**] This work was supported by the National Institutes of Health.

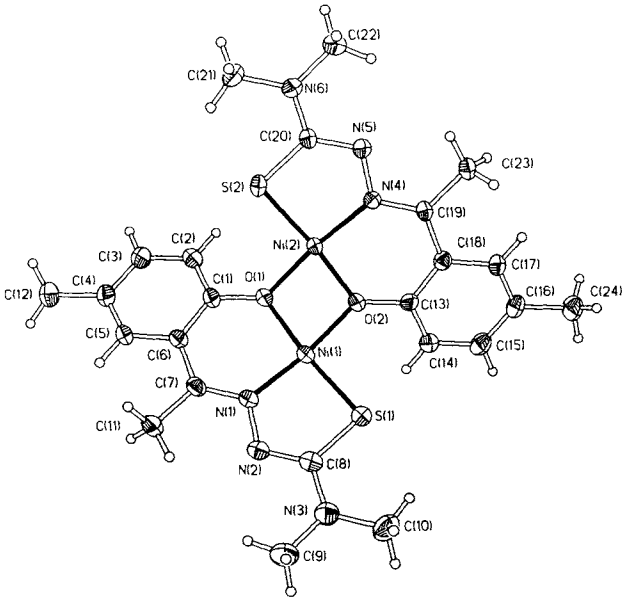

Fig. 1. Molecular structure of **1b** (ORTEP). Selected bond lengths [Å] and angles [°]: Ni(1)-Ni(2) 2.729(1), Ni(1)-O(1) 1.851(3), Ni(1)-O(2) 1.912(4), Ni(1)-N(1) 1.855(5), Ni(2)-O(1) 1.898(4), Ni(1)-S(1) 2.129(1), C(8)-S(1) 1.744(6), C(8)-N(2) 1.298(5); Ni(1)-O(2)-Ni(1) 93.0(2), O(1)-Ni(1)-O(2) 76.4. Dihedral angle Ni(1)O(1)O(2)-Ni(2)O(1)O(2), 136.9(2)°.

change in rate, and neither $NiCl_2$ nor Ni metal mediated the reaction.

The system was active even in neutral solution, but the buildup of protons stopped the process under these conditions. The enzyme was also inhibited at low pH.[1] When sodium acetate (20 mM) was used as a proton acceptor, the reaction proceeded faster. The formation of the methylviologen radical and changes in pH (Fig. 2)[6] indicated that the reaction proceeds steadily at 1.0 turnovers per hour at 25 °C.

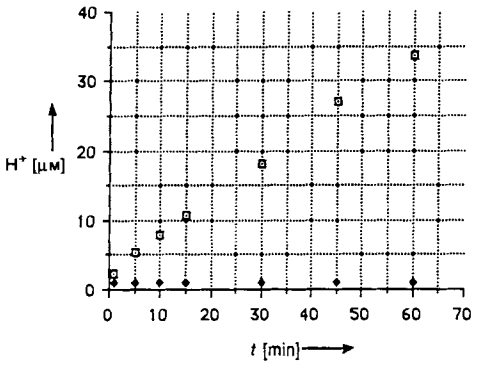

Fig. 2. Release of H^+ in the reduction of MV^{2+} by CO/H_2O with (□) and without (●) catalyst **1a**. [6].

The rate is first order with respect to Ni. Like the enzyme,[1] this system was inhibited both by CN^- (inhibited rate: $3.0 \times 10^{-2}\ h^{-1}$ with 2.5 mM CN^-) and by MeI ($0.78\ h^{-1}$ with 50 mM MeI). This appears to be the first complex to mediate the CODH reaction of Equation (a); stoichiometric model reactions related to the acetylCoA synthase activity of the enzyme have been studied by Holm et al.[7] The water-gas shift reaction, in which CO/H_2O gives CO_2 and H_2, is well known, but not with Ni^{II} as catalyst.[8]

CO reacted with **1a** in CH_2Cl_2 to give a paramagnetic complex **2**, which has an EPR spectrum (Fig. 3, $g_{x,y} = 2.29$, $g_z = 2.05$) consistent with a Ni^I metal center. In the absence of MV^{2+}, Ni^{II} therefore acts as electron acceptor. Complex **2** has so far proved too unstable for a crystal structure to be obtained.

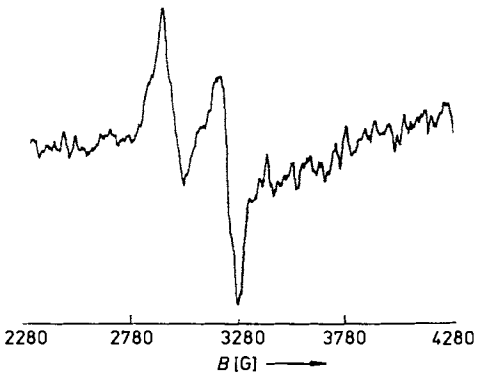

Fig. 3. X band EPR spectrum ($\nu = 9.0519$ GHz) of a frozen solution (5.6 K) of **2**.

The reaction of CN^- and **1a** gave **3**, which has an IR band at 2118 cm^{-1} (νCN) appropriate[9] for a terminal cyanide ligand. CN^- is more resistant to nucleophilic attack than CO, and this may be what allowed us to isolate **3**. The carbonyl analogue of **3**, [Ni^{II}(CO)(tmtss)], could not be prepared or observed spectroscopically, but may be a reactive intermediate in the CO reaction.

$Na[Ni^{II}(CN)(tmtss)]$ **3**

The characteristic blue color of $MV^{\bullet+}$ makes the system a selective sensor for CO when the reaction is conducted under anaerobic conditions as above. Since $MV^{\bullet+}$ is rapidly reoxidized by air to MV^{2+} and the catalyst is not air-sensitive, the acetate-buffered system can be run aerobically for catalytic air oxidation of CO to CO_2 (0.94 turnovers h^{-1}).

Experimental Procedure

$tmtssH_2$: 2'-Hydroxy-4',5'-dimethylacetophenone (1.64 g, 0.01 mol) readily condensed with 4-methylthiosemicarbazide (1.05 g, 0.01 mol) in ethanol (25 mL). Yield 69%, correct C,H,N analysis. ^{1}H NMR (250 MHz, $CDCl_3$): $\delta = 10.50$ (s, 1H; OH), 8.59 (s, 1H; NH), 7.18 (s, 1H; C_6H_2), 6.78 (s, 2H; NH, C_6H_2), 3.25 (d, 3H; CH_3), 2.36 (s, 3H; CH_3), 2.24 (s, 3H; CH_3), 2.21 (s, 3H; CH_3).

1a: To a stirred suspension of $tmtssH_2$ (0.5 g, 2 mmol) in ethanol (20 mL) was slowly added a solution of nickel acetate (0.496 g, 2 mmol) in ethanol (20 mL). After 2 h at reflux, a brownish precipitate was filtered off, washed with cold ethanol, and dried in vacuo. Yield 0.549 g, 89%, correct C,H, analysis. The complex can be recrystallized from CH_2Cl_2/Et_2O. ^{1}H NMR (250 MHz, [D_6]DMSO): $\delta = 7.21$ (s, 1H; C_6H_2), 6.55 (s, 2H; NH, C_6H_2), 2.59 (d, 3H; CH_3), 2.40 (s, 3H; CH_3), 2.11 (s, 3H; CH_3), 2.07 (s, 3H; CH_3). **1b** was prepared analogously.

Received: July 15, 1992
Revised: October 8, 1992 [Z 5468 IE]
German version: *Angew. Chem.* **1993**, *105*, 121

[1] G. Diekert in *The Bioinorganic Chemistry of Nickel* (Ed.: J. R. Lancaster), VCH, Weinheim, **1988**.
[2] H. G. Wood, S. W. Ragsdale, E. Pezacka, *Biochem. Int.* **1986**, *12*, 421; L. Ljungdahl, *Annu. Rev. Microbiol.* **1986**, *40*, 415.
[3] S. W. Ragsdale, H. G. Wood, T. A. Morton, L. G. Ljungdahl, D. DerVartanian in *The Bioinorganic Chemistry of Nickel* (Ed.: J. R. Lancaster), VCH, Weinheim, **1988**.

[4] M. Zimmer, G. Schulte, X.-L. Luo, R. H. Crabtree, *Angew. Chem.* **1990**, *103*, 205; *Angew. Chem. Int. Ed. Engl.* **1991**, *30*, 193.
[5] Structure analysis: **1b**: triclinic, space group $P\bar{1}$, $a = 8.220(2)$, $b = 13.100(3)$, $c = 13.864(3)$ Å; $\alpha = 114.56(3)$, $\beta = 103.59(3)$, $\gamma = 92.07(3)°$, $V = 1304.6(5)$ Å^3, $Z = 2$, $\varrho_{calc.} = 1.568$ g cm^{-3}; 5702 unique reflections, 3637 observed ($F > 5\sigma(F)$), 325 variables, $R = 0.0426$, $R_w = 0.0426$. Further details are available from the Director of the Cambridge Crystallographic Data Centre, University Chemical Laboratory, Lensfield Road, GB-Cambridge CB2 1EW (UK) on quoting the full journal citation.
[6] Conditions: CO (5 mL min^{-1}) was passed at room temperature (20 °C) through a solution of CH_2Cl_2 and CH_3OH (1:1, 60 mL) containing 0.010 g of **1a**, 0.10 g of MV^{2+}, 0.10 g of NaOAc, and 1.0 mL of water. To quantify the proton release, the pH observed (pH meter) was compared with the pH changes found for an identical solution titrated with 0.01 N HCl. Control reactions were run under identical conditions without **1a** and with $tmtssH_2$ but without Ni.
[7] P. Stavropoulos, M. C. Muetterties, M. Carrié, R. H. Holm, *J. Am. Chem. Soc.* **1991**, *113*, 8485.
[8] J. W. Reppe, *Justus Liebigs Ann. Chem.* **1953**, *582*, 121.
[9] M. Sato, F. Sato, T. Yoshida, *J. Organomet. Chem.* **1971**, *31*, 415.

Synthesis and Structure of the First Homoleptic Imidotechnetium Complex: $[Tc_2(NAr)_6]$ (Ar = 2,6-diisopropylphenyl)**

By *Anthony K. Burrell* and *Jeffrey C. Bryan**

Transition metal complexes containing only imido ligands are currently known for niobium, rhenium, osmium, and the Group 6 metals.[1-3] An example especially pertinent to this work is the complex $[Re_2(NtBu)_4(\mu\text{-}NtBu)_2]$, which is formed by reduction of $[Re(NtBu)_3(OSiMe_3)]$ with sodium amalgam.[2] $[Re_2(NtBu)_4(\mu\text{-}NtBu)_2]$ is an edge-bridged tetrahedral dimer, similar to all other structurally characterized M_2E_6 complexes (where E stands for dianionic ligands such as N*t*Bu, S, Se, which form multiple bonds to the metal center).[2-4] We report here the first homoleptic imidotechnetium complex $[Tc_2(NAr)_6]$ (**1**, Ar = 2,6-diisopropylphenyl), which adopts an unprecedented "ethanelike" structure.

Tetrahydrofuran solutions of $[Tc(NAr)_3I]$[5] react quickly at room temperature with sodium metal to form $[Tc_2(NAr)_6]$ (**1**) in high yield (Scheme 1, M = Tc). Complex **1** does not

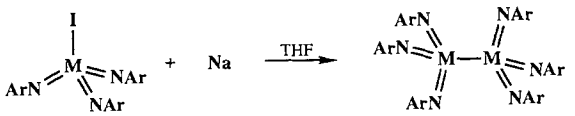

M = Tc, Re
Ar = 2,6-*i*Pr$_2$C$_6$H$_3$

1, M = Tc

Scheme 1. Synthesis of **1**. The analogous Re complex appears to be accessible by the same route.

react with iodine at room temperature to re-form $[Tc(NAr)_3I]$; **1** is air-stable in solution and can be purified on a silica gel column. The ^{1}H NMR spectrum of **1** shows only one set of resonances for the aryl groups, suggesting that all the imido ligands in **1** are chemically equivalent.

X-ray structure analysis of a single crystal of **1**, grown by slow evaporation of a THF/$(Me_3Si)_2O$ solution, reveals an ethanelike structure (Fig. 1).[6] The two Tc atoms are joined

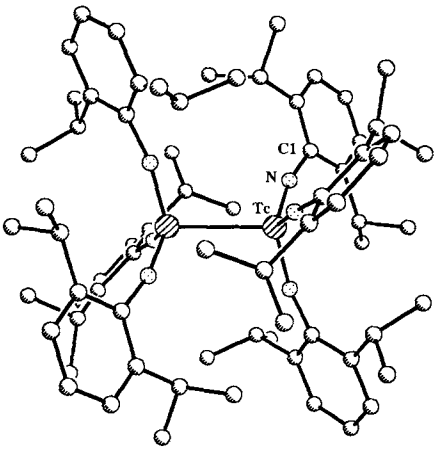

Fig. 1. Crystal structure of $[Tc_2(NAr)_6]$ (**1**). Selected bond angles [°] for **1**, not already mentioned in the text: N–Tc–Tc(A) = 103.6(1), N–Tc–N(A) = 114.6(1).

by an unbridged metal–metal bond, and all six imido ligands are terminally bound, three to each technetium. The Tc–Tc bond lies on a crystallographic S_6 axis making all six imido ligands symmetry equivalent, and requiring a staggered arrangement. If the imido ligands in **1** are counted as dianionic,[7] the Tc atoms can be considered formally to be in the oxidation state +VI. The Tc–Tc bond length of 2.744(1) Å could then only be considered a single bond, consistent with the formulation of **1** as a d^1–d^1 dimer and the diamagnetic behavior of the complex. The Tc–Tc bond is longer than known single bond lengths for Tc^{VI}–Tc^{VI} dimers;[8] this may be due to the sterically demanding Ar groups of the imido ligands. The short Tc–N distances of 1.758(2) Å, and the nearly linear Tc–N–C angles of [167.6(3)°] are consistent with strong multiple bonding between the Tc atom and the imido ligands.[7]

All previous examples of structurally characterized M_2E_6 complexes are edge-bridged tetrahedral dimers with sterically less demanding ligands such as S, Se, and N*t*Bu (Scheme 2).[2-4] Simple molecular mechanics calculations[9] on $[Tc_2(NAr)_6]$ clearly indicate that the observed ethanelike structure is strongly preferred over the dimeric configuration of edge-bridged tetrahedra.

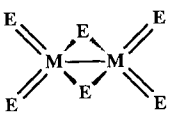

Scheme 2. M_2E_6 complexes which can be considered edge-bridged tetrahedral dimers.

This preference has been extensively demonstrated for M_2X_6 complexes, where X is a *mono*anionic ligand; they adopt a dimeric structure of edge-bridged tetrahedra for nonbulky X ligands and an ethanelike structure for bulky X ligands.[10] Since $[Re_2(NtBu)_4(\mu\text{-}NtBu)_2]$ adopts an edge-bridged tetrahedral dimer structure, we attempted to prepare $[Tc_2(NtBu)_4(\mu\text{-}NtBu)_2]$, without immediate success. However, preliminary work indicates that reduction of [Re-

[*] Dr. J. C. Bryan
Inorganic and Structural Chemistry Group, INC-1, C346
Los Alamos National Laboratory
Los Alamos, NM 87545 (USA)
Dr. A. K. Burrell
Nuclear and Radiochemistry Group, Los Alamos National Laboratory

[**] This work was supported by the Laboratory Directed Research and Development program Los Alamos National Laboratory. We also thank Dr. David L. Clark for helpful discussions.

$(NAr)_3I]$[11] with sodium gives ethanelike $[Re_2(NAr)_6]$ in good yield (Scheme 1, M = Re).[12] These results suggest that steric factors determine the structure of the M_2E_6 complexes.

Experimental Procedure

Caution: The isotope ^{99}Tc used in the synthesis is a low-energy β emitter (E_{max} = 0.29 MeV) with a very long half life (2.1×10^5 years) and without nuclide-specific γ radiation. All preparative procedures were carried out in a glove box.

$[TcI(NAr)_3]$: Iodotrimethylsilane (0.6 mL, 0.42 mmol) was added to a solution of $[Tc(OSiMe_3)(NAr)_3]$ (100 mg, 0.14 mmol) in toluene (15 mL). The mixture was stirred for approximately 1 h, after which the solvent was removed in vacuo. The residue was then extracted with hot $(Me_3Si)_2O$ (15 mL) and filtered through Celite. The solution was cooled at -40 °C for 12 h and then filtered to give the product as a dark green solid (97 mg, 92%). ^{1}H NMR (250 MHz, C_6D_6, 25 °C): δ = 6.97 (m, 9H; ArH), 3.72 (hep, ^3J(H,H) = 6.8 Hz, 6H; CH), 1.09 (d, ^3J(H,H) = 6.8 Hz, 36H; CH_3). Correct elemental analyses (C,H,N).

1: Na (3 mg, 0.13 mmol) was added to a solution of $[TcI(NAr)_3]$ (100 mg, 0.13 mmol) in THF (15 mL). The mixture was stirred for approximately 3 h, after which the solvent was removed in vacuo. The residue was then extracted with $(Me_3Si)_2O$ (15 mL) and filtered through Celite. Evaporation of the $(Me_3Si)_2O$ gave the product as a green solid. Compound **1** was then purified by column chromatography with silica gel by using hexane:toluene (9:1) as eluent. ^{1}H NMR (250 MHz, C_6D_6, 25 °C): δ = 6.97 (m, 18H; ArH), 3.94 (hep, ^3J(H,H) = 7.5 Hz, 12H; CH), 1.08 (d, ^3J(H,H) = 7.5 Hz, 72H; CH_3); ^{13}C NMR (62.8 MHz, CD_2Cl_2, 25 °C): δ = 144.3 (NC), 128.1 (Ar), 126.8 (Ar), 123.5 (Ar), 28.3 (CH), 24.0 (CH_3). Correct elemental analysis (C,H,N).

Received: August 17, 1992 [Z 5519 IE]
German version: *Angew. Chem.* **1993**, *105*, 85

[1] a) M. H. Schofield, T. P. Kee, J. T. Anhaus, R. R. Schrock, K. H. Johnson, W. M. Davis, *Inorg. Chem.* **1991**, *30*, 3595–3604; b) A. A. Danopoulos, G. Wilkinson, M. B. Hursthouse, B. Hussain, *Polyhedron* **1989**, *8*, 2947–2949; A. A. Danopoulos, W.-H. Leung, G. Wilkinson, B. Hussain-Bates, M. B. Hursthouse, *ibid.* **1990**, *9*, 2625–2634; A. A. Danopoulos, G. Wilkinson, *ibid.* **1990**, *9*, 1009–1010; c) $Li_3[Nb(Nmes)_4]$, D. E. Wigley, University of Arizona, personal communication.

[2] A. A. Danopoulos, C. J. Longley, G. Wilkinson, B. Hussain, M. B. Hursthouse, *Polyhedron* **1989**, *8*, 2657–2670.

[3] A. A. Danopoulos, G. Wilkinson, B. Hussain-Bates, M. B. Hursthouse, *J. Chem. Soc. Dalton Trans.* **1991**, 269–275, 1855–1860.

[4] Y.-j. Lu, M. A. Ansari, J. A. Ibers, *Inorg. Chem.* **1989**, *28*, 4049–4050; A. I. Hadjikyriacou, D. Coucouvanis, *ibid.* **1987**, *26*, 2400–2408; "MO_3" (M = Re etc.) forms polymeric structures lacking any metal–metal interaction, see F. A. Cotton, G. Wilkinson, *Advanced Inorganic Chemistry*, 5th ed., Wiley, New York, **1988**; see also ref. [10].

[5] J. C. Bryan, C. J. Burns, A. P. Sattelberger, *Isotope and Nuclear Chemistry Division Annual Report FY*, **1990**, pp. 40–41. National Technical Information Service, US Department of Commerce, LA-12143-PR.

[6] Crystal data for $C_{72}H_{102}N_6Tc_2$ (**1**): rhomohedral space group $R\bar{3}$, a = 13.264(3), c = 33.284(12) Å, V = 5069(3) Å^3, Z = 3, ρ_{calcd} = 1.226 gcm^{-3}, μ ($Mo_{K\alpha}$) = 4.53 cm^{-1}, T = 203 K; 1496 independent reflections with $4 < 2\theta < 55$ were collected, of which 1222 reflections with $F_0 > 4\sigma(F_0)$ were used in the refinement. R = 0.0326, R_w = 0.0407, GOF = 1.12. Further details of the crystal structure investigation are available on request from the Director of the Cambridge Crystallographic Data Centre, University Chemical Laboratory, Lensfield Road, GB-Cambridge CB 21EW (UK), on quoting the full journal citation.

[7] W. A. Nugent, B. L. Haymore, *Coord. Chem. Rev.* **1980**, *31*, 123; W. A. Nugent, J. M. Mayer, *Metal-Ligand Multiple Bonds*, Wiley, New York, **1988**.

[8] To the best of our knowledge three other Tc^{VI}–Tc^{VI} dimers have been structurally characterized with Tc–Tc bond lengths of 2.543(1) Å [8a], 2.5617(3) Å [8b], and 2.694(1) Å [8c]. Tc atoms are bridged in all three examples. a) J. Baldas, J. F. Boas, J. Bonnyman, S. F. Colmanet, G. A. Williams, *J. Chem. Soc. Chem. Commun.* **1990**, 1163–1165; b) W. A. Herrmann, R. Alberto, P. Kiprof, F. Baumgärtner, *Angew. Chem.* **1990**, *102*, 208–210; *Angew. Chem. Int. Ed. Engl.* **1990**, *29*, 189–191; c) $[Tc_2(NAr')_4(\mu\text{-}NAr')(CH_3)_2]$ (Ar' = 2,6-dimethylphenyl), A. K. Burrell, D. L. Clark, C. J. Burns, J. C. Bryan, unpublished results.

[9] CAChe™, August 2, 1991, CAChe Scientific, Inc.

[10] M. H. Chisholm, J. F. Corning, K. Folting, J. C. Huffman, *Polyhedron* **1985**, *4*, 383–390; R. H. Summerville, R. Hoffmann, *J. Am. Chem. Soc.* **1976**, *98*, 7240–7254.

[11] Prepared in a manner analogous to $[Tc(NAr)_3I]$, see Experimental Procedure, and R. Toreki, R. R. Schrock, W. M. Davis, *J. Am. Chem. Soc.* **1992**, *114*, 3367–3380.

[12] The fact that NAr is "less prone to bridge between metals than, for example, a *tert*-butylimido ligand" has been previously observed [1a].

Synthesis and Reactivity of $Me_2P(ZrCp_2Cl)$=NAr, the First Iminozirconiophosphorane, a Masked Iminophosphide**

By *Alain Igau, Nathalie Dufour, Armelle Mahieu,* and *Jean-Pierre Majoral**

Little is known about the interactions of derivatives of unsaturated main group elements and Group 4 metallocenes.[1, 2] We recently investigated the reactivity of phosphaalkenes and iminophosphanes towards the Schwartz reagents $[Cp_2ZrHCl]$,[3, 4] $[Cp_2ZrH_2]$,[4] and $[Cp_2ZrMe_2]$.[4] We now report the surprising synthesis of the first linear *P*-metalated iminophosphorane **3** by carbometalation of the chloroiminophosphane ClP=NAr (**1**, Ar = 2,4,5-*t*Bu$_3$-C_6H_2).[5, 6] Up to now only *N*-metalated iminophosphoranes were prepared because of the strong polarization of the phosphorus–nitrogen double bond of compounds of type R_3P=NR'. From the preliminary studies on the reactivity of **3** we found an unprecedented insertion reaction of nitriles into the phosphorus–zirconium bond.

The chloroiminophosphane **1**, and $[Cp_2ZrMe_2]$, (**2**) were allowed to react in pentane at -40 °C. After workup of the reaction mixture, **3** was isolated as a white powder in 85% yield (Scheme 1). Compound **3** was identified by NMR spectroscopy (Table 1). The ^{1}H NMR signal of Cp protons appeared as a doublet with a coupling constant $^3J_{P,H}$ = 1.4 Hz, consistent with a Cp-Zr-P skeleton. The two methyl groups are bonded to the phosphorus atom, as illustrated by the ^{1}H (only one doublet for the two methyl groups, $^2J_{H,P}$ = 6.3 Hz), ^{13}C (also one doublet, $^1J_{C,P}$ = 11.1 Hz), and ^{31}P NMR spectra (doublet of septet, $^2J_{P,H}$ = 6.3 Hz, $^3J_{P,Cp(H)}$ = 1.4 Hz). The formation of **3** might involve the transient intermediate **4**, which rearranges by migration of the chlorine atom and the methyl group at the zirconium.[7] In solution at room temperature **3** afforded the phosphane **5** quantitatively (the migration of $ZrCp_2Cl$ moieties from the phosphorus to the nitrogen atom gives the thermodynamically favored product **5**, Scheme 1). Compound **5** was characterized by NMR spectroscopy: the ^{31}P NMR chemical shift of **5** was in the expected range; the Cp protons appeared as a singlet, and no coupling with the phosphorus atom was observed. Addition of pyridine or PMe_3 to **3** gave **5** instantaneously. In the presence of proton donors (solvent, traces of water), the Zr–N bond in **5** was cleaved to form **6** quantitatively (Scheme 1).

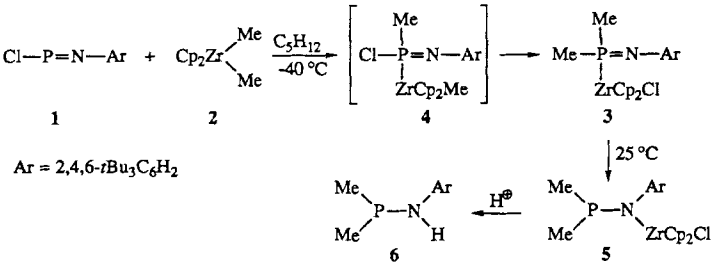

Scheme 1. Synthesis and thermally induced rearrangement of **3**.

[*] Dr. J.-P. Majoral, Dr. A. Igau, Dr. N. Dufour, A. Mahieu
Laboratoire de Chimie de Coordination du CNRS
205, route de Narbonne, F-31077 Toulouse Cédex (France)

[**] This work was supported by the Centre National de la Recherche Scientifique.

Table 1. Selected spectroscopic data of the compounds **3**, **5**, **6**, **7a–c**, **8a,b** [a].

3: $^{31}P\{^1H\}$ NMR (CD_2Cl_2, 25 °C): $\delta = -4.33$; ^1H NMR (CD_2Cl_2, 25 °C): $\delta = 7.28$ (s, CH(Ar)), 6.00 (d, $^3J(HP) = 1.4$ Hz, Cp), 1.53 (s, *o*-*t*Bu), 1.34 (s, *p*-*t*Bu), 0.80 (d, $^2J(HP) = 6.3$ Hz, PCH_3); $^{13}C\{^1H\}$ NMR (CD_2Cl_2, 25 °C): $\delta = 148.8$ (d, $^2J(CP) = 18.0$ Hz, *i*-C(Ar)), 146.5 (d, $^3J(CP) = 6.0$ Hz, *o*-C(Ar)), 138.9 (d, $^5J(CP) = 5.0$ Hz, *p*-C(Ar)), 120.7 (s, *m*-C(Ar)), 110.9 (s, Cp), 36.5 (s, *o*-CCH_3), 36.1 (s, *p*-CCH_3), 33.6 (s, *o*-CCH_3), 30.8 (s, *p*-CCH_3), 16.7 (d, $^1J(CP) = 11.1$ Hz, PCH_3).

5: $^{31}P\{^1H\}$ NMR (CD_2Cl_2, 25 °C): $\delta = 31.8$; ^1H NMR (CD_2Cl_2, 25 °C): $\delta = 7.33$ (s, CH(Ar)), 6.32 (s, Cp), 1.47 (s, *o*-*t*Bu), 1.40 (d, $^2J(HP) = 5.8$ Hz, PCH_3), 1.29 (s, *p*-*t*Bu); $^{13}C\{^1H\}$ NMR (CD_2Cl_2, 25 °C): $\delta = 146.7$ (s, *o*-C(Ar)), 144.8 (s, *p*-C(Ar)), 121.7 (s, *m*-C(Ar)), *i*-C(Ar) not observed, 114.3 (s, Cp), 34.9 (s, *o*-CCH_3), 34.5 (s, *p*-CCH_3), 30.3 (s, *o*-CCH_3), 31.7 (s, *p*-CCH_3), 20.4 (d, $^1J(CP) = 17.5$ Hz, PCH_3).

6: $^{31}P\{^1H\}$ NMR: (CD_2Cl_2, 25 °C): $\delta = 33.3$; ^1H NMR (CD_2Cl_2, 25 °C): $\delta = 7.48$ (s, CH(Ar)), 3.10 (d, $^2J(HP) = 5.8$ Hz, NH), 1.56 (s, *o*-*t*Bu), 1.33 (s, *p*-*t*Bu), 1.09 (d, $^2J(HP) = 6.5$ Hz, PCH_3); $^{13}C\{^1H\}$ NMR (CD_2Cl_2, 25 °C): $\delta = 144.5$ (d, $^2J(CP) = 3.0$ Hz, *i*-C(Ar)), 143.8 (d, $^4J(CP) = 2.2$ Hz, *o*-C(Ar)), 141.9 (d, $^5J(CP) = 14.0$ Hz, *p*-C(Ar)), 123.6 (d, $^2J(CP) = 1.7$ Hz, *m*-C(Ar)), 36.8 (s, *o*-CCH_3), 34.8 (s, *p*-CCH_3), 33.2 (s, *o*-CCH_3), 31.9 (s, *p*-CCH_3), 20.0 (d, $^1J(CP) = 19.5$ Hz, PCH_3); IR (KBr) $\tilde{\nu}$[cm^{-1}] = 3283 (NH).

7a: $^{31}P\{^1H\}$ NMR (C_6D_6, 25 °C): $\delta = 53.8$; ^1H NMR (C_6D_6, 25 °C): $\delta = 7.51$ (s, CH(Ar)), 6.05 (s, Cp), 1.70 (d, $^3J(HP) = 0.9$ Hz, CH_3CP) 1.53 (s, *o*-*t*Bu), 1.25 (s, *p*-*t*Bu), 1.20 (d, $^2J(HP) = 8.8$ Hz, PCH_3); $^{13}C\{^1H\}$NMR (C_6D_6, 25 °C): $\delta = 165.0$ (d, $^1J(CP) = 14.4$ Hz, PC=N), 148.4 (s, *o*-C(Ar)), 148.1 (s, *p*-C(Ar)), 136.60 (s, *i*-C(Ar)), 126.4 (s, *m*-C(Ar)), 111.6 (s, Cp), 35.1 (s, *o*-CCH_3), 34.7, 34.6 (s, *o*-CCH_3), 32.4 (s, *p*-CCH_3), 31.8 (s, *p*-CCH_3), 28.3 (s, $PCCH_3$), 16.9 (d, $^1J(CP) = 25.3$ Hz, PCH_3).

7b: m.p. 126–127 °C (decomp); $^{31}P\{^1H\}$ NMR (C_6D_6, 25 °C): $\delta = 49.3$; ^1H NMR (C_6D_6, 25 °C): $\delta = 7.48$ (s, CH(Ar)), 6.21 (s, Cp), 2.61 (sept, $^3J(HH) = 6.7$ Hz, $CHCH_3$), 1.50 (s, *o*-*t*Bu), 1.34 (s, *p*-*t*Bu), 1.19 (d, $^2J(HP) = 8.8$ Hz, PCH_3), 1.08 (d, $^3J(HH) = 6.7$ Hz, $CHCH_3$); ^{13}C NMR (C_6D_6, 25 °C): $\delta = 171.5$ (d, $^2J(CP) = 15.1$ Hz, PC=N), 148.8 (s, *o*-C(Ar)), 148.3 (s, *p*-C(Ar)), 135.2 (d, $^2J(CP) = 4.5$ Hz, *i*-C(Ar)), 127.1 (s, *m*-C(Ar)), 112.6 (s, Cp), 34.7, 34.6 (s, *o*-CCH_3), 32.4 (s, *p*-CCH_3), 31.8 (s, *o*-CCH_3), 31.7 (s, *p*-CCH_3), 22.8 (s, CH_3CH), 18.6 (d, $^1J(CP) = 27.5$ Hz, PCH_3).

7c: $^{31}P\{^1H\}$ NMR (C_6D_6, 25 °C): $\delta = 56.4$.

8a: ^{31}P NMR (CD_2Cl_2, 25 °C): $\delta = 32.3$ (d, $^1J(PH) = 518.0$ Hz, PH); ^1H NMR (CD_2Cl_2, 25 °C): $\delta = 7.36$ (s, CH(Ar)), 7.31 (d, $^1J(HP) = 518.0$ Hz, PH), 5.83 (d, $^2J(HP) = 9.9$ Hz, NH), 1.86 (d, $^2J(HP) = 14.0$ Hz, PCH_3), 1.40 (s, *o*-*t*Bu), 1.26 (s, *p*-*t*Bu); $^{13}C\{^1H\}$ NMR (CD_2Cl_2, 25 °C): $\delta = 149.9$ (s, *p*-C(Ar)), 134.0 (d, *m*-C(Ar)), 121.9 (d, *o*-C(Ar), *i*-C(Ar) not observed, 36.7 (s, *o*-CCH_3), 34.8 (s, *p*-CCH_3), 32.8 (s, *o*-CCH_3), 30.3 (s, *p*-CCH_3), 7.7 (d, $^2J(CP) = 67.0$ Hz, PCH_3).

8b: $^{31}P\{^1H\}$ NMR (CD_2Cl_2, 25 °C): $\delta = 53.8$; ^1H NMR (CD_2Cl_2, 25 °C): $\delta = 7.34$ (s, CH(Ar)), 6.06 (d, $^2J(HP) = 9.8$ Hz, PCH_3), 1.86 (d, $^2J = 13.0$ Hz, PCH_3), 1.39 (s, *o*-*t*Bu), 1.25 (s, *p*-*t*Bu); $^{13}C\{^1H\}$ NMR (CD_2Cl_2, 25 °C): $\delta = 150.6$ (d, $^5J(CP) = 3.0$ Hz, *p*-C(Ar)), 149.5 (d, $^4J(CP) = 5.0$ Hz, *m*-C(Ar)), 124.5 (d, $^3J(CP) = 2.0$ Hz, *o*-C(Ar), *i*-C(Ar) not observed, 37.0 (s, *o*-CCH_3), 34.9 (s, *p*-CCH_3), 33.3 (s, *o*-CCH_3), 31.2 (s, *p*-CCH_3), 13.6 (d, $^2J(CP) = 67.0$ Hz, PCH_3).

[a] All NMR spectra were recorded on a Bruker AC 200. Standards: $\delta(^{31}P)$: 85% H_3PO_4 external; $\delta(^1H, ^{13}C)$: $(CH_3)_4Si$ external.

The *P*-metalated iminophosphorane **3** was allowed to react with 1.1 equivalents of acetonitrile in CH_2Cl_2 at −40 °C. The iminophosphorane **7a** was formed instantaneously (Scheme 2) by the insertion of MeC≡N into the P–Zr bond. The presence of a third methyl group in **7a** was clearly evident from the ^1H and ^{13}C NMR spectra. In the ^1H NMR spectrum the C–Me group appeared as a doublet at $\delta = 1.70$ ($^3J_{H,P} = 0.9$ Hz) and in the $^{13}C\{^1H\}$ NMR spectrum as a singlet at $\delta = 28.3$. The signal of the imino C atom can also be observed at characteristically low field ($\delta = 165.0$, $^2J_{C,P} = 14.4$ Hz).

The formation of **7a** favored a linear rather than a cyclic structure for **3**, since the azaphosphazirconacyclopropane $[Cp_2Zr(Cl)N(SiMe_3)P(H)N(SiMe_3)_2]$[3] is inert toward nitriles. Other nitriles were treated with **3** under the same conditions. Addition of *i*PrC≡N or PhC≡N to **3** gave the expected insertion products **7b** and **7c**, respectively (Scheme 2). The iminophosphorane **3** reacted formally like an iminophosphide of type **A**, a species never observed until now.[8]

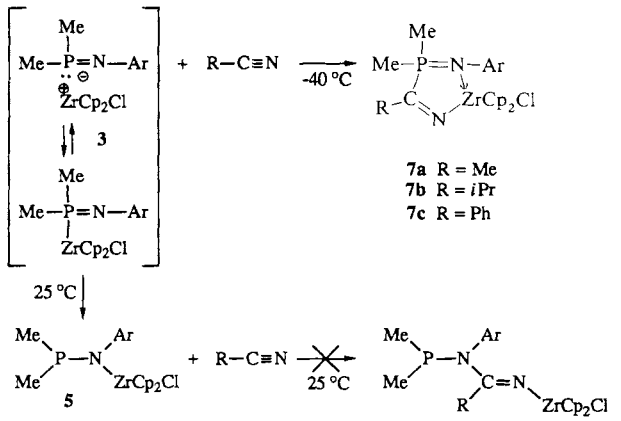

Scheme 2. Reactivity of **3** and **5** toward nitriles.

In marked contrast **5** did not react even with an excess of acetonitrile at room temperature. If **3** is treated with trifluoromethanesulfonic acid or its methylester at −78 °C, the

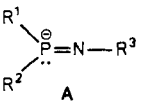

phosphonium compounds **8a** and **8b**, respectively, were obtained in quantitative yield (Scheme 3).

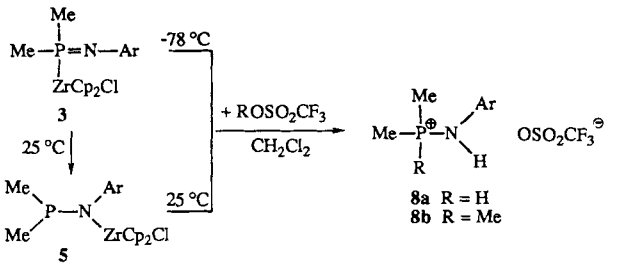

Scheme 3. Reactivity of **3** and **5** toward trifluoromethanesulfonic acid and its methyl ester.

Compounds **8a** and **8b** were also formed by treating **5** with the same reagents (Scheme 3). Like PMe_3 and pyridine ligands, the trifluoromethanesulfonic anion may act as a catalyst for the rearrangement of **3** to **5**. Electrophilic attack of R^+ (H^+, Me^+) at the phosphorus center of **5** followed by cleavage of the Zr–N bond might give rise to the quantitative formation of **8**.

We are currently attempting to determine the scope of the reactions in which **3** reacts as a *P*-metalated iminophosphorane and **5** as a aminozirconiophosphane.

Experimental Procedure

All manipulations were performed in an inert argon atmosphere.

Isolation of **3**: To a solution of **1** (0.326 g, 1.0 mmol) in pentane (10 mL) cooled to −40 °C was added **2** (0.251 g, 1.00 mmol) in pentane (10 ml) at −40 °C. The mixture was stirred for 30 min, after which a white precipitate separated from the solution. The white powder was washed twice with pentane (10 mL, −40 °C), and dried under vacuum. This afforded **3** (0.491 g, 0.850 mmol) in 85% yield.

Decomposition of **3**: A solution of **3** (0.200 g, 0.346 mmol) in CH_2Cl_2 (15 mL) was stirred at room temperature for 4 h, which after removal of the solvent gave a white powder **5** (0.200 g, 0.346 mmol) in quantitative yield. Attempts to iso-

late **5** by treatment of the residue with pentane and THF, gave a mixture of **5** and the phosphane **6**.

Reaction of **3** with nitriles (typical experiment for the isolation of **7a** and **7b**): CH_3CN (10 mL) cooled to −30 °C was added to **3** (0.288 g, 0.50 mmol) through a canula. The reaction mixture was stirred at −40 °C for 1 h, after which a white precipitate separated from the solution. The white powder was washed twice with CH_3CN (10 mL, −30 °C) and pentane (2 × 10 mL), then dried to afford **7a** (0.263 g, 0.425 mmol) in 85% yield.

Typical reaction of **3** with trifluoromethanesulfonic acid: To a solution of **3** (0.577 g, 1.00 mmol) in CH_2Cl_2 (10 mL) cooled to −78 °C was added $HO-SO_2CF_3$ (0.150 mL, 1.00 mmol). The reaction mixture was allowed to warm to room temperature over 30 min. Removal of the solvent gave a white paste. Extraction with pentane (3 × 10 mL) afforded **8a** (0.319 g, 0.98 mmol) as a white powder in nearly quantitative yield.

Received: August 1, 1992 [Z 5497 IE]
German version: *Angew. Chem.* **1993**, *105*, 76

[1] Reactivity of *t*BuC≡P with zirconocenes: a) P. Binger, B. Biedenbach, C. Krüger, M. Regitz, *Angew. Chem.* **1987**, *99*, 798; *Angew. Chem. Int. Ed. Engl.* **1987**, *26*, 764; b) P. Binger, B. Biedenbach, A. T. Herrmann, R. Milczareck, R. Schneider, *Phosphorus Sulfur Silicon Relat. Elem.* **1990**, *49/50*, 337; c) P. Binger, T. Wettling, R. Schneider, F. Zurmühlen, U. Bergsträsser, J. Hoffmann, G. Mass, M. Regitz, *Angew. Chem.* **1991**, *103*, 208; *Angew. Chem. Int. Ed. Engl.* **1991**, *30*, 207.

[2] Reactivity of $R_3P=CH_2$ with Group 4 metallocenes: a) W. C. Kaska, *Coord. Chem. Rev.* **1983**, *48* 1; b) H. Schmidbaur, R. Pichl, *Z. Naturforsch. B* **1985**, *40*, 352; c) G. Erker, P. Czisch, R. Mynott, Y.-H. Tsay, C. Krüger, *Organometallics* **1985**, *4*, 1310; d) G. Erker, P. Czisch, C. Krüger, J. M. Wallis, *ibid.* **1985**, *4*, 2059; e) G. Erker, U. Dorf, P. Czisch, J. L. Petersen, *ibid.* **1986**, *5*, 668.

[3] a) J.-P. Majoral, N. Dufour, F. Meyer, A.-M. Caminade, R. Choukroun, *J. Chem. Soc. Chem. Commun.* **1990**, *6*, 507; b) N. Dufour, J.-P. Majoral, A.-M. Caminade, R. Choukroun, *Organometallics* **1991**, *10*, 45.

[4] N. Dufour, A.-M. Caminade, M. Basso-Bert, A. Igau, J.-P. Majoral, *Organometallics* **1992**, *11*, 1131–1137.

[5] For a review covering the field of iminophosphane chemistry see E. Niecke in *Multiple Bonds and Low Coordination in Phosphorus Chemistry* (Eds.: M. Regitz, O. J. Scherer), Thieme, Stuttgart, **1990**, pp. 293–320; E. Niecke, D. Grudat, *Angew. Chem.* **1991**, *103*, 251; *Angew. Chem. Int. Ed. Engl.* **1991**, *30*, 217.

[6] Reaction of organometallic reagents with $(NPCl_2)_3$ or $(NPF_2)_4$ led to cyclic phosphazenes containing transition metals: H. R. Allcock, *Chem. Eng. News* **1985**, *63* (11), 22–36 and references therein.

[7] Attempts to obtain X-ray quality crystals of **3** failed. Treatment of **1** with $[Cp^*_2ZrMe_2]$ led to unidentified products.

[8] The iminophosphorane structure type was envisaged by Ashby et al. [9] for the ionic, dimeric phosphorus compound $[Li(PhNPPh_2)(OEt_2)]_2$. However, the P–N distance (1.672 Å) determined by X-ray crystallography is in the range of P–N single bond lengths (1.62–1.74 Å).

[9] M. T. Ashby, Li Zhong, *Inorganic Chemistry* **1992**, *31*, 1321.

1,7-Cyclopentenonorbornadiene: Synthesis and Crystal structure**

By *Axel G. Griesbeck,* Thomas Deufel, Karl Peters, Eva-Maria Peters,* and *Hans Georg von Schnering*

Homoconjugative effects[1] are regarded as the reason for the considerable differences in the shifts $\Delta\delta$ of C7 and C8 in the ^{13}C NMR spectra of 7-alkylidenenorbornadienes.[2] Thus, the parent compound 7-methylenenorbornadiene (**1**) shows a resonance signal at $\delta = 177.1$ for C7 and at $\delta = 78.5$ for C8 ($\Delta\delta = 98.6$).[3] In addition, photoelectron spectroscopic results[4] and the peculiar reactivity[5] of analogous compounds indicate an additional interaction between the endocyclic double bonds and the exocyclic double bond.

Paquette and Racheria prepared the 1,7-cyclohexeno-annelated derivative **2**, which also exhibits a considerable low-field shift $\delta(C7) = 170.9$ ($\Delta\delta = 81.8$).[6] We have now synthesized lower homologues by cycloaddition to a 1,3-disubstituted 1,2-dihydropentalene.

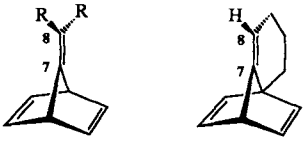

1 (R=H) **3** (R=Me) **2**

Compound **4**, prepared in a one-step reaction from benzylideneacetone,[7] behaves nonuniformly towards dienophiles, in contrast to the 1,5-dihydro- and tetrahydropentalenes[8] derived from it. Like 1,2-dihydropentalene itself,[9] alkene–dienophiles react with **4** to give mixtures of [2 + 2] and [4 + 2] adducts.[10] A markedly higher periselectivity was observed with alkyne–dienophiles. Thus, the reaction of **4** with dimethylacetylenedicarboxylate (after 24 h at 65 °C), followed by chromatographic purification, gave the desired [4 + 2] adduct **5** in 62% yield (Scheme 1).

Scheme 1. E = COOMe

In **5**, as for the known 7-alkylidenenorbornadienes, the ^{13}C NMR signal of C7 is also shifted to low field $\delta = 161.8$; the resonance signal of C8 occurs at $\delta = 103.3$ ($\Delta\delta = 58.5$). In comparison with the cyclohexeno-annelated norbornadiene **2**, the higher homologue, this shift effect is, however, markedly reduced. This is due to the higher degree of substitution at C8, and the electronic effects of the ester groups at C1 and C2. The crystal structure of **5**[11] is shown in Figure 1.

For all cycloadditions to **4** only one diastereomer was formed. Apparently, the phenyl substituent at C1 directs the attack of the dienophile in all cases so that it occurs highly selectively from the opposite side of the molecule, as revealed by the crystal structure analysis of **5**.

The structural parameters are particularly interesting since they can indicate homoconjugative stabilization. However, neither the endocyclic double bonds C2–C3 and C5–C6 (134 and 133 pm, respectively) nor the C7–C8 double bond (131.5 pm) show notable deviations from the corresponding values in norbornene skeletons. According to NMR spectroscopic data, the highly polarized double bond C7–C8 is slightly compressed and not stretched, as expected for a high degree of polarization. The side bonds of the norbornadiene framework are relatively long (average length 155.5 pm)[12] and indicate a high strain within the molecule. This is also evident from the significant distortion of the angle at C7: $\sphericalangle$ C1-C7-C4 = 97.4 and $\sphericalangle$ C4-C7-C8 = 148.2°.

[*] Priv.-Doz. Dr. A. G. Griesbeck, Dipl.-Chem. T. Deufel
Institut für Organische Chemie der Universität
Am Hubland, D-W-8700 Würzburg (FRG)
Dr. K. Peters, E.-M. Peters, Prof. Dr. H. G. von Schnering
Max-Planck-Institut für Festkörperforschung
Heisenbergstrasse 1, D-W-7000 Stuttgart 80 (FRG)

[**] This work was supported by the Fonds der Chemischen Industrie and the Unversitätsbund Würzburg.

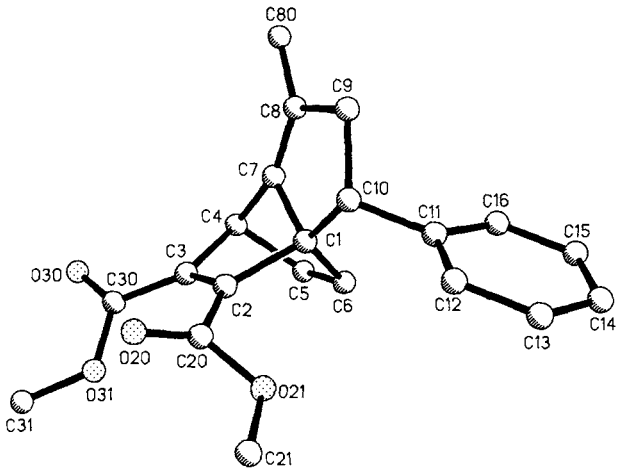

Fig. 1. Crystal structure of **5**. Selected distances [pm] and angles [ ]: C1-C2 155.9(4), C2-C3 134.2(4), C3-C4 155.9(4), C4-C5 155.5(4), C5-C6 132.9(5), C1-C6 155.0(5), C1-C7 151.6(4), C4-C7 151.8(5), C7-C8 131.5(4), C8-C9 151.7(4); C2-C1-C6 104.7(2), C3-C4-C6 104.8(2), C1-C7-C4 97.4(2), C1-C7-C8 114.1(3), C4-C7-C8 148.2(3).

The acetophenone-sensitized irradiation of **5** in pentane affords quantitatively the quadricyclane **6**. The above-mentioned peculiarities for the C7–C8 double bond in the ^{13}C NMR spectrum have disappeared in **6** as expected; the shifts of C7 ($\delta = 144.1$) and C8 ($\delta = 127.3$) are within the range of the values for normal endocyclic double bonds. Since ester

functions at C2 and C3 of 7-alkylidenenorbornadienes reduce the extent of the homoconjugation (again interpreted from the NMR values),[13] we prepared the derivative **9**, which is unsubstituted at the C atoms 2, 3, 5, and 6. For this, **4** was treated with both (*Z*)- and (*E*)-1,2-bis(phenylsulfonyl)ethylene.[14] The cycloaddition with the (*E*)-dienophile was complete after 6 h, in contrast, with the (*Z*)-dienophile this required 48 h. Both cycloadducts were obtained in the diastereomeric pure form, that is, the addition of (*Z*)-1,2-bis(phenylsulfonyl)ethylene led exclusively to the *endo* product **7**, whereas from the reaction with (E)-1,2-bis(phenylsulfonyl)ethylene **8** is formed, in which the phenylsulfonyl group in the neighborhood of the annelated five-membered ring is directed selectively into the *endo* position (Scheme 2).

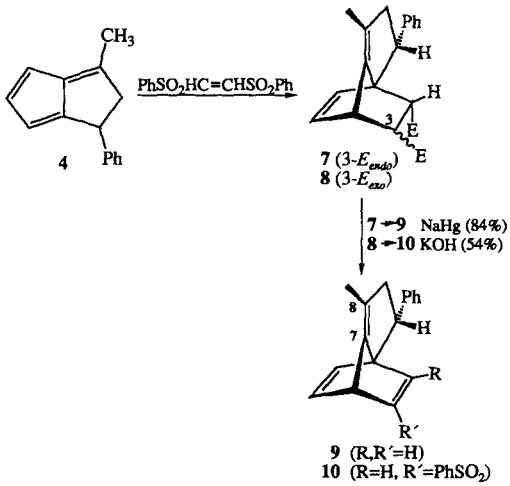

Scheme 2. E = $PhSO_2$

From the adduct **7**, reductive elimination with sodium amalgam led to the norbornadiene **9** in 84% yield. In the ^{13}C NMR spectrum, the signals for C7 ($\delta = 165.7$) and C8 ($\delta = 96.8$) are now even more clearly separated ($\Delta\delta = 68.9$), the bridgehead atom C1 is again markedly shifted to high field $\delta = 78.3$. However, if these values are compared with those of 7-isopropylidenenorbornadiene (**3**) (δ(C7) = 165.6, δ(C8) = 94.2, $\Delta\delta = 71.4$[13]), the additional annelation seems to have only a marginal effect on the polarization of this bond.

The 3-phenylsulfonyl-substituted norbornadiene **10** could (in addition to ca. 40% of the 2-isomer) be synthesized from **8** by KOH-assisted elimination. The resonance signals for C7 and C8 in this case are approximately the same as for compound **5**: $\delta = 161.8$ for C7 and $\delta = 102.9$ for C8 ($\Delta\delta = 58.9$).

1,7-cyclopentenonorbornadienes can be easily constructed according to the synthetic method described here. These compounds exhibit, analogous to the previously described homologous 1,7-cyclohexeno-annelated derivatives,[6] a strongly polarized C7–C8 double bond. However, no indications of homoconjugative effects can be derived from the structural parameters (compound **5**) given here for the first time.

Received: August 19, 1992 [Z 5521 IE]
German version: *Angew. Chem.* **1993**, *105*, 110

Table 1. Selected physical and spectroscopic data[a] of the 1,7-cyclopentenonorbornadienes **5** and **9** as well as the quadricyclane **6** [b].

5: Colorless platelets, m.p. 93–94.5 °C. ^1H NMR: $\delta = 1.61$ (s, 3H), 2.67 (dd, $J = 4.0, 15.8$, 1H), 3.03 (dd, $J = 9.5, 15.8$, 1H), 3.71 (s, 3H), 3.80 (s, 3H), 3.83 (m, 1H), 4.61 (d, $J = 2.8$, 1H), 6.44 (d, $J = 5.0$, 1H), 6.80 (dd, $J = 2.9, 5.0$, 1H), 7.20–7.39 (m, 5H, Ph); ^{13}C NMR: $\delta = 12.7$ (q), 42.4 (d, C10), 49.3 (d, C4), 50.4 (t, C9), 52.5 (q), 81.9 (s, C1), 103.3 (s, C8), 126.7 (d), 128.5 (d), 141.9 (d, C5), 143.6 (d, C6), 143.8 (s), 150.0 (s, C2), 157.5 (s, C3), 161.8 (s, C7), 164.5 (s), 166.4 (s)

6: Colorless oil. ^1H NMR: $\delta = 1.80$ (s, 3H), 2.15 (d, $J = 2.5$, 1H), 2.52 (d, $J = 4.7$, 1H), 2.89 (dd, $J = 4.6, 2.5$, 1H), 2.90 (d, $J = 15.9$, 1H), 3.34 (dd, $J = 8.9, 2.4$, 1H), 3.44 (ddd, $J = 1.1, 8.9, 16.0$, 1H), 3.63 (s, 6H), 7.20–7.40 (m, 5H, Ph); ^{13}C NMR: $\delta = 14.0$ (q), 28.7 (d), 29.3 (d), 32.7 (s), 35.6 (d), 36.9 (s), 37.3 (d), 50.2 (q), 50.7 (q), 54.1 (t), 125.1 (d), 126.4 (d), 127.3 (d), 141.1 (s), 144.1 (s), 168.5 (s), 169.0 (s)

9: Colorless oil. ^1H NMR: $\delta = 1.55$ (s, 3H), 2.67 (dd, $J = 15.4, 5.3$, 1H), 2.95 (dd, $J = 15.4, 9.1$, 1H), 3.75 (dd, $J = 9.1, 5.3$, 1H), 4.10 (t, $J = 2.8$, 1H), 6.37 (d, $J = 5.3$, 1H), 6.66 (d, $J = 5.3, 2.8$, 1H), 6.82 (dd, $J = 5.1, 2.8$, 1H), 6.94 (d, $J = 5.1$, 1H), 7.19–7.36 (m, 5H, Ph); ^{13}C NMR: $\delta = 12.2$ (q), 44.0 (d, C10), 47.2 (d, C4), 49.9 (t, C9), 78.3 (s, C1), 96.8 (s, C8), 125.8 (d), 128.0 (d), 128.2 (d), 141.6 (d, C3), 143.0 (d, C5), 143.9 (d, C2), 144.5 (s), 147.4 (d, C6) [c], 165.7 (s, C7)

[a] ^1H NMR: $CDCl_3$, 250 MHz; ^{13}C NMR: $CDCl_3$, 63 MHz. [b] All new compounds give correct elemental analysis. [c] The assignment (CH-COSY) for C3 and C5, and C2 and C6 is interchangeable.

[1] Review: a) M. N. Paddon-Row, K. D. Jordan, *Modern Models of Bonding and Delocalization* (Eds.: J. F. Liebman, A. Greenberg), VCH, Weinheim, **1988**, pp. 115–194; b) M. J. S. Dewar, *ibid.* pp. 37–38.
[2] H.-D. Martin, B. Mayer, R. W. Hoffmann, A. Riemann, P. Rademacher, *Chem. Ber.* **1985**, *118*, 2514–2543.
[3] R. W. Hoffmann, H. R. Kurz, *Chem. Ber.* **1975**, *108*, 119–127.
[4] R. Gleiter, W. Schäfer, *Acc. Chem. Res.* **1990**, *23*, 369–375, and references therein.
[5] a) L. A. Paquette, L. W. Hertel, R. Gleiter, M. Böhm, *J. Am. Chem. Soc.* **1978**, *100*, 6510–6512; b) T. Sasaki, K. Hayakawa, T. Manabe, S. Nishida, *ibid.* **1981**, *103*, 565–572.

[6] L. A. Paquette, U. S. Racherla, *J. Org. Chem.* **1987**, *52*, 3250–3253.
[7] A. G. Griesbeck, *Chem. Ber.* **1991**, *124*, 403–405.
[8] a) W. Adam, T. Deufel, R. Finzel, A. G. Griesbeck, J. Hirt, *J. Org. Chem.* **1992**, *57*, 3991–3994; b) A. G. Griesbeck, *Chem. Ber.* **1990**, *123*, 549–554.
[9] a) A. Pauli, H. Kolshorn, H. Meier, *Chem. Ber.* **1987**, *120*, 1611–1616; b) H. Meier, A. Pauli, H. Kolshorn, *ibid.* **1989**, *122*, 101–104.
[10] A. G. Griesbeck, T. Deufel, unpublished.
[11] Crystal structure analysis of **3**: Colorless needles crystallized from *tert*-butylmethyl ether/pentane. Triclinic, space group $P\bar{1}$, 4181 measured reflections, 3244 reflections with $F > 3\sigma(F)$ were used for the full-matrix least-squares refinement. Cell constants: $a = 967.8(4)$, $b = 1215.1(5)$, $c = 787.4(4)$ pm, $\alpha = 96.06(4)$, $\beta = 102.63(4)$, $\gamma = 78.37(3)$°, $Z = 2$, $R = 0.077$, $R_w = 0.064$. Further details of the crystal structure investigation may be obtained from the Fachinformationszentrum Karlsruhe, Gesellschaft für wissenschaftlich-technische Information mbH, D-W-7514 Eggenstein-Leopoldshafen 2 (FRG) on quoting the depository number CSD-56411, the names of the authors, and the journal citation.
[12] For a cycloadduct between dimethylacetylenedicarboxylate and a sesquifulvalene, bond lengths of 153 pm were determined: W. Henslee, R. E. Davis, *Acta Crystallogr. Sect. B* **1975**, *31*, 1511.
[13] L. Knothe, J. Werp, H. Babsch, H. Prinzbach, H. Fritz, *Liebigs Ann. Chem.* **1977**, 709–726.
[14] O. De Lucchi, V. Lucchini, L. Pasquato, G. Modena, *J. Org. Chem.* **1984**, *49*, 596–604.

Pentafluorophenylxenon(II) Pentafluorobenzoate: the First Preparative Synthesis and Structural Characterization of an Acyloxy Compound of Xenon(II)**

By *Hermann Josef Frohn,* Angela Klose*, and *Gerald Henkel*

Covalent xenon(II)–oxygen compounds of the type XO–Xe–OX and F–Xe–OX have been described previously.[1] These compounds are stable up to 130 °C when X = TeF_5 and SeF_5, while for X = SO_2F, ClO_3, IOF_4,[2] POF_2, and SO_2CF_3, the upper limit of their thermal stability generally lies below room temperature, and the compounds are explosive. All previous attempts to isolate xenon(II) carboxylates of the type RCO_2–Xe–O_2CR or F–Xe–O_2CR and to characterize them unequivocally by spectroscopy were unsuccessful.[3, 4] We report here the first spectroscopically and structurally characterized xenon(II) carboxylate, C_6F_5–Xe–$O_2CC_6F_5$ (**3**); this compound decomposes exothermically at 85 ± 3 °C.

It has often been suggested both in textbooks and in the literature that only the most electronegative ligands can bond to xenon.[3d, 5] However, we have observed that the xenon(II) carboxylate of the type R–Xe–O_2CR, which we have now prepared, is more stable than the known compounds of the type F–Xe–O_2CR. Thus, F–Xe–O_2CCF_3 is a kinetically unstable compound which detonates readily[3e] and has a half-life of only 10–12 h at room temperature,[3c, 3d] while **3** does not decompose even after 5 days at room temperature.

Our isolation[6] of arylxenon salts with $[C_6F_5Xe]^+$ as the cation[7] and weakly polarizable complex fluorides $[EF_n]^-$ as counterions has provided the basis for a route to new arylxenon compounds with a polar covalent bond, which proceeds by ligand exchange in water(!). Using this principle, **1** was treated with the cesium salt **2** to give the title compound **3** in 80% yield [Eq. (a)]. The compound **3** is insoluble in water but soluble in CH_2Cl_2 and MeCN; as a solid it has an almost unlimited stability at room temperature. In CH_2Cl_2 **3** shows no sign of decomposition after seven days at −45 °C, while at room temperature decomposition takes place within a few hours ($T_{1/2} \approx 3$ h at 35 °C). A CIDNP (chemically induced dynamic nuclear polarization) effect is observed during its slow decomposition at 35 °C in MeCN: the ^{19}F NMR signal of a decomposition product (*o*-F of a C_6F_5 group) is detected at $\delta = -139.4$ as an emission signal (negative peak with increased intensity). The occurrence of this CIDNP effect demonstrates that a radical intermediate of fluoroaromatic nature is formed during the decomposition. The main decomposition product is the ester $C_6F_5CO_2C_6F_5$.

$$[C_6F_5Xe][AsF_6] + Cs[O_2CC_6F_5] \longrightarrow C_6F_5XeO_2CC_6F_5 \quad (a)$$
1 **2** **3**

The xenon compound **3** exists in a covalent form with a strongly polarized Xe–O bond in solution and in the solid state. Both the solubility of **3** in the noncoordinating solvent CH_2Cl_2 (**1** and all previously known salts with an arylxenon cation are completely insoluble in this solvent) and the results from NMR spectroscopy (in particular ^{19}F NMR data) indicate that it cannot be described by the ionic form $[C_6F_5Xe]^+[O_2CC_6F_5]^-$. While in MeCN the cation of **1** exists in the solvated form $[MeCN\cdots XeC_6F_5]^+_{solv}$, that is, coordinated in a manner analogous to that observed in the crystal,[6b] and has a coupling constant $^3J_{Xe,F}$ of 67.2 ± 0.5 Hz, the value of this coupling for **3** in MeCN is 84.0 ± 0.5 Hz. In addition the $^3J_{Xe,F}$ coupling constant for **3** is almost identical in MeCN and CH_2Cl_2, thus **3** must exist in the molecular form in both solvents. The signal due to the *p*-F atom in the C_6F_5Xe moiety is shifted to lower frequency on going from **1** to **3** (in MeCN from $\delta = -141.27$ to $\delta = -146.21$), thus indicating a decrease in the mesomeric interaction between the C_6F_5 group and Xe^{II}, that is, a decrease in the effective charge at Xe^{II} due to replacement of the neutral base MeCN by the anionic base $[C_6F_5CO_2]^-$.

The ^{129}Xe chemical shift for **3** of $\delta = -2029.7$ (with respect to XeF_2) is as far as we are aware the lowest frequency value so far measured (Table 1). As expected, the transition from the base-coordinated cation $[MeCN\cdots XeC_6F_5]^+$ ($\delta = -1956.0$) to the covalent neutral species **3** leads to a shift to lower frequency.

Table 1. ^{129}Xe, ^{19}F, and ^{13}C NMR data for **3** in CD_2Cl_2 at −10 °C [a].

C_6F_5Xe moiety	
^{129}Xe	−2029.7 (t, 84 ± 6 Hz, $\nu_{1/2} = 49$ Hz) [b]
^{19}F	−128.26 (dm, $^3J(F,Xe) = 86.3 \pm 0.5$ Hz, 2; *o*-F), −144.71 (tt, $^3J(F,F) = 20.5$, $^4J(F,F) = 3.7$ Hz, 1; *p*-F), −154.81 (m, 2; *m*-F)
$^{13}C\{^{19}F\}$	144.32 (C4), 143.99 (C2,6), 138.14 (C3,5), 91.25 (C1)
$C_6F_5CO_2$ moiety	
^{19}F	−141.59 (m, 2; *o*-F), −154.39 (t, $^3J(F,F) = 21.0$ Hz, 1; *p*-F), −162.43 (m, 2; *m*-F)
$^{13}C\{^{19}F\}$	163.08 ($-CO_2-$), 144.32 (C2,6), 141.62 (C4), 137.57 (C3,5), 111.63 (C1).

[a] Measured with a Bruker WP 80 SY (^{13}C, Bruker WM 300), $\delta(Xe)$ relative to $\delta(XeF_2)$ in CD_2Cl_2, $\delta(F)$ relative to $\delta(CCl_3F)$. Values in parentheses after the δ values refer to the signal multiplicity, the magnitude of the coupling constant *J*, the signal intensity, and the signal assignment. [b] $\delta = 1327.8$ relative to $\delta(Xe(0))$ in MeCN at −30 °C.

The IR spectrum of the solid also lends no support to the description of **3** as an ionic carboxylate. Asymmetric and symmetric C–O stretching vibrations, as in sodium pentafluorobenzoate (1600 and 1395 cm^{-1}) are not observed. Ab-

[*] Priv.-Doz. Dr. H. J. Frohn, Dipl.-Chem. A. Klose, Prof. Dr. G. Henkel
Fachgebiet Anorganische Chemie der Universität
Lotharstrasse 1, D-W-4100 Duisburg 1 (FRG)

[**] This work was supported by the Deutsche Forschungsgemeinschaft and the Fonds der Chemischen Industrie.

sorptions at 1652 (m), 1626 (s), and 1619 (vs) cm^{-1} are assigned to the C–O stretching vibrations; these values are comparable with those found for the compounds $(C_6F_5)_2IO_2CC_6F_5$[8] (1650 (m) and 1600 (vs) cm^{-1}) and **4**[9] (1707

$C_6F_5I(O_2CC_6F_5)_2$ **4**

(m) and 1658 (vs) cm^{-1}) containing hypervalent iodine. In contrast, the C=O stretching frequency in the ester $C_6F_5CO_2C_6F_5$ lies at 1780 cm^{-1}.[10]

Low-temperature recrystallization from CH_2Cl_2 yielded single crystals of **3**, which according to the results of the X-ray structure analysis[11] consist of neutral molecules (Fig. 1). The xenon atom is linearly coordinated (178.1(1)°) by a carbon atom of the pentafluorophenyl substituent and one of the two oxygen atoms of the pentafluorobenzoyloxy substituent (hypervalent compound[14]). The other oxygen atom of the carboxyl group shows both a weak intramolecular Xe···O interaction (3.142 Å) and an even weaker Xe···O bridge (3.237 Å) to a neighboring molecule. These bridges lead to a pairing of the molecules with an almost square Xe_2O_2 four-membered ring in the crystal (Fig. 1).

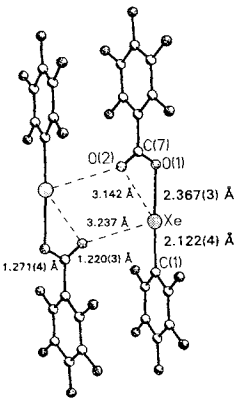

Fig. 1. Crystal structure of **3** with Xe–ligand bond lengths and the relevant intra- and intermolecular Xe–O contact distances. The C–Xe–O bond angle is 178.1(1)°.

According to Alcock[15] these are, however, not secondary bonds, since the intermolecular Xe–F distances *trans* to them do not deviate significantly from the sum of the van der Waals radii (3.47 Å). The length of the Xe–C bond in **3** is 2.122(4) Å; the corresponding bond length in the cation $[MeCN\cdots XeC_6F_5]^+$ is 2.092(8) Å, so that in **3** the Xe–C bond is apparently weakened in favor of the Xe–O bond. However, the Xe–O bond length of 2.367(3) Å in **3** is still considerably longer than that in the other known Xe–O compounds (F_5SeO–Xe–$OSeF_5$ 2.12,[12] F–Xe–$OS(O)_2F$ 2.16,[5] and F–Xe–OS(O)(F)O–Xe–F 2.21 Å[13]). In contrast to purely ionic carboxylate groups with two equal C–O bond lengths of 1.26 Å,[16] the pentafluorobenzoyloxy group in **3** has a longer (O(1), 1.271(4) Å) and a shorter C–O bond (0(2), 1.220(3) Å). A structural comparison with the iodo compound **4**, which exists in solution as discrete molecules and can also be transported in the molecular form in the gas phase,[9] appears appropriate; crystals of **4** contain two primary and two secondary I–O bonds, while the mean C=O and C–O bond lengths are 1.198 and 1.312 Å, respectively.

If we consider the available information on **3** in the solid phase and in solution and in addition take into account that **3** cannot be vaporized in the mass spectrometer without decomposition (decomposition occurs with pressure when the probe is heated), **3** can be described as a covalent compound with a polar, but relatively weak Xe–O bond, which is stabilized more effectively in the solid phase by the intra- and intermolecular contacts than in solution by solvation. The surprisingly high thermal stability of **3** in comparison with F–Xe–O_2CCF_3 cannot at present be explained satisfactorily. Ab initio calculations, as well as further experimental studies, for example by photoelectron spectroscopy, are planned.

Experimental Procedure

1 (81 mg, 166 μmol) was dissolved in D_2O (2 mL) and treated with **2** (60 mg, 174 μmol). After the mixture had been vigorously stirred, **2** dissolved and a voluminous colorless solid was immediately precipitated; the latter was isolated after centrifugation, decantation, and washing three times with D_2O (0.5 mL). The mother liquor contained the by-product $Cs[AsF_6]$. The solid **3** was dried for 3 hours under high vacuum at room temperature and subsequently dissolved in CD_2Cl_2 (≥ 500 μL); **3** crystallized out at −78 °C. Yield: 68 mg (133 μmol, 80%). NMR data are given in Table 1. Single crystals were obtained from CD_2Cl_2 at −45 °C (solubility at room temperature approximately 0.24 M). Differential thermal analysis (stainless steel autoclave): $T_{max} = 85 \pm 3$ °C (exothermic); main decomposition product: $C_6F_5CO_2C_6F_5$. IR(AgCl): $\tilde{\nu}$[cm^{-1}]: 1652 (m, sh), 1635 (m, sh), 1626 (s), 1619 (vs), 1577 (w), 1521 (m, sh), 1505 (vs), 1487 (vs), 1407 (w), 1349 (vs), 1286 (m), 1102 (m), 1082 (s), 1006 (m, sh), 990 (vs), 975 (s), 923 (m), 826 (w), 754 (s), 506 (m) 475 (w), 381 (m).

Received: August 25, 1992
Revised: October 19, 1992 [Z 5532 IE]
German version: *Angew. Chem.* **1993**, *105*, 114

[1] K. Seppelt, D. Lentz, *Prog. Inorg. Chem.* **1982**, *29*, 167–202.
[2] a) R. G. Syvret, G. J. Schrobilgen, *J. Chem. Soc. Chem. Commun.* **1985**, 1529–1530; b) *Inorg. Chem.* **1989**, *28*, 1564–1573.
[3] a) A. Iskraut, R. Taubenest, E. Schumacher, *Chimia* **1964**, *18*, 188; b) J. I. Musher, *J. Am. Chem. Soc.* **1968**, *90*, 7371–7372; c) M. Eisenberg, D. D. DesMarteau, *Inorg. Nucl. Chem. Lett.* **1970**, *6*, 29–34; d) F. O. Sladky, *Monatsh. Chem.* **1970**, *101*, 1571–1577; e) N. Bartlett, F. O. Sladky in *Comprehensive Inorganic Chemistry, Vol. 1* (Ed.: A. F. Trotman-Dickenson), Pergamon Press, Oxford, **1973**, p. 268; f) B. Cremer-Lober, H. Butler, D. Naumann, W. Tyrra, *Z. Anorg. Allg. Chem.* **1992**, *607*, 34–40.
[4] a) L. D. Shustov, T. N. Bocharova, T. I. Yurasova, N. G. Marchenkova, V. A. Legasov, L. N. Nikolenko, *Zh. Obshch. Khim.* **1973**, *43*, 841–843; b) T. N. Bocharova, N. G. Marchenkova, L. D. Shustov, T. Yu. Prokof'eva, L. N. Nikolenko, *ibid.* **1973**, *43*, 1325–1326.
[5] N. Bartlett, M. Wechsberg, F. O. Sladky, P. A. Bulliner, G. R. Jones, R. D. Burbank, *Chem. Commun.* **1969**, 703–704.
[6] a) H. J. Frohn, S. Jakobs, *J. Chem. Soc. Chem. Commun.* **1989**, 625–627; b) H. J. Frohn, S. Jakobs, G. Henkel, *Angew. Chem.* **1989**, *101*, 1534–1536; *Angew. Chem. Int. Ed. Engl.* **1989**, *28*, 1506–1507.
[7] D. Naumann, W. Tyrra, *J. Chem. Soc. Chem. Commun.* **1989**, 47–50.
[8] H. J. Frohn, unpublished results
[9] H. J. Frohn, J. Helber, A. Richter, *Chem.-Ztg.* **1983**, *107*, 169–172.
[10] R. Filler, J. F. White, A. J. Kacmarek, I. J. Solomon, *Can. J. Chem.* **1966**, *44*, 2346–2348.
[11] Crystal structure analysis: Siemens P4RA (four-circle) diffractometer, $Mo_{K\alpha}$ radiation ($\lambda = 0.71073$ Å), graphite monochromator, rotating anode generator, scintillation counter, −117 °C, empirical absorption correction, SHELXTL PLUS programs, direct methods, least-squares refinement; $C_{13}F_{10}O_2Xe$, molecular weight 509.42, monoclinic, space group $P2_1/c$, $a = 11.165(4)$, $b = 10.571(3)$, $c = 12.950(4)$ Å, $\beta = 113.20(2)°$, $V = 1405$ Å^3, $Z = 4$, $\rho_{calcd} = 2.409$ g cm^{-3}, $\mu(Mo_{K\alpha}) = 2.58$ mm^{-1}, transmission range 0.895–0.576, crystal dimensions $0.35 \times 0.32 \times 0.31$ mm^3, ω scan, $2\theta_{max} = 54°$, 3072 independent reflections, $R(R_w) = 0.0274(0.0356)$ for 2803 observed reflections ($I > 2\sigma(I)$), 236 variables, all atoms anisotropic, one scaling factor, one isotropic extinction parameter. Further details of the crystal structure analysis are available on request from the Fachinformationszentrum Karlsruhe, Gesellschaft for wissenschaftlich-technische Information mbH, D-W-7514 Eggenstein-Leopoldshafen 2, quoting the number CSD-56762, the names of the authors and the journal citation.
[12] L. K. Templeton, D. H. Templeton, K. Seppelt, N. Bartlett, *Inorg. Chem.* **1976**, *15*, 2718–2720.
[13] R. J. Gillespie, G. J. Schrobilgen, D. R. Slim, *J. Chem. Soc. Dalton Trans.* **1977**, 1003–1006.
[14] J. I. Musher, *Angew. Chem.* **1969**, *81*, 68–83; *Angew. Chem. Int. Ed. Engl.* **1969**, *8*, 54–68.
[15] N. W. Alcock, *Adv. Inorg. Chem. Radiochem.* **1972**, *15*, 1–58.
[16] A. F. Wells, *Structural Inorganic Chemistry*, 5th edition, Clarendon Press, Oxford, **1984**, p. 920.

A Short, Linear Synthesis of (9*S*)-Dihydroerythronolide A**

By *Rainer Stürmer,* Kerstin Ritter,* and *Reinhard W. Hoffmann**

Recently Mulzer[1] characterized the efforts directed toward the synthesis of erythronolides as a "never-ending story", which is even more amazing as there is no direct need for such syntheses. The motivation is found elsewhere: Since 1956 when Woodward gave his famous appraisal of erythromycin,[2] erythronolide syntheses have become the yardstick for measuring progress in the efficiency of stereoselective synthesis. Almost all of the published syntheses or attempted syntheses of erythronolides A and B were designed to demonstrate the reliability or superiority of a certain methodology or strategy. Thus the history of the development of methods in stereoselective synthesis can be traced from the syntheses of erythronolides.[3]

We present here a stereoselective synthesis of (9*S*)-dihydroerythronolide A (**1**), whose subsequent conversion into erythronolide A is known.[3i,k] In our synthesis, in contrast to that of Woodward et al.,[4] all the stereocenters are generated by external asymmetric induction, for which allylboration and the Sharpless epoxidation were employed (Scheme 1). Although our synthesis is linear with 23 steps (and 16 isolated intermediates) it is the hitherto shortest synthesis of this type of compound.

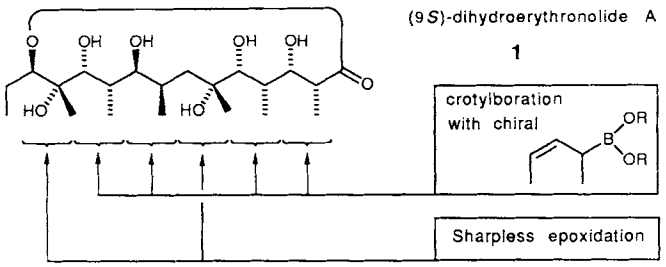

Scheme 1. Strategy for the generation of the stereocenters in (9*S*)-dihydroerythronolide A.

The course of the synthesis is easy to describe. The C11–C15 building block **2** was obtained by Sharpless epoxidation.[5] Reaction with (*S,S,S*)-1-methyl-2-butenylboronic ester **3** led to alcohol **4** in 81% yield (*ds* > 96%).[6]

The hydroxyl group was protected as the *p*-methoxybenzyl ether. Ozonolysis provided aldehyde **5**, which was treated with (*R,R,R*)-1-methyl-2-butenylboronic ester *ent*-**3** to give homoallyl alcohol **6** with > 95% *ds*. The hydroxyl group in **6** was protected as the *p*-methoxylbenzylidene acetal **7** by oxidation with DDQ, and the C–C double bond was subsequently cleaved by ozonolysis. The resulting aldehyde was converted into allyl alcohol **8**, and the next stereocenter was generated by Sharpless epoxidation (Scheme 3). The reaction proceeded with 90% diastereoselectivity in favor of the desired epoxide **9**. The other diastereomer, 6,7-di-*epi*-**9**, was crystalline; its X-ray structure analysis established the correct relative configurations of all of the stereocenters generated up to this point. Epoxy alcohol **9** was oxidized to the

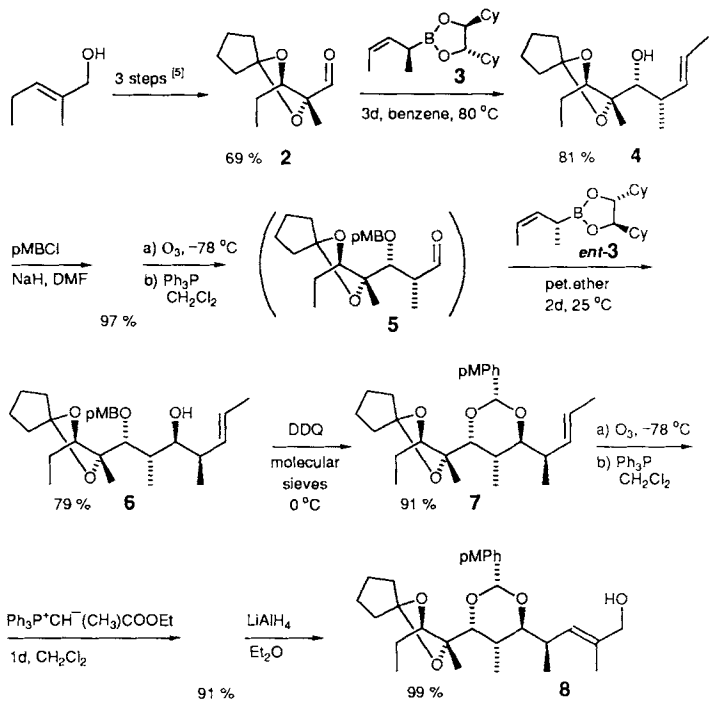

Scheme 2. Synthesis of the C5–C15 section of **1**. Cy = cyclohexyl; pMB = *p*-methoxybenzyl; pMPh = *p*-methoxyphenyl; DDQ = dichlorodicyano-*p*-quinone; NMO = *N*-methylmorpholine-*N*-oxide.

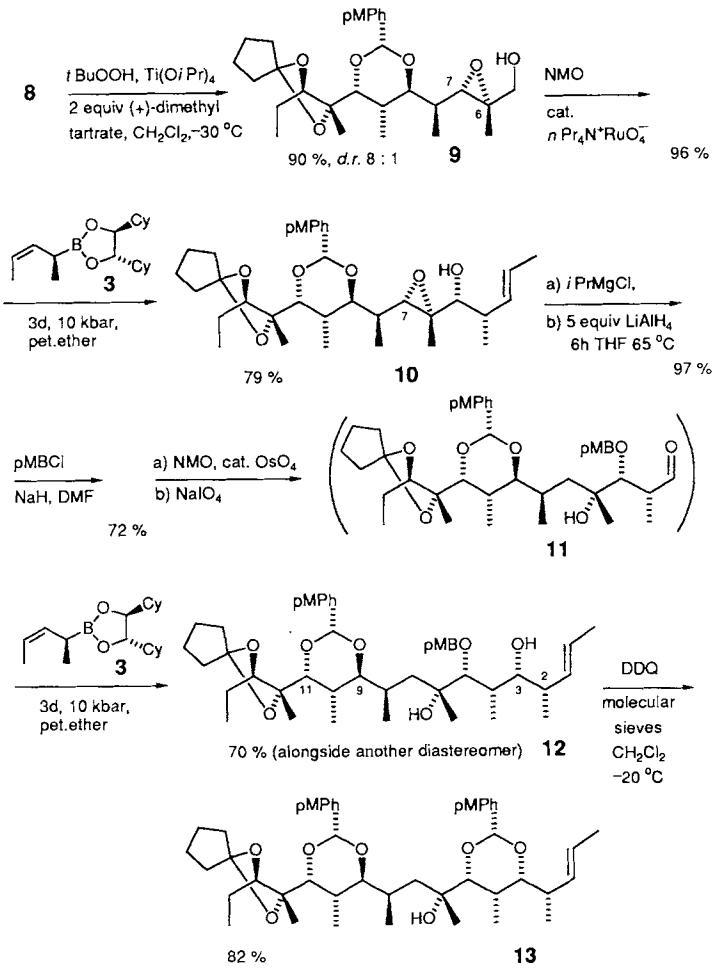

Scheme 3. Synthesis of the C1–C15 section of **1**.

[*] Dr. R. Stürmer, Prof. Dr. R. W. Hoffmann, K. Ritter
Fachbereich Chemie der Universität
Hans-Meerwein-Strasse, D-W-3550 Marburg (FRG)

[**] This research was supported by the Deutsche Forschungsgemeinschaft, the Graduierten-Kolleg "Metallorganische Chemie" at the University of Marburg, and the Fonds der Chemischen Industrie.

aldehyde, which when treated with (*S*,*S*,*S*)-**3** furnished homoallyl alcohol **10** (*ds* > 95%). The 6,7 epimer was removed at this step.

In our attempts to reductively cleave the C7–oxygen bond at the stage of epoxides **9** or **10**, eighteen standard reagents failed. Eventually a solution to this problem was found based on work of Marshall et al.:[7] the epoxide was activated as a magnesium chelate and then cleaved by $LiAlH_4$. The secondary hydroxyl group of the resulting diol was then selectively protected as a *p*-methoxybenzyl ether. Finally, bishydroxylation of the C–C double bond and cleavage with periodate furnished aldehyde **11**. In the next chain extension this aldehyde favors the formation of the *anti*-Cram product (not shown),[8] although the Cram product is desired. Nevertheless, the asymmetric induction of the chiral reagent (*S*,*S*,*S*)-**3** sufficed to provide the Cram product **12** with a diastereoselectivity of 89%. The second diastereomer formed had an *Z*-configurated double bond and should therfore possess the opposite configuration at C2 and C3. The hydroxyl group at C3 of **12** was protected as the *p*-methoxybenzylidene acetal (→**13**) by treatment with DDQ. The subsequent oxidative cleavage of the C–C double bond resulted in the unusually labile derivative **15** of erythronolide A seco acid.

This synthesis, which appears so well-planned and unproblematic, was actually close to failure at a number of stages. The last-resort measures that finally led to success constitute the novelty in this communication. The first critical point was the oxidation of **6** to provide **7**, because for the later macrolactonization the *para*-methoxyphenyl group on the dioxane **7** must be in the α position.[3e, p, 4] This can be achieved with freshly recrystallized DDQ by kinetic control,[9] since the oxonium ion **14** is generated in the conformation with *syn* H atoms as a result of allylic strain.[10] As

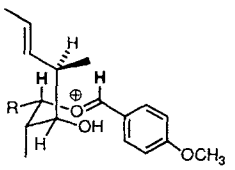

14

soon as equilibration becomes possible acetal **7** isomerizes to the thermodynamically more stable isomer with the aryl substituent in the β position, a compound that is worthless for our synthesis. This happened frequently during the second DDQ oxidation **12**→**13**, because the weakly acidic dichlorodicyanohydroquinone triggered the epimerization of the strained[11] C9/C11 dioxane. We ultimately found that by oxidation with DDQ on molecular sieves (but not on alumina or silica gel) compound **12** could be converted into **13** without epimerization of the other dioxane ring.

The most difficult step was still to come. The seco acid **15** decomposed upon attempted isolation; specifically, the labile C9/C11 and C3/C5 dioxane rings were cleaved. This also occurred in the attempts to hydrolyze the C12/C13 cyclopentylidene moiety selectively in the presence of the *p*-methoxybenzylidene acetals, although this transformation had been successful on model compounds. At this point it was out of the question to start the synthesis over with another protecting group at C12/C13. Therefore a way had to be found to slow down the hydrolysis of the *p*-methoxybenzylidene acetals selectively. While the inclusion of these groups in cyclodextrin did not bring the desired result, a charge-transfer deactivation of the methoxyphenyl groups by trinitrotoluene (10 equiv) in a two-phase system permitted a selective hydrolysis of the cyclopentylidene group of compound **15**.

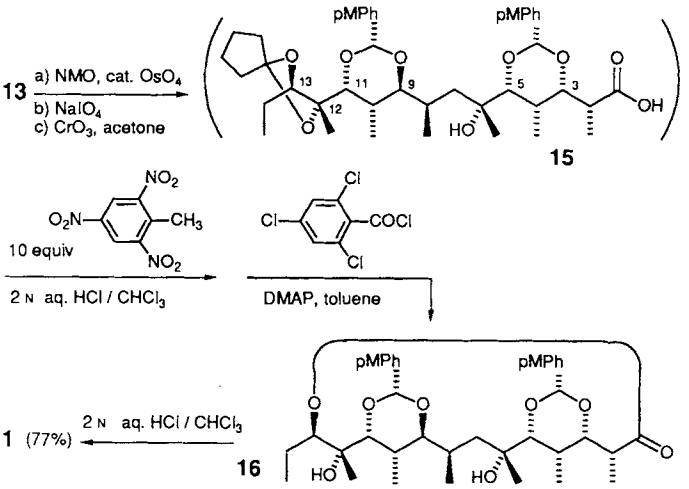

Scheme 4. Final steps in the synthesis of **1**. DMAP = 4-dimethylaminopyridine.

At this stage Yamaguchi lactonization[12] provided macrocycle **16**, whose spectral data are in accord with those of related compounds.[3p] The acetal groups were then hydrolyzed readily under standard conditions. This sequence allowed the generation of (9*S*)-dihydroerythronolide A (**1**) from **13** in 77% yield without isolation of the intermediates (total yield for all steps 10%). The melting point of **1** (201–203 °C)[3l] and its optical rotation (+9.2, $c = 0.7$ in methanol)[3k] are in agreement with the literature values. The ^1H and ^{13}C NMR spectra of **1** are identical to the spectra kindly provided by Dr. I. Paterson (Cambridge, England) and Prof. O. Yonemitsu (Sapporo, Japan).

This does not bring the story of erythronolide synthesis to an end. Inasmuch as our synthesis reflects the present state of the art in the methodology of stereoselective synthesis, more efficient syntheses of erythronolides should become possible with improved methods in the future.

Received: August 14, 1992 [Z 5518 IE]
German version: *Angew. Chem.* **1993**, *105*, 112

[1] J. Mulzer, *Angew. Chem.* **1991**, *103*, 1484–1486; *Angew. Chem. Int. Ed. Engl.* **1991**, *30*, 1452–1455.

[2] R. B. Woodward in *Perspectives in Organic Synthesis* (Ed.: A. Todd), Interscience, London, **1956**, p. 160: „Erythromycin, with all our advantages, looks at present hopelessly complex, particularly in view of its plethora of asymmetric centers."

[3] For a summary of earlier work see: a) I. Paterson, M. M. Mansuri, *Tetrahedron* **1985**, *41*, 3569–3624; for recent work see: b) S. D. Burke, F. J. Schoenen, C. W. Murtiashaw, *Tetrahedron Lett.* **1986**, *27*, 449–452; c) S. D. Burke, F. J. Schoenen, M. S. Nair, *ibid.* **1987**, *28*, 4143–4146; d) S. D. Burke, A. C. Chandler, III, M. S. Nair, O. Campopiano, *ibid.* **1987**, *28*, 4147–4148; e) G. Stork, S. D. Rychnowsky, *J. Am. Chem. Soc.* **1987**, *109*, 1565–1566, 6904; f) T. Nakata, M. Fukui, T. Oishi, *Tetrahedron Lett.* **1988**, *29*, 2219–2222; g) I. Paterson, D. D. P. Laffan, D. J. Rawson, *ibid.* **1988**, *29*, 1461–1464; h) I. Paterson, D. J. Rawson, *ibid.* **1989**, *30*, 7463–7466; i) N. K. Kochetkov, A. F. Sviridov, M. S. Ermolenko, D. V. Yashunsky, V. S. Borodkin, *Tetrahedron* **1989**, *45*, 5109–5136; j) M. C. Born, C. Tamm, *Tetrahedron Lett.* **1989**, *30*, 2083–2086; k) M. Nakata, M. Arai, K. Tomooka, N. Ohsawa, M. Kinoshita, *Bull. Chem. Soc. Jpn.* **1989**, *62*, 2618–2635; l) A. R. Chamberlin, M. Dezube, S. H. Reich, D. J. Sall, *J. Am. Chem. Soc.* **1989**, *111*, 6247–6256; m) S. F. Martin, G. J. Pacofsky, R. P. Gist, W.-C. Lee, *ibid.* **1989**, *111*, 7634–7636; n) Y. G. Kim, K. Whang, R. J. Cooke, J. K. Cha, *Tetrahedron Lett.* **1990**, *31*, 3275–3278; o) D. C. Myles, S. J. Danishefsky, G. Schulte, *J. Org. Chem.* **1990**, *55*, 1636–

1648; p) M. Hikota, H. Tone, K. Horita, O. Yonemitsu, *Tetrahedron* **1990**, *46*, 4613–4628; q) A. F. Sviridov, V. S. Borodkin, M. S. Ermolenko, D. V. Yashunsky, N. K. Kochetkov, *ibid.* **1991**, *47*, 2317–2336; r) N. I. Totah, S. L. Schreiber, *J. Org. Chem.* **1991**, *56*, 6255–6256; s) J. Mulzer, H. M. Kirstein, J. Buschmann, C. Lehmann, P. Luger, *J. Am. Chem. Soc.* **1991**, *113*, 910–923.

[4] R. B. Woodward et al., *J. Am. Chem. Soc.* **1981**, *103*, 3210–3217.

[5] R. Stürmer, *Liebigs Ann. Chem.* **1991**, 311.

[6] R. W. Hoffmann, K. Ditrich, G. Köster, R. Stürmer, *Chem. Ber.* **1989**, *122*, 1783–1789.

[7] J. A. Marshall, R. C. Andrews, *J. Org. Chem.* **1985**, *50*, 1602–1606.

[8] R. W. Hoffmann, U. Weidmann, *Chem. Ber.* **1985**, *118*, 3966–3979.

[9] Y. Oikawa, T. Nishi, O. Yonemitsu, *Tetrahedron Lett.* **1983**, *24*, 4037–4040.

[10] J. L. Broeker, R. W. Hoffmann, K. N. Houk, *J. Am. Chem. Soc.* **1991**, *113*, 5006–5017.

[11] S. L. Schreiber, Z. Wang, G. Schulte, *Tetrahedron Lett.* **1988**, *29*, 4085–4088.

[12] J. Inanaga, K. Hirata, H. Saeki, T. Katsuki, M. Yamaguchi, *Bull. Chem. Soc. Jpn.* **1979**, *52*, 1989–1993.

Synthesis and Structure of the Arsaalkyne Tetramer $(AsC\mathit{t}Bu)_4$ and its $Fe(CO)_4$ Derivative**

By *Peter B. Hitchcock, Julian A. Johnson*, and *John F. Nixon**

Current interest in the chemistry of phosphorus–carbon multiple bonds has arisen, because such compounds were once thought, on theoretical grounds, not to exist.[1–3] In particular, the substitution of CR units by phosphorus in many organic compounds, leading to the formation of novel ring and cage molecules has been widely explored in recent years.[4–8] These molecules include the di- and triphosphacyclopentadienyl anions $(P_2C_3\mathit{t}Bu_3)^-$ (**1**) and $(P_3C_2\mathit{t}Bu_2)^-$(**2**), which have been complexed to several transition metals.[9]

Recently we reported the synthesis of the arsadiphosphacyclopentadienyl anion $(AsP_2C_2\mathit{t}Bu_2)^-$ (**3**) and its η^5-complexation to Mn, Ru, and Co centers.[10] Attempts to prepare similar anions containing more than one As atom resulted in the unexpected formation of an arsaalkyne tetramer $As_4C_4\mathit{t}Bu_4$ (**4**). This has a cubane structure, similar to the analogous phosphaalkyne tetramer **5** reported by Regitz et al.[8]

The yellow, air-stable, sublimable (115 °C, 5×10^{-2} Torr) tetraarsacubane $As_4C_4\mathit{t}Bu_4$ (**4**) is isolated in 35% yield from the reaction of $LiP(SiMe_3)_2$, the arsaalkene (**6**),[11] and $CoCl_2$ at room temperature [Eq. (a)]. The mechanism of the reaction is not yet established, although it is likely that the as yet unknown *tert*-butylarsaalkyne (**7**) is generated as an intermediate by base-catalyzed elimination of hexamethyldisiloxane from the arsaalkene followed by Co-assisted oligomerization of **7**, since no product is obtained in the absence of $CoCl_2$. Efforts to trap **7** as its $[Pt(PPh_3)_2]$ complex have thus far proved unsuccessful.[12]

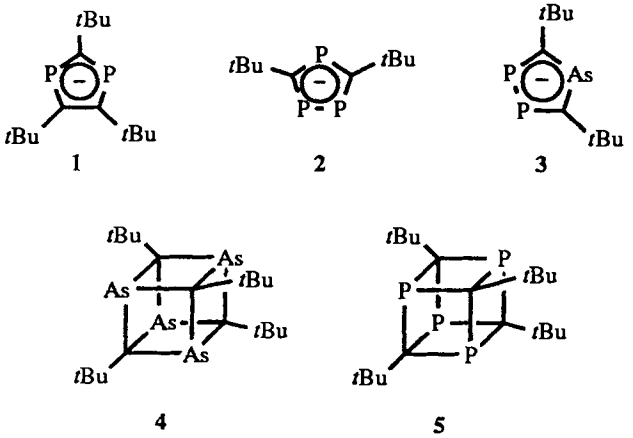

The cubane structure of **4** is proposed on the basis of data from mass spectrometry and NMR spectroscopy. The parent ion (*m/z* 576) is observed in the mass spectrum of **4** together with the expected fragmentation pattern.[13] A singlet at $\delta = 1.01$ is observed in the ^1H NMR spectrum of **4**, and the $^{13}C\{^1H\}$ NMR spectrum shows the expected three singlets at $\delta = -46.5$ (CAs), 21.4 (CCH_3) and 31.4 (CCH_3).

$$Me_3SiAs{=}C(OSiMe_3)\mathit{t}Bu \xrightarrow{LiP(SiMe_3)_2} \mathbf{6} \qquad \text{(a)}$$

$$[\mathit{t}BuC{\equiv}As] \;(\mathbf{7}) \xrightarrow{CoCl_2} \mathbf{4}$$

The high-field shift of the cage C atom is particularly significant and comparable to that observed for the cage C atoms in **5**,[8] implying that there is a shift of electron density from As to C atoms in the cage.

The cubane structure of **4** was confirmed by a single-crystal X-Ray diffraction study (Fig. 1).[14] The cage framework consists of alternate C and As atoms with an average C–As bond length of 2.01 Å. The internal bond angles of the cage (average angles: C-As-C 83.9, As-C-As 95.8°) show the cube to be slightly distorted, and a similar distortion is observed in the analogous phosphorus cage **5**.[8] The exocyclic As-C-C bond angles are on average 120.9°.

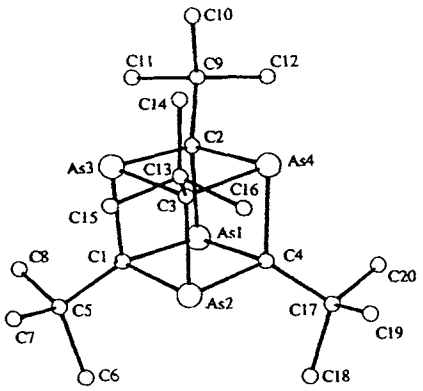

Fig. 1. The molecular structure of **4** [14]. Important bond lengths [Å] and angles [°]: As1-C1 2.021(14), As1-C2 2.022(14), As1-C4 2.024(14), As2-C1 2.001(14), As2-C3 1.990(13), As2-C4 2.002(14), As3-C1 2.010(14), As3-C2 2.006(15), As3-C3 2.013(12), As4-C2 2.047(15), As4-C3 1.988(12), As4-C4 2.023(14); C1-As1-C2 83.8(6), C1-As1-C4 83.5(6), C2-As1-C4 85.3(6), C1-As2-C3 83.7(5), C1-As2-C4 84.5(6), C3-As2-C4 83.8(5), C1-As3-C2 84.5(6), C1-As3-C3 82.9(5), C2-As3-C3 83.9(5), C2-As4-C3 83.5(5), C2-As4-C4 84.7(6), C3-As4-C4 83.0(6), As1-C1-As2 95.8(6), As1-C1-As3 95.5(5), As2-C1-As3 96.2(6), As1-C2-As3 95.6(6), As1-C2-As4 94.3(6), As3-C2-As4 95.2(6), As2-C3-As3 96.4(5), As2-C3-As4 97.3(5), As3-C3-As4 96.8(5), As1-C4-As2 95.7(6), As1-C4-As4 95.0(5), As2-C4-As4 95.7(6).

[*] Prof. Dr. J. F. Nixon, Dr. P. B. Hitchcock, Dr. J. A. Johnson
School of Chemistry and Molecular Sciences
University of Sussex, GB-Brighton BN1 9QJ (UK)

[**] This work was supported by the British Science and Engineering Research Council (SERC).

The arsaalkyne tetramer **4** reacts with $[Fe_2(CO)_9]$ in refluxing THF to give the tetracarbonyl iron(0) complex **8** [Eq. (b)], which has been fully characterized by IR and NMR spectroscopy.[15] The $^{13}C\{^1H\}$ NMR chemical shifts of the cage C atoms adjacent to the coordinated As atom are shifted downfield relative that of the other cage C atom as expected, thus showing a clear reduction in the shift of electron density from the As to the C atom on coordination of **4** to the metal center. Three ν(C=O) bands (2040, 1963, 1942 cm^{-1}) are observed in the IR spectrum of **8**, which are characteristic

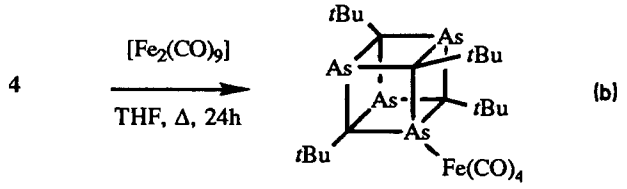

(b)

8

for complexes of the type $[Fe(CO)_4L]$. Interestingly, these values are similar to those in complexes with L = PMe_3 and L = $AsMe_3$,[16] but are considerably less than those for L = $P(OMe)_3$[17] and L = PF_3,[18] suggesting that **4** is not a particularly strong electron-withdrawing ligand.

The molecular structure of **8** (Fig. 2)[19] shows the ligand **4** coordinated, as expected, in an axial position of the trigonal bipyramid; the Fe–As bond length is 2.370(3) Å. This bond

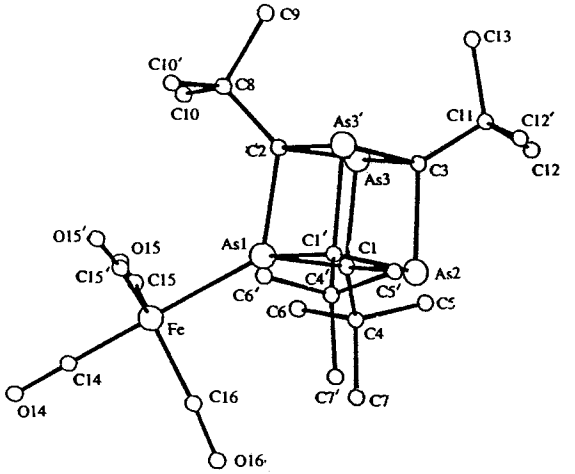

Fig. 2. The molecular structure of **8** [19]. Important bond lengths [Å] and angles [°]: Fe-As1 2.370(1), Fe-C14 1.772(9), Fe-C15 1.802(6), Fe-C16 1.778(9), As1-C1 2.011(6), As1-C2 2.039(7), As2-C1 2.025(6), As2-C3 2.029(8), As3-C1 2.038(5), As3-C2 2.023(5), As3-C3 2.018(6); Fe-As1-C1 128.3(1), Fe-As1-C2 127.0(2), C1-As1-C2 86.3(2), C1-As2-C3 84.7(2), C1-As3-C2 86.0(3), C1-As3-C3 84.6(3), C2-As3-C3 84.3(2), C1-As1-C1' 86.0(2), C1-As2-C1' 85.3(2), As1-C1-As2 94.2(2), As1-C1-As3 93.8(2), As2-C1-As3 94.9(2), As1-C2-As3 93.5(3), As2-C3-As3 95.4(2), As3-C2-As3' 95.3(3), As3-C3-As3' 95.7(3), As1-C1-C4 128.4(3), As1-C2-C8128.6(5), As2-C1-C4 117.8(4), As3-C1-C4 120.0(4), As3-C2-C8119.1(3), As2-C3-C11 121.7(6), As3-C3-C11 121.1(3).

is slightly longer than that observed in $[Fe(CO)_4AsMe_3]$ (2.30(3) Å).[20] The internal bond angles (average angles: C-As-C 85.3, As-C-As 94.7° of the coordinated cage in **8** are comparable to the free ligand; the exocyclic As1-C-C bond angles are increased, presumably to allow the $[Fe(CO)_4]$ metal complex fragment access to the As1 atom. A similar distortion is seen in the tetraphosphacubane **5**, when it is coordinated to an $[Fe(CO)_4]$ fragment.[21] In view of its considerable bulk, the coordination of **4** to other metal centers is currently under investigation.

Experimental Procedure

4: To a solution of $P(SiMe_3)_3$ (0.5 cm^3, 1.75 mmol) in dimethoxyethane (DME) (10 cm^3) was added 2.0 cm^3 of a 1.6 M hexane solution of *n*BuLi (3.2 mmol) at −40 °C. The solution was warmed to room temperature and stirred for 24 h. Arsaalkene **6** (2.0 g, 6.5 mmol) in DME (5 cm^3) was then added, and the resulting red solution was stirred for 72 h. Addition of a 5 cm^3 DME slurry of $CoCl_2$ (0.35 g, 2.7 mmol) gave a dark yellow mixture, which was stirred for a further 48 h. All volatile components were removed in vacuo at room temperature, and the residues were extracted with petroleum ether (PE). Column chromatography of the extracts (Kieselgel/PE) gave a yellow solution from which **4** could be crystallized at −20 °C. Yield: 300 mg (35%), yellow crystalline solid, m.p. 237 °C; satisfactory elemental analysis.

8: A solution of **4** (0.15 g, 0.26 mmol) and $[Fe_2(CO)_9]$ (0.20 g, 0.55 mol) in THF (10 cm^3) was refluxed for 24 h. Removal of solvent afforded a brown residue, which was washed with PE. The residue was redissolved in THF (ca. 3 cm^3) and cooled to −30 °C, which gave **8** as yellow crystals. Yield: 71 mg (46%), m.p. 196–198 °C (decomp); satisfactory elemental analysis.

Received: September 1, 1992 [Z 5548 IE]
German version: *Angew. Chem.* **1993**, *105*, 86

[1] *Multiple Bonds and Low Coordination in Phosphorus Chemistry* (Eds.: M. Regitz, O. J. Scherer), Thieme, Stuttgart, **1990**.
[2] M. Regitz, P. Binger, *Angew. Chem.* **1988**, *100*, 1541; *Angew. Chem. Int. Ed. Engl.* **1988**, *27*, 1485.
[3] J. F. Nixon, *Chem. Rev.* **1988**, *88*, 1327; M. Regitz, *ibid.* **1990**, *90*, 191; J. F. Nixon, *Endeavour*, **1992**, *15*, 49.
[4] D. Hu, H. Schäufele, H. Pritzkow, U. Zenneck, *Angew. Chem.* **1989**, *101*, 929; *Angew. Chem. Int. Ed. Engl.* **1989**, *28*, 900.
[5] R. Bartsch, P. B. Hitchcock, J. F. Nixon, *J. Organomet. Chem.* **1989**, *375*, C31.
[6] R. Bartsch, P. B. Hitchcock, J. F. Nixon, *J. Chem. Soc. Chem. Commun.* **1989**, 1046.
[7] R. Bartsch, P. B. Hitchcock, J. F. Nixon, *J. Chem. Soc. Chem. Commun.* **1989**, 1307.
[8] T. Wettling, J. Schneider, O. Wagner, C. G. Kreiter, M. Regitz, *Angew. Chem.* **1989**, *101*, 1035; *Angew. Chem. Int. Ed. Engl.* **1989**, *28*, 1013; T. Wettling, B. Geissler, R. Schneider, S. Barth, P. Binger, M. Regitz, *ibid.* **1992**, *104*, 761 and **1992**, *31*, 758.
[9] R. Bartsch, P. B. Hitchcock, J. F. Nixon, *J. Chem. Soc. Chem. Commun.* **1987**, 1146; *J. Organomet. Chem.*, **1988**, *356*, C1; *J. Chem. Soc. Chem. Commun.* **1988**, 819; *J. Organomet. Chem.* **1989**, *373*, C17.
[10] R. Bartsch, P. B. Hitchcock, J. A. Johnson, R. M Matos, J. F. Nixon, *Phosphorus Sulfur Silicon Relat. Elem.*, in press.
[11] G. Becker, G. Gutekunst, *Z. Anorg. Allg. Chem.* **1980**, *470*, 144.
[12] To the authors' knowledge only one free arsaalkyne molecule is known, (2,4,6-$tBu_3C_6H_2$)C≡As: G. Märkl, H. Sejpka, *Angew. Chem.* **1986**, *98*, 286; *Angew. Chem. Int. Ed. Engl.* **1986**, *25*, 264.
[13] **4**: MS (70 eV): *m/z* [%] 576 [M^+, 60%], 438 [$M^+ - (tBuC)_2$, 20] 369 [$M^+ - (tBuC)_3$, 100], 300 [$M^+ - (tBuC)_4$, 30], 225 [$M^+ - (tBuC)_4As$, 35], 144 [$M^+ - (tBuCAs)_3$, 15], 69 [$M^+ - (tBuC)_3As_4C$, 75]. We thank Mr. A. Greenway for recording the spectrum.
[14] Crystal data of **4**: $C_{20}H_{36}As_4$, M_r = 576, monoclinic, space group $P2_1/c$, a = 9.959(7), b = 14.345(6), c = 17.188(10) Å, α = 90, β = 92.57(5), γ = 90°, V = 2453.1 Å^3, Z = 4, ϱ_{calcd} = 1.56 g cm^{-3}. The structure was solved by direct methods and refined to R = 0.055 (R' = 0.061) using 1431 reflections with $|F^2| > \sigma(F^2)$ measured on an Enraf–Nonius CAD4 diffractometer [19].
[15] **8**: ^1H NMR (200 MHz, C_6D_6): δ = 0.83 (s, 1H), 1.09 (s, 3H); $^{13}C\{^1H\}$ NMR (62.9 MHz, $CDCl_3$) δ = 213.3 (CO), 33.2, 31.6 (CH_3C), 23.9, 22.0 (CH_3C), −3.08 ($CAsFe(CO)_4$), −45.7 (CAs).
[16] M. Bigorgne, *J. Organomet. Chem.* **1970**, *24*, 211.
[17] H. L. Conder, M. York Darensbourg, *J. Organomet. Chem.* **1974**, *67*, 93.
[18] J. B. P. Tripathi, M. Bigorgne, *J. Organomet. Chem.* **1967**, *9*, 307.
[19] Crystal data of **8**: $C_{24}H_{36}As_4FeO_4$, M_r = 744, monoclinic, space group $P2_1/m$, a = 10.281(4), b = 13.572(1), c = 10.783(1) Å, β = 104.59(2)°, V = 1456 Å^3, Z = 2, ϱ_{calcd} = 1.70 g cm^{-3}. The structure was solved by heavy atom methods and refined to R = 0.035 (R' = 0.041) using 1799 reflections with $|F^2| > \sigma(F^2)$ measured on an Enraf–Nonius CAD4 diffractometer. Further details of the crystal structure investigations are available on request from the Director of the Cambridge Crystallographic Data Centre, University Chemical Laboratory, Lensfield Road, GB-Cambridge CB2 1EW, (UK), on quoting the full journal citation.
[20] J.-J. Legendre, C. Girard, M. Huber, *Bull. Chim. Soc. Fr.* **1971**, 1998.
[21] M. Birkel, J. Schulz, U. Bergsträsser, M. Regitz, *Angew. Chem.* **1992**, *104*, 870; *Angew. Chem. Int. Ed. Engl.* **1992**, *31*, 879.

(Trimethylstannyl)methyllithium as a Source of a Methylene Bridge Connecting Two Acyl Groups: A Potential Route to D-Mycaroside**

By *Tadashi Sato** and *Shigeki Ariura*

A few years ago we reported that compounds with both carbon–lithium and carbon–tin bonds, for example Me_3SnCH_2Li (**1**), could react with electrophiles in two consecutive steps; first as an explicit carbanion because of the carbon–lithium bond, and second as a latent carbanion because of the carbon–tin bond.[1] Consequently **1** is equivalent to a methylene dianion CH_2^{2-}, and we have reported several reactions of **1** with electrophiles.[2]

The reaction of **1** with esters **2** is typical for this reagent.[3] Conventional organometallic compounds react with esters usually producing tertiary alcohols, because the primarily produced ketones are more reactive toward the reagent than the starting esters. The primary product formed with **1**, the α-stannyl ketone **3**, however, is special: the attack of a second molecule **1** occurs preferentially at the electropositive tin atom rather than the carbonyl carbon atom. This attack, supported by the electron-withdrawing effect of the carbonyl group, induces a heterolytic cleavage of the tin–carbon bond to produce enolates **4**. If the resulting enolate is trapped with a suitable electrophile, the net result is a coupling of an acyl group and an E moiety through a methylene unit to give **5** (Scheme 1).

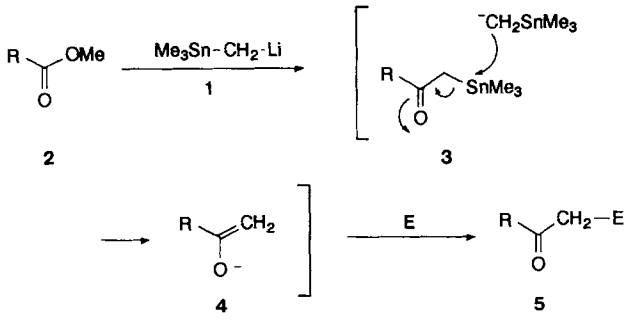

Scheme 1. Coupling of esters and electrophiles E with **1**.

We envisioned a one-step synthesis of β-ketoaldehydes (**5**, E = CHO) using formate as an electrophile, since the β-ketoaldehydes are desirable building blocks for 2-deoxysaccharides. The 2,6-dideoxysaccharides are important constituents of several antibiotics, and many homologues with various stereochemistries and branched carbon skeletons are known.[4] Since the biological activity of the parent antibiotics is influenced by the carbohydrate structure,[5] the development of methods for the synthesis of the deoxysaccharides is important. Frequently the deoxygenation of natural sugars is used; however, sometimes the selectivity of the regiochemical deoxygenation is not good or the starting material from the requisite chiral pool is not available. For instance, the synthesis of D-mycaroside **6** from methyl-α-D-mannopyranoside requires an eight-step reaction sequence (involving some purification processes) with an overall yield of 22%.[6] In contrast, the L-isomer has been synthesized in fewer steps because a suitable starting material, L-rhamnose, is readily

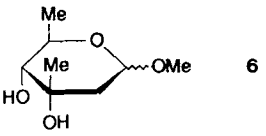

available.[7] Therefore a chiral synthesis from non-carbohydrate starting materials might be required. We have now constructed the major carbon skeleton **7** for the D-mycarose synthesis through the methylene connection reaction (Scheme 2).

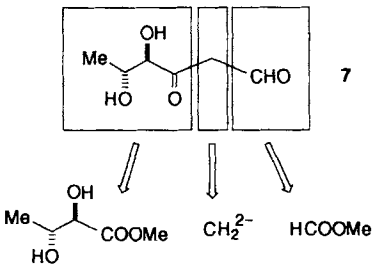

Scheme 2. Retrosynthetic scheme for **7**, the carbon skeleton of D-mycaroside **6**.

When (2*R*,3*R*)-dihydroxybutanoate **8** was treated with two equivalents of **1** at −78 °C, and then with methyl formate at −78 °C to 0 °C, the one-pot reaction proceeded smoothly to afford **9** in 66% yield (Scheme 3). No epimeriza-

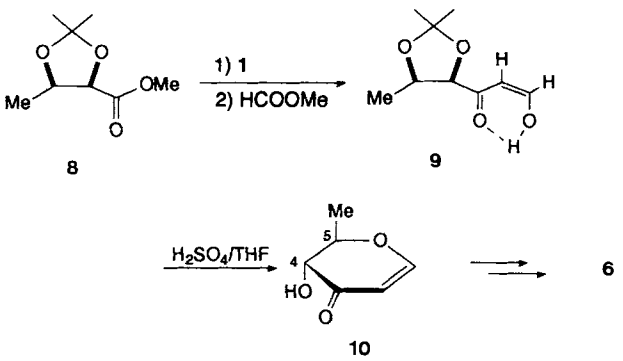

Scheme 3. Synthesis of **10** as a precursor for methyl D-mycaroside **6**.

tion occurred under these conditions, although some degree of epimerization was observed when the reaction temperature was raised to room temperature. The treatment of **9** with H_2SO_4 in THF afforded D-**10** (m.p. 87–88 °C) in 75% yield. In the same way, *rac*-**8** reacts to give *rac*-**10** (m.p. 66 °C). The *trans* arrangement of the substituents at C4 and C5 was confirmed by $J(H^4,H^5) = 13.8$ Hz in the ^1H NMR spectrum (400 MHz). Since the stereoselective synthesis of L-mycarose from L-**10** has been accomplished in two steps,[8] this reaction could provide a convenient route to D-mycaroside.

In addition, we applied the reaction described here to methyl hexanoate and methyl 2-butenoate, which afforded the corresponding β-ketoaldehydes as hydroxymethylene ketone tautomers in 53 and 79% yields, respectively. Although the yields are only moderate, pure products can be isolated when the quenched alkaline reaction mixture is washed with diethyl ether, and the aqueous layer is extracted with $CHCl_3$ after acidification with dilute HCl. Small amounts of the corresponding methyl ketones (**5**, E = H) and tin-containing

[*] Prof. Dr. T. Sato, S. Ariura
Department of Applied Chemistry, Waseda University
Ookubo 3, Shinjuku-ku, Tokyo 169 (Japan)

[**] This work was supported by the Ministry of Education, Science and Culture (Japan).

by-products of unknown structure were obtained from the ether layer.

Experimental Procedure

9: To a solution of bis(trimethylstannyl)methane (5.46 g, 16 mmol) in THF (32 mL) was added *n*BuLi (1.62 *M* hexane solution, 9.9 mL, 16 mmol) at −78 °C. After the mixture had been stirred for 15 min, a solution of **8** [9] (1.43 g, 8 mmol) in THF (8 mL) was added, and the mixture stirred for a further 20 min at this temperature. Methyl formate (3 mL, 49 mmol) was added, and then the reaction mixture was warmed up gradually and stirred for 4 h at 0 °C. The reaction mixture was quenched with aqueous $NaHCO_3$ solution and washed with diethyl ether. The aqueous solution was acidified with 4 *M* HCl and extracted with $CHCl_3$. After evaporation of the solvent pure **9** (981 mg, 66%) was obtained. ^{1}H NMR (60 MHz, CCl_4): δ = 1.15 (d, J = 7 Hz, 3H), 1.32 (s, 3H), 1.50 (s, 3H), 4.23–4.58 (m, 2H), 5.88 (d, J = 5 Hz, 1H), 7.91 (d, J = 5 Hz, 1H), 12.5 (br, 1H).

D-**10**: Compound **9** (365 mg, 2 mmol) was hydrolyzed by adding H_2SO_4 (3 drops) and refluxing in THF (20 mL) for 5 h. The reaction mixture was neutralized with $NaHCO_3$, concentrated in vacuo, and extracted with $CHCl_3$. Purification by sublimation afforded a pure sample of D-**10** (188 mg, 75%). M.p. 87–88 °C (sublimation); $[\alpha]_D^{23}$ = + 218 (c = 1.27, MeOH). ^{1}H NMR (400 MHz, $CDCl_3$): δ = 1.57 (d, J = 7.6 Hz, 3H), 3.58 (s, 1H), 3.97 (d, J = 13.8 Hz, 1H), 4.20 (dq, J = 13.8, 7.6 Hz, 1H), 5.46 (d, J = 7.1 Hz, 1H), 7.38 (d, J = 7.1 Hz, 1H). ^{13}C NMR ($CDCl_3$): δ = 17.91, 72.69, 79.93, 103.4, 164.7, 194.2.

rac-**10**: m.p. 66 °C. Published value for L-**10** [8]: m.p. 86 °C (sublimation); $[\alpha]_D^{28}$ = − 227 (c = 1.3, MeOH).

Received: August 20, 1992 [Z 5525 IE]
German version: *Angew. Chem.* **1993**, *105*, 129

[1] T. Sato, *Synthesis* **1990**, 259–270.
[2] T. Sato, T. Kikuchi, H. Tsujita, A. Kaetsu, N. Sootome, K. Nishida, K. Tachibana, E. Murayama, *Tetrahedron* **1991**, *47*, 3281–3304.
[3] T. Sato, H. Matsuoka, T. Igarashi, M. Minomura, E. Murayama, *J. Org. Chem.* **1988**, *53*, 1207–1212.
[4] Review: J. Thiem, W. Klaffke, *Top. Curr. Chem.* **1990**, *154*, 285–332; K. Toshima, K. Tatsuta, *Yukigosei Kagaku Kyokaishi (J. Synth. Org. Chem. Jpn.)* **1992**, *50*, 303–315.
[5] See for example M. W. Van Dyke, P. B. Dervan, *Biochemistry* **1983**, *22*, 2373–2377.
[6] R. W. Binkley, *J. Carbohydr. Chem.* **1985**, *4*, 227–242 and references therein.
[7] J. Thiem, J. Elvers, *Chem. Ber.* **1978**, *111*, 3514–3515.
[8] H. Paulsen, H. Bünsch, *Chem. Ber.* **1978**, *111*, 3484–3496.
[9] E. Hoff-Jørgensen, *Z. Physiol. Chem.* **1941**, *268*, 194–196; F. W. Bachelor, G. A. Miana, *Can. J. Chem.* **1967**, *45*, 79–80.

Novel Insertions of Carbene Homologues into Metal-η^5–Cp Bonds: Sandwich Complexes with Ge_2Ni and Sn_2Ni Cores**

By *Michael Veith** and *Lothar Stahl*

The carbene homologues $E(NtBu)_2SiMe_2$, E = Ge (**1**), Sn (**2**), are useful ligands for transition metal complexes because of their amphoteric Lewis acidic and Lewis basic properties.[1] It seemed promising to us to investigate their reaction behavior with the paramagnetic 20-electron complex nickelocene $[Cp_2Ni]$. When electrophiles react with $[Cp_2Ni]$ they should attack the Cp rings, in contrast nucleophiles should attack the Ni atom (Scheme 1).[2]

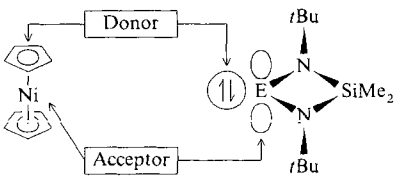

Scheme 1. E = element of Group 14.

If a green solution of $[Cp_2Ni]$ and **1** or **2** in toluene is heated to approximately 80 °C [Eq. (a)], this solution turns black-brown with the formation of the products **3** or **4**.

$$[Cp_2Ni] + 2\,E(NtBu)_2SiMe_2 \xrightarrow{80\ ^\circ C} [CpNi\{E(NtBu)_2SiMe_2\}_2(\mu\text{-}Cp)] \quad (a)$$
1: E = Ge, **2**: E = Sn → **3**: E = Ge, **4**: E = Sn

The NMR spectra (^{1}H, ^{13}C, ^{119}Sn) of **3** and **4**[3] have sharp signals, which indicate that these complexes are diamagnetic. Particularly striking is the occurence of two resonance signals for the Cp ligands with markedly different chemical shifts. The ^{1}H NMR spectrum of **4** shows a singlet at δ = 5.07 typical for η^5-bound Cp ligands, and a signal strongly shifted to low field at δ = 6.54 with tin satellites (J = 8.8 Hz, 27%). Coupling constants and intensities of the satellites indicate that the Cp ligand to which the signal at δ = 6.54 is assigned, is symmetrically π bound to two Sn atoms. As a result of the diastereotopic geminal $SiMe_2$ groups, the hydrogen atoms of the substituents of the SnN_2Si rings appear as three singlets. The NMR spectra hardly change on cooling the NMR samples to −80 °C; also the (cross-polarization magic angle spinning) CP-MAS ^{13}C NMR spectrum of solid **4** is almost identical with the spectrum recorded in solution. The presence of only one sharp signal at $\delta \approx$ 117 in the ^{13}C NMR spectrum shows that the bridging Cp ligand rapidly rearranges haptotropically in solution and in the solid state. The IR spectra, which are almost identical for **3** and **4**, also indicate π-bound Cp units because of the small number of bands for the Cp ligands.

Compounds **3** and **4** crystallize in monoclinic space groups with two molecules in the unit cell; their structures are not isotypic. The molecules lie on inversion centers of the space group $P2_1/c$ (different choice of cell for **3**: $P2_1/n$) which, however, is not in agreement with the NMR spectroscopic data. It became clear during the structure determination that a statistical disorder of a part of the molecules (Cp ligands and the nickel atom) was present as regards the inversion center of the space group; despite this shortcoming, resulting from the packing of the molecules (cf., e.g., ref. [4]), the structures could be refined accurately, and all hydrogen atom positions could be determined from difference Fourier analyses.[5]

The molecular structure of **4**, in which two Cp ligands are bound in different ways, is depicted in Figure 1. The Cp ligands are coordinated sandwichlike to the three metal atoms; Cp^1 (C31–C35) is bound η^5 to the Ni atom. The average Ni–C distance (2.097(9) Å) is shorter than that in $[Cp_2Ni]$ (2.18 Å),[6] indicating a strong Ni–Cp bond (the Ni centers in **3** and **4** each achieve 18-electron configurations). The two Ni–Sn bonds are likewise very short and both almost identical in length (Ni–Sn 2.326(2), Ni–Sn^A 2.369(2) Å); in the compound $[(C_2H_4)_2NiSn\{CH(SiMe_3)_2\}_2]$, in which double bond contributions for the Ni–Sn bond are

[*] Prof. Dr. M. Veith, Dr. L. Stahl
Institut für Anorganische Chemie der Universität
Im Stadtwald 1, D-W-6600 Saarbrücken (FRG)

[**] Cyclic Diazastannylenes, Part 34. This work was supported by the Deutsche Forschungsgemeinschaft and the Fonds der Chemischen Industrie. Part 33: M. Veith, L. Stahl, V. Huch, *Organometallics*, submitted.

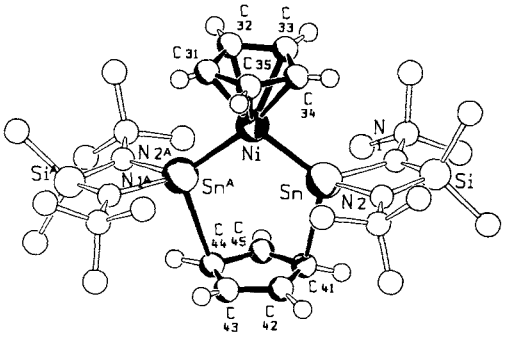

Fig. 1. Molecular structure of **4** (SCHAKAL [11b]). (The atoms labeled with the superscript A are symmetry equivalent [5].) Selected distances [Å] and angles [°] (See also the text): Sn-Ni1,2 2.083(8), Si-N1,2 1.749(5), Sn $\cdots$ Sn^A 3.648(4); Sn-Ni-Sn^A 102.0(1), Ni-Sn-C41 116.7(2), Ni-Sn^A-C44 112.5(2), N1-Sn-N2 75.5(1).

discussed, the Ni–Sn distance is 2.387(1) Å.[7] The center of the Cp^1 ligand, the two tin atoms, and the Ni atom lie almost in one plane. The most unusual structural element in **4** is without doubt the coordination of the second Cp ligand, which symmetrically bridges the two stannylene units via the tin atoms in a π bound manner. One C atom of the Cp^2 ligand (C41–C45) is coordinated to one of the Sn atoms and another C atom of the Cp^2 ligand (C41–C45) is coordinated to the other Sn atom. The distances vary slightly (2.702(12) Å (Sn–C41) and 2.608(11) Å (Sn^A–C44)). The bond lengths correspond to the average Sn–C distance in stannocene (2.71 Å);[8] σ-bound Cp ligands have significantly shorter Sn–C distances (2.15–2.20 Å).[9] To our knowledge this is the first structure in which a Cp ligand bridges μ-η^1:η^1 two main group elements. Both Cp rings are planar and arranged almost parallel (deviation 3.1°); they form dihedral angles of 9.4° (Cp^1) and 6.3° (Cp^2) with the SiN_2Sn metallacycles. The C atoms of Cp^2 bound to the Sn atoms lie, as expected, approximately 0.01 Å above the best plane, the corresponding H atoms (H41, H44) lie relatively far below (approximately 0.38 Å) this plane. The C–C bond lengths of the Cp ligands vary from 1.389(15) to 1.486(17) Å and are typical for Cp ligands with a delocalized π system.

The structure of **3** (Fig. 2) is similar to that of **4**. However, the Ni–Ge and Ge–Cp^2 distances differ considerably more than the corresponding Sn distances in **4**. The Ni–Ge bond

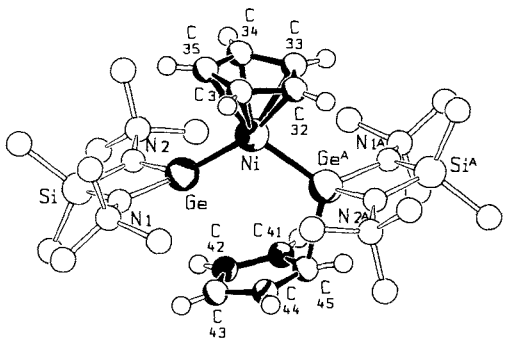

Fig. 2. Molecular structure of **3** (see also legend in Fig. 1). Other selected distances [Å] and angles [°] not discussed in text: Ni-C31-35 2.057(20), Ge-C41 3.007(7), Ge-C44 3.016(8), Ge-N1,2 1.864(3), Si-N1,2 1.729(2), Ge $\cdots$ Ge^A 3.549(7); Ge-Ni-Ge^A 109.6(1), Ni-Ge^A-C45 113.9(2), N1-Ge-N2 81.2(2).

lengths 2.085(3) and 2.258(3) Å differ significantly; the former distance is extremely short. The coordination of the "bridging" Cp^2 ligand (C41–C45) must be described as η^1-π in **3**, since all the Ge–C distances of this ligand are greater than 3.0 Å with the exception of the Ge^A–C45 bond (2.329(8) Å). The Ge–Ni distance is short, but the Ge–Cp^2 distance is long; exactly the opposite is true for the distances to the Ge^A atom. The asymmetry of **3** compared to **4** in the solid state reflects the formation process of the compounds by insertion of the carbene homologue into the Ni–Cp bond far better than the structure of **4**. As for the Sn–Cp^2 bond in **4**, the Ge–Cp^2 interaction in **3**, however, is clearly to be considered as a π bond, which is revealed both by the long Ge–C45 distance compared to usual σ bonds and also the C–H coupling constants.[3]

The structures of **3** and **4** are also interesting in view of the elucidation of the reaction mechanism of a Lewis base attack on $[Cp_2Ni]$.[2] Compounds **3** and **4** can be considered as intermediates of such reactions, which cannot be isolated for usual Lewis bases (CO, PR_3).

Experimental Procedure

$E(NtBu)_2Me_2Si$ (E = Ge (**1**), Sn (**2**) [10]) (6.3 mmol) was added to $[Cp_2Ni]$ (500 mg, 2.65 mmol) in toluene (30 mL), and the mixture was heated to 80 °C. After 36 h, the solution was filtered and concentrated to approximately 25 mL. After 48 h at −20 °C, yellow-brown crystals of **3** (1.91 g, 91.0%, m.p. 155–157 °C) or brown-black, rhombohedral crystals of **4** (1.90 g, 86.8%, m.p. 145–147 °C) were formed. Elemental analyses and mass spectra are in agreement with the empirical formulas.

Received: September 21, 1992 [Z 5588 IE]
German version: *Angew. Chem.* **1993**, *105*, 123

[1] M. Veith, L. Stahl, V. Huch, *Inorg. Chem.* **1989**, *28*, 3278.
[2] H. Werner, *Angew. Chem.* **1977**, *89*, 1; *Angew. Chem. Int. Ed. Engl.* **1977**, *16*, 1.
[3] NMR spectra (200 MHz, C_6D_6, 292K, TMS): **3**: ^{1}H NMR: δ = 0.46 (6H; SiMe), 0.48 (6H; SiMe), 1.29 (36H; *t*Bu), 5.07 (5H; NiCp), 6.35 (5H; (μ-Cp)Ge$_2$); ^{13}C NMR: δ = 6.0 (q, ^1J(C, H) = 117 Hz, 2C; SiMe), 7.4 (q, ^1J(C, H) = 117 Hz, 2C; SiMe), 34.6 (q, ^1J(C, H) = 123 Hz, 12C; C-CH_3), 52.7 (s, 4C; C-CH_3), 91.8 (d, ^1J(C, H) = 175 Hz, 5C; NiCp), 120.4 (d, ^1J(C, H) = 163 Hz, 5C; (μ-Cp)Ge$_2$).
4: ^{1}H NMR: δ = 0.48 (6H; SioMe), 0.55 (6H; SiMe), 1.27 (36H; *t*Bu), 5.07 (5H; NiCp), 6.54 (^2J (H, $^{117/119}$Sn) = 8.8 Hz (27%), 5H; (μ-Cp)Sn$_2$); ^{13}C NMR: δ = 7.9 (q, ^1J(C, H) = 117 Hz, 2C; SiMe), 8.6 (q, ^1J(C, H) = 117 Hz, 2C; SiMe), 35.8 (q, ^1J(C, H) = 132 Hz, 12C; C-CH_3), 53.0 (s, 4C; C-CH_3), 89.1 (d, ^1J(C, H) = 176 Hz, ^1J (C, $^{117/119}$Sn) = 15.2 Hz, 5C; NiCp), 117.4 (d, ^1J(C, H) = 165 Hz, ^2J(C, $^{117/119}$Sn) = 13.2 Hz, 5C; (μ-Cp)Sn$_2$); ^{119}Sn{^{1}H} NMR: δ = 313.3; ^{13}C Cp-MAS NMR: δ = 9.9 (br. s, 4C; SiMe), 36.2 (12C; C-CH_3), 53.6 (d, asymmetric quadrupolar splitting ^{14}N: 100.3 Hz, 4C; C-CH_3), 89.4 (5C; NiCp), 116.9 (5C; (μ-Cp)Sn$_2$).
[4] A. I. Kitaigorodskii, *Organic Chemical Crystallography*, Consultants Bureau, New York, **1961**.
[5] Structure determination with Siemens AED2; $Mo_{K\alpha}$ radiation, SHELXTL program [11]. **3**: monoclinic, $P2_1/n$, a = 9.484(12), b = 11.455(11), c = 16.661(14) Å, β = 91.20(9)°, Z = 2; 1650 reflections with 77 $F_o < 2\sigma$, 183 parameters, R = 0.0309, R_w = 0.0314. **4**: monoclinic, $P2_1/c$, a = 11.749(8), b = 9.886(4), c = 16.567(19) Å, β = 93.64(2)°, Z = 2; 1679 reflections with 39 $F_o < 1\sigma$, 229 parameters, R = 0.0231, R_w = 0.0196. Further details of the crystal structure investigations may be obtained from the Fachinformationszentrum Karlsruhe, Gesellschaft für wissenschaftlich-technische Information mbH, D-W-7514 Eggenstein-Leopoldshafen 2 (FRG) on quoting the depository number CSD-56681, the names of the authors, and the journal citation.
[6] I. A. Ronova, N. V. Alekseev, *Zh. Strukt. Khim.* **1966**, *7*, 886.
[7] C. Pluta, K. R. Pörschke, R. Mynott, P. Betz, C. Krüger, *Chem. Ber.* **1991**, *124*, 1321.
[8] A. Almenningen, A. Haaland, T. Motzfeldt, *J. Organomet. Chem.* **1967**, *7*, 97.
[9] P. G. Harrison, T. J. King, J. A. Richards, *J. Chem. Soc. Dalton Trans.* **1975**, 2097.
[10] a) M. Veith, *Angew. Chem.* **1975**, *87*, 287; *Angew. Chem. Int. Ed. Engl.* **1975**, *14*, 263; b) M. Veith, M. Grosser, *Z. Naturforsch. B.* **1982**, *37*, 1375.
[11] a) G. Sheldrick, SHELXTL; Program for Crystal Structure Determination, Göttingen, **1990**; b) E. Keller, SCHAKAL-88, Fortran Program for the Graphical Representation of Molecular and Crystallographic Models, Freiburg, **1988**.

Bonding in Endohedral Metal–Fullerene Complexes: f-Orbital Covalency in Ce@C_{28}**

By *Notker Rösch,** *Oliver D. Häberlen,* and *Brett I. Dunlap*

The technology for preparing macroscopic amounts of empty fullerenes[1] has been developed to furnish comparable quantities of host–guest complexes with one to three metal atoms inside the fullerene.[2] The host fullerenes for these complexes are the size of C_{82} and larger, providing a single guest atom with a large volume in which to move around.[3] The smallest experimentally relevant fullerene, C_{28},[4] forms endohedral compounds with uranium, hafnium, zirconium, and titanium, which were detected by mass spectrometry.[5] These experiments indicate that the stabilization of this fullerene by tetravalent atoms, as measured by the relative abundance of the endohedral complexes, increases in the order $Ti@C_{28} < Zr@C_{28} < Hf@C_{28} < U@C_{28}$, where the @ notation indicates endohedral complexes.[7,2a] The proposed tetrahedral structure of C_{28}[5] is drawn in Figure 1. Inside C_{28}, titanium, the smallest of these

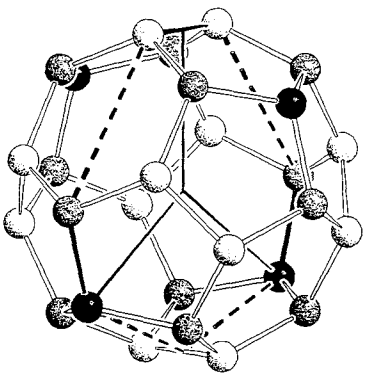

Fig. 1. Structure of the tetrahedral fullerene C_{28}. One of six symmetry-equivalent planes that contain two atoms of each of the three sets of symmetry-equivalent atoms is indicated by solid and dashed lines. In this plane there are two threefold axes from the center to a black atom and one twofold axis from the center to the center of a bond connecting nearest-neighbor white atoms. Gray and white atoms alternate around the circumference of the four hexagons diametrically opposite the four black atoms.

endohedral atoms, is strongly attracted (off-center by about 0.5 Å) to one of the four "black" atoms, which form the corners of a tetrahedron, together with its three nearest-neighboring "gray" atoms.[6] If a larger endohedral atom forms stronger simultaneous bonds to all four corners of the tetrahedron of black atoms, then the experimental trend in the stability of the $M@C_{28}$ complexes could be rationalized.

Such bonding is facilitated by sp^3 or sd^3 (or even sf^3) hybridization on the central atom. Alternatively, C_{28} may be stabilized by bonding between the endohedral atom and the six nearest-neighbor pairs of "white" atoms (see Fig. 1) that form an octahedron around the center of C_{28}. The radial distance from the center of C_{28} to the latter atoms is actually about 0.1 Å shorter than to the black atoms. If the sixfold coordination prevails, then metal–fullerene bonding would be facilitated by sp^3d^2 or sd^2f^3 hybridization on the central atom. The question of f orbital covalency in endohedral fullerene complexes, that is, whether the f orbitals of an endohedral atom contribute to the metal–cage bonding, however, cannot be decided by simply considering localized bonds to atoms (or combinations of atoms). If all possible valence orbitals (s, p, d, and f) of an endohedral f element atom, such as uranium, are employed in the bonding to the cage, then a maximum of 16 localized bonds can be formed. Group theory reveals that all these metal orbitals will be employed when localized bonds are formed to the sets of four black ($a_1 + t_2$) and twelve white (or, alternatively, twelve gray) atoms ($a_1 + e + t_1 + 2\,t_2$).

If a compound exhibits a sufficiently high symmetry then the bonding contributions can be isolated according to the irreducible representations of the molecular orbitals. Historically the di-π-[8]annulene complexes, $[M(C_8H_8)_2]$ where M = Ce, Th, Pa, U, Np, and Pu, have provided fertile ground for such analyses.[7,8] Due to the D_{8h} symmetry, of all the metal atom valence orbitals only the f orbitals can contribute to an e_{3u} HOMO. Indeed, calculations[7,8] and analysis of photoelectron spectra[8c] showed an f orbital contribution to the metal–ring bonding in these sandwich complexes.

Fullerenes are spheroidal shells of atoms often also having high symmetry. Endohedral fullerene complexes may thus be used to assess f orbital covalency with the help of symmetry arguments. At the center of buckminsterfullerene, icosahedral C_{60}, f orbitals can only contribute to g_u and t_{2u} molecular orbitals; at the center of tetrahedral C_{28}, only the f orbitals of the s, p, d, and f valence atomic orbitals can contribute to a t_1 molecular orbital. The f electrons of $Eu@C_{60}$ und $U@C_{60}$ remain localized on the metal atom, however,[9] because the interior volume of C_{60} is too large to allow sufficient overlap between the central f orbitals and the π orbitals of the carbon frame. When the surface of a fullerene is approximated as a sphere with a fixed surface area per carbon atom, the usable interior volume of the fullerene is proportional to the number of carbon atoms to the power 2/3.[10] In this approximation the interior of C_{28} is 40% smaller than the interior of C_{60} (51% smaller than the interior of C_{82}), and even the f electrons of a lanthanide or an actinide atom might participate in the bonding.

This spherical approximation provides yet another, unique way to analyze the electronic structure of fullerenes and endohedral fullerene complexes. The fullerenes can be viewed as spherical shells on which a single π orbital per carbon atom can delocalize forming molecular orbitals to be filled in the order s, p, d, f, etc., according to their nodal character.[11] Real spherical harmonics of rank l have l distinct nodal circles. On a fullerene shell these nodal lines must deform slightly to avoid atomic cores, thus lifting the m_l degeneracy, but the fact that the HOMO and LUMO of C_{60} belong to an incompletely filled h shell ($l = 5$) is obvious from contour plots of those orbitals.[12] This same spherical approximation applied to any isomer of C_{28} suggests that it can be viewed as having four electrons too few to complete its f shell. In particular, the HOMO group of tetrahedral C_{28}, $8a_1$, $14t_2$, and $7t_1$ (see Fig. 2), is ideally set up to overlap with f orbitals on the central atom.

The bonding of a lanthanide atom inside C_{28} is best studied using a scalar-relativistic extension[13] of the first-principles linear combination of Gaussian-type orbitals local density functional (LCGTO-LDF) method.[14] This two-component approximation to the four-component Dirac

[*] Prof. Dr. N. Rösch, Dipl.-Phys. O. D. Häberlen
Lehrstuhl für Theoretische Chemie der Technischen Universität München
Lichtenbergstraße 4, D-W-8046 Garching (FRG)
Dr. B. I. Dunlap
Theoretical Chemistry Section, Code 6179
Naval Research Laboratory
Washington, DC 20375-5000 (USA)

[**] This work was supported by the Deutsche Forschungsgemeinschaft, the Fonds der Chemischen Industrie, and the U.S. Office of Naval Research through the Naval Research Laboratory. The stay of B. I. Dunlap at the TU München, during which this work was done, was made possible by a NATO travel grant (CRG 920132)

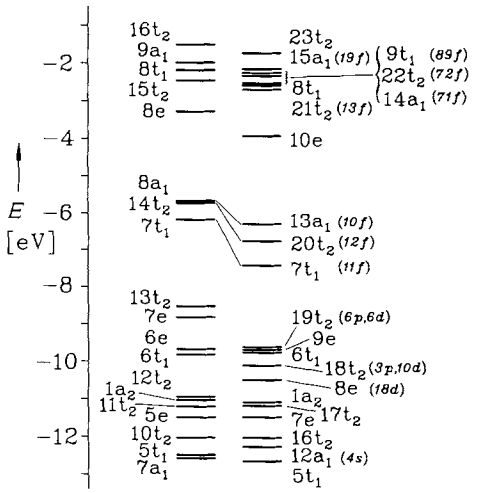

Fig. 2. One-electron energy level diagrams (LDF Kohn–Sham eigenvalues) for C_{28} and Ce@C_{28}. The LUMOs are 8e and 10e, respectively. The empty fullerene has an open-shell quintet ground state; the levels $14t_2$ and $8a_1$ are half filled. The spin-restricted levels are plotted for clarity of presentation; the splittings due to spin-polarization are very small as every orbital is spread out evenly over at least four different symmetry-equivalent atoms. The electronic structure of Ce@C_{28} is closed-shell. The Mulliken contribution of the cerium atom to each level is given in parentheses (in % together with the appropriate angular momentum) where it is significant.

form of the Kohn–Sham equations essentially takes into account the Darwin and mass–velocity terms.[13] We chose cerium as the endohedral atom because it can be tetravalent, because some aspects of its organometallic chemistry are strikingly similar to that of uranium,[7] and because we have a good Gaussian basis set for all-electron quasi-relativistic LCGTO calculations with this atom.[13a] We used an optimized empirical-potential geometry for C_{28}[15] that compares well with the cage geometries of Ti@C_{28} and Zr@C_{28} optimized in tetrahedral symmetry at the Hartree–Fock level of theory.[5b]

We employed a LDF exchange-correlation potential that interpolates between the essentially exact free-electron gas calculations in the completely ferromagnetic and completely paramagnetic limits.[16] The starting orbital basis set for C (9s/5p),[17a] was augmented with a d exponent of 0.6[17b] (all exponents are given in atomic units) and contracted to an atomic 5s/4p/1d basis according to a spin-restricted atomic calculation. The orbital basis set for Ce, 21s/16p/11d/9f,[13a] was contracted similarly to an atomic 11s/10p/8d/5f basis. The 9 C s and the 21 Ce s orbital exponents were scaled by 2 and 2/3 to generate atom-centered s-type functions for the charge density and exchange-correlation fitting bases, respectively.[18] The 5 C p and the 16 Ce p orbital exponents were scaled in the same way to generate the atom-centered r^2-type fitting basis functions. To fit nonspherical contributions around both types of atoms we employed additional fitting functions with higher angular momentum quantum numbers. A geometric series of 5 p-type fitting exponents, 0.1, 0.25, 0.625, 1.5625, and 3.90625, was used in both fitting bases of carbon.[18b] These exponents were scaled by a factor of three to get f-type (the lowest nonzero angular momentum allowed by tetrahedral symmetry at the origin) fitting exponents for Ce that have radial maxima at the same distances.

The symmetry of C_{28} is high enough that a rather complete picture of it may be formed by considering a special single slice through it. Such a plane is indicated by the bold solid and dashed lines in Figure 1. We studied the motion of a Ce atom along the symmetry axes shown in Figure 1 when the structure of the cage was kept fixed at the geometry determined by the empirical potential. The equilibrium position of Ce is at the center to an accuracy of 0.05 Å. The vibrational frequency along the threefold axis is 360 cm^{-1} and that along the twofold axis 350 cm^{-1}. The binding energy of Ce@C_{28} with respect to Ce $f^1d^1s^2$ (the experimental Ce ground state) and C_{28} $^5A_2$ is quite large, 13.7 eV, even if one takes into account that the LDF approximation tends to overestimate binding energies[19] and that the LDF ground state for Ce differs slightly from experiment.

The electronic structures of the empty and filled fullerene show that the spherical approximation is quite good in the case of C_{28}. The energies of the one-electron orbitals of C_{28} and Ce@C_{28} show that two large gaps isolate the f-like orbitals (see Fig. 2). Of these, the $8a_1$ and the three degenerate $14t_2$ orbitals are singly occupied in the ground state of C_{28}. The entire set of corresponding f-like orbitals, $13a_1$, $20t_2$, and $7t_1$, is completely filled in Ce@C_{28}. These f-like orbitals undergo strong downward shifts in energy due to the covalent metal–cage bonding. Similarly, the lower lying d-like orbitals, $13t_2$ and $7e$ of C_{28}, are shifted even lower in energy ($18t_2$ and $8e$ of Ce@C_{28}). These bonding interactions should be reflected in the photoelectron spectrum of the two fullerene compounds. We calculated (as a difference between two all-electron total-energy calculations) the first ionization potentials of C_{28} and Ce@C_{28} to be 7.40 and 8.27 eV, respectively. In their photoelectron spectra both systems are expected to have a gap of similar size (about 2.4 eV) after the first three bands which correspond to the emission of an electron from the HOMO and from the second and third highest levels (C_{28}: $8a_1$, $14t_2$, $7t_1$; Ce@C_{28}: $13a_1$, $20t_2$, $7t_1$). These three orbitals each have significant Mulliken f electron population (approximately 0.1) on the Ce atom and lie within 1.2 eV of each other (see Fig. 2 and Fig. 3 a–c). These bonding f contributions are comparable to those found in uranocene $[U(C_8H_8)_2]$.[7]

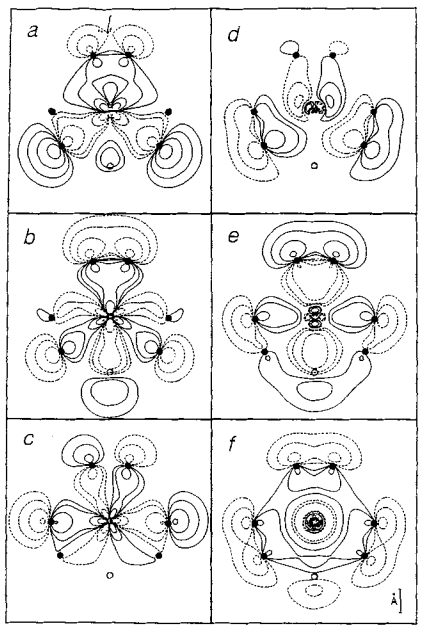

Fig. 3. Contour plots of the LDF one-electron orbitals with significant cerium character (in the plane defined in Fig. 1). The three highest occupied levels, a) the $13a_1$ orbital, b) the $20t_2$ orbital, and c) the $7t_1$ orbital, exhibit Ce f character as can be seen from the nodal patterns at the center of the plots. Orbitals with significant Ce d character are d) the $18t_2$ orbital and e) the $8e$ orbital. The LDF valence orbital with some Ce s character is f) the $12a_1$ orbital. The values of the contour lines are $\pm$ 0.015, $\pm$ 0.03, $\pm$ 0.06, and $\pm$ 0.12 a.u., solid and dashed lines indicate values of opposite sign. The positions of carbon atoms in the plane and the midpoint between out-of-plane white atoms are indicated by black dots and an empty circle, respectively.

 © VCH Verlagsgesellschaft mbH, W-6940 Weinheim, 1993 0570-0833/93/0101-0109 $ 10.00+.25/0

Covalent orbitals with a similar amount of Ce d Mulliken population, the $18t_2$ and $8e$ orbitals, lie roughly 3 eV lower in one-electron energy and within 0.4 eV of each other (see Fig. 2 and Fig. 3 d, e). The near degeneracy of these d shell orbitals indicates that the tetrahedral (four corners) and the octahedral (six pairs of bonds between white atoms) contributions to the ligand field are of comparable strength. Lower still in energy by 2 eV is the only valence orbital with significant Ce s character (0.04) (see Fig. 2 and Fig. 3 f). The LUMOs of C_{28} and $Ce@C_{28}$ are rather similar in nature: they are cage π orbitals. The metal–cage antibonding Ce f orbitals lie higher in energy ($14a_1$, $22t_2$, and $9t_1$) and exhibit a ligand-field splitting of 0.26 eV. All other Ce valence orbitals are pushed to even higher energies than displayed in Figure 2.

A picture of all the bonding contributions in $Ce@C_{28}$ is provided by the charge density difference map (Fig. 4) which is taken with respect to the charge density of the noninteracting fragments Ce and C_{28}. It is clear that cerium forms

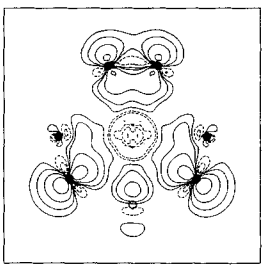

Fig. 4. Contour plot of the charge density difference for $Ce@C_{28}$ with respect to the noninteracting fragments Ce and C_{28}. The values of the contour lines are $\pm 0.003 \times 2.5^n$ a.u. ($n = 0$–3). Solid and dashed lines indicate positive and negative values, respectively. The positions of the cage atoms are marked as in Figure 3.

strong bonds to the tetrahedral (black) atoms as well as to the pairs of octahedral (white) atoms (see Fig. 1). The bonds to the gray atoms are significantly weaker. The net Mulliken charge on the Ce atom is +1.1e.

Our scalar-relativistic, all-electron, total-energy LDF calculations show that in contrast to titanium,[6] cerium is large enough to lie at the center of C_{28}. Because to a good approximation the fullerene is a spherical cage with frontier orbitals of F character, there is significant F covalency as indicated by Ce F population in the three highest occupied orbitals. These metal orbital contributions should be identifiable in variable-energy photoelectron spectra.[8c]

Due to its high symmetry $Ce@C_{28}$ obviously provides an ideal case for a detailed analysis of the metal–cage bonding in endohedral fullerene complexes. The general possibility of overlap characterized by rapid angular modulation will certainly also be found in less symmetric molecules. Strong bonds will arise when the valence orbitals of the enclosed system favorably complements the frontier orbital shell of the fullerene cage and have the proper radial extent, resulting in a closed-shell electronic structure. The isolobality principle[20] with its emphasis on orbital topology comes to mind. For example, in $Sc_3@C_{82}$[2e] an i orbital of C_{82} with its six lobes in one plane might favorably match a molecular orbital of a Sc_3 cluster formed by an antibonding combination of three in-plane d orbitals.

Received: August 27, 1992 [Z 5539IE]
German version: *Angew. Chem.* **1993**, *105*, 78

[1] W. Krätschmer, L. D. Lamb, K. Fostiropoulos, *Nature* **1990**, *347*, 354.
[2] a) Y. Chai, T. Guo, C. Jin, R. E. Haufler, L. P. F. Chibante, J. Flure, L. Wang, J. M. Alford, R. E. Smalley, *J. Phys. Chem.* **1991**, *95*, 7564; b) M. M. Alvarez, E. G. Gillan, K. Holczer, R. B. Kaner, K. S. Min, R. L. Whetten, *ibid.* **1991**, *95*, 10561; c) R. D. Johnson, M. S. de Vries, J. Salem, D. S. Bethune, C. S. Yannoni, *Nature* **1992**, *355*, 239; d) J. H. Weaver, Y. Chai, G. H. Kroll, C. Jin, T. R. Ohno, R. E. Haufler, T. Guo, J. M. Alford, J. Coceicao, L. P. F. Chibante, A. Jain, G. Palmer, R. E. Smalley, *Chem. Phys. Lett.* **1992**, *160*, 460; e) H. Shinohara, H. Sato, M. Ohkohchi, Y. Ando, T. Kodama, T. Shida, T. Kato, Y. Saito, *Nature* **1992**, *357*, 52.
[3] a) J. Cioslowski, E. D. Fleischmann, *J. Chem. Phys.* **1991**, *94*, 3730; b) D. Bakowies, W. Thiel, *J. Am. Chem. Soc.* **1991**, *113*, 3704; c) P. P. Schmidt, B. I. Dunlap, C. T. White, *J. Phys. Chem.* **1991**, *95*, 10537; d) J. L. Ballester, B. I. Dunlap, *Phys. Rev. A* **1992**, *45*, 7985; e) B. I. Dunlap, J. L. Ballester, P. P. Schmidt, *J. Phys. Chem.* **1992**, *96*, 9781.
[4] Q. L. Zhang, S. C. O'Brien, J. R. Heath, Y. Liu, R. F. Curl, H. W. Kroto, R. E. Smalley, *J. Phys. Chem.* **1986**, *90*, 525.
[5] a) T. Guo, M. D. Diener, Y. Chai, M. J. Alford, R. E. Haufler, S. M. McClure, T. Ohno, J. H. Weaver, G. E. Scuseria, R. E. Smalley, *Science* **1992**, *257*, 1661; b) T. Guo, G. E. Scuseria, R. E. Smalley, unpublished.
[6] B. I. Dunlap, O. D. Häberlen, N. Rösch, *J. Phys. Chem.*, **1992**, *96*, 9095.
[7] a) N. Rösch, A. Streitwieser, Jr., *J. Am. Chem. Soc.* **1983**, *105*, 7237; b) N. Rösch, *Inorg. Chim. Acta* **1984**, *94*, 297; c) A. Streitwieser, Jr., S. A. Kinsley, J. T. Rigsbee, I. L. Fragala, E. Ciliberto, N. Rösch, *J. Am. Chem. Soc.* **1985**, *107*, 7786.
[8] a) P. M. Boerrigter, E. J. Baerends, J. G. Snijders, *Chem. Phys.* **1988**, *122*, 357; b) A. H. H. Chang, R. M. Pitzer, *J. Am. Chem. Soc.* **1989**, *111*, 2500; c) J. G. Brennan, J. Green, C. M. Redfern, *ibid.* **1989**, *111*, 2373.
[9] A. H. H. Chang, W. C. Ermler, R. M. Pitzer, *J. Chem. Phys.* **1991**, *94*, 5004.
[10] B. I. Dunlap in *Physics and Chemistry of Finite systems: From Clusters to Crystals* (*NATO ASI Ser. C* **1992**, *374*, 1295).
[11] R. C. Haddon, L. E. Brus, K. Raghavarchari, *Chem. Phys. Lett.* **1986**, *125*, 459.
[12] N. Troullier, J. L. Martins, *Phys. Rev. B* **1992**, *46*, 1754.
[13] a) P. Knappe, N. Rösch, *J. Chem. Phys.* **1990**, *92*, 1153; b) O. D. Häberlen, N. Rösch, *Chem. Phys. Lett.*, **1992**, *199*, 491; c) N. Rösch, O. D. Häberlen, *J. Chem. Phys.* **1992**, *96*, 6322.
[14] B. I. Dunlap, N. Rösch, *Adv. Quantum Chem.* **1990**, *21*, 317.
[15] a) D. W. Brenner, *Phys. Rev. B* **1990**, *42*, 9458; b) Representatives of the three sets of symmetry-equivalent carbon atoms ("black", "gray", and "white", see Fig. 1) of tetrahedral C_{28} have the following coordinates (in Å): (1.451, 1.451, 1.451), (1.737, 1.737, 0.043) and (2.302, 0.527, 0.527).
[16] a) D. M. Ceperley, B. J. Alder, *Phys. Rev. Lett.* **1980**, *45*, 566; b) S. H. Vosko, L. Wilk, M. Nusair, *Can. J. Phys.* **1980**, *58*, 1200.
[17] a) F. B. van Duijneveldt, *IBM Res. Rep. RJ* **1971**, *945*; b) *Gaussian Basis Sets for Molecular Calculations* (Ed.: S. Huzinaga), Elsevier, New York, **1984**.
[18] a) B. I. Dunlap, J. W. D. Connolly, J. R. Sabin, *J. Chem. Phys.* **1979**, *71*, 3396, 4993; b) H. Jörg, N. Rösch, J. R. Sabin, B. I. Dunlap, *Chem. Phys. Lett.* **1985**, *114*, 529.
[19] R. G. Parr, W. Yang, *Density Functional Theory for Atoms and Molecules*, Oxford University Press, New York, **1989**.
[20] a) R. Hoffmann, *Angew. Chem.* **1982**, *94*, 725; *Angew. Chem. Int. Ed. Engl.* **1982**, *21*, 711; b) K. Wade, *Chem. Commun.* **1971**, 792; c) D. M. P. Mingos, *Nature* **1972**, *236*, 99.

Organic Clathrate-Forming Compounds as Highly Selective Sensor Coatings for the Gravimetric Detection of Solvent Vapors**

By *Albert Ehlen, Claus Wimmer, Edwin Weber,** and *Joachim Bargon**

The need for chemical sensors[1] to measure concentrations for medical purposes and industrial process control applications, for warning and safety systems, in environmental analysis, etc. is great.[2] However, the properties of the

[*] Prof. Dr. E. Weber, Dipl.-Chem. C. Wimmer
Institut für Organische Chemie and Biochemie der Universität
Gerhard-Domagk-Strasse 1, D-W-5300 Bonn-1 (FRG)
Prof. Dr. J. Bargon, Dipl.-Chem. A. Ehlen
Institut für Physikalische und Theoretische Chemie der Universität
Wegelerstrasse 12, D-W-5300 Bonn-1 (FRG)

[**] This work was supported by the Fonds der Chemischen Industrie.

chemical sensors already on the market or still in the development stages leave much to be desired. The bottleneck in the construction of chemosensors is the availability of chemically sensitive materials with sufficient stability and high sensitivity.[3] This is particularly pertinent for the gravimetric sensor, which functions either on the principle of the quartz microbalance (QMB) or on the principle of the surface-acoustic oscillator;[4] here a broad selection of selective coatings should rapidly lead to a breakthrough for the method.[2, 3] Among the organic inclusion compounds,[5] only cyclodextrins[6] and a few other macrocyclic compounds containing cavities have found application.[7, 8]

We have discovered that acyclic organic clathrate-forming compounds,[9] which are much more readily accessible and can be structurally modified, can similarly be used to construct active coatings for sensors and now report our initial results on the detection of solvent vapors with the quartz oscillation apparatus (QMB cell). The clathrate-forming compounds **1** and **2** are bulky derivaties of natural lactic acid, which display enantioselective sorption and are suitable for the preparative resolution of organic building blocks.[10] As this investigation shows, the crystalline substances **1** and **2** also proved to be highly selective sorbents for organic solvent vapors. The change in the mass on the formation and dissociation of the clathrates can be determined from the shift of the basic frequency of a quartz oscillator coated with these compounds.

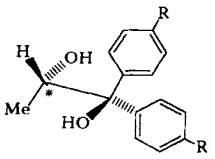

1, R = H
2, R = CMe_3

On applying the simple model of the Langmuir adsorption isotherms to the absorption and adsorption processes,[3, 11] a linear relation between the change in frequency Δf and the concentration c for the system sensor coating/solvent vapor in the region of low partial pressures is obtained [Eq. (a)].[7]

$$\Delta f = -Kc \qquad \text{(a)}$$

The constant K is a measure of the sensitivity of the procedure. For host/guest components that show only unspecific interactions, this configuration is less sensitive than for a clathrate-forming sensor layer/vapor combination (Fig. 1).

The host:guest stoichiometries of the clathrates can also be determined from the measurement of the quartz oscillator frequency. An increase in the vapor concentration to above saturation enables the molar host:guest ratio γ for the saturated crystals to be determined from the quotient of the frequency shift caused by the host coating without guest (Δf_h) and the frequency shift for inclusion of the guest at saturation $\Delta f_{g,sat}$ according to Equation (b) (M_h = molar mass of host, M_g = molar mass of guest). As anticipated, the

$$\gamma \frac{M_h}{M_g} = \frac{\Delta f_h}{\Delta f_{g,Sat}} \qquad \text{(b)}$$

frequency differences $\Delta f_{g,sat}$ at saturation increase linearly with thickness of the coating. This is documented in Figure 2 for the system **1**/dioxane. From the slope of this plot

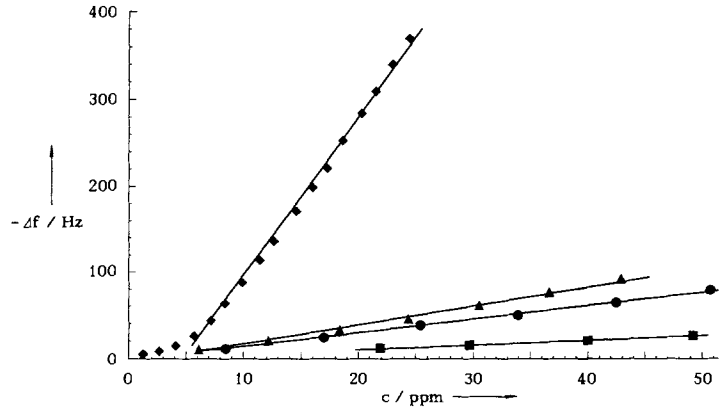

Fig. 1. Concentration dependence of the absorption for the sensor coating **2**. ◆ = 1-butanol, ■ = acetone, ● = methanol, ▲ = 2-propanol.

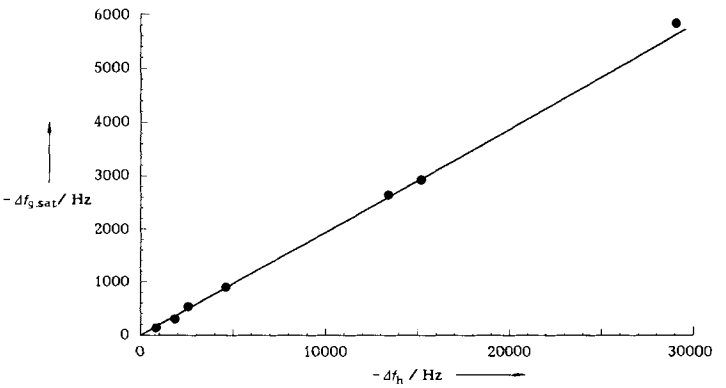

Fig. 2. The dependence of the frequency difference $\Delta f_{g,sat}$ for the inclusion at saturation on the thickness of the coating Δf_h for the system **1**/dioxane. The solid line corresponds to a host:guest inclusion ratio of 2:1.

[$\gamma^{-1} M_g M_h^{-1}$, according to Eq. (b)] a molar inclusion ratio γ of 2:1 (**1**:dioxane) is determined. This corresponds exactly to the stoichiometry of a cocrystallized sample (^{1}H NMR intergration).

Up to this point, a lot of attention was paid when using the quartz microbalance that the electrode coating on the quartz was as smooth and uniform as possible. Agreement with the spectroscopic analysis implies that quantitative measurements are possible also for irregularly crystalline materials. Presumably this is true only for comparative measurements,

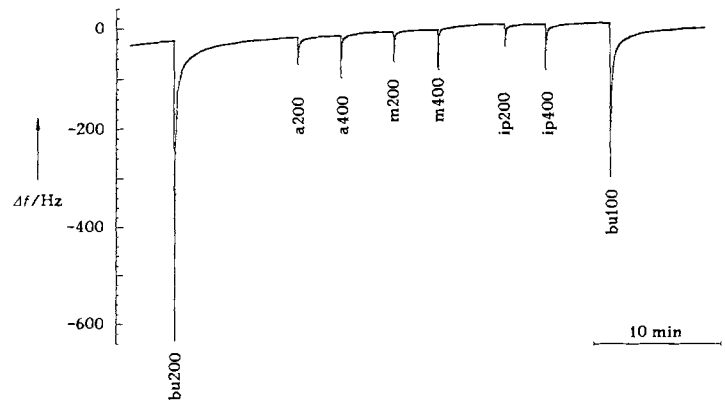

Fig. 3. Flow-through diagram with **2** as sensor coating. The numbers after the letters give the amount of solvent used in μL (bu = 1-butanol, a = acetone, m = methanol, ip = 2-propanol).

since the change in mass (here the inclusion of the guest) adjusts with the unevenness of the quartz coating.

The selective sensor properties of **1** and **2** are particularly obvious when potential guest compounds are compared with other solvent vapors in a series of flow-through experiments. Thus crystalline **2** as sensor coating shows a pronounced affinity for 1-butanol (Fig. 3). In spite of higher polarities and smaller spatial demands, acetone, methanol, and 2-propanol yield much smaller signals even when larger quantities are injected. The high selectivity of **1** for dioxane is demonstrated in Figure 4. Particularly remarkable is the behavior of cyclohexane, which although it has a similar structure to dioxane, gives only small signals.

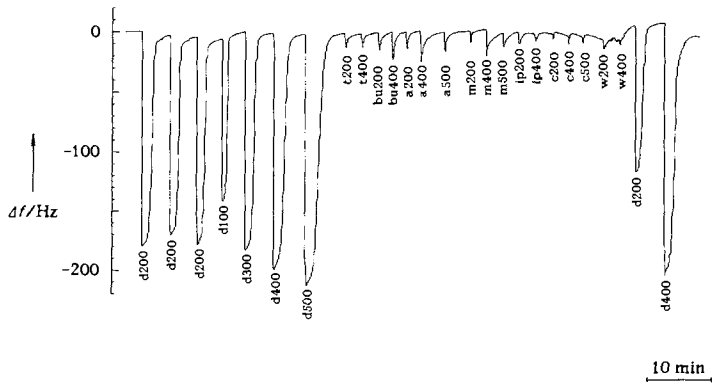

Fig. 4. Flow-through diagram with **1** as sensor coating. The numbers after the letters give the amount of solvent used in μL (bu = 1-butanol, a = acetone, m = methanol, ip = 2-propanol, d = dioxane, c = cyclohexane, t = toluene, w = water).

Thus, the selectivity of the sensor coating depends on the structure of the host molecule, which can be widely varied. The results also encourage the study of clathrate host compounds with other structural characteristics[5, 9] for suitability as sensor coatings.

Experimental Procedure

Apparatus: The quartz oscillator hangs in a cylindrical detector chamber, which is provided with several systems for the introduction of samples and can be evacuated through a suction port. The fundamental frequency of the oscillator used is 5 MHz.

Coating of the quartz oscillator: A solution of the appropriate host substance (100 mg) in THF (2 mL) was transferred in portions to the surface of the electrode. To be certain that the crystallization was complete, the coated electrode was only used on the following day.

Determination of the concentration dependence: For each solvent, a series of volumes of the air/solvent mixture was removed from the saturated vapor phase above the liquid surface in a 20 mL syringe and injected into the evacuated apparatus. The concentrations injected were determined from the equilibrium partial pressures.

Recording the flow-through diagrams: A stream of air enriched with the required solvent vapor was passed through the apparatus. This enrichment of the carrier stream is performed by successively injecting the different solvents from a syringe through a septum into a small flow-through vessel. The diagrams in Figures 3 and 4 were recorded at a flow of several liters per minute. The intensity of each signal reflects the momentary concentration, and the integration of the signals corresponds to the total injected dose (specific for each type of guest molecule) in each case.

Received: August 28, 1992 [Z5544IE]
German version: *Angew. Chem.* **1993**, *105*, 116

[1] K. Cammann, U. Lemke, A. Rohen, J. Sander, H. Wilken, B. Winter, *Angew. Chem.* **1991**, *103*, 519; *Angew. Chem. Int. Ed. Engl.* **1991**, *30*, 516; J. Janata, *Anal. Chem.* **1992**, *64*, 196R.
[2] W. Göpel, *Techn. Messen* **1985**, *52*, 47; *ibid.* **1985**, *52*, 92; *ibid.* **1985**, *52*, 175.
[3] F. L. Dickert, *Chem. Unserer Zeit* **1992**, *26*, 138.
[4] M. S. Nieuwenhuizen, A. Venema in *Sensors – A Comprehensive Survey, Vol. 2* (Eds.: W. Göpel, J. Messe, J. N. Zemel), VCH, Weinheim, **1991**, p. 647.
[5] *Inclusion Compounds, Vol. 4* (Eds.: J. L. Atwood, J. E. Davies, D. D. MacNicol), Oxford University Press, Oxford, **1991**.
[6] F. L. Dickert, P. A. Bauer, *Adv. Mater.* **1991**, *3*, 436.
[7] M. A. F. Elmosalamy, G. J. Moody, J. D. R. Thomas, F. A. Kohnke, J. F. Stoddart, *Anal. Proc. (London)* **1989**, *26*, 12.
[8] R. Lucklum, B. Henning, P. Hauptmann, K. D. Schierbaum, S. Vaihinger, W. Göpel, *Sens. Actuators A* **1991**, *25–27*, 705.
[9] *Molecular Inclusion and Molecular Recognition – Clathrates I, II (Top. Curr. Chem., 140, 149)* (Ed.: E. Weber), Springer, Berlin, **1987** and **1988**.
[10] E. Weber, C. Wimmer, A. L. Llamas-Saiz, C. Foces-Foces, *J. Chem. Soc. Chem. Commun.* **1992**, 733; *Chem. Ind. (London)* **1992**, 364; E. Weber, K. Skobridis, C. Wimmer, *GIT Fachz. Lab.* **1992**, *36*, 740.
[11] A. W. Adamson, *Physical Chemistry of Surfaces*, 5th ed., Wiley, New York, **1990**, Chap. 16.

Metathesis of Sulfur-Containing Olefins with a Metallacyclic Aryloxo(chloro)neopentylidenetungsten Complex**

By *Jean-Luc Couturier, Katsumi Tanaka, Michel Leconte, Jean-Marie Basset,** and *Jean Ollivier*

The application of olefin metathesis[1] to acyclic or cyclic olefins bearing functional groups probably constitutes one of the most promising uses of this reaction, since it allows access to valuable organic products and polymers which are often difficult to obtain by other methods.[2, 3] To date, the metathesis reaction has been applied to olefins containing oxygen, nitrogen, halogen, and silicon heteroatoms, but to our knowledge there are no reports of successful reactions of sulfur-containing acyclic or unstrained cyclic olefins.[4, 5] This lack of data was attributed to the fact that functional groups containing sulfur atom(s) may poison the catalyst; such an effect was reported for some classical heterogeneous and homogeneous catalytic systems.[6] However, this specific application of olefin metathesis could be of particular interest, since it would expand the field of thiochemistry and offer the possibility of synthesizing known or new olefinic compounds containing sulfur by a novel and simple route. We report here on the successful metathesis of olefinic sulfides with a homogeneous catalyst, aryloxo(chloro)neopentylidenetungsten complex **1**, which we recently synthesized and which proved to be highly active in the metathesis of olefins and olefinic esters.[7]

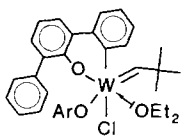

1

[*] Dr. J.-M. Basset, Dr. J.-L. Couturier, Dr. K. Tanaka,[+] Dr. M. Leconte
Institut de Recherches sur la Catalyse, Laboratoire Propre du CNRS
conventionné à l'Université Claude Bernard – Lyon 1,
and
Ecole Supérieure de Chimie Industrielle de Lyon
2 Avenue Albert Einstein, F-69626 Villeurbanne Cedex (France)
Dr. J. Ollivier
Groupement de Recherche de Lacq, SNEA
BP 34, Lacq, F-64170 Artix (France)
[+] Present address:
Department of Electronics Engineering
The University of Electro-Communications
Chofugaoka 1-5-1, Chofu Tokyo, 182 (Japan)

[**] This work was supported by the Société Nationale Elf-Aquitaine.

since the change in mass (here the inclusion of the guest) adjusts with the unevenness of the quartz coating.

The selective sensor properties of **1** and **2** are particularly obvious when potential guest compounds are compared with other solvent vapors in a series of flow-through experiments. Thus crystalline **2** as sensor coating shows a pronounced affinity for 1-butanol (Fig. 3). In spite of higher polarities and smaller spatial demands, acetone, methanol, and 2-propanol yield much smaller signals even when larger quantities are injected. The high selectivity of **1** for dioxane is demonstrated in Figure 4. Particularly remarkable is the behavior of cyclohexane, which although it has a similar structure to dioxane, gives only small signals.

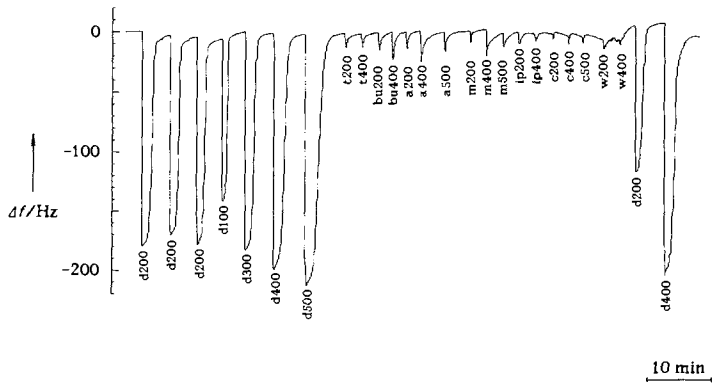

Fig. 4. Flow-through diagram with **1** as sensor coating. The numbers after the letters give the amount of solvent used in μL (bu = 1-butanol, a = acetone, m = methanol, ip = 2-propanol, d = dioxane, c = cyclohexane, t = toluene, w = water).

Thus, the selectivity of the sensor coating depends on the structure of the host molecule, which can be widely varied. The results also encourage the study of clathrate host compounds with other structural characteristics[5, 9] for suitability as sensor coatings.

Experimental Procedure

Apparatus: The quartz oscillator hangs in a cylindrical detector chamber, which is provided with several systems for the introduction of samples and can be evacuated through a suction port. The fundamental frequency of the oscillator used is 5 MHz.

Coating of the quartz oscillator: A solution of the appropriate host substance (100 mg) in THF (2 mL) was transferred in portions to the surface of the electrode. To be certain that the crystallization was complete, the coated electrode was only used on the following day.

Determination of the concentration dependence: For each solvent, a series of volumes of the air/solvent mixture was removed from the saturated vapor phase above the liquid surface in a 20 mL syringe and injected into the evacuated apparatus. The concentrations injected were determined from the equilibrium partial pressures.

Recording the flow-through diagrams: A stream of air enriched with the required solvent vapor was passed through the apparatus. This enrichment of the carrier stream is performed by successively injecting the different solvents from a syringe through a septum into a small flow-through vessel. The diagrams in Figures 3 and 4 were recorded at a flow of several liters per minute. The intensity of each signal reflects the momentary concentration, and the integration of the signals corresponds to the total injected dose (specific for each type of guest molecule) in each case.

Received: August 28, 1992 [Z5544IE]
German version: *Angew. Chem.* **1993**, *105*, 116

[1] K. Cammann, U. Lemke, A. Rohen, J. Sander, H. Wilken, B. Winter, *Angew. Chem.* **1991**, *103*, 519; *Angew. Chem. Int. Ed. Engl.* **1991**, *30*, 516; J. Janata, *Anal. Chem.* **1992**, *64*, 196R.
[2] W. Göpel, *Techn. Messen* **1985**, *52*, 47; *ibid.* **1985**, *52*, 92; *ibid.* **1985**, *52*, 175.
[3] F. L. Dickert, *Chem. Unserer Zeit* **1992**, *26*, 138.
[4] M. S. Nieuwenhuizen, A. Venema in *Sensors – A Comprehensive Survey, Vol. 2* (Eds.: W. Göpel, J. Messe, J. N. Zemel), VCH, Weinheim, **1991**, p. 647.
[5] *Inclusion Compounds, Vol. 4* (Eds.: J. L. Atwood, J. E. Davies, D. D. MacNicol), Oxford University Press, Oxford, **1991**.
[6] F. L. Dickert, P. A. Bauer, *Adv. Mater.* **1991**, *3*, 436.
[7] M. A. F. Elmosalamy, G. J. Moody, J. D. R. Thomas, F. A. Kohnke, J. F. Stoddart, *Anal. Proc. (London)* **1989**, *26*, 12.
[8] R. Lucklum, B. Henning, P. Hauptmann, K. D. Schierbaum, S. Vaihinger, W. Göpel, *Sens. Actuators A* **1991**, *25–27*, 705.
[9] *Molecular Inclusion and Molecular Recognition – Clathrates I, II (Top. Curr. Chem., 140, 149)* (Ed.: E. Weber), Springer, Berlin, **1987** and **1988**.
[10] E. Weber, C. Wimmer, A. L. Llamas-Saiz, C. Foces-Foces, *J. Chem. Soc. Chem. Commun.* **1992**, 733; *Chem. Ind. (London)* **1992**, 364; E. Weber, K. Skobridis, C. Wimmer, *GIT Fachz. Lab.* **1992**, *36*, 740.
[11] A. W. Adamson, *Physical Chemistry of Surfaces*, 5th ed., Wiley, New York, **1990**, Chap. 16.

Metathesis of Sulfur-Containing Olefins with a Metallacyclic Aryloxo(chloro)neopentylidenetungsten Complex**

By *Jean-Luc Couturier, Katsumi Tanaka, Michel Leconte, Jean-Marie Basset,** and *Jean Ollivier*

The application of olefin metathesis[1] to acyclic or cyclic olefins bearing functional groups probably constitutes one of the most promising uses of this reaction, since it allows access to valuable organic products and polymers which are often difficult to obtain by other methods.[2, 3] To date, the metathesis reaction has been applied to olefins containing oxygen, nitrogen, halogen, and silicon heteroatoms, but to our knowledge there are no reports of successful reactions of sulfur-containing acyclic or unstrained cyclic olefins.[4, 5] This lack of data was attributed to the fact that functional groups containing sulfur atom(s) may poison the catalyst; such an effect was reported for some classical heterogeneous and homogeneous catalytic systems.[6] However, this specific application of olefin metathesis could be of particular interest, since it would expand the field of thiochemistry and offer the possibility of synthesizing known or new olefinic compounds containing sulfur by a novel and simple route. We report here on the successful metathesis of olefinic sulfides with a homogeneous catalyst, aryloxo(chloro)neopentylidenetungsten complex **1**, which we recently synthesized and which proved to be highly active in the metathesis of olefins and olefinic esters.[7]

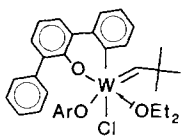

1

[*] Dr. J.-M. Basset, Dr. J.-L. Couturier, Dr. K. Tanaka,[+] Dr. M. Leconte
Institut de Recherches sur la Catalyse, Laboratoire Propre du CNRS
conventionné à l'Université Claude Bernard – Lyon 1,
and
Ecole Supérieure de Chimie Industrielle de Lyon
2 Avenue Albert Einstein, F-69626 Villeurbanne Cedex (France)
Dr. J. Ollivier
Groupement de Recherche de Lacq, SNEA
BP 34, Lacq, F-64170 Artix (France)
[+] Present address:
Department of Electronics Engineering
The University of Electro-Communications
Chofugaoka 1-5-1, Chofu Tokyo, 182 (Japan)

[**] This work was supported by the Société Nationale Elf-Aquitaine.

Table 1. Self-metathesis of allyl methyl sulfide (**2**) and its cometathesis with **5a** and **5b** catalyzed by **1** [a].

2/**1** [b]	**5a**/**1** [b]	**5b**/**1** [b]	T [°C] [c]	t [h] [d]	Conversion of **2** [%]	Yields [%] [e] **3**	**4**	**6**	**7**
25/1	–	–	80	15	40	20	20	–	–
25/1	100/1	–	20	15	95	–	–	95	–
20/1	–	20/1	80	15	60	5	5	30	20

[a] The metathesis reactions were carried out with 0.025 mmol of **1** and 5 mL of C_6H_5Cl as solvent. [b] Initial molar ratios. [c] Reaction temperature. [d] Reaction time. [e] Yields based on initial **2**.

Complex **1** can be prepared by two independent routes starting either from $[WCl_3(CCMe_3)(dme)]$[8] (dme = dimethoxyethane) or from $[WCl_4(2,6\text{-}Ph_2C_6H_3O)_2]$.[9] Complex **1** achieves coordinative saturation by complexing an Et_2O molecule, which also increases the steric shielding of the tungsten center; the coordination sphere is also expected to be extremely rigid due to the metallacyclic structure.

In the presence of **1**, allyl methyl sulfide (**2**) undergoes self-metathesis, leading to **3** and **4**, and cometathesis with *cis*-2-butene (**5a**) and *cis*-2-pentene (**5b**), leading to **6** and **7**[10] (Scheme 1 and Table 1).[11] The turnover rates are lower

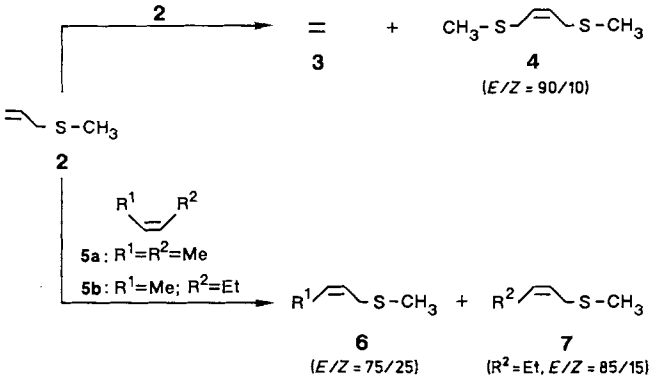

Scheme 1. Metathesis of **2** with acyclic olefins.

than those obtained with **1** in the metathesis of 2-pentene or ethyl oleate,[7] which suggests a reversible coordination of the sulfur compound to **1** and a partial deactivation of the catalyst. Nevertheless, the reaction is highly selective (only the expected metathesis products are detected), and the conversion of **2** can reach a high value when an excess of the coreactant olefin is used.

Cometathesis of **2** with cyclopentene or norbornene in the presence of **1** leads to the dienes depicted in Scheme 2.[10-12] The cross-metathesis reaction is favored with respect to ring-opening metathesis polymerization of cyclopentene or norbornene when an excess of allyl methyl sulfide is used.

Ring-opening metathesis polymerization of various 5-alkylthiocyclooctenes (**8a–e**)[13] leads to the olefinic sulfur polymers **9** (Scheme 3 and Table 2);[14] turnover rates were higher than those observed in the metathesis of allyl methyl sulfide (**2**). The results in Table 2 show that the alkylthio

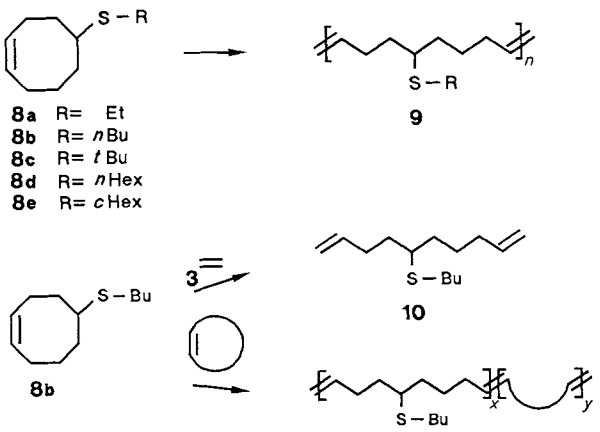

Scheme 3. Metathesis of alkylthio-substituted cyclic olefins.

Table 2. Ring-opening metathesis polymerizations of 5-alkylthiocyclooctenes **8** catalyzed by **1** [a].

8	R	**8**/**1** [b]	T [°C] [c]	t [min] [d]	Conversion of **8** [%]
a	Et	100/1	20	200	97
b	*n*Bu	100/1	20	120	97
c	*t*Bu	100/1	20	10	99
		100/1	80	5	96
		500/1	80	30	96
		100/1 [e]	20	2	(65) [f]
d	*n*Hex	100/1	20	100	99
e	*c*Hex	100/1	20	30	99

[a]–[d] See Table 1. [e] Polymerization performed without solvent. [f] Yield of isolated polymer (M_w = 140100, M_N = 39700, M_w/M_N = 3.5, T_g = – 26 °C).

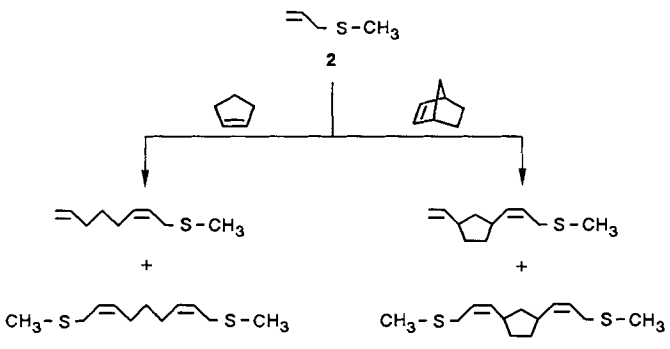

Scheme 2. Metathesis of **2** with cyclic olefins.

substituent strongly affects the rate of polymerization: the greater the steric demands of the alkyl substituent, the faster the polymerization. This confirms the hypothesis that bulky substituents around the sulfur atom could decrease the inhibiting effect induced by a possible coordination of the sulfur to the tungsten atom. The turnover rates can be increased by increasing reaction temperature and/or by performing the polymerization without a solvent. The rather high polydispersity of the polymer obtained from **8c** (M_w/M_N = 3.5) is probably due to the extremely high activity of the catalyst during propagation: this catalyst can open acyclic *and* cyclic double bonds, the consequence being chain-transfer reac-

tions. The catalysts that give living polymers are usually active in metathesis of cyclic olefins and not in that of acyclic olefinic double bonds.[5a, 15, 16]

Reaction of *n*-butylthiocyclooctene **8b** with ethylene (**3**) in the presence of **1** leads to alkylthiodiene **10** (Scheme 3).[10] A decrease of the initial **8b**/**1** molar ratio leads to a slight increase of the final conversion of **8b**, while an increase of the initial **3**/**8b** molar ratio gives, as expected, a higher yield of **10** (Table 3). High reaction temperatures drastically enhance the turnover rates.

Table 3. Cometathesis of **8b** with ethylene (**3**) catalyzed by **1** [a].

8b/**1** [b]	**3**/**1** [b]	*T* [°C] [c]	*t* [h] [d]	Conversion of **8b** [%]	Yield of **10** [%] [e]
200/1	200/1	20	8	82	39
100/1	200/1	20	6	96	59
50/1	200/1	20	6	99	72
50/1	200/1	80	0.25	93	61
25/1	200/1	20	6	99	75

[a]–[d] See Table 1. [e] Yields based on initial **8b**.

Copolymerization of **8b** with various cyclic olefins (cyclopentene, cyclooctene, cyclododecene, 1,5-cyclooctadiene, 1,5,9-cyclododecatriene, norbornene, and dicyclopentadiene) can also be achieved (Scheme 3).[17] The composition of the copolymers (*x*/*y* ratio) depends not only on the initial ratios of the two comonomers, but also on their relative reactivities in metathesis. In reactions with highly reactive comonomers such as norbornene or dicyclopentadiene, the thiocycloolefin is not easily incorporated in the polymer ($x/y \approx 20/80$ starting from an equimolar ratio of the two reactants). Conversely, less active cyclic comonomers (cyclopentene, cyclooctene, etc.) are favorable for incorporating thioolefin ($x/y \approx 50/50$).

Finally, in the presence of **1**, diallyl sulfide (**11**) undergoes an intramolecular metathesis reaction resulting in a cyclization and in the formation of ethylene (**3**) and 2,5-dihydrothiophene (**12**)[18] (Scheme 4).[19] The turnover rates are

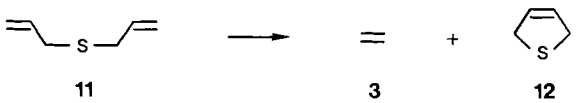

11 **3** **12**

Scheme 4. Intramolecular metathesis of **11**.

rather high and the yield of **12** can reach approximately 90% (Table 4) (the main by-products are most likely oligomers resulting from an intermolecular metathesis reaction of **11**). Interestingly, metathesis of **11** can be easily achieved in the absence of a solvent, which proves to be particularly useful

Table 4. Metathesis of **11** catalyzed by **1** [a].

11/**1** [b]	*T* [°C] [c]	*t* [h] [d]	Conversion of **11** [%]	Yield of **12** [%]
100/1	50	3	98	82
100/1 [e]	80	8	99	85
250/1	50	6	88	78
250/1	80	3	98	88

[a]–[d] See Table 1. [e] Experiment performed without a solvent.

for synthetic purposes. This reaction opens a new route to the synthesis of thiophene.

In summary, we have shown a new property of the neutral metallacyclic neopentylidene–tungsten complex **1** in the catalysis of the metathesis of sulfur-containing olefins. The reactivity of **1** is not completely understood, although it might be due to the high rigidity of the metallacyclic structure and the steric crowding at the tungsten center which prevents strong coordination of the thioether moiety to the metal atom. This hypothesis is corroborated by the observation of a steric effect at the sulfur atom which seems to play a similar role. To our knowledge, it is the first report related to the metathesis of *acyclic* and *unstrained cyclic* olefins containing sulfur. Our results could have a great impact on thiochemistry as well as on polymer science.

The fact that a tungsten-based catalyst could be so active in the metathesis of functionalized olefins deserves some comment. So far, it was implicitly assumed that tungsten-based catalysts with a d^0 configuration, even if they were good metathesis catalysts for simple olefins, could not tolerate functionalized olefins since the heteroatoms would coordinate to the metal center. Therefore, much effort was invested in the recently reported metathesis of functionalized olefins with ruthenium-based catalysts that are obviously less inclined to strongly coordinate heteroatom-containing olefins.[20] The fact that a tungsten-based catalyst with a d^0 configuration is able to catalyze the metathesis of sulfur-containing olefins opens up new possibilities in the choice of the metal best suited for the metathesis of functionalized acyclic and cyclic olefins as well as the ligands for the steric and electronic control of the reactivity of the metal with a d^0 configuration. Obviously, aryloxide ligands are very versatile in this respect.

Received: July 9, 1992 [Z 5454 IE]
German version: *Angew. Chem.* **1993**, *105*, 99

[1] For comprehensive reviews on olefin metathesis, see: a) K. J. Ivin, *Olefin Metathesis*, Academic Press, London, **1983**; b) V. Dragutan, A. T. Balaban, M. Dimonie, *Olefin Metathesis and Ring-Opening Polymerization of Cyclo-Olefins*, 2nd ed., Wiley-Interscience, New York, **1985**.

[2] For a recent review on the metathesis of functionalized acyclic olefins, see: J. C. Mol, *J. Mol. Catal.* **1991**, *65*, 145–162.

[3] For examples of the application of metathesis to the synthesis of polymers containing heteroatoms, see: a) R. H. Grubbs, W. Tumas, *Science* **1989**, *243*, 907–915; b) R. R. Schrock, *Acc. Chem. Res.* **1990**, *23*, 158–165.

[4] To our knowledge, the one mention of the metathesis of an acyclic olefinic sulfide (allyl pentyl sulfide; catalyst Re_2O_7/Al_2O_3-$(CH_3)_4Sn$) was in one sentence and without experimental data. J. C. Mol, *J. Mol. Catal.* **1982**, *15*, 35–45.

[5] Very recently, two examples were reported concerning the ring-opening metathesis polymerization of highly strained cyclic olefins (norbornenes and oxanorbornenes) with sulfur-containing substituents: a) C. C. Cummins, R. R. Schrock, R. E. Cohen, *Chem. Mater.* **1992**, *4*, 27–30; b) E. G. Burns, R. H. Grubbs, poster at the *9th Int. Symp. on Olefin Metathesis and Polymerization*, Collegeville, PA, USA, **1991**.

[6] a) F. Pennella, *J. Catal.* **1981**, *69*, 206–208; b) T. Nishiguchi, K. Fukuzumi, K. Sugisaki, *ibid.* **1981**, *70*, 24–31.

[7] J.-L. Couturier, C. Paillet, M. Leconte, J.-M. Basset, K. Weiss, *Angew. Chem.* **1992**, *104*, 622–624; *Angew. Chem. Int. Ed. Engl.* **1992**, *31*, 628–631.

[8] a) R. R. Schrock, D. N. Clark, J. Sancho, J. H. Wengrovius, S. M. Rocklage, S. F. Pedersen, *Organometallics* **1982**, *1*, 1645; b) R. R. Schrock, J. Sancho, S. F. Pedersen, *Inorg. Synth.* **1989**, *26*, 44–51.

[9] F. Quignard, M. Leconte, J.-M. Basset, L.-Y. Hsu, J. J. Alexander, S. G. Shore, *Inorg. Chem.* **1987**, *27*, 4272–4277.

[10] All the acyclic sulfur-containing products obtained by metathesis were identified by gas chromatography/mass spectrometry (GC-MS).

[11] For clarity, the sulfur-free olefins produced in cometathesis reactions are not shown in the schemes.

[12] The reactions were carried out in chlorobenzene at 80 °C (cyclopentene) or 25 °C (norbornene), with a **2**/**1** molar ratio of 25/1. Unfortunately, the yields could not be accurately determined due to the presence of some polymeric residue.

[13] 5-Alkylthiocyclooctenes **8** are easily synthesized by radical addition of the appropriate thiols to cyclooctadiene: K. Griesbaum, *Angew. Chem.* **1970**, *82*, 276–290; *Angew. Chem. Int. Ed. Engl.* **1970**, *9*, 273–287.
[14] The polymers could be isolated as sticky solids by dilution of the reaction medium with THF and precipitation with methanol. Elemental analyses and NMR spectra (^1H and ^{13}C in $CDCl_3$) of these polymers are in accord with formula **9**. In particular, the ^1H NMR spectrum shows that the double bond is not lost during the reaction, actually proving this to be a ring-opening metathesis polymerization.
[15] a) L. R. Gilliom, R. H. Grubbs, *J. Am. Chem. Soc.* **1986**, *108*, 733–742; b) Z. Wu, D. R. Wheeler, R. H. Grubbs, *ibid.* **1992**, *114*, 146–151.
[16] G. C. Bazan, J. H. Oskam, H. N. Cho, L. Y. Park, R. R. Schrock, *J. Am. Chem. Soc.* **1992**, *113*, 6899–6907.
[17] Copolymerization reactions were performed at 25 °C without a solvent; the initial **8b**/**1** molar ratio was 100/1. The *x*/*y* ratios in the copolymers (Scheme 3) were determined by elemental analysis and ^1H NMR spectroscopy.
[18] 2,5-Dihydrothiophene (**12**) was identified by GC-MS and by ^1H (100 MHz) and ^{13}C (25 MHz) NMR spectroscopy ($CDCl_3$, 25 °C): $\delta(CH) = 5.83$, $\delta(CH_2) = 3.73$; $\delta(CH) = 128.45$, $\delta(CH_2) = 38.88$).
[19] Examples of ring-closing metathesis of oxygen- or nitrogen-containing dienes have been recently reported: G. C. Fu, R. H. Grubbs, *J. Am. Chem. Soc.* **1992**, *114*, 5426–5427, 7324–7325.
[20] a) B. M. Novak, R. H. Grubbs, *J. Am. Chem. Soc.* **1988**, *110*, 960–961, 7542–7543; b) D. V. McGrath, R. H. Grubbs, J. W. Ziller, *ibid.* **1991**, *113*, 3611–3613.

Organometallic Oxides: Lacunary Lindqvist-Type Polyanion-Supported Cyclopentadienylrhodium Complex Fragments**

By *Anna Proust, Pierre Gouzerh,** and *Francis Robert*

In recent years there has been a growing interest in the chemistry of organometallic oxides,[1–3] not least the organometallic clusters derived from polyoxometalates. These can serve as models for metal oxide surfaces and thus help to provide a basic understanding of catalyst-to-support interactions in heterogeneous catalytic processes.[1, 3, 4] Some compounds have been found to display bifunctional catalytic activity.[5] As ligands, polyoxometalates exhibit unique properties.[4] Lacunary anions can be viewed as inorganic-porphyrin analogues[4] and their coordination chemistry has been extensively studied.[6] On the other hand, closed anions are potential polydentate bridging ligands if they use both their terminal and bridging oxygen atoms. For example, the $[V_6O_{19}]^{8-}$,[7] *cis*-$[Nb_2W_4O_{19}]^{4-}$,[8] $[CpTiMo_5O_{18}]^{3-}$,[9] β-$[SiW_9V_3O_{40}]^{7-}$,[10] and $[P_2W_{15}Nb_3O_{62}]^{9-}$[11] anions form stable adducts with cations such as $[M(Cp^*)]^{2+}$ (M = Rh, Ir), $[M(CO)_3]^+$ (M = Mn, Re), $[M(CO)_2]^+$ (M = Rh, Ir), $[Ru(C_6H_6)]^+$, $[Rh(C_7H_8)]^+$, and $[Ir(C_8H_{12})]^+$. Organometallic complexes containing metavanadates[12] and integrated cubane-type clusters[13] have also been characterized.

$(NBu_4)_2[Mo_5O_{13}(OCH_3)_4(NO)\{Na(CH_3OH)\}] \cdot 3CH_3OH$ **1a**

$(NMe_4)_2[Mo_5O_{13}(OCH_3)_4(NO)\{Na(H_2O)\}]$ **1b**

We recently reported the synthesis of **1a**, the anion of which can be viewed as a lacunary Lindqvist-type species.[14] The negative charge density on the terminal oxygen atoms is reduced by the electron-withdrawing effect of the $(MoNO)^{3+}$ unit. Nevertheless, the anion is sufficiently basic to react with various electrophiles; indeed the lacunary species needs some stabilization, otherwise it transforms into the closed $[Mo_6O_{18}(NO)]^{3-}$ anion. The $[Mo_5O_{13}(OCH_3)_4(NO)]^{3-}$ anion has been found to exhibit a rich coordination chemistry. We describe here the synthesis and characterization of two (pentamethylcyclopentadienyl)rhodium(III) complexes of this ligand.

Complexation of $[Rh(Cp^*)]^{2+}$ with $[Mo_5O_{13}(OCH_3)_4(NO)]^{3-}$ was achieved by refluxing a mixture of **1a** and $[\{Cp^*RhCl_2\}_2]$ for several hours in methanol. (Depending on the experiment, chloride was partially or totally removed by prior addition of $AgNO_3$.) The red precipitate of **2a** obtained from this reaction gave red octahedral crystals of **4a** · CH_2Cl_2 upon recrystallization from CH_2Cl_2. Compound **4a** was obtained directly as a red precipitate when 3/4 of the chloride had been removed. Complete removal of the chloride resulted in the precipitation of **3a** as an orange-brown solid; orange-red plates of **3a** subsequently grew from the filtrate. Starting from a sample of **1b**, which turned out to be slightly contaminated with NMe_4Br, red needles of **3c**, and red thin plates of **3b** crystallized successively after the refluxed solution had been cooled. When an excess of NMe_4Br was added to the reactant mixture, a red precipitate of **2b** was obtained, which gave red crystals of **4b** · CH_2Cl_2 upon recrystallization from CH_2Cl_2.

Compounds **2a** and **2b** have not yet been fully characterized. Compounds **3b**, **3c**, and **4b** · CH_2Cl_2 have been identified by X-ray crystallography.[15] Compounds **4a** · CH_2Cl_2 and **4b** · CH_2Cl_2 were found to be isostructural; the composition of **4a** has been confirmed by chemical analysis.

$(NBu_4)[Mo_5O_{13}(OCH_3)_4(NO)\{RhCp^*(solv.)\}]$ **3a**
(solv. = H_2O or MeOH)

$(NMe_4)[Mo_5O_{13}(OCH_3)_4(NO)\{RhCp^*(H_2O)\}] \cdot 2H_2O$ **3b**

$[\{RhCp^*\}_2(\mu\text{-}Br)_3][Mo_5O_{13}(OCH_3)_4(NO)\{RhCp^*(H_2O)\}]$ **3c**

$[Mo_5O_{13}(OCH_3)_4(NO)\{\{RhCp^*\}_2(\mu\text{-}Cl)\}]$ **4a**

$[Mo_5O_{13}(OCH_3)_4(NO)\{\{RhCp^*\}_2(\mu\text{-}Br)\}]$ **4b**

The crystals of **3b** consist of Me_4N^+ cations, water molecules of crystallization, and discrete $[Mo_5O_{13}(OCH_3)_4(NO)\{RhCp^*(H_2O)\}]^-$ anions in which the nitrosyl polyoxomolybdate acts as a bidentate ligand. The anion has $C_s(m)$ crystallographic symmetry (Fig. 1). The $[Mo_5O_{13}(OCH_3)_4(NO)]$ subunit is less symmetrical than that found in **1a**. Indeed, while the Mo–O(Rh) distances are not significantly different from the unperturbed Mo–O_t distances, the two Mo–OMe bonds *trans* to the rhodium-ligated oxygen atoms are significantly shorter than the other ones. Compound **3a** is assumed to contain the same complex anion as **3b** on the basis of analytical and IR spectral data. This anion is also found in **3c** according to a preliminary X-ray study.

The crystals of **4b** · CH_2Cl_2 consist of discrete molecules that have $C_s(m)$ crystallographic symmetry (Fig. 2). Here the $[Mo_5O_{13}(OCH_3)_4(NO)]$ subunit behaves as a symmetrically bridging tetradentate ligand.

In both **3b** and **4b**, the rhodium atoms are approximately octahedrally coordinated and they achieve an 18-electron configuration with two terminal axial oxygen atoms, the Cp* ring, and either a water molecule or a bromide ligand. Compounds **3b** and **4b** represent a new class of complexes sup-

[*] Prof. Dr. P. Gouzerh, A. Proust, F. Robert
Laboratoire de Chimie des Métaux de Transition, URA CNRS 419
Université Pierre et Marie Curie, Casier 42
4 Place Jussieu, F-75252 Paris Cedex 05 (France)

[**] This work was supported by the Centre National de la Recherche Scientifique (URA 419).

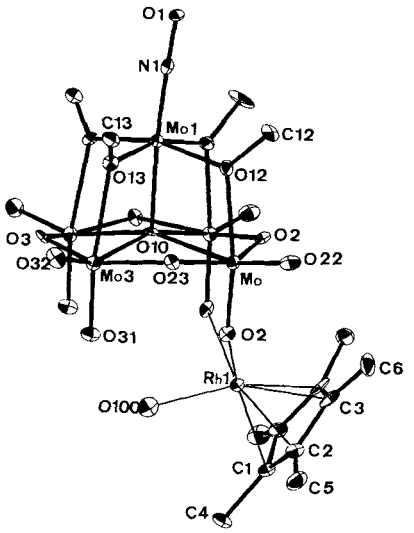

Fig. 1. Structure of the anion of **3b**. The anion lies at a special position with crystallographic *m* symmetry; the mirror plane passes through the Mo1, N1, O1, O10, O2, O3, Rh1, and O100 atoms. Selected bond lengths [Å] and bond angles [°]: Mo1-N1 1.77(3), N1-O1 1.21(4), Mo1-O10 2.14(2), Mo1-O12 2.01(2), Mo2-O12 2.20(1), Mo1-O13 1.94(2) Mo3-O13 2.33(1), Mo2-O22 1.66(2), Mo3-O32 1.69(2), Mo2-O21 1.75(2), Mo3-O31 1.70(1), Rh1-O21 2.11(2), Rh1-O100 2.13(2), Mo1-N1-O1 177.9(27), O10-Mo1-N1 174.8(11), Mo1-O12-Mo2 108.2(7), Mo1-O13-Mo3 106.1(6), O21-Rh1-O100 86.2(7), O21-Rh1-O21′ 82.6(8).

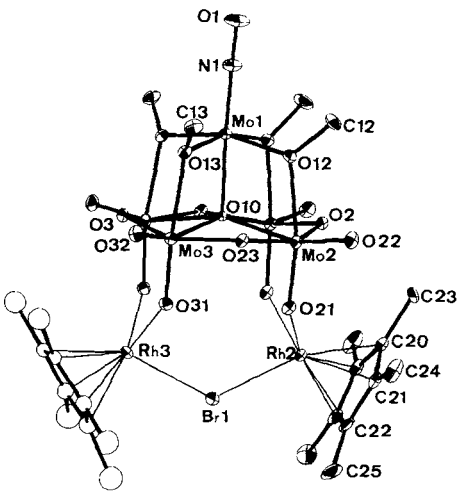

Fig. 2. Structure of the anion of **4b**. The anion lies at a special position with crystallographic *m* symmetry, the mirror plane passes through the Mo1, N1, O1, O10, O2, O3, Rh2, Rh3, and Br1 atoms. The Cp* ligand attached to Rh3 is disordered. Selected bond lengths [Å] and bond angles [°]: Mo1-N1 1.78(1), N1-O1 1.16(2), Mo1-O10 2.123(9), Mo2-O21 1.753(8), Mo3-O31 1.740(8), Mo2-O22 1.688(8), Mo3-O32 1.683(8), Rh2-O21 2.100(8), Rh3-O31 2.118(8), Rh2-Br1 2.539(2), Rh3-Br1 2.550(3), Mo1-N1-O1 178.7(19), O10-Mo1-N1 177.5(7), O21-Rh2-Br1 91.4(2), O31-Rh3-Br1 92.4(2) O21-Rh1-O21′ 82.6(4), O31-Rh3-O31′ 81.4(2), Rh2-Br1-Rh3 125.70(8).

ported on polyoxomolybdates where the organometallic fragment is bound to the terminal oxygen atoms of the open face of a lacunary polyoxoanion. They demonstrate the unique properties of $[Mo_5O_{13}(OCH_3)_4(NO)]^{3-}$ as a ligand.

Experimental Procedure

3a: $AgNO_3$ (0.084 g, 0.5 mmol) was added to a solution of $[\{RhCp^*Cl_2\}_2]$ (0.078 g, 0.125 mmol) dissolved in CH_3OH (10 mL). After the solution had been stirred for approximately 30 min, AgCl was filtered off and washed with methanol (5 mL); the filtrate was added to a solution of **1a** (0.34 g, 0.25 mmol) in methanol (5 mL). The mixture was refluxed for 7 h, during which time **3a** was deposited as an orange-brown solid. It was collected by filtration (yield: 35%). IR(KBr): $\tilde{\nu}[cm^{-1}]$ = 1625 (NO); 935, 895, 855 (MoO_t).

4a: Compound **4a** was similarly prepared from $AgNO_3$ (0.375 mmol), $[\{RhCp^*Cl_2\}_2]$ (0.125 mmol), and **1a** (0.25 mmol) (yield: 50%). IR (KBr): $\tilde{\nu}[cm^{-1}]$ = 1635 (NO); 940, 855 (MoO_t).

Received: August 4, 1992 [Z 5502 IE]
German version: *Angew. Chem.* **1993**, *105*, 81

[1] W. A. Herrmann, *Comments Inorg. Chem.* **1988**, *7*, 73.
[2] F. Bottomley, L. Sutin, *Adv. Organomet. Chem.* **1988**, *28*, 339.
[3] V. W. Day, W. G. Klemperer, *Science* **1985**, *228*, 533.
[4] M. T. Pope, A. Müller, *Angew. Chem.* **1991**, *103*, 56; *Angew. Chem. Int. Ed. Engl.* **1991**, *30*, 34.
[5] A. R. Siedle, C. G. Markell, P. A. Lyon, K. O. Hodgson, A. L. Roe, *Inorg. Chem.* **1987**, *26*, 220.
[6] For recent work, see: a) D. K. Lyon, W. K. Miller, T. Novet, P. J. Domaille, E. Evitt, D. C. Johnson, R. G. Finke, *J. Am. Chem. Soc.* **1991**, *113*, 7209; b) L. A. Combs-Walker, C. G. Hill, *Inorg. Chem.* **1991**, *30*, 4016; c) C. Rong, M. T. Pope, *J. Am. Chem. Soc.* **1992**, *114*, 2032.
[7] a) H. K. Chae, W. G. Klemperer, V. W. Day, *Inorg. Chem.* **1989**, *28*, 1424; b) Y. Hayashi, Y. Ozawa, K. Isobe, *ibid.* **1991**, *30*, 1025.
[8] a) C. J. Besecker, V. W. Day, W. G. Klemperer, M. R. Thompson, *Inorg. Chem.* **1985**, *27*, 44; b) C. J. Besecker, V. W. Day, W. G. Klemperer, M. R. Thompson, *J. Am. Chem. Soc.* **1984**, *106*, 4125; c) C. J. Besecker, W. G. Klemperer, V. W. Day, *ibid.* **1982**, *104*, 6158; d) W. G. Klemperer, D. J. Main, *Inorg. Chem.* **1990**, *29*, 2345 and 2355.
[9] V. W. Day, M. F. Fredrich, M. R. Thompson, W. G. Klemperer, R. S.Liu, W. Shum, *J. Am. Chem. Soc.* **1981**, *103*, 3597.
[10] R. G. Finke, M. W. Droege, *J. Am. Chem. Soc.* **1984**, *106*, 7274; R. G. Finke, B. Rapko, P. J. Domaille, *Organometallics* **1986**, *5*, 175.
[11] a) D. J. Edlung, R. J. Saxton, D. K. Lyon, R. G. Finke, *Organometallics* **1988**, *7*, 1692; b) R. G. Finke, D. K. Lyon, K. Nomiya, S. Sur, N. Mizuno, *Inorg. Chem.* **1990**, *29*, 1784.
[12] V. W. Day, W. G. Klemperer, A. Yagasaki, *Chem. Lett.* **1990**, 1267.
[13] a) Y. Hayashi, K. Toriumi, K. Isobe, *J. Am. Chem. Soc.* **1988**, *110*, 3666; b) Y. Do, X.-Z. You, C. Zhang, Y. Ozawa, K. Isobe, *ibid.* **1991**, *113*, 5892.
[14] P. Gouzerh, Y. Jeannin, A. Proust, F. Robert, *Angew. Chem.* **1989**, *101*, 1377; *Angew. Chem., Int. Ed. Engl.* **1989**, *28*, 1363.
[15] **3b**: orthorhombic, *Pmnn*, M_r = 1208.16, Z = 4, a = 10.969(5), b = 13.227(5), c = 27.762(10) Å, V = 4028(3) Å^3, ϱ_{calcd} = 1.99 g cm^{-3}, $1 < \theta < 23$, $\lambda(Mo_{K\alpha})$ = 0.71069 Å, μ = 19.40 cm^{-1}, R = 0.054, R_w = 0.062. 2863 unique reflections collected; direct methods; 1232 reflections ($I \geq 3\sigma(I)$) were used for the least-squares refinement; 242 refined parameters. **4b** · CH_2Cl_2: orthorhombic, *Pmnb*, M_r = 1482.94, Z = 4, a = 15.884(4), b = 16.512(4), c = 17.650(4) Å, V = 4629(2) Å^3, ϱ_{calcd} = 2.13 g cm^{-3}, $1.5 < \theta < 28$, $\lambda(Mo_{K\alpha})$ = 0.71069 Å, μ = 29.99 cm^{-1}, R = 0.045, R_w = 0.054. 5771 unique reflections collected; direct methods; 3164 reflections ($I \geq 3\sigma(I)$) were used for least-squares refinement; 274 refined parameters. For both structures final refinement was carried out with anisotropic thermal parameters for all atoms except the carbon atoms in one disordered Cp* ring of **4b** · CH_2Cl_2; hydrogen atoms were not introduced. Further details of the crystal structure investigations may be obtained from the Fachinformationszentrum Karlsruhe, Gesellschaft für wissenschaftlich-technische Information mbH, D-W-7514 Eggenstein-Leopoldshafen 2 (FRG), on quoting the depository number CSD-56624, the names of the authors and the journal citation.

Axial Ligation of Diazacyclooctanenickel and -Zinc Complexes**

By *Dawn C. Goodman, Thawatchai Tuntulani, Patrick J. Farmer, Marcetta Y. Darensbourg,** and *Joseph H. Reibenspies*

The 1,5-diazacyclooctane (daco) molecule has proven to be a useful precursor for building ligands with various donor atoms, including those of import to the biological chemistry

[*] Prof. Dr. M. Y. Darensbourg, D. C. Goodman, T. Tuntulani, P. J. Farmer, Dr. J. H. Reibenspies
Department of Chemistry, Texas A & M University
College Station, TX 77843 (USA)

[**] This work was supported by the National Institutes of Health (RO1 GM44865-01) and the National Science Foundation (CHE-8513273 for purchase of the X-ray diffractometer and crystallographic computing system; CHE-8912763 for the EPR spectrometer). We thank Prof. Paul Lindahl for helpful discussions.

of nickel—N, S, and O.[1-5] The coordination of a metal center M results in the formation of two diazametallacyclohexane rings which share an N-M-N unit. A plethora of X-ray crystal structures has established that the common form of the two six-membered rings in metal-bound daco is the boat/chair form (see **1**, Equation (a)). Due to the steric hindrance of the β-methylene CH_2 group in the boat/chair form, axial ligation at the metal is blocked on one side, thus accounting for examples of tetra- and pentacoordinate Ni^{II},[1-3] and pentacoordinate Co^{II} and Co^{III} complexes.[4] This conformational preference is rationalized as avoiding cross-ring methylene C–H interactions that might result from the chair/chair form of the metalladiazacyclohexane rings. Nevertheless, MM2 calculations that we[6] and others conducted suggest that, in the absence of C–H/metal agostic interactions, the differences between the two conformers represented in structure **1** are minor. In fact, the conformation lower in energy, the chair/chair conformation, is the one typically *not* seen in the X-ray crystal structures thusfar reported.[2-6, 8-10] Although disorder in the structure of 1,5-diazacyclooctane-1,5-diylbis(ethylthiolato)nickel(II) (**1**)[5] may be indicative of a mixture of chair/chair and boat/chair conformers, bona fide examples of exclusive chair/chair conformers are rare.[6]

The methylation of **1** yields *N,N'*-bis(3-thiabutyl)-1,5-diazacyclooctanenickel(II) iodide (**2**),[5] suggesting that the nucleophilic character of the nickel-bound thiolate sulfur atoms may be engaged to extend the denticity of the N_2S_2 ligand by the introduction of additional donor atoms that can bind to the Ni atom in axial positions. We report here on the X-ray crystal structure of a Ni complex with a hexadentate $N_2S_2O_2$ ligand and that of a Zn complex with a pentadentate N_2S_2O ligand. These structures aptly illustrate that the steric shielding of the metal center by the daco ligand may be overcome when the metal atoms can attain a preferable coordination number and when ligands with strong binding abilities are employed.

Blue, paramagnetic Δ-1,5-diazacyclooctane-1,5-diylbis (3-thiapentanoato)nickel(II) (**3**), analytically pure as the trihydrate, was obtained as illustrated in Equation (a) and crystallized in the tetragonal space group $P4_32_12$ (no. 96) or $P4_12_12$ (no. 92).[11] Analysis of structural refinement indicated that

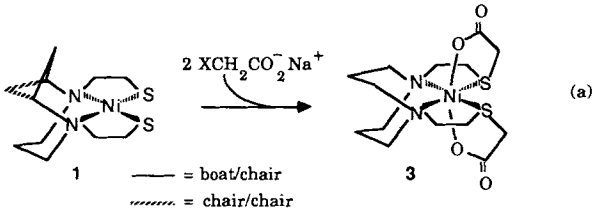

(a)

$P4_32_12$ was the correct space group.[11] Each chiral nickel complex molecule in the asymmetric unit cell possesses a C_2 axis and is hydrogen-bonded through the distal oxygen of the carboxyl group into a three-dimensional network of water molecules. This serpentine of hydrogen bonds through the lattice has no influence on the hydrocarbon portion of the hexadentate ligand and its directionality results from the chirality of the space group of **3**. As illustrated in Figure 1, the Ni^{II} resides in a slightly distorted octahedron whose equatorial positions are taken up by N_2S_2 units and the apexes by O_2 donor atoms. The Ni–S distance of 2.435(2) Å is within the usual range reported for six-coordinate Ni^{II}–SR_2 complexes (d = 2.416 Å),[12] but more than 0.22 Å

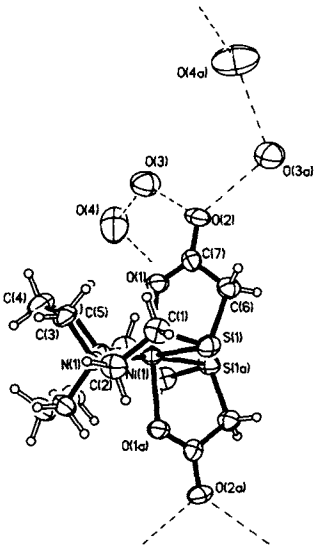

Fig. 1. Crystal structure of **3** · $3H_2O$ (thermal ellipsoids at 50% probability). The atoms labeled **a** are related to the corresponding unlabeled atoms by a C_2 axis; hydrogen atoms on waters removed for clarity. Selected bond lengths [Å] and angles [°]: Ni(1)-S(1) 2.435(2), Ni-O(1) 2.067(3); Ni-N(1) 2.094(4), O(1)-C(7) 1.261(6); C(7)-O(2) 1.254(6); S(1)-Ni-S(1a) 98.5(1). N(1)-Ni-N(1a) 85.7(2); S(1)-Ni-N(1) 88.6(1), O(1)-Ni-O(1a) 170.6(2); O(1)-Ni-S(1) 80.9(1), O(1)-Ni-N(1) 96.7(1); C(3)-C(4)-C(5) 118.2(5); C(3)-N(1)-C(5a) 112.5(4); Ni-S(1)-C(6) 95.0(2).

longer in **3** as compared to the tetradentate square-planar complex **2** (d = 2.211(3), 2.204(3) Å).[5] The C–O bonds have essentially the same length, regardless of whether the O atom is bound directly to nickel or distal to the metal center and hydrogen-bonded to water molecules. The $-CH_2-CO$ unit eclipses the Ni–S bond, creating fairly planar five-membered $NiSC_2O$ rings whose planes form a dihedral angle of 100°; in other words, there is an opening of the S-Ni-S angle by about 10° as compared to complexes **1** or **2**, which show regular 90° angles in the N_2S_2Ni plane.

The most striking feature of the structure of **3** is the uncommon chair/chair conformation of the diazametallacyclohexane rings. Some steric repulsion of the β-CH_2 groups in the folded-back daco ring is evident by the distortion of the bond angles at C5 and C4 from tetrahedral; bond angles of 118.0(4)° and 118.2(5)° are obtained for N1a-C5-C4 and C3-C4-C5, respectively.

Attempts to generate a pentacoordinate Ni^{II} complex by addition of only one equivalent of ICH_2CO_2Na to **1** led to a green product, which on subsequent addition of a second equivalent of ICH_2CO_2Na yielded blue **3**. Elemental analysis of the green material showed it to be the sodium salt of the complex anion iodo(5-sulfidoethyl-1,5-diazacyclooctyl)-3-thiapentanoatonickelate(II). This indicates that the axial oxygen donor atom promotes hexacoordination to the Ni center.[6] In contrast, ICH_2CO_2Na did not react with the dimeric zinc complex **4**.[10] However, from the reaction of **4** with a fourfold excess of $ClCH_2CO_2H$, low yields of **5** · H_2O were obtained [Eq. (b)].

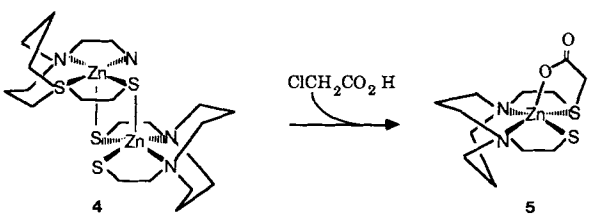

(b)

 © VCH Verlagsgesellschaft mbH, W-6940 Weinheim, 1993 0570-0833/93/0101-0117 $ 10.00+.25/0

The X-ray structure[11] of **5** (Fig. 2) provides interesting structural contrasts to that of compound **3**. Notably, the

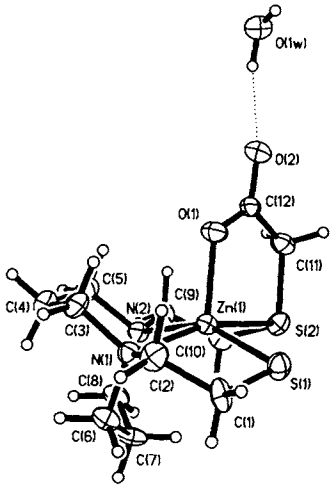

Fig. 2. Crystal structure of $5 \cdot H_2O$ (thermal ellipsoids at 50% probability). Selected bond lengths [Å] and angles [°]: Zn-S(1) 2.295(3); Zn-S(2) 2.584(2); Zn-N(1) 2.184(6); Zn-N(2) 2.189(7), Zn-O(1) 2.005(5) O(1)-C(12) 1.279(9); C(12)-O(2) 1.232(8), O(2)-O(1w) 2.85(1); S(1)-Zn-S(2) 95.6(1); N(1)-Zn-N(2) 83.8(2); S(1)-Zn-N(1) 88.5(2); S(2)-Zn-N(2) 84.3(2); S(1)-Zn-N(2) 153.6(2); S(2)-Zn-N(1) 161.0(2); O(1)-Zn-S(2) 82.6(1); S(1)-Zn-O(1) 112.1(2); C(3)-N(1)-C(6) 111.2(6); C(3)-C(4)-C(5) 115.8(7), Zn-S(2)-C(11) 93.5(2).

diazametallacyclohexane rings are in their usual chair/boat configuration with tetrahedral bond angles at the C atoms. The zinc ion is 0.431 Å above the N_2S_2 best plane, and shows a distinct difference in distances to sulfur: d ($Zn-S_{thioether}$) = 2.584(2) Å, whereas d ($Zn-S_{thiolate}$) = 2.295(3) Å. In contrast to **3**, there is a difference in the lengths of the two C–O bonds; that directed toward the zinc atom is some 0.05 Å shorter than that whose oxygen atom forms a hydrogen bond to the one water of crystallization. The NCH_2CH_2S arms are eclipsed across the MN_2S_2 plane in **4**; in **3**, they are staggered.

In contrast to **1** and **2** (as well as to other sulfidoalkyl- or thioether/daco derivatives), which have electrochemically accessible $Ni^{II/I}$ couples,[5] complex **3** shows no reduction to −2.0 V (cyclic voltammogram in acetonitrile referenced to $Ag^{\circ}/AgCl$). However, the oxidation at +0.99 V is reversible (Fig. 3a) and, as shown by the following EPR results, takes place at the metal center.

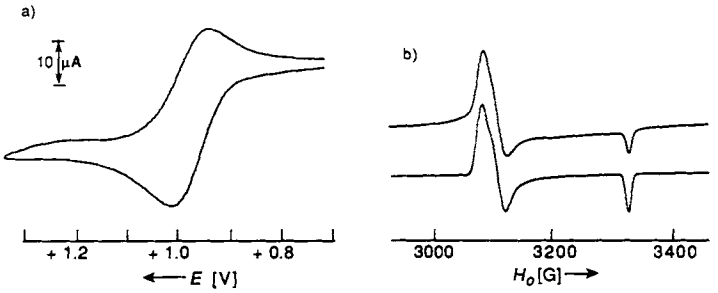

Fig. 3. a) Cyclic voltammogram of **3** (2 mM) in CH_3CN, 0.1 M Bu_4NPF_6. $E_{1/2}$ = 989 mV (Ag/AgCl reference), with $\Delta E_{a/c}$ = 65 mV, i_{pa}/i_{pc} = 0.91. b) Observed and calculated X-band EPR spectra for **3** (4 mM) in CH_3OH bei 10 K (ν = 9.419 GHz). Calculated g-values: 2.190, 2.170, 2.024.

Chemical oxidation of **3** with cerium ammonium nitrate produced an air-sensitive, brick-red, paramagnetic compound which is long-lived even at 22 °C. The simple features of its EPR spectrum, measured on a frozen solution sample, are consistent with a single EPR-active species with nearly axial symmetry (Fig. 3b). Spectral simulation (Fig. 3b) reveals a small anisotropy in the $g_{\perp}$ feature; the best-fit values are $g_{xx} = 2.190$, $g_{yy} = 2.170$, and $g_{zz} = 2.026$.[13, 14] These EPR features indicate that the unpaired electron resides in the d_{z^2} metal orbital of an elongated octahedral d^7 metal complex.[15, 16] However, in the absence of any hyperfine interactions from donor atoms, assignment of the z axis and structural inferences based on EPR spectra are equivocal.

Experimental Procedure

Preparation of **3**: Addition of two equivalents of ICH_2CO_2Na dissolved in methanol to a purple solution of **1**, in CH_3CN at 60 °C with stirring results in a color change, first to brown, then gradually to a forest-green, and finally to aquamarine-blue over the course of 4 h. Filtration and slow evaporation of solvent in an open vessel gave blue, paramagnetic crystals of $3 \cdot (H_2O)_3$ (H_2O from the hygroscopic Na acetate and from the air) in over 90% yield. Correct C,H,N analysis. UV/VIS: λ_{max}[nm] (ε) = 600(49), 364(31); IR(KBr): $\tilde{\nu}$ [cm^{-1}] = 1593, 1385.

Preparation of **5**: A solution of $ClCH_2CO_2H$ (70 mg, 0.67 mmol) in 5 mL of anhydrous CH_3OH was added to **4** (100 mg, 0.17 mmol) in a 50:50 mixture of hot CH_3OH/CH_3CN and refluxed for 1 h. A small amount of white solid precipitated upon cooling and stirring overnight. Recrystallization from pyridine/ether yielded colorless crystals in 15% yield. Correct C, H, N, analysis. IR(KBr): $\tilde{\nu}$[cm^{-1}] = 1633, 1344.

Oxidation of **3** for EPR sample: A 42 mg (91 mmol) sample of **3** was dissolved in 20 mL of anhydrous, degassed MeOH and stirred under N_2. To this blue solution was added with stirring one equivalent of cerium ammonium nitrate dissolved in MeOH. A 500 µL brick-red sample for EPR study was withdrawn and immediately frozen at −70 °C. The red color of the frozen sample remains indefinitely; however, in the course of 30 min at 22 °C, the reaction mixture changed from red back to the original blue. EPR data on frozen solutions were obtained at 77 K on a Bruker ESP 300 spectrometer equipped with an Oxford Instruments ER910 A cryostat. An NMR gaussmeter (Bruker ERO35M) and Hewlett Packard frequency counter (HP5352B) were used to calibrate the field and microwave frequency, respectively.

Received: July 27, 1992 [Z 5482 IE]
German version: *Angew. Chem.* **1993**, *105*, 72

[1] W. K. Musker, M. S. Hussain, *Inorg. Chem.* **1966**, *5*, 1416.
[2] J. C. A. Boeyens, C. C. Fox, R. D. Hancock, *Inorg. Chim. Acta* **1984**, *87*, 1; D. J. Royer, V. H. Schievelbein, A. R. Kalyanaraman, J. A. Bertrand, *ibid.* **1972**, *6*, 307.
[3] D. O. Nielson, M. L. Larsen, R. D. Willett, J. I. Legg, *J. Am. Chem. Soc.* **1971**, *93*, 5079; D. F. Averill, J. I. Legg, D. L. Smith, *Inorg. Chem.* **1972**, *11*, 2344.
[4] W. E. Broderick, K. Kanamori, R. D. Willett, J. I. Legg, *Inorg. Chem.* **1991**, *30*, 3875; K. Kanamori, W. E. Broderick, R. F. Jordan, R. D. Willett, J. I. Legg, *J. Am. Chem. Soc.* **1986**, *108*, 7122.
[5] D. K. Mills, J. H. Reibenspies, M. Y. Darensbourg, *Inorg. Chem.* **1990**, *29*, 4364.
[6] Complex **3** is the first reported example of a complex with diazametallacyclohexane rings with a common N-M-N unit which is exclusively in the chair/chair configuration. A second example of a hexacoordinate nickel derivative prepared by alkylation of **1** with $ICH_2CH_2OCH_2CH_2I$ has been prepared recently: M. Y. Darensbourg, I. Font, D. K. Mills, M. Pala, J. H. Reibenspies, *Inorg. Chem.*, **1992**, *31*, 4965.
[7] R. D. Hancock, M. P. Ngwenya, A. Evers, P. W. Wade, J. C. A. Boeyens, S. M. Dobson, *Inorg. Chem.* **1990**, *29*, 264.
[8] P. J. Farmer, T. Solouki, D. K. Mills, T. Soma, D. H. Russell, J. H. Reibenspies, M. Y. Darensbourg, *J. Am. Chem. Soc.* **1992**, *114*, 4601.
[9] D. K. Mills, Y.-M. Hsiao, P. J. Farmer, E. V. Atnip, J. H. Reibenspies, M. Y. Darensbourg, *J. Am. Chem. Soc.* **1991**, *113*, 1421.
[10] T. Tuntulani, J. H. Reibenspies, P. J. Farmer, M. Y. Darensbourg, *Inorg. Chem.* **1992**, *31*, 3497.
[11] Crystal structure (296 K) data for $3 \cdot 3H_2O$: $C_{14}H_{30}N_2O_7S_2Ni$, M = 461.2, tetragonal crystals, space group $P4_32_12$, $a = b$ = 8.0290(10), c = 30.209(12) Å, V = 1948 Å^3, Z = 4, ρ_{calcd} = 1.573 g cm^{-3}, μ = 1.242 mm^{-1}; 1450 reflections with $F > 4\sigma(F)$, R = 0.043 and R_w = 0.044. – $4 \cdot H_2O$ (193 K): $C_{12}H_{24}N_2O_3S_2Zn$, M = 373.8, monoclinic crystals, space group $P2_1c$, a = 12.479(4), b = 9.322(3), c = 13.702(5) Å, β = 106.35(3)°, V = 1530 Å^3, Z = 4, ρ_{calcd} = 1.623 g cm^{-3}, μ = 1.913 mm^{-1}; 1941 reflections with $F > 4\sigma(F)$, R = 0.064, R_w = 0.063. For both struc-

tures, carbon-bound hydrogen atoms were idealized while hydrogens in water were located in a difference Fourier analysis and not refined. Further details of the crystal structure investigations are available on request from the Director of the Cambridge Crystallographic Data Centre, University Chemical Laboratory, Lensfield Road, GB-Cambridge CB2 1EW, (UK), on quoting the full journal citation.

[12] A. G. Orpen, L. Brammer, F. H. Allen, O. Kennard, D. G. Watson, R. Taylor, *J. Chem. Soc. Dalton Trans.* **1989**, S.1.

[13] Spectral simulations were performed using the program XPOW for $S = 1/2$ paramagnets. [14a] The latest update is described in ref. [14b].

[14] a) R. L. Belford, M. J. Nilges, *Computer Simulation of Powder Spectra EPR Symposium*, 21st Rocky Mountain Conference, Denver, CO, August 1979; b) E. P. Duliba, Ph.D. Thesis, University of Illinois, **1983**.

[15] S. A. Jacobs, D. W. Margerum, *Inorg. Chem.* **1984**, *23*, 1195.

[16] F. V. Lovecchio, E. S. Gore, D. H. Busch, *J. Am. Chem. Soc.* **1974**, *96*, 3109.

A Self-Assembling, Hydrogen-Bonded Helix**

By *Steven J. Geib, Cristina Vicent, Erkang Fan,* and *Andrew D. Hamilton**

In memoriam Margaret Etter

The design of molecular subunits that self-assemble into defined structures in solution or in the solid state is an area of intense current interest.[1] A key to controlling the shape of the aggregate lies in manipulating the type and orientation of the noncovalent interactions between the subunits.[2] The strong and directional nature of hydrogen bonds has led to their widespread use in self-assembling systems. In the solid state, rules have been delineated to allow the reasonable prediction of hydrogen-bonding packing patterns in crystals.[3] This has led to a search for molecular components that because of their hydrogen-bonding characteristics will form persistent packing motifs in well-defined shapes or patterns. Recent results have demonstrated the formation of two- and three-dimensional networks of di- and tetrapyridones;[4] extended sheet structures of ureylenedicarboxylic acids;[5] molecular tapes or (3 + 3) cyclic aggregates made up of alternating melamine and barbiturate derivatives;[6, 7] and variable molecular ribbons composed of hydrogen-bonded acylaminopyridine and acid subunits.[8] In this paper we report the design and structural properties of a molecule that in the presence of an aliphatic dicarboxylic acid of the correct length will self-assemble into a helical arrangement of alternating components held together by a network of hydrogen bonds.[9–11]

We have previously shown[12] that a receptor molecule made up of two 2-amino-6-methylpyridine units separated by a terephthalate spacer and in a *syn* orientation will form strong complexes with dicarboxylic acids of appropriate length with four hydrogen bonds as in **1** with adipic acid. Increasing the length of the dicarboxylic acid beyond the optimum leads to the *anti* conformation of the receptor molecule and formation of ribbon structures with bidentate hydrogen bonding between the two alternating components.[8b] We were interested in investigating the recognition properties of the related isophthalate receptor molecule **2** (formed from isophthaloyl dichloride and 2-amino-6-methylpyridine) since this now has three primary conformations (due to rotation about the phenyl-CO bond); *syn-syn* (see **2**), *syn-anti*, and *anti-anti*. In the *syn-syn* conformation the hydrogen-bonding cavity of **2** is appropriate for binding to urea or barbiturate derivatives[13] but would be too small to form 1:1 complexes with dicarboxylic acids. The carboxylic acid groups on two different molecules could, however, bind to **2**

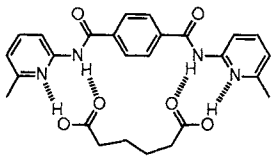

1

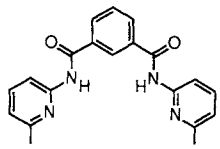

2

with one aminopyridine unit directed above and the other below the plane of the binding cavity. Propagation of this arrangement with a dicarboxylic acid would lead to an extended helical structure, as shown in **3**.

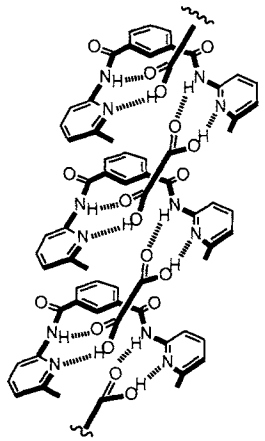

3

Crystallization of a 1:1 mixture of **2** and pimelic acid (heptanedioic acid) by slow diffusion of hexane into $CHCl_3$ gave colorless triclinic needles. X-ray diffraction analysis[14, 15] showed a polymeric cocrystal composed of alternating units of **2** and pimelic acid linked by a network of hydrogen bonds (Fig. 1). Compound **2** is not planar in the

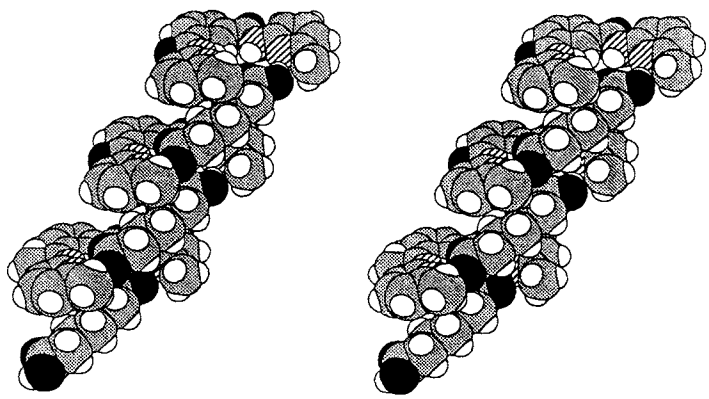

Fig. 1. Section of the X-ray structure of the polymeric 1:1 complex of **2** and pimelic acid (stereoview).

[*] Prof. A. D. Hamilton, S. J. Geib, C. Vicent, E. Fan
Materials Research Center and Department of Chemistry
University of Pittsburgh
Pittsburgh, PA 15260 (USA)

[**] This work was supported by the AFOSR (University of Pittsburgh, Materials Research Center) the Army Research Office and the National Science Foundation. We are also grateful to the Spanish Ministerio de Educacion y Ciencia for a postdoctoral fellowship to C. V.

complex; one acylaminopyridine is 20.5° above and the other 9.4° below the plane of the isophthalate ring. Each pimelic acid molecule retains its preferred all-*trans* conformation and forms two pairs of hydrogen-bonding interactions (NH···O 2.18, N···HO 1.86 Å) to different receptor units.[8b] However, the U-turn shape of the *syn-syn* conformer of **2** enforces an overall helical arrangement onto the strand. A top view of the structure (Fig. 2) shows the perfect alignment of the individual subunits with a spacing of 7.04 Å between each isophthalate ring on neighboring receptor molecules. There are substantial helix–helix contacts in the crystal lattice. Most importantly, each hydrogen-bonded helix is interlocked with a second helix of opposite handedness, as seen in Figure 3. This interaction involves the isophthalate groups of one helix in a face-to-face stacking arrangement (ring–ring distance 3.44 Å)[16] with the corresponding groups of the second helix. Such an intercalation is only possible between right-handed and left-handed helices.

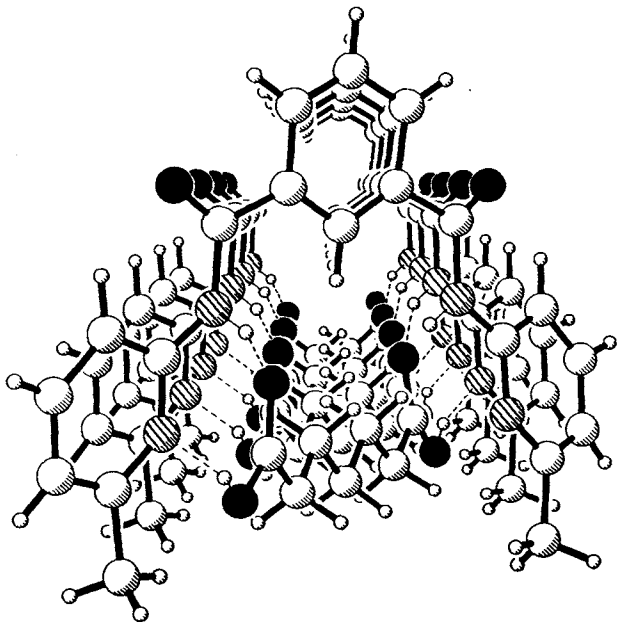

Fig. 2. A top view of the X-ray structure of the polymeric 1:1 complex of **2** and pimelic acid.

One important question is whether a helix of type **3** can exist in solution as well as the solid state. The NMR spectrum of a 0.01 M solution of **2** and pimelic acid (1:1) in D_8[THF]/CD_2Cl_2 (5%) shows large downfield shifts for the pyridine-NH protons indicative of hydrogen-bond formation in solution. Cooling the solution from 298 to 223 K led to upfield shifts of the pimelate-β and -γ CH_2 resonances ($\Delta\delta$ = 0.14 and 0.20) and the observation of NOEs between them and the pyridine-3,-4, and -5 proton resonances. While not conclusive, both of these observations are consistent with a helix-like conformation in solution in which the pimelate alkyl chain is positioned below the plane of one of the pyridine rings.[17]

The stability of the helix structure in the solid state appears to be dependent on the length of the dicarboxylic acid used. Shortening the dicarboxylic acid will reduce the distance between neighboring isophthaloyl rings and inhibit the intercalation interaction seen in Figure 3. Crystals of the 1:1 complex between **2** and glutaric acid were grown from THF (vapor diffusion of hexane), and X-ray analysis was carried out.[15, 18] The structure (Fig. 4) shows the same extended, hydrogen-bonding motif as seen in **3**, reflecting its persistence despite changes in the components and their orientation.[12] In this case, however, **2** has taken up a *syn,anti* conformation, and the glutaric acid displays one *trans* and one *gauche* conformation about its CH_2–CH_2 bonds. The result is a planar ribbon structure stabilized by a hydrogen-bonding network in the plane and stacking interactions between the planes. Figure 4 represents a "squashed" form of the helix in **3** which can, in theory, be converted back to the helix by a rotation of each *anti* phenyl-CO bond by 180° in the same direction towards the center of the spiral.

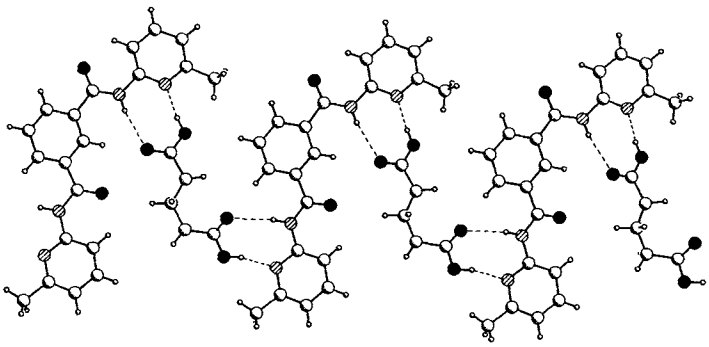

Fig. 4. X-ray structure of the polymeric 1:1 complex of **2** and glutaric acid.

In summary, we have shown that a simple monomeric subunit can be induced, by means of controlling the direction of hydrogen-bonding sites, to interact with aliphatic dicarboxylic acids and self-assemble into an extended helical structure.

Received: July 27, 1992 [Z 5481 IE]
German version: *Angew. Chem.* **1993**, *105*, 83

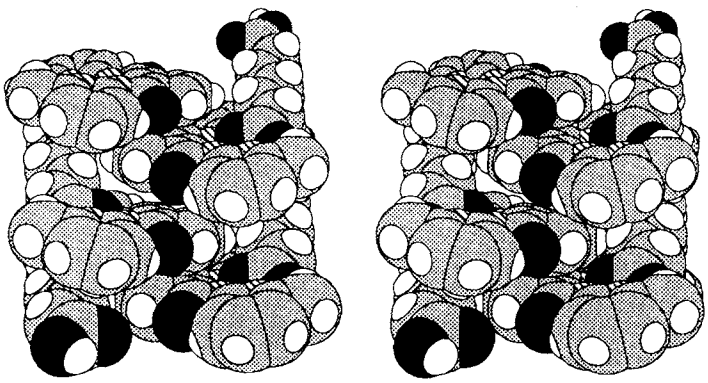

Fig. 3. Stereorepresentation of the side view of a section of the polymeric 1:1 complex of **2** and pimelic acid showing intercalating helices.

[1] For recent reviews on self-assembly see: a) J. S. Lindsey, *New J. Chem.* **1991**, *15*, 153; b) G. M. Whitesides, J. P. Mathias, C. T. Seto, *Science (Washington, DC)* **1992**, *254*, 1312.
[2] For general references see: J. D. Wright, *Molecular Crystals*, Cambridge University Press, Cambridge, **1987**; G. D. Desiraju, *Crystal Engineering: The Design of Organic Solids*, Elsevier, New York, **1989**.
[3] M. C. Etter, *Acc. Chem. Res.* **1990**, *23*, 120; M. C. Etter, Z. Urbanczyk-Lipkowska, M. Zia-Ebrahimi, T. W. Panunto, *J. Am. Chem. Soc.* **1990**, *112*, 8415; L. Leiserowitz, A. T. Hagler, *Proc. R. Soc. London A* **1983**, *388*, 133; L. Leiserowitz, M. Tuval, *Acta Crystallogr. Sect. B* **1978**, *24*, 1230.
[4] Y. Ducharme, J. D. Wuest, *J. Org. Chem.* **1988**, *53*, 5789; M. Gallant, M. T. Phan Viet, J. D. Wuest, *ibid.* **1991**, *56*, 2284; M. Simard, D. Su, J. D. Wuest, *J. Am. Chem. Soc.* **1991**, *113*, 4697.
[5] X. Zhao, Y.-L. Chang, F. W. Fowler, J. W. Lauher, *J. Am. Chem. Soc.* **1990**, *112*, 6627.
[6] J. A. Zerkowski, C. Seto, D. A. Wierda, G. M. Whitesides, *J. Am. Chem. Soc.* **1990**, *112*, 9025; J.-M. Lehn, M. Mascal, A. DeCian, J. Fisher, *J. Chem. Soc. Chem. Commun.* **1990**, 479.

[7] J.-M. Lehn, M. Mascal, A. DeCian, J. Fisher, *J. Chem. Soc. Perkin Trans. 2* **1992**, 461.
[8] a) S. J. Geib, S. C. Hirst, C. Vicent, A. D. Hamilton, *J. Chem. Soc. Chem. Commun.* **1991**, 1283; b) F. Garcia-Tellado, S. J. Geib, S. Goswami, A. D. Hamilton, *J. Am. Chem. Soc.* **1991**, *113*, 9265.
[9] The formation of helical structures in solid-state inclusion complexes has been reviewed: R. Bishop, I. G. Dance, *Top. Curr. Chem.* **1988**, *149*, 137.
[10] Several self-assembling helices based on metal template effects have been reported: E. C. Constable, *Angew. Chem.* **1991**, *103*, 1482; *Angew. Chem. Int. Ed. Engl.* **1991**, *30*, 1450; A. F. Williams, C. Piguet, G. Bernardinelli, *ibid.* **1991**, *103*, 1530 and **1991**, *30*, 1490; U. Koert, M. M. Harding, J. M. Lehn, *Nature* **1990**, *346*, 339; C. O. Dietrich-Buchecker, J. Guilhem, C. Pascard, J.-P. Sauvage, *Angew. Chem.* **1990**, *102*, 1202; *Angew. Chem. Int. Ed. Engl.* **1990**, *29*, 1154; E. C. Constable, M. D. Ward, D. A. Tocher, *J. Chem. Soc. Dalton Trans.* **1991**, 1675.
[11] For examples of covalently linked molecules that take up a helical structure see: K. Deshayes, R. D. Broene, I. Chao, C. B. Knobler, F. Diederich, *J. Org. Chem.* **1991**, *56*, 6787 and references therein; R. Fritsch, E. Hartmann, D. Andert, A. Mannschreck, *Chem. Ber.* **1992**, *125*, 849; D. Gange, P. Magnus, L. Bass, E. V. Arnold, J. Clardy, *J. Am. Chem. Soc.* **1980**, *102*, 2134.
[12] F. Garcia-Tellado, S. Goswami, S. K. Chang, S. J. Geib, A. D. Hamilton, *J. Am. Chem. Soc.* **1990**, *112*, 7393.
[13] S. K. Chang, A. D. Hamilton, *J. Am. Chem. Soc.* **1988**, *110*, 1318; S. K. Chang, E. Fan, D. Van Engen, A. D. Hamilton, *ibid.* **1991**, *113*, 7640.
[14] Crystal data for $C_{27}H_{30}N_4O_6$: triclinic, $P\bar{1}$; $a = 9.156(2)$, $b = 11.860(2)$, $c = 12.355(2)$ Å, $\alpha = 79.89(3)$, $\beta = 78.30(3)$, $\gamma = 81.88(3)°$, $V = 1285.5(4)$ Å^3, $Z = 2$, $\varrho_{calcd} = 1.309$ g cm^{-3}, $T = 23$ °C. A Rigaku AFC5R diffractometer was used to collect 4276 data points, of which 2095 with $F > 5.0\sigma(F)$ were used in the solution and refinement. No absorption correction was necessary ($\lambda(Cu_{K\alpha}) = 1.54178$ Å). Structure was solved by direct methods which located all non-hydrogen atoms. Hydrogen atom positions were calculated (d(C–H) = 0.96 Å) except for N-bound hydrogen atoms which were located and refined. Structure refined to $R = 0.0811$ and $R_w = 0.1166$; GOF = 1.38, highest final difference peak, 0.36 eÅ^{-3}.
[15] Further details of the crystal structure investigations are available on request from the Director of the Cambridge Crystallographic Data Centre, University Chemical Laboratory, Lensfield Road, GB-Cambridge CB2 1EW (UK), on quoting the full journal citation.
[16] A. V. Muehldorf, D. Van Engen, J. C. Warner, A. D. Hamilton, *J. Am. Chem. Soc.* **1991**, *113*, 1318.
[17] Repeated attempts to confirm helix formation in solution by adding chiral shift reagents were unsuccessful, even at low temperature, presumably due to the fast exchange between right- and left-handed helical forms.
[18] Crystal data for $C_{25}H_{26}N_4O_6$: triclinic, $P\bar{1}$; $a = 8.300(2)$, $b = 11.422(2)$, $c = 12.833(3)$ Å, $\alpha = 81.78(3)$, $\beta = 84.88(3)$, $\gamma = 71.99(3)°$, $V = 1143.8(4)$ Å^3, $Z = 2$, $\varrho_{calcd} = 1.389$ g cm^{-3}, $T = 23$ °C. A Rigaku AFC5R diffractometer was used to collect 4296 data points, of which 2254 with $F > 5.0\sigma(F)$ were used in the solution and refinement. No absorption correction was necessary ($\lambda(Cu_{K\alpha}) = 1.54178$ Å). Structure was solved by direct methods which located all non-hydrogen atoms. Hydrogen atom positions were calculatd (d(C–H) = 0.96 Å) except for N-bound hydrogen atoms which were located and refined. Structure refined to $R = 0.0532$ and $R_w = 0.0736$; GOF = 1.39, highest final difference peak, 0.30 eÅ^{-3}.

Preparation and Structure of Two Highly Reactive Intermediates: $[Li(thf)_4][Cu_5Cl_4R_2]$ and $[Li(thf)_4][AlCl_3R]$, R = $Si(SiMe_3)_3$**

By *Andreas Heine* and *Dietmar Stalke**

The large steric requirement and the good solubility of the products in organic solvents make the tris(trimethylsilyl)silyl ligand developed by Gilman and Smith[1] a versatile ligand both in transition metal chemistry[2–4] and main group metal chemistry.[5–8] With this information and the electron-releasing properties of the $Si(SiMe_3)_3$ unit, we thought that this ligand would also be suitable for the stabilization of intermediates.

The importance of silyl groups in organic synthesis is undoubted, however, very little is known about the structures of the intermediates involved in lithium cuprate reactions.[9, 10] This and a report by Eaborn et al. in 1983 on the preparation and structure of the lithium cuprate $[Li(thf)_4][Cu\{C(SiMe_3)_3\}_2]$[11] encouraged us to react $[(Me_3Si)_3SiLi(thf)_3]$[12] with Cu^ICl at −78 °C. The reaction mixture was stored without workup at −30 °C. A brown powder precipitated (LiCl, $Cu^{II}Cl_2$, and elemental copper), in which deep purple crystals grew. After 14 days these crystals were suitable for an X-ray crystallographic study and were mounted directly on the goniometer head from the mother liquor at approximately −30 °C. At temperatures slightly above −30 °C they decompose instantaneously.

The structure analysis reveals the formula **1**[13] (Fig. 1).

$[Li(thf)_4][Cu_5Cl_4\{Si(SiMe_3)_3\}_2]$ **1**

This empirical formula can be rationalized a posteriori as $[Li(thf)_4][Cu\{Si(SiMe_3)_3\}_2]$ containing four additional Cu^ICl units. At the end of the reaction this lithium silylcuprate, similar to that described by Eaborn et al., might be the main product, although we have been unable to confirm that unequivocally. Figure 1 shows the cuprate anion. To

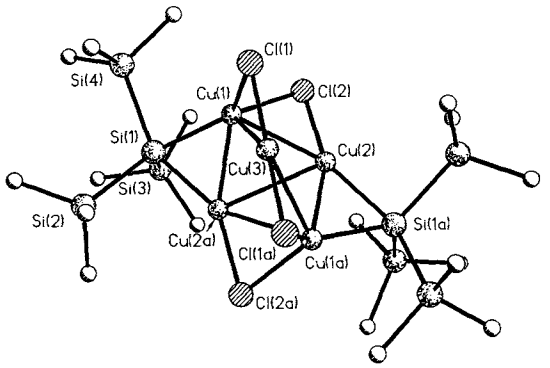

Fig. 1. The structure of the anion in **1** in the solid state. Selected bond lengths [Å] and angles [°]: Si(1)-Cu(1) 2.348(3), Si(1)-Cu(2a) 2.334(3), Cu(1)-Cu(2a) 2.403(2), Cu(1)-Cu(2) 2.654(2), Cu(1)-Cu(3) 2.736(2), Cu(2)-Cu(2a) 2.952(3), Cu(1)-Cl(1) 2.321(3), Cu(3)-Cl(1) 2.127(4), Cu(1)-Cl(2) 2.358(3), Cu(2)-Cl(2) 2.185(3), Si-Si 2.353(4)*; Cu(1)-Si(1)-Cu(2a) 61.75(7), Si(1)-Cu(1)-Cu(2a) 58.86(8), Si(1)-Cu(2a)-Cu(1) 59.40(8), Si-Si-Si 109.96(16)*. Those marked with an asterisk are average values.

our knowledge **1** is the first structurally characterized lithium silylcuprate,[14] a class of compound which is used more and more in situ in organic synthesis. As yet only one other Si–Cu bond length has been determined by X-ray analysis; that found in $[Ph_3SiCu(PMe_3)_3]$.[15] The central silicon atom Si(1) in **1** is in a very unusual bonding situation; it is bonded to three trimethylsilyl groups and two copper atoms, and is thus pentacoordinated. The μ_2-bridging mode for silyl groups is very rare,[16] analogously bound alkyl and aryl groups are, however, well known. The two Si–Cu bonds in **1** are approximately the same length (2.348(3) and 2.334(3) Å) and very similar to the Si–Cu bond length in $[Ph_3SiCu(PMe_3)_3]$ (2.340(2) Å).

The molecule has C_2 symmetry. The bridged Cu(1)–Cu(2a) bond (2.403(2) Å) is by far the shortest of the Cu–Cu bonds in **1** and 0.25 Å shorter than the next longest Cu–Cu bond (Cu(1)–Cu(2) 2.654(2); Cu(1)–Cu(3) 2.736(2); Cu(2)–Cu(2a) 2.952(3) Å). Although slightly shorter Cu–Cu distances are known in complexes where the Cu atoms are forced to come into close contact by chelating ligands

[*] Dr. D. Stalke, Dipl.-Chem. A. Heine
Institut für Anorganische Chemie der Universität
Tammannstrasse 4, D-W-3400 Göttingen (FRG)

[**] This work was supported by the Deutsche Forschungsgemeinschaft and the Fonds der Chemischen Industrie.

(2.348(1) and 2.361(1) Å)[17–19], to our knowledge this distance is the shortest in a Cu_5 complex.[20] Thus the bonding in the almost equilateral triangle $SiCu_2$ can be described in terms of a three-center two-electron bond. The Cu(1)-Cu(2) and Cu(1)-Cu(3) bonds are μ_2-bridged by chlorine atoms. The long Cu(2)···Cu(2a) vector remains unbridged.

In another reaction we treated $[(Me_3Si)_3SiLi(thf)_3]$ with $AlCl_3$ at −78 °C. The reaction mixture was allowed to warm up to room temperature and after the white precipitate that formed had been filtered off the solution was stored at −30 °C. After 2 days at this temperature colorless crystalline blocks began to grow. Single crystals suitable for an X-ray structure analysis were mounted directly on the goniometer head from the mother liquor at about −50 °C. At temperatures slightly above −15 °C these blocks transform into a white insoluble powder. Presumably coordinated THF leaves the lattice and the lithium cation is coordinated to the anion in the form of a contact ion pair.

The reaction product is the aluminate in **2**,[13] where $[Li(thf)_4]$[4] is again the cation (Fig. 2). This molecule may be

$[Li(thf)_4][AlCl_3Si(SiMe_3)_3]$ **2**

interpreted as an intermediate in the reaction to form $[(SiMe_3)_3SiAlCl_2]_2$, which would be of the same structural type as Al_2Cl_6. The structure of **2** proves that the Si–Li bond

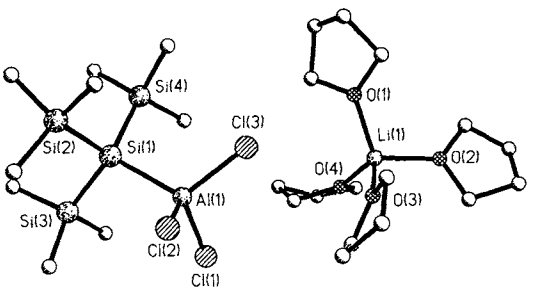

Fig. 2. The structure of **2** in the solid state. Selected bond lengths [Å] und angles [°]: Si(1)-Al(1) 2.446(1), Si-Si 2.341(1).* Al-Cl 2.165(1),* Si-Si-Si 109.96(4),* Cl-Al-Cl 106.34(6)*. Those marked with an asterisk are average values.

in the starting material $[(Me_3Si)_3SiLi(thf)_3]$ is cleaved, and a new Si–Al bond is formed leaving the $AlCl_3$ unit intact, and that LiCl does not precipitate out. Evidently, $AlCl_3$ is a better Lewis acid than the relatively hard lithium atom. The Si(1)-Al(1) bond length (2.446(1) Å) is in good agreement with known values,[21] however, approximately 0.2 Å shorter than the average Si–Li bond length in $[(Me_3Si)_3SiLi(thf)_3]$ (2.644 Å).[22] The average Si-Si-Si angle (109.96°) in **2** indicates than the Si–Al bond is much more covalent than the Si–Li bond. The Si-Si-Si angle in $[(Me_3Si)_3SiLi(thf)_3]$ (102.43(8)°) and in $(Me_3Si)_3SiLi \cdot 1.5$ DME (DME = dimethoxyethane) (104°)[23] indicate that the bond in each case has to be more ionic. The lone pair at the silicon atom $\geqslant Si:^{-}$ $^{+}Li(thf)_3$ fragment reduces the Si-Si-Si angle compared to that in $[(Me_3Si)_3SiAlCl_3]^-$ by more than 7°. The less sterically demanding $-Si-AlCl_3$ covalent bond leads to an Si-Si-Si angle of approximately 110° (**2**). We are currently trying to isolate further intermediates in both reactions.

Experimental Procedure

1: A solution of $[(Me_3Si)_3SiLi(thf)_3]$ (modified preparation ref. [12]) (1.88 g, 4.0 mmol) in pentane (5 mL) was added to $Cu^{I}Cl$ (1 g, 10.1 mmol) in THF at −78 °C over 2 h. A dark purple solution was formed and, after removal of the pentane/THF solvent, cold toluene added, and the solution was cooled to −30 °C. A brown powder of LiCl, $Cu^{II}Cl_2$, and Cu precipitated slowly. After 14 d at −30 °C, cubic, air-sensitive, and extremely thermolabile blocks, identified as **1**, were isolated. Yield ≤ 20%, decomp $T > -30$ °C, color: deep purple. Because of the extreme sensitivity of the compound it was not possible to obtain any spectroscopic data.

2: A solution of $[(Me_3Si)_3SiLi(thf)_3]$ (modified preparation ref. [12]) (2.0 g, 4.3 mmol) in toluene (25 mL) was added to a suspension of $AlCl_3$ (0.5 g, 3.8 mmol) in toluene (20 mL) at −78 °C over 2 h. The solution was stirred for 7 h at −78 °C, then for 10 h at 0 °C, and finally for 7 h at room temperature. The white precipitate, which formed during stirring, was filtered off. A white precipitate was formed from the clear solution at −30 °C, which was redissolved by adding cold THF (3 mL). After 2 days clear, colorless crystals of **2** were obtained at −30 °C. ^1H NMR ([D$_8$]toluene, 25 °C): $\delta = 0.217$ (s, 27H, $Si(SiMe_3)_3$); 1.776, 3.618 (32H, THF); ^{29}Si NMR (THF/[D$_8$]toluene, 25 °C): δ −155.66 ($Si(SiMe_3)_3$), −11.468 ($SiMe_3$).

Received: September 3, 1992 [Z 5554 IE]
German version: *Angew. Chem.* **1993**, *105*, 90

[1] a) H. Gilman, C. L. Smith, *J. Organomet. Chem.* **1967**, *8*, 245–253; b) H. Gilman, C. L. Smith, *ibid.* **1968**, *14*, 91–101.
[2] J. Arnold, T. D. Tilley, A. L. Rheingold, S. J. Geib, *Inorg. Chem.* **1987**, *26*, 2106–2109.
[3] J. Meyer, J. Willnecker, U. Schubert, *Chem. Ber.* **1989**, *122*, 223–230.
[4] H. Piana, H. Wagner, U. Schubert, *Chem. Ber.* **1991**, *124*, 63–67.
[5] A. M. Arif, A. H. Cowley, T. M. Elkins, *J. Organomet. Chem.* **1987**, *325*, C11–C13.
[6] S. P. Mallela, R. A. Geanangel, *Inorg. Chem.* **1990**, *29*, 3525–3528.
[7] A. M. Arif, A. H. Cowley, T. M. Elkins, R. A. Jones, *J. Chem. Soc. Chem. Commun.* **1986**, 1776–1777.
[8] S. P. Mallela, R. A. Geanangel, *Inorg. Chem.* **1991**, *30*, 1480–1482.
[9] H. O. House, *Acc. Chem. Res.* **1976**, *9*, 59–67.
[10] M. M. Olmstead, P. P. Power, *Organometallics* **1990**, *9*, 1720–1722.
[11] C. Eaborn, P. B. Hitchcock, J. D. Smith, A. C. Sullivan, *J. Organomet. Chem.* **1984**, *263*, C23–C25.
[12] G. Gutekunst, A. G. Brook, *J. Organomet. Chem.* **1982**, *225*, 1–3.
[13] Crystal Data of **1**: $C_{34}H_{86}Si_8Cu_5Cl_4O_4Li$, $M_r = 1250.19$, monoclinic, space group $C2$, $a = 26.103(6)$, $b = 9.320(3)$, $c = 14.758(4)$ Å, $\beta = 123.97(2)°$, $V = 2977.6(10)$ Å^3, $Z = 2$, $\varrho_{calcd} = 1.394$ Mg m^{-3}, $F(000) = 1300$, $\lambda = 0.71073$ Å, $T = 153$ K, $\mu(Mo_{K\alpha}) = 2.13$ mm^{-1}, data were collected on a Stoe-Siemens-AED diffractometer. Intensities of a rapidly cooled crystal (dimensions 0.5 × 0.4 × 0.2 mm) in an oil drop were collected by the $2\theta/\omega$ method in the range $8 \leq 2\theta \leq 45°$. Of the 2095 collected reflections, 2083 were independent and corrected for absorption with a semiemperical method, largest difference maximum and minimum: 0.85 and −0.45 eÅ^{-3}. $R_1 = 0.044$ and $wR_2 = 0.113$ (all data). The absolute structure has been determined by refining the Flack parameter to 0.02(3) (H. D. Flack, *Acta Crystallogr. Sect. A* **1983**, *A39*, 876). **2**: $C_{25}H_{59}AlCl_3LiO_4Si_4$, $M_r = 676.35$, triclinic, space group $P\bar{1}$, $a = 10.606(2)$, $b = 13.699(2)$, $c = 13.754(2)$ Å, $\alpha = 87.40(2)$, $\beta = 86.59(2)$, $\gamma = 89.33(2)°$, $V = 1992.7(3)$ Å^3, $Z = 2$, $\varrho_{calcd} = 1.127$ Mg m^{-3}, $F(000) = 728$, $\lambda = 0.71073$ Å, $T = 153$ K, $\mu(Mo_{K\alpha}) = 0.397$ mm^{-1}, data were collected on a Stoe-Siemens-AED. Intensities of a rapidly cooled crystal (dimensions 0.6 × 0.6 × 0.4 mm) in an oil drop were collected by the $2\theta/\omega$ method in the range of $8 \leq 2\theta \leq 50°$. Of a total of 7543 reflections, 7012 were independent and corrected for absorption, largest difference maximum and minimum: 0.34 and −0.20 eÅ^{-3}, respectively. $R_1 = 0.045$ and $wR_2 = 0.109$ (all data). Both structures were solved with direct methods (SHELXS-90) [24] and refined by full-matrix least-squares of F^2 (SHELXL-92) [25]. The hydrogen atom positions were refined with a riding model where the CH_3 groups were free to rotate around their local threefold axis. Further details of the crystal structure investigations are available on request from the Director of the Cambridge Crystallographic Data Centre, University Chemical Laboratory, Lensfield Road, GB-Cambridge CB2 1EW (UK), on quoting the full journal citation.
[14] Cambridge Crystallographic Database, Version **1992**.
[15] A. H. Cowley, T. M. Elkins, R. A. Jones, C. M. Nunn, *Angew. Chem.* **1988**, *100*, 1396–1397; *Angew. Chem. Int. Ed. Engl.* **1988**, *27*, 1349.
[16] J. C. Calabrese, L. F. Dahl, *J. Am. Chem. Soc.* **1971**, 6042–6047.
[17] J. Beck, J. Strähle, *Angew. Chem.* **1985**, *97*, 419–420; *Angew. Chem. Int. Ed. Engl.* **1985**, *24*, 409.
[18] R. Schmid, J. Strähle, *Z. Naturforsch. B* **1988**, *44*, 105–109.
[19] G. van Koten, *J. Organomet. Chem.* **1990**, *400*, 283–301, and references therein.
[20] P. G. Edwards, R. W. Gellert, M. W. Marks, R. Bau, *J. Am. Chem. Soc.* **1982**, *104*, 2072–2073.
[21] M. L. Sierra, V. S. J. de Mel, J. P. Oliver, *Organometallics* **1989**, *8*, 2312–2316.
[22] A. Heine, R. Herbst-Irmer, G. M. Sheldrick, D. Stalke, *Inorg. Chem.*, in press.
[23] G. Becker, H.-M. Hartmann, A. Münch, H. Riffel, *Z. Anorg. Allg. Chem.* **1985**, *530*, 29–42.
[24] G. M. Sheldrick, *Acta Crystallogr. Sect. A* **1990**, *46*, 467–473.
[25] G. M. Sheldrick, *SHELXL-92*, Göttingen, **1992**.

On the Shape of a Diels–Alder Ladder Polymer**

By *Britta L. Schürmann,* Volker Enkelmann,* Matthias Löffler*, and *Arnulf-Dieter Schlüter**

We have developed a new generation of double-stranded (ladder) polymers, which have poly-Diels–Alder addition reactions as a basis for their synthesis.[1] Polymers **1** and **2** were studied extensively as representatives of this group of polymers and found to be extremely soluble in common organic solvents. Not only was their double-strandedness unambiguously proven.[2] but for the first time in the history of ladder polymers, comprehensive information on the molecular weights,[3] the nature of end groups,[3] and configurational and conformational aspects[4] was also obtained. In addition, a model for the shape of polymer **1** was proposed, according to which, the polymer attains the structure of a three-dimensional coil.[4] In this paper, we mostly provide

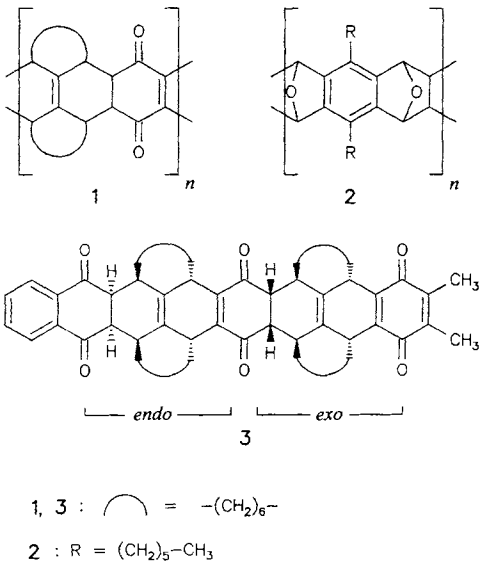

1, 3 : ⌒ = $-(CH_2)_6-$

2 : R = $(CH_2)_5-CH_3$

theoretical evidence that certain ladder polymers in solution may attain the unprecedented shape of a two-dimensional coil, as is illustrated by the computer-generated structure of polymer **2** (Fig. 1).

The formulas of **1** and **2** suggest that both double-stranded polymers have a symmetry plane (σ_{xy}) perpendicular to the plane sketched here, which cuts the bonds that connect the two strands. However, for **1**, model studies clearly show that this is not the case. In constrast to the *endo*-configurated unit (see **3**), the cyclohexene ring of the *exo*-configurated repeat units exists in one of the two possible staggered conformations,[5] which are both nonsymmetrical about σ_{xy}. Figure 2a shows the (published[4]) molecular structure of model compound **3** in the crystal to visualize the consequences for the shape of **1**. Whereas the *endo*-unit has plane symmetry, the *exo*-unit does not. It is this unit that forces the backbone of **1** into the third dimension.

[*] Dr. B. Schürmann, Dr. habil. V. Enkelmann, Prof. Dr. A.-D. Schlüter,[+] Dipl.-Chem. M. Löffler[+] Max-Planck-Institut für Polymerforschung Postfach 3148, D-W-6500 Mainz (FRG)

[+] New Address: Institut für Organische Chemie der Freien Universität, Takustrasse 3, D-W-1000 Berlin 33 (FRG)

[**] This work was supported by the Bundesministerium für Forschung und Technologie and the Fonds der Chemischen Industrie. We are grateful to Prof. G. Wegner, Mainz, for his interest in and support of this work.

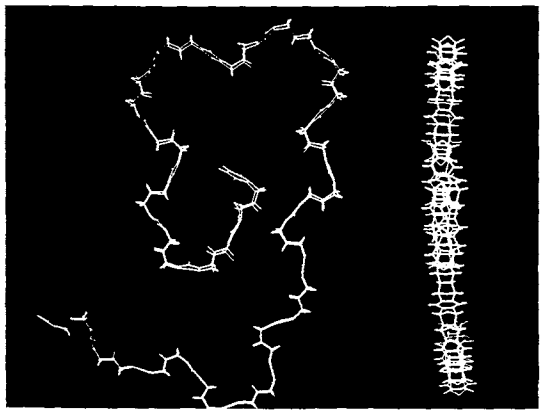

Fig. 1. Top and side view of a computer-generated structure of **2** (alkyl substituents omitted) with a statistical sequence of *syn*- and *anti*-oriented oxygen bridges.

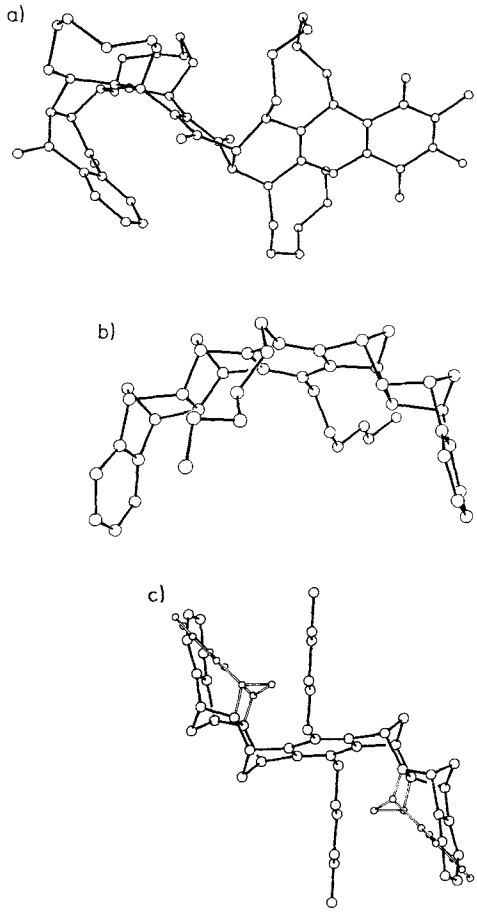

Fig. 2. ORTEP representations of the structures in the crystal of **3** (a), all-*syn*-**6** (b), and all-*anti*-**6** and *syn*/*anti*/*syn*-**6** (mixed crystal) (c).

The structural characteristics of polymer **2** differ distinctly from those of **1**, even though its backbone also consists of linearly annulated, all-carbon, six-membered rings. However, all these rings are now conformationally rigid and have the proper symmetry elements for the polymer to show plane symmetry. Compound **6**, a model for **2**, was selected to demonstrate this point. The three diastereoisomers, all-*anti*-**6**, all-*syn*-**6**, and *syn*/*anti*/*syn*-**6** were synthesized by reacting the bisdienophile **4**[6] with two equivalents of a precursor for isobenzofuran (**5**),[7] single crystals were grown, and the structures in the crystal determined. All-*anti*-**6** and *syn*/*anti*/

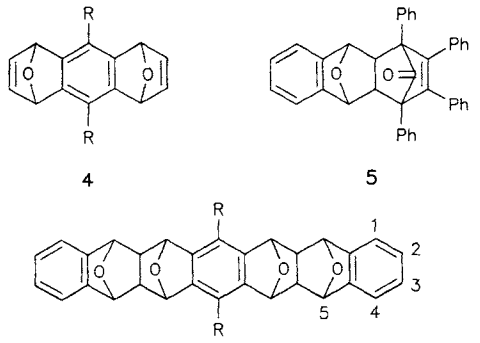

4, 6 : R = $(CH_2)_5$–CH_3

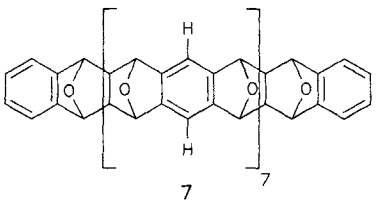

7

syn-**6** are unique cases because they form mixed crystals with statistical disorder.[8] As can be expected, all isomers have a symmetry plane in which the oxygen atoms lie (Fig. 2b, c).[9–11] These structures, however, and the vague description of the fragments of **2** as being rigid are not sufficient to lead to the conclusion that **2** attains the shape of a (snake-like) two-dimensional coil. This would depend upon the degree of anisotropy of the flexibility of **2** in the plane and out of the plane.[12] All-atom molecular dynamics (MD) is an appropriate method to gain information on the fluctuations of the atoms' positions in molecules. It takes into account the chemical structure as well as all the interactions between each two particles of a given ensemble. Hence, we applied this method (AMBER program[13]) to help solve the problem of the shape of polymer **2** in solution. An assessment of the reliability of this method has been published, in which structural predictions based on MD are compared with results obtained from, for example, 2D NMR or X-ray investigations.[14]

Polymer **7**, which consists of seven repeat units carrying no alkyl chains[15] and terminated by benzene rings, was selected as a model for **2**.[16, 17] The MD studies were carried out a) with two different starting conformations of **7** (A and B) to avoid a dependence of the result upon the initial structure and b) in the presence of solvent molecules (benzene), since polymer/solvent effects have considerable influence on the conformation of a polymer chain.[18] The starting structure A of model **7** was constructed by using bond lengths and angles from the X-ray structures of **6** and the AMBER data bank which gives it plane symmetry.[13, 19] Conformation B is an equilibrated structure (after 30 ps) which was created from A by performing a MD calculation in vacuo. During the calculation (without solvent) the initially two-dimensional coil starts to deviate significantly from planarity, which is initiated by higher fluctuations of the termini. This can be seen from the values of the moments of inertia (I_x, I_y, I_z) about the x, y, and z axes which remain similar and constant (over 65 ps) after equilibrium is reached (Fig. 3a).

Both initial structures were placed in a box of constant volume filled with benzene molecules of realistic density at 300 K, and the molecular dynamics were simulated under periodic boundary conditions.[20] The results are as follows: Conformation A keeps its two-dimensional shape over the entire period of simulation (130 ps). This was derived from the dependence of I_x, I_y, and I_z on time. As is required for a nonspherical structure, the values of I_x and I_y are significantly larger than those of I_z (Fig. 3b). Visualization of the molecular dynamics in a movie showed that the structure, on a time average, retains the symmetry plane σ_{xy}. To avoid the local minimum problem, the calculations were repeated at

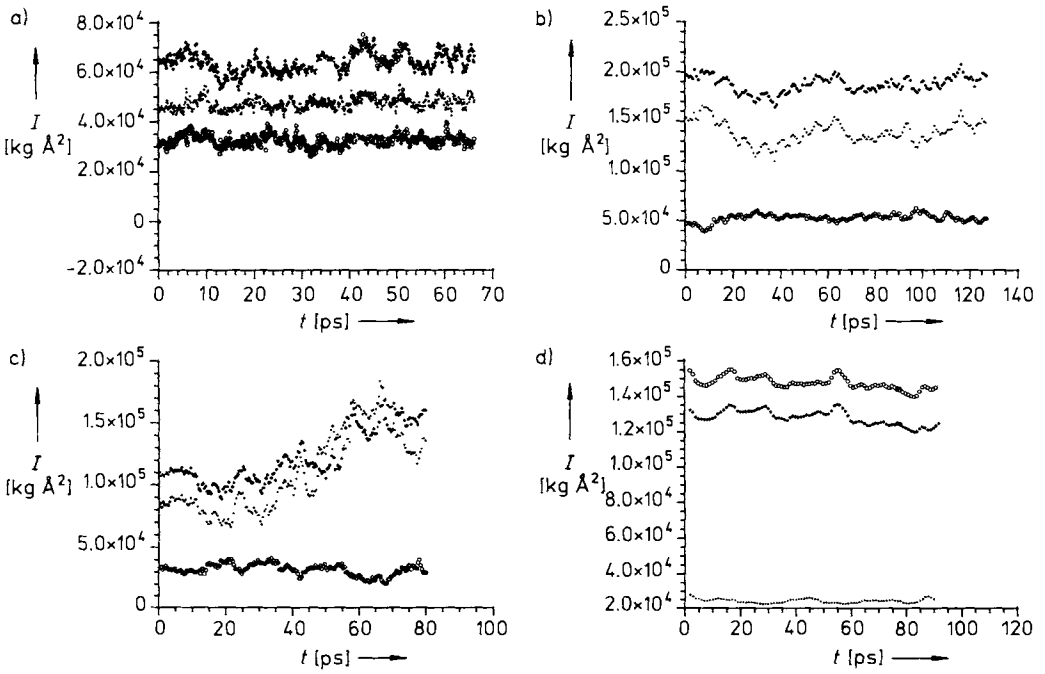

Fig. 3. Dependence of the moments of inertia I_x ◆, I_y (○), and I_z (●) about the x, y and z axes on time (t) of the two different starting conformations A and B (see text) of compound **7**. a) B obtained from A in vacuo, and b) A in benzene (both runs at 300 K after equilibrium is reached). c) B at 700 K during equilibration, and d) B at 300 K after heating to 700 K (d).

400, 500, 600, and 700 K[21] followed by cooling to 300 K, which yielded results in full agreement with those obtained at 300 K.

For starting structure B, the simulation in benzene at 300 K did not lead to any significant change of the gross conformation even at extended simulation time (200 ps). Therefore, the system was heated to 700 K in steps of 100 K. After each run had equilibrated, the system was cooled to 300 K. Finally, in the 700 K case for this conformation, a change in a plane-symmetrical geometry takes place. Figure 3c shows that the moments of inertia about the three axes split into two sets of values (I_x, I_y, and I_z), which are retained upon cooling (Fig. 3d).[22] As in the case of conformation A, the visualization of the molecular motion revealed that conformation B was not spherical anymore but, in fact, two-dimensional and disc-like (on a time average). However, the end-to-end distance was now smaller by a factor of approximately 2 and did not converge within 100 ps to that of the equilibrated conformation A. Undoubtedly, this is due to the large time scale within which the backbone is stretched out.

Regardless of the starting conformation, **7** in benzene solution equilibrates to a two-dimensional conformation, which indicates a unique structural feature of **2** and other ladder polymers of comparable rigidity and symmetry. It is important, however, to realize that this calculation does not account for other effects which might play a role during synthesis of the polymer. It may well be the case that, as the polymer chain grows, larger fragments of the same polymer chain overlap each other irreversibly or that intermolecular effects (for example: formation of entanglements) prevent the polymer from relaxing into a two-dimensional geometry. Small-angle X-ray scattering is an appropriate method with which one can approach this problem experimentally.[23]

Experimental Procedure

A suspension of a mixture of *anti*-**4** and *syn*-**4** [6] (3.0 g, 7.9 mmol) and **5** (8.38 g, 15.8 mmol) in toluene (80 mL) is heated at reflux for 24 h under nitrogen, whereupon the solvent is removed. The crude material obtained is chromatographed through silica gel with petroleum ether (60/40)/ethyl acetate (9/1) as eluent to remove 1,2,3,4-tetraphenylbenzene. A mixture of at least four of the six possible diastereomeric adducts (NMR) is then recovered from the column by using THF as eluent. Yield: 4.37 g (90%). Correct elemental analysis. Fractionating crystallization from chloroform affords pure all-*anti*-**6**, whose solubility is the lowest of all diastereomers obtained, pure all-*syn*-**6**, as well as mixed crystals of all-*anti*-**6** and *syn*/*anti*/*syn*-**6**. ^{1}H NMR (300 MHz, $CDCl_3$): all-*anti*-**6**: δ = 2.38, 2.49 (2m; 4H; α-CH_2), 2.64 (dd, J_1 = 3.2, J_2 = 1.7 Hz; 4H, H-5a, 8a, 14a, 17a), 4.61 (s; 4H, H-6, 8, 15, 17), 5.25 (dd, J_1 = 3.2, J_2 = 1.7 Hz; 4H, H-5, -9, -14, -18); all-*syn*-**6**: δ = 1.87 (s; 4H, H-5a, 8a, 14a, 17a), 2.57 (t, J = 7.6 Hz; 4H, α-CH_2), 5.39 (s; 4H, H-5, 9, 14, 18), 5.40 (s; 4H; H-6, 8, 15, 17); *syn anti syn*-**6**: δ = 1.95 (s; 4H, H-5a, 8a, 14a, 17a), 2.45–2.67 (m; 4H, α-CH_2), 5.44, 5.46 (2s; 8H; H-5, 6, 8, 9, 14, 15, 17, 18).

Received: July 4, 1992 [Z 5446 IE]
German version: *Angew. Chem.* **1993**, *105*, 107

[1] A.-D. Schlüter, *Adv. Mater.* **1991**, *3*, 284; for more recent, related work, see U. Scherf, K. Müllen, *Synthesis* **1992**, 23.

[2] K. Blatter, A.-D. Schlüter, *Macromolecules* **1989**, *22*, 3506; T. Vogel, K. Blatter, A.-D. Schlüter, *Makromol. Chem. Rapid Commun.* **1989**, *10*, 427; A. Godt, A.-D. Schlüter, *Angew. Chem.* **1989**, *101*, 1704; *Angew. Chem. Int. Ed. Engl.* **1989**, *28*, 1680.

[3] A. Godt, A.-D. Schlüter, *Makromol. Chem.* **1992**, *193*, 501.

[4] A. Godt, V. Enkelmann, A.-D. Schlüter, *Chem. Ber.* **1992**, *125*, 433.

[5] E. L. Eliel, *Stereochemistry of Carbon Compounds* McGraw-Hill, New York, **1962**.

[6] K. Blatter, A.-D. Schlüter, *Chem. Ber.* **1989**, *122*, 1351.

[7] In analogy to L. F. Fieser, M. J. Haddadin, *Can. J. Chem.* **1965**, *43*, 1599.

[8] As a consequence, corresponding segments in a polymer chain can replace each other without altering the shape of the polymer.

[9] X-ray structure data of compounds **6**: Enraf–Nonius CAD-4 diffractometer, room temperature, $Cu_{K\alpha}$ radiation, λ = 1.5405 Å, graphite monochromator. The structure was solved by direct methods (MULTAN) and by vector search methods (DIRDIF). Empirical absorption correction, anisotropic temperatur factors for O and C, refinement of the H atoms in the "riding mode" with fixed isotropic temperature factors. All-*anti*-**6** (at 273 K): monoclinic, space group $P2/c$, a = 14.4470(9), b = 6.0272(8), c = 23.9443(15) Å, β = 91.995(8), V = 2083.7 Å^3, Z = 4, ρ_{calcd} = 1.360 g cm^{-3}, 3583 reflections, 2392 observed [$I > 3\sigma(I)$], R = 0.058, R_w = 0.056; all-*syn*-**6** (at 273 K): orthorhombic, space group $Pna2_1$, a = 24.2156(10), b = 10.673(2), c = 29.358(1), V = 7588 Å^3, Z = 8, ρ_{calcd} = 1.225 g cm^{-3}, 6369 reflections, 3092 observed [$I > 3\sigma(I)$], R = 0.083, R_w = 0.085; *syn*-*anti*-*syn*-**6** from a mixed crystal (at 195 K): monoclinic, space group $P2_1/n$, a = 13.671(1), b = 22.387(2), c = 5.6060(5), β = 100.308(4), V = 1688 Å^3, Z = 4, ρ_{calcd} = 1.210 g cm^{-3}, 2177 reflections, 1158 observed [$I > 3\sigma(I)$], R = 0.068, R_w = 0.070.

[10] Further details of the crystal structure investigations may be obtained from the Fachinformationszentrum Karlsruhe, Gesellschaft für wissenschaftlich-technische Information mbH, W-7514 Eggenstein-Leopoldshafen 2 on quoting the depository number CSD-56902, the names of the authors, and the journal citation.

[11] All other stereoisomers should show plane symmetry.

[12] For this specific type of double-stranded polymers, a new theoretical definition of persistence length is required.

[13] S. J. Weiner, P. A. Kollman, D. A. Case, U. C. Singh, C. Ghio, G. Alagona, S. Profeta, P. Weiner, *J. Am. Chem. Soc.* **1984**, *106*, 765.

[14] B. L. Schürmann, M. Depner, *Mol. Phys.* **1991**, *74*, 715; B. L. Schürmann, B. Jung, *Liquid Cryst. Mol. Cryst.* **1990**, *185*, 141. For reviews, see W. F. van Gunsteren, H. J. C. Berendsen, *Angew. Chem.* **1990**, *102*, 1020; *Angew. Chem. Int. Ed. Engl.* **1990**, *29*, 992; H. Frühbeiß, R. Klein, H. Wallmeier, *ibid.* **1987**, *99*, 413 and **1987**, *26*, 403.

[15] The alkyl chains containing six C atoms are expected to have only minor influence on the conformation of the backbone.

[16] The sequence of the relative configurations of neighboring oxygen bridges in **7** is *anti*/*anti*/*syn*/*syn*/*syn*/*syn*/*anti*/*syn*/*anti*/*anti*/*anti*/*syn*/*syn*/*anti*/*anti*.

[17] The structure shown in Figure 1, though having all features required for the formation of a two-dimensional coil, could not be used for simulations *in solution* because of the large number of atoms.

[18] For example see M. Depner, B. L. Schürmann, *J. Comput. Chem.* **1992**, *13*, 1210.

[19] The partial charges used to describe Coulombic interactions were obtained from MNDO calculations and scaled by the empirical factor of 1.3, a factor generally used to obtain consistency with the AMBER force field. [13]

[20] An appropriate distance (1.2 Å) between the solvent and solute molecules was chosen to ensure the correct physical density of the solvent. For a more detailed description, see ref. [18].

[21] The heating was performed to explore the conformational space in the sense that kinetic energy pumped into the ensemble is used to overcome the energy barriers separating the different local minima. Bond breaking cannot occur because of the particular mathematical expression used for the potential.

[22] The I_x, I_y, and I_z values of the two-dimensional coils obtained from starting conformations A and B, respectively (Fig. 3b and d), vary due to differences in the shape of these coils as reflected by the different end-to-end distances.

[23] G. Urban, M. Ballauff, Karlsruhe, private communication.

Book Reviews are written by invitation from the editor. Suggestions for books to be reviewed and for book reviewers are welcome. Publishers should send brochures or (better) books to the following address: Redaktion Angewandte Chemie, Postfach 101161, D-W-6940 Weinheim, Federal Republic of Germany. The editor reserves the right of selecting which books will be reviewed. Uninvited books not chosen for review will not be returned.

Inorganic Chemical Nomenclature. By *B. P. Block, W. H. Powell,* and *W. C. Fernelius.* American Chemical Society, Washington, DC, 1990. 224 pp., hardcover $ 59.95.—ISBN 0-8412-1697-5; paperback $ 39.95.—ISBN 0-8412-1689-3

The task of chemical nomenclature is to provide a systematic method for naming chemical substances. It is in the nature of things that the rules developed for this purpose cannot remain static, but must continually grow to accommodate new classes of substances and increasingly complex structures. How and to what extent this is done are matters that must be kept continually under review. These questions are the particular concern of the IUPAC nomenclature panels, whose members published in 1990 a considerably enlarged and thoroughly revised new edition of the 'Red Book' that has, since 1970, contained the IUPAC recommendations for inorganic chemical nomenclature (see the book review by G. B. Kauffman: *Angew. Chem.* **1991**, *103*, 738; *Angew. Chem. Int. Ed. Engl.* **1991**, *30*, 721). Almost simultaneously with the latter publication the book reviewed here appeared. It is the result of an initiative by the nomenclature committees of the American Chemical Society (ACS), and is intended to be complementary to the book "Nomenclature of Organic Compounds, Principles and Practice", published by the ACS in 1974.

A question that must arise is whether a useful purpose is served by now having two books available on the same topic. There can be no doubt that as a compilation of rules this book must be measured against the 1990 version of the IUPAC recommendations. If in addition it succeeds, as the introduction claims, in equipping the reader with the knowledge required to undertake searches in the older literature, and in conveying a fundamental understanding of the principles of modern inorganic nomenclature, then it should certainly be regarded as a valuable addition to the Red Book.

The problem of dealing with the older literature and with compound names that are no longer in common use has been solved effectively, by including notes scattered throughout the book explaining the older naming conventions, and citing the earliest use of the names that have replaced them. Also the coverage of the individual subject areas could hardly be bettered as regards being complete and up-to-date. The weaknesses of this work lie rather in the method of treatment: the authors devote a disproportionate amount of space to their specialist fields at the expense of topics of more general interest. For example, one finds just four pages on organometallic compounds (Chapter 12), compared with 16 pages on boron hydrides (Chapter 11), 10 on quasi-single-strand polymers (Chapter 7), and 14 on isotopically labeled compounds (Chapter 15).

Unfortunately the care that has been devoted to the latter chapters is lacking in some other parts of the book. After an introductory first chapter, which discusses in a very general way the relationship between language and nomenclature, Chapter 2 launches into the main subject. Here it would undoubtedly have been more sensible to place the explanations of important terms used in inorganic chemistry (oxidation number, binary, ligand, etc.) before the section on "Nomenclature—Conventions" rather than after it. Unfortunately also the description of different systems of nomenclature has been limited to merely listing them, which fails to convey the advantages of particular methods, such as general applicability and simplicity. It should have been pointed out at this stage that the additive nomenclature for inorganic compounds is the most universally applicable. The discussion of the "Grammar of Nomenclature", in which the components of chemical names, such as multiplicative prefixes and locants, is very comprehensive, except for free radical points. The comparatively rare use of the symbol Δ in organic chemistry is explained in detail, whereas its much more important use in inorganic chemistry as a structural descriptor for polyhedral compounds (Ch. 11) is not mentioned. Here, as also in other parts of the book, there is a lack of coherent structure within the individual chapters. After reading Chapter 3 on "Homoatomic Species", one feels compelled to make a case for trivial names. Where these are simple and concise they are definitely preferable to overelaborate systematic names. Otherwise one might in future have to worry about a *catena*-trioxygen hole in the stratosphere! Two lines further on from this example one ought, for consistency, to refer to *tetrahedro*-tetraphosphorus as the systematic name for white phosphorus.

Here in passing is another curiosity. If at any time one needs to give names to 'elemental associates', one should refer to Section 3.2.7. Here one learns, for example, that a particle made up of a muon and an electron is nearly always called 'muonium'. In Chapter 4, which deals with the nomenclature of heteroatomic species, the term 'radical' is applied exclusively to species with unpaired electrons, which is certainly a sensible usage. However, systematizations such as that in Section 4.3.3 ("Binary Oxo Groups") are more likely to confuse; it would have been sufficient to list them. Names such as '... ferrocyanide' (Section 4.3.3) should now be a thing of the past, and radicals should be clearly identified as such (Section 4.5.4).

Chapter 5 has the title "Additive Nomenclature". Here it would certainly have been useful for quick reference to include the nomenclature of coordination compounds. In Section 5.3.5.2 where the κ convention is introduced, it would have been better in the reader's interest to completely avoid the abbreviated way of writing the formulas; in this and certain other cases (Section 5.3.5.3 and parts of Chapter 6, "Multinuclear Complexes") structural formulas are clearly preferable. This would also avoid the need to label the coordinating centers with an asterisk, a symbol that is best reserved for chiral centers and excited states. Also it would have been better to stick to examples in which the use of the κ convention is essential—it is unnecessary in $K_4[Fe(CN)_6]$ and in the symmetrically bridged carbonyl compound $[(CO)_3Co(\mu\text{-}CO)_2Co(CO)_3]$. In Section 5.3.6.3, where the structural prefixes *fac* and *mer* are introduced, it should have

been mentioned that these are no longer to be used as parts of names, but only as general descriptions of complexes of this type; for more complex systems one should use the procedures described in Chapter 16.

Oxo acids, which are treated in Chapter 8, "Acids and Bases", belong to the classical territory of inorganic chemistry, so it is not surprising that this area has a liberal scattering of trivial and non-systematic names. If one adopts from the start such rather unusual structure-based formulas as $ClO_3(OH)$ or $SO_2(OH)_2$ (despite the fact that clear IUPAC recommendations exist for these also), one should then use these forms consistently, and avoid later writing, for example, H_3PO_2 or H_2MnO_4. Here again a too rigorous systematization does not make for easy comprehension; for example, the prefixes ortho and meta were used to distinguish acids that differ in their water content, a terminology that has persisted to the present day in names such as metaboric acid and (less commonly) orthophosphoric acid. But when one finds 'orthosulfurous acid', $S(OH)_4$, alongside 'metasulfurous acid', with an explanation in a footnote that 'meta' can usually be omitted, this is too much of a good thing. Also it is noticeable that whereas the 1957 and 1970 IUPAC inorganic rules and the 1979 IUPAC organic rules are cited frequently, there are only a few references to the 1990 rules. This is especially irksome in cases where discrepancies arise, as in the heteropolyanion $[O_3SOCrO_3]^{2\ominus}$, where the latest IUPAC recommendations now specify that the constituents should no longer be given in alphabetical order, but with the ligand first followed by the transition metal; this results in different names.

In Chapter 9, which is concerned with the application of the substitution nomenclature system for inorganic compounds, especially molecular hydrides, it would have been better to use the names consistently for the parent compounds that are listed in Table AVIII. This applies especially to Section 9.4, dealing with the naming of ions, where the names derived from the parent compounds have important advantages. Of the four names given for the $NH_2^{\ominus}$ ion, the systematic name 'azanide' is the most unambiguous, while the trivial name 'amide' and the radiofunctional name 'azanyl anion' are also acceptable. On the other hand a name such as 'dihydronitride' should be avoided. 'Hydro' is only permissible for complex borates, and it would have been better to omit the rules that are given for constructing such names. Even if one were to describe the ion by a name of this kind, the correct form would be 'dihydrogen nitride' (in analogy to dihydrogen sulfide). The use of 'hydro' becomes very confusing when $H_2NNH^{\ominus}$ is called 'trihydrodinitride'.

Chapter 10 on "Chains and Rings" gives a brief account of methods such as the 'a' nomenclature and the Hantzsch–Widmann nomenclature that are already familiar from organic chemistry, and of names based on repeated identical subunits. Here it would have been useful to also refer briefly to alternative methods such as the recent (1989) IUPAC proposals for inorganic systems, in which W. H. Powell was himself involved. The short Chapter 13 on "Addition Compounds" is followed by one on "Nonstoichiometric Species"; this chapter could usefully have been extended to include polyoxoanions and zeolites. The latter are mentioned in Chapter 13, but only briefly. Topics such as the Niggli notation or the 'i/a' notation (Schäfer, von Schnering) might also have been covered briefly.

Lastly, the final Chapter 16 is in a style that would have been preferable for the entire book. A short historical introduction to the topic is followed by a selection of examples with plenty of illustrations and an informative commentary.

Thus, the overall impression left by the book is rather mixed. Specialists will probably pick up answers to specific problems here and there, but the book only meets the needs of beginners to a limited extent. It forms an acceptable complement to the Red Book, which is, however, due to be followed by a further volume dealing with specialist topics. One is left wondering whether, in the interests of more effective communication between chemists, it might not have been better to combine the efforts to produce a single authoritative book of rules on nomenclature.

Gerhard Karger
Angewandte Chemie
Weinheim (FRG)

The Historical Development of Chemical Concepts. By *R. Mierzecki*. Kluwer Academic Publishers, Dordrecht, 1991. XI, 281 pp., hardcover HFl 240.00.—ISBN 0-7923-0915-4.

This book is a translation from the Polish original published in 1985. It gives silent testimony to the difficulties of scholarship in Eastern Europe. For instance, the index fails to give J. Desmond Bernal's year of death (1971), presumably through lack of documentation. The book does not rise to its ambition, it is a textbook on the history of chemistry, not a scholarly monograph. The viewpoint is that of Whig historiography, truth arising gradually from misconceptions. It has the merit of stressing the contributions of Eastern scientists, sometimes neglected in standard treatments. An example is the Russian pioneer Mikhail Lomonossov. Conversely, the coverage of Western chemists is inadequate. One may ask how any serious historical study of the history of chemistry can fail to mention the likes of Max Born, Lazare Carnot, Georges Darzens, Victor Grignard, Fritz Haber, René-Just Haüy, Roald Hoffmann, Hans Meerwein, R. S. Mulliken, Joseph Needham, Robert B. Woodward...

Besides the absence of such great names, treatment of the concepts is skeletal. It has not been fleshed out with the excitement of the actual history. Take catalysis as an example. It is given a little over a page, focussing only on Wilhelm Ostwald, the Arrhenius activation energy, autocatalytic reactions, and the notion of chain reactions (Nernst–Hinshelwood–Semenov). What a pity, when the actual discovery makes such wonderful history. I cannot resist, as a positive contribution in this review, recapitulating it for the reader. Kirchhoff decomposed starch with sulfuric acid into dextrin and saccharose in 1811. Thénard decomposed hydrogen peroxide in the presence of manganese dioxide or platinum in 1818. Thénard had earlier (1813) reported decomposition of ammonia over heated metals. Then Humphrey Davy found (1817) that preheated platinum wire would continue to glow in mixtures of flammable gases. His cousin Edmund Davy, who had been his assistant at the Royal Institution, carried on this line of work. Then came a crucial set of observations. Johann Wolfgang Döbereiner, who had been interested for years in platinum chemistry, repeated the 1820 experiments of Edmund Davy, ascertained that Davy's powder was platinum suboxide, and showed that it was unchanged by the process it took part in. On July 27, 1823, Döbereiner prepared finely divided platinum metal on filter paper and exposed it to hydrogen gas. He witnessed such a strong reaction that it could extract in a few minutes all the oxygen from its mixture with 99% nitrogen. Two days later, Döbereiner wrote to his friend Goethe, then a Privy Councillor and Minister of State to Duke Carl-August in Weimar,

bursting with excitement about the new phenomenon. Goethe was not a total stranger to catalysis—as the phenomenon would be termed by Berzelius in 1835; in his chemical novel *Wahlverwandtschaften* (Elective Affinities) in 1809, the arrival on the scene of Mittler (the "go-between") triggers all sorts of catastrophes!

Pierre Laszlo
Laboratoire de Chimie
École Polytechnique
Palaiseau (France)

Basic Principles of Membrane Technology. By *M. Mulder*. Kluwer Academic Publishers, Dordrecht, 1991. XII, 363 pp., hardcover HFl 200.00.—ISBN 0-7923-0978-2

Membrane separation methods are rapidly gaining in importance in many areas of chemical and biochemical process technology. Regrettably, there has up to now been no textbook to make it easier for advanced students of chemistry, process technology, or related disciplines to become involved in this field. This book claims to fill that gap, according to the author's preface.

Unfortunately, however, large parts of the book fail to justify that claim. This failure is mainly due to the book's many didactic shortcomings, beginning with the visual presentation. The small line spacing does not make for easy readability, and the absence of spaces beneath the headings accentuates the impression of a tightly cramped text. Moreover, this is not always accompanied by a high density of information, as the author's style is long-winded and inclined towards repetition. The introductory chapter is frankly confusing; for example, terms such as "ultrafiltration", "dialysis", and "pervaporation" are first encountered in a table in which separation techniques are related to molecular properties. The newcomer to membrane technology who starts to read the book from the beginning will learn very little from this table. Often the explanations of symbols used in equations, in terms of the common descriptions of the quantities represented, come too late after their first appearance (e.g., p. 150: coupling coefficient). Basic chemical and physical concepts are sometimes repeated, while on the other hand one often comes across equations that appear from nowhere, or whose derivation is not properly explained. The list of inadequacies of presentation could be continued.

The many omissions are also a source of annoyance; the following are a few examples. Permeation by vapors is only mentioned in passing. In the discussion of the individual methods, no indication is given as to which of these are already established as the state of the art and which are still at the development stage. The amount of space devoted to discussions of individual membrane techniques in Mulders' book gives no clue as to their relative importance; for example, seven pages are devoted to membrane distillation, which has long been of little importance, whereas for the widely used method of dialysis one finds only two-and-a-half pages. In most cases the author does not discuss the capabilities and limitations of the various theories for describing material transport through membranes; for example, it would be useful to have comparisons between theory and experiment in the form of graphs or tables.

Lastly, this reviewer noticed a few inaccuracies. The first example occurs in the introduction, where density, vapor pressure, and freezing point are incorrectly referred to as "molecular properties". On page 224 one finds the sentence: "The dimensions for permeability coefficients indicate that they depend on the membrane thickness, the membrane area, and the driving force." In fact, exactly the opposite is true. On page 236, the unsuitability of polydimethylsiloxane membranes for removing water from trichloroethylene is due not to the organophilic character of these membranes, but to the fact that they undergo severe swelling in solutions containing trichloroethylene as the main component. On pages 334 ff., diafiltration is compared to a process in a continuous stirred reactor. This comparison is incorrect, as the depletion of one component through diafiltration is analogous to the conversion of a component in a discontinuous stirred reactor, as the equations (VIII-28) to (VIII-34) make clear. Regrettably, this list of inaccuracies too could be further extended.

Nevertheless, the positive aspects of the book must not be overlooked. The manufacture of membranes is treated in great detail, including the thermodynamics of the process. The treatment of ultrafiltration (UF) includes a critical discussion of the "cut-off" value. Some very useful X-ray microanalysis results on UF membranes are included. The discussions of facilitated-transport processes and concentration polarization are highly instructive. In the chapter on "Applications", the author meets the needs of the reader who wants quick information by providing brief summaries in note form at the ends of the sections. Other good features are the section on calculating the required membrane areas for gas permeation plants, and the numerical examples on plant layouts at the end of the book.

To summarize, it must be concluded that, despite a few bright points, the various errors, inaccuracies, omissions, and most of all the shortcomings in presentation, prevent the book from fulfilling the claim mentioned at the beginning. A good, comprehensive textbook on membranes is still awaited.

Stefan Bitterlich
ZAV/Verfahrenschemie Trennverfahren
BASF, Ludwigshafen (FRG)

Atoms in Molecules. A Quantum Theory. (International Series Monographs on Chemistry, Vol. 22). By *R. F. W. Bader*. Clarendon Press, Oxford, 1990. XVIII, 438 pp., hardcover £ 50.00.—ISBN 0-19-855168-1

In a series of papers Richard Bader has developed a view on molecules, often referred to as "Bader analysis", which is based on a mathematical description of the electron density as a function of the spatial coordinates, and which allows one to get relevant information on bonding within a molecule. One can thus define a "molecular structure" that is quite distinct from the molecular geometry. One can further construct boundary surfaces that divide a molecule into its constituent atoms in such a way that the same atom looks similar in different but related molecules. Changes in the electron density due to changes in the geometry, e.g. in chemical reactions, can be described by means of catastrophe theory. More recently Bader's interest has shifted to the field generated by applying the Laplacean $\nabla^2 = \frac{\partial^2}{\partial x^2} + \frac{\partial^2}{\partial y^2} + \frac{\partial^2}{\partial z^2}$ to the electron density. This field, referred to as the "Laplacean of the density", contains information about, for example, the localization of electron pairs.

The fact that this very useful method of analysis has currently found only little acceptance in main-stream quantum chemistry, and is usually regarded as some kind of curiosity, is partly due, paradoxically, to Bader's claim that his approach is unique and universal. In this very spirit one reads

in the introduction that nowhere in this book must the reader accept arbitrary assumptions or the author's personal view; nevertheless, this book is very personal. But it does present a both valid and unconventional introduction to theoretical chemistry, based on the Bader analysis of electron density.

One may argue that it is unsatisfactory to insist on analyzing the electron density without first worrying about its physical origin, in other words, without first considering the solution of the Schrödinger equation. In fact, the presentation given here is essentially based on a classical picture (the electron density as a classical variable). The Schrödinger equation is mentioned for the first time on page 130. The subtitle "A Quantum Theory" is nevertheless not unjustified, if one considers some of the discussions in Chapters 5, 6, and 8.

For someone working in the field of theoretical chemistry, Bader's book is stimulating, though sometimes hard to read. It is, again paradoxically, the claim that it should be understandable even for the uninitiated reader which makes the access to this book difficult. In fact in addition to a presentation of the author's own work, one finds a great deal of well-known material, which is often so disguised that one does not recognize it immediately. Perhaps a naive reader who reads this book as it is intended--as an introduction to theoretical chemistry--will not mind this.

Werner Kutzelnigg
Lehrstuhl für Theoretische Chemie
der Ruhr-Universität Bochum (FRG)

Manganese Redox Enzymes. Edited by *V. L. Pecoraro*. VCH Publishers, New York/VCH Verlagsgesellschaft, Weinheim, 1992. X, 290 pp., hardcover $ 110.00/DM 186.00--ISBN 0-89573-729-9/3-527-27934-2

This volume presents a detailed overview of the current state of knowledge of manganese containing metalloenzymes that participate in oxidation/reduction processes, most of which evolve dioxygen in their reactions. Heavy emphasis is given to the oxygen evolving complex (OEC) from photosystem II which performs the light driven four-electron oxidation of water to dioxygen, the reverse of the more commonly studied reaction of dioxygen reduction. The problem is presented primarily from a bioinorganic perspective, with emphasis on biophysical measurements which depend on metal centered physical properties and on manganese coordination chemistry.

Based on the contents of this book, the field of manganese redox biochemistry has made significant progress and is poised to make solid advances in understanding this central and highly complex chemistry. The current level of understanding is significantly behind that of iron sulfur, iron porphyrin, copper metalloprotein, and photosynthetic reaction center chemistry in that there is relatively little structural information on the proteins and there are no clearly correct low molecular weight model compounds. However, the amount of physical information on the proteins and low molecular weight compounds and the general knowledge of the coordination chemistry of polynuclear Mn compounds with oxidation states above II is increasing rapidly. The readers of this book will get a good feeling for the level of knowledge and the excitement of the field, as well as the controversies and uncertainties.

Technically, the book is well produced in a consistent typeface. There are few typographical errors, and figures are generally clear except for several of the crystal structure (ORTEP) representations which are poorly labeled and reproduced.

There are 12 chapters in the book. The first is a general review (E. L. Larson and V. L. Pecoraro) of Mn coordination chemistry and magnetic properties of Mn-containing molecules, as well as a summary of the properties of Mn-containing biomolecules and the current candidates for low molecular weight model systems. Chapter 2 (J. E. Penner-Hahn) concerns Mn catalases and presents kinetic as well as structural and magnetic data. Chapter 3 (W. D. Frasch) presents kinetic data on OEC reactions with alternate substrates and inhibitors (H_2O_2, alcohols, NH_2OH, CN^-, Ca^{2+}) and is concerned with photosystem 2 preparations which contain more components than those discussed by other authors. Chapter 4 (C. F. Yocum) discusses the requirement for Ca^{2+} and Cl^- by the OEC. Chapter 5 (J. P. Dekker) concerns interpretation of an optical signal in the 250–350 nm range which varies with oxidation state change in the OEC. Chapter 6 (T. Vänngård, Ö. Hansson, and A. Håddy) is particularly focussed on the complex problem of the EPR signals generated by OEC preparations. Chapter 7 (G. W. Brudvig and W. F. Beck) reviews, particularly up to late 1989, the available information on the interactions of "ligands" (Cl^-, amines, ammonia, NH_2OH, hydrazine, H_2O_2) with the OEC. Chapter 8 (K. Sauer, V. K. Yachandra, R. D. Britt, and M. P. Klein) provides a discussion of the particularly important EXAFS results that many of the other authors quote in order to focus the speculation regarding the structure of the Mn center(s). Further EPR results are also extensively discussed. The use of solvent NMR relaxation as a probe is presented in Chapter 9 (R. R. Sharp). Chapter 10 (V. L. Pecoraro) presents a detailed overview of known low molecular weight Mn complexes and discusses the limitations on Mn–Mn distances provided by various bridging atom arrangements. Chapter 11 (M. K. Stern and J. T. Groves) discusses a separate issue in small molecule Mn chemistry, oxygen transfer by oxo-Mn porphyrins. The last chapter (W. H. Armstrong) presents more results and the motivation behind the construction of some polynuclear model compounds.

Scot Wherland
Washington State University
Pullman, WA (USA)

Reflections on Symmetry in Chemistry ... and Elsewhere. By *E. Heilbronner* and *J. D. Dunitz*. Verlag Helvetica Chimica Acta and VCH, Basel and Weinheim, 1993, 154 pp., hardcover DM 58.00—ISBN 1-56081-254-0

The book seems to have come out at the wrong time, just *after* Christmas! But there are Christmases to come and this marvelous, handsomely produced volume will find a place under many (slightly unsymmetrical) trees, a token of affection from the chemist's significant other (or vice versa). Like other gifts under those trees, it is almost certain to be wrapped in multicolored paper decorated with some repeating pattern. I remember well as a child looking for the repeat in the paper. The revealable mysteries of these patterns are the melody of this book. Each motif in the Christmas wrap is unique (though designers do tend to copy each other), but if it is to be repeated regularly ("translated") throughout the plane, the pattern, in its symmetries, is constrained by the geometry of our space. There is an infinite variety of designs for the basic unit, but only 17 ways to propagate them in the plane.

"Reflections on Symmetry" is the best popular exposition ever written on symmetry and its role in chemistry. What makes it so good? First, the mastery of the authors, two chemists who have thought more deeply about symmetry and structure (geometrical and electronic) than most of us. Their expertise is a gift to us. Then, the authors are both master tellers of stories, chemical raconteurs. They will not pass up a tale of folly, you can be sure. One wonderful and instructive story they relate is of some crystallographers who took too seriously (or were too lazy to build a model) a distorted journal drawing of a cyclohexane ring. Or the incensed reaction of Henry Edward Armstrong to W. L. Bragg's "failure" to find NaCl molecules in the structure of solid salt: "Chemistry is neither chess nor geometry, whatever X-ray physics may be ...". Third, Dunitz and Heilbronner are master teachers. They know how to rivet our attention with a cigar game (most appropriate to one of the authors, who once gave me a twisty Havana I couldn't find in Havana) that teaches us the importance of perceiving inversion symmetry. Or a striking way of solving a chessboard tiling problem as a lead-in to orbital symmetry control, that phenomenon illustrated with patented blue and yellow orbitals. Only rarely, once in a blue moon (or in a yellow, purple and brown tiling of scalene and equilateral triangles), do the authors misjudge the abilities of lesser mortals to juggle shapes.

The story, that of the role of symmetry in chemistry, is told by Dunitz and Heilbronner with immense wit, best characterized as Scottish/Bavarian. The great and utterly untranslatable German humorist, Karl Valentin, would have been proud of his disciples. So the way an enzyme deals differently with two seemingly symmetrical faces of a molecule is made crystal clear by a photo of a tea cup worn asymmetrically after many years of use by one of the authors. And a hand holding a handed molecule in an illustration sports a bloodied bandage, perhaps the result of a right-hander coping with a left-handed scissors.

The authors, in love with structure, following the pictorial nature of chemistry, of course use a multitude of drawings and photographs. Ruth Pfalzberger deserves great credit for these. The drawings are effortlessly integrated into the text. And it is striking the way they too partake of the wit and pedagogic sensitivity of Dunitz and Heilbronner. Thank God, there are not too many Escher reproductions.

What would I fault? Nothing in the book itself, only an attitude, one I can understand, that gives more value to simplicity and symmetry than it deserves. Symmetry is beautiful (in a simple way), symmetry elicits a sense of peace, repose, and stability. But it's really asymmetry that's interesting. In asymmetry is variety and tension. And richness. Especially in chemistry should we value diversity and difference—what's interesting about steroids is not the underlying molecular skeleton, but the variety of function and biological activity that comes from asymmetrical substitution. Perhaps I'm not entirely fair. Asymmetry without an inkling of order is chaos. Whatever beauty is, the tense edge of symmetry and asymmetry contributes to it. Heilbronner and Dunitz sing the praises of symmetry, but in a closing sentence to a chapter they say "... it could appear that the Gods, unlike humans, have a long-term preference for low symmetry".

It is rare that a book that teaches fundamentals of a science carries the clear stylistic mark of its authors. On every page this gem of exposition does: I read it, and I see the white-haired gentleman who asks hard questions about structures while walking up a Swiss mountain trail; I hear the jovial raconteur of orbital follies handing me a cigar and a glass of wine. I see and hear, and you can read, both of them telling, with deep affection, the wonderful story of symmetry in chemistry.

Roald Hoffmann
Department of Chemistry
Cornell University
Ithaca, NY (USA)

Registered names, trademarks, etc. used in this journal, even when not marked as such, are not to be considered unprotected by law.

© VCH Verlagsgesellschaft mbH, D-W-6940 Weinheim, 1992. – Printed in the Federal Republic of Germany by Konrad Triltsch Druck- und Verlagsanstalt Würzburg.

All rights reserved (including those of translation into foreign languages). No part of this issue may be reproduced in any form — by photoprint, microfilm, or any other means — nor transmitted or translated into a machine language without written permission from the publishers. Only single copies of contributions, or parts thereof, may be made for personal use. This journal was carefully produced in all its parts. Nevertheless, authors, editors, and publisher do not warrant the information contained therein to be free of errors. Readers are advised to keep in mind that statements, data, illustrations, procedural details, or other items may inadvertently be inaccurate.

Valid for users in the USA: The appearance of the code at the bottom of the first page of an article (serial) indicates the copyright owner's consent that copies of the article may be made for personal or internal use, or for the personal or internal use of specific clients. This consent is given on the condition, however, that the copier pay stated per-copy fee through the Copyright Clearance Center, Inc. (CCC), for copying beyond that permitted by Sections 107 or 108 of the U.S. Copyright Law. This consent does not extend to other kinds of copying, such as copying, for general distribution, for advertising or promotional purposes, for creating new collective works, or for resale. For copying from back volumes of this journal see 'Permissions to Photo-Copy: Publisher's Fee List' of the CCC.

Editorial office: Postfach 10 11 61, D-W-6490 Weinheim, Federal Republic of Germany, Telephone (06201) 606 315, Telex 465 516 vchwh d, Telefax (06201) 606 328, E-Mail Z16@ DHDURZ2 in Earn Bitnet.

Editor: *Peter Gölitz*

Associate editors: *N. A. Compton, R. H. Schmidt-Radde, K. J. Schneider.* **Editorial assistant:** *E. Schweikart*

Publishers: VCH Verlagsgesellschaft mbH. (Managing Directors: *Hans Dirk Köhler, Dr. Karlheinz Köpfer*), Pappelallee 3, D-W-6940 Weinheim, Federal Republic of Germany.

Advertising office (Advertising Manager: *N. Schippel*): Postfach 10 11 61, D-W-6940 Weinheim, Federal Republic of Germany, Telephone (0 62 01) 606 312, Telefax (0 62 01) 606 328.

ANGEWANDTE CHEMIE
International Edition in English
Volume 32 · Number 2
February 1993
Pages 131–312

Sequential Transformations in Organic Chemistry: A Synthetic Strategy with a Future

New Synthetic Methods (88)

By Lutz F. Tietze* and Uwe Beifuss

Dedicated to Professor Burchard Franck

Organic-chemical synthesis has always fascinated chemists and will not lose its importance in the future. It is a truism that all chemists—and others too—are dependent on the synthesis of those compounds with which they want to work. As a result, organic-chemical synthesis today is more than ever before the cutting edge of organic chemistry, biology, biochemistry, medicine, physics, and material science. Synthesis is also the basis of the chemical industry. For the passionate synthetic chemist, however, synthesis is much more than just a method for obtaining compounds; it is the expression of his creativity, intelligence, ability, and also his perseverance.

Introduction[**]

In the early days of organic synthesis only simple molecules were prepared. In the meantime, the complexity of target molecules has increased considerably. The current pinnacle has been reached with the synthesis of palytoxin with 64 stereogenic centers,[1] of which, in principle, over 10^{19} stereoisomeric forms can exist. For this reason it has been necessary to develop chemical transformations with increasingly higher selectivity. Thus, in the past few years a wealth of chemo-, regio-, diastereo-, and enantioselective reactions has been discovered and developed, the selectivity of which frequently approaches that of enzymatic processes. Nevertheless, if we compare our synthetic performance to date with that of Nature, then we must recognize that Nature is not just highly selective, but also very efficient, often employing sequential transformations. By this we understand a series of reaction steps in which several bonds are formed or broken, without the isolation of any intermediates.

Important examples include the biosynthesis[2] of alkaloids,[2a] terpenes,[2b] and steroids.[2c] The bicyclic tropane skeleton, an important constituent of numerous alkaloids such as cocaine and atropine, is obtained by a double Mannich reaction of a Δ^1-pyrrolinium salt (formed from ornithine) with an acetoacetate derivative.[3] The analysis of the biogenesis led to an elegant preparation of tropinone **4** by a sequential transformation of succinaldehyde **1**, methylamine **2**, and acetonedicarboxylic acid **3**.[4] Another

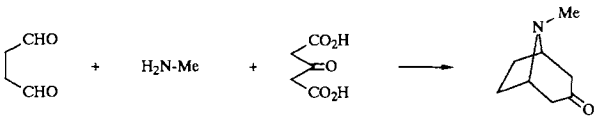

1 2 3 4

particularly fascinating example from Nature is the cyclization of squalene oxide **5** to give lanosterol **6**, a starting material for steroids.[5]

Sequential reactions are characterized by their great elegance, frequently high stereoselectivity, and by the simple manner in which they may be carried out. They permit complex molecules to be constructed in only a few steps. Moreover, the development of this type of synthetic method can lead to a reduction in the amount of undesired by-products, thereby contributing to the protection of the environment.

[*] Prof. Dr. L.F. Tietze, Dr. U. Beifuss
Institut für Organische Chemie der Universität
Tammannstrasse 2, D-W-3400 Göttingen (FRG)

[**] The sections of this review are not numbered systematically; the numbering which begins in the section after next is oriented according to the classification of sequential transformations given in Table 1

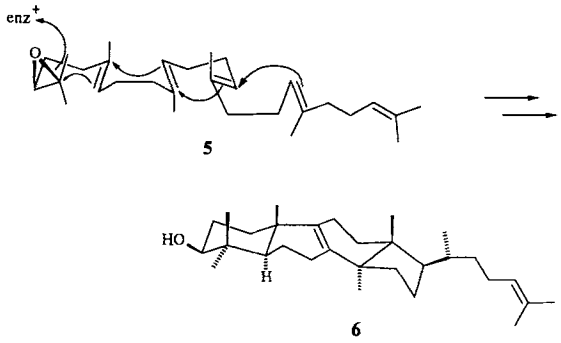

For example, the quantity of solvents and eluents required in comparison with stepwise processes is considerably reduced. Sequential reactions should, therefore, be more frequently included in future synthetic planning. In some cases biogenesis could serve as a prototype, but fundamentally new reaction sequences must be developed. In this review we attempt to classify sequential transformations and, with the help of examples from the literature and from our own work, to demonstrate their possibilities. It is not possible, of course, to discuss all known examples. We show, however, that the map of sequential transformations contains numerous gray areas, which should serve to stimulate new discoveries.

Definitions and Classification

Sequential transformations, which are known to every chemist under the all-embracing term "one-pot reactions", can be divided into two groups:

1. Domino Reactions
2. Consecutive Reactions

This division, as well as the following definitions of terms, are of course not compulsory, but appear to us to be sensible and useful. By a *domino reaction*,[6] frequently also described as *tandem or cascade reaction*, we understand a process involving two or more consecutive reactions in which subsequent reactions result as a consequence of the functionality formed by bond formation or fragmentation in the previous step. The preliminary formation of a reactive intermediate such as a carbocation or a carbanion is not counted here as a reaction step. On the other hand, the formation of a diene by a retro-Diels–Alder reaction with a subsequent cycloaddition would be considered as a domino reaction. In the ideal case the individual reaction steps should have comparable rates; for noncomparable rates it should be possible—with or without catalyst or mediator—to carry out reactions at a single temperature. Enrichment of an intermediate, therefore, does not occur. Rather, a "steady-state" concentration of the intermediate is formed, as we have been able to show by NMR spectroscopy for the tandem Knoevenagel hetero-Diels–Alder reaction.[6d]

In a *consecutive reaction* another reagent, mediator, or catalyst is added after the first transformation without isolation of the first formed product; the subsequent reaction steps then lead to the final product. Strictly speaking, sequences in which the individual steps are carried out at different temperatures should also be included in this group; we have not, however, applied too stringent criteria. Finally, the term *iterative process* is also found in the literature; by this term we understand the reiteration of a given transforma-

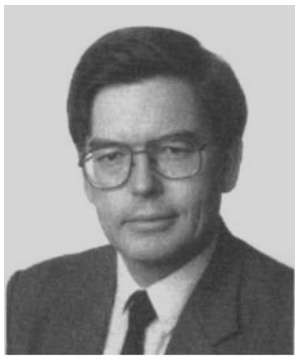

Lutz F. Tietze was born in Berlin in 1942, studied chemistry at the Universities of Kiel and Freiburg (1961–1966), and received his doctorate in 1968 with B. Franck in Kiel on the biomimetic synthesis of alkaloids. After a two-year post-doctoral period with G. Büchi at Massachusetts Institute of Technology in Cambridge, USA, and a brief research study with A. R. Battersby in Cambridge, England, he obtained his habilitation in 1975 in Organic Chemistry at the University of Münster. In 1977 he was appointed Professor in Dortmund, and in 1978 Full Professor and Director of the Institute of Organic Chemistry of the University at Göttingen, Germany, where he still works. He has been a Guest Professor at Madison, Wisconsin, USA, is a Member of the Scientific Academy in Göttingen, a Fellow of the Royal Society of Chemistry, holder of the Karl-Winnacker prize and the Literature Prize of the Fonds der Chemischen Industrie (together with T. Eicher). His research interests include the development of selective and efficient synthetic methods, reactions under high pressure, photochemical transformations, the stereoselective syntheses of natural products, and also the development of new concepts for a selective cancer therapy, based on phenotypic differences of normal and cancer cell population.

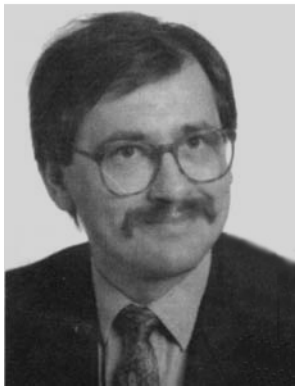

Uwe Beifuss was born in Tornesch/Holstein in 1957 and during the period 1975–1982 studied chemistry at the Universtity of Kiel, the Swiss Federal Institute of Technology (ETH) in Zürich, and at the University of Göttingen. He obtained his doctorate in 1987 with Prof. L.F. Tietze with a dissertation on highly diastereoselective ene reactions for the synthesis of sesquiterpenoids. He spent the period 1987–1988 as a post-doc with Prof. A. R. Battersby in Cambridge, England, where he worked on the biosynthesis of porphyrins. He has been at Göttingen since the end of 1988, working towards his habilitation. In addition to investigating selective reactions with thiocarbenium ions, he is working on the development of new types of dyes for photodynamic cancer therapy.

tion, which can also be carried out as domino, consecutive, or individual reaction.

In this review emphasis will be placed on the domino reaction, because it is often quite elegant and efficient. A typical example of this is the tandem Knoevenagel hetero-Diels–Alder reaction[6a, c] we have developed. In the first step of this process an aldehyde undergoes condensation with a 1,3-dicarbonyl compound to give an activated heterodiene, which then reacts with a dienophile in the second step. Vicinal difunctionalizations,[7] to which the Diels–Alder reaction, 1,3-dipolar cycloadditions, carbene additions to alkenes, and [2 + 2] photoadditions formally belong, are not regarded as domino reactions. In principle, however, all those reactions in which more than one bond is formed can also be classified as multistep processes. In this way, Diels–Alder reactions can frequently be formulated as tandem Michael reactions, which, according to our classification, are genuine domino reactions.

To classify domino reactions we have developed a frame that permits systematic arrangement, taking as a basis the reaction type of the first two synthetic steps (Table 1). Initially four groups are defined, each of which, according to the assignment of the second transformation, can then be classified into four subgroups. Because it is not possible to classify every reaction under this scheme, additional groups must be inserted. The main criteria of the schematic classification were the reactive species, such as cations, anions, or radicals, which can generally be formed in a preliminary reaction. The term cation here is a synonym for electrophile and that of anion for nucleophile. The addition of a nucleophile to a C=C or a C=X group—whether protonated or not—is formulated as an anionic transformation. The Mannich reaction, one of the oldest domino reactions, is thereby classified as an anionic–anionic process. For most domino reactions the first two transformations are of the same type, and anionic–anionic reactions are most common. In the overwhelming majority of domino reactions the second and subsequent steps are intramolecular. Every synthetic chemist knows that this can only be an advantage.

Table 1. Classification of domino reactions [a].

Section	1. Transformation	2. Transformation
1.1	cationic	cationic
1.2	cationic	anionic
1.3	cationic	radical
1.4	cationic	pericyclic
2.1	anionic	anionic
2.2	anionic	cationic
2.3	anionic	radical
2.4	anionic	pericyclic
3.1	radical	radical
3.2	radical	cationic
3.3	radical	anionic
3.4	radical	pericyclic
4.1	pericyclic	pericyclic
4.2	pericyclic	cationic
4.3	pericyclic	anionic
4.4	pericyclic	radical
5.	photochemical	
6.	carben(oid)	
7.	transition metal-induced	

[a] The division is a schematic classification. For example, cationic polyene cyclization is treated under cationic–cationic, without considering the possibility that a concerted process is also feasible.

1. Cationic Primary Step

In this process a carbocation is formed, either formally or in reality. This cation can be formed, for example, by elimination of water from alcohols, of alcohols from acetals, or by addition of a positive particle such as a proton to an alkene or an epoxide. The carbocation then reacts with a nucleophile to form a new carbocation, that undergoes one or more comparable further transformations in a cationic–cationic process (Section 1.1), finally being trapped by a nucleophile or stabilized by elimination of a proton (Scheme 1). Rearrangement reactions, in which numerous cationic species appear, similarly belong to this type of reaction.

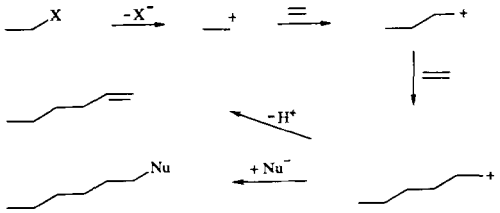

Scheme 1. Cationic–cationic domino reaction.

Formally, in the cationic–anionic (Section 1.2) and in the cationic–radical process (Section 1.3) a two-electron or a single electron transfer, respectively, must take place intermediately. No examples of this type of process have been reported. In the cationic–pericyclic process (Section 1.4) the cation formed by reaction with a nucleophile reacts either as an activated allyl cation or, after loss of a proton, as an alkene in a pericyclic reaction. No examples have been found of the first of these reaction types; the well-known acid-catalyzed reaction of allyl alcohols with orthoesters can be assigned to the second reaction type, although this reaction will not be treated in this review.

1.1. Cationic–Cationic Sequences

An iterative cationic–cationic domino process of considerable biological importance is the cyclotetramerization of porphobilinogen **7a**, the biosynthetic precursor of the "Pigments of Life" protoheme, chlorophyll, and vitamin B_{12}.[8] The acid-catalyzed cyclotetramerization of **7a** is so effi-

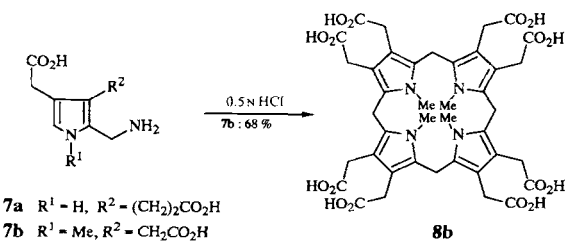

7a R^1 = H, R^2 = $(CH_2)_2CO_2H$
7b R^1 = Me, R^2 = CH_2CO_2H

8b

cient[9] that even strongly sterically hindered cyclotetramers of pyrrole can be constructed. Thus, Franck and Wegner found[8a, 10] that the pyrrole derivative **7b** gave a 68% yield of crystalline **8b** within 30 minutes by heating in 0.5 N hydrochloric acid. Interestingly, all attempts to synthesize *N,N,N,N*-tetramethyl compounds of this type by methylation of the corresponding cyclotetramers with free NH groups failed. This result underlines once again the efficiency of biosynthetic transformations. We have recently been able to show, by calculations and experimentally, that this self-organizing process of cyclotetramerization can be traced back to the substitution pattern on the pyrrole moiety.[11]

The biomimetic cyclization of polyenes, which often shows a high diastereoselectivity, is equally of great biological importance. Considering the stereochemical course of the abiotic cyclization of squalene oxide as a *trans-anti-parallel* electrophilic addition, a concept developed by Eschenmoser et al.[12] and Stork et al.,[13] van Tamelen and Corey conducted in vitro experiments[5, 14] that culminated in the elegant terpene and steroid syntheses of Johnson.[15] The principle of cationic cyclization of polyenes has been used intensively in many areas.[16] In an earlier synthesis of (±)-progesterone (**12**) by Johnson et al., hydroxypolyenyne (**9**) underwent acid-catalyzed cyclization to give **10** in the presence of ethylene carbonate. Subsequent hydrolysis gave ke-

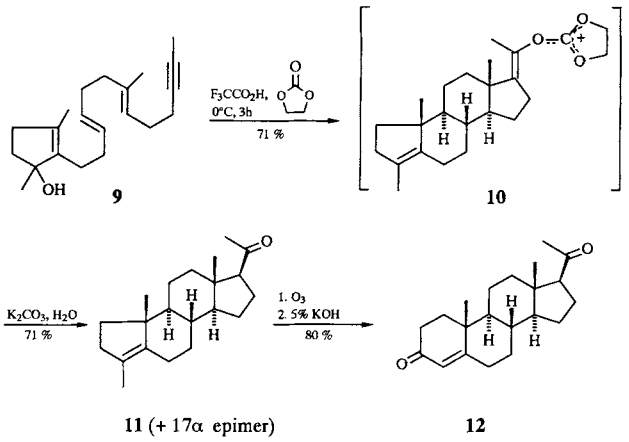

tone **11** in 71% yield. Ozonolysis of **11** led to (±)-progesterone (**12**) in 80% yield.[17] A new piece of work involves the synthesis of tetracyclic euphane–triterpenes,[18] which uses dienediynol **13** as substrate. Methanolysis of **13**, followed by treatment with acid, gave a mixture of two isomeric tetracyclic compounds, from which the ketone **14** could be separated by crystallization as the major product. It is assumed that the vinyl cation **15** is formed first, reacting to form **14** via conformation **15A**. The tetracyclic triterpene euphol **16**, from the group of euphanes, was obtained by cleavage of the C–C double bond in **14** with ozone followed by an aldol reaction. Cyclization products with the configuration of lanostane **17**, which could be formed from the vinyl cation **15** via **15B**, were not found. It should not be forgotten that in polyene cyclizations—as elegant as they are—the synthesis of the precursors is frequently difficult and the yields of cyclization products are not always satisfactory.

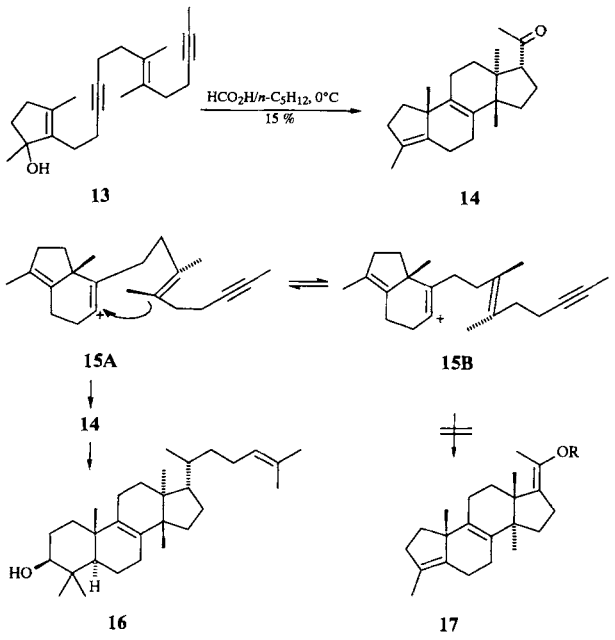

Allyl- and vinylsilanes are often used as terminators in cationic polyene cyclizations.[19] One of several interesting examples from the group of Burke[20] is the Lewis acid-induced formation of the enantiomerically pure acetal **18**,[21] which was formed by enantioselective reduction of a propargylketone with BINAL-H followed by an Ireland–Claisen rearrangement. Reaction of **18** with titanium tetrachloride at −78 °C gave the *trans*-coupled octahydronaphthaline **19** as major product in 74% yield, in addition to other diastereomers as by-products. Compound **19** was used as a precursor for dihydrocompactin. The carbocations **20** and **21** could be considered as intermediates.

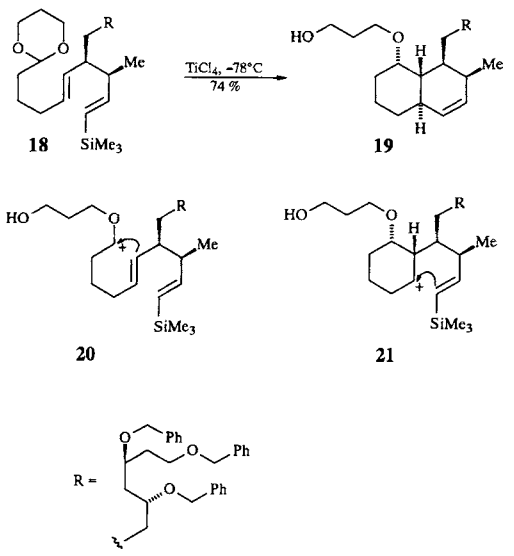

Another cyclization sequence, in which the first step is intermolecular, is the Lewis acid-induced reaction of a trimethylsilyl enol ether **22** with an acetal **23**, which contains an allylsilane unit.[22] In this way the ketone **24**, formed by cationic C–C coupling, underwent intramolecular reaction

with the allylsilane group to give the bicycle **25**. In this fashion annelated ring systems of various sizes can be constructed. Interestingly, the intramolecular cyclization of the bifunctional substrate **23** with $n = 0$, 1, and 2 occurs more slowly than the intermolecular reaction with the enol ether **22**. On the other hand, acetal **23d** leads exclusively to the 3-methylenecyclohexyl methyl ether by an intramolecular process. As an explanation for the different reactivities of the acetals **23a–c** and **23d**, it is assumed that the intramolecular cyclization of **23a–c** is not kinetically favored as a result of stereoelectronic effects.[23]

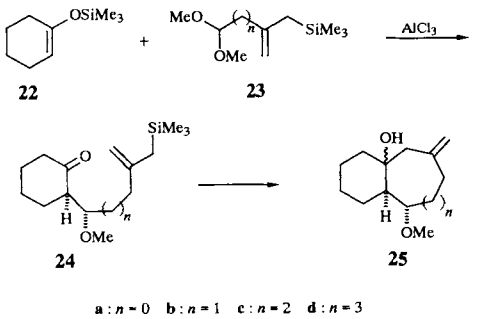

A comparable reaction is the Lewis acid-induced reaction of allylstannane **26** with an α,β-unsaturated acyl iron complex **27**.[24] Depending on the configuration of the double bond in **27** *cis*- and *trans*-1,2-disubstituted cyclopentanes **29** can be formed highly stereoselectively. For example, the (*E*)-crotonyl iron complex **27** gave exclusively the *trans*-cyclopentane derivative **29** (41% yield), which could be converted into **30** in three steps.

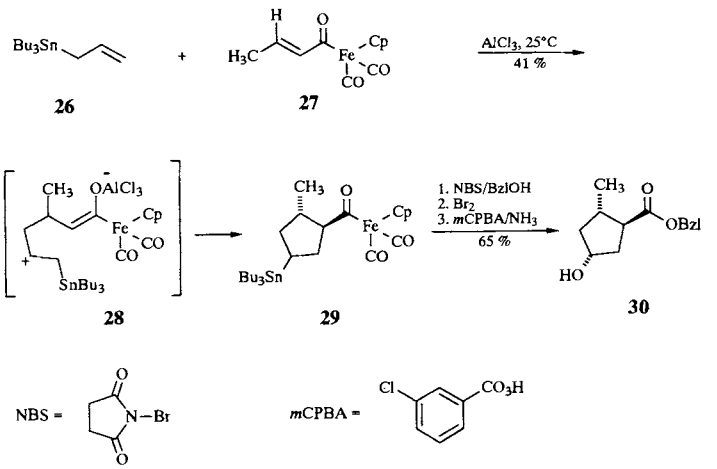

A nice example of a cationic domino reaction is the biomimetic cyclization of polyepoxides[25] for the construction of polyether–ionophores.[26] In the synthesis of polyethers like monensin and etheromycin Paterson and Craw[27] converted the bisepoxide **31** directly into the polyethers **32a** and **32b** (5:1), which contain two tetrahydrofuran groups and one spiroacetal group, in 47% yield by treatment with aqueous hydrofluoric acid in acetonitrile at room temperature. Compound **32b** could be transformed into **32a** by epimerization with potassium carbonate in methanol. When camphorsulfonic acid (CSA) was used as catalyst the reaction of **31** stopped at the stage of the bis(tetrahydrofuran) **33**, since the *tert*-butyldimethylsilyl protecting group was not cleaved under these conditions and, therefore, the spiroacetal unit could not be formed. Reaction of **33** with hydrofluoric acid then gave **32a** and **32b** (2.2:1).

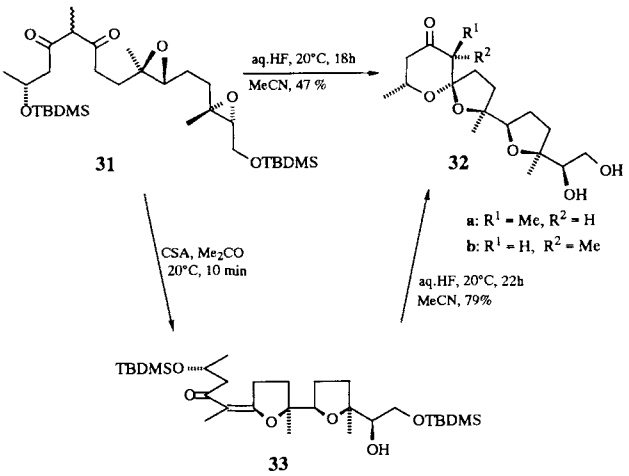

TBDMS = *t*BuSiMe$_2$

Cationic rearrangements such as 1,2-shifts in spiroketones or the Pinacol rearrangement can also be used very efficiently for domino reactions. Fitjer and Quabeck[28] observed multiple cationic 1,2-shifts by treatment of the tetraspiroketone **34** with *p*-toluenesulfonic acid in benzene. Compound **34** isomerized quantitatively within 30 minutes, possibly via the intermediates **35** and **36**, to give the bridged ketone **37**, photochemically induced decarbonylation of which concluded an elegant synthesis of [4.5]coronane **38**.

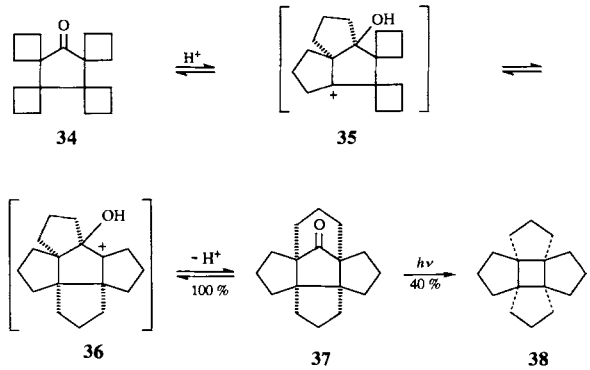

The cationic cyclizations with subsequent Pinacol rearrangement of compounds of type **39**, developed by Overman et al.,[29] are of great synthetic value. Compound **39** can be used for the construction of annelated carbocycles and heterocyclic five-membered rings **41**. The cation **40** is assumed to be an intermediate, undergoing a 1,2-shift with enlargement of ring A. Thus, reaction of acetal **42** with $SnCl_4$ gave the diastereomers of tricyclic ketone **43** (2:1, 70%).

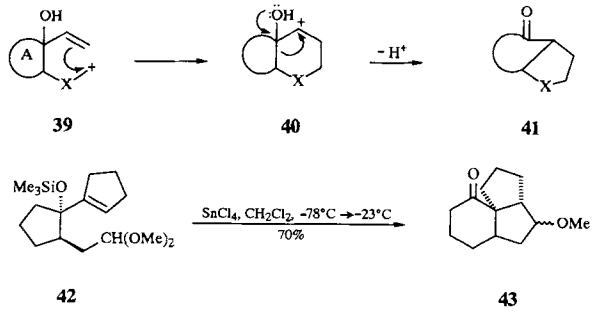

2. Anionic Primary Step

In reactions of this type the primary step is the formation of an anion or a nucleophile. The majority of cases involve the deprotonation of a CH group with the formation of a carbanion, which then reacts with an electrophile to form a new anionic functionality. This anion then attacks another electrophile in an anionic–anionic process. The sequence is completed by reaction with an electrophile, for example, a proton, or by elimination of an X^- group (Section 2.1). In the increasingly important anionic–pericyclic process, the anion formed in the anionic step is converted into a compound containing a multiple bond, which is then capable of undergoing a pericyclic reaction (Section 2.4). For the anionic–cationic and anionic–radical reaction sequences no examples are known.

2.1. Anionic–Anionic Sequences

Polymerizations such as anionic polymerization of α-activated olefins[30] involve an iterative process, which is concluded by chain termination steps. To use such processes for the synthesis of homogeneous compounds of low molecular weight, the chain growth must be stopped after a defined number of steps. As Posner et al. have demonstrated, intramolecular cyclizations, in which the possibility of further polymerization is excluded, are suitable for this purpose,[6c] for example, in the synthesis of cyclohexanone **46** by an intramolecular Dieckmann reaction. After the iterative Michael addition of two molecules of acrylate to the lithium enolate of **44**, with formation of the probable intermediate **45**, potential polymerization was hindered.[31] Termination of the reaction after two additions can also be achieved by an intramolecular Wittig reaction.[32]

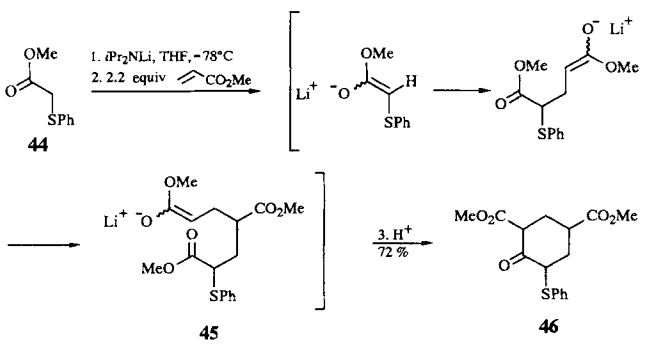

The versatility of this approach could be increased considerably by achieving consecutive reactions with two different electrophiles. For example, the enolate obtained by reaction of 2-cyclohexenone **47** with tributylstannyllithium underwent a Michael addition with ethyl vinyl ketone to give **48**. The subsequent aldol reaction with acetaldehyde gave **49** followed by the intramolecular formation of a hemiacetal led to the annelated tetrahydropyran **50**. Oxidative fragmentation to give **51** completed this novel access to unsaturated macrocyclic lactones. The stereoselectivity of the individual steps is, however, low. The macrocyclic lactone was obtained as a mixture of two diastereoisomers (*trans*:*cis* = 0.7 (**51**)–5.3:1).[33c]

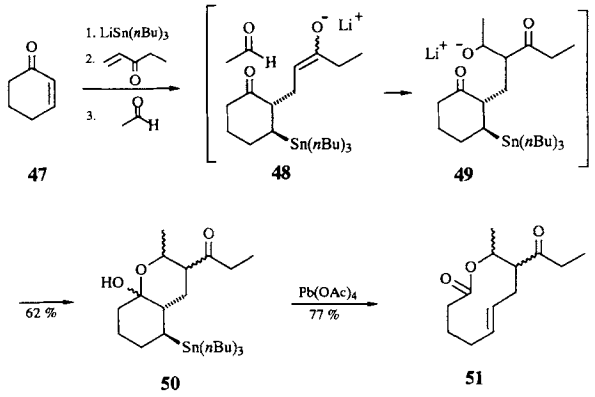

The synthesis of polycyclic systems has shown itself to be the domain of Michael–Michael reactions,[34] for example, in the preparation of the bicyclo[2.2.2]octane[35] and tricyclo[5.3.1.$0^{3,8}$]undecane skeletons,[36] and other framework types,[37] which are important intermediates in the construction of sesquiterpenoids. An attractive example is the synthesis of seychellene **57** from **52** and **53**, reaction of which with diethylaluminum chloride gave the tricyclic ketone **56** in 43% yield. Compounds **54** and **55** could be considered as intermediates. Compound **56** can be converted into **57** in a few steps.[36]

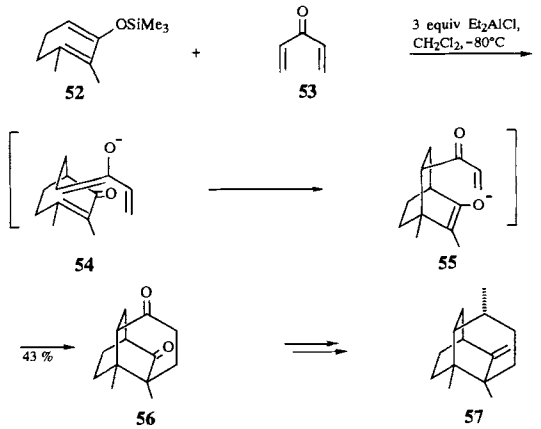

The key sequence in the synthesis of the diterpene (+)-atisirene **58** and the diterpene alkaloid atisine **59** by Fukumoto et al. is also a tandem Michael reaction.[38,39] Reac-

tion of **60** with lithium hexamethyldisilazide gave, via **61**, the tetracycle **62** with high diastereoselectivity. The latter could be converted into **58**.[38]

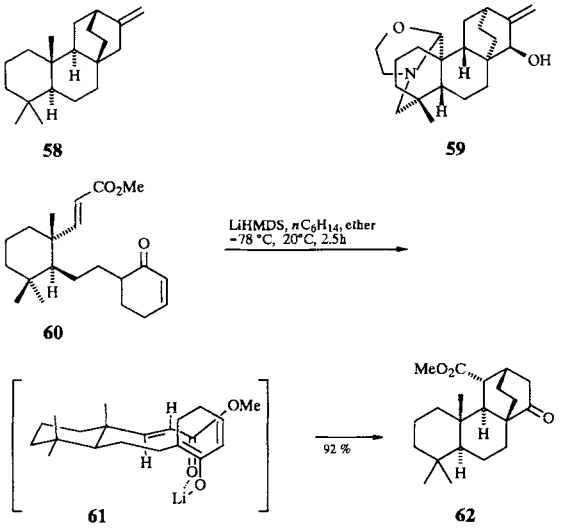

The synthesis of bicyclo[2.2.1]heptanes of type **65** possibly involves three consecutive Michael additions. Compound **64** was generated by an intermolecular 1,4-addition of the thiophenol anion to **63**, which then reacted with methyl acrylate in two further additions to give **65**.[40] The two intramolecular Michael reactions, however, can also be regarded as a Diels–Alder reaction of a cyclopentadiene with acrylate.

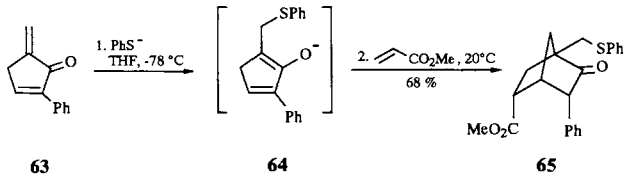

Tricyclo[7.3.0.$0^{1,5}$]dodecanes such as **68** are accessible by double Michael additions. With appropriate functionalization these compounds undergo rearrangement by ring contraction to give tricyclo[6.3.0.$0^{4,8}$]undecanes (e.g. **69**), the

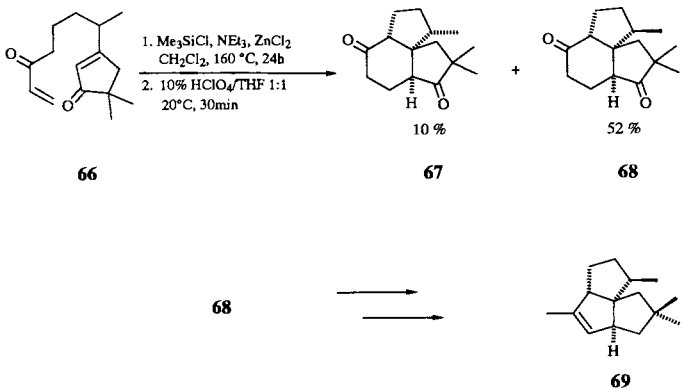

skeleton of some triquinane sesquiterpenes. Compound **66**, heated with chlorotrimethylsilane, trimethylamine, and zinc chloride in a sealed tube gave, in addition to **67** (10%), a 52% yield of **68**, a useful building block for the synthesis of some pentalenes, such as (±)-pentalenene **69**.[41]

Nevertheless, the potential of the tandem Michael reaction is not exhausted with the preparation of bicyclic and tricyclic systems. It can also be used for the efficient synthesis of highly functionalized carbo- and heterocyclic ring systems.[42–44] The synthesis of pentasubstituted cyclopentanes such as **72** from the L-tartaric acid derivative **70** is characterized by excellent diastereoselectivity (*ds* > 99%). The conformation of the transition state is presumably controlled by the *anti*-periplanar arrangement of the two bulky silyl ether groups. Thus, initial 1,4-nucleophilic attack of the cuprate reagent on **70** to give **71** can only take place on one of the two outward facing homofacial alkenoate groups. The subsequent intramolecular 1,4-addition of the ester enolate on the "inner side" of the remaining alkenoate group in **71** then led to the product **72**.[42]

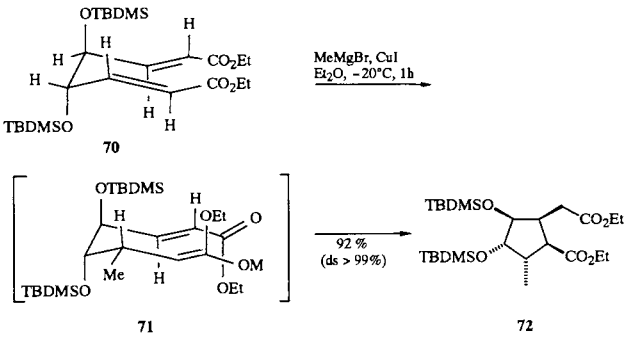

An example of a tandem Michael reaction for the formation of *N*-heterocycles[44] is the synthesis of (−)-α-kainic acid **77**.[44a] Reaction of γ-amino-α,β-unsaturated ester **73** (from D-serine methyl ester) with the nitrobutadiene **74** in ethanol at room temperature gave the pyrrolidine **76** as the only product in quantitative yield with the configuration required for synthesis of **77**.

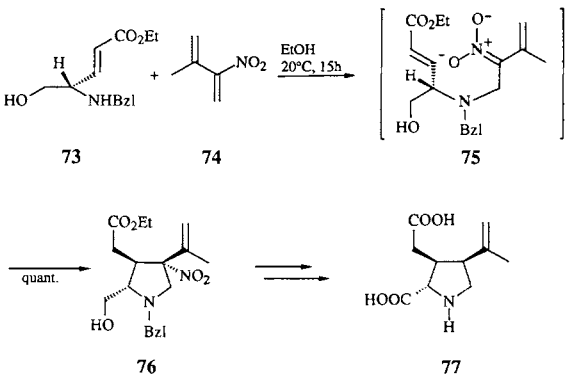

The nitro group can ultimately be removed with retention of configuration by hydride transfer. The excellent diastereoselectivity in the cyclization of the intermediate **75**

to **76** can probably be traced to the addition of nitronate to the acrylate being under the control of the existing stereogenic center in an *anti*-periplanar process.

Tandem Michael reactions have also found much importance in the synthesis of decalines,[45] steroids,[46] and steroid precursors.[47] A consecutive double Michael addition was employed by Takahashi, Tsuji et al. in a synthesis of an enantiomerically pure steroid CD-ring building block by transformation of 2-methyl-2-cyclopentenone **78** with an enantiomerically pure (*Z*)-vinylcuprate such as **79**. The intermediary enolate **80** was trapped by the subsequently added Michael acceptor **81** to give **82**, which was not isolated. The following aldol condensation and removal of the protecting group gave the notable yield of 56% **83** and only 6% **84** for this one-pot reaction.[47a, b]

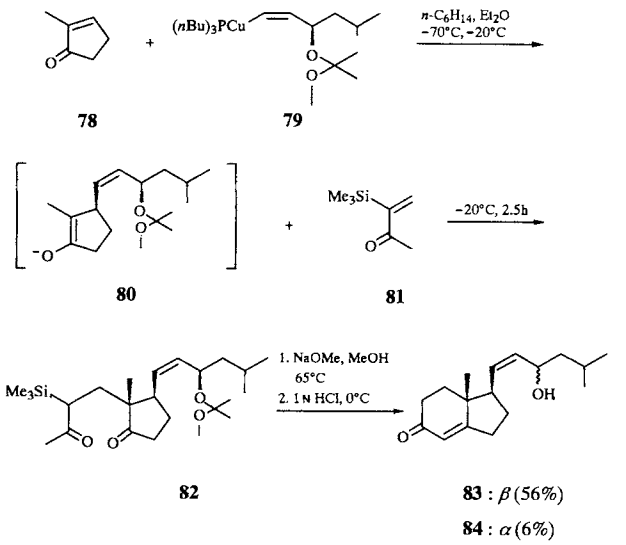

A simple synthesis of the phenanthroindolizidine alkaloid (−)-tylophorine **87** could be realized by an intramolecular tandem Michael sequence of the starting material **85**. Reaction with *tert*-butyldimethylsilyl trifluoromethanesulfonate under very mild conditions gave **86** in 76% yield, which could then be converted into **87**.[48] A glucose derivative was employed as chiral auxiliary in **85**. The diastereoselectivity of the transformation is > 99:1; only one product was found. The quinolizidine alkaloid (±)-epilupinine could be synthesized in the same manner.[49]

Michael and aldol reactions can also be coupled by allowing them to run one after the other. This principle has been used on numerous occasions, for example, for the synthesis of pyrones,[50] pseudoguanolides,[51] lignanes,[52] oxapropellanes,[53] and cyclopentane derivatives.[54] A particularly spectacular example is the synthesis of prostanoids.[55] Noyori et al. effected a "three-component coupling" as the target of a convergent prostaglandin synthesis. The strategy involved the introduction of a β-side chain by 1,4-addition to a cyclopentenone and trapping of the enolate by reaction with a functionalized α-side chain building block, which can be used as an iodide, a nitroolefin, or as an aldehyde. For the synthesis of the prostaglandin derivative **92** the enantiomerically pure cyclopentenone **88** was treated with the enantiomerically pure building block **89** (in the form of the

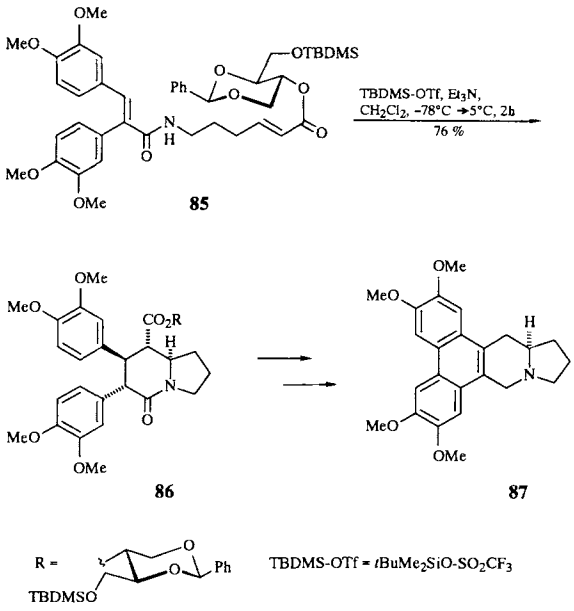

cuprate) in tetrahydrofuran at −78 °C, and the intermediate enolate trapped with **90** to give **91** as a 1:1 mixture in 83% yield.[55]

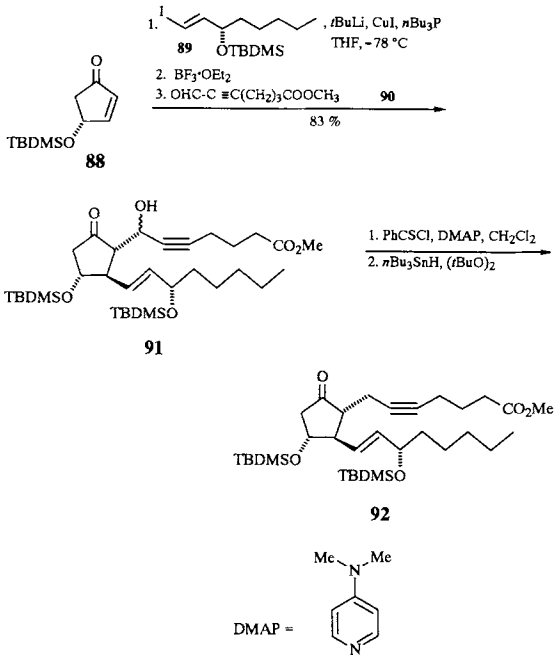

An elegant construction of the skeleton of the corynanthe alkaloids was achieved by Winterfeldt et al. by the reaction of the enantiomerically pure vinylic urethane **93** with the Michael acceptor **94**. Compound **95** was formed in the sequence composed of a diastereoselective Michael reaction (88:12), carbinol–amine formation, and a diastereoselective Pictet–Spengler reaction. Subsequent reduction, methylene–lactam rearrangement and isomerization permitted synthesis of (+)-geissoschizine **96** and (−)-geissoschizol.[56]

Another genuine domino reaction is the cycloalkylation sequence employed by Hudlicky et al. for the synthesis of

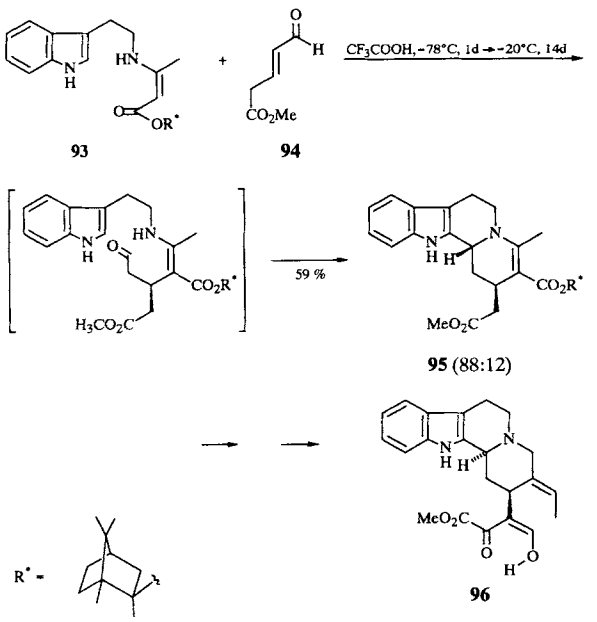

(−)-retigeranic acid (**100**). Michael addition of the dienolate **97** to the bicyclic enone **98** followed by intramolecular substitution with elimination of bromide gave the cyclopropane derivative **99** as a 1:1.5 mixture of the *exo/endo* isomers. Vinylcyclopropane rearrangement of **99** then led to the basic skeleton of **100** in one step.[57] Further related methods for the preparation of cyclopropanes[58] and higher cycloalkenes are known. The consecutive Michael alkylation sequence is established as one of the best methods for the synthesis of steroids and cyclopentanoid natural products.[59]

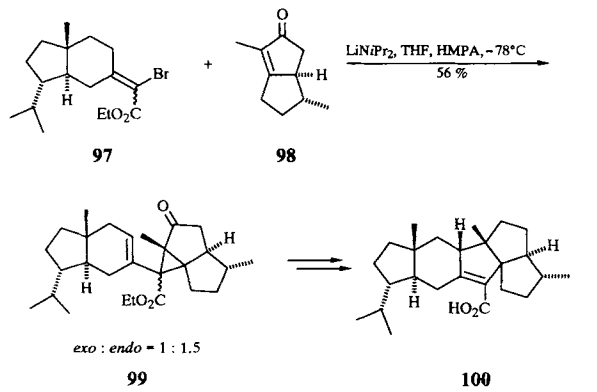

Meyers et al. have used naphthyloxazolines to serve in such sequences as a chiral template for the synthesis of enantiomerically pure substituted 1,2-dihydronaphthalines.[60] In model investigations for the synthesis of aphidicolin and scopadulcic acid, compound **101**, for example, was vinylated in a 1,4-addition to the suspected intermediate lithium azaenolate **102**, which could then be trapped in a diastereoselective reaction with the iodide **103** to give **104**.[60b]

Organobisthiocuprates have emerged as extremely useful nucleophiles in the one-pot synthesis of spiro compounds, as Wender et al. have demonstrated in the reaction of **105** with **106** to give **107**. The reaction sequence is thought to consist

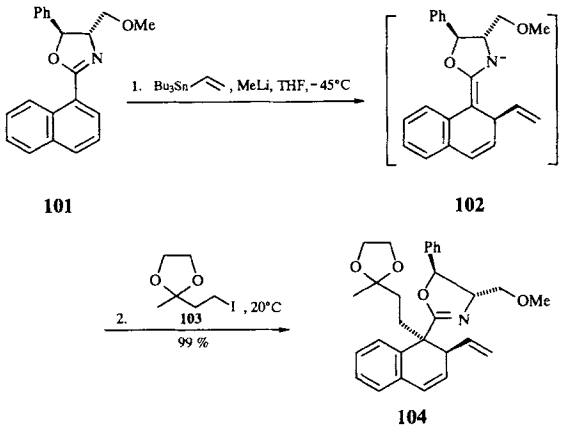

of a Michael addition, an elimination, and another Michael addition.[61]

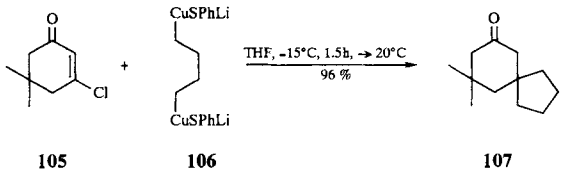

An unusual concept for the synthesis of heteromacrocycles such as **111** is based on the sequence of 1,6-Michael addition, an elimination, and finally a 1,4-Michael addition. Reaction of **108** with butanedithiol gave the enolate **109**, which underwent elimination to give the highly reactive cross-conjugated Michael acceptor **110**. Subsequent addition of the remaining SH group then led to the eleven-membered ring **111**.[62] A multitude of heteromacrocycles is available by variation of the starting materials.

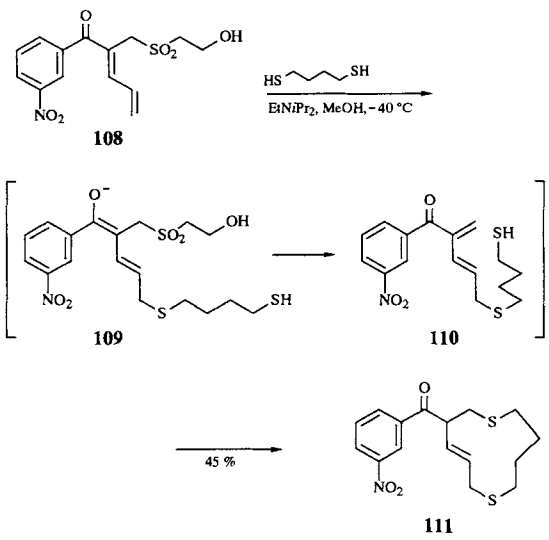

In a similar manner to the 1,4-additions, Reetz et al. have combined 1,2-additions with a series of other anionic processes to give domino sequences.[63] The transformation of *N,N*-dibenzyl-protected α-aminoaldehydes, such as **112**, with the *O*-silylketene acetal **113**, via **114** and **115**, gave

diastereo- and enantiomerically pure 4-substituted 3-amino-γ-lactones **116** in the sequence nonchelate controlled aldol addition, a lactonization and finally stereospecific dyotropic rearrangement.[63]

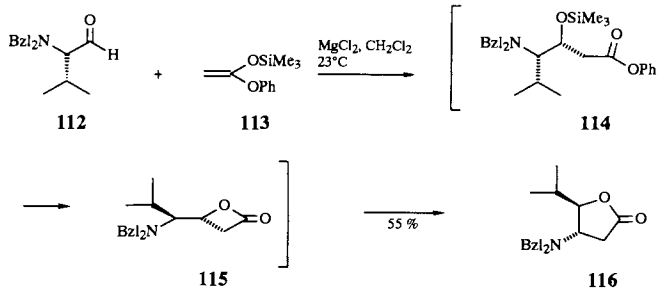

112 **113** **114** **115** **116**

Seebach et al. were able to show that the sequential reaction of enamines with pivaloates of 2-nitroallylic alcohols permits synthesis of six-membered rings.[64] Reaction of **117** with **118**, by way of numerous intermediates, gave **119** in 59% yield and high diastereoselectivity ($ds > 95\%$).[64]

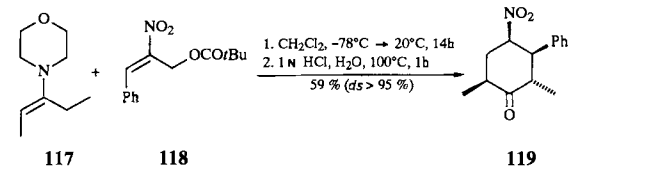

117 **118** **119**

An attractive anionic domino olefin cyclization,[65,66] which, in contrast to the cationic and radical variants, was hitherto something of a sleeping beauty, was described by Bailey et al. with the reaction of **120** with *tert*-butyllithium. The intermediate **121** was formed first, cyclizing to **123** via **122**. Quenching with methanol gave **124** in 81% overall yield.[66]

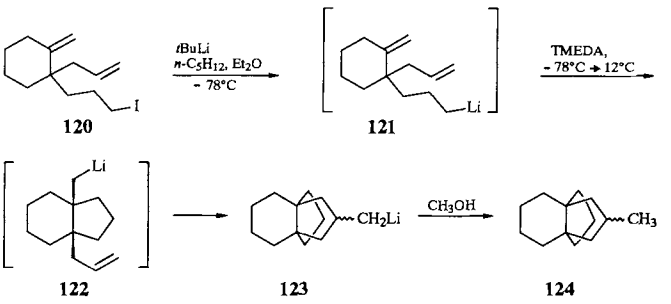

120 **121** **122** **123** **124**

TMEDA = *N,N,N',N'*-tetramethylethylendiamine

One of the oldest domino transformations is the Mannich reaction, which, together with its modern variants, is one of the most important reactions for the formation of nitrogen-containing compounds. The abundance of material is almost limitless.[29c,67] We have selected only two examples, which involve further transformations after the Mannich reaction. The highly diastereoselective construction of the precoccinelline skeleton by Stevens et al. resulted from an intermolecular Mannich reaction of the aminodialdehyde liberated from **125** with methyl acetonedicarboxylate **127**. Compounds **126** and **128**–**130** are suspected intermediates.[68]

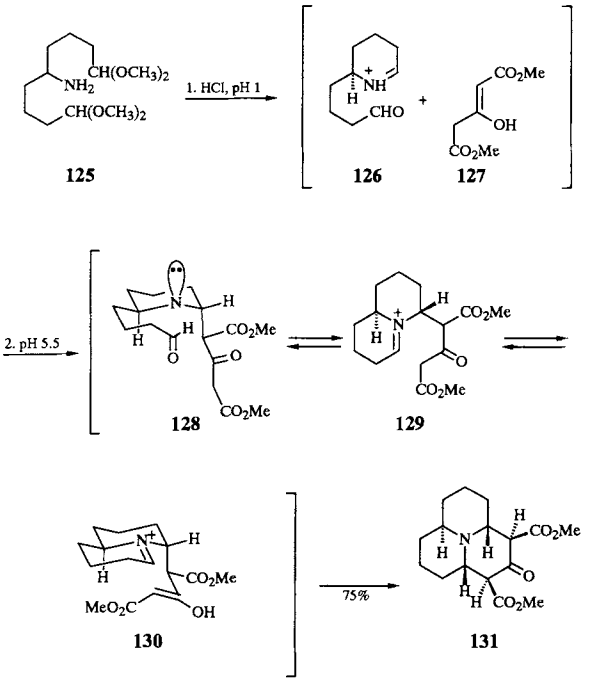

125 **126** **127** **128** **129** **130** **131**

The combination of a Mannich reaction and a polyene cyclization with an allylsilane as terminator was used by Grieco et al. for a synthesis of (±)-yohimbone **134**. The *trans*-coupled D/E ring system **133** in the target molecule was generated diastereoselectively by treatment of **132** with formaldehyde and trifluoroacetic acid.[69]

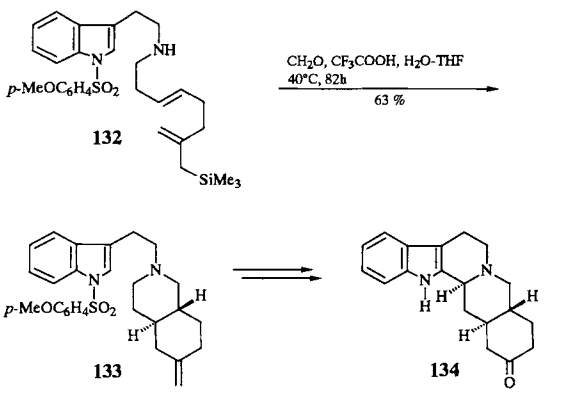

132 **133** **134**

The range of application of the Mannich reaction could be extended considerably if the development of stereoselective variants were attained. Kunz at al. were recently able to demonstrate this with a synthesis of piperidine alkaloids. Reaction of the *O*-pivaloyl-protected galactopyranosylamine **135** with butanal gave the imine **136**. Treatment of this with the silylenol ether **137** led, with high diastereoselectivity, to the Mannich adduct **138** (demonstrated by TLC), which cyclized directly to the Michael product **139** on acidic

workup. Compound **139** can, after removal of the galactosyl auxiliary, be converted in a few steps to the piperidine alkaloid (*S*)-coniine.[70]

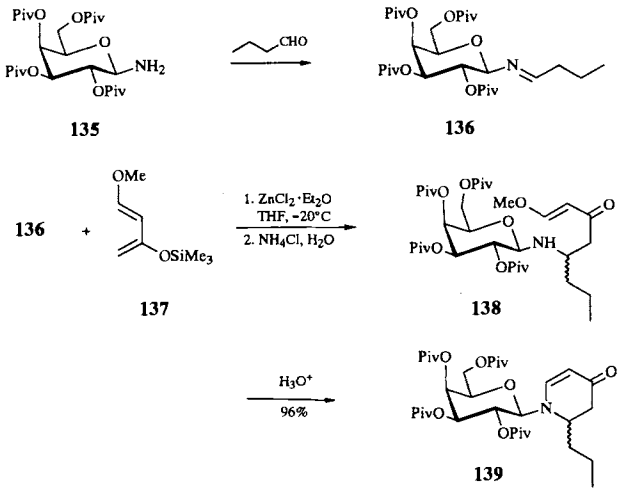

Piv = $(CH_3)_3CCO$-

($\alpha:\beta = 97.5:2.5$)

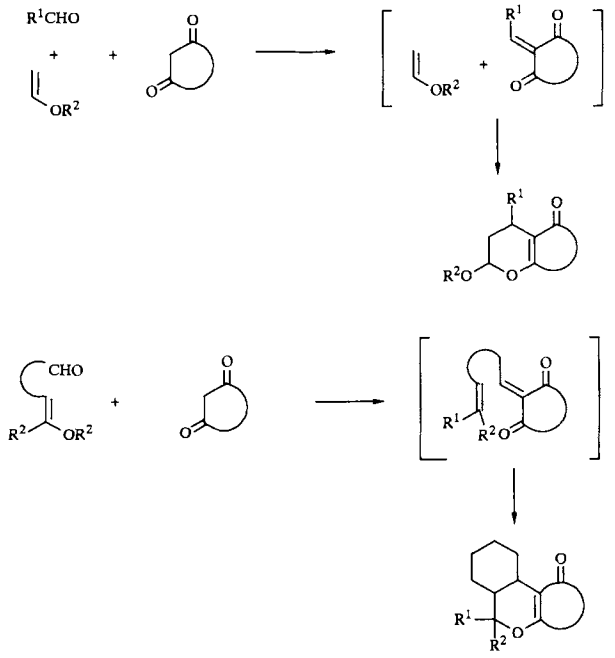

Scheme 2. Three- and two-component tandem Knoevenagel hetero-Diels–Alder reaction.

2.4. Anionic–Pericyclic Sequences

Three well investigated and versatile anionic–pericyclic domino reactions that we have developed are the tandem Knoevenagel hetero-Diels–Alder reactions,[6a, d] tandem Knoevenagel-ene reactions[71] and tandem Knoevenagel-allylsilane cyclizations.[72] With suitable choice of substrate an intramolecular-Prins reaction can be added to the sequence.[71a] All three sequences are characterized by being simple to carry out and—when the second reaction step is intramolecular—by very high stereoselectivity. In the tandem Knoevenagel hetero-Diels–Alder reaction a 1-oxa-1,3-butadiene is first formed[73] in situ by condensation of an aldehyde with a cyclic or highly reactive acyclic 1,3-dicarbonyl compound. The oxabutadiene then undergoes cycloaddition with a dienophile in the second step. Azabutadienes and diazabutadienes can also be formed in a comparable reaction involving condensation of amines with aldehydes. The sequence can be conducted as a three- or two-component reaction. In the first case, a mixture of aldehyde, 1,3-dicarbonyl compound, and dienophile, for example an enol ether, is used. In the second case, a 1,3-dicarbonyl compound is treated with an aldehyde that already contains a dienophile component; the Diels–Alder reaction then takes place intramolecularly.

In a similar fashion 1,3-dicarbonyl compounds such as malonate or malonodinitrile, which cannot undergo hetero-Diels–Alder reactions, are used in the tandem Knoevenagel-ene reaction; for the tandem Knoevenagel-allylsilane cyclization, aldehydes containing an allylsilane unit are used, which are easily available by photochemical Norrish type I cleavage of α-trimethylsilylmethylalkanones.[74] It is frequently advantageous to choose a consecutive reaction process for the tandem Knoevenagel-ene and the -allylsilane sequences, although this is not absolutely necessary (Section 5). The range of applications of these reactions is very large. Numerous aldehydes and 1,3-dicarbonyl compounds can be employed; limitations are not known. Enantiomerically pure products can be obtained by the use of enantiomerically pure aldehydes, enantiomerically pure 1,3-dicarbonyl compounds, or with chiral Lewis acids.

Three factors are essential for the high efficiency and the wide applicability of these sequences:

1. Simple preparation of reactive acceptor components by a Knoevenagel reaction[73] from easily available starting materials.
2. High reactivity of the acceptor components because of a low-lying LUMO and favorable coefficients. AM1 calculations[75] on CN-substituted acroleins show that the highest reactivity is expected for the C-3-substituted compound, as a result of the favorable coefficients, although the LUMO energies of the 4-substituted acroleins are slightly lower (Scheme 3).

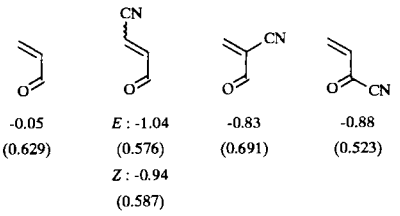

Scheme 3. AM1(CI) calculations for CN-substituted acroleins (LUMO energies in eV, coefficients refer to the 4-position of the 1-oxa-1,3-butadiene).

3. In the Knoevenagel condensation of aldehydes with 1,3-dicarbonyl compounds a trisubstituted double bond is formed. Molecules with this structural element thereby always contain both a *Z* orientation of the substituents at the double bond; as a result of this *Z* orientation a 1,3-

allylic strain generally appears.[76] We assume that in the following cyclization this allylic strain effects a conformative restriction on the transition state, thereby leading to the excellent stereoselectivity observed for the intramolecular reaction. According to the results of AM1 calculations, the ground state conformation A of the propylidene malonate is 10.2 kJ mol^{-1} more stable than conformation B (Scheme 4). This effect involves a common phenomenon that can generally be observed with intramolecular reactions of trisubstituted C=C and C=N bonds; for this reason we have named the spatial control that is obtained by geminal substitution at the terminus of a C=C or a C=N double bond the *sp²-geminal effect*.[71b]

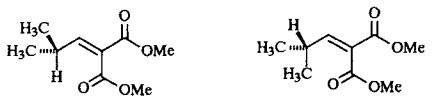

Scheme 4. AM1 calculations of the relative ground state energies for conformations of propylidene methyl malonate.

In the sequential reactions with an intramolecular second step two new rings are formed, connected either *cis* or *trans*. For example, the tandem Knoevenagel hetero-Diels–Alder reaction of aromatic aldehydes **140** with Meldrum's acid **141** gave (via the intermediate benzylidene-1,3-dicarbonyl compound **142**) the *cis*-coupled cycloadduct **143** exclusively (> 99:1),[77a] whereas aliphatic aldehydes such as **144**, for example with dimethylbarbituric acid **145** (or also with **141**), led predominantly to the *trans*-coupled product such as **147** (*trans*/*cis* = 98.2:1.8) via **146**.[77b-d]

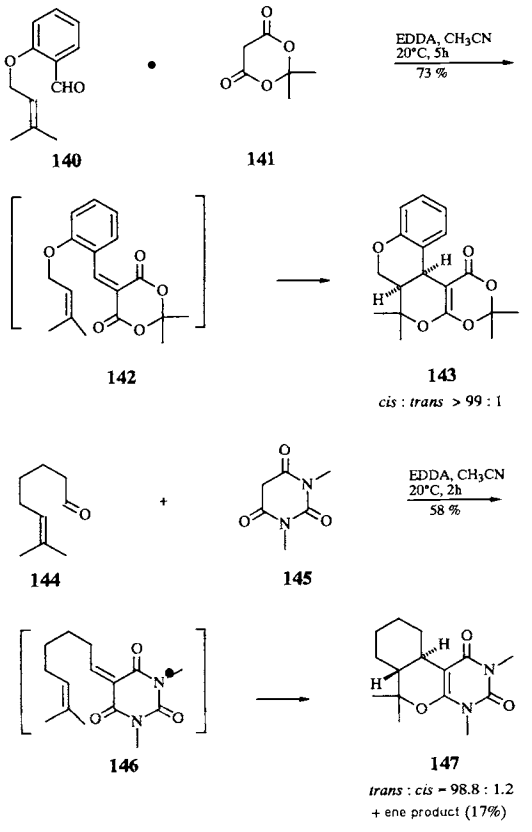

Heterocyclic analogues such as pyrazolones **148** or isoxazolones can also be used as the 1,3-dicarbonyl compound in this reaction. The stereoselectivity is controlled here by the substituent R; in the reaction of aldehyde **140** to give the cycloadduct **149**, the *cis*-selectivity decreases with the decrease in the size of R (R = *tert*-butyl: *cis*/*trans* = 50.2:1; R = Me: *cis*/*trans* = 17.0 : 1; R = H: *cis*/*trans* = 4.6:1).[78]

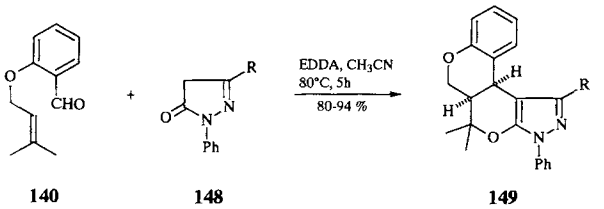

A 1-oxa-1,3-butadiene component with both *Z* and *E* configurations exists simultaneously in the intermediates **142** and **146**. Four different transition state structures can therefore be postulated (Scheme 5); for the classification, it has been decided here that the reacting CO group has the higher priority. The *trans* cycloadduct is formed via the *exo-E-anti* structure **A**, as the *endo-Z-anti* arrangement **D** exhibits too high an energy in the intramolecular reaction on steric grounds. The *cis* annelated compound can be formed from *endo-E-syn* or *exo-Z-syn* geometry, **B** and **C**, respectively. We assume, on the basis of calculations[79] and experiments,[77b,78,80] that *cis* cycloadducts, such as **143** or **149**, obtained from α,β-unsaturated aliphatic and aromatic aldehydes like **140**, are formed via *endo-E-syn* geometry. In contrast, an *exo-Z-syn* transition state must be considered for the reaction of the α,β-saturated aldehyde **144** to give the *cis*-annelated by-products.

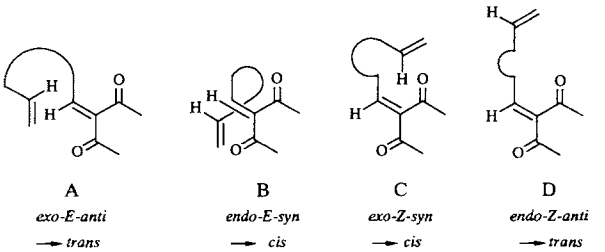

Scheme 5. Transition state structures for the hetero-Diels–Alder reaction of alkylidene- and benzylidene-1,3-dicarbonyl compounds.

These examples make quite clear that it is necessary to consider *E* and *Z* dienes in the discussion when analyzing the selectivity of Diels–Alder reactions. Thus, *trans*-substituted cycloadducts can generally be formed via a transition state with *exo-E-anti* or *endo-Z-anti* geometry, and *cis*-substituted compounds via *endo-E-syn* or *exo-Z-syn* geometry. Clearly also the possibility of isomerization of the diene or the heterodiene must be taken into consideration when discussing the stereochemical outcome of a Diels–Alder reaction.[81]

Annelated cyclopentanes and cycloheptanes can also be prepared by shortening or lengthening the chain attached to the reacting π-electron systems. As a consequence of the unfavorable geometry in the transition states, however, a higher reaction temperature is required. A mixture of **150** and **151**, in the presence of ethylenediammonium diacetate (EDDA) at 187°C gave exclusively the adduct **152** (*cis* > 99%) in 84% yield; reaction of **153** and **151** gave **154** and **155** in the ratio 99:1.[82]

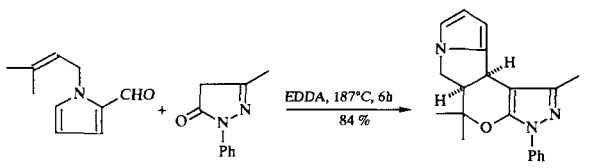

150 **151** **152**

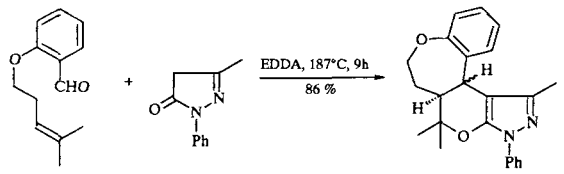

153 **151** **154** : α-H
155 : β-H

If an aldehyde is condensed with a compound formally containing an enamine structure such as **157**, 2-azabutadienes can be obtained as intermediates that can undergo an intramolecular cycloaddition. In this reaction one finds a surprising dependence of the selectivity on the substituents R^1–R^4. Reaction of **156a** with **157** in refluxing xylene gave exclusively *trans*-annelated **159a** in 67% yield, obtained from the first formed cycloadduct by a 1,3-hydrogen shift. If the reaction is conducted at 80°C, the 2-azabutadiene **158a** (postulated as an intermediate) can be isolated. Reaction of **156b** with **157** led to the *cis*-adduct **160b**. The varying selectivity can be traced back largely to changes in the dominant

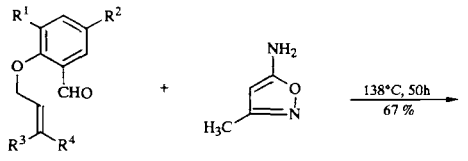

156 **157**

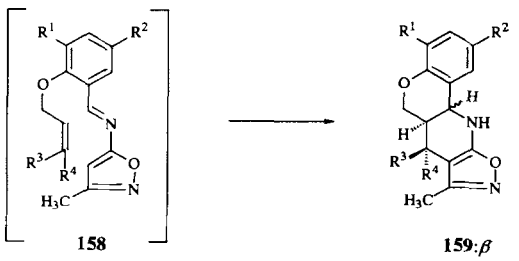

158 **159**:β
160:α

a: R^1=R^2=R^3=H, R^4=CO_2Me; **b**: R^1=R^2=Cl, R^3=R^4=CH_3

orbital interactions (normal → inverse Diels–Alder reaction) arising from the substituents on the dienophile.[83]

Alkylidenemalonates such as **161** and **164**, which can be obtained from the corresponding aldehydes and malonates in good yield in the presence of piperidinium acetate, can be converted (without isolation) into cyclohexane and cyclopentane derivatives thermally at 180°C, with $ZnBr_2$ at 20°C, or with other Lewis acids such as $FeCl_3$ or Et_2AlCl at −78°C.[71, 84] The selectivity is again very high, thus the *trans*-1,2-disubstituted cyclohexane **162** is obtained exclusively (**162**/**163** > 99:1) from **161** under all conditions.[71e, 84] Surprisingly, by the reaction of **164**, also the *trans*-1,2-disubstituted cyclopentane derivative **165** is preferentially formed ($ZnBr_2$/20°C: **165**/**166** = 96.5:3.5).[71b] Our method was recently applied by Corey et al. for the synthesis of pseudopterosin-type sesquiterpenes.[85] Similar results were found with the allylsilanes **167** and **170**, although formation of the cyclohexane was less and that of the cyclopentane more selective (Table 2).[72]

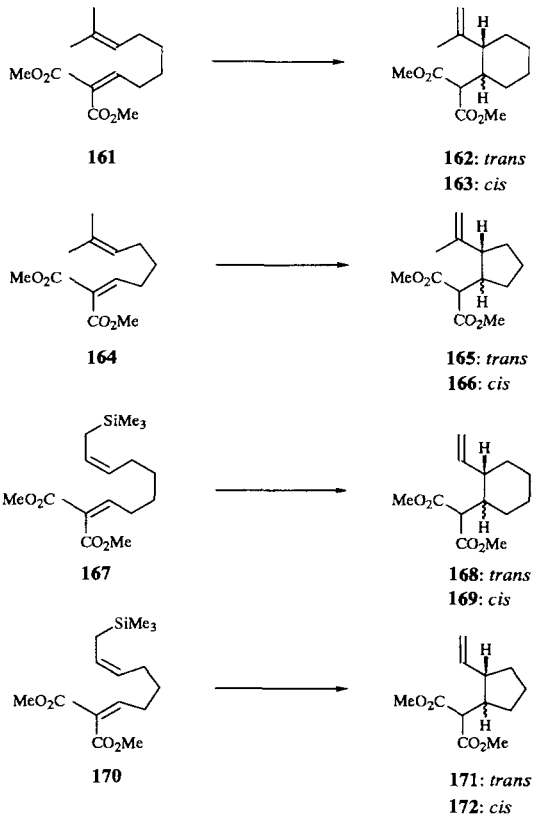

161 **162**: *trans*
163: *cis*

164 **165**: *trans*
166: *cis*

167 **168**: *trans*
169: *cis*

170 **171**: *trans*
172: *cis*

Table 2. Lewis acid-induced reaction of **167** and **170**.

Starting materials	Products	Reaction conditions: $ZnBr_2$ (20°C)	$TiCl_4$ (−78°C)	Me_2AlCl (−78°C)	TMS-OTf (−78°C)
		Product ratio [yield in %]			
167	**168**/**169**	95.2:4.8 [56]	95.9:4.1 [70]	94.4:5.6 [90]	–
170	**171**/**172**	95.8:4.2 [54]	96.6:3.4 [81]	99.7:0.3 [86]	99.6:0.4 [97]

The particular importance of the sp^2 geminal effect (*geminal* substitution at the terminus of a C=C or a C=N bond) is shown by a comparison of the cyclization of **164** and **170**

with the reaction of the monoacceptor-substituted compounds **173** and **175a–d**. Thermal reaction of **173** gave **174** as an almost 2:1 mixture of the *cis* and *trans* isomers.[86] Reaction of **175a–d** with fluoride led to a 63.3–81.2:36.7–18.8 mixture of the corresponding *trans*- and *cis*-1,2-disubstituted cyclopentanes **176**. Reaction of **175** with Lewis acids resulted in desilylation.[87]

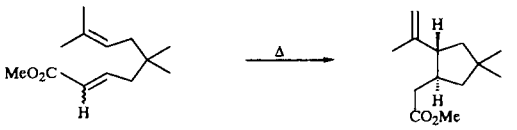

173 (*E*, *Z*)

174
trans : *cis* = 30 : 70

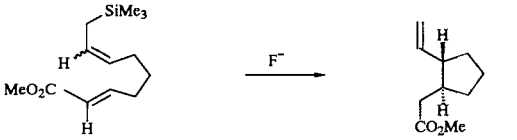

175

	trans : *cis*
a: 2*E*, 7*E*	66.2 : 33.8 (100%)
b: 2*E*, 7*Z*	63.3 : 36.7 (74%)
c: 2*Z*, 7*E*	63.5 : 36.5 (73%)
d: 2*Z*, 7*Z*	81.2 : 18.8 (78%)

176

Oxazepandiones **177**, accessible from malonates and ephedrine, can be used as chiral 1,3-dicarbonyl compounds.[88] Reaction of **140** and **177** with ethylenediammonium diacetate and diethylaluminum chloride, in a consecutive sequence via the (*Z*)-benzylidene compound **178**, gave almost exclusively the *cis*-cycloadduct **179** (asymmetric induction > 99:1). The high diastereoselectivity of the hetero-Diels–Alder reaction can be traced back to a pseudo-boat conformation of the oxazepane ring in **178**, which hinders attack on the *Si* face.[89] It should be pointed out that reaction thereby occurs syn to the sterically more demanding groups at both stereogenic centers in **178**.[90] Our interpretation of the stereochemical control has since been confirmed by Trost et al. in their work with **177** as a chiral auxiliary.[91]

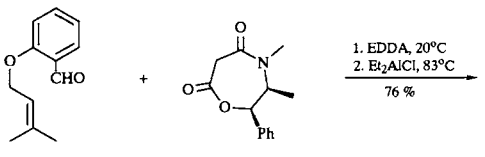

140 **177**

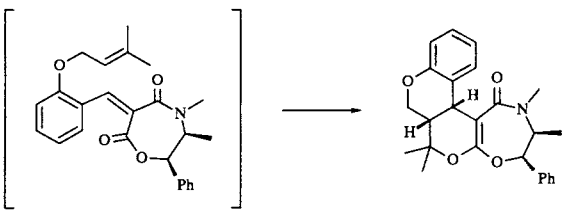

178 **179**

A high induced diastereoselectivity is also found in the tandem Knoevenagel hetero-Diels–Alder reaction with the aldehydes **180**, **182**, **184**, and **186**, which contain a substituent in the α, δ, β, or γ position, respectively. It is necessary here to differentiate between "steric interactions" of the substituents with the diene or the dienophile component and "conformation effects" of the chain. The steric interaction dominates in the case of the α- and δ-substituted aldehydes, the conformation effect for the β- and γ-substituted compounds. For the intermediate alkylidene compounds from **180** and **145** or **182** and **145**, a rigid conformative restriction in the transition state to the cycloadduct as a result of the 1,3-allylic strain (sp^2 geminal effect[71b]) must be assumed with preference of, for example, **188-K2** compared to **188-K1**. Thus, the induced diastereoselectivity in formation of

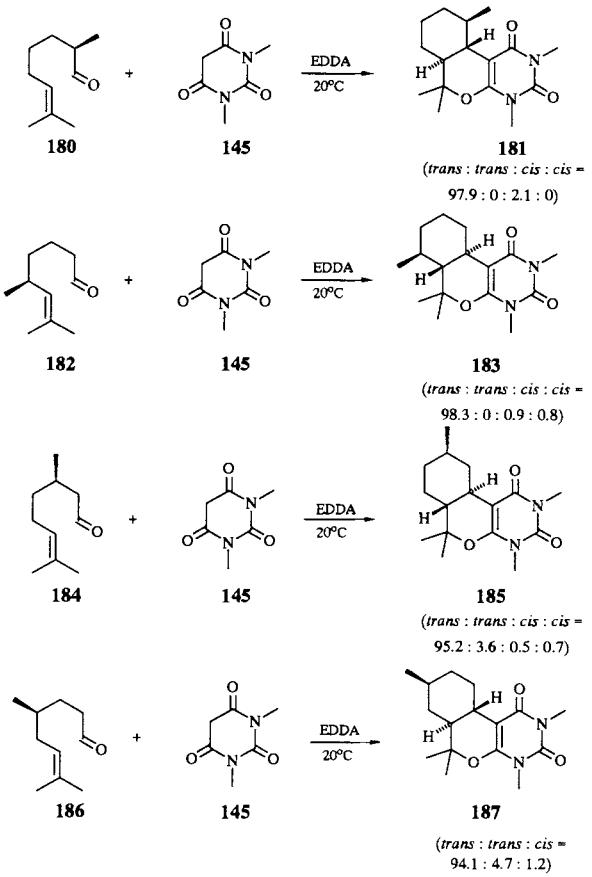

180 **145** **181**
(*trans* : *trans* : *cis* : *cis* = 97.9 : 0 : 2.1 : 0)

182 **145** **183**
(*trans* : *trans* : *cis* : *cis* = 98.3 : 0 : 0.9 : 0.8)

184 **145** **185**
(*trans* : *trans* : *cis* : *cis* = 95.2 : 3.6 : 0.5 : 0.7)

186 **145** **187**
(*trans* : *trans* : *cis* = 94.1 : 4.7 : 1.2)

the products **181** or **183** is > 99%. For the alkylidene compounds formed from **184** and **145** and from **186** and **145**, for example **189-K1**/**189-K2**, the driving force for the selectivity

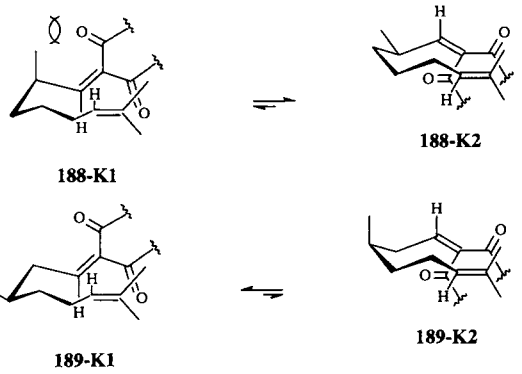

188-K1 **188-K2**

189-K1 **189-K2**

is the formation of a chair-like transition state with an equatorial arrangement of the substituents, as in **189-K1**. Thus, **185** and **187** are formed preferentially.[77b]

Yet higher selectivity is observed with the Lewis acid-initiated ene reaction of the Knoevenagel products of the aldehydes **180**, **182**, **184**, and **186** with malonates. Thus, reaction of the alkylidine malonates from **180** and **182**, initiated either by a Lewis acid or thermally at 180 °C, led in each case to only a single *trans*-1,2-disubstituted cyclohexane derivative;[92] use of the alkylidenemalonate from **184**, with catalytic amounts of $FeCl_3$ on Al_2O_3 (0.1 equiv), led to both possible *trans* products in the ratio 98.8:1.2.[93] An efficient and diastereoselective decalin synthesis based on this reaction was achieved with a Knoevenagel-ene-Prins sequence.[71a] The initially formed Knoevenagel product **192**, from citronellal **191** and methylacetoacetate **190**, reacted under the influence of $ZnBr_2$ to give **194** in 45% yield via the ene-product **193**. In addition, one obtained 20% of the double bond isomers of **194**, small amounts of a diastereomer (< 3%), together with the Diels–Alder product and the ene product **193**.

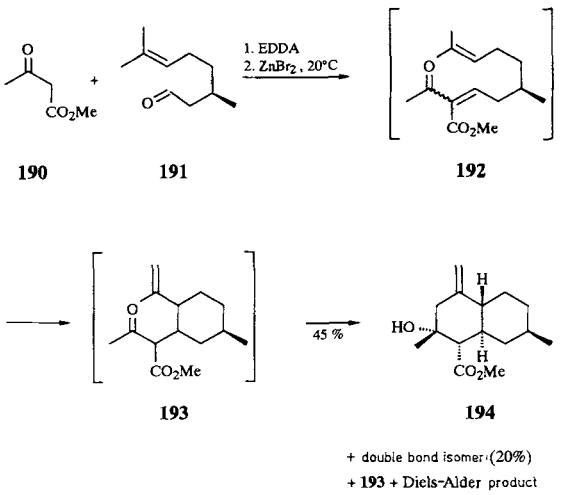

190 **191** **192** **193** **194**

Recently we achieved the development of an enantioselective variant of the tandem Knoevenagel hetero-Diels–Alder reaction by using a chiral Lewis acid. To date, enantioselective intramolecular reactions involving chiral catalysts or mediators have met with little success. As a result, it was hardly surprising that the first experiments with known chiral Lewis acids gave only very small enantiomeric excess (*ee* < 20%). In contrast, with the new chiral Lewis acid **195** (stoichiometric formula), easily available from 1,2:5,6-di-*O*-isopropylidene-α-D-glucofuranose (diacetone glucose), titanium tetraisopropoxide, and titanium tetrachloride (8:3:1), good enantiomeric excesses could be observed in the reaction of the aromatic aldehyde **196** with dimethylbarbituric acid **145** as a model process. The best results were observed with the domino reaction of 4-methoxybenzaldehyde **196a** with **145**, in which **197a** was formed with an *ee* of 88%.[94] The Lewis acid **195** catalyzed both transformations in the Knoevenagel Diels–Alder sequence; without the addition of **195** no Knoevenagel product was formed.

The tandem Knoevenagel hetero-Diels–Alder sequence and tandem Knoevenagel-ene sequence have already been

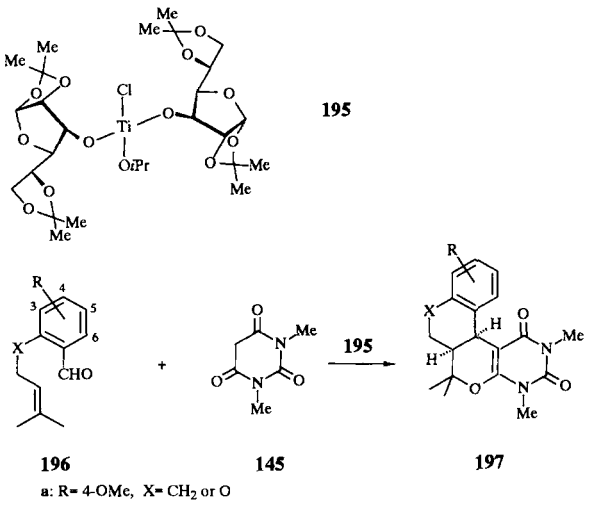

196 **145** **197**

a: R = 4-OMe, X = CH_2 or O

widely used in the synthesis of natural products. It has thus been possible to construct the basic framework of secologanin **202b** from a sequence involving a three-component reaction. (Secologanin possesses great importance as a key compound in the biosynthesis of monoterpene indole alkaloids as well as the ipecacuanha, cinchona, and pyrroloquinoline alkaloids.[95]) Thus, the mono-protected malondialdehyde **198**, the reactive 1,3-dicarbonyl compound **199** (equivalent to formyl acetate), and the enol ether **200** were mixed together in the presence of potassium fluoride as base. The domino reaction led directly to the dihydropyran **201**, which, after conversion of the trichloromethylcarbonyl into a methyoxycarbonyl group, elimination, hydrolysis of the thioacetal, and chromatographic purification, gave 1-ethoxysecologanin-aglucon **202a** in an overall yield of 12%.[96]

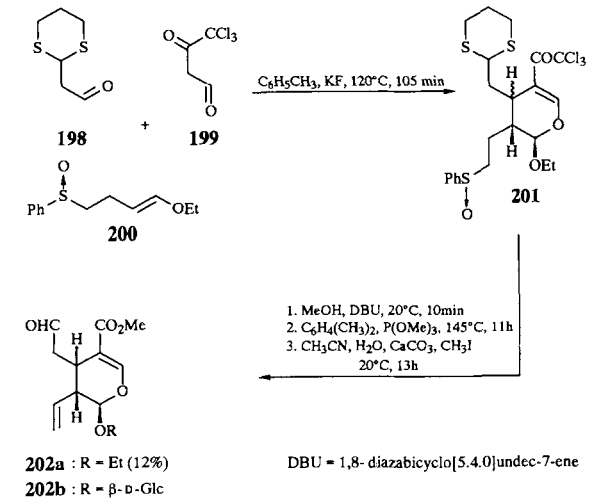

198 **199** **200** **201**

202a : R = Et (12%)
202b : R = β-D-Glc

DBU = 1,8-diazabicyclo[5.4.0]undec-7-ene

A comparable synthetic sequence was used in the construction of the strictosidine analogue **207**. Strictosidine, total synthesis of which has not yet been achieved, is the first nitrogen-containing precursor of the monoterpenoid indole alkaloids and is formed in vivo by enzymatic condensation of tryptamine and secologanin.[97] Reaction of the enantiomerically pure aldehyde **203** with dimethylbarbituric acid **145** and the enol ether **204** in the presence of ethylenedi-

ammonium diacetate and by using ultrasound led to a 92% yield of **205** within 4 h at 20 °C. Hydrogenation of the crude diastereomeric mixture obtained with H_2/Pd/C, in a type of biomimetic transformation, with cleavage of both protecting groups, opening of the hemiacetal formed, condensation of N-4 with the aldehyde formed, and hydrogenation of the resulting iminium salt or the enamine, gave the dihydrocorynanthine derivative **207** (45%, based on **203**), with the correct relative and absolute configurations at all stereogenic centers.[98] In addition, 7% of the *allo*-compound **206a** and

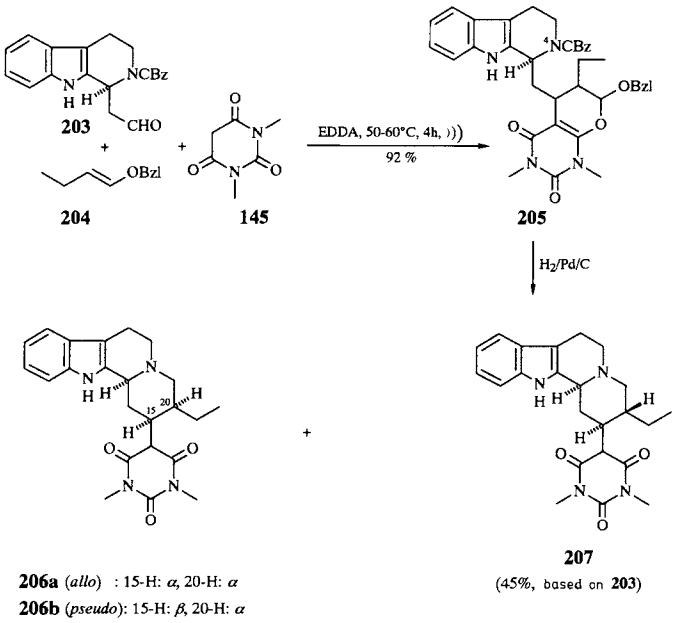

203 + **204** + **145** → **205** → **206a** + **206b** + **207**

206a (*allo*) : 15-H: α, 20-H: α
206b (*pseudo*): 15-H: β, 20-H: α
207 (45%, based on **203**)

12% of the pseudo-compound **206b** were also obtained. In a similar manner, we synthesized the natural product dihydroantirhine **210** from **203**, **204**, and Meldrum's acid **141**, via the intermediates **208** and **209**.[99]

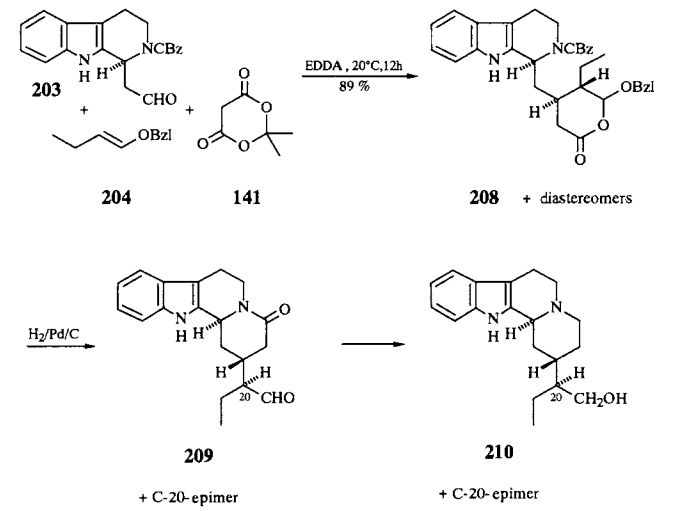

203 + **204** + **141** → **208** + diastereomers → **209** → **210**

209 + C-20-epimer
210 + C-20-epimer

The tandem Knoevenagel hetero-Diels–Alder reaction with an intramolecular second step has, amongst other examples, been used for the synthesis of enantiomerically pure hexahydro-[100] and tetrahydrocannabinol **214**,[101] deoxyloganin **217**,[102] ajmalicine **220**,[103] tetrahydroalstonine **221**,[103] furofuran lignans,[104] heterosteroids **223**,[105] and D-homosteroids **225**.[106]

Reaction of **211**, from linalool, with 5-*n*-pentyl-1,3-cyclohexanedione **212** gave the adduct **213**, from which **214** was obtained in two steps.

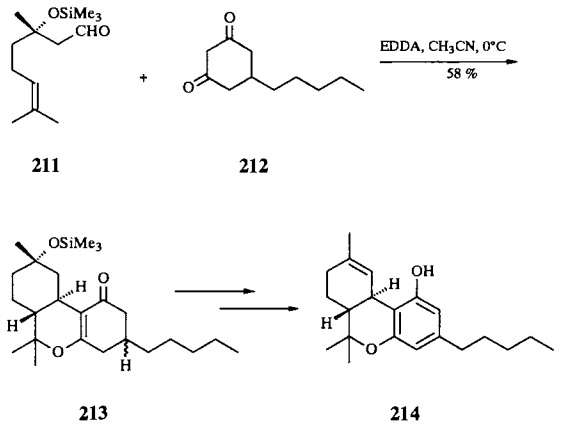

211 + **212** → **213** → **214**

The condensation of aldehyde **215**, accessible from (*S*)-citronellal, proceeded similarly with Meldrum's acid **141** to give the tricycle **216** (*cis*/*trans* = 10:1) in 77% yield, which could be transformed to deoxyloganin **217** in four steps.

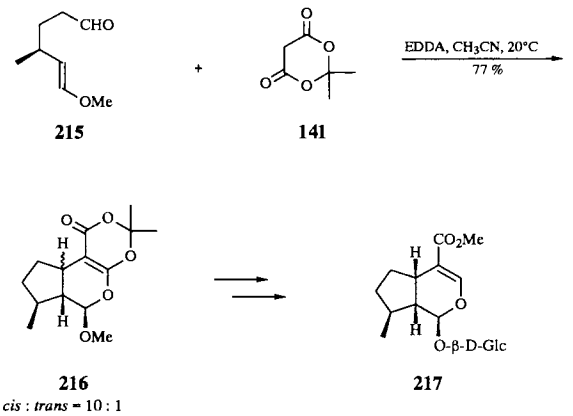

215 + **141** → **216** → **217**

216 *cis* : *trans* = 10 : 1

Other groups have also employed our tandem Knoevenagel hetero-Diels–Alder sequence for the synthesis of natural products, as demonstrated by the work of Takano, Ogasawara et al. in the preparation of furofuran–lignanes[104] and indole alkaloids.[103] Reaction of the enantiomerically pure aldehyde **218** with Meldrum's acid **141** gave the cycloadduct **219**, from which **220** and **221** were obtained.

We have synthesized numerous heterosteroids, such as **223**, by using domino reactions of enantiomerically pure **222** with 1,3-dicarbonyl compounds like, for example, *N*,*N*-dimethylbarbituric acid (**145**).[105] A further interesting example is the preparation of D-homosteroids **225** from Meldrum's acid **141** and aldehyde **224**, which can be obtained from estrone methyl ether.[106] In this case, the bridged cy-

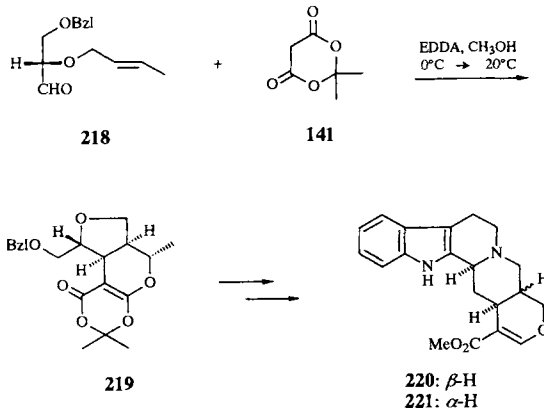

218 **141** **219** **220: β-H** **221: α-H**

cloadduct **225**, rather than the annelated compound, is formed exclusively as a result of the electron density distribution in the dienophile. In general, by suitable choice of the substituents on the dienophile, one can obtain at will either the bridged or the annelated products with the tandem Knoevenagel hetero-Diels–Alder sequence.[77a]

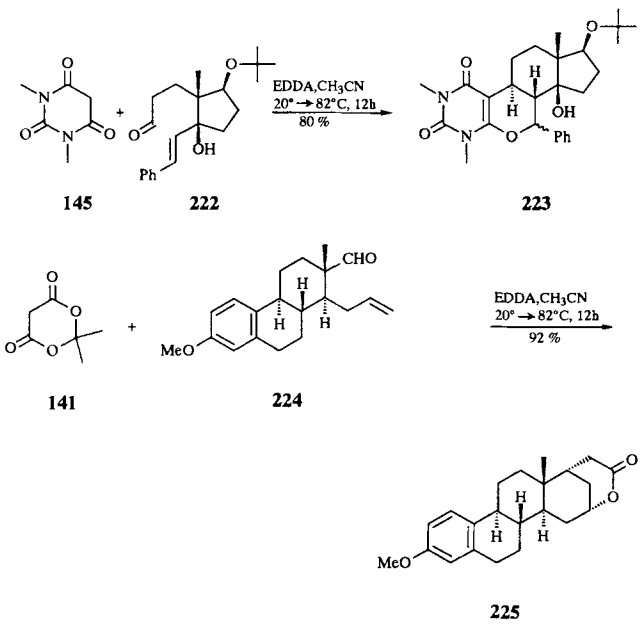

145 **222** **223** **141** **224** **225**

There are also, however, other possibilities to use anionic–pericyclic sequences. This principle was employed by Heathcock et al. in one of the best examples of the use of a domino reaction for the synthesis of a natural product. From simple starting materials they were able to construct, amongst others, the complex hexacyclic alkaloid daphnilactone A **231** in few steps and with high selectivity.[107] Thus, in one sequence, four rings and six new stereogenic centers were formed. Swern oxidation (oxalyl chloride/dimethylsulfoxide (DMSO)/Et_3N) of the easily accessible diol **226** led to the nonisolable dialdehyde, which cyclized to 3,4-dihydropyridine **227** on addition of NH_3. Compound **227** reacted as an 2-aza-1,3-butadiene in a type of Diels–Alder reaction with the central configuratively homogeneous olefinic double bond in the side chain to form the tetracycle **228**. The last step in the sequence to **229** is an intramolecular aza-Prins reaction of the imine formed in situ by the Diels–Alder reaction. A characteristic of the quality of this sequence is the high stereoselectivity of the indivual steps; thus only one diastereoisomer is formed, the absolute configuration of which is based on the stereochemistry of the quaternary C*atom in the substrate **226**. The structure of the carefully chosen starting material forces the subsequent steps to follow the desired route. The synthesis of daphnilactone A **231** was concluded by catalytic hydrogenation of the isopropenyl group, reductive fragmentation with diisobutylaluminum hydride (DIBAH) with formation of an unsaturated seven-membered ring, oxidation of the resulting alcohol to the acid, and finally reaction with formaldehyde to the iminium salt, which gave **231** by a double intramolecular cyclization.

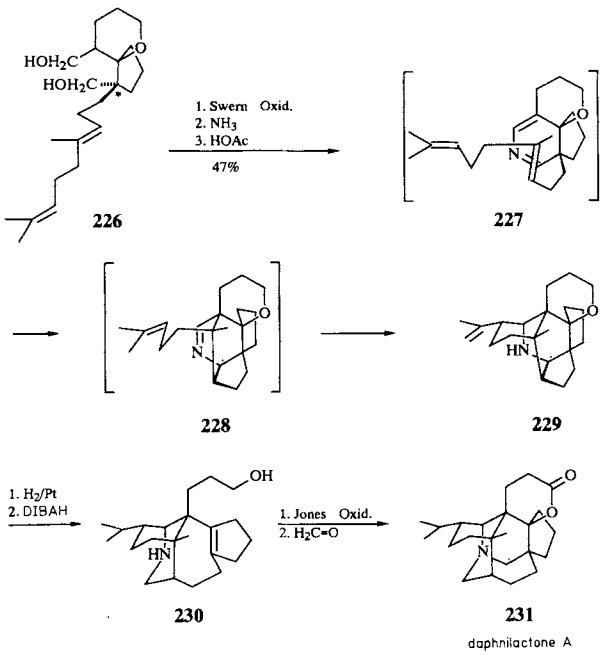

226 **227** **228** **229** **230** **231**
daphnilactone A

Similarly, sequential transformations that start with formation of an imine or an enamine have been developed by Blechert et al. for the synthesis of alkaloids.[108] Reaction of alkenylindole **232** with butanal was used to form the desired tetrahydrocarbazole structure **235**, to build the basic skeleton of the indole alkaloid *epi*-dasycarpidone. We have interpreted this sequence as an anionic–pericyclic process, where-

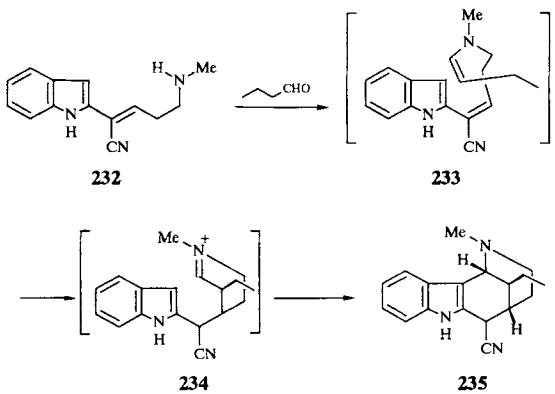

232 **233** **234** **235**

by the enamine **233** reacts to form **235** in a type of Diels–Alder reaction. It is, of course, also possible that **233** reacts first in a Michael reaction to **234**, which then undergoes a Mannich reaction. The alkenylindoles have also been prepared from aromatic hydroxylamines, an aldehyde, and an allene in a sequential process involving 1,3-dipolar cycloaddition and a 2,3-sigmatropic rearrangement.[108]

We have developed a sequence consisting of a Pictet–Spengler and an ene reaction for the synthesis of indole alkaloids of the corynanthe group, such as corynantheine **237**, from simple precursors corresponding to the retrosynthesis **237** ⇒ **236**. Thus, we have prepared, with high diastereoselectivity, the *trans*-indol[2,3-*a*]quinolizidine **239**, which can be further converted in a few steps into the racemic indole alkaloids corynantheine **237**, dihydrocorynantheine, corynantheol, and dihydrocorynantheol. Sequential treatment of **236** with trifluoroacetic acid and tin tetrachloride gave the tricycle **239** as solitary product in 42% yield.[109] The transi-

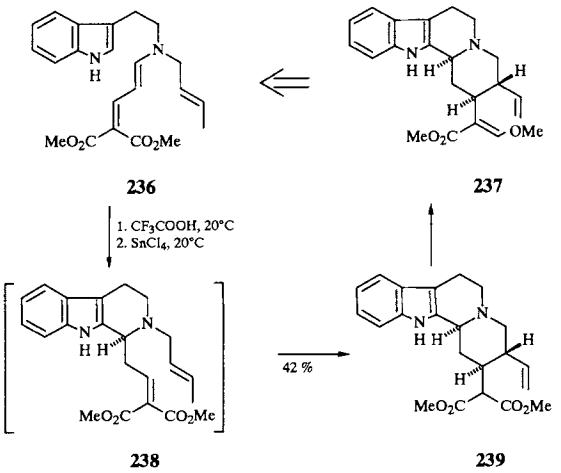

236 **237** **238** **239**

tion structure for the ene reaction **238** to **239** is assumed to have the conformation **240**, which is largely fixed because of the 1,3-allylic strain from the two terminal ester groups on the enophile (sp^2 geminal effect[71b]), thereby leading to the high selectivity observed.

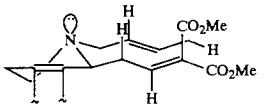

240

Another new sequence in organic synthesis is the combination of a Sakurai with a carbonyl-ene reaction, which we have developed for the synthesis of 7-methylsubstituted steroids.[110] Compounds of this type frequently display, in contrast to the unsubstituted steroids, a higher biological activity. For example, 7α-methylprednisolone showed a five-fold greater antiphlogistic effect than cortisone.[111] For the synthesis of these compounds we started from the enantiomerically pure Hajos–Wiechert ketone **241**,[112] which can be converted via **242** into the aldehyde **243** required for

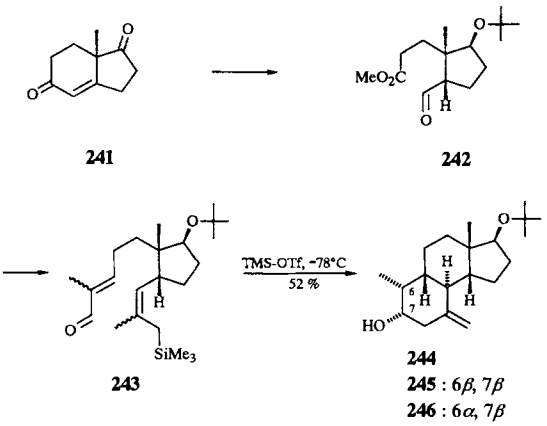

241 **242** **243** **244** **245** : 6β, 7β **246** : 6α, 7β

the domino reaction. Treatment of the isomeric mixture with trimethylsilyl trifluoromethanesulfonate (TMS-OTf) gave exclusively enantiomerically pure **244** with formation of four stereogenic centers. Interestingly, the stereoselectivity of the tandem Sakurai–Prins reaction can be controlled by the choice of the Lewis acid. Thus, treatment of **243** with Et_2AlCl leads to diastereomer **245**; nevertheless, the transformation is not as selective as that with TMS-OTf, as **246** is also obtained (**245**:**246** = 3:1). A new type of tandem Michael Diels–Alder sequence has been used by Naruta et al. for the synthesis of daunomycinone derivatives.[113]

3. Radical Primary Step

For those sequences that start with a radical primary step, we have found exclusively examples of radical–radical transformations (homosequence, Section 3.1). Thus an abundance of possibilities for further investigations exists in this area; the radical–pericyclic sequence in particular appears to us to be of great interest.

3.1. Radical–Radical Sequences

In the last decade radical reactions have gained importance, also for the synthesis of natural products. As with the cationic, anionic, and transition metal-catalyzed sequential cyclization of polyenes or polyenynes, a radical sequence is also possible for suitable substrates. The formation of the primary radical can result by reaction of halogens, phenylthio- and phenylselenium compounds with stannanes such as nBu_3SnH, silanes, and germanes.[114] Redox processes may also be employed; thus, the Mn^{III} oxidation[115,116] of C–H bonds, activated by one or two electron acceptor groups, is well established. Snider et al. used the reaction of **247** with $Mn(OAc)_3$ to form the tricycle **248** in 50% yield.[115c]

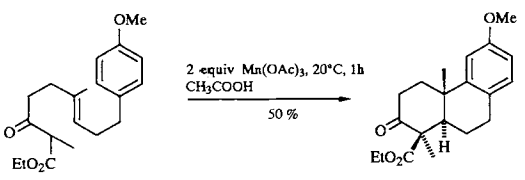

247 **248**

The syntheses of hirsutene,[117] $\Delta^{9,12}$-capnellene,[118] and silphiperfolene[119] are attractive examples of domino radical cyclizations involving halogen compounds. Curran et al. prepared a mixture of triquinanes **251** in 66% yield by reaction of the bromide **249** (obtained from 3-ethoxy-2-cyclopentenone in three steps) with nBu$_3$SnH via the radical **250**. Silphiperfolene **252** was then obtained by Wolff–Kishner reduction and separation of the resulting epimers by gas chromatography.[119]

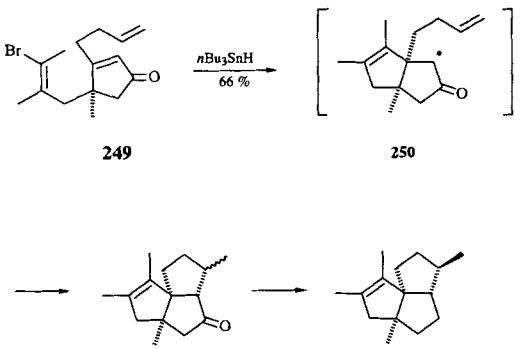

249 **250**

251 **252**

$\alpha:\beta = 3:1$

Acyl radicals can also be used for the domino polycyclization; these can be generated from phenylselenoesters with nBu$_3$SnH, among other methods. The efficiency of this method is demonstrated by diastereoselective formation of **255** from **253** via **254**.[120]

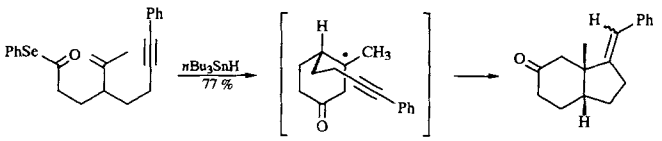

253 **254** **255**

> 98% *cis*

Tandem radical reactions, in which rapid intramolecular cyclization is followed by a slow intermolecular addition, are of particular synthetic interest. This method was successfully used by Stork et al. in the synthesis of prostaglandins.[121] In this case, in contrast to the three-component cuprate addition to enones, bond formation takes place first at C2 and then at C3. Reaction of the α-iodoacetal **256**, synthesized from cyclopentadiene, with seven equivalents of the α-trimethylsilylenone **257** and 0.1 equivalents nBu$_3$SnCl in the presence of NaBH$_3$CN led to a 58% yield of **261**, which could be converted into the prostaglandin precursor **262** by a Saegusa oxidation.[122] The radicals **258**, **259**, and **260** can be formulated as intermediates; the reaction sequence was concluded by transfer of a hydrogen atom from nBu$_3$SnH to **260**. The rapid intramolecular cyclization of **258** to **259**, in comparison with the addition of **257** to **258**, is of decisive importance for the success of this domino reaction. Among other factors, this result can be attributed to the oxygen atom in the chain.

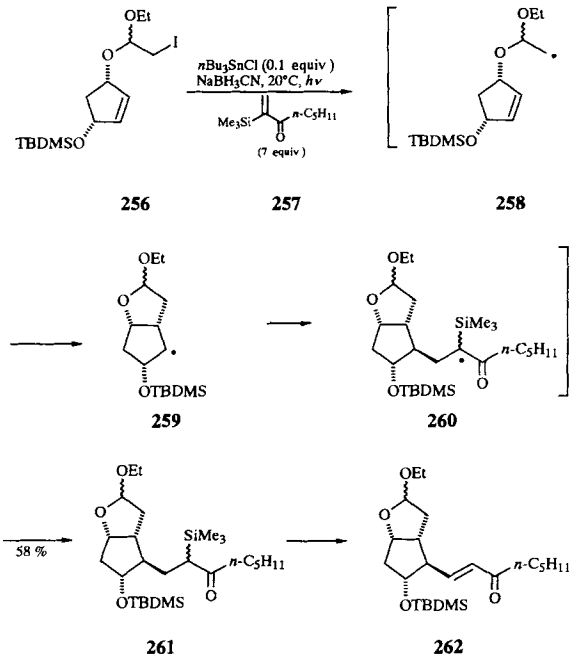

256 **257** **258**

259 **260**

261 **262**

Electrochemical processes may also be applied for the generation of radicals; such methods have the advantage, in contrast to the chemical methods, that toxic reagents such as nBu$_3$SnH are not required and that less waste is produced. Radicals can be formed very simply from carboxylic acids by Kolbe electrolysis (anodic decarboxylation). If coelectrolysis with a second acid is carried out, one obtains—as Schäfer et al. have shown—coupled products in a sequential transformation. Compound **263**, from 2-cyclopentene-1,3-diol, underwent electrochemical double decarboxylation with, for example, four equivalents of methyl succinate to give a 33% yield of **264**, which was used for prostaglandin synthesis.[123a] In similar fashion, perhydropentalene **266** was formed in 64% yield as a 1.25:1 mixture by coelectrolysis of **265** with methyl succinate.[123b]

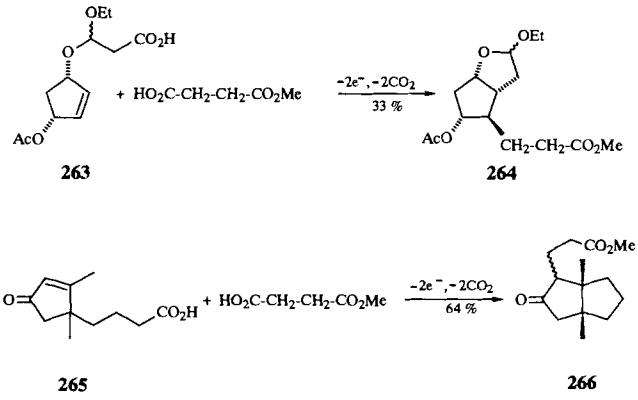

263 **264**

265 **266**

Radicals can also be formed by cathodic reduction of ketones. At a potential of −2.80 V electrolysis of **267** via **268** gave a 54% yield of the perhydropentalene **269**.[124]

The thermal elimination of nitrogen from diazenes, according to Little et al., is a simple method for the production of diradicals, which can undergo sequential reactions with

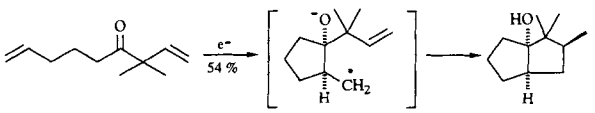

267 268 269

compounds containing multiple bonds. The diazenes required can be prepared by a Diels–Alder reaction of fulvenes with azodicarboxylates. Thermolysis of **270** at 82 °C gave the tricycle **271** in 80–90% yield. The diradical **272**, which reacts to form **271** by way of **273**, can be formulated as the reactive starting molecule in this highly diastereoselective cyclization, in which four stereogenic centers are constructed.[125]

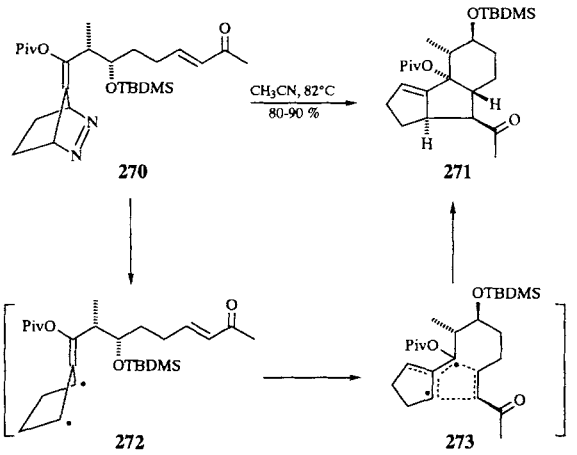

270 271 272 273

A certain amount of detective work is necessary to clarify the details of the conversion of **274** to **275**, which was observed under the classical conditions with nBu$_3$SnH and AIBN.[126]

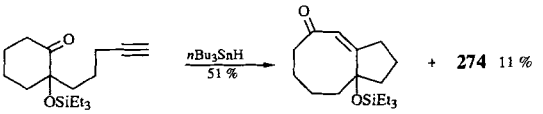

274 275

The reaction of **276** to **277** and **278** in 64% yield in the presence of nBu$_3$SnH and AIBN, described by Wilcox et al., although not a genuine domino reaction according to our definition, is nevertheless an attractive one-pot multiple cyclization.[127]

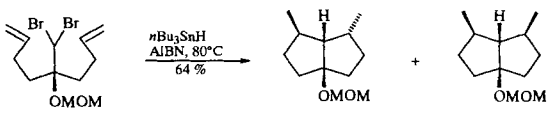

276 277 278

MOM = CH_2OCH_3 AIBN = α,α'-azobisisobutyronitrile

Other interesting radical sequences, also employing carbohydrates as chiral substrates, have been described.[128]

4. Pericyclic Primary Step

Pericyclic reactions can be combined easily with other pericyclic reactions to give sequences. This is particularly the case for the Diels–Alder reaction. Whether inter- or intramolecular, the all-carbon atom or the heteroatom variant, normal, neutral, or with inverse electron demand, this reaction is one of the most efficient methods in the repertoire of the organic chemist.[6a, 6d, 129] There are, however, also methods in which a pericyclic process is coupled with an anionic process (Table 1, Section 4.3). On the other hand, no examples are known for the pericyclic–cationic (Table 1, Section 4.2) or the pericyclic–radical sequence (Table 1, Section 4.4).

4.1. Pericyclic–Pericyclic Sequences

A domino Diels–Alder process is the key step in the synthesis of pagodane **283** by Prinzbach et al., in which the bisdiene **279** reacts with malonic anhydride **280** to give the cycloadduct **282** with excellent yield. Initially, attack of the

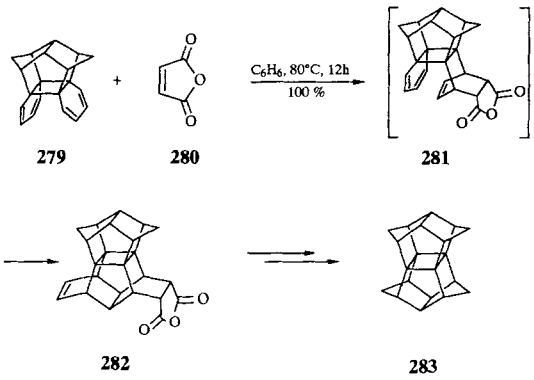

279 280 281 282 283

activated dienophile onto the outer face of **279** takes place by an intermolecular Diels–Alder reaction to give **281**, which could not be isolated, but which reacts further in an intramolecular cycloaddition to give **282**. Compound **282** can be converted to **283**.[130] If **279** is allowed to react with acetylenic dienophiles, in certain cases compounds of type **B** can be isolated in addition to those of type **A** (Scheme 6).[130]

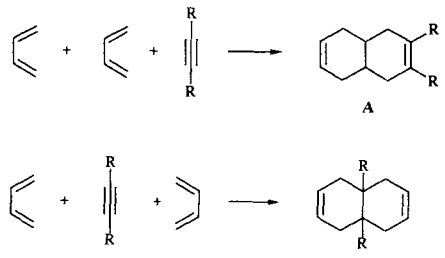

Scheme 6. Types of Diels-Alder sequences A B

A comparable sequential transformation, which is composed of a Diels–Alder reaction and a subsequent dimerization, was used by Hopf et al for the elegant synthesis of

[2.2]paracyclophanes **287**. In this case, a 1,2,4,5-hexatetraene **284** reacts as a 4π-electron component with an electron-deficient acetylene **285**. The highly reactive *p*-xylylene **286** is formed initially, dimerizing with itself to give **287**.[131]

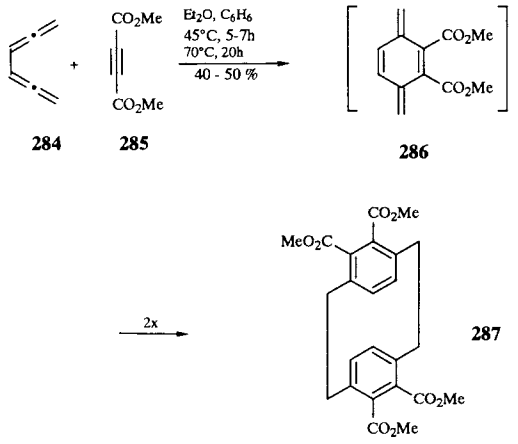

284 **285** **286** **287**

Diels–Alder reactions can also be coupled with retro-Diels–Alder reactions[132] to form interesting sequences. An illustrative example is the reaction of **288** to give **290** via the nonisolable Diels–Alder adduct **289** used by Jacobi et al. in a synthesis of paniculide A **291**. The elimination of acetonitrile from the primary cycloadduct **289** in this sequence is worthy of note.[133]

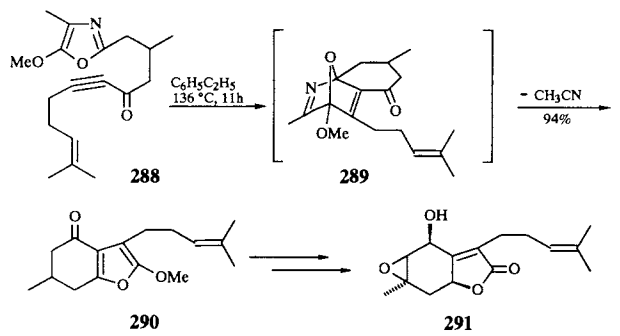

288 **289** **290** **291**

The synthesis of ansa compounds from steroids by Winterfeldt et al., in which the steroid framework is almost completely dismantled, is an attractive example of a Diels–Alder retro-Diels–Alder process. Thus, reaction of ergosterolacetate **292** with propargylaldehyde **293** in refluxing toluene led directly to the ansa compound **295**. On the other hand, the primary cycloadduct **294** can be isolated if Lewis acids are used at room temperature. Heating leads again to **295**.[134]

The reverse order, the retro-Diels–Alder Diels–Alder sequence, is also known.[135] In experiments aimed at the synthesis of the antibiotic indanomycin, Burke et al. unexpectedly isolated the indene derivative **299** in the reaction of **296** with lithium diisopropylamide and chlorotrimethylsilane. The silylketeneacetal **297** and the retro-Diels–Alder adduct **298** are assumed as intermediates.[135a]

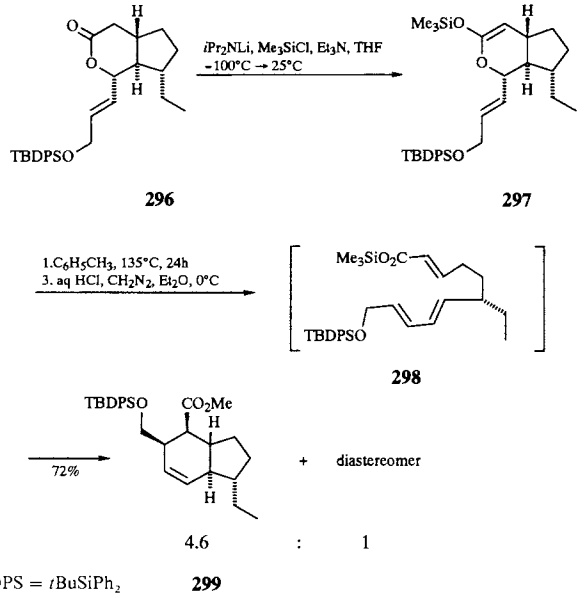

296 **297** **298** **299**

TBDPS = *t*BuSiPh$_2$

To the best of our knowledge, Diels–Alder-ene[136] and retro-Diels–Alder-ene[137] sequences have not been investigated systematically, although isolated examples are known, for example, the reaction of **300** to **302** for the synthesis of alkaloids containing the perhydroindole skeleton, reported by Keck et al. Presumably a retro-Diels–Alder reaction leads to intermediate formation of the acylnitroso-olefin **301**, which then reacts to form **302** in a hetero-ene reaction.[137a]

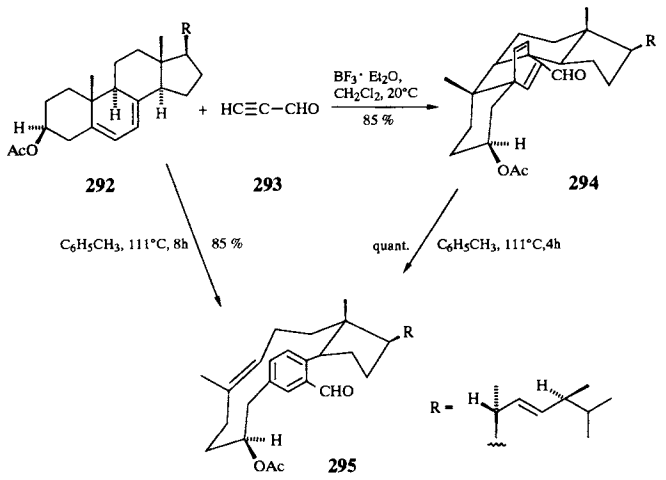

292 **293** **294** **295**

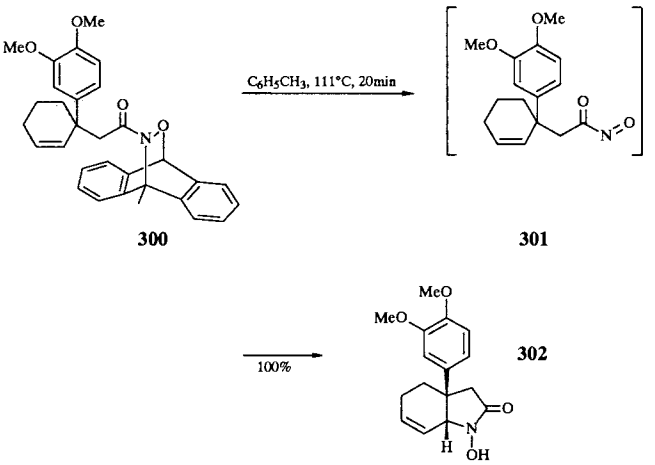

300 **301** **302**

Heterocycles can be constructed by the sequence of Diels–Alder reaction and 1,3-dipolar cycloaddition of functionalized nitroalkenes or nitrodienes.[138] For example, Denmark et al. have obtained the nitrosoacetal **305** with high-induced (98.3%) and noninduced (99%) diastereoselectivity from the enantiomerically pure vinyl ethers **304** and **303**. Compound **305** could be converted into the α-hydroxylactam **306** by reduction with elimination of the chiral auxiliary.[139]

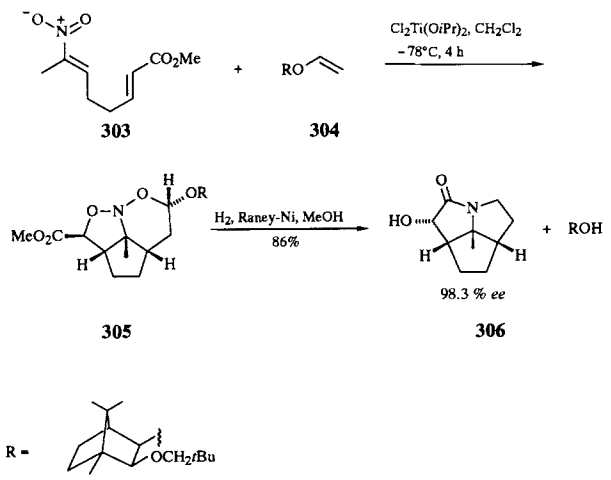

The ene-reaction[140] can, as with the Diels–Alder reaction, be combined with itself or with other pericyclic and related processes. Snider et al. have introduced a new type of annelation method with the reaction of **307** with acrolein to give **309** by way of **308**. Use of an excess of acrolein led to a subsequent Oppenauer oxidation.[141]

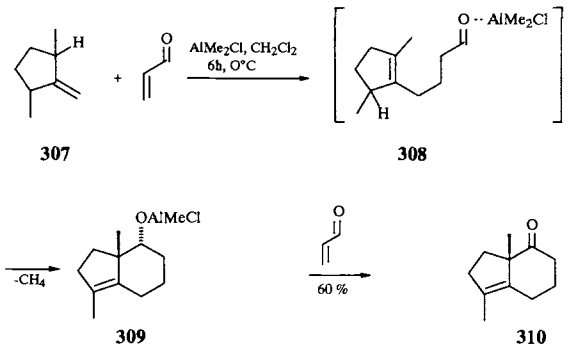

The ene-Diels–Alder sequence was first described 40 years ago with the reaction of 1,4-cyclohexadiene **311** with acetylene dicarboxylate **285** to give **313** via **312**.[142a] In the intervening period the process has been improved.[142b,c]

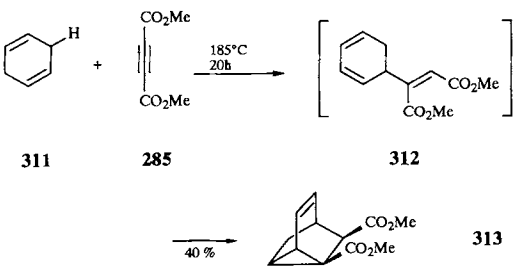

This sequence was adopted by Giguere et al. for the synthesis of the basic framework of khusimone and zizaene. Heating **314** with **285** in xylene under reflux in the presence of $ZnCl_2$ gave **315** (58%) and **316** (34%). The major product can be transformed into the desired tricyclo[6.2.1.$0^{1,5}$]undecane derivative **317** by a subsequent acid-catalyzed reaction.[143]

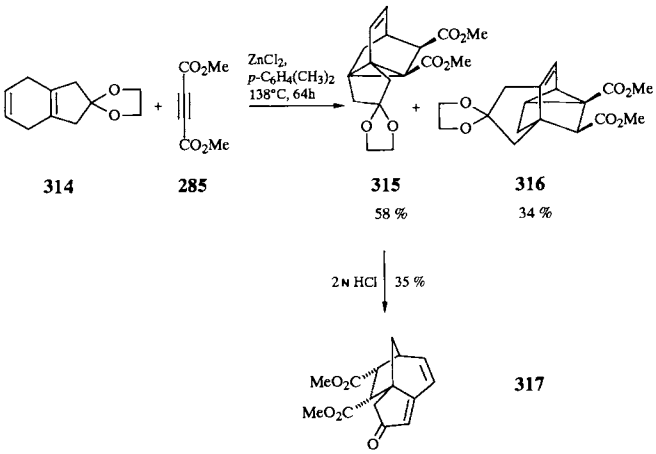

The coupling of Claisen and Cope reactions has already been used on numerous occasions for the synthesis of natural products. Thomas et al. successfully used the Claisen–Cope sequence[144] for the synthesis of sesquiterpenes such as β-sinensal.[145] The efficiency of the Cope–Claisen sequence[144a,146,147] has been demonstrated by Raucher et al. with a synthesis of the germanocrolide (+)-dihydrocostunolide **324**. Thermolysis of the keteneacetal **319**, ob-

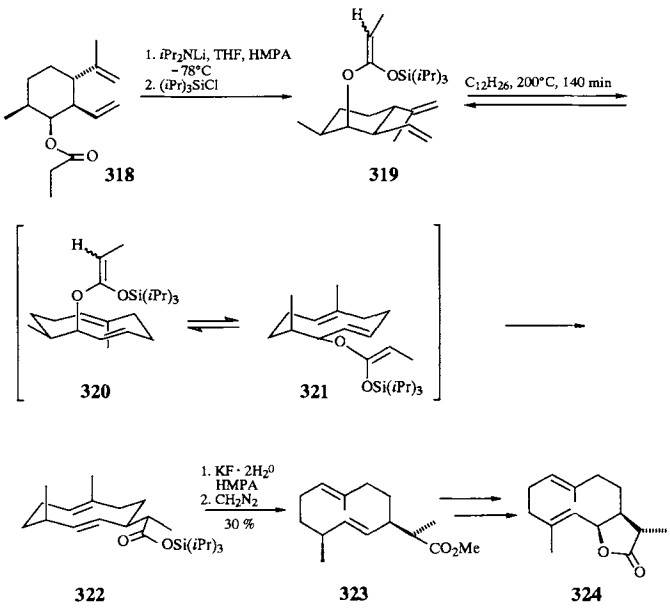

tained by deprotonation of the corresponding propionate **318** in tetrahydrofuran/hexamethylphosphoric acid amide (HMPA) followed by trapping of the enolate with chlorotriisopropylsilane, gave the decadiene **322** via **320** and **321**. Subsequent hydrolysis and esterification led to **323** as a single stereoisomer in 30% yield.[147a]

Examples of the Oxy-Cope–Claisen and Oxy-Cope–Cope sequences are also known.[148] In the synthesis of the tumor inhibitor gnididione **328** by Jacobi et al., the intramolecular Oxy-Cope rearrangement forms the prelude for the conversion of **325** to **327**. The isolable Oxy-Cope product **326**, obtained by heating **325** at 110 °C, underwent a Diels–Alder retro-Diels–Alder reaction at 160 °C to form **327**. Finally, hydrolysis delivered the target molecule **328** in 45% yield.[149]

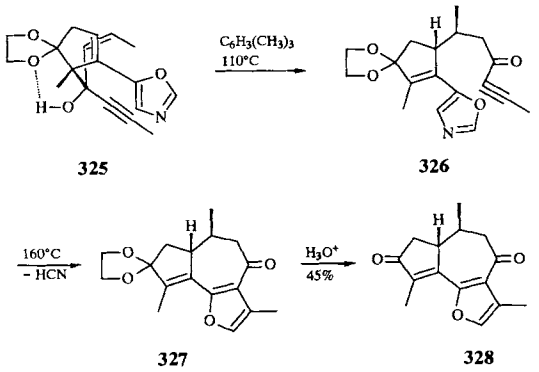

325 **326** **327** **328**

Claisen–Diels–Alder sequences have been applied by Kraus et al. for the synthesis of anthracyclines, for example, 11-deoxydaunomycinon.[150] Another example of this sequence is the diastereoselective synthesis of *trans*-decalines by Mulzer et al. Heating the secondary alcohol **329** with ethyl orthoacetate in the presence of propionic acid at 160 °C first gave the Claisen products **330** and **331**. Whereas **331** can be isolated, **330** reacts further under the reaction conditions to give **332** by an intramolecular Diels–Alder reaction.[151]

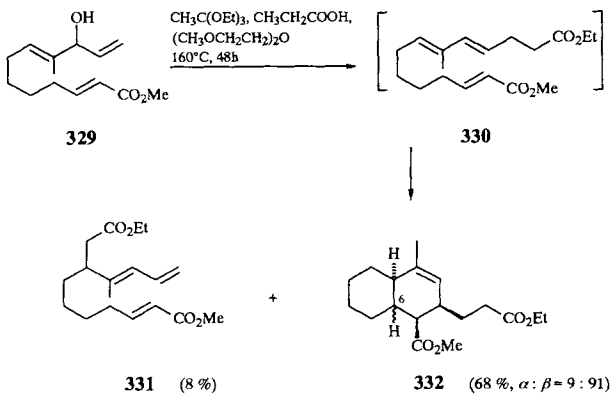

329 **330** **331** (8 %) **332** (68 %, $\alpha:\beta = 9:91$)

Okamura et al. found that allenylsulfoxides and allenylphosphaneoxides could be prepared from sulfenates or phosphinates, respectively, by a [2,3]-sigmatropic rearrangement, and used to react with dienophiles as part of a diene in a Diels–Alder reaction.[152] This strategy formed the key feature in the synthesis of the sesquiterpene (+)-sterpurene **337**. Thus, **333** was allowed to react with phenylsulfenylchloride to give **334**, which then led to the tricyclic **336** in 70% via the suspected intermediate **335**.[153]

A 1,5-hydrogen shift followed by a Diels–Alder reaction formed the starting point for the synthesis of the naturally

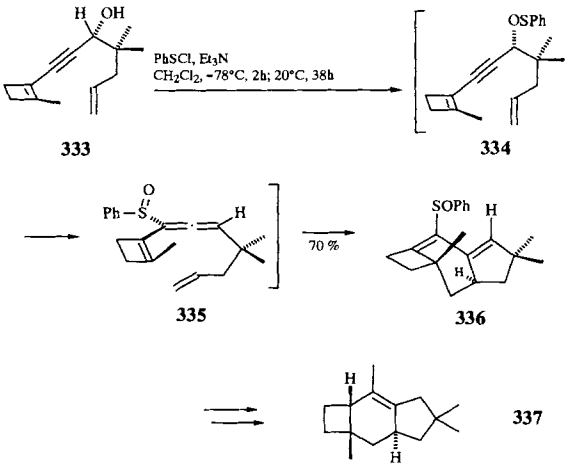

333 **334** **335** **336** **337**

existing isocedrene derivatives in racemic form by Bohlmann et al. Condensation of the tetrahydropyranyl ether of 1-hydroxy-6-methyl-5-hepten-2-one **338** with cyclopentadiene **339** afforded the pentafulvene **340**, which gave the substituted cyclopentadiene **341** as a tautomeric mixture on treatment with $LiAlH_4$. The isomers exist in a dynamic equilibrium through a 1,5-hydrogen shift. In the subsequent intramolecular Diels–Alder reaction only one of the isomers reacts, with constant adjustment of the equilibrium, to form the tricyclic product **342**, which gave **343** on hydrolysis.[154]

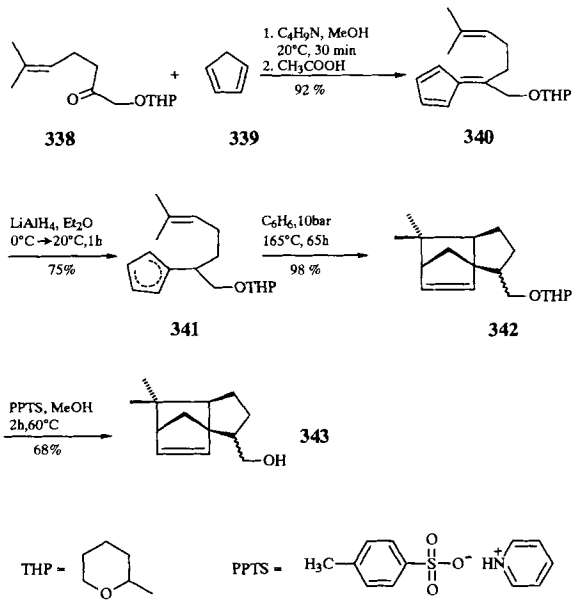

338 **339** **340** **341** **342** **343**

The Claisen-ene strategy can also be used for the synthesis of complex molecules.[140, 155] Thus, the acid-catalyzed reaction of the cyclic enol ether **344** with the enantiomerically pure (*S*)-(*Z*)-allylic alcohol **345** at 180 °C, according to Mikami et al., gave, after acidic workup, the cyclopentane derivative **349** with high diastereoselectivity (C13/C14:100% *trans*; C8/C14:90% *cis*). Compound **349** was subsequently converted to the (+)-dehydroestrone derivative **350**. The Claisen reaction of **346** to give **347**, in which the configuration of the two stereogenic centers C8 and C14 are formed with a *syn* selectivity of 9:1, presumably takes place

via a chair-like transition structure, the following intramolecular ene reaction leads to only one diastereomer, such as **349**, as major product.[156]

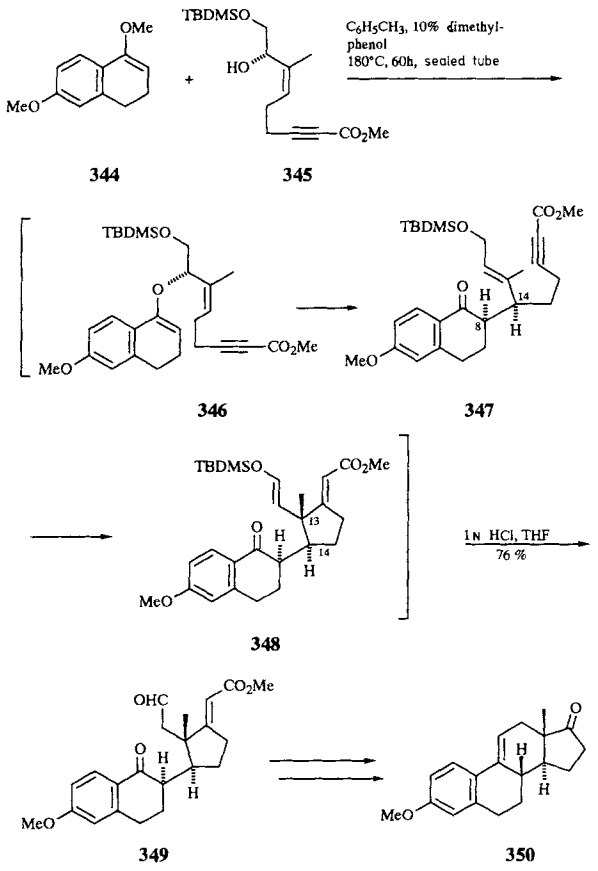

Most of the 1,3-dipoles employed in 1,3-dipolar cycloadditions are generated in situ from suitable precursors.[157] Thus, the classical entry to azomethine-ylides is the electrocyclic ring opening of aziridines.[157b] Thermolysis of the

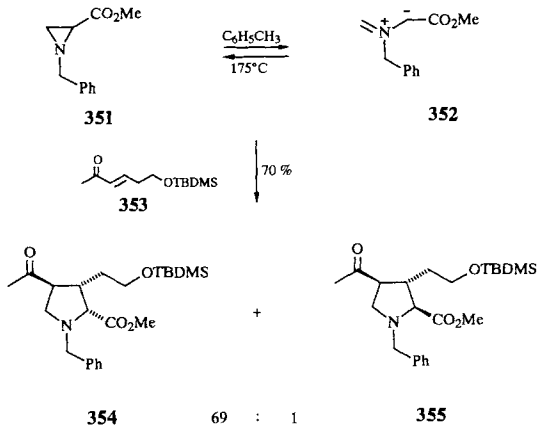

aziridine **351** to give **352**, followed by 1,3-dipolar cycloaddition to the (*E*)-enone **353** in toluene at 175 °C gave the pyrrolidines **354** and **355** regio- and diastereoselectively in 70% yield. Compound **354** was converted by DeShong et al. into the amino acid (±)-*allo*-kainic acid.[158]

As it is well known, orthoquinonedimethanes play a prominent role as 1,3-dienes in domino processes.[159] They can be generated in a great variety of ways, including thermally allowed, conrotatory, electrocyclic ring opening of benzocyclobutenes.[159] With a subsequent intramolecular Diels–Alder reaction it was possible to achieve the formation of numerous complex molecular frameworks.[129, 159] Classic examples include the numerous syntheses of steroids carried out by this route.[59c, 160] Fukomoto et al. showed with the synthesis of some alkaloids from calabar beans that orthoquinodimethanes do not just find application as 1,3-dienes in Diels–Alder reactions.[161] The key step in the synthesis of (±)-geneserine **360** is the thermal reaction of **356**. Thus, electrocyclic ring opening with formation of **357** took place first, followed by electrocyclic ring closure to give **358**, and finally a [3,3] sigmatropic rearrangement afforded **359**.[161]

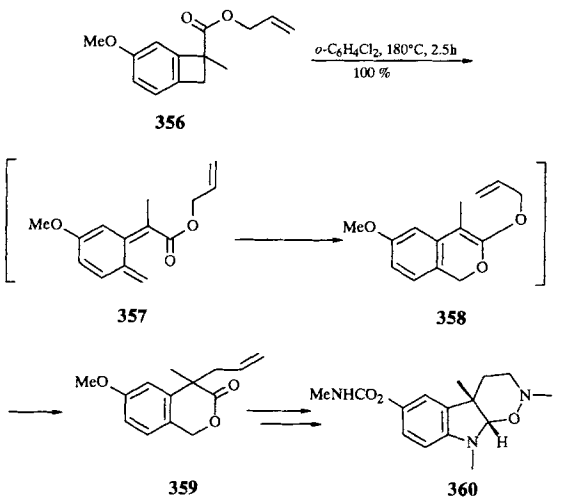

Orthoquinodimethanes and other 1,3-dienes can also be formed by cheletropic reactions. The reaction most used synthetically is the extrusion of SO_2 from sulfones.[162] In the synthesis of elaeokanine A **364** by Weinreb et al. thermolysis of **361** at 370–390 °C gave the bicyclic lactam **363**, formation of which presumably takes place via nonisolable **362**.[163]

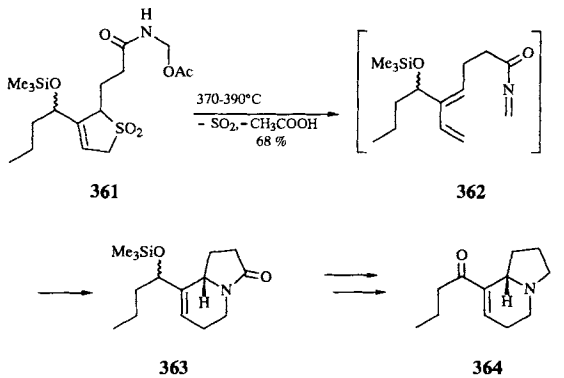

4.3. Pericyclic–Anionic Sequences

Combinations of a pericyclic with a non-pericyclic process have hitherto not been investigated very frequently. That

such a sequence is possible was shown by Grigg et al. with the reaction of a mixture of methyl vinyl ketone, **365**, and **366** in xylene at 80 °C. Initially, the cycloadduct **367** was formed from **365** and **366** in an intermolecular Diels–Alder reaction. At 140 °C **367** and methyl vinyl ketone underwent an intermolecular Michael addition to form the 1,3-dipole **368**, which ultimately reacted by an intramolecular process to give **369**.[164]

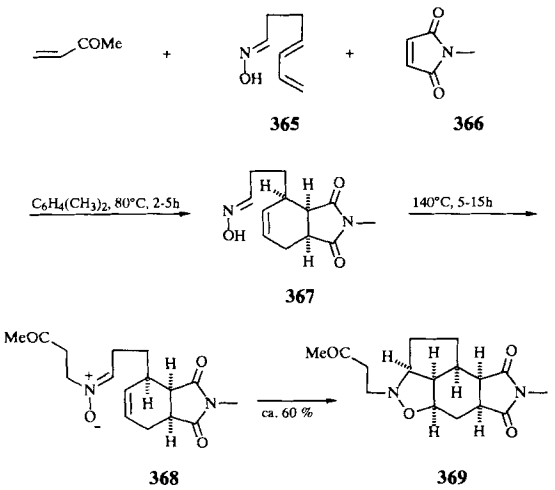

A domino process, consisting of an anionic Oxy-Cope reaction followed by an S_N' reaction for the synthesis of hydroazulenones, was realized by Paquette et al. for the reaction of **370**. Reaction of **370** with potassium hydride in tetrahydrofuran in the presence of [18]crown-6 led, after formation of the alcoholate **371** via a chair-like transition structure with an axial oxyanion group, to *trans,trans*-cyclodecadiene **374**. In this orientation a transannular S_N' substitution resulted in formation of the hydroazulenone **373**. Nevertheless, under the reaction conditions an enolate was formed that, on quenching with aqueous ammonium chloride solution at −78 °C, gave a 2:1 mixture of **372** and **373**.[165]

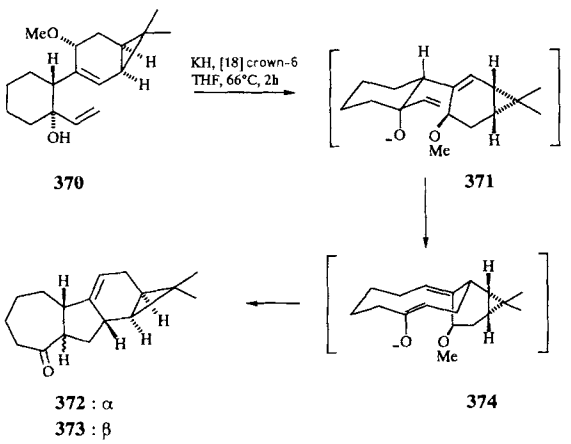

5. Photochemical Sequences

The combination of photochemical and thermal reactions has not been investigated much so far, although there is considerable potential. The reagent "*hν*" can tolerate many functional groups and reagents and can be very effective. Isomerizations, additions, eliminations, and also rearrangements can be initiated by light.

An elegant sequential synthesis of enantiomerically pure estrone was achieved by Quinkert et al. by the application of a photochemical isomerization. They showed that reactive *o*-quinonedimethanes are not just available by electrocyclic ring opening of benzocyclobutenes, but can also be prepared by light-induced tautomerization from *o*-alkyl-substituted derivatives of acetophenones. Irradiation of **375** with light of wavelength > 340 nm led initially to **376**, which then underwent a stereoselective intramolecular Diels–Alder reaction to give **377** as main product. Compound **377** was not isolated because of its instability, but was dehydrated with oxalic acid directly to the constitutionally isomeric steroids **378** and **379** (**378**:**379** = 95:5).[166]

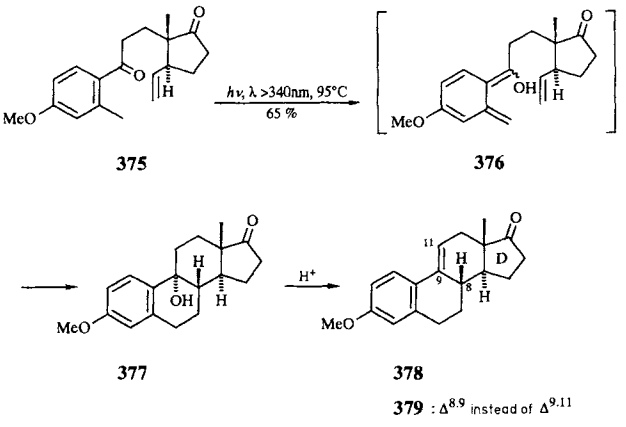

The [2+2] cycloaddition of olefins and cyclic enones or 1,3-dicarbonyl compounds count as one of the most productive photoreactions. In the photoaddition of 1,3-dicarbonyl compounds, known as the de Mayo reaction, a retroaldol reaction and recyclization to dihydropyrans generally follows.[167] This strategy has been used in a variety of ways for the synthesis of iridoids and secoiridoids.[168]

We have recently shown that substituted 1,4-dihydropyridines can also be synthesized with very good yields by the photochemical cycloaddition of enaminecarbaldehydes and alkenes.[169] An example of this is the preparation of the NADH analogue **381** from **380** and ethene.[169b] In these reactions a 2-hydroxytetrahydropyridine is formed as the first isolable compound that gives (via an iminium ion) a 1,4-dihydropyridine in the presence of acid. The iminium salt can also be trapped intramolecularly by allylsilane or propargylsilane moieties in the substrate.[170] Strictly speak-

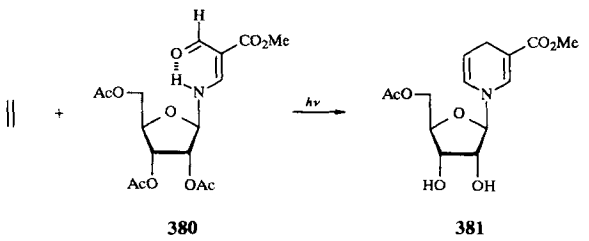

ing this does not, however, represent a domino reaction as the cycloaddition partner (added in excess) must first be removed before the Lewis acid required for the second cyclization step can be added. The allyl- or propargylsilane unit can be present either in the alkene or in the enaminecarbaldehyde. Quinolizidines, cyclohexanopyridines, pyridinoazepines and cyclopentanopyridines can also be constructed by altering the chain length. All reactions proceed with high stereoselectivity: for example, in the reaction of **382** and **383** via the intermediate **384**, only one of the eight possible diastereoisomers was formed, namely **385**.[170a] Irradiation of a mixture of methyl acrylate and **386** gave **387**, which, after distillation of the excess acrylate, led to allene **388** on treatment with trimethylsilyl trifluoromethanesulfonate.[170b]

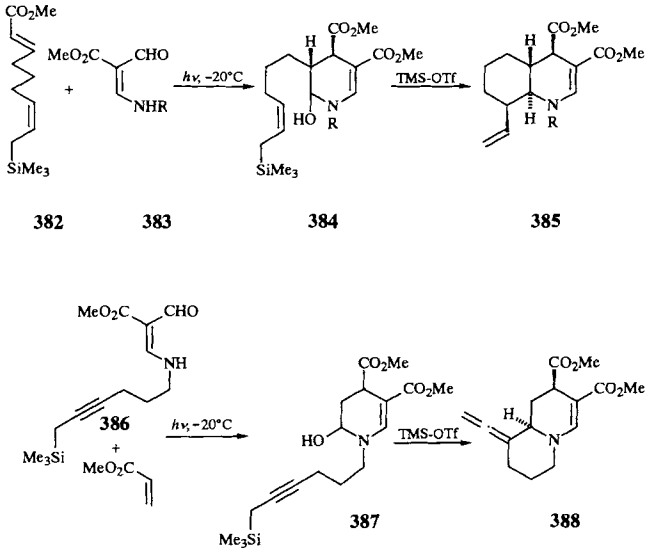

The photochemical *meta* cycloaddition of arenes and alkenes, in which three C–C bonds are formed, is a powerful sequence for the construction of complex molecules.[171] The photoaddition, starting from simple substrates, proceeds with almost quantitative yield. The process has already been employed by Wender et al. in various ways for the synthesis of natural products such as silphenes, subergorgic acids, grayanotoxin and retigeranic acid **392**.[172] The *meta*

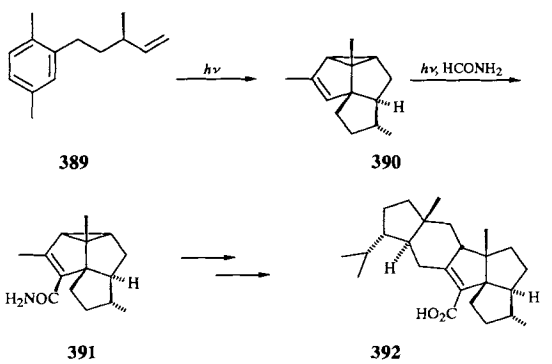

photoaddition of enantiomerically pure **389** led to the angular annelated tricylcopentane system **390**, which, after addition of formamide, gave triquinane **391** in a second photochemical step with opening of the vinylcyclopropane. The complex pentacyclic retigeranic acid **392** can then be formed from **391** in a few steps;[172b] the process includes an intramolecular Diels–Alder reaction for the formation of the 5,6-ring system.

The combination of photochemical cleavage with thermal reactions can also be employed. We have shown that allylsilanes containing an aldehyde group are photochemically accessible by Norrish type I cleavage of trimethylsilylmethylcycloalkanones.[174a] The combination of this reaction with the tandem Knoevenagel-allylsilane cyclization permits an efficient and stereoselective entry to *trans*-substituted cyclopentanes and cyclohexanes from simple precursors.[173] Irradiation of a mixture of **393**, dimethyl malonate and dimethylammonium chloride with a high-pressure mercury lamp ($\lambda > 280$ nm) led directly to **394**. The aldehyde **395** and

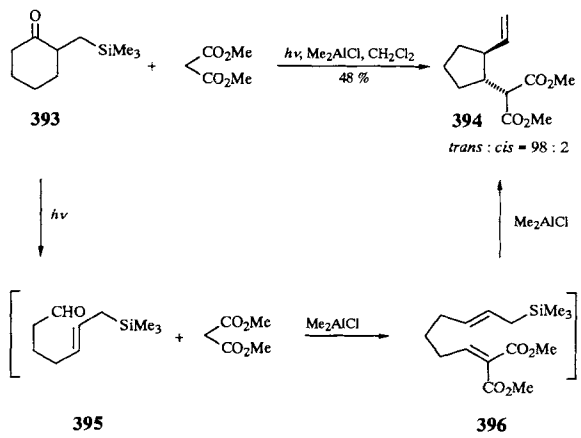

the Knoevenagel product **396** appeared as intermediates in this sequence.

6. Sequences Involving Carbenes

As is well known, carbenes and carbenoids can react with a series of functional groups, whereby a more reactive intermediate is frequently formed that can undergo further subsequent reactions. Cyclic carbonyl ylides, for example, can be prepared by intramolecular reaction of metal carbenoids with carbonyl groups, and subsequently used with dipolarophiles in inter- or intramolecular 1,3-dipolar cycloadditions. This sequence permits the synthesis of a multitude of

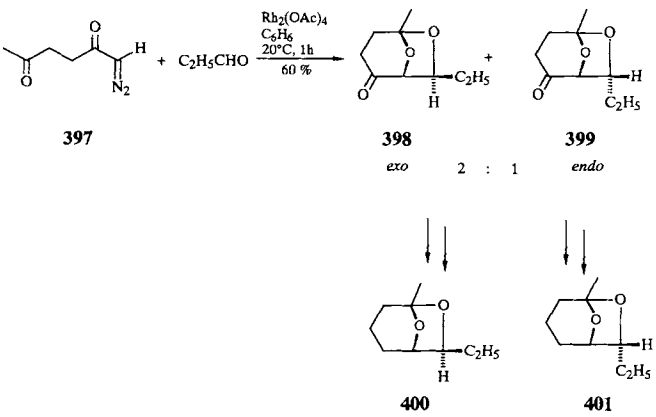

substituted furans.[174] Padwa et al. obtained a 2:1 mixture of the *exo* and *endo* products **398** and **399**, which could be converted into *exo*- or *endo*-brevicomin **400** and **401**, respectively, by the reaction of **397** and propionaldehyde with rhodium(II) acetate.[175]

The in situ formation of sulfonium ylides by an inter- or intramolecular reaction of a sulfide with a carbene forms the basis of a strategy by Kametani et al., which has so far permitted synthesis of penems, carbapenems, and pyrrolizidine alkaloids.[176] Compound **406** was synthesized, from **402** and **403**, presumably via **404** and **405**, and ultimately transformed into (+)-heliotridine **407**.[176a]

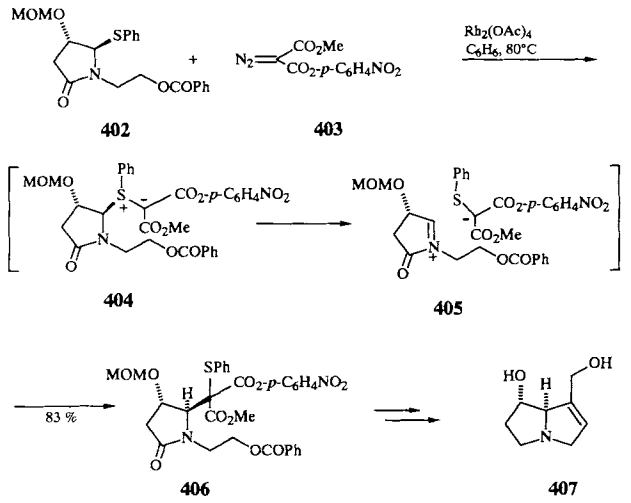

402 **403** **404** **405** **406** **407**

Davies et al. have shown that various ring systems, such as [3.2.1]bicycloocta-2,6-dienes, cyclopentenes, and cycloheptadienes are accessible by a stereoselective rhodium(II)-catalyzed intramolecular cyclopropanation followed by a Cope rearrangement.[177] In the synthesis of cycloheptadiene **411**, a stereospecific intramolecular cyclopropanation took place after formation of the styrylcarbenoid **409** from the diazocompound **408**. Under the prevailing reaction conditions the *cis*-divinylcyclopropane **410** then underwent an intramolecular Cope rearrangement to give **411**.[177a]

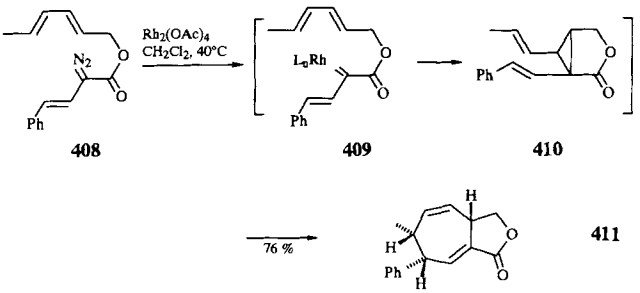

408 **409** **410** **411**

7. Sequences Involving Catalysis by Transition Metals

For a long time transition metal-catalyzed reactions have played a subordinate role in the synthesis of complex organic molecules; in the meantime this picture has been altered completely.[178] The magnesium-ene reaction and related stoichiometric processes possess considerable importance in organic synthesis, in particular for the construction of carbocycles.[179] On the other hand, the catalytic variants, such as the palladium-ene reaction followed by irreversible β elimination or insertion and subsequent reductive elimination, are even more attractive.[180] In some cases it is even possible to generate the system capable of cyclization in situ. Thus, **414** was formed in the reaction of **412** with **413** by Pd^0-catalyzed alkylation; **414** cyclized to the ene-product **417**, presumably via **415** and **416**. The subsequent β elimination to give **418** completed the reaction series.[181]

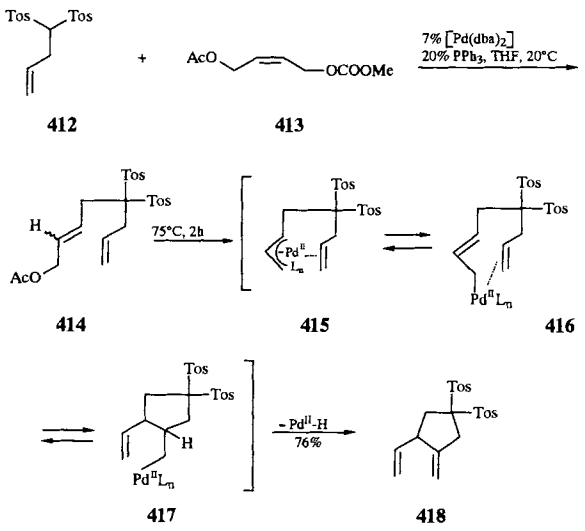

412 **413** **414** **415** **416** **417** **418**

[Pd(dba)$_2$] = bis(dibenzylidenacetone)palladium

It has since been discovered that the intramolecular Heck reaction can compete successfully with the β elimination. Thus, the palladium-catalyzed reaction of the 1,4-*trans*-substituted cycloheptene **419** gave the tetracycle **422** in 50% yield. As a result, ring A is closed first with the formation of **420**, presumably in a palladium-ene reaction. Rings C and D are then constructed in two intramolecular Heck reactions (**420** → **421** → **422**). Surprisingly, in the metal-ene reaction

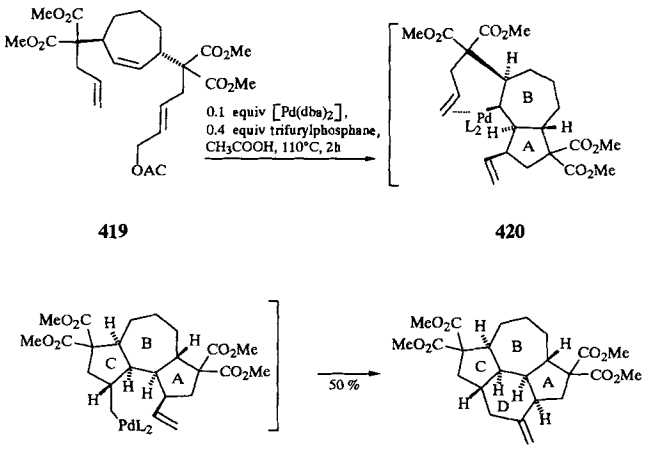

419 **420** **421** **422**

attack of the allyl-palladium component takes place on the *Re* side of the cycloheptene, leading to formation of a *trans*-annelated perhydroazulene. With the corresponding cyclohexene derivative attack takes place "from below".[182]

The alkyl-, alkenyl-, or allyl-palladium species appearing in the inter- and intramolecular Heck reaction can be trapped by a variety of nucleophiles, for example, C, N, and O nucleophiles.[183]

Two rings can be formed in a single synthetic operation when the first Heck reaction is followed by a second Heck reaction, that is, when the palladium species obtained in the first C–C bond forming step reacts with another double or a triple bond in the molecule (e.g. **423** → **424**).[184] The reactive intermediate formed by the second Heck coupling can also be trapped with nucleophiles.[185]

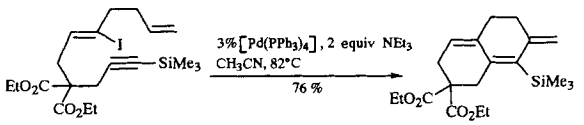

423 **424**

Recently it could be shown that three and even four rings can also be formed in a synthetic sequence with the help of such intramolecular domino Heck cyclizations (e.g. **425** → **426**).[186]

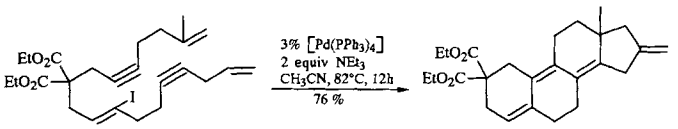

425 **426**

More recently the palladium-catalyzed reactions have been enriched by one more facet, in particular by Trost et al., namely the cycloisomerization of enynes and related systems.[187] Thus, the 1,3-diene **429**, which cyclized under the reaction conditions in the following intramolecular Diels–Alder reaction to give **430**, was formed by treatment of the dienyne **427** with $Pd(OAc)_2$. Compound **428** is a suspected intermediate in this cycloisomerization.[187a] The palladium-

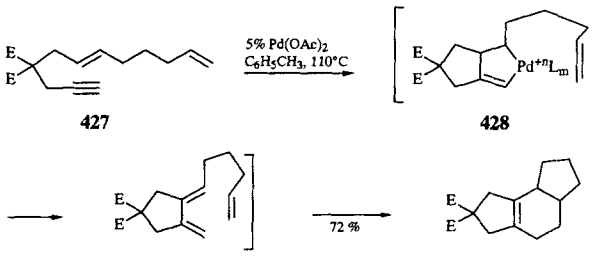

427 **428** **429** **430**

catalyzed alkylation cyclization of enynes[188] and the palladium-catalyzed trimethylenemethane cycloadditions,[189] also developed by Trost et al., are of considerable use.

The synthesis of *o*-bis-annelated arenes by domino cyclization of enediynes, achieved by de Meijere et al., also takes place under Heck conditions.[190] Thus, the reaction of **431** with $Pd(OAc)_2/PPh_3$ under basic conditions (K_2CO_3) led probably to the initial formation of the corresponding alkenyl-palladium derivative **432**, which presumably reacted to give **433** in two consecutive *exo-dig* cyclizations. Compound **433** led to **434** either by Heck coupling or by an electrocyclic reaction with subsequent elimination.[190c]

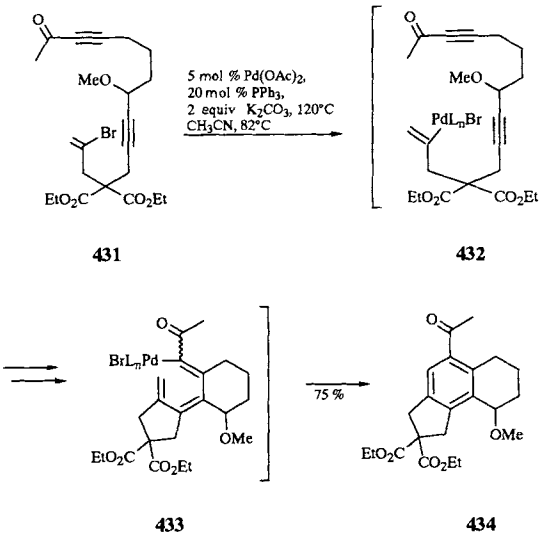

431 **432** **433** **434**

Efficient sequential reactions catalyzed by transition metals are not restricted to organopalladium reactions.[191] Keese et al. used two consecutive intramolecular Pauson–Khand reactions to convert the open-chain enediyne **435** into the tetracyclic fenestrendione **436**.[192]

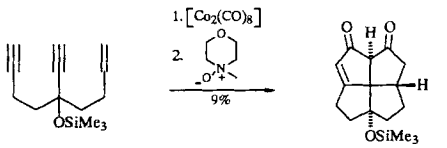

435 **436**

The construction of steroids with an aromatic B ring in only one step from the acyclic precursor **437** by using $CpCo(CO)_2$ as catalyst is an attractive example of the efficiency of organometallic reagents. Thus, an intramolecular

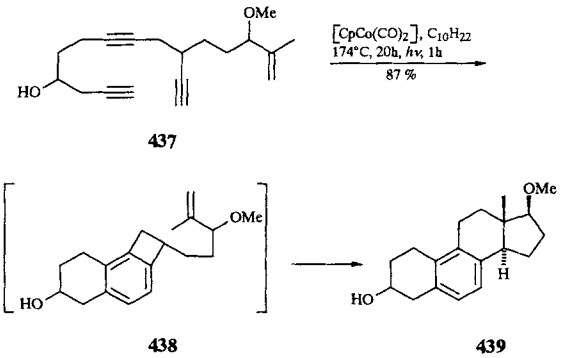

437 **438** **439**

alkyne cyclization with formation of the isolable cyclobutahydronaphthalene **438** takes place first. Electrocyclic ring opening and intramolecular Diels–Alder reaction then gives the steroid derivative **439** in high yield.[193] However, compound **438** can also be isolated by slightly altering the reaction conditions. Cobalt-catalyzed reactions have been used by Vollhardt et al. in a variety of ways, also for the synthesis of other interesting compounds.[194]

8. What Else is There?

In the preceding chapters we have shown that sequential reactions can be started by cationic, anionic, radical, pericyclic, photochemical, or with metal-catalyzed processes. Nevertheless, there is also an abundance of other possibilities, namely rearrangements, fragmentations, oxidations, reductions, and enzymatic processes. The only requirement here is again the formation of a highly reactive group in the presence of one or several other functional groups.

A domino-Beckmann rearrangement-allylsilane cyclization has been described by Schinzer et al. A reactive iminium ion **441** was formed from the (*Z*)-oximesulfonate **440** (R = Ms) and four equivalents of DIBAH; the iminium ion underwent a stereoselective intramolecular reaction with the allylsilane component in **441** to give **443**. In contrast, the (*E*)-oxime **440** (R = H) led surprisingly to **442**, as the allylsilane cyclization takes place more rapidly than the Beckmann rearrangement.[195]

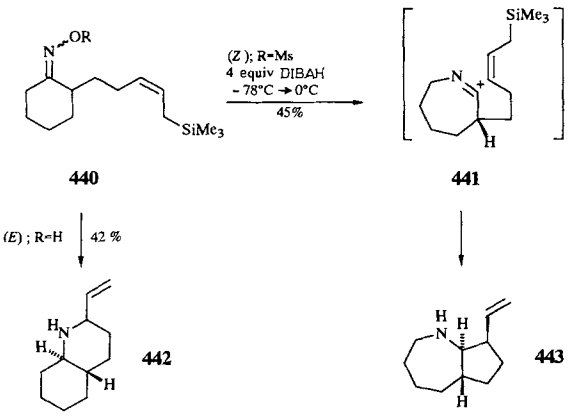

440 **441** **442** **443**

Interesting routes are also opened up when, after a preliminary fragmentation of a bicycle to give a ring extended intermediate, a recyclization takes place. Thus, Kende et al. described the formation of **446** by Grob fragmentation of **444** via **445**; **446**, depending on the choice of base, underwent either an aldol-like reaction to give **448** via **447** or a 1,4-addition to form **450** by way of **449**.[196]

Ziegler and Sobolov found a domino fragmentation retroaldol reaction in the synthesis of the tricycle **454** in attempts to prepare the trichothecene anguidine. The $^1O_2$ cycloadduct **451** fragmented on treatment with $LiAlH_4$ to give **452**, which underwent a retroaldol reaction to give **453** and double C=O addition with formation of **454**.[197]

Oxidative and reductive processes are frequently preliminaries to complex sequence reactions in biosynthesis. One

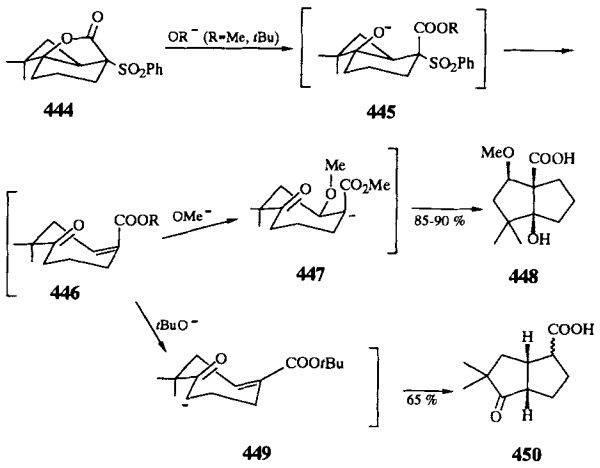

444 **445** **446** **447** **448** **449** **450**

needs only think of the oxidation of phenols,[198] the arachidonic acid cascade,[199] and photosynthesis.[200] Of particular interest in this connection is the toxicity of natural products containing an enediyne group, such as neocarzinostatin, which alludes to the intermediate formation of an aryldiradical.[201] Reductions[202, 203] and oxidations[204, 205] can also initiate processes in organic synthesis.

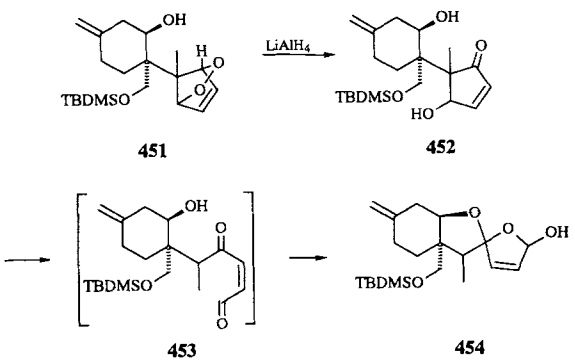

451 **452** **453** **454**

Yates et al. synthesized twistane by a sequence consisting of Wessely oxidation and an intramolecular Diels–Alder reaction. The phenol **455** was oxidized with lead tetraacetate to the intermediate **456**, which reacted to form **457** at 140 °C. Compound **457** was converted into (±)-coronafacic acid **458** in the course of further synthesis.[204b]

Furans can be easily oxidized to γ-keto-α,β-unsaturated esters, which can undergo Diels–Alder reactions as electron-

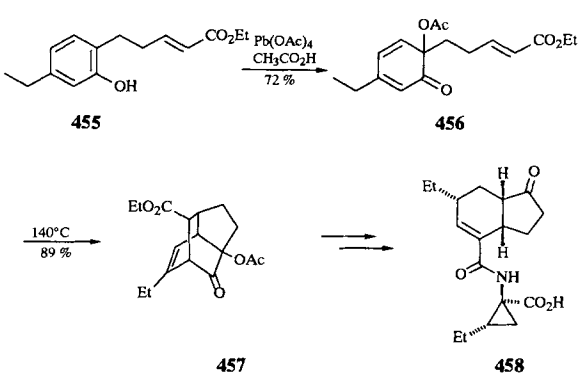

455 **456** **457** **458**

poor dienophiles.[205] In a notable one-pot reaction Feringa et al. achieved formation of the endoperoxide **460** by selective photooxidation of the bisfuran **459** with $^1O_2$; **460** opened to give **461**, which cyclized to **462** after addition of ZnI_2.[205a]

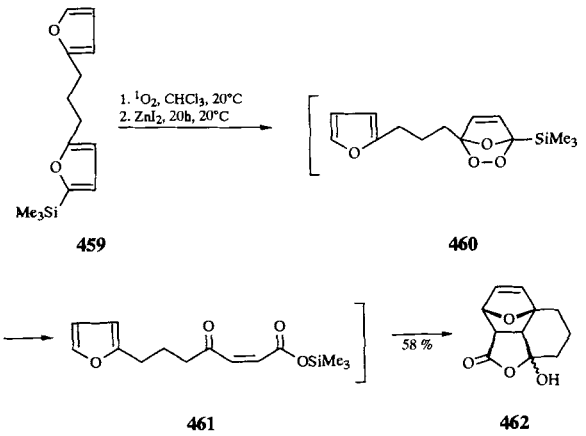

459 **460** **461** **462**

In a model study for the synthesis of (±)-fredericamycin A **466**, the dihydrolactone **463** was reduced with DIBAH to give the enolate **464**, which then cyclized in situ to the spiroketol **465** in an intramolecular 5-(enol-*endo*)-*exo*-*trig* reaction of the aldol type. A corresponding series of reduction and aldol reaction could also be employed for construction of the skeleton of this natural product.[203]

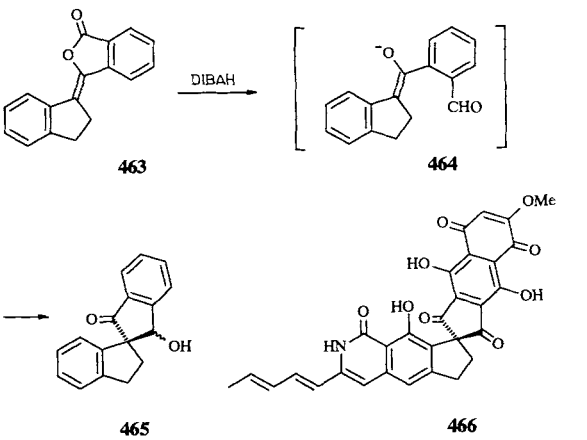

463 **464** **465** **466**

Summary and Outlook

Sequential transformations permit a simple, elegant, efficient and often highly selective entry to a multitude of complex compounds; several reactions are combined here to form a sequence, which then takes place in a sort of domino or consecutive process. Cationic, anionic, radical, pericyclic, organometallic, photochemical, oxidative, and reductive processes can be employed as the first step. The following steps may be of the same or a different type; sequences with identical processes are frequently found, but other reaction series, in particular the anionic–pericyclic sequence, can also be used with much success.

Nevertheless, sequential transformations are not simply efficient and aesthetic; they also make a contribution to the protection of the environment. We are concerned here with a new synthetic strategy, one that can help reduce the production of waste. Thus, numerous workup steps, such as chromatographic purification, extraction, recrystallization, etc. can be avoided with sequential transformations. Of course, the same demands must be met as those of a conventional synthesis: the reactions must be highly selective, give high yields, and it must be possible to carry them out without using highly toxic reagents or solvents. It is also understood that it makes no sense to develop sequences—even elegant sequences—when the synthesis of the starting materials required for the sequence demands a longer route than that for the synthesis of the target molecule by single step processes. The requirements set out here are met in, for example, the tandem Knoevenagel hetero-Diels–Alder reaction, developed by us, in exemplary fashion. They proceed with good yields and under mild conditions, generally at 25 °C and pH 7.0 with the application of a catalytic amount of an ammonium salt, with almost complete regio- and stereoselectivity. The range of application is immense and the starting materials—simple aldehydes and 1,3-dicarbonyl compounds—are readily available.

In this review the legitimacy of sequential transformations is demonstrated, which provides the basis for the discovery of hitherto unknown reactions of this type. There are numerous gray areas on the map of sequential transformations—particularly those involving combinations of nonidentical reactions. These gray areas should stimulate new activity. Sequential transformations must be included in future to a much greater extent in synthetic planning. The development and application of new, efficient, and selective reaction sequences will certainly form an interesting and topical research area over the coming years.

It is a particular pleasure for one of us (L.F.T.) to warmly thank my co-workers for their commitment and their excellent performance, as reflected in the numerous scientific publications. We would like to thank Mrs Sharon Williams and Mrs Vivian Reither for their help in the preparation of the manuscript and the drawings and Mr Jens Fennen for numerous literature searches. We would also like to express our gratitude to the Deutsche Forschungsgemeinschaft, the Fonds der Chemischen Industrie, Bayer AG, BASF AG, Degussa AG, Hoechst AG, and Merck AG for support of the work described here.

Received: April 14, 1992 [A 891 IE]
German version: *Angew. Chem.* **1993**, *105*, 137

Translated by Dr. Michael Ravenscroft, Bischwiller, France

[1] Y. Kishi, *Pure Appl. Chem.* **1989**, *61*, 313.
[2] a) R. B. Herbert, *Nat. Prod. Rep.* **1991**, *8*, 185; b) M. H. Beale, *ibid.* **1991**, *8*, 441; c) D. M. Harrison, *ibid.* **1990**, *7*, 459; d) B. Franck, *Angew. Chem.* **1979**, *91*, 453; *Angew. Chem. Int. Ed. Engl.* **1979**, *18*, 429.
[3] E. Leete, *Planta Med.* **1990**, *56*, 339.
[4] R. Robinson, *J. Chem. Soc.* **1917**, 762; *ibid.* **1917**, 876; C. Schöpf, G. Lehmann, W. Arnold, *Angew. Chem.* **1937**, *50*, 779.
[5] a) E. E. van Tamelen, J. D. Willet, R. B. Clayton, K. E. Lord, *J. Am. Chem. Soc.* **1966**, *88*, 4752; b) E. E. van Tamelen, *ibid.* **1982**, *104*, 6480; c) E. J. Corey, W. E. Russey, P. R. Ortiz de Montellano, *ibid.* **1966**, *88*, 4750; d) E. J. Corey, S. C. Virgil, *ibid.* **1991**, *113*, 4025; e) E. J. Corey, S. C. Virgil, S. Sars *ibid.* **1991**, *113*, 8171; f) E. J. Corey, S. C. Virgil, D. R. Liu, S. Sarshar, *ibid.* **1992**, *114*, 1524.

[6] a) L. F. Tietze, *J. Heterocycl. Chem.* **1990**, *27*, 47; b) F. Ziegler, *Chem. Rev.* **1988**, *88*, 1423; c) G. H. Posner, *ibid.* **1986**, *86*, 831; d) L. F. Tietze in *Selectivity – A Goal for Synthetic Efficiency* (Eds.: W. Bartmann, B. M. Trost), Verlag Chemie, Weinheim, **1984**, p. 299.

[7] M. J. Chapdelaine, M. Hulce, *Org. React.* **1990**, *38*, 225.

[8] a) B. Franck, *Angew. Chem.* **1982**, *94*, 327; *Angew. Chem. Int. Ed. Engl.* **1982**, *21*, 343; b) A. Eschenmoser, *ibid.* **1988**, *100*, 5 and **1988**, *27*, 5; c) P. R. Alefounder, G. J. Hart, A. D. Miller, U. Beifuss, C. Abell, F. J. Leeper, A. R. Battersby, *Biorg. Chem.* **1989**, *17*, 121; d) F. J. Leeper, *Nat. Prod. Rep.* **1989**, *6*, 171; e) A. R. Battersby, F. J. Leeper, *Chem. Rev.* **1990**, *90*, 1261; f) A. I. Scott, *Acc. Chem. Res.* **1990**, *23*, 308; *Angew. Chem.* **1993**, *105*, in press; *Angew. Chem. Int. Ed. Engl.* **1993**, *32*, in press.

[9] a) G. H. Cookson, C. Rimington, *Biochem. J.* **1954**, *57*, 476; b) D. Mauzerall, *J. Am. Chem. Soc.* **1960**, *82*, 2601, 2605.

[10] B. Franck, C. Wegner, *Angew. Chem.* **1975**, *87*, 419; *Angew. Chem. Int. Ed. Engl.* **1975**, *14*, 424.

[11] L. F. Tietze, H. Geissler, unpublished.

[12] A. Eschenmoser, L. Ruzicka, O. Jeger, D. Arigoni, *Helv. Chim. Acta* **1955**, *38*, 1890.

[13] G. Stork, A. W. Burgstahler, *J. Am. Chem. Soc.* **1955**, *77*, 5068.

[14] Reviews: a) E. E. van Tamelen, *Acc. Chem. Res.* **1975**, *8*, 152; b) R. Bohlmann, *Angew. Chem.* **1992**, *104*, 596; *Angew. Chem. Int. Ed. Engl.* **1992**, *31*, 582.

[15] W. S. Johnson, *Angew. Chem.* **1976**, *88*, 33; *Angew. Chem. Int. Ed. Engl.* **1976**, *15*, 9.

[16] a) J. K. Sutherland in *Comprehensive Organic Synthesis, Vol. 3* (Ed.: B. M. Trost), Pergamon Press, Oxford, **1991**, p. 342; b) R. L. Snowden, J.-C. Eichenberger, S. M. Linder, P. Sonnay, C. Vial, K. H. Schulte-Elte, *J. Org. Chem.* **1992**, *57*, 955; c) S. D. Burke, D. N. Deaton, *Tetrahedron Lett.* **1991**, *32*, 4651; d) J. M. Begley, P. V. Fish, G. Pattenden, S. T. Hodgson, *J. Chem. Soc. Perkin Trans. 1*, **1990**, 2263; e) S. D. Burke, S. M. S. Strickland, H. M. Organ, L. A. Silks, *Tetrahedron Lett.* **1989**, *30*, 6303.

[17] a) W. S. Johnson, M. B. Gravestock, B. E. McCarry, *J. Am. Chem. Soc.* **1971**, *93*, 4332; b) W. S. Johnson, W. F. Huffmann, S. G. Boots, *Recl. Trav. Chim. Pays-Pas* **1979**, *98*, 125.

[18] W. R. Bartlett, W. S. Johnson, U. S. Plummer, V. R. Small, Jr., *J. Org. Chem.* **1990**, *55*, 2215.

[19] T. A. Blumenkopf, L. E. Overman, *Chem. Rev.* **1986**, *86*, 857.

[20] S. D. Burke, K. Takeuchi, C. W. Murtiashaw, D. W. M. Liang, *Tetrahedron Lett.* **1989**, *30*, 6299.

[21] Acetals in polyene cyclization. P. A. Bartlett in *Asymmetric Synthesis, Vol. 3* (Eds.: J. D. Morrison), Academic Press, New York, **1984**, p. 341.

[22] T. V. Lee, F. S. Roden, H. T.-L. Yeoh, *Tetrahedron Lett.* **1990**, *31*, 2063.

[23] J. E. Baldwin, M. J. Lusch, *Tetrahedron* **1982**, *38*, 2939.

[24] J. W. Herndon, C. Wu, *Tetrahedron Lett.* **1989**, *30*, 5745.

[25] a) D. O'Hagan, *Nat. Prod. Rep.* **1989**, *6*, 205; b) D. E. Cane, W. D. Celmer, J. W. Westley, *J. Am. Chem. Soc.* **1983**, *105*, 3594.

[26] *Polyether Antibiotics: Naturally Occuring Acid Ionophores, Vol. 1, 2* (Ed.: J. W. Westley), Dekker, New York, **1983**.

[27] I. Paterson, P. A. Craw, *Tetrahedron Lett.* **1989**, *30*, 5799.

[28] a) L. Fitjer, U. Quabeck, *Angew. Chem.* **1987**, *99*, 1054; *Angew. Chem. Int. Ed. Engl.* **1987**, *26*, 1023; b) D. Wehle, L. Fitjer, *ibid.* **1987**, *99*, 135 and **1987**, *26*, 130.

[29] a) G. C. Hirst, P. N. Howard, L. E. Overman, *J. Am. Chem. Soc.* **1989**, *111*, 1514; b) E. J. Jacobsen, J. Levin, L. E. Overman, *ibid.* **1988**, *110*, 4329; c) L. E. Overman, D. J. Ricca in *Comprehensive Organic Synthesis, Vol. 2* (Ed.: B. M. Trost), Pergamon Press, Oxford, **1991**, p. 1007.

[30] a) M. T. Reetz, *Angew. Chem.* **1988**, *100*, 1026; *Angew. Chem. Int. Ed. Engl.* **1988**, *27*, 994; b) M. Fontanille, A. Guyot, *Recent Advances in Mechanistic and Synthetic Aspects of Polymerization*, Reidel, Dordrecht, **1987**; c) M. Morton, *Anionic Polymerization, Principles and Practice*, Academic Press, New York, **1983**; d) M. T. Reetz, T. Knauf, U. Minet, C. Bingel, *Angew. Chem.* **1988**, *100*, 1422; *Angew. Chem. Int. Ed. Engl.* **1988**, *27*, 1373; e) O. W. Webster, W. R. Hertler, D. Y. Sogah, W. B. Farnham, T. V. Rajan Babu, *J. Am. Chem. Soc.* **1983**, *105*, 5706.

[31] G. H. Posner, E. M. Shulman-Roskes, *J. Org. Chem.* **1989**, *54*, 3514.

[32] G. H. Posner, S.-B. Lu, *J. Am. Chem. Soc.* **1985**, *107*, 1424.

[33] a) G. H. Posner, R. D. Crouch, *Tetrahedron* **1990**, *46*, 7509; b) G. H. Posner, K. S. Webb, E. Asirvatham, S.-S. Jew, A. Degl'Innocenti, *J. Am. Chem. Soc.* **1988**, *110*, 4754; c) G. H. Posner, E. Asirvatham, K. S. Webb, S.-S. Jew, *Tetrahedron Lett.* **1987**, *28*, 5071.

[34] D. A. Oare, C. H. Heathcock, *Top. Stereochem.* **1989**, *19*, 227.

[35] a) H. Ahlbrecht, M. Dietz, C. Schön, V. Baumann, *Synthesis* **1991**, *133*; b) R.-B. Zhao, Y.-F. Zhao, G.-Q. Song, Y.-L. Wu, *Tetrahedron Lett.* **1990**, *31*, 3559; c) D. Spitzner, I. Klein, *Liebigs Ann. Chem.* **1990**, 63; d) D. Schinzer, M. Kalesse, *Synlett* **1989**, 34; e) M. Asaoka, H. Takei, *Tetrahedron Lett.* **1987**, *28*, 6343; f) H. Nagaoka, K. Kobayashi, T. Okamura, Y. Yamada, *ibid.* **1987**, *28*, 6641; g) H. Hagiwara, H. Uda, *J. Chem. Soc. Perkin Trans. 1* **1986**, 629; h) M. R. Roberts, R. H. Schlessinger, *J. Am. Chem. Soc.* **1981**, *103*, 724; i) K. B. White, W. Reusch, *Tetrahedron* **1978**, *34*, 2439; j) D. Spitzner, *Tetrahedron Lett.* **1978**, 3349; k) R. A. Lee, *ibid.* **1973**, 3333.

[36] H. Hagiwara, A. Okano, H. Uda, *J. Chem. Soc. Chem. Commun.* **1985**, 1047.

[37] a) D. Spitzner, A. Engler, P. Wagner, A. de Meijere, G. Bengtson, A. Simon, K. Peters, E.-M. Peters, *Tetrahedron* **1987**, *43*, 3213; b) H. Hagiwara, H. Uda, T. Kodama, *J. Chem. Soc. Perkin Trans. 1* **1980**, 963; c) W. Weber, D. Spitzner, W. Kraus, *J. Chem. Soc. Chem. Commun.* **1980**, 1212.

[38] M. Ihara, M. Toyota, K. Fukumoto, T. Kametani, *J. Chem. Soc. Perkin Trans. 1* **1986**, 2151.

[39] M. Ihara, M. Suzuki, K. Fukumoto, C. Kabuto, *J. Am. Chem. Soc.* **1990**, *112*, 1164.

[40] C. Thanupran, C. Thebtaranonth, Y. Thebtaranonth, *Tetrahedron Lett.* **1986**, *27*, 2295.

[41] M. Ihara, M. Katogi, K. Fukumoto, T. Kametani, *J. Chem. Soc. Perkin Trans. 1* **1988**, 2963.

[42] S. Saito, Y. Hirohara, O. Narahara, T. Moriwake, *J. Am. Chem. Soc.* **1989**, *111*, 4533.

[43] R. A. Bunce, E. J. Wamsley, J. D. Pierce, A. J. Shellhammer, Jr., R. E. Drumright, *J. Org. Chem.* **1987**, *52*, 464.

[44] a) A. Barco, S. Benetti, G. P. Pollini, G. Spalluto, V. Zanirato, *J. Chem. Soc. Chem. Commun.* **1991**, 390; b) A. Barco, S. Benetti, A. Casolari, G. P. Pollini, G. Spalluto, *Tetrahedron Lett.* **1990**, *31*, 4917; c) A. Barco, S. Benetti, A. Casolari, G. P. Pollini, G. Spalluto, *ibid.* **1990**, *31*, 3039.

[45] a) C. Spino, P. Deslongchamps, *Tetrahedron Lett.* **1990**, *31*, 3969; b) J. F. Lavallée, P. Deslongchamps, *ibid.* **1988**, *29*, 5117.

[46] R. Ruel, P. Deslongchamps, *Tetrahedron Lett.* **1990**, *31*, 3961.

[47] a) T. Takahashi, H. Okumoto, J. Tsuji, *Tetrahedron Lett.* **1984**, *25*, 1925; b) T. Takahashi, Y. Naito, J. Tsuji, *J. Am. Chem. Soc.* **1981**, *103*, 5261; c) R. K. Haynes, J. P. Stokes, T. W. Hambley, *J. Chem. Soc. Chem. Commun.* **1991**, 58.

[48] M. Ihara, Y. Takino, M. Tomotake, K. Fukumoto, *J. Chem. Soc. Perkin Trans. 1* **1990**, 2287.

[49] M. Ihara, T. Kirihara, A. Kawaguchi, M. Tsuruta, K. Fukumoto, T. Kametani, *J. Chem. Soc. Perkin Trans. 1* **1987**, 1719.

[50] a) T. Mukayama, M. Tamura, S. Kobayashi, *Chem. Lett.* **1986**, 1817; b) S. Kobayashi, T. Mukayama, *ibid.* **1986**, 1805.

[51] S. P. Tanis, M. C. McMills, T. A. Scahill, D. A. Kloosterman, *Tetrahedron Lett.* **1990**, *31*, 1977.

[52] T. Ogiku, M. Seki, M. Takahashi, H. Ohmizu, T. Iwasaki, *Tetrahedron Lett.* **1990**, *31*, 5487.

[53] C. Fang, K. Suganuma, H. Suemune, K. Sakai, *J. Chem. Soc. Perkin Trans. 1* **1991**, 1549.

[54] U. Groth, W. Halfbrodt, unpublished.

[55] a) R. Noyori, M. Suzuki, *Angew. Chem.* **1984**, *96*, 854; *Angew. Chem. Int. Ed. Engl.* **1984**, *23*, 847; b) M. Suzuki, T. Kawagishi, R. Noyori, *Tetrahedron Lett.* **1982**, *23*, 5563.

[56] C. Bohlmann, R. Bohlmann, E. G. Rivera, C. Vogel, M. D. Manandhar, E. Winterfeldt, *Liebigs Ann. Chem.* **1985**, 1752.

[57] T. Hudlicky, A. Fleming, L. Radesca, *J. Am. Chem. Soc.* **1989**, *111*, 6691.

[58] a) D. Arlt, M. Jautelat, R. Lantzsch, *Angew. Chem.* **1981**, *93*, 719; *Angew. Chem. Int. Ed. Engl.* **1981**, *20*, 703; b) J. S. Nowick, R. L. Danheiser, *Tetrahedron* **1988**, *44*, 4113; c) C. Chen, Y.-Z. Huang, Y. Shen, *Tetrahedron Lett.* **1988**, *29*, 1033; d) M. B. Cooke, Jr., J. Y. Jaw, *J. Org. Chem.* **1986**, *51*, 758; e) J. H. Babler, K. P. Spina, *Tetrahedron Lett.* **1985**, *26*, 1923; f) J. Martel, C. Huynh, *Bull. Soc. Chim. Fr.* **1967**, 985.

[59] a) R. C. F. Jones, R. F. Jones, *Tetrahedron Lett.* **1990**, 3367; b) T. Doi, K. Shimizu, T. Takahashi, J. Tsuji, K. Yamamoto, *ibid.* **1990**, *31*, 3313; c) M. B. Groen, F. J. Zeelen, *Recl. Trav. Chim. Pays-Bas* **1986**, *105*, 465, and references therein; d) M. Yamaguchi, M. Tsukamoto, I. Hirao, *Tetrahedron Lett.* **1985**, *26*, 1723.

[60] a) A. I. Meyers, G. P. Roth, D. Hoyer, B. A. Barner, D. Laucher, *J. Am. Chem. Soc.* **1988**, *110*, 4611; b) A. J. Robichaud, A. I. Meyers, *J. Org. Chem.* **1991**, *56*, 2607.

[61] P. A. Wender, A. W. White, *J. Am. Chem. Soc.* **1988**, *110*, 2218.

[62] S. J. Brocchini, M. Eberle, R. G. Lawton, *J. Am. Chem. Soc.* **1988**, *110*, 5211.

[63] M. T. Reetz, A. Schmitz, X. Holdgrün, *Tetrahedron Lett.* **1989**, *30*, 5421.

[64] a) D. Seebach, M. Missbach, G. Calderari, M. Eberle, *J. Am. Chem. Soc.* **1990**, *112*, 7625; b) J. M. Lapierre, D. Gravel, *Tetrahedron Lett.* **1991**, *32*, 2319.

[65] a) A. R. Chamberlain, S. H. Bloom, L. A. Cervini, C. H. Fotsch, *J. Am. Chem. Soc.* **1988**, *110*, 4788; b) M. P. Cooke, Jr., R. K. Widener, *J. Org. Chem.* **1987**, *52*, 1381.

[66] W. F. Bailey, K. Rossi, *J. Am. Chem. Soc.* **1989**, *111*, 765.

[67] a) E. F. Kleinmann in *Comprehensive Organic Synthesis, Vol. 2* (Ed.: B. M. Trost), Pergamon Press, Oxford, **1991**, p. 893; b) H. Heaney, *ibid.*, p. 953.

[68] R. V. Stevens, A. W. M. Lee, *J. Am. Chem. Soc.* **1979**, *101*, 7032.

[69] P. A. Grieco, W. F. Fobare, *J. Chem. Soc. Chem. Commun.* **1987**, 185.

[70] H. Kunz, W. Pfrengle, *Angew. Chem.* **1989**, *101*, 1041; *Angew. Chem. Int. Ed. Engl.* **1989**, *28*, 1067.

[71] a) L. F. Tietze, U. Beifuss, M. Ruther, *J. Org. Chem.* **1989**, *54*, 3120; b) L. F. Tietze, U. Beifuss, M. Ruther, A. Rühlmann, J. Antel, G. M. Sheldrick, *Angew. Chem.* **1988**, *100*, 1200; *Angew. Chem. Int. Ed. Engl.*

1988, *27*, 1186; c) L. F. Tietze, U. Beifuss, *ibid.* **1985**, *97*, 1067 and **1985**, *24*, 1042.
[72] L. F. Tietze, M. Ruther, *Chem. Ber.* **1990**, *123*, 1387.
[73] L. F. Tietze, U. Beifuss in *Comprehensive Organic Synthesis, Vol. 2* (Ed.: B. M. Trost), Pergamon Press, Oxford, **1991**, p. 341.
[74] a) L. F. Tietze, J. R. Wünsch, *Synthesis* **1990**, 985; b) J. R. Hwu, B. A. Gilbert, L. C. Lin, B. R. Liaw, *J. Chem. Soc. Chem. Commun.* **1990**, 161.
[75] M. J. S. Dewar, S. Olivella, J. J. P. Stewart, *J. Am. Chem. Soc.* **1986**, *108*, 5771.
[76] R. W. Hoffmann, *Chem. Rev.* **1989**, *89*, 1841.
[77] a) L. F. Tietze, H. Stegelmeier, K. Harms, T. Brumby, *Angew. Chem.* **1982**, *94*, 868; *Angew. Chem. Int. Ed. Engl.* **1982**, *21*, 863; b) L. F. Tietze, S. Brand, T. Brumby, J. Fennen, *ibid.* **1990**, *102*, 675 and **1990**, *29*, 665; c) L. F. Tietze, T. Brumby, S. Brand, M. Bratz, *Chem. Ber.* **1988**, *121*, 499; d) L. F. Tietze, G. von Kiedrowski, K. Harms, W. Clegg, G. Sheldrick, *Angew. Chem.* **1980**, *92*, 130; *Angew. Chem. Int. Ed. Engl.* **1980**, *19*, 134.
[78] L. F. Tietze, T. Brumby, M. Pretor, G. Remberg, *J. Org. Chem.* **1988**, *53*, 810.
[79] a) L. F. Tietze, J. Fennen, H. Geissler, V. Schulz, unpublished; b) L. F. Tietze, J. Fennen, E. Anders, *Angew. Chem.* **1989**, *101*, 1420; *Angew. Chem. Int. Ed. Engl.* **1989**, *28*, 1371.
[80] L. F. Tietze, M. Bratz, R. Machinek, G. von Kiedrowski, *J. Org. Chem.* **1987**, *52*, 1638.
[81] G. Jefford, *Helv. Chim. Acta* **1992**, in press.
[82] L. F. Tietze, T. Brumby, T. Pfeiffer, *Liebigs Ann. Chem.* **1988**, 9.
[83] L. F. Tietze, J. Utecht, *Chem. Ber.* **1992**, *125*, 2259.
[84] L. F. Tietze, U. Beifuss, *Liebigs Ann. Chem.* **1988**, 321.
[85] E. J. Corey, P. Carpino, *Tetrahedron Lett.* **1990**, *31*, 3857.
[86] S. K. Thompson, C. H. Heathcock, *J. Org. Chem.* **1990**, *55*, 3004.
[87] L. F. Tietze, M. Ruther, unpublished..
[88] a) T. Mukaiyama, T. Takeda, M. Osaki, *Chem. Lett.* **1977**, 1165; b) T. Mukaiyama, T. Takeda, K. Fujimoto, *Bull. Chem. Soc. Jpn.* **1978**, *51*, 3368.
[89] L. F. Tietze, S. Brand, T. Pfeiffer, J. Antel, K. Harms, G. M. Sheldrick, *J. Am. Chem. Soc.* **1987**, *109*, 921.
[90] Mukaiyama et al. [88] had erroneously assumed the (*E*)-configuration for the benzylideneoxazepandione from **177**, and thereby formulated an incorrect transition state structure for the reaction with the Grignard reagent.
[91] B. M. Trost, B. Yang, M. L. Miller, *J. Am. Chem. Soc.* **1989**, *111*, 6482.
[92] L. F. Tietze, G. Schulz, unpublished.
[93] L. F. Tietze, U. Beifuss, *Synthesis* **1988**, 359; *Org. Synth.* **1992**, *71*, 167.
[94] L. F. Tietze, P. Saling, *Synlett* **1992**, 281.
[95] L. F. Tietze, *Angew. Chem.* **1983**, *95*, 840; *Angew. Chem. Int. Ed. Engl.* **1983**, *22*, 828.
[96] a) L. F. Tietze, H. Meier, H. Nutt, *Liebigs Ann. Chem.* **1990**, 253; b) L. F. Tietze, H. Meier, H. Nutt, *Chem. Ber.* **1989**, *122*, 643.
[97] a) J. F. Treimer, M. H. Zenk, *Eur. J. Biochem.* **1979**, *101*, 225; b) A. R. Battersby, A. R. Burnett, P. G. Parsons, *Chem. Commun.* **1968**, 1280.
[98] L. F. Tietze, J. Bachmann, W. Schul, *Angew. Chem.* **1988**, *100*, 983; *Angew. Chem. Int. Ed. Engl.* **1988**, *27*, 971.
[99] L. F. Tietze, J. Bachmann, J. Wichmann, unpublished.
[100] L. F. Tietze, G. von Kiedrowski, B. Berger, *Angew. Chem.* **1982**, *94*, 222; *Angew. Chem. Int. Ed. Engl.* **1982**, *21*, 221.
[101] L. F. Tietze, G. von Kiedrowski, unpublished results.
[102] L. F. Tietze, H. Denzer, X. Holdgrün, M. Neumann, *Angew. Chem.* **1987**, *99*, 1309; *Angew. Chem. Int. Ed. Engl.* **1987**, *26*, 1295.
[103] a) S. Takano, *Pure Appl. Chem.* **1987**, *59*, 353; b) S. Takano, S. Satoh, K. Ogasawara, *J. Chem. Soc. Chem. Commun.* **1988**, 59.
[104] S. Takano, T. Ohkawa, S. Tamori, S. Satoh, K. Ogasawara, *J. Chem. Soc. Chem. Commun.* **1988**, 189.
[105] L. F. Tietze, U. Beifuss, M. Lökös, M. Rischer, A. Göhrt, G. M. Sheldrick, *Angew. Chem.* **1990**, *102*, 545; *Angew. Chem. Int. Ed. Engl.* **1990**, *29*, 527.
[106] L. F. Tietze, J. Wölfling, G. Schneider, *Chem. Ber.* **1991**, *124*, 591.
[107] a) R. B. Ruggeri, K. F. McClure, C. H. Heathcock, *J. Am. Chem. Soc.* **1989**, *111*, 1530; b) C. H. Heathcock, M. M. Hansen, R. B. Ruggeri, J. C. Kath, *J. Org. Chem.* **1992**, *57*, 2544; c) C. H. Heathcock, J. A. Stafford, D. L. Clark, *J. Org. Chem.* **1992**, *57*, 2575; d) C. H. Heathcock, R. B. Ruggeri, K. F. McClure, *J. Org. Chem.* **1992**, *57*, 2585; e) Review: C. H. Heathcock, *Angew. Chem.* **1992**, *104*, 675; *Angew. Chem. Int. Ed. Engl.* **1992**, *31*, 665.
[108] a) S. Blechert, *Synthesis* **1989**, 71; b) S. Blechert in *40 Jahre Fonds der Chemischen Industrie 1950–1990*, Frankfurt, **1990**, p. 41.
[109] L. F. Tietze, J. Wichmann, *Angew. Chem.* **1992**, *104*, 1091; *Angew. Chem. Int. Ed. Engl.* **1992**, *31*, 1079.
[110] L. F. Tietze, M. Rischer, *Angew. Chem.* **1992**, *104*, 1269; *Angew. Chem. Int. Ed. Engl.* **1992**, *31*, 1221.
[111] A. R. Daniewski, E. Piotrowska, *Liebigs Ann. Chem.* **1989**, 571.
[112] a) U. Eder, G. Sauer, R. Wiechert, *Angew. Chem.* **1971**, *83*, 492; *Angew. Chem. Int. Ed. Engl.* **1971**, *10*, 496; b) Z. G. Hajos, D. R. Parrish, *J. Org. Chem.* **1974**, *39*, 1615.
[113] Y. Naruta, Y. Nishigaichi, K. Maruyama, *J. Chem. Soc. Chem. Commun.* **1989**, 1203.
[114] a) C. P. Jasperse, D. P. Curran, T. L. Fevig, *Chem. Rev.* **1991**, *91*, 1237; b) B. Giese, *Angew. Chem.* **1989**, *101*, 993; *Angew. Chem. Int. Ed. Engl.* **1989**, *28*, 969; c) D. P. Curran, *Synthesis* **1988**, 417; **1988**, 489; d) B. Giese, *Radicals in Organic Synthesis: Formation of Carbon-Carbon-Bonds*, Pergamon Press, Oxford, **1986**; e) H. M. R. Hoffmann, *Angew. Chem.* **1992**, *104*, 1361; *Angew. Chem. Int. Ed. Engl.* **1992**, *31*, 1332.
[115] a) M. A. Dombroski, B. B. Snider, *Tetrahedron* **1992**, *48*, 1417; b) M. A. Dombroski, S. A. Kates, B. B. Snider, *J. Am. Chem. Soc.* **1990**, *112*, 2759; c) B. B. Snider, R. Mohan, S. A. Kates, *J. Org. Chem.* **1985**, *50*, 3659.
[116] a) E. J. Corey, M. Kang, *J. Am. Chem. Soc.* **1984**, *106*, 5384; b) E. J. Corey, A. W. Gross, *Tetrahedron Lett.* **1985**, *26*, 4291; c) E. J. Corey, A. K. Ghosh, *ibid.* **1987**, *28*, 175.
[117] D. P. Curran, D. M. Rakiewicz, *J. Am. Chem. Soc.* **1985**, *107*, 1448.
[118] D. P. Curran, M.-H. Chen, *Tetrahedron Lett.* **1985**, *26*, 4991.
[119] D. P. Curran, S.-C. Kuo, *J. Am. Chem. Soc.* **1986**, *108*, 1106; *Tetrahedron* **1987**, *43*, 5653.
[120] a) D. L. Boger, R. J. Mathvink, *J. Org. Chem.* **1992**, *57*, 1429; b) *J. Am. Chem. Soc.* **1990**, *112*, 4003.
[121] a) G. Stork, P. M. Stier, H.-L. Chen, *J. Am. Chem. Soc.* **1986**, *108*, 6384; b) G. E. Keck, D. A. Burnett, *J. Org. Chem.* **1987**, *52*, 2958; c) R. C. Larock, N. H. Lee, *J. Org. Chem.* **1991**, *56*, 6253.
[122] Y. Ito, T. Hirao, T. Saegusa, *J. Org. Chem.* **1978**, *43*, 1011.
[123] a) L. Becking, H.-J. Schäfer, *Tetrahedron Lett.* **1988**, *29*, 2801; b) G. Dralle, *Synthese von Cyclopentanen durch intramolekulare Addition von Kolbe Radikalen*, dissertation, Universität Münster, **1990**.
[124] E. Kariv-Miller, H. Maeda, F. Lombardo, *J. Org. Chem.* **1989**, *54*, 4022.
[125] a) R. D. Little, M. R. Masjedizadeh, K. D. Moeller, I. Dannecker-Doerig, *Synlett* **1992**, 107; b) J. I. McLoughlin, R. Brahma, O. Campopiano, R. D. Little, *Tetrahedron Lett.* **1990**, *31*, 1377.
[126] A. Nishida, H. Takahashi, H. Takeda, N. Takada, O. Yonemitsu, *J. Am. Chem. Soc.* **1990**, *112*, 902.
[127] M. Nagai, J. Lazor, C. S. Wilcox, *J. Org. Chem.* **1990**, *55*, 3440.
[128] H. Pak, I. I. Canalda, B. Fraser-Reid, *J. Org. Chem.* **1990**, *55*, 3009.
[129] a) D. L. Boger, S. M. Weinreb, *Hetero-Diels-Alder Methodology in Organic Synthesis*, Academic Press, San Diego, **1987**; b) T. Kametani, S. Hibino, *Adv. Heterocycl. Chem.* **1987**, *42*, 245; c) G. Helmchen, R. Karge, J. Weetman in *Modern Synthetic Methods, Vol. 4* (Ed.: R. Scheffold), Springer Verlag, Berlin, **1986**, p. 261; d) S. J. Danishefsky, M. P. DeNinno, *Angew. Chem.* **1987**, *99*, 15; *Angew. Chem. Int. Ed. Engl.* **1987**, *26*, 15; e) R. R. Schmidt, *Acc. Chem. Res.* **1986**, *19*, 250; f) E. Ciganek, *Org. React.* **1984**, *32*, 1; g) W. Oppolzer, *Angew. Chem.* **1984**, *96*, 840; *Angew. Chem. Int. Ed. Engl.* **1984**, *23*, 876; h) D. F. Taber, *Intramolecular Diels-Alder and Alder Ene Reactions*, Springer, Berlin, **1984**; i) A. G. Fallis, *Can. J. Chem.* **1984**, *62*, 183; j) G. Brieger, J. N. Bennett, *Chem. Rev.* **1980**, *80*, 63; k) J. Sauer, R. Sustmann, *Angew. Chem.* **1980**, *92*, 773; *Angew. Chem. Int. Ed. Engl.* **1980**, *19*, 779; l) G. Desimoni, G. Tacconi, *Chem. Rev* **1975**, *75*, 651.
[130] a) F.-G. Klärner, U. Artschwager-Perl, W.-D. Fessner, C. Grund, R. Pinkos, J.-P. Melder, H. Prinzbach, *Tetrahedron Lett.* **1989**, *30*, 3137; b) W.-D. Fessner, C. Grund, H. Prinzbach, *ibid.* **1989**, *30*, 3133; c) W.-D. Fessner, G. Sedelmeier, P. R. Spurr, G. Rihs, H. Prinzbach, *J. Am. Chem. Soc.* **1987**, *109*, 4626.
[131] a) H. Hopf, I. Böhm, J. Kleinschroth, *Org. Synth.* **1981**, *60*, 41; b) H. Hopf, F. T. Lenich, *Chem. Ber.* **1974**, *107*, 1891.
[132] a) A. Ichihara, *Synthesis* **1987**, 207; b) D. L. Boger, *Chem. Rev.* **1986**, *86*, 781.
[133] P. A. Jacobi, C. S. R. Kaczmarek, U. E. Udodong, *Tetrahedron Lett.* **1984**, *25*, 4859.
[134] P. K. Chowdhury, A. Prelle, D. Schomburg, M. Thielmann, E. Winterfeldt, *Liebigs Ann. Chem.* **1987**, 1095.
[135] a) S. D. Burke, D. M. Armistead, K. Shankaran, *Tetrahedron Lett.* **1986**, *27*, 6295; b) S. D. Burke, A. D. Piscopio, J. L. Buchanan, *ibid.* **1988**, *29*, 2757; c) G. E. Keck, D. G. Nickell, *J. Am. Chem. Soc.* **1980**, *102*, 3632.
[136] B. M. Trost, P. G. McDougal, K. J. Haller, *J. Am. Chem. Soc.* **1984**, *106*, 383.
[137] a) G. E. Keck, R. R. Webb, II, *J. Org. Chem.* **1982**, *47*, 1302; b) G. E. Keck, R. R. Webb, II, *J. Am. Chem. Soc.* **1981**, *103*, 3173.
[138] a) S. E. Denmark, M. E. Schnute, *J. Org. Chem.* **1991**, *56*, 6738; b) S. E. Denmark, Y.-C. Moon, C. B. W. Senanayake, *J. Am. Chem. Soc.* **1990**, *112*, 311; c) A. P. Kozikowski, K. Hiraga, J. P. Springer, B. C. Wang, Z.-B. Xu, *ibid.* **1984**, *106*, 1845.
[139] S. E. Denmark, C. B. W. Senanayake, G.-D. Ho, *Tetrahedron* **1990**, *46*, 4857.
[140] a) K. Mikami, M. Shimizu, *Chem. Rev.* **1992**, *92*, 1021; b) B. B. Snider in *Comprehensive Organic Synthesis, Vol. 5* (Ed.: B. M. Trost), Pergamon Press, Oxford, **1991**, p. 1; c) B. B. Snider, *Acc. Chem. Res.* **1980**, *13*, 426; d) W. Oppolzer, V. Snieckus, *Angew. Chem.* **1978**, *90*, 506; *Angew. Chem. Int. Ed. Engl.* **1978**, *17*, 476; e) H. M. R. Hoffmann, *ibid.* **1969**, *81*, 597 and **1969**, *8*, 556.
[141] a) B. B. Snider, B. E. Goldman, *Tetrahedron* **1986**, *42*, 2951; b) B. B. Snider, E. A. Deutsch, *J. Org. Chem.* **1983**, *48*, 1822.
[142] a) C.-H. Bong, dissertation, Universität Köln, 1952; b) C. F. Huebner, E. Donoghue, L. Dorfman, F. A. Stuber, N. Danieli, E. Wenkert, *Tetrahe-*

dron Lett. **1966**, 1185; c) R. J. Giguere, A. M. Namen, B. O. Lopez, A. Arepally, D. E. Ramos, G. Majetich, J. Defauw, *ibid.* **1987**, *28*, 6553.
[143] R. J. Giguere, P. G. Harran, B. O. Lopez, *Synth. Commun.* **1990**, *20*, 1453.
[144] a) F. E. Ziegler, *Chem. Rev.* **1988**, *88*, 1423; b) R. Baker, D. L. Selwood, *Tetrahedron Lett.* **1982**, *23*, 3839; c) Y. Fujita, T. Onishi, T. Nishida, *Synthesis* **1978**, 532; d) R. C. Cookson, N. R. Rogers, *J. Chem. Soc. Perkin Trans. 1* **1973**, 2741; e) A. F. Thomas, G. Ohloff, *Helv. Chim. Acta* **1970**, *53*, 1145.
[145] A. F. Thomas, *J. Am. Chem. Soc.* **1969**, *91*, 3281.
[146] a) F. E. Ziegler, H. Lim, *J. Org. Chem.* **1984**, *49*, 3278; b) F. E. Ziegler, J. J. Piwinski, *J. Am. Chem. Soc.* **1982**, *104*, 7181.
[147] a) S. Raucher, K.-W. Chi, K.-J. Hwang, J. E. Burks, Jr., *J. Org. Chem.* **1986**, *51*, 5503; b) S. Raucher, J. E. Burks, Jr., K.-J. Hwang, D. P. Svedberg, *J. Am. Chem. Soc.* **1981**, *103*, 1853.
[148] a) K. Mikami, S. Taya, T. Nakai, Y. Fujita, *J. Org. Chem.* **1981**, *46*, 5447; b) K. Mikami, N. Kishi, T. Nakai, Y. Fujita, *Tetrahedron* **1986**, *42*, 2911.
[149] P. A. Jacobi, H. G. Selnick, *J. Am. Chem. Soc.* **1984**, *106*, 3041.
[150] a) G. A. Kraus, S. H. Woo, *J. Org. Chem.* **1987**, *52*, 4841; b) G. A. Kraus, B. S. Fulton, *ibid.* **1985**, *50*, 1782.
[151] J. Mulzer, H. Bock, W. Eck, J. Buschmann, P. Luger, *Angew. Chem.* **1991**, *103*, 450; *Angew. Chem. Int. Ed. Engl.* **1991**, *30*, 414.
[152] W. H. Okamura, M. L. Curtin, *Synlett* **1990**, 1.
[153] R. A. Gibbs, W. H. Okamura, *J. Am. Chem. Soc.* **1988**, *110*, 4062.
[154] A. Steinmeyer, W. Schwede, F. Bohlmann, *Liebigs Ann. Chem.* **1988**, 925.
[155] a) T. Mandai, S. Matsumoto, M. Kohama, M. Kawada, J. Tsuji, S. Saito, T. Moriwake, *J. Org. Chem.* **1990**, *55*, 5671; b) F. E. Ziegler, J. J. Mencel, *Tetrahedron Lett.* **1984**, *25*, 123.
[156] K. Mikami, K. Takahashi, T. Nakai, *J. Am. Chem. Soc.* **1990**, *112*, 4035.
[157] a) A. Padwa, *1,3-Dipolar Cycloaddition Chemistry, Vol. 1, 2*, Wiley, New York, **1984**; b) R. Huisgen, H. Mäder, *J. Am. Chem. Soc.* **1971**, *93*, 1777.
[158] a) P. DeShong, D. A. Kell, *Tetrahedron Lett.* **1986**, *27*, 3979; b) P. DeShong, D. A. Kell, D. R. Sidler, *J. Org. Chem.* **1985**, *50*, 2309.
[159] a) W. Oppolzer, *Synthesis* **1978**, 793; b) J. L. Charlton, M. M. Alauddin, *Tetrahedron* **1987**, *43*, 2873.
[160] a) R. L. Funk, K. P. C. Vollhardt, *Chem. Soc. Rev.* **1980**, *9*, 41; b) T. Kametani, H. Nemoto, *Tetrahedron* **1981**, *37*, 3.
[161] a) K. Shishido, K. Hiroya, H. Komatsu, K. Fukumoto, T. Kametani, *J. Chem. Soc. Perkin Trans. 1* **1987**, 2491; b) K. Shishido, E. Shitara, H. Komatsu, K. Hiroya, K. Fukumoto, T. Kametani, *J. Org. Chem.* **1986**, *51*, 3007.
[162] a) W. Oppolzer, D. A. Roberts, *Helv. Chim. Acta* **1980**, *63*, 1703; b) K. C. Nicolaou, W. E. Barnette, P. Ma, *J. Org. Chem.* **1980**, *45*, 1463.
[163] H. F. Schmitthenner, S. M. Weinreb, *J. Org. Chem.* **1980**, *45*, 3372.
[164] G. Donegan, R. Grigg, F. Heaney, *Tetrahedron Lett.* **1989**, *30*, 609.
[165] a) L. A. Paquette, R. Guevel, D. R. Sauer, *Tetrahedron Lett.* **1992**, *33*, 923; b) L. A. Paquette, Y.-J. Shi, *J. Org. Chem.* **1989**, *54*, 5205.
[166] a) G. Quinkert, H. Stark, *Angew. Chem.* **1983**, *95*, 651; *Angew. Chem. Int. Ed. Engl.* **1983**, *22*, 637; b) G. Quinkert, U. Schwartz, H. Stark, W.-D. Weber, F. Adam, H. Baier, G. Frank, G. Dürner, *Liebigs Ann. Chem.* **1982**, 1999.
[167] a) P. E. Eaton, *Acc. Chem. Res.* **1968**, *1*, 50; b) P. de Mayo, *ibid.* **1971**, *4*, 41; c) M. T. Crimmins, *Chem. Rev.* **1988**, *88*, 1453.
[168] a) G. Büchi, J. A. Carlson, J. E. Powell, Jr., L. F. Tietze, *J. Am. Chem. Soc.* **1970**, *92*, 2165; **1973**, *95*, 540; b) J. J. Partridge, N. K. Chadha, M. R. Uskokovic, *ibid.* **1973**, *95*, 532; c) L. F. Tietze, K.-H. Glüsenkamp, M. Nakane, C. R. Hutchinson, *Angew. Chem.* **1982**, *94*, 81; *Angew. Chem. Int. Ed. Engl.* **1982**, *21*, 70.
[169] a) L. F. Tietze, A. Bergmann, K. Brüggemann, *Synthesis* **1986**, 190; b) L. F. Tietze, A. Bergmann, *Angew. Chem.* **1985**, *97*, 135; *Angew. Chem. Int. Ed. Engl.* **1985**, *24*, 127; c) L. F. Tietze, K. Brüggemann, *ibid.* **1979**, *91*, 575 and **1979**, *18*, 540.
[170] a) L. F. Tietze, J. R. Wünsch, M. Noltemeyer, *Tetrahedron* **1992**, *48*, 2081; b) L. F. Tietze, J. R. Wünsch, *Angew. Chem.* **1991**, *103*, 1665; *Angew. Chem. Int. Ed. Engl.* **1991**, *30*, 1697.
[171] a) A. Gilbert, *Pure Appl. Chem.* **1980**, *52*, 2669; b) D. Bryce-Smith, *ibid.* **1973**, *34*, 193; c) J. Mattay, *Angew. Chem.* **1987**, *99*, 849; *Angew. Chem. Int. Ed. Engl.* **1987**, *26*, 825; d) P. A. Wender, L. Siggel, J. M. Nuss, *Org. Photochem.* **1989**, *10*, 357.
[172] a) P. A. Wender, R. Ternansky, M. deLong, S. Singh, A. Olivero, K. Rice, *Pure Appl. Chem.* **1990**, *62*, 1597; b) P. A. Wender, S. K. Singh, *Tetrahedron Lett.* **1990**, *31*, 2517.
[173] L. F. Tietze, J. R. Wünsch, C. Schünke, unpublished.
[174] a) A. Padwa, *Acc. Chem. Res.* **1991**, *24*, 22, and references therein; b) A. Padwa, R. L. Chinn, S. F. Hornbuckle, Z. J. Zhang, *J. Org. Chem.* **1991**, *56*, 3271.
[175] A. Padwa, G. E. Fryxell, L. Zhi, *J. Am. Chem. Soc.* **1990**, *112*, 3100.
[176] a) T. Kametani, H. Yukawa, T. Honda, *J. Chem. Soc. Chem. Commun.* **1988**, 685; b) T. Kametani, S.-D. Chu, A. Itoh, T.-C. Wang, A. Nakayama, T. Honda, *ibid.* **1988**, 544; c) T. Kametani, H. Yukawa, T. Honda, *ibid.* **1986**, 651.
[177] a) H. M. L. Davies, M. J. McAfee, C. E. M. Oldenburg, *J. Org. Chem.* **1989**, *54*, 930, and references therein; b) H. M. L. Davies, T. J. Clark, L. A. Church, *Tetrahedron Lett.* **1989**, *30*, 5057; c) see also: W. D. Wulff, D. C. Yang, C. K. Murray, *J. Am. Chem. Soc.* **1988**, *110*, 2653.
[178] a) P. J. Harrington, *Transition Metals in Total Synthesis*, Wiley, New York, **1990**; b) J. P. Collman, L. S. Hegedus, J. R. Norton, R. G. Finke, *Principles and Applications of Organotransition Metal Chemistry*, University Science Books, Mill Valley, CA, **1987**; c) A. J. Pearson, *Metallo-organic Chemistry*, Wiley, Chichester, **1985**; d) S. G. Davies, *Organotransition Metal Chemistry, Applications to Organic Synthesis*, Pergamon Press, Oxford, **1982**.
[179] a) H. Lehmkuhl, *Bull. Soc. Chim. Fr. Part II* **1981**, 87; b) W. Oppolzer, *Angew.Chem.* **1989**, *101*, 39; *Angew. Chem. Int. Ed. Engl.* **1989**, *28*, 38.
[180] a) W. Oppolzer, *Pure Appl. Chem.* **1990**, *62*, 1941; b) *ibid.* **1988**, *60*, 39.
[181] W. Oppolzer, J.-M. Gaudin, *Helv. Chim. Acta* **1987**, *70*, 1477.
[182] W. Oppolzer, R. J. De Vita, *J. Org. Chem.* **1991**, *56*, 6256.
[183] a) R. Grigg, V. Sridharan, S. Sukirthalingam, T. Worakun, *Tetrahedron Lett.* **1989**, *30*, 1139; b) B. Burns, R. Grigg, V. Sridharan, P. Stevenson, S. Sukirthalingam, T. Worakun, *ibid.* **1989**, *30*, 1135; c) B. Burns, R. Grigg, P. Ratananukul, V. Sridharan, P. Stevenson, S. Sukirthalingam, T. Worakun, *ibid.* **1988**, *29*, 5565; d) B. Burns, R. Grigg, P. Ratananukul, V. Sridharan, P. Stevenson, T. Worakun, *ibid.* **1988**, *29*, 4329; e) B. Burns, R. Grigg, V. Sridharan, T. Worakun, *ibid.* **1988**, *29*, 4325; f) R. C. Larock, N. G. Berrios-Pena, C. A. Fried, *J. Org. Chem.* **1991**, *56*, 2615; g) R. C. Larock, C. A. Fried, *J. Am. Chem. Soc.* **1990**, *112*, 5882; h) R. C. Larock, N. Berrios-Pena, K. Narayanan, *J. Org. Chem.* **1990**, *55*, 3447; i) R. C. Larock, E. K. Yum, *Synlett*, **1990**, 529; j) E. Negishi, Y. Noda, F. Lamaty, E. J. Vawter, *Tetrahedron Lett.* **1990**, *31*, 4393.
[184] a) N. E. Carpenter, D. J. Kucera, L. E. Overman, *J. Org. Chem.* **1989**, *54*, 5846; b) M. M. Abelman, L. E. Overman, *J. Am. Chem. Soc.* **1988**, *110*, 2328; c) Y. Zhang, E. Negishi, *ibid.* **1989**, *111*, 3454; d) G. Wu, F. Lamaty, E. Negishi, *J. Org. Chem.* **1989**, *54*, 2507.
[185] R. Grigg, M. J. Dorrity, J. F. Malone, *Tetrahedron Lett.* **1990**, *31*, 1343.
[186] Y. Zhang, G. Wu, G. Agnel, E. Negishi, *J. Am. Chem. Soc.* **1990**, *112*, 8590.
[187] a) B. M. Trost, *Acc. Chem. Res.* **1990**, *23*, 34; b) B. M. Trost, Y. Shi, *J. Am. Chem. Soc.* **1992**, *114*, 791; c) B. M. Trost, Y. Shi, *ibid.* **1991**, *113*, 701; d) B. M. Trost, M. Lautens, C. Chan, D. J. Jebaratnam, T. Mueller, *ibid.* **1991**, *113*, 636.
[188] a) B. M. Trost, J. Dumas, *J. Am. Chem. Soc.* **1992**, *114*, 1924; b) B. M. Trost, W. Pfrengle, H. Urabe, J. Dumas, *ibid.* **1992**, *114*, 1923.
[189] B. M. Trost, T. A. Grese, *J. Org. Chem.* **1992**, *57*, 686.
[190] a) F. E. Meyer, J. Brandenburg, P. J. Parsons, A. de Meijere, *J. Chem. Soc. Chem. Commun.* **1992**, 391; b) F. E. Meyer, P. J. Parsons, A. de Meijere, *J. Org. Chem.* **1991**, *56*, 6487; c) F. E. Meyer, A. de Meijere, *Synlett* **1991**, 777.
[191] N. E. Schore, *Chem. Rev.* **1988**, *88*, 1081.
[192] A. van der Waals, R. Keese, unpublished results; see also M. Thommen, P. Gerber, R. Keese, *Chimia* **1991**, *45*, 21; R. Keese, R. Guidetti-Grept, B. Herzog, *Tetrahedron Lett.* **1992**, *33*, 1207.
[193] S. H. Lecker, N. H. Nguyen, K. P. C. Vollhardt, *J. Am. Chem. Soc.* **1986**, *108*, 856.
[194] a) J. Germanas, C. Aubert, K. P. C. Vollhardt, *J. Am. Chem. Soc.* **1991**, *113*, 4006; b) E. P. Johnson, K. P. C. Vollhardt, *J. Am. Chem. Soc.* **1991**, *113*, 381; c) K. P. C. Vollhardt, *Lect. Heterocycl. Chem.* **1987**, *9*, 59; d) K. P. C. Vollhardt, *Pure Appl. Chem.* **1985**, *57*, 1819; e) K. P. C. Vollhardt, *Angew. Chem.* **1984**, *96*, 525; *Angew. Chem. Int. Ed. Engl.* **1984**, *23*, 539.
[195] D. Schinzer, Y. Bo, *Angew. Chem.* **1991**, *103*, 727; *Angew. Chem. Int. Ed. Engl.* **1991**, *30*, 687; see also K. Maruoka, Y. Matsumura, J. Fujiwara, H. Yamamoto, *Heterocycles* **1984**, *21*, 655; K. Maruoka, T. Miyazaki, M. Ando, Y. Matsumura, S. Sakane, K. Hattori, H. Yamamoto, *J. Am. Chem. Soc.* **1983**, *105*, 2831.
[196] A. S. Kende, I. Káldor, *Tetrahedron Lett.* **1989**, *30*, 7329, and references therein.
[197] F. E. Ziegler, S. B. Sobolov, *J. Am. Chem. Soc.* **1990**, *112*, 2749.
[198] a) B. Franck, G. Blaschke, G. Schlingloff, *Angew. Chem.* **1963**, *75*, 957; *Angew. Chem. Int. Ed. Engl.* **1964**, *3*, 192; b) H. Musso, *ibid.* **1963**, *75*, 965 and **1963**, *2*, 723.
[199] E. J. Corey, *Pure Appl. Chem.* **1987**, *59*, 269.
[200] a) D. W. Lawlor, *Photosynthese*, Thieme Verlag, Stuttgart, **1990**; b) R. Huber, *Angew. Chem.* **1989**, *101*, 849; *Angew. Chem. Int. Ed. Engl.* **1989**, *28*, 848; c) J. Deisenhofer, H. Michl, *ibid.* **1989**, *101*, 872 and **1989**, *28*, 829.
[201] K. C. Nicolaou, W.-M. Dai, *Angew. Chem.* **1991**, *103*, 1453; *Angew. Chem. Int. Ed. Engl.* **1991**, *30*, 1387.
[202] R. B. Gammill, L. T. Bell, S. A. Mizsak, *Tetrahedron Lett.* **1990**, *31*, 5301.
[203] T. R. Kelly, S. H. Bell, N. Ohashi, R. J. Armstrong-Chong, *J. Am. Chem. Soc.* **1988**, *110*, 6471.
[204] a) N. K. Bhamare, T. Granger, C. R. John, P. Yates, *Tetrahedron Lett.* **1991**, *32*, 4439; b) N. K. Bhamare, T. Granger, T. S. Macas, P. Yates, *J. Chem. Soc. Chem. Commun.* **1990**, 739; c) K. C. Majumdar, S. K. Chattopadhyay, A. T. Khan, *J. Chem. Soc. Perkin Trans. 1* **1989**, 1285.
[205] B. L. Feringa, O. J. Gelling, L. Meesters, *Tetrahedron Lett.* **1990**, *31*, 7201; b) H.-J. Wu, K. Pan, *J. Chem. Soc. Chem. Commun.* **1987**, 898, and references therein.

Chemistry of and with Highly Reactive Metals

By Alois Fürstner*

New Synthetic Methods (89)

Today, the synthetic chemist has a large repertoire of metal activation methods at his disposal. After a first breakthrough was made at the beginning of the seventies with the introduction of the Rieke metals, a series of further, in part more efficient methods were described, based on which not only classical metal-induced reactions could be substantially improved but also completely new reactions could be discovered. In this article the individual activation methods are discussed and compared as far as is possible using the currently available data. Especially noteworthy are the metal–graphite combinations because of their unsurpassed reactivity and concomitant easy preparation and manipulation. As shown by numerous applications of these reagents on polyfunctional substrates, particularly natural products, high reactivity of the metal and excellent selectivity are by no means precluded. Besides the purely preparative aspects also insights gained so far into the general principles and limits of metal activation are outlined, and attempts at determining the morphology of highly dispersed systems are reported.

1. Introduction

"Sometimes I have the distinct feeling that organometallic chemists think of both solid state chemistry and surface science as the other side of the moon.
Roald Hoffmann et al. [1]

The simplest way to activate a solid is to dissolve it in a suitable solvent. Reactions in the homogeneous phase are generally easy to reproduce and control, and permit (comparatively) straightforward determination of the reaction mechanism at the molecular level with the repertoire of spectroscopic and kinetic methods developed for this purpose. In general these advantages do not apply to heterogeneous processes. Therefore it is hardly surprising that the marked qualitative and quantitative impetus in organic chemistry in the last decades has changed little in the preference for homogeneous reactions.

Many reasons call for reconsidering this general paradigm. Not only in technical application and industrial production but also in the chemistry of the cell, heterogeneous reactions such as reactions with carrier-bound (e.g. membrane-bound) reagents are notably frequent. Here and there the reasons are similar: enrichment of a reaction partner on a carrier can lead to higher reaction rates and to improved selectivities by synergic effects, the stability of the reagents is increased, manipulation made more reliable, and simple filtration generally suffices for workup of the reaction mixtures.[2] However, phase interfaces have many parameters and it is difficult to determine their properties precisely, especially since they may change when the reaction proceeds.[1] Thus, chemists often depend on purely empirical work as the only means to improve the preparative results. This also holds true for the large range of metal-induced heterogeneous processes to which the following progress report is devoted. Since more or less "activated" forms of almost every metal of the periodic table of the elements have been described, this paper gives preference to a methodological classification rather than a mere descriptive account of various activation techniques.[3]

1.1. General Principles of Metal Activation

Studies on the solid-state chemistry of metal-induced reactions have long been neglected; this is clearly illustrated, for example, in the case of the Grignard reaction. More than seven decades (!) after its discovery and after numerous empirical improvements Whitesides et al., in a series of notable studies, made the first clear statements on the influence of the nature of the magnesium on the course of the reaction; thus, they have also thrown light on the, in part, rather alchemistic practice of metal activation.[4] According to these studies, the initiation of a Grignard reaction takes place *exclusively* at physical defects on the metal surface, that is, at dislocations, edges, and corners. The "chemical" activators[5] (iodine, bromine, 1,2-dibromoethane etc.) commonly used by preparative chemists can only accelerate corrosion; however, they are not capable of creating initial sites for the reaction, whose density is dependent only on the surface structure of the magnesium sample used. Since Grignard reactions of alkyl iodides and bromides are diffusion-controlled after their "initiation", the reaction rate is directly proportional to the available metal surface area.[4]

The fact that those atoms of the surface with the smallest number of direct neighbors (Fig. 1) are the most reactive is reminiscent of the basic concepts of complexation chemistry, according to which the presence of free coordination sites at the central atom is a prerequisite for the chemical reactivity of a complex.[6] In addition, the easier steric accessibility of the atoms on the corners and edges has to be taken into account.

Metal activation thus consists in the creation of a high density of reactive dislocations on a surface that is as large as possible and not passivated. Extrapolation of this definition could lead to the assumption that a metal reaches its maximum reactivity when monatomically distributed. This sup-

[*] Univ. Doz. Dr. A. Fürstner
Institut für Organische Chemie der Technischen Universität Graz
Stremayrgasse 16, A-8010 Graz (Austria)
New address:
Max-Planck-Institut für Kohlenforschung
Kaiser-Wilhelm-Platz 1
D-W-4330 Mülheim a.d. Ruhr (FRG)

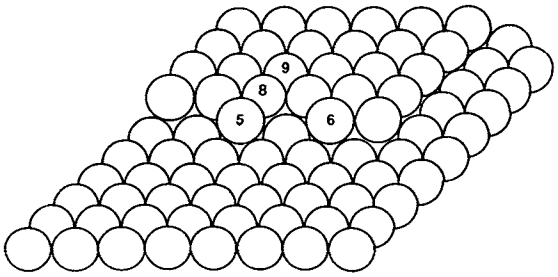

Fig. 1. Schematic representation of a metal surface. The number of nearest neighbors of the atoms at corners, edges, and on terraces is given.

position, however, has been disproved at least for oxidative insertions with magnesium and calcium (Table 1). Both experimental as well as theoretical studies indicate that clusters are more reactive than single atoms, and that larger clusters are more reactive than smaller ones;[7] the decisive factor is possibly the lower ionization potential. Furthermore, more favorable geometries of the transition state are possible for the insertion of a cluster into a C–X bond.[7]

Table 1. Overview of the reactivity of magnesium and calcium atoms and clusters towards methyl halides CH_3X under matrix isolation conditions (according to Klabunde et al. [7b]). (+): oxidative insertion; (–): inert; (?): data obtained are not conclusive.

CH_3X	Ca	Ca_2	Ca_x	Mg	Mg_2	Mg_3	Mg_4	Mg_x
CH_3I	+	+	+	–	+	+	+	+
CH_3Br	–	+	+	–	+	+	?	+
CH_3Cl	–	+	+	–	–	?	–	–
CH_3F	+	+	+	–	–	–	+	+

This set target in physical chemistry, to search for the maximum reactivity of a metal in the area of larger clusters, underscores the insufficiency of the classical repertoire of metal activation. Preparative chemists' current "tricks" for enforcing the initiation of metal-induced reactions are confined to the modification or post-treatment of commercial metal samples by chemical or physical means (e.g., additives such as iodine, 1,2-dibromoethane, CCl_4 etc.; amalgamation, metal/metal coupling, removal of oxide layers by washing with mineral acids; filing, grinding, milling).[5] The production of the finest particles or, in the ideal case, even of large clusters is far from being achieved in this way. High activation results only upon severe attack on the texture of the solid. However, the preparative effort inevitably associated with achieving this goal must in each case be weighed against the increase in efficiency of the metal-induced reaction. Some of the activation methods outlined in the following sections differ considerably with respect to such a preparative "balance" whereby high efficiency does not necessarily exclude user convenience.

2. Methods for the Preparation of Highly Reactive Metals

2.1. Rieke Methods

Rieke et al. made a first breakthrough in the area of high activation of metals in the early seventies with the in situ preparation of highly reactive metal powders by reduction of metal salts by using alkali metals in an inert solvent (Scheme 1).[8, 9] The boiling point of the solvent must exceed

$$MX_n + nK \xrightarrow{\Delta} M^* + nKX$$

Scheme 1. Preparation of Rieke metals M*.

the melting point of the alkali metal (e.g. potassium/THF, sodium/dimethoxyethane (DME) or xylene). Ethereal solvents are generally preferred because of the better solubility of the metal salts. However, in the preparation of aluminum, chromium, indium, or uranium, cleavage of ether was observed under these conditions,[9] so that these metals can only be obtained from the corresponding halides in hydrocarbons (xylene is mostly used because of its higher boiling point).[9] Apart from these few exceptions the Rieke process is nevertheless a universally applicable method that has proven very useful in a series of mechanistically different metal-induced reactions and has often been reviewed.[9] Consequently, only recent developments and improvements of the original procedure will be outlined in this article.

A considerable disadvantage of this method is that the metal salts and the reducing agent must be heated together until the alkali metal melts, but the ensuing exothermic reduction might well be difficult to control. Particular attention must be paid to this when the reaction is performed on a large scale.[9c, d] Moreover, with fine metal powders there is the danger that their reactivity is strongly impaired by agglomeration, sintering, and recrystallization of the particles, particularly at higher temperatures and with long reduction times. Hence, no effort has been spared to make the original Rieke method better controllable, and to avoid subsequent loss of activity by use of more suitable reducing agents.

Alois Fürstner, born 1962 in Bruck/Mur, Austria, studied chemistry at the Technische Universität Graz, where he gained his doctorate under the supervision of Prof. Hans Weidmann. After postdoctoral studies with Prof. W. Oppolzer's research group at the Université de Genève, Switzerland (1990–1991), he returned to Graz to complete his habilitation in Organic Chemistry (1992). He was awarded the Angewandte Chemie *prize in 1992 for the best presentation at the Chemiedozententagung in Heidelberg. His research interests include carbanion chemistry, homogeneous catalysis, and natural product synthesis.*

Both these goals can be achieved by the use of alkali metal/naphthalene ($M^+C_{10}H_8^-$) or alkali metal/biphenyl as a substitute for metallic potassium. Two kinds of applications must be distinguished: the addition of merely catalytic amounts of naphthalene (5–10 mol%) to a mixture of lithium and the metal salt in THF already suffices to effect its reduction.[9, 10] As shown in Scheme 2 the arene functions as

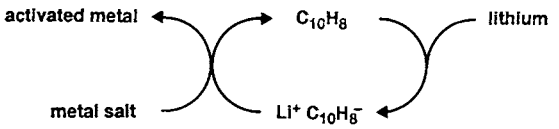

Scheme 2. Modified Rieke method. Naphthalene ($C_{10}H_8$) as single-electron transfer agent.

an electron-transfer agent. Since one is working at room temperature this modified Rieke method is safe in its application and mostly affords more active metal samples than the original method. Disadvantageous are the usual, very long reduction times. However, stoichiometric amounts of $M^+C_{10}H_8^-$ can also be used as reducing agent,[9, 11] and almost any salt can be rapidly reduced thereby to highly reactive metal suspensions even at low temperatures. But the complete removal of large amounts of naphthalene before or after the desired metal-induced reaction can be tedious.

The use of complex metal hydrides as reducing agents for metal salts also represents a variant of the Rieke method. Besides $LiAlH_4$, which has been recommended for the preparation of activated tin[12] and titanium,[13] tetraalkylammonium (or alkali) hydrotriorganoborates in particular offer preparative advantages.[14] With their help transition metal colloids with a narrow particle size range could be obtained which are stabilized by interactions of surface charges on the metal particles with the large tetraalkylammonium ions or the boron complexes occurring in the reduction. Such colloids can also be fixed on inert carriers, thus offering the prospect of promising applications in heterogeneous catalysis (see Section 4.7).[14] A series of other reducing agents such as sodium/potassium alloy[15] or potassium–crown ether mixtures[16] have also been used.

Furthermore, the activity of the Rieke metals obtained can be influenced by the type of metal salt to be reduced as well as by additives. This effect is particularly evident in the preparation of Rieke copper, which serves for the direct preparation of functionalized organocopper compounds (see Section 4.3). Rieke-Cu, obtained by reaction of CuI and potassium in the presence of naphthalene (10 mol%), is especially susceptible to sintering.[15] Only the reduction of copper salts such as $CuCN \cdot 2LiX$ (X = Cl, Br),[17] $CuI \cdot PR_3$ (R = Et, Bu, Cy, Ph)[18] and lithium 2-thienylcyanocuprate,[19] which are readily soluble in THF, with stoichiometric amounts of $Li^+C_{10}H_8^-$ affords adequately active metal samples for achieving direct oxidative insertion into carbon–halogen bonds in good yields. The lower the temperature in the reduction of $CuCN \cdot 2LiX$, the more active the metal suspension obtained.[17]

Also the use of additives (Table 2)[20] or of ultrasound during the reduction process[21] can increase the activity of Rieke metals significantly. To simplify workup of the reaction mixture the use of polymer-bound Rieke metals has also been reported.[22] The need for tailor-made polymers, however, limits the practical use of this approach.

Table 2. Effect of diverse additives on the reactivity of Rieke magnesium in the reaction with *p*-chlorotoluene at 0 °C [20].

Additive	Mg/Additive	% of Grignard reagent after 10 min	120 min
–	–	0	0
KI	10	17	85
KI	4	29	88
KI	2	46	91
KI	1	42	93
KI	0.5	45	93
LiI	2	0	11
NaI	2	6	70
CsI	2	12	89
I_2	20	10	64

2.2. Magnesium–Anthracene Methods

Upon reaction with anthracene derivatives in THF, metallic magnesium readily forms complexes of type **1** (Scheme 3), the spectroscopic and chemical properties of which have been investigated in detail.[23] The X-ray structure analysis

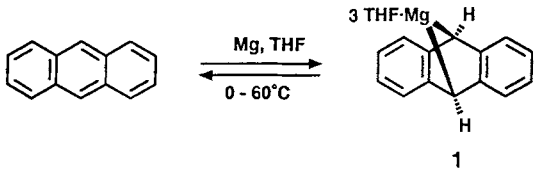

1

Scheme 3. Preparation of the magnesium-anthracene complex **1**.

of a representative of this series shows pentacoordinated magnesium with unusually long bonds to the carbon atoms (2.32 Å) and a significantly bent dihydroanthracene ligand.[24] In view of these structural features the low thermal stability of the metallacycle is evident, which is further reduced by substituents, especially in the 9- and/or 10-position of the anthracene.[25] The unusual structure of this complex is paralleled by its widely diverse chemical behavior. Complex **1** reacts with many electrophiles (e.g. CO_2, alkyl halides, ketones, oxetanes, dichlorosilanes and dichlorostannanes, and Cp_2TiCl_2) as a (di)nucleophile, but acts as an electron donor for aryl halides and as a source of "soluble" magnesium for allyl and benzyl halides, thus enabling these substrates to be converted efficiently into the corresponding Grignard reagents.[26] Even toluene is suitable as solvent. Further, in contrast to Rieke magnesium, **1** permits the metalation of a polystyrene bearing *p*-(chloromethyl) groups.[27] Propargyl chloride is smoothly converted into allenylmagnesium chloride by **1**, which is quite remarkable given the considerable difficulties with which the preparation of this reagent was formerly associated.[26] This "magnesium source" can also be polymerically bound to a polystyrene functionalized with anthracene residues.[28]

As already mentioned, complex **1** is thermally unstable and affords highly reactive pyrophoric magnesium powders with extraordinarily high specific surface areas (up to 110 $m^2 g^{-1}$) and correspondingly high reactivity upon heat-

ing in inert solvents or upon heating neat under vacuum.[23, 29] These powders likewise give Grignard reagents in very good yields upon reaction with a series of different halohydrocarbons in THF, toluene, and in some cases even in heptane. Magnesium powder obtained in the thermal decomposition of activated MgH_2 has proven to be only slightly less reactive.[29]

In any case the activity of such magnesium samples is far superior to that of commercially available metal turnings and compares favorably with that of Rieke magnesium or of magnesium that has been activated by metal vapor techniques (cf. Section 2.3). This has been clearly demonstrated for example by a comparative study of a magnesium–ene reaction (Scheme 4, Table 3).[30] Since the preparative outlay

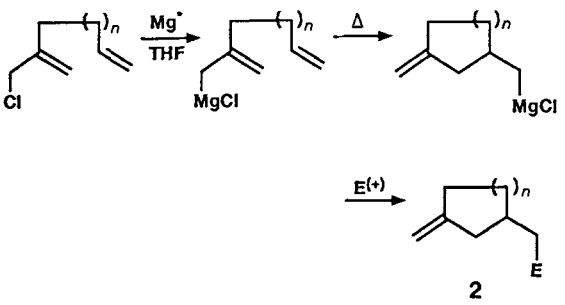

Scheme 4. Magnesium–ene reaction (see Table 3).

Table 3. Comparison of the activity of various magnesium samples in the formation of compound **2** according to Scheme 4 [30].

n	E	Vapor-activated Mg[%]	Anthracene–Mg[%]	Rieke Mg[%]
1	OH	55	56	55
1	CONHPh	71	67	64
2	OH	57	51	48
2	CONHPh	72	69	64

for each of the individual activation methods differs considerably yet the results achieved are comparable, their respective "economy" can be estimated.

In the Rieke process for the reduction of salts, magnesium is suitable only in exceptional cases as a substitute for potassium. However, the ready formation of the anthracene com-

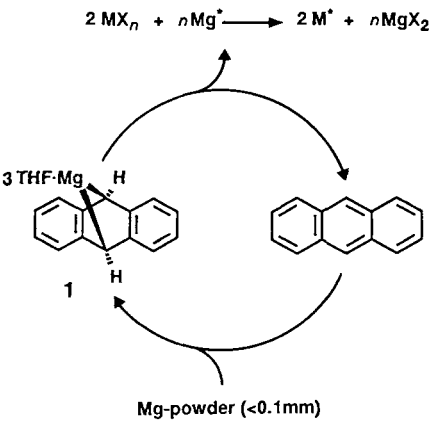

Scheme 5. Preparation of activated metals with the help of magnesium–anthracene complex **1**.

plex **1** can also be exploited for this purpose. As shown in Scheme 5 not only activated metals can be generated by a catalytic cycle, but, in the presence of suitable ligands, also complexes with a zero- or low-valent central atom such as $[M(cod)_2]$ (M = Ni, Pt), $[Cp_2M]$ (M = V, Co, Fe), and $[Pd(PPh_3)_4]$, [Mo(butadiene)$_3$].[31]

2.3. Metal Vapor–Solvent Cocondensation Techniques

Metals are largely monoatomic after vaporization.[32] Although partial dimerizations and oligomerizations of the atoms to clusters have already been observed upon precipitation of such vapors in noble-gas matrices,[32] unprecedentedly high degrees of metal distribution as are required for studying the physics of highly disperse systems can be obtained reproducibly in this way. As has already been mentioned in Section 1.1 spectroscopic studies on matrices doped with alkyl halides have provided insights into the limits of metal activity.[7, 33]

Vaporization can also be used for preparative purposes as a method for the activation of metals.[34–37] It is generally achieved by resistance heating of an appropriate metal block in a high vacuum; in special cases, however, (Table 4) evaporation by electron bombardment or lasers must be resorted to, which increases the cost of equipment tremendously.[36]

Table 4. Vaporization temperature ranges *T* of metals in high vacuum (according to P. L. Timms [36]).

T[°C]	Metal
<1000	Li, Na, K, Rb, Mg, Ca, Zn, Sr, Cd, Sm, Eu
1000–1400	Be, Mn, Cu, Ag, Au, Sn, Pr, Nd, Gd, Tb, Dy, Ho, Er, Tm
1400–1700	Cr, Fe, Co, Ni, Pd, La, Ce, Lu
1700–2000	Ti, V, U
2000–2500	Zr, Ru, Rh, Pt
>2500	Nb, Mo, Hf, Ta, W, Re, Os, Ir

The vapor generated is condensed at low temperatures into a suitable solvent and then the desired reaction is carried out with the resulting suspension. A relatively simple apparatus for this purpose related to a rotary evaporator has been described in detail.[36, 37a]

One of the advantages of this method is that, in contrast to most other methods, metal suspensions completely free of halogens and arenes are obtained. With the proper apparatus even larger amounts of metal can easily be activated.

One of the main areas of employment of the metal-vapor activation technique was in the preparation of metal complexes form "naked" transition metal atoms.[32, 34–36] Also in the field of Grignard reagents progress could be made, inter alia, in the synthesis of allylmagnesium halides and labile reagents, for example cyclopropylmethyl- and benzocyclobutenylmethylmagnesium bromides **3** which undergo ring-opening under conventional conditions (Scheme 6, Table 5). As the previously mentioned comparative study has shown, the magnesium activated by such vaporization is however neither superior to Rieke magnesium nor to magnesium–anthracene (Table 3).[30] Linked with the undoubtedly greater cost of the equipment, this could be responsible for the few recent applications of this technique in organic synthesis.[35d, f]

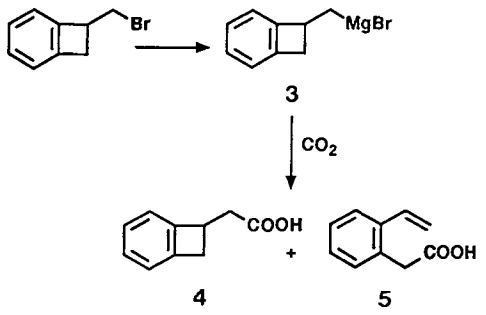

Scheme 6. Labile Grignard compounds. Preparation and reaction of benzocyclobutenylmagnesium bromide **3** (see Table 5).

Table 5. Comparison of the efficiency of magnesium activated by vaporization with that of commerically available metal for the synthesis of benzocyclobutenylacetic acid **4** (Mg* = magnesium activated by vaporization) [37a].

Mg sample	Solvent	T[°C]	Yield [%]	**4**:**5**
Mg turnings	THF	+30	61	0:100
Mg*	THF	−75	82	45:55
Mg*	Et_2O	−50	80	100:0

2.4. Metal–Graphite Reagents

Many factors speak in favor of immobilization of reagents on inert carriers:[2] the simple workup of the reaction mixture by filtration is manifested in high yields; the greater stability and safer manipulation of carrier-bound materials make the preparative work easier. In addition, there is the concentration effect by local enrichment of the reagent, the lowering of the activation energy observed in some cases, and the sometimes remarkable concentration of the dissolved reaction partner at the phase boundary by interactions with polar or charged units on the surface.[2] These advantages are already exploited in many instances in industrial production, where the trend to heterogenization of homogenous reactions continues without diminishing.

The choice of carrier material is of considerable importance. It should be inexpensive, readily available, and essentially inert, although synergic effects with the bound agent are possible. Of the materials in question graphite assumes a special position, since it not only can serve as simple carrier but is also capable of intercalating atoms or molecules between its layers, which are held together only by weak van der Waals forces.[38] The intercalation compounds thus obtained are characterized as "laminar", "covalent", or "residual" compounds according to the kind of interaction between host and guest. All applications of graphite are determined by an interplay of interlaminar events and reactions at the surface (see Section 3).[38]

Although metal–graphite reagents have been known for some decades, they have nevertheless long been underestimated as regards their preparative potential. For example, potassium–graphite (C_8K)[39] first described as long ago as 1926, was still classed in the late seventies as being too aggressive because of its extraordinarily high reactivity;[40] extensive application in organic synthesis was thus excluded. Nevertheless, this bronze-colored substance (Fig. 2) has a number of interesting features: 1) C_8K is easily prepared in a few minutes by stirring a dry mixture of potassium and graphite at 150 °C under argon (Scheme 7). 2) C_8K has an extremely high (compared to potassium even increased) reducing power. 3) Since the 4s electrons of the potassium are delocalized in the conduction band of the graphite, C_8K can be regarded as a polymeric analogue of alkali metal/naphthalene ($M^+C_{10}H_8^-$).[38,40] 4) Through its characteristic coloration both the formation as well as the conversion of C_8K are self-indicative. 5) The undoubtedly most serious yet readily controllable disadvantage of C_8K is its pyrophoric character.

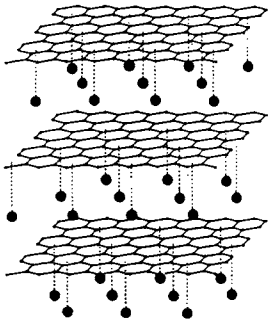

Fig. 2. Structure of C_8K.

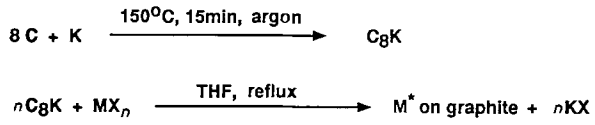

Scheme 7. Preparation of C_8K and metal–graphite reagents.

Apart from its use as a reagent in organic (organometallic) reactions[38] its properties suggest the use of C_8K as a reducing agent for various metal salts.[38,41] It thus provides an activation method which in expense and performance is similar to the Rieke process, which it may clearly surpass, however, with respect to reactivity. Since the reducing agent concomitantly affords the carrier material the metals obtained are protected against subsequent sintering from the moment of their formation. Instead of the limited surface of the molten potassium in the Rieke method the reduction reaction with C_8K can take place at any site on the extended graphite surface, resulting in smaller particle sizes of the metal powder formed (cf. Section 3). C_8K thus combines the favorable reducing properties of alkali metal/naphthalene with the advantage of a conceivably simple workup by filtration.

Metal–graphite combinations prepared as in Scheme 7 first received attention as potential reagents in organic and organometallic synthesis in the seventies, but were mostly tested on simple achiral substrates.[38] Their extraordinary potential for the chemo-, regio-, and stereoselective derivatization of highly functionalized and enantiomerically pure products was fully exploited only recently. An overview of this development with emphasis on our own work in this field is given in Sections 4.2 and 4.4–4.6 of this article.

In some cases a noteworthy chemical enhancement of activation in addition to the activation as a result of the extremely fine distribution of the particles formed on graphite is achieved by the *coreduction* of a mixture of two salts with C_8K. Such synergistic effects have been observed for the metal couples Zn/Ag on graphite ($ZnCl_2$:AgOAc = 10:1)[42]

and Ni/Cu on graphite ($NiBr_2$:$CuCl_2$ = 8:1).[43] However, the reasons for these effects are entirely different for each of the two metal couples, as shown by electron microscopic investigations: In the case of the Ni/Cu couple the reduction of $NiBr_2$ and $CuCl_2$ by C_8K is incomplete (with formation of Ni(0) and CuBr) and the better activity observed in the dimerization of benzyl halides upon using Ni/Cu–graphite instead of Ni–graphite is therefore associated with the catalytic influence of monovalent copper on such Wurtz-type couplings.[44] In the case of Zn/Ag–graphite, on the other hand, which forms an intimate conglomerate of very fine zinc and silver particles on graphite, the increase in activity achieved is not due to alloy- but rather to half-element formation. The interface between the two metals proved to be the preferred site for attack by halogen compounds.[45]

Finally, it should be noted that graphite powder accelerates decomposition of the magnesium–anthracene complex **1**, whereby the liberated metal precipitates on the graphite surface. Again no signs of intercalation have been found in this preparation of a magnesium–graphite combination.[46]

2.5. Metal Activation by Ultrasound

In solutions ultrasound causes "cavitation", that is, the formation, growth, and final collapse of very fine bubbles of gas.[47] In multiphase systems this produces shockwaves which increase mass transfer and can lead to erosion at the surface of a solid. In addition, the strong turbulence gives rise to collisions of the particles distributed in the solvent, which can lead to considerable morphological changes, either by disintegration of the particles or even by their fusing together due to local overheating upon collision.[48] Such collisions are also said to be responsible for the degradation or even the complete destruction of surface oxide layers. In such cases sonication of the metal prior to its use has comparable activation effect as sonication of the whole reaction mixture. This was demonstrated experimentally in Reformatsky reactions, copper-induced Ullmann couplings, and in the preparation of activated nickel powder.[47, 48]

Besides these examples, in which ultrasound essentially exercises a mechanical effect on the solid,[48] reactions whose mechanism is fundamentally changed upon sonication are also known in the literature. Thus, for example, in lithium-induced Barbier reactions the profound influence of ultrasound on the metal surface, which consists in the perpetual creation of new initiation sites for the reaction, has been clearly demonstrated by electron microscopy. Yet this effect does not suffice for an exclusive explanation of all experimental data.[49] Rather, it must be assumed that ultrasound strongly accelerates single-electron transfer (SET) from the metal to the substrate.[50] It was therefore important to seek cases in which a SET mechanism can be increased in such a way by sonication that it overcomes a dominating ionic pathway under thermal reaction conditions. The lithium-induced cyclization of *ortho*-allylbenzamides is one of several examples of such a "sonochemical switching"[50] between competing mechanisms (Scheme 8).

A practical advantage of metal activation by ultrasound lies in the fact that in many cases the conventional ultrasonic purification baths used in the laboratory already suffice to

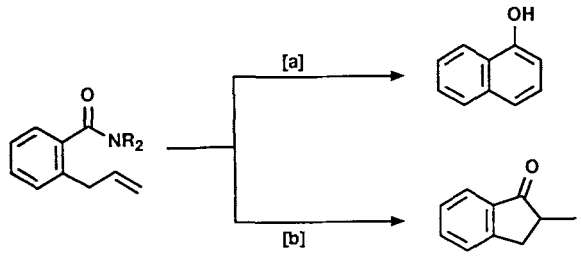

Scheme 8. "Sonochemical switching" in the lithium-induced cyclization of *o*-allylbenzamides: [a] Li, reflux, ionic reaction; [b] Li, ultrasound, radical reaction.

achieve a satisfactory effect. This, however, in no way approaches the performance of the most efficient high-activation methods presented above, but can be further increased by applying higher energetic ultrasound (immersion horns). Also the simple and harmless application of ultrasound on a large-scale is sure to guarantee further use and development of this technique in the future.

2.6. Special Methods

Many metals (e.g. magnesium) are mechanically less stable. Thus, a commonly used magnetic stirring rod suffices to grind down such metals to a finely divided and, in the case of magnesium, blackish-gray powder within about 15 hours under inert gas. This powder is excellently suited for the preparation of Grignard compounds from benzyl, allyl, and propargyl halides.[51]

Attempts were made to exploit the advantages of carrier-bound systems with finely dispersed potassium on aluminum oxide[52] and sodium on active charcoal[53] in the reductive decyanation of alkyl nitriles and the alkylation of ketones. Also the generation of colloidal potassium in toluene using ultrasound has been described.[54]

3. The Morphology of Highly Reactive Metals

Although a detailed knowledge of the morphology of activated metals is undoubtedly a prerequisite for an understanding of their reactivity, the information available so far is in many respects inadequate. Thus, the structural investigations on Rieke metals were almost exclusively carried out with samples that had been filtered and dried before the analyses, without the effect of such treatment on the results obtained being considered more closely.[9] As the electron microscopic and X-ray diffraction data measured on these powders show, in the case of Rieke metals the samples were microcrystalline or X-ray amorphous solids having particle sizes in the micrometer or submicrometer range which may aggregate in a spongelike manner.[9] Also BET analyses indicate a favorable mass/surface area ratio. In the case of Rieke cobalt considerable sintering upon thermal loading of the sample has been demonstrated.[55] Exact correlations between genesis and morphology of the metal powders, however, have yet to be carried out.

A knowledge of the particle size distribution of an activated metal is in itself insufficient for an understanding of the properties of the metal. Since one knows from elemental

analyses about the complex composition of highly reactive metal powders, it follows that investigation of the surface properties is equally essential.[55, 56] Thus, in the case of Rieke nickel (NiI_2, lithium, THF, ultrasound, 30 °C, 10–30 min) carbonyl ligands were found to be tightly bound to the Ni atoms of the metal surface. These ligands originate from cleavage of ether during the preparation of the metal, as control experiments with toluene as solvent have confirmed, and they are essential for the catalytic activity of the nickel sample.[57]

The interrelation between preparation of activated magnesium and its preparative properties is well documented for the anthracene method outlined in Section 2.2. Besides publishing detailed elemental analyses Bogdanović et al.[29] reported a beautiful correlation between increasing X-ray amorphous character and the increasing specific surface area of differently prepared magnesium powders with a wealth of preparative results in the field of Grignard compound formation and the hydrogenation of Mg to MgH_2. Precise analyses are also available for metal samples prepared by the reduction of salts with hydrotriorganoborates.[14] Investigations of the mechanical effect of ultrasound on diverse metals (Li, Zn, Cu, Ni) by scanning electron microscopy[47–49] were already referred to in Section 2.5.

The misconceptions prevailing in the older literature about the morphology of metal–graphite combinations[58] have recently been cleared up. The combined use of electron microscopic (TEM = transmission electron microscopy, HREM = high-resolution electron microscopy, EDX = energy dispersive X-ray spectrometry. EELS = electron energy loss spectroscopy, SAED = selected area electron diffraction) and X-ray diffraction techniques has shown beyond doubt that the reagents prepared according to Scheme 7 are extremely finely divided metals *on* graphite as inert carrier (average particle sizes: Zn 2–10 nm; Ni 2–7 nm; Pd 2–5 nm; Ti 1–2 nm; Pt 3–5 nm etc).[44, 45, 59–61] In none of the cases investigated was there any indication of the postulated intercalation of the metal atoms between the graphite layers.[58] Since these compounds do not have a well-defined structure in the sense of the laminar potassium–graphite C_8K, they are referred to as metal–graphite "combinations". In these structural investigations the expected but up to now neglected effect of the sample preparation was apparent for the first time, since such finely divided metals are extremely readily oxidized and aggregated on exposure to air.[59] In the case of nickel it emerged that this oxidation takes place only superficially on larger particles with formation of a 2–3 nm thick $Ni(OH)_2$ layer, whose composition was determined by photoelectron spectroscopy (XPS) and EELS.[44] This finding explains why the catalytic activity of nickel–graphite as hydrogenation catalyst clearly diminishes upon washing with H_2O but is not completely removed (see Section 4.7).

According to these structural investigations, the method for activating metals by reduction of their salts with potassium–graphite laminate C_8K affords particles a few nanometers in diameter with little outlay, which approaches the optimum regarding metal reactivity at reasonable preparative expense. Since the 4s electrons of the potassium atoms, the actual reducing agent, are delocalized in the conduction band of the graphite and are available on its whole surface, the metal

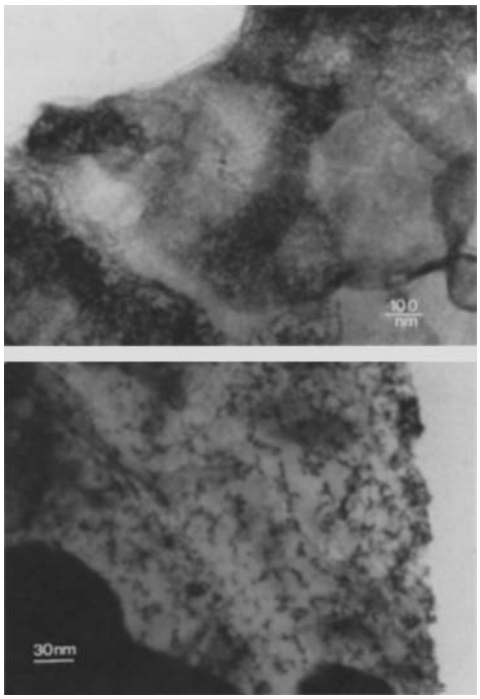

Fig. 3. Top: Transmission electron microscopic (TEM) images of zinc on graphite. Bottom: TEM image of palladium on graphite. Especially in the top picture the uniform coating of the graphite surface with fine particles of metal is evident.

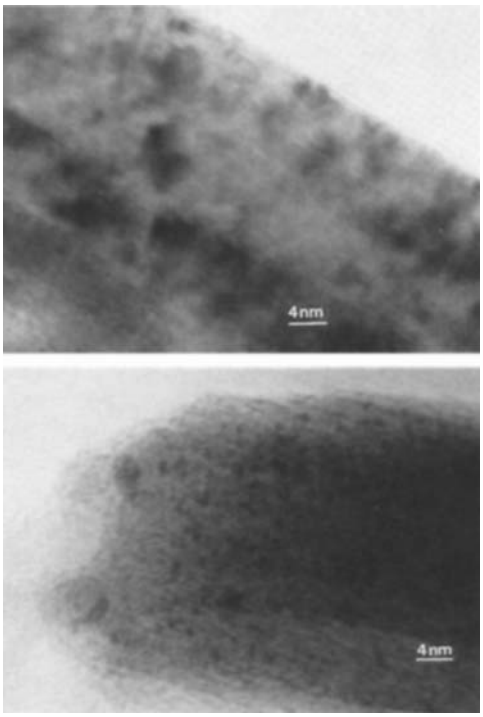

Fig. 4. Top: High-resolution electron microscopic (HREM) image of synthetic graphite (Lonza KS-5-44) shows a regular ordering of graphite layers with constant interlamellar distances. Bottom: HREM image of palladium–graphite. The severe dislocations of the graphite lattice and irregular interplanar distances are a result of the potassium intercalation/deintercalation during the preparation of this surface compound with promising catalytic properties (see Section 4.7).

coating of the graphite platelets should be uniform.[44, 59, 60] As shown in Figure 3 this is largely the case upon using natural graphite. With synthetic graphite, on the other hand,

the metal deposition, for example of palladium (Fig. 3, bottom), preferably takes place along the defects of a clearly imperfect surface.[45]

In the preparation of metal–graphite reagents outlined in Scheme 7 the graphite remains chemically unchanged, whereas its lattice structure suffers considerable damage, as is evident upon comparison of the HREM images of synthetic graphite before and after preparation of palladium–graphite (Fig. 4).[45]

4. Recent Applications of Highly Reactive Metals in Synthetic Chemistry

4.1. Recent Developments in the Use of Alkaline Earth Metals in Organic Synthesis

The skill and intuition of the preparative chemist have long been materially decisive for the success or failure of Grignard reactions. Not only the synthetic potential of this classical reaction but also its reliability has profited considerably from the use of highly reactive magnesium. As the examples presented in the previous sections of this article have shown, activated magnesium can be used to convert substrates such as benzyl, allyl, *tert*-alkyl, cycloalkyl, and long-chain alkyl halides as well as aryl chlorides, and in some cases even fluorohydrocarbons, all previously considered to be problematic, into Grignard reagents in high yields[5, 9, 10, 20, 26, 27, 29, 37, 62] The preparation of highly reactive metals has also contributed appreciably to the study of the elementary steps in the oxidative insertion of metal atoms into carbon–halogen bonds and in the synthesis of chiral organomagnesium halides from enantiomerically pure alkyl halides.[63, 4g]

The possibilities of the applications to more complex reactions increase with this increased efficiency. The intramolecular magnesium-ene reactions which have been systematically investigated by Oppolzer (Scheme 9) represent an obvious example of such sophistication. Their high preparative value

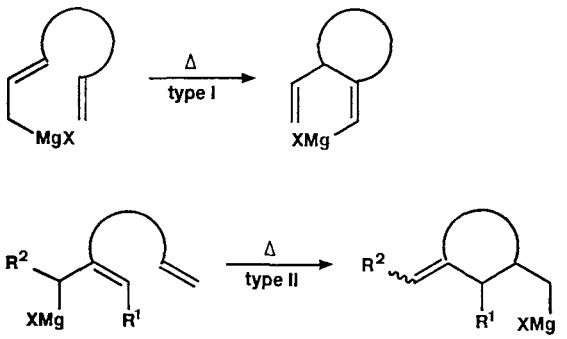

Scheme 9. The two possible types of magnesium–ene reactions.

has already clearly been proven in numerous syntheses of natural products.[64] A prerequisite for their success is a reliable entry to allylmagnesium halides which react thermally with suitably positioned C=C bonds in the sense of an Alder–ene reaction with transfer of the metal. Since allyl halides tend to undergo Wurtz coupling on reaction with magnesium turnings under conventional conditions, the use of high-activation methods (Rieke process, Mg–anthracene method, metal vapor–solvent cocondensation techniques, see Table 3) forms a conditio sine qua non for the success of this process. Where the compatibility of the Grignard reagents with the functional groups in the substrate did not suffice, stoichiometric zinc-ene reactions and especially transition metal catalyzed ene processes further extended the synthetic possibilities.[64]

That metallic magnesium is able to react with conjugated alkadienes has been known for some time, and this branch of organomagnesium chemistry has recently also received great impetus through the use of activated metals. For example, reaction of Rieke magnesium with substituted butadienes in THF at room temperature leads to excellent yields of metallacycles of type **6**–**9** (Scheme 10, M = Mg), which function as dinucleophiles (Scheme 11).[65] They can be converted with

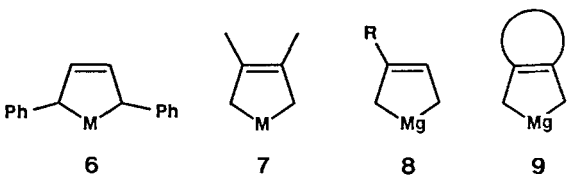

Scheme 10. Metallacyclopentenes from alkadienes and Rieke metals. **6a**, **7a**: M = Mg; **6b**, **7b**: M = Ca; **8**: R = Me, Ph, $CH_2CH_2HC{=}CMe$.

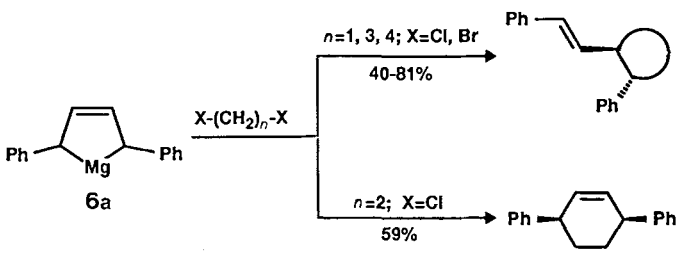

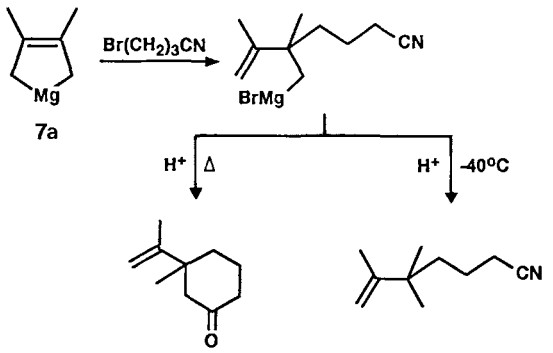

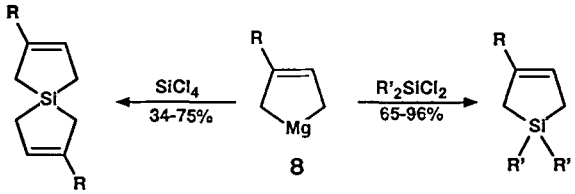

Scheme 11. Reactions of magnesiacyclopent-3-ene derivatives with electrophiles. Selected examples.

α,ω-dihaloalkanes into carbocycles, whereby the substituents on the metallacycle and the chain length of the electrophile determine the regiochemistry of the ring-closure.[65b,c] The conversion with ω-haloalkyl(aryl) nitriles, after aqueous workup of the reaction mixture, affords cyclanones as reaction products, whose formation is explained in terms of alkylation of the magnesiacyclopentene and subsequent intramolecular attack of the resulting Grignard compound at the cyano group (Scheme 11).[65b] When 1,2-dimethylenecycloalkanes are used as dienes, spiroannelated ring systems are formed in an analogous way via metallacycle **9**.[65d] With compound **7** the consecutive conversion with two different electrophiles is also possible, whereas all magnesiacycles react with dichlorosilane or $SiCl_4$ as electrophiles to give (spiro)silacyclopent-3-ene derivatives (Scheme 11).[65a,b]

Rieke calcium, which is prepared by reduction of CaX_2 (X = Br, I) with lithium/biphenyl, likewise reacts with butadiene derivatives with formation of the hitherto unknown calcium metallacycles **6b** and **7b** (M = Ca).[66] Their behavior towards electrophiles resembles qualitatively that of the magnesium analogues, but surpasses the latter in reactivity. Further, the fact that Rieke calcium reacts smoothly with all kinds of halohydrocarbons to give organocalcium reagents seems remarkable.[66] The oxidative insertion already takes place at low temperatures (alkyl halides at −78 °C, aryl halides at −30 to −20 °C) and even problematic substrates such as 1-bromoadamantane, halogenated polystyrene, and even aryl fluorides react without difficulty, the latter, however, first at room temperature. The organocalcium compounds thus formed combine good thermal stability with high reactivity towards carbonyl compounds and can be transmetalated in the usual way with copper(I) salts to organocalcium cuprates (Table 6).[66,67] These promising results are supplemented by H. Yamamoto's observation that the reaction of allyl chlorides with carbonyl compounds induced by highly reactive barium is distinguished by excellent regioselectivity and practically complete retention of the stereochemistry of the allyl double bond (Scheme 12).[68] In view of the hitherto insignificance of the higher alkaline earth metals in organic chemistry, the Grignard reaction may possibly arouse an unexpected competition from this corner of the periodic table.

Table 6. Reactivity of organocalcium compounds [66]

Halogen compound	Yield [%] [a]	Yield [%] [b]	Halogen compound	Yield [%] [a]	Yield [%] [b]
$C_8H_{17}Cl$	83	84	*p*-chlorotoluene	86	86
$C_8H_{17}Br$	79	[c]	bromoanisole	79 [d]	71 [e]
$Br(CH_2)_3OPh$	75	[c]	fluorobenzene	85	[c]
$Br(CH_2)_5OPh$	[c]	76	1-bromo-adamantane	80	[c]
cyclohexyl-bromide	75	82			

[a] Upon reaction of the organocalcium compounds with cyclohexanone. [b] After transmetalation with CuCN · 2 LiBr and reaction of the organocalcium cuprate with benzoyl chloride. [c] Not reported. [d] *meta*-Bromoanisole. [e] *para*-Bromoanisole.

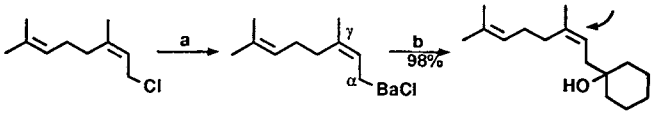

Scheme 12. Preparation and reaction of configuratively stable allylbarium reagents: [a] Rieke barium, THF, −78 °C; [b] cyclohexanone, −78 °C (*Z*): (*E*) > 99:1, α:γ = 91:9.

4.2. Actualization of Classical Synthetic Methods Exemplified by the Reformatsky Reaction

The Reformatsky reaction (Scheme 13) consists in the oxidative insertion of a metal into a carbon–halogen bond activated by neighboring carbonyl groups and the subsequent reaction of the resulting enolates with electrophiles. The reaction was traditionally confined to α-haloesters as donors, zinc as metal, and carbonyl compounds as acceptors, but has seen considerable extension in recent years.[69] The contribution that the high activation of metals has made to the improvement of this classical and, to many, conventional synthesis can be gleaned from the model experiments summarized in Table 7. Thus, on using highly reactive zinc instead of the usual procedure (Zn dust, etheral solvent or aromatic hydrocarbons, reflux), a lowering of the temperature by up to 160 °C (!) is possible with concomitant increase in the yields, increase in the reaction rate, and complete suppression of side reactions.

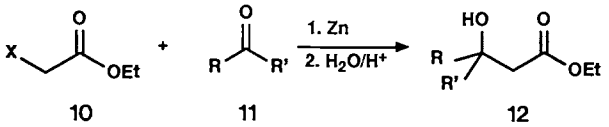

Scheme 13. Principle of the Reformatsky reaction.

Table 7. Comparison of the activity of variously activated zinc samples in simple Reformatsky reactions (Scheme 13) [69].

Zinc sample	Electrophile **11**	Donor X in **10**	Solvent	*T* [°C]	*t* [min]	Yield [%] of **12**
Zn dust	cyclohexanone	Br	benzene	+80	[a]	56
Zn dust	benzaldehyde	Br	benzene	+80	720	61
Zn/Cu couple	cyclohexanone	Br	THF	+66	60	82
Zn/Cu couple	cyclohexanone	Cl	benzene	+80	[b]	52
Zn/Cu couple	benzaldehyde	Br	THF	+66	60	82
Rieke Zn	cyclohexanone	Br	Et_2O	+25	60	95
Rieke Zn	cyclohexanone	Cl	THF	[a]	[a]	65
Rieke Zn	benzaldehyde	Br	Et_2O	+25	60	98
Zn/ultrasound	benzaldehyde	Br	dioxane	+25	5–300	98
$ZnCl_2$/Li–naphthalene	cyclohexanone	Cl	Et_2O	+35	120	85–90
$ZnCl_2$/Li–naphthalene	cyclohexanone	Br	Et_2O	+25	60	95–98
$ZnCl_2$/Li/ultrasound	benzaldehyde	Br	Et_2O	+25	60	90
Zn–graphite	cyclohexanone	Br	THF	0	120	75
Zn/Ag–graphite	cyclohexanone	Cl	THF	−20	10	86
Zn/Ag–graphite	cyclohexanone	Br	THF	−78	20	92

[a] Not determined. [b] 6–8 h.

Highly reactive zinc has also been used in more complex applications. Thus, with the drastic lowering of the reaction temperature there is a considerable gain in stereoselectivity upon reaction of the resulting zinc enolates prepared in situ with diastereotopic carbonyl compounds. This became apparent in the Zn/Ag–graphite-induced stereoselective branching of uloses[42,70] and chain-extension of aldonolactones[71] as well as in an elegant total synthesis of *N*-acetylneuraminic

acid based on a Reformatsky-type reaction of bromomethyl acrylate with an acyclic sugar aldehyde.[72]

Also the use of other haloalkanoates has contributed to the progress made in this field. Thus, for example, reaction of α-dihaloesters with Zn/Ag–graphite and carbonyl compounds at low temperatures leads to glycidates (Scheme 14),[73]

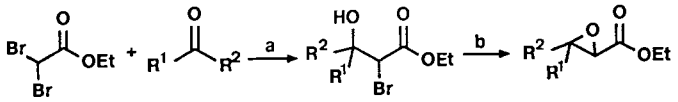

Scheme 14. Reformatsky-type Darzen's glycidate synthesis: [a] Zn/Ag–graphite, THF, −78 °C; [b] base.

whereas α-bromo-α-trimethylsilyl acetate under the same conditions affords 2-alkenoates regioselectively via a Peterson elimination spontaneously following the Reformatsky step.[73] Complementary to this reaction, in the conversion of silylmethyl ketones with zinc ester enolates 3-alkenoates can be obtained by the same sequence from Reformatsky reaction and subsequent Peterson olefination (Scheme 15).[74] The use of acylsilanes as a novel class of electrophiles has also been described.[74]

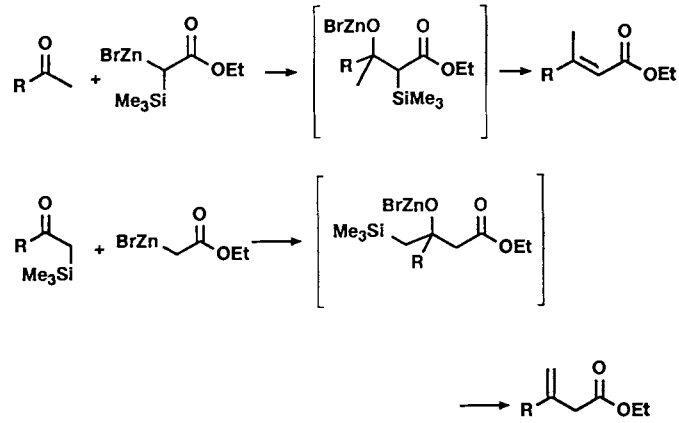

Scheme 15. Complementary syntheses of 2- and 3-alkenoates by Reformatsky–Peterson sequences.

Owing to the high efficiency of Reformatsky reactions with highly reactive zinc, they are also potentially useful as key steps in natural product syntheses. Illustrative examples in this context are the intramolecular reactions based on the use of Rieke zinc which have led to the formation of the 11-membered ring of cytochalasan (**13** → **14**) (Scheme 16)[75] and to the synthesis of the tricyclic skeletal framework of daphnilactone.[76] The latter synthesis is based on an etherification of the zinc aldolate (**16** → **17**) with the terminal bromide following the Reformatsky reaction with 2,5-dibromopentanoate or pentanamide **15**. Further developments in this field are summarized in ref. [69].

4.3. Functionalized Carbanions

The preparation of carbanions by oxidative insertion of metals into carbon–halogen bonds has so far been limited to

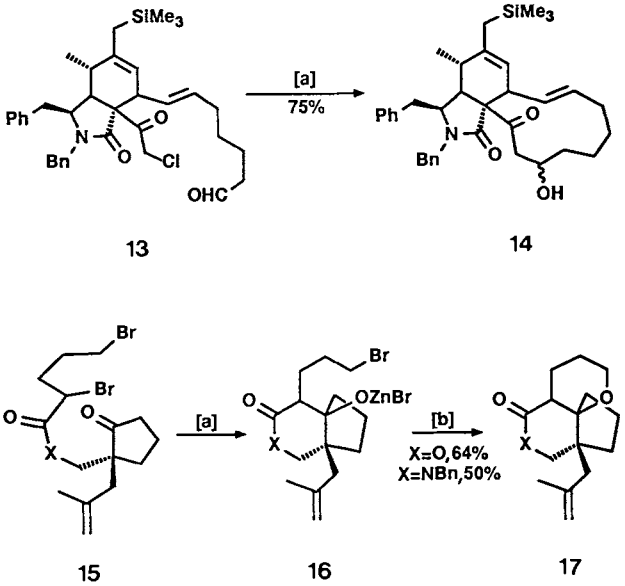

Scheme 16. Reformatsky reactions in natural product synthesis [a] Rieke Zn; [b] Addition of hexamethylphosphonic triamide.

a few elements, of which lithium and magnesium have played by far the most important role. Because of the relatively polar bond character the C-nucleophiles that are formed are, as a rule, very reactive and rarely tolerate electrophilic groups on themselves. However, the ability to undergo oxidative insertion into polarized bonds is a priori in no way confined to the electropositive metals, and in an appropriately activated form a wealth of main and sub-group elements are capable of such insertions.[3, 9, 34, 35, 38] This makes the generation and the chemoselective reaction of previously unknown highly functionalized organometallic compounds feasible.

Zinc, which in its conventional form is relatively unreactive, can be sufficiently activated without great effort that it reacts with many halohydrocarbons under mild conditions to give the corresponding organozinc compounds. In many cases the pretreatment of zinc dust with 1,2-dibromoethane (4 mol%) and Me_3SiCl (3 mol%) suffices for this purpose. The following trends were evident:[77, 78] 1) The insertion of the metal into C–X bonds (X = halogen) is in many cases *facilitated* by neighboring functional groups; with suitable substitution even alkyl bromides or chlorides can be used. 2) Secondary alkyl iodides react with the pretreated zinc in THF at lower temperature (25–30 °C) than primary alkyl iodides (35–45 °C). 3) For the reaction of aryl and heteroaryl iodides, polar solvents (DMF, DMA) are necessary. 4) The amount of Wurtz coupling in the preparation of benzyl- and allylzinc compounds is in general small. The tendency of allyl bromides to dimerize increases with increasing electron density at the double bond.[79a] 5) The distance between metalated carbon atom and heteroatom is of decisive importance. Thus, e.g., all attempts to synthesize β-*S*-substituted alkylzinc compounds failed because of their high tendency to elimination. 6) Most important appears to be the fact that the preparation and reaction of the organozinc compounds are compatible with a large spectrum of functional groups.[78] Even compounds with moderately acidic protons (terminal alkynes, indoles, alkylamides etc.) can be employed.[79b]

Regarding the oxidative insertion, Rieke zinc, which was prepared from ZnX_2 (X = Cl, Br, I) and $Li^+C_{10}H_8^-$ in THF or DME, is still more efficient. This is evident, inter alia, from the fact that it is also capable of reacting smoothly with alkyl, vinyl, and aryl bromides which can likewise be substituted by a series of electrophilic groups.[80] The functionalized organozinc compounds prepared in this way (Scheme 17) react after transmetalation with Cu^I salts, in the presence of catalytic amounts of Pd^0 complexes, or under assistance of Lewis acids, with numerous electrophiles (inter alia, acid chlorides, vinyl, aryl, and alkynyl halides, 3-iodoenones, aldehydes, enones, alkynoates, nitroolefins, Bu_3SnCl) in good to very good yields.[78-80] Allylzinc compounds, which can be prepared with zinc–graphite in THF at 0 °C, react with nitriles to give the corresponding β,γ-unsaturated ketones after hydrolysis of the intermediary metalloaldimines.[81]

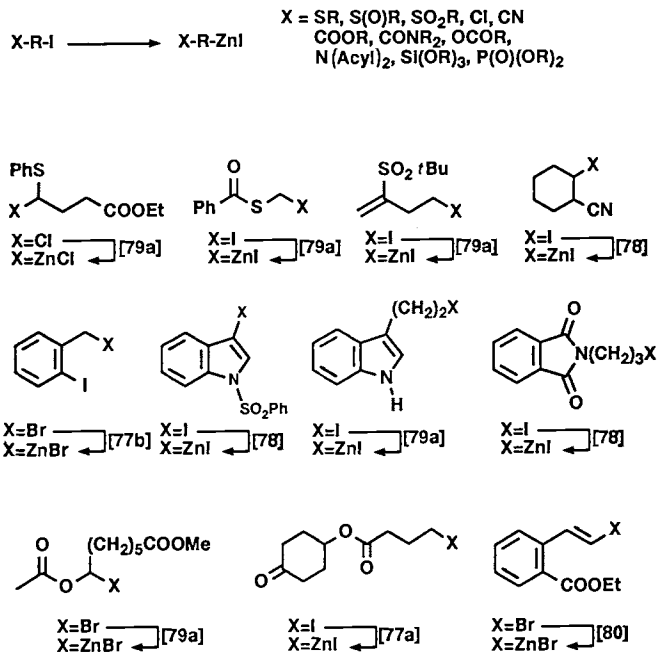

Scheme 17. Selected examples for the synthesis of functionalized organozinc compounds by oxidative insertion.

The situation is similar in the case of activated copper, which is capable of insertion into alkyl, aryl, and allyl halides as well as into allyl acetates.[17-19] In this way the usual transmetalation of reactive organolithium compounds can be avoided, and functionalized organocopper compounds can be prepared that are not accessible by the conventional route. In view of the importance of cuprates for the selective C–C bond formation[82] this new possibility is of particular interest. However, this example highlights the great deal of empirical optimization necessary before a synthetic method using highly reactive metals reaches preparative maturity. The strong tendency of conventional Rieke copper (CuI, potassium, 10 mol% naphthalene, DME, 8 h)[15] to agglomerate made the systematic search for more stable and thus more reactive forms of this metal necessary. The choice of the salt to be reduced thereby plays a decisive role. Particularly active copper samples are obtained in the reduction of $CuI \cdot PR_3$ (R = Et, Bu, Ph)[18] and of $CuCN \cdot 2LiX$[17] with $Li^+C_{10}H_8^-$ at low temperatures (< −100 °C) ($CuCN \cdot 2LiX$ is readily soluble in THF). Thus, reagents were prepared which contained, inter alia, ester, nitrile, carbamate, chloride, and in some cases even ketone, enone, and epoxy groups (Scheme 18), but otherwise showed the usual reaction profile of organocopper compounds.[17-19] They can be

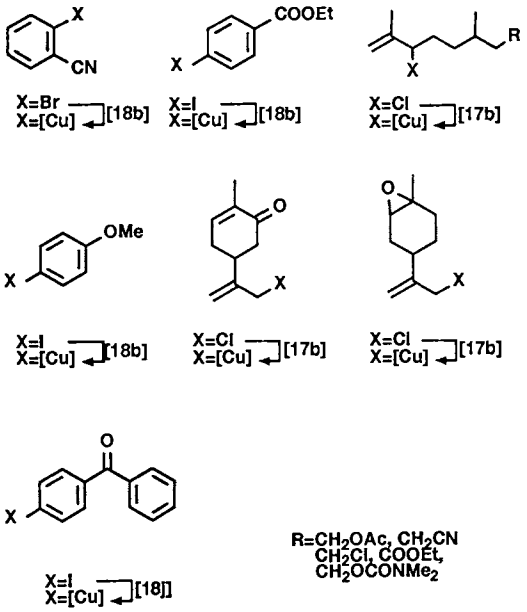

Scheme 18. Synthesis of functionalized organocopper compounds by oxidative insertion of activated copper into carbon–halogen bonds. Selected examples.

converted with acid chlorides in good yields into substituted ketones, be cross-coupled with allyl halides, undergo 1,4-additions to enones, and afford epoxide openings in overall respectable yields. When, however, the distance between metalated carbon and oxirane group is appropriate, intramolecular epoxide openings with formation of carbocycles such as **18** and **19** take place (ring sizes from 3 to 7) (Scheme 19).[17b, 18b, c, f] The observed regiochemistry can in some cases be varied considerably by changing the solvent (Table 8).[18b, c] In the reduction of $CuI \cdot PR_3$, for example, the choice of phosphane not only determines the activity of the metal obtained but also influences the nucleophilicity of the carbanions formed.[18] Further applications of activated

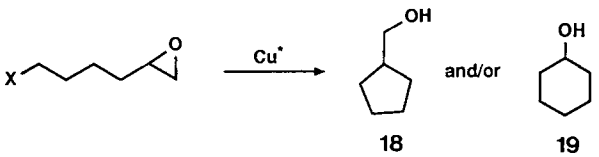

Scheme 19. Rieke Cu induced intramolecular epoxide openings.

Table 8. Influence of the solvent and of phosphanes on Rieke Cu induced intramolecular epoxide openings [18b].

Phosphane [a]	Solvent	**18**:**19**	Yield [%]
PBu_3	THF	1:6	56
PBu_3	toluene	1:0	45
PPh_3	THF	1:4	37
PPh_3	toluene	1:1.5	62

[a] 2.3 equiv. of PBu_3 or 2.0 equiv. PPh_3.

copper are the Wurtz coupling of halogen compounds (Section 4.5.1) and the formation of benzoin and benzil derivatives from aromatic acid chlorides.[83]

Rieke nickel is also capable of oxidative insertions into substituted halogen compounds. Applications to the synthesis of functionalized ketones and in the field of Ullmann biaryl synthesis are summarized in Section 4.5.1

4.4. Enantiomerically Pure Synthetic Building Blocks from Carbohydrates

Despite the proven versatility and reliability of highly reactive metals as tools in organic chemistry, the number of applications to complex substrates or in natural product synthesis has so far remained comparatively small. A few exceptions are found in the previous sections of this review. That high reactivity must not be equated with inadequate selectivity, however, is also demonstrated by the successful use of activated metals in the field of carbohydrate chemistry.

Glycals have long played a prominent role among the enantiomerically pure building blocks derived from sugars.[84] As cyclic enol ethers of the carbohydrate series, they combine an easily functionalizable anchor group with a skeletal framework of chiral centers. Their synthesis could be considerably improved in many respects by the use of graphite reagents. Thus, Zn/Ag–graphite is equally suitable for the reduction of pyranoid and furanoid glycosyl bromides (chlorides) (Scheme 20).[85] Since all operations are

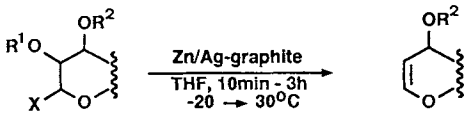

Scheme 20. Principle of the first Fischer–Zach-type glycal synthesis in an aprotic solvent. X = Cl, Br; R^1 = acyl, alkylidene; R^2 = acyl, alkyl, alkylidene.

carried out in an aprotic solvent (THF) at low temperatures and under neutral conditions, not only are all important protecting groups compatible with this method but also the furanoid glycals (**26**–**28**) that rearrange allylically even in weakly acidic media are readily accessible. The latter could virtually not be obtained with the classical Fischer–Zach method (Zn dust in acetic acid). Zn/Ag–graphite has also proven useful in the synthesis of the labile L-fucal **25**[86] and of thioglucal **24**[87] (Scheme 21). In this context it should be pointed out that Rieke zinc, in contrast to Zn/Ag–graphite, is capable of reducing very unstable glycosyl iodides to glycals only.[88]

Besides this first Fischer–Zach-type method for glycal synthesis in aprotic solvent, C_8K is also well suited for this purpose. Its advantages are found in the first direct synthesis of per-*O*-alkylated glycals (Scheme 22) and in the one-pot synthesis of differently protected building blocks by selective protonation, alkylation, acetalization, silylation, or glycosidation of the intermediate potassium alkoxide formed in the fragmentation of 2,3-alkylidenated glycosyl halides (Scheme 23, Table 9).[89] The self-indicative character (by the color change from bronze (C_8K) to black (graphite)), the short

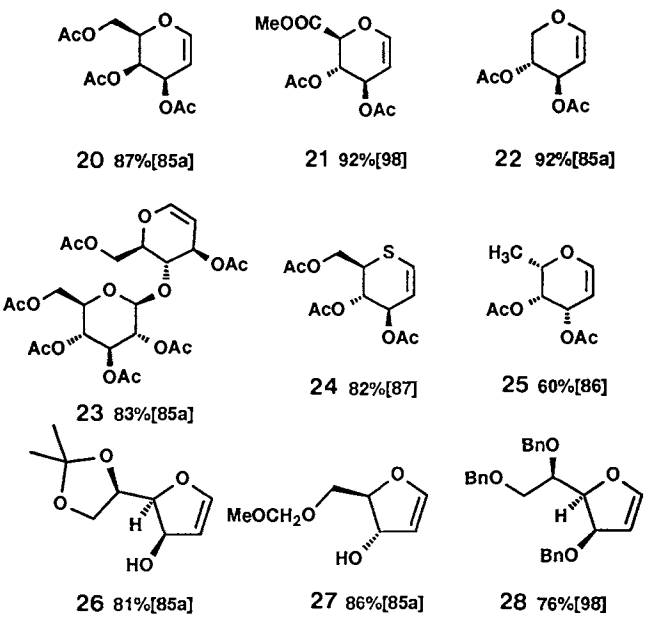

Scheme 21. Selected examples of glycals synthesized with the help of Zn/Ag–graphite.

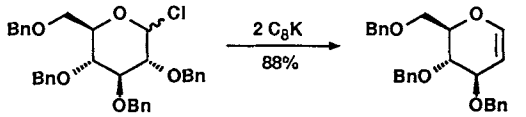

Scheme 22. Direct formation of 3,4,6-tri-*O*-benzyl-D-glucal.

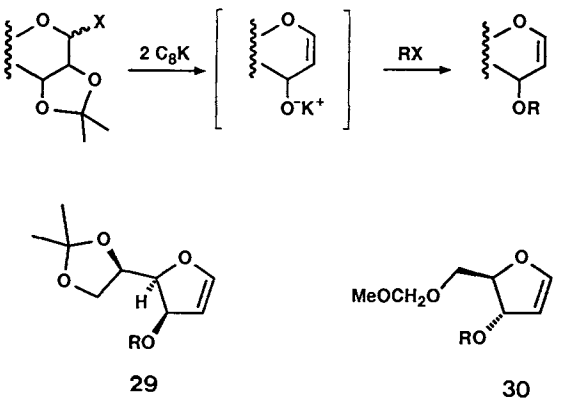

Scheme 23. One-pot synthesis of differently protected furanoid glycals using C_8K. Selected examples.

reaction times, and the simple workup procedure by filtration are further advantages of this novel glycal synthesis. Moreover, it disproves the opinion put forward in the litera-

Table 9. Synthesis of differentially protected furanoid glycals with C_8K (Scheme 23) [89].

Product	RX	Yield [%]	Product	RX	Yield [%]
29	H_2O	96	**30**	H_2O	92
29	$C_6H_5CH_2Br$	84	**30**	$C_6H_5CH_2Br$	86
29	$MeOCH_2Cl$	77	**30**	$MeOCH_2Cl$	80
29	$Ph_2MeSiCl$	90	**30**	$Ph_2MeSiCl$	90
29	2,3:5,6-di-*O*-isopropyliden-α-D-mannofuranosyl chloride	86			

ture[40] that C_8K is far too reactive and therefore unsuitable for the transformation of sensitive starting materials.

The benefits of using highly reactive metals are also clear in the reactions of other carbohydrate derivatives. Scheme 24 illustrates, with the model substrate **31**, possibilities for chemoselective conversions by suitable choice of the respective metal–graphite compound.[90] In the case illustrated

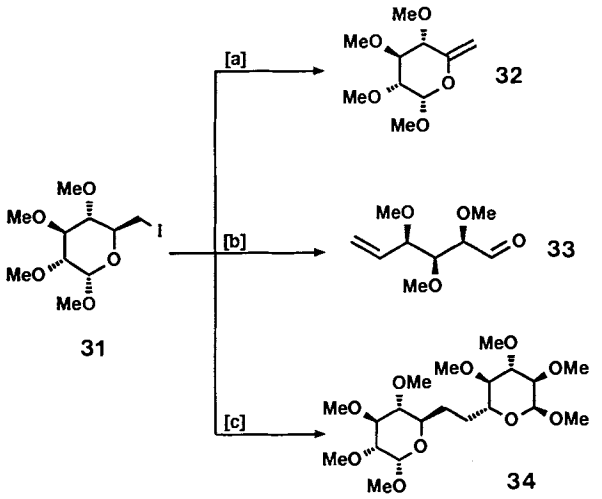

Scheme 24. Chemoselective reaction of 6-deoxy-6-iodopyranoside **31** with metal–graphite reagents: [a] C_8K, THF, 0 °C, 10 min, 94%; [b] Zn/Ag–graphite, room temperature, 10 min, THF, 93%; [c] Mg–graphite, THF, reflux, 3 h, 68%.

C_8K acts as a polymeric Lewis base, which leads to the dehydrohalogenation of the starting compound (**31** → **32**), whereas on using Mg–graphite Wurtz coupling of the substrate occurs (**31** → **34**). Zn/Ag–graphite deserves special attention because it represents by far the most appropriate agent for the reductive ring-opening of deoxyhalo sugars (**31** → **33**). Such dealkoxyhalogenations, in which both the ring oxygen as well as the halogen atom act as leaving groups (Scheme 25), can in principle be achieved even with less ac-

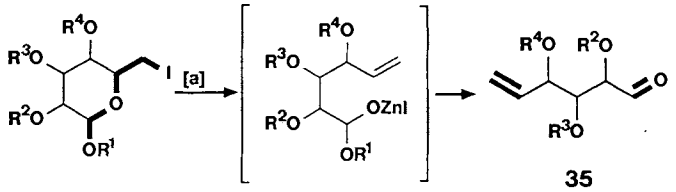

Scheme 25. Zn/Ag–graphite-induced dealkoxyhalogenation of deoxyhalo sugars; [a] Zn/Ag–graphite, THF or DME, ca. 25 °C, < 10 min.

tive zinc samples.[91] Zn/Ag–graphite in THF is, however, the only reagent operative in aprotic solvents; it consequently permits the synthesis of products sensitive to hydrolysis, it induces such reductions under comparatively mild conditions, and it surpasses all classical alternatives in terms of efficiency, suppression of side reactions, and reliability.[90, 92–94] This is clearly demonstrated, inter alia, by those cases in which conventional methods lead to decomposition of the substrate or to an unforseen reaction course, while Zn/Ag–graphite effects regular dealkoxyhalogenations (Scheme 26, Table 10).[92]

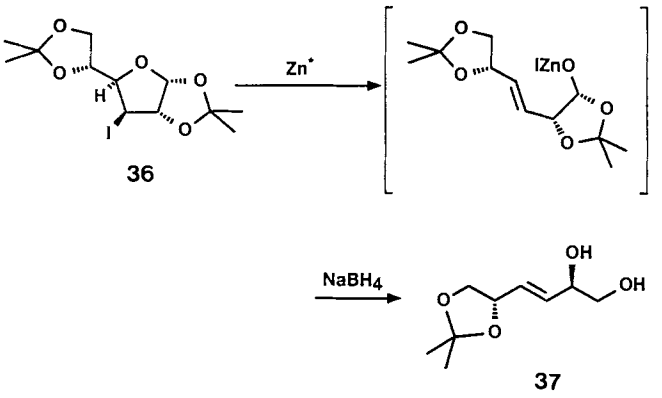

Scheme 26. Dealkoxyhalogenation of 3-deoxy-3-iodo-1,2;5,6-di-*O*-isopropylidene-α-D-glucofuranose and subsequent reduction of the resulting enal (see Table 10).

Table 10. Zinc-induced dealkoxyhalogenation of 3-deoxy-3-iodo-1,2;5,6-di-*O*-isopropylidene-α-D-glucofuranose **36** to enitol **37** (Scheme 26) [90, 92b].

Reagent	Solvent	T[°C]	t[min]	Yield [%]
Zn/Ag–graphite	THF	20	10	83
Rieke Zn	THF	20	10	9
Rieke Zn	THF	70	45	78
Zn dust/ultrasound	THF	20	60	0
Zn dust	EtOH/H_2O	70	240	– [a]

[a] Affords 2,3-dideoxy-5,6-*O*-isopropylidene-D-*erythro*-hex-3-enose (63%) instead of **37**.

In numerous cases Zn/Ag–graphite-induced fragmentations of this kind have proven to be independent of the configuration and conformation of the carbohydrate precursor as well as of the leaving group at the anomeric center (e.g. glycoside, acetal, lactone); they take place in primary and secondary halides at comparable rates.[92, 93] Generally, they occur more readily in iodides than in bromides and more efficiently with pyranoses than furanoses, where simple dehalogenation can compete with ring-opening (Scheme 29).[92]

Their initiation is halogen-selective, which makes a series of other protecting and functional groups compatible with such reductive ring-openings (e.g. *O*-acyl, *O*-alkoxycarbonyl, *O*-alkyl, *O*-silyl, *O*-alkylidene, deoxy, deoxyfluoro, epoxy, nitrile, thioether, acylamido groups) (Schemes 25–29, Tables 11, 12).[90, 92, 93] The transformation **38** → **39** uses this principle for synthesizing substituted tetrahydrofuran derivatives from carbohydrates (Scheme 27).[92a]

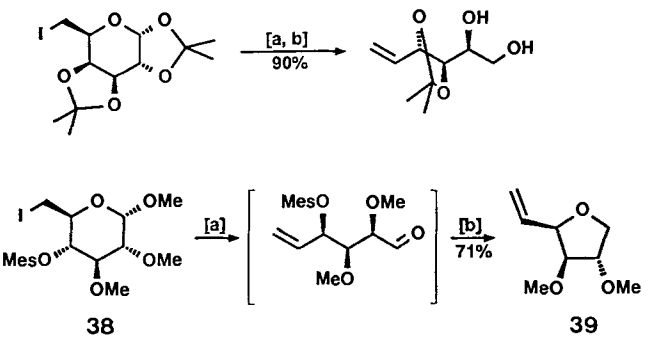

Scheme 27. Preparation of building blocks by reductive ring-opening and subsequent reduction of the resulting enal. [a] Zn/Ag–graphite, THF; [b] $NaBH_4$.

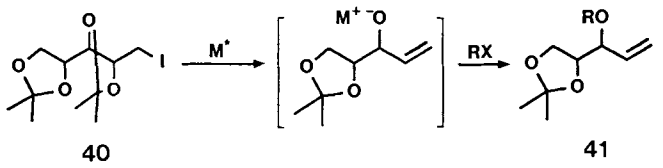

Scheme 28. Dealkoxyhalogenation of 1-deoxy-1-iodo-2,3;4,5-di-*O*-isopropylidenepentitols (see Table 12).

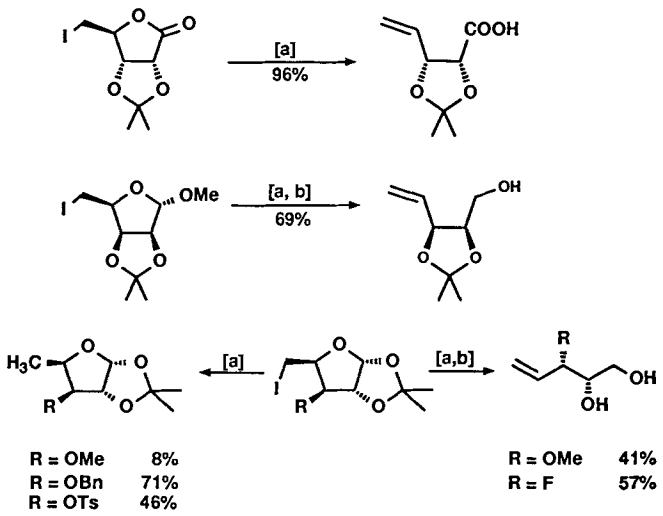

Scheme 29. Synthesis of 5-C building blocks by fragmentation of furanoses. [a] Zn/Ag–graphite, THF; [b] $NaBH_4$.

Table 11. Enantiomerically pure, substituted hex-5-enals **35** by Zn/Ag–graphite-induced ring-opening of 6-deoxy-6-iodopyranosides. Bn = benzyl, Bz = benzoyl, Ts = tosyl.

R^1	R^2	R^3	Configuration	Yield [%]	Ref.
OMe	OMe	OMe	D-*xylo*	93	[90]
OMe	OMe	OMe	D-*lyxo*	88	[100]
OMe	OMe	OMe	D-*ribo*	86	[100]
OMe	OMe	OMe	L-*arabino*	95	[100]
OAc	OAc	OAc	D-*xylo*	87	[92a]
OBz	OBz	OBz	D-*xylo*	81	[92a]
OMe	OMe	OBz	D-*xylo*	66	[92a]
OMe	OMe	OCOOEt	D-*xylo*	83	[92a]
NHAc	OAc	OAc	D-*arabino*	76	[92a]
OBn	H	OBn	D-*threo*	91	[93]
OAc	$OSiPh_2tBu$	OAc	D-*xylo*	85	[93]
$OSiMe_2tBu$	H	OAc	D-*threo*	90	[93]
$OSiPh_2tBu$	H	OAc	D-*erythro*	91	[93]
- O -		OBz	D-*ribo*	90 [a]	[92a]
H	OMe	OTs	D-*threo*	75 [b]	[92a]

[a] Aldehyde reduced in situ with $NaBH_4$. [b] Aldehyde unstable: $t_{1/2} = 20$ min.

Table 12. Synthesis of enantiomerically pure 5-C building blocks. The full set of all stereomeric 1,2-*O*-isopropylidenepent-4-enitols (**40**→**41**) (Scheme 28) [92c].

Reagent	Electrophile (RX)	R	Configuration	Yield [%]
Zn/Ag–graphite	H_2O	H	L-*threo*	90
Zn/Ag–graphite	H_2O	H	D-*threo*	90
Zn/Ag–graphite	H_2O	H	L-*erythro*	92
C_8K	H_2O	H	D-*threo*	95
C_8K	H_2O	H	D-*erythro*	93
C_8K	H_2O	H	L-*erythro*	87
C_8K	MeI	Me	D-*threo*	91
C_8K	ClCOOEt	COOEt	D-*threo*	90
C_8K	Ac_2O	Ac	D-*erythro*	81
C_8K	$C_6H_5CH_2Br$	Bn	D-*erythro*	86
C_8K	$Ph_2MeSiCl$	$SiMePh_2$	L-*erythro*	50

Regarding this high compatibility of the method with diverse functionalities, azidodeoxy groups form an interesting exception to the rule.[93] Although the azide itself generally emerges unchanged from the reaction with highly active zinc, it fundamentally changes its pathway, since instead of the ring-opening only dehalogenation of the substrate is observed (Scheme 30). This holds even when an azide is merely admixed with a starting material that normally undergoes

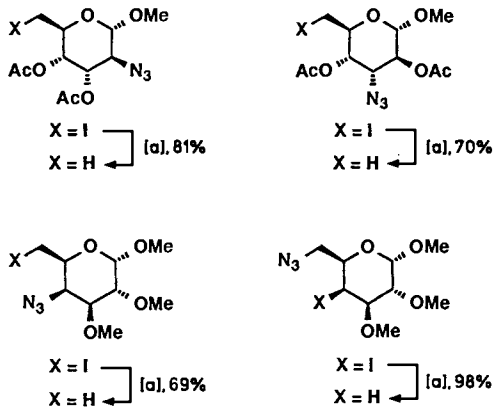

Scheme 30. The azide effect on zinc-induced reactions: [a] Zn/Ag–graphite, THF, room temperature.

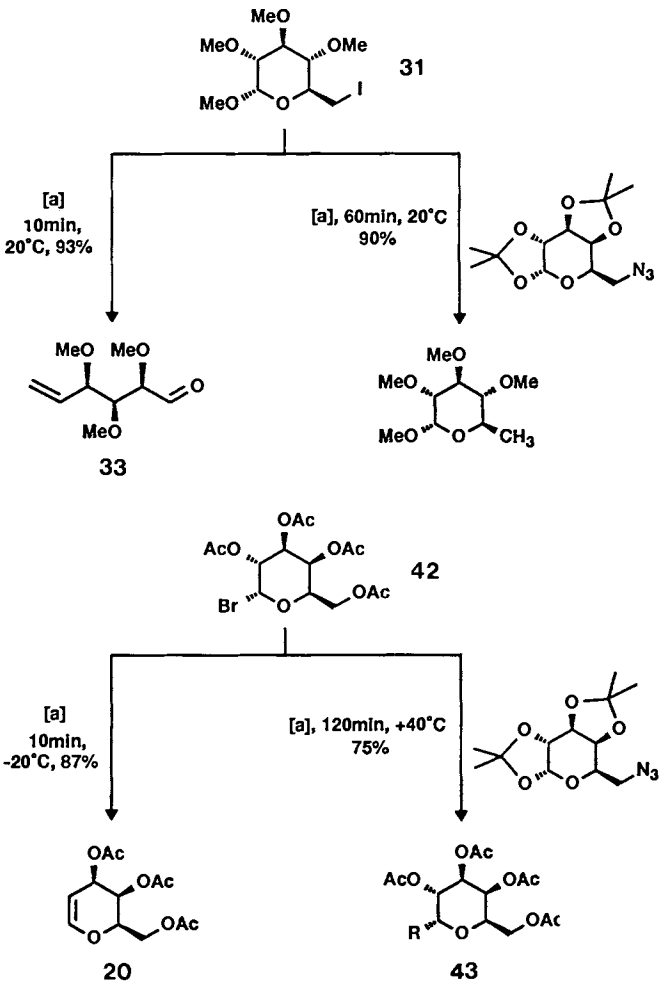

Scheme 31. Effect of external azides on zinc-induced reductions of deoxyhalo sugars; the azide (1 equiv) is recovered unchanged after completion of the reaction: [a] Zn/Ag–graphite [93]. R = H, D.

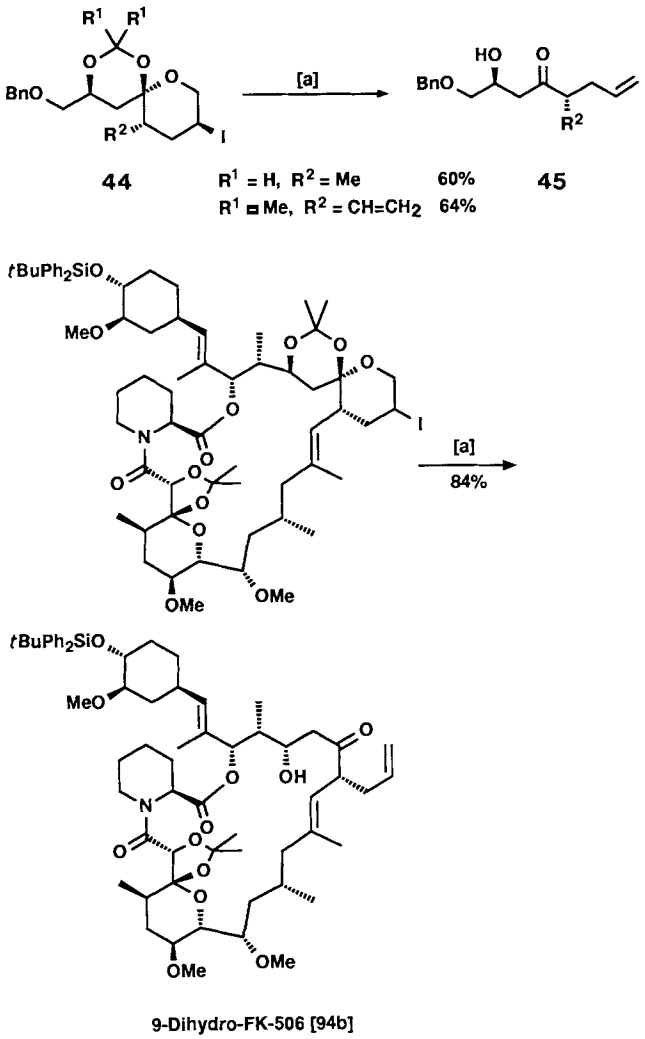

Scheme 32. Aldols by fragmentation of spiroketals [94]: [a] Zn/Ag–graphite, THF. R^1 = H, R = Me, yield 60%; R^1 = Me, R = $HC=CH_2$, yield 64%. Application to the synthesis of 9-dihydro-FK506.

facile ring-opening such as **31**. Likewise, the Zn/Ag–graphite-induced glycal synthesis (**42** → **20**) also fails in the presence of external organic azides (Scheme 31). Instead, dehalogenation with formation of the corresponding 1,5-anhydro sugar derivative (**42** → **43**) occurs. As could be confirmed by a labeling experiment, these simple reductive C–X bond cleavages proceed via radical intermediates for which the THF used as solvent serves as source of hydrogen.[93]

The high efficiency of the Zn/Ag–graphite-induced dealkoxyhalogenations is also the basis for a new, indirect entry to aldols by fragmentation of spiroketals such as **44** (Scheme 32).[94] The versatility and scope of this approach was impressively illustrated in a recent total synthesis of a derivative of the immunomodulator FK506.[94b]

The reactivity of graphite reagents in aprotic solvents is also the prerequisite for the synthesis of products such as the exocyclic enol ethers **47** and **49** (Scheme 33, Table 13),[92b] which are extremely sensitive to hydrolysis, and for the transformation of labile starting compounds. The recently described anomeric bromoimines (e.g. **51**)[95] prepared from glycosyl azides and NBS are in many respects most unstable substances but are nonetheless cleanly transformed by metal–graphite reagents in THF into aldononitriles (Scheme 34).[96] If, in this case, C_8K is employed instead of Zn/Ag–graphite

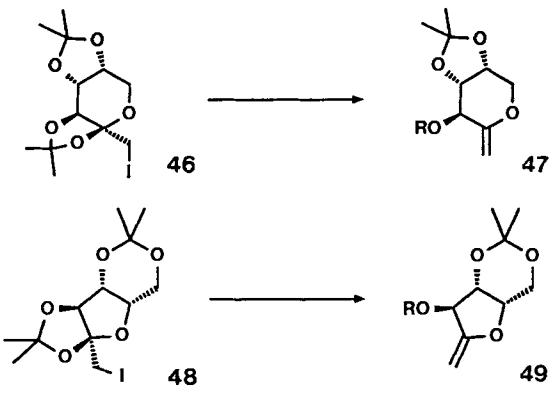

Scheme 33. Synthesis of exocyclic enol ethers from keto sugars (see Table 13).

Table 13. Synthesis of exocyclic enol ethers from keto sugars (Scheme 33) [92b].

Substrate	Reagent	Product	Electrophile	Yield [%]
46	Zn/Ag–graphite	**47** (R = Ac)	Ac_2O [a]	70 [b]
46	C_8K	**47** (R = Ac)	Ac_2O	82
46	C_8K	**47** (R = $SiPh_2Me$)	$Ph_2MeSiCl$	88
46	C_8K	**47** (R = Bn)	$C_6H_5CH_2Br$	72
48	C_8K	**49** (R = Bn)	$C_6H_5CH_2Br$	68

[a] Acetylation in presence of pyridine/dimethylaminopyridine. [b] 1-Deoxy-2,3:5,6-di-*O*-isopropylidene-β-D-fructopyranose (5%) as by-product.

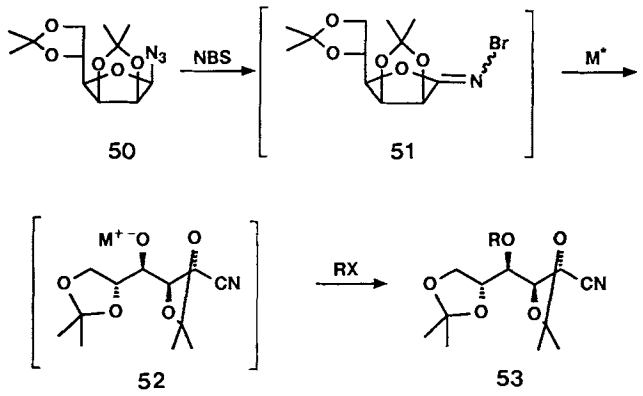

Scheme 34. Synthesis of mannononitriles from glycosyl azides (see Table 14).

Table 14. Synthesis of mannononitriles **53** according to Scheme 34 [96].

Reagent	Electrophile	Yield [%]
Zn/Ag–graphite	H_2O	87 (R = H)
C_8K	H_2O	90 (R = H)
C_8K	benzyl bromide	76 (R = Bn)
C_8K	benzoyl chlomide	80 (R = Bz)
C_8K	$Ph_2MeSiCl$	86 (R = $SiPh_2Me$)

as reducing agent then the intermediary potassium alkoxide **52** ($M^+ = K^+$) can be trapped in situ by addition of a variety of electrophiles (Table 14). To our knowledge there is no precedence to the sequence glycosyl azide–bromimine–aldononitrile (**50** → **51** → **52** → **53**).

The substituted enals formed in the reductive ring-opening of ω-halo sugars find many applications as enantiomerically pure synthetic building blocks with adequate terminal differentiation. Their preparative use can be increased still further by direct functionalization of the terminal double bond. For

this purpose one exploits the well-known property of thioethers to be halogenated in a radical reaction at the α-position[97] in suitably protected 6-deoxy-6-*S*-phenylglycosides. Reaction of **54** with *N*-chlorosuccinimide (NCS) affords the hydrolysis-sensitive α-chlorothioether **55**, which, without further purification, is allowed to react with Zn/Ag–graphite in DME to give the acyclic thioenol ether **56** [(*Z*):(*E*) = 1:2] (Scheme 35).[98] This strategy forms the basis for the enan-

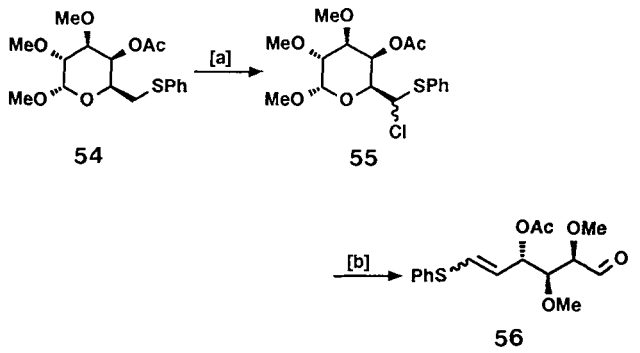

Scheme 35. [a] NCS, CCl_4, room temperature; [b] Zn/Ag graphite, DME, 60 °C, 64% (both steps).

tioselective synthesis of the C9–C14 fragment of trienomycin and mycotrienin antibiotics. This "chiral core" is identical in all members of this group of *ansa*-macrolides, and its relative and absolute stereochemistry has been determined by degradation of trienomycin A (Scheme 36).[99] A few standard steps permit conversion of the substrate **57**, accessible in gram amounts from D-glucose, into the thiophenyl ether **58** with the desired configuration at all the chiral centers. In situ halogenation with NCS followed by Zn/Ag–graphite-induced ring-opening affords compound **59**, which can be converted by chemoselective reaction of its aldehyde group with tris(isopropoxy)methyltitanium and subsequent oxidation of the alcohol formed with pyridinium chlorochromate (PCC) to give the final methyl ketone **60** (Scheme 37).[98] Both the two carbonyl groups as well as the alcohol functions are suitably differentiated, as is required for an intermediate of a total synthesis.

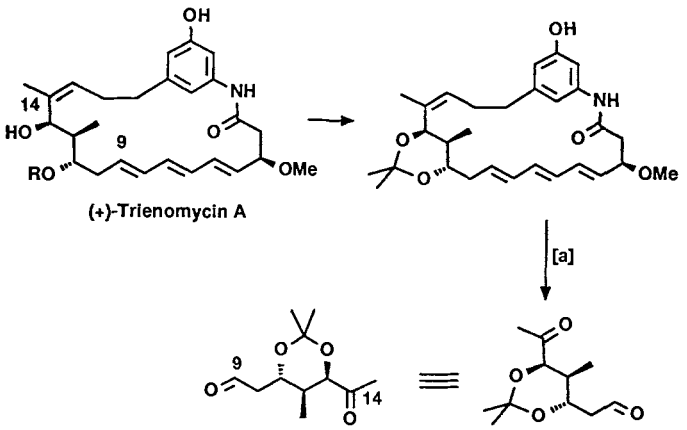

Scheme 36. Degradation of trienomycin A for the determination of the stereochemistry of the C9–C14 fragment [99]: [a] ozonolysis, 35%.

The advantage of the enantiomeric purity of carbohydrate-derived building blocks is limited by the relatively small number of sugars which are sufficient enough in nature to be likely starting compounds for multistep syntheses.[84] In particular, the lack of most sugars of the L series limits the accessible chiral building blocks drastically. This basically holds true also for the enal synthons dealt with herein. However, for these a practical way out of this dilemma is found

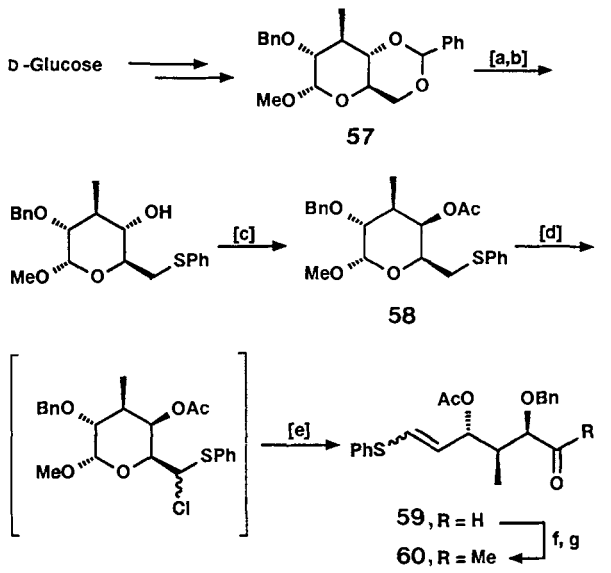

Scheme 37. Synthesis of the differentially protected C9–C14 fragment of the trienomycin and mycotrienin antibiotics: [a] *p*-TsOH · H_2O, THF, quant.; [b] PhSSPh, pyridine, Bu_3P, 83%; [c] (1) trifluoromethanesulfonic anhydride, pyridine, 0 °C; (2) $Bu_4N^+AcO^-$, acetonitrile, 78%; [d] *N*-chlorosuccinimide, CCl_4, 40 °C; [e] Zn/Ag–graphite, DME, 60 °C, 66% (via steps d and e); [f] $(iPrO)_3TiMe$, THF, 81%; [g] PCC, MS 3 Å, NaOAc, CH_2Cl_2, 72%.

with the sequence for transposition of their terminal groups as outlined in Schemes 38 and 39.[100] This method for the formal inversion of the configuration of the synthon, in which no *meso* form is passed through, consists in a well-tuned sequence of a nucleophilic attack at the aldehyde group by trimethylsilylmethylmagnesium chloride and dihydroxylation of the terminal double bond, followed by a Peterson elimination at the "head" of the molecule and subsequent periodate cleavage at its "tail". Since all intermediates do not have to be isolated, the overall yields of this reaction sequence

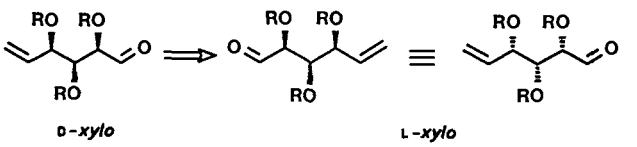

Scheme 38. Retrosynthetic analysis for the transposition of enals.

are satisfactory. In this way, for example, the complete set of all eight stereoisomeric 2,3,4-tri-*O*-methylhex-5-enoses was obtained from readily available parent sugars (D-glucose, D-mannose, D-galactose, D-allose) (Scheme 40).[100]

An application in natural product chemistry of this interplay of Zn/Ag–graphite-induced dealkoxyhalogenation and subsequent inversion of the stereochemistry of the building block obtained is the convergent synthesis of the C1–C13 fragment of amphoteronolide B (Fig. 5), the aglycone of the macrolide antibiotic amphotericin B used clinically as a fungicide.[101] Based on the hidden symmetry of this fragment,

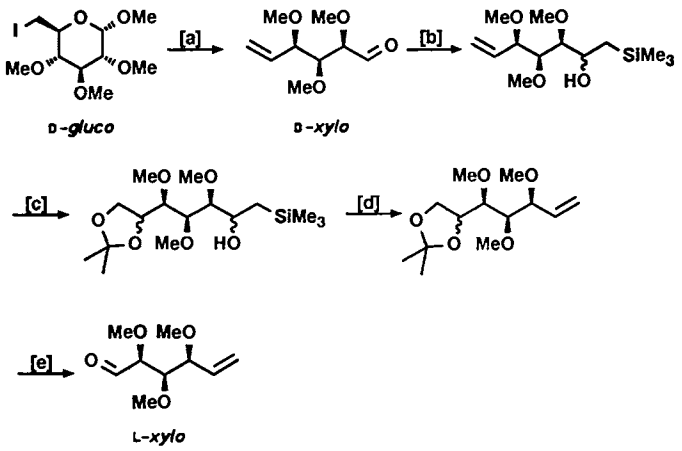

Scheme 39. [a] Zn/Ag–graphite, 10 min, 93%; [b] Me_3SiCH_2MgCl, THF, 60 min, 87%; [c] (1) OsO_4 cat., *N*-methylmorpholine *N*-oxide, 12 h, quantitative; (2) 2,2-dimethoxypropane, *p*-TsOH · H_2O, 15 min, quantitative; [d] $BF_3 \cdot Et_2O$, 10 min, quantitative; [e] (1) *p*-TsOH · H_2O, 10 min, quantitative; (2) $NaIO_4$, 15 min, quantitative.

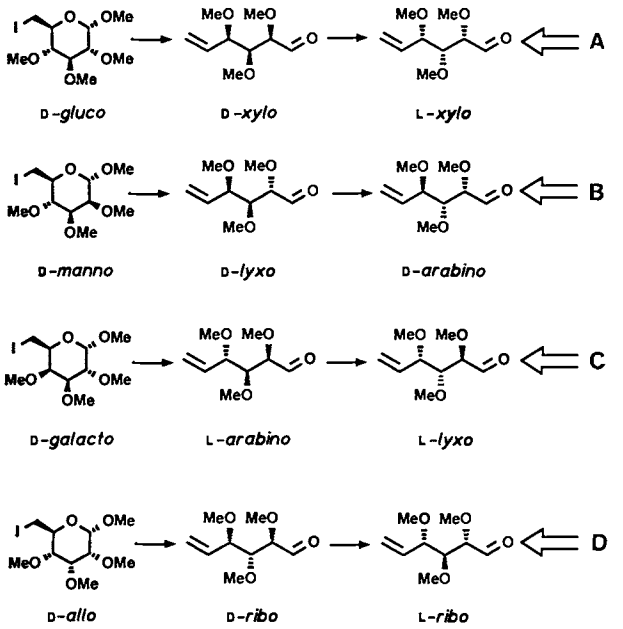

Scheme 40. The complete set of all stereoisomeric 2,3,4-tri-*O*-methylhex-5-enals by Zn/Ag–graphite-induced ring-opening and subsequent transposition. **A**: 6-deoxy-6-iodo-D-idopyranoside and 6-deoxy-6-iodo-L-glucopyranoside; **B**: 6-deoxy-6-iodo-D-altropyranoside and 6-deoxy-6-iodo-L-galactopyranoside; **C**: 6-deoxy-6-iodo-D-gulopyranoside and 6-deoxy-6-iodo-L-mannopyranoside; **D**: 6-deoxy-6-iodo-D-talopyranoside and 6-deoxy-6-iodo-L-allopyranoside.

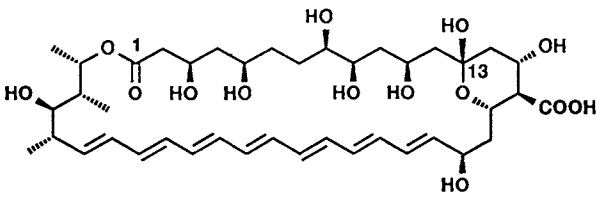

Fig. 5. Amphoteronolide B.

the synthesis of the carbon chain is achieved via a ketophosphonate–aldehyde coupling (**62** + **63** → **61**), followed by conversion of the resulting enone **61** into the target compound essentially according to the precedence of Nicolaou's total synthesis (Scheme 41). Each of the units **62** and **63**

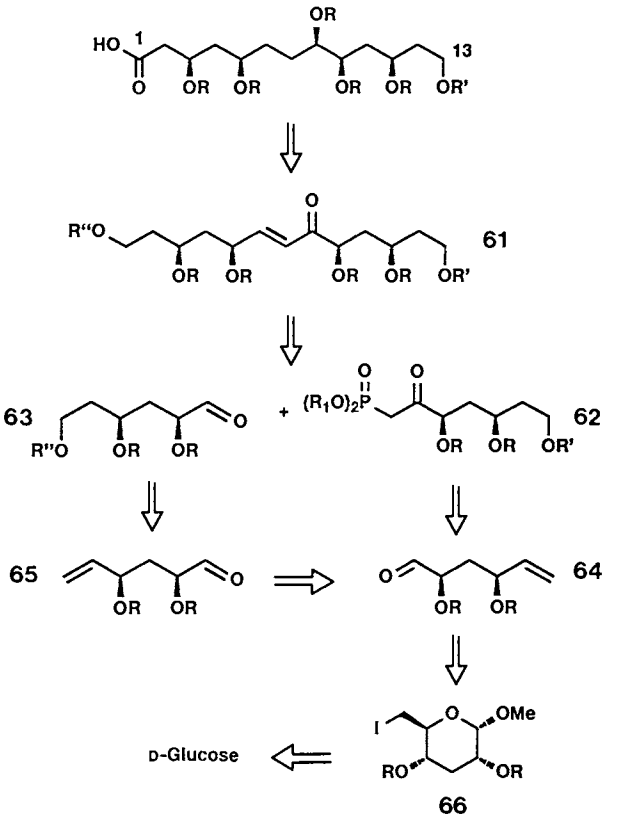

Scheme 41. Retrosynthetic analysis of the C1–C13 fragment of amphoteronolide B.

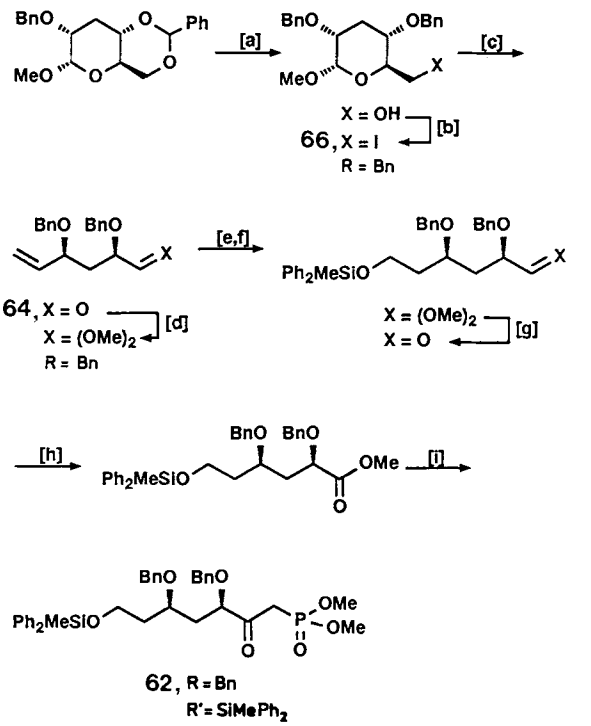

Scheme 42. Amphoteronolide B. Synthesis of the C7–C23 segment from D-glucose, **62′** = **62** with R = Bn, R′ = $SiMePh_2$, R_1 = Me; **64′** = **64** with R = Bn; **66′** = **66** with R = Bn. [a] $BH_3 \cdot NMe_3$, toluene, room temperature, 66%; [b] I_2, PPh_3, imidazole, toluene, room temperature, 88%; [c] Zn/Ag–graphite, THF, room temperature, 86%; [d] $HC(OMe)_3$, *p*-TsOH · H_2O, 97%; [e] (1) 9-BBN, THF; (2) NaOH, H_2O_2; [f] *t*$BuPh_2SiCl$, imidazole, CH_2Cl_2, 86% over both steps; [g] *p*-TsOH, acetone, room temperature, 95%; [h] PCC, CH_2Cl_2, 4 equiv. MeOH, 68%; [i] $(MeO)_2P(O)CH_3$; *n*BuLi, −78 → 0 °C, THF, 90%.

required for the coupling is obtained in a few steps from an enal; the latter are enantiomeric to each other and consequently are both accessible by ring-opening/transposition from the same central intermediate **66**, which in turn can be readily obtained in large amounts from D-glucose (Schemes 42 and 43).[102]

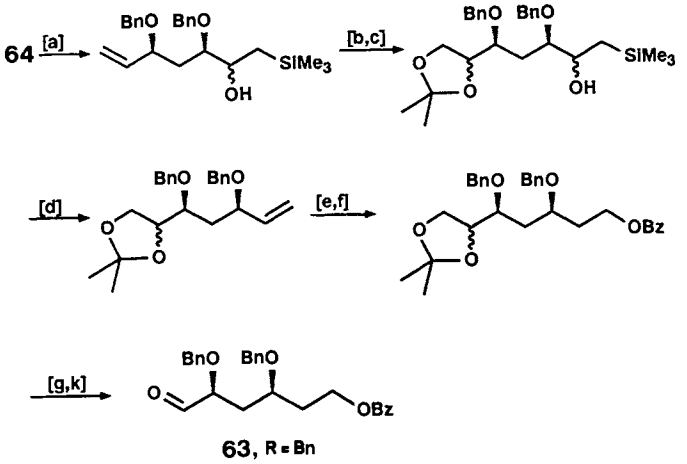

Scheme 43. Amphoteronolide B. Synthesis of the C1–C6 fragment **63'** from enal **64'** (see Scheme 42: **63'** = **63** with R = Bn, R'' = Bz). [a] Me_3SiCH_2MgCl, THF, room temperature; [b] OsO_4 cat., *N*-methylmorpholine *N*-oxide, acetone, 91% over both steps; [c] 2,2-dimethoxypropane, *p*-TsOH · H_2O, CH_2Cl_2, 87%; [d] $BF_3 \cdot Et_2O$, CH_2Cl_2, 68%; [e] (i) 9-BBN, THF; (ii) NaOH (3 M), H_2O_2, 93%; [f] benzoyl chloride, pyridine, 4,4-dimethylaminopyridine cat., 89%; [g] *p*-TsOH, aqueous THF, room temperature; [h] $NaIO_4$, ether/water, room temperature, 78% over both steps.

4.5. Reductive Coupling Reactions

4.5.1. Coupling of Halogen Compounds

Copper powder is the reagent of the classical Ullmann biaryl synthesis.[103] In highly reactive form as Rieke copper it dimerizes allyl, benzyl, alkynyl, aryl, and primary alkyl halides in good yields and tolerates a remarkable spectrum of functional groups in the substrates.[15, 18a, g, i, 21] The coupling of secondary and tertiary alkyl halides and intramolecular reactions can be accomplished only in execptional cases (e.g. 1,3-dibromoalkanes) in good yields.[18i] Passage of oxygen through the solution of the intermediate organocopper compounds leads to their dimerization already at room temperature.[18g] The effect of additives and the importance of the choice of the copper salt to be reduced in such Wurtz couplings have been studied in detail.[21] The activation of commercially available copper powder with ultrasound, which is due to destruction of the oxide layer on the metal, likewise leads to substantial improvements of the Ullmann synthesis by the elimination of the induction period and an up to 64-fold increase in the reaction rate.[48c]

Similarly, activated nickel, either in the form of Rieke nickel[104] or nickel/copper–graphite,[43] dimerizes benzyl halides and aryl iodides in good yields, whereby the substrate can be likewise substituted by a series of functional groups. Bromobenzene derivatives are less suited for nickel-induced Ullmann reactions which are normally facilitated by electron-withdrawing substituents on the phenyl ring. On reaction of benzal halides or benzotrichloride with Rieke nickel the corresponding stilbene derivatives[104] are formed, whereas 1,1-dihalogenoethenes dimerize to allenes or cyclooligomerize to radialenes.[105]

If, on the other hand, a mixture of a benzyl, allyl, vinyl, or pentafluorophenyl halide and an acid chloride is allowed to react with Rieke nickel, cross-coupling preferably occurs with formation of ketones.[106] Mechanistically , this synthesis, which again is distinguished by wide applicability with numerous differently substituted starting compounds, proceeds via oxidative insertion of the nickel into both coupling partners.[106] Due to this ability to form acylnickel compounds and its suitability for the direct preparation of π-allylnickel complexes from allyl halides,[107] activated nickel is a likely substitute for soluble Ni^0 complexes (e.g. $[Ni(CO)_4]$, $[Ni(cod)_2]$), which in some cases are toxic and difficult to handle.

Wurtz-type couplings can also be carried out on a series of structurally different halogen compounds with lithium activated by the use of ultrasound.[108] Table 15 gives a comparison of the above-mentioned methods.

Table 15. Selected examples of the dimerization of halohydrocarbons with activated metals.

Substrate	Reagent	Conditions	Yield [%] coupling	reduction	Ref.
benzyl chloride	Rieke Ni	70 °C, 0.5 h	86	10	[104a]
benzyl chloride	Ni/Cu-graphite	85 °C, 20 h	87 [a]	4	[43]
benzyl chloride	lithium [d]	RT, 40 h	60 [e]		[108a]
benzyl bromide	Rieke Ni	RT, 1 h	77	23	[104a]
benzyl bromide	Ni/Cu-graphite	85 °C, 20 h	99 [a]	1	[43]
benzyl bromide	Rieke Cu	25 °C	95 [a]	-	[18i]
3-$MeOC_6H_4CH_2Cl$	Rieke Ni	RT, 6 h	69	[b]	[104a]
3-$MeOC_6H_4CH_2Cl$	Ni/Cu-graphite	85 °C, 20 h	85	-	[43]
4-$O_2NC_6H_4CH_2Cl$	Rieke Ni	RT, 1 h	78	[b]	[104a]
4-$O_2NC_6H_4CH_2Cl$	Ni/Cu-graphite	85 °C, 20 h	54	[b]	[43]
4-$NCC_6H_4CH_2Br$	Rieke Ni	RT, 1 h	68	[b]	[104a]
4-$NCC_6H_4CH_2Br$	Ni/Cu-graphite	85 °C, 20 h	62	1	[43]
4-$BrC_6H_4CH_2Br$	Rieke Ni	RT, 6 h	70	[b]	[104a]
4-$BrC_6H_4CH_2Br$	Ni/Cu-graphite	85 °C, 20 h	90	0	[43]
4-$MeOOCC_6H_4CH_2Cl$	Rieke Ni	RT, 1 h	73	14	[104a]
4-$MeOOCC_6H_4CH_2Cl$	Ni/Cu-graphite	85 °C, 20 h	85	0	[43]
iodoobenzene	Rieke Ni	85 °C, 2 h	83 [a]	15 [a]	[104b]
iodobenzene	Rieke Cu	85 °C, 1 h	66 [a]		[18a]
iodobenzene	lithium [d]	RT, 12 h	73%		[108a]
chlorobenzene	lithium [d]	RT, 12 h	70%		[108a]
2-$O_2NC_6H_4I$	Rieke Ni	85 °C, 6 h	< 1	< 1	[104b]
2-$O_2NC_6H_4I$	Rieke Cu	65 °C	87		[18a]
4-NCC_6H_4I	Rieke Ni	85 °C, 2 h	85	< 1	[104b]
4-NCC_6H_4Br	Rieke Ni	85 °C, 21 h	71	[b]	[104b]
2-NCC_6H_4Br	Rieke Cu	25 °C, 1 h	76 [c]		[18a]
C_6F_5I	Rieke Ni	85 °C, 2 h	100		[104b]
C_6F_5Br	Rieke Ni	85 °C, 4 h	49	22	[104b]
C_6F_5I	Rieke Cu	101 °C, 24 h	91 [a]		[18a]
PhCCBr	Rieke Cu	25 °C	30 [a]		[18g]
allyl bromide	Rieke Cu	25 °C	99		[18g]
allyl iodide	Rieke Cu	25 °C	92		[18i]
heptyl iodide	Rieke Cu	25 °C	83 [a]		[18g]
1-chloropropane	lithium [d]	RT, 17 h	72%		[108a]
2-iodoopropane	Rieke Cu	25 °C	41		[18i]

[a] Yields determined by gas chromatography. [b] Not determined. [c] O_2 passed through reaction solution to ensure coupling. [d] Ultrasound activation. [e] Determined by NMR.

4.5.2. Coupling of Carbonyl Compounds

In the years 1973 and 1974 three research groups reported independently of one another on carbonyl coupling reactions with formation of alkenes using zero- or low-valent titanium

reagents (Scheme 44).[13, 109] This reductive dimerization, generally referred to as the McMurry reaction[110] demonstrates quite clearly the problems of metal activation. Com-

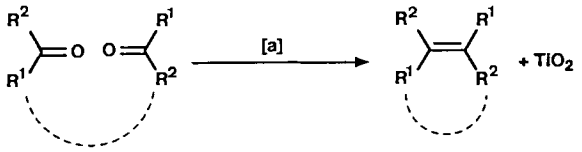

Scheme 44. Principle of the McMurry reaction: [a] low-valent titanium compound.

mercially available titanium powder is unsuitable for this reaction, and the highly reactive metal shows considerably different degrees of activity depending on its genesis. Despite intensive efforts the structure of the metal samples generated in situ is still unclear.[111] These morphological studies are hampered by the complex redox behavior of low-valent titanium compounds, the tendency to ether cleavage, the high oxophilicity, and the potential danger of artefacts during sample preparation. There are numerous indications that $TiCl_4$ is not reduced to metallic titanium by conventional reducing agents in solution.[112–114] In the case of the reaction of $TiCl_3$ with $LiAlH_4$ recent investigations confirm the formation of chlorohydridotitanium complexes as the actual active species.[115] Model investigations on single crystals of titanium dioxide, whose surfaces are partially reduced by ion bombardment likewise show that the presence of zero-valent titanium is not an essential prerequisite for reductive alkene syntheses from carbonyl compounds.[116] Summarizing, these results further strengthen the view that structurally different McMurry agents might be present and could be active, depending on their preparation.

In view of the great preparative potential of the McMurry reaction much empirical work has been devoted to its improvement and standardization by variation of the titanium halide, the solvent, the reducing agent, and the reaction time, as well as by addition of additives (pyridine, triethylamine).[110] Of the numerous procedures, three recent developments deserve special mention. Firstly, McMurry et al. have worked out an optimized procedure for the intra- and intermolecular coupling of (di)carbonyl compounds based on the use of $TiCl_3 \cdot DME_{1.5}$ as source of titanium, Zn/Cu couple as reducing agent, and DME as solvent which affords reproducible results in all the cases investigated.[117] Also the coupling of diisopropyl ketone to tetraisopropylethylene could be considerably improved under these conditions (87% in contrast to 37% with $TiCl_3$/Zn–Cu and 12% with $TiCl_3/LiAlH_4$).

Secondly, studies on the influence of the solvent on the (*Z*)/(*E*) ratio of the alkene formed and the influence of ultrasound on the course of the reaction have been reported.[118] According to these studies, in the intermolecular coupling of acetophenone in DME the (*E*) alkene is preferably formed, whereas in THF, the (*Z*) alkene is the major product. When ultrasound is used the reaction that normally takes place under reflux already occurs at 30 °C, whereby the alkene is only formed in THF (again the (*Z*) isomer predominates), while in DME the reaction stops at the pinacol stage.[118] The general validity of these observations needs to be checked on further examples.

Finally, regarding methodological developments, the high activity of titanium–graphite prepared from $TiCl_3$ and C_8K in all types of McMurry reactions should be mentioned.[114, 119–121] This is an extremely efficient reagent for the inter- and intramolecular coupling of aromatic and aliphatic aldehydes, ketones, dialdehydes, and diketones to alkenes or cycloalkenes, respectively. Since C_8K reduces titanium trichloride much more rapidly (1.5 h) than other reducing agents (e.g. 12–16 h for potassium) the overall reaction time is shortened considerably.[114] Titanium–graphite also proved to be very efficient in the synthesis of *ansa*–titanocene derivatives by dimerization of acylcyclopentadienyl anions.[120] Furthermore, slightly modified titanium–graphite ($TiCl_3$:C_8K = 1:2) has been described as the most suitable reagent for the coupling of highly oxygenated substrates and for annelation reactions.[121]

When titanium tetrachloride is reduced with C_8K a chemoselective titanium reagent is obtained which without reservation dimerizes aromatic carbonyl compounds to alkenes, but reacts with aliphatic carbonyl compounds to give only pinacols.[114] This clearly indicates the presence of different low-valent titanium species depending on the chosen source of titanium. Moreover, in the course of these investigations there were indications that the tertiary amines widely used as additives owe their activity to disproportionations of the low-valent metal.[114]

Since the previous applications of the McMurry reaction in organic synthesis have already been summarized in several excellent review articles,[110] only more recent developments in this field will be dealt with here. From the total syntheses using this reaction in a key step it is clear that the preparation of highly substituted natural products is increasingly approaching the realm of the possible. Thus, intramolecular couplings of highly oxygenated dicarbonyl compounds have been carried out, which in view of the exceptional affinity of low-valent titanium for oxygen are by no means trivial (Scheme 45). For example, of all the reagents tested for the

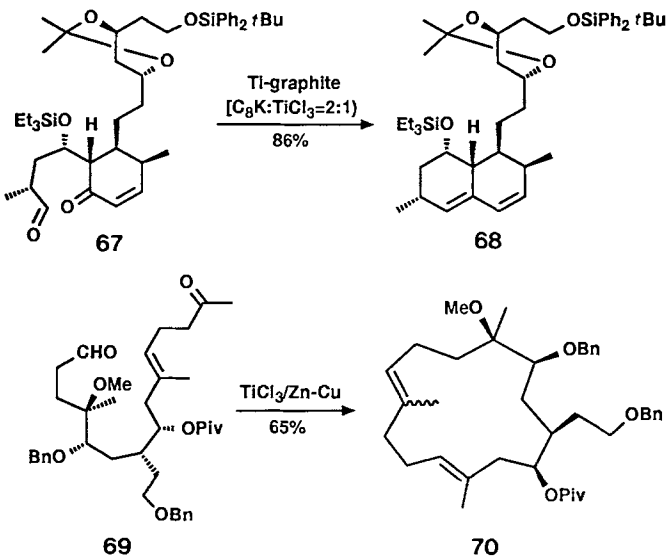

Scheme 45. Intramolecular McMurry reactions with polyoxygenated dicarbonyl compounds. Compound **70** reacts further to give the crassinacetate methyl ether. Piv = pivaloyl.

annelation of the A ring (**67** → **68**) in a late intermediate of a synthesis of (+)-compactin and (+)-mevindin, respectively, only titanium–graphite (C_8K:$TiCl_3$ = 2:1) promoted the desired coupling reaction.[122] Macrocyclization (**69** → **70**) with $TiCl_3$/Zn–Cu plays a central role in the synthesis of crassinacetate methyl ether, a representative of the cembran diterpenes.[123] However, in contrast to a SmI_2-induced pinacolization, all attempts to carry out a titanium-supported cyclization of a polyoxygenated ketoaldehyde in the synthesis of grayanotoxin failed.[124]

Although low-valent titanium compounds do not promote any acyloin condensations of diesters, they are capable of reductively coupling ketoesters to enol ethers, which upon acidic workup of the reaction mixture afford cyclanones as final products (Scheme 46). Such oxoalkanoate cyclizations have proven to be rather sensitive with regard to the titanium sample used. Successful applications have previously only been reported with a Rieke titanium modified by addition of triethylamine[125] and with titanium–graphite.[114] In contrast to other intramolecular McMurry couplings the success of this cyclanone synthesis is somewhat dependent on the ring size of the carbocycle synthesized;[125] also the chain length of the alcohol part of the ester (R^2 in Scheme 46) also appears to be of decisive importance for the outcome of the reaction.[126] This method of titanium-induced ketoester coupling has found uses in natural product chemistry in the syntheses of capnellene[127] and isocarophyllene.[128]

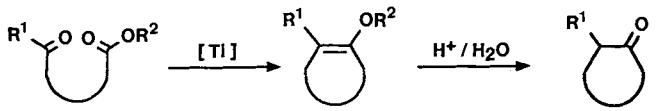

Scheme 46. Titanium-induced cyclization of oxoalkanoates.

Comparable *inter*molecular alkylidenations of acid derivatives with low-valent titanium compounds are the syntheses of enol ethers, enol thioethers, and enamines from carboxylic acid esters, thiol esters, and acid amides, respectively, upon reaction with geminal dibromides (Scheme 47).[129] However, these transformations presumably proceed via titanium carbenes and mechanistically resemble reactions with the Tebbe–Evans–Grubbs reagent.[130]

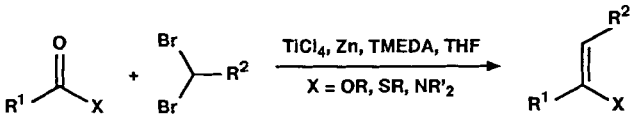

Scheme 47. Intermolecular alkylidenation of esters, thiol esters, and amides induced by low-valent titanium.

The efficiency of the titanium-induced ketoester cyclizations offers the possibility to extend this reaction to the related acyloxycarbonyl compounds (Scheme 48, X = O). This opens up a novel entry to heterocycles, as shown by the syntheses of furans (**73** → **74**) and benzofurans (**71** → **72**) summarized in Table 16 (Scheme 49).[126, 131] Although carboxylic acid amides were previously considered as largely inert under McMurry conditions, this completely new entry to aromatic heterocycles could also be extended to the formation

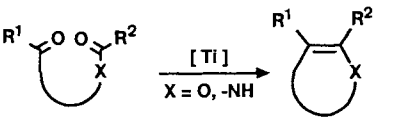

Scheme 48. Principle of the heterocycle synthesis with titanium–graphite.

Table 16. Synthesis of (benzo)furan derivatives with low-valent titanium compounds (Scheme 49).

Substrate	R^1	R^2	R^3 [a]	Product	Method [b]	Yield [%]	Ref.
71	Ph	Ph	H	**72**	A	88	[131a]
71	Ph	Me	H	**72**	A	85	[131a]
71	Me	Ph	H	**72**	A	80	[131a]
71	Me	Ph	H	**72**	B	55	[131b]
71	Me	3-MeOPh	H	**72**	B	60	[131b]
71	Me	Ph	4-OMe	**72**	B	45	[131b]
71	Me	Ph	5-OMe	**72**	B	56	[131b]
71	Me	Ph	6-OMe	**72**	B	58	[131b]
71	Me	Ph	4,5-$(OMe)_2$	**72**	B	24	[131b]
71	Me	Me	H	–	A	[c]	[131a]
71	H	Me	H	–	A	[c]	[131a]
71	H	Ph	H	**72**	A	89	[131a]
71	H	3-MeOPh	4-OMe	**72**	A	[c]	[126]
71	H	[d]	4-OMe	**72**	A	[c]	[126]
73	Ph	Ph	H	**74**	A	92	[131a]
73	Me	Me	H	**74**	A	58	[131a]

[a] Numbering refers to the starting material. [b] Method A: Ti-graphite, THF, reflux; Method B: $TiCl_4$/Zn/dioxane, reflux. [c] Decomposition. [d] 3,5-Dimethoxyphenyl.

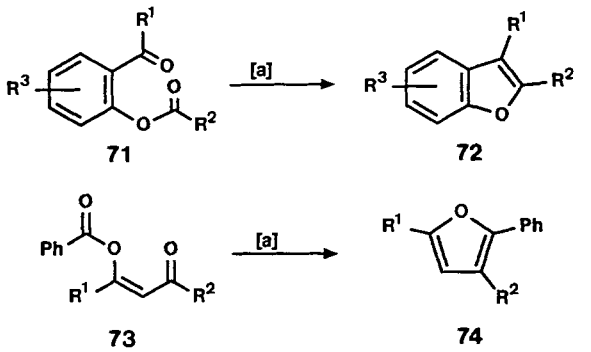

Scheme 49. Titanium-induced cyclization of acyloxycarbonyl compounds to furans or benzo[*b*]furans: [a] Ti-graphite or $TiCl_4$/Zn (see Table 16).

of indoles from acylamidocarbonyl compounds (**75** → **76**) (Scheme 50, Table 17).[126, 131a] This reaction has some remarkable characteristics. For example, the high-dilution technique commonly used in cyclizations is unnecessary, the indole formation can even be carried out at high concentrations in good yields and short reaction times without intermolecular coupling reactions competing. All kinds of amides, from formamide up to fatty acid amide, including aromatic and heteroaromatic ones, undergo comparatively rapid reac-

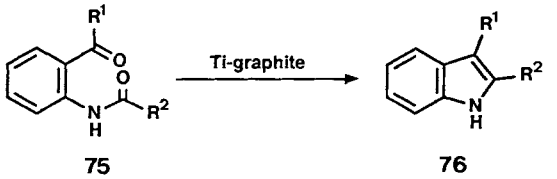

Scheme 50. Principle of the reductive indole snythesis with titanium–graphite [126, 131a].

Table 17. Synthesis of indoles **76** from acylamidocarbonyl compounds **75** using titanium–graphite (Scheme 50) [126].

R^1	R^2	Yield [%]	R^1	R^2	Yield [%]
Me	Ph	75	Ph	[a]	79
Me	Me	70	Ph	*m*-FPh	94
Ph	Ph	90	Ph	*p*-ClPh	86
Ph	Me	87	Ph	*m*-BrPh	81
Ph	H	92	Ph	*p*-IPh	80 [b]
Ph	$(CH_2)_{14}CH_3$	92	Ph	*m*-MeOPh	86
H	Ph	90	Ph	*p*-F_3CPh	83
Ph	*t*Bu	84	Ph	*p*-NCPh	76
Me	H	69	Ph	HC=CHPh	68

[a] Thiophen-2-yl. [b] Together with 2,3-diphenylindole (<10%).

tions. More importantly, this indole synthesis based on a McMurry-type coupling can also be carried out with compounds bearing potentially reducible functional groups. The smooth synthesis of tricyclic skeletal frameworks is also possible, as shown by the reactions **77** → **79** and **80** → **81** (Scheme 51). Last not least, it should be mentioned that this reaction is insensitive with regard to steric hindrance (cf. Table 17, R^1 = Ph, R^2 = *t*Bu).[126]

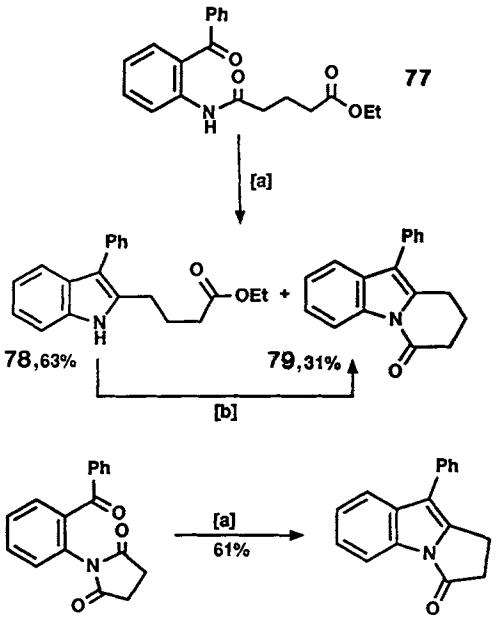

Scheme 51. [a] Ti–graphite, DME; [b] NaH, THF, (**78** → **79**, quantitative).

As is evident in the synthesis of salvadoricine (**83**) (Scheme 52) such indole formations occur in good yields even if, as in compound **82**, an intramolecular diketone cyclization were possible, which would likewise lead to a highly stable heterocycle (quinolin-2-one).[132] This unpredented preference for keto–amide cyclization corresponds to a *complete reversal of the previously known chemoselectivities of titanium-induced reactions*. This also holds true for the preparation of compounds **85**, well-documented precursors (R = Me) for diazapam and (R = CH_2CN) for histamine and serotonin antagonists, by chemoselective keto–amide couplings, without the likewise conceivable keto–ester cyclization in substrate **84** competing (Scheme 53).[132] With this new approach to the indole nucleus by closure of the

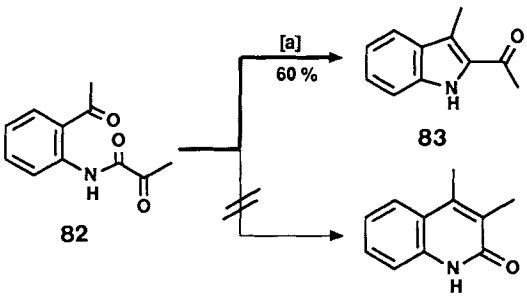

Scheme 52. Chemoselective keto–amide coupling in the synthesis of salvadoricine (**83**) [132]. [a] Ti-graphite (4 equiv.), DME, reflux, 30 min.

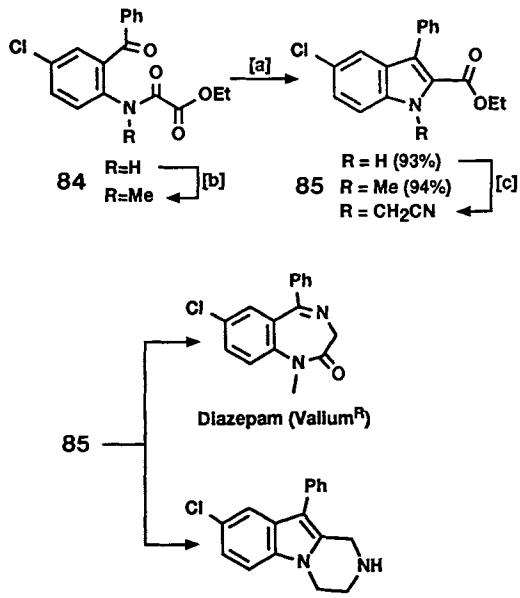

Scheme 53. Chemoselective indole syntheses [132]. [a] Ti-graphite, 4 equiv., DME, reflux; [b] MeI, NaH, THF, 61%; [c] chloroacetonitrile DMF, 80%.

C2–C3 bond, the synthesis of zindoxifen (**86**), known to be strongly tumor-inhibiting, and a series of structural analogues (**86b–d**) of this pharmacologically important compound was also possible (Scheme 54).[133]

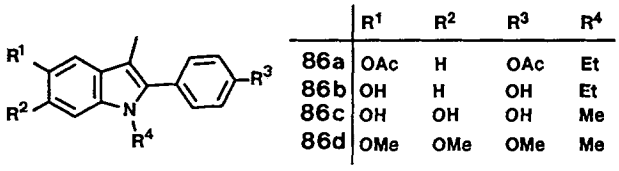

	R^1	R^2	R^3	R^4
86a	OAc	H	OAc	Et
86b	OH	H	OH	Et
86c	OH	OH	OH	Me
86d	OMe	OMe	OMe	Me

Scheme 54. Zindoxifen (**86a**) and zindoxifen analogues **86b–86d**.

4.5.3. Pinacol Coupling and Preparation of vic-Diamines

The McMurry reaction proceeds by the dimerization of ketyl radical anions to titanium pinacolates and their subsequent deoxygenation to the alkene and TiO_2.[110] In view of the striking shortcomings of the classical pinacol reduction there has been much effort to stop the McMurry reaction at the stage of the *vic*-diols. In general this can be accomplished by lowering the reaction temperature. The titanium-based pinacolization methods have contributed considerably to the development of this approach,[109, 113, 114, 134] though the complete suppression of alkene formation has proven difficult in some cases.[135]

In analogy to the classical agents for pinacol formation, aluminum and magnesium amalgam, the corresponding graphite combinations of these metals were examined with regard to their SET abilities. Aluminum–graphite was found to be unsuitable.[136] Magnesium–graphite, however, reduced all kinds of carbonyl compounds to pinacols in consistently high yields.[114b, 137] Its activity manifested itself quite clearly in a comparison with other one-electron transfer agents and in the intramolecular pinacolization of dicarbonyl compounds to cycloalkyl-1,2-diols of different ring size.[114b] The incompatability with chloro and nitro groups is its most serious disadvantage compared to SmI_2 as pinacol-forming agent. With magnesium on graphite, amalgamation is not necessary for promoting the latent single-electron transfer tendency of this metal. Thus, the fine distribution of the magnesium has in this case not only a quantitative but also a quality-changing effect.

Other approaches for a modern pinacolization methodology utilize the redox potential of the rare-earth metals or of transition metal complexes.[138] Of the numerous reagents which have been described in this context samarium diiodide[139] and vanadium(II) salts[140] deserve particular attention because of their versatility and efficiency.

The single-electron transfer reagents leading to the pinacolization of carbonyls, above all low-valent titanium, are also suitable for the reductive dimerization of aldimines or iminium salts to *vic*-diamines.[141]

4.6. Disilanes, Nucleophilic Silylations, Coordination Chemistry

Similarly to the Wurtz coupling of halohydrocarbons, activated metals permit also the efficient dimerization of chlorosilanes and chlorostannanes to disilanes and distannanes. Table 18 shows the exceptional effectivity of C_8K as reducing agent in such reactions.[142] Once again, when this reagent is used the reaction can be monitored easily by the change in color from bronze to black, and the workup consists merely of a filtration.

Also in the cleavage of phenyl-substituted disilanes to silylmetal compounds C_8K proves superior to the conventional methods (Scheme 55). The silylpotassium reagents **87** so obtained can be transmetalated in situ and their reactivity may thus be finely tuned to diverse electrophiles.[142a] Silylpotassium cuprates, manganates, and vanadates prepared in this way react with carboxylic acid chlorides directly to give acylsilanes **88** (Scheme 56, Table 19) and permit 1,4-additions to enones as well as to enoates.[142a]

Table 18. Synthesis of disilanes and distannanes ($R^1R^2R^3M$-$MR^1R^2R^3$) from chlorosilanes (-stannanes) using activated metals. RT = room temperature.

R^1	R^2	R^3	M	Reagent	Conditions	Yield [%]	Ref.
Ph	Ph	Ph	Si	C_8K	0 °C, 5 min	90	[142a]
Ph	Ph	Ph	Si	Li [a]	RT, 10 h	73	[108b]
Ph	Ph	Me	Si	C_8K	0 °C, 5 min	94	[142a]
Ph	Ph	*t*Bu	Si	C_8K	0 °C, 5 min	96	[142a]
Ph	Ph	H	Si	Li [a]	RT, 10 h	68	[108b]
Ph	Me	Me	Si	C_8K	0 °C, 5 min	95	[142a]
Mes	Me	Me	Si	C_8K	0 °C, 40 min	64 [c]	[142b]
Me	Me	Me	Si	C_8K	25 °C, 60 min	88	[142a]
Me	Me	Me	Si	Li [b]	RT, 2 h	42	[108b]
Et	Et	Et	Si	Li [b]	RT, 2 h	58	[108b]
Me	Me	*t*Bu	Si	C_8K	25 °C, 60 min	92	[142a]
Ph	Ph	Ph	Sn	C_8K	0 °C, 5 min	96	[98]
Bu	Bu	Bu	Sn	C_8K	0 °C, 30 min	88	[98]
Bu	Bu	Bu	Sn	Li [a]	RT, 2 h	94	[108b]
Me	Me	Me	Sn	Li [a]	RT, 2 h	60	[108b]

[a] Activation by ultrasound. [b] Activation by ultrasound in the presence of anthracene. [c] Mes = mesitylene; using the silyl bromide instead of the silyl chloride.

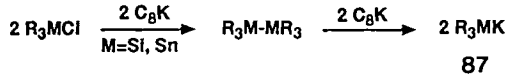

87

Scheme 55. C_8K-induced reduction of chlorosilanes and chlorostannanes.

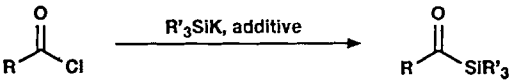

88

Scheme 56. Synthesis of acylsilanes from acid chlorides and silylpotassium reagents (see Table 19).

Table 19. Transmetalation of silylpotassium compounds followed by reaction with acid chlorides affording acylsilanes **88** (Scheme 56).

R	R'_3Si-	Additive	Yield [%]	Ref.
Ph	Ph_2MeSi	CuCN	54	[142]
Ph	Ph_2MeSi	MnI_2	74	[142]
Ph	Ph_2MeSi	VCl_3	67	[142]
C_6H_{11}	Ph_2MeSi	MnI_2	79	[142]
C_6H_{11}	Ph_2MeSi	VCl_3	80	[142]
Me	$PhMe_2Si$	MnI_2	75	[98]
$C_6H_5CH_2$	Ph_2MeSi	MnI_2	78	[98]

New impetus has been given also to the use of C_8K as reducing agent for metal complexes. Hegedus et al. have recently pointed out the advantages of using this reagent as "polymeric" analogue of $M^+C_{10}H_8^-$ (M = Li, Na, K).[143] Reduction of $[Cr(CO)_6]$ with C_8K to $[K_2Cr(CO)_5]$ and its subsequent reaction with amides in the presence of Me_3SiCl provides simple access to aminochromium carbenes **89** (Scheme 57) and their multifarious chemistry. With 4-chloro-

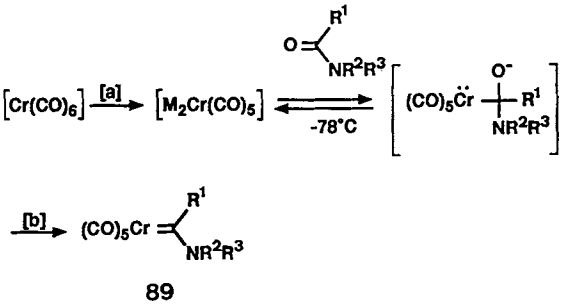

89

Scheme 57. Synthesis of chromocarbenes. [a] 2.2 equiv. C_8K or sodium/naphthalene; [b] Me_3SiCl (see Table 20).

butyryl chloride instead of the amide, pentacarbonyl[(tetrahydrofuran-2-yl)carbenechromium(0) can be prepared in this way. Since not only the yields are generally better than when using $Na^+C_{10}H_8^-$ (Table 20) but also the workup is much more straightforward, this approach based on C_8K

Table 20. Synthesis of chromocarbenes **89** according to Scheme 57 [143b].

R^1	R^2	R^3	Yield [%] C_8K	Yield [%] $Na^+C_{10}H_8$
H	Me	Me	93%	84%
Ph	Me	Me	87%	93%
Me	Bn	Bn	50%	44%
o-ClPh	Et	Et	50%	[a]
3-furyl	Et	Et	63%	[a]
H	Ph	Ph	35% [b]	33% [b]
$CH_3(CH_2)_{10}$	Me	Me	74%	[a]
$-(CH_2)_4-$		Bn	78%	8%
Me	$-(CH_2)_2O(CH_2)_2-$		54%	78%
H	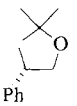		96%	93%
H			63%	[a]

[a] Not reported. [b] Prepared from the Vilsmeier salt instead of the formamide.

is the method of choice for the synthesis of such metal carbenes.[143]

Further, it should be pointed out that both the magnesium–anthracene complex **1** as well as C_8K have enabled entry to a new class of η^4-nickel–anthracene complexes **90** with pronounced dynamic behavior (Scheme 58).[144]

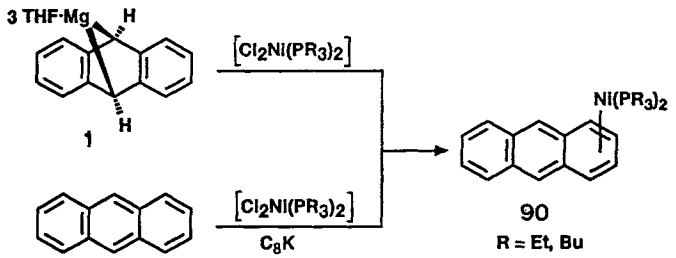

Scheme 58. Activated metals in complex chemistry [144].

4.7. Highly Reactive Metals as Catalysts

Sonication of commercially available nickel powder affords a catalyst which is a nonpyrophoric substitute for Raney nickel.[48a] The Rieke nickel formed in the reduction of NiI_2 with lithium in THF using ultrasound catalyzes both the hydrosilylation of alkenes at room temperature as well as the reductive coupling of phenylhydrosilanes to give di-, tri-, and tetrasilanes.[145] Essential for the activity of this nickel sample are the carbonyl ligands that are formed during the reduction of the salt by ether cleavage and are chemically bound to the metal surface.[57] Nickel–graphite, after addition of ethylenediamine, is a substitute for the classical Lindlar catalyst for the semihydrogenation of alkynes at room temperature and 1 atm H_2 with good to excellent (*Z*) selectivity ((*Z*):(*E*) = 93.6–98.9:6.4–1.1).[146] Upon exposure to air and washing of the catalyst (H_2O, THF) the finely divided nickel particles on the graphite surface are coated with a hydroxide layer a few nanometers thick (see Section 3);[44] though this reduces its catalytic activity, the selectivity with regard to the hydrogenation of different reducible groups or various substituted alkenes is increased.[146] Furthermore, the nickel–graphite treated in this way is storable for months without loss of activity.

High selectivity in the hydrogenation of aromatic halonitro compounds characterizes platinum–graphite as a catalyst.[60] Dehalogenation as well as hydrogenation of the arene remains low even with larger amounts of the catalyst and long reduction times. After the catalyst was used twenty times neither any noticeable decrease in the catalytic activity could be established nor could electron microscopic changes in the morphology of the catalyst be observed. Regarding both its structure as well as its catalytic properties platinum–graphite prepared from $PtCl_2$ and $2C_8K$ is largely identical[60] with the commericially available Platinum–Graphimet®, often erroneously referred to as an intercalation compound. The latter is obtained by low-temperature reduction of $PtCl_4$-laminate with lithiumdiphenyl in THF (Scheme 59).

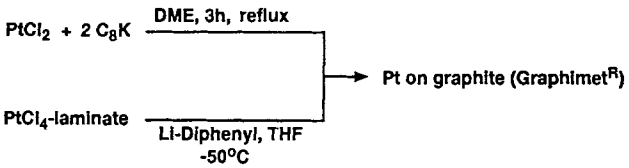

Scheme 59. Two syntheses of Pt–graphite [60].

Highly dispersed metal colloids generated from transition metal salts and tetraalkylammoniumhydrotriorganoborates also exhibit interesting properties as hydrogenation catalysts.[114] After fixing to activated charcoal and doping with bis(η^6-toluene)titanium such catalysts (Rh,Pd,Pt) are far superior to the standard industrial systems with equal metal contents used for the hydrogenation of fatty acids and cinnamic or crotonic acid.[114]

In the semihydrogenation of alkynes, palladium–graphite, like nickel–graphite, produces the corresponding (*Z*) alkenes with high selectivity.[147] Even more interesting is its ability to catalyze organometallic reactions for which hitherto soluble palladium(0) catalysts seemed to be reserved. For example, Heck reactions of aryl and vinyl iodides with activated alkenes using palladium–graphite have been reported to proceed in good yields and with high selectivity.[148] Rieke palladium is also suitable for oxidative insertions into activated carbon–halogen bonds.[56] In the presence of triphenylphosphane, palladium–graphite also permits nucleophilic substitutions of allyl esters with sodium benzenesulfinate, malonates, and enamines in complete analogy to π-allylpalladium chemistry employing soluble palladium complexes.[149] Even commercially available palladium/activated charcoal and palladium/Al_2O_3 can be used for such reactions, although their activity is lower. Since palladium–graphite can be reused after the reaction, these results show good promise for the heterogenation of homogeneous reactions with all perspectives for potential industrial applications.

The catalytic properties of C_8K and related intercalation compounds have been described in detail in relevant review articles.[38]

4.8. Miscellaneous

Finally, a few recent, potentially important applications of highly reactive metals in organic chemistry will be commented on. The first concerns the successful conversion of α,α'-dihalogeno-*o*-xylene derivatives into highly reactive xylylenes (**91** → **92**, Scheme 60) by activated nickel at room temperature; the xylylenes **92** can function as dienes for Diels–Alder reactions. Such metal-induced 1,4-dehalogenations are compatable with OMe, Br, and CN groups on the arene.[150]

Vedejs et al. report on reductive desulfenylation of a cyclic sulfide by treatment with $MeO^+BF_4^-$ and Rieke zinc in their total synthesis of zygosporin E.[151]

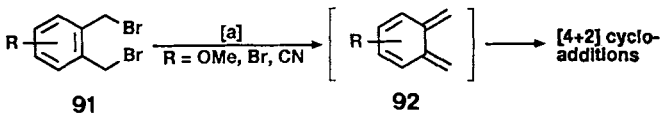

91 **92**

Scheme 60. Synthesis of xylylenes **92**: [a] Rieke Ni, THF, room temperature.

A more recent work describes the reduction of the triple bond of conjugated enynes and of propargyl alcohols to (*Z*) alkenes with Rieke zinc in THF/MeOH/H_2O at 65 °C. These reactions occur in high yields and with very good stereoselectivity, and proceed without overreduction to the alkane, which is difficult to avoid in catalytic hydrogenations on a Lindlar catalyst. Isolated alkyne groups are, however, inert under these conditions.[152]

6. Summary and Outlook

Today, a rich reservoir of methods of metal activation of various efficiency and demand are at the synthetic chemist's disposal. High reactivity of a metal in no way means unselective activity toward organic substrates. On the contrary, some of the results presented here prove that it is the availability of reactive metal samples that allows sensitive and/or highly substituted compounds to be selectively transformed. The exceptional performance of these synthetic tools not only resulted in substantial improvements of numerous classical processes, but also in the development of hitherto unknown reactions. Because of the amazingly high compatability with diverse functional groups these methods should find increasing attention in natural product chemistry and other multistep syntheses.

However, a certain backlog exists regarding the characterization of the metal powders generated in different ways. Without an in-depth consideration of the solid-state chemical aspects of metal-induced reactions and the increased use of modern analytical techniques to answer the associated physico-chemical questions, a better understanding and, consequently, a rational design of highly reactive metals are not to be expected. In view of the wealth of metals in the periodic system and of the reactions effected by them this topic may well continue to be of some importance in the future.

I sincerely thank all my co-workers and colleagues, whose enthusiasm has contributed considerably to the success of the "Graphite Project". Their names are to be found in the literature citations. Special thanks are due to Prof. Dr. H. Weidmann for his continuous advice. Our studies were financially supported by the Fonds zur Förderung der Wissenschaftlichen Forschung, Vienna, and by the Jubiläumsfonds der Österreichischen Nationalbank.

Received: August 7, 1992 [A 893 IE]
German version: *Angew. Chem.* **1993**, *105*, ■

[1] A discussion of the interrelationship of organometallic chemistry and chemistry on surfaces can be found, for example, in: R. Hoffmann, S. D. Wijeyesekera, S. S. Sung, *Pure Appl. Chem.* **1986**, *58*, 481, and references cited therein.
[2] P. Laszlo in *Preparative Chemistry using Supported Reagents* (Eds.: P. Laszlo), Academic Press, New York, **1987**, pp. 3–12.
[3] a) Short reviews are given in: A. Fürstner, *Österr. Chem. Ztg.* **1987**, *88*, 30, 56; b) A. Fürstner *GIT Fachz. Lab.* **1989**, *33*, 350.
[4] a) C. L. Hill, J. B. Vander Sande, G. M. Whitesides, *J. Org. Chem.* **1980**, *45*, 1020; b) K. S. Root, J. Deutch, G. M. Whitesides, *J. Am. Chem. Soc.* **1981**, *103*, 5475; c) H. R. Rogers, C. L. Hill, Y. Fujiwara, R. J. Rogers, H. L. Mitchell, G. M. Whitesides, *ibid.* **1980**, *102*, 217; d) H. R. Rogers, J. Deutch, G. M. Whitesides, *ibid.* **1980**, *102*, 226; e) H. R. Rogers, R. J. Rogers, H. L. Mitchell, G. M. Whitesides, *ibid.* **1980**, *102*, 231; f) J. J. Barber, G. M. Whitesides, *ibid.* **1980**, *102*, 239. g) The mechanism of electron transfer from the metal to the alkyl halide, on the other hand, is still the subject of controversial discussion, of inter alia: H. M. Walborsky, *Acc. Chem. Res.* **1990**, *23*, 286; J. F. Garst, *ibid.* **1991**, *24*, 95, and references cited therein.
[5] For a review see: Y. H. Lai, *Synthesis* **1981**, 585, and references cited therein.
[6] For a review see: J. P. Collman, L. S. Hegedus, J. R. Norton, R. G. Finke, *Principles and Applications of Organotransition Metal Chemistry*, University Science Books, Mill Valley, **1987**, and references cited therein.
[7] a) Y. Tanaka, S. C. Davis, K. J. Klabunde, *J. Am. Chem. Soc.* **1982**, *104*, 1013; b) K. J. Klabunde, A. Whetten, *ibid.* **1986**, *108*, 6529; c) Y. Imizu, K. J. Klabunde, *Inorg. Chem.* **1984**, *23*, 3602; d) P. G. Jasien, C. E. Dykstra, *J. Am. Chem. Soc.* **1983**, *105*, 2089.
[8] a) R. D. Rieke, P. M. Hudnall, *J. Am. Chem. Soc.* **1972**, *94*, 7178; b) R. D. Rieke, P. M. Hudnall, S. Uhm, *J. Chem. Soc. Chem. Commun.* **1973**, 269.
[9] a) R. D. Rieke, *Science* **1989**, *246*, 1260; b) R. D. Rieke, T. P. Burns, R. M. Wehmeyer, B. E. Kahn in *High Energy Processes in Organometallic Chemistry* (Ed.: K. S. Suslick), (*ACS Symposium Series* **1987**, *333*, 223); c) R. D. Rieke, *Top. Curr. Chem.* **1975**, *59*, 1; d) R. D. Rieke, *Acc. Chem. Res.* **1977**, *10*, 301.
[10] R. D. Rieke, P. T. J. Li, T. P. Burns, S. T. Uhm, *J. Org. Chem.* **1981**, *46*, 4323.
[11] R. T. Arnold, S. T. Kulenovic, *Synth. Commun.* **1977**, *7*, 223.
[12] T. Harada, T. Mukaiyama, *Chem. Lett.* **1982**, 161, 467.
[13] J. E. McMurry, M. P. Fleming, *J. Am. Chem. Soc.* **1974**, *96*, 4708.
[14] a) H. Bönnemann, W. Brijoux, R. Brinkmann, E. Dinjus, T. Joussen, B. Korall, *Angew. Chem.* **1991**, *103*, 1344; *Angew. Chem. Int. Ed. Engl.* **1991**, *30*, 1312; b) H. Bönnemann, W. Brijoux, T. Joussen, *ibid.* **1990**, *102*, 324 and **1990**, *29*, *273*.
[15] R. D. Rieke, L. D. Rhyne, *J. Org. Chem.* **1979**, *44*, 3445.
[16] K. L. Tsai, J. L. Dye, *J. Am. Chem. Soc.* **1991**, *113*, 1650.
[17] a) D. E. Stack, B. T. Dawson, R. D. Rieke, *J. Am. Chem. Soc.* **1991**, *113*, 4672; b) *ibid.* **1992**, *114*, 5110.
[18] a) G. W. Ebert, R. D. Rieke, *J. Org. Chem.* **1988**, *53*, 4482; b) R. D. Rieke, R. W. Wehmeyer, T. C. Wu, G. W. Ebert, *Tetrahedron* **1989**, *45*, 443; c) T. C. Wu, R. D. Rieke, *Tetrahedron Lett.* **1988**, *29*, 6753; d) R. M. Wehmeyer, R. D. Rieke, *ibid.* **1988**, *29*, 4513; e) T. C. Wu, R. M. Wehmeyer, R. D. Rieke, *J. Org. Chem.* **1987**, *52*, 5056; f) R. M. Wehmeyer, R. D. Rieke, *ibid.* **1987**, *52*, 5057; g) G. W. Ebert, R. D. Rieke, *ibid.* **1984**, *49*, 5280; h) G. W. Ebert, J. W. Cheasty, S. S. Tehrani, E. Aouad, *Organometallics* **1992**, *11*, 1560; i) F. O. Ginah, T. A. Donavan, S. D. Suchan, D. R. Pfennig, G. W. Ebert, *J. Org. Chem.* **1990**, *55*, 584; j) G. W. Ebert, W. R. Klein, *ibid.* **1991**, *56*, 4744.
[19] R. D. Rieke, T. C. Wu, D. E. Stinn, R. M. Wehmeyer, *Synth. Commun.* **1989**, *19*, 1833.
[20] R. D. Rieke, S. E. Bales, *J. Am. Chem. Soc.* **1974**, *96*, 1775.
[21] P. Boudjouk, D. P. Thompson, W. H. Ohrbom, B. H. Han, *Organometallics* **1986**, *5*, 1257.
[22] R. A. O'Brien, R. D. Rieke, *J. Org. Chem.* **1990**, *55*, 788.
[23] a) B. Bogdanović, *Acc. Chem. Res.* **1988**, *21*, 261; b) *Angew. Chem.* **1985**, *97*, 253; *Angew. Chem. Int. Ed. Engl.* **1985**, *24*, 262.
[24] For the X-ray structure of magnesium 1,4-dimethylanthracene · 3 THF see: B. Bogdanović, N. Janke, C. Krüger, R. Mynott, K. Schlichte, U. Westeppe, *Angew. Chem.* **1985**, *97*, 972; *Angew. Chem. Int. Ed. Engl.* **1985**, *24*, 960.
[25] B. Bogdanović, N. Janke, H. G. Kinzelmann, K. Seevogel, J. Treber, *Chem. Ber.* **1990**, *123*, 1529.

[26] a) B. Bogdanović, N. Janke, H. G. Kinzelmann, *Chem. Ber.* **1990**, *123*, 1507; b) S. Harvey, P. C. Junk, C. L. Raston, G. Salem, *J. Org. Chem.* **1988**, *53*, 3134.
[27] S. Itsuno, G. D. Darling, H. D. H. Stöver, J. M. J. Frechet, *J. Org. Chem.* **1987**, *52*, 4644.
[28] S. Harvey, C. L. Raston, *J. Chem. Soc. Chem. Commun.* **1988**, 652.
[29] E. Bartmann, B. Bogdanović, N. Janke, S. Liao, K. Schlichte, B. Spliethoff, J. Treber, U. Westeppe, U. Wilczok, *Chem. Ber.* **1990**, *123*, 1517.
[30] W. Oppolzer, P. Schneider, *Tetrahedron Lett.* **1984**, *25*, 3305.
[31] a) H. Bönnemann, B. Bogdanović, R. Brinkmann, D. W. He, B. Spliethoff, *Angew. Chem.* **1983**, *95*, 749; *Angew. Chem. Int. Ed. Engl.* **1983**, *22*, 728; b) recent applications of the Mg-anthracene method, coupling of C-B bonds: H. Michel, D. Steiner, S. Wocadlo, J. Allwohn, N. Stamatis, W. Massa, A. Berndt, *Angew. Chem.* **1992**, *104*, 629 and **1992**, *31*, 607; c) synthesis of a highly effective phosphane ligand for asymmetric syntheses: G. Wilke, *ibid.* **1988**, *100*, 189 and **1988**, *27*, 185.
[32] E. P. Kündig, M. Moskovits, G. A. Ozin, *Angew. Chem.* **1975**, *87*, 314; *Angew. Chem. Int. Ed. Engl.* **1975**, *14*, 292, and references cited therein.
[33] Further examples: a) B. S. Ault, *J. Am. Chem. Soc.* **1980**, *102*, 3480; b) G. H. Jeong, K. J. Klabunde, *ibid.* **1986**, *108*, 7103.
[34] a) K. J. Klabunde, *Chemistry of Free Atoms and Particles*, Academic Press, New York, **1980**; b) J. R. Blackbrow, D. Young, *Metal Vapor Synthesis in Organometallic Chemistry*, Springer, Berlin, **1979**; c) W. Romanowski, *Highly Dispersed Metals*, Ellis Horwood/Wiley, Chichester, **1987**.
[35] For a review see, inter alia a) K. J. Klabunde, *Acc. Chem. Res.* **1975**, *8*, 393; b) E. A. Körner von Gustorf, O. Jaenike, O. Wolfbeis, C. R. Eady, *Angew. Chem.* **1975**, *87*, 300; *Angew. Chem. Int. Ed. Engl.* **1975**, *14*, 278; c) K. J. Klabunde, *ibid.* **1975**, *87*, 309 and **1975**, *14*, 287; for recent applications in coordination chemistry see, inter alia: d) U. Zenneck, **1990**, *102*, 171 and **1990**, *29*, 138; e) J. J. Schneider, R. Goddard, C. Krüger, *Organometallics* **1991**, *10*, 665; f) C. Elschenbroich, J. Schneider, M. Wünsch, J. L. Pierre, P. Baret, P. Chautemps, *Chem. Ber.* **1988**, *121*, 177; f) J. J. Schneider, R. Goddard, C. Krüger, S. Werner, B. Metz, *Chem. Ber.* **1991**, *124*, 301, and references cited therein.
[36] The apparatus used for metal vaporization are described in: P. L. Timms, *Angew. Chem.* **1975**, *87*, 295; *Angew. Chem. Int. Ed. Engl.* **1975**, *14*, 273.
[37] a) E. P. Kündig, C. Perret, *Helv. Chim. Acta* **1981**, *64*, 2606; b) K. J. Klabunde, H. F. Efner, L.Satek, W. Donley, *J. Organomet. Chem.* **1974**, *71*, 309; c) W. Oppolzer, E. P. Kündig, P. M. Bishop, C. Perret, *Tetrahedron Lett.* **1982**, *23*, 3901.
[38] For a review see: a) R. Csuk, B. I. Glänzer, A. Fürstner, *Adv. Organomet. Chem.* **1988**, *28*, 85; b) D. Savoia, C. Trombini, A. Umani-Ronchi, *Pure Appl. Chem.* **1985**, *57*, 1887; c) H. B. Kagan, *ibid.* **1976**, *46*, 177; d) R. Setton in *Preparative Chemistry Using Supported Reagents* (Ed.: P. Laszlo), Academic Press, New York, **1987**, p. 255.
[39] K. Fredenhagen, G. Cadenbach, *Z. Allg. Anorg. Chem.* **1926**, *158*, 246.
[40] D. E. Bergbreiter, J. M. Killough, *J. Am. Chem. Soc.* **1978**, *100*, 2126.
[41] D. Braga, A. Ripamonti, D. Savoia, C. Trombini, A. Umani-Ronchi, *J. Chem. Soc. Chem. Commun.* **1978**, 927.
[42] R. Csuk, A. Fürstner, H. Weidmann, *J. Chem. Soc. Chem. Commun.* **1986**, 775.
[43] P. Marceau, F. Beguin, G. Guillaumet, *J. Organomet. Chem.* **1988**, *342*, 137.
[44] A. Fürstner, F. Hofer, H. Weidmann, *Carbon* **1991**, *29*, 915.
[45] A. Fürstner, F. Hofer, unpublished results.
[46] W. M. Brooks, C. L. Raston, R. E. Sue, F. J. Lincoln, J. J. McGinnity, *Organometallics* **1991**, *10*, 2098.
[47] For a review of the physical principles and applications of ultrasound in preparative chemistry see for example a) *Ultrasound. Its Chemical, Physical and Biological Effects* (Ed.: K. S. Suslick), VCH, Weinheim, **1988**; b) S. V. Ley, C. H. R. Low, *Ultrasound in Synthesis*, Springer, Berlin, **1989**; c) *Chemistry with Ultrasound* (Ed.: T. J. Mason), Critical Reports on Applied Chemistry, Vol. 28, Elsevier, Essex, **1990**; d) J. Lindley, T. J. Mason, *Chem. Soc. Rev.* **1987**, *16*, 275; e) C. Einhorn, J. Einhorn, J. L. Luche, *Synthesis* **1989**, 787; f) R. F. Abdulla, *Aldrichimica Acta* **1988**, *21*, 31; g) K. S. Suslick in *Modern Synthetic Methods, Vol. 4* (Ed.: R. Scheffold), Springer, Berlin, **1986**, p. 1.
[48] For a discussion of the mechanical effects of ultrasound on diverse metal powders see for example a) K. S. Suslick, D. J. Casadonte, *J. Am. Chem. Soc.* **1987**, *109*, 3459; b) K. S. Suslick, S. J. Doktycz, *ibid.* **1989**, *111*, 2342; c) K. S. Suslick, D. J. Casadonte, S. J. Doktycz, *Chemistry of Materials* **1989**, *1*, 6.
[49] J. C. de Souza-Barboza, C. Petrier, J. L. Luche, *J. Org. Chem.* **1988**, *53*, 1212.
[50] a) J. L. Luche, C. Einhorn, J. Einhorn, J. V. Sinisterra-Gago, *Tetrahedron Lett.* **1990**, *31*, 4125; b) C. Einhorn, J. Einhorn, M. J. Dickens, J. L. Luche, *ibid.* **1990**, *31*, 4129.
[51] K. V. Baker, J. M. Brown, N. Hughes, A. J. Skarnulis, A. Sexton, *J. Org. Chem.* **1991**, *56*, 698.
[52] D. Savoia, E. Tagliavini, C. Trombini, A. Umani-Ronchi, *J. Org. Chem.* **1980**, *45*, 3227.
[53] H. Hart, B. L. Cheng, C. T. Peng, *Tetrahedron Lett.* **1977**, 3121.
[54] a) J. L. Luche, C. Petrier, C. Dupuy, *Tetrahedron Lett.* **1984**, *25*, 753; b) T. S. Chou, S. H. Hung, M. L. Peng, S. J. Lee, *ibid.* **1991**, *32*, 3551, and references cited therein.
[55] G. L. Rochfort, R. D. Rieke, *Inorg. Chem.* **1986**, *25*, 348.
[56] A. V. Kavaliunas, A. Taylor, R. D. Rieke, *Organometallics* **1983**, *2*, 377.
[57] W. L. Parker, P. Boudjouk, A. B. Rajkumar, *J. Am. Chem. Soc.* **1991**, *113*, 2785.
[58] D. Braga, A. Ripamonti, D. Savoia, C. Trombini, A. Umani-Ronchi, *J. Chem. Soc. Dalton Trans.* **1979**, 2026.
[59] A. Fürstner, F. Hofer, H. Weidmann, *J. Chem. Soc. Dalton Trans.* **1988**, 2023.
[60] A. Fürstner, F. Hofer, H. Weidmann, *J. Catal.* **1989**, *118*, 502.
[61] a) A. Messaoudi, R. Erre, F. Beguin, *Carbon* **1991**, *29*, 515; b) R. Erre, A. Messaoudi, F. Beguin, *Synth. Met.* **1988**, *23*, 493; c) H. Schäfer-Stahl, *J. Chem. Soc. Dalton Trans.* **1981**, 328; d) F. Beguin, A. Messaoudi, *J. Mater. Chem.* **1992**, *2*, 957; e) A. Messaoudi, F. Beguin, *J. Mater. Res.* **1992**, *7*, 418.
[62] a) T. P. Burns, R. D. Rieke, *J. Org. Chem.* **1983**, *48*, 4141; b) R. D. Rieke, S. E. Bales, P. M. Hudnall, G. S. Poindexter, *Org. Synth.* **1979**, *59*, 85.
[63] J. Rachon, H. M. Walborsky, *Tetrahedron Lett.* **1989**, *30*, 7345.
[64] a) W. Oppolzer, *Angew. Chem.* **1989**, *101*, 39; *Angew. Chem. Int. Ed. Engl.* **1989**, *28*, 38; b) W. Oppolzer in *Comprehensive Organic Syntheses, Vol. 5* (Eds.: B. M. Trost, I. Fleming), Pergamon, Oxford, **1991**, p. 29.
[65] a) R. G. Salomon, *J. Org. Chem.* **1974**, *39*, 3602; b) R. D. Rieke, H. Xiong, *ibid.* **1991**, *56*, 3109; c) H. Xiong, R. D. Rieke, *ibid.* **1989**, *54*, 3247; d) *Tetrahedron Lett.* **1991**, *32*, 5269.
[66] T. C. Wu, H. Xiong, R. D. Rieke, *J. Org. Chem.* **1990**, *55*, 5045.
[67] R. A. O'Brien, T. Chen, R. D. Rieke, *J. Org. Chem.* **1992**, *57*, 2667.
[68] A. Yangisawa, S. Habaue, H. Yamamoto, *J. Am. Chem. Soc.* **1991**, *113*, 8955.
[69] A. Fürstner, *Synthesis* **1989**, 571.
[70] R. Csuk, A. Fürstner, H. Sterk, H. Weidmann, *J. Carbohydr. Chem.* **1986**, *5*, 459.
[71] R. Csuk, B. I. Glänzer, *J. Carbohydr. Chem.* **1990**, *9*, 797.
[72] R. Csuk, M. Hugener, A. Vasella, *Helv. Chim. Acta* **1988**, *71*, 609.
[73] A. Fürstner, *J. Organomet. Chem.* **1987**, *336*, C33.
[74] A. Fürstner, G. Kollegger, H. Weidmann, *J. Organomet. Chem.* **1991**, *414*, 295.
[75] E. Vedejs, S. Ahmed, *Tetrahedron Lett.* **1988**, *29*, 2291.
[76] a) R. B. Ruggeri, C. H. Heathcock, *J. Org. Chem.* **1987**, *52*, 5745; b) C. H. Heathcock, R. B. Ruggeri, K. F. McClure, *ibid.* **1992**, *57*, 2585.
[77] a) P. Knochel, M. C. P. Yeh, S. C. Berk, J. Talbert, *J. Org. Chem.* **1988**, *52*, 2390; b) S. C. Berk, P. Knochel, M. C. P. Yeh, *ibid.* **1988**, *53*, 5789.
[78] Review: P. Knochel in *Comprehensive Organic Syntheses, Vol. 1* (Eds.: B. M. Trost, I. Fleming), Pergamon, Oxford, **1991**, p. 211.
[79] Recent advances: a) S. A. Rao, T. S. Chou, I. Schipor, P. Knochel, *Tetrahedron* **1992**, *48*, 2025; b) H. P. Knoess, M. T. Furlong, M. J. Rozema, P. Knochel, *J. Org. Chem.* **1991**, *56*, 5974; c) T. S. Chou, P. Knochel, *ibid.* **1990**, *55*, 4791; d) H. G. Chen, C. Hoechstetter, P. Knochel, *Tetrahedron Lett.* **1989**, *30*, 4795.
[80] L. Zhu, R. M. Wehmeyer, R. D. Rieke, *J. Org. Chem.* **1991**, *56*, 1445.
[81] P. Marceau, L. Gautreau, F. Beguin, G. Guillaumet, *J. Organomet. Chem.* **1991**, *403*, 21.
[82] a) G. H. Posner, *An Introduction to Synthesis Using Organocopper Reagents*, Wiley, New York, **1980**; b) G. H. Posner, *Org. React.* **1972**, *19*, 1; *ibid.* **1975**, *22*, 253; c) B. H. Lipshutz, *Tetrahedron* **1984**, *40*, 5005; d) B. H. Lipshutz, *Synthesis* **1987**, 325; e) J. F. Normant, *ibid.* **1972**, 63.
[83] T. C. Wu, R. D. Rieke, *J. Org. Chem.* **1988**, *53*, 2381.
[84] a) S. Hanessian, *Total Synthesis of Natural Products. The Chiron Approach*, Pergamon, Oxford, **1983**; b) A. Vasella in *Modern Synthetic Methods* (Ed.: R. Scheffold), Sauerländer-Salle, Frankfurt, **1980**, p. 173; c) F. W. Lichtenthaler in *New Aspects of Organic Chemistry* (Eds.: Z. Yoshida, T. Shiba, Y. Ohshiro), VCH, Weinheim, **1990**, p. 351.
[85] a) R. Csuk, A. Fürstner, B. I. Glänzer, H. Weidmann, *J. Chem. Soc. Chem. Commun.* **1986**, 1149; b) R. Csuk, B. I. Glänzer, A. Fürstner, H. Weidmann, V. Formacek, *Carbohydr. Res.* **1986**, *157*, 235.
[86] P. Pudlo, J. Thiem, V. Vill, *Chem. Ber.* **1990**, *123*, 1129.
[87] R. Csuk, B. I. Glänzer, *IV Eur. Symp. Carbohydr. Chem.*, Darmstadt, FRG, **1987**, Abstract A-28.
[88] C. W. Holzapfel, J. M. Koekemoer, G. H. Verdoor, *S. Afr. J. Chem.* **1986**, *39*, 151.
[89] A. Fürstner, H. Weidmann, *J. Carbohydr. Chem.* **1988**, *7*, 773.
[90] A. Fürstner, H. Weidmann, *J. Org. Chem.* **1989**, *54*, 2307.
[91] B. Bernet, A. Vasella, *Helv. Chim. Acta* **1979**, *62*, 1990; for a summary and discussion of the various methods of dealkoxyhalogenation of sugar derivatives see [92, 93].
[92] a) A. Fürstner, D. N. Jumbam, J. Teslic, H. Weidmann, *J. Org. Chem.* **1991**, *56*, 2213; b) A. Fürstner, U. Koglbauer, H. Weidmann, *J. Carbohydr. Chem.* **1990**, *9*, 561; c) A. Fürstner, *Tetrahedron Lett.* **1990**, *31*, 3735.
[93] A. Fürstner, J. Baumgartner, D. N. Jumbam, *J. Chem. Soc. Perkin Trans. 1*, in press.
[94] a) R. E. Ireland, P. Wipf, M. Miltz, B. Vanasse, *J. Org. Chem.* **1990**, *55*, 1423; b) for an application of a Zn/Ag-graphite induced fragmentation in

the synthesis of 9-dihydro-FK506 see: R. E. Ireland, T. K. Highsmith, L. D. Gegnas, J. L. G. Gleason, *J. Org. Chem.* **1992**, *57*, 5071.
[95] J. P. Praly, C. Di Stefano, L. Somsak, G. Descotes, *J. Chem. Soc. Chem. Commun.* **1992**, 200.
[96] A. Fürstner, J. P. Praly, unpublished results.
[97] L. A. Paquette, W. D. Klobucar, R. A. Snow, *Synth. Commun.* **1976**, *6*, 575, and references cited therein.
[98] A. Fürstner, unpublished results.
[99] A. B. Smith III, J. L. Wood, W. Wong, A. E. Gould, C. J. Rizzo, S. Funayama, S. Omura, *J. Am. Chem. Soc.* **1990**, *112*, 7425.
[100] A. Fürstner, H. Weidmann, *J. Org. Chem.* **1990**, *55*, 1363.
[101] A summary review of the previous syntheses of amphotericin and amphotericin segments is given in: a) J. M. Beau in *Recent Progress in the Chemical Synthesis of Antibiotics* (Eds.: G. Lukacs, M. Ohno), Springer, Berlin, **1990**, p. 135; b) K. C. Nicolaou, W. W. Ogilvie, *Chemtracts* **1990**, *3*, 327, and references cited therein.
[102] Part of the dissertation by J. Baumgartner, Technische Universität Graz, **1992**.
[103] a) P. E. Fanta, *Chem. Rev.* **1964**, *64*, 613; b) D. W. Knight in *Comprehensive Organic Syntheses, Vol. 3* (Eds.: B. M. Trost, I. Fleming), Pergamon, Oxford, **1991**, p. 481; c) for a general overview of biaryl syntheses see: M. Sainsbury, *Tetrahedron* **1980**, *36*, 3327.
[104] a) S. I. Inaba, H. Matsumoto, R. D. Rieke, *J. Org. Chem.* **1984**, *49*, 2093; b) H. Matsumoto, S. I. Inaba, R. D. Rieke, *ibid.* **1983**, *48*, 840; c) S. I. Inaba, H. Matsumoto, R. D. Rieke, *Tetrahedron Lett.* **1982**, *23*, 4215.
[105] a) M. Iyoda, A. Mizusuna, H. Kurata, M. Oda, *J. Chem. Soc. Chem. Commun.* **1989**, 1690; b) M. Iyoda, A. Mizusuna, M. Oda, *Chem. Lett.* **1988**, 149.
[106] S. I. Inaba, R. D. Rieke, *J. Org. Chem.* **1985**, *50*, 1373; b) S. I. Inaba, R. D. Rieke, *Tetrahedron Lett.* **1983**, *24*, 2451.
[107] R. D. Rieke, A. V. Kavaliunuas, L. D. Rhyne, D. J. J. Fraser, *J. Am. Chem. Soc.* **1979**, *101*, 246.
[108] a) B. H. Han, P. Boudjouk, *Tetrahedron Lett.* **1981**, *22*, 2757; b) P. Boudjouk, B. H. Han, *ibid.* **1981**, *22*, 3813.
[109] a) T. Mukaiyama, T. Sato, J. Hanna, *Chem. Lett.* **1973**, 1041; b) S. Tyrlik, I. Wolochowicz, *Bull. Soc. Chim. Fr.* **1973**, 2147.
[110] For a review see: a) J. E. McMurry, *Chem. Rev.* **1989**, *89*, 1513; b) D. Lenoir, *Synthesis* **1989**, 883; c) C. Betschart, D. Seebach, *Chimia* **1989**, *43*, 39; d) J. E. McMurry, *Acc. Chem. Res.* **1983**, *16*, 405; e) G. M. Robertson in *Comprehensive Organic Syntheses, Vol. 3* (Eds.: B. M. Trost, I. Fleming), Pergamon, Oxford, **1991**, p. 563.
[111] For ESR studies see: a) R. Dams, M. Malinowski, I. Westdorp, H. Y. Geise, *J. Org. Chem.* **1982**, *47*, 248; b) R. Dams, M. Malinowski, H. Y. Geise, *Transition Met. Chem.* **1982**, *7*, 37.
[112] D. Lenoir, *Synthesis* **1977**, 553.
[113] E. J. Corey, R. L. Danheiser, S. Chandrasekaran, *J. Org. Chem.* **1976**, *41*, 260.
[114] a) A. Fürstner, H. Weidmann, *Synthesis* **1987**, 1071; b) A. Fürstner, R. Csuk, C. Rohrer, H. Weidmann, *J. Chem. Soc. Perkin Trans. 1* **1988**, 1729.
[115] B. Bogdanović, S. Becke, unpublished results; S. Becke, Dissertation, Universität Bochum, **1991**. I thank Prof. Bogdanović for this information.
[116] H. Idriss, K. Pierce, M. A. Barteau, *J. Am. Chem. Soc.* **1991**, *113*, 715.
[117] J. E. McMurry, T. Lectka, J. G. Rico, *J. Org. Chem.* **1989**, *54*, 3748.
[118] S. K. Nayak, A. Banerji, *J. Org. Chem.* **1991**, *56*, 1940.
[119] G. P. Boldrini, D. Savoia, E. Tagliavini, C. Trombini, A. Umani-Ronchi, *J. Organomet. Chem.* **1985**, *280*, 307.
[120] P. Burger, H. H. Brintzinger, *J. Organomet. Chem.* **1991**, *407*, 207.
[121] a) D. L. J. Clive, C. Zhang, K. S. K. Murthy, W. D. Hayward, S. Daigneault, *J. Org. Chem.* **1991**, *56*, 6447; b) D. L. J. Clive, K. S. K. Murthy, C. Zhang, W. D. Hayward, S. Daigneault, *J. Chem. Soc. Chem. Commun.* **1990**, 509.
[122] D. L. J. Clive, K. S. K. Murthy, A. G. H. Wee, J. S. Prasad, G. V. J. da Silva, M. Majewski, P. C. Anderson, C. F. Evans, R. D Haugen, L. D. Heerze, J. R. Barrie, *J. Am. Chem. Soc.* **1990**, *112*, 3018.
[123] W. G. Dauben, T. Z. Wang, R. W. Stephens, *Tetrahedron Lett.* **1990**, *31*, 2393.
[124] T. Kan, F. Matsuda, M. Yanagiya, H. Shirahama, *Synlett* **1991**, 391.
[125] J. E. McMurry, D. D. Miller, *J. Am. Chem. Soc.* **1983**, *105*, 1660.
[126] A. Fürstner, D. N. Jumbam, *Tetrahedron* **1992**, *48*, 5991.
[127] M. Iyoda, T. Kushida, S. Kitami, M. Oda, *J. Chem. Soc. Chem. Commun.* **1987**, 1607.
[128] J. E. McMurry, D. D. Miller, *Tetrahedron Lett.* **1983**, *24*, 1885.
[129] a) M. Mortimore, P. Kocienski, *Tetrahedron Lett.* **1988**, *29*, 3357; b) K. Takai, O. Fujimura, Y. Kataoka, K. Utimoto, *ibid.* **1989**, *30*, 211; c) K. Takai, Y. Kataoka, T. Okazoe, K. Utimoto, *ibid.* **1988**, *29*, 1065; d) T. Okazoe, K. Takai, K. Oshima, K. Utimoto, *J. Org. Chem.* **1987**, *52*, 4410.
[130] a) K. A. Brown-Wensley, S. L. Buchwald, L. Cannizzo, L. Clawson, S. Ho, D. Meinhardt, J. R. Stille, D. Straus, R. H. Grubbs, *Pure Appl. Chem.* **1983**, *55*, 1733; b) S. H. Pine, R. Zahler, D. A. Evans, R. H. Grubbs, *J. Am. Chem. Soc.* **1980**, *102*, 3270; c) F. N. Tebbe, G. W. Parshall, G. S. Reddy, *ibid.* **1978**, *100*, 3611.
[131] a) A. Fürstner, D. N. Jumbam, H. Weidmann, *Tetrahedron Lett.* **1991**, *32*, 6695; b) A. Banerji, S. K. Nayak, *J. Chem. Soc. Chem. Commun.* **1990**, 150.
[132] A. Fürstner, D. N. Jumbam, *J. Chem. Soc. Chem. Commun.*, in press.
[133] A. Fürstner, D. N. Jumbam, unpublished results; for the pharmacology of 2-phenylindoles, see for example: E. von Angerer, J. Prekajac, J. Strohmeier, *J. Med. Chem.* **1984**, *27*, 1439.
[134] a) J. E. McMurry, J. G. Rico, *Tetrahedron Lett.* **1989**, *30*, 1169.
[135] M. P. Mundy, R. Shrinivasa, Y. Kim, T. Dolph, J. R. Warnet, *J. Org. Chem.* **1982**, *47*, 1657.
[136] Cleavage of ether might be responsible for this in the attempted synthesis of Al-graphite from $AlCl_3$ and $3\,C_8K$ in THF.
[137] R. Csuk, A. Fürstner, H. Weidmann, *J. Chem. Soc. Chem. Commun.* **1986**, 1802.
[138] For reviews see: a) J. M. Pons, M. Santelli, *Tetrahedron* **1988**, *44*, 4295; b) B. E. Kahn, R. D. Rieke, *Chem. Rev.* **1988**, *88*, 733 as well as Ref. [110e] and literature citations in Ref. [114b].
[139] Further literature: a) J. Souppe, L. Danon, J. L. Namy, H. B. Kagan, *J. Organomet. Chem.* **1983**, *250*, 227; b) J. L. Namy, J. Souppe, H. B. Kagan, *Tetrahedron Lett.* **1983**, *24*, 765; c) J. L. Chiara, W. Cabri, S. Hanessian, *ibid.* **1991**, *32*, 1125; d) G. A. Molander, C. Kenny, *J. Org. Chem.* **1988**, *53*, 2132; e) E. J. Enholm, A. Trivellas, *Tetrahedron Lett.* **1989**, *30*, 1063.
[140] Further literature: a) A. S. Raw, S. F. Pedersen, *J. Org. Chem.* **1991**, *56*, 830; b) A. W. Konradi, S. F. Pedersen, *ibid.* **1990**, *55*, 4506; c) J. H. Freudenberger, A. W. Konradi, S. F. Pedersen, *J. Am. Chem. Soc.* **1989**, *111*, 8014; d) R. Annunziata, M. Cinquini, F. Cozzi, P. Giaroni, *Tetrahedron: Asymmetry* **1990**, *1*, 355.
[141] Synthesis of *vic*-diamines using low-valent titanium: a) C. Betschart, D. Seebach, *Helv. Chim. Acta* **1987**, *70*, 2215; b) C. Betschart, B. Schmidt, D. Seebach, *ibid.* **1988**, *71*, 1999; c) P. Mangeney, F. Grosjean, A. Alexakis, J. F. Normant, *Tetrahedron Lett.* **1988**, *29*, 2675; d) P. Mangeney, T. Tejero, A. Alexakis, F. Grosjean, J. Normant, *Synthesis* **1988**, 255, and references cited therein.
[142] a) A. Fürstner, H. Weidmann, *J. Organomet. Chem.* **1988**, *354*, 15; b) H. Müller, U. Weinzierl, W. Seidel, *Z. Anorg. Allg. Chem.* **1991**, *603*, 15.
[143] a) L. S. Hegedus, *Pure Appl. Chem.* **1990**, *62*, 691; b) M. A. Schwindt, T. Lejon, L. S. Hegedus, *Organometallics* **1990**, *9*, 2814.
[144] A. Stanger, K. P. C. Vollhardt, *Organometallics* **1992**, *11*, 317.
[145] a) P. Boudjouk, B. H. Han, J. R. Jacobsen, B. J. Hauck, *J. Chem. Soc. Chem. Commun* **1991**, 1424; b) P. Boudjouk, A. B. Rajkumar, W. L. Parker, *ibid.* **1991**, 245.
[146] a) D. Savoia, E. Tagliavini, C. Trombini, A. Umani-Ronchi, *J. Org. Chem.* **1981**, *46*, 5340 and 5344.
[147] D. Savoia, C. Trombini, A. Umani-Ronchi, G. Verardo, *J. Chem. Soc. Chem. Commun.* **1981**, 540.
[148] D. Savoia, C. Trombini, A. Umani-Ronchi, G. Verardo, *J. Chem. Soc. Chem. Commun.* **1981**, 541.
[149] G. P. Boldrini, D. Savoia, E. Tagliavini, C. Trombini, A. Umani-Ronchi, *J. Organomet. Chem.* **1984**, *268*, 97.
[150] S. I. Inaba, R. M. Wehmeyer, M. W. Forkner, R. D. Rieke, *J. Org. Chem.* **1988**, *53*, 339.
[151] E. Vedejs, J. D. Rodgers, S. J. Wittenberger, *J. Am. Chem. Soc.* **1988**, *110*, 4822.
[152] W. N. Chou, D. L. Clark, J. B. White, *Tetrahedron Lett.* **1991**, *32*, 299.

Aminoacyl-tRNA Synthetases: The Division into Two Classes Predicted by the Chemistry of Substrates and Enzymes

By Friedrich Cramer* and Wolfgang Freist*

In biological systems, almost all chemical reactions are catalyzed by enzymes. In order to understand the mode of action of these biocatalysts, we need to know precise details of their structures, their active sites, and their functional groups. Most important are those parts of the protein molecule that are responsible for precise recognition of the substrates, for the specific interaction between the enzymes and their reactants. Decades can pass between the isolation of an enzyme and the determination of its exact structure by X-ray analysis. For the chemist, however, means are known by which initial information may be gathered relatively quickly: the synthesis of modified substrates and affinity labeling. During the last twenty five years these two methods have been put to the test on aminoacyl-tRNA synthetases. Today, we know enough about the structures of these enzymes to evaluate the success of this "chemistry on macromolecules," or their substrates. Chemists have had some successes, which provided the structural analysts with valuable preliminary results.

1. Introduction

Aminoacyl-tRNA synthetases make up an important part of the translation apparatus, which transforms the information stored in the nucleotide sequences in every cell into the amino acid sequences of protein. They catalyze the esterification of a particular transfer-RNA (tRNA) with a particular amino acid. In the first reaction step, amino acid **1** and ATP **2** react to form an enzyme-bound aminoacyl-adenylate **3** [Eq. (a)]; the "activated" amino acid **3** is esterified in a second step with one of the two terminal OH groups of the tRNA[1-3] [Eq. (b)].

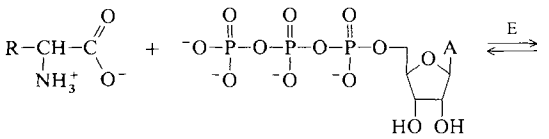

aa ATP

1 **2**

(a)

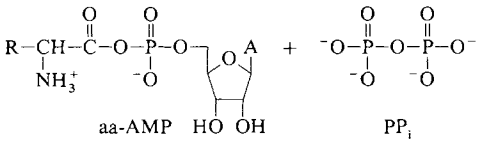

aa-AMP PP_i

3 **4**

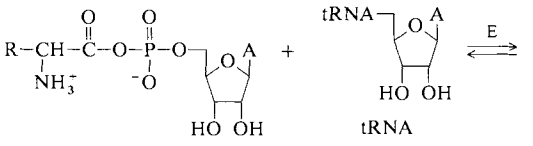

aa-AMP tRNA

3 **5**

(b)

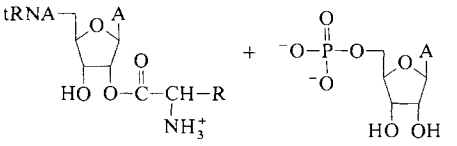

aa-tRNA AMP

6 **7**

Both steps make great demands on the specificity of the enzymes; they must recognize one particular amino acid from 20, some very similar with one another, and must select one particular tRNA from 40-60 (also very similar tRNA molecules), since otherwise faulty and possibly functionless proteins will be synthesized.

The high specificity of the aminoacyl-tRNA synthetases aroused great interest amongst chemists soon after the discovery of the enzymes, particularly with regard to their catalytic mechanism, the functional groups involved, and the position of the active site within the protein molecule. Thus, long before the structures of the enzymes were elucidated, modified substrates were synthesized, in order to identify the groups of atoms important for substrate recognition. At the same time, the essential groups in the active site were sought with affinity labeling.

[*] Prof. Dr. F. Cramer, Dr. W. Freist
Max-Planck-Institut für experimentelle Medizin
Hermann-Rein-Strasse 3, D-W-3400 Göttingen (FRG)

2. Primary Structures of the Aminoacyl-tRNA Synthetases

Soon after the isolation of the first aminoacyl-tRNA synthetases, work began on determining their amino acid sequences by using the classical methods of protein sequencing. But even before a primary structure had been completely elucidated in this way, the route via sequencing of the synthetase genes proved to be quicker and more profitable. Thus, the partial structures obtained by Edman degradation of the isoleucyl-tRNA synthetase (containing 939 amino acids) from *Escherichia coli*[4, 5] were confirmed and completed with data obtained by DNA sequencing.[6] Despite the advances in the technique of gene sequencing, classical Edman degradation has not become redundant, since it has proved useful also to sequence a part of the protein by the

classical method. In this way a check is maintained that the individual amino acids of the protein sequence have indeed been assigned the correct nucleotides as triplets of the genetic code.[7]

In the meantime, all primary structures of the aminoacyl-tRNA synthetases, or their genes, are known from *E. coli*, and most of them are also known for the enzymes isolated from yeast. They are stored in accessible data banks such as the European Molecular Biology Organization (EMBO) library in Heidelberg, or the Genebank in Los Alamos. In solution, the enzymes are either monomeric (α) or exist as dimers with a quaternary structure of the type (α_2), or in one and two cases, respectively, as α_4 or $\alpha_2\beta_2$ (see Table 1).[8, 9] The molecular weights of the α units vary between 37000 and 126000, corresponding to about 300 and 1100 amino acid residues, respectively. Very few similarities were found between synthetases specific for different amino acids, but from the same organism, or from different organisms, but specific for the same amino acid. In most cases only about 20% of the amino acid residues were identical, after the total sequences had been suitably aligned with each other.[10]

2.1. Classification into Class I and Class II Enzymes

Despite the low sequence homologies of the synthetase primary structures, it was possible to classify the enzymes into two groups of ten enzymes each, on the basis of relatively short, common, partial sequences, so-called "consensus or signature sequences". These groups were named class I and class II.[11-13]

Adopting one-letter codes for amino acids, the two consensus sequences for class I were named "HIGH" (His-Ile-Gly-His) and "KMSKS" region (Lys-Met-Ser-Lys-Ser). From the three X-ray structure analyses that are available to date, these sequences point to a structural domain which is known as the "Rossman" or "nucleotide binding" fold.[11-19] This has previously been found in several dehydrogenases as the binding site for nicotinamideadeninedinucleotide (NAD^+),[20] and generally consists of two halves, each comprising three (or two) parallel β-strands, and two (or three) α-helices (Fig. 1). In all the class I aminoacyl-tRNA synthetases studied to date, the binding sites for ATP or the aminoacyladenylate and for the C-C-A end of the tRNA lie in this region.[11-19] An example of the structure of a class I synthetase is shown in Figure 2, the methionyl-tRNA synthetase of *E. coli*.[17] In this case, the complete, dimeric synthetase molecule could not be crystallized, but only a monomeric tryptic fragment which, although it was missing 125 *C*-terminal amino acid residues, nonetheless possessed complete enzymatic activity.[17, 26] The methioyl-tRNA synthetase consists of two domains and a *C*-terminal polypeptide. The first, *N*-terminal domain contains the "Rossman" fold, comprising six parallel β-strands and five α-helices (amino acid residues 1-360). The second domain (positions 361-525) consists predominantly of α-helices; the *C*-terminal polypeptide, which extends to position 551, is partially folded back in the direction of the *N*-terminus, and thus

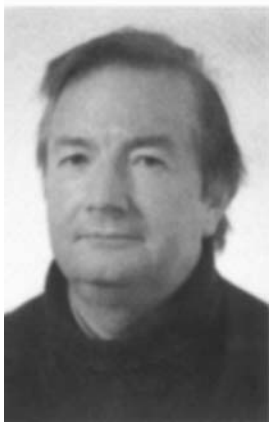

Friedrich Cramer, emeritus Director at the Max-Planck-Institut (MPI) for Experimental Medicine in Göttingen, honorary Professor at the Universities of Göttingen and Braunschweig, was born in 1923. He studied chemistry in Heidelberg from 1944-1949, where he received his doctorate under the supervision of K. Freudenberg and habilitated in 1953. In 1953 and 1954 he was a guest docent at the University of Cambridge (UK), and in 1959 he was appointed Professor at the Technische Hochschule Darmstadt (FRG). From 1962 to 1991, he was Director at the MPI in Göttingen. He is a scientific member of the Max-Planck-Gesellschaft and a member of the Göttingen Academy of Science, the Heidelberg Academy of Science, the Polish Academy of Science and the European Molecular Biology Organization as well as an Honorary Fellow of the American Society of Biological Chemists. In 1990 he received the Bavarian state prize for Literature (Karl-Vossler-Prize) and in the same year the Kopernikus Medal of the Polish Academy of Science. He is the main author of approximately 400 publications and a series of books on a wide variety of topics including inclusion compounds, the synthesis of nucleic acids, the structure of transfer-ribonucleic acids, protein biosynthesis, molecular genetics and cell-cell specificity.

Wolfgang Freist, born in 1940, in Bremen, studied chemistry at the University of Kiel, where he received his doctorate in 1968 under the supervision of R. Greve for work concerning alkaloids. Since 1968 he has been a member of the Department of Chemistry at the Max-Planck-Institut for Experimental Medicine in Göttingen. His fields of interest include the syntheses of modified nucleotides as substrate analogues, the substrate specificity of enzymes of protein biosynthesis and enzyme kinetics.

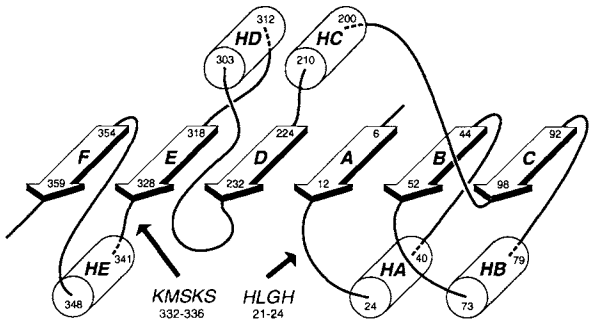

Fig. 1. Schematic diagram of the *N*-terminal domain of *E. coli* methionyl-tRNA synthetase. It displays the Rossman fold typical of class I synthetases, in which the binding sites for ATP and the C-C-A end of the tRNA are found. The numbers correspond to the number of the amino acids, beginning at the *N*-terminus. In this region of the enzyme one also finds the typical consensus sequences for class I, KMSKS and HIGH (HLGH in methionyl-tRNA synthetase). The β-strands (A,B,C,D,E,F) and helices (HA, HB, HC, HD, HE) are named as usual manner for methionyl-tRNA synthetase; for sheet F and for helix HE it is not clear whether they can generally be counted as part of the nucleotide binding fold [17]. (The diagram is a modified version of Figures 2, 3, 1 and 7 in references [16, 17, 103, 104].)

connects the *C*-terminal polypeptide with the *N*-terminal domains.

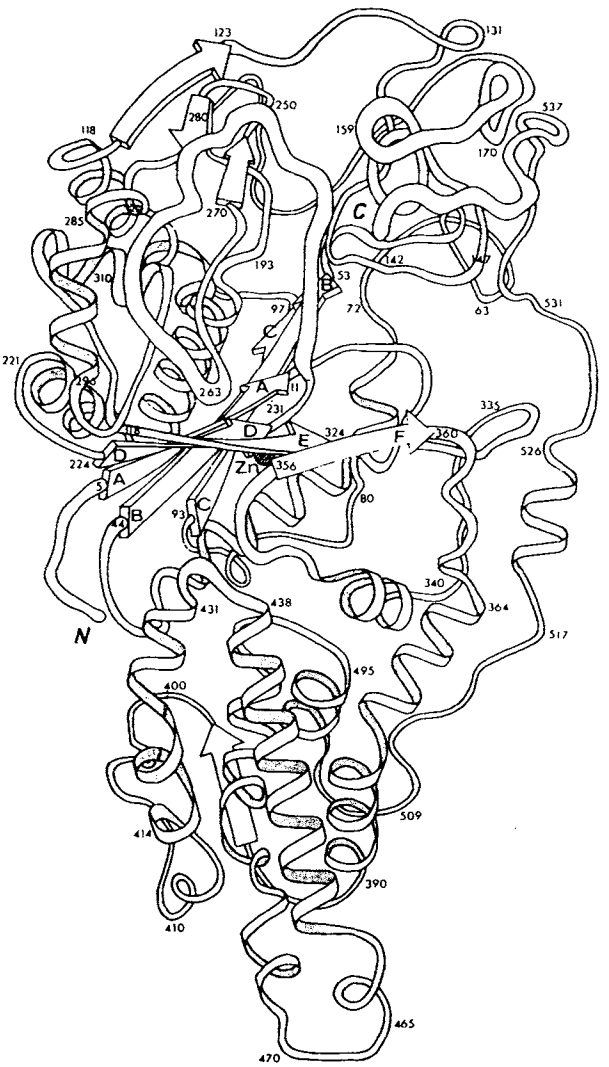

Fig. 2. Schematic diagram of the structure of a tryptic fragment of the methionyl-tRNA synthetase from *E. coli*, taken from ref. [17].

The synthetase structures known to date have recently been discussed in a review article by Moras.[21] Class I contains the synthetases that are specific for valine, leucine, isoleucine, glutamic acid, glutamine, arginine, tyrosine, tryptophan, methionine, and cysteine (Table 1). A more detailed comparison of the structure and sequence allows the class I enzymes to be further divided into three subclasses,[13] which here will be called Ia, Ib, and Ic. Subclass Ia consists of the tyrosyl- and arginyl-tRNA synthetases, subclass Ib contains the glutaminyl-, glutamyl-, and tryptophanyl-tRNA synthetases, while subclass Ic comprises those enzymes which react with leucine, isoleucine, valine, methionine, and cysteine.

The class II enzymes have three "sequence motifs" in common, called motifs 1, 2, and 3; however, two enzymes show motif 3 only (Table 1).[11, 12] Each motif has a prerequisite amino acid at its center. In motif 1 this is a prolyl P; "before" it are two, single, hydrophobic residues ϕ, each followed by two random aminoacyl groups x, and at the start of the motif is usually a glycyl g. "After" the proline residue one finds two hydrophobic groups ϕ:

gϕxxϕxxP$\phi\phi$ motif 1

Motif 2 consists of two parts. The first begins with a phenylalanyl F, tyrosyl Y, or histidyl H, followed by an unchangeable, central arginyl R, a variable residue x, and a glutamyl E, or aspartyl D:

(F/Y/H)Rx(E/D) motif 2, part 1

The second part of the motif begins between four and twelve aminoacyl groups "upstream", and consists of an arginyl R or histidyl H, followed by three variable residues x, and an unchangeable, central phenylalanine F. This is followed by three variable groups x, and an aspartyl D, or glutamyl residue E:

(R/H)xxxFxxx(D/E) motif 2, part 2

Motif 3 begins with the acyl residue of a short-chain amino acid λ, followed first by a variable x and a hydrophobic residue ϕ, and then by two pairs of the common glycyl residue g and a hydrophobic one ϕ. In front of the central arginyl R there is usually a glutamyl e (where the small letter means that this group can be varied), and the end of the motif consists of four hydrophobic residues ϕ:

λxϕgϕgϕeR$\phi\phi\phi\phi$ motif 3

The X-ray structure analyses of class II enzymes which are available, namely those of seryl-tRNA synthetase from *E. coli* and aspartyl-tRNA synthetase from yeast, show that the molecules are constructed of two domains, an *N*-terminal, "helical" domain, and a *C*-terminal, "catalytic" domain.[22-24] The three characteristic motifs are all found in the catalytic domain, which is built up around a heptastranded antiparallel β-pleated sheet[22-24] (Fig. 3). In Figure 4 the structure of the seryl-tRNA synthetase from *E. coli* is presented as an example.[23, 25] This enzyme belongs to the α_2 quaternary structure type, and each of the two subunits con-

Table 1. Classification of the aminoacyl-tRNA synthetases in classes and subclasses (the further subclassification of the enzymes is indicated by the broken line in row four and corresponds to a further subclassification after precise sequence comparisons [13,25]), as well as quaternary structures, aminoacylation positions, specificity in relation to the ATP analogues **A** (base modified) and **B** (sugar modified) and evolutionary tree of the aminoacyl-tRNA synthetases after sequence comparisons. s denotes that the substance for the corresponding enzyme is substrate. i denotes that the substance acts an inhibitor. A dash shows that the substance is neither a substrate nor an inhibitor.

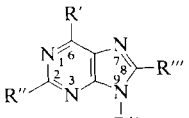

A

	R′	R″	R‴
2-Cl-ATP	NH_2	Cl	H
8-Br-ATP	NH_2	H	Br
TuTP	= 7-deazaadenosin-triphosphate		

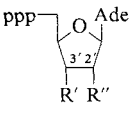

B

	R′	R″
2′-d-ATP	OH	H
3′-d-ATP	H	OH
2′-OCH_3-ATP	OH	OCH_3
3′-OCH_3-ATP	OCH_3	OH

Class	I										II									
Consensus sequences	HIGH + KMSKS										motifs 1, 2, 3					motif 3		motifs 1, 2, 3		
Subclasses according to refs. [13, 25]	Ib			Ia		Ic					IIa					IIc		IIb		
Amino acid specificity	Glu	Gln	Trp	Arg	Tyr	Cys	Ile	Leu	Val	Met	Ser	Thr	His	Pro	Ala	Gly	Phe	Asp	Asn	Lys
Quaternary structure	α	α	α_2	α	α_2	α	α	α	α	α_2	α_2	α_2	α_2	α_2	α_4	$\alpha_2\beta_2$	$\alpha_2\beta_2$	α_2	α_2	α_2
Position of the esterified tRNA OH group	2′	2′	2′	2′	2′,3′	2′,3′	2′	2′	2′	2′	3′	3′	3′	3′	3′	3′	2′	3′	3′	3′
ATP analogues specificity:																				
TuTP	s	s	i	s	s	s	s	s	s	s	–	–	–	–	–	–	–	–	–	–
2-Cl-ATP	i	i	s	i	–	–	s	s	s	s	s	s	s	–	–	s	s	s	s	s
8-Br-ATP	i	i	i	i	–	–	–	–	–	–	–	–	–	–	–	–	–	–	–	–
2′-d-ATP	i	i	s	s	–	–	–	–	–	–	s	s	–	–	–	s	s	s	s	s
3′-d-ATP	i	i	s	s	s	s	s	s	s	s	s	s	i	i	i	s	s	s	s	s
2′-OCH_3-ATP	i	i	s	–	–	–	–	–	–	–	–	–	–	i	i	–	–	–	–	–
3′-OCH_3-ATP	i	i	–	–	–	–	–	–	–	–	–	–	–	i	i	–	–	–	–	–
Aminoacyl-tRNA synthetases evolutionary tree according to ref. [44]																				

sists of 430 amino acid residues. The structure reveals a *C*-terminal, catalytic subunit of 330 amino acid residues, which contains the heptastranded β-pleated sheet; the 100 *N*-terminal amino acid residues form a long arm, built up of two antiparallel helices. The active site is presumably formed from parts of the β-pleated sheet and of the connecting, single strands. An unstructured single strand which contains motif 2 appears to form a flexible "cap" over the active site.[25]

Motif 1 probably has only indirect importance for the active site through stabilization of its conformation.[23] From a

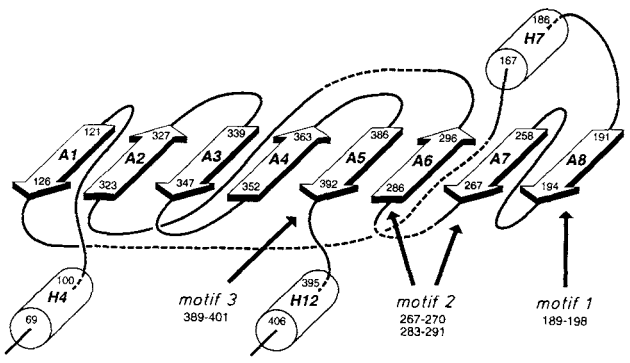

Fig. 3. Schematic diagram of the *C*-terminal, catalytic domain of the seryl-tRNA synthetase from *E. coli*. It is constructed of seven antiparallel β-strands, a structure considered typical of class II aminoacyl-tRNA synthetases. In the shaded regions, differences are found between this structure and that of the only other class II synthetase yet determined by X-ray crystallography, aspartyl-tRNA synthetase from yeast. The *C*-terminal domain of the enzyme contains the typical sequence motifs for class II. The numbers correspond to amino acids, numbered from the *N*-terminus; the nomenclature for strands and helices is the usual one for seryl-tRNA synthetase. (The diagram is based on Figures 7, 5, and 1 in refs [23, 24, 25]).

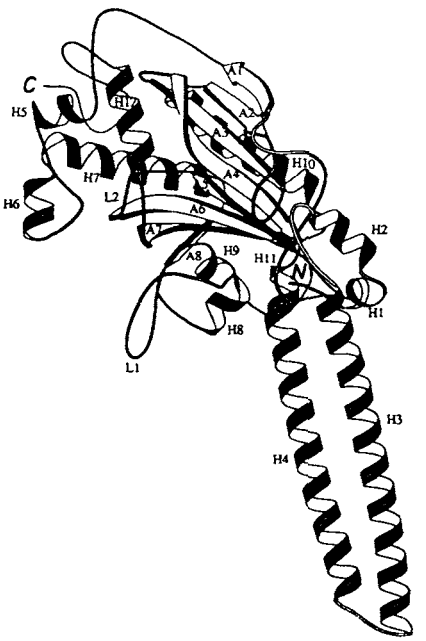

Fig. 4. Schematic diagram of the structure of *E. coli* seryl-tRNA synthetase; from ref. [25].

comparison of the seryl-tRNA synthetase amino acid sequence with those of other class II enzymes,[25] motif 1 is probably responsible for the association of the monomeric subunits of the enzyme to the α_2 quaternary structural type; the class II enzymes with four subunits generally lack this motif (see Table 1). Motifs 2 and 3, by contrast, are likely to be parts of the catalytic center presumed to be located in the *C*-terminal domain.[25] Comparison of the amino acid sequences of the class II enzymes also gave rise to a more detailed subdivision into subclass IIa, comprising the enzymes specific for serine, threonine, proline, and histidine, subclass IIb, comprising the tetrameric enzymes specific for aspartic acid, asparagine and lysine, and subclass IIc, comprising tetrameric enzymes specific for phenylalanine, glycine, and alanine (see Table 1).[25] Of the latter, the phenyl- and glycyl-tRNA synthetases show partial similarity with the enzymes of subclass IIb, while alanyl-tRNA synthetase has homologies to those of subclass IIa (see Table 1).

3. Synthetic Substrate Analogues

Influenced by Emil Fischer's "lock and key" model for enzyme–substrate interactions, chemists have long been synthesizing analogues of enzyme substrates, hormones, antibiotics, and plant substances. This has led not only to the development of new, highly potent pharmaceuticals, but has also yielded understanding of the mechanisms of enzyme-catalyzed reactions, and of the structures of substrate binding sites or receptors for hormones and pharmaceuticals.

Since aminoacyl-tRNA synthetases transform three substrates, they offer many possibilities to affect the course of catalysis by introducing chemical modifications in the substrates. Conclusions about the classification of the synthetases into different classes can only be expected from analogues of common substrates, such as ATP or the C-C-A end of the tRNA; amino acid derivatives can only yield information about their specific synthetase.

3.1. tRNA Analogues

Experiments with modified tRNAs proved to be unusually informative for detailed elucidation of the mechanism of the aminoacylation, and, as can now be seen, also for the classification of the synthetases. The terminal adenosine unit of these tRNAs **8**–**11** either lacks one of the free hydroxyl groups, or is replaced by an amino group.[26–32]

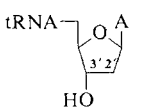

2'-deoxy-tRNA

8

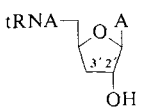

3'-deoxy-tRNA

9

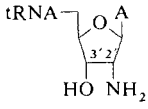

2'-deoxy-2'-amino-tRNA

10

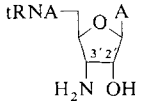

3'-deoxy-3'-amino-tRNA

11

These tRNA analogues were not, however, synthesized by direct chemical modification of the tRNA, but by enzymatic incorporation of the altered, terminal nucleotide N (as triphosphate NTP) after enzymatic removal of the terminal adenosine monophosphate of the tRNA[26–32] [Eq. (c)].

$$\underset{\textbf{12}}{\text{tRNA–C–C}} \xrightleftharpoons{\text{tRNA-Nucleotidyl-transferase, NTP}} \underset{\textbf{13}}{\text{tRNA–C–C–N}} + \text{PP}_i \qquad \text{(c)}$$

It was found that almost all the synthetases esterified only one of the two deoxy or amino-tRNAs with the amino acid (see Table 1).[26–32] From this it was concluded that the naturally occurring tRNA in the cell is also charged on only one of the OH groups of the terminal ribose, and that the primary product isomerizes spontaneously to give a mixture of the 2'- and 3'-*O*-aminoacyl esters.[32–34] When the synthetases were classified into 2'- and 3'- "chargers" (information obtained by modification of the tRNAs), an astonishing agreement was found with the classification into class I and class II enzymes: the class I synthetases esterify the tRNA on the 2'-OH group, while the class II synthetases use the 3'-OH group (see Table 1). This characteristic must therefore be defined by the principally different structure of the two aminoacyl-tRNA synthetase groups. The only exceptions are the phenylalanyl-tRNA synthetase which, as a class II enzyme, charges the 2'-OH group of the ribose, and the cysteinyl- and tyrosyl-tRNA synthetases, which appear to be able to esterify both groups.

Attempts to explain the observed 2',3'-specificity of the aminoacyl-tRNA synthetases, however, remained inconclusive. A speculative model published in 1983[35] considered the observation made on crystalline tyrosyl-tRNA synthetase; if it is alone in solution, AMP can also bind to the tyrosine binding site.[36] This finding led to the assumption that the adenosine monophosphate moiety of the aminoacyladenylate could also, possibly, bind both to the nucleotide and the amino acid binding sites. The change in position of the aminoacyladenylate thus made possible, could bring the carbonyl group of the aminoacyl residue into proximity of either the 2'- or the 3'-OH group.

The first X-ray structure analyses of complexes of tRNA, synthetase, and ATP, which are now available for the glutaminyl system (class I)[19] and the aspartyl system (class II)[24] show, however, that this cannot be the case.

The glutaminyl-tRNA synthetase, a monomeric enzyme built up of 553 amino acid residues, was crystallized as a complex with its cognate tRNA and ATP.[19] The X-ray structure analysis of this complex showed that the enzyme consists of four domains, of which three appear to be responsible for recognition of the tRNA, and one contains the active site (cf. Fig. 5). The latter is located at the *N*-terminus, and shows the Rossman fold typical of class I enzymes, consisting here of three β-strands and two α-helices in the first "half", and two β-strands and two α-helices in the second. Both the single strand connecting the two "halves", and the

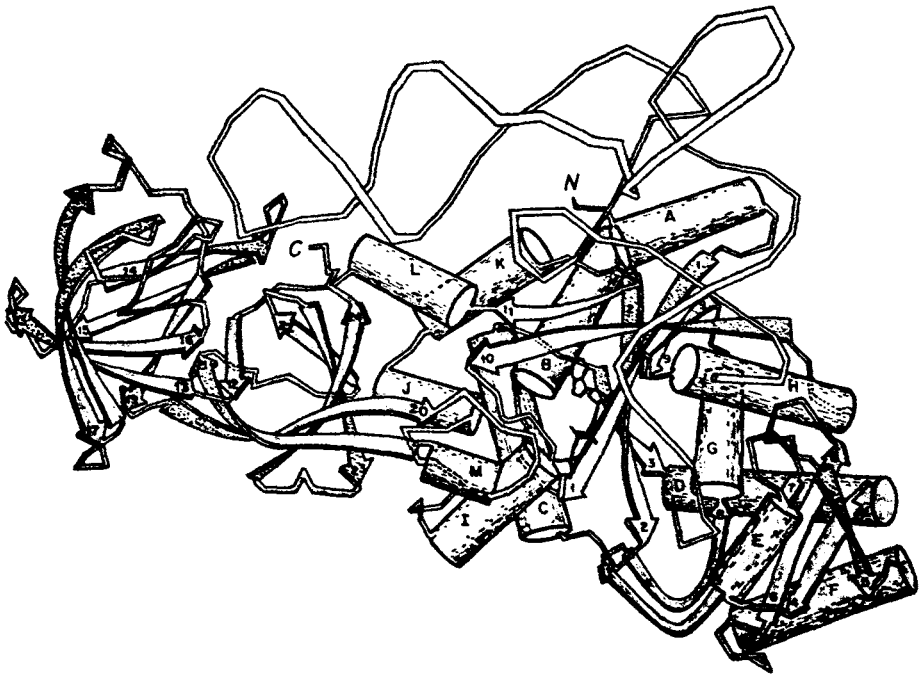

Fig. 5. Schematic diagram of the structure of *E. coli* glutaminyl-tRNA synthetase, complexed with $tRNA^{Gln}$ and ATP; from ref. [19].

second "half" of the Rossman fold are responsible for binding of the tRNA.

The α-phosphate group of the ATP molecule is situated at a distance from the 2′-hydroxy group of the terminal adenosine of the tRNA suitable for hydrogen bonding. The β- and γ-phosphate groups lie close to the two histidyl residues of the HIGH consensus sequence of the class I enzymes.

The first base pair of the aminoacyl acceptor stem of the $tRNA^{Glu}$-cloverleaf structure is opened, and the 3′ end of the tRNA forms a "hairpin" structure in which the unpaired bases form a loop bent back in the direction of the anticodon. The 2′-hydroxyl group of the terminal adenosine is thereby brought into the proximity of the carbonyl group of the glutaminyladenylate.

The aspartyl-tRNA synthetase from yeast, a dimeric enzyme of α_2 quaternary structure, with 557 amino acid residues per subunit, was crystallized as a complex with $tRNA^{Asp}$.[24] The dimeric enzyme binds two tRNA molecules. The X-ray analysis showed that the monomeric unit is composed of two domains, of which the *C*-terminal one contains the active site (cf. Fig. 6). Similarly to the seryl-tRNA synthetase, the catalytic subunit consists of an antiparallel β-pleated sheet surrounded by α-helices, and contains the motifs 1–3 characteristic for class II. Motif 1 causes the dimerization and motifs 2 and 3 the binding of the C-C-A end of the tRNA to ATP.

The C-C-A end of the $tRNA^{Asp}$ has a normal helical structure in the enzyme–tRNA complex. This ought to position the terminal adenosine so that aminoacylation of the tRNA on the 3′-hydroxyl group is made possible.[24] In a figurative sense, then, it is not the change in the position of the aminoacyladenylate which is responsible for the 2′,3′-specificity of the aminoacyl-tRNA synthetases, but that of the terminal hydroxy groups of the tRNA.

Fig. 6. Schematic diagram of the *C*-terminal domain of the aspartyl-tRNA synthetase, complexed with $tRNA^{Asp}$; from ref. [24].

3.2. ATP Analogues

The classification of the aminoacyl-tRNA synthetases, and indeed even a more detailed subclassification, was also carried out in extensive studies on numerous ATP analogues, before the elucidation of the first primary structures.[37–43] Since these results have already been described in detail elsewhere[3, 42, 43] only a few particularly characteristic findings that are important for the classification of the enzymes will be mentioned here (see Table 1). The clearest distinction between classes I and II is seen in the behavior of tubercidin triphosphate (TuTP) in the aminoacylation reaction (see Table 1). This modified ATP, in which the nitrogen atom in position 7 of the purine system is replaced by a carbon atom, can replace ATP as a substrate for the class I enzymes; for tryptophanyl-tRNA synthetase, however, it acts as an inhibitor (see Table 1). From six further ATP analogues, whose specificities are presented in Table 1, subclass Ib can be clearly distinguished from subclasses Ia and Ic. Even the possible

subdivision of subclass Ib, by which tryptophanyl-tRNA synthetase is separated from glutamyl- and glutaminyl-tRNA synthetase on the basis of the length of the the so-called "CP1" sequence,[13] is hinted at in the specificity table.

In class II, the subclasses IIb and IIa reveal the same specificities, with the exception of prolyl-tRNA synthetase. In the subclass of tetrameric enzymes, IIc, glycyl- and phenylalanyl-tRNA synthetases show the same ATP specificity as the enzymes of subclasses IIa and IIb. This agrees with the observation derived from sequence comparisons, that these proteins are related to subclass IIa.[25] Alanyl-tRNA synthetase, in contrast, displays the same specificity pattern as prolyl-tRNA synthetase, which is the single exception in subclass IIa. Here it should be mentioned that on the basis of sequence comparisons, alanyl-tRNA synthetase possesses a certain resemblance to the enzymes of subclass IIa.[25]

With the help of detailed sequence comparisons, the first trees have now been developed which show the evolutionary relationships between the two classes of aminoacyl-tRNA synthetases.[44] Since each of the two groups contains members of the entire spectrum of amino acid types (hydrophobic, basic, acidic), one can assume that today's system of twenty amino acid–synthetase pairs developed from two independent families of ten each. The evolutionary trees for classes I and II are shown in Table 1. They are also in good agreement with the classification that was developed earlier from the ATP specificities. The only exception in class I is the relationship between the tryptophanyl- and tyrosyl-tRNA synthetases, while in class II there are two exceptions, alanyl- and prolyl-tRNA synthetase, these are not related to each other but to the histidyl and threonyl enzymes, respectively. However, since the specificities towards ATP analogues probably depend on a small number of amino acid residues which are crucial for binding, divergences from relationships which are found by comparison of longer sequences are not unusual. All in all, the findings worked out from modified tRNA's and ATP analogues agree very well with the classification arrived at later by sequence comparison.

3.3. Amino acid analogues

Exact recognition of the amino acids by the aminoacyl-tRNA synthetases is a prerequisite for the biosynthesis of functional proteins. The first experiments on the in vivo specificity of protein biosynthesis showed that valine, isoleucine, leucine, tyrosine, and phenylalanine are replaced by each other in less than one in 3000 cases.[45] In more recent work, however, error rates of 1:100 to 1:1000 have been found for the exchange of arginine and tryptophan for cysteine.[46] The specificities of individual enzymes has been studied with respect to the twenty amino acids that occur naturally in proteins, and error rates both higher and lower than those mentioned above have been determined.[47-52] In contrast, amino acids that do not occur naturally seem to be distinguished less well in principle from the cognate substrates normally transformed by the enzymes.[45, 53] Clearly, the high specificity of the aminoacyl-tRNA synthetases has developed during the course of biological evolution primarily towards the twenty natural amino acids.

Systematic studies of the substrate characteristics of noncognate amino acids with individual enzymes can only ever yield information on the topography of the amino acid binding site of the protein concerned. Nonetheless, unifying principles of amino acid recognition can be determined, which may also divide classes I and II.[48-52]

According to the so-called "Stopper-model", four class I enzymes, whose amino acid specificity has been studied in detail, possess an amino acid binding pocket, which allows a particularly "tight" packing, and leads to strong hydrophobic interactions.[48-52, 54] The binding pocket is limited in length by an organic group or an amino acid side chain. In addition, other side chains extend into the binding pocket, and must be "pushed to the side" on binding of the substrate. Noncognate amino acids also displace the size-limiting group, and possibly others. The binding energy for the amino acid side chain is composed of positive energy contributions from hydrophobic interactions and, when possible, hydrogen bonding, and of negative contributions arising from the necessary displacement of the groups of atoms projecting into the binding site. In this model, the amino acid is so to speak assessed the by "fingers" of the protein. Noncognate amino acids either achieve fewer hydrophobic interactions, cannot form the corresponding hydrogen bonds, or have to displace additional amino acid side chains from their positions (Fig. 7). Their binding energy can be predicted to

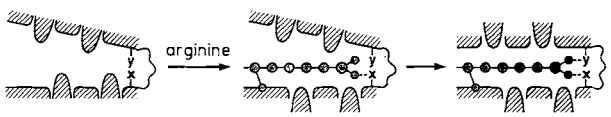

Fig. 7. Schematic diagram of the binding of arginine to arginyl-tRNA synthetase, as an example of one of the four class I enzymes studied. The binding takes place in two steps.

a good approximation by using the laws found for the natural amino acids.[48-50]

For all of the class I enzymes that have been studied in detail, kinetic and stoichiometric data lead to the conclusion that amino acid binding takes place in two steps (Fig. 7).[48-52] The first binding step is probably followed by a conformational change in the enzyme,[55] which leads to the structure described as "especially dense packing",[48-52, 54] which has strong hydrophobic interactions. These are approximately twice as strong as those otherwise found in the literature, 25 cal $Å^{-2}$ (10.5 kJ nm^{-2}).[56-58]

However, in addition to the "assessing" of the amino acid by the specific binding site, two hydrolytic test steps are also responsible for the amino acid specificity. In these, aminoacyladenylates of noncognate amino acids and the aminoacyl-tRNA's formed from them can be rehydrolyzed.[48-52] In most cases the first, pretransfer–correction step is predominant, while the second, posttransfer step plays virtually no role.

Of the class I enzymes, only the lysyl-tRNA synthetase has been studied in detail with respect to its amino acid specificity. It also performs the two hydrolytic correction steps, although rather less effectively.[59] The binding of the amino acid seems, however, to occur in a single step, and the binding site presumably already has a structure with dense pack-

ing (Fig. 8).The entire recognition process consists of only three steps, rather than four as in the class I enzymes. The specificity of the lysyl-tRNA synthetase towards noncognate amino acids is significantly less than that of the studied class I enzymes, but it is too early to tell whether similar results may be expected for all the class II enzymes, and whether this is a general difference between the class I and class II enzymes.

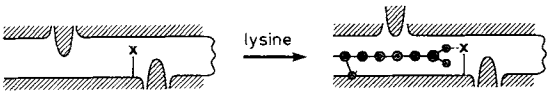

Fig. 8. Schematic diagram of the binding of lysine to lysyl-tRNA synthetase, the only class II enzyme yet studied in a similar manner to the four class I enzymes. Binding takes place in one step.

4. Affinity labeling

In order to determine which parts of the enzyme molecule are essential for specific substrate recognition, substrate molecules were provided with reactive groups capable of forming a covalent bond between substrate and enzyme. Partial degradation or sequencing of labeled enzymes can then be used to obtain information about which subunit or amino acid of the enzyme is responsible for binding the reactive group of the substrate. Here one assumes, not always quite correctly, as will be shown below, that the enzyme is labeled predominantly at the substrate binding site.

Successful experiments have been carried out with modified tRNAs and ATP analogues containing reactive halogen atoms such as bromine in bromoacetates,[60, 61] or chlorine in *N*-chloroethyl groups,[62] or with the azide group in *p*-azidoanilide residues.[62-65] Further reactive groups which have been used less frequently include 5,5′-dinitro-2,2′-dithiodibenzoate and *p*-nitrophenylchloroformate,[66] ^{3}H-labeled acetic anhydride,[67] pyridoxal phosphate,[68] 2,4,6-trimethylbenzoyl-AMP ("mesitoyl-AMP")[69] 3,3′-dithiobis(succinimidopropionate,[70] and adenosine(5′)triphospho(5′)pyridoxal **18** (see Section 4.3).[71] Covalent bonds in tRNA synthetase complexes have also been obtained by direct irradiation with UV light; these bonds probably arise between the bases of the nucleotides and the SH groups of the proteins.[72, 73]

The most informative experiments, however, were carried out with the dialdehydes **14** obtained by periodate oxidation of ATP **2** and tRNA **5**.[74-91] These aldehydes were originally reduced with sodium borohydride in order to obtain ATP and tRNA derivatives with a cleaved C2′–C3′ bond **15** [Eq. (d)].[92, 93]

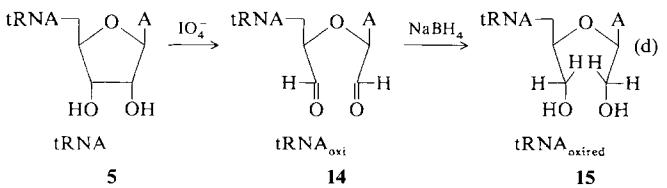

5 **14** **15**

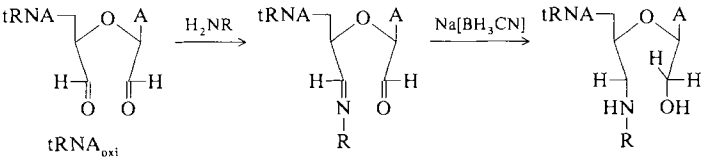

14 **16** **17**

On affinity labeling, the aldehyde groups react with the amino groups of lysine side chains to form Schiff bases **16**. These are then reduced to the amines **17** with sodium cyanoborotrihydridoborate,[80] to stabilize the label.

These stable, covalently bound labels survive degradation of the proteins and allow the identification of the single, reactive lysine side chain concerned.

The following sections will primarily discuss the results obtained with these dialdehyde-affinity labels.

4.1. Labeling with $tRNA_{oxi}$

The first results obtained from affinity-labeling experiments with the dialdehydes synthesized from tRNAs pertained to the composition of the enzyme–tRNA complexes. For methionyl- and tyrosyl-tRNA synthetases (quaternary structure α_2), the complexes found were composed of one covalently bound tRNA and the dimeric enzyme;[78, 84, 85] for leucyl-tRNA synthetase (quaternary structure α), one oxidized tRNA ($tRNA_{oxi}$ **14**) was found per monomeric enzyme.[90] In contrast, arginyl-tRNA synthetase (quaternary structure α) forms not only a 1:1 complex, but also approximately equal quantities of a compound consisting of two $tRNA_{oxi}$ units and the enzyme.[91] For the tetrameric phenalanyl-tRNA synthetase (quaternary structure $\alpha_2\beta_2$) two $tRNA_{oxi}$ were found to be bound; the bond was first postulated to be to the small β subunit,[79, 83] and later to the larger α subunit.[86]

A comparison of these stoichiometric ratios with values obtained by other methods is most interesting. The formation of an enzyme-tRNA complex in a ratio 1:1 was also found for the methionyl-tRNA synthetase by using fluorescence spectroscopy.[94] For tyrosyl-tRNA synthetase, anticooperative binding (i.e. binding hindered in the second step) of two tRNA molecules per enzyme molecule was found in one binding study between tRNA and enzyme,[95] while in another study, under catalytic conditions (i.e. in the presence of all three substrates), only one tRNA molecule was found to bind per enzyme molecule.[96] From a fluorescence titration, a stoichiometry of 1:1 was determined for the binding of tRNA to the arginyl-tRNA synthetase enzyme.[97] Here it is noteworthy that with $tRNA_{oxi}$, compounds are also formed from two $tRNA_{oxi}$ molecules and one enzyme molecule of quaternary structure α. This might confirm the possibility that even the monomeric enzymes operate in catalytic cycles, in the course of which two tRNA molecules can bind to the enzyme. Such cycles have until now only been postulated, on the basis of kinetic studies with, for example, isoleucyl-tRNA synthetase.[3, 98, 99] For methionyl-tRNA synthetase, the value of two bound tRNA molecules per enzyme molecule obtained by physical methods[99-101] agrees with the ratio obtained by affinity labeling.

For alanyl-,[87] phenylalanyl-,[86] tyrosyl-,[85] and methionyl-tRNA synthetases[88] even the individual amino acid to which the $tRNA_{oxi}$ covalently binds has been identified. In most cases it is a lysyl residue,[85-88] in some cases, though, an arginyl residue.[88] As expected in advance by critics of the method, the $tRNA_{oxi}$ is not bound to a single amino acid residue by the individual enzymes, but in several positions.[84-86,88] However, in the cases where an X-ray structure analysis of the enzyme is available (Tyr, Met),[85,88] the labeled amino acids are spatially not far apart.

After covalent binding of $tRNA_{oxi}$, the tyrosyl-tRNA synthetase from *E. coli* loses both its so-called ATP-pyrophosphate exchange ability (the reverse of the activation reaction [Eq. (a)]) and its ability to catalyze the aminoacylation of $tRNA^{Tyr}$.[85] Degradation of the labeled enzyme with chymotrypsin and degradation of the tRNA with ribonuclease A leads to isolation of two oligopeptides (positions 227-235 and 236-244) containing covalently bound adenosine. In the first peptide, which contains two lysyl residues (positions 229 and 234), it is primarily lysine 234 that reacts, and lysine 229 is less active. In the second peptide the sole lysine present (lysine 237) is completely labeled.

Comparison with the structure determined by X-ray diffraction of tyrosyl-tRNA synthetase from *Bacillus stearothermophilus*,[14,15] shows that the labeled lysyl residues belong to an unstructured part of the sequence which connects the *N*-terminal α/β-domains and an α-helical domain. The former contains the mononucleotide binding site, while the second is responsible for binding of the tRNA. The intervening portion containing lysine (and hence positively charged) is suitable for binding of the C-C-A end of the $tRNA^{Tyr}$, both because of possible interactions with the negative charges of the tRNA and because of its position. The lysyl residue 229 belongs to the KMSKS sequence which is characteristic of class I enzymes.

The fact that $tRNA^{Tyr}_{oxi}$ can react with three different lysyl residues suggests that several lysyl residues may be involved in binding of the C-C-A end, but also that it is not strongly fixed in the enzyme-tRNA complex and possesses a certain mobility, made possible by conformational changes in the tRNA, the enzyme, or both.

Similar results have also been obtained by affinity labeling of methionyl-tRNA synthetase with $tRNA^{fMet}$, which is specific for formyl methionine.[78,84,88] After reaction of the enzyme with $tRNA^{fMet}_{oxi}$, the resultant 1:1 complex loses its ability to catalyze ATP-pyrophosphate exchange and to charge the tRNA.[78] Digestion with chymotrypsin and Ribonuclease A yields three oligopeptides, which contain a covalently bound adenosine arising from the tRNA. Two of these contained one completely labeled lysyl residue (positions 61 and 335), while in the third oligopeptide fraction one of the lysyl residues 142, 147, or 149 was labeled. All of these lysyl residues belong to the *N*-terminal domain of the enzyme (position 1-360), which contains the nucleotide binding site fold; lysine 335 is part of the KMSKS signature sequence. According to the X-ray structure analysis of the crystallized enzyme, all the lysine residues lie within a radius of 5.5 Å ($\approx$ 1/10 of a domain radius), thus in this case it is possible to draw conclusions concerning the relative mobility of the C-C-A end of the tRNA in the enzyme-tRNA complex.

The amino acid residues that react with oxidized tRNA have been determined not only for the class I enzymes specific for tyrosine and methionine, but also for the phenylalanine and alanine-specific class II enzymes. In contrast to the class I enzymes, the class II retain their ability to catalyze ATP-pyrophosphate exchange, despite the presence of covalently bound tRNA.[86,87] For phenylalanyl-tRNA synthetase the $tRNA^{Phe}_{oxi}$ reacts with three lysyl residues (positions 2, 61, and 106), for alanyl-tRNA synthetase only with one (lysine 73). All of these lysine-positions lie within the *N*-terminal domains of the enzymes. However, since no X-ray structures of phenylalanyl- or alanyl-tRNA synthetase are available, no conclusions can be drawn about the spatial arrangement of the labeled lysyl-residues in the enzyme molecule.

Thus, one is tempted to assume that class I and class II enzymes may also be differentiated on the basis that the class II enzymes retain the ability to catalyze ATP-pyrophosphate exchange despite the covalent binding of a tRNA molecule. However, the number of enzymes studied is still too small for such a statement to be made. In addition, the results obtained with leucyl-tRNA synthetase are contrary to such a conclusion.[90] This class I enzyme appears also to catalyze amino acid activation after reaction with $tRNA^{Leu}_{oxi}$.

4.2. Labeling with ATP_{oxi}

Aminoacyl-tRNA synthetases can also react with ATP oxidized to a dialdehyde,[74,75,77] just as they can with oxidized tRNA. Methionyl-, tyrosyl-, and tryptophanyl-tRNA synthetases (quaternary structure α_2) can no longer catalyze ATP-pyrophosphate exchange after binding of two molecules of ATP_{oxi}.[74] Phenylalanyl-tRNA synthetase (quaternary structure $\alpha_2\beta_2$) is only completely inactivated after binding of the second ATP_{oxi} molecule; isoleucyl-tRNA synthetase (quaternary structure α) is inactivated by binding of an ATP_{oxi} molecule, but if the Mg^{2+} ions required for catalysis were strictly excluded, a second ATP_{oxi} molecule was incorporated into the enzyme.[74]

This affinity-labeling method initially appeared promising, but proved later to be unsuitable. Detailed experiments with lysyl- and phenylalanyl-tRNA synthetases from *E. coli* showed that these enzymes can bind up to five and fifty ATP_{oxi} molecules per enzyme molecule, respectively.[75] Similar effects to those with ATP_{oxi} can also be achieved with oxidized GTP or uridine.[75] One tryptophanyl-tRNA synthetase (quaternary structure α_2) from bovine pancreas was able to form the tryptophanyl adenylate even after binding of two molecules of ATP_{oxi}.[77] From these findings one must conclude that ATP_{oxi} does not react specifically with lysyl residues in the ATP binding site, but additionally or predominantly with other, easily accessible lysyl residues on the enzyme surface.

4.3. Labeling with Adenosine(5′)triphospho(5′)pyridoxal (AP_3-PL)

The ATP derivative **18**, in which the γ-phosphate group of the ATP is esterified to the 5′-hydroxy group of a pyridoxal

unit, proved to be much better suited for affinity-labeling of the ATP binding site.[71] The aldehyde group of the pyridoxal unit can react with lysyl residues in the enzyme in a similar manner to the aldehyde groups of $tRNA_{oxi}$ or ATP_{oxi}.

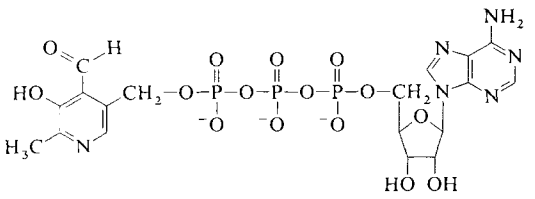

adenosine(5')triphospho(5')pyridoxal (AP_3-PL)

18

Methionyl- and valyl-tRNA synthetases form a 1:1-complex with this reagent, and lose their ability to catalyze ATP-pyrophosphate exchange and the charging of tRNA.

In methionyl-tRNA synthetase a total of three lysyl residues are labeled, in positions 335, 402, and 528. The first lysyl residue (335) is still in the *N*-terminal domain of the enzyme, and belongs to the KMSKS consensus sequence. It also reacts with $tRNA_{oxi}^{fMet}$ during affinity labeling of the same enzyme. No conclusions can be drawn about the exact role of this lysyl residue during catalysis, but one can assume that it may be important either as a ligand for the C-C-A end of the tRNA, or for the phosphate groups of the ATP, or possibly both.[71]

The lysyl residue 528 is only 4 Å removed from Lys335, according to the X-ray structure analysis of the enzyme, thus its protonated NH_2 group can presumably interact (as can lysine 335) with both the phosphate groups of the tRNA end and those of the ATP. According to the X-ray structure analysis, lysyl residue 402 lies some 30 Å away from the active site of the molecule. It is presumed normally to be involved in binding of the tRNA, and that in this case nucleotides can also be bound instead of the tRNA.

In valyl-tRNA synthetase, three lysyl residues were also registered by the labeling reagent (positions 557, 593, and 909). Of these, lysine 557 once again belongs to the KMSKS consensus sequence. Since no X-ray structure is available for a valyl-tRNA synthetase, nothing can yet be said about the position of the other two lysyl residues in the tertiary structure of the enzyme. It can only be presumed that the *C*-terminal domain of the enzyme is similarly folded to that of the methionyl-tRNA synthetase. A similarity between the tertiary structures of the two class I enzymes is thus suggested, but there is almost no material to support a classification of the aminoacyl-tRNA synthetases on the basis of ATP-affinity labeling.

5. Summary and Outlook

The aminoacyl-tRNA synthetases represent a group of enzymes which are present in every cell and catalyze the same reactions. They are therefore particularly suited for testing the usefulness of experiments with modified substrates or reactive groups mounted on substrate analogues, once sufficient experimental data is available. In each case, systematic studies on a number of enzymes are necessary; however, due to the limits set by material and time, studies are often forced to focus on a few, selected enzymes, as seen here for affinity labeling.

By studying the substrate characteristics of tRNA and ATP analogues, it was possible to define a division of the synthetases into two classes of enzymes more than fifteen years before elucidation of the primary structures, obtained only recently, by gene sequencing. The value of this information was at first underestimated, and is only now discernible to its full extent, by comparisons with X-ray structure analyses. The evolutionary trees derived from the primary structures,[44] according to which the aminoacyl-tRNA synthetases are descended from two "primeval synthetases", provides a simple explanation of the division of the enzymes into two main groups, predicted by us.

Affinity labeling does not afford information in every case about the amino acid residues which are essential for substrate binding, but it almost always provides some indications about the neighborhood of the substrate binding site. Because of the small number of enzymes studied to date, the results from this work do not yet allow any detailed statement on a classification of the synthetases. However, the findings observed so far appear, in part, to confirm the division of the synthetases into class I and class II enzymes.

Despite decades of research, the exact catalytic mechanism of the aminoacyl-tRNA synthetases is still largely unknown. To date, we know neither all the amino acid residues involved in catalysis, nor the conformational changes which occur in the course of the catalytic cycle. Here, substrate analogues which react with specific amino acid residues, yet to be developed, could play an important part in final elucidation.

The knowledge of the structures and complex mechanisms of aminoacyl-tRNA synthetases which has been obtained through simple chemistry, gives one courage to develop these methods further, and also to apply them to other enzymes.

Received: March 31, 1992 [A 892 IE]
German version: *Angew. Chem.* **1993**, *105*, 198

[1] L. L. Kisselev, O. O. Favorova, *Adv. Enzymol. Relat. Areas. Mol. Biol.* **1974**, *40*, 141–238.
[2] D. Söll, P. Schimmel in *The Enzymes, Vol. 10, 3rd. Ed.* (Ed.: P. D. Boyer), Academic Press, New York, **1974**, p. 489–538.
[3] W. Freist, *Angew. Chem.* **1988**, *100*, 795–811; *Angew. Chem. Int. Ed. Engl.* **1988**, *27*, 773–778.
[4] M.-R. Kula, *FEBS Lett.* **1973**, *35*, 299–302.
[5] H. Tsai, M.-R. Kula, W. Lindemaier in *Genetic Engineering Techniques: Recent Developments* (Eds.: P. C. Huang, T. T. Kuo, R. Wu), Academic Press, New York, **1982**, p. 159–172.
[6] T. Webster, H. Tsai, M.-R. Kula, G. A. Mackie, P. Schimmel, *Science* **1984**, *226*, 1315–1317.
[7] U. Englisch, S. Englisch, P. Markmeyer, J. Schischkoff, H. Sternbach, H. Kratzin, F. Cramer, *Biol. Chem. Hoppe Seyler* **1987**, *368*, 971–979.
[8] A. Joachimiak, I. Barciszewski, *FEBS Lett.* **1980**, *119*, 201–204.
[9] M. Mirande, *Prog. Nucleic Acid Res. Mol. Biol.* **1991**, *40*, 95–143.
[10] D. L. Gatti, A. Tzagoloff, *J. Mol. Biol.* **1991**, *218*, 557–568.
[11] G. Eriani, M. Delarue, O. Poch, J. Gangloff, D. Moras, *Nature* **1990**, *347*, 203–206.
[12] P. Schimmel, *Trends Biochem. Sci.* **1991**, *16*, 1–3.
[13] J. J. Burbaum, P. Schimmel, *J. Biol. Chem.* **1991**, *266*, 16965–16968.
[14] T. N. Bhat, D. M. Blow, P. Brick, *J. Mol. Biol.* **1982**, *158*, 699–709.
[15] P. Brick, T. N. Bhat, D. M. Blow, *J. Mol. Biol.* **1988**, *208*, 83–98.
[16] J. L. Risler, C. Zelwer, S. Brunie, *Nature* **1981**, *292*, 384–386.
[17] S. Brunie, C. Zelwer, J. L. Risler, *J. Mol. Biol.* **1990**, *216*, 411–424.
[18] T. Meinnel, Y. Mechulam, F. Dardel, J. M. Schmitter, C. Hountoudji, S. Brunie, P. Dessen, G. Fayat, S. Blanquet, *Biochimie* **1990**, *72*, 625–632.
[19] M. A. Rould, J. J. Perona, D. Söll, T. A. Steitz, *Science* **1989**, *246*, 1135–1142.

[20] M. G. Rossman, A. Liljas, C. I. Brändén, L. J. Banaszak in *The Enzymes, Vol. 11*, 3rd ed. (Ed.: P. D. Boyer), Academic Press, New York **1975**, p. 61–102.
[21] D. Moras, *Trends Biochem. Sci.* **1992**, *17*, 154–164.
[22] S. Cusack, C. Berthet-Colominas, M. Härtlein, N. Nassar, R. Leberman, *Nature* **1990**, *347*, 249–255.
[23] R. Leberman, M. Härtlein, S. Cusack, *Biochim. Biophys. Acta* **1991**, *1089*, 287–298.
[24] M. Ruff, S. Krishnaswami, M. Boeglin, A. Poterszman, A. Mitschler, A. Podjarny, B. Rees, J. C. Thierry, D. Moras, *Science* **1991**, *252*, 1682–1689.
[25] S. Cusack, M. Härtlein, R. Leberman, *Nucleic Acids Res.* **1991**, *19*, 3489–3498.
[26] M. Sprinzl, F. Cramer, *Nature* **1973**, *246*, 3–5.
[27] F. Cramer, H. Faulhammer, F. von der Haar, M. Sprinzl, H. Sternbach, *FEBS Lett.* **1975**, *56*, 212–214.
[28] M. Sprinzl, F. Cramer, *Proc. Natl. Acad. Sci. USA* **1975**, *72*, 3049–3053.
[29] A. C. Chinault, K. H. Tan, S. M. Hassur, S. M. Hecht, *Biochemistry* **1977**, *16*, 766–775.
[30] B. Alford, S. M. Hecht, *J. Biol. Chem.* **1978**, *253*, 4844–4850.
[31] T. H. Fraser, A. Rich, *Proc. Natl. Acad. Sci. USA* **1973**, *70*, 2671–2675.
[32] T. H. Fraser, A. Rich, *Proc. Natl. Acad. Sci. USA* **1975**, *72*, 3044–3048.
[33] M. Sprinzl, K. H. Scheit, H. Sternbach, F. von der Haar, F. Cramer, *Biochem. Biophys. Res. Commun.* **1973**, *51*, 881–887.
[34] S. Chladek, M. Sprinzl, *Angew. Chem.* **1985**, *97*, 377–398; *Angew. Chem. Int. Ed. Engl.* **1985**, *24*, 371–392.
[35] W. Freist, F. Cramer, *Eur. J. Biochem.* **1983**, *131*, 65–80.
[36] C. Monteilhet, D. M. Blow, *J. Mol. Biol.* **1978**, *122*, 407–417.
[37] W. Freist, F. von der Haar, M. Sprinzl, F. Cramer, *Eur. J. Biochem.* **1976**, *64*, 389–393.
[38] W. Freist, F. von der Haar, H. Faulhammer, F. Cramer, *Eur. J. Biochem.* **1976**, *64*, 493–497.
[39] W. Freist, H. Sternbach, F. von der Haar, F. Cramer, *Eur. J. Biochem.* **1978**, *84*, 499–502.
[40] W. Freist, F. Cramer, *Eur. J. Biochem.* **1980**, *107*, 47–50.
[41] W. Freist, H. Wiedner, F. Cramer, *Bioorg. Chem.* **1980**, *9*, 491–504.
[42] W. Freist, H. Sternbach, F. Cramer, *Hoppe-Seyler's Z. Physiol. Chem.* **1981**, *362*, 1247–1254.
[43] W. Freist, *Chem. Unserer Zeit* **1990**, *24*, 143–150.
[44] G. M. Nagel, R. F. Doolittle, *Proc. Natl. Acad. Sci. USA* **1991**, *88*, 8121–8125.
[45] R. B. Loftfield, *Prog. Nucleic Acid Res. Mol. Biol.* **1982**, *12*, 87–128.
[46] F. Bouadloun, D. Donner, C. G. Kurland, *EMBO J.* **1983**, *2*, 1351–1356.
[47] S. X. Lin, M. Baltzinger, P. Remy, *Biochemistry* **1984**, *23*, 4109–4116.
[48] W. Freist, H. Sternbach, F. Cramer, *Eur. J. Biochem.* **1987**, *169*, 33–39.
[49] W. Freist, H. Sternbach, F. Cramer, *Eur. J. Biochem.* **1988**, *173*, 27–34.
[50] W. Freist, H. Sternbach, *Eur. J. Biochem.* **1988**, *177*, 425–433.
[51] W. Freist, H. Sternbach, F. Cramer, *Eur. J. Biochem.* **1989**, *186*, 535–541.
[52] W. Freist, F. Cramer, *Eur. J. Biochem.* **1990**, *191*, 123–129.
[53] G. L. Igloi, F. von der Haar, F. Cramer, *Biochemistry* **1978**, *17*, 3459–3468.
[54] A. R. Fersht, *Proc. R. Soc. London B* **1981**, *212*, 351–379.
[55] E. Holler, M. Calvin, *Biochemistry* **1972**, *11*, 3741–3752.
[56] C. Chothia, *Nature* **1974**, *248*, 338–339.
[57] C. Chothia, *Nature* **1975**, *254*, 304–308.
[58] C. Chothia, *J. Mol. Biol.* **1976**, *105*, 1–14.
[59] W. Freist, H. Sternbach, F. Cramer, *Eur. J. Biochem.* **1992**, *204*, 1015–1023.
[60] V. Z. Akhverdyan, L. L. Kisselev, *J. Mol. Biol.* **1977**, *113*, 475–501.
[61] S. N. Khodyreva, N. A. Moor, V. N. Ankilova, O. J. Lavrik, *Biochim. Biophys. Acta* **1985**, *830*, 206–212.
[62] O. Leon, LaDonne H. Schulman, *Biochemistry* **1987**, *26*, 7113–7121.
[63] V. N. Ankilova, D. G. Knorre, V. V. Kravchenko, O. I. Lavrik, G. A. Nevinsky, *FEBS Lett.* **1975**, *60*, 172–175.
[64] I. I. Gorshkova, D. G. Knorre, O. I. Lavrik, G. A. Nevinsky, *Nucleic Acids Res.* **1976**, *3*, 1577–1589.
[65] R. Wetzel, D. Söll, *Nucleic Acids Res.* **1977**, *4*, 1681–1694.
[66] C. I. Bruton, B. S. Hartley, *J. Mol. Biol.* **1970**, *52*, 165–178.
[67] H. R. Bosshard, G. L. E. Koch, B. S. Hartley, *J. Mol. Biol.* **1978**, *119*, 377–389.
[68] M. Baltzinger, F. Fasiolo, P. Remy, *Eur. J. Biochem.* **1979**, *97*, 481–494.
[69] I. A. Madoyan, O. O. Favorova, G. K. Kovaleva, N. I. Sokolova, Z. A. Shaborova, L. L. Kisselev, *FEBS Lett.* **1981**, *123*, 156–160.
[70] D. Valenzuela, LaDonne H. Schulman, *Biochemistry* **1986**, *25*, 4555–4561.
[71] C. Hountondji, J.-M. Schmitter, T. Fukui, M. Tagaya, S. Blanquet, *Biochemistry* **1990**, *29*, 11266–11273.
[72] E. J. Ackerman, A. Joachimiak, V. Klinghofer, P. B. Sigler, *J. Mol. Biol.* **1985**, *181*, 93–102.
[73] J. J. Rosa, M. D. Rosa, P. B. Sigler, *Biochemistry* **1979**, *18*, 637–647.
[74] G. Fayat, M. Fromant, S. Blanquet, *Proc. Natl. Acad. Sci. USA* **1978**, *75*, 2088–2092.
[75] A. H. Mehler, J. P. Kim, A. A. Olsen, *Arch. Biochem. Biophys.* **1981**, *212*, 475–482.
[76] R. Parfait, *Eur. J. Biochem.* **1973**, *38*, 572–580.
[77] M. Fournier, B. Labouesse, J. Labouesse, *Eur. J. Biochem.* **1987**, *167*, 533–540.
[78] G. Fayat, C. Hountondji, S. Blanquet, *Eur. J. Biochem.* **1979**, *96*, 87–92.
[79] M. Baltzinger, F. Fasiolo, P. Remy, *Eur. J. Biochem.* **1979**, *97*, 481–494.
[80] C. Hountondji, G. Fayat, S. Blanquet, *Eur. J. Biochem.* **1979**, *102*, 247–250.
[81] E. Gerlo, J. Charlier, *FEBS Lett.* **1979**, *99*, 25–27.
[82] C. Hountondji, G. Fayat, S. Blanquet, *Eur. J. Biochem.* **1980**, *107*, 403–407.
[83] M. Renaud, F. Fasiolo, M. Baltzinger, Y. Boulanger, P. Remy, *Eur. J. Biochem.* **1982**, *123*, 267–274.
[84] C. Hountondji, S. Blanquet, *Biochemistry* **1985**, *24*, 1175–1180.
[85] C. Hountondji, F. Lederer, P. Dessen, S. Blanquet, *Biochemistry* **1986**, *25*, 16–21.
[86] C. Hountondji, J.-M. Schmitter, C. Beauvallet, S. Blanquet, *Biochemistry* **1987**, *26*, 5433–5439.
[87] K. Hill, P. Schimmel, *Biochemistry* **1989**, *28*, 2577–2585.
[88] C. Hountondji, J.-M. Schmitter, Ch. Beauvallet, S. Blanquet, *Biochemistry* **1990**, *29*, 8190–8198.
[89] Y. Mechulam, F. Dardel, D. Le Corre, S. Blanquet, G. Fayat, *J. Mol. Biol.* **1991**, *217*, 465–475.
[90] S.-T. Huang, S.-X. Lin, J.-P. Shi, Y.-L. Wang, *Sci. Sin. Ser. B (Engl. Ed.)* **1987**, *12*, 1298–1304.
[91] X.-D. Cheng, S.-X. Lin, I.-P. Shi, Y.-L. Wang, *Sci. China Ser. B* **1991**, *34*, 297–305.
[92] F. Cramer, F. von der Haar, E. Schlimme, *FEBS Lett.* **1968**, *2*, 136–139.
[93] F. von der Haar, E. Schlimme, M. Gómez-Guillen, F. Cramer, *Eur. J. Biochem.* **1971**, *24*, 296–302.
[94] S. Blanquet, M. Iwatsubo, J.-P. Waller, *Eur. J. Biochem.* **1973**, *36*, 213–226.
[95] A. Pingoud, D. Boehme, D. Riesner, R. Kownatzki, G. Maass, *Eur. J. Biochem.* **1975**, *56*, 617–622.
[96] R. Jakes, A. R. Fersht, *Biochemistry* **1975**, *14*, 3344–3350.
[97] S. S. Lin, Q. Wang, Y. L. Wang, *Biochemistry* **1988**, *27*, 6348–6353.
[98] W. Freist, H. Sternbach, F. Cramer, *Eur. J. Biochem.* **1982**, *128*, 315–329.
[99] W. Freist, *Biochemistry* **1989**, *28*, 6787–6797.
[100] F. Fasiolo, P. Remy, J. Pouyet, J. P. Ebel, *Eur. J. Biochem.* **1974**, *50*, 227–236.
[101] G. Krauss, D. Riesner, G. Maass, *Eur. J. Biochem.* **1976**, *68*, 81–93.
[102] P. Bartmann, T. Hanke, E. Holler, *Biochemistry* **1975**, *14*, 4777–4786.
[103] R. M. Starzyk, T. A. Webster, P. Schimmel, *Science* **1987**, *237*, 1614–1618.
[104] C. Zelwer, I. L. Risler, S. Brunie, *J. Mol. Biol.* **1982**, *155*, 63–81.

Computer-Assisted Solution of Chemical Problems—The Historical Development and the Present State of the Art of a New Discipline of Chemistry

By Ivar Ugi,* Johannes Bauer, Klemens Bley, Alf Dengler, Andreas Dietz, Eric Fontain, Bernhard Gruber, Rainer Herges, Michael Knauer, Klaus Reitsam, and Natalie Stein

Dedicated to Professor Karl-Heinz Büchel

The topic of this article is the development and the present state of the art of computer chemistry, the computer-assisted solution of chemical problems. Initially the problems in computer chemistry were confined to structure elucidation on the basis of spectroscopic data, then programs for synthesis design based on libraries of reaction data for relatively narrow classes of target compounds were developed, and now computer programs for the solution of a great variety of chemical problems are available or are under development. Previously it was an achievement when any solution of a chemical problem could be generated by computer assistance. Today, the main task is the efficient, transparent, and non-arbitrary selection of meaningful results from the immense set of potential solutions—that also may contain innovative proposals. Chemistry has two aspects, constitutional chemistry and stereochemistry, which are interrelated, but still require different approaches. As a result, about twenty years ago, an algebraic model of the logical structure of chemistry was presented that consisted of two parts: the constitution-oriented algebra of be- and r-matrices, and the theory of the stereochemistry of the chemical identity group. New chemical definitions, concepts, and perspectives are characteristic of this logic-oriented model, as well as the direct mathematical representation of chemical processes. This model enables the implementation of formal reaction generators that can produce conceivable solutions to chemical problems—including unprecedented solutions—without detailed empirical chemical information. New formal selection procedures for computer-generated chemical information are also possible through the above model. It is expedient to combine these with interactive methods of selection. In this review, the Munich project is presented and discussed in detail. It encompasses the further development and implementation of the mathematical model of the logical structure of chemistry as well as the experimental verification of the computer-generated results. The article concludes with a review of new reactions, reagents, and reaction mechanisms that have been found with the PC-programs IGOR and RAIN.

1. Introduction

Chemistry is concerned with the analysis and synthesis of chemical substances, the elucidation of molecular structures, and the reactivity and physical properties of chemical compounds. Apart from the fundamental gain in scientific knowledge, the manifold applications of chemistry justify the endeavors and expenditure of chemical research. The search for compounds with desirable effects, functions, and properties and the development of optimal methods for their synthesis, purification, and quality control are characteristic of research in applied chemistry.

Progress in chemistry is generally due to systematic research. It is evolutionary and takes place in small steps.[1] The rare revolutionary jumps of innovation are produced by new ways of thinking or expertly recognized and systematically exploited, fortunate, incidental observations. Examples are the insight into the significance of conformations[2] by Sachse[3] and Mohr,[4] Meerwein's concept of ionic reaction mechanisms,[5] the discovery of the first organometallic catalysts containing transition elements by Reppe et al.[6a] and Roelen,[7a] the solution of the absolute configuration problem by Bijvoet et al.,[8] and the development of the chemistry of superacids by Olah et al.[9]

For progress in applied chemistry, serendipity and initial misunderstandings can play an important role. Spectacular examples are the introduction of the sulfonamides by Domagk, Mietsch, and Klarer,[10] who thereby revolutionized chemotherapy of bacterial infections, and the discovery of the azole fungizides by Büchel and Plempel[11] that enabled efficient and broad chemotherapy of fungal infections.

The diversity of applications for computers in chemistry reflects the variety in chemical research. They have been used since they have been available and have become indispensable in all areas of chemistry. In 1959 Konrad Zuse,[12] the inventor of the computer, sold the first commercially available machine, the magnetic drum computer Z22, to Bayer AG, who used it partly for scientific purposes.

[*] Prof. Dr. I. Ugi, Dr. J. Bauer, Dr. K. Bley, Dr. A. Dengler, Dipl.-Chem. A. Dietz, Dr. E. Fontain, Dr. B. Gruber, Dr. M. Knauer, Dipl.-Chem. K. Reitsam, Dipl.-Chem. N. Stein
Organisch-chemisches Institut der Technischen Universität München
Lichtenbergstrasse 4, D-W-8046 Garching (FRG)
and
Dr. R. Herges,
Organisch-chemisches Institut der Universität, Henkestr. 42,
D-W-8520 Erlangen (FRG)

Initially computers were exploited exclusively for numerical computations, an application that is still on the increase. The term computational chemistry[13-15] is used for such applications, in which the calculation of molecular energy levels and geometries prevails. Their numerical capabilities make computers an indispensable tool of quantum chemistry and analytical chemistry, which include the elucidation of molecular structure by spectroscopic and X-ray methods. However, they are also useful in the determination of properties of substances, the design of experiments, the collection, evaluation, graphic display, and interpretation of experimental data, as well as in the visualization of molecular structures whose atomic coordinates are obtained from measurements, by quantum chemical computations, or by force-field methods.

To a larger extent these applications of computers in chemistry —mostly computations according to fixed "recipes"— can be automated. With the exception of molecular modeling where both the numerical and graphic capabilities of computers are exploited, an interactive participation of the user is not needed.

Many types of chemical problems can, however, not be solved by numerical computations. The solution of these chemical problems requires another kind of approach, incorporating the logical and combinatorial capabilities of computers. This discipline is called computer chemistry.[16-20] The latter term is not too well chosen, but is now widely used.

The oldest and best known computer programs for the direct solution of chemical problems serve to design syntheses and elucidate molecular structures from spectroscopic data. The search for synthetic routes or reaction mechanisms and the elucidation of molecular structures from spectroscopic data belong to the "classical" problems of chemistry. The solution of such problems involves finding molecules that have certain characteristic chemical features. Generally, the classical chemical problems have a significant combinatorial aspect, and have many solutions that cannot be obtained by numerical computations, although such computations may be of indirect use.[21] The best solutions are often found by intuition, creative thinking, or trial and error. The computer-assisted solution of chemical problems requires the interactive participation of the user, because there are always many potential solutions and no generally applicable rules. Therefore, a nonarbitrary selection of the practicable solutions is needed. The methods for solving such problems are, as a rule, nondeterministic in nature.

Joshua Lederberg and George Vleduts, who died in 1990, are the founding fathers of computer chemistry. Lederberg[22] initiated the DENDRAL project[23] to develop a computer program that determines the significant structural features of a molecule from spectroscopic data and then assembles its complete structure from its substructures.[24] Although, the DENDRAL project was terminated before all its goals were achieved, it nevertheless represents an important milestone in the development of computer chemistry.[13] It was the first computer program that exploited formal means for the solution of chemical problems. DENDRAL also promoted the notion artificial intelligence.[23]

In 1963, Vleduts[25] proposed the design of computer programs for planning multistep organic syntheses (CAOS: Computer-Assisted Organic Synthesis),[26] that is, for finding a way to synthesize a given target molecule from available starting materials in the best possible way according to the criteria that are applicable. As a pioneer of data banks of chemical reactions,[27] Vleduts was the first to discuss in detail how the reverse of stored chemical reactions, the so-called retroreactions, can be used to generate synthetic routes that lead from the target molecule via precursors to available starting materials. For instance, the structural feature **1** in a target molecule leads to the chapter of aldol condensations in the reaction library and thus to the precursors **2** and **3**.

From the precursors of the target molecule their precursors are obtained in turn, until the starting materials are reached. Thus, a tree of syntheses results that generally con-

Ivar Ugi was born in Arensburg in Estonia in 1930. The family moved to Dillingen an der Donau (Germany) in 1941, where Ivar Ugi completed his Abitur in 1949. In the fall of the same year he began his study of chemistry at the University of Tübingen, which he completed with a doctorate at the University of Munich in 1954 under Prof. Huisgen. He obtained his habilitation in 1959 for his work on pentazoles and isonitriles and continued as a research associate at the university for a further two years. In 1962 he joined the company Bayer in Leverkusen and rose to Director and Chairman of the Kommission für Grundlagenforschung. After six years his spirit of research led him to the USA: in 1968 Ugi became Full Professor of Chemistry at the University of Southern California in Los Angeles. In July 1971 he accepted a chair rich in tradition at the Technische Universität München, the Lehrstuhl I für Organische Chemie. Ivar Ungi is a member of committees for many foundations and has been a full member of the Swedish Royal Society for Science since 1987 and the Estonian Academy of Sciences since 1990. His scientific endeavors have been acknowledged with many awards: in 1964 he received the research prize of the Akademie der Wissenschaft in Göttingen and in 1988 the Philip Morris research prize for the Dugandji–Ugi model which he had developed with the topologist Dugandji. His life's work was honored in 1992 with the Emil-Fischer-Medaille der Gesellschaft Deutscher Chemiker not only for the development of mathematical models of the logical structure of chemistry, but also for the many new preparative methods arising from his isonitrile chemistry, four-component condensation, and stereochemical models, which open several new fields of research. These synthetic methods give strong impetus in particular to the chemistry of peptides, nucleotides, and β-lactam antibiotics.

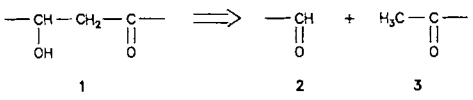

1 2 3

tains many pathways from which one has to be selected. Corey[28] introduced the term retrosynthetic analysis for this procedure.

Bilateral synthesis design is an alternative to the retrosynthetic approach. When both the target molecule and a suitable set of starting materials are known, it suffices to find pathways that lead from the starting materials to the target molecule.

Computers can only be used for the solution of chemical problems when sufficient knowledge and experience are available for model concepts and reasoning by analogy. In the exploration of new domains in chemistry and in areas of incipient research, novel insights, visions, new ideas, and fortunate coincidences are still indispensable. Computers are here, at best, of indirect use, especially as a chemist would probably reject an "imaginative" computer-generated proposal as nonsensical artifact, even if it were completely realizable, instead of checking it in the laboratory.

Since computers do not have any creative intelligence, they are neither able to generate revolutionary ideas nor capable of pioneering scientific achievements. However, as an "amplifier of intelligence" a computer can, within the given body of knowledge, accelerate the progress of science, and also give impetus to research work that would not be feasible without computer-assistance. Even if a computer were able to generate all the conceivable solutions for a given chemical problem, the meaningful and creative solutions could not be selected without the participation of a qualified user.

2. Computer-Assisted Synthesis Design

2.1. Empirical Synthesis Design Assisted by Reaction Libraries

The programs for retrosynthetic design strategy based on data from reaction libraries LHASA,[29, 30] Wipke's SECS,[31] and Gelernter's SYNCHEM,[32] as well as the Leverkusener Peptide Synthesis Design Program, which operates along the bilateral principle,[33, 34] belong to the first computer programs for the solution of chemical problems. Since then, many groups have tried to develop computer programs with various success for the design of syntheses[18, 35].

Since the beginning of organic synthesis, chemists have planned syntheses by retrosynthetic reasoning,[36] mentally dissecting the target molecule while bearing in mind known synthetic reactions. Sir Robert Robinson[37] employed retrosynthetic reasoning particularly systematically. The disconnection method as recommended by Warren[38] also exercises retrosynthetic reasoning.

The early synthetic chemists did not attach a name to their procedure of synthesis design. Since the introduction of the terms synthon, transform, and retrosynthesis (also called antithesis), as well as the transform arrows (⇒) by Corey,[28] publications often contain a retrosynthetic analysis performed after completion of the synthesis. Multistep syntheses are certainly all based on some plan; however, the complex multistep synthetic pathways that are successfully executed in the laboratory cannot yet be planned to the last detail. They evolve from the set of proposed syntheses by trial and error and by successive adjustment of the design to what is feasible.

The empirical retrosynthetic programs are typical expert systems[39] with a knowledge basis and a set of rules. The empirical retrosynthetic programs generate synthetic pathways according to the perceived structural features of the target by application of the transforms, rules, and schemes. The precursors of a given target molecule are generated from it by breaking and making bonds according to stored information on chemical reactions and heuristic rules (see **1**–**3**). The process is iterated for each precursor until available starting materials are reached.

An empirical retrosynthetic program that is not confined to a narrow field of applications and a small repertoire of chemistry requires a large reaction library and a powerful computer. The creation and updating of large error-prone reaction libraries and the incorporation of synthesis-related experience into empirical synthesis design programs is time-consuming and costly. Reactions that are sequences of individual steps are particularly difficult to handle, because redundant information is stored. An advantage of empirical retrosynthetic programs is that they exploit existing chemical experience and therefore yield plans of syntheses that are combinations of known reactions and thus likely to succeed in the laboratory. The reaction library also determines the limits of the program, which is unable to break new territory. Moreover, since it is impossible to store all known reactions, reaction libraries provide to a more or less arbitrary choice of reactions.

Conceivable precursors can exist at any level of synthesis design. Thus, a rapidly expanding tree of synthetic pathways is generated. It is necessary—as in chess—to select particularly promising precursors with a view to finding the next precursors. Within the framework of programs for retrosynthetic analysis, this selection is based on heuristic strategies and selection rules.

The empirical retrosynthesis programs reached a very high level of perfection about 10 years ago. The most advanced example is CASP,[40] a modification and extension of SECS,[31] which was developed by large German and Swiss chemical companies at great expense. It is hardly conceivable that, apart from details, synthesis design programs based on reaction libraries will significantly surpass the present state of the art.

CASP was not sufficiently accepted by potential users, probably because its extremely large reaction library needs a powerful computer. It therefore cannot be directly accessed by bench chemists, but requires a computer specialist as a middleman. It also seems that chemists prefer to use stored information directly instead of having it manipulated by an empirical synthesis design program.

2.1.1. Which Are the Strategic Bonds in Ring Systems?

Many interesting target molecules contain complex polycyclic systems for which suitable strategies need to be planned

first.[41] Corey et al.[42,43] developed heuristic strategies for the synthesis of carbocyclic systems, which were particularly important computer-assisted retrosynthetic analysis. Their rules refer to "strategic" bonds that are preferentially broken and made, and can be summarized as follows (see Section 4.3.2):

1. A bond is strategic if it belongs to a four-, five-, six-, or seven-membered primary ring. A ring is primary if it does not contain two or more smaller rings.
2. A bond is strategic if it is directly connected to another ring (exo to another ring), unless this ring has only three members.
3. A strategic bond should belong to the ring that contains the highest number of bridged positions (bridgehead atoms).
4. If a ring of seven or more members is formed when a bond is broken, this bond is not strategic.
5. Bonds of an aromatic system are not strategic.
6. If a bridge contains a chiral center, none of its bonds are strategic, unless directly connected to the chiral center.

Bonds between carbon and heteroatoms are treated differently. Only rules 4, 5, and 6 apply, and rule 2 if a three-membered ring is involved.

2.1.2. *Difficulties in Identifying Strategic Bonds*

If the rules for strategic bonds are applied to bridged systems with four or more rings (according to Frèrejacques counting[44]) the results are sometimes less than satisfactory, especially when heteroatoms are present. This is because no hierarchy was defined for these rules, and they were conceived without sufficient attention to heteroatoms. As a consequence, in many cases several bonds are recognized as "strategic", with equal priority. An example is ajmaline (**4**),[45] for which six strategic bonds (bonds 9, 10, 15, 16, 23, and 24) are found according to the rules. Breaking bonds 9

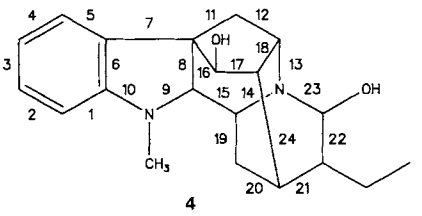

4

and 10 does not simplify the molecular structure, while breaking only one bond does not lead to the formation of an accessible precursor, so other strategic bonds have to be determined. However, this does not necessarily lead to a simplification of the problem, because a burgeoning number of bonds qualify as strategic when the complexity of the ring system decreases. This leads to ever more precursors that have to be processed. Thus, breaking bond 16 of **4** produces seven new strategic bonds.

As mentioned above, the dissection of a bond does not necessarily lead to a "simplified" molecule. Corey's rules also lack a criterion for terminating ring fragmentations. Termination of the procedure after dissection of all bridges between rings would be advantageous; thus, nonbridging bonds such as 9 and 10 in **4** would not be considered.

Heuristic rules are not equally valid in all areas of chemistry, and usually their domains of validity cannot be clearly defined. The automated use of heuristic rules is therefore rather arbitrary and may lead to errors.[21]

Moderate amounts of data can be examined interactively by the user. This is widely applicable, and in computer-assisted synthesis design the interactive selection of synthetic routes by a knowledgeable chemist will yield better results than any automated, heuristic selection procedure. In automated retrosynthetic analysis, synthetic routes with favorable final steps will invariably be preferred over those with less favorable final steps.[46]

2.2. Semiformal Synthesis Design and Prediction of Reactions

The most severe limitations in "creativity" of the present semiformal synthesis design programs are their automated heuristic selection procedures; they are neither transparent nor well-founded.[21] Therefore, the full set of conceivable solutions can not be taken into account.

In principle, semiformal synthesis design programs can carry out all kinds of retrosynthetic analyses. However, they do not have selection procedures that can scan very large sets of solutions. Accordingly, the semiformal approach is limited to relatively small synthetic problems that fall within the domain of validity of the applicable rules and the underlying schematic procedures of the programs. Without a suitable formalism no interactive ordering and classification of the conceivable solutions is possible. For semiformal synthesis design programs, the selection procedures for precursors and retroreactions can still be substantially improved, but no major progress in generating the synthetic pathways seems possible.

In contrast to the empirical synthesis design programs, the semiformal and in particular the formal synthesis design programs have considerable innovative abilities. The semiformal programs cannot intentionally be used to "invent" new reactions (in contrast to the formal programs, e.g. IGOR; see Section 4.4.3), but can invent new types of molecules and chemical reactions when they are needed as a part of a synthetic route that is generated.

To our knowledge, no new compounds or reactions that have been predicted by a semiformal synthesis design program have been subsequently verified by experiment.

The program CAMEO of Jorgensen et al.[47] was developed for the prediction of reaction products, but it can also be used for the design of syntheses. CAMEO is based on the idea that most organic reactions can be represented by a combination of a few mechanistic elementary reactions (see also ref. [48]). The required chemical information is incorporated into individual program modules. Since CAMEO generates chemical reactions from their mechanistic steps, it is more capable of innovation than the retrosynthesis programs based on reaction libraries.[49]

Hendrickson[50] introduced the so-called half-reactions that can be combined to full chemical reactions according to valency considerations, without employing reaction mechanisms. Moreau[51] developed the semiformal synthesis design program MASSO on this principle. Shortly afterwards, Hen-

drickson et al.[52] completed SYNGEN, a similar program that is able to generate convergent syntheses from, at most, four subunits of the target molecule.

Modification and extension of the feasibility study CICLOPS[53] led to the first versions of the synthesis design program EROS,[54] which are of the formal type. Later versions of EROS[55] are essentially semiformal.

The selection processes of EROS for synthetic routes are heuristic in nature. They are based on assumptions on the lability of bonds and on physical data, which restricts the scope of reactions by defining, certain bonds as "breakable". In the course of multistep syntheses, often more than ten bonds are broken or made. Under the assumption that one to three bonds are broken or made per reaction, there are more than 7×10^6 synthetic routes that differ in the sequence of their operations, and that are by no means always equivalent (they would only be equivalent if all operations were independent of each other).

The semiformal synthesis design program TOSCA[56] is most remarkable because it is based on Evans' concept of consonant and dissonant molecules. In a lecture at the University of California at Los Angeles (UCLA) on 6th May 1971, D. A. Evans demonstrated the importance of consonant and dissonant structural features of molecules. Evans documented this concept in a paper with the title "Consonant and Dissonant Relationships—An Organizational Model for Organic Syntheses".[57] Although this paper was never published, its contents became well known in the chemical community, because in 1972 Evans distributed many copies among interested colleagues.

Evans' concept is based on Lapworth's polarity patterns of organic molecules that contain heteroatoms.[58] Evans termed these charge affinity patterns. Molecules like **5** and **6** are called consonant. They have alternating sites of positive and negative charge affinity, which can react as a nucleophile or an electrophile respectively. Molecules like **7** and **8** to

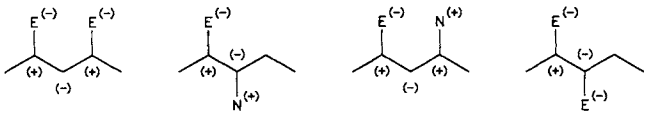

5 **6** **7** **8**

which no such patterns can be assigned are called dissonant. The syntheses of **16** from **9** and **10**, **11**, **12**, and **13**, and **14** and **15** are examples of consonant syntheses.

Evans showed that the conversion of consonant molecules into dissonant molecules and vice versa by ionic reactions requires "inversion operations", which correspond to Umpolung as defined by Seebach.[59] Recognition of consonant and dissonant structural features in the starting material and products of a synthesis is very important for the design of syntheses because the need for inversion operations must be taken into account. We use the Evans–Lapworth schemes in our bilateral synthesis design program RAIN (Reaction And Intermediate Networks).[60–63] With his consonance/dissonance concept Evans has made a far-reaching contribution to computer-assisted synthesis design.

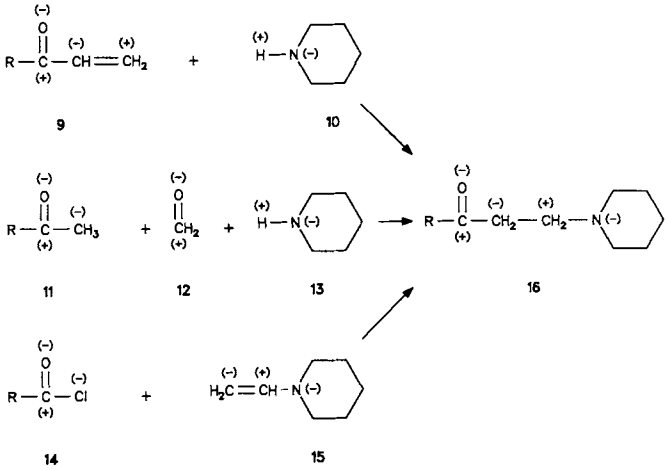

9 **10** **11** **12** **13** **14** **15** **16**

2.3. Synthesis Design with Formal Foundations

2.3.1. What Does "Formal" Mean?

The disadvantages of programs for empirical, semiformal synthesis design can only be avoided by a comprehensive mathematical theory of chemistry that can be used to generate and to select by formal means all molecular systems and chemical reactions that must be accounted for in the selection of a given chemical problem.[21]

Different disciplines use the term formal differently. D. Hilbert and Bernays[64] called mathematics "the science of the formal systems". In informatics formal descriptions require a language (syntax), which may be mathematics, and a mathematically expressed meaning (semantics) together with definitions of rules for transformations and proofs. The validity and domain of a formal algorithm must be proven like a theorem. In chemistry, the term formal is not defined precisely, and is used quite randomly for all kinds of generalizations and classifications, as well as for more or less abstract representations and algorithms. As an empirical science, chemistry is not subject to any rigorously formal approaches in the sense understood in mathematics and informatics. However, our group attempts to put computer-assistance in chemistry onto a formal basis, as far as this is possible. Whenever this is not feasible, we avoid the use of heuristic rules with unpredictable consequences, leaving the required decisions to interactive user participation. The formal description of chemistry requires an adequate, detailed translation of chemistry, including its dynamic aspect, into the language of mathematics, and also a transparent translation of mathematical representations of chemical objects and facts back into the language of chemistry. This is accomplished through a mathematical model of the logical structure of chemistry that represents the molecular systems as well as the chemical changes that they may undergo (see Section 3).

Such a mathematical model can be implemented in computer programs whose applications are not restricted to a single type of problems and that can generate and select, through a formal algorithm, solutions of chemical problems without files of stored, detailed chemical information.[21] Such computer programs are well suited to explore new chemical terri-

tory, because they can propose molecules and chemical reactions that are without precedent, in particular when in dialogue with a creative, knowledgeable, and experienced chemist.

With suitable computer programs all of the combinatorially possible solutions of chemical problems, including those without precedent, can be taken into account. This is, however, of little use if the generated data cannot be ordered and the desired information cannot be extracted. To some extent, this is possible by formal means, but the interactive participation of the user is still required. His intuition and expertise are not only needed to formulate the problem, but also to select the best solutions.

The widespread opinion that a computer does not produce anything that has not been previously provided as data sounds plausible. It is, however, only strictly true for data banks and expert systems that rely solely on stored data.

2.3.2. *Mathematization of Chemistry*

Quantum chemistry has contributed a great deal to the mathematization of chemistry via physics. Quantum chemistry, a branch of molecular theoretical physics, is indispensable for understanding chemistry and for computing the numerical, measurable properties of well-defined molecular systems. The goal of mathematical chemistry is the mathematization of chemistry without the intermediacy of physics and the direct solution of chemical problems by qualitative mathematical methods. The traditional approaches for treating chemical problems by qualitative formulations of discrete mathematics are confined to a static perspective. Such mathematical chemistry does not reach beyond a group theoretical visualization and interpretation of the chemical constitution of molecules and of families of isomers[65-68] and the graph theoretical classification and enumeration of isomers and products of isomerizations.[69-77]

Neither quantum chemistry, which is often called theoretical chemistry, nor traditional mathematical chemistry are suitable as a theoretical basis for the solution of chemical problems with a strong combinatorial aspect, such as the search for molecules or chemical reactions that meet given chemical requirements. The computer-assisted solution of chemical problems by formal means requires global mathematical modeling of chemistry beyond the treatment of individual chemical objects. The model must represent the relations between the objects and the logical structure of chemistry as a whole. Constitutional chemistry and stereochemistry belong together, and yet they are so different that they require distinct mathematical perspectives and approaches. A global mathematical model of chemistry must therefore consist of two parts, one that represents constitutional chemistry and one that describes stereochemistry.

The theory of the be- and r-matrices[78] is an algebraic model of the logical structure of constitutional chemistry (see Section 3.2). It is also cited[79-81] as the "Dugundji–Ugi Model" or "Dungundji–Ugi Theory", abbreviated to the DU model. Besides the algebraic DU model, a graph theoretical model that was published later by Kvasnička et al.[80,81] can serve as a mathematical foundation of formal synthesis-design programs. The logical structure of stereochemistry can be represented by the theory of the Chemical Identity Group (CIG theory),[82] which is based on the notion of permutational isomerism.[76]

In contrast to traditional mathematical chemistry, the above models not only refer to, but even emphasize the dynamic aspect of chemistry. Within the framework of the DU model, chemical reactions are described by transformations of be-matrices. The be-matrices represent constitutional formulas which, in turn, correspond to graphs of the chemical constitution of molecules. In the CIG theory, the set-valued maps represent dynamic processes by which the stereochemical features of molecules are changed. These mathematical devices for the direct modeling of chemical processes are the theoretical foundation of the computer-assisted, deductive solution of a wide variety of chemical problems without reference to detailed empirical chemical information.

In the DU model and the CIG theory, the direct translation of chemistry into mathematics and vice versa is more important than the actual mathematical basis. Mathematics thus becomes part of the language of chemistry bringing its semantics and syntax, just as chemical formulas have been for decades.

2.4. Programs for Formal Synthesis Design

Through the DU model the objects of chemistry (molecules, ensembles of molecules (EM), chemical reactions) can be represented by objects of mathematics (matrices). Thus, chemical problems can be translated into mathematical problems, whose solutions are the solutions of the chemical problems.

This model started the development of formal algorithms, reaction generators, and computer programs for the deductive solution of chemical problems by mathematical means. The formal algorithms can not only generate solutions for many types of chemical problems but are also useful in the classification and selection of these solutions.[21]

The development of programs for formal synthesis design began with the feasibility study CICLOPS.[53] The purpose of CICLOPS was to ascertain whether chemical problems could, in principle, be solved with the DU model. In this respect the CICLOPS study was successful. However, it was also found that CICLOPS was bound to fail under the conditions of practical synthesis design of problems incorporating the combinatorial aspect. Gasteiger and Jochum[54] developed the first versions of EROS from CICLOPS, by reducing the reaction generator (see below) of CICLOPS from approximately 100 potential to the three most important r-classes (see Section 3.2.2) of chemical reactions and by adding a selection procedure for chemical reactions. In analogy to the selection procedure of Stevens and Brownscombe,[83] the choice is made on the basis of reaction enthalpy estimations.

Reaction matrices can be assembled from basic elements that correspond to the elementary reactions of mechanisms.[78] These can be used to create reaction generators that build chemical reactions from their elementary steps. The synthesis design program ASSOR[48] contains a reaction generator of this type and is therefore able to account for the mechanistic aspects of chemical reactions.

The DU model can be used in many ways as the theoretical foundation of monolateral synthesis design programs that

generate synthetic routes either from the target molecule in a retrosynthetic mode, or from the starting material in a synthetic mode. However, the possibilities that the DU model provides for the bilateral design of syntheses[84,85] seem to be more promising. The obvious combinatorial advantages of bilateral synthesis design have also been recognized by other authors. Johnson et al.[86] developed a bilateral synthesis-design program on the basis of LHASA, and recently Hendrickson and Parks[87] combined SYNGEN with the synthesis program FORWARD into a bilateral synthesis-design program.

In bilateral synthesis design, the synthetic routes are spread from both ends, the starting materials and target. At the moment, we are developing a system of computer programs for bilateral synthesis design that operates in three stages.[85,88,89] The partitioning of the problems by such a system provides substantial combinatorial advantages. First, a set of suitable starting materials is selected for the target molecule from a list of available compounds by the substructure correlation program CORREL-S (see Section 4.3.2). Then the co-products (ancillary products formed besides the target molecule) are determined (program STOECH, see Section 4.3.3). The result is a target EM that is isomeric (in terms of Section 3.1) to the EM of starting materials. In a third step, the computer program RAIN (see Section 4.4) generates a network of synthetic routes that connect both ends of the synthesis.

Other formal synthesis-design programs are FLAMINGOES,[90] PEGAS,[91] and MAPOS.[92] Hippe[93] tried to combine the advantages of the formal and empirical approaches in their programs SCANSYNTH, SCANMAT, and SCANPHARM. So did Johnson et al.[94] in their system SYNLMA.

3. The Logical Structure of Chemistry

3.1. The Hierarchy of Isomerisms

Chemistry is an empirical science. Nevertheless, its objects have a consistent logical structure, because all molecules are constructed according to uniform principles.[95] This logical structure is a system of equivalence relations. The most important relations are the various types of isomerism and the interconvertibility of isomeric molecules and ensembles of molecules. The logical structure is determined by the valence properties of the chemical elements and a few general principles. When chemistry is compared to a language, the chemical facts, objects, phenomena, and events correspond to the vocabulary, while the logical structure of chemistry corresponds to the grammar.

The backbone of the logical structure is the classification of molecules according to the various types of isomerism.[96] Isomers contain the same number and type of atoms and accordingly have the same empirical formula. The term "isomer" can be applied to molecules as well as to substances. From the existence of distinct isomers A. von Humboldt inferred that molecules must have an intrinsic structure. Otherwise substances with the same element composition would not be distinguishable.[97]

Those molecular systems that consist of the same collection of atoms—or more exactly, the same collection of atomic cores (i.e., nucleus plus electrons of the inner shells) and valence electrons—are isomeric EMs. The EMs may consist of one or more molecules. This extension of the notion of isomerism from molecules to EMs is one of the conceptual foundations of a mathematical representation of the logical structure of chemistry.[78]

The chemical constitution of molecules corresponds to the atomic neighborhood relations defined by covalent bonds. Isomers that differ by their chemical constitutions are called constitutional isomers.

By their classical definition stereoisomers are molecules with the same chemical constitution but different relative spatial arrangements of their constitutient atoms.[82,98] This definition is of limited usefulness, since many stereoisomers are nonrigid molecules that can not be adequately represented by rigid geometric models. A generally valid definition of stereoisomers that also accounts for flexible molecules is possible on the basis of the concept of chemical identity described in the next paragraph. This equivalence relation can also account for nonrigid chiral molecules.[73,98]

Molecules are chemically identical if they interconvert spontaneously under the given observation conditions and belong to the same uniform chemical compound. Two films showing the time-dependent changes of geometry of a molecule and of a chemically identical molecule will not be the same. However, the sets of molecular frames that are shown in the two films are identical. The same set will be obtained if a snapshot of a sufficiently large number of molecules of the corresponding compound is taken.

If molecules with the same chemical constitution are not chemically identical they are stereoisomers.[73,82,98] Stereoisomerism as defined thus is a principle of classification in its own right and is subordinate to constitutional isomerism.

3.2. An Algebraic Model of the Logical Structure of Constitutional Chemistry

The logical structure of constitutional chemistry follows from the following statements that were used by J. Dugundji and I. Ugi[78] as the axiomatic foundations of the theory of the be- (*b*ond and *e*lectron) and r-matrices (*r*eaction) published in 1973:

> Molecules consist of atomic cores and valence electrons, held together by covalent bonds. A covalent bond corresponds to a pair of valence electrons that simultaneously belongs to two adjacent atoms. A chemical reaction is the conversion of an EM into an isomeric EM by redistribution of valence electrons. During a chemical reaction the atomic cores and the total number of valence electrons remain the same.

The logical structure of constitutional chemistry can be illustrated by the chemistry of a fixed collection $A = \{A_1, \ldots A_n\}$ of atoms. Since any collection of atoms can serve as A, a model of the logical structure of the chemistry of A is valid for all chemistry.

The chemistry of A is given by the family of isomeric EM(A). EM(A) is an EM which contains every atom of A precisely once.[93]

Within the framework of the DU model, an EM of n atoms is described by its symmetric $n \times n$ be-matrix. The ith row

(and column) of a be-matrix is assigned to the atom A_i ($1 \leq i \leq n$). The entry b_{ij} ($= b_{ji}$, $i \neq j$) of the ith row and the jth column of a be-matrix $\boldsymbol{B}$ is the formal bond order of the covalent bond between the atoms A_i and A_j. The diagonal entry b_{ii} is the number of free valence electrons at the atom A_i. The entries $b_{12} = b_{21} = 2$ of the be-matrix of EM(**17**, **18**) signify that the C atom no. 1 and O atom no. 2 are connected by a covalent double bond, while $b_{22} = 4$ represents four free valence electrons at the O atom no. 2 (Scheme 1).

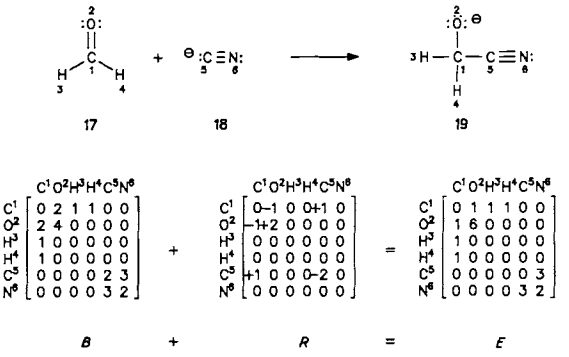

Scheme 1. A reaction and its matrix description.

The rows and columns of the be-matrices represent the number and position of the electrons (valence schemes) of the relevant atoms. It follows that all rows (columns) of be-matrices of stable EMs must correspond to allowable valence schemes of the represented chemical elements. They are the valence boundary conditions of the be-matrices.

The adjacency and connectivity matrices[99] that are used in chemical documentation differ from the be-matrices in their diagonal entries. These matrices are merely tables of bonds that represent chemical constitution. In contrast, the be-matrices do not only represent single molecules but also multimolecular EMs, and are genuine mathematical objects. The algebra of the be- and r-matrices forms a free additive abelian group.[78]

The redistribution of valence electrons by which the starting materials $EM_{\boldsymbol{B}}$ of chemical reactions are converted into their products $EM_{\boldsymbol{E}}$ is customarily indicated by "electron-pushing arrows", which are represented by r-matrices $\boldsymbol{R}$. The chemical reaction $EM_{\boldsymbol{B}} \rightarrow EM_{\boldsymbol{E}}$ corresponds to the additive transformation of the be-matrices $\boldsymbol{B}$ of the educts by the reaction matrix $\boldsymbol{R}$ into the be-matrix $\boldsymbol{E}$ of the products. $\boldsymbol{B} + \boldsymbol{R} = \boldsymbol{E}$ is the fundamental equation of the DU model.

The addition of matrices proceeds entry by entry, that is, $b_{ij} + r_{ij} = e_{ij}$. Since there are no formal negative bond orders or negative numbers of valence electrons, the negative entries of $\boldsymbol{R}$ must be matched by positive entries of $\boldsymbol{B}$ of at least equal values.

3.2.1. Chemical Distance

When the n^2 entries of the be-matrices are interpreted as coordinates of points in an n^2-dimensional euclidean space, the algebraic model of the logical structure of chemistry can be visualized as a geometric model.[78, 100] The EMs correspond to be-points and chemical reactions are described by connecting r-vectors. The L_1 length $d(\boldsymbol{B}, \boldsymbol{E})$ of an r-vector is the sum of the absolute values of the differences of the coordinates of the be-points $P(\boldsymbol{B})$ and $P(\boldsymbol{E})$. The L_1 distance ("taxi driver distance")[101] between the two be-points $P(\boldsymbol{B})$ and $P(\boldsymbol{E})$ is called the chemical distance (CD) between $EM_{\boldsymbol{B}}$ and $EM_{\boldsymbol{E}}$. It is twice the number of valence electrons that are redistributed when $EM_{\boldsymbol{B}}$ and $EM_{\boldsymbol{E}}$ are interconverted (see Table 1).[100]

$$d(\boldsymbol{B},\boldsymbol{E}) = \sum_{ij} |b_{ij} - e_{ij}| = \sum_{ij} |r_{ij}| \qquad (1)$$

When the lattice of points representing a family of all isomeric EM with paired valence electrons is viewed from any of its EMs, then the be-points are surfaces of concentric L_1 shells whose radii differ by four units. The radius of the largest sphere is the total number of valence electrons of the underlying collection of atoms. This aesthetic geometric picture of the logical structure of chemistry is a "map" of the

Table 1. Corresponding representations of the logical structure of constitutional chemistry.

Chemical Representation	Algebraic Representation	Geometric Representation
constitutional formula of $EM_{\boldsymbol{B}}(A)$ ($A = \{A_1, \ldots A_n\}$)	symmetric $n \times n$ be-matrix $\boldsymbol{B} = \langle b_{ij} \rangle$ of $EM_{\boldsymbol{B}}(A)$.	be-point $P(\mathbf{B})$ with the coordinates $(b_{11}, \ldots b_{1n}, \ldots b_{n1}, \ldots b_{nn})$ in an n^2-dimensional euclidian space.
up to $n!$ permutations of atomic indices in $EM_{\boldsymbol{B}}(A)$	up to $n!$ equivalent be-matrices $\boldsymbol{B}'$ can be obtained by row (or column) permutations of $\boldsymbol{B}$ according to $\boldsymbol{B}' = \boldsymbol{P} \cdot \boldsymbol{B} \cdot \boldsymbol{P}^{-1}$. $\boldsymbol{P}$ is a $n \times n$ permutation matrix.	b-cluster of the up to $n!$ equivalent be-points $P(\boldsymbol{B}')$ of $EM_{\boldsymbol{B}}(A)$.
chemical reaction $EM_{\boldsymbol{B}}(A) \rightarrow EM_{\boldsymbol{E}}(A)$ by redistribution of valence electrons	the additive transformation of $\boldsymbol{B}$ in $\boldsymbol{E}$. The entries r_{ij} of $\boldsymbol{R}$ represent the redistribution of valence electrons.	r-vectors in the n^2-dimensional space which connects the be-points, $P(\boldsymbol{B})$ and $P(\boldsymbol{E})$, of the participating EMs, $EM_{\boldsymbol{B}}(A)$ and $EM_{\boldsymbol{E}}(A)$.
the number of redistributed valence electrons in a reaction $EM\boldsymbol{B}(A) \rightarrow EM_{\boldsymbol{E}}(A)$ (corresponds to the CD)	$d(\boldsymbol{B}, \boldsymbol{E}) = \Sigma\lvert r_{ij}\rvert$; that is, the sum of the absolute values of the entries of the r-matrix $\boldsymbol{R} = \boldsymbol{E} - \boldsymbol{B}$.	L_1 distance ("taxi driver distance") between the be-points $P(\boldsymbol{B})$ and $P(\boldsymbol{E})$.
the chemistry of A that is given by the family of all EM(A) and the mutual interconversions of EM(A)	the groups of be-matrices of EM(A) with their transformations under given boundary conditions.	sets of points which correspond to the elements of the family of all EM(A) and the connecting r-vectors.
chemical reactions preferentially proceed by a minimal redistribution of valence electrons.	the atom-onto-atom correlations $EM_{\boldsymbol{B}}(A)$ and $EM_{\boldsymbol{E}}(A)$ with minimal $d(\boldsymbol{B}, \boldsymbol{E})$ are preferred.	preferred r-vectors for $EM_{\boldsymbol{B}}(A) \rightarrow EM_{\boldsymbol{E}}(A)$ lead from one point of the $\boldsymbol{B}$-cluster to the "nearest" point of the $\boldsymbol{E}$-cluster.

energy minima of the potential energy surface of the given collection of atoms.[102]

The solutions of the basic equation $\boldsymbol{B} + \boldsymbol{R} = \boldsymbol{E}$ of the DU model correspond to the solutions of a great variety of chemical problems. Accordingly, the DU model can serve as the universal theoretical foundation of computer programs for the deductive solution of constitution-related chemical problems. Furthermore, it is suitable as a basis of strictly formal, transparent procedures for the selection of chemically meaningful solutions from very large sets of conceivable solutions.[21] Here the Principle of Minimal Chemical Distance[78, 103-107] plays an important role. This principle is a quantitative version of the classical qualitative principle of minimum structure change:[108] The interconversion of isomeric EM by chemical reactions preferentially proceeds by redistribution of the minimum number of valence electrons.

The minimal CD corresponds to one or more atom-to-atom maps of the EM, because the CD between isomeric EMs depends on the correlation of their atoms. In a broad sense this is also true for sequences of reactions, that is, the CD of reaction sequences is rarely more than four units above the minimum of CD.

The principle of minimal CD can not only select the "shortest" pathways of chemical reactions but can also help to determine reactive centers, that is, those atoms whose covalent bonds and free valence electrons are immediately affected by the reaction. The complete set of reactive centers is called the core of the reaction. The bonds that are broken or made during a reaction are determined by the atom-to-atom maps of the interconnected EMs.

Various distance functions and measures of similarity have been published for molecular systems. In essence, they all rely on the fact that chemical reactions correspond to vectors (see Table 1) and have metric properties.[78] Other examples, besides CD,[100] are reaction distance that was defined differently by Kvasnička et al.[80, 81, 109] and by Hendrickson et al.,[87] synthetic proximity of Johnson et al.,[110] and adjacency distance, the sum of the absolute values of the t-matrices (differences of adjacency matrices) of Fontain.[111]

3.2.2. The Hierarchic Classification of Chemical Reactions

A hierarchic classification of chemical reactions by similarity classes[100] follows from the principle of minimal CD (see Scheme 2).

The position of a chemical reaction, for example **25** → **26**, in this hierarchic classification system is determined by stepwise neglect of its characteristic features. First, the reaction is reduced to its core of reactive centers by omitting all substructures that do not directly participate in the reaction. The result is the ra-subclass of the reaction, whose members have the same reaction core but different invariant molecular substructures.

The next step of abstraction is to neglect the differences between the chemical elements of the atoms of the core. This leads to the rb-subclasses (basic reactions). Their members are characterized by the same arrangement of covalent bonds between the atoms of the core (see **27**) and can be represented by the so-called intact be-matrix (Scheme 3).[79]

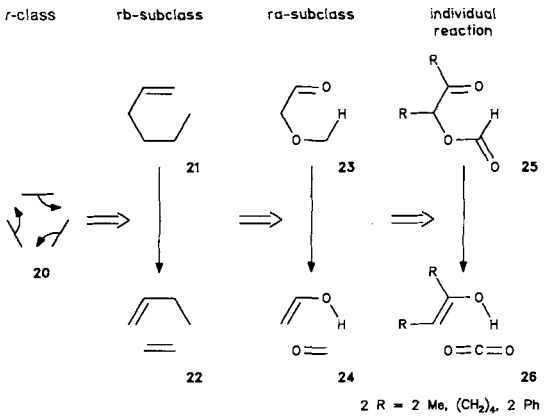

Scheme 2. The procedure for the hierarchic classification of chemical reactions. The individual reaction **25** → **26** is reduced to the electron redistribution scheme **20**.

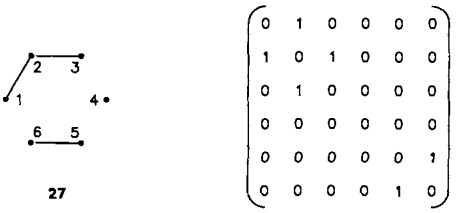

Scheme 3. Intact be-matrix of the rb-subclass **21** → **22**.

Reactions with the same electron redistribution scheme and therefore the same irreducible r-matrix[100, 112, 113] belong to the same r-class. The r-matrix is converted into its irreducible r-matrix by removing all rows and columns that only contain zeros. The rows (and columns) of the irreducible r-matrix belong to the reactive centers of the reactants. The hierarchic classification of chemical reactions ends with the CD-classes.[79, 100, 112-114] Reactions belong to the same CD-class if the same number of valence electrons is redistributed during the course of the reaction and thus the same CD is covered.

Scheme 2[100, 114] illustrates the hierarchic classification of chemical reactions for the example of the extrusion reaction **21** → **22**. The rb-subclass is represented by the bonding scheme **27** and the corresponding 6 × 6 intact be-matrix of Scheme 3.

The classification described above does not only open new ways of documenting chemical reactions,[79, 100, 112, 113] but also plays an important role in the computer program IGOR (*I*ntermediate *G*eneration of *O*rganic *R*eactions).[114-116] It is used to select computer-generated chemical reactions and to assess their degree of novelty.[88, 117] The degree of novelty is determined by assigning classes and subclasses of the reaction in question and ascertaining the level of hierarchy above which no published reactions can be found. The higher this level is, the higher the degree of novelty of the reaction.[88, 113, 114, 117] The reaction **25** → **26** of Scheme 2 was discovered with computer-assistance. It belongs to the extrusion reactions **21** → **22**[114] (see Section 4.1.4.3) that are characterized by the bond system **27**, and that is contained in r-class **20** with 12 rb-subclasses.

No representatives of ra-class **23** → **24** are known. Accordingly the reaction **25** → **26**[114, 118] is novel up to the level of the ra-subclasses.

Almost twenty years ago, Brownscombe and Stevens[83] reported a computer program that was capable of generating any elements of the rb-subclass of extrusion reactions by permuting the chemical elements of the core of the reaction. Reaction **25** → **26** could have already been found with that computer program.

4. The Munich project

The applications of the DU model are not restricted to the design of syntheses. After the CICLOPS study[53] was terminated in 1974 (see Section 2.4) a comprehensive plan, the Munich project, was devised. Its aim was to extend and improve the DU model and to exploit it in as many ways as possible as a formal basis for the computer-assisted solution of chemical problems.[119] During its implementation, the Munich project was changed so much that only its basic ideas are left. However, it initiated the development of computer programs for the solution of chemical problems on a broad front. The Munich project, whose goals have nearly been reached, consists of the following subprojects:

a) Improvement and extension of the DU model, in particular for EMs with multicenter bond systems of delocalized electrons.

b) Development of a computer-oriented mathematical theory of stereochemistry that is able to account for the stereochemical aspect of chemical reactions.

c) Development of a software infrastructure for programs according to d).

d) Development of computer programs for the deductive solution of chemical problems. These programs should not only use the DU model for the generation of solutions of problems, but also for screening and selecting these solutions.

e) Testing and use of programs according to d) and improvement of these programs on the basis of gathered experience.

f) Experimental realization and verification of the results of e).

Progress on individual steps of the Munich project has been described together, as far as possible, with details of the computer programs, which often included the source codes, in order to ensure reproducibility. Here we give a survey of the subprojects of the Munich project, in the order a)–f), covering its historical development and current status.

4.1. Extension of the DU model

For a long time neither we nor others succeeded in extending the DU model as planned in a). Recently, however, a formalism was found through which EMs with multicenter bonds and delocalized valence electron systems (DE systems)[95] can be represented. The xbe-matrix (extended be-matrix) of an EM corresponds to its be-matrix which is extended by additional rows and columns. The be-matrix with n rows and columns refers to the localized covalent bonds whose formal bond orders and free valence electrons can be assigned to the individual atoms. The additional rows and columns with the indices $n + k$ belong to DE systems, for example, multicenter bond systems or delocalized π-electron systems. The off-diagonal entries $b_{i,\,n+k} = b_{n+k,\,i} = 1$ of the kth additional rows and columns indicate that the atom A_i participates in the $(k - n)$th DE system. The diagonal entries $b_{n+k,\,n+k}$ are the numbers of valence electrons that belong to the $(k - n)$th DE system. The xbe-matrix of π-allyl nickel bromide (**28**)[120] may serve as an example in Scheme 4; for the sake of simplicity, the CH bonds and the corresponding entries are omitted.

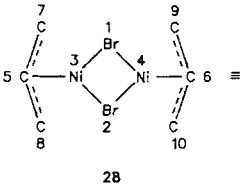

28

≡

4	0	1	1	0	0	0	0	0	0	0	0
0	4	1	1	0	0	0	0	0	0	0	0
1	1	8	0	0	0	0	0	0	0	1	0
1	1	0	8	0	0	0	0	0	0	0	1
0	0	0	0	0	0	1	1	0	0	1	0
0	0	0	0	0	0	0	0	0	0	0	1
0	0	0	0	1	0	0	0	1	1	1	0
0	0	0	0	1	0	0	0	0	0	1	0
0	0	0	0	0	0	1	0	0	0	0	1
0	0	0	0	0	0	1	0	0	0	0	1
0	0	1	0	1	0	1	1	0	0	4	0
0	0	0	1	0	1	0	0	1	1	0	4

Scheme 4. Structural formula of **28** showing numbering and the xbe-matrix representing it. The row and column of the DE systems are indicated by dashed lines.

In analogy to the original DU model, chemical reactions are represented by addition of xr-matrices[95] to the xbe-matrices. The 18 theorems of the DU model are equally valid for the algebra of the xbe- and the xr-matrices, which is named the model of the chemistry of *d*elocalized *e*lectron (DE) systems.

In order to adapt this system to computers, a new data structure was introduced. At the moment, a reaction generator for reactions in which DE systems may also participate is being developed.[121] Here the particular properties of the DE systems must be accounted for by formulation of suitable boundary conditions.

4.2. Computer-Oriented Formalization of Stereochemistry—the Theory of the Chemical Identity Group and Accumulations

Stereochemistry is the science of the spatial structure of molecules and its observable consequences. The differences in the formation, reactions, and properties of stereoisomers are the central issues of stereochemistry. Stereoselective syntheses belong to the most attractive current topics of organic chemistry.[1] Therefore, the stereochemical aspect of computer-assisted chemistry is of particular interest. The large numbers of combinatorial possibilities create huge amounts of data in solving stereochemical problems, which can only be handled if the mathematical structures behind the problems are fully recognized and exploited. It is advantageous to introduce some suitable new concepts and approaches for this purpose.

4.2.1. *Traditional Approaches*

Corey et al.[122] supplemented the transforms of the individual reactions with detailed stereochemical information. This approach is very cumbersome; just the treatment of the stereochemistry of six-membered rings requires a large program of its own. Wipke and Dyott[123] proposed to solve stereochemical problems by assuming sufficiently rigid reactants that are determined by a procedure based on steric bulk. Hanessian et al.[124] assign chiral starting materials to chiral target molecules through their program CHIRON. In the early stages of the Munich project the stereochemical features of EMs with stereogenic subunits with coordination numbers ≤ 4 were represented by parity vectors.[125]

None of these approaches leads to a generally applicable method for the computer-assisted solution of stereochemical problems. The comprehensive computer-oriented formal treatment of stereochemistry requires a fundamentally different approach.

4.2.2. *A Nongeometric Alternative*

In traditional stereochemistry the facts and phenomena are interpreted and predicted on the basis of rigid geometric models. Thus, stereochemistry is reduced to elementary geometry. Molecular geometries and point group symmetries are drastically overemphasized. Widely applicable computer-assisted methods for the solution of stereochemical problems, however, require a theory that treats the static and dynamic aspects in a uniform way.

Many molecules are not rigid. Since their shapes vary with time, they are in general not adequately represented by geometric models. For instance, at 20 °C the methyl groups in ethane **29** rotate around the C–C bond with a frequency of $10^9\ s^{-1}$.[126, 127] This molecule can not be represented by a rigid geometric model.

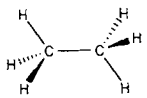

29

The first prerequisite for a comprehensive and uniform theoretical treatment of stereochemistry is that the traditional definition of stereoisomers should be replaced by a definition that is also able to account for flexible stereoisomers. This definition should be based on the notion of chemical identity (see Section 3.1) and should not refer explicitly to any geometry.

Permutation isomerism, as defined in 1970,[76] and the theory of the *c*hemical *i*dentity *g*roup (CIG theory), which was published in 1984,[82] have played an important role in the formalization of stereochemistry. The CIG theory is a group theoretical model of the logical structure of stereochemistry that not only accounts for the energy-related and geometric properties of the molecules, but also includes the valid observation conditions. It avoids explicit reference to rigid geometric models and their point group symmetries. In contrast to the traditional applications of group theory (see Section 2.3.2), the CIG theory does not only cover molecular objects, but also stereochemical relations and processes between molecular systems.

4.2.3. *The Basic Ideas of the CIG Theory*

A molecule can be dissected in the imagination into a molecular skeleton and a set of ligands. The distinct molecules that differ by positioning of the ligands at the skeletal sites, are the permutation isomers. The set of all permutation isomers that can be obtained from a reference isomer is called a family of permutation isomers.

Let m be a snapshot of a molecule. The conceptual separation of m into a molecular skeleton and a set L of ligands yields a reference model. The reference model belongs to an isomer X which serves as the reference isomer. In contrast to a molecule, a model in the present sense has a fixed spatial orientation. The chemical identity of a molecule is independent of its spatial orientation. There are permutations of ligands that convert one model into another that belongs to the same molecule (see Scheme 5). The chemical identity of X is preserved by all permutations of ligands through which models of X are converted into other models of X, for example, permutations that may be interpreted as rotations of the molecule as a whole.

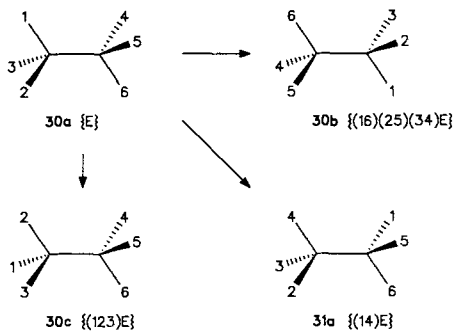

Scheme 5. Ligand permutations of **30a**, the reference model of an arbitrarily substituted ethane molecule.

If all ligands in the set L are distinguishable, the identity-preserving permutations generally form a group $S(E)$. This is the CIG of the reference isomer X that is represented by the model E. $S(E)$ is a subgroup of the symmetric permutation group $Sym(L)$ of L. The distinct permutation isomers of X are represented by the left cosets $\lambda S(E)$ ($\lambda \in Sym(L)$) of $S(E)$ in $Sym(L)$.[*]

For a molecule with n ligands $Sym(L)$ consists of $n!$ permutations. This is the cardinality of the family of permuted models $P(E)$. The maximum number of chemically distinct permutation isomers is $n!/|S(E)|$, because all cosets have the same cardinality $|S(E)|$. The left cosets of the CIG in $Sym(L)$ or any of their elements can serve as nomenclature descriptors for the permutation isomers.[76] The left coset of a CIG corresponds to the permutation isomer of the reference isomer, whose models are obtained from the reference model by ligand permutations from the CIG, followed by a permutation from the considered left coset.

[*] For readers who are less familiar with mathematical concepts and symbols there is an appendix with brief explanations.

Permutations are customarily written as cycles,[128] for example, (123); the vector [123] of numbers is permuted into [231] by mapping $1 \rightarrow 2$; $2 \rightarrow 3$; $3 \rightarrow 1$. The combination (12)(123) of the permutations (12) and (123) corresponds to the action of (12) on the result of (123), that is (12)(123) transforms [123] into [132] and is thus equivalent to (23).

For example, the reference model **30a** of the ethane derivative **30** is converted into the model **30b** by the permutation (16)(25)(34) of the ligands; this corresponds to a rotation by 180° of **30a** around an axis that is perpendicular to the plane of the paper. Note that this rotation of the model **30a** does not superimpose the ethane skeleton onto itself, according to D_{3d} point group symmetry, since the different ligands destroy the symmetry of the skeleton (see Chapter 3 of ref. [82]).

Since the chemical identity of a molecule is independent of its spatial orientation, **30a** and **30b** are chemically identical. The model **30c** also belongs to **30** if the internal rotation around the C–C axis belongs to the spontaneous intramolecular motions, under the given observation conditions. This permutation can be represented by (123).

The CIG (2) contains all ligand permutations that preserve the chemical identity of **30**. The ligand permutations of

$$S(30a) = \{(), (123), (132), (456), (465), (123)(456), (123)(465), (132)(456), (132)(465), (14)(26)(35), (15)(24)(36), (16)(25)(34), (142635), (143526), (152436), (153624), (162534), (163425)\} \quad (2)$$

$S(30a)$ generate further models of $S(30a) \cdot$ **30a** from any model that belongs to $S(30a) \cdot$ **30a**. The ligand permutation (14) converts **30a** into **31a** which represents a permutation isomer of **30**. Likewise the ligand permutation (14) converts any model of **30** into a model of **31**. They can also be obtained by any other permutation of $S(30a)$, followed by any permutation of (14) $\cdot$ $S(30a)$. **30** and **31** are distinct permutation isomers if the ligands 1 and 4 are distinguishable.

In the following sections we will describe set-valued maps (SVM) and accumulations. These operations are very useful for representing permutation isomers with indistinguishable ligands and isomerizations which convert permutation isomers into each other.

4.2.4. Implementation and Applications of the CIG Theory

Within the framework of the CIG theory stereochemical equivalence relations are represented by surjective set-valued maps (SVM) of permutations onto sets of permutations that may be unions of cosets or Wigner subclasses[129] of subgroups of $Sym(L)$. The direct consideration of the dynamic aspect of stereochemistry is the most important contribution of the CIG theory to the mathematical treatment of stereochemistry.

The SVM were introduced into chemistry as a part of the CIG theory. They are a most versatile device for the solution of stereochemical problems that can be formulated as equivalence relations between permutation isomers. Such equivalence relations correspond to equivalence spaces that are generated by SVM.

Let M be a set which is partitioned into equivalence classes in two distinct ways (Fig. 1). The SVM of a class B from the partition $\mathscr{B}$ yields the union of those equivalence classes

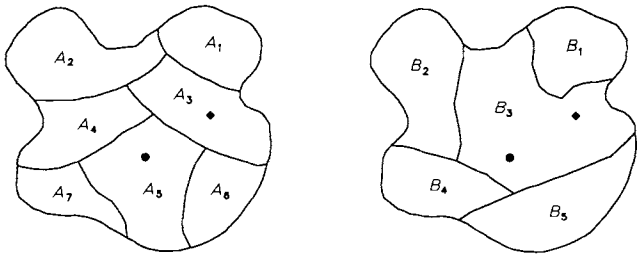

Fig. 1. Two partitions $\mathscr{A}$ and $\mathscr{B}$ of set M.

from partition $\mathscr{A}$ whose intersection with B is non-empty [Eq. (3)].

$$\mathrm{SVM}(\mathscr{A}, B) = \bigcup_{A \cap B \neq \{\}, A \in \mathscr{A}} A \quad (3)$$

For example, ♦ is an element of class A_3 and ● is an element of A_5. These elements also belong to class $B_3 \in \mathscr{B}$. All elements of class A_3 are equivalent to ♦. The elements of class A_5 are equivalent to ●. The elements ♦ and ● are also equivalent since they both belong to class B_3.

Equivalence relations are reflexive, symmetric, and transitive (p. 14 of ref. [128]). The equivalence classes A_3 and A_5 (and any further equivalence classes of $\mathscr{A}$ that intersect B_3) form a single equivalence class. We have the SVM given by (4).

$$(\mathscr{A}, B_3) = A_1 \cup A_2 \cup A_3 \cup A_4 \cup A_5 \cup A_6 \quad (4)$$

In recent years the CIG theory has been modified and extended. It is now more suitable as a foundation for the computer-assisted solution of a great variety of stereochemical problems. In particular, (equivalence) accumulations[130, 131] represent significant progress in practical computer-assisted stereochemistry.

The CIG and its cosets form a space of equivalence classes in $Sym(L)$. Since, by definition, cosets are disjoint, each coset can be interpreted as an equivalence class that represents a permutation isomer. One permutation is sufficient to represent the whole family of permutation isomers. Thus, the amount of data to be processed for stereochemical problems is reduced to a small fraction.

We consider a equivalence space A of molecular models and some independent information I about further equivalences of models, for example, from equivalences of ligands or interconvertibilities of models. According to the additional information I, there exists an equivalence space U which differs from A in that some of the equivalence classes of A merge into a single equivalence class. The information I is an equivalence relation corresponding to group theoretical relations between the individual models. Within the framework of the CIG theory, I can be expressed by a few generating elements that follow directly from the chemical properties of the molecules. An example for such information is the coset space of the CIG $S(30a)$ in $Sym(L)$ mentioned in Section 4.2.3: For each coset $\lambda S(30a)$, $\lambda S(30a) \cdot$ **30a** is an equivalence class of chemically identical models. All pairs of models in the equivalence class are elements of the equivalence relation I, that is, for all models $m, n \in \lambda S(30a) \cdot$ **30a** we have $(m, n) \in I$.

For a given set of models M that is partitioned according to the equivalence space A, and the information I, the accu-

mulation Acc(A, I) is defined according to (5)–(7) (+ represents the transitive closure[132] of a relation):

$$\mathrm{Acc}(A,I) := \{[m]_R \mid m \in M\} \tag{5}$$

$$\text{where} \quad R = (I \cup a \times a \mid a \in A)^+ \tag{6}$$

$$\text{and} \quad [m]_R = \{n \in M \mid (m,n) \in R\} \tag{7}$$

Ligands are considered to be equivalent, if their chemical interpretations are the same and their permutation does not affect the chemical identity of molecules. The permutations of equivalent ligands form the ligand equivalence group Σ. The right cosets of Σ in $Sym(L)$ represent those models that are potentially distinct if all ligands were distinguishable, but are chemically identical because of the equivalence of some of the ligands.

A ligand permutation that converts a reference model into a model of a distinct permutation isomer, followed by a ligand permutation from Σ, corresponds to a ligand permutation that belongs to a right coset of Σ.

Thus, the right coset space of Σ in $Sym(L)$ also contains the following information: the models λE in each equivalence class $\Sigma\mu$ are mutually chemically identical.

If this equivalence class $\Sigma\mu$ intersects with the equivalence classes $\lambda S(E)$ and $\sigma S(E)$ of the coset space of the CIG of E, permutations ρ and τ exist such that $\rho \in \Sigma\mu \cap \lambda S(E)$ and $\tau \in \Sigma\mu \cap \sigma S(E)$. Since $\rho \in \lambda S(E)$, the model ρE is chemically identical to all models $\lambda S(E)E$, and τE is chemically identical to all models $\sigma S(E)E$, because $\tau \in \sigma S(E)$. On the other hand, ρE and τE are chemically identical, because ρ and τ belong to the same right coset $\Sigma\mu$, that is the molecules that are represented by ρE and τE are chemically identical, because models ρE and τE differ only by a permutation of equivalent ligands.

Because as an equivalence relation chemical identity is reflexive, symmetrical, and transitive, all models belonging to $\lambda S(E)E$ are also chemically identical to τE (because ρE is chemically identical to all of those models). The right coset $\Sigma\mu$ contains the information that all models $\Sigma\mu E$ are chemically identical. Thus, the representatives $\lambda S(E)E$ and $\sigma S(E)E$ (and all further equivalence classes $\xi S(E)E$, with $\xi S(E) \cap \Sigma\mu \neq \{\}$) of the permutation isomers that were initially considered to be distinguishable, merge into the class of permuted models described by (8). This class models represents a single permutation isomer. Since such SVM do not take into account the full right coset space of Σ, in some cases the results may be incomplete. A coset $\lambda S(E)$ can exist whose intersection with $\Sigma\mu$ as well as with a further right coset $\Sigma\omega$ is non-empty. Then the SVM of $\Sigma\mu E$ does not yield the complete set of chemically identical models: The expression (9) states that the $\lambda S(E)$ models are chemically identical with all models from (10) and also with all models from (11).

$$\bigcup_{\xi S(E) \cap \Sigma\mu \neq \{\}} \xi S(E) \cdot E = \mathrm{SVM}(\{\lambda S(E) \cdot E \mid \lambda \in Sym(L)\}, \Sigma\mu \cdot E) \tag{8}$$

$$\lambda S(E) \cap \Sigma\mu \neq \{\} \wedge \lambda S(E) \cap \Sigma\omega \neq \{\} \tag{9}$$

$$\bigcup_{\xi S(E) \cap \Sigma\mu \neq \{\}} \xi S(E) \cdot E \tag{10}$$

$$\bigcup_{\xi S(E) \cap \Sigma\omega \neq \{\}} \xi S(E) \cdot E \tag{11}$$

Accordingly, all models that belong to any one of the above molecules are chemically identical. Such problems are avoided by the accumulation (12) by forming the transitive envelope (13).

$$\mathrm{Acc}(\{\lambda S(E) \cdot E \mid \lambda \in Sym(L)\}, \{\Sigma\mu \cdot E \times \Sigma\mu \cdot E \mid \Sigma\mu \cdot E \in \{\Sigma\mu \cdot E \mid \mu \in Sym(L)\}\}) \tag{12}$$

$$R = (\{\Sigma\mu \cdot E \times \Sigma\mu \cdot E \mid \Sigma\mu \cdot E \in \{\Sigma\mu \cdot E \mid \mu \in Sym(L)\}\} \cup \{\lambda S(E) \cdot E \times \lambda S(E) \cdot E \mid \lambda S(E) \cdot E \in \{\lambda S(E) \cdot E \mid \lambda \in Sym(L)\}\})^+ \tag{13}$$

Thus, finally, a family of permutation isomers with a ligand set containing equivalent ligands is represented as a union of the double cosets $\Sigma\lambda S(E)$ ($\lambda \in Sym(L)$). In these cases the customary methods for the enumeration and classification of isomers[70, 72, 74] must be used with caution. In contrast to these methods, the CIG theory also indicates which isomers are involved, which isomers merge into a single isomer due to ligand equivalences, and which chiral isomers in turn yield chiral isomers.

The accumulation is a generalization of the SVM. It takes all of the available information I into account to determine the distinct permutation isomers. In this case this is the whole right coset space of Σ. Besides equivalence of ligands there are other reasons why permutation isomers that were initially regarded as distinguishable are to be classified as chemically identical.

Isomerizations of a permutation isomer X into a permutation isomer of the same family that proceed via a permutation isomer Y of a different family (see Scheme 6) are of particular interest. Let E and F be the reference models of X

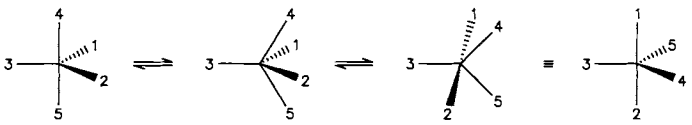

Scheme 6. The reference reaction for the generation of graphs of the Berry pseudorotation and the turnstile rotation.

and Y. The reaction $E \rightleftharpoons F$ is used as the reference reaction, that is, it is assumed that any mutual interconversion between λE and λF (for all $\lambda \in Sym(L)$) is possible. When the permutation isomers of X are considered, the left coset spaces of the CIG $S(E)$ and $S(F)$ are generated. The left coset space of $S(E)$ corresponds to the distinct permutation isomers of X, as long as no isomerization takes place. The left coset space of $S(F)$ in $Sym(L)$ yields the information on the permutation isomers of X that are interconvertible by isomerization and that can thus be viewed as chemically identical. The procedure for determining the distinct permutation isomers of X under the given isomerization conditions corresponds to the procedure for the investigation of the equivalence classes of $S(E)$ when some of the ligands are equivalent.

The reaction schemes (or reaction graphs) that represent all interconversions of permutation isomers are obtained by the SVM of the left cosets $\lambda S(E)$ and $\lambda S(F)$ of the two CIGs $S(E)$ and $S(F)$.[82]

The generation of the graph of all Berry pseudorotations[133] and turnstile rotations[82, 134, 135] of the family **32** of permutation isomers from the reference reaction **32a** $\rightleftharpoons$ **32b** by SVM of the left cosets of $S(32a)$ and $S(32b)$ may

serve as an illustration (Scheme 6). For this, each of the individual members of the family **32** are represented by a left coset of *S(32a)* and also by a left coset of *S(32b)*. A SVM of the two left coset spaces is established.

The isomerization processes involving two or more families of permutation isomers like **32** and **33** can be represented by (equivalence) accumulations, if permutation isomers with the same set of ligands participate in the reference reaction. When **32a**$\rightleftharpoons$**33a** is the reference reaction, a graph of the Berry pseudorotation results, in which the reactants **32** are connected by transition states **33** (see p. 132 of ref. [82]).

Ligand permutations that belong to the same Wigner subclass[129] of the relevant CIG correspond to permutation isomerizations with analogous intramolecular motions, that is the same reorganization mechanism.[96, 134] The union of left cosets of a CIG that intersect with a Wigner subclass of this CIG represent a Musher mode.[82, 136, 137] The latter corresponds to those permutation isomers that are formed directly from a reference isomer by a given reorganization mechanism (or an equivalent mechanism). Berry pseudorotations and turnstile rotations yield equivalent results and thus belong to the same Musher mode. They are represented by the same isomerization graph (see p. 132 of ref. [82]).

Since the result of an (equivalence) accumulation is in turn a space of equivalence classes the procedure of accumulations can be restarted with further information (for example additional ligand equivalencies or isomerization processes). Finally an equivalence class space is obtained whose cardinality yields information about the number of distinct permutation isomers, and, through inclusion relations, also about chirality and hyperchirality.[138]

Since the accumulation algorithm is applied in steps, isomerization graphs can be obtained. Thus, accumulations are well suited for the analysis and description of stereoselective reactions. If the ligands 1 and 2 as well as 3 and 4 of **32** are chemically equivalent, then the equivalence space (14) is subjected to a further accumulation by the right coset space of the ligand equivalence group (15). The result is the new equivalence group (16).

$$A = \mathrm{Acc}(\{\lambda S(32a) \cdot \mathbf{32a} \,|\, \lambda S(32b) \cdot \mathbf{32b} \in \{\lambda S(32b) \cdot \mathbf{32b} \,|\, \lambda \in Sym(L)\}\}) \tag{14}$$

$$\Sigma = \{(), (12), (34), (12)(34)\} \tag{15}$$

$$B = \mathrm{Acc}(A, \{\Sigma\mu \cdot E \times \Sigma\mu \cdot E \,|\, \Sigma\mu \cdot E \in \{\Sigma\mu \cdot E \,|\, \mu \in Sym(L)\}\}) \tag{16}$$

The graph of Berry pseudorotations/turnstile rotations changes accordingly (see p. 133 of ref. [82]).

Analogously it is also possible to determine which stereoisomers can be formed by a ligand-preserving reaction that affects the chemical constitution of the reactants. The formation of one of the stereoisomers can serve as the reference reaction, and the change in chemical constitution is treated as a transition from one family of permutation isomers to another. The representation of all Diels–Alder reactions that **34** and **35** may undergo in analogy to the reference reaction of Scheme 7 is an example.[98]

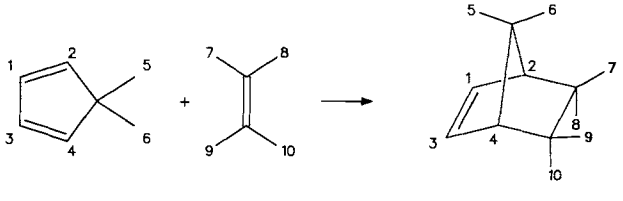

34 **35** **36**

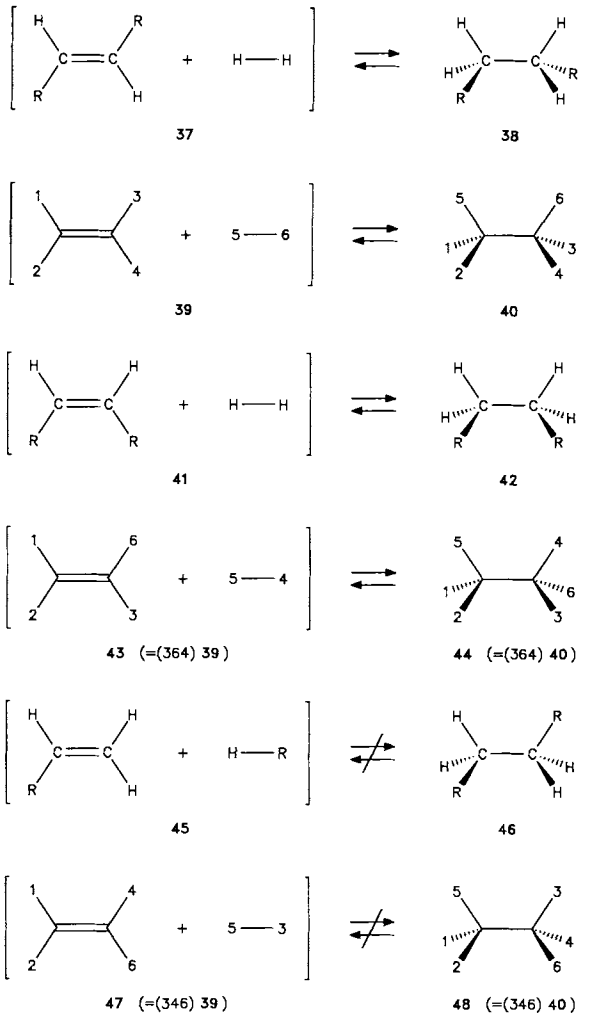

37 **38** **39** **40** **41** **42** **43** (=(364) **39**) **44** (=(364) **40**) **45** **46** **47** (=(346) **39**) **48** (=(346) **40**)

Scheme 7. The *cis–trans* isomerization of alkenes.

The applications of accumulations described above emphasize the wide variety of problems that can be treated by SVM and reaction schemes.[94, 95, 97, 124]

In addition, even the isomerizations which interconvert the members of two families of permutation isomers X and Y (with reference models E and F) that have different sets of ligands can be treated by accumulations. In such cases a reference isomerization $E \rightleftharpoons F$ does not necessarily imply that all processes $\lambda E \rightleftharpoons \lambda F$ must take place. The *cis–trans* isomerizations of an alkene that proceed via an alkane may serve as a simple example (Scheme 8).

It is assumed that internal rotations around the C–C axis of the alkane take place freely under the given observation conditions. It follows that the models (346)**40** (= **48**), (364)**40** (= **44**) and **40**, are interconvertible, that is, "equivalent" in the present sense.

The CIG $S(40)$ contains the permutations (346) and (364). They belong to different left cosets of $S(39)$. Accordingly, the intersections $S(39) \cap (346)S(39)$, $S(39) \cap (364)S(39)$, and $(346)S(39) \cap (364)S(39)$ are empty. However, $S(40)$ intersects with each of these left cosets of $S(39)$: $( ) \in S(40) \cap S(39)$, $(346) \in S(40) \cap (346)S(39)$ and $(364) \in S(40) \cap (364)S(39)$.

It follows that **39**, (346)**39** (= **47**) and (364)**39** (= **43**) are chemically identical. This is certainly true for **39** and (364)**39**, because **37** can be converted into **40** by the hydration route **39** → **40** → (364)**40** → (364)**39**, followed by an internal rotation and subsequent formation of **41** by dehydrogenation.

The *cis–trans* isomers that were initially rated as distinguishable now become interconvertible and thus equivalent (according to the left coset space of $S(39)$ the internal rotation about the C–C bond is not allowable in this case).

In contrast to **39** ⇌ **40** and (364)**39** ⇌ (364)**40** the reaction (346)**39** ⇌ (346)**40** does not represent a hydrogenation/dehydrogenation. Therefore, even though **46** is equivalent to **38** and **42** it cannot be converted into **45**, and (346)**39** ⇌ (346)**40** does not correspond to a model reaction of a hydrogenation/dehydrogenation. In this case a straightforward determination of the intersections is not suitable for establishing the mutual interconvertibilities.

In the description of intermolecular relations chemical reality can be accounted for by so-called filters, which "filter" the feasible interconversions from the set of conceivable or theoretically possible interconversions $\lambda E \rightleftharpoons \lambda F (\lambda \in Sym(L))$. These "allowable" individual isomerizations $\lambda E \rightleftharpoons \lambda F$ are distinguished by characteristic placements of the ligands at the skeletal sites, which are specified as follows: In a reference model M ligand 1 is located at the skeletal site a(M), ligand 2 at the skeletal site b(M), etc. In the hydrogenation/dehydrogenation of Scheme 7, the assignment of the skeletal sites is shown in Scheme 8, in which **39a** = E and **40a** = F are the reference models.

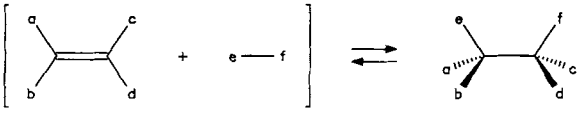

39a (E) **40a** (F)

Scheme 8. Labeling of skeletal sites for the isomerization of Scheme 7.

The *syn* mechanism of hydrogenation/dehydrogenation requires that the skeletal sites e(F) and f(F), and also e(E) and f(E) are occupied by H atoms. The remaining skeletal sites may, in principle, bear any ligands. The only condition is that the corresponding skeletal sites, for example, a(E)/a(F), b(E)/b(F), must bear the same ligands. The filter for this isomerization is formulated in (17).

$$\Phi := \{a(E) = a(F) \wedge b(E) = b(F) \wedge c(E) = c(F) \wedge d(E) = d(F) \wedge e(E) = e(F) = H \wedge f(E) = f(F) = H\} \quad (17)$$

The statement ⟨skeletal site⟩ = ⟨skeletal site⟩ expresses that the two specified skeletal sites must carry the same ligands (e.g., a(E) = a(F)). The condition ⟨skeletal site⟩ = ⟨skeletal site⟩ = ⟨ligand⟩ states that a specific ligand must be present (e.g., e(E) = e(F) = H). Thus, the individual isomerizations $E \rightleftharpoons F$ and $(364)E \rightleftharpoons (364)F$ meet the criterion of the above filter, whereas $(346)E \rightleftharpoons (346)F$ does not.

There are also isomerizations that interconnect members of families which do not have the same set of ligands. Let E and F be the reference models of the participating compounds X and Y. The ligand set $L(E) = \{1, 2, 3, 4\}$ belongs to model E while $L(F) = \{1, 2, 3, 4, 5\}$ belongs to F. Evidently, the permutation (15) only acts on F, because E does not have a fifth ligand. Furthermore, ligand 4 may represent different chemical residues in E and F (e.g., 4(E) = Me; 4(F) = Et). Therefore, the chemical meaning of the permutation may differ depending on the model to which it is applied. In such cases interconvertible isomers of X and Y cannot be determined by intersecting the coset spaces of $S(E)$ and $S(F)$. Filters must be employed to pick the allowable isomerizations. This is an advantage of accumulations[130, 131] over SVM and reaction schemes.[82, 100] The automated elucidation of relations (e.g. interconvertibility) between permutation isomers (which may belong to different families) merely according to the non-empty intersections of equivalence classes restricts the range of applications of reaction schemes and SVM significantly. This restriction is overcome by accumulations which exploit any relation between models in families of permutation isomers.

For four years, we have been developing computer programs to solve stereochemical problems on the basis of the present mathematical concepts.[130, 131]

4.3. The Software Infrastructure

A suitable software infrastructure needed to be created for the computer programs for the deductive solution of chemical problems on the basis of the DU model and the CIG theory.

4.3.1. Canonical Indexing of Atoms

The algorithm and computer program CANON[139, 140] were developed for internal documentation. The algorithm CANON refers to the atomic numbers and coordination numbers of atoms as well as their covalently bound neighbors.

The principle of CANON is illustrated by a simple example (Scheme 9).

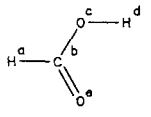

49

1. Atomic indices:	a: 3	b: 2	c: 1	d: 3	e: 1
1. Atomic descriptors:	a: 3.2	b: 2.113	c: 1.23	d: 3.1	e: 1.2
2. Atomic indices:	a: 5	b: 3	c: 2	d: 4	e: 1
2. Atomic descriptors:	a: 5.3	b: 3.125	c: 2.34	d: 4.2	e: 1.3

Scheme 9. An example to illustrate the principle of CANON.

CANON begins by arbitrarily labeling the atoms. In the example of **49**, the letters a–e serve as these arbitrary labels. The first atomic indices are assigned by starting with 1 for the atom with the highest atomic number and proceding in order with decreasing atomic numbers (O:1; C:2; H:3). The first atomic descriptors are formed from the first atomic in-

dices of the considered atom and in numerical order the indices of its covalently bound immediate neighbors (e.g., b: 2.113; c: 1.23; e: 1.2). Subsequently, the order of the first atomic descriptors taken as decimal numbers (lexicographic order) is used to determine the second atomic indices (e.g., b: 3; c:2; e: 1). The second atomic descriptors are formed analogously to the first atomic descriptors from the second atomic indices. Since the lexicographic order of the second atomic descriptors already corresponds to the second atomic indices, the latter are the final atomic indices according to CANON for this example. If this were not so, a further cycle would begin with the computation of the next atomic descriptors. If constitutionally equivalent atoms are present, any representative of their equivalence class can be selected arbitrarily without introducing ambiguity to the indexing procedure.

With CANON atomic indices are unequivocally assigned to atoms in molecules as well as to the corresponding rows (and columns) of the be-matrices with due consideration of chemical constitution and constitutional symmetries. Redundancies are thereby avoided.[21] For our purposes CANON is superior to the Morgan algorithm that is used by the Chemical Abstracts Service.[141] Since CANON recognizes constitutionally equivalent atoms, it is also suitable for ligand indexing in stereochemistry[140,142] and for predicting the chemical shift patterns of NMR spectra. When stereochemical problems are solved with computer-assistance, CANON-based ligand indexing has some significant advantages over the system of CIP rules.[143] In contrast to CANON, the system of CIP rules takes into account the formal bond orders instead of the coordination numbers of the atoms. CANON is simpler and unambiguous in all cases. In addition, CIP is based on a comparison of the individual ligands instead of an analysis of the whole chemical constitution of the considered molecules. The computer program CANON will soon be available for interested users.[144]

4.3.2. Recognition and Correlation of Substructures

For the computer-assisted solution of chemical problems the presence or absence of certain specified substructures in the generated molecules is often required. Therefore, the substructure search algorithm CABASS[145] based on central atoms and a computer program were developed. CABASS serves as a functional subunit in IGOR2.[115]

Substructure search systems, such as the DARC system of Dubois et al.,[146] often operate through a screening procedure and a subsequent atom-onto-atom mapping. The first procedures for atom-onto-atom mappings were published by the Chemical Abstracts Service[147] and by Sussenguth.[148] In its screening procedure, the DARC system uses spherical fragments that are coded as byte strings and embedded in tree structures for storage in a data bank. The search for substructures exploits this tree structure. The method of spherical fragmentation is also used by Lynch et al.[149] for the generation of screening systems for substructure search in structural data files. When Friedrich[150] analyzed the customary substructure search methods[146,151] he found that they are not suitable for the correlation of molecules according to common substructures. This is particularly the case when large files of data must be analyzed, because computing time and memory space increase more steeply than a polynominal curve with the size of the problem.[152]

Recently Ihlenfeldt[153] developed a computer program for structure-oriented correlation of molecules. Although this program is hampered by the disadvantages of the common procedures, it is capable of processing moderate amounts of data quite efficiently.

Fortunately, the complexity of molecular graphs is generally only moderate. Thus, it is possible to devise algorithms to correlate molecules through their substructures so that the need for memory space and computing time increases at worst polynomially (degree ≤ 5) with size and number of molecules that are to be considered. These algorithms are based on stepwise fragmentation of molecules and imbed the resulting fragments in a network of father–son relations which includes all the listed molecules. Based on this concept J. Friedrich[150] tested CORREL, a substructure correlation program for bilateral synthesis design. Improvements of CORREL led to CORREL 2,[154] which is more suitable for routine use. Recently, CORREL-S was employed for bilateral synthesis design;[155] it is based on a selection of substructures.

A special version of CORREL has been used for documentation and sequence matching of peptides[156] and is now being extended to include nucleotide sequences, as well as their correlation with peptide sequences.

The basic design of CORREL, published[150] with its source code, stimulated the implementation of several substructure search and correlation programs of similar design like RESY,[157] KOWIST,[158] HTSS,[159] S4,[151,160] and a program by Klopman.[161,162] The latter program as well as RESY and KOWIST are particularly suitable for structure–activity studies.[158]

Strategic Bonds and Substructures Relevant for Syntheses

For bilateral synthesis design it is necessary to find suitable starting materials for the synthesis of given target molecules. Here the largest common substructures are used as a guideline. CORREL-S was developed for this purpose.[89,155]

When a data bank of substructures relevant for synthesis is assembled, a set of rules about "breakable" bonds is required to reduce the size of the file in a meaningful way.[163] To establish this set, Corey's rules about strategic bonds were modified, hierarchically ordered, and provided with a termination criterion: the procedure is terminated when all nonaromatic rings have been dissected. A strategic bond must fulfill the following criteria:

1. The bond does not belong to a carbocyclic aromatic system. This does not apply to heteroarenes, which are often assembled in the course of a synthesis.
2. A bond is ranked by the number of rings its rupture will open. The higher this number, the higher the bond's preference; the number of rings is determined by CANON[139] and enumerated according to the Frèrejacques formula.[44]
3. If there are more than two bonds that qualify by rule 2, those that generate the fewest new rings are given priority.
4. Bonds at heteroatoms are strategic.
5. A bond is preferred if it is *exo* to other rings.
6. The bond must involve at least one carbon atom with more than two neighboring non-hydrogen atoms. This essentially corresponds to rule 5 when polycyclic structures are

present. However, rule 6 becomes relevant when only isolated single rings are left over.

7. A multiple bond is strategic.

8. The bond is a direct or next neighbor to a bond according to rule 4 or 7.

With these rules it is possible to process simple and complex ring systems. The preference rules help to restrict the number of strategic bonds and to establish the priorities for bond rupture in order to reach substructures relevant for the synthesis in available starting materials as soon as possible.

4.3.3. Stoichiometric Completion of Truncated Reaction Equations

The co-products of the target molecule of a synthesis, its stoichiometric complements in the target EM, are found with the computer program STOECH.[164] STOECH is based on a matrix formalism that was used in the elucidation of the reaction mechanism[165] of the four component condensation (4CC; α-addition of iminium ions and anions to isocyanides, followed by secondary reactions;[166] Ugi reaction[167]). Stoichiometric completion of truncated reaction equations[168] is now also of interest for the systematic documentation of chemical reactions based on their hierarchic classification (see Section 4.3.5).

4.3.4. Determination of Minimal Chemical Distance and the Corresponding Atom-onto-Atom Mappings

The repeated determination of the chemical distances (CDs) between isomeric EMs is a prerequisite for the optimization of reaction networks.[21, 100, 169] The associated atom-onto-atom mappings are needed in hierarchic reaction documentation.[79, 100, 112] Since the computer program PMCD[105] for the approximate determination of the minima of CD, which is based on a heuristic "branch-and-bound" algorithm,[170] does not always yield satisfactory results the computer program PEMCD[106] for the exact determination of the minima of CD was tested. A reaction core with 16 contiguous reaction centers is the upper limit for the present version of the PEMCD. We are therefore presently developing a more powerful computer program as a sucessor of PEMCD.

The CD between EMs with up to 100 reactive centers can be determined with a program that was recently implemented by Fontain.[107] This program is based on the "genetic algorithms".[171] Unfortunately this CD-minimization program does not yield all atom-onto-atom mappings that belong to the minima of CD.

4.3.5. Reaction Documentation

In the customary commercially available reaction documentation systems, chemical reactions are represented by their starting materials and products. This does not suffice to solve the reaction documentation problem satisfactorily.[172] Until recently ORAC[173] outstripped the available reaction documentation systems, but it is unfortunately no longer available. Since the deficiencies of traditional reaction documentation are known, and since reaction documentation belongs to the most important, yet unsolved problems of computer chemistry, many new approaches have been mooted in this field.[174, 175] Therefore within the Munich project, a hierarchically ordered system has been developed[79, 112] that refers directly to the processes of the chemical reactions as such; up to now this system has not found appreciable acceptance. The main reason is that the considered reactions must be stoichiometrically balanced, that is, they must be representable as isomerizations of EMs. In the chemical literature, reactions are often published in truncated form, where some of the participating reactants are omitted and would have to be stoichiometrically completed. This is now possible through the recently published program STOECH (see Section 4.3.3).

4.3.6. Graphic Output of Results

Since the results of the computer-assisted deductive solution of chemical problems are be-matrices, the graphic output program MDRAW[176] was developed. This converts the be-matrices into the graphic constitutional formulas that are more familiar to chemists. ARGOS, a similar program that was tested by J. Bauer and E. Fontain, is part of the user interface of IGOR and RAIN, and it has also been used routinely for several years by the Beilstein Institute for the conversion of connectivity lists into constitutional formulas.

4.4. The Multipurpose Programs IGOR and RAIN[*]

4.4.1. Formal Reaction Generators

The fundamental equation $\boldsymbol{B} + \boldsymbol{R} = \boldsymbol{E}$ of the DU model can be solved from a given be-matrix $\boldsymbol{B}$ by determining those pairs $(\boldsymbol{R}, \boldsymbol{E})$ which fulfill $\boldsymbol{B} + \boldsymbol{R} = \boldsymbol{E}$ under the given boundary conditions. We call these solutions the b-solutions. They are found by *r*eaction *g*enerators (RG) of the type RGB.[169, 177, 178] The equation $\boldsymbol{B} + \boldsymbol{R} = \boldsymbol{E}$ can also be solved from a given r-matrix $\boldsymbol{R}$. These r-solutions correspond to the pairs $(\boldsymbol{B}, \boldsymbol{E})$ for which $\boldsymbol{B} + \boldsymbol{R} = \boldsymbol{E}$ is fulfilled and are obtained by reaction generators of the type RGR.[114–116]

The two complementary types of solutions of the equation $\boldsymbol{B} + \boldsymbol{R} = \boldsymbol{E}$ and the respective RGs correspond to the two basic types of computer programs for the solution of chemical problems on the basis of the DU model. The centerpiece of the present version IGOR2[115] of the computer program IGOR[114–116] is an RGR. Recently RAIN[60–62, 169, 177, 178] also became generally available; the "engine" of RAIN is an RGB.

The RG of IGOR and RAIN are guided by *t*ransition *t*ables (TTs).[62, 63, 177, 178] A standard TT or a TT that is defined by the user is assigned to each chemical element that is taken into account. The allowable transitions are recorded in these TTs (see Fig. 2).

The computer programs IGOR and RAIN operate with strictly formal reaction generators, and are thus not restricted to the solution of a particular type of problem, such as retrosynthetic analysis. In combination with suitable auxil-

[*] IGOR and RAIN are available from the authors on request.

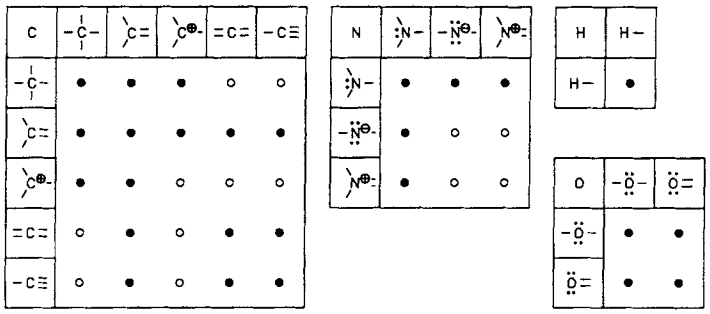

Fig. 2. Examples of transition tables. • = allowed transition, o = forbidden transition.

iary programs, both IGOR and RAIN can deal with a wide variety of chemical problems and deserve to be called multipurpose problem-solving programs. The solutions that they generate can belong to known chemistry, or they can be entirely without precedent, because these programs are independent of detailed empirical chemical information.

The first TT-guided RG (TRG) was the TRGR of IGOR, which solves the equation $\boldsymbol{B} + \boldsymbol{R} = \boldsymbol{E}$ from an r-matrix $\boldsymbol{R}$ and a list of the TTs of all relevant chemical elements. The user selects a suitable collection of TTs for each row/column pair of the potential solutions ($\boldsymbol{B}$, $\boldsymbol{E}$). The TRGR checks whether the entries of the TTs are compatible with $\boldsymbol{R}$ to provide a reduced collection of TTs, which are used to generate the be-matrix $\boldsymbol{B}$, row by row, column by column. From the rows and columns of $\boldsymbol{B}$, $\boldsymbol{R}$ generates rows and columns of $\boldsymbol{E}$. Now all row/column combinations of ($\boldsymbol{B}$, $\boldsymbol{E}$) are verified through use of the TTs. The novelty of each generated pair ($\boldsymbol{B}$, $\boldsymbol{E}$) is checked by CANON[139] in order to avoid redundancies. Subsequently the pairs of matrices are analyzed by CABASS[145] for forbidden or required substructures. The acceptable solutions are finally represented graphically on the screen or printed.

IGOR's TRGR generates pairs of starting materials and products according to a given irreducible r-matrix $\boldsymbol{R}$, which represents the redistribution of electrons (see Section 3.2.2). Thus, IGOR uses given "electron-pushing" patterns to "invent" chemical reactions. The r-matrices of such electron-pushing patterns can be produced by an independent computer program.[179] The reactions that are generated by IGOR are subjected to an interactive selection procedure that follows the hierarchic classification system for chemical reactions.[114]

In the structure-generating mode, a zero matrix $\boldsymbol{R} = \{\}$ is used as an r-matrix. IGOR then produces be-matrices $\boldsymbol{B}$ of molecules or EMs with $\boldsymbol{B} = \boldsymbol{E}$. Sets of molecules with the specified structural features can be obtained by restricting IGOR's output.[114, 177, 180, 181]

An RGB generates all EMs into which a given EM is directly convertible. Since an RGB may also use $-\boldsymbol{R}$ instead of $\boldsymbol{R}$, it can also generate the EMs from which the input EM can be obtained. When incorporated into a retrosynthetic program, an RGB can play the same role as a reaction library in combination with a structure-perceiving module, that is, the RGB finds the precursors of a given target molecule and their precursors, etc.

A TRGB operates in two steps: the first step is to determine the allowable valence schemes of those chemical elements that are assigned to the rows and columns of $\boldsymbol{E}$. They are obtained from the rows and columns of $\boldsymbol{B}$ through the TT. Subsequently, all $\boldsymbol{E}$s are generated that fulfill $\boldsymbol{B} + \boldsymbol{R} = \boldsymbol{E}$ under the given boundary conditions.

RAIN's TRGB[60, 63, 178] generates isomeric EMs from an $EM_{\boldsymbol{B}}$ that is represented by its be-matrix $\boldsymbol{B}$. The isomeric EMs correspond to the products that can be directly formed from $EM_{\boldsymbol{B}}$, or to starting materials for the $EM_{\boldsymbol{B}}$. RAIN is capable of simultaneously generating two trees of successive chemical reactions that consist of sequences of isomeric EMs. The "geometric" properties of the family of all isomeric EMs are exploited to direct the trees so that they grow from $EM_{\boldsymbol{B}}$ and $EM_{\boldsymbol{E}}$ and meet as soon as possible to form a contiguous network of reaction pathways; this bilateral generating process guides each reaction pathway to meet by checking the CD of the intermediate EMs[21, 100, 107, 182, 183] and is terminated as soon as an EM is reached from both sides. Thus, RAIN produces reaction networks that connect isomeric EMs.[60, 63, 177, 184, 185] By interactively specifying the lower and upper bounds and other characteristics of the reaction pathways (number and structural features of the intermediates, number of redistributed electrons per reaction step, etc.), the user can determine the nature of the network.[21] Depending on whether only the valence schemes of stable compounds are admitted, or also those of unstable intermediates, the networks that are generated contain only stable molecules or also short-lived intermediates.

Accordingly, RAIN may be used for mono- and bilateral synthesis design,[84, 88, 89] for planning and predicting reactions, and also for the elucidation of biosyntheses and complex reaction mechanisms (see Section 4.4.4).

Recently, Valdés-Pérez[186] presented the system MECHEM that is capable of generating networks of reaction pathways by symbolic computation. However, the latter program can only take empirical formulas into account, and not constitutional formulas.

4.4.2. Structure Generation by IGOR and RAIN

In their structure-generating modes, IGOR and RAIN produce all constitutional formulas that meet the specified conditions. Thus, for instance, all 23 EMs with the formula $(CH)_8$ and all 18 1,3-dipoles[187] of the elements C, N, and O are generated.[114] In order to demonstrate how the number of isomers increases when the C and H atoms of hydrocarbons are partially replaced by heteroatoms, the number of constitutional formulas of compounds with the empirical formula $C_2H_2N_2O_2$ (nonionic; no triple bonds or cumulated double bonds in rings; ammonium or iminium N^+ or amide N^- and O^- allowable as electronically charged atoms) were enumerated by IGOR and RAIN. Both programs found 1806 EMs, whereas there are only six hydrocarbons C_4H_4. When these molecules are generated by RAIN, the network of all constitutional isomers was generated from two atoms of each of the elements C, H, N, and O. For comparison nonionic $C_2H_2N_2O_2$ isomers were also generated that have a five-membered ring and formally one positive and one negative electrical charge. Sydnone **50** and 51 of its analogues result.

At present the customary reagents for the synthesis of oligonucleotides are derivatives of phosphorous acid[188] because, in general, the alternative phosphoric acid derivatives

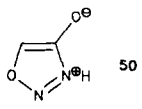

50

do not react sufficiently quickly with nucleoside derivatives. However, five-membered cyclic phosphoric acid derivatives react 10^5–10^7 times faster with nucleophiles or apicophiles than their acyclic analogues.[189, 190] Since 1973, the research groups of F. Ramirez and I. Ugi endeavoured to exploit this fact for syntheses by attempting to develop highly reactive five-membered phosphorylating reagents based on P^V for oligonucleotide syntheses.[191] These reagents would have some advantages over customary P^{III} reagents.[192]

After some initial success[193] the development stagnated, mainly because new ideas were lacking. Only after Ugi et al.[180] decided to review all of the candidate P^V compounds as defined by **51a** and **51b** with the aid of IGOR was progress again rapid.

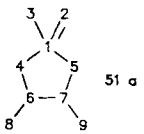

51 a

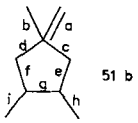

51 b

The following atoms were admitted for **51a**: 1 = P; 2 = O; 3 = X; 4, 5 = O, N, S; 6 = C, N, O, S; 7 = sp^2-C; 8, 9 = C, Cl, N, O, S. H atoms are placed according to valence rules. The covalent bonds are distributed as indicated by **51b**: a double bond; b, c, d: single bond; e, f, g: single or double bond; h, i: single or no bond. IGOR found 278 formulas **51** that complied with the restricting definitions.[180]

Five of these candidates were chosen to be investigated experimentally.[194] Already, two promising phosphorylating reagents, **52**[192] and **53**,[195] have resulted from these studies.

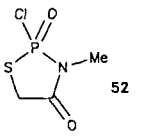

52

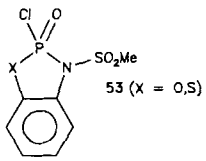

53 (X = O,S)

Lipscomb used the rules that he had established for the structure of boron hydrides to postulate structure **54** for B_6H_{14}, containing open (a) and closed three-center bonds (b).[196] Recent NMR data indicate that two kinds of B atoms (based on first-sphere neighbors) are present.[197] The formulas of Figure 3 generated by RAIN for B_6H_{14} agree with the observations.

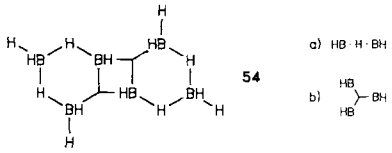

54

Computer-assisted structure elucidation à la DENDRAL employing analytical data is a particularly promising application of IGOR and RAIN. The experimental evidence can be used as restricting conditions when molecular structures are generated. All constitutional formulas that are compatible with the measured data are obtained.

The graph theoretical representation of chemical constitution has already been successful within the DENDRAL pro-

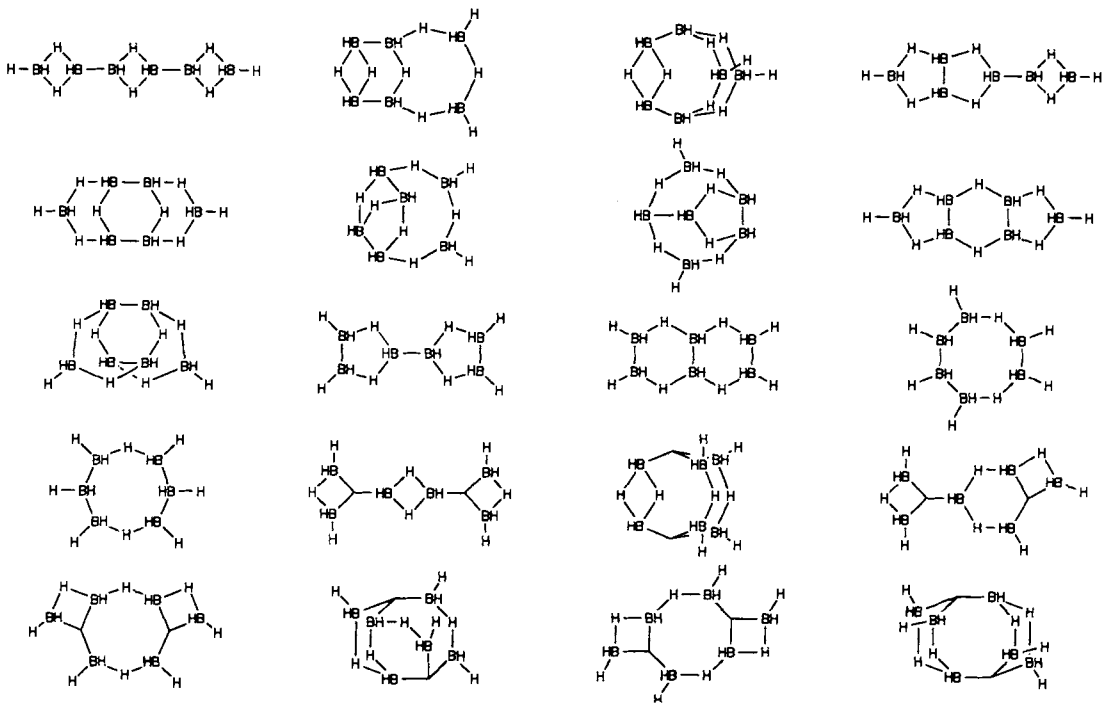

Fig. 3. Proposed structures of B_6H_{14} generated with RAIN.

ject as a mathematical foundation of the computer programs CONGEN[198] and GENOA,[199] and also later in the comparable programs RASTR,[200] MOLGRAPH,[201] ESSESA,[202] and GEN,[203] which generate families of constitutional formulas. GENOA was the first functioning program within this category. The computer-assisted elucidation of chemical constitution of walburganal **55** with the aid of GENOA is one of the most impressive applications of DENDRAL.[24]

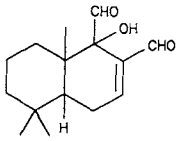

55

RAIN and GENOA generate the same set of 42 constitutional formulas, when the empirical formula $C_{15}H_{22}O_3$ of walburganal **55** and the substructures that are required or forbidden by the spectroscopic data are input. A substance with the empirical formula $C_{13}H_{22}N_2O_2S$ results from the reaction of ethyl β-aminocrotonate **56** and α-mercaptoisobutyraldehyde **57** with *tert*-butyl isocyanide **58**.[204]

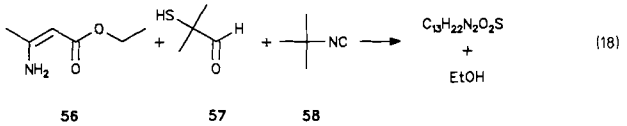

(18)

56 **57** **58**

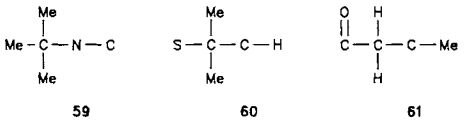

59 **60** **61**

Assuming that the substructures **59**–**61** in the starting materials are also present in the product, RAIN proposes the constitutional formulas of Figure 4.

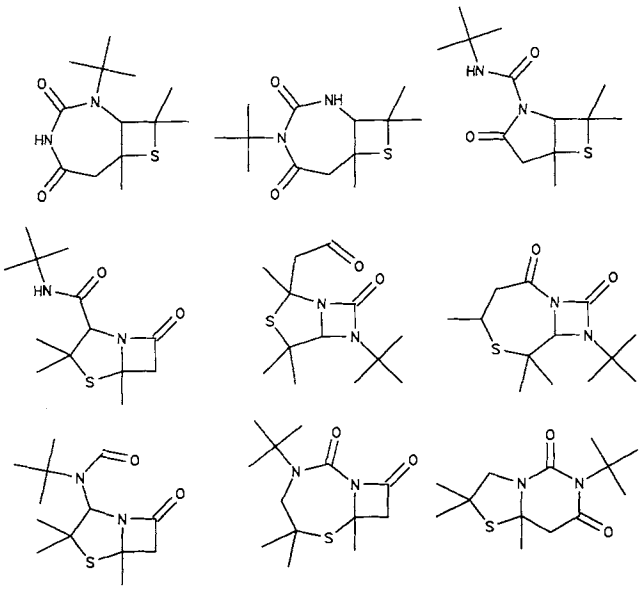

Fig. 4. Structures generated by RAIN as proposed products of reaction (18).

During routine runs, RAIN automatically recognizes the chemical equivalence of prototropic tautomers and resonance structures. For example, the tautomers and resonance structures of Figure 5 are obtained for the nucleobase cytosine.

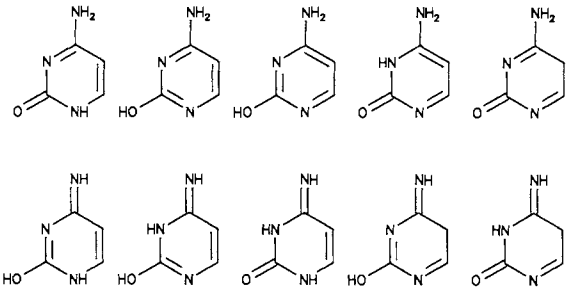

Fig. 5. The tautomers and resonance structures generated by RAIN for cytosine.

4.4.3. Generating Reactions with IGOR

Recently, Barton[205] published a very remarkable article on the systematic search for new reactions without computer-assistance. In this section the computer-assisted discovery of new reactions is described.

About ten years ago, R. Herges was given the task—as a part of his doctoral thesis—to find unprecedented reactions with the aid of the computer program IGOR,[116] which was then still under development, and to verify these reactions in the laboratory. The experience and suggestions gathered in the course of the investigations substantially improved the efficiency and user-friendliness of IGOR.

One of the results was that the chemist's participation varies strongly.[206] Computers only gave the inspiration for the development of cycloadditions of homodienes.[207] The systematic investigation of the r-class of the pericyclic 6-center 6-electron reactions demonstrated that in this 6,6 r-class of 13 basis reactions, only **25** → **26** with C atoms in the core of the reaction had not been studied much, although it was plausible. The reaction **62** + **63** → **64** was selected as an example according to heuristic criteria (ring strain, polarization, molecular geometry, etc.); this reaction succeeded in the laboratory.[114, 118]

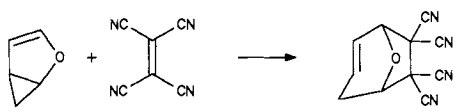

62 **63** **64**

In this context, our experience was that it is very difficult to ensure the unprecedentedness of a reaction in terms of the chemical literature. The data banks of molecular structures (CAS online, Beilstein online, etc.), which contain data on almost all compounds that have ever been synthesized, are easy to research. The commercially available data banks of chemical reactions, however, are not sufficiently structured and far from complete, and precedence must be determined by searching for all potential starting materials and products of the considered reaction.

H. Prinzbach informed us that Fowler[208] carried out the cycloaddition of *N*-methylcarbonylhomopyrrole **65** to dimethyl acetylenedicarboxylate in 1971. This reaction is related to **62** + **63** → **64** because the reactants **62** and **65** are similar. We had overlooked this reaction.

The extrusion reaction **25** → **26** (Scheme 2) is a further example of an experimentally verified reaction that was found by IGOR through the hierarchic classification system of chemical reactions. Hydrogen was chosen as the group to be transferred, since hydrogen transfer reactions generally proceed with particular ease; a carbonyl oxygen atom appeared to be favorable as an sp^2 center. All other reactive centres of **25** → **26** were allowed to be C or O. Furthermore, the chemically meaningful condition was introduced that the extruded molecule must be CO_2. This led to four types of reactions, of which three were already known. One, however, was not, namely the pyrolysis of α-formyloxy ketones **25** to **26**. Three examples of this reaction were successfully carried out in the laboratory[114, 118] (see Scheme 2).

This reaction is of moderate novelty, because the rb-subclass of the extrusion reactions was put in. Accordingly, at best, a further extrusion reaction could be discovered as a "new" reaction. Nevertheless, reaction **25** → **26** is still interesting, novel, and even of preparative value. In the synthesis of cyclic ketones by acyloin condensation[209] it is superior to the customary reduction of acyloins by Zn/HCl.[210] Obviously, the above reaction could also have been found without computer-assistance, but it is interesting and surprising that an probable reaction in the intensively studied field of extrusion reactions had been overlooked. This demonstrates that the systematic search for new reactions is more successful with computer-assistance than without.

There are many conceivable reactions from the CD-class 8 (see Section 3.2.2) that are novel up to the level of the ra-subclasses.[114] Some years ago, a systematic search for pericyclic reactions whose basic reactions are without precedence was conducted with IGOR. The CD-class 20 (reactions with five redistributed electrons) was the first in which a new experimentally realizable pericyclic reaction was found[88, 117] (**65** + **66** → **67**).

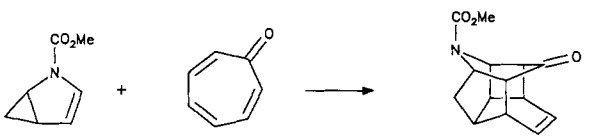

65 **66** **67**

Further reactions found through IGOR are a carbene rearrangement,[211] and a method for the synthesis of isocyanides containing electron-withdrawing groups.[206]

Besides systematic screening of classes of reactions for new reactions, a systematic search can be conducted for reactions that may be used for the synthesis of a given class of compounds. Herges and Hoock[212, 213] scanned the 7-center, 8-electron pericyclic reactions for syntheses of 1,3-dienes. The restrictions were given in the irreducible r-matrix and the valence schemes of the participating atoms (Scheme 10).

Of a total of 72 basic reactions generated (when triple bonds are admitted 470 basic reactions are generated), only three

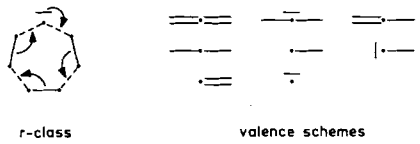

Scheme 10. Pericyclic 7-center, 8-electron reactions.

(Scheme 11) are suitable for the synthesis of 1,3-dienes (a butadiene fragment is produced in these cases).

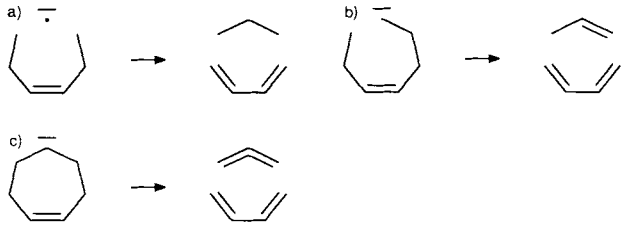

Scheme 11. Potential reactions for the synthesis of 1,3-dienes according to Scheme 10. The arrow in a) indicates an atom possessing a lone pair of electrons (symbolized by a short line).

Only reaction a) is known through some variants involving heteroatoms. One example is the reduction of 1,4-dichloro-2-butene with Zn. To our knowledge, the basis reactions b) and c) have not been published. The variant **68** → **69** of basis

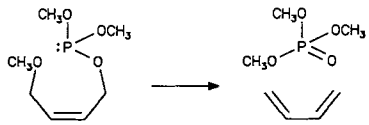

68 **69**

reaction b) was carried out recently, and yields 40% of butadiene in the gaseous phase at 0.40 Torr and 350 °C. It is not useful for syntheses, but is a novel type of 1,4-elimination.

The example **70** → **71**[212] was verified as a representative of c).

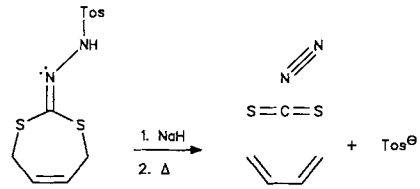

70 **71**

Not only pericyclic reactions can be generated in this way, but also reactions from other areas of organic chemistry. This can be seen in the example in Scheme 12 of a search for a novel carbene reaction.[214]

The first four basis reactions of Scheme 13 are illustrated in published examples. The fragmentations of cyclopropyl and 2-cyclopropyl carbene (a and b) have been thoroughly investigated.[215, 216] Also, reactions of carbenes with strained

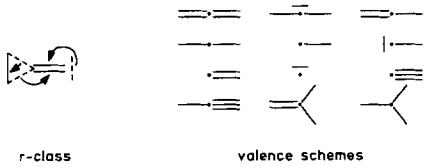

Scheme 12. Carbene reactions.

three-membered rings (c)[217] and the carbene rearrangement (d)[218] are already known. Herges[214] experimentally realized the unprecedented basis reaction (c) for two different carbene precursors (**72** + **73** → **74** → **75**; **76**–**77**).

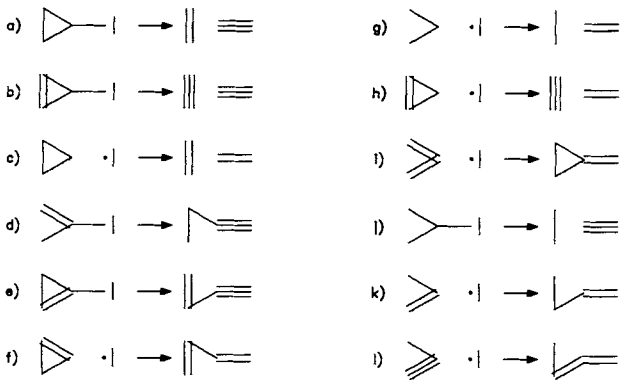

Scheme 13. Potential carbene reactions. Lone pairs of electrons are symbolized by short lines.

Recently, using IGOR2, Fisher, Juarez-Brambila, Goralski, Wipke, and Singaram[219] found and experimentally verified a novel rearrangement of α-aminoalkylboranes to the corresponding β-dialkylaminomonoalkylboranes.

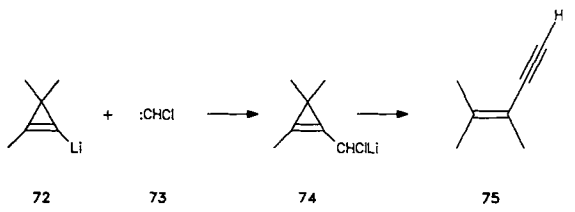

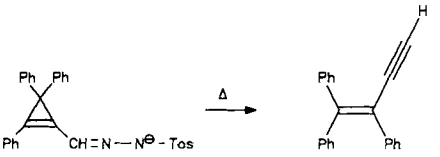

4.4.4. *Generation of Reaction Networks with RAIN*

In the summer of 1982, a reaction mechanisms contest took place at the University of California at Los Angeles. The topic of this contest was the proposal of a plausible reaction mechanism for the newly published Streith–Defoin reaction **78** + **79** → **80**.

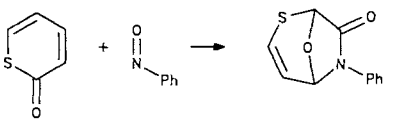

M. Jung, who organized the contest, asked I. Ugi to make some computer-generated proposals for the mechanism of for the Streith–Defoin reaction. We succeeded only after RAIN was available.[21, 60, 63] The Streith–Defoin reaction[220, 221] played an important role as a "fitness bicycle" in the development of RAIN. The network that RAIN generates under suitably chosen boundary conditions[63] contains the four best proposals of that contest; one of these corresponds to the reaction mechanism that has since been elucidated.[221]

Ried and Dietrich's indazole synthesis,[222] the thiazole synthesis by Hantsch,[223] and the Favorskii rearrangement[224] belong to the first applications of RAIN. Initially, a surprisingly large network of conceivable reaction mechanisms was found for the Favorskii rearrangement—116 intermediates at six levels and 43 intermediates at its "widest" level. Besides the published reaction mechanism,[224] this network contained many other mechanisms that are compatible with the known experimental results. When a suitable set of restrictions is input to the present version of RAIN, it generates a single reaction mechanism for the Favorskii rearrangement—the published one.

RAIN finds only one reaction mechanism for the rearrangement of benzocyclobutene **81** into isochroman **84**[62] that was studied by Kametani et al.[225] The intermediates were **82** and **83**.

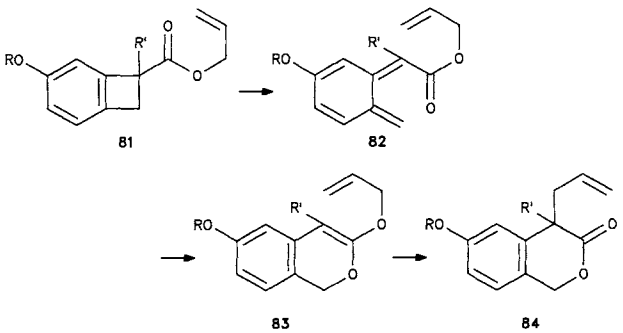

Recently the mechanism of an undesirable side reaction of the four component condensation was elucidated with RAIN.[184, 185] The formation of **89** and the malonamide

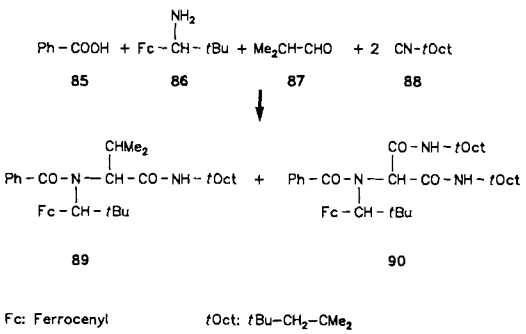

derivative **90** from **85**–**88** served as a model reaction. Experimental evidence in combination with suggestions from RAIN leads to the assumption that **90** is formed by the reaction mechanism depicted in Scheme 14 via the intermediates **91**–**98**.

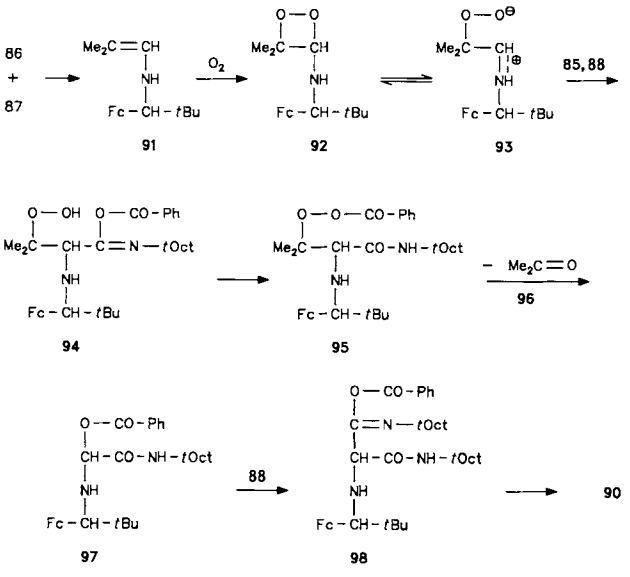

Scheme 14. Mechanism for the formation of **90**.

The elucidation of the mechanism of the hypothetical prebiotic synthesis of adenine from five molecules of hydrogen cyanide[226] is still open-ended, since the experimental evidence is not enough to decide which of the conceivable mechanistic alternatives proposed by RAIN is valid.

5. Perspectives

Nowadays computers belong to the standard instrumentation of chemical research, and it is safe to predict that computers will increasingly contribute to progress in chemistry in ever more diverse ways. The importance of numerical applications in chemistry, in particular in quantum chemistry and chemometrics but also in the planning, executing, and evaluating of measurements and in molecular modeling, will continue to soar. The use of computers in the documentation of chemistry-related data and information will develop vigorously in volume and efficiency.

It is foreseeable that computer programs for the direct solution of chemical problems will become routine in chemical research. In this context, formal algorithms will play an increasingly important role, even in expert systems that rely on stored detailed information. Empirical data will primarily be used for comparison with the results of computer programs that operate on a formal basis.

As a consequence of inquisitiveness of the potential users, computer programs with innovative capabilities will be preferred if the offered software has a convenient user interface and is suitable for widely available hardware. It is also important that such programs operate in an interactive mode, because an intelligent and experienced user wants to participate in the problem-solving process. With the aid of a suitable computer program it is, in principle, possible to generate all the conceivable solutions of a given chemical problem, including the most imaginative ones, but these solutions are worthless if they are hidden under enormous amounts of insignificant data; the meaningful and nonarbitrary selection of the solutions cannot be accomplished without the participation of a qualified user. The computer is able to provide assistance in arriving at new chemical ideas, but chemists must recognize their value and select them from a large number of conceivable alternatives. Thus, innovation may switch from the generation of proposals to their evaluation and selection, but new chemistry cannot be produced without the participation of human creativity. Progress in computer chemistry is based on new insights, ways of reasoning, formalisms, algorithms, software techniques, and also advances in computer hardware. Since the development of computers is still vigorous, it is too early to evaluate the future importance of single projects and tendencies. Much of what now looks impressive will be forgotten tomorrow, and what now seems to be excentric or irrelevant may turn out to be the beginning of a useful and important development.

We would like to thank the Deutsche Forschungsgemeinschaft, the Volkswagen-Stiftung, the Alexander-von-Humboldt-Stiftung, the Commission of the European Community, the Bundesministerium für Forschung und Technologie, and the Fonds der Chemischen Industrie for the generous financial support of our work.

Received: July 6, 1991
Revised: July 14, 1992 [A 894 IE]
German version: *Angew. Chem.* **1993**, *105*, 210

Mathematical Concepts and Notations

Boolean Algebra (let a and b be Boolean values)

$\mathbb{B}$	set of Boolean values {O, L}
$\wedge$	conjunction (logical and): connective $\wedge: \mathbb{B} \times \mathbb{B} \rightarrow \mathbb{B}$ according to the table

$\wedge$	O	L
O	O	O
L	O	L

$\vee$	inclusive disjunction (logical or): connective $\vee: \mathbb{B} \times \mathbb{B} \rightarrow \mathbb{B}$ according to the table

$\vee$	O	L
O	O	L
L	L	L

$\Rightarrow$	implication ($a \Rightarrow b$: "if a then b"): connective $\Rightarrow$: $\mathbb{B} \times \mathbb{B} \rightarrow \mathbb{B}$ according to the Table

$\Rightarrow$	O	L
O	L	L
L	O	L

$\Leftrightarrow$	equivalence ($a \Leftrightarrow b$: "a is equivalent to b", "a has the same value as b"): connective $\Leftrightarrow: \mathbb{B} \times \mathbb{B} \rightarrow \mathbb{B}$ according to the Table

$\Leftrightarrow$	O	L
O	L	O
L	O	L

$\neg$	negation (logical not): $\neg: \mathbb{B} \rightarrow \mathbb{B}$ with $\neg(0) = L$ and $\neg(L) = O$.

Quantifiers

$\exists$	existential quantifier ("there exists at least one ...")
$\forall$	universal quantifier ("for all ...")

Sets (let A, B, M and N be sets)

$\in$	$m \in M$ signifies that m is an element of M.
$\cap$	The intersection $A \cap B$ of two sets contains the elements that belong to both sets A and B.
$\cup$	The union $A \cup B$ of two sets A and B contains those elements that belong either to A or to B.
$\setminus$	The difference $A \setminus B$ of two sets A and B contains those elements of A that do not belong to B.
$\{m: P(m)\}$	The set of all objects, for which the predicate P holds. For example, the expression $\{n: n = 2m;\ m \in \mathbb{N}\}$ describes the set of all even natural numbers.
$\lvert M \rvert$	Cardinality: the number of elements in a set M
$M \times N$	The set of all ordered pairs (m, n) that can be formed from the elements $m \in M$ and $n \in N$ of two sets M and N.
$\mathrm{SVM}(\mathscr{A}, B) = \bigcup_{A \cap B \neq \{\}, A \in \mathscr{A}} A$	The union of all sets A that belong to the family of sets $\mathscr{A}$ and have a nonempty intersection with the set B.

Relations, Mappings

binary relation A binary relation R associates pairwise the elements of two sets X and Y. Accordingly, R is the set of ordered pairs $X \times Y$, expressed by $(x, y) \in R$, or in infix terminology: xRy. A binary relation R may be defined by a predicate P that is valid for all pairs $R = \{(x, y) \in X \times Y: P(x, y)\}$; otherwise all pairs are stated explicitly.

transitive closure The transitive closure R^+ of a (binary) relation R is defined as follows:
(1) $(a, b) \in R \Rightarrow (a, b) \in R^+$
(2) $(a, b) \in R^+ \wedge (b, c) \in R \Rightarrow (a, c) \in R^+$
(3) R^+ contains only what follows from (1) and (2).
R^+ is the smallest transitive relation that comprises R.

equivalence relation Special case of a binary relation $R \subseteq X \times Y$ for which the sets X and Y are identical and which is also endowed with the following three properties:
(1) reflexivity: $\forall x \in X: xRx$ (i.e. each element is in relation with itself).
(2) symmetry: $\forall x, y \in X: xRy \Rightarrow yRx$ (i.e. a relation between elements x and y implies a relation between y and x).
(3) transitivity: $\forall x, y, z \in X: xRy \wedge yRz \Rightarrow xRz$ (i.e. if there is a relation between x and y, and between y and z, then there is also a relation between x and z).

Due to the symmetry of an equivalence relation R on X, for some pair $(x, y) \in R$, the phrase "x has a relation R to y" is generally replaced by "x and y have a relation R"; for any x the set $[x] = \{y: xRy\}$ is the equivalence class of x with regard to R. For z the equivalence class $[z]$ is either identical with $[x]$ if $z \in [x]$, or the equivalence classes are disjoint (i.e. without common elements). The partition $\{[x]: x \in X\}$ of X that is induced by the set of all equivalence classes is called a space of equivalence classes or a quotient set.

$[m]_R$ The equivalence class of m with regard to the equivalence relation R, that is, all elements that are equivalent to m according to the property that is represented by R. Whenever it is necessary to declare the equivalence of some permuted models within a family with regard to a given property, the equivalence relations are of interest in the theory of the CIG.

permutations In the present article permutations are denoted by lowercase Greek letters. A permutation of n elements is a bijective map $\lambda: L \to L$ of a set L onto itself. A permutation $\lambda(l_a) = l_b$, $\lambda(l_b) = l_c, \ldots, \lambda(l_s) = l_a$ can be written in cycle notation as $(l_a l_b \ldots l_s)$. All further elements $l \in L \setminus \{l_a, l_b, \ldots, l_s\}$ are mapped to themselves by λ.

Groups

group A group $G = (M, \bullet)$ consists of a set M and an operation $\bullet$ in M with the following properties:
(1) closure: The combination of any two elements $a, b \in M$ yields again an element of M.
(2) associativity: For all elements $a, b, c \in M$ we have $a \bullet (b \bullet c) = (a \bullet b) \bullet c$.
(3) existence of an identity element: There exists an identity element $e \in M$ such that we have for all elements $a \in M$: $a \bullet e = e \bullet a = a$.
(4) existence of an inverse element: For any element $a \in M$ there exists an element a^{-1} such that: $a \bullet a^{-1} = a^{-1} \bullet a = e$.

In the context of a group the operation symbol $\bullet$ is omitted and one writes "ab" instead of "$a \bullet b$". The cardinality of a group is also called its order. A subgroup of the group $G = (M, \bullet)$ is a group $U = (N, \bullet)$ with $N \subseteq M$.

coset The set aU that belongs to an element $a \in G$ is called a left coset of U; it comprises all elements au with $u \in U$. If the multiplication by a takes place from the right hand side, the right coset Ua result. If the direction of the multiplication follows from the context or is irrelevant, the term coset is used. The set of the (left/right) cosets of the subgroup U in the group G form a (left/right) coset space. A coset space of U in G is a partitioning of G. Any coset space is a space of equivalence classes.

transversals A minimal set T with the property $TU = G$ is called a complete left transversal of U in G, and analogously as a complete right transversal, if $UT = G$. If it follows from the context whether a left or right transversal is meant, the term transversal or system of representatives is used. If U is nontrivial—that is, U does not only contain the identity element—the transversal is ambiguous. The complete transversal of U in G contains precisely one representative from each coset of U in G. Any element of a coset may serve as its representative. The term leading elements of cosets is often used for representatives.

generators In order to define a group G, it suffices to specify the nature of the group operation $\bullet$ and a few elements that, together with their inverses, can be combined to yield G. The latter elements are called the generators of the group G. If the elements of a group are permutations, the term permutation group is used. The set P of all permutations on a set L of n symbols, together with the consecutive execution of permutations as the group operation $\bullet$, form a group $Sym(L) = (P, \bullet)$ with $n!$ permutations; it is called the symmetric group of degree n. Often it is not relevant which elements of L are permuted, but how many. Thus one writes $S_{|L|}$ instead of $Sym(L)$. In the theory of the CIG, permutation group have direct applications. Any family of permuted models $P(E)$ with a set of ligands L is isomorphic to the symmetric group $Sym(L)$, since the action of distinct permutations from $Sym(L)$ on the reference model E leads to distinct models in $P(E)$; any model from P(E) can be obtained by the action of a permutation of $Sym(L)$ on the reference model.

conjugates For $\lambda \in G$ the product $\lambda U \lambda^{-1}$ is called the $(\lambda -)$ conjugate of U in G. The conjugate of a group is itself a group. For $\mu \in G$, the set $\{\lambda\mu\lambda^{-1}: \lambda \in U\}$ is called a Wigner subclass of U in G. The set $\{\{\lambda\mu\lambda^{-1}: \lambda \in U\}: \mu \in G\}$ of the Wigner subclasses forms a space of equivalence classes of G.

[1] D. Seebach, *Angew. Chem.* **1990**, *102*, 1363; *Angew. Chem. Int. Ed. Engl.* **1990**, *29*, 1320.
[2] a) E. L. Eliel, N. L. Allinger, S. J. Angyel, G. A. Morrison, *Conformational Analysis*, Interscience, New York, **1965**; b) M. Hanack, *Conformational Theory*, Academic Press, New York, **1965**; c) G. Chiurdoglu, *Conformation Theory*, Academic Press, New York, **1971**.
[3] H. Sachse, *Ber. Dtsch. Chem. Ges.* **1890**, *23*, 1323; *Z. Phys. Chem.* **1892**, *10*, 203.
[4] E. Mohr, *J. Prakt. Chem.* **1918**, *98*, 315.
[5] H. Meerwein, K. van Emster, *Ber. Dtsch. Chem. Ges.* **1922**, *55*, 2500.
[6] a) W. Reppe, O. Schlichting, K. Klager, T. Toepel, *Justus Liebigs Ann. Chem.* **1948**, *560*, 1; for a retrospective comment see [6b]; b) G. Schröder, *Cyclooctatetraen*, Verlag Chemie, Weinheim, **1965**.

[7] a) O. Roelen, *Angew. Chem.* **1948**, *60*, 213; for reviews see [7b]; b) J. Falbe, *Carbon Monoxide in Organic Synthesis*, Springer, Heidelberg, **1970**; W. A. Herrmann, Kontakte (Darmstadt) **1991**, (1), 22.
[8] J. M. Bijvoet, A. F. Peerdeman, A. J. Bommel, *Nature* **1951**, *168*, 271; J. M. Bijvoet, *Endeavour* **1955**, *14*, 7.
[9] G. A. Olah, G. K. S. Prakash, J. Sommer, *Superacids*, Wiley, New York, **1985**.
[10] G. Domagk, *Klin. Wochenschr.* **1937**, *16*, 1412; F. Mietsch, *Ber. Dtsch. Chem. Ges. B* **1938**, *71*, 15; *Chem. Zentralbl.* **1938**, 120.
[11] K. H. Büchel, *Bayer. Landwirtsch. Jahrb.* **1981**, *58*, 27; K. H. Büchel, M. Plempel, *Chron. Drug Discovery* **1983**, *2*, 235.
[12] K. Zuse, *Der Computer, mein Lebenswerk*, Springer, Heidelberg, **1984**.
[13] *Computer Applications in Chemical Research and Education* (Eds.: J. Brandt, I. Ugi) Hüthig, Heidelberg, **1989**.
[14] *Computational Methods in Chemistry* (Ed.: J. Bargon), Plenum, New York, **1980**.
[15] M. D. Johnston, Jr., *Computational Chemistry*, Elsevier, Amsterdam, **1988**; D. M. Hirst, *A Computational Approach to Chemistry*, Blackwell, Oxford, **1990**; *Modern Techniques in Computational Chemistry: MOTECC-90* (Ed.: E.Clementi), ESCOM, Leiden, **1990**.
[16] *Computer Aids to Chemistry* (Eds.: G. Vermin, M. Chanon), Ellis-Horwood, Chichester, **1986**; B. Adler, *Computerchemie – eine Einführung*, VEB Leipzig, **1986**.
[17] M. A. Ott, J. H. Noordik, *Recl. Trav. Chim. Pays-Bas* **1992**, *111*, 239.
[18] J. Zupan, *Algorithms for Chemists*, Wiley, New York, **1985**.
[19] *PC for Chemists* (Eds.: J. Zupan, D. Hadzi), Elsevier, Amsterdam, **1990**.
[20] I. Ugi, J. Bauer, K. Bley, A. Dengler, A. Dietz, E. Fontain, B. Gruber, M. Knauer, K. Reitsam, N. Stein, *Labor 2000* (special issue of *Labor Praxis*) **1992**, 170.
[21] I. Ugi, E. Fontain, J. Bauer, *Anal. Chim. Acta* **1990**, *235*, 155.
[22] J. Lederberg, *Proc. Natl. Acad. Sci. USA* **1990**, *53*, 134; *How DENDRAL was conceived and born* (ACM Symposium on the History of Medical Informatics 1987), National Library of Medicine, p. 270.
[23] R. K. Lindsay, B. G. Buchanan, E. A. Feigenbaum, J. Lederberg, *Applications of Artificial Intelligence for Organic Chemistry: The DENDRAL Project*, McGraw-Hill, New York, **1980**.
[24] N. A. B. Gray, *Computer-assisted Structure Elucidation 2*, Wiley-Interscience, New York, **1986**.
[25] G. Vleduts, *Inf. Storage Retr.* **1963**, *1*, 117.
[26] A. Dengler, E. Fontain, M. Knauer, N. Stein, I. Ugi, *Recl. Trav. Chim. Pays-Bas* **1992**, *111*, 262.
[27] G. Vleduts, K. A. Finn, *Proc. Dept. of Mechanization and Automation of Information Work*, Acad. Sci. USSR, Moskau, **1960**, p. 66.
[28] E. J. Corey, *Pure Appl. Chem.* **1967**, *14*, 19; see also *Angew. Chem.* **1991**, *103*, 469; *Angew. Chem. Int. Ed. Engl.* **1991**, *30*, 455.
[29] E. J. Corey, W. T. Wipke, *Science* **1991**, *166*, 178; E. J. Corey, X.-M. Cheng, *The Logic of Chemical Synthesis*, Wiley, New York, **1989**.
[30] E. J. Corey, A. K. Long, S. D. Rubenstein, *Science* **1985**, *228*, 4089; see also E. J. Corey, A. K. Long, G. I. Lotto, S. D. Rubenstein, *Recl. Trav. Chim. Pays-Bas* **1992**, *111*, 304.
[31] W. T. Wipke, D. Rogers, *J. Chem. Inf. Comput. Sci.* **1984**, *24*, 71.
[32] H. Gelernter, N. S. Sridharan, A. J. Hart, S. C. Yen, F. W. Fowler, H. J. Shue, *Top. Curr. Chem.* **1973**, *41*, 113; H. Gelernter, J. R. Rose, *J. Chem. Inf. Comput. Sci.* **1990**, *30*, 492.
[33] The computer program for planning peptide syntheses, developed by G. Kaufhold and I. Ugi at Bayer AG in Leverkusen (FRG) is described in [34].
[34] I. Ugi, *Rec. Chem. Prog.* **1969**, *30*, 389; *Intra-Sci. Chem. Rep.* **1971**, *5*, 229.
[35] M. Bersohn, *Computer Assisted Organic Synthesis* (*ACS Symp. Ser.* **1977**, *61*); S. Sasaki, K. Funatsu, *Tetrahedron Comput. Methodol.* **1988**, *1*, 39; R. Barone, M. Arbelot, M. Chanon, *ibid.* **1988**, *1*, 3; E. S. Blurock, *ibid.* **1989**, *2*, 207; A. Weise, *J. Chem. Inf. Comput. Sci.* **1990**, *30*, 228; I. Dogane, T. Takabatake, M. Bersohn, *Recl. Trav. Chim. Pays-Bas* **1992**, *111*, 291; L. Baumer, I. Compagnari, G. Sala, G. Sello, *ibid.* **1992**, *111*, 297; P. Hamm, P. Jauffret, G. Kaufmann, *ibid.* **1992**, *111*, 317.
[36] E. Hjelt, *Geschichte der Organischen Chemie*, Vieweg, Braunschweig, **1916**.
[37] a) R. Robinson et al., *J. Chem. Soc.* **1916**, *109*, 1029, 1039; *ibid.* **1917**, *111*, 958; *ibid.* **1918**, *113*, 639; *ibid.* **1919**, *115*, 943; *ibid.* **1921**, *120*, 545; b) Sir R. Robinson, *The Structural Relations of Natural Products*, Clarendon Press, Oxford, **1955**.
[38] S. G. Warren, *Organic Synthesis: The Disconnection Approach*, Wiley, New York, **1982**.
[39] P. H. Winston, *Artificial Intelligence*, Addison-Wesley, Reading, MA, USA, **1984**; B. A. Hohne, T. H. Pierce, *Expert system Applications in Chemistry* (*ACS Symp. Ser.* **1989**, *408*).
[40] H. W. Brown, *Chem. Ind. London* **1988** (5), 43.
[41] G. M. Downs, V. J. Gillet, J. D. Holliday, M. F. Lynch, *J. Chem. Inf. Comput. Sci.* **1989**, *29*, 172.
[42] E. J. Corey, G. Petersson, *J. Am. Chem. Soc.* **1972**, *94*, 460.
[43] E. J. Corey, W. J. Howe, H. W. Orf, D. A. Pensak, G. Petersen, *J. Am. Chem. Soc.* **1975**, *97*, 6116.
[44] M. Frèrejaques, *Bull. Soc. Chim. Fr. Mem.* **1939**, *5*, 1008.
[45] R. B. Woodward, *Angew. Chem.* **1956**, *68*, 13.
[46] M. Hicks, *J. Chem. Inf. Comput. Sci.* **1990**, *30*, 352.
[47] M. G. Bures, W. L. Jorgensen, *J. Org. Chem.* **1988**, *53*, 2504.
[48] W. Schubert, *MATCH* **1979**, *6*, 213.
[49] G. Grethe, T. E. Moock, *J. Chem. Inf. Comput. Sci.* **1990**, *30*, 505.
[50] J. B. Hendrickson, *Top. Curr. Chem.* **1976**, *62*, 49.
[51] G. Moreu, *Nouv. J. Chim.* **1978**, *2*, 187.
[52] J. B. Hendrickson, A. G. Toczko, *Pure Appl. Chem.* **1988**, *60*, 1583; J. B. Hendrickson, *Anal. Chim. Acta* **1990**, *235*, 103; *Recl. Trav. Chim. Pays-Bas* **1992**, *111*, 323.
[53] J. Blair, J. Gasteiger, C. Gillespie, P. D. Gillespie, I. Ugi in *Computer Representation and Manipulation of Chemical Information* (Eds.: W. T. Wipke, S. R. Heller, R. J. Feldman, E. Hyde), Wiley, New York, **1974**, p. 129.
[54] J. Gasteiger, C. Jochum, *Top. Curr. Chem.* **1978**, *74*, 93.
[55] J. Gasteiger, M. G. Hutchings, B. Christoph, L. Gann, C. Hiller, P. Löw, M. Marsili, H. Saller, K. Yuki, *Top. Curr. Chem.* **1987**, *137*, 19; J. Gasteiger, W. D.-Ihlenfeldt, P. R. Röse, *Recl. Trav. Chim. Pays-Bas* **1992**, *111*, 270.
[56] R. Doenges, B. T. Groebel, H. Nickelsen, J. Sander, *J. Chem. Inf. Comput. Sci.* **1985**, *25*, 425.
[57] D. A. Evans, *unpublished manuscript*, **1972**.
[58] A. Lapworth, *J. Chem. Soc.* **1921**, *120*, 543.
[59] D. Seebach, *Angew. Chem.* **1979**, *91*, 259; *Angew. Chem. Int. Ed. Engl.* **1979**, *18*, 239.
[60] E. Fontain, J. Bauer, I. Ugi, *Chem. Lett.* **1987**, 37.
[61] E. Fontain, *Tetrahedron Comput. Methodol.* **1990**, *3*, 469.
[62] E. Fontain, *Dissertation*, Technische Universität München, **1987**.
[63] E. Fontain, J. Bauer, I. Ugi, *Z. Naturforsch. B* **1987**, *42*, 297.
[64] D. Hilbert, P. Bernays, *Grundlagen der Mathematik*, Teubner, Berlin, **1934**.
[65] A. Cayley, *Ber. Dtsch. Chem. Ges.* **1875**, *8*, 172; F. Herrmann, *ibid.* **1880**, *13*, 792.
[66] *Chemical Applications of Graph Theory* (Ed.: A. T. Balaban), Academic Press, London, **1976**.
[67] *Chemical Applications of Topology and Graph Theory* (Ed.: R. B. King), Elsevier, Amsterdam, **1983**.
[68] R. E. Merrifield, H. E. Simmons, *Topological Methods in Chemistry*, Wiley, New York, **1989**.
[69] H. R. Henze, C. M. Blair, *J. Am. Chem. Soc.* **1931**, *53*, 3077.
[70] A. Polyá, *Acta Math.* **1937**, *68*, 145.
[71] *The Permutation Group in Physics and Chemistry* (Ed.: J. Hinze), Springer, Heidelberg, **1979**.
[72] A. Kerber, K.-J. Thürlings, *Symmetrieklassen von Funktionen and ihre Abzähltheorie* (Bayreuther Math. Schriften), Bayreuth, **1983**.
[73] J. Dugundji, R. Kopp, D. Marquarding, I. Ugi, *Top. Curr. Chem.* **1978**, *75*, 165.
[74] E. Ruch, W. Hässelbarth, B. Richter, *Theor. Chim. Acta* **1970**, *19*, 288; W. Hässelbarth, E. Ruch, *ibid.* **1973**, *29*, 259; W. Hässelbarth, E. Ruch, D. J. Klein, T. H. Seligman in *Group Theoretical Methods in Physics* (Eds.: R. T. Sharp, B. Kolman), Academic Press, New York, **1977**, p. 617.
[75] J. Dugundji, J. Showell, R. Kopp, D. Marquarding, I. Ugi, *Isr. J. Chem.* **1980**, *20*, 20.
[76] I. Ugi, D. Marquarding, H. Klusacek, G. Gokel, P. D. Gillespie, *Angew. Chem.* **1970**, *82*, 741; *Angew. Chem. Int. Ed. Engl.* **1970**, *9*, 703.
[77] I. Ugi, B. Gruber, N. Stein, A. Demharter, *J. Chem. Inf. Comput. Sci.* **1990**, *30*, 485.
[78] J. Dugundji, I. Ugi, *Top. Curr. Chem.* **1973**, *39*, 19.
[79] J. Brandt, J. Bauer, R. M. Frank, A. von Scholley, *Chem. Scr.* **1981**, *18*, 53; J. Brandt, A. von Scholley, *Comput. Chem.* **1983**, *7*, 51.
[80] J. Koča, M. Kratochvil, V. Kvasnička, L. Matyska, J. Pospichal, *Lect. Notes Chem.* **1989**, *51*; E. Hladka, J. Koča, M. Kratochvil, V. Kvasnička, L. Matyska, J. Pospichal, V. Potuček, *Top. Curr. Chem.*, in press.
[81] V. Kvasnička, M. Kratochvil, J. Koča, *Coll. Czech. Chem. Commun.* **1983**, *48*, 2284; J. Koča, *ibid.* **1988**, *53*, 1007, 3108, 3119; *J. Math. Chem.* **1989**, *3*, 73, 91; V. Kvasnička, J. Pospichal, *ibid.* **1989**, *3*, 161; *Int. J. Quantum Chem.* **1990**, *38*, 253; V. Kvasnička, J. Pospichal, *J. Math. Chem.* **1990**, *5*, 309.
[82] I. Ugi, J. Dugundji, R. Kopp, D. Marquarding, *Lect. Notes Chem.* **1984**, *36*.
[83] T. F. Brownscombe, R. V. Stevens, private communication to I. Ugi; T. F. Brownscombe, *Dissertation*, Rice University, Houston, TX, **1972**.
[84] I. Ugi, J. Bauer, J. Brandt, J. Friedrich, J. Gasteiger, C. Jochum in [14], p. 275.
[85] I. Ugi, J. Bauer, K. Bley, A. Dengler, E. Fontain, M. Knauer, S. Lohberger, *J. Mol. Struct. (Theochem)* **1991**, *230*, 73.
[86] A. P. Johnson, C. Marshall, P. N. Judson, *Recl. Trav. Chim. Pays-Bas* **1992**, *111*, 310; *J. Chem. Inform. Comput. Chem.*, in press; A. P. Johnson, C. Marshall, *ibid.*, in press.
[87] J. B. Hendrickson, C. A. Parks, *J. Chem. Inf. Comput. Sci.* **1992**, *32*, 209.
[88] I. Ugi, J. Bauer, R. Baumgartner, E. Fontain, D. Forstmeyer, S. Lohberger, *Pure Appl. Chem.* **1988**, *60*, 1573.
[89] I. Ugi, E. Fontain, M. Knauer, N. Stein, *Recl. Trav. Chim. Pays-Bas* **1992**, *111*, 262.

[90] N. S. Zefirov, E. V. Godeeva, *Usp. Khim.* **1954**, *54*, 1753; N. S. Zefirov, *Acc. Chem. Res.* **1987**, *20*, 237; S. S. Tratch, I. I. Baskin, N. S. Zefirov, *Zh. Org. Khim.* **1988**, *24*, 1121; N. S. Zefirov, S. S. Tratch, *Anal. Chim. Acta* **1990**, *235*, 115.

[91] L. Matyska, J. Koča, *J. Chem. Inf. Comput. Sci.*, in press.

[92] L. Matyska, J. Koča, *J. Chem. Inf. Comput. Sci.* **1991**, *31*, 380.

[93] Z. Hippe in [13], p. 165.

[94] P. Y. Johnson, I. Burnstein, J. Crary, M. Evens, T. Wang, *Expert Systems Application in Chemistry* (*ACS Symp. Ser.* **1988**, 408).

[95] I. Ugi, N. Stein, M. Knauer, B. Gruber, K. Bley, R. Weidinger, *Top. Curr. Chem.* **1993**, *166*, 199; R. Weidinger, *Diplomarbeit*, Universität Passau, **1991**.

[96] J. Gasteiger, P. D. Gillespie, D. Marquarding, I. Ugi, *Top. Curr. Chem.* **1974**, *48*, 1.

[97] E. O. von Lippmann, *Chem.-Ztg.* **1909**, *1*, 1; R. Grund, A. Kerber, R. Laue, *Bayreuther Universitätsblätter*, in press.

[98] I. Ugi, *Chimia* **1986**, *40*, 340.

[99] L. Spialter, *J. Chem. Doc.* **1964**, *4*, 261.

[100] I. Ugi, M. Wochner, E. Fontain, J. Bauer, B. Gruber, R. Karl in *Concepts and Applications of Chemical Similarity* (Eds.: M. A. Johnson, G. M. Maggiora), Wiley, New York, **1990**, p. 239.

[101] J. Dugundji, *Topology*, Allyn and Bacon, Boston, **1966**.

[102] W. Preuss, *Int. J. Quantum Chem.* **1969**, *3*, 123, 131.

[103] M. Wochner, *Dissertation*, Technische Universität München, **1984**.

[104] M. Wochner, I. Ugi, *J. Mol. Struct. (Theochem)* **1988**, *165*, 229.

[105] C. Jochum, J. Gasteiger, I. Ugi, *Angew. Chem.* **1980**, *92*, 503; *Angew. Chem. Int. Ed. Engl.* **1980**, *19*, 495; C. Jochum, J. Gasteiger, I. Ugi, J. Dugundji, *Z. Naturforsch. B* **1982**, *37*, 376.

[106] M. Wochner, J. Brandt, A. von Scholley, I. Ugi, *Chimia* **1988**, *42*, 217.

[107] E. Fontain, *Anal. Chim. Acta* **1992**, *265*, 227.

[108] H. Kolbe, J. Liebig, *Ann. Chem. Pharm.* **1850**, *75*, 211; *ibid.* **1850**, *76*, 1.

[109] J. Pospichal, V. Kvasnička, I. Gutman, *Collect. Sci. Pap. Kragujevac*, **1991**, *12*, 109–125; V. Baláz, J. Pospichal, V. Kvasnička, *Discrete Appl. Math.* **1992**, *35*, 1–19.

[110] A. P. Johnson, C. Marshall, *J. Chem. Inf. Comput. Sci.*, in press.

[111] E. Fontain, *Dissertation*, Technische Universität München, **1987**.

[112] I. Ugi, J. Brandt, A. von Scholley, S. Minker, M. Wochner, H. Schönmann, B. Straupe, *Hierarchisch strukturierte Speicherung and Ermittlung von chemischen Reaktionen* (Forschungsbericht, Information and Dokumentation, BMFT-FB-ID85-005), FIZ Karlsruhe, **1985**.

[113] J. Brandt, J. Friedrich, J. Gasteiger, C. Jochum, W. Schubert, I. Ugi in *Computer Assisted Organic Synthesis* (*ACS Symp. Ser.* **1977**, *61*).

[114] J. Bauer, R. Herges, E. Fontain, I. Ugi, *Chimia* **1985**, *39*, 43.

[115] J. Bauer, *Tetrahedron Comput. Methodol.* **1989**, *2*, 269.

[116] J. Bauer, I. Ugi, *J. Chem. Res. Synop.* **1982**, 298; *J. Chem. Res. Miniprint* **1982**, 3101; J. Bauer, *Dissertation*, Technische Universität München, **1981**.

[117] D. Forstmeyer, J. Bauer, E. Fontain, R. Herges, R. Herrmann, I. Ugi, *Angew. Chem.* **1988**, *100*, 1618; *Angew. Chem. Int. Ed. Engl.* **1988**, *27*, 1558; J. Bauer, E. Fontain, D. Forstmeyer, I. Ugi, *Tetrahedron Comput. Methodol* **1988**, *1*, 129.

[118] R. Herges, *Dissertation*, Technische Universität München, **1984**.

[119] I. Ugi, J. Bauer, J. Brandt, J. Friedrich, J. Gasteiger, C. Jochum, W. Schubert, *Angew. Chem.* **1979**, *91*, 99; *Angew. Chem. Int. Ed. Engl.* **1979**, *18*, 111.

[120] E. O. Fischer, G. Bürger, *Z. Naturforsch. B* **1961**, *16*, 77; G. Wilke, B. Bogdanović, P. Hardt, P. Heimbach, W. Keim, M. Kröner, W. Oberkirch, K. Tanaka, E. Steinrücke, D. Walter, H. Zimmermann, *Angew. Chem.* **1966**, *78*, 157; *Angew. Chem. Int. Ed. Engl.* **1966**, *5*, 159.

[121] N. Stein, proposed *Dissertation*, Technische Universität München.

[122] E. J. Corey, W. J. Howe, D. A. Pensak, *J. Am. Chem. Soc.* **1974**, *96*, 7724.

[123] W. T. Wipke, T. M. Dyott, *J. Am. Chem. Soc.* **1974**, *96*, 4825, 4834.

[124] S. Hanessian, J. Franco, G. Gagnon, D. Laramée, B. Laroade, *J. Chem. Inf. Comput. Sci.* **1990**, *30*, 413.

[125] J. Blair, J. Gasteiger, C. Gillespie, P. D. Gillespie, I. Ugi, *Tetrahedron* **1974**, *30*, 1845.

[126] C. E. Wintner, *Strands of Organic Chemistry*, Holden-Day, San Francisco, **1979**, p. 9.

[127] H. C. Longuet-Higgins, *Mol. Phys.* **1963**, *6*, 445.

[128] S. McLane, G. Birkhoff, *Algebra*, McMillan, New York, **1967**, p. 91; T. A. Whitelaw, *Introduction to Abstract Algebra*, Blackie, Glasgow, **1988**, p. 124.

[129] E. P. Wigner, *Proc. R. Soc. A* **1971**, *322*, 181.

[130] B. Gruber, *Dissertation*, Technische Universität München, **1992**; A. Dietz, *Dissertation*, Technische Universität München, **1993**.

[131] B. Gruber, A. Dietz, I. Ugi, as yet unpublished.

[132] J. E. Hopcroft, J. D. Ullman, *Einführung in die Automatentheorie, formale Sprachen und Komplexitätstheorie*, 2nd ed., Addison-Wesley, Bonn, **1990**, p. 8.

[133] R. S. Berry, *J. Chem. Phys.* **1960**, *32*, 933.

[134] P. Gillespie, P. Hoffmann, H. Klusacek, D. Marquarding, S. Pfohl, F. Ramirez, E. A. Tsolis, I. Ugi, *Angew. Chem.* **1971**, *83*, 493; *Angew. Chem. Int. Ed. Engl.* **1971**, *10*, 503.

[135] P. Lemmen, R. Baumgartner, I. Ugi, F. Ramirez, *Chem. Scr.* **1988**, *28*, 451.

[136] M. Gielen, N. van Lautem, *Bull. Soc. Chim. Belges* **1970**, *79*, 679; J. I. Musher, *J. Am. Chem. Soc.* **1972**, *94*, 5662.

[137] J. Brocas, M. Gielen, R. Willem, *The Permutational Approach to Dynamic Stereochemistry*, McGraw-Hill, New York, **1983**.

[138] J. Dugundji, D. Marquarding, I. Ugi, *Chem. Scr.* **1976**, *9*, 74.

[139] W. Schubert, I. Ugi, *J. Am. Chem. Soc.* **1978**, *100*, 37; *Chimia* **1979**, *33*, 183.

[140] See [96], Chapter 8.

[141] H. L. Morgan, *J. Chem. Doc.* **1965**, *5*, 107.

[142] N. Stein, I. Ugi, as yet unpublished.

[143] R. S. Cahn, C. K. Ingold, *J. Chem. Soc.* **1951**, 612; R. S. Cahn, C. K. Ingold, V. Prelog, *Experientia* **1966**, *78*, 413; V. Prelog, G. Helmchen, *Angew. Chem.* **1982**, *94*, 614; *Angew. Chem. Int. Ed. Engl.* **1982**, *21*, 567; H. Dodziuk, M. M. Mirowicz, *Tetrahedron Asymmetry* **1990**, *3*, 171.

[144] E. Fontain, as yet unpublished.

[145] A. Dengler, I. Ugi, *Comput. Chem.* **1991**, *15*, 103; *J. Chem. Res. Synop.* **1991**, 162; *J. Chem. Res. Miniprint* **1991**, 1279.

[146] J. E. Dubois, *J. Chem. Doc.* **1973**, *13*, 8; R. Attias, J. E. Dubois, *J. Chem. Inf. Comput. Sci.* **1990**, *30*, 2.

[147] W. E. Cossum, G. M. Dyson, M. F. Lynch, R. N. Wolfe, *Mimeographed Report*, Chemical Abstracts Service, **1963**.

[148] E. H. Sussenguth, Jr., *J. Chem. Doc.* **1965**, *5*, 36.

[149] G. W. Adamson, J. Cowell, M. F. Lynch, A. H. W. McLure, W. G. Town, A. M. Yapp, *J. Chem. Doc.* **1973**, *13*, 153.

[150] J. Friedrich, *Dissertation*, Technische Universität München, **1979**; J. Friedrich, I. Ugi, *J. Chem. Res. Synop.* **1980**, 70; *J. Chem. Res. Miniprint* **1980**, *1301*.

[151] M. G. Hicks, C. Jochum, *J. Chem. Inf. Comput. Sci.* **1990**, *30*, 191.

[152] A. V. Aho, J. E. Hopcroft, P. Ullma, *The Design and Analysis of Computer Algorithms*, Addison-Wesley, Reading, **1974**.

[153] W. D. Ihlenfeldt, *Dissertation*, Technische Universität München, **1991**.

[154] K. Bley, *Dissertation*, Technische Universität München, **1991**; E. Fontain, *Diplom thesis*, Technische Universität München, **1986**; K. Bley, I. Ugi, as yet unpublished.

[155] M. Knauer, *Dissertation*, Technische Universität München, **1992**.

[156] H. Thalhammer, *Diplom thesis*, Technische Universität München, **1991**.

[157] B. Raspel, G. Roden, B. Woost, C. Zirz in *Software-Entwicklung in der Chemie 3* (Ed.: G. Gauglitz), Springer, Heidelberg, **1989**, p. 33; W. T. Donner, in [13], p. 9.

[158] E. Meyer, E. Sens, *Anal. Chim. Acta* **1988**, *210*, 135.

[159] P. Bruck in *Chemical Structures - The International Language of Chemistry* (Ed.: W. A. Warr), Springer, Heidelberg, **1988**, p. 113.

[160] M. Hicks, C. Jochum, *Anal. Chim. Acta* **1990**, *235*, 87; M. G. Hicks in *Software-Entwicklung in der Chemie 3* (Ed.: G. Gauglitz), Spinger, Heidelberg, **1989**, p. 9.

[161] G. Klopman, *J. Am. Chem. Soc.* **1984**, *106*, 7315; *Mutat. Res.* **1984**, *126*, 139, 227; *J. Comput. Chem.* **1985**, *6*, 28.

[162] G. Klopman, *J. Math. Chem.* **1991**, *7*, 187.

[163] M. Knauer, I. Ugi, as yet unpublished.

[164] A. Dengler, I. Ugi, *J. Math. Chem.* **1992**, *9*, 1.

[165] I. Ugi, G. Kaufhold, *Justus Liebigs Ann. Chem.* **1967**, *709*, 11.

[166] I. Ugi, *Angew. Chem.* **1962**, *74*, 9; *Angew. Chem. Int. Ed. Engl.* **1962**, *1*, 8.

[167] I. Ugi, S. Lohberger, R. Karl in *Comprehensive Organic Synthesis: Selectivity of Synthetic Efficiency 2* (Eds.: B. M. Trost, C. H. Heathcock), Pergamon Press, Oxford, **1991**, Chapter 4.6.

[168] G. A. Blakley, *J. Chem. Educ.* **1982**, *59*, 728; C. Behnke, J. Bargon, *J. Chem. Inf. Comput. Sci.* **1990**, *30*, 228.

[169] J. Bauer, E. Fontain, I. Ugi, *Anal. Chim. Acta* **1988**, *210*, 123.

[170] R. E. Burkhard, *Methoden der ganzzahligen Optimierung*, Springer, Wien, **1972**; R. E. Burkhard, K. H. Stratmann, *Nav. Res. Logistics Qu.* **1978**, *25*, 129.

[171] D. E. Goldberg, *Genetic Algorithms in Search, Optimisation and Machine Learning*, Addison-Wesley, Reading, **1989**.

[172] *Modern Approaches to Chemical Reaction Searching* (Ed.: P. Willett), Gower, Aldershot, **1986**; D. Bawden, *J. Chem. Inf. Comput. Sci.* **1991**, *31*, 212.

[173] A. P. Johnson, *Chem. Br.* **1985**, *21*, 59; E. Zass, S. Müller, *Chimia* **1986**, *40*, 38; J. H. Borkent, F. Oukes, J. H. Noordik, *J. Chem. Inf. Comput. Sci.* **1988**, *28*, 148.

[174] W. T. Wipke, G. Vladutz, *Tetrahedron Comput. Methodol.* **1990**, *3*, 83.

[175] C. Tonnelier, P. Jauffret, T. Hanser, G. Kaufmann, *Tetrahedron Comput. Methodol.* **1990**, *3*, 351.

[176] K. Bley, J. Brandt, A. Dengler, R. Frank, I. Ugi, *J. Chem. Res.Synop.* **1991**, 261; *J. Chem. Res. Miniprint* **1991**, 2601.

[177] I. Ugi, J. Bauer, E. Fontain in *Personal Computers for Chemists* (Ed.: J. Zupan), Elsevier, Amsterdam, **1990**, p. 135.

[178] E. Fontain, K. Reitsam, *J. Chem. Inf. Comput. Sci.* **1991**, *31*, 96.

[179] We have access to an unpublished program developed by J. Bauer, which generates r-matrices from their defined mathematical properties.

[180] I. Ugi, *Chem. Scr.* **1986**, *26*, 205.

[181] J. Bauer, E. Fontain, I. Ugi, *MATCH* **1992**, *27*, 31.

[182] I. Ugi, *Proc. Estononian Acad Sci.* **1989**, *38*, 225; *ibid.* **1990**, *39*, 193.

[183] E. Fontain, *J. Chem. Inf. Comput. Sci.*, **1992**, *32*, 748.
[184] I. Ugi, J. Bauer, K. Bley, A. Dengler, E. Fontain, M. Knauer, S. Lohberger, *J. Mol. Structure (Theochem)* **1991**, *230*, 73.
[185] S. Lohberger, E. Fontain, I. Ugi, G. Müller, J. Lachmann, *New J. Chem.* **1991**, *15*, 913; *Acta Crystallogr. Sect. C* **1991**, *47*, 2444.
[186] R. E. Valdés-Pérez, *Tetrahedron Comput. Methodol.* **1990**, *5*, 277.
[187] R. Huisgen *Angew. Chem.* **1963**, *75*, 604, 742; *Angew. Chem. Int. Ed. Engl.* **1963**, *2*, 565, 633; *J. Org. Chem.* **1976**, *41*, 403.
[188] S. L. Beaucage, M. H. Caruthers, *Tetrahedron Lett.* **1981**, *22*, 1859; L. J. McBride, M. H. Caruthers, *ibid.* **1983**, *24*, 245.
[189] D. Marquarding, F. Ramirez, I. Ugi, P. D. Gillespie, *Angew. Chem.* **1973**, *85*, 99; *Angew. Chem. Int. Ed. Engl.* **1973**, *12*, 91.
[190] F. Westheimer, *Acc. Chem. Res.* **1968**, *11*, 70.
[191] F. Ramirez, S. Glaser, P. Stern, P. D. Gillespie, *Angew. Chem.* **1973**, *85*, 39; *Angew. Chem. Int. Ed. Engl.* **1973**, *12*, 66; F. Ramirez, J. F. Marecek, I. Ugi, *Synthesis* **1975**, 99.
[192] W. Richter, R. Karl, I. Ugi, *Tetrahedron* **1990**, *46*, 3167.
[193] F. Ramirez, I. Ugi, *Phosphorus Sulfur* **1976**, *1*, 231.
[194] I. Ugi, P. Jacob, B. Landgraf, C. Rupp, P. Lemmen, U. Verfürth, *Nucleosides Nucleotides* **1988**, *7*, 605; I. Ugi, N. Bachmeier, R. Herrmann, P. Jacob, R. Karl, P. Lemmen, W. Richter, U. Verfürth, *Phosphorus Sulfur Silicon* **1990**, *51/52*, 57.
[195] P. Jacob, W. Richter, I. Ugi, *Liebigs Ann. Chem.* **1991**, 519; R. Karl, P. Lemmen, W. Richter, I. Ugi, B. Werner, *Synthesis*, submitted.
[196] W. N. Lipscomb, *Boron Hydrides*, Benjamin, New York, **1966**, p. 57.
[197] B. Brellochs, H. Binder, *Angew. Chem.* **1988**, *100*, 270; *Angew. Chem. Int. Ed. Engl.* **1988**, *27*, 262.
[198] R. E. Carhart, D. H. Smith, H. Brown, C. Djerassi, *J. Am. Chem. Soc.* **1975**, *97*, *5755*.
[199] R. E. Carhart, D. H. Smith, N. A. B. Gray, J. G. Nourse, C. Djerassi, *J. Org. Chem.* **1981**, *46*, 1708.
[200] V. V. Serov, L. A. Gribov, M. E. Elyashberg, *J. Mol. Struct. (Theochem)* **1985**, *129*, 183.
[201] A. Kerber, R. Laue, D. Moser, *Anal. Chim. Acta* **1990**, *235*, 221.
[202] H. Huixiao, X. Xinguan, *J. Chem. Inf. Comput. Sci.* **1991**, *31*, 116.
[203] S. Bohanec, J. Zupan, *J. Chem. Inf. Comput. Sci.* **1991**, *31*, 531.
[204] I. Ugi, E. Wischhöfer, *Chem. Ber.* **1962**, *95*, 136.
[205] D. H. R. Barton, *Aldrichimica Acta* **1990**, *23*, 3.
[206] R. Herges, *Tetrahedron Comput. Methodol.* **1988**, *1*, 15; K. M. T. Yamada, M. W. Markus, G. Winnewesser, W. Joentgen, R. Kock, E. Vogel, H.-J. Altenbach, *Chem. Phys. Lett.* **1989**, *160*, 113.
[207] R. Herges, I. Ugi, *Angew. Chem.* **1985**, *97*, 596; *Angew. Chem. Int. Ed. Engl.* **1985**, *24*, 594; *Chem. Ber.* **1986**, *119*, 829.
[208] F. W. Fowler, *Angew. Chem.* **1971**, *83*, 148; *Angew. Chem. Int. Ed. Engl.* **1971**, *10*, 135.
[209] S. M. McElvain, *Org. React. (NY)*, **1948**, *4*, 256.
[210] M. Stoll, *Helv. Chim. Acta* **1947**, *30*, 1837.
[211] R. Herges, *J. Chem. Inf. Comput. Sci.* **1990**, *3*, 377.
[212] R. Herges, C. Hoock, *Science* **1992**, *255*, 711.
[213] R. Herges in *Proc. 4th Chem. Congr. North Am.*, Division of Chemical Information, New York, **1991**, in press.
[214] R. Herges, *J. Chem. Inf. Comput. Sci.* **1990**, *30*, 37.
[215] J. Arct, U. H. Brinker, *Methoden Org. Chem. (Houben-Weyl) 4th ed. 1952–Vol. E19b*, **1989**, p. 337.
[216] H. Dürr, E. M. Frühauf, *Methoden Org. Chem. (Houben-Weyl) 4th ed. 1952–Band E19b*, **1989**, p. 775.
[217] W. von E. Doering, J. F. Coburn, Jr., *Tetrahedron Lett.* **1965**, 991.
[218] C. Wentrup, R. Harder, *Top. Curr. Chem.* **1976**, *62*, 173.
[219] G. B. Fisher, J. J. Juarez-Brambila, C. T. Goralski, W. T. Wipke, B. Singaram, *J. Am. Chem. Soc.*, submitted.
[220] G. Augelman, H. Fritz, G. Rihs, J. Streith, *J. Chem. Soc. Chem. Commun.* **1982**, 1112.
[221] A. Defoin, G. Augelman, H. Fritz, G. Geoffroy, C. Schmidlin, J. Streith, *Helv. Chim. Acta* **1985**, *68*, 1998.
[222] W. Ried, R. Dietrich, *Angew. Chem.* **1963**, *75*, 476; *Angew. Chem. Int. Ed. Engl.* **1963**, *2*, 495.
[223] J. Metzger in *Comprehensive Heterocyclic Chemistry 6* (Eds.: A. R. Katritzky, C. W. Rees, K. T. Potts), Pergamon Press, Oxford, **1984**, p. 294.
[224] A. Baretta, B. Waegell, *React. Intermed. (Plenum)* **1982**, *3*, 527.
[225] K. Shishido, E. Shitara, K. Fukumoto, T. Kametani, *J. Am. Chem. Soc.* **1985**, *107*, 5810.
[226] J. Oró, A. P. Kimball, *Arch. Biochem. Biophys.* **1961**, *94*, 217; J. Oró, S. S. Amat, *Nature* **1961**, *190*, 442; R. E. Dickerson, *Sci. Am.* **1978**, *239*, (9) 70; *Spektrum Wiss.* **1979** (9) *98*; see also S. Drenkard, J. Ferris, A. Eschenmoser, *Helv. Chim. Acta* **1990**, *73*, 1373.

Extending the Metal Cluster–Metal Surface Analogy

By *Bruce C. Gates**

By the early 1970s, the chemistry of metal clusters—compounds with metal–metal bonds stabilized by ligands such as carbonyls—was emerging from its infancy, as described in the seminal work of Chini.[1] In 1975 Muetterties[2] proposed analogies between metal clusters and metal surfaces and speculated that molecular metal clusters would be found to be catalysts with novel properties. A central argument was that clusters have reactivities different from those of complexes with a single metal atom because they have neighboring metal centers, and the unique metal–ligand bonding patterns in clusters could be expected to facilitate reactions like those occurring on metal surfaces.

In 1975, the western world had just undergone one of its periodic oil supply crises, and a result of this was a surge in interest in catalysis related to production of synthetic fuels; research on the chemistry of catalytic hydrogenation of CO to give hydrocarbons (Fischer–Tropsch chemistry) went through one of its periodic spikes of activity. Simultaneously, metal cluster chemistry became a "hot" topic, with much of the research motivated by the prospect of finding novel catalysts for CO hydrogenation, among other reactions.

A few years later, Muetterties et al.[3] published a detailed, quantitative assessment of the analogies in structure and bonding between metal clusters and metal surfaces, but reactivity and catalysis were largely missing from the assessment. A consensus emerged, articulated by Ertl,[4] that the cluster–surface analogy, although imperfect,[5] includes structure and bonding but does not extend to reactivity and catalysis. Surface scientists, building from this analogy, have now come to rely primarily on comparisons of vibrational spectra of adsorbed species with those of molecular metal clusters characterized by crystallography as the basis for determining structures of adsorbates on metal surfaces.[6] Thus the merging of organometallic chemistry and surface chemistry is well underway.[7]

The anticipated evidence of catalysis by metal clusters, however, has not emerged,[8] and the few examples of cluster catalysis are neither very well understood nor of practical importance; the prospects are limited by the lack of stability of most metal clusters. One consequence of the lack of practical successes has been a marked decrease in the attention paid to research on metal clusters, although progress had continued to be rapid.[9]

Now a pair of recent papers[10, 11] illustrates that the analogy between metal carbonyl clusters and metal surfaces with adsorbed CO ligands extends beyond structure and bonding: The reactivity of a CO molecule bridging metal atoms in a metal cluster reported by Chisholm et al.[10] is analogous to that of a CO molecule bridging metal atoms on a metal surface, reported by Yates et al.[10] The bridging CO dissociates into carbido and oxido ligands (Scheme 1). This step is important in the Fischer–Tropsch reaction catalyzed by metal surfaces.

Scheme 1. Dissociation of a bridging CO molecule.

Both the CO bound to alkoxidotetratungsten $[W_4(OR)_{12}]$ clusters[10] and the CO adsorbed on a sparsely covered Mo(110) surface react with dissociation to give carbido and oxo ligands bonded to neighboring metal centers. The evidence for this reactivity in molecular metal clusters is based on NMR spectra and crystallographic data for a family of clusters, including $[W_4(\mu_4\text{-C})(O)(O\mathit{i}Pr)_{12}]$, the skeleton of which is shown in Figure 1.[10] The carbido ligand is bonded to four tungsten atoms in a butterfly arrangement; the oxo ligand (O6) is bonded to two tungsten atoms. The species on the Mo(110) surface were characterized by vibrational (electron energy loss) spectroscopy, and indications of reactivities of variously bonded CO species were obtained by temperature-programmed desorption (thermal desorption) with analysis of the desorbed products by mass spectrometry.[11]

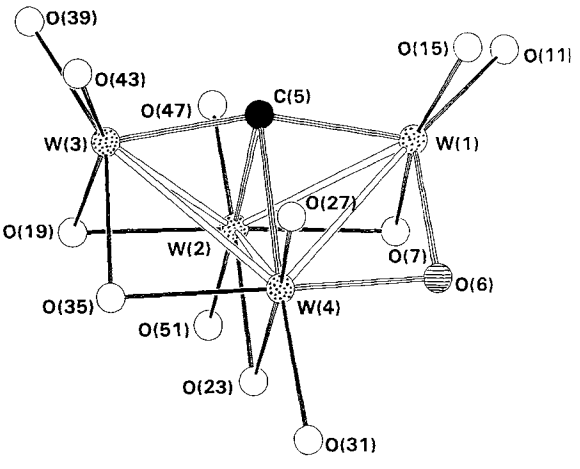

Fig. 1. The $W_4(C)(O)_{13}$ core of the $[W_4(\mu_4\text{-C})(O)(O\mathit{i}Pr)_{12}]$ cluster. O(6) is the oxo ligand (from ref. [10]).

The analogy between the reactivity of CO in the cluster and that of CO on the surface is thus clearly evident, confirming what had been supposed by Muetterties.[12] However, there are differences between the reactivity in the cluster and on the surface. Chisholm et al.[10] identified a cluster with a bridging $(\eta^2,\mu_4\text{-CO})$ group. This structural feature is most pertinent to the cleavage of a CO ligand; however, they found no direct evidence of the reaction of CO with the coordinatively unsaturated tungsten clusters to give $[W_4(OR)_{12}(CO)]$ intermediates, and they could only speculate that the CO may initially bind to one of the W atoms of the cluster framework. The results imply that the bonding of CO to the cluster must be the rate-determining step in the CO

[*] Prof. Dr. B. C. Gates
Department of Chemical Engineering
University of California
Davis, CA 95616 (USA)

dissociation. As the temperature was raised, indications of carbido ligands in the cluster appeared at 243 K.

In contrast, Yates et al.[11] observed variously bonded CO ligands on Mo metal at fractional surface coverages of less than 1. Some ligands were conventionally bound, and one of the CO ligands, characterized by a ν_{CO} band at 1130 cm^{-1}, was inferred (on the basis of a comparison with the IR spectra of carbonylmetal clusters) to bridge two Mo atoms: Mo–C–O–Mo. This is a stable intermediate in the dissociation reaction on the surface. At a surface coverage by CO of about 0.23, the only observed CO species was inferred to be inclined (ν_{CO} = 1345 cm^{-1}), with the C atom bonded to a Mo atom and the O atom interacting with a neighboring Mo atom but not bonded to it. This CO was converted to the bridging species (ν_{CO} = 1130 cm^{-1}), and at least some of the dissociation of adsorbed CO proceeded through this bridged intermediate. When the surface coverage was 0.17, the adsorbed CO was converted into C and O at about 200 to 250 K; the surface reaction was rate determining.

In summary, the data reveal differences in reactivity of the cluster and surface, characterized by different rate-determining steps and different rates of reaction—although these are not determined quantitatively. It is known[4, 10] that the rate of a reaction induced by a molecular cluster is usually less than that induced by a sparsely covered surface of the same metal. The initial step of bonding of a ligand to a cluster requires coordinative unsaturation of the cluster. Since most stable metal clusters are coordinatively saturated, reaction steps such as dissociation of a ligand or reaction of a pair of bound ligands with each other to free a coordination site are prerequisites. In contrast, relatively clean surfaces present arrays of rigid, stable coordinatively unsaturated sites where ligands can be readily bonded and activated.

Thus, although the reaction path of a ligand bonded to a molecular metal cluster and that of a ligand on a metal surface may sometimes be similar, the catalytic activity of a molecular metal cluster is usually expected to be less than that of a sparsely covered surface with a comparable arrangement of metal atoms. However, metal surfaces are usually largely covered with adsorbates during catalysis, and one might still be justifiably tempted to seek similarities between the catalytic properties of such surfaces and those of metal clusters. If metal cluster–metal surface analogies in catalysis are to be found, they are expected to be closest when the metals are dispersed in the form of small particles ("clusters") on solid supports, as was recognized early by Basset and Ugo.[13] This is precisely the form of many industrial metal catalysts. Relatively robust carbonylmetal clusters such as $[H_3Os_4(CO)_{12}]^-$ have been observed on surface suring catalysis of CO hydrogenation,[14] but their role in catalysis remains to be assessed. Furthermore, some industrial supported metal catalysts have such small clusters (typically, five or six Pt atoms in clusters supported in L zeolite[15] used to convert *n*-hexane into benzene) that they may be regarded as virtually molecular in character.

German version: *Angew. Chem.* **1993**, *105*, 240

[1] P. Chini, *Inorg. Chim. Acta Rev.* **1968**, *2*, 31; *Pure Appl. Chem.* **1970**, *23*, 489; P. Chini, G. Longoni, V. G. Albano, *Adv. Organomet. Chem.* **1976**, *14*, 285; P. Chini, *Gazz. Chim. Ital.* **1979**, *109*, 225.

[2] E. L. Muetterties, *Bull. Soc. Chim. Belg.* **1975**, *84*, 959.

[3] E. L. Muetterties, T. N. Rhodin, E. Band, C. Brucker, H. Pretzer, *Chem. Rev.* **1979**, *79*, 91.

[4] G. Ertl in *Metal Clusters in Catalysis* (Eds.: B. C. Gates, L. Guczi, H. Knözinger), Elsevier, Amsterdam, **1986**, p. 577.

[5] M. Moskovits, *Acc. Chem. Res.* **1979**, *12*, 229.

[6] G. A. Somorjai in *Perspectives in Catalysis* (Eds.: J. M. Thomas, K. I. Zamaraev), Blackwell, London, **1992**, p. 147.

[7] M. R. Albert, J. T. Yates, Jr., *A Surface Scientist's Guide to Organometallic Chemistry*, American Chemical Society, Washington, DC, **1987**.

[8] W. L. Gladfelter, K. J. Rosselet in [9], p. 329.

[9] *The Chemistry of Metal Cluster Complexes* (Eds.: D. F. Shriver, H. D. Kaesz, R. D. Adams), VCH, Weinheim, **1990**.

[10] M. H. Chisholm, C. E. Hammond, V. J. Johnston, W. E. Streib, J. C. Huffman, *J. Am. Chem. Soc.* **1992**, *114*, 7056.

[11] M. L. Colaianni, J. G. Chen, W. H. Weinberg, J. T. Yates, Jr., *J. Am. Chem. Soc.* **1992**, *114*, 3735.

[12] E. L. Muetterties, *Science* (Washington, DC) **1977**, *196*, 839.

[13] J.-M. Basset, R. Ugo in *Aspects of Homogeneous Catalysis, Vol. III* (Ed.: R. Ugo), Reidel, Dordrecht, **1977**, p. 137.

[14] H. H. Lamb, B. C. Gates, *J. Am. Chem. Soc.* **1986**, *108*, 81; H. H. Lamb, T. R. Krause, B. C. Gates, *Proc. Int. Congr. Catal. 9th* **1988**, *3*, 1378.

[15] M. Vaarkamp, J. V. Grondelle, J. T. Miller, D. J. Sajkowski, F. S. Modica, G. S. Lane, B. C. Gates, D. C. Koningsberger, *Catal. Lett.* **1990**, *6*, 369.

 © *VCH Verlagsgesellschaft mbH, W-6940 Weinheim, 1993* *0570-0833/93/0202-0229 $ 10.00+.25/0*

Pentazole and Other Nitrogen Rings

By *Rudolf Janoschek**

Although the road of the pentazoles through chemistry has not only just begun, its end is not yet in sight; they have proved that they can stay the distance. Their history began in 1903 when Hantzsch[1] tried in vain to form phenylpentazole (**2**) by rearrangement of benzenediazonium azide (**1**).[**]

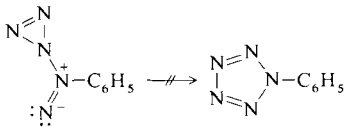

1 **2**

Dimroth and de Montmollin[2] also had no luck when they planned to prepare phenylpentazole from a chain of six nitrogen atoms (**3**). Then in 1915 success seemed to be at

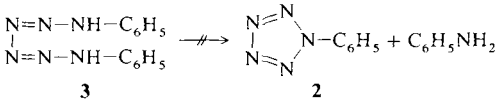

3 **2**

hand when Lifschitz[3] believed he had synthesized pentazolyl acetic acid amidrazone (**5**) from tetrazolecarbonitrile (**4**). But in the same year came a rebuttal from Curtius

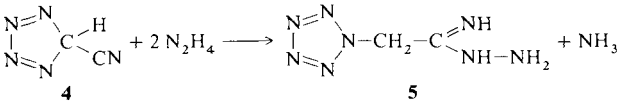

4 **5**

et al.[4] with the title "Die sogenannten Pentazol-Verbindungen von Lifschitz" ("The so-called pentazole compounds of Lifschitz"). They did not mince their words: "Ein derartiger Reaktionsverlauf wäre im höchsten Grade überraschend ... Lifschitz glaubt die Richtigkeit seiner Auffassung 'mit vollkommener Sicherheit' folgern zu müssen ... ohne weitere Prüfung in das Reich des Unmöglichen zu verweisen ... daß alle seine Beobachtungen und Folgerungen auf Irrtum beruhen ... von Pentazol keine Rede sein kann."[***]

Dispute, misunderstanding, and failure dogged the pentazoles from the beginning. Curtius's verdict hit hard. Almost half a century passed before anyone again ventured a search for pentazole. Huisgen and Ugi[5] thus solved a classic problem in 1956 when they proved that they could link the benzenediazonium ion (**6**) with the azide ion to form benzenediazoazide (**7**), which on ring-closure yielded phenylpentazole (**2**).

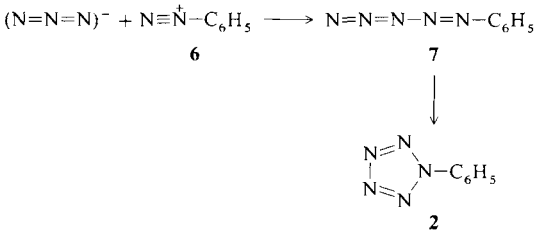

6 **7** **2**

The first structure determination by X-ray diffraction on a pentazole was performed in 1983 by Dunitz and Wallis.[6] The N–N bond lengths in the five-membered ring were all similar (1.31–1.35 Å) and lie between the standard values for N–N (1.449 Å) and N=N (1.252 Å), which can be interpreted as a clear sign of an aromatic ring with six π electrons. This information does not, however, close the chapter on the pentazoles. In fact quite to the contrary, it is now all the more puzzling why the parent compound of the pentazoles, HN_5 (**8**), is still unknown. After all, it would be the final

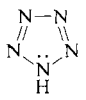

8

member of a well-known series that begins with pyrrole and breaks off prematurely at tetrazole. Perhaps theory can help solve the enigma.

The interest of the quantum chemists in pentazoles was only recently aroused by Ferris and Bartlett.[7] They employed ab initio calculations such as the *n*th order *m*any-*b*ody *p*erturbation *t*heory, abbreviated to MBPT(n), whose better known variant is the *n*th order Møller–Plesset perturbation theory, MPn. The MBPT(n) procedure takes account of *all* the terms to a predetermined final order *n* for the electron correlation. In the *c*oupled *c*luster (CC) theory, on the other hand, certain contributions from the MBPT formalism are summated for *all* orders *n*. Use of the DZP basis set with these procedures yielded the anticipated structural parameters for cyclic HN_5 (**8**) with C_{2v} symmetry and proof that it represents a minimum on the energy hypersurface. The energy barrier for potential decomposition into HN_3 and N_2 was given on the MBPT(2) level as 19.8 kcal mol^{-1}.

The question in the title of reference [7], "Does it exist?", can, of course, not yet be answered on these grounds alone. Experience shows that the MBPT procedure yields energy barriers that are too high. This will be demonstrated later in this highlight for the N_4 molecule. To estimate the kinetic stability of **8** more accurately, other calculation methods such as MP2, MP4, CC, or MCSCF-CI should also be employed. I therefore applied myself to the problem of the uncertainty in this decomposition barrier of 19.8 kcal mol^{-1}. Table 1 collates some of the results.

If electron correlation is considered, the height of the barrier varies between 13.7 and 20.9 kcal mol^{-1}, which might cast doubt on the kinetic stability. Furthermore, the energy hypersurface for the triplet state may not be ignored, because it might cross energy barriers leading to spin-forbidden processes (intersystem crossing) and thus to other decomposi-

[*] Prof. Dr. R. Janoschek
Institut für Theoretische Chemie der Universität
Mozartgasse 14, A-8010 Graz (Austria)

[**] Formerly the azide structure was assumed to be a three-membered ring. This is documented on the Curtius monument in Heidelberg (FRG).

[***] "Such a course for the reaction would be extremely surprising ... Lifschitz believes he must conclude that his interpretation is correct 'in perfect confidence' ... without further proof it must be relegated to the realm of the impossible ... all his observations and conclusions are based on error ... there can be no question of pentazoles in this case."

Table 1. The activation barrier ΔE [kcal mol^{-1}] incorporating the zero-point vibrational correction for the decomposition $HN_5 \rightarrow HN_3 + N_2$, calculated with several methods.

Method [a]	ΔE
HF/6-31G*	36.9
MP2/6-31G*	13.7
MP4/6-31G*	18.9
MBPT(2)/DZP [7]	19.8
CCSD/6-31G*	20.9

[a] The calculations with the 6-31G* basis set were performed with the program GAUSSIAN 92.

tion pathways. Only one issue is definite: theory has pointed the way; the next step must be left to experiment. Matrix isolation has provided many a surprise in the past.

As dramatic as the tale of the pentazoles is the story of the vain attempt to detect a six-membered nitrogen ring. The first calculations were performed in the early seventies. In 1980 Vogler et al.[8] found indications that N_6 is cleaved on UV irradiation from *cis*-$[Pt(N_3)_2(PPh_3)_2]$ embedded in a matrix, but it is only stable at low temperature. At that time hexaazabenzene (**9**) was considered the only feasible structure for N_6. This report loosed an avalanche of quantum chemical calculations, in particular because **9** is isoelectronic with benzene and thus should likewise display aromatic stabilization. The calculations over the decade produced every conceivable answer: hexaazabenzene has D_{6h} symmetry ... has D_{3h} symmetry ... does not exist, because **9** is the transition structure for nitrogen exchange for $3N_2$. The latest MBPT calculations of Bartlett et al.[9] nullified all previous

9

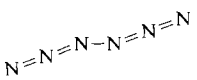

10

labors. According to them, hexaazabenzene cannot exist because this arrangement of atoms (D_{6h}) gives two imaginary frequencies for the out-of-plane vibrations. The naive view and the conclusions from it that *all* cyclic compounds with six π electrons must be aromatic had already been convincingly disproved by Shaik et al.[10] The idea that Vogler's N_6 could be diazide (**10**), which was shown by recent calculations[11] to be 35 kcal mol^{-1} more stable than **9**, was supported repeatedly during the past ten years.

Now that the birth of the five-membered nitrogen rings has been announced only after a long labor, and a six-membered nitrogen ring has even been disputed by theory, it is the turn of three- and four-membered nitrogen rings. In 1977 triaziridine N_3H_3 was discovered in small amounts bound as a complex to a zeolite crystal. X-ray diffraction confirmed the ring structure.[12] More recent ab initio calculations suggest that this compound can also exist in uncomplexed form, since the three-membered nitrogen ring represents a minimum on the energy hypersurface.[13] The authors of this paper, however, are even self-critical and issue a warning that applies to all the theoretical investigations considered here: "... but we must do more work to understand the kinetic lability of these compounds".

In the form of **11**, a structure isoelectronic with cyclobutadiene, N_4 is shown in the SCF approximation to be distinctly more stable than tetraazatetrahedrane (**12**). If the electron

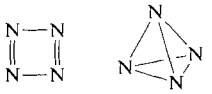

11 **12**

correlation is taken into account, the order is reversed.[9] For this reason, and also because of the homology to the known tetrahedral P_4, more attention has been paid to structure **12** than to **11**. After the most thorough theoretical study yet undertaken,[14] Lee and Rice calculate a considerable energy barrier of 61 kcal mol^{-1} for the decomposition $N_4 \rightarrow 2N_2$. The authors exploited all possibilities both with the basis set (DZP, [4s, 3p, 2d, 1f]) and with the methods of calculation (CASSCF, MP2, CC) to separate the less appropriate methods from the better ones by comparing the different results. In the process, the energy barrier for the decomposition was lowered from 80 to 61 kcal mol^{-1}. Bartlett et al.[9] report a quite high value of 79 kcal mol^{-1} from only one MBPT calculation, which leads to the conclusion that energy barriers calculated with MBPT are too high as a result of a systematic error, and the kinetic stability of all the compounds covered here is therefore overemphasized. The lower, but nevertheless still substantial barrier for N_4 decomposition must not lead to a premature euphoria,[9] because the triplet energy hypersurface intersects this barrier low down,[14] as can be seen in Figure 1. A fast spin-forbidden process (double intersystem crossing) can therefore annihilate N_4. Incidentally, it should be said that a decomposition barrier of only 1 kcal mol^{-1} has been calculated with the semiempirical AM1 method.

This trail through the territory of the nitrogen rings should not end without mention of the latest candidates for experimental proof. Minima have been located on the energy hypersurface for bipentazole N_5–N_5[7] and octaazacubane N_8,[9] and structural data have been reported.

Have nitrogen rings or cages any interesting property that makes the effort to synthesize them worthwhile? A glance at the reaction energies on decomposition to N_2 gives an answer. The energy released per N_2 unit on decomposition of N_4 is 93 kcal mol^{-1} and of N_8, 112 kcal mol^{-1}. Such high energy density makes these compounds promising rocket

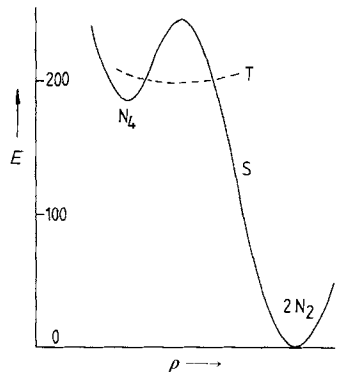

Fig. 1. The energy profile E [kcal mol^{-1}] for the decomposition of N_4 (T_d) to $2N_2$ along the reaction coordinate ρ. Solid line: singlet state (S); broken line: triplet state (T) (from [14]).

fuels. In fact, theory predicts a better efficiency for N_8 than for the conventional fuel, which is based on H_2 and O_2.

The intention of this short report was to show the advance of theory through ab initio calculations in the field of nitrogen rings. Although the calculated molecular properties can still be extended and refined, already a quite clear picture emerges. Nitrogen rings, and in particular nitrogen cages, are extremely energy-rich and kinetically labile systems. In comparison with the results of theoretical studies, the yield of the experimental investigations is as yet small. N_3H_3 and N_6 were unintentional successes. Well-targeted photochemical studies under matrix conditions will probably still expose several surprises.

German version: *Angew. Chem.* **1993**, *104*, 242

[1] A. Hantzsch, *Ber. Dtsch. Chem. Ges.* **1903**, *36*, 2056.
[2] O. Dimroth, G. de Montmollin, *Ber. Dtsch. Chem. Ges.* **1910**, *43*, 2904.
[3] J. Lifschitz, *Ber. Dtsch. Chem. Ges.* **1915**, *48*, 410.
[4] T. Curtius, A. Darapsky, E. Müller, *Ber. Dtsch. Chem. Ges.* **1915**, *48*, 1614.
[5] R. Huisgen, I. Ugi, *Angew. Chem.* **1956**, *68*, 705; *Chem. Ber.* **1957**, *90*, 2914.
[6] J. D. Wallis, J. D. Dunitz, *J. Chem. Soc. Chem. Commun.* **1983**, *16*, 910.
[7] K. F. Ferris, R. J. Bartlett, *J. Am. Chem. Soc.* **1992**, *114*, 8302.
[8] A. Vogler, R. E. Wright, H. Kunkely, *Angew. Chem.* **1980**, *92*, 745; *Angew. Chem. Int. Ed. Engl.* **1980**, *19*, 717.
[9] W. J. Lauderdale, J. F. Stanton, R. J. Bartlett, *J. Phys. Chem.* **1992**, *96*, 1173.
[10] S. S. Shaik, P. C. Hiberty, J. M. Lefour, G. Ohanessian, *J. Am. Chem. Soc.* **1987**, *109*, 363.
[11] M. T. Nguyen, *J. Phys. Chem.* **1990**, *94*, 6923.
[12] Y. Kim, J. W. Gilje, K. Seff, *J. Am. Chem. Soc.* **1977**, *99*, 7057.
[13] D. H. Magers, E. A. Salter, R. J. Bartlett, C. Salter, B. A. Hess, Jr., L. J. Schaad, *J. Am. Chem. Soc.* **1988**, *110*, 3435.
[14] T. J. Lee, J. E. Rice, *J. Chem. Phys.* **1991**, *94*, 1215.

Enantioselective Transition Metal-Catalyzed Hydrogenation for the Asymmetric Synthesis of Amines

By *Carsten Bolm**

Catalyzed asymmetric reductions of functionalized olefins and ketones occur very selectively, in contrast reductions of C=N bonds have so far only led to low enantioselectivities.[1] In two recent publications Burk and Feaster[2] and also Willoughby and Buchwald[3] reported new transition metal catalysts for homogeneous asymmetric hydrogenation, with which optically active amines can be obtained with high enantiomeric excesses.

Following the investigations of the enantioselective hydrogenation of functionalized olefins with chiral bis(phospholane)rhodium(I) complexes,[4] Burk and Feaster have now used the new transition metal catalysts for the asymmetric synthesis of primary amines.[2] With 0.1 mol% of the catalyst system (Et-duphos)Rh^I $[Rh(\mathbf{5})]^+$, *N*-aroylhydrazones **3** of arylalkyl ketones and α-keto esters are reduced under mild reaction conditions (20 °C, 1–4 atm H_2, 1–36 h, in 2-propanol) to give the corresponding optically active *N*-aroylhydrazines **4** (Scheme 1).

In comparison with other chiral diphosphanes such as binap,[5] chiraphos,[5] or bdpp,[5] **5** proved to be the most effective ligand for the transition metal catalysts; enantioselectivities of up to 97% *ee* were achieved with **5**. If compound **4** is allowed to react with samarium iodide (≥2 equiv), the N–N bond can be cleaved and the corresponding amine **2** is obtained with no loss of optical purity. Thus, synthetically valuable primary amines are obtained as reaction products. The chiral α-hydrazino acid derivatives are of particular interest. These derivatives are obtained from α-keto esters and their hydrogenolysis leads to the optically active α-amino acids.

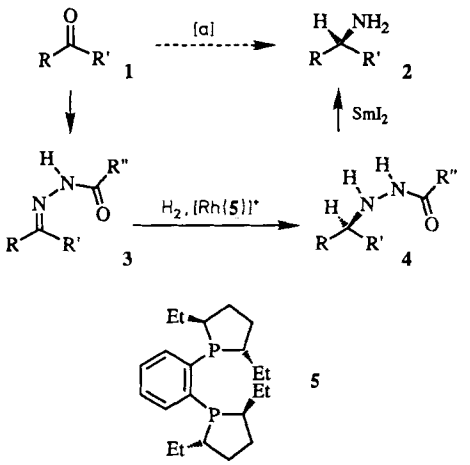

Scheme 1. [a] Reductive amination. R = aryl, CO_2Me, CO_2Et; R′ = alkyl, aryl; R″ = aryl; Et-duphos = **5**.

In their new work[2] Burk and Feaster refer to a series of experiments on the asymmetric reduction of C=N bonds with rhodium(I) catalysts for which molecular hydrogen[6] and silanes[7] were used as reducing agents.[8] In contrast to these known methods, which usually lead to the formation of secondary amines, the asymmetric reductive amination with the $[Rh^I(duphos)]$ complexes now introduced is also distinguished by an extended substrate range, higher enantio- and chemoselectivity as well as milder reaction conditions. Nitriles, imines, halides as well as carbonyl and nitro compounds are not reduced, nonfunctionalized olefins and alkynes are only hydrogenated in small amounts (<2%). Two factors are proposed to be responsible for this high chemoselectivity. A substrate chelation at the cationic transition metal center increases the rate of hydrogenation of the *N*-

[*] Dr. C. Bolm
Departement Chemie der Universität Basel
St. Johanns-Ring 19, CH-4056 Basel (Switzerland)

aroylhydrazones selectively, and the reduction of other functional groups is inhibited by the *N*-aroylhydrazines formed. The *N*-phenylimine and *N*-phenylhydrazone of acetophenone are correspondingly not hydrogenated under these mild reaction conditions. Osborn et al. previously reported[9a, b] similar high chemoselectivities in metal-catalyzed hydrogenations of *N*-arylketimines. The diphosphaneiridium complexes used here are very active, as Spindler et al. have also shown,[9c] but result in products with lower enantiomeric excesses.[9b, c] The optically active secondary and cyclic amines prepared with the iridium catalyst system are important intermediates in the synthesis of herbicides.

Willoughby and Buchwald have investigated[3] a fundamentally different catalyst system for the asymmetric reduction of C=N bonds. If 2–10 mol% of the chiral *ansa*-titanocene **6** is used as the catalyst for the hydrogenation of cyclic imines with molecular hydrogen excellent enantioselectivites (up to 98% *ee*; Scheme 2) are achieved. In contrast, the

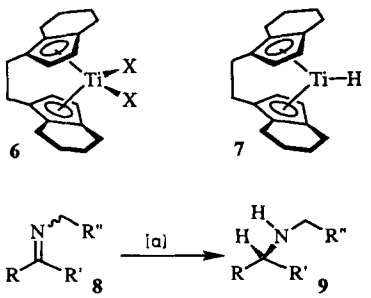

Scheme 2. X_2 = 1,1'-binaphthyl-2,2'-diolate. [a] H_2 pressure, 2–10 mol% **6**; R,R',R" = alkyl, aryl.

reactions of acyclic compounds with C=N bonds occur less selectively; starting from *N*-benzylimines the products are only obtained with *ee* values of between 58 and 87%. Steric factors in the formation of diastereomeric transition states and competitive hydrogenations of stereochemically different substrate/catalyst complexes are thought to be responsible for this.

The authors assume that the hydridotitanium(III) complex **7** is the active form of the catalyst; **7** is prepared by the reaction of the stable complex **6** with *n*-butyllithium in situ and is stabilized by phenylsilane. The hydrogenation of the ketimines occurs in THF at 65 °C under increased hydrogen pressure (ca. 135 atm).

Willoughby and Buchwald have thus shown for the first time that the *ansa*-metallocenes[10] developed by Brintzinger et al. can also be used for the asymmetric hydrogenation of ketimines and thus for the enantioselective synthesis of amines. In the corresponding asymmetric reduction of olefins, structurally related *ansa*-zirconocene binaphtholates were previously tested by Waymouth and Pino as precursors for homogeneous Ziegler–Natta systems (65% ee_{max} for the deuteration of styrene).[11a] This reaction is also catalyzed by a cationic *ansa*-zirconocene hydride structurally analogous to **7**.[11b] The idea of using *ansa*-metallocenes as asymmetric catalysts[12a–d] or chiral reagents[12e, f] is based on their unusually high stereochemical control for the polymerizations and oligomerization reactions of olefins,[13] which can be used both for the formation of stereoregular products[14] of high molecular weight and also for the synthesis of optically active oligo- and polymers.[15]

The enantioselective syntheses of amines of Burk and Feaster,[2] and Willoughby and Buchwald[3] introduced here again illustrate the extraordinary potential of modified chiral transition metal complexes for asymmetric catalysis. Thus, they are not only interesting contributions to modern synthetic chemistry but also important steps on the often difficult path to a more selective and more efficient chemistry.

German version: *Angew. Chem.* **1993**, *105*, 245

[1] a) *Comprehensive Organic Synthesis, Vol. 8* (Eds.: B. M. Trost, I. Fleming), Pergamon, Oxford, **1991**; b) K. Harada, T. Munegumi in [1a], pp. 139–158; c) M. Nishizawa, R. Noyori in [1a], pp. 159–182; d) H. Takaya, R. Noyori in [1a], pp. 443–469.

[2] M. J. Burk, J. E. Feaster, *J. Am. Chem. Soc.* **1992**, *114*, 6266–6267.

[3] C. A. Willoughby, S. L. Buchwald, *J. Am. Chem. Soc.* **1992**, *114*, 7562–7564.

[4] a) M. J. Burk, J. E. Feaster, R. L. Harlow, *Organometallics* **1990**, *9*, 2653–2655; b) *Tetrahedron: Asymmetry* **1991**, *2*, 569–592; c) M. J. Burk, *J. Am. Chem. Soc.* **1991**, *113*, 8518–8519.

[5] binap = 2,2'-bis(diphenylphosphino)-1,1'-binaphthyl, chiraphos = bis(diphenylphosphino)butane, bdpp = bis(diphenylphosphino)pentane.

[6] a) A. G. Becalski, W. R. Cullen, M. D. Fryzuk, B. R. James, G.-J. Kang, S. J. Rettig, *Inorg. Chem.* **1991**, *30*, 5002–5008; b) W. R. Cullen, M. D. Fryzuk, B. R. James, J. P. Kutney, G.-J. Kang, G. Herb, I. S. Thorburn, R. Spogliarich, *J. Mol. Catal.* **1990**, *62*, 243–253; c) G.-J. Kang, W. R. Cullen, M. D. Fryzuk, B. R. James, J. P. Kutney, *J. Chem. Soc. Chem. Commun.* **1988**, 1466–1467; d) J. Bakos, Á. Orosz, B. Heil, M. Laghmari, P. Lhoste, D. Sinou, *ibid.* **1991**, 1684–1685; e) J. Bakos, I. Tóth, B. Heil, G. Szalontai, L. Párkányi, V. Fülöp, *J. Organomet. Chem.* **1989**, *370*, 263–276.

[7] a) N. Langlois, T. P. Dang, H. B. Kagan, *Tetrahedron Lett.* **1973**, 4865–4868; b) H. B. Kagan, N. Langlois, T. P. Dang, *J. Organomet. Chem.* **1975**, *90*, 353–365; c) R. Becker, H. Brunner, S. Mahboobi, W. Wiegrebe, *Angew. Chem.* **1985**, *97*, 969–970; *Angew. Chem. Int. Ed. Engl.* **1985**, *24*, 995–996.

[8] To a [Ru(binap)]-catalyzed imine reduction: W. Oppolzer, M. Wills, C. Starkemann, G. Bernardinelli, *Tetrahedron Lett.* **1990**, *31*, 4117–4120.

[9] a) Y. Ng Cheong Chan, D. Meyer, J. A. Osborn, *J. Chem. Soc. Chem. Commun.* **1990**, 869–871; b) Y. Ng Cheong Chan, J. A. Osborn, *J. Am. Chem. Soc.* **1990**, *112*, 9400–9401; c) F. Spindler, B. Pugin, H.-U. Blaser, *Angew. Chem.* **1990**, *102*, 561–562; *Angew. Chem. Int. Ed. Engl.* **1990**, *29*, 558–559.

[10] a) F. R. W. P. Wild, L. Zsolnai, G. Huttner, H. H. Brintzinger, *J. Organomet. Chem.* **1982**, *232*, 233–247; b) F. Wochner, L. Zsolnai, G. Huttner, H. H. Brintzinger, *ibid.* **1985**, *288*, 69–77; c) P. Burger, K. Hortmann, J. Diebold, H. H. Brintzinger, *ibid.* **1991**, *417*, 9–27; d) S. Collins, B. A. Kuntz, N. J. Taylor, D. G. Ward, *ibid.* **1988**, *342*, 21–29; e) P. Burger, J. Diebold, S. Gutmann, H. U. Hund, H. H. Brintzinger, *Organometallics* **1992**, *11*, 1319–1327, and references therein.

[11] a) R. Waymouth, P. Pino, *J. Am. Chem. Soc.* **1990**, *112*, 4911–4914; b) R. B. Grossman, R. A. Doyle, S. L. Buchwald, *Organometallics* **1991**, *10*, 1501–1505.

[12] a) M. R. Gagné, L. Brard, V. P. Conticello, M. A. Giardello, C. L. Stern, T. J. Marks, *Organometallics* **1992**, *11*, 2003–2005; b) V. P. Conticello, L. Brard, M. A. Giardello, Y. Tsuji, M. Sabat, C. L. Stern, T. J. Marks, *J. Am. Chem. Soc.* **1992**, *114*, 2761–2762; c) S. L. Colletti, R. L. Halterman, *Tetrahedron Lett.* **1992**, *33*, 1005–1008; d) S. C. Berk, K. A. Kreutzer, S. L. Buchwald, *J. Am. Chem. Soc.* **1991**, *113*, 5093–5095; e) S. Collins, B. A. Kuntz, Y. Hong, *J. Org. Chem.* **1989**, *54*, 4154–4158; f) R. B. Grossman, W. M. Davis, S. L. Buchwald, *J. Am. Chem. Soc.* **1991**, *113*, 2321–2322.

[13] a) W. Kaminsky, K. Külper, H. H. Brintzinger, F. R. W. P. Wild, *Angew. Chem.* **1985**, *97*, 507–508; *Angew. Chem. Int. Ed. Engl.* **1985**, *24*, 507–508; b) W. Röll, H. H. Brintzinger, B. Rieger, R. Zolk, *ibid.* **1990**, *102*, 339–340 and **1990**, *29*, 279–280; c) W. Spaleck, M. Antberg, V. Dolle, R. Klein, J. Rohrmann, A. Winter, *New J. Chem.* **1990**, *14*, 499–503; d) J. A. Ewen, *J. Am. Chem. Soc.* **1984**, *106*, 6355–6364.

[14] W. Spaleck, M. Antberg, J. Rohrmann, A. Winter, B. Bachmann, P. Kiprof, J. Behm, W. A. Herrmann, *Angew. Chem.* **1992**, *104*, 1373–1376; *Angew. Chem. Int. Ed. Engl.* **1992**, *31*, 1347–1350.

[15] a) P. Pino, P. Cioni, J. Wei, *J. Am. Chem. Soc.* **1987**, *109*, 6189–6191; b) W. Kaminsky, A. Ahlers, N. Möller-Lindenhof, *Angew. Chem.* **1989**, *101*, 1304–1306; *Angew. Chem. Int. Ed. Engl.* **1990**, *28*, 1216–1218; c) G. W. Coates, R. M. Waymouth, *J. Am. Chem. Soc.* **1991**, *113*, 6270–6271; d) P. Pino, M. Galimberti, P. Prada, G. Consiglio, *Makromol. Chem.* **1990**, *191*, 1677–1688; e) short review: J. Okuda, *Angew. Chem.* **1992**, *104*, 49–50; *Angew. Chem. Int. Ed. Engl.* **1992**, *31*, 47–48.

 © VCH Verlagsgesellschaft mbH, W-6940 Weinheim, 1993 0570-0833/93/0202-0233 $ 10.00+.25/0

Communications may be submitted in English *or* in German. Further details regarding the submission of communications can be found in the "Notice to Authors" reproduced in the January issue of the journal. Copies thereof may be obtained from the editorial office upon request.

An Evaluation of the Peer Review Process at *Angewandte Chemie***

By *Hans-Dieter Daniel**

It is common practice in the sciences for peers (technical experts working in, or close to, the field or specialization in question) to be requested to assess the qualifications of applicants for academic positions, the merit of research proposals, and the quality of manuscripts submitted for publication in professional journals. For a number of years these "gatekeepers of science", as such reviewers or referees are often called,[1] have themselves been the subject of sharp criticism. Indeed, the publishing world has been asked to dispense with manuscript review altogether, substituting in its place a system of "uncensored" publication.[2] Critics of the peer review system contend that:

- the judgments of reviewers show very little agreement (a charge against poor "reliability" in the reviewing process),
- reviewers are often incorrect in their assessment of the significance of a piece of work (an accusation of low "predictive validity" for reviewer judgments), and
- reviewers' recommendations are frequently influenced by external considerations unrelated to the quality of the work and inconsistent with a fair review of the manuscript (the assertion that reviewers' judgments may be subject to "bias").[3]

In view of the significance that has been attached to the peer review process as a mechanism for self-regulation within science, it must come as some surprise that the process itself has rarely been the subject of empirical investigation. Empirical research has concentrated primarily on questions of reliability and fairness in the peer review process. By contrast, there has been little research into the validity of reviewer judgments and editorial decisions.

This communication describes an empirical study into the extent to which criticism of the peer review process is justified, and uses as an example manuscript reviews carried out for *Angewandte Chemie*. At the heart of the study are the three criteria for professional judgment: inter-referee agreement (reliability), fairness, and predictive validity (as measured by mean citation frequencies for accepted manuscripts and rejected manuscripts later published elsewhere).

[*] Priv.-Doz. Dr. H.-D. Daniel
Fachgruppe Psychologie der Universität
Postfach 5560, D-W-7750 Konstanz (FRG)
New address: Das Rektorat der Universität
Postfach 103462, D-W-6800 Mannheim 1 (FRG)

[**] This work was supported by the Deutsche Forschungsgemeinschaft within the priority program "Science of Science".

The present evaluation is based on all 449 communications received from throughout the world for possible publication in *Angewandte Chemie* during the year 1984. Each communication was evaluated by two external referees working with fully structured reviewing forms and operating under the principle of one-sided anonymity (i.e., the referees knew the names of the authors, but the authors did not know those of the referees).

The year 1984 was chosen for our study of peer review at *Angewandte Chemie* since it represented the first year after the system was introduced in which all communications were judged by two independent experts according to a uniform questionnaire. Moreover, the selection of communications from 1984 resulted in a sufficiently long period of time thereafter to permit an analysis of the frequency of citation for both accepted communications and those that were rejected by *Angewandte Chemie* but subsequently published elsewhere.

All communications submitted to *Angewandte Chemie* first undergo an internal evaluation. Thus, the editor-in-chief indicates on an appropriate form whether in his judgment the manuscript should be accepted or rejected, or if he is uncertain as to the proper course of action. This initial assessment is generally accompanied by a brief comment: "good work"; "very nice"; "interesting reaction...quite poorly written"; "straightforward and brief, perhaps useful"; "provided the structure is correct, then everything is fine"; "much speculation, but little that is verifiably new"; "nothing new"; "too specialized"; "there's not enough here".

With respect to the manuscripts submitted for publication as communications in the year 1984, the editor-in-chief initially regarded 35% as suitable for acceptance and 8% worthy of rejection. He was in doubt about the appropriate fate for 57% of the submissions. After taking into account the recommendations of the referees, this same editor-in-chief ultimately accepted 72% of the submitted communications, while 26% were rejected and 2% were withdrawn by the authors themselves.

Table 1 shows the extent to which communications submitted for publication in *Angewandte Chemie* received consistent appraisals from the given pairs of referees ("first" and "second" is not meant to imply a hierarchical relationship, since the two worked independently and were accorded equal status). Inter-referee agreement in responses to the

Table 1. Concurrence and discrepancy in referees' response to the question: "Do you recommend acceptance of the communication?" [a].

Referee 1 (no. = 392) \ Referee 2 (no. = 392)	Yes, without alterations (no. = 77)	Yes, after minor alterations (no. = 154)	Yes, but only after major alterations (no. = 70)	No (no. = 91)
Yes, without alterations (no. = 79)	**20**	**38**	9	12
Yes, after minor alterations (no. = 167)	**33**	**75**	**31**	28
Yes, but only after major alterations (no. = 58)	10	**22**	**15**	**11**
No (no. = 88)	14	19	**15**	**40**

[a] Total agreement (main diagonal) and minor deviations (upper and lower off-diagonals) in referees' recommendations are in boldface.

 © VCH Verlagsgesellschaft mbH, W-6940 Weinheim, 1993 0570-0833/93/0202-0234 $ 10.00+.25/0

question "Do you recommend acceptance of the communication?" is (after correction for chance agreement) actually quite low: the kappa coefficient,[4] which may assume values between -1.0 and $+1.0$, is 0.14 for the reviewer recommendations (the weighted kappa coefficient is 0.20, the intraclass correlation coefficient 0.25). A kappa coefficient of 0.14 indicates that referees agreed in their evaluations on 14% more of the manuscripts than would have been expected on the basis of pure chance.

The highest level of agreement was associated with the recommendation "Reject": On the question "Do you recommend acceptance of the communication?" the category-specific agreement coefficient for the response "No" is 0.28. The corresponding agreement coefficients for the three response categories "Yes, without alterations", "Yes, after minor alterations", and "Yes, but only after major alterations" are only 0.07, 0.10, and 0.09, respectively.

The coefficients established for reviewer agreement in the case of *Angewandte Chemie* are comparable in magnitude to chance-corrected agreement coefficients reported for professional journals in the fields of medicine, psychology, and sociology, which generally range from 0.20 to 0.40.[5] Walling[6] unfortunately does not provide any concordance coefficients for a study based on the *Journal of the American Chemical Society* (*JACS*). A former editor of *JACS*, he analyzed reviewer agreement from a random sample of 121 communications and a second random sample of 85 full papers submitted to that journal for publication in the year 1977. In the case of the communications, 43 (36%) were recommended for acceptance by both referees, 31 (26%) received two negative votes, and 47 (39%) obtained mixed reviews. In the case of the full papers, 45 (53%) were recommended for acceptance by both referees, 12 (14%) were opposed by both reviewers, and 28 (33%) received mixed reviews. Walling summarized his experience with referee judgments in the following observation:[6] "The correlation within pairs (of referees) isn't very good."

From a statistical point of view, the observed extent of referee agreement must be regarded as rather unsatisfying. According to Landis and Koch,[7] kappa coefficients between zero and 0.40 point to a relatively low level of agreement. Kappa coefficients between 0.41 and 0.80 are described as reflecting substantial agreement, and values >0.81 indicate excellent agreement. Nevertheless, no basis exists for dramatizing these low concordance coefficients, for the following reasons:

- Major discrepancies between referee votes are relatively rare: in only about seven percent of all cases did one referee recommend acceptance without alterations while the other recommended rejection.
- The true level of existing agreement is systematically underestimated, because diverging recommendations generally reflect not only the discordance component, the factor of interest, but also dislocational components.[8] Differences in the frames of reference on which reviewers' ratings are based (e.g., referee A may be fundamentally inclined to rate all manuscripts one level lower than referee B) must not be interpreted as truly discordant judgments. Data available for the present study unfortunately do not permit a clear separation of these two components by a one-way analysis of variance with repeated measures, because in most cases a given pair of reviewers had only a single manuscript to evaluate. For this reason, the observed reliability coefficients suggest a greater degree of discordant judgment than exists in reality.
- If one follows the recommendation of Crandall[9] and treats slightly differing votes as fully concordant (i.e., cases in which the reviewers' recommendations differ by only a single category), then the resulting concordance coefficients are much higher. In our study such a "kappa with scores computed as agreement if within one point"[10] is 0.67. A concordance coefficient of this magnitude is generally interpreted as reflecting a substantial degree of reviewer agreement.
- Editors of professional journals usually appoint as their reviewers one specialist and one generalist. A content analysis of reviewer comments indicates that the arguments provided by two reviewers examining the same manuscript rarely touch on the same points—a result entirely consistent with the intentions of the editors.[11] A high level of agreement in the recommendations cannot be expected if editors select their reviewers according to the principle of complementarity as a way of avoiding redundant comments.[12]
- A high level of agreement between two reviewers actually proves relatively little, because the reviewers might be equally mistaken in their judgments. In other words, high reliability provides no assurance whatsoever of valid conclusions.[13]

Editors of professional journals are often confronted with the assertion that external factors (so-called biases) influence the fairness of manuscript reviews. From among the many publication biases that have been discussed in the literature, I have chosen the subject-matter bias for a quantitative analysis. Thus, H. Werner,[14] for example, has suggested in a letter to *Angewandte Chemie* that the journal has an editorial bias in favor of communications dealing with organic chemistry.

In order to analyze whether or not the journal is subject to a publication bias a comparison of accepted manuscripts with those that were rejected was undertaken. Manuscripts rejected by *Angewandte Chemie* were divided for the following analyses into two groups: ones that were later published by another journal and those that were not. The bibliographic databases *Chemical Abstracts* and *Science Citation Index* were examined to ascertain whether a particular manuscript rejected by *Angewandte Chemie* was subsequently published elsewhere and, if so, where. Of the 115 communications rejected for publication by *Angewandte Chemie*, together with the 9 manuscripts withdrawn voluntarily by their authors, a total of 88 (71%) later appeared in other periodicals.

The subject area to which a particular communication should be assigned was established with the help of the abstracting service *Chemical Abstracts*. Results from this analysis reveal a very distinctive publication profile for *Angewandte Chemie*: 60% of all communications published in this journal in the year 1984 fall into only three of the *Chemical Abstracts* subject sections: Section 29 (Organometallic and Organometalloidal Compounds, including not only classical organometallic topics, often regarded as essentially inorganic, but also many papers related to organic synthesis, in which organolithium and organotin reagents, for example, play an important role), which comprised 40% of all the published communications; Section 22 (Physical Organic Chemistry), incorporating 10% of all the communications, and Section 78 (Inorganic Chemicals and Reactions), also 10% of all communications. If one also adds typical papers from the field of organic chemistry (Sections 23–28), constituting a 20% share, then these four areas alone account for 80% of all the published communications. In 1984 three of the five major fields of chemical research were either not represented at all in *Angewandte Chemie* (macromolecular chemistry) or represented only to a very limited extent (biochemistry and applied chemistry or chemical technology).

However a thematic analysis of communications rejected by *Angewandte Chemie* in 1984 also reveals a complete absence of submissions for 44 of the subject sections. Communications accepted for publication in *Angewandte Chemie* display a distribution across *Chemical Abstracts* sections similar to that of manuscripts which were rejected but later published by another journal. Thus, the "goodness of fit" chi square test shows that the two distributions of papers across the sections of *Chemical Abstracts* are very similar (chi square value of 48.995, with 35 degrees of freedom). The highly distinctive publication profile of *Angewandte Chemie* can therefore not be attributed to discriminatory decisions on the part of the editors. Instead, the observed distribution of research papers published in *Angewandte Chemie* more nearly reflect the types of manuscripts submitted.

Due to the high degree of thematic concentration in manuscripts submitted for publication, the analysis that follows regarding relationships among subject area, reviewers' recommendations, and editorial decisions must be limited to Sections 22, 23–28, 29, and 78 of *Chemical Abstracts*. The less frequently represented sections have been grouped together into an "Other" category.

Table 2 shows that organometallic communications (Section 29) achieve the highest marks from the referees—a phenomenon that applies to both first and second referees, and to an equal extent. Nevertheless, the observed differences in mean ratings are statistically not significant; the most one can say is that second referees tend to rate organometallic communications more highly (mean rating = 2.27 on a scale of 1–4) relative to physical organic communications (2.71; t-value = 2.48, $p \leq .10$).

Table 2. First and second referees' mean recommendations by sections of *Chemical Abstracts*.

Section of *Chemical Abstracts*	"Do you recommend acceptance of the communication?" [a]			
	First referee mean vote	No.	Second referee mean vote	No.
Organometallic and Organometalloidal Compounds	2.20	136	2.27 [b]	137
Inorganic Chemicals and Reactions	2.31	42	2.39	41
Physical Organic Chemistry	2.47	45	2.71 [b]	42
Organic Chemistry (Sections 23–28)	2.51	88	2.50	82
Other sections	2.33	79	2.36	76

[a] Four-category rating scale: 1) "Yes, without alterations", 2) "Yes, after minor alterations", 3) "Yes, but only after major alterations", 4) "No". [b] Two sample tests for equal means and variances have been carried out for all pairs of CA sections (the Bartlett test statistics and the single tests for equal variances are statistically not significant). Communications on Organometallic and Organometalloidal Compounds receive on average slightly better recommendations by second referees relative to communications on Physical Organic Chemistry (second referees: t-value of 2.48; first referees: 1.60). All differences in mean ratings are statistically not significant (n. s.).

Communications in the field of organometallic chemistry not only tend to receive the highest rating, they also have the (statistically significant) highest publication rate: 88% of all organometallic communications submitted to *Angewandte Chemie* in 1984 were accepted for publication (cf. Tables 3 and 3a). By way of comparison, communications covering organic chemistry (Sections 23–28), physical organic chemistry (Section 22), and inorganic chemicals and reactions (Section 78) enjoyed acceptance rates of only 70%, 72%, and 73%, respectively (average for all sections: 74%)

However, this remarkably strong emphasis on organometallic chemistry is not limited to communications in *Angewandte Chemie*. Indeed, organometallic chemistry is a subject pursued very successfully and intensively throughout the Federal Republic of Germany. Thus, *Chemical Abstracts* records a total of 18426 organometallic publications in the time period 1988–1990, 2975 of which originated in the Federal Republic of Germany—corresponding to a 16.1% share of world output.[16] Based on the total number of entries in the *Chemical Abstracts* database, the overall (West) German share of world research in chemistry as a whole amounted to only 6.1%. The 16.1% statistic for papers in organometallic chemistry therefore far exceeds the proportional contribution of the Federal Republic of Germany to worldwide research in chemistry generally. If one arranges the 80 sections of *Chemical Abstracts* in descending order according to number of contributions, organometallic chemistry is found to occupy 5th place in Germany, whereas worldwide it ranks 35th in number of publications.

Table 3. Publication outcome of communications submitted to *Angewandte Chemie* in 1984 by sections of *Chemical Abstracts* (in %) [a].

Section of *Chemical Abstracts*	Communication published in *Angewandte Chemie*	Other journals
[1] Organometallic and Organometalloidal Compounds (no. = 147)	88	12
[2] Inorganic Chemicals and Reactions (no. = 44)	73	27
[3] Physical Organic Chemistry (no. = 46)	72	28
[4] Organic Chemistry (no. = 91) (Sections 23–28)	70	30
[5] Other Sections (no. = 83)	77	23

[a] Chi-square value of 14.448, 4 degrees of freedom, $p \leq .01$.

Table 3a. Partition of chi-square value of Table 3 in specific components with one degree of freedom (df) each according to Kimball [15].

Model of independence	df	Chi^2-value	p
$3 \times 4 \div A \times B$	1	0.036	n. s.
$[3 + 4] \times 2 \div A \times B$	1	0.073	n. s.
$[2 + 3 + 4] \times 5 \div A \times B$	1	1.152	n. s.
$[2 + 3 + 4 + 5] \times 1 \div A \times B$	1	13.187	$\leq .01$
Total	4	14.448	$\leq .01$

Germany's leading role in the scientifically and technically very significant field of organometallic chemistry has doubtless played a role in the fact that *Angewandte Chemie* received in the past—and continues to receive—a large number of excellent manuscripts submitted for publication, especially since the most important specialized journals in this field (*Organometallics* and the *Journal of Organometallic Chemistry*) have markedly lower "ISI Journal Impact Factors" than *Angewandte Chemie*. Given this background, the publication bias of *Angewandte Chemie* in favor of this particular specialty cannot be regarded as grounds for broad-based criticism.

Finally, I turn to an aspect of the peer review process that has heretofore been only rarely investigated: validity. The validity of peer review was ascertained in the present study by the methods of Wilson[17] and Lock.[18] I began by identifying those journals in which manuscripts rejected by *Angewandte Chemie* were published, and noting their circulations and the corresponding ISI Journal Impact Factors.[19] I then conducted citation analyses for the individual papers, and citation frequencies for accepted manuscripts were compared with those for communications that were rejected by *Angewandte Chemie* but later published elsewhere.

Citation frequencies are obviously not the sole criterion for quality in a scientific paper. However, studies published

to date—and in keeping with the criticisms leveled against peer review—have without exception relied on citation frequency as their criterion for validity. Despite this fact, citation frequency remains a controversial measure of both quality and scientific progress.[20] The Chemistry Division of the American National Science Foundation (NSF) conducted a citation analysis in 1973 with the goal "to explore the use of this relatively new tool for what it might tell about the discipline, and its practitioners". The results of the NSF study "generally support the idea that citations are meaningful".[21]

Table 4 provides a list of all those journals in which more than one of the manuscripts rejected by *Angewandte Chemie* were subsequently published.

Communications rejected by *Angewandte Chemie* were ultimately published in a total of 39 journals, two-thirds of them in the 10 journals listed in Table 4. Only two of the papers appeared in journals with circulations exceeding that of *Angewandte Chemie* (Ulrich's[19a] reports the circulation for the German edition of the latter to be 5705 and 3000 additional copies were ascribed to the English edition): one publication each in the *Journal of the American Chemical Society* (with a circulation of 13019) and the *Journal of Organic Chemistry* (circulation 9907).

Table 4. List of journals that published more than one communication rejected by *Angewandte Chemie* in 1984, in descending order of number of publications [a].

Journal	Circulation [b]	Impact factor 1986	No. of publications
Tetrahedron Letters	3380	2.158	10
Inorganica Chimica Acta	–	2.439 [c]	8
Journal of Organometallic Chemistry	–	1.792	8
Journal of the Chemical Society, Chemical Communications	4000	2.385	8
Zeitschrift für Naturforschung, Section B (Chemistry)	3200	1.405	7
Chemische Berichte	2140	1.680	5
Chemistry Letters	4650	1.612	4
Synthesis [d]	3300	1.290	4
Journal of Fluorine Chemistry	–	0.905	3
Zeitschrift für Anorganische und Allgemeine Chemie	2450	1.326	2

[a] 29 other journals that published one communication rejected by *Angewandte Chemie* are not included in this table. [b] Source: Ref. [19a]. The circulations of journals published by Elsevier are not provided by this directory. [c] Impact factor 1987. [d] In the section Communications.

Impact Factors for the journals in which papers rejected by *Angewandte Chemie* later appeared range from 0.029 (*National Academy of Sciences, India. Science Letters*) to 4.435 (*Journal of the American Chemical Society*), with a weighted mean of 1.747.

It is worth noting that 83% of the communications that were rejected but subsequently published elsewhere appeared in their original form (i.e., as short papers: communications, letters, notes, etc.). Only 15 of the manuscripts (=17%) were published as full papers.

Based on ISI Journal Impact Factors the decisions of the *Angewandte Chemie* editors can be described as highly valid: none of the rejected manuscripts appeared in a journal with an Impact Factor higher than that of *Angewandte Chemie* itself – in one of the multidisciplinary "high-impact journals", for example. The mean Impact Factor for journals accepting the rejected manuscripts was 1.747, a value significantly lower than that assigned to *Angewandte Chemie* (1986: 5.335).[22]

Journal Impact Factors represent only a very crude measure of validity, since all contributions published in a given journal are characterized by a single mean value. This in turn means that frequently cited contributions are undervalued, whereas contributions that are rarely or never cited are overvalued. For this reason I went beyond the Journal Impact Factors to ascertain how frequently individual papers themselves were cited subsequent to their publication. The results of this citation analysis are presented in Figure 1. Based on the data, communications submitted in 1984 and published in *Angewandte Chemie* were cited twice as frequently on average as those that were rejected by *Angewandte Chemie* but published elsewhere.

Whereas by the end of 1989 only two percent of the communications published in *Angewandte Chemie* had never received a single citation, ten percent of the rejected publications appearing in other periodicals remained uncited. Communications published in *Angewandte Chemie* accumulated as many as 60 citations, as compared with a maximum of 35 for those published in other journals. The observed difference in mean citation frequency is statistically very significant ($F_{1/408} = 11.17$, $p \leq .001$). The analysis of covariance took into account an average delay period from the time of rejection by *Angewandte Chemie* to publication in another journal of almost exactly six months, resulting in a somewhat narrower time window for citation. The statistical significance of the findings becomes even more striking when

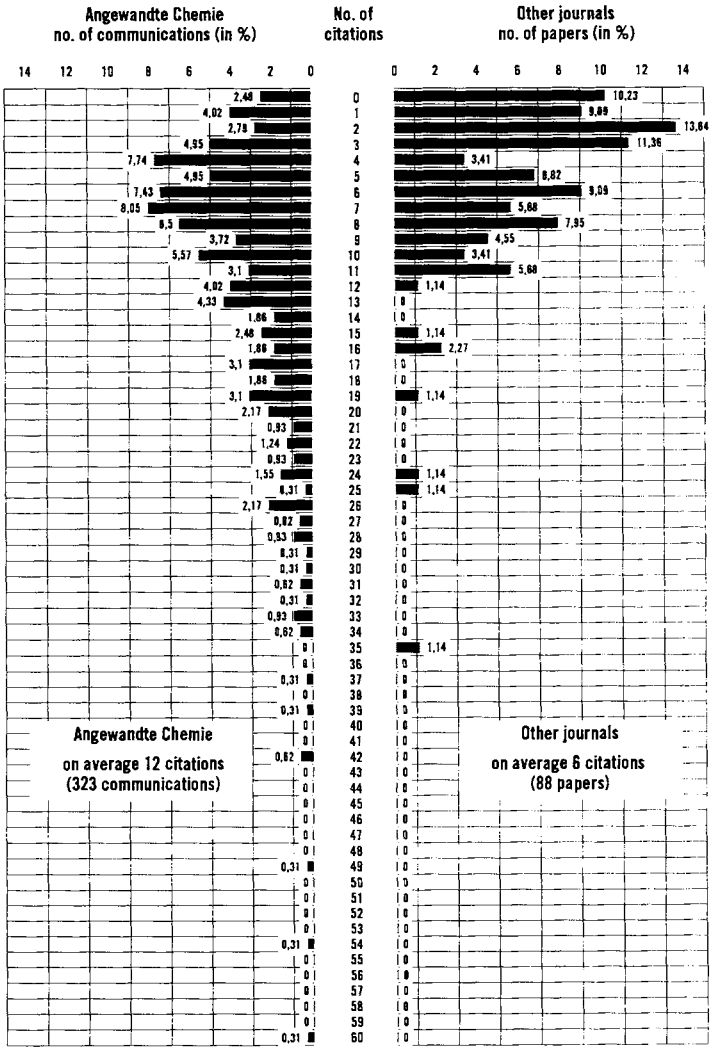

Fig. 1. Comparison of mean citation rates for communications accepted by *Angewandte Chemie* and those rejected by *Angewandte Chemie* but published elsewhere.

the citation frequencies are transformed logarithmically in order to obtain scores with a roughly normal distribution and homogeneous variances ($F_{1/408} = 20.41$, $p \leq .001$).

The results of our citation analysis are in very good agreement with those reported by Wilson,[17] who compared average citation frequencies of manuscripts accepted for publication in the year 1970 by the *Journal of Clinical Investigation* with those that were rejected but published in other journals during 1971. Articles in the *Journal of Clinical Investigation* were cited during the first four years after their publication roughly twice as often as papers that were rejected but later published in other journals. Lock[18] established very similar results for the *British Medical Journal*.

Based on average citation frequencies for accepted manuscripts and manuscripts that were rejected but later published elsewhere, the decisions of the editors in all the cases subjected to scrutiny appear to reflect a consistently high degree of predictive validity. These findings with respect to editorial predictive validity therefore suggest considerable exaggeration in the statement made by Ross[3] that "the data about validity against the single criterion of citation of a work urge that current editing-refereeing processes cannot distinguish a 'good' paper from a 'bad' paper" (p. 46). Indeed, all existing studies rather suggest that highly rated manuscripts are in fact cited more frequently after publication than those rated negatively.

The literature on reliability, fairness, and predictive validity of the peer review process has so far completely neglected one important function of manuscript refereeing, namely the improvement of a piece of work on the basis of reviewer comments. In a contribution by Abelson[23] on the occasion of the 100th anniversary of the journal *Science*, the author observes that virtually every manuscript is subjected to changes in response to reviewer suggestions. The same applies to communications appearing in *Angewandte Chemie*. The editors routinely record whether a given communication has been published without change or only after it has been supplemented or revised by the original authors. Nearly two-thirds (63%) of all communications published in *Angewandte Chemie* are revised by their authors. Comparisons based on mean citation frequencies reveal that revised manuscripts are cited with precisely the same frequency as manuscripts that were not subject to revision (t-test for difference between means, unequal variances, t-value = 0.45, not significant). This may be taken as evidence that reviewers' suggestions for improvement have had a significant impact on a large fraction of the published manuscripts.

Our appraisal is supported by a linguistic analysis carried out by Kretzenbacher and Thurmair[24] on a subset of reviewers' comments prepared for *Angewandte Chemie* in 1984: "It is apparent that efforts have been made to improve the final publications, thereby serving the interests of the entire scientific community, through often very detailed suggestions for changes in both content and style."

Received: October 5, 1992 [Z 5611 IE]
German version: *Angew. Chem.* **1993**, *105*, 247

[1] D. Crane, *Am. Sociologist* **1967**, *2*(4), 195–201; W. A. P. Luck, *Phys. Bl.* **1981**, *37*(2), 37–38.
[2] H. H. Kornhuber in *Evaluation von Forschung: Methoden - Ergebnisse – Stellungnahmen* (Eds.: H.-D. Daniel, R. Fisch), Universitätsverlag Konstanz, Konstanz, **1988**, p. 361–382.
[3] P. F. Ross, *The Sciences' Self-Management: Manuscript Refereeing, Peer Review, and Goals in Science*, The Ross Company, Lincoln, *Massachusetts*, MA 01773, USA, **1980**.
[4] J. L. Fleiss, *Statistical Methods for Rates and Proportions*, Wiley, New York, **1981**, p. 212–236.
[5] D. V. Cicchetti, *Behav. Brain Sci.* **1991**, *14*, 123.
[6] C. Walling, *The Refereeing of Scientific Manuscripts – Does the Peer System Work?*, unpublished manuscript, obtained from the Archives of the National Academy of Sciences, Washington, DC, USA, no date.
[7] J. R. Landis, G. G. Koch, *Biometrics* **1977**, *33*, 159–174.
[8] G. A. Lienert, *Schulnoten-Evaluation*, Athenäum, Frankfurt am Main, **1987**, p. 320.
[9] R. Crandall, *Am. Psychol.* **1978**, *33*, 623–624.
[10] A. Tolman, N. Farrier, K. Farrier, *DynaStat's Kappa Program*, Eugene, OR, **1988**, p. 3–4.
[11] V. Bakanic, C. McPhail, R. J. Simon, *Sociol. Q.* **1989**, *30*(4), 639–654; D. W. Fiske, L. Fogg, *Am. Psychol.* **1990**, *45*(5), 591–598.
[12] L. L. Hargens, *Behav. Brain Sci.* **1991**, *14*(1), 150–151.
[13] H. C. Kraemer, *Behav. Brain Sci.* **1991**, *14*(1), 152–154.
[14] Cf. *Angew. Chem.* **1991**, *103*(4), A-118.
[15] A. W. Kimball, *Biometrics* **1954**, *10*, 452–458.
[16] H.-D. Daniel, *Nachr. Chem. Tech. Lab.* **1991**, *39*(9), 978–980.
[17] J. D. Wilson, *J. Clin. Invest.* **1978**, *61*(4), 1697–1701.
[18] S. Lock, *A Difficult Balance: Editorial Peer Review in Medicine*, Nuffield Provincial Hospitals Trust, London, **1985**, p. 64.
[19] a) *Ulrich's International Periodicals Directory 1992–93*, Bowker, New Providence, NJ, **1992**; b) E. Garfield, *SCI Journal Citation Reports: A Bibliometric Analysis of Science Journals in the ISI Data Base*, Institute for Scientific Information, Philadelphia, PA, **1984** ff.
[20] M. H. MacRoberts, B. R. MacRoberts, *J. Am. Soc. Inf. Sci.* **1988**, *40*(5), 342–349; A. L. Porter, D. E. Chubin, X.-Y. Jin, *Scientometrics* **1988**, *13*(3–4), 103–124.
[21] T. W. Dewitt, R. S. Nicholson, M. R. Wilson, *Scientometrics* **1980**, *2*(4), 265–275.
[22] For example, the 1986 ISI Journal Impact Factor for *Angewandte Chemie* is computed as follows: the total number of citations in SCI source journals during 1986 referring to papers published in *Angewandte Chemie* in 1984 and 1985 is divided by the total number of source items published in *Angewandte Chemie* in 1984 and 1985: 3612/677 = 5.335.
[23] P. H. Abelson, *Science* **1980**, *209*(4452), 60–62.
[24] H. L. Kretzenbacher, M. Thurmair in *Kontrastive Fachsprachen-Forschung* (Eds.: K.-D. Baumann, H. Kalverkämper), Narr, Tübingen, **1992**, p. 144.

New Cu–Te Clusters**

By *Dieter Fenske** and *Jörg-Christian Steck*

PR_3 complexes (R = Et, *i*Pr, *t*Bu) of CuCl react with $Se(SiMe_3)_2$ in organic solvents with the loss of Me_3SiCl to give metal-rich copper clusters; examples include the complexes **A**–**D**.[1] Investigations previously carried out by us have

$[Cu_{20}Se_{13}(PEt_3)_{12}]$ **A** $[Cu_{30-x}Se_{15}(PiPr_3)_{12}]$ **B**, $x = 0,1$
$[Cu_{36}Se_{18}(PtBu_3)_{12}]$ **C** $[Cu_{70}Se_{35}(PEt_3)_{22}]$ **D**

shown that the structure of the cluster is dependent on the phosphane ligands and the conditions employed for the synthesis.[2] The reaction temperature, and the solvent are particularly important; a tendency toward the formation of Cu_2Se is observed even at room temperature. Although the structures of Cu_2Se and the cluster complexes are unrelated, the latter may be considered as possible intermediates for the synthesis of metastable, binary copper selenides. We have now studied analogous reactions of $Te(SiMe_3)_2$ with PR_3 complexes (Scheme 1).

No reaction occurs in THF or ether at $-78\,^{\circ}C$. Only after slowly increasing the temperature of the reaction are dark solutions formed over the course of several days, from which fine crystalline solids precipitate. Crystals suitable for struc-

[*] Prof. Dr. D. Fenske, Dipl. Chem. J.-C. Steck
Institut für Anorganische Chemie der Universität
Engesserstrasse, Geb.-Nr. 30.45, D-W-7500 Karlsruhe (FRG)

[**] This work was supported by the Deutsche Forschungsgemeinschaft (Sonderforschungsbereich 195) and the Fonds der Chemischen Industrie.

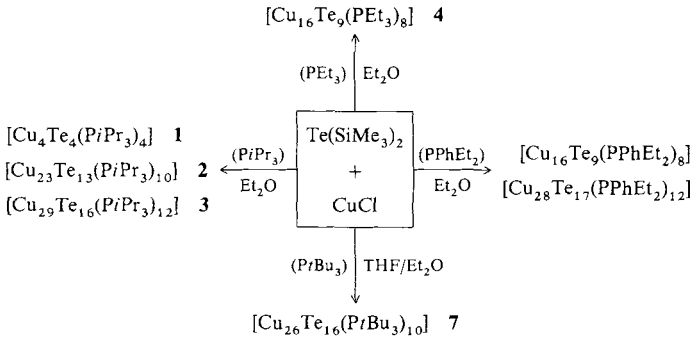

Scheme 1. Reactions of CuCl with phosphanes PR_3 and $Te(SiMe_3)_2$.

tural analysis are obtained if the volatile reaction products are distilled at $-40\,^{\circ}C$, and the residue is dissolved in a little THF or ether.[3]

Compound **1** forms red crystals and **2**–**7** from crystals displaying a metallic luster, which are sparingly soluble in organic solvents. The IR spectra are not very informative, since they only contain characteristic vibrations for the PR_3 ligands in the range 400–4000 cm^{-1}. Thus, X-ray crystal structure analyses were carried out to determine the molecular structures of **1**–**7**.[4]

If CuCl is allowed to react with $Te(SiMe_3)_2$ in the presence of $PiPr_3$, high yields of **1** are initially obtained. However, **1** is converted in ether into a crystalline mixture of **2** and **3** within a few days. In **1** (Fig. 1), the four Cu atoms form a butterfly structure, which is bridged by two μ_4-Te_2^{2-} ligands (Te–Te 280.0(3), 281.2(3) pm and Cu–Cu 279.4–309.5(4) pm). In addition, each Cu atom is bound to the P

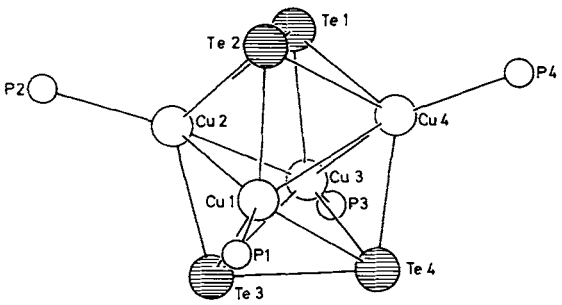

Fig. 1. Crystal stucture of **1** (without C atoms); Cu–Cu distances and Te–Cu distances up to 290 pm are drawn as bonds.

atom of a $PiPr_3$ ligand. Thus, each Cu is surrounded in a distorted tetrahedral manner by three Te atoms and one P atom. The Cu–Te distances are of different length and can be separated into a shorter one (257.4(2)–258.5(2) pm) and two longer ones (265.8(3)–285.6(4) pm). Other authors have already reported on tetranuclear metal clusters with butterfly structures; examples are summarized in Scheme 2.[5, 6]

$[Mo_4I_{11}]^{2-}$	$[Mo_4F_4(OtBu)_8]$
$[Mo_4X_8(PR_3)_4]$, X = Cl, Br; R = Ph, *i*Pr	
$[Os_4(CO)_{12}C_9H_4]$	$[Ru_4(CO)_{12}(\mu_2\text{-}C_2R_2)]$
$[Fe_4C(CO)_{12}]$	$[Ni_4Te_4(PPh_3)_4]$

Scheme 2. Tetranuclear metal clusters with butterfly structures.

Assuming that Te_2^{2-} ligands occur in **1**, the Cu centers must have the charge +1. Whereas several dichalcogenido-bridged complexes with S and Se are known, for example, $[Cp_2V_2Se_5]$ and $[(Co_3S(CO)_7)_2(S_2)I]$,[7] few compounds with Te–Te bridging ligands are known. In the complex $[\{(triphos)M\}_2Te_2]$ (M = Co, Ni; triphos = [2-{diphenylphosphino)methyl}-2-methyl-1,3-propanediyl]bis(diphenylphosphane)) the Te–Te distance is 280.2 pm,[8] in $[Cp_2Mo_2Fe_xTe_2(CO)_7]$ ($x = 1,2$) 313 pm,[9] in $[(Cp_2HfTe_2)_2]$ 280.2 pm,[10] and in the Ni_4Te_4 cluster (see Scheme 2) 286.1 pm. If the Te_2^{2-} ligands are considered eight-electron donors, **1** contains 64 valence electrons, which is in agreement with the 18-electron rule for butterfly structures.[11]

In **2** (Fig. 2 top), the Cu atoms form a nearly spherical cluster with approximately threefold symmetry. With the exception of Te4, which lies in the center of the molecule and is surrounded by nine Cu atoms, the other Te atoms occupy the cluster periphery and function as μ_5 (Te3, Te5–Te10,

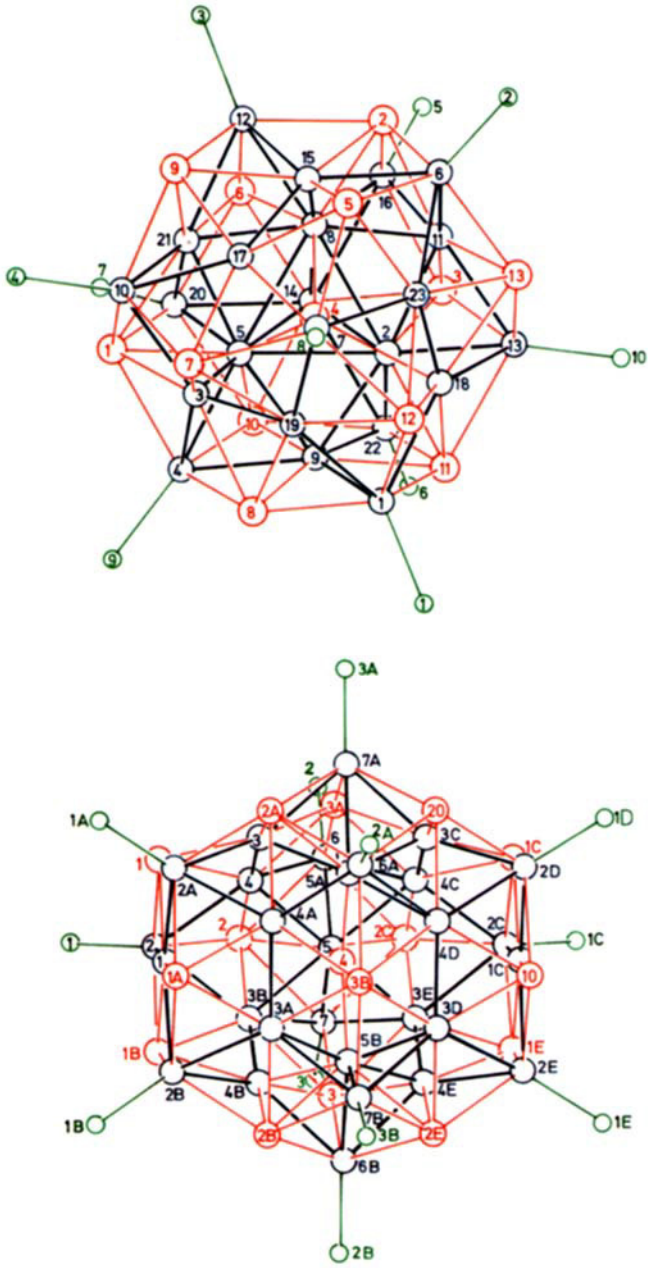

Fig. 2. Crystal structures of **2** (top) and **3** (bottom) (without C atoms); Cu: blue, Te: red, P: green. Cu–Cu bonds (blue) up to 300 pm and Cu–Te bonds (red) up to 290 pm are drawn. The Cu, Te, and P atoms are labeled only with blue, red, and green numbers, respectively. Important distances in **2** in pm (±1 pm): Te4–Cu 254–300, (μ_5-Te)-Cu 253–284, (μ_6-Te)-Cu 259–290; Cu–Cu distances about the Cu atoms (2, 5, 8): 254–263, about the Cu atoms (1, 4, 6, 7, 10, 12, 13, 16, 20, 22): 251–298; about the Cu atoms (17, 19, 23): 252–273; about the Cu atoms (3, 15, 18): 252–276, about the Cu atoms (9, 11, 21): 258–297, and about the Cu atom (14): 257–298.

Te 12, Te 13) or μ_6 bridging ligands (Te 1, Te 2, Te 11). The Cu atoms also occur in different bonding forms. The atoms Cu 2, Cu 5, and Cu 8 are within the cluster, and are each bound to three Te and eight Cu atoms. The Cu atoms (Cu 1, Cu 4, Cu 6, Cu 7, Cu 10, Cu 12, Cu 13, Cu 16, Cu 20, Cu 22) coordinated to P*i*Pr$_3$ are each surrounded by three Cu and three Te atoms. The remaining ten Cu atoms each contain three Te ligands in the coordination sphere and additionally, three Cu(Cu 17, Cu 19, Cu 23), four Cu(Cu 3, Cu 15, Cu 18), five Cu (Cu 9, Cu 11, Cu 21), or six Cu atoms (Cu 14) at a distance of 254–300 pm.

In an alternative description, the structure of **2** can also be derived from a distorted icosahedron, which is formed from the twelve peripheral Te atoms (Te–Te 393.7(7)–472.2(7) pm). Above the twenty Te$_3$ faces lie ten Cu atoms bound to P*i*Pr groups, and below the remaining faces ten further Cu atoms are arranged. The cavity formed in this way is occupied by three additional Cu atoms (Cu 2, Cu 5, Cu 8) and Te 4.

The cluster **2** is probably an intermediate in the formation of **3** (Fig. 2 bottom), which shows threefold symmetry and is constructed from five parallel, planar layers; **B**, $x = 1$ also has this structure.[1] The middle layer is a mirror plane and has the composition [Cu$_9$Te$_4$(P*i*Pr$_3$)$_6$] (Cu 5, Cu 6, Cu 7, Te 3, Te 4, P 2, P 3), the second layers bound to this comprise six Cu (Cu 3, Cu 4) and three Te atoms (Te 2), and the outer layers have the composition [Cu$_4$Te$_3$(P*i*Pr$_3$]. This latter structural fragment is also found in the structure of **2**. As in **2**, Te 4 is situated at the center of the cluster in **3**, and is bound to three Cu atoms (Cu–Te 255.1(3) pm) in a trigonal planar arrangement. The fifteen peripheral Te atoms form a Frank–Kasper polyhedron (Te–Te 392–480 pm) with 26 Te$_3$ faces.[12] Above twelve of the triangular faces of this polyhedron, Cu atoms (Cu 2, Cu 6, Cu 7; Cu–Te 266.7(3)–275.7(3) pm) are bound to P*i*Pr$_3$ groups. Below the remaining fourteen faces are found fourteen Cu atoms, which are generated by symmetry operations from Cu 1, Cu 3, and Cu 4 (Cu–Te 256.7(3)–259.9(3) pm). The Cu–Cu distances in **3** (256.3(3)–276.3(4) pm) are approximately 10–20 pm longer than in **B**, $x = 1$.[1]

Completely different products are obtained if triethyl- or diethylphenylphosphane is used as ligand, instead of the sterically demanding triisopropyl ligand.[13] Consequently, the clusters **4** and **5**, respectively, are obtained, which crystallize in the form of dark green needles (yield 40%).

Figure 3 shows the structure common to both clusters **4** and **5** (**4** is used as the example). Cluster **4** possess a mirror plane, which is formed from the atoms Te 4, Te 5, Te 6, Cu 8, and Cu 9. The structure of the Cu cluster can be derived from a distorted, trigonal Cu$_6$ prism (Cu 6–Cu 11, Cu–Cu 249.1(5)–306.0(5) and 329.2(4) pm), in which six edges are bridged by Cu atoms (Cu 2, Cu 4, Cu 12, Cu 14) or Cu$_2$ units (Cu 3/Cu 5, Cu 13/Cu 16). The framework of the cluster is completed by Cu 1 and Cu 16. Thus, butterfly structure fragments analogous to **1** are obtained, which are formed from the Cu atoms 1, 3, 5, and 6 as well as 11, 13, 15, and 16. The Te ligands function (with the exception of the μ_6-Te$_5$) as μ_5 bridging ligands.

In order to describe the structure of **6** (Fig. 4 top), it is appropriate to consider the sixteen phosphane-free Cu atoms (Cu 4, Cu 5, Cu 8, Cu 11, Cu 17–Cu 28) first. These

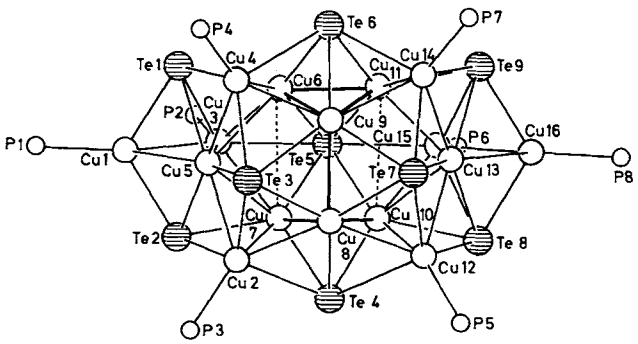

Fig. 3. Crystal structure of **4** (without C atoms). Important distances in pm (+ 0.4 pm): Cu 6–Cu 7 = Cu 11–Cu 12 329.2 (dashed), Cu 8–Cu 9 255.9, Te 5–Cu 258.0–275.4; Cu–Cu distances in the butterfly structure fragments Cu 1, Cu 3, Cu 5, Cu 6 257.3(4)–268.3(5), and Cu 11, Cu 13, Cu 15, Cu 16 258.9(5)–272.4(5).

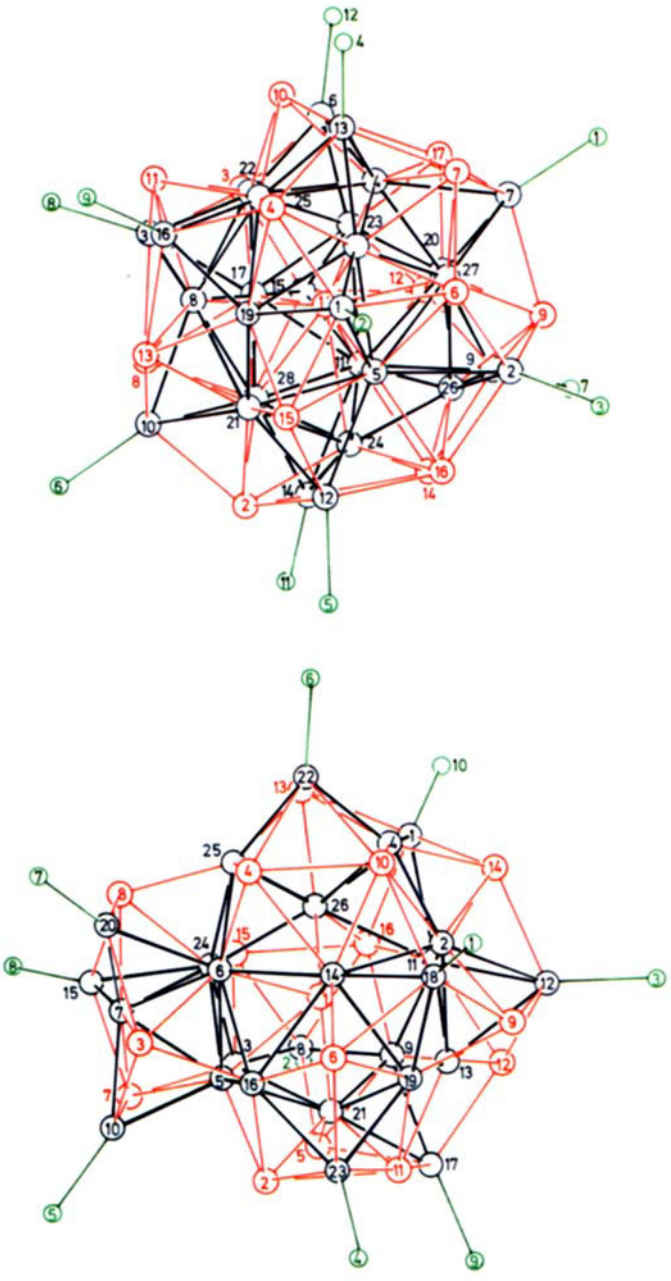

Fig. 4. Crystal structures of **6** (top) and **7** (bottom) (without C atoms); Cu: blue, Te: red, P: green. Cu–Cu bonds (blue) up to 300 pm and Cu–Te bonds (red) up to 290 pm are drawn. The Cu, Te, and P atoms are labeled only with blue, red, and green numbers, respectively. Important distances in pm (±0.5 pm): **6**: Cu–Cu 238.0–311.5, Te–Cu (1–3, 6, 7, 9, 10, 12–16) 260.0–273.1, Te–Cu (19–26) 242.0–260.7, Te–Cu (17, 18, 27, 28) 250.0-284.0, Te–Cu (4, 5, 8, 11) 269.2–283.4, Te 5–Te 8 287.9, Te 6–Te 7 289.3. **7**: Cu–Cu 258.1–290.7, Te–Cu (10, 15, 20) 261.0–269.6, Te–Cu (1, 8, 12, 17, 18, 22, 23) 264.7–297.7 Te–Cu (2–7, 9, 11, 13, 16, 19, 24, 25) 252.2–273.7, Te–Cu (14, 21, 26) 255.5–289.2.

 © VCH Verlagsgesellschaft mbH, W-6940 Weinheim, 1993 0570-0833/93/0202-0240 $ 10.00+.25/0

define a distorted, Frank–Kasper polyhedron with a central Te1 with 28 triangular faces, which are occupied by twelve Cu atoms (Cu1–Cu3, Cu6, Cu7, Cu9, Cu10, Cu12–Cu16) coordinated to $PPhEt_2$ and 16 peripheral Te ligands, which also describe a Frank–Kasper polyhedron, which is strongly distorted because of the Te–Te bonds (Te–Te 287.9(3)–469.8(7) pm).

The Cu–Cu distances vary greatly and are between 238(2) and 311.5 pm. Of the 28 Cu atoms, those twelve which are coordinated to phosphane are bound to three Cu and three Te atoms, the remaining have higher coordination numbers: Cu19–Cu26 form bonds to five Cu and three Te; Cu17, Cu18, Cu27, and Cu28 form bonds to five Cu and four Te, and Cu4, Cu5, Cu8, and Cu11 to six Cu and four Te atoms. The Te ligands function as μ_5 (Te2–Te4, Te9–Te16) or μ_8 ligands (Te1). Only Te5 and Te8 as well as Te6 and Te7 form Te_2^{2-} bridges, which are each bound to eight Cu atoms.

As in **3** and also in the complex **7** with the bulky ligand tris(*tert*-butyl)phosphane (Fig. 4 bottom), the fifteen peripheral Te atoms (Te2–Te16) form a Frank–Kasper polyhedron with a central Te1. However, this polyhedron is very strongly distorted because of the formation of Te–Te bonds (Te2–Te11, Te4–Te10, and Te15–Te16 287.7–289.5(5) pm). All the remaining Te–Te distances lie in the range of 418–488.3 pm. Above ten of these faces are found the Cu atoms (Cu1, Cu8, Cu10, Cu12, Cu15, Cu17, Cu18, Cu20, Cu22, Cu23) bound to $PtBu_3$, which are coordinated in different ways: Cu10, Cu15, and Cu20 form bonds to two Cu and two Te atoms, Cu8, Cu17, Cu18, Cu22, and Cu23 are surrounded by two Cu and three Te atoms, and Cu1 and Cu12 by three Cu and three Te atoms. Below the remaining 16 Te_3 faces, 16 Cu atoms are arranged (Cu2–Cu7, Cu9, Cu11, Cu13, Cu14, Cu16, Cu19, Cu21, Cu24–Cu26), which also have different coordination numbers: seven (three Te and four Cu atoms) is found for Cu3, Cu4, Cu9, Cu16, Cu19, and Cu25; Cu2 and Cu13 are bound to three Te and five Cu atoms, whereas Cu7 and Cu11 are surrounded by three Te and six Cu atoms, and Cu14, Cu21, and Cu26 by four Te and five Cu atoms. The highest coordination numbers are found for Cu5, Cu6, and Cu24, which are surrounded by three Te and seven Cu atoms. The Cu–Cu distances in **7** lie in the range 258.1–290.7(7) pm.

The Cu–Te fragments in **1**–**7** are not related to the structure of Cu_2Te.[14] In Cu_2Te a two-dimensional network of layers of hexagonal Cu_6 prisms is found, which are connected by Te_2 bridges. In contrast, **2**, **3**, **6**, and **7** have a much more shell-like construction, the Cu atoms, which form the inner shell, are surrounded by Te^{2-} in the first sphere and by Cu atoms coordinated to PR_3 in the second sphere; their structure principles, however, show striking similarities with those of intermetallic phases, for example, Laves phases.[15] In both cases, Frank–Kasper polyhedrons can be used to describe the structure. To illustrate this principle, the structure of the Te_{15} polyhedron in **3** and the Cu cluster, which penetrates this polyhedron, is given in Figure 5.

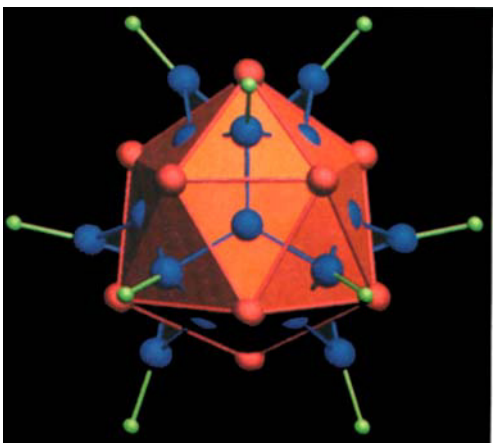

Fig. 5. Structure of the Te_{15} Frank–Kasper polyhedron (red) in **3** and of its penetrating Cu cluster (blue) [17].

The bonding in **2**–**7** can no longer be described with simple counting rules. On the understanding that Te^{2-} and Te_2^{2-} ligands occur, the Cu atoms in **1** would receive the formal charge +1 (d^{10} configuration), whereas mixed-valent conditions have to be assumed in **2**–**7**. Since the Cu–Cu distances in **1**–**7** (257–309 pm) are significantly longer than those discussed for Cu–Cu bonding, it can be assumed that binding Cu–Cu interactions are of little significance.[16] At present we are trying to calculate the electronic structures of the discussed clusters.

Received: August 11, 1992 [Z 5508 IE]
Publication delayed at author's request
German version: *Angew. Chem.* **1993**, *105*, 254

[1] D. Fenske, H. Krautscheid, S. Balter, *Angew. Chem.* **1990**, *102*, 799; *Angew. Chem. Int. Ed. Engl.* **1990**, *29*, 796; D. Fenske, H. Krautscheid, *ibid.* **1990**, *102*, 1513 and **1990**, *29*, 1452.

[2] D. Fenske, H. Krautscheid, M. Müller, *Angew. Chem.* **1992**, *104*, 309; *Angew. Chem. Int. Ed. Engl.* **1992**, *31*, 321.

[3] General description for the synthesis of **1**–**7**: CuCl (1 mmol) was suspended in the solvent (50 mL)(THF, diethyl ether) and dissolved by the addition of the phosphane (CuCl:P = 1: 2.5–5.0). The clear, colorless solution was cooled to −78 °C and allowed to react with half an equivalent $Te(SiMe_3)_2$ (relative to CuCl) and subsequently allowed to warm up slowly. At approximately −40 °C, the reaction mixture darkens, and at this point volatile reaction products were distilled at constant temperature over approximately half an hour; a highly viscous oil remained. This oil was taken up in a little precooled solvent and the mixture was stirred shortly to allow complete homogenization. Thereafter, the solution was allowed to warm to room temperature under the exclusion of light over several days.

[4] X-ray crystal structure analyses: STOE IPDS; $Mo_{K\alpha}$; 200 K; data sets of **1**–**3** were measured on a four-circle diffractometer (Stoe Stadi IV) (MoK_α, empirical absorption correction). Further details of the crystal structure investigation may be obtained from the Fachinformationszentrum Karlsruhe, Gesellschaft für wissenschaftlich-technische Information mbH, D-W-7514 Eggenstein-Leopoldshafen 2 (FRG) on quoting the depository number CSD-56621, the names of the authors, and the journal citation. **1**: $a = 1313.2(8)$, $b = 2524.6(9)$, $c = 1703.2(8)$ pm, $\beta = 111.66(5)°$, $V = 5247.9 \times 10^6$ pm^3; space group $P2_1/n$ (no. 14), $Z = 4$; $\mu(Mo_{K\alpha}) = 37.16$ cm^{-1}, $2\theta_{max} = 56.3°$; 40403 reflections, of which 10056 were independent with $I > 3\sigma(I)$; 435 parameters (Cu, Te, P, C refined anisotropically; positions of the H atoms of the iPr groups calculated); $R = R_w = 0.072$. **2**: $a = 1659.7(8)$, $b = 2524.6(9)$, $c = 1703.2(8)$ pm, $\beta = 98.59(4)°$, $V = 14547.2 \times 10^6$ pm^3; space group $P2_1/c$ (no. 14), $Z = 4$; $\mu(Mo_{K\alpha}) = 61.64$ cm^{-1}, $2\theta_{max} = 48.4°$; 47088 reflections, of which 12959 were independent with $I > 3\sigma(I)$; 1222 parameters (Cu, Te, P, C refined anisotropically; positions of the H atoms of the iPr groups calculated); $R = R_w = 0.066$. **3**: $a = 1982.3(10)$, $c = 2696.9(17)$ pm, $V = 10512.5 \times 10^6$ pm^3; space group $P6_3/m$ (no. 176), $Z = 2$; $\mu(Mo_{K\alpha}) = 45.55$ cm^{-1}, $2\theta_{max} = 52°$; 86723 reflections, of which 5123 were independent with $I > 4\sigma(I)$; 204 parameters (Cu, Te, P anisotropic, C calculated isotropically; H atoms of the iPr groups could not be localized); $R = R_w = 0.074$. **4**: $a = 1286.1(8)$, $b = 2251.8(24)$, $c = 3077.1(24)$ pm, $\beta = 101.72(4)°$, $V = 8008.1 \times 10^6$ pm^3; space group $C2/c$ (no. 15), $Z = 4$; $\mu(Mo_{K\alpha}) = 66.28$ cm^{-1}, $2\theta_{max} = 54°$; 34314 reflections, of which 15015 were independent with $I > 4\sigma(I)$; 518 parameters (Cu, Te, P, refined anisotropically, C isotropically calculated; positions of the H atoms of the ethyl groups calculated); $R = R_w = 0.070$. **5**: $a = 1229.3(10)$, $b = 1294.0(10)$, $c = 3626.6(54)$ pm, $\alpha = 90.41(8)$, $\beta = 93.22(5)$, $\gamma = 113.76(5)°$, $V = 5212.0 \times 10^6$ pm^3; space group $P\bar{1}$ (no. 2), $Z = 2$; $\mu(Mo_{K\alpha}) = 65.15$ cm^{-1}, $2\theta_{max} = 54°$; 36170 reflections; as a result of the poor quality of the crystal only the heavy metal framework could be refined; the organic groups bound to P are disordered; $R = R_w = 0.160$. **6**: $a = 1904.4(15)$, $b = 1921.5(11)$, $c = 2210.4(13)$ pm, $\alpha = 97.35(4)$, $\beta = 93.22(5)$, $\gamma = 90.68(5)°$, $V = 8008.1 \times 10^6$ pm^3; space group $P\bar{1}$ (no. 2), $Z = 2$; $\mu(Mo_{K\alpha}) = 65.15$ cm^{-1}; 103524 reflections, of which 17550 were independent with $I > 4\sigma(I)$; 1583 parameters (Cu, Te, P, C refined anisotropically; positions of the H atoms were calculated); $R = R_w = 0.096$. **7**: $a = 2533.9(17)$, $b = 2967.9(28)$, $c = 2833.9(10)$ pm, $\beta = 92.27(4)°$, $V = 21294.9 \times 10^6$ pm^3; space group $P2_1/n$ (no. 14), $Z = 4$; $\mu(Mo_{K\alpha}) = 45.70$ cm^{-1};

 © VCH Verlagsgesellschaft mbH, W-6940 Weinheim, 1993 0570-0833/93/0202-0241 $ 10.00+.25/0

56104 reflections, of which 17800 were independent with $I > 4\sigma(I)$; 1776 parameters (Cu, Te, P, C refined anisotropically; positions of the H atoms were calculated); $R = R_w = 0.082$.
[5] S. Stensvad, B. J. Helland, M. W. Babich, R. A. Jacobson, R. E. McCarley, *J. Am. Chem. Soc.* **1978**, *100*, 6257; M. H. Chisholm, R. J. Errington, K. Folting, J. C. Huffman, *ibid.* **1982**, *104*, 2025; M. H. Chisholm, J. C. Huffman, R. L. Kelly, *ibid.* **1979**, *101*, 7100; R. E. McCarley, T. R. Ryan, C. C. Torardi, in *Reactivity of Metal-Metal-Bonds* (*ACS Symp. Ser.* **1981**, *155*, 41); H. Chen, B. F. G. Johnson, J. Lewis, P. R. Raithby, *J. Chem. Soc. Chem. Commun.* **1990**, 373; G. Granozzi, R. Bertoncello, M. Acampora, D. Ajò, D. Osella, S. Aime, *J. Organomet. Chem.* **1983**, *244*, 383; P. L. Stanghellini, M. J. Sailor, P. Kusnesof, K. H. Whizmire, J. A. Hriljac, J. W. Kolis, Y. Zheng, D. F. Shriver, *Inorg. Chem.* **1987**, *26*, 2950.
[6] D. Fenske, J. Steck, unpublished.
[7] D. Fenske, P. Maué, *Z. Naturforsch. B* **1989**, *44* 531; A. Müller, W. Jagermann, J. H. Enemark, *Coord. Chem. Rev.* **1982**, *46*, 245.
[8] M. Di Vaira, M. Peruzzini, P. Stoppioni, *J. Chem. Soc. Chem. Commun.* **1986**, 374.
[9] L. E. Bogan, Jr., T. B. Rauchfuss, A. L. Rheingold, *J. Am. Chem. Soc.* **1985**, *107*, 3843.
[10] A. Grissinger, Dissertation, Universität Karlsruhe, **1991**.
[11] J. Wachter, *Angew. Chem.* **1989**, *101*, 1645; *Angew. Chem. Int. Ed. Engl.* **1989**, *28*, 1613.
[12] F. C. Frank, J. S. Kasper, *Acta Crystallogr.* **1958**, *11*, 184; *ibid.* **1959**, *12*, 483.
[13] C. A. Tolmann, *Chem. Rev.* **1977**, *77*, 313.
[14] H. Nowotny, *Metallforschung* **1946**, *1*, 40; *Struct. Rep.* **1945–1946**, 50.
[15] W. B. Pearson, *Acta Crystallogr. Sect. B* **1968**, *24*, 1415.
[16] F. A. Cotton, X. Feng, M. Matusz, R. Poli, *J. Am. Chem. Soc.* **1988**, *110*, 7077; R. Mason, D. M. P. Mingos, *J. Organomet. Chem.* **1973**, *50*, 53; P. K. Mehrotra, R. Hoffmann, *Inorg. Chem.* **1978**, *17*, 2187; C. Kölmel, R. Ahlrichs, *J. Phys. Chem.* **1990**, *94*, 5536; K. M. Merz, R. Hoffmann, *Inorg. Chem.* **1988**, *27*, 2120.
[17] We thank Prof. R. Nesper (ETH Zürich) for making available the program to draw the polyhedra.

New Phosphido-Bridging Copper Clusters**

By *Andreas Eichhöfer, Dieter Fenske,** and *Werner Holstein*

Dedicated to Professor Hartmut Bärnighausen on the occasion of his 60th birthday

Silylated phosphanes react with transition metal halides with the formation of trimethylsilyl halides and multinuclear cluster complexes. In 1968 Abel reported that CuCl and $NiCl_2$ react with Ph_2PSiMe_3 to give insoluble, apparently oligomeric phosphides such as $[CuPPh_2]_n$ and $[Ni(PPh_2)_2]_n$, whose structures could not be elucidated.[1]

Recently, however, we showed that the reaction of $NiCl_2$ with $PhP(SiMe_3)_2$ afforded the nickel cluster $[Ni_{12}Cl_2(PPh)_2(P_2Ph_2)_4(PHPh)_8]$.[2] In contrast, if analogous reactions are carried out with $[MCl_2(PPh_3)_2]$ (M = Ni, Co) and $PhP(SiMe_3)_2$, $[Ni_8Cl_4(PPh)_6(PPh_3)_4]$ and $[Co_4(PPh)_4(PPh_3)_4]$ are isolated in very high yields.[3] Apparently, the structure of the cluster formed is influenced by the PR_3 ligands.

For this reason, we have now investigated systematically the reactions of CuCl with $RP(SiMe_3)_2$ (R = Ph), R_2PSiMe_3 (R = Ph, Me), and $KPPh_2$ in the presence of tertiary phosphanes. The multinuclear Cu cluster complexes **1**–**9** were isolated from these reactions (see Experimental Procedure).

Compounds **1**–**3** are formed as yellow crystals in yields of 80–90% (Schema 1). According to the X-ray crystal structure analysis,[4] **1** (Fig. 1a) contains a threefold axis and consists of a puckered Cu_3P_3 six-membered ring (Cu2 and P2), which is bridged by Cu1. The P atoms of the PPh_2 groups (P2) are thus μ_3-bridging atoms (Cu–P 233.5–243.0(3) pm). The coordination numbers of the Cu atoms vary; Cu2 is surrounded by P2 and the phosphorus atom of the $PnPrPh_2$ ligand (P1) in a trigonal-planar fashion, and Cu1 is surrounded by three PPh_2 ligands (P2) and one Cl ligand and exhibits a distorted tetrahedral coordination geometry. Recently Stelzer et al. reported a compound analogous to **1**, containing PMe_3 ligands.[5]

$$CuCl + Ph_2PSiMe_3 \xrightarrow{PnPrPh_2} [Cu_4Cl(PPh_2)_3(PnPrPh_2)_3] \quad \mathbf{1}$$
$$\xrightarrow{PHPh_2} [Cu_4(PPh_2)_4(PHPh_2)_4] \quad \mathbf{2}$$
$$\xrightarrow{PMe_3} [Cu_5(PPh_2)_5(PMe_3)_3] \quad \mathbf{3}$$

Scheme 1.

A topological relationship exists between the structures of **1** and **3**. Apparently **1** is a reactive intermediate on the way to the cluster **3**. Accordingly, the pentanuclear **3** (Fig. 1c) may be formed as a result of a reaction at the CuCl bond in **1**. With the exception of Cu4, which is coordinated in a distorted tetrahedral manner to four PPh_2 ligands (P1–P3, P5), Cu1–Cu3 and Cu5 exhibit a trigonal-planar coordination geometry.

The influence of the tertiary phosphanes on the formation of the structure of **2** is quite evident. As a result of the coordination of two sterically demanding $PHPh_2$ ligands (P5–P8) at Cu1 and Cu3, the formation of the structure type found in **1** is no longer possible. A nearly planar Cu_4P_4 ring exists in **2** (Fig. 1b), consisting of Cu1–Cu4 and the P atoms of the μ_2-PPh_2 groups (P1–P4). The deviations of these atoms from the best-fit plane are 3–20 pm. The Cu atoms in **2**, like those in **1** and **3**, have varying coordinations. Cu1 and Cu3 are tetrahedrally, and Cu2 and Cu4 are approximately linear (P1-Cu2-P2 166.2(3), P3-Cu4-P4 166.4(3)°) bound to the P ligands. The Cu–Cu distances indicate that no bonding interactions exist between these atoms (Cu1–Cu3 389–395, Cu2–Cu4 317.0(6) pm). In contrast, Cu–Cu distances of 244.5–255.8(2) pm are found in **1** and **3**.

The compounds $[Cu_4(PPh_2)_4(dppm)_2]$ (dppm = bis(diphenylphosphino)methane) and $[Cu_4(StBu)_4(PPh_3)_2]$[7] are structurally related to **2**.

A completely different structure is obtained if the sterically less demanding PMe_2 bridging ligands are used instead of PPh_2. Compound **4** crystallizes from the reaction solution of CuCl with PMe_3 and Me_2PSiMe_3 (in THF) [Eq. (a)], in the form of red needles (yield 90%).

$$CuCl \xrightarrow{PMe_3 + Me_2PSiMe_3} \underset{\mathbf{4}}{[Cu(PMe_3)_4]_2[Cu_{13}Cl_6(PMe_2)_9]} \qquad (a)$$

Compound **4** consists of two $[Cu(PMe_3)_4]^+$ cations and one $[Cu_{13}Cl_6(PMe_2)_9]^{2-}$ anion (Fig. 2 top). The basic cluster framework of the anion ($\bar{6}$ symmetry) is formed from a vertex-linked Cu_7 bitetrahedron (Cu1–Cu2), to whose basal faces six further Cu atoms (Cu3) are bound (Cu–Cu 247.4–257.4(3) pm). The polyhedron formed from thirteen Cu atoms is bridged by μ_3-PMe_2 ligands (P1, P2), and the six peripheral Cu3 atoms are additionally bound to Cl1. Thus Cu3 is linear coordinated (Cl1-Cu3-P1 176.6(2)°) to PMe_2 and Cl1, whereas Cu1 and Cu2 are each surrounded by three PMe_2 ligands (Cu–P 230.5–241.8(4) pm) in a distorted trigonal planar fashion.

[*] Prof. Dr. D. Fenske, Dipl.-Chem. A. Eichhöfer, Dipl.-Chem. W. Holstein
Institut für Anorganische Chemie der Universität
Engesserstrasse, Geb.-Nr. 30.45, D-W-7500 Karlsruhe (FRG)

[**] This work was supported by the Deutsche Forschungsgemeinschaft (Sonderforschungsbereich 195) and the Fonds der Chemischen Industrie.

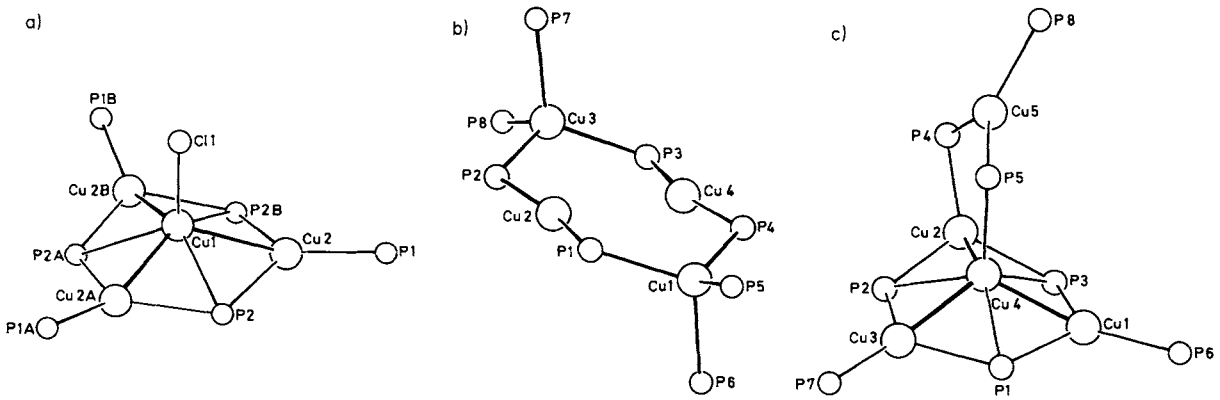

Fig. 1. Crystal stuctures of **1** (a), **2** (b), and **3** (c) (without C atoms). In **1**: P2 corresponds to the P atom of the PPh_2 and P1 to the P atom of the P*n*PrPh$_2$ ligand. In **2**: P1–P4 are the P atoms of the PPh_2 and P5–P8 the P atoms of the $PHPh_2$ ligands. In **3**: P1–P5 are the P atoms of the PPh_2 and P6–P8 the P atoms of the PMe_3 ligands.

Compound **4** is probably a sparingly soluble intermediate of the cluster condensation, whose end product would be $[CuPMe_2]_n$. In agreement with this is the observation that the initially formed red **4** rearranges when allowed to react longer into a completely insoluble, violet residue of the formula $[CuPMe_2]$.

The controlling influence of the bridging ligands on the structure of the cluster is also shown for the reaction of CuCl with $PHPh_2$ and a mixture of Ph_2PSiMe_3 and $PhP(SiMe_3)_2$ [Eq. (b)].

$$CuCl \xrightarrow{PHPh_2 + PhP(SiMe_3)_2 + Ph_2PSiMe_3} \underset{\mathbf{5}}{[Cu_{18}(PPh)_4(PPh_2)_{10}(PHPh_2)_3]} \quad (b)$$

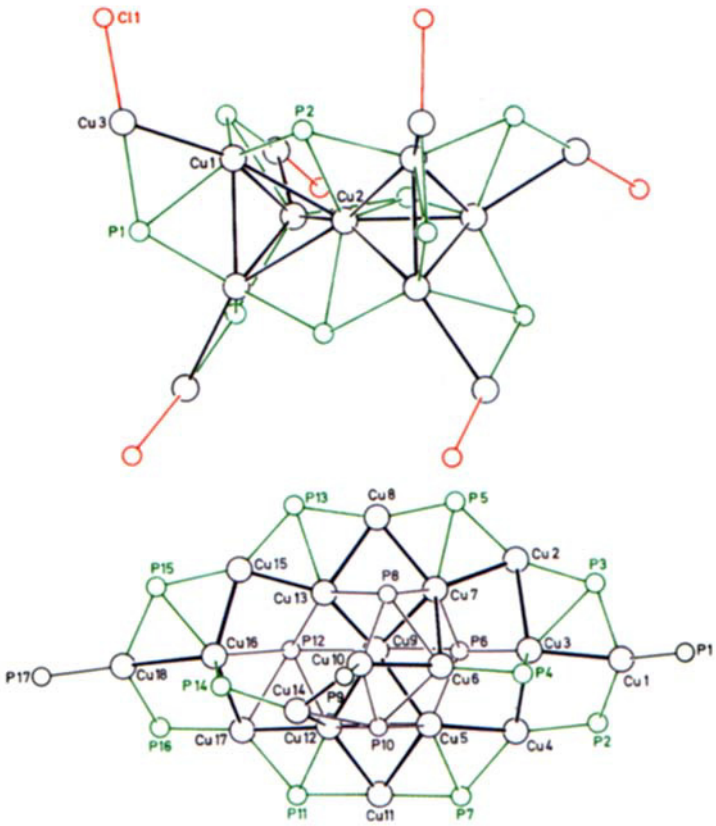

Fig. 2. Crystal structures of the anions in **4** (top) and **5** (bottom) (without C atoms). Cu: blue, Cl: red, P atoms of the PR_2 groups: green, P atoms of the PPh ligands: violet, P atoms of the $PHPh_2$ ligands: black.

Compound **5** crystallizes from THF in the form of black rhombuses (yield 30%). Figure 2 (bottom) shows that **5** is not a spherical cluster. The 18 Cu atoms (Cu–Cu 244.9–271.8(1) pm) are bridged by PPh_2 groups differently: P2, P4, P14, and P16 are the bridging atoms of μ_2 ligands (Cu–P 221.0–229.1(2) pm); P3, P5, P7, P11, P13, and P15 are the bridging atoms of μ_3 ligands (Cu–P 224.0–265.9(2) pm).

The PPh groups are also bound in different ways: P6 and P8 are the bridging atoms of μ_4 ligands (Cu–P 227.2–244.9(2) pm) and P10 and P12 are the bridging atoms of μ_5 ligands (Cu–P 230.1(2)–254.9(2) pm). The Cu atoms of the cluster periphery (Cu1, Cu10, Cu18) are in addition coordinated to terminal $PHPh_2$ ligands (ν(PH) = 2310 cm^{-1}). As a result Cu2, Cu4, Cu8, Cu11, Cu14, and Cu15 are each coordinated to two P atoms of the PPh_2 groups, and all other Cu atoms are coordinated to three P atoms of the phosphane ligands.

The reaction of CuCl with PR_3 (R = Me, Ph) and PhP-$(SiMe_3)_2$ (Scheme 2) analogous to Equation (b) shows the

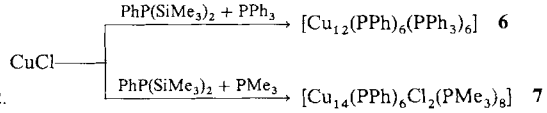

Scheme 2.

effect of the tertiary phosphanes and of the silylphosphane, on the structure of the cluster formed. A rapid coloring of the solution from colorless to black is observed when THF is used as the solvent, and **6** and **7** can be isolated as black crystals in yields of 30 and 80%, respectively.

Figure 3 (top) shows that **6** contains a Cu_{12} polyhedron ($\bar{1}$ symmetry), which is formed by linkage of three penetrating, planar Cu_6 rings (Cu2, Cu3, Cu4; Cu1, Cu2, Cu5; Cu1, Cu3, Cu6; Cu–Cu 256.3–278.3(2) pm). Alternatively **6** can be described as a compressed Cu_{12} cuboctahedron, which is surrounded by a distorted P_6 octahedron of the P atoms of the PPh ligands (P–P 387–453 pm). In the cuboctahedron, the distances between the Cu atoms (Cu4, Cu5, and Cu6) are extended to a nonbonding distance of 348–351 pm as a result of the bridging by the PPh ligands (P1–P3). These Cu atoms are each bound to a P atom of the PPh_3 ligands (P4–P6) and to two P atoms of the μ_4-PPh ligands (P1–P3) and exhibit a distorted trigonal planar coordination geometry. In contrast, the Cu atoms of the Cu_3 faces (Cu1, Cu2, Cu3) are coordinated to two μ_4-PPh ligands in an approximately linear (P-Cu-P 170.5(8)°) fashion. These coordination situations are a result of the steric shielding of these Cu atoms by the phenyl groups.

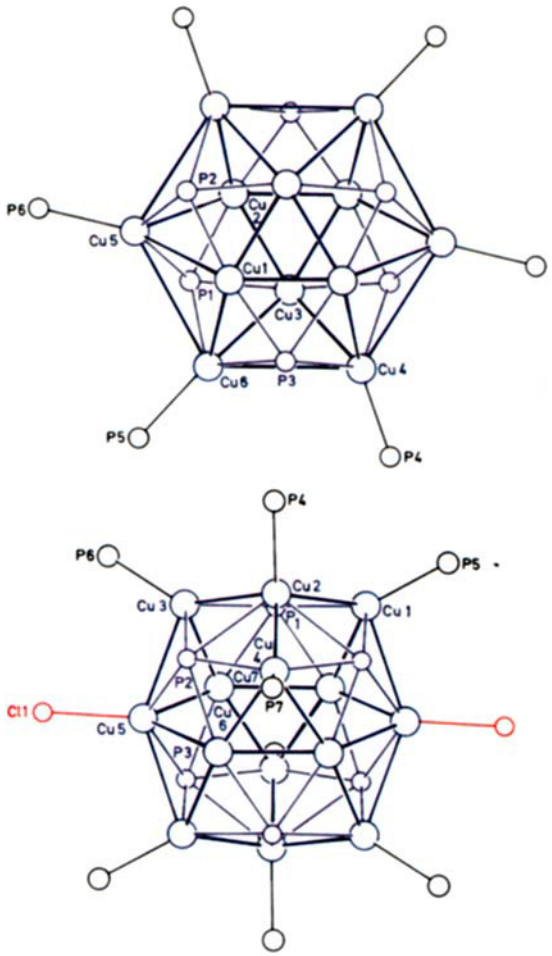

Fig. 3. Crystal structures of **6** (top) and **7** (bottom) (without C atoms). Cu: blue, P atoms of the PPh bridges: violet, P atoms of the PR_3 groups (**6**: R = Ph; **7**: R = Me): black.

The structure of the Cu cluster ($\bar{1}$ symmetry) in **7** (Fig. 3 bottom) can be derived from **6** by insertion of two further Cu atoms (Cu 2) into the Cu_{12} cuboctahedron. The Cu_{14} polyhedron formed is bordered by planar Cu_5 and Cu_3 rings. The pentagonal faces of this polyhedron are bridged by μ_5-PPh ligands (P 1–P 3), and the Cu atoms show differing coordination geometries: Cu 6 and Cu 7 are bound to two PPh ligands in a nearly linear fashion (P 1-Cu 6-P 2 159.9(3), P 1-Cu 7-P 3 161.3(1)°); Cu 1, Cu 3, and Cu 4 are coordinated in a trigonal planar manner to two PPh ligands and PMe_3; Cu 5 is also surrounded by two PPh ligands and one Cl ligand in a trigonal planar fashion; Cu 2 is tetrahedrally coordinated by the P atoms of three PPh ligands and one PMe_3 ligand. The Cu–Cu distances in **6** and **7** are 256.3–278.3(2) and 248.4–253.8(3) pm, respectively.

$[Cu_{12}S_8]^{4-}$, a cluster which has a cuboctahedral arrangement of the Cu atoms, was reported by Krebs et al.[7] As previously shown by Issleib, metalated phosphanes are also suitable for the preparation of polymeric Cu phosphides.[8] Because the structures of these compounds were as yet unknown, we studied the reactions of CuCl with $KPPh_2$ (in the presence of PPh_3), and $CuCl_2$ with $KPPh_2$ (at −75 °C), which led to the compounds **8** and **9**, respectively (Scheme 3).

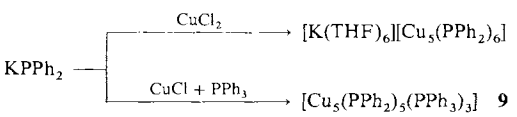

Scheme 3.

A trigonal Cu_5 bipyramid (Cu–Cu 332.9–412.2(2) pm) exists in **8** (Fig. 4) with a twofold axis. The edges to the axial positions are bridged by the P atoms of the PPh_2 groups. The Cu atoms are thereby coordinated either in a linear (Cu 1,Cu 3) (P-Cu-P 172.5(7)°) or trigonal planar fashion (Cu 2).

The geometry of the anion in **8** thus corresponds to that of $[Cu_5(StBu_6]^-$ previously described by Dance.[9] Thus it is clear that a similarity exists between the structures of clusters with PR_2 or SR ligands (R = organic group), which is derivable from the isolobal principle.[11]

Compound **9** forms yellow crystals; its $Cu_5(PPh_2)_5$ framework is analogous to that built in **3**.

A dark red colored amorphous powder is formed by the reaction of CuCl with Ph_2PX (X = K, $SiMe_3$) at room temperature, which corresponds to the formula $[CuPPh_2]$. The sparingly soluble $[CuPPh_2]$, however, can be dissolved in the presence of tertiary phosphanes. The previously discussed cluster complexes can be isolated from these solutions. Similar results were previously obtained by Stelzer et al., who reported multinuclear Cu complexes such as $[Cu_4(R_2PCH_2PR)Cl_3py]$ (R = *i*Pr, py = pyridine) and $[Cu_8(RPCH_2PR)_2Cl_2(py)_5]$.[5,12]

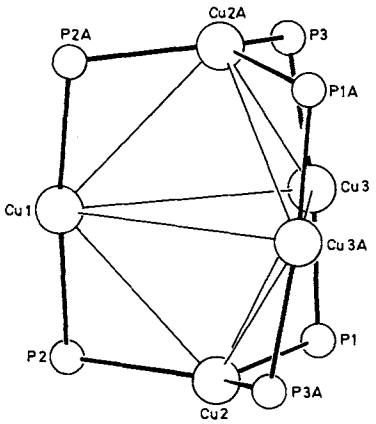

Fig. 4. Crystal structure of the anion in **8** (without C atoms).

If it is assumed that the ligands in **1**–**9** can be considered as Cl^-, PPh_2^-, PMe_2^-, and PPh^{2-}, the copper atoms in all compounds should have the formal oxidation state I (d^{10} configuration). Although the contribution of d^{10}–d^{10} interactions to the metal–metal bonding is controversial, examples are known which show that this can be significant.[12] The following range of Cu–Cu distances exist in **1**–**9**: **1**: 246.6(2), **2**: 317–395, **3**: 244.5–255.8(2), **4**: 247.4–257.4(3), **5**: 244.9–271.8(1), **6**: 256.3–278.3(2), **7**: 248.4–253.8(3), **8**: 332.9–412.2(2), **9**: 249.6–251.9(3) pm. These distances correspond to the values that have been found in other multinuclear Cu clusters and multinuclear Cu complexes with I^-, S^{2-}, Se^{2-}, SR^- ligands.[7,13]

The application of simple counting rules, for example the noble gas rule, is difficult for **1**–**9**. This is connected with the fact that it is not possible to make definite statements with regard to whether a Cu–Cu bond exists or not due to the varying metal–metal distances.

The bonding in **2** and **8** is relatively clear. The cluster complex **2** 64 valence elctrons (VE) at its disposal, which, as a result of the different coordinations, can be distributed to Cu 1–Cu 4, such that the nearly linear coordinated Cu atoms (Cu 2, Cu 4) have 14 VE, and the tetrahedrally coordinated Cu atoms Cu 1 and Cu 3 have 18 VE. Three linear coordinat-

ed (Cu1, Cu3, Cu3A) and two trigonal planar coordinated Cu atoms (Cu2, Cu2A) exist in **8**. Consequently, it could be assumed that Cu1, Cu3, and Cu3A with their ligands can each be described as 14 VE, as well as Cu2 and Cu2A correspondingly as 16 VE metal complex fragments. The fact that the 18-electron configuration is not attained, which is also observed in other coinage metal compounds, is apparently a characteristic of multinuclear complexes of these elements.

Initial studies into the reactivity of AgCl, $CdCl_2$, and $ZnCl_2$ with silylated phosphanes R_2PSiMe_3 (R = Ph) show that the previously described reaction type is a generally applicable method for the preparation of multinuclear, phosphido-bridged metal complexes. So far the following compounds could be isolated and structurally elucidated: $[Ag_4(PPh_2)_4(PMe_3)_4]$, $[Ag_6(PPh_2)_6(PtBu_3)_2]$, $[Zn_4Cl_4(PPh_2)_4(PnPr_3)_2]$, $[Cd_4Cl_4(PPh_2)_4(PnPr_3)_2]$.[14]

Experimental Procedure

1–**3**: CuCl (1.15 g, 0.012 mmol) was dissolved in THF (50 mL) with $PR'R_2$ (0.012 mmol, **1**: R' = *n*Pr, R = Ph; **2**: R' = H, R = Ph; **3**: R' = Me, R = Me). Subsequently Ph_2PSiMe_3 (2.8 mL, 0.012 mmol) was pipetted into the solution. On stirring, the solution turned yellow. Crystals suitable for X-ray structure analysis were obtained for **1** by layering the reaction solution with THF/heptane. Compound **2** crystallized from ether, and **3** from ether, after the addition of heptane (yields 80–90%).

4: CuCl (0.53 g, 5.35 mmol) was dissolved in THF (100 mL) with PMe_3 (0.55 mL, 5.35 mmol). Subsequently Me_2PSiMe_3 (0.8 mL, 5.35 mmol) was pipetted into the solution. After 3 h thin red needles crystallized from the red solution. At the end of the crystallization, the solution was clear and colorless (yield 90%).

5: CuCl (0.8 g, 8.1 mmol) was dissolved by the addition of $PHPh_2$ (1.5 mL, 8.1 mmol) in THF (75 mL). Subsequently Ph_2PSiMe_3 (0.46 mL, 2.03 mmol) and $PhP(SiMe_3)$ (0.46 mL, 2.03 mmol) were pipetted simultaneously into the solution and this was then stirred. The solution darkened after 15 min. After two days, the reaction solution was covered with a heptane layer, and black, rhombohedral, partly dendritic crystals were formed within a week at the solvent interface (yield 30%).

6: CuCl (0.4 g, 4 mmol) and PPh_3 (0.52 g, 2 mmol) were suspended in THF (50 mL). After the addition of $PhP(SiMe_3)_2$ (0.52 mL, 2 mmol), the solution turned black, and the reaction solution was stirred for 8 h. Crystals of **6** were obtained from the concentrated reaction solution or by layering the solution with heptane (yield 10%).

7: CuCl (0.65 g, 6.56 mmol) was dissolved in PMe_3 (1.4 mL, 6.56 mmol) in THF (50 mL). Subsequently $PhP(SiMe_3)_2$ (0.75 mL, 3.28 mmol) was pipetted into the solution with stirring. The solution quickly darkened in color through yellow to black, and **7** precipitated as a fine black crystalline solid. Crystals suitable for X-ray structure analysis were obtained when the reaction solution was layered with heptane (yield 80%).

8: CuCl (1.346 g, 0.0138 mol) was suspended with PPh_3 (7.24 g, 0.0276 mol) in THF (75 mL). It formed a white voluminous precipitate. Subsequently a solution of $KPPh_2 \cdot 2$dioxane (5.52 g, 0.0138 mol) in THF (25 mL) was added dropwise, and the mixture was stirred. After it had been stirred for two days, the yellow precipitate which formed was filtered off. The reaction solution was layered with THF/heptane, and yellow, rhombohedral crystals of **8** were formed at the solvent interface within two days (yield 80%).

9: A solution of $KPPh_2 \cdot 2$dioxane (22.62 g, 0.0565 mol) in THF (40 mL) was added dropwise to a suspension of $CuCl_2$ (3.8 g, 0.0283 mol) in THF (100 mL) at −75 °C, and stirred. Over 24 h the cold bath was warmed to room temperature, and the KCl formed was filtered off. The orange reaction solution was layered with THF/heptane, and yellow-orange crystals of **9** were formed at the solvent interface (yield 60%).

Received: September 5, 1992 [Z 5560 IE]
German version: *Angew. Chem.* **1993**, *105*, 257

[1] E. W. Abel, *J. Chem. Soc. A* **1968**, 2371.
[2] D. Fenske, J. Magull, *Z. Anorg. Allg. Chem.* **1991**, *594*, 29–35.
[3] D. Fenske, R. Basoglou, J. Hachgenei, F. Rogel, *Angew. Chem.* **1984**, *96*, 160; *Angew. Chem. Int. Ed. Engl.* **1984**, *23*, 160.
[4] X-ray crystal structure analyses: Stoe Stadi IV or Stoe IPDS diffractometer, empirical absorption correction; data collection and refinement: ω scan (profile analysis) Stadi IV). **1**: Cell constants (190 K): $a = b = c = 2476.2(19)$ pm, $\alpha = \beta = \gamma = 90°$, $V = 15183 \times 10^6$ pm^3; space group $Pa\bar{3}$ (no. 205), $Z = 8$; $\mu(Mo_{K\alpha}) = 12.45$ cm^{-1}, $2\theta_{max} = 52.3°$; 16629 reflections, of which 3184 were independent with $I > 2\sigma(I)$; 278 parameters (Cu, P, Cl, C refined anisotropically, the positions of the H atoms were calculated); $R = 0.068$. **2**: Cell constants (220 K): $a = 1521.3(20)$, $b = 1626.5(15)$, $c = 1853.3(29)$ pm, $\alpha = 74.83(10)$, $\beta = 82.00(10)$, $\gamma = 75.73(9)°$, $V = 4275.7 \times 10^6$ pm^3; space group $P\bar{1}$ (no. 2), $Z = 2$; $\mu(Mo_{K\alpha}) = 11.15$ cm^{-1}, $2\theta_{max} = 54.2°$; 64643 reflections, of which 7209 were independent with $I > 2\sigma(I)$; 494 parameters (Cu, P refined anisotropically, C isotropically, the positions of the H atoms in the phenyl rings were calculated, H atoms of the $HPPh_2$ groups could not be localized); $R = 0.075$. **3**·2THF: Cell constants (200 K): $a = 2011.7(8)$, $b = 2050.7(11)$, $c = 3786.8(7)$ pm, $\alpha = \beta = \gamma = 90°$, $V = 15622.03 \times 10^6$ pm^3; space group *Pbca* (no. 61), $Z = 8$; $\mu(Mo_{K\alpha}) = 14.77$ cm^{-1}, $2\theta_{max} = 46.2°$; 66408 reflections, of which 9699 were independent with $I > 2\sigma(I)$; 784 parameters (Cu, P, C refined anisotropically, C, O of the solvent isotropically, the positions of the H atoms were calculated); $R = 0.056$. **4**: Cell constants (200 K): $a = b = 1538.9(8)$, $c = 2647.1(22)$ pm, $\alpha = \beta = 90$, $\gamma = 120°$, $V = 5430 \times 10^6$ pm^3; space group $P6_3/m$ (no. 176), $Z = 2$; $\mu(Mo_{K\alpha}) = 39.48$ cm^{-1}, $2\theta_{max} = 56°$; 8243 reflections, of which 3783 were independent with $I > 2\sigma(I)$; 137 parameters (Cu, P, Cl, C refined anisotropically, the methyl groups C3 and C4 were refined as rigid groups, the positions of the H atoms were calculated); $R = 0.063$. **5**·1.5THF: Cell constants (190 K): $a = 1875.1(4)$, $b = 3703.1(10)$, $c = 2591.7(5)$ pm, $\beta = 93.56(2)°$, $V = 17961 \times 10^6$ pm^3; space group $P2_1/m$ (no. 11), $Z = 4$; $\mu(Mo_{K\alpha}) = 21.99$ cm^{-1}, $2\theta_{max} = 52.3°$; 94280 reflections, of which 19898 were independent with $I > 2\sigma(I)$; 2009 parameters (Cu, P, C refined anisotropically, C, O of the solvent refined isotropically with half occupation factors, the positions of the H atoms were calculated); $R = 0.048$. **6**·2.5THF: Cell constants (200 K): $a = 1643.9(8)$, $b = 1772.6(9)$, $c = 1835.6(9)$ pm, $\alpha = 107.17(4)$, $\beta = 114.75(5)$, $\gamma = 100.32(5)°$, $V = 4349 \times 10^6$ pm^3; space group $P\bar{1}$ (no. 2), $Z = 2$; $\mu(Mo_{K\alpha}) = 30.52$ cm^{-1}, $2\theta_{max} = 56.3°$; 74331 reflections, of which 14636 were independent with $I > 2\sigma(I)$; 860 parameters (Cu, P, C refined anisotropically, C, O of the solvent refined with half occupation factors isotropically, the positions of the H atoms were calculated); $R = 0.067$. **7**: Cell constants (230 K): $a = 1385.8(19)$, $b = 1569.2(9)$, $c = 2000.7(18)$ pm, $\alpha = 88.72(6)$, $\beta = 88.28(7)$, $\gamma = 87.75(6)°$, $V = 4344 \times 10^6$ pm^3; space group $P\bar{1}$ (no. 2), $Z = 2$; $\mu(Mo_{K\alpha}) = 33.95$ cm^{-1}, $2\theta_{max} = 50°$; 16007 reflections, of which 9985 were independent with $I > 2\sigma(I)$; 816 parameters (Cu, Cl, P, C refined anisotropically, the positions of the H atoms were calculated); $R = 0.052$. **8**: Cell constants (200 K): $a = 1436.0(8)$, $b = 1356.0(7)$, $c = 2419.3(9)$ pm, $\beta = 101.97(3)°$, $V = 4608 \times 10^6$ pm^3; space group $P2/n$ (no. 13), $Z = 4$; $\mu(Mo_{K\alpha}) = 12.71$ cm^{-1}, $2\theta_{max} = 56°$; 11697 reflections, of which 7199 were independent with $I > 2\sigma(I)$; 546 parameters (Cu, P, C, O, K refined anisotropically, the positions of the H atoms were calculated); $R = 0.054$. **9**·1.5THF: Cell constants (200 K): $a = 2583.6(23)$, $b = 1712.3(13)$, $c = 2811.1(21)$ pm, $\beta = 108.17(6)°$, $V = 1170 \times 10^6$ pm^3; space group $P2_1/a$ (no. 14), $Z = 4$; $\mu(Mo_{K\alpha}) = 9.97$ cm^{-1}, $2\theta_{max} = 50°$; 19584 reflections, of which 14443 were independent with $I > 2\sigma(I)$; 1182 parameters (Cu, P, C refined anisotropically, C, O of the solvent refined isotropically with half occupation factors, the positions of the H atoms were calculated); $R = 0.071$. Further details of the crystal structure investigations may be obtained from the Fachinformationszentrum Karlsruhe, Gesellschaft für wissenschaftlich-technische Information mbH, D-W-7514 Eggenstein-Leopoldshafen 2 (FRG) on quoting the depository number CSD-56699, the names of the authors, and the journal citation.
[5] D. J. Brauer, G. Hessler, P. C. Knüppel, O. Stelzer, *Inorg. Chem.* **1990**, *29*, 2370.
[6] T. A. Annan, R. Kumar, D. Tuck, *J. Chem. Soc. Dalton Trans.* **1991**, 11; I. G. Dance, L. J. Fitzpatrick, D. C. Craig, M. L. Scudder, *Inorg. Chem.* **1989**, *28*, 1853.
[7] P. Betz, B. Krebs, G. Henkel, *Angew. Chem.* **1984**, *96*, 293–294; *Angew. Chem. Int. Ed. Engl.* **1984**, *234*, 311.
[8] K. Issleib, H.-O. Fröhlich, *Chem. Ber.* **1962**, *95*, 374.
[9] I. G. Dance, *J. Chem. Soc. Chem. Commun.* **1976**, 68.
[10] D. J. Brauer, P. C. Knüppel, O. Stelzer, *J. Chem. Soc. Chem. Commun.* **1990**, *123*, 653.
[11] R. Hoffmann, *Science* **1981**, *211*, 995; *Angew. Chem.* **1982**, *94*, 725; *Angew. Chem. Int. Ed. Engl.* **1982**, *21*, 711.
[12] F. A. Cotton, X. Feng, M. Matusz, R. Poli, *J. Am. Chem. Soc.* **1988**, *110*, 7077; R. Mason, D. M. P. Mingos, *J. Organomet. Chem.* **1973**, *50*, 53; P. K. Mehrotra, R. Hoffmann, *Inorg. Chem.* **1978**, *17*, 2187; C. Kölmel, R. Ahlrichs, *J. Phys. Chem.* **1990**, *94*, 5536; K. M. Merz, R. Hoffmann, *Inorg. Chem.* **1988**, *27*, 2120.
[13] J. Beck, J. Strähle, *Angew. Chem.* **1985**, *97*, 419; *Angew. Chem. Int. Ed. Engl.* **1985**, *24*, 409; S. Gambarotta, C. Floriani, A. Chiesi-Villa, C. Guastini, *J. Chem. Soc. Chem. Commun.* **1983**, 1156; J. A. J. Jarvis, B. T. Kilbourn, R. Pearce, M. F. Lappert, *idid.* **1973**, 475; H. Hartl, F. Mahdjour-Hassan-Abadi, *Angew. Chem.* **1984**, *96*, 359; *Angew. Chem. Int. Ed. Engl.* **1984**, *23*, 378; G. Henkel, P. Betz, B. Krebs, *J. Chem. Soc. Chem. Commun.* **1984**, 314; I. G. Dance, J. C. Calabrese, *Inorg. Chim. Acta* **1976**, L 41; D. Coucouvanis, C. N. Murphy, S. K. Kanodia, *Inorg. Chem.* **1980**, 2993; M. Gernon, H. Kang, S. Liu, J. Zubieta, *J. Chem. Soc. Chem. Commun.* **1988**, 1031; D. Fenke, H. Krautscheid, S. Balter, *Angew. Chem.* **1990**, *102*, 799; *Angew. Chem. Int. Ed. Engl.* **1990**, *29*, 796; D. Fenske, H. Krautscheid, *ibid.* **1990**, *102*, 1513 and **1990**, *29*, 1452.
[14] A. Eichhöfer, D. Fenske, J. Eisenmann, F. Simon, unpublished.

Synthesis and Characterization of a High Molecular Weight Stiff Dendrimer**

By *Zhifu Xu* and *Jeffrey S. Moore**

The synthesis and characterization of macromolecules with defined structure[1] such as dendrimers[2] are of widespread interest. The ability to manipulate molecular weight[3] and chemical constitution[4] precisely is typical with dendrimer syntheses; however, it is also important to begin to design approaches to macromolecules that have tailored conformations and well-defined three-dimensional architectures. This paper reports on the synthesis and characterization of a tridendron[5] based on phenylacetylene monomeric units. This macromolecule has a molecular weight in excess of 14 kDa and thus represents the largest pure hydrocarbon known.[6] Key to its synthesis is the proper choice of peripheral functionality (to aid solubility) and careful optimization of reaction conditions. Complete ^{1}H NMR assignment has made it possible to confirm the exact chemical structure. In spite of the high arene content and stiffness of this macromolecule, it is extremely soluble in pentane at room temperature.

In a preliminary report, we described a synthetic scheme for the preparation of triconnected phenylacetylene monodendrons.[7] Difficulties arising from poor solubility and low chemical reactivity hampered our efforts in extending this scheme to high molecular weight generations of monodendrons and tridendrons. In our original communication, we noted that *para-tert*-butylphenyl peripheral groups promoted better solubility than the other groups that we examined. However, during further investigations with this system, we discovered that tridendrons and monodendrons possessing this peripheral group but containing more than 15 monomeric units were poorly soluble in common organic solvents. This behavior severely hampered our efforts to synthesize, purify, and characterize higher generation members of this series.

Here we report that a small change in the peripheral group functionality provides rather dramatic improvement in solubility. In particular, this involves the use of 3,5-di-*tert*-butylphenyl group instead of *para-tert*-butylphenyl as peripheral functionality, which has made it possible to continue the synthesis leading to the high molecular weight tridendron described below. In fact, all members of the phenylacetylene dendrimer series containing the di-*tert*-butylphenyl periphery and up to 94 monomer units are soluble in *pentane* at room temperature. Qualitatively, we note that the solubility is lowest for tridendrons and monodendrons having 10–15 monomer units and *improves* as the molecular size grows beyond this range. Powder X-ray diffraction shows that those dendrimers having only 10–15 monomers are partly crystalline while the higher members are totally amorphous.

One side reaction common to palladium-catalyzed cross-coupling chemistry is the formation of a self-coupling product. For cross-coupling chemistry involving 1-alkynes, the side reaction gives a diacetylene derivative. This side reaction is likely to be catalyzed by adventitious molecular oxygen. We observed that the amount of diacetylene product increases in higher generations, presumably due to the increasing steric congestion around the core. For the highest generations, diacetylene formation is significant even when molecular oxygen is rigorously excluded. Minimizing this side reaction is key to the successful syntheses of these dendrimers and their subsequent purifications. In our earlier publication, we demonstrated that enlarging the monomer for the higher generations is one way to overcome this problem.[7] Here we report reaction conditions that have proven to be successful at minimizing self-coupling without enlarging the monomer or core size.

Aryl iodides are greatly preferred to aryl bromides for the cross-coupling chemistry, since the coupling reaction must be performed at as low a temperature as possible. Long reaction times are required under these conditions, but the yield of the cross-coupling product is substantially higher. Moreover, as the molecular weight increases, substantially larger quantities of catalyst are necessary, which makes it extremely important to run the reaction at low temperature (35–40 °C) for longer periods of time (2 days). At higher temperatures (e.g. 80 °C) and with high catalyst concentrations, side reactions occur which predominately lead to the self-coupling side-product and to unidentified high molecular weight impurities.

Using the optimized reaction conditions described above and 3,5-di-*tert*-butylphenyl peripheral groups, we have successfully prepared the phenylacetylene tridendron containing 94 monomer units (Fig. 1) by coupling 4.0 equivalents of 31-mer monodendron with 1,3,5-triiodobenzene [Eq. (a),

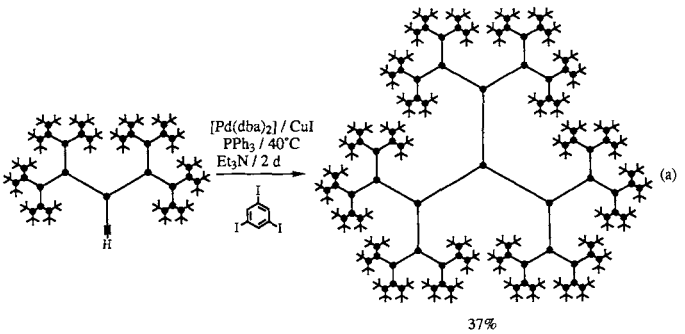

dba = dibenzylideneacetone]. The yield of the final coupling step was 37% after purification by silica gel chromatography. This hydrocarbon dendrimer has the molecular formula $C_{1134}H_{1146}$ and a molecular weight of 14776, which represents the largest pure hydrocarbon reported. Molecular models indicate the diameter of this dendrimer to be about 55 Å. Space-filling molecular models (Fig. 1, right) show that the monomeric units in the outer tier of one arm can come into close contact with those of another arm. The overall structure is thus spherical or globular. Even so, the interior remains open with large voids and niches.

Confirmation of the chemical structure has been obtained through a variety of experiments. Analytical thin-layer chromatography (TLC) of the 94-mer reaction mixture reveals the presence of two new products in addition to the 30-mer diacetylene side-product carried over from the previous generation and a small amount of excess starting material. Separation of this mixture is possible by careful silica gel chromatography. Size exclusion chromatography (SEC) of the two new products shows that they are nearly identical in size. The SEC elution profile in each case is a single sharp peak ($M_w/M_n = 1.03$) and corresponds to a molecular weight of 9.0×10^3 relative to narrow molecular weight polystyrene standards. This value is significantly larger than the value of 6.1×10^3 observed for the starting monodendron which possesses 31 monomer units. The new product of higher R_f ac-

[*] Prof. J. S. Moore, Z. Xu
The Willard H. Dow Laboratories, The University of Michigan
Ann Arbor, MI 48109-1055 (USA)

[**] Stiff Dendritic Macromolecules, Part 2. This work was supported by the National Science Foundation (grant DMR-9212054), the NSF Young Investigator Program and the 3M company (awards program for untenured faculty). Part 1. See reference [7].

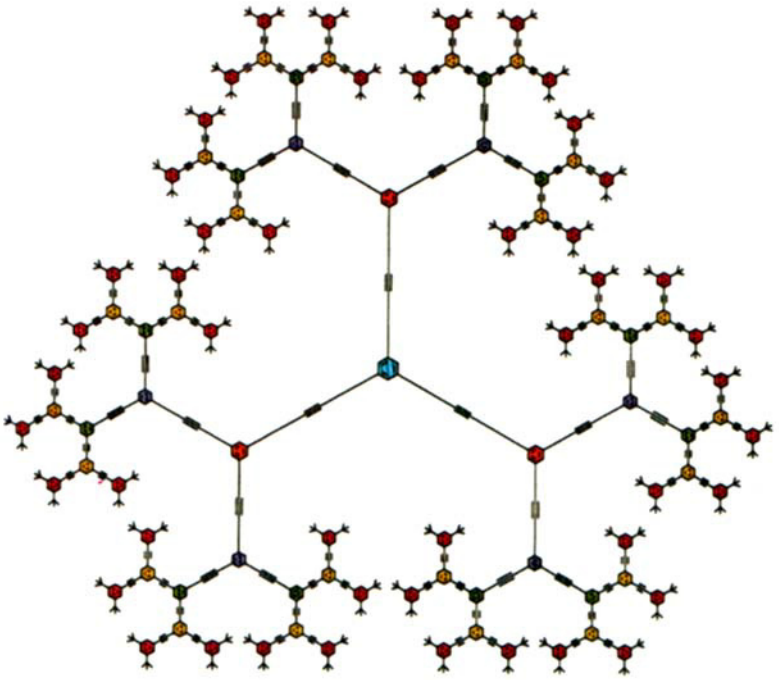

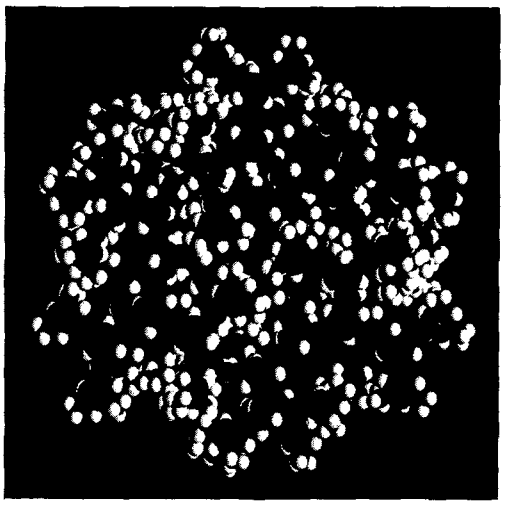

Fig. 1. Structural formula and molecular model of the 94-mer tridendron synthesized as shown in [Eq. (a)]. Equivalent aromatic rings are denoted by a common color, assuming rapid torsional rotation about the sp–sp^2 single bonds.

counts for about 20% of the mixture and is identical (^{1}H NMR, TLC) to the 62-mer diacetylene we synthesized independently. The major product (lower R_f) should thus correspond to the desired 94-mer, although we have also considered the possibility that this substance may be a 63-mer in which only two monodendrons coupled to triiodobenzene. However, the major product gave an elemental composition by combustion analysis of that expected for the 94-mer. This result disfavors the possibility that we isolated the 63-mer, since this monoiodide would have a carbon content 1% lower than the theoretical value of the desired tridendron (Calcd for 63-mer $C_{758}H_{765}$ I: C 91.02, H 7.71. Calcd. for 94-mer $C_{1134}H_{1146}$: C 92.18, H 7.82. Found: C 91.96, H 7.75).

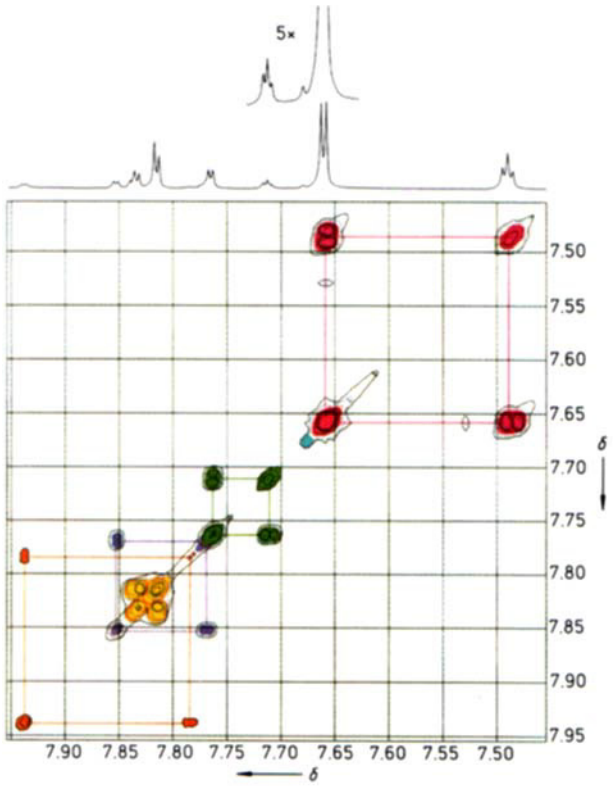

Fig. 2. ^{1}H NMR COSY-45 spectrum of the 94-mer tridendron recorded at 360 MHz in [D_6]benzene at 295 K. Resonances and cross peaks corresponding to the five different AB_2 spin systems and to the lone A_3 spin system are colored to match the structure shown in Figure 1.

Strong evidence in support of this conclusion has been obtained by extensive ^{1}H NMR experiments. In the aliphatic region, only a sharp singlet resonance corresponding to the *tert*-butyl protons is observed. In the aromatic region, adequate chemical shift dispersion for complete assignment has been realized by recording the NMR spectra in several solvents and at several temperatures. Good chemical shift dispersion is found for spectra recorded with [D_6]benzene or [D_8]THF. Spectra recorded in $CDCl_3$, on the other hand, are very congested and contain little information. The COSY-45 spectrum of the 94-mer in [D_6]benzene at 295 K is shown in Figure 2. Five cross peaks corresponding to the five different AB_2 (nearly AX_2) spin systems expected for this compound can clearly be identified. Two-dimensional *J*-resolved spectroscopy has established that each of these cross peaks correlates a triplet–doublet pair. The relative integral intensity of these spin systems follows the predicted ratio of 1:2:4:8:16. Most importantly, a small singlet is observed at $\delta = 7.68$, confirming the presence of a C_3 rotational axis in this molecule. This singlet displays a fairly strong, temperature-dependent chemical shift to lower field at higher temperatures. At 300–330 K, it is possible to separate the singlet from the intense doublet at $\delta = 7.66$ and obtain accurate integral intensities. Careful integration of the singlet against the doublet further downfield gives the expected 1:2 ratio. We believe that the complete assignment of the ^{1}H NMR signals together with the elemental composition data constitutes unambiguous proof of the chemical structure of the 94-mer.[8] We are continuing to explore other synthetic strategies for stiff dendrimers with novel architectures and will report these findings in due course.

Experimental Procedure

A single-neck Schlenk flask was charged with the deprotected 31-mer monodendron (140 mg, 0.0286 mmol), triiodobenzene (3.3 mg, 0.007 mmol),

$[Pd(dba)_2]$ (1.6 mg, 0.003 mmol), triphenylphosphane (6 mg, 0.023 mmol), copper(I) iodide (0.6 mg, 0.003 mmol), and dry triethylamine (3 mL). The flask was stoppered, degassed under vacuum, back-filled with nitrogen and stirred at 40 °C for 2 days. The consumption of the 1-alkyne was monitored by TLC. After completion, the reaction mixture was diluted with dichloromethane, washed with water (3 ×) and saturated aqueous sodium chloride, dried over anhydrous $MgSO_4$, and filtered. The crude mixture was separated by gravity column chromatography by eluting with hexane/CH_2Cl_2 (7:1 increasing to 6:1) to give the major product as a clear, colorless glass (40 mg).

^{1}H NMR (360 MHz, [D_6]benzene, 295 K): δ = 7.94 (d, 6H), 7.86 (d, 12H), 7.84 (t, 24H), 7.81 (d, 48H), 7.79 (t, 3H), 7.77 (t, 6H), 7.76 (d, 24H), 7.71 (t, 12H), 7.68 (s, 3H), 7.66 (d, 96H), 7.49 (t, 48H), 1.37 (s, 864H); ^{13}C NMR (90 MHz, $CDCl_3$): δ = 150.86, 134.69, 134.45, 134.31, 134.06, 133.88, 133.32, 125.95, 124.69, 124.36, 123.84, 123.73, 123.64, 123.34, 123.05, 121.77, 91.84, 89.41, 89.08, 88.87, 88.54, 86.61, 34.78, 31.29. Correct elemental analysis.

Received: September 15, 1992 [Z 5574 IE]
German version: *Angew. Chem.* **1993**, *105*, 261

[1] For a recent review see: J. S. Moore, *Polymer News*, in press.

[2] For reviews see: a) D. A. Tomalia, A. M. Naylor, W. A. Goddard III, *Angew. Chem.* **1990**, *102*, 119–157; *Angew. Chem. Int. Ed. Engl.* **1990**, *29*, 138–175; b) G. R. Newkome, C. N. Moorefield, G. R. Baker, *Aldrichim. Acta* **1992**, in press; c) J. Mulzer, H.-J. Altenbach, M. Braun, K. Krohn, H.-U. Reißig, *Organic Synthesis Highlights*, VCH, Weinheim, **1991**, pp. 378–383 (a contribution from K. Krohn).

[3] a) G. R. Newkome, A. Nayak, R. K. Behera, C. N. Moorefield, G. R. Baker, *J. Org. Chem.* **1992**, *57*, 358–362; b) G. R. Newkome, R. K. Behera, C. N. Moorefield, G. R. Baker, *ibid.* **1991**, *56*, 7162–7167; c) G. R. Newkome, C. N. Moorefield, G. R. Baker, A. L. Johnson, R. K. Behera, *Angew. Chem.* **1991**, *103*, 1205–1207; *Angew. Chem. Int. Ed. Engl.* **1991**, *30*, 1176–1178; d) G. R. Newkome, X. Lin, *Macromolecules* **1991**, *24*, 1443–1444; e) G. R. Newkome, Z. Yao, G. R. Baker, V. K. Gupta, P. S. Russo, M. J. Saunders, *J. Am. Chem. Soc.* **1986**, *108*, 849–850; f) G. R. Newkome, Z. Yao, G. R. Baker, V. K. Gupta, *J. Org. Chem.* **1985**, *50*, 2003–2004; g) K. L. Wooley, C. J. Hawker, J. M. J. Fréchet, *J. Am. Chem. Soc.* **1991**, *113*, 4252–4261; h) C. J. Hawker, J. M. J. Fréchet, *J. Chem. Soc. Chem. Commun.* **1990**, 1010–1013; i) *J. Am. Chem Soc.* **1990**, *112*, 7638–7647; j) G. J. Kallos, D. A. Tomalia, D. M. Hedstrand, S. Lewis, J. Zhou, *Rapid Commun. Mass Spectrom.* **1991**, *5*, 383–386; k) A. B. Padias, H. K. Hall, D. A. Tomalia, J. R. McConnell, *J. Org. Chem.* **1987**, *52*, 5305–5312; l) D. A. Tomalia, H. Baker, J. Dewald, M. Hall, G. Kallos, S. Martin, J. Roeck, J. Ryder, P. Smith, *Macromolecules* **1986**, *19*, 2466–2468; m) *Polym. J. (Tokyo)* **1985**, *17*, 117–132; n) T. M. Miller, T. X. Neenan, R. Zayas, H. E. Bair, *J. Am. Chem. Soc.* **1992**, *114*, 1018–1025; o) E. W. Kwock, T. X. Neenan, T. M. Miller, *Chem. Mater.* **1991**, *3*, 775–777; p) T. M. Miller, T. X. Neenan, *ibid.* **1990**, *2*, 346–349; q) G. D. Mendenhall, S. X. Liang, E. H. T. Chen, *J. Org. Chem.* **1990**, *55*, 3697–3699; r) H. Uchida, Y. Kabe, K. Yoshino, A. Kawamata, T. Tsumuraya, S. Masamune, *J. Am. Chem. Soc.* **1990**, *112*, 7077–7079.

[4] a) C. J. Hawker, J. M. J. Fréchet, *Macromolecules* **1990**, *23*, 4726–4729; b) K. L. Wooley, C. J. Hawker, J. M. J. Fréchet, *J. Chem. Soc. Perkin Trans. 1* **1991**, 1059–1076.

[5] Mono-, di- and tridendrons refer to dendritic architectures radiating outward from a point of singule, double, or triple connectivity, respectively. T. H. Mourey, S. R. Turner, M. Rubinstein, J. M. J. Fréchet, C. J. Hawker, K. L. Wooley, *Macromolecules* **1992**, *25*, 2401–2406.

[6] I. Bidd, D. W. Holdup, M. C. Whiting, *J. Chem. Soc. Perkin Trans. 1* **1987**, 2454–2463.

[7] J. S. Moore, Z. Xu, *Macromolecules* **1991**, *24*, 5893–5894.

[8] We have considered other explanations consistent with our synthetic chemistry to account for the appearance of the signal at δ = 7.68; however, on the following basis, we rule out these possibilities. First, we note that the T_1 value for this signal is similar to the T_1 values of protons on neighboring aromatic rings (ca. 4 s). Second, by comparison to the ^{1}H NMR spectrum of authentic 62-mer diacetylene, we rule out the possibility of its presence. Third, if only two monodendrons coupled to triiodobenzene, then the innermost ring should have structure I or, if reductive deiodination occurred then structure II is possible. Resonances due to protons of I or II would only

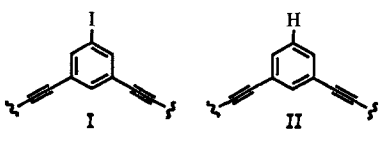

show the appearance of a singlet if theses spin systems were strongly second order. Given the expected chemical shifts of I and II (based on model compounds), this is not likely. Moreover, integration of the signal at δ = 7.68 with respect to the furthermost downfield doublet would be 3:4 and 4:4 for I and II, respectively, instead of the observed 1:2 ratio.

Self-Assembly and Liquid Crystal Formation of Folic Acid Salts**

By *Stefania Bonazzi, Monica Miranda DeMorais, Giovanni Gottarelli,* Paolo Mariani,** and *Gian Piero Spada*

Molecular recognition and self-organization processes are of great interest; in some cases they may lead to the formation of liquid crystalline mesophases.[1] A few biologically relevant molecules are known to exhibit such behavior.[2] Ordered mesophases are also useful for obtaining information, by X-ray diffraction studies, on the supramolecular architecture afforded by self-assembly.[3] Here we report that in water dipotassium folate[4] forms a hexagonal lyotropic liquid crystalline phase by a self-organization process which generates supramolecular objects with a chiral columnar shape.

CD spectra of folate recorded at low and high concentration are shown in Figure 1; these spectra are significantly different. Also the absorption spectra at high concentration

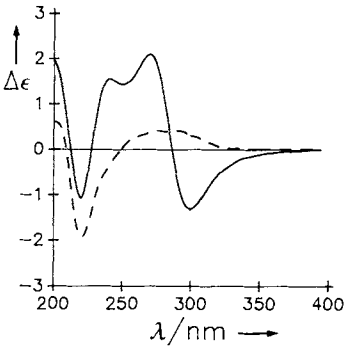

Fig. 1. CD spectra of dipotassium folate in water for concentration $c = 8.4 \times 10^{-5}$ mol L^{-1} (dashed line; recorded at 20 °C; the spectrum does not change on heating to 80 °C) and $c = 8.4 \times 10^{-2}$ mol L^{-1} (solid line; recorded at 5 °C). Measurements were performed with a Jasco J-710 dichrograph in cells fitted with a thermostat and with path length ranging from 0.001 to 1 cm.

show considerable hypochromicity. The CD spectrum of the concentrated solution displays exciton patterns characteristic of a helical arrangement of the chromophoric groups. At a concentration of about 35 wt%, the solution at 25 °C becomes birefringent and textures (Fig. 2) similar to those for the hexagonal mesophases formed by homoguanylic oligodeoxynucleotides,[3, 5] DNA,[6] and "chromonic" phases are observed with a microscope.[7]

In previous research we have shown that several deoxyguanosine derivatives form liquid crystalline phases.[3, 5, 9] The building block of these phases is a chiral columnar aggregate composed of a stacked array of Hoogsteen-bonded guanosine tetramers. Considering the similarity of guanine and pterin (Fig. 3), it seems natural to propose that also for the folate self-assembly leads to the formation of chiral columnar aggregates composed of a stacked array of folic acid tetramers. The stereogenic center in the side chain of the chromophoric groups generates the supramolecular chirality of the columns as revealed by CD spectroscopy. The CD

[*] Prof. G. Gottarelli, Dr. S. Bonazzi, Prof. G. P. Spada
Dipartimento di Chimica Organica "A. Mangini"
Università di Bologna
via S. Donato, 15, I-40127 Bologna (Italy)
Dr. P. Mariani, Dr. M. M. De Morais
Istituto di Scienze Fisiche
Università di Ancona
via Ranieri, 65, I-60131 Ancona (Italy)

[**] This work was supported by CNR and MURST.

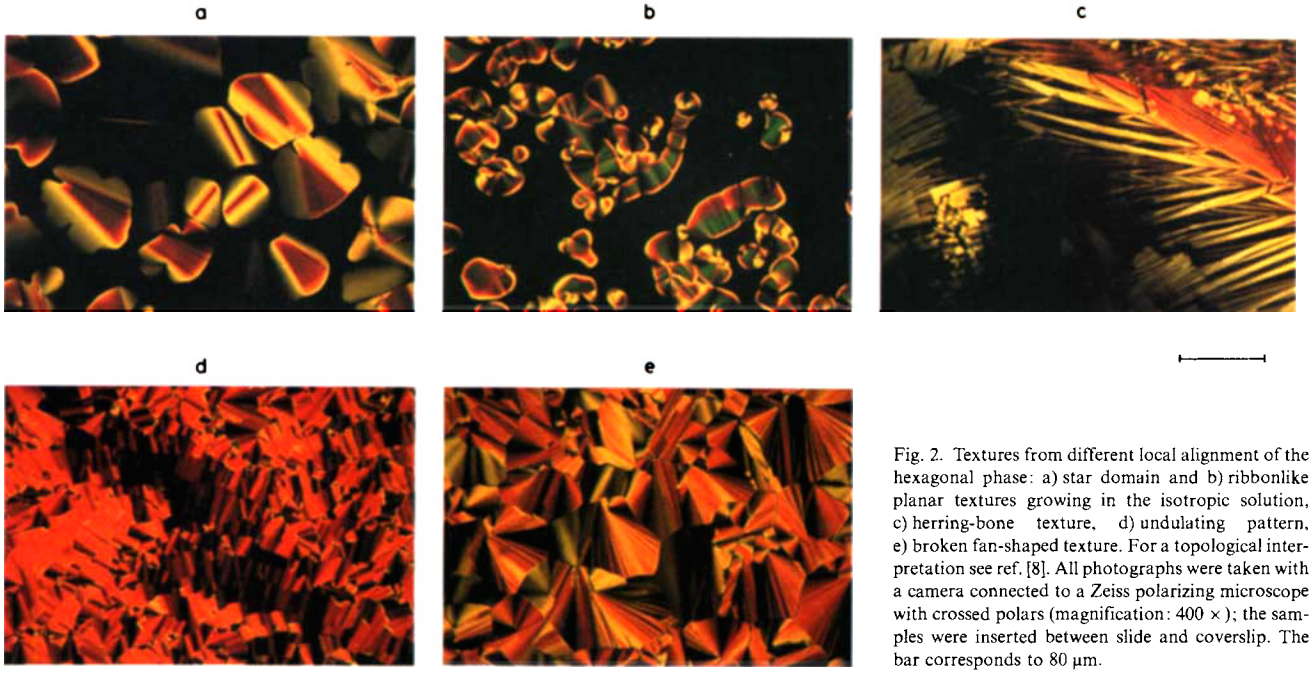

Fig. 2. Textures from different local alignment of the hexagonal phase: a) star domain and b) ribbonlike planar textures growing in the isotropic solution, c) herring-bone texture, d) undulating pattern, e) broken fan-shaped texture. For a topological interpretation see ref. [8]. All photographs were taken with a camera connected to a Zeiss polarizing microscope with crossed polars (magnification: 400 ×); the samples were inserted between slide and coverslip. The bar corresponds to 80 μm.

spectra show that the planar chromophoric tetramers are not exactly superimposed, but are rotated with respect to the one another in a way similar to that found in poliguanylic acid tetramers.[10-12]

The X-ray diffraction profile observed at 25 °C in the concentration range between 35 and 70 wt% is characterized by several low-angle narrow peaks; from the ratios of their spacings in values of s ($s_{hk} = 2\sin\theta/\lambda$, where 2θ is the scattering angle and λ the x-ray wavelength) of $1:3^{1/2}:4^{1/2}:7^{1/2}:9^{1/2}\ldots$, a hexagonal two-dimensional lattice is clearly derived. In such a concentration range, the high-angle region of the diffraction pattern ($s > (10\ \text{Å})^{-1}$) shows a sharp peak centered at $s = (3.3\ \text{Å})^{-1}$. According to the structural model outlined above and proposed previously for the liquid crystalline mesophases of guanosine derivatives,[3, 5, 9] such an X-ray diffraction pattern indicates that this phase could consist of parallel columnar aggregates packed in a two-dimensional hexagonal lattice. Each rod is composed of a stacked array of tetramers,[13] equally spaced at a distance of 3.3 Å and formed by four hydrogen-bonded folate residues. By assuming cylindrical-like aggregates embedded in the water matrix, but not penetrated by water molecules,[3, 9, 14] the cylinder radius was calculated: it is almost independent of the water content and is about 14.5 Å.[15]

It is interesting to analyze the effects of the concentration on the x-ray diffraction profile characteristics. The length a of the hexagonal unit cell appears to be a function of the concentration, changing from 36.2 Å ($c = 70$ wt%) to about 48.6 Å ($c = 36$ wt%) (Fig. 4). Moreover, when the isotropic liquid phase transition is approached (in particular for concentrations lower than ca. 45%), only the first low-angle peak still remains and becomes broad and diffuse. This observation could indicate a transition to a nematic, columnar phase when the water content increases. Quite surprisingly, dilution also modifies the high-angle pattern: in particular the position of the peak appears to change as a function of the folate concentration (Fig. 4 right). In the vicinity of the isotropic liquid phase transition, the peak becomes very large and diffuse. However, studies by optical microscopy seem to support the presence of a direct isotropic liquid to

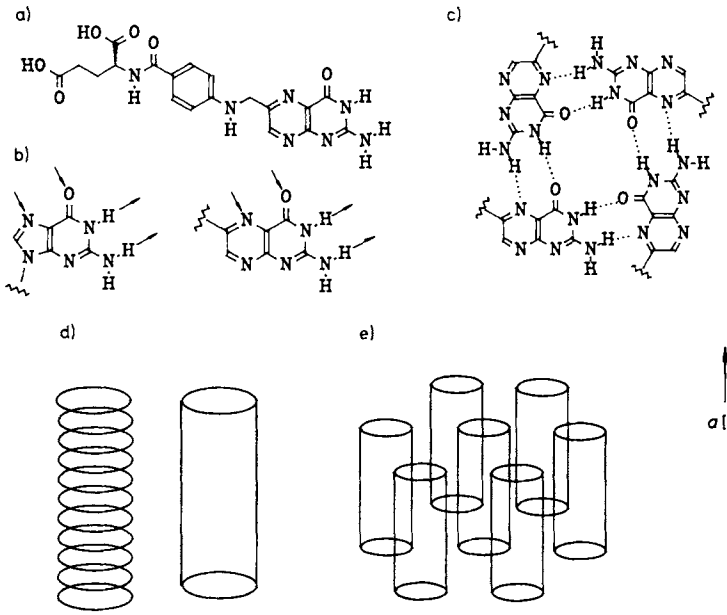

Fig. 3. a) Structure of folic acid and b) the similarity between the guanine and the pterin moieties; c) the proposed tetramers formed by four folic acid molecules. These tetramers may stack to form cylindrical aggregates (d) that in the liquid crystalline phase exhibit a hexagonal order (e).

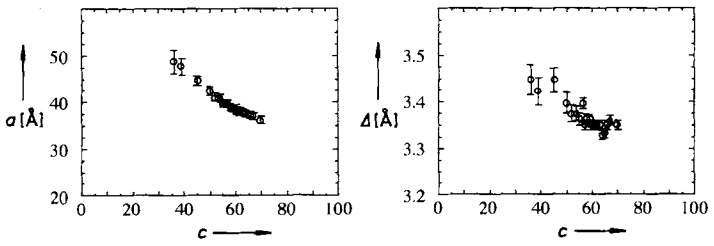

Fig. 4. Variations of two of the structural parameters of the columnar hexagonal phase at 25 °C as a function of folate concentration. Left: hexagonal unit cell parameter a, as calculated from the spacings of the x-ray diffraction low-angle peaks. Right: distance between the stacked tetrameric disks, as determined from the position of the high-angle peak. c = concentration of dipotassium folate in wt%. Range of angles for low-angle peaks $2.5 < 2\theta < 10°$ and for high-angle peaks $25 < 2\theta < 27°$.

hexagonal liquid crystal phase transition. Therefore, from a structural point of view, it appears that dilution establishes a large disordering of the hexagonal packing which completely disappears only when the isotropic phase is reached. Since the previously investigated guanosine derivatives[3, 5, 9] also form a cholesteric phase, this behavior is quite new and could correspond to a loose conformation of the columnar folate aggregates. In particular, the constant cylinder radius and the continuous change of position of the high-angle peak when the water content increases, suggest that the loss of aggregate rigidity could arise from a stacking interaction between the disks, weaker than that for the previously reported guanosine derivatives.[3, 5] The change in position of the high-angle peak might be due to an interaction of water with the polar groups in the side chain. Also a small temperature effect is observed on the hexagonal structural parameters: in particular, when the temperature increases, the dimesions of the unit cell do not change, but the tetramer repeat distance increases (from 3.32 to 3.42 Å in a sample with a folate concentration of 52 wt% when the temperature is raised from 2 to 60 °C).

The electron density map of the sample with a folate concentration of 59.5 wt% calculated from the diffracted intensities by performing a swelling experiment[3, 5, 9, 16] is reported in Figure 5. The map clearly shows the electron-dense rod cross-sections, surrounded by a smooth region of lower electron density, which is associated with the water.[17] There is an excellent agreement between the diameter of the rod determined directly from the map and the one calculated from our model (see above). The central region of the rod cross-section is characterized by a minimum in electron density, corresponding to the "hole" in the tetramer folate arrangement, which is in agreement with the assumption that the central region of the tetramer could contain the K^+ ion.[3, 9]

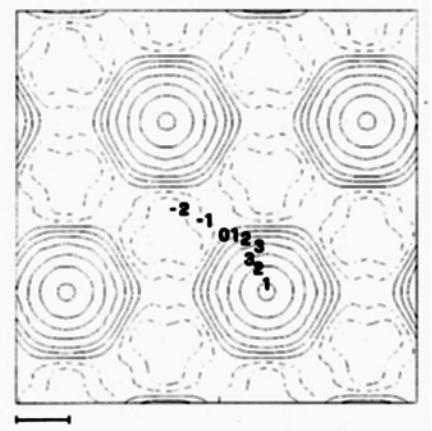

Fig. 5. Electron density distribution of the hexagonal phase in a sample with 59.5 wt% folate concentration. The electron density scale is arbitrary: the intensity data have been normalized so that the sum of the scattered intensity is equal to 1 [17]. Therefore, the corresponding electron density map is a normalized, dimensionless expression of the electron density fluctuation. The density lines are equally spaced: the dotted lines correspond to the region of lower electron density (i.e. to negative values in our data normalization), while the solid lines correspond to the higher electron density region (i.e. to positive values) (see ref. [17]). The structure factors $F(h,k)$, where h and k are the Miller indices, are $F(1,0) = +0.348$, $F(2,1) = -0.165$, $F(2,0) = -0.055$, $F(3,1) = -0.077$, $F(3,0) = 0$, $F(4,2) = +0.029$, $F(4,1) = +0.036$. The bar corresponds to 10 Å.

Since the critical concentration at which the liquid crystalline phase appears is not markedly affected by exchanging potassium for sodium, the ion dependence is not as specific as for guanosine derivatives, and also water molecules may fit into the central cavity.

The presence of small folate aggregates in the isotropic phase is also confirmed by a preliminary analysis of the small-angle neutron scattering: The scattering observed in sample with a folate concentration of 1 wt% is in accord with the existence of rod-like scattering particles with an average length of about 80 Å and a sectional gyration radius of about 14.5 Å. According to the results of similar experiments,[18] a model with cylindrical-like aggregates formed by stacking about 20 folate tetramers seems to fit these data.

Received: September 12, 1992 [Z 5570 IE]
German version: *Angew. Chem.* **1993**, *105*, 251

[1] J. M. Lehn, *Angew. Chem.* **1990**, *102*, 1347; *Angew. Chem. Int. Ed. Engl.* **1990**, *29*, 1304.
[2] S. Hoffmann, *Z. Chem.* **1987**, *27*, 395.
[3] S. Bonazzi, M. Capobianco, M. M. De Morais, A. Garbesi, G. Gottarelli, P. Mariani, M. G. Ponzi Bossi, G. P. Spada, L. Tondelli, *J. Am. Chem. Soc.* **1991**, *113*, 5809.
[4] Dipotassium folate was obtained from commercial folic acid (Aldrich) by neutralization with a stoichiometric amount of sodium hydroxide.
[5] S. Bonazzi, M. M. De Morais, A. Garbesi, G. Gottarelli, P. Mariani, G. P. Spada, *Liq. Cryst.* **1991**, *10*, 495.
[6] F. Livolant, A. M. Levelut, J. Doucet, J. P. Benoit, *Nature* **1989**, *339*, 724.
[7] T. K. Attwood, J. E. Lydon, F. Jones, *Liq. Cryst.* **1986**, *1*, 499.
[8] F. Livolant, Y. Bouligand, *J. Phys. (Paris)* **1986**, *47*, 1813.
[9] P. Mariani, C. Mazabard, A. Garbesi, G. P. Spada, *J. Am. Chem. Soc.* **1989**, *111*, 6369.
[10] S. Arnott, R. Chandrasekaran, C. A. Martila, *Biochem. J.* **1974**, *141*, 537.
[11] S. B. Zimmermann, G. H. Cohen, D. R. Davies, *J. Mol. Biol.* **1975**, *92*, 181.
[12] G. Gottarelli, P. Palmieri, G. P. Spada, *Gazz. Chim. Ital.* **1990**, *120*, 101.
[13] W. Saenger, *Principles of Nucleic Acid Structure*, Springer, New York, **1984**, pp. 315–320.
[14] V. Luzzati in *Biological membranes* (Ed.: D. Chapman), Academic Press, London, **1968**, Chapter 3.
[15] The volume concentrations necessary for the calculation were determined assuming 1.000 and 0.649 $cm^3 g^{-1}$ as specific volumes for the water and folic acid respectively; D. Mastropaolo, A. Camerman, N. Camerman, *Science* **1980**, *210*, 334.
[16] N. P. Franks, *J. Mol. Biol.* **1976**, *100*, 345.
[17] P. Mariani, V. Luzzati, H. Delacroix, *J. Mol. Biol.* **1988**, *204*, 165.
[18] F. Carsughi, M. Ceretti, P. Mariani, *Eur. Biophys. J.* **1992**, *21*, 155.

The Application of Au_{55} Clusters as Quantum Dots**

By *Ulrich Simon, Günter Schön,* and *Günter Schmid**

The availability of smallest solids like larger transition metal clusters[1] opens a field of research raising basic questions: How small must the number of atoms be in order for the typical properties of the original bulk metal to be lost? What can be anticipated in the application of metal clusters in nanotechnology, that is, in microelectronic quantum devices? The nonpareils of miniaturization in microelectronics are the so-called quantum dots, zero-dimensional (0D) quantum devices with diameters on the nanometer scale, whose response is based on single-electron processes. Current investigations worldwide concentrate on tailoring the mesoscopic semiconductor regions in a surrounding bulk material with a broader band gap. However, until now,

[*] Prof. Dr. G. Schmid, Dipl.-Chem. U. Simon, Prof. Dr. G. Schön
Institut für Anorganische Chemie der Universität
Universitätsstrasse 5–7, D-W-4300 Essen 1 (FRG)

[**] This work was supported by the Fonds der Chemischen Industrie. We thank Prof. Dr. U. Kreibig and Dr. M. Herrmann for the STM images (Fig. 1), R. Blümel for providing the fitting program, and the Deutsche Gesellschaft für das Chemische Apparatewesen und Biotechnologie (DECHEMA) for valuable discussions on particle size effects.

quantum devices as small as clusters have not been obtained. We believe that they could be better prepared from metal clusters with semiconducting behavior: With respect to electrical conductivity, Nimtz et al.[2] defined the SIMIT, the Size-Induced Metal–Insulator Transition observed when the volume of metallic particles is reduced down to a diameter of about 20 nm. This size-dependent quantization effect may be considered the beginning of a possible metal–semiconductor transition at the very end of metallic behavior or—with respect to the molecular state—at the beginning of metallic behavior.

Recently numerous physical investigations such as Mössbauer[3] and solid-state NMR spectroscopy,[4] conductivity[5] and susceptibility[6] measurements, and EXAFS[7,8] and optical investigations[9] were performed on transition metal clusters. The results, which depend somewhat on the method, suggest that for ligand-stabilized transition metal clusters about 50–100 metal atoms and a cluster diameter between 1 and 2 nm are necessary for metallic behavior. At this transition from molecular to bulk material, metal particles in the microcluster domain are expected to have novel electronic properties when the boundary conditions given by their dimensions (e.g. the diameter x) reach the order of magnitude of the de Broglie wavelength λ of the valence electrons.[2] Indeed, metal clusters with such diameters can be regarded as custom-made 0D quantum dots, in which a few free electrons are localized geometrically as well as from the point of view of quantum mechanics. By means of Impedance Spectroscopy (IS) it has been shown that as a result of this Quantum Size Effect (QSE), the first (or the last) two metallic valence electrons of cluster **1** are trapped in a quantum box consisting of its own Au_{55} metal core.[10]

$[Au_{55}(PPh_3)_{12}Cl_6]$ **1**

The main difficulty in the application of metal clusters in microelectronic 0D quantum devices seemed to be how to insulate them and simultaneously keep them in contact with their neighbors: This procedure is necessary to build up a so-called cellular automaton[11] or to make a 1D quantum channel (quantum wire) from a chain of single clusters or aggregates of clusters without coalescence to materials with solid-state properties. Figure 1 shows a quantum wire which happened to be observed by means of Scanning Tunneling Microscopy (STM).[12] The single quantum dots most probably consist of molecules of **1** which are aggregated to superclusters $[(\mathbf{1})_{13}]$.

We report here on some of the experimental findings and describe a practical construction of quantum devices with ligand-stabilized metal clusters. The way to a new generation of single-electron devices[13] consisting of the smallest building blocks possible may be opened. In such devices "switchable" quantum dots and quantum channels with correlated electrons could reduce the dimensions of classic electronic switches and memories by many orders of magnitude, possibly resulting in a new generation of computers with tremendous, multidimensional capacity or very simple miniature lasers.[11]

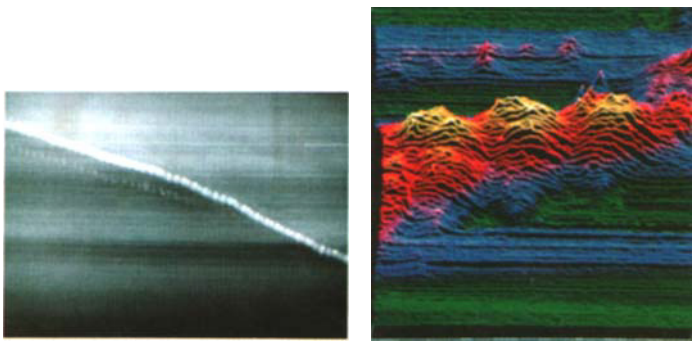

Fig. 1. Left: A quantum wire formed from a solution of **1** which happened to be detected by Scanning Tunneling Microscopy (STM). The diameter of the single particles is about 6 nm. This corresponds to an aggregate of 13 molecules of **1** forming a $[(\mathbf{1})_{13}]$ supercluster. Right: A magnified section of this quantum wire showing three superclusters.

Impedance Spectroscopy (IS) has become a powerful method for tracing macroscopic properties of different, even heterogeneous, materials back to their origins, even if these properties result from a variety of microscopic processes.[14] In analogy to hopping ion processes, electronic relaxation processes can also occur in the low-frequency range. Here, too, coupling with the environment plays a decisive role. One speaks of hopping electrons, or of localized electrons in traps, in which (excited) electronic states such as long-lived exitons can have lifetimes up to seconds. Such localized states are well known from disordered structures like glassy materials.[15–17] We recently demonstrated[10] that this type of phenomenon is also expressed in or on stabilized clusters by electron resonances which reveal fine structures in the low-frequency immittance spectra.[10]

The powdery samples of **1**, whose particles can be regarded as monodisperse within the limits of the following interpretation, were pressed up to an average, gravimetrically defined density of 3.37 $g\,cm^{-3}$. This value approaches that of a theoretical closest sphere packing (3.704 $g\,cm^{-3}$) by a factor of 0.91. Measurements were performed between 253 and 333 K by means of a fully automatic impedance spectrometer, which has been described in detail elsewhere.[18] For the measurements the sample, which looks like a disk of silicon, was placed under N_2 between various noble metal electrodes. As shown in Figure 2, the measurements on compact samples of **1** reveal a depressed arc in the Argand diagram with relaxation frequencies in the range of 10^4 to 10^5 Hz.

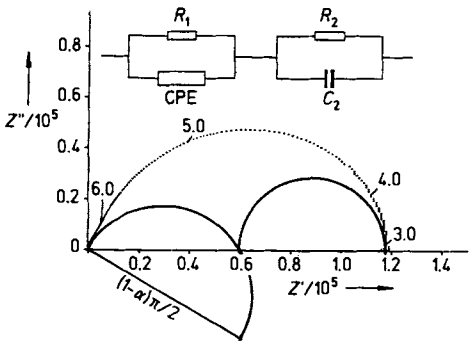

Fig. 2. Result (dotted line) of an impedance measurement on **1** at 293 K. In this unscaled Argand diagram the real part of the impedance Z' is plotted versus the imaginary part of the impedance Z'' in the complex plane. The numbers along the plot indicate the logarithm of the measuring frequency ν. In the upper section a circuit equivalent for the electric behavior of the sample is given. Below the measured plot are the Argand circles belonging to each separate link (solid lines).

By means of a novel mathematical fitting program for immittance data,[19] a circuit equivalent for the sample behavior of **1** was calculated. This yielded an error less than 1.8%. As shown in Figure 2, it consists of a parallel (ideal) Debye R,C link with the resistance R_2 and the capacitance C_2 (low-frequency resonance process 2), and a Cole–Cole R,

CPE link (higher frequency process 1) with the resistance R_1 and a parallel capacity element (Constant Phase Element, CPE).[13]. A Cole–Cole parameter $\alpha \approx 2/3$ is obtained from the fitting data. This value is typical for a percolation mechanism usually described by power laws for the frequency-dependant conductivity (with α as an exponent).[14] The Argand diagram provides the total resistance $R_t = R_1 + R_2$, and because $R_1 \approx R_2$, $R_t = 2R_1$. For the two different conductivity processes the specific conductivities are $\sigma_1 = 1.61 \times 10^{-4}\ \mathrm{Ohm^{-1}\,m^{-1}}$ and $\sigma_1 = \sigma_2 = 3.23 \times 10^{-4}\ \mathrm{Ohm^{-1}\,m^{-1}}$ at 298 K. From the temperature dependance of the conductivities were calculated activation enthalpies EA for the thermally activated processes; for the Debye relaxation process $EA_2 = 0.16 \pm 0.03$ eV and for the Cole–Cole process $EA_1 = 0.15 \pm 0.03$ eV. This means that within the limits of experimental accuracy $EA_2 \approx EA_1$. The relaxation times $\tau_{1/2}$ and the relaxation frequencies $\nu_{1/2}$, however, differ by a factor of two. For both processes $\tau_{1/2}$ shows the same temperature dependance as the resistance $R_{1/2}$, and it follows from the relation $\tau = R \cdot C$ that the capacitances C_2 and CPE must be independent of temperature. This resembles the electronic response of semiconductor–insulator interfaces, in which capacitances are built up and show relaxation in the low-frequency range.[13, 20]

In refs. [5, 9] the frequency dependance of the conductivity of **1** was measured and interpreted by means of a stochastic multiple-site hopping mechanism (a percolation process in which electrons tunnel between clusters), which was predicted to change into a two-site process at higher frequencies. Accordingly, we want to interpret the (higher frequency) Cole–Cole process 1, which we measured as a relaxation of an *inter*cluster process. This is supported by the occurrence of a distributed capacitance element (CPE instead of a single capacitance) caused by a distribution in hopping lengths (or jump times) between clusters, since in the transition of single electrons from one core of a cluster to the core of a neighboring cluster a fluctuating ligand shell must be passed through by tunneling.

We wish to interpret the Debye process 2, proven for the first time in our work, as an *intra*cluster step, which in concentrated samples is necessarily coupled to the intercluster process previously mentioned. In the immittance spectra the Debye process 2 is evident from a sharp resonance beside the broadened intercluster relaxation.

According to the SIMIT experiments, electronic resonance processes in particles with diameters on the nanometer scale should proceed in the range of microwaves, whereas we observe them by impedance spectroscopy already in the kHz range. That means that resonances in this low-frequency range can only be detected on densely packed samples of **1** because of the coupling of the electron processes to the environment. The low-frequency Debye process 2 is determined by the intracluster conductivity $\sigma_2 \approx 1/R_2$, which for **1** is dependent on dimension[10] like the SIMIT. Consequently, the cause of the low-frequency appearance is the capacitance $C_2 = 48$ pF, built up at the ligand shells. Its value is determined by the structure and the polarizability of the shell, for which an exact geometrical picture is not necessary. According to the formula $\tau_2 = R_2 \cdot C_2$ the relaxation time τ_2 is 2.6×10^{-6} s.

The value of the average Cole–Cole relaxation time is smaller by a factor of two and can be explained correspondingly. Both processes show equal conductivities, so that the distributed capacitance CPE equals a mean effective capacitance $C_{1\mathrm{eff}} \approx 1/2\,C_2 \approx 24$ pF. This would be in accordance with the idea that in a tunneling step both ligand shells of a cluster pair must be passed through. Such a single-electron transition corresponds chemically to a disproportionation step, for which a Coulomb energy contribution of ≈ 0.2 eV has already been estimated in comparison to its measured enthalpy of 0.3 ± 0.1 eV.[9] In our experiment the energy of disproportionation must equal the sum of the activation enthalpies $EA_1 + EA_2 = 0.31$ eV. In Figure 3 the total sequence of processes is shown in a simplified manner.

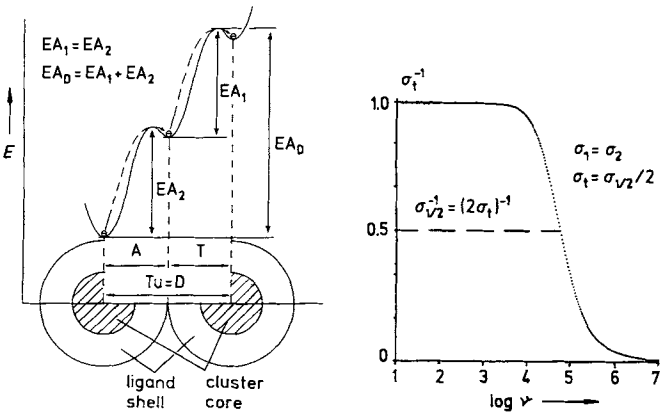

Fig. 3. Left: Scheme of the potential profile for a cluster pair. Activation step (A) and transport Step (T) cause the tunneling step (Tu) which is equal to a disproportionation step (D) with an activation enthalpy EA_D. Distance is plotted on the x axis. Right: A sequence of both steps leads to a total conductivity σ_t which is doubled under resonance conditions to $\sigma_1 = \sigma_2$.

Supposing that in the concentrated samples of **1** partial capacitances are produced in the area of the ligand shell(s) of one cluster or two neighboring clusters, we may determine an experimental density of the electronic states participating at the Debye process 2 $D_{ex} = \mathrm{d}N/\mathrm{d}\varepsilon$ from the capacitance C_2 (see ref. [13]). Assuming an approximately closest sphere packing of the clusters of **1** within the sample and scaling the capacitance $C_2 = 48$ pF to the capacitance of an unit volume, we obtain $D_{ex} \approx 10.75\ \mathrm{eV^{-1}}$. Therefore $\mathrm{d}N$ has the meaning of a number in a partial volume per cluster with its energy contribution $\mathrm{d}\varepsilon$. No other assumptions were made with regard to the effective cluster diameter x or to the distances of the charges.

According to the investigations cited in the introduction it seems possible that the quantum box of **1** has a minimum size, in which the last free electrons of the metal in the form of a free-electron gas are fenced in the cluster interior at the very end of the SIMIT. Due to the Pauli principle, the number of electronic states $N_{(ex)}$ participating in the resonance process would then be one *or* two with energies $E_{ex1/2}$ from D_{ex}. According to the formula for the 3D electron gas in a quantum box consisting of one cluster, an expression for the lateral extension x can be derived [Eq. (a)], where m is the

$$x = \hbar \cdot \pi (2m\,E_F)^{-1/2} \qquad \text{(a)}$$

electron mass and E_F is the Fermi energy. For $E_{ex1} = 0.093\ \mathrm{eV} = E_{F1}$ the lateral extension x_1 is 2.01 nm, and for $E_{ex2} = 0.186\ \mathrm{eV} = E_{F2}$ x_2 is 1.42 nm.

These two values are very close to the diameter of the cluster **1** with ligands (2.1 nm) and the metal core (1.4 nm), respectively. In the first case the quantum box should contain one electron, in the second two electrons (Fig. 4). It seems that the metal core is completely occupied with $N_{(ex)} = 2$ free electrons with a Fermi energy of $E_F \approx 0.19$ eV in the ground state. Free electrons with higher energies can no longer be bound in the cluster. Thus for **1** the density of

states (DOS) on the Fermi plane of a 3D electron gas can be estimated according to Equation (b). The experimental value

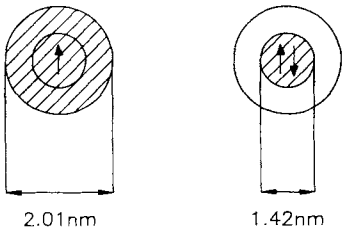

Fig. 4. Illustration of the two possibilities for the occupation of the quantum dot **1** with free electrons according to experiment.

$$D(E_F) = (m/6\,\hbar^2)x^2 \qquad \text{(b)}$$

of 1.42 nm for the diameter of the metal core leads to a density of states of 4.40 eV^{-1} per cluster.

Our experimental results disclose that **1**, a collective of 55 metal atoms within a ligand shell, still displays metallic properties. The effect of the QSE seems to be that in the frontier of the transition from metallic to molecular behavior in the range from 1 to 2 nm the last metallic valence electrons are localized in a quantum box with the lateral dimension of the cluster and that they move freely in this box independent of the particular nature of the respective cluster. The realization of such a quantum dot, in other words its chemical stability, depends on whether the binding energy of these electrons exceeds the de Broglie energy. In **1**, the quantum box is occupied by two electrons from the metal core according to the Pauli principle and may then serve as an electron source. If another electron is added, the nucleus may operate as an electron sink. The particle size implies that two electrons may be charge carriers for the intracluster conductivity, whereas the intercluster conductivity is determined by the tunneling of single electrons.

Compact samples of **1** are handy devices with astonishing electronic quantum properties even at room temperature. In principle, the following microelectronic quantum devices can now be realized by size reduction or/and precise addressing:

1) A Tunnel Resonance Resistance (TRR, see Fig. 5 left), a complete device, the total resistance of which is halved by applying a suitable resonance frequency at ambient temperature. The minimum working unit is as small as a pair of cluster molecules (see Figs. 3 and 6a) with a diameter of 4 nm. (In contrast, the smallest devices currently available have a lateral dimension of about 250 nm.) The resistance of one cluster is coupled to that of a chain of consecutive of single clusters, resulting in 1D quantum channels for correlated electrons (Fig. 6b). According to theory, the total resistance should only change with multiples of the fundamental quantum resistance $\pi\hbar/2e^2$. We will return to this problem later when we attempt to derive a phase relation between the Single-Electron Tunneling (SET) oscillations[13] and our resonance frequencies.

2) A cellular automaton (TRCA) with contacts only at the marginal points (see Fig. 5 right). Due to the tunnel conductivity, however, each quantum dot corresponds with twelve neighbors in strong parallelism.

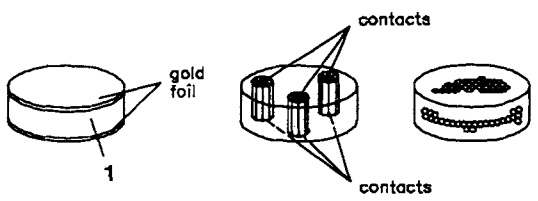

Fig. 5. Compressed disc of ligand-stabilized metal clusters which may be contacted facially by gold foils to build up a Tunnel Resonance Resistance (TRR) (left) or contacted by microscopic scanning patterns to include quantum channels (middle). The contacts may be placed facially and laterally (right).

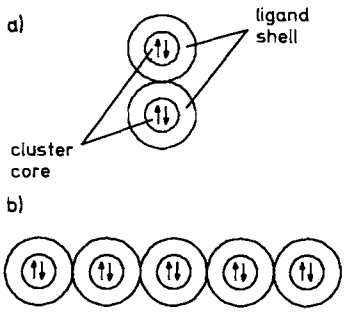

Fig. 6. a) Quantum device consisting of two clusters of **1**. This is also the smallest functional unit of a Tunnel Resonance Resistance (TRR). b) 1D quantum channel made up of clusters of **1** (section of the closest sphere packing in a compressed disc).

Finally, some advantages of the above devices should be mentioned: Firstly, these components can be operated with a defined (tunnel) current which can be doubled when switched by resonance. For this purpose, an additional rest current can be neglected. Furthermore, defects in single clusters and in the package of the pellets as well as single disorders (vacancies of clusters) do not substantially affect the function of the whole device. If single quantum dots or channels fail, they are omitted or possibly repaired by the formation of neighboring bypasses. Secondly, although with the present technology only larger areas of about 50 nm as shown in Figure 5 middle can be addressed and not single quantum dots, only the material between or within the contact areas is wasted.

Besides possible applications of these or similar quantum devices one should keep in mind that our investigations prove that for suitably tailored metals a clear transition to molecular behavior exists in range of 1 to 2 nm. Thus, the present concentration on semiconducting materials with these dimensions, which then should be beyond this transition, is probably not the best approach to ultimate miniaturization.

Received: July 17, 1992 [Z 5470 IE]
German version: *Angew. Chem.* **1993**, *105*, 264

[1] G. Schmid, *Mater. Chem. Phys.* **1991**, *29*, 133.
[2] G. Nimtz, P. Marquard, H. Gleiter, *J. Cryst. Growth* **1988**, *86*, 66.
[3] A. H. Smit, R. C. Thiel, L. J. de Jongh, G. Schmid, N. Klein, *Solid State Commun.* **1988**, *65*, 915.
[4] L. J. de Jongh, J. Baak, H. B. Brom, D. van der Putten, J. M. van Ruitenbeck, R. C. Thiel, *Proc. Int. Symp. Phys. Chem. Finite Systems: From Clusters to Crystals* (Eds.: P. P. Jena, S. N. Khanna, B. K. Rao), Kluwer, Dordrecht, **1992**, p. 839.
[5] H. B. Brom, M. P. J. van Staveren, L. J. de Jongh, *Z. Phys. D.* **1991**, *20*, 281.
[6] L. J. de Jongh, J. A. O. de Agular, H. B. Brom, G. Longoni, J. M. van Ruitenbeck, G. Schmid, M. P. J. van Staveren, R. C. Thiel, *Z. Phys. D* **1989**, *12*, 445.
[7] M. C. Fairbanks, R. E. Benfield, R. J. Newport, G. Schmid, *Solid State Commun.* **1990**, *73*, 431.
[8] M. A. Marcus, M. P. Andrews, J. Zegenhagen, A. S. Bommannavar, P. Montano, *Phys. Rev. Sect. B* **1990**, *42*, 3312.

[9] U. Kreibig, K. Fauth, C.-G. Granquist, G. Schmid, *Z. Phys. Chem.* **1990**, *169*, 11.
[10] U. Simon, G. Schmid, G. Schön, *Proceedings of the MRS Spring Meeting*, San Francisco, **1992**.
[11] E. Corcoran, *Sci. Am.* **1990**, *263(5)*, 74; *Spektr. Wiss.* **1991**, *226(1)*, 76.
[12] U. Kreibig, M. Herrmann, unpublished results.
[13] K. K. Likharev, T. Claeson, *Sci. Am.* **1992**, *266(6)*, 50; *Spektr. Wiss.* **1992**, *8*, 62–67.
[14] J. R. MacDonald, *Impedance Spectroscopy*, Wiley, New York, **1987**, p. 246.
[15] N. F. Mott, E. A. Davis, *Electronic Processes in Noncristalline Materials*, Calrendon, Oxford, **1971**.
[16] O. Madelung, *Festkörpertheorie III*, Springer, Berlin, **1973**.
[17] S. Summerfield, *Philos. Mag.* **1985**, *52(1)*, 9–22.
[18] G. Kelemen, W. Lortz, G. Schön, *J. Mater. Sci.* **1989**, *24*, 333.
[19] R. Blümel, Dissertation, Universität Essen, **1992**.
[20] J. L. Diot, J. Joseph, J. R. Matin, P. Clechet, *Electroanal. Chem.* **1985**, *199*, 75–88.

Superconductivity and Phase Separation in Na_xNbO_2 ($x < 1$)**

By *Maria A. Rzeznik, Margret J. Geselbracht, Mark S. Thompson,* and *Angelica M. Stacy**

The superconductors with the highest known transition temperatures, T_c, are copper oxides with strong covalent bonding between the copper and oxygen atoms within layers, and no copper–oxygen bonds between these layers. The prevalence of layered structures among the copper oxide superconductors has led us to search for new oxide superconductors with anisotropic structures. We recently reported that the layered phase Li_xNbO_2 ($x \approx 0.5$) exhibits superconductivity below 5.5 K.[1] This phase has a hexagonal structure, consisting of $(NbO_2)_n^{n-}$ layers of edge-shared NbO_6 trigonal prisms, analogous to MoS_2; the lithium atoms occupy a portion of the octahedral holes between the layers.[2] $NaNbO_2$[3] is isostructural with $LiNbO_2$ (see Fig. 1). We have now found that Na_xNbO_2 is a superconductor, and that the sodium content of this niobate cannot be varied continuously.

Sodium-deficient samples of Na_xNbO_2 were prepared by partial deintercalation of $NaNbO_2$. Pure $NaNbO_2$ was obtained by reacting sodium metal and NbO_2 in a 1:1 ratio in a sealed tantalum tube. Subsequently, products with nominal compositions of $Na_{0.90}NbO_2$, $Na_{0.80}NbO_2$, $Na_{0.70}NbO_2$, and $Na_{0.65}NbO_2$, were prepared by reaction of $NaNbO_2$ with I_2 in acetonitrile at 298 K. Analyses of the Na:Nb ratio in the products by atomic emission spectroscopy with inductively coupled plasma excitation (AES-ICP) gave values for x within approximately 10% of the nominal values as shown in Table 1.

The powder X-ray diffraction patterns[4] indicate that a phase which is isostructural with $NaNbO_2$ is present in all of the sodium-deficient products; we refer to this as Phase I. As shown in Table 1, the lattice parameter a obtained for Phase I is identical to that of $NaNbO_2$, but c is about 0.1 Å larger. Since a second phase appears in samples with $x < 0.9$, we conclude that $Na_{0.9}NbO_2$ is located at a phase boundary.

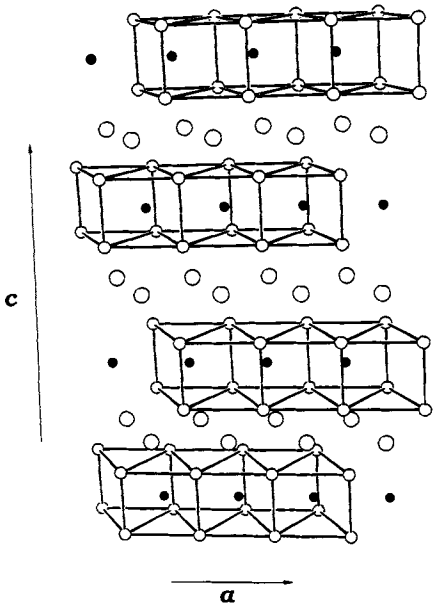

Fig. 1. Schematic representation of the structure of $NaNbO_2$. The layered structure consists of a hexagonal array of niobium atoms (solid circles) sandwiched between hexagonal arrays of oxygen atoms (small open circles). The coordination geometry of oxygen atoms around the niobium atoms is trigonal prismatic. The sodium atoms (large open circles) are located in octahedral sites between the oxygen–niobium–oxygen layers.

A second phase with a related structure is observed for samples with $x < 0.9$, as shown in Figure 2; we refer to it as Phase II. The new reflections can be indexed to a hexagonal unit cell with the same indices as the corresponding reflections in the diffraction pattern for Phase I. Based on this assignment of Miller indices, the lattice parameter a of Phase II is 0.01 Å smaller than that obtained for $NaNbO_2$, and c is approximately 0.4 Å larger, as shown in Table 1.

Table 1. Composition and lattice parameters [Å] for Na_xNbO_2.

Sample	Composition [a]	Phase I		Phase II	
		a	c	a	c
$NaNbO_2$	$Na_{1.1}NbO_2$	2.949(2)	11.556(2)	–	–
$Na_{0.90}NbO_2$	$Na_{0.92}NbO_2$	2.949(2)	11.657(4)	–	–
$Na_{0.80}NbO_2$	$Na_{0.82}NbO_2$	2.949(3)	11.666(3)	2.939(3)	12.005(5)
$Na_{0.70}NbO_2$	$Na_{0.68}NbO_2$	2.947(3)	11.696(2)	2.935(3)	11.964(2)
$Na_{0.65}NbO_2$	$Na_{0.60}NbO_2$	2.946(3)	11.685(5)	2.932(2)	11.984(1)

[a] Determined by AES-ICP.

The intensities of the reflections associated with Phase II increase relative to those of Phase I as x decreases. Therefore, we conclude that the amount of Phase II increases as the sodium content decreases, and that Phase II is sodium-poor compared with Phase I. Since samples with an average value of $x = 0.65$ contain both phases, the sodium-poor phase must have a composition with $x < 0.6$.

The large increase in the lattice parameter c also supports the claim that Phase II is comparatively sodium-poor. Simi-

[*] Prof. Dr. A. M. Stacy, M. A. Rzeznik, Dr. M. J. Geselbracht
Department of Chemistry
University of California, Berkeley, CA 94720 (USA)
Dr. M. S. Thompson
Raychem Corporation, Menlo Park, CA 94025 (USA)

[**] This work was supported by the Electric Power and Research Institute (Contract RP8009-19) and the Director, Office of Basic Energy Research, Office of Basic Energy Sciences, Materials Science Division of the United States Department of Energy (Contract DE-AC03-76SF0009) as well as by Raychem. A. M. S thanks the Alfred P. Sloan and the Camille and Henry Dreyfus Foundation for their support.

lar increases in c by approximately 0.4 Å have been observed for Na_xTiS_2 as x is decreased.[5] The structure may remain identical to that of $NaNbO_2$, or a related polytype may form instead. For example, in Na_xTiS_2, a change in the coordination sphere about the sodium atoms from octahedral to trigonal prismatic is observed as x decreases.

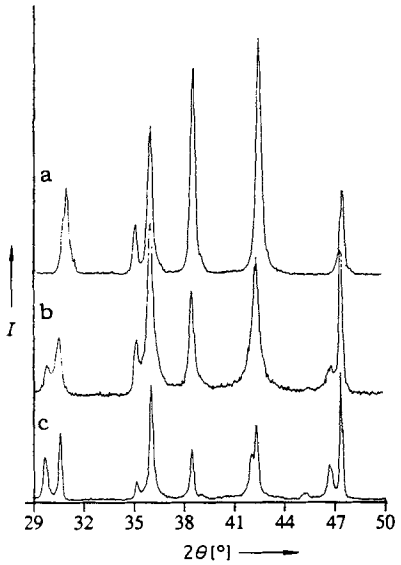

Fig. 2. Powder X-ray diffraction patterns of a) $NaNbO_2$, b) $Na_{0.80}NbO_2$, and c) $Na_{0.65}NbO_2$. The latter two samples contain both a phase that is isostructural with $NaNbO_2$ plus a second phase with a related hexagonal structure. The intensities of the peaks associated with the second phase increase with decreasing sodium content. I = intensity in arbitrary units.

Attempts to isolate a pure sample of Phase II by reactions similar to those described above have not been successful thus far. When greater than 0.2 equivalents of I_2 were used to prepare samples with an average value of $x < 0.6$, the powder diffraction pattern showed many broad reflections of low intensity indicating that the product was poorly crystalline; the peaks associated with Phase I and Phase II were not observed. Clearly, the sodium-deficient phase is not very stable in the presence of oxidizing agents.

The magnetic properties of $NaNbO_2$, $Na_{0.90}NbO_2$, $Na_{0.80}NbO_2$, $Na_{0.70}NbO_2$, and $Na_{0.65}NbO_2$ were measured by cooling samples in magnetic fields of less than 20 G.[6] Although we do not observe superconductivity down to 2 K for $NaNbO_2$, the susceptibility of $Na_{0.65}NbO_2$ drops steeply to diamagnetic values below 4.2 K as shown in Figure 3; this transition indicates the onset of superconductivity. The gram susceptibility at 2 K is -2.8×10^{-3} emu g^{-1}, corresponding to a 25% Meissner fraction.[7] This value of the susceptibility is sufficiently negative to conclude that a substantial fraction of the material is a bulk superconductor.

Superconductivity was also observed for $Na_{0.90}NbO_2$, $Na_{0.80}NbO_2$, and $Na_{0.70}NbO_2$ with a T_c (onset) = 4.2 K, identical to that observed for $Na_{0.65}NbO_2$. However, the magnitude of the diamagnetic signal decreased dramatically as the sodium content increased. Since the magnitude of the diamagnetic signal correlates with the amount of Phase II observed in the powder diffraction patterns, we propose that it is the sodium-poor phase that exhibits superconductivity. Furthermore, the observation that T_c is invarant points to the existence of a single superconducting material with a fixed sodium content in the samples we have prepared.

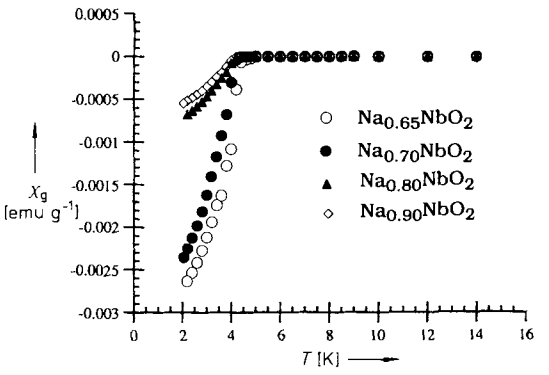

Fig. 3. Meissner effect of $Na_{0.90}NbO_2$, $Na_{0.80}NbO_2$, $Na_{0.70}NbO_2$, and $NaNb_{0.65}NbO_2$ prepared by deintercalation of $NaNbO_2$ with I_2. The onset of superconductivity occurs at 4.2 K. The magnitude of the diamagnetic signal increases as the sodium content decreases.

We conclude that the sodium composition in $NaNbO_2$ cannot be changed continuously by deintercalation reactions with varying amounts of I_2 at 298 K; rather, the products obtained are a two-phase mixture consisting of a nonsuperconducting sodium-rich material and a superconducting sodium-poor material. It is notable that phase separation is often associated with the transition to the superconducting state as the composition is varied in transition metal oxides.[8] Therefore, Na_xNbO_2 is a valuable system for further study of the stability of oxide superconductors.

Experimental Procedure

$NaNbO_2$ was prepared by reacting sodium metal (0.312 g, 13.6 mmol) and NbO_2 (1.70 g, 13.6 mmol). The reactants were loaded under inert conditions into a tantalum tube that was welded shut under an argon atmosphere in an arc furnace. The sealed tantalum tube was placed inside a fused silica ampoule that was evacuated to 4×10^{-5} Torr and sealed. After the ampoule had been heated at 850 °C for three days, a free flowing dark violet powder was obtained. Since this product turned black rapidly upon exposure to air, all sample manipulations were performed under an inert atmosphere. The product obtained was single phase as determined by powder X-ray diffraction, and lattice parameters similar to those reported previously (see ref. [3]) were obtained.

For the deintercalation reactions, the $NaNbO_2$ powder was placed in contact with a stoichiometric amount of a 0.068 M solution of I_2 dissolved in acetonitrile (distilled over calcium hydride) for five to seven days. The product was filtered, washed with acetonitrile and ethanol, and dried under vacuum.

Received: August 12, 1992 [Z 5512 IE]
German version: *Angew. Chem.* **1993**, *105*, 277

[1] a) M. J. Geselbracht, T. J. Richardson, A. M. Stacy, *Nature* **1990**, *345*, 324; b) M. J. Geselbracht, Ph. D. Thesis, University of California, Berkeley, USA, **1991**.
[2] G. Meyer, R. Hoppe, *J. Less Common Met.* **1976**, *46*, 55.
[3] G. Meyer, R. Hoppe, *Z. Anorg. Allg. Chem.* **1976**, *424*, 128.
[4] A Siemens D500 diffractometer was used with $Cu_{K\alpha}$ radiation. The hexagonal lattice parameters were derived by a least squares fit of the data; silicon was used as an internal standard.
[5] See for example: a) E. Sandre, R. Brec, J. Rouxel, *J. Solid. State Chem.* **1990**, *88*, 269; b) A. Leblanc-Soreau, M. Danot, L. Trichet, J. Rouxel, *Mater. Res. Bull.* **1974**, *9*, 191.
[6] A SQUID magnetometer of Quantum Design was used to measure the magnetic susceptibility. Data were collected as samples were cooled from 15 K. The field was calibrated prior to data collection by measuring the superconducting properties of a tin sphere.
[7] The % Meissner effect was calculated assuming a density of 6.0 gcm^{-3}, and ignoring demagnetization corrections.
[8] See for example: a) P. W. Anderson, *Science* **1987**, *235*, 1196; b) A. W. Sleight, J. L. Gillson, D. E. Bierstedt, *Solid State Commun.* **1975**, *17*, 27; c) R. J. Cava, R. B. van Dover, B. Batlogg, E. A. Rietman, *Phys. Rev. Lett.* **1987**, *58*, 408; d) D. C. Johnston, *J. Low Temp. Phys.* **1976**, *25*, 145.

 © VCH Verlagsgesellschaft mbH, W-6940 Weinheim, 1993 0570-0833/93/0202-0255 $ 10.00+.25/0

A New Layered Ternary Sulfide: Formation of Cu_2WS_4 by Reaction of WS_4^{2-} and Cu^+ Ions**

By *Eugene A. Pruss, Barry S. Snyder,* and *Angelica M. Stacy**

The tetrathiometalates MS_4^{2-}, where M = V, Mo, W, and Re, have been used extensively for the synthesis of a wide variety of transition metal sulfides. Products that have been obtained range from small metal sulfide ions to heterometal clusters.[1] Here we show that solid-state sulfides with extended structures also can be prepared by using thiometallates as reactants. Cu_2WS_4, a new layered ternary sulfide, is obtained by reaction of $[Cu(CH_3CN)_4]BF_4$ and $(NH_4)_2WS_4$ in a mixture of *N,N*-dimethylformamide and butyronitrile; in this phase, the WS_4^{2-} units remain intact and are linked into layers of Cu^I ions.

Layered transition metal chalcogenides have attracted much attention because they have many useful properties that are a direct consequence of their low-dimensional structures.[2] Specifically, these materials consist of covalently bound layers of metal atoms bridged by sulfur atoms, and have only weak van der Waals interactions between these layers. Although there are a wide variety of applications for these "two-dimensional" materials, including uses in batteries[3] and as catalysts,[4] only a limited number of phases and structure types are known; these are almost exclusively binary phases.

Typically, the binary layered phases are prepared by direct reaction of the elements at temperatures above 400 °C. Since few ternary sulfides have been prepared under similar conditions, precipitation from organic solvents at lower temperatures is an attractive route to their preparation. Cu_2WS_4 is obtained by reaction of $[Cu(CH_3CN)_4]BF_4$ and $(NH_4)_2WS_4$ in a 2:1 ratio in a mixture of *N,N*-dimethylformamide and butyronitrile at 135 °C. The CH_3CN ligands which are relatively labile, are readily displaced by the WS_4^{2-} ions. After 24 h a bright orange precipitate formed, and was subsequently isolated. The product was found to be diamagnetic, as expected for Cu^I and W^{VI}.

Since we were unable to grow single crystals, the structure solution was obtained by analysis of powder X-ray diffraction data. The calculated and difference profiles of the Rietveld refinement are shown in Figure 1. Atomic coordinates and temperature factors are listed in Table 1, and bond lengths and angles are given in Table 2. Müller and Menge have reported the preparation of an amorphous form of Cu_2WS_4;[5] the properties of the amorphous form are not the same as those observed for the crystalline form reported here.[6]

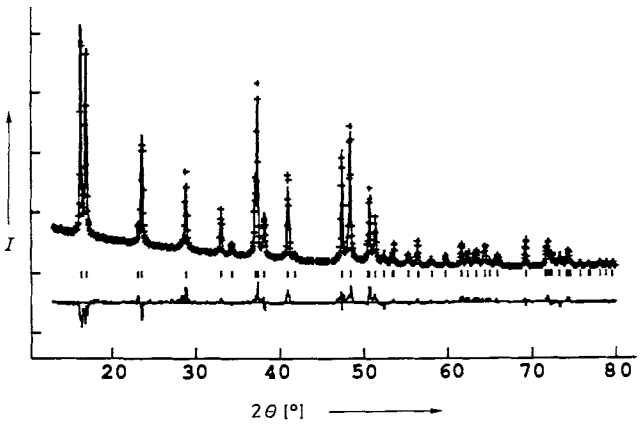

Fig. 1. Powder X-ray diffraction pattern for Cu_2WS_4, including observed (+) and calculated (−) profiles, as well as the difference profile (observed − calculated).

Table 1. Positional parameters and isotropic temperature factors of Cu_2WS_4; space group: $P\bar{4}2m$, lattice parameters: a = 5.4244(2) and c = 5.2336(3) Å

Atom	Site	x	x	z	B_{iso} (Å^2)
W	1a	0	0	0	0.499(8)
Cu	2e	0	0.5	0	1.075(8)
S	4n	0.2482(7)	0.2482(7)	0.2617(5)	0.552(7)

Table 2. Selected bond lengths [Å] and angles [°] of Cu_2WS_4.

Bond lengths		Bond angles	
W-Cu	2.712(1)	S-W-S	109.9(1)
W-S	2.345(1)	S-W-S	108.6(1)
Cu-S	2.356(1)	S-Cu-S	110.3(1)
S-S	3.808(1) [a]	S-Cu-S	108.9(1)
	3.855(1) [b]	S-Cu-S	109.16(1)
	3.841(1) [c]	W-S-Cu	70.45(1)
	3.699(1) [d]		

[a] S–S bond lengths for adjacent S atoms both coordinated to W and in the planes parallel to the a direction. [b] S–S bond lengths for adjacent S atoms both coordinated to Cu and in the planes parallel to the a direction. [c] S–S bond length for the intralayer distance for adjacent S atoms that lie above and below the metal atom planes. [d] S–S bond length for the interlayer distance between adjacent S atoms in different layers.

The structure of Cu_2WS_4 can be viewed as layers of Cu_2WS_4 as shown in Figure 2; the layers are perpendicular to the c direction. The atoms within the layers are covalently bound, while there are only van der Waals interactions between the layers. Each layer consists of W atoms in a square array; the Cu atoms lie along the edges of the square between the W atoms. Each S atom is μ_3-bridging, and spans a W atom and two adjacent Cu atoms; the S atoms alternate above and below the metal atom planes. In comparison, while Cu atoms link WS_4^{2-} units into layers in Cu_2WS_4, WS_4^{2-} units are linked into $CuWS_4^-$ chains in NH_4CuWS_4.[5]

The distances in the WS_4^{2-} units in Cu_2WS_4 deviate slightly from those of the isolated anion. The distortion at the metal center from tetrahedral is manifest in the S-W-S angles which range from 108.6(1) to 110.3(1)°; the S-Cu-S angles are similar (see Table 2). The W–S bond length of 2.345(1) Å is longer than has been observed previously. In comparison, the W–S bond length is 2.177 Å in isolated WS_4^{2-} ions with terminal S atoms.[1a] For S atoms bridging Cu and W in the polynuclear clusters $(PPh_3)_3[Cu_2WS_4] \cdot 0.8\ CH_2Cl_2$[7] and $(PPh_4)_2[Cu_2Cl_2WS_4]$,[8] the bond lengths are 2.217(8) and 2.228(7) Å, respectively. Additionally, the S atoms in $(PPh_3)_3S[Cu_3WS_3Cl]$,[7] $(PPh_4)_2[Cu_{2.5}Cl_{2.5}WS_4]$,[8] and $(PPh_3)_4O_2[Cu_4W_2S_6]$[9] are in a similar environment to that observed in Cu_2WS_4; however, the W–S bond lengths in

[*] Prof. Dr. A. M. Stacy, E. A. Pruss
Department of Chemistry
University of California
Berkeley, CA 94720 (USA)
Dr. B. S. Snyder
Rohm & Haas Co.
Springhouse, PA 19477-0904 (USA)

[**] This work was supported by the Office of Naval Research (Contract N00014-87-0660). The authors thank K. Schwartz of Raychem for collecting the powder X-ray diffraction data. A.M.S thanks the Alfred P. Sloan and the Camille and Henry Dreyfus Foundation for their support.

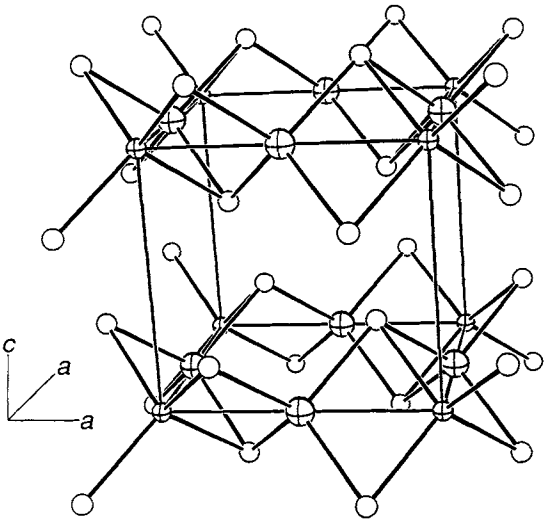

Fig. 2. View of the unit cell of Cu_2WS_4. The small circles with crosses are the W atoms, the large circles with crosses are the Cu atoms, and the open circles are the S atoms.

these polynuclear clusters of 2.261(4), 2.256(3), and 2.206(1) Å, respectively, are also significantly shorter. In contrast, the Cu–S bond length of 2.356(1) Å in Cu_2WS_4 is comparable to the Cu^I–S lengths observed in the five polynuclear clusters mentioned previously (e.g., 2.328(8)[7] 2.240(9),[8] 2.343(4),[7] 2.234(6),[8] and 2.358(4) Å,[9] respectively).

Another description of the structure follows from the recognition that the sulfide lattice can be viewed as a distorted cubic close-packed array of S atoms. The two-dimensional structure results from metal atom occupation of 3/4 of the tetrahedral holes in alternating layers along the *c* direction; only 3/8 of the total number of tetrahedral holes are filled. The interlayer distances between the planes of S atoms that lie parallel to the *a* direction are approximately 2.5(1) Å, while the intralayer distances are 2.7(1) Å. Therefore, the layers containing the metal atoms are expanded along the *c* direction compared with the distance between layers. For actual S–S distances see Table 2.

Although occupation of only 3/8 of the tetrahedral holes has been reported for Al_2CdS_4, β-Ag_2HgI_4, β-Cu_2HgI_4, and In_2CdSe_4, which contain cubic close-packed anions, these structures consist of tetrahedra linked by their vertices in three dimensions.[10] The most analogous structure type to Cu_2WS_4 is that of $K_2Mn_3S_4$, which consists of $[Mn_3S_4]$ tetrahedral layers separated by alkali metal ions.[11] However, since the precise ordering of the tetrahedral vacancies in the $[Mn_3S_4]$ layers is not known, a direct comparison cannot be made. The structure of Cu_2WS_4 can also be described as a defect anti-PbO type with 3/4 of the oxygen positions occupied by the metal atoms.[10]

It is notable that Cu_2WS_4 cannot be prepared by reaction of the elements at elevated temperatures; only binary sulfides are obtained. Furthermore, Cu_2WS_4 decomposes in argon above approximately 175 °C. We conclude that thiometalates are useful reactants in the synthesis of solid-state sulfides, and in particular, new layered ternary phases. Three other new materials, $CuReS_4$, $CsCuWS_4$, $[(CH_3CH_2)_4N]AgWS_4$, prepared by similar methods will be reported in the near future.

Experimental Procedure

All manipulations prior to product formation were performed under a pure dinitrogen atmosphere by using standard Schlenk techniques.

Cu_2WS_4: Butyronitrile (15 mL) was added with a syringe to a flask containing $[Cu(MeCN)_4]BF_4$ (0.14 g, 0.6 mmol) [12] and *N,N*-dimethylformamide (15 mL) was added with a syringe to a flask containing $(NH_4)_2WS_4$ (0.10 g, 0.30 mmol) [13]. After dissolution of the reactants, the Cu complex was transferred via cannula into the flask containing WS_4^{2-}. The resulting solution was stirred for 15 min, and then heated in an oil bath at 135 °C for 24 h. Subsequently, a bright orange, polycrystalline precipitate was isolated from an orange solution. The yield was 0.088 g (67%). The solution became clear, and the yield could be increased to 100% by addition of acetonitrile; however, the product obtained was poorly crystalline as determined by powder X-ray diffraction. Elemental analysis (atomic absorption spectroscopy) gave Cu:W = 2:1.04. One absorption band was observed in the IR spectrum at 443 cm^{-1} [14], and three absorption bands were observed in the diffuse reflectance UV/VIS spectrum, at 22000, 29000, and 34000 cm^{-1}.

Structure Determination: The structure solution was obtained by analysis of powder X-ray diffraction data (SIEMENS D500 diffractometer, θ-2θ geometry, flat-plate sample, curved Ge single-crystal monochromator (λ = 1.542 Å), position-sensitive detector operating in constant scan mode at 1° min^{-1} over the range $10° < 2\theta < 120°$). The diffractometer zero-point was determined from an external Si standard. The autoindexing program TREOR [15] was used to determine the unit cell parameters; a good fit was obtained with a tetragonal unit cell with a = 5.4244(2) and c = 5.2336(3) Å. There are no systematic absences to narrow the choice of space groups; however, if we assume that the WS_4^{2-} tetrahedral ion remains intact, the most reasonable choices are the noncentrosymmetric space groups: $P\bar{4}$, $P422$, $P\bar{4}2m$, and $P\bar{4}m2$. The structure determination proceeded by trial and error methods. Rietveld refinement was carried out by using the software package GSAS [17]. The usual profile parameters were refined (scale factor, lattice parameters, peak profile coefficients, atomic coordinates, and isotropic thermal parameters). Linear interpolation between data points was used to fit the background. The peak profiles were modeled with a pseudo-Voigtian function which included a small linear Gaussian contribution, nonlinear Lorentzian components, and an asymmetry correction. Refinement of the powder diffraction data was attempted for all of the non-centrosymmetric space groups. However, only two ($P\bar{4}2m$ and $P\bar{4}$) of the four possible space groups gave a satisfactory fit to the diffraction pattern. Since the R values for both of these space groups were identical, the higher symmetry space group, $P\bar{4}2m$ was chosen. The final agreement factors were $R_P = 0.097$, $R_{WP} = 0.0643$, and $\chi^2 = 5.3$ for 11 variables and 7 parameters.

Received: August 20, 1992 [Z 5524 IE]
German version: *Angew. Chem.* **1993**, *105*, 279

[1] See for example: a) A. Müller, E. Diemann, R. Jostes, H. Bögge, *Angew. Chem.* **1981**, *93*, 957; *Angew. Chem. Int. Ed. Engl.* **1981**, *20*, 934; b) D. Coucouvanis, *Acc. Chem. Res.* **1981**, *14*, 201; c) R. H. Holm, E. D. Simhon in *Molybdenum Enzymes* (Ed.: T. G. Spiro), Wiley-Interscience, New York, **1985**, Chapter 2; d) A. Müller, H. Bögge, U. Schimanski, *Inorg. Chim. Acta* **1983**, *69*, 5; e) K. E. Howard, J. R. Lockemeyer, M. A. Massa, T. B. Rauchfuss, S. R. Wilson, X. Yang, *Inorg. Chem.* **1990**, *29*, 4385; f) D. Coucouvanis, A. Toupadakis, S.-M. Koo, A. Hadjikyriacou, *Polyhedron* **1989**, 1705.
[2] Examples: a) M. S. Whittingham, *Prog. Solid State Chem.* **1978**, *12*, 41; b) D. W. Murphy, P. A. Christian, *Science* **1979**, *205*, 651.
[3] J. Rouxel, R. Brec, *Annu. Rev. Mater. Sci.* **1986**, *16*, 137.
[4] R. R. Chianelli, T. A. Pecoraro, T. R. Halbert, H. W. Pan, E. I. Stiefel, *J. Catal.* **1984**, *86*, 226.
[5] A. Müller, R. Menge, *Z. Anorg. Allg. Chem.* **1972**, *393*, 259.
[6] The amorphous Cu_2WS_4 was prepared by reaction of $CuCl_2 \cdot 2H_2O$ and $(NH_4)_2WS_4$ in H_2O. The product was red and gave three IR absorption bands at 482, 440, 415 cm^{-1}.
[7] A. Müller, H. Bögge, U. Schimanski, *Inorg. Chim. Acta* **1983**, *69*, 5.
[8] F. Secheresse, M. Salis, *Inorg. Chim. Acta* **1986**, *114*, L19.
[9] A. Müller, H. Bögge, T. K. Hwang, *Inorg. Chim. Acta* **1980**, *39*, 71.
[10] A. F. Wells, *Structural Inorganic Chemistry*, 5th ed., Oxford University Press, Oxford, **1987**, p. 269.
[11] A. Völker, *Liebigs Ann. Chem.* **1846**, *59*, 35.
[12] G. J. Kubas, *Inorg. Synth.* **1979**, *19*, 90.
[13] J. W. McDonald, G. D. Friesen, L. D. Rosenheim, W. E. Newton, *Inorg. Chim. Acta* **1983**, *72*, 205.
[14] Although we only observe one band in the IR spectrum, there should be two bands, a stronger (E) band and a weaker (B_2) band (see A. Müller, W. Jaegermann, W. Hellman, *J. Mol. Struct.* **1983**, *100*, 559).
[15] P. E. Werner, *Z. Kristallogr.* **1964**, *120*, 375.
[16] A. C. Larson, R. B. von Dreele, *GSAS – Generalized Crystal Structure Analysis System*, Los Alamos Report LAUR 86-748, Los Alamos National Laboratory, USA, **1988**.

Cyanosulfines: An Unexpected Reaction of *N,N*-bis(trimethylsilyl)ynamines**

By *Thomas Schmid, Michael Hanack,* Cäcilia Maichle,* and *Joachim Strähle*

In 1988 we detected an alkynyl cation on tritium decay of a 1-tritiumalkyne.[1] Alkynediazonium salts might also generate alkynyl cations, although it is not certain from calculations whether they decompose to nitrogen and alkynyl cations.[2] We have described alkynediazonium salts, which are, however, not stable in either protic or nucleophilic media.[3] The most common syntheses for alkane- or arenediazonium compounds can therefore not be applied.

Alkane- and arenediazonium salts can also be obtained from sulfinylamines **1** on reaction with NO^+X^- (Scheme 1).[4, 5]

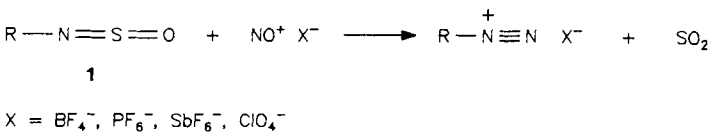

Scheme 1. Formation of diazonium ions from sulfinylamines.

Sulfinylamines **1** are easily prepared from amines (also bissilylated amines) and thionyl chloride.[6] We intended to synthesize alkynylsulfinylamines **3** from bissilylated alkynylamines **2a–d** by reaction with thionyl chloride and to transform these into alkynediazonium salts. To our surprise we obtained not the alkynylsulfinylamines **3**, but the cyanosulfines **4** (Scheme 2).

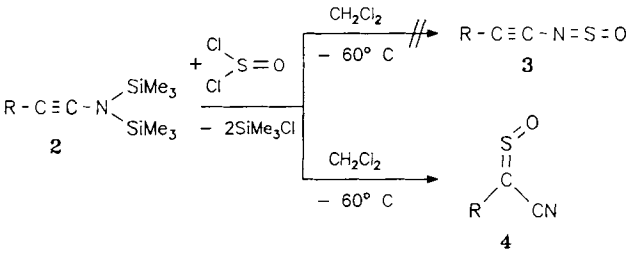

a: R = Ph, **b**: R = *t*Bu, **c**: R = *n*Pr, **d**: R = cyclohexyl

Scheme 2. Reaction of *N,N*-bis(trimethylsilyl)ynamines **2** with $SOCl_2$.

Phenyl cyanosulfine (α-sulfinylbenzylcyanide) **4a** is known; it was synthesized from phenylacetonitrile by reaction with thionyl chloride under HCl catalysis, as well as by an alkylation of SO_2 with α-silylated carbanions.[7] Compound **4a** proved to be identical with an independently synthesized sample of phenyl cyanosulfine.[7b] The cyanosulfines **4a–d** smell unpleasant to repulsive. For **4c** and **4d**, *cis/trans* isomers were detected by gas chromatography and NMR spectroscopy, but **4a** and **4b** are sterically uniform.

Sulfinylamines **3** and the cyanosulfines **4** are distinguishable by spectroscopy only with difficulty. To confirm the structure, **4a** was therefore treated with 2,3-dimethyl-1,3-butadiene. The product was 2-cyano-2-phenyl-4,5-dimethyl-3,6-dihydro-2*H*-thiopyran-1-oxide (**5**), which can only form from cyanosulfine **4a**, but not from sulfinylamine **3a**. Compound **5** was reduced with $LiAlH_4$ to the amine **6**, which was characterized by spectroscopy (Scheme 3).

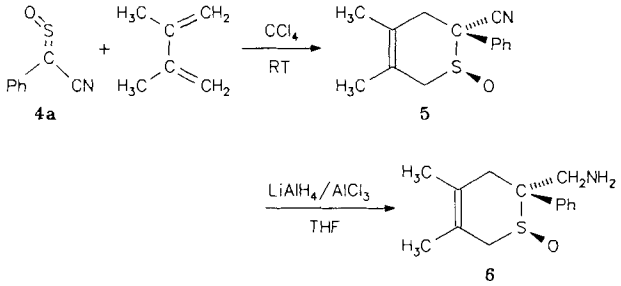

Scheme 3. Diels–Alder reaction of phenyl cyanosulfine **4a** with 2,3-dimethyl-1-3-butadiene and reduction of the resulting dihydrothiopyran-*S*-oxide **5** with $LiAlH_4$. RT = room temperature.

According to X-ray structural analysis, **5** is clearly a dihydrothiopyran-*S*-oxide (Fig. 1). The structure of **5** also shows that the phenyl cyanosulfine **4a** is present in the *E* form.[8]

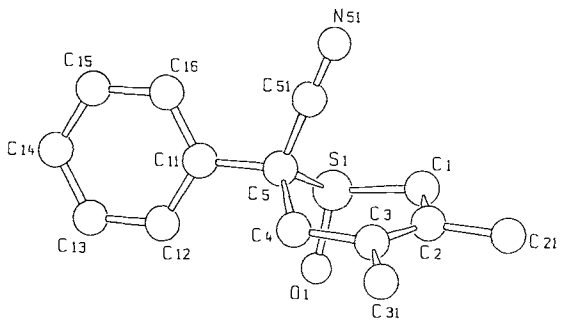

Fig. 1. Crystal structure of the dihydrothiopyran-*S*-oxide **5** (H atoms omitted for clarity).

The unexpected formation of cyansulfines is attributed to the strongly nucleophilic character of the β-C-atom of the *N,N*-bis(trimethylsilyl)ynamine **2**. The $SOCl_2$ thus attacks at this C atom.[9] Scheme 4 shows a proposed mechanism for the formation of cyanosulfines.

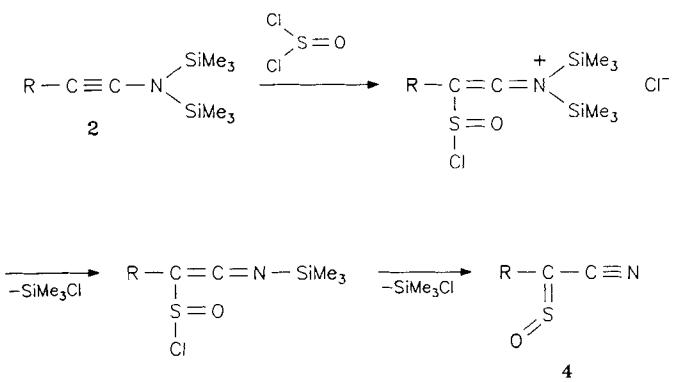

Scheme 4. Mechanism of the cyanosulfine formation.

Experimental Procedure

2: The ynamines **2c,d** were synthesized by adapting the procedure described in [10].

4: To a solution of $SOCl_2$ (6.4 mmol) dissolved in CH_2Cl_2 (10 mL) and cooled to −80 °C was added dropwise a solution of **2a** (6 mmol) in CH_2Cl_2 (4 mL).

[*] Prof. Dr. M. Hanack, Dipl.-Chem. T. Schmid
Institut für Organische Chemie der Universität
Auf der Morgenstelle 18, D-W-7400 Tübingen (FRG)
Prof. Dr. J. Strähle, Dr. C. Maichle
Institut für Anorganische Chemie der Universität Tübingen

[**] Sulfine is the trivial name of the *S*-oxide of the thioaldehyde and -ketone, cyanosulfine of α-sulfinylalkylcyanide.

The solvent was removed under reduced pressure, and the yellow solid purified by sublimation. The bright yellow solid with characteristic odor decomposes in solution. Yield 75.7%; m.p. 65 °C; IR (KBr): ν[cm^{-1}] = 2206 (C≡N), 1146, 1113 (S=O); UV/VIS (CH_3CN): λ_{max} [nm] = 340.8, 226.5, 209.0; after 24 h: 339.4, 274.8, 209.7; ^{1}H NMR (250 MHz, CCl_4, ext. standard D_2O): δ = 8.25 (d), 7.60 (m); ^{13}C NMR (63 MHz, CCl_4, ext. standard D_2O): δ = 111.71 (CN), 127.85 (C3), 129.11 (C2), 131.57 (C1), 133.28 (C4), 159.30 (CSO), (124.71, 129.80 decomposition product). **4b–d** were synthesized analogously.

5: A solution of **4a** (1.84 mmol) in CCl_4 (13 mL) was stirred at room temperature with 2,3-dimethyl-1,3-butadiene for 72 h. The colorless solid **5** precipitates in analytically pure form. Yield after chromatographic workup of the mother liquor: 84.3%; m.p. 150–152 °C; IR (KBr) ν[cm^{-1}] = 2237 (C≡N), 1065 (S=O); ^{1}H NMR (250 MHz, $CDCl_3$): δ = 1.72 (s, 6H), 2.91 (m, 2H), 3.58 (m, 2H), 7.34–7.52 (m, 5H); ^{13}C NMR (100 MHz, $CDCl_3$): δ = 19.49 (q; CH_3), 20.0 (q; CH_3), 39.73 (dt; C3), 53.93 (dt; C6), 62.22 (t; C2), 116.39 (dd; CN), 119.36 (m; C4), 125.74 (m; C5), 127.05 ($C3_{Ar}$), 129.58 ($C2_{Ar}$), 129.90 ($C4_{Ar}$), 131.72 ($C1_{Ar}$).

6: $LiAlH_4$ (1 mmol) and $AlCl_3$ (1 mmol) were stirred for a few minutes in THF (6 mL), after which a solution of **5** (1 mmol) in THF (4.5 mL) was added dropwise. After 1.5 h at room temperature the reaction mixture was worked up with $CHCl_3$ and chromatographed on silica gel ($CHCl_3$/MeOH 10/1). Yellow oil; yield 18.6%; IR (NaCl): ν[cm^{-1}] = 3379, 3319 (NH); ^{1}H NMR (250 MHz, $CDCl_3$): δ = 1.58 (s, 3H), 1.69 (s, 3H), 2.46–3.03 (m, 6H), 7.14–7.42 (m, 5H), (250 MHz, [D$_6$]DMSO): δ = 2.86 (d, NH_2); ^{13}C NMR (63 MHz, $CDCl_3$): δ = 19.19 (q; CH_3), 20.56 (q; CH_3), 30.05 (qt; C3), 41.15 (qt; C6), 51.49 (s; C2), 51.93 (tt; CH_2NH_2), 123.08 (m; C4), 125.72 (C5), 126.76 ($C4_{Ar}$), 127.04 ($C3_{Ar}$), 128.31 ($C2_{Ar}$), 142.59 (s; $C1_{Ar}$).

Received: September 18, 1992 [Z 5581 IE]
German version: *Angew. Chem.* **1993**, *105*, 300

[1] G. Angelini, M. Hanack, M. Speranza, J. Vermehren, *J. Am. Chem. Soc.* **1988**, *110*, 1298.
[2] R. Glaser, *J. Am. Chem. Soc.* **1987**, *109*, 4237.
[3] J. Vermehren, M. Hanack, *Chem. Ber.* **1989**, *122*, 331.
[4] K. Bott, *Angew. Chem.* **1965**, *77*, 132; *Angew. Chem. Int. Ed. Engl.* **1965**, *4*, 148.
[5] G. A. Olah, N. Friedman, J. M. Bollinger, J. Lukas, *J. Am. Chem. Soc.* **1966**, *88*, 5328.
[6] R. Beckert, R. Mayer in *Methoden Org. Chem. (Houben-Weyl) 4th Ed. 1952-*, Vol. E11, Part 1, Thieme, Stuttgart, **1985**, p. 558.
[7] a) M. Ohoka, T. Kojitani, S. Yanagida, M. Okahara, S. Komori, *J. Org. Chem.* **1975**, *40*, 3540; b) M. van der Leij, P. A. T. W. Porskamp, B. H. M. Lammerink, B. Zwanenburg, *Tetrahedron Lett.* **1978**, 811.
[8] Further details of the crystal structure investigation may be obtained from the Fachinformationszentrum Karlsruhe, Gesellschaft für wissenschaftlich-technische Information mbH, D-W-7514 Eggenstein-Leopoldshafen 2 (FRG) on quoting the depository number CSD-56716, the names of the authors, and the journal citation.
[9] R. H. Weigmann, E.-U. Würthwein, *Tetrahedron Lett.* **1990**, *31*, 3082.
[10] R. H. Weigmann, E.-U. Würthwein, *Tetrahedron Lett.* **1989**, *30*, 6147.

Selective Photolabeling near the Middle of Bilayers with a Photosensitive Transmembrane Probe

By *Masakuni Yamamoto, William A. Warnock, Alain Milon, Yoichi Nakatani*, and *Guy Ourisson**

In the 1970s Khorana et al.[1] and Breslow et al.[2] attempted to explore the internal structure of membranes by using photoreactive molecular probes designed so as to be incorporated and oriented properly in the phospholipid bilayer. These amphiphilic molecules contained the photosensitive group positioned at a certain distance from the head group such that it should, when activated, label carbon atoms of the membrane constituents situated near the middle of the bilayer. However, the results were disappointing, as the distribution of cross-linking sites after irradiation was broad both when the probe was used to label phospholipids, and when it was used to label proteins (for the proteins, the attack depended more on the nature of the amino acids than on their localization). These results indicated extensive dynamic disorder of the phospholipid matrix, or disorder induced by the incorporation of the probe or of the protein, or a combination of all these factors.

We have tried to improve the regioselectivity of such probes by selecting as the photosensitive group a 4,4'-dialkoxybenzophenone unit, well known for the high quantum yield of its photoreaction with C–H bonds,[3] and by placing it in the middle of a carbon chain terminated at either end by a lecithin head group, and long enough (about 30 Å) to span the usual biomembranes. We have described previously the synthesis of a transmembrane probe of this type, **1**,[4] and

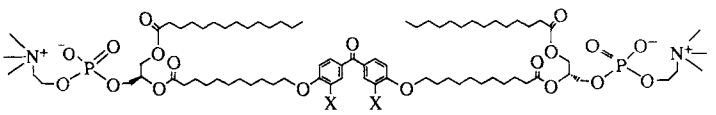

1, X = H; **2**, X = D

have shown that it has some very favorable properties: mixtures of **1** and 1,2-dimyristoyl-*sn*-glycero-3-phosphocholine (DMPC) form vesicles by sonication in water; over the concentration range of 2–20 mol%, **1** is almost completely incorporated into DMPC vesicles and its benzophenone chromophore appears from its absorption spectrum to be localized in a lipidic environment, that is inside the bilayer. We now show that its incorporation into DMPC vesicles is accompanied by complete miscibility in the fluid phase, that it is oriented mostly perpendicularly to the bilayer, and that it photolabels neighboring molecules (phospholipids, sterols, and also proteins as will be reported later) very efficiently and regioselectively near the middle of the membrane. This regioselectivity is extremely high (ca. 90% labeling within 3 Å of the middle of the membrane), when, and only when, the DMPC vesicles also contain cholesterol in normal bioconcentrations.

The phase diagram of mixtures of DMPC (T_m = 25 °C, ΔH = 24 kJ mol^{-1}) and **1** (T_m = 51 °C, ΔH = 70 kJ mol^{-1}) was studied by differential scanning calorimetry (DSC) with increasing concentrations of **1** (Fig. 1). The phase transition of DMPC at about 25 °C remains sharp, its intensity decreasing progressively with increasing content of the probe. Thus, the solidus line is indicative of monotectic phase behavior, that is immiscibility in the gel state. Another transition (liquidus line) appears at temperatures increasing from 25 to 51 °C as the relative content of **1** in the mixture increases from 0 to 100%. This implies complete miscibility of the two

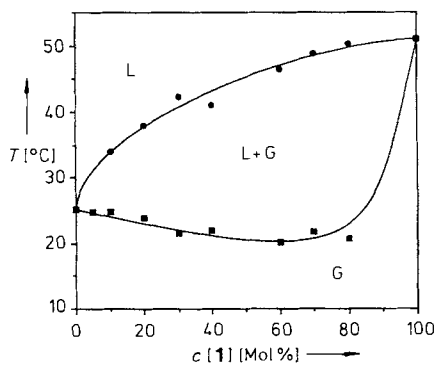

Fig. 1. Phase diagram for aqueous dispersions of DMPC + **1**. G: gel state, L: liquid crystal state. ■: Solidus value; ●: Liquidus value.

[*] Prof. G. Ourisson, M. Yamamoto, Dr. W. A. Warnock, Prof. A. Milon,[+] Prof. Y. Nakatani
Laboratoire de Chimie Organique des Substances Naturelles
associé au CNRS, Université Louis Pasteur
5 rue Blaise Pascal, F-67084 Strasbourg (France)
[+] Present address: CRBGC, CNRS, 118 route de Narbonne, F-31062 Toulouse (France)

lipids in the liquid crystal phase, which corroborates well with the results of the study by UV spectroscopy on these liposomes.[4] Therefore, we have used the liquid crystal state for the photoaffinity labeling experiments.

In order to define the orientation of the probe in the membrane, the deuterated probe **2** was synthesized from its 3,3'-diiodo derivative. The solid-state ^{2}H NMR spectrum was measured (Bruker MSL-300 spectrometer) on an oriented multibilayer sample obtained from a solution of DMPC (90 mol%) and the probe **2** (10 mol%) in 2-propanol, according to a procedure described previously.[5] The ^{2}H NMR spectrum of the multibilayer system (oriented at 90° to the magnetic field, $T = 318$ K; Fig. 2) shows two quadrupolar splittings: $\Delta\nu_{Q_A} = 2.75$ kHz (ca. 90% intensity) and $\Delta\nu_{Q_B} = 10.75$ kHz (ca. 10% intensity). After taking into account the internal flexibility and geometry of the benzophenone structure,[6] the first splitting (A) was interpreted as corresponding to the transmembrane orientation of the probe **2**, and the second one (B) to a U-shaped conformation, in which both head groups are on the same face of the membrane. ^{2}H NMR experiments were also performed with the unlabeled probe **1** inserted into deuterated DMPC. The quadrupolar splittings (angle 90°, 313 K) of oriented bilayers of pure 1-myristoyl-2-[D_{27}]myristoyl-*sn*-glycero-3-phosphocholine ([D_{27}]DMPC) and of [D_{27}]DMPC + 10 mol% probe **1** were compared, and found to differ by less than 8% at each position of the 2-myristoyl chain in [D_{27}]DMPC, thus showing that, at this concentration, the probe causes practically no perturbation of the internal mobility of chains of DMPC in the vesicles.

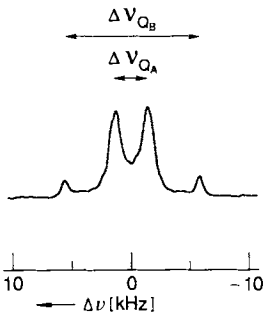

Fig. 2. ^{2}H NMR spectrum of 90° oriented multibilayers of DMPC + 10 mol% **2** at 318 K.

Irradiation (125 W HPK mercury lamp, Philips) of a suspension of vesicles from 1,2-dipalmitoyl-*sn*-glycero-3-phosphocholine (DPPC, 95 mol%) and **1** (5 mol%) at 50 °C for 3.5 hours resulted in the complete disappearance of the benzophenone absorption band in its UV spectrum.

After lyophilization, sodium methoxide in methanol was added to cleave the polar heads by transmethylation. The photolabeled compounds were separated from the crude product on a Sephadex LH-20 column ($CHCl_3$/MeOH = 1/1), and the photolabeled mixture was analyzed by FAB mass spectrometry (ZAB-HF double-focussing mass spectrometer). Examination of the intensity of the fragments derived from the photolabeled palmitate (from DPPC) and myristate (from **1**) (4:1) indicated that the intermolecular and intramolecular reactions are almost equally efficient. This is easily explained in a compact system, where intra- and intermolecular reactions do not differ entropically, and where the probe is largely diluted in the phospholipid matrix: assuming that each transmenbrane chain is surrounded by six fatty acid chains, one of which is that of the probe molecule, the expected ratio of intensities would then be 5:1. This slight difference between the intra and intermolecular reactions is crucial, since it is the intermolecular reaction which will be used for topographical analysis.

The distribution of the positions of attack in the myristoyl chains in DMPC/**1** vesicles was next investigated (Fig. 3). The crude product from the photoreaction was separated by chromatography into fractions of various molecular sizes, and the fraction containing tertiary alcohols was dehydrated with iodine, and then cleaved with sodium periodate and catalytic amounts of ruthenium chloride, using Breslow's procedure.[2] For attack at any atom other than C-14, a

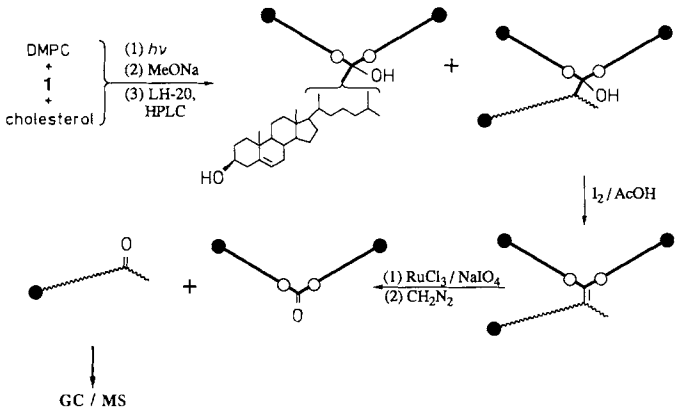

Fig. 3. Reaction sequence for the determination by the photoreaction of the functionalized positions in the myristoyl chains. Irradiation of the DMPC vesicles containing probe **1** and cholesterol gives photolabeled cholesterol and photolabeled methyl myristates, which are separated by chromatography. According to the results from mass spectrometry the label is exclusively on the side chain of cholesterol. The photolabeled methyl myristates are dehydrated with I_2 and oxidatively cleaved with $NaIO_4$ to give the dimethyl ester of the diacid formed from **1**, and a series of methyl *n*-oxomyristates ($n = 4-13$) (analyzed by GC-MS). The black circles symbolize methyl ester groups; the open circles, phenoxy groups (see **1**).

mixture of oxo-esters is produced, with the keto group located at the site of attack; after attack of the terminal C-14 position, the monoester of an α,ω-diacid is obtained, the treatment of which with diazomethane converts it to an α,ω-diester. The reaction mixture was analyzed by GC–MS. With vesicles comprising only DMPC and the probe, attack was mostly observed at C-13 ($\omega-1$: 33%) and C-12 ($\omega-2$: 13%) but was measurable as far from the middle of the bilayer as C-4 (Fig. 4). The small amount observed at C-14 (ω: 0.6%) is consistent with the methyl group being much less reactive than the methylene groups.

The low regioselectivity is not really satisfactory, even though it is higher than those obtained previously.[1, 2] That

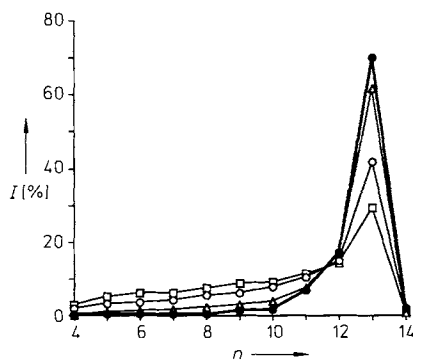

Fig. 4. Distribution of functionalized positions, □: in the absence of cholesterol, ○: with 10 mol% cholesterol, △: with 20 mol% cholesterol, ●: with 33 mol% cholesterol. Percentage of attack at each position of the myristoyl chain: $n = 1$, carboxyl; $n = 14$: C-14 (position ω).

positions as far from the middle layer of the membrane as C-4 are attacked may be due to the presence of the U-shaped conformation of the probe molecule mentioned above, which would make it possible for the excited carbonyl group to "explore" all the carbon atoms of the neighbouring chains. We felt, therefore, that we should attempt to eliminate such a U-shaped conformation; this could be done by selecting more rigid variants of **1**, which are now being synthesized, or by favoring the extended conformation of **1**, which we felt could be achieved by increasing the anisotropy of the bilayer by the addition of a rigidifying partner. Indeed, a spectacular improvement in regioselectivity was observed when cholesterol, a normal constituent of eucaryotic biomembranes, was added to the mixture of phospholipids at progressively higher concentrations until, with 33 mol% of cholesterol,[7] the sum of attack at $(\omega-1)$ and $(\omega-2)$ reached 90% (attack at $\omega-1$: 72%). This remarkable increase in selectivity is of course explainable by the ordering effect of cholesterol on the lipid bilayers, which has been demonstrated previously by different biophysical methods.[8] We have still to check whether the major effect is felt by the probe, or by the phospholipid matrix.

As expected, the inserted cholesterol was also attacked by the photoexcited probe on the side chain, but not at all on the ring system, as shown by FAB-MS analysis of the photolabeled cholesterol fraction. The precise localization of the site(s) of attack of the side chain is presently being studied.

These results show that our transmembrane probe, when used with cholesterol in phospholipid assemblies, can overcome the "inherent" character of lipid bilayers, that is, their disorder above T_m. This should make it possible to investigate more precisely the topography of the polypeptide chains of a membrane-bound protein; in this case, the exceptional topographic specificity of our system should be of crucial importance. Indeed, in collaboration with Dr. F. Pattus (EMBL, Heidelberg) and Dr. A. Van Dorsselaer (Strasbourg), the characterization of the C-terminal, membrane-bound, domain of the bacterial protein colicin A[9] incorporated in a model membrane system has been undertaken and cross-linking between the probe and the polypeptide has been observed. Precise characterization of the site and specificity of labeling is underway.

The principles described here could be extended to a wide variety of probes, differing from **1** by their head groups, the length of the chains, the nature and the position of the photoactive group, etc.

Received: September 10, 1992 [Z 5567 IE]
German version: *Angew. Chem.* **1993**, *105*, 302

[1] a) P. Chakrabarti, H. G. Khorana, *Biochemistry* **1975**, *14*, 5021–5033; b) C. M. Gupta, C. E. Costello, H. G. Khorana, *Proc. Natl. Acad. Sci. USA* **1979**, *76*, 3139–3143; c) A. H. Ross, R. Radhakrishnan, R. J. Robson, H. G. Khorana, *J. Biol. Chem.* **1982**, *257*, 4152–4161, and references therein.

[2] M. F. Czarniecki, R. Breslow, *J. Am. Chem. Soc.* **1979**, *101*, 3675–3676, and references therein.

[3] J. N. Pitts, Jr., H. W. Johnson, Jr., T. Kuwana, *J. Phys. Chem.* **1962**, *66*, 2456–2461.

[4] Y. L. Diyizou, A. Genevois, T. Lazrak, G. Wolff, Y. Nakatani, G. Ourisson, *Tetrahedron Lett.* **1987**, *28*, 5743–5746.

[5] a) I. Schuler, A. Milon, Y. Nakatani, G. Ourisson, A. M. Albrecht, P. Benveniste, M. A. Hartmann, *Proc. Natl. Acad. Sci. USA* **1991**, *88*, 6926–6930; b) M. A. Krajewski-Bertrand, A. Milon, Y. Nakatani, G. Ourisson, *Biochim. Biophys. Acta* **1992**, *1105*, 213–220.

[6] K. M. Gough, T. A. Wildman, *J. Am. Chem. Soc.* **1990**, *112*, 9141–9144.

[7] Up to 33 mol%, cholesterol can be incorporated in DMPC bilayers without perturbation; see R. A. Demel, B. de Kruyff, *Biochim. Biophys. Acta* **1976**, *457*, 109–132.

[8] M. R. Vist, J. H. Davis, *Biochemistry* **1990**, *29*, 451–464.

[9] M. W. Parker, F. Pattus, A. D. Tucker, D. Tsernoglou, *Nature* **1989**, *337*, 93–96.

Polyoxovanadium–Organophosphonates—Properties and Structure of an Unusual Pentavanadate Species with a V=O Group Directed Toward the Interior of the Molecular Cavity**

By *Qin Chen* and *Jon Zubieta**

Metal phosphonates have received significant attention in recent years because of their potential uses as sorbents, catalysts and catalyst supports.[1–5] Numerous new materials have been synthesized including monomolecular coordination compounds,[6, 7] one-dimensional complexes,[8] and layered compounds.[9, 10] Specifically for solid oxovanadium organophosphonates which are members of the structurally rich, general class of V-P-O solids,[11–13] layered structures with alternating organic and inorganic layers have been prepared. These compounds can recognize and selectively discriminate between alcohols.[10, 14] Furthermore, hydrothermal synthesis has been exploited to prepare a number of large polyoxovanadium–organophosphonate anions which form inclusion compounds with cationic and neutral molecules, such as $[(Me_4)N^+ \subset H_6(VO_2)_{16}(CH_3PO_3)_8]^{7-}$[15] and $[(H_2O)_x \subset H_{12}(VO_2)_{12}(PhPO_3)_8]^{4-}$.[16] In contrast to these developments in the solid-state chemistry and the hydrothermal synthesis of large oxovanadium organophosphonate clusters, the chemistry of these compounds in organic solvents under conventional synthetic conditions remains unexplored. We report here the synthesis and structure of a novel pentanuclear oxovanadium organophosphonate $\mathbf{1}\cdot CH_3OH$.

$(C_4H_9)_4N[V_5O_7(OCH_3)_2(PhPO_3)_5]\cdot CH_3OH$ $\quad$ $\mathbf{1}\cdot CH_3OH$

Red, parallelepiped crystals of $\mathbf{1}\cdot CH_3OH$ were prepared in 32.4 yield by the reaction of $[(C_4H_9)_4N]_3[V_5O_{14}]$[17] and $PhPO_3H_2$ in methanol.[18] X-ray structure analysis[19] of $\mathbf{1}\cdot CH_3OH$ revealed the presence of discrete Bu_4N^+ ions and methanol of crystallization in the lattice, as well as a $[V_5O_7(OCH_3)_2(PhPO_3)_5]^-$ ion (Fig. 1). In contrast to the

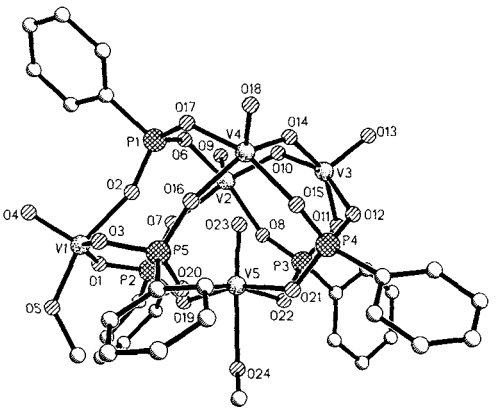

Fig. 1. Molecular structure of the anion $[V_5O_7(OCH_3)_2(C_6H_5PO_3)_5]^{1-}$ of **1**. Selected distances [Å] and angles [°]: V-O(terminal) 1.578(9) (av.); V-O(bridging) 1.805(10) (av.); V-O(P), 1.930(9) for V1–V4 and 1.995(9) for V5; V1-O5, 1.773(7); V5-O23, 1.613(5); V5-O24, 2.201(6); V2···O23, 2.659(6); V3···O23, 2.722(6); V4···O23, 2.885(6); P-C, 1.79(1); P-O, 1.525(12); O23-V5-O24, 177.4(3).

[*] Prof. J. Zubieta, Dr. Q. Chen
Department of Chemistry, Syracuse University
Syracuse, NY 13244 (USA)

[**] This work was supported by a grant from the National Science Foundation (CHE 9119910 to J. Z.).

highly symmetrical toroidal structures of the dodecanuclear and hexadecanuclear V^{IV} species synthesized hydrothermally,[15, 16] the structure of the anion of **1** is distinctly irregular. The core of the structure consists of a trinuclear $[(VO)_3(\mu_2\text{-}O)_2]$ unit connected through four of the five phenylphosphonate ligands to the *endo*-$[(VO)(OCH_3)]$ moiety (V5) and through three phenylphosphonate ligands to the *exo*-$[(VO)(OCH_3)]$ moiety (V1). While vanadium centers V1 to V4 exhibit distorted square pyramidal geometries, V5 displays distorted octahedral geometry with four oxygen donors of the phosphonato ligands occupying the equatorial positions and a terminal oxo group (O23) and a methoxy group in the axial positions.

Several structural motifs common to the solid-state structures of layered vanadium phosphonates[10] and of vanadium phosphates are present in the structure of the anion of **1**.[20, 21] The fusing of dimeric units bridged through two bidentate phosphato ligands $[(VO)_2(\mu_2\text{-}O_2PO(X))_2]$ (X = R, O, or OH) is a common feature of the solid-state structures. This is also observed in the structure of the anion of **1**, where the octahedrally coordinated V5 center displays this type of bridging to the other four vanadium centers. Likewise, the fundamental structural principle of mixed oxophosphonato-bridged binuclear moieties $[(VO)_2(\mu_2\text{-}O)(\mu_2\text{-}O_2PO(X))]$ is observed in the structure of the anion of **1**.[22, 23]

The anion of **1** has a pseudo-mirror plane through V3/V5/O23/P1/V1, resulting in four structurally distinct vanadium centers. The square-pyramidal sites V2 and V4 form the termini of the $[(VO)_3(\mu\text{-}O)_2]$ fragment and are each coordinated to a terminal and a bridging oxo group and to three $(\mu\text{-}O_3PPh)$ ligands. The central vanadium atom V3 of this trinuclear unit is bound to a terminal and two bridging oxo groups and two $(\mu_3\text{-}O_3PPh)$ units. The unique octahedrally coordinated V5 atom caps the bowllike fragment formed by the fusing of the square pyramidal geometries of the vanadium atoms of the central $[(VO)_3(\mu\text{-}O)_2]$ moiety and four (O_3PPh) tetrahedra (P2–P5). The V1 center has "condensed" onto the surface of the cluster so as to satisfy the coordination requirements of the phosphonato ligands P1, P2, and P5.

The most unusual feature of the structure of the anion of **1** is the projection of the oxo group at the V5 atom into the cavity of the molecule, as illustrated by the polyhedral representation in Figure 2. Vanadate clusters form a variety of structures encapsulating different guest molecules or anions;[24] however, the structure of the anion of **1** is unique in providing a primitive prototype of a highly unsymmetrical bowllike structural element folded about a coordinated terminal oxo group. The presence of the fragment at V1 as a unit condensed onto the surface of the bowllike core is also unprecedented.

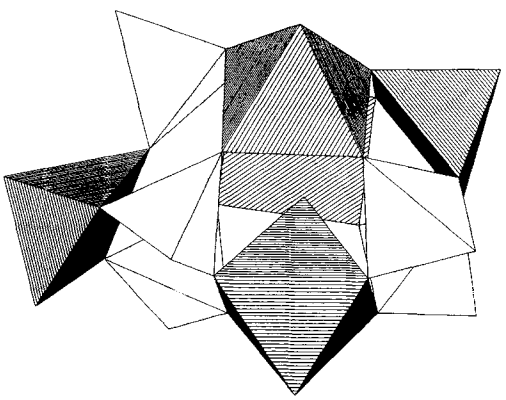

Fig. 2. A polyhedral representation of the structure of the anion of **1**, showing the projection of the terminal oxo group O23 into the central cavity of the cluster.

Protic degradation of **1** in MeOH/HCl yields the binuclear species $[\{VOCl(PhPO_3H)(H_2O)\}_2]$ (**2**),[25] which in turn serves as a simple precursor for condensation reactions of fragments by mild hydrolysis. Controlled hydrolysis of **2** in MeOH yields mixtures of **1** and larger oligomers, whose properties are under investigation. Under more forcing conditions of hydrolysis/condensation, **2** yields the solid phase **3** with a layered structure,[26] which intercalates alcohols to give compounds of the type **4**. Both **1** and **2** are readily reduced to give microcrystalline green products, one of which has been identified as **5**. Compound **5** is structurally analogous to the arsonate derivative recently reported by us, $(Bu_4N)_2[V_6O_{10}(PhAsO_3)_4(PhAsO_3H)_2]$.[27] Cluster **5** may also be employed in hydrolysis/condensation reactions to yield a variety of products.

$[VO(PhPO_3)] \cdot H_2O$ **3**
$[VO(PhPO_3)] \cdot H_2O \cdot ROH$ **4**
$(Bu_4N)_2[V_6O_{10}(PhPO_3)_4(PhPO_3H)_2]$ **5**

Vanadium organophosphonates clearly possess a varied synthetic and structural chemistry which has yet to be fully developed. They afford a variety of polynuclear species of which **1** and **5** have been structurally characterized. The elucidation of these structures may help determine the principles governing the hydrolysis/condensation reaction pathways for this class of compounds and for general reactions of this type, a process of considerable scientific and technological interest.[28]

Received: September 1, 1992 [Z 5550 IE]
German version: *Angew. Chem.* **1993**, *105*, 304

[1] Y. Zhang, A. Clearfield, *Inorg. Chem.* **1992**, *31*, 2821, and references therein.
[2] G. Cao, T. E. Mallouk, *Inorg. Chem.* **1991**, *30*, 1434.
[3] G. L. Rosenthal, J. Caruso, *Inorg. Chem.* **1992**, *31*, 3104.
[4] D. A. Burwell, K. G. Valentine, J. H. Timmermans, M. E. Thompson, *J. Am. Chem. Soc.* **1992**, *114*, 4144.
[5] A. Clearfield, *Chem. Rev.* **1988**, *88*, 125.
[6] E. T. Clark, P. R. Rudolf, A. E. Martell, A. Clearfield, *Inorg. Chim. Acta* **1989**, *164*, 59.
[7] P. R. Rudolf, E. T. Clark, A. E. Martell, A. Clearfield, *J. Coord. Chem.* **1985**, *14*, 139.
[8] B. Bujoli, P. Palvadeau, J. Rouxel, *Chem. Mater.* **1990**, *2*, 582.
[9] G. Cao, H. Lee, V. Lynch, T. E. Mallouk, *Inorg. Chem.* **1988**, *27*, 2781.
[10] G. H. Huan, A. J. Jacobson, J. W. Johnson, E. W. Corcoran, Jr., *Chem. Mater.* **1990**, *2*, 2.
[11] B. L. Hodnett, *Catal. Rev. Sci. Eng.* **1985**, *27*, 373.
[12] O. Centi, F. Trifiro, J. R. Ebnar, V. M. Franchetti, *Chem. Rev.* **1988**, *88*, 55.
[13] G. Villeneuve, K. S. Suh, P. Amoros, N. Casan-Pastor, D. Beltran-Porter, *Chem. Mater.* **1992**, *4*, 108, and references therein.
[14] J. W. Johnson, A. J. Jacobson, W. M. Butler, S. E. Rosenthal, J. F. Brody, J. T. Lewandowski, *J. Am. Chem. Soc.* **1989**, *111*, 381.
[15] G. H. Huan, A. J. Jacobson, V. W. Day, *Angew. Chem.* **1991**, *103*, 426; *Angew. Chem. Int. Ed. Engl.* **1991**, *30*, 422.
[16] G. Huan, V. W. Day, A. J. Jacobson, D. P. Goshorn, *J. Am. Chem. Soc.* **1991**, *113*, 3188.
[17] V. W. Day, W. G. Klemperer, O. M. Yaghi, *J. Am. Chem. Soc.* **1989**, *111*, 4519.
[18] $(Bu_4N)_3V_5O_{14}$ (1.20 g, 1.0 mmol) was added under a nitrogen atmosphere with stirring to a dry methanol solution (35 mL) of phenylphosphonic acid (0.79 g, 5.0 mmol). The solution slowly turned red, and after 24 h of stirring at room temperature, a red solid precipitated. The solid was collected by filtration, washed with anhydrous diethyl ether and dried under vacuum. Recrystallization was accomplished from CH_2Cl_2/MeOH/Et_2O (2:3:1 by volume) at 0 °C. (Yield: 0.48 g, 32.4%). Correct C,H,N analyses. – IR(KBr pellet): $\tilde{\nu}$[cm^{-1}] = 3422(m), 2960(m), 2874(w), 1483(w), 1138(s), 1080(m), 1039(s), 974(s), 756(m), 696(m), 668(w), 630(m), 571(m).
[19] **1**: monoclinic space group $P2_1/n$ with a = 12.167(2), b = 23.348(5), c = 22.508(5) Å, β = 98.49(2)°, V = 6323.9(19) Å^3, Z = 4, (ϱ_{calcd} =

1.558 g cm^{-3}; $\mu(Mo_{K\alpha}) = 9.10$ cm^{-1}) $R = 0.0536$ for 4942 reflections with $2\theta < 45$ and $I \geq 3\sigma(I)$; Rigaku AFC5S diffractometer, graphite monochromated $Mo_{K\alpha}$ radiation. The structure was solved using direct methods with the SHELXTL program package. Further details of the crystal structure investigation may be obtained from the Fachinformationszentrum Karlsruhe, Gesellschaft für wissenschaftlich-technische Information mbH, D-W-7514 Eggenstein-Leopoldshafen 2 (FRG) on quoting the depository number CSD-56814, the names of the authors, and the journal citation.

[20] K. H. Lii, N. S. Wen, C. C. Su, B. R. Chueh, *Inorg. Chem.* **1992**, *31*, 439, and references therein.

[21] P. Amoros, A. LeBail, *J. Solid State Chem.* **1992**, *97*, 283.

[22] D. Beltran-Porter, P. Amoros, R. Ibanez, E. Martinez, A. Beltran-Porter, A. LeBail, G. Ferey, G. Villeneuve, *Solid State Ionics* **1989**, *32/33*, 57, and references therein.

[23] R. C. Haushalter, Z. Wang, M. E. Thompson, J. Zubieta, C. O'Connor, *Inorg. Chem.*, submitted.

[24] W. G. Klemperer, T. A. Marquart, O. M. Yaghi, *Angew. Chem.* **1992**, *104*, 51; *Angew. Chem. Int. Ed. Engl.* **1992**, *31*, 49.

[25] J. Salta, Q. Chen, J. Zubieta, unpublished.

[26] G. Huan, A. J. Jacobson, J. W. Johnson, E. W. Corcoran, *Chem. Mater.* **1990**, *2*, 91.

[27] M. I. Khan, Y. Chang, Q. Chen, H. Hope, S. Parkin, D. P. Goshorn, J. Zubieta, *Angew. Chem.* **1992**, *104*, 1236; *Angew. Chem. Int. Ed. Engl.* **1992**, *31*, 1197.

[28] C. J. Brinker, G. W. Scherer, *Sol-gel Science*, Academic Press, San Diego, **1990**.

Cobalt Tetra(hydroquinone)porphyrin: An Efficient Electron Transfer Reagent in Aerobic Pd-Catalyzed 1,4-Diacetoxylation of 1,3-Cyclohexadiene**

By *Helena Grennberg, Sylvie Faizon,* and *Jan-E. Bäckvall**

The palladium-catalyzed 1,4-diacetoxylation of 1,3-dienes[1] was recently developed into an aerobic process by the use of a one-pot triple catalytic system (Scheme 1).[2] The triple catalytic system involves selective interactions between each consecutive catalyst, and the reoxidation of hydroquinone (HQ) to benzoquinone (BQ) is a crucial step. If a quinone-containing macrocycle is used, an intramolecular electron transfer between the hydroquinone unit and the oxidized metal-containing macrocycle may be achieved.[3]

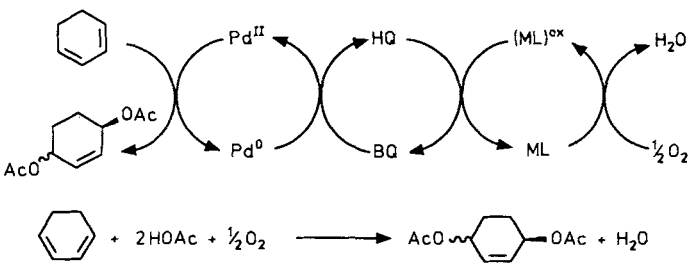

Scheme 1. The triple catalytic system and the overall reaction of the diacetoxylation of 1,3-cyclohexadiene. ML = metal-containing macrocycle.

This was expected to lead to a more efficient overall reaction than that observed for the system with the hydroquinone and metal-containing macrocycle as separate molecules. We report here on the significant increase in the rate of the aerobic 1,4-diacetoxylation of 1,3-cyclohexadiene obtained by the use of a porphyrin with hydroquinone units.

Cobalt tetra(hydroquinone)porphyrin [Co(TQP)] (**3**) was prepared by a Lindsey condensation of 2,5-dimethoxybenzaldehyde and pyrrole. This initially afforded the protected *meso*-tetra(2,5-dimethoxyphenyl)porphyrin (TDMPP), which was then demethylated with BBr_3 and metalated with $[Co(OAc)_2] \cdot 4H_2O$.[4, 5] The new bifunctional catalyst **3** was used for the aerobic 1,4-diacetoxylation of 1,3-cyclohexadiene.[6] The rate of oxygen consumption was measured and compared to that of the corresponding reaction catalyzed by free hydroquinone and **1**.[7] As can be seen in Figure 1, the use of **3** results in a faster oxygen consumption, indicating a more efficient electron transfer. To determine if this rate enhancement was an effect of the electron-rich phenyl groups in **3**, **3** was also compared to **2** + HQ. The overall performance of **2** + HQ was more similar to that of **1** + HQ than **3**, indicating that the increased reaction rate for the catalysis with **3** was not an electronic effect from the substituted phenyls.

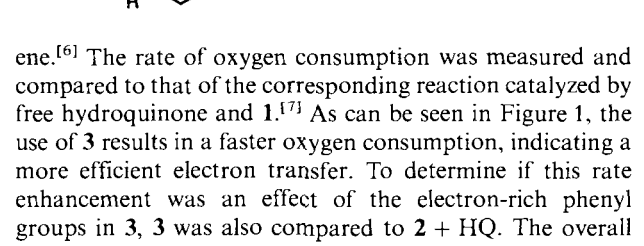

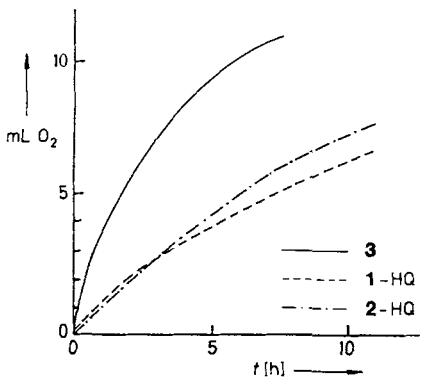

Fig. 1. Aerobic 1,4-oxidation of 1 mmol of 1,3-cyclohexadiene by addition of 2.5 mol% of $[Pd(OAc)_2]$.

Under standard conditions[1, 2] (5 mol% $[Pd(OAc)_2]$), the reaction catalyzed by **3** was complete in 10 h; all substrate was oxidized to give 1,4-diacetoxy-2-cyclohexene **4** and benzene.[2b] The reaction catalyzed by **1** + HQ ceased after 18 h.[8] The yields of **4** are about the same for both reactions (ca. 75%). However, when a smaller amount of $[Pd(OAc)_2]$ (2.5 mol%) was used, the reaction catalyzed by **3** was unaffected, whereas the rate of that catalyzed by **1** + HQ decreased, yielding 65% of **4** after 28 h (Table 1).[8] In addition the reaction catalyzed by **2** + HQ was slow under these conditions, and gave 60% **4** together with benzene after 24 h.[8, 9] The relative stereochemistry of **4**, previously shown to be dependent on both the type and amount of lithium salt

[*] Prof. Dr. J.-E. Bäckvall, Dr. H. Grennberg, S. Faizon
Department of Organic Chemistry, University of Uppsala
Box 531, S-751 21 Uppsala (Sweden)

[**] This work was supported by the Swedish Natural Science Research Council and the Swedish Research Council for Engineering Science. The Region PACA (France) is acknowledged for financially supporting the student exchange between University of Aix-Marseille III (S. F.) and University of Uppsala.

Table 1. Aerobic 1,4-oxidation of 1,3-cyclohexadiene [a].

Catalyst	LiOAc [mol]	Product [b]/Selectivity [%]	Yield [c]/Time [%] [h]
3	0	*trans*-**4**/70	70/10
	0.6	*trans*-**4**/63	70/10
1 + HQ	0	*trans*-**4**/60	65/28
	0.6	*trans*-**4**/ > 90	65/28
2 + HQ	0	*trans*-**4**/65	60/24
	0.6	*trans*-**4**/87	60/24

[a] Conditions: 2.5 mol% of $[Pd(OAc)_2]$, 2–2.5 mol% of [Co(porphyrin)], 10 mol% HQ (for **1** and **2**) in 2 mL HOAc at room temperature and 1 atm O_2. [b] The relative stereochemistry of **4** was determined by ^1H NMR spectroscopy. [c] Isolated yield.

present[1] and the structure of the quinone,[1, 10] was also found to be dependent on whether the reaction was catalyzed by **3** or **1** + HQ. With **1** + HQ,[2] *trans*-**4** was obtained with a stereoselectivity of > 90% whereas with the catalyst **3** only a moderate stereoselectivity (70% *trans*) was achieved.

At least two pathways for the electron transfer in the bifunctional Co(porphyrin-hydroquinone) molecule are possible. The observed efficiency of the quinone-containing porphyrin **3** is best explained by an intramolecular electron transfer from the hydroquinone unit to the oxidized cobalt atom via the π-electron system of the porphyrin. An alternative mechanism would involve intermolecular interactions via a "liquid polymer"[11] coordination of the hydroquinone unit of one porphyrin molecule to the metal center of a second molecule.

Thus the bifunctional catalyst **3** not only accelerates the electron transfer but also acts as an efficient oxygen activating agent in the aerobic palladium-catalyzed *trans*-1,4-diacetoxylation of 1,3-cyclohexadiene.

Experimental Procedure

$TDMPPH_2$ was prepared by a Lindsey condensation [4a]: a solution of trifluoroacetic acid (0.46 g, 4 mmol) in CH_2Cl_2 (50 mL) was added over 15 min to a degassed solution of 2,5-dimethoxybenzaldehyde (1.1 g, 6.6 mmol) and freshly distilled pyrrole (0.51 g, 7.5 mmol) in CH_2Cl_2 (250 mL, distilled from CaH_2). The mixture was stirred under an N_2 atmosphere for about 15 h. A toluene solution of 2,3-dichloro-5,6-dicyano-1,4-benzoquinone (1 g in 10 mL) was added and the mixture was heated at reflux for 1 h, then filtered through basic alumina and evaporated to dryness. The crude product was dissolved in $CHCl_3$ and precipitated with pentane to yield 0.21 g (15%) $TDMPPH_2$. UV (CH_2Cl_2): λ[nm] = 398 (sh), 418, 513, 545, 588, 643. ^1H NMR ([D_6]acetone): δ = 8.80 (br s, 8H, β-pyrrole), 7.64 (m, 4H, *o*-Ph), 7.38 (br s, 8H, m, *p*-Ph), 3.95 and 3.55 (m, 12H each, OCH_3), −2.66 (br s, NH). Correct elemental analysis (C,H,N) for $C_{52}H_{46}N_4O_8$.

$TQPH_2$: To a cooled (−75 °C) solution of $TDMPPH_2$ (0.20 g, 0.23 mmol) in dry CH_2Cl_2 (20 mL) under an N_2 atmosphere was added BBr_3 [4b,c] (20 mL of a 1 M CH_2Cl_2 solution) over 30 min. The green mixture was stirred at −75 °C for 75 min, at room temperature for 1.5 h, and then slowly poured into 300 mL of a crushed ice-H_2O mixture. The biphasic mixture was stirred until the ice had melted. Subsequently EtOH (200 mL) was added and then solid $NaHCO_3$ until the mixture turned red. The mixture was then extracted with CH_2Cl_2 and ether, washed with H_2O, dried over $MgSO_4$, and evaporated to yield 0.15 g (71%) $TQPH_2$. UV (acetone): λ[nm] = 417, 512, 544, 589, 645.

2 and **3** were prepared by treating the porphyrin free bases with an excess of $[Co(OAc)] \cdot 4H_2O$ in refluxing, freshly distilled DMF, in accordance with the literature [4d]. UV (acetone) of **3**: λ[nm] = 407, 530 (unresolved). UV (CH_2Cl_2) of **2**: λ[nm] = 414, 438, 529, 546 (unresolved).

Received: September 11, 1992 [Z 5568 IE]
German version: *Angew. Chem.* **1993**, *105*, 269

[1] J.-E. Bäckvall, S. E. Byström, R. E. Nordberg, *J. Org. Chem.* **1984**, *49*, 4619.

[2] a) J.-E. Bäckvall, A. K. Awasthi, Z. D. Renko, *J. Am. Chem. Soc.* **1987**, *109*, 4750; b) J.-E. Bäckvall, R. B. Hopkins, H. Grennberg, M. M. Mader, A. K. Awasthi, *ibid.* **1990**, *112*, 5160.

[3] Intramolecular electron transfer has been reported in porphyrin-quinone photosynthesis model compounds: M. R. Wasielewski, *Chem. Rev.* **1992**, *92*, 435; J. A. Schmidt, A. R. McIntosh, A. C. Weedon, J. R. Bolton, J. S. Connolly, J. K. Hurley, M. R. Wasielewski, *J. Am. Chem. Soc.* **1988**, *110*, 1733; J. Rodriguez, C. Kirmaier, M. R. Johnson, R. A. Friesner, D. Holten, J. L. Sessler, *ibid.* **1991**, *113*, 1652.

[4] a) J. S. Lindsey, I. C. Schreiman, H. C. Hsu, P. C. Kearney, A. M. Marguerettaz, *J. Org. Chem.* **1987**, *52*, 827; b) J. F. W. McOmie, D. E. West in *Org. Synth. Collect. Vol V*, (Ed.: H. E. Baumgarten), Wiley, New York, **1973**, p. 412; c) E. H. Vickery, L. F. Pahler, E. J. Eisenbraun, *J. Org. Chem.* **1979**, *44*, 4444; d) A. D. Adler, F. R. Longo, R. Kampas, J. Kim, *J. Inorg. Nucl. Chem.* **1970**, *32*, 2443.

[5] a) J. Dalton, L. R. Milgrom, *J. Chem. Soc. Chem. Commun.* **1979**, 609; b) M. A. Bergkamp, J. Dalton, T. L. Netzel, *J. Am. Chem. Soc.* **1982**, *104*, 253.

[6] A Co(salen-HQ) was recently reported as a catalyst in a Pd-catalyzed allylic oxidation of cyclohexene [5b]. When this catalyst was tried and compared to **3** in a 1,4-diacetoxylation, we found that the salene-HQ complex led to a considerably lower reaction rate and was also less stable to the reaction conditions than the porphyrin: S. E. Byström, E. M. Larsson, B. Åkermark, *J. Org. Chem.* **1990**, *55*, 5674.

[7] The oxygen consumption gives a good estimate of the progress of the Pd-catalyzed oxidation; 12 mL of O_2 corresponds to conversion of 1 mmol of the substrate [2b].

[8] In the reaction catalyzed by **1** + HQ, the free quinone was consumed in a Diels–Alder reaction with 1,3-cyclohexadiene, and no benzene formation was observed (by GC or GC-MS).

[9] a) A control experiment employing **2** *without* hydroquinone yielded a very rapid and unexpected [9b] oxygen consumption. In only 4 h all diene was converted to **4** and benzene, of which **4** was isolated in 35% yield. Interestingly, the relative stereochemistry of the product was reversed from the 70% *trans* obtained by using **3** to 75% *cis* with **2**. This mechanistically interesting observation will be the subject of a separate study. b) Employing **1** without a quinone yielded only porphyrin degradation products.

[10] H. Grennberg, A. Gogoll, J.-E. Bäckvall, *J. Org. Chem.* **1991**, *56*, 5808.

[11] E. B. Fleischer, A. M. Shachter, *Inorg. Chem.* **1991**, *31*, 3763.

Surprising Differences in the Cycloaddition Reactions of Cumulenes and Heterocumulenes to Vinylidenetitanocene: Formation of Four- or Five-Membered Titanacycles**

By *Rüdiger Beckhaus,* Isabelle Strauß, Trixie Wagner,* and *Paul Kiprof*

The stabilization of the vinylidene group $H_2C{=}C{:}$, tautomeric to acetylene, by complexation as metallaallene **1** led to an extensive chemistry, particularly for electron-rich transition metals.[1, 2] The methylidene titanacyclobutane **3**, accessible from the divinyltitanocene **2** in almost quantitative yield,[3a, b] is an efficient source for vinylidenetitanocene **4**,[4] which is formed from **3** by heating to cleave ethylene. Extended Hückel MO calculations show that the electronic structure of **4** makes it ideally suited for cycloaddition reactions with multiply bonded systems.[4]

1

[*] Dr. R. Beckhaus, I. Strauß, T. Wagner
Institut für Anorganische Chemie der Technischen Hochschule
Professor-Pirlet-Strasse 1, D-W-5100 Aachen (FRG)
Dr. P. Kiprof[+]
Anorganisch-chemisches Institut der Technischen Universität München
[+] Present address:
Department of Chemistry, University of Wisconsin
Madison (USA)

[**] The experimental studies were partly carried out during a visit to the Anorganisch-chemisches Institut der Technischen Universität München (extraordinary research grant of the Alexander von Humboldt Foundation for RB). RB thanks Prof. P. Hofmann for his continued interest. Financial support from the Fonds der Chemischen Industrie is gratefully acknowledged.

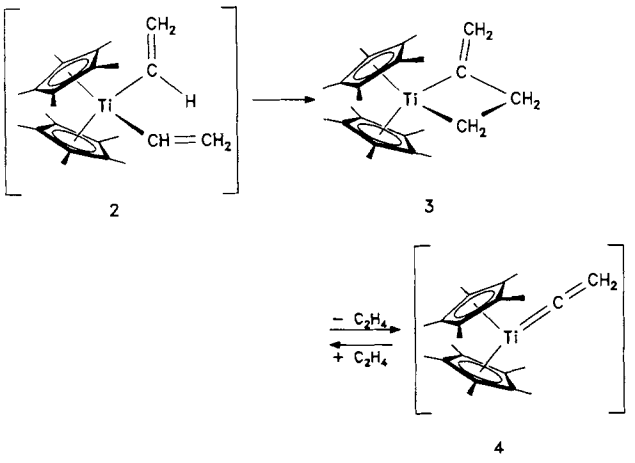

Attempts to stabilize thermally generated **4** with phosphanes were unsuccessful, in contrast to reactions with similar metallacyclobutanes[5, 6] and titanium–carbon double-bond systems.[7, 8] The product of this reaction, the fulvene complex **5**, can also be conveniently prepared as dark green solid by "dry" thermolysis of **3** under vacuum, or in solution from $[Cp^*_2Ti(CH_3)(CH{=}CH_2)]$ ($Cp^* = \eta^5$-$C_5(CH_3)_5$) by elimination of methane.

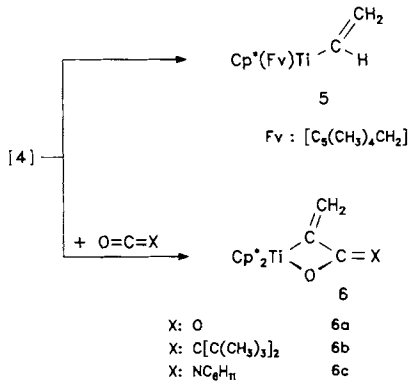

If **3** is heated in the presence of acceptor ligands containing cumulative double bonds, for example carbon dioxide, ketenes, or isocyanates, ethylene is liberated and the cycloreversion products **6a**, **b**, and **c**, respectively, are formed. The NMR spectra of **6** (Table 1) confirm the presence of a metallaoxetane unit. Particularly characteristic are the ^{1}H NMR signals of the exocyclic methylidene group [$\delta = 7.17$, 4.79 (**6a**); 6.49, 4.57 (**6b**), 7.21, 4.68 (**6c**)] and the chemical shift of the ring carbon atoms Ti–C [$\delta = 194.5$ (**6a**); 184.4 (**6b**); 193.7 (**6c**)] and O–C [$\delta = 159.9$ 9 (**6a**); 143.1 (**6b**); 146.7 (**6c**)]. A feature of the crystal structure analysis of **6c** (Fig. 1) is a twisted metallaoxetane in which C 1 lies 0 .090(4) Å above and C 3 0.116(3) Å below the plane defined by the Ti, O, and C 2 atoms. The titanium atom has pseudotetrahedral coordination, as anticipated, with typical Ti–Cp* distances (2.0939(6), 2.0979(6) Å) and a characteristic Cp*-Ti-Cp* angle of 140.78°. The Ti–O and Ti–C bond lengths of 1.983(2) and 2.121(3) Å, respectively, lie in the usual range. Double-bond lengths of 1.325(4) and 1.285(4) Å were found for the exocyclic C=CH_2 and C=N groups.

The use of hexacarbonylchromium, or -tungsten, cymantrene ([CpMn(CO)$_3$]), or methylcymantrene ([Cp′Mn(CO)$_3$], Cp′ = η^5-$C_5(CH_3)H_4$) in reaction with **3** (→ **4**) surprisingly affords the binuclear Fischer carbene complexes **7** containing a five-membered titanacycle. Accordingly, the ^{1}H NMR

Table 1. Spectroscopic data of **5**–**7** [a].

5: ^{1}H NMR (270 MHz): $\delta = 1.73$ (s, 15H, $C_5(CH_3)_5$), 1.22, 1.40, 1.61, 1.97 (s, each 3H, CH_3), 1.31, 1.80 (dd, ^2J(H,H) = 4.2 Hz, each 1H, $C_5(CH_3)_4CH_2$), 4.27 (dd, ^2J(H,H) = 3.4 Hz, ^3J(H,H) = 22.9 Hz, 1H, =CH_2), 5.29–5.11 (m, 1H, =CH), 5.67 (dd, ^2J(H,H) = 3.4 Hz, ^3J(H,H) = 18.5 Hz); ^{13}C{^{1}H} NMR (125 MHz): $\delta = 12.1$ ($C_5(CH_3)_5$), 118.8 ($C_5(CH_3)_5$), 10.6, 10.7, 10.9, 16.6 ($C_5(CH_3)_4CH_2$), 76.1 ($C_5(CH_3)_4CH_2$), 120.7, 124.0, 125.9, 126.6, 129.5 ($C_5(CH_3)_4CH_2$), 113.6 (TiC=CH_2), 208.0 (TiC=CH_2)

6a: ^{1}H NMR (500 MHz): $\delta = 1.61$ (s, 30H), 4.79 (s, 1H, 1H of =CH_2), 7.17 (s, 1H, 1H of =CH_2); ^{13}C{^{1}H} NMR (125 MHz): $\delta = 11.7$ ($C_5(CH_3)_5$), 125.0 ($C_5(CH_3)_5$), 119.6 (=CH_2), 159.9 (C=O), 194.5 (Ti-C); MS (CI): *m/z* 389 ($M^{\oplus}$ + H, 100%), 318 ($M^{\oplus} - C_3H_2O_2$, 10)

6b: ^{1}H NMR (270 MHz): $\delta = 1.71$ (s, 30H, $C_5(CH_3)_5$), 1.65 (s, 9H, $C(CH_3)_3$), 1.72 (s, 9H, $C(CH_3)_3$), 4.57 (s, 1H, 1H of =CH_2), 6.49 (s, 1H, 1H of =CH_2); ^{13}C NMR (67.9 MHz): $\delta = 12.1$ (q, ^1J(C,H) = 126 Hz, $C_5(CH_3)_5$), 122.5 (s, $C_5(CH_3)_5$), 34.0 (q, ^1J(C,H) = 125 Hz, $C(CH_3)_3$), 35.1 (s, $C(CH_3)_3$), 40.0 (s, =$C(C(CH_3)_3)_2$), 114.0 (t, ^1J(C,H) = 154.5 Hz, =CH_2), 143.1 (s, OC=C), 184.4 (s, Ti-C); MS (70 eV): *m/z* 498 ($M^{\oplus}$)

6c: ^{1}H NMR (500 MHz): $\delta = 1.66$ (s, 30H, $C_5(CH_3)_5$), 4.28–4.20 (m, 1H, =NCH), 2.16–2.12 (m, 2H, H_{Chx}), 1.99–1.94 (m, 2H, H_{Chx}), 1.88–1.79 (m, 2H, H_{Chx}), 1.72–1.60 (m, 1H, H_{Chx}, masked), 1.60–1.51 (m, 2H, H_{Chx}), 1.43–1.34 (m, 1H, H_{Chx}), 7.21 (d, $+^2J$(H,H) = 1.8 Hz, 1H of =CH_2), 4.68 (d, $+^2J$(H,H) = 1.8 Hz, 1H of =CH_2); ^{13}C{^{1}H} NMR (125.7 MHz): $\delta = 11.7$ ($C_5(CH_3)_5$), 123.7 ($C_5(CH_3)_5$), 51.5 (C4), 35.6 (C5, C9), 26.1 (C6, C8), 27.0 (C7), 112.8 (C1), 146.7 (C3), 193.7 (C2) (assignment according to Fig. 1); MS (70 eV): *m/z* 469 ($M^{\oplus}$, 91%), 454 ($M^{\oplus} - CH_3$, 78%), 386 ($M^{\oplus} - C_6H_{11}$, 36), 335 ($M^{\oplus} - C_9H_{11}N$, 88), 318 ($M^{\oplus} - C_9H_{13}NO$, 100)

7a: ^{1}H NMR (270 MHz): $\delta = 1.47$ (s, 30H, $C_5(CH_3)_5$), 7.01 (d, ^3J(H,H) = 8.9 Hz, 1H, CH), 7.46 (d, ^3J(H,H) = 8.9 Hz, 1H, CH); ^{13}C{^{1}H} NMR (67.9 MHz): $\delta = 11.6$ ($C_5(CH_3)_5$), 124.6 ($C_5(CH_3)_5$), 151.8 (TiCH=*C*H), 240.1 (TiCH=CH), 325.4 (*C*=Cr); IR (*n*-heptane): $\tilde{\nu}$(CO)[cm^{-1}] = 2040, 1980, 1923; MS (70 eV): *m/z* 564 ($M^{\oplus}$, 10%), 536 ($M^{\oplus}$ − CO, 3) 508 ($M^{\oplus}$ − 2CO, 5), 480 ($M^{\oplus}$ − 3CO, 4%), 452 ($M^{\oplus}$ − 4CO, 10), 424 ($M^{\oplus}$ − 5CO, 100)

7b: ^{1}H NMR (270 MHz): $\delta = 1.49$ (s, 30H, $C_5(CH_3)_5$), 7.20 (d, ^3J(H,H) = 8.8 Hz, 1H, =CH), 7.45 (d, ^3J(H,H) = 8.8 Hz, 1H, =CH); ^{13}C NMR (67.9 MHz): $\delta = 11.7$ ($C_5(CH_3)_5$), 124.6 ($C_5(CH_3)_5$), 155.8 (TiCH=*C*H), 201.5 (CO-*cis*), 205.7 (CO-*trans*), 243.6 (TiCH=CH), 305.5 (C=W); IR (*n*-heptane): $\tilde{\nu}$(CO)[cm^{-1}] = 2050, 1980, 1920; MS (70 eV): *m/z* 697 ($M^{\oplus}$)

7c: ^{1}H NMR (270 MHz): $\delta = 1.57$ (s, 30H, $C_5(CH_3)_5$), 4.56 (s, 5H, C_5H_5), 6.72 (d, ^3J(H,H) = 9.3 Hz, 1H, =CH), 7.17 (d, ^3J(H,H) = 9.3 Hz, 1H, =CH); ^{13}C NMR (67.9 MHz): $\delta = 11.8$ (q, ^1J(C,H) = 126 Hz, $C_5(CH_3)_5$), 86.5 (d, ^1J(C,H)) = 175 Hz, C_5H_5), 123.9 (s, $C_5(CH_3)_5$), 153.8 (d, ^1J(C,H) = 156 Hz, TiCH=*C*H), 227.4 (d, ^1J(C,H) = 143 Hz, TiCH=CH), 236.3 (s, CO), 322.5 (s, Mn=C); IR (*n*-heptane): $\tilde{\nu}$(CO)[cm^{-1}] = 1918, 1852; MS (70 eV): *m/z* 548 ($M^{\oplus}$, 100%), 492 ($M^{\oplus}$ − 2CO, 20)

7d: ^{1}H NMR (500 MHz): $\delta = 1.60$ (s, 30H, $C_5(CH_3)_5$), 1.96 (s, 3H, $(C_5H_4)CH_3$), 4.42, 4.55 (t, J(H,H) = 1.9 Hz, each 2H, $(C_5H_4)CH_3$), 6.73 (d, ^2J(H,H) = 8.8 Hz, 1H, =CH), 7.17 (d, ^3J(H,H) = 8.8 Hz, 1H, =CH); ^{13}C{^{1}H} NMR (125 MHz): $\delta = 11.9$ ($C_5(CH_3)_5$), 124.0 ($C_5(CH_3)5$), 14.5 ($C_5H_4CH_3$), 85.8, 88.2, 101.2 ($C_5H_4CH_3$), 154.0 (TiCH=*C*H), 227.2 (TiCH=CH), 236.8 (CO), 322.6 (C=Mn); IR (*n*-heptane): $\tilde{\nu}$[cm^{-1}](CO) = 1911, 1847; MS (70 eV): *m/z* 563 ($M^{\oplus}$, 25%), 506 ($M^{\oplus}$ − 2CO, 100)

[a] NMR spectra were recorded at 25 °C; solvent C_6D_6, standard TMS.

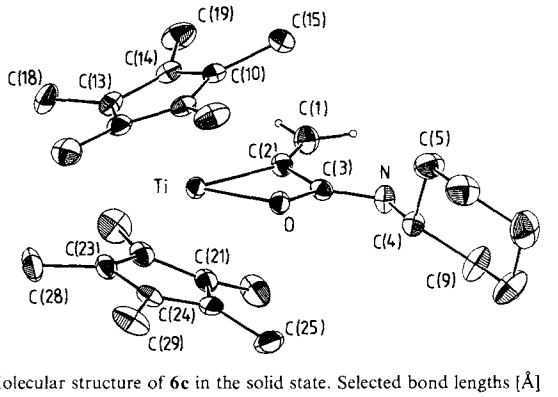

Fig. 1. Molecular structure of **6c** in the solid state. Selected bond lengths [Å] and angles [°] (Cp1 and Cp2 represent the centers of the Cp* ligands at the titanocene fragment: Ti-Cp(1) 2.09339(6), Ti-Cp(2) 2.0979(6), Ti-O 1.983(2), Ti-C(2) 2.121(3), C(2)-C(1) 1.325(4), C(1)-H1$_a$ 0.99(3), C(1)-H1$_b$ 0.95(4), C(2)-C(3) 1.477(4), C(3)-N 1.285(4), N-C(4) 1.459(4), C(4)-C(9) 1.516(4), C(3)-O 1.348(3); Cp(1)-Ti-Cp(2) 140.78, C(2)-Ti-O 67.6(1), Ti-O-C(3) 96.7(2), O-C(3)-C(2) 107.9(2), C(3)-C(2)-Ti 87.2(2), C(1)-C(2)-Ti 147.3(3), H1$_a$-C(1)-H1$_b$ 114.(3) [15].

spectrum contains an AB pattern for the CH=CH–E unit that bridges the titanium and carbon atoms, and the ^{13}C NMR spectrum shows typical $^{1}J_{C,H}$ coupling constants for methine carbon atoms (**7c**: $J = 156$, 143 Hz). The chemical shifts of the carbene carbon atoms lie in the expected low-field region [δ = 325.4 (**7a**); 305.5 (**7b**); 322.5 (**7c**); 322.6 (**7d**)].

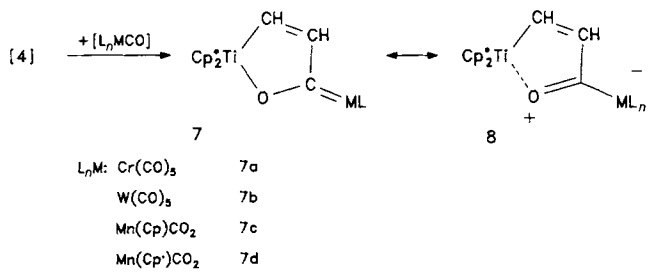

The X-ray structure analysis of **7d** confirms the presence of an almost planar metallacyclopentene unit whose C(4)–C(5) bond is 1.330(5) Å long, which corresponds to a double bond (Fig. 2).

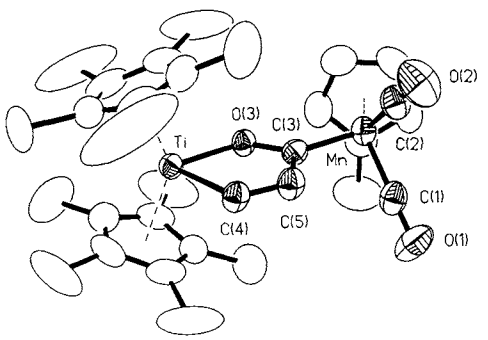

Fig. 2. Molecular structure of **7d** in the solid state. Selected bond lengths [Å] and angles [°] (Cp1 represents the center of the five-membered ring of the methylcyclopentadienyl ligand at the manganese center; Cp2 and Cp3 represent the centers of the Cp* ligands at the titanocene fragment): Mn-C(1) 1.776(3), Mn-C(2) 1.767(4), Mn-C(3), 1.915(4), Ti-O(3) 1.983(2), Ti-C(4) 2.109(3), O(1)-C(1) 1.154(5), O(2)-C(2) 1.156(5), O(3)-C(3) 1.314(4), C(3)-C(5) 1.472(5), C(4)-C(5) 1.330(5), Mn-Cp(1) 1.791, Ti-Cp(2) 2.092, Ti-Cp(3) 2.112, C(1)-MnC(2) 89.3(2), C(1)-Mn-C(3) 90.2(2), C(2)-Mn-C(3) 90.2(2), Cp(1)-Mn-C(2) 126.3, Cp(1)-Mn-C(3) 124.6, Mn-C(1)-O(1) 178.2(4), Mn-C(2)-O(2) 178.8(3), Mn-C(3)-O(3) 125.2(3), Cp(2)-Ti-Cp(3) 141.6, Ti-O(3)-C(3) 122.4(2), Ti-C(4)-C(5) 112.4(3), O(3)-Ti-C(4) 125.0(2), Cp(2)-Ti-O(3) 106.2, Cp(2)-Ti-C(4) 103.7, Cp(3)-Ti-O(3) 105.6, Cp(3)-Ti-C(4) 103.9, O(3)-C(3)-C(5) 125.0(2) [15].

The bond lengths are characteristic for Fischer carbene complexes.[10a] The relatively long Ti–O bond typical for oxatitanacycles (1.983(2) Å) lies opposite a shorter C3–O distance (1.314(4) Å). Similar bonding relationships occur in the cycloaddition product from [Cp$_2^*$Ti(C$_2$H$_4$)] and [Re$_2$(CO)$_{10}$] (Ti–O 2.02(2) Å).[10b] The Ti–O distance in **7d** is larger than in titanium alkoxide [Cp$_2$Ti(Cl)(OCH$_2$CH$_3$)] (Ti–O: 1.855(2) Å)[11] or the titanium enolate [Cp$_2$Ti-(OCH=CH$_2$)$_2$] (Ti–O 1.903(2) Å).[12] Thus the ionic resonance structure **8** may be invoked in the description of **7**.

The carbene complexes **7** are thermally remarkably stable and decompose in the solid state only above 200 °C. In the mass spectra the molecular ions are observed, and their fragmentation patterns are characterized primarily by a stepwise and complete loss of all CO ligands.

The formation of the five-membered metallacycles **7** instead of the four-membered rings **6** corresponds formally to a cycloaddition of an acetylene intermediate to a C–O bond of the metal carbonyl. The transformation of vinylzirconocenes take a similar course.[13] A vinylidene–acetylene rearrangement would correspond to the behavior of the free vinylidene, which very rapidly transforms into the tautomeric acetylene because of the low energy barrier.[14] At present we are investigating the mechanistic aspects of the formation of **7**, such as participation of primary cycloaddition products similar to **6** or to vinyl intermediates **5**.

Experimental Procedure

5: Compound **3** (500 mg, 1.3 mmol) was heated in a sublimation apparatus under vacuum (10^{-3} Torr) to 120–140 °C. The product **5** sublimed as dark green substance. Yield 320 mg (71%).

6a: Compound **3** (500 mg, 1.3 mmol) was dissolved in *n*-heptane (30 mL) and heated in a dry CO_2 atmosphere at 80 °C for 45 min. After concentration at −10–0 °C, red-violet, light-sensitive crystals of **6a** formed. Yield 450 mg (86%).

6b and **6c**: Heating **3** (500 mg, 1.3 mmol) and O=C=C[C(CH$_3$)$_3$]$_2$ (250 mg, 1.6 mmol) or **3** (370 mg, 1 mmol) and cyclohexylisocyanate (150 µL, 1.2 mmol) in *n*-heptane at 70–90 °C for 3 h, followed by filtration and concentration of the solution at 0–10 °C gave, respectively, golden yellow crystals of **6b** (450 mg, 65%, m.p. 143 °C) and red crystals of **6c** (352 mg, 75%, m.p. 128–131 °C).

7a–d: Heating **3** (500 mg, 1.3 mmol) and a stoichiometric amount of [M(CO)$_6$] (M = Cr, W) or [LMn(CO)$_3$] (L = Cp, Cp') in *n*-heptane (100 mL) at 90–100 °C for 4 h, followed by separation of the small amount of insoluble precipitate from the still warm solution by filtration, gave after crystallization at −35 °C red (for **7a**, **b**) or orange-yellow crystals (for **7c**, **d**). Yields (%): for **7a** 30, **7b** 45, **7c** 60, and **7d** 65. All compounds gave correct elemental analyses (C, H, N, Ti).

Received: September 9, 1992 [Z 5564 IE]
German version: *Angew. Chem.* **1993**, *105*, 281

[1] H. Werner, *Nachr. Chem. Tech. Lab.* **1992**, *40*, 435–444.
[2] M. I. Bruce, *Chem. Rev.* **1991**, *91*, 197–257.
[3] a) These results form part of the habilitation thesis of R. Beckhaus, "*Zur Chemie von Vinylverbindungen elektronenarmer Übergangsmetalle*", Technische Hochschule, Merseburg, **1989**; b) R. Beckhaus, K.-H. Thiele, D. Ströhl, *J. Organomet. Chem.* **1989**, *369*, 43–54.
[4] R. Beckhaus, S. Flatau, S. Trojanov, P. Hofmann, *Chem. Ber.* **1992**, *125*, 291–299.
[5] J. D. Meinhart, E. V. Anslyn, R. H. Grubbs, *Organometallics* **1989**, *8*, 583–589.
[6] B. J. J. van de Heisteeg, G. Schat, O. S. Akkerman, F. Bickelhaupt, *J. Organomet. Chem.* **1986**, *310*, C25–C28.
[7] P. Binger, P. Müller, R. Wenz, R. Mynott, *Angew. Chem.* **1990**, *102*, 1070–1071; *Angew. Chem. Int. Ed. Engl.* **1990**, *29*, 1037–1038.
[8] P. Binger, P. Müller, R. Benn, R. Mynott, *Angew. Chem.* **1989**, *101*, 647–648; *Angew. Chem. Int. Ed. Engl.* **1989**, *28*, 610–611.
[9] G. A. Luinstra, J. H. Teuben, *Organometallics* **1992**, *11*, 1793–1801.
[10] a) K. H. Dötz, H. Fischer, P. Hofmann, F. R. Kreissl, U. Schubert, K. Weiss, *Transition Metal Carbene Complexes*, Verlag Chemie, Weinheim, **1983**; b) K. Mahima, K. Jyodoi, A. Ohyshi, H. Takaya, *J. Chem. Soc. Chem. Commun.* **1986**, 1145–1146.
[11] J. C. Huffman, K. G. Moloy, J. A. Marsella, K. G. Caulton, J. Am. Chem. Soc. **1980**, *102*, 3009–3014.
[12] M. D. Curtis, S. Thaneder, W. M. Butler, *Organometallics* **1984**, *3*, 1855–1859.
[13] R. Beckhaus, K.-H. Thiele, *J. Organomet. Chem.* **1989**, *368*, 315–322.
[14] M. M. Gallo, T. P. Hamilton, H. F. Schaefer III, *J. Am. Chem. Soc.* **1990**, *112*, 8714–8719.
[15] X-ray structure analyses: **6c**: red cubic crystals, size 0.3 × 0.4 × 0.5 mm, composition $C_{29}H_{43}NOTi$, M_r = 469.557 g mol^{-1}, a = 9.904(3), b = 13.780(3), c = 19.342(4) Å, β = 95.07(2)°, V = 2629(2) Å^3, Z = 4, ρ_{calcd} = 1.1834 g cm^{-3}, F_{000} = 1016.0; space group $P2_1/c$ (no. 14); Enraf–Nonius CAD4 diffractometer, 5943 measured reflections, 2799 independent reflections with $I > 3\sigma$, $2\theta_{max} = 54°$; 297 refined parameters; R = 0.048, R_w = 0.051.
7d: red-brown cubic crystals, size not determined, composition $C_{31}H_{39}O_3MnTi$, M_r = 562.5 g mol^{-1}, cell constants from least-squares refinement of 25 centered reflections, a = 1148.4(4), b = 1179.5(3), c = 1198.2(3) pm, α = 66.29(3), β = 70.35(2), γ = 82.47(2)°, V = 1399 × 10^6 pm^3, Z = 2, ρ_{calcd} = 1.335 g cm^{-3}, F_{000} = 592; space group $P\bar{1}$ (no. 2). Enraf–Nonius CAD4 diffractometer, 5181 measured reflections (h(0/13), k(−14/15), l(−14/14), $2\theta_{max} = 50°$), 4913 independent reflections of which 4155 with $I > 2.0\,\sigma$ used for refinement; empirical absorption correction with 6 reflections (μ = 7.4 cm^{-1}). 419 parameters refined; R = 0.043, R_w = 0.042; residual electron density + 0.31, −0.21 e Å^{-3}. One of the two Cp* rings of the titanocene fragment is disordered (20%) and was refined in two positions. Further details of the crystal structure investigation may be obtained from the Fachinformationszentrum Karlsruhe, Gesellschaft für wissenschaftlich-technische Information mbH, D-W-7514 Eggenstein-Leopoldshafen 2 (FRG) on quoting the depository number CSD-56734, the names of the authors, and the journal citation.

η^6-(1,2-Dioxocyclobutabenzene)tricarbonylchromium(0): Starting Material for Double Anionic Oxy-Cope Rearrangements under Very Mild Conditions**

By *Michael Brands, Richard Goddard, Hans G. Wey,* and *Holger Butenschön**

Reactions of arenetricarbonylchromium(0) complexes[1] are of great interest in organic synthetic chemistry. We recently found an efficient access to **1**, the tricarbonylchromium(0) complex of 1-oxocyclobutabenzene.[2] The alcohols which are readily accessible from this complex undergo distal[2] and proximal[3] four-membered ring openings under very mild conditions. Because of the increased reactivity of

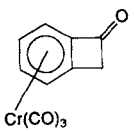

1

the keto group as a result of the coplanarity with the coordinated, electron-deficient arene ring, we have also investigated the corresponding complex **3** of 1,2-dioxocyclobutabenzene. We report here on the synthesis and structure of this complex, and some of its reactions, including double anionic oxy-Cope rearrangements, which occur under remarkably mild conditions.

Attempts at the direct complexation of 1,2-dioxocyclobutabenzene with hexacarbonylchromium(0) were unsuccessful, thus **3** was prepared similar to **1** by hydrolytic cleavage of the easily accessible diacetal **2** (Scheme 1).[4] The

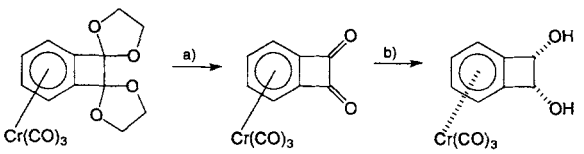

2 **3** **4**

Scheme 1. a: concentrated HCl, 2 h, 25 °C, 80%; b: $Li[AlH_4]$, Et_2O, −78 °C, 90%, *dr* 88%.

treatment of **2** with concentrated hydrochloric acid gave the diketone complex **3** as a burgundy red powder in 80% yield. (NMR data of all new compounds are given in Table 1.) Crystals of **3** suitable for an X-ray structure analysis[5] were obtained from a mixture of dichloromethane and diethyl ether (Fig. 1). In the asymmetric unit are two independent molecules with similar structures.

The annelated four-membered ring in **3** is bent away from the plane of the arene ring toward the chromium atom by about 8° (±1°).[6] The large value (8°)—usually 2 to 3°—can be understood as a result of a stronger coordination of C2a and C6a to the metal center, which leads to a reduction of the ring strain.

Table 1. ^1H NMR data of **3**–**7**, **9**, and **10**.

3: (200 MHz, [D$_8$]THF): δ = 5.76 + 6.26 (AA'BB' system, 2 × 2H, 3(6)-H, 4(5)-H)
4: (200 MHz, [D$_8$]THF): δ = 4.42 (br, 2H, OH), 4.96 [s, 2H, 1(2)-H], 5.25 + 5.48 (AA'BB' system, 2H, 3(6)-H, 4(5)-H)
5: (200 MHz, [D$_6$]acetone): δ = 1.95 (m, 4H, 7(8)-H), 2.73 (m, 4H, 6(9)-H), 5.87 (m, 4H, 1(4)-H, 2(3)-H)
6: (200 MHz, [D$_6$]acetone): δ = 5.33 (dd, 1H, *cis*-8-H, $^3J_{7,cis\ 8}$ = 10.6 Hz, $^2J_{trans\ 8,cis\ 8}$ = −0.8 Hz), 5.40 (dd, 1H, *trans*-8-H, $^3J_{7,trans\ 8}$ = 17.4 Hz), 5.63 (dd, 1H, 4-H or 5-H, J = 5.8, 6.1 Hz), 5.83 (dd, 1H, 4-H or 5-H), 5.87 (d, 1H, 3-H or 6-H), 6.07 (d, 1H, 3-H or 6-H), 6.22 (dd, 1H, 7-H).
7: (200 MHz, [D$_6$]acetone): δ = 1.21 (d, 3H, 11-H, $^3J_{6,11}$ = 6.6 Hz), 1.85 (m, 2H, 7-H or 8-H), 2.10 (m, 2H, 7-H or 8-H), 2.48-2.73 (m, 2H, 9-H), 3.02 (m, 1H, 6-H), 5.60 (d, 1H, 1-H or 4-H, J = 6.1 Hz), 5.74 (dd, 1H, 2-H or 3-H, J = 6.4 Hz), 6.01 (dd, 1H, 2-H or 3-H), 6.08 (d, 1H, 1-H or 4-H)
9: (400 MHz, CD_2Cl_2): δ = 1.15 (d, 3H, 14-H, $^3J_{10,14}$ = 6.8 Hz, 1.39 (s, 3H, 13-H), 1.61-1.70 (m, 2H, 12-H), 1.77 (m, 1H, 10-H or 11-H), 1.87-1.98 (m, 2H, 10-H or 11-H), 5.44 (m, 1H, aromat.), 5.68 (m, 3H, aromat.)
10: (200 MHz, CD_2Cl_2): δ = 0.10 (s, 18H, 11-(13)-H), 1.39 (s, 6H, 12(14)H, 14-H), 2.13 + 3.21 (AA'BB' system, 2 × 2H, *endo*-7(8)-H, *exo*-7(8)-H), 5.38 + 5.81 (AA'BB' system, 2 × 2H, 1(4)-H, 2(3)-H)

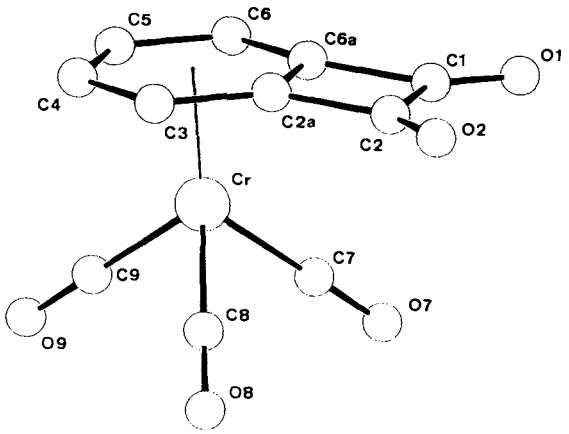

Fig. 1. Structure of **3** [5]. The asymmetric unit contains two independent molecules of similar structure, only one of the two is shown here. Selected average bond lengths [Å]: C1–C2 1.566(7), C1–C6a 1.507(6), C2–C2a 1.504(6), C2a–C6a 1.418(3), Cr–C2a 2.152(23), Cr–C3 2.221(4), Cr–C4 2.208(8), Cr–C5 2.205(14), Cr–C6 2.222(2), Cr–C6a 2.159(16).

Compound **3** reacts with $Li[AlH_4]$ in diethyl ether already at −78 °C to give the diol **4** in 90% yield.[7] The diastereomeric excess (88%) is somewhat less than for the reduction of **1**; in addition to **4**, a small amount of the *trans* reduction product is obtained. The mild conditions and the high yield indicate an increase in the reactivity of the keto group in **3** as a result of the coordination to $Cr(CO)_3$.[2, 8]

If the diketone complex **3** is treated with seven equivalents of vinylmagnesium bromide or better vinyllithium in THF at −78 °C, not the expected double Grignard adduct is obtained after hydrolysis at −78 °C, but the tricarbonylchromium(0) complex **5** of benzoannelated cyclooctan-1,4-dione (87%, m.p. 145–146 °C, Scheme 2) as a result of a double anionic oxy-Cope rearrangement.

Through the double nucleophilic attack from the side of the ligand which faces away from the chromium,[9] the synperiplanar orientation of the two vinyl groups favorable for the double anionic oxy-Cope rearrangement is achieved. This reaction is one of the few double anionic oxy-Cope rearrangements known so far;[10, 11] the reaction occurs at

[*] Priv.-Doz. Dr. H. Butenschön,[+] Dipl.-Chem. M. Brands, Dr. R. Goddard, Dr. H. G. Wey
Max-Planck-Institut für Kohlenforschung
Kaiser-Wilhelm-Platz 1, D-W-4330 Mülheim an der Ruhr 1 (FRG)

[+] New address:
Fachbereich 9, Organische Chemie der Universität-Gesamthochschule Gauss-Strasse 20, D-W-5600 Wuppertal 1 (FRG)

[**] This work was supported by the Fonds der Chemischen Industrie. M. B. thanks the Verband der Chemischen Industrie, H. G. W. the Max-Planck-Gesellschaft for a doctoral grant, H. B. the Deutsche Forschungsgemeinschaft for a Heisenberg Fellowship. Our thanks also go to the Director of the Max-Planck-Institut für Kohlenforschung, Prof. Dr. G. Wilke, for his supporting interest. We thank C. Wirtz for recording the NMR spectra.

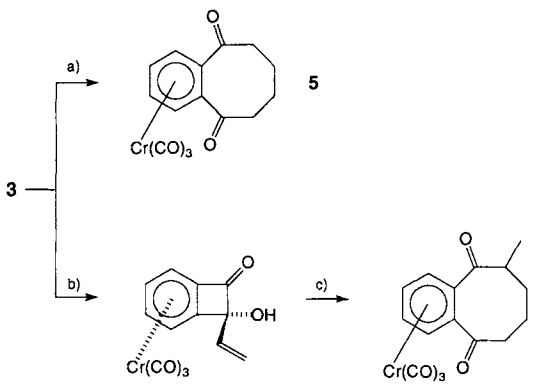

Scheme 2. a: 1) 7 equiv vinyllithium, −78 °C, 2) H_3O^+, −78 °C, 87%; b: 1) 2 equiv vinylmagnesium bromide, −78 °C, 2) H_3O^+, −78 °C, 90%; c: 1) 6 equiv 2-propenyllithium, −78 °C, 2) H_3O^+, −78 °C, 60%.

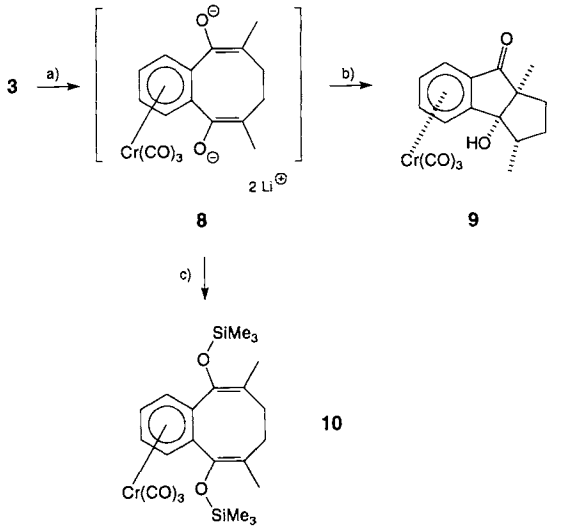

Scheme 3. a: 1) 7 equiv 2-propenyllithium, −78 °C; b: H_3O^+, −78 °C, 48%; c: trimethylsilyl trifluoromethanesulfonate, −40 °C, 70%.

−78°, to our knowledge the lowest temperature so far observed for such a rearrangement, room temperature is usual. In contrast to most known examples,[10, 11] it is not necessary to isolate the diallyl diol; the diolate is produced directly by the double addition of the alkenyl metal reagent to the 1,2-dione. This is the first example of the formation of a cyclooctadione derivative by a double anionic oxy-Cope rearrangement, in which the hydrolysis product itself can be isolated, without immediately undergoing a subsequent reaction (aldol reaction, see below). Remarkably, the reaction of the noncomplexed 1,2-dioxocyclobutabenzene, under the reaction conditions used for **3**, only leads to a complex mixture of products, which contains the ligand of **5** at best in trace amounts.

If **3** is treated with only two equivalents of vinylmagnesium bromide, the adduct **6**[7] is obtained diastereoselectively in 90% yield. This opens up the possibility of obtaining products from "mixed" double anionic oxy-Cope rearrangements by the reaction of **6** with another alkenyl Grignard or alkenyllithium reagent. The corresponding reaction of **6** with 2-propenyllithium gave the methyl-substituted product **7** as a single diastereomer in over 60% yield. In order to investigate this more closely, **3** was treated with a sevenfold excess of 2-propenyllithium with the intention of obtaining a symmetrical, double methyl-substituted derivative. After hydrolysis of the enolate **8** at −78 °C, however, the tricyclic complex **9**, which results from an intramolecular aldol addition, was obtained diastereomerically pure in 48% yield together with two by-products[12] (1:1). Following characterization by NMR spectroscopy, the relative configuration was determined by an X-ray crystal structure analysis.[13] Thereafter protonation of an enolate group occurs followed by the intramolecular nucleophilic attack on the carbonyl group formed, preferably from the side of the bicyclic ligand which faces away from the metal atom.

In order to show that **9** really forms via the dienolate **8** as the primary product of the double anionic oxy-Cope rearrangement, **8** was trapped with trimethylsilyl trifluoromethanesulfonate. The bis(trimethylsilyl enol ether) **10** (70%) thus obtained should be suitable for the introduction of further substituents in the α positions.[14]

We have showed that by the coordination of 1,2-dioxocyclobutabenzene to a tricarbonylchromium(0) unit, double anionic oxy-Cope rearrangements are made possible under very mild conditions, which lead to differently substituted benzocyclooctan-1,4-dione complexes. We are currently investigating the extent to which this reaction could provide an alternative access to eight-membered ring compounds by reactions with other alkenyllithium reagents.[15]

Experimental Procedure

All operations were carried out under an inert atmosphere.

3: Concentrated HCl (125 mL) was added to **2** (2.99 g, 8.4 mmol) [4] at 0 °C and then vigorously stirred for 2 h at 20 °C. The reaction was monitored by thin-layer chromatography (diethyl ether/pentane 2:1, SiO_2). During the reaction the mixture turned deep red and at the end of the reaction time it was red brown. Compound **3** precipitated partly as a burgundy-red solid. The mother liquor was removed with a capillary and retained. The residue was washed with water, dried under vacuum, washed twice with a little cold pentane, and dried once again under vacuum. 1.56 g of **3** remained. The mother liquor was extracted with diethyl ether, the extracts were dried over $MgSO_4$ for 2 h, and the solvent was removed under vacuum. The residue was washed with a little cold pentane and then dried under vacuum. 0.23 g of **3** was obtained. Thus, total yield of **3** was 1.79 g, (6.7 mmol, 80%) (m.p. 132.2 °C).

5: A solution of **3** (304 mg, 1.13 mmol) in diethyl ether/THF (100 mL) (1:1) was added dropwise over 4 h at −78 °C to a 0.5 M solution of vinyllithium in THF (15.8 mL, 7.9 mmol); the reaction mixture immediately turned black after the first few drops had been added. The mixture was stirred for 16 h at −78 °C and subsequently hydrolyzed at −78 °C with saturated aqueous ammonium chloride solution. The red solution obtained was extracted with water, and the organic phase was dried over $MgSO_4$. After the solvent had been removed under vacuum, **5** was obtained as a red oil. Following purification by column chromatography (SiO_2, diethyl ether/pentane 5:1) and crystallization from diethyl ether/pentane **5** was obtained (320 mg, 0.99 mmol, 87%; m.p. 145–146 °C).

Received: September 19, 1992 [Z 5585 IE]
German version: *Angew. Chem.* **1993**, *105*, 285

[1] A. Solladié-Cavallo, *Adv. Met. Org. Chem.* **1989**, *1*, 99–133; M. Uemura, *ibid.* **1991**, *2*, 195–245; S. G. Davies, S. J. Coote, C. L. Goodfellow, *ibid.* **1991**, *2*, 1–57.

[2] H. G. Wey, H. Butenschön, *Angew. Chem.* **1991**, *103*, 871–873; *Angew. Chem. Int. Ed. Engl.* **1991**, *30*, 880–881.

[3] M. Brands, H. G. Wey, H. Butenschön, *J. Chem. Soc. Chem. Commun.* **1991**, 1541–1542.

[4] H. G. Wey, P. Betz, I. Topalovic, H. Butenschön, *J. Organomet. Chem.* **1991**, *411*, 369–374.

[5] Crystal structure analysis of **3**: formula $C_{11}H_4O_5Cr$, $M_r = 268.1$, crystal dimensions $0.28 \times 0.28 \times 0.28$ mm, $a = 7.988(1)$, $b = 19.900(1)$, $c = 13.031(1)$ Å, $\beta = 99.20(1)°$, $V = 2044.9$ Å^3, $\rho_{calcd} = 1.74$ g cm^{-3}, $\mu = 10.94$ cm^{-1}, $F(000) = 1072$ e, $Z = 8$, crystal system monoclinic, space group $P2_1/c$ (no. 14), Enraf-Nonius CAD4 diffractometer, $\lambda = 0.71069$ Å, method of measurement ω–2θ, 5017 measured reflections ($\pm h$, + k, + l), $[(\sin\theta/\lambda)_{max}$ 0.65 Å^{-1}, 4671 independent reflections and 3887 observed reflections with $[I > 2\sigma(I)]$, 339 refined parameters, H atom positions calculated and included in the least-squares refinement, $R = 0.034$, $R_w = 0.044$ $[w = 1/\sigma^2(F_o)]$, maximum residual electron density 0.30 eÅ^{-3}. Further details of the crystal structure investigation may be obtained from the Fach-

informationszentrum Karlsruhe, Gesellschaft for wissenschaftlich-technische Information mbH, D-W-7514 Eggenstein-Leopoldshafen 2 (FRG) on quoting the depository number CSD-56753, the names of the authors, and the journal citation.
[6] a) K. O. Hodgson, K. N. Raymond, *Inorg. Chem.* **1973**, *12*, 458–466; b) M. Elian, M. M. L. Chen, D. M. P. Mingos, R. Hoffmann, *ibid.* **1976**, *15*, 1148–1155; c) D. M. P. Mingos, *Adv. Organomet. Chem.* **1977**, *15*, 1–51.
[7] By analogy to the reduction product of **1** [2] and to a Grignard adduct of **1**, for which a crystal structure analysis exists [13], it is assumed that the nucleophilic attack occurs from the side of the ligand which faces away from the chromium atom. The compounds **6**, **7**, and **9** were obtained as racemates.
[8] M. P. Cava, D. R. Napier, R. J. Pohl, *J. Am. Chem. Soc.* **1963**, *85*, 2076–2080.
[9] Compound **3** reacts under the same conditions with an excess of EtMgBr to give the *cis*-di-Grignard adduct. By analogy to the reduction of **1**, it is assumed that the nucleophilic attack occurs from the side which faces away from the metal, and that the hydroxy groups thus stand on the side of the coordination to $Cr(CO)_3$.
[10] L. A. Paquette, *Angew. Chem.* **1990**, *102*, 642–660; *Angew. Chem. Int. Ed. Engl.* **1990**, *29*, 609–629.
[11] a) P. Geetha, C.A.M.A. Huq, K. Rajagopalan, S. Swaminathan, *Tetrahedron Lett.* **1982**, *23*, 569–570; b) S. Saito, T. Yamamoto, M. Matsuoka, T. Moriwake, *Synlett* **1992**, 239–240; c) R. W. Alder, D. Colclough, F. Grams, A. G. Orpen, *Tetrahedon* **1990**, *46*, 7933–7940.
[12] The spectroscopic data of the by-products are compatible with the eight-membered ring compounds accessible from **8** by protonation (yield 11%).
[13] M. Brands, H. Butenschön, R. Goddard, unpublished.
[14] M. T. Reetz, *Angew. Chem.* **1982**, *94*, 97–109; *Angew. Chem. Int. Ed. Engl.* **1982**, *21*, 97–109.
[15] a) Compare with G. Kaupp, *Angew. Chem.* **1992**, *104*, 435; *Angew. Chem. Int. Ed. Engl.* **1992**, *31*, 422–424, and references therein.; b) N. A. Petasis, M. A. Patane, *Tetrahedron* **1992**, *48*, 5757–5821.

S-Glycosylated Cyclic Peptides**

By *Manfred Gerz, Hans Matter,* and *Horst Kessler**

The biological importance of naturally occurring glycopeptides[1–3] stimulates the idea to use modified glycopeptide structures for pharmaceutical purposes. One goal of chemical modification is to increase metabolic stability. The peptide moiety might be protected against proteolysis caused by exopeptidases by cyclization, whereas the glycosidic bond between the saccharide and peptide can be stabilized by using thioglycosidic analogues. The higher chemical stability of *S*-glycosylated amino acids was proven by Baran and Drabarek.[4] Cyclic *S*-glycopeptides are preferably prepared by peptide synthesis with *S*-glycosylated amino acid building blocks, because glycosylation of cyclic peptides may be difficult for conformational reasons. A comparison of the spatial structure of a cyclic *S*-glycopeptide with analogous *O*- and *N*-glycopeptides permits investigations of peptide–sugar interactions.

Here we describe a new method of preparation of *S*-glycosylated cysteine derivatives (Table 1) and their use in the synthesis of the cyclic glycosylated hexapeptide *cyclo*-(-D-Pro^1-Phe^2-Ala^3-Cys^4(*β*-D-galactopyranosyl)-Phe^5-Phe^6-). The conformation of the peptide in [D_6]DMSO was determined by 2D NMR spectroscopy in combination with molecular dynamics (MD) calculations, and is compared to the structure of analoguous hexapeptides.

Previous syntheses of *S*-glycosyl cysteine derivatives[4–6] yielded products not bearing orthogonal protection of amino, carboxyl, and hydroxyl functions that consequently were not suitable for the synthesis of peptides. An exception is the *S*-glycosylation of *C*-terminally unprotected Fmoc amino acids under Lewis acid catalysis recently published by Eloffson et al.[7] These building blocks were employed in the solid-phase synthesis of linear *S*-glycopeptides.

For the preparation of a *tert*-butoxycarbonyl(BOC)-protected glycosylated cysteine with free carboxyl function *N,N'*-bis(*tert*-butoxycarbonyl)cystine was first reduced by triethylphosphane[8] (92%), and the resulting cysteine derivative treated with sodium hydride to form the S,O-dianion, which reacts with 2,3,4,6-tetra-*O*-acetyl-α-D-galactopyranosyl bromide (acetobromogalactose) to give the *S*-glycosylamino acid in 66% yield (method A). A better yield was obtained by reduction and deprotonation in one step (method B): reduction of *N,N'*-bis(*tert*-butoxycarbonyl)-cystine with sodium in liquid ammonia directly gives the S,O-dianion, which after removal of the ammonia was dissolved in dry THF and treated with acetobromogalactose. The *β*-thiogalactoside was formed in 75% yield (Scheme 1).

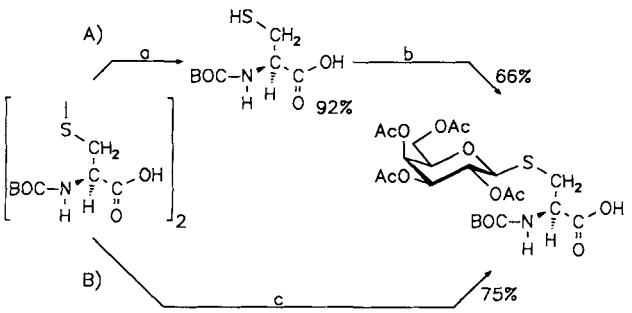

Scheme 1. a) Triethylphosphane, THF/water (9:1); b) 1. NaH, THF, 2. acetobromogalactose; c) 1. Na, liquid ammonia, 2. acetobromogalactose, THF.

Problems in the purification of products with free carboxyl functions prompted us to attempt the synthesis of *S*-glycosylated *C*- and *N*-terminally protected cysteine derivatives which could be purified easily by chromatography on silicagel. Ogawa et al. converted *β*-configurated peracetyl sugars to methyl-*β*-thioglycosides by treatment with Bu_3SnMe and $SnCl_4$.[9] Analogously Z-Cys(Bu_3Sn)-OBzl (Z = benzyloxycarbonyl), prepared by azeotropic stannylation of Z-Cys-OBzl with $(Bu_3Sn)_2O$ in toluene in a Dean–Stark trap,[10] affords the *β*-configurated product in 51% yield when reacted with pentaacetyl-*β*-D-galactose under $SnCl_4$ catalysis. Application of Koenigs–Knorr[11] conditions with $HgBr_2$ as promotor and acetobromogalactose as glycosyl donor raises the yield to 60%. The glycosylation yield depends significantly on the size of the *N*-terminal protecting group: The BOC group totally inhibits glycosylation even when the small allyl group is used to protect the carboxyl group (difficulties with glycosylation of BOC-protected amino acids have already been described by Paulsen et al.[12]). In contrast, the benzyloxycarbonyl group allows the glycosylation of the thiol function in good yields, especially when the carboxyl group is protected as an allyl ester. The preparation of the allyl ester was carried out by esterification of an *N,N'*-diprotected cystine derivative with allyl bromide by using the cesium carbonate procedure[13] and subsequent cleavage of the disulfide bond by triethylphosphane. Introduction of a disaccharide donor does not reduce the yield, as was demonstrated by the reaction of Z-Cys-OAll with acetobromocellobiose (85% yield). However, the tripeptide Boc-Phe-Cys-Ala-OBzl did not react under these conditions, probably because the reactivity of the thiol function was

[*] Prof. Dr. H. Kessler, Dr. M. Gerz, Dr. H. Matter
Organisch-chemisches Institut der Technischen Universität München
Lichtenbergstrasse 4, D-W-8046 Garching (FRG)

[**] This work was supported by the Fonds der Chemischen Industrie and the Deutsche Forschungsgemeinschaft.

reduced by hydrogen bonding. Only β-thioglycosides were isolated, as expected for sugars bearing an acetate function in the 2-position. The results of the glycosylation experiments are summarized in Table 1.

Table 1. Glycosylation yields of different thiolamino acid derivatives under Koenigs–Knorr conditions with $HgBr_2$ promotor.

Acceptor	Donor	Yield [%]
Z-Cys(Bu_3Sn)-OBzl	pentaacetyl-β-D-galactose	51 [a]
Z-Cys(Bu_3Sn)-OBzl	acetobromogalactose	60
Z-Cys-OBzl	acetobromogalactose	71
BOC-Cys-OBzl	acetobromogalactose	-
BOC-Cys-OAll	acetobromogalactose	-
BOC-D-Pen-OAll [b]	acetobromogalactose	-
BOC-Phe-Cys-Ala-OBzl	acetobromogalactose	-
Z-Cys-OAll	acetobromogalactose	77
Z-Cys-OAll	acetobromocellobiose	85

[a] $SnCl_4$ as promotor; [b] D-Pen = D-penicillamine (β,β-dimethylcysteine). Z = benzyloxycarbonyl.

These *S*-glycosylcysteine derivatives were used for the synthesis of the cyclic hexapeptide *cyclo*-(-D-Pro^1-Phe^2-Ala^3-Cys^4(β-D-galactopyranosyl)-Phe^5-Phe^6-). As depicted in Scheme 2, the synthesis was performed by [3 + 3] fragment condensation, cyclization (azidodiphenylphosphate/$NaHCO_3$), and deacetylation (NaOMe/MeOH). The compound is an analogue of the previously described *N*- and *O*-glycopeptides[14, 15] *cyclo*-(-D-Pro^1-Phe^2-Ala^3-Xaa^4-Phe^5-Phe^6-) [with Xaa = Gln(*N*-2-acetamido-2-deoxy-β-D-glycopyranosyl) or Ser(*O*-β-lactopyranosyl)].

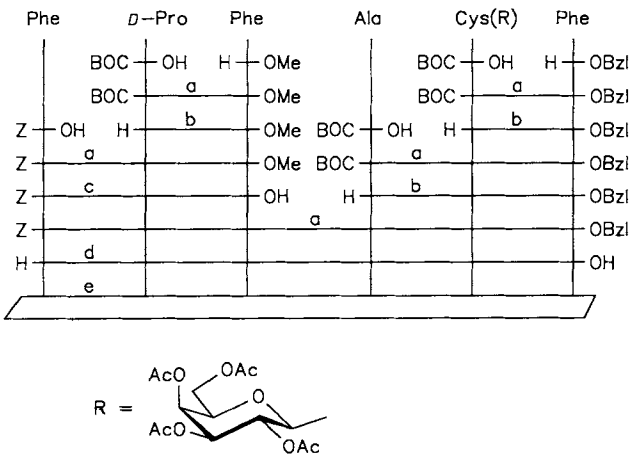

Scheme 2. Synthesis of the cyclic glycopeptide *cyclo*-(-D-Pro^1-Phe^2-Ala^3-Cys^4(β-tetra-*O*-acetylgalactopyranosyl)-Phe^5-Phe^6-). a) EtN=C=N-$(CH_2)_3NMe_2$·HCl (EDCl), 1-hydroxy-1*H*-benzotriazole (HOBt), THF/dimethylacetamide (2:1); b) trifluoroacetic acid (TFA), CH_2Cl_2; c) 1 N NaOH, isopropanol; d) H_2, Pd/C, methanol; e) azidodiphenylphosphate, $NaHCO_3$, dimethylformamide (DMF). Z = benzyloxycarbonyl.

For the structure determination of the deprotected glycopeptide all ^1H and ^{13}C resonances were assigned by modern NMR spectroscopic techniques (see refs. [14–16] for methods). Experimental parameters including homo- and heteronuclear coupling constants as well as 43 NOE values were extracted from 1D and 2D spectra. The distances obtained by quantitative evaluation of the NOEs were used as restraints in MD calculations. For the GROMOS force field additional parameters for the thioglycosidic bond were applied: C–S distance of 181 pm and C–S–C angle of 100.2° were taken from an X-ray analysis of a β-thioglycoside.[17] The force constants used were the same as those for *O*-glycosides.

The averaged structure (with additional energy minimization to eliminate physically unrealistic artifacts) of the 70 ps MD trajectory in DMSO as solvent[16] is shown in Figure 1.

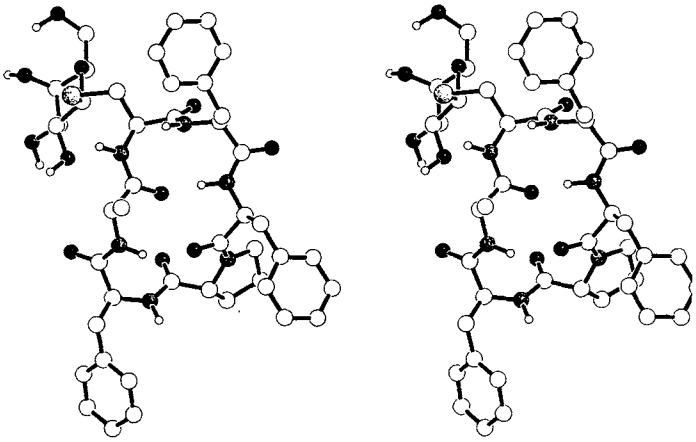

Fig. 1. Stereoplot of the major conformation of the cyclic glycopeptide *cyclo*-(-D-Pro^1-Phe^2-Ala^3-Cys^4(β-D-galactopyranosyl)-Phe^5-Phe^6-) in [D_6]DMSO. This structure is obtained by averaging over the last 70 ps of a 100 ps restrained MD simulation in DMSO using the GROMOS package [18]. Experimental restraints were derived from 600 MHz NOESY data. The calculation follows the protocol previously described [14]. The side chain conformations are shown as the dominating rotamers derived from NMR spectroscopy.

Two transannular hydrogen bonds (Ala^3-NH···OC-Phe^6 and Phe^6-NH···OC-Ala^3) were observed consistent with two standard β-turns: a stable βII′ turn with D-Pro^1 in the i + 1 position and a βI turn about Xaa-Phe^5. A detailed analysis of the NOEs in the latter, however, provides strong evidence for the existence of an equilibrium between two types of turns (βI, βII), as was previously found in several analogous peptides.[14, 15] The hydrogen bond pattern is not changed by glycosylation of the amino acid in the i + 1 position, which can be seen from the comparison with the non-glycosylated peptide *cyclo*-(-D-Pro^1-Phe^2-Ala^3-Ser^4-Phe^5-Phe^6-) in the crystal and in solution.[15]

In conclusion, we have found that *N*-, *O*-, or *S*-glycosylation in the i + 1 position of a β-turn does not influence the structure and dynamics of the peptide moiety. The comparison of a series of glycosylated hexapeptides leads to the conclusion that it should be possible to modify the pharmacokinetic and pharmacodynamic properties of a peptide by introduction of glycosylated amino acids in suitable positions, while maintaining the biological activity of the parent compound. Hence, one can use the "recognition function" of the saccharide substituents for drug targeting as a physiological address (interaction with sugar-binding receptors) to prepare drugs which develop specific activities at defined loci. The chemical and enzymatic stability of the thioglycopeptides presented here should be of importance for the realization of this concept.

Received: October 7, 1992 [Z 5614 IE]
German version: *Angew. Chem.* **1993**, *105*, 311

[1] R. C. Hughes, *Glycoproteins*, Chapman and Hall, New York, **1983**.
[2] H. Kunz, *Angew. Chem.* **1987**, *99*, 297–311; *Angew. Chem. Int. Ed. Engl.* **1987**, *26*, 294–308, and references therein.
[3] H. Paulsen, *Angew. Chem.* **1990**, *102*, 851–867; *Angew. Chem. Int. Ed. Engl.* **1990**, *29*, 823–838, and references therein.
[4] E. Baran, S. Drabarek, *Pol. J. Chem.* **1978**, *52*, 941–946.

[5] M. L. P. Monsigny, D. Delay, M. Vaculik, *Carbohydr. Res.* **1977**, *59*, 589–593.
[6] K. C. Nicolaou, A. Chucholowski, R. E. Dolle, J. L. Randall, *J. Chem. Soc. Chem. Commun.* **1984**, 1155–1156.
[7] M. Eloffson, B. Walse, J. Kihlberg, *Tetrahedron Lett.* **1991**, *32*, 7613–7616.
[8] F. Urpí, J. Vilarrasa, *Tetrahedron Lett.* **1986**, *27*, 4623–4624.
[9] T. Ogawa, M. Matsui, *Carbohydr. Res.* **1977**, *86*, C17–C21.
[10] S. David, S. Hanessian, *Tetrahedron* **1985**, *41*, 643–663, and references therein.
[11] H. Paulsen, *Angew. Chem.* **1982**, *94*, 184–201; *Angew. Chem. Int. Ed. Engl.* **1982**, *21*, 155–197, and references therein.
[12] C. Kolar, U. Knödler, F. R. Seiler, H.-W. Fehlhaber, V. Sinnwell, M. Schultz, H. Paulsen, *Liebigs Ann. Chem.* **1987**, 577–581.
[13] S.-S. Wang, B. F. Gisin, D. P. Winter, R. Makofske, I. D. Kulesha, C. Tzougraki, J. Meienhofer, *J. Org. Chem.* **1977**, *42*, 1286–1290.
[14] H. Kessler, H. Matter, G. Gemmecker, A. Kling, M. Kottenhahn, *J. Am. Chem. Soc.* **1991**, *113*, 7550–7563.
[15] H. Kessler, H. Matter, G. Gemmecker, M. Kottenhahn, J. W. Bats, *J. Am. Chem. Soc.* **1992**, *114*, 4805–4818.
[16] D. F. Mierke, H. Kessler, *J. Am. Chem. Soc.* **1991**, *113*, 9466–9470.
[17] A. Atkinson, J. R. Ruble, G. A. Jeffrey, *Acta Crystallogr. Sect. B* **1981**, *37*, 1465–1467.
[18] W. F. van Gunsteren, H. J. C. Berendsen, *Groningen Molecular Simulation (GROMOS) Library Manual*, Biomos, Groningen, **1987**.

Two New High-Pressure Modifications of NaOH**

By *Horst P. Beck** and *Gunda Lederer*

NaOH crystallizes in three forms, depending on the temperature; listed in order of increasing temperature they are the anti-Tl I type, then a variant that is a deformation thereof, and finally a NaCl-analogous structure ("NaCl I"), in which the OH particles appear isotropic as a result of dynamic disorder.[1–3] Studies under pressure with differential thermal analysis indicate that above 1–2 GPa at least one further form exists.[4] However, no structural information on the high pressure phases was available, because they could not be quenched and thus could only be characterized in situ.[5]

Use of a diamond anvil cell with a heating device in a special X-ray diffractometer[6, 7] enabled us to define the boundaries in the p,T field of two high-pressure modifications, to determine their structures, and to refine one with the Rietveld method. Furthermore, our new techniques yield such good diffraction data even under pressure that the usual structure solution and refinement procedures may be applied.

Figure 1 shows the extended phase diagram for NaOH in which the domains of the known normal pressure modifications are also plotted. At higher temperatures ($T > 70\,^{\circ}C$) and under pressure ($p > 1.3$ GPa), another phase with the NaCl structure ("NaCl II") forms. It appears that its p,T stability range remains distinctly separate from that of NaCl I even at higher temperatures. The bonding in the two phases is therefore different.[8] We propose that this high-pressure phase is a NaCl type with static disorder, which cannot transform continuously into the type with dynamic disorder because the required activation volume for free rotation under pressure can no longer be accommodated.

At higher pressures and lower temperatures the domain of the other new modification, "NaOH II", borders on that of the NaCl II phase. The NaOH II structure[9] is depicted in Figure 2. It is best described as a deformation variant of the NiAs type in which the Na atoms deviate most from the ideal positions in the aristotype. Because of the high density under these conditions, the OH groups have no chance of rotating freely. We find them in defined orientations, and this forces the cations to shift from their positions. Although the sites of the hydrogen atoms have not yet been detected experimentally, the analysis of the cation shifts shows that the positive ends of the OH dipoles probably point between two Na ions related by translation perpendicular to the plane viewed in Figure 2 rather than toward an adjacent OH group. The suspected orientation of the OH groups is included in the figure.

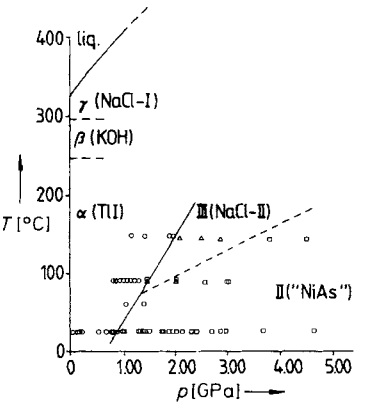

Fig. 1. p,T diagram for NaOH. Normal pressure phases are indicated by Greek letters, high pressure phases by Roman numerals; the assigned structural type appears in brackets.

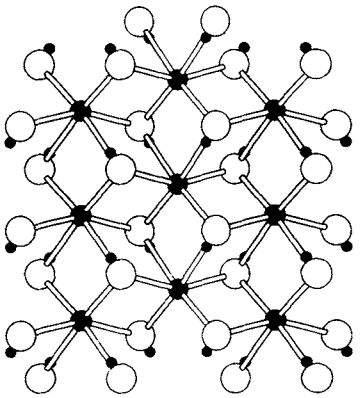

Fig. 2. Structure of the high-pressure phase NaOH II viewed along [001]. Solid circles represent Na, large open circles O, and small solid circles the presumed hydrogen positions.

The diversity of the structural chemistry of the alkali metal hydroxides is governed by the quotient of the radii and the variety of orientations for the OH groups, which leads to hydrogen bonds of different strength. Since their contribution to the energy is relatively small, slight temperature changes can lead to a reorganization of the OH dipoles. Under high-pressure conditions the possibility of hydrogen bond formation becomes less important than the drive to minimize the volume and the interatomic repulsion. To achieve a more dense packing, the phase is forced into an electrostatically less favorable constellation.

[*] Prof. Dr. H. P. Beck, Dr. G. Lederer
Fachrichtung Anorganische und Analytische Chemie und
Radiochemie der Universität
Im Stadtwald, D-W-6600 Saarbrücken 11 (FRG)

[**] This work was supported by the Deutsche Forschungsgemeinschaft and the Fonds der Chemischen Industrie.

Received: September 23, 1992 [Z 5592IE]
German version: *Angew. Chem.* **1993**, *105*, 292

[1] H. Stehr, *Z. Kristallogr. Kristallgeom. Kristallphys. Kristallchem.* **1967**, *125*, 332.
[2] H.-J. Bleif, H. Dachs, *Acta Crystallogr. Sect. A* **1982**, *38*, 470.
[3] C. W. F. T.Pistorius, *Progr. Solid. State Chem.* **1978**, *11*, 1.
[4] H. Jacobs, J. Koekelkorn, T. Tacke, *Z. Anorg. Allg. Chem.* **1985**, *531*, 119.
[5] A paper by M. P. Krobok, P. G. Johansen, and W. B. Holzapfel (*J. Phys.: Condens. Matter* **1992**, *4*, 8141) published after the submission of this communication reports on a study of the same region of the phase diagram with IR and Raman methods and confirms the results presented here.
[6] R. Haberkorn, Dissertation, Universität Erlangen-Nürnberg, **1988**.
[7] G. Lederer, Dissertation, Universität Erlangen-Nürnberg, **1992**.
[8] The NaCl I phase at normal pressure and 320 °C has the same molar volume as the NaCl III phase at 2 GPa and 120 °C. A continuous transition from NaCl III to NaCl I on increasing the temperature and subsequently reducing the pressure would certainly lead to a distinct increase in volume. The volume changes can only be explained if along the described route a domain of another modification is traversed, which must form by contraction from the phase of type NaCl III on raising the temperature. Such a process implies that $\Delta U > 0$. In fact, differential thermal analysis [3] indicates that other phases exist in the region of the p,T field in question, but their structures are unknown.
[9] Orthorhombic, *Pbcm*, $a = 314.8(1)$, $b = 595.8(2)$, $c = 612.8(2)$ pm, Rietveld refinement with program DWB [10] from digitalized data from a powder diagram in the region $12° < 2\theta < 27°$, recorded with $Mo_{K\alpha 1}$ radiation (quartz monochromator), Gauss profile function with half-width correction; Na(4c): $x = 0.359(2)$; O(4d): $x = 0.800(3)$, $y = 0.043(2)$; $R/Rw/R_{Bragg} = 4.6/7.1/15.5$. Further details of the crystal structure investigation may be obtained from the Fachinformationszentrum Karlsruhe, Gesellschaft für wissenschaftlich-technische Information mbH, D-W-7514 Eggenstein-Leopoldshafen 2 (FRG) on quoting the depository number CSD-56766, the names of the authors, and the journal citation.
[10] D. B. Wiles, A. Sakthivel, R. A. Young, *Program DBW 3.2S V87.11 for Rietveld Analysis of X-ray and Neutron Powder Diffraction Patterns*, Georgia Institute of Technology, Atlanta **1987**.

A Simple Route from Glucal to Cerny Epoxides

By *Gilbert Lauer* and *Franz Oberdorfer**

Ring opening of the conformationally fixed "Cerny epoxides" **1** and **2**[1, 2] takes place regio- and stereoselectively with formation of the corresponding Fürst–Plattner products in which the resulting substituents are aligned in *trans*-diaxial fashion. Numerous selectively substituted pyranoses, which are valuable chiral starting materials for enantiospecific syntheses, can be obtained by using this strategy.

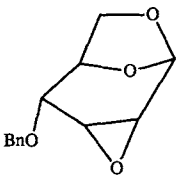

1

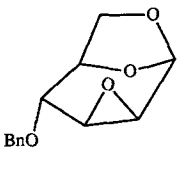

2

Our interest in these diastereomeric compounds came about for the following reason: they force the hexoses out of the stable $^1C_4$ conformation into the ^5H_O conformation, which is higher in energy and easily attacked by nucleophiles, thus enabling a variety of applications. Compounds **1** and **2** are, therefore, ideal starting materials for the selective formation of pyranose derivatives functionalized at C2, C3 or C4. The preparation of such compounds by other methods is usually tedious.

[*] Dr. F. Oberdorfer, Dipl.-Chem. G. Lauer
Deutsches Krebsforschungszentrum
Abteilung Radiochemie und Radiopharmazeutische Chemie
Im Neuenheimer Feld 280, D-W-6900 Heidelberg (FRG)

The known syntheses of **1** and **2** start either from levoglucosan,[2] which is either commercially available but expensive, or only accessible by pyrolysis or from dimers of acrolein.[3] These syntheses are laborious, multistep processes requiring costly separations and providing less than satisfactory yields. As a result, it is hardly surprising that the obvious synthetic potential of the Cerny epoxides has been little used.

We describe here an elegant, short, and new synthetic route to **1** and **2**, which provides both diastereomeric oxiranes without difficulty and in good yield from the readily available tri-*O*-acetyl-D-glucal (Scheme 1).

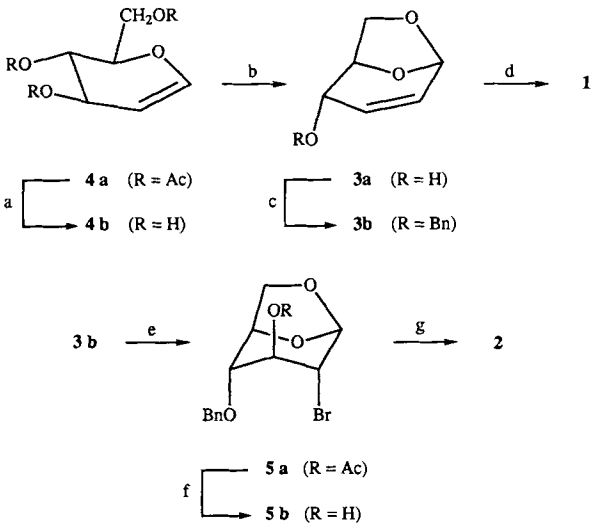

Scheme 1. Synthesis of **1** and **2** (room temperature, if not stated otherwise). a: **4a**, CH_3OH/LiOH, 10 min, according to Zemplen et al.[4] gave 94% **4b** (colorless needles); b: **4b**, THF, $CuSO_4$ (anhydrous, 7 equiv), reflux, 6 h, gave 42% **3a** (colorless crystals) after chromatography [5]; c: **3a**, DMF, NaH, benzyl bromide, 15 min, according to Bovin et al.[6] gave 61% **3b** (colorless, thin oil); d: **3b**, *m*CPBA (excess), CH_2Cl_2, reflux, 24 h, gave 54% **1** (faintly yellow oil) [7]; e: **3b**, AcOBr, CCl_4, ice bath, 25 min, gave 62% **5a** (colorless, viscous oil) [8]; f: **5a**, K_2CO_3 (2 equiv), CH_3OH/H_2O, 9/1, 3 h, gave **5b** in quantitative yield (colorless oil, slowly separating as crystals when cooled) [9]; g: **5b**, K_2CO_3, CH_3OH/H_2O 9/1, 5 d, gave 85% **2** (colorless crystals) [7].

A retrosynthetic analysis showed that the key compound 1,6-anhydro-2,3-dideoxy-β-D-*erythro*-hex-2-enose **3a**—a derivative of pseudoglucal that is generally obtained from the pyrolysis products of the ivory nut (*phytelephas macrocarpa*) or from cellulose[10]—should also be accessible from glucal **4b** by an intramolecular vinylogous substitution. We have now been able to carry out this reaction, not previously observed with the complex glucal chemistry. The primary alcohol group in glucal was activated for the intramolecular reaction in a dipolar aprotic medium in the presence of a considerable excess of anhydrous $CuSO_4$. Under these conditions compound **4b** underwent condensation with allylic rearrangement to give the bridged glucoside **3a** (42% yield). 2-(D-Glycero-1,2-dihydroxyethyl)furan was formed, as expected, as a side product (22% yield) that was easily separated from **3a** by column chromatography.[5] After subsequent benzylation in the presence of NaH in dimethylformamide (DMF) **1** and **2** could be prepared as desired by selective epoxidation of the double bond in **3b**.

The *exo* oxirane **1** was obtained easily from **3b** by a Prilezaev reaction with an excess of almost anhydrous *m*-chloroperbenzoic acid (*m*CPBA) (54% yield). This method has already proven to be reliable with similar bicyclic unsaturated acetals.[11] The isomeric *endo* oxirane **2** was formed in only

small amounts (< 5%). The *exo*/*endo* ratio did not depend on the steric requirements of the substituents on C4 ($OSiPh_3$, $OSiBn_3$, $OSitBuMe_2$). The *exo*-directing influence arose exclusively from the effect of the 1,6-anhydro configuration. This observation has been confirmed with related monocyclic pseudoglucal derivatives. The oxirane ring was preferentially oriented *trans* to the alkoxy substituent on C1.[12]

The *endo* oxirane **2** was formed stereoselectively from the same starting material if a formally analogous hypobromite was used for the electrophilic attack on the double bond in **3b** instead of a peracid. The addition of acetylhypobromite (AcOBr) to **3b** in CCl_4 gave the hitherto unknown compound **5a** with a *trans*-diaxial arrangement of the newly introduced substituents. Compound **5a** could be isolated from the reaction mixture by chromatography in 62% yield.[8] The bromohydrin **5b** was obtained quantitatively by mild, selective hydrolysis of the acetyl group with K_2CO_3 in aqueous methanol (90%). After complete reaction (about 3 h, monitored with TLC), **5b** was converted (without workup) in a slow (5 d) and clean reaction into the *endo* oxirane **2**.[9] The latter was obtained in 85% yield, based on **5a**.

In the fully analyzed ^{1}H NMR spectrum of compound **5a**[8] all vicinal ^3J couplings are less than 2 Hz, with the exception of $^3J(5,6_{exo})$, 5.8 Hz. The relatively high values for ^4J and ^5J (0.7–1.7 Hz) are quite remarkable and indicate a largely coplanar arrangement of the bonds. These results corroborate an exclusive and rigid $^1C_4$ conformation for the acetate, in which all ring protons are in equatorial positions and the substituents are in an antiperiplanar arrangement. An equilibrium with the possible $B_{0,3}$ conformation (equatorial substituents) in **5a** does not exist, at least not at room temperature. The considerable shift of the resonance frequency of proton H3 to lower field ($\Delta\delta$ ca. 2) in comparison with that in **1** and **2** is caused by the deshielding effect of the carbonyl group of the axial acetyl substituent on C3. This observation confirms the correct position of the acetyl group and our original assumption that the addition of hypobromite to **3b** takes place regio- and stereoselectively. Thus, **5a** is predestined for ring closure to the *endo* oxirane.

The most notable aspect of our new synthetic route for the Cerny epoxides is the evident simplicity of the methods employed. Laborious protecting group chemistry is not needed for preparing the synthetic building blocks **1**, **2**, **3**, and **5** from tri-*O*-acetyl-D-glucal. These compounds, which were previously unknown or could only be prepared by complicated routes, now provide an easy and generally accessible entry to hexoses selectively substituted at C2 to C4.

Received: September 10, 1992 [Z 5566 IE]
German version: *Angew. Chem.* **1992**, *104*, 271

[1] M. Cerny, J. Stanek Jr., *Adv. Carbohydr. Chem.* **1977**, *34*, 107–164. In addition to numerous examples of the chemistry of Cerny epoxides, this review includes a more detailed explanation of the conformation nomenclature used in the text. Text books on the chemistry of sugars also provide similar information. See, for example, J. Lehmann, *Chemie der Kohlehydrate*, Thieme, Stuttgart, **1976**. The capital letters *C* (chair), *H* (half-chair), *B* (boat), etc. indicate the ring conformation of the pyranose. The indices indicate the numbers of the ring atoms (carbohydrate notation), those which lie above (in tbe direction of the observer, superscript) or those below (away from the observer, subscript) a reference plane. The corresponding reference planes for each of the conformations is formed out of four ring atoms. The index "O" designates the oxygen atom in the pyranose ring.

[2] M. Cerny, T. Trnka, P. Beran, J. Pacak, *Collect. Czech. Chem. Commun.* **1969**, *34*, 3377–3382; M. Cerny, J. Stanek, J. Pacak, *ibid.* **1969**, *34*, 849–856; T. Trnka, M. Cerny, *ibid.* **1971**, *36*, 2216–2225; J. Pecka, M. Cerny, *ibid.* **1973**, *38*, 132–142; J. Stanek, M. Cerny, *Synthesis* **1972**, 698–699; T. B. Grindley, G. J. Reimer, J. Karlovec, R. G. Brown, M. Anderson, *Can. J. Chem.* **1987**, *65*, 1065–1071.

[3] T. P. Murray, U. P. Singh, R. K. Brown, *Can. J. Chem.* **1974**, *49*, 2132–2138; K. Ranganayakulu, U. P. Singh, T. P. Murray, R. K. Brown, *ibid.* **1974**, *52*, 988–992; K. Ranganayakulu, R. K. Brown, *J. Org. Chem.* **1974**, *39*, 3941–3943.

[4] G. Zemplen, A. Gerecs, I. Hadacsy, *Ber. Dtsch. Chem. Ges.* **1936**, *69*, 1827–1829.

[5] MPLC: Silica gel 60 LiChroprep 15–25 μm, 350 × 15 mm, 17 mL min^{-1} CH_2Cl_2/ethyl acetate (EE) 70/30, RI detection, t_R = 18.5 min for the furan (k' = 2.7), t_R = 13.5 min for **3a** (k' = 1.7); HPLC: LiChrospher Si 100/II 5 μm, 250 × 4 mm, 1 mL min^{-1} CH_2Cl_2/ethyl acetate 70/30, RI detection, t_R = 8.2 min for **3a** (k' = 1.6). ^{1}H NMR Ref. [3, 10]; ^{13}C NMR (62.89 MHz, $CDCl_3$, 300 K): **3a**: δ = 130.16 (C=*C*, C2), 126.28 (*C*=C, C3), 95.52 (C1), 76.82 (C4), 67.2 (C5), 62.56 (C6).

[6] N. V. Bovin, S. E. Zurabyan, A. Y. Khorlin, *Carbohydr. Res.* **1981**, *98*, 25–35.

[7] ^{1}H NMR (250 MHz, $CDCl_3$, 300 K, TMS): **1**: Lit. [3]; **2** (identical with that of a genuine sample, for which we thank Prof. Dr. J. Pacak, Prague): δ = 7.37 (m, 5H; C_6H_5), 5.71 (dddd, $^3J(1,2)$ = 3.1, $^4J(1,3)$ = 0.7, $J(1,6exo)$ = $J(1,6endo)$ = 0.6 Hz, 1H; H1), 4.73 (s, 2H; CH_2Ph), 4.51 (dddd, $^3J(5,6exo)$ = 6.6, $^3J(5,6endo)$ = 2.1, $^3J(5,4)$ = 1.1, $^4J(5,3)$ = 1.6 Hz, 1H; H5), 3.71 (ddd, $^2J(6exo,6endo)$ = 7.2 Hz, 1H; H6*exo*), 3.67 (ddd, 1H; H6*endo*), 3.66 (dd, $^3J(4,3)$ = 0, $^4J(4,2)$ = 0.8 Hz, 1H; H4), 3.45 (ddd, $^3J(2,3)$ = 3.8 Hz, 1H; H2), 3.19 (ddd, 1H; H3); ^{13}C NMR (62.89 MHz, $CDCl_3$, 300 K): **1**: δ = 137.4–127.96 (Ph), 97.2 (C1), 75.51 (C5), 72.02 (C4), 70.79 (CH_2Ph), 65.55 (C6), 47.94 (C2), 47.65 (C3); **2**: analogous to **1**; MS (70 eV), high resolution: **1** and **2**: 234.088448 (calc. 234.089209 $C_{13}H_{14}O_4$), *m/z* 234 (M^+, 9%), 91 (100).

[8] ^{1}H NMR (250 MHz, $CDCl_3$, 300 K, TMS): **5a**: δ = 7.37 (m, C_6H_5), 5.62 (ddddd, $^3J(1,2)$ = 1.5, $^4J(1,3)$ = 1.3, $^5J(1,4)$ = 0.7, $J(1,5)$ = 0.4, $J(1,6exo)$ = 0.5, $J(1,6endo)$ = 0.3 Hz, 1H; H1), 5.34 (dddd, $^3J(3,2)$ = $^3J(3,4)$ = 1.3, $^4J(3,5)$ = 1.7 Hz, 1H; H3), 4.77 (d, ^2J = 12.4 Hz, 2H; CH_2Ph), 4.62 (dddddd, $^3J(5,6exo)$ = 5.8, $^3J(5,6endo)$ = 1.1, $^3J(5,4)$ = 1.9, $^5J(5,2)$ = 0.6 Hz, 1H; H5), 3.88 (ddd, $^2J(6exo,6endo)$ = 7.5 Hz, 1H; H6*exo*), 3.61 (ddd, 1H; H6*endo*), 3.46 (dddd, $^4J(4,2)$ = 1.4 Hz,m 1H; H4), 3.09 (dddd, 1H; H2), 2.09 (s, 3H; CH_3); ^{13}C NMR (62.89 MHz, $CDCl_3$, 300 K): **5a**: δ = 169.29 (C=O), 137.35–127.94 (Ph), 101.16 (C1), 74.7 (C5), 74.36 (C4), 71.1 (CH_2Ph), 70.87 (C3), 65.36 (C6), 43.75 (C2), 20.91 (CH_3); MS (70 eV), high resolution: **5a**: 356.026413 (calc. 356.025943 $C_{15}H_{17}O_5Br$), *m/z* (M^+, 5%), 91 (100); **5b**: 314.017066 (calc. 314.016916 $C_{13}H_{15}O_4Br$), *m/z* 314 (M^+, 63.5%), 91 (100). Chromatography: **5a**: silica gel 40–63 μm, 250 × 20 mm, petroleum ether (PE)/EE 75:25.

[9] Neither the addition product **5a** nor the bromohydrin **5b** had to be isolated. The yield of **2**, based on **3b**, was more than 53% in this case. In order to stop the reaction at the stage of the bromohydrin **5b** (after ca. 3 h with K_2CO_3), consumption of **5a** was followed by TLC (silica gel, petroleum ether/acetone 70/30, molybdatophosphoric acid as indicator; R_f **5a**: 0.49, R_f **5b**: 0.43).

[10] Previous syntheses of **3a**: F. Shafizadeh, R. H. Furneaux, T. T. Stevenson, *Carbohydr. Res.* **1979**, *71*, 169–191 (from levoglucosenone); P. Köll, T. Schultek, R. W. Rennecke, *Chem. Ber.* **1976**, *109*, 337–344 (from levomannosane); the pyrolytic yields amount to a few percent. For *rac*-**3a** see ref. [3].

[11] F. Sweet, R. K. Brown, *Can. J. Chem.* **1968**, *46*, 2289–2298.

[12] The epoxidation of a monocyclic, 2,3-unsaturated α-methylglycoside with *m*CPBA gave more than 95% of the *trans* (relative to the methoxy substituents) oriented ("*endo*") oxirane: F. Sweet, R. K. Brown, *Can. J. Chem.* **1968**, *46*, 2283–2288.

Total Synthesis of (−)-Pyrimidoblamic Acid and Deglycobleomycin A_2**

By *Dale L. Boger,** *Royce F. Menezes,* and *Takeshi Honda*

The bleomycins are a family of glycopeptide antitumor antibiotics that possess clinically useful activity thought to be mediated by their metal-dependent oxidative cleavage of duplex DNA.[1] Bleoxane, a clinically employed antineoplas-

[*] Prof. D. L. Boger, R. F. Menezes, T. Honda
Department of Chemistry, The Scripps Research Institute
10666 North Torrey Pines Road, La Jolla, CA 92307 (USA)

[**] This work was supported by the National Institutes of Health (CA 42056). We thank Q. Dang for the development of the synthesis of **7** (see ref. [6]) and Dr. T. Doyle of Bristol-Myers Squibb for samples of bleoxane from which an authentic sample of bleomycin A_2 and deglycobleomycin A_2 was obtained.

tic drug, is derived from natural sources, and is composed of a mixture of bleomycins of which bleomycin A_2 (70%) and bleomycin B_2 (20%) are the major constituents. Consequently bleomycin A_2,[2] its naturally occurring congeners,[3] its degradation products and semisynthetic derivatives,[4] and synthetic analogues[5, 6] have been the subject of extensive examination. Herein, we detail an efficient, diastereocontrolled total synthesis of (−)-pyrimidoblamic acid (**2**)[7] and deglycobleomycin A_2 (**1**)[2] by an approach applicable to the preparation of the naturally occurring bleomycins and structural analogues. The key elements of the approach to (−)-pyrimidoblamic acid include a one-step preparation of the functionalized pyrimidine nucleus **5** employing the inverse-electron-demand Diels–Alder reaction[8] of 2,4,6-tris(ethoxycarbonyl)-1,3,5-triazine (**3**)[9] with propionamidine hydrochloride (**4**), and a diastereoselective imine addition reaction constituting the first reported stereocontrolled introduction of the C2 acetamido side chain.

Treatment of **3** with **4** (100 °C, dimethylformamide (DMF), 72 h, 80%) provided pyrimidine **5** in a reaction cascade that proceeds by thermal tautomerization of **4** to 1,1-diaminopropene and its [4 + 2] cycloaddition with **3** (Scheme 1).[10] The sequential elimination of ammonia, tautomerization of the resulting imine, and retro-Diels–Alder loss of ethyl cyanoformate provide **5** directly in excellent yield. Selective reduction of the sterically more accessible and electronically more reactive C2 ethoxycarbonyl group of **5** (1.0 equiv $NaBH_4$, EtOH, 5 °C, 150 h, 70%) provided **6**.[6, 10] Oxidation of **6** (10 equiv MnO_2, CH_3CN, 84 °C, 3 h, 83%) followed by condensation of **7** with **8**[6, 10] (10 wt. equiv. 4 Å molecular sieves, CH_3CN, 25 °C, 6 h, 98–100%) afforded **9**.

Addition of the stannous (*Z*) enolate **10**, generated by treatment of the corresponding oxazolidinone[11] (1 equiv, THF, −20 °C, 1 h) with iPr_2NEt (2.2 equiv) in the presence of $Sn(OTf)_2$ (2.0 equiv), to **9** (0.5 equiv) provided a separable 87:13 mixture of the imine addition products **11a**:**11b** (THF, 0 °C, 12 h, 81–85%). The prescribed reaction conditions were derived only through considerable experimentation, and the reaction was found to proceed with a minimal number of protecting groups for the potentially reactive functionality in imine **9**. Key to the success of the diastereoselective imine addition reaction,[12, 13] which pro-

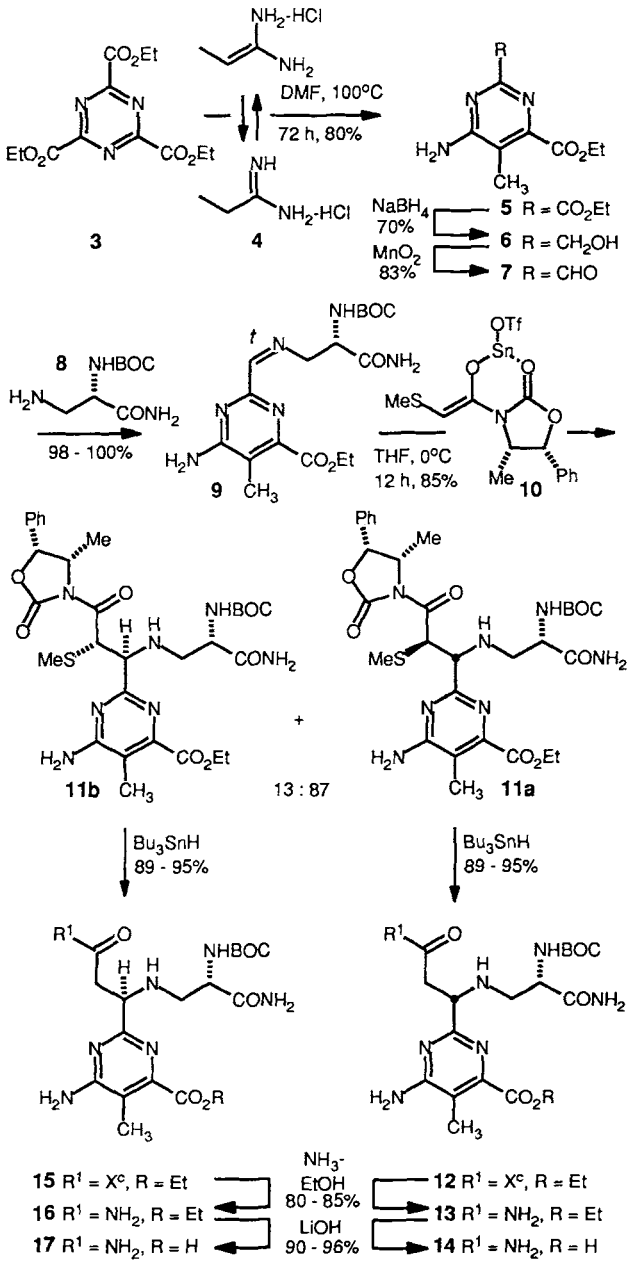

Scheme 1. Synthesis of (−)-pyrimidoblamic acid.

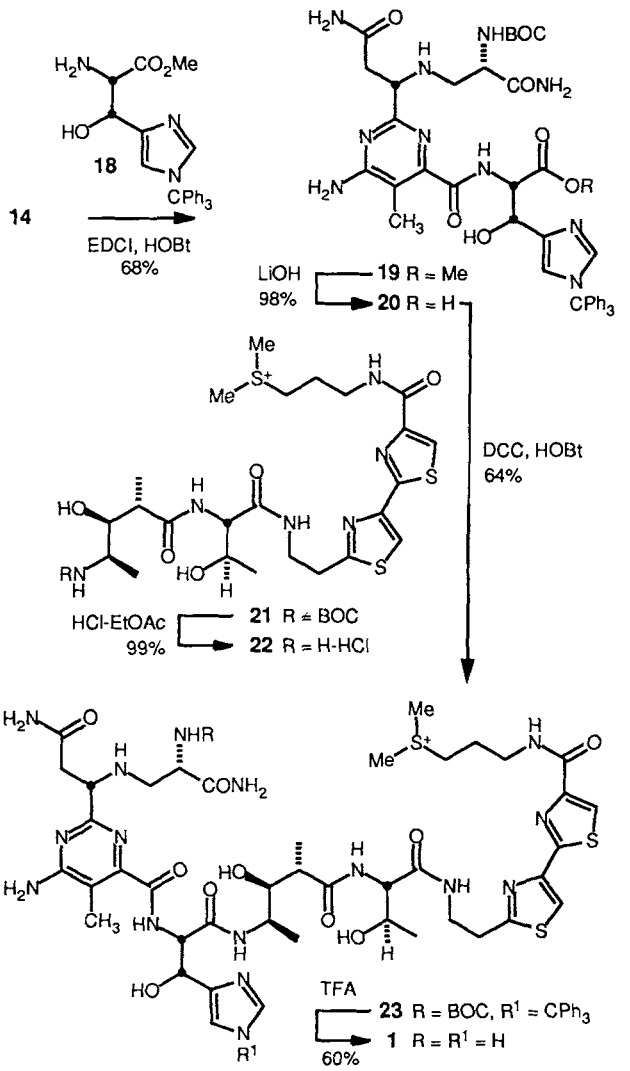

Scheme 2. Synthesis of deglycobleomycin A_2.

vides predominantly the *anti* adduct, was the use of the stannous enolate[14, 15] (2.0 equiv) in the presence of two additional equiv of $Sn(OTf)_2$. Under such conditions the major *anti*-**11a** adduct was found to slowly epimerize to *syn*-**11a** (0 °C, 12 h, 16:1 *anti*:*syn* **11a**; 0 °C, 24 h, 1.8:1 *anti*:*syn* **11a**).[16] Reductive desulfurization of the major diastereomer *anti*-**11a** as well as *syn*-**11a** (3 equiv Bu_3SnH, 0.3 equiv azobisisobutyronitrile (AIBN), C_6H_6, 80 °C, 45 min, 89–95%) followed by aminolysis of **12** (X^c = oxazolidinyl) (16% NH_3–EtOH, 0 °C, 1 h, 80–85%) provided **13**.[18]

Hydrolysis of the ethyl ester **13** (1.5 equiv LiOH, THF/H_2O/CH_3OH 3:1:1, 0 °C, 1 h, 90–95%) provided the well-characterized N^{α}-*tert*-butyloxycarbonyl (Boc) derivative of (−)-pyrimidoblamic acid **14**,[18] and acid-catalyzed deprotection (3 N HCl/EtOAc, 25 °C, 1 h, 100%) of **14** provided (−)-pyrimidoblamic acid (**2**).[18] Subjection of the minor diastereomer **11b** (>20:1 *anti*:*syn*) to the identical sequence provided **15**–**17** and *epi*-(+)-pyrimidoblamic acid.[18]

Direct coupling of **14** with erythro-N^{π}-triphenylmethyl-β-hydroxy-L-histidine methyl ester (**18**)[17] provided **19** (1.05 equiv 1-ethyl-3-[3-(dimethylamino)propyl]carbodiimide (EDCI), 1.0 equiv hydroxybenztriazole (HOBt), THF/DMF 2:1, 25 °C, 55 h, 68%), without protection of the primary or secondary amine of **14** (Scheme 2). Methyl ester hydrolysis (1.5 equiv LiOH, THF/CH_3OH/H_2O 3:1:1, 0 °C, 1.5 h, 98%) followed by *direct* coupling of **20** with synthetic tetrapeptide S (**22**)[17] provided **23**,[18] without additional protection of the adorning functionality (3 equiv dicyclohexylcarbodiimide (DCC), 1.0 equiv HOBt, 2.5 equiv $NaHCO_3$, DMF, 25 °C, 72 h, 64%). Final deprotection of **23** (trifluoroacetic acid (TFA), 25 °C, 45 min, 60%) afforded deglycobleomycin A_2 (**1**)[18] identical in all compared respects with authenic material[19] (^1H NMR and IR spectra, high-resolution mass spectrometry, TLC, HPLC).

Received: October 15, 1992 [Z 5629 IE]
German version: *Angew. Chem.* **1993**, *105*, 310

[1] M. Ohno, M. Otsuka in *Recent Progress in the Chemical Synthesis of Antibiotics* (Eds.: G. Lukacs, M. Ohno), Springer, New York, **1990**, p. 387.
[2] T. Takita, Y. Umezawa, S. Saito, H. Morishima, H. Naganawa, H. Umezawa, T. Tsuchiya, T. Miyake, S. Kageyama, S. Umezawa, Y. Muraoka, M. Suzuki, O. Otsuka, M. Narita, S. Kobayashi, M. Ohno, *Tetrahedron Lett.* **1982**, *23*, 521; Y. Aoyagi, K. Katano, H. Suguna, J. Primeau, L.-H. Chang, S. M. Hecht, *J. Am. Chem. Soc.* **1982**, *104*, 5537; T. Takita, Y. Umezawa, S. Saito, H. Morishima, H. Umezawa, Y. Muraoka, M. Suzuki, M. Otsuka, S. Kobayashi, M. Ohno, *Tetrahedron Lett.* **1981**, *22*, 671; S. Saito, Y. Umezawa, H. Morishima, T. Takita, H. Umezawa, M. Narita, M. Otsuka, S. Kobayashi, M. Ohno, *ibid.* **1982**, *23*, 529; Y. Aoyagi, H. Suguna, N. Murugesan, G. M. Ehrenfeld, L.-H. Chang, T. Ohgi, M. S. Shekhani, M. P. Kirkup, S. M. Hecht, *J. Am. Chem. Soc.* **1982**, *104*, 5237.
[3] H. Umezawa, *Pure Appl. Chem.* **1971**, *28*, 665.
[4] H. Umezawa, T. Takita, S. Saito, Y. Muraoka, K. Takahashi, H. Ekimoto, S. Minamide, K. Nishikawa, T. Fukuoka, T. Nakatani, A. Fujii, A. Matsuda in *Bleomycin Chemotherapy* (Eds.: B. I. Sikic, M. Rozenweig, S. K. Carter), Academic Press, Orlando, FL, USA, **1985**, p. 289.
[5] T. Owa, A. Haupt, M. Otsuka, S. Kobayashi, N. Tomioka, A. Itai, M. Ohno, T. Shiraki, M. Uesugi, Y. Sugiura, K. Maeda, *Tetrahedron* **1992**, *48*, 1193; B. J. Carter, K. S. Reddy, S. M. Hecht, *ibid.* **1991**, *47*, 2463; D. L. Boger, R. F. Menezes, Q. Dang, W. Yang, *BioMed. Chem. Lett.* **1992**, *2*, 261.
[6] D. L. Boger, R. F. Menezes, Q. Dang, *J. Org. Chem.* **1992**, *57*, 4333.
[7] Pyrimidoblamic acid structure determination: a) T. Yoshioka, Y. Muraoka, T. Takita, K. Maeda, H. Umezawa, *J. Antibiot.* **1972**, *25*, 625; Synthesis: b) Y. Umezawa, H. Morishima, S. Saito, T. Takita, H. Umezawa, S. Kobayashi, M. Otsuka, M. Narita, M. Ohno, *J. Am. Chem. Soc.* **1980**, *102*, 6630; c) M. Otsuka, M. Narita, M. Yoshida, S. Kobayashi, M. Ohno, Y. Umezawa, H. Morishima, S. Saito, T. Takita, H. Umezawa, *Chem. Pharm. Bull.* **1985**, *33*, 520; d) H. Arai, W. K. Hagmann, H. Suguna, S. M. Hecht, *J. Am. Chem. Soc.* **1980**, *102*, 6631; e) Y. Aoyagi, M. S. Chorghade, A. A. Padmapriya, H. Sugana, S. M. Hecht, *J. Org. Chem.* **1990**, *55*, 6291.
[8] D. L. Boger, S. M. Weinreb, *Hetero Diels–Alder Methodology in Organic Synthesis*, Academic Press, San Diego, CA, USA, **1987**.
[9] E. Ott, *Chem. Ber.* **1919**, *52*, 656; C. Grundmann, G. Weisse, S. Seide, *Justus Liebigs Ann. Chem.* **1952**, *577*, 77.
[10] D. L. Boger, Q. Dang, *Tetrahedron* **1988**, *44*, 3379; D. L. Boger, Q. Dang, *J. Org. Chem.* **1992**, *57*, 1631.
[11] D. A. Evans, M. D. Ennis, D. J. Mathre, *J. Am. Chem. Soc.* **1982**, *104*, 1737; D. A. Evans, J. Bartroli, T. L. Shih, *ibid.* **1981**, *103*, 2127.
[12] M. Otsuka, M. Yoshida, S. Kobayashi, M. Ohno, Y. Umezawa, H. Morishima, *Tetrahedron Lett.* **1981**, *22*, 2109.
[13] D. J. Hart, *Chem. Rev.* **1989**, *89*, 1447.
[14] Y. Nagao, W.-M. Dai, M. Ochiai, S. Tsukagoshi, E. Fujita, *J. Org. Chem.* **1990**, *55*, 1148; T. Yamada, H. Suzuki, T. Mukaiyama, *Chem. Lett.* **1987**, 293, **1986**, 915.
[15] The stannous enolate **10** proved more effective than the titanium enolate ($TiCl_4$, 20–30% yield, 9:1, **11a**:**11b**) which provided the same products with a comparable level of diastereoselectivity. The di-*n*-butylboronyl enolate proved ineffective.
[16] The isomers *anti*-**11a** and *syn*-**11a** were correlated through their independent conversion to **12**, and the absolute configuration at the newly established amine center was determined with the conversion of **12** to natural (−)-pyrimidoblamic acid (**2**) as well as its incorporation into deglycobleomycin A_2. The assignments of the relative configurations of *anti*-**11a** and *syn*-**11a** were determined through their independent conversion to a cyclic carbamate derived by $NaBH_4$ reduction of the acyl oxazolidinone to the primary alcohol and cyclic carbamate formation through reaction with phosgene. The axial and equatorial disposition of the thiomethyl substituent was determined by ^1H NMR coupling constants, half-width values, and 2D ^1H-^1H NMR spectroscopy. The epimerization of *anti*-**11a** to *syn*-**11a** detailed occurs at the MeS center.
[17] D. L. Boger, R. F. Menezes, *J. Org. Chem.* **1992**, *57*, 4331.
[18] For **12**: $[\alpha]_D^{25} = -19.3$ ($c = 0.29$, $CHCl_3$), m.p. 122–124 °C (EtOAc-hexane); **13**: $[\alpha]_D^{25} = -10.8$ ($c = 0.36$, EtOH), m.p. 157–159 °C (*i*PrOH-hexane), ref. [7e] $[\alpha]_D^{25} = -7.5$ ($c = 1.0$, EtOH, ref. [7e] m.p. 159–162 °C (*i*PrOH); **14**: $[\alpha]_D^{25} = -35.6$ ($c = 0.8$, H_2O), m.p. 220–222 °C (EtOH-hexane), ref. [7e] $[\alpha]_D^{28} = -33.6$ and ref. [7b] −32.8 ($c = 0.75$, H_2O), ref. [7e] m.p. 220–222 °C and ref. [7b] 223–225 °C (EtOH); (−)-pyrimidoblamic acid (**2**): $[\alpha]_D^{25} = -26.7$ ($c = 0.12$, H_2O); **15**: $[\alpha]_D^{25} = -1.1$ ($c = 0.2$, $CHCl_3$), m.p. 121–123 °C (EtOAc-hexane); **16**: $[\alpha]_D^{25} = +37.7$ ($c = 0.6$, EtOH), m.p. 69–72 °C (*i*PrOH-hexane), ref. [7e] $[\alpha]_D^{25} = +14.8$ ($c = 1.0$, EtOH), ref. [7e] m.p. 64–66 °C (*i*PrOH); **17**: $[\alpha]_D^{25} = +20.8$ ($c = 0.4$, H_2O), m.p. 221–223 °C (EtOH-hexane), ref. [7e] $[\alpha]_D^{25} = +20.8$ ($c = 0.65$, H_2O), ref. [7e] m.p. 221 °C (EtOH); *epi*-(+)-pyrimidoblamic acid: $[\alpha]_D^{25} = +20.1$ ($c = 0.1$, H_2O); **19**: $[\alpha]_D^{25} = +18.3$ ($c = 0.08$, CH_3OH); **20**: $[\alpha]_D^{25} = -12.5$ ($c = 0.07$, CH_3OH); **23**: $[\alpha]_D^{25} = -21$ ($c = 0.03$, CH_3OH).
[19] D. L. Boger, R. F. Menezes, W. Yang, *BioMed. Chem. Lett.* **1992**, *2*, 959.

Iodine Azide**

By *Peter Buzek, Thomas M. Klapötke,* Paul von Ragué Schleyer,* Inis C. Tornieporth-Oetting,* and *Peter S. White**

Only four binary iodine nitrogen compounds have been described, all of which are explosive because of the very labile N–I bond[1] and the associated thermodynamic instability: IN_3,[2a, b] $I(N_3)_2^-$,[3] NI_3,[4] and $I_2N_3^+$.[5] Although iodine azide IN_3, the first example of this class of compounds,[2a] has been well known since the beginning of this

[*] Priv.-Doz. Dr. T. M. Klapötke, Dr. I. C. Tornieporth-Oetting
Institut für Anorganische und Analytische Chemie der
Technischen Universität
Strasse des 17. Juni 135, D-W-1000 Berlin 12 (FRG)
Prof. Dr. P. von R. Schleyer, Dipl. Chem. P. Buzek
Institut für Organische Chemie der Universität
Henkestrasse 42, D-W-8520 Erlangen (FRG)
Dr. P. S. White
Department of Chemistry
University of North Carolina
Chapel Hill, NC 27599-3290 (USA)

[**] This work was supported by NATO (T. M. K. and P. S. W., CRG 920034), the Fonds der Chemischen Industrie, the Deutsche Forschungsgemeinschaft (KL 636/2-2) and the Bundesministerium für Bildung und Wissenschaft (program title "Synthesis and structural elucidation of low-molecular-weight compounds").

century, it was only in 1976 that Dehnicke succeeded in its isolation and characterization by vibrational spectroscopy.[2b] Only the $I(N_3)_2^-$ ion could be characterized structurally.[3] $[NI_3 \cdot NH_3]_n$, investigated by Jander et al.[6] by X-ray diffraction methods, consists of chains in the crystal. The N atom is surrounded by I atoms in an almost tetrahedral arrangement. The I atoms have weak covalent bonds (2.53 Å) to NH_3. $[NI_3 \cdot NH_3]_n$ is therefore not a true binary compound. We now report the synthesis of very pure crystalline IN_3, its X-ray structure analysis, and an ab initio calculation of its structure.

The preparation of IN_3 follows a modified literature method.[2a] Iodine and freshly prepared silver azide react in $CFCl_3$ according to Equation (a) to give iodine azide.

$$1.5\,AgN_3 + I_2 \xrightarrow{0\,^\circ C,\ 1\ h,\ CFCl_3} IN_3 + AgI \qquad (a)$$

After removal of AgN_3 and AgI (which are insoluble in $CFCl_3$) by decantation and subsequent evaporation of the solvent at 0 °C (14 Torr), highly pure, bright yellow iodine azide was isolated in yields up to 95% (0.5 g). Sublimation (1 h at 200 Torr N_2 pressure in the sublimation flask) gave single crystals suitable for X-ray analysis. The crude product was kept at 4 °C and the cold finger at 0 °C. The crystals, protected by careful coating with "Kel-F" $(-F_2CCFCl-)_n$, were placed on a glass fiber also coated with Kel-F and mounted immediately on the X-ray diffractometer.

According to the crystal structure analysis IN_3 forms I-N-I-N chains which are arranged along the *a* axis. The terminal N atoms of each N_3 unit (N4, N5) help comprise the chain (Fig. 1). The chains lie roughly in the IN_3 plane and form layers.[7] As expected, the N_3 units are disordered. The

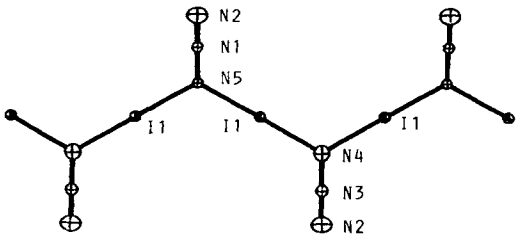

Fig. 1. Structure of IN_3 in the solid state. Selected bond lengths [Å] and angles [°], standard deviation in parentheses: I1-N4 2.264(23), I1-N5 2.30(3), N1-N5 1.19(9), N2-N3 1.05(6), N3-N4 1.28(7), N1-N2 1.09(6); N4-I1-N5 177.2(20), N2-N3-N4 174(6), I1-N4-N3 114.2(14), I1-N5-I1 121(3), I1-N5-N1 117.7(18), N2-N1-N5 171(7).

iodine atoms of different layers lie on top of each other, so that the terminal N atoms of the N_3 unit (N2) are superimposed. Thus the structure could be refined with 100% occupation probability for N2 but with only 50% for the other N atoms. The I and N2 atoms were refined anisotropically, like the remaining N atoms, the latter with only 3.5 electrons on each atom. The insignificantly larger thermal parameters of the N2 atoms are consistent with the slightly different positions of the superimposed atoms.[8f] The N–I distance (2.30 Å) in IN_3 is in remarkable agreement with that observed in the $I(N_3)_2^-$ ion (2.27 Å).[3] Furthermore both IN_3 and $I(N_3)_2^-$ appear to have bent N_3 units with clearly different N–N bond lengths.[3] Only the I-N-N bond angles vary between IN_3 (114°) and $I(N_3)_2^-$ (124°).[3]

We carried out ab initio calculations on the structure of IN_3. The results are in good agreement with the experimental bond lengths and angles of the $(IN_3)_n$ polymer (Fig. 2), as well as with the recently published results of ab initio calcu-

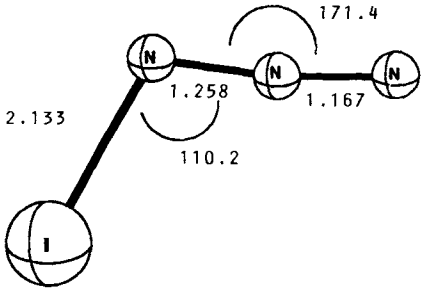

Fig. 2. MP2 optimized structure of IN_3, basis sets: see text, bond lengths in [Å] and angles in [°] [18].

lations on halogen azides.[9] While insignificant, the deviations between the experimental and theoretical values can be attributed to packing effects in the crystal as well as to the twofold coordination of the iodine atom in the chain. Calculations were carried out with the program package Gaussian 90 by using the 6-31 + G* standard basis set for N*,[10, 11] for iodine a quasi-relativistic pseudopotential[12] and a [5s5p1d]/[2s2p1d] (DZ + P) basis set[13] were employed. The geometry was fully optimized, including the effect of dynamic electron correlation, by means of second-order Møller–Plesset (MP(FU)) perturbation theory.

Vapor-pressure measurements at room temperature on solid IN_3 showed that the vapor pressure is about 2 Torr.[14] Consequently a gas-phase IR spectrum could be recorded for the first time.[15] This spectrum, as well as the solution and solid-state spectra,[2b] are in agreement with the C_s molecular symmetry and a bent I-N-N unit. Except for the I-N-N deformation vibration, which is expected to lie below the range of our measurement, all fundamental vibrations could be assigned, and a combination ($\nu_s + \nu_{as}$) and an overtone vibration ($2\nu_s$) observed.[2b, 15] An electron diffraction investigation failed because IN_3 exploded during attempted room-temperature vaporization (lower temperatures are not possible because of the relatively low vapor pressure).[16]

Caution: IN_3 is explosive.[17] The explosive nature increases with greater purity.

Received: October 19, 1992 [Z 5634 IE]
German version: *Angew. Chem.* **1993**, *105*, 289

[1] R. H. Davies, A. Finch, P. N. Gates, *J. Chem. Soc. Chem. Commun.* **1989**, 1461.
[2] a) A. Hantzsch, M. Schüman, *Ber. Dtsch. Chem. Ges.* **1990**, *33*, 522; b) K. Dehnicke, *Angew. Chem.* **1976**, *88*, 612; *Angew. Chem. Int. Ed. Engl.* **1976**, *15*, 553.
[3] U. Müller, R. Dübgen, K. Dehnicke, *Z. Anorg. Allg. Chem.* **1980**, *463*, 7.
[4] I. C. Tornieporth-Oetting, T. M. Klapötke, *Angew. Chem.* **1990**, *102*, 726; *Angew. Chem. Int. Ed. Engl.* **1990**, *29*, 677.
[5] I. C. Tornieporth-Oetting, P. Buzek, P. von R. Schleyer, T. M. Klapötke, *Angew. Chem.* **1992**, *104*, 1391; *Angew. Chem. Int. Ed. Engl.* **1992**, *31*, 1338.
[6] H. Hartl, H. Bärnighausen, J. Jander, *Z. Anorg. Allg. Chem.* **1968**, *375*, 225.
[7] Crystal data: IN_3, $M_r = 168.92$, crystal dimensions $0.25 \times 0.25 \times 0.15$ mm, $a = 4.0033(4)$, $b = 6.5596(13)$, $c = 12.809(7)$ Å, $V = 336.37(20)$ Å^3, $Z = 4$, orthorhombic, space group *Pmcb*, $\rho_{calcd} = 3.336$ Mg m^{-3}, $Mo_{K\alpha}$ ($\lambda = 0.71073$ Å) radiation, $\mu = 9.17$ mm^{-1}, 997 measured reflections, of which 343 symmetry independent, $F(000) = 293.27$, measured at $-168(2)$ °C in the $\theta/2\theta$ range, $2\theta_{max} = 50°$, all data were collected on a Rigaku diffractometer. The structure was solved and refined with 6 atoms, 25 parameters, and 280 out of 343 reflections with NRCVAX [8a–e]; $R_F = 0.070$, $R_w = 0.093$, $F_0 < 2.5\,\sigma(F)$, $R_F = \sum(F_0 - F_c)/\sum F_0$; $R_w = [\sum(w(F_0 - F_c)^2/\sum(w(F_0^2)]^{0.5}$. Further details of the crystal structure investigation may be obtained from the Fachinformationszentrum Karlsruhe, Gesellschaft für wissenschaftlich-technische Information mbH, D-W-7514 Eggenstein-Leopoldshafen 2 (FRG) on quoting the depository number CSD-56735, the names of the authors, and the journal citation.
[8] a) Structure program: E. J. Gabe, Y. Le Page, J.-P. Charland, F. L. Lee, P. S. White, *J. Appl. Cryst.* **1989**, *22*, 384; b) Scattering Factors: *Interna-*

tional Tables for X-ray Crystallography, Vol. 4, Kynoch Press, Birmingham, **1974**; c) ORTEP: C. K. Johnson, *ORTEP – A Fortran Thermal Ellipsoid Plot Program*, Technical Report ORNL-5138, Oak Ridge, Tennessee, USA **1976**; d) Missing Symmetry Treatment: Y. Le Page, *J. Appl. Crystallogr.* **1988**, *21*, 983; e) Grouping of Equivalent Reflections: Y. Le Page, E. J. Gabe, *J. Appl. Crystallogr.* **1979**, *12*, 464; f) Another conceivable disordered structure with bent chains at the I atom does not make chemical sense.

[9] M. Otto, S. D. Lotz, G. Frenking, *Inorg. Chem.* **1992**, *31*, 3647.

[10] M. J. Frisch, M. Head-Gordon, G. W. Trucks, J. B. Foresman, H. B. Schlegel, K. Raghavachari, M. A. Robb, J. S. Binkley, C. Gonzalez, D. J. DeFrees, D. J. Fox, R. A. Whiteside, R. Seeger, C. F. Melius, J. Baker, R. L. Martin, L. R. Kahn, J. J. P. Stewart, S. Topiol, J. A. Pople, *Gaussian 90, Revision F*, Gaussian Inc., Pittsburgh, PA, USA, **1990**.

[11] W. J. Here, L. Radom, P. von R. Schleyer, J. A. Pople, *Ab Initio Molecular Orbital Theory*, Wiley, New York, **1986**.

[12] P. Schwerdtfeger, M. Dolg, W. H. E. Schwarz, G. A. Bowmaker, P. D. W. Boyd, *J. Chem. Phys.* **1989**, *91*, 1762.

[13] M. Kaupp, P. von R. Schleyer, H. Stoll, H. Preuss, *J. Am. Chem. Soc.* **1991**, *113*, 6012.

[14] H. Oberhammer, Universität Tübingen, unpublished.

[15] IR (IN_3, 10 cm gas cuvette, CsI windows coated with Nujol, 2 Torr) $\tilde{\nu}$[cm^{-1}]: 3240 vw, ($\nu_{as} + \nu_s N_3$), 2350 sh (2 $\nu_s N_3$), 2330 m (2 $\nu_s N_3$), 2055 vs ($\nu_{as} N_3$), 1320 w, 1178 sh, ($\nu_s N_3$), 1170 s ($\nu_s N_3$), 648 m (δN_3), 578 m (γN_3), 360 m (νN-I).

[16] H. Oberhammer, *Molecular Structure by Diffraction Methods*, Vol. 4, The Chemical Society, London, **1976**.

[17] With $\Delta H_f^\circ(IN_3, g) = +90.2$ kcal mol^{-1} [5,18], neglecting the heat of sublimation ($\Delta H_{subl.}$: **1** = 0), for IN_3 the following thermodynamic quantities are obtained[19]: Heat of explosion (ΔH) = −490 kcal mol^{-1}, normal gas volume $V = 265$ L kg^{-1}, detonation temperature (T_{ex}) = 6000 K, specific energy $f = 60$ m t kg^{-1}, lead block expansion (standardized to 10 g) = 140 cm^3.

[18] The following non-SI units were employed: 1 Å = 10^{-10} m, 1 cal = 4.18 J, 1 H = 27.2 eV = 627.4 kcal mol^{-1}.

[19] J. Köhler, R. Meyer, *Explosivstoffe*, 7th ed., VCH Verlagsgesellschaft, Weinheim, **1991**.

Nickel(III)-Promoted DNA Cleavage with Ambient Dioxygen**

By *Chien-Chung Cheng, Steven E. Rokita,** and *Cynthia J. Burrows**

Chemical modification of nucleic acids promoted by transition metal complexes sees utility in structure elucidation, gene manipulation, and chemotherapeutics. For in vivo applications, reactions involving transition metal catalyzed DNA oxidation should rely upon the physiologically available oxidant O_2 rather than hydroperoxides and peroxyacids commonly used in vitro.[1, 2] Moderate reactivity of a metal complex with O_2 is desirable since highly reactive species might be too unstable for biological use. Only a few nickel complexes are known to activate O_2.[3] Pentaaminedioxidonickel(II) complexes are excellent candidates for this chemistry; their reactivity with O_2 has been documented by Kimura and co-workers[4] and recently reinvestigated by Martell et al.[5] Although little DNA site-specificity would be expected with these simple compounds, such specificity may not be required for many applications. In fact, most DNA-targeted drugs show little or no sequence-specificity.

[*] Prof. S. E. Rokita, Prof. C. J. Burrows, C. C. Cheng
Department of Chemistry
State University of New York at Stony Brook
Stony Brook, NY 11794-3400 (USA)

[**] Chemistry of Nickel with Nucleic Acids, Part 4. This work was supported by grants from the Stony Brook Center for Biotechnology sponsored by the New York State Science and Technology Foundation, the American Cancer Society, and the National Science Foundation (CHE-9006684). – Part 3: J. G. Muller, X. Chen, A. C. Dadiz, S. E. Rokita, C. J. Burrows, *J. Am. Chem. Soc.* **1992**, *114*, 6407.

Macrocycles **1a** and **1b** were previously reported to form pentacoordinate complexes [Ni^{II}L] (L = **1a**, **1b** − 2H) in mildly basic aqueous solutions.[4] These purple compounds turn brown on exposure to O_2 and are proposed to have the hexacoordinate nickel(III)–superoxido structure shown as **3**.[4] The complexes are stable for minutes to hours depending upon the ligand substituents. Earlier studies demonstrated the capacity of **3a, b** to oxidize benzene to phenol[4a] and hydroxylate its own ligand[5] at the R^1,R^2 position.

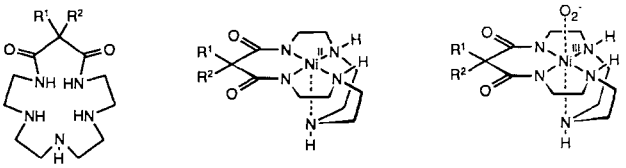

1 **2** **3**

a $R^1 = R^2 = H$
b $R^1 = CH_2C_6H_5$, $R^2 = H$
c $R^1 = F$, $R^2 = H$
d $R^1 = F$, $R^2 = CH_2C_6H_5$
e $R^1 = R^2 = CH_3$

Tetracoordinate nickel(II) complexes have recently been shown to display interesting DNA reactivity in the presence of monopersulfate HSO_5^-, including specific recognition of guanine units in single-stranded regions of DNA.[1] In the present study, the nickel complexes of ligands **1b**–**1e** were examined for reactivity with plasmid DNA in the presence of only O_2 as oxidant. Nickel- and O_2-dependent strand scission was observed for complexes of **1b** and **1c**. These ligands initially form green complexes with Ni^{2+} in H_2O in which only the three amine nitrogen atoms of the macrocycle are coordinated. Raising the pH to about 9 effects amide deprotonation to yield the pentacoordinate purple complexes **2b**[4b] and **2c**, which remain purple on lowering the pH back to 7.5. Complexes **2b** and **2c** have nearly identical properties: $E_{1/2}$ ($Ni^{III/II}$, pH 9.2, K_2HPO_4, vs. Ag/AgCl) = 0.28 V for **2b** and 0.31 V for **2c**; $\lambda_{max}(H_2O)$ = 350 and 520 nm for **2b**, and 344 and 512 nm for **2c**. Both form brown O_2 complexes, **3b** (λ_{max} = 270 and 290 nm) and **3c** (λ_{max} = 269 and 306 nm), on exposure to air for 15 min. Complex **3c** is stable for >1 h at pH 7.5. Most studies were carried out using **3c** because of the ease of ligand synthesis.[6]

In DNA modification studies, circular plasmids were used to monitor the amount of oxidative strand scission. Both **3b** and **3c** were equally reactive and exhibited concentration-dependent single-strand cleavage of supercoiled form I DNA to nicked form II DNA (see Fig. 1 A). Complete DNA

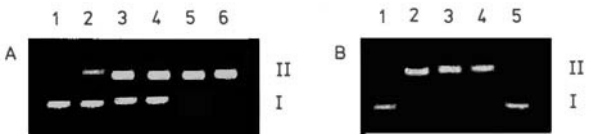

Fig. 1. A: Concentration dependence of the DNA nicking reaction (form I → form II) with complex **3c**. DNA (2.2 μM base pair) alone (lane 1) and treated with 30 μM (lane 2), 60 μM (lane 3), 120 μM (lane 4), 180 μM (lane 5), and 240 μM (lane 6) **3c**. B: Quenching studies of **3c** and comparison of the reactivity of **3d**. Lane 1, DNA only; lanes 2–4, 200 μM **3c**; lane 2, no quenching agents; lane 3, 50 mM mannitol; lane 4, 1.5 M EtOH; lane 5, 200 μM **3d**, no quenching agents.

nicking was observed after 45 min at room temperature when 180 μM **3c** was used with the plasmid pBR322. The reactivity of the precursor complex **2c** was also checked. When **2c** was added directly to a solution containing plasmid

DNA without preforming the O_2 complex, the nickel(II) complex was capable of slowly cleaving DNA under an ambient air atmosphere. The final extent of reaction in either case was the same, but the time required for reaction was 6–8 h for **2c** versus 45 min for **3c**. Higher concentrations of **2c** or **3c** led to further fragmentation of form II DNA. Subsequent reaction did not occur adjacent to the first site of modification since the accumulation of linearized DNA (form III) was not observed. A heterogeneous set of products was formed instead and detected as broad, unstructured bands of DNA derivatives by gel electrophoresis. $Ni(OAc)_2$ (180 μM) had no effect on plasmid DNA under the reaction conditions used for **2c** and **3c**.

Quenching studies were performed to help identify the oxidant responsible for nicking. The reaction was unaffected by 50 mM mannitol and by 1.7 M ethanol (Fig. 1 B, lanes 3 and 4); both typically quench reactions involving $HO^{\bullet}$ radicals. On the other hand, addition of superoxide dismutase (0.94 μM) quenched about 50% of the reaction. This effect did not arise from scavenging of an oxidant by proteins in general, but was instead specific to the catalytic activity of this enzyme. RNase A (1.16 μM), in contrast, had no effect on the reaction of **3c** and plasmid DNA. These experiments suggest that the superoxido complex **3c**, O_2^- itself, or a decomposition product of O_2^- may be involved in DNA oxidation leading to strand scission. In a subsequent study, however, incubation of 520 μM KO_2 (from a DMSO solution containing excess [18]crown-6 for initial solubilization) yielded no detectable DNA scission after 20 min. This initial examination thus suggests a crucial role for **3c**.

In an attempt to optimize the reactivity, the fluorobenzyl ligand **1d** was synthesized. Previous work [4, 5] suggested that the benzyl substituent provides a hydrophobic pocket for stabilization of the O_2 complex and that further substitution at this site might prevent the competing side reaction of ligand hydroxylation and inactivation of the complex. Both ligand **1d** and the known compound **1e** [7] formed green complexes on coordination of Ni^{2+}, but surprisingly, both failed to give stable purple complexes (**2d, e**) at higher pH, turning instead to yellow-brown. Also, both failed to induce plasmid DNA strand scission (e.g. Fig. 1 B, lane 5), indicating the high sensitivity of this overall process to substituents on the ligand. Further mechanistic studies are expected to provide insight in the design of optimum nickel complexes.[8]

Finally, the specificity of the cleavage reaction mediated by **3c** was monitored using the hairpin-forming oligonucleotide d(AGTCTATGGGTTAGACT) previously described.[1b] Strand scission occurred directly after incubation but was enhanced by a final treatment with piperidine.[1] High-resolution gel electrophoresis revealed cleavage at almost all sites and little nucleotide-, conformation-, or sequence-specificity could be discerned. This is consistent with a picture in which an octahedral Ni^{III}–O_2^- complex such as **3** is coordinatively saturated, and the metal is unable to participate in direct DNA binding and recognition. Nevertheless, site-specificity, if desired, should be possible if the standard DNA binding agents are appended to the macrocycle.[9] Such agents would be expected to increase greatly the efficiency of the nickel–superoxido complex for DNA oxidation, making lower concentrations practical.[10]

These results are significant because they show that appropriately designed nickel complexes may cause DNA scission under physiological conditions using only O_2 at ambient pressure. No additional reagents, light, or electrochemistry are required for reaction. Variation of substituents on the macrocycle will now allow careful modulation of the overall activity of the nickel complex.

Experimental Procedure

1c: A solution of diethyl fluoromalonate (6.3 mmol) and tetraethylenepentaamine (6.1 mmol) in anhydrous ethanol (200 mL) was heated to reflux for 24 h. After the reaction mixture was concentrated, the crude material was recrystallized from CH_3CN/CH_3OH to provide a white solid in 42 % yield. ^1H NMR ($CDCl_3$): $\delta = 7.27$ (br s, 2H), 5.22 (d, 1H, $J = 47.4$ Hz, exchangeable with D_2O), 3.61 (m, 2H), 3.35 (m, 2H), 2.56 - 2.86 (m, 12H), 1.65 (br s, 3H); ^{13}C NMR ($CDCl_3$): $\delta = 164.9$, 86.9 (d, $J = 196$ Hz), 48.8, 48.4, 48.3, 39.0. IR (KBr): $\tilde{\nu}$[cm^{-1}] = 3529, 2837, 1695, 1537, 1276, 1127 cm^{-1}. Correct C, H, N analysis.

1d: Diethyl fluoromalonate (6.18 mmol) was added dropwise to excess NaH in THF at 0 °C. After 20 min benzyl bromide (7.02 mmol) was added, and the clear solution was stirred at room temperature for 6 h. Water was added to quench the reaction and the product extracted with CH_2Cl_2. The collected extracts were dried over $MgSO_4$, filtered, and concentrated. Distillation at reduced pressure provided pure diethyl benzylfluoromalonate (38% yield) and recovered diethyl fluoromalonate (60% yield). Diethyl benzylfluoromalonate was used in the same cyclization procedure reported for **1c**. The crude product was chromatographed on silica gel with $CHCl_3$:CH_3OH:NH_4OH = 10:2:0.2 to yield a white solid in 28% yield. ^1H NMR ($CDCl_3$): $\delta = 7.18$ (m, 5H), 7.09 (br s, 2H), 3.5 (m, 2H), 3.48 (d, 2H, $J = 25.5$ Hz), 3.04 (d, 2H), 2.1–2.8 (m, 12H), 1.58 (br s, 3H); ^{13}C NMR (CD_3OD): $\delta = 167.5$, 133.9, 130.1, 127.8, 126.8, 98.6 (d, $J = 202$ Hz), 47.4, 47.1, 38.6, 38.3, 38.1. FAB-MS *m/z* 366 ($M+1$).

DNA Studies: Aqueous solutions (pH 7.5) of nickel complexes **2** were exposed to air for 15 min to provide the O_2 complexes **3**. Plasmid DNA pBR322 (2.2 μM per base pair) and nickel complex (30–240 μM) in 10 mM phosphate (or tris) buffer at pH 7.48 containing 5 mM NaCl was allowed to react under ambient air at room temperature for 45 min. Conversion of form I to form II DNA was detected by gel electrophoresis on 1% agarose with ethidium bromide staining. In control experiments nickel complex was added. Superoxide dismutase from bovine erythrocytes was purchased from Sigma.

Received: June 5, 1992
Revised: August 31, 1992 [Z 5390 IE]
German version: *Angew. Chem.* **1993**, *105*, 290

[1] a) X. Chen, S. E. Rokita, C. J. Burrows, *J. Am. Chem. Soc.* **1991**, *113*, 5884; b) X. Chen, C. J. Burrows, S. E. Rokita, *ibid.* **1992**, *114*, 322.
[2] a) D. P. Mack, P. B. Dervan, *J. Am. Chem. Soc.* **1990**, *112*, 4604; b) D. P. Mack, P. B. Dervan, *Biochemistry* **1992**, *31*, 9399.
[3] For other examples, see a) D. W. Margerum, S. L. Anliker in *The Bioinorganic Chemistry of Nickel* (Ed.: J. R. Lancaster, Jr.) VCH, New York, **1988**, p. 29ff; b) A. Berkessel, J. W. Bats, C. Schwarz, *Angew. Chem.* **1990**, *102*, 81; *Angew. Chem. Int. Ed. Engl.* **1990**, *29*, 106; c) A. Böttcher, H. Elias, L. Müller, H. Paulus, *ibid.* **1992**, *104*, 635 and **1992**, *31*, 623.
[4] a) E. Kimura, R. Machida, *J. Chem. Soc. Chem. Commun.* **1984**, 499; b) E. Kimura, R. Machida, M. Kodama, *J. Am. Chem. Soc.* **1984**, *106*, 5497; c) R. Machida, E. Kimura, Y. Kushi, *Inorg. Chem.* **1986**, *25*, 3461.
[5] a) D. Chen, A. E. Martell, *J. Am. Chem. Soc.* **1990**, *112*, 9411; b) D. Chen, R. Motekaitis, A. E. Martell, *Inorg. Chem.* **1991**, *30*, 1396.
[6] For related work, see: E. Kimura, M. Shionoya, M. Okamoto, H. Nada *J. Am. Chem. Soc.* **1988**, *110*, 3679.
[7] E. Kimura, H. Anan, T. Koike, M. Shiro, *J. Org. Chem.* **1989**, *54*, 3998.
[8] J. G. Muller, X. Chen, A. C. Dadiz, S. E. Rokita, C. J. Burrows, *J. Am. Chem. Soc.* **1992**, *114*, 6407.
[9] P. B. Dervan, *Methods Enzymol.* **1991**, *208*, 497.
[10] As described here the concentration of **3c** in plasmid DNA studies is 82 equivalents per base pair.

Propionyl-Aza(dethia)coenzyme A as Pseudosubstrate of the Biotin-Containing Transcarboxylase

By *Harald Martini* and *János Rétey**

The exact details of how biotin-containing carboxylases work are still a matter of dispute.[1] The ingenious experiments of Lynen et al.[2] established the intermediacy of 1′*N*-carboxybiotin in the carboxylation process. It is, however, still unclear how 1′*N*-carboxybiotin formation is coupled to ATP hydrolysis and how the carboxyl group is transferred to

[*] Prof. Dr. J. Rétey, Dr. H. Martini
Lehrstuhl für Biochemie im Institut für Organische Chemie der Universität
Richard-Willstätter-Allee, D-W-7500 Karlsruhe 1 (FRG)

the substrate, for example, propionyl-coenzyme A (CoA). Retention of configuration in the substitution of a H atom by a carboxyl group[3-7] as well as a distinct tritium transfer from one noncarboxylated substrate to the other (propionyl-CoA and pyruvate) in the transcarboxylase reaction seemed to support a concerted mechanism (Fig. 1).[8] Later results

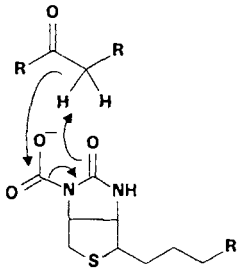

Fig. 1. Concerted mechanism of carboxyl transfer from 1'*N*-carboxybiotin to the substrate.

obtained using β-fluoropropionyl-CoA as pseudosubstrate[9] and more decisively, results from a double isotope fractionation assay[10, 11] showed, however, that the carboxyl transfer —most likely to the enolate of the substrate— is a stepwise process. Figure 2 illustrates the two remaining mechanistic possibilities. Variant *a* represents a direct nucleophilic attack by the substrate enolate on the carboxyl group of 1'*N*-carboxybiotin, whereas according to variant *b* the latter would be first decarboxylated and the CO_2 trapped in situ by the enolate.[1]

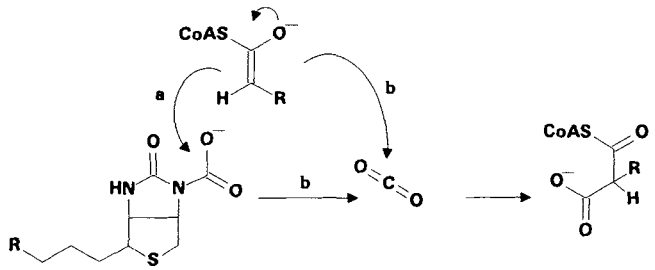

Fig. 2. Stepwise mechanisms of carboxyl transfer from 1'*N*-carboxy-biotin to the substrate. Variant *a*: direct attack of the substrate enolate; variant *b*: prior decarboxylation of 1'*N*-carboxybiotin followed by trapping the locked CO_2 by the substrate enolate.

To distinguish between these two variants we synthesized propionyl-aza(dethia)coenzyme A (**5**) starting from *N*-(2-aminoethyl)propionamide (**1**). We followed essentially the same strategy that has been applied for the synthesis of propionyl-carba(dethia)coenzyme A.[12] Amide **1** was treated with the *p*-NO_2-phenyl ester of (*Z*)-β-alanine to yield **2**. After hydrogenolytic removal of the protecting group the product was condensed by melting with D-pantolactone to obtain **3** (X = H). Phosphorylation of **3** (→ X = PO_3H_2) was performed with β-cyanoethylphosphate.[13] Finally, **3** (X = PO_3H_2) was coupled with adenosine-2',3'-cyclophosphate-5'-morpholidate (**4**). After opening the 2',3'-phosphate ring by acid, the resulting propionyl-aza(dethia)coenzyme A (**5**) was separated from the 2'-phosphoisomer (iso-**5**) by chromatography and was spectroscopically characterized.[14] In a coupled optical enzyme assay **5** seemingly behaved as a substrate of propionyl-CoA-oxaloacetate transcarboxylase (oxaloacetate = 2-oxosuccinic acid) from *P. shermanii*. The kinetic constants, K_m and V_{max}, for propionyl-CoA are 0.47×10^{-4} M and 2.40 μmol min^{-1} mL^{-1}, respectively, and for **5** 1.29×10^{-4} M and 0.11 μmol min^{-1} mL^{-1}, respectively. Investigation of the product by ^{1}H NMR spectroscopy revealed, however, that no methylmalonyl-CoA was formed; that is, the carboxyl group of oxaloacetate was not transferred to **5**. Nevertheless, the coupled enzyme assay proved the formation of pyruvate. It must thus be concluded that **5** induced the enzymatic decarboxylation of oxaloacetate.

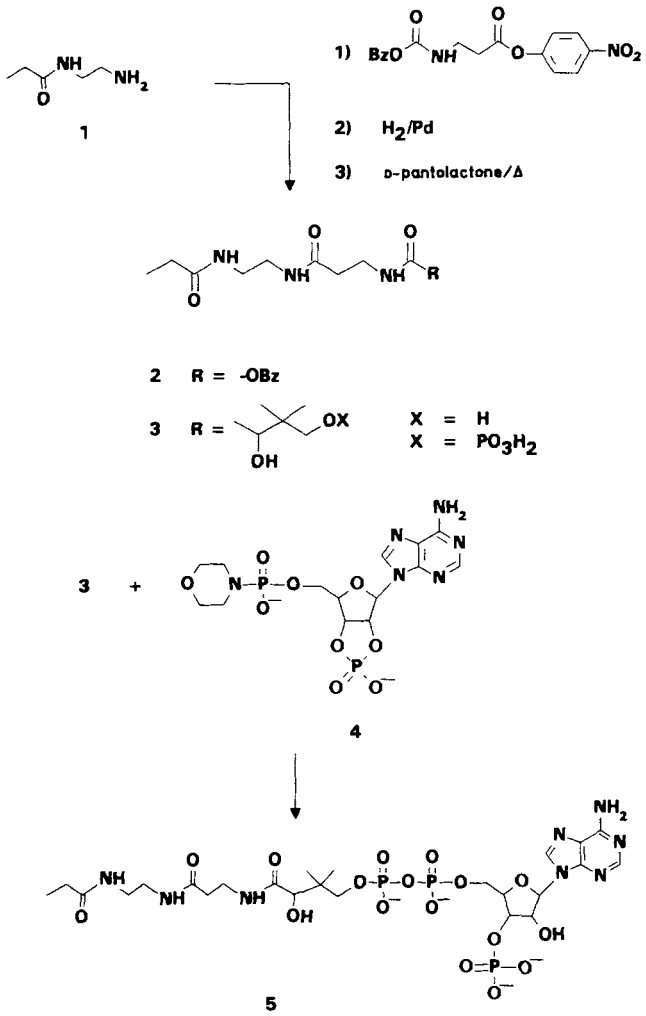

To produce a direct proof for this decarboxylation we applied instead of oxaloacetate its 3-fluoro analogue. 3-Fluorooxaloacetate is a substrate of the transcarboxylase,[15] and its decarboxylation can be monitored directly by ^{19}F NMR spectroscopy. The ^{19}F signal for fluorooxaloacetate appears at $\delta = -204$ (trifluoroacetate $\delta = -77$), that of fluoropyruvate at $\delta = -230$. Monitoring the reaction for 5 hours showed that in the presence of propionyl-aza(dethia)coenzyme A **5** (12 mM) about double as much 3-fluorooxaloacetate was decarboxylated as with transcarboxylase alone.

The induction of decarboxylation can be interpreted as follows: Binding of pseudosubstrate **5** causes a conformational change of the enzyme that is necessary to catalyze the decarboxylation of 1'*N*-carboxybiotin. On the other hand the low acidity of the α-CH_2 group does not allow enolate formation from **5**, and thus its carboxylation by the "naked" CO_2 locked at the active site cannot occur. Our results support a two-step mechanism of the carboxyl transfer: 1) formation of CO_2 from 1'*N*-carboxybiotin, 2) trapping the locked CO_2 by the enolate of the substrate (Fig. 2, variant *b*).

Whether the enolate of biotin, produced on decarboxylation, functions as base for the deprotonation of the substrate, as discussed by J. R. Knowles,[1] is unclear. In contrast to **5**, propionylcarba(dethia)coenzyme A is actually carboxylated to its methylmalonyl derivative in the transcarboxylase reaction.[12]

Received: September 26, 1992 [Z 5599 IE]
German version: *Angew. Chem.* **1993**, *105*, 287

[1] Review: J. R. Knowles, *Annu. Rev. Biochem.* **1989**, *58*, 195–221.
[2] F. Lynen, J. Knappe, E. Lorch, G. Jütting, E. Ringelmann, *Angew. Chem.* **1959**, *71*, 481–486.
[3] J. Rétey, E. Lynen, *Biochem. Z.* **1965**, *342*, 256–271.
[4] D. Arigoni, F. Lynen, J. Rétey, *Helv. Chim. Acta* **1966**, *49*, 311–316.
[5] D. J. Prescott, J. L. Rabinowitz, *J. Biol. Chem.* **1968**, *243*, 1551–1557.
[6] I. A. Rose, *J. Biol. Chem.* **1970**, *245*, 6052–6056.
[7] Y. F. Cheung, C. H. Fung, C. Walsh, *Biochemistry* **1975**, *14*, 2981–2986.
[8] I. A. Rose, E. L. O'Connel, F. Solomon, *J. Biol. Chem.* **1976**, *251*, 902–904.
[9] J. Stubbe, R. H. Abeles, *J. Biol. Chem.* **1977**, *252*, 8338–8340.
[10] S. J. O'Keefe, J. R. Knowles, *Biochemistry* **1986**, *25*, 6077–6084.
[11] P. V. Attwood, P. A. Tipton, W. W. Cleland, *Biochemistry* **1986**, *25*, 8197–8205.
[12] M. Michenfelder, J. Rétey, *Angew. Chem.* **1986**, *98*, 337–338; *Angew. Chem. Int. Ed. Engl.* **1986**, *25*, 366–367.
[13] G. M. Tener, *J. Am. Chem. Soc.* **1961**, *83*, 159–168; M. Shimizu, O. Nagase, J. Hosokawa, H. Tagawa, J. Jotsui, *Chem. Pharm. Bull.* **1970**, *18*, 838–841.
[14] ^{1}H NMR (250 MHz, ^2H_2O): $\delta = 0.76$ (s, 3H), 0.87 (s, 3H), 1.08 (t, $J = 7.6$ Hz, 3H), 2.22 (q, $J = 7.6$ Hz, 2H), 2.45 (t, $J = 6.6$ Hz, 2H), 3.37 (s, 4H), 3.45 (t, $J = 6.6$ Hz, 2H), 3.68 (ABX, $J_{AB} = 9.7$, $J_{AX} = 4.9$ Hz, 2H), 4.01 (s, 1H), 4.24 (m, 2H), 6.18 (d, 6.5 Hz), 8.27 (s, 1H), 8.56 (s, 1H); ^{31}P NMR (121.49 MHz, ^2H_2O); $\delta = 2$ (s, 1P), -10 (m, 2P).
[15] J. A. Goldstein, J. F. Cheung, M. A. Marletta, C. Walsh, *Biochemistry*, **1978**, *17*, 5567–5575.

Ca_2PN_3: A New Phosphorus(v) Nitride with One-Dimensional Infinite Chains of Corner-Sharing PN_4 Tetrahedra**

By *Wolfgang Schnick** and *Verena Schultz-Coulon*

The systematic investigation of binary and higher phosphorus(v) nitrides has uncovered a variety of P–N substructures which, despite the comparatively small number of known compounds, show clear structural analogies to silicates and phosphates.[1–6] The characteristic structural elements found in all the phosphorus(v) nitrides are PN_4 tetrahedra which may be connected by common vertices showing differing degrees of condensation: Isolated PN_4^{7-} anions are found in Li_7PN_4,[1] whereas in $Li_{12}P_3N_9$ three PN_4 units form $P_3N_9^{12-}$ anions, analogously to cyclotrisilicates.[2] The smallest imaginable cage structure that can be formed from corner-sharing PN_4 tetrahedra has been found in $Li_{10}P_4N_{10}$,[3] which contains the $P_4N_{10}^{10-}$ anion, the nitrido analogue of molecular phosphorus(v) oxide. HPN_2, $LiPN_2$,[4, 5] and $Zn_7[P_{12}N_{24}]Cl_2$[6] each exhibit three-dimensional infinite network structures of corner-sharing PN_4 tetrahedra, $_\infty^3[PN_{4/2}^-]$, which can be considered as the topological equivalent of β-crystobalite or of the sodalite framework, respectively. Low-dimensional structures of corner-sharing PN_4 tetrahedra have not yet been proven for phosphorus(v) nitrides. Like silicate compounds with chain or layer structures the analogous phosphorus nitrides are expected to have P:N ratios of 1:3 or 2:5. In contrast, lithium phosphorus nitrides with these ratios contain "dreier" rings or $P_4N_{10}^{10-}$ cages, respectively.

By the reaction of stoichiometric amounts of the binary nitrides Ca_3N_2 and P_3N_5 [Eq. (a)] we have now successfully

$$2\,Ca_3N_2 + P_3N_5 \xrightarrow[\text{W crucible, } N_2 \text{ atm.}]{800\,^\circ C,\ 14\,d} 3\,Ca_2PN_3 \qquad \text{(a)}$$

synthesized pure calcium phosphorus(v) nitride Ca_2PN_3[7] and elucidated its crystal structure.[8] In the solid one-dimensional infinite "zweier" chains exist running parallel [100] (Fig. 1). These chains exhibit a perodicity of two PN_4 tetrahedra and an extreme stretching factor $f_s = 1.0$ similar to that found in johannsenite, $CaMn[Si_2O_6]$, ($f_s = 0.98$).[9] The P–N bond lengths to the terminal nitrogen atoms (average value: 162.5 pm) are shorter than those within the chains (167.4 pm). This finding corresponds qualitatively with the bonding in $Li_{12}P_3N_9$ and $Li_{10}P_4N_{10}$ and can be explained by an increased double bond character or by polar bonding contributions. The Ca^{2+} ions in Ca_2PN_3 are coordinated in a distorted pentagonal bipyramidal manner by the nitrogen atoms of the PN_3 chains, whereby one Ca^{2+} ion connects three chains with one another.[10] The Ca–N contact distances (242–300 pm) lie approximately in the region of the sum of the ionic radii.

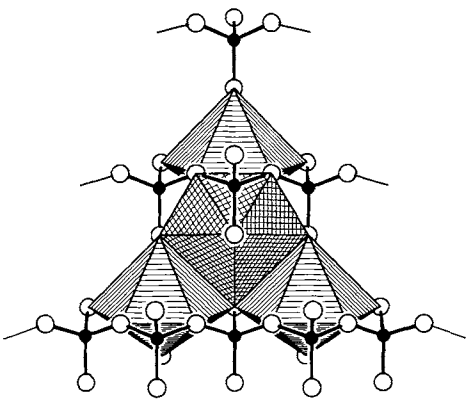

Fig. 1. Crystal structure of Ca_2PN_3 (view along [001]). The PN_3 chains along [100] are clearly visible. The two crystallographically independent Ca atoms are each coordinated in a distorted pentagonal-bipyramidal fashion by nitrogen atoms of the PN_3 chains. The coordination spheres around the Ca^{2+} ions are shown as closed polyhedra. Phosphorus: black, nitrogen: white.

Despite the observed topological similarity of the P–N substructures in this compound (as in other phosphorus(v) nitrides) with isosteric silicate anions, it appears that the structure rules as formulated by Liebau for silicates[11] cannot be applied directly to phosphorus(v) nitrides: cyclic silicate anions are less stable than chainlike arrangements due to electrostatic repulsive forces between the oxygen atoms. In the case of phosphates, this difference is leveled out due to lower charge densities on the PO_4^{3-} units. In contrast, for phosphorus(v) nitrides (PN_4^{7-}), this repulsive effect is expected to be significantly enhanced due to the higher charges. In addition, a significant destabilization of cyclic and branched silicate anions is observed due to the influence of hard electropositive counterions (Li^+, Mg^{2+}), whereas with soft cations (Ca^{2+}, Na^+, K^+) the opposite effect occurs.

Although any generalization is difficult owing to the small number of phosphorus(v) nitrides known to date, the appearance of $_\infty^1[PN_2N_{2/2}^{4-}]$ chains in the calcium compound and $[P_3N_9^{12-}]$ "dreier" rings in the lithium compound is nev-

[*] Priv.-Doz. Dr. W. Schnick, Dipl.-Chem. V. Schultz-Coulon
Institut für Anorganische Chemie der Universität
Gerhard-Domagk-Strasse 1, D-W-5300 Bonn 1 (FRG)

[**] This work was supported by the Deutsche Forschungsgemeinschaft and the Fonds der Chemischen Industrie.

ertheless surprising. Also, the existence of $[P_4N_{10}^{10-}]$ cages in $Li_{10}P_4N_{10}$, for which no isosteric silicate anion is known, is a further example of the divergent structural behavior of phosphorus(v) nitrides compared to silicates. Possible reasons for this could be, in particular, in comparison to the Si–O bonds, the higher covalent character of the P–N bonds, longer P–N bond lengths and, related to this, the larger P–P distances between neighboring tetrahedral centers and a preference for smaller bond angles at the bridging nitrogen atoms. Thus, P–N bonds are on average about 10 pm longer than Si–O bonds of comparable bond strength.[12] A simple estimation of the degree of covalency of the P–N bonds based on the occurring differences in electronegativity (Pauling)[13] gives a distinctly higher value than that found for the more polar Si–O bonds (P–N: 78%, Si–O: 50% covalent). These two factors result in a smaller electrostatic repulsion between centers of neighboring tetrahedra for the phosphorus(v) nitrides. Cosequently, for the P-N-P bond angles an average value of about 120° is observed which is significantly smaller than the ideal value for the Si-O-Si bond angles in silicates (140°) as given by Liebau.[14, 15]

The coordinative requirements of the Ca^{2+} ions in Ca_2PN_3 could be responsible for the formation of the PN_3 "zweier" chains found in this compound. Likewise, in Mg_2PN_3, which crystallizes in an ordered wurtzite superstructure variant,[16] infinite chains of corner-sharing PN_4 tetrahedra are probably present. We are currently working on a more accurate determination of the structural data for this compound.

Experimental Procedure

Stoichiometric amounts of the binary nitrides Ca_3N_2 (synthesized from pure alkaline earth metal in a flow of nitrogen gas, 950°C, 1 h, heating rate 150°C h^{-1}) and P_3N_5 were homogenized in a micro-ball mill under an argon atmosphere (glove box, MBRAUN, Garching (FRG); $O_2 < 0.4$ ppm, $H_2O < 0.1$ ppm). The reaction mixture was sealed under a pure nitrogen atmosphere in a tungsten crucible in a quartz ampoule and finally allowed to react at 800°C (14 days). Under these conditions, Ca_2PN_3 was obtained in a pure form as a light beige microcrystalline powder.

Received: October 5, 1992 [Z 5612 IE]
German version: *Angew. Chem.* **1993**, *105*, 308

[1] W. Schnick, J. Lücke, *J. Solid State Chem.* **1990**, *87*, 101.
[2] W. Schnick, *Phosphorus Sulfur Relat. Elem.*, in press.
[3] W. Schnick, U. Berger, *Angew. Chem.* **1991**, *103*, 857; *Angew. Chem. Int. Ed. Engl.* **1991**, *30*, 830.
[4] W. Schnick, J. Lücke, *Z. Anorg. Allg. Chem.* **1992**, *610*, 121.
[5] W. Schnick, J. Lücke, *Z. Anorg. Allg. Chem.* **1990**, *588*, 19.
[6] W. Schnick, J. Lücke, *Angew. Chem.* **1992**, *104*, 208; *Angew. Chem. Int. Ed. Engl.* **1992**, *31*, 213.
[7] Elemental analyses were performed by first dissolving the product obtained in dilute H_2SO_4 at 180°C and 10 bar. The amount of calcium was determined by complexometric titration with EDTA, phosphorus photometrically as molybdovanadatophosphate, and nitrogen photometrically as indophenol. Parallel to this, the solid product was analyzed by energy dispersive and wavelength dispersive X-ray microanalyses (EDX: Ca, P and WDX: absence of oxygen). The presence of hydrogen (as N-H groups) was excluded by use of IR spectroscopy.
[8] Ca_2PN_3: *Cmca*, $a = 519.14(4)$, $b = 1031.60(8)$, $c = 1128.91(10)$ pm; $Z = 8$, Stoe-Stadi/P-transmission powder diffractometer, $Cu_{K\alpha1}$ radiation, germanium monochromator, linear position-sensitive detector (Stoe-Mini-PSD), capillary measurement, number of data points: 4001, measurement range: $10° \leq 2\theta \leq 90°$, total measurement time: 12 h, structure determination: direct methods (Multan) and difference Fourier (program package C.S.D. from STOE, Darmstadt (FRG)); structure refinement: modified Rietveld method, number of observed reflections: 138, number of refined profile parameters: 14, number of refined positional and temperature parameters: 17, R factors: $R_p = 0.049$, $R_{wp} = 0.0636$, $R_{(I, hkl)} = 0.0939$. Further details of the crystal structure investigation may be obtained from Fachinformationszentrum Karlsruhe, Gesellschaft für wissenschaftlich-technische Information mbH, D-W-7514 Eggenstein-Leopoldshafen 2 (FRG) on quoting the depository number CSD-56915, the names of the authors, and the journal citation.
[9] F. Liebau, *Structural Chemistry of Silicates*, Springer, Berlin, **1985**, p. 80ff.
[10] Ca_2PN_3 is isotypical with Rb_2TiO_3 (see W. Schartau, R. Hoppe, *Z. Anorg. Allg. Chem.* **1974**, *408*, 60) and with alkali metal cobaltates(IV) $[M_2CoO_3]$ where M = K, Rb, Cs (see M. Jansen, R. Hoppe, *Z. Anorg. Allg. Chem.* **1974**, *408*, 75).
[11] F. Liebau, *Structural Chemistry of Silicates*, Springer, Berlin, **1985**, p. 191ff.
[12] N. E. Brese, M. O'Keeffe, *Acta Crystallogr. Sect. B* **1991**, *47*, 192.
[13] L. Pauling, *The Nature of the Chemical Bond*, Cornell University Press, Ithaca, New York, **1960**, p. 97ff.
[14] F. Liebau, *Structural Chemistry of Silicates*, Springer, Berlin, **1985**, p. 168ff.
[15] The P-N-P bond angles at the bridging nitrogen atoms observed to date in phosphorus nitrides vary from 116° to 148° from which the largest value observed is from the "zweier" chains present in Ca_2PN_3 with maximum stretching factor $f_s = 1.0$. The observed range of bond angles at nitrogen for phosphorus(v) nitrides is about the same as the corresponding range in molecular phosphazenes. (H. R. Allcock, *Phosphorus-Nitrogen Compounds*, Academic Press, New York, **1972**, p. 44f.).
[16] R. Marchand, Y. Laurent, *Mater. Res. Bull.* **1982**, *17*, 399.

Reductive Ring-Opening of Oxabicyclic Compounds with Diisobutylaluminum Hydride. Application to the Synthesis of the C_{17}–C_{23} Subunit of Ionomycin**

By *Mark Lautens*,* *Pauline Chiu*, and *John T. Colucci*

The development of methodology for the construction of polypropionate and polyacetate subunits is of critical importance to the preparation of many natural products.[1–3] The aldol condensation and other carbonyl addition approaches have been widely used to address this challenge in spite of the inherently iterative nature of this strategy. We have recently reported an alternative synthetic sequence that utilizes nucleophilic ring-opening of oxabicyclic compounds to generate cyclic and acyclic fragments related to *anti* propionate aldol constructs with up to five contiguous stereocenters.[4, 5] This methodology has been applied to the synthesis of the C_{21}–C_{27} subunit of rifamycin.[6] Herein, we describe a complementary sequence using a reductive ring-opening which assembles stereochemical arrays currently prepared by acetate aldol reactions. We also highlight the efficiency of this strategy in a synthesis of a fragment of the ionophore ionomycin.

In a previous study, we found that Grignard reagents bearing β-hydrogen atoms effect the slow reductive ring-opening of oxabicyclo[3.2.1] and -[2.2.1] substrates.[7] This reaction occurred only in the presence of *excess* magnesium bromide which indicated that a Lewis acidic component was crucial to the success of the reduction. However, the scope and regioselectivity of this reaction was limited. A survey of other hydride sources identified diisobutylaluminum hydride (DIBAH) as a new and effective reagent for reducing oxabicyclic substrates.[8, 9] Cycloalkenols with up to four contiguous stereocenters are generated in one step from readily available starting materials.

In a typical reaction, oxabicyclic substrates such as **1a** were treated with excess DIBAH (1.5–6 equiv) in refluxing hexanes [Eq. (a), TBDS = *tert*-butyldimethylsilyl]. The ma-

[*] Prof. M. Lautens, P. Chiu, J. T. Colucci
Department of Chemistry
University of Toronto
Toronto, Ontario M5S 1A1 (Canada)

[**] The A. P. Sloan Foundation, the Natural Science and Engineering Research Council (NSERC) of Canada, the Merck Frosst Centre for Therapeutic Research, Bio-Mega Inc., the Eli Lilly (USA) Grantee Program, and the Petroleum Research Fund administered by the American Chemical Society are thanked for financial support.

jor product **2a** was accompanied by a minor side product **3a**. The formation of this overreduced product could be minimized by decreasing the amount of DIBAH as well as avoiding prolonged reaction times. Thus, treatment of **1b** with 1.5 equiv DIBAH for 3 h yielded only **2b** and unreacted starting materials (25%). The high yield of **2a** compared to **3a** is significant since it reveals a reversal in the usual rates of hydroalumination of cycloalkenes.[10] Additional strain in the bicyclic dihydrofuran compared to cyclopentene, or complexation of the bridging oxygen to the Lewis acidic DIBAH might be responsible for this reversal. Formation of **3a** and **3b** can also be achieved by increasing the ratio of DIBAH to substrate and the reaction time.[11]

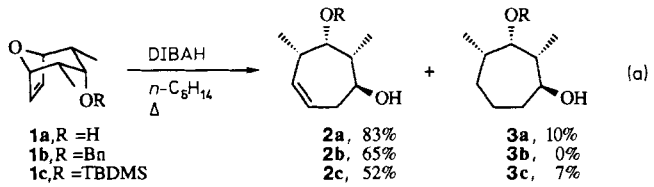

(a)

1a,R =H **2a**, 83% **3a**, 10%
1b,R =Bn **2b**, 65% **3b**, 0%
1c,R =TBDMS **2c**, 52% **3c**, 7%

Table 1. Reductive ring-opening of oxabicyclic compounds.

Entry	Substrate	Reaction time [h]	Product	Yield [c] [%]
1 [a]	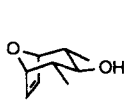 **4**	36	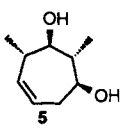 **5**	77
2 [a]	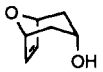 **6**	36	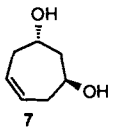 **7**	64 [d]
3 [a]	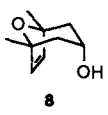 **8**	12	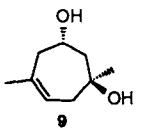 **9**	89
4 [a]	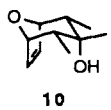 **10**	12	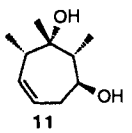 **11**	77
5 [a]	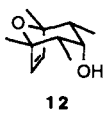 **12**	22	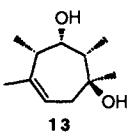 **13**	50
6 [a]	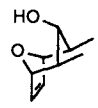 **14**	19	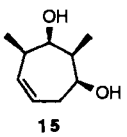 **15**	69
7 [b]	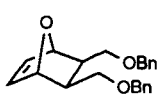 **16**	16	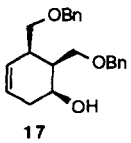 **17**	80

[a] Reaction conditions: 6 equiv DIBAH in refluxing hexanes. [b] 6 equiv DIBAH in refluxing ether. [c] Yields of isolated, analytically pure material. [d] Could not be separated from the doubly reduced product, yield estimated from the ^{1}H NMR spectrum of the mixture.

The data in Table 1 shows the generality of the reaction. Substituents at all positions were tolerated, and every oxabicyclic substrate effectively underwent reductive ring-opening. Substrates included compounds with unprotected hydroxyl groups (entries 1–6), and oxabicyclo[3.2.1] compounds with substituents at the bridgehead positions (entries 3,5). The more strained oxabicyclo[2.2.1] substrate **16** was reduced under even milder conditions and in very good yield (entry 7).

Highly regioselective opening of an unsymmetrical substrate **18** was also achieved; the selectivity of this reaction could be manipulated by varying the substituent at C_3 [Eq. (b)]. Hydroalumination of the protected alcohol **18a** occurred regioselectively placing the bulky dialkylaluminum at the sterically less hindered position. Subsequent elimination of the bridging oxygen atom β to the aluminum atom provided **19a**. Treatment of **18b** with DIBAH alone resulted in virtually no selectivity. However, when **18b** was deprotonated with MeLi prior to hydroalumination, the major product was the regioisomer **20b**. These results demonstrate that the remote *endo* alkoxide group exerts a directing effect on the mode of the hydroalumination reaction. Previous work in our laboratories has established that double bonds in oxabicyclic compounds with an *endo* alkoxide function at C_3 are more reactive toward organolithium reagents.[6] We are currently investigating the stereochemistry of the hydroalumination reaction (i.e. *exo* or *endo* addition) and also examining specific applications for the observed selectivity.

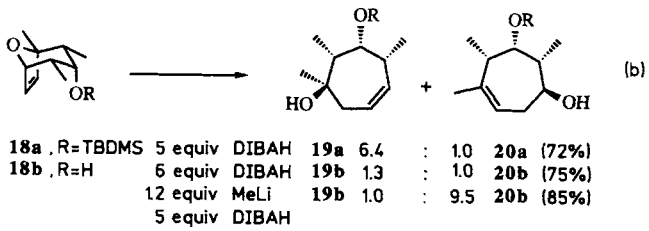

(b)

18a, R=TBDMS 5 equiv DIBAH **19a** 6.4 : 1.0 **20a** (72%)
18b, R=H 6 equiv DIBAH **19b** 1.3 : 1.0 **20b** (75%)
12 equiv MeLi **19b** 1.0 : 9.5 **20b** (85%)
5 equiv DIBAH

The following concise synthesis of the C_{17} to C_{23} subunit of ionomycin serves to highlight the efficiency of the reductive ring-opening reaction (Scheme 1).[12] Cycloheptenol **2b**, obtained from the reductive ring-opening of **1b**, was subjected to an oxidation–reduction sequence to invert the stereochemistry at C_{21}, producing **21** (>10:1 selectivity) in an overall yield of 90%. It is noteworthy that the reductive ring-opening of the less readily available oxabicyclic alcohol **14**[13] directly generated cycloheptenol **15** with the correct stereochemistry (Table 1, entry 6). Protection of the alcohol as a *p*-methoxybenzyl ether (80%), followed by ozonolysis

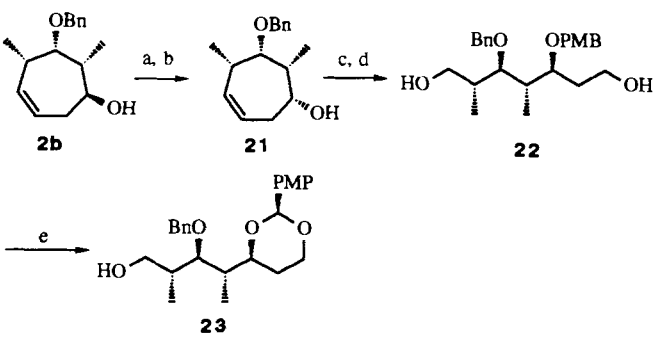

2b **21** **22** **23**

Scheme 1. a) $(COCl)_2$, Et_3N, dimethyl sulfoxide, −78 °C; 93%. b) DIBAH, THF, −78 °C; 97%. c) NaH, dimethylformamide, PMBBr; 80%. d) O_3, MeOH, −78 °C; $NaBH_4$; 93%. e) DDQ, CH_2Cl_2, 0 °C; 72%.

and reductive workup with $NaBH_4$ afforded the acyclic heptanediol **22**. Finally, treatment of **22** with DDQ under anhydrous conditions gave **23**, the product of oxidative cyclization (72%).[14] The synthesis of the fully differentiated ionomycin subunit was accomplished in six steps from the oxabicyclic substrate **1b** (31% overall yield).[15]

Experimental Procedure

The substrate was dissolved in anhydrous hexanes to make a 0.1 M solution. After the solution was cooled to 0 °C, 1–6 equiv neat DIBAH was added dropwise with stirring. Then the reaction mixture was heated to reflux and the progress followed by thin-layer chromatography. When the reaction was complete, the reaction mixture was diluted with ether, cooled to 0 °C, and quenched with a saturated solution of NH_4Cl. Stirring at room temperature for about 15 min produced a white gel which was dissolved by the dropwise addition of 10% H_2SO_4. The organic layer was separated and the aqueous layer was extracted three to five times with ethyl acetate. The combined organics were dried over anhydrous magnesium sulfate, and the solvent was removed in vacuo. The crude product was purified by flash chromatography on silica gel.

2a: ^1H NMR (400 MHz, $CDCl_3$): δ = 5.88 (dddd, J = 10.3, 8.3, 5.4, 2.6 Hz, 1H), 5.32 (dddd, J = 10.3, 4.1, 2.4, 1.0 Hz, 1H), 3.46 (d, J = 7.0 Hz, 1H), 3.36 (ddd, J = 9.3, 9.3, 3.2 Hz, 1H), 2.62 (qm, J = 7.2 Hz, 1H), 2.38 (ddd, J = 14.1, 8.4, 3.2 Hz, 1H), 2.32 (ddddd, J = 14.1, 9.3, 5.4, 2.3, 1.1 Hz, 1H), 1.67 (br, 1H, exchanges with D_2O), 1.66 (dqd, J = 9.3, 6.9, 2.4 Hz, 1H), 1.30 (br d, J = 9.8 Hz, 1H, exchanges with D_2O), 1.18 (d, J = 7.3 Hz, 3H), 1.16 (d, J = 6.8 Hz, 3H); ^{13}C NMR (50 MHz, $CDCl_3$): δ = 135.4, 128.7, 78.3, 68.8, 49.8, 38.4, 37.6, 20.4, 17.6; Correct elemental analysis.

Received: July 7, 1992
Revised: October 28, 1992 [Z 5452 IE]
German version: *Angew. Chem.* **1993**, *105*, 267

[1] For reviews, see: a) C. H. Heathcock, in *Comprehensive Organic Synthesis* (Ed.: B. M. Trost), Pergamon Press, Oxford, **1991**; Vol. 2, p. 133, 181; b) B. Moon Kim, S. F. Williams, S. Masamune, *ibid.* Vol. 2, p. 239; c) I. Fleming, *ibid.*, Vol. 2, p. 563.

[2] For reviews on the reactions of allylmetal compounds with carbonyl groups, see: a) R. W. Hoffmann, *Angew. Chem.* **1982**, *94*, 569; *Angew. Chem. Int. Ed. Engl.* **1982**, *21*, 555; b) Y. Yamamoto, *Acc. Chem. Res.* **1987**, *20*, 243; c) W. R. Roush, in *Comprehensive Organic Synthesis* (Ed.: B. M. Trost, Pergamon Press, Oxford, **1991**, Vol. 2, p. 1.

[3] Recent syntheses of macbecin I serve to illustrate the aldol strategy: a) D. A. Evans, S. J. Miller, M. D. Ennis, P. L. Ornstein, *J. Org. Chem.* **1992**, *57*, 1067; b) S. F. Martin, J. A. Dodge, L. E. Burgess, M. Hartmann, *ibid.* **1992**, *57*, 1070.

[4] a) M. Lautens, C. DiFelice, A. Huboux, *Tetrahedron Lett.* **1989**, *30*, 6817; b) M. Lautens, A. S. Abd-El-Aziz, A. Lough, *J. Org. Chem.* **1990**, *55*, 5305.

[5] For the reactions of [2.2.1] systems with cuprates or organolithium reagents, see: a) M. Lautens, A. C. Smith, A. S. Abd-El-Aziz, A. H. Huboux, *Tetrahedron Lett.* **1990**, *31*, 3253; b) O. Arjona, R. Fernandez de la Pradilla, E. Garci, A. Martin-Domenech, J. Plumet, *ibid.* **1989**, *30*, 6437.

[6] M. Lautens, R. K. Belter, *Tetrahedron Lett.* **1992**, *33*, 2617.

[7] M. Lautens, P. Chiu, *Tetrahedron Lett.* **1991**, *32*, 4827.

[8] The conjugate reduction of vinyl epoxides with DIBAH has been reported, see: R. S. Lennox, J. A. Katzenellenbogen, *J. Am. Chem. Soc.* **1973**, *95*, 957.

[9] For a recent review on the of hydroalumination alkenes and alkynes, see: J. J. Eisch in *Comprehensive Organic Synthesis* (Ed.: B. M. Trost), Pergamon Press, Oxford, **1991**, Vol. 8, p. 733.

[10] Cycloheptene is reported to react at twice the rate of cyclopentene, see: K. Ziegler, H. G. Gellert, H. Martin, K. Nagel, J. Schneider, *Justus Liebigs Ann. Chem.* **1954**, *589*, 91. We are currently investigating whether the ring-opening occurs by hydroalumination followed by elimination of the aluminum alkoxide, or by an S_N2'-type delivery of the hydride.

[11] Reaction of substrate **1b** with DIBAH in refluxing hexanes (ca. 15 h) gave a 75% yield of **3b**.

[12] Previous syntheses of ionomycin: S. Hanessian, N. G. Cooke, B. DeHoff, Y. Sakito, *J. Am. Chem. Soc.* **1990**, *112*, 5276; D. A. Evans, R. L. Dow, T. L. Shih, J. M. Takacs, R. Zahler, *ibid.* **1990**, *112*, 5290, and references therein.

[13] Alcohol **14** was obtained from the L-Selectride reduction of the corresponding ketone, which was a minor product from the synthesis of the ketone precursor of **1a** see: M. R. Ashcroft, H. M. R. Hoffman, *Org. Synth.* **1978**, *58*, 17.

[14] Y. Oikawa, T. Yoshioka, O. Yonemitsu, *Tetrahedron Lett.* **1982**, *23*, 889.

[15] Enantioselective reductive ring-opening utilizing an asymmetric hydroboration [16]–fragmentation [17] strategy was attempted. While the initial hydroboration occurred in 85–95% *ee*, ring-opening was not observed under a variety of conditions.

[16] H. C. Brown, J. V. N. Vara Prasad, *J. Am. Chem. Soc.* **1986**, *108*, 2049.

[17] G. Zweifel, J. Plamondon, *J. Org. Chem.* **1970**, *35*, 898.

Novel Arsaalkenes from an Arsasilene Derivative and Isocyanides**

By *Matthias Driess,* Hans Pritzkow,* and *Michael Sander*

Dedicated to Professor Robert West on the occasion of his 65th birthday

Recently we reported a simple synthetic route to the first arsasilene $Is_2Si{=}AsSiiPr_3$ (**1**) (Is = 2,4,6-$iPr_3C_6H_2$).[1] The high reactivity of **1** allowed the synthesis of new arsasila heterocycles, which are suitable, for example, as synthetic equivalents for alkylidenarsanes ("arsaalkenes"). Thus, the thermolysis of 1,2,3-oxaarsasilacyclobutane **2**,[1] which is accessible from **1** and Ph_2CO, leads to the formation of the arsaalkenes **3** and **4** (Scheme 1). Bickelhaupt et al., Becker et. al, and Tzschach et al.[2] previously reported arsaalkenes, however, their structures and reactivity have been less investigated than phosphaalkenes. To our knowledge the only arsaalkene structurally characterized so far is the arsaalkenyliron complex $[(\eta^5\text{-}C_5H_5)(CO)_2Fe{-}As{=}C(OSiMe_3)tBu]$.[3] We have now found that the Si=As bond is extremely reactive towards organic isocyanides, and that these reactions open a new, unusual route to arsaalkenes.

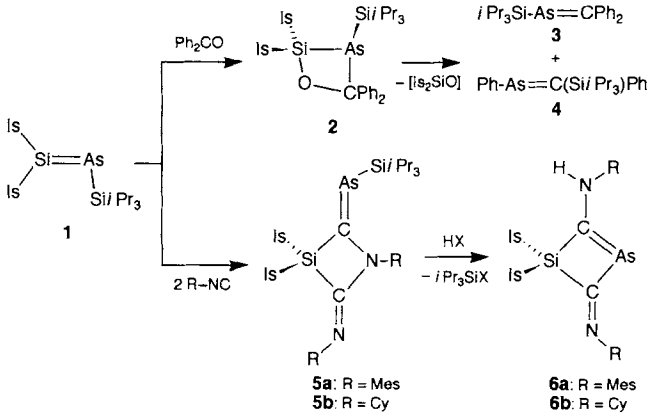

Scheme 1. Syntheses of the arsaalkenes **3**–**6** from **1** and benzophenone or from **1** and isocyanides. Mes = 2,4,6-trimethylphenyl, Cy = cyclohexyl, Is = 2,4,6-triisopropylphenyl.

Compound **1** reacts with RNC (R = Mes, *cyclo*-C_6H_{11}) at −80 °C, independent of the chosen stoichiometry, in the molar ratio 1:2 to give the arsaalkenes **5** (Scheme 1). This reactivity of the Si=As bond towards isocyanides is similar to the behavior of the C=Si bond in silenes. Thus silenes also react with isocyanides in a 1:2 molar ratio leading to 2-alkylidene-4-imino-1-aza-3-silacyclobutanes,[4] which are isostructural with **5**. In contrast, the Si=Si bond in disilenes reacts in a different way with isocyanides depending on the substituents: tetraaryldisilenes afford *thermally* by [2 + 1] cycloaddition exclusively *C*-iminodisilacyclopropanes,[5a] whereas the *photolysis* of tetra-*tert*-butyldisilene in the presence of isocyanides leads to the formation of 3,4-diimino-1,2-disilacyclobutanes and 2,4-diimino-1,3-disilacyclobutanes.[5b]

The constitution of **5a, b** was confirmed by NMR and IR spectroscopy (Table 1) and in the case of **5b** also by X-ray crystallography (Fig. 1).[6] The SiC_2N four-membered ring is planar, and the N atom in the ring is trigonal planar coordinated. The exocyclic C=N bond (1.258(4) Å) has the

[*] Dr. M. Driess, Dr. H. Pritzkow, Dipl.-Chem. M. Sander
Anorganisch-chemisches Institut der Universität
Im Neuenheimer Feld 270, D-W-6900 Heidelberg (FRG)

[**] This work was supported by the Deutsche Forschungsgemeinschaft (Sonderforschungsbereich 247). We thank the referees for valuable hints.

Table 1. Selected NMR, IR spectroscopic, and mass spectrometric data of **5** and **6** [a].

5a ^{1}H NMR: δ = 1.16–1.39 (m, 54H, CHMe_2), 1.39 (sept., 3H, SiCHMe$_2$, J(H,H) = 6.6 Hz), 2.14 (s, 3H, p-Me), 2.19 (s, 3H, p-Me), 2.28 (s, 6H, o-Me), 2.34 (br., 6H, o-Me), 2.79 (sept., 2H, p-CHMe$_2$, J(H,H) = 6.8 Hz), 3.54 (br., 2H, o-CHMe$_2$), 3.91 (br., 2H, o-CHMe$_2$), 6.64 (s, 2H, arom. H), 6.77 (br., 2H, arom. H), 7.23 (br., 4H, arom. H); ^{13}C NMR: δ = 169.54 (s, C=N), 217.75 (s, C=As); ^{29}Si NMR (INEPT): δ = 18.76 (s, SiiPr), 2.66 (s, SiIs); IR: $\tilde{\nu}$[cm^{-1}] = 1120 (s, C=As), 1643 (s, C=N); MS: m/z 956 (M^+, 0.3), 799 ((M − SiiPr$_3$)$^+$, 40), 756 ((M − SiiPr$_3$ − C$_3$H$_7$)$^+$, 70), 119 (Mes$^+$, 100)

5b ^{1}H NMR: δ = 0.364 (d, 6H, CHMe_2, J(H,H) = 6.2 Hz), 0.48 (d, 6H, CHMe_2, J(H,H) = 6.4 Hz), 1.05–2.02 (m, 67H, SiCHMe$_2$, CHMe_2, C$_6$H$_{11}$), 2.65 (m, 2H, p-CHMe$_2$), 3.05 (sept., 1H, o-CHMe$_2$, J(H,H) = 6.4 Hz), 3.49 (sept., 1H, o-CHMe$_2$, J(H,H) = 6.2 Hz), 4.17 (br., 1H, o-CHMe$_2$), 4.78 (sept., 1H, o-CHMe$_2$, J(H,H) = 6.5 Hz), 6.98 (d, 2H, arom. H, J(H,H) = 14.2 Hz), 7.10 (d, 2H, arom. H, J(H,H) = 14.2 Hz); ^{13}C NMR: δ = 169.07 (s, C=N), 220.76 (s, C=As); ^{29}Si NMR (INEPT): δ = 20.14 (s, SiiPr), −3.59 (s, SiIs); IR: $\tilde{\nu}$[cm^{-1}] = 1124 (C=As), 1646 (C=N); MS: m/z 885 (M^+, 88) 728 ((M − SiiPr$_3$)$^+$, 64), 668 ((M − 2C$_6$H$_{11}$NC + 2H)$^+$, 100)

6a ^{1}H NMR: δ = 0.46 (d, 6H, CHMe_2, J(H,H) = 6.2 Hz), 0.59 (d, 6H, CHMe_2, J(H,H) = 6.5 Hz), 1.18–1.63 (m, 24H, CHMe_2), 1.78 (s, 3H, Ar-Me), 1.90 (s, 3H, Ar-Me), 2.09 (s, 3H, Ar-Me), 2.41 (br., 9H, Ar-Me), 2.80 (sept., 2H, p-CHMe$_2$, J(H,H) = 6.7 Hz), 3.12 (sept., 1H, o-CHMe$_2$, J(H,H) = 6.5 Hz), 3.51 (sept., 1H, o-CHMe$_2$, J(H,H) = 6.3 Hz), 3.91 (sept., 1H, o-CHMe$_2$, J(H,H) = 6.6 Hz), 4.40 (sept., 1H, o-CHMe$_2$, J(H,H) = 6.8 Hz), 6.53–7.28 (m, 8H, arom. H), 8.14 (s, 1H, NH); ^{29}Si NMR (INEPT): δ = 4.30 (s); IR: $\tilde{\nu}$[cm^{-1}] = 1101 (w, C=As), 1618 (s, C=N), 3361 (s, NH); MS: m/z 800 (M^+, 0.1), 742 ((M − Me − C$_3$H$_7$)$^+$, 0.1), 668 ((M − MesN + H)$^+$, 10), 451 (100), 435 (Is$_2$SiH$^+$, 98)

6b ^{1}H NMR: δ = 0.45 (d, 6H, CHMe_2, J(H,H) = 6.3 Hz), 0.59 (d, 6H, CHMe_2, J(H,H) = 6.4 Hz), 1.16–2.02 (m, 46H, C$_6$H$_{11}$, CHMe_2), 2.81 (sept., 2H, p-CHMe$_2$, J(H,H) = 6.5 Hz), 3.12 (sept., 1H, o-CHMe$_2$, J(H,H) = 6.6 Hz), 3.52 (sept., 1H, o-CHMe$_2$, J(H,H) = 6.2 Hz), 3.94 (sept., 1H, o-CHMe$_2$, J(H,H) = 6.6 Hz), 4.42 (sept., 1H, o-CHMe$_2$, J(H,H) = 6.8 Hz), 6.91 (d, 2H, arom. H, J(H,H) = 13.7 Hz), 7.10 (d, 2H, arom. H, J(H,H) = 13.7 Hz); ^{29}Si NMR (INEPT): δ = 4.18(s); IR: $\tilde{\nu}$[cm^{-1}] = 1103 (w, C=As), 1614 (s, C=N), 3352 (s, NH); MS: m/z 729 (M^+, 0.1), 671 ((M − Me − C$_3$H$_7$)$^+$, 0.3), 632 ((M − C$_6$H$_{11}$N)$^+$, 17), 435 (Is$_2$SiH$^+$, 100)

[a] NMR spectra in C_6D_6; ^{1}H: 200 MHz, ^{13}C: 50 MHz, ^{29}Si: 39.7 MHz; MS: electron impact ionization, 70 eV; IR spectra in KBr.

same length as the C=N bonds in methylenimine and other Schiff bases.[7] The C–As bond (1.827(3) Å) is considerably shorter than a C–As single bond (1.96 Å)[7] and corresponds to the C–As distance in the arsaalkenyl complex [(η^5-C$_5$H$_5$)(CO)$_2$Fe–As=C(OSiMe$_3$)tBu][3] (1.821(2) Å). In contrast, more conjugated C=As bonds such as those found in arsinines are longer (1.859, 1.884 Å).[8]

A reaction mechanism as given in Scheme 2 is proposed for the formation of **5**; however, no intermediate can be proven by NMR spectroscopy. Compound **1** probably reacts initially with one equivalent of isocyanide to give the intermediate arsasilacyclopropanimine **A**, which isomerizes immediately in a Peterson-like olefination to give the azasilacycloproylidenearsane **B**.[9] The insertion of a further isocyanide molecule into the Si–N bond of **B** could then finally lead to **5**. In the similar reaction of silenes with isocyanides in the molar ratio 1:2, C-alkylidenazasiliridines,[4] that is, compounds analogous to **B**, could be proven as intermediates, which supports the postulated mechanism in Scheme 2.

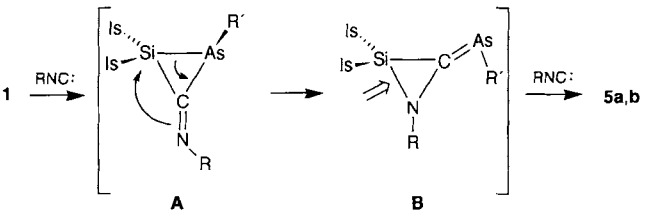

Scheme 2. Hypothetical mechanism for the reaction of **1** with RNC to give **5**.

The reaction of **5** in Et_2O with a stoichiometric amount of HCl etherate or aqueous 40% HF at −50 °C was carried out to investigate whether a 1,2 addition to the C=As bond and/or the exchange of the SiiPr$_3$ groups at the arsenic atom by a hydrogen atom is possible. Surprisingly, in these reactions, however, the novel cyclic arsaalkenes **6** and iPr$_3$SiX (X = F, Cl) are obtained as the only products (Scheme 1, Table 1). The existence of an intermediate could not be proven by spectroscopy, so that only assumptions could be made about the reaction mechanism. The expected low-field signals for the C atoms of the C=As bond are observed in the ^{13}C NMR spectra of **6** (δ = 235.88 (**6a**), 211.86 (**6b**)). The C atoms (positioned in the ring) of the imines also exhibit a singlet signal at very low field (δ = 201.68 (**6a**), 198.52 (**6b**)); this unusually strong deshielding in comparison to **5** (δ = 169.54 (**5a**), 169.76 (**5b**)) is produced by a higher contribution of polar resonance structures in the electronic ground state (Scheme 3).

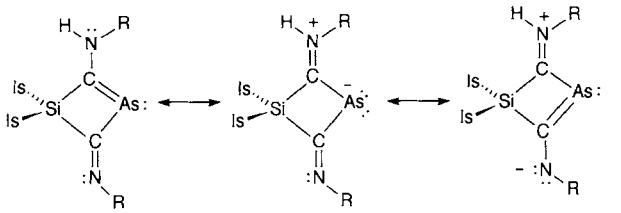

Scheme 3. Mesomeric resonance structures of the arsaalkenes **6**.

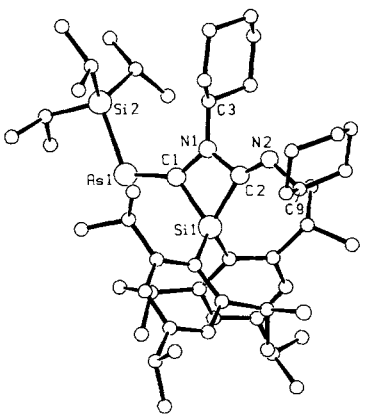

Fig. 1. Molecular structure of **5b**. Selected distances [Å] and angles [°]: As1–Si2 2.384(1), As1–C1 1.827(3), Si1–C1 1.935(3), Si1–C2 1.929(3), N1–C1 1.377(4), N1–C2 1.437(4), N1–C3 1.468(4), N2–C2 1.258(4); C1–As1–Si2 115.5(1), C2–Si1–C1 71.6(1), C2–N1–C1 106.8(2), C3–N1–C1 128.5(2), C3–N1–C2 124.7(2), C9–N2–C2 117.6(2).

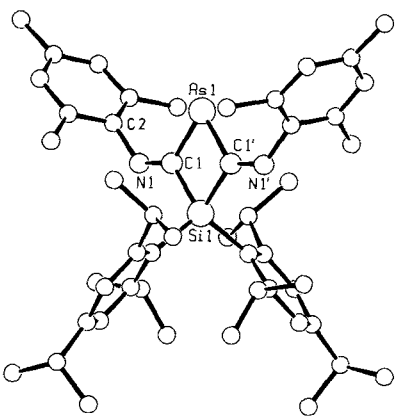

Fig. 2. Molecular structure of **6a**. Selected distances [Å] and angles [°]: As1–C1 1.921(3), Si1–C1 1.887(3), N1–C1 1.302(3), N1–C2 1.433(4); C1–As1–C1' 80.2(1), C1–Si1–C1' 81.9(1), C2–N1–C1 126.9(2), Si1–C1–As1 99.0(1), N1–C1–As1 130.8(2), N1–C1–Si1 130.0(2).

The IR spectra of **6** (Table 1) each show one band for the N–H stretching frequency in the characteristic region for secondary amines.[10] The crystal structure analysis[11] of **6a** confirmed the presence of a four-membered ring with a AsC_2Si skeleton (Fig. 2), but only gives an averaged structure in which the molecule possesses a twofold axis through As1 and Si1. The As1–C1 (1.921(2) Å) and C1–N1 (1.302(3) Å) bond lengths lie between the values for the corresponding single and double bonds,[7] which supports the formulation of **6** as given in Scheme 3.

The rearrangement of **5** into **6** poses the question of whether similar substituted phosphaalkenes lead to analogous products; this is currently under investigation.

Experimental Procedure

5a: **1** (322 mg, 0.48 mmol) in toluene (20 mL) was treated with mesitylisocyanide (139.2 mg, 0.96 mmol) at −80 °C. This caused the color of the reaction solution to change from orange to pale yellow. The solution was warmed to room temperature over 3 h, and subsequently the solvent was removed under vacuum (10^{-2} Torr). The product was obtained quantitatively as a yellow powder (m.p. 227–228 °C). Yellow crystals of the analogue **5b** were obtained from **1** (322 mg, 0.48 mmol) and cyclohexylisocyanide (104.6 mg, 0.96 mmol; m.p. 242 °C).

6a: **5a** (320 mg, 0.35 mmol) in Et_2O at −50 °C was treated with the stoichiometric amount of HCl or with aqueous 40% HF and subsequently warmed to 25 °C. Removal of the volatiles under vacuum (10^{-2} Torr), and uptake of the residue in hexane (5 mL), gave a yellow solution, from which, following filtration, orange-yellow crystals (192 mg, 0.24 mmol, 68%; m.p. 173 °C) were isolated at −30 °C (ca. 7 days). **6b** was obtained in an analogous way from **5b** (138.5 mg, 0.19 mmol, 61%) as a yellow powder (m.p. 186–188 °C).

Received: October 16, 1992 [Z 5631 IE]
German version: *Angew. Chem.* **1993**, *105*, 273

[1] M. Driess, H. Pritzkow, *Angew. Chem.* **1992**, *104*, 350; *Angew. Chem. Int. Ed. Engl.* **1992**, *31*, 316.
[2] T. C. Klebach, H. van Dongen, F. Bickelhaupt, *Angew. Chem.* **1979**, *91*, 423; *Angew. Chem. Int. Ed. Engl.* **1979**, *18*, 395; G. Becker, G. Gutekunst, *Z. Anorg. Allg. Chem.* **1980**, *470*, 131, 144; G. Becker, A. Münch, H.-J. Wessely, *Z. Naturforsch. B* **1981**, *36*, 1080; J. Heinicke, A. Tzschach, *J. Organomet. Chem.* **1978**, *154*, 1; *ibid.* **1979**, *166*, 175.
[3] L. Weber, G. Meine, R. Boese, *Angew. Chem.* **1986**, *98*, 463; *Angew. Chem. Int. Ed. Engl.* **1986**, *25*, 469.
[4] A. G. Brook, Y. K. Kong, A. K. Saxena, J. F. Sawyer, *Organometallics* **1988**, *7*, 2245; A. G. Brook, J. F. Sawyer, A. K. Saxena, *ibid.* **1989**, *8*, 850.
[5] a) H. B. Yokelson, A. J. Millevolte, K. J. Haller, R. West, *J. Chem. Soc. Chem. Commun.* **1987**, 1605; b) M. Weidenbruch, B. Brand-Roth, S. Pohl, W. Saak, *Angew. Chem.* **1990**, *102*, 93; *Angew. Chem. Int. Ed. Engl.* **1990**, *29*, 90; M. Weidenbruch, "Novel Ring Systems from Cyclotrisilanes and Cyclotristannanes" (*Stud. Inorg. Chem.* **1992**, *14*, 51.
[6] X-ray structure analysis of **5b**: space group $P\bar{1}$, $a = 10.244(7)$, $b = 13.643(8)$, $c = 19.922(13)$ Å, $\alpha = 91.29(5)$, $\beta = 98.45(5)$, $\gamma = 97.20(5)°$, $Z = 2$, $V = 2730$ Å^3; four-circle diffractometer ($Mo_{K\alpha}$ radiation, ω scan), 5938 observed reflections ($I > 2\sigma_I$), non-hydrogen atoms anisotropic, H atoms of the methyl groups as part of a rigid group, others refined isotropic in found positions, $R = 0.043$ [12].
[7] F. A. Allen, O. Kennard, D. G. Watson, L. Brammer, A. G. Orpen, R. Taylor, *J. Chem. Soc. Perkin Trans. 2* **1987**, S1; see also [4].
[8] F. Sanz, J. J. Daly, *Angew. Chem.* **1972**, *84*, 679; *Angew. Chem. Int. Ed. Engl.* **1972**, *11*, 630; G. Märkl, S. Dietl, *Tetrahedron Lett.* **1988**, *29*, 535.
[9] J. Peterson, *J. Org. Chem.* **1968**, *33*, 780.
[10] J. Weidlein, U. Müller, K. Dehnicke, *Schwingungsfrequenzen I*, Thieme, Stuttgart, **1981**, p. 252.
[11] X-ray structure analysis of **6a**: space group $C2/c$, $a = 22.849(19)$, $b = 10.066(7)$, $c = 25.006(19)$ Å, $\beta = 126.90(5)°$, $Z = 4$, $V = 4599$ Å^3; four-circle diffractometer ($Mo_{K\alpha}$ radiation, ω scan), 2913 observed reflections ($I > 2\sigma_I$), non-hydrogen atoms anisotropic, H atoms (apart from the methyl groups) refined isotropic in found positions $R = 0.041$. A refinement in Cc showed strong correlations and did not converge [12].
[12] Further details of the crystal structure investigations may be obtained from the Fachinformationszentrum Karlsruhe, Gesellschaft für wissenschaftlich-technische Information mbH, D-W-7514 Eggenstein-Leopoldshafen 2 (FRG) on quoting the depository number CSD-56771, the names of the authors, and the journal citation.

Synthesis of 4-Oxo-L-proline and *cis*-4-Hydroxy-L-proline Derivatives from L-Aspartic Acid**

By *Klaus Burger,* Martin Rudolph,* and *Susanna Fehn*

Every reaction of an amino acid that proceeds with conservation of stereochemistry is preparatively valuable, especially if the conversion can be carried out on amino acids that are readily available in both enantiomeric forms.[1] We have shown that hexafluoroacetone-protected aspartic acid derivatives **2**–**4** are interesting starting materials for the synthesis of amino acids[2] and peptides.[3]

Diazoketone **4**,[2] available in three steps from L-aspartic acid, has the complete sequence of atoms of the framework of 4-oxo-L-proline.[4] To reach the target molecule only a C–N bond must be formed (**4** → **6**). The photochemical transformation **4a** → **6a** was not successful, since the Wolff rearrangement of the α-oxocarbene is much faster than the N–H insertion to form the five-membered ring (Scheme 1).

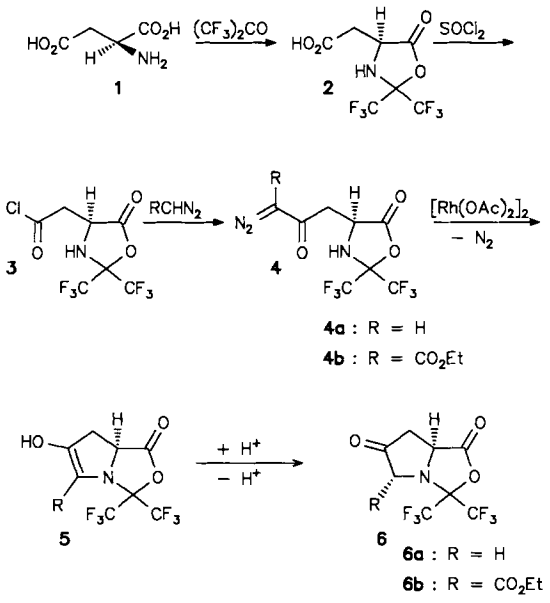

Scheme 1.

Transition metal catalyzed reactions of α-diazocarbonyl compounds proceed via electrophilic Fischer-type carbene complexes.[5] The Wolff rearrangement is thus suppressed, and consequently the insertion takes place exclusively.[6] When a solution of **4a** in chloroform at room temperature was treated with a catalytic amount of dirhodium tetraacetate,[7] the 4-oxo-L-proline derivative **6a** is obtained in 73% yield. The conversion **4a** → **6a** could also be achieved in a mixture of 70% HF/pyridine at −20 °C.[8] Treatment of **4a** with HCl and HBr, on the other hand, yields the corresponding α-haloketones.[2]

In contrast, when α-diazoketone **4a** is treated at room temperature with a catalytic amount of dirhodium tetraacetate for a controlled decomposition, the ^{19}F NMR spectrum shows the initial formation of the single product **5b** with the

[*] Prof. Dr. K. Burger, Dr. M. Rudolph, Dipl.-Chem. S. Fehn
Institut für Organische Chemie der Technischen Universität München
Lichtenbergstrasse 4, D-W-8046 Garching (FRG)

[**] Hexafluoroacetone as a Protecting Group and Activation Reagent in Amino Acid and Peptide Chemistry, Part 12. This research was supported by the Fonds der Chemischen Industrie. We thank Hoechst AG, Frankfurt/Main, for their generous donation of chemicals. – Part 11: K. Burger, M. Rudolph, E. Windeisen, A. Worku, S. Fehn, *Monatsh. Chem.*, in print.

disappearance of starting material; the NMR spectra are in accordance with an enol substructure. Crystalline **5b** can be stored at −28 °C for longer periods. At room temperature in both the solid state and in solution **5b** rearranges to give the expected oxoproline derivative **6a** (monitored by ^{19}F NMR spectroscopy).

The configuration of the newly formed stereogenic center C8 was determined with a heteronuclear NOE experiment (^{19}F–^{1}H HOESY).[9] In the 2D NOE NMR spectrum an NOE was found between the proton at C8 and only one of the trifluoromethyl groups at C2. The configuration of compound **6b** is thus established: relative to the chiral center C5 introduced by the (*S*)-aspartic acid, C8 is also *S*-configurated. The formation of the chiral center at C8 in the keto → enol rearrangement is a thermodynamically controlled self-organization of a sterogenic center.[10] Because of the accessibility of diazo compounds with diverse functionality,[11] this method allows the diastereoselective synthesis of numerous 4-oxoproline derivatives with interesting substitution patterns and may become important in peptide modification and the development of proline dehydrogenase inhibitors (Scheme 2).

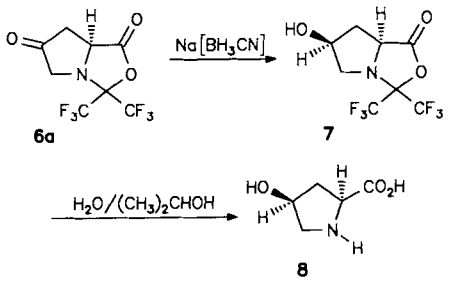

Scheme 2.

Compounds **4**–**6** possess considerable potential not only with regards to the diastereoselective synthesis of 5-substituted 4-oxoproline derivatives. As a result of the concave shape of bicycle **6** whose inner face is also sterically shielded by a trifluoromethyl group,[12] nucleophilic additions to the carbonyl function should display a distinct preference for the *Re* face. This was confirmed by the reduction of the keto function of **6a** with $Na[BH_3CN]$ (*de* > 86%). The stereochemistry of the main product **7** was established by an NOE experiment and shown to correspond to that of *cis*-4-hydroxy-L-proline.

The L-proline derivatives resulting from nucleophilic addition to the keto function or from conversion of the carbonyl function are N-protected amino acids with activated carboxyl groups and can be employed directly for the functionalization of the carboxyl group. The derivatization of the carboxyl group is coupled with the deblocking of the amino function. The free amino acids are obtained in a pH-neutral mixture of 2-propanol and water.[13] The hydrolysis of **7** leads to *cis*-4-hydroxy-L-proline (**8**),[14] which is a proline antagonist in collagen biosynthesis[15] and inhibits the growth of cultured tumor cells that synthesize basal membrane collagen.[16] If the synthetic sequence starts with D-aspartic acid, then the corresponding D-proline derivative is obtained.

We will report elsewhere on other applications of compounds of the type **4**–**7** in the regio- and stereoselective functionalization of the proline framework and the transfer of the concept described here to similar heterocyclic amino acids.

Experimental Procedure

5 (R = $CO_2C_2H_5$): **4b**[2] (5.6 g, 14.8 mmol) was dissolved in $CHCl_3$ (200 mL) at room temperature under N_2 and treated with $[Rh(OAc)_2]_2$ (12 mg, 27 μmol). After 2 d the reaction was complete according to ^{19}F NMR spectroscopy. The solvent was removed under vacuum and the residue extracted with hexane (3 × 100 mL). The hexane extracts were concentrated to dryness giving **5** (4.67 g, 90%) as a crystalline substance which had already undergone partial conversion to **6b** (10%), but which did not appear to react further at −28 °C. ^{1}H NMR ($CDCl_3$): δ = 1.31 (t, J = 7 Hz, 3H; CH_3), 2.93 (dd, J = 9, 18 Hz, 1H; H-C6), 3.24 (dd, J = 10, 18 Hz, 1H; H-C6), 4.31–4.39 (m, 2H; OCH_2), 4.75 (dd, J = 9, 10 Hz, 1H; H-C5), 10.19 (brs, 1H; OH); ^{13}C NMR ($CDCl_3$): δ = 13.6 (CH_3), 33.9 (C6), 59.1 (C5), 61.5 (OCH_2), 92.7 (sept, J = 39 Hz; C2), 109.5 (C8), 119.9 (q, J = 291 Hz; CF_3), 120.2 (q, J = 286 Hz; CF_3), 165.7 (C7), 166.6, 168.7 (C=O ester, C4); ^{19}F NMR ($CDCl_3$): δ = −0.4 (q, J = 9 Hz, 3F; CF_3), 4.5 (q, J = 9 Hz, 3F; CF_3).

6a: A solution of **4a**[2] (3.05 g, 10 mmol) in CH_2Cl_2 (150 mL) was added dropwise under N_2 to a vigorously stirred solution of $[Rh(OAc)_2]_2$ (24 mg, 54 μmol) in anhydrous CH_2Cl_2 (200 mL). After 24 h the ^{19}F NMR spectrum showed the reaction to be complete. The solvent was removed under vacuum. Kugelrohr distillation of the residue (1.3 mbar, oven temperature 80 °C) provided **6a** as a colorless oil (2.02 g, 73%). $[\alpha]_D^{21}$: −168.0 (c = 1.0 $CHCl_3$). IR: $\tilde{\nu}$[cm^{-1}] = 1835, 1770. ^{1}H NMR ($CDCl_3$): δ = 2.66 (dd, J = 9, 19 Hz, 1H; H-C6), 2.83 (dd, J = 9, 18 Hz, 1H; H-C6), 3.68 (d, J = 19 Hz, 1H; H-C8), 3.82 (d, J = 19 Hz, 1H; H-C8), 4.54 (t, J = 9 Hz, 1H; H-C5); ^{13}C NMR ($CDCl_3$): δ = 37.4 (C6), 54.0 (C5), 57.2 (C8), 91.6 (sept, J = 33 Hz; C2), 120.3 (q, J = 291 Hz; CF_3), 120.4 (q, J = 286 Hz; CF_3), 168.8 (C4), 207.7 (C7); ^{19}F NMR ($CDCl_3$): δ = −3.4 (q, J = 9 Hz, 3F; CF_3), 5.0 (q, J = 9 Hz, 3F; CF_3).

6b: Compound **5** (4.67 g, 13.4 mmol) was dissolved in $CHCl_3$, and the solution was filtered through a pad of silica gel (diameter 90 mm, height 70 mm, 0.032–0.063 mm). The silica gel was washed with $CHCl_3$ (5 × 50 mL), the filtrate concentrated to dryness under vacuum, and **6b** obtained as a colorless oil (4.4 g, 94%). $[\alpha]_D^{21}$: −104.5 (c = 2.0 $CHCl_3$). IR: $\tilde{\nu}$[cm^{-1}] = 1830, 1770, 1740. ^{1}H NMR ($CDCl_3$): δ = 1.31 (t, J = 7 Hz, 3H; CH_3), 2.71 (dd, J = 9, 19 Hz, 1H; H-C6), 2.94 (dd, J = 8.5, 19 Hz, 1H; H-C6), 4.23–4.32 (m, 2H; OCH_2), 4.46 (s, 1H; H-C8), 4.77 (dd, J = 8.5, 9 Hz, 1H; H-C5); ^{13}C NMR ($CDCl_3$): δ = 13.9 (CH_3), 37.1 (C6), 56.3 (C5), 62.9 (OCH_2), 66.1 (C8), 91.3 (sept, J = 32 Hz; C2), 120.0 (q, J = 291 Hz, CF_3), 120.1 (q, J = 287 Hz, CF_3), 165.2, 167.9 (C=O ester, C4), 201.9 (C7); ^{19}F NMR ($CDCl_3$): δ = −2.3 (q, J = 9 Hz, 3F; CF_3), 5.9 (q, J = 9 Hz, 3F; CF_3).

7: A solution of **6a** (1.07 g, 3.88 mmol) in anhydrous 2-propanol (10 mL) at 0 °C was stirred and $Na[BH_3CN]$ (0.12 g, 1.94 mmol) added in portions. After the addition of glacial acetic acid (4 mL), the reaction mixture was stirred until no more starting material was evident by ^{19}F NMR spectroscopy (ca. 1 h). $CHCl_3$ was added to the reaction mixture, which was then washed twice with $NaHCO_3$ solution and water, dried over $MgSO_4$, and concentrated to dryness under vacuum. **7** was obtained as a colorless oil (0.74 g, 68%). $[\alpha]_D^{21}$: −28.4 (c = 1.2 $CHCl_3$). IR: $\tilde{\nu}$[cm^{-1}] = 3600–3200, 2960, 1815. ^{1}H NMR ([D_6]acetone): δ = 2.20 (ddd, J = 13.5, 4.5, 2 Hz, 1H; H-C6), 2.35 (ddd, J = 13.5, 9, 4 Hz, 1H; H-C6), 3.29 (dd, J = 13, 9.5 Hz, 1H; H-C8), 3.48 (ddd, J = 13, 4, 2 Hz, 1H; H-C8), 4.24 (m, 1H; H-C5), 4.40 (m, 1H; H-C7); ^{13}C NMR ([D_6]acetone): δ = 37.1 (C6), 57.7 (C5), 60.9 (C8), 69.4 (C7), 92.8 (sept, J = 32 Hz; C2), 120.2 (q, J = 288 Hz; CF_3), 122.2 (q, J = 288 Hz; CF_3), 172.7 (C4); ^{19}F NMR ($CDCl_3$): δ = −1.72 (q, J = 10.5 Hz, 3F; CF_3), 7.28 (q, J = 10.5 Hz, 3F; CF_3).

8: A solution of **7** (1.06 g, 3.79 mmol) in 2-propanol/water (20 mL/20 mL) was stirred at room temperature. After the starting material could not be detected by ^{19}F NMR spectroscopy, the reaction mixture was concentrated to dryness under vacuum and the residue recrystallized from H_2O/CH_3OH to give **8** (0.43 g, 41%). M.p. 241 °C (decomp). $[\alpha]_D^{21}$: −60.9 (c = 1.0 H_2O). ^{1}H NMR (D_2O): δ = 2.31 (m_c, 1H; H-C3), 2.56 (m_c, 1H; H-C3), 3.43 (dd, J = 2.5, 12.5 Hz, 1H; H-C5), 3.53 (m_c, 1H; H-C5), 4.28 (dd, J = 2.5, 10.5 Hz, 1H; H-C2), 4.64 (m_c, 1H; H-C4); ^{13}C NMR (D_2O): δ = 39.8 (C3), 55.6 (C5), 62.4 (C2), 71.8 (C4), 177.2 (CO_2H).

Received: September 18, 1992 [Z 5578 IE]
German version: *Angew. Chem.* **1993**, *105*, 293

[1] D. Seebach, M. Boes, R. Naef, W. B. Schweizer, *J. Am. Chem. Soc.* **1983**, *105*, 5390–5398.
[2] K. Burger, M. Rudolph, H. Neuhauser, M. Gold, *Synthesis* **1992**, 1150; K. Burger, M. Gold, H. Neuhauser, M. Rudolph, E. Höss, *ibid.* **1992**, 1145.
[3] K. Burger, M. Rudolph, *Chem.-Ztg.* **1990**, *114*, 249–251.
[4] A. A. Patchett, B. Witkop, *J. Am. Chem. Soc.* **1957**, *79*, 185–192; R. H. Andreatta, V. Nair, A. V. Robertson, W. R. J. Simpson, *Aust. J. Chem.* **1967**, *20*, 1493–1509.
[5] Reviews: M. P. Doyle, *Chem. Rev.* **1986**, *86*, 919–939; G. Maas, *Top. Curr. Chem.* **1987**, *137*, 75–253; J. Adams, D. M. Spero, *Tetrahedron* **1991**, *47*, 1765–1808.
[6] K. Kondo, I. Ojima, *Chem. Commun.* **1972**, 860–861.

[7] R. W. Ratcliffe, T. N. Salzmann, B. G. Christensen, *Tetrahedron Lett.* **1980**, 31–34.
[8] M. Rudolph, *Dissertation*, Technische Universität München, **1991**.
[9] C. Yu, G. C. Levy, *J. Am. Chem. Soc.* **1984**, *106*, 6533–6537.
[10] Review: R. M. Williams, *Synthesis of Optically Active α-Amino Acids, Self Reproduction of Chirality*, Pergamon, New York, **1989**, pp. 62–84.
[11] Review: M. Regitz, G. Maas, W. Illger, *Diazoalkane, Eigenschaften und Synthese*, Thieme, Stuttgart, **1977**.
[12] The van der Waals volume of the trifluoromethyl group (42.6 Å^3) is more than double that of the methyl group; its van der Waals radius (2.7 Å) is between that of the methyl group (2.0 Å) and the *tert*-butyl group (3.5 Å): D. Seebach, *Angew. Chem.* **1990**, *102*, 1363–1409; *Angew. Chem. Int. Ed. Engl.* **1990**, *29*, 1320–1367, and references therein.
[13] K. Burger, M. Rudolph, H. Neuhauser, *Liebigs Ann. Chem.* **1991**, 1365–1368.
[14] H. Leuchs, K. Bormann, *Ber. Dtsch. Chem. Ges.* **1919**, *52*, 2086–2097.
[15] E. M. L. Tan, L. Ryhanen, J. Uitto, *J. Invest. Dermatol.* **1983**, *80*, 261–267; *Chem. Abstr.* **1983**, *98*, 137603s.
[16] W. D. Klohs, R. W. Steinkampf, M. S. Wicha, A. E. Mertus, J. B. Tunac, W. R. Leopold, *J. Natl. Cancer Inst.* **1985**, *75*, 353–359; *Chem. Abstr.* **1985**, *103*, 115868b.
[17] Melting points (uncorrected): Tottoli apparatus (Büchi). IR spectra: Perkin-Elmer spectrometers 157G and 257. ^{1}H NMR: Bruker AM 360 (360.1 MHz), tetramethylsilane as internal standard; ^{13}C NMR: Bruker AM 360 (90.6 MHz), tetramethylsilane as internal standard; ^{19}F NMR: Jeol C60 HL (56.5 MHz) or Bruker AM 360 (338.8 MHz), trifluoroacetic acid as external standard. Elemental analyses: C,H,N analyzer EA 415/0, Monar system (Heraeus). Correct elemental analyses were obtained for all the compounds described: C ± 0.17, H ± 0.31, N ± 0.12.

Ba[Si(OCH$_2$CH$_2$O)$_3$], a Hexaalkoxysilicate Synthesized from SiO$_2$**

By *Martin L. Hoppe, Richard M. Laine,* Jeffrey Kampf, Mark S. Gordon,* and *Larry W. Burggraf*

Anionic (pentacoordinate) and dianionic (hexacoordinate) organosilicates were first reported more than 60 years ago.[1–4] Pentacoordinate Si complexes have recently received considerable attention because of their role in sol–gel processing of silicate glasses,[4–6] their utility in organic synthesis and polymerization,[7–9] and their use as precursors to organosilicon compounds.[10–12] Pentacoordinate silicates are easily prepared from compounds with tetrasubstituted Si centers.[10–22] Although polyhalogenated anionic silicates are relatively common, only perfluorinated derivatives are found to form hexacoordinate silicate dianions, for example $[SiF_6]^{2-}$.[23] Salts of the dianion $[Si(1,2\text{-}O_2C_6H_4)_3]^{2-}$, first prepared in the early 30s, are the most common nonfluorinated hexacoordinate silicates.[2, 3, 10]

Surprisingly, these salts are thermally and hydrolytically more stable than pentacoordinate alkoxysilicates, possibly because the aromatic rings provide charge delocalization.[1c] Hexacoordinate dianionic germanium complexes $M_2[Ge(1,2\text{-}O_2C_2Me_4)_3]$ (M = K, Li; $1,2\text{-}O_2C_2Me_4$ = dianion of pinacole) have been synthesized directly from GeO_2; however, silicon analogues are still unknown.[24] Polyhedral germanates with four, five, and six oxygen donors at Ge have been prepared, but it has been suggested[25] that the ability of Ge (but rarely Si) to exhibit sixfold O-coordination is because it is a post transition metal element. Materials with sixfold O-coordinated Si atoms are limited to the rare mineral stishovite formed from a meteor impact.

Given that no examples of hexaalkoxysilicates have been described in the literature since the synthesis of the tris(benzenediyldioxido) complexes in 1931, it can be inferred that they do not form readily. However, theoretical calculations suggest that simple silicate dianions with six O ligands without supporting aromatic groups should be stable.[26] We report here the first such example.

We recently reported the synthesis of the pentacoordinate silicates $M[Si(OCH_2CH_2O)_2(OCH_2CH_2OH)]$ and $M_2[Si_2(OCH_2CH_2O)_5]$ (M = Li, Na, K, Cs) by direct reaction of one equivalent of MOH with one equivalent of SiO_2 in excess ethylene glycol.[27] Efforts to delineate the scope of this reaction led to studies of analogues with alkali metals, for example $M[Si_2(OCH_2CH_2O)_5]$ (M = Mg, Ca, Ba), whose stoichiometry would be ideal for the preparation of aluminosilicates such as $CaO \cdot 2SiO_2 \cdot Al_2O_3$ (garnet). These studies provided rather unique and unexpected results. We report here the synthesis of the first example of the heretofore unknown dianionic hexaalkoxysilicate **1** directly from silica, ethylene glycol, and barium oxide.

$Ba[Si(OCH_2CH_2O)_3]$ **1**

When mixtures of BaO (85.2 g, 0.56 mol), SiO_2 (30.0 g, 0.5 mol), and glycol (500 mL) were heated such that excess glycol and the H_2O formed in the reaction distilled off, the SiO_2 dissolved completely in 2–4 h. When the clear solution was cooled, the white microcrystalline methanol-soluble product **1** precipitated (≈ 90% yield).[28] CaO and MgO can be used in place of BaO; the yields are low with MgO because of the low reactivity of MgO with ethylene glycol. X-ray quality single crystals of the Ba complex were grown by vapor diffusion of acetonitrile into a solution of the Ba complex in glycol.

The structure determined by single-crystal X-ray diffraction (Fig. 1)[29] reveals two crystallographically independent $Ba^{2+}[Si(OCH_2CH_2O)_3]^{2-}$ formula units per asymmetric unit. ^{29}Si MAS solid-state NMR data support these findings.[30] Each Si atom has a slightly distorted octahedral coordination environment with three bidentate ethanediolato ligands. Each unit cell contains 13 glycol molecules in the crystal lattice. Coulombic Ba···O interactions and strong hydrogen bonding with the glycol molecules in the lattice[31] likely account for the stability of the complex and also modify the stereochemistry about each silicon atom. One Si atom has a Δ configuration; its three bidentate ethanediolato ligands adopt a $(\lambda\delta\delta)$ configuration. The configuration about the other Si atom is $\Delta(\delta\delta\delta)$. The crystallographic inversion center also generates Si centers with $\Lambda(\delta\lambda\lambda)$ and $\Lambda(\lambda\lambda\lambda)$ stereochemistry.

There are no chemically significant differences in any of the Si–O or C–C bond lengths or angles for the two molecules except for those imposed by stereochemistry. However, the Ba atoms occupy quite different environments in the crystal lattice. Each Ba atom has nine contacts with O atoms < 3.2 Å. For Ba1, two of these contacts are with the Si1–tris-

[*] Prof. R. M. Laine, M. L. Hoppe
Department of Materials Science and Engineering
H. H. Dow Building, 2300 Hayward St.
University of Michigan
Ann Arbor, MI 48109-2136 (USA)
J. Kampf
Department of Chemistry, University of Michigan (USA)
M. S. Gordon
Department of Chemistry,
North Dakota State University, Fargo, ND (USA)
L. W. Burggraf
Air Force Office of Scientific Research, Washington DC (USA)

[**] This work was supported by the Air Force Office of Scientific Research. We would like to thank Prof. Linda Nazar, Waterloo, and Prof. Florence Babonneau, Paris, for continuing collaborations, especially for running solid-state NMR studies; and Prof. R. J. P. Corriu for numerous helpful discussions that have made this publication possible.

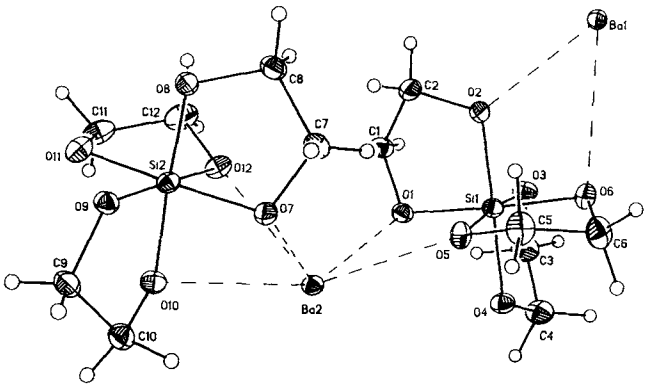

Fig. 1. ORTEP plot of the crystallographically independent formula units of $Ba[Si(OCH_2CH_2O)_3]$ (**1**) (atoms represented as 50% thermal ellipsoids). Selected interatomic distances [Å]: Si(2)-O(7) 1.835(2), Si(2)-O(8) 1.762(2), Si(2)-O(9) 1.753(2), Si(2)-O(10) 1.781(2), Si(2)-O(11) 1.809(2), Si(2)-O(12) 1.770(2), Ba(2)···O(7) 2.772(2), Ba(2)···O(10) 2.956(2), Ba(2)···O(12) 2.682(1), Ba(2)···Si(2) 3.481(1). Mean bond lengths have typical values: Si-O 1.785(1), C-O 1.419(3), C-C 1.516(4).

(ethanediolato)complex (mean distance) (2.904(2)), two are with the Si2 complex (2.739(2)), and five are with glycol molecules in the lattice (2.832(2)Å). For Ba2, two contacts are with the Si1 complex (2.739(2)), three are with the Si2 complex (2.803(2)), and four are with glycol molecules in the lattice (2.827(2)Å). The Ba···Si distances are also quite dissimilar. The Ba1–Si2 and Ba1–Si2 distances are 3.874(1) and 3.768(1) Å, respectively, while the Ba2–Si1 and Ba2–Si2 distances are 3.684(1) and 3.481(1) Å. The closest Ba···Ba distance is quite long, 4.750(1) Å.

Thermogravimetric analyses of **1** reveal the expected weight loss calculated from the chemical analysis,[28] and at temperatures greater than 800 °C lead to the formation of phase-pure $BaSiO_3$ (JCPDS File No. 26-1402).[32]

Because no chemically significant differences in the Si–O bonds are observed in the crystal structure, despite the coulombic interactions with Ba^{2+} ions, we reexamined the synthesis of the analogous hexacoordinate alkali metal silicates with two equivalents of LiOH or KOH; the reactions provided the pentacoordinate complexes in lower yields.[27] The presence of a dication may be required to stabilize dianionic hexaalkoxysilicates; however, this conclusion is not supported by preliminary theoretical studies.[26]

Preliminary ab initio calculations with a minimal basis set (STO-2G)[33] were conducted on the free, isolated $[Si(OCH_2CH_2O)_3]^{2-}$ dianion to determine if it has any inherent asymmetry. Geometry optimization using analytical gradient routines (GAMESS[34]) was conducted with C_1 symmetry. The resulting structure (which has a positive definite hessian) predicts Si–O bond lengths that are within an 0.002 Å range (1.805–1.807 Å). The semiempirical AM1 method[35] predicts all six bond lengths to be 1.794 Å. Both of these results are remarkably close to the average experimental Si–O distance of 1.785 Å in **1**. (EXAFS studies of **1** indicate that the Si–O bond lengths, which range from 1.753 to 1.809 Å, are essentially identical to those in stishovite, 1.757 and 1.809 Å.[39]). Thus, at these levels of theory the isolated dianion exhibits no bond-length distortion. The distortions seen in the X-ray structure of **4** probably result from crystal packing effects, H-bonding, and Ba–O coulombic interactions.

The monomers $M[Si(OCH_2CH_2O)_3]$ (M = Mg, Ca, Ba) and tractable polymeric derivatives may offer access to novel silicon-containing materials, including glasses and ceramics. $Mg(OR)_2/Si(OR)_4$ mixtures have been used to form novel silicates;[36] our work suggests that $Mg[Si(OR)_6]$ may be an intermediate. The Mg analogue of **1** can be used as a tractable cordierite precursor.[37] The isolation of hexaalkoxysilicates also provides support for the formation of hexacoordinate silicate anion intermediates in the nucleophilic reactions of pentacoordinated silicates.[38]

Received: September 5, 1992 [Z 5557 IE]
German version: *Angew. Chem.* **1993**, *105*, 283

[1] a) H. Meerwein, *Justus Liebigs Ann. Chem.* **1929**, *476*, 113; b) R. Müller, L. Heinrich, *Chem. Ber.* **1961**, *94*, 1943; c) C. L. Frye, *J. Am. Chem. Soc.* **1970**, *92*, 1205–1210.
[2] a) A. Rosenheim, B. Raibmann, G. Schendel, *Z. Anorg. Chem.* **1931**, *196*, 160; b) D. W. Barnum, *Inorg. Chem.* **1970**, *9*, 1942; c) *ibid.* **1972**, *11*, 1424.
[3] a) C. L. Frye, *J. Am. Chem. Soc.* **1964**, *86*, 3170; b) J. J. Flynn, F. P. Boer, *ibid.* **1969**, *91*, 5756.
[4] a) R. J. P. Corriu, *Pure Appl. Chem.* **1988**, *60*, 99–106; b) R. R. Holmes, *Chem. Rev.* **1990**, *90*, 17.
[5] C. J. Brinker, G. W. Scherer, *Sol Gel Science*, Academic Press, Boston, **1990**.
[6] R. M. Laine in *Sol-Gel Processing of Glasses Proc. SPIE Int. Soc. Opt. Eng.* **1990**, *1328*, 16.
[7] a) S. K. Chopra, J. C. Martin, *J. Am. Chem. Soc.* **1990**, *112*, 5342–5343; b) M. Kira, K. Sato, H. Sakurai, *Chem. Lett.* **1987**, 2243–2246.
[8] Y. Hatanaka, S. Fukushima, T. Hayama, *Chem. Lett.* **1989**, 1711–1714.
[9] O. W. Webster, W. R. Hertler, D. Y. Sogah, W. B. Farnham, T. V. Rajan Babu, *J. Am. Chem. Soc.* **1983**, *105*, 5706–5708.
[10] A. Boudin, G. Cerveau, C. Chuit, R. J. P. Corriu, C. Reyé, *Angew. Chem.* **1986**, *98*, 473; *Angew. Chem. Int. Ed. Engl.* **1986**, *25*, 473.
[11] R. J. P. Corriu, C. Guérin, B. J. L. Henner, W. W. C. Man, *Organometallics* **1988**, *7*, 237.
[12] A. Boudin, G. Cerveau, C. Chuit, R. J. P. Corriu, C. Reyé, *Organometallics* **1988**, *7*, 1165.
[13] C. Brelière, R. J. P. Corriu, G. Royo, W. W. C. Man, J. Zwecker, *Organometallics* **1990**, *9*, 2633–2635.
[14] R. Tacke, J. Sperlich, C. Strohman, G. Mattern, *Chem. Ber.* **1991**, 124, 1491–1496.
[15] G. Cerveau, C. Chuit, R. J. P. Corriu, N. K. Nayyar, C. Reyé, *J. Organomet. Chem.* **1990**, *389*, 159.
[16] R. Damrauer, B. O'Connell, S. E. Danahey, R. Simon, *Organometallics* **1989**, *8*, 1167–1171.
[17] D. A. Dixon, W. R. Hertler, D. B. Chase, W. B. Farnham, F. Davidson, *Inorg. Chem.* **1988**, *27*, 4012–4019.
[18] M. Kira, K. Sato, H. Sakurai, *J. Am. Chem. Soc.* **1988**, *110*, 4599-4602.
[19] D. Kummer, K.-E. Gaisser, T. Seshadri, *Chem. Ber.* **1977**, *110*, 1950–1962.
[20] R. R. Holmes, R. O. Day, J. S. Payne, *Phosphorous Sulfur Silicon Relat. Elem.* **1989**, *42*, 1–13.
[21] R. R. Holmes, R. O. Day, J. J. Harland, J. M. Homes, *Organometallics* **1984**, *3*, 347–353.
[22] K. C. K. Swamy, V. Chandrasekhar, J. J. Harland, J. M. Homes, R. O. Day, R. R. Holmes, *J. Am. Chem. Soc.* **1990**, *112*, 2341–2348.
[23] S. N. Tandura, M. G. Voronkov, N. V. Alekseev, *Top. Curr. Chem.* **1986**, *131*, 99–186.
[24] G. Cerveau, C. Chuit, R. J. P. Corriu, C. Reyé, *Organometallics* **1991**, *10*, 1510–1515.
[25] R. H. Jones, J. Chen, J. M. Thomas, A. George, M. B. Hursthouse, R. Xu, S. Li, Y. Lu, G. Yang, *Chem. Mater.* **1992**, *4*, 808–812.
[26] L. W. Burggraf, L. P. Davis in *Better Ceramics Through Chemistry II* (*Mater. Res. Soc. Symp. Proc.* **1986**, *73*, 529–542).
[27] R. M. Laine, K. Y. Blohowiak, T. R. Robinson, M. L. Hoppe, P. Nardi, J. Kampf, J. Uhm, *Nature* **1991**, *353*, 642–644.
[28] Simple filtration followed by washing with anhydrous ethanol and acetonitrile and then drying at 100 °C under vacuum 2–6 h provided analytically pure samples. Correct C,H,Ba,Si analysis for $1 \cdot 3.25\ HOCH_2CH_2OH$ [29].
[29] Crystal data for $1 \cdot 3.25\ HOCH_2CH_2OH$: triclinic $P\bar{1}$, $a = 10.151(8)$, $b = 13.865(5)$, $c = 15.709(6)$ Å, $\alpha = 102.90(3)$, $\beta = 91.04(3)$, $\gamma = 109.75(3)°$, $V = 2018(1)$ Å^3, $Z = 4$, $\varrho_{calcd} = 1.70$ g cm^{-3}, $\mu(Mo_{K\alpha}) = 2.08$ mm^{-1}, $F(000) = 1080$, colorless rectangular plate, $0.2 \times 0.5 \times 0.44$ mm^3, 13038 reflections collected with $5° < 2\theta < 50°$, 9298 unique reflections, $R_{merge} = 0.0312$; 8999 reflections with $F_0 \geq 6\,\sigma(F)$ used in the refinement. Data were collected on a Siemens R3/v diffractometer equipped with a LT-2 low-temperature device at 175K and corrected for absorption (φ scans) and secondary extinction. The structure was solved by direct methods and refined using Siemens SHELXTL PLUS. All non-H atoms were refined anisotropically. H atoms were located by difference Fourier synthesis and refined isotropically. The O atom of one glycol of solvation is disordered over two positions at refined occupancies of 0.700(1) and 0.300(1). The related H atom was not placed. 745 parameters were refined with a weighting scheme $[w^{-1} = \sigma^2(F) + 0.000382(F_0)^2]$ to give a final

convergence of $R = 0.0282$, $R_w = 0.0374$, and a final difference electron density max. of $+0.80$ e Å^{-3}, min. -0.82 e Å^{-3}. Further details of the crystal structure investigation are available on request from the Director of the Cambridge Crystallographic Centre, 12 Union Road, GB-Cambridge CB21EZ (UK), on quoting the full journal citation.

[30] Solid-state ^{29}Si MAS NMR: $\delta = -143.3$, -145.5; M. Hoppe, L. Nazar, R. M. Laine, unpublished results.

[31] Significant H-bonding interactions for **1**: Distances [Å] between the hydroxyl proton of a glycol molecule in the lattice and the numbered oxygen of a coordinated glycol. Approximate errors are 0.04 Å. a) O(11) 1.84, O(4) 1.97; b) O(3) 1.60, O(6) 1.94; c) O(7) 1.52, O(4) 1.91, O(13) 1.97; d) O(11) 1.70, O(10) 1.87. Symmetry transformations a) x, y, z; b) $1 + x, 1 + y, z$; c) $1 - x, 1 - y, -z$; d) $2 - x, 1 - y, -z$.

[32] Details of the pyrolysis experiments with the Mg, Cu, and Ba complexes will be described elsewhere. P. Kansal, K. W. Chew, M. L. Hoppe, R. M. Laine, unpublished results.

[33] W. J. Hehre, R. F. Stewart, J. A. Pople, *J. Chem. Phys.* **1969**, *51*, 2657.

[34] M. W. Schmidt, K. K. Baldridge, L. Boatz, J. H. Jensen, S. Koseki, M. S. Gordon, K. A. Nguyen, T. L. Windus, S. T. Elbert, *QCPE Bulletin* **1990**, *10*, 52.

[35] M. J. S. Dewar, E. G. Zoebisch, E. F. Healy, J. J. P. Stewart, *J. Am. Chem. Soc.* **1985**, *107*, 3902.

[36] a) J. M. Burlitch, M. L. Beeman, B. Riley, D. L. Kohlstedt, *Chem. Mater.* **1991**, *3*, 692–698; b) F. D. Duldulao, J. M. Burlitch, *ibid.* **1991**, *3*, 772–773.

[37] Z.-F. Zhang, M. L. Hoppe, J. A. Rahn, S.-M. Koo, R. M. Laine in *Synthesis and Processing of Ceramics: Scientific Issues* (*Mater. Res. Soc. Symp. Proc.* **1992**, *249*, 81–86).

[38] R. J. P. Corriu, C. Guerin, B. J. L. Henner, Q. Wang, *Organometallics* **1991**, *10*, 3200.

[39] J. S. Tse, D. D. Klug, B. X. Yang, X. H. Feng, R. M. Laine, *Phys. Chem. Miner.*, submitted.

A Hemerythrin Model Complex with Catalase Activity**

By *Bert Mauerer, Jonathan Crane, Jürgen Schuler, Karl Wieghardt,** and *Bernhard Nuber*

In the past few years the structural and electronic properties of the active site of the metalloprotein hemerythrin have been modeled successfully with low-molecular-weight systems.[1] Current efforts are concentrated on the preparation of *functional* model complexes. The active form of the enzyme, deoxyhemerythrin, has one penta- and a hexacoordinate, high-spin iron(II) ion bridged by a hydroxy or aqua ligand, whereas in the O_2 containing form, oxyhemerythrin, both Fe ions are in the oxidation state + III and one Fe^{III} ion binds a hydroperoxo ligand (Scheme 1).

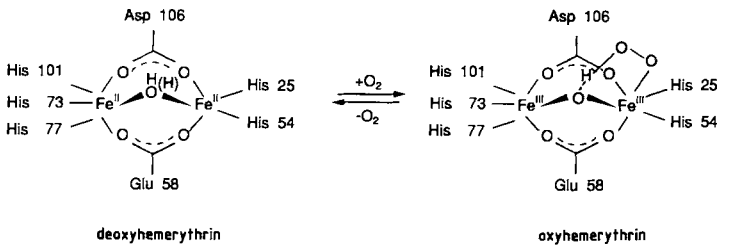

Scheme 1.

[*] Prof. Dr. K. Wieghardt, Dipl.-Chem. B. Mauerer, Dr. J. Crane, Dipl.-Chem. J. Schuler
Lehrstuhl für Anorganische Chemie I der Universität
Postfach 102148, D-W-4630 Bochum (FRG)
Dr. B. Nuber
Anorganisch-chemisches Institut der Universität
Heidelberg (FRG)

[**] This research was supported by the Fonds der Chemischen Industrie. J. C. thanks the Alexander-von-Humboldt-Stiftung for a stipend.

Previous attempts at modeling the active site in oxyhemerythrin proceeded logically from the synthesis of coordinatively unsaturated Fe^{II}_2 complexes, which were treated with O_2 at low temperatures in aprotic solvents in the hope of stabilizing the oxyhemerythrin form.[2] Despite some preliminary success this approach is problematic because of the extreme lability of Fe^{II} complexes. Therefore, we decided to try another approach in which more robust, coordinatively unsaturated Fe^{III}_2 complexes are treated with H_2O_2.[3] We report here on the synthesis and reactivity of a complex of this type.

The dinuclear complex **1**, which is asymmetric with respect to the two Fe^{III} ions with different coordination, was synthesized by the reaction of $[(bpy)_2Fe_4O_2(ac)_7](PF_6)$[4a] (bpy = 2,2′-bipyridine; ac = acetate) with $LFeCl_3$[4b] (L = 1,4,7-trimethyl-1,4,7-triazacyclononane) and 2,2′-bipyridine in acetonitrile. As the X-ray structure analysis[5] shows (Fig. 1 top), one Fe^{III} ion is bound to the tridentate amine L and the other to 2,2′-bipyridine and a terminal choride ion; the two metal ions are connected by an oxo and

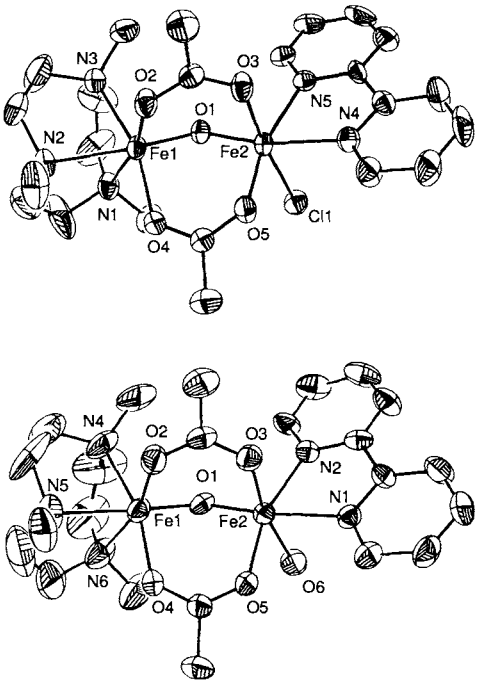

Fig. 1. Crystal structures of the cations in **1** (top) and **2** (bottom). Selected distances [Å] and angles [°]: **1**: Fe2-Cl1 2.376(2); Fe1-O1 1.786(5), Fe2-O1 1.797(5), Fe1···Fe2 3.097(2), Fe2-N4 2.206(6), Fe2-N5 2.146(7), Fe1-N1 2.184(7), Fe1-N2 2.252(7), Fe1-N3 2.211(7); Fe1-O1-Fe2 119.6(3). **2**: Fe1-O1 1.806(8), Fe1-O2 1.995(9), Fe1-O4 2.017(9), Fe1-N4 2.173(12), Fe1-N5 2.242(15), Fe1-N6 2.190(12), Fe2-O1 1.785(7), Fe2-O3 2.048(9), Fe2-O5 2.017(8), Fe2-N1 2.218(10), Fe2-N2 2.148(10), Fe2-O6 2.153(9), Fe1···Fe2 3.102(3); Fe1-O1-Fe2 119.5(4).

two symmetric acetate bridges. Thus, this is an asymmetric methemerythrin model complex. The chloro ligand in **1** can by replaced by H_2O in a reaction with $AgClO_4 \cdot H_2O$ in CH_2Cl_2 giving complex **2**, whose X-ray structure was also

$[LFe(\mu\text{-}O)(\mu\text{-}ac)_2Fe(bpy)Cl]X$ **1a**, X = PF_6, **1b**, X = ClO_4

$[LFe(\mu\text{-}O)(\mu\text{-}ac)_2Fe(bpy)(H_2O)](ClO_4)_2 \cdot CH_2Cl_2$ **2**

determined (Fig. 1 bottom).[5] The structural and electronic properties of **1** and **2** are similar to those of their sym-

metric analogues $[L_2Fe^{III}_2(\mu\text{-}O)(\mu\text{-}ac)_2]^{2+}$,[6a] $[(bpy)_2Fe^{III}_2(\mu\text{-}O)(\mu\text{-}ac)_2Cl_2]$,[4a] and $[(bpy)_2Fe^{III}_2(\mu\text{-}O)(\mu\text{-}ClCH_2CO_2)_2(H_2O)_2]^{2+}$.[6b]

When we treated **2** with an aqueous H_2O_2 solution, we observed an unexpected, vigorous evolution of O_2. Complex **2** catalyzes the disproportionation of H_2O_2 following Equation (a); the complex thus displays catalase activity. Interestingly, the symmetric complex, $[L_2Fe^{III}_2(\mu\text{-}O)(\mu\text{-}ac)_2]^{2+}$ (lacking the labile coordination site), is comparatively unreactive under the same conditions (see below).

$$2H_2O_2 \longrightarrow O_2 + 2H_2O \qquad (a)$$

To our knowledge catalase activity has not been observed for hemerythrin. It is known that deoxyhemerythrin (5×10^{-5} M) reacts with H_2O_2 (ca. 5×10^{-4} M) at pH 6.3–8.3 to give hydroxymethemerythrin,[7] but O_2 evolution was not observed (though possibly also not sought).

We examined the kinetics of the reaction of **2** with H_2O_2 in homogeneous aqueous solution more closely. Compound **2** is stable in pure H_2O for only a few minutes; the formation of $[Fe(bpy)_3]^{2+}$ can be detected by UV/VIS spectroscopy. In contrast, **2** is stable in 0.10 M acetic acid/sodium acetate buffer (1:1) for more than 24 h. We therefore decided to measure the evolution of O_2 from solutions of **2** (buffered acetic acid/sodium acetate) at 20 °C with a manometer with variation of the following parameters: 1) the concentration of **2** (1.3×10^{-5}–1.2×10^{-4} M), 2) the concentration of H_2O_2 (0.27–1.7 M), 3) the pH (3.7–5.6), and finally 4) the concentration of acetate ions (0.14–1.0 M).

Figure 2 shows the O_2 evolution as a function of time, from which the following conclusions can be drawn. From

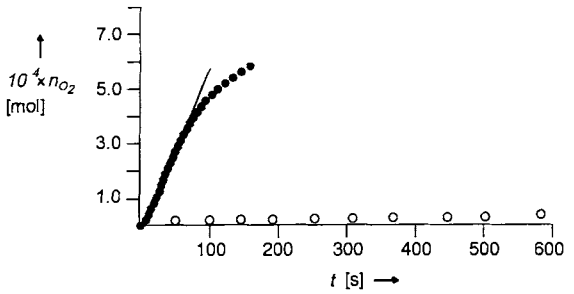

Fig. 2. Plot of the O_2 evolution versus time at 20 °C for catalyst **2** (•) and $[L_2Fe^{II}_2(\mu\text{-}O)(\mu\text{-}ac)_2](ClO_4)_2$ (○). Conditions: $[CH_3CO_2H/CH_3CO_2^-] = 0.07$ M; pH = 5.01; $[H_2O_2] = 1.03$ M; $[\mathbf{2}] = 1.2 \times 10^{-4}$ M. The region in which the plot follows the straight line has zeroth-order kinetics.

the start of the reaction until about 200–300 turnovers the reaction follows zeroth-order kinetics. The O_2 evolution is terminated by decomposition of the catalyst. Plots of the initial rates versus the concentrations of a) **2** and b) H_2O_2 indicate that the reaction is first order in both under constant concentrations of H^+ and $CH_3CO_2^-$ [Eq.(b)].

$$\text{rate} = k[\mathbf{2}][H_2O_2] \qquad (b)$$
$$([H^+] = \text{const.}, [CH_3CO_2^-] = \text{const.})$$

Experiments at constant concentrations of **2**, H_2O_2, and $CH_3CO_2^-$ demonstrate that the rate of evolution of O_2 *decreases* with increasing H^+ concentrations (Fig. 3 bottom). Acetate ions *inhibit* the evolution of O_2 (Fig. 3 top) as well. These observations allow the conclusion that the acetate ions replace the labile H_2O ligand in **2** and compete with H_2O_2 (or HO_2^-) molecules for this coordination site. The observed pH-dependence most probably arises because HO_2^- is a better nucleophile than its protonated form H_2O_2. It is noted that in the experimental pH range (4–6) the spectrum of **2** does not change, that is, protonation at the μ-oxo bridge does not occur.

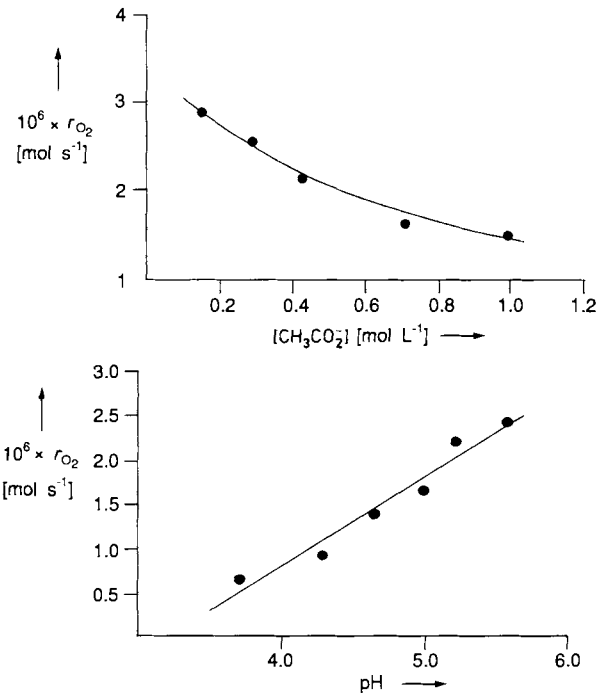

Fig. 3. Plot of the initial rate of O_2 evolution as a function of the concentration of acetate ions (pH = 5.0; $[H_2O_2] = 1.03$ M; $[\mathbf{2}] = 7.2 \times 10^{-5}$ M) (top) and the pH ($[\mathbf{2}] = 6.0 \times 10^{-5}$ M; $[CH_3CO_2^-] = 0.18$ M, $[H_2O_2] = 1.08$ M) (bottom).

A possible catalytic cycle is sketched in Figure 4 which takes into account the known chemistry of hemerythrin and its model complexes as well as the kinetic experiments described here. The rate-determining step may be the substitu-

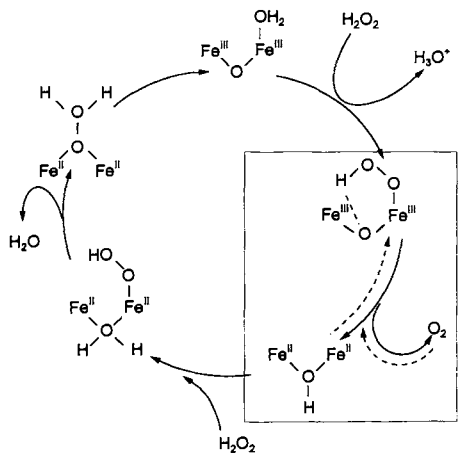

Fig. 4. Proposed mechanism for the disproportionation of H_2O_2 catalyzed by complex **2**. In the framed section hemerythrin–oxygen binding is in the direction of the dashed arrows.

tion step in the binding of H_2O_2 (or HO_2^-) to an Fe^{III} ion in **2**. This cycle is plausible, since it essentially represents steps of the back reaction in hemerythrin–oxygen binding. Finally, only the Fe^{III}/Fe^{II} redox potential of hemerythrin and its model complexes decides if the oxyhemerythrin form can be stabilized or if the coordinated HO_2^- is oxidized with concomitant formation of the deoxyhemerythrin form (Fe^{II}).

Experimental Procedure

Synthesis of the complexes: **1a**: A solution of $[(bpy)_2Fe_4O_2(ac)_2](PF_6)$[4a] (6.0 mmol) $LFeCl_3$[4b] (12 mmol) and bpy (37 mmol) in acetonitrile (200 mL) was heated for 4 h at reflux. The reaction mixture was cooled and filtered, then nBu_4NPF_6 (5.0 g) and diethyl ether (400 mL) were slowly added in portions. After 30–40 min red $[Fe(bpy)_3](PF_6)_2$ precipitated and was filtered off. Ether (100 mL) was again added to the filtrate, and the solution was filtered after 30 min. Within the next 12 h brown crystals of **1a** formed (30%). The perchlorate salt **1b** was prepared analogously by using nBu_4NClO_4.

2: A solution of **1b** (1.0 mmol) and nBu_4NClO_4 (0.50 g) in anhydrous CH_2Cl_2 (80 mL) was treated with a solution of $AgClO_4 \cdot H_2O$ (1.0 mmol) in CH_2Cl_2/toluene (3:1; 3 mL) and stirred. After 5 min AgCl was filtered off. Within 12 h brown crystals of **2** (30%) formed. **1a**, **1b**, and **2** gave satisfactory elemental analyses (C,H,N,Fe).

Physical properties[8]: UV/VIS (CH_3CN) λ_{max} [nm] (ε[$Lmol^{-1}cm^{-1}$]): **1**: 235 (2.6×10^4), 294 (1.3×10^3), 336 (8.6×10^3), 463 (1.1×10^3), 500 (970), 718 (202); **2**: 237 (2.6×10^4), 285 (1.3×10^3), 341 (7.9×10^3), 475 (1.2×10^3), 500 (sh), 766 (228). Magnetic susceptibility (SQUID measurement, 4–298 K): $H = -2JS_1 \cdot S_2$ ($S_1 = S_2 = 5/2$): J[cm^{-1}]: **1**: −124; **2**: −117. Resonance Raman spectrum (506 nm): ν_{as} (Fe-O-Fe), ν_s (Fe-O-Fe) [cm^{-1}]: **1**: 736, 530; **2**: 734, 532. Mössbauer spectrum at 4.2 K (doublet): δ [$mm\,s^{-1}$], ΔE_Q [$mm\,s^{-1}$], **1**: 0.49, 1.59; **2**: 0.51, 1.61.

Received: September 21, 1992 [Z 5586 IE]
German version: *Angew. Chem.* **1993**, *105*, 306

[1] Recent reviews: S. J. Lipppard, *Angew. Chem.* **1988**, *100*, 353; *Angew. Chem. Int. Ed. Engl.* **1988**, *27*, 344; D. M. Kurtz, Jr., *Chem. Rev.* **1990**, *90*, 585; J. B. Vincent, G. L. Olivier-Lilley, B. A. Averill, *ibid.* **1990**, *90*, 1447; L. Que, Jr., A. E. True, *Progr. Inorg. Chem.* **1990**, *38*, 97; J. Sanders-Loehr in *Iron Carriers and Iron Proteins* (Ed.: T. M. Loehr), VCH, Weinheim, **1989**, p. 373.

[2] N. Kitajima, F. Hideno, Y. Moro-oka, Y. Mizutani, T. Kitagawa, *J. Am. Chem. Soc.* **1990**, *112*, 6401; S. Ménage, B. A. Brennan, C. Juarez-Garcia, E. Münck, L. Que, Jr., *ibid.* **1990**, *112*, 6423; Y. Hayashi, M. Suzuki, A. Uehara, Y. Mizutani, T. Kitagawa, *Chem. Lett.* **1992**, 91.

[3] The (μ-peroxo)iron(III) complex $[Fe_6(O)_2(\mu\text{-}O_2)(O_2CPh)_{12}(OH_2)_2]$ was prepared in this fashion: W. Micklitz, S. G. Bott, J. G. Bentsen, S. J. Lippard, *J. Am. Chem. Soc.* **1989**, *111*, 372.

[4] a) J. B. Vincent, H. C. Huffman, G. Christou, Q. Li, M. A. Nanny, D. N. Hendrickson, R. H. Fong, R. H. Fish, *J. Am. Chem. Soc.* **1988**, *110*, 6898; b) K. Wieghardt, K. Pohl, D. Ventur, *Angew. Chem.* **1985**, *97*, 415; *Angew. Chem. Int. Ed. Engl.* **1985**, *24*, 392.

[5] Crystal structure analyses: Syntex R3, $Mo_{K\alpha}$, empirical absorption correction, H atoms at calculated positions. **1**: Crystal data (295 K): $a = 8.852(3)$, $b = 24.824(8)$, $c = 14.740(4)$ Å, $\beta = 95.61(2)°$, $V = 3223.5$ Å^3; space group $P2_1/c$ (no. 14), $Z = 4$, $\mu(Mo_{K\alpha}) = 1.10$ mm^{-1}, $2\theta_{max} = 57.5°$; 9051 reflections, 3875 of which were independent with $I > 2.5\sigma(I)$, 389 parameters (Fe, P, C, N, O, Cl anisotropic), $R_1 = 0.081$, $R_2 = 0.066$. **2**: Crystal data (295 K): $a = 18.275(5)$, $b = 16.847(8)$, $c = 23.571(7)$ Å, $\beta = 92.32(2)°$, $V = 7251$ Å^3; space group $C2/c$ (no. 15), $Z = 8$, $\mu(Mo_{K\alpha}) = 1.01$ mm^{-1}, $2\theta_{max} = 52.5°$; 7789 reflections, 3883 of which were independent with $I > 2.5\sigma(I)$, 410 parameters, ClO_4^- and the solvent molecule are highly disordered, $R_1 = 0.091$, $R_2 = 0.082$. – Further details of the crystal structure investigations may be obtained from the Fachinformationszentrum Karlsruhe, Gesellschaft für wissenschaftlich-technische Information mbH, D-W-7514 Eggenstein-Leopoldshafen 2 (FRG) on quoting the depository number CSD-56752, the names of the authors, and the journal citation.

[6] a) P. Chaudhuri, K. Wieghardt, B. Nuber, J. Weiss, *Angew. Chem.* **1985**, *97*, 774; *Angew. Chem. Int. Ed. Engl.* **1985**, *24*, 778; b) K. L. Taft, A. Masschelein, S. Liu, S. J. Lippard, D. Garfinkel-Shweky, A. Bino, *Inorg. Chim. Acta* **1992**, *198–200*, 627.

[7] a) G. D. Armstrong, A. G. Sykes, *Inorg. Chem.* **1986**, *25*, 3514; b) Z. Bradic, P. C. Harrington, R. G. Wilkins, *Biochemical and Clinical Aspects of Oxygens*, Academic Press, New York, **1979**, p. 557.

[8] We thank Prof. Sanders-Loehr (Oregon Research Center) for recording the resonance Raman spectra, and Dipl.-Phys. C. Butzlaff, Dr. E. Bill, and Prof. Dr. A. X. Trautwein (Medizinische Universität Lübeck (FRG)) for measuring the magnetic susceptibility and recording the Mössbauer spectra.

2,3,7,8,12,13,17,18-Octamethoxyporphyrin**

By *Andreas Merz,* Roland Schropp,* and *Johann Lex*

Dedicated to Professor Emanuel Vogel on the occasion of his 65th birthday

Porphyrins are of considerable biological importance and of interest to theoreticians as aromatic systems; nevertheless, far from all of the imaginable or desirable substitution patterns have been realized for the porphyrin system. While *meso*-tetraarylporphyrins are easily accessible from pyrrole and aromatic aldehydes,[1] the construction of even symmetric octaalkylporphyrins, for example **1c** or **1d**, is laborious,[2] primarily due to the lack of good synthetic routes to the basic pyrrole building blocks such as 3,4-disubstituted pyrroles. Porphyrins with + M substituents, in particular, are hardly known; the descriptions are limited to a few examples having one or two methoxy groups besides six alkyl substituents in the remaining β-pyrrole positions[3] as well as derivatives of octaalkylporphyrins with *meso*-amino substituents.[4, 5] We report here on the synthesis and properties of octamethoxyporphyrin **1a**, the first porphyrin with multiple donor substituents.

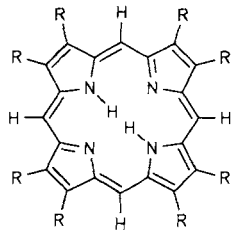

1a (R = OCH_3)
1b (R = H)
1c (R = CH_3)
1d (R = CH_2–CH_3)

3,4-Dimethoxypyrrole (**2**), the basic building block of **1a**, is a stable, crystalline compound that can be oxidized electrochemically to give highly conductive polydimethoxypyrrole films.[6] The facile oxididation of **2** is also reflected in its chemical behavior: treatment of a cold solution (−70 °C) of **2** in THF with *N*-bromosuccinimide leads to oxidative polymerization, not the formation of brominated derivatives. In contrast, the synthesis of porphyrin **1a** from the reaction of **2** with formaldehyde under acid catalysis and air oxidation is remarkably smooth; the best results, approximately 20% yield of **1a**, were hitherto obtained following the method of Treibs and Häberle with mixtures of glacial acetic acid and pyridine.[7] **1a** forms shiny, blue, rectangular prisms (m.p. 307–309 °C) that dissolve in many solvents to give brown solutions, thin layers of which appear red. Irradiation with a UV lamp causes an intense crimson fluorescence. Dilute solutions of **1a** are stable for several weeks without protection from air or light.

The methoxy group can function as an −I and + M substituent on aromatic systems.[8] This is evident from the comparison of the spectroscopic and structural data of **1a** with that of the parent compound porphine (**1b**), octamethylporphyrin **1c**, and octaethylporphyrin **1d**, which is isosteric and isoelectronic to **1a**. In the UV/VIS spectrum of

[*] Prof. Dr. A. Merz, Dipl.-Chem. R. Schropp
Institut für Organische Chemie der Universität
Universitätsstrasse 31, D-W-8400 Regensburg (FRG)
Dr. J. Lex
Institut für Organische Chemie der Universität Köln

[**] This research was supported by the Deutsche Forschungsgemeinschaft and the Fonds der Chemischen Industrie. We thank Dr. W. Bauer, Erlangen, for the ^{13}C NMR measurements.

1a (Table 1) the hypsochromic shift of the Soret bands characteristic for porphyrins by 15 and 20 nm compared to **1b** and **1d**, respectively, is particulary noticeable. The mono-

Table 1. UV/VIS data for porphin (**1b**), octaethylporphyrin **1d**, and octamethoxyporphyrin **1a**[a].

Cmpd.	Soret	Q-IV	Q-III	Q-II	Q-I
1b [b]	395	490	520	569	616
	(261 000)	(16 000)	(3 000)	(4 400)	(890)
1d [c]	400	498	532	568	622
	(159 000)	(14 500)	(10 800)	(6 800)	(5 800)
1a [c]	377	494	530	564	618
	(155 000)	(9 600)	(12 200)	(5 700)	(6 000)

[a] λ_{max} [nm]. [b] In benzene [10]. [c] In toluene.

and dimethoxyporphyrins described in ref.[3] do not show this effect. Since −M substituents (vinyl, formyl, and carboxyl groups) in the β positions often exert a considerable *bathochromic* effect on the Soret bands,[9] the hypsochromic shift observed here is in accord with the + M character of the methoxy group. The differences in the visible part of the spectrum are not as evident. Relative to the spectrum of **1d** the Q bands of **1a** have a slight hypsochromic shift and change from the etio to the rhodo type; the Q-III band, not the Q-IV band, has the greatest intensity. This effect has been observed previously for vinyl and formyl groups, but in those cases is accompanied by a *bathochromic* shift.[9] On irradiation of **1a** at 77 K with light with a wavelength of 400 nm, its fluorescence spectrum exhibits an intense band at 622 nm, flanked by three weaker bands at longer wavelengths, 644, 666, and 683 nm, with 18, 24, and 35% intensities (relative to that of the main band). Phosphorescence was not observed below 900 nm.

The ^{1}H NMR spectrum of **1a** shows only three singlets as expected (Table 2). The resonance frequency of the *meso*

Table 2. ^{1}H and ^{13}C NMR data of **1a**–**d** and **2**.

Cmpd.	$\delta(^1H)$			$\delta(^{13}C)$				Ref.
	meso H	β Subst.	N–H	*meso* C	α C	β C	Other	
1b [a]	10.58	9.74 (H)	−3.76					[11]
1b [b]	11.22	9.92 (H)	−4.40					[11, 12]
1c [b]	10.98	3.77 (CH_3)	−4.82					[12]
1d [a]	10.18	4.14 (CH_2)	−3.74					[13]
		1.95 (CH_3)						
1d [b]	10.98	4.28 (CH_2)	−4.28	96.0	142.2	140.9		[4, 14]
		1.87 (CH_3)						
1a [c]	10.59	4.77 (CH_3)	−4.05	94.3				
1a [a]	10.06	4.79 (CH_3)	−4.41		137.0	143.8	62.3 (CH_3)	
2 [a]		3.80 (CH_3)			99.6	138.1	58.4 (CH_3)	[6]
OAP [d]				95–96	143–144	135–137		[14]

[a] In $CDCl_3$. [b] In CF_3COOD. [c] In $CDCl_3$ + 10% CF_3COOD. [d] Other octaalkylporphyrins in CF_3COOD.

protons in **1a** relative to that of **1d** and **1c** does not indicate any particular effect of the methoxy substituents on this position: steric effects appear to cancel out the electronic effects. The downfield shift of the OCH_3 protons ($\Delta\delta \approx 1$ relative to **2** or anisole) reflects the high diatropism of the porphyrin system, but this value is $\Delta\delta \approx 0.5$ greater than that of the CH_3 groups of **1d** when the chemical shifts of both groups as benzene substituents are used as a comparison. This supports a structure of **1a** in which the OCH_3 groups are oriented more in the porphyrin plane. The upfield shift of the quadrupole-broadened NH signal is also in accord with the electron-donating effect of the OCH_3 group. For **1a** the difference in the chemical shifts of N–H and *meso*-H, $\Delta\delta = 14.47$, is greater than that of porphyrins listed for comparison (Table 2). In contrast to **1b** and **1d**, in the spectrum of the green, double-protonated form of **1a** both the *meso* protons and the N–H protons are shifted to lower fields.

In the ^{13}C NMR spectrum of dimethoxypyrrole **2** relative to that of the unsubstituted parent compound the two OCH_3 groups cause a tremendous downfield shift of the β C atoms and a simultaneous upfield shift of the α C atoms; this corresponds to the −I effect on the C atom directly bound to the oxygen atoms and the + M effect on the neighboring position. This effect is also apparent, although to a lesser degree, in the comparison of octamethoxyporphyrin **1a** and octaalkylporphyrins. Since the quadrupole effect of the ^{14}N nucleus causes the relaxation time of the neighboring C atoms to decrease, the two ^{13}C NMR signals could be assigned because of the signal broadening of the α C atoms.

The crystal structure of porphyrin **1a** has C_i symmetry (Fig. 1, Table 3).[15] Comparison of the structure of **1a** to

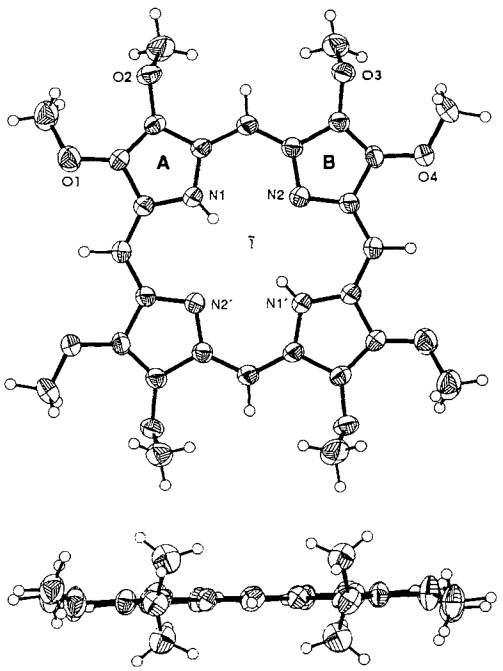

Fig. 1. Crystal structure of **1a** (ORTEP, ellipsoids at the 40% probability level[15]).

those of the other basic types of porphyrins[16] shows the bond lengths and angles to be intermediate to those of the unsubstituted parent compound **1b** and those of **1d**, which is in accord with the reduced steric demands along the

Table 3. Selected bond lengths [Å] and angles [°] of **1a**[a].

d	CαN [a]	CαCβ [a]	CβCβ	CαC*meso*	CβO1 CβO4	CβO2 CβO3
ring A	1.366	1.437	1.361	1.390	1.356	1.369
ring B	1.368	1.450	1.357	1.384	1.349	1.375
Angle	CαNCβ	NCαCβ [a]	CαCβCβ [a]	CαC*meso*Cα	CβO1Me CβO4Me	CβO2Me CβO3Me
ring A	109.4	107.5	107.6	125.7	114.4	117.6
ring B	106.9	109.7	106.8	125.7	114.5	117.7

[a] Mean values; standard deviations: ±0.003 Å and ±0.2°.

perimeter of **1a**. Since the methoxy groups require less space, one methoxy group on each pyrrole ring is almost in the porphyrin plane (i.e. its C–O bond and the porphyrin are close to coplanar). The deviation of the CH_3 carbon atoms of these "planar" methoxy groups from the best plane of the porphyrin ring is only 0.415(O1) and 2.33(O4) Å for **1a**, and 1.144(O2) and 1.068(O3) Å for those twisted out of the plane. The methoxy groups are arranged so that the "planar" methoxy groups point away from the *meso* hydrogen atoms, forcing the neighboring methoxy group on the same pyrrole ring out of the plane. Four of the eight methoxy groups are thus in conjugation with the porphyrin unit; the increased sp^2 character of the oxygen atoms results in markedly shorter porphyrin–O and methyl–O distances and in larger C-O-C bond angles at the "planar" groups.

In summary, **1a** as the first octaalkoxyporphyrin does not show principal changes in the geometry of the porphyrin core; however, all of its spectroscopic properties point to a modified π-electron system, which will certainly be the subject of future investigations.

We have also been able to improve the synthesis of starting material **2** (Scheme 1). *N*-Benzyl-3,4-dihydroxypyrrole (**4**),

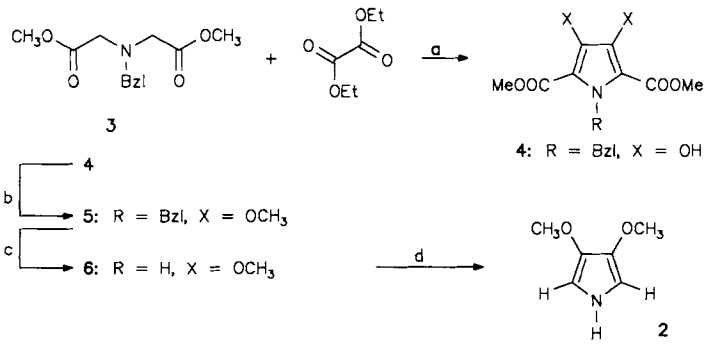

Scheme 1. a: 1. CH_3ONa/CH_3OH, reflux, 2. neutralization (58%); b: $(CH_3)_2SO_4/Na_2CO_3$, acetone, reflux (80%); c: H_2/10% Pd/C, acetic acid, 10 bar (96%); d: ref.[6]. Bzl = benzyl.

obtained from the condensation of dimethyl *N*-benzyliminodiacetate (**3**) and diethyl oxalate, was methylated with dimethyl sulfate to give the dimethoxy derivative **5**. The subsequent selective debenzylation at 10 bar H_2 on Pd/C provided **6** without hydrogenation of the porphyrin core.[17] The final reactions furnishing **2** can be conducted on a 10 g scale without difficulty as already described.[6] The route via **3** also opens the way to other 3,4-dialkoxypyrroles, which may find ample application, for example, in the synthesis of porphyrins with improved solubility properties or with peripheral functionalization.

Experimental Procedure

A solution of **2** (250 mg, 1.96 mmol) in glacial acetic acid (14 mL) and pyridine (7 mL) was treated with 35% formalin solution (0.2 mL) and then heated at reflux for 30 min while air was passed through the reaction mixture. After standing several days at room temperature the reaction mixture was filtered, providing 10–15 mg of **1a**. The filtrate was evaporated to dryness and the residue extracted with hot toluene. The resulting solution was chromatographed on silica gel eluting with ether; the first faction provided another 35–40 mg of **1a**. Correct C,H,N analysis. FAB-MS: *m/z* 551 ($M + H^+$).

Received: September 18, 1992 [Z 5579 IE]
German version: *Angew. Chem.* **1993**, *105*, 296

[1] P. Rothemund, *J. Am. Chem. Soc.* **1935**, *57*, 2010.
[2] "...but the reader is warned that even this synthesis of (**1d**) is necessarily long, and that in inexperienced hands the final product, rather than lustrous purple crystals, is often an intractable black polymer.": J. B. Kim, A. D. Adler, F. R. Longo in *The Porphyrins, Vol. I* (Ed.: D. Dolphin), Academic Press, New York, **1978**, p. 88; see also: J. L. Sessler, A. Mozaffari, M. R. Johnson, *Org. Synth.* **1991**, *70*, 68.
[3] R. Chong, P. S. Clezy, *Aust. J. Chem.* **1967**, *20*, 951; P. S. Clezy, N. W. Webb, *ibid.* **1972**, *25*, 2217.
[4] R. Bonnett, G. F. Stephenson, *J. Org. Chem.* **1965**, *30*, 2791.
[5] B. Evans, K. M. Smith, *Tetrahedron* **1977**, *33*, 629.
[6] A. Merz, R. Schwarz, R. Schropp, *Adv. Mater.* **1992**, *4*, 409.
[7] A. Treibs, N. Häberle, *Liebigs Ann. Chem.* **1968**, *450*, 164.
[8] Hammett constants for the CH_3O substituent: $\sigma_{para} = -0.27$, $\sigma_{meta} = +0.12$: C. D. Ritchie, F. W. Sager, *Prog. Phys. Org. Chem.* **1964**, *2*, 323.
[9] *Porphyrins and Metalloporphyrins* (Ed.: K. M. Smith), Elsevier, Amsterdam, **1975**, p. 20, 872–877.
[10] U. Eisner, R. P. Linstead, *J. Chem. Soc.* **1955**, 3749.
[11] K. N. Solov'ev, V. A. Mashenkov, A. T. Gradyushko, A. E. Turkova, U. P. Legina, *J. Appl. Spectrosc. (Engl. Transl.)* **1970**, *13*, 1106.
[12] R. J. Abraham, A. H. Jackson, G. W. Kenner, D. Warburton, *J. Chem. Soc.* **1963**, 853.
[13] H. H. Inhoffen, J. H. Fuhrhop, H. Voigt, H. Brockmann, *Liebigs Ann. Chem.* **1966**, *695*, 133.
[14] R. J. Abraham, C. E. Hawkies, K. M. Smith, *J. Chem. Soc. Perkin Trans. 2* **1974**, *627*; see also ref. [2], Vol. IV, S. 40.
[15] The structure was determined on an Enraf–Nonius CAD4 four-circle diffractometer with the SDP program system. Crystallographic data: $C_{28}H_{30}N_4O_8$, lattice constants $a = 6.948(2)$, $b = 13.093(3)$, $c = 14.795(3)$ Å, $\beta = 99.85(2)°$; $\rho_{calc} = 1.379$ g cm^{-3}; monoclinic, space group $P2_1/c$, $Z = 2$; $Mo_{K\alpha}$ radiation; range of measurement $\theta_{max} = 30°$; number of reflections: 2617 observed, $I \geq 2\sigma(I)$, 1232 unobserved; 241 refined parameters, C,N,O anisotropic, H isotropic; $R = 0.061$; $R_w = 0.067$. The NH hydrogen atoms were localized unequivocally and assigned to the five-membered rings. Further details of the crystal structure investigation may be obtained from the Fachinformationszentrum Karlsruhe, Gesellschaft für wissenschaftlich-technische Information mbH, D-W-7514 Eggenstein-Leopoldshafen 2 (FRG) on quoting the depository number CSD-56715, the names of the authors, and the journal citation.
[16] J. W. Lauher, J. A. Ibers, *J. Am. Chem. Soc.* **1973**, *95*, 5148.
[17] E. C. Jorgensen, G. C. Windridge, T. C. Lee, *J. Med. Chem.* **1970**, *13*, 352.

$[Fe_2Cl_6]^{2-}$: A Discrete Form of Ferrous Chloride**

By *Kim R. Dunbar** and *Anne Quillevéré*

The important role of iron in biological as well as catalytic processes has spurred a considerable amount of research by bioinorganic and coordination chemists.[1, 2] In order to gain a better understanding of the function of non-heme iron–sulfur proteins in fundamental biological reactions such as the transformation of N_2 into NH_3 by nitrogenase, researchers have designed synthetic analogues to compare their magnetic, spectroscopic, redox, and structural properties to those of the natural enzymes.[3] The dinuclear model compounds have the general formula $[Fe_2S_2(SR)_4]^{2-/3-}$, in which the iron centers in the oxidation states III,III or III,II are bridged by two sulfur atoms in an overall edge-sharing bitetrahedral arrangement.[4] This structural type is atypical for diiron(II) compounds, however, as evidenced by the fact that the only known representatives are $[Fe_2(SEt)_6]^{2-}$ and $[Fe_2Cl_4(OPh)_2]^{2-}$.[5, 6] All other reported fully reduced diiron complexes exhibit either a doubly or triply bridged bioctahedral geometry.[7, 8–11]

[*] Prof. K. R. Dunbar, A. Quillevéré
Department of Chemistry, Michigan State University
East Lansing, MI 48824 (USA)

[**] This research was supported by the National Science Foundation (Grant CHE-89149) and the Camille and Henry Dreyfus Foundation. We thank G. Christou, D. Dunham, and M. Kanatzidis for helpful discussions and D. Dunham for the magnetic data. We also appreciate the help of J. Matonic in obtaining the packing diagram. The X-ray equipment was purchased with funds from the National Science Foundation (CHE-8403823 and CHE-8908088).

While studying the reactivity of ferric chloride with tris(2,4,6-trimethoxyphenyl)phosphane tmpp, we unexpectedly isolated the hitherto unknown ferrous chloride anion $[Fe_2Cl_6]^{2-}$ as the phosphonium salt **1**. In spite of the extensive literature on Fe^{II} and Fe^{III} which documents numerous structures of common units such as $[FeCl_4]^{2-}$ and $[FeCl_4]^-$,[12,13] the title complex is the first homoleptic dinuclear iron(II) chloride species, although the $[Fe_2I_6]^{2-}$ anion is known.[14,21]

$[Htmpp]_2[Fe_2Cl_6]$ **1**

The reaction of anhydrous ferric chloride with one equivalent of tmpp in benzene produced a pale yellow air-sensitive solid identified as **1** (yield 60–65%).[15] In an alternate synthesis the starting materials were dissolved separately in diethyl ether, and the $FeCl_3$ solution was passed through a filter and into the solution containing the phosphane. Single crystals were obtained by slow diffusion of hexanes into a solution of **1** in acetone.[16] The salt appears to be indefinitely stable in acetone in the absence of air, but in alcohols it decomposes to a mixture of $[Fe^{II}Cl_4]^{2-}$ and unidentifiable products. Oxidation to the well-known $[Fe^{III}Cl_4]^-$ is facile in the presence of oxygen or in halogenated solvents.[17] Thus far, no firm evidence for a mixed-valence complex has been found, although an intensely colored intermediate has been observed in O_2-saturated solutions of **1** in CH_2Cl_2 before the $[FeCl_4]^-$ compound is formed; the identity of this species is under investigation.

The X-ray structure unequivocally establishes the identity of the anion in **1** as $[Fe_2Cl_6]^{2-}$ with two phosphonium ions as counterions. An ORTEP representation of $[Fe_2Cl_6]^{2-}$ is presented in Figure 1. The structure of the dianion consists

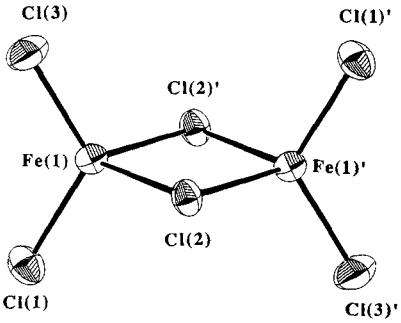

Fig. 1. Selected distances [Å] and angles [°] for the anion in **1**: Fe(1)···Fe(1)′ 3.350(4), Fe(1)-Cl(1) 2.235(2); Fe(1)-Cl(2) 2.38(5); Fe(1)-Cl(3) 2.227(2), Fe(1)-Cl(2)′ 2.409(2); Cl(1)-Fe(1)-Cl(2) 108.02(9); Cl(1)-Fe(1)-Cl(2)′, 110.57(8); Cl(1)-Fe(1)-Cl(3), 120.5(1); Cl(2)-Fe(1)-Cl(2)′; 91.36(8); Cl(2)-Fe(1)-Cl(3), 110.96(9); Cl(3)-Fe(1)-Cl(2)′, 111.50(8); Fe(1)-Cl(2)-Fe(1)′, 88.64(8).

of two edge-sharing tetrahedra with two terminal and two bridging chloro ligands per metal atom with an inversion center at the midpoint of the Fe(1)···Fe(1)′ bond. The Fe(1)···Fe(1)′ distance of 3.350(4) Å, which is much larger than the sum of the covalent radii, precludes the formation of a direct bond and is comparable to the distances of 3.32 Å found in $[Fe_2(\mu\text{-}OH)(OAc)_2(me_3tacn)_2](ClO_4)$[8] and 3.35 Å in $[Fe_2(bpmp)(OPr)_2](BPh_4)$,[9] but shorter than the corresponding value reported for $[Fe_2(biphme)_2(O_2CH)_4]$ (3.585 Å).[10] The Fe···Fe distances reported for the two closely related structures $[Fe_2(SEt)_6]^{2-}$ and $[Fe_2Cl_4(OPh)_2]^{2-}$ are somewhat shorter, 2.978(1) and 3.177(3) Å, respectively.[5,6] The average Fe^{II}–Cl bond length for the terminal chloro ligand (2.231(2)Å) is intermediate between the reported ranges for Fe^{II}–Cl (2.25–2.35 Å)[12] and Fe^{III}–Cl bonds (2.15–2.20 Å).[13] As expected, the average distance for the bridging chloro ligands is longer (2.397(2) Å) than for the terminal groups. The Cl-Fe bond angles are in the range anticipated for tetrahedral geometry (108.02(9) – 120.5(1)°) but the Cl(2)-Fe(1)-Cl(2)′ and the Fe(1)-Cl(2)-Fe(1)′ angles of 91.36(8) and 88.64(8)°, respectively, are considerably distorted from ideal geometry. A three-dimensional packing diagram of **1** (Fig. 2) viewed along the *b* axis illustrates the segregated arrangement of the $[tmpp]^+$ and the $[Fe_2Cl_6]^{2-}$ units and underscores how bulky the unusual cation is. The

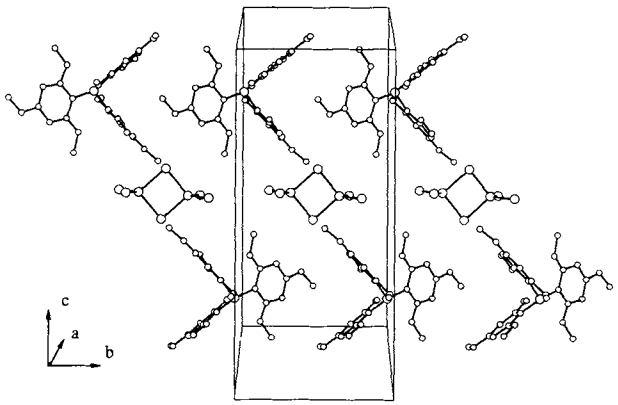

Fig. 2. Packing diagram of **1** viewed along the *b* axis.

identity of the cation and its spatial requirements may affect the structure; therefore, we have sought to prepare other salts of $[Fe_2Cl_6]^{2-}$ with more common counterions. Preliminary results indicate that the corresponding reaction of PPh_3 with $FeCl_3$ in benzene furnishes the analogous product, $[HPPh_3]_2[Fe_2Cl_6]$. We are currently working on syntheses with $FeCl_2$ and salts such as [tmpp]Cl, $[Ph_4P]Cl$, and $[Et_4N]Cl$.

The far-IR spectrum of **1** exhibits four Fe–Cl stretching bands at 360(s), 320(m), 300(m), and 230(w) cm^{-1}, as predicted by a group-theoretical treatment of a molecule with D_{2h} symmetry. The electronic spectrum of **1** ($CHCl_3$) exhibits three features (λ_{max} [nm] (ε [$M^{-1}cm^{-1}$])): 377 (1.80×10^3), 287 (sh), and 260 (6.80×10^4)). The ^1H NMR spectrum (CD_3CN) exhibits the characteristic resonances attributed to the protonated phosphane: $\delta = 3.67$ (s, *o*-OCH_3), 3.85 (s, *p*-OCH_3), 6.24 (d, *m*-H), 8.37 (d, P–H).

The magnetic exchange interactions within the $[Fe_2Cl_6]^{2-}$ unit are being examined by measuring the solid-state temperature-dependence of the magnetic susceptibility. A plot of μ_{eff} versus T[K] is shown in Figure 3. A detailed description of the magnetic behavior of **1** along with its Mössbauer spectrum will be reported in full elsewhere.

Complex **1** reacts with molecular oxygen in a variety of solvents to eventually form the very stable tetracoordinate phosphane oxide adduct (Otmpp) · $FeCl_3$ in high yield.[18] When the reaction was carried out in protic solvents such as MeOH or EtOH the tetrachloroferrate salts $[Htmpp]_2[Fe^{II}Cl_4]$ and $[Htmpp][Fe^{III}Cl_4]$ were isolated as intermediates.[19] These results indicate that the oxidation of phosphane to phosphane oxide in the presence of $FeCl_3$ proceeds by quaternarization of the phosphane and not via dioxygen adducts. We are currently extending this chemistry to other tertiary phosphanes in order to determine the role of $[Fe_2Cl_6]^{2-}$ in the catalytic oxidation of such systems.

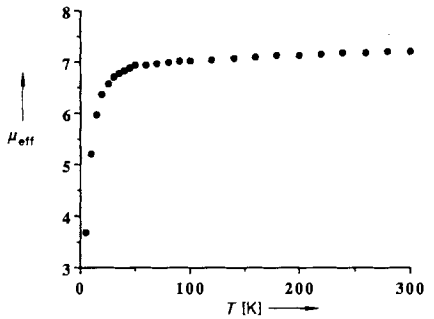

Fig. 3. A plot of μ_{eff} versus temperature for **1**. The curvature in this graph is due to the presence of zero-field splitting terms in the spin Hamiltonian.

The ionic compound reported in this paper contains the remarkably simple yet unknown anion $[Fe_2Cl_6]^{2-}$. While dinuclear complexes of the type $[Fe_2Cl_6(\mu\text{-}O)]^{2-}$ and $[Fe_2Cl_6(\mu\text{-}OR)_2]^{2-}$ are known for Fe^{III} centers [2] and Fe_2Cl_6 is the structure $FeCl_3$ adopts in the gas phase,[20] no discrete unit of $FeCl_2$ has ever been reported to our knowledge.[21] Furthermore, the title compound constitutes one of the few structurally characterized diiron(II) compounds.

Experimental Procedure

Method A: Anhydrous $FeCl_3$ (0.162 g, 0.999 mmol) was added to one equivalent of tmpp (0.532 g, 0.999 mmol) in 30 mL of deoxygenated benzene. The resulting suspension was stirred at room temperature for 24 h, after which time the solvent was decanted from a yellow solid. The product was washed with several aliquots of benzene (3 × 10 mL) and THF (3 × 10 mL) until the washings were colorless. The resulting pale yellow product was dried in vacuo (yield 0.456 g, 65%).

Method B: A solution of $FeCl_3$ (0.062 g, 0.380 mmol) in 15 mL of diethyl ether was filtered into a solution of tmpp (0.203 g, 0.380 mmol) in 25 mL of diethyl ether. The resulting yellow suspension was stirred at room temperature for 24 h. The workup was the same as described in method A. A yellow solid was obtained (yield 0.148 g, 56%).

Received: June 20, 1992
Revised: October 27, 1992 [Z 5413 IE]
German version: *Angew. Chem.* **1993**, *105*, 298

[1] See for example: R. H. Holm, *Acc. Chem. Res.* **1977**, *10*, 427; R. H. Holm, *Chem. Soc. Rev.* **1981**, *10*, 455; B. A. Averill, *Fe-S and Mo-Fe-S Clusters as Models for the Active Site of Nitrogenase* (*Struct. Bonding* (*Berlin*) **1983**, *53*, 59); R. H. Holm, S. Ciurli, J. A. Weigel, *Prog. Inorg. Chem.* **1990**, *38*, 1; J. B. Vincent, G. L. Ollivier-Lilley, B. A. Averill, *Chem. Rev.* **1990**, *90*, 1447.

[2] R. Davis, *Coord. Chem. Rev.* **1985**, *67*, 109; F. A. Cotton, G. Wilkinson, *Advanced Inorganic Chemistry*, 5th ed., Wiley, New York, **1988**; P. Thornton, *Coord. Chem. Rev.* **1992**, *113*, 131.

[3] R. H. Sands, W. R. Dunham, *Q. Rev. Biophys.* **1975**, *7*, 443; J. A. Fee, K. L. Findling, T. Yoshida, R. Hille, G. E. Tarr, D. O. Hearshen, W. R. Dunham, E. P. Day, T. A. Kent, E. Münck, *J. Biol. Chem.* **1983**, *259*, 124; L. Que, Jr., A. E. True, *Prog. Inorg. Chem.* **1990**, *38*, 97.

[4] J. J. Mayerle, S. E. Denmark, B. V. DePamphilis, J. A. Ibers, R. H. Holm, *J. Am. Chem. Soc.* **1975**, *97*, 1032; R. W. Lane, J. A. Ibers, R. B. Frankel, G. C. Papaefthymiou, R. H. Holm, *J. Am. Chem. Soc.* **1977**, *99*, 84; M. A. Bobrik, K. O. Hodgson, R. H. Holm, *Inorg. Chem.* **1977**, *16*, 1851; K. S. Hagen, R. H. Holm, *J. Am. Chem. Soc.* **1982**, *104*, 5496; A. Salifoglou, A. Simopoulos, A. Kostikas, W. R. Dunham, M. G. Kanatzidis, D. Coucouvanis, *Inorg. Chem.* **1988**, *27*, 3394.

[5] K. S. Hagen, R. H. Holm, *Inorg. Chem.* **1984**, *23*, 418.

[6] D. Coucouvanis, K. Greiwe, A. Salifoglou, P. Challen, A. Simopoulos, A. Kostikas, *Inorg. Chem.* **1988**, *27*, 593.

[7] S. L. Lambert, D. N. Hendrickson, *Inorg. Chem.* **1979**, *18*, 2683; C. L. Spiro, S. L. Lambert, T. J. Smith, E. N. Duesler, R. R. Gagne, D. N. Hendrickson, *ibid.* **1981**, *20*, 1229; B. Chiari, O. Piovesana, T. Tarentelli, P. Zanazzi, *ibid.* **1984**, *23*, 3398.

[8] J. R. Hartman, R. L. Rardin, P. Chaudhuri, K. Pohl, K. Wieghardt, B. Nuber, J. Weiss, G. C. Papaefthymiou, R. B. Frankel, S. J. Lippard, *J. Am. Chem. Soc.* **1987**, *109*, 7387; P. Chaudhuri, K. Wieghardt, *Angew. Chem.* **1985**, *97*, 774; *Angew. Chem. Int. Ed. Engl.* **1985**, *24*, 778. me_3tacn = *N,N',N''*-trimethyl-1,4,7-triazacyclononane.

[9] A. S. Borovik, L. Que, Jr., *J. Am. Chem. Soc.* **1988**, *110*, 2345; A. S. Borovik, M. P. Hendrich, T. R. Holman, E. Münck, V. Papaefthymiou, L. Que, Jr., *ibid.* **1990**, *112*, 6031. Hbpmp = 2,6-bis{[bis(2-pyridylmethyl)-amino]methyl}-4-methyl phenol.

[10] W. B. Tolman, A. Bino, S. J. Lippard, *J. Am. Chem. Soc.* **1989**, *111*, 8523. biphme = methoxy-bis(1-methylimidazol-2-yl)phenylmethane).

[11] O. A. Ileperuma, R. D. Feltham, *Inorg. Chem.* **1975**, *14*, 3042; C. Bianchini, P. Dapporto, C. Mealli, A. Meli, *ibid.* **1982**, *21*, 612.

[12] J. W. Lauher, J. A. Ibers, *Inorg. Chem.* **1975**, *14*, 348; T. Toan, L. F. Dahl, *J. Am. Chem. Soc.* **1971**, *93*, 2654; H. C. Freeman, G. H. W. Milburn, C. E. Nockolds, *Chem. Commun.* **1969**, 55; R. Mason, E. D. McKenzie, G. B. Robertson, G. A. Rusholme, *ibid.* **1968**, 1673.

[13] T. Glowiak, E. Durcanska, I. Ondrejkovicova, G. Ondrejovic, *Acta Crystallogr. Sect C.* **1986**, *42*, 1331; F. A. Cotton, C. A. Murillo, *Inorg. Chem.* **1975**, *14*, 2467; G. Constant, J.-C. Daran, Y. Jeannin, *J. Organomet. Chem.* **1972**, *44*, 353; F. A. Cotton, R. L. Luck, K.-A. Son, *Acta Crystallogr. Sect. C* **1990**, *46*, 1424 and references therein; J. D. Walker, R. Poli, *Polyhedron* **1989**, *8*, 1293.

[14] W. Saak, D. Haase, S. Pohl, *Z. Naturforsch.* **1988**, *43b*, 289.

[15] Correct C,H,Cl analysis. The by-product of this reaction was determined to be the oxidized form of the phosphane, [Cltmpp][$FeCl_4$], by NMR and IR spectroscopy as well as by FAB mass spectrometry.

[16] Crystal data for **1** at -100 ± 2 °C: $Fe_2Cl_6P_2O_{18}C_{54}H_{68}$, $M_r = 1391.48$, monoclinic, space group $P2_1/n$, $a = 14.294(8)$, $b = 10.140(9)$, $c = 22.543(8)$ Å, $\beta = 105.76(4)°$, $V = 3144(3)$ Å^3, $Z = 2$, $\varrho_{calcd} = 1.469$ g cm^{-3}, $\mu = 8.32$ cm^{-1}. The intensity data were collected on a Rigaku AFC6S diffractometer in the range $4 < 2\theta < 47°$ ($0/2\theta$ scan). After equivalent reflections were averaged, 4952 unique data remained, of which 3440 with $F_o^2 \geq 3\sigma\,(F_o)^2$ were used to refine 370 parameters to residuals of R (R_w) = 0.046 (0.079), GOF = 2.84. The final difference Fourier map showed a highest peak of 0.96 e/Å^3. Further details of the structure determination are available upon request from the Director of the Cambridge Crystallographic Data Centre, 12 Union Road, GB-Cambridge CB21EZ (UK), on quoting the full journal citation.

[17] $[Fe^{II}Cl_4]^{2-}$ and $[Fe^{III}Cl_4]^-$ were isolated from the decomposition reactions of [Htmpp]$_2$[Fe_2Cl_6] as [Htmpp]$^+$ salts and fully characterized by magnetism measurements, Mössbauer, IR and UV/VIS spectroscopy, and X-ray diffraction investigations.

[18] K. R. Dunbar, S. C. Haefner, A. Quillevéré, *Polyhedron* **1990**, *9*, 1695.

[19] K. R. Dunbar, A. Quillevéré, *Polyhedron*, in press.

[20] M. Hargittai, J. Tremmel, I. Hargittai, *J. Chem. Soc. Dalton Trans.* **1980**, 87.

[21] Note added in proof (Dec. 30, 1992): Recently the structure of [η^6-C_6Me_6)Fe(η^5-C_5H_5)]$_2$[Fe_2Cl_6]·$2CH_2Cl_2$ was reported: K. Ruhlandt-Senge, U. Müller, *Z. Naturforsch.* **1992**, *47b*, 1075.

1-Hetero-3,4-diborolanes and Two New Routes to 1,2-Diboretanes**

By *Ralf Littger, Heinrich Nöth,* Martina Thomann,* and *Matthias Wagner*

The synthetic potential of boryl-substituted alkyllithium compounds (alkylideneborates) has hardly been exploited so far, although compounds of the type R_2BCH_2Li [1] and $(R_2B)_2CHLi$ [2] should allow access to other boryl-substituted organometallic compounds. An even greater variety of reactions is to be expected for the (formally) dianionic 2,3-diboratabutadienes.[3] Thus, for example, **1** should be suitable for the construction of new heterocycles. Indeed, from the reactions given in Scheme 1, not only the methyl derivative **2**, but also the 1-hetero-3,4-diborolanes **3a–c** are obtained in good yields.

For **3b** and **3c** two signals occur for the NMe_2 groups in both the ^{1}H and ^{13}C NMR spectra, in the case of **3a**, however, four signals are observed, because the pyramidal C_2AsCl group causes a decrease in symmetry. Thus, hindered rotation about the B–N bonds occurs in all compounds. Thirteen signals for the fluorenyl groups in the ^{13}C

[*] Prof. Dr. H. Nöth, Dipl.-Chem. R. Littger, Dr. M. Thomann, Dr. M. Wagner
Institut für Anorganische Chemie der Universität
Meiserstrasse 1, D-W-8000 München 2 (FRG)

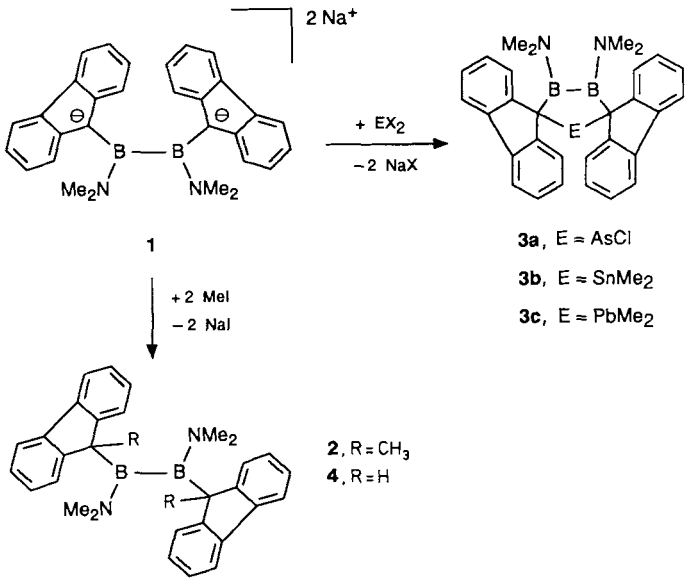

Scheme 1.

NMR spectra of both **3b,c**, and only one signal for the two methyl groups at the Sn and at the Pb atom, respectively, indicate a *twist* conformation with C_2 symmetry for the appropriate B_2C_2E ring framework. Twenty-three signals are found for the fluorenyl groups of **3a**, three of these signals show double intensity; thus two nonequivalent fluorenyl groups exist due to the lower symmetry. The ^{11}B chemical shifts of **3a** ($\delta = 48$), **3b** ($\delta = 48$), and **3c** ($\delta = 50$) lie in the expected range.[4] In the case of **3b** $\delta(^{119}Sn) = 101.4$ indicates a strongly deshielded Sn atom in an SnC_4 environment.[5] Since $\delta(^{119}Sn)$ responds strongly to a change of bond angles at the Sn atom,[5] this value indicates a considerable deviation from the ideal tetrahedral configuration. This corresponds to the "normal" coupling constant[5] to the methyl C atoms $^1J(^{119}Sn,^{13}C = 286$ Hz) and to an unusually small coupling to the endocyclic C atoms (135 Hz).

The X-ray structure analysis[6] of **3b** reveals that the C_2 symmetry deduced from NMR spectroscopy is almost retained in the solid state (Fig. 1). The twisted B_2C_2Sn five-membered ring (ring C atoms above and below the B_2Sn plane) contains Me_2NB groups, whose C_2BN planes strive for orthogonality, like all electron-precise poly(dimethylamino)boranes.[7] The B–B distance in **3b** (1.757(9) Å) is significantly longer than in **1** (1.716 Å)[3a] and the neutral compound **4** (1.697(4) Å).[4] The B–C distances in **3b** (1.606(8), 1.614(9) Å), however, are somewhat shorter than in **4** (1.618(3), 1.624(3) Å). The endocyclic Sn–C bonds are on average 0.11 Å longer than the exocyclic ones. This, and the small endocyclic C-Sn-C angle of the ring (96.1(2)°) indicate ring strain. In the mass spectrum of **3b** a fragmentation leading to $[SnMe_2]^{\cdot+}$ and $[fl{=}B{=}NMe_2]^{\cdot+}$ (fl = fluorenylidene) is dominant, which can be interpreted as a [2 + 2 + 2] cycloreversion. Also with the elimination of $SnMe_2$ the 1,2-diboretane cation is formed during the fragmentation of $M^{\cdot+}$. This contraction of the ring, however, is not achieved either by thermolysis or by photolysis of **3b**.

Since Pb–C bonds are weaker than Sn–C bonds, **3c** should be more readily accessible to elimination of $PbMe_2$ than **3b** is to expulsion of $SnMe_2$. Indeed, the reaction that was only suggested for **3b** in its mass spectrum, can be carried out for **3c**: $PbMe_2$ is eliminated photochemically from **3c** and with contraction of the ring, the 1,2-diboretane derivative **5a**[8] is obtained. The liberated $PbMe_2$ disproportionates into $PbMe_4$ and elemental lead. Compound **5a** is more readily accessible by the oxidative coupling of the disodium salt **1** with C_2Cl_6 (Scheme 2) than by photolysis.

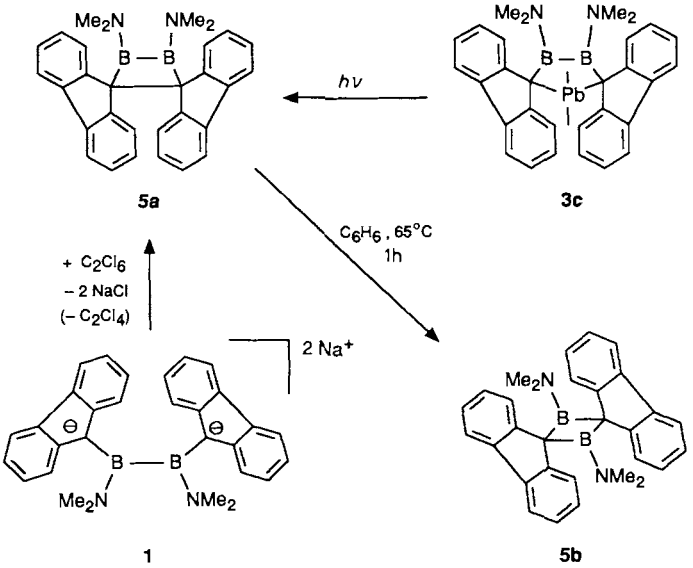

Scheme 2.

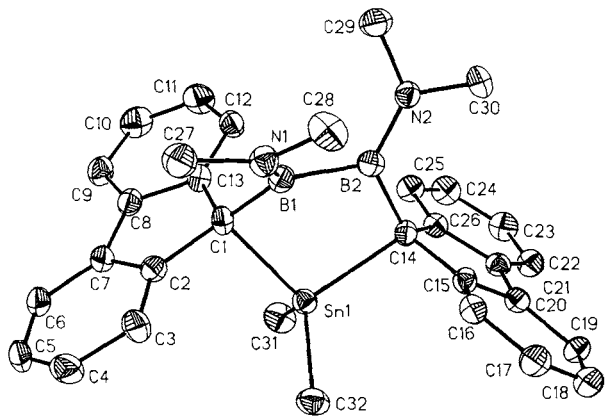

Fig. 1. Crystal structure of **3b**. Selected bond lengths [Å] and angles [°] with standard deviations in parentheses: B1-B2 1.757(9), B1-N1 1.389(8), B2-N2 1.386(6), B1-C1 1.606(8), B2-C14 1.614(9), Sn-C1 2.267(6), Sn-C14 2.225(4), Sn-C31 2.119(7), Sn-C32 2.145(6); B2-B1-N1 123.5(5), B1-B2-N2 124.3(6), N1-B1-C1 122.3(5), N2-B2-C14 119.5(5), B2-B1-C1 114.0(5), B1-B2-C14 116.1(4), Sn-C1-B1 94.9(4), Sn-C14-B2 99.7(3), C31-Sn-C32 114.8(4).

On heating to 65 °C in benzene solution, **5a** rearranges quantitatively into the isomeric 1,3-diboretane derivative **5b** within an hour. Compound **5a** is thus formed under kinetic control, whereas **5b** is thermodynamically the more stable product. This is in agreement with the theoretical prediction.[9] The corresponding rearrangement does not occur for 1,2-bis(diisopropylamino)-1,2-diboretane.[8] It remains an open question whether the rearrangement takes place via radical intermediates, an intermediary B–C double bond system, or a tetrahedral cluster transition state.

Experimental Procedure

The numbering for the fluorenyl C atoms in Figure 1 is also used for the assignment of the NMR spectroscopic data.

2: MeI (0.23 mL, 3.8 mmol) was added to a solution of **1** (0.92 g, 1.9 mmol) [7b] in THF (20 mL) at −30 °C. The orginally blood-red solution immediately brightened. After the solution had been warmed to room temperature, it was

stirred for 1 h, then concentrated to 5 mL under vacuum. The resulting paste-like suspension was treated with benzene (20 mL) and centrifuged, thereafter insoluble products (mainly NaI) were discarded. After removal of all volatiles from the solution under vacuum, the paste-like residue was dissolved in pentane (15 mL). Compound **2** (0.53 g, 60%) crystallized as a yellow solid at −78 °C, m.p. 117–120 °C; $C_{32}H_{34}B_2N_2$ (468.3), correct elemental analysis; ^{11}B NMR (64.16 MHz, C_6D_6, 25 °C, $BF_3 \cdot OEt_2$): $\delta = 52$ ($h_{1/2} = 700$ Hz); ^{1}H NMR (400 MHz, C_6D_6, 25 °C, TMS): $\delta = 7.80$ (m, 6H), 7.50 (m, 2H), 7.30 (m, 8H), 2.69, 1.92 (s, 6H, s, 6H; $N(CH_3)_2$), 1.76 (s, 6H; fl-CH_3); ^{13}C NMR (100.6 MHz, C_6D_6, 25 °C, TMS): $\delta = 155.9$, 155.8 (C2,13), 141.2 (C7,8), 127.5, 127.1 (C5,10), 125.9, 125.8 (C4,11), 125.0, 124.5 (C3,12), 120.3 (C6,9), 49.2 (C1), 47.2, 38.4 ($N(CH_3)_2$), 29.4 (fl-CH_3).

3a: $AsCl_3$ (0.71 g, 3.92 mmol) in THF (10 mL) was added dropwise to a solution of **1** (1.91 g, 3.94 mmol) in THF (15 mL) at −78 °C. After the solution had warmed to room temperature, it was stirred for 12 h. The solvent was removed under vacuum from the orange suspension. The residue was taken up in CH_2Cl_2 (20 mL) and separated from insoluble products by centrifugation, the solvent was removed under vacuum, and the nonvolatile yellow solid precipitated from hexane (15 mL). Yield: 1.42 g **3a** (66%), colorless powder, m.p. 175 °C (decomp); $C_{30}H_{28}AsB_2ClN_2$ (548.6), correct elemental analysis; ^{11}B NMR (64.16 MHz, $CDCl_3$, 25 °C, $BF_3 \cdot OEt_2$): $\delta = 48$ ($h_{1/2} = 850$ Hz); ^{1}H NMR (400 MHz, $CDCl_3$, 25 °C, TMS): $\delta = 7.89$, 7.58, 7.30 (m, 5H, m, 6H, m, 5H; aromatic protons) 2.97, 2.85, 2.29, 1.96 (s, 3H, s, 3H, s, 3H, s, 3H; $N(CH_3)_2$); ^{13}C NMR (100.6 MHz, $CDCl_3$, 25 °C, TMS): $\delta = 149.7$, 145.6, 145.3, 145.2 (C2,13), 140.0, 139.7, 139.2 (C7,8), 128.5, 126.8, 126.7, 126.2, 125.8, 125.7, 125.6, 125.4, 125.1, 123.3 (C3,4,5,10,11,12), 120.8, 120.3, 119.9, 119.8 (C6,9), 61.0, 60.6 (C1), 45.7, 44.9, 41.6, 40.1 ($N(CH_3)_2$).

3b: **1** (1.63 g, 3.4 mmol) in THF (20 mL) at −78 °C was treated (as for **3a**) with a 0.44 M solution of Me_2SnCl_2 (7.6 mL, 3.3 mmol) in THF. After the solution had warmed to room temperature, it was stirred for 12 h. During this time a precipitate formed that did not settle very well and the solution remained tomato red. Following centrifugation the insoluble products were separated and all the volatiles were removed from the solution under vacuum. The remaining red resin was precipitated from hexane (10 mL), which afforded **3b** (1.75 g, 88%; m.p. 280–283 °C) as a colorless powder. Single crystals of **3b** were formed on slow evaporation of a CH_2Cl_2 solution over paraffin chips. ^{11}B NMR (64.16 MHz, $CDCl_3$, 25 °C, $BF_3 \cdot OEt_2$): $\delta = 48$ ($h_{1/2} = 880$ Hz); ^{119}Sn NMR (74.58 MHz, $CDCl_3$, 25 °C): $\delta = 101.4$; ^{1}H NMR (400 MHz, $CDCl_3$, 25 °C, TMS): $\delta = 8.04$, 7.99 (d, 2H, d, 2H; H6,9), 7.79, 7.60 (d, 2H, d, 2H; H3,12), 7.51, 7.38, 7.34, 7.29 (each pseudo-t, 2H; H4,5,10,11), 3.07, 2.26 (s, 6H, s, 6H; $N(CH_3)_2$), −0.63 (s, $^2J(^{117/119}Sn,H) = 48$ Hz, 6H; $Sn(CH_3)_2$); ^{13}C NMR (100.6 MHz, $CDCl_3$, 25 °C, TMS): $\delta = 149.8$, 148.7 ($^2J(^{117/119}Sn,C) = 18$ Hz, $^2J(^{117/119}Sn,C) = 44$ Hz; C2,13), 136.8, 136.6 ($^3J(^{117/119}Sn,C) = 16$ Hz, $^3J(^{117/119}Sn,C) = 17$ Hz; C7,8), 125.7, 125.3 ($^4J(^{117/119}Sn,C) = 11$ Hz, $^4J(^{117/119}Sn,C)$ not resolved; C4,11), 124.6, 121.9 ($^3J(^{117/119}Sn,C) = 15$ Hz, $^3J(^{117/119}Sn,C) = 17$ Hz; C3,12), 122.4 ($^5J(^{117/119}Sn,C)$ not resolved; C5,10), 120.1, 120.0 ($^4J(^{117/119}Sn,C)$ each not resolved; C6,9), 56.3 ($^1J(^{117/119}Sn,C) = 135$ Hz; C1,14), 44.8, 42.2 ($N(CH_3)_2$), −6.9 ($^1J(^{117/119}Sn,C) = 286$, 274 Hz; $Sn(CH_3)_2$).

3c: A solution of **1** (8.13 g, 16.8 mmol) in THF (50 mL) was added dropwise to a suspension of Me_2PbBr_2 (6.66 g, 16.8 mmol) in THF (40 mL) with exclusion of light at −78 °C and continuously stirred. Workup as for **3b**. Yield: **3c** (8.85 g, 78%) as an intense yellow powder, m.p. 110 °C (decomp); $C_{32}H_{34}B_2N_2Pb$ (675.5), correct elemental analysis; UV/VIS (C_6H_6): λ_{max}[nm] = 276, 295, 366; ^{11}B NMR (64.16 MHz, C_6D_6, 25 °C, $BF_3 \cdot OEt_2$): $\delta = 50$ ($h_{1/2} = 930$ Hz); ^{1}H NMR (400 MHz, C_6D_6, 25 °C, TMS): $\delta = 8.03$, 7.96 (d, 2H, d, 2H; H6,9), 7.92, 7.60 (d, 2H, d, 2H; H3,12), 7.54, 7.33 (each pseudo-t, 2H, 2H; H4,11), 7.25, 7.21 (each pseudo-t, 2H, 2H; H5,10), 2.76, 2.09 (s, 6H, s, 6H; $N(CH_3)_2$), −0.01 (s, $^2J(^{207}Pb,H) = 35$ Hz, 6H; $Pb(CH_3)_2$); ^{13}C NMR (100.6 MHz, C_6D_6, 25 °C, TMS): $\delta = 149.7$, 149.0 ($^2J(^{207}Pb,C) = 19$ Hz, $^2J(^{207}Pb,C) = 62$ Hz; C2,13), 137.0, 136.7 ($^3J(^{207}Pb,C) = 30$ Hz, $^3J(^{207}Pb,C) = 26$ Hz; C7,8), 125.9, 125.6 ($^4J(^{207}Pb,C) = 23$ Hz, $^4J(^{207}Pb,C) = 19$ Hz; C4,11), 124.8, 122.3 ($^3J(^{207}Pb,C) = 31$ Hz, $^3J(^{207}Pb,C) = 34$ Hz; C3,12), 123.1, 122.9 ($^5J(^{207}Pb,C) = 28$ Hz, $^5J(^{207}Pb,C) = 22$ Hz; C5,10), 120.5, 120.4 ($^4J(^{207}Pb,C) = 15$ Hz, $^4J(^{207}Pb,C) = 19$ Hz; C6,9), 68.5 ($^1J(^{207}Pb,C)$ not resolved; C1), 44.2, 42.0 ($N(CH_3)_2$), 12.0 ($^1J(^{207}Pb,C) = 8$ Hz; $Pb(CH_3)_2$).

5a: a) By photolysis of **3c**: A solution of **3c** (0.53 g, 0.79 mmol) in benzene (80 mL) was solidified in a cylindrical quartz flask by using a cold finger (isopropanol-dry ice). Afterwards the reaction flask was placed in the sunlight, and the solidified solution was allowed to warm up over 2 h. During this time a black lead mirror formed, and the yellow color of **3c** completely disappeared. Subsequently, the mixture was filtered through a G4 frit, and volatile benzene and $PbMe_4$ were removed under vacuum. Pale pink **5a** was obtained by precipitation from hexane in an analytically pure form. Titration of the amount of lead deposited gave 90% of that expected theoretically. Yield of **5a**: 0.18 g, 51%. b) By oxidative coupling of **1** with hexachloroethane: **1** (2.75 g, 5.68 mmol) was suspended in benzene (70 mL) and a solution of hexachloroethane (1.34 g, 5.66 mmol) in benzene (20 mL) was added over 10 min at room temperature, and the mixture was stirred. Thereafter no undissolved **1** remained. All volatiles were removed from the clear, red-brown solution under vacuum, the residue was suspended in a little benzene and centrifuged from the slimy precipitate. The benzene was removed from the solution under vacuum and the solid residue was reprecipitated from hexane (5–10 mL). Yield of **5a**: (1.0 g, 42%), colorless powder (m.p. 159–161 °C). (The reactions described [a and b] occur quantitatively; the moderate yields of **5a** are a result of the considerable solubility of **5a** in hexane.) $C_{30}H_{28}B_2N_2$ (438.2), correct elemental analysis; ^{11}B NMR (64.16 MHz, C_6D_6, 25 °C, $BF_3 \cdot OEt_2$): $\delta = 49$ ($h_{1/2} = 820$ Hz); ^{1}H NMR (400 MHz, C_6D_6, 25 °C, TMS): $\delta = 7.77$, 7.67, 7.12 (m, 4H, m, 4H, m, 8H; aromatic protons), 2.65, 1.86 (s, 6H, s, 6H; $N(CH_3)_2$); ^{13}C NMR (100.6 MHz, C_6D_6, 25 °C, TMS): $\delta = 148.5$, 140.6 (C2,7), 126.1, 125.6, 124.5, 120.3 (C3,4,5,6), 62.0 (C1), 43.9, 39.2 ($N(CH_3)_2$).

5b: Compound **5a** (0.37 g, 0.84 mmol) was dissolved in benzene (15 mL). The red solution was held at 65 °C for 1 h and stirred. Even at this temperature a little **5b** precipitated as a colorless powder. The solution was cooled to room temperature, and the now colorless solution was concentrated to a third of its volume, and the insoluble **5b** was filtered with a G3 frit. After **5b** had been washed with a few drops of benzene, it was obtained as a colorless powder; yield: 0.23 g (62%); m.p. 245–246 °C; $C_{30}H_{28}B_2N_2$ (438.2), correct elemental analysis; ^{11}B NMR (64.16 MHz, $CDCl_3$, 25 °C, $BF_3 \cdot OEt_2$): $\delta = 46$ ($h_{1/2} = 490$ Hz); ^{1}H NMR (400 MHz, $CDCl_3$, 25 °C, TMS): $\delta = 8.02$, 7.40 (m, 8H, m, 8H; aromatic protons), 1.79 (s, 12H; $N(CH_3)_2$); ^{13}C NMR (100.6 MHz, $CDCl_3$, 25 °C, TMS): $\delta = 150.7$ (C2), 139.7 (C7), 126.3 (C3), 123.7, 123.2 (C4,5), 120.2 (C6), 38.8 ($N(CH_3)_2$, signal of C1 not observed.

Received: September 3, 1992 [Z 55521E]
German version: *Angew. Chem.* **1993**, *105*, 275

[1] a) M. W. Rathke, R. Kow, *J. Am. Chem. Soc.* **1972**, *94*, 6854–6855; b) M. P. Cooke, Jr., R. K. Widener, *ibid.* **1987**, *109*, 931–933.

[2] a) M. V. Garad, J. W. Wilson, *J. Chem. Res. (S)* **1982**, 132–133; b) D. S. Matteson, *J. Am. Chem. Soc.* **1977**, *99*, 3196–3197; c) B. Ederer, Dissertation, Universität München, **1991**.

[3] a) H. Nöth, M. Thomann, M. Wagner, *Chem. Commun.*, in press; b) G. Herberich, B. Hessner, M. Hostalek, *Angew. Chem.* **1986**, *98*, 637–638; *Angew. Chem. Int. Ed. Engl.* **1986**, *25*, 642–643; c) M. Pilz, J. Allwohn, P. Willershausen, W. Massa, A. Berndt, *ibid.* **1990**, *102*, 1085–1087 and **1990**, *29*, 1030.

[4] H. Nöth, M. Wagner, *Chem. Ber.* **1991**, *124*, 1963–1972.

[5] B. Wrackmeyer, *Annu. Rep. NMR-Spectrosc.* **1985**, *16*.

[6] Crystal structure analysis of **3b**·0.5CH_2Cl_2 : triclinic, $a = 11.959(5)$, $b = 14.955(5)$, $c = 18.250(6)$ Å, $\alpha = 94.05(3)$, $\beta = 106.94(3)$, $\gamma = 100.73(3)°$, $V = 3041$ Å^3, space group $P\bar{1}$ (no. 2), $Z = 4$, $\rho_{calcd} = 1.375$ g cm^{-3}, $\mu = 9.54$ cm^{-1}, $Mo_{K\alpha}$ radiation, graphite monochromator, measurements at 20 °C, crystal dimensions: 0.4 × 0.2 × 0.15 mm. Scan width/background: 1.8/0.5°, 2θ range: 3–49° in h, ±k, ±l, 9567 independent reflections, of which 7628 with $F \leq 3\sigma(F_o)$, empirical absorption correction (Ψ scans), solution of structure with direct methods (SHELXTL program), refinement of 881 parameters, $R = 0.0524$, $R_w = 0.0647$. Further details of the crystal structure investigation may be obtained from the Fachinformationszentrum Karlsruhe, Gesellschaft für wissenschaftlich-technische Information mbH, D-W-7514 Eggenstein-Leopoldshafen 2 (FRG) on quoting the depository number CSD-56670, the names of the authors, and the journal citation.

[7] a) D. Loderer, Dissertation, Universität München, **1990**; b) M. Wagner, Dissertation, Universität München, **1992**.

[8] A. Krämer, J.-K. Uhm, S. E. Garner, H. Pritzkow, W. Siebert, *Z. Naturforsch. B* **1990**, *45*, 1019–1021.

[9] K. Krogh-Jespersen, D. Cremer, J. D. Dill, J. A. Pople, P. von R. Schleyer, *J. Am. Chem. Soc.* **1981**, *103*, 2589–2594.

The First Octahedral Zintl Ion: Sn_6^{2-} as a Ligand in $[Sn_6\{Cr(CO)_5\}_6]^{2-}$**

By *Berthold Schiemenz* and *Gottfried Huttner**

Dedicated to Professor Hartmut Bärnighausen on the occasion of his 60th birthday

Octahedral clusters with M_6 skeletons (M = transition metal) appear very frequently in the chemistry of the d block elements.[1] In contrast, in the chemistry of the main group elements, it is only in boron chemistry that the octahedron is known as a framework pattern of clusters.[1] Octahedral clusters have so far not been proven either for Zintl ions E_6^{n-} [2, 3] (E = main group element) or for isopolycations E_6^{n+}.[4] The reason why the octahedron does not occur as a

[*] Prof. Dr. G. Huttner, Dipl.-Chem. B. Schiemenz
Anorganisch-chemisches Institut der Universität
Im Neuenheimer Feld 270, D-W-6900 Heidelberg (FRG)

[**] This work was supported by the Deutsche Forschungsgemeinschaft (Sonderforschungsbereich 247) and the Fonds der Chemischen Industrie.

construction motif in these cases appears to be unknown.[2] Thus, for example, in the chemistry of tin, which shows a rich Zintl ion chemistry,[2, 3] an octahedral ion Sn_6^{2-} is unknown. According to Wade's rules,[5] such an ion could be stable as an octahedral cluster with 14 framework electrons; also its comparatively low charge seems to indicate that it could exist. However such clusters occur neither in the solid state nor in solution.[2, 3] Also attempts to stabilize Zintl ions by using transition metal complex fragments[6] have so far not led to the isolation of aggregates which are not members of the series of the well-known anions E_m^{n-}.[2, 3]

We report now on the synthesis of coordinatively stabilized, octahedral Sn_6^{2-} in $[Sn_6\{Cr(CO)_5\}_6]^{2-}$ (**1**). $K_2[Cr(CO)_5]$[7]

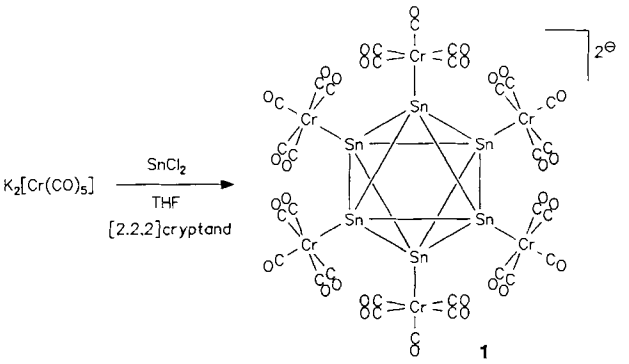

reacts with $SnCl_2$ in THF at $-70\,^{\circ}C$ to give a brown-red solution. After the addition of potassium [2.2.2]cryptand,[8] **1** can be crystallized from this solution as the [2.2.2]cryptand salt.[9] At the same time elemental tin is precipitated from the reaction solution. In addition $[K([2.2.2]cryptand)]_2[Cl_2Sn\{Cr(CO)_5\}_2]$ can be isolated as a crystalline compound.

The structure of the anionic cluster **1** is shown in Figure 1.[10] The six tin atoms form an almost regular octahedron with Sn–Sn distances ranging between 293.0 and 296.0 pm (Fig. 1). The Sn–Sn bond lengths are in the normal range.[3, 11] Each tin atom is coordinated through its "lone pair of electrons" to one $Cr(CO)_5$ fragment. The Sn–Cr bond vectors radiate outwards with Sn–Cr distances of 260.8 to 261.3 pm. The deviations from the ideal radial orientation (ideal value Sn-Sn-Cr: 135°; cf. range of angles for Sn-Sn-Cr angle, Fig. 1) result from the spatial requirement of the bulky $Cr(CO)_5$ "protective groups". On the whole, however, the distortions remain quite small (Fig. 1).

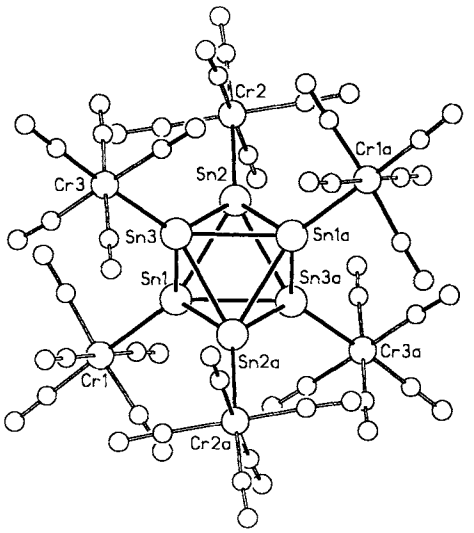

Fig. 1. The crystal structure of the anion $[Sn_6\{Cr(CO)_5\}_6]^{2-}$ (**1**). Selected distances [pm] and angles [°]: Sn1-Sn2 294.0(1), Sn1-Sn3 293.0(1), Sn1-Sn2a 294.8(1), Sn1-Sn3a 294.2(1), Sn2-Sn3 296.0(1), Sn2-Sn1a 294.8(1), Sn2-Sn3a 294.5(1), Sn1-Cr1 260.9(2), Sn2-Cr2 260.8(3), Sn3-Cr3 261.3(2); Cr1-Sn1-Sn2 148.0(1), Cr1-Sn1-Sn3 129.9(1), Cr1-Sn1-Sn2a 121.1(1), Cr1-Sn1-Sn3a 136.6(1), Cr2-Sn2-Sn1 135.1(1), Cr2-Sn2-Sn3 131.6(1), Cr2-Sn2-Sn1a 135.3(1), Cr2-Sn2-Sn3 131.6(1), Cr2-Sn2-Sn1a 135.3(1), Cr2-Sn2-Sn3a 138.7(1), Cr3-Sn3-Sn1 135.3(1), Cr3-Sn3-Sn2 130.5(1), Cr3-Sn3-Sn1a 134.7(1), Cr3-Sn3-Sn2a 139.2(1). The center of the Sn_6 octahedron is a crystallographic inversion center. The atom designators Xi and Xia stand for atoms related by inversion symmetry.

The Zintl ion **1** is not only aesthetically pleasing, but its isolation shows for the first time that octahedral element aggregates such as Sn_6^{2-}, the first octahedral Zintl ion, can exist also in main group chemistry. Evidently, apart from the correct number[5] of 14 framework electrons, a prerequisite for the synthesis of such ions is also the "correct" choice of synthetic method and protective groups.

Experimental Procedure

All experiments were carried out with freshly distilled and dried solvents under an argon atmosphere. IR spectra: Bruker IFS 66. NMR spectra: Bruker AC 200. KC_8 (270 mg, 2 mmol) [7] was suspended in THF (20 mL) and allowed to react with $[Cr(CO)_6]$ (220 mg, 1 mmol) at $-70\,^{\circ}C$. To the dirty green suspension [7] obtained after the mixture had been stirred for 3 h (1 h $-70\,^{\circ}C$, 2 h $0\,^{\circ}C$) was added anhydrous $SnCl_2$ (95 mg, 0.5 mmol) at $-70\,^{\circ}C$. The suspension turned brown immediately; after it had been stirred for 30 min [2.2.2]cryptand (126 mg, 0.3 mmol) was added. The solution was allowed to warm to $0\,^{\circ}C$ and subsequently filtered through diatomeic earth. The brown filtrate was concentrated to 5 mL under vacuum and layered first with a little diethyl ether and then with pentane at $15\,^{\circ}C$. In the course of 7 days elemental tin was deposited; in addition yellow needlelike crystals of $[K([2.2.2]cryptand)]_2[Cl_2Sn\{Cr(CO)_5\}_2]$ could be isolated. Deep red, analytically pure crystals of $[K^+\text{-}([2.2.2]cryptand)]_2$ [1] were found both on the wall of the flask and in the precipitate; they must be picked out by hand. $M = 2695.61\ g\,mol^{-1}$, $C_{66}H_{72}Cr_6K_2N_4O_{42}Sn_6$, yield: 15 mg (7% based on Sn), correct C,H,N analysis, IR (THF): ν_{CO} [cm^{-1}] = 2073 m, 1943 vs, 1918 s; ^1H NMR (293 K, [D_6]acetone: $\delta = 2.61$ (m, 24 H), 3.65 (m, 48 H).

Received: September 18, 1992 [Z 5580 IE]
German version: *Angew. Chem.* **1993**, *105*, 295

[1] N. N. Greenwood, A. Earnshaw, *Chemistry of the Elements*, Pergamon Press, Oxford, **1984**; F. A. Cotton, G. Wilkinson, Advanced Inorganic Chemistry, 5th edition, Wiley, New York, **1988**.
[2] H. G. von Schnering, *Angew. Chem.* **1981**, *93*, 44; *Angew. Chem. Int. Ed. Engl.* **1981**, *20*, 33.
[3] J. D. Corbett, *Chem. Rev.* **1985**, *85*, 383; S. M. Kauzlarich, *Comments Inorg. Chem.* **1990**, 75; P. Sherwood, R. Hoffmann, *J. Am. Chem. Soc.* **1990**, *112*, 2881.
[4] N. Burford, J. Passmore, J. C. P. Sanders in *From Atoms to Polymers: Isoelectronic Analogies* (Eds.: J. F. Liebman, A. Greenberg), VCH, Weinheim **1989**, p. 53.
[5] K. Wade, *Adv. Inorg. Chem. Radiochem.* **1976**, *18*, 1.
[6] B. W. Eichhorn, R. C. Haushalter, W. T. Pennington, *J. Am. Chem. Soc.* **1988**, *110*, 8704.
[7] M. A. Schwindt, T. Lejon, L. S. Hegedus, *Organometallics* **1990**, *9*, 2814.
[8] [2.2.2]cryptand = 4,7,13,16,21,24-hexaoxa-1,10-diazabicyclo[8.8.8]hexacosane.
[9] By an otherwise similar reaction procedure the complex $[Sn\{W(CO)_5\}_3]$ with trigonal planar coordinated tin is obtained from $SnCl_2$ with $Na_2W_2(CO)_{10}$: G. Huttner, U. Weber, B. Sigwarth, O. Scheidsteger, H. Lang, L. Zsolnai, *J. Organomet. Chem.* **1985**, *282*, 331.
[10] $[K^+\text{-}([2.2.2]cryptand)]_2$[**1**]: $a = 1350.1(9)$, $b = 1376.4(7)$, $c = 1574.9(10)$ pm, $\alpha = 83.93(5)$, $\beta = 65.60(5)$, $\gamma = 74.99(5)°$, space group $P\bar{1}$, $Z = 1$, $R = 0.054$, $R_w = 0.053$; Measurement on a Siemens (Nicolet Syntex) R3m/V diffractometer, ($Mo_{K\alpha}$ radiation, graphite monochromator, ω scan, $2° \le 2\theta \le 42°$), 5425 independent reflections with ($I > 2\sigma(I)$), all non-hydrogen atoms anisotropic, solution and refinement of the structure carried out with the SHELX76 program (G. M. Sheldrick, University of Cambridge, **1976**). Further details of the crystal structure investigation may be obtained from the Fachinformationszentrum Karlsruhe, Gesellschaft für wissenschaftlich-technische Information mbH, D-W-7514 Eggenstein-Leopoldshafen 2 (FRG) on quoting the depository number CSD-56787, the names of the authors, and the journal citation.
[11] See for example, d(Sn–Sn) = 294–316 pm in $[Sn_9Cr(CO)_3]^{4-}$ [6]; d(Sn–Sn) = 297–331 pm in Sn_5^{4-}: J. D. Corbett, P. A. Edwards, *J. Am. Chem. Soc.* **1977**, *99*, 3313.

Book Reviews are written by invitation from the editor. Suggestions for books to be reviewed and for book reviewers are welcome. Publishers should send brochures or (better) books to the following address: Redaktion Angewandte Chemie, Postfach 101161, W-6940 Weinheim, Federal Republic of Germany. The editor reserves the right of selecting which books will be reviewed. Uninvited books not chosen for review will not be returned.

New Books to Mark the Coming-of-Age of Bioinorganic Chemistry

Bioinorganic chemistry has now matured into a well established area of research and has become an essential part of the education of new chemists. This is well illustrated by the first four books reviewed below. However, a comparison of these gives a hint of a new development. Whereas three of the books treat bioinorganic chemistry from a classical standpoint which, although interdisciplinary, is predominantly based on the concepts of inorganic chemistry, the book by J. J. R. Fraústo da Silva and R. J. P. Williams strongly emphasizes the *biological* aspects. The latter viewpoint can be characterized as the "biological chemistry of the elements", a broadly based subject ranging from inorganic chemistry (i.e., the chemistry of the elements) to molecular biology; thus it includes bioinorganic chemistry in the conventional sense, but extends beyond it.

Bioanorganische Chemie. (Series: Teubner Studienbücher Chemie.) By *W. Kaim* and *B. Schwederski*. Teubner, Stuttgart, 1991. XII, 450 pp., paperback DM 44.80.—ISBN 3-519-03505-7

At last here is an up-to-date and comprehensive textbook of bioinorganic chemistry! According to the cover blurb it is intended for use by students who have already attended a basic course of lectures in chemistry. In fact, in order to use the book to full advantage it is necessary (and sufficient) for readers to have a basic knowledge of the three core areas of chemistry as well as of biochemistry. However, to suggest only students as potential readers is too restrictive.

The authors have avoided following a rigid plan of arranging the contents according to either chemical elements or biological functions, and have thus freed the readers and themselves from unnecessary restrictions—especially with regard to presenting an overall view of bioinorganic chemistry. The result is an interesting and lively book. The detailed contents mainly follow a sequence that is of proven didactic value: presenting the experimental facts, explaining these on the basis of proposed models, and drawing attention to more far-reaching relationships. The text is supported by over 400 figures, tables, structural formulas, reaction schemes, and equations.

Two introductory chapters, the first giving a historical survey and indicating the present importance, and the second introducing some basic principles, are followed by 17 chapters devoted to special topics such as photosynthesis, hemoproteins, nickel-containing enzymes, biomineralization, and chemotherapy. Practically all the areas of bioinorganic chemistry are covered. The book concludes with a bibliography, a glossary of terms, and a good keyword index.

Particular attention has been given to providing up-to-date literature references, citing publications up to and including 1991. Readers are likely to have different views on whether or not the large number of literature references (over 700) is appropriate—probably those engaged in research will say that it is, whereas students will be less inclined to agree.

The glossary explains just under a hundred terms very briefly, typically in two lines. In view of the assumed previous knowledge of the readers, the extremely short definitions seem unnecessary in many cases; examples are diamagnetism, entropy (" a thermodynamic quantity measuring the degree of disorder in a system"), extinction coefficient, Lewis base, Lewis acid, molecular orbital, and the primary, secondary, and tertiary structure of a protein. Instead of these it would have been better to include expressions that are less familiar to chemists, such as "fakultativ aerob" (facultatively, or optionally, aerobic) on page 326.

A similar difficulty arises with some of the special sections inserted into the text, typically one or two pages in length and distinguished by a gray background, that deal with physical methods or theoretical models. Some of the explanations of complicated measurement and evaluation procedures are too superficial. Expressions such as "data sets", "the phase problem" (in the determination of structures by X-ray diffraction), "a method that is not unambiguous" (in connection with X-ray absorption spectroscopy), and "quadrupole splitting" (in Mössbauer spectroscopy) are used with little or no explanation. However, there are other such sections (e.g., those on the entatic state—catalysis by enzymes, electron spin resonance I + II, mirror image isomers in octahedral complexes) that are well presented.

Factual errors and inaccuracies are very few in relation to the wealth of information contained in the book. Although it is true that thiolates *can* stabilize high oxidation states of metal centers (p. 123), the authors should certainly have mentioned that for this to occur it is necessary for the normal reaction yielding the organic disulfide (with reduction of the metal ion) to be blocked. In Equation (7.11) the reducing agent needed to form $[Fe_4S_4(RS)_4]^{2-}$ is not shown. In Equation (10.10) the formula of the *ortho*-quinone is incorrect. In the catalytic cycle of the Cu,Zn-superoxide-dismutase (p. 218) the imidazole ring coordinated at stages 3 and 4 must be neutral, not anionic. The statement on page 237 that a bridging by N_2 between two metal centers in the nitrogenase is not possible is at least misleading, since an Mo–N_2–Fe configuration has in fact been discussed in the literature for the actual cluster model shown (Eq. (11.23)). Changes in bone structure in cases of chronic cadmium poisoning are probably caused not so much by direct replacement of Ca by Cd as by the indirect effects of kidney damage (through interference with the calcium and phosphate metabolism). On page 348 the impression is given that carcinogenic effects of chromate in humans have not yet been proven. In fact, however, zinc chromate is classified as a human carcinogen (see the MAK register). I found about 30 printing errors in the book.

These minor defects do not alter the favorable overall impression of the book. As already indicated above, the potential readership is not confined to students. The book is of interest to everyone who wishes to obtain an overview of bioinorganic chemistry and already has an adequate knowl-

edge of general chemistry. Advanced chemistry students should definitely have a copy, and the relatively low price should help to make that possible.

It is desirable that an English language edition should be made available very soon, and the book should then have an excellent prospect of gaining a reputation beyond the German-speaking world as a standard work on bioinorganic chemistry.

The Biological Chemistry of the Elements. The Inorganic Chemistry of Life. By *J. J. R. Fraústo da Silva* and *R. J. P. Williams*. Clarendon Press, Oxford, 1991. XXI, 561 pp., hardcover £ 60.00.—ISBN 0-19-855598-9

A preliminary thumbing through this book already reveals some unusual features in form and content. The text is arranged in short sections with headings that stand out clearly, and a liberal use is made of space, all of which makes for excellent clarity. A wide margin occupies the left-hand third of each page, and is frequently used for figures and tables. Quite a number of the figures present biological information; for example, there are diagrams of a hepatocyte and a nerve cell, organelles (mitochondrion, chloroplast, etc.), the skeleton of a lizard, and many schematic diagrams of cells of a wide variety of types, showing cell membranes with material and energy flows.

The interconnections between inorganic chemistry, (bio)-physical chemistry, biochemistry, and molecular biology are emphasized in a wealth of examples. The program of the book can be illustrated by three quotations. Page 147: "The function of an element or a compound in biology has to be seen in the context of where and when it combines and how it moves, is used, and is removed." Page 155: "The complexity of the uses of energy, the fact that the whole system is constantly multiplying and growing or repairing, that it can maintain shape or alter it, and that the several operations are timed require a continuous monitoring, feedback, communication and energy network." Page 527: "The central hypothesis is that the evolving nature of living systems... is a product of an interaction between the properties of inorganic elements... and an ever-evolving organic chemistry dependent on these properties."

The book is divided into three sections containing altogether 22 chapters. The first section is concerned mainly with coordination chemistry and physicochemical and biochemical aspects. Some of the topics discussed are the relative abundance, bioavailability, and speciation of different elements, compartmentelation in biological systems, kinetic and energetic aspects, the special role of hydrogen, and biological macromolecules. The second section is the bioinorganic core of the book, consisting of 12 chapters dealing with individual elements, groups of elements, and the forms in which each element can occur (e.g., iron in the form of heme). The third section is concerned with biominerals and biological shapes, homeostasis, morphogenesis, and evolution, and lastly with the use of the elements by man (ecological, toxicological, and medical aspects). A detailed index completes the book. The lists of references given at the end of most of the chapters have deliberately been kept short, with a high proportion of review articles.

There are about 450 figures and tables, plus many reaction equations and structural formulas. The consistently high quality of the figures and the commendably low incidence of printing errors show that the book has been carefully prepared. Some errors worth pointing out are as follows: on page 44 "1 pm = 100 Å" is wrong; on page 45 the sulfide S-atoms of the Fe_4S_4 cluster cannot have free terminal bonds; on pages 152 and 522 an incorrect formula is given for the anion of shikimic acid; in the formula for glutathione on page 455 the positions of the glycine and cysteine groups should be interchanged.

"The Biological Chemistry of the Elements" is an attractive book and is a pleasure to read. The authors have sought to present a comprehensive picture, including both the biochemical states *and* the processes, covering both the spatial *and* the temporal (e.g., evolutionary) aspects. From the reader's standpoint a broad background knowledge is desirable as a starting basis. This work is not suitable as a student textbook, and is presumably not intended as such; in any case, the high price alone will deter students from buying it. The book should be of great interest to those engaged in research and teaching in chemistry and biology, especially in the areas of complex chemistry, bioinorganic chemistry, biochemistry, and molecular biology. Other books suitable as introductions and accompaniments to the study of this work are: *Bioanorganische Chemie*, by W. Kaim and B. Schwederski (see above) and *Molecular Biology of the Cell*, by B. Alberts, D. Bray, J. Lewis, M. Raff, K. Roberts, and J. D. Watson.

Bioinorganic Chemistry. (Series: Progress in Inorganic Chemistry, Vol. 38.) Edited by *S. J. Lippard*. Wiley, New York, 1990. XV, 535 pp., paperback £ 28.30.—ISBN 0-471-52945-1

This volume contains eight review articles on current areas of research in bioinorganic chemistry, based on contributions to the Fourth International Conference on Bioinorganic Chemistry held in 1989 in Cambridge (USA).

In the first article R. H. Holm, S. Ciurli, and J. A. Weigel begin with a short introduction to the chemistry of iron–sulfur clusters, then go on to describe studies with model compounds aimed at mimicking the effects of the protein matrix on Fe_4S_4 centers. Special attention is then devoted to Fe_4S_4 cubane-type clusters with nonequivalent iron atoms.

O. Hayaishi, O. Takikawa, and R. Yoshida contribute a review of the heme-containing enzyme indoleamine-2,3-dioxygenase. Here, unfortunately, inorganic aspects only receive marginal attention, and therefore a more appropriate place for this article would be in a series on biochemistry.

Iron and manganese proteins containing (μ-oxo)dimetal centers take part in a variety of biochemical processes. Perhaps the best known of these proteins is the dioxygen carrier hemerythrin. L. Que, Jr., and A. E. True describe these metalloproteins and numerous smaller complexes that serve as models for their active centers. This is the longest chapter (104 pp.), and also contains the greatest number of literature references. The authors have succeeded in giving a very clear account of the combined use of spectroscopic, X-ray crystallographic, magnetochemical, and electrochemical methods to study proteins and model complexes.

An article by P. Hendry and A. M. Sargeson deals with biologically important reactions of phosphate derivatives and discusses their mechanisms. Complexes formed by inert metal ions have proved to be especially useful for such mechanistic studies. The central theme is the intramolecular attack of metal-coordinated nucleophiles such as OH^- or NH_2^- on neighboring phosphate ligands.

B. E. Bowler, A. L. Raphael, and H. B. Gray discuss theoretical and experimental aspects of long-range electron transfer (ET) in donor–acceptor complexes and proteins. The ET rate is shown to depend on various factors, such as the electronic coupling, the distance between donor and acceptor,

and the reorganization energy. The authors also discuss ET processes between proteins and inorganic complexes, in modified proteins, and between different proteins.

J. G. Wright, M. J. Natan, F. M. MacDonnell, D. M. Ralston, and T. V. O'Halloran present a detailed review of the state of mercury(II)-thiolate chemistry. As a closely related topic they describe the receptor MerR, which is specific for Hg^{II}; this DNA-binding protein controls the mechanism of the detoxification of Hg^{II} ions in certain bacteria.

Transition metal complexes can be used as probes for investigating nucleic acids, for example as a way of recognizing different types of DNA, or in sequencing. Metal complexes are especially suitable for this purpose since they can react in many different ways, have useful spectroscopic and electrochemical properties, and can if necessary have rigid structures with defined symmetry. This fascinating subject is covered by A. M. Pyle and J. K. Barton.

In the final article S. L. Bruhn, J. H. Toney, and S. J. Lippard discuss the structure and biochemistry of DNA molecules that have been modified by the action of platinum compounds. As expected the main emphasis is on the antitumor agent cisplatin, but the properties of the corresponding *trans* compound are also discussed.

The experiment mentioned in the preface whereby the usual proofreading has been omitted, so as to produce a more up-to-date text, is not without its adverse effects. Even without a systematic search, more than 30 printing errors were noticed, of which more than 20 were in the article by J. G. Wright et al. However, most of these were not very serious. The figures are, with only a few exceptions, of good quality, and the index is adequate.

The potential readership should particularly include advanced students. The idea of publishing the book in a (relatively!) cheap paperback version at the outset was a good one, not only with students in mind. The advanced level of treatment could present problems for the average student, but despite this some of the chapters may be suitable as a basis for student seminar discussions. In any case, however, the students will first need to be familiar with the fundamentals of bioinorganic chemistry, for example through an introductory lecture course or from a textbook such as that by Kaim and Schwederski (see above).

To summarize, everyone interested in the latest developments in bioinorganic chemistry is strongly recommended to buy this book. It is, in any case, a must for every departmental library.

Perspectives on Bioinorganic Chemistry, Volume 1. Edited by *R. W. Hay, J. R. Dilworth*, and *K. B. Nolan*. JAI Press Ltd., London, 1991. XI, 284 pp., hardcover \$ 78.50 (in North America).– ISBN 1-55938-184-1

The new series "Perspectives on Bioinorganic Chemistry" aims to present the current state of research in this field. The first five volumes are already planned, and will appear at approximately yearly intervals, as implied by the subtitle of Volume 1: "A Research Annual". This first volume contains seven review articles varying in length from 26 to 51 pages. The fact that the individual chapters are short and not very broad in scope is perhaps a justification for the absence of an index.

The first topic is the formation of complexes between metal ions and peptides, reviewed by L. D. Pettit, J. E. Gregor, and H. Kozlowski. The article is arranged according to the various metals, with particular emphasis on copper, and the authors limit their treatment essentially to a factual account in the style of the "Specialist Periodical Reports". However, this is not typical of the book as a whole. Surprisingly, there is no mention of the phytochelatins, a class of plant peptides with an important role in the homeostasis of metal ions.

In the second article T. H. Fife describes the action of metal ions in catalyzing the hydrolysis of esters and amides, starting with simple small-molecule systems and then going on to the example of carboxypeptidase A. The author discusses kinetic and mechanistic aspects which are, of course, intimately related to the structures of the complexes, substrates, and ligands.

There are already numerous reviews on the topic of "blue copper proteins", and the article here by S. K. Chapman is therefore to be seen as updating the position. A description of the structural and spectroscopic properties of the blue copper centers is followed by a list of the individual proteins. Lastly several special topics are covered, such as ruthenium-modified proteins.

F. A. Armstrong contributes an article on voltammetry of metal centers in proteins. The versatile capabilities of this technique, which has hitherto been viewed with some skepticism, are well described. Among other aspects, the special importance of the electrode surfaces is emphasized. Of the systems that have been investigated, iron–sulfur proteins receive particular attention.

W. E. Smith and J. Reglinski report on the use of gold compounds for the treatment of rheumatoid arthritis. After briefly describing the nature of the disease and the clinical aspects, the authors discuss the chemistry of gold compounds, especially complexes with sulfur-containing ligands. The distribution of gold in living organisms, reactions with enzymes and cells, clinical trials, and the mechanism of the therapeutic action are also discussed.

R. C. Hider and A. D. Hall deal with iron chelating agents that can be used for therapeutic applications. The discussion centers mainly on derivatives of 3-hydroxypyridin-4-one. The first clinical tests on compounds of this class have yielded promising results. The work reported includes studies on the mobilization of iron from proteins with transport and storage functions.

In the final article R. R. Eady collects together information on nitrogenases that do not depend on molybdenum. The aspects reported on include the genetics of nitrogen fixation, the biochemistry of the nitrogenase, and the iron proteins, VFe proteins, and FeFe proteins.

Some of the figures and formulas are unsatisfactory in their quality and size. However, this criticism definitely does not apply to the chapters by T. H. Fife and by R. C. Hider and A. D. Hall. The incidence of factual and printing errors is tolerably low. Some particularly noticeable examples are as follows: on page 10 rubredoxin has an Fe_2S_2 core; the formulas given for the lysine side-chain on page 21 and for serine on page 274 contain errors; on page 28 "Glu–Cys–Gly" for glutathione is not strictly correct; in the discussion of CH_3Hg^+ complexes on page 30, the stability constants given are for Cd^{2+}; in Figure 5 on page 198 no unit is given for the ordinate axis; Ref. [47] on page 208 gives the names of the authors but not the journal; on page 280 the text refers to Table 5, but this cannot be found.

On the basis of the quality of the contributions in this first volume, the series "Perspectives on Bioinorganic Chemistry" should find a place in every relevant library. Research groups with interests in bioinorganic chemistry are also recommended to buy the series.

Henry Strasdeit
Fachbereich Chemie
der Universität Oldenburg (FRG)

Natural Products. A Laboratory Guide. 2nd Edition. By *R. Ikan*. Academic Press, New York, 1991. XIV, 360 pp., hardcover $ 54.95.—ISBN 0-12-370551-7

Most specialist books are either cheaply produced or too expensive or, in the worst cases, both. The one reviewed here is not cheaply produced; it is typeset in a clear style, printed on good paper, and solidly bound. But what purpose does it serve? More on this later.

The main content of the 17 chapters (about 350 pages altogether) consists of descriptions of 33 isolations of natural products, of which 26 are from the plant kingdom, five from the animal kingdom, and two others. In addition 15 conversion or breakdown reactions and five total syntheses are described. Also included are experimental data on 24 chromatographic separations and six other laboratory processes (color reactions, formation of inclusion complexes, separation of racemates, etc.).

The contents are arranged under four main compound classes: acetogenins, carbohydrates, isoprenoids, and nitrogen compounds. These are further subdivided; for example, the acetogenins are divided into flavones, lipids, lignans, quinones, and phloroglucinols. Each chapter begins with an introduction and ends with questions and a list of recommended books. The middle part describes the individual experiments relating to the subject of the chapter.

Each introduction describes the relevant group of natural products and explains its subdivisions. For example, steroids are subdivided into sterins, bile acids, steroid hormones, compounds with cardiac activity, and sapogenins. On the whole these introductions are very detailed and well illustrated with formula diagrams, although regrettably these are often shown as "flat" structures that are stereochemically ambiguous. These introductions are, of course, no substitute for reading up on natural products chemistry in the relevant textbooks, especially since they do not deal at all with the important aspect of biosynthesis. Nevertheless, they are suitable as a first introduction or for revision, and are presumably meant to be no more than that.

The questions are intended to serve as revision of what has been learnt, but the chemical aspects are not adequately covered. Only rarely does one find questions about reactions or understanding of the principles; instead the emphasis is on names and definitions ("What is ...?" or "Describe ..."). It is doubtful whether this style is suitable as a preparation for examinations.

The descriptions of experiments contain many old favorites, such as Gattermann's methods for the isolation of caffeine from tea and of heme from blood. However, some micropreparations are also included, where the emphasis is not so much on isolating significant quantities as on chromatographic investigations, as in the isolation of pteridines from fruit-flies. Finally, to complete the picture, there are some examples of conversions (e.g., cholesterol to cholestenone, which again is old hat) and total syntheses (e.g., mescalin—was this really necessary?). These experimental descriptions again follow a consistent pattern under standard headings: introduction, principle of the method, apparatus, materials, time required, and execution. The latter usually also includes information on yield, physical properties, test reactions and derivatives, spectroscopic data, and literature references. The latter especially makes it evident that the original edition is now 25 years old.

Some important items that have been added since the first edition are the spectroscopic data given for most of the end products, and details of the flash chromatography of essential oils, HPLC of carotenoids, RP-HPLC of amino acids, HPTLC of carbohydrates, experiments on geoporphyrins, yeast RNA, and the synthesis and breakdown of alkaloids and steroids.

Time and again one asks "Is this necessary?" Not because of the errors, which are very few—for example, in the formula diagrams on pages 201 and 252, in nomenclature (the correct names are citral, not geranial, and sabinene, not sabonene), and on page 240 where the impression is given that strychnine can be extracted from ground-nuts. These are pardonable sins, but more serious faults to my mind are the unnecessarily detailed descriptions of experiments (pp. 280f., preparation of silica gel layers on glass rods and test-tubes for thin-layer chromatography), and sketches of apparatus whose poor print quality alone indicates that they have probably been simply photocopied (p. 197, apparatus for UV irradiation, and p. 200, where the flash chromatography sketch is clearly identical to that in Still's original publication).

Who should buy this book? Obviously it tries to achieve too much. The whole of natural products chemistry, from isolation and structure determination through conversions to the total synthesis of natural products—a subject that should certainly also include biosynthesis—cannot be compressed into 350 pages. If the subtitle "A Laboratory Guide" is intended seriously, a good deal of this could be left out, and perhaps also some of the old familiar stuff could be sacrificed in favor of up-to-date procedures. At this price students are hardly likely to buy the book, and natural products chemists will find in it little that they do not already have in other sources; however, interested scientists from neighboring disciplines can obtain from it a concise impression of the variety of natural products chemistry.

Horst C. Uzar
Fachbereich Organische Chemie
der Universität-Gesamthochschule Siegen (FRG)

Nucleophilic Aromatic Displacement. The Influence of the Nitro Group. (Series: Organic Nitro Chemistry Series). By *F. Terrier*. VCH Publishers, New York/VCH Verlagsgesellschaft, Weinheim, 1991. XI, 460 pp., hardcover DM 239.00.—ISBN 0-89573-312-9/3-527-26746-8

The attention of modern organic chemistry is directed mostly towards control of the stereochemistry of organic reactions, synthesis of natural products, and especially towards life processes. The chemistry of aromatic compounds, particularly nucleophilic substitution in aromatic rings, is presently "out of fashion" in academic research. There are some reasons for such an attitude; nevertheless, since the majority of products of organic chemical industry contain aromatic carbo- or heterocyclic rings, the chemistry of arenes is still of great importance. Moreover, contrary to the common opinion, it also offers a significant intellectual challenge and an interesting field for discoveries.

In this situation the appearance of the monograph by François Terrier is very timely and welcome. In a relatively short volume the author discusses many important effects of the nitro group on the reactivity of aromatic compounds with nucleophilic agents. Thus, such problems as the kinetics and thermodynamics of the formation of σ-adducts, classical nucleophilic aromatic substitution of leaving groups, and many variants of nucleophilic substitution of hydrogen, photosubstitution, etc., are thoroughly discussed, and a rich selection of examples and references is given. As one might expect, the author's own preferences and interests flavor the book to a noticeable extent. Physicochemical and mechanistic problems are discussed in more depth than practical

aspects; nevertheless, the usefulness and applicability of the various reactions in organic synthesis is discussed at an adequate level.

Although I am very favorably impressed by the concept of this book and its content, I cannot refrain from some critical remarks.

The first objection concerns terminology. Although it is commonly accepted to use the term "complexes" for the adducts of nucleophiles to nitroarenes, this is somewhat misleading. It implies a specific nature for the bonds formed in the addition process, whereas they are normal σ-bonds to sp^3 carbon atoms. The term "σ-adduct" should perhaps be used instead of "complex", and in fact the former term is also used occasionally by the author.

The second objection is more important. In the present state of knowledge, it is evident that nucleophilic addition to a carbon atom bonded to hydrogen (to form a σ^H-adduct) takes place more rapidly than to one with another substituent (σ^x-adduct formation), when these carbon atoms are in equally activated positions of the aromatic ring. This fact is well presented in the book, and also in the author's own original papers and earlier reviews. From this one can draw the general conclusion that nucleophilic substitution of a leaving group in the nitroaromatic ring is usually preceded by fast and reversible formation of the isomeric σ^H-adducts. The author justifiably claims that π-complexes are formed in the course of the S_NAr reaction, but does not mention the more important pre-equilibrium of the formation of σ^H-adducts. Such a conclusion would undoubtedly stimulate the search for new reactions, and would give this very interesting book an additional value.

In a relatively concise book such as this, it is necessary to select material, and thus some omissions are unavoidable. However, I think that the important, although not very general, method of converting σ^H-adducts into nitroso compounds should be mentioned as another variant of the nucleophilic substitution of hydrogen.

The general appearance of the book is pleasing, and the high quality of typography and artwork makes reading it not only an interesting, but also an enjoyable excursion into the chemistry of nitroarenes.

There are very few typographical errors; for example, in structure **10** (p. 162), in the side chain NO_2 should instead be Me; on page 179, second line from the bottom, 5% should instead be 50%; on page 163, "dimethylation" (with HMPA) should read dimethylamination. The most serious error can be seen on the back cover!: *neu*cleophilic substitution.

In general, this is a very valuable, interesting, and important book, and I strongly recommend it for all libraries of academic and industrial chemical research laboratories. In spite of the relatively high price, it will undoubtedly also be purchased by many individual chemists. I certainly hope that it will promote a greater interest in the fascinating chemistry of nitroarenes.

Mieczysław Mąkosza
Institute of Organic Chemistry
Polish Academy of Sciences
Warsaw (Poland)

Microbial Degradation of Natural Products. Edited by *G. Winkelmann*. VCH Verlagsgesellschaft, Weinheim/VCH Publishers, New York, 1992. XII, 420 pp., hardcover DM 248.00.—ISBN 3-527-28354-4

Molds and bacteria play a central role in the mineralization of all organic compounds. This book presents an overview of microorganisms and their enzymes that are involved in the degradation of natural products. The importance of such enzymes extends far beyond degradation in the narrower sense. They are involved in many biotechnological processes, and are also present as supplements in various products. Interest in natural products as renewable raw materials has increased in recent years. In Germany, for example, research on renewable raw materials has been supported by grants of about DM 50 million from the Federal Ministry for Research and Technology alone. Therefore the book fills a gap and is likely to be welcomed with considerable interest. No survey of the degradation of natural products has previously been available in this form.

The editor, G. Winkelmann, has succeeded in recruiting a team of expert authors from universities and industry. In twelve chapters they report on the breakdown of starch, pectin, cellulose, hemicellulose, lignin, proteins, nucleic acids, and arenes. In nature these substrates undergo degradation by a wide variety of microorganisms, of which molds play a central role. These organisms synthesize a great variety of amylases, glucoamylases, pectinases, and other enzymes. The current state of knowledge on the microorganisms and enzymes that take part in degradation is brought together here, both in the text and in the numerous tables. The chapters have a clear arrangement of subject matter, and for each substrate there are sections on the physiology and genetics of the microorganisms, and on the properties of the enzymes and methods for their purification and assay. There are also applications-related sections explaining the importance of the enzymes in biotechnology. Enzymes such as amylases, glucose-isomerase, and proteases, which are manufactured on a large scale and are used in the saccharification of starch, in the food industry, and in detergents are described, but the spectrum of applications is much broader, ranging from medicine (collagenases) through fine chemicals manufacture (thermolysin, lipases) to molecular biology (nucleases). Whereas it is not yet clear how or whether lignin-peroxidases will be adopted in biotechnology, the use of P-450 enzymes for selective biotransformations is continually being extended to new processes. Everyone interested in such enzymes will find in this book a wealth of possible organisms for producing them. However, whether or not a particular one is actually obtainable is another question, since many organisms have not been deposited in the available collections, and some of those mentioned in publications are not even accessible through the groups reporting them.

Most of the enzymes involved in the degradation of natural products are exoenzymes, and their synthesis and secretion is therefore reviewed in the first chapter. Two other chapters of special importance are those on arenes, which occur in nature during the breakdown of lignin, and are also present in amino-acids, lignin precursors, antibiotics, flavonoids, phytoalexins, and melanins. One of these chapters is devoted to metabolization in molds, and the other to anaerobic breakdown of arenes. As well as being potentially useful for the detoxification of water and soil, these reactions also offer possibilities for manufacturing fine chemicals by biotransformations that are environmentally friendly and selective.

The book gives the reader an insight into the gaps in present knowledge and the directions of future research. For example, we do not yet have a complete picture of anaerobic degradation. Progress is hampered especially by the slow growth rate of the microorganisms concerned and by the small cell mass per unit volume of the fermentation medium. An important advance in the understanding of lignin break-

down came with the discovery of lignin-peroxidase in 1983, but the fate of the phenoxy radicals that are formed after the initial oxidation step is not yet understood. The topic of how microorganisms interact during degradation raises more questions than answers. Most investigations are carried out using pure cultures, but this book shows very clearly that there are many different isolated strains that can use a given substrate as a carbon source. In contrast to the understanding of the functions of individual microorganisms, little is known about the cooperative functioning of several specialized microorganisms, nor about the ecology of the functionally redundant types. The first insights into these questions are now coming from studies of the degradation of wood in soil and of cellulose in the digestive systems of ruminants. However, studies of the "communication" between microorganisms and their metabolic interactions are only just beginning.

The main emphasis of the book is on microorganisms and their enzymes, whereas there is in general relatively little theoretical discussion of the chemistry and mechanisms of degradation. The book is essentially a literature survey and a work of reference, and the detailed bibliographies citing material for further reading, as well as an index of microorganisms and enzymes at the end, are consistent with this purpose. It can be recommended for everyone interested in studies of microbial degradation, and also especially for users of such processes.

Bernhard Hauer
BASF AG, Ludwigshafen (FRG)

Transition Metal Oxides. An Introduction to their Electronic Structure and Properties. (International Series of Monographs on Chemistry, Vol. 27.) By *P. A. Cox*. Oxford University Press, Oxford, 1992. IX, 284 pp., hardcover £ 37.50.—ISBN 0-19-855570-9

As the author mentions in the preface to this book, interest in the oxides of the transition metals can be traced far back into antiquity. These compounds are nowadays of enormous importance in chemical technology, for example as magnetic pigments, white pigments, laser materials (e.g., garnets), and X-ray fluorescent materials (e.g., $BaWO_4$). They are also an important subject of basic research, which has led to a deeper understanding of many physical properties of the solid state. One of the most significant recent discoveries is that of the new high temperature superconductors (the oxocuprates), the study of which provides a good illustration of the close connection between structure and properties in the solid state.

This book is not so much concerned with describing the great variety of transition metal oxides as with discussing their widely varying electronic properties. The first chapter starts by briefly explaining some basic concepts of solid state chemistry, such as oxidation levels, nonstoichiometric compounds, the phase rule, and phase diagrams. This is followed by an equally concise treatment of the coordination of metal atoms by oxygen, the resulting polyhedral crystal structures, the occurrence of defects in these, and an overview of electronic properties.

Chapter 2 describes the essential features of various models for interpreting electronic structures, ranging from the purely ionic picture of the ligand field theory, through the molecular orbital (MO) theory, to the band structure model. Intermediate models such as the Hubbard model and the Anderson localization theory are also discussed. Chapter 3 begins by discussing band gaps in relation to spectroscopic properties, based on examples of nonconducting oxides of metals with d^0, d^8, or d^{10} electronic configurations. The author then deals with the question of the assignment of bond energies in doped and undoped transition metal oxides, and the various types of magnetic interactions that can occur in these materials. Chapter 4 is concerned with physical effects in semiconducting oxides, such as the properties of the charge carriers, point defect models, carrier binding energies, spectroscopic studies of free and bound charge carriers, and transitions to the metallic state. The fifth and last chapter deals with band structures and with the transport and optical properties of metallic transition metal oxides, and ends with a brief discussion of the new high temperature superconductors and the problems of developing a theoretical understanding of their properties.

A praiseworthy attempt is made in this book to treat the chemistry of transition metal oxides from the standpoint of their physical properties. Although the descriptions of the various theoretical models are brief and sketchy, the understanding of them is helped by numerous tables and diagrams. However, the reader whose interest in the subject goes beyond a superficial level is not well served. Also anyone who hopes for an overview of the whole field of transition metal oxides will be disappointed. Moreover, the treatment of the subject is incomplete insofar as oxides with localized metal–metal bonds, such as reduced oxomolybdates and oxoniobates, are not covered.

Despite these criticisms, the book can be recommended for all whose work is concerned with the structure and properties of solids. The many literature references provide an excellent starting point for more advanced reading in this area.

Jürgen Köhler
Max-Planck-Institut für Festkörperforschung
Stuttgart (FRG)

Oxygen Chemistry. By *D. T. Sawyer*. Oxford University Press, Oxford, 1991. 223 pp., hardcover £ 30.00.—ISBN 0-19-505798-8

Within the *International Series of Monographs on Chemistry* Donald Sawyer has provided a new book on different aspects of the chemistry of oxygen. In a one-page preface, R. J. P. Williams mentions that molecular oxygen is one of the major constituents of the atmosphere and that life depends on the kinetic barriers to oxygen reactions, in the presence of a very strong thermodynamic drive. This stimulating book is an attempt to show how the entire chemistry of oxygen (molecular oxygen and its reduced forms) in aqueous and non-aqueous media can be treated in a unified way, leading to a comprehensive understanding of all the different reaction pathways involving oxygen.

The book is divided into eight chapters. After an introductory chapter dealing with fundamentals such as the central role of oxygen in chemistry, and O_2 as a unique natural product, Chapter 2 describes the redox thermodynamics for oxygen species (ozone, molecular oxygen, $HOO\cdot$, $O_2^-\cdot$, HOOH, HOO^-, O, $O^-\cdot$ and HO^-). This chapter contains useful tables on reduction potentials in aqueous or aprotic solvents which are generally widely scattered throughout the literature. The chemical versatility of dioxygen species (oxido-reduction, atom transfer, or dismutation) is mainly influenced by the reaction medium. Chapter 3 describes the nature of the chemical bonds in oxygen species, on the basis of

electronegativities of elements and valence bond theory. This first half of the book provides the necessary background for the second half, which is focussed more on the chemical reactivity of the different oxygen species. Chapter 4 describes the reactivities of hydrogen peroxide, alkyl hydroperoxides, and peracids. The Lewis acid activation of HOOH and the monooxygenation reactions induced by iron(III) salts in aprotic solvents are described in great detail. The following chapters, 5 and 6, are concerned with the reactivity of oxygen radicals ($HO\cdot$, $RO\cdot$, $HOO\cdot$, $ROO\cdot$ and $RC(O)O\cdot$) and the activation of dioxygen for selective oxygenation reactions, respectively. Biological systems are mentioned in a small section. Chapter 7 is entirely devoted to the reactivity of superoxide ion, a favorite topic of the author ("How super is superoxide?"), and finally Chapter 8 is concerned with the reactivity of oxy-anions (HO^-, RO^-, HOO^-, ROO^-, and $O_2^-\cdot$). References are listed at the end of each chapter. All in all, this book is useful for readers involved in oxygen chemistry. However, it must be noted that some aspects of this monograph are rather controversial by deliberate intent of the author ("the electron is the ultimate nucleophile"). High-valent metal-oxo complexes are usually considered by the author as being not well substantiated, despite the growing evidence provided by various physicochemical methods on several species isolated at low temperatures.

In summary, this book is a good choice for chemists and electrochemists who want to enter the field of oxygen chemistry, and it is recommended for anyone who is not convinced that oxygen chemistry is highly versatile.

Bernard Meunier
Laboratoire de Chimie de Coordination du CNRS
Toulouse (France)

HPLC of Proteins, Peptides and Polynucleotides. Contemporary Topics and Applications. By *M. T. W. Hearn*. VCH Publishers, New York/VCH Verlagsgesellschaft, Weinheim, 1991. XV, 776 pp., hardcover DM 225.00.—ISBN 1-89573-295-5/3-527-26951-7

The great importance of modern high performance liquid chromatography (HPLC) for the analytical and preparative scale separation of peptides, proteins, and polynucleotides has led to the development of many new stationary phases, and these are comprehensively reviewed in this book. Many different chromatographic media are described, for example, those based on agarose, silica, and polyethyleneimine. The capabilities of the method are illustrated by examples, and a wealth of literature references is provided. Also the importance of models for describing the interactions between the peptide or protein and the stationary phase, from which one can predict the retention behavior, is recognized. The author also describes strategies for achieving an optimal separation by progressively changing the composition of the mobile phase. Several of the chapters contain very detailed descriptions of techniques such as reversed phase, ion exchange, exclusion, and hydrophobic interaction chromatography, and combinations of these. In analogy to 2-D electrophoresis, two-dimensional or multidimensional HPLC can be used for protein or peptide mapping. Another chapter is devoted to the use of chromatography for investigating protein–protein interactions. The various methods for determining equilibrium constants using exclusion or affinity chromatography are described in detail. Much attention is also given to preparative techniques. Variants of affinity chromatography using a variety of immobilized ligands, such as dyes, antibodies, lectin, and heparin are thoroughly discussed. Further chapters deal specifically with the separation and purification of individual groups of substances; these include protein hormones, membrane proteins, viral proteins, monoclonal antibodies, physiological amino-acids, oligonucleotides, plasmids, and DNA restriction fragments. The book ends with a chapter on the separation of peptides and proteins by capillary electrophoresis, an alternative to HPLC which combines the high efficiency and ease of automation of HPLC with the special separation mechanisms of electrophoresis.

To summarize, this book gives an excellent survey of the latest developments in the analysis of peptides and proteins, bringing together information that would otherwise be available only by an extensive study of the original literature. Each chapter is supplemented by numerous literature references. The book is definitely intended not for beginners, but for HPLC users interested in extending their knowledge. It does not contain laboratory recipes for particular separations, but instead discusses general relationships and optimization strategies. Every one of the 22 chapters is of a very high standard and contains a wealth of information. Even chromatographers with long experience in the field will gain a lot of useful knowledge from the book.

Christine Schwer
Max-Planck-Institut für Biochemie
Martinsried (FRG)

Phase Diagrams of the Elements. By *D. A. Young*. University of California Press, Berkeley, CA (USA), 1991. XI, 291 pp., hardcover $ 39.95.—ISBN 0-520-07483-1

Our understanding of the chemical bonding in solids and its influence on the properties of materials has, in the past, been greatly helped by structural studies in which the pressure and temperature are systematically altered. The results of such investigations, including the interconversion of different modifications of a substance under conditions of thermodynamic equilibrium, can be displayed especially clearly in the form of p–T phase diagrams, which have a high information content. The structures of the elements in the solid state, and their dependence on pressure and temperature, are of fundamental interest to the chemist, and there is now a wealth of information on these for the majority of elements. By bringing together a comprehensive collection of phase diagrams for the elements that have been investigated up to now, accompanied by brief descriptions of the structures that occur, this book fills an important gap.

The comprehensiveness of the results presented here has been made possible through the considerable developments that have recently taken place in experimental techniques for work at high temperatures and pressures. Most important among these developments is the diamond anvil cell (DAC). This has now made it possible to carry out X-ray crystallographic and spectroscopic studies at pressures up to about 1.1 TPa, or at temperatures up to 5000 K (at 100 GPa pressure). There have also been improvements in theoretical methods for understanding and predicting the occurrence of high pressure or high temperature phases, for example the application of the band theory of solids through the "local density approach" (LDA).

The book begins with a short introduction to modern experimental techniques used in high-pressure studies. This is followed by an equally brief summary of the theoretical methods for predicting the occurrence of phases and inter-

preting the results (band structure calculations, Monte-Carlo methods, molecular dynamics, and the thermodynamics of phase transformations and melting processes).

The main part of the book presents the phase diagrams for the individual elements, arranged according to the groups of the Periodic Table. Experimental results and relevant theoretical studies published between 1960 and 1990 are included; the main emphasis is on results published in the last ten years, stressing the most recent developments. This is followed in each case by a summary of the results in graphical form, in which the high-pressure phases of each element as a function of pressure are shown alongside each other for easy comparison. Each chapter ends with a comprehensive list of literature references. As all the elements of the Periodic Table are covered in barely 190 pages, this usually leaves only a little space for discussing the structures and special physical properties of the modifications that occur. Often the discussion is limited to a brief mention of theoretical considerations to explain the electronic structure and the different crystal structures found, together with literature references. Consequently the book should be regarded not as a comprehensive work of reference, but rather as a concise up-to-date summary of results, with particular emphasis on theoretical approaches to understandig the phase transformations that occur.

Although the book contains much information that should make interesting reading even for students, only certain parts of it are suitable for use as teaching material (in particular the p–T phase diagrams and the structural diagrams). Some of the abbreviations used are rather misleading: for example, the cubic primitive structure of α-Po is described as being of the α-sc(1) type, while the structure of black phosphorus is described as eco(8), and that of solid Cl_2 as eco(4). Thus, the structures are classified according to their Bravais types and the number of atoms per unit cell.

The author (a theoretical physicist) has written the book for a readership that includes solid state chemists with structural interests, but not all of these will find it meets their needs. Despite the brevity of the individual sections, all the important modifications of the elements are mentioned. A particularly interesting feature is that gaps in present knowledge are pointed out in many cases (for example, in the phase diagram for boron, or with regard to experimental evidence for the occurrence of a semimetallic modification of carbon at pressures of 1.1 TPa or greater).

This book is a valuable compilation of p–T phase diagrams and crystal structures of the elements in the solid state, containing information not hitherto available, and with special attention to the theoretical understanding of solids.

Wolfgang Schnick
Institut für Anorganische Chemie
der Universität Bonn (FRG)

Fascinating Molecules in Organic Chemistry. By *F. Vögtle*. Wiley, Chichester, 1992. IX, 304 pp., hardcover £ 80.00. – ISBN 0-471-93147-0

The author is an internationally renowned organic chemist whose diverse research interests include cyclophanes, crown compounds, and supramolecular chemistry. His love for exotic molecules is particularly evident in this volume. Like the companion book, *Supramolecular Chemistry*, this volume is based principally on lectures given at the University of Bonn. Although "fascinating" is a subjective term and beauty truly lies in the eye of the beholder, few modern enthusiasts of organic chemistry would find fault with the selection of organic molecules covered in this book. Key aspects of each parent system or class of molecules are described, including history, synthesis, properties and applications. The book is an excellent source of material for enlivening lectures on introductory organic chemistry and for special topics courses at the graduate level.

The book is organized in five chapters, and Chapter 1 is an introduction to fascinating natural structures and symmetry. Highly symmetrical structures have intrinsic aesthetic appeal. "The Platonic Solids" introduces a discussion that interweaves chemistry with cosmology. The result is not New Age chemistry; rather it is an exploration of the way in which symmetry can excite imagination concerning the structure of the universe as well as structural chemistry. Chapter 2, entitled "Alicyclic Compounds", ties into the previous chapter by beginning with a discussion of the fundamental Platonic hydrocarbon derivatives that are currently known: tetra-*t*-butyltetrahedrane, cubane and dodecahedrane. Icosahedral C_{60} (buckminsterfullerene), while not a Platonic hydrocarbon, should rightly follow dodecahedrane in this discussion of carbon clusters. Unfortunately, most fullerene research is too recent to be included in this book, except for some brief notes at the end of the first chapter. Chapter 2 continues with lively discussions on adamantane, pagodane, and [1.1.1] propellane. The alicyclic compounds presented in this chapter represent milestones in synthetic and structural organic chemistry. In addition to the now classical syntheses of the parent systems, more recent synthetic approaches and commercial applications are also described, including the Idemitsu process for the production of adamantane and pharmaceutical applications of adamantane derivatives.

Chapter 3 presents the highlights of research on fascinating aromatic compounds, including the triphenylcyclopropenylium cation, azulene, biphenylene, circulenes, cycloarenes, and the helicenes. Coverage of these aromatic compounds is somewhat uneven and clearly reflects the author's personal perspective. For example, 25 pages are devoted to the history, synthesis and properties of azulene, whereas kekulene is all but omitted from the interesting discussion on circulenes and cycloarenes. The section on helicenes on the other hand is a very good review and it is an excellent introduction to helically chiral compounds. In Chapter 4 triptycenes, 1,8-methanonapthalene, [2.2.2]phanes, and superphane are grouped together as "aralicyclic compounds". These discussions are just as interesting as those of the preceding sections. Finally Chapter 5, entitled "Heterocycles and Biologically Active Compounds", is more or less a grab bag of interesting molecules that do not clearly fit into the previous categories. It includes excellent discussions of Tröger's base, acetylsalicylic acid, vitamin B_6 (pyridoxine), and phthalocyanines. The discussion on phthalocyanines can be viewed as a bridge between this volume and the companion book (*Supramolecular Chemistry*) since it describes the properties of molecular materials derived from phthalocyanines, including electronic conduction and photochemical hole burning. Also included is a short epilogue on new tetrapyrrole macrocycles concerning porphacenes and other expanded porphyrins of current interest.

Overall, "Fascinating Molecules in Organic Chemistry" is a masterful compilation of challenging synthetic targets, theoretical puzzles, and molecular templates for practical applications. The English is remarkably smooth for a translation from German and there are very few errors. Rare mistakes include the misnumbering of structures on page 197 (duplication of **60**), redundant description of Landa's first isolation of adamantane (pp. 44, 45, 46), and misnaming of [1.1.1]-

propellane as [1.1.1]cyclopropane (p. 69). Good author and subject indexes enhance the utility of this book for reference purposes. This book is a necessary acquisition for relatively complete academic and industrial libraries. It would also be useful as a reserve book and as a source of interesting material in introductory and advanced organic chemistry courses. It could also serve as a textbook in special topics courses, but unfortunately it is priced as an import in the United States. Every effort should be made to reduce the price of this and the companion volume, *Supramolecular Chemistry*, in order to make them useful as textbooks, in accord with the apparent intention of their author.

Thomas W. Bell
Department of Chemistry
State University of New York, Stony Brook, NY (USA)

Properties of Chemically Interesting Potential Energy Surfaces. (Series: Lecture Notes in Chemistry, Vol. 56.) By *D. Heidrich, W. Kleisch,* and *W. Quapp.* Springer, Berlin, 1991. VIII, 183 pp., paperback DM 44.00.—ISBN 3-540-54286-8

The calculation of molecular structures using quantum-chemical computer programs has now become almost a routine procedure in modern theoretical chemistry. The enticing possibilities offered by these methods are not limited to the ability to calculate energy minima on the potential energy hypersurface (PHS), giving results that may be compared with experimental values and are increasingly being used as a substitute for them; one can also determine any other kinds of extrema such as first-order saddle points, which represent transition states and provide the chemist with information that cannot be obtained experimentally. Volume 56 in the excellent series "Lecture Notes in Chemistry" gives an overview of the mathematical basis of calculations on potential hypersurfaces. The main emphasis is on a discussion of the search procedures for determining extrema and of methods for predicting reaction pathways on the PHS. As an example of the application of these techniques, proton transfer processes are treated in detail.

The book is divided into four chapters. Chapter 1 (25 pp.) starts by discussing the concept of the PHS. This chapter is recommended reading for everyone interested in obtaining a brief introduction to current ideas on molecular structure based on the PHS model, and a survey of the most important published work. Conventional theories of molecular structure are based on the Born–Oppenheimer approximation, the validity of which is usually taken to be self-evident. However, there are growing indications that this approximation has its limitations, for example from studies of systems such as the NH_3 molecule. The authors propose some tests of the validity of the Born–Oppenheimer approximation, and suggest that this could lead to a fundamental change in the understanding of molecular structures. However, having put forward these somewhat heretical views, the authors are content to leave it at that, and the rest of the book proceeds along conventional lines within the Born–Oppenheimer approximation. The first chapter is completed by an explanation of some fundamental principles in the theoretical treatment of chemical reactions.

Chapters 2 and 3 (66 and 35 pp., respectively) are devoted to mathematical aspects. Two of the three authors (Kleisch and Quapp) are mathematicians, and these two chapters essentially contain a summary of the mathematical basis of the optimization procedures used in many quantum-mechanical calculations. This is the most important part of the book from the specialist's standpoint, and the comprehensive presentation of so many techniques, such as those for updating the Hesse matrix, is especially valuable since it is the only such compilation available. The fundamentals of these quantum-mechanical methods can be found in many textbooks, but the mathematical details of the computer programs used are often difficult to find. These two chapters are, unavoidably, written in the language of a mathematical textbook. However, this reviewer found that, after a short period of getting accustomed to the style, most of the derivations could be understood without much difficulty. The authors also deserve praise for having taken the trouble to give the mathematical expressions in terms of quantities understandable to chemists, at least pictorially, and to avoid losing the link with the chemical problem. Perhaps we see here the influence of the chemist member of the author team (Heidrich).

The fourth and last chapter (38 pp.) deals with the calculation of potential hypersurfaces and reaction pathways in proton transfer. Here again particular attention has been given to the question of the visualization of the numerical results. To the despair of many theoreticians, chemists respond better to pictorial than to numerical information, and it is found again and again that more attention is paid to a diagram of dubious accuracy than to a good numerical calculation that is difficult to interpret. The fashionable subject of "molecular modeling" provides enough disturbing examples of this. The authors have succeeded very well in bridging this difficult gap; Chapter 4 is not only understandable to the average chemist but is also well worth reading.

The book is a must for all chemists with theoretical interests, while Chapters 1 and 4 can be recommended for reading by chemists from all backgrounds. It should certainly be held by every departmental library. That should be possible even in these times of severe cost-cutting in view of the commendably low price.

Gernot Frenking
Fachbereich Chemie
der Universität Marburg (FRG)

Transition Metal Organometallics for Organic Synthesis. By *F. J. McQuillin, D. G. Parker* and *G. R. Stephenson.* Cambridge University Press, Cambridge, 1991. XX, 594 pp., hardcover £ 100.00.—ISBN 0-521-33353-9

Transition metal organometallics have made very important contributions to the success of organic synthesis in recent years. Nevertheless, many of the available methods are not yet employed as widely as their effectiveness justifies. To remedy this situation, the authors have provided a work of broad scope which describes the various synthetic methods based on transition metal organometallic reactions. Its main purpose is to assist newcomers to the field.

A brief introduction to the basic concepts needed for describing the structure and reactivity of transition metal organic compounds is given, and this is then followed by discussions of major reaction types, such as isomerization and rearrangement reactions, oxidations of multiple bonds, nucleophilic and electrophilic additions to coordinated ligands, carbonylation, and coupling reactions. The chemistry of transition metal-complexed π-ligands as well as σ- and car-

bene complexes is examined in detail and illustrated by a multitude of well selected examples. Catalytic and non-catalytic processes are explained with equally great care, and even enantioselective methods are not neglected. The two concluding chapters deal with "organometallic" strategies for the synthesis of natural products and heterocycles, providing striking illustrations, in the context of specific synthetic problems, of the usefulness of the methods previously introduced. Here, if not earlier, it also becomes evident that "habitual retrosynthetic thinking" must be thrown overboard if one really wants to use the opportunities of transition metal chemistry.

The text is written in a concentrated but very readable style, and is interlarded with valuable information and references. Preparative aspects clearly dominate throughout the book, but are always complemented and connected by mechanistic considerations. The scope and limitations of the individual methods generally become clearly evident, which is of great interest for potential "users".

The impressive wealth of material is backed up by more than 2000 literature references, which are grouped (sorted by chapters) at the end of the book. The literature is continuously covered up to 1988, and partly even up to 1990. It should be mentioned that the appealing quality of the book is also reflected in its appearance (binding, paper, printing, harmony of typesetting and formula diagrams). The book is also provided with an extensive subject index, which, together with the well structured table of contents, facilitates quick orientation even during the search for single facts.

A safety bibliography warns of potential risks associated with the handling of organometallic reagents. However, there is a possibility of an immediate danger of a different kind to the reader of the book, insofar as some misunderstandings could occur. Some readers, especially those not completely well versed in stereochemistry, could possibly be misled by the fact that a clear distinction is not always made between absolute and relative configuration. For instance, not all racemic target compounds are indicated as such, and the diagrammatic representation of stereochemical details (particularly of π-complexes) in many structural formulas could certainly be improved. But these are more or less minor matters: on the whole, the formula diagrams are clearly arranged, and also the number of misprints and other mistakes is small.

Of course, one is tempted to rate the book as overexpensive. However, if one takes into account the excellent quality of its appearance and contents, the enormous wealth of up-to-date, well selected, and conscientiously processed information on almost 600 pages, the price seems reasonable. To the publisher one could make an appeal to also provide a cheaper paperback edition, which would enable a larger circle of private individuals (e.g., students!!) to buy this important work.

To summarize, this generally excellent book entirely fulfills its intention, and is well worth its (high) price. On the back cover is the claim: "This book stands as an invaluable reference work as well as a source for initiating the design of new organometallic procedures, and as such will be of great value to organic chemists and research workers in both universities and industry". I can only agree with this statement and I hope this book will be well received by a wide readership.

Hans-Günther Schmalz
Institut für Organische Chemie
der Universität Frankfurt/M. (FRG)

Chemical Equilibria in Solution. Dependence of Rate and Equilibrium Constants on Temperature and Pressure. (Physical Chemistry Series). By *M. J. Blandamer*. Ellis Horwood/Prentice Hall, Chichester, 1992. 144 pp., hardcover $ 68.50.—ISBN 0-13-131 731-8

This monograph (142 pages) uses a thermodynamics theme to provide arrays of suitable equations which can be used to analyze data from solution equilibrium and kinetics experiments in which pressure or temperature, or both, are varied. It does not purport to, and does not discuss experimental methods or provide interpretative discussion of activation parameters derived from the various treatments. A pleasing feature, and one making for easier reading, is the separation of sets of equations from the narrative.

The author presents a literature survey in addition to contributions from his group, and successfully manages, almost without fault, the unenviable task of providing an orderly and consistent set of symbols throughout. References are cited for each subsection of a chapter, a convenient approach. However, the lack of lists of chapter-end references or of a cumulative reference list could be bothersome for some. There is an index of essential terms and named equations.

Chapters 1, 2, and 3 develop standard thermodynamics in terms of symbolism and application to solution chemistry into the repertoire of needs for the heart of the book (Chapters 4–6). Of these latter chapters, the first examines methods for treatment of pressure dependence results, while Chapters 5 and 6 consider, at length, methods for treating equilibrium and kinetics temperature dependence results. In the seventh and final chapter the dependence of equilibrium composition and rate constants on temperature and pressure is covered. The reader is given a lucid account of recent contributions to characterization of the isochoric condition and to calculations of isochoric activation parameters.

Overall the writing style is direct. There are some minor errors, such as missing words, for example in the first sentence of Section 4.14, and in the second sentence of the first complete paragraph of page 91, a missing letter as in pentaamminecobalt(III) (p. 69), and occasional confusing use of units; in this latter category an enthalpy change $\Delta_r H^\infty$ is given in $J\,mol^{-1}$ on page 102, and in $kJ\,mol^{-1}$ on page 105, and the volume parameter $\Delta_r V^\infty$ is expressed in cm^3mol^{-1} on page 71 but is given (erroneously) as $-35.9\ m^3mol^{-1}$ on page 66. The Tait equation, introduced in Chapter 1 and used again on page 72, contains lower case c, but when it is applied in the context of the Benson–Berson approach (pp. 73–74) a capital C appears.

Given that the author is a renowned thermodynamics expert one might expect that only other thermodynamics specialists will be attracted to this book. This would not be an accurate assessment, since the book can appeal in total, or in selected parts, to chemists and other scientists who have an undergraduate or more advanced knowledge of physical chemistry. It is likely that it could form part of the recommended reading for a graduate student lecture course on solution thermodynamics. The promotional material on the back cover cites among others "researchers in medicinal chemistry and medically related subjects..." as potential readers. While the broad appeal of the text can be lauded, it is not clear why these groups were selected.

Because of its focus only on development of thermodynamics equations for treatment of data, there is, at times, a sense of lack of connection with actual chemical equilibria and various chemical reactions. This is a disappointing aspect, and for some experimentalists could have the effect of

reducing the scope of use of the book. An emphasis could have been placed on the limitations which are not so much a lack of will or skill to fit data, but of suitable instrumentation, time, or amenable reacting systems. Obtaining data of sufficient quality to justify pursuit of calculation of the pressure and temperature derivatives of ΔV^* and ΔH^* respectively is seldom possible. Again, although this would have broadened the purpose of the book, it would have benefited from the inclusion of a section devoted to interpretation of derived parameters, and explaining how this contributes to understanding the chemical processes being studied. However, all the treatments experimentalists require are collected together here in one convenient source with each method easily accessible and referenced. This alone merits a place for this book in chemistry libraries and in the personal collections of thermodynamicists and kineticists.

Colin D. Hubbard
Department of Chemistry
University of New Hampshire
Durham, NH (USA)

Materials Science and Technology. A Comprehensive Treatment. Series editors: *R. W. Cahn, P. Haasen,* and *E. J. Kramer*. VCH Verlagsgesellschaft, Weinheim/VCH Publishers, New York.

Volume 3A: Electronic and Magnetic Properties of Metals and Ceramics (Part I). Edited by *K. H. J. Buschow*, 1991. XIV, 641 pp., hardcover DM 430.00.—ISBN 3-527-26816-2/0-89573-691-8

Volume 4: Electronic Structure and Properties of Semiconductors. Edited by *W. Schröter*, 1991. XVI, 603 pp., hardcover DM 430.00.—ISBN 3-527-26817-0/0-89573-692-6

Volume 7: Constitution and Properties of Steels. Edited by *F. B. Pickering*, 1992. XVI, 824 pp., hardcover DM 430.00.—ISBN 3-527-26820-0/0-89573-695-0

Volume 15: Processing of Metals and Alloys. Edited by *R. W. Cahn*, 1991. XIV, 628 pp., hardcover DM 430.00.—ISBN 3-527-26828-6/0-89573-802-3

The new 18-volume series "Materials Science and Technology" covers the properties, manufacture, and processing of materials, and their specific areas of use. It brings together the know-how of chemists, physicists, and engineers, and shows how fundamental research and applications-orientated research can be made to interact most effectively and fruitfully.

The first volume to appear, in 1991, was Volume 5, "Phase Transformations in Materials", and has already been reviewed in the context of the series as a whole (*Angew. Chem.* **1992**, *104*, 245; *Angew. Chem. Int. Ed. Engl.* **1991**, *30*, 1521). Up to now Volumes 2A, 3A, 4, 5A, 7, 9, 14, and 15 have been published, and four of these (3A, 4, 7, 15) are reviewed here.

During the planning of Volume 3 ("Electronic and Magnetic Properties of Metals and Ceramics") it already became clear that it would hardly be possible to treat all the necessary aspects and phenomena of this subject in a single volume, and it was decided to have two volumes. The second of these (Vol. 3B) has not yet appeared, but the chapter titles have already been given as: "Magnetic Properties of Spinel Ferrite"; "Electronic Properties of Liquid, Amorphous, and Quasicrystalline Alloys"; "Invar Alloys"; "Magnetic Recording Materials"; "Hydrogen in Pure Metals and Solid Solutions"; "Ternary Hydrides"; "Soft Magnetic Metallic Materials"; "Permanent Magnet Materials"; "Magnetostrictive Materials".

The first chapter of Volume 3A deals with the calculation of electronic structures. The ability to perform such calculations for the highly complex systems of interest to materials science has come with the availability of very fast computers. Chapter 2 is concerned with the magnetooptical properties of metals, alloys, and compounds. After an introduction to the fundamentals (theory and measurement techniques), some special materials are described and their properties discussed (alloys and compounds of 3d metals, materials based on lanthanoids and actinoids, and mixed 3d–4f and 3d–5f compounds). Chapter 3 is devoted to electron transport properties of "normal" metals, including the behavior of electrons in magnetic fields, electrical resistivity, the Hall effect, thermoelectric power, etc. Chapter 4 covers superconductivity, with discussions of the Bardeen–Cooper–Schrieffer (BCS) and Ginzburg–Landau (GL) theories; the oxide high-temperature superconductors are also described, of course. In Chapter 5 the focus of interest turns to the magnetic properties of metallic systems, then Chapter 6 deals with ultrathin films and superlattices (epitaxy). The book concludes with Chapter 7 on Fermi surfaces in strongly coupled electronic systems. This, like Chapter 1, treats the topic in a fundamental way, and includes instructive comparisons of experimental results with band structure calculations.

Volume 4 ("Electronic Structure and Properties of Semiconductors") presents the basic concepts of modern semiconductor physics, starting from the fundamentals of ideal semiconductors and continuing through the physics of defects and heterostructures (artificial semiconductors) to amorphous semiconducting systems. Chapter 1 ("Band Theory Applied to Semiconductors") and Chapter 2 ("Optical Properties and Charge Transport") are of an introductory nature. They cover the basic theory needed to understand the formation of energy bands in solids with three-dimensional structures and structures of lower dimensionality and in amorphous materials, the investigation of band structures by measuring intrinsic optical properties, charge transport, and nonlinear optics. Chapter 3 deals with the simplest types of point defects, the intrinsic defects that occur in crystal structures where some atoms have changed their positions or are missing altogether; essentially one is concerned here with vacancies, interstitial sites, and sites at which anions or cations have been changed ("antisites"). As examples of different types the chapter discusses silicon (an elemental semiconductor), ZnSe (a II–VI semiconductor), and GaAs (a III–V semiconductor). In Chapter 4 ("Deep Centers in Semiconductors") the discussion moves on from intrinsic defects to doped materials (e.g., with nitrogen and transition metals as dopants in silicon or compound semiconductors, chalcogens in silicon, and DX centers—in which D represents a donor and X an unknown effect—in the mixed crystal system $Al_xGa_{1-x}As$). Silicon and gallium arsenide are nowadays the most important semiconducting materials used in the manufacture of electronic and optoelectronic components, and Chapter 5 ("Equilibria, Nonequilibria, Diffusion, and Precipitation") is concerned particularly with these materials and the behavior of their point defects (whether intrinsic or produced by doping). Moving on from point defects, Chapters 6 ("Dislocations") and 7 ("Grain Boundaries in Semiconductors") deal with these more extended types of defects and their effects on the physical properties of semiconductor materials, from both the phenomenological and theoretical standpoints. Newer manufacturing techniques, including the now highly developed methods of epitaxial growth, make it possible to produce artificial materials and components with special properties that depend on the presence and concentration of interfaces. Chapter 8 gives the

reader an insight into basic concepts whereby one can describe the structural characteristics of such interfaces and understand how they confer special electronic properties on these materials. The tendency towards increasing miniaturization has also resulted in a move from two-dimensional to one-dimensional systems. Lithographically produced heterostructures such as those of the system GaAs–$Al_xGa_{1-x}As$ are suitable for studying the quantum Hall effect in a quasi-one-dimensional electron gas, as described in Chapter 9 ("The Hall Effect in Quantum Wires").

For nearly twenty years now there has also been much interest in the possibilities of using amorphous silicon (e.g., for photovoltaic devices). However, the pure phase contains such a high concentration of defects that it is unsuitable for electronic components. It was accidentally found during the manufacture of amorphous silicon from silane that the concentration of defects could be considerably reduced by introducing hydrogen to saturate the proportion of free silicon valences that are present, and this proved to be the breakthrough needed. The interesting material thus obtained is described in Chapter 10 ("Material Properties of Hydrogenated Amorphous Silicon"). Lastly Chapter 11 contains an up-to-date review of the doping of silicon with 3d elements (see also Ch. 5). The unusual and interesting physical properties that this gives are, however, accompanied by some disadvantages. Aspects of the behavior of 3d elements in the host structure that are discussed here are solubility, diffusion, electronic structure (at high temperatures), and separating out by nucleation.

Silicon is undoubtedly one of the most important materials in the present "silicon age". A metallic material that still continues to be of great importance to human activities and is produced in vast quantities worldwide is the system that we loosely call "steel", and this is the subject of Volume 7 ("Constitution and Properties of Steels").

The world production of steel in 1989 was 783 million tonnes. The plentiful natural occurrence and availability of iron ores is enough in itself to guarantee this class of materials a long-term future, let alone the unique properties that make steel suitable for such a wide variety of uses. The subject of metallography covers many aspects: chemical constitution, phases, alloys, equilibria and nonequilibria between phases, structure and microstructure, precipitation processes, and many more. Chapter 1 ("Microstructure and Transformations in Steel") introduces the basic tools for understanding the subject: phase diagrams for the iron–carbon system, microstructures such as cementite, ferrite, pearlite, martensite, and bainite, precipitation reactions in ferrite and austenite, etc. Chapter 2 ("Structure–Property Relationships in Steels") is concerned mainly with microstructures (dimensions of the matrix–grain structure, crystallographic texture, and grain size distribution). This provides the essential key to understanding and controlling the mechanical properties. Chapter 3 ("Steelmaking and Non-Metallic Inclusions") describes steel production, then Chapter 4 ("Processing—Conventional Heat Treatments") deals with the heat treatment stages (annealing, normalizing, quenching, tempering, case-hardening) that are used to control the microstructure and phase composition. Thermomechanical processing, which is the subject of Chapter 5, also has an important role in determining the microstructure and phase composition of steels, and the same applies to cold-working and work-hardening, as described in Chapter 6. The factors influencing the malleability of steels and methods for controlling it are discussed in Chapter 7. The following chapters are devoted to steels with special properties and uses, as follows. Chapter 8: high strength low-alloyed steels (building and construction steels with small amounts of vanadium, niobium, or titanium); Chapter 9: steels with medium to high carbon contents (≥ 0.30 wt.% C), used for railway tracks, for example; Chapter 10: heat-treated forging steels (0.45 wt.%C, 1.5 wt.% Mn); Chapter 11: creep-resistant steels for applications at high pressures and temperatures; Chapter 12: stainless steels containing 11 wt.% or more of chromium; Chapter 13: tool steels with especially high strength and hardness; Chapter 14: high temperature resistant "superalloys" with iron, nickel, or cobalt as the main constituent; Chapter 15: cast iron, i.e. iron-based alloys containing C, Si, Mn, S, and P as the main alloying elements, with Al, Bi, and Sb as minor additives, and further additives to influence the matrix structure (Mo, Cu, Ni, Sn) and/or the graphite morphology (Mg, Ce, Ti). To complete and round off Volume 7, Chapter 16 deals with the welding of steel and Chapter 17 with surface treatments.

Volume 15, the last of the four reviewed here, is entitled "Processing of Metals and Alloys". Practical aspects are closely linked to results from basic research, but the main emphasis throughout is on applications. The first task facing the editor of this volume, R. W. Cahn, was to decide which topics to include and which to leave out, since this was to be a concise treatment. Among the aspects excluded was mechanical shaping; Cahn explains this in the preface as follows: "I took the view that these topics have become part of the province of mechanical engineering, of continuum mechanics in particular (just as extractive metallurgy is virtually part of chemical engineering today)". In Chapter 1 ("Solidification Processing") the various types of structures that can result from solidification (dendritic, cellular, planar, single phase or multiphase, etc). are described and are discussed in the context of particular process conditions. Important variables influencing the outcome include the solidification rate and the heat flow. Chapter 2 is devoted exclusively to rapid solidification processes. Methods range from those based on spraying and on falling droplets to atomization and the quenching of molten films. Chapter 3 is concerned with the surface treatment of metals and alloys using laser beams, e.g. from a CO_2 laser. Chapter 4 deals with powder metallurgy (the production, characterization, granulation, and sintering of powders, and molding at high temperatures). Chapter 5 describes how high energy ball-milling can be used not only for uniform mixing but also to produce special alloys not obtainable in any other way. For example, oxide particles can be finely dispersed in metallic systems to give oxide dispersion strengthened (ODS) alloys. This method can be used to significantly increase the mechanical strength of an alloy matrix, as the mobility of dislocations is thereby reduced. Chapter 6 is concerned with ion implantation and mixtures produced using ion beams. The particular interest of this method is that it can be used to form metastable alloys not obtainable in other ways, new compositions and structures, and (not least) new intermediate phases. From Chapter 7 ("The Epitaxy of Metals") and Chapter 8 ("Metallic Multilayers") it becomes evident that the uses of epitaxy and multilayer methods are by no means confined to the semiconductors field, but also extend to metals and alloys. Chapter 9 deals with recrystallization and recovery (the "healing" of defects), and Chapter 10 with the measurement and control of texture. Other aspects that arise here are the growth and migration of grain boundaries, nucleation, deep drawing and molding, and ferromagnetic anisotropy. The last three chapters of Volume 15 are concerned with special processes and materials. Chapter 11 ("Electrodeposition of Metals and Alloys") describes new developments in the surface treatment of metallic materials (coating, etc.). Chapter 12 ("Solidifica-

tion Processing under Microgravity") examines the topical question of whether the modification of solidification processes under weight loss conditions (microgravity) can be usefully applied to make new materials or to optimize properties. Chapter 13 ("Cluster Assembly of Nanophase Materials") describes the preparation, characterization, and properties of materials in which a very high proportion of the atoms are in "grain boundary" type situations (i.e. with "ordered" regions and "grain" dimensions of less than 100 nm).

Despite the fact that the "Materials Science and Technology" series involves over 200 authors from all parts of the world (about 50 in these four volumes alone), the editors have succeeded well in guiding their contributions so as to present a unified overall picture. This in itself is an achievement that should not be underestimated. Moreover, the quality of the contributions is very high, and represents the current state of the art in every case.

It was certainly a good decision on the part of VCH to publish this series. The time was ripe for it; to quote the preface: "This bold new field (Materials Science and Technology) is now in need of an all-inclusive reference source—one that meets the demands of theorists and practitioners from every area of materials research, in research institutes and universities as well as in industrial research and development".

It is this reviewer's conviction that materials science and fundamental research are not opposites but form a unified whole. It is not sufficiently recognized that the problems and questions of basic research are very close to those of materials science, as this series impressively demonstrates. The volumes published so far deserve to reach a wide readership, and one can confidently predict that this assessment will also hold for the series as a whole.

Rüdiger Kniep
Eduard-Zintl-Institut
der Technischen Hochschule Darmstadt (FRG)

Kinetics and Mechanism of Reactions of Transition Metal Complexes. 2nd Edition. By *R. G. Wilkins*. VCH Verlagsgesellschaft, Weinheim/VCH Publishers, New York, 1991. XV, 465 pp., hardcover DM 148.00.—ISBN 3-527-28253-X/1-56081-125-0; Softcover DM 68.00.—ISBN 3-527-28389-7/1-56081-198-6.

The author has thoroughly revised and updated the first edition of this book published in 1974, thereby maintaining its position as one of the classic textbooks dealing with the reaction mechanisms of transition metal complexes. Noticeable changes from the first edition mainly involve recent developments in this area, such as the application of photochemical, NMR, and high pressure techniques to elucidate the intimate details of reaction mechanisms. In addition, more information on biological aspects of coordination chemistry (bioinorganic kinetics) is given and a few examples from organometallic chemistry are included. With this book the author has fulfilled a serious need for a textbook dealing with inorganic reaction mechanisms that is suitable for students up to graduate level.

The approach used in the revised edition is similar to that of the first edition. The first three chapters are devoted to the acquisition of experimental data in order to determine the empirical rate law, and the formulation of theoretical mechanisms that are in agreement with the experimental findings. In these chapters many chemical examples are used to illustrate the meaning of the formal mathematics. The following four chapters present a systematic treatment of the mechanisms of substitution, oxidation–reduction and isomerization reactions, as well as the reactivity of coordinated ligands in transition metal complexes. The last chapter includes a systematic summary of the mechanistic features of complexes of different transition elements. Each chapter contains a detailed list of references (between 96 and 370) and selected bibliography (between 2 and 18), and a set of stimulating and illustrative problems (between 10 and 34). Hints to solutions of these problems are given in a separate chapter.

This is the first mechanistic textbook in which the application of pressure as a kinetic parameter in the study of transition metal complexes is described at an appropriate level. Significantly, the author states on page 65 that "the rate law gives the composition of the activated complex (transition state)—nothing more nor less—but yields no clue about how it is assembled". He emphasizes on page 110 that "a careful compilation of as many kinetic parameters as possible can lead to overwhelming support for a mechanism"; thus all activation parameters ($\Delta H^{\neq}$, $\Delta S^{\neq}$, and $\Delta V^{\neq}$) should be considered. This general philosophy will find strong support from students and researchers in this area.

Highlights of the textbook include an attractive balance between theoretical aspects and real chemical systems, a compact but complete treatment of ligand substitution processes, and a well presented chapter on oxidation–reduction reactions. The numerous references to biochemically-related systems will attract the attention not only of inorganic chemists, but also of biochemists interested in the role of transition metal complexes in biological systems. The book really has something for everyone, and should be well accepted by students.

To summarize, the publication of this textbook has fulfilled the longstanding need for such an updated book in the general area of inorganic reaction mechanisms. The experience of the author in research and teaching on the kinetics and mechanisms of reactions of transition metal complexes has resulted in a well-balanced and well presented textbook. The presentation is of a high technical quality, and the text is easy to follow. The price of the paperback copy is very reasonable and should fit the average student budget. It is highly recommended to students and researchers in this field. Ralph Wilkins will receive a sincere appreciation from many inorganic kineticists for providing this thoroughly revised edition.

Rudi van Eldik
Institut für Anorganische Chemie
der Universität Witten/Herdecke (FRG)

A Wandering Natural Products Chemist. (Series: Profiles, Pathways, and Dreams.) By *K. Nakanishi*. American Chemical Society, Washington, D.C., 1991. XXIII, 230 pp., hardcover $ 24.95.—ISBN 0-8412-1775-0

Seventy Years in Organic Chemistry. (Series: Profiles, Pathways, and Dreams.) By *T. Nozoe*. American Chemical Society, Washington, D.C., 1991. XIX, 267 pp., hardcover $ 24.95.—ISBN 0-8412-1769-6

With the appearance of the autobiographies of Nakanishi and Nozoe the series "Profiles, Pathways, and Dreams" is now half completed. Looking at the half-time score in this 22-volume series, the verdict so far is that the excellent first impression has not diminished in any respect. Gradually the pieces of this mosaic are beginning to fit together to form a

multicolored picture of modern chemistry. These latest two volumes again show how sensible it was of the series editor Jeffrey I. Seaman to construct this "living history" of chemistry on international lines right from the start.

Comparing these two autobiographies one notices another attractive feature, in that they are complementary to each other. Whereas Nozoe represents the old "imperial" Japan, which was obliged to open itself up to the outside world (and indeed wished to do so), Nakanishi is the citizen of the world who has overcome the language and cultural barriers (partly as a result of his unusual upbringing) and has become the archetypal example of the modern scientist. Readers whose acquaintance with the Japanese culture is only superficial, and is nonexistent at the psychological and emotional levels, cannot easily appreciate the importance and sometimes considerable power of the forces of tradition. It is slightly disappointing that Nozoe is reticent on this point, and does not allow the reader an insight into how he overcame his initial language isolation, for example. (At first he spoke no English, and lectures to be given abroad were first translated by a colleague and then learnt by heart—a common situation at that time, and one that does not appear to have been completely overcome even today.) One would also have liked to be told more about the political background, as the author began his scientific career at the Taihoku Imperial University in Formosa (now Taiwan), an island that still belonged to Japan in the thirties. The Japan of the pre-war years and of World War II is only spoken of rarely by Japanese people, and that also applies to this book. Nozoe's main area of research, the chemistry of seven-membered ring compounds derived from tropone and tropolone, is described in great detail—a very suitable title for the book might have been "Seven Decades of Seven-Ring Chemistry". Here the editor could well have intervened with a little tightening up without adversely affecting the book as a whole. On the other hand, this part could well serve as an excellent and sound introduction to the field, on which the now 92-year-old chemist is currently writing a definitive monograph.

Of all the autobiographies that have appeared in the series so far, the Nakanishi volume is the one I like best. The author gives a lively account of a scientific life that can have few equals with regard to its variety. This ranges from the isolation of natural products (on which there is much thought-provoking comment here), through the characterization of products using all kinds of physical methods, to synthetic chemistry, in which very few classes of substances are absent. Moreover, this varied nature is by no means confined to the scientific aspects of Nakanishi's experience. Parochial thinking, a common fault among chemists, is unknown to this author. He is more of a natural philosopher than a chemist, and the word "wandering" in the title could just as well have been spelled with an "o" instead of "a". The two authors are in stark contrast in the breadth of their choice of research topics, but Nakanishi is also well aware of the risks that can come from covering too broad a range. But what a lively and interesting man he turns out to be—whether he is expressing his curiosity about new eating habits and foods, or discussing his hobbies, including his well known skill as a magician, or his shortcomings. His views on policies towards research and education in Japan (and in his host country, the USA), on the relationship between teacher and student, or on choosing research topics that deserve attention, are all well worth reading, not least because they bear the stamp of Nakanishi's human point of view.

Like other books in the series, these are both illustrated by many evocative photographs and by formula schemes. Nozoe also includes extracts from his famous autograph books; these are guest books in which scientific colleagues from all parts of the world have recorded their good wishes, notes, or sketches of their favorite molecules or reactions. This "book within a book" can be read separately, and is a very personal miniature illustrated history of the (mainly organic) chemistry of the last forty years.

Henning Hopf
Institut für Organische Chemie
der Technischen Universität Braunschweig (FRG)

Registered names, trademarks, etc. used in this journal, even when not marked as such, are not to be considered unprotected by law.

© VCH Verlagsgesellschaft mbH, D-W-6940 Weinheim, 1992. – Printed in the Federal Republic of Germany by Konrad Triltsch Druck- und Verlagsanstalt Würzburg.

All rights reserved (including those of translation into foreign languages). No part of this issue may be reproduced in any form — by photoprint, microfilm, or any other means — nor transmitted or translated into a machine language without written permission from the publishers. Only single copies of contributions, or parts thereof, may be made for personal use. This journal was carefully produced in all its parts. Nevertheless, authors, editors, and publisher do not warrant the information contained therein to be free of errors. Readers are advised to keep in mind that statements, data, illustrations, procedural details, or other items may inadvertently be inaccurate.

Valid for users in the USA: The appearance of the code at the bottom of the first page of an article (serial) indicates the copyright owner's consent that copies of the article may be made for personal or internal use, or for the personal or internal use of specific clients. This consent is given on the condition, however, that the copier pay stated per-copy fee through the Copyright Clearance Center, Inc. (CCC), for copying beyond that permitted by Sections 107 or 108 of the U.S. Copyright Law. This consent does not extend to other kinds of copying, such as copying, for general distribution, for advertising or promotional purposes, for creating new collective works, or for resale. For copying from back volumes of this journal see 'Permissions to Photo-Copy: Publisher's Fee List' of the CCC.

Editorial office: Postfach 10 11 61, D-W-6490 Weinheim, Federal Republic of Germany. Telephone (06201) 606 315, Telex 465 516 vchwh d, Telefax (06201) 606 328, E-Mail Z16@ DHDURZ2 in Earn Bitnet.

Editor: *Peter Gölitz*

Associate editors: *N. A. Compton, R. H. Schmidt-Radde, K. J. Schneider.* **Book editor:** *G. Karger.* **Editorial assistant:** *E. Schweikart*

Publishers: VCH Verlagsgesellschaft mbH. (Managing Directors: *Hans Dirk Köhler, Dr. Karlheinz Köpfer*), Pappelallee 3, D-W-6940 Weinheim, Federal Republic of Germany.

Advertising office (Advertising Manager: *N. Schippel*): Postfach 10 11 61, D-W-6940 Weinheim, Federal Republic of Germany. Telephone (0 62 01) 606 312, Telefax (0 62 01) 606 328.

ANGEWANDTE CHEMIE
International Edition in English
Volume 32 · Number 3
March 1993
Pages 313–456

Defect Chemistry: Composition, Transport, and Reactions in the Solid State; Part I: Thermodynamics**

By Joachim Maier*

Dedicated to Professor Hermann Schmalzried on the occasion of his 60th birthday

Within the last few decades—though its foundations were laid over 60 years ago—a direction of research has developed almost unnoticed by the classical chemical disciplines, such that one can now recognize a chemistry *within* the solid state that is analogous to the long-familiar chemistry in the liquid state. It arises from those departures from the ideal structure that are thermodynamically unavoidable, the point defects, and is referred to as defect chemistry. It includes the description of ionic and electronic effects, and it considers diffusion as a special step of the overall reaction. This area of chemistry enables one to describe and treat in a unified way many widely different phenomena such as ionic conduction in crystals, doping effects and p–n junctions in semiconductors, color centers in alkali metal halides, image development in photography, passivation and corrosion of metals, the kinetics of synthesis and sintering of solid materials, problems of rock formation during the earth's evolution, the mechanisms of gas sensors and high temperature fuel cells, the performance of photosensitive electrodes, variations of the electron balance in high-temperature superconductors, elementary processes of heterogeneous catalysis, nonequilibrium transitions and oscillations in semiconductors in electric fields, and many more. In such phenomena the equilibrium concentration of defects has an important double role: it not only determines the disorder and the departure from the Dalton composition in the equilibrium state, but also, together with the mobility as the kinetic parameter, is the key parameter concerning the rates of physicochemical processes. Accordingly, in this first part of the review the emphasis will be on the equilibrium thermodynamics of point defects, whereas the second part will be specifically concerned with the kinetic aspects. Both parts will emphasize the fact that the defect chemistry of solids, as well as being the counterpart of solution chemistry in the liquid state, also provides a unifying approach in which electronic and ionic charge carriers are treated by analogous methods, both in the bulk and in boundary layers, and allows diffusion to be incorporated naturally into the overall kinetics of reactions as an elementary chemical process.

1. Introduction

Whereas the solid state has traditionally always played a prominent role in physics, the chemist still continues to regard it as a special case, despite its importance in everyday life. The importance of structure and bonding in solids is very well acknowledged, as is that of solid-state reactions on a global scale; however, the notion of solid-state chemistry in the sense of a chemistry of processes taking place *within* the solid phase, and being studied as successfully as "wet chemistry" before it, still seems rather fanciful.

[*] Prof. Dr. J. Maier
Max-Planck-Institut für Festkörperforschung
Heisenbergstrasse 1, D-W-7000 Stuttgart 80 (FRG)

[**] Part II: Kinetics will appear in the April issue of *Angewandte Chemie*.

Nevertheless, this chemistry of the solid state is a key discipline on which the fundamental insights and considerable achievements of modern materials science largely depend, and it affords a unified description of the thermodynamics and kinetics of a whole range of important phenomena in such varied fields as catalysis, battery research, corrosion, sensors, and electronics.[1] This review aims to show that "defect chemistry" is in fact a natural extension (and generalization) of chemistry in solutions. Defect chemistry is essentially the study of the nature of point defects in the solid state and of their interactions (but it also includes higher dimensional defects, such as dislocations, interfaces, or pores). The central role of point defects, that is essentially the role of extra particles and of missing particles, is illustrated in Figure 1a, which shows a small region of the structure of water. The successes that have been achieved in understanding the chemistry of water and in modifying its properties depend not so much on a precise knowledge of the basic structure and bonding (which influence phenomenological parameters such as equilibrium constants and rate constants) but on the ability to relate these properties to relevant "particles," such as H_3O^+ and OH^- ions, and foreign molecules or ions. If we formally subtract the underlying perfect water phase (Fig. 1a), we are left with the two "defects" (shown on the right-hand side in Fig. 1a), namely an "extra" proton and a "missing" proton (proton vacancy). This can be described in terms of the formation reactions in Equations (1a)–(1c).

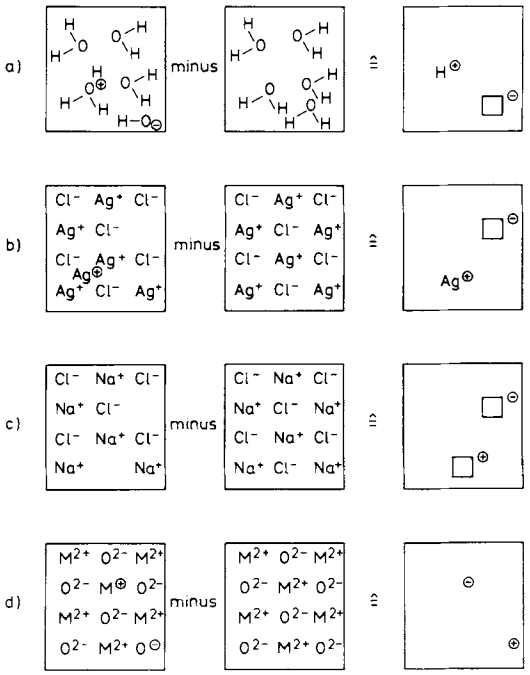

Fig. 1. By "subtracting" the ideal structure (middle column) from the actual structure (left-hand column), the defects remain as the "particles" that determine the behavior.

$$2H_2O \rightleftharpoons H_3O^+ + OH^- \quad | - H_2O \qquad (1a)$$

$$H_2O \rightleftharpoons H^+ + OH^- \quad | - H_2O \qquad (1b)$$

$$\text{nil} \rightleftharpoons H^+ + |H|^- \qquad (1c)$$

From the standpoint of defect chemistry the particles appearing in Equation (1c) (in which the underlying phase has completely disappeared from the description) are the defects in the water structure, namely an extra proton (H^+) and a vacant proton site ($|H|^-$). These particles, together with any dissolved substances, determine the acid-base and redox chemistry in water, and make ionic transport possible.

Figure 1b shows AgCl, a typical solid phase. Here also, the occupation of the sites in the rock salt structure is not perfect at finite temperatures; a small number of the silver ions have left their regular sites to occupy interstitial positions, leaving (in the case of the pure material) an equal number of vacant sites in the crystal lattice [Eq. (2)].[3, 14, 15]

$$\text{nil} \rightleftharpoons Ag^{\bullet} + |Ag|' \qquad (2)$$

In this sense the vacant silver ion site can also be regarded as a negative $Ag^{\bullet}$ particle (or better as a complementary particle). It can be seen that this class of defects, which are said to be formed by a Frenkel reaction (F), corresponds to the autoprotolysis reaction [Eq. (1c)]. In both cases the "defect concentration" is an inevitable consequence of the thermodynamics due to entropy considerations. These internal equilibria can also be treated, as we shall see again later, by using mass action laws, and here too dissolved particles have to be considered. As in the later examples, the existence of the same relevant particles leads to an internal mobility, thus allowing ionic conduction, either by an interstitial lattice mechanism or by a vacancy mechanism (similar to the Grotthus mechanism of proton conduction). The defect chemistry of solids is fundamentally more general than the chem-

Joachim Maier was born in 1955 in Neunkirchen, Saarland. He studied chemistry at the Universität des Saarlandes and received his doctorate there in 1982 in physical chemistry. At the Max-Planck-Institute für Festkörperforschung in Stuttgart he devoted himself to the questions of mass and charge transport in the solid state. In 1988 he completed his habilitation at the Universität Tübingen about "ionic conduction in boundary layers". After a visiting professorship at the Massachusetts Institute of Technology, where he is still a faculty member today, he worked at the Pulvermetallurgischen Laboratorium des Max-Planck-Instituts für Metallforschung on ceramic materials. Since 1991 he has been scientific member of the Max-Planck-Gesellschaft and Director at the Max-Planck-Institut für Festkörperforschung in Stuttgart. Among his awards the Chemidozentenstipendium and the Carl-Duisberg-Gedächtnispreis are particularly worthy of mention. His interests include the thermodynamics and kinetics of the solid state, in particular questions of the boundary layers and of ionic transport.

istry of ions in water, as can be seen from the following features:

1) Since many solids are built up of ions,[16] it is necessary to distinguish between real and relative charges. For example, a vacant cationic site has an effective negative charge relative to the background of the perfect structure. In Equation (2), as commonly used in the literature, this relative charge has been indicated by deliberately using dots and primes instead of plus and minus signs. The systematic notation is explained in the next section.

2) In the solid the particles are assigned fixed positions, and one therefore has to distinguish between several different types of disorder. In addition to Frenkel (F) defects, and anti-Frenkel ($\bar{F}$) disorder, as the corresponding defects in the anion structure (e.g., in halides of alkaline earth metals) are called, there are Schottky defects (S). (See Fig. 1c). Schottky defects occur particularly in the closely packed alkali metal halides;[2, 14] in NaCl this involves the formation of a sodium vacancy and a chlorine vacancy ($|Na|'$ and $|Cl|^{\cdot}$) with the removal of an NaCl molecule [Eq. (3)].

$$nil \rightleftharpoons |Na|' + |Cl|^{\cdot} + NaCl \tag{3}$$

Anti-Schottky defects ($\bar{S}$), believed to occur in yellow lead(II) oxide,[17] conversely involve the incorporation of a lattice molecule PbO with the formation of Pb^{2+} and O^{2-} ions ($Pb^{\cdot\cdot}$ and O'', respectively) in the interstitial lattice [Eq. (4)].

$$PbO \rightleftharpoons Pb^{\cdot\cdot} + O'' \tag{4}$$

In principle, of course, the thermodynamic treatment of a given phase must simultaneously take into account all these equilibria. For water in the liquid state this variability does not exist. In this case no regular and interstitial lattice sites are defined, and therefore the reaction desribed by Equation (1) can be regarded with equal validity as generating Schottky defects (vacant OH^- and H^+ sites), anti-Schottky defects (extra H^+ and OH^- ions), or anti-Frenkel defects (missing OH^- ions and extra OH^- ions).

3) In contrast to the usual situation in chemical kinetics, the low mobility in the solid state means that diffusion processes always constitute an important part of the overall process, and in many cases represents the rate-determining step. This point will be considered in detail in Part II of the review,[97] where it will also be shown that chemical reactions and transport processes can be treated by formally similar methods (see also Fig. 5, and Figs. 2 and 3 in Part II).

4) The thermodynamic and kinetic treatment of the solid state is of a more general nature than that of most liquids since, in addition to ionic defects, one always has to consider electronic charge carriers, which include both conduction electrons (e') and electron holes ($h^{\cdot}$). This leads not only to internal redox processes (which also occur in aqueous systems), but also, more importantly, to an intrinsic electronic conductivity which often predominates. Frequently ionic and electronic conduction are present simultaneously. This general case of a mixed conductor leads to interesting properties, and requires a generalized treatment of electrical transport phenomena. For many ionic compounds, and especially for transition metal oxides, the transfer of a valence electron into the conduction band can often be described as an internal redox reaction of the form shown in Equation (5). In more general terms this again can be considered as the formation of one extra particle, the conduction electron (e') and one vacancy, the electron hole ($h^{\cdot}$) [Eq. (6)].

$$O^{2-} + M^{m+} \rightleftharpoons O^- + M^{(m-1)+} \tag{5}$$

$$nil \rightleftharpoons e' + h^{\cdot} \tag{6}$$

Figure 1d illustrates this in a simplified way by showing a localized picture. As the notation already suggests, the thermodynamics and kinetics for electronic defects can be treated analogously at sufficiently high temperatures.

5) Because of the restricted space in the solid and the associated selective solubility, an aliovalent doping of the ionic crystal nearly always results in a pattern of substitution that involves both an acid-base effect (a change in the concentration of ionic defects) and/or a redox effect (a change in the concentration of electronic defects), whereas this is normally not the case in the aqueous phase as the anions and cations are normally dissolved simultaneously (see Section 2).[18]

2. Notation

The notation introduced here is based on a relative notation; in other words, it describes the changes that take place as one goes from the perfect to the real solid. The notation used in Section 1 (the "building elements" notation[4, 6, 8]) is a precise relative notation with regard to matter and electric charge, and is the most rigorous from a thermodynamic standpoint, but it fails to convey a clear structural picture. The "structural elements" description[19] is a compromise

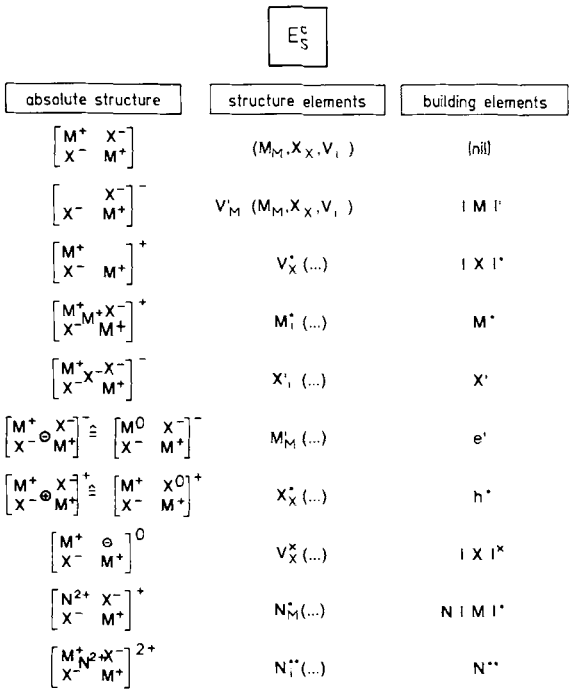

Fig. 2. Simple point defects represented in the form of the absolute structure (left), the structure elements (middle), and the building elements (right).

that comes closer to a chemical representation; it takes the structural picture into account,[20] but is still a relative notation with regard to electric charge. Here, as Figure 2 illustrates, the symbol E_s^c represents a general structural element; E defines the chemical species, for example Ag, Cl, or V for a vacancy. As explained previously, it is important to define the crystallographic site (s); for example, s is Ag, Cl, or i (i denotes an interstitial site). The term c gives the relative charge (the charge in the real state minus the charge in the perfect state); the superscripts ′ and • are used to denote positive and negative charges, respectively. Where the relative charge is zero, the superscript is often omitted or written as "×". Thus Ag_{Ag} or Ag_{Ag}^{x} represents a regular silver ion, V'_{Ag} represents a vacant silver site, $Ag_i^{\bullet}$ a silver ion at an interstitial site, and $Cd_{Ag}^{\bullet}$ a Cd^{2+} ion that has replaced a regular Ag^+ ion. For a compound whose ideal composition is M^+X^-, the formation equations for the different types of defects as discussed previously now take on the clearly descriptive form shown in Equations (7)–(10).

$$M_M + V_i \rightleftharpoons V'_M + M_i^{\bullet} \qquad \text{(Frenkel, F)} \qquad (7)$$

$$X_X + V_i \rightleftharpoons V_X^{\bullet} + X_i' \qquad \text{(anti-Frenkel, } \bar{F}\text{)} \qquad (8)$$

$$M_M + X_x \rightleftharpoons MX + V'_M + V_X^{\bullet} \qquad \text{(Schottky, S)} \qquad (9)$$

$$MX + 2V_i \rightleftharpoons M_i^{\bullet} + X_i' \qquad \text{(anti-Schottky, } \bar{S}\text{)} \qquad (10)$$

For simplicity no distinction has been made between the interstitial lattice sites of anions and cations. It can be seen that the reactions S and $\bar{S}$ result in a coupling between the anion and cation lattices, and involve the uptake or release of a "lattice molecule", which can only take place if dislocations or interfaces are present. In the reactions of defect chemistry, not only must the particles and charges on the two sides of the equation balance, as in conventional chemical reactions, but the lattice sites must also balance.

Although the electronic defect-forming reaction in structure element notation could be described as the transfer of an electron from the valance band to a vacant site in the conduction band, which would generate an electron in the conduction band and a hole in the valence band (in analogy to the Frenkel reaction F), the notation used in Equation (6) will be retained for this case, as the electron shell is already understood as being included in the ionic defects. Moreover, in this way the extent of localization is not specified (Fig. 2).

By rearranging Equations (7)–(10) it can be seen that each of the building elements [see Eqs. (2)–(4)] corresponds to a combination of the structure elements; for example, $Ag^{\bullet} \equiv Ag_i^{\bullet} - V_i$ and $|Ag|' \equiv V'_{Ag} - Ag_{Ag}$. These combinations denote structure elements that can be introduced into the crystal (leaving aside charge effects). For example, the introduction of an extra Ag^+ ion leads to both the loss of a vacant lattice site and the creation of a vacancy by the removal of a regular ion. When the regular constituents Ag_{Ag}, Cl_{Cl}, and V_i are present in large numbers, which provides a virtually inexhaustible supply, the two notations are thermodynamically equivalent.[20, 21]

Since both ionic and electronic defects can occur in a crystal, it is possible to have deviations from the ideal composition M^+X^- (non-stoichiometry). According to the Gibbs phase rule, in thermodynamic equilibrium at a given temperature and pressure the degree of non-stoichiometry is determined by the activities of the components M or X, and therefore by the partial pressures of M or X (or X_2). The interaction can then be derived from a relationship such as, for example, Equation (11a), which represents the incorporation of X, in the form of the X^- anion, into a vacant X site. The effect of this on the other defects, such as $M^{\bullet}$ or $h^{\bullet}$, is then given by Equations (7) to (10). This can, of course, also be obtained directly by expressing the insertion reaction [Eq. (11a)] in appropriate alternative forms. For example, the effect on the concentration of metal vacancies (hole concentration) may be obtained from Equations (11b) or (11c).

$$\tfrac{1}{2}X_2 + V_X^{\bullet} + e' \rightleftharpoons X_X \qquad (11a)$$

$$\tfrac{1}{2}X_2 + M_M + e' \rightleftharpoons MX + V'_M \qquad (11b)$$

$$\tfrac{1}{2}X_2 + M_M \rightleftharpoons MX + V'_M + h^{\bullet} \qquad (11c)$$

However, Equations (11b) and (11c) are redundant if the equilibria expressed by Equations (7) to (11a) are established. Similarly, the effect of an impurity ion N^{2+}, which is usually treated as an irreversible introduction, is sufficiently described by only *one* structure element combination, for example the acid-base reaction given in Equation (12a).

$$NX_2 + 2M_M \rightarrow N_M^{\bullet} + V'_M + 2MX \qquad (12a)$$

(The replacement of an M^+ ion by an N^{2+} ion is compensated by generating a vacancy at an M site.) It can be seen that the greater charge of the N-impurity ion results in an increase in the concentration of M vacancies. As can be seen by combining this with the Schottky reaction [Eq. (9)], the establishment of the equilibrium is accompanied simultaneously by a reduction of the concentration of anion vacancies. Instead of Equation (12a) one could, of course, have chosen to go directly to Equation (12b), which is in fact redundant if the above equilibria apply; here X is introduced into an anion vacancy. Furthermore, combining this with Equation (11a) shows that the e′ concentration is also affected; it is increased as a result of the introduction of N^{2+}. Here again one could have chosen to write the doping reaction immediately as a redox reaction [Eq. (12c)], in which the incorporation of the N^{2+} ion is accompanied by a reduction of the crystal.

$$NX_2 + V_X^{\bullet} + M_M \rightarrow N_M^{\bullet} + MX + X_X \qquad (12b)$$

$$NX_2 + M_M \rightarrow MX + \tfrac{1}{2}X_2 + N_M^{\bullet} + e' \qquad (12c)$$

All this can be summarized as follows: as one can easily see from general considerations that are based ultimately on the irreversibility of Equations (12) and the electrical neutrality of the reactions given, the introduction of an impurity with an effective positive charge causes an increase in the concentrations of all negatively charged defects and a reduction in the concentrations of all positively charged defects, and vice versa. This generalization is very important for materials research, and may be described as the "rule of homogeneous doping", expressed by Equation (13).

$$\frac{z_k}{z_{dop}} \frac{\delta c_k}{\delta c_{dop}} < 0 \qquad (13)$$

Here z_k is the effective charge of the intrinsic crystal defect, z_{dop} is the effective charge of the dopant species, and c is the concentration. (It will be shown in Section 3.2 that a similar relationship can also be derived for "heterogeneous doping".) For example, the doping of AgCl with $CdCl_2$, which involves the formation of $Cd^{\bullet}_{Ag}$ defects, raises the numbers of silver vacancies, and of conduction electrons and lowers the concentrations of interstitial silver ions and of electron holes. The introduction of S^{2-} ions by doping AgCl with Ag_2S, with consequent formation of S'_{Cl} defects, has exactly the opposite effect (see Section 3.1.1, homogeneously doped silver halide).[115]

Here it must be briefly mentioned that in addition to these simple point defects one can have complex defects formed by association between them. An example is the association of two vacancies that neutralize each other electrically [Eq. (14)]; such a pair can be regarded as a preliminary stage in the

$$V'_M + V^{\bullet}_X \rightleftharpoons (V_M V_X)^{\times} \qquad (14)$$

formation of a pore. Another example is the capture of electronic charge carriers by ionic defects, as in Equations (15) or (16).

$$V'_M + h^{\bullet} \rightleftharpoons V^{\times}_M \qquad (15)$$

$$N^{\bullet}_M + e' \rightleftharpoons N^{\times}_M \qquad (16)$$

Ion-electron associates of this kind are of considerable significance when their electronic energy levels lie within the band gap.

Other important examples are color centers, such as those observed in NaCl when subjected to high partial pressures of sodium.[122] These arise from the capture of electrons (e') by Cl^- vacancies, as in Equation (17) (cf. Fig. 2). Such color

$$V^{\bullet}_{Cl} + e' \rightleftharpoons V^{\times}_{Cl} \qquad (17)$$

centers can be described surprisingly well by using the simple quantum mechanical model of an electron in a box with atomic dimensions, and optical absorption measurements can therefore be used to assess the dimensions of the anion vacancy sites.[123]

Evidently, because of the gain in Coulomb energy and the reduction of configurational entropy, such association reactions will usually take place preferentially at low temperatures and high concentrations.

All this occurs within the one phase "MX"—thus it can be seen that the chemistry of the solid state is just as richly varied as the chemistry of the aqueous phase. A characteristic feature is the variation in the M:X ratio, which results from the simultaneous occurrence of electronic and ionic defects, and is determined by the partial pressures of M and X. The defect concentrations are normally very small, and very often their contribution to the total energy of the crystal is negligible, but they are of crucial importance for many properties (equilibrium partial pressures of the M and X components, transport phenomena, and reactivity). The following sections will begin by discussing the thermodynamic equilibrium. If the notation presents difficulties initially, the reader is recommended to always bear in mind the absolute structure (as in the left-hand column of Fig. 2).

3. Thermodynamics

3.1. Behavior in the Bulk Material

The thermodynamic treatment takes a simple form in cases where the defects can be regarded as behaving independently of each other.[23b] This condition is most likely to be satisfied for low defect concentrations and high temperatures.[2] Let us consider, as the simplest example, the formation of vacancies in an elemental crystal (Fig. 3). Since the

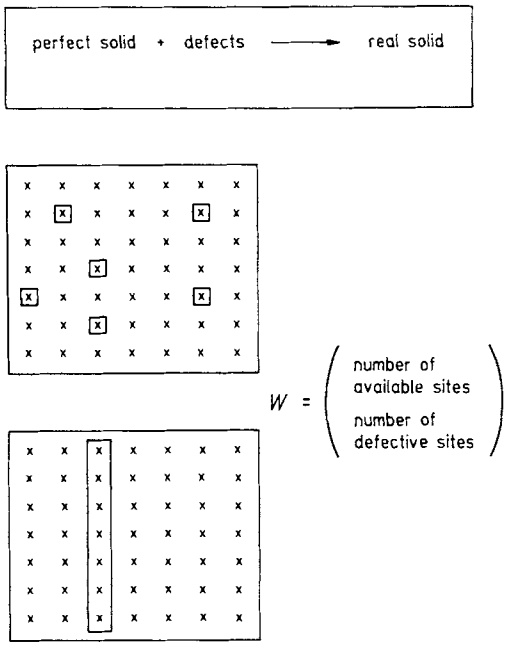

Fig. 3. The introduction of point defects (in this case vacancies) into an elemental crystal.

relevant bonds must be broken in this case, some energy must always be expended. Moreover, the resulting deficit cannot be fully made up by structural changes in the immediate environment that minimize the "damage", nor by any possible increase of the vibrational entropy. Despite this, any crystal in thermodynamic equilibrium at a finite temperature contains a finite number of point defects, because the introduction of such defects makes an enormous number of new configurations possible. The macrostate specified in Figure 3 (six vacancies in a total of 49 sites) can be achieved by any one of W microstates, where W is given by Equation (18).

$$W = \binom{\text{number of available sites}}{\text{number of defective sites}} = \binom{49}{6} = 49!/\{6!(49-6)!\} \qquad (18)$$

The resemblance of Figure 3 to a completed lottery slip (six out of 49) is not accidental. In the German national lottery the probability of winning the top prize ($1/W$) is discouragingly small due to the size of W (about 14 million), and in view of the state's cut of the profits this has led to the lottery being sourly described as a "special tax on fools".

The gain in configurational entropy, ΔS_{conf}, follows directly from the calculation above (see [Eq. (19)]). The total Gibbs energy of the real solid (where N_{def} is the number of point defects) can be broken down into several contributions, as shown in Equation (20).

$$\Delta S_{conf} = k \ln W_{real} - k \ln W_{ideal} = k \ln W_{real} \tag{19}$$

$$\begin{aligned} G_{real}(N_{def}) &= G_{perf} + \Delta G_{def}(N_{def}) \\ &= G_{perf} + N_{def} g^0_{def} - T\Delta S_{conf}(N_{def}) \end{aligned} \tag{20}$$

Here G_{perf} is the Gibbs energy of the perfect solid; this consists essentially of the bonding energy at absolute zero together with the contributions from thermal activation, which is mainly determined by the vibrational specific heat.[5, 13] The quantity g^0_{def} represents the free enthalpy change caused by the introduction of each defect, arising mainly from a bonding enthalpy contribution and a change in vibrational entropy. As already mentioned, structural relaxation processes make the value of g^0 considerably more favorable than the naive picture (Fig. 3) would suggest, but nevertheless it is always positive. Typically it is of the order of 1 eV per defect, which corresponds to 100 kJ mol^{-1} [24] Provided that the point defects do not interact, the factor g^0_{def} is independent of N_{def}, and thus the second term is proportional to the number of defects. However, this is not the case for the negative term $-T\Delta S_{conf}$. As Figure 4 shows, the decrease of this term at small N_{def} values is very pronounced; as a result the curve of free enthalpy against number of defects has a minimum at a small but finite defect number $\hat{N}_{def}$, which is the equilibrium defect number and increases with increasing temperature.[23b]

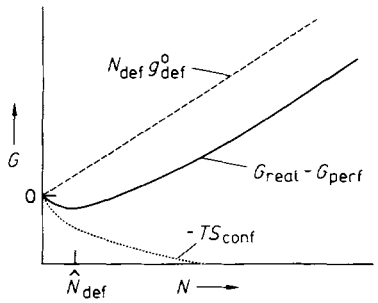

Fig. 4. The main contributions to the free enthalpy G of a real crystal (with a low concentration of defects). The minimum corresponds to the equilibrium concentration of point defects, $\hat{N}_{def}$. [23b] N = number of point defects.

This equilibrium value is given by the condition $\partial G_{real}/\partial N_{def} = 0$. Furthermore, up to the Avogadro number N_A, the partial derivative $\partial G_{real}/\partial N_{def}$ is identical to the chemical potential μ_{def}, which can be regarded as a measure of how much the particles (i.e. the defects) are "disliked" in the phase. This is obtained from Equation (20), in the form that is already familiar for dilute states, as a linear function of the logarithm of the defect concentration [Eq. (21)].

$$\mu_{def} = \mu^0_{def} + RT \ln c_{def} \tag{21}$$

The standard potential μ^0_{def} is given by $N_A g^0_{def}$ and the defect concentration c_{def} by N_{def}/N, where N is the total number of available sites. It will be noticed that N_{def} and N are the same terms as in the expression for W (cf. [Eq. (18)]. The equilibrium concentration $\hat{c}$ can be derived readily, and is given by Equation (22). It is not difficult to see that this is equivalent to the simplest case of a mass action equation, corresponding to the formation reaction [Eq. (23)] (Fig. 5).

$$\hat{c}_{def} = \exp - \left(\frac{\mu^0_{def}}{RT}\right) \equiv K(T) \tag{22}$$

$$\text{nil} \rightleftharpoons \text{defect (vacancy)} \tag{23}$$

The equilibrium constant $K(T)$ contains the standard value of the chemical potential, whereas the contribution arising from the configurational entropy is taken into account by the concentration term [left-hand side of Eq. (22)]. The above result can be easily generalized for the formation of several defects (for example, via a Schottky or Frenkel defect). Because of conservation of the elements, a minimum in G requires that the sums of the chemical potentials on the two sides of the reaction equation cancel each other.[25] From Equation (21) we can obtain the mass action law in its usual form. The mass action constant is then given by the corresponding linear combination of the standard potentials (e.g. $\mu^0_B - \mu^0_A$ in Fig. 5).[25] Provided that, as assumed here, we are concerned with dilute states, it does not matter

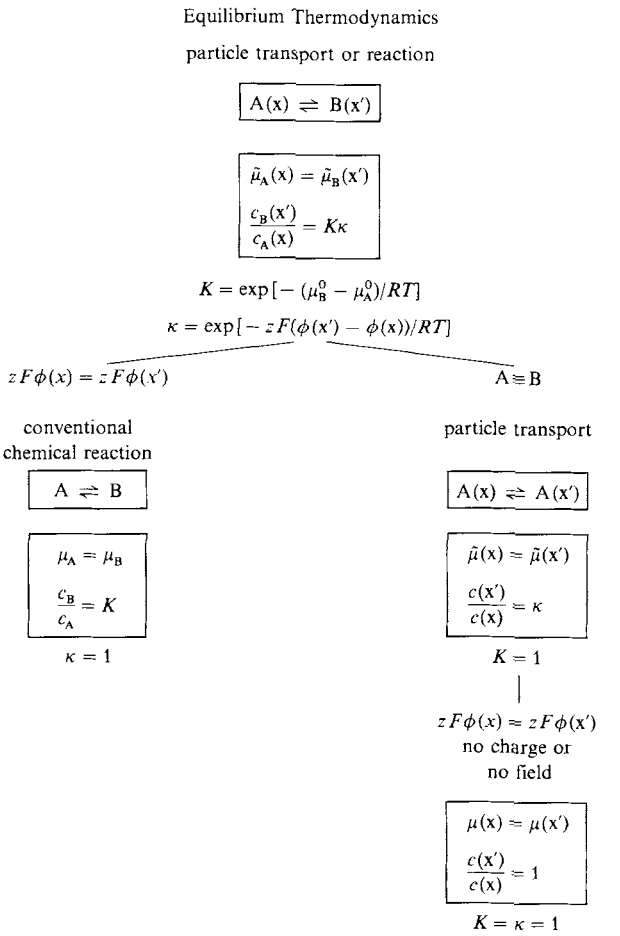

Fig. 5. Diagram summarizing equilibrium thermodynamics. Both the reactions of particles and their transport are included in the general description, so that (conventional) chemical reactions and particle transport appear as two special cases.

whether we use the thermodynamically correct building elements notation, or whether we use the structure element notation and introduce individual virtual potentials for each of the species involved.[20, 21] This is because the virtual chemical potentials of the regular particles remain constant due to their high concentration. For convenience, in the following discussions molar concentrations will be used for c unless otherwise stated. With this convention the mass action constants become dimensional quantities.

Table 1 lists the relevant mass action relationships for the defect equilibria discussed previously. It is well known that

Table 1. Defect reactions, mass action equations, and electroneutrality conditions for the simple bulk defect chemistry of an ionic crystal "M^+X^-" (or $M_{1+\delta}X$).

Simple defect chemistry in $M_{1+\delta}X$	
Reaction (r)	Mass action equation
internal	
Schottky (S)	$[V_X^{\cdot}]\,[V_M'] = K_S$
anti-Schottky ($\bar{S}$)	$[M_i^{\cdot}]\,[X_i'] = K_{\bar{S}}$
Frenkel (F)	$[M_i^{\cdot}]\,[V_M'] = K_F$
anti-Frenkel ($\bar{F}$)	$[V_X^{\cdot}]\,[X_i'] = K_{\bar{F}}$
band-to-band (B)	$[h^{\cdot}]\,[e'] = K_B$
$K_r(T) \propto \exp + \left(\frac{\Delta_r S^0}{R}\right) \exp - \left(\frac{\Delta_r H^0}{RT}\right)$	
external	
reaction with the gas phase (X)	$[h^{\cdot}]\,[V_M'] \, P_{X_2}^{-1/2} = K_X$
electroneutrality condition	
$[V_X^{\cdot}] + [M_i^{\cdot}] + [h^{\cdot}] = [V_M'] + [X_i'] + [e'] \; (\pm D)$	

this formalism can also be applied to electronic defects in solids.[26] These relationships form the basis of a large part of semiconductor physics. Provided that the concentration of defects is sufficiently low and the temperature sufficiently high, the conduction electrons or holes are assumed to be distributed over a large reservoir of available states, as in the previous examples. Again the configurational entropy is as given earlier, resulting in an expression of the same form as Equation (21) for the potential (Boltzmann approximation). However, owing to the band character of the states in this case, the total number of available sites is replaced by an effective density of states. In Table 1 these terms have been included in the mass action constants, wherever electronic concentrations are involved. Also, at lower temperatures and high electron concentrations, Fermi–Dirac statistics must be applied. These corrections can be formally incorporated into the activity coefficients.[27] As shown in Figure 6, the energy levels used in semiconductor physics, namely E_F (Fermi level), E_v (upper edge of valence band), and E_c (lower edge of conduction band), here expressed as molar quantities for convenience, correspond in thermochemical terms to the electrochemical potentials (chemical potential + electrical potential term) or to the electrochemical standard potentials.[28] In particular, bearing in mind Equation (21), one can immediately understand why it is usual in semiconductor physics to determine the concentrations of electrons and holes from the energy differences $E_c - E_F$ and $E_F - E_V$. It can also be seen that the difference between E_V and E_L, the band gap E_g, is almost identical to the expression in Equation (24), in other words to the change of the standard free

$$\mu_{h^{\cdot}}^0 + \mu_{e'}^0 = -RT \ln K_B \qquad (24)$$

energy of the electron-hole reaction in Table 1.[29] It is also evident that the Fermi level for a "pure semiconductor", in which $[e'] = [h^{\cdot}]$, lies approximately in the middle of the band gap. To emphasize the similarities between the two representations, in Figure 6 level schemes for the ionic disorder in AgCl (see also Fig. 7) and for water (with the energy levels E_{exc}, E_{reg}, E_F') have been constructed. The electrochemical potentials of H^+ and Ag^+ lie in the middle between the upper and lower levels, which indicates equal concentrations of negative and positive ionic defects. This condition is fulfilled for both pure H_2O and pure AgCl so far as the ions are concerned, but—as shown by Example 1 (Section 3.1.1) – it is in these compounds normally not fulfilled for electronic defects (E_F lies in the middle of the band gap only in very special cases). Figure 7 shows the level scheme for AgCl at a higher resolution,[31] emphasizing an important characteristic of ion transport in solids: The transport of the interstitial defects (Fig. 7, top) and the transport of vacancies (Fig. 7, bottom) are both affected by free activtion energies for the periodic hopping process ($\Delta_i G^{\neq}$ and $\Delta_v G^{\neq}$), which refer to the transition states in conventional chemical reactions, and are determined by the "bottleneck" (more precisely: saddle-point) associated with the diffusion path or the reaction coordinates.

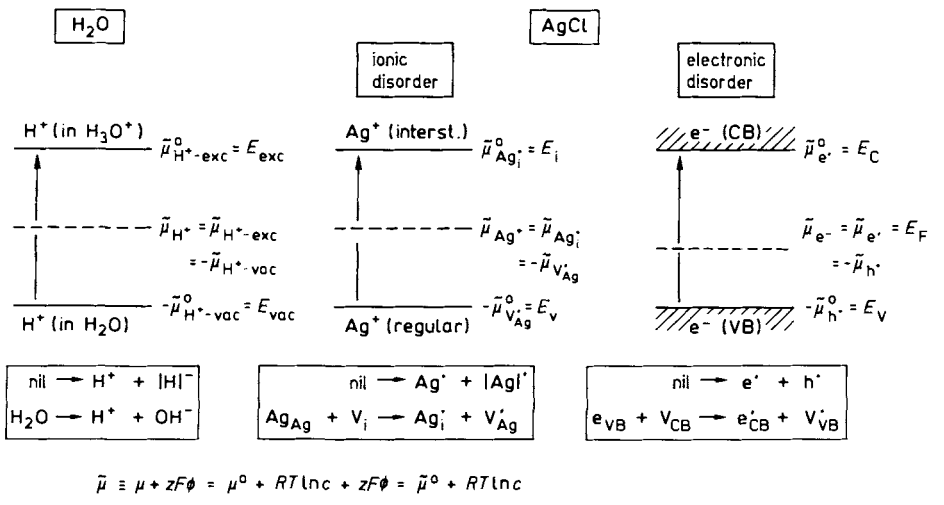

$$\tilde{\mu} \equiv \mu + zF\phi = \mu^0 + RT \ln c + zF\phi = \tilde{\mu}^0 + RT \ln c$$

Fig. 6. The construction of a band diagram and analogous energy level diagrams for the electrons and the Ag^+ ions in AgCl [66] and for the protons in water ($H_{exc}^+ \triangleq H^+$; $H_{vac}^+ \triangleq OH^-$). CB = conduction band, VB = valence band.

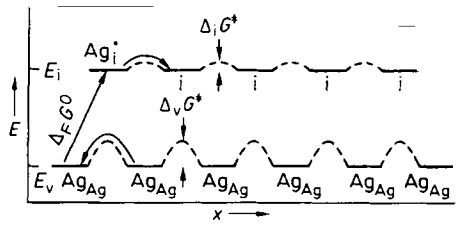

Fig. 7. The generation and transport of ionic defects in silver halides, shown in the form of an energy level diagram (cf. Fig. 6), x = spatial coordinate [66].

Let us, as shown in Figure 3, impose restrictions on the distribution of the defects, in demanding for example that all the defects must form a column as in Figure 3 (bottom), we obtain a crude way of simulating the extended defects such as grain boundaries with respect to the configurational behavior. The probability of the configuration, and consequently also the configurational entropy, are then enormously reduced; in the above case there is a reduction from 14 million to 6 (or to 7 in the example chosen). In the three-dimensional arrangement, and with particle numbers of macroscopic magnitudes, the reductions are even more extreme.[32] From this one can immediately conclude that the equilibrium probabilities for internal surfaces in real crystals are completely negligible. Despite this, such internal boundaries are of great importance due their metastable existence.[33] In summary, the equilibria involved in the chemistry of simple internal defects for a pure compound $M_{1+\delta}X$ are described by the mass action equations given in Table 1.

A closer inspection of the equations in Table 1 reveals that one of them is redundant (for example, one can write $K_{\bar{F}} = K_S K_{\bar{S}}/K_F$). The only additional relationship needed to solve the system with variable defect concentrations (treating P_{X_2} as a parameter) is the local electrical neutrality condition[34] given by Equation (25a), which can also be written in the form of Equation (25b) by using the mass action equations.

$$[V_X^{\bullet}] + [M_i^{\bullet}] + [h^{\bullet}] = [V_M'] + [X_i'] + [e'] \tag{25a}$$

$$[M_i^{\bullet}](K_s/K_F + 1) + [h^{\bullet}] = [V_M'](K_{\bar{S}}/K_F + 1) + [e'] \tag{25b}$$

If aliovalent impurities of fixed valency are present, these must be taken into account by including their doping concentrations (D, normally constant) in Equation (25). The mathematical treatment of systems with a large number of mass action equations (linear when reduced to logarithmic form) also presents no difficulties, nor does that of systems involving association reactions. Complications arise only when we come to the electrical neutrality relationship, (or equations for element conservation) which is not logarithmically linear. However, in many cases, depending on the X_2 partial pressure and also on the temperature, one of the two terms in Equation (25b) can be neglected, so that Equation (25b) becomes linear when expressed in logarithmic form (Brouwer approximation).[30] In such cases one can derive sectional solutions, yielding the equilibrium concentration for each defect species as a function of the controlling parameters $P \equiv P_{X_2}$ (X_2 partial pressure), T (temperature), and D (dopant concentration) in the form of Equation (26).

$$\hat{c}_k(P,T,D) = \alpha_k P^{N_k} D^{M_k} \Pi_r K_r^{\gamma_{rk}}(T) \tag{26}$$

Here α_k, N_k, M_k, and γ_{rk} are characteristic constants, and the mass action constants are given by the usual expressions in terms of the reaction enthalpies and reaction entropies for the reaction r (Table 1). Thus, Equation (26) represents the fundamental solution of the (bulk) problem of defect chemistry in the equilibrium case. The characteristic exponent N_k (not to be confused with the number of particles), is of particular importance, as it represents the dependence of the activity of the components on the partial pressure [Eq. (27a)], and yields valuable information about the defect model on which the theory is based.

$$N_k = \partial \ln \hat{c}_k / \partial \ln P \tag{27a}$$

$$M_k = \partial \ln \hat{c}_k / \partial \ln D \tag{27b}$$

Figure 8a shows schematically the dependence of $\lg \hat{c}_k$ on $\lg P$ in the Brouwer approximation for the case where there is negligible disorder in the anion lattice ($K_s = K_{\bar{s}} = 0$). Thus,

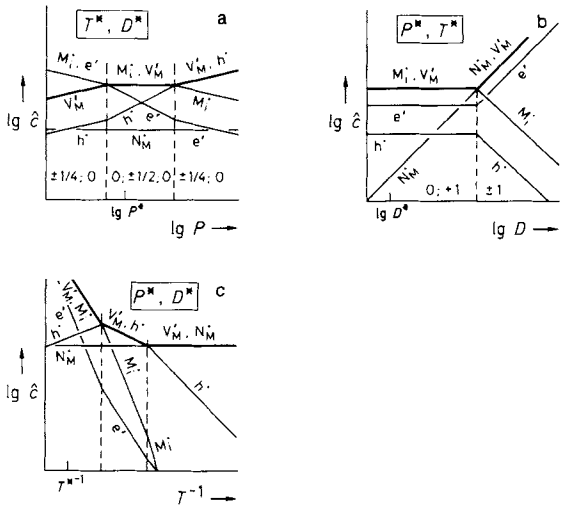

Fig. 8. Defect concentration as a function of the partial pressure (a), dopant concentration (b), and temperature (c) in the Brouwer approximatio (P^*, T^*, D^* are the values at the working point).

Figure 8a describes the "chemistry of the solid state" as one moves through the homogeneous region of the phase in the phase diagram. The straight-line sections correspond to constant values of N, with slopes equal to N_k (in the example chosen here, the exponents have the values 0, $\pm 1/4$, $\pm 1/2$). For very high values of the X_2 partial pressure (high [X]/[M] ratio, right-hand side of Fig. 8a), the concentrations of metal site vacancies are correspondingly high [see Eq. (11c)] and, owing to the oxidizing conditions, the holes predominate, so that the electrical neutrality condition simplifies to that given in Equation (28).

$$[h^{\bullet}] = [V_M'] \tag{28}$$

Equation (11c) then leads directly to Equations (29), and similarly from Equations (7)–(10) we obtain Equations (30),

$$[h^{\bullet}] \propto P^{1/4};\ [V_M'] \propto P^{1/4} \tag{29}$$

$$[e'] \propto P^{-1/4};\ [M_i^{\bullet}] \propto P^{-1/4} \tag{30}$$

as shown in Figure 8a. Provided that the dopant concentration ($[N_M^{\bullet}]$) remains small compared with those of the majority charge carriers ($h^{\bullet}$, V_M'), its effects, even on the minority charge carriers, can be neglected. Analogously for the region of low partial pressures (in which $[e'] = [M_i^{\bullet}]$), the straight-line sections shown in the left-hand side of Figure 8 are obtained. Similarly, for the intermediate regime ionic defects often predominate, as has been assumed in Figure 8a, so that $[M_i^{\bullet}] = [V_M'] =$ constant (constant $= K_F^{1/2}$ according to Table 1), leading to Equations (31). In general the width of the phases is usually insufficient to cover the whole of the defect range shown in the diagram.

$$[h^{\bullet}] \propto P^{1/2};\ [e'] \propto P^{-1/2} \tag{31}$$

The dependence of defect concentration on the degree of doping for constant values of P and T can be derived in an analogous way (Fig. 8b). For the fixed dopant level $D = D^*$ and partial pressure P^* assumed in plotting Figure 8a, the degree of doping is insufficient to cause a detectable effect, as is confirmed by the left-hand half of Figure 8b. Only when the defect concentration D becomes comparable with the concentration of the majority charge carriers (in this case $M_i^{\bullet}$, V_M') does it have a controlling influence on defect chemistry (right-hand side of Fig. 8b). Here, in agreement with the doping rule [Eq. (13)], the concentrations of the metal ion vacancies and of the conduction electrons increase with increasing doping, while those of the interstitial metal ions and electron holes decrease. In this example the resulting values of the exponent M (see Eq. (27b)) are 0, +1, and −1.

The temperature dependence is given in terms of the standard reaction enthalpies of the equilibria involved from Equation (22). This results in Equation (32), in which the

$$W_k \equiv -\partial \ln \hat{c}_k/\partial(1/RT) = +\sum_r \gamma_{rk} \Delta_r H^0 \tag{32}$$

value of $\Delta_r H^0$ for the formation of electron–hole pairs is, to a good approximation, equal to the band gap ($\Delta_B H^0 \simeq \Delta_B G^0 = E_g$), and the factors γ_{rk} are again simple rational numbers. Thus the temperature dependence yields information about the corresponding energy values, and $\ln c$ should be a linear function of T^{-1} over limited temperature ranges. Figure 8c illustrates the chemistry within the solid at different temperatures. The example chosen shows that also in this case a succession of different regimes are possible as the temperature is altered. If we start from the point (T^*, P^*, D^*), we are initially in the ionic-dominated region, as shown by Figure 8a. Since the various reaction enthalpies have different values ($\Delta_F H^0 > \Delta_X H^0 > \Delta_B H^0$ in the example chosen here), the boundaries of the regimes indicated in Figure 8a vary with temperature. In the example shown, reducing the temperature with fixed P results in a shift into the "high-pressure region" ($[V_M'] = [h^{\bullet}]$). Further cooling causes the thermally generated defect concentrations to become less and less, so that eventually the defect chemistry is determined by the level of doping.

A few examples illustrating the behavior in real situations will be described in the following sections. For this we first need to anticipate a result that will be arrived at in Part II of this review, namely that the observed electrical conductivity provides a convenient measure of the (equilibrium) defect concentration, and conversely the conducting properties of solid materials are determined by the (equilibrium) defect chemistry. Although slight departures from equilibrium are unavoidable when measuring the conductivity σ, provided that these are small the conductivity due to a defect k can be expressed in the form given in Equation (33). Here z_k is the

$$\sigma_k(T,P) = |z_k| F u_k(T) \hat{c}_k(T,P) \tag{33}$$

charge number, F is the Faraday constant, u_k is the mobility, and $\hat{c}_k$ is the equilibrium molar concentration. Since u_k is essentially independent of the composition, and therefore of P, for small defect concentrations, σ_k is proportional to the equilibrium concentration. Thus, by measuring the conductivity as a function of the partial pressure and dopant concentration the values of the important exponents N_k and M_k are obtained directly [Eqs. (34)].

$$\partial \ln \sigma_k/\partial \ln P = N_k;\ \partial \ln \sigma_k/\partial \ln D = M_k \tag{34}$$

The temperature dependence is a little more complicated, since the mobility also varies with the temperature. For ionic defects, and also for electronic polaron states, the activation energy controlling the value of u is the migration threshold $\Delta H^{\neq}$ (see Fig. 7 and the more detailed discussion in Part II of this review), and consequently the temperature dependence of the specific conductivity σ is given by a thermodynamic term ($\sum \gamma_{rk} \Delta_r H^0$) and a kinetic term ($\Delta H_k^{\neq}$), as indicated in Equation (35).

$$E_k \equiv -R\partial \ln \sigma_k/\partial(1/T) = W_k + \Delta H_k^{\neq} \tag{35}$$

Figure 7 illustrates very clearly the two contributions that are needed for ionic charge transport to occur. In the first place the necessary defects must be formed (e.g. by generating interstitial ions and lattice vacancies, as controlled by $\Delta_F G^0$), and these must then be transported from their original sites to the nearest equivalent sites over the corresponding migration thresholds (e.g. $\Delta_i G^{\neq}$ for the interstitial lattice mechanism or $\Delta_v G^{\neq}$ for the vacancies mechanism). If band conduction occurs, and k refers to an electronic defect, the mobility of the electronic charge carriers normally decreases slowly with temperature according to a power law (typically $T^{-3/2}$).[26] In such cases the temperature dependence of the concentration term predominates, and Equation (35) is still approximately valid for $\Delta H^{\neq} \simeq 0$. In general the conductivity is the sum of the partial contributions, and this can be separated into an ionic term and an electronic term, as in Equation (36).

$$\sigma = \sigma_{ion} + \sigma_{eon} = \sum \sigma_k \tag{36}$$

An experimental procedure for determining the separate contributions is indicated in Section 3.2.1. The overall changes N, E, and M can be formally expressed as weighted summations of the individual changes by using the transport numbers $t_k \equiv \sigma_k/\sigma$, as in Equation (37).[35]

$$N = \sum_k t_k N_k;\ E = \sum_k t_k E_k;\ M = \sum_k t_k M_k \tag{37}$$

3.1.1. Example 1: Silver Chloride – A Typical Ionic Conductor

Due to the rather low concentration of crystal defects combined with relatively high mobilities, silver chloride is an excellent model substance for studying ionic conduction. Furthermore, it is also a solid of practical interest. One need only mention the importance of silver halides in photography, and the Ag/AgCl electrode that is so useful in electrochemistry, for example, as a reference electrode in water analysis or in gas sensor technology, applications which all depend on its defect chemistry.

Pure silver chloride

In pure silver chloride Frenkel disorder predominates. The conduction is predominantly ionic, involving silver ions. Accordingly, there is a much higher concentration of ionic defects than of electronic defects.[15] Thus the electrical neutrality (EN) relationship is simply given by Equation (38).

$$[V'_{Ag}] = [Ag^{\bullet}_i] \tag{38}$$

The interaction with the adjacent phase can be described by Equations (39). From the Frenkel equilibrium (F) ex-

$$\tfrac{1}{2}Cl_2 + Ag_{Ag} \rightleftharpoons AgCl + V'_{Ag} + h^{\bullet} \tag{39a}$$

$$K_{Cl} = [h^{\bullet}]\,[V'_{Ag}]\,P^{-1/2} \tag{39b}$$

pressed by Equations (40) and the condition of electroneutrality [Eq. (38)] the simple result follows that both ionic defect concentrations are determined by the square root of

$$Ag_{Ag} + V_i \rightleftharpoons Ag^{\bullet}_i + V'_{Ag} \tag{40a}$$

$$K_F = [Ag^{\bullet}_i]\,[V'_{Ag}] \tag{40b}$$

the Frenkel constant [Eq. (41)]. Combining this with Equation (39) gives the more complex expressions in Equations (42) for the concentrations of electronic defects.

$$[Ag^{\bullet}_i] = [V'_{Ag}] = K_F^{1/2} = \exp\left(\frac{\Delta_F S^0}{2R}\right)\exp-\left(\frac{\Delta_F H^0}{2RT}\right) \tag{41}$$

$$[h^{\bullet}] = (K_{Cl}K_F^{-1/2})\,P^{1/2} \tag{42a}$$

$$[e'] = (K_B K_{Cl}^{-1} K_F^{+1/2})\,P^{-1/2} \tag{42b}$$

The concentrations of all the charge carriers are highly temperature dependent, but only those of the electronic charge carriers are also strongly influenced by the chlorine partial pressure, that is by the exact position in the phase diagram. The dependence of the partial pressure of the ionic and electronic contributions on the conductivity is shown in Figure 9. As the abscissa one can use either the logarithm of the chlorine partial pressure or that of the silver activity (a_{Ag}), which are related to each other through the reaction constant for the formation of AgCl. Figure 9 shows the behavior of defect chemistry within the AgCl phase as one moves across the phase diagram. The window accessible in this way corresponds to the middle section of Figure 8a. At the extreme left of Figure 9 AgCl is in equilibrium with silver metal ($a_{Ag} = 1$). This defines the lowest possible Cl_2 partial pressure, whereas the right-hand edge of the diagram is fixed by the chlorine partial pressure of 1 bar.[37] Changes in defect chemistry are thus accompanied by a change of about 12 orders of magnitude in the chlorine partial pressure!

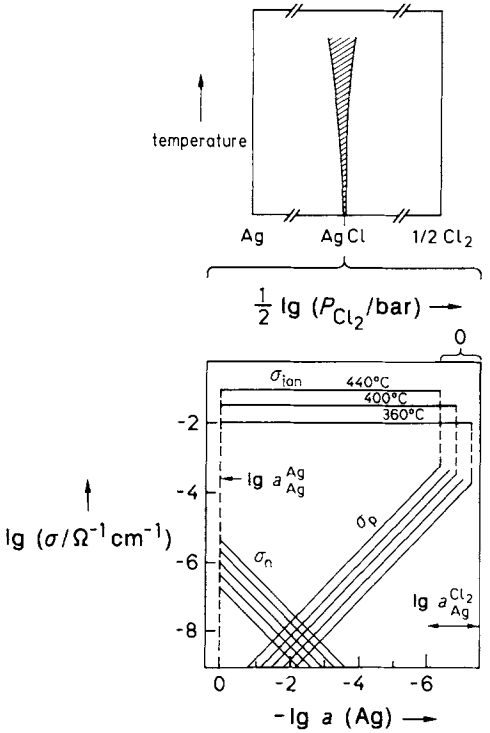

Fig. 9. The ionic and electronic conductivities in AgCl as functions of the silver activity (a_{Ag}) or of the chlorine partial pressure give a picture of the defect chemistry on passing through the width of the phase (data from ref. [36]). The superscripts Ag and Cl_2 denote the boundaries of the phase width (i.e. contact with Ag or with pure Cl_2).

Curve 1 in Figure 10 shows the conductivity (which is entirely ionic) of nominally pure AgCl as a function of temperature.[38] As will be shown later, the interstitial ions are the most mobile, so that $\sigma \simeq \sigma_{ion} \simeq \sigma_{Agi}$. The slope at higher temperatures in Figure 10 is therefore determined by half the

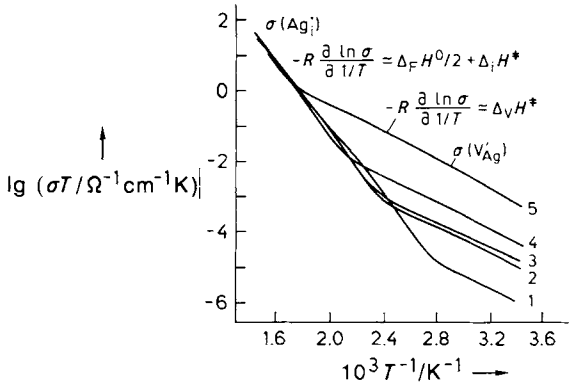

Fig. 10. Ionic conductivity of AgCl with various dopant levels as a function of temperature. Curves 1 and 2: nominally pure AgCl, with calculated dopant concentrations of 0.3 and 0.6 ppm, respectively; curve 3: with 6.9 ppm Mn; curve 4: with 31 ppm Cd; curve 5: with 1200 ppm Cd [38].

Frenkel enthalpy together with the activation energy for transport from one interstitial site to the next [Eq. (43)].

$$E = E_{A_{gi}} = \Delta_f H^0/2 + \Delta_i H^+ \quad (43)$$

Simulations and doping experiments have shown (see next section) that $\Delta_i H^+$ is small, thus the value of 1.45 eV obtained by doubling the slope gives the standard enthalpy of the Frenkel reaction with a good degree of accuracy.[39]

Any real material, even though nominally pure, contains impurities. Since the degree of thermal disorder decreases exponentially on reducing the temperature, the behavior at sufficiently low temperatures is *always* determined by extrinsic conditions (see Fig. 8c). This accounts for the reduced slope of the conductivity curves at low temperatures (curves 1 and 2) in Figure 10.

Homogeneously doped silver halides

If AgCl contains cationic impurities of higher valency such as Cd^+ or Mn^+, (as in curves 3–5 of Fig. 10), an additional term such as $D = [Cd^{\bullet}_{Ag}]$ must be included on the right-hand side of Equation (38). The concentrations of ionic defects are then given by the solution of a quadratic equation [Eq. (44)].

$$[V'_{Agi}] = D + [Ag^{\bullet}_i] = \frac{D}{2} + \sqrt{\frac{D^2}{4} + K_F} \quad (44)$$

For $D \ll \sqrt{K_F}$ (where $\sqrt{K_F}$ = intrinsic ionic defect concentration) the compound effectively behaves like the pure material ($[V'_{Ag}] = [Ag^{\bullet}_i] = \sqrt{K_F}$), whereas in the other extreme case of high defect concentrations one obtains a (high) concentration of vacancies that is independent of partial pressure and temperature ($[V'_{Ag}] \simeq D$), and the concentration of interstitial ions [see Eq. (45)] is reduced to a very low value, which is strongly temperature dependent due to the effect of $\Delta_F H^0$.

$$[Ag^{\bullet}_i] = K_F(T)/D \quad (45)$$

If instead the material is doped with Ag_2S (giving S'_{Cl}), these relationships are expected to be exactly reversed. Figure 11 shows the changes in the ionic conductivity for AgBr with temperature.[15] The minimum in the right-hand half of the figure corresponds to the change from interstitial type conduction to vacancy conduction. The fact that this does not occur at the zero point (pure AgBr) is due to the lower mobility of the vacancies: For very low Cd^{2+} concentrations, even though there is already a greater concentration of vacancies the conduction is still of the interstitial type, and the conductivity is therefore less than that of the pure material. On the other side of the minimum the higher value of $[V'_{Ag}]$ more than compensates for the lower mobility, and vacancy conduction predominates.

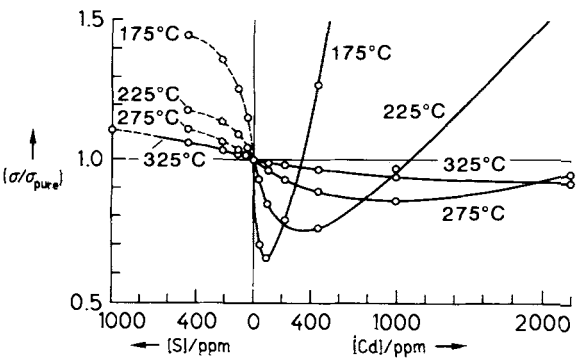

Fig. 11. Ionic conductivity of AgCl as a function of dopant concentration [15].

In Figure 10 the lower (right-hand) part of the conductivity curve corresponds to vacancy conduction, in contrast to the high temperature (left-hand) side. For the reason already explained, there is a characteristic knee in the curve corresponding to the transition region. The slope of the right-hand portion corresponds to 0.3 eV, and since $[V'_{Ag}]$ is constant this can be attributed to the enthalpy of migration of the silver ion vacancies. Thus it can be seen that measurements of this kind allow one to determine thermodynamic quantities such as enthalpies and entropies of formation, and also the enthalpies and entropies of migration that are relevant to kinetic studies. Table 2 summarizes some results.[13, 24]

Table 2. Thermodynamic parameters for the formation and migration of point defects.

Crystal	Disorder type	Enthalpy of formation [MJ mol^{-1}]	Entropy of formation [a]	Migration enthalpy [kJ mol^{-1}]	Migration entropy [a]
LiF	S	0.23	9.6	70 (V'_{Li})	1 (V'_{Li})
LiCl	S	0.21		40 (V'_{Li})	
LiBr	S	0.18		40 (V'_{Li})	
LiI	S	0.11		40 (V'_{Li})	
NaCl	S	0.24	9.8	70 (V'_{Na})	1–3 (V'_{Na})
KCl	S	0.25	9.0	70 (V'_K)	2.4 (V'_K)
RbCl	S	0.21		50–100 (V'_{Rb})	
CsCl	S	0.18	10	60 (V'_{Cs})	19 (V'_{Cs}) (?)
AgCl	F	0.14	9.4	28 (V'_{Ag})	−1 (V'_{Ag})
				1–10($Ag^{\bullet}_i$)	−3($Ag^{\bullet}_i$)
AgBr	F	0.11	6.6	≈30 (V'_{Ag})	
				5–20 ($Ag^{\bullet}_i$)	
CaF_2	$\bar{F}$	0.27	5.5	40–70 ($V^{\bullet}_F$)	1–2 ($V^{\bullet}_F$)
				80–100 (F'_i)	5 (F'_i)
SrF_2	$\bar{F}$	0.17		50–100 ($V^{\bullet}_F$)	
				80–100 (F'_i)	
BaF_2	$\bar{F}$	0.19		40–70 ($V^{\bullet}_F$)	
				60–80 (F'_i)	

[a] In units of R.

Two further comments on this example should be added:

1) Because Equations (2) and (6) both have the same form, exactly analogous considerations apply for a purely electronic (dilute) solid system such as pure silicon, or silicon doped with boron or phosphorus. Detailed descriptions can be found in textbooks on solid-state physics, and these cases are covered by the formalism given above.

2) One type of homogeneously doped ionic conductor of considerable practical importance is ZrO_2 doped with CaO or Y_2O_3. Oxygen vacancies are formed in the material in such a concentration as to give a high oxygen conductivity, which is used in high-temperature fuel cells and in electrochemical oxygen sensors (Fig. 12).[40] If different oxygen partial pressures P_1 and P_2 exist on the two sides of the doped zirconium oxide (to which electrodes are attached as in Fig. 12), a voltage is generated which, according to the Nernst equation, is proportional to $\ln(P_1/P_2)$. This can be used to determine the partial pressure P_1 (e.g., the oxygen

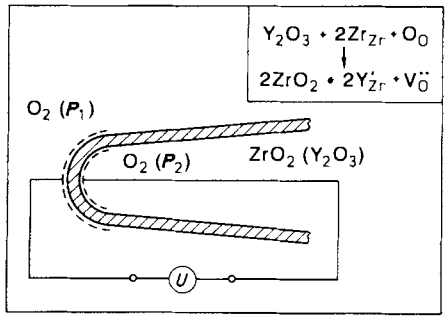

Fig. 12. Schematic arrangement of an oxygen concentration cell based on the ceramic solid electrolyte $ZrO_2(Y_2O_3)$, as used in oxygen sensors, pumps, and fuel cells. (In the latter, the oxygen partial pressure on the anode side is kept very low by a gas such as hydrogen.)

partial pressure in automobile exhaust gases) if P_2 is known, or can even be used to control it (as in the automobile λ-probe). Alternatively, a very large difference in the oxygen potentials, and thus a high cell voltage, can be achieved (by supplying hydrogen to one side[41]) corresponding to an electrochemical conversion of H_2 and O_2 to water. In this way chemical energy can be converted to electrical energy efficiently. Such fuel cells with ceramic solid electrolytes attain an efficiency that is not limited by the conditions of the Carnot cycle, since no heat energy stage is involved. Furthermore, they have the advantage that they can be operated at high temperatures. At these temperatures the electrode reactions are reversible, and this also allows other fuels such as CH_4 or CH_3OH to be electrochemically converted.[42]

3.1.2. Example 2: Tin(IV) Oxide—A Semiconducting Oxide

As a second example of bulk equilibrium thermodynamics the semiconductor SnO_2 is considered.[43,44] The dependence of the conductivity on the oxygen partial pressure (Fig. 13), indicates that n-type conduction predominates, thus "SnO_2" is better described as $SnO_{2-|\varepsilon|}$. The oxygen

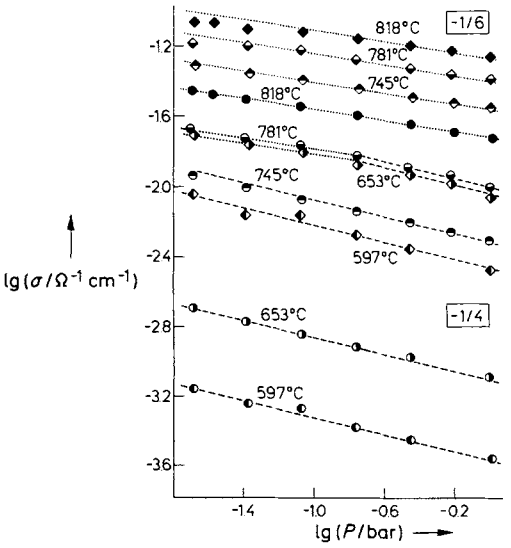

Fig. 13. Electronic conductivity of SnO_2 as a function of the oxygen partial pressure at various temperatures. Circular symbols: nominally pure material which, however, contains high levels of acceptor impurities, mainly Fe^{3+}; square symbols: materials in which this is partly counteracted by additional doping with small amounts of the donor Sb (as Sb^{5+}) [43].

incorporation or removal at high temperatures is understood by oxygen vacancies $V_O^{\cdot\cdot}$ as compensating defects. This is indicated in Equation (46), with Equation (47) as the electroneutrality condition.

$$\tfrac{1}{2}O_2 + V_O^{\cdot\cdot} + 2e' \rightleftharpoons O_O \tag{46}$$

$$2[V_O^{\cdot\cdot}] = [e'] \tag{47}$$

Applying the mass action equation leads directly to the value $-1/6$ for the exponent $N_{e'}$. Figure 13 shows that for nominally pure SnO_2 (circular symbols) these slopes are only found at very high temperatures and/or low partial pressures.[43] This is due to the effects of (acceptor) impurities, in this case Fe^{3+} ions resulting in Fe'_{Sn} defects [see Eq. (13)]. At low temperatures (negative reaction enthalpy for Eq. (46)) and at high oxygen partial pressures (see Eq. (46) and compare with the isotherm for 781 °C in Fig. 13), the e' concentration is suppressed below the impurity level (see Fig. 8c), and the electroneutrality condition is then given by Equation (48), with $N_{e'} = -1/4$, in agreement with the experimentally observed value (see Fig. 13).[46]

$$[Fe'_{Sn}] = 2[V_O^{\cdot\cdot}] = \text{const.} \tag{48}$$

The impurity-controlled range can be extended by doping SnO_2 with In_2O_3 as an acceptor.[43] If SnO_2 containing Fe as an impurity, as described previously, is lightly doped, with a donor $Sb^{\cdot}_{Sn}$ (i.e. Sb^{5+} replacing Sn^{4+}), this reduces the effective acceptor concentration, and thus also the extrinsically determined vacancy concentration, as given by Equation (49).

$$[V_O^{\cdot\cdot}] = [Fe'_{Sn}] - [Sb^{\cdot}_{Sn}] \tag{49}$$

As expected, the transition from the impurity-controlled region to that of virtually pure material then occurs at a lower temperature (the critical isotherm in Fig. 13 is that for 653 °C, square symbols), but at the same conductivity value (i.e. the same electron concentration).[43] An example in which the donor effect predominates is described in reference [44]; here SnO_2 prepared from SnF_4 was studied. Residual fluorine impurities act as donor centers $F^{\cdot}_O$ (F^- replacing O^{2-}), which increases the electron concentration. This results in an electronic conductivity at low temperatures and high partial pressures (due to the electroneutrality condition $[F^{\cdot}_O] = [e']$), whose value is almost independent of partial pressure and temperature. Transitions between the different disorder regimes can also be recognized from the temperature dependence of the conductivity: since the mobility makes only a small contribution, a plot of $\ln \sigma$ vs. T^{-1} yields the slopes $-\Delta_O H^0/3R$ for pure SnO_2, $-\Delta_O H^0/2R$ for acceptor-compensated SnO_2, and zero for donor-compensated SnO_2.[43,44] Here $\Delta_O H^0$ is the reaction enthalpy for Equation (46). At lower temperatures the effects of association between ionic and electronic defects [Eq. (50)] become

$$V_O^{\cdot\cdot} + 2e' \rightleftharpoons V_O^{\cdot} + e' \rightleftharpoons V_O^{\times} \tag{50}$$

important, and these then determine the changes observed in the conductivity.[47] From the energy data obtained in this way a fairly detailed band scheme can be constructed.[43]

Here it must again be noted that in no case does the band gap control the temperature dependence.

3.1.3. Example 3: The High Temperature Superconductors Lanthanum Copper Oxide and Yttrium Barium Copper Oxide

Pure La_2CuO_4, the archetype of the family of high-temperature superconductors,[49] is in one sense the opposite of SnO_2, since it exhibits an excess of oxygen, which results in a p-type conduction. Studies of defect chemistry are generally concentrated on the non-superconducting state for the following reasons. First, at temperatures below 40 K the stoichiometric changes are so slow that equilibrium studies are not possible. More importantly superconducting ceramics are prepared at very high temperatures, where the defect chemistry attains partial equilibrium. The concentrations of ionic and electronic point defects are thus established at these high temperatures according to the relationships discussed previously, and due to the extreme temperature dependence of the kinetic parameters in the superconducting region they remain essentially frozen in (apart from ordering and association processes).[57] To emphasize this point yet again, defect chemical relationships that apply at high temperatures are determined by the quantitative correlation between charge carrier concentration and parameters such as the oxygen partial pressure as discussed previously.

Chemical analysis and neutron scattering studies show that oxygen can be incorporated at interstitial sites.[50, 51, 52] For pure La_2CuO_{4+x} this is expressed by Equation (51), with the electroneutrality condition given by Equation (52).

$$\tfrac{1}{2}O_2 + V_i \rightleftharpoons O_i'' + 2h^{\bullet} \tag{51}$$

$$2[O_i''] = [h^{\bullet}] \tag{52}$$

These two equations lead directly to the value of $+1/6$ for the exponent in the case of hole conduction, in agreement with experiment.[56] As is well known, La_2CuO_4 with a sufficient proportion of excess oxygen is superconducting.[52] Alternatively, the degree of oxidation (generating holes) is raised by the method originally reported,[49] namely by doping with an acceptor, for example by exchanging Sr^{2+} for La^{3+}, as in Equation (53a).

$$2\text{“SrO”} + 2La_{La} + 1/2\,O_2 \rightleftharpoons \text{“}La_2O_3\text{”} + 2Sr'_{La} + 2h^{\bullet} \tag{53a}$$

According to the homogeneous doping rule [Eq. (13)], incorporating Sr not only reduces the oxygen concentration in the interstitial lattice but also (in greater numbers as it turns out) generates oxygen vacancies [Eq. (53b)].

$$2\text{“SrO”} + 2La_{La} + O_O \rightarrow \text{“}La_2O_3\text{”} + 2Sr'_{La} + V_O^{\bullet\bullet} \tag{53b}$$

Only one of these two equations is needed to define the thermodynamic situation, provided the disorder equilibria given in Table 1, which refer to the anion substructure, are established, namely Equation (46) and the anti-Frenkel equilibrium Equation (54). This example provides a very nice

$$O_O + V_i \rightleftharpoons O_i'' + V_O^{\bullet\bullet} \tag{54}$$

illustration of the relationship between the equilibrium concentration and the (fixed) concentration of dopant introduced, which follows directly from the above relationships [cf. M_k in Eq. (27b)].[50] Figure 14 shows how the concentration of defects in $(La,Sr)_2CuO_{4+x}$ varies with the dopant concentration (with constant T and P_{O_2}). In the region of

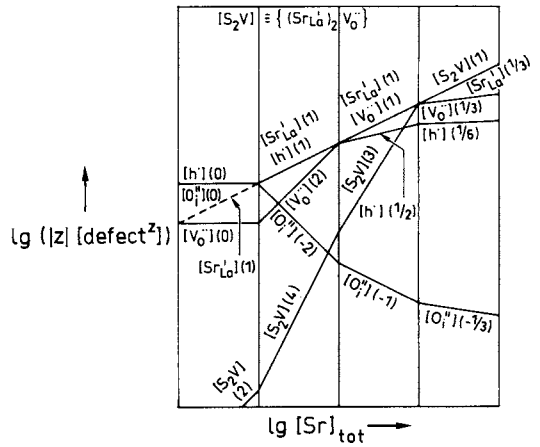

Fig. 14. Defect concentrations in La_2CuO_4 as a function of Sr dopant concentration [50].

negligibly low Sr concentrations (left-hand region), $[Sr'_{La}]$ does not appear in the electroneutrality equation, and $[h^{\bullet}]$, $[V_O^{\bullet\bullet}]$, and $[O_i'']$ do not depend on $[Sr'_{La}]$. With increasing Sr concentration the concentration of the excess oxygen ions is reduced, whereas that of the holes is increased. Eventually a region must be reached in which the impurity concentration is compensated by the hole concentration (inner left region), so that the gradient of the holes curve is given by $M_{h^{\bullet}} = 1$. This can be confirmed experimentally by measurements of the conductivity. The dependence of the concentration of interstitial oxygen ions on the dopant concentration, and the slopes of $M_{O_i''} = -2$ and $M_{V_O^{\bullet\bullet}} = +2$ follow from Equations (55–57).

$$M_{O_i''} = (\partial \ln [O_i'']/\partial \ln D) \tag{55}$$

$$K_O P^{1/2} = [O_i''][h^{\bullet}]^2 \tag{56}$$

$$2M_{h^{\bullet}} + M_{O_i''} = 0 \tag{57}$$

Since $M_{V_O^{\bullet\bullet}} > M_{h^{\bullet}}$, the concentration of vacancies increases very steeply, and a regime is reached in which the impurity concentration is compensated by that of the oxygen vacancies (inner right region). By analogous derivations the remaining quantitative relationships shown in Figure 14 are obtained. It is also found that in this impurity-controlled region the dependence of the hole concentration on oxygen partial pressure is given by $N_{h^{\bullet}} = +1/4$ (since $[V_O^{\bullet\bullet}]$ and $[O_i'']$ are constant), and in the hole-compensated region by $N_{h^{\bullet}} = 0$ ($[h^{\bullet}]$ constant). Both these relationships can be tested by experiment. With regard to the ionic contributions, an analogous transition from the interstitial mechanism to the vacancy mechanism occurs, as confirmed by tracer diffusion and ionic conductivity measurements (see Part II of this reviews). In all the measurements it is found that at very high

Sr concentrations the high temperature conductivity falls off rapidly with increasing Sr content. In this region the simple concept of point defects, in which defect chemistry is treated as a perturbation of the perfect structure, becomes unreliable; structural changes assume an important role, and the equilibrium constants and mobilities discussed above become concentration-dependent. Even if randomly distributed association complexes between Sr'_{La} and $V_O^{\cdot\cdot}$ (or between Sr'_{La} and $h^{\cdot}$) are assumed, this does not explain the behavior adequately, as Figure 14 shows. Although the postulated formation of Sr'_{La}–$V_O^{\cdot\cdot}$ complexes causes a flattening of the curve (right-hand regime), it does not reduce the concentrations of the free charge carriers. The situation here is further complicated by the probable existence of vacant La sites.

The defect chemistry of $YBa_2Cu_3O_{6+x}$ can be described in a similar way, but in this case the high defect concentrations result in interactions between ionic and electronic point defects even at high temperatures [Eq. (58)],[53] so that a significant proportion of the holes are localized.

$$O_i'' + 2h^{\cdot} \rightleftharpoons O_i' + h^{\cdot} \rightleftharpoons O_i^{\times} \tag{58}$$

(The O_6 compound has the appropriate reference composition.)[48] On reducing the temperature, significant ordering effects are observed. It is possible that localization phenomena (which are also expected to occur in La_2CuO_4 at lower temperatures) play an important role in superconductivity. Whether or not that is the case, a high concentration of point defects is a common feature of all high-temperature superconductors, and this must also influence their dynamic properties.[54]

A striking feature of $YBa_2Cu_3O_{6+x}$ (and also of the more complex high-temperature superconductors with higher critical temperatures) is the high degree of disorder in the cationic partial structure, leading to entropy effects which partly compensate for the generally poor stability of these compounds.[55]

These considerations have provided the basis for a quantitative rationalization[53] of the empirical relationships observed between equlibrium partial pressure, composition, and temperature for $YBa_2Cu_3O_{6+x}$.

It is also worth mentioning that for $YBa_2Cu_3O_{6+x}$ in contrast to La_2CuO_4, a transition to n-type conduction at low oxygen partial pressures has been observed.[56]

3.1.4. Example 4: The Transition from n- to p-Type Conduction in $SrTiO_3$

Figure 15 shows a set of conductivity isotherms for $SrTiO_3$.[58] Here again the defect chemistry in the dense perovskite structure can be considered very simply in terms of oxygen vacancies and electronic defects. Any Sr and Ti defects that may be present are immobile at the temperatures used for the measurements. The slopes of $\pm 1/4$ observed in Figure 15 are as expected for a fixed $V_O^{\cdot\cdot}$ concentration, as is the flattening out to an $N_{e'}$ value of $-1/6$ at lower oxygen partial pressures (see the previous Section). Whether the compensation occurring here is mainly due to immobile Sr vacancies or to acceptor impurities is unimportant. The transition from n- to p-type conduction can be clearly seen. At low temperatures it is superposed by the accompanying ionic

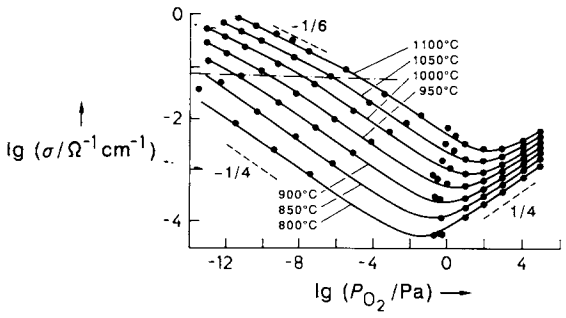

Fig. 15. Electronic conductivity of $SrTiO_3$ as function of the oxygen partial pressure [58].

conduction (see Fig. 8a). From the temperature dependences observed in the different regions of the conductivity curves one can calculate the standard reaction enthalpies for the reactions shown in Equations (59a) and (59b), then from their difference one obtains that of the electronic defect-forming reaction [Eq. (60)], which corresponds to the thermal band gap ($\Delta_B H^0 \simeq E_g$).

$$\tfrac{1}{2}O_2 + V_O^{\cdot\cdot} + 2e' \rightleftharpoons O_O \tag{59a}$$

$$\tfrac{1}{2}O_2 + V_O^{\cdot\cdot} \rightleftharpoons O_O + 2h^{\cdot} \tag{59b}$$

$$\text{nil} \rightleftharpoons e' + h^{\cdot} \tag{60}$$

An alternative way of determining the thermal band gap is to measure the temperature dependence of the conductivity minimum in Figure 15. From Equation (61), and the fact

$$\sigma_{min} = 2\sigma_{n,min} = 2\sigma_{p,min} \tag{61}$$

that the conductivity increases with increasing concentration, and also taking into account Equation (60), the temperature dependence of the minimum yields the band gap directly [Eq. (62)].

$$-R\frac{d \ln \sigma_{min}}{d(1/T)} \cong \tfrac{1}{2}\Delta_B H^0 \simeq \tfrac{1}{2}E_g \tag{62}$$

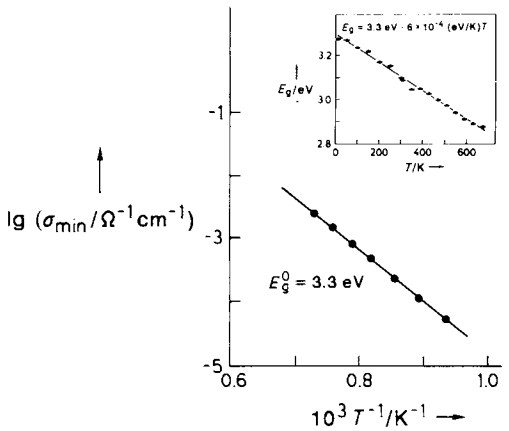

Fig. 16. a) A determination of the thermal band gap at absolute zero for $SrTiO_3$, from the conductivity values at the minima in Figure 15. b) Inset: Temperature dependence of the optical band gap from absorption measurements [59].

A determination by this method is shown in Figure 16.[58] However, it must be noted here that the band gap is temperature dependent, as is evident from the data obtained by in situ optical measurements[59, 60] shown in the inset of Figure 16. The value of E_g yielded by Equation (62) is that for $T = 0$ K, and the same value is obtained by extrapolation of the optical data.

The sensitive and reproducible dependence of the conductivity on the oxygen partial pressure indicated here is of considerable interest and promise as the basis for an oxygen sensor in automobiles, especially as $SrTiO_3$ is stable at high temperatures and less affected by temperature changes than $ZrO_2(Y_2O_3)$.

3.1.5. *Example 5: Proton Conduction in Oxides of the Perovskite Type*

This conduction phenomenon, which has only recently begun to be investigated in detail, provides an excellent example of the importance of foreign elements in ionic conduction.[61] Evidence for proton conduction is found in a number of perovskite materials, particularly in acceptor-doped perovskites such as $(Sr,Fe)TiO_3$,[62] and possibly also in the structurally similar $(La,Sr)_2CuO_4$.[63] The most interesting of these materials is ytterbium-doped $SrCeO_3$.[64a] In all these cases acceptor doping increases the concentration of vacant oxygen sites. It is conceivable that through contact with a moist atmosphere these oxygen vacancies become occupied by OH groups, the remaining proton being taken up by regular O^{2-} ions to form a further hydroxyl group. Such effects at surfaces are already well known. The incorporation reaction can be expressed in the form of Equation (63), in

$$H_2O + O_O + V_O^{\bullet\bullet} \rightleftharpoons 2OH_O^{\bullet} \tag{63}$$

which $OH_O^{\bullet}$ can also be regarded from a phenomenological standpoint as $(O_O + H_i^{\bullet})$. It is not yet clear to what extent this mechanism is in agreement with the observed conductivity phenomena, or how important a role it plays.[64b]

3.2. Boundary Layers

The foregoing thermodynamic description is inadequate for the boundary layers of the M^+X^- crystal. The condition for phase equilibrium, namely that the neutral components must have a constant chemical potential, when combined with the electroneutrality condition, was entirely adequate for understanding the behavior within the bulk material. However, in the boundary regions some limited deviations from electrical neutrality can occur. This means that even the expanded formula $M_{1+\delta}X$ is no longer sufficient and must be replaced by $[M_{1+\delta'}X]^{\varepsilon+}$, in which δ' and ε are position-dependent variables.[65] At the boundary surfaces the distribution of particles is no longer uniform, and the concentrations of the charged constituents differ from those in the bulk material in ways that depend on the chemical nature of the adjacent phase. Local deviations from electrical neutrality can result from an excess or deficiency of any of the ionic or electronic defect centers involved. Electrical neutrality is, of course, retained in a global sense; thus the corresponding opposite charge may be either in the boundary layer itself or in the boundary regions of the adjacent phase. In addition to the condition for phase equilibrium, which requires that the chemical potentials of the neutral components M and X must be spatially invariant [Eq. (64)], for complete contact equilibrium the electrochemical potentials of the ions and electrons must also be spatially invariant, as expressed by Equation (65) (see the general scheme shown in Fig. 5).

$$(\partial/\partial x)\mu_M = (\partial/\partial x)\mu_X = 0 \tag{64}$$

$$(\partial/\partial x)\tilde{\mu}_{M^+} = (\partial/\partial x)\tilde{\mu}_{X^-} = (\partial/\partial x)\tilde{\mu}_{e^-} = 0) \tag{65}$$

It can be shown that the electrochemical potentials of the defects also have zero gradient. This means that only the sum of the concentration and field contributions is required to be spatially invariant. In other words, an adjacent phase (such as A in Fig. 17) which exerts attractive or repulsive forces on cations, anions, or electrons, causes a separation of charges. This chemical effect generates gradients in the chemical potential, and therefore concentration gradients (see Fig. 5), but only up to the point where it is balanced by the opposing charge separation effect (i.e. a gradient in the electrical potential). Since the standard potential in Equation (21) is constant, this condition is expressed quantitatively by Equation (66), in which k refers to the (dilute) defect species.

$$(\partial/\partial x)\mu_k = RT(\partial/\partial x)\ln c_k = -z_k F(\partial/\partial x)\phi \tag{66}$$

Figure 17 shows this both from the thermochemical standpoint (a), and in the form of an "energy level Diagram" (b) which is constructed in analogy to the level schemes of semiconductor physics (see Fig. 6). It is seen that although the (free) energy profiles for the charged defects show a curved region, those for μ_M and $\Delta_F G^0$ (i.e. the difference between E_i and E_v) are spatially invariant.[67]

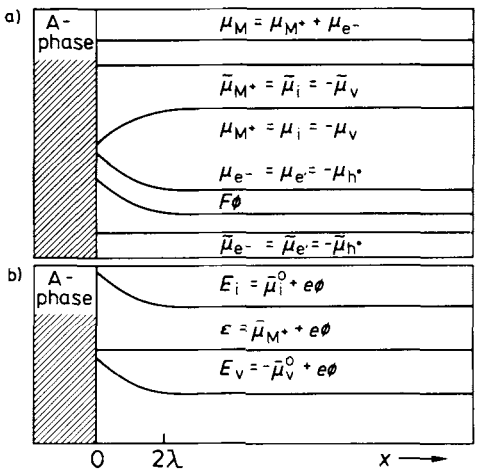

Fig. 17. a) Thermochemical representation of the boundary layer thermodynamics for a mixed conductor (A is the adjacent phase). Both the chemical potential of the neutral component and the electrochemical potential of the charged particles must be spatially invariant. The chemical potentials of the charged species are seen to have gradients (i.e. a gradient of the electrostatic potential ϕ). b) Boundary layer thermodynamics of the ions in the form of an energy level diagram analogous to that for a semiconductor. The separations between the "Fermi level" ε and the energies E_i or E_v correspond to the defect concentrations (i: $M_i^{\bullet}$; v: V_M') [66].

Integration of Equation (66) from the bulk (∞) of the material up to the position x in the boundary layer yields the increase in concentration as a function of the field effect [Eq. (67)].

$$\left(\frac{c_k(x)}{c_k(\infty)}\right)^{1/z_k} = \exp\{-F(\phi(x) - \phi(\infty))\} = \Xi(x) \qquad (67)$$

This can also be seen directly from Figure 5 ($\Xi^{z_k} \equiv \kappa$). As the expression on the right-hand side of Equation (67) is independent of the nature of the defect, it follows from this equation (and is also shown graphically in Fig. 18) that the defect concentrations in the boundary layer are either raised or lowered, depending on the charge of the defect (particle), by a factor $\Xi(x)$ that is independent of the type of defect.

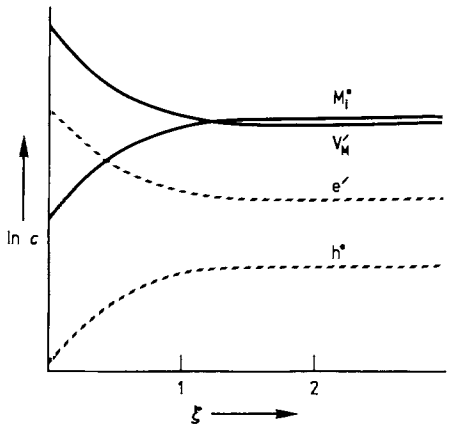

Fig. 18. Defect concentration profiles in the boundary layer for a mixed conductor with Frenkel disorder and a positive charge at the boundary (adsorption of cations) [66]. ξ = spatial coordinate normalized relative to the Debye length.

Taking AgCl as an example, for positive boundary layer potentials ($\phi - \phi_\infty$) the concentrations of the silver ions in the interstitial lattice and of the electron holes must be increased by the factor Ξ, whereas those of the silver lattice vacancies and the conduction electrons must be reduced by the same factor. A comparison with Table 1 will confirm that this behavior is entirely consistent with the conditions for equilibrium between the particles. However, this does not solve the problem for the chemist, since first the space charge potential is not independent of the defect concentrations, and second the chemistry of the adjacent phase needs to be taken into consideration.

The condition of local electroneutrality has, according to electrostatics, to be replaced by Poisson's equation. This takes the form of a relationship [Eq. (68)] between the electric field gradient (the curvature of the electrical potential) and the defect concentrations.

$$(\partial^2/\partial x^2)\phi = \frac{1}{\varepsilon\varepsilon_0}\sum_k z_k F c_k \qquad (68)$$

(In the bulk material $\partial^2\phi_\infty/\partial x^2 = 0$ on grounds of symmetry, and therefore $\sum z_k F c_{k\infty} = 0$, which is the electroneutrality condition.) By taking into account the dependence of the electrical potential on the defect concentrations as given by Equation (67), a parametric solution of Equation (68) is obtained. The concentration profile is then given by an expression of the form shown in Equation (69), where f represents a function of position which has a steep increase or decrease in the boundary layer region. The analytical form of the function is given in reference [65].

$$c_k = f(x;\lambda,\theta) = f(x;c_0,c_\infty) \qquad (69)$$

In a similar way to the Brouwer approximation, this solution is only valid when the charge density depends on only two types of charge carriers (here those with charge numbers $+1$ and -1). For the silver halides these are the defect pair $[Ag_i^{\bullet}]$ and $[V_{Ag}']$ (or, in the heavily Cd-doped material, $[V_{Ag}']$ and $[Cd_i^{\bullet}]$, in silicon they are $h^{\bullet}$ and e', and in SnO_2 $V_O^{\bullet\bullet}$ and e'.

Equation (69) introduces two quantities that are of great importance for the chemist. The first of these is the Debye length λ, which is directly proportional to the square root of the dielectric constant and inversely proportional to the square root of the concentration (for pure AgCl; $c_\infty = [Ag_i^{\bullet}]_\infty = [V_{Ag}']_\infty = \sqrt{K_F}$). The second is the parameter θ,[68] which describes the extent to which the adjacent phase influences the defects under investigation, and is defined by Equation (70). Evidently this quantity varies between $+1$ and -1, that is between the extremes of a greatly increased concentration ($c_0 \gg c_\infty$) and a greatly reduced concentration ($c_0 \ll c_\infty$). The case where $\theta = 0$, corresponding to $c_0 = c_\infty$, is the point of zero charge, where the boundary effect vanishes. In semiconductors this is referred to as the case of a flat band potential. Thus, the chemistry of the boundary layer is determined entirely by the two parameters c_∞ and c_0, namely the concentration in the bulk and that in the atomic layer directly adjacent to the interface where the opposing charge is situated. The solution of the problem in the bulk material, as discussed in the preceding section, corresponds to the state of the art, in contrast to the boundary layer problem considered here. The parameter c_0 contains the interaction with the adjacent phase, and thus describes the contact chemistry. However, the problem of relating c_0 to the properties of the adjacent phase is complicated. It involves considering the potential jump between $x = 0$ and the actual interface, the condition of global electroneutrality (the dielectric displacement must be continuous), and the electrochemical equilibrium at the interface. The procedure is complex, and is described in reference [69]. In such a way c_0 can ultimately be related to the controlling parameters of temperature, dopant content, and partial pressure (in the adjacent phase!).

$$\theta \equiv \frac{(c_0/c_\infty)^{1/2} - 1}{(c_0/c_\infty)^{1/2} + 1} \qquad (70)$$

Although these space charge effects are very important in relation to the electronic states in semiconductor physics, when considering ions in solids—and therefore the composition of the solids!—they are scarcely taken into account. The brief description of boundary layer phenomena that is given here, as well as that of the bulk thermodynamics, is independent of the nature of the defects; it includes the general case of a mixed conductor, and therefore also that of a purely electronic conductor. We start by considering an ionic conductor.

3.2.1. Example 1: The Junction between an Ionic Conductor and a Surface-Active Adjacent Phase: "Heterogeneous Doping"

Of the ionic conductor junctions that have been studied, those between AgCl and ("inert") oxides have yielded most information.[66, 68, 72] The nature of the oxide surface determines whether, and to what extent, silver (or chloride) ions are preferentially accumulated at the interface. Results from detailed electrochemical and spectroscopic studies show that the mechanism of defect formation at the interface is as in Equation (71) (see Fig. 19c).

$$[\text{Oxide}] - \text{OH} + \text{M}_\text{M} \rightleftharpoons [\text{Oxide}] - \text{OHM}^+ + \text{V}'_\text{M} \qquad (71)$$

According to this, cations from the crystal are adsorbed internally at the oxide surface, mainly by OH groups. An analogous reaction is known to occur when aqueous solutions are in contact with oxides such as Al_2O_3 or SiO_2; there it is an expression of the Brønsted acid–base interaction with the solid surface. In that case, the proton of the OH group may also become detached under strongly basic conditions. The pH value for which the surface appears neutral is called the pH of zero charge. This value is reduced as one goes from Al_2O_3 to SiO_2, or from γ-Al_2O_3 to α-Al_2O_3, and this is accompanied by the corresponding reduction in the basicity expressed by Equation (71), and thus in the adsorption effect. However, if the OH groups of γ-Al_2O_3 are deactivated with $(CH_3)_3SiCl$, the above reaction [Eq. (71)] no longer takes place.[66] The use of a silver chloride melt as the contacting phase even allows the study of the effects of different crystallographic orientations of α-Al_2O_3 on the wetting contact angle and the calculation of interaction enthalpies and entropies.[73] It is evident from Figures 18 and 19 that at the junction between (crystalline) AgCl and γ-Al_2O_3 the concentration of silver vacancies must be increased and that of the interstitial ions reduced by the same amount. This means that at very high temperatures, at which according to Section 3.1.1 the ion transport in the bulk is determined by the Ag_i ions, the average conductivity in the boundary layer should be reduced compared with that in the bulk (depleted boundary layer, Fig. 20a). At moderate temperatures, because the boundary layer effect varies only slightly with temperature, and also because vacancy conduction becomes increasingly important as a result of impurity effects, the vacancy conduction in the boundary layer is dominant compared with the interstitial ion conduction characteristic of the bulk (inversion layer, Fig. 20b). Thus, there is a local transition from interstitial ion conduction (i) to vacancy conduction (v); this i–v transition[69] is entirely analogous to an electronic n–p transition. Finally, even in nominally pure AgCl close to room temperature the extrinsic vacancy conduction (caused by impurities with cations of higher valency) is almost always dominant; the vacancy conduction that predominates in the bulk is then further enhanced near the boundary (accumulation with respect to V'_{Ag} layer, Fig. 20c). It is shown in reference [68] that the effective conductivity due to the boundary layer (in the direction parallel to the interface) is given by Equation (72).

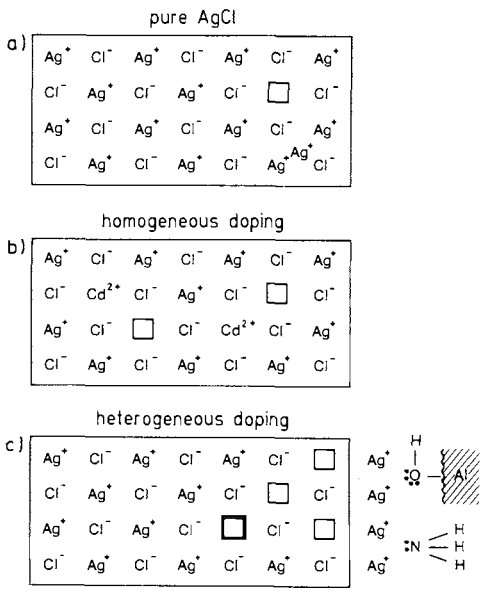

Fig. 19. Comparison of the effects of conventional (homogeneous) doping (b) (with $CdCl_2$ as the dopand), and of heterogeneous doping (c) (with Al_2O_3 or NH_3 as the active adjacent phase), when applied to pure AgCl (a).

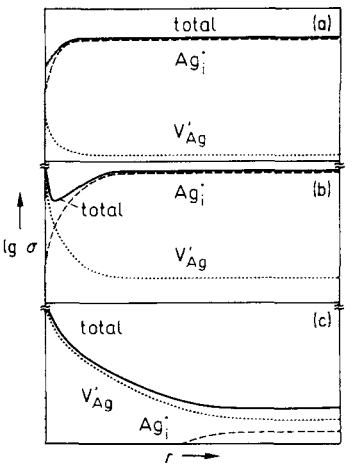

Fig. 20. Ionic conductivity σ in silver halides at the junction with Al_2O_3. At high temperatures (a) an insulating space charge zone is formed, whereas at low temperatures (c) the space charge zone has a higher conductivity than the bulk. At intermediate temperatures (b) an inversion layer is formed, which is characterized by a v–i transition (the ionic equivalent of a p–n transition).

$$\langle\sigma\rangle = \varphi_\text{L} F \sum_{\text{v},i} u_{\text{v},i} \left(2c_\infty \frac{\theta_{\text{v},i}}{1-\theta_{\text{v},i}} \right) \simeq F u_\text{v} (2\lambda)(c_0 c_\infty)^{1/2} \propto u_\text{v} c_{\text{v}0}^{1/2} \qquad (72)$$

Here φ_L is the contribution of the boundary layer to the measured volume, and is determined by the effective thickness of the boundary layer (2λ). For large effects ($|\theta| \to 1$) we obtain the simple expression on the right-hand side, which shows that the conductivity is determined by the effective thickness 2λ and the effective charge carrier concentration, given by the geometric mean of the concentrations in the bulk and in the first layer adjacent to the neighboring phase. Since λ is proportional to $c_\infty^{-1/2}$, the bulk contribution cancels out, and the conductivity is therefore a direct measure of the boundary effect. In particular it is seen that, to a good approximation, impurities do not enter into the calculation; the resulting increase in the bulk concentration, and thus

increase in the effective charge carrier concentration, is compensated by increased screening, resulting in a decreased effective thickness of the boundary layer.

Despite the large increase in charge carrier concentration, the overall effect of a single interface in typical samples is too small to be detected. Thus, measurements must be carried out using a two-phase mixture of the ionic conductor and the oxide. This is best prepared by dispersing a fine Al_2O_3 powder into the melt of an ionic conductor, for example AgCl, which is then cooled. This produces a large number of interfaces. The very small oxide particles are deposited in the AgCl grain boundaries, leading to a network of continuous conduction pathways. A moderate increase of Al_2O_3 content leads to an increase of the interfacial contact area by decreasing the AgCl grain size. It is only at very high Al_2O_3 concentrations (typically above 10%) that the conduction paths gradually become blocked by excess oxide, and the conductivity of the mixture is drastically reduced.

Figure 21 shows the results of conductivity measurements on $AgBr/Al_2O_3$ composite solid electrolytes.[71] These data

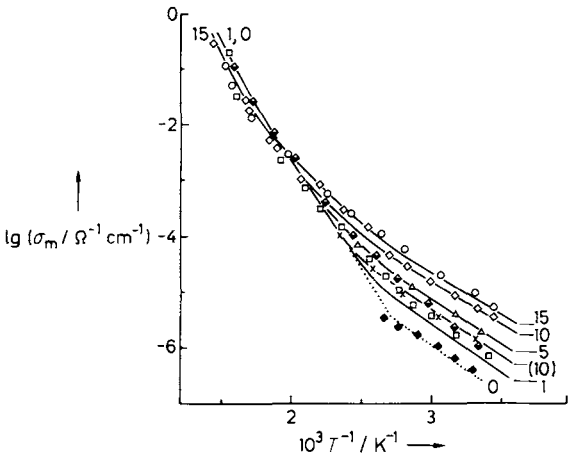

Fig. 21. Total conductivity of two-phase mixtures of AgBr with γ-Al_2O_3 as a function of temperature for various volume ratios (the numbers give the volume percentage of Al_2O_3) and different particle sizes [10: 10 vol% Al_2O_3, 0.03 μm; (10): 10 vol%, 0.05 μm]. The symbols represent experimental data and the solid lines the results of theoretical calculations [71].

indicate that the conductivity increase of one to two orders of magnitude (relative to pure AgBr) that occurs in the low temperature region has an activation energy of about 0.3 eV, a value which corresponds to the migration enthalpy of the vacancies [see Eq. (72)], and results from the fact that $c_{v0}^{1/2}$ varies only slightly with temperature.[68] As is shown by the solid curves in Figure 21, together with detailed discussions,[66, 71] the observed conductivities for the entire range of experimental conditions investigated, variation of the temperature, volume fraction, and γ-Al_2O_3 particle size) can be quantitatively described by assuming the maximum disorder in the first layer of the halide adjacent to the oxide.

A comparison with Figure 11 confirms that there is a similarity to the behavior with conventional (homogeneous) doping. As in that case, here too one has a means of influencing the concentration of defects, and here too it is controlled by the effective charge. Apart from the presence of an electric field, the most important difference from conventional doping is the absence of spatial homogeneity. For this reason insulating regions (e.g., in the moderate- or high-temperature regions for AgBr, see Fig. 20a, b) can be bypassed by using more readily conducting paths in the bulk material, and the knee observed in the case of homogeneous doping is now absent (compare Figs. 21 and 10).[75] It is legitimate to talk of „heterogeneous doping" as an alternative way of modifying the conducting properties of a given phase,[66] and this term is now becoming established in the literature. An example is discussed in reference [76] in which the simultaneous effects of homogeneous and heterogeneous doping were investigated. In an analogous way it is possible to improve the conduction properties of a whole range of similar ionic conductors with moderate defect concentrations (CuCl, CuBr, AgBr, β-AgI, etc.).[66, 72] A system of historical interest is LiI/Al_2O_3, in which such effects were first discovered.[77] Another important system is $TlCl/Al_2O_3$, in which the heterogeneous doping effect of Al_2O_3 converts an anionic conductor into a cationic conductor.[76] Furthermore, in analogy to the fundamental rule of homogeneous doping [Eq. (13)], we can state a rule of heterogeneous doping [Eq. (73)].

$$\frac{\delta(z_k c_{0k})}{\delta \Sigma} < 0 \qquad (73)$$

This expresses the fact that for a positive surface charge Σ the concentrations of all positive mobile defects in the space charge layer are reduced, whereas for a negative surface charge the concentrations of all negative defects are increased. Figure 19b, c illustrates the two basic methods for influencing the defect concentration in the example of the model substance AgCl.

Recently the electrochemical behavior of a single boundary layer of this type has been successfully investigated.[79] This study made use of the depletion effect that is expected at higher temperatures (see Fig. 20) and which can be calculated from Equation (69). The experiments were carried out using sufficiently basic, but electronically conducting, oxides, such as RuO_2 and $(La,Sr)CoO_3$, which could simultaneously serve as electrodes. By impedance spectroscopic measurements in series with the boundary layer it was possible to detect these as layers with a high resistance and, at the same time, a high capacitance (i.e. small thickness). The results showed that, in agreement with quantitative calculations,[79] the activation energy for the space charge resistance is $\Delta_f H^0/2$ and that for the boundary layer capacitance is $\Delta_f H^0/4$.

A question of fundamental interest is that of the behavior of the electronic charge carriers in these materials,[74] since we are then considering the general case of defect thermodynamics of a mixed conductor of the type M^+X^- (provided the behavior of the boundary layer is dominated by no more than two defect concentrations). As already mentioned, the n and p concentrations are expected to react to the electric field in a similar way as $Ag_g^{\bullet}$ and V'_{Ag} [see Eq. (67) and Fig. 18]. In silver halides the ionic defects predominate by several orders of magnitude. Therefore, since only the defects that determine the charge density enter into Poisson's equation, the boundary layer effect and the associated electric field are determined by the interaction of these defects with the adjacent phase. Consequently, the behavior of the electronic charge carriers is determined not by the redox

interaction of the silver halides with the adjacent phase but by the acid-base properties (interaction with the ions). Thus the electronic charge carriers in the boundary layer are under ionic control or better under acid-base control, a fact that may be of considerable importance for many semiconducting materials with high concentrations of ionic point defects (see next Section). In the case of Al_2O_3/AgCl dispersions one can predict from Equation (73) or more quantitatively from Equation (67) in the space charge zones there will be an increase in n-type conduction and a decrease in p-type conduction. Experimental studies are possible by using the Wagner–Hebb method,[80] in which one of the reversible silver electrodes that are normally used for the measurements is exchanged for a graphite electrode which blocks the Ag^+ ions. In the steady state the ion current is completely blocked, so that the minority electronic conduction can be measured and even resolved into its n and p components from the current vs. voltage curve. Furthermore, a quantitative extension of the experiment to inhomogeneous systems[74] allowed the separate measurement of the bulk and boundary layer values for all these contributions. The results agree with the theoretical predictions within the limits of experimental error. Extensive thermodynamic calculations have been carried out for AgCl as a prototype, and up to now the only example;[74] this yields a complete set of data for the defect concentrations as functions of temperature, Ag activity (or Cl_2 partial pressure), and spatial coordinates, and is thus a complete solution of the thermodynamic problem for this case.[69, 74] Figure 22 shows these important results for two of the charge carriers (V'_{Ag} as a majority charge carrier and e' as a minority charge carrier) as a function of the silver activity (or chlorine partial pressure) at a given temperature. A silver activity of 1 corresponds to the left-hand coexistence line in the phase diagram (Fig. 9) that is in contact with silver.

The extremely high defect concentrations that can be obtained by heterogeneous doping also exhibit catalytic activity, as will be described in Part II of this review.[81] Last but not least it is worth mentioning that the very high defect concentrations expected in the space charge regions may possibly lead to phase transformations immediately at the contact.[23b]

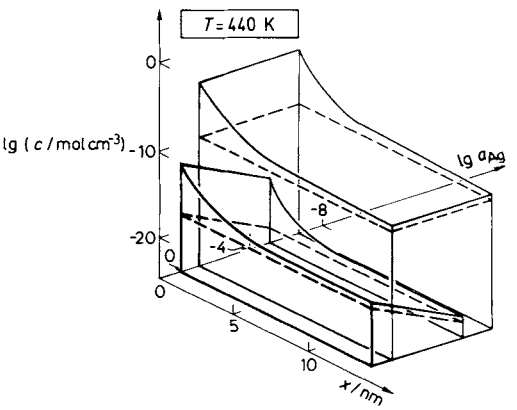

Fig. 22. Defect chemistry in the boundary layer and the bulk for pure AgCl (γ-Al_2O_3 as the adjacent phase) as a function of silver activity of 1 (i.e. exact position in the phase equilibrium). The larger graph gives the concentration of the vacancies and the smaller graph the concentration of the conduction electrons [74]. The dashed lines represent the values for the bulk.

3.2.2. *Example 2: Conductivity Anomalies in Ionic Conductor–Ionic Conductor Systems and in Ceramics*

Here we consider a junction between two ionically conducting phases, such as occurs for mixed silver halide systems in the miscibility gaps of the relevant phase diagram (e.g., β-AgI:AgBr, Fig. 23,[82] or β-AgI:AgCl[83]). In analogy to semiconductor junctions, the equilibrium at the interface results in a transfer of mobile ions from one phase to the adjacent phase, in order to achieve a constant electrochemical potential.[84] This leads to a double space charge effect, associated with an increase in vacancy conduction in one phase and an increase in interstitial ion conduction in the other phase (see Fig. 23). The situation is entirely analogous to the behavior of a semiconductor–semiconductor junction, in which the need to build up a constant Fermi level causes a transfer of electrons at the interface (Fig. 23). Evidently an

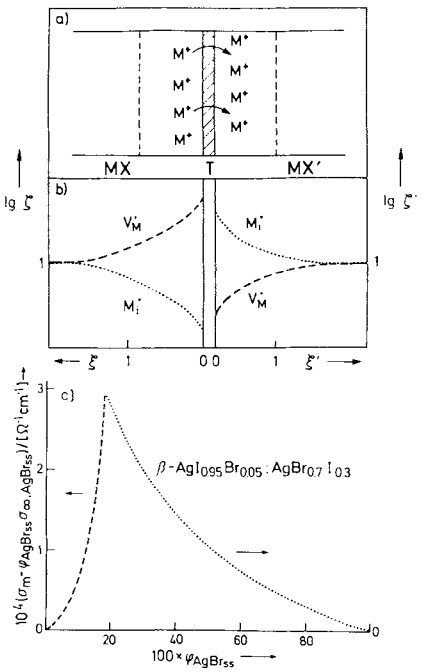

Fig. 23. Boundary effects at the junction between two ionic conductors MX and MX': a) establishment of equilibrium at the junction by redistribution of M^+ ions; b) the resulting defect distribution; c) anomalous increase in conductivity relative to the corresponding boundary phases for the AgI/AgBr system in the miscibility gap (φ = volume fraction, ζ = concentration normalized to the bulk value, ξ = spatial coordinate normalized relative to the Debye length) [66,82].

overall contact equilibrium is only possible if a constant electrochemical potential is maintained for each defect (ionic and electronic). A quantitative treatment of the thermodynamics, concentration profiles, and conductivity behavior is also possible in this case.[84] The conductivity anomalies in the miscibility gaps of the β-AgI:AgCl system can be understood quantitatively in the light of the foregoing discussion.[83] Here the free standard reaction enthalpy of the heterogeneous Frenkel reaction [Eq. (74)] plays a key role.

$$Ag_{Ag}(\text{phase 1}) + V_i(\text{phase 2}) \rightleftharpoons Ag_i^{\bullet}(\text{phase 2}) + V'_{Ag}(\text{phase 1}) \quad (74)$$

More interesting and instructive is the fact that at temperatures above the transition to the superconducting α phase (i.e. in the miscibility gap of the α-AgI/AgCl system) the conduction mechanism shows the classical percolation behavior;[79] this means that the transport of charge occurs by α-AgI_{ss} particles in contact with each other, and not as a result of boundary effects.

Another type of junction that is of fundamental importance in ceramics is the grain boundary itself, that is a contact between two grains of the same chemical composition (a homojunction, in contrast to the heterojunctions discussed above). Since the structure at the (metastable) grain boundaries differs from that of the bulk, thermodynamics requires that there should be a stabilization of cations or anions, in addition to possible electronic effects, associated with a symmetrical space charge zone (Fig. 24).[85, 86, 88] A particularly important result for ceramics is the observation that grain boundaries can act both as blockers and as efficient conductors in the same ceramic material. This is connected with their anisotropy: Owing to the sandwich-like structure of alternating core regions and space charge regions, and to the significant profile character of the space charges, there is a large difference depending on whether the movement of the ions is along the grain boundaries or perpendicular to them.[85] In polycrystalline samples, in priciple, a distinction can be made between the two types of conduction paths: on the one hand, transport through the bulk, interrupted at points where the path crosses grain junctions in a perpendicular direction, and on the other hand bypass conduction, in which the paths lie entirely within grain boundaries. In varistor materials, which are the basis of some important electronic components, the grain boundaries have a blocking function.[90] In the electronic conductor ZnO the grain boundaries determine the observed (DC) resistivity; the energy barrier, and therefore the resistivity (electronic in this case), can be conveniently altered by an externally applied voltage. In the case of SiC, which is a good electronic conductor in its monocrystalline form, the grain boundaries in an SiC ceramic material increase the resistivity to such an extent that these materials have applications as insulators. In studies of silver halides by impedance spectroscopy it was shown that both functions of the grain boundaries (highly conducting and blocking) are present simultaneously, and the reduction of these effects during sintering was monitored.[85] More interestingly, it was found that for AgCl ceramics the greatest increases in conductivity observed occurred for materials prepared from the diammonium complex of AgCl. Traces of NH_3 are adsorbed at the grain boundaries, and these evidently serve to capture Ag^+ ions, in a manner similar to the action of the OH groups in Al_2O_3 in the composite electrolyte, which leads to an enhanced vacancy conduction in the grain boundaries (see Fig. 19c).[66] This behavior is very interesting from the chemist's standpoint. The main difference in comparison with the Al_2O_3 dispersions is that the surface potential in the heterogeneous solid electrolytes has a higher absolute value and is less temperature-sensitive.

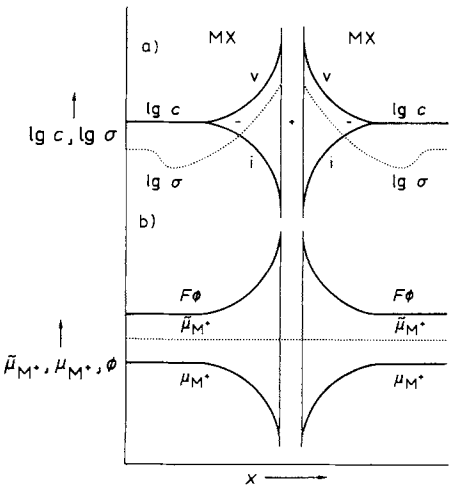

Fig. 24. Interfacial effects at a grain boundary [66]. x = spatial coordinate.

3.2.3. *Example 3: The Interface between an Electrical Conductor and a Gas*

As one might expect, a gaseous phase too not only influences the behavior within the bulk, but also has a direct effect on the space charge potential. From the above example the NH_3/AgCl interface suggests itself as a suitable system for investigation. As anticipated, it is found that under suitable conditions there is an increase in the concentration of vacancies. This effect gives rise to a new sensor principle that can be used to detect (acid–base active) gases through the change in surface conductivity (Fig. 25, bottom).[91]

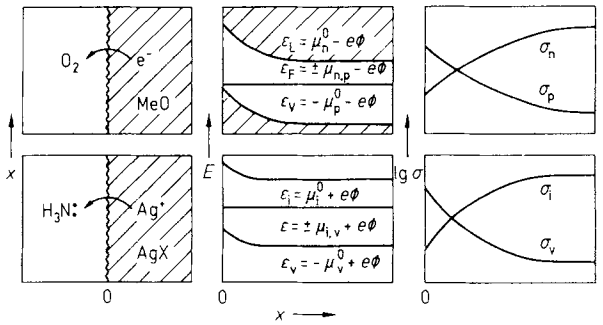

Fig. 25. Top: The interfacial influence of a redox-active gas on the electron distribution in a semiconductor. Bottom: The interfacial influence of an acid–base active gas on an ionic conductor [91]. x = spatial coordinate, E = potential.

This ionic phenomenon again has its electronic counterpart. The change in the surface electronic conductivity in SnO_2 (close to room temperature) has long been used for detecting redox-active gases. Let us first recall the example in the previous section, in which it was shown that the bulk conductivity in SnO_2 or the $SrTiO_3$ is dependent on the oxygen partial pressure. This effect can be used advantageously for measuring oxygen concentrations. Bulk conductivity sensors of this kind could eventually replace the λ-probe used currently in automobiles.[92] (Boundary layer effects are relatively insignificant at these high temperatures owing to the shortness of the Debye length.) In addition SnO_2 can be used conveniently as a gas sensor at room temperature, or better still at slightly elevated temperatures. In

this case the kinetic conditions do not allow a bulk equilibrium (see Part II of this review). On the other hand, the electronic interaction within the space charge zones is rapid enough.[93] The chemical properties of the oxygen adsorbed at the surface cause it to capture electrons, resulting in the band bending shown in the upper half of Figure 25.[67] The surface region of the SnO_2 (an n-type conductor) suffers a depletion of charge carriers, considerably reducing the surface conductivity. Figure 25 shows only the effect on the electronic charge carriers. However, within certain limits determined by the kinetics, the oxygen vacancies [see Eq. (67)] can also migrate in response to the electric field, or at least there may be some ionic charge carrier gradients that have become frozen in during the preparation of the ceramic material. This becomes especially important when the ionic point defects are the majority charge carriers, as is the case in acceptor-doped SnO_2, and usually also in nominally pure SnO_2 at low temperatures. If the interaction of the oxygen with the oxygen vacancies is a significant factor in the formation of the space charge potential, the depletion of the vacancies at the boundary may cause a complete reversal of the field relative to the direction, leading to an enrichment of only the electronic charge carriers. This is one explanation why donor-doped SnO_2 has been found to be preferable in applications as a boundary layer gas sensor.[69]

A further comment is appropriate here: As shown earlier, within the range of validity of the Brouwer approximation, the dependence of the defect concentration in the bulk material on the oxygen partial pressure can be described by a power law with an exponent $N_{k\infty}$. If the behavior in the boundary layers can be described by a power law, it cannot be assumed that the exponents will have the same values. Furthermore, it should be noted that, owing to the proportionality to $\sqrt{c_0}$, the observed boundary layer conductivity does not correspond to $N_{k\infty}$ as in the bulk, nor to N_{k0}, but to $N_{k0}/2$. This explains in a very simple way the observation that the surface conductivity for ZnO[93] follows a power law with an exponent of approximately 0.15 ± 0.03 (about 1/8), whereas N_∞ has the value 1/4.[69]

3.2.4. *Example 4: Nanosystems*

Boundary layer phenomena become very important in cases in which the dimensions are no longer large compared with the Debye length, as in very thin films and ceramics with crystallites of nanometer dimensions. In addition to the obvious reason that the boundary layers then occupy a larger fraction of the total volume, a further aspect of a more fundamental nature is involved.[94] The left-hand part of Figure 26 shows the behavior of the boundary layer as the specimen thickness is reduced. Since the value of c_0 is determined by the interaction with the adjacent phase, the defect concentration profile for nanosystems no longer corresponds to the bulk properties anywhere in the sample. This means that the specimen behaves like a single boundary layer with a single space charge zone, and the properties are determined essentially by the adjacent phase. Thus, much greater conductivity effects are expected to be found than in normal boundary layers. The problem of calculating the profiles is more complicated than before, and can only be solved by numerical

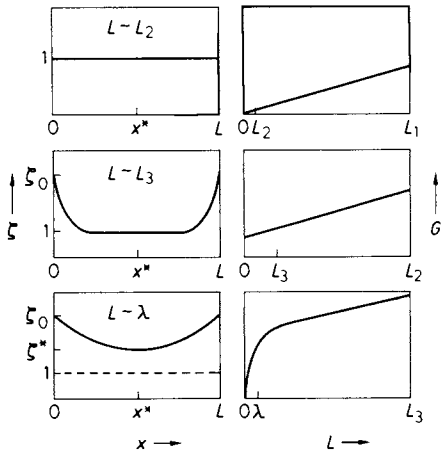

Fig. 26. Left-hand column: defect concentration distribution in thin films of different thicknesses (ζ = concentration normalized relative to the bulk value). Right-hand column: the dependence of the conductance G (parallel to the interface), on film thickness L [66].

methods.[94] The right-hand part of Figure 26 shows that for macroscopic specimens with negligible space charge effects the conductance G (the reciprocal of the resistance) increases in proportion to the thickness, whereas when the space charge effects become appreciable (while remaining independent of the thickness), they show up as a finite intercept on the conductance axis. However, as Figure 26 indicates the behavior in cases in which such size effects (mesoscopic effects) are significant is more complicated. The resulting additional increase in the conductivity (i.e. above that expected from Eq. (72)) can be calculated numerically, but exactly, by introducing a "size effect factor",[94] which in simple cases is approximately $4\,\lambda/L$; thus, for $L \simeq \lambda/2$ the additional effect is an increase by nearly an order of magnitude. There is no doubt that these phenomena can sometimes have appreciable effects even for the heterogeneous solid electrolytes discussed previously, as well as for ceramics with microcrystalline structures of nanometer dimensions. It has been shown that by applying the above relationships together with data on the dependence of the ionic and electronic conductivities on the thickness, various important thermodynamic parameters for the bulk and for the boundary layer can be determined.[94] Some surprises are also possible regarding our knowledge of structures, as illustrated by the observation that LiI layers on SiO_2 can be obtained with a hexagonal structure.[95] For systems with electronic charge carriers the reduction of the specimen dimensions leads to additional quantum-mechanical effects.[96] Apart from these phenomena, the discussion presented here leads to a unified description of ionic and electronic effects. This discussion has concentrated mainly on ionic boundary layer effects, since the corresponding electronic effects (p–n transitions, Schottky barriers) behave in an analogous way and are treated in detail in textbooks on solid-state physics.

Received: April 1, 1992 [A 896 IE]
German version: *Angew. Chem.* **1993**, *105*, 333.

[1] The chemistry of the solid state has been put on a firm scientific footing by the publications of Wagner, Schottky [2], and Frenkel [3]. Most of the basic relationships underlying the subject are reviewed in the monographs by Schmalzried [4], Schmalzried and Navrotsky [5], Hauffe [6], Kröger [7], and Rickert [8], and in special review articles such as that by Lidiard [9]. More

recent developments are described in other publications. For example in those cited in references [10–13].
[2] C. Wagner, W. Schottky, *Z. Phys. Chem. Abt. B* **1930**, *11*, 163; C. Wagner, *ibid.* **1933**, *22*, 181; W. Schottky, *ibid.* **1935**, *29*, 335; W. Schottky, *Halbleiterprobleme, Vol. 44* (Ed.: W. Schottky), Vieweg, Braunschweig, **1958**, p. 235.
[3] J. I. Frenkel, *Z. Phys.* **1926**, *35*, 652.
[4] H. Schmalzried, *Solid State Reactions*, Verlag Chemie, Weinheim, **1981**.
[5] H. Schmalzried, N. Navrotsky, *Festkörperthermodynamik*, Verlag Chemie, Weinheim, **1975**.
[6] K. Hauffe, *Reaktionen in und an festen Stoffen*, Springer, Berlin, **1986**.
[7] F. A. Kröger, *Chemistry of Imperfect Crystals*, North Holland, Amsterdam, **1964**.
[8] H. Rickert in *Electrochemistry of Solids. An Introdution*, Springer Verlag, Berlin, **1988**.
[9] A. B. Lidiard, *Handbuch der Physik, Vol. 20* (Ed.: S. Flügge), Springer, Berlin, **1957**, p. 246.
[10] *Superionic Solids and Solid Electrolytes* (Eds.: A. L. Laskar, S. Chandra), Academic Press, New York, **1989**.
[11] T. Takahashi, *High Conductivity Solid Ionic Conductors*, World Scientific Press, Singapore, **1989**.
[12] *Science and Technology of Fast Ion Conductors* (Eds.: H. L. Tuller, M. Balkanski), Plenum Press, New York, **1989**.
[13] F. Aguillo-Lopez, C. R. A. Catlow, P. D. Townsend, *Point Defects in Materials*, Academic Press, New York, **1988**.
[14] W. Schottky, *Z. Phys. Chem. Abt. B* **1935**, *29*, 335.
[15] J. Teltow, *Ann. Phys. (Leipzig)* **1950**, *5*, 63; *Z. Phys. Chem.* **1950**, *195*, 213.
[16] The analogy with water is even more complete if one considers defects in covalently bonded materials such as Si, Ge, SiC, N, C, or GaAs.
[17] J. Maier, G. Schwitzgebel, *Mater. Res. Bull.* **1982**, *17*; *ibid.* **1983**, *18*, 601; *Mater. Sci. Monogr.* **1985**, *28A*, 415.
[18] An example of an analogous case in the aqueous phase is the replacement of an OH^- ion by another anion in a precipitation reaction, for example $AlCl_3 + 3H_2O \rightleftharpoons Al(OH)_3 + 3HCl$.
[19] The structural elements notation is an exact relative notation only with regard to charge, not with regard to material.
[20] F. A. Kröger, H. J. Vink, in *Solid State Physics, Vol. 3* (Eds.: F. Seitz, D. Turnbull), Academic Press, **1956**.
[21] H. Schmalzried, *J. Phys. (Paris)* **1976**, *37*, C7.
[22] R. W. Pohl, *Proc. R. Soc. London A* **1937**, *49*, 149.
[23] a) E. Mollwo, *Nachr. Ges. Wiss. Göttingen Math. Phys. Kl. Fachgruppe* **1939**, *3*, 199; b) The defect–defect interaction can be expressed in terms of activity coefficients. This corresponds to another free enthalpy contribution in Figure 4 that can lead to a second minimum at high defect concentrations. Under certain conditions, this minimum becomes the absolute minimum. Then a transition from a low defective state into a highly disordered (superionic) state occurs (if the totally molten state is not more favorable).
[24] J. Corish, P. W. M. Junkers, *Surf. Defect Prop. Solids* **1973**, *2*, 160; J. Corish, P. W. M. Jacobs, S. Radhakrishna, *ibid.* **1977**, *6*, 218.
[25] Strictly speaking in the case of charged species, the electrochemical potential should be used to describe the equilibrium condition, as in Figure 5. However, the average electrical potential terms cancel out in cases where the reaction equations relate to (approximately) the same position. ($\kappa = 1$ in Fig. 5.)
[26] O. Madelung, *Grundlagen der Halbleiterphysik*, Springer, Berlin, **1970**, and references therein.
[27] S. Rosenberg, *J. Chem. Phys.* **1960**, *33*, 665; see also ref. [8].
[28] See for example ref. [8].
[29] The electrostatic potential term cancels out in the difference; $\Delta_R S^0$ is small.
[30] G. Brouwer, *Philips Res. Rep.* **1954**, *9*, 386.
[31] J. Maier in *Superionic Solid and Solid Electrolytes, Recent Trends* (Eds.: A. L. Laskar, S. Chandra) Academic Press, New York, **1989**, p. 137.
[32] Also in this case the probability can be calculated from: (number of positions for lines or planes) over (number of lines or planes present). In a cube with n atoms along each edge the number of possible planes in any given direction is $n^{1/3}$. If the value of g^o for one such defect plane containing $n^{2/3}$ individual defects is estimated to be $n^{2/3}g^0_{def}$, we obtain an extremely small equilibrium probability (per particle), given by $\hat{c}^{n^{2/3}}/n^{2/3}$, where $\hat{c}$ is the equilibrium fraction of point defects whose free enthalpy of formation would be g^0_{def}.
[33] In contrast to this, the surface areas of phases are determined by the limited mass. However, here too the equilibrium morphology, as specified by the Wulff conditions, is usually not estblished (see for example C. Herring, *Phys. Rev.* **1951**, *82*, 87).
[34] The electrical neutrality condition is a consequence of electrostatics for the special case of the interior of an extended homogeneous body (in general Poisson's equation applies, see Section 3.2).
[35] G. Schwitzgebel, J. Maier, U. Wicke, H. Schmitt, *Z. Phys. Chem. (Wiesbaden)* **1982**, *130*, 97.
[36] J. Mizusaki, K. Fueki, *Solid State Ionics* **1982**, *6*, 55.
[37] Chlorine partial pressures of more than 1 bar increase the total hydrostatic pressure, whereas lower pressures can be obtained with a total pressure of 1 bar by using mixtures such as chlorine plus argon.
[38] J. Corish, P. W. M. Jacobs, *J. Phys. Chem. Solids* **1972**, *33*, 1799.
[39] In the case of α–AgI, [23b] in which all the Ag^+ ions can be regarded as disordered, the enthalpy of formation term $\Delta_R H^0$ is negligible, and only the (small) migration energy is significant. At lower temperatures this modification is unstable and it becomes converted to the "normal" β phase.
[40] The usual dopant levels of around 10% are well above the regime of low defect concentrations, and interactions between the defects play an important role [9].
[41] If we consider the partial pressure of water vapor in a typical atmosphere, it is seen that an appreciable H_2 partial pressure of 1 atm corresponds to an extremely small oxygen partial pressure, given by $P_{O_2} = K^{-1}P_{H_2}^{-2}P_{H_2O}^2$ (where K is the equilibrium constant for the formation of H_2O).
[42] B. C. H. Steele, P. H. Middleton, R. A. Rudkin, *Solid State Ionics* **1990**, *40/41*, 388.
[43] J. Maier, W. Göpel, *J. Solid State Chem.* **1988**, *72*, 293; W. Göpel, J. Maier, K. Schierbaum, H. D. Wiemhöfer, *Solid State Ionics* **1989**, *32/33*, 440.
[44] C. G. Fonstadt, R. H. Rediker, *J. Appl. Phys.* **1971**, *42*, 2911.
[45] An alternative possibility in principle would be Sn ions in the interstitial lattice, but this is refuted by density measurements, and is also inconsistent with the observed slopes of the isotherms. The Schottky equilibrium only becomes important at very high temperatures.
[46] The occupation of singly charged oxygen vacancies by oxygen would also explain the slope of 1/4 at lower temperatures, but would result in a critical isotherm of a completely different shape [43].
[47] For kinetic reasons the main electron source or sink at low temperatures is no longer the interaction with the gas phase, but is instead the transfer of electrons to or from the vacant sites, as in Equation (50). However, the gas phase still has an effect on the boundary regions, as discussed later (Section 3.2.3).
[48] The transition from n-type to p-type conduction occurs near the composition corresponding to O_6. It is therefore appropriate (except in very complex situations) to choose this composition as the reference point. Thus, any additional oxygen is regarded as being in the interstitial lattice. If ionized, it is compensated by holes. The choice of O_7 for the reference composition leads to an inconsistency, since a lower oxygen content would then correspond to vacancies ($V_O^{\cdot\cdot}$, $V_O^{\cdot}$, $V_O^{\times}$), which would be compensated by conduction electrons. This would then lead (assuming comparable mobilities) to n-type conduction, rather than the p-type conduction that is observed (n and p mobilities are comparable).
[49] K. A. Müller, J. D. Bednorz, *Science* **1987**, *237*, 1133.
[50] J. Maier, G. Pfundtner, H. L. Tuller, E. J. Opila, B. J. Wuensch, *Mater. Sci. Monogr.* **1991**, *70*, 423; J. Maier, G. Pfundtner, *Adv. Mater.* **1991**, *3*, 292.
[51] M. J. Tsai, E. J. Opila, H. L. Tuller in *High Temperature Superconductors Fundamental Properties and Novel Material Processing* (Eds.: D. Christen, L. Schneemeyer), Mater. Res. Soc., Pittsburgh, PA, USA, **1987**, p. 65.
[52] C. Chaillout, S. W. Cheong, Z. Fisk, M. S. Lehmann, M. Marezio, B. Morio, J. E. Schirber, *Physica C: (Amsterdam)* **1989**, *158*, 183; C. Chaillout, S. W. Cheong, Z. Fisk, M. S. Lehmann, M. Marezio, B. Morosin, J. E. Schirber, *Phys. Scr.* **1989**, *129*, 97.
[53] a) J. Maier, P. Murugaraj, G. Pfundtner, W. Sitte, *Ber. Bunsenges. Phys. Chem.* **1989**, *93*, 1350; b) J. Maier, P. Murugaraj, G. Pfundtner, *Solid State Ionics* **1990**, *40/41*, 802.
[54] J. C. Phillips, *Physics of High T_c Superconductors*, Academic Press, New York, **1989**.
[55] Y. D. Tretyakov, I. E. Graboy, *Proc. Int. Conf. Supercond.* Bangalore, **1990**, 121.
[56] G. M. Choi, H. L. Tuller, M. J. Tsai, *Nato ASI Ser.* **1989**, *276*, 451.
[57] The formation of Cooper pairs also amounts to a (phonon-assisted) association of the form $2h^{\cdot} \rightleftharpoons h_2^{\cdot\cdot}$.
[58] G. M. Choi, H. L. Tuller, *J. Am. Ceram. Soc.* **1988**, *71*, 201.
[59] T. Bieger, J. Maier, R. Waser, *Solid State Ionics*, in press; T. Bieger, J. Maier, R. Waser, *Sens. Actuators* **1991**, *7*, 763.
[60] The agreement between the optical and electrical methods does not necessarily prove that direct semiconduction occurs (with a constant wavenumber vector), since indirect transitions in the immediate neighborhood are possible. In connection with the band gap in $SrTiO_3$, see also M. Cardona, *Phys. Rev.* **1965**, *140*, A651.
[61] The incorporation of H_2O into ZrO_2 was previously reported by C. Wagner (*Ber. Bunsenges. Phys. Chem.* **1966**, *70*, 781).
[62] R. Waser, *Ber. Bunsenges. Phys. Chem.* **1986**, *90*, 1223; A. S. Nowick, Columbia University, New York, personal communication.
[63] P. Rudolf, W. Paulus, R. Schöllhorn, *Adv. Mater.* **1991**, *3*, 438.
[64] a) H. Iwahara, T. Esuka, H. Uchida, N. Maeda, *Solid State Ionics* **1981**, *3/4*, 359; b) K. D. Kreuer, E. Schönherr, J. Maier, unpublished.
[65] J. Maier, *Mater. Chem. Phys.* **1987**, *17*, 485; J. Maier in *Science and Technology of Fast Ion Conductors*, (Ed.: H. L. Tuller), Plenum Press, New York, **1988**, p. 345.
[66] J. Maier in *Recent Trends in Superionic Solids and Solid Electrolytes* (Eds.: S. Chandra, A. Laskar), Academic Press, New York, **1989**, p. 137.
[67] It should be noted that a) the band bending means a change in the electrical potential (μ^0 is constant), and b) as a consequence of Equation (21) the distance from the Fermi level gives the corresponding charge carrier concentration.

[68] J. Maier, *J. Phys. Chem. Solids* **1985**, *46*, 309; *Ber. Bunsenges. Phys. Chem.* **1984**, *88*, 1057.
[69] J. Maier, *J. Electrochem. Soc.* **1987**, *134*, 1524; *Solid State Ionics* **1989**, *32/33*, 727. A simplified treatment is given in [70], but this does not properly take into account the spatial structure of the double layer.
[70] K. L. Kliewer, J. S. Köhler, *Phys. Rev. A* **1965**, *140*, 1226.
[71] J. Maier, *Mater. Res. Bull.* **1985**, *20*, 383.
[72] J. B. Wagner, in *High Conductivity Solid Conductors* (Ed.: T. Takahashi), World Scientific, Singapore, *1989*.
[73] U. Riedel, J. Maier, R. J. Brook, *Proc. CIMTEC 90*, Elsevier, Amsterdam, **1991**, 691; *J. Eur. Ceram. Soc.* **1992**, *9*, 205.
[74] J. Maier, *Ber. Bunsenges. Phys. Chem.* **1989**, *93*, 1468; *ibid.* **1989**, *93*, 1474.
[75] In cases where blocking by boundary layers occurs, its effects can often be determined separately by impedance spectroscopy or time-resolved direct current measurements.
[76] J. Maier, B. Reichert, *Ber. Bunsenges. Phys. Chem.* **1986**, *90*, 666.
[77] C. C. Liang, *J. Electrochem. Soc.* **1973**, *120*, 1289.
[78] J. B. Wagner, *Mater. Res. Bull.* **1980**, *15*, 1691.
[79] U. Lauer, J. Maier, *Solid State Ionics*, in press; *J. Electrochem. Soc.* **1992**, *139*(5), 1472.
[80] C. Wagner in *Proc. 7th Meet. Int. Comm. Electrochem. Thermodyn. Kin.* (Lindau (1955)), Butterworth, London, **1957**.
[81] J. Maier, P. Murugaraj, *Solid. State Ionics* **1990**, *40/41*, 1017, *ibid.* **1989**, *32/33*, 993.
[82] J. B. Wagner, *Mater. Res. Bull.* **1980**, *15*, 1691.
[83] U. Lauer, J. Maier, *Solid State Ionics* **1992**, *51*, 209; *Ber. Bunsenges. Phys. Chem.* **1992**, *96*, 111.
[84] J. Maier, *Ber. Bunsenges. Phys. Chem.* **1985**, *89*, 355.
[85] J. Maier, *Ber. Bunsenges. Phys. Chem.* **1986**, *90*, 26; J. Maier, S. Prill, B. Reichert, *Solid State Ionics* **1988**, *28*, 1465.
[86] Analogous electronic phenomena are treated thoroughly in publications on semiconductor junctions, see for example [87].
[87] H. J. Queisser, J. H. Werner, *Mater. Res. Soc. Symp. Proc.* **1988**, 53; *Polycrystalline Semiconductors* (Eds.: H. J. Möller, H. P. Strunk, J. Werner), Springer, Berlin, **1989**.
[88] Segregation of ions at grain boundaries plays an important role in sintering behavior. However, the literature is inconclusive on this point, see for example ref. [89].
[89] S. B. Desu, D. A. Payne, *J. Am. Ceram. Soc.* **1990**, *73*, 3391.
[90] F. Greuter, G. Blatter, M. Rossinelli, F. Stucki, *Adv. Varistor Tech., Ceram. Trans. Vol. 3*, The American Ceramic Soc., Westerville, **1989**.
[91] J. Maier, U. Lauer, W. Göpel, *Solid State Ionics* **1990**, *40/41*, 463.
[92] Ch. Tragut, K. H. Härdtl, *Sen. Actuators* **1991**, *B4*, 425.
[93] See for instance: W. Göpel, *Progr. Surf. Sci.* **1986**, *20*, 6447.
[94] J. Maier, *Solid State Ionics* **1987**, *23*, 59; *Phys. Status Solidi A* **1989**, *112*, 115; see also ref. [85]. The functional relationship can only be expressed in implicit form, as explained in these publications.
[95] B. Wassermann, T. P. Martin, J. Maier, *Solid State Ionics* **1988**, *28–30*, 1514.
[96] G. H. Döhler, *Spektrum Wiss.* **1984**, *7*, 32; K. von Klitzing, *Festkörperprobleme* **1990**, *30*, 25.
[97] J. Maier, *Angew. Chem.* **1993**, *105*, no. 4; *Angew. Chem. Int. Ed. Engl.* **1993**, *32*, no. 4.

Carbohydrates as Chiral Auxiliaries in Stereoselective Synthesis

New Synthetic Methods (90)

By Horst Kunz* and Karola Rück

Carbohydrates are inexpensive natural products in which numerous functional groups and stereogenic centers are combined in one molecule. By directed regio- and stereoselective formation of derivatives they can be converted into efficient chiral auxiliaries for controlling asymmetric syntheses. Stereoelectronic effects and pre-orientation of the reactive and shielding groups through formation of complexes can often be used for effective diastereofacial differentiation. In aldol reactions and alkylations on carbohydrate ester enolates intramolecular complexation promotes simultaneous elimination with formation of ketene. The steric, stereoelectronic, and coordinating properties of carbohydrate templates can also be used selectively to attain high levels of asymmetric induction in processes such as Diels–Alder reactions, hetero-Diels–Alder reactions, [2 + 2] cycloadditions, cyclopropanations, and Michael additions. It was possible with bicyclic, strongly stereodifferentiating carbohydrate auxiliaries to achieve a diastereoselective synthesis of carboxylic acid derivatives branched in the β position by a new 1,4-addition of alkylaluminum halides to α,β-unsaturated *N*-acylurethanes, in which methylaluminum halides and higher alkyl- or arylaluminum compounds behave mechanistically in a strikingly different manners. As complex ligands in chiral reagents and promoters, carbohydrates allow highly stereoselective reductions and aldol reactions that lead, amongst others, to chiral alcohols and β-hydroxy-α-amino acids in excellent enantiomeric excesses. Glycosylamines offer the possibility of versatile stereoselective applications: in the presence of Lewis acids the corresponding aldimines permit high-yielding syntheses of enantiomerically pure α-amino acids by Strecker and Ugi reactions, controlled by steric and stereoelectronic effects and by complex formation. They can be used with equal efficiency for asymmetric syntheses of chiral homoallylamines and for asymmetric Mannich syntheses of β-amino acids and chiral heterocycles, for example alkaloids.

1. Carbohydrates in Natural Selection Processes

Carbohydrates are widespread chiral natural products. Many are produced continuously in considerable quantity in nature, for example in sugar cane, sugar beets, and trees, and in chitin. They are cheap and frequently easy to obtain in the pure form. As a result of these useful qualities, carbohydrates have been transformed into diverse, interesting chiral products in ex-chiral pool syntheses. However, carbohydrates were not used for a long time as chiral auxiliaries in stereoselective syntheses. For this purpose they were regarded as too complex, constructed of too many chiral centers, and with too many functional groups. The chiral information they contain could not be exploited in stereodifferentiating selection processes in an organized and surveyable fashion. In addition, carbohydrates long had the reputation of fulfilling more general, less selective roles in biological processes. In analogy to the main representatives of the polysaccharides, starch and cellulose, they were regarded largely as biological stores of energy and as skeletal components. Only during the last two decades has it been increasingly recognized that the carbohydrate portions of glycoconjugates play a decisive role in processes of biological selection – in particular those pertaining to biological recognition on membranes.[1] Selective interactions of carbohydrates with receptors regulate, for example, the uptake of serum proteins into cells[2] and the intracellular transport of enzymes;[3] they are of decisive importance for infection[4] and numerous immunological processes,[5] cell adhesion,[6a] and the regulation of cell growth.[6b] These highly interesting findings from research in cell biology, immunology, and biochemistry have strongly stimulated chemists' interest in glycoconjugates. These results have made researchers aware that carbohydrates contain a considerable amount of regio- and stereochemical information,[7] which nature employs in diverse selection and directed distribution processes in multicellular organisms. Apparently, it is not just chirality or the functional groups capable of forming hydrogen bonds that are responsible for this selection potential. Lemieux has pointed out the amphiphilic character of those monosaccharides frequently involved in recognition processes, D-galactose **1**, D-galactosamine **2**, and L-fucose **3**.[8]

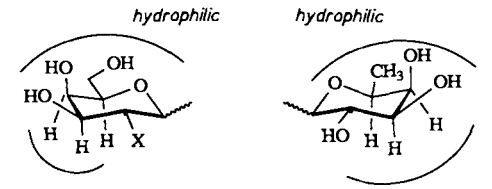

1: X = OH
2: X = NHAc

3

It is obvious that saccharide structures with peripheral galactose, galactosamine, and/or fucose units can undergo not only polar but also hydrophobic interactions. In consideration of biological selection processes of this type it may be

[*] Prof. Dr. H. Kunz, Dr. D. K. Rück
Institut für Organische Chemie der Universität
Johann-Joachim-Becher-Weg 18–20
D-W-6500 Mainz (FRG)

more appropriate, in view of the high pressure under which organic molecules exist in a biological, aqueous environment, to speak of the ability to minimize the hydrophobic volume instead of simply the hydrophobic interaction. In this context saccharides **1**–**3**, in which the arrangement of the hydrophobic and hydrophilic groups divides the molecules into sections, fit much better into a hydrophobic receptor counterpart than, for example, glucose or mannose.

This faculty for recognition displayed by oligosaccharides in glycoconjugates, further magnified by formation of antenna- or clusterlike accumulations, has induced considerable interest in the synthesis of glycoconjugates, which are of enormous importance for immunology, infection processes, and the development of directed pharmaceuticals that are more stable toward proteases. They have also stimulated our efforts in the synthesis of glycopeptides.[9] In these syntheses of *O*-glycosylserine- and -threonine-glycopeptides, a major problem is the facile β-elimination of the carbohydrate portion, for example when the protecting groups are removed.[10] The explanation of this reaction directs attention to a further property of carbohydrates that in addition to chirality and polyfunctionality is also of interest for stereoselective processes: their ability to form complexes. According to recent findings, the complex-forming ability of carbohydrates is also important for processes of biological recognition, for example, in the interaction of the calcium-dependent carbohydrate-recognizing domains of mammalian lectines with saccharides.[11]

2. Carbohydrates—Chiral Matrices Able to Form Complexes

The β-elimination of carbohydrates derived from *O*-glycosylserine and -threonine derivatives takes place even under mildly basic conditions, as shown by the example of glucosaminylthreonine ester **4**.[12] Seen from the viewpoint of peptide chemistry, this smooth, base-catalyzed elimination, long known in carbohydrate chemistry,[13] is surprising.

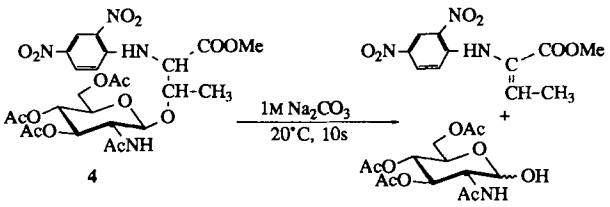

Usually serine and threonine esters protected in the side chain as benzyl or *tert*-butyl ethers can be saponified under much more forcing conditions without β-elimination. The reaction of *O*-benzylthreonine benzyl ester **5** underlines this difference.[14]

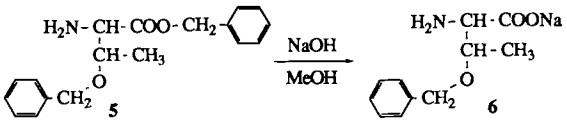

Confronted with these contradictory experiences from carbohydrate and peptide chemistry, we explained the greater tendency of carbohydrates of *O*-glycosylserine and -threonine derivatives to undergo elimination by the complex-forming properties that carbohydrates can display towards cations.[9]

Complexation of the cation in **7** increases the ability of the carbohydrate to function as a leaving group, because the

Karola Rück was born in 1963 in Hargesheim near Bad Kreuznach (Rhineland-Palatinate). She started her chemistry studies in 1983 at the University of Mainz and received her Ph.D. in 1992 for her work with Horst Kunz on stereoselective reactions of organoaluminum compounds. In 1989 she received the Adolf-Todt-Preis of the University of Mainz and a doctoral stipend from the Fonds der Chemischen Industrie. Since October 1992 she has been working with Steven Ley at the University of Cambridge in Great Britain as a postdoctoral fellow supported by the Deutscher Akademischer Austauschdienst.

Horst Kunz was born in 1940 in Frankenhausen near Zwickau (Saxony). He studied chemistry at the Humboldt University in (formerly East) Berlin and at the University of Mainz. He received his Ph.D. in 1969 for his work with Leopold Horner on the synthesis of organophosphorus compounds. He acquired his "Habilitation" in 1977 for his work on ester analogues of acetylcholine and their application in protecting group chemistry. He was appointed Associate Professor for Organic Chemistry in 1979 at the University of Mainz and was promoted to Full Professor for Bioorganic Chemistry in 1988. His research centers on stereoselective synthesis, methods in peptide and carbohydrate chemistry, and the synthesis, elaboration, and development of glycopeptides, for which he recieved the Max-Bergmann-Medaille in 1992.

developing charge is neutralized. This complex-forming ability of carbohydrates is also reflected in the considerably higher rate of saponification of carbohydrate esters compared with that of analogous alkyl esters.[15] By complexation carbohydrate esters gain the properties of active esters to a certain extent, which could be developed into a new process for the synthesis of peptides.[16] It should be noted that anomeric selection effects in glycoside synthesis by alkylation of carbohydrates not protected at the anomeric position could also be explained by complexation.[17]

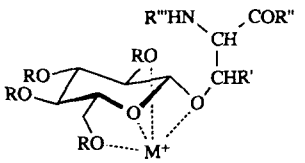

7

For us the explanation of the rapid β-elimination of the carbohydrate component of glycosylserine and -threonine derivatives by formation of complex **7** was the starting point for the development of a concept, according to which inexpensive carbohydrates can be employed in stereoselective syntheses as chiral matrices organized by complexation.[18] This is even more promising, as a diverse spectrum of methods is now available for the regioselective modification of the functional groups and the stereochemistry of carbohydrates.

At this point some studies had already appeared in which carbohydrate components were used for stereodifferentiation.[19] The early experiments of Landor et al.[20] are representative: lithium alkoxyaluminum hydrides were prepared from $LiAlH_4$ and used as enantioselective reducing agents. This strategy was employed for the stereoselective reduction of propiophenone to 1-phenylpropanol by means of reagent **8**, which was prepared from 3-*O*-alkyl-1,2-*O*-cyclohexylidene-α-D-glucofuranose. Whereas the 3-*O*-methyl (**8a**) and 3-*O*-ethyl (**8b**) derivatives showed little induction, the 3-*O*-benzyl derivative **8c** gave an enantioselectivity of 79:21 in favor of the (*S*) alcohol.

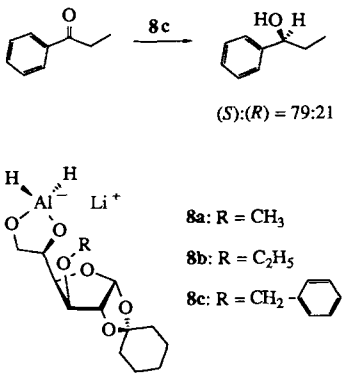

Although the role of the carbohydrate ligands was difficult to explain in most cases, very interesting effects could be observed. For example, addition of one equivalent of ethanol to **8c** gave a less reactive, apparently monohydrido complex that reacted with propiophenone with reversal of the direction of selectivity to give the (*R*) alcohol [(*R*):(*S*) = 73:27].

Other individual examples of the use of carbohydrates for stereoselection involve, for example, aldol reactions, cycloadditions, and 1,2- and 1,4-additions of Grignard reagents and will be discussed in the following sections. Nevertheless, it should be mentioned here that in 1,3-dipolar cycloadditions of *N*-(α-mannofuranosyl)nitrones, for example, considerable stereoselectivity was observed without the addition of complex-forming reagents.[21] An influence of the carbohydrate complexation on aldol reactions and related processes must certainly be assumed; consequently, these will be discussed first.

3. Stereoselective Reactions of Carbohydrate Ester Enolates

In order to keep this review a reasonable length, the scope must be restricted to stereoselective reactions in which the carbohydrate serves as a chiral auxiliary removed at the end of the process. The extensive investigations in which carbohydrates have been used in ex-chiral pool syntheses[22]—2,3-*O*-isopropylideneglyceraldehyde alone has been applied on countless occasions in this regard[23–25]—cannot be treated here. As early as 1981 Heathcock et al.[26] investigated enolates of carbohydrates both in chiral pool syntheses and also in auxiliary-supported stereoselective reactions. The lithium enolate of ketone **9** (prepared from D-fructopyranose) reacted with benzaldehyde in the first sense (i.e. ex-chiral pool) to give the diastereomeric aldols **10** with high, simple diastereoselectivity but modest asymmetric induction (Scheme 1). This example is the best of a whole series of analogous cases.

The same enolate reacted with (*S*)-*O*-isopropylideneglyceraldehyde (**11**) with double diastereodifferentiation to give aldol **12**, which was formed with high selectivity as one of the two *syn* diastereoisomers (presumably 2*R*,3*R*). In contrast, the analogous reaction with the (*R*) glyceraldehyde gave three diastereomers in the ratio 5.5:2.5:1. In other examples,

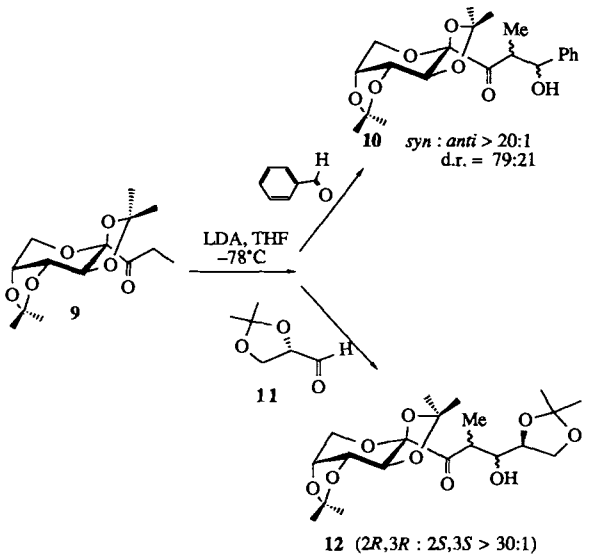

Scheme 1. LDA = Lithium diisopropylamide.

as already seen in the reaction of benzaldehyde, even less stereodifferentiation was observed. All in all, the results of Heathcock et al.[26] provide an interesting picture, but one that is nevertheless complicated and difficult to interpret and tends to confirm the preconceived view expressed earlier that carbohydrates are too chiral and too polyfunctional for directed stereoselection. This impression is reinforced by the results obtained in the same work on ester enolates with carbohydrates as removable auxiliaries, as shown by the example of propionate **13** derived from D-fructopyranose.[26] Apart from a small *anti*/*syn* preference, practically no diastereodifferentiation was found with the enolate, and a mixture of all four diastereomeric aldol adducts **14** resulted.

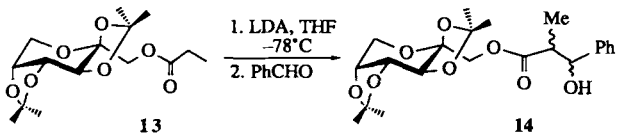

13 **14**
syn (17+10) : *anti* (37+36) = 27 : 73

In another early example of the use of carbohydrates as chiral auxiliaries Brandänge et al.[27] subjected the 3-*O*-acetate of diacetoneglucose (**15**) to aldol reactions under various conditions. The highest diastereoselectivity was obtained by deprotonation of **15** with lithium *N*-isopropyl-(−)-menthylamide (Li-IMA) and reaction with acetophenone as the prochiral partner.

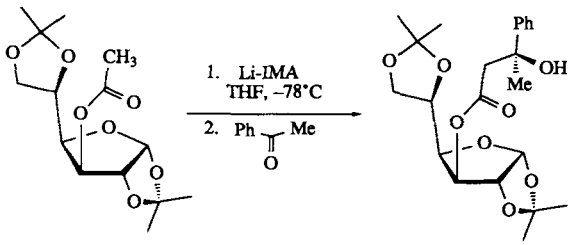

15 **16** (3*S* : 3*R* = 3:1)

The influence of the complexation of Li^+ in these processes is evident, since addition of magnesium chloride to the enolate of **15** (generated with LDA) with acetophenone favored the (*R*) diastereomer of **16** with lower selectivity. In contrast, an analogous Reformatsky reaction starting from the bromoacetic acid ester corresponding to **15** (with zinc in refluxing THF) gave predominantly the (*S*) diastereomer **16**.

The complex-forming ability of the carbohydrate auxiliary strongly affects the alkylation of the prochiral ester enolate of 3-*O*-propionyl diacetone glucose **17**. Reaction of the enolate **18** (formed with LDA) with ethyl iodide at −70 °C gave 2-methylbutyrate **19** with low selectivity and yield. In addition, an O-alkylation product and **20**, surprisingly the product of an apparent ester condensation, were formed.[28] Closer investigation of the unexpected reaction revealed that enolate **18** starts to decompose reversibly into ketene and carbohydrate alkoxide even at −70 °C, a reaction that is otherwise only observed with ester enolates at considerably higher temperatures.[29] With this behavior the carbohydrate once again shows its ability to form intramolecular complexes, which increases its tendency to function as a leaving group. The ketene formed reacts with the intact enolate **18** to give the condensation product **20**. As a consequence of the reversibility of the enolate decomposition, **18** exists as a mixture of *E*/*Z* isomers, which was demonstrated by NOE measurements on the corresponding silylketene acetals. The slow alkylation of enolate **18** at −70 °C and the competing isomerization of **18** by the reversible decomposition account for the low stereoselectivity observed.

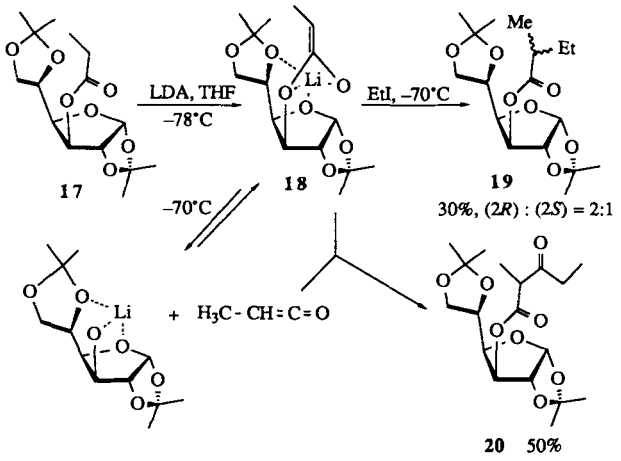

17 **18** **19**
30%, (2*R*) : (2*S*) = 2:1
20 50%

In contrast to enolate **18**, the enolates of esters of 3-epimeric 1,2;5,6-di-*O*-isopropylidene-α-D-allofuranose (**21**) are considerably more reactive.[28] Deprotonation at −90 °C led to (*Z*) enolates **22** (proven by silylketene acetals), which reacted with methyl iodide even at −95 °C to give the chiral α-methylcarboxylic acid esters **23**. At such a low temperature formation of ketene was not observed. In comparison with that of **18** both the yield and the stereoselectivity of the alkylation of **22** are considerably higher. High yields and stereoselectivities were found in particular with bulky substituents R. The different reactivity and selectivity of carbohydrate ester enolates like **18** and **22** indicate not only the complex-forming effect of the carbohydrate function, but also the steering influence of the lithium ion during attack of the electrophile.[28]

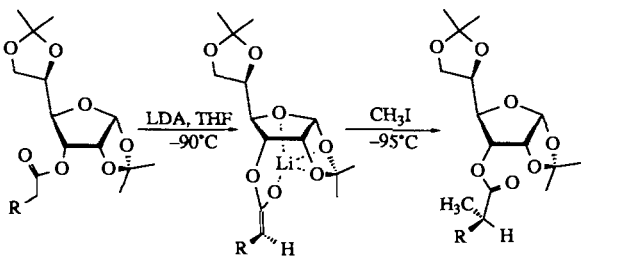

21 **22**
23a: R = Et, 65%, (*R*):(*S*)=82:18
23b: R = *t*Bu, quant., (*R*):(*S*)=91:9

Intramolecular complexation that does not promote decomposition into ketene and an alcohol might exist in enolates that are formed by deprotonation of Schiff bases **24**, themselves prepared from protected galactodialdehyde and

Table 1. D-Galactodialdehyde as a chiral auxiliary in the stereoselective synthesis of methyl esters of α-alkylamino acids [30].

Amino acid residue R	R'-I	Yield (**25**)	*de*
$CH(CH_3)_2$	$CH_2C_6H_5$	91%	80
$CH(CH_3)_2$	$CH_2CH{=}CH_2$	91%	>95
$CH_2CH(CH_3)_2$	$CH_2C_6H_5$	93%	75

amino acid esters (Table 1).[30] For these reactions the configuration of the enolate formed was not given, however.[31] Moreover, the ratios of the diastereomers of the alkylation products **25** could not be determined directly, but were obtained by ^{1}H NMR measurements in the presence of chiral shift reagents after hydrolysis to give the free amino acids. Interpretation of the results regarding the complexation and the stereodifferentiating factors was therefore not possible.

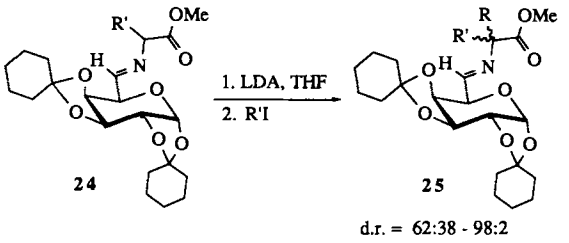

On the other hand, for the alkylation of ester enolates of branched carbohydrate carboxylic acids, which belong, strictly speaking, to ex-chiral pool syntheses, a transfer of chirality was postulated that is not effected by chelation.[32] Following the principles of stereoselective enolate formation,[33] ester **26** (obtained from the corresponding 3-ulose by Horner olefination and subsequent hydrogenation) reacted with LDA/THF to give the (*Z*) enolate (*Z*)-**27** (*Z*/*E* = 97:3) and with LDA/hexamethylphosphoric triamide (HMPA)/THF to give predominantly the (*E*) enolate (*E*)-**27** (*Z*/*E* = 15:85).

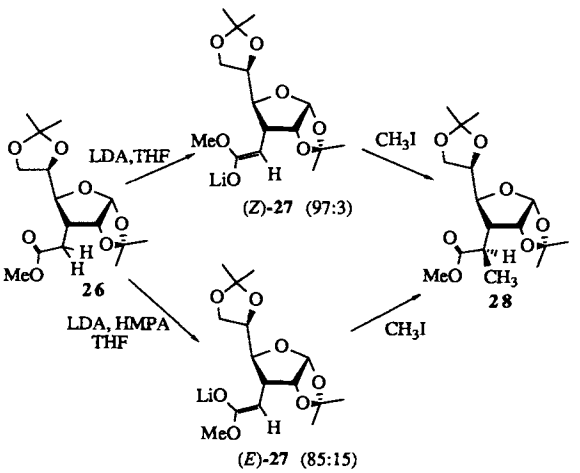

Both enolates reacted selectively with methyl iodide to give the (*R*)-α-methyl derivative **28**. From this and the even higher induction observed in alkylation of analogous ester enolates containing 5-deoxy- or 2,5-dideoxyfuranose structures, the authors[32] concluded that chelate formation with the carbohydrate functions cannot be responsible for the stereoselectivity in these reactions. As the intramolecular complexation of Li^+ in the (*Z*) enolate (*Z*)-**27** is sterically unfavorable, this enolate should form aggregates. Complexation with the ring oxygen atom in (*E*)-**27** cannot be ruled out, so that the alkylations of (*Z*)-**27** and (*E*)-**27**, which lead to product **28** with high selectivity, could have a different cause in each case. In the reaction of (*E*)-**27** chelate control could exist, whereas in the reaction of the other enolate this is clearly not the case. Intramolecular complexation of these enolates at least does not promote decomposition into ketene and alcohol.

The intramolecular chelation and formation of ketene characteristic of O-bound carbohydrate ester enolates considerably limit the range of application of carbohydrates as removable auxiliaries in the reactions of enolates. As a result, asymmetric reactions of enolates with carbohydrates as auxiliaries can compete only in isolated cases with the well-known, very successful concepts for asymmetric syntheses based on ester and amide enolates.[34]

This limitation is not, however, valid for silyl derivatives of carbohydrate ester enolates attached to diacetone glucose,[35] as shown by recent results in the synthesis of α-chlorocarboxylic acid esters **30** from silylketene acetals **29**.

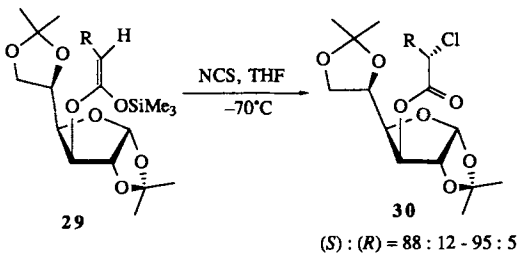

The sterically more favorable frontal attack of *N*-chlorosuccinimide (NCS) on **29** effected the preferential formation of the (*S*) diastereomer of 2-chlorocarboxylic acid ester **30** with notable stereoselectivity.

4. Cycloadditions

Cycloadditions in which the carbohydrate unit itself acts as the cycloaddition component will not be treated here, although such ex-chiral pool transformations can lead to interesting products.[36–38] However, the role of the carbohydrate in de novo disaccharide syntheses from 1-butadiene ethers of monosaccharides such as **31** and reactive carbonyl

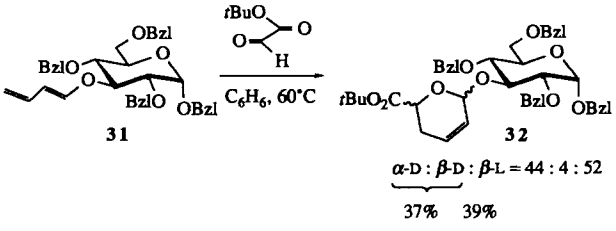

compounds such as esters of glyoxylic acid[39] could also be regarded as that of an auxiliary.

In spite of the elevated reaction temperature the carbohydrate-bound diene component **31** reacted with high diastereofacial differentiation (96:4), although with only a low *endo*/*exo* selectivity, to give a mixture of epimeric and anomeric disaccharides **32**. The diastereomeric ratios were determined by chromatographic separation (sometimes after chemical transformation). 2,3,4-Trideoxy-L-glycerohexopyranoses could be obtained from the β-L diastereomers of **32** by reduction of the ester with lithium aluminum hydride, hydrogenation of the double bond, and subsequent acidic hydrolysis. The product contains no carbon atoms from the carbohydrate auxiliary employed.[39]

4.1. Diels–Alder Reactions

As in the reaction described above with a heterodienophile, carbohydrate-bound dienes have also been used successfully in asymmetric Diels–Alder reactions. In connection with tetracycline syntheses it was shown that the electron-rich 1-glucosyloxydiene **33a** reacts, for example, with 2-methoxycarbonyl-*p*-benzoquinone with considerable stereoselectivity to give the hydrolysis product **34a** via the Diels–Alder adduct.[40,41] From NOE experiments the authors[41] deduced a preferred conformation of the glucosyloxydiene, which is in agreement with the *exo*-anomeric effect and which corresponds to the transoid conformation of **33a**. The higher selectivity observed in the reaction of the analogous 2-methyldiene **33b** proves that the cisoid form of **33a** is not decisive. On the assumption that an *endo* addition occurs, the dienophile must in this case preferentially attack from the front side, that is, from that direction in which the steric interaction with the 2-acetoxy group must be overcome.[40]

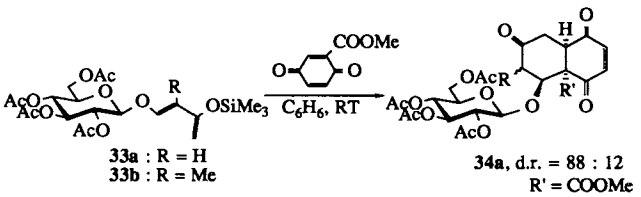

High stereoselectivities were reported for the asymmetric Diels–Alder reactions of 1,4-naphthoquinone with cyclohexanedienols bound to diacetone glucose.[42]

Anomeric glucosyloxy-butadienes such as **35** with unprotected hydroxyl groups enable interesting Diels–Alder reactions to be carried out in water. Compound **35** reacted with methyl acrylate with complete *endo* selectivity but modest diastereofacial differentiation to give the diastereomeric cyclohexenol ethers **36**.[43] The corresponding α-anomeric diene reacted with methacrolein to give the cycloadduct with lower and opposing *Re*/*Si* facial differentiation. On the assumption that the cisoid conformation of **35** is preferred, the predominant attack of the dienophile would be from the *Re* side (C1), again with approach from the front side.[43] When an *O*-benzyl ether protecting group was introduced selectively to the 2-position of **35**, the cycloaddition with methacrolein proceeded with reversal of the direction of induction but also with lower selectivity (34:66).[44]

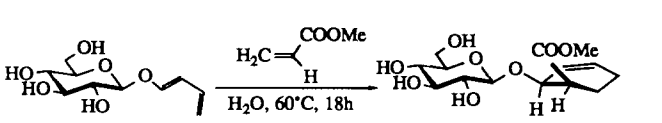

A stereoselective Claisen rearrangement of an allyl vinyl ether attached to an unprotected glucose is related to these Diels–Alder reactions. This process also showed a selectivity of only 60:40.[45]

Diels–Alder reactions of dienes attached to carbohydrates have been carried out without Lewis acid catalysis, which may be one reason for the generally modest asymmetric inductions observed. When the dienophile was attached to a carbohydrate auxiliary, the reactivity was increased by Lewis acid catalysis and the Diels–Alder reaction could be conducted at a lower temperature. Results obtained to date show that the dienophile can be shielded by coordinative fixing to the carbohydrate framework to give effective diastereodifferentiation. Intermediate **38**, formed from the 3-*O*-acryl-glucofuranose derivative **37** and titanium tetrachloride at −78 °C, contains both the dienophile and the Lewis acid catalyst bound to the carbohydrate matrix. The dienophile is oriented by intramolecular coordination in the chiral matrix in such a manner that it reacts with cyclopentadiene preferentially on the *Si* side.[46] Thus, the *endo* adduct **39** was formed with high stereoselectivity as the (*R*) diastereomer. The analogous reaction with a 5-*O*-trimethylsilylxylofuranose derivative gave the diastereomeric (*R*) adduct exclusively.[46] The reactions of dienes with lower reactivity must be conducted at ambient temperature and are thus less selective.

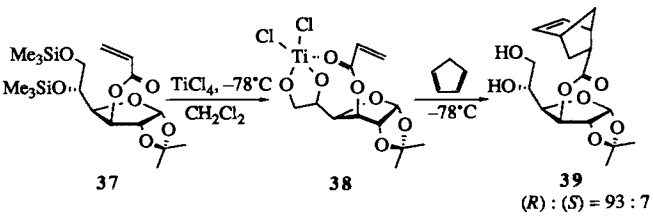

2-*O*-Acrylates derived from β-L-arabinopyranosides were used by Shing et al.[47] in Et_2AlCl catalyzed Diels–Alder reactions. The reason for the moderate inductions observed, compared with those from the titanate complexes **38** mentioned above, may be that the functional groups in the carbohydrate residue in **40** carry protecting groups which exhibit a reduced coordination tendency towards the Lewis acid catalyst.

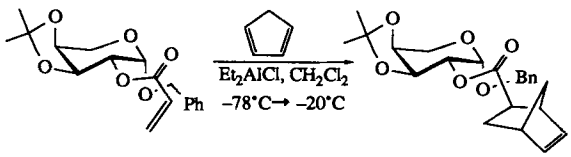

In agreement with this conclusion it was possible, using another concept, to coordinate the Lewis acid with great effect to the carbohydrate matrix by acyl protecting groups. In this case it is possible to vary the strength of the Lewis acid over a wide range, thus permitting the stereoselective reaction of less reactive dienes.[48] Compound **42**, an acrylate bound to a dihydroglucal template (Scheme 2), reacted with cyclopentadiene under $TiCl_2(OiPr)_2$ catalysis at $-30\,^{\circ}C$ to give the cycloadduct **43a** in high yield and stereoselectivity (98:2). However, cycloaddition of **42** with anthracene required activation from the stronger Lewis acid $TiCl_4$ at $0\,^{\circ}C$. Adduct **43d** was then obtained as almost exclusively one diastereomer (Table 2). The examples in Table 2 show that reactive as well as less reactive dienes can be converted to chiral cycloadducts according to this flexible principle with efficient stereoselectivity and in high yield.

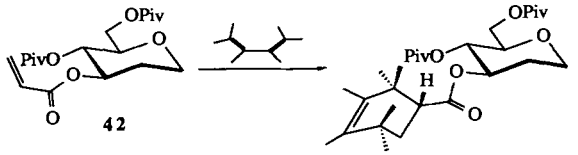

Scheme 2. Piv = Pivaloyl. For products of analogous reactions see text and Table 2.

Table 2. Stereoselective Diels–Alder reaction of acrylate **42** bound to dihydro-D-glucal [48].

Diene (10 equiv)	Lewis acid (3 equiv)	T [°C]/ t [h]	Adduct	Yield [%]	$(R):(S)$
cyclopentadiene	$TiCl_2(OiPr)_2$	−30/1.5	**43a**	92	98:2
isoprene	$TiCl_3(OiPr)$	0/48	**43b**	94	95:5
buta-1,3-diene	$TiCl_3(OiPr)$	0/6	**43c**	90	92:8
anthracene	$TiCl_4$	0/4	**43d**	87	99:1

The range of application of this stereoselection method has been extended considerably, since cycloadducts of the opposite configuration could also be prepared with high selectivity. In the case of dienophile **44** a dihydro-L-rhamnal unit served as the chiral template, to which the acrylate function was attached as an ester.[48]

Comparison of the two auxiliaries **42** and **44** illustrates that the structural and functional versatility of the carbohydrates provides a flexible concept for the alternative stereoselective synthesis of both enantiomeric configurations of a chiral target molecule, even though most sugars do not exist naturally in both enantiomeric configurations. The essential coordinating and shielding groups of the auxiliaries obtained from glucose and L-rhamnose mirror each other perfectly (Scheme 3). The trick of using quasi-enantiomeric carbohydrate templates was employed earlier in amino acid syntheses for selective formation of either the D or the L enantiomer (see Section 7.1).[18]

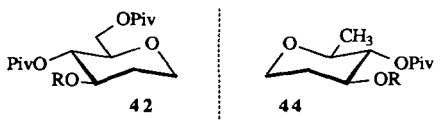

Scheme 3. R = Acryloyl.

Compound **44** (R = acryloyl) reacted with dienes to give (*S*)-configurated cycloadducts such as **45**, again in high selectivity and yield (Table 3); the strength of the Lewis acid and the reaction temperature were varied.

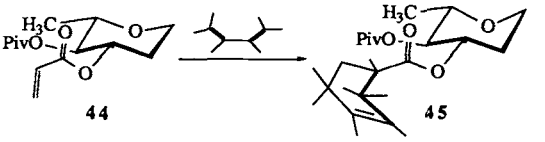

Table 3. Stereoselective Diels–Alder reaction of acrylate **44** bound to dihydro-L-rhamnal [48].

Diene (10 equiv)	Lewis acid (3 equiv)	T [°C]/ t [h]	Yield [%]	$(R):(S)$
cyclopentadiene	$TiCl_2(OiPr)_2$	−30/2	80	6:94
isoprene	$TiCl_3(OiPr)$	−30/18	60	10:90
butadiene	$TiCl_4$	−30/4	68	5:95
anthracene	$TiCl_4$	0/18	52	1:99

The anomeric acrylate **46** could be converted into the corresponding adduct (here **47**) at $-30\,^{\circ}C$ only with more reactive dienes such as cyclopentadiene. $TiCl_2(OiPr)_2$ was sufficient as Lewis acid; stronger Lewis acids such as $TiCl_4$ caused cleavage of the anomeric ester.[49] In contrast to the reactions of dienes attached to carbohydrates, attack on the back side clearly dominates in this Lewis acid catalyzed Diels–Alder reaction of the carbohydrate-bound dienophile. An *endo/exo* selectivity of 96:4 and stereoselectivity in favor of the (*R*) diastereomer of **47**, also 96:4, were obtained.[49] The α-anomeric acrylate corresponding to **46** reacted more slowly with cyclopentadiene and with a lower selectivity. Interestingly, in this case the diastereomeric (*S*) adduct was formed preferentially.[49]

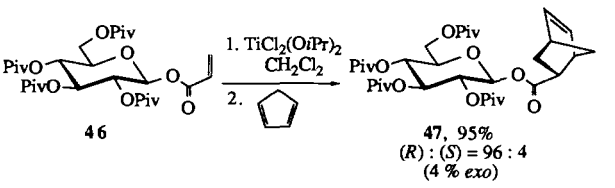

Methyl-3,4-*O*-methylene-β-D-arabinopyranoside, in which the 2-hydroxyl group was esterified with acrylic acid to give **48**, was recently used as auxiliary in a Lewis acid catalyzed Diels–Alder reaction.[50] Compound **48** reacted with cyclopentadiene and 2,3-dimethylbutadiene in the presence of $TiCl_4$ or $SnCl_4$ to give adducts such as **49** with high stereoselectivity and *endo* preference. Only modest or low induction was achieved when the reaction was conducted with boron trifluoride or ethylaluminum dichloride as the catalyst and with isoprene as the diene. Nevertheless, the authors[50] traced the diastereofacial differentiation in favor of the *Re* face in **48** back exclusively to the steric shielding caused by the β-methoxy group.

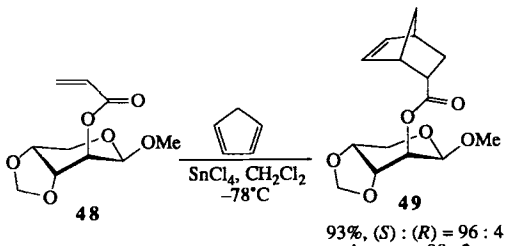

48 49

93%, (*S*) : (*R*) = 96 : 4
endo : *exo* = 98 : 2

The crotonates corresponding to the acrylates **42**, **44**, and **46** do not generally react at sufficiently low temperature to give the cycloadducts stereoselectively. However, crotonates were successfully employed in diastereoselective Diels–Alder reactions with various auxiliaries not derived from carbohydrates.[51]

Crotonate **50**, containing a bicyclic oxazolidinone unit (developed for another purpose, see Section 5.2) derived from galactosamine, underwent Diels–Alder reactions with high *endo* preference and practically complete diastereoselectivity.[52] The reaction required catalysis by Lewis acids like

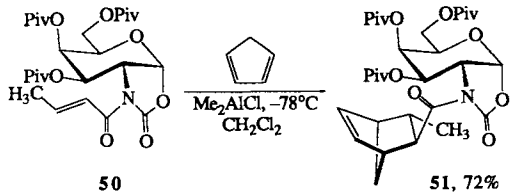

50 **51**, 72%

dimethylaluminum chloride and gave the *endo* adduct **51** (*endo*:*exo* = 20:1). The *endo* adduct was detected as only a single diastereoisomer by capillary GC.[52]

4.2. Heteroanalogous [4+2] Cycloadditions

The α-chloronitroso compound **52**, formed by reaction of the hydroxyimino-γ-lactone of the isopropylidene-protected mannonic acid with *tert*-butylhypochlorite, reacted with dienes at −70 °C with high stereoselectivity to give 3,4-dihydro-2*H*-1,2-oxazines such as **53**.[53] The configuration of **52** was determined by X-ray analysis. The intermediate adduct was hydrolyzed during the reaction or the subsequent workup to give the free oxazine hydrochloride **53**.

Stereoselectivities of more than 98:2 have been attained in numerous examples. Heterodienophile **52** is characterized by

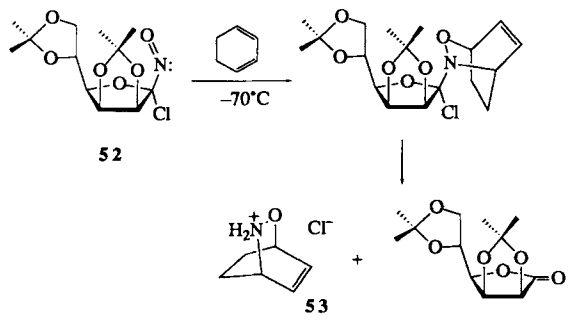

52 **53**

a high reactivity at low temperature. It seems that, as in the solid state, a conformation of **52** is preferred that is stabilized by $n \rightarrow \sigma^*$ delocalization of the lone pair on the nitrogen atom into the C1–O bond. The result is a very effective stereofacial differentiation in favor of attack on the sterically more accessible back side of the N=O bond, while the *anti* orientation of the diene relative to the furanose ring is preferred.

These favorable properties could also be employed in a stereoselective ene reaction. When the chloronitrosoribose derivative **54** was used instead of the mannose compound, the alternative enantiomeric series could be prepared (Scheme 4).[54] The enantiomeric ratios for both **53** and **55** were determined after chemical transformation.

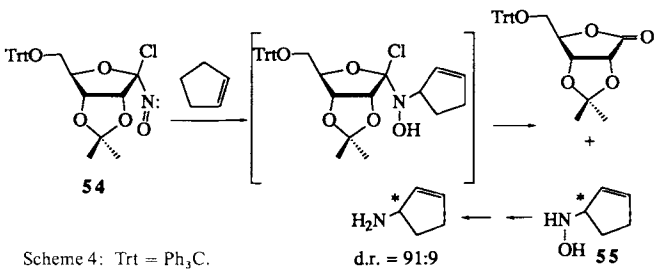

54 **55**

Scheme 4: Trt = Ph_3C. d.r. = 91:9

Isoquinolinium salts have been used as heterodienes in Diels–Alder reactions with inverse electron demand with vinyl glycosides.[55] In one case, the reaction of **56**, a high induction was observed. The given diastereomeric ratios of products **57** (DNP = dinitrophenyl) were obtained after isolation of the diastereomer mixtures. As neither reaction nor

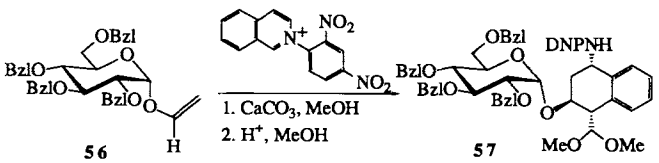

56 **57**

70%, d.r. > 98 : 2

workup conditions were given, enrichment effects cannot be excluded. The synthesis offers, after conversion of acetal **57** into a dithiane and cleavage of the carbohydrate unit with trimethylsilyl iodide, an interesting route to homochiral trisubstituted tetralines. Diacetone glucose enol ethers reacted stereoselectively with nitrosoalkenes (generated in situ) as heterodienes to give chiral 1,2-oxazine derivatives **58**.[56] The

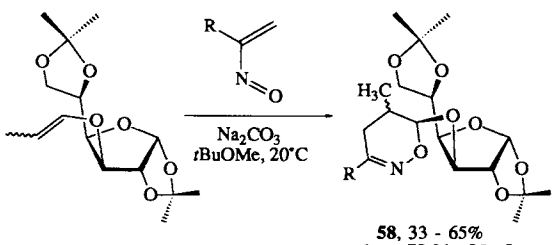

58, 33 - 65%
d.r. = 79:21 - 95 : 5

reported results allow the conclusion that the (*E*) enol ethers generally react with greater selectivity than the (*Z*) analogues.

The stereoselective synthesis of 2-substituted piperidine derivatives was achieved by the hetero-Diels–Alder reaction of *N*-galactosylimine **59** with dienes such as isoprene.[57] The reaction required catalysis by zinc chloride, as imines are usually too unreactive for cycloadditions.

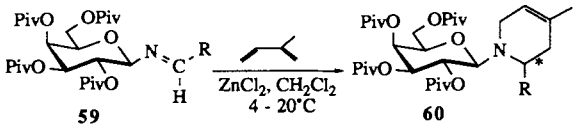

59 **60**

Although the absolute configuration of the major diastereomers of didehydropiperidines **60** has not been clarified, the NMR data for the imine and its zinc complexes[18] for R = aryl indicate that a (2*S*) configuration is probable. A few examples of these stereoselective syntheses of didehydropiperidines are listed in Table 4. Although the diastereomeric ratio reaches a value of 10:1 in only a few cases, the process offers the advantage that most of the products **60** can be obtained in good yield and diastereomerically pure by recrystallization or by flash chromatography.

Table 4. Aza-Diels–Alder reaction of Schiff bases **59** with isoprene; stereoselective synthesis of 2-substituted piperidine derivatives [57]. RT = room temperature.

R	*T* [°C]/*t*	Yield [%]	Diastereomeric ratio	Pure diastereomer
p-ClC_6H_4	+4/12 h	95	87:13	60%
p-FC_6H_4	+4/12 h	90	91:9	52%
2-furyl	RT/4 d	98	80:20	65%
2-thienyl	RT/4 d	95	84:16	56%

According to recent results the reaction can also be catalyzed by tin tetrachloride. Imines of D-arabinopyranosylamine, which are quasi-mirror images of **59**, can be used for the synthesis of chiral piperidines that, in comparison to **60**, have the opposite configuration.[58]

In the 1,3-dipolar cycloaddition of *N*-manno- and *N*-ribofuranosylnitrones to alkenes, Vasella et al.[59, 60] found an interesting stereoselective route to isoxazolines with a chiral center at C5. As an example, the addition of nitrone **61** (prepared from *O*-isopropylidene-protected *N*-mannofuranosylhydroxylamine and formaldehyde) to methyl methacrylate is given.

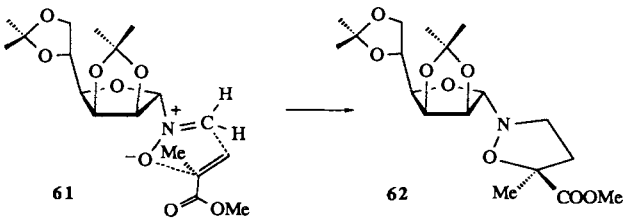

61 **62**

98%, (5*S*) : (5*R*) = 87.5 : 12.5

The preferred formation of the (5*S*) diastereomer was explained,[60] in that **61** reacts from a predominantly O-*endo* conformation. Moreover, a methyl-*endo* geometry in the approach to the methacrylate was concluded from similar reactions of other nitrones[61]. Attack of the dipolarophile follows with high selectivity from the back side, that is, from the direction of the furanose C1–O bond, because delocalization of the *n* orbital developing on the nitrogen atom (in **62**) into the σ^* orbital of the ring C–O bond can occur at an early phase and in the transition state (kinetic *exo*-anomeric effect). In analogous cycloadditions prochiral nitrones of type **61**, for example that of acetaldehyde, were not very diastereoselective with regard to the configuration at C3 of the isoxazolidine. This effect could be traced back to the low configurative stability of the nitrone itself. Nitrone **61** and its pseudo-enantiomeric ribofuranosyl analogues with N-protected L-vinylglycine esters were employed in a double diastereodifferentiation.[60] Whereas **61** gave the diastereomeric isoxazolidines in a ratio of only 3:1, L-vinylglycine esters and the D-ribose analogue apparently form a "matching pair" and react to give a single stereoisomer, which was subsequently transformed into the antibiotic acivicin.[62]

4.3. [2 + 2] Cycloadditions

In addition to [2 + 2] cycloadditions in which the carbon atoms of the carbohydrate unit are incorporated into the ring structure,[38, 63] syntheses of four-membered rings have recently been reported in which carbohydrates act as chiral auxiliaries. For the purpose of this review, stereoselective Paterno–Büchi reactions should also be included here,[64] although such photochemical processes are not concerted but take place via 1,4-diradicals. Irradiation of the carbohydrate phenylglyoxylic acid ester **63** and furan gave the diastereomeric dioxabicycloheptenes **64a** and **64b** in the ratio 9:1. An interesting observation in this reaction was that a somewhat higher diastereoselectivity was found with increasing reaction temperature.[64]

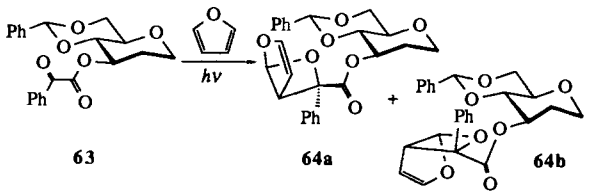

63 **64a** **64b**

80%, 64a : 64b = 9 : 1

Asymmetric [2 + 2] cycloadditions that permit access to chiral β-lactams are of particular interest. In this context the vinyl ether of diacetone glucose **65** was treated with tosyl isocyanate in ether at room temperature.[65] The (4*R*) diastereomer of β-lactam **66** was obtained predominantly with a diastereoselectivity of 86:14.

The yields in these and similar processes are moderate.[65] In several other cases the (4*S*) diastereomer of the lactam was formed, albeit with lower selectivity. *N*-Trichloroacetyl isocyanate underwent almost exclusively [4 + 2] cycloaddi-

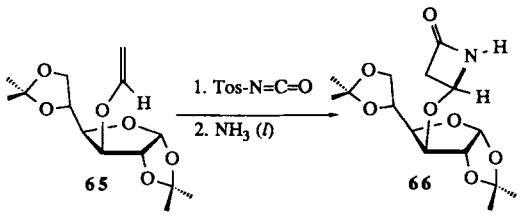

tion with vinyl ethers like **65** and showed only little or no diastereofacial differentiation.[65]

Another route to chiral β-lactams is provided by the Staudinger reaction of ketenes with imines prepared from chiral amines. Imine **67**, derived from glucosamine and cinnamic aldehyde, reacted with ketenes generated in situ to give the *cis* β-lactams **68**.[66] Whereas *N*-phthalimidoketene gave the (3*S*,4*S*) adduct in high yield and complete stereoselectivity, the analogous reaction of the methoxyketene (R = MeO) showed hardly any selectivity. The glucosamine auxiliary was cleaved by abstraction of the dithianyl proton with butyllithium and β-elimination of the lactam (yield: 35%).

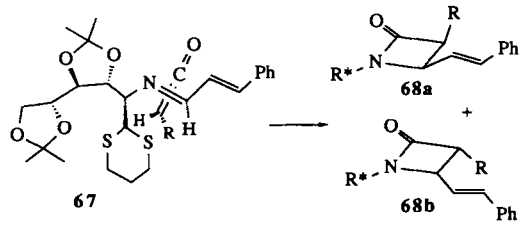

R = PhtN, 92%, **68a**
R = OMe, 94%, **68a** : **68b** = 65 : 35

Galactosylimines[18, 57] display only slight stereodifferentiation in the Staudinger reaction with aryloxyketenes according to the observations of G. Georg et al.[67] As shown, for instance, in the reaction of imine **69**, obtained from *p*-chlorobenzaldehyde, both *cis* products **70a** and **70b** were formed in good yield. The *cis* α,α-diastereomer **70a** generally predominated in the ratio 3:2.[67b]

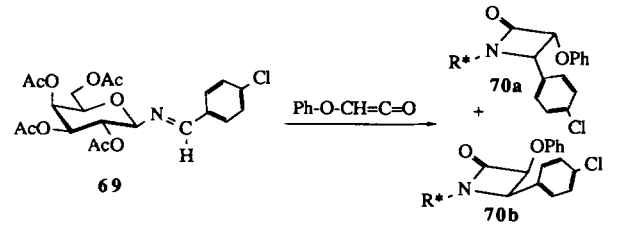

85%, **70a** : **70b** = 60 : 40

Recently, a stereoselective Staudinger reaction with the chiral, carbohydrate-bound ketene from *O*-glycosylglycolic acid **71** was described.[68] Both *cis* β-lactam diastereomers were formed selectively; the *cis* α,α-diastereomer **72** dominated in a ratio of about 85:15. The reason for the observed facial differentiation could be the unhindered attack on the *Re* side of the ketene formed in situ as a result of the 2-deoxy structure of **71**. The importance of stereoselective β-lactam syntheses does not need to be underlined here; a large number of important types of antibiotics belong to this group of compounds.

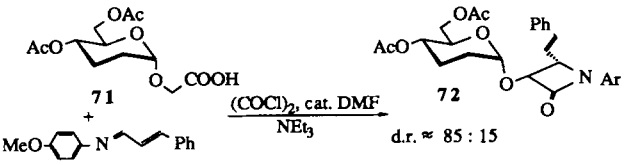

d.r. ≈ 85 : 15

4.4. Cyclopropanations

Cyclopropanations by addition of carbenes (or carbenoids) can be regarded as [2π + 2ω] or [2π + 2σ] processes and are thereby categorized as [2 + 2] cycloadditions.[69, 70] The geometric and stereoelectronic factors in these reactions are so different from those of the [2s + 2a] additions of compounds with cumulated double bonds discussed previously that the stereodifferentiating influence of auxiliaries in these reactions may be quite different.

An interesting and efficient asymmetric synthesis of chiral cyclopropyl compounds was described by Charette et al.[71] in the reaction of allyl β-D-glucopyranosides **73** with diethyl zinc/diiodomethane. The chiral cyclopropylmethylglucosides **74** were obtained in high yields and generally with excellent diastereoselectivity (ca. 100:1). Some appropriate examples are given in Table 5.

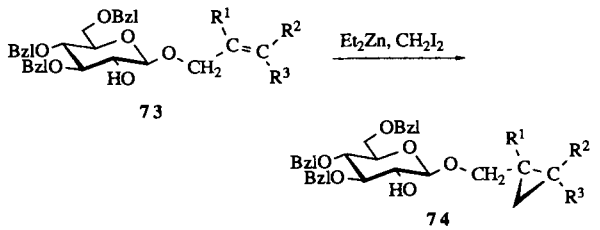

Table 5. Cyclopropanation of allyl-2-hydroxyglucopyranosides **73** [71].

R	*T* [°C]	Diastereomeric ratio [a]
-OCH$_2$-(Pr)	−35 → 0	>50:1 (124:1)
-OCH$_2$-(Me)	−35 → 0	>50:1
-OCH$_2$-(Ph)	−35 → 0	>50:1 (130:1)
-OCH$_2$-(Ph)	−35 → 0	>50:1 (114:1)
-OCH$_2$-(Me, Me)	−35 → 0	>50:1 (111:1)

[a] Values in brackets refer to ratios obtained from the ^{13}C NMR spectra.

The unprotected 2-hydroxyl group is important for the diastereofacial differentiation in **73**. This group reacts with diethyl zinc and forms a coordinative anchor for the Simmons–Smith intermediate with the iodomethyl zinc unit.

When diethyl zinc was used in only equimolar amounts rather than a tenfold excess, the diastereomeric ratio dropped to about 60:40. In addition, allylglucopyranosides in which the 2-position is protected showed only a modest asymmetric induction in cyclopropanation under standard conditions.[71a]

When this reaction was conducted with the auxiliary "L-**75**", which is pseudo-enantiomeric to D-glucose (D-**75**; see Section 4.1, **42**/**44**) and easily accessible from L-rhamnal, cyclopropanes with the opposite configuration were obtained stereoselectively. Similarly, in the reaction with the α-anomeric allyl glucosides corresponding to **73**, preferential formation of the cyclopropylmethylglucoside with the opposite configuration to that of **74** was observed.

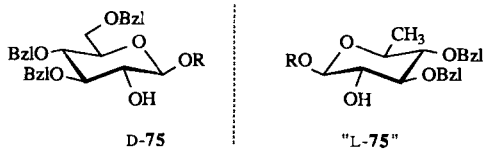

The examples described above show that because of their steric and chelating potential carbohydrates are effective agents for the asymmetric shielding of the diastereotopic sides of components in cycloadditions. Initial results of hetero-Cope rearrangements of derivatives of diacetone glucose show that this selection principle can be successfully extended to other types of pericyclic processes.[72] The structure of the selected auxiliary must, of course, fit the reaction to be stereochemically controlled. Otherwise, the induction will be unsatisfactory. High selectivity is generally always obtained when unequivocal facial differentiation can be guaranteed by the regio- and stereoselective attachment of both the reacting functionality and the shielding groups. Without additional means this is frequently attained by attachment of the substrate structure to a secondary hydroxyl group of the carbohydrate auxiliary, and indeed especially when spatial requirements clearly favor a preferred conformation of the substrate. Fixing the reactive and shielding groups by complexation frequently leads to decisive increases in the stereoselectivity. This is particularly the case for substrates that are attached to the auxiliary at the anomeric position. Moreover, in this type of attachment, stereoelectronic effects (anomeric effects) also promote selectivity in the cycloaddition.

Nevertheless, in some cases the reaction takes an unexpected course. It makes sense to clarify the structures of unexpected products, as their formation could provide stimulus for further investigations. This is illustrated by work on the Diels–Alder reaction of the *N*-acryloxazinone **76** derived from xylofuranose.[73] The cycloaddition catalyzed by diethylaluminum chloride[51] was not only slow and incomplete, but also showed disappointingly low stereoselectivity. In addition to the Diels–Alder adduct **77** a side product **78** was isolated. The latter emerged[73] as a 1,4-adduct (a "Michael" adduct) of the catalyst and the acceptor **76**. The formation of this adduct led to a new route to the synthesis of β-branched carboxylic acids, which will be discussed in the following section.

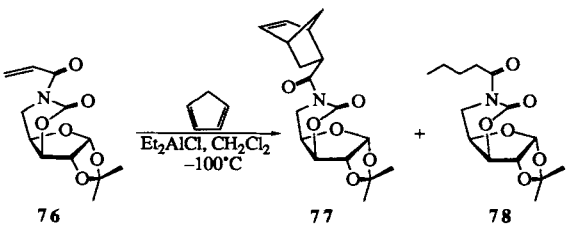

5. Michael Additions

5.1. Michael Additions of Enolates and Cuprates

Carbohydrate derivatives can also be applied successfully for stereodiscrimination in Michael additions. Thus, chiral 1,3-dithian-2-carboxylic acid ester **79** (derived from diacetone glucose) was added, after deprotonation with LDA (at −30 °C), to benzylidenemalonic ester at −85 °C as a prochiral component. The diastereomeric ratios for the resulting ketoglutaric acid derivatives **80** lie between 90:10 and 93:7.[18, 73]

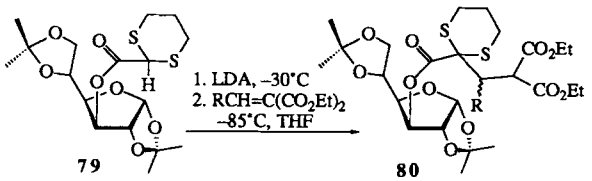

R = *m*-ClC$_6$H$_4$, (*S*):(*R*) = 90:10
R = Ph, (*S*):(*R*) = 93:7

In a sequence of reactions, consisting of a 1,4-addition of the silylcuprate $(PhMe_2Si)_2CuLi_2CN$ to the α,β-unsaturated ester derivative **81** of diacetone allose and subsequent methylation of the intermediate enolate with methyl iodide, a mixture of four diastereomeric products **82** was formed in the ratio 72:23:4:1.[74] After the carboxylic acid products were cleaved from the auxiliary, a 95:5 ratio of the *anti* and *syn* isomers was found. This result indicates that although the alkylation indeed takes place with high *anti* selectivity, the preceding Michael addition of the cuprate occurs with only moderate diastereoselectivity.

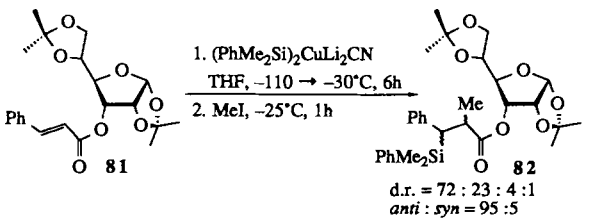

The Cu^{I}Cl catalyzed conjugate addition of Grignard reagents to the corresponding α,β-unsaturated esters was first considered in an early study on stereodifferentiation

with carbohydrates.[75] The reaction of the 3-*O*-crotonic ester prepared from 1,2;5,6-di-*O*-cyclohexylideneglucofuranose with phenylmagnesium iodide gave, after removal of the auxiliary, 3-phenylbutyric acid in 74% optical and 58% chemical yield.

Conjugate addition of organocuprates to Michael acceptors bound to carbohydrates, giving good yields and with a diastereoselectivity of 79:21 to 95:5 (Table 6), could be achieved by suitable modification of the carbohydrate structure.[76] Steric shielding by the benzyl group is apparently the sole factor responsible for the selectivity of the addition to **83**.

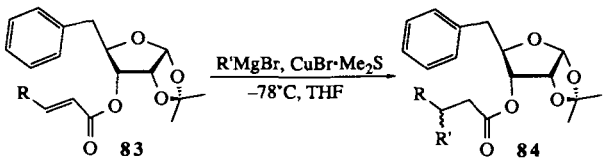

Table 6. Conjugate addition of cuprates to substrate **83** [76].

R	R′	Yield (**84**) [%]	Diastereomeric ratio
Me	Ph	74	(*S*):(*R*) = 97.5:2.5
Me	Et	65	(*R*):(*S*) = 95:5
Me	*i*Pr	72	(*S*):(*R*) = 95:5
Ph	Et	89	(*R*):(*S*) = 79:21
Ph	*i*Pr	69	(*S*):(*R*) = 87.5:12.5

5.2. 1,4-Additions of Alkylaluminum Compounds to Carboxylic Acid Derivatives

A new route to β-alkyl-substituted carboxylic acid derivatives has been provided by the 1,4-addition of diorganoaluminum chlorides to α,β-unsaturated *N*-acylurethanes. This route was developed based on the analysis of the by-products formed in the Diels–Alder reaction of oxazinone dienophiles catalyzed by aluminum Lewis acids (see Section 4.4, reaction of **76**). The cinnamic acid derivative **85** reacted in this new synthesis to give, when at least two equivalents of Et_2AlCl were employed, exclusive 1,4-addition and the 3-phenylvaleric acid derivative **85** in high yield and with a diastereoselectivity of 87:13.[77]

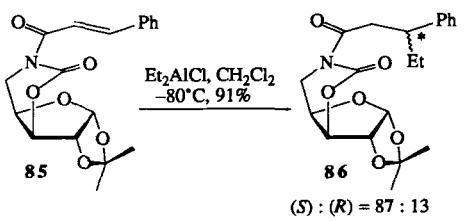

Further investigations into the preparative applicability of the reaction and its extension to other diorganoaluminum chlorides were first carried out on achiral[77] and chiral *N*-acyloxazolidinones (derived from the amino acid (*S*)-phenylalanine).[78] Whereas the higher homologues nPr_2AlCl, iBu_2AlCl, and Ph_2AlCl reacted smoothly at low temperature to give the 1,4-adduct exclusively, the transfer of a methyl group from Me_2AlCl was possible only with photochemical initiation or in the presence of atmospheric oxygen.[78] This unexpected contrast between the mode of reaction of methylaluminum compounds and that of higher alkylaluminum compounds is a striking characteristic of this 1,4-addition. Because of the moderate diastereoselectivity obtained with auxiliaries such as oxazinones like **85** or oxazolidinones derived from (*S*)-phenylalanine, bicyclic oxazolidinones **87** from 2-aminodeoxy sugars were developed in order to attain effective steric shielding of one side of the α,β-unsaturated acceptor and thereby higher diastereoselectivity in the 1,4-addition. After deprotonation of the nitrogen atom, the oxazolidinones **87** were treated with acid chlorides to give Michael acceptors **88** and **89**. The examples of the reactions

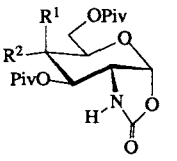

87a: R^1 = OPiv, R^2 = H
87b: R^1 = H, R^2 = OPiv

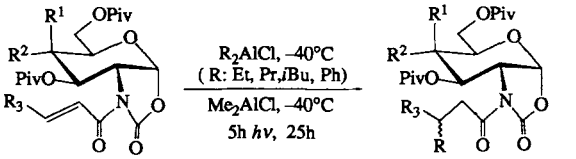

88: R^1 = OPiv, R^2 = H
89: R^1 = H, R^2 = OPiv
R_3 = CH_3,C_6H_5

90: R^1 = OPiv, R^2 = H
91: R^1 = H, R^2 = OPiv

carried out with these acceptors listed in Table 7 illustrate the stereodifferentiating efficiency of the carbohydrate auxiliaries derived from galactosamine and glucosamine. The β-branched carboxylic derivatives **90** and **91** were formed with excellent diastereoselectivity, in particular with the galactosamine auxiliary **87a**; both configurational series are accessible by choice of the groups R^3 and R.[79] The selectivity in the case of the glucosamine-oxazolidinone derivatives **89** is somewhat lower.

Table 7. Stereoselective Michael addition of diorganoaluminum chlorides with bicylic carbohydrate-oxazolidinones **87** as chiral auxiliaries [79].

R^1	R^2	R^3	R_2AlCl	*T* [°C]/ *t* [h]	Yield [%]	(*R*):(*S*)
H	OPiv	Ph	Et_2AlCl	–40/8	90	90:10
H	OPiv	Ph	iBu_2AlCl [a]	–40/28	73	92:8
H	OPiv	Me	iBu_2AlCl [a]	–40/48	82	15:85
OPiv	H	Ph	Et_2AlCl	–78/2.5	84	96:4
OPiv	H	Ph	Pr_2AlCl	–40/5	74	97:3
OPiv	H	Me	Ph_2AlCl	–40/20	56	>2:98
OPiv	H	Me	Et_2AlCl	–30/20	70	90:10
OPiv	H	Ph	Me_2AlCl	–40/30 [b]	82	>98:2
OPiv	H	Ph	iBu_2AlCl [a]	–40/24	87	>99:1

[a] Activation with 1 equiv Me_2AlCl. [b] Photochemical initiation.

As in the Diels–Alder reactions already discussed, the sterically demanding pivaloyl protecting group also offers an advantage. This group is inert towards strong aluminum Lewis acids and, in addition, permits the desired, pronounced steric control of the reaction. The diastereomerically pure β-branched carboxylic acid derivatives can generally be isolated in good yields after flash chromatography or by recrystallization. For substrate **90** (R^3 = Ph), for example, cleavage of the acid from the auxiliary with $LiOH/H_2O_2$ in THF/water proceeded in high yield (> 87%) and with almost quantitative recovery of the carbohydrate template.

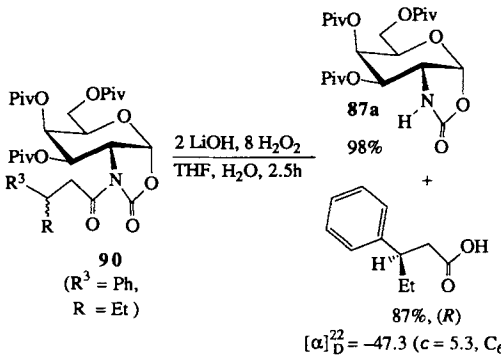

Trapping the intermediate aluminum enolate formed in the 1,4-addition of higher organoaluminum compounds with *N*-chloro- or *N*-bromosuccinimide gave chiral β-branched α-halocarboxylic acid derivatives such as **92** with high *anti* selectivity.[80]

Based on the results obtained so far, the high diastereofacial selection potential of the bicyclic carbohydrate-oxazolidinone **87** provides a number of routes to chiral β-branched carboxylic acid derivatives. The use of various electrophiles

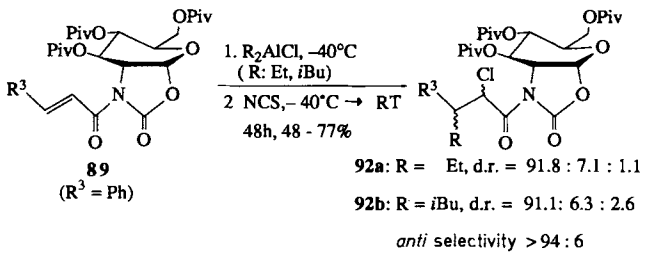

for the subsequent reaction with the enolates formed permits access to a wide spectrum of interesting products.

6. Carbohydrates as Components of Chiral Reagents and Promoters

6.1. Complex Hydrides

Carbohydrates were employed quite early as chiral ligands for complex organoaluminum reducing agents.[20] In reactions with carbohydrate alcohols, preferably diacetone glucose **93**, modified complex borohydrides also proved to be efficient in the enantioselective reduction of prochiral ketones.[81] These reactions are influenced by temperature, molar ratios, solvent, and other additives in a complex way. Addition of Lewis acids such as zinc chloride raises the level but reverses the direction of induction.[82] The addition of carboxylic acids such as butyric acid was found to be of value;[83, 84] the direction of induction did not change but a higher enantiofacial differentiation was attained. The reduction of propiophenone (**94**) is a favorable example.[84]

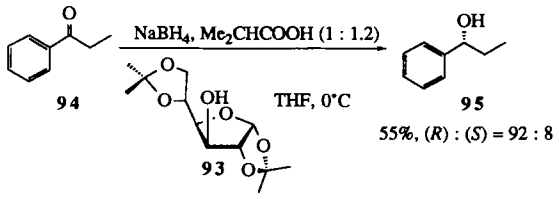

Since several of the species formed from the reaction components could be responsible for the asymmetric induction,[83] interpretation of the steric course of the process is hardly possible. The use of dicyclohexylideneglucofuranose instead of **93** and of chiral carboxylic acids failed to bring about an increase in the stereoselectivity.[85]

Sterically demanding complex borohydrides of defined structure such as **96**, capable of reducing ketones even at –78 °C, were obtained from 9-borabicyclo[3.3.1]nonane, diacetone glucose, and potassium hydride in THF.[86] Propiophenone (**94**) was reduced to (*R*)-1-phenylpropanol (**95**) by **96** with excellent enantioselectivity. Under the same conditions the sterically demanding *tert*-butyl phenyl ketone gave practically pure (*R*)-carbinol. α-Keto esters could also be reduced with **96** to give the corresponding α-hydroxycarboxylic acids with high enantioselectivity.[87] α-Aminoketones were converted with **96** into chiral 2-aminoalcohols with the same direction of induction, but nevertheless with significantly lower enantiofacial differentiation.[88]

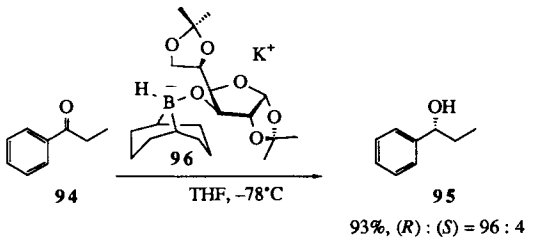

Phosphines and phosphinites[89–91] derived from carbohydrates have been used on numerous occasions as chiral ligands in asymmetric hydrogenations. For reasons of space, we are unable to consider this application in this review.

6.2. Chiral Titanates as Promoters in Aldol Reactions

As is the case for reductions with complex hydrides, it is also an advantage in other stereoselective syntheses when the inducing chirality of the auxiliary resides in the reagent, which, during the reaction, transfers a group diastereoselec-

tively to the substrate, but itself does not appear in the enantioselectively formed product. This is particularly the case for processes in which the covalent attachment of a chiral auxiliary is difficult to realize or causes undesired side reactions, as shown, for example, in the case of the carbohydrate enolate reactions (see Section 3).

A good solution to this problem, precisely for aldol reactions and related processes, was provided by Riediker, Duthaler, et al.[92-94] with the introduction of dialkoxy(chloro)cyclopentadienyltitanate **97**. In reactions with allyl Grignard reagents in ether/THF at 0 °C, **97** was converted into the chiral allyltitanate **98**. This complex reacted with

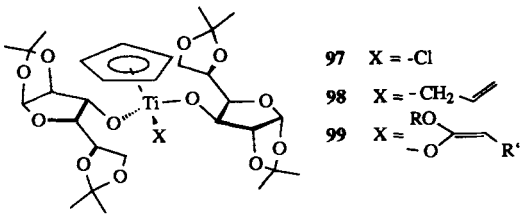

aldehydes at −78 °C in high yield and enantioselectivity to give the (*R*)-homoallylic alcohols **100**.[92, 95] Some examples of this reaction are listed in Table 8.

Table 8. Enantioselective syntheses of homoallylalcohols **100** using chiral allyltitanium reagent **98**[92].

R [a]	Yield (**100**)	*ee*	Config.	R [a]	Yield (**100**)	*ee*	Config.
phenyl	85%	90	(*R*)	*n*-propyl	78%	93	(*S*)
1-naphthyl	83%	88	(*R*)	isobutyl	55%	85	(*R*)
vinyl	61%	86	(*R*)	cyclohexyl	78%	92	(*R*)

[a] R (aldehyde).

Substitution in the cyclopentadienyl ligand of complex **98** had hardly any effect on the selectivity of the reaction. In contrast, exchange of the diacetone glucose ligand **93** for other carbohydrate alcohols always led to considerable loss of stereoselectivity. When diacetone-L-idose (5-epimer of **93**) was employed as the ligand, the (*S*)-configurated homoallylic alcohol was indeed formed preferentially, but with a diastereomeric ratio of only about 70:30.[96]

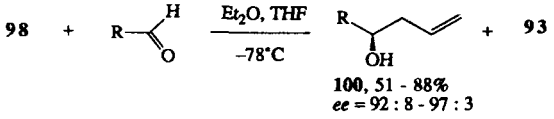

The diacetone glucose titanate complex also displays a high stereoselection potential in aldol reactions of ester enolates. The lithium enolate of the *tert*-butylacetate was treated with **97** to provide titanium enolate **99a** (R = *t*Bu, R' = H; DAG = diacetone glucose), which reacted with aldehydes to give chiral β-hydroxycarboxylic acid esters in enantiomeric ratios of 95:5 to 98:2 at −78 °C.[93, 95] A few examples demonstrating the efficiency of this process are given in Table 9.

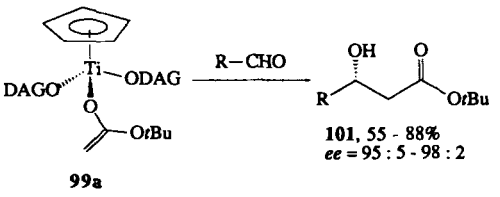

Table 9. Enantioselective aldol addition with titanium ester enolates **99a** [93].

R [a]	Yield (**101**)	*ee*	R [a]	Yield (**101**)	*ee*
n-propyl	51%	94	cyclohexyl	70%	92
isobutyl	81%	94	α-styryl	64%	96
isopropyl	66%	95	phenyl	62%	95

[a] R (aldehyde)

The preparative range of this aldol addition could be extended since both the (*Z*) and (*E*) series of titanium propionyl ester enolates (**99b** and **99c**, respectively; R = $C_5H_3Me_2$, R' = Me) are available. These complexes reacted with aldehydes with high diastereo- and enantioselectivity to give α-methyl-β-hydroxycarboxylic acid esters **102**.[93, 94]

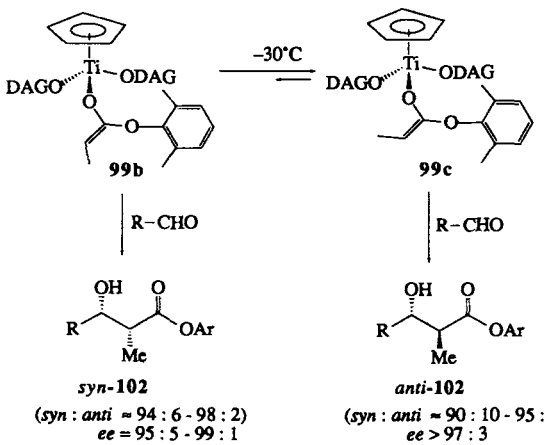

The aldol reaction with titanium enolate **99d** (R = Et, R' = $C_6H_{16}NSi_2$), obtained from the N-protected glycine ethyl ester, gave β-hydroxy-α-amino acid esters **103** with high enantioselectivity .[94, 96] In some cases the reaction provided one of the four possible stereoisomers almost exclusively. β-Hydroxyamino acids are of interest for synthesis of drugs.

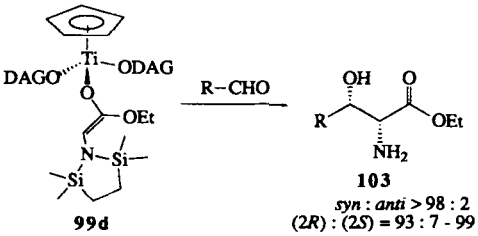

The modified diacetone glucose titanate **106** has recently been described as an effective Lewis acid catalyst in a tandem Knoevenagel–Diels–Alder reaction sequence.[97] The tetracyclic product **107** was formed with considerable enantioselectivity from aldehyde **104** and *N,N'*-dimethylbarbituric acid (**105**) via the Knoevenagel condensation product followed by its intramolecular cycloaddition.

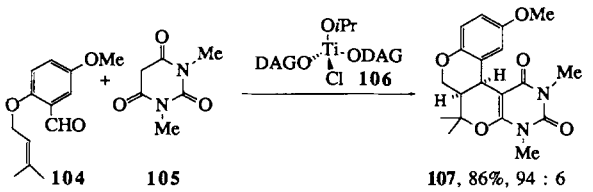

6.3. Electrophilic Reagents Bound to Carbohydrates

In contrast to the titanium and complex hydrido complexes, the mixed sulfate **108** from diacetone glucose reacts as a chiral electrophile. Lithium enolate **109** (obtained from the glycine methyl ester protected as a Schiff base) was alkylated with **108** to give the corresponding alanine derivative with predominant formation of the L enantiomer **110** (70:30).[98]

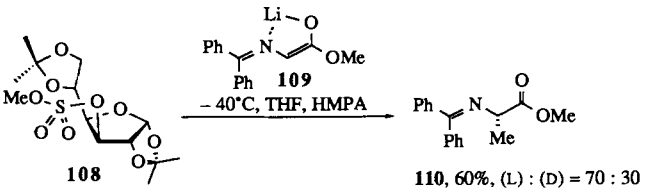

A powerful synthesis of chiral sulfoxides was attained by using diacetone glucose **93**, which was treated with methylsulfinyl chloride either in the presence of diisopropylethylamine to give the (*S*) diastereomeric product, sulfinate (*S*)-**111**, or in the presence of pyridine to give (*R*)-sulfinate (*R*)-**111**. As both diastereomeric sulfinates react with Grignard reagents with inversion at sulfur, one could obtain both enantiomeric series of the chiral sulfoxides **112**.[99]

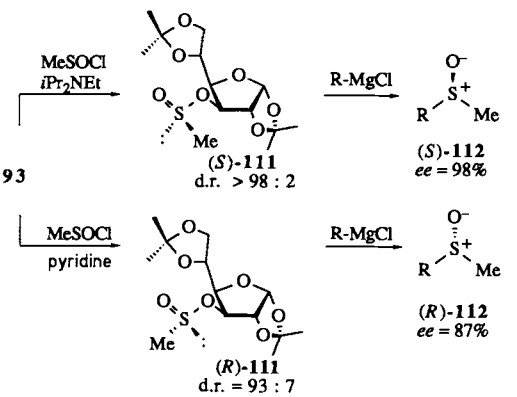

Finally, we should mention that, in addition to other chiral compounds, carbohydrates also have been employed in experiments aimed at enantioselective protonation.[100, 101] In these and related[102] protonations with chiral proton sources, however, enantiomeric ratios of 80:20 have rarely been exceeded.

7. Stereoselective Syntheses with Glycosylamines

Glycosylamines are chiral cyclic aminoacetals, the nitrogen atom of which can be carried into the product being synthesized. Since the N-glycosidic bonds in these products are easy to cleave, separation of the selectively prepared chiral compound from the chiral carboxhydrate matrix can generally be achieved under mild conditions. As previously discussed in Section 4.2, glycosylamine Schiff bases **59** can act as heterodienophiles in aza-Diels–Alder reactions, thereby providing a stereoselective route to chiral nitrogen-containing heterocycles.[57] Even before these investigations, glycosylamines had been examined as chiral templates in the asymmetric synthesis of amino acids.

7.1. Strecker and Ugi Syntheses of α-Amino Acid Derivatives

The increasing importance of biomimetic drugs during the last few years has stimulated interest in the stereoselective synthesis of enantiomerically pure natural and non-natural amino acids.[103, 104] Among the known amino acid syntheses, the Strecker synthesis offers the advantage that it does not require the use of organometallic reagents and that only inexpensive components are employed.

In the stereoselective Strecker synthesis, tetra-*O*-pivaloyl-β-D-galactosylamine (**113**) has been shown to be the best of those derived from glycosylamines.[105] It could be converted with aldehydes to *N*-galactosylimines **59**, which reacted with trimethylsilylcyanide in the presence of either zinc chloride in isopropanol or tin tetrachloride in THF in a few hours to give nearly quantitative yields of *N*-galactosyl-α-aminonitriles **114**. The D-aminonitriles were thus formed in excess

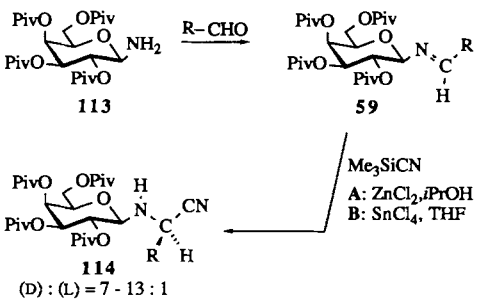

in the ratio 87:13 to 93:7.[106, 107] Still more fundamental for the preparation of enantiomerically pure amino acids was the discovery that pure D-aminonitrile diastereomers **114** can be obtained in high yields (75–90%) by simple recrystallization from *n*-heptane. As bases are not used, D-phenylglycine derivatives can be efficiently produced in this fashion (Table 10).

Table 10. Stereoselective Strecker synthesis of D-aminonitriles **114** with galactosylamine **113** as chiral auxiliary [106,107].

R	Method [a]	T [°C]/ t [h]	Yield [b] [%]	D:L
$CH(CH_3)_2$	**B**	−18/5	74	8:1
$C(CH_3)_3$	**B**	−18/3	86	13:1
C_6H_5	**A**	0/1.5	70	4:1
C_6H_4-4-CH_3	**A**	−18/8	87	12:1
C_6H_4-4-Cl	**B**	−18/6	84	11:1

[a] **A**: $ZnCl_2$, isopropanol; **B**: $SnCl_4$, THF. [b] Yield of pure D diastereomer.

The free D-amino acids were obtained by treating the diastereomerically pure aminonitriles **114** with HCl/formic acid or HBr/acetic acid/dichloromethane. As shown with the example of 4-chlorophenylglycine **115**, the carbohydrate matrix could be removed without measurable racemization.[107]

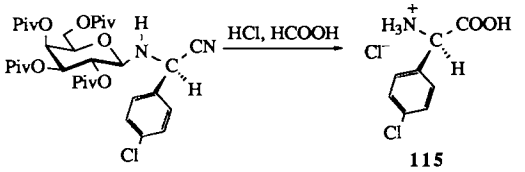

115

An interesting characteristic of the Strecker synthesis with galactosylimines **59** is that the direction of induction can be reversed by a change in solvent. Reaction of **59** with trimethylsilylcyanide in the presence of zinc chloride in chloroform led to preferential formation of L-aminonitrile **116**.[108] Moreover, Strecker synthesis with imines **59** in chloroform showed a remarkable dependence on the temperature; the (*S*) selectivity (for R = *i*Pr) increased from 60:40 at −20 °C to 84:16 at +20 °C.[109]

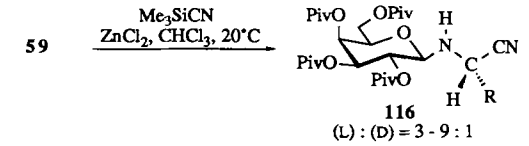

116

(L) : (D) = 3 - 9 : 1

The stereoselectivity in these Strecker syntheses of **114** and **116** and the opposing inductions observed in isopropanol and chloroform have been explained with the aid of zinc complex **117**. As a result of the delocalization of the π electrons in the C=N bond into the σ^* orbital of the C1–O bond, the Schiff bases **59** adopt the conformation illustrated in **117**. This was shown by a significant NOE in the ^{1}H NMR spectrum between the aldimine proton and 1-H. According to the NMR measurements this conformation is retained in the zinc complex (in both $[D_8]$THF and $CDCl_3$).

In polar media the cyanide released from the silylcyanide reacts with complex **117** preferentially by attack on the free back side to give D-aminonitriles.[106,107] In chloroform, however, free cyanide is not formed. In this case the nucleophilicity of the CN group must first be developed by interaction between the *exo* chloro ligand on zinc and the silyl group. After completion of this electronic circuit, which can only take place on the front side of the C=N bond, the CN group is sufficiently electron-rich to react with the imine, which in turn is activated by complexation. This geometry favors formation of L-aminonitriles **116**.[108] This alternative mode of reaction was confirmed in several other reactions. This process depends on whether a free nucleophile, or one that must first be developed during the process, reacts with the zinc complex of imines such as **59**.

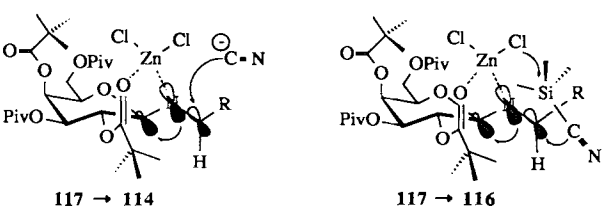

117 → **114** **117** → **116**

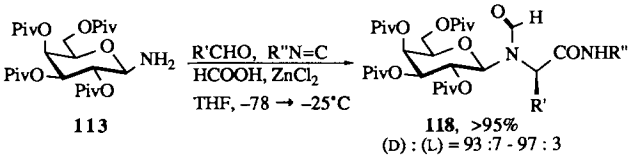

113

118, >95%

(D) : (L) = 93 :7 - 97 : 3

Another amino acid synthesis in which galactosylamine acts as chiral template is the Ugi reaction.[110] When galactosylamine **113** was allowed to react with an aldehyde, an isocyanide, and a carboxylic acid (preferably formic acid) in the presence of zinc chloride in THF, *N*-galactosyl-amino acid amide derivatives **118** were obtained almost quantitatively. At −25 °C (for aliphatic imines −78 °C) the D-amino acid diastereomers **118** were formed with a diastereoselectivity of about 95:5.[110,111]

Phenylglycine derivatives **118**, even those containing electron-withdrawing groups, were furnished with high stereoselectivity. Diastereomerically pure D-amino acid amides **118** could be isolated in yields of 75–95% by simple recrystallization from heptane or heptane/dichloromethane. Aliphatic amino acid amides were recovered in diastereomerically pure form by recrystallization from methanol/water or by flash chromatography. A few examples are listed in Table 11.

Table 11. Diastereoselective Ugi synthesis of amino acid amides **118** using D-galactosylamine **113** as the chiral auxiliary and *tert*-butyl isocyanide [110, 111].

R'	T [°C]/ t	D:L	Yield [%] [a]
n-propyl	−78/2 d	94:6	80
isopropyl	−78/2 d	95:5	86
tert-butyl	−25/3 d	96:4	80
phenyl	−25/24 h	95:5	80
styryl	−25/24 h	95:5	75

[a] Yield of pure 2-D-**118**.

Similarly high stereoselectivities were observed in Ugi reactions with *O*-acetyl-protected galactopyranosylamine.[111] The high differentiation in this one-pot reaction can also be explained with the aid of the zinc complex of the intermedi-

ate imine (**117**). The free isocyanide nucleophile attacks this complex with a strong preference for the back side, where it encounters no steric repulsion. Thus, the D-amino acid amide diastereomers **118** are formed with high selectivity. In agreement with this interpretation, no reversal of the direction of induction was obtained when this Ugi reaction was carried out in chloroform. Nevertheless, in order to obtain the interesting L-amino acid derivatives by the stereoselective Ugi reaction, the pivaloyl-protected D-arabinopyranosylamine **119** was used as a chiral template, quasi-enantiomeric to **113**.[112]

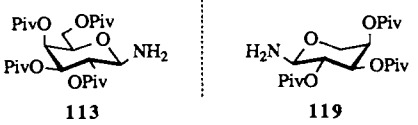

113 **119**

The comparison shows that **119**, although belonging to the D series, is almost the mirror image of galactosylamine **113** used hitherto. The Ugi reaction of D-arabinopyranosylamine **119** with aldehydes, *tert*-butyl isocyanide, and formic acid in the presence of zinc chloride in THF gave the L-amino acid amide derivatives **120** in excellent diastereoselectivity and in high yield. Diastereomerically pure compounds **120**

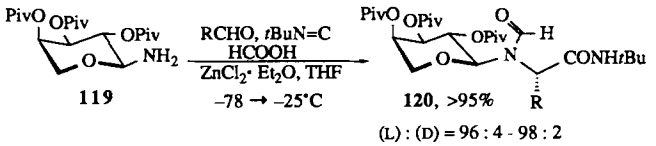

119

were recovered in yields of 85–95% by recrystallization or flash chromatography.[113] The examples given in Table 12 illustrate that diastereomerically pure aliphatic, branched, aromatic, and heteroaromatic L-amino acid derivatives **120** can be prepared according to this process with high efficiency.

Table 12. Diastereoselective Ugi synthesis of L-amino acid amides using D-arabinopyranosylamine **119** as chiral matrix [112,113].

R	T [°C]/t [h]	L:D	Yield [%] [a]
tert-butyl	–25/72	97:3	85
benzyl	–78/24	97:3	87
4-chlorophenyl	–25/24	98:2	91
2-furyl	–25/24	96:4	85
2-thienyl	–25/24	4:96	85 (2*D*)

[a] Yield of pure 2-L-**120**.

Exchange of the *O*-acyl protecting group in the glycosylamine for an *O*-methyl protecting group generally leads to a reduction in the stereoselection in this Ugi reaction.[114] This observation indirectly confirms the importance of the mechanism of differentiation via complexes such as **117**.

7.2. Stereoselective Syntheses of α-Aminophosphonic Acids

Chiral α-aminophosphonic acids are drawing increasing attention as enzyme inhibitors and building blocks for drugs. Stereoselective synthesis of such compounds by means of carbohydrate auxiliaries was achieved by Vasella et al.[115] These authors treated *N*-mannofuranosylnitrones such as **121**, already employed in 1,3-dipolar cycloadditions,[59] with phosphites like tris(trimethylsilyl)phosphite.

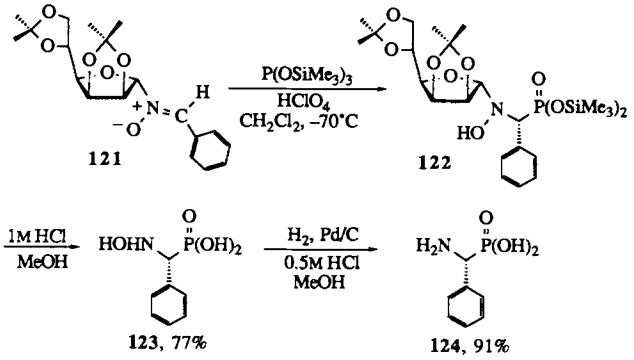

121 **122** **123, 77%** **124, 91%**

When the reaction was catalyzed with $HClO_4$, (*R*)-*N*-hydroxyphenylphosphaglycine (**123**) was obtained in high yield and with an optical purity of 87.5% after acidic workup. The latter could be increased to 95% by recrystallization. Hydrogenolysis of **123** (optical purity 95%) gave (*R*)-phenylphosphaglycine (**124**), the optical purity of which amounted to 88%.[115] For another aromatic aldehyde and three aliphatic aldehydes similar stereoselective syntheses of the corresponding aminophosphonic acids have been described. The reaction, the stereochemistry of which can be explained under the conditions given above by a kinetic *exo*-anomeric effect, shows a striking dependence on the Lewis acid catalyst employed, the amount of catalyst, and on the solvent. For example, **121** reacted selectively with the phosphite with catalysis by 0.01 equivalents of zinc chloride in benzene (78 °C) to give (*S*)-*N*-hydroxyphosphaglycine (*S*)-**123** (enantiomeric ratio 94:6). When the amount of zinc chloride was increased to 1 equivalent, the (*R*) enantiomer was again obtained in excess (o.p. > 83%).[115] To explain this effect it was assumed that the catalyst can influence both the conformational equilibrium of the nitrone and also the direction of approach of the phosphite. Based on NMR spectroscopic measurements on the nitrone **121**, it was concluded that zinc chloride can form a complex with both the *N*-oxide oxygen and with the O2 atom of the furanose component, in spite of the 1,2-*trans* arrangement of the ligands on the five-membered ring.

Complexation of a Lewis acid exerts an unmistakable influence on the facial differentiation in the formation of α-aminophosphonic acid esters from diethylphosphite and the Schiff bases **59** derived from galactosylamine **113**.[116] In the presence of catalytic amounts of tin tetrachloride in THF the four diastereomeric *N*-galactosyl-4-chlorophenylphosphaglycine esters **126** were formed from *N*-galactosylimine **125**. The β diastereoisomer **126** (83%) clearly predominated,

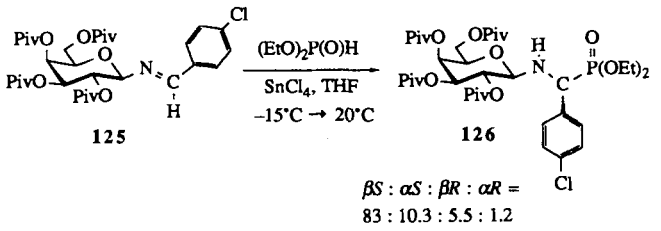

and overall a ratio of (*S*)/(*R*) diastereomers of 93:7 was found. The preferential formation of β-*S*-**126** is apparently due to tin complex **127**, in which the *Re* side of the imine **125** is effectively shielded. The phosphite attacks this complex as a free nucleophile (see the interpretation of the Strecker synthesis, Section 7.1) from the back side (*Si* side).

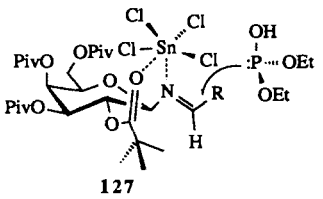

127

The reaction could also be carried out as a one-pot process, almost without loss of stereoselectivity, starting from galactosylamine **113**, the respective aldehyde, and phosphite. In addition, with fucosylamine **128** as a quasi-enantiomeric auxiliary, it was possible to prepare the series of (*R*)-diastereomeric α-aminophosphonic acid esters **129** with similar efficiency.[116] In reactions with the fucosyl derivatives

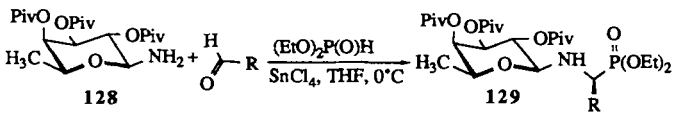

R = 4-MeC$_6$H$_4$: 81%
βR : αR : βS : αS = 85 : 4 : 10 : 1

the major diastereomers ((*R*) configuration) crystallized slowly. Since the corresponding *N*-glucosylaminophosphonic acid esters show a stronger inclination to crystallize, the major diastereomers, with (*S*) configuration, could be obtained in pure form.[116] This tendency to crystallize is effected largely by the pivaloyl protecting group.[117] The utility of this group for the isolation of enantiomerically pure α-amino acids[105–113] has already been documented.

7.3. Chiral Homoallylamines

Although the utility of the quasi-enantiomeric pair D-galactose and L-fucose had already been demonstrated in earlier stereoselective syntheses of (*S*)-[118,119] and (*R*)-homoallylamines,[120] the reaction of aldimines with allyltrimethylsilane had not yet been described for the simple, achiral case. The achievement of the reaction with *N*-glycosylimines such as **59** with Lewis acid catalysis can probably be traced back to the higher electrophilicity of these Schiff bases of semiaminal ethers such as **113** and **128**. In THF, however, the reaction must be initiated with 2.2 equivalents of tin tetrachloride and conducted at 0–25 °C. Nevertheless, high to excellent stereoselectivity was attained, and the (*S*)-homoallylamine derivatives **130** were preferentially formed from galactosylimines **59** in a ratio of 7–27:1. In this manner, however, the process was possible only with imines **59** derived from aromatic aldehydes. Some examples are listed in Table 13.

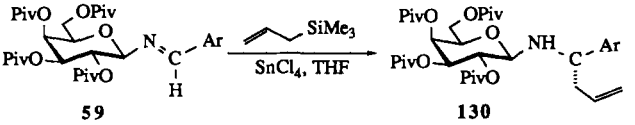

Table 13. Diastereoselective synthesis of *N*-galactosyl-1-arylhomoallylamines **130** [119].

Ar	*t* [d]	Yield [%]	(*S*):(*R*)
4-ClC$_6$H$_4$	2	49	22:1
C$_6$H$_5$	3	65	14:1
4-O$_2$NC$_6$H$_4$	2.5	73	8:1
4-MeC$_6$H$_4$	4.5	55	22:1
4-NCC$_6$H$_4$	3	49	15:1

Under these conditions the analogous imines **59** of aliphatic aldehydes undergo anomerization and decomposition. Their conversion to homoallylamines **131** was achieved, however, at −78 °C with allyltributylstannane instead of allylsilane, again in the presence of $SnCl_4$ (1.2 equivalents). Thus, (*R*)-homoallylamines **131** were obtained selectively with the same direction of induction.[118,119] The α anomers of **131** appeared as side products, formation of which occurred with lower stereoselectivity.

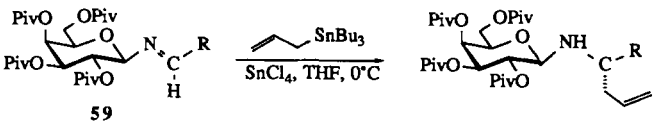

131a: R = *n*-C$_3$H$_7$, 32%, (*R*) : (*S*) = 24 : 1
131b: R = *n*-C$_9$H$_{19}$, 37%, (*R*) : (*S*) = 8 : 1

If these reactions are conducted with the *O*-pivaloyl-protected L-fucosylimines **132** instead of the quasi-enantiomeric *N*-galactosylimines **59**, then selective formation of the (*R*)-configurated homoallylamines **133** (R = aryl) and the (*S*)-homoallylamines (R = unbranched alkyl group) is possible.[120] The (*R*)-homoallylamines **133** were formed with high selectivity from imines derived from aromatic amines, whereas the aliphatic compounds again reacted only with allyltributylstannane to form **133** at −78 °C in low yields

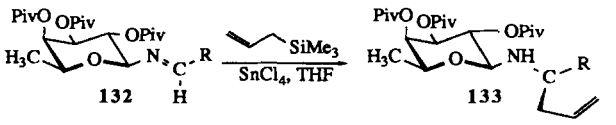

and in this case with only moderate selectivity. A few examples can be found in Table 14.

Table 14. Stereoselective synthesis of *N*-(L-fucosyl)-homoallylamines **133**[120].

R	*T* [a]/*t*	Yield [%]	(*R*):(*S*)
4-ClC$_6$H$_4$	RT/36 h	66	9:1
C$_6$H$_5$	RT/4 d	44	23:1
4-O$_2$NC$_6$H$_4$	RT/2 d	68	20:1
4-MeC$_6$H$_4$	RT/60 h	43	49:1
4-NCC$_6$H$_4$	RT/2 d	56	13:1
n-C$_3$H$_7$	−30 °C/36 h	26	4.5:1

[a] RT = room temperature.

Most *N*-fucosylhomoallylamines **133** are crystalline and can be obtained as the pure (*R*) diastereomer or as a strongly enriched mixture simply by recrystallization. The homoallylamines **130**, **131**, and **133** can be converted in a variety of ways into other chiral products.

1-Phenylhomoallylamine **135** was released quantitatively from the carbohydrate auxiliary by treatment of the phenyl derivative **134** with aqueous methanolic hydrochloric acid. After introduction of the Boc protecting group (Boc = *tert*-butoxycarbonyl) and oxidation of the double bond, the Boc-protected *β*-phenyl-*β*-alanine **136** was obtained; acidolysis provided free (*S*)-*β*-phenyl-*β*-alanine (**137**).

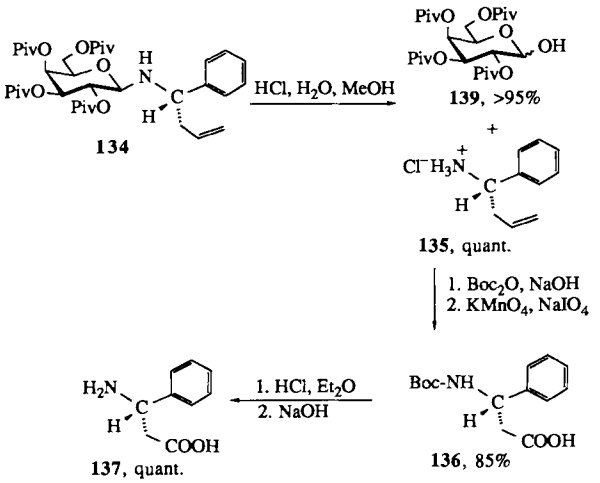

After its removal the carbohydrate auxiliary was recovered almost quantitatively. (*S*)-*β*-Phenyl-*β*-alanine (**137**), a precursor to Winterstein's acid,[121] was thus obtained from galactosamine **113** in six steps with an overall yield of 41%. In contrast, a 15-step synthesis from L-diethyltartrate provided (*S*)-**137** in 4.3% yield and with a lower optical purity.[122] This comparison illustrates the utility of allylsilane additions to *N*-glycosylimines.[118–120]

7.4. Syntheses of Chiral *β*-Amino Acids

Glycosylimines, for example those of type **59**, offer an alternative, direct, and highly stereoselective synthesis of chiral *β*-amino acids. They react with silylketene acetals in THF under catalysis by zinc chloride in the fashion of a Mannich reaction to give *N*-glycosyl-*β*-amino acid esters **138**, as shown by the reaction with the silylketene acetal of isobutyric acid methyl ester.[123] The reaction proceeded with high

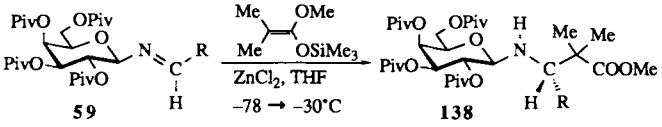

stereocontrol and frequently produced products with a diastereomeric ratio of over 100:1. An effective stereoselection was observed even at room temperature. Some examples are listed in Table 15.

Table 15. Diastereoselective synthesis of *N*-galactosyl-*β*-amino acid esters **138** using an asymmetric Mannich reaction[123].

R	*T* [°C]/*t* [h]	Yield [%]	L:D
3-ClC$_6$H$_4$	−30/24	90	68:1
C$_6$H$_5$	−30/24	89	150:1
4-FC$_6$H$_4$	−30/24	88	105:1
2-naphthyl	+30/72	90	10:1
n-C$_3$H$_7$	−30/24	83	250:1

The preferred formation of the (*S*)-diastereomeric *β*-amino acid ester **138** was proven by conversion of the phenyl derivative **138a** into free *β*-phenyl-*α*,*α*-dimethyl-*β*-alanine (**141**), the (*R*) enantiomer of which is known in the literature.[124] Treatment of **138a** with HCl in methanol led to quantitative cleavage of the N-glycosidic bond. The auxiliary **139** was completely recovered. Warming the *β*-amino acid ester **140** in aqueous HCl gave the free (*S*)-amino acid **141**. This procedure is generally applicable for the synthesis of free enantiomerically pure *β*-amino acids from diastereomers **138**.

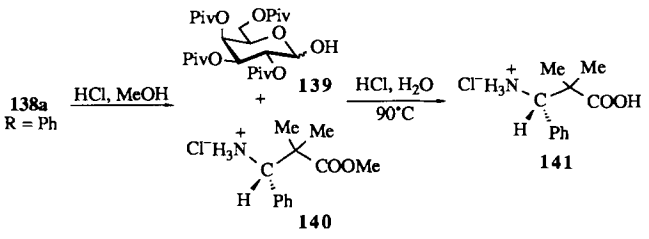

Attack on the *Re* side of the *N*-galactosylimine–zinc complex **117** is a prerequisite for the highly selective formation of the (*S*)-configurated *β*-amino acid diastereomers **138**. This result can be explained by an initiatiating interaction of the silyl group in the silylketene acetal with one of the chloro ligands on the zinc atom (**142**) similar to the case of the (*S*)-selective Strecker synthesis in chloroform (see **117** → **116**, Section 7.1). Attaching the reaction partners steers the approach such that it occurs selectively on the *Re* side of the imine (front side in **142**). This interaction between Cl and Si, illustrated for **142**, generates the required nucleophilicity of

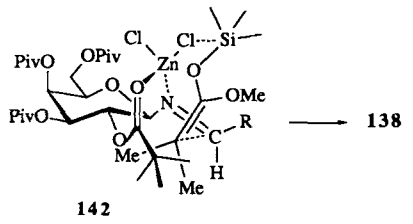

142 → 138

the ketene acetal and leads the way to the C–C bond forming electron transfer. This interpretation was prompted by the stereochemistry observed in presumed hetero-Diels–Alder reactions between galactosylimines **59** and silyloxydienes (see Section 7.5).[125]

7.5. Chiral 2-Substituted Piperidines and Mannich Bases

In the course of investigations on the hetero-Diels–Alder reaction of *N*-galactosylimines **59**[57] (see Section 4.2), 1-methoxy-3-trimethylsiloxybuta-1,3-diene[126] was employed as an electron-rich diene. As a result of the high reactivity of the latter, the reaction proceeded under catalysis by zinc chloride in THF at low temperature (−40 to −20 °C). After hydrolysis with dilute hydrochloric acid, *N*-galactosyl-2,3-dehydropiperidin-4-one derivatives **143** were obtained in high yield and excellent stereoselectivity. The reaction does not proceed as a concerted cycloaddition, as only shown when the products were hydrolyzed with ammonium chloride solution. The initially formed Mannich base **144** could then be isolated and characterized. The diastereomeric ratios

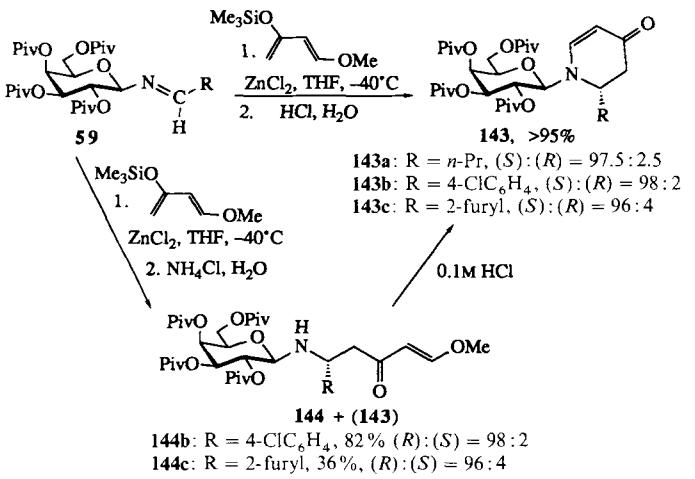

were obtained by analytical HPLC of the hydrolyzed reaction solution and gave the same values for **143** and **144**.[125] According to this, the formation of the chiral piperidinones **143** proceeds as a tandem Mannich–Michael addition, which is terminated by the elimination of methanol in the condensation step. The major diastereomers of the chiral heterocycles **143** were obtained in pure form in yields of 60–90% by recrystallization or flash chromatography.[125]

Piperidinones are starting materials for further transformations. In this context reduction and deoxygenation of **143a** gave *N*-galactosylconiine **145**. After the straightforward removal of the carbohydrate matrix, (*S*)-coniine (**146**) was obtained in enantiomerically pure form. The absolute configuration of the Mannich bases **144** and the piperidinones **143** were thereby clarified at the same time.

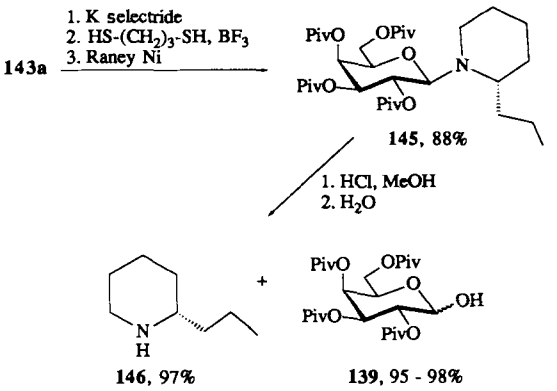

The Schiff base (**59**) of 3-pyridinaldehyde **147** underwent the tandem Mannich–Michael process with 1-methoxy-3-silyloxybutadiene with similarly high stereoselectivity (96:4). Two equivalents of zinc chloride were required, however, and the opposite direction of induction was shown with formation of (*S*)-piperidinone **148**.

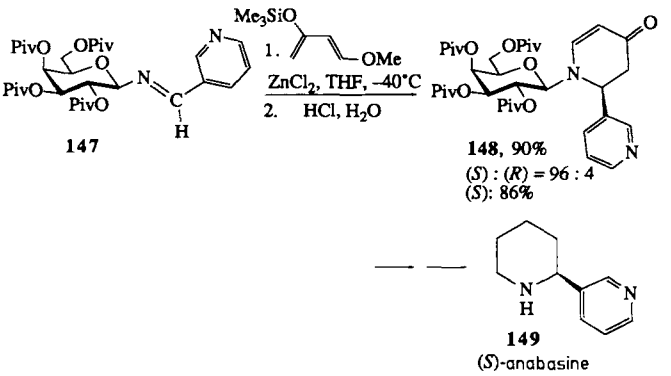

The pure major diastereomer **148** was again isolated in high yield by simple flash chromatography. By means of an analogous reaction series as that used for coniine, compound **148** was converted into enantiomerically pure (*S*)-anabasine (**149**). This process brought to light the surprising opposing direction of induction and initiated the more detailed investigation of the presumed cycloadditions. The opposite diastereofacial selectivity in the preliminary Mannich reaction leading to **145** and **148** was explained by the reaction of the zinc complexes **150** and **151** with the silyldienol ether.[125]

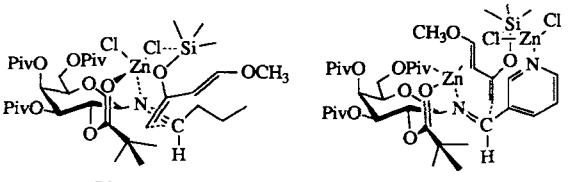

The reactions of the Schiff bases **59** with the silyloxydiene required only one equivalent of zinc chloride. The stereochemistry of the products **143** formed can be explained by a reaction pathway (**150**) analogous to that of the silylketene acetal reaction (**142**). In the reaction with 3-pyridylaldimine **147** the first equivalent of zinc chloride coordinates to the more nucleophilic nitrogen atom of the pyridine. This equivalent of zinc chloride is thus no longer available for activation of the imine, but carries the more nucleophilic chloro ligands that favor the interaction with the silyloxydiene molecule in **151** and effect the alternative introduction of the nucleophile to the *Si* side (back side) of the imine. These interpretations of the course of the reaction are working hypotheses, which nevertheless permit systematic conclusions to be made regarding the selection processes taking place on carbohydrate auxiliaries, and which also stimulate new experiments. In this fashion, concepts have been developed, in particular for the reactions of glycosylamines, that permit predictions to be made concerning the stereochemistry expected from the envisaged processes involving carbohydrate auxiliaries.

8. Characteristics of Stereoselection with Carbohydrates

As stereodiscriminating auxiliaries carbohydrates offer a variety of possibilities for spatial differentiation at a reactive group. In principle, numerous parameters are provided for adjustment of a desired stereoselectivity—the choice of carbohydrate, the regioselective attachment of the substrate unit, the selected introduction of sterically shielding groups, the epimerization at chiral centers, and the organization of reactive groups and the functional groups on the carbohydrate by formation of complexes. Steric shielding predominantly characterizes, for example, the function of diacetone glucose in chiral complex borohydrides,[81-88] and in the chiral titanium Lewis acids,[92-96] which sterically control aldol reactions and the nucleophilic transfer of allyl groups to carbonyl compounds very effectively. The stereoselectivity of cycloadditions is also sterically controlled in the absence of coordinating Lewis acids; the effects of attachment at, for example, the 3-position of diacetone glucose[45, 56] are generally greater than those obtained by attachment at the anomeric center.[40, 41, 43-45]

If steric and complexation effects can be combined to give a strong facial differentiation, then high stereoselectivity can be attained, as has been shown, for example, for Diels–Alder reactions[46-48, 50] and cyclopropanations.[71]

A particular characteristic of carbohydrate auxiliaries is provided by the striking stereoelectronic effects, in particular those that involve the anomeric substituents. Thus, the excellent stereoselectivity in the cycloaddition to anomeric chloronitroso-mannofuranoses[53] can be traced back to an *exo*-anomeric effect that fixes the heterodienophile spatially. If steric, stereoelectronic, and complexing influences can be cooperatively combined, an effective stereoselection can be established, especially for attachment of the reacting species at the anomeric center. This is underlined by the Strecker and Ugi syntheses of α-amino acid derivatives and [105-113] the Mannich reactions to give β-amino acid esters[123] and chiral piperidine derivatives, which open up routes to stereoselective syntheses of alkaloids.[125] The high stereoselectivities of the reactions of allylsilanes and -stannanes with glycosylimines result from the same sources.[118-120] Bicyclic carbohydrate auxiliaries generate a particularly effective facial differentiation that permits, for example, the 1,4-addition of alkylaluminum compounds to unsaturated carboxylic acid derivatives to be steered with high selectivity.[79] Furthermore, carbohydrates offer the possibility of synthesizing both series of enantiomers of a chiral product alternatively and selectively, as was demonstrated for the pair galactosylamine and D-arabinosylamine in the Strecker and Ugi syntheses[110-113] and later also in cycloadditions.[48, 71]

A multitude of interesting chiral products are accessible in diastereo- or enantioselective fashion, either with carbohydrate auxiliaries or with carbohydrate reagents. These include chiral carbocycles, heterocycles, branched carboxylic acids, secondary alcohols, β-lactams, and α- and β-amino acids. The interest in the stereodifferentiating potential of carbohydrates may continue to increase, so that in addition to the well-developed ex-chiral pool syntheses, in which carbohydrate units are built into chiral products, the use of carbohydrates as versatile and easily modified chiral auxiliaries in stereoselective synthesis will be established as an independent research area. In the field of enantioselective catalysis[127] the hitherto rarely considered carbohydrates (neglecting hydrogenation catalysts) also appear to bear interesting potential.[128] In an early study Inch et al.[129] employed diacetone glucose **93** as an equimolar solvent additive to steer a Grignard–carbonyl reaction stereoselectively. In the addition of MeMgBr to cyclohexyl phenyl ketone the corresponding methylcarbinol was obtained in 70% optical and 95% chemical yield.

Chiral Lewis acids such as **153**, derived from D-mannitol, were used successfully as equimolar additives in asymmetric Diels–Alder reactions of cyclopentadiene with *N*-crotonyl-4,4-dimethyloxazolidin-2-one (**152**).[130]

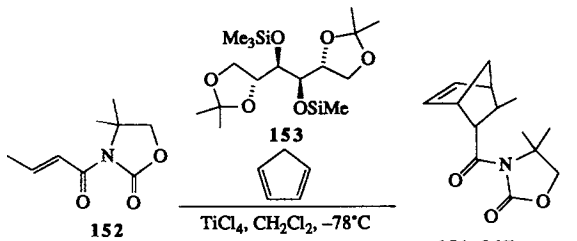

In the field of catalytic enantioselective processes, application of macrocyclic lactose derivatives leads to asymmetric Michael additions. Thus, phenylacetic acid methyl ester underwent smooth addition to methyl acrylate at −78 °C in the presence of potassium *tert*-butylate and catalyst **155** to give **156** in 70% optical and 73% chemical yield.[131]

Catalysis of the addition of diethyl zinc to aldehydes such as benzaldehyde can be influenced enantioselectively by carbohydrate catalysts. Addition of penta-*O*-pivaloyl-β-D-galactopyranose (**157**) to the reaction of benzaldehyde with

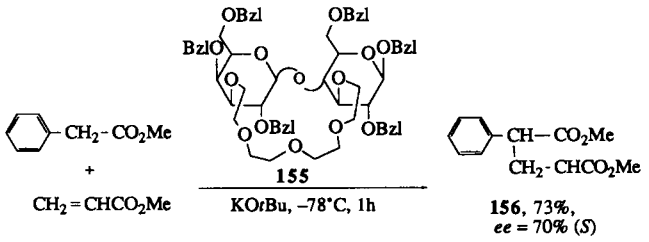

diethyl zinc in toluene gave 1-phenylpropanol with considerable excess of the (*R*) enantiomer **158**.[132] It is remarkable that **157** is not only relatively planar but also contains no acidic functional groups, as usually required for catalysis of reactions of diethyl zinc.

When the more complex diamide **159**,[133] obtained simply from pyridine-2,6-dicarboxylic acid and glucosamine, was employed in this reaction as catalyst, a completely chemoselective reaction was observed. No benzyl alcohol was formed by hydride transfer. The transfer of an ethyl group

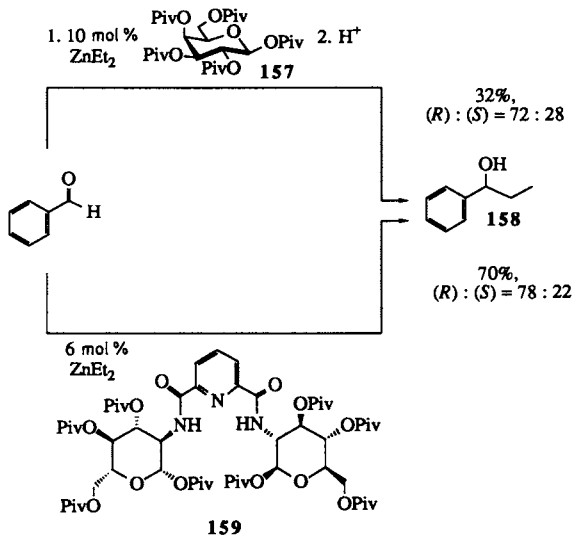

proceeded with an enantioselectivity of 4:1 in favor of the (*R*) enantiomer **158**.[133] It is easy to see that carbohydrates can be converted into highly selective catalysts for enantioselective synthesis and that these generally inexpensive, naturally occurring, regenerable compounds will open up a further, attractive field of application.

We thank the Deutsche Forschungsgemeinschaft, the Bundesminister für Forschung und Technologie, and the Fonds der Chemischen Industrie for the financial support of our work. K. R. thanks the Adolf-Todt-Stiftung of the University of Mainz for a stipend and the Fonds der Chemischen Industrie for a doctoral stipend. H. K. expresses his gratitude for the stimulating teamwork of all those co-workers whose ability and enthusiam have helped to further the cause of stereoselective syntheses with carbohydrates. In addition to the coauthor these include Joachim Weissmüller, Bernd Müller, Jürgen Mohr, Wilfried Sager, Klaus-Jürgen Pees, Waldemar Pfrengle, Matthias Decker, Wolfgang Stähle, Dirk Schwanzenbach, Sabine Laschat, Stefan Engel, Ingo Ganz, Michael Puhl, Helmut Haning, Dominique Hebrault, Andreas Burgard, Markus Weymann, and Arnim Stamm.

Received: July 23, 1992 [A 895IE]
German version: *Angew. Chem.* **1993**, *105*, 355
Translated by Dr. M. D. Ravenscroft, Bischwiller (France)

[1] Recent brief overviews: K.-A. Karlsson, *Trends Biochem. Sci.* **1991**, *12*, 265.
[2] G. Ashwell, A. G. Morell, *Adv. Enzymol. Relat. Areas Mol. Biol.* **1974**, *41*, 99.
[3] a) G. N. Sando, E. F. Neufeld, *Cell* **1977**, *12*, 619; b) A. Kaplan, D. T. Achord, W. S. Sly, *Proc. Natl. Acad. Sci USA* **1977**, *74*, 2026.
[4] For a review see, for example: K.-A. Karlsson, *Annu. Rev. Biochem.* **1989**, *58*, 309.
[5] For a review on tumor-associated antigens, see, for example: S. I. Hakomori, *Adv. Cancer Res.* **1989**, *52*, 257.
[6] a) See, for example: M. L. Phillips, E. Nudelman, F. C. A. Gaeta, M. Perez, A. K. Singhal, S.-I. Hakomori, J. C. Paulson, *Science* **1990**, *250*, 1130; b) R. J. Wieser, F. Oesch, *J. Cell. Biol.* **1986**, *103*, 361.
[7] R. R. Schmidt, *Angew. Chem.* **1986**, *98*, 213; *Angew. Chem. Int. Ed. Engl.* **1986**, *25*, 212.
[8] R. U. Lemieux, *Chem. Soc. Rev.* **1989**, *18*, 347.
[9] H. Kunz, *Angew. Chem.* **1987**, *99*, 297; *Angew. Chem. Int. Ed. Engl.* **1987**, *26*, 294.
[10] R. D. Marshall, A. Neuberger, *Adv. Carbohydr. Chem. Biochem.* **1970**, *25*, 407.
[11] W. I. Weis, R. Kahn, R. Fourme, K. Drikamer, W. A. Hendrickson, *Science* **1991**, *254*, 1608.
[12] J. R. Vercellotti, R. Fernandez, C. J. Chang, *Carbohydr. Res.* **1967**, *5*, 97.
[13] R. Kuhn, I. Löw, *Ber. Dtsch. Chem. Ges.* **1941**, *74*, 219.
[14] T. Mizoguchi, G. Levin, D. W. Woolley, J. M. Stewart, *J. Org. Chem.* **1968**, *33*, 903.
[15] H. Kunz, R. Kullmann, unpublished; R. Kullmann, Diplomarbeit, Universität Mainz, **1987**.
[16] H. Kunz, R. Kullmann, *Tetrahedron Lett.* **1992**, *33*, 6115.
[17] R. R. Schmidt, U. Moering, M. Reichrath, *Chem. Ber.* **1982**, *115*, 39.
[18] H. Kunz in *Selectivities in Lewis Acid Promoted Reactions* (Ed.: D. Schinzer), Kluwer, Amsterdam, **1989**, p. 189.
[19] T. D. Inch, *Synthesis* **1970**, 466.
[20] a) S. R. Landor, B. J. Miller, A. R. Tatchell, *J. Chem. Soc. C* **1966**, 1922, 2280; b) S. R. Landor, B. J. Miller, A. R. Tatchell, *ibid.* **1967**, 197.
[21] A. Vasella, R. Voeffrey, *Helv. Chim. Acta* **1982**, *65*, 1953.
[22] S. Hanessian in *Organic Synthesis – an Interdisciplinary Challenge* (Eds.: J. Streith, H. Prinzbach, G. Schill), (*Proc. 5th IUPAC Symp. Org. Synth.*), Blackwell, Oxford, **1985**, p. 267.
[23] C. H. Heathcock, C. T. Buse, W. A. Kleschik, M. C. Pirrung, J. E. Sohn, J. Lampe, *J. Org. Chem.* **1980**, *45*, 1066.
[24] Review: J. Jurczak, S. Pikul, T. Bauer, *Tetrahedron* **1986**, *2*, 447.
[25] K. L. Yu, S. Hand, R. Tsang, B. Fraser-Reid, *Tetrahedron* **1991**, *47*, 189.
[26] C. H. Heathcock, C. T. White, J. J. Morrison, D. van Derveer, *J. Org. Chem.* **1981**, *46*, 1296.
[27] S. Brandänge, S. Josephson, L. Mörch, S. Vallèn, *Acta Chem. Scand. Ser. B* **1981**, *35*, 273.
[28] H. Kunz, J. Mohr, *J. Chem. Soc. Chem. Commun.* **1988**, 1315.
[29] A review on the structure and properties of lithium enolates can be found in: D. Seebach, *Angew. Chem.* **1988**, *100*, 1685; *Angew. Chem. Int. Ed. Engl.* **1988**, *27*, 1624.
[30] a) U. Schöllkopf, T. Tölle, E. Egert, M. Nieger, *Liebigs Ann. Chem.* **1987**, 399; b) I. Hoppe, U. Schöllkopf, T. Tölle, *Synthesis* **1984**, 789.
[31] In reference [30b] the configuration of the (*E*) ester enolate probably involved could not be proven and is formulated in an unlikely conformation. Analysis of the results was also made more difficult because the alkylation products **25** of the Schiff bases of alanine ester [30b] and leucine ester, on the one hand, and those of valine and isoleucine ester [30a], on the other, are given throughout as having predominantly the (*S*) configuration.
[32] J. Mulzer, U. Steffen, L. Rorn, C. Schneider, E. Weinhold, W. Münch, R. Rüdert, P. Luger, H. Harth, *J. Am. Chem. Soc.* **1988**, *110*, 4640.
[33] R. E. Ireland, R. H. Mueller, A. K. Willard, *J. Am. Chem. Soc.* **1976**, *98*, 2868.
[34] Review: D. A. Evans in *Asymmetric Synthesis* (Ed.: J. D. Morrison), Academic Press, New York, **1984**, p. 1; C. H. Heathcock, *ibid.*, p. 111.
[35] L. Duhamel, P. Angiland, J. R. Desmurs, J. Y. Valuot, *Synlett* **1991**, 807.
[36] D. Horton, T. Machinami, *J. Chem. Soc. Chem. Commun.* **1981**, 88.
[37] a) S. J. Danishefsky, W. H. Pearson, D. F. Harvey, C. J. Maring, J. P. Springer, *J. Am. Chem. Soc.* **1985**, *107*, 1256; b) S. J. Danishefsky, R. Hungate, *J. Am. Chem. Soc.* **1986**, *108*, 2486.
[38] a) M. Chmielewski, Z. Kaluza, *Carbohydr. Res.* **1987**, *167*, 143; b) H. Redlich, J. B. Lenfers, J. Kopf, *Angew. Chem.* **1989**, *101*, 764; *Angew. Chem. Int. Ed. Engl.* **1989**, *28*, 777.

[39] S. David, A. Lubineau, A. Thieffry, *Tetrahedron* **1978**, *34*, 299, and references therein.
[40] R. C. Gupta, A. M. Z. Slawin, R. J. Stoodley, D. J. Williams, *J. Chem. Soc. Chem. Commun.* **1986**, 668.
[41] R. C. Gupta, D. S. Larsen, R. J. Stoodley, A. M. Z. Slawin, D. J. Williams, *J. Chem. Soc. Perkin Trans. 1* **1989**, 739.
[42] S. W. Bird, A. Lewis, *Tetrahedron Lett.* **1989**, *30*, 6227.
[43] A. Lubineau, Y. Queneau, *J. Org. Chem.* **1987**, *52*, 1001.
[44] A. Lubineau, Y. Queneau, *Tetrahedron* **1989**, *45*, 6697.
[45] A. Lubineau, J. Augé, N. Bellanger, S. Caillebourdin, *Tetrahedron Lett.* **1990**, *31*, 4147.
[46] H. Kunz, B. Müller, D. Schanzenbach, *Angew. Chem.* **1987**, *99*, 269; *Angew. Chem. Int. Ed. Engl.* **1987**, *26*, 267.
[47] T. K. Shing, P. Lloyd-Williams, *J. Chem. Soc. Chem. Commun.* **1987**, 423.
[48] W. Stähle, H. Kunz, *Synlett* **1991**, 260.
[49] H. Kunz, W. Stähle, unpublished; W. Stähle, Dissertation, Universität Mainz, **1991**.
[50] R. Nouguier, J.-L. Gras, B. Girard, A. Virgili, *Tetrahedron Lett.* **1991**, *32*, 5529.
[51] a) D. A. Evans, K. T. Chapman, J. Bisaha, *J. Am. Chem. Soc.* **1988**, *110*, 1238; b) G. Helmchen, R. Karge, J. Weetman in *Modern Synthetic Methods* (Ed.: R. Scheffold), Springer, Berlin, **1986**, p. 261.
[52] H. Kunz, B. Müller, W. Pfrengle, K. Rück, W. Stähle in *Cycloaddition Reactions in Carbohydrate Chemistry* (Ed.: R. M. Giuliano), (*ACS Symp. Ser.* **1992**, *494*, p. 131).
[53] a) H. Felber, G. Kresze, R. Prewo, A. Vasella, *Helv. Chim. Acta* **1986**, *69*, 1137; b) H. Braun, R. Charles, G. Kresze, M. Sabuni, J. Winckler, *Liebigs Ann. Chem.* **1987**, 1129.
[54] H. Braun, H. Felber, G. Kresze, A. Ritter, F. P. Schmidtchen, A. Schneider, *Tetrahedron* **1991**, *47*, 3313.
[55] A. Choudhury, R. W. Frank, R. B. Gupta, *Tetrahedron Lett.* **1989**, *37*, 4921.
[56] a) H. U. Reissig, *Angew. Chem.* **1992**, *104*, 295; *Angew. Chem. Int. Ed. Engl.* **1992**, 288; b) T. Arnold, B. Orschel, H.-U. Reissig, *ibid.* **1992**, *104*, 1084 and **1992**, 1033.
[57] W. Pfrengle, H. Kunz, *J. Org. Chem.* **1989**, *54*, 4261.
[58] H. Kunz, D. Hebrault, unpublished (Abstract 243, XVI. Int. Carbohydr. Symp., Paris, July 6–10, **1992**).
[59] A. Vasella, *Helv. Chim. Acta* **1977**, *60*, 1273.
[60] H. Huber, A. Knierzinger, E. Krawzcyk, J.-P. Obrecht, A. Vasella in *Organic Synthesis – an Interdisciplinary Challenge* (Eds.: J. Streith, H. Prinzbach, G. Schill), (*Proc. 5th IUPAC Symp. Org. Synth.*) Blackwell, Oxford, **1985**, p. 255, and references therein.
[61] P. M. Wovkulich, F. Barcelos, A. D. Batcho, J. F. Sereno, E. G. Baggiolini, B. M. Hennessy, M. R. Uskokovic, *Tetrahedron* **1984**, *40*, 2283.
[62] S. Mzengeza, R. A. Whitney, *J. Org. Chem.* **1988**, *53*, 4074.
[63] T. Matsui, T. Morooka, M. Nakayama, *Bull. Chem. Soc. Jpn.* **1987**, *60*, 417.
[64] a) R. Pelzer, P. Jütten, H.-D. Scharf, *Chem. Ber.* **1989**, *122*, 487; b) H. Buschmann, H.-D. Scharf, N. Hoffmann, P. Esser, *Angew. Chem.* **1991**, *103*, 480–518; *Angew. Chem. Int. Ed. Engl.* **1991**, *30*, 477–515.
[65] Z. Kaluza, W. Fudong, C. Belzecki, M. Chmielewski, *Tetrahedron Lett.* **1989**, *38*, 5171.
[66] D. H. R. Barton, A. Gateau-Olesher, J.-A. Mateos, J. Cleophax, S. D. Gero, A. Chiaroni, C. Riche, *J. Chem. Soc. Perkin Trans. 1* **1990**, 3211.
[67] a) G. I. Georg, P. M. Mashava, E. Akgün, M. W. Milstead, *Tetrahedron Lett.* **1991**, *32*, 3152; see also Corrigendum *ibid.* **1992**, *33*, 152; b) G. I. Georg, E. Akgün, P. M. Mashava, M. Milstead, H. Ping, Z.-J. Wu, D. Vander Velde, F. Takusagawa, *ibid.* **1992**, *33*, 2111.
[68] B. C. Borer, D. W. Balogh, *Tetrahedron Lett.* **1991**, *32*, 1039.
[69] a) R. B. Woodward, R. Hoffmann, *Angew. Chem.* **1969**, *81*, 797; *Angew. Chem. Int. Ed. Engl.* **1969**, *8*, 781; b) K. N. Houk, Y. Li, J. D. Evanseck, *ibid.* **1992**, *104*, 711 and **1992**, *31*, 682.
[70] I. Fleming, *Frontier Orbitals and Organic Chemical Reactions*, Wiley, London, **1976**.
[71] a) A. B. Charette, B. Cotè, J.-F. Marcoux, *J. Am. Chem. Soc.* **1991**, *113*, 8166; b) A. B. Charette, J.-F. Marcoux, B. Cotè, *Tetrahedron Lett.* **1991**, *32*, 7215.
[72] K. Kakinuma, T. Koudate, H.-Y. Li, T. Eguchi, *Tetrahedron Lett.* **1991**, *32*, 5801.
[73] H. Kunz, K.-J. Pees, unpublished; K.-J. Pees, Dissertation, Universität Mainz, **1987**.
[74] H. Kunz, S. Laschat, unpublished; S. Laschat, Dissertation, Universität Mainz, **1990**.
[75] M. Kawana, S. Emoto, *Bull. Chem. Soc. Jpn.* **1966**, *39*, 910.
[76] Y.-S. Hon, F.-L. Chen, Y.-P. Huang, T.-J. Lu, *Tetrahedron: Asymmetry* **1991**, *2*, 879.
[77] H. Kunz, K.-J. Pees, *J. Chem. Soc. Perkin Trans. 1* **1989**, 1169.
[78] H. Kunz, K. Rück, *Angew. Chem.* **1991**, *103*, 712; *Angew. Chem. Int. Ed. Engl.* **1991**, *30*, 694.
[79] H. Kunz, K. Rück, *Synlett* **1992**, 343.
[80] H. Kunz, K. Rück, unpublished; K. Rück, Dissertation, Universität Mainz, **1992**.
[81] A. Hirao, H. Mochizuki, S. Nakahama, N. Yamazaki, *J. Org. Chem.* **1979**, *44*, 1720.
[82] A. Hirao, S. Itsuno, H. Mochizuki, S. Nakahama, N. Yamazaki, *Bull. Chem. Soc. Jpn.* **1981**, *54*, 1424.
[83] A. Hirao, S. Nakahama, H. Mochizuki, S. Itsuno, N. Yamazaki, *J. Org. Chem.* **1980**, *45*, 4231.
[84] A. Hirao, S. Itsuno, M. Owa, S. Nagami, H. Mochuzuki, H. H. A. Zoorov, S. Nakahama, N. Yamazaki, *J. Chem. Soc. Perkin Trans. 1* **1981**, 900.
[85] J. D. Morrison, E. R. Gandbois, S. I. Howard, *J. Org. Chem.* **1980**, *45*, 4229.
[86] a) H. C. Brown, W. S. Park, B. T. Cho, *J. Org. Chem.* **1986**, *51*, 1936; b) H. C. Brown, W. S. Park, B. T. Cho, P. V. Ramachandran, *J. Org. Chem.* **1987**, *52*, 5402.
[87] H. C. Brown, B. T. Cho, W. S. Park, *J. Org. Chem.* **1988**, *53*, 1231.
[88] B. T. Cho, Y. S. Chun, *Tetrahedron: Asymmetry* **1992**, *3*, 341.
[89] See, for example: M. Fiorini, G. M. Giongo, *J. Mol. Catal.* **1980**, *7*, 411.
[90] See, for example: D. Sinon, G. Descotes, *React. Kinet. Catal. Lett.* **1980**, *14*, 463, and references therein.
[91] R. Selke, *J. Organomet. Chem.* **1989**, *370*, 249.
[92] M. Riediker, R. O. Duthaler, *Angew. Chem.* **1989**, *101*, 488; *Angew. Chem. Int. Ed. Engl.* **1989**, *28*, 494.
[93] R. O. Duthaler, P. Herold, W. Lottenbach, K. Oertle, M. Riediker, *Angew. Chem.* **1989**, *101*, 490; *Angew. Chem. Int. Ed. Engl.* **1989**, *28*, 495.
[94] G. Bold, R. O. Duthaler, M. Riediker, *Angew. Chem.* **1989**, *101*, 497; *Angew. Chem. Int. Ed. Engl.* **1989**, *28*, 497.
[95] R. O. Duthaler, P. Herold, S. Wyler-Helfer, M. Riediker, *Helv. Chim. Acta* **1990**, *73*, 659.
[96] a) R. O. Duthaler, A. Hafner, M. Riediker, *Pure Appl. Chem.* **1990**, *62*, 631; b) A. Hafner, R. O. Duthaler, R. Marti, P. Rothe-Streit, F. Schwarzenbach, *J. Am. Chem. Soc.* **1992**, *114*, 2321.
[97] L. F. Tietze, P. Saling, *Synlett* **1992**, 281.
[98] P. Duhamel, J. J. Eddine, J.-Y. Valnot, *Tetrahedron Lett.* **1987**, *28*, 3801.
[99] J. M. Lera, J. Fernandez, F. Aleudia, *Tetrahedron Lett.* **1991**, *32*, 7299.
[100] F. M. Stoyanovich, E. P. Zakharov, Y. L. Goldfarb, M. M. Kraynshkin, *Izv. Akad. Nauk SSSR Ser. Khim.* **1986**, 1455.
[101] U. Gerlach, S. Hünig, *Angew. Chem.* **1987**, *99*, 1323; *Angew. Chem. Int. Ed. Engl.* **1987**, *26*, 1283.
[102] a) L. Duhamel, J.-C. Plaquevent, *J. Chem. Soc.* **1978**, *100*, 7415; b) see also: *Tetrahedron Lett.* **1980**, *21*, 2521.
[103] Review: R. M. Williams, *Synthesis of Optically Active α-Amino Acids*, Pergamon, Oxford, **1989**.
[104] Review: P. Cintas, *Tetrahedron* **1991**, *47*, 6079.
[105] H. Kunz, W. Sager, W. Pfrengle, M. Decker, DE-A 3624376 A1, **1986**; *Chem. Abstr.* **1988**, *111*, 39830.
[106] H. Kunz, W. Sager, *Angew. Chem.* **1987**, *99*, 595; *Angew. Chem. Int. Ed. Engl.* **1987**, *26*, 557.
[107] H. Kunz, W. Sager, D. Schanzenbach, M. Decker, *Liebigs Ann. Chem.* **1991**, 649.
[108] H. Kunz, W. Sager, W. Pfrengle, D. Schanzenbach, *Tetrahedron Lett.* **1988**, *29*, 4397.
[109] H. Kunz, D. Schanzenbach, unpublished.
[110] H. Kunz, W. Pfrengle, *J. Am. Chem. Soc.* **1988**, *110*, 651.
[111] H. Kunz, W. Pfrengle, *Tetrahedron*, **1988**, *44*, 5487.
[112] H. Kunz, W. Pfrengle, W. Sager, *Tetrahedron Lett.* **1989**, *30*, 4109.
[113] H. Kunz, W. Pfrengle, K. Rück, W. Sager, *Synthesis* **1991**, 1039.
[114] M. Göbel, I. Ugi, *Synthesis* **1991**, 1095.
[115] R. Huber, A. Vasella, *Helv. Chim. Acta* **1987**, *70*, 1461, and references therein.
[116] S. Laschat, H. Kunz, *Synthesis* **1992**, 90.
[117] H. Kunz, A. Harreus, *Liebigs Ann. Chem.* **1982**, 41.
[118] S. Laschat, H. Kunz, *Synlett* **1990**, 51.
[119] S. Laschat, H. Kunz, *J. Org. Chem.* **1991**, *56*, 5883.
[120] S. Laschat, H. Kunz, *Synlett* **1990**, 629.
[121] E. Graf, H. Boeddeker, *Liebigs Ann. Chem.* **1958**, *613*, 111.
[122] T. Kaseda, T. Kichuchi, C. Kibayashi, *Tetrahedron Lett.* **1989**, *30*, 4539.
[123] H. Kunz, D. Schanzenbach, *Angew. Chem.* **1989**, *101*, 1042; *Angew. Chem. Int. Ed. Engl.* **1989**, *28*, 1068.
[124] M. Furukawa, T. Okawara, H. Noguchi, Y. Terawaki, *Heterocycles* **1977**, *6*, 1323.
[125] H. Kunz, W. Pfrengle, *Angew. Chem.* **1989**, *101*, 1041; *Angew. Chem. Int. Ed. Engl.* **1989**, *28*, 1067.
[126] S. Danishefsky, *J. Am. Chem. Soc.* **1974**, *96*, 7807.
[127] a) H. Brunner, *Synthesis* **1988**, 645; b) R. Noyori, M. Kitamura, *Angew. Chem.* **1991**, *103*, 34; *Angew. Chem. Int. Ed. Engl.* **1991**, *30*, 49, and references therein.
[128] H.-U. Blaser, *Chem. Rev.* **1992**, *92*, 925.
[129] T. D. Inch, G. J. Lewis, G. L. Sainsbury, D. J. Sellers, *Tetrahedron Lett.* **1969**, *41*, 3657.
[130] C. Chapuis, J. Jurczak, *Helv. Chim. Acta* **1987**, *70*, 436.
[131] M. Alonso-Lopez, M. Martin-Lomas, S. Penadés, *Tetrahedron Lett.* **1986**, *27*, 3551.
[132] H. Kunz, S. Engel, unpublished.
[133] H. Kunz, M. Puhl, unpublished.

Dynamic Solvent Effects on Electron-Transfer Reactions

By Hans Heitele*

Electron-transfer processes in solution are among the most important reactions in chemistry and biology. The huge number of redox reactions of transition metal ions and complexes, many preparatively important oxidations and reductions of organic compounds, photosynthesis, and metabolism are only a few examples where electron-transfer reactions play a pivotal role. This ubiquity, as well as their relative simplicity, makes them excellent models for the study on a molecular level of chemical reactions in solution. A particularly important question in chemical reaction dynamics in solution is the influence of the solvent on the reaction rate. In this context one distinguishes between static and dynamic solvent effects. Static effects refer to the stabilization of reactants, transition state, and products, that is, how the solvent affects the free energies of these species and the energy of activation. This interpretation of solvent effects on all kinds of chemical reactions is well established. A more recent development is the investigation of the influence of solvent dynamics on the rate of a reaction. The transfer of an electron is usually thought to be triggered by a fluctuation of the dielectric polarization in the surrounding solvent. The dynamics of such fluctuations is determined by the finite response time of the orientational polarization of the solvent. Under certain conditions this dielectric response time can become the rate-determining factor of the reaction. In this article I intend to give a review of these modern developments in the theory and experimental study of electron-transfer processes. We shall see that solvent dynamics may lead to a whole plethora of phenomena in reaction dynamics. The concepts needed for their description are not limited to electron transfer but bear relevance to many other chemical reactions in solution.

1. Introduction

Electron-transfer (ET) reactions in solution have been one of the most thoroughly investigated subjects in chemical reaction dynamics over the last decade.[1-12] Advances in the synthesis of tailor-made, artifical electron donor–acceptor systems and the availability of spectroscopic techniques for dynamic measurements with high temporal resolution have led to a wealth of new experimental results. Major progress has been made on the dependence of ET rates on the free energy of reaction (driving force),[13-17] on the donor–acceptor distance,[14, 18-26] as well as on the static properties of the solvent.[27-32] Some elements of ET research such as energetic control of ET rates or the Marcus cross-relation have already become part of textbook chemistry.[33]

More recently, the development of ultrafast optical spectroscopy and intensive theoretical research have shifted interest on effects of solvent dynamics on ET. It has become increasingly evident that many basic assumptions in ET theory will no longer obtain when the actual transfer step occurs on a shorter time scale than the dynamics of the surrounding solvent. In this case the solvent dynamics during the reaction has to be taken into account explicitly. Because of the many-body nature of the interaction between the reacting species and a large number of solvent molecules, this dynamics is essentially stochastic in character. Although stochastic barrier crossing has been a well-known concept in reaction dynamics at least since Kramers's work in 1940,[34] its application to ET reactions is a fairly recent development. An additional complication here is that there are adiabatic as well as nonadiabatic reactions involving one or two potential energy surfaces (PESs). The proper description of a reaction will crucially depend on the intimate relationship between stochastic motion across the activation barrier and hopping between PESs.

On the other hand the comparatively advanced degree of understanding of electron-transfer processes promises a very detailed insight into the basic mechanisms of the dynamic interaction of reacting species with the surrounding solvent. Thus the more general importance of these ET studies is as a test case for some of the most fundamental concepts of reaction dynamics in solution.

Progress in the study of dynamic solvent effects is extensively documented (see refs [35-55] for theory and refs. [56-77] for experiment). In addition to many research papers, a number of reviews of the subject have appeared recently. Maroncelli et al.[78] and Simon[79] focus on time-resolved studies of polar solvent dynamics. Weaver and McManis[80] discuss recent results on bimolecular electron self-exchange (i.e., symmetrical) reactions. Barbara and Jarzeba[81] extensively review their own work on ultrafast intramolecular electron-transfer reactions and solvation of the excited state. Bagchi[82] summarizes mostly theoretical developments in the dynamics of polar solvation and briefly discusses charge-transfer reactions.

However, despite these authoritative accounts of the state of progress of dynamic solvent effects an experimentalist or an interested nonexpert might look for a more general presentation of fundamental theoretical aspects, as well as a critical assessment of the present state of experimental verification. This does not require a rigorous derivation of these effects. Instead, the following article will focus on qualitative arguments using characteristic length and time scales.[39-41, 83-85] In this respect it borrows heavily from the seminal paper by Frauenfelder and Wolynes[83] on the

[*] Dr. H. Heitele
Institut für Physikalische
und Theoretische Chemie der Technischen Universität München
Lichtenbergstrasse 4, D-W-8046 Garching (FRG)

effects of friction and nonadiabaticity on barrier crossing phenomena.

The organization of this paper is as follows: Section 2 develops general concepts of ET reactions and their description within a transition-state (TS) theory. How dielectric friction effects on ET reactions arise and how they affect the reaction rate is discussed next. This is shown in terms of the two basic theoretical models used in this context. Section 3 presents the fundamental ideas of Kramer's approach to barrier crossing in the presence of friction and modifications due to nonadiabaticity of the reaction. Section 4 explains the physical aspects of the (apparently) very different model of Sumi and Marcus.[45] These theories require a detailed knowledge of the dynamic dielectric response of the solvent used. Recent results on the characterization of the dielectric relaxation of polar liquids are briefly discussed in Section 5. Section 6 finally gives a critical, although necessarily incomplete review of recent experiments and how they fit into the predictions of Sections 3 und 4.

In ET reactions accompanied by bond breaking, bond formation, or by a significant conformational change ("large amplitude motion"), the overall reaction rate is very often limited by the progress of these structural changes and not by the actual electron transfer. In order to avoid such complications we shall focus on ET reactions of the outer-sphere type[2, 4-6, 8] with the reactants kept at a fixed distance in a well-defined geometry.

2. Transition-State Theory of Electron Transfer

In TS theory the system is assumed to be in (quasi-) equilibrium between the reactant state and the activation maximum. ET is described as the crossing of the activation barrier along a specific coordinate in a straight trajectory. It must be borne in mind that the electronic change itself may be a rate-limiting factor.

2.1. Potential Energy Surfaces in Electron Transfer

Like most other chemical reactions, ET processes can be discussed as motions on, and transitions between, potential energy surfaces (PESs).[1-7, 54] These PESs represent the potential energy of the nuclei of the entire system consisting of electron donor, acceptor, and solvent environment, as a function of the nuclear coordinates. Reactants or products in (quasi-)equilibrium correspond to local minima on PESs.

In general the potential energy of the entire system is a complex function of a very large number of these coordinates specifying bond lengths and bond angles within the donor and acceptor themselves (intramolecular coordinates), as well as the position and orientation of the surrounding solvent molecules (solvent coordinates). An explicit inclusion of all these coordinates in a theoretical treatment is impossible. In most cases they are summarily combined into one or a small number of high-frequency (intramolecular) vibrational coordinates to be treated by quantum mechanics and a one classical (solvent) coordinate. The choice of the solvent coordinate is explained in Section 2.2. However, this reduction of the degrees of freedom necessitates a reinterpretation of PESs as free energy surfaces (FESs) as will be argued in Section 2.2.

It is customary to distinguish diabatic and adiabatic PESs (or FESs) (see Fig. 1). The motivation is as follows. In order to speak of reactants and products at all, these states must be metastable for a short time. The idea is that the total Hamiltonian $\boldsymbol{H}$ of the system can be partitioned into a zeroth-order part $\boldsymbol{H}_0$ and a weak perturbation $\boldsymbol{V}$. Reactants or products are eigenfunctions (stable states) of $\boldsymbol{H}_0$ in which the electron to be transferred is localized either on the donor or the acceptor.[86]

A Born–Oppenheimer approximate wave function to these zeroth-order Hamiltonians gives the diabatic PESs U_R and U_P for the two states. The shift of the minima for reactants and products takes account of the change in the solvent and

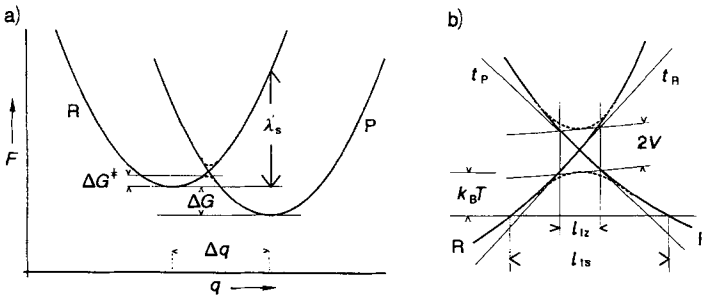

Fig. 1. a) Free energy surfaces (FESs) F used in the discussion of electron-transfer reactions as functions of a generalized solvent coordinate q. Solid lines: diabatic FESs of reactants R and products P: $F_R = 1/2 f_s q^2$, $F_P = 1/2 f_s (q - \Delta q)^2 + \Delta G$; dashed lines: adiabatic FESs in the Landau–Zener (LZ) region. λ_s = solvent reorganization energy. b) Definition of LZ and transition state (TS) regions and estimate of the corresponding lengths l_{Iz} and l_{Is} (t_R, t_P: tangents to the diabatic FESs R and P at the intersection).

Hans Heitele was born in Friedrichshafen am Bodensee in 1956. He studied chemistry at the University of Constance and later at the Technical University in Munich where he earned his Ph.D. in 1986 for research on photoinduced electron-transfer reactions under the supervision of Prof. M. E. Michel-Beyerle. Since 1986 he has been working on his habilitation in physical chemistry.

intramolecular equilibrium coordinates upon oxidation and reduction of the reacting species. Motion on a diabatic surface does not change the electronic state of the system. In the diabatic picture ET is induced by the perturbation term V, which couples reactant and product electronic states ($|R\rangle$ and $|P\rangle$). The strength of this coupling is characterized by the matrix element $V = \langle P|V|R\rangle$.

On the other hand adiabatic PESs are Born–Oppenheimer approximate solutions to the full Hamiltonian of the system. In contrast to the diabatic PES, on the adiabatic PES the electronic state changes smoothly from that of the reactants to products upon the proper change of the nuclear coordinates. Adiabatic states can be constructed as linear combinations of diabatic states coupled by the perturbation. In the two-state approximation of Figure 1b this perturbation leads to an avoided crossing and a splitting of the diabatic PESs by about $2V$.

A useful criterion in the discussion below is the extent of the region with significant interaction between the diabatic PESs of reactants and products. A crude estimate of this Landau–Zener (LZ) region is obtained with simple geometric arguments (see Fig. 1b). The diabatic PESs in the vicinity of the activation maximum are approximated by their tangents at the crossing. Sizable mixing of reactant and product electronic states occurs where the energies of the respective diabatic PESs differ by less than $2V$. As is evident from Figure 1b this is the case on a length l_{lz} [eq. (1)] near the top of the barrier. U_R' and U_P' denote the slopes of the diabatic PESs of reactants and products at the crossing point. The derivatives for the determination of the tangents are taken along the coordinate to be defined in the next section.

$$l_{lz} = \frac{2V}{|U_R' - U_P'|} \tag{1}$$

2.2. Definition of the Reaction Coordinate q

We begin with a simplified description of ET ignoring high-frequency vibrations. In general, electronic motion is much faster than nuclear motion, which confines the actual ET step to a narrow region on the PES where the nuclear momenta and the potential energy are nearly conserved (Franck-Condon principle). Consequently, an adjustment of the nuclear configuration prior to the ET reaction is required to achieve a situation where the PESs of reactants and products intersect (see Fig. 1). This process gives rise to the activation barrier. The narrow reaction zone is nothing but the LZ region of Section 2.1.

A crucial step is the identification of the mode of nuclear rearrangement—the reaction coordinate q—by which this intersection is effected. Usually the reaction coordinate is constructed by finding the minimum energy path between the minima for reactants and products on the multidimensional PESs.[37] A very convenient alternative approach[54, 55, 87–95] is to define the reaction coordinate q directly as the vertical energy gap [eq. (2)]. $U_R(X)$ and $U_P(X)$ denote the values on

$$q(X) = U_R(X) - U_P(X) \tag{2}$$

the microscopic, multidimensional, diabatic PESs of reactants and products for a solvent arrangement (the solvent configuration) characterized by the set of coordinates X. In general there exists a huge number of different configurations leading to the same value of $q(X)$. The energy gap q is the difference in the collective, mainly electrostatic interaction of many solvent molecules with reactants or products and depends on the position and orientation of these solvent molecules. The temporal change of q [that is, $q(X(t))$] reflects the very complex dynamics $X(t)$ of the solvent environment. Motion within the potential wells along q away from the minima essentially corresponds to a (nonequilibrium) dielectric polarization fluctuation. Yet, nonequilibrium only exists with respect to that part of the polarization which is due to the orientation of permanent dipoles; electronic polarization is always at equilibrium with the momentary charge distribution on electron donor and acceptor.

The reaction coordinate defined according to equation (2) changes its sign at the intersection of the diabatic PESs and intuitively is a useful parameter for the characterization of processes that occur near this intersection. Yet, the definition in equation (2) reveals its usefulness and full power only in explicit multibody molecular dynamics calculations.[54, 55, 87–95]

A change in the description of the potential energy from the microscopic coordinates X to the reaction coordinate q does not merely correspond to a simple one-dimensional profile of the multidimensional PESs $U_{R,P}(X)$. Instead it implies a statistical weighting of all the solvent configurations X that give the same value of $q(X)$. This procedure leads to the FESs mentioned in Section 2.1, which we shall denote by the symbols $F_{R,P}(q)$.

The microscopic construction of the diabatic FESs $F_{R,P}(q)$ can be carried out as follows: For a fixed charge distribution on the reacting species (corresponding to either reactants or products) a molecular dynamics calculation for the solvent environment generates an equilibrium probability distribution $p_{R,P}(X)$ of the solvent configurations and, on application of equation (2), one of $q(X)$, namely $p_{R,P}(q)$.[54, 55, 87–95] Use of these distributions enables the functions F of the diabatic FESs to be defined according to equations (3a) and (3b), where k_B = Boltzmann's constant and T = absolute temperature; for ΔG see Section 2.3. Very often no clear distinction is made between the PESs $U_{R,P}$ and the FESs $F_{R,P}$.[96]

$$F_R(q) = -k_B T \ln [p_R(q)] \tag{3a}$$
$$F_P(q) = -k_B T \ln [p_P(q)] + \Delta G \tag{3b}$$

2.3. Characterization of the Activation Barrier

For simplicity it is usually assumed that the diabatic FESs $F_{R,P}(q)$ are quadratic functions of the reaction coordinate with equal force constants f_S for reactants and products.[97] Recent Monte Carlo simulations in model systems have shown this approximation to be surprisingly accurate.[88]

Several parameters characterizing $F_{R,P}(q)$ are shown in Figure 1. The free energy of reaction ΔG is the difference in the free energies between the minima of products and reactants. In general a polar medium provides better solvent stabilization of a more polar species. Thus a polar environment increases the driving force of a charge-separation reaction, but reduces it for charge recombination.[31] Another

useful quantity is the solvent-reorganization energy $\lambda_S = 1/2 f_S \Delta q^2$ where Δq is the shift between the free energy minima. It is approximately given by equation (4),[98,99] where $r_\pm$ are the effective radii of the reactants at distance d, n is the refractive index, and ε_S the static dielectric constant of the solvent. The energy parameter λ_S in equation (4) has the same form as that part of the solvation energy (of an ion pair) that results from the *orientational* polarization of the solvent. The free energy of activation $\Delta G^{\neq}$ can be expressed in terms of the free energy of reaction ΔG and the solvent reorganization energy λ_S [(5)], by solving the quadratic equation for the point of intersection of two parabolas. The splitting V is often neglected in $\Delta G^{\neq}$.

$$\lambda_s = e^2 \left(\frac{1}{2r_+} + \frac{1}{2r_-} - \frac{1}{d} \right) \left(\frac{1}{n^2} - \frac{1}{\varepsilon_s} \right) \tag{4}$$

$$\Delta G^{\neq} \approx \frac{(\Delta G + \lambda_s)^2}{4\lambda_s} - V \tag{5}$$

In the following we shall distinguish the transition-state (TS) region from the LZ region of Section 2.1. The TS region denotes the neighborhood of the activation maximum differing in energy by less than $k_B T$ (see Fig. 1b). For many purposes the TS region can be considered as (energetically) flat. On the other hand, once the system has left the TS region on either side it can be considered as thermally stabilized. We characterize its extent by the length l_{ts}. Its estimate depends on the strength of the electronic coupling V (see Fig. 2). A

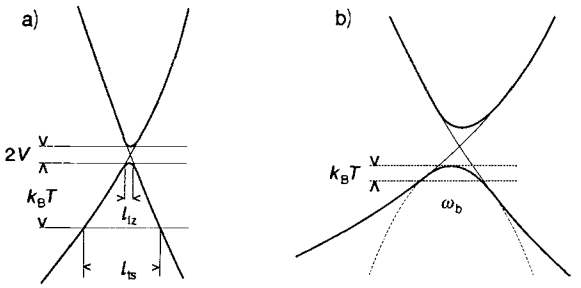

Fig. 2. Shape of the barrier top for different electronic couplings V. a) Nonadiabatic reaction for $V \ll k_B T$ (cusped barrier). A stepwise linear approximation gives $l_{ts} = k_B T(1/|F_R'| + 1/|F_P'|) \approx 4k_B T/\sqrt{2\lambda_s M\omega_0^2}$ and $l_{lz} = 2V/\sqrt{2\lambda_s M\omega_0^2}$. Here we assume that $F_{R,P}' \approx U_{R,P}'$. b) Strongly adiabatic reaction. For the inverse parabolic barrier with the force constant $f_b = M\omega_b^2$, the length l_{ts} is defined by $l_{ts} = \sqrt{8k_B T/M\omega_b^2}$.

small splitting of the diabatic FESs leaves the adiabatic FESs rather sharp (cusped barrier) on the length scale l_{ts}. Strong electronic coupling leads to a broad maximum, which is often described by an inverse parabola.

2.4. The Electron-Transfer Rate k in Transition-State Theory

Interpreted as a motion on FESs, the picture of electron transfer is the following: Most of the time the reactants are at or near equilibrium with the solvent environment; that is, the system moves near the minimum of the reactant FES. Once in a while a solvent fluctuation drives the system up the activation barrier where reactant and product FESs intersect. Within the LZ region near the intersection an electron may hop from the electron donor to the acceptor; with a certain probability the system changes to the product FES and subsequently relaxes to the bottom of the well. Thus we have to take account of changes in the nuclear coordinates as well as of the electronic structure.

The derivation of the reaction rate in the framework of conventional TS theory presupposes the validity of the following assumptions:

a) Throughout the course of the reaction the system maintains a quasi-equilibrium distribution along the reaction coordinate on the reactant FES up to the TS region. This in general requires that vibrational and solvent relaxation in the reactant FES are much faster than ET.

b) Upon crossing the activation barrier along the reaction coordinate the system moves uniformly through the TS region. Reactive trajectories on the FES cross the barrier top once and only once.

c) Once the system has crossed the TS region and a reaction (with probability P) has occurred, excess energy is dissipated fast enough to trap the system on the products side.

The ET rate k is then given by the product of three factors [eq. (6)]: firstly the occurrence probability of the system in the TS region moving in forward direction, secondly the (average) inverse time it takes to cross the TS region "in straight flight", and thirdly the electronic transition probability P for a transition from reactant to product FESs whenever the system traverses the TS region.[100-102]

$$k = P \frac{k_B T}{h} \frac{1}{Z_0} e^{-\frac{\Delta G^{\neq}}{k_B T}} \approx P \frac{\omega_0}{2\pi} e^{-\frac{\Delta G^{\neq}}{k_B T}} = P k_{ts} \tag{6}$$

Z_0 is the partition function of a classical, one-dimensional motion in the initial well with the oscillation frequency $\omega_0 = \sqrt{f_s/M}$; M is the effective mass associated with the motion near the well bottom[97] (h = Planck's constant). A typical value of ω_0 is $10^{13}\ s^{-1}$[103].

The preexponential factor $\omega_0/2\pi$ is somewhat misleading in the sense that it seems to count the number of attempted barrier crossings per unit time. Yet, equation (6) does not hold when the system undergoes a simple oscillation on the FES as will be argued in Section 3. The factor $\omega_0/2\pi$ is just the ratio $k_B T/hZ_0$.

2.5. Estimate of the Electronic Transition Probability P

It is intuitively obvious that the likelihood of a successful electronic transition increases the longer the system remains in the LZ region and the faster an electronic transition takes place there. Thus, P depends on the ratio of the traversal time τ_{lz} of the system through the LZ region to the duration τ_{hop} of the change of the electron distribution from that of the reactants to that of the products.[1] The traversal time is the ratio l_{lz}/v_{th} where v_{th} is the thermal velocity of the motion along the reaction coordinate through the LZ region. The duration of an electronic transition is about $\hbar/V$. When using l_{lz} from equation (1) the ratio τ_{lz}/τ_{hop} thus is directly proportional to the square of the electronic coupling V and inversely proportional to the average thermal velocity v_{th} along the reaction coordinate [eq. (7)].

$$\frac{\tau_{lz}}{\tau_{hop}} \approx \frac{l_{lz}/v_{th}}{\hbar/V} = \frac{2V^2}{\hbar v_{th}|U_R' - U_P'|} := \gamma_{lz} \tag{7}$$

where $v_{th} = \sqrt{2k_B T/\pi M}$ and γ_{lz} is the (Landau-Zener) adiabaticity parameter[104].

For a sufficiently small electronic coupling V we have a nonadiabatic reaction with $\gamma_{lz} \ll 1$, where P is proportional to γ_{lz} ($P = 2\pi\gamma_{lz}$).[105] If l_{lz} is used for the cusped barrier (Fig. 2a), the explicit expression is equation (8). Alternative-

$$k_{na} = \frac{2\pi}{\hbar} \frac{1}{\sqrt{4\pi\lambda_s k_B T}} V^2 e^{-\frac{(\Delta G + \lambda_S)^2}{4\lambda_S k_B T}} \tag{8}$$

ly, equation (8) can be derived in the framework of nonadiabatic ET theory based on time-dependent perturbation theory[107-109] (see also the semiclassical trajectory approach in ref. [55]). The characteristic feature of ET reactions with small couplings is the proportionality of the rate to V^2. In the nonadiabatic case the system moves too fast through the LZ region for the electrons to form the product state. It will most likely stay on the diabatic FES of the reactants. A successful reaction is a rare jump to the product FES among many futile crossings of the LZ region.

In the opposite case of a large electronic coupling $\gamma_{lz} \gg 1$, $P = 1$ (adiabatic reaction). Every crossing of the LZ region leads to products. The traversal time is long enough to form the electronic state of lowest energy; the reaction can be discussed on the lower adiabatic FES alone. For arbitrary values of γ_{lz}, P is a geometric series[1, 110] in the Landau-Zener probability p_{lz} [eq. (9)] where $p_{lz} = 1 - e^{-\pi\gamma_{lz}}$.[106]

$$P = \frac{2p_{lz}}{1 + p_{lz}} \tag{9}$$

2.6. Concluding Remarks

The free energies of reaction and activation [eq. (5)] depend on the relative stabilization of the reactants, the transition state, and the products by the solvent environment. This stabilization of charged species is mainly determined by static properties of the solvent such as the polarity and the refractive index. The force constant f_S and the effective mass M for the frequency ω_0 are equilibrium properties as well[97] (see also eq. (25) in Section 5.1). Thus the rate in equation (6) as a whole is determined by the static properties of the solvent. Solvent dynamics can be completely ignored.

3. Kramers's Theory of Barrier Crossing and Beyond

The rapidly fluctuating, collective interaction between the reacting species and the solvent environment may have a profound influence on the rate of energetic (de)activation of the system and on the character of the trajectories over the activation barrier. Under certain circumstances the basic assumptions of TS theory in Section 2.4 are no longer fulfilled and corrections to the ET rate in TS theory are necessary.

3.1. Electron Transfer as a Problem of Random Walk and Solvent Dielectric Response

We immediately recognize the importance of solvent dynamics if we remember that the reaction coordinate $q(X)$ is itself a function of a great number of coordinates X characterizing the position and orientation of mutually interacting solvent molecules. The projection of the highly irregular dynamics of many solvent molecules onto a single reaction coordinate results in the occurrence of frictional and random forces in the equation of motion for q.

Two consequences of frictional and random forces on the dynamics along the reaction coordinate are important: 1) They provide a mechanism for the exchange of energy between the reaction coordinate and the other degrees of freedom (mostly of the solvent) functioning as a heat bath. Without such an energy flow the system could neither acquire the necessary energy along the reaction coordinate to overcome the activation barrier nor get rid of excess energy to become stabilized on the products' side once it has crossed the barrier. 2) They change the character of the motion along the reaction coordinate. They are able to effect a crossover from deterministic to stochastic motion which resembles a random walk (or Brownian motion) on the FESs.

In view of the complexity of this motion its dynamics is usually described phenomenologically by a Langevin equation[111] for the reaction coordinate [eq. (10)].[37, 112] The

$$M\frac{\partial^2 q}{\partial t^2} = -\frac{\partial F_{R,P}(q)}{\partial q} - \zeta\frac{\partial q}{\partial t} + R(t) \tag{10}$$

first term on the right hand side is the potential force in the relevant FES $F_{R,P}$ (for parabolic FESs $\partial F_R(q)/\partial q = M\omega_0^2 q$), the second the dielectric friction with the microscopic friction constant ζ, and the third the random force $R(t)$ exerted by the rapidly fluctuating solvent environment. The many-body aspect of the solvent dynamics is incorporated into the friction constant ζ and the random force $R(t)$ which is defined by its stochastic properties, that is, its moments and autocorrelation functions.[111-113] The fluctuation–dissipation theorem shows these two quantities to be closely related.[111-113] In the treatment below they are used as input information known from experiments or other theories. This is discussed further in Section 5.

It has to be kept in mind, however, that friction along the reaction coordinate is, a priori, unrelated to the hydrodynamic friction that is exerted on a molecule rotating or drifting in a liquid. Motion along the reaction coordinate reflects the dynamics of polarization fluctuations; that is, it is governed by the dielectric response of the solvent.

In much of the following we assume that the second derivative on the left hand side of equation (10) is negligible. This neglect of inertial effects in solvent dynamics is reasonable in the presence of strong friction and results in overdamped motion (of a harmonic oscillator, for example). In dielectric relaxation it corresponds to the important special case of a Debye liquid in which the frequency-dependent dielectric constant is defined by equation (11),[114, 115] where ε_S is the static and ε_∞ the high-frequency dielectric constants of the solvent (very often $\varepsilon_\infty \approx n^2$). The resulting dielectric response

exhibits a single-exponential time dependence with the Debye relaxation time τ_d. Nevertheless, the characteristic time scale of interest here is the longitudinal (or constant charge) dielectric relaxation time τ_l, related to τ_d by equation (12).

$$\varepsilon(\omega) = \varepsilon_\infty + \frac{\varepsilon_s - \varepsilon_\infty}{1 + i\omega\tau_d} \tag{11}$$

$$\tau_l = \frac{\varepsilon_\infty}{\varepsilon_s}\tau_d \tag{12}$$

Thus in polar solvents τ_d can exceed τ_l by more than an order of magnitude (see Table 1)! Both refer to the same underlying molecular relaxation mechanisms; they differ by the boundary condition under which the response of the medium is measured. The dielectric relaxation time τ_d is the response

Table 1. Selection of representative dielectric relaxation times τ_d and τ_l (in ps) in common solvents from [67, 69]. The values τ_1 and τ_2 and the corresponding amplitudes in parentheses are biexponential fits to the function $C(t)$ in equation (26) from TDSS experiments [81, 144].

Solvent	τ_d	τ_l	τ_1	τ_2	τ_s
acetonitrile	3.3	≃0.2	0.07 (80) [b]	0.2 (20)	
CH_2Cl_2	1.5	≃0.4			
methanol	48 [a]	8.2 [a]	1.2 (40)	9.6 (60)	6.2
propanol	390 [a]	42 [a]	14 (30)	40 (70)	33
acetone	3.3	0.3	0.3 (47)	1.0 (53)	0.7
water		0.2	0.25 (50)	1.0 (50)	0.6
DMSO		2.4	0.3 (57)	2.3 (43)	1.2

[a] τ_d and τ_l for methanol and propanol refer to the dominant slowest component of the dielectric response. [b] The data for acetonitrile in [139] were fitted by the sum of a Gaussian with a fwhm = 120 fs and an exponential with a decay time of 200 fs.

time when a fixed electric field is suddenly turned on (E-jump) whereas τ_l characterizes the response when a fixed (external) charge is added (D-jump).[116] As defined in equation (2), the reaction coordinate describes the change in the solute–solvent interaction upon an instantaneous (virtual) change of the charge distribution on the reacting species. Consequently τ_l is taken as the relevant relaxation time.[117] For most common liquids τ_l falls in the range from 250 fs to 10 ps (see Table 1) and is identified with the relaxation time of the overdamped harmonic motion resulting from equation (10) for a parabolic FES.[50] This gives the simple relationship $\zeta = M\omega_0^2\tau_l$ between the friction constant ζ and τ_l in a Debye liquid.

3.2. Adiabatic Reactions

The influence of friction on the dynamics along the reaction coordinate and on the adiabaticity of the reaction leads to corrections to the TS value k_{ts} to yield the ET rate $k(\zeta)$. We define $k(\zeta)/k_{ts}$ as a measure of frictional effects. At first we shall focus on intrinsically adiabatic reactions where the motion is confined to the lower adiabatic FES in Figure 1 leading continuously from reactants to products. This is the realm of Kramers's theory[34] and its more recent generalizations;[102, 112, 118–120] its results are illustrated in Figure 3 and explained in the following.

For weak frictional or random forces the system will undergo several oscillations between the reactant and product wells before finally settling down in one of them. The reaction rate is limited by how fast the necessary activation energy is acquired and how fast excess energy in the reaction coordinate is dissipated to trap the system in either well (regime of energy diffusion, Fig. 3a). This is achieved by an exchange of energy between the reaction coordinate and the heat bath. The energy dissipation of a weakly damped oscillator, which is directly proportional to the friction constant ζ serves as a crude estimate of this flow of energy, that is, $k(\zeta)/k_{ts} \propto \zeta$. This is the equivalent of the low-pressure regime of unimolecular reaction theory. The proportionality constant[102] need not concern us here. A consequence of slow energy exchange is that, in contrast to TS theory, a quasi-stationary Boltzmann distribution in the initial state is never achieved. The distribution is significantly depleted well below the TS region.

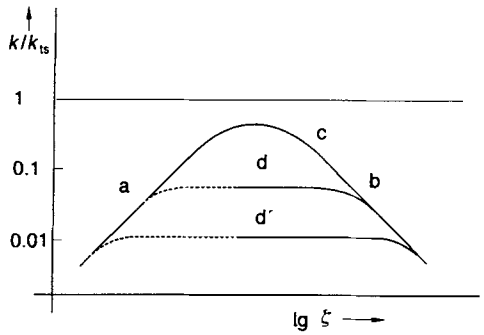

Fig. 3. Qualitative dependence of the ratio $k(\zeta)/k_{ts}$ as a function of the microscopic dielectric friction constant ζ experienced by the system upon barrier crossing. a) Regime of energy diffusion, b) regime of spatial diffusion, c) adiabatic reaction ($P \approx 1$); d) and d') indicate the influence of nonadiabaticity ($P < 1$) on the rate. The dashed sections are not treated here but were added for completeness.

With increasing frictional and random forces the motion in q becomes steadily more statistical; it changes direction on a shorter length scale (characterized by the mean free path l_f) and in a random fashion resembling a diffusive motion. This will lead to a rapid equilibration of the reactants to a Boltzmann distribution. On the other hand, once the mean free path l_f of the motion is shorter than l_{ts}, such a randomly moving system will change direction several times even within the TS region and recross the barrier top repeatedly before finally settling on the products' side (see Fig. 4).

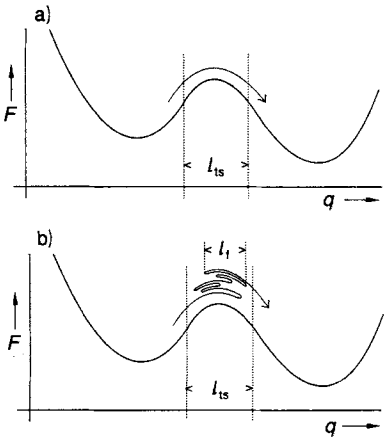

Fig. 4. Influence of frictional and random forces on the barrier-crossing dynamics: a) uniform or ballistic crossing for weak frictional forces, b) repeated back scattering of the system within the TS region in the presence of strong frictional and random forces ($l_f \ll l_{ts}$).

This "back scattering" reduces and finally dominates the rate.[121] The ratio $k(\zeta)/k_{ts}$ then approximately equals the inverse ratio of the traversal times $\tau_{ts,diff}$ of diffusive and $\tau_{ts,uni}$ of uniform or ballistic motion through the TS region [spatial diffusion limit, Fig. 3b, eq. (13)]. The diffusive traversal time

$$\frac{k(\zeta)}{k_{ts}} \approx \left(\frac{\tau_{ts,diff}}{\tau_{ts,uni}}\right)^{-1} \tag{13}$$

$\tau_{ts,diff}$ can be estimated as the time a random walker (with diffusion constant D) needs to cover a distance equal to the length of the TS region l_{ts}: $\tau_{ts,diff} = l_{ts}^2/2D$[111]. Thus one derives equation (14) using $\tau_{ts,uni} = l_{ts}/v_{th}$ and the Einstein relation $D = k_B T/\zeta$.[111] This simple estimate with l_{ts} from Figure 2 reproduces the correct ratio $k(\tau_1)/k_{ts} = \sqrt{\pi \lambda_s/4 k_B T}\,1/\omega_0\tau_1$ for the cusped barrier (Fig. 2a) and yields the exact result $\omega_b/\omega_0^2\tau_1$ for the parabolic barrier (Fig. 2b) up to a factor of $2/\sqrt{\pi} \approx 1.13$. The important point is that the rate is *inversely* proportional to the friction constant ζ or the relaxation time τ_1: $k(\zeta)/k_{ts} \propto 1/\zeta,\ 1/\tau_1$.

$$\frac{k(\zeta)}{k_{ts}} \approx \left(\frac{\tau_{ts,diff}}{\tau_{ts,uni}}\right)^{-1} = \left(\frac{l_{ts}^2/2D}{l_{ts}/v_{th}}\right)^{-1} = \frac{2k_B T}{v_{th} l_{ts}}\frac{1}{\zeta} = \frac{2k_B T}{v_{th} l_{ts}}\frac{1}{M\omega_0^2}\frac{1}{\tau_1} \tag{14}$$

The crossover from the energy diffusion to the spatial diffusion regimes results in the nonmonotonic dependence of the rate on friction in Figure 3. The limit predicted by TS theory of $k(\zeta)/k_{ts} = 1$ is never achieved but is approached in a region of intermediate friction (Kramers turnover). TS theory is thus a useful approximation when friction is strong enough for rapid equilibration in the initial state but still weak enough to allow a quasi-uniform or ballistic crossing of the TS region.

To assess what kind of motion is realized in any specific case is a major problem. Yet, at present it appears unlikely that the energy diffusion limit is ever achieved in ET reactions in solution. It would imply a collective oscillatory motion of many solvent molecules in a system as disordered as a liquid. Current estimates[41, 103] indicate that most liquids belong either to the turnover or spatial diffusion regimes. Henceforth the energy diffusion regime can be omitted.

3.3. Inclusion of Nonadiabaticity

3.3.1. A Modified Landau–Zener Parameter

Let us next turn to a nonadiabatic reaction where $V \ll k_B T$. This in general implies a cusped barrier with $l_{ts} \gg l_{lz}$ (Fig. 2a). A thorough discussion would require a case distinction depending on the relative size of l_f, l_{ts}, and l_{lz} and p_{lz}; this has been done,[39–41, 84] but since from an experimentalist's point of view several of these cases are practically indistinguishable, we shall focus on the gross features instead.

As long as TS theory is approximately valid, weak electronic coupling reduces the rate by a factor equal to the electronic transition probability P [eq. (6)]. Its effect in the spatial diffusion regime is a priori not clear since the derivation of P assumes uniform a motion through the LZ region. Yet, the interpretation of the adiabaticity parameter γ_{lz} as the ratio of the residence time τ_{lz} and the hopping time τ_{hop} in equation (7) indicates that, in the end, not the character of the motion but the total time spent in the LZ region is the crucial aspect.[39]

In order to obtain the analogous adiabaticity parameter κ for diffusive motion along the reaction coordinate we have to remember two important differences from the uniform case: 1) The residence time in the LZ region has to be estimated by using random walk arguments. 2) Since by assumption $l_{ts} \gg l_{lz}$, the system will leave and reenter the LZ region many times before it finally drifts out of the TS region and settles in either the reactant or the product well. The total residence time τ_{lz} in the LZ region is, therefore, the fraction of the residence time τ_{ts} in the TS region given by equation (15a), from which follows (15b) and (15c). Inserting l_{lz} and l_{ts} for the cusped barrier (Fig. 2a) we obtain equation (16).[41] The factor of 2π is included with a view to the later derivation of equation (18).

$$\tau_{lz} = \frac{l_{lz}}{l_{ts}}\tau_{ts} \tag{15a}$$

$$\tau_{lz} = \frac{l_{ts} l_{lz}}{2k_B T}\zeta \propto V\tau_1 \tag{15b}$$

$$\frac{\tau_{lz}}{\tau_{hop}} \propto V^2\tau_1 \tag{15c}$$

$$\kappa(\tau_1) = \frac{4\pi V^2}{\hbar\lambda_s}\tau_1 \approx 2\pi\frac{\tau_{lz}}{\tau_{hop}} \tag{16}$$

3.3.2. Interpolation of the Transfer Rate

As long as $\kappa \ll 1$, a transition from one diabatic FES to the other during a crossing of the TS region is an improbable event, and the reaction is nonadiabatic, be the motion uniform or diffusive.[39] Although the number of traversals of the TS region is greater for uniform motion (because the system moves faster) the system stays in this region longer *per traversal* for diffusive motion. The fraction of time the system spends in the LZ region is given by the Boltzmann distribution and is the same in both cases. On the other hand if $\kappa \gg 1$, the system always stays in the LZ region long enough for a change of electronic states to occur. Once the system drifts out of the TS region on the product side it will, for energetic reasons, always do so on the lower FES leading to products. The rate of the reaction is no longer limited by the change of electronic states as in a normal nonadiabatic reaction but by the escape rate from the TS region! Thus we return to the adiabatic case where Kramers's theory is valid (solvent-controlled adiabatic reaction)! For the cusped barrier equations (6) and (14) give equation (17) when $\kappa \gg 1$. In practice A will most likely be of the order of 0.1 to 1. Thus, equation (17) sets an upper limit of $1/\tau_1$ to the rate for all reactions!

$$k(\tau_1) = \sqrt{\frac{\lambda_s}{16\pi k_B T}}\frac{1}{\tau_1}e^{-\frac{(\Delta G + \lambda_S)^2}{4\lambda_s k_B T}} = \frac{A}{\tau_1}e^{-\frac{\Delta G^{\ddagger}}{k_B T}} \tag{17}$$

To estimate the rate between these extremes we simply interpolate between the nonadiabatic rate constant k_{na} [eq. (8)] and Kramers's prediction $k(\tau_l)$ [eq. (17)] for a Debye liquid. In fact, the proportionality constant in equation (16) was defined in such a way that $\kappa = k_{na}/k(\tau_l)$, from which we derive (18).[41]

$$k = \left(\frac{1}{k_{na}} + \frac{1}{k(\tau_l)}\right)^{-1} = \frac{1}{1+\kappa(\tau_l)} k_{na} = \frac{1}{1+\frac{4\pi V^2}{\hbar \lambda_S}\tau_l} k_{na} \quad (18)$$

The result is depicted in Figure 3 as well. At first the rate is practically independent of friction, but it finally merges with Kramers's prediction for a friction-limited adiabatic reaction. Another essential feature of equation (18) is that the reaction rate may be proportional to V^2 for fast relaxation [eq. (8)], but with increasing τ_l finally becomes independent of the electronic coupling.

3.4. Generalizations

3.4.1. Inclusion of (Intramolecular) Quantum Modes

So far we have ignored intramolecular degrees of freedom. The excitation of intramolecular vibrations provides a way for the system to dispose of large amounts of energy.[55, 108, 122] We can easily include them into our described framework when we remember that their frequencies in general satisfy the condition $\hbar\omega_i \gg k_B T$; that is, in contrast to solvent dynamics, intramolecular motion has a quantum-mechanical nature. The appropriate description of these degrees of freedom is not in terms of position and momentum on a FES, but as discrete quantum states enumerated by quantum numbers. For most practical purposes a single intramolecular mode will suffice; that is, we specify its vibronic state by the number of phonons in this mode. Instead of a single FES for reactants and products each, we get two sets of FESs where every FES is characterized by the electronic state (reactant or product) *and* the phonon number defining the vibronic state with respect to the intramolecular high-frequency mode (see the nested FESs in Fig. 11). Since by physical argument $\hbar\omega_i \gg k_B T$, only the vibronic ground state of the reactants is occupied. We then define individual reaction rate constants $k_{0,n}$ between the reactant ground state and every vibronic substate of the set of product states [eq. (19)].[39, 44, 51]

$$k_{0,n} = \frac{1}{1+\frac{4\pi\tau_l}{\hbar\lambda_S}V_{0,n}^2} \frac{2\pi}{\hbar} \frac{1}{\sqrt{4\pi k_B T \lambda_S}} V_{0,n}^2 \, e^{-\frac{(\Delta G + \lambda_S + n\hbar\omega_i)^2}{4\lambda_S k_B T}} \quad (19)$$

The individual rate constants differ in two ways from equations (8) and (18) which ignore high-frequency intramolecular vibrations: 1) The effective free energy of reaction $\Delta G_{0,n} = \Delta G + n\hbar\omega_i$ corrects for the part of the driving force taken up by the intramolecular mode. 2) Since a transition from the reactant FES to a product FES involves a change of the electronic state as well as of the intramolecular vibronic state, the purely electronic transition matrix element V has to be multiplied by the vibronic overlap matrix element $\langle 0|n\rangle$ between the vibronic ground state of the reactants $|0\rangle$ and the nth vibronic product state $|n\rangle$; that is, the square of the effective matrix element $V_{0,n}^2$ is the product of the purely electronic coupling V^2 times the Franck–Condon factor for the transition between the respective vibronic states: $V_{0,n}^2 = V^2 |\langle 0|n\rangle|^2$.

$|\langle 0|n\rangle|^2$ is a function of the intramolecular reorganization energy $\lambda_i = 1/2\, f_i \Delta x^2$ where f_i is the force constant and Δx the shift of the equilibrium position of the intramolecular mode from reactants to products. The overall rate constant is the sum over all these rate constants for the different vibronic channels: $k = \sum_n k_{0,n}$. For $\tau_l \to 0$ we recover the rate in the nonadiabatic limit[108, 109] and thereby generalize equation (8) in the presence of high-frequency intramolecular vibrations.

Very often one of the channels predominates. This is particularly important for reactions with a very high driving force (reactions in the inverted region with $-\Delta G > \lambda_s + \lambda_i$). In these cases nuclear tunneling in the high-frequency modes favors the transition to that electronic–vibronic state whose FES intersects the reactant FES in the minimum resulting in an almost activationless reaction[122] (see for example Figure 11) but with a considerably lower rate!

In addition to the well-established quantum effects in intramolecular vibrations, potential quantum effects in solvent motion have recently attracted increasing attention.[55, 93, 103, 123] Current estimates predict only small or mutually compensating corrections to classical solvent dynamics.[103] Possible exceptions are protic solvents where the motions of hydrogen atoms can be dominated by tunneling.[123]

3.4.2. Influence of Frequency-Dependent Friction

So far, we have assumed a single characteristic time scale of dielectric response. Yet, the description of the dielectric relaxation dynamics of most liquids requires a whole spectrum of relaxation times. The underlying molecular mechanisms are usually discussed in terms of the two extremes of polar media, those with static and those with dynamic disorder.

In a medium with (pure) dynamic disorder, solvent dielectric relaxation is the same in the microscopic environment of every electron donor–acceptor pair but nevertheless nonexponential. In the Langevin equation of the reaction coordinate this implies a finite correlation time of the random force $R(t)$ and a memory effect of the friction [eq. (20)].[112, 113, 124] Fourier transformation converts $\zeta(t)$ into a frequency-dependent friction constant $\zeta(\omega)$ or relaxation time $\tau_l(\omega)$.[50]

$$\zeta \frac{\partial q}{\partial t} \to \int_0^t \zeta(t-\tau) \frac{\partial q}{\partial \tau} \, d\tau \quad (20)$$

The barrier top for many ET reactions with weak electronic coupling, especially of those with a high activation barrier, is rather sharp (cusped barrier) and l_{lz} and l_{ts} small. As a consequence the required solvent fluctuation to traverse the TS region is also small. In these cases the short but finite correlation time of the frictional force could be important. In a molecular picture, the underlying relaxation mechanism could involve small amplitude motions of individual solvent molecules that will experience only weak friction with the

surrounding liquid.[112] The strong curvature of the barrier top therefore probes the short time dynamics of solvent relaxation, which accelerates the transition of the system over the barrier top but does not necessarily assist in acquiring the activation energy or in the deactivation on the products' side.[112]

The quantitative formulation of this problem is still a matter of active research. A theoretical treatment by Hynes et al.[50, 124] predicts that the actual crossing of the activation maximum in ET reactions with a cusped barrier is determined by a friction constant $\zeta(\omega \gg \omega_0)$ at high frequencies that is small and not rate-determining, whereas energetic (de)activation is somewhat slowed by dielectric friction. Altogether a weak dependence of the rate on the relaxation properties is expected.[50] This finding is in contradiction to numerical simulations by Straub, Borkovec, and Berne[125] and more recent theoretical treatments of Kramers's problem by Pollack, Grabert, and Hänggi,[126] which give a rather strong dependence of the overall barrier-crossing rate on frequency-dependent friction. Yet, the latter results rest very much on specific assumptions on the shape of the barrier which may or may not be justified in ET reactions. This problem was also discussed by several other groups[36, 41, 52, 127–129] who arrive at different conclusions. In summary, the influence of frequency-dependent dielectric friction on barrier crossing in general, and ET reactions in particular, is still an open question.

In a solvent with (pure) static disorder, the dielectric relaxation of the microscopic solvent environment of any electron donor–acceptor pair is exponential but the relaxation times τ_l in the environment of different pairs are not identical. This corresponds to an inhomogeneous medium with a distribution of relaxation times $g(\tau_l)$. The observed survival probability of the reactants $P(t)$ is an ensemble average of systems with individual reaction rate constants $k(\tau_l)$ over $g(\tau_l)$ [eq. (21)].[43, 47] This averaging can result in a strongly nonexponential time-dependence. An example is given in ref. [43].

$$P(t) = \int_0^\infty \mathrm{e}^{-k(\tau_l)t} g(\tau_l)\, \mathrm{d}\tau_l \qquad (21)$$

3.4.3. Nonequilibrium Effects

Another mechanism leading to a nonexponential time dependence comes into play when the crossing of the activation barrier is able to compete effectively with equilibration to a quasi-steady-state distribution on the reactant FES. This is expected for adiabatic reactions with a very low activation barrier or when the initially prepared distribution of the reactants is far from an equilibrium distribution. In this case the concept of a (time-independent) reaction rate constant is no longer meaningful. In general, the kinetics of the reaction has to be determined by explicit numerical solution of a Langevin or an equivalent equation for the motion along the reaction coordinate.[130]

3.5. Additional Remarks

The interplay of electronic coupling, dielectric friction, and the character of the motion along the reaction coordinate is illustrated in the triangle in Figure 5 formed by the extreme cases of a uniform adiabatic, a nonadiabatic, and a solvent-controlled adiabatic reaction. Transitions between these limiting cases are governed by the respective adiabaticity parameters κ and γ_{lz}, and the ratio l_{ts}/l_f. A closed interpolation formula encompassing all three limits was proposed by Rips and Jortner.[131]

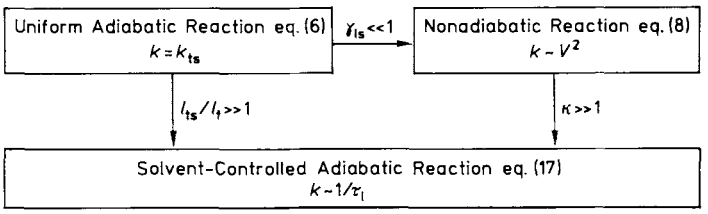

Fig. 5. Schematic representation of the relationship between uniform adiabatic, nonadiabatic, and solvent-controlled adiabatic electron-transfer reactions based on the extension of Kramers's one-dimensional approach as described in Section 3. Transitions between these limiting cases are controlled by the Landau–Zener adiabaticity parameter γ_{lz} for uniform motion [eq. (7)], the adiabaticity parameter κ for diffusive motion [eq. (16)], and the ratio of the width l_{ts} of the TS region and of the mean free path l_f of the motion along the reaction coordinate (see Fig. 4).

The formal treatment of the influence of solvent dynamics on ET has been attempted in many different ways, for example,

- in the framework of quantum-mechanical propagators by path integral calculations for a two-level system coupled to a heat bath of harmonic oscillators by Garg et al.[38] and Onuchic,[39] or to a dielectric by Rips and Jortner[41]
- by the solution of a stochastic Liouville equation for a two-level system where the reaction coordinate is described by a Smoluchowski equation (Zusman,[35] Rips and Jortner[42])
- with Greens function methods for the Liouville equation of the density matrix reminiscent of optical line-shape theory by Mukamel and coworkers[52]
- with Greens functions for the solution of a Fokker–Planck equation for the reaction coordinate by Cukier et al.[53] and
- within the mean first passage times approach by Friedman and Newton.[49]

The comparability of these approaches is difficult to assess. Except for minor corrections they seem to agree in the gross features of the effect of solvent dynamics and in particular in the crossover from nonadiabatic to solvent-controlled adiabatic behavior. The interested reader is referred to the original papers.

4. Two-Dimensional Approach of Sumi and Marcus

An essential feature of Kramers's model is the assumption that the barrier crossing is overwhelmingly undertaken along or close to the minimum energy path on the PES, and thus an essentially one-dimensional treatment of the motion is sufficient. This approximation may break down when the curvature of the PES at the barrier perpendicular to the reaction coordinate is weak or the motions along the reaction coordinate and perpendicular to it are characterized by

very different time scales. In this case the system may follow a trajectory over the barrier with a higher energy of activation, that for reasons of dynamics, however, is more easily accessible than the minimum energy path.

4.1. Basic Assumptions

This possibility of an alternative route across the activation barrier is the basis of the model for dynamic solvent effects suggested by Marcus, Sumi, and Nadler,[45, 46] which is related to earlier work of Agmon and Hopfield.[132] In this approach it is assumed that in addition to solvent fluctuations a low-frequency intramolecular vibration mode ($\hbar\omega_{i,cl} \leq k_B T$) exists, along which the activation barrier can be overcome. Thus, the FES is a two-dimensional function of an intramolecular (Y) and a solvent coordinate (X) (Fig. 6). The solvent motion is taken to be purely diffusive.

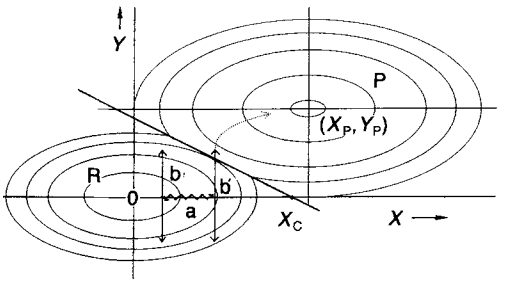

Fig. 6. Contour plot of the two-dimensional FES as a function of a diffusive solvent coordinate X and a low-frequency intramolecular coordinate Y. The diagonal line marks the intersection between the diabatic FESs. a) Diffusive motion along the solvent coordinate X; b), b') classical oscillation and barrier crossing along the intramolecular coordinate Y.

Furthermore, the relaxation along Y is assumed always to be fast enough compared to that along X to maintain thermal equilibrium with respect to Y. In contrast to the situation in Sections 2 and 3, the barrier is surmounted along the nondiffusive, intramolecular coordinate. Nevertheless, diffusive motion along the solvent coordinate changes the barrier height $\Delta G^{\neq}(X)$ of the reaction, which has to be overcome by intramolecular vibration. Again, if a (step wise) parabolic dependence of the FES on X and Y is assumed, a simple calculation shows that $\Delta G^{\neq}$ is given by equation (22). The reorganization energies λ_s and $\lambda_{i,cl}$ are for the solvent and the low-frequency intramolecular mode, respectively. They are defined by $\lambda_s = 1/2 f_s (X_R - X_P)^2$ and $\lambda_{i,cl} = 1/2 f_{i,cl} (Y_R - Y_P)^2$, where $f_s (= M\omega_0^2)$ and $f_{i,cl}$ are force constants and $X_{R,P}$ and $Y_{R,P}$ the appropriate equilibrium positions for reactants and products. X_c is the position of the barrier top on the X axis (see Fig. 6). A crucial quantity in this approach is the ratio $r = \lambda_{i,cl}/\lambda_s$. For $r \gg 1$, $\Delta G^{\neq}(X)$ is only weakly dependent on X; the barrier can be overcome for a wide range of X (wide reaction window), whereas for $r \ll 1, \Delta G^{\neq}(X)$ rapidly increases with the distance $(X - X_c)$ and confines the actual barrier crossing to a narrow gate near X_c (narrow reaction window).

$$\Delta G^{\neq}(X) = \frac{1}{2}\frac{\lambda_s}{\lambda_{i,cl}} f_s (X - X_c)^2 = \frac{1}{2r} f_s (X - X_c)^2 \qquad (22)$$

The quantitative formulation of this combination of diffusive and reactive motion leads to the Smoluchowski equation (23) for the time-development of the probability distribution $P(X,t)$ of the system along the solvent coordinate X.[45]

$$\frac{\partial P}{\partial t} = \frac{k_B T}{M\omega_0^2 \tau_l}\frac{\partial^2 P}{\partial X^2} + \frac{1}{M\omega_0^2 \tau_l}\frac{\partial}{\partial X}\left(P\frac{\partial F}{\partial X}\right) - k(X)\,P \qquad (23)$$

The first two terms on the right-hand side describe one-dimensional diffusion in a potential $F(X)$, that is taken as the cross section through the FES at $Y = Y_R$. The last term simulates the actual ET along Y. Since the distribution along Y is (by assumption) always at quasi-equilibrium, it need not be treated explicitly. $k(X)$ is taken from TS theory; its dependence on X refers to the fact that the activation barrier that the system has to overcome along the low-frequency mode is a function of X [eq. (22)].

4.2. Some Predictions

The details of the solution of the basic equation (23) are beyond the scope of this paper. Qualitatively the reaction dynamics is an interplay of two processes: 1) The system crosses the activation barrier along the low-frequency intramolecular mode Y into the product well at a rate $k(X)$. This reaction depletes the distribution $P(X, t)$ in the reactants' well for values of X that have a low activation barrier. 2) Diffusive motion along the solvent coordinate X repopulates the distribution for depleted values of X. This situation is illustrated in Figure 6.

Depending on r and on the initial preparation of the system, a very rich dynamic behavior is expected. The two limiting cases for very fast and very slow relaxation (fast and slow diffusion) are immediately obvious. In the first case the equilibrium distribution in X is always maintained; the effective rate k_{eq} is a thermal average of $k(X)$ over the equilibrium distribution $P_{eq}(X, t)$ and corresponds to the TS limit in equation (6). In the slow diffusion limit, the dynamics can be considered an ensemble average over a frozen distribution of X. More general cases have to be treated numerically. In general, the predicted time dependence of the reaction is nonexponential. Nevertheless, approximate relationships can be derived for the average survival time τ_a and the first moment τ_b of the survival probability $P(t)$ [$P(X, t)$ integrated over X] of the reactants. For large τ_l, both survival times τ_a and τ_b of the reactants are proportional to a (fractional power of) τ_l [eq. (24)].[46]

$$\tau_a = \int_0^\infty P(t)\,dt \propto \tau_l^\alpha \qquad (24a)$$

$$\tau_b = \frac{1}{\tau_a}\int_0^\infty t\,P(t)\,dt \propto \tau_l^\beta \quad \text{with} \quad 0 < \alpha, \beta \leq 1 \qquad (24b)$$

The exponents α and β decrease with increasing r. In the narrow reaction-window limit ($r \to 0$, meaning predominant influence of solvent reorganization), α and β approach 1; in the wide reaction-window limit α and β approach 0 for very large r. This is a plausible but important finding: Low-frequency intramolecular degrees of freedom may dampen the

influence of friction. They widen the range of X that has a low activation barrier and thereby reduce the need for sizable polarization fluctuations along X. In the narrow reaction-window limit the functional dependence on τ_l is very much like that in equation (18) in Section 3.3.2.

4.3. Generalizations

High-frequency intramolecular vibrational modes can be incorporated into the scheme in an analogous way to that discussed in Section 3.4.1. Instead of a single adiabatic FES or a pair of diabatic FESs one considers a set of FESs each characterized by a particular vibronic state (with index n) with respect to the high-frequency mode and defines vibronic reaction channels with individual rate constants $k(0 \rightarrow n,X)$. As in equation (19), high-frequency modes are important as accepting modes for large reaction energies.

In the original Sumi–Marcus approach, the classical low-frequency mode is thought of as an intramolecular vibration. Such vibrations often exist in transition metal complexes but not necessarily in rigid organic donor–acceptor molecules. Yet, another interpretation of this degree of freedom is as a fast relaxation mode of the solvent. In fact, under certain simplifying assumptions the Langevin equation (10) with memory friction [eq. (20)] characterized by two relaxation times can be cast into the form of equation (23).[133] Thus the Sumi–Marcus approach can be interpreted, too, as an alternative way to incorporate more than one time scale for the dielectric response.

4.4. Further Comments

In the preceding sections we have seen that effects of dielectric relaxation on ET reactions are the result of an interplay of three factors: 1) the degree of electronic coupling between reactant and product states as described by the parameter V; 2) the dynamics of dielectric response of the solvent and its effect on the nature of the motion along the reaction coordinate; and 3) the relative importance of intramolecular and solvent reorganization during the reaction.

Although the two theoretical models discussed so far differ in important assumptions, they agree in several qualitative predictions.

1) For fast relaxing solvents the reaction rate is independent of the relaxation properties of the solvent. With increasing relaxation time the system undergoes a continuous crossover and the rate finally becomes inversely proportional to (a fractional power of) τ_l.

2) The relaxation time at which this transition occurs depends on the electronic coupling V.

3) Unless the activation barrier is high, nonexponential kinetics are likely.

4) The overall dependence of the rate on the dielectric response of the solvent is sensitive to details of the dielectric relaxation spectrum as well as to intramolecular vibrational modes.

A general deficiency of most theoretical models is that they treat the solvent as an unstructured continuum and include molecular aspects of the solvent and its interaction with the solute insufficiently. Solvent properties enter the theory as empirical input parameters. Some progress towards a molecular theory has been made by using a description of the solvent beyond the simple continuum model.[134] One approach is the mean spherical approximation;[135, 136] another is molecular dynamics simulations of model charge-transfer reactions.[54, 55, 87–95]

5. Characterization of Solvent Dielectric Relaxation

Dielectric response enters the theories in Sections 3 and 4 as necessary input information. Although considerable progress has been achieved lately, the lack of reliable data in particular on the short-term behavior of dielectric relaxation is one of the main sources of uncertainty and ambiguity in the interpretation of possible dielectric relaxation effects on electron-transfer processes.

5.1. Qualitative Description

Historically, dielectric relaxation has been attributed to rotational diffusion of permanent dipoles[114, 115] or clusters of dipoles (region (a) in Fig. 7). This is the mechanism related to the Debye relaxation time τ_d. As a purely dissipative process, rotational diffusion represents a strongly overdamped motion with an exponential (possibly multiexponential) response function. In many cases the relevant time scale is correlated with the shear viscosity of the liquid[114, 115] and can vary by orders of magnitude (see Table 1). Additionally, translational diffusion of polar molecules (region (b) in Fig. 7) surrounding an electric charge was found to speed up dielectric relaxation considerably in solvents such as methanol.[82, 137] As long as these diffusional mechanisms dominate the dielectric response, the neglect of the second derivative in equation (10) is a valid approximation. More recently, however, inertial motion turned out to be important in simple liquids such as acetonitrile.[138–140] This motion is mainly associated with free rotation of individual solvent molecules (region (c) in Fig. 7) in the cage formed by surrounding molecules. Its characteristic time scale is the inverse well frequency ω_0^{-1} of Section 2. As is shown in equation (25), ω_0 is related[50, 103] to the thermal free rotational frequency ω_f given by $\omega_f^2 = 2k_BT/I$. I is the solvent molecular moment of inertia I. The prefactor to ω_f^2

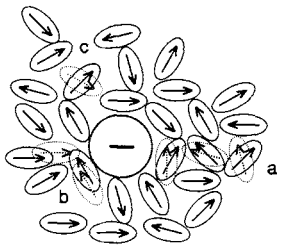

Fig. 7. Schematic representation of different mechanisms of dielectric response in a polar liquid: a) (strongly hindered) rotational diffusion, b) translational diffusion, and c) free (inertial) rotation of polar molecules.

in equation (25) accounts for the effect on the free rotation of the local electric field induced by the surrounding dielectric. The Kirkwood correlation parameter g is of the order of 1 in many solvents.[115] An ensemble average over many molecules leads to a Gaussian time dependence for the inertial part of the dielectric response function. There is also some speculation about a weak oscillatory contribution to the response function.[138-140]

$$\omega_0^2 = \frac{2\varepsilon_s + \varepsilon_\infty}{3g\varepsilon_\infty}\frac{2k_B T}{I} \tag{25}$$

5.2. Measurement of Dielectric Response

The most common experimental method for the determination of dielectric relaxation times is based on the measurement of dielectric loss spectra[141] in a macroscopic sample of the dielectric. Numerous experiments of this kind have shown that dielectric relaxation in many liquids—especially in alcohols[142, 143]—occurs on a whole distribution of time scales. Nevertheless, there are major disadvantages of these methods: a) They measure bulk properties; structural changes of the solvent and short-range correlation effects around the solute are ignored. b) In general the achievable microwave or millimeter wave frequency is insufficient to probe the dielectric response on the relevant time scale of a few picoseconds and below. Fortunately, progress is being made to extend the frequency range into the far infrared.[141] c) In liquids with nonexponential dielectric response, the relationship between resonances in dielectric loss spectra and microscopic relaxation times is not as simple as in equation (12), but requires a model for the coupling of the various relaxation components to the microscopic charge distribution.

More recent experimental methods are based on time-dependent shifts of fluorescence[144-147] or absorption[148] spectra of molecules undergoing a considerable change in dipole moment upon emission or optical excitation. The principle of these measurements is illustrated in Figure 8.

When a fluorophor is excited from a weakly polar ground state in equilibrium with the solvent environment to a strongly polar excited state, the electronic polarization of the solvent will instantly adjust to the new charge distribution on the solute. On the other hand the orientational polarization immediately after excitation will be the same as before, which represents a nonequilibrium situation in the excited state. The solvent will respond by dielectric relaxation to the equilibrium configuration with respect to the excited state. Analogously, fluorescence from the excited state will preserve the orientational polarization of the excited state present at the instant of the transition. The time-resolved fluorescence spectrum consequently experiences a time-dependent red-shift (see Fig. 8), which is usually cast into the normalized function $C(t)$ [eq. (26)].

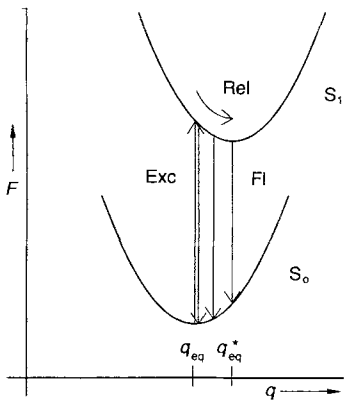

Fig. 8. Schematic representation of the influence of solvent relaxation (Rel) on the time-dependent red-shift of the fluorescence (Fl) of molecules undergoing a large change of dipole moment upon optical excitation (Exc).

$$C(t) = \frac{\nu(t) - \nu(\infty)}{\nu(0) - \nu(\infty)} \tag{26}$$

The frequencies $\nu(0)$, $\nu(t)$, and $\nu(\infty)$ represent the intensity maximum of the fluorescence spectrum immediately after excitation, at time t, and for the fully relaxed spectrum. The advantages of time-dependent spectral shift (TDSS) measurements are threefold: 1) These solutes are direct microscopic probes of the solvent environment. 2) The temporal resolution of these experiments is as high as 100 fs. 3) $C(t)$ directly mirrors the motion along the solvent coordinate on the excited state FES. In fact, $C(t)$ can be considered the (properly normalized) solvent coordinate q[149] [see eq. (2) and Fig. 8]!

A great number of such investigations allow some generalization to be made. a) With the exception of strongly associated liquids such as higher alcohols, dielectric relaxation in many common solvents occurs on a time scale of 10 ps and less. A number of representative results is compiled in Table 1. b) The dynamics is nonexponential in most cases. For simplicity an average solvation time τ_s is then introduced as an approximate time constant of dielectric relaxation. c) At least in acetonitrile there is indeed a very fast relaxation component with a characteristic decay time of about 100 fs, which constitutes almost 80% of the overall dielectric response of the solvent.[139] This is strong evidence for the kind of inertial motion depicted in Figure 7 (c).

Nevertheless, any attempt to translate experimental data into molecular mechanisms is rather speculative at present. In this context, molecular dynamics simulations of solvation[140] constitute a powerful and very promising tool. Although numerical difficulties in these calculations require serious simplifications, these techniques offer several advantages. First, such simulations achieve a theoretical temporal resolution that is still far beyond experimental means. This is particularly important for the short-time behavior of dielectric relaxation. Second, they provide a very detailed picture of the microscopic molecular motion of the solvent. Different types of motion such as rotation of dipoles, translation of molecules, and diffusional motion can be distinguished, and their relative importance in different stages of relaxation can be evaluated.

6. Experiments on Dielectric Relaxation Effects

Most relevant experiments measure the dependence of the ET rate on the longitudinal dielectric relaxation time τ_l (or τ_s). A glance at Table 1 and equation (17) shows that such an

experiment will either require a temporal resolution on a (sub)picosecond time scale or a reaction with a sizable activation barrier. The relaxation time τ_l is varied either by the use of different solvents, or in the same solvent by a change of temperature or external pressure.[150] This procedure leads to additional complications since other solvent parameters such as dielectric constant, refractive index, and density cannot be kept constant. Several of these parameters affect the rate through the free energy of activation. This dependence has to be eliminated experimentally or theoretically before a meaningful comparison with theoretical predictions can be made.

6.1. Evidence for Solvent-Controlled Adiabatic Electron Transfer

A popular method is the investigation of intermolecular electron exchange between molecules and their anions or cations:

$$A^{\bullet -} + A \rightleftharpoons A + A^{\bullet -} \quad \text{or} \quad C^{\bullet +} + C \rightleftharpoons C + C^{\bullet +}$$

A small fraction of the molecules in solution is oxidized or reduced chemically or electrochemically. These species are expected to form precursor complexes $A/A^{\bullet -}$ or $C/C^{\bullet +}$ within which the electron exchange, which is investigated with ESR[72] and NMR techniques[68] or electrochemical methods, occurs.[65, 66] The electron exchange leads to a broadening of ESR or paramagnetic NMR lines, which can be measured as a function of solvent, temperature, etc. Typical examples are TMPD/TMPD$^{\bullet +}$ (TMPD = *N,N,N',N'*-tetramethylphenylenediamine), TCNE/TCNE$^{\bullet -}$ (TCNE = tetracyanoethylene), and $[Cp_2Co]/[Cp_2Co]^{\bullet +}$ (Cp = cyclopentadienyl). Grampp et al.[72] and Weaver et al.[65, 68] have indeed found some cases where the rate of exchange is inversely proportional to τ_l as is expected for a solvent-controlled adiabatic reaction [eq. (17)]. Great care was taken to correct the data for solvent effects on the barrier height $\Delta G^{\ddagger}$.

A characteristic feature of most electron-exchange reactions is that they are processes with weak electronic coupling and a high activation barrier (of the order of 0.2 eV); that is, a steady-state distribution in the reactants is likely. In fact, the latter is a necessary condition to slow the reaction down sufficiently to make it accessible to magnetic resonance methods. Although these systems constitute good models for a verification of the above theoretical predictions, ESR and NMR methods have serious drawbacks. 1) They are limited to practically thermoneutral reactions. 2) The rate is indirectly inferred from the linewidth; no explicit time dependence is monitored. 3) On the time scale of the electron-transfer reaction in many of these systems, other processes occur, potentially obscuring or in any case complicating the interpretation of experimental data,[151, 152] among them decay and reformation of the precursor complex of the reactants and structural changes within it.

Some of these disadvantages were avoided in a few time-resolved fluorescence experiments of photoinduced charge-transfer reactions. Among the first examples were fluorescence measurements by Kosower et al.[56] with the *N*-arylaminonaphthalenesulfonate derivative **1**.

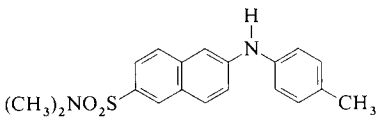

1

The reaction is initiated by optical excitation of the naphthalenesulfone-*N,N*-dimethylamide. In polar solvents the fluorescence of the excited state is quenched by intramolecular ET from the arylamino residue to the excited sulfonamide to form a charge-separated state. Back ET from the sulfonamide anion to the arylamino cation to form the ground state of the molecule completes the reaction cycle. The charge-separated state is fluorescent, too. Time-resolved measurements of the fluorescence decay from the excited state and the charge-separated state reveal the kinetics of charge-separation and recombination. Measurements were carried out in the series of alkanols from methanol to decanol as solvent. The dielectric response of these linear alcohols is best described by a sum of three exponentials where the slowest relaxation component covers a range of τ_l from 3 to 500 ps. The intramolecular charge separation was nonexponential but the average electron-transfer time τ_{et} was found to be about the same as τ_l within 30% when τ_l was calculated with this longest dielectric relaxation component of the alkanols. Obviously the faster components are irrelevant in this case. ET reactions on such a short time scale are necessarily processes with a low activation barrier.

In another series of experiments Huppert et al.[57] focus on the explicit time dependence of the charge separation in **1** and related derivatives in several pentanediols. They found that the fluorescence intensity is well fitted by a stretched exponential function and attribute it to a perturbation of the local solvent structure by the presence of the fluorophor.

Still, electron transfer in many of these systems is expected to be accompanied by the rotation of part of the molecule. Such conformational changes are known to exhibit a dependence on the viscosity of the solvent,[153] which may be difficult to distinguish from dielectric relaxation effects. In fact, much of the formalism in Section 4 was originally developed[132] as a model for an intramolecular reaction accompanied by slow conformational changes!

6.2. Evidence for the Crossover from Nonadiabatic to Solvent-Controlled Adiabatic Transfer

Evidence for the transition from nonadiabatic to solvent-controlled adiabatic behavior is still scarce. Weaver et al.[68] investigated a series of electron-exchange reactions between metallocenes with different metal atoms and with substituents of different size and their cations. The different substituents and central atoms influence the intermolecular electronic coupling V between the reactants in the precursor complex. In the solvents used, τ_l increased from about 250 fs to 10 ps. The qualitative dependence of the rate was similar to that defined in equation (18) with a regime with practically constant rate that then falls off roughly as $1/\tau_l$. Furthermore, the larger the substituents on the ferrocene the later this crossover occurred. This is consistent with a weaker donor–acceptor coupling V the further apart the reactants are kept by bulky ligands.

Higher alcohols exhibit a very strong temperature dependence of τ_l. This property was utilized by several groups[58, 73, 74, 76] to test equation (18) with intramolecular donor–acceptor compounds that exhibit photoinduced nonadiabatic ET at room temperature. Upon lowering the temperature, τ_l increases sufficiently to effect a crossover from nonadiabatic to solvent-controlled adiabatic behavior. An example of this kind is shown in Figure 9 where the

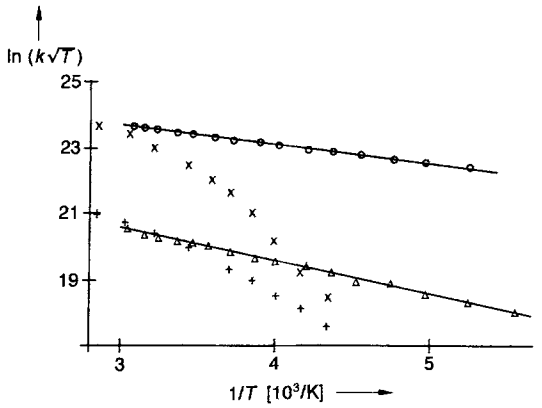

Fig. 9. Temperature-dependent electron-transfer rates in **2** in propionitrile (o, Δ) and propylene glycol (x, +). o,x: $n = 1$; Δ, +: $n = 2$.

temperature-dependent rates of the photoinduced intramolecular ET in the two compounds (**2**, $n = 1$, 2) are compared in propylene glycol and propionitrile.[74]

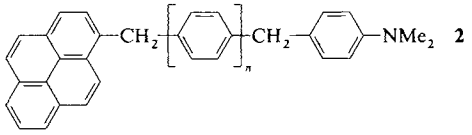

2

Optical excitation of the pyrene moiety induces an ET from the dimethylanilino residue to the excited acceptor. The kinetics of the ET is inferred from the increased fluorescence decay rate relative to that of a reference compound lacking the electron donor. The longer bridge between the donor dimethylaniline and the acceptor pyrene in **2** ($n = 2$) results in weaker electronic coupling V than in **2** ($n = 1$). The temperature dependence of the rates determined by $\Delta G^{\neq}$ is expected to be quite similar in both solvents and is empirically corrected in the ratio of the rates in both solvents, k_{diol}/k_{nitr}. On the other hand, in contrast to propionitrile, dielectric relaxation in propylene glycol is enormously slowed down at lower temperatures. Furthermore, it exhibits a broad distribution of relaxation times of the Davidson–Cole type.[143] The data in Figure 9 show that at elevated temperatures the rates for each compound are about the same in the two solvents. At lower temperatures they rapidly diverge. The temperature at which this deviation sets in increases, that is, the corresponding τ_l decreases, the stronger the electronic coupling V. This is predicted by equation (18). The strong temperature dependence of the ratio k_{diol}/k_{nitr} translates into $k_{diol} \propto 1/\tau_l^{\alpha}$, $\alpha = 0.3-0.6$. This exponent is possibly related to the distribution of relaxation times in propylene glycol.[43, 47, 48]

A similar qualitative change in behavior was observed in other experiments.[58, 76] However, as with **2**, all these donor–acceptor systems are rather flexible molecules undergoing conformational changes, which in turn can overlay the actual ET reaction and lead to a dependence on temperature and viscosity not unlike the one predicted by equation (18). Nevertheless, no systematic study seems to have been undertaken with rigid compounds yet.

6.3. Examples of an Unexpected Absence of Solvent Control

Despite such examples of reasonable agreement between experiment and theory there is a significant number of apparent failures, in the sense that very little correlation was found between charge-transfer rates and published relaxation times. These examples include intermolecular electron-exchange reactions, charge transfer in certain intramolecular systems with a twisted charge-transfer state (TICT), and fairly rigid intramolecular donor–acceptor compounds. In many of these cases k_{et} is much faster than the inverse of τ_l or τ_s, although according to equation (17), $1/\tau_l$ is an upper bound for the rate!

In several of their measurements on bimolecular electron exchange Weaver et al.[67, 69–71] explain this discrepancy with a predominant coupling of the charge transfer to fast relaxation components of the solvents that are even now difficult to measure and were left out in older relaxation data. According to Hynes[50] these components can speed up the rate significantly (see Section 3.4.2). Yet it is less than obvious what distinguishes these systems from similar ones such as those in Sections 6.1 and 6.2 that do behave as expected. A major drawback for attempts at clarification is the insufficient knowledge of the relevant intramolecular and solvent parameters of most ET systems, which allows no detailed comparison with existing theories without additional ad hoc assumptions.

Kobayashi et al.[77] measured the intermolecular ET rate in a solution of nile blue (**3**) in *N,N*-dimethylaniline. In this

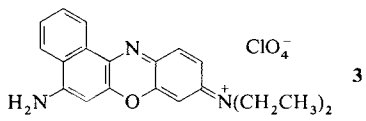

3

system *N,N*-dimethylaniline is both solvent and electron donor, which quenches the fluorescence of nile blue. The reaction is thought to occur in a close face-to-face configuration of donor and acceptor. The kinetics of the reaction is biphasic; the dominant decay time is 100 fs (95%) and the second component 2.5 ps (5%). The faster component implies an ET rate of 10^{13} s^{-1}, which is about 50 times faster than the inverse of the (estimated) τ_l of about 5ps in *N,N*-dimethylaniline! On the grounds of estimated reorganization energies of $\lambda_s \approx \lambda_i \approx 0.3$ eV, the authors classify their system as belonging to the intermediate reaction-window regime ($r \approx 1$, see Section 4.2). In the Sumi–Marcus model intramolecular vibrations offer an "escape route" over the activation barrier independent of frictional effects. Results of nu-

merical calculations for the average survival times τ_a and τ_b of equation (24) in this regime are indeed consistent with experimental decay times in this case (assuming $k_{eq} = 2 \times 10^{14}\ s^{-1}$). Yet their estimate of the intramolecular reorganization energy[77] yields only the high-frequency part of λ_i, whereas, strictly speaking, the ratio r in Section 4 refers to low-frequency vibrations. Thus the straightforward application of the Sumi–Marcus theory appears somewhat questionable.

Similar behavior was revealed for the cyclophane-like compound **4** containing a porphyrin and two dichloroquinone units in a cofacial orientation.[75] The optically excited

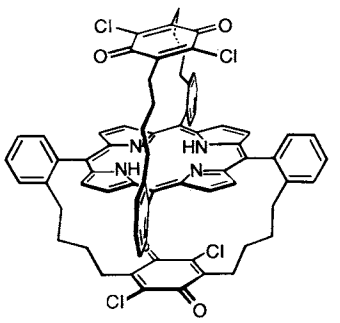

4

porphyrin acts as the electron donor, the quinones as acceptors. The kinetics is again monitored by the fluorescence quenching of the porphyrin. The reorganization energies λ_s and λ_i in this compound are comparable to those of system **3**.[154] The intramolecular ET rate is about $10^{12}\ s^{-1}$ and almost independent of solvent polarity in solvents ranging from hexane to acetonitrile and those with dielectric relaxation times as large as $\tau_l \approx 100-300$ ps such as glycerol triacetate and octanol. The very fast ET even in the nonpolar solvent hexane indicates that the reaction coordinate does not necessarily involve significant polarization fluctuations.

In addition to these cases of "missing" frictional effects there are several examples where initially a good correlation of ET rates and dielectric relaxation was postulated, which later turned out to be a simple effect of solvent on the barrier height ΔG^{+} (a static solvent effect)[155, 156] or were questioned for other reasons.[157] A general problem in this context is that the accessible range of τ_l (or other parameters) in most systems is rather narrow because of experimental difficulties. This leads to small variations of the rate which can be fitted by any theory showing the same qualitative behavior (and vice versa).

6.4. Recent Results from Ultrafast Spectroscopy

A significant step forward towards a sufficient characterization of the system under investigation was recently made by Barbara et al. at the University of Minnesota in a series of experiments in which solvent and intramolecular parameters could be determined independently. One example is the photoinduced charge separation in bianthryl (**5**, A–A)[59, 60] (see Fig. 10).

An ultrashort light pulse excites the molecule into a nonpolar locally excited (excitonic) (LE) state (A–A $\rightarrow$A*–A $\leftrightarrow$A–A*). In a polar liquid an asymmetric fluctuation in the solvent environment breaks the symmetry of the system

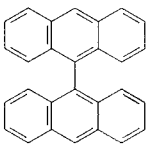

5

and induces an intramolecular charge separation leading to one of two possible dipolar charge-transfer (CT) states (A*–A $\leftrightarrow$A–A* $\rightarrow$A$^+$–A$^-$,A$^-$–A$^+$). The stronger solvent stabilization of the polar CT state compared to the nonpolar LE state leads to self-trapping of the CT state.

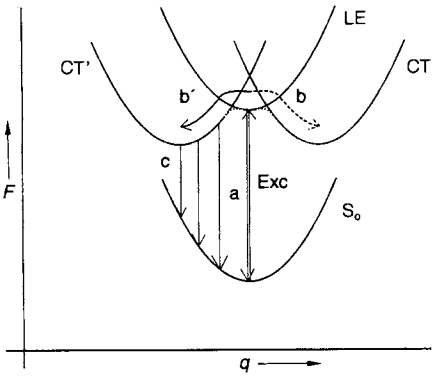

Fig. 10. Schematic representation of diabatic and adiabatic FESs for **5** in a polar solvent in the ground state S_0 (A–A), the nonpolar LE state (A*–A $\leftrightarrow$A–A*), and the two polar charge-transfer states CT (A$^-$–A$^+$) and CT' (A$^+$–A$^-$). a) Fluorescence from the LE state, b), b') intramolecular charge separation to the CT states and solvent relaxation, c) time-dependent red-shift of the charge recombination fluorescence from CT'.

The kinetics of this system was extensively investigated by the time dependence of the fluorescence spectra of the LE state (A*–A $\leftrightarrow$A–A* $\rightarrow$A–A) and of the CT states (A$^-$–A$^+$, A$^+$–A$^-$ $\rightarrow$A–A) in many solvents with very high temporal resolution.[59] The average electron-transfer times τ_{et} of the reaction LE $\rightarrow$ CT vary from 0.85 ps in acetone to 450 ps in pentanol at 273 K and agree with average solvation times τ_s within 40%. As in the system depicted in Figure 8, the temporal change of the fluorescence spectrum from the charge-separated state directly mirrors the motion on the FES. This motion was simulated[60] with a Langevin equation and a frequency-dependent friction term determined in TDSS experiments (see Section 5.2). The agreement between experimental spectra and numerical simulations was surprisingly good. The experimental data show that the charge-separation reaction is adiabatic, practically activationless, and nonexponential in most cases. Yet one distinctive feature of this system should be kept in mind: Sizable solvent fluctuations are indispensible for creating the asymmetry necessary in the system if a charge separation is to occur. Otherwise there is no reaction; that is, polarization fluctuation dynamics is necessarily rate-determining. It is hard to see how some intramolecular vibration could have the same effect.

A very similar analysis was performed by the Minnesota group on the photoinduced charge separation in the (unsymmetrical) molecule 9-(4-*N*,*N*-dimethylaminophenyl)anthracene (**6**).[61] The ET in this compound can be considered as a two-step process. The first step comprises most of the change of the electronic charge distribution on **6**, occurs on a time scale of less than 150 fs, and is independent of solvent

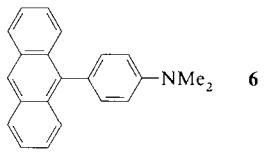

6

relaxation properties. The second one essentially mirrors the time-dependent solvent stabilization of the resulting charge-separated state with the characteristic time constant τ_s and involves only a minor further separation of the total charge transferred. Thus the ET reaction as a whole is only weakly affected by dynamic solvent effects.

A common feature of systems **5** and **6** is that the explanation of the ET dynamics requires the explicit simulation of the time dependence of the probability distribution of the reactants along the reaction coordinate. A discussion in terms of rate constants is clearly insufficient.

A very different behavior was found[62-64] for the photo-induced charge separation in the compound betaine-30 (**7**).

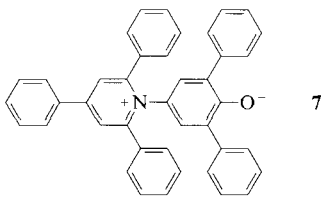

7

This molecule is directly excited from a charge-separated ground state into a higher, weakly polar state (see Fig. 11).

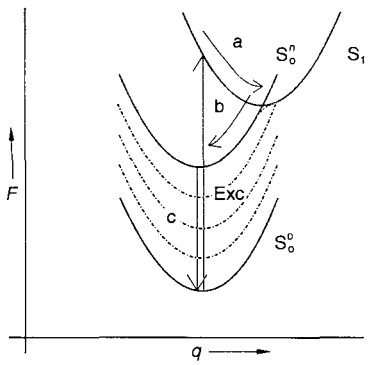

Fig. 11. FESs representing the vibronic ground state S_0^0 and the manifold of nth vibrationally excited states S_0^n of the charge-separated ground state S_0 and the weakly polar, optically excited state S_1 of **7**. The various states S_0^n are vertically shifted by the phonon energy $\hbar\omega_i$. Note: The classical coordinate q refers to two different degrees of freedom for step a and b: a) dielectric relaxation of the solvent in the excited state, b) charge-transfer reaction induced by a low-frequency (intramolecular) vibration, c) vibrational relaxation to the ground state with respect to high-frequency modes.

The large change in dipole moment will necessarily lead to a nonequilibrium initial polarization in the excited state. The reverse reaction from the weakly polar excited state to the charge-separated ground state was monitored by the recovery of the ground-state absorption (temporal resolution of about 100 fs). Room temperature measurements in simple solvents such as acetonitrile and methyl acetate cover a range of average solvation times τ_s between 250 fs and about 10 ps.[62, 63] Temperature-dependent measurements in glycerol triacetate from 228 to 318 K extend the upper limit of τ_s from 10 ps to μs.[64] A drawback of the experiments on temperature dependence is that the dielectric response of glycerol triacetate is less well characterized than that of the other solvents. The reliability of the data for fast and slow relaxation is therefore not strictly comparable.

The relevant solvent parameters and intramolecular parameters were estimated by fitting model band-shape functions to stationary ground-state absorption spectra in many solvents.[158] The band shape is statisfactorily reproduced if, in addition to a structureless continuous dielectric, an effective high-frequency ($\hbar\omega_i \approx 1600\ cm^{-1}$) intramolecular mode and a low-frequency ($\hbar\omega_{i,el} \leq 200\ cm^{-1}$) mode are included. The nature of the latter mode is not yet understood, however. Furthermore, the band-shape analysis yields estimates of the energies λ_s, λ_i, and $\lambda_{i,el}$ (see Sections 2.3, 3.4.1, and 4.1) referring to solvent continuum and high-frequency and low-frequency mode reorganization. The electronic coupling V was estimated at about $2500\ cm^{-1}$, which guarantees an adiabatic reaction under all circumstances.

The overall dependence on relaxation properties is as follows: In solvents with solvation times τ_s of less than 3 ps, the survival time of the excited state rapidly rises with τ_s from 0.2 to about 2 ps, but then remains almost constant at 2–5 ps in "slower" solvents with solvation times greater than 10 ps (even by several orders of magnitude). This kind of crossover of the ET rate with increasing dielectric relaxation time of the solvent is the exact opposite of the one in equation (18)!

The interpretation offered by the authors[63] is the generalized Sumi–Marcus model including a classical and a high-frequency, quantum-mechanical intramolecular mode. The high-frequency mode serves as an accepting mode for the high driving force and enables an almost activationless course of this ET reaction in the inverted regime. The low-frequency mode of the band-shape analysis is taken as the Y coordinate in Figure 6. Furthermore, the initial nonequilibrium polarization prepared upon optical excitation is explicitly taken into account.

The qualitative explanation of the biphasic dependence of the rate on τ_s is as follows: Optical excitation of the betaine initially prepares a state within a range of the diffusive solvent coordinate X that has a sizable activation barrier in $k(X)$. In "fast" solvents ($\tau_s \leq 3$ ps) the solvent polarization will at first "diffuse" to a solvent configuration for which the activation barrier is lower, and then the system reacts to form products very rapidly along the classical nondiffusive coordinate. The rate-determining step is the polarization diffusion, and the survival time of the excited state is therefore proportional to τ_s. In "slow" solvents ($\tau_s \geq 10$ ps), the system will react over the barrier that it experiences in its initial solvent configuration before it can diffuse to another configuration characterized by a lower barrier. Naturally the rate will be almost independent of τ_s in this limit. Although the time scale is only 10 ps, this already corresponds to the frozen limit of Section 4.2.

On comparison of **5**, **6**, and **7**, a very specific dynamic solvent effect is found in each compound. Nevertheless, these systems represent only the special case of an almost barrierless reaction with an intrinsically very strong donor–acceptor interaction. The crossover between the nonadiabat-

ic/solvent-controlled adiabatic/uniform adiabatic cases has not yet been treated in the same detail.

7. Conclusions and Prospects

In general, the finite dielectric response time of a polar solvent exerts a retarding influence on the change of the charge distribution on a solute that is a reactant of an ET reaction. Such a reaction is described as the crossing of a particle (the "system") over an activation barrier between two wells on a FES. The rapidly fluctuating interaction with many solvent molecules is modeled by frictional and random forces and results in a highly stochastic motion of the particle over the barrier.

A fairly general consequence of diffusive barrier crossing is that the retardation in the rate of crossing is proportional to the longitudinal dielectric relaxation time τ_l of the solvent. Thus for a long time the proportionality of the rate to $1/\tau_l$ has been considered the trademark of dielectric relaxation effects, and early experimental results seemed to confirm this picture. In fact, theory suggested that dynamic solvent control of ET can be attained in every reaction if it is carried out in solvents with sufficiently slow dielectric relaxation. Yet, this early enthusiasm may have been premature. It has become increasingly evident that reality is much more complex. This behavior results from an interplay of electronic coupling (nonadiabaticity), stochastic barrier crossing, and the possibility of several time scales for dielectric response and intramolecular reorganization. Nevertheless, current theoretical models are still too crude to offer reliable criteria in practical cases. In this respect a lot remains to be done to develop a truly molecular theory.

On the other hand it is precisely the uncertainty of relaxation data and the lack of reliable molecular information in combination with the flexibility of current theories that has hitherto allowed researchers to declare agreement of theory with practically every experimental outcome. Consequently, the crucial question is: What are the conditions an ideal experiment has to fulfill to remedy this somewhat unsatisfactory state of affairs?

First, fixed distance and orientation of electron donor and acceptor are highly desirable. This condition is realized in rigidly bridged intramolecular donor–acceptor compounds and ensures a well-defined electronic coupling and excludes conformational and other structural changes likely to interfere with the ET.

Second, a full characterization of intramolecular and static solvent parameters independent of the measurement of dynamic solvent effects on ET is indispensible. The electronic coupling can be estimated from a global analysis of the dependence of the rate on the driving force and the distance[14] and in some cases from static charge-transfer absorption spectra.[18, 159, 160] Band-shape analysis of charge-transfer transitions can provide estimates of relevant reorganization energies and vibronic frequencies.[158, 161] Raman studies of these systems[162] could further improve our knowledge on these parameters.

Third, detailed information on the time scales and mechanisms of dielectric response and its coupling to the reacting species is essential. In this context, ultrafast optical spectroscopy has reached a stage where one is beginning to understand solvent dynamics on a molecular level.

Fourth, there is important information in the explicit time depencence of ET. This necessitates a time-resolved measurement of ET kinetics on a time scale comparable to dielectric response. In summary, only a combination of several static and dynamic measurements will provide the necessary information to construct the relevant FESs of the system and the motion thereon.

Fortunately, the enormous progress in spectroscopic instrumentation and the synthesis of suitable donor–acceptor systems have brought these ambitious goals within reach. Furthermore, advances in computer power are beginning to enable realistic simulations of ET reactions in solution, which promise to close the gap between experiment and theory.

This encouraging prospect is of far-reaching importance for reaction dynamics in solution as a whole. Although the general ideas of dynamic solvent effects such as diffusive barrier crossing and adiabaticity have been discussed in the context of ET, they are of a much wider validity and pertain to other reactions such as proton transfer, isomerizations,[163] ligand binding in enzymes,[83] ionic and radical association/dissociation,[164] and to nucleophilic substitution[117, 165] as well.

Most of all I would like to thank my academic teacher Prof. M. E. Michel-Beyerle, Technische Universität München (TUM). Her enthusiasm has been a source of inspiration over many years. Without her ceaseless commitment I would have had neither the means nor the conceptual background for my work on electron-transfer reactions. It was at her instigation that I began writing this review. It is also with great pleasure that I acknowledge the continuous support and encouragement by Prof. J. Jortner, Tel Aviv University. He introduced me to the subject and has generously shared his comprehensive knowledge and latest results with me ever since. Much of the success in our work at the TUM is a direct result of his advice. Without the enormous synthetic effort and the close cooperation with Prof. H. A. Staab and his co-workers at the Max-Planck-Institut in Heidelberg, we could not have carried out our most recent measurements with the porphyrin–quinone compounds. Furthermore, I have benefited much from the critical reading of the manuscript and many stimulating discussions with Prof. M. Bixon, Tel Aviv University, and Prof. N. Rösch, Technische Universität München. I would also like to thank Prof. P. F. Barbara, University of Minnesota, for making available several preprints prior to publication. The financial support by the Deutsche Forschungsgemeinschaft and the Bundesministerium für Forschung und Technologie is gratefully acknowledged. Last but not least, I am heavily indebted to Prof. G. L. Hofacker, TUM, for the kind hospitality I have experienced at his institute.

Received: February 7, 1992 [A 897 IE]
German version: *Angew. Chem.* **1993**, *105*, 378

[1] J. Ulstrup, *Charge Transfer Processes in Condensed Media*, Springer, Berlin, **1979**.
[2] R. D. Cannon, *Electron Transfer Reactions*, Butterworths, London, **1980**.
[3] V. Balzani, F. Scandola, *Supramolecular Photochemistry*, Ellis Horwood, New York, **1991**.
[4] H. Taube, *Angew. Chem.* **1984**, *96*, 315; *Angew. Chem. Int. Ed. Engl.* **1984**, *23*, 329.
[5] M. D. Newton, N. Sutin, *Annu. Rev. Phys. Chem.* **1984**, *35*, 437.
[6] R. A. Marcus, N. Sutin, *Biochim. Biophys. Acta* **1985**, *811*, 265.

[7] K. V. Mikkelsen, M. A. Ratner, *Chem. Rev.* **1987**, *87*, 113.
[8] A. Haim, *Prog. Inorg. Chem.* **1983**, *30*, 273; T. J. Meyer, *ibid.* **1983**, *30*, 389; N. Sutin, *ibid.* **1983**, *30*, 441.
[9] J. Kavarnos, *Top. Curr. Chem.* **1990**, *156*, 21.
[10] F. Scandola, M. T. Indelli, C. Chiorboli, C. A. Bignozzi, *Top. Curr. Chem.* **1990**, *158*, 73.
[11] *Photoinduced Electron Transfer. Part A–D* (Eds.: M. A. Fox, M. Chanon), Elsevier, Amsterdam, **1988**.
[12] J. S. Connolly, J. R. Bolton in [11], *Part D*, p. 303.
[13] M. R. Wasielewski, M. P. Niemczyk, W. A. Svec, E. B. Pewitt, *J. Am. Chem. Soc.* **1985**, *107*, 1080; G. L. Gaines, M. P. O'Neill, W. A. Svec, M. P. Niemczyk, M. R. Wasielewski, *ibid.* **1991**, *113*, 719.
[14] G. L. Closs, L. T. Calcaterra, N. J. Green, K. W. Penfield, J. R. Miller, *J. Phys. Chem.* **1986**, *90*, 3673.
[15] I. R. Gould, R. H. Young, R. E. Moody, S. Farid, *J. Phys. Chem.* **1991**, *95*, 2068.
[16] T. Asahi, N. Mataga, Y. Takahashi, T. Miyashi, *Chem. Phys. Lett.* **1990**, *171*, 309; T. Asahi, N. Mataga, *J. Phys. Chem.* **1991**, *95*, 1956.
[17] P. Chen, R. Duesing, D. K. Graff, T. J. Meyer, *J. Phys. Chem.* **1991**, *95*, 5850.
[18] D. E. Richardson, H. Taube, *J. Am. Chem. Soc.* **1983**, *105*, 40.
[19] Systematic studies on electron transfer in modified biomolecules are described in: S. L. Mayo, W. R. Ellis, R. J. Crutchley, H. B. Gray, *Science* **1986**, *233*, 948; B. E. Bowler, A. L. Raphael, H. B. Gray, *Prog. Inorg. Chem.* **1990**, *38*, 259, and references therein.
[20] Systematic studies on synthetic oligopeptides are described in: S. S. Isied, *Prog. Inorg. Chem.* **1984**, *32*, 443; M. R. DeFelippis, M. Faraggi, M. H. Klapper, *J. Am. Chem. Soc.* **1990**, *112*, 5640; K. S. Schanze, L. A. Cabana, *J. Phys. Chem.* **1990**, *94*, 2740.
[21] J. M. Warman, M. P. de Haas, M. N. Paddon-Row, E. Cotsaris, N. S. Hush, H. Oevering, J. W. Verhoeven, *Nature* **1986**, *320*, 615; H. Oevering, M. N. Paddon-Row, M. Heppener, A. M. Oliver, E. Cotsaris, J. W. Verhoeven, N. S. Hush, *J. Am. Chem. Soc.* **1987**, *109*, 3258.
[22] A. D. Joran, B. A. Leland, P. M. Felker, A. H. Zewail, J. J. Hopfield, P. B. Dervan, *Nature* **1987**, *327*, 508.
[23] H. Heitele, M. E. Michel-Beyerle, P. Finckh, *Chem. Phys. Lett.* **1987**, *134*, 273.
[24] G. L. Closs, M. D. Johnson, J. R. Miller, P. Piotrowiak, *J. Am. Chem. Soc.* **1989**, *111*, 3751.
[25] M. R. Wasielewski in [11], *Part A*, p. 161.
[26] M. D. Newton, *Chem. Rev.* **1991**, *91*, 767, and references therein.
[27] M. J. Powers, T. J. Meyer, *J. Am. Chem. Soc.* **1978**, *100*, 4393; *ibid.* **1980**, *102*, 1289.
[28] A. Weller, *Z. Phys. Chem. (Munich)* **1982**, *133*, 93.
[29] G. Grampp, W. Jaenicke, *Ber. Bunsenges. Phys. Chem.* **1984**, *88*, 325, 335.
[30] J. A. Schmidt, A. Siemiarczuk, A. C. Weedon, J. R. Bolton, *J. Am. Chem. Soc.* **1985**, *107*, 6112; J. A. Schmidt, J.-Y. Liu, J. R. Bolton, M. D. Archer, V. P. Y. Gadzekpo, *J. Chem. Soc. Faraday Trans. 1* **1989**, *85*, 1027.
[31] H. Heitele, S. Weeren, F. Pöllinger, M. E. Michel-Beyerle, *J. Phys. Chem.* **1989**, *93*, 5173; H. Heitele, F. Pöllinger, S. Weeren, M. E. Michel-Beyerle, *Chem. Phys.* **1990**, *143*, 325; *Chem. Phys. Lett.* **1990**, *168*, 598.
[32] J. Burgess, E. Pelizzetti, *Prog. React. Kinet.* **1992**, *17*, 1.
[33] K. F. Purcell, J. C. Kotz, *Inorganic Chemistry*, W. B. Saunders, Philadelphia, USA, **1977**; F. A. Cotton, G. Wilkinson, *Advanced Inorganic Chemistry*, Wiley, New York, **1988**.
[34] H. A. Kramers, *Physica (Amsterdam)* **1940**, *7*, 284.
[35] L. D. Zusman, *Chem. Phys.* **1980**, *49*, 295.
[36] L. D. Zusman, *Chem. Phys.* **1988**, *119*, 51; *ibid.* **1990**, *144*, 1.
[37] D. F. Calef, P. G. Wolynes, *J. Phys. Chem.* **1983**, *87*, 3387.
[38] A. Garg, J. N. Onuchic, V. Ambegaokar, *J. Chem. Phys.* **1985**, *83*, 4491.
[39] J. N. Onuchic, *J. Chem. Phys.* **1987**, *86*, 3925.
[40] J. N. Onuchic, P. G. Wolynes, *J. Phys. Chem.* **1988**, *92*, 6495.
[41] I. Rips, J. Jortner, *J. Chem. Phys.* **1987**, *87*, 2090.
[42] I. Rips, J. Jortner, *J. Chem. Phys.* **1987**, *87*, 6513.
[43] I. Rips, J. Jortner, *Chem. Phys. Lett.* **1987**, *133*, 411.
[44] J. Jortner, M. Bixon, *J. Chem. Phys.* **1988**, *88*, 167.
[45] H. Sumi, R. A. Marcus, *J. Chem. Phys.* **1986**, *84*, 4272, 4894.
[46] W. Nadler, R. A. Marcus, *J. Chem. Phys.* **1987**, *86*, 3906.
[47] W. Nadler, R. A. Marcus, *Chem. Phys. Lett.* **1988**, *144*, 24.
[48] W. Nadler, R. A. Marcus, *Isr. J. Chem.* **1990**, *30*, 69.
[49] H. L. Friedman, M. D. Newton, *Faraday Discuss. Chem. Soc.* **1982**, *74*, 73; M. D. Newton, H. L. Friedman, *J. Chem. Phys.* **1988**, *88*, 4460.
[50] J. T. Hynes, *J. Phys. Chem.* **1986**, *90*, 3701.
[51] A. B. Helman, *Chem. Phys.* **1982**, *65*, 271.
[52] M. Sparpaglione, S. Mukamel, *J. Chem. Phys.* **1988**, *88*, 3263, 4300; Y. J. Yan, M. Sparpaglione, S. Mukamel, *J. Phys. Chem.* **1988**, *92*, 4842.
[53] R. I. Cukier, *J. Chem. Phys.* **1988**, *88*, 5594; M. Morillo, R. I. Cukier, *ibid.* **1988**, *89*, 6736; M. Morillo, D. Y. Yang, R. I. Cukier, *ibid.* **1989**, *90*, 5711; D. Y. Yang, R. I. Cukier, *ibid.* **1989**, *91*, 281.
[54] A. Warshel, *J. Phys. Chem.* **1982**, *86*, 2218.
[55] A. Warshel, J.-K. Hwang, *J. Chem. Phys.* **1986**, *84*, 4938.
[56] D. Huppert, H. Kanety, E. M. Kosower, *Faraday Discuss. Chem. Soc.* **1981**, *74*, 161; E. M. Kosower, D. Huppert, *Chem. Phys. Lett.* **1983**, *96*, 433.
[57] D. Huppert, V. Ittah, E. M. Kosower, *Chem. Phys. Lett.* **1988**, *144*, 15; D. Huppert, V. Ittah, A. Masad, E. M. Kosower, *ibid.* **1988**, *150*, 349.
[58] A. Masad, D. Huppert, E. M. Kosower, *Chem. Phys.* **1990**, *144*, 391.
[59] T. J. Kang, M. A. Kahlow, D. Giser, S. Swallen, V. Nagarajan, W. Jarzeba, P. F. Barbara, *J. Phys. Chem.* **1988**, *92*, 6800.
[60] T. J. Kang, W. Jarzeba, P. F. Barbara, T. Fonseca, *Chem. Phys.* **1990**, *149*, 81.
[61] K. Tominaga, G. C. Walker, W. Jarzeba, P. F. Barbara, *J. Phys. Chem.* **1991**, *95*, 10475.
[62] E. Akesson, G. C. Walker, P. F. Barbara, *J. Chem. Phys.* **1991**, *95*, 4188.
[63] P. F. Barbara, G. C. Walker, T. P. Smith, *Science* **1992**, *256*, 975.
[64] E. Akesson, A. E. Johnson, N. E. Levinger, G. C. Walker, T. P. DuBruil, P. F. Barbara, *J. Chem. Phys.* **1992**, *96*, 7859.
[65] M. J. Weaver, T. Gennett, *Chem. Phys. Lett.* **1985**, *113*, 213.
[66] T. Gennett, D. F. Milner, M. J. Weaver, *J. Phys. Chem.* **1985**, *89*, 2787.
[67] G. E. McManis, M. N. Golovin, M. J. Weaver, *J. Phys. Chem.* **1986**, *90*, 6563.
[68] G. E. McManis, R. M. Nielson, A. Gochev, M. J. Weaver, *J. Am. Chem. Soc.* **1989**, *111*, 5533.
[69] R. M. Nielson, G. E. McManis, M. N. Golovin, M. J. Weaver, *J. Phys. Chem.* **1988**, *92*, 3441.
[70] G. E. McManis, M. J. Weaver, *Chem. Phys. Lett.* **1988**, *145*, 55.
[71] M. J. Weaver, G. E. McManis, W. Jarzeba, P. F. Barbara, *J. Phys. Chem.* **1990**, *94*, 1715.
[72] W. Harrer, G. Grampp, W. Jaenicke, *Chem. Phys. Lett.* **1984**, *112*, 263; G. Grampp, W. Harrer, G. Hetz, *Ber. Bunsenges. Phys. Chem.* **1990**, *94*, 1343; G. Grampp, W. Jaenicke, *ibid.* **1991**, *95*, 904.
[73] H. Heitele, M. E. Michel-Beyerle, P. Finckh, *Chem. Phys. Lett.* **1987**, *138*, 237.
[74] P. Finckh, H. Heitele, M. E. Michel-Beyerle, *Chem. Phys.* **1989**, *138*, 1.
[75] F. Pöllinger, H. Heitele, M. E. Michel-Beyerle, C. Anders, M. Futscher, H. A. Staab, *Chem. Phys. Lett.* **1992**, *198*, 645.
[76] U. Rempel, B. von Maltzan, C. von Borczyskowski, *Z. Phys. Chem.* **1991**, *170*, 107.
[77] T. Kobayashi, Y. Takagi, H. Kandori, K. Kemnitz, K. Yoshihara, *Chem. Phys. Lett.* **1991**, *180*, 416.
[78] M. Maroncelli, J. McInnis, G. R. Fleming, *Science* **1989**, *243*, 1674.
[79] J. D. Simon, *Acc. Chem. Res.* **1988**, *21*, 128.
[80] M. J. Weaver, G. E. McManis, *Acc. Chem. Res.* **1990**, *23*, 294.
[81] P. F. Barbara, W. Jarzeba, *Adv. Photochem.* **1990**, *15*, 1.
[82] B. Bagchi, *Annu. Rev. Phys. Chem.* **1989**, *40*, 115.
[83] H. Frauenfelder, P. G. Wolynes, *Science* **1985**, *229*, 337.
[84] R. E. Cline, P. G. Wolynes, *J. Chem. Phys.* **1987**, *86*, 3836.
[85] D. F. Calef, in [11], *Part A*, p. 362.
[86] In fact, two different ways to partition the full Hamiltonian into zeroth-order and perturbation parts for reactants and products each are presumed to exist [1, 5, 26].
[87] A. Yoshimori, T. Kakitani, Y. Enomoto, N. Mataga, *J. Phys. Chem.* **1989**, *93*, 8316.
[88] The direct simulation of FESs far from the minima of reactants or products turns out to be impracticable. Instead, a free energy perturbation approach must be used as described in G. King, A. Warshel, *J. Chem. Phys.* **1990**, *93*, 8682.
[89] J.-K. Hwang, A. Warshel, *J. Am. Chem. Soc.* **1987**, *109*, 715.
[90] A. Warshel, Z.-T. Chu, W. W. Parson, *Science* **1989**, *246*, 112.
[91] A. Warshel, Z.-T. Chu, *J. Chem. Phys.* **1990**, *93*, 4003.
[92] A. Warshel, W. W. Parson, *Annu. Rev. Phys. Chem.* **1991**, *42*, 279.
[93] R. A. Kuharski, J. S. Bader, D. Chandler, M. Sprik, M. L. Klein, R. W. Impey, *J. Chem. Phys.* **1988**, *89*, 3248.
[94] D. A. Zichi, G. Ciccotti, J. T. Hynes, M. Ferrario, *J. Phys. Chem.* **1989**, *93*, 6261.
[95] E. A. Carter, J. T. Hynes, *J. Phys. Chem.* **1989**, *93*, 2184; *J. Chem. Phys.* **1991**, *94*, 5961.
[96] A difficult question is whether the equilibrium averaging in equation (3) of the solvent configurations (X) remains meaningful even in a dynamic process far from equilibrium. Eventually, nonequilibrium dynamics has to be treated explicitly on higher dimensional (free) energy surfaces, for example, along the lines of Section 4.
[97] A harmonic free energy surface $F(q)$ corresponds to a Gaussian probability distribution $p(q)$ in equation (3). Its force constant f_s is determined by the width of the Gaussian $f_s = k_B T/\langle (q - \langle q \rangle)^2 \rangle$; the effective mass M is defined through the equipartition theorem $M = k_B T/\langle (\partial q/\partial t - \langle \partial q/\partial t \rangle)^2 \rangle$, where the brackets $\langle\ \rangle$ indicate equilibrium averages [95].
[98] R. A. Marcus, *J. Chem. Phys.* **1956**, *24*, 988; *ibid.* **1965**, *43*, 679.
[99] N. S. Hush, *Trans. Faraday Soc.* **1961**, *57*, 557.
[100] H. Eyring, S. H. Lin, S. M. Lin, *Basic Chemical Kinetics*, Wiley, New York, **1980**.
[101] D. G. Truhlar, W. L. Hase, J. T. Hynes, *J. Phys. Chem.* **1983**, *87*, 2664.
[102] P. Hänggi, P. Talkner, M. Borkovec, *Rev. Mod. Phys.* **1990**, *62*, 251, and references therein.
[103] G. E. McManis, A. Gochev, M. J. Weaver, *Chem. Phys.* **1991**, *152*, 107.
[104] There are other conventions for γ_{1L} differing from equation (7) by factors of 2, $\pi/2$, $\sqrt{\pi/2}$ etc.

[105] The justification of the factor of π requires an explicit quantum-mechanical calculation of the transition probability for a single crossing of the LZ region [100, 106]. The factor of 2 accounts for the fact that in a nonadiabatic reaction the system usually crosses the LZ region twice: once on the way up the reactant PES and, unless a transition has occurred during the first crossing, once on the return trip, each contributing $\pi\gamma_{lz}$ to the overall transition probability P for a successful reaction.

[106] L. Landau, *Phys. Z. Sovietunion* **1932**, *1*, 88; *ibid.* **1932**, *2*, 46; C. Zener, *Proc. R. Soc. London A* **1932**, *137*, 696; *ibid.* **1933**, *140*, 660.

[107] V. O. Levich, *Adv. Electrochem. Electrochem. Eng.* **1966**, *4*, 249; R. R. Dogonadze, A. M. Kuznetsov, *Sov. Electrochem. (Engl. Transl.)* **1967**, *3*, 1189.

[108] R. P. Van Duyne, S. F. Fischer, *Chem. Phys.* **1974**, *5*, 183; N. R. Kestner, J. Jortner, J. Logan, *J. Phys. Chem.* **1974**, *78*, 2148; J. Ulstrup, J. Jortner, *J. Chem. Phys.* **1975**, *63*, 4358; J. Jortner, *ibid.* **1976**, *64*, 4860.

[109] Practically all analytical results in quantum-mechanical ET theory were derived only for reactions with a negligible entropy change. In applications, however, entropy effects are included in rate expressions by simply substituting free energies for ordinary energies. For equation (8) this substitution is discussed in R. A. Marcus, *J. Chem. Phys.* **1984**, *81*, 4494. In general, this procedure is only justified by the lack of alternatives. In simulations, free energies enter in a more natural way [55].

[110] The Landau–Zener probability p_{lz} is the transition probability upon a single crossing of the LZ region for arbitrary γ_{lz}. The derivation of the geometric series is a generalization of the argument in [105]: After an unsuccessful crossing of the LZ region on the way up the reactant PES the system may be trapped above the crossing point by repeated hopping between the diabatic PESs on the way down. The overall transition probability is the sum over all transition probabilities for an arbitrary number n of hops: $P = p_{lz} + (1\text{-}p_{lz})p_{lz}(1\text{-}p_{lz}) + \cdots + (1\text{-}p_{lz})p_{lz}^{2n-1}(1\text{-}p_{lz}) + \cdots = 2p_{lz}/(1 + p_{lz})$. See for example, [1] and T. Holstein, *Ann. Phys. (N.Y.)* **1959**, *8*, 343. Yet, the LZ transition probability is only valid between one-dimensional PESs. Its application to FESs must be seen in the spirit of the remark in [109].

[111] S. Chandrasekhar, *Rev. Mod. Phys.* **1943**, *15*, 1; C. W. Gardiner, *Handbook of Stochastic Methods*, Springer, Berlin, **1983**.

[112] J. T. Hynes in *Theory of Chemical Reaction Dynamics* (Ed.: M. Baer), CRC Press, Boca Raton, FL, **1985**, p. 171.

[113] S. A. Adelman, *Adv. Chem. Phys.* **1980**, *44*, 143; *ibid.* **1983**, *53*, 61; and references therein.

[114] P. Debye, *Polar Molecules*, Dover, New York, **1929**; H. Fröhlich, *Theory of Dielectrics*, Oxford, London, **1949**.

[115] C. F. Böttcher, P. Bordewijk, *Theory of Electric Polarization, Vol. 2*, Elsevier, Amsterdam, **1978**.

[116] H. L. Friedman, *J. Chem. Soc. Faraday Trans. 2* **1983**, *79*, 1465; D. Kivelson, H. L. Friedman, *J. Phys. Chem.* **1989**, *93*, 7026.

[117] This statement tacitly ignores an important aspect: In an adiabatic reaction the solvent "sees" a gradual shift of the charge from the donor to the acceptor in the LZ region, which leads to an additional coupling between the dynamics of the solvent and of the change of the electronic structure [55]. This observation seems to have been overlooked in practically all analytical treatments of dynamic solvent effects on ET. Yet, the coupling was explicitly taken into account in computer simulations of S_N2-reactions (J.-K. Hwang, G. King, S. Creighton, A. Warshel, *J. Am. Chem. Soc.* **1988**, *110*, 5297; J.-K. Hwang, S. Creighton, G. King, D. Whitney, A. Warshel, *J. Chem. Phys.* **1988**, *89*, 859) and in the simulation of the model ET reaction in [94].

[118] T. Fonseca, J. A. N. F. Gomes, P. Grigolini, F. Marchesoni, *Adv. Chem. Phys.* **1985**, *62*, 389.

[119] A valuable collection of articles on Kramers's and related problems can be found in *J. Stat. Phys.* **1986**, *42* (1/2) and in *Ber. Bunsenges. Phys. Chem.* **1991**, *95*, (3).

[120] B. J. Berne, M. Borkovec, J. E. Straub, *J. Phys. Chem.* **1988**, *92*, 3711.

[121] This back scattering is classical and unrelated to quantum-mechanical resonance and coherence phenomena in barrier-crossing problems. Although such effects have been discussed in connection with friction [40], they should be limited to very special cases unlikely to be encountered in systems of interest here.

[122] S. Efrima, M. Bixon, *Chem. Phys. Lett.* **1974**, *25*, 34; M. Bixon, J. Jortner, *J. Phys. Chem.* **1991**, *95*, 1941.

[123] J. S. Bader, R. A. Kuharski, D. Chandler, *J. Chem. Phys.* **1990**, *93*, 230.

[124] R. F. Grote, J. T. Hynes, *J. Chem. Phys.* **1980**, *73*, 2715.

[125] J. E. Straub, M. Borkovec, B. J. Berne, *J. Chem. Phys.* **1985**, *83*, 3172; *ibid.* **1986**, *84*, 1788.

[126] E. Pollack, H. Grabert, P. Hänggi, *J. Chem. Phys.* **1989**, *91*, 4073.

[127] S. Okuyama, D. W. Oxtoby, *J. Chem. Phys.* **1986**, *84*, 5824, 5830.

[128] G. E. McManis, M. J. Weaver, *J. Chem. Phys.* **1989**, *90*, 912.

[129] T. Fonseca, *Chem. Phys. Lett.* **1989**, *162*, 491; *J. Chem. Phys.* **1989**, *91*, 2869.

[130] B. Bagchi, G. R. Fleming, *J. Phys. Chem.* **1990**, *94*, 9, and references therein.

[131] I. Rips, J. Jortner in *Perspectives in Photosynthesis* (Eds.: J. Jortner, B. Pullman), Kluwer, Dordrecht, 1990, p. 293.

[132] N. Agmon, J. J. Hopfield, *J. Chem. Phys.* **1983**, *78*, 6947.

[133] M. V. Basilevski, G. E. Chudinov, *Mol. Phys.* **1988**, *65*, 1121; *ibid.* **1990**, *71*, 461.

[134] D. F. Calef, P. G. Wolynes, *J. Chem. Phys.* **1983**, *78*, 470.

[135] P. G. Wolynes, *J. Chem. Phys.* **1987**, *86*, 5133.

[136] I. Rips, J. Klafter, J. Jortner, *J. Chem. Phys.* **1988**, *88*, 3246; *ibid.* **1988**, *89*, 4288; A. L. Nichols, D. F. Calef, *ibid.* **1988**, *89*, 3783; Y. Zhou, H. L. Friedman, G. Stell, *ibid.* **1989**, *91*, 4885; *Chem. Phys.* **1991**, *152*, 185.

[137] G. van der Zwan, J. T. Hynes, *Chem. Phys. Lett.* **1983**, *101*, 367.

[138] A. Chandra, B. Bagchi, *J. Chem. Phys.* **1991**, *94*, 3177.

[139] S. J. Rosenthal, X. Xie, M. Du, G. R. Fleming, *J. Chem. Phys.* **1991**, *95*, 4715; M. Cho, S. J. Rosenthal, N. F. Scherer, L. D. Ziegler, G. R. Fleming, *ibid.* **1992**, *96*, 5033.

[140] M. Maroncelli, G. R. Fleming, *J. Chem. Phys.* **1988**, *89*, 5044; M. Maroncelli, *ibid.* **1991**, *94*, 2084; P. VijayaKumar, B. L. Tembe, *J. Phys. Chem.* **1991**, *95*, 6430.

[141] J. K. Vij, F. Hufnagel, *Adv. Chem. Phys.* **1985**, *63*, 751, and references therein.

[142] S. K. Garg, C. P. Smyth, *J. Phys. Chem.* **1965**, *69*, 1294.

[143] D. W. Davidson, R. H. Cole, *J. Chem. Phys.* **1950**, *18*, 1417; *ibid.* **1951**, *19*, 1484.

[144] W. Jarzeba, G. C. Walker, A. E. Johnson, P. F. Barbara, *Chem. Phys.* **1991**, *152*, 57; M. A. Kahlow, T.-J. Kang, P. F. Barbara, *J. Chem. Phys.* **1988**, *88*, 2372; M. A. Kahlow, W. Jarzeba, T.-J. Kang, P. F. Barbara, *J. Phys. Chem.* **1989**, *90*, 151.

[145] E. W. Castner, M. Maroncelli, G. R. Fleming, *J. Chem. Phys.* **1987**, *86*, 1090; M. Maroncelli, G. R. Fleming, *ibid.* **1987**, *86*, 6221.

[146] S.-G. Su, J. D. Simon, *J. Phys.Chem.* **1987**, *91*, 2693; J. D. Simon, S.-G. Su, *Chem. Phys.* **1991**, *152*, 143.

[147] A. Declemy, C. Rulliere, P. Kottis, *Chem. Phys. Lett.* **1983**, *101*, 401; *ibid.* **1987**, *133*, 448; A. Declemy, C. Rulliere, *ibid.* **1988**, *146*, 1.

[148] N. P. Ernsting, *Chem. Phys. Lett.* **1990**, *166*, 221.

[149] G. van der Zwan, J. T. Hynes, *J. Phys. Chem.* **1985**, *89*, 4181.

[150] D. Huppert, P. M. Rentzepis, *J. Phys. Chem.* **1988**, *92*, 5466; H. Lueck, M. W. Windsor, W. Rettig, *ibid.* **1990**, *94*, 4550.

[151] D. N. Beratan, J. N. Onuchic, *J. Chem. Phys.* **1988**, *89*, 6195.

[152] A. Gochev, G. E. McManis, M. J. Weaver, *J. Chem. Phys.* **1989**, *91*, 906.

[153] E. Lippert, W. Rettig, V. Bonačić-Koutecký, F. Heisel, J. A. Miehe, *Adv. Chem. Phys.* **1987**, *68*, 1, and references therein.

[154] H. Heitele, F. Pöllinger, K. Kremer, M. E. Michel-Beyerle, M. Futscher, G. Voit, J. Weiser, H. A. Staab, *Chem. Phys. Lett.* **1992**, *188*, 270.

[155] S.-G. Su, J. D. Simon, *Chem. Phys. Lett.* **1989**, *158*, 423.

[156] J. D. Simon, S.-G. Su, *J. Phys. Chem.* **1990**, *94*, 3656, and references therein.

[157] P. C. M. Weisenborn, A. H. Huizer, C. A. G. O. Varma, *Chem. Phys.* **1989**, *133*, 437, and references therein.

[158] A. M. Kjaer, J. Ulstrup, *J. Am. Chem. Soc.* **1987**, *109*, 1934; E. M. Itskovich, J. Ulstrup, M. A. Vorotyntsev in *The Chemical Physics of Solvation, Part B* (Eds.: R. R. Dogonadze, E. Kalman, A. A. Kornyshev, J. Ulstrup), Elsevier, Amsterdam, 1986, p. 223, and references therein.

[159] N. S. Hush, *Prog. Inorg. Chem.* **1967**, *8*, 391; C. Creutz, *ibid.* **1983**, *30*, 1, and references therein.

[160] K. W. Penfield, J. R. Miller, M. N. Paddon-Row, E. Cotsaris, A. M. Oliver, N. S. Hush, *J. Am. Chem. Soc.* **1987**, *109*, 5061.

[161] E. M. Kober, J. V. Caspar, R. S. Lumpkin, T. J. Meyer, *J. Phys. Chem.* **1986**, *90*, 3722; L. A. Worl, R. Duesing, P. Chen, L. Della Ciana, T. J. Meyer, *J. Chem. Soc. Dalton Trans.* **1991**, 849; K. R. Barqawi, Z. Murzata, T. J. Meyer, *J. Phys. Chem.* **1991**, *95*, 47.

[162] S. K. Doorn, J. T. Hupp, *J. Am. Chem. Soc.* **1989**, *111*, 1142.

[163] J. Schroeder, J. Troe, *Annu. Rev. Phys. Chem.* **1987**, *38*, 163, and references therein; D. H. Waldeck, *Chem. Rev.* **1991**, *91*, 415, and references therein.

[164] G. Ciccotti, M. Ferrario, J. T. Hynes, R. Kapral, *J. Chem. Phys.* **1990**, *93*, 7137.

[165] B. J. Gertner, K. R. Wilson, J. T. Hynes, *J. Chem. Phys.* **1989**, *90*, 3537.

Nitric Oxide, NO, an Intercellular Messenger

By *Hans-Joachim Galla**

Nitric oxide, NO, is a colorless, relatively stable gas. It is not very reactive chemically, even though it has an unpaired electron and thus shows radical character. This can be equated with the fact that the ground state of the molecule at low temperatures is diamagnetic because of the interaction between the orbital moment and the spin moment of 1/2. Since the energy difference between the ground state and the excited paramagnetic state is around $1/2\,kT$ at room temperature NO exists as a gaseous highly paramagnetic free radical. NO reacts readily with oxygen in the air to form NO_2. NO is thermally unstable and under high pressures breaks down to yield N_2O and NO_2. In contrast to NO_2, pure NO evokes no physiological irritation. It is, however, able to convert hemoglobin to methemoglobin by oxidizing Fe^{2+} to Fe^{3+}. Since methemoglobin is unable to bind and transport oxygen NO is potentially toxic. The solubility of NO in water is low and is of the same order of magnitude (about 1 mM) as that of O_2 and CO_2. NO can, however, easily diffuse across the cell membrane. In physiological media the NO radical has a half-life of only a few seconds. Although it could not be deduced from its chemical and physical properties, we know today that NO is one of the most important and widely used messenger molecules in biological systems.[1] Endogenous NO is synthesized enzymatically in various mammalian cells by so-called NO synthases, during this process the amino acid L-arginine reacts with oxygen to give citrulline. This pathway is a shortened version of the urea cycle (Fig. 1). Hitherto the amino acid arginine has not been considered to be important in signal transduction, however, as a precursor of NO it takes on a completely new role. This is particularly interesting when one considers the role of the urea cycle in the brain; here two key enzymes of the urea cycle have so far not been found, namely ornithine carbamoyl transferase and carbamoyl phosphate synthase.[2] This is despite the fact that all the imtermediates of the urea cycle including citrulline, which is synthesized from carbamoyl phosphate and ornithine, have been identified in brain tissue. This finding can be explained partly by the shortened cycle through NO synthase. However, how arginine is transported into the brain remains unclear.

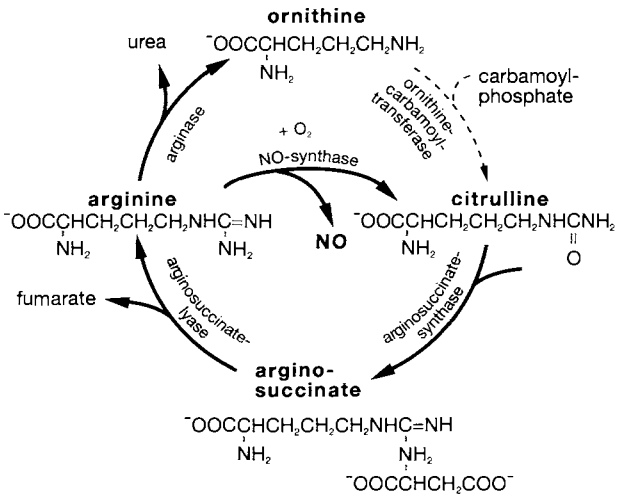

Fig. 1. Urea cycle and NO synthesis (taken from [2]).

The first indications that NO is a new kind of messenger molecule came from studies on the cell-mediated immune response. About ten years ago it was established that the expression of the cytotoxicity of activated macrophages on tumor cells can be induced and is dependent on L-arginine.[3] It has been known even longer that the activated macrophages inhibit DNA replication and the mitochondrial respiratory chain as well as the citrate cycle in their tumor target cell. The inhibited enzymes such as the proximal oxidoreductases of the mitochondrial membrane or the enzyme aconitase of the citrate cycle all contain 4Fe4S clusters as prosthetic groups. Therefore it was proposed that intracellular iron was the site of the attack. The identification of nitrosyl–iron–sulfur complexes two years ago supported the hypothesis that the arginine NO pathway is involved in the immune response. It is now known that in addition to the cytotoxicity on mammalian cells, NO possesses antimicrobial activity. It has therefore been proposed that the NO synthesis induced by cytokines or lipopolysaccharides (LPS) is an important biochemical defense mechanism against intracelluar microorganisms and pathogens.[4] An inducable NO synthase occurs in neutrophilic granulocytes.

Vascular endothelial cells[5, 6] release a wide variety of vasoactive substances, of these the so-called endothelial-derived relaxing factor (EDRF) is believed to be the most important. The EDRF is very unstable with a half-life of around 5 s. It activates a soluble guanylate cyclase in vascular smooth muscle cells and in blood platelets. This activation results in an increased level of the concentration of cyclic 3',5'-guanosine monophosphate (cGMP), which in turn inhibits the contraction of smooth muscles and the activation of blood platelets by a reduction in the level of intracellular free calcium. A number of well-known vasoactive substances, among them the platelet-derived compounds ADP, ATP, and serotonin (5-hydroxytryptamine), or the neurotransmitter substance *P*, bradykinin, acetylcholine, and histamine exert their dilatory effect by causing the endothelial release of the EDRF. This in turn leads to a relaxation of the smooth muscle surrounding the blood vessel by increasing the level of cGMP. In 1986, after years of intensive research into the chemical structure of EDRF, it was first proposed by Furchgott during a conference that EDRF is in fact nitric oxide.[7] Although other nitrogen compounds such as dinitrosyl Fe^{2+} complexes, S-nitrosothiols, or hydroxylamine remain in contention as the EDRF, it is now accepted that NO is the primary and direct product formed from the guanidino nitrogen of L-arginine. This was estab-

[*] Prof. Dr. H.-J. Galla
Institut für Biochemie der Universität
Wilhelm-Klemm-Strasse-2
D-W-4400 Münster (FRG)

lished by Mülsch and Busse[5] using electron paramagnetic resonance (EPR) spectroscopy. They were able to trap any NO produced in the form of a ferrous diethyldithiocarbamate mononitrosyl complex, which exhibits a characteristic EPR signal. The presence of a nitrosyl-Fe^{2+}–S complex in macrophages activated by cytokines was also established by EPR spectroscopy. In addition to the effect NO has on muscle cells, it also plays an important role in the regulation of the blood flow by the blood platelets. Mediated by cGMP, NO acts as an endogenous antithrombic substance by preventing the adhesion and the aggregation of the thrombocytes on the endothelium.

The identification of NO as EDRF stimulated experiments on brain tissue, in which likewise NO was liberated from L-arginine.[8, 9] The highest levels of NO synthesis were observed in the cerebellum, in which the excitatory neurotransmitter glutamate increases the level of cGMP by binding to the *N*-methyl-D-aspartate (NMDA) receptor. The addition of glutamate or NMDA leads to a threefold increase of the NO synthase activity, addition of NO synthase inhibitors prevents the increase in NO synthase activity and cGMP concentration. This clearly shows that NO plays a role in the effect of the neurotransmitter glutamate. Interestingly, in the brain the NO synthesis occurs preferably in populations of neurons that are selectively resistant to neurotoxic damage, for example in Huntington's disease (St Vitus'dance) or in a stroke. Since glutamate stimulates the formation of NO it seems paradoxical that those neurons which contain NO synthase are resistant to the neurotoxicity of the glutamate. This finding only makes sense if we assume that glutamate stimulates the production of NO in neurons but that then NO diffuses out of these cells and affects neighboring cells. This is supported by the fact that the destruction of neurons due to the neurotoxic activity of NMDA, which is for example released in the case of a stroke, can be prevented effectively by the use of NO synthase inhibitors, such as nitroarginine. A significant level of NO synthesis has been found in the peripheral nervous system in populations of neurons that regulate peristalsis in the intestine, in the nerves to erectile organs, and in neurons to the posterior pituatory gland and to the adrenal medulla. In these systems NO acts as a neurotransmitter: the synthase enzyme causes NO release upon nerve stimulation.

The NO-synthesizing enzyme, NO synthase, is a NADPH-dependent dioxygenase, which requires tetrahydrobiopterin as a cofactor. The enzyme is widely distributed and its activity is linked mostly to the activation of a soluble guanylate cyclase in the NO-producing cell itself or in other target cells (Fig. 2). This means that NO is both an intercellular messenger and an autocrine signal. The synthase occurs in at least two isoforms. The basal level of NO synthase activity in macrophages or in neutrophilic granulocytes is low. After stimulation of the macrophages by lipopolysaccharides or γ-interferon there is a drastic increase in NO synthesis.[10] At the same time oxygen free radicals are formed, that can combine with NO to form, for example, peroxynitrite, which is broken down to yield hydroxyl and nitrogen dioxide radicals. These are the actual cytotoxic substances (Fig. 2).

In endothelial cells a constitutive Ca^{2+}/calmodulin-dependent NO synthase occurs.[5] This enzyme produces physiological amounts of NO, which regulates the resting blood

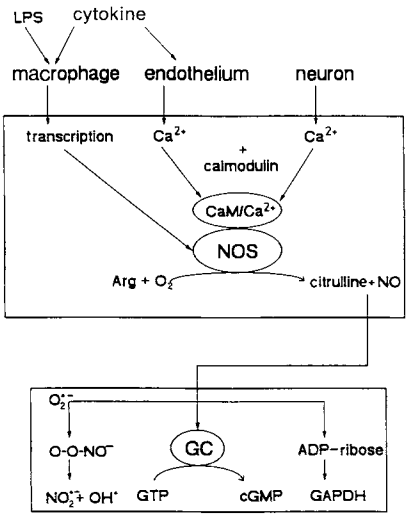

Fig. 2. Overview of the production and effects of NO on macrophages, endothelium, and neurons. Abbreviations: CaM, calmodulin; LPS, lipopolysaccharide; NOS, NO synthase; GC, guanylate cyclase; Arg, arginine; GAPDH, glycerine aldehyde-3-phosphate dehydrogenase (taken from [1]).

pressure through the smooth muscle of the blood vessel walls. The constitutive NO release can be divided up into continuous basal release and stimulated release. The stimulated NO synthesis can be increased by a factor of 2 to 3 receptor-dependent by agonists like acetylcholine, ATP, or bradykinin, or receptor-independent by Ca^{2+} ionophores, polycations, or Ca^{2+} ATPase inhibitors. This leads, however, to a short release of NO for only a few seconds. Both receptor-dependent and receptor-independent pathways require an increase in the intracellular Ca^{2+} concentration for NO synthesis. This transmembrane calcium flux remains little understood. Well understood, on the other hand, is the process in which the binding of an agonist to a receptor leads to the release of inositol-1,4,5-trisphosphate (IP_3) by the action of a membrane-bound phospholipase C on phosphatidylinositol-4,5-bisphosphate. IP_3 causes the release of Ca^{2+} from intracellular storage, as well as an influx of Ca^{2+} through voltage-independent Ca^{2+} channels. The resulting Ca^{2+}/calmodulin complex activates the NO synthase. Apart from this constitutive isoform, the endothelial cells, as well as granulocytes, and macrophages contain a NO synthase which can be induced in response to immune stimulation. A cardiovascular collapse which sometimes occurs after the application of cytokines such as tumor necrose factor (TNF) or interleukin-2 is in all probability caused by a pathological overproduction of NO. The same also applies to septic shock during which the endogenous level of cytokines drastically increases.

In the central nervous system, nerve stimulation leads to an increase in the cGMP level. Glutamate is released from the presynaptic terminal and affects the excitatory amino acid receptors, namely the NMDA and the AMPA receptors, which are named after their selective antagonists, *N*-methyl-D-aspartate and α-amino-3-hydroxy-5-methyl-4-isoxazole propionate. Both receptors are classed as ionotropic receptors, that is, they contain an integral ion channel. The NMDA channel of the glutamatergic synapse is normally blocked by Mg^{2+}. If, however, the postsynaptic membrane becomes sufficiently depolarized, the Mg^{2+} is released from

the NMDA channel and the channel is then open for an influx of Ca^{2+}. The Ca^{2+}, which enters the postsynapse, is complexed by calmodulin and activates the NO synthase. NO can then diffuse into neighboring cells, for example astrocytes, or diffuse back to the presynaptic nerve ending and activate the guanylate cyclase present there. The cGMP formed can in turn affect ion channels, stimulate phosphorylation by cGMP-dependent kinases, lower the cAMP level through cGMP-stimulated phosphodiesterases, and raise the level of cAMP through cGMP-inhibited phosphodiesterases (Fig. 2). A coherent overall picture of these interactions is not available at present.

Since the successful cloning of the cDNA of the neuronal NO synthase by Bredt et al.[11] much information has come to light about the structure and regulation of this enzyme. The NO synthases from brain tissue, endothelial cells, and macrophages show a 50% homology in their amino acid sequences, although the neuronal NO synthase is longer at both the C and N terminal than the endothelial and macrophage NO synthase. Cytochrome P_{450} reductase shows a significant sequence homology with NO synthase. Cytochrome P_{450} reductase transfers electrons to cytochrome P_{450}, which plays an important role in the detoxification of xenobiotic compounds. The NO synthases have the same binding sites for the coenzymes nicotinamide adenine dinucleotide phosphate (NADPH), flavin adenine dinucleotide (FAD), and flavin mononucleotide (FMN).[12] Such flavonucleotide binding sites are typical of the family of electron transfer proteins. In cytochrome P_{450} reductase these flavin nucleotides together with NADPH form an electron tranport chain through the isoalloxazine rings. It is assumed that electron transfer between the flavins also plays a role in NO synthase. The fact that the purified enzyme binds heme groups tightly and that after binding of carbon monoxide light is absorbed at 450 nm, leads to the conclusion that NO synthase must be a cytochrome P_{450} enzyme.

All three synthases have binding sites for calmodulin, however, the macrophage NO synthase is insensitive to Ca^{2+}. It is also interesting that the NO synthases have consensus sequences for cAMP-dependent phosphorylation sites. The neuronal NO synthase is phosphorylated by cAMP-dependent protein kinase A, protein kinase C, and by a Ca^{2+}/calmodulin-dependent protein kinase. Each of these three enzymes phosphorylates different serine residues in the NO synthase. Phosphorylation by protein kinase C leads to a drastic reduction in the catalytic activity of the NO synthase.

Bredt et al.[12] postulated an interesting mechanism for the regulation of the NO synthesis and deduced a connection between the IP_3 signal chain and the signal chain of NO as a messenger in neurons and endothelial cells. The receptor-controlled hydrolysis of phosphatidylinositolbisphosphate yields two messengers IP_3 and diacylglycerine (DAG). IP_3 causes an increase in the concentration of intracellular Ca^{2+}, leading to the formation of a Ca^{2+}/calmodulin complex which then activates NO synthase. The down regulation could then take place through DAG which activates protein kinase C, and decreases the rate of NO synthesis by phosphorylation of the NO synthase.

The physiological importance of the NO system is emphasized by a further consideration. Based on the sequence homology with cytochrome P_{450} reductase, which only applies to the C terminal of NO synthase, and the observation that NO synthase also exhibits cytochrome P_{450} properties, Lowenstein and Snyder[1] concluded that both enzymatic functions are present in NO synthase. One function of cytochrome P_{450} reductase is electron transfer to hemoxygenase, which breaks down the heme group into biliverdin and carbon monoxide. CO could function as a messenger in a very similar way to NO.[13] This idea is supported by the fact that hemoxygenase has the same distribution in neurons in the brain as guanylate cyclase. This could indicate that CO also regulates the endogenous cGMP level, so that the question has to be asked whether CO instead of NO is really the physiological regulator of guanylate cyclase activity in the brain. This naturally leads to the question of whether other target molecules exist for NO. In the meantime many other regulatory effects of NO have come to light, for example an increase in ADP-ribosylation of proteins in blood platelets. A further possible metabolic target is glycolysis. In this case NO increases the ADP-ribosylation of glycerine aldehyde-3-phosphate dehydrogenase (Fig. 2), which leads to an inhibition of the enzyme. This is also a possible explanation for the neurotoxicity of NO.

In view of the enormous increase in popularity of messenger NO, (it was for example voted "Molecule of the Year 1992" by *Science*),[14] it is not surprising that much effort has been directed towards developing a direct method for determining NO in situ. The way ahead has been shown by Malinski and Taka[15] who have taken advantage of the ease of oxidation of NO for the determination of its concentration. The authors used polymeric porphyrins with nickel as the central metal ion. By coating the polymer with a substance which is permeable to NO but blocks the diffusion of nitrite they created a detector specific for NO and able to measure a concentration down to 10 nM in solution. The authors successfully applied their method to the measurement of NO in blood vessels. Such a sensor will certainly help to answer questions about the intracellular localization of NO synthase and the nature of the target molecules for NO in the not too distant future.

German version: *Angew. Chem.* **1993**, *105*, 399

[1] C. J. Lowenstein, S. H. Snyder, *Cell* **1992**, *70*, 705–707.
[2] J. Garthwaite, *Trends Neurosci.* **1992**, *14*, 60–67.
[3] D. L. Granger, R. R. Taintor J. L. Cook, J. B. Hibbs, *J. Clin. Invest.* **1980**, *65*, 357–370.
[4] J. B. Hibbs, *Res. Immunol.* **1991**, *142*, 565–569.
[5] R. Busse, A. Mülsch in *Molecular Aspects of Inflammation*, Springer, (Eds.: H. Sies, L. Flohé, G. Zimmer) **1991**, pp. 189–205.
[6] R. Busse, A. Mülsch, I. Flemming, M. Hecker, *Circulation* **1993**, in press.
[7] R. F. Furchgott in *Mechanism of Vasodilatation* (Ed.: P. M. Vanhoutte) *Vol. 4*, Raven, New York, 1988, pp. 401-404.
[8] T. M. Dawson, D. S. Bredt, M. Fotuhi, P. M. Hwang, S. H. Snyder, *Proc. Natl. Acad. Sci. USA*, **1991**, *88*, 7797–7801.
[9] V. L. Dawson, T. M. Dawson, E. D. London, D. S. Bredt, S. H. Snyder, *Proc. Natl. Acad. Sci. USA*, **1991**, *88*, 6368–6371.
[10] C. F. Nathan, J. B. Hibbs, *Curr. Opin. Immunol.* **1991**, *3*, 65–70.
[11] D. S. Bredt, P. H. Hwang, Ch. E. Glatt, C. Lowenstein, R. R. Reed, S. H. Snyder, *Nature* **1991**, *351*, 714–718.
[12] D. S. Bredt, C. Ferris, S. H. Snyder, *J. Biol. Chem.* **1992**, *267*, 10976–10981.
[13] For the most recent developments see A. Verma, D. J. Hirsch, C. E. Glatt, G. V. Ronnett, S. H. Snyder, *Science* **1993**, *259*, 381-384.
[14] E. Culotta, D. E. Koshland, *Science* **1992**, *258*, 1862-1865.
[15] T. Malinski, Z. Tada, *Nature* **1992**, *358*, 676-677.

Heterogeneous Catalysis—Still Magic or Already Science?**

By *Robert Schlögl**

The optimization of industrial heterogeneous catalytic processes with respect to the minimization of energy consumption and pollution is of increasing importance. Although the results of these efforts may be put into operation only slowly because of the high capital costs, the scientific efforts required for these optimizations, though rewarding, are very substantial. The underlying problem is understanding the operation of a catalytic system at an atomic level; it is not adequate to have only a model. In the historic approach to catalysis research the complexity of a practical reaction system is reduced to a level that can be adequately described. This approach was very successful in the analysis of a large number of details of heterogeneous catalysis, giving rise to the hope that someday entire processes may be understood. This was thought to be possible by extrapolations of experimental details from model investigations to the real world of an operating system.

Studies on ammonia synthesis, the traditional testing ground for catalysis science, are the best known examples of this strategy.[1] The culminating success of decades of research was a kinetic theory that allowed the precise prediction of the yield of ammonia under technical conditions using as parameters experimentally determined properties and a set of experimentally verified elementary reaction steps.[2]

Unfortunately, this strategy was not successful in any other practical application as yet. Actual heterogeneous catalytic processes could not be designed up to now. All of the catalytic processes vital to industry were developed by purely empirical methods and countless screening experiments. This heuristic approach has led to the opinion that catalysis research is not a science but rather "black magic". Industrial chemists tend to be rather skeptical towards inductive-scientific strategies in heterogeneous catalysis, since it is evident that our understanding of the relationships between structure and reactivity is inadequate.

One significant obstacle to understanding structure–reactivity relationships is the complexity of the solid catalyst. Active materials are multiphase compounds with dynamic behavior with respect to both surface and bulk structure. These dynamics were recognized only recently and relate to geometric structure, composition, and the local electronic state[1] of the active center. The analyst of a catalyst should thus not be preoccupied with a priori distinctions between important and unimportant components of the system but should consider all constituents (active components, support, impurities, poisons, promotors) of a practical catalyst. The long history of catalyst characterization should have taught the lesson that all analysis should be done in situ; all monographs on the subject repeat this statement.[3] Nevertheless only a fraction of the analyses are conducted under in situ conditions, since only few techniques can be used for such investigations and even then the technical reaction conditions must be modified.

Thus these experiments place certain technical constraints on the reaction conditions. A realistic description of an in situ experiment may be that a property of a catalyst is investigated as a function of reaction conditions characteristic of the practical application under simultaneous observation of the reaction kinetics (conversion, selectivity). Only then is it ensured that the active state of the catalyst is characterized and that the data are relevant to the reaction mechanism.

Knowing the mechanism is crucial to understanding the catalyst operation, which in turn is central to the scientific approach towards catalyst optimization. Extrapolations from experimental to real operation conditions must be limited, as the mechanism is dependent on interconnected sets of parameters whose quantitative relations are unknown (Fig. 1). Quantitative knowledge of these interconnections allows the full understanding of the mode of catalyst operation.

Activity and selectivity data do not allow conclusions concerning the reaction mechanism. The kinetics are determined by chemisorption processes (only a part of the mechanism) and by the micro- and macrotexture of the catalyst. The limitations of mass- and energy-exchange processes and noncatalytic consecutive reactions tend to obscure the relationship between kinetics and mechanism. The same holds for the relationship between the elementary steps and the microkinetics composed of them.

Analytical in situ experiments and all non in situ studies require deviations from the empirically optimized reaction conditions which affect the four groups of parameters in Figure 1 simultaneously. These deviations cause parameter gaps. If the gaps are closed by inadequate extrapolations the interconnection of all factors may lead to possibly dramatic

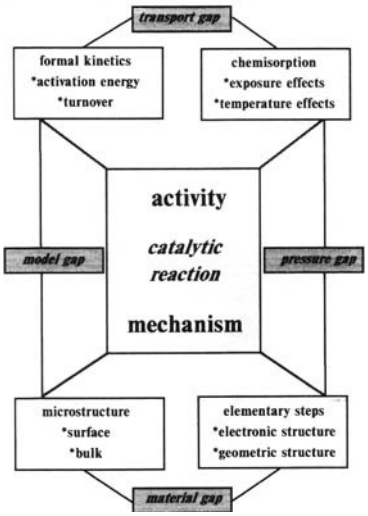

Fig. 1. Relationships between the catalytic performance of a solid (middle) and the main determining factors. The gaps arise from simplifications in the parameter sets that are required for catalysis experiments. Extrapolations from the data obtained from the simplified model to the actual catalytic reaction may endanger the relevance of a whole mechanistic reconstruction.

[*] Prof. Dr. R. Schlögl
Institut für Anorganische Chemie der Universität
Niederurseler Hang, D-W-6000 Frankfurt 50 (FRG)

[**] This work was supported by the Deutsche Forschungsgemeinschaft, the Max-Planck Society, and the Fonds der Chemischen Industrie. The author thanks the many co-workers involved with the projects mentioned. We also thank BASF (Ludwigshafen) for a longstanding cooperation.

mechanistic errors. This is the reason for the failure of catalysis research as a science which has to prove its validity in the industrial application. As an example, much information has been accumulated on the elementary steps of chemical reactions on single crystals under high-vacuum conditions. Yet the "pressure gap" and "material gap" have been bridged inadequately, and an interpretation of the formal kinetics is not possible. As a further illustration for this point, the famous prediction arising from surface science of a theoretical limit for the selectivity of ethylene epoxidation was proven false in industrial practice.

The gaps shown in Figure 1 are all relevant in the design of in situ experiments. The transport gap describes the influences of mass- and energy-transport limitations on the kinetics. These phenomena are different for a catalyst in a fixed-bed reactor, for transparent wafers of the same material, and for catalysis experiments with single crystals. The pressure gap describes differences in the total pressure in experiments. The reaction mechanism frequently changes profoundly in a pressure range between millibars and ultrahigh-vacuum conditions because of threshold limits in the chemical potential of the gas-phase species.[4] The material gap[5] describes the difference in local microstructure and defect properties between single crystals (well-defined, easy to analyse, low dynamics) and polycrystalline materials (ill-defined, highly reactive, difficult to analyze). The model gap finally addresses the problem of finding the physical relevance of parameters obtained in a formal mathematical analysis of catalyst performance. Typically, gradients of specific activity, chemical transformations, and structural modifications are assumed to exist along the reactor tube or within a single grain of catalyst. Their experimental verification is in most cases, however, not possible.

In a fashionable approach to understanding a process a model system whose complexity is intermediate to that of a single crystal and a real system is defined and examined. Although this approach is partly successful, experimental verification of the relation between model and reality is very difficult.

This list of interconnected problems was addressed in a recent study of the methanol synthesis catalyst,[7] in which the authors describe their attempts at determining the nature of the active material of the catalyst experimentally. It is not known if in the hydrogenation of CO the active copper surface is metallic or oxidic. This reaction is the present testing ground in catalysis research, in analogy to the ammonia synthesis.[8] Certainly if the chemical nature of the active species is not known,[9] the mechanism of this reaction cannot be worked out scientifically.

For the difficult task of determining the valence state of the active copper species, which was attempted frequently before, a new spectroscopic technique has been developed which can provide information concerning the catalyst surface in situ. The results of the method are compared to and calibrated against the results obtained by more traditional techniques. The crucial experiment is a variation of the well-known extended X-ray absorption fine structure spectroscopy (EXAFS) experiment. This method allows the determination of the local geometric structure of a solid for a specific element without requiring long-range order as in conventional diffraction experiments. For metal atoms the specific X-ray radiation is hard enough to penetrate a gas atmosphere and the windows of a reaction cell, allowing in situ experiments on supported metal catalysts. In these studies of the Cu catalyst for the hydrogenation of CO the bond lengths determined allowed the differentiation between copper metal and copper oxides.

The experiment was conducted with a technical, polycrystalline, supported catalyst at ambient pressure in a gas atmosphere typical for industrial conditions (ca. 60 bar pressure). The bulk-sensitive EXAFS data clearly show that the catalyst is present in the metallic form under the conditions chosen. This was confirmed in a similar in situ experiment with conventional X-ray diffraction. The two sets of complementary structural information indicate that neither crystalline nor amorphous oxide are present in the catalyst.

Nothing has been said so far about the state of the copper surface, the essential interface for catalytic operation. The new experiment helped here: X-ray absorption was detected by measuring the yield of secondary electrons caused by the photoabsorption process, which converted the method from bulk-sensitive to surface-sensitive (information from a few monolayers instead of several micrometers). This technique also showed very convincingly that no copper oxide was present on the surface.

The nature of the active catalyst would have been clarified at this point if the experiments had been truely in situ. Unfortunately, as the authors did not determine the activity and selectivity of their catalyst, they describe an arbitrary state of the catalyst and give no evidence that the catalyst was indeed active. This point is not trivial (in the light of the gas phase applied), as the complexity of a working catalyst system outlined in Figure 1 does not permit this far-reaching extrapolation. It is frequently observed that the top layer of a catalyst bed is deactivated by poisons from the feed. In the experiments discussed only the top layer of the catalyst bed was investigated. No information on the gas purity, the shape of the catalyst bed, and the influence of the catalyst geometry (differential flow reactor) on the kinetic performance was given. Because of this lack of experimental information the investigation is not an in situ experiment, and the nature of the active copper species is open for further discussion.

At this stage the question arises of which other methods may be used to obtain information relevant to catalysis. Instationary conversion experiments are often suitable. In such truely in situ experiments the catalytic performance is analyzed as function of a process variable that changes with a defined time profile. The determination of dissolved atomic nitrogen in the catalysts used in the technical ammonia synthesis serves as an example.[10] Its interpretation required, however, a detailed knowledge of the surface chemistry of elemental iron.[11]

Such detailed chemical information is a prerequisite for a mechanistic analysis of a catalytic process and can only be obtained with certain reliability if several complementary methods are used for their determination. Only then can misinterpretations occurring as internal inconsistencies within one dataset be recognized and possibly corrected. An example of the erroneous overinterpretation of a single analytical method is the theory of paracrystallinity in catalysis. Carefully measured X-ray powder diffraction data of ammo-

nia synthesis catalysts revealed characteristic anomalies in the lineprofiles.[12] These were correlated with molecular dispersions of promoter oxides within the bulk iron, and special catalytic effects were ascribed to this unusual state of matter. Today we know[13] that the lineprofile anomalies were caused by special crystallographic artifacts which were known to exist then but were not considered. No correlation exists between the bulk X-ray diffraction data and the catalytic performance.

A further example of incorrect structural data from an in situ experiment on the active phase of the ammonia synthesis catalyst was caused by the inadvertant activation of the catalyst within the X-ray diffraction system. The resulting amorphous state was concluded[14] to be the active principle in ammonia synthesis, again without testing the catalytic activity during the diffraction experiment. Today we know that the activated catalyst contains highly oriented, crystalline iron metal particles.[10]

As outlined in Figure 1 the detailed knowledge of microstructure alone is inadequate for a complete understanding of the mode of operation of a catalyst; information about its surface constitution is essential. Unfortunately, all surface science techniques require ultrahigh-vacuum conditions because of the nature of the information-bearing particles (photoelectrons, ions, atoms). Real on-line in situ experiments with these techniques are thus not possible. The most adequate solution to this dilemma is the combination of a high-pressure microreactor with a surface analytical instrument. The suitable design of the transfer system between the high-pressure and ultrahigh-vacuum sections ensures that the working catalyst surface is frozen.[15] Any reactive chemisorbed molecular species will, however, be lost in the evacuation process. This technique was used for the investigation of the nature of the active phase[16] of the iron oxide catalyst used for the dehydrogenation of ethylbenzene to styrene. A published model of the catalyst operation[17] predicted that the conversion should increase with the surface abundance of potassium (an essential promoter) and should decrease as the surface becomes covered with carbon (from the products). A summary of X-ray photoelectron spectroscopic data collected from catalysts operated at various levels of conversion in a steady state prior to analysis[18] is given in Figure 2. It can be seen that both predictions from the catalyst model are incorrect. The parameter controlling the conversion is the abundance of hydroxyl ions indicating the presence of potassium in the deactivated form of KOH, which results from disintegration of the active ternary iron oxide $KFeO_2$.[16] A number of other promoters that are added to technical catalyst systems to improve the selectivity and stability of the catalyst are either not abundant at the surface or their bulk concentration does not appear to correlate with the surface catalytic process. This example demonstrates the value of an in situ experiment including simultaneous characterization of the catalyst performance. Its results were corroborated by a variety of complementary experiments probing both the bulk and the surface of the catalyst.[16]

In consideration of this discussion if we try to answer the question asked in the title the realistic reply must be—still magic. The obstacles to a scientific understanding of heterogeneous catalysis are considerable. The perspectives of penetrating the magic of catalysis by scientific means is, however, promising owing to the increasingly frequent attempts at circumventing these obstacles. Catalysis research today is on its way to becoming an interdisciplinary science incorporating in a rational way the knowledge from surface science, solid-state physics, and chemical engineering. Its progress will be measured by its contribution to the efficient solution of the strategies problems of future catalyst applications.

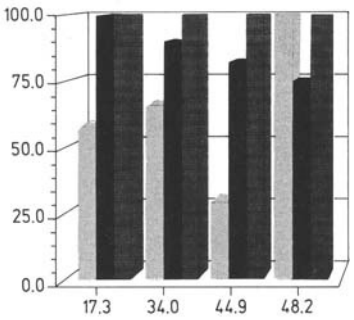

Fig. 2. Results of quantitative XPS analyses on an iron oxide catalyst active in the dehydrogenation of ethylbenzene to styrene. The data were measured at given steady-state conversion levels. The conversions were carried out under technical conditions (873 to 893 K, 6:1 mixture of water ethylbenzene, 1 bar total pressure, liquid hourly space velocity (LHSV) 0.5 Lh^{-1}). XPS data were obtained after rapid transfer of a fraction of the catalyst sample into ultrahigh vacuum. All numbers are normalized to 100. *x* Axis: Conversion to ethylbenzene in %. *y* Axis: Spectroscopic parameter in arbitrary units. Light gray columns: carbon abundance, dark gray columns: potassium to iron ratio, black columns: hydroxyl abundance.

German version: *Angew. Chem.* **1993**, *105*, 403

[1] G. Ertl, *Angew. Chem.* **1990**, *102*, 1258; *Angew. Chem. Int. Ed. Engl.* **1990**, *29*, 1219.
[2] P. Stoltze, *Phys. Scr.* **1987**, *36*, 824.
[3] *Characterization of Catalysts* (Eds.: J. M. Thomas, R. M. Lambert), Wiley, New York, **1980**; J. R. Anderson, K. C. Pratt, *Introduction to Characterization and Testing of Catalysts*, Academic Press, **1985**; *Characterization of Heterogeneous Catalysts* (Ed.: F. Delannay), Dekker, New York, **1984**.
[4] C. Rehren, M. Muhler, X. Bao, R. Schlögl, G. Ertl, *Z. Phys. Chem.* **1991**, *174*, 11.
[5] R. Schlögl, R. C. Schoonmaker, M. Muhler, G. Ertl, *Catal. Lett.* **1988**, *1*, 237.
[6] See for example: D. R. Strongin, G. A. Somorjai in *Catalytic Ammonia Synthesis* (Ed.: J. R. Jennings), Plenum, New York, **1991**, p. 133; G. A. Somorjai, *Chemistry in Two Dimensions*, Cornell University Press, Ithaca, **1981**.
[7] G. T. Moggridge, T. Rayment, R. M. Ormerod, M. A. Morris, R. M. Lambert, *Nature* **1992**, *358*, 658.
[8] G. Ertl, *J. Vac. Sci. Technol. A* **1983**, *1*, 1247; A. Ozaki, K. Aika in *Catalysis, Science and Engineering, Vol. 1* (Eds.: J. R. Anderson, M. Boudart), Springer, Berlin, **1981**, p. 88.
[9] B. S. Clausen, *J. Catal.* **1991**, *132*, 524; G. C. Chincen, M. S. Spencer, K. Waugh, D. A. Whan, *J. Chem. Soc. Faraday Trans. 1* **1987**, *83*, 2193.
[10] W. Mahdi, J. Schütze, G. Weinberg, R. Schoonmaker, R. Schlögl, G. Ertl, *Catal. Lett.* **1991**, *11*, 19.
[11] F. Bozso, G. Ertl, M. Weiss, *J. Catal.* **1977**, *50*, 519.
[12] R. Hosemann, A. Preisinger, W. Vogel, *Ber. Bunsen Ges. Phys. Chem.* **1966**, *70*, 797.
[13] W. S. Borghard, M. Boudart, *J. Catal.* **1983**, *80*, 194.
[14] T. Rayment, R. Schlögl, J. M. Thomas, G. Ertl, *Nature* **1985**, *315*, 311.
[15] M. Muhler, R. Schlögl, S. Eder, G. Ertl, *Surf. Sci.* **1987**, *189*, 69.
[16] M. Muhler, R. Schlögl, A. Reller, G. Ertl, *Catal. Lett.* **1989**, *2*, 201; M. Muhler, R. Schlögl, G. Ertl, *SIA Surf. Interface Anal.* **1988**, *12*, 233; M. Muhler, J. Schütze, M. Wesemann, T. Rayment, A. Dent, R. Schlögl, G. Ertl, *J. Catal.* **1990**, *128*, 339.
[17] D. Mross, *Catal. Rev. Sci. Eng.* **1983**, *25*, 591; W. Mross in *DECHEMA Statusseminar Fortschritte der Katalyseforschung*, **1987**, p. 173.
[18] C Abundance: Integral of the C-1s line; K:Fe ratio: ratio of the corrected integrals of the K-2p and Fe-2p line; OH abundance: relative area of the OH emission in the O-1s spectrum at 531.7 eV relative to the emission of the metal oxides at 529.9 eV.

Communications may be submitted in English *or* in German. Further details regarding the submission of communications can be found in the "Notice to Authors" reproduced in the January issue of the journal. Copies thereof may be obtained from the editorial office upon request.

BNC Isosteres of Cyclopropane and a Borylated Diazoester from Diazo Compounds and (Dimethylamino)bis(trifluoromethyl)borane**

By *Andreas Ansorge, David J. Brauer, Hans Bürger,* Thomas Hagen,* and *Gottfried Pawelke*

Dedicated to Professor Dietrich Mootz on the occasion of his 60th birthday

The electron-withdrawing effect of the CF_3 groups is responsible for the reactivity of the BN bond of (dimethylamino)bis(trifluoromethyl)borane (**1**), which is significantly different from that of other aminoboranes.[1] Compound **1**, like other aminoboranes, adds H-acid compounds such as hydrogen halides and H_2O;[2] furthermore, like isosteric alkenes, **1** is capable of [2 + 2] cycloadditions with isocyanates and isothiocyanates,[3] [2 + 4] cycloadditions with dienes and enones,[4] and ene reactions with carbonyl compounds and nitriles.[5] Consequently, it was also to be expected that **1** would react with carbenes and thus, we investigated its reaction with diazomethane and two derivatives. We found that **1** reacts readily with diazoalkanes $R^1R^2C{=}N{=}N$ to give the novel azoniaboratacyclopropanes **2**–**4** in high yields.

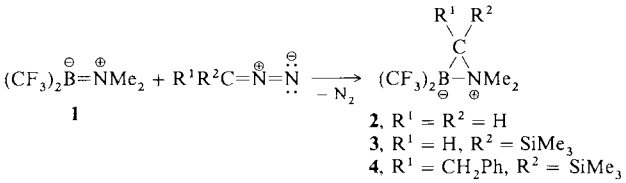

1 → (− N_2) → **2**, $R^1 = R^2 = H$; **3**, $R^1 = H$, $R^2 = SiMe_3$; **4**, $R^1 = CH_2Ph$, $R^2 = SiMe_3$

The products **2**–**4** are sublimable and stable up to about 90 °C. Their constitution was derived from the NMR spectra (Table 1). We carried out an X-ray crystal structure investigation for **4**.[6] This shows (Fig. 1) that the B–N bond in the three-membered ring is the shortest found so far between tetracoordinated boron and nitrogen atoms.[4] Several short contacts occur between the ring substituents; as a result the exocyclic valency angles are below the tetrahedral value, despite the small angles in the three-membered ring. The substituent planes B,C(1),C(2) and C,C(5),Si do not bisect the corresponding angles in the three-membered ring, but, as a result of steric interactions between the B and C substituents, are twisted by 9.5(5)° and 8.3(5)°, respectively, in the direction of the NMe_2 group. This strain has different effects on the distances in the three-membered ring. Whereas the N–C bond is 0.08(1) Å longer than the average $N–CH_3$ distance, the B–C bond (1.595(5) Å)) is as yet the shortest in a ring system containing $(CF_3)_2B$ (cf. $B–CH_2$ in 1,1,4,5-tetramethyl-2,2-bis(trifluoromethyl)-1-azonia-2-borata-4-cyclohexene: 1.599(3) Å[4]). The similarity of the lengths of different bonds in the three-membered ring is remarkable, as is the fact that the Si–C bond is 0.072(7) Å longer than the average $Si–CH_3$ distance.

Ethyl diazoacetate, in contrast, reacts in an entirely different way with **1**. The borylated ethyl diazoacetate **5** is formed at −120 °C in almost quantitative yield. Compound **5** is as

Table 1. Selected spectroscopic data of **2**–**5** [a].

2: ^1H NMR: $\delta = 2.01$ (s, 2H; CH_2), 2.78 (s, 6H; CH_3); $^{13}C\{^1H\}$ NMR: $\delta = 40.7$ (broad), 47.18 (sept, $^4J(C,F) = 2.1$ Hz); ^{11}B NMR: $\delta = -16.3$ (sept. $^2J(B,F) \approx 30$ Hz); ^{19}F NMR: $\delta = -59.4$ (q, $^2J(F,B) \approx 30$ Hz); IR(gas): $\tilde{\nu}$[cm^{-1}] = 1140, 1100 (C–F).

3: ^1H NMR: $\delta = 0.20$ (s, 9H; CH_3), 1.35 (s, 1H; CH), 2.82 (s, 3H; CH_3), 2.84 (s, 3H; CH_3); $^{13}C\{^1H\}$ NMR: $\delta = -0.15$ (q, $^5J(C,F) = 1.7$ Hz), ≈44.4 (broad), 45.46 (q $^4J(C,F) = 2.6$ Hz), 50.14 (q, $^4J(C,F) = 2.4$ Hz); ^{11}B NMR: $\delta = -15.3$ (sept, $^2J(B,F) \approx 34$ Hz); ^{19}F NMR: $\delta = -57.3$ ("d", −60.5 ("d"); IR (KBr): $\tilde{\nu}$[cm^{-1}] = 1108, 1085 (C–F).

4: ^1H NMR: $\delta = 0.08$ (s, 9H; CH_3), 2.83 (s, 3H, CH_3), 3.00 (s, 3H; CH_3), 3.30 (d, 16.6 Hz, 1H; CH_2) 3.54 (d, 16.6 Hz, 1H; CH_2), 7.20–7.33 (m, 5H; C_6H_5); $^{13}C\{^1H\}$ NMR: $\delta = 2.64$ (q, $^5J(C,F) = 1.9$ Hz), 34.65 (q, $^4J(C,F) = 2.1$ Hz), 43.27 (q, $^4J(C,F) = 2.4$ Hz), 47.94 (q, $^4J(C,F) = 2.8$ Hz), ≈50.5 (broad), 126.4(s), 128.1(s), 128.6(s), 138.1(s); ^{11}B NMR: $\delta = -14.2$(s); ^{19}F NMR: $\delta = -55.7$(s), −56.1(s); IR (KBr): $\tilde{\nu}$[cm^{-1}] = 1100, 1076 (C–F).

5: ^1H NMR: $\delta = 1.31$ (t, $^3J(H,H) = 7.1$ Hz, 3H; CH_3), 2.78 (d, $^3J(H,H) = 5.6$ Hz, 6H; CH_3), 4.22 (q, $^3J(H,H) = 7.1$ Hz, 2H; CH_2), 7.18 ((broad), 1H; NH); $^{13}C\{^1H\}$ NMR: $\delta = 14.69$(s), 40.50 (sept, $^4J(C,F) = 1.4$ Hz), ≈44.9 (broad), 62.06(s), 133.18 (q,q $^1J(C,F) = 306$ Hz, $^1J(C,B) = 78$ Hz), 172.04 (s); ^{11}B NMR: $\delta = -8.4$(s); ^{19}F NMR: $\delta = -63.8$ (q, $^2J(B,F) \approx 33$ Hz); IR (KBr): $\tilde{\nu}$[cm^{-1}] = 2100, (C=N=N); 1650, (C=O); 1091, (C–F).

[a] ^1H NMR: 250 MHz, $CDCl_3$, 25 °C, $\delta(CHCl_3) = 7.27$; ^{13}C NMR: 62.9 MHz, **2**–**4**: $CDCl_3$, 25 °C, $\delta(CDCl_3) = 77.0$, **5**: CD_3CN, 25 °C, $\delta(CD_3CN) = 1.30$; ^{11}B NMR: 25.52 MHz, $CDCl_3$, 25 °C, $BF_3 \cdot OEt_2$ external; ^{19}F NMR: 84.67 MHz, $CDCl_3$, 25 °C, $CFCl_3$.

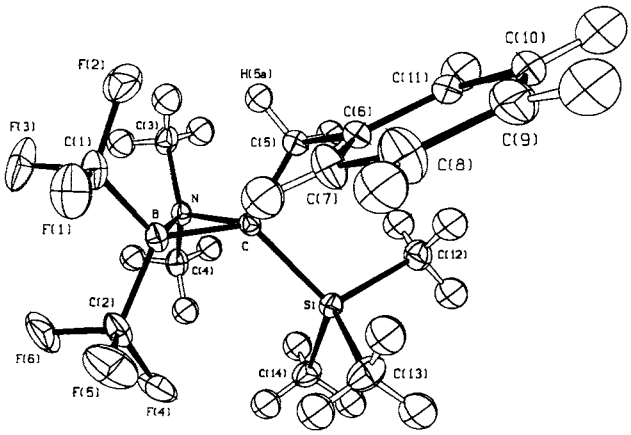

Fig. 1. Crystal structure of **4** (in perspective). Selected distances [Å] and angles [°] with standard deviations in parentheses: B-C 1.595(5), B-N 1.560(5), B-C(1) 1.614(6), B-C(2) 1.609(6), C-N 1.567(4), C-C(5) 1.540(5), C-Si 1.941(3), N-C(3) 1.493(4), N-C(4) 1.477(4); C-B-N 59.2(2), C(1)-B-C(2) 107.9(3), B-C-N 59.1(2), C(5)-C-Si 108.3(2), B-N-C 61.3(2), C(3)-N-C(4) 107.8(3)

[*] Prof. Dr. H. Bürger, Dipl.-Chem. A. Ansorge, Prof. Dr. D. J. Brauer, Dipl.-Chem. T. Hagen, Dr. G. Pawelke
Anorganische Chemie, FB 9 der Universität-Gesamthochschule
Postfach 100127 D-W-5600 Wuppertal 1 (FRG)

[**] This work was supported by the Ministerium für Wissenschaft und Forschung Nordrhein-Westfalen and the Fonds der Chemischen Industrie.

thermally stable as diazoacetate itself and melts at 84 °C without decomposition. The constitution of **5** is deduced

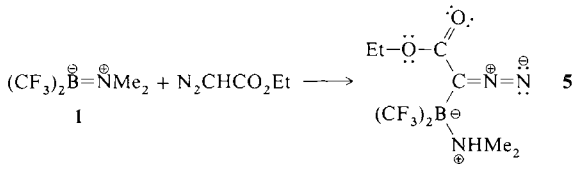

from the IR and NMR spectra as well as from an X-ray structure analysis.[8] The latter shows (Fig. 2) that the ethoxycarbonyldiazomethane group including the B atom is planar within ±0.06 Å. This planarity and the short C(3)–C(4) bond length (1.441 Å) are characteristic for a delocalized π-electron system in this part of the molecule. The B–C(3) distance is normal.[7] Noteworthy is the intramolecular hydrogen bonding.

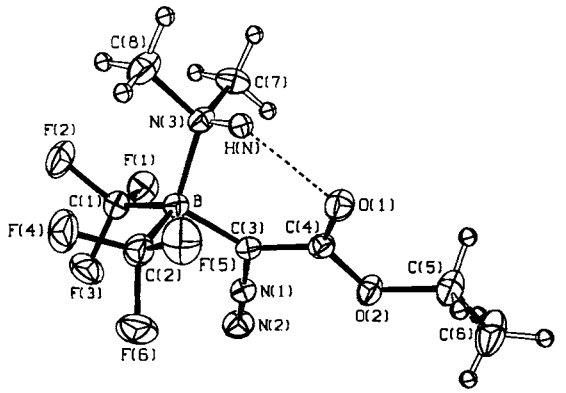

Fig. 2. Crystal structure of **5** (in perspective). Selected distances [Å] and angles [°] with standard deviations in parentheses: B-N(3) 1.612(4), B-C(1) 1.615(5), B-C(2) 1.624(5), B-C(3) 1.608(4), C(3)-C(4) 1.441(4), C(3)-N(1) 1.321(4), N(1)-N(2) 1.123(3), C(4)-O(1) 1.217(3), C(4)-O(2) 1.341(3), H(N)-O(1) 2.18(3); C(3)-B-N(3) 107.0(2), C(1)-B-C(2) 109.0(3), B-C(3)-C(4) 124.6(3), B-C(3)-N(1) 120.2(3), C(4)-C(3)-N(1) 115.0(2), C(3)-N(1)-N(2) 178.6(3), N(3)-H(N)-O(1) 141(3).

The azoniaboratacyclopropanes **2**–**4** are the first BNC three-membered rings in which boron and nitrogen occur with the coordination number four. Thus, they are the first BN isosteres of cyclopropane, whereas the corresponding isosteres of the cyclopropene have been known for some time.[9] The cyclopropanation of the B–N double bond is unprecedented, since with diazomethanes, boranes usually insert CH_2 into the boron–element bonds with retention of the coordination number three for the boron atom.[10] The inductive effect of the two trifluoromethyl groups makes a boron atom so electronically poor that it strives for saturation by increasing its coordination number to four. The reaction that **1** undergoes with ethyl diazoacetate follows the same principle and corresponds to the known reaction with carbonyl compounds $R^1CH_2COR^2$, during which dimethylamino-stabilized bis(trifluoromethyl)boranes of the type $(CF_3)_2B(R^1CHCOR^2)\cdot HNMe_2$ are formed.[5] In contrast, borylated diazomethane derivatives with boron with the coordination number three are well known.[9]

Experimental Procedure

2–**4**: An ethereal solution of diazomethane (11.8 mmol), trimethylsilyldiazomethane, or benzyl(trimethylsilyl)diazomethane (for the synthesis of **2**, **3**, and **4**, respectively) was added dropwise to **1** (2.0 g, 10.3 mmol), dissolved in dry pentane (15 mL), at −10 °C. **2**, **3**: The reaction mixture was stirred for 1 h at room temperature and subsequently condensed in a high vacuum fractionating apparatus. Compounds **2** and **3** were frozen out in a trap at −10 °C. **4**: The reaction mixture was stirred for 1 h at room temperature and subsequently the solvent was removed under vacuum. Compound **4** was isolated from the remaining black residue by sublimation at 40 °C in a high vacuum apparatus and recrystallized from CH_2Cl_2/petroleum ether.

5: Ethyl Diazoacetate (11.0 mmol) was added dropwise to **1** (2.0 g, 10.3 mmol), dissolved in dry CH_2Cl_2 (15 mL), at −120 °. The solvent was removed under vacuum while the reaction mixture was warmed from −70 °C to room temperature, and the residue recrystallized from acetone/petroleum ether. Yields/m.p.: **2**: 95%/30 °C; **3**: 97%/35 °C; **4**: 56%/74 °C; **5**: 98%/84 °C. Spectroscopic data of **2**–**5** are given in Table 1.

Received: October 22, 1992 [Z 5637 IE]
German version: *Angew. Chem.* **1993**, *105*, 429

[1] R. Köster, in *Methoden Org. Chem. (Houben-Weyl) 4th. Ed. 1952 (Organoborverbindungen)* Vol. 13/3a/3b/3c, Thieme, Stuttgart, **1982**, **1983** and **1984**.
[2] D. J. Brauer, H. Bürger, F. Dörrenbach, G. Pawelke, W. Weuter, *J. Organomet. Chem.* **1989**, *378*, 125–137.
[3] A. Ansorge, D. J. Brauer, H. Bürger, F. Dörrenbach, T. Hagen, G. Pawelke, W. Weuter, *J. Organomet. Chem.* **1991**, *407*, 283–300.
[4] A. Ansorge, D. J. Brauer, H. Bürger, F. Dörrenbach, T. Hagen, G. Pawelke, W. Weuter, *J. Organomet. Chem.* **1990**, *396*, 253–267.
[5] A. Ansorge, D. J. Brauer, H. Bürger, T. Hagen, G. Pawelke, *J. Organomet. Chem.*, in press.
[6] a) Single crystals of **4** were obtained from dichloromethane/petroleum ether: $a = 7.396(3)$, $b = 10.840(4)$, $c = 12.277(6)$ Å, $\alpha = 92.93(3)$, $\beta = 95.66(4)$, $\gamma = 108.71(3)°$, $V = 924.1(7)$ Å^3, $Z = 2$, $\rho_{calcd} = 1.327$ g cm^{-3}, $P\bar{1}$ (no. 2); $T = 299$ K; measurement range $3° \le 2\theta \le 50°$; $Mo_{K\alpha}$; 3249 independent reflections, R = 0.055 for 2185 observed reflections ($F_o \ge 4\sigma(F_o)$) and 246 parameters, $R_w = 0.068$ ($w = 1/(\sigma^2(F_o) + 0.0003\,F_o^2)$). b) Further details of the crystal structure investigation may be obtained from the Fachinformationszentrum Karlsruhe, Gesellschaft für wissenschaftlich-technische Information mbH, D-W-7514 Eggenstein-Leopoldshafen 2 (FRG) on quoting the depository number CSD-56793, the names of the authors, and the journal citation.
[7] See also A. Ansorge, D. J. Brauer, H. Bürger, F. Dörrenbach, B. Krumm, G. Pawelke, *Z. Naturforsch. B* **1992**, *47*, 772–782.
[8] Single crystals of **5** were obtained from acetone/petroleum ether: $a = 15.125(2)$, $b = 12.678(1)$, $c = 14.406(3)$ Å, $V = 2762.5(7)$ Å^3, $Z = 8$, $\rho_{calcd} = 1.476$ g cm^{-3}, *Pbcn* (no. 60); $T = 300$ K; measurement range $5° \le 2\theta \le 50°$; $Mo_{K\alpha}$; 2427 independent reflections, R = 0.053 for 1557 observed reflections ($F_o \ge 4\sigma(F_o)$) and 198 parameters, $R_w = 0.052$ ($w = 1/(\sigma^2(F_o) + 0.0002\,F_o^2)$). See also [6b].
[9] R. Boese, P. Paetzold, A. Tapper, *Chem. Ber.* **1987**, *120*, 1069–1071; A. Tapper, T. Schmitz, P. Paetzold, *ibid.* **1989**, *122*, 595–601; B. Glaser, H. Nöth, *ibid.* **1985**, *97*, 424–425; M. Arthur, A. Baceiredo, G. Bertrand, *J. Am. Chem. Soc.* **1991**, *113*, 5856–5857.
[10] H. S. Turner, *Chem. Ind. (London)* **1958**, 1405; J. Goubeau, K. H. Rohwedder, *Justus Liebigs Ann. Chem.* **1957**, *604*, 168–178.

Stereochemistry of Norbornyl → Norpinyl Rearrangements

By *Wolfgang Kirmse** and *Dirk Minkner*

The ionization of *exo*-2-norbornyl derivatives **1b** occurs with the participation of the C1–C6 bond (**1b** → **3**).[1] For *endo*-2-norbornyl derivatives **1a** corresponding participation of the C1–C7 bond (**1a** → **4**) should likewise be possible. However, the ring strain thereby increases,[2] so that the k_c process **1a** → **2** → **3** is often preferred over the k_Δ route **1a** → **4**[3] (Scheme 1). Charge destabilizing groups at C3[4] or C2, and similarly, charge stabilizing groups at C1[5] or C6[6] can cause (partial) rearrangement to give norpinyl derivatives, particularly when nitrogen ($X = N_2^+$) serves as the leaving group. To date it remains unclear whether the

[*] Prof. Dr. W. Kirmse, Dipl.-Chem. D. Minkner
Fakultät für Chemie der Universität
Postfach 102148, D-W-4630 Bochum (FRG)

 © VCH Verlagsgesellschaft mbH, W-6940 Weinheim, 1993 0570-0833/93/0303-0385 $ 10.00+.25/0

norpinyl derivatives **6** arise from the bridged cation **4** or the open cation **5**. However, since **4** is chiral, but **5** is achiral, we have now answered this question by stereochemical investigations.

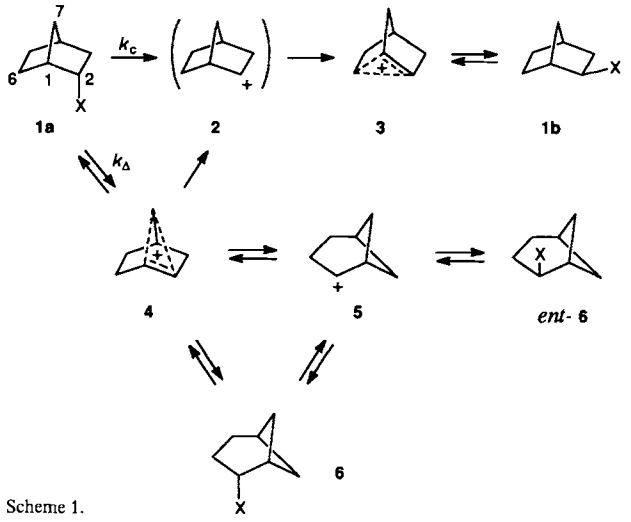

Scheme 1.

The deamination of *endo*-2-aminobicylo[2.2.1]heptan-*exo*-2-carbonitrile **12** ($NaNO_2$, $H_2O/HClO_4$, pH4) gives among other products, 2-hydroxybicyclo[3.1.1]heptan-1-carbonitrile **13** in 9% yield.[7] For the synthesis of optically active **11** we used the enzymatic cleavage of bicyclo-[2.2.1]hept-5-en-*endo*-2-yl-acetate **7** by lipase from *Candida cylindracea*.[8] From **8** we obtained the desired starting material by oxidation (→ **9**), hydrogenation (→**11**), and Strecker synthesis[7] (Scheme 2). The enantiomeric purity (*ee* values) of **11**, **12** (88 ± 1%), and **13** (81 ± 2%) was determined by gas chromatography (GC) on a chiral phase.[9] During the rearrangement **12** → **13** the enantiomeric purity is retained (92 ± 2%).

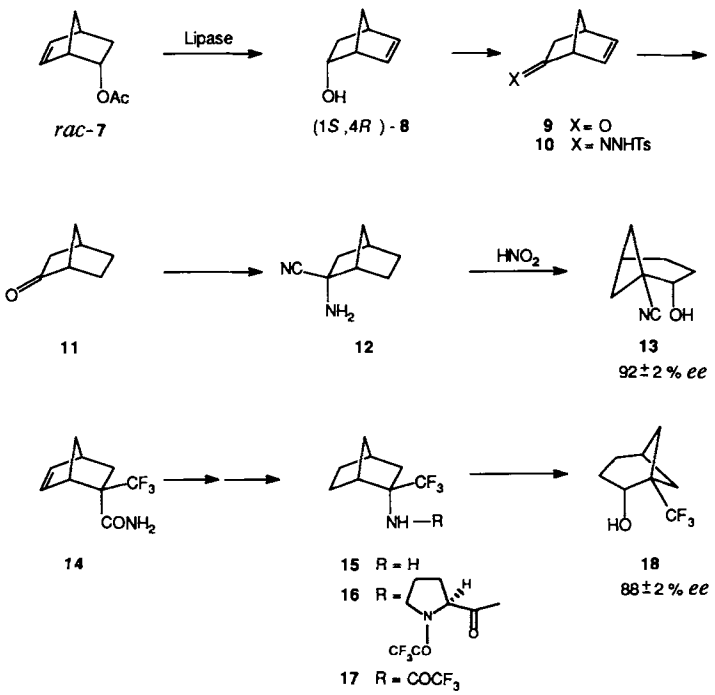

Scheme 2. Ts = *p*-toluenesulfonate

Among other products, 1-trifluoromethylbicyclo[3.1.1]-heptan-2-ol **18** is obtained in 11% yield from the deamination of *exo*-2-trifluoromethylbicyclo[2.2.1]heptyl-*endo*-2-amine **15**.[10] The starting material **15** was synthesized by a Diels–Alder reaction of cyclopentadiene with 2-trifluoromethylacrylamide, followed by hydrogenation and Hofmann degradation.[10] HPLC of the *N*-trifluoroacetyl-(*S*)-prolylamides **16** allowed the resolution of **15**, whose *ee* value (92 ± 1%) was determined by GC of the trifluoroacetamide **17**. From this starting material, **18** (81 ± 2% *ee*) was obtained with 88% retention of the enantiomeric purity. The formation of **13** and **18** thus results predominantly from bridged ions of the type **4**.

As an example demonstrating the contrary we investigated the photolysis of optically active bicyclo[2.2.1]hept-5-en-2-one-tosylhydrazones **10** in 0.5 N NaOH. The protonation of the initially generated diazo compound occurs nonselectively; however, bicyclo[3.1.1]hept-3-en-2-ol (**21**) (6%) is formed only from the *endo*-diazonium ion.[11, 12] The formation of predominantly racemic **21** (5 ± 2% *ee*) indicates that the achiral allyl cation **20** is a product-determining intermediate. The bridged structure **19** is only a transition state on the way to **20** (Scheme 3).

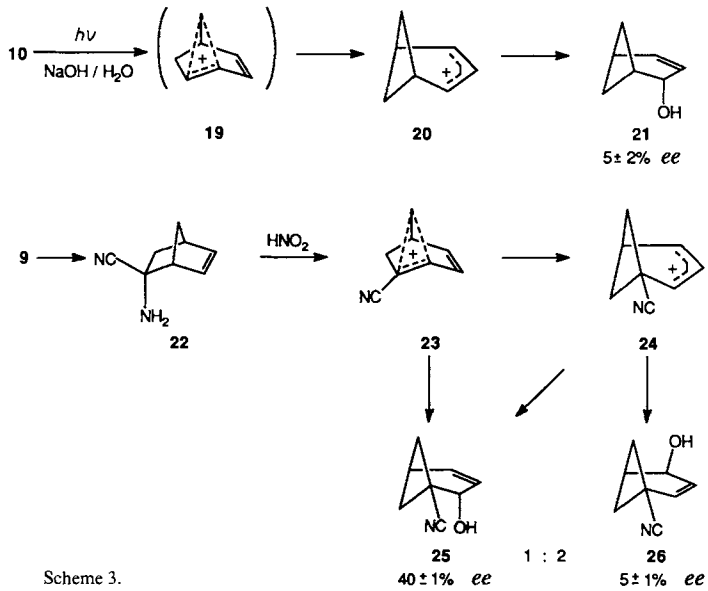

Scheme 3.

Particularly interesting is the combination of structural elements with opposite effects (CN group and C–C double bond) in **22**, which was obtained from optically active **9** (91 ± 1% *ee*) by Strecker synthesis. The achiral allyl cation **24**, which is derived from **22**, affords the isomeric allyl alcohols **25** and **26**, of which only **25** can be formed from the bridged ion **23**. Whereas almost racemic **26** (5 ± 1% *ee*) was obtained as expected, for **25** (37 ± 1% *ee*) the enantiomeric purity of the starting material was partially retained (40 ± 1%). Evidently, in addition to **24** also **23** participates in the formation of **25**.

As our results show, the stereochemistry of norbornyl → norpinyl rearrangements is strongly influenced by the choice of substituents. In contrast to the *exo*-selective 2-norbornyl cations, 2-norpinyl cations have no inherent stereopreference. The effects observed here genuinely reflect

the σ or π delocalization of the cationic intermediates. In favorable cases (**23**, **24**), both structural types can appear successively in one rearrangement and can be trapped by nucleophiles.

Received: October 20, 1992 [Z 5635IE]
German version: *Angew. Chem.* **1993**, *105*, 466

[1] Reviews: G. D. Sargent in *Carbonium Ions* (Eds.: G. A. Olah, P. von R. Schleyer), *Vol. III*, Wiley, New York, **1972**, p. 1099; H. C. Brown: *The Nonclassical Ion Problem* (with comments by P. von R. Schleyer), Plenum, New York, **1977**; W. Kirmse, *Top. Curr. Chem.* **1979**, *80*, 125; V. A. Barkhash, *ibid.* **1984**, *116*, 1; P. Vogel: *Carbocation Chemistry*, Elsevier, Amsterdam, **1985**; D. Lenoir, Y. Apeloig, D. Arad, P. von R. Schleyer, *J. Org. Chem.* **1988**, *53*, 661.

[2] According to force field calculations the strain energy of bicyclo[3.1.1]heptane (norpinane, **5**, X = H) is 143.8 kJ mol^{-1}, that of bicyclo[2.2.1]heptane (norbornane, **1**, X = H) is 63.2 kJ mol^{-1}: W. F. Maier, P. von R. Schleyer, *J. Am. Chem. Soc.* **1981**, *103*, 1981.

[3] Review: W. Kirmse, *Acc. Chem. Res.* **1986**, *19*, 36.

[4] P. Yates, R. J. Crawford, *J. Am. Chem. Soc.* **1966**, *88*, 1561; R. A. Blattel, P. Yates, *Tetrahedron Lett.* **1972**, 1069, 1071; C. J. Collins, I. T. Glover, M. D. Eckart, V. F. Raen, B. M. Benjamin, B. S. Bemjaminov, *J. Am. Chem. Soc.* **1972**, *94*, 899; R. Siegfried, *Chem. Ber.* **1974**, *107*, 1472.

[5] W. Kirmse, G. Arend, R. Siegfried, *Angew. Chem.* **1970**, *82*, 174; *Angew. Chem. Int. Ed. Engl.* **1970**, *9*, 165; W. Kirmse, G. Arend, *Chem. Ber.* **1972**, *105*, 2738, 2746; W. Kirmse, R. Siegfried, *ibid.* **1972**, *105*, 2754; W. Kirmse, K. Loosen, *ibid.* **1981**, *114*, 400; W. Kirmse, N. Knöpfel, K. Loosen, R. Siegfried, H.-J. Wroblowsky, *ibid.* **1981**, *114*, 1187; K. Banert, W. Kirmse, H.-J. Wroblowsky, *ibid.* **1983**, *116*, 3591.

[6] W. Kirmse, F. Söllenböhmer, *Angew. Chem.* **1989**, *101*, 1728; *Angew. Chem. Int. Ed. Engl.* **1989**, *28*, 1667.

[7] Strecker synthesis afforded a mixture of **11** and *exo*-2-aminobicyclo[2.2.1]heptan-*endo*-2-carbonitrile: H. S. Tager, H. N. Christensen, *J. Am. Chem. Soc.* **1972**, *94*, 968. Details for the separation of isomers and their deamination products (R. Siegfried) will be published in *Chem. Ber.*

[8] G. Eichberger, G. Penn, K. Faber, H. Griengl, *Tetrahedron Lett.* **1986**, *27*, 2843.

[9] Heptakis(2.6-di-*O*-methyl-3-*O*-trifluoroacetyl)-β-cyclodextrin in OV 1701: H. P. Nowotny, D. Schmalzing, D. Wistuba, V. Schurig, *J. High Resolut. Chromatogr.* **1989**, *12*, 393. Compound **12** was analyzed as an N-trifluoroacetyl derivative.

[10] K.-R. Gassen, dissertation, Universität Bochum, **1985**.

[11] W. Kirmse, N. Knöpfel, K. Loosen, R. Siegfried, H.-J. Wroblowsky, *Chem. Ber.* **1981**, *114*, 1187.

[12] For the preparation of **21** from bicyclo[3.1.1]hept-2-ene see W. Kirmse, H.-J. Wroblowsky, *Chem. Ber.* **1983**, *116*, 2486.

Synthesis, Properties, and Structure of $[L_xLi_2Pt(CH_2CH_2CH_2CH_2)_2]$—A New Type of Pt^{II} Metallacyclopentane Complexes**

By *Hans-Otto Fröhlich,* Ralf Wyrwa,* and *Helmar Görls*

Metallacycles containing d-block elements are of great significance as intermediates of numerous catalytic reactions such as the [2 + 2] cycloaddition of olefins,[1-3] the oligomerization of 1,2- and 1,3-dienes,[4-8] the isomerization of strained cyclic hydrocarbons,[9] and olefin metathesis.[10] Mechanistic and structural investigations, in particular on Pt^{II} and Pt^{IV} metallacyclopentanes of the known types $[L_2Pt(CH_2CH_2CH_2CH_2)]$ and $[L_nXYPt(CH_2CH_2CH_2CH_2)]$ (L = neutral ligand; X = CH_3, I; Y = Cl, Br, I; n = 1, 2), have contributed considerably to a better understanding of the catalytic behavior and the reasons behind the fact that these metallacycles are thermally more stable than noncyclic compounds of corresponding composition.[11-15] These investigations, particularly those on the platinum(II) compounds, show the influence of the neutral ligands L on the structure and thermal stability of the platinacyclopentane system. Thus, it was of interest to prepare Pt^{II} metallacycles in which exclusively butane-1,4-diyl ligands are bound to the central atom. Herein we report on the first synthesis of complexes of the type $[L_xLi_2Pt(CH_2CH_2CH_2CH_2)_2]$ (L = diethyl ether, x = 1: **1**; L = *N*,*N*,*N*′,*N*′-tetramethylethylenediamine (TMEDA), x = 2: **2**) as well as on the results of ^1H and ^{13}C NMR spectroscopic investigations, differential thermal analyses (DTA), and X-ray structure analyses of these substances.

Compound **1** is obtained from the reaction of dichloro(1,5-cyclooctadiene)platinum(II) with 1,4-dilithiobutane [Eq. (a)]. By substituting the diethyl ether in **1** for other neutral mono-, bi-, and terdentate ligands, derivatives such as **2** are easily obtained [Eq. (b)].

$$[(cod)PtCl_2] + 2\,Li_2(C_4H_8) \xrightarrow[-78 \rightarrow 25\,^\circ C]{Et_2O} [(Et_2O)Li_2Pt(CH_2CH_2CH_2CH_2)_2] + cod + 2\,LiCl \quad \mathbf{1},\ 75\% \qquad (a)$$

$$\mathbf{1} + 2\,TMEDA \xrightarrow[-Et_2O]{} [(tmeda)_2Li_2Pt(CH_2CH_2CH_2CH_2)_2] \quad \mathbf{2},\ 82\% \qquad (b)$$

According to DTA studies,[16] the decomposition temperatures of **1** and **2**, surprisingly vary considerably. Whereas **1** decomposes already at 85 °C, **2** decomposes at 249 °C. Evidently, bidentate tertiary amines such as TMEDA contribute particularly to the stabilization of these platinum(II) complexes.

After the DTA measurements, the gas phases above the solid decomposition residues of compounds **1** and **2** were analyzed. The hydrocarbon mixtures were found to have the following compositions (percentage in parentheses): Sample of **1**: ethene (18), but-1-ene (66), (*Z*/*E*)-but-2-ene (4), butane (12); sample of **2**: ethene (10), but-1-ene (13), (*Z*/*E*)-but-2-ene (38), butane (39). Neither the presence of cyclobutane nor butadiene could be proven. A comparison of these results with those of the thermal decomposition (under similar conditions) of Pt^{IV} metallacyclopentanes[14] shows that in the gaseous decomposition products of the latter no ethene is present, which indicates that their decomposition occurs without cleavage of the C–C bond.

Compound **2** was characterized by ^1H and ^{13}C NMR spectroscopy (Table 1) and by an X-ray structure analysis (Fig. 1).[17]

Table 1. ^1H and ^{13}C NMR data of **2** in C_6D_6 at room temperature.

^1H NMR data (200 MHz)	^{13}C NMR data (50 MHz)
δ(Pt-CH_2, 8H, t) = 1.33	δ(Pt-CH_2) = 19.2
$^2J(^{195}Pt\text{-}^1H)$ = 35.4 Hz	$^1J(^{195}Pt\text{-}^{13}C)$ = 498 Hz
$^3J(^1H\text{-}^1H)$ = 5.9 Hz	
δ(β-CH_2, 8H, m) = 2.26	δ(β-CH_2) = 38.2
δ(N-CH_2, 8H, s) = 1.78	δ(N-CH_2) = 56.6
δ(N-CH_3, 24H, s) = 2.08	δ(N-CH_3) = 45.6

[*] Prof. Dr. H.-O. Fröhlich, Dipl.-Chem. R. Wyrwa
Institut für Anorganische Chemie der Universität
August-Bebel-Strasse 2, D-O-6900 Jena (FRG)
Dr. H. Görls[+]
Max-Planck-Gesellschaft
Arbeitsgruppe "CO_2-Chemie" an der Universität Jena

[+] Crystal structure analysis

[**] Contributions to the chemistry of organometallic metallacyclic compounds of the d block elements, Part 7. This work was supported by the Fonds der Chemischen Industrie, the Volkswagen-Stiftung, and the Buna AG. Part 6: [16]

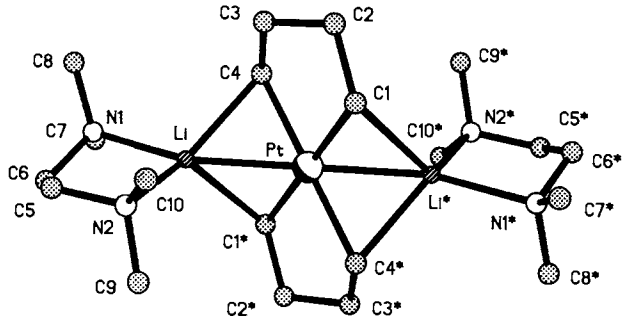

Fig. 1. Crystal structure of **2**. Selected distances [Å] and angles [°]: Pt-C1 2.114(4), Pt-C4 2.141(4), C1-C2 1.543(7), C2-C3 1.487(7), C3-C4 1.489(7), Pt-Li 2.453(7), Li-C4 2.302(8), Li-C1* 2.455(8), Li-N1 2.136(8), Li-N2 2.100(8); C1-Pt-C4 81.8(2), C1*-Pt-Li 64.5(2), C4-Pt-Li 59.7(2), Pt-C1-C2 110.0(3), C1-C2-C3 110.3(4), C2-C3-C4 109.8(4), Pt-C4-C3 108.9(3), Pt-C4-Li 66.9(2), Pt-Li-N1 161.6(4), Pt-Li-N2 112.6(3).

The molecule is centrosymmetric. The platinum atom occupies the center of symmetry. The central atom is surrounded in a planar manner by four anionic centers C1, C4, C1*, and C4*. The average Pt–C distance is 2.128 Å and the angle of inclination of the axis Li–Pt–Li* toward the coordination plane 44.3(2)°. The distances Li–C4 (2.302(8) Å) and Li–C1* (2.455(8) Å) differ significantly, showing that the Li atom interacts more strongly with one of the adjacent C atoms. This is also shown by the longer Pt–C4 distance. The shorter of the two Li–C distances, Li–C4, is similar to the one in $(LiCH_3)_4$ (2.28 Å[18]). The Li–Pt distances are 2.453(7) Å, and are thus shorter than the sum of the covalent radii Pt–Li (2.53 Å). By binding one tmeda ligand at each lithium atom the coordination number is increased to five. The intensive interaction of the lithium atoms, which are extensively shielded by the tmeda ligands, with the bis(butane-1,4-diyl)platinum(II) system apparently contributes to the thermal stabilization of the complex, as does the fact that the distances of the hydrogen atoms of the tmeda ligands from the platinum are ≥ 3.5 Å. Thus, an oxidative addition of C–H groups of the diamine at the Pt^{II} center, which would enhance the thermal decomposition, as for the thermal decomposition of bis(tricyclopentylphosphane)platinacyclopentane (in this case it is C–H groups of the cyclopentyl moieties) is probably made more difficult.[11]

Experimental Procedure

All operations were carried out under an argon atmosphere.

1: 1,4-dilithiobutane (35.8 mmol) was dissolved in diethyl ether (250 mL) and stirred at −78 °C in a Schlenk flask. Over 30 min [(1,5-cod)$PtCl_2$] (6.7 g, 17.9 mmol) was added to this solution. The reaction mixture was stirred for 2 h at −40 °C and subsequently slowly warmed to room temperature. Lithium chloride was separated, the pale yellow filtrate concentrated to 50 mL under vacuum, and finally cooled to −78 °C. The colorless crystals formed were washed with cold diethyl ether and dried under vacuum at room temperature. When required the compound can be purified by recrystallization from diethyl ether. Compound **1** was obtained in the form of colorless crystals (5.3 g, 74.9%).

2: **1** (2 g) was dissolved in diethyl ether (75 mL) cooled to −20 °C. The solution was stirred and TMEDA (3.5 mL) was added. The mixture was allowed to warm to 20 °C and then left to crystallize at −78 °C. The colorless crystals were collected on a frit and dried. Yield of **2**: 2.3 g (82.1%).

Received: October 24, 1992 [Z 5644 IE]
German version: *Angew. Chem.* **1993**, *105*, 425

[1] R. Noyori, T. Ishigami, N. Hyashi, H. Takaya, *J. Am. Chem. Soc.* **1973**, *95*, 1674–1676.
[2] A. R. Fraser, P. H. Bird, S. A. Bezman, I. R. Shapley, R. White, J. A. Osborn, *J. Am. Chem. Soc.* **1973**, *95*, 597–598.
[3] J. M. Doyle, J. McMeeking, P. Binger, *J. Chem. Soc. Chem. Commun.* **1976**, 376–377.
[4] M. Green, J. A. K. Howard, P. Mitrprachachon, M. Pfeffer, J. L. Spencer, F. G. A. Stone, P. J. Woodward, *J. Chem. Soc. Dalton Trans.* **1979**, 306–314.
[5] P. W. Jolly, C. Krüger, R. Saltz, J. C. Sekutowsky, *J. Organomet. Chem.* **1979**, *165*, C39–C42.
[6] A. Borrini, G. Ingrosso, *J. Organomet. Chem.* **1977**, *132*, 275–289.
[7] P. W. Jolly, G. Wilke, *The Organic Chemistry of Nickel, Vol. II*, Academic Press, New York, **1975**.
[8] G. K. Barker, M. Green, J. A. K. Howard, J. L. Spencer, F. G. A. Stone, *J. Am. Chem. Soc.* **1976**, *98*, 3373–3374.
[9] K. C. Bishop, *Chem. Rev.* **1976**, *76*, 461–486.
[10] N. Calderon, J. P. Lawrence, E. A. Ofstead, *Adv. Organomet. Chem.* **1979**, *17*, 449–492.
[11] T. M. Miller, G. M. Whitesides, *Organometallics* **1986**, *5*, 1473–1480.
[12] C. G. Biefeld, H. A. Eick, R. H. Grubbs, *Inorg. Chem.* **1973**, *12*, 2166–2170.
[13] J. X. McDermott, J. F. White, G. M. Whitesides, *J. Am. Chem. Soc.* **1976**, *98*, 6521–6528.
[14] M. P. Brown, A. Hollings, K. J. Houston, R. J. Puddephatt, M. Rashidi, *J. Chem. Soc. Dalton Trans.* **1976**, 786–791.
[15] A. K. Cheetham, R. J. Puddephatt, A. Zalkin, D. H. Templeton, L. K. Templeton, *Inorg. Chem.* **1976**, *15*, 2997–2999.
[16] H.-O. Fröhlich, B. Kosan, B. Müller, W. Hiller, *J. Organomet. Chem.*, **1992**, 441, 177–184.
[17] Crystal structure analysis of **2** ($C_{20}H_{48}Li_2N_4Pt$, $M_r = 553.4$): $P1$, $a = 7.799(5)$, $b = 8.673(6)$, $c = 10.264(6)$ Å, $\alpha = 79.59(5)$, $\beta = 86.89$, $\gamma = 69.86(5)°$, $V = 641(1)$ Å^3, $Z = 1$, $\rho_{calcd} = 1.43$ g cm^{-3}, $\mu = 55.37$ cm^{-1}, $\lambda = 0.71069$ Å, 3083 measured reflections, 2917 symmetry-independent reflections, all observed [$I > 2\sigma(I)$], 124 refined parameters, $R = 0.026$, $R_w = 0.031$. ($w = 1/\sigma^2(F_o)$), residual electron density 1.42 e Å^{-3}. Further details of the crystal structure investigation may be obtained from the Fachinformationszentrum Karlsruhe, Gesellschaft für wissenschaftlich-technische Information mbH, D-W-7514 Eggenstein-Leopoldshafen 2 (FRG) on quoting the depository number CSD-56790, the names of the authors, and the journal citation.
[18] E. Weiss, E. A. C. Lucken, *J. Organomet. Chem.* **1964**, *2*, 19.

An Al–Al One-Electron π Bond**

By *Christian Pluta, Klaus-R. Pörschke,* Carl Krüger,* and *Knut Hildenbrand*

For several years we have been interested in coordination compounds of (alkene)nickel(0) complexes with main group metal alkanides (LiR,[1a, 1b] MgR_2,[1c] SnR_2,[1d]) and hydrides [M_AH,[2] $M_AH_nM_BR_{4-n}$,[3] (M_A = Li, Na; M_B = Al, Ga), $HAlMe_2$[4]]. These studies were prompted by the "nickel effect" observed by Ziegler et al.,[5a] which according to Wilke et al. is founded in an interaction between nickel(0) and trialkylaluminum compounds.[5b] However, till today no compounds with defined nickel–aluminum bonds have been synthesized.[6] Thus, in a further attempt at this goal, we treated the dialane(4) **1** prepared by Uhl[7] with $[Ni(C_2H_4)_3]$[8] or $[\{(tmeda)Li\}_2Ni(C_2H_4)_3]$ (tmeda = tetramethylethylenediamine).[9] Whereas $[Ni(C_2H_4)_3]$ did not react, a dark red solution was obtained with the lithiated complex, from which, however, no uniform product could be isolated. We therefore treated **1** directly with lithium.[10]

The dialane **1** reacts with one lithium atom in ether at −30 °C to give a blue-violet solution,[11] from which large black-violet crystals of **2** precipitate slowly at −78 °C. If the

[*] Priv.-Doz. Dr. K.-R. Pörschke, Dr. C. Pluta, Prof. Dr. C. Krüger
Max-Planck-Institut für Kohlenforschung
Postfach 101353, D-W-4330 Mülheim an der Ruhr (FRG)
Dr. K. Hildenbrand
Max-Planck-Institut für Strahlenchemie
Postfach 101365, D-W-4330 Mülheim an der Ruhr (FRG)

[**] The title implies a close relation between this work and ref.[25]. We thank Prof. Dr. H. Sabrowsky, Ruhr-Universität Bochum, for the magnetic susceptibility measurements and the Fonds der Chemischen Industrie for support.

reaction solution containing **2** is treated with tmeda at 0 °C, fine, black-violet crystals of the ionic compound **3** form. Both compounds are *extremely* air-sensitive and decompose with decoloration.

$$\underset{\mathbf{1}}{Al_2\{CH(SiMe_3)_2\}_4} + Li \xrightarrow[Et_2O]{-30\,^\circ C} \underset{\mathbf{2}}{[(Et_2O)_3Li][Al_2\{CH(SiMe_3)_2\}_4]^\bullet}$$

$$\xrightarrow[tmeda]{0\,^\circ C} \underset{\mathbf{3}}{[Li(tmeda)_2]^+[Al_2\{CH(SiMe_3)_2\}_4]^{\bullet -}}$$

Solid **2** decomposes slowly with decoloration at 20 °C. Apparently the ether ligands are easily cleaved to form the starting materials **1** (colorless) and Li. In contrast, solid **3** is stable at 20 °C; the shielding of the lithium ion by two tmeda ligands precludes a reverse reaction as in **2**. The complexes behave similarly in aromatic solvents.[12] Compounds **2** and **3** afford blue-violet solutions in THF that appear unchanged after several weeks at room temperature. Presumably the ionic compound $[Li(thf)_4]^+[Al_2\{CH(SiMe_3)_2\}_4]^{\bullet -}$ **4** is present. It may be deduced from these findings that the radical ion pair $Li^+[Al_2R_4]^{\bullet -}$ is stabilized by a strong solvent coordination of the lithium ion.

On protolysis of **2** with 2-propanol (undiluted, −78/20 °C), 1.46 H_2 per two Al is released,[13] which is in accord with an oxidation of aluminum from the formal oxidation state 1.5 to Al^{III}. Compounds **2** and **3** cannot be vaporized without decomposition; their mass spectra (70 eV, 100 °C) correspond to that of dialane **1**. Informative NMR spectra have not been obtained.[14] Magnetic measurements on **3** revealed a paramagnetism that displays a temperature dependence in accord with the Curie-Weiss law.[15]

The ESR spectrum of **4** obtained at 60 °C[16] (Fig. 1a, $g = 2.0035 \pm 0.0005$) comprises eleven signal groups 1.19 mT apart. The 11-fold splitting is explained by a coupling of the unpaired electron with the two magnetically equivalent ^{27}Al nuclei ($I = 5/2$; abundance 100%; $a^{Al} \approx 1.19$ mT, 60 °C). Each of the eleven signals is flanked by ^{29}Si sidebands ($I = 1/2$; abundance 4.67%; $a^{Si} = 0.4$ mT, 60 °C). A coupling of the unpaired electron with the four β-AlCH protons does not occur, because of its predominant occupation of a π orbital, the SOMO, which forms a dihedral angle of 90 °C with the C–H bonds that lie in the nodal plane of the SOMO[17] (see molecular structure of **3**).

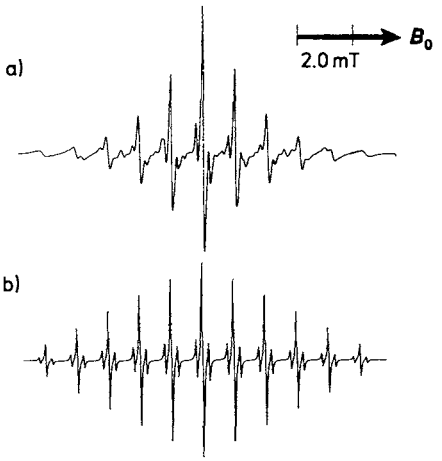

Fig. 1. a) ESR spectrum of **4** in THF at 60 °C; b) sum of the simulated ESR spectra for two isotopomeric forms of the radical anion in **4**, one with only magnetically inactive Si nuclei and one with a ^{29}Si nucleus. A complete averaging of the anisotropy was assumed. Based on the binomial distribution the following isotopic abundance is calculated: molecules with only magnetically inactive Si, 68.2%; molecules with one ^{29}Si, 26.7%. The others have two or more ^{29}Si (not taken into account in the simulaton).

The width of the signals of the high-temperature ESR spectrum is about 0.09 mT in the middle of the spectrum and increases with increasing distance from the center. The signal broadening is attributable to the anisotropy of the Al coupling, which is particularly noticeable in the outer regions of the spectrum. The effect is enhanced by lowering the temperature: at −30 °C only five and at −70 °C three signal groups may still be distinguished; the rest are very broad. One possible explanation is the decrease in the rate of the molecule's rotation in solution which therefore renders the averaging of the anisotropy less feasible (similar line-broadening is observed for an Al–ethyne adduct in neon matrix[18]). The result of a simulation of the spectrum in which anisotropy effects were not taken into account is depicted in Figure 1b.

Whereas **2** appears amorphous, the structure of **3** was determined by X-ray crystal structure analysis.[19] Its ionic structure is composed of a $[Li(tmeda)_2]$ cation and an $[Al_2\{CH(SiMe_3)_2\}_4]$ radical anion $\mathbf{1}^{\bullet -}$ (Fig. 2). Two independent molecules of the radical anion (Mol 1 and Mol 2) are arranged centrosymmetrically about an inversion center in the unit cell ($C_i \equiv \bar{1}$); the anions contain ideally planar C_2Al–AlC_2 units. Molecules 1 and 2 have similar bond lengths and

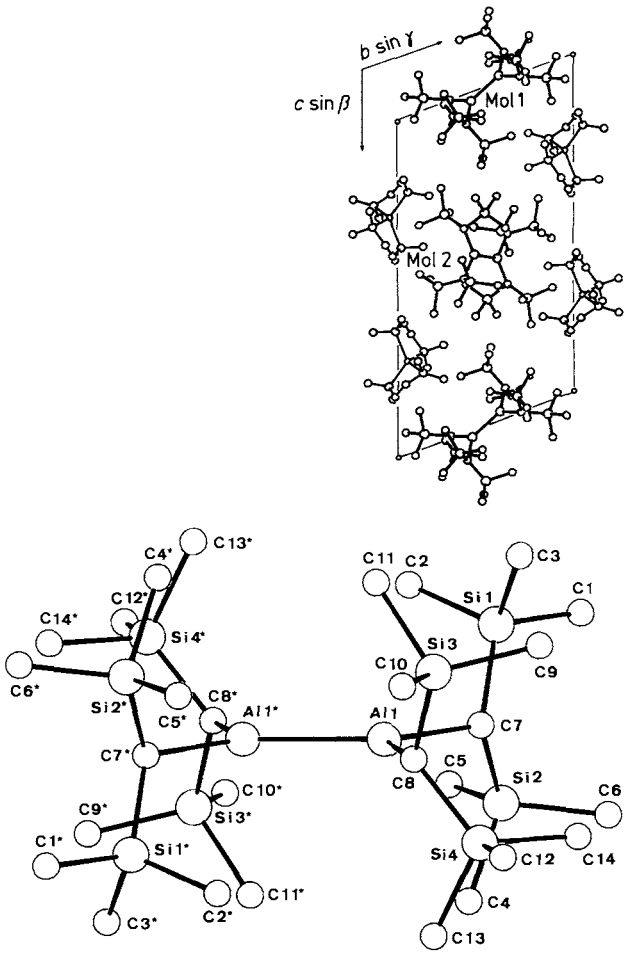

Fig. 2. Top: Unit cell of **3**. Bottom: Structure of the radical anion in **3** in the crystal (H atoms omitted). Averaged bond lengths [Å] and angles [°]: Al1*–Al1 2.53(1), Al1–C7 2.042(5), Al1–C8 2.038(6); Al1*-Al1-C7 127(1), Al1*-Al1–C8 121(1), C7-Al1-C8 111.9(2); interplanar angles Al1,C7,C8/C7,Si1,Si2 88.9/85.0; Al1,C7,C8/C8,Si3,Si4 79.3/83.3.

 © VCH Verlagsgesellschaft mbH, W-6940 Weinheim, 1993 0570-0833/93/0303-0389 $ 10.00+.25/0

angles, but their torsion and interplanar angles for the SiCSi groups differ marginally because of packing effects. The four $CH(SiMe_3)_2$ substituents in each molecule are so positioned that the H atoms at C7 and C8 (situated at idealized calculated positions) lie approximately in the C_2Al–AlC_2 plane, pointing in the same direction. The structure of the anion $\mathbf{1}^{\bullet-}$ thus corresponds to that of the neutral dialane **1**,[7] but in detail the structures of $\mathbf{1}^{\bullet-}$ and **1** reveal significant differences. In anion $\mathbf{1}^{\bullet-}$ the angle C-Al-C of 111.9(2)° is smaller than in neutral **1** (116.7(1)°); the remaining angles at the trigonal-planar aluminum atom are 127(1)° for Al1*–Al1–C7 and 121(1)° for Al1*–Al1–C8. The Al–C bond lengths of the anion (2.040(5) Å) are distinctly elongated (by 0.06 Å) relative to those of the neutral dialane (1.982(5) Å), and the central Al–Al bond in $\mathbf{1}^{\bullet-}$ of 2.53(1) Å is considerably shortened (by 0.13 Å) from the 2.660(1) Å of the same bond in **1**.[20]

The change in the structural parameters on one-electron reduction of the neutral dialane **1** to the radical anion $\mathbf{1}^{\bullet-}$ is in accord with an Al–Al π bond of partial multiple bond character in $\mathbf{1}^{\bullet-}$. On the transformation $\mathbf{1} + e \rightarrow \mathbf{1}^{\bullet-}$, the unoccupied p_z orbitals of the sp^2 hybridized aluminum atoms in **1** take up the electron, which becomes delocalized in a *bonding* orbital. The center of gravity of the charge lies between the aluminum nuclei, as their equivalence in the ESR spectrum shows. The reaction of **1** with lithium accordingly leads to a *strengthening of the Al–Al bond*.[21] The results of MO calculations agree with the experimental findings.[22] The bonding situation of the one-electron π bond[23, 24] in $\mathbf{1}^{\bullet-}$ is analogous to that in the very stable anions $[R_2B{-}BR_2]^{\bullet-}$[25] and $[R_2B{=}BR_2]^{2-}$[26] (MO calculations[27]). Furthermore, the radical anion $\mathbf{1}^{\bullet-}$ is isoelectronic with a $[R_2C{-}CR_2]^{\bullet+}$ ion. In view of the lower tendency of the main group elements of the third and higher periods to form multiple bonds, the existence of this bonding type for aluminum is surprising.

Experimental Procedure

2: A solution of **1** (1.38 g, 2.0 mmol) in ether (60 mL) was treated with an excess of lithium (50 mg) at −78 °C. The reaction mixture was stirred while it warmed slowly (2 h) to −30 °C. The color changed to dark blue-violet. After the excess lithium was filtered off, large black-violet crystals formed at −78 °C in about 24 h. After removal of the mother liquor with a capillary tube, the crystals were dried in vacuum. Yield: 1.2 g (65%); correct elemental analysis.

3: The reaction solution of **2** was treated at 0 °C with tmeda (2 mL) in ether (10 mL). Fine, black-violet crystals separated, which were filtered off, washed in 10 mL ether, and dried under high vacuum at 0 °C. Yield: 875 mg, (47%); correct elemental analysis.

Received: November 11, 1992 [Z 5677 IE]
German version: *Angew. Chem.* **1993**, *105*, 451

[1] a) K.-R. Pörschke, K. Jonas, G. Wilke, R. Benn, R. Mynott, R. Goddard, C. Krüger, *Chem. Ber.* **1985**, *118*, 275; b) K.-R. Pörschke, K. Jonas, G. Wilke, *ibid.* **1988**, *121*, 1913; c) W. Kaschube, K.-R. Pörschke, K. Angermund, C. Krüger, G. Wilke, *ibid.* **1988**, *121*, 1921; d) C. Pluta, K.-R. Pörschke, R. Mynott, P. Betz, C. Krüger, *ibid.* **1991**, *124*, 1321.

[2] a) K.-R. Pörschke, W. Kleimann, G. Wilke, K. H. Claus, C. Krüger, *Angew. Chem.* **1983**, *95*, 1032; *Angew. Chem. Int. Ed. Engl.* **1983**, *22*, 991; b) R. Goddard, C. Krüger, K.-R. Pörschke, G. Wilke, *J. Organomet. Chem.* **1986**, *308*, 85; c) K.-R. Pörschke, G. Wilke, *ibid.* **1988**, *349*, 257.

[3] a) K.-R. Pörschke, G. Wilke, *Chem. Ber.* **1985**, *118*, 313; b) W. Kleimann, K.-R. Pörschke, G. Wilke, *ibid.* **1985**, *118*, 323; c) K.-R. Pörschke, G. Wilke, *J. Organomet. Chem.* **1988**, *358*, 519.

[4] K.-R. Pörschke, W. Kleimann, Y.-H. Tsay, C. Krüger, G. Wilke, *Chem. Ber.* **1990**, *123*, 1267.

[5] a) K. Ziegler, *Brennst. Chem.* **1954**, *35*, 321; K. Ziegler, E. Holzkamp, H. Breil, H. Martin, *Angew. Chem.* **1955**, *67*, 541; b) K. Fischer, K. Jonas, P. Misbach, R. Stabba, G. Wilke, *ibid.* **1973**, *85*, 1002; *Angew. Chem. Int. Ed. Engl.* **1973**, *12*, 943; G. Wilke, *ibid.* **1988**, *100*, 189 and **1988**, *27*, 185, and references therein.

[6] Nickel–aluminum interactions confirmed by crystal structure analyses: a) See [4]; b) C. Krüger, J. C. Sekutowski, H. Hoberg, R. Krause-Göing, *J. Organomet. Chem.* **1977**, *141*, 141.

[7] W. Uhl, *Z. Naturforsch. B* **1988**, *43*, 1113.

[8] K. Fischer, K. Jonas, G. Wilke, *Angew. Chem.* **1973**, *85*, 620; *Angew. Chem. Int. Ed. Engl.* **1973**, *12*, 565.

[9] a) K. Jonas, *Angew. Chem.* **1975**, *87*, 809; *Angew. Chem. Int. Ed. Engl.* **1975**, *14*, 752; b) K.-R. Pörschke, Dissertation, Universität Bochum, **1975**.

[10] C. Pluta, Dissertation, Universität Düsseldorf, **1992**.

[11] The cyclic voltammogram of **1** in THF (0.1 M NBu_4ClO_4) at 20 °C shows only one wave in the potential range from +1.6 to −3.2 V (glassy carbon electrode) with a peak potential at $E_p = -2.85$ V vs. SCE. This current overlaps with that from the decomposition of the electrolyte, the former resulting in a weak shoulder. In fact the corresponding electrode process (reduction) is irreversible at a sweep rate of 200 Vs^{-1}; the subsequent reaction (decomposition) of the reduction product must be extremely fast. Cyclic voltammetry thus shows that the dialane is reduced, but no deduction about whether it is a one- or two-electron reduction is possible.

[12] On dissolving **2** in benzene an immediate decolorization is observed; besides the evolution of ether, **1** is again formed. However, a suspension of **3** in benzene is stable over a long period. A suspension of **3** in toluene, stirred at 20 °C, decolorizes completely within one day, which we attribute to a radical reaction with the solvent.

[13] With MeOD, 90% D_2 was formed besides 10% HD (determined by mass spectrometry).

[14] The signals of the ^1H NMR spectra of the solutions of **2** and **3** in [D_8]THF (they contain **4**) are broad at −80 °C, and the $CH(SiMe_3)_2$ groups have only about 10–20% of their potential intensity relative to the ether or tmeda signals. With increasing temperature the signals become sharper and increase in intensity, but cannot be interpreted in more detail up to 27 °C. Probably these NMR signals arise from (diamagnetic) decomposition products of the highly reactive (paramagnetic) radical ion in **4**.

[15] Gouy method; temperature range 81–293 K; the magnetic moment is largely temperature-independent. At 293 K, $\mu = 1.85\ \mu_B$.

[16] Spectrometer: Varian E-9; X band, 100 kHz modulation.

[17] This is valid on the assumption that the β-AlCH hyperfine constant a^H can be explained by a hyperconjugation mechanism, and its value is thus dependent on the angle ($a = a_0 + a_1 \cos^2\theta$). C. Heller, H. M. McConnell, *J. Chem. Phys.* **1960**, *32*, 1535.

[18] P. H. Kasai, *J. Am. Chem. Soc.* **1982**, *104*, 1165.

[19] Crystallographic data of **3**: Formula $C_{28}H_{76}Al_2Si_8 \cdot C_{12}H_{32}LiN_4$, $M_r = 930.9$; crystal size $0.35 \times 0.67 \times 0.35$ mm, $a = 12.100(2)$, $b = 13.239(2)$, $c = 22.817(3)$ Å, $\alpha = 106.50(1)$, $\beta = 98.03(1)$, $\gamma = 109.07°$, $V = 3201.5$ Å^3, $\rho_{calcd} = 0.97$ g cm^{-3}, $\mu = 2.16$ cm^{-1}, $F(000) = 1034$, $Z = 2$, crystal system triclinic, space group $P\bar{1}$ (no. 2), Enraf–Nonius CAD4 diffractometer, $\lambda = 0.71069$ Å, $\omega-2\theta$ scan, 19211 measured reflections ($\pm h$, $\pm k$, $+l$), $[(\sin\theta)/\lambda]_{max} = 0.70$ Å^{-1}, 18615 independent and 8437 observed reflections [$I > 3\sigma(I)$], 476 refined parameters, heavy metal method, positions of hydrogens calculated and not included in the least-squares refinement, $R = 0.069$, $R_w = 0.088$ [$w = 1/\sigma^2(F_0)$], maximum residual electron density 0.49 e Å^{-3}; the tmeda molecules are disordered (50:50). Further details of the crystal structure investigation may be obtained from the Fachinformationszentrum Karlsruhe, Gesellschaft für wissenschaftlich-technische Information mbH, D-W-7514 Eggenstein-Leopoldshafen 2 (FRG) on quoting the depository number CSD-56868, the names of the authors, and the journal citation.

[20] Other Al–Al bond lengths: a) metallic aluminum 2.86 Å: W. P. Davey, *Phys. Rev.* **1925**, *25*, 761; b) Al_7Te_{10} 2.60 Å: R. Nesper, J. Curda, *Z. Naturforsch. B* **1987**, *42*, 557; c) $[Al(\eta^5\text{-}C_5Me_5)]_4$ 2.77 Å: C. Dohmeier, C. Robl, M. Tacke, H. Schnöckel, *Angew. Chem.* **1991**, *103*, 594; *Angew. Chem. Int. Ed. Engl.* **1991**, *30*, 564; d) $K_2[Al_{12}tBu_{12}]$ 2.68 Å: W. Hiller, K.-W. Klinkhammer, W. Uhl, J. Wagner, *ibid.* **1991**, *103*, 182 and **1991**, *30*, 179; e) The inter-aluminum distance of 2.56(1) Å found for a Sm_4Al_4 cluster compound was taken by the authors as nonbonding: V. K. Belsky, Y. K. Gun'ko, B. M. Bulychev, G. L. Soloveichik, *J. Organomet. Chem.* **1991**, *420*, 43.

[21] We expected a reductive fission of the Al–Al bond in **1** and formation of two equivalents of $Li^+[Al\{CH(SiMe_3)_2\}_2]^-$, which did not occur.

[22] For $Al_2H_4^-$ a D_{2h} energy minimum is calculated with Al–Al 2.503 Å and H-Al-H 110.3° (MP2/6-31G*) or Al–Al 2.490 Å and H-Al-H 110.7° (MP2/6-31 + G**); for $Al_2H_2^{2-}$ values of 2.465 Å for Al–Al and 106.0° for H-Al-H are obtained (MP2/6-31G*). We thank Prof. Dr. P. von R. Schleyer for these data.

[23] A similar bond possibly also exists in the blue product that arises from the reduction (with alkali metal or electrochemically) of $AlCl_3$ in pyridine. a) R. Köster, G. Benedikt, H. W. Schrötter, *Angew. Chem.* **1964**, *76*, 649; *Angew. Chem. Int. Ed. Engl.* **1964**, *3*, 514; b) H. Lehmkuhl, G. Fuchs, R. Köster, *Tetrahedron Lett.* **1965**, 2511; c) E. Ziegler, G. Fuchs, H. Lehmkuhl, *Z. Anorg. Allg. Chem.* **1967**, *355*, 145.

[24] Uhl et al. arrived at analogous results: W. Uhl, A. Vester, W. Kaim, J. Poppe, *J. Organomet. Chem.*, in press.

[25] H. Klusik, A. Berndt, *Angew. Chem.* **1981**, *93*, 903; *Angew. Chem. Int. Ed. Engl.* **1981**, *20*, 870.

[26] a) A. Moezzi, M. M. Olmstead, P. P. Power, *J. Am. Chem. Soc.* **1992**, *114*, 2715; b) A. Moezzi, R. A. Bartlett, P. P. Power, *Angew. Chem.* **1992**, *104*, 1075; *Angew. Chem. Int. Ed. Engl.* **1992**, *31*, 1082.

[27] E. Kaufmann, P. von R. Schleyer, *Inorg. Chem.* **1988**, *27*, 3987.

Superexchange through Orthogonal Magnetic Orbitals in π-Type Organic Triradicals: Quartet Ground State in Ga(3,5-dtbsq)$_3$**

By *David M. Adams, Arnold L. Rheingold, Andrea Dei,* and *David N. Hendrickson**

The design of molecular ferromagnets is a topic of considerable interest.[1] Paramagnetic building blocks must be connected together in such a way that their magnetic orbitals[2] are effectively orthogonal. This has been achieved with Cu^{II}–V^{IV} chains,[3] polycarbenes,[4] and a Ti^{IV} complex with two tridentate ligands analogous to semiquinone anion.[5] We report here that ferromagnetic exchange interactions between the three *ortho*-semiquinone ligands exist in [Ga(3,5-dtbsq)$_3$] (**1**), where 3,5-dtbsq$^-$ = 3,5-di-*tert*-butyl-1,2-benzosemiquinone anion, a ligand with $S = 1/2$.

Gallium metal (0.570 g) and 3,5-di-*tert*-butyl-1,2-benzoquinone (1.00 g) were added to 50 mL of degassed toluene under an atmosphere of argon. The heterogeneous reaction mixture was refluxed for 3 h. A noticeable color change from the yellow-green of the quinone to the blue-green of the semiquinone was noted. After the mixture was allowed to cool to room temperature and left for 24 h, the excess gallium was filtered off and the mother liquor subjected to slow evaporation under a steady flow of N_2 for two days to give black-green cubic crystals of **1** (0.30 g). The X-ray crystal structure of **1** is shown in Figure 1.[6] The gallium is octahedrally coordinated by three 3,5-dtbsq$^-$ ligands, which are related by a crystallographic C_3 axis. The bond lengths in complexed *ortho*-quinone units are characteristic of the various oxidation states of the ligand.[7] In **1** the C–O distances are 1.271(12) and 1.315(10) Å and the C–C bond length between the chelating oxygen atoms is 1.439(12) Å; all of these indicate that the three ligands are *ortho*-semiquinones. In isostructural [Cr(3,5-dtbsq)$_3$] the C–O distances are 1.280 and 1.299 Å, and the central C–C distance is 1.433 Å.[8]

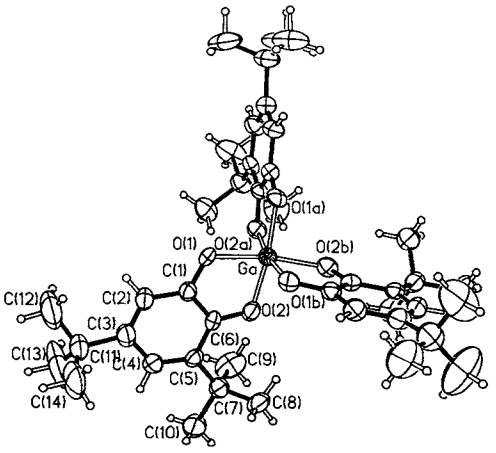

Fig. 1. Crystal structure of **1**. Important bond lengths [Å] and angles [°]: Ga-O(1) 1.963(8), Ga-O(2) 1.992(6); O(1)-Ga-O(2) 82.6(3), O(1)-Ga-O(1a) 92.6(3), O(1)-Ga-O(2a) 95.8(3), O(1)-Ga-O(2b) 170.4(3), O(2)-Ga-O(2a) 89.7. The torsion angle between the GaO_2C_2 planes is 95.7° clockwise around the threefold axis.

Ferromagnetic exchange interactions between 3,5-dtbsq$^-$ ligands in **1** are evident from the magnetic susceptibility data obtained for a polycrystalline sample in a 10.0 kG field (Fig. 2). As the temperature is decreased the effective magnetic moment per molecule increases from 2.95 μ_B at 320 K to a maximum of 3.58 μ_B at 9 K and then drops to 3.26 μ_B at 2 K. The magnetic moment at 320 K is slightly less than the value of 3.00 μ_B expected for three noninteracting, unpaired electrons. There may be a small diamagnetic impurity (the bulk sample smells of toluene). Only the data in the 60–320 K range could be fit to the Curie–Weiss equation with a Curie constant $C = 1.048$ emu K mol^{-1} and $\theta = +8.94$ K. The data from 9 to 320 K were fit by least-squares refinement to the susceptibility expression derived by assuming pairwise magnetic exchange interactions between the three $S = 1/2$ ligands on each complex with the spin Hamiltonian $\hat{H} = -2J\sum\hat{S}_i \cdot \hat{S}_z$. The C_3 site symmetry of **1** dictates one exchange parameter J; this gives one quartet and two accidentally degenerate doublet states. An expression for the molar paramagnetic susceptibility for such a complex is given in Equation (a).

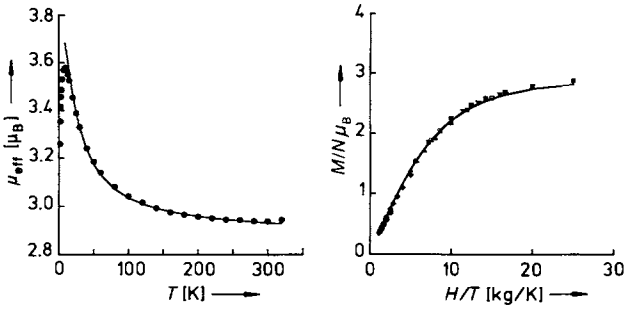

Fig. 2. Left: Plot of effective magnetic moment versus temperature for a polycrystalline sample of **1** in a magnetic field of 10.0 kG. Solid line: theoretical fit of the data in the 9–320 K range. Right: Plot of reduced magnetization, $M/N\mu_B$ (N is Avogadro's number and μ_B is the Bohr magneton), versus H/T. Data were collected at field strengths of 5.00 kG (●), 10.0 kG (♦), 20.0 kg (Δ), 30.0 kG (□), 40.0 kG (▼), and 50.0 kG (■) in the range of 2.0–4.0 K. For measurements at 10.0 and 50.0 kG data were collected in the 2.0–9.0 K range.

$$\chi_M = \frac{Ng^2\beta^2}{4kT}\left[\frac{1 + 5\exp(3J/kT)}{1 + \exp(3J/kT)}\right] \qquad (a)$$

Fitting the susceptibility data to Equation (a) gives $J = 7.8$ cm^{-1} and $g = 1.92$. The solid line in Figure 2 left shows that the data in the 9–320 K range are accommodated by Equation (a). The relatively low g-value reflects the small diamagnetic impurity and does not affect the accurate determination of J. Thus, **1** has a $S = 3/2$ ground state with two $S = 1/2$ states at an energy of 23.4 cm^{-1}.

The $S = 3/2$ ground state was confirmed by variable-field (5.00, 10.0, 20.0, 30.0, 40.0, and 50.0 kG) magnetization data in the 2.0–4.0 K range (Fig. 2). The solid line is a theoretical fit of the data accounting for Zeeman interactions in an isolated $S = 3/2$ state with $g = 1.92$ and where there is no zero-field interaction. This fit was obtained by assuming that only the $S = 3/2$ ground state is thermally populated; on each iteration of the fit the full spin Hamiltonian matrix including the Zeeman interaction was diagonalized. These data clearly indicate a $S = 3/2$ ground state experiencing a small zero-field splitting.

[*] Prof. Dr. D. N. Hendrickson, D. M. Adams, Prof. A. Dei[+]
Department of Chemistry-0506
University of California at San Diego
La Jolla, CA 92093-0506 (USA)
Prof. Dr. A. L. Rheingold
Department of Chemistry, University of Delaware
Newark, DE 19716 (USA)
[+] On sabbatical leave from the Universitá di Firenze, Firenze (Italy).

[**] This work was supported by the U.S. National Science Foundation (CHE-9115286 to D. N. H.).

In order to fit the full range of data collected from 2 to 320 K at a field strength of 10.0 kG it would be necessary to set up the full Hamiltonian matrix for **1** including magnetic exchange, and Zeeman and zero-field interactions and then diagonalize the matrix on each iteration. Such an effort is in progress. Simulations with full-matrix diagonalization of the Hamiltonian for an isolated $S = 3/2$ state show that most of the decrease in μ_{eff}/molecule occurring below 9 K at 10.0 kG is attributable to saturation effects. Thus, at temperatures below 9 K the Zeeman interaction is strong enough so that only the $M_s = -3/2$ component of the $S = 3/2$ state is thermally populated. Comparison with the experimental data suggests there may be very weak intermolecular exchange interactions present, which will be examined in the full report.

The ferromagnetic ligand–ligand interactions in **1** can be rationalized by proposing a dominant ferromagnetic superexchange interaction that is propagated by empty 4p orbitals on the Ga^{III} ion. The magnetic orbital of each semiquinone anion ligand is a π^* antibonding orbital. It is known[7] that the spin density of each unpaired electron is delocalized over each 3,5-dtbsq$^-$ ligand; however, there is little leakage onto the metal ion. A schematic representation of how the three Ga^{III} 4p orbitals interact with the p(π) orbitals on the six oxygen atoms of the three ligands is shown in Figure 3. It is possible to see that the orbital overlap that

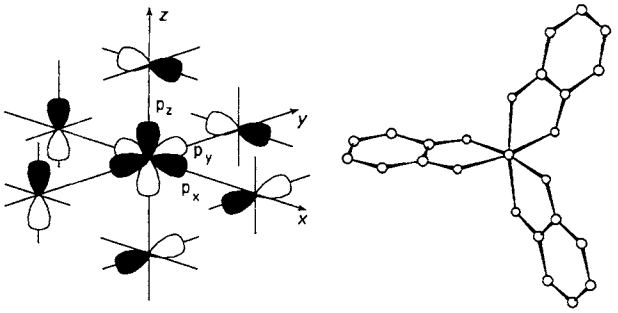

Fig. 3. Schematic drawing showing the overlap of the π^* orbitals of the three 3,5-dtbsq$^-$ ligands containing unpaired electrons with the three 4p orbitals of the Ga^{III} ion. For the ligand π^* orbitals only the 2p orbital contributions from the oxygen atoms are shown.

determines a (3,5-dtbsq$^-$) $\cdots$ (3,5-dtbsq$^-$) exchange interaction is orthogonal if the 4p orbitals of the Ga^{III} ion provide the main superexchange pathway. From the perspective of a configuration interaction, this pathway involves a virtual excited state in which the bridging gallium ion is reduced by the semiquinone anion ligand. This shows that when diamagnetic metal ions are octahedrally coordinated by *ortho*-semiquinone anion ligands paramagnetic building blocks may be assembled so that ferromagnetic spin alignments are maintained.

Received: September 23, 1992 [Z 5593 IE]
German version: *Angew. Chem.* **1993**, *105*, 434

[1] *Magnetic Molecular Materials* (Eds.: D. Gatteschi, O. Kahn, J. S. Miller, F. Palacio), Kluwer, Dordrecht, **1991**.
[2] *Magneto-Structural Correlations in Exchange Coupled Systems* (Eds.: R. D. Willett, D. Gatteschi, O. Kahn), Reidel, Dordrecht, **1985**.
[3] O. Kahn, J. Galy, Y. Journaux, J. Jaud, I. Morgenstern-Badarau, *J. Am. Chem. Soc.* **1982**, *104*, 2165.
[4] a) A. Sugawara, S. Bandow, K. Kimura, H. Iwamura, K. Itoh, *J. Am. Chem. Soc.* **1986**, *108*, 368; b) K. Teki, T. Takui, K. Itoh, H. Iwamura, K. Kobayashi, *ibid.* **1986**, *104*, 2147; c) I. Fujita, Y. Teki, T. Takui, T. Kinoshita, K. Itoh, F. Miko, Y. Sawaki, H. Iwamura, A. Izuoka, T. Sugawara, *ibid.* **1990**, *112*, 4074.
[5] A. Caneschi, A. Dei, D. Gatteschi, *J. Chem. Soc. Chem. Commun.* **1992**, 630.
[6] Crystal data for **1**: $C_{42}H_{60}GaO_6$, $M_r = 730.6$, rhombohedral, $R\bar{3}$, $a = 16.419(2)$, $c = 13.899(3)$ Å, $V = 3244(9)$ Å^3, $Z = 3$, $\rho_{calc} = 1.122$ g cm^{-3}, $\mu(Mo_{K\alpha}) = 6.71$ cm^{-1}, $T = 298$ K. Of 1070 independent reflections collected ($2\theta_{max} = 45^\circ$, Siemens P4 diffractometer, $Mo_{K\alpha}$), 886 were observed ($4\sigma F_0$). Systematic absences in the reflection data supported all of the rhombohedral space groups except for $R3c$ and $R\bar{3}c$. The E-statistics ($|E^2 - 1| = 0.727$) suggested one of the noncentrosymmetric space groups $R3$, $R3m$, or $R32$. As the only anticipated molecular symmetry element was a three-fold rotational axis, the first of the alternatives was chosen initially, and later confirmed by the results of refinement. The structure was solved by a Patterson synthesis. All non-hydrogen atoms were refined with anisotropic thermal parameters, and hydrogen atoms were placed in idealized locations. $R(F) = 0.049$ (0.0631 for all data), $R(wF) = 5.43$ for 148 refined parameters. The maximum/minimum residual electron density was less than ± 0.3 eÅ^{-3}. Further details of the crystal structure investigations are available on request from the Director of the Cambridge Crystallographic Data Center, 12 Union Road, GB-Cambridge CB2 1EZ (UK), on quoting the complete journal citation.
[7] a) C. G. Pierpont, S. K. Larsen, S. R. Boone, *Pure Appl. Chem.* **1988**, *60*, 1331; b) C. G. Pierpont, R. M. Buchanan, *Coord. Chem. Rev.* **1981**, *38*, 45; c) W. Kaim, *Coord. Chem. Rev.* **1987**, *76*, 187.
[8] S. R. Sofen, D. C. Ware, S. R. Cooper, K. N. Raymond, *Inorg. Chem.* **1979**, *18*, 234.

Synthesis and Structure of a Trimeric Cyclometalated Coordination Compound with a Hydrophobic Cavity**

By *Stéphane Rüttimann, Gérald Bernardinelli,* and *Alan F. Williams**

The rapidly developing field of supramolecular coordination chemistry offers synthetic routes to complex molecular structures formed by the combination of structured ligands with cations showing clear stereochemical requirements. Although particular attention has been paid to the synthesis of helical systems[1] and molecular knots,[2] in principle a wide variety of structures may be generated by suitable choice of ligands and metal ions. We report here on the synthesis and structure of a trinuclear complex with a hydrophobic cavity formed by a cyclometalation reaction followed by self-assembly.

Palladium(II) readily undergoes cyclometalation reactions,[3] and cyclometalation of the ligand 1,3-bis(1-methylbenzimidazol-2-yl)benzene mbzimpH **1**[4] could give rise to two products corresponding to the closed system (2-metalation, **2a**) or the open system (6-metalation, **2b**), in which the product possesses a free benzimidazole group which may complex another cation and thereby allow the construction of a larger supramolecular unit. Reaction of **1** with $Pd(OAc)_2$ in acetic acid gives a yellow solution from which a yellow solid **3** may be isolated in 88% yield. The chemical analysis of **3** is consistent with its formulation as the cyclometalated product [Pd(mbzimp)(OAc)], and the ^{1}H NMR spectrum (400 MHz, [D$_6$]DMSO) shows 11 different aromatic protons, confirming the loss of one hydrogen in the cyclometalation reaction, and excluding structure **2a** in which the ligand would be symmetrically coordinated.

[*] Dr. A. F. Williams, Dr. S. Rüttimann
Département de Chemie Minérale, Analytique et Appliquée
Université de Genève
30 quai Ernest Ansermet, CH-1211 Genève 4 (Switzerland)
Dr. G. Bernadinelli
Laboratoire de Cristallographie aux Rayons-X, Université Genève

[**] This work was supported by the Swiss National Science Foundation (Grant No. 20.30139.90).

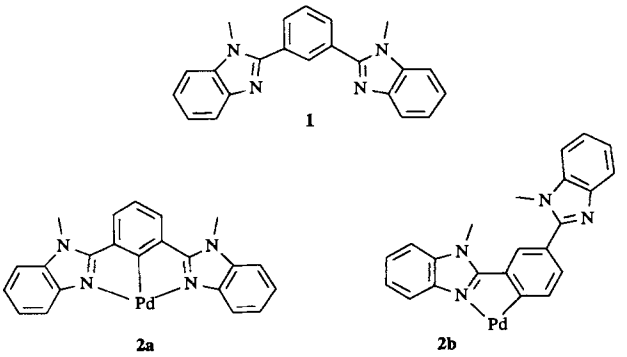

Scheme 1. The ligand mbzimpH **1** and the two possible modes of cyclopalladation: in the 2-position (**2a**) and the 6-position (**2b**).

Crystals of **3** could be grown from acetonitrile solution and were shown by X-ray crystallography to have the composition $[Pd_3(mbzimp)_3(OAc)_3]\cdot 9CH_3CN$, containing the cyclic complex $[Pd_3(mbzimp)_3(OAc)_3]$. This complex may be regarded as a trimer of the 6-metalated product **2b** in which the acetato ligands occupy the fourth coordination site of each palladium atom. The trimer may be described crudely as an equilateral triangle with a palladium atom at each vertex and a ligand making up each side (Fig. 1). The coordination sphere of each palladium atom is approximately square planar and is made up of the N–C chelate ring formed by the cyclometalation reaction, the free benzimidazole group of a second ligand (*trans* to the nitrogen of the chelate ring), and a monodentate acetato ligand (*trans* to the carbon of the chelate ring) (Fig. 2). The four atoms bound to Pd are not perfectly coplanar, but show a slight distortion of approximately 0.1 Å out of the least-squares plane towards a tetrahedral geometry; the palladium atom lies within 0.1 Å of this plane. The Pd–O bonds (average 2.15 Å) are significantly longer than the Pd–C (average 1.98 Å) and Pd–N (2.03 Å) bonds, presumably as a result of the strong *trans* influence of the Pd–C *T* bond. The chelate bite angle (81.1°) and Pd–N and Pd–C bond lengths are comparable to those previously reported for cyclopalladation of 6-phenyl-2,2′-bipyridine.[5] The three palladium sites are essentially identical within experimental error; the greatest deviations are observed for the weakly bound acetato ligands (Table 1).

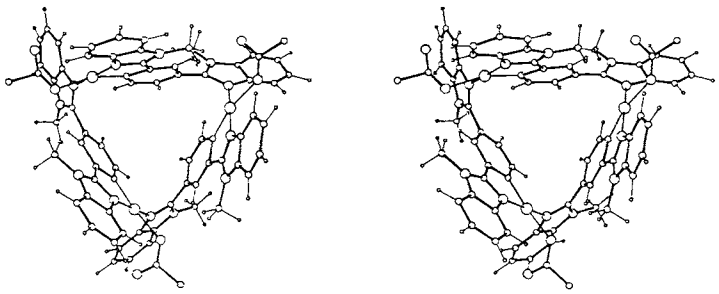

Fig. 1. ORTEP[11] stereoview of the trimer. The guest molecule of acetonitrile has been removed for clarity.

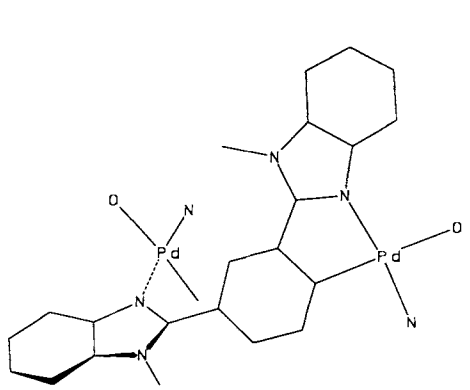

Fig. 2. View of one ligand unit of **3** showing the coordination sphere of the palladium atom and the conformation of the ligand.

Table 1. Structural data for **3**[a].

Parameter	Position A	Position B	Position C	Average
Pd-N1 [Å]	2.00(1)	2.01(2)	2.04(1)	2.02
Pd-C [Å]	1.98(1)	1.99(1)	1.96(1)	1.98
Pd-N2 [Å]	2.02(1)	2.04(1)	2.06(1)	2.04
Pd-O [Å]	2.21(2)	2.12(2)	2.12(1)	2.15
N1-Pd-C [°]	81.0(6)	81.7(7)	80.5(5)	81.1
N1-Pd-N2 [°]	172.0(5)	174.4(5)	174.0(5)	173.5
N1-Pd-O [°]	99.5(6)	95.0(5)	92.7(4)	95.7
C-Pd-N2	91.9(6)	93.2(6)	93.6(5)	92.9
C-Pd-O	165.7(5)	171.9(6)	167.0(5)	168.2
N2-Pd-O	88.3(5)	90.3(5)	93.6(5)	92.9
ligand deviation [Å] [b]	0.19	0.12	0.15	
Pd deviation [Å] [c]	0.11	0.06	0.07	
ph-bzim$_{chelate}$ [°]	1.6(4)	7.5(6)	6.9(5)	5.3
ph-bzim$_{pendant}$ [°]	47.7(5)	49.2(6)	48.5(5)	48.5

[a] N1: nitrogen donor in chelate ring; N2: nitrogen donor of the free benzimidazole unit; ph-bzim$_{chelate}$: angle formed by the planes of the phenyl ring and the benzimidazole unit of chelate ring; ph-bzim$_{pendant}$: angle formed by the phenyl ring and the second benzimidazole unit. [b] Maximum deviation of the four coordinated atoms from the least-squares plane. [c] Deviation of the Pd atom from the least-squares plane of the coordinated atoms.

The benzimidazole and phenyl rings of the ligands show no significant deviations from planarity. The phenyl ring and the benzimidazole unit of the chelate ring are almost coplanar (average angle between planes 5°), while the free benzimidazole is inclined at an average angle of 48.5° toward the phenyl group. The similarity of the three coordination sites and of the three ligand conformations results in a non-crystallographic C_3 symmetry for the trimer, which is chiral, although the enantiomers have not been separated. Figure 1 shows the trimer to possess a cavity at its center, which is occupied in the crystal by an acetonitrile molecule, as shown in the MOLCAD[6] view in Figure 3. The methyl group of the acetonitrile molecule lies at the bottom of the cavity, but the Pd–C_{methyl} distances are all greater than 4 Å, and agostic Pd–H interactions may therefore be excluded.

The apparent specificity for 6-metalation is probably caused by the steric hindrance of the second benzimidazole group; the only available crystal structure of a complex of mbzimpH shows the hydrogen atom on C6 to be closest to the metal ion coordinated to the benzimidazole.[4] Although the tridentate coordination mode arising from 2-metalation would be expected to be more favorable, the second chelate ring can only form after the metalation; if metalation takes place irreversibly at the 6-position, then **2a** will not be formed. The initial product of metalation will thus be **2b**, which possesses a pendant benzimidazole group able to act as a donor and two labile coordination sites on palladium; an oligomerization reaction is therefore possible. The assembly in high yield to give only the trimer presumably results from the rather rigid spatial arrangement of the donor and acceptor sites: **2b** has only one degree of internal freedom,

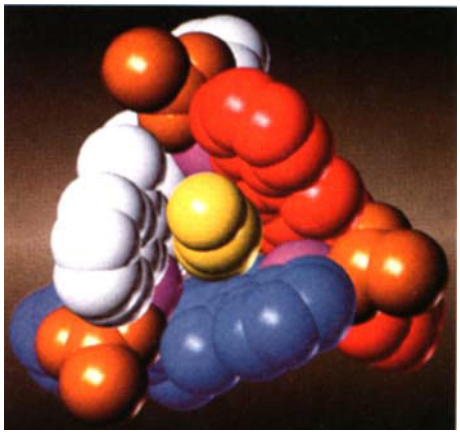

Fig. 3. MOLCAD[6] view of the trimer. The individual three ligand units are colored red, white, and blue respectively, the palladium pink, the acetato ligands brown, and the guest acetonitrile yellow.

that of torsion about the bond joining the phenyl ring and the nonchelating benzimidazole. It should be noted that the pendant benzimidazole occupies the site *trans* to the chelating nitrogen rather than the activated site *trans* to the aromatic carbon atom.

The chiral nature of the cavity in this complex offers the prospect of an interesting host–guest chemistry which is currently being investigated in solution. Further details, including the verification of the trimeric structure in solution, will be published elsewhere.[7]

Experimental Procedure

Palladium(II) acetate[8] and mbzimpH[4] were prepared according to literature methods. A solution of 0.112 g (0.5 mmol) of palladium(II) acetate in acetic acid (5 mL) was added to a solution of 0.169 g (0.5 mmol) of mbzimpH in acetic acid and refluxed for 26 h. The yellow mixture was cooled and filtered to remove a lemon-yellow precipitate (40 mg). The filtrate was evaporated to give 220 mg of **3** as a yellow-green powder (88%). Yellow crystals suitable for X-ray diffraction were obtained by slow evaporation of a solution of **3** in acetonitrile at 40°C. Analysis correct for $PdC_{24}H_{20}N_4O_2$.

A yellow crystal ($0.20 \times 0.20 \times 0.35$ mm) was sealed in a capillary with some of the mother liquor. $M_r = 626$, triclinic, space group $P\bar{1}$, $a = 14.241(2)$, $b = 16.962(2)$, $c = 19.467(4)$ Å, $\alpha = 82.40(1)$, $\beta = 84.73(1)$, $\gamma = 70.94(1)^\circ$ based on 25 reflections ($14^\circ < 2\theta < 26^\circ$), $V = 4400(1)$ Å^3, $Z = 2$. Intensity data were collected at room temperature on a Philips PW100 diffractometer with $Mo_{K\alpha}$ radiation ($\lambda = 0.71069$ Å), $6^\circ < 2\theta < 40^\circ$, 8174 unique reflections measured. Structure solved by direct methods[9], other calculations made using the XTAL system[10] and ORTEP[11] programs. Full matrix refinement was performed successively on a third of the atoms in the asymmetric unit (maximum number of variables = 280). All non-hydrogen atoms other than solvent molecules were refined with anisotropic thermal displacement parameters. One carbon atom of one of the nine solvent molecules could not be located. Final R factor = 0.072 ($R_w = 0.050$, $w = 1/\sigma^2(F_o)$), for 5704 observed reflections ($|F_o| > 4\sigma(F_o)$). Further details of the crystal structure investigation are available on request from the Director of the Cambridge Crystallographic Data Centre, 12 Union Road, GB-Cambridge CB2 1EZ (UK) on quoting the full journal citation.

Received: August 31, 1992 [Z 5546 IE]
German version: *Angew. Chem.* **1993**, *105*, 432

[1] J.-M. Lehn, A. Rigault, J. Siegel, J. MacB. Harrowfield, B. Chevrier, D. Moras, *Proc. Natl Acad. Sci. USA* **1987**, *84*, 2565; J.-M. Lehn, A. Rigault, *Angew. Chem.* **1988**, *100*, 1121; *Angew. Chem. Int. Ed. Engl.* **1988**, *27*, 1095; E. C. Constable, M. D. Ward, *J. Am. Chem. Soc.* **1990**, *112*, 1256; A. F. Williams, C. Piguet, G. Bernardinelli, *Angew. Chem.* **1991**, *103*, 1530; *Angew. Chem. Int. Ed. Engl.* **1991**, *30*, 1490.

[2] J.-P. Sauvage, *Acc. Chem. Res.* **1990**, *23*, 319; C. O. Dietrich-Buchecker, J. Guilhem, C. Pascard, J.-P. Sauvage, *Angew. Chem.* **1990**, *102*, 1202; *Angew. Chem. Int. Ed. Eng.* **1990**, *29*, 1154.

[3] A. D. Ryabov, *Chem. Rev.* **1990**, *90*, 403.

[4] S. Rüttimann, C. Piguet, G. Bernardinelli, B. Bocquet, A. F. Williams, *J. Amer. Chem. Soc.* **1992**, *114*, 4230.

[5] E. C. Constable, R. P. G. Henney, T. A. Leese, D. A. Tocher, *J. Chem. Soc. Chem. Commun.* **1990**, 513.

[6] J. Brickmann, MOLCAD molecular modeling package, Technische Hochschule, Darmstadt (FRG), **1990**.

[7] R. F. Carina, A. F. Williams, unpublished.

[8] R. F. Heck: *Palladium Reagents in Organic Synthesis*, Academic Press, London, **1985**, p. 17.

[9] P. Main, S. J. Fiske, S. E. Hull, L. Lessinger, G. Germain, J.-P. Declercq, M. M. Woolfson *MULTAN 87*, Universities of York, Great Britain, and Louvain, Belgium, **1987**.

[10] *XTAL 3.0 User's Manual* (Eds.: S. R. Hall, J. M. Stewart), Universities of Western Australia and Maryland, **1990**.

[11] C. K. Johnson, ORTEPII Report ORNL-5138, Oak Ridge National Laboratory, Tennessee, USA, **1976**.

Stereodivergent Enantioselective Synthesis by Exploiting Unusually Large Kinetic H/D Isotope Effects on Deprotonation**

By *Dieter Hoppe,** *Mario Paetow,* and *Folker Hintze*

We report here a new strategy in enantioselective synthesis that is based on the discrimination by a base between protons and deuterons in an otherwise identical chemical environment. Primary kinetic H/D isotope effects on the deprotonation of C–H acids usually fall within the range $k_H/k_D = 2-7$.[1] Only in exceptional cases are higher values obtained, which are attributed to the participation of quantum mechanical tunnel effects.[2] For example, for the deprotonation of 2-nitropropane with 2,6-dimethylpyridine a value of $k_H/k_D = 24$ is given.[3] The larger effective radius predicted by the Heisenberg Uncertainty Principle for the lighter proton should be particularly noticeable as a pronounced isotope effect at low temperature, for sterically shielded centers, and in aprotic media.

In an attempt to lithiate the (*S*)-(1-deuterioethyl) carbamate (*S*)-**3**, prepared by the deprotonation of **1** with *sec*-butyllithium/(−)-sparteine[4, 5] in ether (4 h, −78 °C) and subsequent deuteration with [D$_1$]methanol, for a second time under the same conditions, we noticed that the reaction was extremely slow: the product (*S*)-**5**, anticipated on capture of the lithium carbanion (*S*)-**2** with chlorotrimethylsilane, was obtained in only 6% yield, while the sample of (*S*)-**5** prepared in the same manner from **1** was formed in 86% yield and greater than 96% *ee*[6] (Scheme 1).[7, 8] Since the deuterium atom in (*S*)-**3** occupies a sterically more favorable position than the 1-H atom for abstraction by the chiral base,[9] the low rate of the reaction has its origin in an unusually high isotope effect.

In the next experiment the configurational restraint was removed by treating (*S*)-**3** (> 99% D)[10] in the presence of the achiral complex-forming agent *N*,*N*,*N*′,*N*′-tetramethylenediamine (TMEDA) instead of (−)-sparteine. The isotope effect alone then determined the rate of the abstraction of 1-H and 1-D in (*S*)-**3**, and the product (*R*)-**7** was obtained with greater than 95% *ee*[6, 7] after silylation. The content of 1-H was 1.3%.[11] Therefore the quotient k_H/k_D

[*] Prof. D. Hoppe
Organisch-chemisches Institut der Universität
Corrensstrasse 40, D-W-4400 Münster (FRG)
M. Paetow, F. Hintze
Institut für Organische Chemie der Universität Kiel

[**] This work was supported by the Fonds der Chemischen Industrie and the Deutsche Forschungsgemeinschaft.

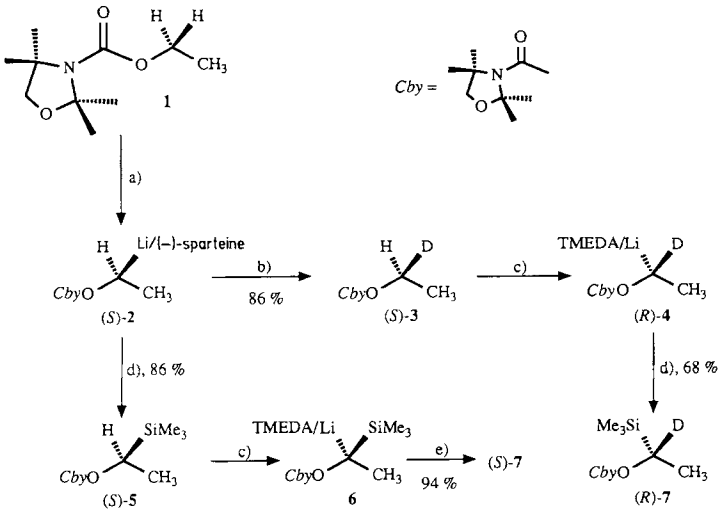

Scheme 1. a) 1.4 equiv *s*BuLi/(−)-sparteine, ca. 0.2 M in ether, −78 °C, 4 h; b) 1.6 equiv CH_3OD at −78 °C; c) 1.4 equiv *s*BuLi/TMEDA, −78 °C, 4 h; d) 1.6 equiv Me_3SiCl at −78 °C; e) 1.6 equiv CH_3COOD at −78 °C.

must be at least 70. For comparison, the enantiomer (*S*)-**7** was formed on deprotonation and deuterolysis of the isotopomer (*S*)-**5** via the anion (*S*)-**6** (95% *ee*).[7, 12–14]

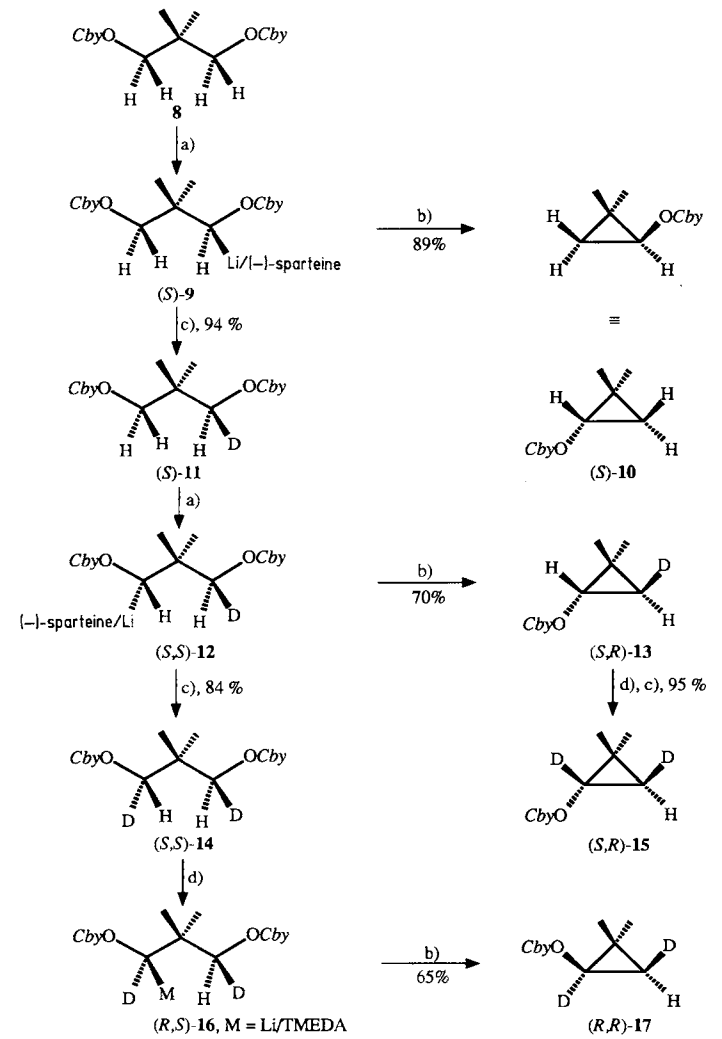

Scheme 2. a) 2.0 equiv *s*BuLi/(−)-sparteine, in ether, −78 °C, 2.5 h; b) 2.2 equiv Me_3SiCl at −78 °C; c) 3.0 equiv CH_3OD at −78 °C; d) 2.0 equiv *s*BuLi/TMEDA, −78 °C, 2.5 h, in ether.

Propanediyl dicarbamates such as **8**[15] bear two homotopic methylene groups each with enantiotopic protons (Scheme 2). In a series of experiments we demonstrate how the achiral starting material **8** can be used for the synthesis of almost enantiomerically pure, specifically deuterated cyclopropanes. The (−)-sparteine complex (*S*)-**9**, generated in the usual way,[15] reacts under the influence of chlorotrimethylsilane by 1,3-elimination to form cyclopropyl carbamate (*S*)-**10**,[15, 16] while deuterolysis yields the labeled dicarbamate (*S*)-**11** (97% D_1).[17] The second deprotonation of (*S*)-**11**, followed by cyclization, affords the *trans*-cyclopropane (*S,R*)-**13**[16] with 97% *ee*[18] and 96.1% D.[17] After the correction for the original degree of deuteration, the ratio of the lithiation of the 3-CH_2 to the 1-CHD group in (*S*)-**11**, which gives (*S,S*)-**12** and (*S*)-**9**, respectively, is calculated to be about 70:1. (*S,R*)-**13** was converted into the deuteriocyclopropane (*S,R*)-**15**[16] by lithiation and deuterolysis (93% D_2).[17] The epimer (*R,R*)-**17**[16] (96.1% D_2)[17] is distinguished from (*S,R*)-**15** only in the configuration of the isotope pattern; we synthesized it by deuterolysis of (*S,S*)-**12** to give (*S,S*)-**14** (96.7% D_2)[17] followed by TMEDA-assisted lithiation and subsequent 1,3-cycloelimination. (*S,R*)-**15** and (*R,R*)-**17** have the same numerical value for the optical rotation, but opposite signs.[16]

We have therefore discovered a simple method for the stereodivergent synthesis of almost enantiomerically pure and stereospecifically labeled alcohol derivatives. It is based on the following prerequisites, which are excellently fulfilled in the chosen system:

1. possibility of generating the carbanion by deprotonation at low temperature,
2. large H/D isotope effects, amplified by tunneling,
3. configurational stability of the carbanionic intermediate.

General Experimental Procedure

(See also the legends to the schemes.)

To a stirred solution of (−)-sparteine (1.4 equiv) or TMEDA (2.0 equiv) in ether (10 mL) at −70 to −78 °C was injected a solution of *s*BuLi in cyclohexane/isopentane (1.4 N, 2.0 equiv); the solution was treated at this temperature with the carbamate (2 mmol) dissolved in ether (2–4 mL) and stirred for 4 h (2.5 h for TMEDA) below −70 °C. Thereafter the required amount of CH_3OD, Me_3SiCl, or CH_3COOD was added, and the solution was stirred for 24 h, while it warmed to room temperature. After an aqueous workup, the product was purified by chromatography on silica gel (ether/pentane)[4].

Received: October 22, 1992 [Z 5636 IE]
German version: *Angew. Chem.* **1993**, *105*, 430

[1] Reviews: a) G. Lamaty in *Isotopes in Organic Chemistry, Vol. 2* (Eds.: E. Buncel, C. C. Lee), Elsevier, Amsterdam, **1976**, p. 33; b) K. T. Leffek, *ibid.* p. 89.

[2] Reviews: a) P. P. Bell, *The Tunnel Effect in Chemistry*, Chapman and Hall, London, **1980**; b) L. B. Sims, D. E. Lewis in *Isotopes in Organic Chemistry, Vol. 6* (Eds.: E. Buncel and C. C. Lee), Elsevier, Amsterdam **1984**, p. 161.

[3] E. S. Lewis, L. H. Funderburk, *J. Am. Chem. Soc.* **1967**, *89*, 2322, and references therein.

[4] a) F. Hintze, P. Tebben, D. Hoppe, *Angew. Chem.* **1990**, *102*, 1457; *Angew. Chem. Int. Ed. Engl.* **1990**, *29*, 1422; b) F. Hintze, D. Hoppe, *Synthesis* **1992**, 1216; c) J. Schwerdtfeger, D. Hoppe, *Angew. Chem.* **1992**, *104*, 1547; *Angew. Chem. Int. Ed. Engl.* **1992**, *31*, 1505.

[5] Short review: P. Knochel, *Angew. Chem.* **1992**, *104*, 1486; *Angew. Chem. Int. Ed. Engl.* **1992**, *31*, 1459.

[6] Determined by ^1H NMR spectroscopy (300 MHz) in the presence of 3.3 mol% of tris[3-(heptafluoropropylhydroxymethylene)-(+)-camphorato]praseodymium(III). Because of line broadening a more precise value cannot be obtained.

[7] $[\alpha]_D^{19}$: (*S*)-**5** −26.6 (c = 1.7, CH_2Cl_2), (*R*)-**7** + 26.0 (c = 1.2, CH_2Cl_2); $[\alpha]_D^{16}$: (*S*)-**7** −27.4 (c = 1.1, CH_2Cl_2).

[8] At the same time this finding presents the proof for the following assumptions: The selection by the chiral base system *s*Bu/(−)-sparteine is kinetically controlled. The incoming deuteron takes up the position of the abstracted proton as a result of double stereoretention and the configurational stability of the carbanion.

[9] For all the deprotonations of the achiral alkyl carbamates assisted by (−)-sparteine observed till now, a strong preference for the selection of the *pro-S*-proton was noticed [4, 5, 15].
[10] A complete monodeuteration (> 99% D_1, determined by mass spectrometry) was achieved by performing the procedure twice.
[11] Determined by ^1H NMR spectroscopy (300 MHz).
[12] Degree of deuteration 98.4% (^1H NMR, 300 MHz). Some of the product (*S*)-**7** decomposed on use of CH_3OD. Yield 55–58%.
[13] This is also the first proof of a configurationally stable 1-oxy-1-silyl carbanion persisting in solution [14].
[14] For former experimental indications of a slow rate of enantiomerization of racemic 1-methoxy-1-trimethylsilylmethyllithium, see: G. Schmid, W. Hofheinz, *J. Am. Chem. Soc.* **1983**, *105*, 624.
[15] a) M. Paetow, H. Ahrens, D. Hoppe, *Tetrahedron Lett.* **1992**, *33*, 5323; b) H. Ahrens, M. Paetow, D. Hoppe, *ibid.* **1992**, *33*, 5327.
[16] (*S*)-**10**: 300 MHz ^1H NMR ($CDCl_3$): $\delta = 3.75$ (dd, 1-H_1), 0.66 (dd, $^2J(H,H) = 6.1$ Hz, $^3J(H,H$; *trans*$) = 3.4$ Hz, $^3J(H,H$; *cis*$) = 6.7$ Hz, 3-H_1), 0.50 (dd, 3-H_1); $[\alpha]_D^{20}$ +9.2 ($c = 1.0$, acetone); (*S,R*)-**13**: 200 MHz ^1H NMR ($CDCl_3$): $\delta = 3.75$ (d, $^3J(H,H$; *trans*$) = 3.3$ Hz, 1-H_1), 0.48 (0.45) (d, 3-H_1); $[\alpha]_D^{23}$ +11.8 ($c = 1.0$, acetone); (*S,R*)-**15**: 200 MHz ^1H NMR ($CDCl_3$): $\delta = 0.48$ (0.46) (s, 3-H_1); $[\alpha]_D^{20}$ +7.0 ($c = 1.1$, ether); (*R,R*)-**17**: 300 MHz ^1H NMR ($CDCl_3$): $\delta = 0.64$ (s, 3-H_1); $[\alpha]_D^{20}$ −6.9 ($c = 1.1$, ether).
[17] Determined by GC-MS, chemical ionization with NH_3 and integration over the whole peak area. We thank Dr. F. Luftmann, Münster, for these measurements.
[18] Determined by ^1H NMR spectroscopy in the presence of tris[3-(heptafluoropropylhydroxymethylene)-(+)-camphorato]europium(III) (5.3 mol-%) after conversion into the corresponding methyl 1-carbamoyloxy-1-cyclopropanecarboxylate via the configurationally stable 1-anion of (*S,R*)-**13**.

under argon, **3** is obtained. This is the pathway followed by the reduced species **2** in the absence of an appropriate concentration of N_2. The reduction of **1** in presence of N_2 produces **6** nearly quantitatively (97%). The stepwise formation of **6** through the intermediacy of the ion pair **4** and complex **5** is suggested mainly by the product from the reduction with potassium.

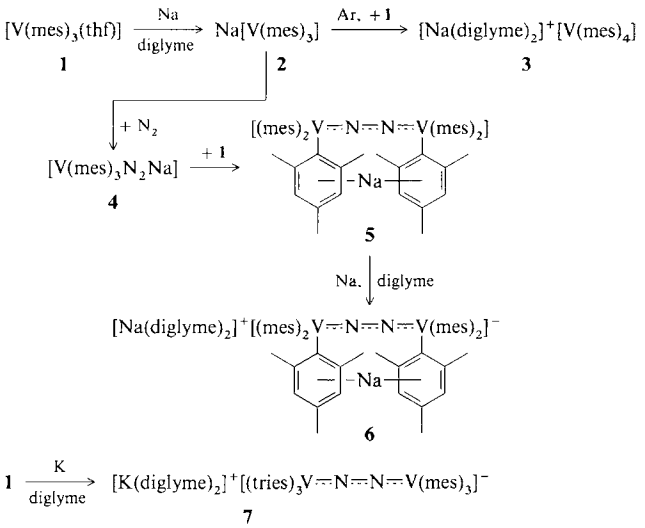

Scheme 1. Reduction of **1** with sodium and potassium. diglyme = $MeOCH_2CH_2OCH_2CH_2OMe$.

Fixation and Reduction of Dinitrogen by Vanadium(II) and Vanadium(III): Synthesis and Structure of Dinitrogenmesitylvanadium Complexes**

By *Richard Ferguson, Euro Solari, Carlo Floriani,* Angiola Chiesi-Villa*, and *Corrado Rizzoli*

Reduction of homoleptic alkyl- and arylmetal compounds should produce very reactive low-valent, bifunctional ion pairs, having exclusively σ-donor ligands incapable of accommodating electron density from the metal. With this in mind we approached dinitrogen activation by early transition metals. This is a preliminary report on vanadium–nitrogen chemistry, which is a field of major interest for several reasons: 1) The first widely known bifunctional system for converting N_2 into NH_3 and N_2H_4 is based on a V^{II}/Mg^{II} system;[1, 2] 2) a vanadium-containing nitrogenase was recently discovered;[3] 3) vanadium model compounds in this area are very rare.[4] Some significant precedents in the use of low-valent homoleptic aryliron compounds in dinitrogen reduction exist, though no dinitrogeniron species has been clearly identified.[5]

The results on reductions of $[V(mes)_3(thf)]$ (**1**)[6] [mes = 2,4,6-$Me_3C_6H_2$] by alkali metals are summarized in Scheme 1. When the reaction of **1** with Na is carried out

With potassium the reaction affords complex **7** in good yield (68%). Reduction of **7** with sodium did not give the complex analogous to **6** as expected. Also, when the reduction of **1** is carried out with only 0.5 equivalents of Na, the product is still **6**. The sodium ion pair **4** is expected to be much more stable than an analogous potassium intermediate in presence of oxygen donors (e.g. diglyme), and the reduction of the neutral species **5** much easier than the reduction of the anion in **7**.

Some of the hypotheses outlined above have been greatly supported by the X-ray analysis on **3**, **6**, and **7**. Structural details are reported only for the anion in complex **6** (Fig. 1).[7] The anion has an imposed crystallographic C_2 symmetry. The V–N distance [1.763(15) Å] is very short and shows multiple-bond character, while the N–N bond [1.280(21) Å] is significantly longer than the N–N bond in free dinitrogen [1.0968 Å]. The bond lengths of all the V–N_2 complexes reported[4] to date, including **6** and **7**, should be compared, since these few complexes represent a series where dinitrogen is either simply coordinated to the metal, or significantly polarized or reduced by the metal.[4] The sodium cation is inserted into a cavity formed by two bent phenyl rings and the dinitrogen molecule. A close resemblance exists between the structure of **6** and the intermediate in the V^{II}/Mg^{II} system proposed by Shilov.[1] The structural parameters of **7**[8] are very close to those of **6**, and strongly support a significant degree of reduction of N_2.

The magnetic properties of **6** and **7** are unexpected[4c, 9] and give information on the degree of reduction of N_2 and the formal oxidation state of the metal. Coordination of N_2 usually does not change the magnetic properties of the original vanadium ion;[4c] however, in complexes **6** and **7** the magnetic moments do not correspond to a pair of d^3–d^3

[*] Prof. Dr. C. Floriani, Dr. R. Ferguson, Dr. E. Solari
Section de Chimie, Université de lausanne
Place du Château 3, CH-1005 Lausanne (Switzerland)
Prof. Dr. A. Chiesi-Villa, Dr. C. Rizzoli
Istituto di Strutturistica Chimica
Centro di Studio per la Strutturistica Diffrattometrica del CNR
Università di Parma

[**] This work was supported by the Fonds National Suisse de la Recherche Scientifique (Grant No. 20-28470.90) and Ciba-Geigy SA (Basel, Switzerland). Professor C. Fiorani (I. T. S. E., Rome, Italy) is acknowledged for carrying out the magnetic measurements.

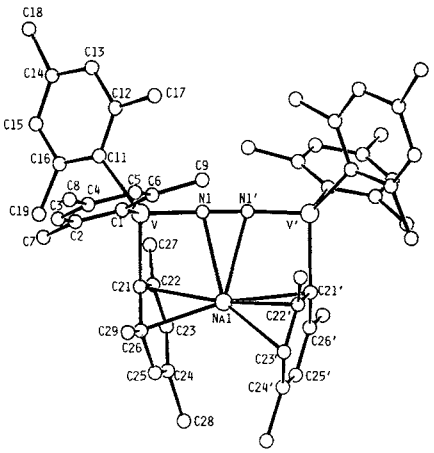

Fig. 1. A view (SCHAKAL) of the anion in complex **6**. Selected bond lengths [Å] and angles [°]: V-C1 2.131(15), V-C11 2.176(17), V-C21 2.179(17), V-N1 1.763(15), N1-N1′ 1.280(21), Na1-N1 2.55(3), Na1-N1′ 2.63(3), Na1-C21 2.59(4); Na1-C26 2.49(4), Na1-C21′ 2.50(4), Na1-C22′ 2.35(4), Na1-C23′ 2.56(3); C11-V-C21 118.5(7), C1-V-C21 114.7(7), C1-V-C11 106.2(7), N1-V-C21 91.5(7), N1-V-C11 119.2(8), N1-V-C1 106.1(11), V-N1-N1′ 174.1(25). Symmetry transformation: ′ = − x, y, −1/2 − z. The disordered Na1′ position has been omitted for clarity.

(complex **6**) or a d^3–d^2 (complex **7**) ions. Complex **6** (magnetic moment of 1.69 BM per vanadium at 293 K) has two unpaired electrons while **7** (μ_{eff} of 1.83 BM at 293 K) contains a single unpaired electron per two vanadium atoms. These reduced magnetic moments can be the consequence of either a strong electronic coupling of the two vanadium atoms through the N_2 bridge or a change in the oxidation state of vanadium. That the electron density on the N_2 unit is increased is additionally supported by the results from its protonation in **6** and **7**. The reaction of **6** with 0.1 M HCl (see Experimental Procedure) gave reproducible results which revealed on average of 49% N_2, 36% N_2H_4, and 11% NH_3, as decomposition products from the bridging N_2 unit, whereas with **7** the results were 70% N_2, 22% N_2H_4, and 7% NH_3.[10]

Experimental Procedure

3: A large excess of Na sand (0.430 g, 18.7 mmol) was added to a solution of **1** (4.089 g, 8.49 mmol) in diglyme (200 mL) under argon, and stirred for two hours. The brown filtrate was concentrated under vacuum to 50 mL to give, upon cooling to 0 °C, a microcrystalline solid that was recrystallized from hot diglyme. Correct elemental analysis for $C_{48}H_{72}NaO_6V$, $\mu_{eff} = 2.84$ BM at 293 K.

6: Diglyme (200 mL) and **1** (3.277 g, 6.82 mmol) were combined in a 1000 mL round-bottomed flask. The mixture was cooled to −5 °C, and then solid Na spheres (av. diameter 1.2 mm) (0.142 g, 6.18 mmol) were added. This mixture was stirred vigorously under 1–2 atm N_2 in a closed system for 14 h at −5 °C, then for 4 hr at room temperature. The black microcrystalline substance (97%, extremely air- and water-sensitive, pyrophoric) was recrystallized from benzene at about 60 °C. Correct elemental analysis for $C_{72}H_{100}N_2Na_2O_6V_2$. The N_2 content of **6** determined by reaction with iodine in THF was 98% of the expected value.

7: The procedure for **6** was used for the preparation of **7**, with 100 mL of diglyme, 4.29 g (8.92 mmol) of **1**, and a single ball of potassium (0.42 g, 10.8 mmol, excess recovered at end) (yield 68%). Correct elemental analysis for $C_{66}H_{94}KN_2O_6V_2$. The N_2 content determined as for **6** was 95% of the expected value.

Reaction of **6** and **7** with HCl: A 250 mL round-bottomed flask was charged with 0.1 M HCl (100 mL), and then degassed with N_2. A thin glass vial containing the sample (0.5–1.0 g) was placed in the flask, and the flask connected to a device for measuring gas evolution. The vial was broken by stirring and the volume of N_2 evolved measured. The solution containing decomposition products (typically light-blue) was filtered to remove bits of glass. The solution was analyzed spectrophotometrically for NH_2NH_2 on addition of Kovac's reagent [11] at μ = 42 nm and as a check at μ = 482 nm. The mixture was then distilled over KOH into a flask containing 0.1 M HCl. This distillation eliminated NH_2NH_2, while liberating NH_3. The distillate was analyzed spectrophotometrically for NH_3 after addition of Nessler's reagent [12] at μ = 524 nm.

Received: October 29, 1992 [Z 5656 IE]
German version: *Angew. Chem.* **1993**, *105*, 453

[1] N. T. Denisov, O. N. Efimov, N. I. Shuvalova, A. K. Shilova, A. E. Shilov, *Zh. Fiz. Khim.* **1970**, *44*, 2694; A. E. Shilov, D. N. Denisov, O. N. Efimov, N. F. Shuvalov, N. I. Shuvalova, A. E. Shilova, *Nature (London)* **1971**, *231*, 460; N. P. Luneva, L. A. Nikonova, A. E. Shilov, *Kinet. Katal.* **1980**, *21*, 1041.

[2] S. I. Zones, T. M. Vickery, J. G. Palmer, G. N. Schrauzer, *J. Am. Chem. Soc.* **1976**, *98*, 1289; G. N. Schrauzer, N. Strampach, L. A. Hughes, *Inorg. Chem.* **1982**, *21*, 2184; G. N. Schrauzer, M. R. Palmer, *J. Am. Chem. Soc.* **1981**, *103*, 2659; S. I. Zones, M. R. Palmer, J. G. Palmer, J. G. Doemeny, G. N. Schrauzer, *ibid.* **1978**, *100*, 2113.

[3] P. E. Bishop, D. M. L. Jarlenski, D. R. Hetherington, *J. Bacteriol.* **1982**, *150*, 1244; R. L. Robson, R. R. Eady, T. H. Richardson, R. W. Miller, M. Hawkins, J. R. Postgate, *Nature (London)* **1986**, *322*, 388; J. M. Arber, B. R. Dobson, R. R. Eady, P. Stevens, S. S. Hasnain, C. D. Garner, B. E. Smith, *ibid.* **1986**, *325*, 372; G. N. George, C. L. Coyle, B. J. Hales, S. P. Cramer, *J. Am. Chem. Soc.* **1988**, *110*, 4057; J. E. Morningstar, B. J. Hales, *ibid.* **1987**, *109*, 6854.

[4] a) D. Rehder, C. Woitha, W. Priebsch, H. Gailus, *J. Chem. Soc. Chem. Commun.* **1992**, 364; b) C. Woitha, D. Rehder, *Angew. Chem.* **1990**, *102*, 1495; *Angew. Chem. Int. Ed. Engl.* **1990**, *29*, 1438; c) J. J. H. Edema, A. Meetsma, S. Gambarotta, *J. Am. Chem. Soc.* **1989**, *111*, 6878; d) G. J. Leigh, R. Prieto-Alcón, J. R. Sanders, *J. Chem. Soc. Chem. Commun.* **1991**, 921.

[5] Some significant precedents in the use of low-valent homoleptic aryl iron compounds in dinitrogen reduction exist, though no dinitrogen iron species has yet been clearly identified: a) A. E. Shilov, *New J. Chem.* **1992**, *16*, 213 and references therein. b) T. A. Bazhenova, L. M. Kachapina, A. E. Shilov, *J. Organomet. Chem.* **1992**, *428*, 107; c) A. E. Shilov in *Perspectives in Coordination Chemistry* (Eds.: A. F. Williams, C. Floriani, A. Merbach), VCH, Weinheim, **1992**, p. 233.

[6] S. Gambarotta, C. Floriani, A. Chiesi-Villa, C. Guastini, *J. Chem. Soc. Chem. Commun.* **1984**, 886.

[7] Crystal structure analysis of **6**, $C_{54}H_{66}N_2NaV_2 \cdot C_{12}H_{28}NaO_6 \cdot C_6H_6$, M = 1237.5, orthorhombic, space group $C222_1$, a = 11.823(4), b = 21.651(2), c = 28.696(6) Å, V = 7346(3) Å^3, Z = 4, ρ_{calcd} = 1.119 g cm^{-3}, $Cu_{K\alpha}$ radiation (λ = 1.54178 Å), $\mu(Cu_{K\alpha})$ = 26.24 cm^{-1}, crystal dimensions 0.16 × 0.26 × 0.35 mm. For 851 unique observed structure amplitudes [$I > 2\sigma(I)$] collected on a Rigaku AFC6S diffractometer in the range $5 < 2\theta < 120°$, corrected for absorption, the current R value is 0.081 (R = 0.093 for the incorrect enantiomorph). The structure was solved by the heavy atom method. The low percentage of observed reflections and the consequent low accuracy of the analysis could be related to the intrinsic low scattering power of the crystal due to the presence of three different molecular species. Only vanadium, nitrogen, oxygen, and non-disordered sodium atoms [Na(2)] were allowed to vary anisotropically. Na(1) was found to be statistically distributed over two positions about a twofold axis. All hydrogen atoms were placed in calculated positions prior the last stage of refinement (U_{iso} = 0.12 Å^2). The collection of the Friedel's pairs would have given a better overdetermination ratio and smaller esd.'s for all parameters. However, the presence in the structure of an element (vanadium) showing a remarkable dispersive effect with the $Cu_{K\alpha}$ wavelength enables the determination of the absolute configuration with a high degree of confidence, as indicated by the final R factors resulting from the refinement carried out on the enantiomers: R = 0.081, R_G = 0.083 for one and R = 0.093, R_G = 0.094 for the other. (W. C. Hamilton, *Acta Crystallogr.* **1965**, *18*, 502). All calculations were carried out with SHELX-76. Further details of the crystal structure investigation are available on request from the Director of the Cambridge Crystallographic Data Centre, 12 Union Road, GB-Cambridge CB2 1EZ (UK), on quoting the full journal citation.

[8] Preliminary results from an X-ray analysis on **7**.

[9] a) J. Chatt, J. R. Dilworth, R. L. Richards, *Chem. Rev.* **1978**, *78*, 589, and references therein; b) R. A. Henderson, J. Leigh, C. J. Pickett, *Adv. Inorg. Radiochem.* **1983**, *27*, 197; c) *New Trends in the Chemistry of Nitrogen Fixation* (Eds.: J. Chatt, L. M. da Camara Pina, R. L. Richards), Academic, New York, **1980**.

[10] For the protonation of metal-bonded dinitrogen see: G. J. Leigh, *Acc. Chem. Res.* **1992**, *25*, 177 and references therein. See also [1], [2], [4 a,d], and [5c].

[11] L. C. Thomas, G. J. Chamberlain, *Colorimetric Chemical Analytical Methods*, 9th ed., Wiley, New York, **1980**, p. 193.

[12] *Vogel's Textbook of Quantitative Chemical Analysis*, 5th ed., Longman, London, **1989**, p. 679.

Stereoselective Protonation of Boron Enolates**

By *Thomas Haubenreich, Siegfried Hünig,** and *Hans-Joachim Schulz*

In most enantioselective protonations of formal carbanions a chiral protonic acid HX* attacks a prochiral C atom.[1] Noncovalent interactions between the substrate, which occur in the unknown, strongly variable ion aggregates, and HX* have a decisive influence on the (diastereomeric) transition states, and thus on the stereochemical course of the protonation. On the one hand, numerous possibilities exist which can influence the outcome of the protonation (temperature, choice of solvent, additives, and auxiliaries, etc.), on the other hand, the lack of knowledge about the true nature of the reacting aggregate necessitates a great deal of experience when carrying out the experiment.

Thus, we decided to extend the stereoselective protonation to enol derivatives of the type **A** according to the principle formulated in Scheme 1. As a first example we describe the

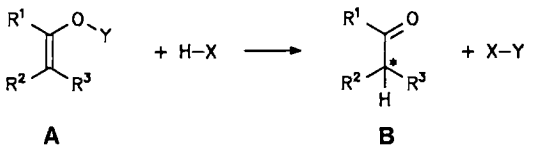

Scheme 1. Stereoselective protonation of the enol derivatives **A**. X and/or Y are chiral.

protonation of **A**, with the loss of a chiral auxiliary Y*, by achiral proton sources. For this we generated the boron enolates **3** and **4** in situ from *rac*-**1** and *rac*-**2** (Scheme 2).

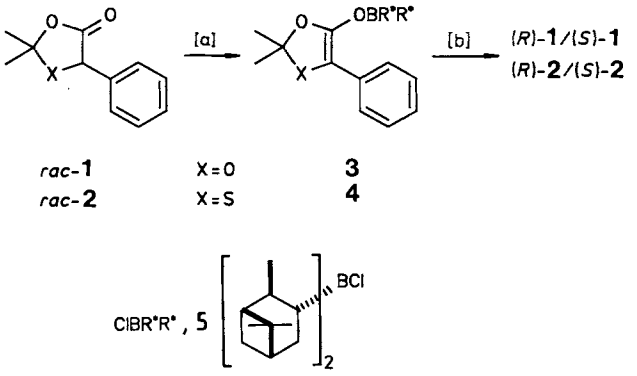

Scheme 2. [a] 1. lithium hexamethyldisilazane (0.2 mmol), THF, 30 min, −40 to −50 °C; 2. ClBR*R* **5** (0.3 mmol) 2–3 min, −70 °C. [b] 1. addition, 30 min, −70 °C; 2. HX (0.4 mmol), 30 min, −70 °C; 3. AcOH or TFA (0.2 mL), −70 °C.

A boron-containing auxiliary should be able to bind (achiral) OH and NH acids coordinatively, and thus generate a defined, though transient compound between substrate and proton source. With a similar approach stereoselective C–C couplings between enol borates[2] as well as enol borinates[3] and carbonyl compounds have been well established. As a model for the planned protonations we chose chiral boron enolates, produced from commercially available (−)-*B*-chlorodiisopinocampheylborane (**5**) and ketones, which undergo stereoselective aldol reactions.[3a]

For **1** and **2**, however, it was not possible to produce the boron enolates **3** and **4** by direct reaction with **5** and the aid of tertiary amine. This commonly used method fails if the proton abstraction should occur at a tertiary carbon atom.[4] In contrast, the roundabout way via the lithium or potassium enolates of **1** and **2** was successful. Their reaction with **5** at approximately −50 °C yielded the desired chiral boron enolates, which were protonated in situ with the acids listed in Table 1.

Table 1. Protonations of the boron enolate **4**, produced in situ, in THF at −70 °C. Abbreviations are explained in [a].

Entry	Addition (equiv)	Proton source	Reaction stopped by	2% *ee* [b] (config.)
1	–	AcOH	–	54 (*R*)
2	–	TFA	–	32 (*S*)
3	–	TClA	–	40 (*S*)
4	–	MeOH	AcOH	0
5	–	MeOH	TFA	0
6	–	F_3EtOH	AcOH	0
7	–	*t*BuOH	AcOH	56 (*R*)
8	–	*t*BuOH	TFA	34 (*S*)
9	–	PhOH	TFA	4 (*S*)
10	–	$(MeCO)_2CH_2$	AcOH	46 (*S*)
11	–	$MeCOCH_2CO_2Et$	TFA	19 (*R*)
12	(*S*)-PEA (5)	AcOH	–	43 (*R*)
13	(*S*)-PEA (5)	TFA	–	19 (*S*)
14	(*R*)-PEA (5)	AcOH	–	2 (*R*)
15	(*R*)-PEA (10)	AcOH	–	5 (*R*)
16	(*S*)-EPEA (4)	AcOH	–	57 (*R*)
17	(*S*)-EPEA (4)	TFA	–	37 (*S*)
18	Pip (4)	AcOH	–	41 (*R*)
19	TMP (4)	AcOH	–	76 (*R*)
20	TMP (4)	TFA	–	39 (*S*)
21	Et_3N (10)	AcOH	–	47 (*R*)
22	*i*Pr(NEt_2) (4)	AcOH	–	51 (*R*)

[a] AcOH = acetic acid, TFA = trifluoroacetic acid, TClA = trichloroacetic acid, F_3EtOH = trifluoroethanol, PEA = α-phenylethylamine, EPEA = *N*-ethylphenylethylamine, Pip = Piperidine. [b] HPLC (Merck, ChiraSpher), reproducibility ±1%.

The boron enolate produced in situ was proven by ^{11}B NMR spectroscopy.[5] Since the measurements were to be carried out at +5 °C, the somewhat more thermostable boron enolate **3** was used. In addition to the signal for the reagent **5** (used in excess) at $\delta = 70.4$ ($\delta = 74$ in THF/Et_2O, 0 °C[6]), a new peak occurs at $\delta = 53.9$ which must be assigned to **3**. This signal lies within the range typical for dicyclohexylboron enolates ($\delta = 50–54$ in CCl_4).[7] Thus, the generation of optically active **1** or **2** for the subsequent protonation can be attributed to the attack of HX on the boron enolates **3** and **4**, respectively.

To avoid racemizations of the product formed from the protonation with weak acids, each reaction was stopped by neutralization with acetic acid (in some cases with trifluoroacetic acid). The enantiomeric excess of (*R*)- or (*S*)-enriched **1** and **2** was determined by chromatography with a chiral column (Merck, ChiraSpher), without further workup of the reaction mixture.

Since almost the same *ee* values were obtained for the products from *rac*-**1** and *rac*-**2** (AcOH and TFA as HX), only the results for the lactone **2** are listed in Table 1 and will be discussed in the following.

Interestingly, the results in Table 1 show that the protonation of **4** with acetic acid leads to an enrichment of (*R*)-**2** (entry 1), whereas the reaction with the stereochemically

[*] Prof. Dr. S. Hünig, Dr. T. Haubenreich, Dr. H.-J. Schulz
Institut für Organische Chemie
Am Hubland, D-W-8700 Würzburg (FRG)

[**] This work was supported by the Deutsche Forschungsgemeinschaft and the Fonds der Chemischen Industrie.

very similar trifluoroacetic acid favors the formation of the (*S*)-isomer (entry 2). Evidently, the lactone is protonated by two different reaction mechanisms. Thus, this is a further example of a reversal of stereoselectivity on changing from a methyl to a trifluoromethyl group in a reaction partner.[8]

The results can be explained if it is assumed that owing to the nucleophilicity of the carbonyl oxygen atom, the acetic acid forms a dative bond with the boron atom. This adduct transfers the acidic proton to the enol in a cyclic transition state, for example **6**, whereby the (*R*)-isomer is formed. A similar cyclic transition state was also postulated by Brown et al. for the protolysis of *B*-crotyl-9-borabicyclo-[3.3.1]nonane.[9]

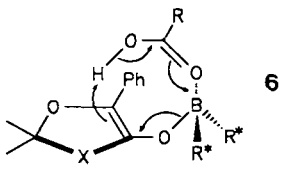

6

In contrast, trifluoroacetic acid (TFA) protonates the enolate without prior binding at the boron atom. The reason for the reduced capability for coordination of TFA is the reduced nucleophilicity of the carbonyl oxygen atom due to the accepting ability of the trifluoromethyl group. Thus, in contrast to the IR spectra of trifluoroacetoxydibutylborane, the IR spectra of acetoxydibutylborane indicate an intramolecular coordination of the carbonyl oxygen atom to the boron atom.[10] Interestingly, the reaction rates for the protolytic cleavage of the B–C bond are less influenced by the acidity of the acid than by its nucleophilicity. Thus, the protolyses with trifluoro- and trichloroacetic acid occur extremely slowly, whereas carbonic acids which can coordinate to the boron atom cause cleavage very rapidly.[11] Indeed, after the protonation of **4** with trichloroacetic acid, (*S*)-**2** is enriched even more (entry 3).

Evidently, noncoordinating acids directly attack the enol β-C atom of **4** preferably from the less shielded *si* side. In contrast, proton sources capable of coordinating at the boron atom form an adduct with **4**, from whose *re* side the proton is transferred. Thus, different protonation mechanisms can be used in such a way that with the same chiral auxiliary opposite stereoselectivities are achieved.[12]

Sterically less demanding alcohols (methanol, trifluoroethanol) protonate **4** unselectively. The stopping of the reaction with acetic acid and with TFA both produce the same result—a racemic mixture (entries 4,5). Thus, the protonation has occurred before the addition of the acids. The same applies for the more acidic trifluoroethanol (entry 6). In contrast, the bulky *tert*-butyl alcohol is inert towards **4**. This is revealed by the change in configuration on addition of TFA and AcOH (entries 7,8). Thus, if a reaction is stopped with acetic or trifluoroacetic acid this allows a simple examination of the effect of a proton source. Stereoselective protonation of **4** is observed with β-dicarbonyl compounds. Strangely, the configuration of the product changes with the transfer from acetylacetone ((*S*)-**2**, 46% *ee*) to acetoacetic ester ((*R*)-**2**, 19% *ee*, entries 10,11).

The experiments with amines (entries 12–22) reveal that primary and secondary amines influence the stereoselective protonation considerably (tertiary amines have no or only a weak effect), without functioning as a proton source. The different effects of the antipodes of chiral amines indicate that amines are inserted—probably via noncovalent interactions—in the transition state. Direct coordination of amines with the boron enolate **4**, however, seems ruled out: Particularly highly shielded 2,2,6,6-tetramethylpiperidine (TMP) shows the strongest effects (76% *ee*, entry 19). For the protonation of **3** with acetic acid, under the addition of TMP, (*R*)-**1** could be enriched to almost 80% *ee*! A reaction with chlorodiisopinocampheylborane **5** in excess cannot serve as an explanation for the amine effect. It is already known that **5** does not add sterically hindered amines.[6]

A further optimization of the auxiliary-induced stereoselective protonation via boron enolates can be expected from the variation of the chiral boron moiety. Thus, the conformatively flexible boron diisopinocampheyl group could be substituted by cyclic, chiral, C_2 symmetrical boron ligands, as has already proved successful for stereoselective aldol reactions.[3b, c]

Protonation of the boron enolates **4** applied can be described as an auxiliary-induced stereoselective reaction. Normally, in such reactions the auxiliary is only removed in a subsequent reaction. Thus, for example, in the previously mentioned aldol addition[3] the boron-containing auxiliary is first seized by the alcoholate function formed and subsequently removed by hydrolysis.

The protonation described herein, however, belongs to the rare examples in which the construction of the new stereocenter is coupled with the removal of the auxiliary—an important step of enantioselective catalytic synthesis.

Received: November 19, 1992 [Z 5691 IE]
German version: *Angew. Chem.* **1993**, *105*, 443

[1] H. Waldmann, *Nachr. Chem. Tech. Lab.* **1991**, *39*, 413–418.
[2] M. W. Andersen, B. Hildebrandt, G. Dahmann, R. W. Hoffmann, *Chem. Ber.* **1991**, *124*, 2127–2139.
[3] a) I. Paterson, J. M. Goodman, M. A. Lister, S. M. Riseman, I. Shinkai, *Tetrahedron* **1990**, *46*, 4663–4684; b) S. Masamune, T. Sato, B. M. Kim, T. A. Wollmann, *J. Am. Chem. Soc.* **1986**, *108*, 8279–8281; c) M. T. Reetz, F. Kunisch, P. Heitmann, *Tetrahedron Lett.* **1986**, *27*, 4721–4724.
[4] H. C. Brown, R. K. Dhar, K. Ganesan, B. Singaram, *J. Org. Chem.* **1992**, *57*, 2716–2721.
[5] We thank Prof. Dr. Wrackmeyer, Universität Bayreuth, for enabling us to carry out the measurements and for his help with the interpretation.
[6] H. C. Brown, J. Chandrasekharan, V. Ramachandran, *J. Am. Chem. Soc.* **1988**, *110*, 1539–1546.
[7] H. C. Brown, R. K. Dhar, K. Ganesan, B. Singaram, *J. Org. Chem.* **1992**, *57*, 499–504.
[8] M. Gautschi, D. Seebach, *Angew. Chem.* **1992**, *104*, 1061–1062; *Angew. Chem. Int. Ed. Engl.* **1992**, *31*, 1083–1085.
[9] G. W. Kramer, H. C. Brown, *J. Organomet. Chem.* **1977**, *132*, 9–27.
[10] L. A. Duncanson, W. Gerrard, M. F. Lappert, H. Pyszora, R. Shafferman, *J. Chem. Soc.* **1958**, 3652–3656.
[11] L. H. Torporcer, R. E. Dessy, S. I. E. Green, *J. Am. Chem. Soc.* **1965**, *87*, 1236–1240.
[12] D. Seebach, *Angew. Chem.* **1990**, *102*, 1363–1409; *Angew. Chem. Int. Ed. Engl.* **1990**, *29*, 1320–1367.

DBU and DBN are Strong Nucleophiles: X-Ray Crystal Structures of Onio- and Dionio-Substituted Phosphanes**

By *Robert Reed, Régis Réau, Françoise Dahan*, and *Guy Bertrand**

Base-induced intra- or intermolecular dehydrohalogenation reactions play a key role in organic and inorganic chemistry. Since the 1970s the efficiency of DBU (1,8-diazabi-

[*] Dr. G. Bertrand, Dr. R. Reed, Dr. R. Réau, Dr. F. Dahan
Laboratoire de Chimie de Coordination du CNRS
205, route de Narbonne, F-31077 Toulouse Cédex (France)
[**] This work was supported by the Centre National de la Recherche Scientifique.

cyclo[5.4.0]undec-7-ene) and DBN (1,5-diazabicyclo[4.3.0]-non-5-ene) has been widely demonstrated,[1] although many authors have reported unexplained phenomena.[2] In this paper we report that these bicyclic amidines, known as "non-nucleophilic strong bases"[1, 3] can behave as strong nucleophiles; X-ray crystal structures of onio- and dionio-substituted phosphanes (Weiss-type compounds)[4] are presented.

In dichloromethane solution chlorobis(diisopropylamino)phosphane (**1**) and DBN or DBU are in equilibrium with the cationic phosphanes **2a** or **3a**. This equilibrium is shifted towards the products in acetonitrile, or by exchanging the chloride for hexafluorophosphate to yield **2b** and **3b**.[5]

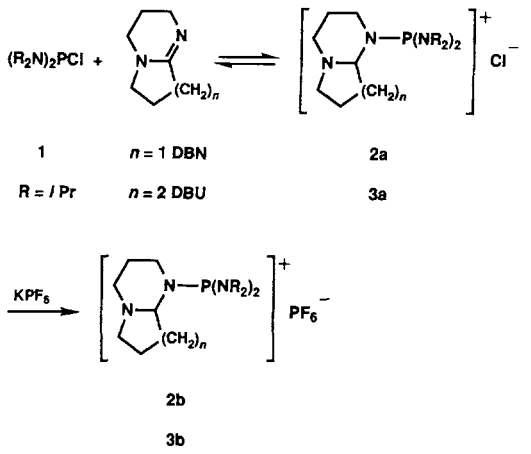

Scheme 1.

The ^{31}P NMR chemical shifts observed for these compounds [$\delta = +108$ (**2b**), $+107$ (**3b**)] are consistent with triaminophosphanes; furthermore in the ^{13}C NMR spectra, phosphorus coupling to the bridgehead carbons [$^2J_{C,P} = 31.1$ (**2b**) and 21.1 Hz (**3b**)] confirms that the bicyclic amidines are bound to the phosphorus. To establish the exact nature of the interaction between the amidine and the phosphorus atom, a single crystal X-ray diffraction study was performed on **2b**.[6] The ORTEP view (Fig. 1) reveals the phosphorus atom in a pyramidal environment in which the three substituents are arranged in a propeller fashion to minimize the steric interactions. The P1–N3 and P1–N4 bond lengths [1.666(4) and 1.661(4) Å] are classical, longer than those observed in phosphanylium ions where 2pπ–3pπ interaction between the phosphorus and the nitrogens atom takes place.[7] Of particular interest are the very long P1–N1 bond [1.796(3) Å] and the almost equal C1–N1 [1.322(5) Å] and C1-N2 [1.298(5) Å] bond lengths. The structure of this cationic phosphane is comparable to that of borylium ions in which a cationic bivalent boron atom is stabilized by an electron pair donor and the positive charge is delocalized on the cluster.[8]

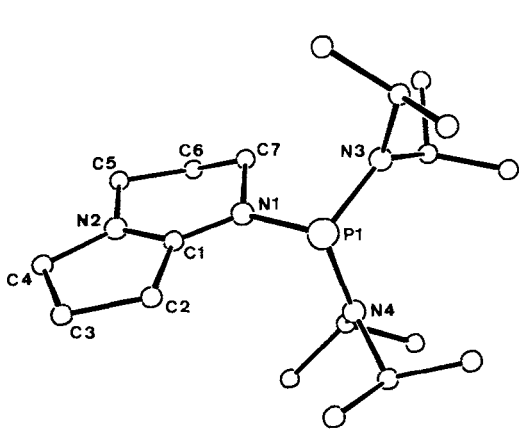

Fig. 1. Structure of cation **2b** (ORTEP). Selected bond lengths [Å] and angles [°]: P1-N1 1.796(3), P1-N3 1.661(4), P1-N4 1.666(4), N1-C1 1.322(5), C1-N2 1.298(5); N1-P1-N3 101.6(2), N1-P1-N4 99.1(2), N3-P1-N4 109.3(2), P1-N1-C1 120.3(3), P1-N1-C7 124.0(3), C7-N1-C1 114.9(3), N1-C1-C2 123.7(4), N2-C1-C2 110.0(4), N1-C1-N2 126.2(4), C1-N2-C5 123.7(4), C1-N2-C4 115.3(3), C4-N2-C5 120.9(4).

As expected, a similar ionic adduct **2c** can be obtained by treating bis(diisopropylamino)phosphanylium tetrachloroaluminate[9] with DBN. In addition, the free bis(diisopropylamino)phosphanylium salt can be cleanly regenerated by the addition of one equivalent of borontrifluoride-etherate complex to **2b**.

Most importantly, the nucleophilic behavior of DBU and DBN is very general (Table 1) and also allows the preparation of dionio-substituted phosphanes **6**–**9**, which formally result from the interaction of two DBU or DBN molecules with monocoordinated phosphorus dications (RP^{2+}).

Table 1. Spectroscopic data of the compounds $(R^1R^2R^3P)^+PF_6^-$ **2b**–**5b** and $(R^1R^2R^3P)^{2+}2PF_6^-$ **6b**–**9b** [a].

No.	R^1	R^2	R^3	$\delta^{31}P$ [b]	$\delta^{13}C$ [b] NCN	^2J(C,P)	Yield [%] [c]	M.p. [°C]
2b	iPr_2N	iPr_2N	DBN	108	165.5	31	64	128–130
3b	iPr_2N	iPr_2N	DBU	107	168.1	21	50	110–116
4b	Ph	Ph	DBN	71	169.8	33	12	193–195
5b	Ph	Ph	DBU	71	169.8	26	30	140–143
6b	Cy_2N [d]	DBN	DBN	109	166.8	35	23	180–183
7b	Cy_2N [d]	DBU	DBU	100	163.5	10	43	212–216
8b	Ph	DBN	DBN	102	171.5	38	14	214–217
9b	Ph	DBU	DBU	98	173.2	31	[e]	[e]

[a] The spectroscopic data of compounds **2a**–**9a** (isolated as viscous oils, Cl^- as counter anion) and **2c** ($AlCl_4^-$ as counter anion) are essentially identical to **2b**–**9b** (PF_6^- as counter anion). [b] Spectra of cations in $CDCl_3$ solution, dications in CD_3CN solution. Coupling constants are in Hz. [c] Yields after recrystallization. The yields determined by ^{31}P NMR spectroscopy are essentially quantitative; no other phosphorus products were observed. [d] Cy = cyclohexyl. [e] Compound not isolated.

The X-ray crystal structure of **6b** is shown in Figure 2.[10] The P1–N1 and P1–N3 bonds are rather long [1.766(5) and 1.752(4) Å], and the C–N bond lengths of the NCN moieties [1.339(6), 1.304(8) and 1.334(7), 1.290(7) Å] are between single and double bonds. Here also, the positive charges are strongly delocalized.

This new understanding of the behavior of DBU and DBN towards halogenated derivatives of main group elements[11] led us to reconsider the mechanism of dehydrohalogenation in the presence of these cyclic amidines. For example, addition of DBU to a mixture of chlorodiphenylphosphane and diphenylphosphane gives the tetraphenyldiphosphane. In fact, no reaction between diphenylphosphane and DBU is observed by ^{31}P NMR spectroscopy, whereas adduct **5a** reacts with diphenylphosphane to yield the diphosphane quantitatively.

In contrast to what is generally admitted, these results show that DBU and DBN can act as strong nucleophiles. This new understanding will help to clarify the superior utility and frequently observed unexplained behavior of these highly popular reagents in "base-induced" dehydrohalogenation reactions.

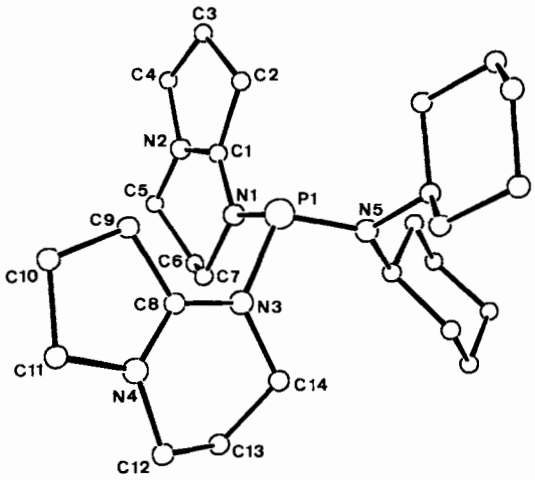

Fig. 2. Structure of cation **6b** (ORTEP). Selected bond lengths [Å] and angles [°]: P1-N1 1.766(5), P1-N3 1.752(4), P1-N5 1.628(5), N1-C1 1.339(6), C1-N2 1.304(8), N3-C8 1.334(7), C8-N4 1.290(7); N1-P1-N3 95.9(2), N1-P1-N5 104.7(2), N3-P1-N5 106.5(2), P1-N1-C1 117.2(4), P1-N1-C7 125.1(3), C1-N1-C7 116.3(5), N1-C1-N2 123.9(5), N1-C1-C2 125.6(6), C2-C1-N2 110.5(5), C1-N2-C4 113.6(5), C1-N2-C5 125.3(4), C4-N2-C5 121.1(5).

Experimental Procedure

Representative synthesis of compounds **2a–9b**, example **2a** and **2b**: An acetonitrile solution (20 mL) of DBN (5.6 mL, 45 mmol) was added dropwise at room temperature to an acetonitrile solution (20 mL) of chlorobis(diisopropylamino)phosphane **1** (12.0 g, 45 mmol) to afford **2a** as an extremely hygroscopic, viscous oil. ^{31}P NMR (32 MHz, CH_3CN, 35 °C): $\delta = 106.7$; ^{13}C NMR (50 MHz, $CDCl_3$, 25 °C): $\delta = 18.8$ (s, CH_2), 19.5 (s, CH_2), 23.8 (t, $^3J(C,P) = 7$ Hz, CH_3), 31.2 (d, $^2J(C,P) = 27$ Hz, CH_2), 42.5 (s, CH_2), 43.6 (s, CH_2), 47.5 (d, $^2J(C,P) = 12$ Hz, CH), 53.8 (s, CH_2), 165.1 (d, $^2J(C,P) = 31$ Hz, NCN). This solution was added slowly at 0 °C to an acetonitrile solution (20 mL) of KPF_6 (8.5 g, 46 mmol) and stirred for 24 hrs. The precipitated KCl was filtered off, and the solvent removed under vacuum. Compound **2b** was crystallized at −40 °C from CH_2Cl_2/Et_2O (14.5 g, 64%). ^{31}P NMR (32 MHz, $CDCl_3$, 35 °C): $\delta = 108.4$, −143.6 (sept, $^1J(P,F) = 709$ Hz); ^{13}C NMR (50 MHz, $CDCl_3$, 25 °C): $\delta = 18.7$ (d, $^3J(C,P) = 4$ Hz, CH_2), 19.3 (s, CH_2), 23.8 (t, $^3J(C,P) = 7$ Hz, CH_3), 31.2 (d, $^2J(C,P) = 27$ Hz, CH_2), 42.5 (d, $^3J(C,P) = 3$ Hz, CH_2), 43.1 (s, CH_2), 47.9 (d, $^2J(C,P) = 14$ Hz, CH), 53.5 (s, CH_2), 165.4 (d, $^2J(C,P) = 31$ Hz, NCN).

Received: November 6, 1992 [Z 5669 IE]
German version: *Angew. Chem.* **1993**, *105*, 464

[1] H. Oediger, F. Möller, K. Eiter, *Synthesis* **1972**, 591–598; I. Hermecz, *Adv. Heterocycl. Chem.* **1987**, *42*, 83; A. H. Cowley, *Acc. Chem. Res.* **1984**, *17*, 386–392.

[2] C. N. Smit, Dissertation, Vrije Universiteit te Amsterdam, **1987**; T. C. Klebach, R. Lourens, F. Bickelhaupt, *J. Am. Chem. Soc.* **1978**, *100*, 4886–4888; A. H. Cowley, J. E. Kilduff, J. G. Lasch, S. K. Mehrotra, N. C. Norman, M. Pakulski, B. R. Whittlesey, J. L. Atwood, W. E. Hunter, *Inorg. Chem.* **1984**, *23*, 2582–2593; J. Escudié, C. Couret, H. Ranaivonjatovo, J. Satgé, *J. Chem. Soc. Chem. Commun.* **1984**, 1621–1622; T. R. Juneja, D. K. Garg, W. Schäfer, *Tetrahedron* **1982**, *38*, 551–556; L. L. McCoy, D. Mal, *J. Org. Chem.* **1981**, *46*, 1016–1018; H. O. House, M. B. de Tar, D. Von Derveer, *ibid.* **1979**, *44*, 3793–3800; T. A. Van Der Knapp, F. Bickelhaupt, *Phosphorus Sulfur* **1984**, *21*, 227–236; S. Kim, H. Chang, *Bull. Chem. Soc. Jpn.* **1985**, *58*, 3669–3670.

[3] H. A. Muathen, *J. Org. Chem.* **1992**, *57*, 2740–2741; P. Wolkoff, *ibid.* **1982**, *47*, 1944–1948.

[4] R. Weiß, S. Engel, *Synthesis* **1991**, 1077–1079; R. Weiß, S. Engel, *Angew. Chem.* **1992**, *104*, 239–240; *Angew. Chem. Int. Ed. Engl.* **1992**, *31*, 216–217.

[5] It should be noted that chlorophosphane **1** is inert towards triethylamine, and even towards 4-dimethylaminopyridine.

[6] Crystal data for **2b**: Space group $P2_1/n$, $a = 7.877(1)$, $b = 9.638(1)$, $c = 34.066(3)$ Å, $\beta = 92.62(1)°$, $V = 2583.5(8)$ Å^3, $Z = 4$; 4540 measured reflections, 2852 independent reflections observed [$F_o^2 > 3\sigma(F_o^2)$], 280 refined parameters, $R(F_o) = 0.044$ ($R_w = 0.045$).

[7] M. Sanchez, M. R. Mazière, L. Lamandé, R. Wolf in *Multiple Bonds and Low Coordination in Phosphorus Chemistry* (Eds.: M. Regitz, O. J. Scherer), Thieme, Stuttgart, **1990**, S. 129–148; A. H. Cowley, M. C. Kemp, *Chem. Rev.* **1985**, *85*, 367–382.

[8] P. Kölle, H. Nöth, *Chem. Rev.* **1985**, *85*, 399–418.

[9] A. H. Cowley, M. C. Cushner, J. S. Szobota, *J. Am. Chem. Soc.* **1978**, *100*, 7784–7786.

[10] Crystal data for **6b**: Space group $P2_1/n$, $a = 17.341(2)$, $b = 9.715(1)$, $c = 24.032(2)$ Å, $\beta = 109.99(1)°$, $V = 3805(1)$ Å^3, $Z = 4$; 5950 measured reflections, 3294 independent reflections observed [$F_o^2 > 3\sigma(F_o^2)$], 289 refined parameters, $R(F_o) = 0.046$ ($R_w = 0.048$). Further details of the crystal structure investigation may be obtained from the Fachinformationszentrum Karlsruhe, Gesellschaft für wissenschaftlich-technische Information mbH, D-W-7514 Eggenstein-Leopoldshafen 2 (FRG), on quoting the depository number CSD-56813, the names of the authors, and the journal citation.

[11] Preliminary experiments show that DBU and DBN can act as nucleophiles towards a variety of halogenated compounds of main group elements.

Perspirocyclopropanated [3]Rotane—A Section of a Carbon Network Containing Spirocyclopropane Units?**

By *Sergei I. Kozhushkov, Thomas Haumann, Roland Boese,* and *Armin de Meijere**

Dedicated to Professor Emanuel Vogel on the occasion of his 65th birthday

Twenty years ago the synthesis[1, 2] of [3]rotane (**1**)[3] may have been seen as the end of the development of highly strained cyclopropane derivatives with unusual structural[4–8] and spectroscopic properties.[9] However, more recent reports on branched [*n*]triangulanes[10] like **2**[11–13] and **3**[12, 13] containing a [3]rotane subunit show that **1** is actually the starting point of a larger group of star-shaped, branched hydrocarbons with nothing but spirocyclic linkages between three-membered rings. Accordingly, the perspirocyclopropanated [3]rotane **4**,[14] a [10]triangulane[10] with D_{3h} symmetry, which we describe here, is also just another peak on a possible route to higher summits.

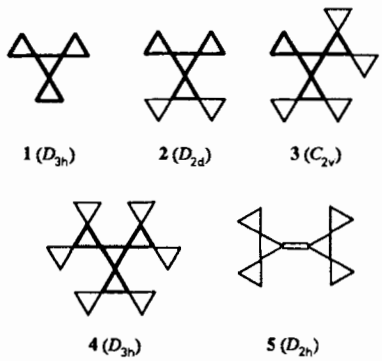

The starting material for the successful route[15] to **4** (Scheme 1, Table 1) was the recently described bi(dispiro-[2.0.2.1]heptylidene) **5**.[12] Cyclopropanation of **5** with two

[*] Prof. Dr. A. de Meijere, Dr. S. I. Kozhushkov
Institut für Organische Chemie der Universität
Tammannstrasse 2, D-W-3400 Göttingen (FRG)
Priv. Doz. Dr. R. Boese, Dipl.-Chem. T. Haumann
Institut für Anorganische Chemie der Universität-Gesamthochschule
Essen

[**] This work was supported by the Fonds der Chemischen Industrie. We thank the companies BASF, Bayer, Hoechst, and Degussa AG for gifts of chemicals. S.I.K. is grateful to the Alexander von Humboldt Foundation for a research fellowship.

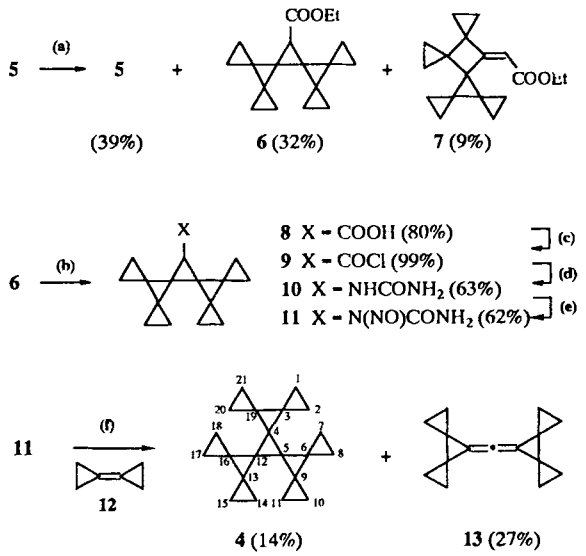

Scheme 1. a) 2 equiv $N_2CHCOOEt$, CH_2Cl_2, $[\{Rh(OAc)_2\}_2]$ (1 mol%), 0 °C, 12 h. b) 1.2 equiv NaOH, H_2O, 100 °C, 6 h. c) $SOCl_2$, 80 °C, 2 h. d) 1) NaN_3, Me_2CO, 0 °C, 2 h; 2) C_6H_6, 80 °C, 2 h; 3) NH_3, 5 °C. e) N_2O_4, Et_2O, 0 °C, 2 h. f) 10 equiv NaOMe, 0 °C, 10 h.

equivalents of ethyl diazoacetate in the presence of dirhodium tetraacetate[18] yielded, besides the desired carboxylate **6**[19] (32%), also 9% of the rearranged product **7**.[20] The products **6** and **7** were separated by chromatography over silica gel. The hydrolysis of the ester **6** afforded the acid **8** (80% yield), which was transformed into the acid chloride **9** (99%) with thionyl chloride. Analogous to the synthesis of *N*-nitroso-*N*-cyclopropylurea,[21] the nitrosourea **11** was obtained from **9** in 39% yield. The crucial step—the in situ generation of the diazo[7]triangulane from **11**—was achieved with ten equivalents of solid sodium methyl alcoholate at 0 °C[22] in a large excess of bicyclopropylidene (**12**).[23] The perspiro-cyclopropanated [3]rotane **4** could be separated from the allene **13**[19] (see ref. [15]) by chromatography on silica gel and was isolated in 14% yield.

[3]Rotane **4** precipitated on slow concentration of a dilute solution in ethanol in the form of crystals suitable for X-ray structure analysis (Fig. 1).[24] Comparison of the structural parameters of **4** (averaged over D_{3h} symmetry) with those of **1**,[4c] **2**,[8b, 11] and **3**[12] shows, on one hand, the known effects for branched triangulanes:[8a, c] the difference in length between the distal [1.525 (**1**), 1.532 (**2**), 1.516 and 1.512 (**3**), 1.529 Å (**4**)] and proximal bonds [1.477 (**1**), 1.483 (**2**), 1.475 and 1.472 (**3**), 1.481 Å (**4**)] in the outer cyclopropane rings, as well as the shortening of all C–C bonds in the trispiro-annelated rings [for the central rings: 1.475 (**1**), 1.477 and 1.481 (**2**), 1.471 and 1.483 (**3**), 1.484 Å (**4**)].[4c, 8b, 11, 12] The reason is to be found in hybridization changes involving an increased angular strain.[4c, 12, 25] To this extent the bond lengths of branched [*n*]triangulanes can be estimated according to an empirical increment system.[26] On the other hand, the bonds in the central three-membered ring of **4** (1.484 Å with a standard deviation of 0.001 Å) are significantly longer than those in the central ring of [3]rotane **1** [1.475(2) Å].[4c] This might be attributable to an additional electronic interaction in terms of a spiro conjugation between the six outer rings and the central three-membered ring.[27]

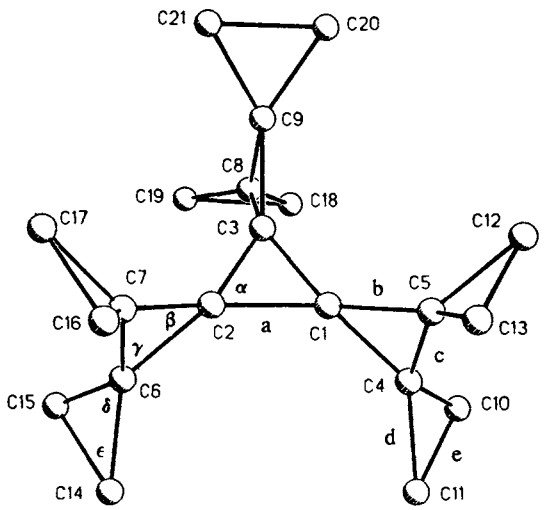

Fig. 1. Structure of **4** in the crystal. The numbering in this figure is not the same as the systematic numbering according to IUPAC nomenclature. Bond lengths [Å] and angles [°] (averaged over D_{3h} symmetry): a = 1.484(1), b = 1.479(1), c = 1.476(2), d = 1.481(1), e = 1.529(1); α = 60.0(1), β = 59.9(1), γ = 60.1(1), δ = 62.2(1), ε = 58.9(1).

Table 1. Physical and spectroscopic data of important new compounds [16]. NMR spectra: $CDCl_3$, 250 MHz (^1H); 62.9 MHz (^{13}C, additional DEPT).

4: White solid, m.p. 200–201 °C. ^1H NMR: δ = 0.69, 0.75 (AA'BB', 24H); ^{13}C NMR: δ = 6.52 (12 CH_2), 18.24 (6 C), 28.82 (3 C); high resolution MS: *m/z* calcd for $C_{21}H_{28}N$ ($M^+ + NH_4$), 294.4601, found 294.4374 (100%).

6: White solid, m.p. 80–82 °C. ^1H NMR: δ = 0.52–0.63 (m, 2H), 0.63–0.91 (m, 12H), 0.91–1.0 (m, 2H), 1.22 (t, J = 7.0 Hz, 3H), 2.09 (s, 1H), 4.05 (q, J = 7.0 Hz, 2H); ^{13}C NMR: δ = 3.51, 4.98, 6.64, 6.99 (2 CH_2), 14.08 (CH_3), 25.59 (CH), 59.88 (CH_2), 18.07, 18.49 (2 C), 172.49 (C).

7: White solid, m.p. 66–68 °C. ^1H NMR: δ = 0.05–0.12 (m, AB, J = 5.0 Hz, 2H), 0.45–0.54 (m, 2H), 0.64–0.73 (m, 4H), 0.75–0.87 (m, 4H), 0.95–1.05 (m, 4H), 1.25 (t, J = 7.1 Hz, 3H), 4.11 (q, J = 7.1 Hz, 2H), 5.20 (s, 1H); ^{13}C NMR: δ = 2.78, 4.12, 6.23, 14.36 (2 CH_2), 14.57 (CH_3), 26.45 (2 C), 29.60, 31.99, 39.10, 165.33, 175.55 (C), 59.27 (CH_2), 104.11 (CH).

8: White solid, m.p. 204–206 °C (decomp.). ^1H NMR: δ = 0.53–0.62 (m, 2H), 0.67–0.76 (m, 6H), 0.76–0.93 (m, 6H), 1.01–1.10 (m, 2H), 2.03 (s, 1H), 10.50 (s, 1H); ^{13}C NMR: δ = 3.33, 5.11, 6.69, 7.06 (2 CH_2), 25.39 (CH), 18.08, 18.65, 32.46 (2 C), 179.68 (C).

9: Clear oil. ^1H NMR: δ = 0.58–0.71 (m, 4H), 0.71–0.79 (m, 8H), 1.12–1.29 (m, 4H), 2.55 (s, 1H); ^{13}C NMR: δ = 3.42, 5.35, 6.70, 7.30 (2 CH_2), 18.23, 19.05, 36.34 (2 C), 36.10 (CH), 172.42 (C).

10: White solid, m.p. 176–178 °C (decomp.). ^1H NMR: δ = 0.60–1.12 (16H), 2.93 (s, 1H), 4.70 (s, 1H), 4.79 (s, 2H); ^{13}C NMR: δ = 3.76, 4.48, 6.55, 6.79 (2 CH_2), 17.54, 18.70, 28.71 (2C), 34.03 (CH), 160.62 (C).

11: Yellow solid, m.p. 124–125 °C (decomp.). ^1H NMR: δ = 0.55–1.15 (m, 16H), 3.21 (s, 1H), 5.20 (s, 2H); ^{13}C NMR: δ = 5.04, 6.13, 6.59, 6.71 (2 CH_2), 18.72, 19.29, 29.54 (2 C), 36.12 (CH), 175.14 (C).

13: White solid. ^1H NMR: δ = 0.97, 1.18 (AA'BB', 16H); ^{13}C NMR: δ = 8.38 (8 CH_2), 20.99 (4 C), 95.27 (2 C), 165.02 (C).

On comparison of the ^{13}C NMR data of **1**–**4**, a shift to lower field for the signals of the central C atoms is observed for each addition of two spiroannelated three-membered rings onto [3]rotane: δ = 18.3 for **1**,[1a] 23.1 for **2**,[11–13] 25.9 for **3**,[12] and 28.8 for **4**.[28]

Particularly notable is the high thermal stability of the [10]triangulane **4** with D_{3h} symmetry. Although its total strain of at least 1130 kJ mol^{-1}[29] makes **4** more highly strained than cubane,[30] it is stable for a long time even at its melting point of 200–201 °C. As the DSC curve shows,[31] a thermal transformation or decomposition occurs only above 250 °C. Accordingly, from the point of view of stability, higher aggregates of spiropentane units should be no

problem. Model calculations show that four spirocyclopropane units can be linked to construct a cyclic [8]triangulane without significant angular distortion; two [8]triangulanes in turn linked in a spiro fashion by four three-membered rings form a sort of cube ([20]triangulane), and five such cubes can be linked through common triangular faces (Fig. 2). A carbon network comprising only spiro-

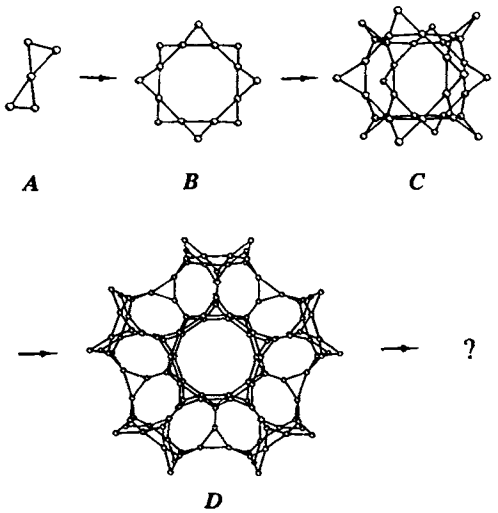

Fig. 2. *A*: spiropentane C_5H_8. ***B***: [8]cyclotriangulane $C_{16}H_{16}$. ***C***: [20]triangulane $C_{36}H_{24}$. ***D***: [80]triangulane $C_{135}H_{60}$.

linked three-membered rings is therefore conceivable.[32] Whether such a network can actually be realized is a different matter.

Received: November 23, 1992 [Z 5697 IE]
German version: *Angew. Chem.* **1993**, *105*, 426

[1] a) L. Fitjer, J.-M. Conia, *Angew. Chem.* **1973**, *85*, 349; *Angew. Chem. Int. Ed. Engl.* **1973**, *12*, 334; b) L. Fitjer, *Chem. Ber.* **1982**, *115*, 1047, and literature therein.

[2] Cf. also: a) I. Erden, *Synth. Commun.* **1986**, *16*, 117; b) N. S. Zefirov, K. A. Lukin, S. J. Kozhushkov, T. S. Kuznetsova, A. M. Domarev, I. M. Sosonkin, *Zh. Org. Khim.* **1989**, *25*, 312; *J. Org. Chem. USSR* **1989**, *25*, 278.

[3] Systematic name of [3]rotane: trispiro[2.0.2.0.2.0]nonane.

[4] a) C. Pascard, T. Prange, A. de Meijere, W. Weber, J.-P. Barnier, J.-M. Conia *J. Chem. Soc. Chem. Commun.* **1979**, 425; b) T. Prange, C. Pascard, A. de Meijere, U. Behrens, J.-P. Barnier, J.-M. Conia, *Nouv. J. Chim.* **1980**, *4*, 321; c) R. Boese, T. Miebach, A. de Meijere, *J. Am. Chem. Soc.* **1991**, *113*, 1743.

[5] a) M. Randić, L. Kumar, *J. Mol. Struct.* **1975**, *26*, 145; b) M. Randić, L. Jakab, *Croat. Chim. Acta* **1970**, *42*, 425; c) K. Kovačević, Z. B. Maksić, A. Moguš, *ibid.* **1979**, *52*, 249; d) Z. B. Maksić, M. Eckert-Maksić, K. Rupnik, *ibid.* **1984**, *57*, 1295.

[6] a) S. P. Zil'berg, A. I. Ioffe, O. M. Nefedov, *Izv. Akad. Nauk SSSR Ser. Khim.* **1983**, 261; *Acad. Sci. USSR Bull. Chem. Sci.* **1983**, *32*, 228; b) A. I. Ioffe, V. A. Svyatkin, O. M. Nefedov, *ibid.* **1987**, 801 and **1987**, *36*, 727.

[7] K. Rasmussen, C. Tosi, *J. Mol. Struct. (Theochem)* **1985**, *121*, 233.

[8] a) D. S. Yufit, S. I. Kozhushkov, K. A. Lukin, A. de Meijere, Yu. T. Struchkov, N. S. Zefirov, *Dokl. Akad. Nauk SSSR* **1991**, *320*, 357; b) S. I. Kozhushkov, D. S. Yufit, K. A. Lukin, A. de Meijere, R. Boese, Yu. T. Struchkov, N. S. Zefirov, *ibid.* **1991**, *320*, 104; c) D. S. Yufit, K. A. Lukin, S. I. Kozhushkov, Yu. T. Struchkov, N. S. Zefirov, *ibid.* **1991**, *320*, 653.

[9] R. Gleiter, R. Haider, J.-M. Conia, J.-P. Barnier, A. de Meijere, W. Weber, *J. Chem. Soc. Chem. Commun.* **1979**, 130.

[10] For an explanation of the term [*n*]triangulane, see: a) N. S. Zefirov, S. I. Kozhushkov, T. S. Kuznetsova, O. V. Kokoreva, K. A. Lukin, B. I. Ugrak, S. S. Tratch, *J. Am. Chem. Soc.* **1990**, *112*, 7702; b) K. A. Lukin, S. I. Kozhushkov, A. A. Andrievsky, B. I. Ugrak, N. S. Zefirov, *J. Org. Chem.* **1991**, *56*, 6176.

[11] N. S. Zefirov, S. I. Kozhushkov, B. I. Ugrak, K. A. Lukin, O. V. Kokoreva, D. S. Yufit, Yu. T. Struchkov, S. Zoellner, R. Boese, A. de Meijere, *J. Org. Chem.* **1992**, *57*, 701.

[12] a) S. Zöllner, H. Buchholz, R. Boese, R. Gleiter, A. de Meijere, *Angew. Chem.* **1991**, *103*, 1544; *Angew. Chem. Int. Ed. Engl.* **1991**, *30*, 1518; b) S. Zöllner, *Dissertation*, Universität Hamburg, **1991**.

[13] K. I. Lukin, S. I. Kozhushkov, A. A. Andrievsky, B. I. Ugrak, N. S. Zefirov, *Mendeleev Commun.* **1992**, 51.

[14] Systematic name: nonaspiro[2.0.0.0.2.0.2.0.0.0.2.0.2.0.0.0.2.0]henicosane.

[15] Four other attempted routes did not yield **4**: 1) 7-diazodispiro[2.0.2.1]-heptane generated in situ did not react with **5**, but with bicyclopropylidene **12** instead. In the presence of **5** only bis(cyclopropylidene)methane formed while in the presence of **12** the cyclopropanation product **2** was obtained in 28% yield. 2) The alkene **5** did not react with 1-chloro-1-(2-alkoxyethyl)carbene in analogy to ref. [11]. 3) The dibromocarbene adduct of **5** was, in fact, obtained in 94% yield, but the carbenoid formed by treatment with methyllithium in the presence of bicyclopropylidene (**12**) [17] was not trapped by this adduct [16], but reacted under ring opening via the corresponding carbene to afford exclusively the allene **13**. 4) The reaction of **6** with ethylmagnesium bromide/titanium tetra(isopropyl alcoholate) according to Kulinkovich indeed furnished the 1'-hydroxycyclopropyl derivative (93% yield) [17], but it could not be converted into the bromide, and thus the prerequisite for elimination and subsequent further cyclopropanation was not attained.

[16] Cf. M. Bertrand, A. Tubul, C. Ghiglione, *J. Chem. Res. (Synop.)* **1983**, 250; *(M)* 2274.

[17] A. de Meijere, S. I. Kozhushkov, T. Spaeth, N. S. Zefirov, *J. Org. Chem.* **1993**, *58*, in press, and literature therein.

[18] a) A. J. Hubert, A. F. Noels, A. J. Anciaux, P. Teyssie, *Synthesis* **1976**, 600; b) M. P. Doyle, D. van Leusen, W. H. Tamblyn, *ibid.* **1981**, 787.

[19] All new compounds were completely characterized by spectroscopic methods and by elemental analysis or crystal structure analysis. The crystal structure analysis of the head-to-head dimer of **13** was performed in Moscow (Dr. D. S. Yufit, Nesmeyanov Institute for Organo-Element Compounds).

[20] The rearranged product **7** indicates that in part a 1,3-dipolar cycloaddition of ethyl diazoacetate to **5** has taken place. Cf. L. Fitjer, D. Wehle, *Chem. Ber.* **1982**, *115*, 1061 and reference [1b] therein.

[21] W. Kirmse, H. Schutte, *Chem. Ber.* **1968**, *101*, 1674.

[22] Analogous to the spirocyclopropanation of cyclopropylidene(dispiro-[2.0.2.1]heptylidene)methane to form **5** with diazocyclopropane generated in situ. Cf. [12].

[23] It was helpful that a new three-step synthesis made **12** conveniently accessible in multigram amounts. Cf. [17].

[24] Structure determination of **4**: diffractometer Nicolet R 3m/V, $\lambda(Mo_{K\alpha})$, graphite monochromator, ω scan, $3° \leq 2\theta \leq 57°$, direct methods (SHELXTL-PLUS). Crystal dimensions $0.5 \times 0.4 \times 0.25$ mm^3, space group $P2_1/n$, $Z = 4$, $T = 120$ K; cell dimensions: $a = 9.559(2)$, $b = 14.473(3)$, $c = 12.268(3)$ Å, $\alpha = \gamma = 90°$, $\beta = 94.59(2)°$. 4103 independent reflections, of which 2886 observed ($F_0 \geq 4\sigma(F)$), 286 parameters for the structure refinement, all non-hydrogen atoms anisotropic, $R = 0.051$, $Rw = 0.054$. Further details of the crystal structure investigation may be obtained from the Fachinformationszentrum Karlsruhe, Gesellschaft für wissenschaftlich-technische Information mbH, D-W-7514 Eggenstein-Leopoldshafen 2 (FRG) on quoting the depository number CSD-320568, the names of the authors, and the journal citation.

[25] M. Eckert-Maksić, S. Zöllner, W. Göthling, R. Boese, L. Maksimović, R. Machinek, A. de Meijere, *Chem. Ber.* **1991**, *124*, 1591, and literature therein

[26] a) F. H. Allen, *Acta Crystallogr. Sect. B* **1980**, *36*, 81; b) K. A. Lukin, S. I. Kozhushkov, N. S. Zefirov, D. S. Yufit, Yu. T. Struchkov, *ibid.* **1992**, in press.

[27] Cf. a) H. E. Simmons, T. Fukunaga, *J. Am. Chem. Soc.* **1967**, *89*, 5208; b) H. Dürr, R. Gleiter, *Angew. Chem.* **1978**, *90*, 591; *Angew. Chem. Int. Ed. Engl.* **1978**, *17*, 559.

[28] The signals for **4** at $\delta = 28.8$ are shifted further downfield than those of all other unsubstituted [*n*]triangulanes. Cf. K. A. Lukin, S. I. Kozhushkov, N. S. Zefirov, *Magn. Res. Chem.* **1991**, *29*, 774.

[29] Under the usual assumption of additivity of strain energies of all subunits (cf. [6, 10a]) the total strain energy of **4** should be at least tenfold that of cyclopropane.

[30] G. W. Griffin, A. P. Marchand, *Chem. Rev.* **1989**, *89*, 997; P. E. Eaton, *Angew. Chem.* **1992**, *104*, 1447; *Angew. Chem. Int. Ed. Engl.* **1992**, *31*, 1421.

[31] DSC = differential scanning calorimetry. We thank Ms. A. Dreier, Max-Planck-Institut für Kohlenforschung, Mühlheim a. d. Ruhr, for the DSC measurements.

[32] The concept of constructing a network from spiropentane units has not yet been mooted. Cf. F. Diederich, Y. Rubin, *Angew. Chem.* **1992**, *104*, 1123; *Angew. Chem. Int. Ed. Engl.* **1992**, *31*, 1101.

Activation of the C2 Position of Purine by the Trifluoromethanesulfonate Group: Synthesis of N^2-Alkylated Deoxyguanosines**

By *Thomas Steinbrecher, Christa Wameling, Franz Oesch,* and *Albrecht Seidel**

The covalent bonding of electrophilic metabolites to nucleophilic centers of pyrimidine and purine bases in DNA plays a central role in the biological activity of chemical carcinogens.[1] For carcinogenic epoxides, which are formed in the cell predominantly under catalysis of the cytochrome P450 enzymes from olefinic or aromatic structures, often attack the exocyclic amino group of deoxyguanosine (**1**) in vivo.[2] In contrast, N^2-alkylated deoxyguanosines are accessible selectively only with difficulty through a direct reaction with electrophilic reagents.[3] They are therefore usually synthesized through transformation of the appropriate substituted amines with 2-halohypoxanthines.[4] An alternative approach was recently described by Casale and McLaughlin.[5] They employed the chemoselective alkylation of 2'-deoxy-4-demethylwyosine at the N^5 position and subsequently transformed the products into N^2-alkyldeoxyguanosine derivatives. We now report on a very efficient general synthesis of fully protected N^2-alkylated deoxyguanosines. The protecting groups are chosen so that the deoxyguanosine derivatives can be used in an oligonucleotide synthesis.

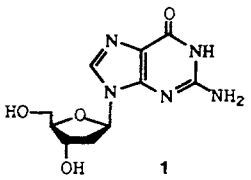

1

Deoxyguanosine (**1**) is transformed into O^6-(*p*-nitrophenylethyl)-3',5'-bis(*tert*-butyldimethylsilyl)deoxyguanosine (**2a**). For this purpose the hydroxyl groups are protected by silylation with *tert*-butyldimethylsilyl chloride (TBDMS-Cl) and the O^6 position of the purine moiety through a Mitsunobu reaction with 2-(*p*-nitrophenyl)ethanol (NPE-OH)[6] or with allyl alcohol (→ **2b**). Till now **2b** was considerably more laborious to prepare by nucleophilic displacement of the mesitylenesulfonate residue, used to activate the C6 position, with allyl alcohol.[7] Allyl ethers can be cleaved under mild conditions.[7, 8] The deoxyxanthosine derivatives **3a,b** are obtained from **2a** and **2b** by a deamination with *n*-pentyl nitrite. Compounds **3a** and **3b** are transformed into **4a** and **4b**, respectively, with trifluoromethanesulfonyl chloride (Tf-Cl). Derivative **4a** reacts with the amines **5**–**7** and the amino alcohols **8** and **9** in dimethylformamide (DMF) under mild conditions and in excellent yields to give the corresponding N^2-substituted deoxyguanosines **5a**–**7a** and **8a** and **9a** (Table 1).

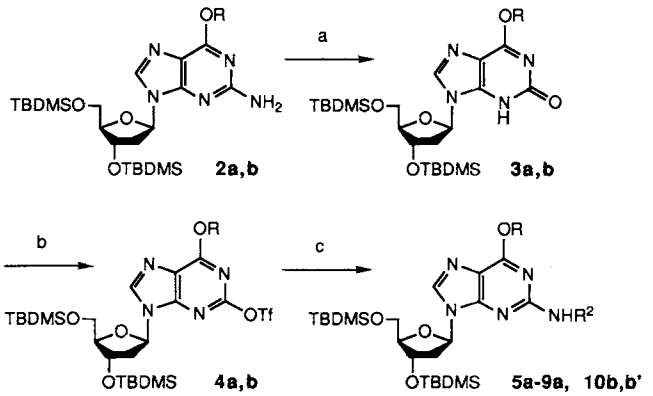

Scheme 1. a) *n*-$C_5H_{11}ONO$; b) CF_3SO_2Cl, NEt_3, CH_2Cl_2; c) R^2NH_2, DMF; **a**: R = *p*-nitrophenylethyl; **b**: R = allyl.

The reaction of **4a** with 1-aminomethylpyrene **6** and (*S*)-(+)-2-amino-2-phenylethanol **9** affords the protected N^2-deoxyguanosine adducts **6a** and **9a** in 81% and 88% yields, respectively. In contrast, Lee et al. reported[9a] a yield of 70% for the reaction of **6** with O^6-NPE-2-fluorodeoxyinosine under comparable conditions, while for a similar transformation of a partially protected 2-fluorodeoxyinosine with *trans*-configurated 1-amino-2-hydroxy-1,2,3,4-tetrahydrophenanthrene, Zajc et al.[9b] recently reported a yield of 55%.

Table 1. Experimental conditions and yields of the reaction of **4a** and **4b** with amines and amino alcohols according to Scheme 1. Selected physical data of the products are given in Table 2.

Amine (R^2NH_2)	Product	*T* [°C]	Yield [%]	R^1
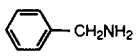	**5**	25	75	NPE
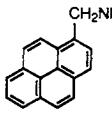	**6**	25	81	NPE
	7	25	81	NPE
$HO\text{-}CH_2\text{-}CH_2\text{-}NH_2$	**8**	25	82	NPE
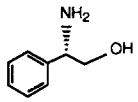	(+)-**9**	25	88	NPE
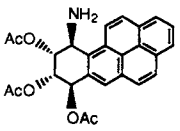	(±)-**10**	60	5	allyl

The structures **6a** and **9a** are derivatives of deoxyguanosine adducts proven to be products of the DNA alkylation by 1-pyrenylmethylsulfate[10] and 1-styreneoxide,[11] respectively. The reaction of **4b** with the acetylated *trans* amino alcohol (±)-**10**[12] of benzo[*a*]pyrene, which is only weakly nucleophilic due to the axially oriented amino group in the bay region,[13] yields a diastereomeric mixture of the N^2-deoxyguanosine adducts **10b** and **10b'**. These

[*] Dr. A. Seidel, Dr. T. Steinbrecher, Dipl.-Chem. C. Wameling, Prof. Dr. F. Oesch
Institut für Toxikologie der Universität
Obere Zahlbacher Strasse 67, D-W-6500 Mainz (FRG)

[**] Chemistry of Carcinogenic Metabolites, Part 2. This work was supported by the Deutsche Forschungsgemeinschaft (SFB 302). We thank the company Boehringer Mannheim for gifts of chemicals. T. S. is indebted to the German National Scholarship Foundation for a postgraduate fellowship. Part 1: W. Bochnitschek, A. Seidel, H. Kunz, F. Oesch, *Angew. Chem.* **1985**, *97*, 703; *Angew. Chem. Int. Ed. Engl.* **1985**, *24*, 699.

compounds are fully protected derivatives of the adducts formed in vivo from (±)-*r*-7,*t*-8-dihydroxy-*t*-9,10-epoxy-7,8,9,10-tetrahydrobenzo[*a*]pyrene [(±)-*anti*-BPDE], which is metabolically produced by cyctochrome P450-dependent monooxygenases.[14] Both diastereomers **10b**/**10b′** can be separated by preparative HPLC on a silica gel column. The absolute configuration of **10b** and **10b′** was confirmed by a qualitative comparison with the known CD spectra of the *trans*-configurated adducts[14] that were prepared by in vitro transformations of (+)- and (−)-*anti*-BPDE with calf thymus DNA, followed by enzymatic degradation and separation of the resulting *cis*/*trans* products. While the diastereomer eluted first (**10b** which has a 10*R* configuration) is ascribed to the *trans*-opened adduct of (−)-*anti*-(7*S*,8*R*,9*R*,10*S*)-BPDE, the more polar diastereomer **10b′** (10*S* configuration) corresponds to the analogous adduct of the ultimate carcinogenic (+)-*anti*-(7*R*,8*S*,9*S*,10*R*)-BPDE.[14]

The synthetic strategy described here enables the preparation of deoxyguanosines specifically alkylated at the exocyclic amino group. N^2-deoxyguanosine derivatives of epoxides with a defined structure are thus accessible. This method using the trimethanesulfonate group provides advantages over the common method using fluoro substituents with regard to reactivity and the use of inert silyl protecting groups at the deoxyribose moiety. The orthogonality of the protecting groups opens the possibility of sequence-selective incorporation of these adducts into oligonucleotides,[9a, 9b] which can serve as interesting tools for mechanistic studies of the mutation events in DNA initiated by adducts with defined structures.

Table 2. Selected physical data of the N^2-alkylated deoxyguanosines **5a**–**9a** and **10b**,**b′**.

5a: M.p. 77–79 °C; ^{1}H NMR (400 MHz, $CDCl_3$), δ = 8.09 (d, 2H, Ph), 7.83 (s, 1H, purine), 7.38–7.23 (m, 7H, Ph), 6.28 (pseudo-t, 1H, $H_{1'}$), 5.28 (t, 1H, NH), 4.65 (t, 2H, $CH_2C_6H_4NO_2$), 4.59 (d, 2H, CH_2-NH), 4.54–4.51 (m, 1H, $H_{3'}$), 3.96–393 (m, 1H, $H_{4'}$), 3.78 (dd, 1H, $H_{5'}$), 3.72 (dd, 1H, $5_{5'*}$), 3.19 (t, 2H, O-CH_2), 2.58–2.53 (m, 1H, $H_{2'}$), 2.30–2.26 (m, 1H, $H_{2'*}$), 0.88 (s, 9H, *t*Bu), 0.87 (s, 9H, *t*Bu), 0.05 (s, 6H, $SiCH_3$), 0.04 (s, 6H, $SiCH_3$); MS (FD): *m*/*z* 735 (M^+)

6a: M.p. 104–106 °C; ^{1}H NMR (400 MHz, $CDCl_3$), δ = 8.31 (d, 1H, H_{10}), 8.18–7.86 (m, 9H, aromat.), 7.43 (d, 2H, Ph-NO_2), 6.37 (pseudo-t, 1H, $H_{1'}$), 5.21 (d, 2H, CH_2-NH_2), 4.58–4.54 (m, 3H, CH_2-Ph-NO_2, $H_{3'}$), 3.96–3.94 (m, 1H, $H_{4'}$), 3.83–3.74 (m, 2H, $H_{5'}$, $H_{5'*}$), 3.10–3.01(m, 2H, OCH_2), 2.62–2.57 (m, 1H, $H_{2'}$), 2.36–2.30 (m, 1H, $H_{2'*}$), 0.89 (s, 9H, *t*Bu), 0.88 (s, 9H, *t*Bu), 0.06 (s, 6H, $SiCH_3$), 0.05 (s, 6H, $SiCH_3$); MS (FD): *m*/*z* 860 (M^+)

7a: M.p. 141–143 °C; ^{1}H NMR (400 MHz, $CDCl_3$), δ = 8.12 (d, 2H, Ph), 7.79 (s, 1H, purine), 7.44 (d, 2H, Ph), 6.28 (pseudo-t, 1H, $H_{1'}$), 4.69 (t, 2H, $CH_2C_6H_4NO_2$), 4.56–4.54 (m, 1H, $H_{3'}$), 3.94–3.92 (m, 1H, $H_{4'}$), 3.76–3.72 (m, 6H, $H_{5'}$, $H_{5'*}$), 3.25 (t, 2H, CH_2-CH_2-C_6H_4-NO_2), 2.66–2.62 (m, 1H, $H_{2'}$), 2.31–2.29 (m, 1H, $H_{2'*}$), 1.62–1.57 (m, 6H, CH_2-CH_2-CH_2), 0.89 (s, 18H, *t*Bu), 0.87 (s, 18H, *t*Bu), 0.08 (s, 6H, $SiCH_3$), 0.05 (s, 6H, $SiCH_3$); MS (FD): *m*/*z* 713 (M^+)

8a: viscous oil; ^{1}H NMR (400 MHz, $CDCl_3$), δ = 8.11 (d, 2H, Ph), 7.86 (s, 1H, purine), 7.43 (d, 2H, Ph), 6.27 (pseudo-t, 1H, $H_{1'}$), 5.35 (t, 1H, NH), 4.66 (t, 2H, CH_2-C_6H_4-NO_2), 4.55-4.52 (m, 1H, $H_{3'}$), 3.95–3.92 (m, 1H, $H_{4'}$), 3.88–3.78 (m, 4H, $H_{5'}$, $H_{5'*}$, CH_2-NH), 3.59–3.54 (m, 2H, CH_2OH), 3.23 (t, 2H, CH_2-CH_2-Ph-NO_2), 2.51–2.46 (m, 1H, $H_{2'}$), 2.34–2.59 (m, 1H, $H_{2'*}$), 0.87 (s, 18H, *t*Bu), 0.06 (s, 6H, $SiCH_3$), 0.05 (s, 6H, $SiCH_3$); MS (FD): *m*/*z* 689 (M^+)

9a: M.p. 124–125 °C; ^{1}H NMR (400 MHz, $CDCl_3$), δ = 8.09 (d, 2H, Ph-NO_2), 7.80 (s, 1H, purine), 7.35–7.21 (m, 7H, Ph-NO_2, Ph), 6.20 (pseudo-t, 1H, $H_{1'}$), 5.73 (d, 1H, NH), 5.04–5.00 (m, 1H, *CH*-NH), 4.65 (m, 3H, Ph-NO_2, $H_{3'}$), 3.96–3.88 (m, 3H, $H_{4'}$, CH_2OH), 3.79 (dd, 1H, $H_{5'}$), 3.72 (dd, 1H, $H_{5'*}$), 3.12 (t, 2H, CH_2-CH_2-C_6H_4-NO_2), 2.53–2.15 (m, 1H, $H_{2'}$) 2.32–2.15 (m, 1H, $H_{2'*}$), 0.89 (s, 9H, *t*Bu), 0.88 (s, 9H, *t*Bu), 0.07 (s, 6H, $SiCH_3$), 0.06 (s, 6H, $SiCH_3$) MS (FD): *m*/*z* 764 (M^+)

10b (derived from (−)-*anti*-BPDE): decomp. 125 °C, $[\alpha]_D^{20} = -179$ (*c* = 0.076, CH_3OH); $[\theta]_{281} = -265°$, $[\theta]_{244} = +346°$; UV(CH_3OH) λ_{max} [nm] (ε[cm^{2}mmol^{-1}]) = 245 (90660) 278 (63920); ^{1}H NMR (400 MHz, $CDCl_3$), δ = 8.20–7.99 (m, 8H, aromat.), 7.95 (s, 1H, purine), 6.75 (d, 1H, H_7), 6.35–6.25 (m, 1H, $H_{1'}$), 6.14 (pseudo-t, 1H, H_{10}), 6.10 (dd, 1H, H_9), 6.15–6.08 (m, 1H, allyl-H_γ), 5.95 (dd, 1H, H_8), 5.40 (d, 1H, allyl-H_t), 5.20 (d, 2H, allyl-H_c, OCH_2), 5.10–4.92 (m, 1H, OCH_2), 4.53 (s, 1H, $H_{3'}$), 3.92 (s, 1H, $H_{4'}$), 3.74–3.80 (m, 2H, $H_{5'}$, $H_{5'*}$), 2.27–2.33 (m, 2H, $H_{2'}$, $H_{2'*}$), 2.28 (s, 3H, $COCH_3$), 2.08 (s, 3H, $COCH_3$), 2.00 (s, 3H, $COCH_3$), 0.85 (s, 9H, *t*Bu), 0.80 (s, 9H, *t*Bu), 0.05 (s, 6H, $SiCH_3$), 0.03 (s, 6H, $SiCH_3$); MS (FAB): *m*/*z* 964 (MH^+)

10b′ (derived from (+)-*anti*-BPDE): decomp. 102 °C, $[\alpha]_D^{20} = +25.6$ (*c* = 0.12, CH_3OH); $[\theta]_{281} = +298°$, $[\theta]_{246} = -143°$; UV(CH_3OH) λ_{max} [nm] (ε[cm^{2}mmol^{-1}]) = 245 (75500) 278 (56570); ^{1}H NMR (400 MHz, $CDCl_3$), δ = 8.20–7.99 (m, 9H, purine, aromat.), 6.75 (d, 1H, H_7), 6.23–6.10 (m, 4H, H_9, H_{10}, allyl-H_γ, $H_{1'}$), 5.94 (dd, 1H, H_8), 5.38–5.31 (m, 1H, allyl-H_t), 5.24–5.10 (m, 2H, allyl-H_c, OCH_2), 5.11–4.95 (m, 1H, OCH_2), 4.54 (s, 1H, $H_{3'}$), 4.00–3.91 (m, 1H, $H_{4'}$), 3.86–3.68 (m, 2H, $H_{5'}$, $H_{5'*}$), 2.53 (m, 1H, $H_{2'}$), 2.28 (m, 4H, $COCH_3$, $H_{2'*}$), 2.08 (s, 3H, $COCH_3$), 2.01 (s, 3H, $COCH_3$), 0.88–0.81 (m, 18H, *t*-Bu), 0.05–0.04 (m, 12H, $SiCH_3$); MS (FAB): *m*/*z* 964 (MH^+)

Experimental Procedure

3a: **2a** (2.00 g, 3.1 mmol) was stirred in portions into *n*-pentyl nitrite (25 mL) at 0 °C. On warming to room temperature the solid went into solution, accompanied by nitrogen evolution. The solution was immediately evaporated to dryness under high vacuum and the crude product purified by flash chromatography (SiO_2; ethyl acetate/petroleum ether, 1:1). The product **3a** was obtained as viscous oil. Yield: 0.95 g (50%), $[\alpha]_D^{20} = +4.5$ (*c* = 0.3, methanol; NMR (400 MHz, $CDCl_3$): δ = 8.12 (d, 2H,Ph), 7.89 (s, 1H, purine), 7.46 (d, 2H, Ph), 6.33 (pseudo-t, 1H, $H_{1'}$), 4.84 (t, 2H, CH_2-C_6H_4-NO_2), 4.55–4.51 (m, 1H, $H_{3'}$), 3.94 (m, 1H, $H_{4'}$), 3.89 (dd, 1H, $H_{5'}$), 3.77 (dd, 1H, $H_{5'*}$), 3.25 (t, 2H, OCH_2), 2.52–2.49 (m, 1H, $H_{2'}$), 2.48–2.26 (m, 1H, $H_{2'*}$), 0.80 (s, 18H, *t*Bu), 0.03 (s, 12H, $SiCH_3$); MS(FD): *m*/*z* 646 (M^+).

4a: **3a** (0.50 g, 0.77 mmol) was dissolved in CH_2Cl_2 (25 mL) and treated with triethylamine (1 mL). The solution was stirred at 0 °C, and trifluoromethanesulfonyl chloride (130 mg, 0,77 mmol) was added. After 15 min the reaction mixture was concentrated and purified by flash chromatography (SiO_2, ethyl acetate/petroleum ether, 1:2). The initially oily product **4a** crystallized at −20 °C within 24 h. Yield: 510 mg (85%), m.p. 72 °C, $[\alpha]_D^{20} = +5.9$ (*c* = 2.6, methanol); ^{1}H NMR (400 MHz, $CDCl_3$): δ = 8.31 (s, 1H, purine), 8.15 (d, 2H, Ph), 7.46 (d, 2H, Ph), 6.35 (pseudo-t, 1H, $H_{1'}$), 4.81 (t, 2H, CH_2-C_6H_4-NO_2), 4.57 (m, 1H, $H_{3'}$), 4.00 (m, 1H, $H_{4'}$), 3.84 (dd, 1H, $H_{5'}$), 3.75 (dd, 1H, $H_{5'*}$), 3.30 (t, 2H, CH_2-CH_2-C_6H_4-NO_2), 2.59–2.54 (m, 1H, $H_{2'}$), 2.45–2.41 (m, 1H, $H_{2'*}$), 0.89 (s, 9H, *t*Bu), 0.87 (s, 9H, *t*Bu), 0.08 (s, 6H, $SiCH_3$), 0.06 (s, 6H, $SiCH_3$); MS(FAB): *m*/*z* 778 (M^+, 65%).

General procedure for the treatment of **4a**,**b** with amines and amino alcohols: **4a**,**b** (0.13 mmol) and amines **5**–**7** or amino alcohols **8**–**10** were stirred in DMF (10 mL) (for reaction temperatures see Table 1) until no more **4a**,**b** could be detected by thin-layer chromatography. The DMF was distilled off under high vacuum. The crude products were purified by flash chromatography (SiO_2, ethyl acetate/petroleum ether, 1:3 for the amine derivatives and 1:1 for the amino alcohol derivatives); the separation into diastereomeric adducts **10b** and **10b′** was achieved by preparative HPLC (5 µm, SiO_2) with a solvent mixture of dichloromethane/acetone (98.5:1.5) as eluent (**10b** is the product eluted first).

Received: July 8, 1992
Revised: December 11, 1992 [Z 5453 IE]
German version: *Angew. Chem.* **1993**, *105*, 408

[1] Reviews: a) E. C. Miller, J. A. Miller, *Pharmacol. Rev.* **1966**, *18*, 805; b) J. A. Miller, *Cancer Res.* **1970**, *30*, 559.
[2] Reviews: a) R. G. Harvey, *Acc. Chem. Res.* **1981**, *14*, 218; b) A. Dipple, R. C. Moschel, C. A. H. Bigger in *Chemical Carcinogens* (*ACS Monogr.* **1984**, *182*), S. 41.
[3] R. C. Moschel, W. R. Hudgins, A. Dipple, *J. Org. Chem.* **1986**, *51*, 4180.
[4] a) Reviews: P. C. Srivastava, R. K. Robins, R. B. Meyer in *Chemistry of Nucleosides and Nucleotides*, *Vol. 1* (Ed.: L. B. Townsend), Plenum, New York, **1988**, p. 113–281; b) G. E. Wright, E. F. Baril, V. M. Brown, N. C. Brown, *Nucleic Acids Res.* **1982**, *10*, 4431; c) G. E. Wright, L. W. Dudycz, *J. Med. Chem.* **1984**, *27*, 175; d) J. F. Gerster, R. K. Robins, *J. Am. Chem. Soc.* **1965**, *87*, 3752; e) M. J. Robins, B. Uznanski, *Can. J. Chem.* **1981**, *59*, 2608.
[5] R. Casale, L. W. McLaughlin, *J. Am. Chem. Soc.* **1990**, *112*, 5264.
[6] F. Himmelbach, B. S. Schulz, T. Trichtinger, R. Charubala, W. Pfleiderer, *Tetrahedron* **1984**, *40*, 59.
[7] Y. Hayakawa, M. Hirose, R. Noyori, *Nucleic Acids. Res. Symp. Ser.* **1990**, *22*, 1.
[8] E. J. Corey, J. W. Suggs, *J. Org. Chem.* **1973**, *38*, 3224.
[9] a) H. Lee, M. Hinz, J. J. Stezowski, R. G. Harvey, *Tetrahedron Lett.* **1990**, *31*, 6773; b) B. Zajc, M. K. Lakshman, J. M. Sayer, D. M. Jerina, *ibid.*

1992, *33*, 3409; the authors also report on a reaction of (±)-10-amino-7,8,9-trihydroxy-7,8,9,10-tetrahydrobenzo[*a*]pyrene with a silylated 2-fluorodeoxyinosine derivative but characterization of the products and yields are not given.

[10] S. Monnerjahn, A. Seidel, P. Steinberg, F. Oesch, M. Hinz, J. J. Stezowski, A. Hewer, D. H. Phillips, H. R. Glatt in *Proc. Int. Meet. Postlabelling Methods for the Detection of DNA Adducts*, Lyon (France), **1992**, in press.

[11] a) L. Latif, R. C. Moschel, K. Hemminki, A. Dipple, *Chem. Res. Toxicol.* **1988**, *1*, 364; b) K. Pongracz, S. Kaur, A. L. Burlingame, W. J. Bodell, *Carcinogenesis* **1992**, *13*, 315.

[12] For the stereoselective synthesis of (±)-**10**, see M. Lakshman, D. V. Nadkarni, R. E. Lehr, *J. Org. Chem.* **1990**, *55*, 4892. A O–N migration of an acyl group was not observed under these conditions.

[13] M. K. Lakshman, J. M. Sayer, D. M. Jerina, *J. Am. Chem. Soc.* **1991**, *113*, 6589.

[14] a) S. C. Cheng, B. D. Hilton, J. M. Roman, A. Dipple, *Chem. Res. Toxicol.* **1989**, *2*, 334; b) J. M. Sayer, A. Chadha, S. K. Agarwal, H. J. C. Yeh, H. Yagi, D. M. Jerina, *J. Org. Chem.* **1991**, *56*, 20.

[15] A. K. Basu, J. M. Essigmann, *Chem. Res. Toxicol.* **1988**, *1*, 1.

Stable [12]- and [18]Annulenes Derived from Tetraethynylethene**

By *John Anthony, Carolyn B. Knobler,* and *François Diederich**

In memoriam Franz Sondheimer

We recently described the synthesis of tetraethynylethene (**1a**)[1] along with geminally bisdeprotected (**1b**, **c**),[1] monodeprotected (**1d**),[2] and *trans*-bisdeprotected (**1e**)[2] derivatives and now wish to report the completion of the series with the first synthesis of a *cis*-bisdeprotected tetraethynylethene (**1f**).[3] Compound **1f** with a free *cis*-enediyne unit is of special interest because it could lead, by oxidative cyclization, to the hexaethynylhexadehydro-[18]annulene **2a** and after deprotection to **2c**, to the planar all-carbon network **3**.[4] Here, we report that Hay coupling of **1f** leads not only to the [18]annulene **2a** but also to the [12]annulene **4a** and discuss the very different properties of these macrocycles.

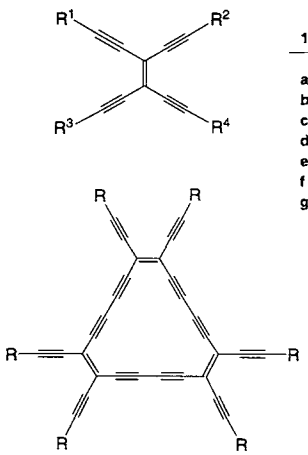

1	R^1	R^2	R^3	R^4
a	H	H	H	H
b	Ph	Ph	H	H
c	TIPS	TIPS	H	H
d	TIPS	TIPS	TIPS	H
e	Ph	H	H	Ph
f	TIPS	H	TIPS	H
g	TMS	H	TMS	H

2a R = TIPS
2b R = TMS
2c R = H

TIPS = $Si(iPr)_3$, TMS = $SiMe_3$

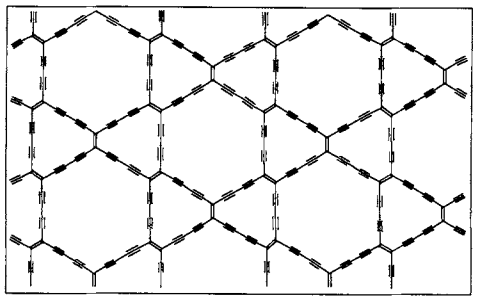

3

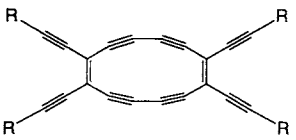

4a R = TIPS
4b R = TMS

cis-Enediyne **1f** proved to be far more difficult to prepare than the tetraethynylethene derivatives **1b–e** previously synthesized. The simplest route to **1f** started from *cis*-2,3-dichloro-2-buten-1,4-diol (**5**), obtained by exhaustive reduction of mucochloric acid,[5] and followed the pathway previously used for the synthesis of the *trans* derivative **1e** (Scheme 1).[2] However, this route was abandoned after oxidation of *cis*-diol **6** led preferentially to the dialkynyl lactone **7**[6] and since dialdehyde **8** could not be transformed into tetrabromide **9**.

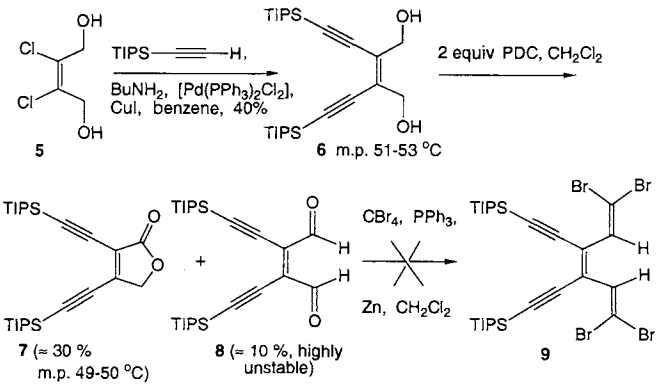

Scheme 1. Attempted direct synthesis of *cis*-enediyne **1f** from precursor **9**. TIPS = triisopropylsilyl, PDC = pyridinium dichromate.

To avoid the problems associated with the preparation and reactivity of dialdehyde **8**, a route to **1f** was chosen by which the key intermediate **9** was prepared by sequential introduction of the two dibromomethylene residues (Scheme 2). The key steps in this synthesis are the preparation of orthoester **11** and its selective reduction to the monoprotected diol **12**.[7] Since compound **13** and all other intermediates with dibromomethylene groups on the way to **1f** underwent facile *cis–trans* isomerizations in the presence of acid, acidic reaction and workup conditions had to be strictly avoided. As an example, removal of the methoxy-

[*] Prof. F. Diederich, J. Anthony
Laboratorium für Organische Chemie
ETH-Zentrum
Universitätstrasse 16, CH-8092 Zürich (Switzerland)
Dr. C. B. Knobler
Department of Chemistry and Biochemistry
University of California
Los Angeles, CA 90024-1569 (USA)

[**] We thank the U.S. National Science Foundation, the American Chemical Society (A.C.S. graduate student fellowship to J. A.) and the ETH (set-up funds) for support of this work. According to IUPAC nomenclature tetraethynylethene should be called 3,4-diethynyl-3-hexene-1,5-diyne. The trivial name tetraethynylethene is easier to remember, however, and equally unambiguous.

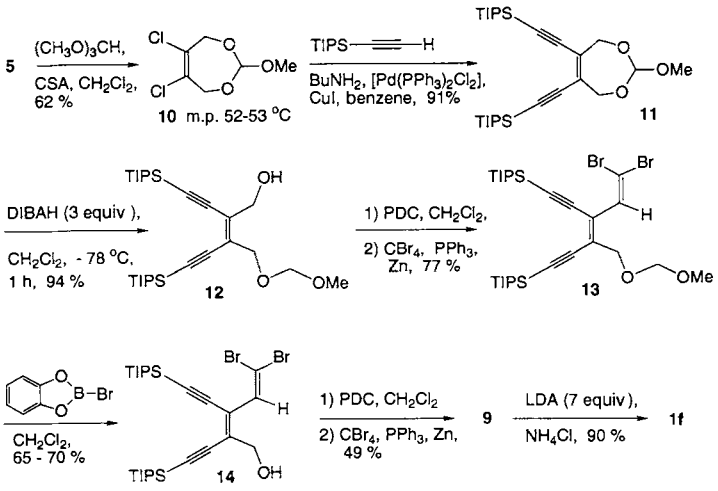

Scheme 2. Synthesis of *cis*-enediyne **1f**. Except for **10**, all compounds are oils. CSA = camphorsulfonic acid, DIBAH = diisobutylaluminum hydride, LDA = lithium diisopropylamide.

methylene protecting group in **13** with bromotrimethylsilane[8] afforded **14** in addition to a significant amount of the corresponding *trans*-enediyne, whereas no isomerization of **14** was detected with *B*-bromo-1,3,2-benzodioxaborole ("*B*-bromocatecholborane") as the deprotecting agent.[9]

Tetrabromide **9** was obtained as a yellow oil which, upon standing on the lab bench, yielded pale yellow crystals. Surprisingly, X-ray analysis of these crystals showed them to be *trans*-tetrabromide **15** (m.p. 78 °C, Fig. 1)![10] Further study showed that *cis*-tetrabromide **9** can be stored safely for several days in solution in the dark at −20 °C when traces of acid are strictly eliminated.

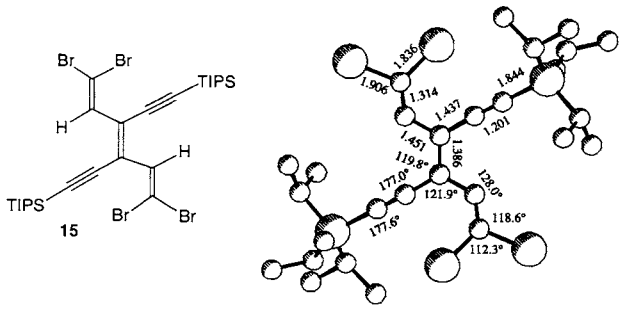

Fig. 1. X-ray crystal structure of **15**.

Upon treatment of **9** with an excess of LDA at −78 °C, a deep purple solution of the *cis*-di(lithium acetylide) formed, which was quenched at 0 °C with saturated NH_4Cl. The free *cis*-enediyne **1f** was obtained as a yellow oil which is quite stable at room temperature in dilute solution. When a solution of **1f** in benzene was heated at reflux for 6 h, 80 % of the compound was recovered; heating the neat oil to 60 °C gave immediate decomposition. Whether intramolecular Bergman cyclizations[11] or intermolecular processes are responsible for the decomposition of **1f** is currently under investigation.[12]

Hay coupling of **1f** (0.002 M in acetone) yielded the [12]annulene **4a** (28 %) and the [18]annulene **2a** (12 %) as readily separable and isolable compounds.[13] The 18-membered cycle **2a** is a stable yellow solid (m.p. 215 °C decomp.), and its ^{13}C and ^1H NMR data strongly support the cyclic trimeric structure. In addition, the characteristic electronic absorption spectrum of **2a** (Fig. 2) closely resembles those of other hexadehydro[18]annulenes with planar aromatic perimeters.[14] Based on this strong spectral correlation, we also assign aromatic character to the cyclic [4n + 2] π-electron system in **2a**.

The [12]annulene **4a** (m.p. 200 °C, decomp) crystallizes readily from pentane to give dark red needles suitable for X-ray crystallography (Fig. 3).[10] Except for the isopropyl groups, **4a** is planar with a mean out-of-plane deviation of the conjugated 20-carbon framework of 0.089(6) Å. Considerable strain in the 12-membered ring is expressed by the

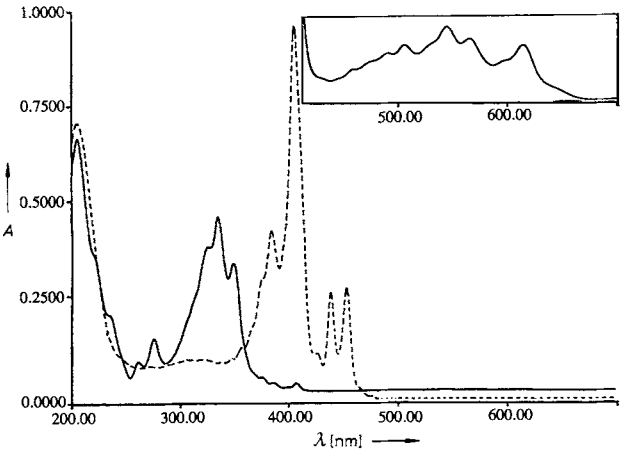

Fig. 2. Electronic absorption spectra of **2a** (----) and **4a** (——) recorded in pentane, $T = 298$ K, $d = 1$ cm, $c = 4.23 \times 10^{-6}$ M for **2a** and $c = 1.024 \times 10^{-5}$ M for the shorter wavelength and 2.56×10^{-6} M for the longer wavelength absorptions (insert) of **4a**. Inset is scaled up 25 ×. A = Absorbance.

strong bend in the two butadiyne units[4, 15b] and by the reduction of the inner C–C≡C bond angles to 117.6 and 118.5°. Despite this ring strain, the molecule is quite stable. At room temperature, dilute pentane solutions remain unchanged over weeks and crystals can be kept in air for several days without decomposition. However, if a solution of **4a** is concentrated without crystallization, significant decomposition occurs.

Both [18]annulene **2a** and [12]annulene **4a** have planar rigid chromophores, and correspondingly, their electronic absorption bands show considerable vibrational fine struc-

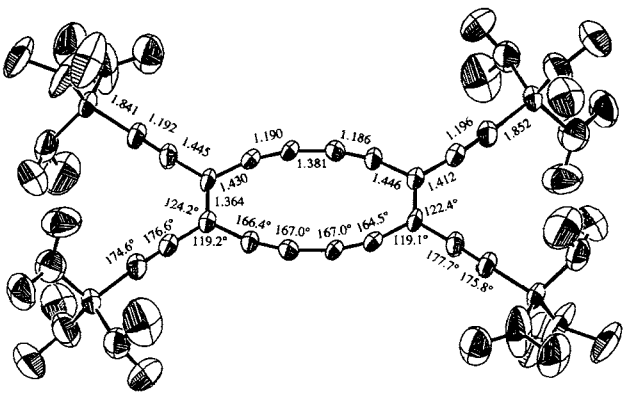

Fig. 3. X-ray crystal structure of **4a**.

ture. The spectra of the two compounds are otherwise strikingly different (Fig. 2). The end absorption in **2a** occurs near 480 nm (2.57 eV), while **4a** shows a characteristic weak absorption band at longer wavelengths which extends to 660 nm (1.87 eV) (Fig. 2). Solutions of **2a** are bright yellow, whereas compound **4a** gives purple solutions that, when dilute, look remarkably similar to solutions of buckminsterfullerene C_{60}.

Although the absence of protons in proximity to the [12]annulene perimeter of **4a** prevents a direct experimental determination of its paratropic character by ^{1}H NMR spectroscopy, a comparison of optical properties suggests that **4a** is antiaromatic. The strong redshift of the end absorption in the UV/VIS spectrum of **4a** as compared to **2a**, can be explained by the smaller HOMO–LUMO gap in an antiaromatic system. The spectrum of **4a** is indeed extremely similar in shape and structure to the spectrum of [12]annulene **16** which has an end absorption at approximately 620 nm (1.99 eV) and is paratropic according to its ^{1}H NMR spectrum.[16, 17] In contrast, [12]annulene **18** does not exhibit a paramagnetic ring current as a result of the benzannelation and shows optical properties that differ entirely from those of **4a** and **16**.[15a] Compound **18** is pale yellow and its end absorption in the UV/VIS spectrum already occurs at 450 nm (2.74 eV).[18] Together with the results of previous comparative studies on [18]- and [24]annulenes[4, 14, 19] these findings suggest that in series of planar, structurally related annulenes, careful correlations of electronic absorption spectra can be used to evaluate their aromatic or antiaromatic character.

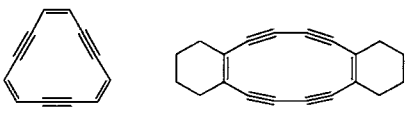

16

17

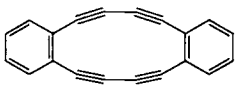

18

The deprotection of **2a** to give compound **2c** and the preparation of planar all-carbon networks by oxidative polymerization are now under investigation.

Experimental Procedure

12: To a solution of 7.35 g (15.0 mmol) of **11** in CH_2Cl_2 (150 mL) at $-78\,^\circ$C was added slowly 45 mL of a 1.0 M solution of DIBAH in hexanes (45 mmol). After 15 min, the solution was warmed rapidly to $0\,^\circ$C and stirred at that temperature for 15 min. The solution was quenched by careful addition of water until the entire mixture solidified. The product was dissolved in 50 mL of CH_2Cl_2, and the resulting solution was dried over $MgSO_4$. The grainy solid was removed by filtration, and the product-containing solution was concentrated to yield crude (96% pure) **12** (7.0 g, 94% yield) as a pale yellow oil which was used in the next reaction without further purification. Analytically pure **12** was obtained as a colorless oil by flash chromatography (SiO_2, CH_2Cl_2): IR (neat): $\tilde{\nu}$[cm^{-1}] = 3440 (O–H), 2146, 2127 (C≡C); ^{1}H NMR (200 MHz, $CDCl_3$): δ = 1.07 (s, 42H), 3.38 (s, 3H), 4.24 (s, 2H), 4.66 (s, 2H); ^{13}C NMR (50.32 MHz, $CDCl_3$): δ = 11.40, 18.86, 55.70, 62.04, 66.15, 95.86, 99.48, 101.02, 105.63, 106.55, 126.80, 132.49. MS (EI, 20 eV) *m/z* 492.3 (M^+).

2a/4a: To a solution of **1f** (0.89 g, 0.002 mol) in 500 mL of acetone was added 1 mL of Hay catalyst (prepared by stirring CuCl (2.5 g) and TMEDA (1.25 mL) in acetone (45 mL) for 30 min). After 1 h, the black solution was poured into pentane and extracted first with 0.1 N HCl, then with water and saturated NaCl solution. The solution was filtered with pentane through a short silica gel plug. The rapid elution of the deep purple fraction of **4a** (0.24 g, 28%) was followed by elution of the bright yellow fraction of **2a** (0.104 g, 12%). Compound **4a**: dark red needles (pentane), m.p. ≈ 200 °C (decomp); IR (KBr) $\tilde{\nu}$[cm^{-1}] = 2107 (C≡C); ^{1}H NMR (360 MHz, $CDCl_3$) δ = 1.00 (s, 84H); ^{13}C NMR (90.6 MHz, $CDCl_3$): δ = 11.06, 18.51, 87.80, 94.05, 99.67, 106.79, 124.37; MS (Desorption Electron Impact (DEI)), 20 eV) *m/z* 868 (M^+): UV/VIS (pentane) λ_{max} (ε) = 614 (270), 598 (sh) (190), 564 (300), 546 (370), 531 (sh) (290), 506 (290), 491 (254), 477 (225), 461 (195), 407 (1540), 402 (sh) (565), 385 (1690), 374 (sh) (3110), 349 (32650), 335 (44700), 326 (36900), 276 (13200), 262 (7210), 233 (sh) (19600), 220 nm (sh) (35200). Compound **2a**: m.p. 215 °C (decomp). IR (neat): $\tilde{\nu}$[cm^{-1}] = 2122 (C≡C); ^{1}H NMR (360 MHz, $CDCl_3$) δ = 1.17 (s, 126H); ^{13}C NMR (90.6 MHz, $CDCl_3$); δ = 11.31, 18.69, 83.81, 85.09, 102.25, 107.38, 118.00. MS (DEI, 20 eV) *m/z* = 1303.7 (M^+). UV/VIS (pentane) λ_{max} (ε) = 453 (56000), 438 (53700), 425 (sh) (22500), 405 (189700), 383 (84300), 375 (59400), 367 (35400), 356 (sh) (24100), 323 nm (17600).

Received: November 13, 1992 [Z 5686 IE]
German version: *Angew. Chem.* **1993**, *105*, 437

[1] Y. Rubin, C. B. Knobler, F. Diederich, *Angew. Chem.* **1991**, *103*, 708–710; *Angew. Chem. Int. Ed. Engl.* **1991**, *30*, 698–700.

[2] A. M. Boldi, J. Anthony, C. B. Knobler, F. Diederich, *Angew. Chem.* **1992**, *104*, 1270-1273; *Angew. Chem. Int. Ed. Engl.* **1992**, *31*, 1240–1242.

[3] a) Y. Hori, N. Noda, S. Kobayashi, H. Taniguchi, *Tetrahedron Lett.* **1969**, 3563–3566; b) H. Hauptmann, *Angew. Chem.* **1975**, *87*, 490–491; *Angew. Chem. Int. Ed. Engl.* **1975**, *14*, 498–499; c) H. Hauptmann, *Tetrahedron Lett.* **1975**, 1931–1934; d) H. Hopf, M. Kreutzer, *Angew. Chem.* **1990**, *102*, 425–426; *Angew. Chem. Int. Ed. Engl.* **1990**, *29*, 393–395; e) H. Hopf, M. Kreutzer, P. G. Jones, *Chem. Ber.* **1991**, *124*, 1471–1475.

[4] F. Diederich, Y. Rubin, *Angew. Chem.* **1992**, *104*, 1123–1146; *Angew. Chem. Int. Ed. Engl.* **1992**, *31*, 1101–1123.

[5] B. A. Arbuzov, E. N. Klimovitskii, M. B. Timirbaev, *Zh. Obshch. Khim.* **1986**, *13*, 150–155.

[6] All new compounds were fully characterized by ^{1}H and ^{13}C NMR, IR, and UV/VIS spectroscopy, and mass spectrometry. Correct elemental analyses were obtained for all stable derivatives; high-resolution mass spectra were measured for instable compounds.

[7] M. Takasu, Y. Naruse, H. Yamamoto, *Tetrahedron Lett.* **1988**, *29*, 1947–1950.

[8] S. Hanessian, D. Delorme, Y. Dufresne, *Tetrahedron Lett.* **1984**, *25*, 251–254.

[9] R. K. Boeckman, Jr., J. C. Potenza, *Tetrahedron Lett.* **1985**, *26*, 1411–1414.

[10] X-ray crystal data for **15** ($C_{28}H_{44}Br_4Si_2$); M_r = 756.45, triclinic space group $P\bar{1}$, Z = 1 (centrosymmetric molecule); a = 8.310(2), b = 9.514(2), c = 11.899(3) Å, α = 112.204(7), β = 97.872(7), γ = 90.175(7)°, V = 861 Å^3, $Mo_{K\alpha}$ radiation, $2\theta \leq 50°$, 3029 unique reflections; the structure was solved by heavy-atom methods, yielding R = 0.054, R_w = 0.072 for 1439 independent reflections with $I > 3\sigma(I)$. X-ray crystal data for **4a** ($C_{56}H_{84}Si_4$); M_r = 867.64, triclinic space group $P\bar{1}$, Z = 1 (centrosymmetric molecule); a = 11.739(3), b = 12.445(3), c = 12.438(3) Å, α = 101.262(8), β = 105.936(7), γ = 117.635(7)°, V = 1433 Å^3, $Cu_{K\alpha}$ radiation, $2\theta \leq 115°$, 3929 unique reflections; the structure was solved by statistical methods (SHELXS90), yielding R = 0.080, R_w = 0.101 for 2827 independent reflections with $I > 3\sigma(I)$. Further details of the crystal structure investigations are available on request from the Director of the Cambridge Crystallographic Data Centre, 12 Union Road, GB-Cambridge CB2 1EZ (UK), on quoting the full journal citation.

[11] T. P. Lockhart, P. B. Comita, R. G. Bergman, *J. Am. Chem. Soc.* **1981**, *103*, 4081–4090.

[12] The TMS-protected *cis*-enediyne **1g** was also obtained as a colorless oil following the synthetic route shown in Scheme 2. The TMS-protected [12]annulene **4b** (ready decomposition) and [18]annulene **2b** (m.p. 170 °C, decomp) have also been prepared and their spectral properties closely resemble those of the two TIPS derivatives **4a** and **2a**, respectively; J. Anthony, F. Diederich, unpublished results.

[13] The yield of the oxidative cyclization reaction is strongly dependent on concentration as was shown in more systematic studies with the TMS-protected *cis*-enediyne **1g**: Whereas a 0.006 M solution of **1g** in acetone gave a product ratio of 12:5:1 (**4b**:**2b**: larger macrocycles), a 0.045 M solution led to a higher yield of the larger cycles [product ratio: 1:4:2 (**4b**:**2b**: larger macrocycles)]. Generally, the overall yield of isolable cyclic products increased with increasing concentration of **1g**. In the coupling of the TIPS derivative **1f**, higher cyclic oligomers beyond **2a** are not formed presumably for reasons of steric crowding of the TIPS groups in the larger macrocycles.

[14] a) F. Diederich, Y. Rubin, C. B. Knobler, R. L. Whetten, K. E. Schriver, K. N. Houk, Y. Li, *Science (Washington, D.C.)* **1989**, *245*, 1088–1090; b) Y. Rubin, C. B. Knobler, F. Diederich, *J. Am. Chem. Soc.* **1990**, *112*, 1607–1617.

[15] a) O. M. Behr, G. Eglinton, A. R. Galbraight, R. A. Raphael, *J. Chem. Soc.* **1960**, 3614–3623; b) W. K. Grant, J. C. Speakman, *Proc. Chem. Soc. London* **1959**, 231.
[16] a) K. G. Untch, D. C. Wysocki, *J. Am. Chem. Soc.* **1966**, *88*, 2608–2610; b) F. Sondheimer, R. Wolovsky, P. J. Garratt, I. C. Calder, *ibid.* **1966**, *88*, 2610.
[17] Some degree of paratropicity has been assigned to **17** by using the ^{1}H NMR criterion, although the conformational flexibility of the cyclohexene rings seems to influence the rigidity of the 12-membered ring as suggested by the reduced vibrational fine structure in the electronic absorption spectrum which extends to approx. 550 nm (2.24 eV); G. M. Pilling, F. Sondheimer, *J. Am. Chem. Soc.* **1971**, *93*, 1970–1977.
[18] For the cancellation of the paramagnetic ring current in other benzannelated [12]annulenes, see H. A. Staab, R. Bader, *Chem. Ber.* **1970**, *103*, 1157–1167 and references therein.
[19] Y. Li, Y. Rubin, F. Diederich, K. N. Houk, *J. Am. Chem. Soc.* **1990**, *112*, 1618–1623.

$[Mo_2(CCH)_4(PMe_3)_4]$, the Parent Dimetallapolyyne**

By *Timothy C. Stoner, Steven J. Geib,* and *Michael D. Hopkins**

We are presently exploring the syntheses, structures, bonding, and properties of transition metal complexes and transition metal-containing polymers with conjugated electron systems.[1–3] As part of this work, we recently reported the preparation of alkynyl-substituted complexes with quadruple bonds of the types $[M_2(CCR)_4(PMe_3)_4]$ (M = Mo, W; R = alkyl, C_6H_5, $SiMe_3$)[1] and $[1,1\text{-}W_2(CCMe)_2Cl_2(PMe_3)_4]$,[2] and we noted that the electronic absorption spectra of these dimetallapolyynes manifest δ(MM)–π(CC) conjugation. Unfortunately, we were neither able to characterize the $[M_2(CCR)_4(PMe_3)_4]$ class by X-ray crystallography,[4] nor to prepare the parent $[M_2(CCH)_4(PMe_3)_4]$ derivatives by the otherwise general synthetic route to these compounds. The study of the parent ethynyl compounds, which possess the electronically simplest alkynyl R group with the highest symmetry, is crucial to understanding the dimetallapolyyne class as a whole, since their bonding and properties provide benchmarks against which the symmetry and inductive effects of organic and inorganic R groups can be evaluated. We now wish to report the synthesis and crystal structure of the dimetallapolyyne **1**, as well as spectroscopic evidence that **1**

$[Mo_2(CCH)_4(PMe_3)_4]$ **1**

is, in fact, electronically distinct from other $[Mo_2(CCR)_4(PMe_3)_4]$ complexes.

We have successfully prepared a variety of $[M_2(CCR)_4(PMe_3)_4]$ complexes from the reaction between $[M_2Cl_4(PMe_3)_4]$ and LiCCR (4 equiv).[1, 2] In contrast, no tractable products were obtained under comparable conditions from the reactions between $[Mo_2Cl_4(PMe_3)_4]$ and either $LiCCH \cdot (H_2NCH_2CH_2NH_2)$ or MgCl(CCH). Given that protodesilylation of alkynylsilanes is a standard synthetic route to terminal alkynes,[5] it seemed plausible to us that **1** might be similarly generated from **2**.[1] Although the use of

$[Mo_2(CCSiMe_3)_4(PMe_3)_4]$ **2**

this method to generate transition metal ethynyl complexes has not, to our knowledge, been reported,[6] and there is scant precedent in the chemistry of complexes with quadruple bonds for ligandlocalized reactivity,[7] the reaction of **2** with $[nBu_4N][HF_2]$[8] in dimethoxyethane at room temperature affords **1** cleanly in high yield. The use of $[nBu_4]F \cdot 3H_2O$ as the protodesilylation reagent slows down the reaction, and lowers the yield of **1**. Compound **1** was identified by elemental analyses, ^{1}H, ^{13}C, and ^{31}P NMR spectroscopy, and X-ray crystallography.

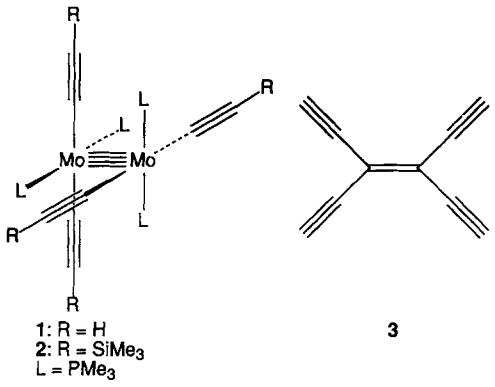

Crystals of **1** are free of disorder, unlike those of all other $[M_2(CCR)_4(PMe_3)_4]$ compounds that we have examined,[4] allowing the first high-quality single-crystal X-ray diffraction study for this class of compounds.[9] The structure of **1** (Fig. 1) is typical of those of the $[M_2X_4(PMe_3)_4]$ class:[7, 10] it possesses idealized D_{2d} symmetry, and the bond lengths and angles of the $Mo_2C_4P_4$ core lie within the expected ranges. The C≡C (1.18 Å) and C–H (0.93 Å) bond lengths of **1** are similar to those of $[Fe(\eta^5\text{-}C_5Me_5)(CO)_2(CCH)]$ (1.17

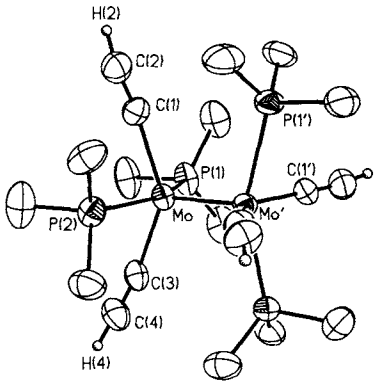

Fig. 1. Molecular structure of **1** (ORTEP, thermal ellipsoids at the 50% probability level). For clarity, all hydrogen atoms are omitted except H(2) and H(4), which are represented by spheres of arbitrary size. Selected bond lengths [Å] and bond angles [°] (standard deviations in parentheses): Mo-Mo' 2.134(1), Mo-P(1) 2.509(1), Mo-P(2) 2.515(1), Mo-C(1) 2.153(4), Mo-C(3) 2.161(4), C(1)-C(2) 1.183(6), C(3)-C(4) 1.174(6), C(2)-H(2) 0.950(39), C(4)-H(4) 0.909(35); Mo'-Mo-P(1) 103.2(1), Mo'-Mo-P(2) 103.1(1), Mo'-Mo-C(1) 110.5(1), Mo'-Mo-C(3) 110.1(1), Mo-C(1)-C(2) 171.7(3), Mo-C(3)-C(4) 171.9(4), C(1)-C(2)-H(2) 172.1(24), C(3)-C(4)-H(4) 166.7(24), Mo-Mo' torsion angle = 1.1.

[*] Prof. M. D. Hopkins, T. C. Stoner, Dr. S. J. Geib
Department of Chemistry, University of Pittsburgh
Pittsburgh, PA 15260 (USA)

[**] This research was supported by the National Science Foundation, the Camille and Henry Dreyfus Foundation, and the David and Lucile Packard Foundation (M. D. H.), and by an Andrew W. Mellon Graduate Fellowship (T. C. S.).

and 0.87 Å, respectively),[11] the only other related metal complex for which both lengths are known, and to those of acetylene.[12] The Mo–C≡C (ca. 172°) and C≡C–X (172, 167°) units in **1** are slightly bent, which may reflect the fact that relatively little energy is necessary to bend a C≡C–H unit.[13] The difference of 5° between the two crystallographically independent C≡C–H bond angles is not statistically significant, although the ethynyl groups do lie in very different environments in these chiral crystals: C(1)≡C(2)–H(2) is pointed at the ethynyl β-carbon atom of an adjacent molecule, forming a T-shaped structure, while the ethynyl ligand of a third molecule is directed similarly at C(4) of C(3)≡C(4)–H(4). This interesting arrangement is reminiscent of one found in crystalline[12] and surface-bound[14] acetylene, as is the CCH ··· C distance (2.99 Å for **1**, 3.05 Å for C_2H_2).[12]

We have proposed previously that the structural parameter most sensitive to π(CC)–δ(MM)–π(CC) conjugation in dimetallapolyynes is the M–C bond length.[2] The difference between the Mo–C bond lengths of **1** and $[Mo_2Me_4(PMe_3)_4]$[10] is 0.09 Å, which can be attributed solely to the difference (0.08 Å) between the single-bond covalent radii of sp- and sp^3-hybridized carbon atoms. Thus, the structure of **1** does not manifest a π(Mo–C) bonding interaction. In contrast, the more sensitive ^{1}H NMR and electronic spectroscopic probes of such interactions strongly support the formulation of **1** as a system with π(CC)–δ(MM)–π(CC) conjugation. Specifically, the signal of the proton of the C≡C–H unit in **1** appears as a complex multiplet in the ^{1}H NMR spectrum and as a singlet in the $^1H\{^{31}P\}$ spectrum, indicative of long-range spin-spin coupling between these nuclei and phosphorus; this coupling is facilitated by π(CC)–δ(MM) electron delocalization.[2] Moreover, the $^1(\delta \rightarrow \delta^*)$ absorption band in the electronic spectrum of **1** ($\tilde{\nu}_{max} = 15150\ cm^{-1}$, $\varepsilon = 4550$) is red shifted by about 1800 cm^{-1} from that of $[Mo_2Me_4(PMe_3)_4]$,[1] and is nearly 2.5 times as intense, consistent with π–δ–π conjugation.

Although the properties of **1** are largely similar to those of other $[Mo_2(CCR)_4(PMe_3)_4]$ compounds, there also appear to be electronic differences between the parent compound and the substituted derivatives, as evidenced by the distinctive vibronic structure that the $^1(\delta \rightarrow \delta^*)$ band of **1** displays at low temperature. Whereas all other $[Mo_2(CCR)_4(PMe_3)_4]$ derivatives that we have examined display a prominent 360-cm^{-1} progression as the major vibronic feature, **1** displays a 400-cm^{-1} progression (Fig. 2). We have suggested that the 360-cm^{-1} progression corresponds to the excited-state ν(Mo–C) mode, based on the ground-state vibrational frequencies for **2** (ν(Mo–Mo) = 362, ν(Mo–C) = 397 cm^{-1}).[1] While we have not been able to obtain Raman data for **1** due to its photochemical instability (see below), this conclusion applies to **1** better still, given the closer match in frequency between its vibronic progression and ν(Mo–C), and we thus conclude that the 360-cm^{-1} progression observed for other dimetallapolyynes is a combination of the vibrations of both ν(Mo–Mo) and ν(Mo–C), and that the 400-cm^{-1} progression for **1** is almost exclusively based on ν(Mo–C). Since the $\delta(M_2)$ and $\delta^*(M_2)$ orbitals are nonbonding with respect to the σ(CCR) orbitals, the different relative vibronic activities of the ν(Mo–C) and ν(Mo–Mo) modes for **1** as compared to other $[Mo_2(CCR)_4(PMe_3)_4]$ compounds would appear to reflect fundamental differences in ground- and/or $^1(\delta\delta^*)$ excited-state M–C π bonding among these complexes. That **1** is electronically distinct from other dimetallapolyynes is also borne out by its reactivity in the excited state; while solutions of **2** are indefinitely stable towards irradiation into the $^1(\delta \rightarrow \delta^*)$ band, **1** decomposes rapidly under comparable conditions. The question of whether these differences between **1** and substituted $[Mo_2(CCR)_4(PMe_3)_4]$ derivatives arise from σ or π effects of the R group is under investigation.

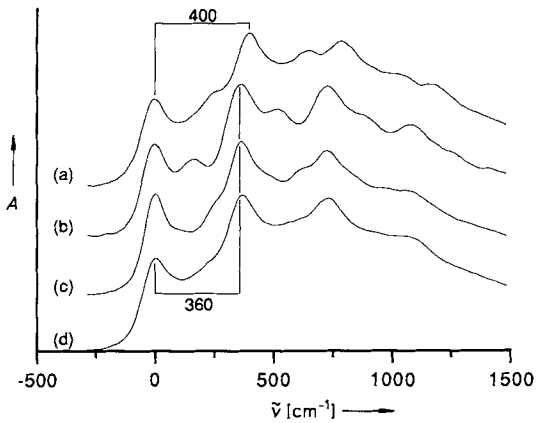

Fig. 2. Electronic absorption spectra (in the region of the $^1(\delta \rightarrow \delta^*)$ band) of compounds of the type $[Mo_2(CCR)_4(PMe_3)_4]$ at 77 K in 2-methylpentane, normalized to the energies of their 0–0 vibronic transitions: a) R = H, b) R = Me, c) R = *t*Bu, d) R = $SiMe_3$. *A* = absorbance. Vibronic spacings are in cm^{-1}.

In closing, it is interesting to compare the structure, spectra, and bonding of **1** with those of the recently reported tetraethynylethene (**3**),[15] its closest organic analogue and archetype of the tetraalkynylethene class of compounds.[16] Aside from the lack of planarity among the ethynyl groups of **1**, these cross-conjugated tetraethynyl compounds differ largely in the elemental and frontier-orbital composition of their dinuclear cores; the δ(Mo≡Mo) fragment of **1**[17] is replaced by a π(C=C) subunit in **3**. Spectroscopic similarities between **1** and **3** include the fact that they exhibit identical ^{1}H NMR chemical shifts for the proton of the C≡C–*H* unit ($\delta = 4.38$), well downfield from that of acetylene ($\delta = 1.80$), and that the energies of the lowest lying electronic transitions of the $[Mo_2(CCR)_4(PMe_3)_4]$ and $C_2(CCR)_4$ classes both stand in the order H > $SiMe_3$ > Ph.[1, 15, 16c] In addition, the molecular structures of these classes both display distinct bond-order alternation along their conjugated backbones. These similarities support our earlier suggestions[1–3] that the electronic structures of conjugated organic and transition metal compounds parallel each other, and they encourage us to believe that other physical properties common to dimetallapolyynes and tetraalkynylethenes will track each other as well. Work is in progress to explore these analogies further.

Experimental Procedure

1: A dimethoxyethane solution of $[nBu_4N][HF_2]$ [8] (excess) was added to a solution of **2** [1] (5.08 g, 5.73 mmol) in the same solvent at 25 °C. The color of the resulting solution changed little over the course of the reaction; monitoring by UV/VIS spectroscopy revealed that the reaction was complete within about 30 min. The volatile components of the reaction mixture were removed under vacuum, yielding a viscous liquid; this was extracted with pentane, which was then decanted from the reaction mixture, filtered, and evaporated under vacuum. Recrystallization of the resulting blue powder by slow addition of acetonitrile to an ether solution at room temperature gave 3.19 g (93%) of **1** as blue needles. Crystals suitable for single-crystal X-ray diffraction were obtained by slow cooling of a hexamethyldisiloxane solution of **1** to −35 °C. ^{1}H NMR (500 MHz, C_6D_6, 25 °C): $\delta = 4.38$ (m, C*CH*), 1.72 (virtual t, ^2J(H,P) + ^4J(H,P) = 7.65 Hz, PMe_3); $^1H\{^{31}P\}$ NMR (500 MHz): $\delta = 4.38$ (s, 4H, CCH), 1.72 (s, 36H, PMe_3); ^{13}C NMR (75.4 MHz): $\delta = 133.8$ (d, ^1J(C,H) = 219 Hz, *C*CH), 133.4 (br, *C*CH), 15.3 (q, ^1J(C,H) = 129 Hz, PMe_3); $^{31}P\{^1H\}$ NMR

(202 MHz): $\delta = -4.39$ (s). UV/VIS (*n*-hexane): λ_{max} [nm] (ε) = 660 (4550), 520 (290), 362 (5140). Correct C, H analysis.

Received: June 17, 1992 [Z 5397 IE]
German version: *Angew. Chem.* **1993**, *105*, 457

[1] T. C. Stoner, R. F. Dallinger, M. D. Hopkins, *J. Am. Chem. Soc.* **1990**, *112*, 5651.
[2] T. C. Stoner, S. J. Geib, M. D. Hopkins, *J. Am. Chem. Soc.* **1992**, *114*, 4201.
[3] a) T. P. Pollagi, T. C. Stoner, R. F. Dallinger, T. M. Gilbert, M. D. Hopkins, *J. Am. Chem. Soc.* **1991**, *113*, 703; b) J. Manna, S. J. Geib, M. D. Hopkins, *ibid.* **1992**, *114*, 9199.
[4] T. C. Stoner, M. D. Hopkins, W. P. Schaefer, R. E. Marsh, *Acta Crystallogr. Sect. B*, submitted.
[5] E. W. Colvin, *Silicon Reagents in Organic Synthesis*, Academic Press, London, **1988**.
[6] Protodesilylations of other C–SiMe$_3$ ligands have been reported: A. Wong, P. C. W. Kang, C. D. Tagge, D. R. Leon, *Organometallics* **1990**, *9*, 1992; G. M. Janison, A. E. Bruce, P. S. White, J. L. Templeton, *J. Am. Chem. Soc.* **1991**, *113*, 5057.
[7] F. A. Cotton, R. A. Walton, *Multiple Bonds Between Metal Atoms*, Wiley, New York, **1982**.
[8] R. K. Sharma, J. L. Fry, *J. Org. Chem.* **1983**, *48*, 2122.
[9] X-ray crystallographic data for **1**: $P4_32_12$; $a = 12.013(2)$, $c = 20.623(4)$ Å, $V = 2976.1(10)$ Å^3, $Z = 4$, $\rho_{calcd} = 1.331$ g cm^{-3}, $T = -55$ °C. All 2639 independent reflections ($4° \le 2\theta \le 53°$) were used in the solution and refinement of the structure. A semi-empirical absorption correction (XABS) was applied to all data ($\mu(Mo_{K\alpha}) = 10.61$ cm^{-1}). The structure was solved by direct methods, which located the Mo and two P atoms; remaining non-hydrogen atoms were located from subsequent difference Fourier syntheses and refined anisotropically. All hydrogen atoms were located and refined isotropically. The structure refined to $R_F = 0.0319$ and $R_{wF} = 0.0199$; $\Delta/\rho = 0.46$ e Å^{-3}. Further details of the crystal structure investigation are available on request from the Director of the Cambridge Crystallographic Data Centre, 12 Union Road, GB-Cambridge CB2 1EZ (UK), on quoting the full journal citation.
[10] F. A. Cotton, K. J. Wiesinger, *Inorg. Chem.* **1990**, *29*, 2594, and references therein.
[11] M. Akita, M. Terada, S. Oyama, Y. Moro-oka, *Organometallics* **1990**, *9*, 816.
[12] G. J. H. van Nes, F. van Bolhuis, *Acta. Crystallogr. Sect. B* **1979**, *35*, 2580.
[13] E. B. Wilson, Jr., J. C. Decius, P. C. Cross, *Molecular Vibrations*, McGraw-Hill, New York, **1955**, p. 176.
[14] S. K. Dunn, G. E. Ewing, *J. Phys. Chem.* **1992**, *96*, 5294, and references therein.
[15] Y. Rubin, C. B. Knobler, F. Diederich, *Angew. Chem.* **1991**, *103*, 708; *Angew. Chem. Int. Ed. Engl.* **1991**, *30*, 698.
[16] a) Y. Hori, K. Noda, S. Kobayashi, H. Taniguchi, *Tetrahedron Lett.* **1969**, 3563; b) H. Hauptmann, *Angew. Chem.* **1975**, *87*, 490; *Angew. Chem. Int. Ed. Engl.* **1975**, *14*, 498; c) H. Hopf, M. Kreutzer, P. G. Jones, *Chem. Ber.* **1991**, *124*, 1471.
[17] See also footnote 19 in ref. [1].

Tetracyanohydroquinone and its Dimorpholinium Salt: Hydrogen Bonds O–H···N or $O^{\ominus}\cdots H\text{–}^{\oplus}N$ to Nitrogen Bases of Different Strengths**

By *Hans Bock,* Wolfgang Seitz, Zdenek Havlas,* and *Jan W. Bats*

Dedicated to Professor Meir Lahav

Multiple hydrogen bonding in[1] and between[2–4] molecules exert a structure-determining influence especially if their usually small individual energy contributions are increased by cooperative effects. Furthermore, the H-bond dynamics $(A\text{–}^{\oplus}H\cdots B)\leftrightarrow(A\cdots H^{\oplus}\text{–}B)$ within the time domain of about 10^{-9} s allows, through molecular recognition, the fast and biochemically important[2] optimization of self-organization processes, which is presently topic of extensive studies on selected suitable model compounds.[2, 3] The morphology of molecules and molecular aggregates containing structure-determining hydrogen bonds can also be modified by the relative electron densities at their proton donor and acceptor centers:[1–4] Thus the exchange of chloride anions as *external*, electron-rich H-bond acceptors ($Cl^{\ominus}\cdots H\text{–}^{\oplus}N$) in tetrapyridylpyrazine dihydrochloride by non-protonatable tetraphenylborate anions produces a flattened molecular skeleton with extremely short *intramolecular* $N\cdots H\text{–}^{\oplus}N$ bridges between adjacent pyridine rings[1]. Here we report drastic structural changes (Fig. 1) caused by reorganization of hydrogen bonds on treatment of tetracyanohydroquinone with the considerably stronger nitrogen base, morpholine [Eq. (a)].

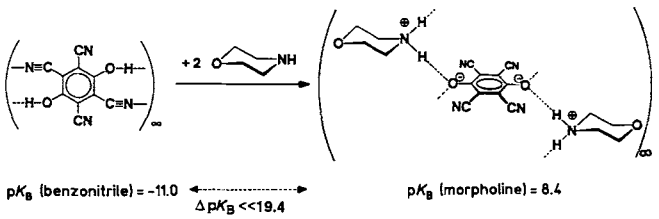

(a)

According to the general reaction scheme between Brønsted acids AH and bases B via proton transfer—$AH + B \rightleftharpoons (A\text{–}H\cdots B) \rightleftharpoons (A^{\ominus}\cdots H\text{–}^{\oplus}B)$—the acidic hydroquinone AH_2 crystallizes in a form containing four H bonds to its weakly basic cyanogen substituents, the H acceptors (Fig. 1a, b). After addition of the almost 20 pK_B units stronger (!) base, morpholine,[5] a double proton transfer generates the dimorpholinium salt $(HB^{\oplus})_2A^{2\ominus}$ under formation of its energetically favorable dianion $A^{2\ominus}$. In this process, four O–H···N hydrogen bonds, two on either side of the six-membered rings, are each substituted by $O^{\ominus}\cdots H\text{–}^{\oplus}N$ bonds outside of the planes of the rings (Fig. 1c, d).

A search of the literature for known hydrogen bonds to nitrile acceptors[8] yielded almost a thousand references in which the shortest O(H)···NC distances of 279 pm were found for both cyanoacetic acid[8g] and for hexacyanocobalt(III) dihydrate.[8h] The O(H)···NC distances of only 277 pm in tetracyanohydroquinone (Fig. 1b) are therefore the shortest O–H···NC hydrogen bonds observed so far. Remarkable are also the enlarged angles CCO of 125° and COH of 115°, which result in an approximately linear O(H)···NC arrangement (angle at H of about 162°). The O–H bond lengths have to be corrected (based on neutron diffraction data[1, 2, 4]) to about 100 pm; the H···N distances should therefore amount to about 180 pm (Fig. 1b).

On recrystallization of tetracyanohydroquinone in the presence of the stronger nitrogen base, morpholine,[5] a double proton transfer produces the tetracyanohydroquinone dianion and two morpholinium cations [Eq. (a)], which again form a hydrogen-bonded aggregate. Its low-temperature crystal structure analysis (Fig. 1c, d) proves that polar bonds $O^{\ominus}\cdots H\text{–}^{\oplus}N$ are now present below and above the planes of the six-membered rings. At both participating centers, the hydroquinone dianion oxygen and the

[*] Prof. Dr. H. Bock, Dipl.-Chem. W. Seitz
Institut für Anorganische Chemie der Universität
Niederurseler Hang, D-W-6000 Frankfurt am Main 50 (FRG)
Dr. Z. Havlas
Institute of Organic Chemistry and Biochemistry
of the Czechoslowakian Academy of Sciences in Prague (Czech Republic)
Dr. J. W. Bats
Institute of Organic Chemistry, University of Frankfurt

[**] Structures of Charge-Perturbed and Sterically Overcrowded Molecules, Part 19. This work was supported by the Deutsche Forschungsgemeinschaft, the Fonds der Chemischen Industrie and the State of Hesse. – Part 18: Z. Havlas, S. Nick, H. Bock, *J. Int. Quantum Chem.* **1992**, *44*, 449.

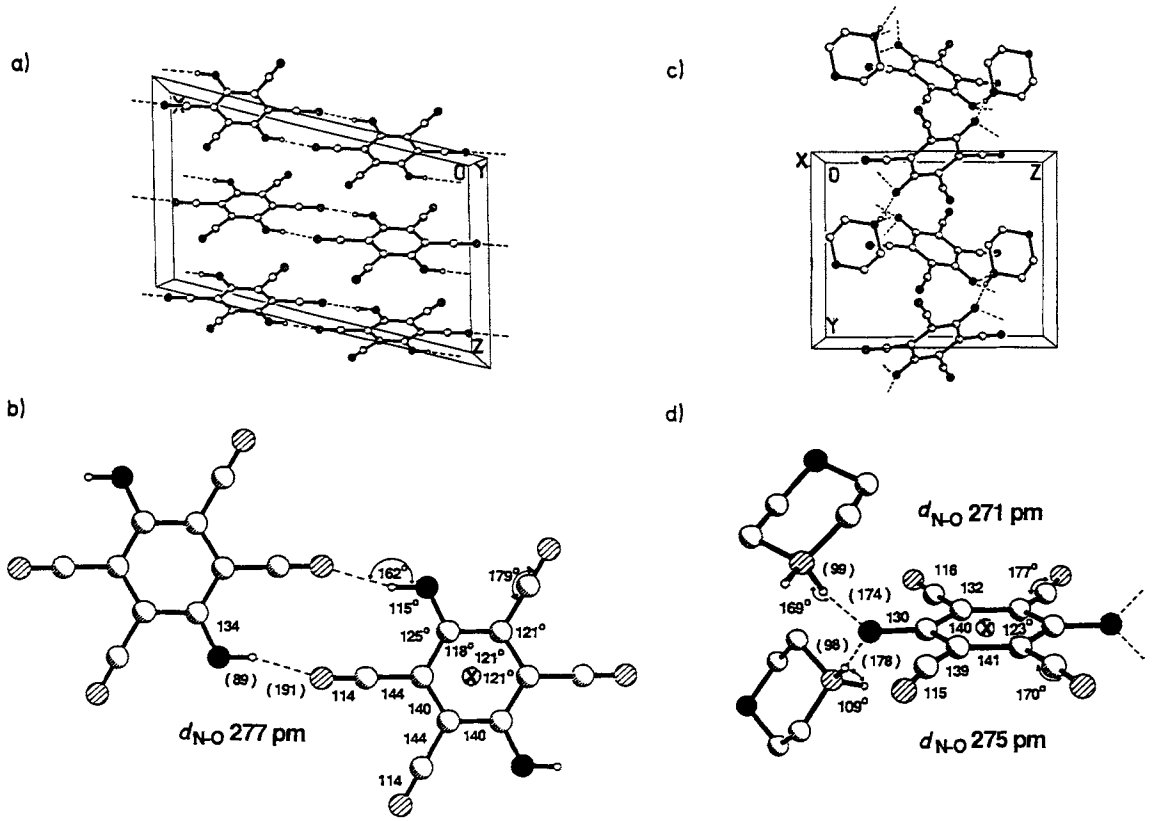

Fig. 1. Single crystal structures of tetracyanohydroquinone [6] and its dimorpholinium salt [7]: a) Unit cell of hydroquinone showing strings in the (110) direction ($Z = 4$; shortest interchain distance 308 pm) and b) section with four O–H ··· NC hydrogen bonds and the essential structural data. c) Packing of the morpholinium salt in the x direction showing unit cell ($Z = 2$) and d) section with four $O^{\ominus} \cdots H\text{–}{}^{\oplus}N$ hydrogen bonds and the essential structural data. (● = O, ▨ = N; ⊗: crystallographic inversion center.)

morpholinium nitrogen, bifurcation[2–5,9] ($H \cdots O^{\ominus} \cdots H$) and ($\cdots H\text{–}{}^{\oplus}N\text{–}H \cdots$) is observed. The $O^{\ominus} \cdots H\text{–}{}^{\oplus}N$ distances of 271 and 275 pm are shorter than in tetracyanohydroquinone (Fig. 1b,d); the same holds for the average $O^{\ominus}$–C ($\Delta d_{OC} = -4$ pm) and (N)C–C distances ($\Delta d_{CC} = -9$ pm). Eye-catching is also the decrease in the benzene *ipso* angle by 114° caused by the $O^{\ominus}$ donor substituent.[10]

For rationalization of these unexpected structural findings, extensive and mostly geometry-optimized PM3 calculations[11] provide the following clues:

1) Monomeric tetracyanohydroquinone should exhibit a gas-phase structure[11a], which except for the angles COH (calcd 109°) and the O–H bond lengths (calcd 95 pm) satisfactorily agrees with the crystal structure data (Fig. 1) and, therefore, does not change significantly in the H-bonded aggregate. The PM3 enthalpy of formation calculated from the crystal structure data for the dimer and trimer, is lower than that for the monomer by $\Delta\Delta H_f^{PM3} = -27$ and -53 kJ mol^{-1},[11a] and yields for each O–H ··· NC hydrogen bond an average value of -13 kJ mol^{-1}.

2) The question pertinent to self-organization phenomena whether the structurally proven paired formation of $(O\text{–}H \cdots NC)_2$ bridges (Fig. 1a, b) is favored by a cooperative effect[2] can be elaborated upon by calculations of potential surfaces for the considerably smaller model system of two molecules of (*Z*)-2-hydroxyethenecarbonitrile, which reflects all essential structural facets (Scheme 2, left). Its selection is supported by the PM3 geometry-optimized structures[11b]: Of the two dimers, interconvertible by a 180° rotation around one H bond and containing either a single O–H ··· NC hydrogen bond (symmetry C_s, Scheme 1a: ---) or a pair of them (symmetry C_{2h}; Scheme 1, left: ——), the structure calculated for the latter satisfactorily resembles that for tetracyanohydroquinone determined experimentally (Fig. 1, right). Moving each H center along the geometry-optimized O ··· N distance of about 280 pm generates asymmetric double minimum potentials (see [1]). The distinct well on the OH side of each double minimum potential occurs about 100 pm from O, while on the NH side the well is considerably shallower because of the necessary charge separation. For each hydrogen bond within the nonpolar subunits $(O\text{–}H \cdots NC)_{1,2}$, the differences in enthalpy of formation $\Delta\Delta H_f^{PM3}$ are calculated to be 17 kJ mol^{-1} for single hydrogen-bond links ($n = 1$, C_s) and 19 kJ mol^{-1} for the doubly H-bonded dimer ($n = 2$, C_{2h}): the cooperative effect should therefore amount to approximtely 10%.

3) The PM3 enthalpies of formation[11] for the model dimers composed of the subunits ($NCHC{=}CH\text{–}O^{\ominus} \cdots H\text{–}{}^{\oplus}N(CH_3)_2\text{–}H$; Scheme 1, right) exhibit a different dependence on the distance parameter $d_{O \cdots H}$ (Fig. 1c and d) because of the structurally proven charge separation. For a constant O ··· N distance of 280 pm, the polar structures $(O^{\ominus} \cdots H\text{–}{}^{\oplus}NH)_{1,2}$ are clearly more stable, although for $(O\text{–}H \cdots N)_{1,2}$ hydrogen bonds on the other side of the rather high barrier of about 130 kJ mol^{-1} (Scheme 1, right, C_{2h}), a distinct minimum at $d_{O\text{–}H} \approx 100$ pm results. The bond energies calculated for each hydrogen bond amount to 37 kJ mol^{-1} for the dimer with one H bond ($n = 1$, C_s) and 55 kJ mol^{-1} for the dimer with H-bond pairs ($n = 2$, C_{2h}): Accordingly, the cooperative effect of about 32% exceeds the one estimated for nonpolar O–H ··· N bonds (Scheme 1a) considerably.

The comparison of the structural data (Fig. 1) and the additional calculations (Scheme 1) thus confirms

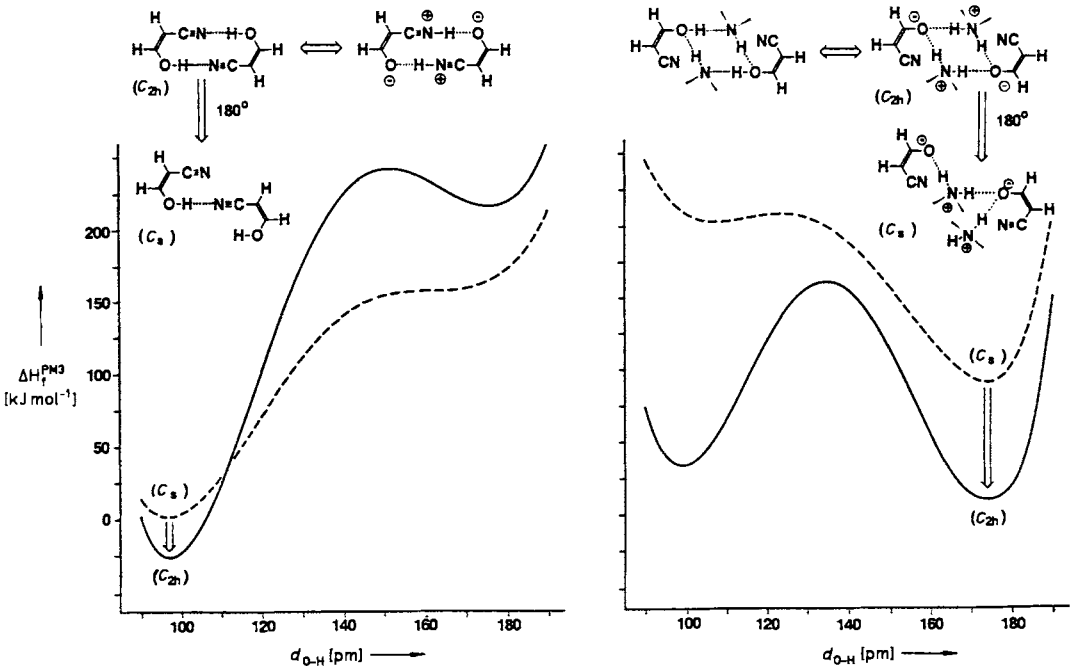

Scheme 1. Results of PM3 potential calculations (ΔH_f^{PM3}) for the model dimers of two molecules (*Z*)-2-hydroxyethenecarbonitrile (left) as well as two molecules each of (*Z*)-2-hydroxyethenecarbonitrile and dimethylamine (right) and their dependence on the distance $d_{O\cdots H}$ (– – –: dimers with a single H-bond of C_s symmetry; ——: dimers with H-bond pairs of C_{2h} symmetry).

unanimously that both the strength of the H bonds and the cooperative effect increase as their polarity ($O-H\cdots N) \Rightarrow (O^{\ominus}\cdots H-^{\oplus}N$) increases. The dependence of the morphology of H-bonded molecular aggregates on the basicity of the proton acceptor center,[1–4] which has far-reaching biochemical consequences,[2] can be tested further for many hydrogen-bonded molecular aggregates by adding suitable stronger bases.[1,2]

Received: March 9, 1992
Revised version: July 29, 1992 [Z 5487 IE]
German version: *Angew. Chem.* **1993**, *105*, 410

[1] H. Bock, T. Vaupel, C. Näther, K. Ruppert, Z. Havlas, *Angew. Chem.* **1992**, *104*, 348; *Angew. Chem. Int. Ed. Engl.* **1992**, *31*, 299, and references therein, especially Q.-C. Yang, M. F. Richardson, J. D. Dunitz, *Acta Crystallogr. Sect. B* **1988**, *45*, 312.

[2] G. A. Jeffrey, W. Saenger, *Hydrogen Bonding in Biological Structures*, Springer, Heidelberg, **1992**.

[3] Further selected examples of structures with multiple hydrogen bonding between building blocks: a) On self-organization of five building blocks containing cyanuric acid and melamine subunits connected through alkyl chains, molecular aggregates result that have two layers each with 18 hydrogen bonds (C. T. Seto, G. M. Whitesides, *J. Am. Chem. Soc.* **1991**, *113*, 71 and *ibid.* **1992**, *114*, 5473). b) Guanidium benzo-[27]crown-9 salts contain six H bonds (J. W. H. M. Uiterwijk, S. Harkema, J. Geevers, D. N. Rheinhoudt, *J. Chem. Soc. Chem. Commun.* **1982**, 200. c) 5-Methylhypoxanthine hydrochloride hydrate consists of dimeric structural units containing five H bonds (J. Gao, S. Bondon, G. Wipf, *J. Am. Chem. Soc.* **1991**, *113*, 9610 and references therein. d) Tetramethylammonium salts can crystallize in clathrates $[R_4N^{\oplus}(H_2O)_{20}]OH^{\ominus}$ containing 36 H bonds (D. Mootz, R. Seidel, *J. Inclusion Phenom.* **1990**, *8*, 139). e) D-Alanine crystals grow in the (001) direction (I. Weissbuch, L. Addadi, M. Lahav, L. Leiserowitz, *Science* **1992**, *253*, 638).

[4] Selected reviews on hydrogen bonds: a) A. F. Wells, *Structural Inorganic Chemistry*, 5th ed., Clarendon Press, Oxford, **1987**, p. 355–376; b) J. Elmsley, *Chem. Soc. Rev.* **1980**, *9*, 91–124; c) R. Taylor, O. Kennard, *Acc. Chem. Res.* **1984**, *17*, 320; d) R. Desiraju, *Acc. Chem. Res. ibid.* **1991**, *24*, 290.

[5] Cf. for example, R. Stewart, *The Proton: Applications to Organic Chemistry*, Academic Press, New York, **1985**.

[6] a) The synthesis of tetracyanohydroquinone (K. Wallenfels, G. Bachmann, D. Hoffmann, R. Kern, *Tetrahedron* **1965**, *21*, 2239) advantageously starts from the dichloro derivative, because for the cyanation a tenfold increase in batch size is possible, which increases the yield above 90%. Single crystals can be grown from dimethoxymethane (DME) in an *n*-hexane atmosphere and within 12 h yellow needles are obtained, m.p. = 251 °C (decomp.). b) Crystal structure analysis ($C_{10}H_2N_4O_2$), M_r = 210.15 g mol^{-1}, a = 1600.5(1), b = 573.45(4), c = 1009.8(1) pm, β = 105.494(9)°, V = 893.1(3) × 10^6 pm^3 (293 K), Z = 4, ρ_{calcd} = 1.563 g cm^{-3}, $\mu(Cu_{K\alpha})$ = 9.4 cm^{-1}, monoclinic, space group $C2/c$ (no. 15 Int. Tab.), Enraf-Nonius-CAD4 diffractometer, 3325 reflections within $2° < 2\theta < 132°$, of which 775 are independent with $I > 0(I)$. Solution with direct methods (MULTAN 80), N = 770, N_p = 78, R = 0.030; R_w = 0.045, $\omega = 4F^2/[\sigma^2(I) + (0.03\,F^2)^2]$. C, N, O positions anisotropically refined, H found by difference Fourier analysis and refined isotropically with a constant temperature factor. Empirical absorption correction program, DIFABS (factors between 0.94 and 1.07); residual electron density < 0.16 e Å^{-3}. The molecule is situated at a crystallographic inversion center. c) Further details of the crystal structure determination may be obtained from the Fachinformationszentrum Karlsruhe, Gesellschaft für wissenschaftlich-technische Information mbH, D-W-7514 Eggenstein-Leopoldshafen 2, (FRG) on quoting the deposit number CSD-56 968, the names of the authors and the journal citation.

[7] a) The dimorpholinium salt of tetracyanohydroquinone precipitated on adding 2 equivalents of morpholine to a solution of tetracyanohydroquinone in diethyl ether at room temperature, and was recrystallized from methanol. Red needles, m.p. > 300 °C. b) Crystal structure analysis ($C_{10}N_4O_2 \cdot 2C_4H_{10}NO$), M_r = 384.39 g mol^{-1}, a = 872.0(3), b = 939.6(3), c = 1167.4(5) pm, β = 91.23(3)°, V = 956(1) × 10^6 pm^3 (115 K), Z = 2, $\rho_{calc.}$ = 1.385 g cm^{-3}, $\mu(Cu_{K\alpha})$ = 9.4 cm^{-1}, monoclinic, space group $P2_1/(a)C$ (no. 14 Int. Tab.), Enraf Nonius CAD4 diffractometer, 1643 reflections within $2° < 2\theta < 120°$, of which 1418 are independent with $I > 0(I)$. Structure solution by direct methods (SHELXS), N = 1412, N_p = 110, R = 0.076; R_w = 0.074, $\omega = 4F^2/[\sigma^2(I) + (0.003\,F^2)^2]$. C, N, O positions anisotropically refined, hydrogen-bonded H found by difference Fourier analysis and refined isotropically with a constant temperature factor, morpholine H at idealized positions. Empirical absorption correction program, DIFABS (factors between 0.81 nd 1.15); residual electron density < 0.35 e Å^{-3}. The salt is situated at a crystallographic inversion center in the middle of the benzene rings. See also [6c].

[8] A search through the Cambridge Structural Data File yields altogether 956 entries for structural units EH···NC (E: elements of main groups 5 to 7) and after distance limitation ($d_{E\cdots N}$ < 300 pm) still 72 entries. Selected in the order of decreasing E···N distances are a) (HCN)$_x$ 318 pm (W. J. Dulmagge, W. N. Lipscomb, *Acta Crystallogr.* **1951**, *4*, 330); b) cyanoacetamide 314 pm (P. C. Chieh, J. Trotter, *J. Chem. Soc. A* **1970**, 184; c) 2-amino-1,1,3-tricyanopropene 295 pm (B. Klewe, *Acta Chem. Scand.* **1972**, *26*, 317); d) bis(ammonium) salts of octacyano cyclobutane dianion and of 1,2,4-tricyanocyclopentadienide, each 291 pm (B. Gerecht, T. Kampchen, K. Kohler, W. Massa, G. Offermann, R. E. Schmitz, G. Seitz, R. Sutrisno, *Chem. Ber.* **1984**, *117*, 2714 and S. Buchholz, K. Harms,

W. Massa, G. Boche, *Angew. Chem.* **1989**, *101*, 58; *Angew. Chem. Int. Ed. Engl.* **1989**, *28*, 73); e) 2,5-dicyanophenol hexahydrate 282 pm (E. K. Andersen, I. G. K. Andersen, *Acta Crystallogr. Sect. B* **1975**, *31*, 379); f) *p*-cyanophenol 282 pm (T. Higashi, K. Osaki, *Acta Crystallogr. Sect. B.* **1977**, *33*, 607); g) *ibid.* **1978**, *34*, 1393, 1396); h) bis(diethylenetriamine)-cobalt(III)/hexacyanocobaltate(III)dihydrate 279 pm (M. Konno, F. Marumo, Y. Saito, *ibid.* **1973**, *29*, 739); i) dimeric *N*-methylene-*N*,*N*,*N*'-trimethyl-*p*-phenylenediamine)-7,7,8,8-tetracyanoperfluoro-*p*-quinodimethane 271 pm (J. S. Miller, J. C. Calabrese, *J. Chem. Soc. Chem. Commun.* **1988**, *63*).

[9] Cf. also the doubly H_2O-bridged $Cl^{\ominus}$ ions in 8,9-difluoro-6-oxo-6*H*-benzene[*c*]quinolizine hemihydrate hemihydrochloride (E. F. Kleinmann, J. Bordner, B. J. Newhouse, K. MacFerrin, *J. Am. Chem. Soc.* **1992**, *114*, 4945).

[10] Cf. H. Bock, K. Ruppert, C. Näther, Z. Havlas, H.-F. Herrmann, C. Arad, I. Göbel, A. John, J. Meuret, S. Nick, A. Rauschenbach, W. Seitz, T. Vaupel, B. Solouki, *Angew. Chem.* **1992**, *104*, 564; *Angew. Chem. Int. Ed. Engl.* **1992**, *31*, 550, and references therein.

[11] The PM3 calculations (J. J. Stewart, *J. Comput. Chem.* **1989**, *10*, 209, 221) have been performed with SCAMP Version 4.1 (T. Clark, Erlangen) on an IBM RISC 6000/300 work station (CPU: 32 MB). a) Optimized gas-phase structure of tetracyanohydroquinone: $\Delta H_f = 380\ kJ\,mol^{-1}$; selected structural parameters CC(ring) 141, CC 143, CN 116, CO 136 pm, ∢ CCO 124°, COH 109°, OH 95 pm. Dimer and trimer based on crystal structure data: $\Delta H_f = 734$ and 1088 $kJ\,mol^{-1}$. b) (*Z*)-2-hydroxy ethene carbonitrile: $\Delta H_f = 5.5\ kJ\,mol^{-1}$, C=C 135, CC 142, CN 116, CO 135 pm, ∢ CCO 127°, COH 110°, OH 95 pm. Dimer C_s: $\Delta H_f = -6\ kJ\,mol^{-1}$; dimer C_{2h}: $\Delta H_f = -27\ kJ\,mol^{-1}$, C=C 135, CC 141, CN 116, CO 133 pm, ∢ CCO 129°, COH 114°, OH 97, O···N 275 pm, ∢ OHN 166°. c) $(NC)HC{=}CHO^{\ominus}\cdots HN^{\oplus}(CH_3)_2H$: $\Delta H_f = 59\ kJ\,mol^{-1}$, C=C 138, CC 140, CN 117, CO 127, O···N 270, $N^{\oplus}$-H(···O) 107, NH 100 pm, ∢ CCO 126°. Dimer C_{2h}: $\Delta H_f = 9\ kJ\,mol^{-1}$, O···N 275 pm; dimer C_s: $\Delta H_f = 81\ kJ\,mol^{-1}$. Dimer with nonpolar H bonds O-H···N after geometry optimization: $\Delta H_f = 27\ kJ\,mol^{-1}$, O···N = 271 and 278 pm.

[12] H. Bock, W. Seitz, J. W. Bats, unpublished results. Cf. also M. C. Etter, S. M. Reutzel, *J. Am. Chem. Soc.* **1991**, *113*, 25876, and references therein.

"Supersilyl" Compounds $(R_3Si)_3SiSi(SiR_3)_3$ and $(R_3Si)_3SiC_6H_4Si(SiR_3)_3$: Structures and Properties**

By *Hans Bock,** *Jochen Meuret,* and *Klaus Ruppert*

Dedicated to Professor Richard Müller

Tris(trimethylsilyl)silyl ("supersilyl") and tris(trimethylsilyl)methyl groups, according to space-filling structure models, should shield the central molecular skeleton in **1** and **3** completely or almost completely by a "H_3C-skin". In addition, special substituent effects are expected from the subunits $SiSi_3$ containing a local threefold axis, because of the low effective nuclear charge of their four Si centers.

Since their first syntheses[1a,b] supersilyl compounds have revealed many remarkable facts: Thus tris(trimethylsilyl)acyl silane $(R_3Si)_3SiC(=O)R'$ has been rearranged photochemically to $(R_3Si)_2Si{=}CR'OSiR_3$ to yield the first silaethene kinetically stabilized by alkyl shielding. Both thermally stable iminoborane $(R_3Si)_3SiB{\equiv}NCR_3$[1d] or the first formylsilane $(R_3Si)_3SiC(=O)H$[1e] could be isolated (R always refers to CH_3). According to a gas-phase electron diffraction structure determination of the spherical molecule $Si(SiR_3)_4$, the R_3Si groups still can rotate.[1f] The now commercially available $(R_3Si)_3SiH$ is used in organic syntheses as a reducing agent.[1g] Numerous metallorganic derivatives[1h] such as $(R_3Si)_3Si{-}Zn{-}Si(SiR_3)_3$[1i] have been prepared and their structures determined.

In contrast to the structurally related compounds containing $(R_3C)_3Si$ or $(R_3Si)_3C$ groups, which in $(R_3C)_3SiSi(CR_3)_3$, for instance, stretch the Si–Si bond by 35 pm (!)[2a] (Scheme 1) or in the 1,4-benzene derivative $(R_3Si)_3CC_6H_4C(SiR_3)_3$ decrease its first vertical ionization energy to a value of only 7.45 eV[2b] (Scheme 3), corresponding measurements for the analogous supersilyl-substituted compounds are lacking. Therefore, we report and discuss the single crystal structure of $(R_3Si)_3SiSi(SiR_3)_3$[3,4] (Fig. 1), the ionization energies of both title molecules determined by photoelectron spectroscopy (Scheme 3), and the spin distribution, determined by ESR spectroscopy, in the radical anion of the 1,4-disubstituted benzene[5b] (Scheme 4), which has been synthesized for the first time.

In "hexakis(trimethylsilyl)disilane" (Fig. 1), the two half-shells of the space-filling substituents $Si[Si(CH_3)_3]_3$ are con-

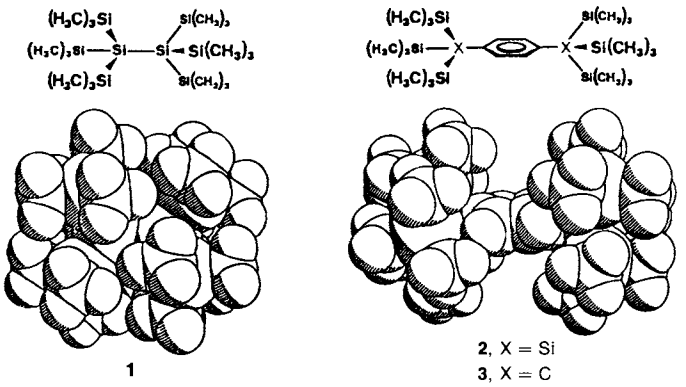

1 **2**, X = Si **3**, X = C

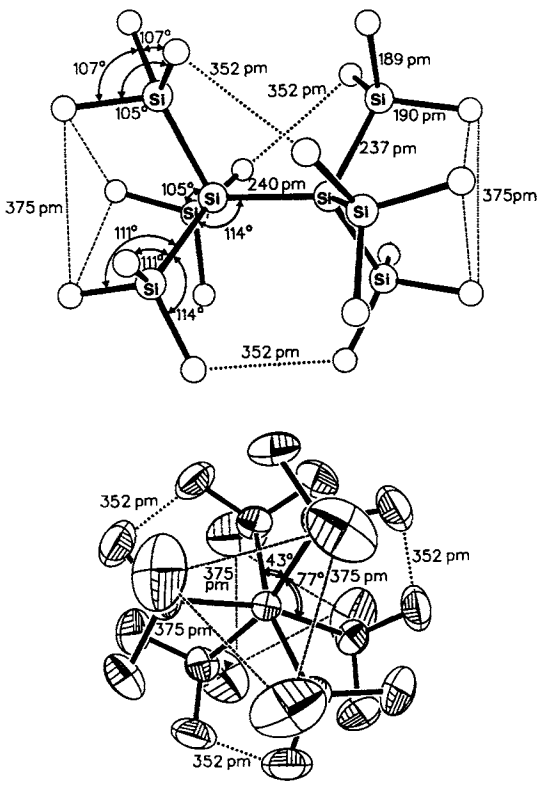

Fig. 1. Single crystal structure of $[(H_3C)_3Si]_3Si{-}Si[Si(CH_3)_3]_3$ (**1**). Top: side view with essential bond lengths, bond angles, and the shortest nonbonding C···C distances; bottom: axial view (50% thermal ellipsoids) with different dihedral angles ω(SiSi–SiSi).

[*] Prof. Dr. H. Bock, Dipl.-Chem. J. Meuret, Dr. K. Ruppert
Institut für Anorganische Chemie der Universität
Niederurseler Hang, D-W-6000 Frankfurt am Main 60 (FRG)

[**] Structures of Charge-Perturbed or Sterically Overcrowded Molecules, Part 22. This work was supported by the Deutsche Forschungsgemeinschaft, the State of Hesse, and the Fonds der Chemischen Industrie. Part 21.: H. Bock, C. Näther, K. Ruppert, B. Havlas, *J. Am. Chem. Soc.* **1992**, *114*, 6907.

nected by a Si–Si bond elongated to 240 pm. Some of the C···C distances between the two molecular halves amount to only 352 pm; that is, they are shortened by 12% relative to the sum of the van der Waals radii of two methyl groups (each 200 pm).[4] The molecular skeleton of $Si_3Si-SiSi_3$ exhibits D_3 symmetry and, unexpectedly, two different dihedral angles of 43 and 77° (Fig. 1 and Scheme 1). For a structural comparison based on a model in which the two substituent half-shells are separated along the central C_3 axis by spacers of different lengths (Scheme 1), the following molecules have been selected: hexakis(*tert*-butyl)disilane, which has a 270 pm (!) long Si–Si bond,[2a] linear (!) hexakis(*tert*-butyl)disiloxane,[5a] di[tris(trimethylsilyl)silyl]zinc[1i] and the acetylene and 1,4-benzene derivatives with tris(trimethylsilyl)methyl substituents on both sides.

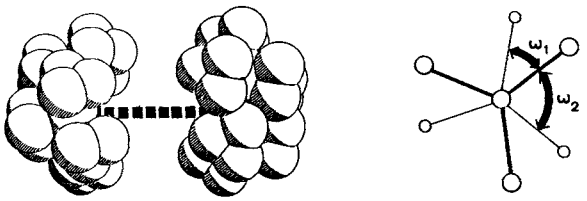

molecular framework	distance	$\omega(X_3Y\cdots YX_3)$
$Si_3Si-SiSi_3$	240 pm	43 + 77°
$C_3Si-SiC_3$	270 pm	45 + 75°
$C_3Si-O-SiC_3$	333 pm	45 + 75°
$Si_3C-C\equiv C-CSi_3$	414 pm	60°
$Si_3Si-Zn-SiSi_3$	468 pm	60°
$Si_3C-C_6H_4-CSi_3$	604 pm	60°

Scheme 1. Half-shell structural model for organosilicon compounds with spacers of different lengths, viewed along the substituent C_3 axis, and dihedral angles $\omega(X_3Y-YX_3)$ of the molecular skeletons.

As may be seen in Scheme 1, the dihedral angles ω_1 and ω_2 between the groups that are staggered when viewed down the spacer linking the half-shells are different if the substitution centers are less than 333 pm apart, but identical if more than 414 pm apart. The twisting $D_{3d} \rightarrow D_3$ of the molecular skeletons from the optimal conformation with $\omega(X_3Y-YX_3) = 60°$ is therefore an appropriate criterion for steric overcrowding, which leads to the extremely short C···C van der Waals distances between the methyl groups (Fig. 1, top), as a result of the additional cogwheel-meshing of these groups in the interior of the molecule.

Spatial overcrowding especially due to tris(*tert*-butyl)silyl substituents with C–C distances, which are approximately 40 pm shorter than C–Si distances,[6] stretches the standard Si–Si bond length of 235 pm in hexamethyldisilane to 270 pm[6] and lowers the corresponding Pauling bond order from 1.0 to 0.26[2a, 7] (Scheme 2). It has been proposed,[7] therefore, that the weakened central Si–Si bonds (in some cases the weakening is extreme) are strengthened by additional attractive van der Waals interactions in the enveloping

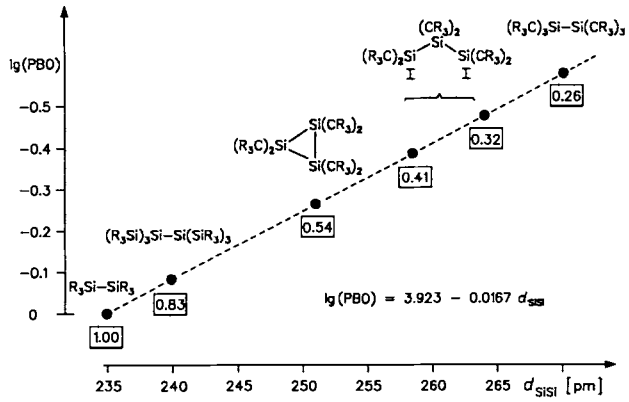

Scheme 2. Si–Si bond lengths in di- and trisilane derivatives and the respective Pauling bond orders lg (PBO) = $[d(1)-d(X)]/60$ (PBO values are framed).

hydrocarbon "skin". This assumption would also be compatible with the structure of hexakis(trimethylsilyl)disilane, in which some of the intramolecular C···C distances only amount to 352 pm (Fig. 1, top).

The discussion on structure raises the question about how supersilyl substituents will modify especially the ground states of molecular ions. A comparison of the first vertical ionization energies of both title molecules[5b] (determined by PE spectroscopy) with those of other disilane or 1,4-benzene derivatives[8, 9] reveals the strongest lowering within each class of compounds for **1** and **2** (Scheme 3): apparently, in the ground states of the resulting radical cations the delocalization of the positive charge into the half-shells $Si(SiR_3)_3$ is energetically favorable. These half-shells are excellent donor substituents on account of the low effective nuclear charge of the Si centers.

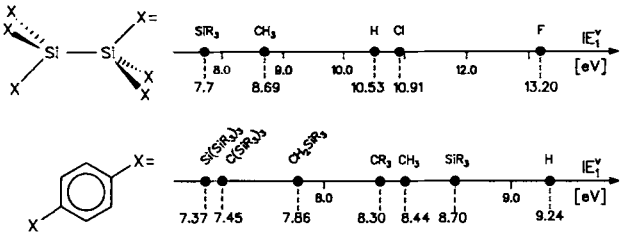

Scheme 3. First vertical ionization energies of selected disilane and 1,4-benzene derivatives.

Supersilyl substituents are also well suited to stabilize negative charges considerably: in the radical anion of the 1,4-benzene derivative, more than half of the π-spin population ρ_μ^π is located in the $[(H_3C)_3Si]_3Si$ groups, according to ESR/ENDOR experiments[5b] and augmented by HMO estimates $(c_{J\mu})^2$ for the "blind" centers (Scheme 4: o).

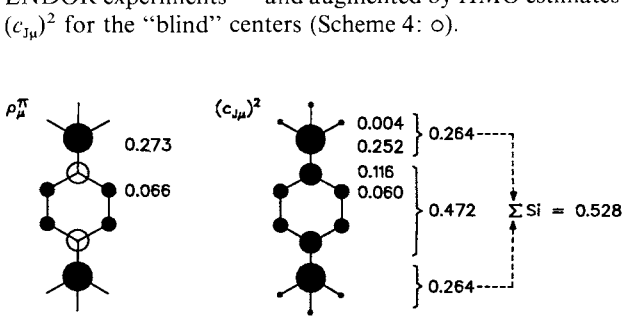

Scheme 4. ESR/ENDOR π-spin populations ρ_μ^π in the radical anion of 1,4-di-[tris(trimethylsilyl)silyl]benzene and corresponding squared HMO coefficients $(c_{J\mu})^2$.

The steric and electronic effects of supersilyl substituents that are demonstrated here for the selected title molecules, stabilize radical cations as donors and radical anions as acceptors and are worth further investigation in other appropriately chosen organosilicon compounds.

Experimental Procedure

2: To a suspension of 0.25 g (10.2 mmoles) Mg turnings in 3 mL dry THF were added under Ar 0.5 mL of a solution of 1.2 g (5.1 mmoles) *p*-dibrombenzene in 4 mL dry THF until the exothermic reaction started. Subsequent addition of 3.07 g (10.8 mmoles) of tris(trimethylsilyl)chlorosilane and the remaining *p*-dibrombenzene yielded an opalescent solution, which was stirred 24 h at RT and then boiled for 50 h under reflux. The solution first turned green then red, and a white precipitate ($MgCl_2$) formed. After hydrolysis with 30 mL H_2O, triple extraction with 30 mL portions of diethyl ether, and drying with Na_2SO_4, filtration and removal of the solvent yielded an oily residue, which crystallized after addition of acetone. Chromatographic purification of a 4:1 solution of hexane and methyl acetate over silica gel (60 Å) enabled the isolation of white crystals (0.15 g, 5%), m.p. = 272 °C. ^{1}H NMR ($CDCl_3$/TMS): $\delta = 0.12$ (s, 54H), 7.21 (s, 4H); MS: *m/z* 571 ($M^{\oplus}$), 556 ($M^{\oplus} - CH_3$), 498 ($M^{\oplus} - Si(CH_3)_3$).

Received: August 3, 1992 [Z 5500 IE]
German version: *Angew. Chem.* **1993**, *104*, 413

[1] a) H. Gilman, C. L. Smith, *J. Am. Chem. Soc.* **1964**, *86*, 1454; *J. Organomet. Chem.* **1967**, *8*, 245; *ibid.* **1968**, *14*, 91; b) H. Gilman, R. L. Harrell, *ibid.* **1966**, *5*, 199; *ibid.* **1967**, *9*, 67; c) A. G. Brook, S. Nyberg, F. Abdesaken, B. Gutekunst, R. K. M. R. Kallury, Y. C. Poon, Y.-M. Chang, W. Wong-Ng, *J. Am. Chem. Soc.* **1982**, *104*, 5668; d) M. Haase, U. Klingebiel, R. Boese, M. Polk, *Chem. Ber.* **1986**, *119*, 1117; e) F. H. Elsner, H.-G. Woo, T. D. Tilley, *J. Am. Chem. Soc.* **1988**, *110*, 314; f) L. S. Bartell, F. B. Clippard, T. L. Boates, *Inorg. Chem.* **1970**, *9*, 2436; g) Cf. C. Chatgilialoglu, D. Griller, M. Lesage, *J. Org. Chem.* **1989**, *54*, 2492; h) Cf. the summary in H. Bock, J. Meuret, K. Ruppert, *J. Organomet. Chem.*, in print; i) J. Arnold, T. D. Tilley, A. L. Rheingold, S. G. Geib, *Inorg. Chem.* **1987**, *26*, 2106.

[2] a) N. Wiberg, H. Schuster, A. Simon, K. Peters, *Angew. Chem.* **1986**, *98*, 100; *Angew. Chem. Int. Ed. Engl.* **1986**, *25*, 79. We are grateful to Prof. A. Simon (Stuttgart) for additional structural information; b) H. Bock, *Angew. Chem.* **1989**, *101*, 1659; *Angew. Chem. Int. Ed. Engl.* **1989**, *18*, 1627.

[3] Hexakis(trimethylsilyl)disilane should be termed 1,4-hexamethyl-2,3-bis(trimethylsilyl)tetrasilane, according to IUPAC rules. It is prepared according to [1b] from $Si[Si(CH_3)_3]_4$, $LiCH_3$, and BrH_2CCHBr_2 and recrystallized from acetone; yield 46%. White, air-stable crystals with m.p. = 372 °C; ^{1}H NMR ($CDCl_3$, TMS): $\delta = 0.30$ (s, 54H); MS: *m/z* 495 ($M^{\oplus}$), 480 ($M^{\oplus} - CH_3$), 422 ($M^{\oplus}$-$Si(CH_3)_3$). Crystal structure analysis: $C_{18}H_{54}Si_8$ (M_r 495.3), $a = b = 1614.5(8)$, $c = 2285.9(13)$ pm, $\alpha = \beta = 90°$, $\gamma = 120°$, $V = 51532 \times 10^6$ pm^3 (300 K), $Z = 6$, $\rho_{calcd} = 0.955$ g cm^{-3}, $\mu(Mo_{K\alpha}) = 3.1$ cm^{-1}, rhombohedral, space group $R\bar{3}c$ (no. 167 Int. Tab.), Siemens AED-II four cycle diffractometer, 3261 measured reflections within $3° < 2\theta < 48°$, of which 598 are independent with $I > 2\sigma(I)$. Structure solution by direct methods (SHELXTL-PLUS), $N = 598$, $N_p = 41$, $R = 0.065$, $R_w = 0.067$, $\omega = 1/\sigma^2(F) + 0.003F^2$, residual electron density +0.34/−0.21 e_0Å^{-3}. C and Si atoms anisotropically refined, H atoms at idealized positions. The central Si–Si bond isolated on a threefold axis. Further details of the crystal structure investigation are available on request from the Fachinformationszentrum Karlsruhe, Gesellschaft für wissenschaftlich-technische Information mbH, W-7514 Eggenstein-Leopoldshafen 2 (FRG) on quoting the depository number CSD-56427, the names of the authors, and the journal citation. The structure has been independently determined in the interim both by S. P. Mallela, I. Bernal, R. A. Geanangel (*Inorg. Chem.* **1992**, *31*, 1626; R_w only 0.20) and by F. R. Fronzek, P. D. Lickiss, Brighton, England (personal communication).

[4] Cf. H. Bock, K. Ruppert, C. Näther, Z. Havlas, H.-F. Herrmann, C. Arad, I. Göbel, A. John, J. Meuret, S. Nick, A. Rauschenbach, W. Seitz, T. Vaupel, B. Solouki, *Angew. Chem.* **1992**, *104*, 564; *Angew. Chem. Int. Ed. Engl.* **1992**, *31*, 550 and references therein.

[5] a) N. Wiberg, E. Kühnel, K. Schurz, H. Borrmann, A. Simon, *Z. Naturforsch. B* **1988**, *43*, 1075. b) J. Meuret, *Ph.D. thesis*, University Frankfurt, **1992**; cf. also [1h].

[6] Cf. W. Sheldrick in *"The Chemistry of Organic Silicon Compounds"* (Eds.: S. Patai, Z. Rappoport), Wiley, Chichester, **1989**, p. 227–303.

[7] a) A. Schäfer, M. Weidenbruch, K. Peters, H. G. von Schnering, *Angew. Chem.* **1984**, *96*, 311; *Angew. Chem. Int. Ed. Engl.* **1984**, *23*, 302; b) M. Weidenbruch, B. Flintjer, K. Peters, H. G. von Schnering, *ibid.* **1986**, *98*, 1090, and **1986**, *25*, 1129.

[8] Cf. H. Bock, *Angew. Chem.* **1989**, *101*, 1659; *Angew. Chem. Int. Ed. Engl.* **1989**, *28*, 1627 and references therein.

[9] Cf. a) H. Bock, B. Solouki *"Photoelectron Spectra of Silicon Compounds"* in *"The Chemistry of Organic Silicon Compounds"* (Eds.: S. Patai, Z. Rappoport), Wiley, Chichester, **1989**, p. 555–653 and references therein; b) H. Bock, W. Kaim, *Acc. Chem. Res.* **1982**, *15*, 9 and references therein.

The Triplet Biradical Tris(3,5-di-*tert*-butyl-4-oxophenylene)methane: Crystal Structure, and Spin and Charge Distribution

By *Hans Bock,* Andreas John, Zdenek Havlas,* and *Jan W. Bats*

Dedicated to Professor Rudolf Zahradnik

Trimethylenemethane can be generated in a methylenecyclopropane single crystal at 77 K by γ irradiation and according to the ESR spectrum is a triplet biradical with axial symmetry.[1a] As a simplification, this observation can be rationalized by its alternating π system of D_{3h} symmetry with twofold degenerate e'' molecular orbitals,[1b] which according to the Pauli principle are each occupied by one electron of parallel spin (Scheme 1a). The energy difference between the triplet ground state $\tilde{X}(^3A_2')$ and the first excited singlet state $\tilde{A}(^1E')$ according to ab initio GVB/CI calculations is 110 kJ mol^{-1}[1c] (Scheme 1b).

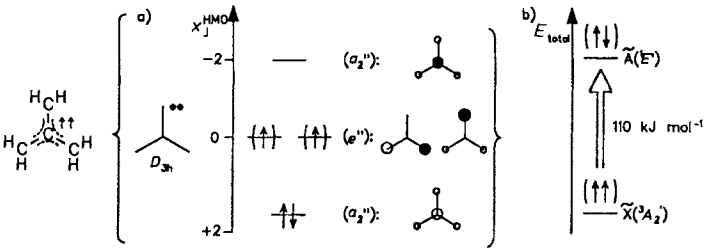

Scheme 1. a) Topological (HMO) coefficients of π eigenvalues x_j^{HMO} as well the corresponding orbital diagrams of trimethylenemethane. b) Total energy difference (ab initio GVB/CI) between the triplet ground state $\tilde{X}(^3A_2')$ and the first excited singlet state $\tilde{A}(^1E')$.

Many paramagnetic compounds of the same structural type have been characterized by ESR/ENDOR spectroscopy,[2a] inter alia the dark violet title compound **1**, often referred to as Yang's biradical.[2b, c] It can be synthesized in three steps from 2,6-di-*tert*-butyl-4-lithiophenoxy(trimethyl)silane and diethyl carbonate[2d, 5a] [Eq. (a)].

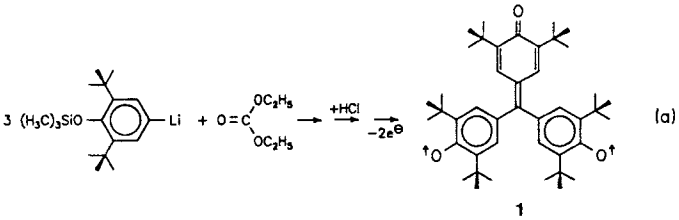

1

Two electron/connection line formulas as drawn for **1**, correctly reflect neither the structure nor the properties of

[*] Prof. Dr. H. Bock, Dipl.-Chem. A. John
Institut für Anorganische Chemie der Universität
Niederurseler Hang, D-W-6000 Frankfurt am Main 50 (FRG)
Dr. Z. Havlas
Institute of Organic Chemistry and Biochemistry of the Czechoslowakian Academy of Sciences, CS-16610 Prag (Czech Republic).
Dr. J. W. Bats
Institut für Organische Chemie der Universität Frankfurt

[**] Structures of Charge-Perturbed and Sterically Overcrowded Molecules, Part 25. The research project is supported by the Deutsche Forschungsgemeinschaft, the State of Hesse, and the Fonds der Chemischen Industrie. Part 24. H. Bock, J. Meuret, K. Ruppert, *J. Organomet. Chem.*, in press.

triplet biradicals, which are of actual interest because of their potential ferromagnetism.[3] We report here the first[4] single crystal structure analysis of such a compound[5b] (Fig. 1) and the calculations based on it of its spin and charge distributions[7] (Scheme 2).

According to the structure determination (Fig. 1) and in contrast to the misleading valence line formula in Eq. (a), the triplet biradical exhibits approximately D_3 symmetry: steric interactions of the *ortho* hydrogen substituents (shortest distance H···H 235 pm) twist the six-membered rings in the same direction out of the central trimethylenemethane C_4 plane by 31, 31, and 34°. Within this plane the angles around

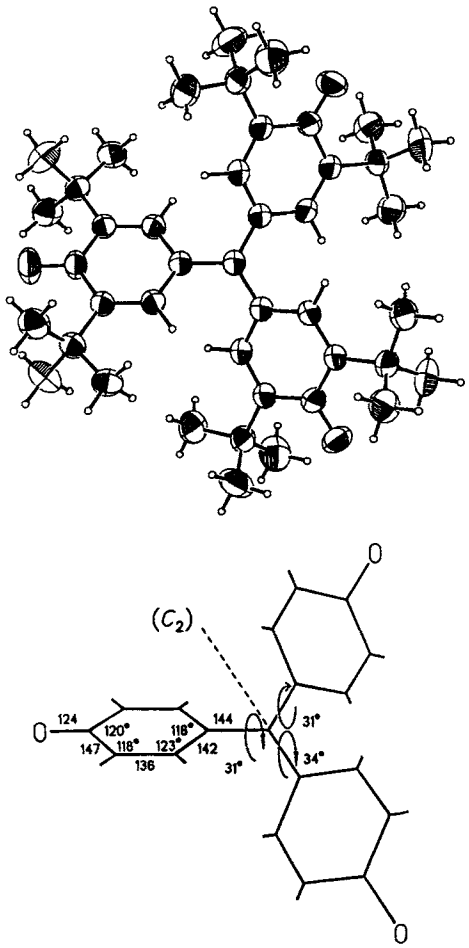

Fig. 1. Single crystal structure of tris(3,5-di-*tert*-butyl-4-oxopheylene)methane. Top: view in the *x* direction (50% thermal ellipsoids); bottom: molecular skeleton (without *tert*-butyl substituents) showing the twofold axis (C_2) and essential average bond lengths and angles (standard deviations: ±1 pm, ±0.5°).

its C center are 120° and the C–C lengths 144 pm each. The six-membered rings are considerably quinoidally perturbed as inferred from the alternating CC bond lengths of 142, 136, and 147 pm, as well as from the inner angles of 118, 123, 118, and 120°. The average CO distances of 124 pm exceed those of electron-rich quinones[6] and approach those observed for the dimer of fluorenone radical anion (128 pm[6]), thereby indicating a substantial negative charge at the oxygen centers. The structure of the biradical **1** in its triplet ground state (Fig. 1), which except for the smaller phenyl twisting angles of only 12° resembles that of the diphenylene monoradical galvinoxyl $[HC(C_6H_2(CR_3)_2O)_2]^{\bullet}$,[8] illustrates the shielding and, therefore, kinetic stabilizing effect of the wrapping of the six *tert*-butyl substituents (Fig. 1).

In the crystal lattice the individual triplet biradicals occur as isolated species[5b] because of the inclusion of the solvent *n*-hexane into the interstices on crystallization.[5a] Therefore AM1/CI calculations[7] starting from the structural parameters (Fig. 1) could be performed, in part with additional geometry optimization. The (6 × 6)CI wave function composed of 225 configurations reproduces the propeller-like structure of **1** even in details such as the differing bond lengths or the inner angles of the six-membered rings.[7] The first excited singlet state $\tilde{A}(^1B)$, which exhibits only C_{2v} symmetry on account of the perpendicular conformation of one ring, should be 36 kJ mol^{-1} = 0.37 eV above the triplet ground state $\tilde{X}(^3B)$ of the C_3 symmetric triplet biradical according to the AM1/CI enthalpies of formation. This result is supported by the ESR/ENDOR measurements[2a–c] and suggests that it would be interesting to calculate in addition both the spin population and the charge distribution, which by definition,[9] represent different properties of the overall electron cloud and, therefore, are neither identical nor directly proportional to one another.[10]

The differences in the approximate spin densities and charge distributions calculated for the neutral biradical (Scheme 2) are amazing: Almost half the spin of the two unpaired electrons is expected at the outer centers of the trimethylenemethane group (see Scheme 1), whereas their charge orders are rather negligible. The connecting carbon center is no longer situated in a (zero) spin nodal plane because of the symmetry lowering $D_{3h} \rightarrow D_3$ (see Scheme 1) and according to the ESR/ENDOR data,[2a–c] exhibits a ^{13}C coupling of 0.86 mT. On insertion of the AM1/CI spin densities calculated for the adjacent centers and normalized with respect to the number of unpaired electrons[7] (Scheme 2 left: $\rho_{c'} = 0.30$) into the Karplus/Fraenkel equation,[2a] the values calculated ($a_{^{13}C} = |Q|\rho_c + \sum|Q_{cc'}|\rho_{c'} = [0 + 3 \times (-0.14) \times 0.3]/2 = -0.63$ mT) are in satisfactory agreement with the spectroscopic data.

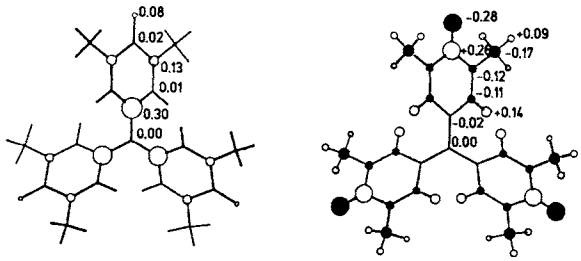

Scheme 2. Spin densities $\rho_{\mu,\pi}^{AM1/CI}$ (left) and charge orders $q_{\mu}^{AM1/CI}$ (right) of **1**.

The charge orders (Scheme 2 right) confirm carbonyl groups polarized according to the effective nuclear charges that is, containing partial negative charge on the oxygen and partial positive charge on the carbon centers, as well as negatively charged *ortho* and *meta* ring centers, which partly reflect the electron-donor effects of the *tert*-butyl substituents.

Structural analyses of biradicals, often unjustifyingly classified as "exotic", thus provide interesting information on the paramagnetic individual molecule, especially if the lattice packing does not enforce intermolecular contacts.[5b] They supplement the ESR/ENDOR measurements in solution or in low-temperature glasses and the structural data are preferable as a basis for quantum chemical calculations. For all of these reasons, further crystal structure determination of known biradicals would be desirable, for example for the sterically less shielded 6-chloro-bis(*N*,*N*-diphenylhydrazyl)-

1,3,5-benzene tricarbonitrile, from which dark green single crystals with a metallic luster can be grown.[11]

Received: August 27, 1992 [Z 5540 IE]
German version: *Angew. Chem.* **1993**, *105*, 416

[1] a) O. Claesson, A. Lund, T. Gillbro, T. Ichikawa, O. Edlund, H. Yoshida, *J. Chem. Phys.* **1980**, *72*, 1463, and references therein; b) E. Heilbronner, H. Bock, The HMO Model and Its Appplication, Wiley, Chichester, **1979**; c) J. H. Davis, W. A. Goddard III, *J. Am. Chem. Soc.* **1977**, *99*, 4242, and references therein; d) Cf. also R. Zahradnik, J. Fabian, *Angew. Chem.* **1989**, *101*, 693–710; *Angew. Chem. Int. Ed. Engl.* **1989**, *28*, 677–694.

[2] a) Cf. for example, H. Kurreck, B. Kirste, W. Lubitz, *Electron Nuclear Double Resonance Spectroscopy of Radicals in Solution*, VCH Publishers, New York, **1988**, pp. 253–277; b) N. C. Yang, A. J. Castro, *J. Am. Chem. Soc.* **1960**, *82*, 6208; cf. also D. Kearns, S. Ehrenson, *ibid.* **1962**, *84*, 739; c) ESR/ENDOR: H. van Willingen, B. Kirste, H. Kurreck, M. Plato, *Tetrahedron* **1982**, *38*, 759, and references therein; cf. also [2a] and K. Mukai, K. Ishizu, M. Nakahara, Y. Deguchi, *Bull. Chem. Soc. Jpn.* **1980**, *53*, 3363; d) W. Harrer, H. Kurreck, J. Reusch, W. Gierke, *Tetrahedron* **1975**, *31*, 625.

[3] Cf., for example, a) L. Y. Chiang, R. B. Upasani, H. S. Shen, S. P. Goshorn, C. H. Lee, *J. Chem. Soc. Chem. Commun.* **1992**, 959; b) J. R. Morton, K. F. Preston, Y. Le Page, A. J. Williams, M. D. Ward, *J. Chem. Phys.* **1990**, *93*, 2222.

[4] A CAS-on-line search with the key-words "bi/diradical" and "crystal structure" produced 32 citations, but none for a biradical in its triplet ground state. Examples of more recent crystal structures of diradicals with $S = 0$ (and a potentially temperature-dependent admixture of $S = 1$) are eightfold *tert*-butyl-substituted 2,5-dihydro-2,5-di(4-oxocyclohexadienylidene)-3,6-di(4-hydroxyphenyl)-thieno[3,2-*b*]thiophene (T. Sugimoto, M. Sakaguchi, H. Ando, T. Tanaka, Z. Yoshida, J. Yamauchi, Y. Kai, N. Kanehisa, N. Kasai, *J. Am. Chem. Soc.* **1992**, *114*, 1893), bis(1,3,2,4,6-thiaphosphatriazinyl)-1,4-phenylene (K. Bestari, G. Fergison, J. F. Gallagher, R. T. Oakley, *Inorg. Chem.* **1992**, *31*, 442; cf. also *J. Am. Chem. Soc.* **1992**, *114*, 1729). For Chichibabin and Thiele's biradicals a singlet ground state has also been proven (L. K. Montgomery, J. C. Huffmann, E. A. Jurczak, M. P. Grendze, *J. Am. Chem. Soc.* **1986**, *108*, 6004). For the complex $[Fe^{2\oplus}(mesitylene)_2][C_3(C(CN)_2)_3^{\ominus}]_2$ containing two hexacyanotriradialene anions, a triplet ground state has been detected by solid-state ESR spectra [3b].

[5] a) Preparation of **1** (according to [2d]) proceeded by reaction of the trimethylsilyl-blocked 2,6-di-*tert*-butyl-4-bromophenol with *n*-butyllithium and diethyl carbonate in *n*-hexane with addition of tetramethylethylenediamine TMEDA, followed by hydrolysis with aqueous HCl in methanol, and oxidation of the isolated bis(3,5-di-*tert*-butyl-4-hydroxyphenyl)-3,5-di-*tert*-butyl)-4-oxophenylenemethane with $K_3[Fe(CN)_6]$ in a degassed water/benzene mixture. The organic phase yields a violet powder on removal of benzene. Crystal growth is achieved by slow evaporation of the green *n*-hexane solution and yields dark violet rhombusses after 2 days. At room temperature, the ESR data for the compound dissolved in toluene $g = 2.0046$ and $a_H = 0.087$ mT for the septet of the six *ortho*-ring-hydrogens; the signal intensities provide no evidence for an additional quintet expected when a monoradical impurity is present. b) Crystal structure analysis $(C_{43}H_{60}O_3 \cdot C_6H_{14})$, $M_r = 711.13\ g\,mol^{-1}$, $a = 1150.4(5)$, $b = 1770.0(9)$, $c = 2253.0(2)$ pm, $\beta = 100.62(2)^\circ$, $V = 4509(5) \times 10^6\ pm^3$ (298 K), $Z = 4$, $\rho_{calcd} = 1.047\ g\,cm^{-3}$, $\mu(Cu_{K\alpha}) = 9.4\ cm^{-1}$, monoclinic, space group $C2/c$ (no. 15 Int. Tab.). Enraf-Nonius CAD4 diffractometer, 7055 reflections within $2^\circ < 2\theta < 120^\circ$, of which 3266 are independent with $I > 0$. Structure solution with direct methods (SHELXS), $N = 3266$, $N_P = 243$, $R = 0.059$, $R_w = 0.056$, $w = 1$. The crystal proved to be partially twinned; only reflections of the main domain, which amounts to 88% of the crystal volume, have been recorded. C,O positions anisotropically refined, H positions of the biradical are detected by difference Fourier analysis and are kept on calculated positions; residual electron density $< 0.26\ e_0 Å^{-3}$. The crystal packing does not show any short intermolecular contact distances; in the biradical crystal interstices *n*-hexane molecules are found disordered along a twofold axis. Further details of the crystal structure analysis can be obtained from the Fachinformationszentrum Karlsruhe, Gesellschaft für wissenschaftlich-technische Information mbH, W-7514 Eggenstein-Leopoldshafen 2, on quoting the deposition number CSD-56 969, the authors, and the full journal citation.

[6] Cf. H. Bock, K. Ruppert, C. Näther, Z. Havlas, H.-F. Herrmann, C. Arad, I. Göbel, A. John, J. Meuret, S. Nick, A. Rauschenbach, W. Seitz, T. Vaupel, B. Solouki, *Angew. Chem.* **1992**, *104*, 564; *Angew. Chem. Int. Ed. Engl.* **1992**, *31*, 560, and references therein.

[7] a) The calculations have been performed with the program SCAMP 4.1 (T. Clark, University Erlangen) on an IBM RISC 6000 workstation. For the triplet biradical a CI wave function (6 × 6, 225 configurations) has been applied. The matrix elements $P_{\mu\mu} = \sum_K a_K^2 P_{\mu\mu}^K$ of the configurations K yield for the individual centers X, according to $P_{XX}^{spin} = \sum_\mu P_{\mu\mu}^{spin}$, the spin populations, and according to $P_{XX} = \sum_\mu^X P_{\mu\mu} - Z_X$, the charge orders. In addition, all structures have been geometry-optimized. b) Triplet ground state (D_3): $\Delta H_f^{AM1/CI} = 42\ kJ\,mol^{-1}$, $d_{C\cdots C} = 143$ pm, $\omega = 29^\circ$, rings: $d_{CC} = 145, 137, 150$ pm, $\sphericalangle CCC = 117, 124, 120, 118^\circ$, eigenvalue $\varepsilon_j(e'') = -5.56$ eV. First excited singlet state (C_2!): $\Delta H_f^{AM1/CI} = 78\ kJ\,mol^{-1}$, $d_{C\cdots C} = 147, 147, 136$ pm, $\omega = 30, 30, 90^\circ$, eigenvalues $\varepsilon_j = -5.40, -5.68$ eV. c) Closed shell singlet state (C_2): $\Delta H_f^{AM1} = 144\ kJ\,mol^{-1}$, $d_{C\cdots C} = 146, 146, 134$ pm, $\omega = 30, 30, 90^\circ$, eigenvalues -2.94 eV (unoccupied), -7.89 eV (doubly occupied).

[8] D. E. Williams, *Mol. Phys.* **1969**, *16*, 145.

[9] Cf., for example, W. Kutzelnigg, *Einführung in die Theoretische Chemie*, Vol. 1 and 2, Verlag Chemie, Weinheim, **1975** and **1978**, respectively.

[10] The dependency between spin and charge distribution, which is often complex, can be illustrated by selection the contact ion pairs of the [15]crown-5-2-aminonaphthosemiquinone radical anion (**2**), which also contains a quinoid six-membered ring as in the title compound (Fig. 1). Alkali

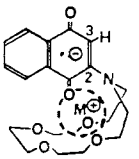

2

metal counter cations $M^\oplus$ polarize the crown-side carbonyl group $>C^{\delta\oplus}O^{\delta\ominus}\cdots M^\oplus$ differently on account of their different effective ionic charges. Therefore, at the carbonyl oxygen negative partial charges result, which increase when the cation changes from $Cs^\oplus$ to $Li^\oplus$. The ring proton couplings $a_{H,3}$ determined by ENDOR-spectroscopy confirm that the spin density in the quinone six-membered ring increases with the negative partial charge at the oxygen centre (Scheme 2) and that its spin component therefore decreases (H. Bock, B. Hierholzer, F. Vögtle, G. Hollmann, *Angew. Chem.* **1984**, *96*, 74; *Angew. Chem. Int. Ed. Engl.* **1984**, *23*, 57).

[11] J. Bretschneider, K. Wallenfels, *Tetrahedron* **1968**, *24*, 1063.

Enantioselective Synthesis of α-Amino Acetals and α-Amino Acids by Nucleophilic 1,2-Addition to Diethoxyacetaldehyde SAMP Hydrazone**

By *Dieter Enders,* Rudolf Funk, Martin Klatt, Gerhard Raabe*, and *Eric R. Hovestreydt*

Dedicated to Professor Joachim Goerdeler on the occasion of his 80th birthday

Protected, enantiomerically pure α-aminoaldehydes are of great interest as chiral synthetic building blocks because they are bifunctional, and this results in a wide range of application.[1] Although the synthesis and applications of N-protected α-aminoaldehydes are well known, the analogous carbonyl-protected compounds have attracted little attention.[2–6] The standard syntheses of carbonyl- and N-protected α-aminoaldehydes generally start from the naturally occurring α-amino acids. Asymmetric synthesis of carbonyl-protected α-aminoaldehydes has only recently become known.[7–9] One of the methods most frequently employed in this respect for the generation of the amino group is the addition of organometallic compounds to the CN double bond[10] of imines,[11] acylimines,[12] nitrones,[13] sulfen-

[*] Prof. Dr. D. Enders, Dr. R. Funk, Dipl.-Chem. M. Klatt, Dr. G. Raabe
Institut für Organische Chemie der Technischen Hochschule
Professor-Pirlet-Strasse 1, D-W-5100 Aachen (FRG)
Dr. E.R. Hovestreydt
Siemens AG, D-W-7500 Karlsruhe 21 (FRG)

[**] This work was supported by the Fonds der Chemischen Industrie and contains important parts of the dissertation of R.F., Technische Hochschule Aachen, **1990**. We are grateful to Degussa AG, BASF AG, Bayer AG, and Hoechst AG for gifts of chemicals. – SAMP = (*S*)-1-Amino-2-methoxymethylpyrrolidine.

imines,[14] sulfonylimines,[15] sulfoxyimines,[16] oxime ethers,[17] and hydrazones.[8, 9, 18–21] Organolanthanoid compounds are used with increasing frequency for this purpose.[22]

We report here an enantioselective synthesis of α-amino acetals **A** starting from α-SAMP or -RAMP hydrazone acetals **B**. The key step is the diastereoselective nucleophilic 1,2-addition of organocerium and organolithium compounds to the hydrazone double bond. Oxidative transformation of the acetal into an acid group thereby provides a new, highly enantioselective entry to α-amino acids **C**.

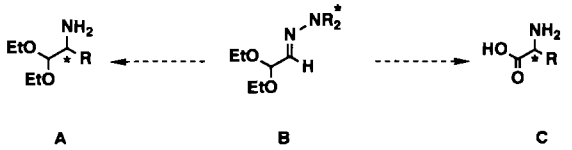

The reaction of diethoxyacetaldehyde **1**[23] with SAMP[24] gave the SAMP hydrazone (*S*)-**2** in very good yield. The latter was treated at −100 °C with organocerium or lithium compounds in THF. The organocerium compounds were obtained according to a procedure of Imamoto et al.,[25] in which anhydrous $CeCl_3$ is treated in THF with the appropriate organolithium or Grignard reagent. The 1,2-additions, which occurred in very good yields (72–98%) and with very high diastereomeric excess (78–98%), provided the sensitive hydrazines (*S*,*R*)-**3** after aqueous workup. After chromatographic separation of the minor diastereomers, the almost diastereomerically pure hydrazines (*S*,*R*)-**3** were converted to the α-amino acetals (*R*)-**4** by reductive cleavage with Raney nickel/hydrogen in methanol. The chiral amine (*S*)-**2**-methoxymethylpyrrolidine (SMP, recovery of the auxiliary) was separated by chromatography, and after subsequent distillation (kugelrohr) the pure, colorless α-amino acetals (*R*)-**4** were obtained (Scheme 1, Table 1).

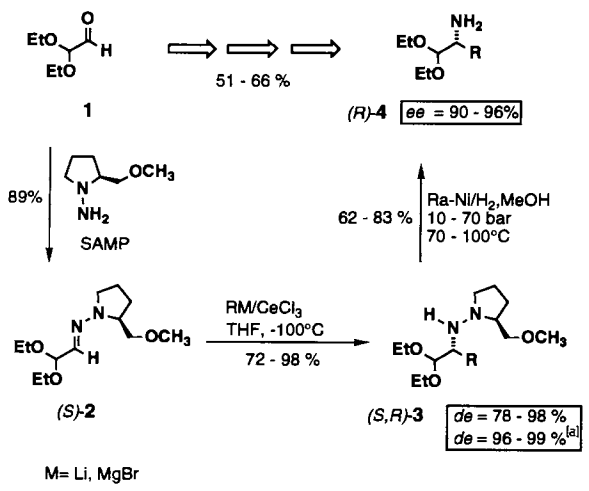

Scheme 1. Enantioselective synthesis of α-amino acetals **4**. $RM/CeCl_3$ was employed in excess (5 equiv). [a] After chromatography.

Table 1. SAMP α-amino acetals **3** (prepared by nucleophilic 1,2-addition to diethoxyacetaldehyde SAMP hydrazone) and their cleavage to **4**.

	R	$M/CeCl_3$	Yield of **3** [a] [%]	*de* [b] [%]	Yield of **4** [%]	$[\alpha]_D^{RT}$ **4** (*c*, EtOH)	*ee* [c] [%]
a	Me	Li	91	98	78	−18.9° (1.2) [d]	96.7 (*R*)
a [e]	Me	Li	92	97.5	62	+16.4° (1.0) [d]	95.3 (*S*)
b	Et [f]	MgBr	98	100 (94)	83	+1.4° (1.0)	94.0 (*R*)
c	*n*Pr [f]	MgBr	92	100 (86)	75	+8.8° (0.9)	90.0 (*R*)
d	*i*Pr	MgBr	89	100 (95)	80	−8.3° (1.2)	94.0 (*R*)
e	*n*Bu	Li	92	100 (95)	62	+8.3° (1.1)	91.0 (*R*)
f	*t*Bu	Li [g]	89	100 (78)	72	−26.0° (1.1)	94.0 (*R*)
g	Ph	MgBr	72	>96	80 [h]	+3.3° (neat)	96.0 (*R*)

[a] Yields of the major diastereomers (*R*,*S*)-**3a–h**. [b] Determined by gas chromatography (GC) (OV-1-CB, FID). The *de* values of the crude hydrazines before chromatographic purification are in parentheses. [c] Determined by ^{19}F NMR or GC analysis of the MTPA amide. The absolute configurations are in parentheses. [d] The solvent used was 0.1 N HCl. [e] RAMP was employed as chiral auxiliary. [f] Yields of both diastereomers. [g] Without addition of $CeCl_3$. [h] R = *cyclo*-C_6H_{11}.

contrast to many of the corresponding N-protected compounds, are completely configurationally stable. Even after several weeks at room temperature no loss in optical activity could be observed. The enantiomeric excess for the amino acetals (*R*)-**4** was determined in all cases by comparison with the racemates via the 3,3,3-trifluoro-2-methoxy-2-phenylpropionic acid (MTPA) amides[26] by gas chromatography or NMR spectroscopy. The racemates were synthesized in similar fashion via the corresponding dimethylhydrazones. The absolute configuration of the α-amino acetals (*R*)-**4** could be determined by two independent methods: The optical rotation was compared with that of the known compound (*S*)-**4a**,[3] and an X-ray crystal structure analysis of the (*S*)-MTPA derivative of the compound (*R*)-**4g** gave the (*R*) configuration for the newly generated stereogenic center (Fig. 1).[27, 28] The enantiomers (*S*)-**4** are accessible by simply changing the auxiliary (RAMP instead of SAMP) (see (*S*)-**4a**, Table 1).

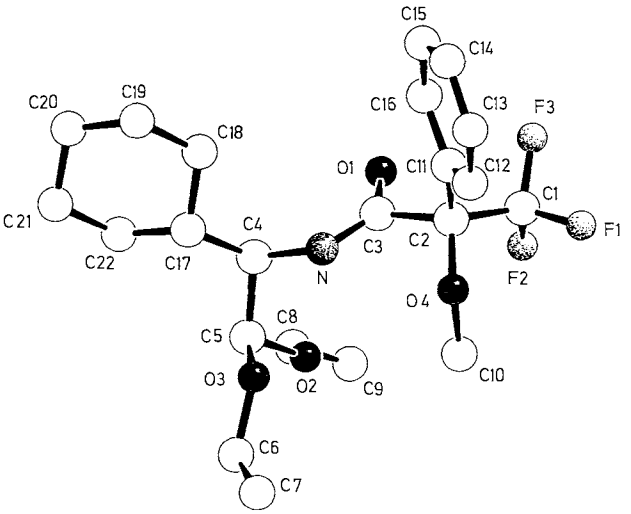

Fig. 1. Crystal structure of the MTPA amide of **4g**[7,28].

Cleavage of the N–N bond in hydrazines (*S*,*R*)-**3** by hydrogenolysis occurred with little racemization, so that the enantiomeric excess lies slightly below that of the diastereomeric excess. During hydrogenolysis of (*R*)-**3g** the phenyl ring was also hydrogenated. The α-amino acetals, in

As demonstrated in Scheme 2 for the example of the enantioselective synthesis of (*R*)-alanine (*R*)-**7**, diethoxyacetaldehyde SAMP hydrazone (*S*)-**2** can also function as an equivalent for the glycine cation, thereby permitting a new entry to α-amino acids. The key to success lies in the use of ozono-

lysis for the cleavage of the cyclic acetal with the 1,3-dioxolane structure to the hydroxyethylester, according to the method of Deslongchamps et al.[29] After addition of the organocerium compound from MeLi/$CeCl_3$ to (*S*)-**2** and trapping with acetylchloride, the N–N bond was cleaved reductively without racemization by reaction with Li/NH_3.[30] Finally, the *N*-acetyl-protected α-amino acetal was converted into the cyclic acetal (*R*)-**5** (*ee* = 97.0%) with ethylene glycol in a yield of 83%. After introduction of the *tert*-butoxycarbonyl (Boc) protecting group with $(Boc)_2O$ and hydrazinolysis, the carbamate-protected α-amino acetal was obtained. Ozonolysis, requiring only a few minutes at −78°C, gave the α-amino acid ester (*R*)-**6** quantitatively. The protecting group was removed by treatment with three equivalents of trimethylsilyliodide and the ester group hydrolyzed simultaneously. The amino acid, after purification by ion-exchange chromatography (Lewatit SP 112), was obtained in an overall yield of 34% and an enantiomeric excess of 95.3%.[31]

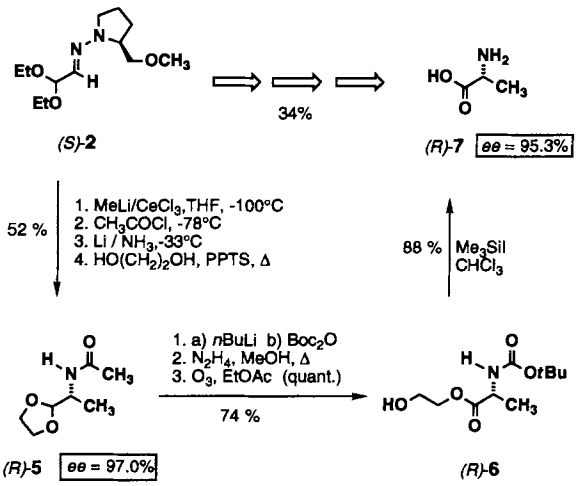

Scheme 2. Enantioselective synthesis of (*R*)-alanine. PPTS = pyridinium *para*-toluenesulfonate. Me_3SiI was used in excess (3 equiv).

The methods described here provide a new, highly enantioselective entry to both enantiomers of α-amino acetals and α-amino acids. Initial results show that the process is also applicable for homologous β-SAMP hydrazone acetals, thereby leading to the corresponding β-amino acetals and β-amino acids.[32]

Experimental Procedure

α-Amino acetals **4**: 5 Equiv $CeCl_3 \cdot 7H_2O$ was dried in a Schlenk flask with stirring for 2 h at 140 °C/0.1 Torr. After cooling, the anhydrous $CeCl_3$ was stirred at room temperature under argon with dry THF (3 mL mmol^{-1} $CeCl_3$) for 2 h and then for 1 h in an ultrasound bath. The colorless suspension was cooled to −78 °C and treated dropwise with 5 equiv RLi or RMgX. Upon addition of RLi a bright yellow suspension was obtained, whereas addition of RMgX caused the color to change to light gray. After the resulting suspension was stirred for 2 h at −78 °C, the reaction mixture was cooled to −100 °C (ethanol/liquid nitrogen). The SAMP hydrazone (*S*)-**2**, dissolved in THF (3 mL mmol^{-1}), was added to the suspension very slowly (10 mL h^{-1}; syringe pump). The reaction mixture was first held at −100 °C for 2 h and then allowed to warm to room temperature over ca. 15 h. The mixture was hydrolyzed with ca. 40 mL saturated $NaHCO_3$ solution, the organic phase separated, and the residue extracted several times with ether. The combined organic phases were concentrated, dissolved in 50 mL ether, washed with water, and finally dried over Na_2SO_4. After concentration, the sensitive hydrazines (*R*)-**3** were purified by flash chromatography (silica gel, ether:petroleum ether 2:1 to 1:3). A solution of the hydrazine in methanol (5–10 mL mmol^{-1}) was treated with freshly prepared Raney nickel[33] (0.5–1.0 g Ni-Al alloy per mmol of hydrazine) and hydrogenated in an autoclave with stirring at 70–100 °C and a hydrogen pressure of 70 bar for 20–60 h (monitored by thin-layer chromatography). After completion of the reaction, the catalyst was removed by filtration through celite, the solvent removed from the filtrate, the residue dissolved in ether, and the resulting ethereal solution dried over Na_2SO_4 and concentrated to dryness. The α-amino acetals were purified by flash chromatography (silica gel, anhydrous methanol) followed by removal of the methanol and distillation (kugelrohr).

α-Amino acids **7**: The product resulting from nucleophilic 1,2-addition to the SAMP hydrazone (*S*)-**2** (see above) was trapped at −78 °C with 5.5 equiv acetyl chloride and then stirred for 1 h at 0 °C. The product was worked up with 40 mL saturated Na_2CO_3 solution and ether. The hydrazines were purified by flash chromatography (silica gel, ether:petroleum ether 2:1). A solution of the *N*-acylated hydrazine in anhydrous THF (1 mL mmol^{-1}) was mixed with ammonia (15 mL mmol^{-1}) at −78 °C, and the mixture treated with clean Li wire (4 mmol mmol^{-1}). The resulting solution rapidly turned blue. The cooling bath was removed, the solution allowed to stir for 1 h at −33 °C, the reaction stopped by addition of NH_4Cl (12 mmol mmol^{-1}), and the ammonia allowed to evaporate. The residue was dissolved in 40 mL water and extracted several times with ether. After the combined organic phases were dried and concentrated, the *N*-acetylated α-amino acetals were obtained. These were dissolved in glycol (3 mL mmol^{-1}), treated with 0.1 g pyridinium *p*-toluenesulfonate (PPTS), and stirred for 3 h at 80 °C. After distillation of the volatile components, the whole was taken up in 40 mL water and extracted with CH_2Cl_2. The combined organic phases were dried over Na_2SO_4 and concentrated, and the α-amino acetals (*R*)-**5** were purified by flash chromatography (silica gel, ethyl acetate). A solution of (*R*)-**5** in anhydrous THF (5 mL mmol^{-1}) was treated with 1.1 equiv *n*BuLi at −78 °C, stirred for 4 h at this temperature, and then trapped with $(Boc)_2O$ (5 mmol mmol^{-1}). The crude solution was concentrated and the residue taken up in methanol (5 mL mmol^{-1}), treated with anhydrous hydrazine (3 mL mmol^{-1}), and stirred for 4 h at reflux. After aqueous workup and extraction with ether the α-amino acetals, protected as carbamates, were obtained. Purification was by flash chromatography (silica gel, ether:petroleum ether 2:1). The acetals were dissolved in ethyl acetate (15 mL mmol^{-1}) and treated with ozone at −78 °C (reaction followed by thin-layer chromatography). The solvent was removed to provide the pure ester (*R*)-**6**, which was allowed to react with 3 equiv Me_3SiI in $CHCl_3$ (5 mL mmol^{-1}) under argon (3–5 min). Workup was with 1 N HCl, and the amino acids were purified by ion-exchange chromatography (Lewatit SP 112, 2 N aqueous NH_3 solution).

Received: September 23, 1992 [Z 5594 IE]
German version: *Angew. Chem.* **1993**, *105*, 418

[1] a) M. T. Reetz, *Angew. Chem.* **1991**, *103*, 1559; *Angew. Chem. Int. Ed. Engl.* **1991**, *30*, 1531; b) J. Jurczak, A. Golebiowski, *Chem. Rev.* **1989**, 149; c) L. E. Fisher, J. M. Muchowski, *Org. Prep. Preoced. Int.* **1990**, *22*, 399.
[2] a) E. Fischer, T. Kametaka, *Justus Liebigs Ann. Chem.* **1909**, *365*, 7; b) E. Fischer, *Ber. Dtsch. Chem. Ges.* **1908**, *41*, 1019.
[3] a) K. Balenovic, N. Bregant, D. Cerar, D. Fles, J. Jambresic, *J. Org. Chem.* **1953**, *18*, 297; b) K. Balenovic, N. Bregant, T. Galijan, Z. Stefanac, V. Skaric, *ibid.*, **1956**, *21*, 115.
[4] M. Gacek, K. Undheim, *Tetrahedron* **1974**, *30*, 4233.
[5] a) S. Kano, T. Yokomatsu, H. Iwasawa, S. Shibuya, *Heterocycles* **1987**, *26*, 2805; b) S. Kano, T. Yokomatsu, H. Iwasawa, S. Shibuya, *Chem. Lett.* **1987**, 1531.
[6] G. Bringmann in *The Alkaloids, Vol. 29* (Ed.: A. Brossi), Academic Press, New York, **1987**, p. 141.
[7] G. Bringmann, J. P. Geisler, *Synthesis* **1989**, 608.
[8] M. Thiam, F. Chastrette, *Tetrahedron Lett.* **1990**, *31*, 1429.
[9] A. Alexakis, N. Lensen, P. Mangeney, *Tetrahedron Lett.* **1991**, *32*, 1171.
[10] K. Harada in *The Chemistry of the Carbon Nitrogen Double-Bond* (Ed.: S. Patai), Interscience, London, **1970**.
[11] Reviews: a) D. J. Hart, D.-C. Ha, *Chem. Rev.* **1989**, *89*, 1447; b) M.-J. Brown, *Heterocycles* **1989**, *29*, 2225; c) Y. Yamamoto, *Acc. Chem. Res.* **1987**, 243. Recent examples: d) S. Laschat, H. Kunz, *Synlett* **1990**, 51; e) M. T. Reetz, R. Jaeger, R. Drewlies, M. Hübel, *Angew. Chem.* **1991**, *103*, 76; *Angew. Chem. Int. Ed. Engl.* **1991**, *30*, 103; f) K. Tomioka, I. Inoue, M. Shindo, K. Koga, *Tetrahedron Lett.* **1991**, *32*, 3095; g) Y. Ukaji, J. Watai, T. Sumi, T. Fujisawa, *Chem. Lett.* **1991**, 1555; h) G. Cainelli, D. Giacomini, E. Mezzina, M. Pannuzio, P. Zarantonello, *Tetrahedron Lett.* **1991**, *32*, 2967; i) R. Annunziata, M. Cinquini, F. Cozzi, P. G. Cozzi, *ibid.*, **1992**, *33*, 1113.
[12] a) P. Münster, W. Steglich, *Synthesis* **1987**, 223; b) R. Kobes, K. Papadopoulos, W. Miltz, D. Enders, W. Steglich, H. Reuter, H. Puff, *Tetrahedron* **1985**, 1693; c) P. Ermert, I. Meyer, C. Stucki, J. Schneebeli, J. P. Obrecht, *Tetrahedron Lett.* **1988**, *29*, 1265.
[13] a) Z.-Y. Chang, R. M. Coates, *J. Org. Chem.* **1990**, *55*, 3475; b) M. A. Schwartz, X. Hu, *Tetrahedron Lett.* **1992**, *33*, 1689.
[14] C. Fuganti, P. Grasselli, G. Pedrocchi-Fantoni, *J. Org. Chem.* **1983**, *48*, 909.
[15] a) F. A. Davis, M. A. Giangiordano, W. E. Starner, *Tetrahedron Lett.* **1986**, *27*, 3957; b) J. Siske, S. M. Weinreb, *J. Org. Chem.* **1990**, *55*, 393.
[16] D. H. Hua, S. W. Miao, J. S. Chen, S. Iguchi, *J. Org. Chem.* **1991**, *56*, 4.

[17] H. Fujioka, M. Fuji, Y. Okaichi, T. Yoshida, H. Annoura, Y. Kita, Y. Tamura, *Chem. Pharm. Bull.* **1989**, *37*, 602.
[18] H. Takahashi, H. Inagaki, *Chem. Pharm. Bull.* **1983**, *31*, 4295, and references therein.
[19] D. A. Claremon, P. K. Lumma, B. T. Phillips, *J. Am. Chem. Soc.* **1986**, *108*, 8265.
[20] a) D. Enders, H. Schubert, C. Nübling, *Angew. Chem.* **1986**, *98*, 1118; *Angew. Chem. Int. Ed. Engl.* **1986**, *25*, 1109; b) D. Enders, D. Bartzen, *Liebigs Ann. Chem.* **1991**, 569.
[21] a) S. E. Denmark, T. Weber, D. W. Piotrowski, *J. Am. Chem. Soc.* **1987**, *109*, 2224; b) S. E. Denmark, T. Weber, J. P. Edwards, *Synlett*, **1989**, *1*, 20.
[22] G. A. Molander, *Chem. Rev.* **1992**, 29.
[23] H. Stetter, K. H. Mohrmann, *Synthesis* **1981**, 129.
[24] a) D. Enders in *Asymmetric Synthesis, Vol. 3*, (Ed.: J. D. Morrison), Academic Press, Orlando, FL, USA **1984**, p. 275; b) D. Enders, P. Fey, H. Kipphardt, *Org. Synth.* **1987**, *65*, 173, 183; b) D. Enders, P. Fey, H. Kipphardt, *Org. Prep. Proced. Int.* **1985**, *17*, 1.
[25] a) T. Imamoto, N. Takiyama, K. Nakamura, *Tetrahedron Lett.* **1985**, *26*, 4763; b) T. Imamoto, Y. Sugiura, *J. Organomet. Chem.* **1985**, *C21*, 285; c) T. Imamoto, Y. Sugiura, N. Takiyama, *Tetrahedron Lett.* **1984**, *25*, 4233; d) T. Imamoto, T. Kusumoto, Y. Tawarayama, Y. Sugiura, T. Mita, Y. Hatanaka, M. Yokoyama, *J. Org. Chem.* **1984**, *49*, 3904.
[26] J. A. Dale, H. S. Mosher, *J. Am. Chem. Soc.* **1973**, *95*, 512.
[27] Suitable crystals were obtained from EtOAc/cyclohexane (2:1) at $-20\,^{\circ}C$. Monoclinic, space group $P2_1(4)$, $a = 10.758(5)$, $b = 10.336(4)$, $c = 11.720(6)$ Å, $\beta = 113.73(4)^{\circ}$. The cell volume is 1193.0(9) Å^3, $Z = 2$ and $M_r = 431.5$, leading to a density $\varrho_{calc} = 1.201\ g\,cm^{-3}$. The total number of electrons per unit cell $F(000) = 460$, $Mo_{K\alpha}$ irradiation ($\lambda = 0.71069$ Å, graphite monochromator), $m = 0.91\ cm^{-1}$. Siemens R3m/V four-circle diffractometer, 2 θ-θ scans, 23 °C. A total of 2241 independent reflections ($+h + k \pm l$) were recorded, of which 1074 were observed ($I > 2\sigma(I)$), $R_m = 0.07$, $\sin\theta/\lambda_{max} = 0.597$. The structure solution was obtained using direct methods (Siemens SHELXTL PLUS) and the refinement using the XTAL3.0 program [28]. Positions of hydrogen atoms were calculated. A total of 270 parameter refinements were used, $R = 0.073$ ($R_w = 0.029$), residual electron density 0.5 e Å^{-3}. Further details of the crystal structure investigation may be obtained from the Fachinformationszentrum Karlsruhe, Gesellschaft für wissenschaftlich-technische Information GmbH, D-W-7514 Eggenstein-Leopoldshafen 2 (FRG) on quoting the depository number CSD-56669, the names of the authors, and the journal citation.
[28] *XTAL3.0 User's Manual* (Eds.: S. R. Hall, J. M. Stewart), Universities of Western Australia und Maryland, **1990**.
[29] P. Deslongchamps, P. Atlani, D. Frehel, A. Malaval, C. Moreau, *Can. J. Chem.* **1974**, *52*, 3651.
[30] a) C. Nübling, *Dissertation*, Technische Hochschule Aachen, **1987**; b) S. E. Denmark, O. Nicaise, J. P. Edwards, *J. Org. Chem.* **1990**, *55*, 6219.
[31] All new compounds gave correct elemental analysis and NMR, IR, and mass spectra.
[32] D. Enders, M. Klatt, R. Funk, unpublished.
[33] *Organikum*, 16th ed., VEB Deutscher Verlag der Wissenschaften, Berlin, **1986**.

Enantioselective Aldol Reactions with a Phosphoenolpyruvate Equivalent: Asymmetric Synthesis of 4-Hydroxy-2-oxocarboxylic Acid Esters**

By *Dieter Enders*,* *Hubert Dyker*, and *Gerhard Raabe*

Dedicated to Professor Rudolf Hoppe on the occasion of his 70th birthday

The aldol reaction is the preferred method for the stereoselective synthesis of 1,3-dioxygenated building blocks.[1] Enantiofacial differentiation in the enolates can be diastereoselectively controlled by covalently bound auxiliaries, which permit formation of one or two stereogenic centers with high selectivity and predictable configuration.

[*] Prof. Dr. D. Enders, Dr. H. Dyker, Dr. G. Raabe
Institut für Organische Chemie der Technischen Hochschule
Professor-Pirlet-Strasse 1, D-W-5100 Aachen (FRG)

[**] This work was supported by the Deutsche Forschungsgemeinschaft and the Fonds der Chemischen Industrie. We thank Degussa AG, BASF AG, Bayer AG, and Hoechst AG for donating samples of chemicals. H.D. thanks the Fonds der Chemischen Industrie for a Kekulé stipend.

Enzyme-catalyzed aldol reactions are used in nature, for example, in the stereoselective formation of monosaccharides. The transfer of the pyruvate unit as phosphoenolpyruvate (PEP) to aldoses with the generation of 4-hydroxy-2-oxocarboxylic acids **A** in the biosynthesis of ulosonic acids[2] and sialic acids[3] is one of the most important synthetic routes of this type. Aldolases, which catalyze this reaction, have recently been used in the biocatalytic synthesis of natural and unnatural higher monosaccharides from PEP or pyruvate and aldehydes.[4-8]

Several achiral metalated pyruvic derivatives (d^2 synthons **B**) have been used as chemical equivalents for PEP in imitation of the synthetic principle used in nature.[9] Stereoselective reactions of these reagents are nevertheless limited to diastereoselective aldol reactions with enantiomerically pure aldehydes.[9g-9i]

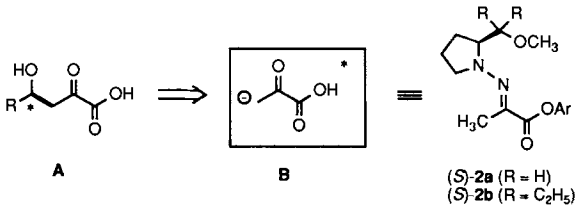

A **B** (*S*)-**2a** (R = H) (*S*)-**2b** (R = C_2H_5)

Ar = 2,6-di-*tert*-butyl-4-methoxyphenyl

We recently reported on the development of an enantiomerically pure, homologous PEP equivalent[10] in which our SAMP/RAMP hydrazone method[11,12] was employed and on its use in the enantioselective synthesis of 3-substituted 2-oxacarboxylic acid esters. We now introduce an enantiomerically pure, chemical PEP equivalent, which permits the biomimetic enantioselective synthesis of 4-hydroxy-2-oxocarboxylic acid esters **A**. The key step is the diastereoselective aldol reaction of (*S*)-**2** with achiral and chiral aldehydes.

In initial investigations of the metalation and alkylation conditions, simple alkylation of SAMP hydrazone (*S*)-**2a** was examined. The uniformly (*E*) hydrazone was obtained in 96% yield as light yellow solid (m.p. 84 °C) by reaction of the appropriate pyruvic acid ester **1**[10] with (*S*)-1-amino-2-methoxymethylpyrrolidine (SAMP).[12,13] Employing the 2,6-di-*tert*-butyl-4-methoxyphenyl ester[14] to avoid the self-condensation of the corresponding azaenolate is decisive.[10]

Surprisingly, the alkylation of hydrazone (*S*)-**2a** with benzylbromide by metalation with 1.1 equivalents of lithium diisopropylamide (LDA) was incomplete. The alkylated product was isolated in 71% yield, together with 21% unreacted starting material. The use of 2.2 equivalents of LDA gave both the monoalkylated and the bisalkylated products in variable yield. Complete conversion in the alkylation (98% yield) was achieved only when 1.1 equivalents of base were employed in the presence of 2 equivalents of lithium bromide at $-78\,^{\circ}C$ in THF. Similar effects have been described for related systems.[9j,15] The aldol reaction of the SAMP hydrazone (*S*)-**2a** metalated in this manner with 3-methylbutanal at $-90\,^{\circ}C$ gave the aldol product (*S,R*)-**3a** in similar good yield, albeit with only moderate stereoselectivity (84 °% yield, *de* = 36 °%). The stereoselectivity of the aldol reaction could be increased considerably when SAMP was exchanged for the sterically more demanding auxiliary (*S*)-1-amino-2-(1-ethyl-1-methoxypropyl)pyrrolidine (SAEP)[16] (Scheme 1, Table 1).

The condensation of pyruvic acid ester **1** with the hydrazine SAEP gave the (*E*)-configurated hydrazone (*S*)-**2b**

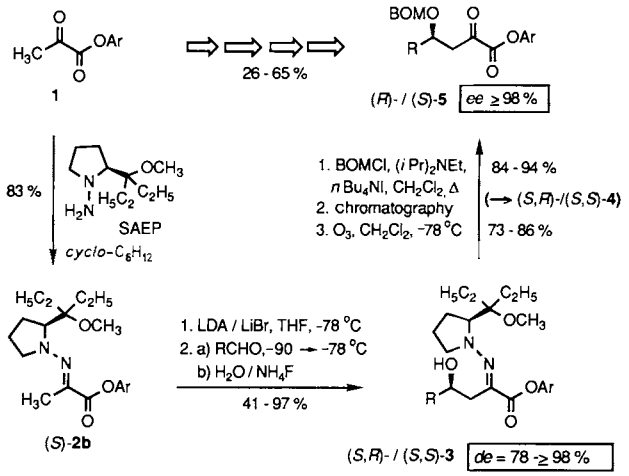

Scheme 1. Four-step enantioselective synthesis of BOM-protected 4-hydroxy-2-oxocarboxylic acid ester **5** (BOM = $PhCH_2OCH_2$).

in 83% yield as a viscous yellow oil. Metalation of the hydrazone with LDA in the presence of lithium bromide under the conditions given above, and reaction of the resulting reactive azaenolates with aldehydes at temperatures between −90 and −78 °C gave hydrazones (*S*,*R*)-/(*S*,*S*)-**3** in very good yield (86–97%) and with high diastereomeric excess (*de* = 78– ≥ 98%) as highly viscous yellow substances that could be purified by chromatography and characterized. Only the reaction with the isopropylidene-protected (*R*)-glyceraldehyde gave a low yield (41%, *de* ≥ 98%, (*S*,*S*,*R*)-**3h**).

Table 1. Enantiomerically pure BOM-protected 4-hydroxy-2-oxocarboxylic acid esters **5** synthesized by the enantioselective aldol reaction of the SAEP hydrazone (*S*)-**2b** prepared from pyruvic acid ester **1**.

	R	Yield at **3** [%]	*de* [a] [%]	Yield at **4**/**5** [b] [%]	**5** $[\alpha]_D^{RT}$ [c]	**5** *ee* [d] [%]
a [e]	$(H_3C)_2CHCH_2$	84	36	94/81	+3.6	36(*R*)
a	$(H_3C)_2CHCH_2$	96	90	93/76 [f]	+11.0	≥98(*R*)
b	n-C_4H_9	93	93	93/86	+5.0	≥98(*R*)
c	n-C_5H_{11}	86	90	91/76	+6.1	≥98(*R*)
d	$PhCH_2CH_2$	87	78	84/82	+1.9	≥98(*R*)
e	C_6H_5	95	≥98	90/84	−59.3	≥98(*S*)
f	p-H_3C-C_6H_5	92	≥98	94/73	−55.8	≥98(*S*)
g	p-H_3CO-C_6H_5	97	≥98	94/86	−77.3	≥98(*S*)
h		41	≥98	89/85	+8.8	≥98(*S*,*R*)

[a] Diasteromeric excess determined by ^{13}C NMR. [b] Yield of the major diastereomer **5** after flash chromatography. [c] $c = 1$, $CHCl_3$. [d] Determined as *de* at the stage of hydrazone **4** by ^{13}C NMR spectroscopy. The absolute configuration is given in parentheses. [e] SAMP was employed as chiral auxiliary. The diastereomers were not separated at the hydrazone stage. [f] M.p. 57–59 °C.

As 4-hydroxy-2-oxocarboxylic acid esters **5**, the final products of the reaction sequence described here, are inclined toward elimination and side reactions during the chromatographic purification,[9k,l] introduction of a protecting group was necessary. Use of *O*-silyl and *O*-acetyl protecting groups was unsuccessful. Isolation of the final products **5** without decomposition was achieved, however, by the introduction of the *O*-benzyloxymethyl (BOM) protecting group. The BOM group was introduced with very good yield (generally over 90%) by reaction of the aldol products **3** with excess benzyloxymethylchloride in the presence of Hünig base. Separation of the diastereomers was possible by simple flash chromatography, so that after chromatographic purification products **4** were obtained diastereomerically pure (*de* ≥ 98%) and in yields of 84–94% as light yellow, highly viscous oils. A further isomer could not be detected by ^{13}C NMR spectroscopy.

The protected aldol products **4** could be converted without racemization and in good yield by oxidative cleavage with ozone to give the enantiomerically pure final products (*R*)- and (*S*)-**5**, which were purified by rapid flash chromatography (73–86% yield).

The diastereomeric excesses of the hydrazones **3** and the BOM-protected aldol products **4** were determined by ^{13}C NMR spectroscopy. The values given for the enantiomeric excesses of the final products **5** refer to the diastereomeric excesses of the BOM-protected aldol products **4** determined by ^{13}C NMR spectroscopy. Isolation of (*S*,*R*)-**5h** in diastereo- and enantiomerically pure form verified that the introduction of the protecting group and cleavage of the hydrazone proceed without racemization.

The absolute configurations given for the hydrazones and, thereby, the final products **5** are based on a crystal structure analysis of a single crystal of hydrazone (*S*,*R*)-**4a** (Fig. 1),[17] the only product obtained as a solid (m.p. 57–59 °C), and the assumption of a uniform reaction mechanism. The (*R*) configuration determined for the newly generated stereogenic center ((*S*) configuration for R = Ar and in case **h**) is in agreement with the stereochemical process previously observed in aldol reactions with SAMP/RAMP hydrazones.[18–20]

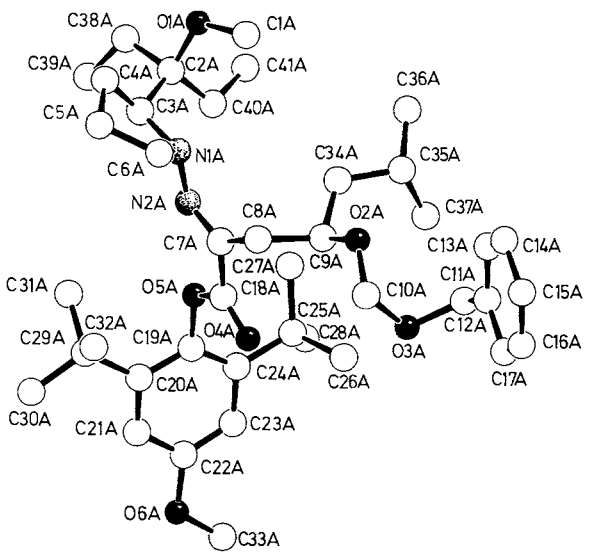

Fig. 1. Crystal structure of one of the two independent molecules of (*S*,*R*)-**4a** (Schakal plot[21]).

The methods described here permit the efficient, highly enantioselective transfer of the pyruvate unit to achiral and chiral aldehydes.[22] The synthesis of natural products, demonstrated with the example of the protected 2-keto-3-deoxygluconate (KDG) **5h**,[4] and their analogues is the subject of current investigations, which include the extension of this new synthetic process to homologous phosphoenolpyruvate equivalents.

Experimental Procedure

To 2.2 mmol of an LDA/LiBr solution (prepared by addition of 1.47 mL of a 1.5 M solution of *n*-butyllithium in *n*-hexane to a solution of 0.22 g (2.2 mmol)

diisopropylamine and 0.35 g (4 mmol) LiBr in 15 mL anhydrous THF at 0 °C under argon) cooled to −78 °C was slowly added dropwise a solution of 0.95 g (2 mmol) hydrazone (*S*)-**2b** dissolved in 3–4 mL THF, and the reaction mixture was stirred at this temperature for 1–2 h. The resulting solution was cooled to −90 °C and 2.2 mmol of the aldehyde dissolved in 2 mL THF added slowly. The reaction mixture was held at −90 °C for 1–2 h, allowed to warm to −78 °C, stirred at this temperature for 1 h, and then hydrolyzed with 2 mL saturated NH_4Cl solution. The mixture was warmed to room temperature and diluted with 150 mL ether. The organic phase was washed with 10 mL water, buffer solution (pH 7), and saturated NaCl solution, and dried over $MgSO_4$. After removal of the solvent in vacuo the product was purified by flash chromatography (silica gel, petroleum ether/ethyl acetate 4:1). For the introduction of the benzyloxymethyl (BOM) protecting group, 1 mmol of the aldol product was dissolved together with 14 mg (0.1 mmol) nBu_4NI in 10 mL anhydrous CH_2Cl_2, and 0.52 g (4 mmol) *N*-ethyldiisopropylamine and 0.47 g (3 mmol) benzylchloromethylether were slowly added in that sequence. The resulting solution was heated at reflux for 12–15 h. After the reaction was complete the solution was treated with 2 mL methanol to quench the excess chloride, stirred for 2 h at room temperature, and concentrated. The residue was dissolved in 150 mL ether, the solution then washed with 10 mL of saturated NH_4Cl solution and 10 mL saturated NaCl solution, dried over $MgSO_4$, and concentrated. The product was purified by flash chromatography (silica gel, petroleum ether/ethyl acetate 95:5). For cleavage of the auxiliary, 1 mmol of the hydrazone was dissolved in ca. 50 mL CH_2Cl_2 and cooled to −78 °C under argon. Ozone was passed through the solution at this temperature until the reaction was complete. After removal of the excess ozone by purging with a stream of argon, the reaction mixture was warmed to room temperature, and concentrated. The product was purified by flash chromatography (silica gel, petroleum ether/ethyl acetate/2-propanol 90:10:1).

Received: September 29, 1992 [Z 5604 IE]
German version: *Angew. Chem.* **1993**, *105*, 420

[1] a) C. H. Heathcock in *Asymmetric Synthesis, Vol. 3* (Ed.: J. D. Morrison), Academic Press, Orlando, **1984**, p. 111; b) S. Masamune, W. Choy, J. S. Petersen, L. R. Sita, *Angew. Chem.* **1985**, *97*, 1; *Angew. Chem. Int. Ed. Engl.* **1985**, *24*, 1; c) M. Braun, *ibid.* **1987**, *99*, 24 and **1987**, *26*, 24; d) R. W. Hoffmann, *ibid.* **1987**, *99*, 503 and **1987**, *26*, 489; e) *Comprehensive Organic Synthesis, Vol.2* (Eds.: B. M. Trost, I. Fleming, C. H. Heathcock), Pergamon, Oxford, **1991**, Chaps. 1.5–1.7, 1.9 and 1.15.

[2] F. M. Unger, *Adv. Carbohydr. Chem. Biochem.* **1980**, *38*, 323.

[3] a) R. Schauer, *Adv. Carbohydr. Chem. Biochem.* **1982**, *40*, 132; b) R. Schauer, A. P. Cornfield in *Sialic Acids, Chemistry, Metabolism and Function (Cell Biol. Monogr. 10*, Ed.: R. Schauer), Springer, Wien, **1982**; c) R. Schauer, *Pure Appl. Chem.* **1984**, *56*, 907.

[4] S. T. Allen, G. R. Heintzelmann, E. J. Toone, *J. Org. Chem.* **1992**, *57*, 426.

[5] L. M. Reimer, D. L. Conley, D. L. Pompliano, J. W. Frost, *J. Am. Chem. Soc.* **1986**, *108*, 8010.

[6] a) M. D. Bednarski, C. D. Crans, R. Dicosimo, E. S. Simon, P. D. Stein, G. M. Whitesides, M. J. Scheider, *Tetrahedron Lett.* **1988**, *29*, 427; b) C. Auge, B. Bouxom, B. Cavaye, C. Gautheron, *ibid.* **1989**, *30*, 2217.

[7] a) C. Auge, S. David, C. Gautheron, A. Malleron, B. Cavaye, *New J. Chem.* **1988**, *12*, 733; b) M.-J. Kim, W. J. Hennen, H. M. Sweers, C.-H. Wong, *J. Am. Chem. Soc.* **1988**, *110*, 6481; c) A. Schrell, G. M. Whitesides, *Liebigs Ann. Chem.* **1990**, 111; d) U. Kragl, D. Gygax, O. Ghisalba, C. Wandrey, *Angew. Chem.* **1991**, *103*, 854; *Angew. Chem. Int. Ed. Engl.* **1991**, *30*, 827.

[8] a) C. Auge, C. Gautheron, S. David, *Tetrahedron* **1990**, *46*, 201; b) C. Gautheron-LeNarvor, Y. Ichikawa, C.-H. Wong, *J. Am. Chem. Soc.* **1991**, *113*, 7816.

[9] a) C. G. Wermuth, *Bull. Soc. Chim. Fr.* **1986**, 1435; b) R. R. Schmidt, R. Betz, *Angew. Chem.* **1984**, *96*, 420; *Angew. Chem. Int. Ed. Engl.* **1984**, *23*, 430; c) A. Esswein, R. Betz, R. R. Schmidt, *Helv. Chim. Acta* **1989**, 213; d) R. Metternich, W. Lüdi, *Tetrahedron Lett.* **1988**, *29*, 3923; e) I. Tapia, V. Alcazar, J. R. Moran, C. Caballero, M. Grande, *Chem. Lett.* **1990**, 697; f) I. Tapia, V. Alcazar, J. R. Moran, *Can. J. Chem.* **1990**, *68*, 2190; g) A. Dondoni, G. Fantin, M. Fogagnolo, *Tetrahedron Lett.* **1989**, *30*, 6063; h) *ibid.* **1990**, *31*, 4513; i) A. Dondoni, P. Merino, *J. Org. Chem.* **1991**, *56*, 5294; j) D. R. Williams, J. W. Benbow, *ibid.* **1990**, *31*, 5881; k) H. Sugimura, Y. Shigekawa, M. Uematsu, *Synlett* **1991**, 153; l) C. Chen, D. Crich, *J. Chem. Soc. Chem. Commun.* **1991**, 1289.

[10] D. Enders, H. Dyker, G. Raabe, *Angew. Chem.* **1992**, *104*, 649; *Angew. Chem. Int. Ed. Engl.* **1992**, *31*, 618.

[11] D. Enders in *Asymmetric Synthesis, Vol. 3* (Ed.: J. D. Morrison), Academic Press, Orlando, FL, USA, **1984**, p. 275.

[12] D. Enders, P. Fey, H. Kipphardt, *Org. Synth.* **1987**, *65*, 173, 183.

[13] a) D. Enders, P. Fey, H. Kipphardt, *Org. Prep. Proc. Int.* **1985**, *17*, 1; b) D. Enders, H. Eichenauer, *Chem. Ber.* **1979**, *112*, 2933.

[14] a) C. H. Heathcock, M. C. Pirrung, S. H. Montgomery, J. Lampe, *Tetrahedron* **1981**, *37*, 4087; b) C. H. Heathcock, M. C. Pirrung, S. D. Young, J. P. Hagan, E. T. Jarvi, U. Badertscher, H.-P. Märki, S. H. Montgomery, *J. Am. Chem. Soc.* **1984**, *106*, 8161; c) R. Häner, D. Seebach, *Chimia* **1985**, *39*, 356; d) T. Vettiger, D. Seebach, *Liebigs Ann. Chem.* **1990**, 189; e) M. P. Cooke, Jr., *J. Org. Chem.* **1986**, *51*, 1638.

[15] a) M. Murakata, M. Nakajima, K. Koga, *J. Chem. Soc. Chem. Commun.* **1990**, 1657; b) N. DeKimpe, L. D'Hondt, E. Stanoeva, *Tetrahedron Lett.* **1991**, *32*, 3879.

[16] D. Enders, H. Kipphardt, P. Gerdes, L. J. Breña-Valle, V. Bushan, *Bull. Soc. Chim. Belg.* **1988**, *97*, 691.

[17] Suitable crystals for the X-ray structure analysis were obtained by crystallization from methanol at 2 °C. Monoclinic, space group $P2_1(4)$, $a = 10.940(1)$, $b = 15.822(2)$, $c = 23.817(4)$ Å, $\beta = 92.42(1)°$. From the cell volume of 4118.9 Å^3, two independent molecules in the asymmetric unit, and $M_r = 680.98$ a density of $\varrho_{calc} = 1.098$ g cm^{-3} can be calculated. Total electron count per unit cell $F(000) = 1488$. Enraf-Nonius CAD4 four-circle diffractometer, graphite monochromator, $\Omega/2\theta$ scans, −50 °C, $Cu_{K\alpha}$ irradiation ($\lambda = 1.54179$ Å), $\mu = 5.42$ cm^{-1}. A total of 7218 independent reflections ($\pm h + k + l$), of which 6518 were observed ($I > 2\sigma(I)$), $R_m = 0.008$, $\sin\theta/\lambda_{max} = 0.620$. The structure solution was obtained with direct methods (SHELXS-86 [23]) and the refinement by application of the routines of the SDP program package [24]. The two independent molecules differ considerably in the conformation of the substituents at C3A,B of the five-membered ring. For the phenyl groups C12A,B-C17A,B the ideal positions were calculated because of disorder in the atoms C14A,B-C16A,B and the substituents refined isotropically as rigid groups. Hydrogen atom positions were calculated. For the refinement 783 parameters were used, $R = 0.089$ ($R_w = 0.120$). Isotropic extinction coefficient $a = 2.2 \times 10^{-6}$. Residual electron density is largely localized in the region of the phenyl groups C12A,B-C17A,B, maximum value 0.45 e Å^{-3}. Further details of the crystal structure investigation may be obtained from the Fachinformationszentrum Karlsruhe, Gesellschaft für wissenschaftlich-technische Information GmbH, D-W-7514 Eggenstein-Leopoldshafen 2 (FRG) on quoting the depository number CSD-56869, the names of the authors, and the journal citation.

[18] H. Eichenauer, E. Friedrich, W. Lutz, D. Enders, *Angew. Chem.* **1978**, *90*, 219; *Angew. Chem. Int. Ed. Engl.* **1978**, *17*, 206.

[19] D. Enders, H. Eichenauer, R. Pieter, *Chem. Ber.* **1979**, *112*, 3703.

[20] D. Enders, *Chem. Scr.* **1985**, *25*, 139.

[21] E. Keller, *Chem. Unserer Zeit* **1986**, *20*, 178.

[22] All new compounds gave correct elemental analyses, IR spectra, and ^1H and ^{13}C NMR spectra.

[23] G. M. Sheldrick in *Crystallographic Computing 3* (Eds.: G. M. Sheldrick, C. Krüger, R. Goddard), Oxford University Press, **1985**, p. 175–189.

[24] B. A. Frenz and Ass., Inc., *Structure Determination Package (VAX SDP)*, College Station, TX 77840, USA, and Enraf-Nonius, Delft, The Netherlands.

Diastereo- and Enantioselective Synthesis of C_2-Symmetrical HIV-1 Protease Inhibitors**

By *Dieter Enders*,* *Udo Jegelka*, and *Barbara Dücker*

Since the Center for Disease Control in Atlanta (USA) defined[1] the diagnostic term AIDS (Acquired Immunodeficiency Syndrome) in 1982 only three medications have been authorized for treatment of AIDS: 3′-azido-3′-deoxythymidine (AZT, Wellcome, 1987), 2′,3′-dideoxyinosine (DDI, Bristol Myers Squibb, 1992), and 2′,3′-dideoxycytosine (DDC, Hoffmann LaRoche, 1992), which was recently introduced for limited use. These drugs inhibit the enzyme reverse transcriptase of the human immunodeficiency virus (HIV). Nevertheless, they are only able to prolong somewhat the survival of patients with advanced cases of AIDS. They also lead to considerable side effects (bone marrow damage, neuropathy) and to the generation of more resistant strains of the virus.[2]

Since the solution of its structure in 1989[3] HIV-1 protease has become a new, highly favored target for chemotherapy.[4] This protease belongs to the class of acidic aspartate proteases and has an unusual homodimeric C_2-

[*] Prof. Dr. D. Enders, Dr. U. Jegelka, Dipl.-Chem. B. Dücker
Institut für Organische Chemie der Technischen Hochschule
Professor-Pirlet-Strasse 1, D-W-5100 Aachen (FRG)

[**] This work was supported by the Deutsche Forschungsgemeinschaft and the Fonds der Chemischen Industrie. We thank Degussa AG, BASF AG, Bayer AG, and Hoechst AG for gifts of chemicals.

symmetrical structure. Starting from the Phe-Pro cleavage point most frequently preferred by the enzyme, Erickson and Kempf et al.[5] developed the C_2-symmetrical, highly selective HIV-1 protease inhibitor A-74704 (*S,S*)-**1a**. They demonstrated that the marked inhibiting effect of the inhibitor relies on its optimal fit in the active center of the C_2-symmetrical protease. Derivatives with other substituents at the amino group, for example (*S,S*)-**1b** and -**1c**,[6] are also active compounds.

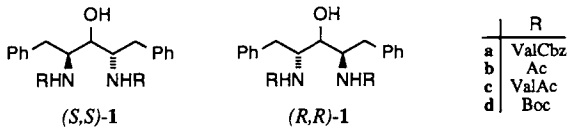

A-74704 (R=ValCbz)

We report here on a new, highly diastereo- and enantioselective entry to C_2-symmetrical HIV-1 protease inhibitors of type **1**. To demonstrate the process both enantiomers of the *tert*-butyloxycarbonyl (Boc)-protected diaminoalcohol **1d** and the racemate *rac*-**1d** (dimethylhydrazone method[11]) were synthesized from the dibenzylated ketones (*R,R*)- and (*S,S*)-**3** (*de*, *ee* = 98%). The compounds (*R,R*)- and (*S,S*)-**3** were prepared from the dihydroxyacetone derivative **2**[7-9] according to the SAMP/RAMP-hydrazone method[10] in four steps and in over 60% yield.

As shown in Scheme 1 (Route A), ketone (*R,R*)-**3** was reduced with lithium aluminum hydride to provide the alcohol, which was then protected as the benzylether, and hydrolyzed under acidic conditions to release diol (*R,R*)-**4** (*de*, *ee* = 98%, overall yield 92%). Attempts to obtain bisazide (*S,S*)-**5** via a bismesylate, itself available quantitatively, with sodium azide in dimethylformamide (20 h, 90 °C), gave **5** and the corresponding HN_3-elimination product in the unfavorable ratio of 1:1. We produced (*S,S*)-**5** with double inversion in 85% yield (*de*, *ee* = 98%) by converting **4** into the bistriflate with trifluoromethanesulfonic acid anhydride (Tf_2O) and substituting with tetramethylguanidinium azide[12] in dichloromethane. In both cases the elimination product could be separated easily by chromatography. The bisazide was ultimately converted to the Boc_2-protected diamine by hydrogenation in the presence of a catalytic amount of Pd/C and 2.4 equivalents of Boc_2O. When ethyl acetate was employed as solvent, then the completely *N*-Boc- and *O*-Bn-protected diaminoalcohols were obtained in 75% yield. Subsequent hydrogenation in methanol led quantitatively to (*S,S*)-**1d** in almost diastereo- and enantiomerically pure form; (*R,R*)-**1d** was prepared by use of the corresponding auxiliary SAMP (Route B). The overall yield of **1d**, best characterized as the 3,3,3-trifluoro-2-methoxy-2-phenylpropionic acid (MTPA) ester,[13] is 58–59% starting from **3** and 36% based on **2** (Scheme 1).

When the hydrogenation of (*S,S*)-**5** was conducted in methanol, a 75% yield of the unprotected diaminoalcohol (*S,S*)-**1** (R = H) was obtained, which can be converted into the C_2-symmetrical HIV-1 protease inhibitor A-74704 (*S,S*)-**1a** according to Kempf et al.[6] and Dreyer et al.[14] Since in the previously described syntheses either L-phenylalanine[6] or D-arabitol[14] were incorporated into the final product, Route A described here provides an entry to the first asymmetric synthesis of A-74704, and at the same time Route B allows a flexible and efficient access to its enantiomer.

For synthesis of the racemate of **1d** the *meso* compound **7** was first prepared in four steps from **2** by the dimethylhydrazone method[11] with an overall yield of 44%. In contrast to the *trans* double alkylation of simple cyclic ketones via the *N,N*-dimethylhydrazone (DMH) derivatives, the α,α-dibenzylation of **2** via *rac*-**6** provided the *cis* product and thereby *meso*-**7** (*de* = 98%) diastereoselectively. After conversion to the mono-protected triol *meso*-**8** (*de* = 98%) analogous to that shown in Scheme 1, bisazide *rac*-**5** was obtained in 71% yield by a Mitsunobu reaction in the presence of zinc azide and diisopropylazidocarboxylate.[15] In this Mitsunobu reaction only one stereogenic center is generated by inversion and the other with retention. This can be explained by invoking an S_Ni reaction: initially, the 1,3-diol is converted into an oxetane ring, which is opened by azide with assistance by Zn^{2+} (retention). The azidoalcohol formed then undergoes substitution with inversion to give the bisazide.[16] After subsequent hydrogenation in the presence of Boc_2O in analogy to that in Scheme 1, *rac*-**1d** was obtained (*de* = 98%) (Scheme 2).

The asymmetric syntheses described here provide an efficient and stereochemically flexible entry to C_2-asymmetric HIV-1 protease inhibitors. The inhibiting effect and the pharmacological properties of these new agents may possibly be improved further for the treatment of AIDS, as certain properties can be varied almost at will:[17] the stereogenic center, which can be selected by the choice of the

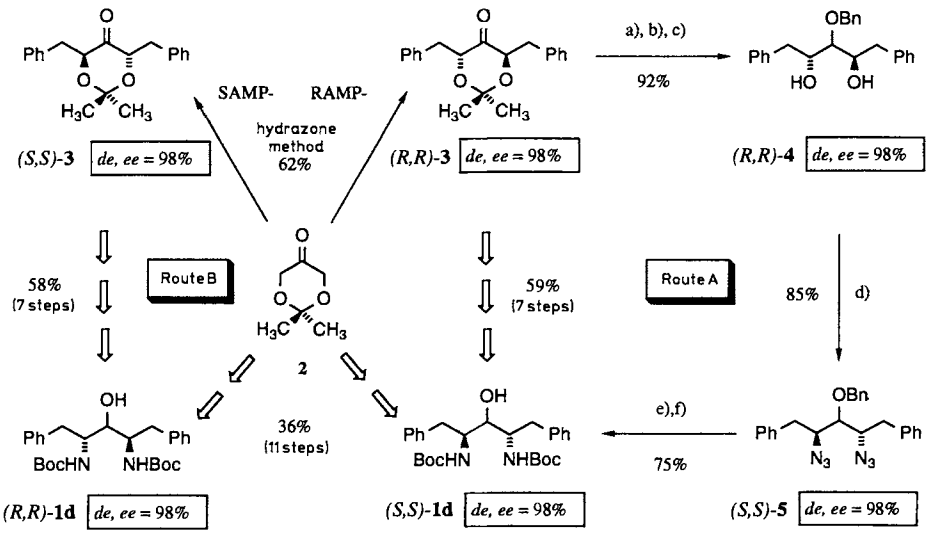

Scheme 1. Enantioselective synthesis of C_2-symmetrical protease inhibitors. a) $LiAlH_4$, Et_2O, room temperature (RT), 99%; b) NaH, BnBr, Bu_4NI, THF, 15 h, quant.; c) 3N HCl, MeOH, RT, 93%; d) 1. Tf_2O, 2,6-lutidine, CH_2Cl_2, −78 °C, 1 h, 2. tetramethylguanidinium azide, CH_2Cl_2, −78 → 0 °C; e) H_2, Pd/C, Boc_2O, EtOAc, RT, 12 h, 75%; f) H_2, Pd/C, MeOH, RT, quant.

 © VCH Verlagsgesellschaft mbH, W-6940 Weinheim, 1993 0570-0833/93/0303-0424 $ 10.00+.25/0

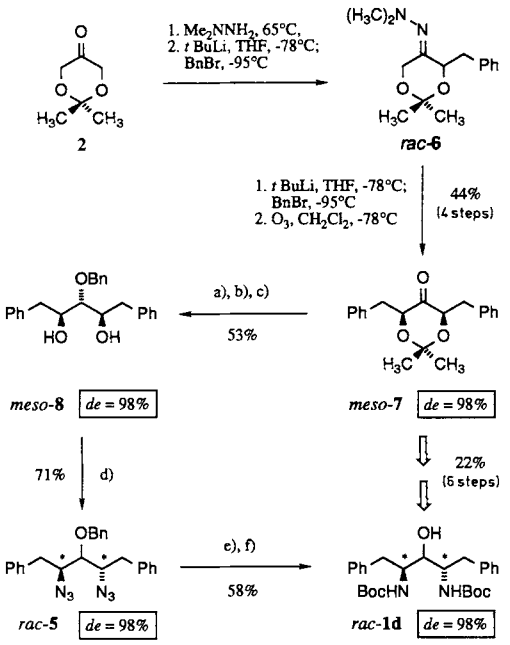

Scheme 2. Synthesis of the racemic protease inhibitor *rac*-**1d**. a), b), c), e), f) as in Scheme 1; d) $Zn(N_3)_2 \cdot Py$, Ph_3P, $iPrO_2C-N=N-CO_2iPr$, toluene, RT, 5 h.

auxiliary (SAMP/RAMP); the side chain (here $PhCH_2$), by the choice of electrophile;[7-9] and the substituents on the amino group.[3, 6]

Experimental Procedure

(*S,S*)- and (*R,R*)-**1d**: Compound **3** [9] (1.50 g, 4.8 mmol) was dissolved in 3 mL Et_2O and added dropwise to a suspension of 0.5 equiv (0.09 g) lithium aluminum hydride in 25 mL Et_2O at room temperature (RT). After 3 h the reaction mixture was hydrolyzed with 100 mL water, stirred for 15 min, and extracted with ether (3 × 200 mL). The organic phase was washed with saturated solutions of $NaHCO_3$ and NaCl, then dried over $MgSO_4$. After removal of the solvent and chromatography (silica gel, ether/petroleum ether 1:2), 1.50 g (99%) of the alcohol was obtained. This compound was dissolved in 60 mL THF, and treated with 2 equiv NaH and 0.02 equiv Bu_4NI at 0°C. After the reaction mixture was allowed to warm to RT, 4.9 mmol benzylbromide was added dropwise. After 15 h, 9.6 mL of a 20% KOH solution and a spatula tip of SiO_2 were added. The gelatinous precipitate was removed by filtration, the aqueous phase extracted with ether, and the combined organic phases dried over $MgSO_4$. After concentration and chromatography (silica gel, ether:petroleum ether 1:20), 1.93 g (100%) of the benzylether was obtained. This was dissolved in 10 mL methanol, stirred for 0.5 h with 10 mL of 3N HCl, and then neutralized with solid $NaHCO_3$. After the crude mixture was extracted with ether, the organic phase was dried over $MgSO_4$ and concentrated. Chromatographic purification (silica gel, ether/petroleum ether 2:1) gave 1.61 g (93%) **4**. After dissolution in 22 mL CH_2Cl_2, **4** was treated with 2.0 mL trifluoromethanesulfonic acid anhydride (Tf_2O) at −78°, then 5 min later with 1.5 mL 2,6-lutidine. The reaction mixture was stirred for 30 min, before a further 0.2 mL Tf_2O and 0.15 mL 2,6-lutidine were added. After a further 30 min a solution of tetramethylguanidinium azide (4.1 g dissolved in 22 mL CH_2Cl_2) was added dropwise. The reaction mixture was left to stand for 15 min, allowed to warm to 0°C, and stirred at this temperature for a further 2 h. The crude mixture was filtered through silica gel and evaporated to dryness. Chromatography (silica gel, ether/petroleum ether 1:10) gave 1.54 g (85%) **5** as a colorless oil. To a mixture of 0.05 g Pd/C (10%) in 1 mL ethyl acetate at RT under hydrogen was added dropwise a solution of 0.24 mmol **5** and 2.4 equiv Boc_2O in 4 mL ethyl acetate. After stirring for 12 h, filtration through Celite, and chromatography (silica gel, ether/petroleum ether 1:4), 0.1 g (75%) of the triply protected diaminoalcohol was obtained as colorless crystals, m.p. 125°C (petroleum ether); $[\alpha]_D^{23}$ + 23.5 (*c* = 1.0, $CHCl_3$) for the compound with (*R,R*) configuration. Subsequent debenzylation by hydrogenation [0.05 g Pd/C (10%), H_2, 5 mL MeOH, 3 h] gave 0.08 g **1d** (quantitative); MTPA derivative [18]: colorless oil, $[\alpha]_D^{23}$ + 19.39 (*c* = 0.98, $CHCl_3$) (*R,R*).

rac-**1d**: Compound **2** (26.0 g, 0.2 mol) was heated with 3 equiv *N,N*-dimethylhydrazine under reflux at 65°C for 20 h. The reaction mixture was concentrated and dissolved in 400 mL ether and washed with water. The organic phase was dried over $MgSO_4$, the solvent removed, and the residue purified by distillation to give 29.9 g (87%) of the DMH derivative of **2** (pale yellow oil, b.p. 57°C/2.25 Torr). This compound (20 mmol) was treated with *t*BuLi and BnBr (under the conditions given ref. [9] for the SAMP hydrazones) and the crude α,α-bisalkylated product oxidatively cleaved with ozone in CH_2Cl_2 at −78°C. After chromatography (silica gel, ether/petroleum ether 1:30), 2.94 g (44% based on **2**) of *meso*-**7** (*de* = 98%) was obtained as a colorless oil. Conversion into *meso*-diol **8** was achieved in similar manner to that described for **4**. For the substitution with zinc azide according to Mitsunobu [16] 0.63 g (1.71 mmol) *meso*-**8** was used. Chromatographic purification gave 0.42 g (71%) of *rac*-**5** (*de* = 98%) as colorless crystals, m.p. 91°C (petroleum ether). Conversion to *rac*-**1d** followed in similar fashion to that used for (*R,R*)-**1d**; 0.33 g (58%).

Received: October 1, 1992 [Z 5606IE]
German version: *Angew. Chem.* **1993**, *105*, 423

[1] M. G. Koch, *AIDS, Vom Molekül zur Pandemie*, Spektrum der Wissenschaften, Heidelberg, **1989**.
[2] a) D. Häbich, *Chem. Unserer Zeit* **1991**, *25*, 295; b) R. M. Baum, *Chem. Eng. News* **1992**, 24. August, p. 26.
[3] a) M. A. Navia, P. M. D. Fitzgerald, B. M. McKeever, C. T. Leu, J. C. Heimbach, W. K. Herber, I. S. Sigal, P. L. Darke, J. P. Springer, *Nature* **1989**, *337*, 615; b) R. Lapatto, T. Blundell, A. Hemmings, J. Overington, A. Wilderspin, S. Wood, J. R. Merson, P. J. Whittle, D. E. Danley, K. F. Geoghegan, S. J. Hawrylik, S. E. Lee, K. G. Scheld, P. M. Hobart, *ibid.* **1989**, *342*, 299; c) A. Wlodawer, M. Miller, M. Jaskólski, B. K. Sathyanarayana, E. Baldwin, I. T. Weber, L. M. Selk, L. Clawson, J. Schneider, S. B. H. Kent, *Science* **1989**, *245*, 616.
[4] a) J. R. Huff, *J. Med. Chem.* **1991**, *34*, 2305; b) GDCh-Symposium HIV-Infektion, Chemotherapeutische Entwicklungen, Frankfurt am Main, **1992**.
[5] J. Erickson, D. J. Neidhart, J. VanDrie, D. J. Kempf, X. C. Wang, D. W. Norbeck, J. J. Plattner, J. W. Rittenhouse, M. Turon, N. Wideburg, W. E. Kohlbrenner, R. Simmer, R. Helfrich, D. A. Paul, M. Knigge, *Science* **1990**, *249*, 527.
[6] D. J. Kempf, D. W. Norbeck, L. M. Codacovi, X. C. Wang, W. E. Kohlbrenner, N. E. Wideburg, D. A. Paul, M. Knigge, S. Vasavanonda, A. Craig-Kennard, A. Saldivar, W. Rosenbrock, J. J. Clement, J. J. Plattner, J. Erickson, *J. Med. Chem.* **1990**, *33*, 2687.
[7] D. Enders, B. Bockstiegel, *Synthesis* **1989**, 493.
[8] D. Enders, W. Gatzweiler, E. Dederichs, *Tetrahedron* **1990**, *46*, 4757.
[9] D. Enders, W. Gatzweiler, U. Jegelka, *Synthesis* **1991**, 1137.
[10] a) D. Enders in *Asymmetric Synthesis, Vol. 3* (Ed.: J. D. Morrison), Academic Press, Orlando, **1984**, p. 275; b) D. Enders, P. Fey, H. Kipphardt, *Org. Synth.* **1987**, *65*, 173, 183.
[11] a) E. J. Corey, D. Enders, *Tetrahedron Lett.* **1976**, 3, 11; b) E. J. Corey, D. Enders, *Chem. Ber.* **1978**, *111*, 1337, 1362. The reasons for the variable stereoselectivity in the α,α-dialkylation of **2** via the dimethylhydrazone and the SAMP/RAMP hydrazones are not yet known, see also: D. B. Collum, D. Kahne, S. A. Gut, R. T. DePue, F. Mohamadi, R. A. Wanat, J. Clardy, G. Van Dyne, *J. Am. Chem. Soc.* **1984**, *106*, 4865; R. A. Wanat, D. B. Collum, *ibid.* **1985**, *107*, 2078.
[12] a) R. Wagner, J. W. Tilley, K. Lovey, *Synthesis* **1990**, 785; b) A. Y. Papa, *J. Org. Chem.* **1966**, *31*, 1426.
[13] J. A. Dale, H. S. Mosher, *J. Am. Chem. Soc.* **1973**, *95*, 512.
[14] B. Chenera, J. C. Boehm, G. B. Dreyer, *Bioorg. Med. Chem. Lett.* **1991**, *1*, 219.
[15] M. C. Viaud, P. Rollin, *Synthesis* **1990**, 130.
[16] O. Mitsunobu, *Synthesis*, **1981**, 1. We thank one of the referees for making this plausible suggestion.
[17] All new compounds gave correct elemental analyses and NMR and IR spectra in agreement with their structures.
[18] R. Tanikaga, T. X. Jun, A. Kaji, *J. Chem. Soc. Perkin Trans. 1* **1990**, 1185.

Silylamines with Pyramidal Coordination at Nitrogen**

By *Karin Ruhlandt-Senge, Ruth A. Bartlett, Marilyn M. Olmstead*, and *Philip P. Power**

The nature of the Si–N bond in silylamines has been a subject of considerable interest[1] since the planar structure of $N(SiH_3)_3$ was originally established in 1951.[2] For several

[*] Prof. P. P. Power, Dr. K. Ruhlandt-Senge, R. A. Bartlett, Dr. M. M. Olmstead
Department of Chemistry, University of California
Davis, CA 95616 (USA)

[**] This work was supported by the National Science Foundation and the Petroleum Research Fund.

years, it was argued that characteristics such as short Si–N bonds, planar nitrogen coordination, and poor amine basicity could be plausibly accounted for in terms of an N–Si p–d π-bonding model. The importance of this bonding has been questioned, particularly from a theoretical standpoint, for a number of years.[3–5] It is now thought that multiple N–Si interactions, if they occur in silylamines, involve a p–σ^* rather than a p–d interaction.[4, 6]

With regard to the planarity of EX_3 species (E = main group 5 element, X = substituent), it has been shown experimentally[7b, c] and theoretically[7d] that an increase in the electropositive character (e.g. replacing C by Si) of the substituents X reduces the inversion barrier at E, thereby making planar coordination at E more probable. This may be illustrated by noting that the inversion barrier in NH_3 is 5.8 kcal mol^{-1} whereas in H_3SiNH_2 it is calculated to be almost 1 kcal mol^{-1}.[8] If it is accepted that the introduction of a single silyl group in ammonia reduces the inversion barrier to about 1 kcal mol^{-1}, the observation of a pyramidal geometry at nitrogen in such a compound would tend to imply that Si–N π bonding (which tends to favor planar geometry in order to maximize overlap) should be quite weak. In this paper the synthesis and structural characterization of the silylamines **1**–**3** are described.

H_2NSiPh_3 **1** $(H_2N)_2SiMes_2$ **2** $(H_2N)_3SiTriph$ **3**

Mes = 2,4,6-$Me_3C_6H_2$, Triph = 2,4,6-$Ph_3C_6H_2$

These compounds were chosen for study because steric effects at the nitrogen are minimized through the use of two hydrogen substituents. In addition, electronic effects are minimized through the use of only one electropositive ligand. Such considerations maximize the chances of observing a nonplanar geometry and the effects of this strategy are seen in the structures of **1**–**3** which display varying degrees of pyramidicity at nitrogen.

H_2NSiPh_3 (**1**) was synthesized by using a literature procedure.[9] The new species **2** and **3** were synthesized as described in the Experimental Procedure. The X-ray crystal structures[10] of **1**–**3** are illustrated in Figures 1–3. Important bond lengths and angles for **1**–**3** are given in Table 1. Clearly, the nitrogen centers in **1**–**3** are pyramidal to varying degrees and have substantial out of plane angles ϕ. There is

Table 1. Important Structural Parameters **1**–**3**.

Parameter	1	2	3
Si-N [Å]	1.711(2)	1.713(2), N(1) 1.717(2), N(2)	1.710(6), N(1) 1.710(7), N(2) 1.708(7), N(3)
$\Sigma \sphericalangle$ N[°][a]	351.9	350.2, N(1) 344.8, N(2)	344.1, N(1) 349.2, N(2) 358.1, N(3)
ϕ [b]	25.5	30.5, N(1) 33.9, N(2)	37.0, N(1) 29.9, N(2) 14.6, N(3)

[a] Sum of angles at N; [b] ϕ is the out of plane angle at N, see **A**.

A

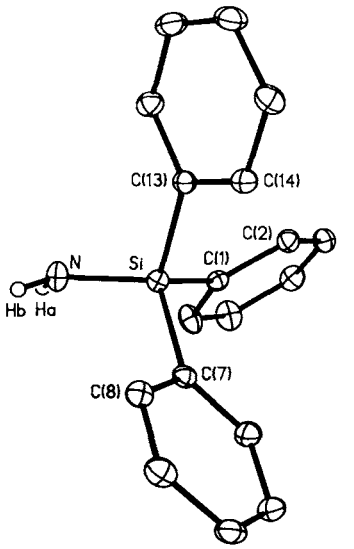

Fig. 1. Computer-generated plot of **1** (50% ellipsoids). H atoms have been omitted for clarity.

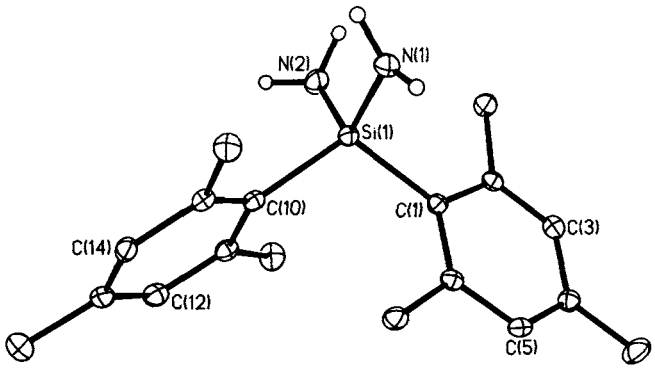

Fig. 2. Computer-generated plot of **2** (50% ellipsoids). H atoms have been omitted for clarity.

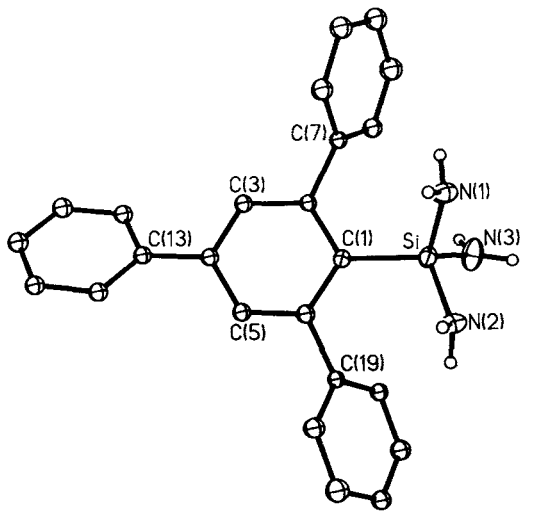

Fig. 3. Computer-generated plot of **3** (50% ellipsoids). H atoms have been omitted for clarity.

neither a dramatic variation in the observed Si–N distances in the three compounds, nor are the Si–N distances outside the normal range.[11] Other structural parameters such as Si–C and C–C distances are also unremarkable. There are also no unusual angles or evidence of severe steric crowding or interactions with the N–H groups that would readily account for the pyramidicities at the nitrogen atoms.

The structures of **1**–**3** represent the first X-ray crystal structures of acyclic[12] silylamines which show a substantial pyramidal character at nitrogen. Compound **3** is also unique in the sense that it is the first stable compound that has three NH_2 groups bound to one silicon atom. Pyramidal coordination at nitrogen in silylamines has been previously intimated in H_3SiNMe_2 and related species by an electron diffraction study.[13] The structure of H_3SiNMe_2 was later questioned and the data were said not to rule out planar geometry at nitrogen.[14] Further work indicated planar geometry in the gas phase for H_3SiNMe_2 and slightly pyramidal geometry at nitrogen (sum of the angles at N ca. 358°) in the crystal.[15] An important feature of the data in Table 1 is the consistency of the Si–N distance in all three compounds. Taken together, the pyramidicity at nitrogen and lack of variation in Si–N distances indicate that the π component (whether it is of a p–σ* or p–d type) in the Si–N bonds of silylamines must have an extremely small, even negligible, effect on the structural parameters. In arguments regarding π bonding in Si–N systems considerable significance has often been attached to the planarity at nitrogen and shortness of the N–Si bonds. However, as noted previously, the inversion in silylamines is quite low (ca. 1 kcal mol^{-1}).[8] Yet, in neither **1**, **2**, nor **3** are all the nitrogen centers capable of attaining planar geometry in order to maximize π overlap. The confinement of the N–Si distances to the narrow range 1.708(7)–1.717(2) Å also suggests that N → Si electron pair π donation is not very significant.[11] A greater variation might have been expected since the amount of lone-pair electron donation (and π bonding) by each individual nitrogen atom is expected to decrease as the number of nitrogen atoms increases, owing to negative charge buildup at silicon.

The N–Si distances in **1**–**3** are somewhat shorter than the value predicted (1.75 Å) when the ionic contribution is taken into account.[11] However, they are closer to the Si–N bond length (1.735(1) Å) observed in the sterically relaxed species $N(SiH_2Ph)_3$.[16]

It is unlikely that pyramidicity at the nitrogen atom in **1**–**3** is induced exclusively by extrinsic forces such as packing effects, since pyramidicity at nitrogen is observed in the three different molecules. A more likely explanation is that pyramidal coordination can be observed even in the presence of a very low inversion barrier because of the lowered steric congestion[16] (hydrogen substituents) and because inductive effects are minimized (only one silyl substituent).

Experimental Procedure

2: Under anaerobic and anhydrous conditions Mes_2SiCl_2 [17] (3.37 g, 10 mmol) was dissolved in liquid ammonia (100 mL) and refluxed for 4 h (dry ice condenser). The ammonia was evaporated and the white residue taken up in warm diethyl ether (100 mL). Filtration followed by reduction of the solution volume to 20 mL and storage at −40 °C gave colorless crystals of **2** in quantitative yield. M.p. 125–126 °C (NH_3 evolved > 200 °C); IR: νN–H = 3495, 3455, 3449, 3430, 3370, 3350 cm^{-1}. ^{1}H NMR (300 MHz, C_6D_6) δ = 0.831 (s, 4H, NH), 2.137 (s, 6H, *p*-CH_3), 2.392 (s, 12H, *o*-CH_3), 6.738 (s, 4H, *m*-H).

3: $Li(OEt_2)_2$Triph (5.71 g, 10 mmol) [18] was dissolved in a mixture of *n*-hexane (100 mL) and diethyl ether (100 mL) and cooled with an ice bath. Freshly distilled $SiCl_4$ (1.7 g, 10 mmol) in diethyl ether (20 mL) was added dropwise. A white precipitate was formed immediately and the mixture was refluxed for 18 h. Filtration followed by removal of solvents afforded crude $TriphSiCl_3$ as a white solid. This was cooled in a dry ice/acetone bath and ammonia (150 mL) was added. The reaction commenced immediately as indicated by the formation of a copious white precipitate. The mixture was refluxed for 4 h (dry ice condenser). The ammonia was evaporated and the residue was extracted into 100 mL of warm diethyl ether and filtered. The volume was reduced to 30 mL and cooled to −20 °C. This afforded **3** as colorless crystals. Yield 2.72 g, 71%. M.p. 118–120 °C (NH_3 evolution). IR: νN–H = 3465, 3460, 3440, 3378, 3345, 3335 cm^{-1}. ^{1}H NMR (300 MHz, C_6D_6): δ = 0.284 (s, 6H, NH), 6.9 (m, 17H, Triph).

Received: October 15, 1992 [Z 5630 IE]
German version: *Angew. Chem.* **1993**, *105*, 459

[1] a) H. Kwart, K. King, *d-Orbitals in the Chemistry of Silicon, Phosphorus and Sulfur*, Springer, Berlin **1977**; b) Y. Apeloig, *The Chemistry of Organosilicon Compounds, Vol. 1* (Eds.: S. Patai, Z. Rappoport), Wiley, New York, **1989**, Chapter 2.

[2] K. Hedberg, *J. Am. Chem. Soc.* **1955**, *77*, 6491. The structure of $N(SiH_3)_3$ was disclosed at the XII International Congress of Pure and Applied Chemistry, New York, September, **1951** and at the International Congress of Crystallography, Stockholm, July, **1951**.

[3] J. M. Lehn, B. Munsch, *J. Chem. Soc. Chem. Commun.* **1970**, 994.

[4] C. G. Pitt, *J. Organomet. Chem.* **1973**, *61*, 49.

[5] B. T. Luke, J. A. Pople, M.-B. Krogh-Jespersen, Y. Apeloig, Y. Chandrasekhar, P. von R. Schleyer, *J. Am. Chem. Soc.* **1986**, *108*, 260.

[6] T. A. Albright, J. K. Burdett, M. H. Whangbo, *Orbital Interactions in Chemistry*, Wiley, New York, **1985**.

[7] a) J. D. Andose, J. M. Lehn, K. Mislow, J. Wagner, *J. Am. Chem. Soc.* **1970**, *92*, 4050; b) J. Stackhouse, R. D. Baechler, K. Mislow, *Tetrahedron Lett.* **1971**, 3437, 3441; c) S. J. Brois, *Trans. NY Acad. Sci.* **1969**, *31*, 931; d) K. Mislow, *ibid.* **1973**, *34*, 227; d) C. C. Levin, *J. Am. Chem. Soc.* **1975**, *97*, 5649.

[8] M. S. Gordon, *Chem. Phys. Lett.* **1986**, *126*, 45. According to these calculations (6–31 G*), H_2NSiH_3 has Si–N = 1.729 Å and $\sum$N = 350.8° (cf. corresponding values for H_2NSiPh_3 in Table 1). Furthermore, no multiple d-p π-character is evident in the Si–N bond.

[9] C. A. Kraus, R. Rosen, *J. Am. Chem. Soc.* **1925**, *47*, 2739.

[10] Crystal data for **1**–**3** at 130 K with $Mo_{K\alpha}$ radiation (λ = 0.71069 Å). **1**: *a* = 8.912(1), *b* = 9.302(2), *c* = 10.798(2) Å, α = 66.58(1), β = 82.27(1), γ = 65.99(1)°, space group, $P\bar{1}$, 2719 reflections ($I > 2\sigma(I)$), *R* = 0.037. **2**: *a* = 10.113(1), *b* = 16.908(4), *c* = 19.545(4) Å, space group *Pbca*, 2612 reflections ($I > 3\sigma(I)$), *R* = 0.040. **3**: *a* = 10.394(3), *b* = 6.190(5), *c* = 31.599(11) Å, β = 99.65(2)°, space group $P2_1/c$, 964 reflections ($I > 3\sigma(I)$), *R* = 0.055. Further details of the structures may be obtained form the Fachinformationszentrum Karlsruhe, Gesellschaft für wissenschaftlich-technische Information mbH, D-W-7514 Eggenstein-Leopoldshafen 2 (FRG), on quoting the depository number CSD-56886, the names of the authors and the journal citation.

[11] a) E. Lukevics, O. Pudova, R. Sturkovich, *Molecular Structure of Organosilicon Compounds*, Ellis-Horwood, Chichester, **1989**; b) W. S. Sheldrick, *The Chemistry of Organosilicon Compounds, Vol. 1* (Eds.: S. Patai, Z. Rappoport), Wiley, New York, **1989**, Chapter 3. Most neutral silylamines have Si–N distances in the range 1.70–1.76 Å. This is considerably shorter than the sum of the radii of silicon (1.17 Å) and sp^2 hybridized nitrogen (0.7 Å) that is, 1.87 Å. When this value is corrected for ionic contributions by using Allred–Rochow electronegativities and the Schomaker–Stevenson equation ($r_{AB} = r_A + r_B - 0.09|EN_A - EN_B|$) and Si–N distance of 1.75 Å is calculated. If the modified equation ($r_{AB} = r_A + r_B - 0.085|EN_A - EN_B|^{1.4}$) of Haaland and Blom (R. Blom, A. Haaland, *J. Mol. Struct.* **1985**, *129*, 21) is used the Si–N distance is also calculated to be 1.75 Å.

[12] A pyramidal coordination for a silylamine nitrogen (sum of angles at N = 346.8°) has been observed in the bicyclic compound NSi*t*Bu$_2$Si*t*Bu$_2$CHCMe$_2$SCH*i*Pr)). The constraints on the nitrogen geometry may significantly increase the inversion barrier in this case [7]: M. Weidenbruch, B. Flintzer, S. Pohl, D. Haase, J. Martens, *J. Organomet. Chem.* **1988**, *338*, C1.

[13] C. Glidewell, D. W. H. Rankin, A. G. Robiette, G. M. Sheldrick, *J. Mol. Struct.* **1970**, *6*, 231.

[14] P. Livant, M. L. McKee, D. Worley, *Inorg. Chem.* **1983**, *22*, 895.

[15] A. J. Blake, E. A. V. Ebsworth, D. W. H. Rankin, H. E. Robinson, D. E. Smith, A. J. Welch, *J. Chem. Soc. Dalton Trans.* **1986**, 91.

[16] It is possible to achieve an essentially planar geometry at nitrogen through steric effects alone as in $NiPr_3$: H. Bock, I. Göbel, Z. Havlas, S. Liedle, H. Oberhammer, *Angew. Chem.* **1991**, *103*, 193; *Angew. Chem. Int. Ed. Engl.* **1991**, *30*, 187. In contrast, the relaxation of steric crowding in trisilylamines such as $N(SiH_2Ph)_3$ still affords an essentially planar geometry at the nitrogen atom in the crystal phase: N. Mitzel, A. Schier, H. Schmidbaur, *Chem. Ber.* **1992**, *125*, 2711.

[17] N. Wiberg, B. Neruda. *Chem. Ber.* **1966**, *99*, 740.

[18] M. M. Olmstead, P. P. Power, *J. Organomet. Chem.* **1991**, *408*, 1.

Nucleophilic Substitution of Bis(cyclopentadienyl)-tin(II); Synthesis, Structure, and Solution Dynamics of *trans*-$[(\eta^3\text{-Cp})Sn\{\mu_2\text{-}N{=}C(NMe_2)_2\}]_2$

By *Dietmar Stalke, Michael A. Paver,* and *Dominic S. Wright**

Recently we have been interested in the occurrence and nature of bonds between later main group metals (Groups 3–5) and early main group metals (Groups 1 and 2). These studies have led to the synthesis and characterization of $Ph_3ELi \cdot$ pmdeta complexes (E = Sn,[1] Pb;[2] pmdeta = $MeN(CH_2CH_2NMe_2)_2$), the first compounds in which such bonding has been identified. With a view to finding other related complexes, we have more recently been investigating the reactions of cyclopentadienyl complexes of heavy p block metals (as convenient and stabilized precursors) with nucleophiles. Nucleophilic *addition* of CpNa to bis(cyclopentadienyl)tin(II)[3] in the presence of pmdeta (mol ratio 1:1:1) resulted in the formation of the unusual trigonal-planar "paddle wheel" triorganostannate complex $[(\eta^5\text{-Cp})_2\text{-}Sn(\mu\text{-}\eta^5\text{-Cp})Na \cdot \text{pmdeta}]$.[4]

We report here the outcome of the reaction of $[LiN{=}C(NMe_2)_2]_6$,[5] which contains a more potent nucleophile, with $[Cp_2Sn]$ (mol ratio 1:1). The result is the nucleophilic *substitution* of just one of the Cp ligands and the formation of the dimeric mixed-ligand organotin(II) complex *trans*-$[(\eta^3\text{-Cp})Sn\{\mu_2\text{-}N{=}C(NMe_2)_2\}]_2$ (**1**). This is the first iminotin(II) complex and the first structurally characterized oligomeric cyclopentadienyl organotin(II) complex. Nucleophilic substitution of cyclopentadienyl complexes of heavy p block metals provides a clean and potentially general route to such mixed-ligand metal complexes.

Addition of a solution of $[Cp_2Sn]$[3] in THF to a solution of $[LiN{=}C(NMe_2)_2]_6$[5] in THF (mol ratio 1:1) [Eq. (a)] produces a bright yellow solution which affords colorless crystals of **1** (see Experimental Procedure).

$$[Cp_2Sn] + [LiN{=}C(NMe_2)_2] \xrightarrow{THF} \underset{\mathbf{1}}{[CpSnN{=}C(NMe_2)_2]} + CpLi \quad (a)$$

An X-ray crystallographic study of complex **1**[6] (the crystal was mounted wet from solution) shows it to be a centrosymmetric dimer $[(\eta^3\text{-Cp})Sn\{\mu_2\text{-}N{=}C(NMe_2)_2\}]_2$ with a Sn_2N_2 ring (Fig. 1). One THF molecule per dimer unit is found in the crystal lattice; it is readily removed when the crystals are placed under vacuum for a short period of time (10^{-1} bar, 15 min), although the crystals are then destroyed. In the planar ring of each dimer, the imino groups bridge the two Sn centers almost symmetrically (Sn(1)–N(1) 2.196(3) Å, Sn(1)–N(1a) 2.185(3) Å, cf. typical Sn–N lengths in amidotin complexes, e.g., 2.202(1) Å in $[Sn(NtBu)]_4$[7]). There is extreme rhombic distortion within this ring (N-Sn-N, 75.36(12)°, Sn-N-Sn, 104.64(12)°). To our knowledge, more acute angles at Sn have been observed only in the heptaatomic species $[Sn_3(NtBu)_2(OtBu)_2]$ (N-Sn-N, 68.0(2)°).[8] The terminal η^3-Cp ligands have a *trans* orientation with respect to this ring (the shortest Sn–C contact is Sn(1)–C(4), 2.432(5) Å). The essentially flat imino anions are eclipsed in order to avoid the *trans* Cp ligands. They fit into the "slot" left to them by the Cp ligands, and are inclined to the Sn_2N_2 ring plane by approximately 37°.

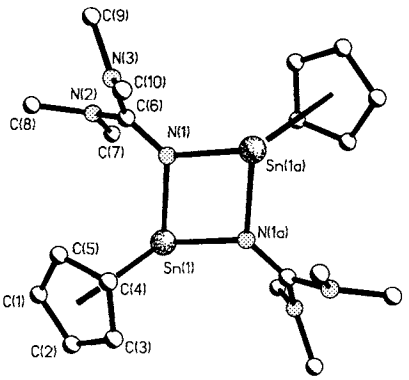

Fig. 1. Crystal structure of **1**; selected bond lengths [Å] and angles [°]: Sn(1)-N(1) 2.196(3), Sn(1)-N(1a) 2.185(3), Sn(1)-C(4) 2.432(4), Sn(1)-Cp(center) 2.432(4), N(1)-C(6) 1.294(5), C(6)-N(2) 1.371(5), C(6)-N(3) 1.370(5), average N-Me 1.445(7); N(1)-Sn(1)-N(1a) 75.4(1), Sn(1)-N(1)-Sn(1a) 104.6(1), N(1)-Sn(1)-C(4) 91.6(2), N(1a)-Sn(1)-C(4) 93.8(2).

The structure of **1** is unprecedented among the structures of cyclopentadienyltin(II) complexes. Most other structurally characterized compounds are mononuclear, for example, neutral $[Cp_2Sn]$ and compounds related to the cationic $[CpSn]^+$ system.[9] In polymeric $[(\eta^5\text{-Cp})SnCl]_\infty$, prepared from $[Cp_2Sn]$ and $SnCl_2$ (mol ratio 1:1), alternating monomer units are associated by bridging Sn···Cl contacts.[10] The structure of **1** can be compared to those of iminoaluminum complexes in which μ_2-bridging imino groups connect the metal centers.[11, 12] In the latter, the Al_2N_2 rings show a similar rhombic distortion to that seen in **1**, although with less sharp angles at their metal centers (N-Al-N, ca. 83°).

Studies of the temperature- and concentration-dependence of the ^1H NMR spectra of **1** in THF (400.13 MHz) indicate that an equilibrium exists between the *cis*- and *trans*-Cp isomers. At +25 °C both isomers coexist in an approximately 1:1 ratio. In the *trans* form, the same structure as that in the solid state, the steric demands lead to restricted rotation of the Me_2N groups of the imino ligands; the Me groups are consequently nonequivalent (δ = 2.73, 2.68 (1:1)). In the *cis* form, presumably because of their less sterically crowded environment, these Me groups are free to rotate and are equivalent (δ = 3.11). Two separate Cp signals for the *cis* and *trans* isomers (δ = 5.98 and 5.91) are also observed. Reducing the temperature leads to a broadening of the Me resonances of the *cis* isomer and, at approximately −95 °C, this signal begins to split. At −125 °C, these Me groups are fully resolved into two (1:1) signals. This is consistent with the less restricted rotation of the imino groups of the *cis* isomer compared to those in the *trans*, and consequently the lower activation energy for rotation in the former. The fact that the same ratio of intensities for the signals of both species in solution is observed regardless of concentration supports an intramolecular *cis–trans* equilibrium. An alternative interpretation of an intermolecular dimer–monomer equilibrium can be ruled out, as the ratio of the solution species would then be expected to vary with concentration.

[*] Dr. D. S. Wright, M. A. Paver
University Chemical Laboratory
Lensfield Road, GB-Cambridge CB2 1EW (UK)
Dr. D. Stalke
Institut für Anorganische Chemie der Universität
Tammannstrasse 4, D-W-3400 Göttingen (FRG)

[**] This work was supported by the SERC (M. A. P., D. S. W.), the Associated Octel Co. Ltd., U.K. (M. A. P., D. S. W.), the Royal Society (D. S. W.), the Nuffield Foundation (D. S. W.), the Deutsche Forschungsgemeinschaft (D. S.), and the Fonds der Chemischen Industrie (D. S.).

Variable-temperature ^{119}Sn NMR spectra of **1** in THF (148.89 MHz) showed only one resonance at all the temperatures investigated.[13] Although this observation does not allow firm conclusions, two very distinct signals would be expected in an alternative equilibrium involving dimers and solvated monomers of **1**. ^1H NMR spectroscopy and molecular mass measurements in aromatic solvents suggest that only the *cis* isomer is present. Only one Cp ($\delta = 5.28$) and one Me resonance ($\delta = 2.62$) are seen at $+25\,^{\circ}C$ in the ^1H NMR spectra of **1** in toluene. The Me signal begins to broaden at approximately $-80\,^{\circ}C$, and this resonance resolves into two signals (1:1 ratio) at $-95\,^{\circ}C$ as rotation of the Me_2N group is frozen out. Cryoscopic measurement of a saturated solution of **1** in benzene confirms that **1** is dimeric ($n = 2.05 \pm 0.07$ (0.026 M)). The behavior of **1** is similar to that of $[Sn(\mu\text{-}Cl)NCMe_2(CH_2)_3CMe_2]_2$ for which *cis* and *trans* isomers were identified in toluene at low temperature, while in THF only one (unidentified) isomer was found.[14]

The synthesis of **1** by a nucleophilic substitution reaction of $[Cp_2Sn]$ with $[LiN{=}C(NMe_2)_2]_6$ is worthy of note. Previous studies have centered on the reactions of electrophiles with $[Cp_2Sn]$.[9] Although nucleophilic disubstitution of $[Cp^*_2Sn]$ ($Cp^* = C_5Me_5$) with organolithium compounds has been reported, monosubstitution does not appear to be possible; the reaction of $[Cp^*_2Sn]$ and $(Me_3Si)_2CHLi$ gives a mixture of Cp*Li, $[(Me_3Si)_2CH]_2Sn$, and unreacted Cp^*_2Sn.[15] We are currently examining reactions of $[Cp_2E]$ (E = Sn,[3] Pb[16]) with a variety of nucleophiles (containing C, O, S, N, and P centers), and combined addition[4] and substitution reactions with $[Cp_2Sn]$ for the syntheses of new triorganostannate reagents containing three different organic groups.

Experimental Procedure

A solution of $[Cp_2Sn]$ [3] in THF (0.500 g, 2.0 mmol in 1.5 mL) was added to a solution of $[LiN{=}C(NMe_2)_2]_6$ (2.0 mmol in 5 mL THF) under nitrogen atmosphere. A bright yellow solution was formed, and after removal of ca. 1 mL of solvent under vacuum, the solution was cooled to 5 °C for 24 h. Crystalline, colorless, air-sensitive rods, identified as **1**, were isolated. These contain one molecule of THF per unit of **1**. Placing these crystals under vacuum (10^{-1} bar, 15 min) gave a dry powder in which THF lattice solvation is completely removed. The following analytical and spectroscopic data were obtained on this dry, unsolvated material. First batch yield (0.25 g (42%); m.p. 179–181 °C (decomp to brown liquid). Satisfactory C,H,N-analysis. IR (solid): $\tilde{\nu}[cm^{-1}] = 3066$, 1512 (cf. 1600 cm^{-1} in $(Me_2N)_2C{=}NH$). ^1H NMR (25 °C, 400.13 MHz, [D$_8$]THF): $\delta = 5.98$, 5.91 (5H each; Cp in *cis* and *trans* isomers of **1**), 3.11 (s, 12H; Me_2N groups in *cis* isomer), 2.73, 2.68 (12H each; separate Me groups of *trans* isomer). ^1H NMR (25 °C, 400.13 MHz, [D$_8$]toluene): $\delta = 5.28$ (s, 5H; Cp of *cis* isomer), 2.62 (s, 12H; Me_2N in *cis* isomer).

Received: August 10, 1992
Revised version: October 20, 1992 [Z 5505 IE]
German version: *Angew. Chem.* **1993**, *105*, 445

[1] D. Reed, D. Stalke, D. S. Wright, *Angew. Chem.* **1991**, *103*, 1539–1540; *Angew. Chem. Int. Ed. Engl.* **1991**, *30*, 1459–1460.
[2] D. R. Armstrong, M. G. Davidson, D. Moncrieff, D. Stalke, D. S. Wright, *J. Chem. Soc. Chem Commun.* **1992**, 1413.
[3] a) E. O. Fischer, H. Gruber, *Z. Naturforsch. B* **1956**, *11*, 423–424; b) A. Almenningen, A. Haaland, T. Motzfeld, *J. Organomet. Chem.* **1967**, *7*, 97–104.
[4] M. G. Davidson, D. Stalke, D. S. Wright, *Angew. Chem.* **1992**, *104*, 1265–1267; *Angew. Chem. Int. Ed. Engl.* **1992**, *31*, 1226–1227.
[5] a) I. Pattison, K. Wade, B. K. Wyatt, *J. Chem. Soc. A* **1968**, 837–842; b) W. Clegg, R. Snaith, H. M. M. Shearer, K. Wade, G. Whitehead, *J. Chem. Soc. Dalton Trans.* **1983**, 1309–1317.
[6] Crystal data for **1**: $C_{10}H_{17}N_3Sn + 0.5$ thf, $M = 329.98$, monoclinic, space group $C2/c$, $a = 14.654(1)$, $b = 16.517(2)$, $c = 11.971(2)$ Å, $\beta = 94.73(3)^{\circ}$, $V = 2887.6(6)$ Å^3, $Z = 8$, $\rho_{calc} = 1.518$ mg m^{-3}, $F(000) = 1312$, $\lambda = 0.71073$ Å, $T = 223$ K, $\mu(Mo_{K\alpha}) = 1.755$ mm^{-1}. Data were collected on a Siemens-Stoe AED diffractometer using an oil-coated, rapidly cooled crystal of dimensions $0.5 \times 0.3 \times 0.15$ mm by the $2\theta/\omega$ method ($8^{\circ} \le \theta \le 52^{\circ}$). Of a total of 7346 collected reflections, 2853 were unique and corrected for absorption with semiempirical methods. The structure was solved by direct methods (SHELX-90, G. M. Sheldrick, *Acta Crystallogr. Sect. A* **1990**, *46*, 467–473) and refined by full-matrix least-squares of F^2 (SHELXL-92, G. M. Sheldrick, Göttingen, **1992**); $wR1 = 0.031$, $wR2 = 0.102$; largest difference between maximum and minimum 0.66 and -0.69 eÅ^{-3}. All hydrogen atoms were located in a difference Fourier map and their positions were refined by using a riding model, in which CH_3 groups were free to rotate about their local threefold axes. Further details of the crystal structure investigation are available on request from the Director of the Cambridge Crystallography Data Centre, 12 Union Road, GB-Cambridge, CB2 1EZ (UK), by quoting the full journal citation.
[7] M. Veith, O. Rechtenwald, *Z. Naturforsch. B* **1983**, *38*, 1054–1061.
[8] M. Veith, W. Frank, *Angew. Chem.* **1984**, *96*, 163–164; *Angew. Chem. Int. Ed. Engl.* **1984**,*23*, 158–159.
[9] a) P. Jutzi, *Adv. Organomet. Chem.* **1989**, *26*, 217–288; b) J. W. Connely, C. Hoff, *Adv. Organomet. Chem.* **1981**, *19*, 123–153.
[10] K. D. Bos, E. J. Bulten, J. G. Noltes, *J. Organomet. Chem.* **1975**, *99*, 71–77.
[11] W. S. McDonald, *Acta Crystallogr. Sec. B* **1969**, *25*, 1385–1391.
[12] S. J. Bryan, W. Clegg, R. Snaith, K. Wade, E. H. Wong, *J. Chem. Soc. Chem. Commun.* **1987**, 1223–1224.
[13] The chemical shift of the ^{119}Sn signal was characteristically temperature dependent; the signal shifted linearly from $\delta = 2068.5$ at 25 °C to $\delta = 2090.4$ at $-60\,^{\circ}C$ (external standard $[Cp_2Sn]$ in THF at $+25\,^{\circ}C$). The full width at half height of this resonance was ca. 243 Hz at 25 °C but sharpened to ca. 104 Hz at $-60\,^{\circ}C$.
[14] R. W. Chorley, P. B. Hitchcock, B. S. Jolly, M. F. Lappert, G. A. Lawless, *J. Chem. Soc. Chem. Commun.* **1991**, 1302–1303.
[15] P. Jutzi, B. Hielscher, *Organometallics* **1986**, *5*, 2511–2514.
[16] a) E. O. Fischer, H. Gruber, *Z. Anorg. Allg. Chem.* **1956**, *286*, 237–242; b) C. Pannattoni, G. Bombieri, U. Croatto, *Acta Crystallogr.* **1966**, *21*, 823–826.

Facile Formation of Hexahydroporphyrin Complexes by Reduction of Octaethylisobacteriochlorinnickel(II)**

By *Goutam K. Lahiri* and *Alan M. Stolzenberg**

Dedicated to Professor Richard H. Holm on the occasion of his 60th birthday.

The isobacteriochlorin macrocycle is remarkable for its ability to form isolable complexes of Ni(I) and Cu(I), oxidation states which are not commonly attained in a tetrapyrrole environment.[1, 2] The accessibility of these complexes reflects, in part, their resistance to further reduction. The nickel(I) and copper(I) octaethylisobacteriochlorin-(OEiBC) anions exhibit no cathodic processes in cyclic voltammograms in acetonitrile or dimethylformamide (DMF) and resist reduction by sodium amalgam. During recent studies, we had occasion to conduct amalgam reductions of [Ni(OEiBC)] (**1**) in the presence of proton donors and in a wider range of solvents than previously examined.[3] Unexpectedly, we observed the facile formation and interconversion of the two isomeric hexahydroporphyrin complexes **2** and **3**. Compounds **3** and **4**, the free base of **2**, were first prepared during Eschenmoser's investigations of chemistry relevant to the prebiotic origin and biosynthesis of Vitamin B_{12}.[4] Precorrins 2 (15,23-dihydrosirohydrochlorin) and 3, which are intermediates in the biosynthesis of Vitamin B_{12} and of Factor F430, have chromophores identical to **2**.[5]

A red-brown colored solution of **2**, whose UV/VIS spectrum is shown in Figure 1, is obtained by reduction of **1** with

[*] Prof. A. M. Stolzenberg, Dr. G. K. Lahiri
Department of Chemistry, West Virginia University
PO Box 6045, Morgantown, WV 26506-6045 (USA)

[**] The Reductive Chemistry of Nickel Hydroporphyrins, Part 3. This work was supported by the National Institutes of Health (grant GM 33882). Part 2.: [1].

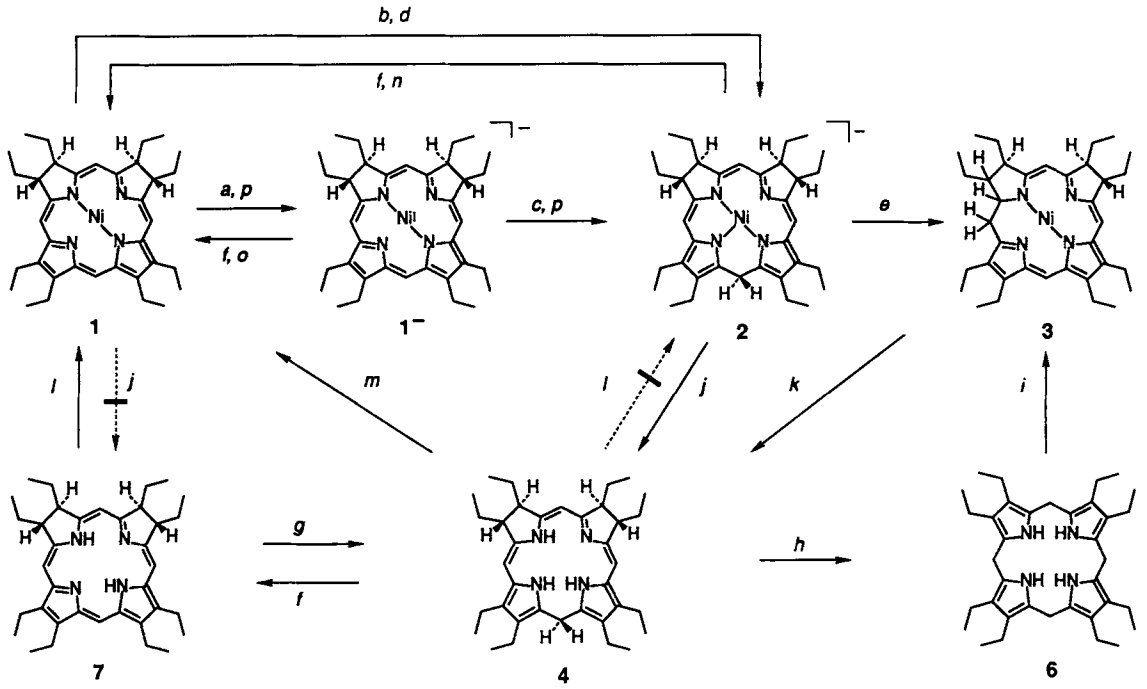

Scheme 1. All reactions were conducted at room temperature unless noted. *a*: Solution of **1** in various solvents (excluding those listed in *b*) + excess sodium amalgam (1% sodium). *b*: 2,5-Dimethyl-THF, TMEDA, or *N*-methylformamide solution of **1** + excess sodium amalgam (1% sodium) about 30 min–2 h. *c*: Acetonitrile, tetrahydropyran, THF, or 2-methyl-THF solution + excess sodium amalgam (1% sodium), about 2–48 h. *d*: Excess sodium amalgam (1% sodium) and $[(n\mathrm{Bu})_3\mathrm{NH}][\mathrm{ClO}_4]$, about 10 min. *e*: $[(n\mathrm{Bu})_3\mathrm{NH}][\mathrm{ClO}_4]$, about 2 min. *f*: O_2 or other oxidants. *g*: H_2, Pt on carbon (5%), in ethyl acetate solution [10]. *h*: In pyridine/acetic acid (1:1), 60 °C, evacuated tube, 40 h [10]. *i*: 7.3 equiv $[\mathrm{Ni(OAc)_2}]\cdot 4\mathrm{H_2O}$ in *p*-xylene + 2 vol.% $\mathrm{AcOH/Et_3N}$ (4:1), 140 °C, evacuated tube, 15–21 h [7]. *j*: AcOH, CF_3CO_2H, or HBF_4. *k*: Excess HBF_4 and $[(n\mathrm{Bu})_3\mathrm{NH}][\mathrm{ClO}_4]$. *l*: 3 equiv $[\mathrm{Ni(acac)_2}]$ in benzene or THF under reflux; see [13]. *m*: 3 equiv $[\mathrm{Ni(acac)_2}]$ + more than 3 equiv Et_3N in benzene or THF. *n*: $[\mathrm{Ni(acac)_2}]$ or $NiClO_4$. *o*: Excess H_2O, AcOH, CH_3OH, or C_6H_5SH; see [3]. *p*: Sodium naphthalide.

an excess of 1% sodium amalgam in specific solvents (Scheme 1).[6] In some solvents, the formation of $[\mathrm{Ni^I(OEiBC)}]^-$ ($\mathbf{1}^-$) is not observed during the reduction. However, in others the reduction initially affords $\mathbf{1}^-$, which later converts to **2**. Conversion of $\mathbf{1}^-$ to **2** requires 12–48 h in THF and acetonitrile, the solvents used in our original studies.[1] Ion $\mathbf{1}^-$ is stable to further reduction in dimethoxyethane, *N*-methylpyrrolidinone, dimethylformamide (DMF), and hexamethylphosphoric triamide (HMPA) even in the presence of a large excess of amalgam. The complex **2** could not be obtained by electrolysis in bulk solution or in an optically transparent thin-layer electrode electrochemical cell.

Reduction of **1** in the presence of the proton donor salt $[(n\mathrm{Bu})_3\mathrm{NH}][\mathrm{ClO}_4]$ requires significantly less time. If amalgam is present in large molar excess relative to salt, the final product is **2**. When salt is in excess, reduction affords a green solution of the known nickel(II) complex of octaethyl-1,2,3,7,8,20-hexahydroporphyrin (**3**).[7] Complex **3** also can be obtained within minutes at room temperature by addition of the perchlorate salt to a solution of **2** in the absence of amalgam.

Solutions of **2** are extraordinarily air-sensitive and are more difficult to handle than $[\mathrm{Ni^I(OEiBC)}]^-$. Partial oxidation of **2** to **1** invariably occurs upon transfer, dilution, or standing in the absence of amalgam. Analysis or purification of **2** by chromatography or isolation as a pure solid is not possible. In contrast, solutions of **3** are relatively stable. They can be purified by chromatography and can withstand brief exposure to air without sigificant reoxidation to **1**.

As initially obtained, **2** appears to be a single compound. NMR data and the similarity of the UV/VIS absorption bands of **2** prepared in widely varying solvents speak against a mixture of compounds with different saturation levels and sites. The ^{1}H NMR spectrum of **2** in $[D_8]$THF shows *meso* proton signals, which give a 1:2 ratio on integration, at $\delta = 5.55$ (C5) and 6.05 (C10 and C20). Each signal is partially resolved into two singlets of unequal height, which suggests that **2** is a mixture of diastereomers, like **1**.[7, 8] No signals are observed at lower field, with the exception of the *meso* protons of the [Ni(OEiBC)] impurity.[9] The twofold symmetry of **2** that is required by the *meso* proton signals, the rearrangement of **2** to the hexahydroporphyrin **3** in the absence of a reducing agent, and the facile and apparently quantitative oxidation of **2** to **1** establish that **2** is an anionic complex formed by saturation of C15 of **1**.

Complex **2** is the first metal complex of a 2,3,7,8,15,23-hexahydroporphyrin. Known free bases of compounds with this type of chromophore include precorrins 2 and 3,[5] **4**,[10] and 5-cyano-3,3,7,7,15,23-hexahydro-2,2,8,8,12,13,17,18-octamethylporphyrin (**5**).[11] The chemical shifts of the C5, 10, and 20 *meso* protons of these free bases fall exclusively in the range $5.0 \leq \delta \leq 6.1$, which distinguishes 2,3,7,8,15,23-hexahydroporphyrins from all other hexahydroporphyrin tautomers as well as from all tetrahydro- and dihydroporphyrin tautomers. The close correspondence of the ^{1}H NMR spectra of **2** and **4** and the absence in the spectrum of **2** of an NH proton peak near $\delta = 7.9$ are consistent with **2** being the nickel complex of **4**.

Eschenmoser et al. demonstrated that hexahydroporphyrins of type **4**, saturated at C15, are not favored in equilibria with other hexahydroporphyrins. Compound **4** tautomerizes to octaethylporphyrinogen (**6**).[10] Hexahydroporphyrin **5** can be transformed to a free base or nickel hexahydroporphyrin of the same chromophoric type as **3**.[11] Similar conditions can affect conversion of **6** to **3**.[7] All of

these conversions require extreme conditions: several days at temperatures of 60–140 °C. Thus, the facile conversion of **2** to **3** at room temperature is extraordinary.

The UV/VIS spectrum of **4** prepared by the literature method[10] is shown in Figure 1. Reaction of **2** with a small excess of acid results in immediate formation of a yellow compound whose UV/VIS spectrum is identical to that of **4**. In contrast to the rapid demetalation of **2**, solutions of purified **3** are unaffected by acid. However, in the presence of a large excess of both HBF_4 and $[(n\text{Bu})_3\text{NH}][ClO_4]$, **3** is rapidly demetalated to afford **4**. Thus, hexahydroporphyrins saturated at C15 are not always disfavored in equilibria with other hexahydroporphyrin tautomers.

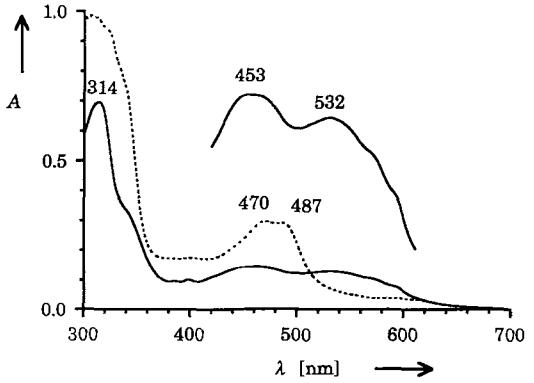

Fig. 1. UV/VIS spectra of nickel complex **2** (——) and free base **4** (– – – –) in THF. A = absorbance. Scales of the y axis for the two spectra are not the same. Inset: expansion of the spectrum of **2**.

Attempts to prepare **2** by metalation of **4** or catalytic hydrogenation of **1** were unsuccessful. Smith et al. used hydrogenation catalyzed by Raney nickel to prepare nickel hexahydroporphyrin complexes of the same type as **3** from Ni(II) anhydromesorhodochlorin and pyropheophorbide complexes.[12] Because solutions of **4** are easily reoxidized (but less readily than solutions of **2**) to octaethylisobacteriochlorin (**7**), a gentle method of inserting metals with $[M(acac)_2]$ complexes was investigated.[13] No reaction occurs when M = Ni, Cu, or Zn, even after hours at reflux in THF or benzene. Addition of base to assist in deprotonation of **4** results in immediate formation of the [M(OEiBC)] complex. Separate experiments showed that **2** is oxidized to **1** by either $[Ni(acac)_2]$ or $NiClO_4$ and is, therefore, unstable to the metalation conditions. Complex **1** suffers partial dehydrogenation to nickel octaethylchlorin, [Ni(OEC)], during catalytic hydrogenation in the presence of Pt/C catalyst. Raney Ni (Aldrich, pH > 9, slurry) completely bleaches solutions of **1** or of [Ni(OEC)]. Neither **6** nor any other identifiable compound can be isolated from the reaction.

It is curious that proton donors and potentially acidic solvents favor the reduction of **1** to **2** because proton donors oxidize $\mathbf{1}^-$, [Eq. (a)].[3] Indeed, more than 7 mol of H_2 are produced per mol of **2**, when **2** is prepared in *N*-methylformamide (NMF). This might implicate a hydrido-[Ni(OEiBC)] intermediate as the reagent that reduces **1** to **2**. However, the failure of $LiAlH_4$ to react with **1** and the lengthy reaction time (3 days) required for reduction of **1** to **2** by $Li(Et_3BH)$ suggest otherwise.

$$\underset{\mathbf{1}^-}{[Ni^I(OEiBC)]^-} + HA \longrightarrow \underset{\mathbf{1}}{[Ni(OEiBC)]} + 0.5\,H_2 + A^- \qquad (a)$$

In an effort to understand the reaction sequence that leads to **2**, we examined the cyclic voltammetry of **1** in THF, a solvent that has a potential limit of nearly −3 V vs. a saturated Calomel electrode (SCE) with $[(n\text{Bu})_4\text{N}][ClO_4]$ as electrolyte. The totally irreversible second reduction process observed at −2.56 V (cathodic peak) would appear to be beyond the range of sodium amalgam, whose potential is approximately −2.05 V vs. SCE in acetonitrile and THF.[14] However, this is a standard reduction potential, not the potential in the absence of electrolyte (i.e. $[Na^+] = 0$). We determined that the potential of 1% sodium amalgam in organic solvents (solutions 0.1 M in $[(n\text{Bu})_4\text{N}][ClO_4]$, but 0 M in added Na^+) is typically −2.25 V vs. SCE. Furthermore, the position of the cathodic peak includes a contribution from an overpotential. The peak underwent a 200 mV anodic shift when a hanging Hg drop electrode was used in place of a Pt electrode. Finally, ion pairing with the small Na^+ cation, the only counterion present during amalgam reduction, could cause significant anodic shifts in reduction potential as has been observed for aromatic dianions.[15] Thus, the thermodynamic potential of the second reduction of **1** and the potential of sodium amalgam under actual experimental conditions may be close enough to permit partial formation of $[Ni^I(OEiBC^{\bullet})]^{2-}$ [Eq. (b)]. Isobacteriochlorin anion radicals have unprecedentedly large spin density at C15.[16] Protonation of the strongly basic radical dianion at C15 accompanied by internal electron transfer from Ni^I to the π system [Eq. (c)] should be irreversible and drive formation of **2**. Consistent with this sequence, titration of **1** by sodium naphthalide sequentially produces $\mathbf{1}^-$ and **2**.

$$\underset{\mathbf{1}^-}{[Ni^I(OEiBC)]^-} + e^- \longrightarrow [Ni^I(OEiBC^{\bullet})]^{2-} \qquad (b)$$

$$[Ni^I(OEiBC^{\bullet})]^{2-} + H^+ \longrightarrow \mathbf{2} \qquad (c)$$

Reductions of zinc, copper, and palladium octaethylisobacteriochlorin (**8**–**10**) were reexamined in light of our results for **1**. The zinc complex **8** has a reversible second reduction at −2.13 V. Complexes **9** and **10** have irreversible second reductions with cathodic peaks at −2.57 and −2.68 V, respectively. All three are reduced by sodium amalgam to species with UV/VIS spectra similar to that of **2** in solvents that favor formation of **2**. These species reoxidize more readily than **2**. Proton donors appear to assist the formation of these species. Reduction of **8** or **9** does not proceed beyond $[Zn(OEiBC^{\bullet})]^-$ or $[Cu^I(OEiBC)]^-$, respectively, in 'dry' DMF. In 'wet' DMF,[17] **9** is reduced partially and **8** completely to species analogous to **2**.

Received: October 8, 1992 [Z 5616 IE]
German version: *Angew. Chem.* **1993**, *105*, 440

[1] A. M. Stolzenberg, M. T. Stershic, *J. Am. Chem. Soc.* **1988**, *110*, 6391.
[2] A. M. Stolzenberg, L. J. Schussel, *Inorg. Chem.* **1991**, *30*, 3205.
[3] G. K. Lahiri, L. J. Schussel, A. M. Stolzenberg, *Inorg. Chem.*, **1992**, *31*, 4991.
[4] A. Eschenmoser, *Angew. Chem.* **1988**, *100*, 5; *Angew. Chem. Int. Ed. Engl.* **1988**, *27*, 5.
[5] a) A. R. Battersby, K. Frobel, F. Hammerschmidt, C. Jones, *J. Chem. Soc. Chem. Commun.* **1982**, *455*; b) A. R. Battersby, *Acc. Chem. Res.* **1986**, *19*, 147; c) F. J. Leeper, *Nat. Prod. Rep.* **1989**, *6*, 171.
[6] Solvents and reagents were rigorously purified, dried, and degassed. All manipulations and reactions were performed under nitrogen in a Vacuum Atmos. Co. dry-box.
[7] J. E. Johansen, C. Angst, C. Kratky, A. Eschenmoser, *Angew. Chem.* **1980**, *92*, 141; *Angew. Chem. Int. Ed. Engl.* **1980**, *19*, 141.

[8] A. M. Stolzenberg, L. O. Spreer, R. H. Holm, *J. Am. Chem. Soc.* **1980**, *102*, 364.
[9] The C15 *meso* protons and other protons cannot be assigned because of overlap between $\delta = 0$ and $\delta = 4$ of the NMR spectra of **1**, **2**, and solvent.
[10] C. Angst, K. Masahiro, E. Zass, A. Eschenmoser, *Angew. Chem.* **1980**, *92*, 139; *Angew. Chem. Int. Ed. Engl.* **1980**, *19*, 140.
[11] P. Naab, R. Lattmann, C. Angst, A. Eschenmoser, *Angew. Chem.* **1980**, *92*, 143; *Angew. Chem. Int. Ed. Engl.* **1980**, *19*, 143.
[12] a) K. M. Smith, D. A. Goff, *J. Am. Chem. Soc.* **1985**, *107*, 4954; b) K. M. Smith, D. J. Simpson, *ibid.* **1987**, *109*, 6326.
[13] G. K. Lahiri, J. S. Summers, A. M. Stolzenberg, *Inorg. Chem.* **1991**, *30*, 5049.
[14] L. Horner, R.-E. Schmitt, *Z. Naturforsch. B* **1982**, *37*, 1163.
[15] A. J. Fry, C. S. Hutchins, L. L. Chung, *J. Am. Chem. Soc.* **1975**, *97*, 591.
[16] a) K. M. Barkigia, C. K. Chang, J. Fajer, M. W. Renner, *J. Am. Chem. Soc.* **1992**, *114*, 1701; b) M. W. Renner, E. Fujita, I. Fujita, A. D. Procyk, D. F. Bocian, J. Fajer *J. Phys. Chem.*, **1992**, *96*, 9597.
[17] 'Wet' DMF means Burdick and Jackson DMF (0.013% H_2O) that was not dried further.

Regiospecific Conversion of 3,4-Bis(trimethylsilyl)furan to 3,4-Disubstituted Furans: A Novel Suzuki-Type Cross-Coupling of Boroxines**

By *Zhi Zhong Song, Zhong Yuan Zhou, Thomas C. W. Mak,* and *Henry N. C. Wong**

Polysubstituted furans are important building blocks for natural and nonnatural product synthesis.[1] However, the tendency of furans to undergo both lithiation and electrophilic substitution at C2 or C5[2] makes the synthesis of 3,4-disubstituted furans an exceedingly difficult task. To circumvent this, several special methods have been developed.[3] Recently we reported the preparation of 3,4-bis(trimethylsilyl)furan (**1**) and some of its conversions.[4] In this communication, we disclose that **1** can be converted regiospecifically into various boroxines,[5] which in turn undergo the well-established Suzuki-type cross-coupling reactions[6] to give 3,4-disubstituted furans.

The yield of **1** was optimized to 80% by heating equimolar quantities of bis(trimethylsilyl)acetylene and 4-phenyloxazole[7] in 5 mol% of triethylamine at 250 °C in a sealed tube for 2 days (Scheme 1). The presence of triethylamine is essential for retarding the rearrangement of **1**.[8, 9] In a separate experiment, trifluoroacetic anhydride containing a catalytic amount of trifluoroacetic acid was found to promote the rearrangement of **1** efficiently,[8, 9] which furnished 2,4-bis(trimethylsilyl)furan as the only isolable product in 85% yield.[10]

Attempts to displace the trimethylsilyl groups of **1** directly with aryl or alkenyl groups by palladium-catalyzed coupling have so far been unfruitful, although similar reactions on fluorinated silanes are well-documented.[11] Furthermore,

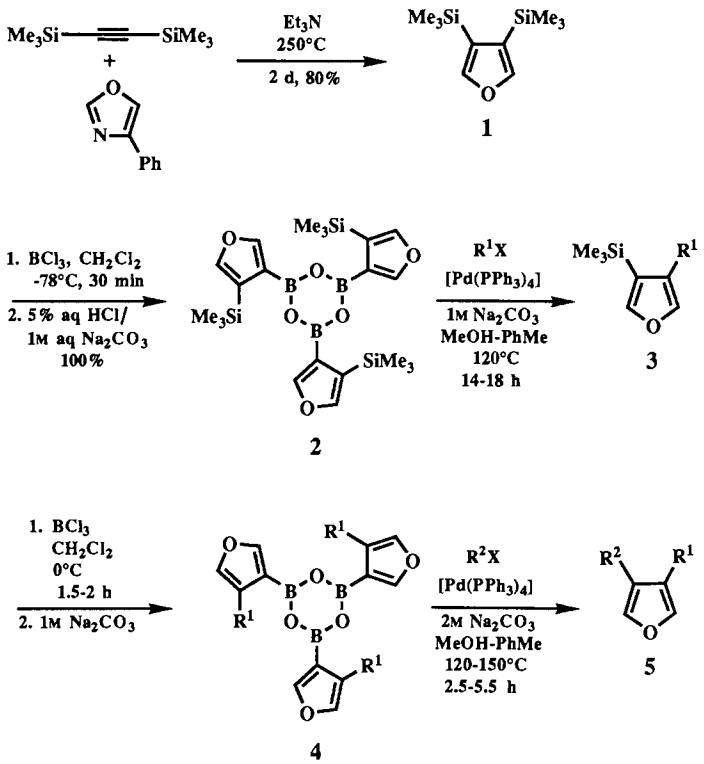

Scheme 1. The reaction of bis(trimethylsilyl)acetylene and 4-phenyloxazole was performed in a sealed tube.

Friedel–Crafts acylation of **1** with various acid chlorides only led to mixtures of compounds with substitution at both C2 and C3.[10] After several manipulations, we eventually discovered that **1** underwent regiospecific *ipso*-substitution[12] with one to two equivalents of boron trichloride at 0 °C to room temperature.[13] Subsequent workup[14] of the resulting dichloroborane by addition of either 5% HCl or 1 M Na_2CO_3 afforded unexpectedly the air-stable tris[(4-trimethylsilyl)furan-3-yl]boroxine **2** in quantitative yield (Scheme 1). The structure of **2** has been substantiated by NMR spectrometry and shown to exhibit approximate C_{3h} symmetry by an X-ray crystallographic study (Fig. 1).[15]

Although the trimeric anhydrides of boronic acids, the boroxines, have been known for more that fifty years,[5] their synthetic applications[16] have been restricted mainly to characterization and purification of the corresponding

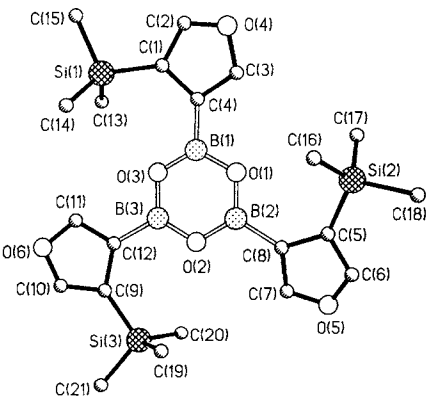

Fig. 1. Perspective view of the molecular structure of **2** with atom numbering. In the boroxine ring the average B–O bond lengths are 1.372(6) Å and O-B-O angles are 119.3(5)°.

[*] Dr. H. N. C. Wong, Z. Z. Song,[+] Prof. Z. Y. Zhou,[++] Prof. Dr. T. C. W. Mak
Department of Chemistry, The Chinese University of Hong Kong, Shatin, New Territories (Hong Kong)
[+] Permanent address: Lanzhou University, Lanzhou (China)
[++] Permanent address: Analysis and Testing Center, The Chinese Academy of Sciences, Chengdu (China)

[**] 3,4-Disubstituted Furans, Part 4. This work was supported financially by Hong Kong University and Polytechnic Grants Committee Earmarked Grants for Research (Acc. No. 221300110 and Acc. No. 221600010). Part 3: Y. Yang, H. N. C. Wong, *J. Chem. Soc. Chem. Commun.* **1992**, 1723–1725.

Table 1. Preparation of furans **3** from boroxine **2** and R^1X, and boroxines **4** from furans **3**, as well as furans **5** from boroxines **4** and R^2X [a].

R^1X	Product (yield [%])	Product (yield [%])	R^2X	Product (yield [%])
C_6H_5Br	**3a**, $R^1 = C_6H_5$ (97)			
4-MeC_6H_4I	**3b**, R^1 = 4-MeC_6H_4 (97)	**4b** (47)	**B**	**5b** (54)
4-$MeCOC_6H_4Br$	**3c**, R^1 = 4-$MeCOC_6H_4$ (96)			
1-bromonaphthalene	**3d**, R^1 = 1-naphthyl (98)	**4d** (42)	*trans*-$C_5H_{11}CH{=}CHI$	**5d**, R^1 = 1-naphthyl, R^2 = *trans*-$C_5H_{11}CH{=}CH$ (92)
2-(4-MeC_6H_4)-C_6H_4I	**3e**, R^1 = 2-(4-MeC_6H_4)-C_6H_4 (95)	**4e** (41)	bromocyclooctatetraene	**5e**, R^1 = 2-(4-MeC_6H_4)-C_6H_4, R^2 = cyclooctatetraenyl (90)
2-bromothiophene	**3f**, R^1 = 2-thienyl (96)			
4-$BrCH_2COC_6H_4Br$	**3g**, R^1 = 4-$BrCH_2COC_6H_4$ (91)			
A	**3h**			
9-bromofluorene	**3i**, R^1 = 9-fluorenyl (45)			
4-$O_2NC_6H_4CH_2Br$	**3j**, R^1 = 4-$O_2NC_6H_4CH_2$ (95)	**4j** (61)	9-bromophenanthrene	**5j**, R^1 = 4-$O_2NC_6H_4CH_2$, R^2 = 9-phenanthryl (87)
		4j	C	**5k** (90)
		4j	**D**	**5l** (61)

[a] For structural formulas, see Scheme 2.

boronic acids.[17] However, we found that boroxine **2** smoothly underwent regiospecific Suzuki-type cross-coupling reaction[6] catalyzed by 10 mol% of $[Pd(PPh_3)_4]$ to afford furans **3** (Table 1, Scheme 2). With only one notable exception (**3i**), which might perhaps be attributed to steric hindrance, the yields of **3** are generally higher than 90%.

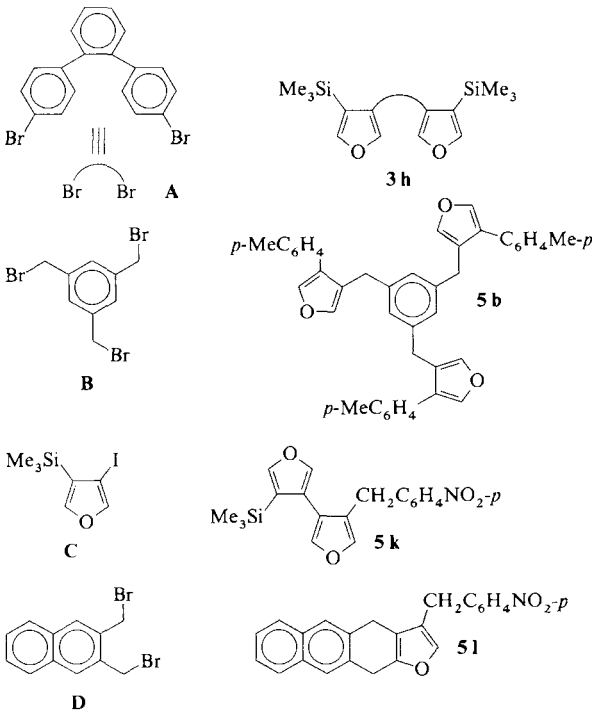

Scheme 2. Structures of the halides **A**–**D** and the furans **3h**, **5b**, **5k**, and **5l**.

To achieve our ultimate goal of preparing 3,4-disubstituted furans, the remaining trimethylsilyl groups of **3** were replaced by the dichloroboranyl group with boron trichloride, and the reaction mixtures were subsequently worked up by addition of 1 M Na_2CO_3. As expected, boroxines **4** were obtained, albeit in somewhat inferior yields (Table 1). Apparently the displacement of the second trimethylsilyl group in **3** by boron trichloride is less facile. Again, boroxines **4** readily underwent Suzuki-type cross-coupling reactions catalyzed by 10 mol% of $[Pd(PPh_3)_4]$ to furnish 3,4-disubstituted furans **5** in good yields (Table 1). As can be seen, the intriguing generation of **5b** aptly demonstrates the versatility of boroxine in the cross-coupling reaction. The formation of **5l**, on the other hand, shows that palladium(0) is able to trigger an unexpected intramolecular Heck-type coupling at C2 of the furan nucleus.

In conclusion, we have shown that the cross-coupling reaction for boroxines is quite efficient in terms of the ease of product workup and yields. However, in practice, it should be noted that R^1 must be insensitive to Lewis acid. The choice of R^2 is less demanding, depending solely on the limitation of the Suzuki reaction. A number of 3,4-disubstituted furans, which are otherwise difficult to realize, have been prepared. This palladium-catalyzed silicon–boron strategy for synthesis of 3,4-disubstituted furans is expected to have interesting uses in organic synthesis.

Experimental Procedure

1: A mixture of 4-phenyloxazole (0.1 mol), bis(trimethylsilyl)acetylene (0.12 mol), and triethylamine (5 mmol) was heated in a sealed tube at 300 °C for 7 days. Vacuum distillation gave a colorless liquid. Purification by column chromatography (SiO_2, 350 g, hexanes) yielded **1** (17 g, 80%) as colorless oil, b.p. = 30–32 °C (0.6 mmHg). ^1H NMR (250.132 MHz, $CDCl_3$, 25 °C): δ = 0.25 (s, 9H, $Si(CH_3)_3$), 7.41 (s, 1H, H2); ^{13}C NMR (62.896 MHz, $CDCl_3$): δ = 0.42 (q, $Si(CH_3)_3$), 121.90 (s, C3), 149.61 (d, C2); EI-MS (70 eV): *m/z* 212 (M^+, 60%), 73 ($Si(CH_3)_3$, 100).

2: *To a solution of* **1** *(0.05 mol) in* CH_2Cl_2 *(100 mL)* was added slowly a 1.0 M solution of BCl_3 in CH_2Cl_2 (50 mL) under a nitrogen atmosphere at room temperature. The reaction was quenched with 2 M Na_2CO_3 solution, and the mixture extracted with ether (3 × 20 mL). The organic layer was dried ($MgSO_4$), and the solvent evaporated. The crude product was chromatographed (SiO_2, 250 g, hexanes/ether, 2:1). Colorless crystals of **2** were obtained (8.1 g, 98%), m.p. = 167–168 °C. ^1H NMR (250.132, $CDCl_3$, 25 °C): δ = 0.38 (s, 9H, $Si(CH_3)_3$), 7.43 (d, 1H, J = 1 Hz, H5), 8.17 (d, 1H J = 1 Hz, H2); ^{13}C NMR (62.896 MHz, $CDCl_3$): δ = – 0.42 (q, $Si(CH_3)_3$), 117.05 (br. s, C3), 122.21 (s, C4), 149.10 (d, C5), 156.55 (d, C2); EI-MS (70 eV): *m/z* 498 (M^+, 13%), 483 (M^+ – Me, 90), 275 (48), 73 ($Si(CH_3)_3$, 100).

3j: A mixture of **2** (10 mmol), *p*-nitrobenzyl bromide (30 mmol) and $[Pd(PPh_3)_4]$ (0.5 mmol) in methanol/toluene (70 mL, 1:1) was stirred. After 5 min, a 2 M Na_2CO_3 solution (4 mL) was added. The reaction mixture was then stirred while heating at reflux for 5 h at 140 °C. After addition of water (100 mL) and cooling to room temperture, the mixture was extracted with ether (3 × 25 mL). The combined organic solution was washed with water, dried ($MgSO_4$) and concentrated. Purification by column chromatography (SiO_2, 200 g, hexanes/ether, 10:1) yielded **3j** (7.8 g, 95%) as a colorless oil. ^1H NMR (250.132 Hz, $CDCl_3$, 25 °C): δ = 0.11 (s, 9H, $Si(CH_3)_3$), 3.93 (s, 2H, CH_2), 7.19 (d, 1H, J = 1.2 Hz, H5), 7.31 (d, 1H, J = 1.2 Hz, H2), 7.34 (d, 2H, J = 8.7 Hz, *m*-H(NO_2)), 8.11 (d, 2H, J = 8.7 Hz, *o*-H(NO_2)); ^{13}C NMR (62.896 Hz, $CDCl_3$): δ = – 0.81 (q, $Si(CH_3)_3$), 31.52 (t, CH_2), 118.90 (s, C4), 123.22, 123.35

(each d, each 1C, *o*-C(NO_2)), 126.02 (s, C3), 129.29, 129.58 (each d, each 1C, *m*-C(NO_2)), 141.34 (d, C2), 146.58 (s, *p*-C(NO_2)), 148.05 (s, CNO_2), 148.88 (d, C5); EI-MS (70 eV): *m/z* 275 (M^+, 29%), 260 (M^+ − Me, 100), 199(30), 180(33), 137(18), 73 ($Si(CH_3)_3$, 27).

4j: To a solution of **3j** (7 mmol) in CH_2Cl_2 (200 mL) was added slowly a 1.0 M solution of BCl_3 in CH_2Cl_2 (14 mL) under a nitrogen atmosphere at room temperature. The reaction was quenched with 2 M Na_2CO_3 solution, and the mixture extracted with ether (3 × 20 mL). The organic layer was dried ($MgSO_4$), and the solvent evaporated off. The crude product was chromatographed (SiO_2, 250 g, hexanes/ether, 1:1) to give **4j** (0.98 g, 61%) as a semisolid. ^1H NMR (250.132 Hz, $CDCl_3$, 25 °C): δ = 4.11 (s, 2H, CH_2), 7.16 (s, 1H, H5), 7.34 (d, 2H, J = 8.6 Hz, *m*-H(NO_2)), 7.83 (s, 1H, H2), 8.08 (d, 2H, J = 8.6 Hz, *o*-H(NO_2)); ^{13}C NMR (62.896 Hz, $CDCl_3$): δ = 30.80 (CH_2), 113.85 (br. s, C3), 123.45, 123.61 (each d, each 1C, *o*-C(NO_2)), 126.11 (s, C4), 129.11, 129.33 (each d, each 1C, *m*-C(NO_2)), 141.98 (d, C5), 146.80 (s, *p*-C(NO_2)), 148.17 (s, CNO_2), 155.19 (d, C2); EI-MS (70 eV): *m/z* 687 (M^+, 19%), 203(75), 128(100).

5j: A mixture of **4j** (0.32 mmol), 9-bromophenanthrene (0.96 mmol), and [Pd(P-$Ph_3)_4$] (0.1 mmol) in methanol/toluene (30 mL, 1:1) was stirred for 5 min, where upon 2 M Na_2CO_3 solution (3 mL) was added. The reaction mixture was again stirred while heating at reflux for 5 h at 140 °C. After addition of water (50 mL) and cooling to room temperature, the mixture was extracted with ether (3 × 20 mL). The combined organic solution was washed with water, dried ($MgSO_4$), and concentrated. Purification by column chromatography (SiO_2; 20 g, hexanes/ether, 7:1) yielded **5j** (317 mg, 87%) as semisolid. ^1H NMR (250.132 Hz, $CDCl_3$ 25 °C): δ = 3.51 (s, 2H, CH_2), 6.80 (d, 2H, J = 8.5 Hz, *m*-H(NO_2)), 7.24–7.68 (m, 10H), 8.53 (t, 2H, J = 8.0 Hz, *o*-H(NO_2)); ^{13}C NMR (62.896 Hz, $CDCl_3$): δ = 30.23 (CH_2), 122.52, 122.85, 123.13, 126.41, 126.57, 126.90, 128.40, 128.89, 129.25 (each d, each 1C), 124.21, 124.89, 127.98, 130.15, 130.42, 131.25, 131.54, (each s, each 1C), 140.43 (d, C2), 141.52 (d, C5), 146.31 (s, *p*-C(NO_2)), 147.37 (s, CNO_2); EI-MS (70 eV): *m/z* 379 (M^+, 100%), 255(26), 184(33), 119(42), 118(42).

Recieved: October 5, 1992 [Z 5613 IE]
German version: *Angew. Chem.* **1993**, *105*, 406

[1] W. Kreiser, *Nachr. Chem. Tech. Lab.* **1981**, *29*, 118–120; B. H. Lipshutz, *Chem. Rev.* **1986**, *86*, 795–819.
[2] H. W. Gschwend, H. R. Rodriguez, *Org. React. (NY)* **1979**, *26*, 1–360; F. M. Dean, *Adv. Heterocycl. Chem.* **1982**, *30*, 167–238; F. M. Dean, *ibid.* **1982**, *31*, 237–344; D. M. X. Donnelly, M. J. Meegan, in *Comprehensive Heterocyclic Chemistry, Vol. 4, Part 3* (Eds.: C. W. Bird, G. W. H. Cheeseman), Pergamon, Oxford, **1984**, p. 657–712.
[3] M. E. Garst, T. A. Spencer, *J. Am. Chem. Soc.* **1973**, *95*, 250–252; E. J. Corey, D. N. Crouse, J. E. Anderson, *J. Org. Chem.* **1975**, *40*, 2140–2141; J. Hutton, B. Potts, P. F. Southern, *Synth. Commun.* **1979**, *9*, 789–797; H. König, F. Graf, V. Weberndörfer, *Liebigs Ann. Chem.* **1981**, 668–682; H. J. Reich, R. E. Olson, *J. Org. Chem.* **1987**, *52*, 2315–2317; M. E. Price, N. E. Schore, *ibid.* **1989**, *54*, 2777–2778; S. Y. Yu, B. A. Keay, *J. Chem. Soc. Perkin Trans. 1* **1991**, 2600–2601; B. A. Keay, J.-L. J. Bontront, *Can. J. Chem.* **1991**, *69*, 1326–1330; V. N. Kalinin, *Synthesis* **1992**, 413–432.
[4] M. S. Ho, H. N. C. Wong, *J. Chem. Soc. Chem. Commun.* **1989**, 1238–1240.
[5] W. Gerrard, *The Organic Chemistry of Boron*, Academic Press, London, **1961**, p. 68; A. G. Avent, M. F. Lappert, B. Skelton, C. L. Raston, L. M. Engelhardt, S. Harvey, A. H. White, in *Heteroatom Chemistry*; (Ed.: E. Block), VCH, Weinheim, **1990**, Chapter 15, p. 275–285; P. A. McCusker, E. C. Ashby, H. S. Makowski, *J. Am. Chem. Soc.* **1957**, *79*, 5179–5181; P. A. McCusker, H. S. Makowski, *ibid.* **1957**, *79*, 5185–5188; L. Barton, F. A. Grimm, R. F. Porter, *Inorg. Chem.* **1966**, *5*, 2076–2078; R. Boese, M. Polk, D. Bläser, *Angew. Chem.* **1987**, *99*, 239–241; *Angew. Chem. Int. Ed. Engl.* **1987**, *26*, 245–247.
[6] N. Miyaura, T. Yanagi, A. Suzuki, *Synth. Commun.* **1981**, *11*, 513–519; N. Miyaura, K. Yamada, H. Suginome, A. Suzuki, *J. Am. Chem. Soc.* **1985**, *107*, 972–980; A. Suzuki, *Pure Appl. Chem.* **1991**, *63*, 419–422.
[7] H. Bredereck, R. Gompper, *Chem. Ber.* **1954**, *87*, 700–707.
[8] T. J. Barton, G. P. Hussmann, *J. Am. Chem. Soc.* **1983**, *105*, 6316–6318.
[9] D. Seyferth, D. L. White, *J. Am. Chem. Soc.* **1972**, *94*, 3132–3138; *J. Organomet. Chem.* **1972**, *34*, 119–128; D. Seyferth, D. L. White, *J. Organomet. Chem.*, **1972**, *34*, 119–128.
[10] Z. Z. Song, H. N. C. Wong, unpublished.
[11] Y. Hatanaka, T. Hiyama, *J. Org. Chem.* **1988**, *53*, 918–920; Y. Hatanaka, S. Fukushima, T. Hiyama, *Chem. Lett.* **1989**, 1711–1714; Y. Hatanaka, T. Hiyama, *J. Org. Chem.* **1989**, *54*, 268–270; Y. Hatanaka, T. Hiyama, *Tetrahedron Lett.* **1990**, *31*, 2719–2722.
[12] F. H. Pinkerton, S. F. Thames, *J. Heterocycl. Chem.* **1970**, *7*, 747–750; C. Eaborn, *J. Organomet. Chem.* **1975**, *100*, 43–57; F. Effenberger, D. Häbich, *Liebigs Ann. Chem.* **1979**, 842–857; J. B. Lambert, *Tetrahedron* **1990**, *46*, 2677–2689.
[13] M. J. Sharp, W. Cheng, V. Snieckus, *Tetrahedron Lett.* **1987**, *28*, 5093–5096; D. Kaufmann, *Chem. Ber.* **1987**, *120*, 853–854; *ibid.* **1987**, *120*, 901–905.
[14] B. P. Roques, D. Florentin, M. Callanquin, *J. Heterocycl. Chem.* **1975**, *12*, 195–196; D. Florentin, M. C. Fournie-Zaluski, M. Callanquin, B. P. Roques, *ibid.* **1976**, *13*, 1265–1272.
[15] Crystal data for **2**: orthorhombic, $P2_12_12_1$ (no. 19), a = 10.685(5), b = 11.524(2), c = 23.752(7) Å, V = 2149.5(1.5) Å^3, Z = 4; R = 0.054, R_w = 0.070 for 298 parameters and 1495 observed reflections [$|F_0| > 6\sigma(|F_0|)$] collected at 18 °C ($Mo_{K\alpha}$, 3° < 2θ < 52°) on a Nicolet R3m diffractometer. All non-hydrogen atoms were refined anisotropically. The hydrogen atoms were included in fixed calculated positions with assigned isotropic temperature factors. Further details of the crystal structure investigation are available on request from the Director of the Cambridge Crystallographic Data Centre, 12 Union Road, Cambridge CB2 1EZ (UK), on quoting the full journal citation.
[16] R. P. Dickinson, B. Iddon, *J. Chem. Soc. C* **1970**, 1926–1928; H. C. Brown, C. G. Rao, S. U. Kulkarni, *Synthesis* **1979**, 704–705.
[17] *Vogel's Textbook of Practical Organic Chemistry*, 5th ed. (Revised B. S. Furniss, A. J. Hannaford, P. W. G. Smith, A. R. Tatchell), Longman, Harlow, Essex, England, **1989**, p 971–975.

A Short Synthetic Route towards a Biologically Active Heparin-like Pentasaccharide with a Pseudo-Alternating Sequence**

By *Hans Lucas, Jan E. M. Basten, Peter Konradsson* and *Constant A. A. van Boeckel**

It is now well established that only a small heterogeneous pentasaccharide domain[1, 2] of the anti-thrombotic drug heparin (a glycosaminoglycan) is responsible for the inactivation of blood coagulation factor Xa (αXa-activity) mediated by antithrombin III (AT III). The synthetic pentasaccharide **15a**, which has an extra sulfate group at the 3 position in unit H[3] (Fig. 1), was found to be one of the most active counterparts of the unique heparin domain, eliciting an αXa-activity of 1250 U mg^{-1}.

Recently, it was discovered that the replacement of all "N-sulfate" groups in **15a** by "O-sulfate" functions and methylation of all free hydroxyl groups[4] to give the highly modified "nonglycosamino" glycan analogue **15b** actually increased the biological activity (compound **15b** displayed an αXa-activity of 1323 U mg^{-1}). In comparison with the syntheses of pentasaccharides corresponding to the unique heparin domain, the preparation of the nonglycosamino glycan analogue is much easier: a) The free hydroxyl groups are permanently blocked as methyl ethers meaning that the protecting group strategy required for the preparation of heparin fragments can be abandoned; it is not necessary to discriminate between sulfated (acyl esters) and nonsulfated (benzyl ethers) hydroxyl groups. b) No α-coupled glucosamines are present which require elaborate synthetic routes towards azide-containing building blocks. c) Selective N-sulfation need not be performed at the end of the synthesis.

Having the simplified derivative **15b** at our disposal, we wondered whether even shorter synthetic routes could be devised towards this compound or closely related analogues. With this in mind we designed analogue **15c** (Fig. 1), which has a pseudo-alternating sequence, that is, because of the

[*] Dr. C. A. A. van Boeckel, H. Lucas, J. E. M. Basten, Dr. P. Konradsson
AKZO Pharma Division
Organon Scientific Development Group
P. O. Box 20, NL-5340 BH Oss (The Netherlands)

[**] This work was supported by the Eureka Programme of the European Community (EU 237). We wish to thank the SANOFI Recherche Carbohydrate Chemistry Group (Maurice Petitou) for useful discussions and Theo van Dinther of the Department of Vascular Pharmacology for determining the αXa-activities.

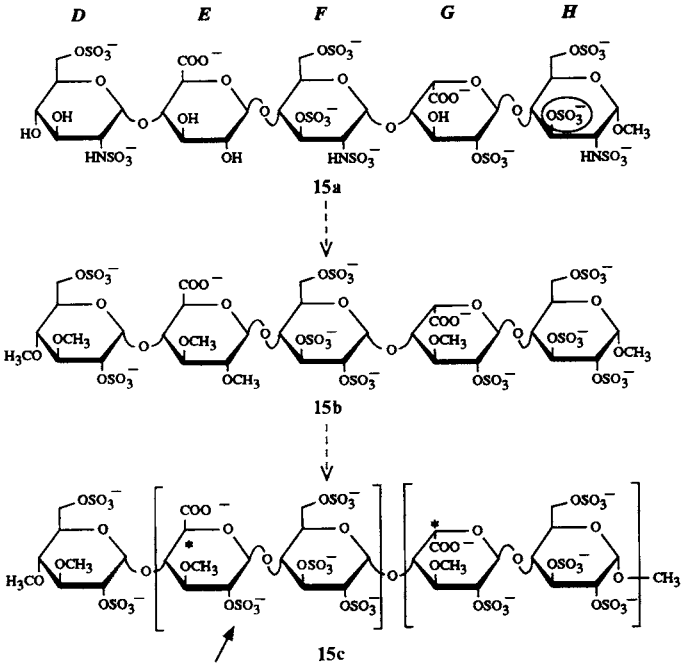

Fig. 1. Replacement of all *N*-sulfate groups in **15a** with *O*-sulfate groups and methylation of all free OH functions gives the active nonglycosaminoglycan analogue **15b**. In analogue **15c** an extra sulfate group in the 2-position of unit E (see arrow) has been introduced to create a pseudo-alternating sequence. The disaccharide fragments between brackets only differ in their configuration at C5 of the uronic acid moieties (*).

2-sulfate group at unit E, the disaccharide fragments EF and GH have the same substitution pattern.

The only remaining difference between the disaccharide fragments EF and GH of compound **15c** is the opposite configuration at C5 of the uronic acid moieties. Hence, a shorter synthetic route[5] to **15c** could be developed in which the disaccharide fragment EF is obtained from its counterpart GH by epimerization.[6] In the transformation of the epimerized GH building block into an appropriate EF glycosyl donor the acetolysis of the locked anomeric center also plays a pivotal role (Scheme 1).

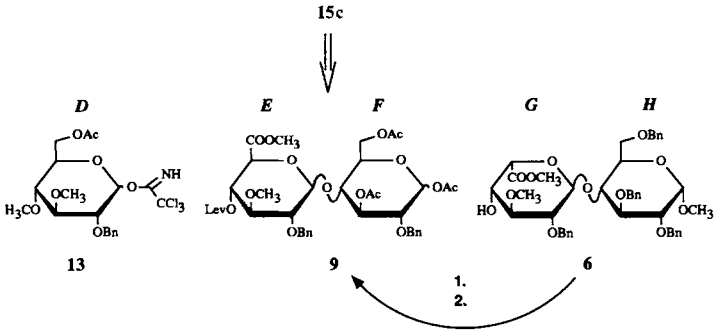

Scheme 1. The retrosynthetic analysis for pentasaccharide **15c** shown here is based on the epimerization (1.) and acetolysis (2.) of an iduronic acid GH disaccharide acceptor **6** to give an EF donor.

The key intermediate in the synthesis of pentasaccharide **15c** is the suitably protected iduronic acid building block **6**. Since the required epimerization is carried out under strongly basic conditions we had to protect the GH building block **6** exclusively with benzyl groups. Fortunately, this does not present a problem in this new series of pentasaccharides (in contrast to the synthesis of the natural fragments), as we can select ether or ester protecting groups for all hydroxyl groups to be sulfated. Glycosylation of the glycosyl acceptor **2**[7] with the known 3-*O*-methyl idopyranosyl fluoride **1**[4a] in the presence of $BF_3 \cdot OEt_2$ and 4 Å molecular sieves in dichloromethane at 0 °C gave the disaccharide fragment **3** in 90% yield (Scheme 2). Saponification of the ester functions of compound **3** and subsequent introduction of the 4′,6′-benzylidene acetal afforded intermediate **4** in an overall yield of 64%. Next, the free hydroxyl group of compound **4** was quantitatively benzylated to afford crystalline **5**. According to well-established reaction sequences[4a, 8] compound **5** could be converted into the key intermediate **6** in 41% overall yield. Compound **6** was then treated with sodium methoxide in methanol under reflux (16 h) to accomplish the C5′ epimerization. Despite the strictly anhydrous conditions, hydrolysis of the methyl ester could not be avoided during the epimerization reaction. Hence, after neutralization of the reaction mixture with DOWEX H^+, the free carboxylate group was methylated with CH_3I in *N*,*N*-dimethylformamide (DMF) and in the presence of $KHCO_3$ to give a mixture of **7** and **6** (ratio 10:1). After purification over silica gel the glucuronic acid fragment **7** was isolated in about 73% yield together with recovered **6** (7%). Protection of the free

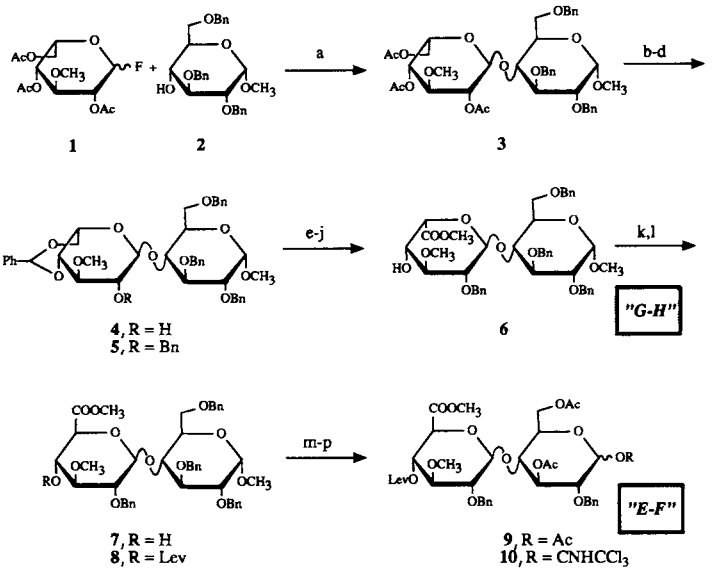

Scheme 2. a) $BF_3 \cdot OEt_2$, CH_2Cl_2, 4 Å molecular sieves (MS 4 Å), 0 °C, 1 h (90%); b) KO*t*Bu, MeOH, dioxane, room temperature (RT), 1 h (92%); c) $C_6H_5CH(OCH_3)_2$, *p*-TsOH, RT, 1.5 h (70%); d) BnBr, NaH, DMF, RT, 2 h (100%); e) 70% trifluoroacetic acid (TFA), CH_2Cl_2, RT, 1 h (82%); f) *tert*-butyldimethylsilylchloride (TBDMSiCl), pyridine, RT, 16 h; g) levulinic acid, *N*,*N*-dicyclohexylcarbodiimide (DCC) dioxane, dimethylaminopyridine (DMAP), RT, 2 h; h) CrO_3, H_2O, H_2SO_4, acetone, RT, 3 h; i) $KHCO_3$, CH_3I, DMF, MS 4 Å, RT, 3 h; j) $H_2NNH_2 \cdot H_2O$, HOAc, pyridine, RT, 6 min. (50%, steps f–j); k) NaOMe, MeOH, reflux, 16 h; l) $KHCO_3$, CH_3I, DMF, MS 4 Å, RT, 3 h (73%, steps k–l); m) levulinic acid, DCC, dioxane, DMAP, RT, 2 h (97%); n) HOAc/Ac_2O/TFA 1/25/3.5, RT, 2 d; o) piperidine, THF, RT, 16 h; p) Cs_2CO_3, $NCCCl_3$, CH_2Cl_2, RT, 0.5 h (75%, steps n–p). Lev = $OC(O)CH_2CH_2C(O)CH_3$.

4′-hydroxyl group in **7** as a levulinoyl ester afforded compound **8**, which was acetolyzed in a mixture of trifluoroacetic acid/acetic anhydride/acetic acid (3.5/25/1, v/v/v). Under the aforementioned conditions we observed the acetolysis of the anomeric center as well as of the 3- and 6-benzyl ethers.[9, 10] Fortunately, the 2-benzyl ether essential for the subsequent introduction of an α-glycosidic linkage remained unaffected.

After two days at room temperature disaccharide **9** was formed in nearly quantitative yield. The anomeric acetate of compound **9** was selectively removed by treatment with piperidine in THF. The trichloroacetimidate function was then introduced in a mixture of dichloromethane and trichloroacetonitrile and in the presence of cesium carbonate[11] to give the desired EF glycosyl donor **10** in 75% overall yield. Coupling of disaccharide donor EF (compound **10**, 1.2 equiv) and acceptor GH (compound **6**) in dichloromethane with trimethylsilyltriflate as promoter in the presence of 4 Å molecular sieves at −15 °C afforded tetramer **11** in a yield of 75% (Scheme 3). Selective removal

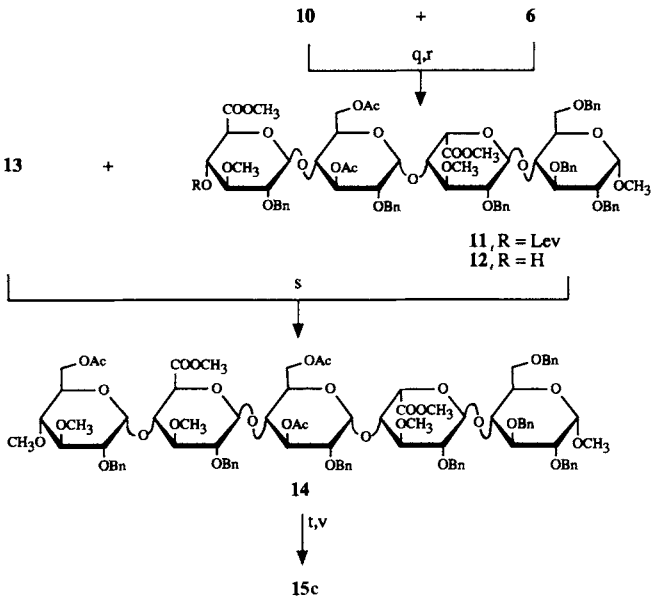

Scheme 3. q) $Me_3SiO_3SCF_3$(TMSOTf), CH_2Cl_2, MS 4 Å, −15 °C, 1 h (75%); r) $H_2NNH_2 \cdot H_2O$, HOAc, pyridine, RT, 6 min. (90%); s) TMSOTf, CH_2Cl_2, MS 4 Å, −20 °C, 1 h (65%); t) LiOOH, THF, 0 °C, 16 h, NaOH, MeOH, RT, 16 h (90%); u) Pd/C, H_2, RT, 16 h (94%); v) $Et_3N \cdot SO_3$ complex, DMF, 55 °C, 16 h, G-25 Sephadex chromatography (90%).

of the levulinoyl function of **11** afforded acceptor **12**, which was then glycosylated with the known glycosyl donor **13**[4c] at low temperature under the same conditions as described for the preparation of **11**. The fully protected pentasaccharide **14** was obtained in a yield of 65% after chromatography. Successive saponification, hydrogenolysis, and sulfation of compound **14** according to described procedures[12, 13] afforded the *O*-methylated/sulfated analogue **15c** in about 76% overall yield. Pentasaccharide **15c**[14] displayed a high αXa-activity of 1025 U mg^{-1} in an amidolytic assay.

In comparison with the synthesis of the analogues of the natural product (e.g. compound **15a**), which requires about 60 steps, this preparation of a biologically active pentasaccharide is much more efficient and opens new perspectives for the development of biologically active heparin-like drugs.

Received: September 30, 1992 [Z 5605 IE]
German version: *Angew. Chem.* **1993**, *105*, 462

[1] U. Lindahl, G. Backstrom, L. Thunberg, *Carbohydr. Res.* **1982**, *100*, 393.
[2] J. Choay, J.-C. Lormeau, M. Petitou, P. Sinay, J. Fareed, *Ann. N. Y. Acad. Sci.* **1981**, *370*, 664.
[3] C. A. A. van Boeckel, T. Beetz, S. F. van Aelst, *Tetrahedron Lett.* **1988**, *29*, 803.
[4] a) G. Jaurand, J. Basten, I. Lederman, C. A. A. van Boeckel, M. Petitou, *Bioorg. Med. Chem. Lett.* **1992**, *2*, 897; b) J. Basten, G. Jaurand, B. Olde-Hanter, M. Petitou, C. A. A. van Boeckel, *ibid.* **1992**, *2*, 901; c) J. Basten, G. Jaurand, B. Olde-Hanter, P. Duchaussoy, M. Petitou, C. A. A. van Boeckel, *ibid.* **1992**, *2*, 905.
[5] A similar synthetic route can be used for a methylated/sulfated analogue which contains 2,3-di-*O*-methyl-substituted uronic acid moieties. The preparation of this compound and others in the series of methylated/sulfated analogues will be published elsewhere.
[6] Apparently the configuration of the glucuronic acid moiety is lower in energy than the corresponding iduronic acid. Epimerization attempts on glucuronic acid model compounds led to little if any of the iduronic acid entities.
[7] P. J. Garegg, H. Hultberg, *Carbohydr. Res.* **1981**, *93*, C10.
[8] C. A. A. van Boeckel, T. Beetz, J. N. Vos, A. J. M. de Jong, S. F. van Aelst, R. H. van den Bosch, J. M. R. Mertens, F. A. van der Vlugt, *J. Carbohydr. Chem.* **1985**, *4*, 293.
[9] R. Eby, S. J. Sondheimer, C. Scheurch, *Carbohydr. Res.* **1979**, *73*, 273.
[10] J. Sakai, T. Takeda, Y. Ogihara *Carbohydr. Res.* **1981**, *95*, 125.
[11] F. J. Urban, B. S. Moore, R. Breitenbach, *Tetrahedron Lett.* **1990**, *31*, 4421.
[12] M. Petitou, P. Duchaussoy, I. Lederman, J. Choay, P. Sinaÿ, J.-C. Jacquinet, G. Torri, *Carbohydr. Res.* **1986**, *147*, 221.
[13] H. Lucas, J. E. M. Basten, T. G. van Dinther, D. G. Meuleman, S. F. van Aelst, C. A. A. van Boeckel, *Tetrahedron* **1990**, *46*, 8207.
[14] ^{1}H NMR data (360 MHz, D_2O, HOD standard): The ^{1}H NMR spectrum of **15c** was completely assigned using 2D-COSY techniques. The following signals are important: unit H: δ = 5.14 (d, J = 3.8 Hz, 1 H, H1), 4.59 (m, 1 H, H3), 3.46 (s, 3 H, OCH_3); unit G: δ = 5.16 (d, J = 5.0 Hz, 1 H, H1), 4.41 (dd, J = 9.0, 5.0 Hz, 1 H, H2), 3.81 (dd, J = 4.2, 9.0 Hz, 1 H, H3), 4.96 (d, J = 3.6 Hz, 1 H, H5); unit F: δ = 5.48 (d, J = 4.0 Hz, 1 H, H1), 4.35 (c, 1 H, H2), 4.59 (c, 1 H, H3); unit E: δ = 4.75 (d, J = 8.1 Hz, 1 H, H1), 3.63 (c, 1 H, H3), 3.80 (t, J = 9.6 Hz, 1 H, H5); unit D: δ = 5.53 (d, J = 3.6 Hz, 1 H, H1), 4.20 (dd, J = 3.6, 10.0 Hz, 1 H, H2), 3.67 (c, 1 H, H3), 3.41 (t, J = 9.6 Hz, 1 H, H4); $[\alpha]_D$ = +39.8 (c = 1.05, H_2O). MS (FAB$^+$): m/z 2013 $[M + Na]^+$, 1991 $[M + H]^+$; MS (FAB$^-$): m/z 1967 $[M - Na]^-$.

A Simple One-Step Synthesis of Symmetrical Thiocrown Ethers and the Molecular Structure of an Unusual Sandwich-like Tetrametallic Silver Thiocrown Ether Complex**

By *Jilles J. H. Edema,* H. Thijs Stock, Jan Buter, Richard M. Kellogg,* Wilberth J. J. Smeets, Anthony L. Spek*, and *Fre van Bolhuis*

Many heavy metal ions are known to complex easily with thiocrown ethers.[1–7] This phenomenon has stimulated wide interest in the design of ion-selective receptors for heavy metals like Ag, Cd, Cu, and Hg,[1–4] which has led to significant improvements in the syntheses of macrocyclic thioethers during the past two decades. In particular, Mo-,[5] Ru-,[6] and Cs-based[7, 8] syntheses along the lines of the 1 + 1 approach depicted in Scheme 1 have allowed the isolation of preparative quantities of the desired macrocycles. The key point in these cyclizations is the experimentally enforced preference for cyclization over polymerization.[7] We now report a new simple method for the one-pot preparation of cyclic oligothioethers, which, in many cases, are formed

[*] Dr. J. J. H. Edema, Prof. Dr. R. M. Kellogg, H. T. Stock, J. Buter
Department of Organic and Molecular Inorganic Chemistry
University of Groningen
Nijenborgh 4, NL-9747 AG Groningen (The Netherlands)
W. J. J. Smeets, Dr. A. L. Spek
Bijvoet Research Center, Department of Crystal and Structural Chemistry
University of Utrecht
Padualaan 8, NL-3584 CH Utrecht (The Netherlands)
F. van Bolhuis
Molecular Structure Center, University of Groningen
Nijenborgh 4, NL-9747 AG Groningen (The Netherlands)

[**] The crystallographic facilities in Utrecht are supported by the Netherlands Foundation for Chemical Research (S. O. N.).

by a 2+2 coupling (Scheme 1, method b). An advantage of this new method, in addition to the good yields, is its applicability in the presence of functional groups such as ketones and alkenes.

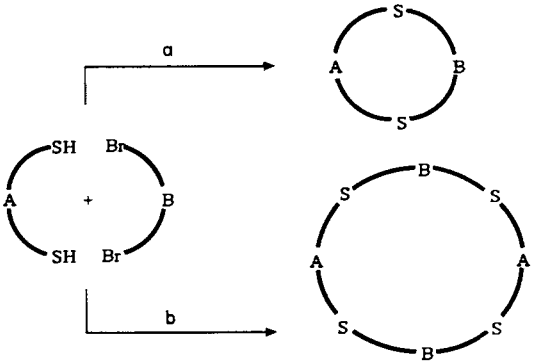

Scheme 1. Syntheses of thiocrown ethers. a) 1+1 approach, for example, with Cs_2CO_3 in dimethylformamide (DMF); b) 2+2 approach with $B(OiPr)_3$/$Al(OiPr_3)$.

Reaction of **1** with 1,3-dibromopropane (**2a**) in THF/alcohol mixtures in the presence of a 5:1 B/Al-alkoxide couple afforded 1,4,7,11,14,17-hexathiaicosane (**3a**) in 52% yield. In contrast the corresponding 10-membered ring system (the 1+1 product) is formed exclusively by the reaction of the Cs salt of **1** with **2a** in DMF;[7d] **3a** was contaminated with only traces of the 1+1 product.

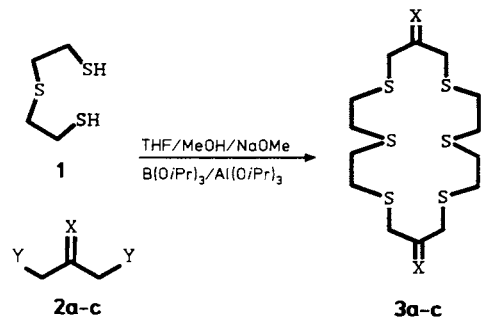

a, X = H_2, Y = Br, **b**, X = O, Y = Cl, **c**, X = CH_2, Y = Cl

Somewhat in contrast to the above results, the analogous reaction of **1** with 1,4-dibromobutane gave rise to the formation of a 1:4 mixture of 11- and 22-membered (1+1 and 2+2 products, respectively) rings.[10] The ratios of the products were determined by ^1H NMR and ^{13}C NMR spectroscopy. The 1+1 products (S_3-cyclophanes) are formed exclusively in yields of 85% or higher from the reaction of **1** with *ortho, metha*, and *para*-α,α'-xylylene dibromides.[11]

The molecular structure of **3a** is illustrated in Figure 1. The molecule is centrosymmetric; the sulfur atoms adopt an overall *anti* arrangement with respect to each other and point away from the molecular cavity. This arrangement is found in most large macrocyclic thioethers containing S-C-C-S linkages.[1, 7-9]

The reactions of **1** with 1,3-dichloroacetone (**2b**) or 3-chloro-2-(chloromethyl)propene (**2c**) proceed essentially as with (**2a**), leading to the formation of 9,19-dioxo-1,4,7,11,14,17-hexathiaicosane (**3b**) and 9,19-dimethylene-1,4,7,11,14,17-hexathiaicosane (**3c**) in 42 and 67% yields

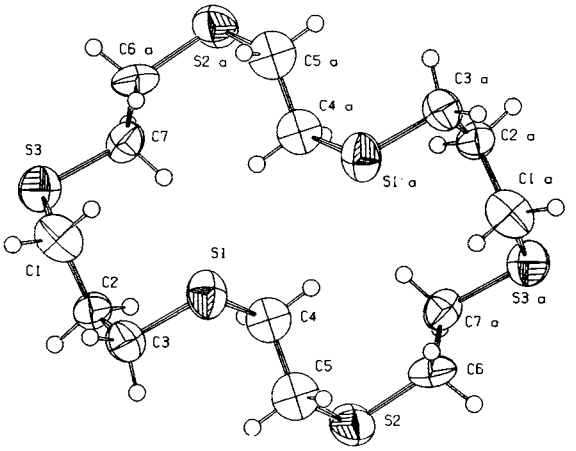

Fig. 1. Molecular structure of **3a** (thermal ellipsoids for 50% probability). Selected dihedral angles [°]: S1-C4-C5-S2 176.2(11), S2-C6-C7a-S3a −175.2(6), S3-C1-C2-C3 164.0(10) [15].

(non-optimized), respectively. Only minor quantities (<5%) of 1+1 products could be detected.

The molecular structure of **3b**, as determined by us, is shown in Figure 2. The highly symmetrical molecule possesses an inversion center. As in **3a**, the sulfur atoms point away from the molecular cavity, but the two carbonyl groups point inward into the cavity. As found for **3a** and other large cyclic oligothioethers, the S-C-C-S linkages are nearly perfectly *anti*:[1-4, 8, 9, 12] The dihedral S-C-C-S angles have values ranging from 175 to 177° and these compare well with those found in **3a**. During the course of the investigations reported here, we became aware of an alternative synthesis and solid-state structure of **3b** (in 6% yield) reported by Setzer et al.[13]

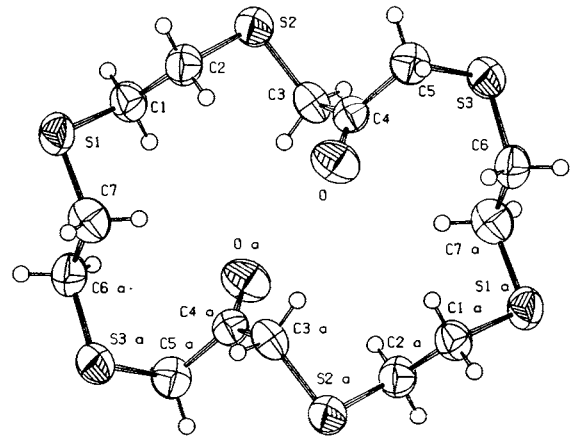

Fig. 2. Molecular structure of **3b** (thermal ellipsoids for 50% probability). Selected dihedral angles [°]: S1-C1-C2-S2 −176.3(2), S3-C6-C7a-S1a 175.7(2), O-C4-C5-S3 108.3(4), S2-C3-C4-O 104.4(4) [16].

Suitable crystals of the free ligand **3c** have not yet been obtained. Comparison of the spectroscopic data of **3c** with those of a sample prepared by an unambiguous multistep synthesis employing Cs thiolates, established the 2+2 composition of **3c**; this was further confirmed by mass spectrometry.

The mechanism of cyclization is unclear. Aggregates involving B and Al dithiolates are thought to form under the conditions used. Understanding of the nature of this aggre-

gate structure is necessary before the factors that determine 1+1 or 2+2 cyclization can be defined. Experiments with 1+1 products in the presence of the B/Al alkoxido couple indicated no trace of interconversion into 2+2 products.

It has recently been reported that in the presence of the Lewis acid $BF_3 \cdot Et_2O$, 1,4-dihydro-2,3-benzodithiin reacts with alkenes to form mixtures of 2+2 and 1+1 products.[14]

Complexation of **3b** with $Ag(CF_3SO_3)$ in THF/MeCN proceeds smoothly and forms irreversibly the tetracation $[(\mathbf{3b})_2Ag_4]^{4+}$ as the $CF_3SO_3^-$ salt, in the form of colorless crystals. From conductometric titration experiments[19] in MeCN, the direct formation of 2:4 adducts was established without detectable formation of 1:1 adducts. Furthermore, conductometric experiments with preformed salt established that the $[(\mathbf{3b})_2Ag_4]^{4+}$ fragment is stable in solution. The sandwich-like structure probably prevents nucleophilic attack of solvent molecules at the metal centers.

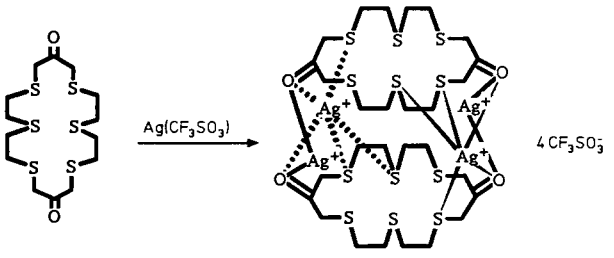

3b $[(\mathbf{3b})_2Ag_4](CF_3SO_3)_4$

The molecular structure of $[(\mathbf{3b})_2Ag_4](CF_3SO_3)_4$ has been established by X-ray diffraction methods (Fig. 3). The cation is centrosymmetric and consists of four Ag^+ ions that are arranged in a quadrangular fashion. The two thiocrown ethers are positioned above and below the Ag_4 plane. The four $CF_3SO_3^-$ ions are placed rather loosely around the molecular core of the cation without any significantly short Ag–O contacts in accord with the results of the conductometric experiments.

The thioether ligand is slightly folded as a result of coordination to the silver ions. In contrast with free **3b** the sulfur atoms are arranged *gauche* to each other (S-C-C-S angles ranging from 60–120°). Thus a major conformational rearrangement occurs on complexation.

The Ag–S bond lengths are reasonably similar and range from 2.52 to 2.61 Å, and thus compare well with those found in other Ag^+–thiocrown ether complexes and related compounds.[1, 2, 5, 6, 7d, 12]

The simultaneous bridging coordination of the carbonyl groups to the two Ag^+ ions is unexpected. The Ag–O bond lengths range from 2.56 to 2.76 Å and are comparable with those in the closely related Ag^+ complexes of 3-oxo-1,4,8,11-tetrathiacyclotetradecane[6] and 3-oxo-1,5-dithiacycloheptane.[12]

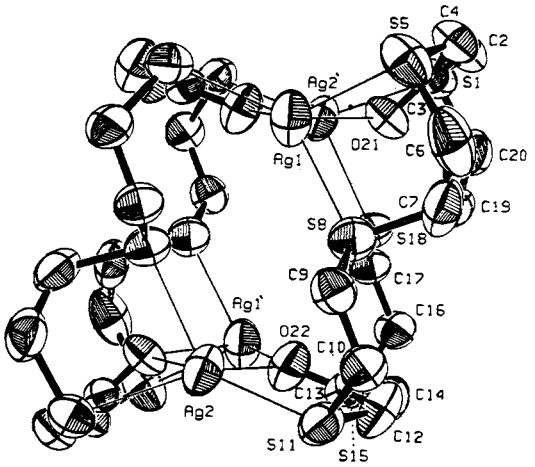

Fig. 3. Molecular structure of the cation in $[(\mathbf{3b})_2Ag_4](CF_3SO_3)_4$ (thermal ellipsoids for 50% probability). Selected bond lengths [Å] and angles [°]: Ag2'-O21 2.817(3), Ag2-O22 2.669(3), Ag1-O21 2.175(3), Ag1'-O22 2.527(3); S1-C2-C3-C4 −171.90(30), S1-C2-C3-O21 8.6(6), S5-C6-C7-S8 −60.07(47), S8-C9-C10-S11 −66.18(36), S15-C16-C17-S18 67.83(37), S18-C19-C20-S1 59.43(45), S11-C12-C13-O22 18.45(5), S11-C12-C13-C14 −161.73(32), O21-C3-C4-S5 −6.35(57) [17].

Experimental Procedure

$Ag(CF_3SO_3)$, **1**, **2a**, **2b**, **2c**, and MeCN (HPLC grade) were purchased from Aldrich and used without further purification. ^1H NMR and ^{13}C NMR spectra were recorded on a Varian 200 MHz spectrometer. IR spectra were obtained from a Perkin Elmer 768 spectrophotometer.

Synthesis of **3a** as a typical example: To a solution of $B(OiPr)_3$ (5 mmol) in THF (250 mL) was added $Al(OiPr)_3$ (1 mmol) and MeOH (40 mL). The mixture was refluxed for 30 min, after which Na (20 mmol) was added. The mixture was then refluxed until the sodium had dissolved. After the mixture had been cooled to 20 °C, **1** (10 mmol) was introduced over 15 min. The solution was subsequently refluxed again for 60 min. The mixture was kept at reflux and a solution of **2a** (10 mmol) in THF (75 mL) was added dropwise over a period of 8–10 h. After the addition was complete, the stirring was continued for 4 h. The mixture was evaporated to dryness and the residue was redissolved in CH_2Cl_2. The organic layer was washed with brine to remove the borate and aluminum salts. The solvent was removed in vacuo and the residual solid was chromatographed over silica gel with CH_2Cl_2/hexane 2/1 as eluent. The organic layer was evaporated to provide the product, yield 52%. ^1H NMR (200 MHz, $CDCl_3$, 25 °C): δ = 1.83 (quint.), 2.66(t), 2.76(m); ^{13}C NMR (50.3 MHz, $CDCl_3$, 25 °C): δ = 29.52(t), 30.62(t), 32.17(t), 32.34(t); IR(KBr): ν[cm^{-1}] = 2950m, 1400s, 1280s, 1210m, 1080s, 920w; MS (70 eV): *m/z* 388.031 (theor. 388.032).

3b: Yield 42%. ^1H NMR (200 MHz, $CDCl_3$, 25 °C): δ = 2.72(s), 3.54(m); ^{13}C NMR (50.3 MHz, $CDCl_3$, 25 °C): δ = 31.17(t), 31.85(t), 37.51(t), 204.01(s); IR (KBr): $\tilde{\nu}$[cm^{-1}] = 2995m, 1734m, 1689s, 1646m, 1558w, 1425s, 1400s, 1393s, 1297s, 1278s, 1255s, 1222m, 1204s, 1195s, 1147s, 1076s, 945s, 890w, 880m; MS (70 eV): *m/z* 416.010 (theor. 416.010).

3c: Yield 53%. ^1H NMR (200 MHz, $CDCl_3$, 25 °C): δ = 2.75(m), 3.33(s), 5.11(s, br); ^{13}C NMR (200 MHz, $CDCl_3$, 25 °C): δ = 31.18(t), 31.83(t), 35.51(t), 115.99(t), 140.87(s); IR (KBr): $\tilde{\nu}$[cm^{-1}] = 2930s, 1719m, 1636m, 1524w, 1425s, 1380w, 1268m, 1230m, 1198s, 1120s, 1020w, 917s, 784m; MS (70 eV): *m/z* 412.051 (theor. 412.051).

$[(\mathbf{3b})_2Ag_4](CF_3SO_3)_4$: To a solution of **3b** (5 mmol) in THF/MeCN (50 mL) was added $Ag(CF_3SO_3)$ (2 mmol) in MeOH (40 mL). The mixture was refluxed for 50 min. The mixture was evaporated to dryness and the residue was redissolved in MeCN. The solution was layered with diethyl ether after which white crystals separated; yield 67%. ^1H NMR (200 MHz, CD_3CN, 25 °C): δ = 2.99 (s, 16H), 3.57(s, 8H); ^{13}C NMR (50.3 MHz, CD_3CN, 25 °C): δ = 33.21(t), 33.62(t), 41.49(t), 214.01(s); IR (KBr): $\tilde{\nu}$[cm^{-1}] = 2995m, 1734m, 1689s, 1646m, 1558w, 1425s, 1400s, 1393s, 1297s, 1278s, 1255s, 1222m, 1204s, 1195s, 1147s, 1076s, 945s, 890w, 880m.

Received: October 26, 1992
Revised version: November 30, 1992 [Z 5650/5651 IE]
German version: *Angew. Chem.* **1993**, *105*, 448

[1] S. C. Rawle, S. R. Cooper, *Struct. Bonding (Berlin)* **1991**, *72*, 1.
[2] a) B. de Groot, S. J. Loeb, *Inorg. Chem.* **1990**, *29*, 4084; b) B. de Groot, H. A. Jenkins, S. J. Loeb, *ibid.* **1992**, *31*, 203; c) B. de Groot, S. J. Loeb, *ibid.* **1989**, *28*, 3573; d) B. de Groot, G. K. H. Shimizu, *J. Chem. Soc. Chem. Commun.* **1991**, 1119; e) B. de Groot, G. R. Giesbrecht, S. J. Loeb, G. K. H. Shimizu, *Inorg. Chem.* **1991**, *30*, 177.
[3] A. J. Blake, E. C. Pasteur, G. Reid, M. Schroeder, *Polyhedron* **1991**, 1546.
[4] A. J. Blake, M. Schroeder, *Adv. Inorg. Chem.* **1990**, *35*, 1.
[5] D. Sellmann, L. Zapf, *Angew. Chem.* **1984**, *96*, 799; *Angew. Chem. Int. Ed. Engl.* **1984**, *23*, 807.
[6] D. Sellmann, F. Knoch, C. Wronna, *Angew. Chem.* **1988**, *100*, 710; *Angew. Chem. Int. Ed. Engl.* **1988**, *27*, 691.
[7] a) J. Buter, R. M. Kellogg, *J. Chem. Soc. Chem. Commun.* **1980**, 466; b) *J. Org. Chem.* **1987**, *46*, 4481; c) *Org. Synth.* **1987**, *65*, 150; d) J. Buter, R. M. Kellogg, F. van Bolhuis, *J. Chem. Soc. Chem. Commun.* **1991**, 910.
[8] B. de Groot, H. A. Jenkins, S. J. Loeb, *Inorg. Chem.* **1992**, *31*, 203.
[9] W. N. Setzer, Y. Tang, G. J. Grant, D. G. VanDerveer, *Inorg. Chem.* **1991**, *30*, 3652.

[10] Considerable amounts of 1,4-dithiane and some tetrahydrothiophene are present as side products. The latter is probably formed as result of intramolecular nucleophilic displacement of tetrahydrothiophene from the intramolecularly cyclized sulfonium ion. See for instance: a) E. S. Gould, *Mechanism and Structure in Organic Chemistry*, Holt, Rinehart, and Winston, New York, **1959**, p. 572, and references cited therein; b) L. A. Ochrymowycz, C. P. Mak, J. D. Michna, *J. Org. Chem.* **1974**, *39*, 2079.

[11] The structure of the cyclization product of para-α,α'-xylylene dibromide with **1** has been confirmed unambiguously by X-ray crystallography after molecular weight determinations indicated an 1+1 structure for all the cyclization products of **1** with the xylylene dibromides, J. J. H. Edema, H. T. Stock, J. Buter, R. M. Kellogg, A. L. Spek, W. J. J. Smeets, unpublished.

[12] J. J. H. Edema, J. Buter, R. M. Kellogg, F. van Bolhuis, *Inorg. Chem.*, submitted.

[13] W. N. Setzer, E. Cacioppo, E. G. Grant, R. S. Glass, *Phosphorus Sulfur Silicon* **1989**, *45*, 223.

[14] R. Sato, J. Kumagai, K. Yonesaka, S. Sato, *Tetrahedron Lett.* **1992**, *33*, 947.

[15] Crystal data for **3a**: $C_{14}H_{28}S_6$, $M = 388.77$, monoclinic space group $C2/c$, $a = 22.485(4)$, $b = 5.4334(10)$, $c = 17.894(3)$ Å, $\beta = 117.63(2)^\circ$, $V = 1936.9(7)$ Å^3, $Z = 4$, $\rho_{calcd} = 1.333$ g cm^{-3}, $\mu(Mo_{K\alpha}) = 6.7$ cm^{-1}. Data were collected on a CAD 4 ($Mo_{K\alpha}$, Zr-filtered, $\theta_{max} = 27.5^\circ$) for a colorless transparent crystal. The structure was solved with the TREF option of the SHELXS-86 program. An empirical absorption correction was carried out with DIFABS. The structure was refined by full-matrix least-squares on F with SHELX-76. A disorder model was used to describe a 53:47 conformational disorder in part of the ring. Convergence was reached at $R = 0.078$ ($R_w = 0.053$, $w^{-1} = \sigma^2(F) + 0.000043F^2$) for 592 reflections with $I > 2.5\sigma(I)$ [18].

[16] Crystal data for **3b**: $C_{14}H_{24}S_6O_2$, $M = 416.74$, monoclinic space group $P2_1/c$, $a = 10.3406(5)$, $b = 9.3270(4)$, $c = 11.1102(5)$ Å, $\beta = 108.363(3)^\circ$, $V = 1016.98(8)$ Å^3, $Z = 2$, $\rho = 1.361$ g cm^{-3}, $\mu(Mo_{K\alpha}) = 6.5$ cm^{-1}. Data were collected on a CAD 4T with a rotating anode ($Mo_{K\alpha}$, 9 kW, $\theta_{max} = 27.5^\circ$) for a colorless crystal. The structure was solved with DIRDIF92 and refined by full-matrix least-squares on F with SHELX-76 to $R = 0.047$ ($R_w = 0.038$, $w^{-1} = \sigma^2(F)$) for 1395 reflections with $I > 2.5\sigma(I)$ [18].

[17] Crystal data for $[(\mathbf{3b})_2Ag_4](CF_3SO_3)_4$, $M = 930.61$, monoclinic space group $P2_1/n$ (approximate dimensions $0.45 \times 0.20 \times 0.15$ mm), $a = 14.920(1)$, $b = 12.237(2)$, $c = 16.426(1)$ Å, $\beta = 92.12(1)^\circ$, $V = 2996.9(9)$ Å^3, $Z = 4$, $\rho_{calcd} = 2.062$ g cm^{-3}, $\mu(Mo_{K\alpha}) = 19.06$ cm^{-1}. Data were collected on a CAD 4 ($Mo_{K\alpha}$, Zr-filtered, $\theta_{max} = 27.5^\circ$) for a colorless transparent crystal. The structure was solved by direct methods and refined with full-matrix least-squares techniques to $R = 0.043$ and $R_w = 0.042$; $w^{-1} = \sigma^2(F)$ for 4430 reflections $I > 3.0\sigma(I)$ [18] including 361 parameters.

[18] Further details of the crystal structure determinations are available on request from the Director of the Cambridge Crystallographic Data Centre, 12 Union Road, GB-Cambridge CB2 1EZ (UK), on quoting the full journal citation.

[19] a) C. J. Pedersen, H. K. Frensdorff, *Angew. Chem.* **1972**, *84*, 16; *Angew. Chem. Int. Ed. Engl.* **1972**, *11*, 16; b) P. G. Sears, G. R. Lester, L. R. Dawson, *J. Phys. Chem.* **1956**, *60*, 1433.

Structure of Diamagnetic $[W(O\text{-}4\text{-}Me\text{-}C_6H_4)_2Cl_2(PMePh_2)_2]$ and Comparison with Related Paramagnetic 2,6-Diphenylphenoxido Complexes: A Steric Effect on π-Bonding and Electronic Structure**

By *Lauren M. Atagi* and *James M. Mayer**

Sterically demanding ligands have become increasingly important in modern inorganic and organometallic chemistry. Bulky ligands including phosphanes[1] and alkyl, aryl,[2] cyclopentadienyl,[3] alkoxide,[4] aryloxide,[5] amide,[6] and imido groups,[7] to mention just a few, have been utilized in advances ranging from carbon monoxide and arene hydrogenation[3-5] to well-defined olefin metathesis catalysts[7] to the study of multiple bonds between the heavier main group elements.[2] Bulky groups are typically selected for their steric properties, but can have a substantial electronic influence as well. For instance, the five methyl groups in η^5-C_5Me_5 (Cp*) make it a much more electron-donating ligand than η^5-C_5H_5 (Cp).[8] We describe here a new kind of electronic difference between bulky and unencumbered ligands, revealed by a comparison of tungsten(IV) aryloxido complexes $[W(OAr)_2Cl_2(PR_3)_2]$. In the complex with the small *para*-cresolato ligand, a short W–OAr bond is formed, whereas such a close approach is more difficult for the large 2,6-diphenylphenoxido ligand and results in weaker W–O π-bonding. As a result, the complexes have substantially different bond lengths and, most interestingly, different electronic ground states.

The phenoxido and cresolato complexes **1a** and **1b** were prepared by reaction of $[WCl_2(PMePh_2)_4]$ with phenol and

$[W(OPh)_2Cl_2(PMePh_2)_2]$ **1a**

$[W(O\text{-}4\text{-}Me\text{-}C_6H_4)_2Cl_2(PMePh_2)_2]$ **1b**

cresol, respectively.[9] Spectral and analytical data clearly indicate the compositions of the materials and that they are diamagnetic. The ^{1}H, ^{31}P, and ^{13}C NMR spectra are consistent with either all-*trans* (D_{2h}) or *trans-cis-cis* (C_{2v}) structures. We originally favored the latter because similar complexes **2** containing 2,6-diphenylphenoxido ligands were

$[W(O\text{-}2,6\text{-}Ph_2\text{-}C_6H_3)_2Cl_2(PMe_2Ph)_2]$ **2a**

$[W(O\text{-}2,6\text{-}Ph_2\text{-}C_6H_3)_2Cl_2(PMePh_2)_2]$ **2b**

reported by Rothwell and co-workers[5a] to have the all-*trans* configuration and to be paramagnetic (contact shifts in the ^{1}H NMR spectra).

We were therefore surprised when an X-ray crystal structure of **1b**[10] showed it to have the all-*trans* geometry (Fig. 1). Crystals of both **1b** and **2a** contain isolated mole-

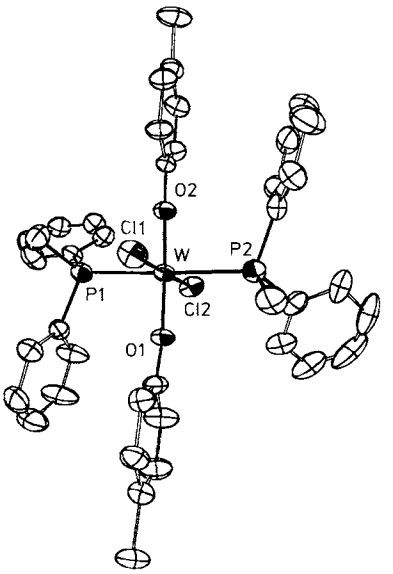

Fig. 1. Crystal structure of **1b** (ORTEP).

[*] Prof. J. M. Mayer, Dr. L. M. Atagi
Department of Chemistry BG-10, University of Washington
Seattle, WA 98185 (USA)

[**] This work was supported by the (U.S.) National Science Foundation. We thank P. Farrall for his work on this system.

cules with close to regular octahedral geometries. The *trans* angles in **1b** are 177.5(3) (O-W-O), 177.5(1) (Cl-W-Cl), and 174.7(1)° (P-W-P), in **2a** they are crystallographically imposed 180° angles; the *cis* angles in both compounds range from 87 to 95°. The bond lengths, however, are quite different (see Table 1 which also contains data for the related tungsten(v) aryloxido complex **3**[5a]). The W–O distances in

$[W(O\text{-}2,6\text{-}Ph_2\text{-}C_6H_3)_2Cl_3(PMe_2Ph)]$ **3**

the cresolato complex **1b** are 0.12 Å shorter than those in the 2,6-diphenylphenoxido complex **2a**, while the W–Cl distances are ≈0.1 Å longer. The W–O bond lengths in **1b** are more comparable to those in the d^1 complex **3** (Table 1). The

Table 1. Bond lengths [Å] and angles [°] of complexes **1b**, **2a**, and **3**.

	1b [a]	**2a** [b]	**3** [b]
W-O	1.848(5), 1.840(5)	1.966(4)	1.853(4), 1.877(4)
W-Cl	2.471(2), 2.440(2)	2.354(2)	2.351(2), 2.356(2), 2.392(2)
W-P	2.526(3), 2.534(3)	2.551(2)	2.579(2)
W-O-C	166.3(6), 171.7(5)	140.0(4)	[c]

[a] This work. [b] Ref. [5a]. [c] Not reported.

W-O-C bond angles are larger in the less crowded *para*-cresolato complex (average 169° in **1b**, 140° in **2a**); Rothwell et al. have shown that this parameter does not correlate with metal–oxygen distance or bond order but is rather primarily the result of steric or packing interactions.[11] The conformation in **1b** may be influenced by π-stacking interactions between the cresolato ligands and phenyl groups of the phosphane ligands, since the phenyl planes are close (3.47(2) and 3.77(2) Å apart, vs. 3.35 Å in graphite) and almost parallel (dihedral angles of 13(2) and 15(2)°).

What is the origin of these structural differences and why are compounds **1** diamagnetic and **2** paramagnetic? These are very similar compounds: **1** and **2b** differ only in their aryloxido ligands, small OPh and O-*para*-tolyl versus 2,6-diphenylphenoxide (**2a** has a slightly different phosphane ligand, PMe_2Ph instead of $PMePh_2$). The fact that the W–O bonds in **1b** are 0.1 Å shorter than those in **2a** suggests a stronger bond in **1b**, most likely due to increased O → W π-bonding.[11] This π-bonding splits the three tungsten d_π orbitals—the octahedral "t_{2g}" set of orbitals that are roughly degenerate in the absence of π interactions. If the O-W-O axis is assigned as the *z* axis, π-donation from the aryloxido ligands raises the level of the d_{xz} and d_{yz} orbitals (Scheme 1). In compounds **1**, this splitting (Δ_π) is enough to cause the electrons to pair in the one nonbonding orbital, d_{xy}. But in **2**, the steric bulk of the aryloxido ligands makes it energetically costly for them to approach the metal closely enough to make strong π bonds, so the splitting Δ_π is smaller and the electrons unpair to give a paramagnetic ground state. This situation is analogous to the classical high-spin/low-spin dichotomy in octahedral d^4–d^7 complexes, except that here π-bonding alone accounts for the splitting within the octahedral t_{2g} manifold. As a result of the large bending of the aryloxido ligands in **2a** (W-O-C 140°) the d_{xz} and d_{yz} orbitals are also split; the O → W π-bonding is concentrated in the one unoccupied orbital and the π-antibonding interaction between the oxygen lone pairs and the unpaired electron in d_{xz} or d_{yz} is minimized. This antibonding interaction may contribute to the long W–O distances in **2a**.[12] In the d^1

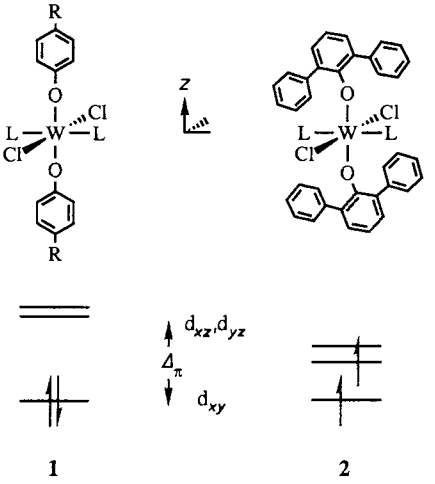

Scheme 1. Qualitative energy level diagram illustrating the splittings of the d_π orbitals in **1** and **2**.

complex **3**, the electron occupies the nonbonding d_{xy} orbital and short W–O bonds are observed.

The key difference between **1** and **2** is *not* that the *para*-cresolato ligand is more electron rich than the 2,6-diphenylphenoxido ligand. Such substituent effects are typically invoked to explain differences between more and less bulky ligands, as in comparisons between Cp and Cp*. But complexes analogous to **1** with 4-phenylphenoxido and 4-bromophenoxido ligands are, like **1**, diamagnetic, even though 4-bromophenoxide is less electron-rich than 2,6-diphenylphenoxide. Similarly, a related tungsten complex with cyclometalated phenylphenoxido ligands (**4**, L = $PMePh_2$) is diamagnetic and has short W–O bonds comparable to those of **1b** because there is little steric penalty for a close approach of the aryloxido oxygen atom to the tungsten center.[13] The essential difference between **1** and

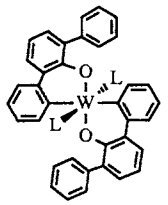

4

2 is that the 2,6-diphenylphenoxido ligand is so bulky that it cannot come close enough to the tungsten center to form strong π bonds. This may be the first clear example of a steric influence on metal–ligand π-bonding.

Experimental Procedure

$[WCl_2(PMePh_2)_4]$ (0.40 g, 0.38 mmol), toluene (17 mL), and *p*-cresol (0.44 g, 4.07 mmol, 11 equivalents) were stirred in a sealed tube at 25 °C for two weeks. The volatiles were removed and the residue washed with pentane and ether to give 0.20 g (61%) **1b**. For ^1H and ^{31}P NMR spectra see ref. [9]. $^{13}C\{^1H\}$ NMR (C_6D_6): δ = 162.2 (s, C-O), 140.0 (t, 20 Hz, *ipso* C-P), 133.5, 131.6, 129.7, 129.2, 116.9 (s, Ph), 20.6 (s, aryl-Me), 15.8 (t, 13 Hz, PMe). Satisfactory C,H,O-analysis.

The 4-phenylphenoxido and 4-bromophenoxido complexes were prepared by addition of $4\text{-}PhC_6H_4OH$ and $4\text{-}BrC_6H_4OH$ to $[WCl_2(PMePh_2)_4]$ in benzene. For $[W(O\text{-}4\text{-}Ph\text{-}C_6H_4)_2Cl_2(PMePh_2)_2]$ ^1H NMR (300 MHz, C_6D_6, 25 °C): δ = 7.5–6.8 (m, 38H), 1.83 (t, 3 Hz, 6H; PMe); ^{31}P NMR: δ = −87.0 (s, $J_{(W,P)}$ = 310 Hz); MS (FAB): *m/z* 995, 993 ($M + H^+$, 70%), 794, 792 ($M^+ - PMePh_2$, 100%). For $[W(O\text{-}4\text{-}Br\text{-}C_6H_4)_2Cl_2(PMePh_2)_2]$ ^1H NMR: δ = 7.60 (m, 8H; PPh_2), 7.06 (d, 9 Hz, 4H; OC_6H_4Br), 6.87 (m, 12H; PPh_2),

6.40 (d, $J = 9$ Hz, 4H; OC_6H_4Br), 1.56 (t, $J = 3$ Hz, 6H; PMe); ^{31}P NMR: $\delta = -104.6$ (s, $J_{(W,P)} = 306$ Hz); MS: m/z 1000, 998 (M^+, 80%), 800, 798 ($M^+ - PMePh_2$, 100%).

Received: October 12, 1992 [Z 5620 IE]
German version: *Angew. Chem.* **1993**, *105*, 455

[1] C. A. Tolman, *Chem. Rev.* **1977**, *77*, 313–348.
[2] A. H. Cowley, N. C. Norman, *Prog. Inorg. Chem.* **1986**, *34*, 1; *Multiple Bonds and Low Coordination in Phosphorus Chemistry* (Eds.: M. Regitz, O. J. Scherer), Thieme, Stuttgart, **1990**; R. West, *Angew. Chem.* **1987**, *99*, 1231; *Angew. Chem. Int. Ed. Engl.* **1987**, *26*, 1201; P. P. Power, *ibid.* **1990**, *102*, 527 and **1990**, *29*, 449; G. Raabe, J. Michl in *The Chemistry of Organosilicon Compounds* (Eds.: S. Patai, Z. Rappoport), Wiley, New York, **1989**.
[3] J. E. Bercaw, H. H. Brintzinger, *J. Am. Chem. Soc.* **1971**, *93*, 2045; P. T. Wolczanski, J. E. Bercaw, *Acc. Chem. Res.* **1980**, *13*, 121–127.
[4] C. C. Cummins, G. D. Van Duyne, C. P. Schaller, P. T. Wolczanski, *Organometallics* **1991**, *10*, 164–170, and references therein; D. R. Neithamer, R. E. LaPointe, R. A. Wheller, D. S. Richeson, G. D. Van Dyne, P. T. Wolczanski, *J. Am. Chem. Soc.* **1989**, *111*, 9056–9072.
[5] For example, see: a) J. L. Kershner, P. E. Fanwick, I. P. Rothwell, *Inorg. Chem.* **1989**, *28*, 780–786; b) J. S. Yu, B. C. Ankianiec, M. T. Nguyen, I. P. Rothwell, *J. Am. Chem. Soc.* **1992**, *114*, 1927–1929; c) M. H. Chisholm, I. P. Rothwell in *Comprehensive Coordination Chemistry, Vol. 2* (Eds.: G. Wilkinson, R. D. Gillard, J. A. McCleverty), Pergamon, New York, **1987**, pp. 335–364.
[6] S. J. Simpson, H. W. Turner, R. A. Andersen, *Inorg. Chem.* **1981**, *20*, 2991–2995; ref. [5c], pp. 161–188.
[7] H. H. Fox, K. B. Yap, J. L. Robbins, S. Cai, R. R. Schrock, *Inorg. Chem.* **1992**, *31*, 2287–2289, and references therein; R. R. Schrock, *Acc. Chem. Res.* **1990**, *23*, 158.
[8] J. L. Robbins, N. Edelstein, B. Spencer, J. C. Smart, *J. Am. Chem. Soc.* **1982**, *104*, 1882–1993; P. G. Gassman, C. H. Winter, *Organometallics* **1991**, *10*, 1592–1598.
[9] S. Jang, L. M. Atagi, J. M. Mayer, *J. Am. Chem. Soc.* **1990**, *112*, 6413–6414.
[10] Crystal data for **1b**: $C_{40}H_{40}Cl_2O_2P_2W$, triclinic, $P\bar{1}$, $a = 11.576(2)$, $b = 11.962(3)$, $c = 15.279(4)$ Å, $\alpha = 88.90(2)$, $\beta = 83.34(2)$, $\gamma = 63.64(2)^\circ$, $V = 1881.8(17)$ Å^3, $Z = 2$. 4639 unique, observed reflections ($I > 3\sigma(I)$) were refined to $R = 0.046$, $R_w = 0.051$ after correction for absorption ($\mu = 33.939$ cm^{-1}) and decay (6.5%). Further details of the crystal structure investigation may be obtained from the Fachinformationszentrum Karlsruhe, Gesellschaft für wissenschaftlich-technische Information mbH, D-W-7514 Eggenstein-Leopoldshafen 2 (FRG), on quoting the depository number CSD-56812, the names of the authors, and the journal citation.
[11] Ref. [5a], J. W. Coffindaffer, I. P. Rothwell, J. C. Huffman, W. Streib, *J. Chem. Soc. Chem. Commun.* **1985**, 1519.
[12] J. M. Mayer, *Comments Inorg. Chem.* **1988**, *8*, 125.
[13] J. L. Kershner, P. E. Fanwick, I. P. Rothwell, *Organometallics* **1988**, *7*, 1871.

A New Photoreaction of γ,δ-Unsaturated Ketones: The Oxadi-π-ethane(ODPE) Rearrangement

By *Johannes Leitich* and *Kurt Schaffner* *

The readily accessible *endo*-Diels–Alder adducts **1** from 1,3-cyclopentadiene and *cis*- or *trans*-1-cyclohexenyl methyl (or phenyl) ketone or methyl vinyl ketone were prepared by us during an investigation of the photochemistry of these ketones.[1] Unexpectedly, we found a novel photoisomerization of **1**, which leads to the strained tricyclo[3.2.0.0][3,6]-heptane framework and, in some cases, occurs in high chemical yields.

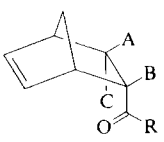

1	A	B	C	R
a	$(CH_2)_4$		H	Ph
b	$(CH_2)_4$		H	Me
c	H	H	H	Me
d	H	$(CH_2)_4$		Me
e	H	$(CH_2)_4$		Ph

[*] Prof. Dr. K. Schaffner, Dr. J. Leitich
Max-Planck-Institut für Strahlenchemie
Stiftstrasse 34–36, D-W-4330 Mülheim an der Ruhr (FRG)

The intramolecular photoreactions of γ,δ-unsaturated ketones known so far include, depending on structural type, oxetane formation,[4, 5] oxa-ene addition,[4] cyclopentane ring closure,[4] β cleavage with the formation of allyl and oxaallyl radicals,[6] and *Z*/*E* isomerization of the C=C bond.[7] Sauers et al. observed the smooth formation of the oxetanes **2** on irradiation of numerous *endo*-bicyclo-[2.2.1]hept-2-en-5-yl-ketones of the type **1** (e.g. of **1c**[8]), and investigated these reactions in detail.[5] Correspondingly, we also found that **2a** and **2b**[9] form in a uniform way from **1a** and **1b**, respectively, on direct irradiation (conditions see Table 1); for **1a** also on triplet sensitization (Scheme 1).

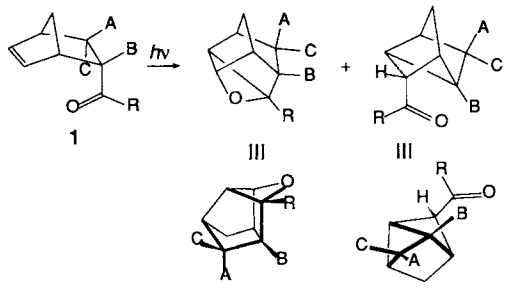

Scheme 1.

However, on triplet sensitization of **1b**, surprisingly, the isomeric ketone **3b** was formed in approximately 60% yield and the expected product **2b** only in about 20% yield. The E_T value (triplet energy in kcal mol^{-1}) of the sensitizer benzonitrile (76.5[10]) indicates an excitation of the C=C bond (norbornene: $72.3 \leq E_T \leq 76$[11]), and not of the C=O bond (E_T value for acetone: 79–82).[12] In contrast to **1b**, under the same sensitization conditions **1c** only slowly formed the oxetane **2c** as the main product in addition to a mixture of undefined by-products. For **1d** and **1e** the formation of products of type **3** predominates: triplet-sensitized **1d** affords exclusively **3d**; on direct irradiation **1d** affords **2d** and **3d** in about equal yields. Finally, **1e**, in sharp contrast to **1a**, exclusively forms **3e** under both sets of conditions. These results are summarized in Table 1.

On direct irradiation **3e** undergoes an efficient secondary photoreaction to give **4** (R = Ph) and **5**; these products are formed in a ratio of 1:1.2. Correspondingly, **3d** is transformed into **4** (R = Me).[13] These secondary photoreactions are prevented completely by addition of the triplet quencher 1,3-pentadiene (1 M); in contrast, the formation of **3** (and **2**) is not influenced by this addition.

The decision whether **1** reacts to give **2** or **3** is influenced by at least three factors: first, by the electronic excitation

Table 1. Products (fractions were determined by ^{1}H NMR spectroscopy; 1.0 = 100% of the treated starting material) after direct irradiation and after triplet sensitization of compounds of the type **1**.

Compound	Direct irradiation [a]		Triplet-sensitized		
1	**2**	**3**	**2**	**3**	Conditions
a	1.0	0.0	1.0	0.0	[b]
b	1.0	0.0	0.2 [c]	0.6	[d]
c	1.0	0.0	0.8 [c]	0.0	[d]
d	0.5	0.5	0.0	1.0	[d, e, f]
e	0.0	1.0	0.0	1.0	[b, f]

[a] $\lambda > 300$ nm; Hg high-pressure lamp, hexane or acetonitrile. [b] Acetophenone as solvent $\lambda > 300$ nm. [c] At present it cannot be excluded that the formation of **2** in these cases is a result of singlet sensitization by benzonitrile and/or the direct absorption of light occurring to < 1%. [d] Benzonitrile in *tert*-butyl alcohol, $\lambda = 254$ nm. [e] Acetone as solvent or acetophenone in benzene, $\lambda > 300$ nm. [f] Benzophenone in benzene, $\lambda > 300$ nm.

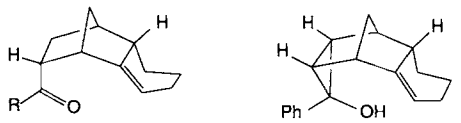

4 **5**

used, as shown by the examples **1b,d**; second, by the degree of alkylation at the C atom from which the acyl group shifts to form ultimately **3**, as shown by the comparison of **1b**/**1c**; third, the proximity of carbonyl C atom to the C=C bond (particularly in **1d,e**) favors the formation of **3**. This particular proximity of carbonyl C atom to the C=C bond in **1d,e** gives rise to a bathochromic shift of the longest wave ($n\pi^*$) UV absorptions by 450–500 cm^{-1} with respect to those of the corresponding hydrogenated ketones (for **1a,b** and **1c** a much smaller shift is observed). It also appears to lead to a large decrease in the energy of the lowest triplet state, as shown by the efficient sensitization of the formation of **3d,e** by benzophenone (E_T = 68.6); by contrast, for the formation of **3b**, benzonitrile (E_T = 76.5) is required.

The designation (in the title) "oxadi-π-ethane" rearrangement for the formation of **3** is derived from the analogy to the "di-π-ethane"[14] and the "oxadi-π-methane" (ODPM) rearrangements. The latter rearrangement, which has been known for a long time,[15] formally differs from the one described herein only by the presence of a second saturated C atom between the C=C and the C=O unit; as a result a 1,3 shift instead of a 1,2 shift of the acyl moiety occurs and a cyclobutane ring closure instead of a cyclopropane ring closure takes place. To our knowledge, a non-allylic 1,3 shift of the acyl moiety has not been observed so far. In addition to the described similarity there is a clear analogy to the ODPM rearrangement with regard to the dependence of the reactivity on the electronically excited state,[15] suggesting that the two rearrangements have similar mechanisms. Thus, the two-step mechanism formulated in Scheme 2, which uses **1e** as an example, is assumed.

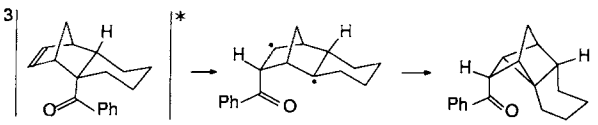

^{3}[**1e**]* **3e**

Scheme 2.

Received: October 15, 1992 [Z 5628 IE]
German version: *Angew. Chem.* **1993**, *105*, 436

[1] **1c** see ref. [8] **1e** see ref. [2]. **1d** see ref. [3].
[2] J. Leitich, I. Heise, S. Werner, C. Krüger, K. Schaffner, *J. Photochem. Photobiol. A* **1991**, *57*, 127–151.
[3] P. E. Eaton, *Acc. Chem. Res.* **1968**, *1*, 50–57.
[4] A. Pascual, N. Bischofberger, B. Frei, O. Jeger, *Helv. Chim. Acta* **1988**, *71*, 374–388, and references therein; J. Berger, M. Yoshioka, M. P. Zink, H. R. Wolf, O. Jeger, *ibid.* **1980**, *63*, 154–190, and references therein.
[5] R. R. Sauers, A. A. Hagedorn, S. D. van Arnum, R. P. Gomez, R. V. Moquin, *J. Org. Chem.* **1987**, *52*, 5501–5505, and references therein; R. R. Sauers, A. D. Rousseau, B. Byrne, *J. Am. Chem. Soc.* **1975**, *97*, 4947–4953, and references therein.
[6] K. J. Crandall, J. P. Arrington, R. J. Watkins, *J. Chem. Soc. Chem. Commun.* **1967**, 1052.
[7] H. Morrison, *J. Am. Chem. Soc.* **1965**, *87*, 932.
[8] R. R. Sauers, W. Schinski, M. M. Mason, *Tetrahedron Lett.* **1969**, 79–82.
[9] The molecular structures and the stereochemistry of all compounds were derived from their 400 MHz ^{1}H and 100 MHz ^{13}C NMR spectra (broad band decoupling, DEPT sequence) including ^{13}C/^{1}H COSY, ^{1}H/^{1}H spin-spin decouplings and NOE spectra. In these spectra all the resonance signals (except the badly resolved ones of the central sections of the tetramethylene bridges) could be assigned unequivocally. In addition, the molecular structure of **3e** was confirmed by a single-crystal X-ray structure analysis (I. Ortmann, C. Krüger, unpublished).
[10] Unless otherwise stated all E_T values are from: S.L. Murov, *Handbook of Photochemistry*, Dekker, New York, **1973**.
[11] T. Ni, R. A. Caldwell, L. A. Melton, *J. Am. Chem. Soc.* **1989**, *111*, 457–464; R. A. Caldwell, University of Texas, Dallas, private communication.
[12] Acetophenone (E_T = 73.7) had no effect as sensitizer; acetone (as solvent, E_T = 79–82) led to a complex mixture, containing no **2b** and only a little **3b**; instead it contained mainly products which seem to have resulted from a hydrogen transfer from acetone to the excited C=C bond.
[13] These reactions are apparently induced by a δ-H abstraction by the oxygen atom of the excited carbonyl group. The resulting 1,5 diradical stabilizes by fragmentation of a strained C–C bond to give a 1,3 diradical, which reacts to give **4** and **5**.
[14] W. C. Schumann, D. B. Vashi, J. A. Ross, R. W. Binkley, *J. Org. Chem.* **1972**, *37*, 21–24.
[15] Reviews: D. I. Schuster in *Rearrangements in Ground and Excited States, Vol. 3* (Eds.: P. DeMayo), Academic Press, New York, **1980**, pp. 232–279; K. Schaffner, *Tetrahedron* **1976**, *32*, 641–653; K. N. Houk, *Chem. Rev.* **1976**, *76*, 1–74; see also: M. J. C. M. Koppes, H. Cerfontain, *Recl. Trav. Chim. Pays-Bas* **1988**, *107*, 549–562; T. J. Eckersley, N. A. J. Rogers, *Tetrahedron* **1984**, *40*, 3759–3768, and references therein; D. E. Sadler, J. Wendler, G. Olbrich, K. Schaffner, *J. Am. Chem. Soc.* **1984**, *106*, 2064–2071; Review on synthetic applications: M. Demuth, *Org. Photochem.* **1991**, *11*, 37–109.

Organometallic Titanium Complexes with Unpaired Electrons: Syntheses and Structures of $[\{(\eta^5\text{-Cp})_2TiF_2\}_3Ti]$ and $[\{(\eta^5\text{-Cp}')_2TiF_2\}_3Al]$**

By *Feng-quan Liu, Heinz Gornitzka, Dietmar Stalke,* and *Herbert W. Roesky**

Dedicated to Professor Jean'ne M. Shreeve on the occasion of her 60th birthday

The polynuclear titanium complexes previously reported[1] all contain titanium in its highest oxidation state. Well-known paramagnetic d^1 electron systems such as $[\{Cp(C_5H_4)TiOH\}_2]$[2] (Cp = η^5-C_5H_5), $[\{Cp_2Ti(\mu\text{-}H)_2\}_2AlCl]$,[3] $[\{Cp_2TiX\}_2ZnX_2]$[4] (X = Cl, Br), or $[\{Cp_2TiCl\}_2MnCl_2]\cdot 2OC_4H_8$[5] are formed with a maximum of two titanium atoms. All these complexes have oxo, hydrido, chloro, or bromo bridging ligands. Since fluorine atoms have a marked tendency to form bridges, the syntheses of the corresponding fluorotitanium complexes should be possible.[6]

The reaction of $[Cp_2Ti(CO)_2]$[7] with $[Cp_2TiF_2]$[8] in a 1:1 ratio leads to the formation of the complexes **1** and **2**[9] (Scheme 1), as well as brown insoluble precipitate. Com-

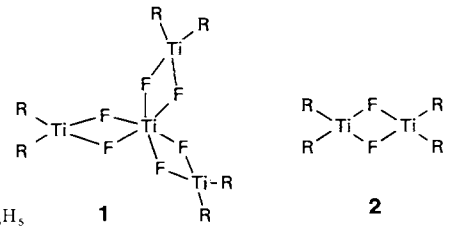

Scheme 1. R = η^5-C_5H_5 **1** **2**

[*] Prof. H. W. Roesky, Dr. F. Liu, Dipl.-Chem. H. Gornitzka, Dr. D. Stalke
Institut für Anorganische Chemie der Universität
Tammannstrasse 4, D-W-3400 Göttingen (FRG)

[**] This work was supported by the Deutsche Forschungsgemeinschaft, the Volkswagenstiftung, and the Fonds der Chemischen Industrie. We would like to thank D. F. Koch (Riedel-de-Haen, Seelze, FRG) for supplying the perfluorinated polyethers for the crystal application.

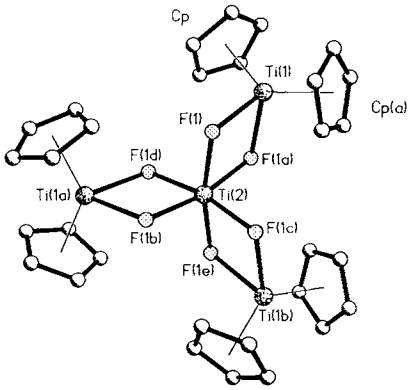

Fig. 1. Molecular structure of **1**. Selected distances [pm] and angles [°]: Ti2-T1 197.5(1), Ti1-F1 209.4(1), Ti1-Cp 204.4(1); F1-Ti2-F1a 76.18(6), Ti2-F1-Ti1 106.34(5), F1-Ti1-F1a 71.15(6), Cp-Ti1-Cp(a) 135.8; the planes of the three four-membered Ti_2F_2 propeller blades intersect with an angle of 86.5°.

pound **1** crystallizes as blue crystals, whereas those of the known complex **2** are green. The X-ray structure analysis[10] reveals the characteristic structural feature of complex **1**; a distorted octahedral TiF_6 moiety at the central Ti2 atom (Fig. 1).

We replaced the central Ti atom with aluminum because for the latter the formation of an octahedral AlF_6 group is particularly favored. Indeed, $[Cp_2TiF_2]$ or $[Cp'_2TiF_2]$ ($Cp' = \eta^5$-C_5H_4Me) reacts with activated aluminum to give the compounds **3** and **4**, respectively (Scheme 2). The blue

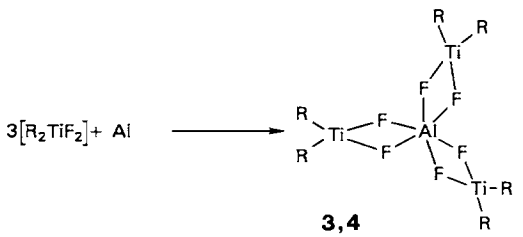

Scheme 2. **3**: R = η^5-C_5H_5; **4** = η^5-C_5H_4Me.

complex **3** is slightly soluble in THF and toluene, and as expected **4** is more soluble in these solvents.

The structure of **4** was determined by X-ray structure analysis (Fig. 2) and found to be isostructural with that of **1**. The

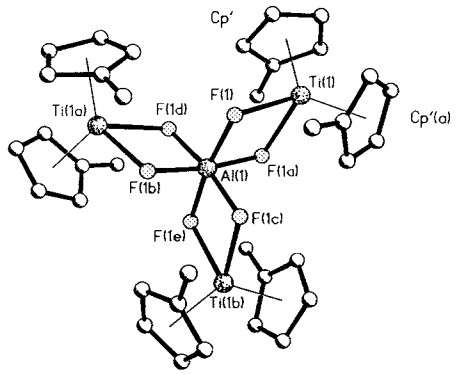

Fig. 2. Molecular structure of **4**. Selected distances [pm] and angles [°]: Al1-F1 181.2(2), Fi1-F1 209.5(2), Ti1-Cp 204.2(1), F1-Al1-F1a 80.91(10), Al1-F1-Ti1 105.40(8), F1-Ti1-F1a 68.29(9), Cp-Ti1-Cp(a) 134.3; the planes of the three four-membered $AlTiF_2$ propeller blades intersect with an angle of 86.9°.

four-membered Ti_2F_2 (**1**) and $AlTiF_2$ (**4**) rings in the two structures are unsymmetrical [**1**: Ti2–F1 197.5(1), Ti–F1 209.4(1) and **4**: Al1–F1 181.2(2), Ti1–F1 209.5(2) pm]; the octahedral coordination of the central atoms Ti2 and Al1, respectively is significantly distorted, and they are surrounded by the four-membered rings (Ti_2F_2 and $AlTiF_2$) in a propeller-like manner. The "propeller blade angle" between the planes of the four-membered rings is 86.5° in **1** and 86.9° in **4**. Because of the distortion of these rings [**1**: F1-Ti2-F1a 76.18(6)° and Ti2-F1-Ti1 106.34(5)°; **4** F1-Al1-F1a 80.91(10)° and Al1-F1-Ti1 105.40(8)°] a metal–metal bonding interaction can be excluded (**1**; Ti1 ··· Ti2 325.77(10); **4**: Al1 ··· Ti1 311.3(2) pm). A comparable nonbonding Ti ··· Ti distance of 319.5(4) pm was found in $[\{Cp(C_5H_4)TiOH\}_2]$.[2, 10] A similar coordination to the aluminum atom in **4** was found in $[\{(Me_3Si)_2N\}_2Al(NH_2)_2\}_3Al]$.[11]

The ESR spectra of the complexes **1** and **4** confirm the paramagnetic behavior. In toluene a very broad resonance signal is observed for each compound;[12] similar observations were made for $[\{Cp_2TiCl_2\}_2Zn]$.[4] Although, organometallic titanium and zirconium compounds, in combination with aluminum compounds, are mainly used as catalysts in the polymerization of olefins, very little is known to date about their interactions.[13, 14] Compounds **1**, **3**, and **4** are interesting examples of the symbiosis of classical Werner coordination and organometallic chemistry.

Experimental Procedure

1: A mixture of $[Cp_2Ti(CO)_2]$ (0.35 g, 1.5 mmol) and $[Cp_2TiF_2]$ (0.33 g, 1.5 mmol) in THF (50 mL) was stirred for 24 h at room temperature and 6 h at 70 °C. The solution turned green. After removal of the solvent and the volatile reaction products under vacuum the residue was crystallized from a hexane/THF (1:1) mixture. A brown amorphous solid remained. Blue crystals of **1** (0.11 g, 0.14 mmol) formed from the solution and subsequently green crystals of **2** [9] (0.23 g, 0.58 mmol). **1**: M.p. > 310 °C (decomp), MS(EI) *m/z* 197 (Cp_2TiF) biggest fragment; IR (Nujol) $\tilde{\nu}[cm^{-1}]$ = 3108, 1024m, 1012m, 804s, 498s, 405s; correct elemental analysis of $C_{30}H_{30}F_6Ti_4 \cdot C_4H_8O$ (768.2).

2: M.p. > 228 °C (decomp) MS(EI) *m/z* 216 (Cp_2TiF_2), 197 (Cp_2TiF). IR (Nujol): $\tilde{\nu}[cm^{-1}]$ = 3091m, 1093m, 793st, 471s; weak bands are not reported.

3: A solution of $[Cp_2TiF_2]$ (0.43 g, 2 mmol) in THF (50 mL) was added to Al (0.2 g) and stirred for 40 h at room temperature. A green solution and a blue solid were formed. The solution was filtered and the solid was extracted with toluene (50 mL). Yield of **3** 0.25 g (55%). M.p. > 320 °C (decomp) IR (Nujol) $\tilde{\nu}[cm^{-1}]$ = 3100m, 1017m, 800s, 617m, 552m, 397m; correct elemental analysis for $C_{30}H_{30}AlF_6Ti_3$ (675.2).

4: $[Cp'_2TiF_2]$ (0.5 g, 2 mmol) was dissolved in THF (50 mL) and treated with aluminum (0.1 g). The mixture was stirred for 2 d at room temperature, during which time the solution turned dark green. After the solution had been filtered the solvent was removed under vacuum. The residue was crystallized from hexane/THF (1:1); yield of **4** 0.35 g (70%). M.p. > 172 °C (decomp), IR (Nujol): $\tilde{\nu}[cm^{-1}]$ = 3119m, 1498m, 1353m, 1027m, 899m, 861m, 814m, 789m, 582s, 541m, 446s, 405m; correct elemental analysis for $C_{36}H_{42}AlF_6Ti_3$ (759.3).

Received: September 19, 1992 [Z 5583 IE]
German version: *Angew. Chem.* **1993**, *105*, 447

[1] *Gmelin Handbook of Inorganic Chemistry, Organotitanium Compounds, part 1–5*, Springer, Berlin, **1977–1990**; *Comprehensive Organometallic Chemistry, Vol. 3* (Eds.: G. Wilkinson, F. G. A. Stone, E. W. Abel), Pergamon, Oxford, **1982**.
[2] L. J. Guggenberger, F. N. Tebbe, *J. Am. Chem. Soc.* **1976**, *98*, 4137.
[3] A. I. Sizov, I. V. Molodniskaya, B. M. Bulychev, E. V. Evdokimova, G. L. Soloveichik, A. I. Guser, E. B. Chuklanova, V. I. Adrianov, *J. Organomet. Chem.* **1987**, *335*, 323.
[4] D. Gourier, D. Vivien, E. Samuel, *J. Am. Chem. Soc.* **1985**, *107*, 7418.
[5] D. Sekutowski, R. Jungst, G. D. Stucky, *Inorg. Chem.* **1978**, *17*, 1848.
[6] M. Witt, H. W. Roesky, *Prog. Inorg. Chem.* **1992**, *40*, 353.
[7] B. Demerseman, G. Bouquet, M. Biqorgne, *J. Organomet. Chem.* **1975**, *101*, C24.
[8] P. M. Druce, B. M. Kingston, M. F. Lappert, T. R. Spalding, R. C. Srivastava, *J. Chem. Soc. A* **1969**, 2106.

[9] R. S. P. Coutts, P. C. Wailes, R. L. Martin, *J. Organomet. Chem.* **1973**, *47*, 375. $[Cp_2TiF]_2$ was prepared by the reduction of $[Cp_2TiF_2]$ with aluminum.

[10] Crystal Data: **1** crystallized with one molecule THF: $C_{30}H_{30}F_6Ti_4 \cdot C_4H_8O$, $M = 768.3$, rhombohedral, space group $R\bar{3}c$, $a = b = 16.174(2)$, $c = 21.371(5)$ Å, $V = 4841.6$ Å^3, $Z = 6$; $\rho_{calcd} = 1.581$ Mgm^{-3}, $F(000) = 2352$, $\lambda = 0.71073$ Å, $T = 153$ K, $\mu(Mo_{K\alpha}) = 1.02$ mm^{-1}. Data were collected on a Stoe-Siemens-AED diffractometer. Intensities of a rapidly cooled crystal (dimensions $0.3 \times 0.4 \times 0.3$ mm) in an oil drop were collected by the $2\theta/\omega$ method in the range $8° \leq 2\theta \leq 55°$. Of the 4551 collected reflections 1245 were independent and corrected for absorption and 1049 observed with $F_0 > 4\sigma(F_0)$. 118 parameters were refined on F^2 with all data (SHELXL-92) [15]. Largest difference maximum and minimum: 0.29 and -0.26 eÅ^{-3}, respectively, $R1 = 0.029$ and $wR2 = 0.080$ (all data). – **4**: $C_{36}H_{42}AlF_6Ti_3$, $M = 759.3$, rhombohedral, space group $R\bar{3}c$, $a = b = 16.549(5)$, $c = 20.912(11)$ Å, $V = 4959.9$ Å^3, $Z = 6$; $\rho_{calcd} = 1.525$ Mgm^{-3}, $F(000) = 2346$, $\lambda = 0.71073$ Å, $T = 153$ K, $\mu(Mo_{K\alpha}) = 0.79$ mm^{-1}, data were collected on a Stoe-Siemens-AED diffractometer. Intensities of a rapidly cooled crystal (dimensions $0.4 \times 0.4 \times 0.3$ mm) in an oil drop were collected by the $2\theta/\omega$ method in the range of $8° \leq 2\theta \leq 45°$. Of a total of 1415 reflections 725 were independent and corrected for absorption and 594 were observed with $F_0 > 4\sigma(F_0)$. 72 parameters were refined on F^2 with all data (SHELXL-92) [15]. Largest difference maximum and minimum: 0.22 and -0.50 eÅ^{-3}, respectively, $R1 = 0.033$ and $wR2 = 0.90$ (all data). Both structures were solved with direct methods (SHELXS-90) [16] and refined by full-matrix least-squares of F^2 (SHELXL-90) [15]. Further details of the crystal structure investigations are available on request from the Director of the Cambridge Crystallographic Data Centre, 12 Union Road, GB-Cambridge CB2 1EZ (UK), on quoting the full journal citation.

[11] K. J. L. Paciorek, J. H. Nakahara, L. A. Hoferkamp, C. George, J. L. Flippen-Anderson, R. Gilardi, W. R. Schmidt, *Chem. Mat.* **1991**, *3*, 82.

[12] Examinations carried out by Dr. Marsh, Max-Planck-Institut, Göttingen.

[13] H. Sinn, W. Kaminsky, *Adv. Organomet. Chem.* **1980**, *18*, 99.

[14] W. Kaminsky, K. Külper, H. H. Brintzinger, F. R. W. P. Wild, *Angew. Chem.* **1985**, *97*, 507; *Angew. Chem. Int. Ed. Engl.* **1985**, *24*, 507.

[15] G. M. Sheldrick, Universität Göttingen **1992**.

[16] G. M. Sheldrick, *Acta Crystallogr.* **1990**, *A46*, 467.

BOOKS

This section contains book reviews and a list of new books received by the editor. Book reviews are written by invitation from the editor. Suggestions for books to be reviewed and for book reviewers are welcome. Publishers should send brochures or (better) books to the Book Editor, Dr. Gerhard Karger, Redaktion Angewandte Chemie, Postfach 101161, D-W-6940 Weinheim, Federal Republic of Germany. The editor reserves the right of selecting which books will be reviewed. Uninvited books not chosen for review will not be returned.

Book Reviews

Following the Trail of Light: A Scientific Odyssey. (Series: Profiles, Pathways, and Dreams. Series editor: *J. I. Seeman.*) By *M. Calvin.* American Chemical Society, Washington, DC, 1992. XXIII, 175 pp., hardcover $ 24.95.—ISBN 0-8412-1828-5

As a young assistant professor enamoured of coordination chemistry, I had occasion to refer frequently to Professor Calvin's 1952 monograph *Chemistry of the Metal Chelate Compounds* (coauthored with Arthur E. Martell). Therefore I regarded Calvin as an inorganic chemist. When he was awarded the 1961 Nobel Prize in chemistry "for his research on the carbon dioxide assimilation in plants", I began to think of him as an organic chemist. After reading his latest book, I have come to realize that this multidisciplinary scientist defies categorization. In explaining the book's title, "Following the Light", he states "The word 'light' was not meant in its literal sense, but in the sense of following an intellectual concept or idea to where it might lead" (p. 134). In promoting this goal, he assembled in his laboratory "scientists whose disciplines ranged from psychology to botany, from organic photochemistry to chemical evolution" (p. xxii).

Born on April 8, 1911 in St. Paul, Minnesota of emigrant parents (father from Lithuania; mother from Russian Georgia) of limited financial means, Calvin showed an early interest in science, dismantling his toys and reassembling them after understanding how they worked. The family moved to Detroit, Michigan, where he attended high school. With the aid of a scholarship he attended the Michigan College of Mining and Technology (now Michigan Technological University) but interrupted his studies there for a year to earn money as an analyst in a brass factory to continue his education. After receiving his B. S. degree in chemistry (1931) he worked on the electron affinity of halogen atoms under George C. Glockler at the University of Minnesota, from which he received his Ph.D. degree (1935). He spent the academic years 1935–1937 at the University of Manchester in England, where he worked on coordination catalysis, activation of molecular hydrogen, and metalloporphyrins with chemist, political scientist, economist, and philosopher Michael Polanyi, who introduced him to the advantages of the interdisciplinary approach to science that was to characterize Calvin's scientific career. In 1937, at the invitation of Gilbert Newton Lewis, whose intuitive approach to science also exerted a great influence on him, Calvin became an Instructor at the University of California, Berkeley, the first chemist not a UC graduate to be hired since 1912. He has remained at Berkeley ever since and is now University Professor of Chemistry.

Calvin's collaboration with G. E. K. ("Gerry") Branch resulted in the publication of *The Theory of Organic Chemistry* (1941), the first book on the subject written in the United States to employ quantum mechanics. Its publication marked the advent of theoretical organic chemistry in the United States and made Berkeley one of its foremost centers. The World War II years saw his work on the use of cobalt complexes that reversibly bond with molecular oxygen applied to an oxygen-generating machine for destroyers or submarines. He also became involved in the Manhattan Project, applying his expertise in chelation and solvent extraction to the problems of decontaminating (purifying) the irradiated uranium in fission products and isolating and purifying plu-

 © VCH Verlagsgesellschaft mbH, W-6940 Weinheim, 1993 0570-0833/93/0303-0444 $ 10.00+.25/0

tonium. In 1942 he married Genevieve Jemtegaard, with whom he had two daughters and a son. Following the death of their first child because of R_h incompatibility, he collaborated with his wife to determine the chemical factors causing this problem. After the 1973 oil embargo the two worked together to seek plants, such as those of the genus *Euphorbia*, that would convert solar energy to hydrocarbons to be used as fuels, an area of research in which Calvin is still active.

When the radioisotope carbon-14 became available, Calvin, in 1946, begin his Nobel-winning work on tracing the path of carbon in photosynthesis. Simultaneously he investigated the electronic, photoelectronic, and photochemical behavior of porphyrins; molecular genetics; chemical evolution and organic geochemistry, including examination of organic constituents of lunar rocks; free radicals in reactions; the effect of deuterium in biological reactions; chemical and viral carcinogenesis; and artificial photosynthesis ("synthetic chloroplasts"). Calvin discusses all these topics as well as those previously mentioned. The history of the Bio-Organic Chemistry Group is related, from its inception in 1945 through its move to the new Laboratory of Chemical Biodynamics (1964) and, following Calvin's retirement as director in 1980, its present activity as the Melvin Calvin Laboratory, one of the world's first and foremost interdisciplinary laboratories. Calvin's numerous awards, honors, services, memberships, consultantships, books, and family relationships are discussed. The Nobel Prize ceremonies are described in detail by his wife, who died of cancer in 1987.

The book abounds with many of the maxims for which Calvin is justly famous, e.g., "It is better to act in relative ignorance than not to act at all" and "We are here to learn, and as chemists we can learn better than most". In addition to structural formulas, equations, reaction schemes, and figures, it contains 52 illustrations—not only formal photographs and informal snapshots but also congratulatory telegrams from the Nobel Foundation Secretary and U.S. President John F. Kennedy, as well as building plans (the circular Laboratory of Chemical Biodynamics, colloquially referred to as the "Round House" or "Calvin Carousel", with open laboratories, many windows, and few walls was specifically designed to promote Calvin's research philosophy of interaction, discussion, and cooperation). The volume is a gold mine of scientific and autobiographical data lacking in most scientific articles; Calvin even recollects the exact moment when his sudden insight into the cyclic character of the path of carbon in photosynthesis occurred (he was sitting at the wheel of his car waiting for his wife) (p. 68). Although scrupulously documented (101 numbered references, many of which are multiple ones), the book is eminently readable. A 12-page (2 columns per page) index facilitates access to specific information. I heartily recommend these engrossing memoirs of a fascinating, multifaceted scientific pioneer to scientists, historians of science, and all persons interested in research and its practice.

George B. Kauffman
California State University
Fresno, CA (USA)

Semiclassical Mechanics with Molecular Applications. (International Series of Monographs on Chemistry, Vol. 25.) By *M. S. Child.* Oxford University Press, Oxford, 1991. X, 417 pp., hardcover £ 50.00.—ISBN 0-19-855654-3

To come straight to the point, this (long overdue!) monograph by Child meets the needs of theoretical chemists and molecular physicists who want a thorough, modern treatment of this important borderline area between classical mechanics and quantum mechanics, and may also wish to apply the knowledge. Although Child's treatment includes the traditional territory of semiclassical mechanics, such as the Bohr model of the atom, the Landau–Zener model for nonadiabatic transitions, the relationship between quantum-mechanical wave functions and classical trajectories based on the work of Jeffreys, Wentzel, Kramers, and Brillouin (JWKB theory), the quantization of nonseparable systems according to Einstein, Brillouin, and Keller (EBK theory), and the procedure for determining molecular potential curves from spectroscopic data based on the work of Rydberg, Klein, and Rees (RKR method), he goes far beyond this. Of even greater significance are the descriptions of important new developments and applications of semiclassical mechanics, few of which can yet be found in applications-orientated textbooks. Examples are the problems of the quantization of classical chaotic behavior, the classification of semiclassical approximation methods using catastrophe theory, modern semiclassical theories of reaction dynamics as developed by Marcus, Miller, and others, and Heller's revolutionary time-dependent approach to dynamics and spectroscopy based on Gaussian wavepackets. In brief, the book covers just about everything that one could wish for in semiclassical matters, clearly set out, and supported by about 500 carefully chosen references and useful author and keyword indexes.

However, some criticisms must also be mentioned. First, the level of treatment is not sufficiently uniform; depending on the topic under discussion it varies from elementary introductions for students to the sort of erudite information that passes from one expert to another. Just one example of this: Chapter 11 on "Wavepackets" begins with a very detailed explanation of Heller's concept of wavepackets described by properties and variables that are partly classical (trajectories) and partly quantum-mechanical (dispersion, coherence, interference). A well motivated student working through the first ten pages or so of this should be able to master the basic principles as applied to important areas of current research, and is also provided with a guide to the relevant original literature. But then things change—there follows in Section 11.4 ("Franck–Condon Transitions, Raman Spectroscopy, and Photodissociation") a four-page description of applications in spectroscopy and molecular reaction dynamics. Not a single example of photodissociation is given (there are so many interesting ones that could have been described!), and in all of this the relevant equations are presented to the unprepared reader without explaining the background.

A second weakness of the book is that some sections mention examples from the original literature without placing them within an appropriate larger context, as one should in a monograph. For example, in Section 7.3 ("Uniform Quantization at a Resonance") a system of coupled Morse oscillators is treated semiclassically using action angle variables, but the connection with the important Thiele and Wilson model for molecular vibrations is not explained. It would have been useful even to relate it to the nowadays common representation in terms of local, normal, and hyperspherical modes of vibration.

The third criticism is that Child's treatment is occasionally just a little slipshod. Apart from the incorrect spellings of some authors' names (Beidenharn, Engleke, Romelt, etc.), a more serious fault is that diagrams or even model systems are often reproduced from the original papers without taking the necessary care with detailed figure legends, labeling and scaling of graph axes, specifying the model Hamiltonian operator on which the analysis is based, etc.

The last criticism concerns a rather fundamental point. None of the examples of applications involves systems of more than one or two dimensions, except for a few rare literature references to systems of higher dimensionality. It might be argued that this is justified from a didactic standpoint, insofar as one starts with the simpler cases. On the other hand, students faced with the arduous task of ploughing through some of the more demanding parts of semiclassical theory may well ask themselves whether it is worth the effort, since the model systems treated in the book can nowadays be handled numerically by quantum-mechanical methods right from the start, with good accuracy and in a clearly understandable way. Child has undoubtedly succeeded here in clearly showing how semiclassical theory can explain many molecular phenomena. On the other hand, he has occasionally succumbed to the temptation to let formulas run riot, with results that can only be appreciated by readers who are already thoroughly familiar with the subject.

What is missing, in my view, is a clear and well-founded statement of the future outlook for semiclassical theory; one might claim, for example, that it offers the prospect of providing a satisfactory description of the dynamics and spectroscopy of complex multidimensional molecular systems that seem likely to remain untreatable by pure quantum-mechanical methods. But is this in fact true?

To summarize, this monograph is a must for departmental libraries concerned with theoretical chemistry and molecular physics. There is no other remotely comparable treatment of this topical field. However, the book should be read with a critical attitude.

Jörn Manz
Institut für Physikalische und Theoretische Chemie
der Freien Universität Berlin (FRG)

Photochemistry in Organized and Constrained Media. Edited by *V. Ramamurthy*. VCH Publishers, New York/VCH Verlagsgesellschaft, Weinheim, 1991. XVI, 875 pp., hardcover DM 236.00.—ISBN 0-89573-775-2/3-527-27936-9

How are photochemical and photophysical processes affected when one arranges for them to take place not in one of the usual solvents, but in a medium that restricts the mobility of the reactive molecules? For example, how is the selectivity of the [2+2]-photocycloaddition of cinnamic acid altered if, instead of irradiating the molecules in solution, one irradiates them in the ordered crystalline form, or how are the proportions of the different products altered when photolytic α-cleavage occurs within a zeolite? Can one control the selectivity of a photoreaction by first aligning the reacting molecules in an ordered environment? What types of media are suitable as matrices for ordering the molecules in this way? Such questions are not only of interest for potential applications in synthesis; their answers also yield new information about the mechanisms of photoreactions and the structures of the media. One of the scientists who has made important contributions to the progress of research in this area is V. Ramamurthy. His experience and knowledge of this subject was summarized several years ago in a comprehensive review article (*Tetrahedron* **1986**, *42*, 5753–5839). An updated and greatly augmented treatment has now been published in book form. Ramamurthy has brought together as authors 29 well-known specialists from the disciplines of organic chemistry, physical chemistry, and biochemistry. The resulting work can be read either in its entirety, as a definitive account of organic chemistry in "non-classical" reaction media, or selectively to learn about one or more of the specific topics covered in the 19 chapters. Although it is intended mainly for photochemists, it can also be recommended to other chemists who are interested in finding new ways of obtaining enhanced selectivity.

In Chapter 1, M. Garcia-Garibay and N. J. Turro explain their ideas for describing organized, supramolecular systems in terms of topological geometry. Taking as an example the α-cleavage of dibenzylketones, they show how different reaction media can be classified and compared from a topological standpoint. The reader thus obtains an insight into the concepts that underlie the studies described in the later chapters, and also an aid to interpreting the data that are presented.

Chapters 2, 3, 12, and 13 describe modern spectroscopic methods for studying ordered systems. K. Kalyanasunderam describes all the most important molecules that can be incorporated into micelles, vesicles, or biological membranes, or into cyclodextrins or zeolites, to act as fluorescence probes. He explains how such probes can be incorporated, and classifies them according to their interactions with the surrounding medium. C. Bohne, R. W. Redmond, and J. C. Scaiano describe experimental arrangements for laser spectroscopic studies, and show how these methods can be used to determine the physical properties of microheterogeneous systems; the main emphasis is on determining physical and kinetic parameters for micelles. D. Avnir and M. Ottolenghi discuss photophysical processes involving molecules adsorbed on the surfaces of heterogeneous catalysts. They start from the assumption that these surfaces are fractal in nature, and show that the effects of the surface properties on the reactivity of adsorbed substances can be calculated using exponential relationships of the kind that occur in fractal geometry. To conclude this group, W. R. Ware shows the kinds of information that time-resolved spectroscopy can yield regarding the kinetics of fluorescence quenching in microheterogeneous systems. Here again the main emphasis is on micelles, but work on cyclodextrins, silica gel, and biological systems is also featured.

The treatment of true photo*chemistry* starts with Chapter 4. Chapters 4–6, consisting altogether of about 170 pages, deal with photoreactions in crystals, subdivided into biomolecular photoreactions (Ch. 4, K. Venkatesan, V. Ramamurthy), monomolecular photoreactions (Ch. 5, J. R. Scheffer, P. R. Pokkuluri), and the preparation of chiral products in crystals (Ch. 6, M. Vaida, R. Popovitz-Biro, L. Leiserovitz, M. Lahav). The last-mentioned chapter contains a particularly interesting account of experiments aimed at using crystal symmetry to produce chiral products from achiral educts. Unfortunately, however, the quality of reproduction of some of the figures is poor.

Chapter 7 (V. Ramamurthy) is concerned with photoprocesses involving host–guest complexes in the solid phase. The center-point of this chapter is Ramamurthy's own work on Norrish reactions and photochemically-induced Fries rearrangements in cyclodextrins, but all the other important systems are also given an appropriate amount of space. It is regrettable that some of the guest systems described as being suitable for photoreactions are not accompanied by examples of reactions for which they have been used, and also that some of the figures are of poor quality: even readers already familiar with the subject will be unable to recognize in Figure 18 the effect referred to in the text.

Chapters 8–11 could be summarized under the general heading "Photoprocesses of Molecules Adsorbed on the Surface and in the Interior of Metal Oxides". In Chapter 8, L. J. Johnston has collected together the reactions of molecules adsorbed on silica gel and alumina, and arranged them according to reaction types. W. Jones then describes in Chap-

ter 9 photophysical processes involving molecules intercalated between the layers of clays, micas, and other metal oxide phases with layer structures. Chapter 10 (V. Ramamurthy) contains a review of photochemical reactions within zeolites, which is especially worth reading. Like Chapter 8, Chapter 11, by H. Al-Ekabi, dealing with photoelectron transfer induced reactions on the surface of semiconductor catalysts, is again classified according to reaction types.

Photophysical and photochemical processes in liquid crystals form the subject of Chapter 14 (R. G. Weiss). The author begins by considering photophysical processes in mesophases, and shows how the analysis of spectroscopic data yields information on the structures of excimers and exciplexes in these phases. This is followed by detailed descriptions of various chemical reactions, in particular of Norrish Type II reactions and [2+2]-cycloadditions.

Chapter 15, in which S. P. Spooner and D. G. Whitten deal with photoreactions in Langmuir–Blodgett films, is again logically divided into a physical part and a chemical part. The authors explain how the structure of the film determines which types of energy and electron transfer mechanisms are effective, and they describe some of the most important types of photochemical reactions for chromophores that are incorporated as subunits into the amphiphiles used to form the films. Examples of such reactions are the *cis–trans* isomerization of azobenzene, (reversible) [2+2]-cycloadditions, and reactions of merocyanine dyes. However, the authors do not give details of possible applications of Langmuir–Blodgett films, such as in information storage or in biochemical analysis.

In Chapter 16, A. Ueno and T. Osa describe two particularly interesting types of host–guest complexes, namely cyclodextrin complexes and systems containing crown ether structures. The section on the photochemistry of cyclodextrin complexes in solution is complementary to the discussion in Chapter 7, where the corresponding solid-phase reactions were described. That on crown ether systems contains a review of metal complexes that are of potential interest in relation to the development of an ion-specific photometric analysis method and the photoinduced transport of ions through membranes.

Chapters 17 and 18 discuss examples of photochemical processes in biological systems. C. V. Kumar reports some findings on details of the photochemistry of photosynthesis, and describes the use of DNA as an organized medium for influencing the selectivity of photochemical processes. R. S. H. Liu and Y. Shichida show how the *cis–trans* isomerization of retinal in rhodopsin is influenced by the protein environment. The collection ends with an article by D. F. Eaton (Chapter 19), giving some interesting examples of potential technological applications of photochemistry in organized media.

It is unfortunate that this otherwise very comprehensive and detailed collection of articles on photochemistry in organized systems includes nothing on the particularly important topic of micelles. The explanation given in the preface is that to include this would have exceeded the planned size of the book, and also some up-to-date reviews are already available. This is not very convincing, since every chapter in the book begins by referring to other relevant review articles, some of which are very recent. Indeed, the particular advantage of this book is that it gathers together information from a wide range of specialist areas and journals, so that one can recognize parallels leading to ideas for new experiments.

However, despite this gap in coverage, the principle of having an expert to report on each specialist topic means that the reader gets a wealth of up-to-date information at first hand. Ramamurthy has succeeded remarkably well in matching together the individual contributions and avoiding repetition. Frequent cross-references to related areas of work in other chapters are included. The incidence of printing errors is remarkably small, and there are no really serious errors that could lead to misunderstandings. This demonstrates the wisdom of Ramamurthy's practice of having each article cross-checked by three expert referees, and the work as a whole checked again by P. de Mayo and N. J. Turro. Finally, Ramamurthy has collected all the manuscripts together and used the computer to put them into a uniform format. Only someone who has previously undertaken such a task will appreciate how much time and patience it requires. The version finally seen by the reader is a photographically reduced and bound copy of the computer printout. Nevertheless, it must be said that, although the printout appears superficially very neat with a close resemblance to a normal printed text, it is appreciably less agreeable to read than, for example, a typewritten transcript of a lecture. The characters produced by the laser or ink-jet printer are simply too thick and lacking in sharpness when reproduced in the size that is appropriate for a book page. It would have been better, and perhaps more economical, if the text could have been typeset directly from the computer.

Thomas Rumbach
Organisch-Chemisches Institut
der Universität Münster (FRG)

State Selected and State-to-State Ion–Molecule Reaction Dynamics. Part 1: Experiment, Part 2: Theory. (Series: Advances in Chemical Physics, Vol. 82.) Edited by *C.-Y. Ng* and *M. Baer*. Wiley, Chichester, 1992. Pt. 1: XIII, 686 pp., hardcover £ 109.00, $ 164.00.—ISBN 0-471-53258-4; Pt. 2: XIII, 561 pp., hardcover £ 109.00, $ 164.00.—ISBN 0-471-53263-0

The time is ripe for the publication of a textbook on the subject described by the above title, and in these two volumes the editors have achieved an important step in that direction. It is a collection of soundly prepared review articles, eight in each volume, on experimental investigations into ion–molecule reactions (Pt. 1) and their theoretical treatment (Pt. 2), which presents the current state of research in this field, and also discusses promising new methods of investigation. Research into the reaction dynamics of ions is important not only in relation to processes occurring in interstellar space, the atmosphere, and plasmas, but also for contributing to a better fundamental understanding of reactions between neutral species.

The dynamics of ion–molecule reactions is, of course, predominantly influenced by long-range ion–multipole interactions, and probably the most important difference compared with reactions between neutral reactants is in the mechanisms of charge transfer. Nevertheless, many of the experimental and theoretical methods used are similar in the two cases. For example, resonance enhanced multiphoton ionization (REMPI) provides a bridge between studies of neutral–neutral and of ion–molecule reactions, serving in the former case as a state-selective detection method, and in the latter as a means of state selection for the ionic reactants.

The absolute reaction cross-section for an ion–molecule reaction can be determined relatively easily up to very high collision energies. However, it is more difficult to investigate collisions with low energies in the meV range. The problems can be partly overcome by using well-defined ion beams in conjunction with inhomogeneous radiofrequency (RF) fields

and ultrasonic excitation, a technique described by D. Gerlich in the first chapter of Part 1. This review of the theory and applications of inhomogeneous RF field studies of low energy ion–molecule reactions contains much useful technical information and practical advice. The discussion of the integration of RF ion optics into such experiments, and of other variants such as single and multiple photon ionization, photodissociation, chemiluminescence, chemical ionization, and coincidence techniques, gives an insight into applications in other areas besides the specific dynamics of particular collision processes.

In Chapter 2 S. Anderson describes multiphoton ionization (MPI) methods for preparing reactant ions in selected states. As well as explaining the principles of the MPI method, he describes its successful application to a number of individual ionic species. However, it would have been useful from the experimentalist's point of view if information on the laser power needed in each case had been included. In Chapter 3 J. Weishaar describes further applications of the MPI method, with particular emphasis on cations of transition metals. Studies of these reactants should help to elucidate the influence of electronic states on the chemical reactivity of systems with partially filled d-shells. Such investigations should also yield information about the chemistry of metal clusters, whose much more complex electronic structures are still largely unknown.

In Chapter 4 I. Koyano and K. Tanaka report on an extension of the now well-established photoelectron–photoion coincidence (PEPICO) technique for the state- or energy-resolved analysis of dissociation processes. In this method, threshold photoelectron secondary ion coincidence (TESICO), the reactant ions are formed by photoionization at a fixed wavelength, and one detects the ionic products that appear in coincidence with the photoelectrons emitted at the energy threshold. The data thus obtained give direct information about the reaction of ions in a particular electronic state, which is selected by the choice of wavelength.

In Chapter 5 J.-Cl. Brenot and M. Durup-Ferguson discuss aspects of multiple coincidence methods. Present limitations of electronics and data processing techniques mean that the use of such methods to determine absolute state-to-state cross-sections is still in the future, but hopefully is not too far away.

The article by C.-Y. Ng (Chapter 6) definitely belongs in the present, being mainly concerned with the determination of state selected and state-to-state cross-sections for simple ion–molecule reactions and comparison of the results with the theory. This makes possible, for the first time, a critical test of theoretical calculations. The experiments reported by Ng on state-to-state cross-sections are probably the most significant carried out so far.

Chapter 7 is a review by J. Futrell of the most recent experiments on charge transfer processes of monatomic and diatomic ions in crossed molecular beams. In the final chapter of this part G. Niedner-Schatteburg and P. Toennies review 15 years of high resolution studies of the scattering of protons by atoms and molecules, yielding important information about interaction potentials and dynamic vibrational coupling mechanisms. Using a time-of-flight method one can achieve an energy resolution of 10 meV, which gives an impressive indication of the capabilities of this state-of-the-art technique.

In Part 2, dealing with theory, the first three chapters discuss various methods for calculating potential energy hypersurfaces. Charge transfers are nonadiabatic processes, since the reactant and product systems carry different charges and are therefore also in different electronic states. In the transition between these states the system must pass through a small region where there are strong electronic interactions which are nonadiabatic. For large regions, however, an adiabatic treatment involving different hypersurfaces may be permissible. B. Lengsfield III and D. Yarkony provide an answer to the important question of which variables need to be determined in order to describe an electronic nonadiabatic process. They also discuss effective methods for locating crossovers and avoided crossovers. V. Sidis then deals with diabatic descriptions of the potential energy hypersurface. This chapter includes a detailed account of a method for calculating the potential energy hypersurface and coupling terms from first principles, so that the corresponding nonadiabatic coupling terms are kept relatively small. F. A. Gianturco and F. Schneider calculate model potentials by means of the diatomics-in-molecules (DIM) method, in which information from various asymptotic electronic states of atoms and diatomic fragments is used to construct a basis set, from which wave functions, energies, and couplings of electronic states can then be obtained using the variational principle.

The last five chapters deal with the dynamics of the species of interest on the potential hypersurface, beginning with an account by M. Baer of quantum-mechanical calculations. The calculated total and differential state-to-state cross-sections are compared with experimental results. H. Nakamura then describes a semiclassical approach to the problem of the charge transfer process.

E. A. Gilason, G. Parlant and M. Sizun describe classical calculations of pathways for charge transfer processes in ion–molecule collisions. The computational techniques are discussed in detail, giving an insight into the most suitable numerical methods for such calculations. S. Chapman describes special types of classical trajectory calculations; in regions where the Born–Oppenheimer approximation is valid the normal methods are used for calculating the trajectories, whereas in the limited regions of strong nonadiabatic couplings the trajectories are allowed to jump between the coupled energy hypersurfaces.

For all the dynamic calculations described an important prerequisite is a precise knowledge of the potential hypersurfaces, which unfortunately is only available for very few reactions. For this reason statistical theories, which are reviewed in detail by J. Troe in the last chapter, may be extremely useful. The author gives derivations of rate constants and cross-sections for uni- and bimolecular reactions, and nonadiabatic corrections are also included.

In summary, the appearance of this two-volume work was already overdue. Both books can be recommended for everyone working in this or related fields. However, there is as yet no introductory text giving an overview of ion–molecule reaction dynamics for nonspecialists or advanced students wishing to learn something about this subject.

Karl-Heinz Gericke
Institut für Physikalische und Theoretische Chemie
der Universität Frankfurt am Main (FRG)

Biosynthesis of Tetrapyrroles. (Series: New Comprehensive Biochemistry, Vol. 19. Series editors: *A. Neuberger, L. L. M. van Deenen.*) Edited by *P. M. Jordan.* Elsevier, Amsterdam, 1991. XII, 309 pp., hardcover HFl 225.00.—ISBN 0-444-89285-0

Tetrapyrroles such as chlorophyll, heme, the cytochromes, and vitamin B_{12} fulfill key roles in the world of living organisms, and can be appropriately described as the "pigments of

life". Consequently their structures, functions, synthesis, and biosynthesis attract much attention as research topics. The aim of this book is to outline the progress achieved during the last twenty years in understanding the biosynthesis of tetrapyrroles. The editor, P. M. Jordan, has enlisted the help of a number of expert authors who, like himself, are active in this field of research.

In the first chapter (66 pp.) P. M. Jordan deals with the early stages in the biosynthesis of tetrapyrroles that are common to the different cases, by describing the biosynthesis of 5-aminolevulinic acid and its conversion to uroporphyrinogen III. The depth of treatment of the different biosynthetic steps varies considerably; thus, whereas the tetramerization of porphobilinogen to hydroxymethylbilane is described in detail, other conversions such as the cyclization of hydroxymethylbilane to uroporphyrinogen III are given relatively scant attention. Again, in the discussion of possible mechanisms of action of uroporphyrinogen-III-synthase the reader is only referred to a review article, which is quite inadequate. The impression of a lack of balance is intensified by the fact that the published work treated in most detail is Jordan's own. In Chapter 2 (33 pp.) M. Akhtar is concerned with the conversion of uroporphyrinogen III to the red blood pigment heme. The mechanistic and stereochemical studies that have been carried out are thoroughly described, and the author also draws attention to aspects that still need to be investigated. The problem of understanding the biosynthesis of vitamin B_{12} is certainly one of the most difficult that nature has posed for biosynthetic research. In Chapter 3, which is regrettably rather short (38 pp.), A. I. Scott and P. J. Santander clearly show that the important advances outlined here would have been inconceivable without the use of modern NMR spectroscopic methods. However, this is not a review article in the conventional sense, since here again rather large sections are devoted to the authors' own work. Thus, whereas the authors describe their "pulse labeling" experiments to elucidate the methylation sequence between uroporphyrinogen III and cobyrinic acid, they unfortunately neglect to mention the pioneering work of Battersby's group (H. C. Uzar, A. R. Battersby, *J. Chem. Soc. Chem. Commun.* **1982**, 1204). Chapter 4, by H. C. Friedmann, A. Klein, and R. K. Thauer, (16 pp.) is devoted to the biochemistry of the porphinoid nickel complex coenzyme F 430, which is found in methanogenic archebacteria. F 430 is the prosthetic group of the enzyme, which catalyzes the final step of methane formation in these bacteria. It is pleasing to note that the authors have included the determination of the configurations at C-17, C-18, and C-19, which was reported as recently as 1991, but unfortunately not all the formula diagrams have been altered to take account of this. In Chapter 5 (81 pp.) S. I. Beale and J. D. Weinstein give a very detailed account of the magnesium-containing chlorophylls and the bilins, which are the photosynthetic pigments present in plants and algae. As well as describing the individual biosynthetic steps they also explain the mechanism whereby the formation of the pigments is regulated. Chapter 6 (19 pp.) is devoted to the bacteriochlorophylls. Here K. M. Smith briefly discusses their occurrence and structures, and the rather scanty knowledge that exists about their biosynthesis. In the last chapter (38 pp.) the editor again makes an appearance. Here he and B. I. A. Mgbeje give a lucid and masterly summary of present knowledge regarding the genes involved in the biosynthesis of tetrapyrroles. The discussion underlines the importance of the contributions that molecular biology is now making to studies of biosynthetic pathways.

In this book it is impressively shown that progress in biosynthetic studies is only possible by ingeniously combining physical methods such as NMR spectroscopy with enzymology and the methods of molecular biology and organic synthesis. However, as in many multiauthor books there is a lack of consistency in style and in the use of abbreviations and naming conventions. Some of the articles are quite short, whereas others are rather long, and there is inevitably some overlapping of subject matter. The numbers of illustrations and their quality also vary considerably from one chapter to another; unfortunately not all the contributions are as well illustrated as that by Scott and Santander. Also the formulas in some of the chapters are not numbered in sequence, which is inconvenient for the reader. However, the book succeeds on the whole in presenting a good account of recent and very recent results on the biosynthesis of tetrapyrroles. About 1300 references to original papers and reviews are included, covering the literature up to late 1990 and early 1991. Unfortunately the index is incomplete, and the question arises as to whether it is appropriate to publish books on areas of research that are in a state of very rapid development, as this book demonstrates.

However, despite the above criticisms, this very well produced (though by no means cheap) book can be recommended to all readers with an interest in the biosynthesis of tetrapyrroles.

Uwe Beifuss
Institut für Organische Chemie
der Universität Göttingen (FRG)

Physical Chemistry. By *R. A. Alberty* and *R. J. Silbey*. Wiley, Chichester, 1992. XIII, 898 pp., paperback £ 35.95.—ISBN 0-471-55220-8

This well known textbook of physical chemistry traces its origins back 79 years to a book entitled "Outlines of Theoretical Chemistry" written by F. Getman in 1913. The title of the book was changed to "Physical Chemistry" in 1955 when R. Alberty became coauthor of the book together with F. Daniels. For the new edition the responsibility is shared between R. J. Silbey and the senior author R. A. Alberty.

Like earlier editions the book is still divided into four parts. The chapter on thermodynamics begins by describing the interconversion of various kinds of energy and the changes in physical properties that are involved (first law of thermodynamics). Based on the second law of thermodynamics and the definition of entropy the natural direction of physical and chemical processes is investigated in more detail, and the question of whether a process may occur or not is answered. This leads to the definition of the equilibrium constant of a chemical reaction and its dependence on temperature, pressure, and concentration. The concept of chemical equilibrium is then applied to the equilibrium between different phases, electrochemical cells, and biochemical reactions.

The second chapter introduces the basic concepts of quantum mechanics and applies them to atoms and molecules to deduce their spectroscopic properties and to get an understanding of the nature of the chemical bond. Methods for calculating energy levels and the molecular geometry are discussed in detail for atoms and small molecules. Symmetry is introduced as a concept to simplify these calculations for larger and more complicated systems. Various spectroscopic techniques, ranging from NMR to UV spectroscopy, are described in detail. These techniques are used to identify individual atoms and molecules and to collect information about their physical and chemical properties. The importance of the development of the laser for atomic and molec-

ular spectroscopy is discussed, and the increasing importance of NMR spectroscopy is recognized by dedicating a separate section to this powerful technique.

In the chapter on statistical mechanics and kinetics the information provided by quantum mechanical calculations and spectroscopic measurements is used to calculate thermodynamic properties for simple systems. Intermolecular interactions are then taken into account to extend these ideas to dense gases, liquids, and solids. The kinetic theory provides insight into transport properties of gases and the control of chemical reaction rates in the gas phase. After the discussion of complex mechanisms in chemical reactions, the potential energy surface and the concept of the transition state is introduced. Photochemical methods to create and study highly reactive species are described in detail. Finally the basic concepts of chemical kinetics are extended to the liquid phase, where viscosity, diffusion, and electrical transport of ions must be taken into account.

The last chapter, on macroscopic and microscopic structures, deals with macromolecules having a molar mass from 10^4 to 10^6 $g\,mol^{-1}$. Different methods for gaining more insight into these systems are discussed. X-ray diffraction is described as a method to study the structure of solids. Electrical conductivity and its dependence on crystallographic properties is used to introduce the concept of semiconductors. A separate section is dedicated to the study of processes occurring at the interface between the solid and gas phases to get a better understanding of catalytic reactions.

The book is completed by a number of useful appendixes containing information about physical quantities and units, values of physical constants, thermodynamic tables, mathematical relationships, and symbols for physical quantities and their SI units. The whole book places emphasis on the meaning and the importance of using appropriate units for the measurement and interpretation of physical quantities.

Compared to previous editions some improvements and changes have been made. The section on the second law of thermodynamics has been changed completely. A thermodynamic temperature scale is introduced at an early stage, and the second law is deduced from the Clausius theorem. In general more emphasis has been put on the understanding of entropy and the solution of problems concerning chemical equilibrium. The difference between intensive and extensive properties has been clarified by using a new notation for molecular quantities. In the chapter on quantum mechanics and spectroscopy linear operators are introduced earlier than before and are used exclusively. Quantum mechanical ideas are applied throughout the chapter to deduce molecular properties and spectroscopic parameters. In the chapter on statistical mechanics the Maxwell–Boltzmann distribution is introduced right at the beginning. Thermodynamic properties of the ideal gas are then derived in a straightforward way. The basic idea of theoretical kinetics has been combined with the section on photochemistry to form a unified treatment. The photochemical destruction of the stratospheric ozone layer and the importance of femtosecond pulsed laser studies to improve the understanding of the transition state region are described in detail in a separate section. In the last chapter two complete new sections on macromolecules and surface dynamics have been added, to take account of the importance and rapid growth in these fields. The number of examples within the text has been increased by 30% as an aid to understanding the theoretical principles, and a number of problems have been updated.

Even though there are special sections about important and fast growing fields such as biochemical reactions, nuclear magnetic resonance, macromolecules, and surface dynamics one might get the impression that there is not much emphasis on the description of developments of new theoretical concepts and of new experimental techniques and possibilities. But it is clearly beyond the scope of this textbook to give a survey of all the new activities going on in physical chemistry. The real merit of this textbook consists more in a well presented descripton and deduction of basic ideas and fundamental concepts, and therefore it is strongly recommended for students seeking a well founded understanding of physical chemistry.

Georg Seyfang
Laboratorium für Physikalische Chemie
der Eidgenössischen Technischen Hochschule
Zürich (Switzerland)

Molecular Design: Chemical Structure Generation from the Properties of Pure Organic Compounds. (Studies in Physical and Theoretical Chemistry Series, No. 75). By *A. L. Horvath*. Elsevier, Amsterdam, 1992. XII, 1489 pp., hardcover $ 295.00/HFl 575.00—ISBN 0-444-89217-6.

It was in the early part of the nineteenth century that chemists first began to understand that molecules are tiny architectural edifices that can be broken down, reconstructed and modified in a variety of different ways. Almost as soon as this discovery had been made, physicists such as André Ampère, and physical chemists such as Hermann Kopp, started to develop methods that could be used to predict the properties of chemical substances from their molecular structure. Initially the focus was on physical properties, but over the intervening years methods have been evolved for the prediction of an enormous range of properties. In fact, it may now be said after over one and a half centuries of unrelenting endeavor that we have reached the point where it is possible to predict virtually any property with reasonable accuracy, provided that the substance has a well-defined molecular structure. Included among the methods that have been devised are a great variety of so-called additivity methods that exploit either atom, bond, or cluster additivities within a molecule, quantum-theoretical methods that make use of models of differing levels of sophistication, and methods that rely on mathematical descriptors of molecules such as topological indices or geometrical parameters.

The work under review here purports to provide a comprehensive survey of such methods, and is even ambitious enough to state that its prime aim is "to summarize the present state-of-the-art information on the generation and discovery of new and useful chemicals." Clearly a tall order, for such a mammoth undertaking would tax even the most inspired of authors to accomplish within the confines of a single monograph. It comes therefore as no surprise that the author fails in his mission. This work is not only tiresome and tedious but its contents are anything but state-of-the-art. No enlightening discussion on nonlinear structure–activity relationships, no introduction to the plethora of exciting new software now coming on to the market, no elucidation of the intricacies of hierarchical clustering, and no mention of the rapidly growing use of neural networks is to be found herein. Instead, what we are offered is a dreary and long-winded recital of additivity methods that would not be out of place in a text dating from the last century. If the reader's interest extends no further than this, he or she would do much better to consult Lyman's 1982 *Handbook of Chemical Property Estimation Methods*, which is at least entertainingly written. Given the author's eccentric notion of what constitutes state-

of-the-art, is there any merit in a detailed treatment of methods that are now largely of historical interest?

The first thing that strikes one about this book is its enormous size. The book is over 2½ inches (6.4 cm) thick, weighs over 5½ pounds (2.6 kilos), and contains 1500 pages. The text has been reproduced from camera-ready copy that is not justified on the right. Many pages are only partially filled and diagrams typically take up a whole page. It is my impression that this book represents a monumental waste of paper, for the entire contents could have been contained in a work of less than half the present length if the book had been typeset in the conventional way. The text may be roughly divided up into three sections each of some 500 pages in length. The first third concerns itself with a description of methods used for predicting the properties of pure organic compounds, the middle third discusses the characterization of molecular structure by means of various molecular descriptors, and the final third lists all of the literature references cited in the book and also includes ten appendixes. Roughly speaking, the first 500 pages are devoted to discussion of now dated methods (such as additivity methods), the next 500 pages make brief mention of more modern methods (such as the use of topological indices, pattern recognition, and molecular orbital theory), and the remaining 500 pages contain an assortment of references, many of which are irrelevant to modern molecular design. Lacking completely is any treatment of really modern methods or of exciting new approaches such as the use of neurocomputing.

The style in which this book is written is at least as eccentric as the choice of material it contains. Among other things, we are introduced to radically new ways of spelling English words, e.g. isomerizm (isomerism), algoritm (algorithm), approximative (approximate), occurence (occurrence), and valance (valence). Leading workers in the field also have their names misspelt, e.g. Bollzmann (Boltzmann) and Boncher (Bonchev), and names always appear without accents, e.g. Randić and Trinajstić never have their accents. British and American spellings are completely mixed up, e.g. odor on page 748 becomes odour on page 1486 and vapor on page 585 becomes vapour on page 620. Moreover, symbols are used inconsistently, e.g. the Wiener index is represented by w on page 63, but becomes W on page 181 and ΔW on page 278. In addition this work contains much redundant or useless information, e.g. we are told on page 283 that "the boiling point temperature is known for a large number of substances" and on page 747 that "more and more sophisticated methods are needed for the reduction and effective analysis of data." Worse still, the information that this work proffers is often so vague as to be misleading, e.g. on page 55 we learn that "in chemistry, the symmetry plays a great role for the estimation of structural regularities which are the foundations of many thermodynamic systems at various conditions" and on page 861 that "structure generation is the inverse problem of the estimation methods for physical properties of substances with well defined structure." On occasion, the text degenerates into pure gibberish, examples of which are to be found on page 606 in the sentence: "The molecular structures may be examined at a three-dimensional level, and studying the overlapping each other and to compare the molecular shapes quantitatively", and on page 799 in the sentence: "The objective with all collected data is to use them for establishing or proving some phenomenon which is expected or demonstrating that the data do not characterize the inter-relationships for the parameters under study."

In short, it may be said that Horvath's book is a misbegotten attempt to treat the highly complex and tremendously fascinating subject of molecular design. The failure is to be laid at the door of both the author and the publisher. The author has quite clearly sought to write a work that is beyond him. The publisher should have noticed that the manuscript was written in atrocious English and unfit for publication. The end result is a massive book that contains practically nothing of interest to the modern designer of molecular species. This work deserves to be forgotten and to sink without a trace—a prospect that is happily quite likely in view of the great weight of this volume.

Dennis H. Rouvray
University of Georgia
Athens, Georgia (USA)

Pulsed Magnetic Resonance: NMR, ESR, and Optics. A Recognition of E. L. Hahn. Edited by *D. M. S. Bagguley*. Clarendon Press, Oxford, 1992. XV, 550 pp., hardcover £ 65.00—ISBN 0-19-853962-2

Pulsed excitation is nowadays standard for acquisition of NMR spectra. In fact the availability of pulsed excitation has made possible the development of most modern NMR methods and extended the range of applications from conventional one-dimensional spectra to multidimensional NMR spectra for structure determination of biological macromolecules in solution, solid state NMR, and NMR imaging. Pulsed excitation is now conquering ESR spectroscopy, following a similar route as in NMR. It is even used in optical spectroscopy, where many phenomena analogous to magnetic resonance can be observed as well as additional, new effects.

Why is pulsed excitation special? Old-fashioned continuous excitation with a narrow-band irradiation source requires simultaneous detection of the response. Each frequency interval has to be measured in successive steps. By pulsed excitation all frequency components of the spectrum are measured simultaneously, resulting in far shorter acquisition times or better signal-to-noise ratios. Furthermore, excitation and detection are separated into different periods on the time axis. Thus sophisticated pulse sequences can be developed, which are tailored to the properties to be interrogated in the experiment. The Nobel Prize in Chemistry was awarded to Professor Richard Ernst in 1991 for the development of pulsed NMR into a routine method and for an abundance of pioneering new NMR methods.

But pulsed magnetic resonance was born as early as 1949 in the discovery of the spin echo by Professor Erwin Hahn, just four years after the first successful NMR experiments. It turned out that the echo provided confirmation of the famous "Umkehreinwand" of Lohschmidt against Boltzmann's irreversible increase of entropy. After the decay of the initial pulse response, the signal could be made to reappear following a second pulse some time later. The reappearing signal is the echo, which Erwin Hahn discovered accidentally during his PhD work and subsequently explained and exploited for use in NMR, ESR, and optics. The echo can be explained by a time reversal. The decay of the echo amplitude as a function of the echo time measures the homogeneous linewidth or the phase relaxation time T_2. This quantity is of great interest for molecular dynamics, as it characterizes translation and reorientation processes.

A second important contribution of Erwin Hahn to magnetic resonance spectroscopy is the development of cross-polarization, the transfer of magnetization from one nuclear species to another by matching the precession frequencies of the two species in the applied radiofrequency fields. Here the

Hartmann–Hahn condition must be satisfied, a rule well known to every solid state NMR spectroscopist. These and many other contributions to pulse spectroscopy have led to the conclusion of Richard Ernst quoted on page 117 of this book: "The influence of Erwin Hahn on the development of time domain magnetic resonance during the past forty years has been very significant. Even some of the roots of two-dimensional spectroscopy may be found in his early work together with Maxwell".

Erwin Hahn reached his 70th birthday in 1991. An international symposium was held in his honor. The editor of this book, Dr. Bagguley, spent considerable time and effort to have many speakers of this symposium contribute scientific articles on current developments in physics and chemistry which have, in one way or another, been inspired by earlier work of Erwin Hahn and his colleagues. This book is an excellent birthday present, not only to Erwin Hahn, but to the entire magnetic and optical resonance community. It contains 22 contributions from well-known scientists, mainly dealing with the fundamentals and the use of echoes and polarization transfer in NMR, ESR, optical spectroscopy, and magnetic resonance imaging. Many of them are written in a personal fashion, from a friend to a friend, spiced with some reminiscences of the past. Some of the highlights are "The Echo Phenomenon" by D. M. S. Bagguley, "Pulsed NMR in Solids—Then and Now" by C. P. Slichter et al., "New Angles in Motional Averaging" by A. Pines et al., "The Multidimensional Importance of Time Domain Magnetic Resonance" by R. R. Ernst, "Spin Echoes and Thermodynamics" by J. S. Waugh, "Thermodynamics of Hartmann–Hahn Cross-Polarization" by M. H. Levitt, "Spin Choreography" by R. Freeman, "Imaging by Nuclear Magnetic Resonance" by P. Mansfield, "Pulsed Electron–Nuclear Spectroscopy and the Study of Metalloprotein Active Sites" by H. Thomann and W. B. Mims, "Coherent Raman Beats in Electron Paramagnetic Resonance Spectroscopy" by M. K. Bowman et al., and "Optical Excitation and Detection of Spin Precession" by M. Mehring et al. The editor has succeeded in bringing together a coherent and stimulating account of research that has grown out of the original papers by Erwin Hahn. The book will be of benefit not just for the specialist, but for a wide range of students and research workers. The practical use of the book is enhanced by a list of Hahn's published papers, a glossary of abbreviations, an author index, and a subject index. It is highly recommended for acquisition by libraries, and by individuals who enjoy accounts of modern pulse spectroscopy with a historical perspective.

Bernhard Blümich
Max-Planck-Institut für Polymerforschung
Mainz (FRG)

Chemical Information Management. By *W. A. Warr* and *C. Suhr*. VCH Verlagsgesellschaft, Weinheim, 1992. XIII, 261 pp., hardcover DM 128.00.—ISBN 3-527-28366-8

In the preface to this book two things already become apparent. Firstly, advantage has been taken (unusually) of the facility for listing additional recent publications that appeared too late to be mentioned in the text. Secondly, it is explained that the book consists mainly of a reprint of a chapter on the same subject in *Ullmann's Encyclopedia of Industrial Chemistry* (Vol. B1, Ch. 12). Therefore the question at once arises as to whether double publication of this kind is helpful from the standpoint of the reader and/or purchaser. In this case it is, since (to anticipate the favorable verdict of this reviewer) the high quality and information content of this text by two authors who are well known in the field merits ensuring that it reaches as wide a readership as possible. In my experience most chemists are (unfortunately!) not likely to seek information of this kind in "Ullmann", and therefore this book offers the only realistic possibility of having it constantly to hand in the laboratory or in private collections. The book's high price, combined with its compactness and the demanding standard of the contents, means that chemistry students are unlikely to buy it, but for the same reasons no chemistry departmental library should be without it. In contrast to the well-known guides to the chemical literature by Wolman, Mücke, Skolnik, Maizell, and others, which concentrate on practical aspects (e.g., where and how to seek information on a specific topic), this book presents a survey of the whole field of chemical information and of the basic principles that is concise, informative, and up-to-date, but by no means limited to digital data processing. In the absence of any other suitable up-to-date and comprehensive treatment, it could even be used as a more advanced, though very compact, textbook on chemical information and literature sources, to follow an initial introduction using a book such as *Communication, Storage and Retrieval of Chemical Information*, by Ash et al. In addition to giving a practically orientated guide to the literature, the book provides the background information that is essential to understanding the subject, and predictions about likely future developments. The teaching institutions are notorious for their neglect of this area of chemistry, and it is remarkable that it has been left to these two authors from industry to fill a gap that existed.

Right at the beginning of the book one finds a very useful and comprehensive list of common acronyms, the numbers of which continue to grow on an epidemic scale in this as in other fields. The comprehensive bibliography of more advanced literature is given in complete form for each chapter—this means that a particular reference can appear several times if cited in different chapters. Unfortunately, however, instead of giving these lists of references at the ends of the relevant chapters, which would have made the book easier to use and would have justfied the redundancy just mentioned, they are collected together at the end of the book.

The first three chapters present a concise and readable survey of the primary, secondary, and tertiary literature. The following two chapters are fairly detailed, and deal with matters that often cause problems and are unfamiliar to many chemists, namely the "gray literature" and commercial information. Chapters 6 ("Computer Hardware") and 7 ("Software") are rather brief and superficial, but Chapter 8 ("Information Retrieval") and those that follow contain more detailed treatments appropriate to their subjects. The chapter on data banks is a highlight of the book; all the latest developments receive at least a brief mention, including the SPECINFO system and the Gmelin data bank. Chapter 10, on the handling of chemical structures, is typical, consisting of an introduction to the basic principles with references to more advanced reading (6 pp.), followed by a review of current developments (6 pp.) then, as the main material, a 16-page description of operational systems, including relevant PC software (although naturally the latter compilation already needs to be extended). The following chapter on "Artificial Intelligence" presents a survey encompassing neuronal networks as well as hypermedia. This is immediately followed by a topic that might be regarded as the opposite extreme: Chapter 12 and the subsequent ones deal with patents and make up nearly a third of the book. The detailed treatment of this subject is certainly appropriate to its impor-

tance in industry, and its length has been approximately doubled compared with its predecessor in "Ullmann". Guides to the literature often devote very little space to patents (perhaps as a consequence of the bias that exists against patent information in the teaching institutions where there is no relevant expertise), and therefore this part of the book is nearly enough in itself to justify buying it. The discussion of legal aspects is confined to matters that are essential for an understanding. From Chapter 14 onwards the emphasis is on patents as an information source. Chapter 15 briefly discusses some of the less obvious differences between patents and other publications. Chapters 16–22 then deal with the layout of patent specifications, storage of patent information (including new storage media such as CD-ROM), patent searches, patent information services, and data banks.

The book concludes in Chapter 23 ("The Future of Patent Information Management") by inviting its readers ".... to soon render it obsolete by making their own creative contributions to the fascinating world of information management". Some of the fascination that the subject holds for the authors is conveyed as one reads this book. It is to be hoped that the word "Management" in the title will not deter chemists in teaching and technology from reading this book, which will be of great value to them in view of the growing importance of information in their day-to-day work.

Engelbert Zass
Laboratorium für Organische Chemie
der Eidgenössischen Technischen Hochschule
Zürich (Switzerland)

Graphics and Animation in Surface Science. Edited by *D. D. Vvedensky* and *S. Holloway*. Adam Hilger, Bristol (UK), 1992. VIII, 117 pp., hardcover £ 27.50.—ISBN 0-7503-0188-X

For many years now the computer has been an indispensable tool of experimental science, not only for the recording and interpretation of data, but also for preparing manuscripts and disseminating results. Recently, however, another way of using computers has become increasingly important. This is computer graphics, which not only enables one to present experimental results in clever and visually appealing forms, but also often reveals new scientific relationships not previously apparent. For example, very rapid processes can be studied in a slowed-down presentation, allowing intermediate states to be observed for the first time. Conversely, very slow processes can be presented as a rapid sequence of images, so that the effects of interest can be much more easily recognized.

The advantages that can result from using such computer graphics can be particularly well illustrated by examples from the physics and chemistry of surfaces. That is the purpose of the book reviewed here, in which the editors have collected together seven individual contributions on computer techniques applied mainly to various research topics in surface physics. The results, some of which are quite spectacular, would hardly have been possible without effective graphics and animation techniques.

The book begins with a general introduction by the editors in which they mention, among other aspects, the application of graphics methods to ab initio calculations of total energy, to describing dynamic molecular processes, for Monte-Carlo simulations, and for studying surface reactions.

In Chapter 2 N. M. Harrison gives a concise account of the use of advanced graphics computers in surface research, with particular attention to technical aspects of the choice of computer systems (hardware and software), the problems of generating hard copies suitable for reproduction, and some possible applications of individual graphics user packages in surface physics.

Chapter 3 by O. H. Nielsen has the title "Animation in Surface Science". In this context animation implies that experimental or theoretical results that do not convey a clear picture in the form of tabulated data or a two-dimensional diagram, or are even quite incomprehensible in these forms, are reprocessed to yield a suitable multidimensional representation and/or a sequence of colored images (a movie) that makes them understandable. As an example to illustrate the use of computer animation in surface physics the author chooses the perspective representation of a solid surface. The rest of the chapter is mainly concerned with the computational and technical problems of animation.

In Chapter 4 M. W. Rickets deals with a more specialized topic, describing the well known WINSOM software package and its application to some selected problems in molecular modeling, liquid crystals, potential fields, and complex biological structures.

Chapter 5 by P. Stolze is likely to be of special interest to surface physicists; this emphasizes the immense value of graphics and animation techniques for simulating dynamic molecular processes. One aspect of this is the presentation in graphic form of the results of numerical calculations. A very good example is the visual representation of the trajectories of interacting atoms or molecules over long periods (e.g., in a liquid or a crystal undergoing melting). Such graphics methods have contributed especially to the understanding of crystal growth, premelting phenomena, and roughening transitions.

In Chapter 6, "Animation of Large-Scale Simulations", M. R. Wilby and S. Clarke are mainly concerned with the graphical representation of Monte-Carlo simulations of the molecular beam epitaxy (MBE) process, which is of great technological importance. As in the previous chapter, the aim here is to compute and display the trajectories of the atoms taking part in the growth over a period of time for different values of the variables, in this case the (anisotropic) interaction energies with the substrate, so as to give a better understanding of the macroscopic growth processes.

The book ends with a chapter on "Animation of Quantum Scattering Events using Hypercard", by D. M. Halstead and S. Holloway. The authors discuss the theoretical problem of quantum scattering at potential barriers, which is important for calculating the trajectories of molecules undergoing adsorption, for example, and they explain how the theoretical results are presented graphically.

First, a few critical comments. The title of the book is rather general, and appears at first to promise the reader a snapshot of the whole topic of computer animation in surface research. However, it quickly becomes obvious that such a slim volume can only cover a small selection of topics or applications. Thus, some extremely useful graphics and animation programs known to this reviewer, such as those for displaying structures of surfaces and adsorbates, or for visualizing lattice vibrations (phonons in the bulk and at the surface), are not included. Again, there is no mention of programs for the processing and display of scanning tunneling microscopy images, probably now the most topical and fruitful of the techniques used in surface physics. However, the editors have taken on the risky task of opening to a wider readership a field that is undergoing very rapid development, and the fact that they have not only attempted this but have produced a worthwhile result is greatly to be welcomed. Every

physicist and chemist who wishes to learn about computer animation in surface research should buy this little book, despite the risk that parts of it may be overtaken by computer developments within a few years. Moreover, the affordable price for this well produced book (containing many colored figures) should have an *animating* effect on readers.

Klaus Christmann
Institut für Physikalische und Theoretische Chemie
der Freien Universität Berlin (FRG)

The Meaning of Quantum Theory. By *J. Baggott*. Oxford University Press, Oxford, 1992. XIV, 230 pp., hardcover £ 11.95. ISBN 0-19-855575-X

In recent years there has been a growing trend towards the publication of books on technical aspects of quantum mechanics and quantum chemistry for chemists with theoretical interests. Although these differ greatly in emphasis and degree of difficulty, most of them follow a common pattern. Their central theme is to provide the reader with quantum theoretical methods—thus they present quantum theory in the form of a technological toolkit. Any reader who approaches J. Baggott's book expecting something of this kind will certainly be disappointed. The author's purpose here is to examine the meaning of quantum theory as a conceptual structure from a scientific and philosophical standpoint. The most important message can be summarized in one succinct statement: the central elements of quantum theory are open to more than one possible interpretation. Baggott illustrates this by the example of the old controversy between, on the one hand, the positivist school of Bohr and the young Heisenberg, and on the other hand the realistic interpretation based on wave mechanics, as put forward by Einstein and Schrödinger. The positivist approach to quantum theory is a conceptual structure of a puristic kind. Baggott describes positivism as a view based on the premise that any observation on a quantum-mechanical system involves a disturbance of the system, and therefore the description requires a Hamiltonian operator that includes both the quantum-mechanical system itself and the spectrometer or observer.

Baggott characterizes the realistic viewpoint by the concept of "local realities". In this framework an experimental system can also be described by restricting the treatment to localized subfragments. Baggott explains the scientific controversy in terms of certain imaginary experiments of historical importance, such as the Einstein–Podolsky–Rosen theorem, the Bell inequality, and the intellectual construction known as Schrödinger's cat.

The book is divided into five chapters. In Chapter 1 the author summarizes the historical facts that led to the development of quantum mechanics, and discusses in detail the wave–particle duality hypothesis of de Broglie. This chapter provides an easily readable introduction to the theoretical ideas, and also introduces a number of novel relationships. Chapter 2 begins with an explanation of the operator concept of quantum mechanics. Here Baggott also describes lucidly the considerations that led to the formulation of the Schrödinger equation. In this chapter, which is orientated mainly towards mathematical techniques and formalisms, the author explains in an easily understandable way the elements of quantum mechanics, such as state vectors in Hilbert space and the Pauli exclusion principle. Chapter 3 moves on from the technical background to an examination of the meaning of the quantum theory. The reader learns that the controversies between the positivists and the realists were often emotional and heated. Chapter 4 takes up the subject of the conceptual "experiments" mentioned above, that were put forward in support of either the positivist or the realist interpretations.

Unfortunately, after about the first 100 pages, the book loses some of its initial excitement and conciseness. In the opinion of this reviewer, the last part could have been tightened up and condensed to about half its length. In Chapter 5 Baggott moves away from the themes of the previous chapters and focuses attention on the relationships between quantum theory and philosophy. He also discusses, among other topics, the ideas of Karl Popper and of René Descartes. The chapter concludes with some metaphysical considerations. The question of the existence of a deity, which is introduced carefully and dicreetly at this point, rests on the same philosophical basis of the debate between determinism and indeterminism as do the fundamentals of quantum theory—hence the excursions into matters of religion. The merit accorded to this part of the book will no doubt vary from reader to reader.

Some of the comments that Baggott includes are trenchant and worthy of attention. One of the best passages is that on page 79: "It would, perhaps, be very difficult for high-energy physicists to justify the financial investments ... if they were not convinced of the reality of the objects on which they wish to make measurements".

In this book Baggott presents a skillful analysis of those concepts of quantum mechanics with which we have, in the course of time, learned to be "comfortable". He succeeds in opening the reader's mind to new questions about quantum mechanics and thereby taking a fresh look at hitherto accepted conceptual models. The book can be recommended for readers interested in the philosophical aspects of quantum theory. Large parts of it are stimulating to work through. However, this requires a good deal of concentration, apart from the "technical information" parts. Unfortunately Baggott's treatment is not at a consistent level throughout, but against this it must be said that the aim was very ambitious. The minor criticisms above should not deter anyone from buying this interesting and stimulating book. It is desirable that as many chemists and physicists as possible should concern themselves with aspects of quantum theory other than technological applications, and this book offers a good introduction to the subject.

Michael C. Böhm
Institut für Physikalische Chemie
der Technischen Hochschule Darmstadt (FRG)

Transuranium Elements: A Half Century. Edited by *L. R. Morss* and *J. Fuger*. American Chemical Society, Washington, DC, 1992. XXIV, 562 pp., hardcover, $ 99.95.—ISBN 0-8412-2219-3

When news of Otto Hahn and Fritz Strassmann's discovery of nuclear fission in 1939 reached the University of California, scientists at Berkeley began experiments to reproduce the unexpected results. By May, 1940 Edwin M. McMillan, an assistant professor of physics, and Philip H. Abelson, a recent Berkeley physics alumnus, succeeded in producing the first transuranium element (at. no. 93) by bombarding uranium (at. no. 92) with neutrons from Ernest O. Lawrence's cyclotron. They named it neptunium after Neptune, the next planet after uranium. A mere seven months later, on December 14, 1940, Berkeley chemistry instructors Glenn T. Seaborg and Joseph W. Kennedy and graduate student Arthur C. Wahl synthesized the second transuranium element (at. no. 94) by bombarding uranium with deuterons from the

same cyclotron. They named it plutonium after Pluto, the planet beyond Neptune. Seaborg and McMillan shared the 1951 Nobel Prize in Chemistry for their accomplishments.

As is well known, the discovery of plutonium led to the second nuclear bomb ("Fat Man"), while the discovery of these first two transuranium elements added a new dimension to the Periodic Table and changed forever the world in which we live. A half century later the discovery was celebrated by articles, books, conferences, and meetings. One of the most prominent of the meetings, a Symposium to Commemorate the 50th Anniversary of the Discovery of Transuranium Elements, was sponsored by the Divisions of Nuclear Chemistry and Technology, the History of Chemistry, and Inorganic Chemistry of the American Chemical Society and was held at the 200th National ACS Meeting, Washington, DC, August 26–31, 1990. The volume reviewed here, dedicated to Glenn T. Seaborg "in recognition of his inspiring leadership in the discovery of the transuranium elements and in the elucidation of their chemical properties", contains 51 of the 67 papers presented at the symposium by 109 internationally renowned authorities from the United States (many from nuclear research centers such as the Los Alamos, Argonne, Brookhaven, and Oak Ridge National Laboratories, the Lawrence Berkeley Laboratory, and the University of California, Berkeley) as well as from Australia, Belgium, China, Finland, France, Germany, India, Japan, Portugal, Russia, and Switzerland. Many of the chemists, physicists, materials scientists, and engineers who pioneered the historic research on transuranium elements during the 1940s are among the contributors.

The book is divided into eight sections—(1) Introduction: Transuranium Elements: Their Impact on Science and Technology, by the editors; (2) Historical Viewpoints (12 papers by Seaborg, Abelson, Connick, Katz, and other early pioneers); (3) Spectroscopy, Photophysics, and Photochemistry (7 papers); (4) Chemistry (7 papers); (5) Separations and Thermodynamics (6 papers); (6) Materials Physics (4 papers); (7) Materials Chemistry (10 papers); and (8) Analytical Chemistry (4 papers). Each paper is prefaced by an abstract, and the volume is replete with 310 tables, figures, reaction schemes, and photographs of great historical significance, such as portraits of the discoverers and crucial pages from laboratory notebooks.

The papers reflect the unique and challenging nuclear, spectroscopic, physical, chemical, and solid-state behavior of the transuranium elements and present predictions and perspectives for the conduct of future research, including that on the "superheavy" elements (atomic numbers above 111). They discuss the impact of fundamental and applied physical research on the characterization and properties of elements caused by the filling of the 5f electron subshell. Seaborg's celebrated actinide concept, postulating that transuranium elements constitute a second rare earth series, which accounted for their position in an expanded Periodic Table and predicted conditions for their synthesis and isolation, is featured prominently in many of the contributions, but important differences between the actinides and lanthanides are not neglected.

A judicious balance is struck between papers presenting first-hand historical accounts and anecdotes, review papers, and reports describing the most recent contemporary research (synthesis of new derivatives, corrosion studies, thermodynamic interpretations, and methods for detecting and disposing of radioactive fuel waste, both on a laboratory scale and plant scale). Despite the multiplicity of authors from various laboratories, which often results in the inconsistent format, uneven appearance, and large number of mis spellings usually associated with symposium proceedings, the book is most attractive and virtually error-free, thanks to the efforts of the editors and the staff of the ACS Books Department, which maintains exacting editorial and production standards. A detailed name and subject index (27 pp., 2 columns per page) makes the contents readily accessible.

In reflecting the dynamics and trends of research on the actinides, this excellent collection of papers of historical and contemporary value is a major contribution to the scientific community. I recommend it highly to historians of science and technology, practicing chemists, physicists, and engineers, as well as to anyone interested in this family of fascinating elements whose unusual and complex chemical, physical, and nuclear properties pose a multitude of challenging problems for scientists and whose control has created thorny issues for the world's politicians and statesmen.

George B. Kauffman
California State University
Fresno, CA (USA)

New Books
see next page

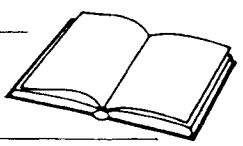

 © *VCH Verlagsgesellschaft mbH, W-6940 Weinheim, 1993* *0570-0833/93/0303-0455 $ 10.00+.25/0*

New Books

Asymmetric Synthesis. Edited by **R.A. Aitken, S.N. Kilényi**. Blackie A & P, Glasgow, **1992**. 233 pp., hardcover, £ 59.—ISBN 0-7514-0059-9

The Organic Chemistry of Drug Design and Drug Action. By **R.B. Silverman**. Academic Press, New York, **1992**. 422 pp., hardcover, $ xxx.—ISBN 0-12-643730-0

Phthalocyanines. Properties and Applications, Vol 2. Edited by **C.C. Leznoff, A.B.P. Lever**. VCH Verlagsgesellschaft, Weinheim, **1993**. 305 pp., hardcover, DM 268.—ISBN 3-527-89544-2

Chemistry of Iron. Edited by **J. Silver**. Blackie A & P, London, **1993**. 306 pp., hardcover, £ 69.—ISBN 0-7514-0062-9

Super-Acids and Acidic Melts as Inorganic Chemical Reaction Media. By **T.A. O'Donnell**. VCH Verlagsgesellschaft, Weinheim, **1993**. 243 pp., hardcover, DM 184.—ISBN 3-527-28092-8

Macrocyclic Chemistry. Aspects of Organic and Inorganic Supramolecular Chemistry. By **B. Dietrich, P. Viout, J.M. Lehn**. VCH Verlagsgesellschaft, Weinheim, **1993**. 384 pp., hardcover, DM 148.—ISBN 3-527-28330-7

Determination of Thermodynamic Properties. Physical Methods of Chemistry, Vol. VI. Edited by **B.W. Rossiter, R.C. Baetzold**. Wiley, Chichester, **1992**. 743 pp., hardcover, £ 157.—ISBN 0-471-57087-7

Solid Supports and Catalysts in Organic Synthesis. Organic Chemistry Series. Edited by **K. Smith**. Ellis Horwood, New York, **1992**. 338 pp., hardcover, $ 85.—ISBN 0-13-639998-3

Theoretical Treatment of Liquids and Liquid Mixtures. Studies in Physical and Theoretical Chemistry, Vol. 80. By **C. Hoheisel**. Elsevier, Amsterdam, **1992**. 362 pp., hardcover, FL 320.—ISBN 0-444-89835-2

Reviews in Computational Chemistry, Vol. 3. Edited by **K.B. Lipkowitz, D.B. Boyd**. VCH Verlagsgesellschaft, Weinheim, **1992**. 271 pp., hardcover, DM 128.—ISBN 3-527-89619-8

Molecular Recognition: Chemical and Biochemical Problems II. Edited by **S.M. Roberts**. Royal Society of Chemistry, Cambridge, **1992**. 200 pp., hardcover, £ 39.50.—ISBN 0-85186-226-8

Kevlar Aramid Fiber. By **H.H. Yang**. Wiley, Chichester, **1992**. 200 pp., hardcover, £ 39.95.—ISBN 0-471-93765-7

Chemical Safety Data Sheets, Vol. 5. Flammable Chemicals. By/Edited by **R. Allen**. Royal Society of Chemistry, Cambridge, **1992**. 288 pp., paperback, £ 54.95.—ISBN 0-85186-411-2

Bioanalytical Approaches for Drugs, Including Antiasthmatics and Metabolites. Methodological Surveys in Biochemistry and Analysis, Vol. 22. Edited by **E. Reid, I.A. Wilson**. Royal Society of Chemistry, Cambridge, **1992**. 356 pp., hardcover, £ 75.—ISBN 0-85186-236-5

Extraction of Natural Products Using Near-Critical Solvents. Edited by **M.B. King, T.R. Bott**. Blackie A & P, London, **1992**. 325 pp., hardcover, £ 69.—ISBN 0-7514-0069-6

Compendium of Organic Synthetic Methods, Vol. 7. By **M.B. Smith**. Wiley, Chichester, **1992**. 547 pp., hardcover, £ 47.50.—ISBN 0-471-60713-4

Chemical Safety Matters. Edited by **P.H. Bach, J.A. Heines, B.C. McKusick, S.S. Brown, R.M. Joyce, H.G.J. Worth**. Cambridge University Press, Cambridge, **1992**. 284 pp., paperback, £ 19.95.—ISBN 0-521-41375-3

Secondary Ion Mass Spectrometry SIMS VIII. Edited by **A. Benninghoven, K.T.F. Janssen, J. Tümpner, H.W. Werner**. Wiley, Chichester, **1992**. 915 pp., hardcover, £ 115.—ISBN 0-471-93064-4

Hazards in the Chemical Laboratory, 5th Ed.. Edited by **S.G. Luxon**. Royal Society of Chemistry, Cambridge, **1992**. 676 pp., paperback, £ 45.—ISBN 0-85186-229-2

The Chemical Industry – Friend to the Environment?. Edited by **J.A.G. Drake**. Royal Society of Chemistry, Cambridge, **1992**. 191 pp., hardcover, £ 25.—ISBN 0-85186-477-5

Risk Management of Chemicals. Edited by **M.L. Richardson**. Royal Society of Chemistry, Cambridge, **1992**. 392 pp., hardcover, £ 47.50 .—ISBN 0-85186-467-8

Photochemistry, Vol. 23. Specialist Periodical Reports. By **D. Bryce-Smith, A. Gilbert**. Royal Society of Chemistry, Cambridge, **1992**. 556 pp., hardcover, £ 145.—ISBN 0-85186-215-2

Particle Size Analysis. Edited by **N.G. Stanley-Wood, R.W. Lines**. Royal Society of Chemistry, Cambridge, **1992**. 538 pp., hardcover, £ 57.50.—ISBN 0-85186-487-2

Clean Air at Work. New Trends in Assessment and Measurement for the 1990s. Edited by **R.H. Brown, M. Curtis, K.J. Saunders, S. Vandendriessche**. Royal Society of Chemistry, Cambridge, **1992**. 508 pp., hardcover, £ 65.—ISBN 0-85186-217-9

General and Synthetic Methods, Vol. 14. Specialist Periodial Reports. Edited by **G. Pattenden**. Royal Society of Chemistry, Cambridge, **1992**. 492 pp., hardcover, £ 147.50.—ISBN 0-85186-954-8

Chemicals Control in the European Community. Edited by the **Commission of the European Community**. Royal Society of Chemistry, Cambridge, **1992**. 120 pp., hardcover, £ 32.50.—ISBN 0-85186-197-0

Industrial Applications of Surfactants III. Edited by **D.R. Karsa**. Royal Society of Chemistry, Cambridge, **1992**. 278 pp., hardcover, £ 47.50.—ISBN 0-85186-227-6

Total Quality in the Chemical Industry. Edited by **J.M. Askey, G.R. Turner**. Royal Society of Chemistry, Cambridge, **1992**. 102 pp., hardcover, £ 29.50.—ISBN 0-85186-497-X

Progress in Heterocyclic Chemistry, Vol. 4. Edited by **H. Suschitzky, E.F.V. Scriven**. Pergamon Press Ltd., Oxford, **1992**. 296 pp., hardcover, £ 60.—ISBN 0-08-040612-2

Dibenzaanthracenes and Environmental Carcinogenesis. Cambridge Monographs of Cancer Research. By **W. F. Karcher**. Cambridge University Press, Cambridge, **1992**. 271 pp., hardcover, £ 75.—ISBN 0-521-30382-6

Einführung in die organische Chemie. By **S. Hauptmann**. Deutscher Verlag für Grundstoffindustrie, Leipzig, **1992**. 378 pp., hardcover, DM xxx .—ISBN 3-342-00635-8

Einführung in die chemische Laboratoriumspraxis. By **E. Fanghänel**. Deutscher Verlag für Grundstoffindustrie, Leipzig, **1992**. 304 pp., paperback, DM xxx.—ISBN 3-342-00394-4

Dairy Rheology. A Concise Guide. By **J.H. Prentice**. VCH Verlagsgesellschaft, Weinheim, **1992**. 165 pp., hardcover, DM 158.—ISBN 3-527-28349-8

Modern Methodology in Organic Synthesis. Edited by **T. Shono**. VCH Verlagsgesellschaft, Weinheim, **1992**. 463 pp., hardcover, DM 218.—ISBN 3-527-28407-9

New Aspects of Organic Chemistry II. Organic Synthesis for Materials and Life Sciences. Edited by **Z. Yoshida, Y. Ohshiro**. VCH Verlagsgesellschaft, Weinheim, **1992**. 521 pp., hardcover, DM 174.—ISBN 3-527-29014-1

Registered names, trademarks, etc. used in this journal, even when not marked as such, are not to be considered unprotected by law.

© VCH Verlagsgesellschaft mbH, D-W-6940 Weinheim, 1992. – Printed in the Federal Republic of Germany by Konrad Triltsch Druck- und Verlagsanstalt Würzburg.

All rights reserved (including those of translation into foreign languages). No part of this issue may be reproduced in any form — by photoprint, microfilm, or any other means — nor transmitted or translated into a machine language without written permission from the publishers. Only single copies of contributions, or parts thereof, may be made for personal use. This journal was carefully produced in all its parts. Nevertheless, authors, editors, and publisher do not warrant the information contained therein to be free of errors. Readers are advised to keep in mind that statements, data, illustrations, procedural details, or other items may inadvertently be inaccurate.

Valid for users in the USA: The appearance of the code at the bottom of the first page of an article (serial) indicates the copyright owner's consent that copies of the article may be made for personal or internal use, or for the personal or internal use of specific clients. This consent is given on the condition, however, that the copier pay stated per-copy fee through the Coypright Clearance Center, Inc. (CCC), for copying beyond that permitted by Sections 107 or 108 of the U.S. Copyright Law. This consent does not extend to other kinds of copying, such as copying, for general distribution, for advertising or promotional purposes, for creating new collective works, or for resale. For copying from back volumes of this journal see 'Permissions to Photo-Copy: Publisher's Fee List' of the CCC.

Editorial office: Postfach 10 11 61, D-W-6490 Weinheim, Federal Republic of Germany, Telephone (06201) 606 315, Telex 465 516 vchwh d, Telefax (06201) 606 328, E-Mail Z16@DHDURZ2 in Earn Bitnet.

Editor: *Peter Gölitz*

Associate editors: *N. A. Compton, R. H. Schmidt-Radde, K. J. Schneider.* **Book editor:** *G. Karger.* **Editorial assistant:** *E. Schweikart*

Publishers: VCH Verlagsgesellschaft mbH. (Managing Directors: *Hans Dirk Köhler, Dr. Karlheinz Köpfer*), Pappelallee 3, D-W-6940 Weinheim, Federal Republic of Germany.

Advertising office (Advertising Manager: *N. Schippel*): Postfach 10 11 61, D-W-6940 Weinheim, Federal Republic of Germany, Telephone (0 62 01) 606 312, Telefax (0 62 01) 606 328.

ANGEWANDTE CHEMIE
International Edition in English
Volume 32 · Number 4
April 1993
Pages 457–628

Optical Spectroscopy of Single Impurity Molecules in Solids

By W. E. Moerner* and Thomas Basché*

Optical spectroscopy of a single impurity molecule provides the first truly local probe of host–guest interactions in doped solids. In conventional optical high-resolution experiments with many molecules only ensemble averages of the microscopic parameters can be obtained. In the single-molecule regime, the exquisite sensitivity of an individual dopant molecule to both the local environment and to external perturbations has been exploited in recent experiments to reveal a wealth of fascinating novel phenomena such as spectral diffusion in crystals and polymers, optical modification of a single impurity molecule (spectral hole-burning), local field measurements at the site of a single impurity molecule, and quantum optics in a solid.

1. Introduction[**]

Significant progress in the optical spectroscopy of single quantum systems confined in traps or on surfaces has occurred in the last decade. For example, imaging and spectroscopy of single ions confined in electromagnetic traps has led to novel measurements that test the foundations of quantum physics. In particular, various workers have reported direct measurement of quantum jumps, Doppler sidebands, photon antibunching, extremely narrow optical linewidths, and other fundamental phenomena such as ion crystallization and chaos.[1–3] The original work on trapped single electrons and on the Paul trap led to the Nobel Prize in physics for Dehmelt, Paul, and Ramsey in 1989.[4]

At the other extreme, recent advances in various near-field spectroscopies such as scanning tunneling microscopy (STM)[5, 7b] have provided detailed images of single atoms, of single molecules of benzene and CO on Rh surfaces,[6] and of liquid crystal molecules on graphite[7] to name only a few examples. The invention of STM earned Binnig and Rohrer[5] the Nobel Prize in physics in 1986, and many workers around the world are applying this technique to a large variety of systems. Moreover, the STM work has inspired a broad array of sensitive surface measurements based on the atomic force microscope.[7b, 8] A requirement of STM is the need for a strong bond between the molecule of interest and the underlying surface so that the molecule can remain in a fixed configuration long enough for the tunneling spectrum to be obtained.

By contrast, the relatively new field of single-center optical spectroscopy in condensed matter is only now beginning to provide novel chemical and physical insights. For single molecules in liquids, the emphasis has been on the detection of single molecules labeled with fluorophores for analytical applications without recording detailed spectra. In the early work, use of laser-induced fluorescence and a hydrodynamically focused flow to reduce the scattering volume allowed the detection of single molecules of the protein B-phycoerythrin, whose fluorophore is equivalent to 25 rhodamine 6G molecules.[9, 10] Recent enhancements of the method have

[*] Dr. W. E. Moerner
IBM Research Division, Almaden Research Center
San Jose, CA 95120-6099 (USA)
Dr. T. Basché
Institut für Physikalische Chemie der Universität
Sophienstrasse 11, D-W-8000 München 2 (FRG)

[**] Important terms and abbreviations are listed in a glossary (Section 10) at the end of the review.

 © VCH Verlagsgesellschaft mbH, W-6940 Weinheim, 1993 0570-0833/93/0404-0457 $ 10.00+.25/0

allowed the detection of single molecules of rhodamine 6G in a flowing liquid.[11, 12] One distinct advantage here is that the experiments are usually conducted at room temperature; however, the fluorescent molecule and the solution must be chosen carefully to maximize photostability. In the first work to go beyond digital (present/not present) detection of a molecule, two fluorescent species were distinguished by the difference in fluorescence lifetime.[13]

This review concerns single-center spectroscopy when the center of interest is a molecular or ionic dopant (defect) hidden deep inside a solid. The detection and spectroscopy of a single absorber in a solid (in the case of a molecular impurity called single-molecule detection, SMD) provides a natural complement to the earlier hole-burning and coherent transient spectroscopy of impurities in solids.[14–17] Single-center spectroscopy in solids provides a useful tool for the study of local host–guest interactions where the absorbing center is essentially at rest, confined by the host lattice, and where the normal averaging over many "equivalent" centers is removed. Although this paper focuses on molecular impurity centers, the physical concepts apply equally well to ions, color centers, and other defect absorptions in solids.

As an important first step toward single-molecule detection (SMD), it was necessary to make a very detailed examination of the inhomogeneously broadened optical absorption line of a defect in a solid with large numbers of absorbers (the usual regime). In this limit, a fundamental effect called statistical fine structure (SFS) was observed for the first time.[18, 19] SFS results from (static) fluctuations in the spectral density of absorbers with optical wavelength, and therefore scales as the square root of the number of absorbers in resonance. The observations of SFS and other steps toward SMD will be described in Section 2. Crucial to these measurements was the use of a powerful zero-background laser technique called frequency modulation (FM) spectroscopy, first described by Bjorklund[20] in 1980.

With a firm understanding of SFS in inhomogeneous lines, it became possible to approach the ultimate limit of single-molecule detection (SMD) and spectroscopy. One motivation for the development of SMD comes from the fact that for an inhomogeneously broadened line, the centers located within a homogeneous width of a given laser frequency are located at that particular spectral position for a variety of possible reasons. This intrinsic multidimensional inhomogeneity cannot be removed with spectral hole-burning or coherent transient techniques. However, with SMD the absorption spectrum of a unique individual absorber in its particular environment can become directly accessible, as long as no other centers absorb at the same frequency. This is the primary reason for pursuing the spectroscopy of individual centers in condensed matter. The use of powerful spectroscopic methods (FM spectroscopy) and the properties of the inhomogeneous line itself make SMD feasible; the first successful SMD experiments[21–24] will be described in Section 3.

The advent of a superior technique, fluorescence excitation with extremely high collection efficiency,[25] allowed greatly increased signal-to-noise ratio (SNR) for single-molecule spectra. Examples of precise measurements of the optical linewidth[26] and other phenomena which then became observable will be presented in Section 4. In studies of pentacene molecular defects in crystalline *para*-terphenyl, a novel physical effect called spectral diffusion was observed,[27, 28] which will be summarized in Section 5. Section 6 describes how extensions of SMD to polymeric hosts[29, 30] allow direct observations of hole-burning and stochastic kinetics for an individual center. Section 7 presents results of very recent single-molecule spectroscopy in which spectral shifts due to external electric fields (the Stark effect) have been measured in both crystalline and amorphous materials.[31, 32] Finally, Section 8 reviews a novel new experiment on quantum optics in solids, where the fundamental photon antibunching expected for the fluorescence emission from a single molecule in a solid has been observed.[33] With these results, a new regime of optical spectroscopy may be envisioned in which some of the scientific

W. E. Moerner was born in 1953 in Pleasanton, California. After receiving three Bachelor's degrees in 1975 from Washington University, St. Louis, he obtained M. S. (1978) and Ph.D. (1981) degrees in physics from Cornell University, where he worked with A. J. Sievers. He joined the IBM Research Division, Almaden Research Center in 1981, and worked extensively in the area of spectral hole-burning. He received the Roger I. Wilkinson Outstanding Young Electrical Engineer Award from the Eta Kappa Nu Honorary Electrical Engineering Society of the U.S. in 1984 and an Outstanding Technical Achievement Award from IBM in 1988 and in 1992. He is a Fellow of the Optical Society of America and the American Physical Society, a Senior Member of the Institute of Electrical and Electronics Engineers, and a member of the American Chemical Society. His current interests include single-molecule spectroscopy in solids, optical storage, and polymeric photorefractive materials.

Thomas Basché, born 1959 in Bingen, Germany, did his undergraduate studies in chemistry at the University of Munich where he received his Ph.D. in 1990 for his work with C. Bräuchle. In 1991 and 1992 he was a postdoctoral fellow with W. E. Moerner at the IBM Almaden Research Center in San Jose. His current research interests include optical line-narrowing experiments with adsorbed molecules and single-molecule spectroscopy in condensed phases.

advances and observations of physical effects made possible by the ion trap and STM techniques may be applied to condensed matter.

2. First Steps toward Single-Molecule Spectroscopy

2.1. Background on Inhomogeneously Broadened Optical Lines

It is well known that absorbing guest centers in solids with zero-phonon transitions give rise to inhomogeneously broadened lines[34, 35] where the overall line profile is caused by an approximately Gaussian distribution of center frequencies for the individual absorbers that is broader than the (usually Lorentzian[36]) homogeneous lineshape of the individual absorbers. This situation is shown schematically in Figure 1 and by simulation in Figure 2, which will be described in Section 2.2. The distribution of center frequencies is caused by dislocations, point defects, or random internal electric and strain fields and field gradients in the host material. Inhomogeneous broadening is not only a universal feature of high-resolution laser spectroscopy of defects in solids,[15, 37] but it also appears in a fundamental way in other spectroscopies of impurity centers such as NMR, ESR, and Mössbauer spectroscopy. Inhomogeneous broadening also occurs in amorphous hosts, where the (generally broad) center frequency distribution is caused by the large multiplicity of local environments. Although the work reviewed here is focused mainly on the lowest electronic transition of the absorbing molecule, all of the concepts apply equally well to inhomogeneously broadened vibronic lines as well as to inhomogeneously broadened purely vibrational zero-phonon lines.

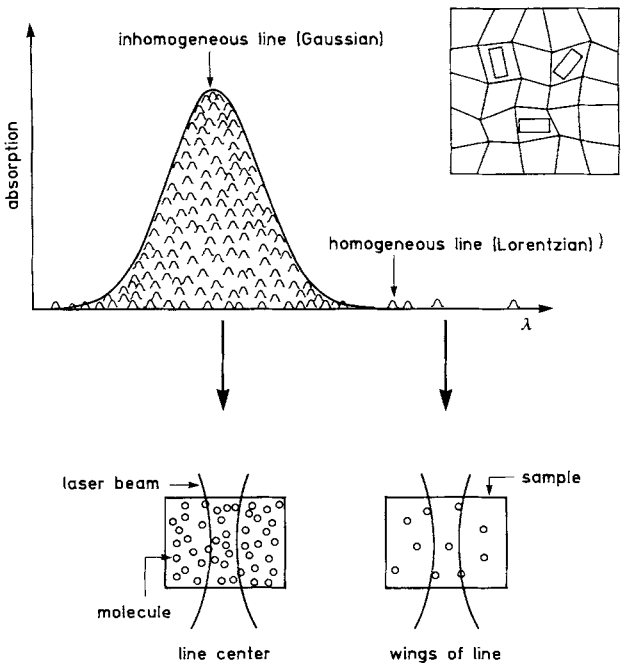

Fig. 1. Top: Schematic representation of an inhomogeneous absorption band at low temperatures and the principle of single-molecule detection in solids. The entire band is formed as a superposition of Lorentzian profiles of the individual absorbers; a distribution of center resonance frequencies is caused by random strains and imperfections. The lower part of the figure shows how the number of impurity molecules in resonance in the probed volume can be varied by changing the laser wavelength. The laser linewidth ($\simeq 3$ MHz) is negligible (after ref. [23]).

Inhomogeneous broadening generally dominates at low temperatures, because the homogeneous zero-phonon lines become much narrower than the inhomogeneous distribution of center frequencies only when the host phonons are quenched. For example, for pentacene in *p*-terphenyl, the homogeneous width of the lowest electronic transition at 593 nm is 7.8 MHz at 1.5 K,[38] while the overall inhomogeneous line is 42 GHz in width in crystals grown by the Bridgman method.[39] In the single-molecule spectroscopy to be described in Section 3, inhomogeneous broadening will be used to select one single absorber for study by proceeding out into the wings of the inhomogeneous line as shown on the right side of Figure 1.[40] Since the center frequencies for these absorbers are displaced very far from the most common center frequencies near the center of the inhomogeneous line, such absorbers have highly unique and strained sites. For this reason, various recent SMD experiments have also considered the situation where the concentration of impurity centers is lowered and single molecules are measured much closer to the center of the inhomogeneous line.

2.2. Statistical Fine Structure

Before the single-molecule limit can be approached, however, it is necessary to review the statistical properties of inhomogeneous lines. To quantify the number of impurity centers absorbing at a particular frequency or wavelength, it is useful to define the quantity $\bar{N}_H$, which is the average number of centers in the probed volume whose center frequencies are within one homogeneous width of the laser wavelength. Due to the unavoidable randomness associated with the imperfections in solid hosts even for a single molecular orientation or "site", inhomogeneous absorption lines (at least where $\bar{N}_H \gg 1$) are often approximated by smooth, Gaussian profiles.[34, 39] However, since the inhomogeneous line on a microscopic scale is simply a superposition of discrete homogeneous lines with widths as much as 1000 times narrower than the overall inhomogeneous profile, the true shape of the inhomogeneous line cannot be a smooth function. In fact, unavoidable fluctuations in the number of absorbers per unit wavelength interval should give rise to a "spectral noise" on the overall Gaussian background that scales as the square root of the mean number of centers in resonance. In other words, there should be a statistical fine structure (SFS) present on the absorption profile scaling in absolute magnitude as $\sqrt{\bar{N}_H}$ (in the limit of $\bar{N}_H \gg 1$). Since SFS arises from the absorption of many overlapping impurity absorptions, the absolute magnitude of the SFS is clearly larger than a single-molecule absorption signal (where $\bar{N}_H \simeq 1$). Therefore, observations of SFS would be expected to precede true single-molecule or single-center detection. This is more than just a pedagogical point: in fact, in any experiment with sensitivity capable of reaching the single-molecule limit, SFS should be observed first and used as a "test signal" to optimize the detection conditions.

Figure 2 shows a computer simulation of an inhomogeneous lineshape for various total numbers of centers N and

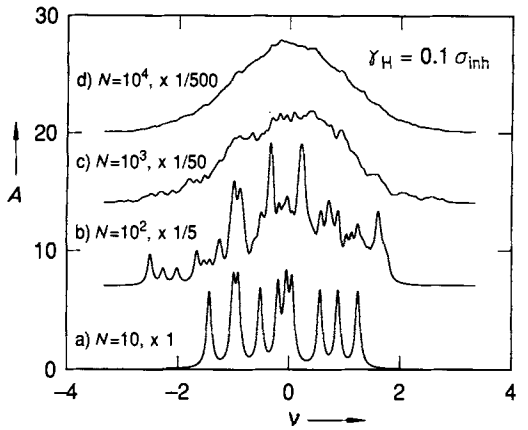

Fig. 2. Simulated absorption spectra with different total numbers of absorbers N. A Gaussian random variable was used to select center frequencies. The homogeneous linewidth is one-tenth of the standard deviation of the inhomogeneous distribution. A = absorption in arbitrary units, ν = frequency in units of σ_{inh} (see text).

hence different values of $\bar{N}_H$. Here γ_H is the (assumed Lorentzian) homogeneous width (full width at half-maximum absorption, FWHM), and σ_{inh} is the standard deviation of the normally distributed distribution of center frequencies. For clarity, a small value of the ratio $\sigma_{inh}/\gamma_H = 10$ was chosen for the simulation; in real solids, this ratio usually ranges from 10^2–10^5. The main point here is that even though the center frequencies were chosen by sampling from a (smooth) normally distributed random variable, the actual center frequencies never form a smooth uniform covering of the allowed frequency space. This is merely a statement that the usual number fluctuations encountered in many areas of physics and chemistry must occur here as well. As Figure 2 shows, the average absorption $\bar{\alpha}$ grows linearly with $\bar{N}_H$, while the relative fluctuations in absorption $\Delta\alpha/\bar{\alpha}$ decrease with $(\bar{N}_H)^{-1/2}$. Therefore, in terms of relative changes in absorption it appears that low-concentration samples ($\bar{N}_H < 10$, for example) might be expected to be optimal for the observation of SFS. While this is true for most techniques, SFS was in fact first observed in a different regime.

2.3. Detection of Statistical Fine Structure with Laser Frequency Modulation Spectroscopy

The limit $\bar{N}_H \to 1$ is in fact the single-molecule regime itself. In the early work, it was realized that statistical fine structure could be measured without completely solving the problem of single-molecule detection. The zero-background technique of laser frequency modulation (FM) spectroscopy[20] provides a solution, because the variable measured is $\Delta\alpha$ itself, which increases with $(\bar{N}_H)^{1/2}$. In other words, statistical fine structure is easier to detect at large $\bar{N}_H$ if FM spectroscopy is used. A glance at Figure 2d verifies that the size of the absorption variations due to SFS in terms of departures from the average absorption is indeed far larger than the size of the absorption signal from a single molecule. Rather than describe the details[41] of FM spectroscopy here, it is more useful to describe the characteristics of the method: 1) The laser is phase-modulated at the radio frequency ν_m, and the transmitted beam is detected with a radio frequency lock-in amplifier at ν_m. 2) The background is zero in the absence of residual amplitude modulation (RAM). 3) The noise on the signal is derived from the laser noise at ν_m, which may be at the quantum limit if no excess noise is introduced by the detector. 4) The signal is largest when the width of the spectral feature is comparable to or less than ν_m; broad spectral features produce no signal. More precisely, in FM spectroscopy the detected signal (in the cosine phase) is proportional to $[\alpha(\nu + \nu_m) - \alpha(\nu - \nu_m)]L$, where ν is the laser frequency and L is the sample thickness. Thus the FM signal measures the difference in αL at the two sideband frequencies. It can easily be shown[19] that as long as the optical density is not too large the FM signal resulting from statistical fine structure is described by Equation (a), where σ is the

$$(\Delta\alpha)L = \sigma(\bar{N}_H)^{1/2}/A = \sigma(\rho_H L/A)^{1/2} \quad \text{(a)}$$

peak absorption cross section, A is the beam area, and the volume density per homogeneous linewidth is given by $\rho_H = \bar{N}_H/AL$. Therefore, the FM signal increases if the concentration of absorbers or the sample length increases, and increases for smaller laser spots. Further, centers with higher cross section lead to larger FM signals.

For the well-studied model system[15,42] pentacene in p-terphenyl crystals statistical fine structure can be easily detected by FM spectroscopy at 1.5 K.[18,19] A schematic illustration of the location of the pentacene molecules in the p-terphenyl host crystal is shown in Figure 3. Pentacene can

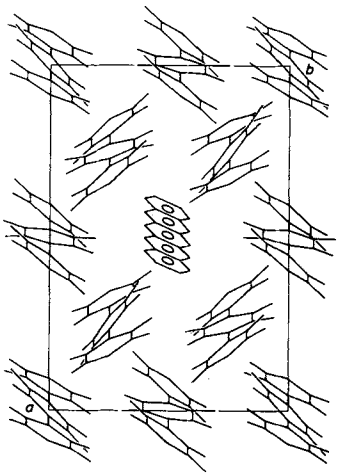

Fig. 3. Schematic representation of the crystal struture of p-terphenyl showing one possible location for a pentacene dopant molecule. This depiction of the pseudomonoclinic crystal structure (projected onto the ab plane) was adapted from ref. [43].

substitute for any one of the four p-terphenyl molecules in the low-temperature unit cell[39,43] giving rise to four $S_1 \leftarrow S_0$ optical absorption origins near 593 nm, called O_1, O_2, O_3, and O_4. It is convenient to focus on the inhomogeneously broadened origins O_1 and O_2, because the homogeneous linewidths are smaller here than for the other origins.

An example of the static nature (and repeatability) of the SFS spectra measured with FM spectroscopy is shown in Figure 4, where the bottom panel shows a 5-GHz-wide scan near the peak of the O_1 line. The spectra were acquired by

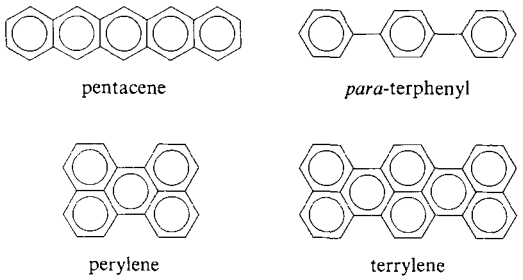

repeatedly scanning the desired frequency range with a Rhodamine 6G single-frequency dye laser (2.8 MHz linewidth). Contrary to what the reader might think, this is not a recording of some noisy signal. The many peaks and valleys are actual, repeatable fine structure as is demonstrated by the two expanded traces in the top panel of Figure 4, the lower

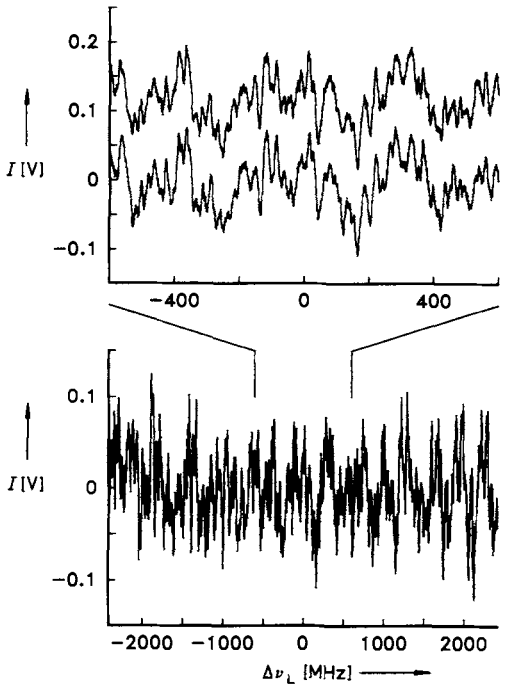

Fig. 4. Frequency modulation spectrum over a wide scan range showing statistical fine structure. The lower panel shows the result of 64 averages of a 5 GHz region of the inhomogeneous line of pentacene in *p*-terphenyl ($T = 1.4$ K). The upper panel shows a portion of the same spectrum on an expanded frequency-scale together with another acquisition of the spectrum taken 20 min later, offset for clarity. Laser power 3 μW, focal spot diameter 20 μm (after ref. [19]). *I* is the intensity of the SFS signal in Volts.

of which is an expansion of the trace in the bottom panel and the upper of which is a subsequent acquisition of the same spectral region more than 20 min later. The agreement is quite good, indicating that at 1.4 K there is little or no rearrangement or annealing of the strains and other imperfections in the *p*-terphenyl crystal which defined the inhomogeneous distribution when the crystal was cooled. Most, if not all, of the slight differences between the spectra are due to the quantum and avalanche noise of the detection system. As expected from Equation (a), the root mean square amplitude of the SFS spectra should grow as $(\bar{N}_H)^{1/2}$, and indeed a measured dependence of $(\bar{N}_H)^{0.54\pm0.05}$ has been observed experimentally.[18]

More insight into the source of SFS can be derived from spectra from different sample volumes. The formation of a specific set of center frequencies for a given sample volume is a random process which reflects the underlying probability distribution for center frequencies; thus SFS should be different for different sample volumes. A "SFS landscape" of the sample can be generated by acquiring multiple SFS spectra as a function of the position of the laser spot, as shown in Figure 5. This display allows one to search for "mi-

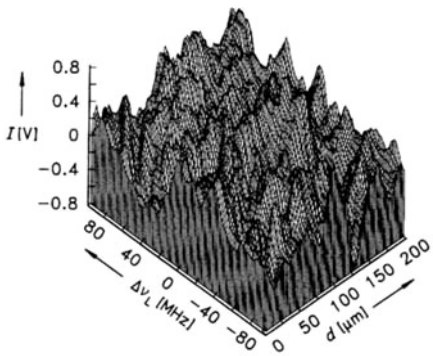

Fig. 5. Statistical fine structure (SFS) versus laser spot position *d* and laser frequency ν_L (0 MHz = 592.32 nm) near the inhomogeneous line center for pentacene in *p*-terphenyl. A sequence of 100 spectra were obtained; the 20 μm laser spot was moved by 2 μm after each spectrum, and the results plotted as a three-dimensional plot of the SFS signal to show the SFS "landscape" (after ref. [19]).

crosites", special (more probable) frequencies that would appear as ridges in this three-dimensional plot. No evidence for microsites or departures from the statistical source for SFS have been observed in this system. As a final point, the value of the underlying homogeneous linewidth can be determined directly by an autocorrelation analysis of the SFS spectra.[19] In systems with weak spectral hole-burning and weak spectral diffusion, this method of obtaining the homogeneous width should work as well as the older, more established techniques of coherent transients or hole-burning, as long as the signal-to-noise ratio of the SFS spectrum is reasonable.

2.4. Further Steps Toward the Single-Center Limit

Subsequent to the first observations of statistical fine structure, other researchers utilized both FM spectroscopy and fluorescence excitation to observe SFS in other classes of materials at smaller and smaller values of $\bar{N}_H$. Lange et al.[44] relied upon fluorescence excitation of Sm^{2+} ions in CaF_2 at 77 K with a fixed-frequency laser in tightly focused spots. They saw Poisson fluctuations in the detected fluorescence as a function of the position of the focal spot, and concluded that they had reached the level $\bar{N}_H = 5$. In a particularly novel approach, developed by the Yen group at the University of Georgia,[45,46] laser fluorescence excitation was used in a glass fiber doped with Nd^{3+} ions. Here the fiber geometry effectively maintained a small focus and a small sample volume, and background signals from the host were reduced. The measured SFS led these researchers to conclude that they had reached $\bar{N}_H$ values on the order of a few tens of ions,

although the spectral features were somewhat broad. In both of these cases, special detection geometries were required to reduce interfering background fluorescence from Rayleigh and Raman scattering.

Equation (a) shows that SFS becomes harder and harder to detect when σ decreases. The drop in signal can be partially offset by increasing the concentration of centers, but for constant optical density the signal still suffers as the square root of the cross section. Nevertheless, FM techniques with the addition of secondary Stark modulation to remove residual amplitude modulation (RAM) allowed the observation of SFS for Cr^{3+} ions in alexandrite.[47] Another approach when σ is low is maintaining a focused spot over a long distance in an optical fiber. In this case the SFS signal increases as the square root of the fiber length, as long as the optical density is less than unity. Using this approach and FM spectroscopy techniques, Brocklesby et al.[48] observed SFS for Nd^{3+} ions in a silica fiber. These experiments demonstrated that SFS can indeed be detected for absorbers in amorphous hosts and for relatively weakly absorbing centers.

3. Detection of Single Molecules in Solids with Absorption Techniques

3.1. Detection with FM Double-Modulation Techniques

Compared to the previous single-absorber experiments on ions in traps, molecules on surfaces, and molecules in hydrodynamic flows, single-molecule detection in solids provides a different set of experimental challenges. The problem can be likened to finding a needle in a haystack, because unlike the ion-trap experiments, for example, the molecule of interest is hidden within a solid containing a large number ($\approx 10^{12} - 10^{18}$) of nonabsorbing, potentially interfering host molecules within the laser focal volume. If laser-induced fluorescence excitation were used for SMD and the host molecules had appreciable Raman (or Rayleigh) scattering cross sections, the signal from the one absorbing molecule could be swamped by the scattering signal from the host.

The first successful SMD experiment,[21] also performed on the pentacene/*p*-terphenyl system, avoided the problem of fluorescence background from the host "haystack" by using the powerful zero-background properties of FM spectroscopy.[20] This method also has the advantage that it is sensitive only to spectral features with widths on the order of the modulation frequency ν_m. Therefore, any impurity molecules in the host matrix with wide absorption lines as a result of stronger electron–phonon coupling or much shorter excited state lifetimes than that of pentacene do not contribute to the observed signal. In this method narrow spectral features in the sample are used to convert the frequency- (phase-) modulated light beam into an amplitude-modulated beam. Since the method directly measures the conversion of frequency into amplitude modulation, any residual amplitude modulation (RAM) from imperfections in the modulator can give rise to a spurious background signal. To overcome this, a secondary modulation of the spectral feature itself was implemented by using oscillating Stark (or separately, ultrasonic) fields.

In the case of pentacene, the applied secondary Stark modulation with oscillating electric fields at frequency f (in the kHz range) shifts the absorption profile twice each cycle by the quadratic Stark effect.[49, 50] The secondary modulation with demodulation at $2f$ generates the first derivative of the FM signal. Because the physical effects giving rise to the RAM are insensitive to the Stark modulating field, this detection system yields a signal that is free from RAM background. It is clear that other local perturbations of the impurity molecule might also be used for double-modulation detection. Other RAM suppression methods that do not require secondary modulation could also be utilized.[51, 52]

The size of the expected absorption signal from a single molecule in an FM spectrum is straightforward to estimate.[21] The change in absorbance, $(\Delta\alpha)L$, is given by the probability of absorption of a photon in the incident beam by the molecule, σ/A, where σ is the peak absorption cross section and A is the area of the laser beam. Clearly, then, one would prefer tightly focused laser spots and molecules with strong absorptions. In the first experiments, the focal spot was $\simeq 3$ μm in diameter, and the peak (low-temperature) absorption cross section for pentacene is 9.3×10^{-12} cm^2, yielding an absorbance change of $\simeq 10^{-4}$. This is not an extremely small signal, but detection must be performed with a light intensity that does not produce extreme power broadening. To meet this constraint in a tightly focused spot, the measurements were performed with only 0.1 μW of light at the detector, which is an extremely small laser power for FM spectroscopy. Such a low light level required an avalanche photodiode to avoid detector Johnson (thermal) noise and resulted in detection approximately 3 dB above the quantum limit.

In spite of these limitations, the FM/Stark and FM/ultrasound methods can be used to detect the optical absorption of a single molecule of pentacene in a solid crystal of *p*-terphenyl.[21, 23] Figure 6 shows examples of the spectra for the FM/Stark case. The first three traces are simulations to illustrate the expected single-molecule lineshape for either Stark or ultrasonic double-modulation. Trace a shows a Lorentzian absorption profile of width γ, trace b the expected simple FM signal:[41] two copies of the absorption line with opposite sign, spaced by $2\nu_m = 150$ MHz (in the limit $\gamma \ll \nu_m$, where ν_m is the rf modulating frequency). With secondary modulation that causes frequency shifts less than the linewidth, the resulting double-modulation lineshape is the derivative of the simple FM lineshape (trace c). Thus the signature of a single molecule is a W-shaped feature with a large negative slope and a large positive slope separated by $2\nu_m$.

In a typical experiment, the laser frequency was set near the center of the inhomogeneous line, and the resulting strong SFS signal was used to optimize the optical and electronic configuration. Then as the laser wavelength was moved out into the wings of the line, the SFS amplitude dropped uniformly. Eventually spectra that appear to be superpositions of two to five single-molecule spectra were observed. Finally, sufficiently far out into the wings of the line, true single-molecule spectra could be recorded. Trace d in Figure 6 shows a set of eight FM/Stark double–modulation spectra of a strong in-focus molecule far out in the long-wavelength edge of O_1, along with several unavoidable,

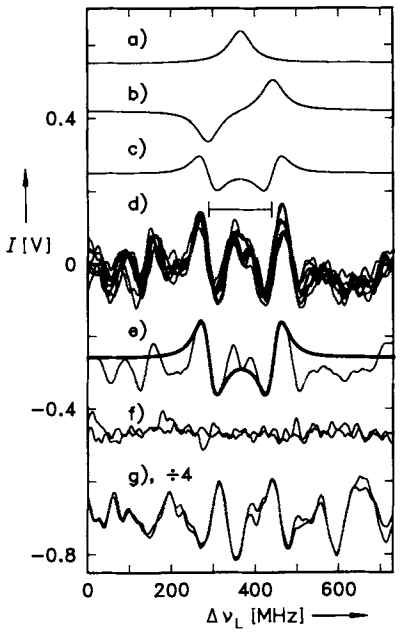

Fig. 6. Single-molecule spectra obtained with the FM/Stark technique (quadratic Stark effect) for pentacene in *p*-terphenyl. a) Simulation of the absorption line. b) Simulation of the FM spectrum with $\nu_m = 75$ MHz. c) Simulation of FM/Stark double-modulation lineshape. d) SMD spectra at $\lambda = 592.423$ nm, 512 averags, 8 traces overlaid; the bar corresponds to $2\nu_m = 150$ MHz. (O_1 line center is at 592.326 nm.) e) Average of traces in (d) and the fit to the in-focus molecule (smooth curve). f) Signal at $\lambda = 597.514$ nm very far from the line center; same conditions. g) Traces of SFS at the O_2 line center, $\lambda = 592.186$ nm, 128 averages each. The vertical scale is correct for trace d; the other traces have the same scale but are offset vertically for clarity (after ref. [21]). I = intensity of the double-modulation signal.

weak, repeatable features from out-of-focus molecules at the left and right edges of the laser scan range. These out-of-focus features were caused by molecules not located at the peak of the laser intensity profile. The fiducial bar in Figure 6 marks a spectral range equal to $2\nu_m$. Trace e shows the average of the eight scans in trace d, along with a fit to the central feature generated by a simple model for the double-modulation process.[23] The fit to the essential features of the SMD lineshape is reasonable, and the homogeneous width required by the fitting process is somewhat larger than the low-power homogeneous width, as expected.

Trace f in Figure 6 shows the detected signal from a laser wavelength so far away from the pentacene site origins that no absorptions are expected to lie in the laser scan range; this is the background shot and avalanche noise. In samples of undoped pure *p*-terphenyl, only a baseline noise level similar to the off-line data in trace f was observed, even near the center of the inhomogeneous line. Trace g shows spectra of the strong SFS observed near the center of the inhomogeneous line for which a smaller number of averages were used. This spectrum is composed of a superposition of many W profiles similar to trace d in Figure 6 with many different center frequencies, illustrating the qualitative difference between spectra of large numbers of molecules (trace g) and spectra of one molecule (trace d). By using the related FM/ultrasound technique and both longitudinal and transverse (shear) ultrasonic waves,[21, 23] single-molecule detection was confirmed.

In summary, the shape of the observed features, the position relative to the pentacene in *p*-terphenyl origins, the lack of such signals in undoped samples, and the appearance of single-molecule spectra with both the FM/Stark and FM/ultrasound techniques, led to the conclusion that the recorded spectra were indeed due to single molecules of pentacene. However, in both cases, the signal-to-noise ratio (SNR) was only approximately 3–5, and further improvements in this SNR proved difficult since the measurements were already performed near the quantum limit and power broadening was already present. Indeed, one cannot underestimate the difficulty in acquiring spectra like those in Figure 6, especially since later work to be described in Section 4 showed that many molecules spectrally diffuse within seconds. The single molecules observed by FM spectroscopy must have been class I (see Section 4) stable pentacene molecules with no spectral diffusion.

3.2. Signal-to-Noise Limits in FM Detection

The characteristics of the signal-to-noise ratio (SNR) for nonsaturating absorbers in FM spectroscopy have been described in ref. [41]. We will outline here the additional complications of avalanche photodiode detection and saturation of the optical transition as they affect single-molecule detection.[*] The analysis in this section is the result of unpublished work by W. P. Ambrose and one of the authors (W. E. M.). For simplicity, the signal-to-noise ratio for simple frequency modulation will be presented, with the assumption that the principal effect of the double-modulation is to remove residual amplitude modulation (RAM) and that the secondary modulation is strong enough to provide maximal signal.

The signal-to-noise ratio (SNR) of simple frequency modulation (FM) can be expressed in terms of a voltage or current ratio [Eq. (b)], where the (homogeneous) saturation of the absorption is described by Equation (c). P_0 is the laser

$$\mathrm{SNR} = \left[C \frac{P_0^2 (\Delta\alpha L)^2}{P_0 + J} \right]^{1/2} \tag{b}$$

$$(\Delta\alpha L) = \sigma/A = \frac{\sigma_0/A}{1 + I_+/I_s} \tag{c}$$

power at the detector, σ_0 is the unsaturated peak cross section, I_s is the saturation intensity, and $I_+ = \beta^2 P_0/4AT_w$ is the laser intensity in the first-order sideband at the sample, β is the modulation index, and T_w is the total transmittance of all optical components between the sample and the detector.

The SNR limits of FM spectroscopy derive from the two noise terms in the denominator of Equation (b), which represent the contributions of the shot noise of the laser beam (carrier) and the Johnson (thermal) noise of the detector, respectively. The constant J is given by $4kT/2eR_L RG_a^2 F_e$ with k Boltzmann's constant, T the absolute temperature, e the electron charge, R_L the load resistance, R the detector responsivity in AW^{-1}, G_a the avalanche gain, and F_e the avalanche excess noise factor. As one can see, the effect of the Johnson noise in reducing SNR is suppressed due to the

[*] Readers not interested in this particular problem may move on to the next section.

gain of the avalanche photodiode. Similarly, the constant C is given by $R\beta^2/16eBF_e$, with B the detection bandwidth. While FM spectroscopy has been shown to be capable of detecting absorption changes as small as 10^{-7} in a 1 Hz bandwidth if several mW of power is available at the detector, the severe limitations on the laser power in single-molecule detection greatly reduce the sensitivity of the technique. When the best possible gains for Si avalanche detectors of approximately 100 and F_e factors near 2.2 are used, the peak FM SNR is on the order of 1 for a saturation intensity of 70 mWcm^{-2}, which is the value for pentacene in *p*-terphenyl including triplet saturation. This SNR is consistent with the observed SNR in the FM experiments, and can be improved only by the use of laser beams with reduced quantum noise. As will be shown below, many pentacene centers have smaller values of saturation intensity and thus were probably not observable in the FM experiments.

4. Improvements in Signal-to-Noise Ratio by Fluorescence Excitation

4.1. Signal-to-Noise Limits in Fluorescence Excitation

The relatively low signal-to-noise ratio (SNR) available from FM absorption spectroscopy and the high powers required to attain this SNR placed severe limits on the physical and chemical information that could be obtained. The demonstration by Orrit et al. (see Section 4.2) that fluorescence excitation with high collection efficiency can be accomplished with acceptable background scattering levels provided greatly increased SNR at lower probing intensity, thus opening the door for additional detailed spectroscopic studies. In the fluorescence excitation method the frequency of a single-mode laser is tuned across the molecular absorption line, and the Stokes-shifted fluorescence intensity is monitored as a function of the excitation wavelength. The fluorescence excitation spectrum then represents an image of the absorption spectrum. An example of the experimental arrangement used by the IBM group is shown in Figure 7. (In the original setup by Orrit et al. a focusing lens was not used and the sample was placed at the end of a single-mode optical fiber.) For optimal collection of the emitted photons, the sample is placed at the joint focus of a lens focusing the laser beam and a paraboloid with numerical aperture near 1.0. The sample is mounted on a transparent substrate made of an alkali metal halide to reduce the possibility of first-order Raman scattering from the substrate. The emitted radiation passes through a long-pass color filter before detection with photon-counting apparatus.

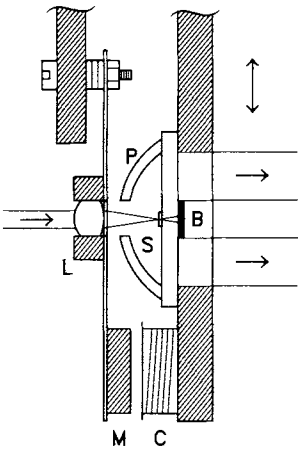

Fig. 7. Experimental set-up for single-molecule fluorescence excitation spectroscopy in a solid at liquid helium temperatures. The excitation laser beam enters from the left and is focused by a lens (L) with a 10 mm focal length into the sample (S), which is mounted on an alkali metal halide plate. The excitation beam is terminated with a piece of black tape (B). The fluorescence from the sample is collected by a parabolic mirror (P), which collimates the emission into a beam propagating to the right in the figure. Fine positioning of the lens (L) relative to the sample is accomplished with an electromagnetic actuator consisting of a coil (C) and magnet (M). Vertical displacement of the sample relative to the laser focal spot (resolution: 10 μm) is performed with a translation stage and micrometer screw (not shown) (after ref. [28]).

The attainable signal-to-noise ratio (SNR) for single-molecule detection in a solid by fluorescence excitation can be approximated by Equation (d), where S_1 is the peak fluorescence signal from one molecule, Φ_f is the fluorescence quantum yield, σ ist the peak absorption cross section on resonance, P_0 is the laser power, τ is the integration time (counting interval), $h\nu$ is the photon energy, N_d is the dark count rate, and C_b is the background count rate per Watt of excitation power. The factor $D = \eta_Q F_p F_f F_i$ describes the overall efficiency for the detection of emitted photons, where η_Q is the photomultiplier tube quantum efficiency, F_p is the fraction of the total emission solid angle collected by the paraboloid, F_f is the fraction of emitted fluorescence which passes through the long-pass filter, and F_i is the total transmission of the windows and collection optics along the way to the photomultiplier. The three terms in the denominator of Equation (d) represent shot noise contributions from the emitted fluorescence, background, and dark signals, respectively.

$$\frac{S_1}{(\text{noise})_{\text{rms}}} = \frac{D\Phi_f\sigma P_0\tau/Ah\nu}{\left[\frac{D\Phi_f\sigma P_0\tau}{Ah\nu} + C_b P_0\tau + N_d\tau\right]^{1/2}} \quad \text{(d)}$$

According to Equation (d) there are several important criteria that have to be fulfilled for optimum SNR, once the collection efficiency D is maximized. First, the peak absorption cross section σ and the fluorescence quantum yield Φ_f of the impurity in the matrix should be as high as possible. Further, the area of the laser spot at the sample plane should be as small as possible, which requires tight focusing of the probing laser beam. The power P_o cannot be increased arbitrarily because saturation causes the peak absorption cross section to drop,[53] $\sigma \rightarrow \sigma(I) = \sigma_o/(1 + I/I_S)$, where I is the laser intensity. For maximum I_S for organic molecules, it is favorable to have the triplet quantum yield low and the triplet lifetime short (expressions for I_S are given in ref. [54]).

To give a concrete example of the application of Equation (d) to a specific material we now consider the parameters appropriate for the model system pentacene in *p*-terphenyl at 1.5 K. Prior work has established that $\Phi_F = 0.78$[57] and that $\sigma_o = 9 \times 10^{-12}$ cm^2.[23] For I_S we use the measured[55] value of 2.5 mW cm^{-2}, which is lower than the value one would calculate using published photophysical parameters.[28, 57] The collection optics and GaAs photomultiplier tube yielded a collection efficiency of $D = 0.01$, and background and dark count parameters of $C_b = 7 \times 10^{10}$

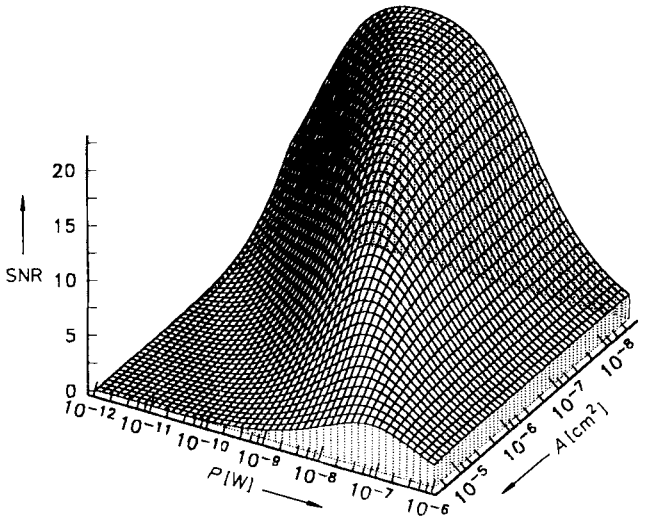

Fig. 8. Signal-to-noise ratio (SNR) for fluorescence excitation of pentacene in *p*-terphenyl versus laser power P and laser beam cross-sectional area A.

counts $W^{-1}\,s^{-1}$ and $N_d = 30$ cps, respectively. With these values, a three-dimensional plot of SNR for an integration time of 1 s versus laser power and beam area can be produced (Fig. 8). It is clear that for a fixed laser spot area, an optimal power exists which maximizes the tradeoff between the saturating fluorescence signal and the linearly increasing (with P) background signal. The lens focusing arrangement shown in Figure 7 produced a spot size of $\approx (5\,\mu m)^2$ located at the midpoint of the area axis. The SNR values predicted by Equation (d) are in reasonable agreement with the experimentally obtained values. One final fact to recognize from Figure 8 is that the best-case SNR at smaller and smaller beam areas levels off. This is due to the effect of saturation and shot noise; at smaller and smaller areas the power must be reduced eventually to the point where the SNR is controlled by the shot noise of the detected signal [first term in the denominator of Eq. (d)].

Of course, in single-molecule studies in solids, a crucial physical effect not included in Equation (d) must be taken into account. Persistent spectral hole-burning (PSHB), which can be observed for certain impurities in crystals and which is a more or less general phenomenon in amorphous hosts,[114] can cause the single impurity to change its absorption frequency before it emits enough photons to be detected above the noise level. The amount of hole-burning that can be tolerated depends upon the total number of molecular excitations required to achieve adequate SNR. A general rule of thumb for practical situations with collection efficiency D near 1% is that approximately 10^5 excitations are required to achieve a SNR on the order of 10 with 1 s integration time. This means that the hole-burning quantum efficiency should be $\leq 10^{-6}$. This indeed may be the most important factor limiting the number of materials systems suitable for single-molecule studies.

4.2. Fluorescence Excitation Measurements for Pentacene in *p*-Terphenyl

Recognizing from the SMD experiments using FM detection that pentacene in *p*-terphenyl is nearly ideal for such studies, Orrit et al. were the first to apply fluorescence excitation with high-efficiency collection to this system.[25] Figure 9 shows the first spectra generated with apparatus similar to that in Figure 7 except that an optical fiber rather than a lens was used. The sample itself was a thin sublimed platelet which helped to reduce the volume available for scattering. In the upper traces, the single-molecule signals appear as isolated dots; expansion of the scan range in the lower trace shows a clear, well-defined single-molecule profile with much improved SNR. These results led most investigators to subsequently use the fluorescence excitation method.

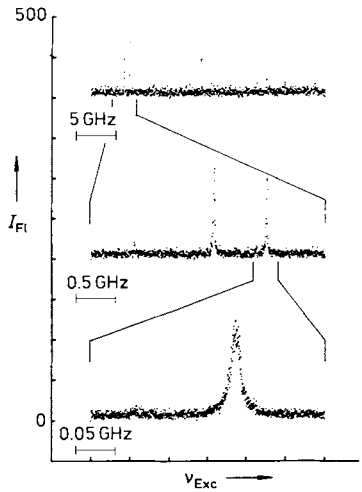

Fig. 9. Fluorescence excitation spectra of single molecules of pentacene in *p*-terphenyl ($T = 1.8$ K) (after ref. [25]). ν_{Exc} = excitation frequency, I_{Fl} = fluorescence intensity in arbitrary units.

The entire inhomogeneous line may now be measured over a wide wavelength range in order to provide specific data that can be contrasted with the schematic picture in Figure 1. Figure 10 shows data for a ≈ 10-μm-thick, low-concentration, sublimed sample of pentacene in *p*-terphenyl at 1.5 K,[28] which was carefully mounted to avoid strain. This 18 GHz spectrum, obtained by scanning a 3 MHz linewidth dye laser, contains 20000 points; showing all the fine structure usually requires several meters of linear space. Figure 10 top shows the frequency region covering the central part of the inhomogeneous line for the O_1 site at 592.321 nm. The structures appearing to be noise are not; they are direct measurements of the statistical fine structure (SFS) as described in Section 2. This structure is static and repeatable and arises directly from statistical variations in the spectral density of absorbers with laser frequency. It is immediately obvious that the inhomogeneous line is far from Gaussian in shape and that there are tails extending out many standard deviations from the center both to the red and to the blue.

More interesting are the spectral features in the wings of the inhomogeneous line (Fig. 10 bottom). At a detuning of -2.7 GHz and elsewhere, clearly resolved, individual single-molecule peaks can be observed. Similar single-molecule peaks are present on the blue edge of the inhomogeneous line. There is a slight variation in the height of the single-molecule peaks since some molecules are not exactly in the center of the Gaussian intensity profile of the laser beam.

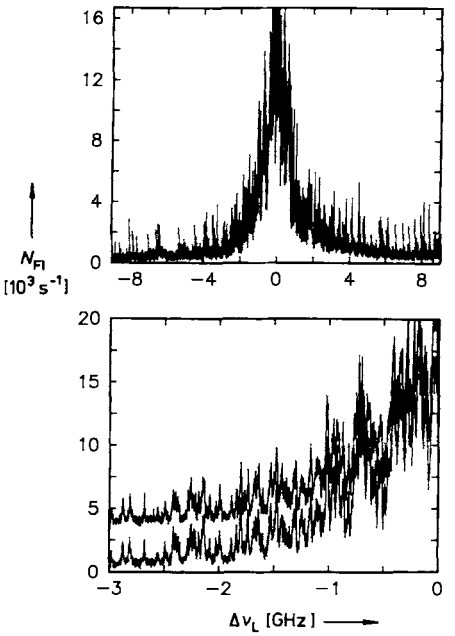

Fig. 10. Fluorescence excitation spectrum of pentacene in *p*-terphenyl (T = 1.5 K). The value of 0 on the frequency axis corresponds to a wavelength of 592.321 nm, which is near the center of the O_1 site inhomogeneous distribution. N_{FI} = Fluorescence count rate, $\Delta\nu_L$ = laser detuning. The unit $10^3\ s^{-1}$ means 10^3 counts per second. Top: An excitation spectrum obtained over 10 min with 2 nW of laser power. Bottom: Two spectra on an expanded scale (the upper trace is displaced from the lower) in the wing of the O_1 site inhomogeneous distribution. The isolated peaks out in the wing are excitation peaks for single pentacene defects (after ref. [28]).

The total pentacene concentration for the sample can be estimated directly by counting the number of molecules in the spectrum; a value of $1.7\times10^{13}\,cm^{-3}$ or 8×10^{-9} mol mol^{-1} is obtained. At different concentrations and in samples with differing levels of strain from mounting, the inhomogeneous linewidth can be varied over a wide range. It has been observed (as in Fig. 9 and confirmed by the IBM group) that in some samples epoxied to the end of an optical fiber the strain can become so great as to spread out the inhomogeneous line over several hundred GHz in frequency space.

Upon close examination of an individual single-molecule peak, the lifetime-limited linewidth of 7.8 ± 0.2 MHz can be observed[26] (Fig. 11). This value is in excellent agreement with previous photon echo measurements on large ensembles of pentacene molecules.[38, 58] The single-molecule excitation profile is well described by a Lorentzian function, as would be expected, since all inhomogeneous broadening has been removed. The laser intensity required for this measurement was 0.5 mW cm^{-2} (laser power 89 pW), and special care was required to remove the interfering effect of laser frequency drift during the measurements.

In general the homogeneous linewidth (full width at half-maximum, FWHM) of an optical transition in a solid is given by Equation (e), where T_1 is the excited state lifetime

$$\Delta\nu_H = \frac{1}{2\pi T_1} + \frac{1}{\pi T_2^*} \qquad \text{(e)}$$

and T_2^* is the (pure) relaxation time (dephasing time). Pure dephasing effects alter the phase of the excited transition without causing excited state decay, as for example when a lattice phonon scatters off the impurity molecule. In the pentacene/*p*-terphenyl system T_2^* goes to infinity for low temperatures ($T < 4$ K), because the host phonons and local modes are essentially quenched. Therefore, the homogeneous width as shown in Figure 11 is given solely by the

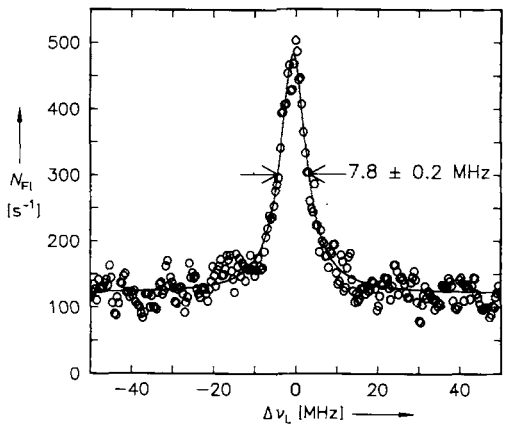

Fig. 11. Low-power fluorescence excitation spectrum for a single pentacene molecule in a sublimed crystal of *p*-terphenyl (T = 1.5 K). 0 MHz ≡ 592.407 nm, which is in the wing of the O_1 site inhomogeneous line. The solid line is a Lorentzian fit to the data (after ref. [26]).

lifetime contribution T_1. It is important to recall that in hole-burning experiments[16] the width of a spetral hole is given in principle by twice the homogeneous width, because a spectral hole is a convolution of the population hole (with width $\Delta\nu_H$, produced during the burning step) and the homogeneous lineshape (produced during the readout step). In many real (especially amorphous) systems, the hole width, however, can be much larger than $2\Delta\nu_H$ due to spectral diffusion occurring on a broad range of timescales.[59] The effect of spectral diffusion on the single-molecule lineshape in a polymeric host is described in Section 6. The point here is that the lineshape in Figure 11 shows neither spectral diffusion nor pure dephasing effects; the width has reached the smallest value allowed by Equation (e) and thus is the true homogeneous linewidth.

By slowly translating the laser focal spot across the face of the crystal and obtaining spectra at each position, one may observe single-molecule peaks localized in both frequency and position. It is thus possible to acquire a "spectral landscape" from the fluorescence excitation spectrum of the sample similar to that obtained for the statistical fine structure at high concentration near the inhomogeneous line center (see Fig. 5). Figure 12 shows a three-dimensional color plot of spectra taken at a series of overlapping laser spots 0.568 μm apart, in which the displacement was accomplished by translating the incident laser beam across the sample.[28] Within the 300 MHz tuning range shown, isolated single-molecule excitation peaks occur at laser detunings of +20, +130, and −120 MHz (relative to the center of the scan) at different positions in the crystal of 30, 35, and 40 μm. The shape of an excitation peak along the position axis is a direct measure of the (Gaussian) intensity profile of the laser beam in the crystal, as probed with the fluorescence emitted by a single molecule. In Figure 12, the spatial width (FWHM) of

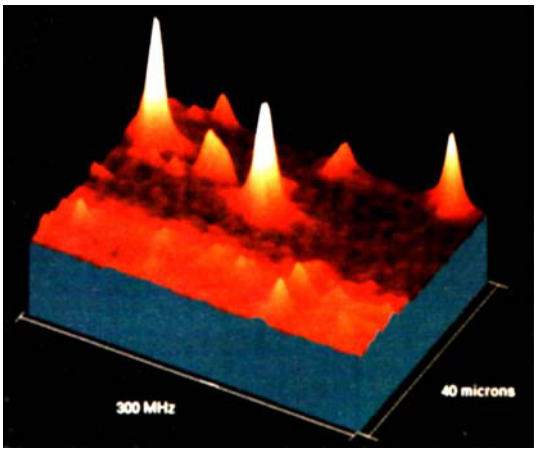

Fig. 12. "Spectral landscape" of the fluorescence excitation of a single pentacene molecule in a crystal of *p*-terphenyl ($T = 1.5$ K). The horizontal axis covers 300 MHz; the center of the axis corresponds to 592.544 nm. The axis extending into the page was generated by measuring successive, excitation spectra (scan time 2 min). The laser focal spot was displaced laterally by 0.57 μm between each measurement to cover a total distance of 40 μm. The intensity of the fluorescence is plotted on the vertical axis.

a single-molecule peak, and hence that of the laser focal spot is $\approx 5 \pm 0.5$ μm. The fluorescence peaks have different sizes because the molecules do not pass directly through the center of the laser focus and "experience" different peak laser intensities. The frequency widths of the peaks in Figure 12 are slightly larger than the lifetime-limited width (Fig. 11) due to the higher probing intensity used. The other oddly shaped peaks in the figure result from molecules that are spectrally diffusing. This effect will be discussed in more detail in the next section.

Spectra like those shown in Figure 11 are ideal for detailed measurements. For example, the intensity saturation behavior of both the linewidth and the emission rate for several single molecules in the wings of the inhomogeneous line was measured,[28] yielding a (free-space) value for the saturation intensity of $I_s = 2.5\ \mathrm{mWcm^{-2}}$. Usually, absolute intensity measurements are difficult because of the Gaussian shape of the laser spot and the difficulty in determining the size of the laser spot in the sample. Here, however, the laser spot diameter may be easily determined simply by using the single molecule as a probe. In the high-intensity limit, the peak fluorescence emission rate saturates at $(7.2 \pm 0.7) \times 10^5$ photons per second. As the peak emission rate saturates, the emission rate in the wings of the line continues to increase with intensity, and the homogeneous linewidth broadens according to the expected form [Eq. (f)].[60] It is remarkable that the value

$$\Delta\nu_{\mathrm{FWHM}}(I) = \Delta\nu_{\mathrm{FWHM}}(0)[1 + I/I_S]^{1/2} \qquad \text{(f)}$$

of I_s expected based on previously determined photophysical parameters for pentacene in *p*-terphenyl is larger than the measured value by more than a factor of 20. The exact reason for this discrepancy is unknown, although it is reasonable that some of the photophysical parameters are modified for the single molecules located in the wings of the inhomogeneous line. It is likely that the intersystem-crossing rate and/or triplet lifetime are affected rather than the fluorescence lifetime, since the intersystem-crossing process is more likely to be affected by strain.[56]

It is also possible to measure the linewidths (FWHM) of the signals of single pentacene molecules as a function of temperature. Such data have been acquired at temperatures up to 10 K where the linewidth increases by almost a factor of 100 compared to the value at low temperatures.[28] The data are in excellent agreement with previous photon echo experiments[15, 61, 62] in which the temperature dependence of the echo decay time was found to follow a form described by dephasing via a single pentacene librational mode[61] with librational energy $\Delta E/k = 38 \pm 1\ \mathrm{K} = 27 \pm 0.7\ \mathrm{cm^{-1}}$. To date, this same temperature dependence was found for all single molecules studied, indicating that the local mode is intrinsic to the defect center and is not influenced by the specifics of the local environment. This is to be contrasted with the local electric fields which do show a distribution (Section 7).

5. Detection of Spectral Diffusion of a Single Molecule in a Solid

In the course of the fluorescence excitation studies by Ambrose et al. on pentacene in *p*-terphenyl, an unexpected physical effect was observed: spectral diffusion of individual pentacene impurity molecules in a crystal at 1.5 K.[27] Here, spectral diffusion means changes in the resonance frequency of a defect at low concentration due to changes in the nearby host, rather than the energy transfer effects that can occur for impurity centers at high concentration.[37] Two distinct classes of impurity molecules were identified: class I, which have center frequencies that are stable in time, and class II, which show spontaneous, discontinuous jumps in resonance frequency of 20–60 MHz on a timescale of 1–420 s. Class II molecules were responsible for the distorted single-molecule peaks in Figure 12 which appeared to change shape between the individual laser scans. Figure 13 shows the behavior of a particular class II defect more clearly; the laser scan speed was increased to 1 scan every 2.7 s so that the spectral position of the molecule could be recorded with improved time resolution. The upper part of the figure shows how the resonance frequency of a spectrally "jumping" class II defect evolved with time, where each trace was digitally smoothed. A digital waveform recorder located the peak in each scan and recorded this resonance frequency as a function of time in the lower part the figure. For this defect, the optical transition energy appears to have a preferred set of values, and the defect performs spectral jumps between these values that are discontinuous on the one-second timescale of the measurement. This type of jumping behavior occurred for some tens of class II defects. In one case, one single molecule was observed that discontinuously jumped between only two allowed frequencies, but spectral jumps between a larger number of allowed frequencies was much more common (see below).

Before summarizing other types of behavior, we should present two crucial observations: First, the occurrence of class II defects was quite common in the wings of the inhomogeneous line (increasing to 40% of the studied molecules at a distance of +0.23 nm from line center), but only class I

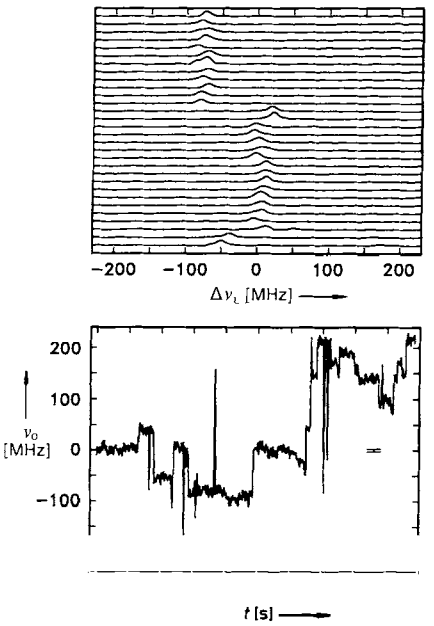

Fig. 13. Spectral jumps in the resonance frequency ν_0 of a class II single pentacene defect in p-terphenyl ($T = 1.5$ K). In the upper half of the figure are individual excitation spectra measured successively (scan time 2.7 s). The peak in each spectrum is represented as a function of time t in the lower half of the figure (after ref. [28]). $\Delta\nu_L$ is the laser detuning.

defects were observed in a spectral region from 0.003 to 0.01 nm from line center. The fraction of pentacene molecules showing class II behavior increased for wavelengths further and further from line center, suggesting that disorder in the crystal is partially responsible for the spectral migration. Second, the jumping rate did not depend upon the laser power used to measure the fluorescence excitation spectrum. This is the main reason that the observed changes in resonance frequency were attributed to a spontaneous process rather than a light-induced spectral hole-burning ef-

The behavior shown in Figure 13 shows relatively discontinuous resonant frequency changes, but in fact a wide array of characteristics was observed. Figure 14 provides an example that also illustrates the general effect of increasing temperature. These measurements of the time dependence of the resonance frequency of a single molecule were taken on a sample mounted on the end of a single-mode optical fiber placed at the focus of the collection paraboloid. This "wandering" defect spectrally diffused rapidly, and was found at a new frequency in every laser scan. During the 1600-second measurement at 1.5 K (Fig. 14 top), the spectral wandering for this defect was confined to a 500 MHz region. At 4.0 K (Fig. 14 bottom), the wandering range expanded to 700 MHz, and the spectral diffusion rate also appears to be higher. This could have been due to a larger number of small jumps between the laser scans, or the spectral jump sizes may have increased with temperature.

Of course, a detailed study of the temperature dependence of an appropriately defined average jumping rate would help to identify the source of the spectral diffusion effect. Such data have not been obtained to date for technical reasons relating to the difficulty of following the same single molecule over the entire temperature range. In samples attached to the end of the optical fiber molecules with wandering behavior like that in Figure 14 were found almost exclusively, which reflects the increased disorder in these samples. In future work, it should be possible to obtain useful temperature-dependence data even with the lens arrangement (Fig. 7) by cooling below 1.5 K with ^{3}He or a dilution refrigerator.

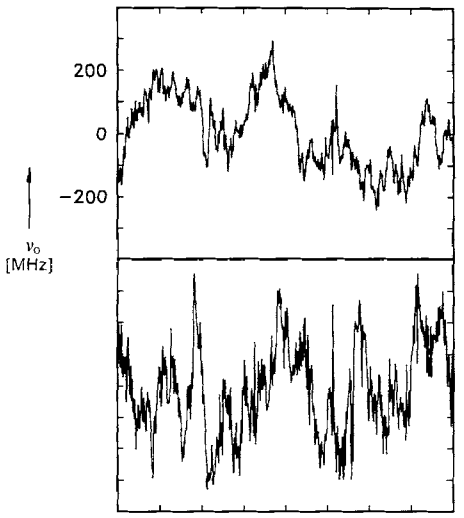

Fig. 14. Qualitative increase in spectral diffusion rate with temperature. In both traces the resonance frequencies ν_0 for a spectrally jumping molecule near the 592.582 nm excitation wavelength are shown. This molecule jumps often, appearing at a new frequency in each spectrum (scan time 2.7 s). Raising the temperature from 1.5 K (top trace) to 4.0 K (bottom trace) appears to increase the spectral diffusion rate and jumping range (after ref. [28]).

As a final illustration of the fascinating spectral diffusion phenomenon, Figure 15 shows the peak frequency trend of another pentacene defect over 1.6 h at 1.5 K. For this defect, which is on the low-frequency side of the inhomogeneous distribution, the overall trend can be described as "creeping" by successive jumps towards higher optical frequencies. As

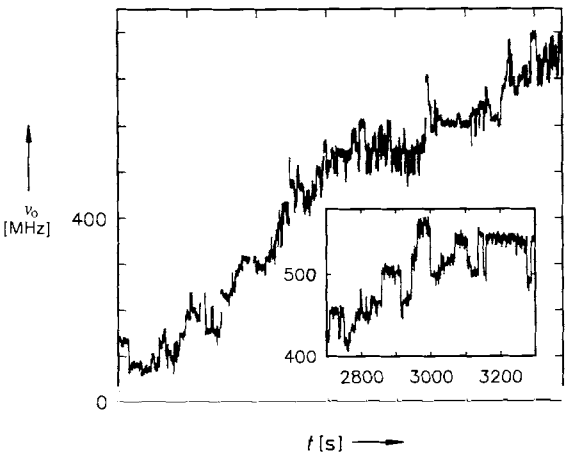

Fig. 15. Frequency "creep" of a spectrally jumping pentacene defect over an extended time. The peak frequency ν_0 of a class II defect near 592.544 nm (on the long-wavelength side of the O_1 inhomogeneous distribution) spectrally jumps no more than 100 MHz on short timescales, but tends towards higher frequencies over 1.6 h. The inset, an expansion of the trace recorded over 600 s, shows the individual jumps < 80 MHz. (after ref. [28]).

shown in the inset, there are residence times on the order of 30 s, and the molecule appears at new, higher frequencies at later times. This "creeping" pentacene defect may be in an environment that is structurally relaxing at 1.5 K into an environment more typical of those found at the center of the inhomogeneous line.

The resonance frequency of an impurity molecule in an inhomogeneously broadened line is extremely sensitive to the strain at the position of the molecule. Thus the spectral jumps appear to occur because the class II pentacene molecules are coupled to an (unidentified at present) ensemble of two-level systems (TLS) in the host crystal undergoing phonon-assisted tunneling or thermally activated barrier crossing. One possible source for the tunneling transitions could be discrete librations of the central ring of the nearby *p*-terphenyl molecules about the molecular axis. As Figure 3 shows, the *p*-terphenyl molecules have a particular dihedral angle between the central and outer phenyl rings, depending upon the specific position in the crystal.[43] When the monoclinic, room-temperature crystal strucure becomes triclinic below 170 K, it is not unreasonable to postulate that the sample may contain several single-crystal domains even though the phase transition is not destructive to the sample.[63] The *p*-terphenyl molecules in a domain wall may have lowered barriers to such central-ring tunneling motions, and the pentacene molecules near the domain walls would "sense" such local motions and show class II behavior. Further experiments are necessary to conclusively identify the molecular motions responsible for the effect. Of course, the spectral diffusion surprisingly observed here in a crystalline system is analogous to spectral diffusion processes that play a crucial role in the physics of glasses and other amorphous materials.[64] Most importantly, with the single-molecule detection technique the spectral changes can be followed in real time for each individual impurity molecule; no ensemble averages over "equivalent" centers need be made.

6. Single-Molecule Spectroscopy in Polymeric Hosts

6.1. Physical Properties of Glasses and Polymers at Low Temperatures

The experiments described so far were performed with single impurity molecules doped into a crystalline matrix. Amorphous systems such as glasses and polymers have a number of interesting physical properties at low temperatures that are quite different from those for crystalline materials.[65] A wealth of information on the low-temperature dynamics of amorphous systems was obtained by doping these materials with optical impurities and probing them with optical line-narrowing techniques such as fluorescence line-narrowing,[37] persistent spectral hole-burning,[14] and photon echoes.[59]

To understand the optical properties of these systems, a brief description of the amorphous state is in order. A glassy or amorphous material is characterized by a complex, multidimensional potential energy surface. According to the two-level system (TLS) model, the potential energy surface can be approximated by a distribution of asymmetric double-well potentials or so-called two-level systems. The TLS model assumes that at low temperatures only the two lowest energy levels of each double-well are important. Transitions from one side of the double-well to the other occur by phonon-assisted tunneling and represent changes in the local structure of the glass. As a result of the broad distribution of barrier heights and well-asymmetries, structural relaxation processes can occur on a wide distribution of timescales. When an impurity molecule is doped in an amorphous solid, its optical transition can couple to the TLSs (e.g. by dipole–dipole coupling), and the lineshape of the optical transition reflects the dynamical processes of the host.[66]

One important physical effect that occurs often in amorphous hosts is persistent spectral hole-burning (PSHB). In PSHB experiments, narrow bandwidth laser irradiation is used to select a reasonantly absorbing subensemble of molecules out of the inhomogeneously broadened absorption band. The optical excitation induces either photochemical changes in the excited centers or photophysical (nonphotochemical) alterations in the nearby host, and a narrow spectral hole can develop in the absorption because the altered centers no longer absorb at the laser wavelength. While photochemical hole-burning can occur in amorphous or crystalline systems, the nonphotochemical process is an almost general phenomenon in amorphous systems and is most likely caused by TLS transitions induced by the laser excitation.[67] By measuring the hole-shape as a function of temperature and/or thermal cycling,[16] information on the host dynamics can be obtained.

6.2. Detection of Single Perylene Molecules in Polyethylene

Aromatic hydrocarbons in non-hydrogen-bonding matrices are systems that show nonphotochemical hole-burning and have low PSHB quantum efficiencies. Taking this important prerequisite into account, perylene in a polyethylene matrix was found to be a suitable candidate for single-molecule detection.[29] Furthermore, the photophysical parameters for this system are favorable: the homogeneous linewidth of the optical transition is narrow, the absorption cross section ($\sigma_0 = 3.5 \times 10^{-11}$ cm^2) and the fluorescence quantum yield $\Phi_F = 0.98$ are high, and the triplet yield and lifetime are low.

The maximum of the inhomogeneous line for the lowest electronic transition of perylene in polyethylene lies at approximately 440 nm. The width of the inhomogeneous distribution is much larger than in a crystalline system, and single molecules were detected in the red wing of this distribution between 445 and 450 nm. In Figure 16 a fluorescence excitation "spectral landscape" of a perylene-doped thin film of polyethylene is shown at 1.5 K. This picture was taken with the same procedure as Figure 12. The signal sizes of the six strong single-molecule fluorescence peaks are again different, partly because the molecules "experience" different peak laser intensities. In an amorphous matrix, however, the orientations of the impurity transition dipoles are statistically distributed, and with a fixed polarization of the incoming laser the single molecule fluorescence intensities vary as

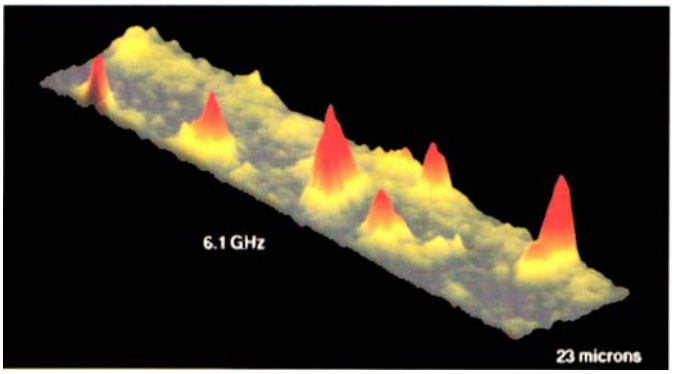

Fig. 16. "Spectral landscape" of the fluorescence excitation of single perylene defects in a polyethylene film. Each "mountain" represents the fluorescence from an individual molecule as the probing laser scans the frequency (6.1 GHz, horizontal axis) and is translated spatially across the face of the sample (23 μm, axis extending up and right).

$\cos^2\theta$, where θ is the angle between the laser polarization and the transition dipole axis. Hence, in this case there are two mechanisms that can lead to varying signal intensities. A close examination of the signal shapes along the frequency axis reveals that these shapes are slightly distorted. This distortion is due to a real physical effect, namely spectral diffusion, the various manifestations of which will be described in the next section.

6.3. Spectral Diffusion in a Polymeric Host

In the pentacene/*p*-terphenyl system the observation of spectral diffusion of single molecules was quite surprising, as the phenomenon occurred in an ordered crystalline material. By contrast, in disordered, amorphous matrices spectral diffusion is a well-known phenomenon.[59, 68] In the TLS picture spectral diffusion occurs due to spontaneous (phonon-driven) transitions in the double-well potentials of the host when the impurity molecules are in their electronic ground states. In hole-burning experiments spectral diffusion is observable by the time-evolution of the hole shapes (broadening) after the burning process.[69] How does spectral diffusion manifest itself in single-molecule experiments in a polymer?

In the perylene/polyethylene system spectral diffusion appeared in two ways in single-molecule spectra.[70] First, discontinuous jumps in frequency space on the scale of several hundred MHz between or during consecutive laser scans (scan time 2.86 s) were observed which were similar to the effects observed with pentacene/*p*-terphenyl (Section 5). Second, a broadening of the single-molecule lineshape was observed which varied from molecule to molecule. The observed linewidths ranged from 52 MHz to 142 MHz, and all these values were larger than the lifetime-limited width of 22.7 MHz. It should be mentioned that part of the observed line-broadening could be due to pure homogeneous dephasing by fast, global (non-local) TLS transitions. According to standard theories, this contribution to the width, however, is generally assumed to be the same for all molecules.

These results give direct evidence that spectral diffusion may occur over a range of frequencies and timescales. When the TLS model is employed, the experimental findings can be qualitatively explained by a hierarchy of TLSs surrounding the impurity. Distant TLSs produce fast shifts that are small in magnitude; in this case spectral diffusion appears as a broadening of the linewidth on the one-second timescale of the measurement. The closer TLSs produce larger shifts that are more infrequent; in this case spectral diffusion appears as frequency jumps which can be resolved on the experimental timescale.

6.4. Spectral Hole-Burning of a Single Molecule

A spectral hole usually refers to a dip in the inhomogeneously broadened absorption spectrum of many molecules when light irradiation alters the absorption frequencies of a portion of the resonant absorbers. In the single-molecule regime, however, only the isolated absorption profile of a single center is present. When photochemical or photophysical changes occur as a result of optical excitation, the absorption line simply appears to vanish as the resonance frequency of the single center shifts away from the laser frequency. As the underlying mechanisms are the same in both cases, we will continue to use the term persistant spectral hole-burning (PSHB) even for the single-molecule case.

An example of spectral hole-burning of a single perylene molecule in a polyethylene host is presented in Figure 17.

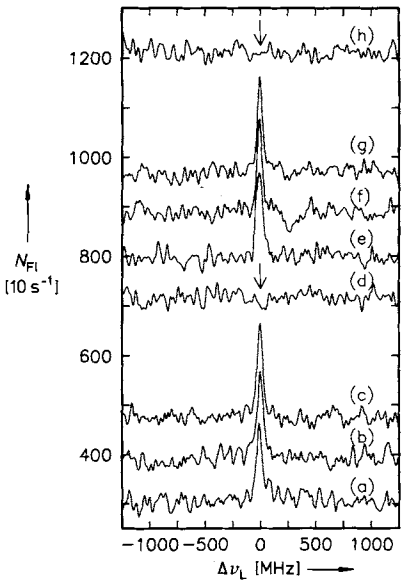

Fig. 17. Persistent spectral hole-burning (PSHB) of a single perylene molecule in a polyethylene film at 1.5 K (see text). 0 MHz ≡ 488.021 nm. The laser power for burning and scanning is 9 nW, and the scan time is 25 s (after ref. [29]). The vertical scale is correct for trace a, the other traces have the same scale but are offset vertically for clarity.

Before the traces shown in the figure were recorded, the molecule was scanned five times, and no significant changes were observed. Traces a, b, and c show three additional scans of the molecule. After trace c the laser was tuned into resonance with the molecule until the fluorescence decreased suddenly. Trace d was then acquired, which showed that the resonance frequency had shifted by more than ±1.25 GHz

as a result of the light-induced change; in other words, PSHB had occurred. A further scan some minutes later (trace e) showed that the molecule surprisingly returned to the burning frequency. After trace g the molecule was "burnt" again, and the whole sequence could be repeated several times.

The exact location of the new resonance frequency, however, could not be determined in these experiments. By analogy with previous nonphotochemical hole-burning studies of large ensembles of molecules,[17] the shift may be expected to be as much as 100 cm^{-1}. Besides the reversible single-molecule hole-burning illustrated in Figure 17, it was possible to observe other single molecules where the light-induced change was irreversible on the timescale of the experiment. The irreversible process was more common at high light power levels.

The possibility of burning one and the same molecule several times was used to determine the power dependence of single-molecule PSHB and to measure the kinetics of this process. Figure 18 shows that with increasing power, the burning time, although stochastically distributed, decreases. The power dependence of the hole-burning process was confirmed in this way for many single molecules. The experiments unambiguously showed that the single-molecule hole-burning is truly a light-driven process in contrast to excitation-power-independent spectral diffusion.

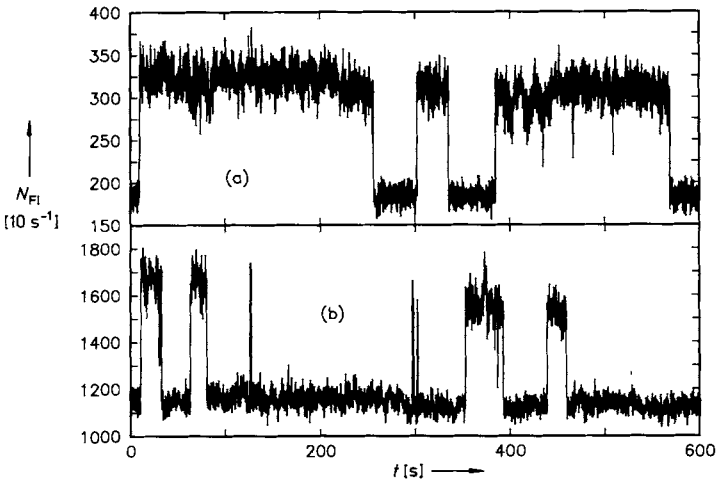

Fig. 18. Illustration of the power dependence of the hole-burning process for a single perylene molecule in a polyethylene film. a) The laser is tuned to resonance (λ = 448.159 nm) with the single molecule in the first 10 s at a power level of 4.5 nW. The abrupt drop of the fluorescence signal at 260 s is the hole-burning event; the return of the fluorescence signal indicates that the molecule has returned to its original frequency, only to be burnt again, and so on. b) The laser power level was increased to 27 nW; now the time in resonance, although stochastic, is clearly shorter (after ref. [29]).

In Section 6.3 two types of TLSs interacting with the impurity were discussed, those producing broadened single-molecule lineshapes, and those producing resonance frequency jumps. There are, however, also the so-called external TLSs which are created by doping the host with the impurity molecules.[71] These TLSs are thought to be in the close vicinity of the impurity and effectively locked because the barrier to configurational changes is too high. A common model for nonphotochemical hole-burning[17] assumes that by optical excitation of the impurity this barrier is lowered and a transition of the TLS can take place. The spontaneous return of perylene molecules after a burning event to exactly the same wavelength was somewhat surprising, though not absolutely unexpected. It suggests that coupling to exactly one dominant nearby TLS, rather than a succession of TLS configurations, is involved in the hole-burning process. In this picture optical excitation induces a (phonon-assisted) transition in the double-well potential in one direction which is reverted by a spontaneous (phonon-assisted) transition at some time later when the molecule is in its electronic ground state.

6.5. Measurement of the Stochastic Phototransformation Kinetics of a Single Molecule

The single-molecule hole-burning experiments are measurements with a single quantum system, although the molecule and its surrounding matrix cage have to be regarded as a kind of "supermolecule". Therefore, it is not surprising that the burning time for one molecule at a fixed power level is a stochastic quantity. By measuring a large number of burning events for one and the same perylene molecule in a polyethylene host it was shown that the burning times are exponentially distributed (Fig. 19).[70] This may be understood by the following simple argument.

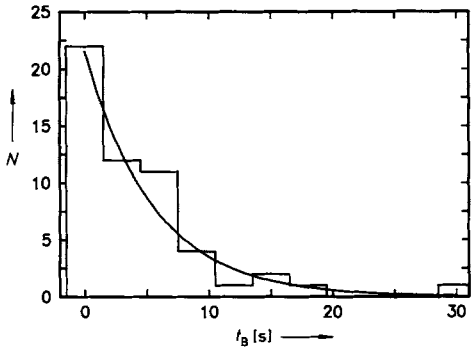

Fig. 19. Histogram of a random sample of 54 burning events measured for a single perylene molecule in a polyethylene matrix by using a power level of 4.5 nW (T = 1.5 K, λ = 448.156 nm). The plotted curve is the result of an exponential fit to the data (after ref. [70]). N is the number of events per time interval.

Single-molecule hole-burning is an example of a Poisson random process. The probability distribution for r successes (hole formation) in a finite time interval τ is therefore given by $P(r,\tau) = \exp(-\lambda\tau)/(\lambda\tau)^r r!$. In the hole-burning experiment, however, the waiting time before the first burning event (i.e. $r = 0$) was measured, and this waiting time therefore has the probability distribution $P(0,\tau) = \exp(-\lambda\tau)$. This corresponds to the familiar result that the distribution of waiting times between Poisson random events is exponential. The smooth curve in Figure 19 is a result of a fit of a simple exponential to the data. The histogram of the random sample of burning times is reasonably well approximated by an exponential distribution function with rate parameter $\lambda = 0.18\ s^{-1}$. This also means that the single perylene molecule investigated has an average hole-burning quantum efficieny of 2.9×10^{-7} per photon absorbed.

It is interesting to point out a formal analogy between these experiments and "quantum-jump" measurements with single trapped ions in a vacuum. In the latter investigations the bright fluorescence from a strong (allowed) transition ceases when the single atom "jumps" into a dark state which is weakly coupled to the ground state by a forbidden transition. In this case the number of quantum jumps per unit time is given by a Poisson distribution and the waiting times between quantum jumps by an exponential distribution as well.[72, 73]

7. Stark Effect Studies with Single Molecules

The fact that spectra of a single molecule in a solid can be obtained with high signal-to-noise ratios naturally leads to measurements of such spectra under the influence of external fields. One can imagine that Zeeman effects, Stark effects, and stress-induced splittings and shifts can be observed. In recent work, two groups have completed Stark effect studies on single molecules, in one case in a crystalline host and in the other case, a polymeric host.

7.1. Pentacene in *p*-Terphenyl Crystals

The first single-molecule Stark effect studies of the pentacene/*p*-terphenyl system were performed by Wild et al. using a longitudinal geometry in which the sample was held between a thin metal plate with a 5 μm pinhole and a SnO_2-coated glass plate.[31] (In fact, both the linear and quadratic Stark effects for this single-molecule system were utilized in the double-modulation scheme reported in Section 3 for the initial detection of single molecules with FM absorption.) In the recent work, fluorescence excitation spectra of single molecules were recorded with various DC external electric fields applied in order to determine specific values for the polarizability change and the internal field. In all cases, only shifts and no splittings of the single molecule spectra were observed.

Figure 20 shows the energy shifts recorded for four single molecules, along with best-fits to the data using second-order polynomials.[31] In general, a quadratic shift was observed with an offset from zero which was different for different molecules. The high symmetry of the pentacene molecule is consistent with a quadratic shift, and the linear term was attributed to different internal crystal fields at the positions of the various single molecules. The data were used to determine that the internal fields ranged from -1.6×10^3 kVcm^{-1} to $+0.8\times10^3$ kVcm^{-1}, and that the polarizability change $\Delta\alpha$ ranged from 1.1×10^{-39} Fm^2 to 2.5×10^{-39} Fm^2. The unambiguous observation of a quadratic shift, which was relatively constant from molecule to molecule, and a first-order shift, which varied considerably from molecule to molecule, gives direct evidence for one underlying source of inhomogeneous broadening that has been long postulated—randomness in the local crystal field.

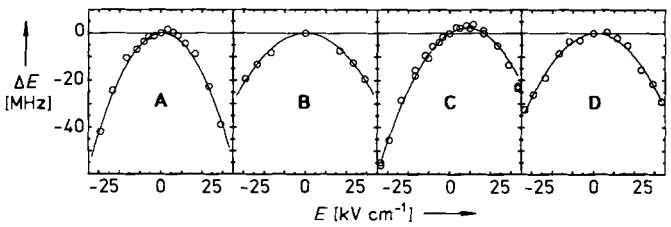

Fig. 20. Stark shift of four molecules of pentacene **A–D** in *p*-terphenyl as a function of electric field. The plotted curves are the result of second-order polynomial fits to the data (after ref. [31]).

7.2. Terrylene in Polyethylene

Numerous Stark effect studies of impurity molecules in amorphous materials have been performed over the last decade by using hole-burning techniques.[74, 75] Even with centrosymmetric molecules, only linear Stark effects were observed, due to the reduction of symmetry caused by local fields. To address the important question as to whether or not linear Stark effects persist down to the single-molecule level, Orrit et al. have recently studied a new system composed of terrylene molecules in low-density polyethylene.[32] The terrylene molecule is similar to perylene, except that three rather than two naphthalene molecules are condensed at the peri positions. This modification conveniently shifts the first electronic transition to longer wavelengths. The thin films were sandwiched between two transparent conducting plates for the optical measurements. As with pentacene in *p*-terphenyl, only shifts of the single-molecule lines were observed.

Figure 21 shows the observed frequency shifts for a selection of six single molecules. Only linear Stark shifts were detected, suggesting that the local fields were quite effective

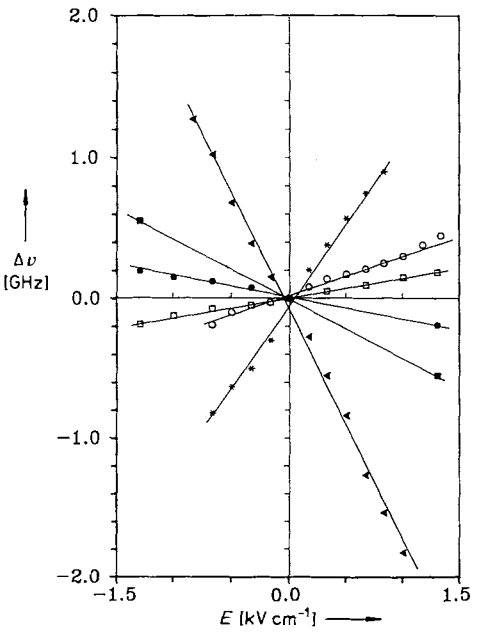

Fig. 21. Stark shift of single terrylene molecules in polyethylene as a function of electric field. The plots are linear to within experimental error; the magnitudes and signs of the slopes depend upon the orientation of the field relative to the molecule and the matrix cage. The largest slope corresponds to a change in dipole moment of several Debye (after ref. [32]).

in lowering the molecular symmetry. By studying a large number of single molecules, the distribution of Stark coefficients could be sampled, and positive coefficients were found to be more common than negative coefficients. It is certainly clear that these results provide individual measurements of the local fields, and that such perturbations are averaged in the conventional measurements at large values of $\bar{N}_H$. If it will be possible to measure the splitting coefficients for a single molecule with several directions of applied field, more specific information about the local symmetries may be obtained.

8. Measurements of Quantum Effects with Single Molecules in Solids

In all the experiments described in the preceding sections the single molecule served as an ultrasensitive probe for measuring truly local host–guest interactions. A single molecule can also be used to study the fundamental interaction of light and matter in experiments in which the fully quantum-mechanical nature of this interaction is revealed. So far investigations of this type with single particles were limited to single atoms stored in radio-frequency traps by photon-recoil cooling. A variety of fascinating experiments such as quantum jumps, quantum collapse and revival, photon antibunching, and many others were realized with laser-cooled ions.[1, 2] However, for all molecules, even diatomic species, the internal degrees of freedom prevent laser-cooling, and therefore trapping of a single molecule in a vacuum has not been achieved to date. As illustrated in the earlier part of this paper, however, single molecules can be easily "trapped" and observed optically in a solid. When the molecules are impurities in a solid and the samples are cooled to liquid-helium temperatures, the solid acts as a "trap" for the single impurity molecules. They are effectively held at rest, and in many cases, rotation of the impurity molecule is quenched and recoil effects are usually small (less than the optical linewidth).[35, 76]

One interesting aspect of the interaction of light and matter concerns the correlation between photons radiated by a single atom or molecule. As was shown for Na atoms in a weak atomic beam[77] or a single trapped Mg^+ ion,[78] the correlation between successive photons emitted by a single atom (ion) decreases near $t = 0$ (photon antibunching). This is in marked contrast to the case for coherent light, where the correlation is independent of the time separation between photons, and for thermal light, which shows an increase in correlation (photon bunching) near $t = 0$.

Photon antibunching in the resonance fluorescence of a single atom was predicted by Carmichael and Walls.[79] This phenomenon is a true signature of a quantum-mechanical radiation field which can be nicely rationalized with the following simple picture. In the correlation measurement the joint probability for the arrival of a photon at time $t = 0$ and the arrival of a photon at $t > 0$ is recorded. After emission of a photon at $t = 0$ the quantum system is in its ground state since it just emitted the photon. The probability of emitting a second photon at $t = 0$ is zero because the molecule cannot emit from the ground state. On the average, a time of half a Rabi period must elapse for the molecule to have a finite probability of being in the excited state and hence emitting a second photon.

Photon antibunching must be observed on a short timescale comparable to the excited singlet-state lifetime. Correlation measurements on the nanosecond timescale, or to be more specific, measurements of the second-order or intensity correlation function $g^{(2)}(\tau)$ were performed with single pentacene molecules in a *p*-terphenyl host.[33] The exciting laser pumped the lowest zero-phonon purely electronic transition $S_1 \leftarrow S_0$, and the photon correlation properties of the vibronically shifted fluorescence from the excited singlet state S_1 were analyzed. As in the single-atom experiments, the delay time distribution of consecutive pairs, $N(\tau)$, which is proportional to $g^{(2)}(\tau)$, was measured in a Start–Stop experiment, that is, by using a beamsplitter and two photomultipliers (PMTs) to record the emitted fluorescence. Detection of a photon from the first PMT starts a delay time counter, and the detection of a photon by a second PMT stops the counter. The distribution of such delay times is recorded for many Start–Stop pairs.

Plots of $N(\tau)$ are shown in Figure 22 for different levels of Rabi frequency (which is proportional to the square root of the intensity). The antibunching in the correlation function is clearly evident at short times $t \rightarrow 0$. With increasing power the background due to accidental pair correlations increases, leading to an increasing deviation of $N(\tau)$ from zero at the origin. The solid lines in Figure 22 show the results of numerical fits to the data using the solutions of the optical Bloch equations for a three-level system. At the highest power level (Fig. 22c) the correlation function shows, besides the antibunching, the expected Rabi oscillations which are damped out during the excited state lifetime.

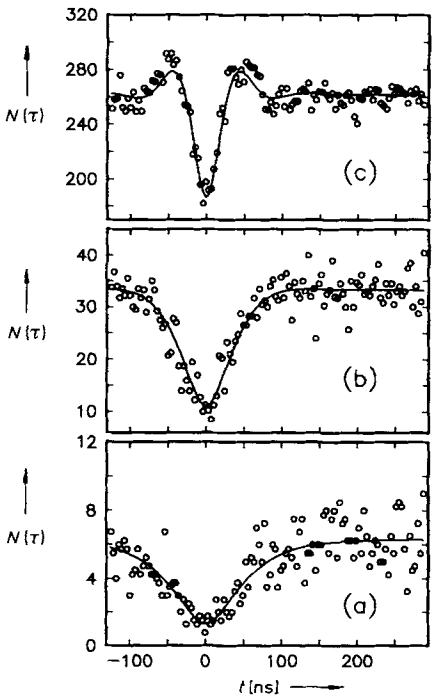

Fig. 22. Measured intensity correlation $N(\tau)$ [in counts per 0.9 ns] for a single pentacene molecule ($\lambda \approx 593.4$ nm). The antibunching is clearly seen for $t \rightarrow 0$. Rabi frequencies Ω: a) 11.2 MHz; b) 26.2 MHz; c) 68.9 MHz. The solid lines are fits to the data with $\Omega = 1-10$ MHz (a), 25.5 MHz (b), and 71.3 MHz (c) (after ref. [33]).

Since pentacene in *p*-terphenyl is effectively a three-level system when lowest triplet state is included, photon bunching should be observed for much longer times, comparable to the 40 μs triplet lifetime. This is a consequence of the fact that on average, the pentacene molecule emits roughly 200 photons due to singlet–singlet excitation before intersystem crossing into the "dark" triplet state occurs (the triplet yield is 0.0047[57]). This purely classical effect was observed clearly by Orrit et al.[25] and used to prove that the spectra in the early experiments arose from single molecules.

These first results on quantum optics in a solid demonstrate that single-molecule spectroscopy in solids can be used to investigate truly quantum-mechanical effects for multiatom molecules with zero-phonon optical transitions. Here the experimental data were not affected by transit time or secular motion effects as are the beam or ion-trapping methods. However, background signals and intersystem crossing into the triplet state did limit the single-molecule antibunching signal and must be controlled in each specific case. As long as the lowest electronic transition of the molecule is pumped, the presence of vibrational levels in the ground state and the detection of nonresonant fluorescence does not prevent the observation of photon antibunching.

9. Summary and Outlook

By utilizing the near-quantum-limited performance and low background of laser frequency modulated (FM) spectroscopy, the intrinsic fine structure on inhomogeneous lines in solids, statistical fine structure (SFS), was detected for the first time. With a detailed understanding of SFS and improvements to FM spectroscopy to remove residual amplitude modulation (RAM), it thus became possible to measure the optical absorption spectrum of a single molecule of pentacene in *p*-terphenyl. Dramatic improvements in the signal-to-noise ratio resulting from the use of fluorescence excitation with high-efficiency collection led to the observation of lifetime-limited widths, to saturation and dephasing studies, and to the surprising observation of spectral diffusion for a single impurity molecule in a crystal. Extensions of these investigations to systems with polymeric hosts allowed study of the spectral diffusion process widely postulated in amorphous materials, as well as to the observation of spectral hole-burning and stochastic kinetics for a single molecule. Stark effect studies in both crystals and polymers have yielded important new information about local symmetries and local fields. Fially, single-molecule techniques in recent work have led to the first quantum optics in a solid—the detection of photon antibunching for a single molecule.

The success of single-molecule detection and spectroscopy in solids opens up a new frontier of single-absorber experiments in which the measured properties of the absorbing center are not averaged over many "equivalent" absorbers. Here the absorbing entity is exquisitely sensitive to the symmetry and perturbations introduced by the local environment such as the local vibrational modes and the true local fields. While as a general technique the method presented here is not applicable to all molecular impurities, it can be applied to the large number of absorbing ions and molecules in solids that have zero-phonon transitions, reasonable absorption strength, and efficient fluorescence. The detectability of the resulting single-center signal, which ultimately depends upon the specific sample and weak or absent spectral hole-burning, must be evaluated in each case.

A number of fascinating future experiments based on the single-molecule detection techniques presented here may be contemplated. The temperature dependence of the spectral diffusion process in crystals may help to identify the source of the effect. It would be particularly interesting to measure the temperature dependence of the linewidth in a polymeric host to attempt to resolve the current controversy about dephasing processes in these systems. Nonlinear spectroscopy to measure the dynamic Stark effect for a single isolated molecule may also be performed. With the proper choice of lifetimes, one would expect quantum jumps and other processes observed for single ions in vacuum electromagnetic traps to become directly observable. The door is also open to true photochemical experiments on single absorbers, measurements of the dispersed fluorescence from a single molecule, and the possibility of optical storage with single molecules.[29]

In one novel experiment now possible the emission from a single molecule could be used as a light source of subnanometer-dimensions for near-field optical microscopy. Another possibility would be to perform cavity quantum electrodynamics studies with a single molecule in a solid. It is to be expected that single-molecule spectra will be obtained at higher and higher temperatures to extend the applicability of these studies to a wider range of materials. In all cases, improvements in the signal-to-noise ratio would be expected to open up a new class of applications. Because this field is only in its infancy, the possibilities are only limited at present by the imagination and the persistence of the experimenter and the continuing interest of the theoretician in the properties of single-quantum systems in solids.

10. Glossary

Coherent transient spectroscopy and photon echoes: In the present context we will limit our short explanation to the case of optical coherent spectroscopy where only two levels, the ground and excited electronic state of an atom or molecule, are involved. Coherent excitation of such a system with sufficiently high intensity lasers creates a coherent superposition of the ground and excited state wave functions. The coherent superposition, which is characterized by a well-defined phase relation between the two levels, leads to interference effects whose time evolution can be monitored with special spectroscopic techniques. The coherent state is described by the off-diagonal elements of the two-level density matrix in the optical Bloch equation formalism. The coherence is a transient phenomenon which is destroyed rapidly by population and phase relaxation processes. One example of coherent transient spectroscopy is the photon echo where the decaying coherence initially created by a first intense light pulse can be reestablished by a properly timed second light pulse. The photon echo can be formally described by the time evolution of a pseudo-spin vector in a fashion equivalent to the spin echo in magnetic resonance spectroscopy.

The time decay of the photon echo amplitude also gives information about the underlying homogeneous width when inhomogeneous broadening is present. See for example, L. Allen, J. H. Eberly, *Optical Resonance and Two-Level Atoms*, Dover, New York, **1987**.

Electron–phonon coupling and zero-phonon transition: When an impurity molecule in a solid matrix is electronically excited, the host vibrations (phonons) can couple to the electronic excitation (electron–phonon coupling) in the same way as is well known for the intramolecular vibrations of the impurity. Linear electron–phonon coupling, where the coupling strength is given by the displacement of the excited state potential surface with respect to the ground state potential surface, gives rise to phonon sidebands of the purely electronic transition line in absorption and emission. The purely electronic transition with no net creation or destruction of phonons is called the zero-phonon transition and can be viewed as the optical analogue of the recoil-free Mössbauer line. Quadratic electron–phonon coupling leads to a broadening of the zero-phonon line by phonon scattering. See for example, A. M. Stoneham, *Rev. Mod. Phys.* **1969**, *41*, 82; R. H. Silsbee, in *Optical Properties of Solids*, (Eds.: S. Nudelman, S. S. Mitra), Plenum, New York, **1969**, p. 607; K. K. Rebane, *Impurity Spectra of Solids*, Plenum, New York, **1970**, p. 99.

Frequency modulation (FM) spectroscopy: In FM spectroscopy the laser is frequency-modulated at a high frequency, narrow spectral features in the sample convert the frequency modulation into amplitude modulation, and the amplitude modulation of the light beam is detected with a high-speed detector and a lock-in amplifier. See G. C. Bjorklund, M. D. Levenson, W. Lenth, C. Ortiz, *Appl. Phys. B* **1983**, *32*, 145.

FWHM: Full width at half-maximum; a convention for measuring the width of spectral lines or of laser beam profiles.

Photon antibunching: A purely quantum-mechanical correlation property of a light beam which states that the probability of detecting two photons separated by a small time interval Δt approaches zero as $\Delta t \rightarrow 0$. See for example, R. Loudon, *The Quantum Theory of Light*, Clarendon, Oxford, **1983**, pp. 226–229.

Rabi period: In the time evolution of a two-level atomic system pumped by light, the Rabi period is the time required for the superposition of the two states to go from pure ground state, through the excited state, and back to the pure ground state again. See L. Allen, J. H. Eberly, *Optical Resonance and Two-Level Atoms*, Dover, New York, **1987**.

Residual amplitude modulation (RAM): Unwanted amplitude modulation of the laser beam in FM spectroscopy which represents a spurious background signal that can limit sensitivity. See for example, E. A. Whittaker, M. Gehrtz, G. C. Bjorklund, *J. Opt. Soc. Am. B* **1985**, *2*, 1320.

Statistical fine structure (SFS): This effect refers to the intrinsic variations in absorption coefficient versus wavelength which occur for inhomogeneously broadened transitions due to number fluctuations in the spectral density of absorbers. See T. P. Carter, M. Manavi, W. E. Moerner, *J. Chem. Phys.* **1988**, *89*, 1768.

SMD: Single-molecule detection.

SNR: Signal-to-noise ratio.

Spectral hole-burning: In spectral hole-burning experiments, narrow-bandwidth laser irradiation is used to select the resonantly absorbing subensemble of molecules out of an inhomogeneously broadened absorption profile. The optical excitation induces either photochemical changes in the excited centers or photophysical (nonphotochemical) alterations in the nearby host, and a narrow dip (spectral hole) can develop in the absorption spectrum because the altered centers no longer absorb at the laser wavelength. The width of the spectral hole can provide information about the underlying homogeneous linewidth when spectral diffusion effects are absent. Peristent spectral hole-burning (PSHB) refers to the situation in which the spectral hole lasts longer than any excited state lifetime. See for example, J. Friedrich, D. Haarer, *Angew. Chem.* **1984**, *96*, 96; *Angew. Chem. Int. Ed. Engl.* **1984**, *23*, 113; R. Jankowiak, G. J. Small, *Science* **1987**, *237*, 618–625; *Persistent Spectral Hole-Burning: Science and Applications* (*Top. Curr. Phys.* **44**), (Ed.: W. E. Moerner), Springer, Berlin, **1988**.

We are grateful to the Research Division of International Business Machines Corporation and to the U. S. Office of Naval Research for support of this research. We also acknowledge our colleagues, Drs. W. P. Ambrose, T. P. Carter, and L. Kador for their work which laid the foundations for single-molecule spectroscopy in solids.

Received: August 13, 1992 [A 898 IE]
German version: *Angew. Chem.* **1993**, *105*, 537

[1] W. M. Itano, J. C. Bergquist, D. J. Wineland, *Science* **1987**, *237*, 612, and references therein.
[2] F. Diedrich, J. Krause, G. Rempe, M. O. Scully, H. Walther, *IEEE J. Quantum Electron.* **1988**, *24*, 1314, and references therein.
[3] R. G. Brewer, J. Hoffnagle, R. G. DeVoe, L. Reyna, W. Henshaw, *Nature* **1990**, *344*, 305.
[4] a) H. Dehmelt, *Angew. Chem.* **1990**, *102*, 774; *Angew. Chem. Int. Ed. Engl.* **1990**, *29*, 734; b) W. Paul, *ibid.* **1990**, *102*, 780 and **1990**, *29*, 739; c) N. F. Ramsey, *ibid.* **1990**, *102*, 790 and **1990**, *29*, 725.
[5] G. Binnig, H. Rohrer, *Angew. Chem.* **1987**, *99*, 622; *Angew. Chem. Int. Ed. Engl.* **1987**, *26*, 606.
[6] H. Ohtani, R. J. Wilson, S. Chiang, C. M. Mate, *Phys. Rev. Lett.* **1988**, *60*, 2398.
[7] a) J. S. Foster, J. E. Frommer, *Nature* **1988**, *333*, 542; b) Review: J. E. Frommer, *Angew. Chem.* **1992**, *104*, 1325; *Angew. Chem. Int. Ed. Engl.* **1992**, *31*, 1298.
[8] D. Sarid, *Scanning Force Microscopy*, Oxford, New York, **1991**.
[9] D. C. Nguyen, R. A. Keller, J. H. Jett, J. C. Martin, *Anal. Chem.* **1987**, *59*, 2158.
[10] K. Peck, L. Stryer, A. N. Glazer, R. A. Mathies, *Proc. Natl. Acad. Sci. USA* **1989**, *86*, 4087.
[11] E. B. Shera, N. K. Seitzinger, L. M. Davis, R. A. Keller, S. A. Soper, *Chem. Phys. Lett.* **1990**, *174*, 553.
[12] S. A. Soper, E. B. Shera, J. C. Martin, J. H. Jett, J. H. Hahn, H. L. Nutter, R. A. Keller, *Anal. Chem.* **1991**, *63*, 432.
[13] S. A. Soper, L. M. Davis, E. B. Shera, *J. Opt. Soc. Am. B* **1992**, *9*, 1761.
[14] See *Persistent Spectral Hole-Burning: Science and Applications (Top. Curr. Phys. 44)* (Ed.: W. E. Moerner), Springer, Berlin, **1988**.
[15] D. A. Wiersma in *Photoselective Chemistry, Part 2 (Adv. Chem. Phys. 47)* (Eds.: J. Jortner, R. D. Levine, S. A. Rice), Wiley, New York, **1981**, pp. 421–485.
[16] J. Friedrich, D. Haarer, *Angew. Chem.* **1984**, *96*, 96; *Angew. Chem. Int. Ed. Engl.* **1984**, *23*, 113.
[17] R. Jankowiak, G. J. Small, *Science* **1987**, *237*, 618–625.
[18] W. E. Moerner, T. P. Carter, *Phys. Rev. Lett.* **1987**, *59*, 2705.
[19] T. P. Carter, M. Manavi, W. E. Moerner, *J. Chem. Phys.* **1988**, *89*, 1768.
[20] G. C. Bjorklund, *Opt. Lett.* **1980**, *5*, 15.
[21] W. E. Moerner, L. Kador, *Phys. Rev. Lett.* **1989**, *62*, 2535.
[22] W. E. Moerner, L. Kador, *Anal. Chem.* **1989**, *61*, 1217A.
[23] L. Kador, D. E. Horne, W. E. Moerner, *J. Phys. Chem.* **1990**, *94*, 1237.
[24] For a "highlight" see D. Haarer, L. Kador, *Angew. Chem.* **1991**, *103*, 553; *Angew. Chem. Int. Ed. Engl.* **1991**, *30*, 540.
[25] M. Orrit, J. Bernard, *Phys. Rev. Lett.* **1990**, *65*, 2716–2719.

[26] W. E. Moerner, W. P. Ambrose, *Phys. Rev. Lett.* **1991**, *66*, 1376.
[27] W. P. Ambrose, W. E. Moerner, *Nature* **1991**, *349*, 225–227.
[28] W. P. Ambrose, T. Basché, W. E. Moerner, *J. Chem. Phys.* **1991**, *95*, 7150.
[29] T. Basché, W. E. Moerner, *Nature* **1992**, *355*, 335.
[30] For a "highlight" see C. Bräuchle, *Angew. Chem.* **1992**, *104*, 431; *Angew. Chem. Int. Ed. Engl.* **1992**, *31*, 426.
[31] U. P. Wild, F. Güttler, M. Pirotta, A. Renn, *Chem. Phys. Lett.* **1992**, *193*, 451.
[32] M. Orrit, J. Bernard, A. Zumbusch, R. I. Personov, *Chem. Phys. Lett.* **1992**, *196*, 595.
[33] T. Basché, W. E. Moerner, M. Orrit, H. Talon, *Phys. Rev. Lett.* **1992**, *69*, 1516.
[34] A. M. Stoneham, *Rev. Mod. Phys.* **1969**, *41*, 82.
[35] K. K. Rebane, *Impurity Spectra of Solids*, Plenum, New York, **1970**, p. 99.
[36] A (normalized) Lorentzian lineshape is given by $(\Gamma/\pi)/(\omega^2 + \Gamma^2)$, where Γ is the full width at half-maximum.
[37] See *Laser Spectroscopy of Solids (Top. Appl. Phys. 49)* (Eds.: W. M. Yen, P. M. Selzer), Springer, Berlin, **1981**.
[38] F. G. Patterson, H. W. H. Lee, W. L. Wilson, M. D. Fayer, *Chem. Phys.* **1984**, *84*, 51.
[39] R. W. Olson, M. D. Fayer, *J. Phys. Chem.* **1980**, *84*, 2001.
[40] It would also be possible to drastically lower the impurity concentration and work near the center of the inhomogeneous line, and this has also been done. The present approach is somewhat more useful experimentally, since by tuning to the center of the inhomogeneous line where N is large, a convenient alignment signal results that can be used to optimize the detection system. Then, by tuning out into the wings, single-molecule absorptions can be observed.
[41] G. C. Bjorklund, M. D. Levenson, W. Lenth, C. Ortiz, *Appl. Phys. B* **1983**, *32*, 145.
[42] T. E. Orlowski, A. H. Zewail, *J. Chem. Phys.* **1979**, *70*, 1390.
[43] J. L. Baudour, Y. Delugeard, H. Cailleau, *Acta Crystallogr. Sect. B.* **1976**, *32*, 150.
[44] R. Lange, W. Grill, W. Martienssen, *Europhys. Lett.* **1988**, *6*, 499.
[45] W. M. Yen, *Proc. SPIE Int. Soc. Opt. Eng.* **1988**, *1033*, 183.
[46] W. M. Yen in *Laser Spectroscopy of Solids II (Top. Appl. Phys. 65)* (Ed.: W. M. Yen), Springer, Berlin, **1989**, p. 23.
[47] T. P. Carter, D. E. Horne, W. E. Moerner, *Chem. Phys. Lett.* **1988**, *151*, 102.
[48] W. S. Brocklesby, B. Golding, J. R. Simpson, *Phys. Rev. Lett.* **1989**, *63*, 1833.
[49] J. H. Meyling, D. A. Wiersma, *Chem. Phys. Lett.* **1973**, *20*, 383.
[50] J. H. Meyling, W. H. Hesselink, D. A. Wierma, *Chem. Phys.* **1976**, *17*, 353.
[51] M. Gehrtz, G. C. Bjorklund, E. A. Whittaker, *J. Opt. Soc. Am. B* **1985**, *2*, 1510.
[52] N. C. Wong, J. L. Hall, *J. Opt. Soc. Am. B* **1985**, *2*, 1527.
[53] See for example P. N. Butcher, D. Cotter, *The Elements of Nonlinear Optics*, Cambridge Univ. Press, Cambridge, **1990**, p. 180.
[54] H. de Vries, D. A. Wiersma, *J. Chem. Phys.* **1980**, *72*, 1851.
[55] The I_s value measured in ref. [28] for single molecules in the wings of the inhomogeneous line is altered, presumably by distortion of the molecule in the highly strained local environment. See ref. [56].
[56] C. Kryschi, H.-C. Fleischhauer, B. Wagner, *Chem. Phys.* **1992**, *161*, 485.
[57] H. de Vries, D. A. Wiersma, *J. Chem. Phys.* **1979**, *70*, 5807.
[58] H. de Vries, D. A. Wiersma, *J. Chem. Phys.* **1978**, *69*, 897.
[59] L. R. Narasimhan, K. A. Littau, D. W. Pack, Y. S. Bai, A. Elschner, M. D. Fayer, *Chem. Rev.* **1990**, *90*, 439.
[60] See for example A. Yariv, *Quantum Electronics*, 3rd ed. Wiley, New York, **1989**, Chap. 8.
[61] W. H. Hesselink, D. A. Wiersma, *J. Chem. Phys.* **1980**, *73*, 648.
[62] F. G. Patterson, W. L. Wilson, H. W. H. Lee, M. D. Fayer, *Chem. Phys. Lett.* **1984**, *110*, 7.
[63] B. A. Bolton, P. N. Prasad, *Chem. Phys.* **1978**, *35*, 331.
[64] B. Golding, J. E. Graebner in *Amorphous Solids – Low-Temperature Properties (Top. Curr. Phys. 24)* (Ed.: W. A. Phillips), Springer, Berlin, **1981**, pp. 107–134.
[65] See *Amorphous Solids—Low-Temperature Properties (Top. Curr. Phys. 24)* (Ed.: W. A. Phillips), Springer, Berlin, **1981**.
[66] R. Silbey, K. Kassner, *J. Lumin.* **1987**, *36*, 283.
[67] J. M. Hayes, R. P. Stout, G. J. Small, *J. Chem. Phys.* **1981**, *74*, 4266.
[68] J. Friedrich, D. Haarer in *Optical Spectroscopy of Glasses* (Ed.: I. Zschokke), Reidel, Dordrecht, **1986**, p. 49.
[69] S. Jahn, K.-P. Müller, D. Haarer, *J. Opt. Soc. Am. B* **1992**, *9*, 925.
[70] T. Basché, W. P. Ambrose, W. E. Moerner, *J. Opt. Soc. Am. B* **1992**, *9*, 829.
[71] B. L. Fearey, G. J. Small, *Chem. Phys.* **1986**, *101*, 269.
[72] W. Nagourney, J. Sandberg, H. Dehmelt, *Phys. Rev. Lett.* **1986**, *56*, 2797.
[73] T. Sauter, R. Blatt, W. Neuhauser, P. E. Toschek, *Opt. Commun.* **1986**, *60*, 287; *Phys. Scr.* **1988**, *T22*, 128.
[74] F. A. Burkhalter, G. W. Suter, U. P. Wild, V. D. Samoilenko, N. V. Rasumova, R. I. Personov, *Chem. Phys. Lett.* **1983**, *94*, 483.
[75] U. Bogner, P. Schätz, R. Seel, M. Maier, *Chem. Phys. Lett.* **1983**, *102*, 267.
[76] R. H. Silsbee in *Optical Properties of Solids* (Ed.: S. Nudelman, S. S. Mitra), Plenum, New York, **1969**, p. 607.
[77] H. J. Kimble, M. Dagenais, L. Mandel, *Phys. Rev. Lett.* **1977**, *39*, 691.
[78] F. Diedrich, H. Walther, *Phys. Rev. Lett.* **1987**, *58*, 203.
[79] H. J. Carmichael, D. F. Walls, *J. Phys. B.* **1976**, *9*, L43.

Poly(hydroxyalkanoates): A Fifth Class of Physiologically Important Organic Biopolymers?**

By Hans-Martin Müller and Dieter Seebach *

Along with polyisoprenoids, polypeptides, polysaccharides, and polynucleotides, Nature contains a further group of biopolymers, the poly(hydroxyalkanoates). The commonest member of this group, poly[(*R*)-3-hydroxybutyrate] P(3-HB), had been identified by Lemoigne as early as the 1920s, as a storage substance in the microorganism *Bacillus megaterium* made up of more than 12000 (3-HB) units. However, the widespread distribution and significance of these biopolymers has only become clear recently. The work of Reusch, in particular, has shown that low molecular weight P(3-HB) (100–200 3-HB units) occurs in the cell membranes of prokaryotic and eukaryotic organisms. The function of P(3-HB) in the latter sources is largely unknown; it has been proposed that a complex of P(3-HB) and calcium polyphosphate acts as an ion channel through the membrane. Indeed, it has even been speculated that P(3-HB) plays a role in transport of DNA through the cell wall. In the present article, the following subjects will be discussed: metabolism of P(3-HB) and analogous polyesters in the synthesis and degradation of storage materials; P(3-HB) as a starting material for chiral synthetic building blocks; synthesis of cyclic oligomers (oligolides) of up to ten 3-HB units, and their crystal structure; high molecular weight bio-copolymers of hydroxybutyrate and hydroxyvalerate (BIOPOL) as biologically degradable plastics; nonbiological production of polyhydroxyalkanoates from 3-hydroxy carboxylic acids and the corresponding β-lactones; specific synthesis of linear oligomers with a narrow molecular weight distribution, consisting of about 100 (*R*)-3-hydroxybutyrate units, by using an exponential coupling procedure; structure of the polyesters, and a comparison with other polymers; the experimental results which led to the postulation of a P(3-HB) ion channel through the cell wall; modeling of P(3-HB) helices of various diameters, by using the parameters obtained from the crystal structures of oligolides; formation of a crown ester complex and ion transport experiments with the triolide of 3-HB. The article describes one example of the contributions that synthetic organic chemists can make to important biological problems in an interdisciplinary framework.

1. Introduction: Occurrence and Significance of Polyhydroxyalkanoates in Nature

Polyhydroxy acids (PHAs[1]) are synthesized by microorganisms under conditions of nutrient limitation in the presence of an excess carbon and energy source. Due to their low solubility and their high molecular weight PHAs do not cause an increase in osmotic pressure, and they are therefore ideal storage compounds.[2] In this role they are much more common in microorganisms than are glycogen, polyphosphates, or fats, for example.[3,4] The most prominent PHA is poly[(*R*)-3-hydroxybutyrate] [P(3-HB)], a linear, unbranched homopolymer built up of (*R*)-3-hydroxybutyric acid units. The molecular weight values given in the literature vary considerably, and are dependent on microorganism, cultivation conditions, and the method of isolation. Typically, the values lie between 1×10^5–7.5×10^5 g mol^{-1} ($n = 2500$–9000, polydispersity (M_w/M_n) = 1.7–2.9[5]), but they can be greater than one million g mol^{-1}. The copolymer from (*R*)-3-hydroxybutyrate and (*R*)-3-hydroxyvalerate P(3-HB/3-HV) has achieved a certain economic importance because of its polypropylene-like material properties, and is marketed by ICI under the tradename "BIOPOL". P(3-HB) and P(3-HB/3-HV) are both biodegradable, and their synthesis is based on renewable materials.[6] Great things are expected of them because of these qualities; this is apparent by their regular appearance in the press,[7] review articles which are published ever more frequently,[1b,4,5,8–13] and the increasing number of patents.[14]

P(3-HB) was first described by Lemoigne in 1925,[15] who later isolated and identified the material from *Bacillus megaterium*.[16] Since then, P(3-HB) has been discovered in a large number of different microorganisms,[11] for example in Archaebacteria, in both gram-negative and gram-positive bacteria, and in Cyanobacteria. Apart from a few phototrophic microorganisms, *Clostridium* and *Syntrophomonas* are the only strict anaerobes in which P(3-HB) has been found. Interestingly, enterobacteria (gut bacteria) such as *Escherichia coli* do not normally synthesize P(3-HB) as a storage compound.[11,17,18]

Apart from its occurrence as a storage compound, P(3-HB) is also found—in a low molecular weight form—in bacterial membranes and in the tissues of plants and animals, where it presumably forms part of an ion channel (see Section 7).[19–23] Recently it has also been detected in relatively large amounts in human blood plasma (between 0.6 and 18.2 mg per liter blood), where it is bound mainly to the so-called "low density lipoproteins" (20–30%), and to albumin (70–80%).[24]

[*] Prof. Dr. D. Seebach, Dr. H.-M. Müller
Laboratorium für Organische Chemie
der Eidgenössischen Technischen Hochschule
ETH Zentrum
Universitätstrasse 16, CH-8092 Zürich (Switzerland)

[**] This review article contains part of the dissertation of H.-M. Müller (dissertation no. 9685, ETH Zürich, 1992).

Schulz and Toft have shown that in certain species of spiders from the Linyphia family, (*R*,*R*)-hydroxybutyrate dimers act as pheromones. They lead the male to roll up the web of unfertilized females, possibly in order to demonstrate that the female is now occupied. This behavior is not observed with the webs of already fertilized females.[25] P(3-HB) has also been discussed as a possible energy source for nitrogen fixation in *rhizobia*.[12, 17a, 26]

2. Polyhydroxy Acids as Cellular Storage Materials

Quantitatively, the most important role of poly(3-hydroxyalkanoates) is to store carbon-containing material and reductase equivalents in the cells of prokaryotic microorganisms (up to 90% of cell dry weight!). The biochemistry of the synthesis and degradation of high molecular weight P(3-HB) has therefore been subject to intensive studies. These have demonstrated which other hydroxy acids can be incorporated into the polymer, in natural or synthetic growth media. The enzymes involved in the biosynthesis have been identified, transferred to other microorganisms, and expressed by gene technological methods.

2.1. Intracellular Distribution of Polyhydroxy Acid Esters

PHAs occur in the cytoplasm of the cell in the form of inclusion bodies, so-called granules. Typically, these have a diameter of 100–800 nm, and have been shown to be surrounded by a kind of micelle ("monolayer"), but not by a double layered structure (typical membrane, lipoprotein bilayer).[27] Depending on the bacterium, the PHA-synthase and depolymerase system may also be bound to this envelope. Purified granules from *B. megaterium* consist of 97.7% P(3-HB), 1.8% protein, and 0.5% lipid.[5, 28]

The structure of P(3-HB) within the granules has been subject to debate until recently. All that was previously known was that treatment with solvents, bases or acids, as well as cooling or heating inhibited their enzymatic digestion.[29] More recently Doi et al.[30] by X-ray diffraction and Sanders et al. ([31a], but also[31b]) by high-resolution ^{13}C NMR spectroscopy have shown that the P(3-HB) within the native granules is present in an amorphous form. This is surprising, since isolated P(3-HB) normally reveals between 60 and 70% crystallinity.[32] The reasons for this are not yet clear; Sanders et al. postulate water as a plasticizer, whereas Doi et al. attribute an inhibitory effect on crystallization to an as yet unknown lipid component. Because of its thermodynamically less favorable state, amorphous P(3-HB) is probably more amenable to enzymatic degradation than P(3-HB) with a high content of crystalline domains.

2.2. Poly[(*R*)-3-hydroxybutyrate] Metabolism

Intracellular P(3-HB) metabolism is a cyclic process, involving seven enzymes, as shown in Scheme 1. It has been investigated primarily by Schlegel et al. and Dawes et al. in *Alcaligenes eutrophus*,[33–40] by Dawes et al. in *Azotobacter beijerinckii*,[41–43] by Fukui et al. and Tomita et al. in *Zoologea ramigera*,[44–49] and in somewhat less detail by Merrick et al. and Doudoroff et al. in *Rhodospirillum rubrum* and *Bacillus megaterium*.[29, 50–56] It has also been studied in other microorganisms.[1b, 12]

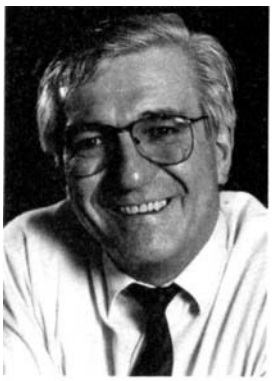

Dieter Seebach was born in Karlsruhe in 1937, he studied chemistry at the University of Karlsruhe. He received his Ph.D in 1964 with a thesis on small-ring compounds and peroxides (supervisor R. Criegee). After a stay of almost two years at Harvard University as a postdoctoral fellow with E. J. Corey and lecturer of chemistry, he returned to Karlsruhe and his research led to a habilitation on S- and Se-stabilized carbanion and carbene derivatives in 1969. In 1971 he became a full professor at the University of Giessen and since 1977 he has been a full professor at the Eidgenössische Technische Hochschule in Zürich. He has had visiting professorships at the Universities of Madison (Wisconsin), Strasbourg, München (TU), Kaiserslautern, as well as Caltech (Pasadena) and the Max-Planck-Institut in Mülheim. His main areas of research are the development of new synthetic methods, mechanistic studies, structure determinations, and natural product syntheses. Recently his research has been concerned more and more with the topic discussed in this review.

Hans-Martin Müller was born in Herisau/Appenzell Ausserrhoden, Switzerland in 1962. After training as a chemistry laboratory assistant he studied chemistry at the Ingenieurschule in Basel (Diplom 1985). He subsequently studied chemistry at the ETH Zürich (Diplom 1988). He received his doctorate with D. Seebach with a thesis on polyhydroxybutyric acid in 1992 and in the same year joined the company Sandoz.

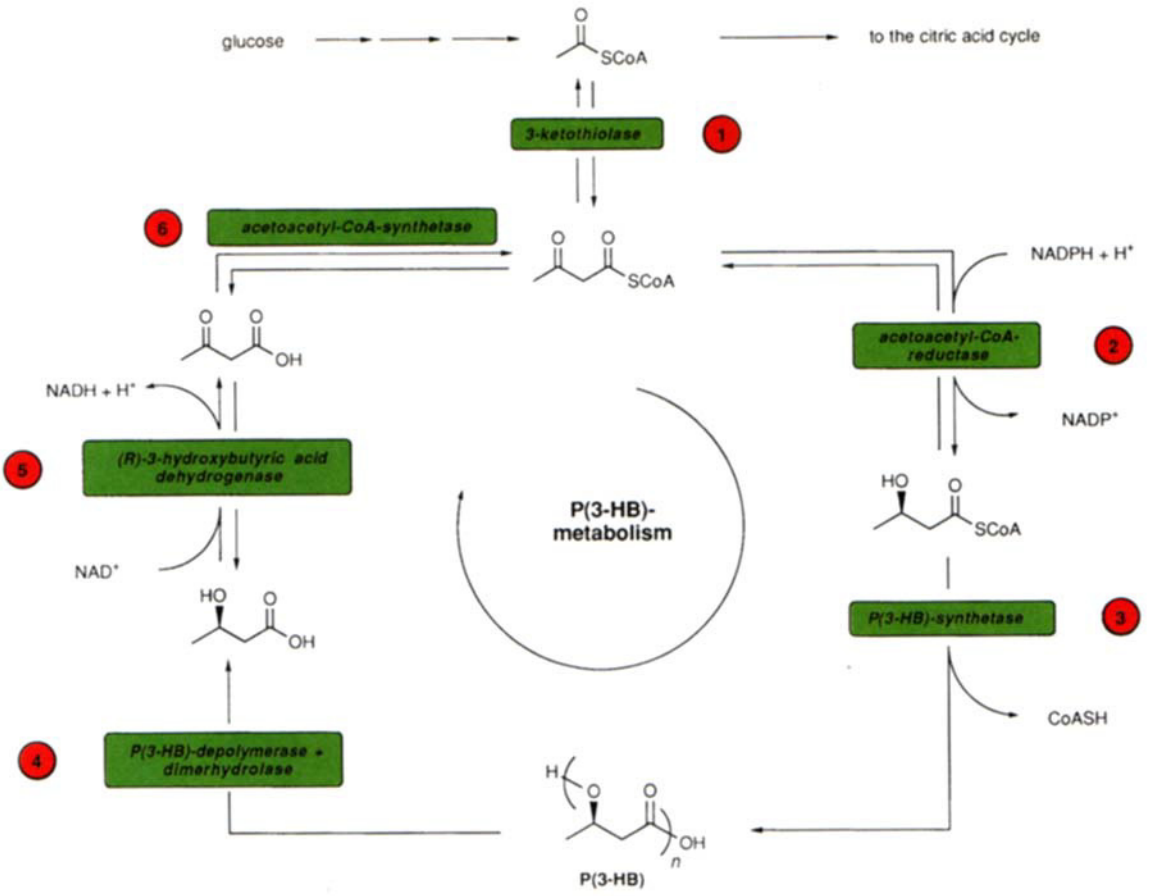

Scheme 1. The best known and probably most widely distributed P(3-HB) metabolic pathway, which also occurs in *A. eutrophus*, *Z. ramigera*, and *A. beijerinckii*.

A metabolic pathway slightly different from that in Scheme 1 has been proposed for *A. eutrophus* by Doi et al,[57] which uses butyric acid (and probably also the higher carboxylic acids) as substrate. Here, butyric acid is first esterified with coenzyme A (CoA) and then converted stepwise into acetoacetyl-CoA via crotonyl-CoA and (*S*)-3-hydroxybutyryl-CoA. The remainder of the pathway is identical to that shown in Scheme 1. In other bacteria, further metabolic variants have been found (see [58] and Section 2.3.1).

2.2.1. Biosynthesis

The following section will discuss primarily the P(3-HB) biosynthetic pathway observed in *A. eutrophus*, since this microorganism, as the basis of the production of BIPOL by the ICI process, has the greatest commercial importance.[59] The *A. eutrophus* strains NCIB11599[5] and N9A[60] produce more than 90% of their dry weight as P(3-HB), when the C source provided is glucose or fructose, respectively. In contrast to *Pseudomonas oleovorans* and other bacteria, only polyesters with C_3–C_5 monomer units are synthesized, from a variety of substrates.[61]

A. eutrophus possesses two 3-ketothiolases,[36] which catalyze the Claisen reaction of two carboxylic thioesters to the corresponding 3-ketocarboxylate. The mechanism of this reversible reaction has been studied in detail by Masamune et al.[62] Enzyme A acts predominantly on acetoacetyl-CoA, and is somewhat less active with 3-ketopentanoyl-CoA; it is therefore responsible for P(3-HB) metabolism. Enzyme B prefers higher 3-ketoacetyl-CoA substrates (C_4 to C_{10}), and is presumably more concerned with fatty acid metabolism. It is the only enzyme in Scheme 1 which is involved in both the biosynthesis and the biodegradation of polyesters.

For the second step, the reduction of acetoacetyl-CoA, two enzymes are again present in *A. eutrophus*,[37] an NADH- and an NADPH-dependent reductase. The NADH-dependent enzyme can oxidize both (*R*)- and (*S*)-3-hydroxybutyryl-CoA, whereas reduction affords only (*S*)-3-hydroxybutyryl-CoA. The NADPH-reductase is stereoselective in both the oxidation and reduction reactions, and is active only with (*R*)-3-hydroxybutyrate, which is also the exclusive product in the reduction. It is therefore only this reductase that is involved directly in P(3-HB) metabolism.

P(3-HB)-synthase, the last enzyme associated with the biosynthesis, is found in a soluble form and a "granule-associated" form.[39] Under normal growth conditions one finds only the soluble synthase, which is transformed to the granule-associated form under conditions of nitrogen limitation. This enzyme can only polymerize certain hydroxy acids, and therefore governs the composition of the polymer.[40]

2.2.2. Cloning and Expression of the Poly[(R)-3-hydroxybutyrate] Biosynthetic Pathway of Alcaligenes eutrophus

The transfer of an entire biosynthetic pathway into a foreign organism is always advantageous when an industrially

more robust strain is required, when different (cheaper) raw materials are sought, or in order to investigate mechanistic questions.[63] Often the genes coding for the biosynthesis lie close to each other, making transfer to another organism somewhat simpler. When one considers the great expectations placed on PHAs, it is hardly surprising that no fewer than three research groups have cloned and expressed the *A. eutrophus* P(3-HB) biosynthetic genes (steps 1–3, Scheme 1) in *E. coli*.[17b, 64–66] *E. coli* does not normally synthesize PHAs, but in this case can produce about 50% of its dry weight as P(3-HB) (with some strains up to 80%). Here, too, it appears in the form of intracellular granules. The three enzymes responsible for the synthesis are organized in a P(3-HB)-synthesis-operon, which is controlled from one promoter.[66] If the P(3-HB)-synthase gene is transferred alone into *E. coli*, no polyester can be produced. Clearly, *E. coli* is itself not capable of synthesizing (*R*)-3-hydroxybutyryl-CoA.[17b]

In addition to the P(3-HB)-operon, Lubbitz et al.[67] also built in a lysis gene, which is expressed at higher temperatures in the presence of divalent cations. The P(3-HB) granules are thus released into the surrounding medium through openings in the cell wall, and can be separated from the cell debris. This elegant method of isolation is also applicable to *Alcaligenes* species, and has recently been patented.[68]

Other projects are at present probably more visions of the future than reality. Somerville et al.,[69a] for example, plan to insert the P(3-HB)-synthesis genes of *A. eutrophus* into potatoes or other plants, in order to harvest a type of "plastic potato" after expression of the genes. A first realization of this idea has just been reported, but the transgenic plants were only able to produce tiny quantities of P(3-HB). The 3-ketothiolase is present in higher plants, but genes for both the reductase and P(3-HB)-synthase genes must also be introduced here for P(3-HB) production.

Apart from the PHA-structural genes from *A. eutrophus*, those of several other microorganisms, such as *Z. ramigera*[70] and *P. oleovorans*,[71] have also been identified and their nucleotide sequence determined.

2.2.3. Depolymerization

Depolymerization (step 4 in Scheme 1) of the granular, amorphous P(3-HB) to (*R*)-3-hydroxybutyric acid is catalyzed by a depolymerase which degrades P(3-HB) predominantly to dimers. Only in *A. eutrophus* is the direct product (*R*)-3-hydroxybutyric acid.[72] In other microorganisms, the dimers are subsequently cleaved by a dimer hydrolase to the monomers. The depolymerase has been isolated from *A. eutrophus*,[33] *B. megaterium*,[53] and *R. rubrum*.[29] However, its mode of action is still only poorly understood. In contrast to the depolymerase, the mechanism of the dimer hydrolase reaction is quite well known. This enzyme has been isolated from *Z. ramigera*[47] and *R. rubrum*,[52] and hydrolyzes not only the (*R*,*R*) dimers,[73] but, depending on the bacterium, also the (*R*,*S*) dimers (*R. rubrum*, *Z. ramigera*) and the (*S*,*R*) dimers (*Z. ramigera*). The latter are cleaved more slowly, however. The other enantiomers are not saponified by the respective organism. Higher oligomers (pentamers, for example) can also be attacked. As Tomita et al. have shown, these are degraded in *Z. ramigera* in an exo-fashion[74] from the alcohol end; the longer the chain, the greater the reaction rate. Even the corresponding methyl esters are hydrolyzed (except for those of the dimeric or monomeric compound).[47]

The oxidation of (*R*)-3-hydroxybutyric acid to acetylacetate (step 5 in Scheme 1) is catalyzed by a dehydrogenase. The enzymes have been isolated from *A. eutrophus*,[33] *A. beijerinckii*,[43] and *Z. ramigera*,[48] and are very similar with respect to optimum pH values, inhibitors, and the K_m value with (*R*)-3-hydroxybutyric acid. NAD^+ functions as cofactor in all cases.

Two different mechanisms have been found for the esterification of acetoacetate with coenzyme A (step 6 in Scheme 1). In *A. eutrophus* and *A. beijerinckii* the enzyme responsible is a 3-ketoacid-CoA transferase, and the CoA unit is supplied by succinyl-CoA.[43] In *Z. ramigera*, the same step is catalyzed by an acetoacetyl-CoA synthase, and involves ATP.[49]

2.2.4. Regulation of the Poly[(R)-3-hydroxybutyrate] Cycle

The control of PHA metabolism shown in Scheme 1 has been studied most extensively by Dawes et al. in *A. beijerinckii*. It proceeds analogously in *A. eutrophus* and *B. megaterium*, but cannot be extended generally to all bacteria.[12]

3-Ketothiolase is the only enzyme which participates in both the synthesis (Claisen reaction of two acetyl-CoA units) and degradation (retro-Claisen reaction of acetoacetyl-CoA) of P(3-HB), and it plays a central role in the control of the cycle. The Claisen reaction is inhibited by high concentrations of CoASH, while the retro-Claisen reaction is inhibited by acetoacetyl-CoA. The latter inhibition can be overcome by addition of high CoASH concentrations.

Normally, acetyl-CoA is used predominantly in the citric acid cycle, releasing CoASH; that is, the concentration of acetyl-CoA is low, that of CoASH is high, and the 3-ketothiolase is therefore inactive.

Limitation of a nutrient (either nitrogen, oxygen, or phosphorus, depending on bacterium[111]) has the effect of increasing NADH concentration, leading to less efficient degradation of acetyl-CoA by the citric acid cycle. The acetyl-CoA concentration therefore rises, and that of CoASH begins to fall. The inhibition of 3-ketothiolase is thereby overcome, and acetoacetyl-CoA can react with excess NADH according to Scheme 1, to yield P(3-HB). Synthesis of P(3-HB) acts to a certain extent as a sink for acetyl and reduction equivalents.

Degradation is initiated if too little C source is present; the high CoASH levels associated with this situation can override the inhibition of the 3-ketothiolase by acetoacetyl-CoA, and acetyl-CoA units can be released from P(3-HB). The details of regulation of the degradative pathway are still largely unclear, since not enough is known about the P(3-HB)-depolymerase.[75]

For *A. eutrophus*, Doi et al. have shown that under nitrogen limitation P(3-HB) biosynthesis and degradation can take place simultaneously. To what extent the released

monomer units are reused for polymer synthesis has not yet been clarified.[76]

2.3. Microbiologically Accessible Polyesters

A large number of studies have been made with various carbon sources in the growth medium, using different microorganisms capable of producing polyester storage materials. These have been carried out primarily with the aim of synthesizing enantiomerically pure starting materials required for organic synthesis, as discussed below, and in the search for biodegradable materials with a variety of structure-dependent characteristics.

2.3.1. Synthesis of Polyesters Containing no Further Functional Groups with Alcaligenes eutrophus and Pseudomonas oleovorans

A. eutrophus synthesizes only unsubstituted polymers, even when chlorinated or unsaturated acids, for example, 2-chloropropionic acid,[5] 5-chlorovaleric acid,[77] or 4-pentenoic acid[78] are used as substrate. Polyesters with C_4/C_5 hydroxy acid units are produced from almost all C sources, and C_3 structural units have till now been discovered in only a few cases (Table 1, no. 4); C_6 units have never been found.

Table 1. Preparation of polyesters with structural units 3-HP (3-hydroxypropionate), 3-HB (3-hydroxybutyrate), 4-HB (4-hydroxybutyrate), 3-HV (3-hydroxyvalerate), and 5-HV (5-hydroxyvalerate) from various carbon sources by *Alcaligenes eutrophus*.

No.	Substrate	3-HP	3-HB	4-HB	3-HV	5-HV
1	glucose	–	+	–	–	–
2	glucose + propionate	–	+	–	+	–
3	γ-butyrolactone [5, 79, 80] [a]	–	+	+	–	–
4	3-hydroxypropionate or 1,5-pentanediol [5]	+	+	–	–	–
5	5-chlorovalerate [77]	–	+	–	+	+

[a] In addition 4-hydroxybutyrate, 1,4-butanediol, 1,6-hexanediol, or 4-chlorobutyrate can also be used.

Glucose and propionic acid are the substrates which ICI employ for the production of P(3-HB) and P(3-HB/3-HV), and the limiting nutrient is phosphate in each case.[81] By changing the glucose/propionate ratio, the proportion of 3-HV can be varied between 0–20%. These polymers are available commercially under the tradename "BIOPOL".[82] The P(3-HV) homopolymers appear not to be microbiologically accessible; the highest 3-HV content found was about 90%, using valeric acid as C source.[57]

By using [D_3]acetate as substrate in H_2O or D_2O, P(3-HB) with varying degrees of deuteration can be synthesized.[83] Higher levels of deuteration can be achieved in *Rhodobacter sphaeroides*, which affords a maximum of 16% [D_6]3-HB with acetate in D_2O/H_2O (92:8).[84] Under the same conditions, [D_3]acetate leads to synthesis of 6% [D_6]3-HB, 73% [D_5]3-HB, and 16% [D_4]3-HB units.[85]

By use of suitably labeled C sources, ^{13}C- and ^{14}C-P(3-HB) can also be synthesized,[1b, 8] from which either crotonic acid or hydroxybutyrate derivatives of (*R*) configuration can be obtained.

Doi, Kunioka et al.[79, 80] discovered in 1988 that with certain substrates a copolymer of 3-HB and 4-hydroxybutyrate (4-HB) is synthesized (Table 1, no. 3). Depending on the composition of the C source, a 4-HB content between 9% and 40% can be achieved,[86] with the polymer constituting up to 30% of the dry cell mass. Both biodegradability[86] and material properties[87] are different from those of P(3-HB) or P(3-HB/3-HV).

The last two polymers in Table 1 have been relatively little studied, but help to demonstrate the variety of microbiologically accessible PHAs.

Witholt et al.[88] discovered in 1983 that *Pseudomonas oleovorans* also produces intracellular PHA granules, by using *n*-octane as substrate. However, they did not find P(3-HB), but exclusively poly-(*R*)-3-hydroxyoctanoic acid. Several groups subsequently investigated the potential of *P. oleovorans* and other pseudomonads to synthesize unusual PHAs.[40, 89, 90] *P. oleovorans* can metabolize straight-chain aliphatic hydrocarbons, their alcohols and carboxylic acids as substrates,[91] but cannot utilize glucose. In general, statistical copolymers of C_6 to C_{12} (*R*)-3-hydroxy acid units are formed. Units with a chain length smaller than C_6 or longer than C_{12} are only found in small quantities (Table 2).

Table 2. Composition of the PHAs from *Pseudomonas oleovorans* with carboxylic acids as carbon sources (from [89b]). The homologous series starting from 3-*hydroxy*caproate to 3-*hydroxydod*ecanoate is denoted by 3-HC–3-HDD.

Substrate	PHA [a] [%]	Repeating unit in the polyester [%] 3-HC	3-HH	3-HO	3-HN	3-HD	3-HUD	3-HDD
(*R*)-3-hydroxybutyrate	1.2	–	–	22	–	57	–	21
caproate	3.3	95	–	5	–	–	–	–
heptanoate	2.3	–	100	–	–	–	–	–
octanoate	8.7	8	–	91	–	1	–	–
nonanoate	9.1	–	35	–	65	–	–	–
decanoate	12.5	8	–	75	–	17	–	–
undecanoate	9.8	–	28	–	59	–	13	–
dodecanoate	6.6	6	–	57	–	32	–	5
pentadecanoate	5.3	–	32	–	47	8	13	–
heptadecanoate	–	–	–	–	–	–	–	–

[a] Given as percentage of the cell dry weight. The isolated PHA quantities are also only given in ref. [90b]. Evidently, the highest PHA quantites (0.7 $g L^{-1}$) are obtained with nonanoate as substrate.

With C_{2n+1} acids, polyesters with C_7, C_9, and C_{11} hydroxy acid units are produced, though the C_9 units predominate. C_{2n} acids result in analogous polymers built up of the even-numbered C_6, C_8, C_{10}, and C_{12} hydroxy acid units; the C_8 acid playing the major part. Polymers with relatively uniform side chain lengths are also formed from the hydrocarbons hexane, heptane, and octane.[40, 89a]

The longer the side chains of the hydroxy acids, the more elastic and the less crystalline are the polymers produced.[92a] On the other hand, the higher PHAs are no longer biodegradable, as has been shown for poly-(*R*)-3-hydroxyoctanoate or poly-(*R*)-3-hydroxynonanoate![1b, 5, 11]

Presumably, PHA biosynthesis developed from P(3-HB) metabolism in pseudomonads when various strains developed the ability to utilize substrates with more than four C atoms. The direct polymerization of such substrates is en-

ergetically more sensible than first degrading them to the C_4 acids.[89a] Alkanes, however, can only be utilized by microorganisms possessing the so-called OCT-plasmid. This plasmid encodes the genetic information for those enzymes responsible for transforming alkanes to the corresponding alcohols.[93]

2.3.2. *Production of Polyesters with Further Functional Groups by Microorganisms*

With all the polyhydroxy acids described so far, subsequent modifications in the structure of the polymer are not possible; however, functionalized polymers are accessible by so-called polymer-analogous reactions. Certain bacteria can synthesize polyesters from functionalized substrates without loss of the functionality during construction, as does *A. eutrophus*. Here, too, the synthesis of homopolymers is the exception rather than the rule, since the biosynthesis of polyesters allows the incorporation of 3-hydroxy acid units with side chains shortened by C_2 or C_4 units. If, for instance, 3-hydroxy-7-octenoate is treated under analogous conditions to those given in Scheme 2b, a polymer is obtained which contains 23% 3-hydroxyhexanoic acid units.[94]

The first polyester with an additional functional group was isolated from *Nocardia* in 1964, though the enol ester structure of this polymer was only determined by IR spectroscopic studies.[98] In general, the functional groups may not lie too close to the main chain. Thus, for instance, no cell growth is observed with the substrates 6-bromohexanoic acid,[83] 3-phenylpropionic acid,[97] and 3-hydroxy-3-phenylpropionic acid.[97] The only substrate which can be converted to a homopolymer is 5-phenylvaleric acid (when 6-octenoic acid is used, the polymer shown in Scheme 2b contains only 80% of the given structural unit, whereas the remainder is composed of a mixture of other units.[94]). Surprisingly, a mixture of nonanoic and phenylvaleric acid yields the two corresponding homopolymers, and no copolymer![99] The yields are unsatisfactory in all cases.

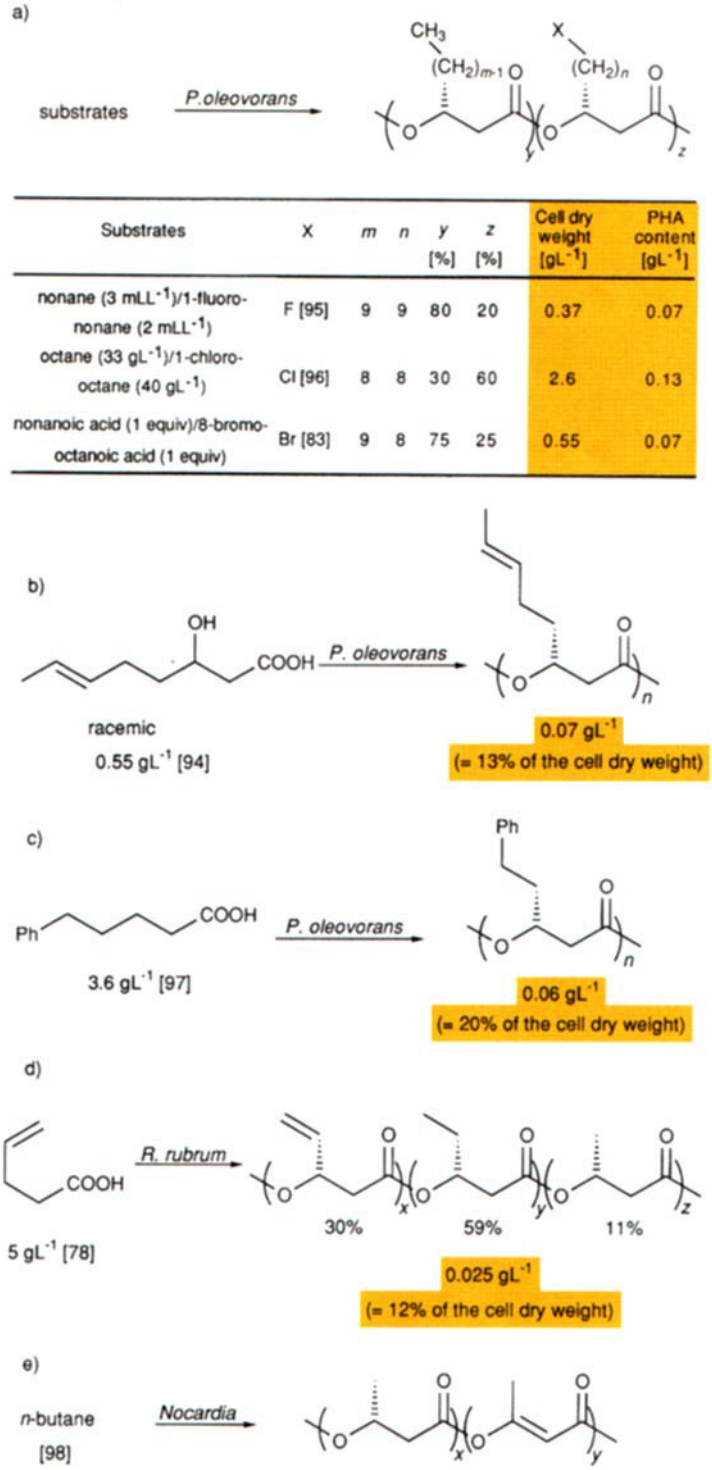

Substrates	X	m	n	y [%]	z [%]	Cell dry weight [gL^{-1}]	PHA content [gL^{-1}]
nonane (3 mLL^{-1})/1-fluoro-nonane (2 mLL^{-1})	F [95]	9	9	80	20	0.37	0.07
octane (33 gL^{-1})/1-chloro-octane (40 gL^{-1})	Cl [96]	8	8	30	60	2.6	0.13
nonanoic acid (1 equiv)/8-bromo-octanoic acid (1 equiv)	Br [83]	9	8	75	25	0.55	0.07

Scheme 2. Microbially accessible polyesters with functional groups in the side chain.

3. Polyhydroxy Acids as Starting Materials for Chiral Compounds of Low Molecular Weight

Ten years ago, this subject brought our research group into contact with P(3-HB) for the first time, since we saw P(3-HB) as a welcome source of C_4 synthetic units with (*R*) configuration. We began to search for suitable procedures for the preparative degradation of P(3-HB) to the monomers, and were soon interested in the directed synthesis of oligomers from the monomers thus isolated.

3.1. Degradation of Poly[(R)-3-hydroxybutyrate] and the Chemistry of the Monomer

Because of their stereoregularity, microbially synthesized polyesters are extremely attractive sources of chiral building blocks. The investigations carried out for this reason were all limited to the polymers P(3-HB) or P(3-HB/3-HV), since these two were the only two polyhydroxy esters available in large quantities at the time. Depending on the aims of the study, either the oligomer mixtures or the monomers could be of interest. Various mixtures of oligomers can be formed by partial hydrolysis or alcoholysis, for example, or by ester pyrolysis at temperatures >175 °C, where the average molecular weight is determined by the length of the heating period.[100–103] At the alcohol end, the pyrolysis products all carry a crotonyl group, as is to be expected for mechanistic reasons. Product mixtures of the same type have also been obtained by Brändli et al.[104] by treating P(3-HB) or P(3-

HB/3-HV) in the presence of an excess of lithium diisopropylamide/LiCl at low temperatures. Even after repeated treatment of the same sample under the same conditions, one sees only a slight shift in the distribution maxima (assumed to be bimodal) to lower molecular weights (Fig. 1 b). Similarly, the yields of isolated oligomers change very little (ca. 75% for each degradation step). The mechanism of the degradation is not yet satisfactorily understood, but probably does not go through the poly-enolates originally postulated,[104] since no alkylation products could be identified with a variety of electrophiles (Fig. 1 a).

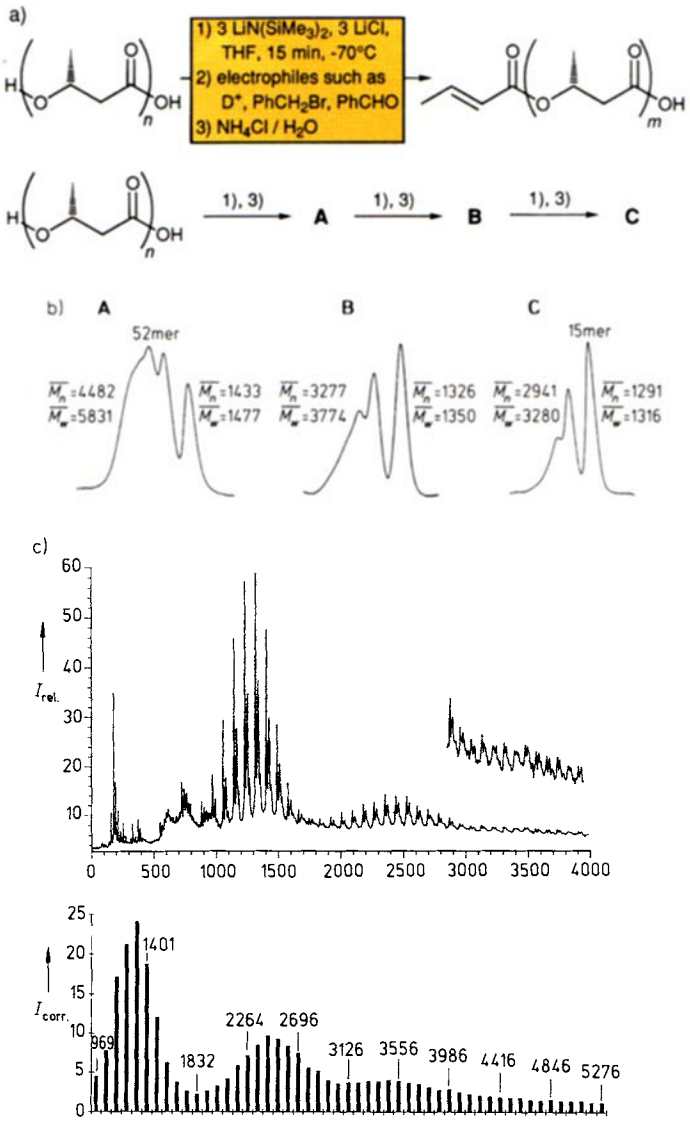

Fig. 1. Degradation of P(3-HB) ($M_n = 7.5 \times 10^5$) with $LiN(SiMe_3)_2$ in tetrahydrofuran at low temperature. Since the products arising from base treatment cannot be alkylated with electrophiles, polyenolates cannot be present as intermediates [104]. b) Gel permeation chromatograms of oligomer mixtures obtained by one (**A**), two (**B**), or three (**C**) repetitions of the reaction sequence shown in a). The two maxima are displaced only slightly towards lower molecular masses. The signal at high molecular weight corresponds to a 52mer for **A**, and to a 36mer for **C**, while the low molecular weight peak is a 17mer for **A** and a 15mer for **C**. The chromatograms shown were obtained by fractionation of a mixture on Shodex columns K-802, K-802.5, and K-803, by using chloroform as eluent. c) Top: matrix-supported laser desorption ionization spectrum (LDI) of the triple degradation product **C**. The insert is increased fivefold: the corresponding bar spectrum obtained when the [M + H] and [M + Na] peaks are counted together, and the area rather than the relative peak height is measured. Each m/z is given on the x axis. We thank Dr. K. Börnsen and Dr. M. Schär (Ciba-Geigy, Basel) for recording the LDI-spectra for us [105,106].

The work of Züger et al.[107] and Vanlautem et al.[108] has also made available the monomeric (*R*)-3-hydroxybutyric acid and its corresponding ester (**A** in Scheme 3), by acid-catalyzed saponification or transesterification of P(3-HB).[109] The reaction conditions were later optimized by Breitschuh et al.,[110] so that the monomers can now be obtained by a simple procedure in about 80% yield. Similarly, reduction of P(3-HB) with lithium aluminum hydride or its treatment with organometallic reagents leads directly to the 1,3-butanediols with (*R*) configuration of type **B** (Scheme 3).

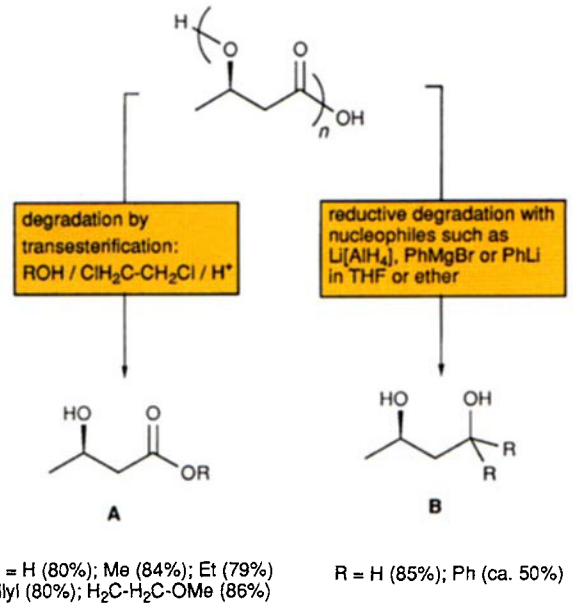

Scheme 3. Depolymerization of P(3-HB) by transesterification or by reduction of the ester carbonyl groups.

Derivatives as accessible as this can certainly be interpreted as an extension of the "pool of chiral building blocks".[111a] Natural product syntheses beginning from (*R*)-hydroxybutyric acid are being published continually,[111b] as shown by recent syntheses of gloeosporon,[112] grahamimycin A_1,[113] and (*R*)-lasiodiplodin.[114]

By now, any of the hydrogen atoms in (*R*)-3-hydroxybutyric acid can be replaced by other groups (product types **A**–**H** in Scheme 4).[115] The most notable developments in this area are the chiral acetoacetic ester derivative (*R*)-*tert*-butyl-6-methyl-2*H*,4*H*-1,3-dioxin-4-one[116] (this cycle yields compounds of type **D** and in principle also of type **C**, with regeneration of the stereogenic center[117]), and the diastereoselective synthesis of 2,5,5,6,6-pentaalkyl-substituted dioxanones[118] (see **E**; this corresponds formally to the product of an enantioselective aldol reaction of a α-branched carboxylic acid with a ketone).

The alcohol function of 3-hydroxybutyric acid can be substituted nucleophilically by other groups with inversion of configuration, either via the corresponding tosylate or via the β-butyrolactone[124, 125] (the former compound requires weakly basic nucleophiles such as $LiAlD_4$,[126] $Bu_4N^+NO_3^-$,[127] or NaN_3;[128a] the lactone can be opened with S-nucleophiles such as HS^- or $tBuS^-$,[129] for example, or with N-nucleophiles like benzylamine or NaN_3[129a]). Diastereoselective opening of dioxanones from HB by S_N2

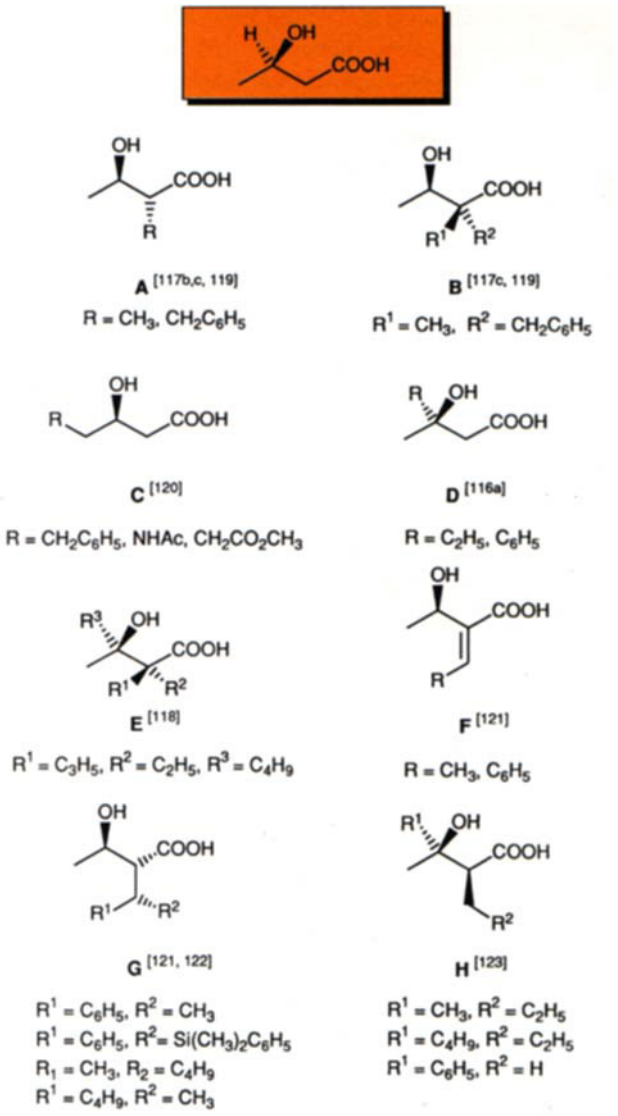

Scheme 4. Products of the transformation of (*R*)-3-hydroxybutyric acid while retaining the acid and alcohol functions.

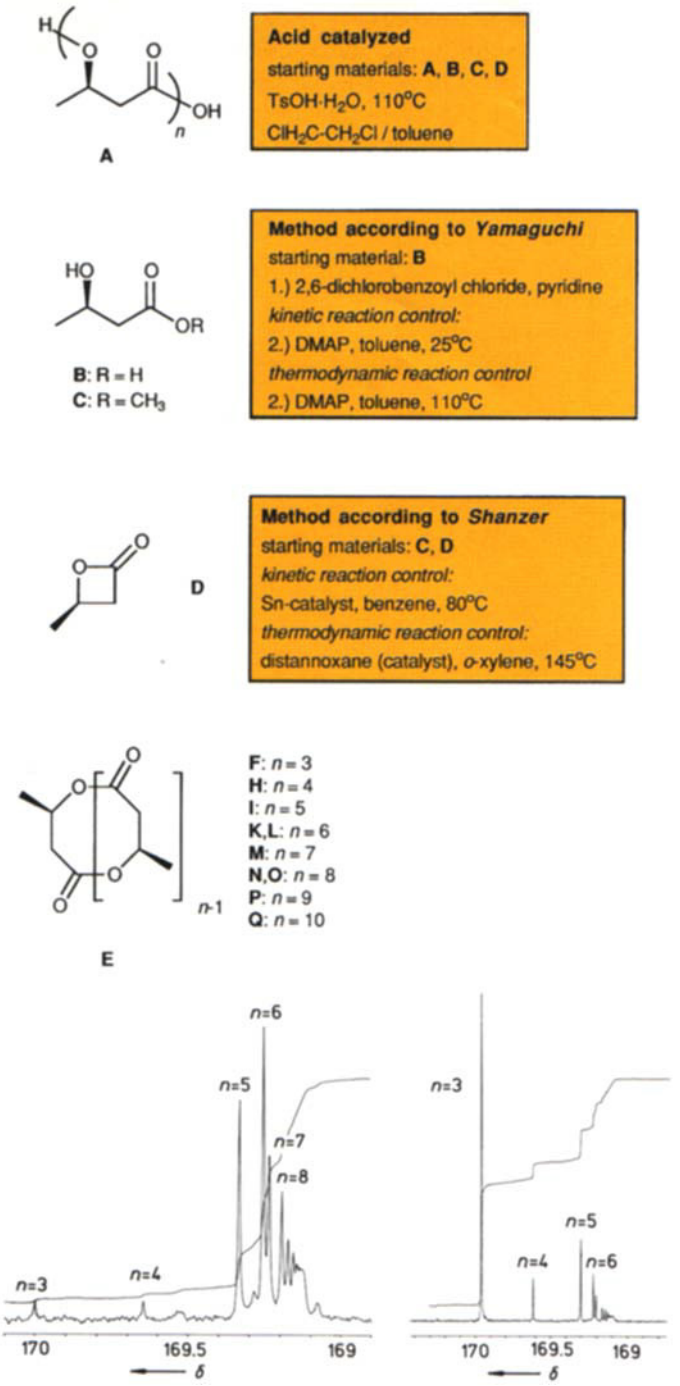

Scheme 5. Top: Synthesis of macrocycles of type E according to the methods of Yamaguchi, (via the mixed anhydride with 2,6-dichlorobenzoyl chloride) Shanzer, (by using the tin catalyst 1,1,6,6-tetrabutyl-1,6-distanna-2,5,7,10-tetraoxacyclodecane [136] (= template)), or by acid catalysis with toluenesulfonic acid monohydrate ($TsOH \cdot H_2O$). DMAP: *N*,*N*-dimethylaminopyridine. Bottom: ^{13}C NMR spectra of the carbonyl region of oligolide mixtures obtained under the conditions specified in a) by Yamaguchi lactonization (left) of (*R*)-3-hydroxybutyric acid (kinetic control) and acid catalyzed (right) by degradation of P(3-HB) (thermodynamic control). For completeness, it should be mentioned that the β-butyrolactone **D** of (*R*) configuration was never used as starting material, but rather its enantiomer, which is also formed by known methods from (*R*)-3-hydroxybutyric acid [124]. The (*R*) form was preferred here only for graphic reasons. Measurement conditions for the ^{13}C NMR spectra (100 MHz): Inverse-gated experiment with a relaxation delay of 3 s, an acquisition time of 3.2 s, and a pulse angle of 45°.

reaction at the acetal C atom is a greatly improved variant of the Johnson method with regard to selectivity and ease of execution in greater quantities as well as in the presence of groups sensitive to oxidation, in which hydroxybutyric acid is converted into crotonic acid, and thus sacrificed (*immolative* enantioselective reaction sequence).[117b,c,128]

3.2. Synthesis of Oligolides from 3-Hydroxybutyric Acid, and Structural Studies

Chiral macrolides of type **E** (Scheme 5) can be obtained directly from P(3-HB) **A** either by acid-catalyzed transesterification or from the monomeric building blocks **B**–**D**, by the methods of Yamaguchi,[130–133] Shanzer.[132–134] or again by acid catalysis.[135] Depending on the reaction conditions, the oligolides are obtained in various proportions, and can be separated from each other by careful chromatography.[133] Under thermodynamic control, triolide **F** (in Scheme 5) predominates; thus, acid-catalyzed transesterification of P(3-HB) affords this really quite complex compound in about 50% yield by simple distillation of the product mixture.[135]

Single crystals of the oligolides **F**–**O** in Scheme 5 were grown, and their structures were determined. For both the

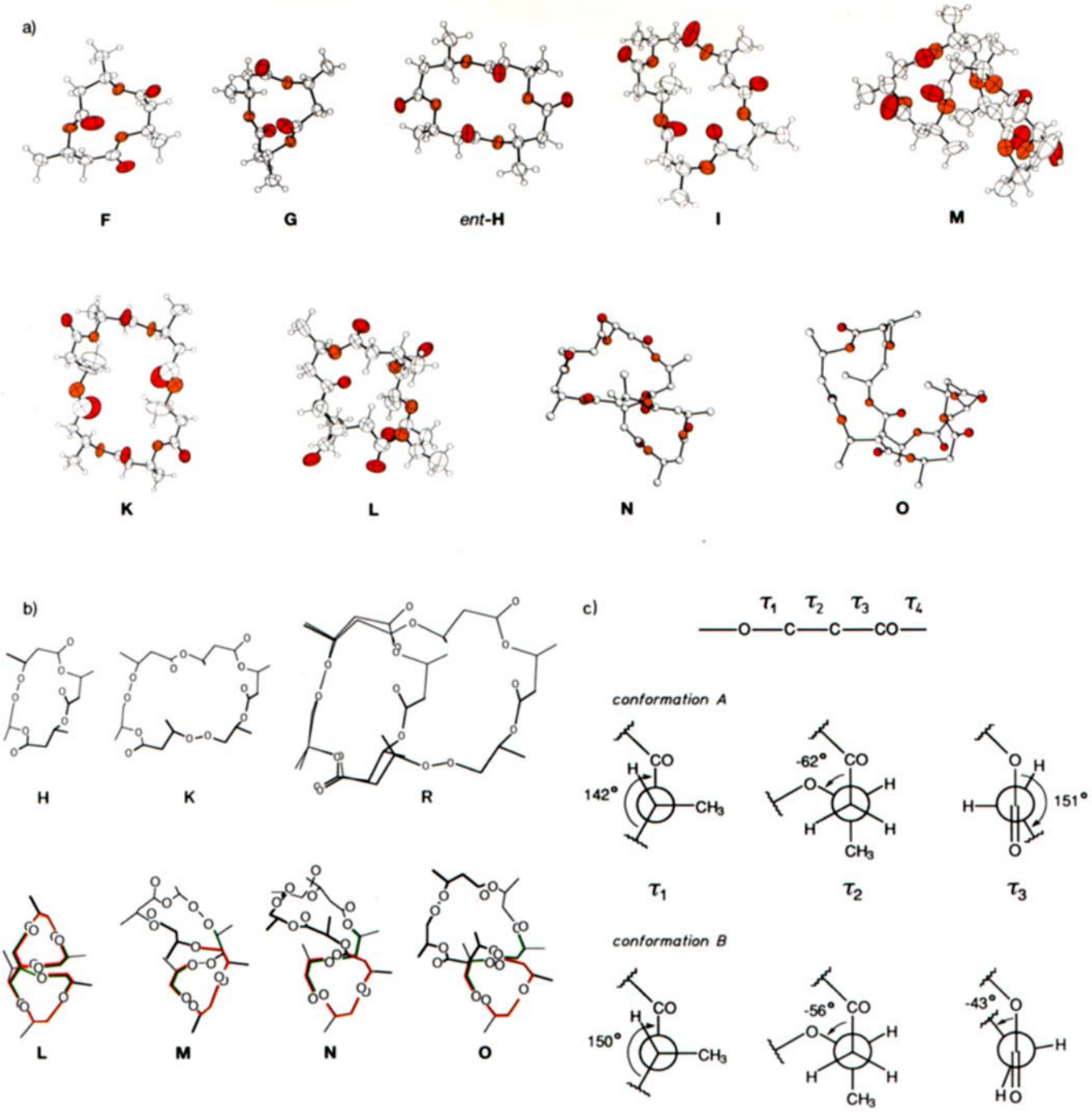

Fig. 2. a) Structures of the oligolides **F–O**, all in the all-*R*-form with the exception of *ent*-**H**, which is depicted in the all-*S*-configuration (**F**–**M** as ORTEP diagrams, and **N**,**O** as PLUTO plots). The *rac-epi* triolide **G** (shown here in the (*R*,*R*,*S*) form) is obtained, for example, by acid-catalyzed lactonization of *rac*-β-butyrolactone in boiling toluene/1,2-dichloroethane together with the racemic triolide *rac*-**F** in a 3:1 ratio. Red spheres are oxygen atoms of the CO functional groups, orange are OR oxygens on the ester groups. For synthesis and characterization of the oligolides see [131–135]. b) Structural similarities between the macrolides. MacMoMo views of the all-(*R*)-tetrolide **H** and of the C_2 symmetrical hexolide **K** and its superposition **R**. The higher macrolides **L–O** all contain as common structural fragments a Δ-shaped portion (red) and an S-shaped moiety (green). In the hexolide L they even appear twice [133]. c) Mean torsion angles τ_1–τ_3 and Newman projections of the bonds of the (*R*)-3-hydroxybutyric acid units in conformations **A** (the Δ-shaped building block) and conformation **B** (the S-shaped fragment) of the higher macrolides **L–O** [133,135b]. The torsion angles are given according to the IUPAC-IUB definition [138]; a zero-value represents a synperiplanar arrangement for the main chain.

hexolide ($n = 6$)[132] and the octolide ($n = 8$), two conformers were found (**K**, **L**, and **N**, **O**, respectively, see Fig. 2a). The structures show remarkable similarities (Fig. 2b). Comparison of the two C_2 symmetric conformations of the tetrolide **H** and the hexolide **K** show that the latter can be constructed from **H** by halving and introducing two hydroxybutyric acid units. The larger macrolide structures **L–O** are all constructed of folded rings and contain an S-shaped (Fig. 2b, green), and a Δ-shaped region (Fig. 2b, red) as common structural elements. A study of the interdependence of the torsion angles τ_1, τ_2, and τ_3 reveals two preferred configurations of the (*R*)-hydroxybutyric acid units in these cycles (Fig. 2c). Conformation **A** (which forms the Δ-shaped structural element) occurs about three times more frequently than **B** (which forms part of the S-shaped fragment).[137]

The potential of polyesters as precursors of chiral building blocks has certainly not yet been exhausted, as can be seen from the continuing publication of syntheses of further compounds from them.[139]

4. Polyhydroxy Acids as Biologically Degradable Plastics

Plastics make up about seven percent by weight and over thirty percent by volume of the total garbage produced today in the USA and Japan.[140] This can be explained in part by the fact that plastics are more and more replacing glass, paper, or metal as packaging materials. In principle, there are three possibilities for the disposal of plastics: incineration, recycling, and degradation in the environment. Each of these will presumably find future applications.

Several countries, such as Italy for example, have introduced legislation which requires all plastic packaging materials to be degradable by 1991.[141] The growth rate in the market for degradable polymers is expected to increase by 75% per year, representing a turnover in 1992 of about 400000 tons of polymer and approximately US$ 340 million. By then, some 15% of plastic refuse will be biodegradable, compared with 1% in 1987.[141, 142]

In principle, a macromolecule can be degraded by chemical, biological, or physical methods.[143] Cleavage by light is the most important degradative pathway for C–C main chain polymers, and is accelerated by the introduction of carbonyl groups[144] (which can be brought about by copolymerization of an olefin with carbon monoxide, for example[145]), or by photoactive additives such as benzophenone[146] (degradation by Norrish type I and II cleavage). Oxidative chain fission can be achieved by addition of hydrogen peroxide or suitable transition metals, and is important particularly with unsaturated polymers.[147]

The production of polymer mixtures (blends) of largely undegradable and biologically degradable materials (usually starch) is also widespread. In this way, the advantages of petrochemically derived plastics can be combined with those of biopolymers. During degradation, the biologically utilizable part of the mixture is dissolved, and the remainder must then be dealt with by nonbiological systems.

4.1. Requirements for Biodegradable Polymers

In contrast to chemical processes, microbial degradation processes are to a certain extent autocatalytic, since the substrate being degraded leads to an increase in the organism population. The bacteria concerned profit from the degradation; that is, the fragments produced must also be able to be utilized. Many monomers of synthetic polyesters and polyamides are in principle microbially degradable, but since the corresponding microorganisms do not have suitable depolymerases available, degradation is impossible. The same is true if the polymerase is present, but the resulting fragments cannot be broken down or metabolized. The most important type of cleavage is the hydrolysis of ester, amide, and glycosidic bonds. The corresponding hydrolases require only water as a reaction partner, and are therefore more common in the extracellular environment, since no complex cosubstrates are needed. Polyesters with easily degradable monomers such as glycolate, lactate, malate, caprolactone, and 3-hydroxy acid derivatives therefore have a good chance of being biodegraded.[149] Pure C-chain polymers are less suitable, though their degradation has been demonstrated.[150]

4.2. Extracellular Polyhydroxy Acid Degradation

A remarkable property of many microbially synthesized PHAs is their biodegradability in the environment, which proceeds more rapidly under anaerobic conditions than aerobically. For *A. eutrophus*, Doi et al.[5, 76] found that under anaerobic conditions the main intracellular metabolites are acetate and (*R*)-3-hydroxybutyrate. The conversion of acetyl-CoA to acetate is presumably coupled to the phosphorylation of ADP to ATP in this case. Under aerobic conditions, acetyl-CoA is broken down to CO_2 and H_2O by the citric acid cycle, releasing 12 ATP equivalents and allowing a far more economic use of the polyester.

Many bacteria and fungi possess extracellular depolymerases,[151] with which they can degrade PHAs and if necessary utilize them as a sole C source. Enzymes of this nature have been found in *Alcaligenes faecalis*,[152–155] *Pseudomonas lemoignei*,[156–160] *Pseudomonas delafieldii*,[161] *Penicillium simplicissimum*,[162] and *Eupenicillium sp.*,[162] though the enzymes of the first two species have been by far the best studied.

A. faecalis has two extracellular esterases, a P(3-HB) depolymerase and an oligomer hydrolase. The depolymerase degrades both P(3-HB) and water soluble oligomers. However, it displays significantly higher activity towards the longer oligomers, and attacks in an endo fashion at the second ester bond from the hydroxy terminus.[152] An octolide (i.e. a ring constructed of eight (*R*)-3-hydroxybutyrate units) is attacked in a similar fashion, but the open-chain trimer protected on the alcohol function with *tert*-butyldimethylsilyl groups is not degraded.[154]

The oligomer hydrolase attacks only water-soluble oligomers, but with approximately ten times higher activity than the depolymerase. Longer polymer chains are more rapidly degraded than the dimers. Of the four possible stereoisomers of 3-hydroxybutyrate dimers, the (*R*,*R*) form and the (*R*,*S*) form are hydrolyzed, the latter rather more slowly.[73] The monomeric methyl ester is also attacked, while the corresponding ethyl and benzyl esters are practically inert. Degradation occurs in an exo manner from the acid end.[153]

The gram-negative organism *P. lemoignei* also possesses two enzymes which are involved in extracellular degradation, but differs from *A. faecalis* in that only the depolymerase is exported from the cell. P(3-HB) is broken down outside the cell to a trimer/dimer/monomer mixture which is then transported through the cell wall and is only fully saponified to the monomer by a dimer hydrolase within the cell. Here too, the depolymerase attacks in an endo fashion at the second or third ester bond from the hydroxy terminus, though in this case both oligomers and P(3-HB) can be hydrolyzed.[160] In contrast to *A. faecalis*, the dimer hydrolase degrades the (*S*,*R*) dimer as well as the (*R*,*R*) form, while

their enantiomers are not saponified. (*R*)-3-(butanoyloxy)butyric acid is also attacked.[157]

Despite numerous investigations, many questions remain unanswered. It is not clear, for instance, how the depolymerase can attack both the water soluble oligomers and the hydrophobic P(3-HB), which in contrast to the intracellular case (see Section 2.2.3) is present here in a crystalline form! From a chemical point of view, it would also be interesting to investigate the influence of various end groups on the degradability; synthetically produced (all-*S*)-P(3-HB) is no longer biodegradable, and neither is a stereoblock-P(3-HB) built up of (*R*) and (*S*) residues.[111]

5. Synthesis of Poly[(*R*)-3-hydroxybutyrate] and Derivatives

P(3-HB) was produced by synthetic means far earlier than by biotechnological methods. Processes of this sort are becoming ever more attractive, due to the facile methods now available for the synthesis of (*R*)- and (*S*)-hydroxy acids. In principle, two types of monomers are available for the polymerization, the 3-hydroxy acids and the corresponding β-butyrolactones. Because of their tendency to crotonize, the acids have never been used, however, since polyesters of high average molecular weight can only be obtained by polycondensation of very pure starting materials.[163] All the studies published to date have therefore started from β-butyrolactones, and have polymerized these with simultaneous ring-opening. β-Propiolactone can be polymerized easily with either anionic or cationic initiators, and the α-monosubstituted and α,α-disubstituted β-lactones react cleanly. Substituents in the β-position reduce the reactivity dramatically, so that conversion is often incomplete even after extended reaction periods.[164]

In all the studies published up till now, P(3-HB) was synthesized by one of the following procedures: a) from racemic β-butyrolactone and an achiral initiator, b) from racemic β-butyrolactone and a chiral initiator, or c) from enantiomerically pure β-butyrolactone and an achiral initiator.

5.1. Polymerization of Racemic β-Butyrolactone with an Achiral Initiator

Biologically degradable (all-*R*)-polymers cannot, of course, be obtained in this manner. However, suitable reaction conditions were thus developed with the readily available racemic β-butyrolactone,[165] and some of these could also be used for polymerization of enantiomerically pure lactone.

The step determining stereoselectivity in the ring-opening polymerization is the insertion of a monomer into the end position of the polymer-initiator complex.[166] In principle, this can lead to isotactic (*-RRR-/-SSS-*), syndiotactic (*-SRSRSR-*), or atactic (*-SSRSRRS-*) polyesters. β-Butyrolactone, however, yielded only isotactic and atactic P(3-HB). The result can be either a stereoblock polymer or an isotactic chain with periodic defects, depending on whether the polymer chain end or the initiator determines selectivity; atactic polymers are obtained when neither is dominant (Scheme 6).

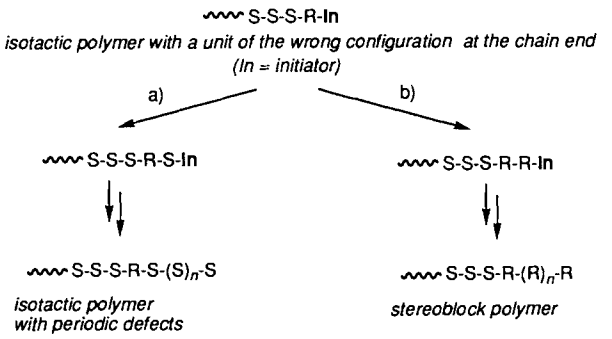

Scheme 6. Stereoselectivity of monomer insertion into the terminal initiator-polymer bond. *R,S*: (*R*) configuration or (*S*) configuration unit in the polymer. In case a) the initiator is responsible for the selectivity, in b) the terminal monomer unit.

The tacticity was determined in earlier times by fiber X-ray diffraction,[167, 168] but today is much simpler to measure from the ^{13}C and ^{1}H NMR spectra. Isotactic and stereoblock-P(3-HB) cannot yet be distinguished either by X-ray diffraction analysis or by high-field NMR spectroscopy.[169] For this reason, whenever isotactic polyesters are mentioned in the following sections, stereoblock polymers may also be present.

Atactic and isotactic fractions may be separated by fractional crystallization from acetone or methanol, where the atactic polymer remains in solution. Initiators which have been applied with more or less success are summarized in Table 3. Classical Brønsted or Lewis acids such as CF_3SO_3H,[170] $BF_3 \cdot OEt_2$,[171, 172] $Et_3O^+BF_4^-$,[164] Et_2AlCl,[171] or nucleophiles like *n*BuLi,[171] pyridine,[173] NEt_3,[171, 173] PPh_3,[173] NaOMe,[170] and tetraethylammonium benzoate[170] afford oily mixtures of oligomers, at best.

In 1971, Agostini et al.[174] described in detail for the first time a synthesis of P(3-HB) from β-butyrolactone and $AlEt_3 \cdot H_2O$; Inoue et al. had briefly mentioned such a reaction in 1961, as part of a communication on polymerization of β-butyrolactone with $ZnEt_2/O_2$.[172] Tani et al.[170, 171] later improved the reaction conditions for the Al-initiated ring-opening polymerization, which was subsequently adopted by several other research groups. The long reaction times and the generally unsatisfactory conversions (Table 3) are conspicuous; the yield of isotactic P(3-HB) reaches 50% at best. The molecular weights achieved are comparable with those for microbiologically produced P(3-HB), depending on the catalyst used, but the molecular weight distribution is much broader. Exceptions are the two last systems (Table 3, nos. 8 and 9), in which relatively narrow molecular weight distributions are obtained. In no. 9, the actual initiator is potassium crotonate which, like potassium acetate or potassium benzoate, can be applied in the presence of [18]crown-6[177] or dibenzo[18]crown-6[173] instead of potassium naphthalide as a starter.

5.2. Polymerization of Racemic β-Butyrolactone with a Chiral Initiator

Polymerization of a racemic monomer with a suitable chiral initiator ought in the ideal case to yield only one enantiomer of the product, while the other enantiomer remains in

Table 3. Polymerization of *rac*-β-butyrolactone with achiral iniators.

No.	Initiator	Reaction conditions T [°C]	t [d]	solvent	Yield polymer [%]	of the isotactic fraction [%]	$M_n \times 10^{-3}$ (of the isotactic fraction)	M_w/M_n [d]	Ref.
1	$AlEt_3:H_2O = 1:1$ [a]	53	4	without	52	–	–	–	[174]
2	$AlEt_3:H_2O$:epichlorohydrin = 1:0.8:1 [a]	60	10	toluene	52	37	–	–	[171]
3	$AlEt_3:H_2O = 1:1$ [a]	60	7	toluene	–	28	21.4 [d]	5.6	[175]
4	EAO [b]	60	7	toluene	78	52	400 [d]	–	[170]
5	EAO [b]	60	14	toluene	51	20	110 [d]	8.0	[169]
6	$Zn(OEt)_2 \cdot Al(OiPr)_3$	40	14	toluene	45	–	–	–	[164]
7	Bu_3SnOMe	50	2	without	–	–	ca. 6 [e]	–	[173]
8	TPPAlCl [c]	25	33	CH_2Cl_2	60	–	4.4 [f]	1.05	[176]
9	potassium naphthalide + cryptand [2.2.2]	25	8	THF	95	0	11 [f]	1.29	[177]

[a] The initiator is synthesized from $AlEt_3$ and H_2O before the addition of the monomer in toluene. [b] The *ethyl*a*l*uminum *o*xide (EAO) initiator was synthesized as in [a], then the solvent was removed, and the residue dried at 180 °C/10^{-3} Torr, and this was then redissolved in toluene. [c] Initiator from 5,10,15,20-tetraphenylporphin and Et_2AlCl. [d] Determined with gel permeation chromatography by comparison with a polystyrene standard. [e] Estimated from the ^1H NMR spectrum. [f] Determined with vapor pressure osmometry. The monomer/initiator ratio for no. 8 is 100 and for no. 9 150.

the reaction mixture (the yield of polymer can therefore only be 50%, at most). LeBorgne and Spassky et al. have polymerized oxiranes and thiiranes with considerable success, by using as initiator a complex of (*R*)-3,3-dimethyl-1,2-butanediol and $ZnEt_2$.[178] However, with β-butyrolactone the reaction is far less selective (Table 4).

Table 4. Polymerization of *rac*-β-butyrolactone with the chiral initiator *A* (complex from (*R*)-3,3-dimethyl-1,2-butanediol and $ZnEt_2$) and *B* (*N*,*N*′-disalicylidene-(1*R*,2*R*)-1,2-cyclohexanediaminatocobalt(II)-$AlEt_3$ complex).

Catalyst	Reaction conditions T [°C]	t [d]	solvent	Conversion [%]	Isotactic fraction [%]	$[\alpha]_D$ of the polymer [a]	$M_n \times 10^{-3}$	M_w/M_n
A [179]	25	0.25	toluene	84	27	−0.6 ($CHCl_3$) [b]	ca. 20	–
B [180]	30	14	benzene	41	–	−46.1 (benzene) [c]	–	9.4

[a] Optical rotation of microbial all-(*R*)-P(3-HB): $[\alpha]_D = -1.8$ ($CHCl_3$). [b] $[\alpha]_D$ of the unreacted monomer: −12.8 ($CHCl_3$); (*S*)-β-butyrolactone: $[\alpha]_D = -34.8$ ($CHCl_3$). [c] $[\alpha]_D$ of the unconverted monomer: −1.65 (benzene); (*S*)-β-butyrolactone: $[\alpha]_D = -50.8$ (benzene).

The selectivities achieved by this strategy are definitely not yet satisfactory. In the second case, the compound obtained is presumably a strongly atactic polyester or an isotactic P(3-HB) of low molecular mass, since (all-*R*)-P(3-HB) oligomers of size >1000 g mol^{-1} are almost insoluble in benzene.

5.3. Polymerization of Enantiomerically Pure β-Butyrolactone with an Achiral Initiator

Enantiomerically pure β-butyrolactone can be synthesized either by cyclization of 3-bromobutyric acid[124d] or 3-mesyloxybutyric acid,[124e] or by pyrolysis of the cyclic orthoester of 3-hydroxybutyric acid and triethyl orthoacetate,[124a,b] though with a maximal yield of 35%. Four-membered ring lactones can be opened by nucleophiles either with retention (path **a** in Table 5) or with inversion (path **b** in Table 5)[181] of configuration, and hence P(3-HB) constructed by this procedure does not necessarily consist entirely of units with identical configuration (i.e. 100% isotactic) (Table 5).

Once again, it was Agostini et al.[124d] who were the first to polymerize (*R*)-β-butyrolactone with $AlEt_3 \cdot H_2O$ to give P(3-HB) of preferentially (*R*) configuration, opening the lactone with retention of configuration. Lenz et al.[182] later found inversion, exactly the opposite reaction mechanism, in the same system (no. 2 in Table 5). They explained the change in mechanism with a different method of producing the aluminum complex.[183] In all cases, no stereoregular P(3-HB) was obtained, probably because of the polymeric nature of the initiators used, which can contain various active centers (see [183], but also [178a]). On the basis of the optical rotation

Table 5. Polymerization of chiral β-butyrolactone with achiral initiators.

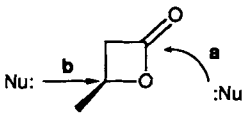

No.	Initiator	Lactone configuration	Polymer	$[\alpha]\lambda_i$ in $CHCl_3$ [a]	$M_n \times 10^{-3}$	M_w/M_n	Ref.
1	$AlEt_3 \cdot H_2O$ (1:1)	(*R*)	(*R*)-P(3-HB)	+4.0 [b]	–	–	[124d]
2	$AlEt_3 \cdot H_2O$ (1:1)	(*S*)	(*R*)-P(3-HB)	+6.9	30	8.0	[182]
3	$ZnEt_2 \cdot H_2O$	(*S*)	(*S*)-P(3-HB)	−7.0	14	1.5	[182]
4	EAO [c]	(*S*)	(*S*)-P(3-HB)	−5.8	24	7.8	[182]

[a] For λ_i all-(*R*)-P(3-HB) has an optical rotation of +7.4 (the wavelength (λ = 589 nm) given in ref.[182] (no. 2–4) is probably incorrect). [b] $[\alpha]_{365}$ of all-(*R*)-P(3-HB): +10.2 ($CHCl_3$). (*R*)-β-butyrolactone with an optical purity of 73% was used as monomer. [c] EAO see footnote [b] in Table 3.

of the polymers obtained and the reproducibility of the experiments, the Zn system seems to be the best one. Recently Doi et al. used this system to show that in the polymerization of enantiomeric β-butyrolactone mixtures, the (*R*) and (*S*) units are statistically distributed in the polyester.[184]

With the ethylaluminum oxide (EAO) initiator, the attainable molecular weights decrease as the size of the residue on the β-butyrolactone increases. In this way, Tani et al. were able to polymerize γ-mono, di-, and trichloro-substituted β-lactones in 1977,[170] which by now are also accessible in the enantiomerically pure form by the Wynberg method.[185] A further functionalized polymer was synthesized by Lenz et al. from racemic or from (*R*)-β-alkoxycarbonyl-β-propiolactone. The resulting malic acid polyesters are biodegradable.[186]

5.4. Synthesis of Defined Oligomers and Polymers from (*R*)-3-Hydroxybutyric Acid

Oligomers of uniform molecular mass have also been produced by directed synthesis. Such compounds were of interest in the past for a variety of reasons; they were used to obtain more detailed information about the intra- and extracellular degradation mechanism for P(3-HB),[152, 154, 187] or for synthesis of the corresponding straight-chain oligolide precursors.[131] In all previous syntheses, chain extension proceeded by stepwise addition of monomer units. Our aim was to study the structure and function of the presumed P(3-HB)-containing ion channel, already mentioned above, which required polymers with a length of 100–150 monomer units. For the synthesis of such large molecules, a stepwise technique is, of course, no longer practical. Polymerization of enantiomerically pure β-butyrolactone would probably lead to P(3-HB) samples with a relatively narrow size distribution (Table 3, nos 8 and 9), but from the results described above, these would not be likely to possess uniform configuration. A possible alternative was the segment condensation strategy, in which the two protecting groups on an unasymmetrically protected oligomer are selectively removed. The deprotected portions are then coupled to afford a molecule of "twice the size". The tetramers used as starting material in Scheme 7 were synthesized by one of the procedures described earlier,[131] though with some modifications. However, the coupling step via the acid chloride, and the benzyl ether and *tert*-butylester protecting groups were retained.

Characterization of the purified products becomes more and more difficult with increasing chain length, since because of their structural similarity, they display more or less identical analytical properties. Luckily, great progress has been made recently in the area of mass spectrometry, with the so-called soft ionisation methods.[189] In the case of P(3-HB), however, not all of these methods were equally useful, and larger molecules could finally only be characterized by means of matrix-supported laser desorption ionization (LDI) mass spectrometry (Fig. 3a,b).

For the fully protected 32mer **M**, the mass spectra each show three signals (as isotope distributions) with approximately the same *m/z* values and relative intensities (Fig. 3a). Such peaks were not observed with the smaller oligomers. They do not come about by fragmentation, but represent the

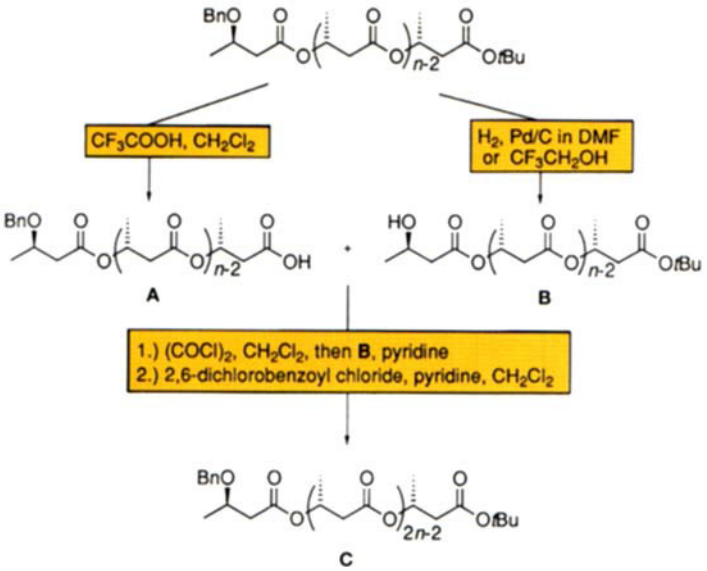

n	*n*mer acid **A**/ *n*mer alcohol **B**	2*n*	2*n*mer **C**	Yield [%] after the acid chloride coupling
4	**D/E**	8	**F**	>95
8	**G/H**	16	**I**	90
16	**K/L**	32	**M**	60
32	**N/O**	64	**P**	45
64/32	**Q/R**	96	**S** (96mer)	45

Scheme 7. Segment condensation algorithm for the synthesis of defined oligomers of (*R*)-3-hydroxybutyric acid. An *n*mer acid **A** is coupled to an *n*mer alcohol **B**, giving rise to a 2*n*mer product **C** of "twice the size". The yield after the acid chloride coupling step decreases with increasing size of the compounds. To improve the total yield for the larger molecules (**M**, **P**, and **S**), we "recoupled" with 2,6-dichlorobenzoyl chloride. This method allows activation of an acid in the presence of an alcohol [188].

molecular composition of the sample. A more detailed study of the reaction sequence showed that under the deprotection conditions specified in Scheme 7, terminal subunits may be cleaved off. For this reason, the average degree of polymerization (X_n) of the polymer mixture obtained was only 93, though this was distributed over a narrower range than would have been the case under ideal polymerization conditions[190] (Fig. 3b, see also reference to our own work in [106] and ref.[135b]).

These synthetic P(3-HB) oligomers represent a series of compounds, which can be used as standards to determine the molecular masses of polymers with similar constitution and configuration, by using gel permeation chromatography. For us, this was of special interest with respect to the ion channel already mentioned. Comparing molecular weights with those obtained after standardization with polystyrene or polyisoprene showed that the molecular weight values derived by using the latter standards can be appreciably higher (Fig. 3c).

5.5. Possible Future Applications of Polyhydroxyalkanoates

Up till now, the polyesters P(3-HB) and P(3-HB/3-HV) are the only PHAs that have been produced on a large scale

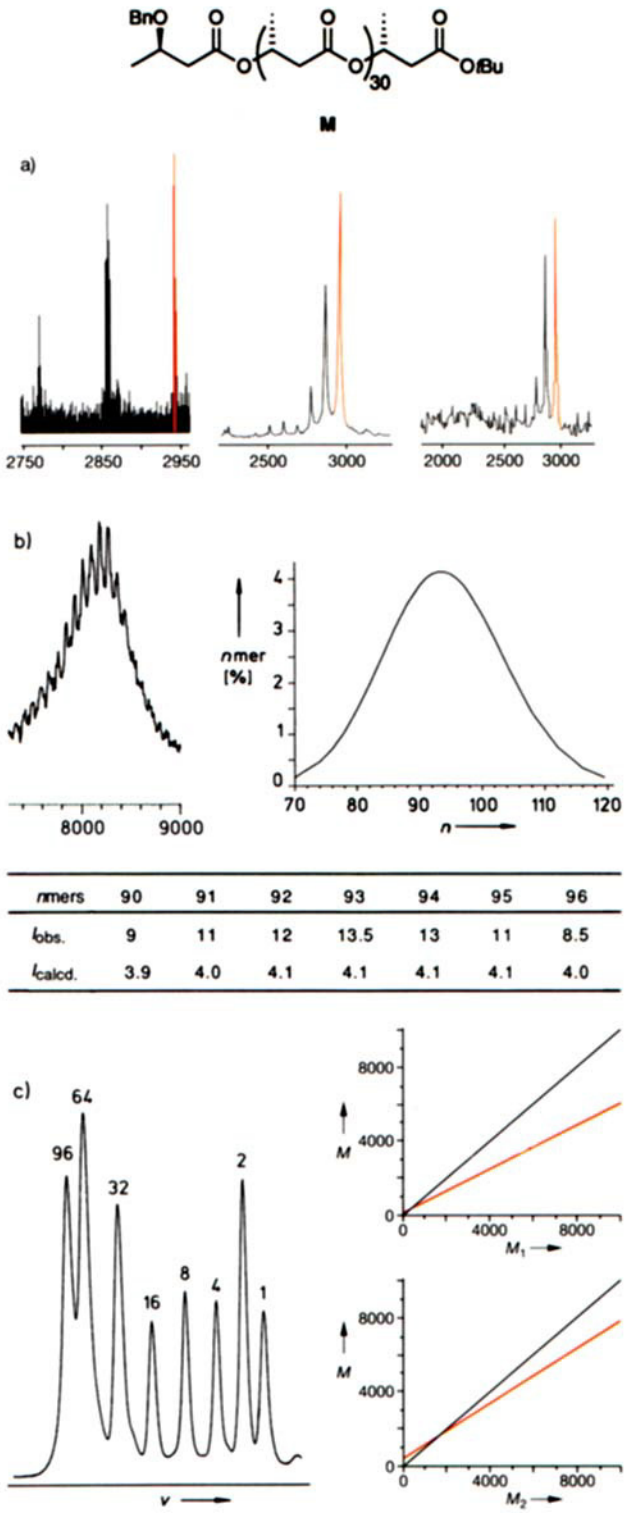

Fig. 3. a) Secondary ionization MS (in a 3-nitrobenzyl alcohol matrix, left), Plasma desorption ionization (PDI)-MS (center), and laser desorption ionization (LDI)-MS (in a 2,6-dihydroxy benzoic acid matrix, right) of the fully-protected 32mer (**M** in Scheme 7). We thank Prof. Dr. M. Przbylski and K. Schneider, University of Constance, for recording the PDI spectrum, and Dr K. Börnsen and Dr. M. Schär (Ciba-Geigy, Basel) for the LDI-spectra. b) Left: LDI mass spectrum of the fully-protected "96mer" (**S** in Scheme 7). The commonest compound in the distribution (right) is no longer the 96mer but the 93mer. In the distribution diagram the x axis is the degree of polymerization n; and the y axis is the share of $n$mer in %. Table: Comparison of the measured distribution of the "96mer" with that calculated for ideal polymerization conditions with a polymer length of 93 ($M_w/M_n = 1.01$) [163]. c) Gel permeation chromatogram of the fully protected P(3-HB) compounds (left). v = current. Comparison with the molecular masses determined after standardization using polystyrene or polyisoprene (right). M = real molecular mass; M_1 = apparent molecular mass with polystyrene; M_2 = apparent molecular mass with polyisoprene.

by using biotechnology. From 2.5 kg glucose, about 1 kg P(3-HB) can be synthesized in this way.[191a] In the middle of the nineties, the annual production of BIOPOL will be increased from about 300 tons to 5000–10000 tons.[191b] The production costs at present constitute about 50 DM per kilogram; the future aim is a kilo-price of 5–10 DM.[141]

By employing phototrophic microorganisms, it is even possible to utilize sunlight as energy source. Thus, *Rhodobacter sphaeroides* synthesizes up to 70% of its dry weight as P(3-HB).[192] Microbiological production of PHAs with a great variety of compositions and material properties is therefore possible, even if at present the yields are unsatisfactory, and the starting materials are oil-derived. How far these disadvantages can be countered by the use of genetechnologically modified organisms remains to be determined.

Synthetic methods are at present not well enough developed to compete with biotechnological production, at least of BIOPOL. On the other hand, a broad range of (*R*)- and (*S*)-hydroxy acids is now readily available, by enantioselective hydrogenation of the corresponding 3-keto esters.[193] We can therefore expect that in future synthetic processes will be developed which will be a match for microbial methods. With such a procedure, a variety of polymers would probably be accessible without great changes of the reaction conditions. In addition, workup of these reactions would be likely to prove far more simple than for biotechnological production methods, since it would be possible to work at high concentrations and in organic solvents.

With respect to molecular weight, melting region, crystallinity, flexibility, and tensile strength, BIOPOL and polypropylene are quite similar, though the former has disadvantages in its low tensile strength, poor solvent resistance,[194] limited resistance to acids, bases, and heat, and last but not least, its high price. It can be moulded thermoplastically, and processed to sheets and fibers,[195] but till now has been used primarily for the production of shampoo bottles (Fig. 4). Other applications for such polyesters can be found in agriculture (e.g. as cold frame sheeting, seed capsules, or formulations for the controlled release of pesticides or herbicides[1b]), or in human and veterinary medicine, because of their biocompatibility. Thus, numerous patents

Fig. 4. Shampoo bottles made of BIOPOL, after 0, 3, and 9 months in compost. The slower degradation of the printed areas is clearly visible. Doi et al. [92b] have shown that degradation occurs from the surface, and proceeds more quickly the larger the surface area. Nonenzymatic hydrolysis is several orders of magnitude slower than enzymatic depolymerization.

have already been registered, in which such materials are used for surgical implants to support organ and tissue healing processes,[196] as supports for "slow-release" systems,[10, 197] for the production of powders,[198] or as a component of membranes.[199] A process for elimination of nitrate from drinking water using P(3-HB) has also been developed.[200]

Recently attempts have been made to extend the field of application of P(3-HB) and P(3-HB/3-HV) by preparing degradable block copolymers with polystyrene and polyethers,[201] or "blends" with polyethylene, polystyrene, polyvinyl chloride, or polyethylene oxide.[202] Films of P(3-HB) act as a gas barrier in a similar way to polyvinyl chloride or polyethylene terephthalate.[202a] Because of these properties, P(3-HB) could well play an important role as a packaging material.

Judging by the increasing number of publications, the area is in the midst of great developments. How well PHAs can assert themselves against other biopolymers remains to be seen.

6. What is Known About the Structure of Polyesters?

The structures of many polyesters have been determined from fiber X-ray diffraction experiments.[203] In contrast to polyamides, polyesters cannot form hydrogen bonds, and so the force field is composed only of torsion, nonbonding, and electrostatic energy terms.[204] Figure 5 presents the structures that are known for aliphatic polyesters of hydroxy acids and their amino acid analogues, as far as the latter are known. Depending on the method of workup, solids with differing conformations are often isolated; for poly-β-propionolactone and polyglycine not all of these structures have been determined.

Prediction of the secondary structure of peptides and proteins is well established.[221] It has turned out that certain rules can also be derived for polyesters:

- polymers of the type -[O-(CH_2)n-CO-]- assume a staggered conformation (zigzag chain), at least for $n = 1$, 2, and 5 (**A**, **D**, and **L**, respectively in Fig. 5).[203]
- substituted poly-β-propiolactones always form a 2_1-helix (**M**–**Q** in Fig. 5). The pitch (axial spacing) of the helix decreases with increasing substituent size in the β-substituted poly-β-propionolactone series (**N**, **O**, and **P** in Fig. 5). According to Marchessault et al. a lower limit of 4.5 Å exists, below which changes in the helix geometry must occur.[217]

In the following sections, a few selected structures will be presented in more detail:

6.1. Structural Comparison of Homopolymers of α-Hydroxy Acids and α-Amino Acids

For polylactides, two conformations were found, a 10_3- and a 3_1-helix. These have practically the same energy content, and the latter is strongly reminiscent of the 3_1-helix of polyglycine (Table in Fig. 6), which forms no hydrogen bonds in this modification.[207] The α-helix of polyalanine

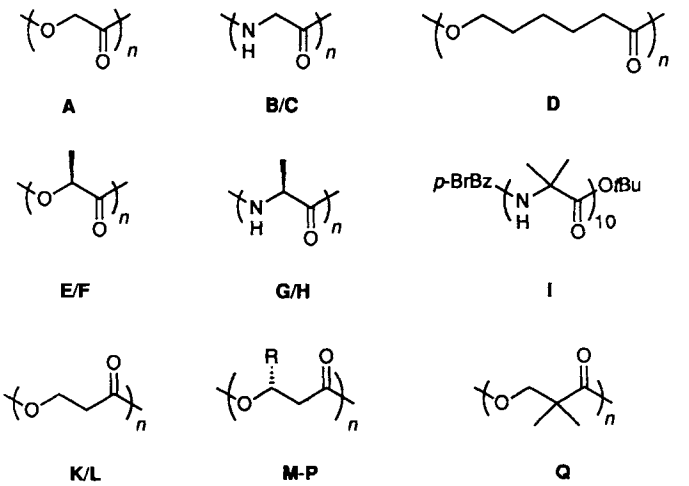

Name		Conformation [a]	Identity period [Å]	Ref.
A	polyglycolide	staggered	7.02	[205]
B	polyglycine I	?	–	[206]
C	polyglycine II	3_1-helix	9.3	[207]
D	polycaprolactone	staggered	17.05	[208]
E	β-poly-(*S*)-lactide	3_1-helix	9.00	[209b]
F	α-poly-(*S*)-lactide	10_3-helix	28.8	[209]
G	α-poly-(*S*)-alanine	β-staggered sheet	6.9	[210]
H	β-poly-(*S*)-alanine	4^7_{13}-helix [b]	70.3	[211]
I	deca-α-aminoisobutyrate	16_5-helix [c]	31.5	[212]
K	poly-β-propiolactone I	?	–	[213]
L	poly-β-propiolactone II	staggered	4.77	[214]
M	polydiketene (R: =CH_2)	2_1-helix	7.75	[215]
N	p(3-HB) (R: -CH_3)	2_1-helix	5.96	[167, 204,216]
O	p(3-HV) (R: -C_2H_5)	2_1-helix	5.56	[168]
P	p(3-HO) (R: -C_5H_{11})	2_1-helix	4.55	[217]
Q	poly-α,α-dimethylpropiolactone	2_1-helix	6.03	[218]

[a] On the basis of the crystallographic designation of screw axes the helix symmetry is expressed in the form n_r, which means that within an identity period n structural units form r rotations [219, 220]. This classification differs from the usual nomenclature for proteins; there in a n_r helix n denotes the number of amino acids per rotation and r the atom number of the ring formed from a hydrogen bond and its associated main chain segment [138]. [b] Corresponds to an α-helix. [c] Corresponds to a 3_{10}-helix.

Fig. 5. The known solid structures of polyesters of bifunctional monomers known to date, and those of the corresponding poly-(α-amino acid)amides, as far as these have been studied.

(**H** in Figs. 5 and 6), whose structure is stabilized by intramolecular hydrogen bonds, is not found with polyesters.

α-Aminoisobutyric acid (Aib) is a non-proteinogenic amino acid which is nonetheless found in many natural peptides (e.g. in peptaibols).[222] Single crystals have been grown from the fully protected oligomers containing up to ten Aib units.[212, 223] Because of the substitution pattern of Aib, the preferred secondary structure of such oligomers is not an α-helix but a 3_{10}-helix with a somewhat smaller internal diameter, which with the decamer **I** (Figs. 5 and 6) is almost ideal in form. The structure is also stabilized by intramolecular hydrogen bonds, and therefore has no analogue in the polyester series. Surprisingly, oligomers of α,α-diethylglycine (Deg) and α,α-dipropylglycine (Dpg) have staggered conformations, stabilized by intramolecular hydrogen bonds between the amide H atoms and the adjacent carbonyl groups, which are obviously energetically more favorable than a 3_{10}-helix.[223]

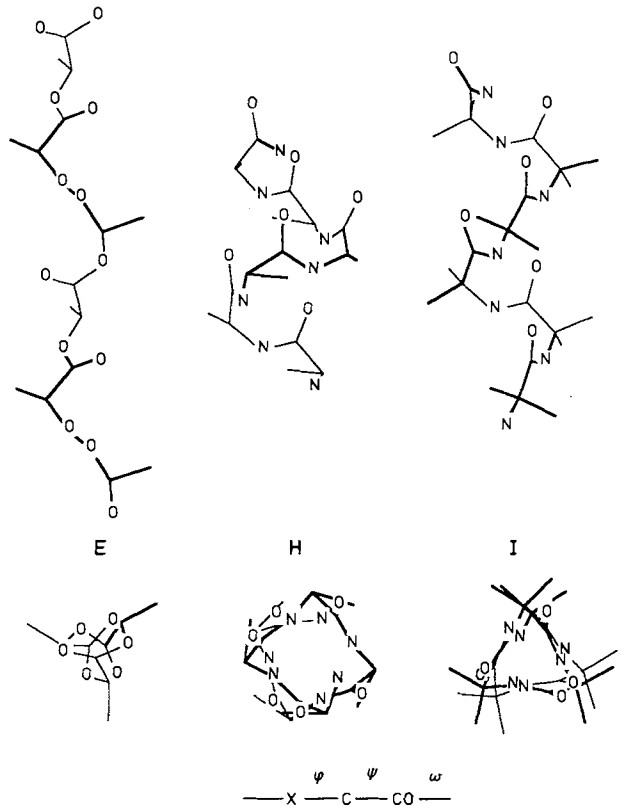

Polymer	Pitch [Å]	φ [°]	ψ [°]	ω [°]
poly-(*S*)-lactide : 3_1-helix **E**	9.0	-74	+144	180
polyglycine : 3_1-helix **C**	9.3	+/-80	-/+150	180
poly-(*S*)-alanine **H**	5.4	-66	-44	+179
p-BrBz-(Aib)$_{10}$-O*t*Bu **I**	6.3	+/-54	+/-31	+/-176

Fig. 6. MacMoMo views and a comparison of the 3_1-helix torsion angles of poly-(*S*)-lactide **E**, the α-helix of poly-(*S*)-alanine **H** and the 3_{10}-helix of deca-α-aminoisobutyrate **I**. The torsion angles are defined as for Figure 2c; the letters **E**, **H**, and **I** refer to the compounds in Figure 5.

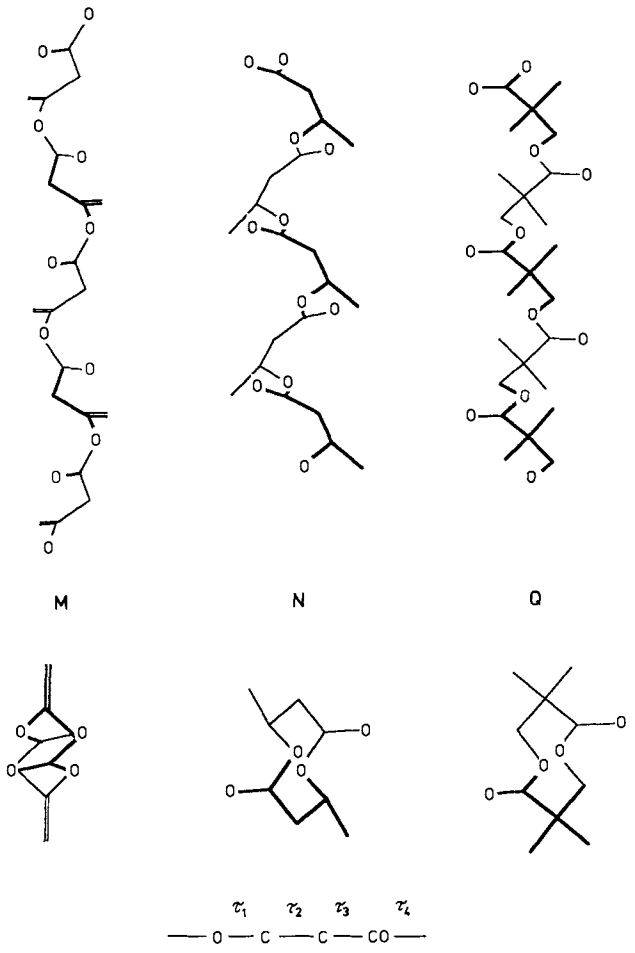

Polymer	Pitch [Å]	τ_1 [°]	τ_2 [°]	τ_3 [°]	τ_4 [°]
poly-α,α-dimethyl-β-propiolactone **Q**	6.03	+/-178	+/-41	+/-61	-/+164
polydiketene **M**	7.75	+/-84	+/-74	+/-147	+/-177
poly-(*R*)-3-hydroxybutyrate **N**	5.96	+162	-52	-42	-175
poly-(*R*)-3-hydroxyvalerate **O**	5.56	+136	-60	-21	179
poly-(*R*)-3-hydroxyoctanoate **P**	4.55	+111	-68	+15	-161

Fig. 7. MacMoMo views, and a comparison of the 2_1-helix torsion angles of polydiketene **M**, poly-(*R*)-3-hydroxybutyrate **N**, and poly-α,α-dimethyl-β-propiolactone **Q**. In each case, five structural units are shown. The torsion angles are defined as for Figure 2c; the letters **M**, **N**, and **Q** refer to the compounds in Figure 5. The values for P(3-HB) are taken from ref.[170].

6.2. Structural Comparison of Homopolymers of 3-Hydroxy Acids: Modeling Studies with the Structural Parameters from Oligolides of (*R*)-3-Hydroxybutyric Acid

The same left-handed 2_1-helix with an identity period of 5.9 Å has been derived independently by three different groups[167, 204, 216] from the diffraction pattern of P(3-HB) fibers, by using different algorithms.[224a] Depending on the method, slight variations in the torsion angles were found, but they still lie quite close to each other ($\tau_1 = +142°$ to $+152°$, $\tau_2 = -52°$ to $-59°$, $\tau_3 = -31°$ to $-42°$, $\tau_4 = -173°$ to $-180°$; Fig. 7).

So far, it has not been possible to grow suitable crystals of P(3-HB) or of linear (3-HB) oligomers,[224b] and so the P(3-HB)-helix has never been directly "seen". The only exact structural parameters available at present are those of (3-HB) oligolides (see above, Fig. 2). Thus, from the S-shaped partial structure (Fig. 2b, green) a left-handed helix with approximately two units per turn (2_1-helix) may be constructed, while the Δ-shaped structural element (Fig. 2a, red) can be used to make a right-handed helix with about three units per turn (3_1-helix) and a correspondingly larger internal diameter (Fig. 8).[133, 135b]

In the 2_1-helix the ester carbonyl plane is almost perpendicular to the helix axis. For the 3_1-helix, in contrast, it lies almost parallel to the axis. The latter structural type has not yet been found in solid P(3-HB), though this does not preclude its presence in solution. The structure in solution was and is the subject of numerous studies, with somewhat controversial results.[225]

Under tension, the identity periods of the polyesters change, presumably because either the helix or the amorphous regions of the polymer assume a staggered conformation (zigzag chain).[167, 204b] Recently Marchessault et al. have calculated the conformation of such a zigzag structure for P(3-HB), by energy minimization with an MM2 force field.[226] The chain is not ideally staggered, and the torsion angles are $\tau_1 = +113°$, $\tau_2 = -169°$, $\tau_3 = -113°$, and

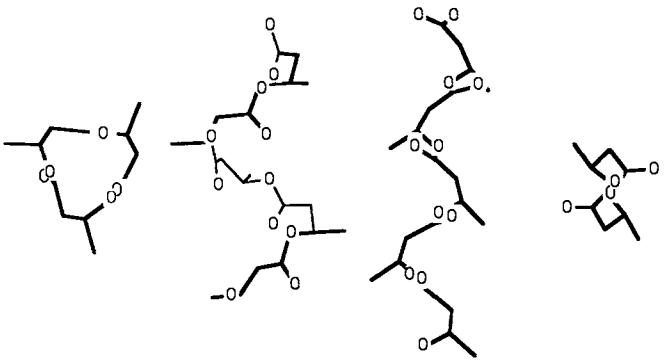

Fig. 8. MacMoMo views of the 2_1-helix (right) constructed from the S-shaped structural moiety (Fig. 2b, green), and the 3_1-helix (left) derived from the Δ-shaped spiral (Figure. 2b, red). In the middle, the two projections along the helical axes are shown (in each case only one turn of the helix is depicted).

$\tau_4 = +172°$ (identity period: 4.60 Å, for ideal staggering it would be 4.74 Å).

By using X-ray diffraction and ^{13}C NMR spectroscopy, it has been shown that the copolymer P(3-HB/3-HV) crystallizes in a P(3-HB)-helix up to 40% HV content, and in a P(3-HV)-helix above 55% HV (isodimorphism).[5, 227] Poly-β-isopropyl-β-propiolactone probably also crystallizes in a 2_1-helix, though all that is known about it is the identity period of 6.49 Å.[228] Unfortunately, at present it is not possible to compare the structure of the PHAs with the corresponding β-amino acid homopolymers, since there appear to be no structures known for the latter.[229]

7. Poly-(*R*)-3-hydroxybutyric Acid–Calcium Polyphosphate [P(3-HB)Ca-polyP$_i$] Complex: A Natural, Non-Proteinogenic Ion Channel?

Every cell has its own "microclimate". In order to preserve the special conditions required inside each cell, it surrounds itself with membranes. Biological membranes are essentially lipid bilayers containing interspersed proteins, usually about 75 Å thick. The hydrophobic interior is usually about 25 Å in size, but depending on the number of double bonds in the lipid chains can be up to 35 Å in breadth.[230] Because of their structure, lipid bilayers are practically impermeable for ions and most polar molecules. Nonetheless, these must somehow be able to pass through the membrane, since they play an important part in many physiological processes. Two transfer modes exist, carriers and channel mechanisms, whereby the latter is the more efficient and widespread of the two. Ion channels are mostly composed of proteins, with the channels themselves formed by ringlike conformations of several amphiphilic helices. The channel may consist of a single protein or of an aggregate of similar or identical subunits.[231] In addition, channel-forming peptides are also known, such as gramicidin,[232] for example, or alamethicin.[233]

Because of their great physiological importance, ion channels are at present the subject of intensive research; their importance was demonstrated in 1991 by the presentation of the Nobel Prize for medicine to Neher and Sakmann.

7.1. Findings which Led to the Postulation of an PHB-Containing Ion Channel

In 1983, Reusch et al. observed abrupt changes between 50 and 60 °C in the fluorescence intensity of *N*-phenyl-1-naphthylamine in the membranes of a variety of quite unrelated, genetically competent[234] gram-negative and gram-positive bacteria (*Azotobacter vinelandii*, *Bacillus subtilis*, and *Haemophilus influenzae*).[235] In each case, P(3-HB) was detected in the cell membranes, in significantly higher concentrations than were found in the noncompetent state. On the basis of these observations, the authors concluded that the characteristic changes in the fluorescence intensity must be somehow connected with P(3-HB).[19] Further experiments with *E. coli* showed that in the competent state, considerable quantities of P(3-HB) can be isolated (see Table 6).[235] The jump in fluorescence intensity at 50–60 °C was more intense if the competence protocol, which had been arrived at by "trial and error", was adhered to rigorously. A transition of this sort was not observed when biosynthesis of P(3-HB) was blocked with acetaldehyde, or if P(3-HB) was incorporated into liposomes. Clearly, the genetic transformability is connected with P(3-HB), but the P(3-HB) is not present by itself, but in the form of a quite unstable complex.[20] The authors later showed by freeze-fracture electron microscopy that in the plasma membranes of competent *A. vinelandii* and *E. coli* bacteria, islands with a visibly different structure are present.[21] Reusch and Sadoff were later able to isolate a labile complex from genetically competent *E. coli* bacteria, whose constituents were identified as P(3-HB), polyphosphate,[236] and calcium ions, and postulated a complex structure (see Figs. 9 and 10).[22, 23] In addition, they were able to show that the complex can be incorporated in vitro into liposomes, again using fluorescence spectroscopy.[22] Recently Reusch has also detected the complex more or less convincingly in plant and animal tissues (above all in the mitochondria and microsomes, to a lesser extent in the plasma membranes), though at significantly lower levels than in competent bacteria (see Table 6).[23]

Table 6. Occurrence of the complexes identified as [P(3-HB)Ca-polyP$_i$] in selected prokaryotes and eukaryotes [22,23].

Source	P(3-HB)$_{total}$ [μg g^{-1}]	Complex components [a] P(3-HB) [ng g^{-1}]	PolyP$_i$ [ng g^{-1}]	Ca^{2+} [ng g^{-1}]
E. coli log. phase	0.26	–	–	–
E. coli competent	156	9600	4200	2000
spinach leaves	6.5	435	232	126
cow heart	9.2	662	353	178
cow liver	0.86	163	88	47

[a] The given numbers are based on the wet weight.

7.2. Composition and Possible Structure of the PHB-Containing Complex

According to Reusch, in the complex isolated from *E. coli*, 3-HB, phosphate, and Ca^{2+} occur in a ratio of 1:1:0.5. In contrast, the eukaryotic complex contains a longer polyP$_i$ chain (see Table 7). On the basis of molecular modeling and

Table 7. Chain lengths of the P(3-HB) and polyphosphate chains in organisms. (Determined from the gel permeation chromatogram by comparison of the retention times with standards) [22,23].

Complex	Chain length in monomer units	
	P(3-HB)	PolyP$_i$ [a]
prokaryotic complex	120–200 [b]	130–170
eukaryotic complex	120–200 [c]	170–220

[a] Gel: Showdex B804; standard: polyethylene glycol. [b] Gel: Altex m-Spherogel; standard: polyisoprene. [c] Gel: Altex m-Spherogel; standard: *erroneously given as polystyrene* [23]! According to a personal communication from Reusch, however, they too used polyisoprene.

energy minimization considerations (with the force field program Charmm), Reusch et al. postulate the exolipophilic-endopolarophilic structure shown in Figure 9.

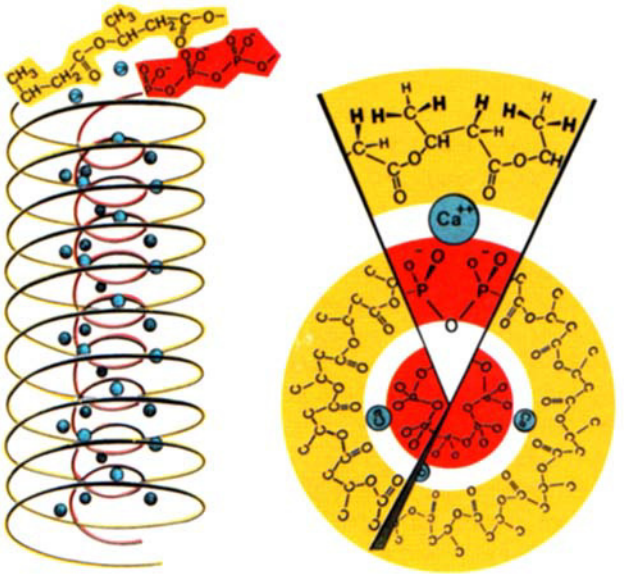

Fig. 9. Structure of a [P(3-HB)Ca-PolyP$_i$] complex suggested by Reusch [23].

The Ca^{2+} coordination geometry was decisive for the postulated spatial configuration. The external, right-handed P(3-HB)-helix must contain 14 units per turn, and the internal, also right-handed polyP$_i$-helix 7 units per turn, in order to bring the carbonyl and phosphate oxygen atoms into a suitable geometry for complexation with the Ca^{2+} ions (Fig. 10).[237] The Ca^{2+} ions lie vertically one above the other within the P(3-HB) cylinder. On the outside face, the methyl and methylene groups of the hydroxybutyric acid units also lie one above the other.

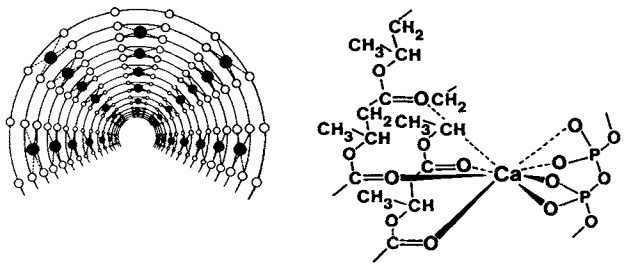

Fig. 10. Coordination geometry of the calcium in the postulated [P(3-HB)Ca-PolyP$_i$] complex [22].

A diameter of 24 Å,[238] and a length of 45 Å have been calculated, with an identity period of 4 Å, representing about 150 3-HB units and 80 P$_i$ units. To traverse the hydrophobic part of a membrane, 45 Å ought to be more than sufficient. However, in the projection shown in Figure 9, the ester bonds of the P(3-HB)-helix appear to assume at best the less favorable *E* conformation, which is about 3 kcal mol^{-1} less stable than the *Z* form.[239]

According to Reusch, the complex is quite labile in vitro, and extremely water-sensitive, probably due to the absence of stabilization of the postulated exolipophilic-endopolarophilic structure by the hydrophobic lipid bilayer.[240]

7.3. Possible Functions of the Ion Channel: DNA Transport?

The presumed exolipophilic–endopolarophilic structure is the ideal arrangement for an ion channel. Reusch assumes that such a channel would, above all, transport Ca^{2+} ions and polyphosphates across the plasma membrane. The inner, Ca-polyP$_i$-helix twists like a screw through the outer P(3-HB)-helix, and the Ca^{2+} ions are progressively transferred from one carbonyl group to the next. The transport of the neutral Ca-polyP$_i$ salt requires less energy than that of Ca^{2+} and polyP$_i$ ions separately. The interdependence of genetic transformability and complex concentration led Reusch to postulate DNA transport as well. However, for this to take place, the polyP$_i$ would first need to be removed from the P(3-HB)-helix. The outer P(3-HB)-helix remains intact as long as sufficient glucose is available as an energy source. According to Reusch and Sadoff, the internal diameter is sufficient to permit transport of single-stranded DNA. The structural requirements used to calculate this remain open—must the DNA be transported as a linear strand, or are secondary structures allowed? The secondary structures of single-stranded polynucleotides can display a considerable diameter. Thus, for example, the helix of polyadenosine has a diameter of 19 Å, only slightly less than that of double-stranded DNA (A-form: ca. 21 Å , B-form: ca. 22 Å, and Z-form: ca. 19 Å).[220] In addition, in transformation experiments, plasmids (cyclic, double-stranded DNA) are usually used, which in their supercoiled form have a far larger diameter! The role of calcium in genetic transformation, which is emphasized repeatedly by the authors, must also be somewhat modified, since transformation was obviously carried out according to the Hanahan protocol, where calcium plays only a subsidiary role![241] It is also unclear how such a channel could be opened and closed.

Nonetheless, this possible DNA-transport system through cell membranes is very intriguing, also with a view to future development of antisense medicaments.[242] The transport of charged oligonucleotides through cell membranes is still largely not understood.[242a, 243]

8. Complexation and Transport Experiments with Metal Ions and Polyesters

In the [P(3-HB)Ca-polyP$_i$] structure postulated by Reusch et al. the calcium ions are coordinated both to four

polyphosphate oxygen atoms and to four ester carbonyl oxygen atoms (Fig. 10). Complexes in which several ester carbonyl groups of the same acyclic molecule are coordinated to one cation are not known, to our knowledge. On the other hand, relatively many complexes exist between various cations and cyclic ligands, in which the ester carbonyl oxygen atoms cooperate with other functional groups. In nonactin, these are the ether oxygen atoms of the tetrahydrofuran rings.[244] Interestingly, these alkali metal complexes are very similar to the folded structure of the octolide of (*R*)-3-hydroxybutyric acid **O** (in Fig. 2), which in contrast to nonactin is not, however, active as an antibiotic (Fig. 11).[245] In the case of the depsipeptides, such as valinomycin, it is only the ester carbonyl groups which take part in complexation, but the structure is additionally stabilized by hydrogen bonds between the amide groups.[244]

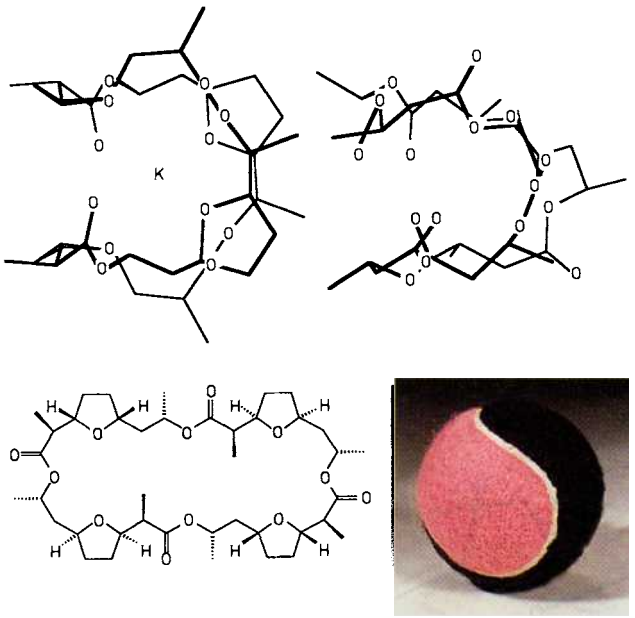

Fig. 11. MacMoMo views of the potassium complex of nonactin (top left) and the octolide structure **O** (top right) from Figure 2, and of the formula for nonactin (bottom left). Both 32-membered rings resemble the seam of a tennis ball in their structure (bottom right). The K^+ ion in the nonactin complex is surrounded by the four O atoms of the tetrahydrofuran rings and the four ester carbonyl O atoms in approximately cubic geometry. In the uncomplexed form nonactin has a different conformation to that in the potassium complex, and no longer resembles the octolide [244].

With the synthesized linear and cyclic P(3-HB) compounds in hand, we were in a position to investigate the complexing ability of polyesters of (*R*)-3-hydroxybutyric acid in more detail. All attempts at crystallization of such complexes with the open-chain molecules and larger cycles were unsuccessful, but promising results were obtained with the triolide **F** (in Fig. 2). Its structure is almost ideal for complexation, since the carbonyl groups are all practically parallel to each other, in the same hemisphere. Solutions of the triolide with sodium or potassium rhodanide in acetonitrile led to precipitation of solids whose structures could be determined.[135] For KSCN, crystals were only formed after the solution had been left open to air moisture for a little time: this proved that a little water was required for crystal formation. Both complexes are polymeric, and only in exceptional cases, for the sodium complex, were three ester carbonyl groups of one triolide molecule chelated to the same cation. Both the sodium and the potassium ions showed no particular preference for one coordination geometry with the ester carbonyl oxygen atoms (Fig. 12). Schreiber et al. made the same observation for alkali metal complexes with other carbonyl ligands.[246]

On the basis of ^{1}H NMR studies, and measurements of the dipole moment, the triolide appears to have a similar structure in solution to that in the crystal. In methanol, an interaction was observed with the alkali metal ions, which disappeared progressively, however, with gradual dilution. P(3-HB) also seems to undergo a certain degree of complexation with lanthanides in solution. Delsarte and Weill have suggested a structure for P(3-HB) in solution,[225c] by using the geometric data which they obtained from the McConnell–Robertson relationship of the pseudocontact complex of P(3-HB) with $Eu(fod)_3$ (fod = 1,1,1,2,2,3,3-heptafluoro-7,7-dimethyl-4,6-octadienato).

Okada et al.[247] and Burke et al.[248] have studied the transport of alkali metal picrates through an organic medium, by using cyclic polyesters which also contained additional acetal or ether oxygen atoms. Analogous experiments with triolide **F** showed increasing transport efficiency as the radius of the alkali metal ion increased (Fig. 13).[104b] These results can be explained readily by the increasing lipophilicity of the ions. The lack of ion selectivity could be connected to the rigidity of the triolide skeleton, whose structure remains almost unchanged even in the complexes with NaSCN and KSCN (Fig. 13). Similarly, high molecular weight P(3-HB) and linear oligomers of about 35 (3-HB) units also transported Cs^+ ions through a CH_2Cl_2 phase.[104b]

9. Conclusions and Outlook

After the discovery of P(3-HB) by Lemoigne about seventy years ago, interest in this biopolymer was at first very limited. The existence of this compound was known only to a few specialists. Because of the accessibility of polymers of this type from regenerable carbon sources, by using fermentation, an explosive development took place in this field at the time of the oil crisis about twenty years ago. Recently this has been strengthened by the fact that the poly(hydroxyalkanoates) are biodegradable and biocompatible polymers. Review articles and books have been written, and conferences held, whose participants from industry, academia, and state institutions were a more colorful interdisciplinary mixture than even the more experienced of us had ever seen. In a very recent international symposium on bacterial polyhydroxyalkanoates (ISBP '92, 1–5. June 1992) in Göttingen, the speakers and audience comprised biologists, microbiologists, geneticists, botanists, chemists, physicists, polymer scientists and polymer engineers, biotechnologists, pharmaceutical and medical scientists, many of whom came from institutes for raw materials and agrotechnology, food sciences,[249] groups concerned with waste disposal, housing and water management,[250] catalyst and surface research, even construction and building![251] Interest was concentrated almost exclusively (35 of 37 lectures) on high molecular

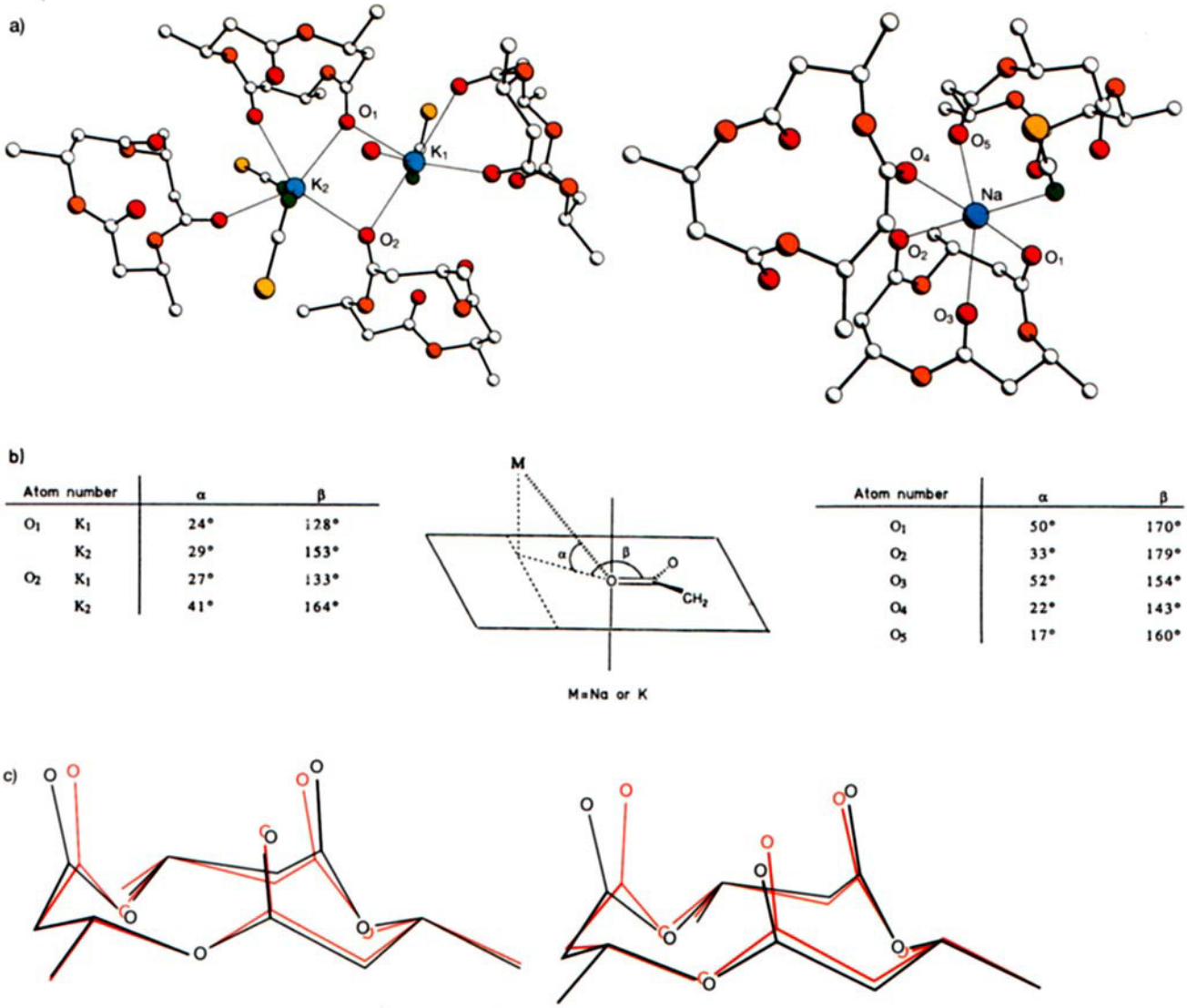

Atom number		α	β
O_1	K_1	24°	128°
	K_2	29°	153°
O_2	K_1	27°	133°
	K_2	41°	164°

Atom number	α	β
O_1	50°	170°
O_2	33°	179°
O_3	52°	154°
O_4	22°	143°
O_5	17°	160°

Fig. 12. a) PLUTO diagram of sections of the crystal structures of the triolide complex with KSCN (left) and with NaSCN (right). All potassium and sodium ions are hexacoordinated with the ester carbonyl O atoms of the triolides and the N atoms of the rhodanide ions as ligands. In the potassium complex, an additional water molecule is complexed to K_1. Red spheres are oxygen atoms of the CO functional groups, orange are OR oxygen atoms of the ester groups, white are carbon atoms, yellow are sulfur atoms, and green are nitrogen atoms. b) Coordination geometries of the potassium and sodium ions in the two complexes with selected ester carbonyl groups. For comparison: In the C_2 symmetrical nonactin–potassium complex, the angles are about α 61° and 67°, β 154° and 150°. c) Superposition of the free triolide (black) on the threefold coordinated triolide (red) in the Na complex (right), and on the twofold coordinated triolide (red) in the K complex (left).

weight polyhydroxyalkanoates, the bacterial storage materials made up of over 10000 (3-HB) units (referred to in the following as s-PHA or s-P(3-HB)[252]): their genesis, production, structure, material properties, applications, and biological degradation.[253]

Besides high molecular weight P(3-HB) in granules in microorganisms, the work of Reusch et al. has shown that short-chain P(3-HB), consisting of 100–200 (3-HB) units is also present in prokaryotic and eukaryotic organisms (referred to in the following as c-P(3-HB)[254]). It is always found in a complexed form, for example, in the cell membranes with Ca ions and probably a polyphosphate [19–23] and in human blood plasma with albumin and the so-called "low-density lipoproteins" (LDL).[24] In *E. coli*, which normally does not produce s-P(3-HB) (see also ref.[18]), the c-P(3-HB)-containing complex is only found in the inner cell membrane in the genetically competent state of the microbe, while in eukaryotes the complex is concentrated primarily in the mitochondria (the "microorganisms of the eukaryotic cell") and the microsomes; these facts suggest that c-P(3-HB) has important effects and functions. The results of our studies on the structure and properties of linear and cyclic (3-HB) oligomers do not contradict the hypothesis that c-P(3-HB) could be a component of an ion channel through cell membranes. It is notable that it should occur specifically as part of a complex with Ca polyphosphate, especially in view of a proposal made by Lipmann in 1965; he suggested that the first organisms on our planet may have used not ATP as their energy carrier, but inorganic polyphosphate or pyrophosphate (Polyphosphate – "a metabolic fossil"!).[255]

If one disregards inorganic polyphosphate [251, 257] and the aromatic amino acid-derived plant polymer lignin, which is non-uniform and difficult to classify,[258, 259] there are four classes of physiologically important biopolymers ("biomacromolecules"): polyisoprenoids, polynucleotides,

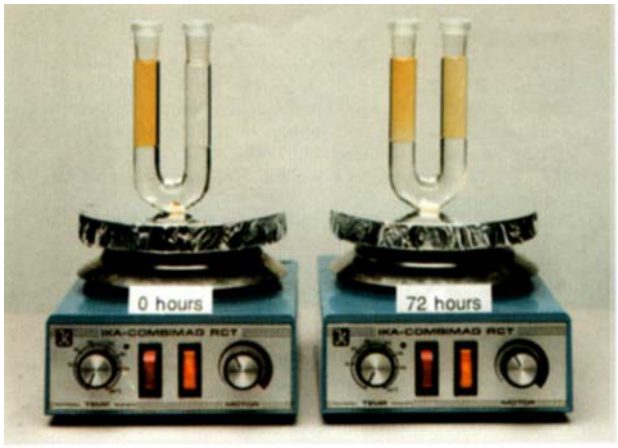

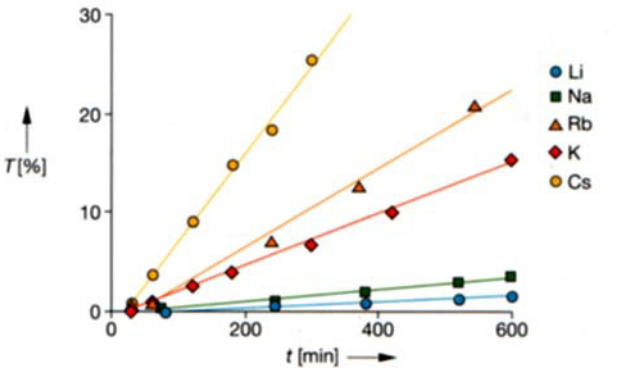

Fig. 13. Top: Apparatus for performing transport experiments through a "fluid membrane". The ions are transported out of a Tris-buffered (0.1 M) solution initially containing 1 mM alkali metal picrate/0.1 M alkali metal chloride, in the left side of the U-tube, through a 0.1 M triolide/CH_2Cl_2 solution into the other arm of the U-tube, whose water phase becomes progressively more yellow as the experiment proceeds. The picrate concentration is determined spectroscopically at λ_{max} = 356 nm. Bottom: Relative transport velocity T of the various alkali metal ions. These represent a so-called lipophilic series (without selectivity for a certain ionic radius!) [104b].

polypeptides, and polysaccharides. All four are distinguished by the facts that a) their monomeric building blocks are fundamental metabolic intermediates of the organisms, b) the respective oligomers display important effects, for example, as cofactors, hormones, or vitamins, in signal transduction or information transfer, or in recognition mechanisms, and c) the high molecular weight forms possess important functions, for example, as catalysts and receptors, as information carriers, as transport vehicles, storage materials, or structural elements. According to these criteria, poly(hydroxyalkanoates) must now also be regarded as a fifth important class of biopolymers. a) Their building blocks, the hydroxycarboxylic acids, in the simplest case hydroxybutyric acid, are a part of fatty acid metabolism; like the isoprenoids and polyketides[260] they are eventually derived from acetic acid. b) The oligomers, called c-P(3-HB) above, occur as components of complexes with other molecules, with effects as yet unknown; c-P(3-HB) is involved in the modification of cell membrane properties (phase transition, fluidity, permeability). c) The high molecular weight s-P(3-HB) is a microbial storage material (carbon reservoir, NADH-equivalents). In Table 8, examples are given of the five classes of biopolymers, and the polymers are contrasted with their low molecular weight equivalents.

Last of all, we come to the question of why low molecular weight c-PHA was discovered so late, and why its importance is only now slowly being recognized. Clearly, it was overlooked in the lipid fractions of cell extracts because of its chemical (heat, acid, base) and biochemical (ester-cleaving enzymes) instability. c-P(3-HB) occurs in *E. coli*, for example, only in very small amounts; it is synthesized to achieve a specific effect (membrane modification) and is then degraded again. It is probably subject to rapid anabolism/catabolism in the organism. The situation is therefore similar to that for hormones, whose stable representatives have been known and identified for a long time, while such important molecules as those of the arachidonic acid cascade (also lipids!), namely the leukotrienes, prostaglandins, thromboxanes etc. have only been isolated, characterized, synthesized, and their full importance recognized in the last few years (several have half-lives in serum or in tissues of less than a minute!).

Table 8. Comparison of monomers, oligomers, and polymers in chemistry and biochemistry of natural products.

Monomer *metabolic intermediates* biosynthesis and degradation from and to other low molecular weight building blocks	**Oligomers** *action* e.g. as hormone, cofactor, vitamin, information carrier, signal, recognition	**Polymers** *function* catalyst, receptor energy, storage material, transport vehicle, structural elements
amino acids	oligopeptides e.g. endorphines,bradykinin	polypeptides, e.g. fatty acid synthase hemoglobin, immunoglobulins skin, nails, hair, silk
monosaccharides, sugars	oligosaccharides e.g. blood group determinants heparin, sugar part of the glycoprotein dextrin	polysaccharides e.g. cellulose, starch chitin, glucan, glycogen murein
acetic acid, mevalonic acid isopentenyl pyrophosphate	isoprenoids carotinoids, rhodopsin, vitamin A, E, squalene, steroids, steroid hormones	polyisoprenoids, rubber, gutta-percha
purine and pyrimidine bases nucleosides, nucleotides, phosphate	oligonucleotides NADH, NADPH, tRNA	polynucleotides *m* and *r*RNA, DNA
hydroxycarboxylic acids	low molecular weight P(3-HB) (c-PHB, complexation)	high molecular weight P(3-HB) (s-PHB, storage)

We thank Silvia Sigrist for her tireless efforts in producing the manuscript. Without the help of Hans-Michael Bürger, Andreas Brunner, and Urs Lengweiler in preparing the final versions of Figures, Schemes, and Tables, the work would not have succeeded!

Received: July 29, 1992 [A 900 IE]
German version: *Angew. Chem.* **1993**, *105*, 483

[1] a) The expression poly(hydroxy acid) (PHA) was coined in 1983 by Findlay and White (R. H. Findlay, D. C. White, *Appl. Environ. Microbiol.* **1983**, *45*, 71) when it was realized that homopolymeric poly-(*R*)-3-hydroxybutyric acid occurred as the exception rather than the rule. Polymers with various hydroxy acid units are far more common. b) Recently the German term Polyhydroxyfettsäuren (PHF) has been proposed by Steinbüchel (A. Steinbüchel, *Nachr. Chem. Tech. Lab.* **1991**, *39*, 1112-1124)
[2] M. Doudoroff, R. Y. Stainer, *Nature (London)* **1959**, *183*, 1440.
[3] H. G. Schlegel, Allgemeine *Mikrobiologie*, 6th ed., Thieme, Stuttgart, **1985**.
[4] In this context it was demonstrated that microorganisms with PHA storage materials could survive "starvation periods" much better than those without them. The ability to survive is often directly proportional to the initial PHA content (E. A. Dawes, *Microbial Energetics*, Blakie, London, **1986**).
[5] Y. Doi, *Microbial Polyester*, VCH, Weinheim, **1990**.
[6] J. Schurz, *Nachr. Chem. Tech. Lab.* **1988**, *36*, 388; H. Zoebelein, *Chem. Unserer Zeit* **1992**, *26*, 27-34.
[7] The New York Times of May 3, 1985; Neue Zürcher Zeitung of December 12, 1986; Tagblatt der Stadt Zürich of August 23, 1990; Allgemeiner Hochschulanzeiger **1990**, no. 9, 11; Geo **1990**, no. 10, 224; Geo **1991**, no. 3, 80.
[8] H. G. Schlegel, G. Gottschalk, *Angew. Chem.* **1962**, *74*, 342-347.
[9] E. A. Dawes, P. J. Senior, *Adv. Microb. Physiol.* **1973**, *10*, 135-266.
[10] R. M. Lafferty, B. Korsatko, W. Korsatko, *Biotechnology, Vol. 6b* (Ed.: H. J. Rehm), VCH, Weinheim, **1988**, p. 135-176.
[11] H. Brandl, R. A. Gross, R. W. Lenz, R. C. Fuller, *Adv. Biochem. Eng. Biotechnol.* **1990**, *41*, 77-93.
[12] A. J. Anderson, E. A. Dawes, *Microbiol. Rev.* **1990**, *54*, 450-472.
[13] *Novel Biodegradable Microbial Polymers* (*NATO ASI Ser. Ser. E*, **1990**, *186*).
[14] Annual patent registration according to P(3-HB) substructure search in *Chem. Abstr.*: 29 (1991); 14 (1990); 13 (1989); 20 (1988); 7 (1987); 10 (1986); 9 (1985); 5 (1984); 5 (1983); 7 (1982); 1 (1981); 3 (1980)
[15] M. Lemoigne, *Ann. Inst. Pasteur (Paris)*, **1925**, *39*, 144.
[16] M. Lemoigne, *Bull. Soc. Chim. Biol.* **1926**, *8*, 770; *Ann. Inst. Pasteur (Paris)* **1927**, *41*, 148.
[17] a) W. G. C. Forsyth, A. C. Hayward, J. B. Roberts, *Nature (London)* **1958**, *182*, 800; b) O. P. Peoples, A. J. Sinskey, *J. Biol. Chem.* **1989**, *264*, 15298.
[18] The *E. coli* strain K-12 can produce up to 1.2% of its dry weight as P(3-HB), under suitable nutritional conditions. If it also harbors the R-plasmid RP1, and growth is under C-limiting conditions, this value can reach 5.8% (P. Gilbert, M. R. W. Brown, *J. Bacteriol.* **1978**, *133*, 1062). However, the authors do not comment on whether it is present as a storage material or as a membrane component (see Section 7).
[19] R. Reusch, H. Sadoff, *J. Bacteriol.* **1983**, *156*, 778.
[20] R. Reusch, T. Hiske, H. Sadoff, *J. Bacteriol.* **1986**, 168, 553.
[21] R. Reusch, T. Hiske, H. Sadoff, R. Harris, T. Beveridge, *Can. J. Microbiol.* **1987**, *33*, 435.
[22] R. Reusch, H. Sadoff, *Proc. Natl. Acad. Sci. USA* **1988**, *85*, 4176.
[23] R. Reusch, *Proc. Soc. Exp. Biol. Med.* **1989**, *191*, 377.
[24] R. Reusch, A. W. Sparrow, J. Gardiner, *Biochim. Biophys. Acta* **1992**, *1123*, 33.
[25] S. Schulz, S. Toft, Abstract of a lecture held at the "8th Annual Meeting of the International Society of Chemical Ecology (ISCE)", July 2-7, **1991**, in Dijon. The (*R,R*)-3-hydroxybutyric acid dimer is a very poorly volatile compound, and is odorless to the human nose. Odors could possibly arise from crotonic acid derivatives at concentrations below the NMR detection limit. The ester between crotonic acid and (*R*)-3-hydroxybutyric acid has the same effect as the (*R,R*) dimer: S. Schulz, Institut für Organische Chemie der Universität Hamburg, personal communication.
[26] D. B. Karr, J. K. Warers, F. Suzuki, D. W. Emerich, *Plant Physiol.* **1984**, *75*, 1158.
[27] D. Ellar, D. G. Lundgren, K. Okamura, R. H. Marchessault, *J. Mol. Biol.* **1968**, *35*, 489.
[28] R. Griebel, Z. Smith, J. M. Merrick, *Biochemistry* **1968**, *7*, 3676.
[29] J. M. Merrick, M. Doudoroff, *J. Bacteriol.* **1964**, *88*, 60.
[30] Y. Kawaguchi, Y. Doi, *FEMS Microbiol. Lett* **1990**, *70*, 151.
[31] a) G. N. Barnard, J. K. M. Sanders, *J. Biol. Chem.* **1989**, *264*, 3286. S. B. Amor, T. Rayment, J. K. M. Sanders, *Macromolecules* **1991**, *24*, 4583. - At the conference on PHB held in Göttingen this year (see also [251], [253]), Sanders gave a lecture (K. M. Bonthrone, J. Clauss, D. M. Horowitz, B. K. Hunter, J. K. M. Sanders, *The Biological and Physical Chemistry of Polyhydroxyalkanoates as seen by NMR Spectroscopy*) which are published in the corresponding Congress volume [253]; J. K. M. Saunders, *Chem. Soc. Rev.* **1993**, *22*, 1.
[32] W. J. Orts, M. Romansky, J. E. Guillet, *Macromolecules* **1992**, *25*, 949, and references therein.
[33] J. Schindler, H. G. Schlegel, *Biochem. Z.* **1963**, *339*, 154.
[34] H. Hippe, H. G. Schlegel, *Arch. Mikrobiol.* **1967**, *56*, 278.
[35] V. Oeding, H. G. Schlegel, *Biochem. J.* **1973**, *134*, 239.
[36] G. W. Haywood, A. J. Anderson, L. Chu, E. A. Dawes, *FEMS Microbiol. Lett.* **1988**, *52*, 91.
[37] G. W. Haywood, A. J. Anderson, L. Chu, E. A. Dawes, *FEMS Microbiol. Lett.* **1988**, *52*, 259.
[38] G. W. Haywood, A. J. Anderson, L. Chu, E. A. Dawes, *Biochem. Soc. Trans.* **1988**, *16*, 1046.
[39] G. W. Haywood, A. J. Anderson, E. A. Dawes, *FEMS Microbiol. Lett.* **1989**, *57*, 1.
[40] A. J. Anderson, G. W. Haywood, E. A. Dawes, *Int. J. Biol. Macromol.* **1990**, *12*, 102.
[41] G. A. F. Ritchie, P. J. Senior, E. A. Dawes, *Biochem. J.* **1969**, *112*, 803.
[42] G. A. F. Ritchie, P. J. Senior, E. A. Dawes, *Biochem. J.* **1971**, *121*, 309.
[43] P. J. Senior, E. A. Dawes, *Biochem. J.* **1973**, *134*, 225.
[44] T. Fukui, A. Yoshimoto, M. Matsumoto, S. Hosokawa, T. Saito, H. Nishikawa, K. Tomita, *Arch. Microbiol.* **1976**, *110*, 149.
[45] T. Nishimura, T. Saito, K. Tomita, *Arch. Microbiol.* **1978**, *116*, 21.
[46] H. Shuto, T. Fukui, T. Saito, Y. Shirakura, K. Tomita, *Eur. J. Biochem.* **1981**, *118*, 53.
[47] Y. Tanaka, T. Saito, T. Fukui, T. Tanio, K. Tomita, *Eur. J. Biochem.* **1981**, *118*, 177.
[48] T. Nakada, T. Fukui, T. Saito, K. Miki, C. Oji, S. Matsuda, A. Ushijima, K. Tomita, *J. Biochem.* **1981**, *89*, 625.
[49] T. Fukui, M. Ito, K. Tomita, *Eur. J. Biochem.* **1982**, *127*, 423.
[50] J. M. Merrick, M. Doudoroff, *Nature (London)* **1961**, *189*, 890.
[51] J. M. Merrick, F. P. Delafield, M. Doudoroff, *Fed. Proc.* **1962**, *21*, 228.
[52] J. M. Merrick, C. I. Yu, *Biochemistry* **1966**, *5*, 3563.
[53] R. Gavard, A. Dahinger, B. Hauttecoeur, C. Reynaud, *C. R. Acad. Sci.* **1967**, *265*, 1557.
[54] G. J. Moscowitz, J. M. Merrick, *Biochemistry* **1969**, *8*, 2748.
[55] R. Griebel, J. M. Merrick, *J. Bacteriol.* **1971**, *108*, 782.
[56] J. M. Merrick, *Polym. Prepr. (Am. Chem. Soc. Div. Polym. Chem.)* **1988**, *29(1)*, 586.
[57] Y. Doi, A. Tamaki, M. Kunioka, K. Soga, *Appl. Microbiol. Biotechnol.* **1988**, *28*, 330.
[58] A third variant [Eq. (a)] was found by Merrick et al in *R. rubrum* [54]. The (*S*)-hydroxybutyric acid derivative is first formed from acetoacetyl-CoA, and this is then epimerized to the (*R*) configuration by an enoyl-CoA hydratase. The subsequent reaction sequence proceeds as shown in Scheme 1. Evidently, *R. rubrum* cannot synthesize (*R*)-hydroxybutyryl-CoA directly by reduction of acetoacetyl-CoA.

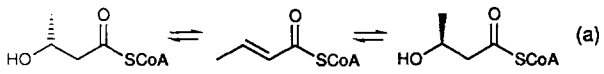

(a)

[59] P. A. Holmes, L. F. Wright, S. H. Collins, *Eur. Pat. Appl.* **1982**, EP 52459 (*Chem. Abstr.* **1982**, *97*, 143 146r); P. A. Holmes, F. Leonard, S. H. Collins, *ibid.* **1983**, EP 69497 (and 1983, *98*, 141 883a).
[60] C. Pedros-Alio, J. Mas, R. Guerrero, *Arch. Microbiol.* **1985**, *143*, 178.
[61] As well as sugars, carboxylic acids (up to and including caproic acid [5]) can be utilized, as can (*S*)-3-hydroxybutyric acid itself. (H. W. Ulmer, R. Gross, P. Weissbach, R. C. Fuller, R. W. Lenz, *Polym. Prepr. (Am. Chem. Soc. Div. Polym. Chem.)* **1989**, *30*, (*2*), 402). As an anaerobe, *A. eutrophus* can also use a mixture of H_2, CO_2 and air as C source, which was originally even considered as a raw material for the industrial production of P(3-HB) (D. Byrom, *Trends Biotechnol.* 1987, 5, 246).
[62] S. Masamune, C. T. Walsh, A. J. Sinskey, O. P. Peoples, *Pure Appl. Chem.* **1989**, *61*, 303-312.
[63] J. E. Bailey, *Science* **1991**, *252*, 1668.
[64] S. C. Slater, W. H. Voige, D. E. Dennis, *J. Bacteriol.* **1988**, *170*, 4431.
[65] P. Schubert, A. Steinbüchel, H. G. Schlegel, *J. Bacteriol.* **1988**, *170*, 5837.
[66] P. Schubert, N. Krüger, A. Steinbüchel, *J. Bacteriol.* **1991**, *173*, 168.
[67] A. Witte, W. Lubitz, *Eur. J. Biochem.* **1989**, *180*, 393.
[68] W. Lubbitz, *Eur. Pat. Appl.* **1990**, EP 435028 A2 (*Chem. Abstr.* **1990**, *115*, 134 2165b).
[69] a) R. Pool, *Science* **1989**, *245*, 1187; b) Y. Poirier, D. E. Dennis, K. Klomparens, C. Somerville, *ibid.* **1992**, *256*, 520.
[70] O. P. Peoples, A. J. Sinskey, *Mol. Microbiol.* **1989**, *3*, 349.
[71] G. W. Huisman, E. Wonink, R. Meima, B. Kazemier, P. Terpstra, B. Witholt, *J. Biol. Chem.* **1991**, *266*, 2191.

[72] The authors could only isolate an enriched depolymerase from *A. eutrophus*. They maintain that the lack of evidence for a dimer can possibly be ascribed to the action of an esterase, which copurifies with the depolymerase [33].

[73] (*R,S*) dimer, or (3*R*)-3-[(3′*S*)-3′-hydroxybutyryloxy]butyric acid **I**:

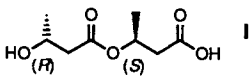

I

The (*R,S*) dimer is identical with the compound described as 3-L-[3-D-hydroxybutyryloxy]butyric acid (= LD dimer) in earlier publications [47, 52].

[74] Exoenzymes attack the polymer chains from the ends, in contrast to endoenzymes, which can also cleave within the polymer chain (*Lexikon der Biochemie*, (Eds. : H. D. Jakubke, H. Jeschkeit), VCH, Weinheim, **1974**).

[75] Merrick et al. have shown that the depolymerase is normally deactivated by an inhibitor whose action can be neutralized by an activator protein. The inhibitor can also be destroyed or removed by treating the P(3-HB) granules with trypsin, or extracting with alkali [55, 56]. The activities of the other enzymes are also affected by certain metabolic products. Thus, for example, NADH, pyruvate, and in some organisms oxaloacetate [35] or 2-oxo-glutarate inhibit 3-hydroxybutyrate dehydrogenase [43].

[76] Y. Doi, Y. Kawaguchi, Y. Nakamura, M. Kunioka, *Appl. Environ. Microbiol.* **1989**, *55*, 2932.

[77] Y. Doi, A. Tamaki, M. Kunioka, K. Soga, *Macromol. Chem. Rapid. Commun.* **1987**, *8*, 631.

[78] R. A. Gross, H. Brandl, H. W. Ulmer, M. A. Posada, R. C. Fuller, R. W. Lenz, *Polym. Prepr. (Am. Chem. Soc. Div. Polym. Chem.)* **1989**, *30*, 492.

[79] M. Kunioka, Y. Nakamura, Y. Doi, *Polym. Commun.* **1988**, *29*, 174.

[80] Y. Doi, M. Kunioka, Y. Nakamura, K. Soga, *Macromolecules*, **1988**, *21*, 2727.

[81] D. Byrom, *Trends Biotechnol.* **1987**, *5*, 246.

[82] BIOPOL. Nature's Plastic, ICI Bio Products & Fine Chemicals, PO Box 1, GB-Billingham, Cleveland TS23 1LB.

[83] R. W. Lenz, B.-W.Kim, H. Ulmer, K. Fritsche, R. C. Fuller, *Polym. Prepr. (Am. Chem. Soc. Div. Polym. Chem.)* **1990**, *31(2)*, 408.

[84] In pure deuterium oxide bacterial growth is too slow, see ref. [85].

[85] R. A. Gross, H. Brandl, H. W. Ulmer, D. J. Tshudy, P. C. Uden, R. C. Fuller, R. W. Lenz, *Polym. Prepr. (Am. Chem. Soc. Div. Polym. Chem.)* **1989**, *30(2)*, 398.

[86] A mixture of butyric acid and γ-butyrolactone as C source affords a polymer mixture made up of 3-HB- and 4-HB-rich polymers, which can comprise up to 80% 4-HB units (Y. Doi, A. Segawa, M. Kunioka, *Int. J. Biol. Macromol.* **1990**, *12*, 106).

[87] M. Scandola, G. Ceccorulli, Y. Doi, *Int. J. Biol. Macromol.* **1990**, *12*, 112.

[88] M. J. Smet, G. Eggink, B. Witholt, J. Kingma, H. Wynberg, *J. Bacteriol.* **1983**, *154*, 870.

[89] a) R. G. Lageveen, G. W. Huisman, H. Preusting, P. Ketelaar, G. Eggink, B. Witholt, *Appl. Environ. Microbiol.* **1988**, *54*, 2924; b) G. W. Huisman, O. Leeuw, G. Eggink, B. Witholt, *ibid.* **1989**, *55*, 1949.

[90] a) H. Brandl, R. A. Gross, R. W. Lenz, R. C. Fuller, *Appl. Environ. Microbiol.* **1988**, *54*, 1977; b) R. A. Gross, C. DeMello, R. W. Lenz, H. Brandl, R. C. Fuller, *Macromolecules* **1989**, *22*, 1106.

[91] Substituted carboxylic acids can also be utilized, but the branch position may not lie too close to the main chain. (K. Fritzsche, R. W. Lenz, R. C. Fuller, *Int. J. Biol. Macromol.* **1990**, *12*, 92).

[92] a) R. H. Marchessault, C. J. Monasterios, *Biotechnology and Polymers* (Ed.: C. G. Gebelein), Plenum, New York, **1991**, pp. 47–52. b) Y. Doi, Y. Kanesawa, M. Kunioka, T. Saito, *Macromolecules* **1990**, *23*, 31.

[93] G. Eggink, P. H. Lelyveld, A. Arnberg, N. Arfman, C. Witteveen, B. Witholt, *J. Biol. Chem.* **1987**, *262*, 6400.

[94] K. Fritsche, R. W. Lenz, R. C. Fuller, *Int. J. Biol. Macromol.* **1990**, *12*, 85.

[95] C. Abe, Y. Taima, Y. Nakamura, Y. Doi, *Polym. Commun.* **1990**, *31*, 404.

[96] Y. Doi, C. Abe, *Macromolecules* **1990**, *23*, 3705.

[97] K. Fritsche, R. W. Lenz, R. C. Fuller, *Makromol. Chem.* **1990**, *191*, 1957.

[98] J. B. Davis, *Appl. Microbiol.* **1964**, *12*, 301.

[99] Y. B. Kim, R. W. Lenz, R. C. Fuller, *Macromolecules* **1991**, *24*, 5256.

[100] F. E. Küng, US-A 2361036 **1944** (*Chem. Abstr.* **1944**, *38*, 6301).

[101] B. Hauttecoeur, M. Jolivet, R. Gavard, *C. R. Hebd. Seances Acad. Sci. Ser. D.* **1975**, *280*, 2801; S. Coulombe, P. Schauwecker, R. H. Marchessault, B. Hauttecoeur, *Macromolecules* **1978**, *11*, 279; H. Morikawa, R. H. Marchessault, *Can. J. Chem.* **1981**, *59*, 2306.

[102] N. Grassie, E. J. Murray, P. A. Holmes, *Polym. Degrad. Stab.* **1984**, *6*, 47, 95, 127.

[103] M. Kunioka, Y. Doi, *Macromolecules* **1990**, *23*, 1933.

[104] a) U. Brändli, dissertation (Herstellung und Charakterisierung cyclischer und offenkettiger Oligomerer von 3-Hydroxybutter- und -valeriansäure sowie Versuche zur Racematspaltung von 3,3,3-Trifluormilchsäure; dissertation no. 8680), ETH Zürich, **1988**; D. Seebach, *Angew. Chem.* **1988**, *100*, 1685–1715; *Angew. Chem. Int. Ed. Engl.* **1988**, *27*, 1624–1654; D. Seebach, A. K. Beck, U. Brändli, D. Müller, M. Przybylski, K. Schneider, *Chimia* **1990**, *44*, 112; b) H. M. Bürger, as yet unpublished experiments from the dissertation, ETH Zürich, **1990–1993**.

[105] K. O. Börnsen, M. Schär, H. M. Widmer, *Chimia* **1990**, *44*, 412; M. Schär, K. O. Börnsen, E. Grossmann, H. Widmer, *ibid.* **1991**, *45*, 123, and references therein.

[106] Mass spectrometric methods are becoming more and more established as new methods for determination of molecular weight distribution see, for example, J. V. Bletsos, D. M. Hercules, D. vanLeyen, B. Hagenhoff, E. Niehuis, A. Benninghoven, *Anal. Chem.* **1991**, *63*, 1953, and references therein. As yet, there are relatively few publications concerned with the mass spectrometric determination of P(3-HB): A. Ballistreri, D. Garozzo, M. Giuffrida, G. Impallomeni, G. Montaudo, *Macromolecules*, **1989**, *22*, 2107; A. Balliestreri, D. Garozzo, M. Giuffrida, G. Montaudo in ref.[13], p. 49–64; A. Ballistreri, G. Montaudo, D. Garozzo, M. Giuffrida, M. S. Montaudo, *Macromolecules*, **1991**, *24*, 1231; ref. 104; H. M. Bürger, H.-M. Müller, D. Seebach, K. O. Börnsen, M. Schär, *Macromolecules* submitted: here P(3-HB)-oligomer distributions determined by GPC analysis are compared with those obtained by matrix-supported LDI mass spectrometry.

[107] D. Seebach, M. Züger, *Helv. Chim. Acta* **1982**, *65*, 495; P. Schnurrenberger, M. F. Züger, D. Seebach *ibid.* **1982**, *65*, 1197; D. Seebach, M. F. Züger, *Tetrahedron Lett.* **1984**, *26*, 2747 (preparation of (*R*)-3-hydroxyvalerate from P(3-HB/3HV) copolymer).

[108] N. Vanlautem, G. Jacques, *Eur. Pat. Appl.* **1982**, EP 43 620 A1 (*Chem. Abstr.* **1982**, *96*, 163397f).

[109] Naturally, mixtures of oligomers (without crotonyl endgroups) are also accessible in this way; their mean molecular weight can be determined from the ratio P(3-HB)/alcohol: S. Akita, Y. Einaga, Y. Miyaki, H. Fujita, *Macromolecules* **1976**, *9*, 774; see also ref. [101], articles by Montaudo et al. in [106] and [108].

[110] D. Seebach, A. K. Beck, R. Breitschuh, K. Job, *Org. Synth.* **1992**, *71*, 39-47. Preparation was repeated successfully by E. R. Hickey, L. Paquette.

[111] a) D. Seebach, H. O. Kalinowski, *Nachr. Chem. Techn. Lab.* **1976**, *24*, 415; b) The total syntheses of colletodiol, grahamimycin A_1, pyrenophorin, and elaiophylidin by our group are summarized in Scheme 1 of the following publication: D. Seebach, H.-F. Chow, R. F. W. Jackson, M. A. Sutter, S. Thaisrivongs, J. Zimmermann, *Liebigs Ann. Chem.* **1986**, 1281-1308.

[112] N. R. Curtis, A. B. Holmes, M. G. Looney, N. D. Pearson, G. C. Slim, *Tetrahedron Lett.* **1991**, *32*, 537.

[113] K. Ohta, O. Mitsunobu, *Tetrahedron Lett.* **1991**, *32*, 517.

[114] M. Braun, U. Mahler, S. Houben, *Liebigs Ann. Chem.* **1990**, 513.

[115] D. Seebach, *Angew. Chem.* **1990**, *102*, 1363–1409; *Angew. Chem. Int. Ed. Engl.* **1990**, *29*, 1320–1367.

[116] a) D. Seebach, J. Zimmermann, U. Gysel, R. Ziegler, T. Ha, *J. Am. Chem. Soc.* **1988**, *110*, 4763; b) D. Seebach, U. Gysel, K. Job, A. K. Beck, *Synthesis*, **1992**, 39.

[117] a) D. Seebach, R. Naef, *Helv. Chim. Acta* **1981**, *64*, 2704; b) D. Seebach, R. Imwinkelried, T. Weber, *Mod. Synth. Methods* **1986**, 125–260; c) D. Seebach, S. Roggo, J. Zimmermann in *Stereochemistry of Organic and Bioorganic Transformations* (Eds.: W. Bartmann, K. B. Sharpless), VCH, Weinheim, **1987**, pp. 85–126.

[118] T. Pietzonka, D. Seebach, *Chem. Ber.* **1991**, *124*, 1837.

[119] G. Frater, *Helv. Chim. Acta* **1979**, *62*, 2825, 2829; *ibid.* **1980**, *63*, 1383; *Tetrahedron Lett.* **1981**, *22*, 425; D. Seebach, D. Wasmuth, *Helv. Chim. Acta* **1980**, *63*, 197; M. Sutter, D. Seebach, *Liebigs Ann. Chem.* **1983**, 939; J. Aebi, M. Sutter, D. Wasmuth, D. Seebach, *ibid.* **1983**, 2114.

[120] Y. Noda, D. Seebach, *Helv. Chim. Acta* **1987**, *70*, 2137.

[121] W. Amberg, D. Seebach, *Chem. Ber.* **1990**, *123*, 2413.

[122] W. Amberg, D. Seebach, *Chem. Ber.* **1990**, *123*, 2439.

[123] W. Amberg, D. Seebach, *Chem. Ber.* **1990**, *123*, 2429.

[124] The best method for synthesizing enantiomerically pure β-butyrolactone at present goes through the orthoester **II**, from which the β-butyrolactone can be liberated by pyrolysis, with exclusive inversion of the configuration at C-3, in 30-35% yield. The S_N2 attack on the lactone therefore corresponds formally to retention with respect to the (*R*)-hydroxybutyric

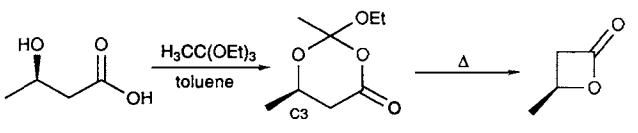

II

acid used as starting material. The original synthetic method, and an improved version: a) A. Griesbeck, D. Seebach, *Helv. Chim. Acta* **1987**, *70* 1320; b) R. Breitschuh, D. Seebach, *Chimia* **1990**, *44*, 216; other synthetic methods: c) A.R. Olson, R.J. Miller, *J. Am. Chem. Soc.* **1938**, *60*, 2687; d) J.R. Shelton, D.E. Agostini, J.B. Lando, *J. Polym. Sci. Part A1* 1971, **9**, 2789; e) R.A. Gross, Y. Zang, R.M. Thomas, R.W. Lenz, *Polym. Prepr.(Am. Chem. Soc. Div. Polym. Chem.)* **1988**, *29(1)*, 596.

[125] β-butyrolactone can be stereoselectively α-alkylated with suitable bases, so that products of the type **III** can be obtained in about 30–40% yield; see ref.[124a]; R. Schwesinger, *Nachr. Chem. Tech. Lab.* **1990**, *38*, 1214-

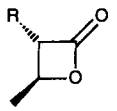

III

1226; H. Schlemper, dissertation (Extrem starke Oligophosphazen-Basen, Synthesen und Anwendungen), Universität Freiburg, **1990**. Similar experiments have been carried out earlier with α,β-substituted β-propiolactones, see J. Mulzer, T. Kerkmann, *J. Am. Chem. Soc.* **1980**, *102*, 3620.

[126] H. Liu, R. Auchus, C. T. Walsh, *J. Am. Chem. Soc.* **1984**, *106*, 5335.

[127] G. Cainelli, F. Manescalchi, G. Martelli, M. Panunzio, L. Plessi, *Tetrahedron Lett.* **1985**, *26*, 3369.

[128] a) R. Imwinkelried, dissertation (Organovanadiumverbindungen und enantiomerenreine Acetalderivate in der Synthese, dissertation no. 8142), ETH Zürich, **1986**; b) D. Seebach, R. Imwinkelried, G. Stucky, *Helv. Chim. Acta* **1987**, *70*, 448-464.

[129] a) A. Griesbeck, D. Seebach, *Helv. Chim. Acta* **1987**, *70*, 1326; b) R. Breitschuh, D. Seebach, *Synthesis* **1992**, 83.

[130] N. Yamaguchi, J. Inanga, H. Saeki, T. Katsuki, *Bull. Chem. Soc. Jpn.* **1979**, *52*, 1989.

[131] D. Seebach, U. Brändli, P. Schnurrenberger, M. Przybylski, *Helv. Chim. Acta* **1988**, *71*, 155.

[132] D. Seebach, U. Brändli, H.-M. Müller, M. Dobler, M. Egli, M. Przybylski, K. Schneider, *Helv. Chim. Acta* **1989**, *72*, 1704.

[133] H.-M. Müller, M. Dobler, P. Zbinden, D. Seebach, *Chimia* **1991**, *45*, 376.

[134] A. Shanzer, J. Libman, F. Frolow, *J. Am. Chem. Soc.* **1981**, *103*, 7339; A. Shanzer, *Bull. Soc. Chim. Belg.* **1983**, *92*, 411; A. Shanzer, J. Libman, F. Frolow, *Acc. Chem. Res.* **1983**, *16*, 60; A. Shanzer, J. Libman, *J. Chem. Soc., Chem. Commun.* **1983**, 846. The natural product Enterobactin contains the structural element of the triolide **F** (Scheme 5); the crystal structure of a vanadium complex of enterobactin has recently been published: T.P. Karpishin, K.N. Raymond, *Angew. Chem.* **1992**, *104*, 486; *Angew. Chem. Int. Ed. Engl.* **1992**, *31*, 466.

[135] a) D. Seebach, H.-M. Müller, H. M. Bürger, D. A. Plattner, *Angew. Chem.* **1992**, *104*, 443; *Angew. Chem. Int. Ed. Engl.* **1992**, *31*, 434; b) D. A. Plattner, A. Brunner, M. Dobler, H.-M. Müller, W. Petter, P. Zbinden, D. Seebach, *Helv. Chim. Acta* **1993**, in press.

[136] T. B. Grindley, R. Thangarasa, *J. Am. Chem. Soc.* **1990**, *112*, 1364, and refences therein.

[137] The results described will be published in more detail at a later point.

[138] IUPAC-IUB Commission on Biochemical Nomenclature, *Biochemistry* **1970**, *9*, 3471.

[139] For example, recently the following compounds **IV**–**VII** have been produced or generated from 3-hydroxy acids. Compound **IV**: D. Seebach, U. Misslitz, P. Uhlmann, *Angew. Chem.* **1989**, *101*, 484; *Angew. Chem. Int.*

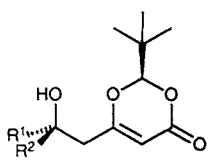

IV

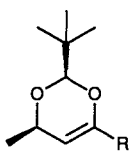

V

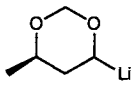

VI

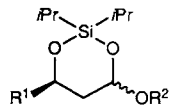

VII

Ed. Engl. **1989**, *28*, 472; D. Seebach, U. Misslitz, P. Uhlmann, *Chem. Ber.* **1991**, *124*, 1845. Compound **V**: U. Gysel, dissertation (Chromatographische Enantiomerentrennung von 1,3-Dioxinonen und Synthese von enantiomerenreinen 1,3-Dioxinen aus 3-Hydroxybuttersäure, dissertation no. 9473), ETH Zürich, **1991**. Configurationally stable 4-lithium-1,3-dioxanones with structure **VI** have been synthesized in several steps from P(3-HB). In THF, the (4*R*, 6*R*) derivative is stable at −78 °C, and the(4*R*, 6*S*) epimer is stable at 0 °C (R. J. Linderman, B. D. Griedel, *J. Org. Chem.* **1991**, *56*, 5491). Lactols of type **VII** have recently been synthesized by hydrosilylation of the corresponding 3-hydroxy acids. They can be diastereoselectively alkylated with allylsilane and suitable Lewis acids (A. P. Davis, S. C. Hegarty, *J. Am. Chem. Soc.* **1992**, *114*, 2745). Numerous pheromones have been synthesized by Mori et al. from 3-hydroxybutyrate and 3-hydroxyvalerate (K. Mori, *Tetrahedron* **1989**, *45*, 3233-3298).

[140] *Agricultural and Synthetic Polymers, Biodegradability and Utilization* (*ACS Symp. Ser.* **1990**, *433*).

[141] J. D. Evans, S. K. Sikdar, *CHEMTECH* **1990**, 38.

[142] In contrast to this, it is emphasized repeatedly at conferences and seminars on the subject that greater application of biodegradable polymers is not to be desired. On the one hand, they can be disposed of without commercial use, and on the other, their degradation products may pollute waterways (e.g. by eutrophication).

[143] Conference on Degradability of Polymers and Plastics, London, **1973**.

[144] R. Leaversuch, *Mod. Plast.* **1987**, *64*, 52.

[145] T.-W. Lai, A. Sen, *Organometallics* **1984**, *3*, 866; A. Sen, J. S. Brumbaugh, *J. Organomet. Chem.* **1985**, *279*, C5; M. Marsacchini, G. Consiglio, L. Medici, G. Petrucci, U. W. Suter, *Angew. Chem.* **1991**, *103*, 992; *Angew. Chem. Int. Ed. Engl.* **1991**, *30*, 989; A. Batistini, G. Consiglio, U. W. Suter, *ibid.* **1992**, *104*, 306 and **1992**, *31*, 303.

[146] C. E. Swanholm, R. G. C. Caldwell, DE-A 2216650, **1973** (*Chem. Abstr.* **1974**, *80*, 37852g).

[147] G. J. L. Griffin, *PCT Int. Appl.* **1988**, WO 8809354-A (*Chem. Abstr.* **1989**, *110*, 76828m).

[148] For example: F. H. Otey, R. P. Westhoff, W. M. Doane, *Ind. Eng. Chem. Prod. Res. Dev.* **1980**, *19*, 592.

[149] I. Tomka, B. Schink in the poceedings for the conference *Werkstoffe für die Bedürfnisse von Morgen* April 17–18, **1991**, Zürich.

[150] J. G. Leahy, R. R. Colwell, *Microbiol. Rev.* **1990**, *54*, 305–315.

[151] A. A. Chowdhury, *Arch. Mikrobiol.* **1963**, *47*, 167.

[152] T. Tanio, T. Fukui, Y. Shirakura, T. Saito, K. Tomita, T. Kaio, S. Masamune, *Eur. J. Biochem.* **1982**, *124*, 71.

[153] Y. Shirakura, T. Fukui, T. Tanio, K. Nakayama, R. Matsuno, K. Tomita, *Biochim. Biophys. Acta* **1983**, *748*, 331.

[154] Y. Shirakura, T. Fukui, T. Saito, Y. Okamoto, T. Narikawa, K. Koide, K. Tomita, T. Takemasa, S. Masamune, *Biochim. Biophys. Acta* **1986**, *880*, 46.

[155] T. Fukui, T. Narikawa, K. Miwa, Y. Shirakura, T. Saito, K. Tomita, *Biochim. Biophys. Acta* **1988**, *952*, 164.

[156] F. P. Delafield, M. Doudoroff, N. J. Palleroni, C. J. Lusty, R. Contopoulos, *J. Bacteriol.* **1965**, *90*, 1455.

[157] F. P. Delafield, K. E. Cooksey, M. Doudoroff, *J. Bacteriol.* **1965**, *240*, 4023.

[158] C. J. Lusty, M. Doudoroff, *Biochem.* **1966**, *56*, 960.

[159] M. W. Stinson, J. M. Merrick, *J. Bacteriol.* **1974**, *119*, 152.

[160] K. Nakayama, T. Saito, T. Fukui, Y. Shirakura, K. Tomita, *Biochim. Biophys. Acta* **1985**, *827*, 63.

[161] D. Davies, R. Y. Stanier, M. Doudoroff, M. Mandel, *Arch. Microbiol.* **1970**, *70*, 1.

[162] D. W. McLellan, P. J. Halling, *FEMS Microbiol. Lett.* **1988**, *52*, 215.

[163] The mean degree of polymerization ($\bar{X}_n$) with a bifunctional monomer can be calculated from Equation (b):

$$\bar{X}_n = 1/(1\text{-functional group conversion}) \qquad \text{(b)}$$

see textbooks of polymer chemistry such as e.g. P.C. Hiemenz, *Polymer Chemistry*, Marcel Dekker Inc., New York, **1984**.

[164] N. C. Billingham, M. G. Proctor, J. D. Smith, *J. Organomet. Chem.* **1988**, *341*, 83.

[165] F. E. Küng, US-A 2356459, **1944**, (*Chem. Abstr.* **1944**, *38*, 6301).

[166] J. P. Collman, L. S. Hegedus, J. R. Norton, R. G. Finke, *Principles and Applications of Organotransition Metal Chemistry*, University Science Books, Mill Valley, **1987**, Chapter 11.

[167] M. Yokouchi, Y. Chatani, H. Tadokoro, K. Teranishi, H. Tani, *Polymer* **1973**, *14*, 267.

[168] M. Yokouchi, Y. Chatani, H. Tadokoro, H. Tani, *Polym. J.* **1974**, *6*, 248.

[169] S. Bloembergen, D. A. Holden, T. L. Blum, G. K. Hamer, R. H. Marchessault, *Macromolecules* **1989**, *22*, 1656.

[170] K. Teranishi, M. Iida, T. Araki, H. Tani, *Macromolecules* **1977**, *10*, 275.

[171] K. Teranishi, M. Iida, T. Araki, S. Yamashita, H. Tani, *Macromolecules* **1974**, *7*, 421.

[172] S. Inoue, Y. Tomoi, T. Tsuruta, J. Furukawa, *Makromol. Chem.* **1961**, *48*, 229.

[173] H. Kricheldorf, N. Scharnagel, *J. Macromol. Sci. Chem. A* **1989**, *26(7)*, 951.

[174] D. E. Agostini, J. B. Lando, J. R. Shelton, *J. Polym. Sci. Part A1* **1971**, *9*, 2775.

[175] R. A. Gross, Y. Zhang, G. Konrad, R. W. Lenz, *Macromolecules* **1988**, *21*, 2657.

[176] T. Yashuda, T. Aida, S. Inoue, *Macromolecules* **1983**, *16*, 1792. T. Yasuda, T. Aida, S. Inoue, *Macromolecules* **1984**, *17*, 2217.

[177] Z. Jedlinski, M. Kowalczuk, W. Glokowski, J. Grobelny, M. Szware, *Macromolecules* **1991**, *24*, 349.

[178] a) N. Spassky, A. LeBorgne, M. Sepulchre, *Pure Appl. Chem.* **1981**, *53*, 1735–1744; b) H. B. Kagan, J. C. Fiaud, *Top. Stereochem.* **1984**, *18*, 249–330.

[179] A. LeBorgne, N. Spassky, *Polymer* **1989**, *30*, 2312.
[180] T. Takeichi, Y. Hieda, Y. Takayama, *Polym. J.* **1988**, *20*, 159.
[181] Ref. [124a], and references therein; L. D. Arnold, T. H. Kalantar, J. C. Vederas, *J. Am. Chem. Soc.* **1985**, *107*, 7105; L. D. Arnold, J. C. G. Drover, J. C. Vederas, *ibid.* **1987** *109*, 4649; L. D. Arnold, R. G. May, J. C. Vederas, *ibid.* **1988**, *110*, 2237.
[182] Y. Zang, R. A. Gross, R. W. Lenz, *Polym. Prepr. (Am. Chem. Soc. Div. Polym. Chem.)* **1989**, *30(2)*, 400.
[183] Y. Zang, R. A. Gross, R. W. Lenz, *Polym Prepr. (Am. Chem. Soc. Div. Polym. Chem.)* **1990**, *31(1)*, 1.
[184] N. Tanahashi, Y. Doi, *Macromolecules* **1991**, *24*, 5732.
[185] P. E. F. Ketelaar, E. G. Staring, H. Wynberg, *Tetrahedron Lett.* **1985**, *26*, 4665, and references therein.
[186] S. C. Arnold, R. W. Lenz, *Makromol. Chem. Macromol. Symp.* **1986**, *6*, 285.
[187] I. Ohlson, J. M. Merrick, I. J. Goldstein, *Biochemistry* **1965**, *4*, 453.
[188] The results described will be discussed in detail in a planned publication.
[189] *Methods Enzymol. (Mass Spectrometry)* **1991**, 193.
[190] The rate of the reaction of the monomer with the initiator must be greater than the rate of the polymerization reaction, and no chain transfer or chain termination reactions may occur. It can then be shown that in such cases the molecular weight follows a Poisson distribution, and the proportion of *n*mers in the mixture can be calculated, as can the polydispersity (M_w/M_n) [163]. In this way, "living polymers" with a relatively narrow distribution can be produced. More recent developments in this area include group transfer polymerization (GTP): D. Y. Sogah, W. R. Hertler, O. W. Webster, G. M. Cohen, *Macromolecules*, **1987**, *20*, 1473; M. T. Reetz, *Angew. Chem.* **1988**, *100*, 1026; *Angew. Chem. Int. Ed. Engl.* **1988**, *27*, 994, ring-opening metathesis polymerization (ROMP): R. Grubbs, *J. Am. Chem. Soc.* **1986**, *108*, 733; R. R. Schrock, *Acc. Chem. Res.* **1990**, *23*, 158, and cationic polymerization: T. Higashimura, S. Aoshima, M. Sawamoto, *Makromol. Chem., Macromol. Symp.* **1988**, *13/14*, 457; *ibid.* **1988**, *13/14*, 513; M. Zsuga, R. Faust, J.P. Kennedy, *Polym. Bull.* (Berlin) **1989**, *21*, 273.
[191] a) From a seminar held by Dr. F. Wynne, ICI (FRG), at a workshop on biodegradable plastics at Zürich University on November 27, 1991; b) *Chimia* **1990**, *44*, 222.
[192] Independent of the C source, this organism also makes primarily P(3-HB) (H. Brandl, R. A. Gross, R. W. Lenz, R. Lloyd, R. C. Fuller, *Arch. Microbiol.* **1991**, *155*, 337)
[193] a) R. Noyori, M. Kitamura, *Mod. Synth. Methods* **1989**, *Vol. 5*, 115-198; R. Noyori, H. Takaya, *Acc. Chem. Res.* **1990**, *23*, 345–350; b) A. Tai, T. Kikukawa, T. Sugimira, Y. Inoue, T. Osawa, S. Fujii, *J. Chem. Soc. Chem. Commun.* **1991**, 795.
[194] P(3-HB) is readily soluble in halogenated solvents, for example dichloromethane, chloroform, 1,2-ethylene dichloride, or trifluoroethanol. On heating, it also dissolves in dimethylformamide, dimethylsulfoxide, xylene, pyridine, dichloroacetic acid, trifluoroacetic acid, and acetic acid, though in the last four of these depolymerization must be reckoned with, especially at higher temperatures. Further discussion of solubility can be found in ref. [1b] and [10].
[195] "BIOPOL" from ICI–A Guide for Processors, ICI Bio Products & Fine Chemicals, PO Box 1, GB-Billingham, Cleveland TS23 1LB.
[196] For example: A. Heimerl, H. Pletsch, K. H. Rademacher, H. Schwengler, G. Winkeltau, K. H. Treutner, *Eur. Pat. Appl.* **1989**, EP 336148 A2 (*Chem. Abstr.* **1990**, *112*, 240568r); F. S. Bowald, E. G. Gunilla, *ibid.* **1990**, EP 349505 A2 (and **1990**, *113*, 46362z); M. Talja, P. Törmälä, P. Rokkanen, S. Vainionpää, T. Pohjonen, *PCT Int. Appl.* **1990**, WO 9004982 (and **1991**, *114*, 88740x).
[197] For example: M. Trau, R. W. Truss, *Eur. Pat. Appl.* **1988**, EP 293172 A2 (*Chem. Abstr.* **1989**, *110*, 90646g); L. Kwan, W. Steber, *ibid.* **1991**, EP 406015 A1 (and **1991**, *115*, 57187p); B. Korsatko, W. Korsatko, K. Wegleitner, *ibid.* **1991**, EP 450262 A1 (and **1992**, *116*, 67196a).
[198] P. A. Holmes, *UK Pat. Appl.* **1985**, GB 2160208 A (*Chem. Abstr.* **1986**, *104*, 230469e).
[199] T. Kamata, R. Numazawa, J. Kamo, JP 60137402 A2, **1983** (*Chem. Abstr.* **1986**, *104*, 39779b).
[200] M. Kloss, DE-A 3711598 A1, **1988** (*Chem. Abstr.* **1989**, *110*, 141188u).
[201] M. S. Reeve, S. McCarthy, R. A. Gross, *Polym. Prepr. (Am. Chem. Soc. Div. Polym. Chem.)* **1990**, *31(1)*, 437.
[202] a) M. Avella, E. Martuscelli, *Polymer* **1988**, *29*, 1731; b) P. Greco, E. Martuscelli, *ibid.* **1989**, *30*, 1475; c) P. B. Dave, N. J. Ashar, R. A. Gross, S. P. McCarthy, *Polym. Prepr. (Am. Chem. Soc. Div. Polym. Chem.)* **1990**, *31(1)*, 442; d) S. N. Bhalakia, T. Patel, R. A. Gross, S. P. McCarthy, *ibid.* **1990**, *31(1)*, 441.
[203] H. Tadokoro, *Structure of Crystalline Polymers*, 2nd edition, R. E. Krieger, Malaba, **1990**.
[204] a) J. Cornibert, R. H. Marchessault, *J. Mol. Biol.* **1972**, *71*, 735; b) J. Cornibert, R. H. Marchessault, *Macromolecules* **1975**, *8*, 296.
[205] Y. Chatani, K. Suehiro, Y. Okita, H. Tadokoro, K. Chujo, *Makromol. Chem.* **1968**, *113*, 215.
[206] C. H. Bamford, L. Brown, E. M. Cant, A. Elliott, W. E. Hanby, B. R. Malcolm, *Nature (London)* **1955**, *176*, 396.
[207] F. H. C. Crick, A. Rich, *Nature (London)* **1955**, *176*, 780; G. N. Ramachandran, V. Sasisekharan, C. Ramakrishnan, *Biochim. Biophys. Acta* **1966**, *112*, 168.
[208] Y. Chatani, Y. Okita, H. Tadokoro, Y. Yamashita, *Polym. J.* **1970**, *1*, 555.
[209] a) P. Desantis, A. J. Kovacs, *Biopolymers* **1968**, *6*, 299; b) W. Hoogsteen, A. R. Postema, A. J. Pennings, G. tenBrinke, P. Zugmaier, *Macromolecules* **1990**, *23*, 634.
[210] S. Arnott, S. D. Dover, A. Elliott, *J. Mol. Biol.* **1967**, *30*, 201.
[211] S. Arnott, A. J. Wonacott, *J. Mol. Biol.* **1966**, *21*, 371.
[212] C. Toniolo, M. Crisma, G. M. Bonora, E. Benedetti, B. Di Blasio, V. Pavone, C. Pedone, A. Santini, *Biopolymers* **1991**, *31*, 129.
[213] S. Okamura, T. Higashimura, A. Tanaka, R. Kato, Y. Kikuchi, *Makromol. Chem.* **1962**, *54*, 226.
[214] K. Suehiro, Y. Chatani, H. Tadokoro, *Polym. J.* **1975**, *7*, 352.
[215] M. Yokouchi, Y. Chatani, H. Tadokoro, *J. Polym. Sci.* **1976**, *14*, 81.
[216] S. Brückner, S. V. Meille, L. Malpezzi, A. Cesaro, L. Navarini, R. Tombolini, *Macromolecules* **1988**, *21*, 967.
[217] R. H. Marchessault, C. J. Monasterios, F. G. Morin, P. R. Sundararajan, *Int. J. Biol. Chem.* **1990**, *12*, 158.
[218] G. Perego, A. Melis, M. Cesari, *Makromol. Chem.* **1972**, *157*, 269.
[219] J. P. Glusker, K. N. Trueblood, *Crystal Structure Analysis*, 2nd edition, Oxford University Press, New York, **1985**.
[220] W. Saenger, *Principles of Nucleic Acid Structure*, 2nd edition, Springer, New York, **1988**.
[221] For example: M. Mutter, S. Vuilleumier, *Angew. Chem.* **1989**, *101*, 551–571; *Angew. Chem. Int. Ed. Engl.* **1989**, *28*, 535–554.
[222] R. Nagaraj, P. Balaram, *Acc. Chem. Res.* **1981**, *14*, 356; I. J. Karle, P. Balaram, *Biochemistry* **1990**, *29*, 6787; H. Heimgartner, *Angew. Chem.* **1991**, *103*, 271–297; *Angew. Chem. Int. Ed. Engl.* **1991**, *30*, 238–264.
[223] C. Toniolo, E. Benedetti, *Macromolecules* **1991**, *24*, 4004.
[224] a) In many articles, P(3-HB) is incorrectly ascribed a right-handed 2_1-helix, for example, in refs. [5,10,11,22], perhaps because Marchessault and Okamura originally proposed this (K. Okamura, R. H. Marchessault, *Conformation of Biopolymers*, (Ed.: G. N. Ramachandran), Academic Press, London, **1967**), though they later corrected themselves [204]. b) For the growth of lamellar crystallites of P(3-HB) and their X-ray and electron microscopic identification, see P. J. Barham, A. Keller, E. L. Otun, P. A. Holmes, *J. Mater. Sci.* **1984**, *19*, 2781.
[225] a) R. Marchessault, K. Okamura, C. Su, *Macromolecules* **1970**, *3*, 737; b) J. Cornibert, R. Marchessault, *J. Mol. Biol.* **1972**, *71*, 735; c) J. Delsarte, G. Weill, *Macromolecules* **1974**, *7*, 343; d) *ibid.* **1974**, *7*, 450; e) S. Akita, Y. Einaga, Y. Miyaki, H. Fujita, *ibid.* **1976**, *9*, 774; f) Y. Doi, M. Kunioka, Y. Nakamura, K. Soga, *ibid.* **1986**, *19*, 1274; g) *ibid.* **1986**, *19*, 2860; h) N. Kamiya, Y. Inoue, Y. Yamamoto, R. Chujo, Y. Doi, *ibid.* **1989**, *22*, 1676; i) P. Dais, M. E. Nedea, F. G. Morin, R. H. Marchessault, *ibid.* **1989**, *22*, 4208; k) N. Kamiya, Y. Inoue, Y. Yamamoto, R. Chujo, Y. Doi, *ibid.* **1990**, *23*, 1313.
[226] W. J. Orts, R. H. Marchessault, T. L. Blum, G. K. Hamer, *Macromolecules* **1990**, *23*, 5368.
[227] M. Scandola, G. Ceccorulli, M. Pizzoli, M. Gazzano, *Macromolecules* **1992**, *25*, 1405.
[228] K. Teranishi, T. Araki, H. Tani, *Macromolecules* **1972**, *5*, 660.
[229] According to a crystal structure search in the Cambridge crystallographic data file and ref. [203].
[230] G. Boheim, W. Hanke, H. Eibel, *Proc. Natl. Acad. Sci. USA* **1980**, *77*, 3403; L. Stryer, *Biochemie*, 3rd edition, Spektrum der Wissenschaften, Heidelberg, **1990**; M. Jain, *Introduction to Biological Membranes*, 2nd edition, Wiley, New York, **1988**.
[231] J. Findlay, *Chem. Br.* **1991**, 724.
[232] D. A. Langs, *Science* **1988**, *241*, 188; F. R. Salemme, *ibid.* **1988**, *241*, 145; B. A. Wallace, K. Ravikumar, *ibid.* **1988**, *241*, 182; D. Buster, J. Hinton, F. Millett, D. Shungu, *Biophys. J.* **1988**, *53*, 145; D. W. Urry, *Membranes and Transport, Vol. 2* (Ed.: A. Martonosi), Plenum, New York, **1982**, pp. 175–218.
[233] K. Voges, G. Jung, W. Sawyer, *Biochim. Biophys. Acta* **1987**, *896*, 64; G. Boheim, W. Hanke, G. Jung, *Biophys. Struct. Mech.* **1983**, *9*, 181; W. Hanke, G. Boheim, *Biochim. Biophys. Acta* **1980**, *596*, 456.
[234] "Genetic transformation" indicates the ability of a cell to take up DNA from the external medium, leading to both a new genotype and—because of expression of the introduced DNA—a new phenotype (W. Wenzel, M. J. Amann, *Lexikon der Gentechnologie*, Springer, Heidelberg, **1985**; H. Smith, D. Danner, R. Deich, *Ann. Rev. Biochem.* **1981**, *50*, 41).
[235] It remains to be investigated how P(3-HB) can be produced by *E. coli* under the conditions described. Sinskey et al. [17b] have shown that only genetically modified *E. coli* containing the ketothiolase, reductase, and synthetase genes is capable of biosynthesis of P(3-HB) according to Scheme 1. The same appears to be true in plants [69b].
[236] As mentioned at the start, polyphosphates occur in many bacteria [4]. Their function is still not clear; they may act as reservoirs of energy or phosphate, or replace ATP in kinase reactions (K. A. Ahn, A. Kornberg, *J. Biol. Chem.* **1990**, *265*, 11734; I. S. Kulaev, *The Biochemistry of Inorganic Polyphosphates*, Wiley, New York, 1979 and ref.[13]). Their common appearance with P(3-HB) is not so surprising, since Doi et al. have

shown that in *A. eutrophus* polyphosphate synthesis and P(3-HB) synthesis are connected [76].

[237] In this approach, the structure of calcium metaphosphate $[Ca(PO_3)_2]_n$ is clearly not critical (four different modifications are known, the α, β, γ, and δ forms) (A. O. McIntosh, W. L. Jablonski, *Anal. Chem.* **1956**, *28*, 1424). The structure of the β form is known; it is zigzag-shaped and not a helix (M. Schneider, K. H. Jost, P. Leibnitz, *Z. anorg. allg. Chem.* **1985**, *527*, 99). However, the rotation barrier of the P-O-P bond is relatively low, so that depending on the cation various conformations have been found, including helical arrangements with $[AgPO_3]_n$ or $[NaPO_3]_n$, in the Kuroll A and B modifications (D. E. C. Corbridge, *The Structural Chemistry of Phosphorus*, Elsevier, Amsterdam, **1974**).

[238] This presumably refers to the external diameter, which was not defined in the article quoted [22].

[239] P. Deslongschamps, *Stereoelectronic Effects in Organic Chemistry*, Pergamon, Oxford, **1983**, and references therein.

[240] Stabilization and a better protection against water could probably be achieved with suitable detergents. Using such a method Huber, Deisenhofer, and Michel were also more able to solubilize the exolipophilic-endopolarophilic photosynthetic reaction center of *Rhodopseudomonas viridis* in water, and subsequently to crystallize it as detergent micelles (see J. Deisenhofer, H. Michel, *Angew. Chem.* **1989**, *101*, 872-892; *Angew. Chem. Int. Ed. Engl.* **1989**, *28*, 829)

[241] D. Hanahan, *J. Mol. Biol.* **1983**, *166*, 557.

[242] a) U. English, D. H. Gauss, *Angew. Chem.* **1991**, *103*, 629–646; *Angew. Chem. Int. Ed. Engl.* **1991**, *30*, 613; b) E. Uhlmann, A. Peyman, *Chem. Rev.* **1990**, *90*, 553–584.

[243] L. A. Yakubov, E. A. Deeva, V. F. Zarytova, *Proc. Natl. Acad. Sci. USA* **1989**, *86*, 6454; S. L. Loke, C. A. Stein, X. H. Zhang, *ibid.* **1989**, *86*, 3474.

[244] M. Dobler, *Ionophores and Their Structures*, Wiley, New York, **1981**.

[245] It shows no antibiotic effect against *Staphylococcus aureus*, *Comamonas terrigena*, *Candida albicans*, and *Aspergillous niger*. We thank Dr. J.-J. Sanglier of Sandoz AG in Basel for carrying out the antibiotic tests for us.

[246] S. Shambayati, W. E. Crowe, S. L. Schreiber, *Angew. Chem.* **1990**, *102*, 273–290; *Angew. Chem. Int. Ed. Engl.* **1990**, *29*, 256.

[247] I. Tajima, M. Okada, H. Sumitomo, *J. Am. Chem. Soc.* **1981**, *103*, 4096.

[248] S. D. Burke, W. J. Porter, J. Rancourt, R. F. Kaltenbach, *Tetrahedron Lett.* **1990**, *31*, 5285.

[249] It has been shown that 3-hydroxybutyrate can replace glucose as brain nutrient, for example, in patients who are required to lose weight before an operation due to excessive obesity, or in coma patients: G. L. S. Pawan, S. J. G. Semple, *The Lancet* **1983**, *1*, 15.

[250] ICI showed many years ago that fermentation of *Alcaligenes eutrophus* can take place in urban wastewater, and can in principle produce s-P(3-HB) [61].

[251] International Symposium on Bacterial Polyhydroxyalkanoates ISBP'92, Göttingen, (FRG), June 1–5, **1992**; Programme and Abstracts, including list and addresses of the participants.

[252] The "s" stands for storage.

[253] The manuscripts of the lectures and posters are published in a special volume of *FEMS-Microbiol. Rev.* **1992**, *103*, 91-376.

[254] The "c" stands for complexed, following a proposal of R. Reusch [251,253].

[255] Pages 151–158 of the book by Dawes [4] and the detailed literature list contained.

[256] Microorganisms are known which can store polyphosphates of molecular weights up to over 10^6 [255].

[257] Literature list to chapter 11 in the book cited in [4].

[258] Apart from cellulose, lignin is probably the most widely distributed natural product on our planet!?

[259] Reviews: K. Freudenberg, *Science* **1965**, *148*, 595; E. Adler, S. Larson, K. Lindquist, G. E. Mikshe, *Abstr. Int. Wood Chem. Symp.* **1969**. See also: *Natural Product Chemistry, Vol. 2* (Eds.: K. Nakanishi, T. Goto, S. Ito, S. Natori, S. Nozoe), Academic Press, New York, **1975**, Chapter 9.16.

[260] Classification of natural products: *Natural Product Chemistry, Vol. 1* (Eds.: K. Nakanishi, T. Goto, S. Ito, S. Natori, S. Nozoe), Academic Press, New York, **1974**, Chapter 1.

Neural Networks in Chemistry

By Johann Gasteiger* and Jure Zupan*

The capabilities of the human brain have always fascinated scientists and led them to investigate its inner workings. Over the past 50 years a number of models have been developed which have attempted to replicate the brain's various functions. At the same time the development of computers was taking a totally different direction. As a result, today's computer architectures, operating systems, and programming have very little in common with information processing as performed by the brain. Currently we are experiencing a reevaluation of the brain's abilities, and models of information processing in the brain have been translated into algorithms and made widely available. The basic building-block of these brain models (neural networks) is an information processing unit that is a model of a neuron. An artificial neuron of this kind performs only rather simple mathematical operations; its effectiveness is derived solely from the way in which large numbers of neurons may be connected to form a network. Just as the various neural models replicate different abilities of the brain, they can be used to solve different types of problem: the classification of objects, the modeling of functional relationships, the storage and retrieval of information, and the representation of large amounts of data. This potential suggests many possibilities for the processing of chemical data, and already applications cover a wide area: spectroscopic analysis, prediction of reactions, chemical process control, and the analysis of electrostatic potentials. All these are just a small sample of the great many possibilities.

1. Introduction

In many areas where complex information needs to be processed--from the stock-market to medical diagnosis and chemistry—people are suddenly talking about "neural networks". Neural networks appear to be a new secret weapon to combat a multitude of problems. In order to illustrate this, Figure 1 shows the dramatic rise in the number of publications on the use of neural networks in chemistry. What makes neural networks so attractive? Are they really a panacea for information processing ?

Neural networks were originally developed as models of information processing within the brain. This explains some of their fascination: The human brain has phenomenal processing power, far beyond that even of supercomputers today. Obviously the human brain processes information in a completely different way from that of today's conventional computers, which are constructed along the lines of the "von Neumann" architecture. A von Neumann computer works through a program (an algorithm) step by step, that is, sequentially.

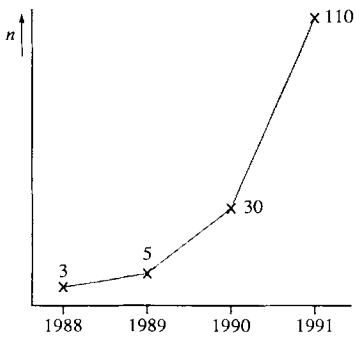

Fig. 1. Increase in the number of publications on the use of neural networks in chemistry over the period 1988-1991.

In contrast the human brain operates largely in parallel: incoming information is channeled through many processing units simultaneously. This can be demonstrated by the "100 Step Paradox": We know from neurophysiology that a nerve cell or neuron recovers approximately one millisecond after firing. On the other hand we also know that the human brain is able to perform intelligent processes, such as recognizing a friend's face or reacting to some danger, in approximately one tenth of a second. Therefore the brain is able to perform difficult tasks in less than 100 sequential steps. This small number of steps is of course insufficient to solve such complex problems, so we conclude that many tasks must be performed simultaneously and in parallel.

Artificial neural networks are nowadays usually implemented as software packages which run on conventional von Neumann computers and merely simulate parallel processing. True parallel processing is only possible on appropriate hardware (Transputers) and is still rare today. The software approach permits the use of the same program for quite different knowledge domains. The same algorithm can be used to study the relationships between chemical structure and the infrared spectrum, to simulate a tennis match, or to predict stock-market trends.

In conventional programming one tries to solve problems by finding a *problem-specific algorithm* where every instruction is tailored to exactly the task at hand. Alternatively one may solve the problem by using an expert system, which distinguishes strictly between the knowledge specific to the task and the mechanism to draw conclusions and make decisions. Neural network algorithms, however, do not belong to

[*] Prof. Dr. J. Gasteiger
Organisch-chemisches Institut
der Technischen Universität München
Lichtenbergstrasse 4, D-W-8046 Garching (FRG)
Prof. Dr. J. Zupan
National Institute of Chemistry
Hajdrihova 19, SLO-61115 Ljubljana (Slovenia)

any particular knowledge domain, but may be used generally to solve certain *classes of problems* from a wide variety of fields.

No longer is it the sequence of instructions that is specific to a task. It is the type of information that is fed into the neural network and the way it is represented there that tailor a study involving a neural network to the task at hand.

Neural networks may be used to solve the following problem types:

- Classification: An object, characterized by various properties, is assigned to a particular category.
- Modeling: Neural networks can output both binary and real values. Through this feature, by combining certain experimental results for an object we can arrive at other properties for it. Statistical methods produce such relationships by using an explicit mathematical equation. Neural networks however are able to express such relationships implicitly; this is especially useful in cases where an explicit equation can not be set up.
- Association: Neural networks can be used for the task of comparing information because they are able to store information of similar kinds. Thus they are able to recognize that two pictures of a face depict the same person, even when one of the pictures is distorted (autoassociation). Furthermore, they can be used for associative tasks where one object has a particular relation to another object (heteroassociation).
- Mapping: Complex information can be transformed into a simpler representation (e.g., projection onto a plane) while preserving all essential information.

In this introductory article we shall first introduce the basic features of the various types of neural networks before giving an overview and selected examples of the application of neural nets in the field of chemistry.[1, 2]

2. Neurons and Networks

In this review the term neural networks always refers to "artificial neural networks", because these were developed in order to emulate the biological neural networks of the human brain. However for simplicity the epithet "artificial" is omitted here.

2.1. A Model of a Neuron

Neural networks consist of subelements, the neurons, which are connected together to form a network. The artificial neuron is supposed to model the functions of the biological nerve cell. Although there are at least five physiologically distinct types of nerve cell, we need only present one type here (Fig. 2), since we discuss only the basic structure of a neuron; the physiological processes—and the chemical processes[3] that cause them—cannot be examined in more detail.

The nerve's cell body possesses a large number of branches, known as dendrites, which receive the signals and pass them on to the cell body. Here the signals are accumulated, and when a particular threshold limit has been exceeded, the neuron "fires". An electrical excitation is transmitted across the axon. At its end each axon has contact with the dendrites of the neighboring neurons; this contact point is called the

Johann Gasteiger was born in Dachau in 1941. He studied chemistry at Munich and Zurich universities with a doctoral thesis (1971) on "Mechanistic Investigations into Reactions in the Cyclooctatetraene System" under R. Huisgen. In his post-doctorate studies (1971–1972) he carried out ab initio calculations on carbanions under A. Streitwieser, Jr. at the University of California in Berkeley. In 1972 he transferred to the Technical University of Munich where he developed, along with a group led by I. Ugi, a prototype for a synthesis-planning program. He received his "habilitation" in chemistry in 1978 with a study on models and algorithms for investigating chemical reactions and reactivity. Since 1989 he has been professor at the Technical University of Munich. His main area of research is the development of methods and computer programs for predicting reactions and planning syntheses, for evaluating and simulating mass spectra, and for the three-dimensional modeling of molecules. From 1987–1991 he was the project manager for the Fachinformationszentrum Chemie in the implementation of a reaction database based on ChemInform, and in 1991 was awarded the Gmelin–Beilstein memorial medal from the German Chemical Society for his achievements in the field of computer chemistry.

Jure Zupan was born in Ljubljana, Slovenia in 1943. He studied physics at the University of Ljubljana, where he received his doctorate in 1972 under D. Hadzi with a thesis on the energy bands in boronitrides. Until 1973 he worked at the Josef Stefan Institute in the field of quantum chemistry and the magnetic properties of ceramic materials. Since 1974 he has led a group at the Institute for Chemistry in Ljubljana. His areas of work include chemometrics, artificial intelligence, and the development of expert systems and algorithms for chemical applications. In 1982 he was visiting professor at Arizona State University/USA, in 1988 at the Vrije Universiteit in Brussels, and 1990–1992 at the TU München in Garching. For his research work (approximately 150 original publications, 2 monographs, and 3 books) he received the highest Slovenian award for research in 1991. He obtained his habilitation in 1975 and has been Professor of Chemometry at the University of Ljubljana since 1988.

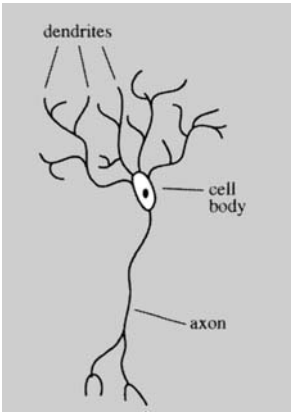

Fig. 2. Much simplified scheme of a nerve cell. The number of dendrites and the number of branches in the dendrites are much higher in reality.

synapse. Neurons are linked with each other across these synapses.

The synapses, however, also present a barrier that alters the intensity of the signal during transmission. The degree of alteration is determined by the synaptic strength. An input signal of intensity x_i has an intensity of s_i after crossing synapse i of strength w_i [Eq. (a), Fig. 3]. The synaptic strength may change, even between one impulse and the next.

$$s_i = w_i x_i \tag{a}$$

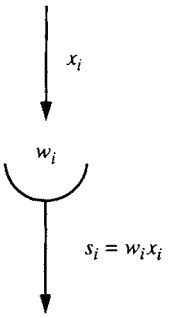

Fig. 3. Transformation of an input signal x_i on passage through a synapse of strength w_i.

Each neuron has a large number of dendrites, and thus receives many signals simultaneously. These m signals combine into one collective signal. It is not yet known exactly how this net signal, termed *Net*, is derived from the individual signals.

For the development of artificial neurons the following assumptions are made:

1. The *Net* is a function of all those signals that arrive at the neuron within a certain time interval, and of all the synaptic strengths.
2. The function is usually defined as the sum of the signals s_i, which in turn is given by the product of the input signals x_i ($i = 1, \ldots m$) and the synaptic strengths w_i ($i = 1, \ldots m$), now referred to as weights [Eq. (b)]. Figure 4 shows the model of a neuron as developed up to this point.

$$Net = s_1 + s_2 + \ldots s_i + \ldots s_m = w_1 x_1 + w_2 x_2 + \ldots w_i x_i + \ldots w_m x_m \tag{b}$$

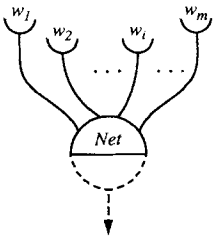

Fig. 4. First stage of a model of a neuron.

The net signal *Net* is, however, not yet the signal that is transmitted, because this collective value *Net* can be very large, and in particular, it can also be negative. It is especially the latter property that cannot be a good reflection of reality. A neuron may fire or not, but what is the meaning of a negative value? In order to attain a more realistic model, the value of *Net* is modified by a transfer function. In most cases a sigmoid function, also known as a logistic or Fermi function, is used. With this transfer function the range of values for the ouput signal *out* [Eq. (c)] is restricted to between zero and one, regardless of whether *Net* is large or small or negative.

$$out = \frac{1}{1 + e^{-(\alpha Net + \vartheta)}} \tag{c}$$

Most important, we now have a nonlinear relationship between input and output signals, and can therefore represent nonlinear relationships between properties, a task which can often only be carried out with difficulty by statistical means. Moreover, in α and ϑ we now have two parameters with which to influence the function of the neuron (Fig. 5).

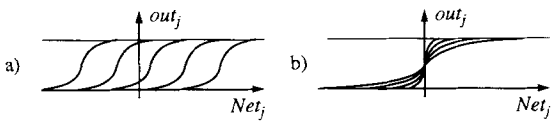

Fig. 5. Influence of α (a) or ϑ on the output signal out_j, defined as in Equation (c).

The transfer function completes the model of the neuron. In Figure 6a the synaptic strengths, or weights w are still depicted as in Figure 4; in the following figures they will no longer be shown, as in Figure 6b, but must of course still be used.

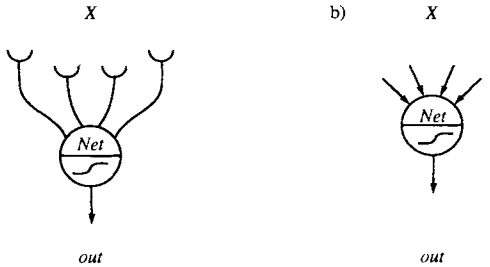

Fig. 6. Complete model of a neuron a) with and b) without explicitly defined synapse strengths w.

Symbols and Conventions

The literature on neural networks uses a confusing array of terminologies and symbols. In order that the reader may better compare the individual networks, a standard nomenclature will be followed throughout this article:

- Magnitudes that consist of a single value (scalar magnitudes) will be represented by lower-case letters in italics x_i. (The only exception is *Net* which is capitalized in order to distinguish it from the English word net. Moreover, though *Net* and *out* are symbols for single pieces of data, they are written with three letters so as to be more easily readable.)
- Data types which consist of several related values (vectors or matrices) are symbolized by a capital letter in bold italics: $\boldsymbol{X}$.
- An input object that is described by several single data (e.g., measured values from sensors) will thus be represented by $\boldsymbol{X}$, whereas the individual values are given by $x_1, x_2, \ldots x_m$. A single input value from this series is specified with the index i, thus x_i. A single neuron from one group (layer) of n neurons will be labeled with the index j; the whole of the output signals from these n neurons will be denoted $\boldsymbol{Out}$ $(out_1, out_2, \ldots out_n)$: The output signal from any one individual thus has the value out_j.
- In a layer of n neurons receiving m input data there are $n \times m$ weights that are organized into a matrix $\boldsymbol{W}(w_{11}, w_{12} \ldots w_{nm})$. A single weight from this matrix will be labeled w_{ji}.
- If there are more than one input objects, they will be distinguished by the index s: thus $\boldsymbol{X}_s$; the individual data will then be x_{si}.
- In a multilayered network the various layers will be labeled with the superscript l, e.g., out_j^l.
- Iterations in a neural network are characterized by the superscripts t, which are written in parentheses, e.g., $\boldsymbol{W}^{(t)}$.

2.2. Creating Networks of Neurons

The 100-step paradox teaches us that the advantage of the human brain stems from the parallel processing of information. The model of a neuron that we have just presented is very simple, but even much more complicated models do not provide any great degree of increased performance. The essential abilities and the flexibility of neural networks are brought about only by the interconnection of these individual arithmetic units, the artificial neurons, to form networks.

Many kinds of networking strategies have been investigated; we shall present various network models and architectures in the following sections. Since the most commonly applied is a layered model, this network architecture will be used to explain the function of a neural net.

In a layered model the neurons are divided into groups or layers. The neurons of the same layer are not interconnected, but are only linked to the neurons in the layers above and below. In a single-layered network all the neurons belong to one layer (Fig. 7). Each neuron j has access to all input data $\boldsymbol{X}$ $(x_1, x_2, \ldots x_i, \ldots x_m)$ and generates from these an output value which is specific to this neuron, out_j.

In Figure 7 the input units are shown at the top. They do not count as a layer of neurons because they do not carry out any of the arithmetic operations typical of a neuron, namely

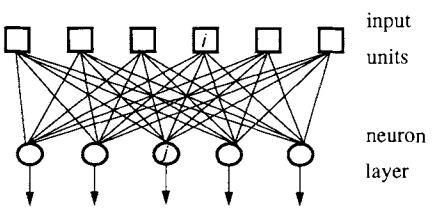

Fig. 7. Neural network with input units (squares) and one layer of active neurons (circles).

the generation of a net signal *Net*, and its transformation by a transfer function into an output signal *out*. In order to distinguish them from neurons, which are represented as circles in the following diagrams, input units will be shown as squares.

The main function of the input units is to distribute input values over all the neurons in the layer below. The values that arrive at the neurons are different, because each connection from an input unit i to a neuron j has a different weight w_{ji}, representing a specific synaptic strength. The magnitudes of the weights have to be determined by a learning process, the topic of Section 4.

The output value out_j of a neuron is determined by Equations (d) and (e), which are generalizations of Equations (b)

$$Net_j = \sum_{i=1}^{m} w_{ji}\, x_i \tag{d}$$

$$out_j = \frac{1}{1 + e^{-(\alpha\, Net_j + \vartheta)}} \tag{e}$$

and (c). The index j covers all n neurons and the index i all m input values.

In a single-layered network the output signals out_j of the individual neurons are already the output values of the neural network.

Equations (d) and (e) suggest a more formal representation for the neuron and the neural network. The input values can be interpreted as a vector $\boldsymbol{X}$ $(x_1, x_2, \ldots x_i, \ldots x_m)$ that is transformed by the matrix of weights $\boldsymbol{W}$ with elements w_{ji} and the transfer function into the vector of output values $\boldsymbol{Out}$ $(out_1, out_2, \ldots out_j, \ldots out_n)$ (Fig. 8).

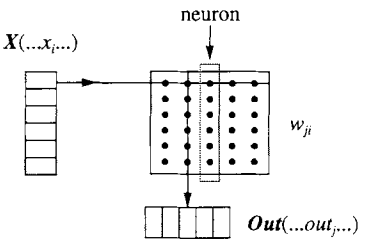

Fig. 8. Matrix representation of a one-layered network, which transforms the input data $\boldsymbol{X}$ into the output data $\boldsymbol{Out}$ by using the weights w_{ji}.

Each neuron represents a column in the matrix in Figure 8. In this matrix representation it is emphasized that every input value is fed into every neuron. The implementation of the layered model as algorithms is also realized in the matrix representation.

A single layer of neurons is known as a perceptron model and offers only limited flexibility as yet for the transformation of input values into output values. These limitations can be overcome by using several single layers in succession.

In a multilayered model the architecture chosen usually connects all the neurons of one layer to all the neurons in the layer above and all the neurons in the layer below. Figure 9 shows a two-layered neural network. (As we mentioned previously, the input units do not count here, because they are not neurons but serve only to distribute the input values across the neuron layer below.) The network user cannot

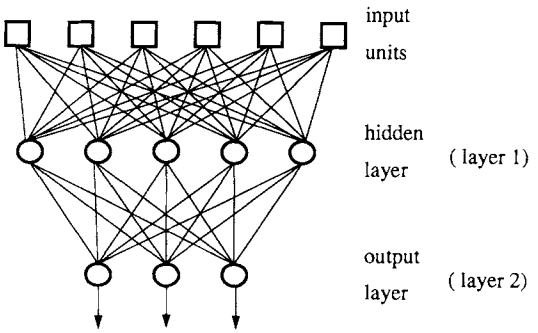

Fig. 9. Neural network with input units and two layers of active neurons.

access the first layer of neurons, which is therefore known as a hidden layer; the neurons in it are called inner neurons. The output values $\boldsymbol{Out}^1$ of the first layer of neurons are the input values $\boldsymbol{X}^2$ of the second layer of neurons. Thus each neuron in the upper layer passes its output value on to every neuron in the layer below. Because of the different weights w_{ji} in the individual connections (synapses) the same output value $\boldsymbol{Out}^1 = \boldsymbol{X}^2$ has a different effect on each individual neuron [Eq. (d)]. The result of the neural network as a whole is only given by the last layer in the network (here $\boldsymbol{Out}^2$). Figure 10 shows a two-layer network in matrix notation.

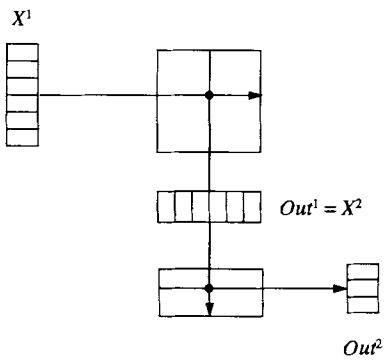

Fig. 10. Matrix representation of a two-layered network.

3. Historical Perspective

The dramatic increase in interest in neural networks does much to disguise the fact that people have been developing them for nearly 50 years.[4] As early as the forties McCulloch and Pitts[5, 6] developed a model of a neuron as a logical threshold element with two possible states. They were forced to leave open the question of how neurons learn, to which Hebb (1949) suggested an answer.[7] This Hebb learning rule states that the synaptic strength of a neuron varies proportionally with the activity in front of and behind the synapse.

Rosenblatt[8] organized a number of neurons in such a way that they corresponded essentially to a one-layered network (Fig. 7), and named this formation a perceptron.

The original enthusiasm for the development of models of biological nervous systems began to wane in the sixties for various reasons. The results with the networks of that time were hardly relevant to solving real-world problems and thus not very encouraging. With the advent of the computer, interest shifted more and more to problem-solving by directly programmed methods. The buzz-word invented for this, "artificial intelligence", shows only too clearly what was expected of this technology, although it was clear from the outset that the method chosen had very little to do with the processing of information as performed by the human brain.

Not surprising therefore that research into neural networks suffered a heavy blow from none other than Marvin Minsky, one of the main proponents of artificial intelligence. In 1969 together with Papert[9] Minsky published a very severe but probably justified criticism of the network models of the time. They showed in their theoretical study that perceptrons—at least as they were being developed at that time—offer only limited possibilities. Moreover they speculated that extending the architecture of perceptrons to more layers would not bring about any significant improvement in results. As a consequence of this criticism from so influential a personage as M. Minsky, research funding for the modeling of biological nervous systems became virtually unavailable.

In the years that followed very little work was done on neural network models; however, even at this time some important advances were made. The work of Albus,[10] Amari,[11] Grossberg,[12] Kohonen,[13] von der Malsburg,[14] and Widrow and Hoff[15] all deserves mention.

A decisive new impetus was given in 1982 by a physicist, Hopfield,[16] who was able to show that network models of binary neurons correspond formally to spin systems, and can be manipulated by the methods already developed for them.

The greatest boost for the application of neural networks then came through the publication of the "back-propagation" algorithm for learning in multilayered models, introduced by Rumelhart, Hinton, and Williams.[17, 18] Even though the back-propagation algorithm had been suggested earlier,[19] credit must go to the research group on "Parallel Distributed Systems"[20] for bringing it to the attention of the public.

Despite all the successes in the development of models for neural information processing, we must clearly acknowledge the fact that we are still very far from an understanding of the way the human brain works. The capacities of artificial neural networks must still be reckoned very rudimentary in comparison with the biological networks they are supposed to emulate. Nevertheless even these elementary models of neural networks have shown new ways of processing information. It is precisely to the possibilities they are opening up, especially in the area of chemistry, that we wish to devote ourselves in this article.

4. Architectures and Learning Processes

Over the years a whole series of research groups have developed their own characteristic artificial neural networks. Some of these models are closer to their biological counterparts than others; some seem to emulate certain processes in the human brain very well, whereas others bear only a slight similarity to their biological forbears.

Our primary concern here however is not the faithfulness to reality of each neural network model. We wish rather to

show which kinds of problems can be processed with the various models, and what capacities these neural networks offer to information processing. An artificial neural network can still have great significance for information processing, even if it bears but little relationship to biological systems.

As we mentioned in the introduction, neural networks can be applied to a whole series of problems: classification, modeling, association, and mapping. Each neural network is more or less suitable for handling these problem types; each has its own characteristic strengths and weaknesses. We wish expound upon this here and to develop some feeling for which network model is best applied to a particular task.

Three elements essentially characterize every neural network model:

1. the arithmetic operation in a neuron
2. the architecture of the net, that is, the way the individual neurons are connected
3. the learning process that adapts the weights so that the correct result is obtained.

The model of a neuron mentioned in Section 2 is only one of many, albeit a very common one. Even the organization of neurons into layers need not necessarily be that described in Section 2. The learning process, though, is very tightly coupled to the architecture of the neural network. There are essentially two types of learning processes: learning with or learning without instruction ("supervised" and "unsupervised" learning).

In supervised learning the neural net is presented with a series of objects. The input data $\boldsymbol{X}$ from these objects is given to the net, along with the expected output values $\boldsymbol{Y}$. The weights in the neural net are then adapted so that for any set p of known objects the output values $\boldsymbol{Y}$ conform as closely as possible to the expected values $\boldsymbol{Y}$ (Fig. 11).

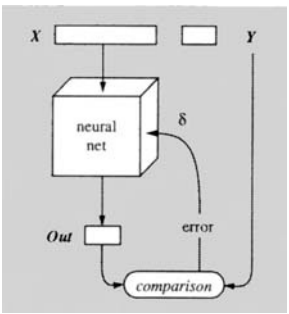

Fig. 11. Supervised learning. A comparison with expected values yields an error δ, which determines whether further adjustment cycles are necessary.

In unsupervised learning the input data are passed repeatedly through the network until it has stabilized, and until the input values map an object into certain areas of the network (Fig. 12).

4.1. The Hopfield Model

The American physicist Hopfield brought new life into neural net research in 1982 with his model.[16] He pointed out analogies between neural networks and spin systems and

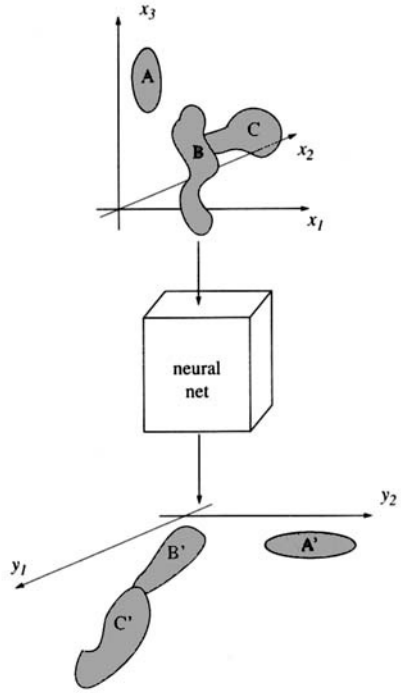

Fig. 12. Unsupervised learning.

was thereby able to apply a whole series of mathematical methods from theoretical physics to research into neural networks. In addition to this he is also responsible for the introduction of nonlinear transfer functions.

The Hopfield net performs one of the most interesting functions of the human brain: it can *associate*. This means that stored pictures (or any other kind of complex information that can be represented as a multidimensional vector or matrix) can be recognized even from partial information or distorted versions of the original picture. For example, one could recognize one particular face from a collection of faces, even if only the eyes and nose are shown.

The Hopfield net is a one-layered model that has exactly the same number of neurons as input nodes. Because every input node is connected to every neuron (Fig. 7), $m \times m$ weights must be determined for m input nodes. The original Hopfield model works with bipolar input data ($+1$ or -1) (f). The net result in neuron j is attained by the multiplication

$$x_i \begin{cases} +1 \\ -1 \end{cases} \tag{f}$$

of all input signals x_i by the weights w_{ji} for that neuron, as in Equation (d). The transfer function here is a simple step function (Fig. 13) as may be produced by the sign of the value.

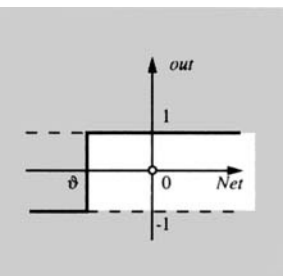

Fig. 13. A step function as a transfer function.

The output signal of a neuron, out_j, in a Hopfield net is given in Equation (g), where as already mentioned, x_i can only assume the values $+1$ and -1.

$$out_j = \text{sign}(Net_j) = \text{sign} \sum_{i=1}^{m} w_{ji}\, x_i \qquad \text{(g)}$$

In order to understand the learning process in Hopfield networks we introduce an example at this point: We require a Hopfield net to learn the four pictures in Figure 14. Each

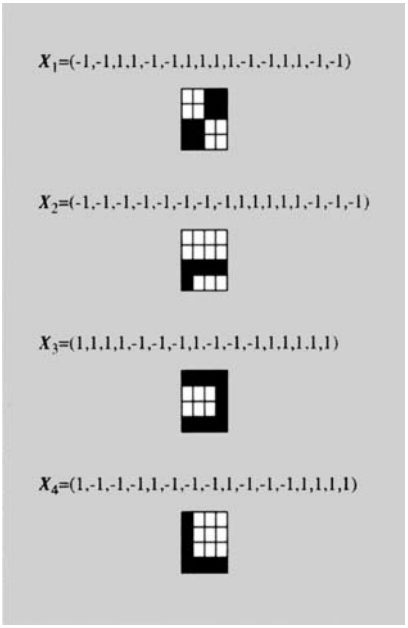

Fig. 14. Four pictures X_1, X_2, X_3, and X_4 used to train a Hopfield network.

picture consists of 4×4 fields (pixels) that are either black ($+1$) or white (-1), so that each picture may be represented as a $4 \times 4 = 16$ dimensional vector. Figure 15 shows the architecture of the corresponding Hopfield net and the input of the first picture with values represented by -1 (for a white pixel) and $+1$ (for a black one). In the picture used for training, the output values are exactly equal to the input values.

The weights w in a Hopfield net do not have to be derived from a costly, iterative learning process, but can be calculated directly from the pictures: If p pictures are presented to the Hopfield net, then the weights w_{ji} for the neuron j may be derived from the input values of the individual pictures s and thus X_s according to (h) and (i). This means that the weight

$$w_{ji} = \sum_{s=1}^{p} x_{sj}\, x_{si} \quad \text{for} \quad j \neq i \qquad \text{(h)}$$

$$w_{ji} = 0 \quad \text{for} \quad j = i \qquad \text{(i)}$$

w_{ji} increases by 1 if, in a particular picture, the pixels j and i are either both black or both white, and decreases by 1 if, in that picture, the ith and jth pixels are of different colors. The more pictures there are in which pixels j and i match, the greater is the weight w_{ji}. The 4×4 pictures from Figure 14 are stored accordingly in a Hopfield net consisting of 16 neurons with 16 weights in a weight-matrix of dimensions 16×16.

We should first test whether a Hopfield net has stabilized. For this purpose an input vector (e.g., one of the four pictures from Fig. 14) is fed into the Hopfield net, and the output values derived from Equation (g). These output values are compared to the input values. If they are equal then the process can terminate, otherwise the output values are fed into the net again as new input values and the process is repeated (Fig. 16). If after a few cycles one receives as output the same values as the original input, then one can say that the net has stabilized. Of course a Hopfield net is not intended simply to reproduce its own input values as output; this is just a stability test.

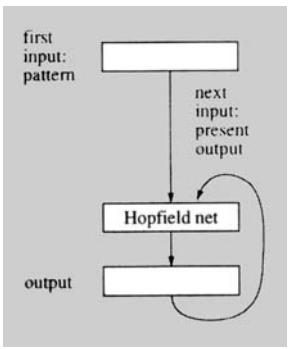

Fig. 16. Testing a Hopfield net for stability.

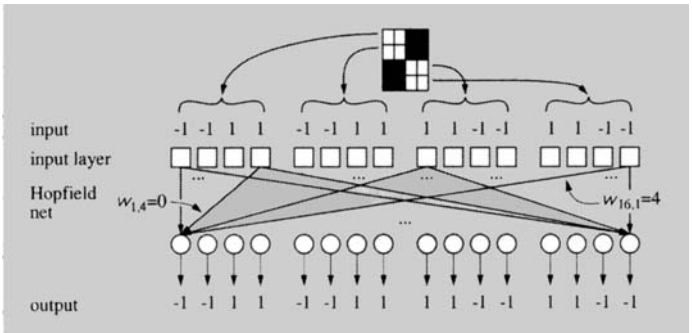

Fig. 15. Architecture of the Hopfield net complete with input and output of the first picture of Figure 14. The given w_{ji} values are determined from Equation (h) for the four pictures of Figure 4.

The true value of a Hopfield net becomes evident in the retrieval of the original stored data from incomplete or distorted data; we can for instance retrieve an original picture in the Hopfield net from a blurred or spoiled picture.

We shall investigate this phenomenon with the four pictures from Figure 14 and a Hopfield net in which they are stored in the form of 16×16 weights. We produce distorted pictures by altering a certain number of pixels in the original pictures, that is, by changing fields from black to white and vice versa. In Figure 17 we have shown the results obtained when each picture is altered by two, five, or indeed even thirteen pixels.

One can see that with a distortion of two pixels the original pictures are retrieved correctly after only 1–2 iterations. When five fields are altered (a noise level of 31%!), the

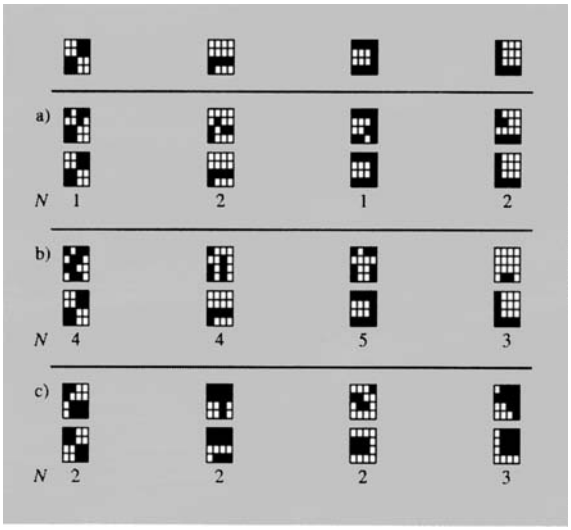

Fig. 17. Search for original pictures (showed at the top) stored in a Hopfield network after input of pictures with a) two, b) five, and c) thirteen altered fields. N is the number of iterations required to arrive at the result (bottom line in a–c) when presented with the erroneous input (top line in a–c).

original pictures are still found successfully, but only after 3–5 iterations. This is not always so; we have observed cases with a five-pixel distortion where the wrong picture is output, or the right picture in negative form (black and white pixels swapped), or an oscillation occurs between two patterns that represent none of the stored pictures, so that the operation has to be aborted.

If thirteen pixels in the pictures are altered (81% distortion) the original pictures are retrieved after 2–3 iterations as negatives. How does this come about? After all, significantly more than half the fields have been altered in color. It is remarkable that the negative of the original picture is returned, and not the negative of some other picture.

Thus we have seen that as simple a model as a Hopfield net can still reproduce one of the human brain's more interesting faculties, namely the power of association. The Hopfield net does however have one significant drawback: The number of patterns (pictures, vectors) that can be stored is severely limited. In order to store more pictures an increased number of neurons is required; thus the size of the weight matrix grows very rapidly.

4.2. An Adaptive Bidirectional Associative Memory

With the Hopfield net we have shown that a neural network has the power to associate. An adaptive bidirectional associative memory (or ABAM)[21] can do this as well. We shall now show, however, that an ABAM is able, in addition, to combine patterns. An ABAM is, like a Hopfield net, a one-layered network. The number of output neurons n is however usually much lower than the number of input units m.

In order to simplify the notation, and because in the case of ABAMs the meanings of input and output are apt to blur, in the following sections we refer to an input vector as $\boldsymbol{X}$ and the output values as $\boldsymbol{Y}$. Thus we always observe pairs of input ($\boldsymbol{X}_s$) and output ($\boldsymbol{Y}_s$) values (the index s characterizes the individual input values and their corresponding outputs):

$$\boldsymbol{X}_s = (x_{s1}, x_{s2}, \ldots x_{sj}, \ldots x_{sm})$$
$$\boldsymbol{Y}_s = (y_{s1}, y_{s2}, \ldots y_{si}, \ldots y_{sn})$$

Given a series of such pairs $\{\boldsymbol{X}_s, \boldsymbol{Y}_s\}$ where it is known which $\boldsymbol{Y}_s$ value is to be expected from a particular $\boldsymbol{X}_s$ value, the weights are determined in a supervised learning process.

First starting values are calculated for the weights according to Equation (j). The weight matrix is now no longer square, as in the Hopfield net, but rather rectangular. It has dimensions $m \times n$.

$$w_{ji} = \sum_{s=1}^{p} x_{sj}\, y_{si} \qquad \text{(j)}$$

The basic idea of learning with an ABAM net is that one can multiply an $m \times n$ matrix in two different ways: the standard way by multiplying by an m-dimensional vector, which results in an n-dimensional vector, or in the alternative transposed form, by multiplying by an n-dimensional vector to give an m-dimensional vector (Fig. 18).

$$\{\boldsymbol{X}^{(0)}, \boldsymbol{Y}^{(0)}\} \longrightarrow \boldsymbol{W}^{(0)}$$
$$\boldsymbol{X}^{(0)}\boldsymbol{W}^{(0)} \longrightarrow \boldsymbol{Y}^{(1)}$$
$$\boldsymbol{Y}^{(1)}\boldsymbol{W}^{(0)\mathrm{T}} \longrightarrow \boldsymbol{X}^{(1)}$$
$$\{\boldsymbol{X}^{(1)}, \boldsymbol{Y}^{(1)}\} \longrightarrow \boldsymbol{W}^{(1)}$$
$$\vdots \longrightarrow$$
$$\boldsymbol{X}^{(t)} = \boldsymbol{X}^{(0)}$$
$$\boldsymbol{Y}^{(t)} = \boldsymbol{Y}^{(0)}$$

Fig. 18. The learning process in an adaptive bidirectional associative memory (ABAM).

The learning process is as follows: An initial weight matrix $\boldsymbol{W}^{(0)}$ is calculated from the predefined pairs $\{\boldsymbol{X}^{(0)}, \boldsymbol{Y}^{(0)}\}$. From $\boldsymbol{X}^{(0)}$ and $\boldsymbol{W}^{(0)}$ the output values $\boldsymbol{Y}^{(1)}$ are produced, which do not as yet correspond to the goal values. Therefore these $\boldsymbol{Y}^{(1)}$ values are multiplied by the transposed matrix $\boldsymbol{W}^{(0)\mathrm{T}}$ to give a set of $\boldsymbol{X}^{(1)}$ values. Applying Equation (j) to the pairs $\{\boldsymbol{X}^{(1)}, \boldsymbol{Y}^{(1)}\}$ we calculate a new weight matrix $\boldsymbol{W}^{(1)}$. This process is repeated until the pair $\{\boldsymbol{X}^{(t)}, \boldsymbol{Y}^{(t)}\}$ corresponds to the predefined values $\{\boldsymbol{X}^{(0)}, \boldsymbol{Y}^{(0)}\}$.

In the procedure the $\boldsymbol{Y}$ values are calculated in the usual way. Here, too, the individual x and y values are bipolar $(+1, -1)$ [Eq. (k) and (l)].

$$Net_j = \sum_{i=1}^{m} w_{ji}\, x_i \qquad \text{(k)}$$

$$y_i = \mathrm{sign}(Net_j) \qquad \text{(l)}$$

As with the Hopfield net we also use simple pictures here as an illustration of how an ABAM may be applied. Pictures made of 5×5 fields, where each field may each be black $(+1)$ or white (-1), will serve as input information. These can

thus be represented by a 25-dimensional vector, so that 25 input units will be required. We use only five such pictures and identify them on the output side by a 5-dimensional vector. Each of the five patterns (pictures) is assigned one of the five positions in the vector, thus in the case of the first picture the first position is 1 and all the others are zero (10000), the second picture is represented by (01000) etc. (We are actually dealing with bipolar values +1 and −1 here, but for clarity's sake we use binary notation (1,0) in the following sections). Figure 19 shows the five patterns and their identifications. The ABAM has a 25×5 architecture, and thus 25×5 weights.

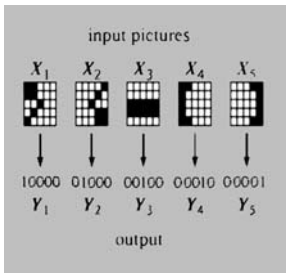

Fig. 19. Five pictures used to train the ABAM, their symbols, and vector representations.

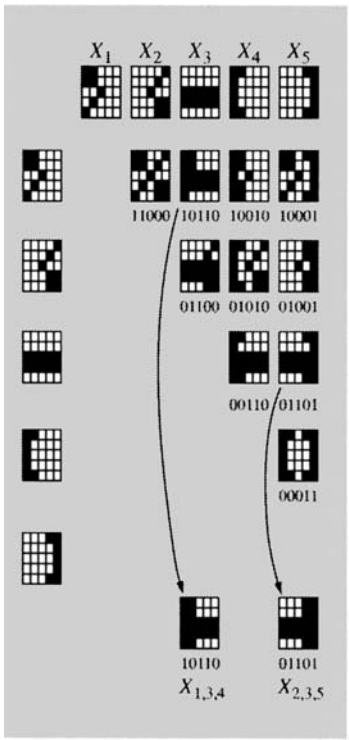

Fig. 20. All combinations of two pictures from Figure 19. The two cases where three bits were activated erroneously are compared with the combination of three pictures drawn in the bottom row (see text for details).

An ABAM was trained with these five pictures and the five-dimensional vector (consisting of four zeros and one 1 in each case). Then the ABAM's ability to associate distorted pictures with stored undistorted ones was put to the test. All possible 1-pixel errors were generated; in the case of five pictures each of 5×5 pixels this makes a total of 125 different distorted pictures. The ABAM identified the correct undistorted output picture in all cases.

Next the ability of the ABAM to combine individual pieces of information was tested: that is, can it recognize, when presented with pictures made of two patterns, which combination of two pictures it is, despite previously having been presented with the patterns only singly? Figure 20 shows all ten permutations of pairs for the five patterns, with the answer from the ABAM written underneath as a five-bit vector. In eight cases the ABAM returns a 1 in exactly the right two positions. Thus, for example, for the first combined pattern, which consists of the patterns 1 and 2, it returns the answer (11000), meaning that first and second patterns are contained in it. In the cases of the other two pattern combinations (1 + 3 and 3 + 5) the ABAM also recognizes which individual patterns are present in the combination, but makes the mistake of identifying a third pattern. If we generate these three-pattern combinations, as demonstrated in the bottom row of Figure 20, they differ very little from the two-pattern combinations (1 pixel difference). The ABAM's answers in these two cases are therefore not very far from the truth.

The ABAM's ability to combine two patterns has been discussed here in more detail for two reasons: Firstly, the ability to recognize that a piece of information is a combination of other pieces of information is, of course, an important capability of the human brain. Therefore if the ABAM can do this too, we have reproduced an important aspect of biological, neural information processing. Secondly, the ability to combine single pieces of information is required in many problem tasks in chemistry, especially in the study of relationships between structure and spectral data: If a neural network learns this relationship from pairs of spectra and structures, it should be able to derive all the component substructures from a new spectrum, even if it has never "seen" this particular combination of substructures previously.

4.3. The Kohonen Network

4.3.1. Principles

T. Kohonen[22, 23] developed a neural network which of all models has the greatest similarity to its biological counterpart.[24] This is especially true of the way in which the brain processes sensory signals.

There is a broad strip of tissue in the cerebral cortex which specializes in the perception of touch and is known as the somatosensory cortex. Particular areas in this tissue are responsible for particular parts of the body; parts of the body that carry the most sensory receptors are assigned correspondingly large, contiguous areas, whereas areas of skin which are supplied with relatively few sensory nerves are assigned only small areas, even if the part of the body in question is actually very large by comparison. In addition, neighboring parts of the body are assigned neighboring regions in the somatosensory cortex, so that for the sense of touch there is a contorted mapping of the body surface onto the brain (Fig. 21).

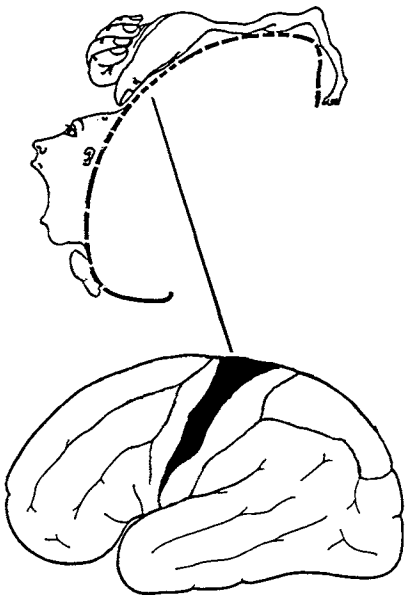

Fig. 21. Map of the human body (top) in the somatosensory cortex of the brain (bottom).

Kohonen introduced the concept of a "self-organized topological feature map" that is able to generate such mappings. Briefly, these are two-dimensional arrays of neurons that reflect as well as possible the topology of information, that is, the relationships between individual pieces of data and not their magnitude. Using the Kohonen model we are able to create a *mapping* of multidimensional information onto a layer of neurons, that preserves the essential content of the information (relationships). The whole process therefore represents a kind of abstraction. Figure 22 shows the two-dimensional organization of the neurons in a Kohonen net.

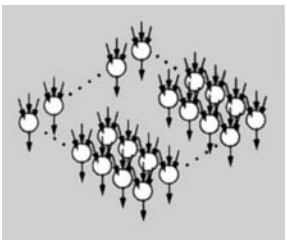

Fig. 22. Two-dimensional assignment of the neurons in a Kohonen network.

In this context mapping of information means that the similarity of a pair of signals is expressed in the proximity or "neighborhood relation" of the neurons activated by them: the more alike two signals are, the closer together the neurons they activate should lie. However, as we are talking here about topological and not Euclidean distance, a neuron in a square array (Fig. 23a) has eight neighbors in the first "sphere", since the neuron has eight direct neighbors. In a Kohonen network where the neurons are arrayed in a square the spheres of neighborhood grow through the network as shown in Figure 23b.

We must take the discussion on the topology of the Kohonen net a little further before we can proceed to the learning algorithm because the topology is the decisive factor in a Kohonen net. If every neuron is to have the same number of neighbors, a square, planar array is poorly suited to the task because the neurons at the edges have fewer neighbors than those in the center of the net (Fig. 23c).

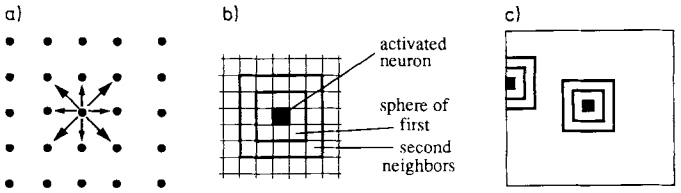

Fig. 23. Proximity relations of the neurons in a Kohonen network. a) First sphere of neighbors; b) growth of the spheres; c) neurons at the edge of the network.

From a square or rectangular array of elements we can nevertheless easily construct a topology in which each element has exactly the same number of neighbors. In order to do this we must wrap the surface around on itself and connect ("glue together") its opposite edges. Thus from the surface we produce first a cylinder and then a torus, as shown in Figure 24.

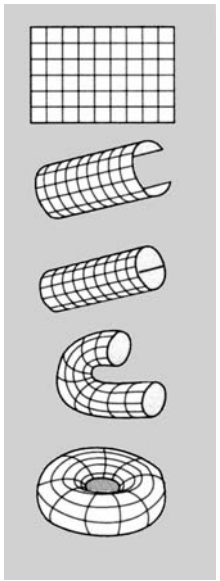

Fig. 24. The transformation of a rectangular array of neurons into a torus in which each neuron has the same number of neighbors.

In a torus each element has the same number of neighbors: eight in the first circle, 16 in the second etc. Of course it is not easy to display in its entirety a mapping onto a torus. We shall therefore continue to represent Kohonen networks as

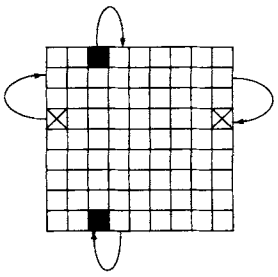

Fig. 25. Representation of the surface of a torus on a plane. The topmost edge wraps onto the bottom, and the left edge wraps onto the right.

flat surfaces in the knowledge that if one arrives at one of the edges the surface carries on over to the opposite edge (Fig. 25). Both the filled-in squares are therefore immediate neighbors. The same is true in the horizontal axis for those fields marked by crosses.

The topology of the Kohonen net has been discussed a little more fully here in order to understand the examples better (see Sections 10.1 and 10.2).

4.3.2. The Learning Process

Learning in a Kohonen net is a competitive process: all the neurons compete to be stimulated by the input signal. The input signal is an object that is described by m single values and can therefore be interpreted as a point in an m-dimensional space, projected onto a plane. Only one single neuron is finally chosen as the "best" ("winner takes all"). Different criteria are applied to find the "best" neuron—the central neuron c. Very often the neuron whose weights are most similar to the input signal $\boldsymbol{X}_k$ is chosen [Eq. (m)].

$$out_c \leftarrow \min \left\{ \sum_{i=1}^{m} (x_{ki} - w_{ji})^2 \right\} \qquad \text{(m)}$$

For this central neuron c, the weights w_{jc} are corrected so that the output value becomes even more similar to the input signal. The weights on the other neurons are also corrected, albeit proportionally less the further they are from the strongly stimulated (central) neuron. Here it is the topological distance which counts, that is, which sphere of neighborhood (as reckoned outwards from the central neuron) includes the neuron under consideration (compare Fig. 23).

Then the process is repeated with the next input data. Every object (that is, every point in the m-dimensional space) stimulates a very specific neuron, so that every object is assigned a definite point in the Kohonen net.

A simple example, the mapping of the surface of a sphere onto a Kohonen net, will explain the workings and the results of the Kohonen net in more detail (Fig. 26). The spherical surface was divided into eight sectors, as shown in Figure 26b; a point on this surface is defined by its three coordinates (x, y, z values). An array of $15 \times 15 = 225$ neurons was used to make a Kohonen net, which therefore had three input units distributing their data over 225 neurons. Thus a total of $3 \times 225 = 675$ weights had to be determined.

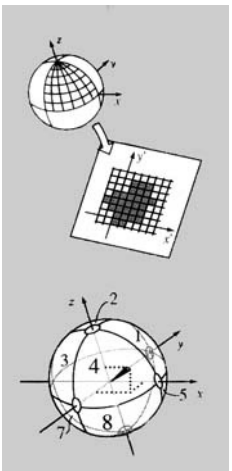

Fig. 26. The representation of the surface of a sphere in a Kohonen network. The sphere's surface is divided into eight sectors. Each point on the surface of the sphere is characterized by its assignment to one of these sectors. The point marked in the sphere at the bottom belongs to sector number 4.

Two thousand points were chosen at random from the spherical surface, and their sets of x, y, and z coordinates used severally to train the Kohonen net. For the graphical representation of the net that had developed after the learning of these 2000 points, each point was identified by the number of the spherical sector from whence it came. (This information was not used in the learning process, however, but only at the end for identifying the points.) Because 2000 points have to be mapped onto 225 fields there are several points mapped onto each field. As it turns out, however, at the end of the learning process only points from the same sector of the sphere arrive at the same field, and points from neighboring regions of the spherical surface are projected onto neighboring fields. Figure 27 shows the resulting Kohonen net.

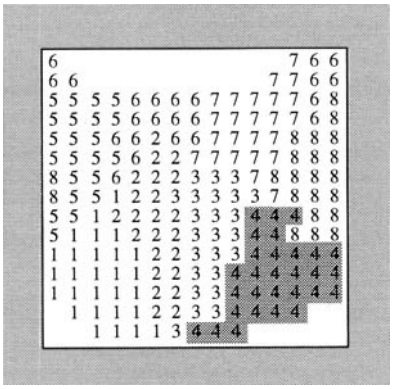

Fig. 27. Result of the projection of a spherical surface onto a Kohonen network.

Fields with the same number, that is, points from the same sector of the sphere, form contiguous areas in the Kohonen net. It must be remembered that the surface shown here actually forms a torus (Fig. 24); therefore points on the left-hand edge are continued over onto the right hand edge (Fig. 25). Thus the two fields on the left-hand edge marked with the number 8 do indeed have a direct connection to the remaining fields with the number 8. Some fields (neurons) in the Kohonen net were not assigned any points from the spherical surface. That the spherical surface was mapped onto the Kohonen net while preserving the neighborhood relations between the points on the sphere may also be seen from the details of the Kohonen net as shown in Figure 28. Sectors on the sphere which meet at lines of longitude or at the equator are also neighbors in their projection on the Kohonen net, and hold whole borders in common. In several regions four fields meet together; these regions or points correspond to the points where the coordinate axes break through the spherical surface. For example at the circle in Figure 28 (bottom row, center) the sectors 1,2,3 and 4 converge. This corresponds to the "North pole" of the sphere.

The mapping of a sphere onto a Kohonen net has been explained in this detail to show how a simple three-dimensional body can be mapped onto a plane. This illustrates well the way a Kohonen net functions as a topology-preserving

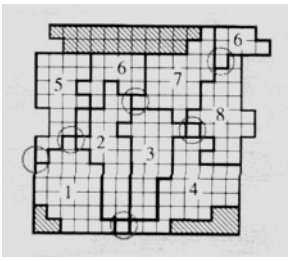

Fig. 28. Areas on the Kohonen map of Figure 27 where four sectors meet, highlighted by circles.

map and lays the foundation for a good understanding of the application of Kohonen networks to examples from the field of chemistry.

4.4. Back-Propagation

The majority of neural net applications uses the "back-propagation" algorithm. This algorithm does not represent any particular kind of network architecture (a multilayered net is generally used) but rather a special learning process. Although this method was not introduced until 1986 by Rumelhart, Hinton, and Williams[17] it quickly gained widespread popularity and contributed decisively in the eventual triumph of neural networks. A few years ago a study carried out on publications about neural networks in chemistry showed that in 90% the back-propagation algorithm was used.[2]

The attraction of learning through back-propagation stems from the fact that adjustments to the neural net's weights can be calculated on the basis of well-defined equations. Nevertheless this procedure for correcting errors has very little in common with those processes responsible for the adjustment of synaptic weights in biological systems.

The back-propagation algorithm may be used for one- or multilayered networks and is a supervised learning process. The input data are passed through the layers; the output data of a layer l, $\boldsymbol{Out}^l$ form the input data $\boldsymbol{X}^{l+1}$ of the layer $l+1$. The results for the input data should eventually be delivered by the final layer. This will, however, not be the case at first. The output data, $\boldsymbol{Out}^{last}$, of the final layer are therefore compared with the expected values $\boldsymbol{Y}$ and the error determined. This error is now used to correct the weights in the output layer. Next the weights in the penultimate layer are corrected with regard to the error from the final layer. Thus the error is fed back layer by layer, from bottom to top, and used to correct the weights at each level (Fig. 29). The error therefore flows counter to the direction of the input data; hence the name back-propagation, or loosely formulated, "error-correction in reverse".[25] In the following sections we demonstrate the basic features of the back-propagation algorithm. For a detailed explanation we refer the reader to the literature.[1, 17, 18, 25]

The back-propagation algorithm is intended to change the weights until the error in the output values $\boldsymbol{Out}$ is minimized; that is, they must correspond as closely as possible to the provided values $\boldsymbol{Y}$.

In the case of the last layer the error can be determined directly because the value $\boldsymbol{Y}$, which is the expected output value, is known. The weight adjustments for the final layer,

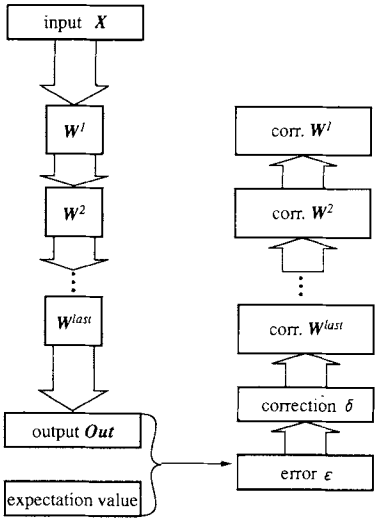

Fig. 29. The learning process of the back-propagation algorithm. The weights are corrected by feeding the errors back into the network.

Δw_{ji}^{last}, are determined by deriving the error ε [Eq. (n)] according to the individual weights. The chain rule leads to Equations (o) and (p).

$$\varepsilon = \sum_{j=1}^{m} (y_j - out_j^{last})^2 \tag{n}$$

$$\delta_j^{last} = -\partial\varepsilon/\partial Net_j^{last} \tag{o}$$

$$\Delta w_{ji}^{last} = \eta\, \delta_j^{last} out_j^{last-1} \tag{p}$$

In the hidden layers the error is not directly known because it is not known what output values, $\boldsymbol{Out}^l$, should be produced by those layers. At this point we make the assumption that the error from the layer below was distributed evenly over all the weights in the layer above. This assumption enables the error in one layer to be calculated from the error in the layer below (which has just been calculated). This is the basis of the back-propagation algorithm: The error is carried back through the individual layers (hence "back-propagation of errors") thus enabling us to correct the weights in each layer.

All in all we derive the closed form (q) for correcting the weights of a single layer. Here η is a parameter, the learning

$$\Delta w_{ji}^{l} = \eta \sum_{k=1}^{r} \delta^{l+1} w_{jk}^{l+1} f'(Net_j^l) out_i^{l+1} \tag{q}$$

rate, that determines how rapidly a neural net learns. Usually a value between 0.1 and 0.9 is chosen for it. Frequently when correcting the weights, the changes in weights from the cycle before (previous) are also taken into account. This is accomplished by extending the Equation (q) by the contribution $\mu \Delta w_{ji}^{l(previous)}$. The parameter μ is the momentum term. It determines the extent to which the previous weight changes are taken into account; it gives the learning process a certain capacity for inertia. The smaller μ is, the quicker previous changes in weights are forgotten. It can be shown that the sum of η and μ should be about 1.[26]

5. Other Neural Network Models

Apart from those mentioned in Section 4, a number of different processes for analyzing data with neural networks are still available. We wish briefly to mention only two more.

The counterpropagation network consists of a Kohonen layer combined with a look-up table in order to give answers.[27]

The *a*ssociative *m*emory *s*ystem (AMS) was developed as a model of information processing in the cerebellum, which is primarily responsible for processing motoric stimuli.[10] The AMS model has been used to predict chemical reactivity data, in particular the polar reactivity of bonds.[28]

6. Overview of Applications in Chemistry

A great many approaches to problems from diverse branches of chemistry have already been investigated by applying neural networks—from very general tasks such as structure-spectrum relationships, chemical reactivity, secondary and tertiary structures of proteins and process monitoring, to such specific questions as the classification of energy levels in the curium atom and the recognition and classification of aerosol particle distributions, as well as the relationship between the physical structure and the mechanical properties of polyethylene–terephthalate fibers.

This diversity underlines the fact that neural networks represent quite general, broadly applicable problem-solving methods. The final, concrete application is determined only by the nature of the data fed into the neural network.

This article is intended to convey some feeling for the kinds of problems best approached with neural networks, so that the reader will be able to decide whether these methods can be used for his particular problem. The goal is therefore to demonstrate the capabilities of the methods and to give incentive to further applications, rather than to give a comprehensive overview of all the work that has gone before. For this reason only a selection of typical neural network applications in chemistry will be given in the following sections; these will not be organized by application area but rather by problem type, that is, according to whether the task in question is one of classification, modeling, association, or mapping.

There is, of course, a whole series of methods that can be used as alternatives to neural networks—and which have been used successfully for many years. Many tasks for which neural networks are used today could be solved equally well by using statistical and pattern-recognition methods such as regression analysis, clustering methods, and principal component analysis. In many cases these methods should be able to deliver results that are every bit as good. What is unfortunately lacking in most papers is a comparison between the capabilities of neural networks and those of more established methods. Comparisons such as these might bring out the advantages of neural networks more. These advantages include the following:

- the mathematical form of the relationship between the input and output data does not need to be provided
- neural networks are also able to represent nonlinear relationships.

On the other hand, the application of neural networks requires exactly the same care in the formulation of the problem, the representation of information, the selection of data, and the division of data into training and test sets as is necessary for pattern-recognition and statistical methods. It must be stated clearly that the quality of the results obtained from neural networks depends crucially on the work and trouble invested in these subtasks.

Essential aspects must be considered before deploying any kind of neural network.

- What is the nature of the task under consideration? Classification, modeling, association, or mapping?
- Which kind of learning process should be chosen? Supervised or unsupervised learning? Is there a set of expected results available for the objects, or must the structure of the information first be found?

In Table 1 the various methods are correlated with problem types and learning processes to make it easier to decide which neural network method should be used for a specific task.

Table 1. Possibilities for applying neural networks.

	Hopfield network	ABAM	Kohonen network	Back-propagation
classification		x	x	x
modeling				x
association	x	x		x
mapping			x	
learning process [a]	unsup.	unsup. + sup.	unsup.	sup.

[a] unsup. = unsupervised learning, sup. = supervised learning (see Section 4).

In chemistry most problems are of the classification or modeling types. This is one of the reasons why multilayered networks trained by the back-propagation algorithm predominate. The results of a survey of those neural network applications in chemistry that appeared before the end of 1990 show that over 90% of studies used the back-propagation algorithm.[2] Hopfield networks were used twice, an adaptive bidirectional associative memory only once, and a Kohonen net coupled with the counterpropagation algorithm likewise only once. This distribution need not hold true in future, however, since ABAM and Kohonen networks as well as the counterpropagation algorithm all offer possibilities that have by no means been exhausted.

If we consider only the multilayered model with the back-propagation algorithm, we still have a broad spectrum for the complexities of the networks used: from networks with only 20 weights up to some with 40000, in one case even 500000 weights! The number of data used for training a net should, in the case of the back-propagation algorithm, be at least as large as the number of weights. This rule was by no means always followed. The number of times the training data-set was passed through the net (number of epochs) also varied considerably: from 20 up to 100000 iterations. As may be imagined, the training times increased greatly in proportion with the number of weights and the number of iterations, from a few minutes on a personal computer up to hours on a Cray supercomputer.

7. Classification

Classification problems are one of the most common areas of application for neural networks. An object is first characterized by various measurements and on that basis assigned to a specific category. Alternatively it may be found not to have a particular characteristic or not to belong to the class in question. Thus the output data are binary in nature: a feature is either present or it is not; the object either belongs to a certain class or it does not. The input data that characterize the object can be binary in nature but can also be real values (measured data). Classification is a traditional domain for the use of statistical and pattern-recognition methods. Neural networks have the advantage that they can still be applied in cases where the relationships between the object data and the classes to which they are to be assigned are highly complex. Neural networks are suitable even for relationships that cannot or can only barely be expressed in terms of explicit equations. In the following sections we show examples from several branches of chemistry where either a single condition is to be diagnosed (Section 7.1) or a single category is to be chosen from a series of others (Section 7.5), or alternatively where an object is to be assigned to several classes simultaneously (Sections 7.2–7.4).

7.1. Chemical Reactivity

The chemist derives his knowledge about the reactivity of bonds and functional groups from a great many observations of individual reactions. How can this process be transferred to a neural network? Let us look at the problem of polar bond breaking (Scheme 1), the first step in many organic reactions.[29]

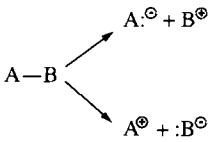

Scheme 1. Polar bond cleavage.

The reactivity is characterized very roughly in this case: namely whether a bond is easy or hard to break heterolytically. For this a single output neuron that is set to one if the bond may be easily broken and to zero if the bond is difficult to break will suffice. We still have to characterize the polar bond breaking by parameters that serve to influence the process. For this purpose a number of energetic and electronic effects were used: bond dissociation energy (BDE), difference in total charge Δq_{tot}, difference in π-charge Δq_π, difference in σ-electronegativity $\Delta\chi_\sigma$, σ-polarity Q_σ, polarizability of bonds α_b, and the degree of resonance stabilization $R^\pm$ of the charges that arise from polar bond breaking. Values for these quantities were calculated by empirical methods.[30–34] For these seven parameters, seven units are required into which are fed the (real) values of the individual quantities. A hidden layer of three neurons completes the architecture for this study (Fig. 30).

A data set that consisted of 29 aliphatic compounds containing 385 bonds was created. As each bond may be broken

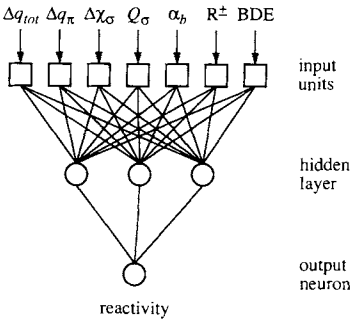

Fig. 30. Architecture and input parameters for a neural network to predict the breaking of bonds. For details see text.

heterolytically in two directions (see Scheme 1), there was a total of 770 possible bond breaks. From these, 149 heterolyses of simple bonds were chosen and 64 of them used to train the net by the back-propagation algorithm; the remaining 85 bond-breaks were used to test the net (the division into training and test data sets will be explained in Section 10.1). Figure 31 shows a selection of molecules from the data set, in which those bonds classified as breakable or unbreakable have been marked.

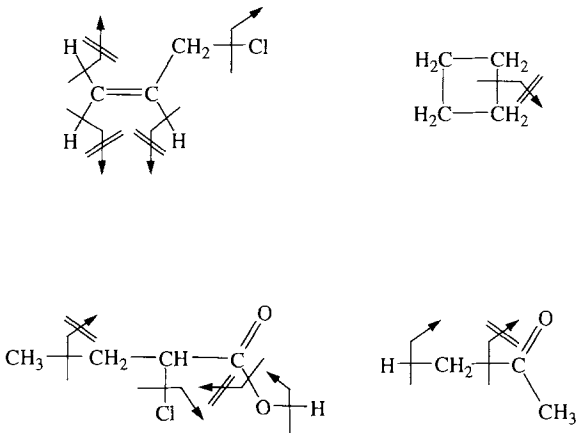

Fig. 31. Selection of structures from the training set indicating which bonds are easy (arrow) or difficult (arrow crossed through) to break heterolytically. The direction of the arrows indicate to which atom the electron pair will be shifted in bond cleavage (that is, which atom will receive the negative charge).

After 1300 cycles (epochs) the net had correctly learned all 64 bond breaks from the training data set. Then the bond breaks from the test data set were passed through the already trained neural net. These 85 bond breaks, about which the net had hitherto received no information, were also classified correctly. The division of the bonds into those easily and those not easily broken was predicted by the net exactly the same way as the chemist had determined them. The net had therefore learned the relationship between electronic and energetic parameters and polar bond-breaking.

The net was then ready to be applied to compounds that were contained neither in the training nor the test data sets. It even made correct predictions about bond types which contained atoms that were not used at all in training. In Figure 32 the predicted reactive bonds of a structure which was not used to train the net are shown. The dissociation of

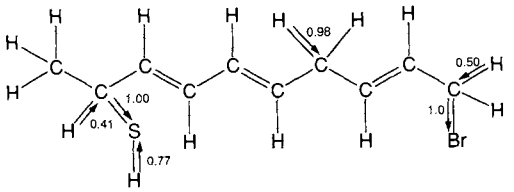

Fig. 32. Bond cleavages predicted by the neural network for a structure which was not used in training. The direction of the arrows indicate the shifts of electron pairs, the values the predicted probability for heterolysis.

a bromide ion and a thiol group, both in allyl position, were found to be especially reactive, as were the removal of a proton from the central allylic position and from the thiol group. The allylic positions at the ends of the system were estimated to be less acidic, whereas the position at which the bromine atom can still function in an inductively stabilizing way receives a higher acidity. Thus all results correspond closely to chemical experience.

It is remarkable that the reactivity of the SH group was correctly judged, even though the training data set did not contain a single structure with a sulfur atom. This is made possible by the use of those electronic and energetic parameters that contain the influence of the atom in general form in the techniques used for calculation of the inputs. Thus even a type of atom which does not occur in the current training set can be taken into consideration, provided that it is contained in the calculation process.

This neural network is able to predict which bonds can easily be broken in a polar manner for a wide range of aliphatic structures.

7.2. Process Control

For many chemical processes the relationship between process data and control parameters can be represented, if at all, only by nonlinear equations. It is therefore very hard to model these processes and to predict their behavior. It therefore comes as no surprise that neural networks are being used intensively for tasks in process control.[35-41] This includes not only the classification of certain events (yes/no decisions), but also the modeling of control parameters (prediction of a real value).

An example in which the task is to choose between membership of different classes will serve to illustrate the possible applications.[36] The goal was to derive individual failure modes from six different sensor values for a continually stirred reaction vessel in which an exothermic reaction was in progress.

The following measurements were taken (cf. Fig. 33): 1) The outlet concentration of the educt C_e, 2) the reactor temperature T_r, 3) the volume of the contents of the reactor V_r, 4) the outlet flowrate FR_p, 5) the temperature of the cooling water T_c, and 6) the flowrate of the cooling water, FR_c. These six parameters were to be used as "symptoms" to diagnose several failure modes of the reactor. Malfunction can be caused by incorrect inlet concentration of the educt C_{eo}, inlet temperature T_e, and inlet flow-rate FR_e. If any of these measurements deviates by more than 5 percent from the normal value, a failure has occurred in the reactor.

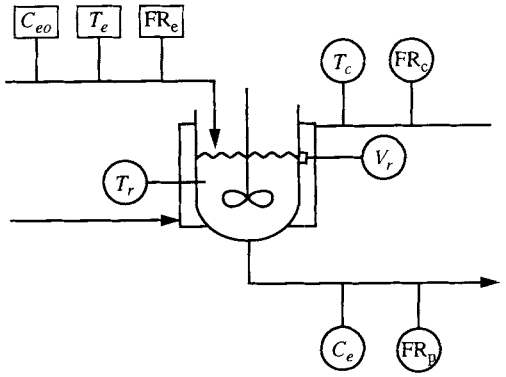

Fig. 33. Diagram of a reactor tank showing the six measured values (C_e, T_r, V_r, FR_p, T_c, FR_c) and the state variables that give rise to a failure mode (C_{eo}, T_e, FR_e).

Each one of the failure modes affects almost all the symptoms, that is, all six measured values, so that a specific failure mode can not be diagnosed directly from a single measurement. Moreover, it is possible for the failure modes to occur not just singly but simultaneously, and for the effects of simultaneous failure modes to compensate in the sensor values, or contrarily to amplify each other synergetically.

Which network architecture was chosen in this case? Because six real measured values are to be input, six input units are required. Likewise the number of output neurons chosen was six; for each of the three crucial inlet parameters (C_{eo}, T_e, and FR_e) one neuron for a deviation over the normal value and one for a deviation below it. Thus if any of the six failure modes occurs the corresponding output neuron should also be activated. Five neurons in a hidden layer complete this multilayered net (Fig. 34).

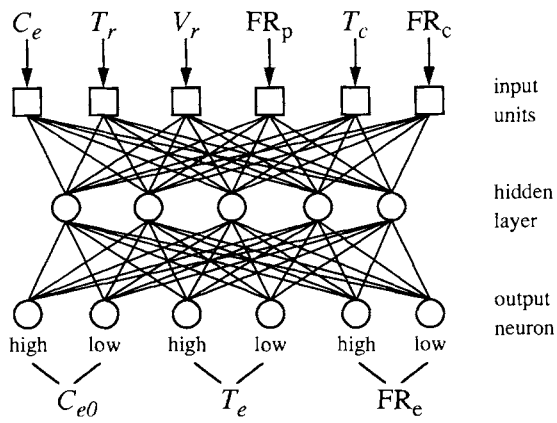

Fig. 34. Neural network for diagnosing failure modes of the chemical reactor depicted in Figure 33.

Accordingly for this neural network $6 \times 5 + 5 \times 6 = 60$ weights were to be determined. Twelve individual failure modes were deliberately produced, and the network trained by using the sensor data measured from them on application of the back-propagation algorithm. The network so trained was able to identify sensor data from the reactor running normally (data which were not used in the training process) as undisturbed behavior. Furthermore, when four multiple

failure modes were produced the neural net was likewise able to derive these correctly from the sensor data taken at the time.

Neural networks will certainly become very important in the area of process control. It should also be possible to take a neural network that has been trained on a specific process, hard-code this onto a chip, and build this chip into the control process.

7.3. The Relationship between Structure and Infrared Spectra

In the examples from Sections 7.1 and 7.2, rather simple neural networks with relatively few weights were used. For the following application a considerably larger network with almost 10000 weights was developed.

Modern structure elucidation is based on spectroscopic methods. However, as the relationships between the structure of an organic compound and its spectroscopic data are too complex to be captured by simple equations, there are a multitude of empirical rules. The enormous amount of spectroscopic data thus available fulfills an important precondition for the training of neural networks. The first steps to store the relationships between structure and spectroscopic data in neural networks have already been taken. Nevertheless, as we shall see, there is still much development to be done in this area.

Munk et al.[42] investigated to what extent conclusions could be drawn by a neural network about the substructures contained in a particular compound from an infrared spectrum. The range of an infrared spectrum between 400 and 3960 cm^{-1} was divided into 256 intervals, and each of these intervals assigned to an input element. If an absorption band was found in such an interval, its intensity was fed into the input element. The neural network had 36 output neurons, each of which was responsible for one of 36 different functional units (primary alcohol, phenol, tertiary amine, ester etc.). If a functional unit was present in the compound under investigation, then the corresponding neuron received the value one, otherwise the value zero. Further, an intermediate layer containing 34 hidden neurons was used, which required $265 \times 34 + 34 \times 36 = 9928$ weights to be determined for this multilayered network. The basic procedure and the architecture of the neural network are sketched in Figure 35.

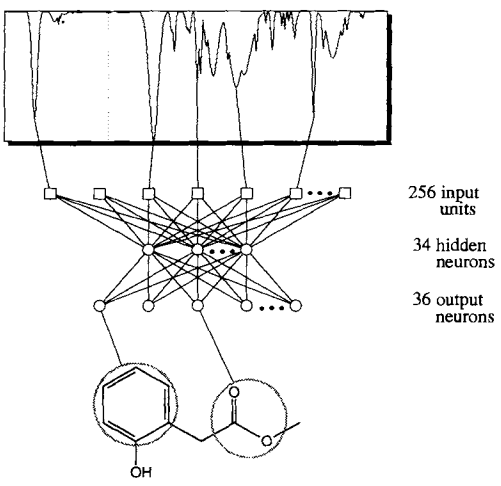

Fig. 35. Neural network to learn the relationships between the infrared spectrum of a compound and the substructures present in it.

To determine the weights of the neural network, 2499 infrared spectra together with their structures, which were broken down into their functional units, were learned through the back-propagation algorithm. Then 416 spectra were used to test the predictive ability of the net. A single cycle through all spectra required 10 min CPU time on a VAX 3500; for a training session with many cycles (called epochs—typically 100 epochs were necessary) a Cray supercomputer was used.

For each functional group the quality of the results was measured by a number, named the A50 value. This value represents the precision at 50% information return, that is, the precision with which a functional group can be ascertained when the threshold value is set to the mean of the distribution curve.

Figure 36 shows a typical result, in this case for primary alcohols. The threshold value here lay at an output value of

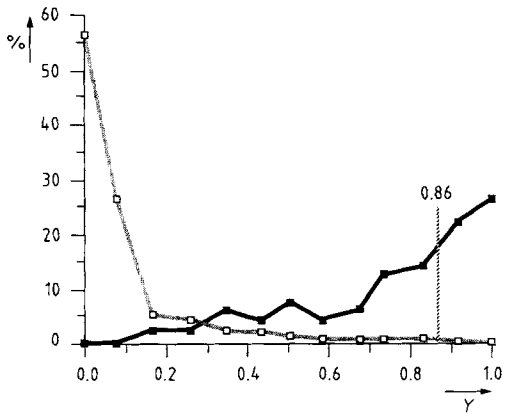

Fig. 36. Percent distribution of the output values Y of the neural network for primary alcohols. The solid line represents compounds which are primary alcohols, the shaded line all other compounds. The mean of the output values for primary alcohols is 0.86.

0.86. At this value 132 of the 265 primary alcohols contained in the training set are correctly identified, but 34 compounds are incorrectly classified as primary alcohols as well. The A50 value for this group is therefore $132/(132 + 34) = 79.5\%$. This value was still deemed to be good. Thirty of the 36 functional groups were able to be predicted with similar or better precision.

The results from this network, which contained a hidden layer, were compared with classification capabilities of a network without a hidden layer.[43] The hidden layer brought about a considerable improvement in results.

This experiment has, of course, not solved the problem of resolving the relationships between infrared spectrum and structure. For the most part, work concentrated on a few important functional groups, and the molecular skeleton was ignored. Even for those groups the predictions were only of moderate quality; to recognize 132 out of 265 primary alcohols in addition to 34 false assignments is disappointing. If one sets the threshold value even higher one can determine to a high degree of certainty whether a functional group is

present or absent, but a large range of compounds remains for which no reliable predictions can be made. In an automatic structure–elucidation system, however, these kinds of predictions allow a considerable reduction of the search space. Herein lies the value of these results.

This is not the last word on the relationship between structure and infrared data. Further experiments should attempt to classify vibrations of the skeleton. This would, however, necessitate a change in the way structures are coded.

7.4. The Relationship between Structure and Mass Spectra

The relationships between mass spectra and structure are even more complex than those between infrared spectra and structure. Nevertheless, this problem also has already been approached with neural networks.

In this case, too, a multilayered network containing a hidden layer was trained with the back-propagation algorithm.[44] The mass spectra were described by 493 features; these included the logarithms of the intensity of the peaks between m/z 40 and 219, the logarithms of the neutral losses between m/z 0 and 179, autocorrelation sums, modulo-14 values, etc. The values for these 493 spectral characteristics were fed into the same number of input units.

Here too the structure of an organic compound was characterized by 36 substructures which, however, differed partly from those used in the study on infrared spectra. Thirty-six output neurons were needed for this. As the number of neurons in the hidden layer was 80, $493 \times 80 + 80 \times 36 = 42320$ weights had to be determined.

Correspondingly larger data sets were investigated: with 31926 mass spectra for training and 12671 mass spectra for testing. With such large data sets and a network with so many weights, the learning process (the back-propagation algorithm was also used here) required a great deal of time. One epoch (that is the process of passing all 32000 spectra once through the net) needed 6 h on a HP 9000/370 or SUN-4 workstation. Typically 50 epochs were needed; thus training alone required two weeks computing time on a high-performance workstation.

The results of the classification from the fully trained neural network, MSnet, were compared with results from STIRS.[45] STIRS, from the group led by McLafferty, is a powerful expert system for determining the presence of functional groups from mass spectra.

The classification results from MSnet were somewhat better than those from STIRS. MSnet offers a few additional advantages however: 1) A probability value can be given for the assignment of a compound to a particular class. 2) Not only the presence but also the absence of a functional group can be diagnosed. 3) The computing time required for queries to MSnet is two orders of magnitude lower than for STIRS.

The following point must be emphasized: Even though the training of a neural network may require a great deal of CPU time, a fully trained neural network can make predictions in minimal time.

In order to satisfy as general a requirement as representing or learning the relationship between molecular structure and spectroscopic data for the entire domain of organic chemistry, we must confront a fundamental problem, the statistical distribution of data. For example, the data set of 32000 compounds contains 33 phthalic acid esters, which give a very characteristic peak at m/z 149. However, most of the spectra which have a peak at m/z 149 happen not to be phthalic acid esters because there are only very few of them in the total set. As a consequence phthalic acid esters are not recognized.

In this paper[44] an interesting attempt is made to overcome this general problem: a hierarchy of neural networks is proposed (Fig. 37). A preliminary network first undertakes

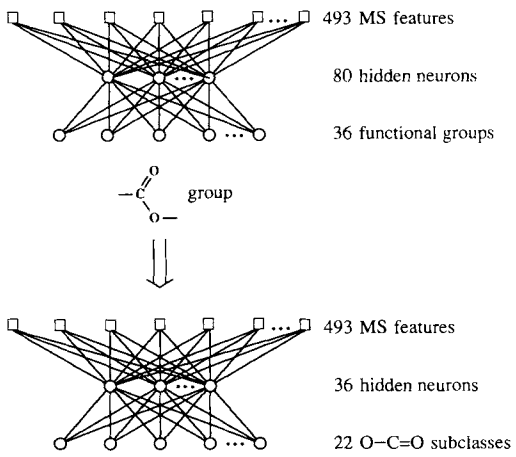

Fig. 37. Hierarchy of neural networks for deriving substructures from mass spectra.

the partitioning according to the most important functional groups, while specialized neural networks carry out further refinements of the compound classes. Thus a special network was developed which divided compounds containing the O–C=O group into 22 subclasses (saturated esters, aromatic esters, lactones, anhydrides etc.).

This idea of using a hierarchy of neural networks could prove very useful in other problem areas.

7.5. Secondary Structure of Proteins

In the example from the previous section we were still dealing with a rather simple network architecture. We now move on to describe cases with a rather extensive coding of the input data. The neural network involved is correspondingly complex, with a large number of weights.

To gain a deeper insight into the physiological characteristics of proteins one must know their secondary structure. For this reason there has been no scarcity of attempts to derive the secondary structure of proteins from their primary structures (that is, from the sequence of amino acids). Chou and Fasman[46] introduced a method which is much used today to decide from the sequence of amino acids what secondary structure the individual parts of a protein will assume. This procedure is able to predict with 50–53% accuracy for the individual amino acids in a protein whether they take part in an α-helix, β-sheet or an irregular coiled struc-

ture.[47] Over the past few years a series of papers have appeared in quick succession[48-56] on applications of neural networks to predict the secondary or even tertiary structure of particular sections of a protein from the sequence of amino acids. Our intention is to demonstrate the principal procedure based on the work of Qian and Sejnowski.[48] Most of the other investigations[49-56] have chosen a very similar strategy.

Both the Chou and Fasman method[46] and the application of neural networks are based on the assumption that the amino acid (AA) itself and its immediate surroundings (that is, the amino acids immediately before and after it in the sequence) decide which secondary structure it will adopt.

In order to take the dependence of the secondary structure on the sequence into account, the amino acid under examination will be fed into the net along with the six amino acids preceding and the six following it in the sequence. Thus from the amino acid sequence, a "window" of 13 amino acids is extracted every time. This window is pushed in steps of single AAs down the entire length of the amino acid sequence, so that each individual AA in turn may find itself in the center.

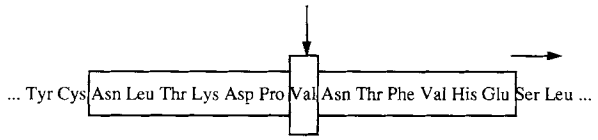

Fig. 38. Section ("window") of 13 amino acids from a protein sequence. The window helps to determine the secondary structure in which the amino acid in question (in this case valine) finds itself.

How are the individual amino acids coded? For each AA in the window of 13 AAs a bit vector of length 21 is used. For each of the 20 naturally occurring amino acids a particular position in the bit vector is reserved (e.g., the 14th bit is set to 1 when the AA proline is present). A last bit is required in order to mark that the window is at the beginning or end of the protein and thus that there are no more AAs at one of its ends. Thirteen input units are needed for the size of the window and 21 for the identity of the AA, thus $13 \times 21 = 273$ input units altogether; each feeds only one bit, a zero or a one, into the network.

The network had three output neurons: one for the presence of an α-helix, one for a β-sheet, and one for a coiled structure. After experimenting with between 0 and 80 hidden neurons, a hidden layer of 40 neurons was chosen as optimal for the net, which meant that $273 \times 40 + 40 \times 3 = 11\,040$ weights were to be determined. Again in this case the back-propagation learning algorithm was chosen. The overall architecture is pictured in Figure 39.

The network was trained with 106 proteins containing a total of 18 105 amino acids. The efficacy of the net was tested with 15 additional proteins, which comprised 3250 AAs in total. A prediction accuracy of 62.7% was achieved.

Thus one could say with 62.7% certainty whether an amino acid was part of an α-helix, a β-sheet or a coiled structure. This is a noticeable improvement over traditional methods for predicting secondary structures but still leaves something to be desired. It is therefore understandable that this area is being researched so actively.[48-56]

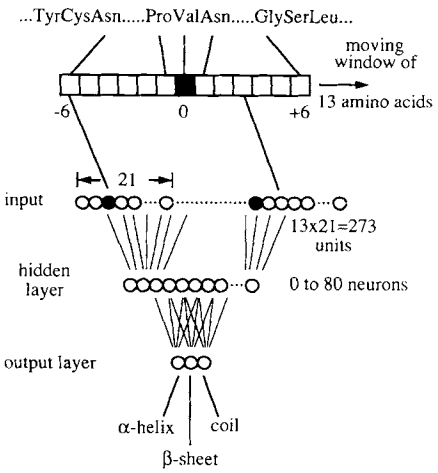

Fig. 39. Neural network for deriving the secondary structure of a protein from the sequence of amino acids.

7.6. Summary

These applications from very different branches of chemistry serve to underline the broad range of possibilities which neural networks offer for classification. In every one of the examples portrayed, a multilayered network was used that was trained by the back-propagation learning process.

The number of neurons in the hidden layer is usually determined by a systematic series of experiments. With too few neurons a problem can not be correctly learned; the larger the number of neurons the smaller the error in learning, but the longer the training times. Too many neurons and too long a training period can lead to another problem: overtraining. This means that a neural net has been trained for so long that, although it can reiterate the training set without error, it may give bad predictions when faced with new data. Multilayered networks usually have many weights, and therefore many degrees of freedom in adapting to a data set. This presents the danger that one might fall into an erroneous local minimum in training, thus reducing the ability to make predictions based on new data.

The complexity of the neural net (mainly the number of weights and the number of training data used) can bring with it a large increase in the training time. One should not be discouraged too much by long training times, however, because ideally a network needs to be trained only once. Once it has finished learning, predictions on new data can be made very rapidly, because these data only have to be passed through the fully trained net once.

In the case of classification problems it is desirable to obtain values of one or zero in the output neurons so that an object belongs unambiguously to a category or not. In reality values between one and zero are obtained, and decisions are made on the basis of threshold values (e.g., 0.8 or 0.2) whether an object belongs to that category. These numeric output values can also be interpreted as probabilities, and as such may be used in a decision support system.

The numerical output clearly points to the transition to modeling problems, which are the subject of the next section. In modeling tasks it is desirable to obtain function values, (i.e., real data). These can be produced by taking those val-

ues between zero and one and transforming them through mathematical functions.

In summary, the most important task when implementing a neural network is to find a suitable representation for the input and output data. The hierarchical ordering of multiple networks (Section 7.4) and the movable window from Section 7.5 demonstrates that the technology sets no limits to the imagination.

8. Modeling

We have already seen that even in the case of classification a neural network returns values between zero and one, that is, a continuum of values. It is also possible, however, to train a neural network with real expectation values and to use the output values in their real magnitudes, just as one might normally calculate the value of a function from a series of variables. This task of using data about an object (compound, reaction, spectrum) and deriving other characteristics of the object from them has commonly come to be called "modeling", and is what we shall use the term to mean in the following sections. The neural network therefore assumes the task of using input variables (data) from an object to find the value of some dependent characteristic (or even several of them). A neural network offers the advantage of not requiring an explicit formulation of the relationship as a mathematical equation. It expresses this relationship implicitly in the connections between the individual neurons.

8.1. HPLC Analysis

A simple example shall serve to represent the potential of this technique in analytical chemistry.

In the HPLC analysis of Spanish wines, the dependence of the separation of the components (expressed as the selectivity factor SF) on the ethanol content (10, 20, or 30%) and the pH value (5.0, 5.5, or 5.6) of the liquid phase was determined. These nine experimental points were fitted to a quadratic equation with standard modeling techniques.[57] The result is given in Equation (r), where x_1 = % ethanol and x_2 = pH value. This functional relationship is also represented in Figure 40 in the form of lines of the same selectivity factor.

$$SF = 0.018\,x_1^2 - 1.42\,x_2^2 + 0.015\,x_1\,x_2 - 0.995\,x_1 + 16.16\,x_2 - 31.86 \qquad (r)$$

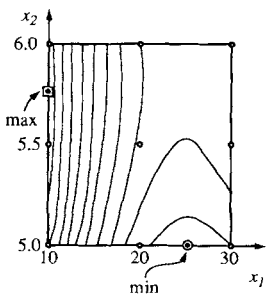

Fig. 40. HPLC analysis of Spanish wines: Shown is the dependence of the selectivity factor SF on the ethanol content x_1 and on the pH value x_2 of the liquid phase. The curved arrows highlight the maximum (left) and minimum SF (bottom).

The same nine experimental data were built into a neural network with two input units (one for the ethanol content and one for the pH value), one output neuron (for the selectivity factor), and six neurons in a hidden layer, which was trained with the back-propagation algorithm.[58]

Values for the ethanol content and the pH were fed into the network and the results entered into the diagram in Figure 41. Here too, just as in Figure 40, lines of the same selectivity factor were drawn in. A comparison between Figures 40 and 41 shows that both standard modeling and neural network techniques arrive at quite similar results. In particular, the positions for the minimum and the maximum values of the selectivity factor are very similar.

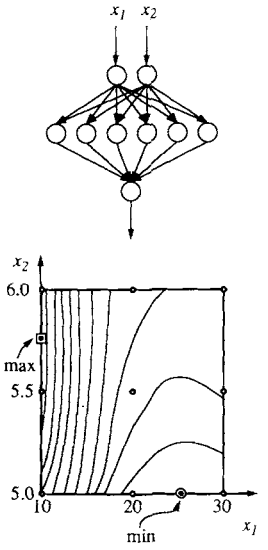

Fig. 41. The results obtained from a neural network (shown at the top) on the selectivity of the HPLC analysis of Spanish wines: dependence of SF on the ethanol content and on the pH value. See also Figure 40.

The advantage of the neural network is clear: in statistical modeling the mathematical form of the functional relationship (here a quadratic equation) had to be given explicitly. With the neural network this is not necessary; it finds the relationship by itself, implicitly, by assigning appropriate weights.

8.2. Quantitative Structure–Activity Relationships (QSAR)

The search for quantitative structure–activity relationships (QSARs) is one of the most important application areas for modeling techniques. A great deal of trouble and effort has been invested, especially in the prediction of pharmacological and biological data. It is therefore all the more surprising that as yet very few studies have been published which employ neural networks to provide quantitative relationships between structure and biological activity.[59, 60] A typical study shall briefly be described here.

For this study a data set that had already been investigated with statistical modeling techniques (a multilinear regression analysis) was deliberately chosen in order to compare the performance of a neural network against a standard method from the field of QSAR. The data set comprised 39 *para*-quinones, some of them anticarcinogenic (Scheme 2).

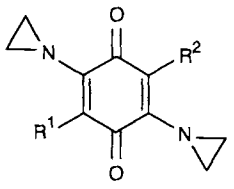

Scheme 2. *para*-Benzoquinones containing two aziridine substituents, a class of compounds which includes some anticarcinogenic members. R^1 and R^2 are, for instance, CH_3, C_6H_5, etc.

The influence of the substituents R^1 and R^2 was described by six physicochemical parameters: the contribution of R^1 or of both substituents to the molar refractivity index, MR_1 and $MR_{1,2}$, their contribution to the hydrophobicity, π_1 and $\pi_{1,2}$, the substituent constants of the field effect (F), and the resonance effect (R). Accordingly for a description of the influences of the substituents, six input units were required (Fig. 42).

The neural network was intended to yield the minimum effective dosage of the medication for a single injection. This minimum effective dosage is given by the amount of substance (as $\lg 1/c$) that leads to a 40% increase in length of life. A single neuron was present in order to output the value of $\lg 1/c$. A hidden layer of 12 neurons completed the network architecture (Fig. 42).

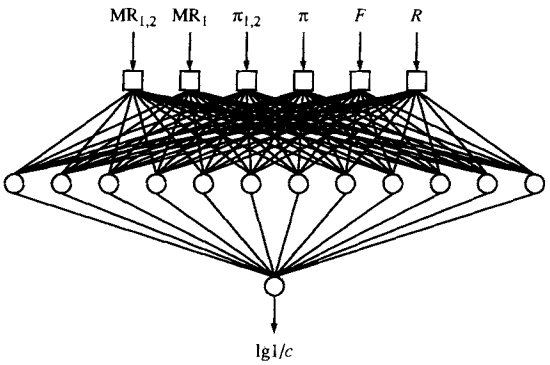

Fig. 42. Neural network for predicting the anticarcinogenic activity of *para*-benzoquinones.

Thirty-five benzoquinones were used to train the multilayered network with the back-propagation algorithm. The values for $\lg 1/c$ obtained from the network were compared with the results calculated from an equation determined by multilinear regression analysis. In 17 cases the results from the neural network were better, for 6 more or less as good, and for 12 worse. In other words, the results from the neural network are significantly better. Nevertheless this problem can be solved quite well by a linear method that leaves little room for improvement by a neural network. In the case of QSAR problems containing nonlinear relationships more might be gained by using neural networks.

8.3. Chemical Reactivity

Whereas in Section 7.1 we were satisfied with a yes/no decision on chemical reactivity (does a bond break easily in a polar manner or not), here we wish to make a quantitative statement about the behavior of a chemical reaction.

The electrophilic aromatic substitution of monosubstituted benzene derivatives can lead in principle to three isomers: *ortho*, *meta*, and *para* products (Scheme 3). The dependence

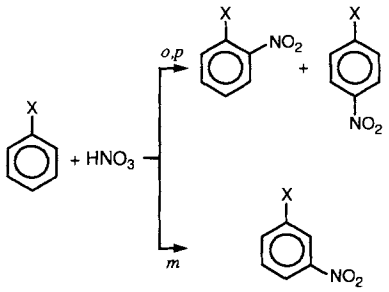

Scheme 3. Isomeric distribution in electrophilic aromatic substitution.

of the isomer distribution on the nature of the substituents X is a classical problem in organic chemistry. Basically the substituents may be divided into two classes: electron-donating substituents (inductive or mesomeric), which prefer to direct into *o*- and *p*-positions, and mesomeric electron acceptors which steer towards the *m*-position. The factors that determine the *o*/*p* ratio are both steric and electrostatic in nature.

In one study[61] into the product ratios for the nitration of monosubstituted benzene derivatives, the amounts of *ortho* and *para* products were combined. Accordingly, one output neuron was used for the $o + p$ content and a second for the percentage of *m*-isomer. As already mentioned, the distribution of product is determined by the nature of the substituent, especially by the electronic effects which it produces. In order to represent this, two codings of the input information were tested. In the first attempt the partial atomic charges on the six carbon atoms of the benzene ring as they are calculated in the semi-empirical quantum mechanical program suite MOPAC[62] according to Mulliken population analysis were used as the six inputs. In addition an intermediate layer with 10 hidden neurons brought the total number of weights to be determined to $6 \times 10 + 10 \times 2 = 80$.

As an alternative method the structure of the substituent was represented directly in the form of a connection table. This had dimensions of 5×5; each row contained first the atomic number of the atom in question then the index of the atom itself followed by the index of the adjacent atom further away from the ring, the order of this bond, and the formal charge on the atom. For each atom of the substituent except a hydrogen atom a new row was used. The first row reflects the situation at the atom which is directly bonded to the ring. With each successive row a further step is taken into the substituent (cf. Fig. 43). If the substituent had fewer than five non-hydrogen atoms then the rest of the 25 entries were filled with zeros. If it had more than five heavier atoms, those atoms which were further away from the point of attachment of the substituent on the ring (atom 1) were left out. Figure 43 explains this coding by connection table for the example of acetanilide. For this coding $5 \times 5 = 25$ input units were required, the intermediate layer had five neurons, and the network thus $25 \times 5 + 5 \times 2 = 135$ weights.

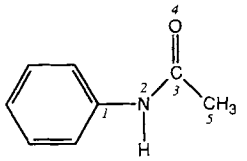

atomic number	relevant bond: reference atom	adjacent atom	bond order	charge
7	2	1	1	0
6	3	2	1	0
8	4	3	2	0
6	5	3	1	0
0	0	0	0	0

Fig. 43. Example illustrating the representation of monosubstituted benzene derivatives by a connection table of the substituent.

The network was trained with 32 monosubstituted benzene derivatives and the back-propagation algorithm; it was then tested with 13 further benzene derivatives. In this example the enormous number of 100000 epochs or training cycles was necessary before the error in the training data set had been reduced to a sufficient degree.

Of the two forms of coding with their networks, the second version—that is, the input of the substituent by means of a connection table—clearly produced the better results. Only the percentages of the *meta* products (Table 2) are necessary

Table 2. Results of attempts at predicting the amount of *meta*-product in the nitration of monosubstituted benzene derivatives. The size of the error in the prediction is quoted [%].

Method	Training data (32 compounds)	Test data (13 compounds)
network based on charge	5.2	19.8
network based on connection table	0.3	12.1
CAMEO	18.0	22.6
estimate by chemists	–	14.7

to judge the quality of the results. The training data set was able to be learned down to an average error of 0.3% for the *m*-isomer content. For the network obtained from the charge values the average error was 5.2%. With the test data of 13 compounds that the network had not seen before, the connection table coding gave an average error of 12.1% in predicting the percentage of *m*-product. For the atomic charge representation the error was noticeably higher at 19.8%

The results from these two neural networks were compared to values produced by CAMEO,[63] an expert system for predicting reactions. They were in every respect better than those produced by CAMEO. Finally the 13 monosubstituted benzene derivatives were given to three organic chemists to predict the expected percentage of *m*-product from the nitration. The values they gave were averaged; this gave an error of 14.7%. The chemists were thus better than the neural network with charge-coding and better than CAMEO, but were beaten by the neural network with the connection-table input!

Though the results for predicting the product ratios from the nitration of monosubstituted benzene derivatives with a neural network based on the coding of the substituents by a 5×5 connection table are very encouraging, they do deserve more detailed comment. First, it is not surprising that the coding by the partial charges on the six ring atoms was rather unconvincing. Apart from the known inadequacies of Mulliken population analysis, the ground-state charge distribution is only one of the factors (not even the most important electronic effect) that influences the product ratios in electrophilic aromatic substitution. For these reasons the charge values can not represent the benzene derivatives sufficiently well to explain the product ratios from nitration.

As satisfactory as its results may be, the coding of the benzene derivatives by a 5×5 connection table can not provide an explanation for the effects responsible for regioselectivity, nor for the influence of the reaction conditions. Nor can it explain the product ratios from di- and polysubstituted benzene derivatives. To do this one must choose a different representation for the benzene compounds, which is indeed feasible.[64] The substituent should not be described globally. Rather its influence on the individual positions on the aromatic ring should be represented directly: for each position on the ring a value for the resonance effect, the local electrostatic potential, and the steric effect should be given. Because this represents the influence of a substituent at every single position on the ring, we can extend inferences from monosubstituted benzene derivatives to di- and polysubstituted compounds. Then we can make predictions about isomer distributions in further substitution. In addition, it is also possible to take account of the influence of the medium by providing a further input unit for the concentration of sulfuric acid. The network is trained with this alongside the descriptors for the influences of the substituents.[64]

8.4. Summary

Modeling tasks are very common in many branches of chemistry. This opens up a wide area for the application of neural networks. At present this area is dominated almost exclusively by multilayered networks and the back-propagation algorithm. This need not be the case. Other neural network architectures, especially the counterpropagation algorithm,[27] can certainly be used just as well for creating models.

The deployment of neural networks for modeling (that is, for predicting some characteristic of an object from a series of other parameters or measurements from that object) should always be considered carefully in relation to the use of statistical methods. If one has a relatively clear idea which variables influence the feature sought, and if there is some largely linear relationship between them, then traditional methods, such as multilinear regression analysis clearly offer advantages: these methods are faster and require less computing time, they give measures for the quality of the discovered relationship, and, above all, the equation derived from the statistical modeling allows a clear interpretation of the individual effects of the feature sought.

Neural networks should be used, however, if it is presumed that nonlinear relationships exist between the dependent and the independent variables, and if it is not possible to specify exactly which parameters influence the characteristic under investigation.

Whether the choice falls on statistical methods or neural networks, the success of a study depends crucially on the selection of the data set, on the representation of the information, and on the methods employed to validate the results. Moreover, when implementing neural networks, the following points are of crucial importance:

- the selection of a homogenous data set for training (e.g., by using experimental design techniques or a Kohonen network – see Section 10.1)
- the partitioning of the data set into training and test data sets
- the selection of suitable parameters as input data to describe the objects.

9. Association

The capacity to associate is closely related to the recognition of similarities between different objects. Neural networks can also be conceived of as memories, because they store the information they have learned from the training data in the form of weights or "synaptic strengths". Should a new object be fed into the neural network whose input data resemble those of an object used in training, some network architectures are able to recognize this and yield the stored object from the training phase as output.

This ability of neural networks to associate, to recognize similarities in given data, has been exploited very little in chemistry up to now. Even the two studies presented here are essentially only feasibility studies. The basic solution to a problem is demonstrated here on small, simply structured data sets. For a real-world application however, larger sets of more complex data would have to be investigated.

9.1. Adjustment of Base Lines

Systematic deviations from the base line may be observed in many spectra and could be caused by impurities, the influence of solvents, or problems with technical equipment. Five different types of base line (normal, ascending, descending, concave, convex) were stored in a Hopfield network as simple black pixel-patterns in a matrix consisting of 6×20 points.[65] Then a simple, simulated spectrum which contained a convex base line was fed into the thus trained Hopfield network. After three iterations the pattern for this baseline was output by the network (Fig. 44).

Afterwards therefore, a background correction could be undertaken for this spectrum. We have already pointed out in this review that a real-world application would need a far higher resolution; thus the base lines would have to be represented by a larger pixel matrix (e.g., 20×250). However, because of the basic limitations on the storage capacity of Hopfield networks, and in order to make good predictions, 2×10^7 matrix elements would need to be checked. It only makes sense to carry out this task by hardware implementations of parallel neural networks.

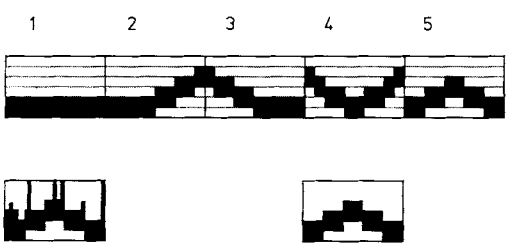

Fig. 44. Five types of base lines of a spectrum (top), a much simplified spectrum with a concave baseline (bottom left) and the concave base line recognized by the neural network after three iterations (bottom right).

Because of the storage and calculation problems presented by Hopfield networks, the same task was also investigated with a Hamming network.[65] A Hamming network,[66] which requires far less memory capacity, was in fact also able to be solve the problem. However, in this case too, only a 7×20 matrix was used to represent the five types of base line; an application which uses experimental data with a high resolution has yet to appear.

9.2. Identification of Spectra

Another feasibility study was made into how slightly altered UV spectra (e.g., through the influence of solvents) might be recognized.[67] Prototypes of UV spectra were represented by a sequence of points (pixels) in two 10×10 fields; the first field containing the band maxima was placed at the input of an adaptive bidirectional associative memory (ABAM), and the second field, comprising the tailing portions, was placed at the output (Fig. 45a). Because of the bidirectional nature of the ABAM the terms input and output are of course purely arbitrary.

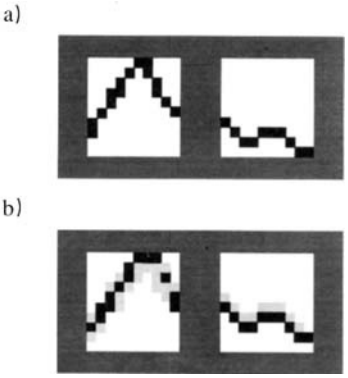

Fig. 45. Grid representation of an ultraviolet spectrum (a) and fuzzy coded forms of this spectrum (gray dotted fields) (b).

The ABAM was trained with five model UV spectra coded in this way. For testing fuzzy codings and slightly altered spectra were used (cf. Fig. 45 b). The recall capability of the ABAM was heavily dependent on the choice of various network parameters; however, in the end a set of parameters was found that was able to recall all five spectra learned from the input of its distorted counterpart.

10. Mapping

Many chemical phenomena are influenced simultaneously by a whole series of factors and depend on many parameters. These parameters can be seen as coordinates in a multidimensional space. Individual observations then represent

points in this multidimensional space. To visualize the structure of this multivariate information in order to make visible the essential relationships between the individual data points, the dimensionality of the space has to be reduced to such a degree that it can be represented graphically and thus analyzed by the human eye. Such a mapping, say onto a two-dimensional plane, should preserve the essential relationships between the individual data points as far as possible.

In Section 4.3 we saw how a three-dimensional space, the surface of a sphere, could be mapped by a Kohonen network onto the surface of a torus, and the neighborhood relationships between the points on the sphere were kept intact. In the following sections we present two examples for the mapping of multidimensional chemical information by a Kohonen network.

10.1. Chemical Reactivity

We wish once more to examine the data set introduced in Section 7.1, which classified a series of single bonds in aliphatic molecules according to whether they were easy or difficult to break heterolytically[29] (cf. Figure 31). Each of the bonds was characterized by seven electronic and energetic parameters, such as difference in charge and polarizability, and bond dissociation energy (cf. Figure 30). The rupture of a bond is thus represented by a point in a seven-dimensional space.

The question now is, are the points with reactive bonds in this seven-dimensional space separated from those of the nonreactive bonds? Moreover, if this is the case, can this separation be retained in a map onto a two-dimensional surface by means of a Kohonen network?

A Kohonen network consisting of 11×11 neurons was trained with the 149 bonds; the values of the seven electronic and energetic factors were used as input data (see Fig. 30).

The results are shown in Figure 46. Indeed the reactive bonds do find themselves predominantly in certain neurons, and the nonreactive bonds in different neurons. Additionally the neurons of the reactive bonds form a contiguous part of the Kohonen network.[29]

It may be concluded from this that the chosen parameters characterize the heterolysis of a bond well (because reactive and nonreactive bonds are separate) and that a Kohonen network is able to preserve this separation even when mapping it onto a surface. It should be emphasized once again that the Kohonen network learns without supervision, and therefore that the information on the reactivity of a bond was not used during the learning process.

Yet another conclusion may be drawn from Figure 46. Bond cleavages that activate the same neuron ought also to contain more or less the same reactivity information; the interaction of the seven parameters ought to produce a similar net effect in reactivity. Accordingly, if the relationships between reactivity and the electronic and energetic parameters are to be investigated further, it is sufficient to choose a single bond out of the many that activate the same neuron. At the same time, at least one bond should be chosen from each occupied neuron in order to cover as much as possible of the reactivity spectrum. In fact the data set that was learned by the back-propagation algorithm (see Section 7.1) was chosen with these considerations in mind. Thus two different neural network models were used: a Kohonen network for the selection of the data set and a multilayered neural network, trained by the back-propagation algorithm, for the task of classification.[29]

The Kohonen method can therefore be used to make balanced selections of data sets for investigations with statistical or pattern-recognition methods, or even used with other neural networks.

10.2. Electrostatic Potential

The electrostatic potential surrounding a molecule has a decisive influence on many physical, chemical, and biological properties. Electrostatic potentials are analyzed in detail, especially in investigations into the interactions between substrate and receptor, but also in studies into chemical reactivity.

If one moves a probe charge, for example a positive unit charge in the form of a point, around a molecule, for every point in space the electrostatic potential may be determined by quantum mechanical or classical electrostatic methods.

Scheme 4 shows a three-dimensional molecular model of 3-chloro-3-methylbutan-1-ol, and Figure 47 the electrostatic potential that a positive point charge experiences on the van der Waals surface of this molecule. The magnitude of the

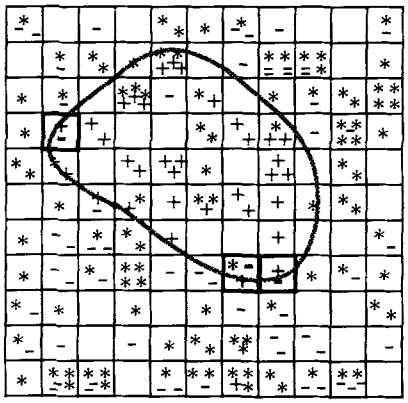

Fig. 46. A Kohonen network that maps polar bond rupture characterized by seven electronic and energetic parameters. + indicates a reactive bond, – a nonreactive bond, and * a bond whose reactivity was not decided.

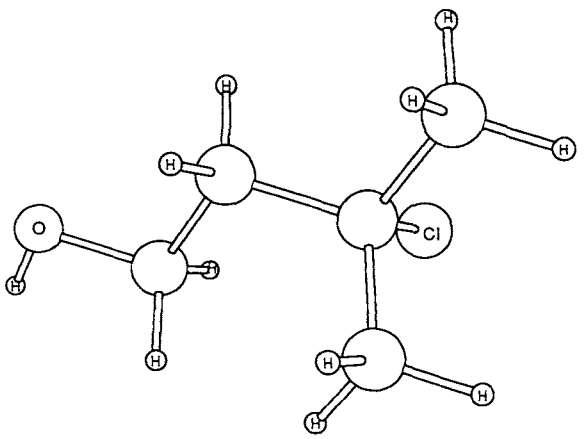

Scheme 4. Molecular model of 3-chloro-3-methylbutan-1-ol.

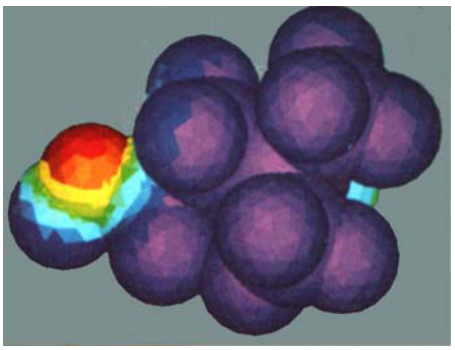

Fig. 47. Electrostatic potential on the van der Waals surface of 3-chloro-3-methylbutan-1-ol. Red regions possess a negative potential, and thus attract a positive charge; blue and violet regions repel this charge.

electrostatic potential is translated into a color code: Strongly negative values of the electrostatic potential (positions to which a positive charge is attracted—that is, nucleophilic positions) are represented by red. Strongly positive values (positions from which a positive charge is repelled—that is, electrophilic positions) are marked in blue or violet. The intermediate values are represented by continuous blends of color. The electrostatic potential was calculated in the classical way by summing the Coulomb interactions of the probe charge with the atomic charges as calculated by the PEOE procedure.[30, 31]

Figure 47 represents a parallel projection of the distribution of the electrostatic potential on the van der Waals surface of the molecule onto the plane of the graphics screen. Of course, only that part of the electrostatic potential that happens to be visible to the observer can be shown. Thus for example, the chlorine atom can barely be seen in Figure 47. A complete view of the distribution of the electrostatic potential can only be obtained by taking a series of such mappings from different observation points. The more complex the form of the van der Waals surface and the variation in electrostatic potential, the more mappings are required. For this reason it will be very difficult to obtain a complete impression of the distribution of the electrostatic potential and the relationships between all electrophilic and nucleophilic centers.

The inadequacies of a parallel projection onto a plane (monitor screen) led us to look for other projection methods that are capable of representing the essential aspects of the potentials on a molecular surface in a single mapping.[68] A Kohonen network is one such projection method.

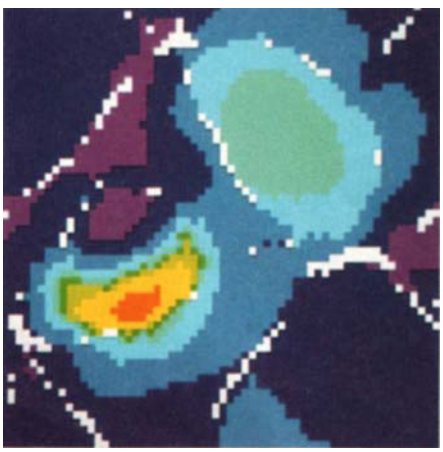

Fig. 48. Kohonen network of the electrostatic potential in Figure 47.

Figure 48 shows the projection of the electrostatic potential of 3-chloro-3-methylbutan-1-ol from Figure 47 onto a Kohonen network. To obtain this mapping, 20000 points were chosen at random from the molecular surface and a Kohonen network of 60×60 neurons was trained with the x, y, and z coordinates of each point. After each point had been passed through the network the neurons were examined to see which points were assigned to which neurons.

Points of the same or similar potential values were indeed found to be located in the same or neighboring neurons. The electrostatic potential on the van der Waals surface of a molecule had therefore been mapped onto the Kohonen map, and the neighborhood relationships on the van der Waals surface were largely preserved intact.

We remind the reader once more that in the case of a Kohonen network the mapping takes place onto a torus, that is onto a surface without beginning or end (cf. Figure 24). The map in Figure 47 can therefore be shifted up, down, to the left or to the right.

A comparison between Kohonen maps of electrostatic potentials of different molecules reflects the essential similarities of the electronic properties on the surface of the molecules, that is, at the places where molecules come into direct contact with their environment. The electrostatic potential on the surface of a molecule is a decisive factor in the interaction of a substrate with a biological receptor. Kohonen maps of electrostatic potentials of different molecules that are bound to the same receptor should therefore indicate certain similarities.

Indeed, it could be shown that Kohonen maps of the electrostatic potential of compounds that bind to the muscarinic receptor have common characteristics. Similarities are also perceived in the Kohonen maps of electrostatic potentials of molecules that bind to the nicotinic receptor, but these characteristics are different from those for molecules bound to the muscarinic receptor.[68]

Kohonen maps show in a single picture essential characteristics of electrostatic potentials. These characteristics are apparently responsible for the binding of a substrate to a biological receptor.

11. Summary and Outlook

Although the development of computational models of information processing in the human brain can look back on a history of almost 50 years, it is only in the last four to five years that neural networks have been applied widely to problem solving. New, efficient algorithms have paved the way for a multitude of applications, and the use of neural networks is still increasing—also in the field of chemistry—by leaps and bounds.

The models of neural networks and their potential applications of classification, modeling, association, and mapping are as diverse as the capabilities of the human brain are varied. The potential in neural networks for the processing of chemical information is very far from being exhausted.

In chemistry the task is often to assign objects to certain categories or to predict the characteristics of objects. This

accounts for the dominance of the back-propagation algorithm. A whole series of other neural network models exists, however, which could be applied successfully to the field of chemistry. This should be explored more widely in future.

Undoubtedly, many of the problems that have been approached with neural networks could also have been solved with statistical or pattern-recognition methods. Neural networks, however, offer capacities which exceed the possibilities of traditional methods of data analysis. Of special importance is the fact that the relationship between input and output data need not be specified in mathematical form, but is derived from the data themselves and represented implicitly. This enables the modeling even of nonlinear relationships.

The use of neural networks still requires much experimentation; guidelines to arrive as quickly as possible at a viable solution to a problem become apparent only gradually. Of crucial importance to the successful application of a neural network is the strategy for data representation; the better the chemical information to be examined is coded, the easier and better the problem may be solved.

The cooperation between our two working teams depended crucially on support from the Bundesministerium für Forschung und Technologie of the Federal Republic of Germany and from the Slovenian Research Ministry. Particularly the provision of a guest-professorship for Jure Zupan at the Technical University of Munich within the framework of BMFT project 08G 3226 has enabled us to develop a productive scientific exchange. We would like to thank especially our co-workers A. Fröhlich, P. Hofmann, X. Li, J. Sadowski, K.-P. Schulz, V. Simon, and M. Novic, who undertook with us the first steps into the Terra Nova of applying neural networks to chemical problems.

Received: July 20, 1992 [A 899 IE]
German version: *Angew. Chem.* **1993**, *105*, 510
Translated by Dr. P. Brittain, Garching (FRG)

[1] A textbook introduction to neural networks will appear shortly: J. Zupan, J. Gasteiger, *Neural networks for Chemists: A Textbook*, VCH, Weinheim, **1993**.
[2] For a detailed overview of neural network applications in Chemistry up to 1990 see J. Zupan, J. Gasteiger, *Anal. Chim. Acta* **1991**, *248*, 1–30.
[3] K. J. Skinner, *Chem. Eng. News* **1991**, *69* (40), 24–41.
[4] A highly recommended collection of publications reflecting milestones in the development of neural networks, each with a short commentary, may be found in *Neurocomputing: Foundations of Research* (Eds: J. A. Anderson, E. Rosenfeld), MIT Press, Cambridge, MA, USA, **1988**.
[5] W. S. McCulloch, W. Pitts, *Bull. Math. Biophys.* **1943**, *5*, 115–133.
[6] W. Pitts, W. S. McCulloch, *Bull. Math. Biophys.* **1947**, *9*, 127–147.
[7] D. O. Hebb, *The Organization of Behaviour*, Wiley, New York, **1949**.
[8] F. Rosenblatt, *Psych. Rev.* **1958**, *65*, 386–408.
[9] M. Minsky, S. Papert, *Perceptrons*, MIT Press, Cambridge, MA, USA, **1969**.
[10] J. S. Albus, *Brain, Behavior and Robotics*, BYTE Books, Peterborough, USA, **1981**.
[11] S.-I. Amari, *Biol. Cybernetics* **1977**, *26*, 175–185.
[12] S. Grossberg, *Biol. Cybernetics* **1976**, *23*, 121–134.
[13] T. Kohonen, *IEEE Trans. Comput.* **1972**, *C-21*, 353–359.
[14] C. von der Malsburg, *Kybernetik* **1973**, *14*, 85–100.
[15] B. Widrow, M. E. Hoff, *IRE ESCON Conv. Rec.* **1960**, 96–104.
[16] J. J. Hopfield, *Proc. Natl. Acad. Sci. USA* **1982**, *79*, 2554–2558.
[17] D. E. Rumelhart, G. E. Hinton, R. J. Williams in *Parallel Distributed Processing, Vol. 1* (Eds.: D. E. Rumelhart, J. L. McClelland, and the PDP Research Group), MIT Press, Cambridge, MA, USA, **1986**, pp. 318–362.
[18] D. E. Rumelhart, G. E. Hinton, R. J. Williams, *Nature* **1986**, *333*, 533–536.
[19] P. J. Werbos, Dissertation, Applied Mathematics, Harvard University, **1974**.
[20] *Parallel Distributed Processing, Vol. 1 + 2* (Ed.: D. E. Rumelhart, J. L. McClelland and the PDP Research Group), MIT Press, Cambridge, MA, USA, **1986**.
[21] B. Kosko, *Appl. Opt.* **1987**, *26*, 4947–4960.
[22] T. Kohonen, *Biol. Cybernetics* **1982**, *43*, 59–69.
[23] T. Kohonen, *Self-Organization and Associative Memory*, Springer, Berlin, **1988**.
[24] H. Ritter, T. Martinetz, K. Schulten, *Neuronale Netze – Eine Einführung in die Neuroinformatik selbstorganisierender Netzwerke*, Addison-Wesley, Bonn, **1990**.
[25] W. Kirchner, *c't* **1990**, *11*, 248.
[26] X. Li, J. Gasteiger, J. Zupan, unpublished results.
[27] R. Hecht-Nielsen, *Appl. Opt.* **1987**, *26*, 4979.
[28] K.-P. Schulz, P. Hofmann, J. Gasteiger in *Software-Entwicklung in der Chemie 2* (Eds.: J. Gasteiger), Springer, Heidelberg, **1988**, pp. 181–196.
[29] V. Simon, J. Gasteiger, J. Zupan, *J. Am. Chem. Soc.*, submitted.
[30] J. Gasteiger, M. Marsili, *Tetrahedron* **1980**, *36*, 3219–3228.
[31] J. Gasteiger, H. Saller, *Angew. Chem.* **1985**, *97*, 699–701; *Angew. Chem. Int. Ed. Engl.* **1985**, *24*, 687–689.
[32] M. G. Hutchings, J. Gasteiger, *Tetrahedron Lett.* **1983**, *24*, 2541–2544.
[33] J. Gasteiger, M. G. Hutchings, *J. Chem. Soc. Perkin Trans. 2* **1984**, 559–564.
[34] J. Gasteiger, M. Marsili, M. G. Hutchings, H. Saller, P. Löw, P. Röse, K. Rafeiner, *J. Chem. Inf. Comput. Sci.* **1990**, *30*, 467–476.
[35] J. C. Hoskins, D. M. Himmelblau, *Comput. Chem. Eng.* **1988**, *12*, 881–890.
[36] V. Venkatasubramanian, R. Vaidyanathan, Y. Yamamoto, *Comput. Chem. Eng.* **1990**, *14*, 699–712.
[37] K. Watanabe, I. Matsuura, M. Abe, M. Kubota, D. M. Himmelblau, *AIChE J.* **1989**, *35*, 1803–1812.
[38] P. Bhagat, *Chem. Eng. Prog.* **1990**, *86*(8), 55.
[39] V. Venkatasubramanian, K. Chan, *AIChE J.* **1989**, *35*, 1993–2002.
[40] L. H. Ungar, B. A. Powell, S. N. Kamens, *Comput. Chem. Eng.* **1990**, *14*, 561–572.
[41] N. Bhat, T. J. McAvoy, *Comput. Chem. Eng.* **1990**, *14*, 573–583.
[42] M. E. Munk, M. S. Madison, E. W. Robb, *Mikrochim. Acta* **1991**, II, 505–514.
[43] E. W. Robb, M. E. Munk, *Mikrochim. Acta* **1990**, I, 131–155.
[44] B. Curry, D. E. Rumelhart, *Tetrahedron Comput. Methodol.* **1990**, *3*, 213–238.
[45] F. W. McLafferty, D. B. Stauffer, *J. Chem. Inf. Comput. Sci.* **1985**, *25*, 245–252.
[46] P. Y. Chou, G. D. Fasman, *Biochemistry* **1974**, *13*, 222–241.
[47] W. Kabsch, C. Sander, *FEBS Lett.* **1983**, *155*, 179–182.
[48] N. Qian, T. J. Sejnowski, *J. Mol. Biol.* **1988**, *202*, 865–884.
[49] L. H. Holley, M. Karplus, *Proc. Natl. Acad. Sci. USA* **1989**, *86*, 152–156.
[50] D. G. Kneller, F. E. Cohen, R. Langridge, *J. Mol. Biol.* **1990**, *214*, 171–182.
[51] H. Bohr, J. Bohr, S. Brunak, R. M. J. Cotterill, B. Lautrup, L. Norskov, O. H. Olsen, S. B. Petersen, *FEBS Lett.* **1988**, *241*, 223–228.
[52] H. Bohr, J. Bohr, S. Brunak, R. M. J. Cotterill, F. Fredholm, B. Lautrup, O. H. Olsen, S. B. Petersen, *FEBS Lett.* **1990**, *261*, 43–46.
[53] H. Andreassen, H. Bohr, J. Bohr, S. Brunak, T. Bugge, R. M. J. Cotterill, C. Jacobsen, P. Kusk, B. Lautrup, *J. Acquired Immune Defic. Syndr.* **1990**, *3*, 615.
[54] J. D. Bryngelson, J. J. Hopfield, S. N. Sothhard, *Tetrahedron Comput. Methodol.* **1990**, *3*, 129–141.
[55] M. S. Friedrichs, P. G. Wolynes, *Tetrahedron Comput. Methodol.* **1990**, *3*, 175–190.
[56] G. L. Wilcox, M. Poliac, M. N. Liebman, *Tetrahedron Comput. Methodol.* **1990**, *3*, 191–211.
[57] J. Zupan, F. X. Rius, *Anal. Chim. Acta* **1990**, *239*, 311–315.
[58] M. Tusar, F. X. Rius, J. Zupan, *Mitteilungsblatt der GDCh-Fachgruppe „Chemie – Information – Computer (CIC)"* **1991**, *19*, 72–84.
[59] T. Aoyama, Y. Suzuki, H. Ichikawa, *J. Med. Chem.* **1990**, *33*, 905–908.
[60] T. Aoyama, Y. Suzuki, H. Ichikawa, *J. Med. Chem.* **1990**, *33*, 2583–2590.
[61] D. W. Elrod, G. M. Maggiora, R. G. Trenary, *J. Chem. Inf. Comput. Sci.* **1990**, *30*, 477–484.
[62] MOPAC, A General Molecular Orbital Program Package V4.0, QCPE.
[63] A. J. Gushurst, W. L. Jorgensen, *J. Org. Chem.* **1988**, *53*, 3397–3408.
[64] A. Fröhlich, J. Gasteiger, unpublished results.
[65] M. Tusar, J. Zupan in *Software Development in Chemistry 4* (Ed.: J. Gasteiger), Springer, Berlin, **1990**, p. 363–376.
[66] R. P. Lippmann, *IEEE ASSP Magazine* **1987**, *April*, 4–22.
[67] M. Otto, U. Hörchner in *Software Development in Chemistry 4* (Ed.: J. Gasteiger), Springer, Berlin, **1990**, p. 377–384.
[68] J. Gasteiger, X. Li in *Software Development in Chemistry 7* (Ed.: D. Ziessow], Springer, Berlin, **1993**; X. Li, J. Sadowski, C. Rudolph, J. Gasteiger, unpublished results.

Defect Chemistry: Composition, Transport, and Reactions in the Solid State; Part II: Kinetics**

By Joachim Maier*

Dedicated to Professor Hermann Schmalzried on the occasion of his 60th birthday

Within the last few decades—though with its beginnings traceable to as early as 60 years ago—a direction of research has developed almost unnoticed by the classical chemical disciplines, such that one can now recognize a chemistry *within* the solid state that is analogous to the long-familiar chemistry in the liquid state. It arises from those departures from the ideal structure that are thermodynamically unavoidable, the point defects, and is referred to as defect chemistry. It includes the description of ionic and electronic effects, and it considers diffusion as a special step of the overall reaction. This area of chemistry enables one to describe and treat in a unified way many apparently widely different phenomena such as ionic conduction in crystals, doping effects and p–n junctions in semiconductors, color centers in alkali metal halides, image development in photography, passivation and corrosion of metals, the kinetics of the synthesis and sintering of solid materials, the problems of rock formation during the earth's evolution, the mechanisms of gas sensors and high temperature fuel cells, the performance of photosensitive electrodes, variations of the electron balance in high temperature superconductors, elementary processes of heterogeneous catalysis, nonequilibrium transitions and oscillations in semiconductors in electric fields, and many more. In such phenomena the equilibrium concentration of defects has an important double role: it not only determines the disorder and the departures from the stoichiometric composition in the equilibrium state, but also, together with the mobility as the kinetic parameter, is the key parameter concerning the rates of physical processes, which are the main subject of the present discussion. Following the account of the thermodynamic fundamentals in Part I, this second part of the review will be concerned with kinetic processes. These are essentially the equilibration processes (physical diffusion, electrical conduction, chemical diffusion, and reactions) that take place under the influence of chemical and electric driving forces. As in Part I, here again the general characteristics of defect chemistry will clearly emerge, including the coexistence of ionic and electronic charge carriers, and the importance of the spatial coordinates. The concluding section will discuss some special characteristics of nonlinear processes that are too often overlooked in solid-state studies.

1. Introduction

Part I of this review[1] consisted of a detailed presentation which showed that in thermodynamic equilibrium all solids contain point defects whose nature and concentration depends not only on the material but also on the temperature, the hydrostatic pressure, and the chemistry of the environment—for example, the oxygen partial pressure in the adjacent phase in the case of a binary oxide. Such defects may take the form of extra "particles" (ions, electrons, etc.), missing particles, or foreign particles. In the same way as the H^+ and OH^- ions or dissolved foreign species in water, these defects determine not only the exact composition of the phase but also its reactivity and in particular and the transport processes within it. Although Part I was essentially confined to equilibrium thermodynamics, we already saw there that the concentrations of defects can be determined by measuring the ionic or electronic conductivities, which result in the ionic case from excess ions, vacancies, or foreign ions, or in the electronic case from excess electrons or electron holes.[2] The conductivity is extremely sensitive to the defect concentration, since it is normally only the defects that contribute, not the regular structural units. Moreover, as will be shown later, the conductivity is the key quantity in understanding the dynamic processes in solids. In this article, therefore, we shall start by considering the kinetic component of conductivity, which is the mobility of the point defects, or in chemical terminology the rate constant for the "hopping reaction". Next we will deal with the self-diffusion of the particles, then with the kinetics of "true" chemical reactions—first, as a simple example, the homogeneous case of the "dissolution" of oxygen in oxides, then as a phase-forming process the corrosion of a metal, and lastly a solid–solid reaction. In cases where such processes are diffusion-controlled the relevant kinetic parameters are the diffusion coefficients, which are closely related to the ionic and electronic conductivities. The concentrations of point defects are also decisive for the rates of local chemical reactions, which occur especially at surfaces (interfacial reactions, heterogeneous catalysis). The article will conclude by discussing nonlinear phenomena that are observed under conditions far removed from equilibrium.

[*] Prof. Dr. J. Maier
Max-Planck-Institut für Festkörperforschung
Heisenbergstrasse 1, D-W-7000 Stuttgart 80 (FRG)

[**] Part I: Thermodynamics appeared in the March issue of *Angewandte Chemie* [1].

2. General Features of Solid-State Kinetics

In contrast to the situation in liquids the regular structural units in solids are immobile, except for vibrations and rotations about their equilibrium positions. Nevertheless, there is a degree of internal mobility due to point defects. Figure 1 illustrates this by taking vacant crystal sites as an example.

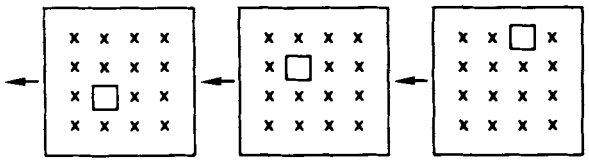

Fig. 1. Schematic representation of the migration of vacancies in a crystalline phase. The mass transport is in the opposite direction.

At sufficiently high temperatures a neighboring atom or ion can move into the vacant site, and the resulting newly formed vacancy then serves as a destination for a jump by another neighbor. From an energetic point of view the new situation does not differ from that existing previously. To be more exact, there is no overall change in the standard free enthalpy between initial and final state. However, it is necessary to supply an activation energy corresponding to the bottleneck (or, more correctly, the saddle point) for the jump process. (A more sophisticated model has been developed for the case of highly disordered materials.)[3] It is evident that the resulting mass transport can be described much more easily as the migration of a vacancy, rather than as a complex superposition of the motions of all the particles involved. In a similar way a particle occupying an interstitial lattice site also confers mobility, but here the direct hopping from one such interstitial site to the nearest equivalent site will nearly always be less energetically favorable than, for example, the jump of an interstitial particle towards an adjacent regular particle which itself is then forced into another vacant interstitial site.

It is a characteristic feature of the solid state that the positional coordinates must always be taken into account. Strictly speaking, all reactions in the solid state are heterogeneous, in other words they are associated with a transport component. So that we can approach the problem from a chemical standpoint, particle transport will be treated formally as a chemical reaction in the following discussion. If we represent such a general reaction by Equation (1), this can include not only

$$A(x) \rightleftharpoons B(x') \tag{1}$$

the case of a conventional homogeneous chemical reaction ($x \equiv x'$) but also that of a simple transport process (from x to x') when A is identical to B. Under equilibrium conditions there is no difference between the chemical potentials $\tilde{\mu}$ on the left- and right-hand sides of Equation (1). Consequently, for the case of particle transport, there must be no gradients in the electrochemical potential (The electrochemical potential is the sum of a chemical potential term and an electrical potential term, as explained in Part I). Conversely, the existence of gradients in the electrochemical potential means that there are driving forces causing a particle flow J, which, in the absence of external influences that may maintain the gradients, will lead to a restoration of the equilibrium. The behavior is depicted in Figure 2. If we express J as a power series in $(\partial/\partial x)\tilde{\mu}$ and neglect all higher terms beyond the linear term, we can describe the kinetic behavior in the neighborhood of equilibrium by Equation (2). Here the factors β_k

$$J_k = -\beta_k(\partial/\partial x)\tilde{\mu}_k \tag{2}$$

are the corresponding kinetic coefficients. This mathematical description[4] of linear irreversible thermodynamics[5, 6] is found in practice to be highly suitable in the case of the transport behavior, but for chemical reactions a linear equation of this kind can only be used in situations very close to equilibrium (Fig. 2). Before examining this in greater detail, let us consider the special cases of pure electrical conduction and pure diffusion (Fig. 2, right-, and left-hand branches, respectively, under "particle transport"). Pure diffusion occurs in the trivial case where the particles or defects concerned carry no charges. The only remaining driving force is then the gradient of the chemical potential μ; for sufficiently low concentrations this is given[7] by Equation (3), and thus

$$(\partial/\partial x)\mu = (RT/c)(\partial/\partial x)c \tag{3}$$

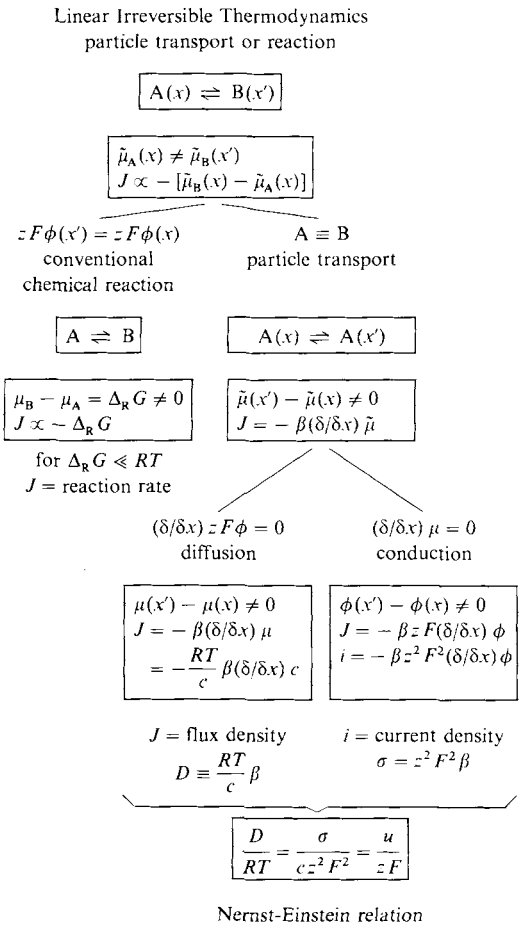

Fig. 2. Diagram summarizing nonequilibrium behavior in solids close to equilibrium. The generalized representation includes both conventional chemical reactions ($x \equiv x'$) and particle transport (A ≡ B) as special cases. Particle transport also includes the cases of pure diffusion ($z\Delta\phi = 0$) and pure electrical conduction ($\Delta\mu = 0$).

the concentration gradient can also be conceived as the driving force. Equations 2 and 3 then lead to Fick's law, in which the diffusion coefficient D is proportional to β/c. The other special case of pure conduction occurs for very high defect concentrations; the gradient of the chemical potential then disappears, resulting in a current that is proportional to the gradient of the electrical potential ϕ. This is obviously Ohm's law, with the conductivity σ proportional to β. It follows from this that the quantities D and σ are related through the coefficient β; for particles with charge number z the relationship is given by Equation (4), which is the Nernst–Einstein

$$\frac{\beta}{c} = \frac{D}{RT} = \frac{\sigma}{cz^2F^2} = \frac{u}{zF}. \tag{4}$$

relation (see bottom to Fig. 2), F is the Faraday constant). Here the quantity u is the mobility, which contains the same information, expressed in electrical units, as does the diffusion coefficient expressed in thermal units.

If we now take a more detailed look at the kinetics (Fig. 3), it becomes possible to specify the conditions under which the treatment given here is valid. It is not necessary to restrict the conditions to near-equilibrium. However, the simple rate equations that are familiar to the chemist, and are applied in the following discussion, are only valid if we assume low concentrations from the outset. We again treat reactions and transport in a unified way [Eq. (1)] with rates for both the forward and reverse processes, as is usual in chemical kinetics. In the general case the free energy profile for the process is assumed to be modified by an electrical potential (Fig. 3). If the variation in the electrical potential from the initial state to the final state is assumed to be linear, its effect is to alter the transition threshold roughly by the amount $\pm zF\Delta\phi/2$ and thus the usual chemical rate constants must be multiplied by $\exp(\pm zF\Delta\phi/2RT)$. In the case of a chemical reaction the linear relationship between "flow rate" (i.e. reaction rate) and driving force ($\Delta_R G$) only applies if $\Delta_R G/RT \ll 1$ (left-hand side of Fig. 3), a condition that is only satisfied very close to equilibrum. In the case of particle transport (right-hand side of Fig. 3) A and B are identical, and the energy profile is symmetrical (apart from the superimposed effect of an electric field, if present), so that $\Delta_R G^0 = 0$, since one is dealing with a shift of a defect from one lattice site to the nearest equivalent site. This involves passing through a saddle point whose energy is higher than that of the initial and final states. The difference between the initial (or final) state and the transition state is the free enthalpy of migration. The reaction coordinate in this case is the positional coordinate. In this sense, therefore, transport can perhaps be regarded as the simplest of chemical reactions, namely a positional rearrangement with a negligible standard affinity. The G^0 profile for this case is defined not by a snapshot, but by scanning the variation in free enthalpy as the defect successively occupies all the different positions. For the case of pure diffusion ($z\Delta\phi = 0$), this leads directly to Fick's first law, in which D corresponds to the chemical rate constant, that is it is proportional to $\exp(-\Delta G^{\neq}/RT)$. Thus the linear theory (as shown in Fig. 2) is found to be entirely valid in this case. For pure electrical conduction we must initially consider a nonlinear law (in fact a sinh $zF\Delta\phi/RT$ law, see Fig. 3).

However, the potential difference applied to the specimen is usually of the order of 1 V or less, and since the jump distance Δx is approximately 10^{-7} cm, compared with a specimen thickness of about 10^{-1} cm or greater, the relevant potential difference $\Delta\phi$ between adjacent sites is about 1 μV or less. In contrast, the quantity F/RT is of the order of 10 V^{-1} even at 1000 K, and thus $F\Delta\phi/RT \ll 1$. It is only necessary to use the high field law for very high voltages or very thin films, or for boundary layers at which there is a voltage drop of typically 0.5 V over the Debye length (typically 10^{-6} cm).[8]

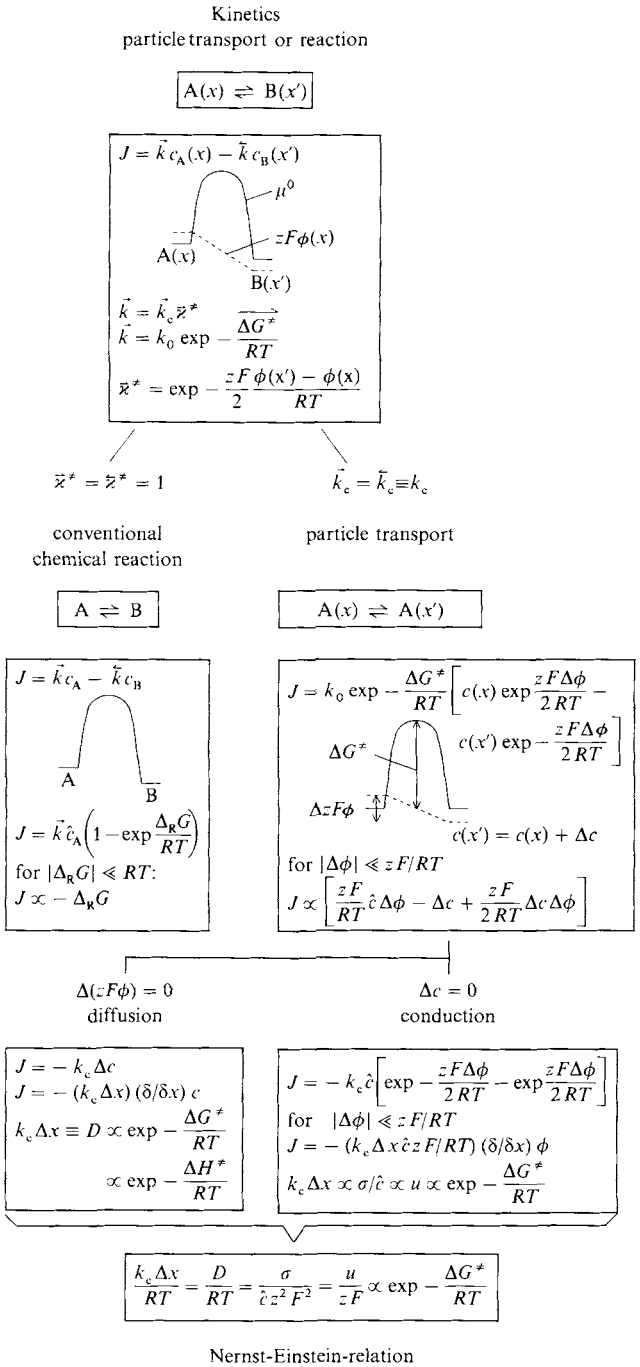

Fig. 3. Diagram summarizing the kinetic treatment of nonequilibrium behavior at low defect concentrations. Chemical reactions, diffusion, and electrical conduction appear as special cases ($\hat{c}$ = equilibrium concentration). In the case of transport, k_c is proportional to Δx.

In particular, in reactions carried out in electrochemical cells the relationship between current and voltage follows the Butler–Volmer equation[9] rather than Ohm's law (see Section 4.7). Ohm's law is obtained for near-equilibrium conditions by expanding the exponential function as a power series and truncating after the linear term. One can then treat c as approximately constant and replace it by the equilibrium concentration (Fig. 3). In addition to the Nernst–Einstein relationship [Eq. (4)], it is found that the mobility corresponds essentially to the rate constant for the hopping reaction (see Fig. 1), and a particular consequence of this is that the temperature dependence of the mobility is determined by the enthalpy of migration [Eq. (5)]. In the above approximation it is necessary to apply an external voltage (i.e. $\Delta\phi \neq 0$) to obtain any measurable effect at all, but $\Delta\phi$ has a negligible effect on the migration threshold.

$$\Delta H^{\neq}/RT = \Delta G^{\neq}/RT + \Delta S^{\neq}/R \qquad (5)$$

3. Chemical Diffusion

Although diffusion processes associated with compositional effects almost exclusively manifest themselves as changes in the positions of neutral components of a system, the defects that are involved carry electric charges, and consequently, such diffusion is always charge-coupled (ambipolar diffusion). For example, the diffusion of oxygen into an oxide (with a change in the "oxygen content") usually involves a coupled diffusion of O^{2-} ions and electrons, in which the electron flux must be twice as great as the ion flux and in the opposite direction.[10, 11] The process can thus be formally regarded as a diffusion of "O". It can be seen that there is a parallel between the treatment of chemical diffusion and that of a chemical equilibrium.[1] Corresponding to the chemical equilibrium conditions ($(\partial/\partial x)\tilde{\mu}_k = 0$), we have in this case the flow equations ($J_k \propto (\partial/\partial x)\tilde{\mu}_k$) and the electroneutrality condition corresponds to the coupling of the particle flows. Just as the potentials are linked to the control parameters in a chemical equilibrium, here the gradients must be so linked. The analysis shows that the oxygen flow J_O resulting from the coupling is given by Equation (6),

$$J_O = J_{O^{2-}} = -\frac{1}{2}J_{e^-} \propto -\frac{\sigma_{e^-}\,\sigma_{O^{2-}}}{\sigma_{e^-} + \sigma_{O^{2-}}}\frac{\partial \mu_O}{\partial x} = -\left(\frac{\sigma_{e^-}\,\sigma_{O^{2-}}}{\sigma_{e^-} + \sigma_{O^{2-}}}\frac{\partial \mu_O}{\partial c_O}\right)\frac{\partial c_O}{\partial x} \qquad (6)$$

and the proportionality constant relating it to the externally applied driving force is thus a mixed-transport coefficient (proportional to $\tilde{D}$).[10, 11] Such mixed-transport coefficients or chemical diffusion coefficients $\tilde{D}$ (essentially the expression in parentheses on the right-hand side of Eq. (6)) play a very important role in solid-state chemical kinetics and result in cases where no redox effects occur, mostly from the coupled, electrically neutral migration of different ionic species.[2, 12] If a current i is applied from an external source, the internal currents no longer cancel each other out. In this case it is also possible to have pure electrical conduction (as is usual in metals or solid electrolytes). In the general case the flow of one of the components k is the sum of a conduction term and a diffusion term (stoichiometry term). The conduction term is given by the external current multiplied by a weighting factor, the fractional contribution of the conductivity σ_k to the total conductivity σ, which results in the expression $(\sigma_k/\sigma)i$. The diffusion term is determined by the concentration gradient and the ambipolar diffusion coefficient.[10, 14]

The principles set out in this and the previous section will now be illustrated by some representative examples.

4. Examples

4.1. Example 1: The Mobility in Electrically Conducting Materials

Numerous examples of conductivity measurements in which the ultimate purpose was to determine the equilibrium concentration of defects have already been discussed in Part I of this review. In measuring the conductivity one automatically excludes diffusion terms, and pure conduction takes place. The electric fields used for such measurements are kept low enough to ensure that the normal Ohm's law behavior can be assumed in the calculations (see Fig. 3). Various elegant DC and AC methods have been developed[2, 11, 13, 14] for resolving the conductivity into its different components, such as electronic p-type or n-type conduction, or ionic conduction by vacancies or by interstitial ions. One such method, based on electrodes with a selective blocking function, has been mentioned in Part I,[1] and this will be referred to again briefly in Section 4.3. Another method, which does not involve measuring an external current, is the concentration cell experiment. This enables one to separate the ionic and electronic parts of the conductivity when these are of similar magnitudes.[15] In general, if a galvanic cell contains a solid electrolyte whose conduction is partly electronic, this acts as an internal short circuit, and consequently the measured e.m.f. is only a fraction of the Nernst value depending on the electronic contribution.[16]

The most important of the kinetic parameters which affect the conductivity is the mobility ($u \propto \sigma/c$), and the present discussion centers on this quantity. We note once again that, from the parallel with chemical kinetics, the mobility corresponds to the rate constant for the hopping reaction, apart from a proportionality factor that is unimportant in this context. The mobility term can be determined separately if the charge carrier concentration is known from measurements of the Hall effect or thermoelectric power, or is simply fixed by the level of doping. Figure 4 shows values for the mobilities of interstitial ions and vacancies in AgCl, determined from conductivity measurements on AgCl specimens with different levels of Cd doping. The Arrhenius plot is seen to be linear, as Figure 3 leads one to expect. The slope of each line yields the corresponding migration enthalpy; in agreement with computer simulations, this is found to be appreciably greater for transport by vacancies than for transport by interstitial ions.

In contrast, conduction by electronic charge carriers through a band mechanism is only slightly temperature dependent. In this case raising the temperature increases the scattering and thus slightly reduces the mobility. In the case

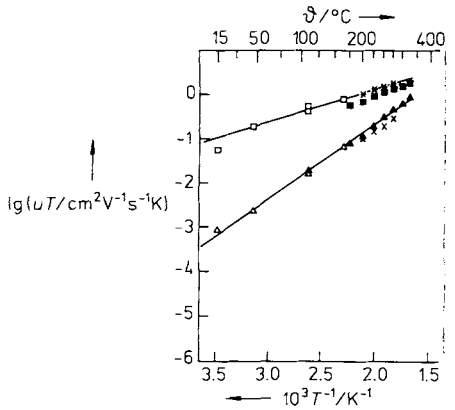

Fig. 4. Mobility of Frenkel defects in AgBr as a function of temperature [18]. (Interstitial mechanism: top line, vacancy mechanism: bottom line).

of acoustic phonon scattering the temperature dependence is typically of the form given in Equation (7). Figure 5 shows

$$u \propto T^{-3/2} \tag{7}$$

mobility data for SnO_2; at sufficiently high temperatures a power law similar to Equation (7) applies. At lower temperatures the mobility is probably limited by polaron transport, in which the polarization of the surrounding medium results in a thermally activated charge transport mechanism, involving a localized hopping process. In superconducting states, of course, u is infinite.

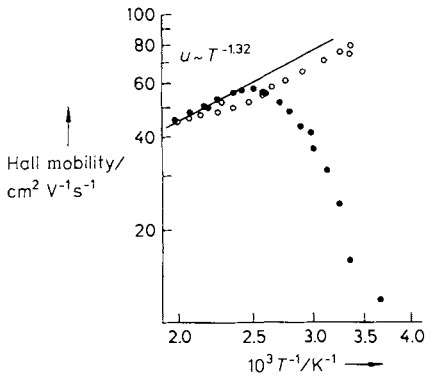

Fig. 5. Mobility of excess electrons as a function of temperature for two different SnO_2 samples, determined by Hall effect measurements [19].

4.2. Example 2: Tracer Diffusion in Oxides

As was shown previously, ionic conduction usually involves only one type of defect. The ionic conductivity is proportional to the concentration of this defect species and to its mobility u_k or diffusion coefficient D_k. Let us suppose that, in the absence of more detailed information about the defect chemistry, we group together all the relevant ions (oxygen ions in our example), regardless of whether they are fixed or mobile (that is, at regular or defect sites). We can then determine from σ_{ion} an average mobility, or more correctly a self-diffusion coefficient, which is, of course, much smaller than the mobility of the defect species.[12] Its value is given by Equation (8), and it therefore bears a simple relationship [Eq. (9)] to the diffusion coefficient D_k of the mobile defects.

$$D_{O^{2-}} = \frac{\sigma_{ion} RT}{c_{O^{2-}} 4F^2} \tag{8}$$

$$D_{O^{2-}} = \frac{c_k}{c_{O^{2-}}} D_k \tag{9}$$

Thus, whereas the diffusion coefficient of the defects, D_k, is proportional to their mobility u_k, $D_{O^{2-}}$ is directly proportional to the ionic conductivity, and thus to the product $u_k c_k$. $D_{O^{2-}}$ can also be determined by a tracer diffusion experiment, in which one observes the mixing of two isotopes, such as ^{16}O and ^{18}O, by the interdiffusion of the corresponding O^{2-} ions. In cases where the gas exchange is sufficiently rapid, the most convenient method is to enrich one portion of the natural O_2 gas with $^{18}O_2$, then to interrupt the experiment after a certain time and measure the change in mass of the gas phase. Alternatively, by using low temperatures one can freeze the concentration profile and analyze it by secondary ion mass spectrometry (SIMS) or by some other method. The ideal procedure would be to place the oxide specimen in contact with a second oxide specimen with a different isotope content, but this is not usually possible. The change of concentration with time in a defined volume is given by the difference between the inward and outward flow rates, and therefore by the flux divergence ($\partial c/\partial t = -\partial j/\partial x$), and since also for tracer diffusion Fick's first law is obeyed we obtain Equation (10). This equation (Fick's second law)

$$\partial c/\partial t = D^{Tr} \partial^2 c/\partial x^2 \tag{10}$$

can be solved to determine D^{Tr} for the appropriate boundary and initial conditions.[122] Except for some small corrections (correlation factors), D^{Tr} is identical to the self-diffusion coefficient mentioned previously, and from it one can calculate $D_{O^{2-}}$ and an ionic conductivity. Figure 6 shows some results from tracer–SIMS diffusion measurements on the $(La,Sr)_2CuO_4$ system. These can be understood on the basis of the defect chemistry described in Part I of this review (see Fig. 14 of Part I).[1] The relationship between D^{Tr} and σ_{ion} is much more complicated in the case of $YBa_2Cu_3O_{6+x}$, as different charge carriers are present (see Section 4.4). Figure 7 shows the results of tracer measurements on isotopically labeled iron in Fe_3O_4 as a function of the oxygen partial pressure.

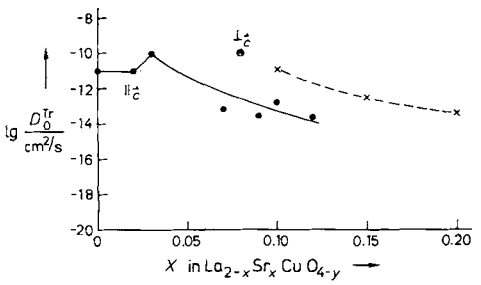

Fig. 6. Tracer diffusion results for monocrystalline (solid) [20] and polycrystalline (dashed line) [21] $(La,Sr)_2CuO_4$ materials at $T = 600\,^{\circ}C$; according to ref. [20].

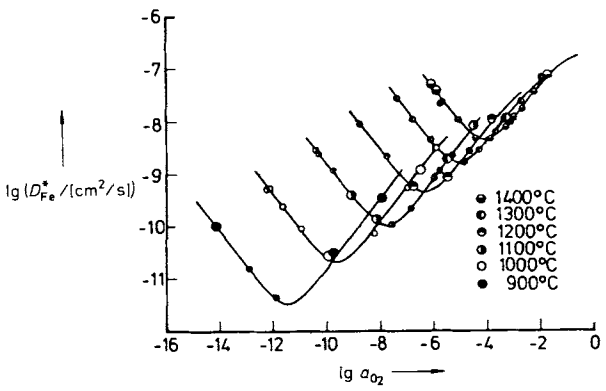

Fig. 7. Tracer diffusion results for ^{59}Fe in magnetite $Fe_{3-\delta}O_4$ [23]. D^* is the tracer diffusion coefficient.

The transition from an interstitial cation mechanism to a cation vacancy mechanism can be clearly seen.[23]

4.3. Example 3: Oxygen Uptake and Release in Oxides: Chemical Diffusion and Surface Reaction

In the previous example no chemical effects are involved; in other words there are no chemical gradients. The situation alters radically when we consider the uptake or release of oxygen in an oxide as a most simple example of a chemical reaction. Leaving aside surface reactions, we are again concerned here with a diffusion process, but one that is associated with a change of composition, namely of the local oxygen concentration. Our example is $SrTiO_3$, which was previously discussed in Part I of this review[1] in connection with the dependence of the electronic defect concentrations, and therefore of the conductivity, on the oxygen partial pressure. The data shown there (see Fig. 15, in ref. [1]) enable one to read off the initial and final concentrations, and hence the respective values of the conductivity, when the oxygen partial pressure is changed from P_1 to P_2. However, to determine the rate of approach to the final state it is necessary to consider the kinetics of the reaction [(Eq. (11)]. A knowledge of

$$SrTiO_{3-\delta} + \frac{\Delta\delta}{2} O_2 \rightarrow SrTiO_{3-\delta+\Delta\delta} \tag{11}$$

this rate is needed if, for example, the sensitive dependence of the electrical conductivity on the oxygen content is to be used as the basis of an oxygen sensor. Here, in contrast to Example 2, (Section 4.2) only the defects are involved in the diffusion. The relevant diffusion coefficient refers to the mobile particles, and is very much greater than $D_{O^{2-}}$. It can easily be seen that the diffusion of "O" into the material is an electrically neutral process involving the coupled migration of O^{2-} ions and electrons (at low oxygen partial pressures the mechanism involves oxygen vacancies, $V_O^{\cdot\cdot}$, and conduction electrons, e', at high partial pressure, $V_O^{\cdot\cdot}$ and holes, $h^{\cdot}$ (for the notation see also Part I,[1] Section 2)). This chemical diffusion coefficient is given by an expression [(Eq. (12)] which, as

$$\tilde{D} = \frac{RT}{4F^2} \frac{\sigma_{eon}\sigma_{ion}}{\sigma c_{O^{2-}}} \frac{\partial \ln a_O}{\partial \ln c_O} \tag{12}$$

expected from the equivalence of the ionic and electronic currents [see Eq. (6)], contains a mixture of ionic and electronic transport terms. It can be seen that for very good electronic conductors ($\sigma \simeq \sigma_{eon}$), the expressions for D^{Tr} [Eq. (8)] and $\tilde{D}$ are identical except for the thermodynamic factor $\partial \ln a_O / \partial \ln c_O$. However, owing to the high oxygen concentration (in contrast to the low defect concentration) and the strong ionic bonding, this factor differs greatly from 1 (a_O is the oxygen activity). Assuming that the defect chemistry is simple, the thermodynamic factor is approximately given by Equation (13), in which c_v and c_n are the concentrations of

$$\left(\frac{\partial \ln a_O}{\partial \ln c_O}\right) \simeq c_{O^{2-}} \left(\frac{1}{c_v} + \frac{4}{c_n}\right) \tag{13}$$

the oxygen vacancies and of the conduction electrons, respectively. For a purely ionic conductor, in which the ionic conductivity, and therefore also the concentration of ionic defects, are much greater than the corresponding electronic quantities, it follows from Equation (13) that $\tilde{D}$ is identical to the diffusion coefficient of the electronic defects (in this case D_n). This means that the rate of diffusion is limited by the electron flux. For an electronic conductor with an abundance of electrons, we have the opposite case in which $\tilde{D}$ is limited by the diffusion coefficient of the ionic defects D_v. However, there are many electronic conductors in which ionic defects predominate, resulting in the mixed case given by Equation (14). In the general case, assuming a simple defect chemistry, $\tilde{D}$ has a value intermediate between D_n and D_v [Eq. (15)].[24] In Equations (14) and (15) n and v are to be

$$\tilde{D} = \left(\frac{\sigma_v}{\sigma_n}\right) D_n = 4\frac{c_v}{c_n} D_v \tag{14}$$

$$\tilde{D} = \left(\frac{\sigma_n}{\sigma}\right) D_v + \left(\frac{\sigma_v}{\sigma}\right) D_n \tag{15}$$

understood as representing the dominant electronic and ionic defect species, respectively. Measuring the variation of the stoichiometry with time is a simple method of estimating the chemical diffusion coefficient, which thus describes the kinetics of the chemical reaction in the solid state (where this is diffusion-limited). Such measurements can be simply performed by using gravimetric or conductometric methods. Two alternative methods are described below.[11, 25]

The defect chemistry of nominally pure $SrTiO_3$ is very often dominated by the presence of iron impurities. A proportion of the iron ions (normally Fe^{3+}) are tetravalent, depending on the oxygen partial pressure, and in interaction with the normal defect chemistry. The associated transfer of an electron from the valence band to the iron level in the band gap can be described by Equation (16). The presence of

$$Fe'_{Ti} + h^{\cdot} \rightleftharpoons Fe^{x}_{Ti} \tag{16}$$

Fe^{4+} ions gives the oxide a reddish color, and their concentration can be measured in situ by optical absorption spectroscopy.[27] It can be shown that here too the chemical diffusion is, to a first approximation, governed by Fick's second law. The solution for small values of the time t, and the

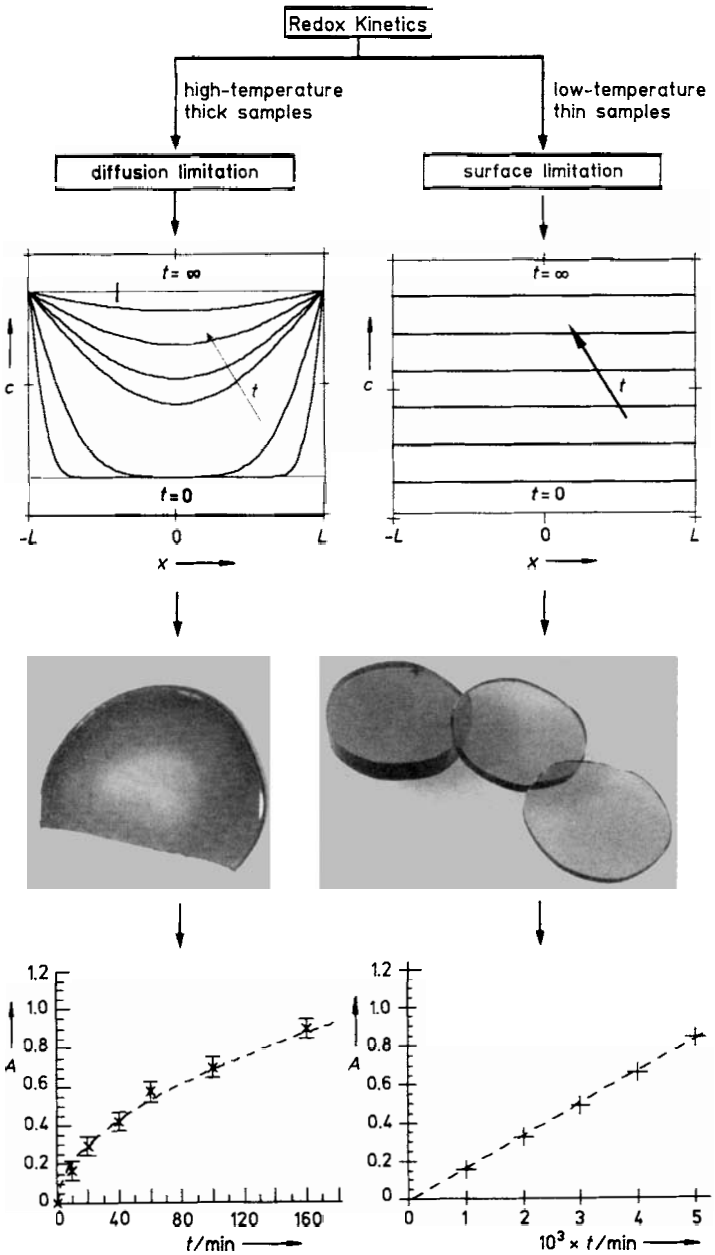

Fig. 8. Kinetics of the uptake and release of oxygen in $SrTiO_3$: theoretically predicted profiles, and experimental data from optical absorption measurements (see text) [25]. c = defect concentration, x = spatial coordinate, A = reduced absorption (arbitrary units).

appropriate boundary and initial conditions, gives a $\sqrt{t}$ law, from which $\tilde{D}$ can be calculated (Fig. 8 left-hand column) (As will be described in the next section, in this and many other cases, internal trapping effects must also be included in the analysis). In practice the overall process of oxygen uptake and release is much more complicated [Eq. (17)]. Following

$$\tfrac{1}{2}O_2(g) \rightleftharpoons \tfrac{1}{2}O_2\ (\text{surface}) \rightleftharpoons O_{ad} \rightleftharpoons O_{ad}^{2-} - 2e^- \rightleftharpoons O \qquad (17)$$

the arrival of the oxygen at the surface by gas diffusion, it must be adsorbed and must dissociate, then become ionized, pass through the phase boundary, and migrate through the space charge zones, before the chemical diffusion within the material can actually begin. The suggested sequence shown here does not show all the individual steps, nor does it take into account other possible reactions proceeding in parallel. The extent to which any one in this succession of migration and reaction processes may become a rate-limiting step depends on the region within which the state parameters fall. In fact it is found that at low temperatures the relative change of (reduced) optical absorption increases linearly with time for small values of t, indicating that under these conditions the rate-limiting step is not diffusion but the reaction at the interface (Fig. 8, right-hand column). For this case the photographic images show uniform coloration, in contrast to those for high temperatures in which color profiles corresponding to concentration profiles can be observed across the sample (diffusion-limited case). Results such as these allow quantitative determination of diffusion coefficients and rate constants.[25]

Another method, whose principle has been described by Yokota,[11] is based on earlier work by Wagner;[13] its application to yellow PbO is described here.[14] A sample of the oxide with a defined composition (corresponding to the value of the external oxygen partial pressure P_{O_2}) is compressed between two purely ionic conducting materials, sealed off from the laboratory atmosphere by a glass coating, and polarized by a constant current (or constant voltage). In contrast to the example described above, an electric current term is here superimposed on the chemical diffusion (as discussed earlier). The ionic and electronic currents cancel each other locally, except for the external current i. The variation with time of the concentration profile is determined, to a first approximation, by Fick's second law. As a consequence of the boundary conditions the development of the profile is symmetrical.[28] The driving force for the variation of the composition within the material arises from the fact that only the oxygen ions can cross the phase boundary between the oxide and the purely ionic conductor. Electrons cannot transfer through the phase boundaries either on one side (negative pole) or on the other (positive pole). The electron concentration profile that is thereby set up must, on electroneutrality grounds, be charge-compensated by an ionic profile. In the steady state only ionic currents exist, even

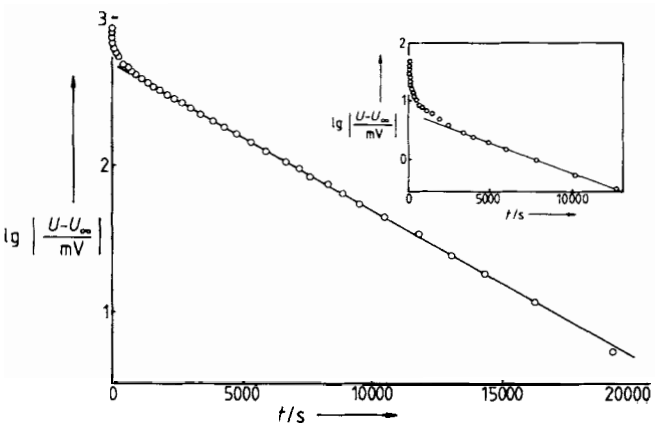

Fig. 9. The voltage of an electrochemical polarization cell consisting of PbO between ZrO_2 electrodes, during polarization with a constant current and during depolarization (i.e., after switching off the current, see insert). In the steady state the internal flow is purely ionic. In the transient state at sufficiently large values of t the voltage follows an exponential law, and from the time constants the chemical diffusion coefficient can be determined. $T = 503\,^{\circ}C$, $i = 21.83\,\mu A\,cm^{-2}$, $\tilde{D}$ (polarization) $= 2.3 \times 10^{-7}\,cm^2\,s^{-1}$, $\tilde{D}$ (depolarization) $= 2.2 \times 10^{-7}\,cm^2\,s^{-1}$.

locally; the ionic conductivity can therefore be separated from the total conductivity (which determines the voltage jump at the start of the experiment), and the chemical diffusion coefficient can be determined from the variation of the profile with time. It can be shown that for small values of t the change in the voltage is a linear function of $\sqrt{t/\tau}$, and for large values of t it is a linear function of $\exp(-t/\tau)$; here $\tilde{D}$ is inversely proportional to the time constant τ, which itself is proportional to the square of the sample thickness. The depolarization after switching off the current behaves similarly (Fig. 9).[10, 11, 14] The same method can also be used to determine ionic conductivities and chemical diffusion coefficients in efficient electronic conductors such as $YBa_2Cu_3O_{6+x}$ (Fig. 10).[26]

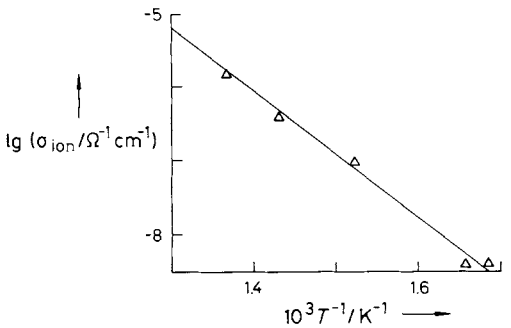

Fig. 10. The steady-state voltage as a function of temperature for an electrochemical polarization cell consisting of $YBa_2Cu_3O_{6+x}$ between ZrO_2 electrodes. The slope yields the ionic conductivity of $YBa_2Cu_3O_{6+x}$ [26].

4.4. Example 4: Modification of Chemical Diffusion by Trapping Effects

The normal relationships need to be radically modified when, in addition to the diffusion process itself, there are reaction processes, especially those associated with the trapping of electronic charge carriers by ionic centers.[29] Localized variations of concentration with time can then also arise from the source and sink terms associated with internal shifts in the equilibria of the trapping reactions, as indicated in Figure 11. These effects require modification not only of the

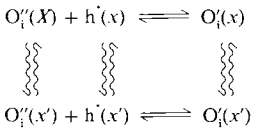

Fig. 11. Diffusion in a solid accompanied by changes in valency represented here as a combined reaction–diffusion process.

flow equations involving the diffusion coefficients, but usually also of the formulas for evaluating these by the electrochemical methods. The details will not be discussed here, but can be found in the literature.[14, 17]

The Fe-doped $SrTiO_3$ material discussed in the last section serves as a relatively simpe application. The usual expression for the chemical diffusion coefficient [Eq. (15)] gives good agreement with the observed temperature dependence at high temperatures, but at lower temperatures the predictions are in error by several orders of magnitude. The trapping reaction shown in Equation (16) is exactly the type of internal reaction that leads to a local particle production through the effects of diffusion, even when there is local equilibrium. It can be shown that Equation (15) must then be modified by including a trapping factor,[17] whose value can be calculated from a knowledge of the defect chemistry. The absolute calculation of $\tilde{D}$ then gives an excellent quantitative fit to the observed temperature dependence (Fig. 12). The underlying

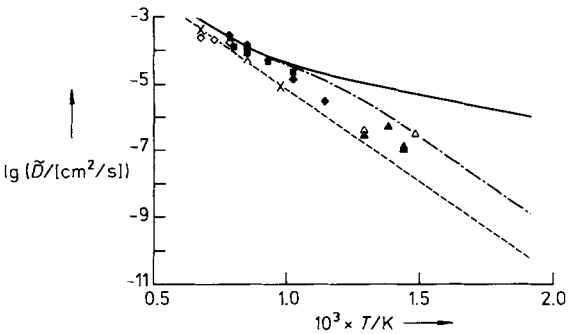

Fig. 12. Temperature dependence of the chemical diffusion coefficient for oxygen in $SrTiO_3$. When dynamic trapping effects are included the theory accounts satisfactorily for the data without recourse to a fitting parameter: —— $\tilde{D}$ without trapping, - - - $\tilde{D}$ with trapping, --- self diffusion coefficient of $V_O^{\cdot\cdot}$; this curve was calculated, symbols are measured values; according to ref. [25].

reason for this is that the process described by Equation (16) provides mobile electronic charge carriers by dissociation of the trapped states for example electron holes from Fe^{4+}, so that a different ($\sigma_{h^{\cdot}} \gg \sigma_{Fe^{4+}} \simeq 0$) effective concentration has to be considered.

For a solid such as YBa_2CuO_{6+x} in which, as explained in Section 3.1.3 of Part I of the review, the differently charged defects O_i'', O_i', and O_i^x must be taken into account, a more general treatment is needed. These defect species are again connected by redox reactions, but can also themselves contribute to the migration process.[14, 17] For this general case Equation (12) is replaced by Equation (18). Here σ_2 and σ_1

$$\tilde{D} = \frac{RT}{8F^2}\left[\frac{(\sigma_2 + 2\sigma_1)(\sigma_e - \sigma_1)}{\sigma} + 2\sigma_1 + 4s\right]\frac{d\mu_{O_2}}{dc_O} \qquad (18)$$

are the respective contributions of O_i'' and O_i' to the conductivity, and s is an analogous quantity that is proportional to the diffusion coefficient for O_i^x. Equation (18) can be put into a generalized form for all types of charge carriers.[14, 17]

For $YBa_2Cu_3O_{6+x}$ also, one can similarly determine the ionic conductivity and the chemical diffusion coefficient by a Wagner–Hebb polarization experiment,[26] and the self-diffusion coefficient of the oxygen ions by tracer experiments.[21] However, to understand the significance of the quantities measured and their interrelationships, a more detailed consideration is necessary, which takes into account

the redox interactions.[14, 17] In particular, the tracer diffusion coefficient is no longer proportional to the ionic conductivity, nor is the ionic conductivity in the polarized state necessarily the same as the normal ionic conductivity, owing to the dissociation processes. Furthermore, neutral defects play an important role in determining the behavior of the tracer and chemical diffusion coefficients. A simple statistical model based on the defect model in Part I (Section 3.1.3) predicts a thermodynamic factor for $YBa_2Cu_3O_{6+x}$ which is good agreement with the experimental results.[26]

For solid-state reactions that are diffusion-controlled, which is very often the case for specimens of macroscopic dimensions (thickness L), since $J \propto L^{-1}$ the most important kinetic parameter is nearly always the chemical diffusion coefficient. A simple example is the oxidation of a metal M, to its oxide, which was discussed many years ago by Carl Wagner.[31] The reaction begins at the gas–metal interface with the formation of a thin oxide layer. If the molar volume of the oxide in this layer differs significantly from that of the metal,[32] this usually results in the formation of islands or cracks allowing the reaction to progress further by gaseous diffusion (Fig. 13, left). If, on the other hand, a dense layer is formed (Fig. 13, right), further reaction is only possible if

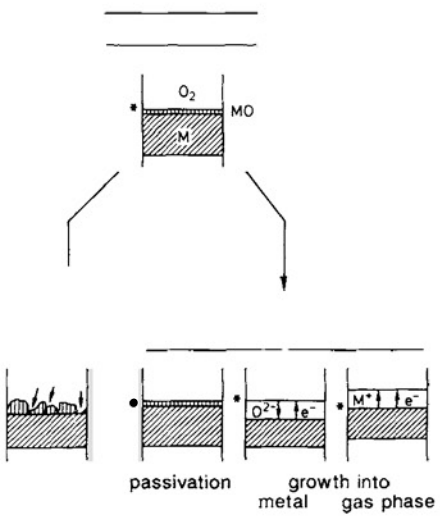

there is a chemical diffusion of either the metal (involving migration of M^+ and e^- in the same direction) or the oxygen (migration of O^{2-} and $2e^-$ in opposite directions). In the former case the oxide grows outward into the gas phase, and in the latter case it grows inward into the metal. If either the ionic or the electronic conductivity is negligibly small at the relevant temperature, as is the case for Al_2O_3 at room temperature, the defect layer has a passivating function.[33] Thus, corrosion of the type described above is only possible if an oxide phase with a mixed conduction mechanism exists. For example, in the case of SnO_2, corrosion would take place through a migration of oxygen vacancies and conduction electrons in the same direction, whereas for ZnO the probable mechanism involves a migration of zinc ions (in the interstitial lattice) and electrons in the same direction (since this is an n-type semiconductor).[34] The effective flow rate of the metal M through the oxide, which determines the rate of reaction, can be determined from Equation (6). This leads to Equation (19). As the flow geometry is known, the rela-

$$J_M = J_{M^+} = J_{e^-} \propto \frac{\sigma_{M^+}\sigma_{e^-}}{\sigma}\frac{\partial \mu_M}{\partial x} \propto \left\langle \frac{\sigma_{M^+}\sigma_{e^-}}{\sigma} \right\rangle \frac{\Delta \mu_M}{L} \qquad (19)$$

tionship can also be expressed in integrated form [Eq. (19), second part]. Here the brackets indicate an average value, since there is usually an appreciable variation in composition, and therefore in conductivity, through the thickness L of the oxide layer. The chemical potential of the metal has its highest (and maximum possible) value on the metal side of the interface, and its lowest value on the gas side; that of the oxygen has its lowest (and minimum possible) value on the metal side, and its highest value on the gas side.

The four main factors influencing the flow rate can be identified (1, 2, 3, and 4 below) from Equation (19). For a high rate the driving force, which is the (average) gradient of the thermodynamic potential for this component ($\Delta\mu_M/L$), must be as large as possible (there is a linear relationship between the flow rate and the driving force). Since there is no gradient on the metal side, this requirement is fulfilled when 1) the oxygen partial pressure is as high as possible, and 2) the layer thickness is as small as possible. However, a high rate also requires that the specific kinetic coefficient (the expression in parentheses) should be sufficiently large; thus the electronic conductivity 3) and the ionic conductivity 4) must both be sufficiently large. (If neutral O atoms can migrate, as is possibly the case in $YBa_2Cu_3O_{6+x}$, then $D_{O_i''}$, represented by s in Eq. (18), also becomes important.) Since the flow rate J, and therefore ultimately the resulting rate of increase of the oxide layer thickness ($\dot{L}$), are both inversely proportional to the thickness ($i \propto L^{-1}$), this yields the well-known square root law [Eq. (20)].[31]

$$L \propto \sqrt{t} \qquad (20)$$

Figure 14 shows that these predictions are confirmed in the case of the oxidation of zinc. The slope is a measure of the

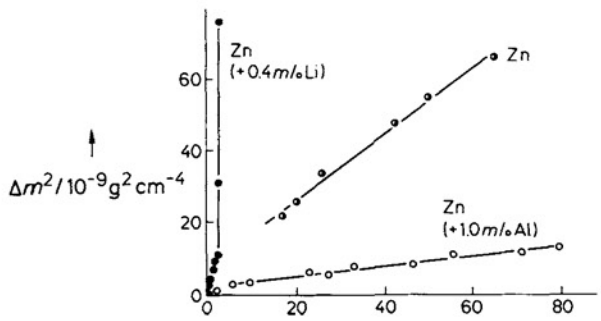

Fig. 14. Progress of corrosion in zinc ($Zn + 1/2\,O_2 \rightarrow ZnO$) with and without doping (Δm = increase in mass, which is proportional to the thickness of the oxide layer; one-dimensional geometry is assumed) [35]. $k_d \propto \langle \sigma_{Zn^{2+}} \rangle$, $\sigma_{Zn^{2+}} \propto [Zn_i^{\cdot\cdot}]$; $T = 390\,^{\circ}C$. (m/o Al: mol % Al).

effective rate constant, which is proportional to $\langle \sigma_{ion}\sigma_{e^-}/\sigma \rangle$. Since electronic conduction predominates in ZnO, this expression reduces simply to $\langle \sigma_{ion} \rangle$. The steep temperature dependence of the ionic conductivity readily explains why the rate of growth of the oxide layer thickness is extremely sensitive to the temperature. The effects of homogeneous doping are clearly evident in Figure 14. In ZnO the ionic conductivity is probably due mainly to zinc ions in the interstitial lattice, although oxygen vacancies are an alternative possibility; in any case, however, the charge carriers are positively charged ionic defects. In either case doping the metal (as in Part I[11]), and therefore also the oxide, with lithium (Li'_{Zn}) causes an increase in the ionic charge carrier concentration. This results, as expected, in much faster corrosion. The effect of the relatively small change in the activity of the metal is insignificant here. Doping with aluminum, which leads to the formation of $Al^{\cdot}_{Zn}$ (or $Al_i^{\cdot\cdot\cdot}$), has the opposite effect, giving a considerable degree of corrosion protection.

Solid–solid reactions can be approached in a similar way. An example is the reaction whereby a spinel is formed from the oxides of two elements[2a] (in this case the mechanism may also involve an ambipolar diffusion of the different cationic species). Figure 15 shows that at large layer thicknesses the growth follows a $\sqrt{t}$ law, whereas for small thicknesses the growth is linear. For small values of L the diffu-

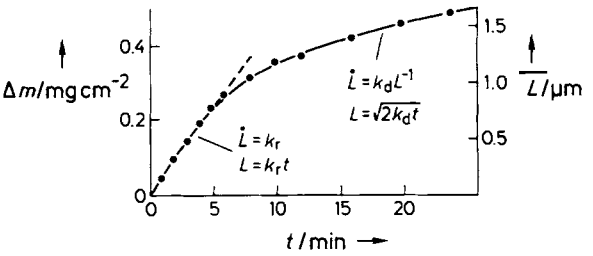

Fig. 15. Growth of the spinel layer ($ZnAl_2O_4$) in the reaction between the oxides ZnO and Al_2O_3 (one-dimensional geometry) [2b]. $T = 1350$ °C.

sion through the thickness is so rapid that the rate of growth $\dot{L}$ is determined by the surface reaction, and is independent of L, and thus $L(t)$ is a linear function. From the foregoing discussion it is clear that, even for the purely diffusion-controlled case, the predicted $\sqrt{t}$ law is based on a number of idealized assumptions (e.g., that space charge effects are negligible, that the interface is planar, and that one-dimensional geometry applies). It would be wrong to suppose that the above approach can lead to a complete and accurate treatment of a real reaction that takes place entirely in the solid state (with complications such as multiple phases, complex – possibly fractal – grain size distributions and geometries, the appearance of new phase boundaries, etc.), even though various attempts at such analyses have been reported. Nevertheless, useful information can be obtained, qualitatively at least, about important parameters, for example the requirements of intimate contact, small grain size, large driving force, or high temperature.

4.6. Example 6: Catalysis at the Surface and in the Interior of Solids

By its presence in a reacting system a catalyst alters the free activation energy but not the position of the equilibrium. This is expressed by Equation (21), where cat represents

$$d\Delta_R G^\circ/d[\text{cat}] = 0 \mp d\Delta G^*/d[\text{cat}] \quad (21)$$

the catalyst. The commonest examples of heterogeneously catalyzed reactions are those in which a solid influences a reaction in the gas state. The usual mechanism involves the adsorption of gas molecules at the surface followed by a reaction in the surface region. The effect of the catalyst in speeding up the reaction relies firstly on the increase in the effective particle concentration. However, in addition to the presence of adsorption centers, it is essential that rapid diffusion should be possible at the surface. Therefore it is not surprising that mixed conductors, a class that includes many transition metal oxides, often have very good catalytic properties.

A surface or interface can be treated as an extended defect, which is characterized by a surface tension; alternatively it can be regarded as an ensemble of interacting point defects, possessing a chemical standard potential different from that of the bulk.[36] In this way, based on the Langmuir theory, the adsorption of a gas molecule G onto the catalyst can be described by Equation (22), in which V_{ad} and G_{ad} are surface

$$G + V_{ad} \rightleftharpoons G_{ad} \quad (22)$$

defects. This might, for example, represent the adsorption of N_2 onto the iron catalyst in the Haber–Bosch ammonia synthesis. By applying the law of mass action to Equation (22) we obtain the familiar Langmuir equation [Eq. (23)], in

$$P_G(1 - \theta) = \theta/K_{ad} \quad (23)$$

which θ is the fraction of the surface sites that are occupied.[37] In many cases the catalyst increases the reaction rate to such an extent that the adsorption becomes the rate-determining step. Since we are dealing with a typical chemical reaction, similarly as in the case of dissociation, recombination, and desorption that might follow, the rate can be adequately described by usual kinetic relationships (for example, forward rate $\propto P_G\theta$) under nonequilibrium conditions. Only when the conditions are very close to equilibrium does this relationship reduce to one of proportionality to the free reaction enthalpy, as is required by linear irreversible thermodynamics (see Figs. 2, 3).

An elegant example of how the defect chemistry influences reaction rates is the HCl elimination reaction of *tert*-butyl chloride, which has been investigated by Simkovich and Wagner.[38] Acid- and base-catalyzed homogeneous elimination reactions are well known in organic chemistry. As described in Part I, doping AgCl with $CdCl_2$ increases the concentration of vacancies that act as bases. It is possible that here it facilitates the detachment of a proton (with subsequent or simultaneous elimination of the chlorine ion). The experiments show that the rate constant is, in fact, proportional to the cadmium concentration.

More recent experiments with AgCl heterogenously doped by contact with Al_2O_3 have yielded a deeper understanding.[39] As expected from the analogy between heterogeneous and homogeneous doping as explained in Part I, the rate of elimination of HCl from *tert*-butyl chloride is in-

creased considerably by the presence of $AgCl:Al_2O_3$ dispersions. Figure 16 shows the pressure increase measured during the reaction. Evidently the increased V'_{Ag} concentration

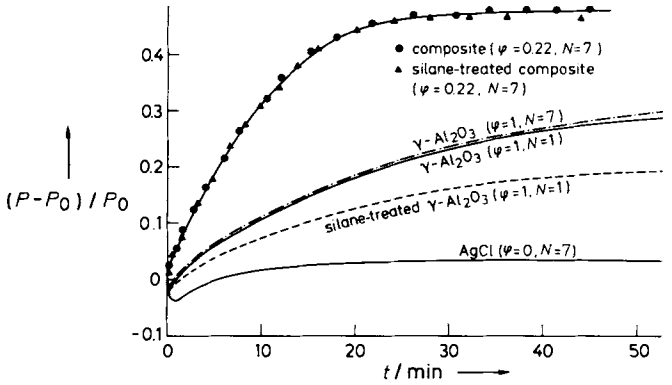

Fig. 16. Fractional pressure increase as a measure of the progress of the reaction during the elimination of HCl from *tert*-butyl chloride, showing the catalytic effect of silver chloride heterogeneously doped with Al_2O_3 (φ = volume fraction of Al_2O_3 in the catalyst, N = number of catalyst pellets). The effects of pure Al_2O_3 and pure AgCl are both very much smaller (despite the greatly increased specific surface area of the former) [39]. T = 423 K, particle size = 0.06 μm.

has the effect of a basic catalyst, facilitating the adsorption of *tert*-butyl chloride and the detachment of a proton. As in the discussion of the boundary effects on the conductivity (see Part I), data on the conductivities of such composite electrolytes[1] yield quantitative information about rate constants as functions of volume fraction, particle size, temperature, and interface chemistry, but restricted space does not allow a detailed description here.

Defect chemistry in the bulk is of special interest in relation to electrocatalysis. In a hydrogen–oxygen fuel cell a considerably higher efficiency is attained than by direct combustion to water, since the chemical energy is converted directly into electrical energy instead of through heat energy. In addition to the importance of the electrolyte (for example, homogeneously doped ZrO_2 as a solid electrolyte oxygen vacancies as charge carriers see Fig. 12 of Part I[1]), the electrodes too play a vital role. If conventional electrodes are used, then the required reaction can only take place at the three-phase junction between the electrode (electron source or sink), the electrolyte (an O^{2-} or H^+ conductor), and the gas phase (O_2–H_2 reservoir), as in the upper diagram of Figure 17. If instead a mixed conductor is used for the electrodes with, for example, O^{2-} and e^- as charge carriers, as is the case for $(La,Sr)CoO_3$, then oxygen can migrate through the solid by chemical diffusion, and oxygen (or hydrogen) can enter at any point on the electrode surface (Fig. 17, lower).

In conclusion it must be mentioned that homogeneous catalysis can also be observed within the solid itself. An example is the more rapid transfer of electrons from the valence band into the conduction band, resulting in the formation of an electron–hole pair (or the reverse process of recombination), that may take place when states within the band gap (recombination centers) are also involved. The process is given, in the structure elements notation, by Equations (24)–(26), where VB and CB represent the valence and conduction bands, respectively. Equation (24) describes the transfer of an electron from the valence band into the redox level, and Equation (25) that of an electron from the redox level into the conduction band. The sum of these two equations is the band-band transfer reaction [Eq. (26)]. In the building elements notation the sum is the pair formation reaction [Eq. (27)] that is already familiar from Part I.

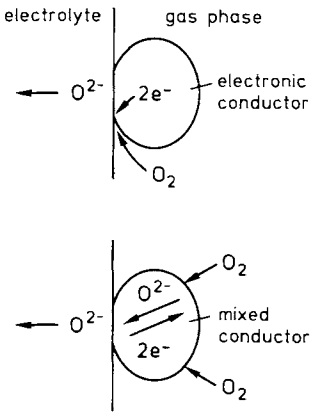

Fig. 17. With conventional metal electrodes, oxygen uptake can only take place at a three-phase junction. With an oxide mixed conductor as the electrode, oxygen can enter at any point on its surface.

$$e'_{VB} + M^{+\,+} \rightleftharpoons M^+ + V_{VB} \quad (24)$$

$$M^+ + V_{CB} \rightleftharpoons M^{+\,+} + e'_{CB} \quad (25)$$

$$e'_{VB} + V_{CB} \rightleftharpoons e'_{CB} + V_{VB} \quad (26)$$

$$\text{nil} \rightleftharpoons e' + h^{\cdot} \quad (27)$$

4.7. Example 7: The Electrochemical Transfer Reaction

The transfer of a charge carrier from the surface into the bulk is neither a conventional reaction ($A \neq B$, $x = x'$ nor a pure transport process ($A = B$, $x \neq x'$). Over the reaction distance there exists a strong electric field as well as a difference in the standard potential. Here, therefore, the analysis of an electrochemical reaction, as represented in Figure 3, must be applied in its most general form [Eq. (1)]. If the current is limited by this transfer step, as is very often the case when the diffusion in the bulk and the sorption at the surface are both rapid, the current–voltage curve takes the form described by the Butler–Volmer equation.[9] Figure 18 shows a current–voltage characteristic measured for CaO-doped CeO_2.[40] At high overvoltages the logarithm of the current, and not the current itself, is a linear function of the overvoltage (i.e. Tafel law instead of Ohm's law). A direct proportionality law only applies close to zero voltage ($U \rightarrow 0$). The resistance corresponding to the ohmic regime is proportional to the exchange current density, which is a measure of the reversibility of the electrode reaction, and can also be interpreted in terms of the defect chemistry.

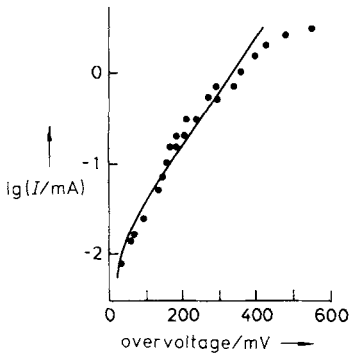

Fig. 18. The steady-state current-voltage characteristic for CaO-doped CeO_2. The kinetic behavior is entirely determined by the phase boundary transfer step, resulting in a markedly nonlinear characteristic [40].

4.8. Example 8: Nonlinear Effects

It has been amply demonstrated here that in transport processes there is normally a linear relationship between rate and driving force (see Fig. 2). Nevertheless, it has been mentioned at several points (e.g., in Section 4.7) that this no longer applies for large driving forces; such behavior is especially common for field effects, and even more so for chemical reactions. In this section, however, the emphasis will be on the type of nonlinear effects that are characteristic of complex systems under conditions far from equilibrum.[41] Even for some quite simple reaction schemes, including those encountered in defect chemistry, conditions leading to nonlinear behavior can arise very easily.

A necessary criterion for equilibrium in a system is that there is no entropy production within the system. In the nonequilibrium case the entropy production is always positive for any process, in accordance with the second law of thermodynamics. Consequently, any (slight) departure from equilibrium results in a retroactive force (negative feedback); this tends to restore the equilibrium state, which is thereby stabilized. Often, however, there are external conditions that hinder the system from attaining its equilibrium state; an example is the previously described case of a specimen through which a current is passed and in which the electron current is blocked by ionic conductor contacts. If a constant voltage is applied in this case, then a steady state becomes established, in which a (reduced) ion current flows through the circuit (cf. the measurement of the ionic part of the conductivity in $YBa_2Cu_3O_{6+x}$, as mentioned in Section 4.3). If the applied voltage is sufficiently small, so that the conditions are close to equilibrium, the entropy production is, of course not zero, but at a minimum according to the principle of Glansdorff and Prigogine.[41] It can also be shown that a steady state close to equilibrium is stable. However, under conditions far from equilibrium we have the interesting situation that a steady state is no longer necessarily stable, and such states can then undergo changes in a variety of ways. The most impressive examples of this are found in living organisms (usually involving chemical reactions).

A kinetic peculiarity that can very easily result in a system becoming nonlinear, and therefore interesting, is autocatalysis (see Fig. 19, top). The process shown here (top row) represents, quite generally, a growth reaction; for example, this might be the multiplication of bacteria, or the growth of a city, as well as impact ionization in a solid (in which an electron already present gives up some energy to form a new electron–hole pair).[41] In such a process the increase in concentration of the product causes an acceleration of the reaction, and the system explodes or produces an allergic response. Here there is a positive feedback mechanism, which drives the system further from equilibrium. It can very easily be shown that Equation (28) then holds. (If the back reaction becomes important, its rate is proportional to $[A]^2$, and in the neighborhood of equilibrium a negative feedback becomes dominant [Eq. (29)], as one expects.) Such a destabi-

$$\delta[A]^{\cdot}/\delta[A] > 0 \tag{28}$$

$$\delta[A]^{\cdot}/\delta[A] < 0 \tag{29}$$

lizing relationship between flow and driving force (e.g., between current and voltage) often occurs in solids when the current density in the system falls with increasing voltage (negative differential conductivity). For example, the impact ionization already mentioned acts in this way.[43] In the second row of Figure 19 the "growth reaction" is accompanied by a competing "decay reaction". Whether or not the species X "survives", to use the biological term, depends not only on the rate constants but also on the "food supply" [A]. If the stationary solution $[X]_{ss}$ (zero or finite) is plotted as a function of [A], it is found that there is a characteristic quantitative change corresponding to a nonequilibrium phase transition. Where there are several species X, the question of whether or not a given species survives is determined entirely by the rate constants and the food concentration, which is assumed to remain constant and is thus inexhaustible. On the other hand, if [A] is not inexhaustible there is a competition situation in which the survival criteria become ever more severe as the process continues, as analyzed by Eigen.[44] If the surviving species now undergo modification, for example through the effects of radiation (mutation in the biological case), these new variants may either replace the old ones or die out. It can be seen that under nonlinear conditions, even very simple reaction sequences can lead to effects analogous to the "biological" phenomena of growth, selection, and mutation. A slightly more complicated reaction scheme can lead to reactions that oscillate with time; examples include the Lotka–Volterra and Belousov–Zhabutinski reactions.[41] The analysis also explains certain spatial effects, especially spatially periodic patterns such as the dissipative structures in the Belousov reaction, or patterns observed in biologial systems.[42] Here the spatial coordinate enters into the analysis due to the fact that diffusion is now an important part of the overall process. Instabilities can destroy the spatial symmetry in such cases. An increasing divergence from equilibrium, passing successively through a number of bifurcation points, can eventually lead to a fractal pattern characterized by a deterministic chaos situation (in which the end result cannot be predicted).

The above discussion obviously has important implications for defect chemistry. Even a small degree of complexity in defect reactions is enough to lead to such effects. Moreover, the reactions are usually linked to diffusion processes. In semiconductor physics especially, effects of the kind de-

autocatalytic reaction	$A + X \longrightarrow 2X$	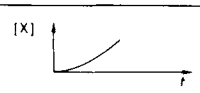	growth, positive feedback
autocatalytic + decay reaction	$A + X \underset{k_2}{\overset{k_1}{\rightleftharpoons}} 2X$ $X \xrightarrow{k_2} Z$	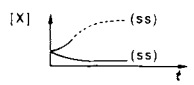	growth or death
no selection pressure	$[A] = \text{const}$ $W_c = k_1[A] - k_2$		nonequilibrium phase transformation bifurcation
autocatalytic + decay + selection pressure (+ perturbation)	$A + X \longrightarrow 2X$ $X \longrightarrow Z$ $[A] \neq \text{const}$ $W_c = f(t)$	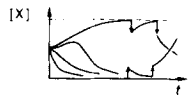	competition selection mutation
Lotka–Volterra reaction scheme	$A + X \longrightarrow 2X$ $X + Y \longrightarrow 2Y$ $Y \longrightarrow Z$	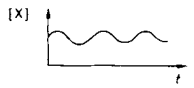	structurally unstable oscillation
Brusselator reaction scheme	$A \longrightarrow X$ $2X + Y \longrightarrow 3X$ $B + X \longrightarrow Y + D$ $X \longrightarrow Y$	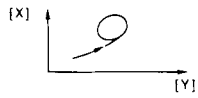	limit cycle oscillation
or catalytic CO oxidation	$(CO + O \rightleftharpoons CO;\ Pt_{hex} \rightleftharpoons Pt_{sq})$	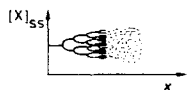	symmetry breaking, deterministic chaos
above reaction scheme + diffusion	(e.g. $X(x) \rightleftharpoons X(x')$	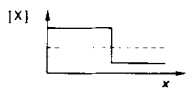	compartmentation, dissipative structure in space

Fig. 19. Summary of chemical kinetics under conditions far from equilibrium, showing that even quite simple reaction sequences can result in typical nonlinear phenomena, such as kinetic phase transformations, dissipative structures, and deterministic chaos (see text). B = bifurcation parameter, x = site.

scribed have been observed.[43] A typical autocatalytic reaction is the impact ionization mentioned earlier. Here, for example, an electron whose energy lies in the conduction band causes the formation of a new electron–hole pair as in Equation (30) (the reverse process of Auger recombination),

$$e' \rightleftharpoons 2e' + h^{\bullet} \tag{30}$$

so that the overall effect is an electron-catalyzed growth in the electron concentration. The departure from equilibrium can also often be controlled by an external voltage (overvoltage). Figure 20 shows a nonequilibrium phase transition observed in gold-doped silicon when the applied voltage exceeds a critical value. This corresponds exactly to the third diagram in Figure 19. Here the relevant growth and decay

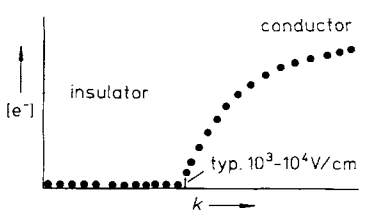

Fig. 20. Nonequilibrium phase transition (from insulator to conductor) in Au-doped silicon, controlled by varying the applied voltage in the nonlinear region [43]. $[e^-]$ = concentration of stationary electrons, k' = rate constant of the impact ionization.

mechanisms are impact ionization [Eq. (30)] and band–band

$$e' + h^{\bullet} \rightleftharpoons 0 \tag{31}$$

recombination [Eq. (31)]. Since the dependent variable in this case is the stationary electron concentration, the effect observed is a (voltage-induced) insulator–conductor transition. Figure 21 shows current oscillations observed with different values of the applied voltage for doped germanium at high electric field strengths, and simultaneous irradiation in the far IR region. As the field is increased the oscillation period is doubled, and eventually deterministic chaos is reached. This is apparent from the "phase portraits" (I vs. $\dot{I}$),

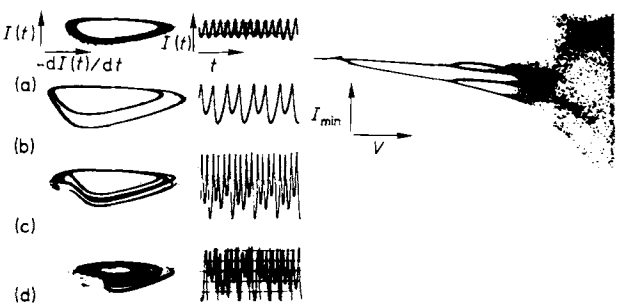

Fig. 21. Periodic structures and chaos phenomena in germanium, controlled by varying the applied voltage in the nonlinear region [45].

from the time evolved $I(t)$, and from the plot of the current minima as a function of the voltage.[45] Finally, Figure 22 shows images from a nonequilibrium structure in p-type germanium, recorded with a scanning electron microscope by using the EBIC (electron-beam-induced current) technique.[46] The bright lines (current filaments) represent zones in which the electron concentration has changed. These are only observed under nonequilibrium conditions, and accordingly disappear when the current is switched off. Spatial (and also temporal) periodic structures and deterministic chaos behavior can also be observed under suitable conditions during the catalytic oxidation of CO on platinum surfaces.[47] The study of nonlinear effects in solids, especially with regard to ionic conduction phenomena, and questions of the morphology can be expected to reveal many more surprises in the future.

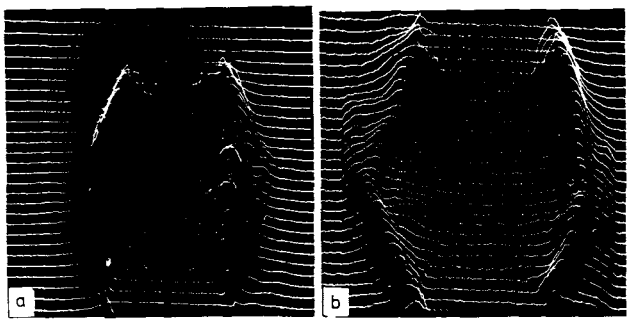

Fig. 22. Current filaments observed by the EBIC (electron-beam-induced current) technique in p-type germanium with two different voltages [46].

5. Summary

The most important points that have been discussed qualitatively in the two parts of this article, the thermodynamic and the kinetic, are the following:

1) All solids with ordered structures exhibit a finite concentration of point defects in thermodynamic equilibrium. Although these are of no consequence for some properties, they play a key role in a wide range of phenomena of importance in chemistry, especially transport and reactivity. With regard to properties such as these, the behavior of a solid cannot be predicted without a prior knowledge of its detailed composition and therefore of the state parameters that control it, for example the oxygen partial pressure in the case of an oxide.

2) Defect chemistry, which is the study and quantitative description of the nature and concentration of such defects and of their interactions, is a logical extension of the solution-state chemistry of the relevant species, of which the most familiar example is the chemistry of aqueous solutions. In an analogous way defect chemistry provides the basis for the thermodynamic and kinetic treatment of solid-state chemistry.

3) As well as leading to a universally valid treatment of the chemistry of ions in the condensed state, the approaches developed in defect chemistry also provide a unified description of ionic and electronic charge carriers, allow boundary layer effects to be incorporated into the overall theory, and enable diffusion to be treated as a special case of an elementary chemical reaction step. In particular, every solid-state chemical reaction must begin at a boundary and extend into the interior by chemical transport.

4) In view of the above, defect chemistry, which is the chemistry of the solid state, is an essential foundation stone of modern materials research. This review has aimed to present the case for defect chemistry, and the examples described are a testimony to its capabilities.

Received: April 1, 1992 [A 896 IE]
German version: *Angew. Chem.* **1993**, *105*, 558

[1] Part I: J. Maier, *Angew. Chem.* **1993**, *105*, 333; *Angew. Chem. Int. Ed. Engl.* **1993**, *32*, 313.
[2] Some recommended textbooks dealing with the field are: a) H. Schmalzried, *Solid State Reactions*, Verlag Chemie, Weinheim, **1981**; b) H. Schmalzried, N. Navrotsky, *Festkörperthermodynamik*, Verlag Chemie, Weinheim, **1975**; c) K. Hauffe, *Reaktionen in und an festen Stoffen*, Springer, Berlin, **1986**; d) F. A. Kröger, *Chemistry of Imperfect Crystals*, North Holland, Amsterdam, **1964**; e) H. Rickert, *Electrochemistry of Solids. An Introduction*, Springer, Berlin **1988**; f) Also strongly recommended is the review by A. B. Lidiard, *Handbuch der Physik* **1957**, 20, 246.
[3] K. Funke, *Solid State Ionics* **1986**, *18/19*, 183.
[4] Strictly speaking Equation (2) should, for greater accuracy, also take into account the electrochemical potential gradients of other particles (see also ref. [5]).
[5] L. Onsager, *Phys. Rev.* **1931**, *37*, 405; *ibid.* **1932**, *38*, 2265.
[6] S. R. de Groot, *Thermodynamics of Irreversible Processes*, North Holland, Amsterdam, **1951**; I. Prigogine, *Etude thermodynamique des phénomènes irreversibles*, Dunod, Paris, **1947**.
[7] As explained in Part I [1] for low concentrations the chemical potential μ is a linear function of the logarithm of the concentration.
[8] J. J. O'Dwyer, *The Theory of Electrical Conduction and Breakdown*, Clarendon, Oxford, **1973**.
[9] J. O. M. Bockris, A. K. Reddy, *Modern Electrochemistry*, Plenum, New York, **1970**.
[10] C. Wagner, *Atom Movements*, American Society for Metals, Cleveland, **1951**, p. 153; *Progr. Solid. State Chem., Vol. 6* (Ed.: F. Reiss), Pergamon, Oxford, **1971**.
[11] I. Yokota, *J. Phys. Soc. Jpn.* **1961**, *16*, 2213.
[12] H. Schmalzried, *Z. Phys. Chem. N. F.* **1962**, *33*, 111.
[13] C. Wagner, *Proc. 7th Meeting Int. Committee Electrochem. Thermodyn. Kinetics, London* **1955**, *7*, 301; I. Riess, *Solid State Ionics* **1992**, *51*, 219.
[14] J. Maier, *Z. Phys. Chem. N. F.* **1984**, *140*, 191.
[15] H. Schmalzried, *Z. Phys. Chem. N. F.* **1963**, *38*, 87.
[16] The modifications to the interpretation and calculation of results from these methods that become necessary when the ionic defects can undergo internal valency changes are described in refs. [14, 17].
[17] J. Maier, *Mat. Res. Soc. Symp. Proc. 210*, Materials Research Society, Pittsburgh, **1991**, p. 499; J. Maier, G. Schwitzgebel, *Phys. Status Solidi B* **1982**, *113*, 535; *J. Amer. Ceram. Soc.* in press.
[18] D. Müller, *Phys. Status Solidi* **1965**, *1312*, 775.
[19] C. G. Fonstadt, R. H. Rediker, *J. Appl. Phys.* **1971**, *42*, 2911.
[20] E. J. Opila, G. Pfundtner, J. Maier, H. L. Tuller, B. J. Wuensch, *Mater. Sci. Eng. B*, in press.
[21] S. J. Rothman, J. L. Routbart, J. E. Baker, *Phys. Rev. B* **1989**, *40*, 8852.
[22] Mathematical solutions to a variety of diffusion problems are given in: J. Crank, *The Mathematics of Diffusion*, University Press, London, **1987**. A more detailed and comprehensive treatment based on the isomorphic heat conduction equation can be found in: H. S. Carslaw and J. C. Jaeger, *Conduction of Heat in Solids*, Clarendon Press, Oxford, **1959**.
[23] R. Dieckmann, H. Schmalzried, *Ber. Bunsenges. Phys. Chem.* **1977**, *81*, 344.
[24] See, for example: L. Heyne in *Solid Electrolytes*, (Ed.: S. Geller), Springer, Berlin, **1977**.
[25] T. Bieger, J. Maier, R. Waser, *Solid State Ionics* **1992**, *53–56*, 578; T. Bieger, J. Maier, R. Waser, *Sensors Actuators* **1991**, *7*, 763.
[26] G. Pfundtner, J. Maier, *Proc. Bilateral German-Soviet Symp. HTSC*, Karlsruhe, September **1990**, 598.
[27] H.-J. Hagemann, Dissertation, Technische Hochschule Aachen, **1980**; K. A. Müller, W. Berlinger, R. S. Rubin, *Phys. Rev.* **1969**, *186*, 361; K. A. Müller; T. von Waldkirch, W. Berlinger, B. W. Faughnan, *Solid State Commun.* **1971**, *9*, 1071.
[28] J. Maier, *J. Phys. Chem. Solids* **1985**, *46*, 197.
[29] Trapping effects can be treated by including trapping reactions in the diffusion process [14, 17], as well as by the inclusions of Onsager coupling terms [30].

[30] M. Martin, H. Schmalzried, *Solid State Ionics* **1986**, *20*, 75; H. D. Wiemhöfer, *ibid.* **1990**, *40/41*, 530.
[31] C. Wagner. *Z. Angew. Chem.* **1936**, *49*, 735.
[32] N. B. Pilling, R. E. Bedworth, *J. Inst. Met.* **1923**, *29*, 529.
[33] Another extreme example is provided by the batteries used in cardiac pacemakers, in which a lithium/iodine contact forms LiI as a solid electrolyte. This results in a (self-repairing) electrochemical cell. For a long operational life the electronic contribution to the conductivity should be negligible, since otherwise rapid self-discharging would occur.
[34] M. H. Sukhar, H. L. Tuller, *Adv. Ceram.* **1984**, *7*, 71.
[35] C. Gensch, K. Hauffe, *Z. Phys. Chem.* **1951**, *196*, 427.
[36] Surfaces and interfaces are not the main topic of this article, and it would be inappropriate to go into more detail here.
[37] A statistical analysis shows that the activity of the occupied fraction of the surface sites can be expressed approximately as $\theta/1-\theta$; from a naive standpoint this reflects, in an idealized model, the structure elements V_{ad} and G_{ad} (which correspond to the terms $(1-\theta)$ and θ, respectively).
[38] G. Simkovich, C. Wagner, *J. Catal.* **1962**, *1*, 521.
[39] P. Murugaraj, J. Maier, *Solid State Ionics* **1989**, *32/33*, 993; J. Maier, P. Murugaraj, *ibid.* **1990**, *40/41*, 463.
[40] D. Y. Wang, A. S. Nowick, *J. Electrochem. Soc.* **1979**, *126*, 1155; *ibid.* **1979**, *126*, 1166.
[41] G. Nicolis, I. Prigogine, *Self-Organizaton in Non-Equilibrium Systems*, Wiley, New York, **1972**; W. Ebeling, *Strukturbildung bei irreversiblen Prozessen*, Teubner, Leipzig, **1976**; H. Haken, *Synergetik*, Springer, Berlin, **1983**.
[42] A. Gierer, M. Meinhardt, *Lect. Math. Life Sci.* **1974**, *7*, 163.
[43] E. Schöll, *Non-Equilibrium Phase Transitions in Semiconductors*, Springer, Berlin, **1987**.
[44] M. Eigen, *Naturwissenschaften* **1971**, *58*, 465.
[45] S. W. Teitsworth, R. M. Westervelt, E. E. Haller, *Phys. Rev. Lett.* **1983**, *51*, 825.
[46] K. M. Mayer, R. Gross, J. Parisi, J. Peinke, R. P. Huebener, *Solid State Commun.* **1987**, *63*, 55.
[47] M. P. Cox, G. Ertl, R. Imbihl, *Phys. Rev. Lett.* **1985**, *15*, 1725; see also the description of research in *Jahrbuch der Max-Planck-Gesellschaft* MPG, **1991**, p. 364.

Peptoids—A New Approach to the Development of Pharmaceuticals

By *Horst Kessler**

Molecular recognition of a target is not only the basis of biological regulation and communication, but also the foundation for rational drug design. For an increasing number of diseases, target systems have been identified whose selective inhibition may prevent the progression of the disease or its symptoms, or even provide a complete cure.

Since most often relatively little is known about the structure and dynamics of the target systems—often macromolecular receptors—the successful direct design of a drug recognized by the target molecule is rare even today. Thus, an efficient screening method is required for testing the effect of a variety of spatial arrangements of different functional groups on the binding and activity against the target molecule. In this respect peptides have been shown to be very suitable because of their modular construction, the large variability of their functional groups, and their rational and automated chemical or biological synthesis.[1, 2] Nowadays, almost every pharmaceutical company has a "peptide group" whose goal is to develop new lead structures for drugs.

The general procedure in the development of peptide mimetics begins with searching for a peptide that binds to the target molecule. Either naturally occurring, biologically active peptides/proteins are used as starting points, or structures are searched for by a systematic screening of peptide libraries.[3] Then the "active sequence" is located by the systematic replacement of each amino acid by Gly, Ala, and/or a D-amino acid.[4] In the next step, the conformational flexibility of this sequence is reduced in order to determine the optimal spatial orientation of the pharmocophors, the groups important for the binding to the receptor.[5] Finally, nonpeptides are sought that have the bioavailability, high selectivity (minimal side effects), high activity (low dosage), and sufficient metabolic stability required for orally administered drugs.

In a recently published report by 16 authors a new, promising concept in the search for active molecules and the localization of the active sequence was suggested:[6] the side chains on the α-carbon atom of the peptide chain are "shifted" by one position along the peptide backbone to the nitrogen atom to give an N-substituted oligoglycine (Scheme 1). The advantages of these new structures, called peptoids, are

- metabolic stability, since natural proteases cannot cleave the N-substituted peptide bond
- great variability in functional groups by simple chemical synthesis
- high flexibility and thus the possibility of probing a large conformational space
- the absence of additional spatial restrictions which are present in peptides due to the chirality of the α-C atom.

The new concept is in some ways reminiscent of the PNAs recently reviewed in this journal:[7] an achiral, flexible backbone is equipped with functional groups (for PNAs, the nucleobases; for peptoids, peptide side chains) spaced at intervals comparable to those in the naturally occurring polymer. This provides a structurally flexible molecule with the properties required for molecular recognition.

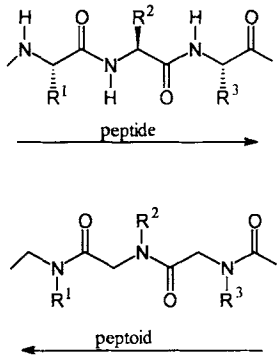

Scheme 1. Comparison of a portion of a peptide chain and a peptoid chain. Note that the direction of the peptide bonds are reversed in the peptoid ("retrosequence") to maintain the relative orientation of the carbonyl groups to the R groups. Peptoids are achiral.

It is evident from inspection of the structures in Scheme 1 that the order of the amino acids must be reversed in the peptoid ("retrosequence") if the carbonyl group contributes to the binding of the target molecule. In fact, the peptide retrosequences had the same behavior as the corresponding peptides in binding to three receptor systems: inhibition of α-amylase by peptides derived from tendamistat, inhibition of the hepatitis A virus 3C protease, and binding to the TAT RNA of the HIV virus.

Two approaches have been used in the chemical synthesis of peptoids. The first synthesis used the technique of Merrifield with Fmoc strategy[8] (Scheme 2). Recently Zuckermann et al. reported an interesting variation using "submonomer" solid-phase synthesis.[9] In both approaches the construction of the peptoid proceeds from the C-terminal to

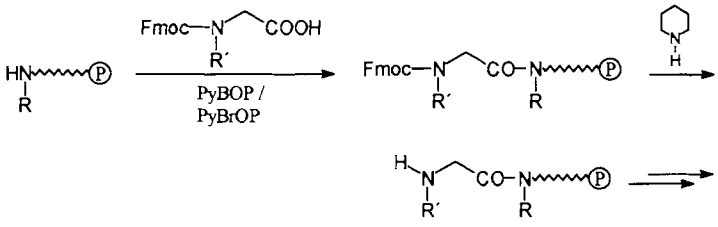

Scheme 2. Synthesis of peptoids according to the Merrifield method. The protected monomer unit is coupled to the growing chain and then deprotected. The [4-{(2,4-dimethoxyphenyl)aminomethyl}phenoxy]methyl residue serves as a linker (Rink resin); the peptoid can be cleaved from this linker under mild acid conditions. PyBOP = benzotriazol-1-yloxy-tris(pyrrolidino)phosphonium hexafluorophosphate, PyBrOP = bromo-tris(pyrrolidino)phosphonium hexafluorophosphate.

[*] Prof. Dr. H. Kessler
Organisch-chemisches Institut der Technischen Universität München
Lichtenbergstrasse 4, D-W-8046 Garching (FRG)

 © VCH Verlagsgesellschaft mbH, W-6940 Weinheim, 1993 0570-0833/93/0404-0543 $ 10.00+.25/0

the N-terminal end. The new method (Scheme 3) does not employ the complete, N-substituted glycine unit; instead the amino group of the growing resin-bound peptide chain is converted into the α-haloamide by treatment with chloroacetic acid under standard conditions. The following side chain protected amino group is then introduced by nucleophilic substitution of the halogen (bromine and iodine give better yields than chlorine).

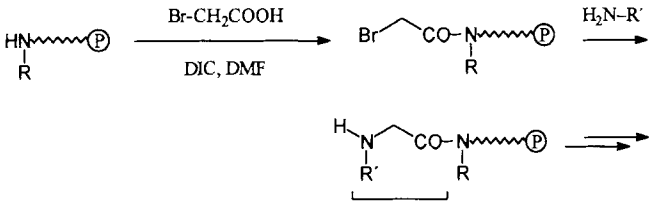

Scheme 3. Synthesis of peptoids by the submonomer solid-phase synthesis. The resin-bound monomer is synthesized stepwise from two building blocks. Since the two steps are different reactions, protecting group chemistry is not necessary and the monomer (designated by ⌴) does not need to be preconstructed. DMF = dimethylformamide, DIC = *N*,*N*'-diisopropylcarbodiimide.

The advantage of this procedure is its flexibility and that it avoids the tedious synthesis and deprotection of the N-terminal Fmoc-protected glycine building block. The efficiency of the method was demonstrated for nine pentapeptoids as well as a 25-mer, which was prepared in 86% yield and 65% purity (by HPLC). It remains to be shown if the problems of purification and the elimination of side products in the submonomer solid-phase synthesis can be solved.

The new class of compounds, the peptoids, opens a new dimension in peptide chemistry. The investigation of their chemical, biological, and structural potential is just beginning. The branch of medicinal chemistry involved with the search for new lead structures for the targeted intervention in pathological processes will certainly benefit from peptoids.

German version: *Angew. Chem.* **1993**, *105*, 572

[1] *Computer-Aided Drug Design* (Eds.: T. J. Perun, C. L. Propst, Marcel Dekker, New York, **1989**.
[2] *Peptide Pharmaceuticals. Approaches to the Design of Novel Drugs*, (Ed.: D. Ward), Open University Press, Milton Keynes, **1991**.
[3] G. Jung, A. G. Beck-Sickinger, *Angew. Chem.* **1992**, *104*, 375–391; *Angew. Chem. Int. Ed. Engl.* **1992**, *31*, 367–383.
[4] See, for example, A. Fourier, R. Conture, J. Magnan, M. Gendreau, D. Regoli, S. St.-Pierre, *Can. J. Biochem.* **1980**, *58*, 272–280; A. G. Beck-Sickinger, W. Gaida, G. Schnorrenberg, R. Lang, G. Jung, *Int. J. Pept. Protein Res.* **1990**, *36*, 522–530.
[5] H. Kessler, *Peptide Engineering: Design of Biologically Active Peptides under Conformational Control* (in *Trends in Drug Research* (Ed.: V. Claassen), Elsevier, Amsterdam, **1990**, pp. 73–84).
[6] R. J. Simon, R. S. Kania, R. N. Zuckermann, V. D. Huebner, D. A. Jewell, S. Banville, S. Ng, L. Wang, S. Rosenberg, C. K. Marlowe, D. C. Spellmeyer, R. Tan, A. D. Frankel, D. V. Santi, F. E. Cohen, P. A. Bartlett, *Proc. Natl. Acad. Sci. USA* **1992**, *89*, 9367–9371.
[7] C. Meier, J. W. Engels, *Angew. Chem.* **1992**, *104*, 1039–1041; *Angew. Chem. Int. Ed. Engl.* **1992**, *31*, 1008–1010.
[8] G. B. Fields, R. L. Noble, *Int. J. Pept. Protein Res.* **1990**, *35*, 161–214.
[9] R. N. Zuckermann, J. M. Kerr, S. B. H. Kent, W. H. Moos, *J. Am. Chem. Soc.* **1992**, *114*, 10646–10647.

Compounds Containing Silicon, Germanium, and Tin Polyhedra: The First Octahedral Tin Cluster

By *Manfred Weidenbruch**

Polyhedral compounds, and in particular the platonic bodies have always aroused a fascination that was founded on the harmony within these molecules. Accordingly, the resonance was large when the platonic hydrocarbons cubane (**1**),[1] tetrahedrane (**2**),[2] and dodecahedrane (**3**)[3] were isolated as derivatives or as the parent compounds.[4]

Polyhedral compounds of the heavy carbon homologues, on the other hand, have not been known for long, and only a few have been prepared. It is certainly not the thermodynamic instability of such compounds that complicates their synthesis, since calculations of the tetrahedrane (X_4H_4), prismane (X_6H_6), and cubane systems (X_8H_8) have shown that the strain energies of these molecules decrease to a different extent from X = carbon to the heavier homologues.[5] The problem is rather one of limited accessibility. Whereas for the formation of **1**–**3** the possibilities of organic synthesis were skillfully employed, mostly only one-pot reactions are available for analogous compounds of heavy homologues, in which many bonds are broken and remade.

So the reductive halogen elimination from **4** affords a series of mono- and oligocyclic compounds. Of these, octasilane **5** contains the most cycles.[6] While in **5** the unfavorable orientation of the two chlorine atoms hinders the formation of the cubane framework by another dehalogenation, the use of bulky R groups in silanes of type **4** or **6** indeed leads to octasilacubane **7**,[7] whose structure was proven by X-ray structure analyses on two derivatives.[8, 9]

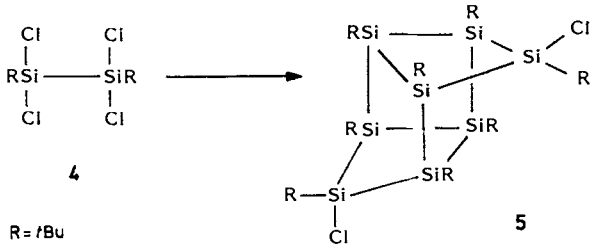

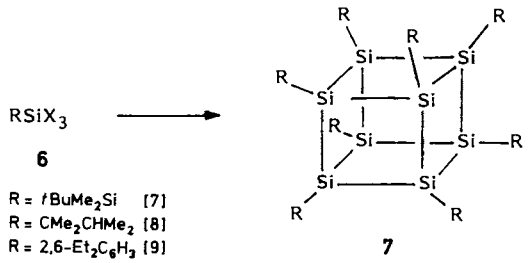

The polycyclic oligogermanes show a similar dependence on substituents. Reductive dehalogenation of *tert*-butyltrichlorogermane or tetrabromo-1,2-di-*tert*-butyldigermane affords the germanium compounds analogous to **5**.[10] The subtle differences in spatial requirements of the substituents R are documented by the reactions of **9** with reducing agents, which either furnish hexagermaprismane **8**[11] or the octagermacubanes **10**.[9]

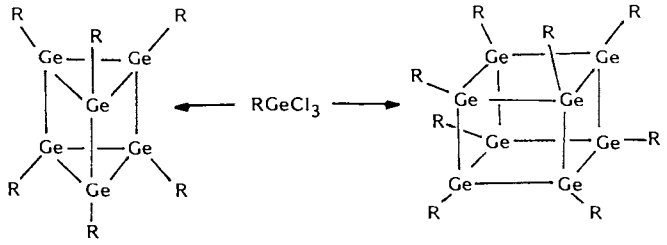

However, the very low yields of these polycyclic compounds signal that care is necessary—besides the isolated materials, other molecules of this sort are also likely to be present. A good example is the thermolysis of cyclotristannane (**11**) in the presence of naphthalene or benzophenone, which leads to reaction mixtures from which a whole range of polycyclic oligostannanes can be isolated in laborious separations. Decastanna[5]prismane **12**,[12] octastannacubane **13**,[13] and pentastanna[1.1.1]propellane **15**[14] are successively isolated together with distannane **14** and other tin-containing products. It is clear from the spectrum of products that the stannylene R_2Sn: resulting from the decomposition of **11** affords compounds both of the type $(RSn)_{2n}$ and other compositions by disproportionation with aryl group migration.

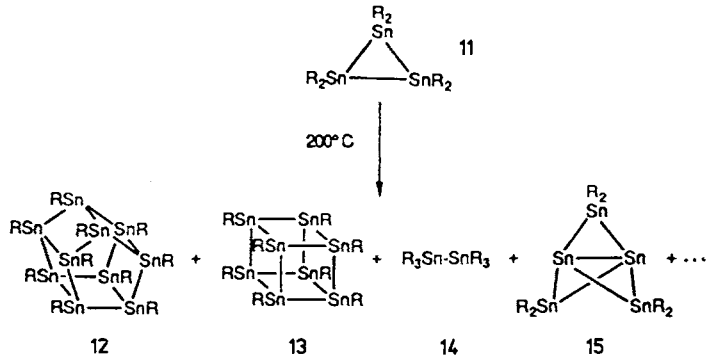

The striking feature of the compounds containing polyhedra of silicon, germanium, and tin is the dominance of the [*n*]prismanes. Results of theoretical studies also predict that these are the preferred products.[5, 15] For example, calculations on Si_6H_6 revealed that hexasilaprismane is more stable

[*] Prof. Dr. M. Weidenbruch
Fachbereich Chemie der Universität
Carl-von-Ossietzky-Strasse 9–11, D-W-2900 Oldenburg (FRG)

than hexasilabenzene, which is, in turn, distinctly lower in energy than hexasilaoctahedrane.[15] This result seems feasible, since in octahedral molecules X_6R_6 the skeletal atoms X would each be five-coordinate.

That with a suitable number of framework electrons and the correct choice of the protecting groups an octahedron can also be the coordination polyhedron has now been demonstrated by Schiemenz and Huttner in a noteworthy paper. Treatment of $SnCl_2$ with $K_2[Cr(CO)_5]$ in the presence of [2.2.2]cryptand yielded the cluster anion **16**, which has an almost perfect octahedral arrangement of the tin atoms.[16]

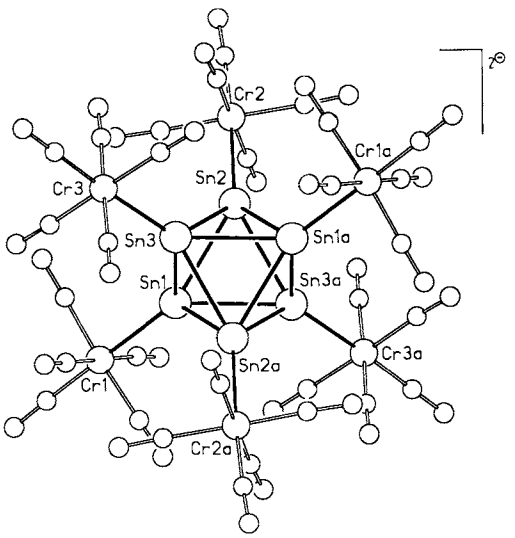

16

Formally **16** is composed of six stannylene-like building blocks, $[(OC)_5CrSn:]$. As a result, on inclusion of the two negative charges with the electron pairs of six skeletal atoms, a total (6 + 1) pairs of electrons are available for the bonds within the cluster. According to the Wade rules, **16** is analogous to $B_6H_6^{2-}$, a *closo* compound that with six skeletal atoms is expected to have the octahedral structure proven here.[17] Interestingly, the octahedral clusters of main group elements were only known in the case of boron. In the field of Zintl ions, which is certainly not lacking in homonuclear polycyclic compounds, the octahedral structure is found as construction principle only in the hexaborides of the CaB_6 type.[18, 19] Even though **16** was in fact formed rather incidentally, and as yet only in low yields, the concept shown here seems to be generalizable and might serve as basis for the synthesis of other polyhedral molecules or molecular ions.

German version: *Angew. Chem.* **1993**, *105*, 574

[1] P. E. Eaton, T. W. Cole, Jr., *J. Am. Chem. Soc.* **1964**, *86*, 3157.
[2] G. Maier, S. Pfriem, U. Schäfer, R. Matusch, *Angew. Chem.* **1978**, *90*, 552; *Angew. Chem. Int. Ed. Engl.* **1978**, *17*, 520.
[3] R. J. Ternasky, D. W. Balogh, L. A. Paquette, *J. Am. Chem. Soc.* **1982**, *104*, 4503.
[4] Reviews: G. Maier, *Angew. Chem.* **1988**, *100*, 317; *Angew. Chem. Int. Ed. Engl.* **1988**, *27*, 309; F. Vögtle, *Reizvolle Moleküle der Organischen Chemie*, Teubner, Stuttgart, **1989**.
[5] G. Nagase, *Angew. Chem.* **1989**, *101*, 340; *Angew. Chem. Int. Ed. Engl.* **1989**, *28*, 329; review: S. Nagase, *Polyhedron* **1991**, *10*, 1299.
[6] Y. Kabe, M. Kuroda, Y. Honda, O. Yamashita, T. Kawase, S. Masamune, *Angew. Chem.* **1988**, *100*, 1793; *Angew. Chem. Int. Ed. Engl.* **1988**, *27*, 1725.
[7] H. Matsumoto, K. Higuchi, Y. Hoshino, H. Koike, Y. Naoi, Y. Nagai, *J. Chem. Soc. Chem. Commun.* **1988**, 1083.
[8] H. Matsumoto, K. Higuchi, S. Kyushin, M. Goto, *Angew. Chem.* **1992**, 104, 1410; *Angew. Chem. Int. Ed. Engl.* **1992**, *31*, 1354.
[9] A. Sekiguchi, T. Yatabe, H. Kamatani, C. Kabuto, H. Sakurai, *J. Am. Chem. Soc.* **1992**, *114*, 6260.
[10] M. Weidenbruch, F.-T. Grimm, S. Pohl, W. Saak, *Angew. Chem.* **1989**, *101*, 201; *Angew. Chem. Int. Ed. Engl.* **1989**, *28*, 198; A. Sekiguchi, H. Naito, H. Nameki, K. Ebata, C. Kabuto, H. Sakurai, *J. Organomet. Chem.* **1989**, *369*, C1.
[11] A. Sekiguchi, C. Kabuto, H. Sakurai, *Angew. Chem.* **1989**, *101*, 97; *Angew. Chem. Int. Ed. Engl.* **1989**, *28*, 55.
[12] L. R. Sita, I. Kinoshita, *J. Am. Chem. Soc.* **1991**, *113*, 1856.
[13] L. R. Sita, I. Kinoshita, *Organometallics* **1990**, *9*, 2865.
[14] L. R. Sita, R. D. Bickerstaff, *J. Am. Chem. Soc.* **1989**, *111*, 6454.
[15] A. F. Sax, R. Janoschek, *Angew. Chem.* **1986**, *98*, 634; *Angew. Chem. Int. Ed. Engl.* **1986**, *25*, 651.
[16] B. Schiemenz, G. Huttner, *Angew. Chem.* **1993**, *105*, 295; *Angew. Chem. Int. Ed. Engl.* **1993**, *32*, 297.
[17] K. Wade, *Adv. Inorg. Chem. Radiochem.* **1976**, *18*, 1.
[18] Reviews: H. G. von Schnering, *Angew. Chem.* **1981**, *93*, 44; *Angew. Chem. Int. Ed. Engl.* **1981**, *20*, 33; *Nova Acta Leopold.* **1985**, *59*, (*264*) 165; J. D. Corbett, *ibid.* **1985**, *59* (*264*) 183.
[19] Layers of *closo*-In_6 octahedra linked by four vertices to one another are contained in the Zintl phase Rb_2In_3: S. C. Sevov, J. D. Corbett, *Z. Anorg. Allg. Chem.* **1993**, *619*, 128.

 © VCH Verlagsgesellschaft mbH, W-6940 Weinheim, 1993 0570-0833/93/0404-0546 $ 10.00+.25/0

Palladium-Catalyzed, Enantioselective Allylic Substitutions

By *Oliver Reiser**

The development of enantioselective-catalyzed reactions has led to great success over the past few years. Numerous chiral metal catalysts have been tested, which have achieved a wide range of selectivities, never thought possible, for a great number of reactions by using tailored ligands.[1] A problem in the catalysis repertoire was palladium-catalyzed, enantioselective allylic substitution.[2] Elegant mechanistic investigations have contributed to the development of this reaction as a valued method of synthesis. The understanding of factors such as the initial conformation of the allylic component,[3] the nature of its leaving group,[4] the conformation of the intermediate allylic palladium complexes,[5] the hardness of the nucleophile,[6] and the electronic and steric properties of the ligands bound to the palladium center,[7] today allow such substitution reactions to be carried out with high regio- and diastereoselectivities.

Most of the asymmetric allylic substitution processes start from racemic allylic components *rac*-**1**-R (where for **1**-R, R designates the general group of the compound, e.g. **1**-Me is **1** with R = Me), which in the absence of chiral ligands form *meso* complexes of the type **2** with palladium(0). Since a nucleophile can attack at either of the two ends of the allylic component, the enantiomers **3**-R and *ent*-**3**-R are formed. The degree of the enantioselectivity of a reaction depends on how well a chiral ligand in **2** can direct the attack of the nucleophile (Nu) to *one* of the two allylic termini.

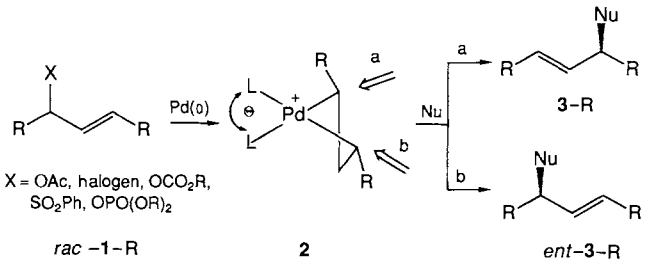

The problem with allylic substitutions, such as reaction (a), is that a soft nucleophile attacks the complexes **2** from the side opposite to the ligands L; as a result the distance between the reaction centers and the chiral inductor is large.

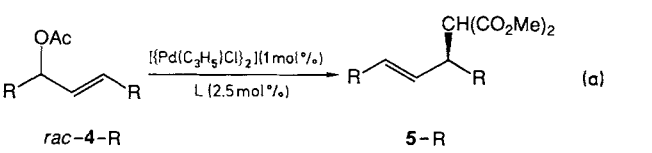

Thus, it is not surprising that ligands which are normally highly selective, such as (+)-DIOP,[8] achieved an enantiomeric excess of only 22% *ee* (Table 1) for the preparation of **5**-Me.[9] Even ligands such as BINAP[8], or Chiraphos[8] have so far only shown a high selectivity for few substrates.[10] As a result, ligands were developed which can "reach over" to the *exo* side of the allylic complexes **2**, for example the ferrocene **6** designed by Hayashi.[11] In the allylic complex **7** a flexible hydroxyl group of the phosphane ligand directs the nucleophile. With this ligand **5**-Ph was synthesized in up to 96% *ee*.

Table 1. Enantioselective allylic alkylation of *rac*-**4**-R according to Equation (a).

4-R	5-R	L	Yield [%]	% *ee*	Ref.
4-Me	5-Me	(+)-DIOP [c]	66–88 [a]	22	[9]
4-Me	5-Me	**17**-*t*Bu	96 [b]	71	[18]
4-*n*Pr	5	**17**-*t*Bu	96 [b]	69	[18]
4-*i*Pr	5	**17**-*t*bu	88 [a]	96	[18]
4-Ph	5-Ph	**6a** [d]	85 [a]	96	[11]
4-Ph	5-Ph	**6b** [d]	97 [a]	90	[11]
4-Ph	5-Ph	**6c** [d]	80 [a]	86	[11]
4-Ph	*ent*-5-Ph	**13**	99 [b]	95	[14b]
4-Ph	5-Ph	**14**	97 [b]	97	[14b]
4-Ph	5-Ph	**16** [e]	63 [a]	68	[17]
4-Ph	5-Ph	**16** [f]	89 [a]	81	[17]
4-Ph	5-Ph	**17**-Ph	99 [b]	99	[18]

[a] $NaCH(CO_2Me)_2$. [b] $CH_2(CO_2Me)_2$, BSA, KOAc. [c] 100 mol% $PdCl_2$, 200 mol% ligand. [d] 0.5 mol% $[\{Pd(C_3H_5)Cl\}_2]$, 1 mol% ligand. [e] 2.5 mol% $[\{Pd(C_3H_5)Cl\}_2]$, 10 mol% ligand. [f] 2.5 mol% $[\{Pd(C_3H_5)Cl\}_2]$, 50 mol% ligand.

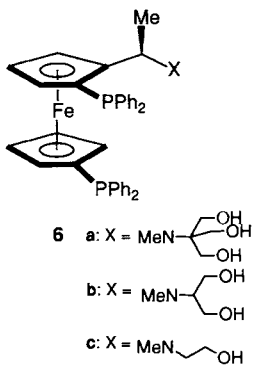

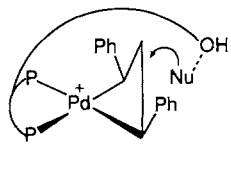

A different concept is pursued with the synthesis of ligands which are derived from 2-diphenylphosphinobenzoic acid.[12] By the coordination of **8** or **9** to palladium a 13-

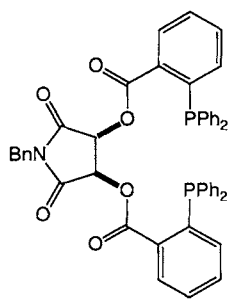

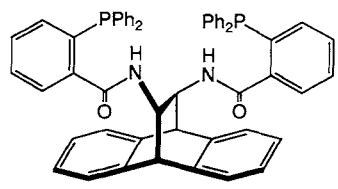

[*] Dr. O. Reiser
Institut für Organische Chemie der Universität
Tammannstrasse 2 D-W-3400 Göttingen (FRG)

membered ring is formed each time. This chelate ring extension causes an increase of the bite angle θ in **2**, whereby the chiral centers of the ligands are positioned closer to the allylic component.

The *meso*-ditosylcarbamate **11**, which is generated in situ from the diol **10**, cyclizes to give the oxazolidinone **12** with up to 88% *ee*; the highest enantioselectivity for this system obtained so far. Unfortunately, there are no selectivity values of **8** or **9** (as yet?) for substitutions at **4**-R, so that a direct comparison of the different ligand concepts is not possible.

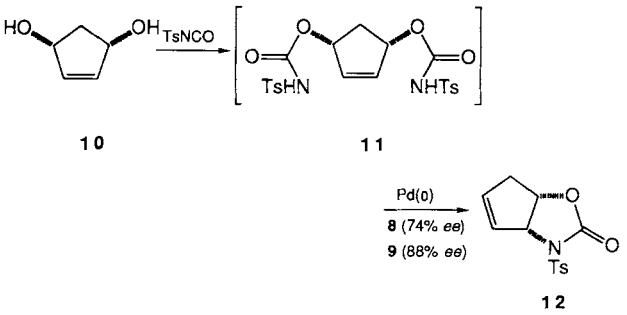

10 **11** **12**

C_2 symmetric, chiral semicorrines[13] and bis(dihydrooxazoles)[14] have given a great boost to catalysis research over recent years. They have also proved to be efficient ligands in the enantioselective synthesis of **5**-Ph and *ent*-**5**-Ph,[14b] although these ligands neither "attack" the *exo* side of the complex **2** nor can they increase the bite angle θ in the macrocyclic chelate. A selectivity of 95% *ee* is achieved for the substitution at **4**-Ph with ligand **13** and with **14** even one of 97% *ee* (see Table 1) in an almost quantitative reaction. For this substitution, instead of sodium dialkylmalonate as nucleophile, the use of a mixture from dimethyl malonate and *N*,*O*-(bistrimethylsilyl)acetamide (BSA) proved successful.[15]

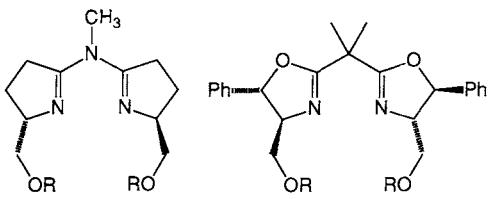

13 R = $SiMe_2tBu$ **14**

These excellent results, supported by an X-ray structure analysis of complex **15**, could be explained convincingly;[16] one benzyl group in the ligand and one phenyl substituent at the allylic terminus repel each other considerably. This steric hindrance is, for example, illustrated by a clear twisting of the dihydrooxazole ring in question and from the lengthening of the corresponding Pd–C bonds. The nucleophile attacks at the allylic terminus which is sterically strained, since in this way, in combination with the rupture of the Pd–C bond, the steric strain can be reduced.

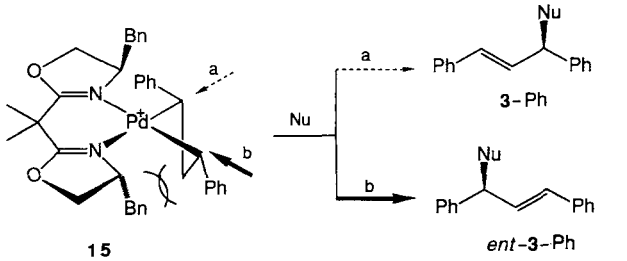

15

If people have so far been under the impression that the basic condition for an efficient ligand is C_2 symmetry, they might have to change their ideas as a result of two very recent publications. The ligand **16**, consisting of a chiral dihydrooxazole and an achiral thiophene unit, leads to only a moderate enantioselectivity of 68–81% *ee* for the reaction of **4**-Ph and sodium dimethylmalonate; however, a new principle is illustrated here, according to which the selectivity in metal-catalyzed reactions can be controlled by steric and stereoelectronic factors.[17]

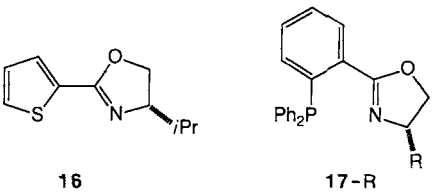

16 **17**-R

The most favorable arrangement sterically between the allylic component and **16** should occur in complex **18**. The thiophene ligand as an electron-rich π system acts as donor and, as a result of the *trans* effect, should transfer electron density to the allylic carbon atom *trans* to the sulphur atom. This carbon atom should less willingly undergo nucleophilic attack because of the increased electron density. Thus, the favorable attack occurs by route a to give **5**-Ph.

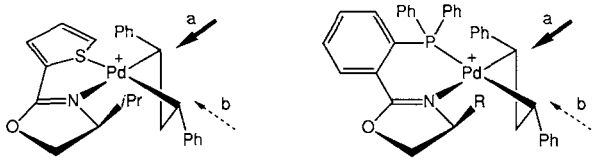

18 **19**

Ligand **17**-R has two different coordination sites, in this case, a triphenylphosphane and a dihydrooxazole unit. Ligand **17**-R shows record selectivities (Table 1) not only for the substitution of **4**-Ph, but for the first time also with alkyl-substituted propenylacetates.[18] If here, too, the most favorable conformation sterically **19** is taken as the starting point, the attack of the nucleophile occurs *trans* to the nitrogen atom. However, this is surprising in view of the model established for **18**, since the triphenylphosphane group should clearly be a better π-acceptor than the dihydrooxazole unit, and this should be transferred to a position at the allylic terminus *trans* to the acceptor.

An interesting NMR study provided an explanation for these stereoelectronic facts.[19] According to this study, in an allylic palladium complex the carbon atoms of the allylic

termini are shifted with increasing acceptor strength of the ligands (e.g., change from nitrogen to phosphorus coordination) to higher field in the ^{13}C NMR spectrum. This effect is particularly marked for the carbon atom in the position *trans* to the ligand. With the necessary caution required when dealing with the correlation of ^{13}C NMR shifts with charge distributions, this is an indication that the electron density of an allylic carbon atom *trans* to the phosphane ligand, in comparison to the nitrogen ligand, should be reduced significantly.

It can be noted that **18** and **19** are attacked by the nucleophile mainly at the same allylic carbon atom, despite their different electronic properties. This might be an indication that neither structure **18** nor **19** is the reactive conformation. Finally, a speculative mechanism may be proposed: is it possible that through a π–σ–π mechanism an equilibrium **18** $\rightleftharpoons$ **20** and **19** $\rightleftharpoons$ **21** predominates, whereby **20** and **21** are significantly more reactive towards nucleophiles than **18** or **19** because of their greater instability? In addition to the

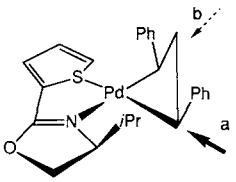

20

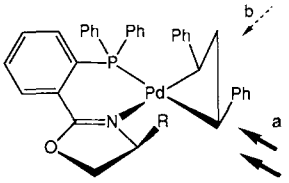

21

stereoelectronic factors, the aspect of reduction of the steric strain during the attack of the nucleophile would again become important. Whereas in **20** steric and stereoelectronic factors work against each other, these problems do not occur in **21**: the attack *trans* to the triphenylphosphane ligand simultaneously reduces the steric strain. This model could explain the superior selectivity of **17** over **16**, despite their very similar steric volume.

Further mechanistic investigations, developments, and applications of ligands such as **16** or **17**-R are eagerly anticipated. Although 1993 has only just begun, **17**-R might already be a promising candidate for the reagent of the year. Without doubt, palladium-catalyzed allylic substitution has been transformed from the cinderella to a princess of catalysis.

German version: *Angew. Chem.* **1993**, *105*, 576

[1] a) R. Noyori, M. Kitamura in *Modern Synthetic Methods* (Ed.: R. Scheffold), Springer, Berlin, **1989**, pp. 115–198; b) H. Brunner, *Top. Stereochem.* **1988**, *18*, 129.

[2] New reviews: a) C. G. Frost, J. Howarth, J. M. J. Williams, *Tetrahedron: Asymmetry* **1992**, *3*, 1089–1122; b) S. A. Godleski in *Comprehensive Organic Synthesis, Vol. 4* (Ed.: B. M. Trost), Pergamon, Oxford, **1991**, p. 585; c) B. M. Trost, *Angew. Chem.* **1989**, *101*, 1199–1219; *Angew. Chem. Int. Ed. Engl.* **1989**, *28*, 1173; d) G. Consiglio, R. Waymouth, *Chem. Rev.* **1989**, *89*, 257.

[3] T. Hayashi, A. Yamamoto, T. Hagihara, *J. Org. Chem.* **1986**, *51*, 723.

[4] a) F. K. Sheffy, J. K. Stille, *J. Am. Chem. Soc.* **1983**, *105*, 7173; b) B. M. Trost, N. R. Schmuff, M. J. Miller, *ibid.* **1980**, *102*, 5979; c) J. Tsuji, I. Minami, *Acc. Chem. Res.* **1987**, *20*, 140; d) N. Greenspoon, E. Keinan, *Tetrahedron Lett.* **1982**, *23*, 241.

[5] B. Akermark, S. Hansson, A. Vitagliano, *J. Am. Chem. Soc.* **1990**, *112*, 4587.

[6] a) J.-C. Fiaud, J.-Y. Legros, *J. Org. Chem.* **1987**, *52*, 1907; b) N. Greenspoon, E. Keinan, *ibid.* **1988**, *53*, 3723; c) B. M. Trost, J. W. Herndon, *J. Am. Chem. Soc.* **1984**, *106*, 6835; d) B. M. Trost, T. R. Verhoeven, *J. Org. Chem.* **1976**, *41*, 3215.

[7] a) B. Akermark, S. Hansson, B. Krakenberger, A. Vitagliano, K. Zetterberg, *Organometallics* **1984**, *3*, 679; b) B. Akermark, S. Hansson, A. Vitagliano, *J. Organomet. Chem.* **1987**, *335*, 133.

[8] Abbreviations of the ligands: DIOP = 2,3-*O*-isopropylidene-2,3-dihydroxy-1,4-bis(diphenylphosphino)butane; Chiraphos: 2,3-bis(diphenylphosphino)butane; BINAP 2,2′-bis(diphenylphosphino)-1,1′-binaphthyl.

[9] B. M. Trost, T. J. Dietsche, *J. Am. Chem. Soc.* **1973**, *95*, 8200.

[10] M. Yamaguchi, T. Shima, T. Yamagishi, M. Hida, *Tetrahedron Lett.* **1990**, *35*, 5049–5052.

[11] T. Hayashi, *Pure Appl. Chem.* **1988**, *60*, 7–12.

[12] a) B. M. Trost, D. L. van Vranken, *Angew. Chem.* **1992**, *104*, 194–196; *Angew. Chem. Int. Ed. Engl.* **1992**, *31*, 228; b) B. M. Trost, D. L. van Vranken, C. Bingel, *J. Am. Chem. Soc.* **1992**, *114*, 9327–9343.

[13] a) A. Pfalz in *Modern Synthetic Methods* (Ed.: R. Scheffold), Springer, Berlin, **1989**, pp. 199–248; b) *Chimica* **1990**, *44*, 202.

[14] a) D. Müller, G. Umbricht, B. Weber, A. Pfaltz, *Helv. Chim. Acta* **1991**, *74*, 232; b) U. Leutenegger, G. Umbricht, C. Farni, P. von Matt, A. Pfaltz, *Tetrahedron* **1992**, *48*, 2143–2156; c) C. Bolm, K. Weikhardt, M. Zehnder, T. Ranff, *Chem. Ber.* **1991**, *124*, 1173; d) C. Bolm, K. Weikhardt, M. Zehnder, D. Glasmacher, *Helv. Chim. Acta* **1991**, *74*, 717; e) D. A. Evans, K. A. Woerpel, M. M. Hinman, M. M. Faul, *J. Am. Chem. Soc.* **1991**, *113*, 726–728; f) G. Helmchen, A. Krotz, K. T. Ganz, D. Hansen, *Synlett* **1991**, 257; g) R. E. Lowenthal, S. Masamune, *Tetrahedron Lett.* **1991**, *32*, 7373–7376; h) C. Bolm, *Angew. Chem.* **1991**, *103*, 556; *Angew. Chem. Int. Ed. Engl.* **1991**, *30*, 542.

[15] B. M. Trost, S. J. Brickner, *J. Am. Chem. Soc.* **1983**, *105*, 568.

[16] A. Pfaltz, *Acc. Chem. Res.* **1993**, in press; b) M. Zehnder, M. Neuburger, P. von Matt, A. Pfaltz, unpublished results.

[17] C. G. Frost, J. M. J. Williams, *Tetrahedron Lett.* **1993**, *34*, in press.

[18] P. von Matt, A. Pfaltz, *Angew. Chem.* **1993**, *105*, 614; *Angew. Chem. Int. Ed. Engl.* **1993**, *32*, 566.

[19] B. Akermark, B. Krakenberger, S. Hansson, A. Vitagliano, *Organometallics* **1987**, *6*, 620.

 © *VCH Verlagsgesellschaft mbH, W-6940 Weinheim, 1993* *0570-0833/93/0404-0549 $ 10.00+.25/0*

Concerning "An Opinion on the Heterogeneous Photoreduction of N_2 with H_2O"

First Letter

By *Vincenzo Augugliaro** and *Javier Soria*

In a recent commentary, Edwards et al.[1] reported on the inefficiency in their attempts to photoreduce molecular nitrogen on heterogeneous surfaces. They used coprecipitated or surface-loaded iron-doped titania and certain single or binary oxide xerogels for performing two types of irradiation experiments in the presence of $N_{2(g)}$ enriched to 99% with ^{15}N and water vapor or liquid water. Though we accept the main conclusion of their work, namely that the authors were unsuccessful in photosynthesizing ammonia, in our opinion, on the basis of the results of their own negative experiments, Edwards et al. should question the reasons for their unsuccessful runs, instead of questioning the reproducibility of this intriguing reaction, which was first described in 1977[2] and which has since been reproduced in different laboratories[3, 4] under similar experimental conditions and with different TiO_2-based photocatalysts.

We believe that readers of Angewandte Chemie should be made aware of the fact Edwards et al. performed most of their experiments under conditions substantially different from those described in the literature and with different and inadequately characterized photocatalysts. Thus, most of their photoreduction experiments were conducted with "single or binary oxide xerogels" whose photocatalytic activity has not been documented in the scientific literature[5] and which, on the basis of our experience, are not expected to be photoactive. Moreover, the great majority of irradiation experiments were conducted in aqueous suspensions in which photoreduction of nitrogen is not generally observed. Only a total of twelve irradiation experiments were apparently performed with iron-doped TiO_2 powders of not reported composition and characterization which were allegedly prepared according to published procedures.[2, 3] We stress the point that the specimen preparation is crucial for the success of the process; this is why all papers in the field of heterogeneous catalysis report details on the specimen preparation and characterization. All researchers working in heterogeneous catalysis are well aware that an undetected contamination can invalidate all the findings. For the preparation of photocatalytically active TiO_2 powders, the iron-doped anatase must be subjected to a heat-treatment to effect a rearrangement of anatase into rutile. This requires carefully controlled conditions, since it is accompanied by drastic changes in crystal sizes and surface areas (see e.g., refs. [3, 6]). It is difficult to assess whether Edwards et al. had catalytically active powders as they did not provide details such as the rutile/anatase ratio, particle size, or the surface areas. Neither were specifications given for the photoreactivity runs. The reaction conditions such as mass of catalyst, time of irradiation, irradiated surface area of catalyst, temperature inside the photoreactor, and method of avoiding warming of catalyst due to the IR radiation of the 450 W lamp used were absent. The authors worked in batch vessels of quartz, which thus were more UV-transparent than our Pyrex vessels or our Pyrex continuous photoreactor. This may have favored the photooxidation of ammonia which becomes a side reaction especially after longer irradiation periods.

The authors are certainly correct in warning against ammonia contamination problems. However, it must be stressed that although contamination could explain random results, it could not explain trends in photoreactivity or changes in activity in response to changes in operating conditions or photocatalyst composition.[3] We call to mind the experiments[4] in which cycles of activation–deactivation of photocatalyst were clearly observed and also explained on the basis of ESR spectra performed contemporaneously with the photoactivity experiments. Only an "intelligent" contamination could explain all the results obtained in the field of dinitrogen photoreduction.

In discussing the possibility of direct nitrogen photooxidation reactions, a previously published paper should have been quoted.[7] Last but not least, the remarks made by Edwards et al. on the photoreduction of nitrogen on desert sands are quite unfounded as Schrauzer et al.[8] clearly explained how they calculated the ammonia yields from their $^{15}N_2$ experiments. Moreover, they also reported the yields of nitrogen photooxidation products, and already pointed out that ammonia photooxidation occurs as a side reaction.

[*] Prof. V. Augugliaro
Dipartimento di Ingegneria Chimica dei Processi e dei Materiali
Univeristy of Palermo
Viale delle Scienze, I-90128 Palermo (Italy)
Prof. J. Soria
Campus de la Universidad Autónoma
Cantoblanco, E-28049 Madrid (Spain)

[1] J. G. Edwards, J. A. Davies, D. L. Boucher, A. Mennad, *Angew. Chem.* **1992**, *104*, 489; *Angew. Chem. Int. Ed. Engl.* **1992**, *31*, 480.
[2] G. N. Schrauzer, T. D. Guth, *J. Am. Chem. Soc.* **1977**, *99*, 7189.
[3] J. Soria, J. C. Conesa, V. Augugliaro, L. Palmisano, M. Schiavello, A. Sclafani, *J. Phys. Chem.* **1991**, *95*, 274.
[4] H. Miyama, N. Fuji, Y. Nagao, *Chem. Phys. Lett.* **1980**, *74*, 523.
[5] In [1] the patent literature quoted is obviously in error: US 4688522, **1987** and US 4799870, **1989** are by H. A. McMaster but do not deal with photoreduction reactions. These patents deal with "Fluid Power Transfer Devices", a totally unrelated matter in our opinion.
[6] G. N. Schrauzer, T. D. Guth, J. Salehi, N. Strampach, Liu Nan Hui, M. R. Palmer in *Homogeneous and Heterogeneous Photocatalysis*, (Eds.: E. Pelizzetti, N. Serpone), D. Reidel, Dordrecht, **1986**, p. 509.
[7] R. I. Bickley, V. Vishwanathan, *Nature (London)* **1979**, *280*, 306.
[8] G. N. Schrauzer, N. Strampach, Liu Nan Hui, M. R. Palmer, J. Salehi, *Proc. Natl. Acad. Sci. USA* **1983**, *80*, 3873.

 © VCH Verlagsgesellschaft mbH, W-6940 Weinheim, 1993 0570-0833/93/0404-0550 $ 10.00+.25/0

Second Letter

By *Leonardo Palmisano, Mario Schiavello,** and *Antonino Sclafani*

Edwards et al.[1] in their communication in essence convey the impression that the photoreduction of dinitrogen on heterogeneous photocatalysts is thermodynamically close to impossible and that the ammonia yields observed by previous workers[2, 3] may have been due to erroneous measurements of background contamination.

The authors furthermore claim to have conducted numerous experiments with promising photocatalysts under conditions identical to those used by the earlier investigators. This is actually not quite true. For example, Edwards et al. performed their experiments in quartz, rather than Pyrex vessels and employed, a medium-pressure Hg lamp; accordingly, the relative contribution of short UV light was higher than in the experiments conducted by us and most other workers in the field. Furthermore, and more seriously, the majority of the experiments seem to have been done with solids that would be expected to have little or no photocatalytic activity. Thus, Edwards et al. performed most of their experiments with "binary oxide xerogels" composed of TiO_2, Fe_2O_3, NiO, Al_2O_3, and SiO_2, which we would judge to have little chance of being photoactive in the first place. Only very few experiments were actually performed with iron-doped TiO_2 under conditions where nitrogen photoreduction could have taken place. In these experiments, the Fe–TiO_2 photocatalysts must first be heat-treated at defined temperatures and for known periods of time and subsequently stored in humid air. From the information given, it is our impression that the authors did not spend enough time and effort to optimize the photocatalyst pretreatment conditions. It should be recalled that only homogeneous samples having Fe^{3+} ions in the lattice of TiO_2 are photoactive. Heterogeneous samples, that is, those in which the surface is covered by iron oxides, or those with mixed iron–titanium oxides such as Fe_2TiO_5 on the surface, are photochemically completely inactive. The heat treatment temperature must be chosen so that the anatase–rutile conversion does not occur too rapidly. Prolonged heating at temperatures that are too high produces large crystals of low or zero photocatalytic activity. The optimal heating temperatures and times must be determined for each batch, as both vary from sample to sample, and numerous samples must be prepared and tested individually prior to the actual photoreduction experiments.

Based on the evidence provided, we can only conclude that Edwards et al. probably never had active photocatalysts at their disposal. Furthermore, we must point out that their discussion of the thermodynamics of dinitrogen photoreduction is also seriously flawed and misleading. They argue that the yields would have to be "absurdly low" (on the order of 10^{-50} M with respect to NH_3 or O_2) in view of the unfavorable thermodynamic equilibrium concentrations of the reactants. This reasoning is naive inasmuch as many thermodynamically "uphill" reactions involving TiO_2 are already well documented. Best known among these is the water splitting reaction (a).[4]

$$3H_2O + h\nu \rightarrow 3H_2 + 3/2\ O_2 \qquad (a)$$

This reaction is possible because the potential corresponding to the band gap in TiO_2 (E_{cb}) is negative vs. the normal hydrogen electrode (NHE) ($E_{cb} < E_{H^+/H_2}$), for any pH value. From the Pourbaix diagram,[5] the reduction potential E_{N_2/NH_3} is positive vs. NHE ($E_{N_2/NH_3} > E_{H^+/H_2}$). Since the formation of NH_3, according to Equation (b) is known, it follows that, irrespective of mechanism, the photoreduction of N_2, according to Equation (c) in feasible given TiO_2' band gap energies.

$$N_2 + 3H_2 \rightarrow 2NH_3 \qquad (b)$$

$$N_2 + 3H_2O + h\nu \rightarrow 2NH_3 + 3/2\ O_2 \qquad (c)$$

Last but not least, we must reject the suggestion that our NH_3 yields were due to background contamination. This source of error was always safely eliminated by conducting blank experiments either in the absence of photocatalyst or in the dark.

[*] Prof. M. Schiavello, Prof. L. Palmisano, Prof. A. Sclafani
Dipartimento di Ingegneria Chimica dei Processi e dei Materiali
University of Palermo
Viale delle Scienze, I-90128 Palermo (Italy)

[1] J. G. Edwards, J. A. Davies, D. L. Boucher, A. Mennad, *Angew. Chem.* **1992**, *104*, 489; *Angew. Chemie Int. Ed. Engl.* **1992**, *31* 480.
[2] G. N. Schrauzer, T. D. Guth, *J. Am. Chem. Soc.* **1977**, *99*, 7189.
[3] J. Soria, J. C. Conesa, V. Augugliaro, L. Palmisano, M. Schiavello, A. Sclafani, *J. Phys. Chem.* **1991**, *95*, 274.
[4] A. Fujishima, K. Honda, *Nature* **1972**, *238*, 37.
[5] M. Pourbaix, *Atlas of Electrochemical Equilibria in Aqueous Solutions*, Pergamon Press, London, **1966**, p. 496.

 © *VCH Verlagsgesellschaft mbH, W-6940 Weinheim, 1993* *0570-0833/93/0404-0551 $ 10.00+.25/0*

Reply: Standards of Demonstration for the Heterogeneous Photoreactions of N_2 with H_2O

By *Julian A. Davies* and *Jimmie G. Edwards**

The claim that ammonia can be synthesized catalytically from nitrogen and water in the presence of simple metal oxide powders by the action of light suggests a process of overwhelming importance to the future of the human race. For that reason, the possibility deserves our utmost attention. For the same reason, it can be very enticing to conduct large numbers of experiments with various potential catalysts that appear to produce tantalizingly small amounts of ammonia, as has been occurring now for fifteen years. If the small amounts are adventitious and not photosynthetic, all the effort has been wasted, and nothing positive has been added to the human condition. The concept of a major discovery that remains continually on the borderline of demonstration is internally inconsistent. It behooves us, then, to settle this issue now by setting guidelines to decide the validity of this putative process. If the claim is valid, we should proceed to fulfill its stupendous promise of a completely renewable, solar-driven source of ammonia. Our communication[1] gave such guidelines and expressed our skepticism about the validity of the claim.

In the correspondence,[3] the authors object to the procedures and conclusions given in our Communication. We are nonplussed by the statements, "Only an 'intelligent' contamination could explain all the results..." and "...irradiated surface area of catalyst..."[2a] and by the unusual coefficients in Equation (a).[2b] We did note that this choice of coefficients makes the reaction have about the same ΔG°(298 K) as that of their putative reaction (c). Both correspondents take us to task for not fully referencing prior published work or providing complete experimental details. We followed the "Instructions to Authors" where the page limit (inclusive of all literature citations) and the instruction to summarize experimental details in Communications for *Angewandte Chemie* are clearly stated. Full experimental details of our work are available elsewhere,[3] and more work is to be published in the near future. A complete review by us of the literature in this field has been accepted for publication.[4] Our Communication included only our statistically most significant results, exactly as stated therein.

The correspondents dismiss our results with the assertion that they are possessed of special arts in catalyst synthesis not known to us and that our reaction conditions were somehow unsuitable for the putative photoreaction: "it is difficult to assess whether Edwards et al. had catalytically active powders..."[2a] and "Edwards et al. probably never had active photocatalysts at their disposal".[2b] We confirm unequivocally that no powder that we examined ever showed any statistically significant catalytic activity for the putative photoreaction under discussion here. Despite the claims that only very special substances prepared under highly controlled conditions will catalyze the putative reaction, a vast array of different materials, prepared and characterized by diverse techniques, has been examined for potential photocatalysts of this reaction, and success with them has been reported by many workers.[4] Low levels of ammonia have been reported from reactions that employed vastly different putative catalysts, among them desert sands, and that were performed under very different experimental conditions. It is stated[2a] that "It should be recalled that only homogeneous samples having Fe^{3+} ions in the lattice of TiO_2 are photoactive." The origin of this statement is obscure to us, especially in the light of the work on desert sands (cited in[2a]) whose precise structure and homogeneity are unknown. In connection with this topic, we note that a review article by Augugliaro and Palmisano cites without critical comment a report that boiling chips catalyze the putative photosynthesis of ammonia.[5]

Statistically significant results that unequivocally confirm the photocatalytic synthesis of ammonia from nitrogen and water over oxide catalysts are not found in the literature.[4] If the correspondents are indeed possessed of special arts in catalyst synthesis, then it would be straightforward for them to prepare catalysts that can generate ammonia from $^{15}N_2$ at a level where unambiguous demonstration is routine[3] and where a statistically significant number of experiments can easily be performed. We note the operational technique[2b] ("....numerous samples must be prepared and tested individually prior to the actual photoreduction experiments") where it seems each batch of catalyst was tested and only those that produced the desired result were reported. The authors state that we "claim to have conducted numerous experiments with promising photocatalysts under conditions identical to those used by the earlier investigators." We made no such claim in our Communication. Here we ask both correspondents to publish the specific conditions necessary to prepare effective catalyst powders, and the specific parameters and their values that identify the powders as effective, so that their operational selection method can be avoided.

We believe that no more effort should be expended on production of tiny amounts of ammonia from natural nitrogen as described in most of the published work. We have demonstrated a variety of ways by which adventitious ammonia and various other contaminants can give false indications of ammonia synthesis at such levels.[3] In view of the enormous importance of the putative photoreaction, the cost of isotopically enriched nitrogen gas is small; furthermore, the use of isotope-ratio mass spectrometers in correctly designed, statistically significant experiments can settle the issue conclusively.

After we have been proven wrong in our skepticism, and this new, extraordinarily important way of catalyzing ammonia synthesis has been firmly established, scientists will then face the challenge of understanding the process. In particular, it will be a demanding task to learn how a material as simple as iron-doped titania (or even a boiling chip) can contain sites so special that they organize at least one molecule of nitrogen, three molecules of water, six electrons, six holes, and enough photons to generate the electrons and

[*] Prof. J. G. Edwards, Prof. J. A. Davies
Department of Chemistry, University of Toledo
Toledo, OH 43606 (USA)

 © VCH Verlagsgesellschaft mbH, W-6940 Weinheim, 1993 0570-0833/93/0404-0552 $ 10.00+.25/0

holes in a way that can drive the reaction uphill by more than 600 kJ mol^{-1}. The energy problem might be worse in Pyrex vessels, to which both the correspondents refer, since in such cases only the lower energy photons can contribute to the energy balance. The thermodynamic and kinetic issues we raised in our Communication cannot be rationalized away, despite the argument that our "discussion of the thermodynamics of dinitrogen reduction is [also] seriously flawed and misleading".[2b] The analogy of water photolysis [$H_2O \rightarrow H_2 + 1/2\ O_2$] is used,[2b] a process that is best conducted photoelectrochemically, and that minimally requires only a single reactant molecule and which can be driven uphill by a single photon of UV radiation unless its equation is balanced in the misleading way of their Equation (a). The analogy fails.

Augugliaro and Soria[2a] raise the issue of photooxidation of ammonia, a process readily catalyzed by every powder we synthesized. This mechanistically fascinating but thermodynamically favorable process has been firmly established since the early work of Gopalarao et al.[6] We observed it whenever we irradiated aqueous ammonia in the presence of gaseous nitrogen and a titania-based powder. We have considered the possibility that titania-based catalysts 1) promote nitrogen reduction at one type of site and ammonia oxidation at a second type of site, or 2) promote nitrogen reduction at one wavelength of incident radiation and ammonia oxidation at a second wavelength; each of these processes would fix nitrogen. However, we found no statistically significant evidence of fixed nitrogen, as reported in our Communication.

In conclusion, we advise those who would continue with this line of research to attend to the standards of demonstration we set in our Communication, this letter, and elsewhere.[3, 4]

[1] J. G. Edwards, J. A. Davies, D. L Boucher, A. Mennad, *Angew. Chem.* **1992**, *31*, 489; *Angew. Chem. Int. Ed. Engl.* **1992**, *31*, 480. The "other work" to which we referred in this paper was in connection with an innovative engine for which one of the proposed fuel systems included ammonia. The criticism in reference [5] of [2a] is unjustified.

[2] a) V. Augugliaro, J. Soria, *Angew. Chem.* **1993**, *105*, 579; *Angew. Chem. Int. Ed. Engl.* **1993**, *32*, 550; b) L. Palmisano, M. Schiavello, A. Sclafani, *ibid.* **1993**, *105*, 581 and **1993**, *32*, 551.

[3] David L. Boucher, *Ph. D. Thesis*, University of Toledo, **1992**, *Diss. Abstr. Int.* **1992**, *53-B*, 2853.

[4] J. A Davies, D. L. Boucher, J. G. Edwards, *Adv. Photochem.* in press.

[5] V. Augugliaro, L. Palmisano in *Photocatalysis and Environment* (*NATO ASI Ser. Ser.* **1988**, **237**, 432).

[6] G. Gopalarao, C. I. Varadanam, *J. Indian Chem. Soc.* **1941**, *18*, 361 and references therein.

 © *VCH Verlagsgesellschaft mbH, W-6940 Weinheim, 1993* *0570-0833/93/0404-0553 $ 10.00+.25/0*

Communications may be submitted in English *or* in German. Further details regarding the submission of communications can be found in the "Notice to Authors" reproduced in the January issue of the journal. Copies thereof may be obtained from the editorial office upon request.

Ti^{IV} Complexes with Bridging Ylide Ligands: Double Oxophiles in Reactions with Aldehydes

By *Karin A. Hughes, Pablo G. Dopico, Michal Sabat,* and *M. G. Finn**

The series of complexes of Group 4 metals with bridging ylide ligands and the general structure **1**, prepared by Schmidbaur and co-workers,[1] comprise an interesting combination of phosphorus and early transition metal oxophiles. We report here two new examples of this class of metallacycles and the selective production of allenes from their reactions with aromatic aldehydes.

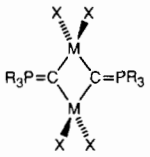

1

When an excess of $(Me_2N)_3P{=}CH_2$ was treated with $TiCl_2(NMe_2)_2$ according to the general procedure of Schmidbaur[1c,d] (by employing the phosphorus methylide as base as well as nucleophile), complex **2** was obtained, the first such compound having different terminal ligands on titanium (Scheme 1). The X-ray crystal structure analysis of **2** revealed the centrosymmetric structure shown in Figure 1, with a *trans* orientation of Cl ligands.[2] While the bond lengths and angles of **2** are similar to those in the analogous complex $[\{(Et_2N)_3P{=}C{-}TiCl_2\}_2]$,[1c] π-donation from the amido ligands results in slightly longer Ti–Cl bonds and shorter Cl–P1 bonds in **2**.

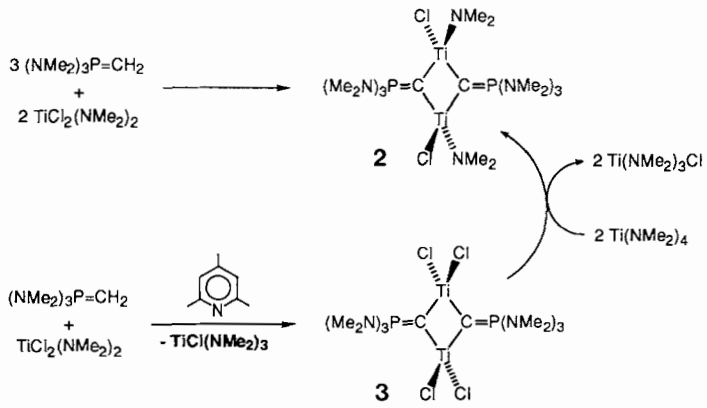

Scheme 1. Synthesis of complexes **2** and **3**.

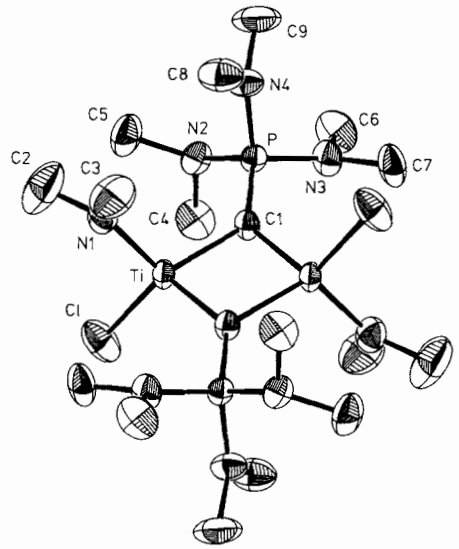

Fig. 1. Crystal structure of **2** (ORTEP). Selected bond lengths [Å] and angles [°]: Ti-Cl 2.303(2), Ti-N1 1.928(4), Ti-Cl 2.014(4), Ti-Cl* 1.936(4), Cl-P 1.693(4), P-N2 1.673(4), P-N3 1.660(4), P-N4 1.650(4); Cl-Ti-Cl 115.5(1), Cl-Ti-Cl* 114.8(1), N1-Ti-Cl 111.7(2), Cl-Ti-Cl* 87.6(2), Ti-Cl-Ti* 92.4(2), Ti-Cl-P 131.8(2), Ti*-Cl-P1 135.5(2).

The addition of 2,4,6-trimethylpyridine to an equimolar mixture of ylide and $TiCl_2(NMe_2)_2$ provided the new metallacycle $[\{(Me_2N)_3P{=}C{-}TiCl_2\}_2]$ (**3**) instead of **2**, in a yield of 17% (Scheme 1). The crude reaction mixture was found to contain a substantial amount of $TiCl(NMe_2)_3$ arising from disproportionation of $TiCl_2(NMe_2)_2$, which implies that the other disproportionation product, $TiCl_3(NMe_2)$, is the active reagent for the synthesis of **3**. However, use of $TiCl_3(NMe_2)$ in place of $TiCl_2(NMe_2)_2$ afforded **3** in the same isolated yield.[3] These observations and the apparent loss of a Ti-bound NMe_2 group in the isolation of **3** suggest that crystallization of the metallacycle is the critical step in the synthesis, proceeding in low yield and driving exchange of chloride for the amido ligand on titanium.

Complex **3** underwent ligand exchange reactions at titanium without disruption of the metallacycle core. Thus, the addition of 2.5 equivalents of $Ti(NMe_2)_4$ to **3** at ambient temperature afforded **2** in quantitative yield. Analysis of this reaction by NMR spectroscopy reveals the formation of an intermediate compound (presumably the ylide metallacycle with one amido group), which disappeared to give **2** over a period of approximately one hour (Scheme 1). This exchange rate is considerably slower than that of many titanium halides, amides, and alkoxides, indicative of steric hindrance at each metal center. This is further demonstrated by the slow decomposition (requiring several days) of **2** and **3** in the presence of a large excess of benzophenone, affording no characterizable organic products.

However, metallacycle **3** reacted immediately with an excess of 4-methylbenzaldehyde or 4-methoxybenzaldehyde in

[*] Prof. M. G. Finn, K. A. Hughes, P. G. Dopico, Dr. M. Sabat
Department of Chemistry
University of Virginia
Charlottesville, VA 22901 (USA)

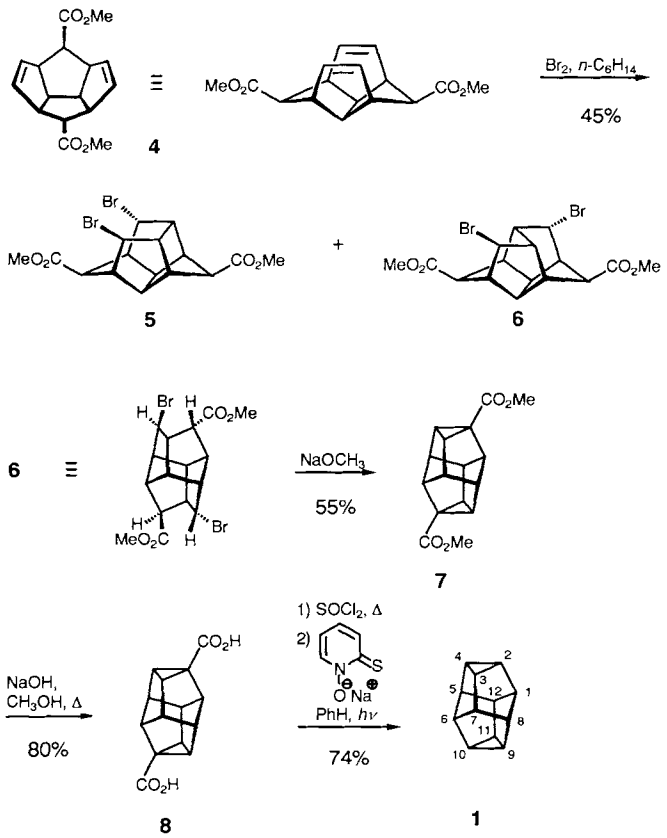

reduced pressure], and its structure was determined by X-ray crystallography (Fig. 1).[15]

p-[$3^2.5^6$]Octahedrane **1** has the point symmetry D_{3d} rare among hydrocarbons; the point symmetry corresponds to the unusual space group $R\bar{3}c$ of the crystals. Its 500 MHz ^{1}H NMR spectrum (in $CDCl_3$) shows only two broad singlets at $\delta = 3.00$ (6H, 1(5,6,7,8,12)-H) and 1.60 (6H, 2(3,4,9,10,11)-H). The coupling between the cyclopropyl protons and those at the central ring, determined from the COSY long-range ^{1}H NMR spectrum, is apparently very small, which must be attributed to the relatively large H-C-C bond angle [H2-C2-C1: 123.5(15)°, H1-C1-C2: 115.3(13)°] at the five-membered rings, which are rigid and folded with an angle of 34.1°.[16] With respect to the ^{1}H NMR signal of dodecahedrane **3** ($\delta = 3.38$, in $CDCl_3$), the signal of the protons belonging to the five-membered rings on the central six-membered ring of **1** undergoes a high-field shift, apparently the effect of the diamagnetic anisotropy of the three-membered rings.[17] This is also manifest in the 125.7 MHz ^{13}C NMR spectrum (in $CDCl_3$) of **1**, which displays two doublets at $\delta = 62.3$ ($^1J_{C,H} = 140$ Hz, C1(5,6,7,8,12))[18] and 33.6 ($^1J_{C,H} = 170$ Hz, C2(3,4,9,10,11)). The relatively large ^{13}C–H coupling constant of 170 Hz at the cyclopropyl positions[19] reflects a different type of hybridization at the cyclopropyl carbon atoms than in simple cyclopropane derivatives, as a result of the bending of the three C–C bonds in each ring that point inward. The increased s character of 34% for the cyclopropylic C–H bonds in **1** that correlates[20] with the coupling constant of $^1J = 170$ Hz probably implies an increased C–H acidity. As a result an independent chemistry for suitable derivatives of the dicarboxylic acid **8** and perhaps also for the hydrocarbon **1** can be predicted.[21] The bond lengths of 1.507(4) Å in the three-membered ring of **1** are normal, and the stretching of the bonds of the three-membered rings proximal to the methoxy carbonyl groups and contraction of the distal bonds in diester **7** corresponds to the usual effect of an electron-withdrawing substituent.[22]

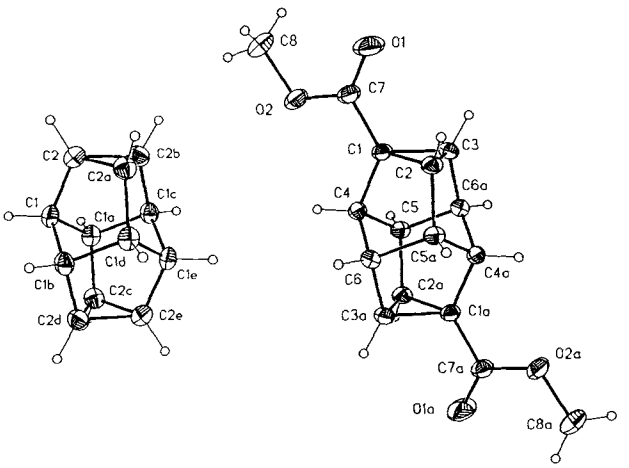

Fig. 1. Crystal structures of the dimethyl ester (**7**) of *p*-[$3^2.5^6$]octahedrane-2,10-dicarboxylic acid (right) and *p*-[$3^2.5^6$]octahedrane (**1**, left) [13]. Bond lengths [Å] and angles [°] (numbering does not conform to IUPAC rules): **7**: (averaged for C_{2h} symmetry): C1-C2 1.529(1), C1-C4 1.527(2), C1-C7 1.476(2), C2-C3 1.495(1), C4-C5 1.551(1), C5-C6a 1.554(1); C1-C3-C2 60.7(1), C2-C1-C4 106.9(1), C2-C1-C7 119.1(1), C4-C1-C7 126.6(1), C1-C4-C6 106.0(1), C2-C1-C3 58.6(1), C5-C4-C6 101.0(1). – **1**: C1-C2 1.520(3), C1-C1a 1.550(3), C2-C2a 1.507(4); C2-C1-C1a 106.4(1), C1a-C1-C1b 100.7(2), C1-C2-C2a 106.9(1), C2-C1-C1b 106.4(2), C2a-C2-C2b 60.0(1), C1-C2-C2b 106.8(1).

Received: December 3, 1992 [Z 5724 IE]
German version: *Angew. Chem.* **1993**, *105*, 611

[1] Cf. *Cage Hydrocarbons* (Ed.: G. A. Olah), Wiley, New York, **1990**, and references therein; *Carbocyclic Cage Compounds* (Eds.: E. Osawa, O. Yonemitsu), VCH, New York, **1992**, and references therein.

[2] Cubane as $(CH)_8$: a) P. E. Eaton, T. W. Cole, Jr., *J. Am. Chem. Soc.* **1964**, *86*, 3157; b) P. E. Eaton, M. Maggini, *ibid.* **1988**, *110*, 7230; c) P. E. Eaton, C.-H. Lee, Y. Xiong, *ibid.* **1989**, *111*, 8016; d) P. E. Eaton, *Angew. Chem.* **1992**, *104*, 1447; *Angew. Chem. Int. Ed. Engl.* **1992**, *31*, 1421. Pentaprismane as $(CH)_{10}$: e) P. E. Eaton, Y. S. Or, S. J. Branca, B. K. Ravi Shankar, *Tetrahedron* **1986**, 1621; dodecahedrane as $(CH)_{20}$: f) L. A. Paquette, *Chem. Rev.* **1989**, *89*, 1051.

[3] a) L. A. Paquette, D. W. Balogh, R. Usha, D. Kountz, G. G. Christoph, *Science* **1981**, *211*, 575; b) L. A. Paquette, D. W. Balogh, *J. Am. Chem. Soc.* **1982**, *104*, 774; c) R. J. Ternansky, D. W. Balogh, L. A. Paquette, *ibid.* **1982**, *104*, 4503; d) W.-D. Fessner, B. A. R. C. Murty, J. Wörth, D. Hunkler, H. Fritz, H. Prinzbach, W. D. Roth, P. von R. Schleyer, A. B. McEwen, W. F. Maier, *Angew. Chem.* **1987**, *99*, 484; *Angew. Chem. Int. Ed. Engl.* **1987**, *26*, 452; e) R. Pinkos, J.-P. Melder, H. Prinzbach, *ibid.* **1990**, *102*, 102 and **1990**, *29*, 92; f) J.-P. Melder, R. Pinkos, H. Prinzbach, *ibid.* **1990**, *102*, 105 and **1990**, *29*, 95; g) J.-P. Melder, H. Prinzbach, *Chem. Ber.* **1991**, *124*, 1271; h) D. Elsässer, K. Hassenrück, H.-D. Martin, B. Mayer, G. Lutz, H. Prinzbach, *ibid.* **1991**, *124*, 2863.

[4] P. J. Garratt, J. F. White, *J. Org. Chem.* **1977**, *42*, 1733.

[5] L. A. Paquette in [1], p. 313 ff., and references therein

[6] Systematic name: heptacyclo[6.4.0.$0^{2,4}$.$0^{3,7}$.$0^{5,12}$.$0^{6,10}$.$0^{9,11}$]dodecane. The trivial name ditriaxane was previously proposed for this hydrocarbon (**1**) [7]. We favor the term introduced by Paquette et al. [8], *p*-[$3^2.5^6$]octahedrane, which enables the symmetry of the molecule and its relationship to other members of the subgroup of $(CH)_{2n}$ hydrocarbons to be recognized more easily.

[7] K.-I. Hirao, Y. Ohuchi, O. Yonemitsu, *J. Chem. Soc. Chem. Commun.* **1982**, 99; K.-I. Hirao, H. Takahashi, Y. Ohuchi, O. Yonemitsu, *J. Chem. Res. (S)* **1992**, 319; *(M)* **1992**, 2601–2611.

[8] Cf. L. A. Paquette, A. R. Browne, C. W. Doecke, R. V. Williams, *J. Am. Chem. Soc.* **1983**, *105*, 4113, and footnote [4] therein.

[9] P. J. Garratt, C. W. Doecke, J. C. Weber, L. A. Paquette, *J. Org. Chem.* **1986**, *51*, 449.

[10] Only the synthesis of the C_2-symmetric 2,9-dimethyl derivative of **1** has been reported [7].

[11] L. A. Paquette, M. J. Wyvratt, H. C. Berk, R. E. Moerck, *J. Am. Chem. Soc.* **1978**, *100*, 5845.

[12] Diffractometer Siemens 3m/V, $Mo_{K\alpha}$, graphite monochromator, Wyckoff scan, $3.0° < 2\theta < 65°$, direct methods (SHELXTL-PLUS). Crystal size $0.35 \times 0.35 \times 0.14$ mm^3, space group $P2_1/c$, $Z = 2$, $T = 293$ K, unit cell: $a = 9.125(1)$, $b = 5.982(1)$, $c = 12.024(1)$ Å, $\alpha = \gamma = 90$, $\beta = 108.41(1)°$,

The Incorporation of C_{60} in Molecular Sieves

By *Andreas Gügel, Klaus Müllen, Horst Reichert, Wolfgang Schmidt, Günter Schön, Ferdi Schüth,* Jochen Spickermann, Jeremy Titman,* and *Klaus Unger*

Fullerenes have attracted wide interest in recent years because of their qualities. Their inclusion in molecular sieves could alter their optical and electronic properties and thus create new materials. In this communication the possibility of including large quantities of fullerenes in molecular sieves was investigated.[1] Zeolites and their analogues are particularly suitable as matrix materials: they have pores from 2.7 (in clathrasils) to 12.1 Å (in VPI-5).[2] We used the aluminophosphates VPI-5, $AlPO_4$-5, and $AlPO_4$-8, which contain one-dimensional pore systems and were prepared according to references [3] and [4]. The free channel diameters are given in Figure 1. High-vacuum activation at elevated temperature removes adsorbed water and leaves the pore system freely accessible.

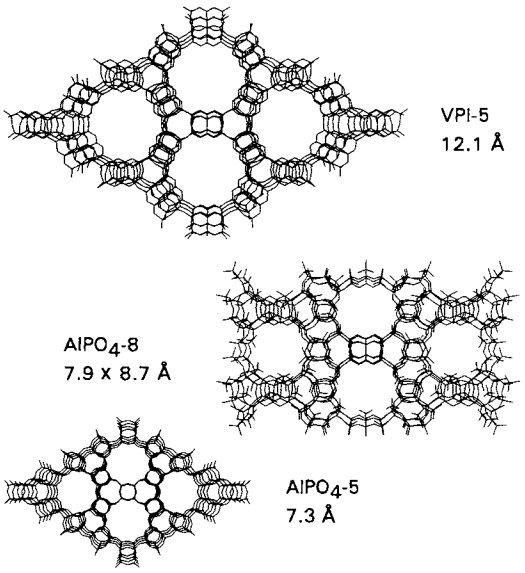

Fig. 1. The aluminophosphates VPI-5, $AlPO_4$-8, $AlPO_4$-5 are constructed from alternating AlO_4 and PO_4 tetrahedra, which are linked by oxygen bridges. The pore diameters are given below the aluminophosphate names.

The loading of the aluminophosphate with C_{60} was studied both by adsorption from the liquid phase and from the gas phase. In no sample treated directly with a concentrated solution of C_{60} in toluene could significant amounts of the fullerene be detected in the pores. However, it was possible to incorporate C_{60} into VPI-5 and $AlPO_4$-8 from the gas phase. The C_{60} used in all experiments still contained toluene that could not be removed by drying in an oil pump vacuum (about 28 wt.%).

The activated aluminophosphate was heated together with C_{60} in vacuum at 450 °C. C_{60} vaporizes and diffuses into the micropores of the aluminophosphate. The experiments were performed with various C_{60} loads (0.1–0.5 g C_{60} per 1 g $AlPO_4$). In this way VPI-5 and $AlPO_4$-8 were loaded with C_{60}, but the pore openings of $AlPO_4$-5 were apparently too small for adsorption of this fullerene. The success of the loading could even be observed optically by a yellow tint in the aluminophosphate crystals under a light microscope. Combined thermogravimetric/differential thermal analysis (TG/DGA) in a stream of air showed that the charged samples lost a considerable amount of their mass (up to 30 mass %) in an exothermic step in the temperature range of 400–900 °C. We attribute this to the burn off of C_{60} and perhaps of the toluene bound more firmly to C_{60}, since pure toluene was completely desorbed from the aluminophosphate channels at 200 °C. Figure 2 shows the IR spectra of C_{60}, C_{60} in $AlPO_4$-8, and unloaded $AlPO_4$-8, recorded on an IR microscope that enabled the study of individual crystals or crystal aggregates. The sharp absorption band of C_{60} at 1429 cm^{-1} broadened when the fullerene was adsorbed in the aluminophosphate and appears at 1432 cm^{-1} as a shoulder on the broader band of the aluminophosphate framework. At a higher C_{60} load both band types were observed. Other IR bands of the adsorbed fullerene could not be detected, because they were either hidden under the lattice vibrations of $AlPO_4$-8 or occurred at too low a frequency (cut-off of the detector, 700 cm^{-1}).

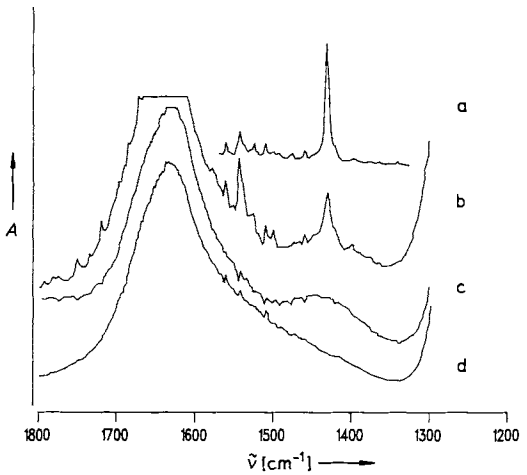

Fig. 2. IR spectra of a) unloaded $AlPO_4$-8, b) $AlPO_4$-8 loaded with C_{60} (0.144 g C_{60} per 1 g $AlPO_4$-8), c) $AlPO_4$-8 loaded with C_{60} (0.500 g C_{60} per 1 g $AlPO_4$-8), d) C_{60} (the signal was reduced by a factor 10) A = absorption units.

The sharp IR band that appeared in addition to the broadened band in more highly loaded samples indicated that here, to a certain extent, C_{60} was adsorbed on the surface of the aluminophosphate. The large amount of C_{60} detected by TG (up to 30 wt % of the samples) was, however, a further indication besides the broadened IR band that the major portion of C_{60} was in the interior of the molecular sieve crystals. Larger quantities of C_{60} outside the micropores could only be contained in mesopores between the individual aluminophosphate crystallites. Bulk C_{60} on the outer surface of the aluminophosphates can be easily detected by X-ray powder diffraction (XRD), since in this case the peaks typical for C_{60} appear beside the aluminophosphate peaks. These additional peaks were no longer present after ultrasonic treatment of the samples in toluene.

N_2 sorption measurements showed that the mesopores of a loaded VPI-5 molecular sieve (0.144 g C_{60} per 1.0 g VPI-5) were freely accessible to N_2. However, the free micropore

[*] Dr. F. Schüth, Dipl.-Chem. H.Reichert, Dipl.-Chem. W. Schmidt, Prof. Dr. K. Unger
Institut für Anorganische Chemie und Analytische Chemie der Universität J.-J.-Becher-Weg 24, D-W-6500 Mainz (FRG)
Dipl.-Chem. A. Gügel, Prof. Dr. K. Müllen, J. Spickermann, Dr. J. Titman
Max-Planck-Institut für Polymerforschung, Mainz
Prof. Dr. G. Schön
Institut für Anorganische Chemie der Universität Essen

volume of the loaded VPI-5 was only about one third of that of an unloaded sample (unloaded: 0.184 cm^{-3}, loaded 0.065 cm^3).

Besides the proof of the inclusion of C_{60} in the micropores, this study also included preliminary investigations on the dynamics of the adsorbed C_{60}. For this purpose solid-state ^{13}C NMR spectra both with and without rotation about the magic angle (magic angle spinning, MAS) were recorded for aluminophosphate samples that have no detectable bulk C_{60} on the outer surface according to XRD. These spectra showed that the C_{60} molecules rotate freely within the channels of the aluminophosphates, because the line-broadening expected for restricted rotation[5] was not unambiguously observed. Nevertheless, the lines were broadened in those spectra recorded without MAS, from which a partial restriction of the free isotropic rotation can be deduced. A further, though only slight, broadening of the lines from 600 to 700 Hz was obtained by cooling the sample from 298 to 230 K. This might point to a transition from the "rotator" phase to the "rachet" phase (the low-temperature phase according to ref. [5]) in the aluminophosphate lattice at relatively high temperatures.[6] It should, however, be mentioned that coadsorbed water can influence the dynamics significantly.

At present we are studying in more detail the electronic and optical properties of the molcular sieves doped with C_{60}. In particular, we are attempting to separate C_{60}, C_{70}, and higher fullerenes in the gas phase by these methods. This would be an alternative to the usual separation by liquid chromatography[7, 8] and is also applicable on larger scales.

Experimental Procedure

Sample preparation: $AlPO_4$-5 and $AlPO_4$-8 were activated by simple heating to 200 °C in air to remove adsorbed water. Under analogous treatment VPI-5 was transformed irreversibly into $AlPO_4$-8 and had therefore to be dehydrated under high vacuum (10^{-5} Torr) [4].

The aluminophosphate samples were placed in one arm of an inverted glass U-tube, and the other was charged with C_{60}. The arm containing aluminophosphate was heated separately, and the sample chamber was evacuated prior to calcination through the opening in the center of the tube. At 10^{-5} Torr the aluminophosphates were first activated at 280 °C for 12 h and then at 480 °C for 1 h. Thereafter under maintenance of the vacuum the glass tube was fused, and the glass ampule containing the activated aluminophosphate and C_{60} was heated for 10 h at 450 °C. The tube was opened, and the sample washed in toluene, filtered off, and again washed for three periods of 15 min in toluene (200 mL portions per 1 g loaded aluminophosphate) in a ultrasonic bath. This procedure removed the last residues of C_{60} from the crystal surface (determined by XRD). The IR spectra were recorded on crushed crystal aggregates with an Analytical Plan IR microscope (SpectraTec) coupled to a Nicolet 5SXB FTIR spectrometer. The N_2 sorption measurements were performed at 77 K with a volumetric sorption apparatus (Omnisorp 100). To remove adsorbed water and toluene, the samples were first heated for 8 h at room temperature, followed by 10 h at 280 °C in vacuum. The NMR spectra were recorded on a Bruker 300 MSL NMR spectrometer (frequency 75.47 MHz, impulse duration 2 μs repeated every 10 s, 3600 scans; rotation frequency in the MAS experiment 2 kHz); the C_{60} signal appears at $\delta = 151$.

Received: September 28, 1992
Revised version: November 19, 1992 [Z 5600 IE]
German version: *Angew. Chem.* **1993**, *105*, 618

[1] The incorporation of very small amounts of C_{60} into the molecular sieve 13X was described by P. N. Keizer, J. R. Morton, K. F. Preston, A. K. Sugden, *J. Phys. Chem.* **1991**, *95*, 7117–7118.
[2] W. M. Meier, D. H. Olson, *Zeolites* **1992**, *5*.
[3] B. Kanz-Reuschel, Dissertation, Universität Mainz, **1991**.
[4] W. Schmidt, F. Schüth, H. Reichert, K. Unger, B. Zibrowius, *Zeolites* **1992**, *1*, 2–8.
[5] R. D. Johnson, G. Meijer, D. S. Bethune, C. S. Yannoni, *Acc. Chem. Res.* **1992**, *25*, 169–175.
[6] Measurements at lower temperatures are planned.
[7] A. Gügel, M. Becker, D. Hammel, L. Mindach, J. Räder, T. Simon, M. Wagner, K. Müllen, *Angew. Chem.* **1992**, *104*, 666–667; *Angew. Chem. Int. Ed. Engl.* **1992**, *31*, 644–645.
[8] M. S. Meier, J. P. Selegue, *J. Org. Chem.* **1992**, *57*, 1924–1926.

Selective Cleavage of a 35-mer Single-Stranded DNA Containing the Initiation Codon of the TAT Gene of HIV-1 by a Tailored Cationic Manganese Porphyrin**

By *Marguerite Pitié, Christiane Casas, C. Jeffrey Lacey, Geneviève Pratviel, Jean Bernadou*, and *Bernard Meunier**

Antisense oligonucleotides have been tested as potential antiviral agents over the last decade. Since the work of Zamecnik and Stephenson[1] on the inhibition of the replication of Rous sarcoma virus with a 13-mer oligonucleotide, it has been shown that HIV can be inhibited by various chemically modified oligonucleotides.[2–4b] Resistance to nucleases has been enhanced by using phosphorothioate oligonucleotides, and cellular uptake has been improved by attaching polylysine[5] or lipophilic groups.[6] However, many of these modified antisense oligonucleotides are active as antiviral agents in a non-sequence-dependent manner.[7] Moreover, the antiviral activity in cell cultures is often in the range of micromolar concentrations, at least two orders of magnitude above the concentration required for a fast development of new antiviral agents based on antisense oligonucleotides. Here we report that a 35-mer corresponding to (+)strand DNA sequence containing the first eight codons of HIV-1 TAT gene is efficiently cleaved in vitro by a cationic manganese porphyrin complex vectorized by a 19-mer complementary to the target, even in the presence of a large excess of random double-stranded DNA. Breaks are observed at low concentrations (10 nM) and with only 2.6 molecules of the metalloporphyrin conjugate per molecule of target.

Among all possible DNA cleavers[8, 9] to be attached to oligonucleotides to prepare active antisense oligonucleotides,[10] the motif tris(*N*-methylpyridinio)porphyrinatomanganese(III) (Mn-trisMPyp) has some significant advantages: 1) the parent molecule *meso*-tetrakis (4-*N*-methylpyridinio)porphyrinatomanganese(III) (Mn-TMPyP) is an efficient DNA cleaver able to hydroxylate C-H bonds at the 1′ and 5′ positions of deoxyribose units,[11, 12] 2) manganese ions are not removed from synthetic porphyrins in vivo,[13] and 3) these cationic manganese porphyrins exhibit a non-negligible anti-HIV activity.[14] Starting from a tris-(*N*-methylpyridinio)porphyrinatomanganese(III) precursor having an acid function at the *para* position of the *meso*-phenyl group (R′ = OH in Scheme 1), the covalent connection to the 19-mer bearing a 5′-amino link was achieved via an active ester prepared by carbonyldiimidazole followed by a transesterification with 1-hydroxybenzotriazole. The manganese porphyrin conjugate Mn-trisMPyP-5′-GGCTC-CATTTCTTGCTCTC (see Scheme 1 for structure) was purified on a short column of a polyacrylamide gel (Bio-Gel P-2(F) from Bio-Rad) and HPLC on Gen Pak-Fax column (Waters). No loss of product was detected on use of these purification methods, whereas sephadex columns led to extensive degradation of the hybrid molecule. The tether has 17 bonds, and its length is sufficient to allow the binding of the cationic manganese porphyrin within the minor groove formed by the 19-mer vector and its complementary sequence contained in the 35-mer target 5′-CAGAGGAGAG-

[*] Dr. B. Meunier, M. Pitié, Dr. C. Casas, Dr. C. J. Lacey, Dr. G. Pratviel, Prof. Dr. J. Bernadou
Laboratoire de Chimie de Coordination du CNRS
205 route de Narbonne, F-31077 Toulouse Cedex, France

[**] This work was supported by the French Agency for AIDS Research (ANRS), Région Midi-Pyrénées, and CNRS. Dr. C. J. Lacey and Dr. C. Casas are indebted to CNRS and to Pierre Fabre Médicaments, respectively, for a research fellowship. We thank Christophe Loup for excellent technical assistance and preparation of metalloporphyrin precursors.

CAAGAAATGGAGCCAGTAGATCCTA. This DNA target corresponds to the region containing the initiation codon of TAT (35 mer = nucleotides 5360 to 5394 according to the numbering of ref. [15]). The expression of the HIV transacting factor TAT or other viral proteins like REV or ENV has been inhibited with antisense oligonucleotides.[16, 17]

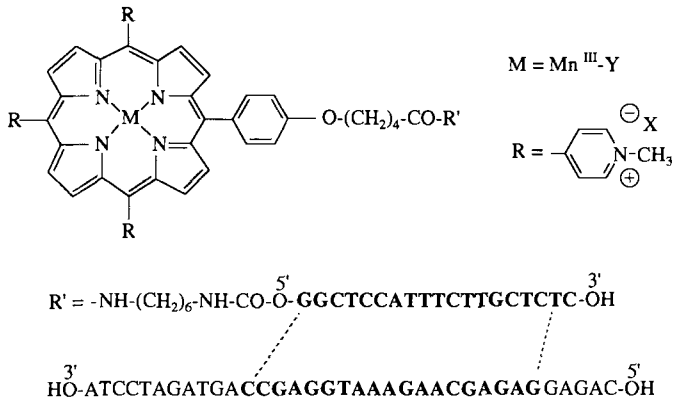

Scheme 1. Structural formulas of the hybrid molecule and the initiation codon region of the HIV-1 TAT gene (R' in the hybrid molecule contains a 19-mer complementary to this initiation codon region with an amino link at the 5' position). The axial ligand Y is a water molecule at pH <7 and a hydroxo group at pH >7. The counter ion X^- of the tris(*N*-methylpyridinio)porphyrin used in the coupling reaction was I^-.

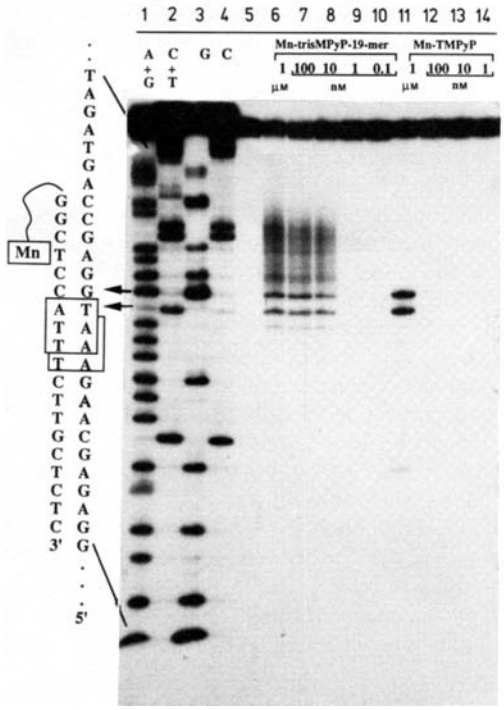

Fig. 1. Analysis by electrophoresis of the cleavage of a 5'-labeled 35-mer single-stranded DNA containing the initiation codon of the TAT gene of HIV-1 by a deliberately designed cationic manganese porphyrin conjugate Mn-trisMPyP 19-mer. Lane 1: Maxam-Gilbert A + G; lane 2: C + T; lane 3: G; lane 4: C; lane 5: 1 μM of the conjugate Mn-trisMPyP 19-mer without $KHSO_5$ (control); lanes 6 to 10: 1 μM, 100, 10, 1, and 0.1 nM of the conjugate Mn-trisMPyP 19-mer, respectively, with 1 mM $KHSO_5$; lanes 11 to 14: the Mn-porphyrin conjugate is replaced by 1 μM of free 19-mer and 1 μM, 100, 10, and 1 nM of Mn-TMPyP, respectively, with 1 mM $KHSO_5$.

In vitro assays of the anti-TAT nuclease activity of the vectorized manganese porphyrin were performed by using potassium monopersulfate, a water-soluble oxygen atom donor that we used to generate activated bleomycin[18] or oxomanganese–porphyrin complexes[11, 12, 19, 20] (such metal–oxo species can be generated in a cell by molecular oxygen and an electron source according to a mechanism similar to that of P-450 enzymes). Under the experimental conditions the manganese porphyrin conjugate Mn-trisMPyP 19-mer cleaves the HIV 35-mer at a very low concentration (10 nM) with only 2.6 equivalents of the vectorized DNA cleaver with respect to the target (lane 8 in Fig. 1). Such remarkable nuclease activity is obtained in the presence of a large excess of a random double-stranded DNA of salmon testes. The main cleavage sites (two discrete bands at T and G preceded by smears of high intensity) on the 35-mer are observed on the 3' side of a 5'-AAAT sequence. This sequence and the complementary strand make two A · T triplets (indicated by two overlapping squares in Fig. 1) which are the highest affinity sites of the parent metalloporphyrin Mn-TMPyP.[12] From previous studies, free Mn-TMPyP was expected to cleave the duplex formed by the 35-mer and the free 19-mer vector only at the vicinal nucleotides on the 3' side of each A · T triplet (T and G in the present case, see arrows in Fig. 1). This is effectively the case (lane 11) for the non-vectorized manganese porphyrin, but at higher concentration (1 μM). No cleavage was detected at nanomolar concentrations (lanes 12–14). The presence of two discrete bands and an intense smear in lanes 6 to 8 suggests that the mechanism of the DNA cleavage by the vectorized manganese porphyrin is not restricted to the specific 5' mechanism observed for the free metalloporphyrin Mn-TMPyP.[12]

Without question, the attachment of the cleaver motif tris(*N*-methylpyridinio)porphyrinatomanganese(III) to a 19-mer vector allowed selective recognition and cleavage of the complementary target, even in the presence of a large excess of random DNA. These data provide support for further investigations with nuclease-resistant manganese porphyrin conjugates on RNA-targets in vitro (an appropriate model for HIV would probably be a single-stranded RNA containing an AUG start codon as in viral RNA) and also at cellular level.

Experimental Procedure

Oligonucleotides were synthetized by standard solid-phase β-cyanoethylphosphoramidite chemistry on Cyclone Plus DNA equipment from Milligen/Biosearch. Both 35-mer and free 19-mer were purified to homogeneity on 20% polyacrylamide denaturating gels. Concentrations of single-stranded oligonucleotides were determined at 260 nm according to ref. [21]. The 35-mer was labeled at the 5' end by treatment with T4 polynucleotide kinase and [γ-^{32}P]ATP.

Synthesis of the manganese porphyrin conjugate Mn-trisMPyP 19-mer: The cationic, functionalized porphyrin (Scheme 1; R = methylpyridinio, R' = OH; for preparation see ref. [22]) was metalated by partially dissolving 5 mg (4.1 μmol) in 600 μL of a solution of $MnCl_2 \cdot 4H_2O$ (10.3 mg, 52 μmol) and heating in a sealed screw-cap Eppendorf tube for 4.5 h. The solution was evaporated to dryness (Speed-Vac), the residue dissolved in dry dimethylformamide (DMF), the solution filtered, and the product precipitated by addition of THF. The mixture was centrifuged (8000 rpm, 25 min), the supernatant drawn off, the pellet triturated with THF, and the mixture centrifuged a second time. The product was dried under vacuum. The metalated cationic porphyrin (2.87 mg, 2.3 μmol) was dissolved in 150 μL of dry DMF, and carbonyldiimidazole (CDI, 7.11 mg, 44 μmol) was added. Formation of the imidazolide was allowed to take place over 13 h. Then 1-hydroxybenzotriazole (12 mg, 88 μmol) was added, and after 4 h at room temperature the excess of CDI was hydrolyzed by addition of 20 μL of 0.2 M Hepes buffer, pH 8. After 30 min the solution was added to 2.1 optical density units (λ = 260 nm, 13.4 nmol) of NH_2-19-mer oligonucleotide in 20 μL of buffer (this oligonucleotide was prepared by the automated phosphoramidite method and functionalized at the 5' position by the method of Wachter et al. [23]). (Note: one optical density unit will yield an absorption of 1.0 in 10 mL of 0.1 M NaCl, pH 7.0 for a 1 cm light path, here at λ = 260 nm.) The solution was incubated at 37 °C for 20 h. The solvents were removed under vacuum (Speed-Vac), the residue taken up in 500 μL of water,

and the solution applied to a column (2.5 g, 10 mL) of Bio-Gel P-2(F) from Bio-Rad equilibrated with water. The crude product was purified by HPLC (Gen Pak-Fax column from Waters; A = 0.025 M Tris · HCl, pH 8.5; B = A + 1 M NaCl; linear gradient: 10 to 90% B over 45 min; flow rate = 0.7 mL min^{-1}; the chromatogram was monitored with a 2-channel diode array detector) and desalted on a bed of Bio-Gel P-2(F) (2 g, water). A comparison of the UV/VIS spectra before and after desalting revealed no loss of product. Spectrophotometric data were: oligonucleotide, $\varepsilon_{260} = 1.6 \times 10^5\ M^{-1}cm^{-1}$; Mn^{III} porphyrin: $\varepsilon_{466} = 0.98 \times 10^5\ M^{-1}cm^{-1}$; hybrid molecule: calculated $\varepsilon_{466}/\varepsilon_{260} = 0.62$, observed $A_{468}/A_{264} = 0.63$. Yield was 25% after final purification and desalting (measured by UV spectroscopy at 264 nm). The HPLC retention time of the conjugate was 20.1 min compared to 22.6 min for the starting oligonucleotide.

Each DNA cleavage reaction (see Fig. 1) was performed with 3.75 nM of the 5'-labeled 35-mer (21 300 cpm $nmol^{-1}$; 9.6 nCi $nmol^{-1}$), from 0.1 nM to 1 μM of Mn-trisMPyP 19-mer (DNA cleaver/target ratio between 0.026 and 260) and 400 μM in nucleotides of double-stranded salmon testes DNA (3000 equivalents with respect to the 35-mer) in a solution of 125 mM NaCl and 50 mM Tris · HCl buffer (pH 8). Annealing of the free Mn-trisMPyP 19-mer with the 35-mer was achieved by heating at 90 °C for 3 min and followed by a cooling to 37 °C within 4 h and overnight storage at 4 °C. All assays (total volume = 16 μL) were performed at 4 °C. For reactions without conjugate, the free 19-mer was hybridized with the 35-mer and then pre-incubated with 1 nM to 1 μM of the parent DNA cleaver without vector Mn-TMPyP (pentaacetate of *meso*-tetrakis(4-*N*-methylpyridinio)porphyrinatomanganese(III); see ref. [11] for preparation) for 15 min at 4 °C before addition of $KHSO_5$. DNA cleavage reactions were initiated by addition of 1 mM $KHSO_5$ and maintained at 4 °C for 1 h. Reactions were then quenched by 40 mM Hepes buffer (pH 8), and the mixtures heated at 90 °C for 30 min (all concentrations listed are final concentrations). After cooling to 4 °C, samples were diluted with 1 μL of yeast tRNA (10 mg mL^{-1}) and 100 μL of 0.3 M sodium acetate (pH 5.2), precipitated with 300 μL of ethanol, and finally rinsed with 75% ethanol and lyophylized. Fragments of DNA were analyzed by 20% polyacrylamide gel electrophoresis under denaturing conditions (7 M urea) as previously described[12].

Received: November 4, 1992
Revised December 22, 1992 [Z 5663/5665 IE]
German version: *Angew. Chem.* **1993**, *105*, 607

[1] P. C. Zamecnik, M. L. Stephenson, *Proc. Natl. Acad. Sci. USA* **1978**, *75*, 280.
[2] S. Agrawal, T. Ikeuchi, D. Sun, A. Konodka, J. Maizel, P. C. Zamecnik, *Proc. Natl. Acad. Sci. USA* **1989**, *86*, 7790.
[3] E. Uhlmann, A. Peyman, *Chem. Rev.* **1990**, *90*, 543.
[4] a) *Prospects for Antisense Nucleic Acid Therapy of Cancer and AIDS* (Ed.: E. Wickstrom), Wiley-Liss, New York, **1991**; b) M. Matsukura, H. Mitsuya, S. Broder in [4a], p. 159.
[5] L. Leserman, G. Degols, P. Machy, J. P. Leonetti, N. Mechti, B. Lebleu in [4a], p. 25.
[6] C. MacKellar, D. Graham, D. W. Will, S. Burgess, T. Brown, *Nucleic Acids Res.* **1992**, *20*, 3411.
[7] C. A. Stein, R. Pal, A. L. DeVico, G. Hoke, S. Mumbauer, O. Kinstler, M. G. Sarngadharan, R. L. Letsinger, *Biochemistry* **1991**, *30*, 2439.
[8] H. E. Moser, P. B. Dervan, *Science* **1987**, *238*, 645.
[9] D. Sigman, *Biochemistry* **1990**, *29*, 9097.
[10] a) V. Vlassov, L. A. Yakubov in [4a], p. 243; b) T. Le Doan, L. Perrouault, C. Hélène, M. Chassignol, N. T. Thuoung, *Biochemistry* **1986**, *25*, 6736; T. Le Doan, L. Perrouault, M. Chassignol, N. T. Thuoung, C. Hélène, *Nucleic Acids Res.* **1987**, *15*, 8643; T. Le Doan, D. Praseuth, L. Perrouault, M. Chassignol, N. T. Thuong, C. Hélène, *Bioconjugate Chem.* **1990**, *1*, 108.
[11] J. Bernadou, G. Pratviel, F. Bennis, M. Girardet, B. Meunier, *Biochemistry* **1989**, *28*, 7268.
[12] M. Pitié, G. Pratviel, J. Bernadou, B. Meunier, *Proc. Natl. Acad. Sci. USA* **1992**, *89*, 3967.
[13] R. J. Fiel, E. Mark, T. Button, S. Gilani, D. Musser, *Cancer Lett.* **1988**, *40*, 23.
[14] L. Ding, J. Balzarini, D. Schols, B. Meunier, E. De Clercq, *Biochem. Pharmacol.* **1992**, *44*, 1675.
[15] S. Wain-Hobson, P. Sonigo, O. Danos, S. Cole, M. Alizon, *Cell* **1985**, *40*, 9.
[16] T. Shimada, H. Fugii, B. Maier, S. Hayashi, H. Mitsuya, S. Broder, A. W. Nienhuis, *Antiviral Chem. Chemother.* **1991**, *2*, 133.
[17] G. Sczakiel, M. Pawlita, *J. Virol.* **1991**, *65*, 468.
[18] G. Pratviel, J. Bernadou, B. Meunier, *Biochem. Pharmacol.* **1989**, *38*, 133.
[19] L. Ding, J. Bernadou, B. Meunier, *Bioconjugate Chem.* **1991**, *2*, 201.
[20] L. Ding, G. Etemad-Moghadam, S. Cros, C. Auclair, B. Meunier, *J. Med. Chem.* **1991**, *34*, 900.
[21] *Handbook of Biochemistry and Molecular Biology-Nucleic Acids* (Ed.: G. Fasman), 3rd ed., CRC Press, **1975**, p. 175.
[22] C. Casas, B. Saint-Jalmes, C. Loup, C. J. Lacey, B. Meunier, *J. Org. Chem.* **1993**, in press.
[23] L. Wachter, J. A. Jablonski, K. L. Ramachandran, *Nucleic Acids Res.* **1986**, *14*, 7985.

p-[$3^2.5^6$]Octahedrane, the $(CH)_{12}$ Hydrocarbon with D_{3d} Symmetry**

By *Chih-Hung Lee, Shelue Liang, Thomas Haumann, Roland Boese,* and *Armin de Meijere**

Dedicated to Professor Klaus Hafner on the occasion of his 65th birthday

As a rule, polycyclic cage hydrocarbons[1] have unusual properties, and research into them is as topical as ever.[1-3] Among the cage molecules with the formula $(CH)_{2n}$, those with the highest symmetry have always exercised the greatest attraction. Back in 1977 Garrat et al. pointed out the formal relationship between the polycycles **1**, **2**, and **3**.[4] All three contain a central *n*-membered ring whose carbon atoms are linked alternately to the corners of an *n*/2-membered ring lying above or below them. Whereas dodecahedrane **3** [$(CH)_{2n}$, where $n = 10$] has been prepared since then,[1,3] and its reactions are at present under intense investigation,[3e-h] no breakthrough could be achieved in the synthesis of *p*-[$4^2.5^8$]decahedrane **2**[5] and the unsubstituted *p*-[$3^2.5^6$]octahedrane **1**.[6,9] We now report a short synthesis of the dimethyl ester of *p*-[$3^2.5^6$]octahedrane-2,10-dicarboxylic acid (**7**) and the parent hydrocarbon **1**.

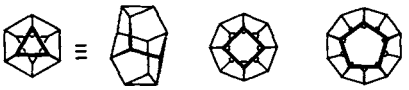

1 **2** **3**

The crucial precursor of the first synthesis of dodecahedrane,[3a] the dimethyl ester **4** of 2a,3,3a,5a,6a,6b,6c-octahydrodicyclopenta[*cd*,*gh*]pentalene-3,6-*endo*,*endo*-dicarboxylic acid,[11] served as starting material. The addition of bromine to **4** afforded a nonseparable mixture of the bromides **5** and **6** in 45% yield in a ratio of 2:1. Heating the mixture of **5** and **6** in methanol with five equivalents of sodium methyl alcoholate for 2 h furnished **7** in 55% yield (based on **6**). Its constitution with C_{2h} symmetry was consistent with the ^1H NMR spectrum (in $CDCl_3$, signals at $\delta = 3.60$ (s, 6 H), 3.56–3.50 (m, 2 H), 3.30–3.20 (m, 4 H), and 2.45–2.35 (br. s, 4 H)), and with the ^{13}C NMR spectrum (in $CDCl_3$, $\delta = 171.9$ (C=O), 61.2 (C1(6) or CH_3), 61.1 (CH_3 or C1(6)), 51.5 (C2(10)), 47.9 (C5(7,8,12)), and 45.8 (C3(4,9,11)). Colorless prisms that were suitable for X-ray structure analysis (Fig. 1)[12] crystallized from dichloromethane/cyclohexane (m.p. 213–214 °C).

The diester **7** was saponified with sodium hydroxide in methanol. Acidification with concentrated hydrochloric acid at 0 °C gave the dicarboxylic acid **8** in 80% yield which was transformed into the acid chloride with thionyl chloride. This was prepared for the decarboxylation according to Barton[14] with sodium pyridine-2-thione-*N*-oxide. Photolysis in benzene of the bis-*O*-acylthiohydroxamate obtained thus afforded the hydrocarbon **1** in 74% yield as a colorless solid [m.p. 134–135 °C (sealed capillary), after sublimation under

[*] Prof. Dr. A. de Meijere, Dr. C.-H. Lee, Dipl.-Chem. S. Liang
Institut für Organische Chemie der Universität
Tammannstrasse 2, D-W-3400 Göttingen (FRG)
Dipl.-Chem. T. Haumann, Priv.-Doz. Dr. R. Boese
Institut für Anorganische Chemie der Universität-GH Essen (FRG)

[**] This work was supported by the state of Niedersachsen and the Fonds der Chemischen Industrie. We thank the companies Bayer, BASF, and Hoechst AG for gifts of chemicals.

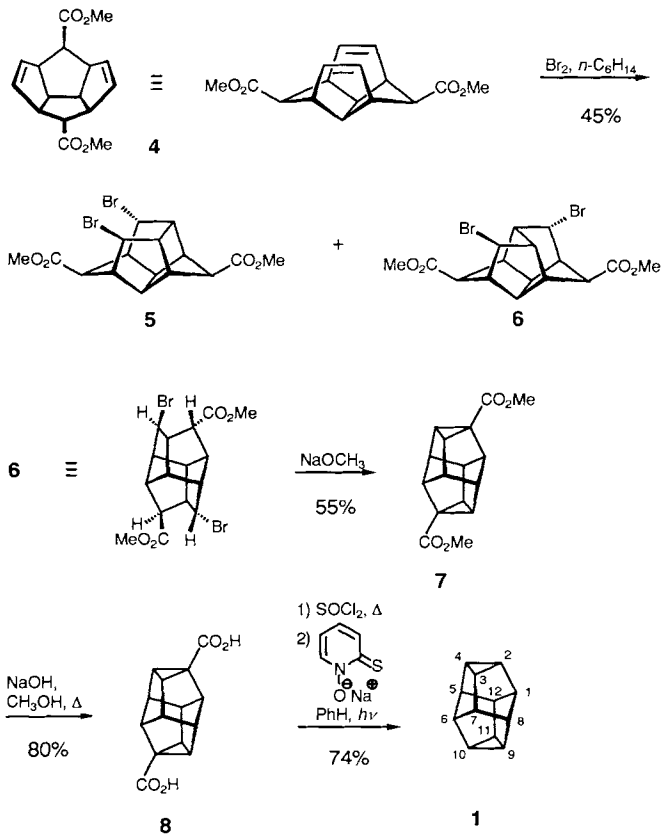

reduced pressure], and its structure was determined by X-ray crystallography (Fig. 1).[15]

p-[$3^2.5^6$]Octahedrane **1** has the point symmetry D_{3d} rare among hydrocarbons; the point symmetry corresponds to the unusual space group $R\bar{3}c$ of the crystals. Its 500 MHz ^{1}H NMR spectrum (in $CDCl_3$) shows only two broad singlets at $\delta = 3.00$ (6H, 1(5,6,7,8,12)-H) and 1.60 (6H, 2(3,4,9,10,11)-H). The coupling between the cyclopropyl protons and those at the central ring, determined from the COSY long-range ^{1}H NMR spectrum, is apparently very small, which must be attributed to the relatively large H-C-C bond angle [H2-C2-C1: 123.5(15)°, H1-C1-C2: 115.3(13)°] at the five-membered rings, which are rigid and folded with an angle of 34.1°.[16] With respect to the ^{1}H NMR signal of dodecahedrane **3** ($\delta = 3.38$, in $CDCl_3$), the signal of the protons belonging to the five-membered rings on the central six-membered ring of **1** undergoes a high-field shift, apparently the effect of the diamagnetic anisotropy of the three-membered rings.[17] This is also manifest in the 125.7 MHz ^{13}C NMR spectrum (in $CDCl_3$) of **1**, which displays two doublets at $\delta = 62.3$ ($^1J_{C,H} = 140$ Hz, C1(5,6,7,8,12))[18] and 33.6 ($^1J_{C,H} = 170$ Hz, C2(3,4,9,10,11)). The relatively large ^{13}C–H coupling constant of 170 Hz at the cyclopropyl positions[19] reflects a different type of hybridization at the cyclopropyl carbon atoms than in simple cyclopropane derivatives, as a result of the bending of the three C–C bonds in each ring that point inward. The increased s character of 34% for the cyclopropylic C–H bonds in **1** that correlates[20] with the coupling constant of $^1J = 170$ Hz probably implies an increased C–H acidity. As a result an independent chemistry for suitable derivatives of the dicarboxylic acid **8** and perhaps also for the hydrocarbon **1** can be predicted.[21] The bond lengths of 1.507(4) Å in the three-membered ring of **1** are normal, and the stretching of the bonds of the three-membered rings proximal to the methoxy carbonyl groups and contraction of the distal bonds in diester **7** corresponds to the usual effect of an electron-withdrawing substituent.[22]

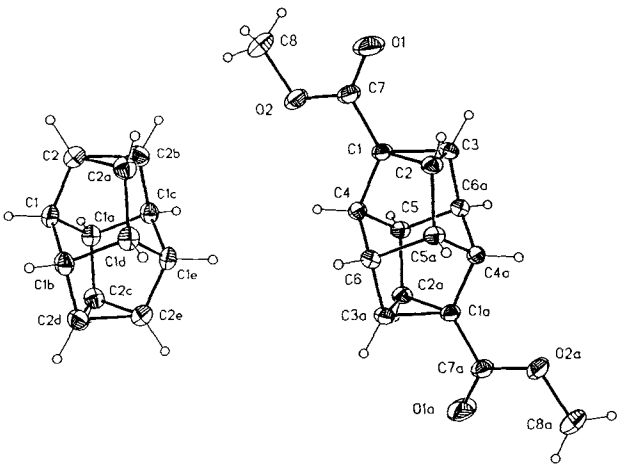

Fig. 1. Crystal structures of the dimethyl ester (**7**) of *p*-[$3^2.5^6$]octahedrane-2,10-dicarboxylic acid (right) and *p*-[$3^2.5^6$]octahedrane (**1**, left) [13]. Bond lengths [Å] and angles [°] (numbering does not conform to IUPAC rules): **7**: (averaged for C_{2h} symmetry): C1-C2 1.529(1), C1-C4 1.527(2), C1-C7 1.476(2), C2-C3 1.495(1), C4-C5 1.551(1), C5-C6a 1.554(1); C1-C3-C2 60.7(1), C2-C1-C4 106.9(1), C2-C1-C7 119.1(1), C4-C1-C7 126.6(1), C1-C4-C6 106.0(1), C2-C1-C3 58.6(1), C5-C4-C6 101.0(1). – **1**: C1-C2 1.520(3), C1-C1a 1.550(3), C2-C2a 1.507(4); C2-C1-C1a 106.4(1), C1a-C1-C1b 100.7(2), C1-C2-C2a 106.9(1), C2-C1-C1b 106.4(2), C2a-C2-C2b 60.0(1), C1-C2-C2b 106.8(1).

Received: December 3, 1992 [Z 5724 IE]
German version: *Angew. Chem.* **1993**, *105*, 611

[1] Cf. *Cage Hydrocarbons* (Ed.: G. A. Olah), Wiley, New York, **1990**, and references therein; *Carbocyclic Cage Compounds* (Eds.: E. Osawa, O. Yonemitsu), VCH, New York, **1992**, and references therein.

[2] Cubane as $(CH)_8$: a) P. E. Eaton, T. W. Cole, Jr., *J. Am. Chem. Soc.* **1964**, *86*, 3157; b) P. E. Eaton, M. Maggini, *ibid.* **1988**, *110*, 7230; c) P. E. Eaton, C.-H. Lee, Y. Xiong, *ibid.* **1989**, *111*, 8016; d) P. E. Eaton, *Angew. Chem.* **1992**, *104*, 1447; *Angew. Chem. Int. Ed. Engl.* **1992**, *31*, 1421. Pentaprismane as $(CH)_{10}$: e) P. E. Eaton, Y. S. Or, S. J. Branca, B. K. Ravi Shankar, *Tetrahedron* **1986**, 1621; dodecahedrane as $(CH)_{20}$: f) L. A. Paquette, *Chem. Rev.* **1989**, *89*, 1051.

[3] a) L. A. Paquette, D. W. Balogh, R. Usha, D. Kountz, G. G. Christoph, *Science* **1981**, *211*, 575; b) L. A. Paquette, D. W. Balogh, *J. Am. Chem. Soc.* **1982**, *104*, 774; c) R. J. Ternansky, D. W. Balogh, L. A. Paquette, *ibid.* **1982**, *104*, 4503; d) W.-D. Fessner, B. A. R. C. Murty, J. Wörth, D. Hunkler, H. Fritz, H. Prinzbach, W. D. Roth, P. von R. Schleyer, A. B. McEwen, W. F. Maier, *Angew. Chem.* **1987**, *99*, 484; *Angew. Chem. Int. Ed. Engl.* **1987**, *26*, 452; e) R. Pinkos, J.-P. Melder, H. Prinzbach, *ibid.* **1990**, *102*, 102 and **1990**, *29*, 92; f) J.-P. Melder, R. Pinkos, H. Prinzbach, *ibid.* **1990**, *102*, 105 and **1990**, *29*, 95; g) J.-P. Melder, H. Prinzbach, *Chem. Ber.* **1991**, *124*, 1271; h) D. Elsässer, K. Hassenrück, H.-D. Martin, B. Mayer, G. Lutz, H. Prinzbach, *ibid.* **1991**, *124*, 2863.

[4] P. J. Garratt, J. F. White, *J. Org. Chem.* **1977**, *42*, 1733.

[5] L. A. Paquette in [1], p. 313 ff., and references therein

[6] Systematic name: heptacyclo[6.4.0.$0^{2,4}$.$0^{3,7}$.$0^{5,12}$.$0^{6,10}$.$0^{9,11}$]dodecane. The trivial name ditriaxane was previously proposed for this hydrocarbon (**1**) [7]. We favor the term introduced by Paquette et al. [8], *p*-[$3^2.5^6$]octahedrane, which enables the symmetry of the molecule and its relationship to other members of the subgroup of $(CH)_{2n}$ hydrocarbons to be recognized more easily.

[7] K.-I. Hirao, Y. Ohuchi, O. Yonemitsu, *J. Chem. Soc. Chem. Commun.* **1982**, 99; K.-I. Hirao, H. Takahashi, Y. Ohuchi, O. Yonemitsu, *J. Chem. Res. (S)* **1992**, 319; *(M)* **1992**, 2601–2611.

[8] Cf. L. A. Paquette, A. R. Browne, C. W. Doecke, R. V. Williams, *J. Am. Chem. Soc.* **1983**, *105*, 4113, and footnote [4] therein.

[9] P. J. Garratt, C. W. Doecke, J. C. Weber, L. A. Paquette, *J. Org. Chem.* **1986**, *51*, 449.

[10] Only the synthesis of the C_2-symmetric 2,9-dimethyl derivative of **1** has been reported [7].

[11] L. A. Paquette, M. J. Wyvratt, H. C. Berk, R. E. Moerck, *J. Am. Chem. Soc.* **1978**, *100*, 5845.

[12] Diffractometer Siemens 3m/V, $Mo_{K\alpha}$, graphite monochromator, Wyckoff scan, $3.0° < 2\theta < 65°$, direct methods (SHELXTL-PLUS). Crystal size $0.35 \times 0.35 \times 0.14$ mm^3, space group $P2_1/c$, $Z = 2$, $T = 293$ K, unit cell: $a = 9.125(1)$, $b = 5.982(1)$, $c = 12.024(1)$ Å, $\alpha = \gamma = 90$, $\beta = 108.41(1)°$,

2249 independent reflections, 1861 of which were observed ($F_0 \geq 4.0\sigma(F_0)$). 102 parameters, all non-hydrogen atoms refined anisotropically, hydrogen atoms as rigid groups, $R = 0.0455$, $R_w = 0.0547$.

[13] Further details of the crystal structure investigation may be obtained from the Fachinformationszentrum Karlsruhe, Gesellschaft für wissenschaftlich-technische Information mbH, D-W-7514 Eggenstein-Leopoldshafen 2 (FRG) on quoting the depository number CSD-400029 (for **7**), and 400005 (for **1**), the names of the authors, and the journal citation.

[14] D. H. R. Barton, Y. Hervé, P. Potier, J. Thierry, *Tetrahedron* **1988**, *44*, 5479.

[15] Diffractometer Siemens 3m/V, $Mo_{K\alpha}$, graphite monochromator, Wyckoff scan. $3.0° < 2\theta < 55°$, direct methods (SHELXTL-PLUS). Crystal size $0.4 \times 0.35 \times 0.2$ mm^3, space group *R*-3*c*, $Z = 6$, $T = 293$ K, unit cell: $a = b = 9.477(2)$, $c = 14.903(3)$ Å, $\alpha = \beta = 90$, $\gamma = 120°$, 301 independent reflections, 223 of which were observed ($F_0 \geq 4.0\sigma(F_0)$). 27 parameters, all non-hydrogen atoms refined anisotropically, $R = 0.0482$, $R_w = 0.0579$.

[16] The analogous vicinal H,H coupling constants in triaxane ([3]peristylane) are about 1.5 Hz: A. Nickon, G. D. Pandit, *Tetrahedron Lett.* **1968**, 3663.

[17] Cf. K. Tori, K. Kitahonoki, *J. Am. Chem. Soc.* **1965**, *87*, 386; C. D. Poulter, R. S. Boikess, J. I. Brauman, S. Winstein, *ibid.* **1972**, *94*, 2291; R. C. Hahn, P. H. Howard, *ibid.* **1972**, *94*, 3143; T. Preuss, Dissertation, Universität Hamburg, **1983**.

[18] The ^{13}C NMR signal of the carbon atoms in the five-membered ring of dodecahedrane **3** lies at $\delta = 66.93$.[3c]

[19] The $^1J_{C,H}$ values of cyclopropanes whose angles are not deformed are found to be approximately 160 Hz. Cf. H. Günther, *NMR-Spektroskopie*, 3rd ed., Thieme, Stuttgart, **1992**, p. 452.

[20] N. Muller, D. E. Pritchard, *J. Chem. Phys.* **1959**, *31*, 768.

[21] For example, one should be able to introduce other functional groups into **8** with the help of proven directing groups (see P. Beak, V. Snieckus, *Acc. Chem. Res.* **1982**, *15*, 306) by deprotonation and electrophilic substitution, as has been impressively demonstrated for cubane and cyclopropane derivatives [2c].

[22] Cf. F. H. Allen, *Acta Crystallogr. Sect. B* **1980**, *36*, 81, and references therein.

[MnM(egta)] · 8 H_2O (M = Mn, Cd): A Novel Type of Two-Dimensional Magnetic Lattice**

By *Juan J. Borrás-Almenar, Eugenio Coronado,* Carlos J. Gómez-García,* and *Lahcène Ouahab*

Research in the field of low-dimensional magnetism has been particularly active in the last decade, and major developments have occurred in both the theoretical and magnetochemical areas.[1] The most remarkable advance is perhaps the preparation and characterization of compounds containing ferrimagnetic chains, also called one-dimensional (1-D) ferrimagnets.[2] Typically, this kind of compound has two alternating metal sites in the structure and a characteristic magnetic behavior: a minimum in the plot of the product of the magnetic susceptibility and temperature versus temperature, arising from the noncompensation of the two alternating magnetic moments. Aside from the interest in 1-D magnetism, some of these compounds are of interest as molecular-based materials exhibiting cooperative magnetic effects (bulk ferro- and ferrimagnets) as a consequence of the interchain interactions.[3]

In this field, coordination chemistry has provided most of the known 1-D ferrimagnets. The next step is now the search for novel compounds of higher magnetic dimensionality. There are two reasons that justify this goal: From the physical point of view, 2-D systems are the most interesting in magnetism,[4] since they form the borderline between ordering and nonordering systems.[5] From the chemical point of view, it is essential to control the transition from 1-D to 2-D systems in order to shift the ordering temperature of a molecular ferromagnet toward higher temperatures. In this context, we previously demonstrated that removing some water from the ferrimagnetic chain compounds MM'[edta] · 6 H_2O (M, M' = Mn^{II}, Co^{II}, Ni^{II}, and Cu^{II}; edta = ethylenediaminetetraacetate) through a hydrothermal treatment results in an interconnection of the chains, and consequently, in an extension of the ferrimgnetic lattice.[6]

An alternative way to increase the dimensionality may consist of introducing more coordinating donor groups into the ligand. We report here such an example obtained by reaction of the ethylenedioxybis(ethylenenitrilo)tetraacetate (egta[7]) with Mn^{II} and Cd^{II} ions. This new series of isomorphous complexes can be formulated as [MnM(egta)] · 8 H_2O and shows an unprecedented puckered, layered structure, which may give rise to a novel type of two-dimensional magnetic lattice.

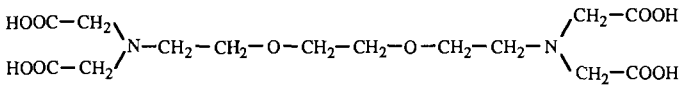

H_4egta

The X-ray crystal structure determination, carried out on Mn–Cd crystals,[8] shows the presence of two different metal sites (Fig. 1a): an eight-coordinate site, with square antiprismatic geometry, in which egta wraps around the cadmium center to form the dianion $[Cd(egta)]^{2-}$, and an octahedral site in which the manganese is surrounded by six oxygen atoms from three water molecules and three carboxylate groups belonging to three different egta ligands. In each

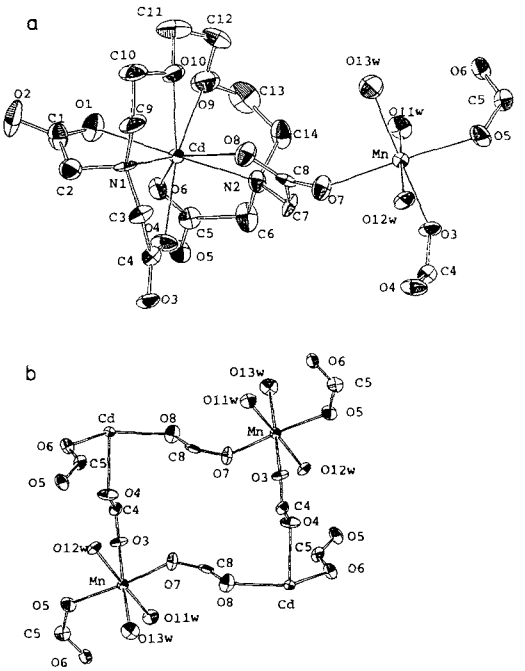

Fig. 1. Crystal structure of [MnCd(egta)] · 8 H_2O (ORTEP). a) First coordination sphere of the Cd and Mn ions. b) View of the tetranuclear centrosymmetrical unit $[MnCd(egta)]_2$.

[*] Prof. Dr. E. Coronado, Dr. J. J. Borrás-Almenar, Dr. C. J. Gómez-García
Departamento de Química Inorgánica
Universidad de Valencia
Dr. Moliner 50, E-46100 Burjasot (Spain)
Dr. L. Ouahab
Laboratoire de Chimie du Solide et Inorganique Moléculaire
Université de Rennes (France)

[**] This work is supported by the Dirección General de Investigación Científica y Técnica (PB91-0652), the Program of Spanish–French Integrated Actions (HF-068), and by the Institució Valenciana d'Estudis i Investigació. J. J. B-A and C. J. G.-G thank the Ministerio de Educación y Ciencia for a Fellowship Grant.

dianion three carboxylate groups act as bridging ligands connecting the cadmium ion to three manganese ions. Two of these three carboxylate groups (O3-C4-O4 and O7-C8-O8) are involved in the construction of a tetranuclear centrosymmetrical unit formed by alternating Cd and Mn sites (Fig. 1b). The third carboxylate (O5-C5-O6) connects these basic units to give, as overall structure, the extended layered network showed in Figure 2. This figure reveals parallel layers well separated from each other: the shortest interlayer metal–metal distances are Mn–Mn = 11.808(2), Mn–Cd = 9.965(2), and Cd–Cd = 8.680(1) Å, while within the layer the nearest neighbor Mn–Cd distances are d_1 = 5.752(2), d_2 = 6.148(2), and d_3 = 5.553(2) Å (corresponding to the three carboxylate bridges).

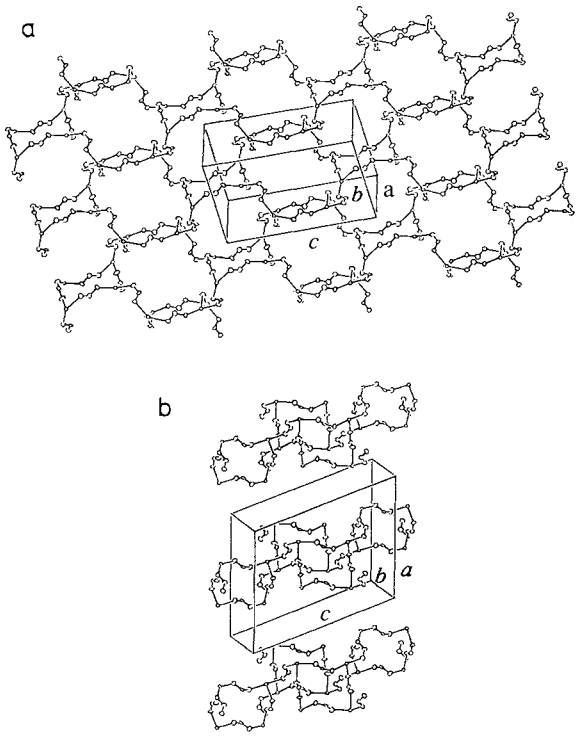

Fig. 2. a) View onto the bc plane of a bimetallic layer. b) The stacking of the layers.

When both sites are occupied by manganese, this unusual structure should give rise to the two-dimensional magnetic lattice sketched in Scheme 1. In this lattice the two magnetic sites (indicated as open and filled circles) alternate in both directions and are coupled by three different exchange interactions (J_1, J_2, and J_3), in accordance with the three different carboxylate bridges. The magnetic behavior for this compound has been investigated with a SQUID susceptometer in a magnetic field of 0.1 T between 298 and 2 K, and is compared in Figure 3 with that obtained for the Mn–Cd compound. While in the Cd-containing compound the product

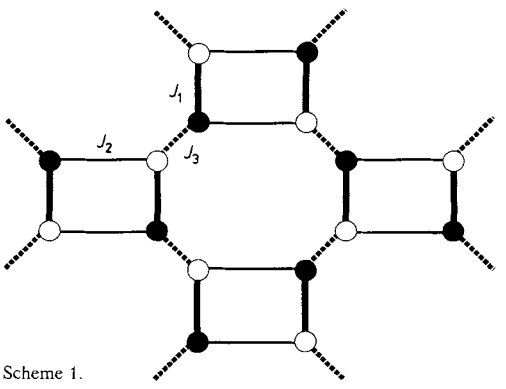

Scheme 1.

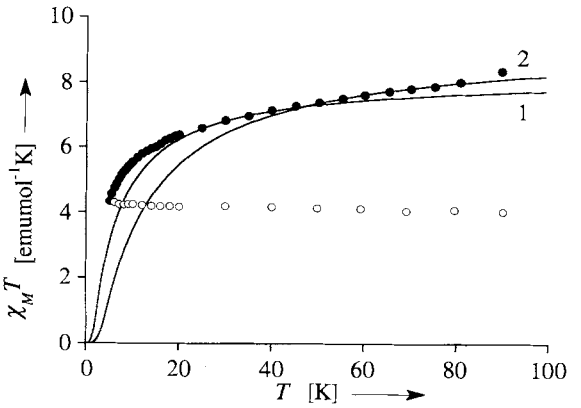

Fig. 3. Plot of $\chi_m T$ versus T for [MnMn(egta)] · 8 H_2O (solid circles) and [MnCd(egta)] · 8 H_2O (open circles). Solid lines correspond to the behaviors of a square S = 5/2 Heisenberg lattice with $J = -0.35\ cm^{-1}$ and $g = 2.14$ (curve 1), and $J = -0.7\ cm^{-1}$ and $g = 2.02$ (curve 2).

$\chi_m T$ is almost temperature-independent, as expected for isolated Mn^{II} ions, the Mn–Mn compound shows a continuous decrease of $\chi_m T$ with decreasing temperature and no evidence of transition to a long-range order in the investigated temperature range. Such behavior is consistent with the presence of short-range antiferromagnetic interactions between Mn^{II} ions through the carboxylate bridges. The lack of a theoretical model for this kind of 2-D system precludes a quantitative analysis of the magnetic data. However, an estimate of the nearest neighbor exchange interactions may be deduced from the model developed for a square spin lattice with a single interaction J.[9] As expected, this model does not give an overall fit to the data, but from the fits obtained by using the low and high temperature data (see curves 1 and 2 in Fig. 3), antiferromagnetic exchange constants in the range 0.35–0.70 cm^{-1} may be derived. These values are similar to that found in the related manganese chain compound [MnMn(edta)] · 9 H_2O[10] for which $J = -0.5\ cm^{-1}$, in agreement with the similar arrangements of the carboxylate bridges. However, it is interesting to notice that whereas the compound with the edta chain undergoes a long-range magnetic ordering at T_c = 1.5 K, no indication of ordering is found down to 2 K in the egta compound despite its higher dimensionality. This result emphasizes the good magnetic isolation of its 2-D lattice.

This preliminary work demonstrates the feasibility of preparing structurally ordered bimetallic layers containing the egta ligand. The versatility of this lattice opens quite interesting possibilities in magnetochemistry, since by variation in the two interacting paramagnetic ions, 2-D ferrimagnetic materials should be isolated. This includes the preparation of compounds formed by rare earth elements and transition metal ions, since the egta ligand has been shown to form very stable complexes with lanthanides. Attempts are in progress.

Experimental Procedure

Synthesis of [MnMn(egta)] · 8 H_2O: $MnCO_3$ (0.3448 g, 3.0 mmol) was added to a warm solution of H_4egta (0.5534 g, 1.5 mmol) in 40 mL of H_2O (final

pH = 5.33). This solution was filtered through paper to remove any insoluble material. A portion (10 mL) of this solution was diluted with 20 mL of H_2O and placed in a U-shaped cell with acetone. After several weeks, slow diffusion of acetone vapor caused a white crystalline powder to deposit.

[MnCd(egta)] · $8H_2O$ was synthesised by a similar procedure. $Cd(NO_3)_2$ (0.3085 g, 1 mmol) was added to a solution of H_4egta (0.3690 g, 1.0 mmol) in 25 mL of H_2O. The pH of this solution was adjusted to 2.5 by adding about 2 mL of 1 M NaOH (2 mmol). $MnCO_3$ (0.1149 g, 1.0 mmol) was then added, and the resulting solution was gently heated for 1 hour (final pH = 4.2). Finally, this solution was allowed to cool at room temperature and placed in a U-shaped cell with acetone. After several weeks of slow diffusion of acetone vapor, white needles formed. IR spectra show the presence of the egta ligand in the white powder and in the single crystals. Both compounds provided a correct elemental analysis and show quite similar X-ray powder patterns.

Received: November 13, 1992 [Z 5684 IE]
German version: *Angew. Chem.* **1993**, *105*, 637

[1] a) *Magneto-Structural Correlations in Exchange-Coupled Systems* (Eds.: R. D. Willett, D. Gatteschi, O. Kahn) (*NATO ASI Ser.* **1985**); b) *Magnetic Molecular Materials* (Eds.: D. Gatteschi, O. Kahn, J. S. Miller, F. Palacio) (*NATO ASI Ser. Ser. E* **1991**), p. 198.

[2] C. P. Landee in *Organic and Inorganic Low Dimensional Crystalline Materials* (Eds.: P. Delhaes, M. Drillon) (*NATO ASI Ser.* **1987**), p. 168.

[3] O. Kahn in *Magnetic Molecular Materials* (Eds.: D. Gatteschi, O. Kahn, J. S. Miller, F. Palacio) (*NATO ASI Ser. Ser. E* **1991**), p. 198; A. Caneschi, D. Gatteschi, R. Sessoli, P. Rey, *Acc. Chem. Res.* **1989**, *22*, 392–398.

[4] L. J. de Jongh in *Magnetic Properties of Layered Transition Metal Compounds, Vol. 9* (Ed.: L. J. de Jongh), Kluwer, Dordrecht, **1990**.

[5] Ordering and nonordering systems refer to the presence or absence of a transition to a long-range ordered state at a finite temperature.

[6] F. Sapiña, E. Coronado, D. Beltrán, R. Burriel *J. Am. Chem. Soc.* **1991**, *113*, 7940.

[7] The chelating properties of the egta ligand with different alkaline earth elements, lanthanides, and transition metals have been recently reported: C. K. Schauer, O. P. Anderson, *Acta Crystallogr. Sect. C* **1986**, *42*, 760; *J. Am. Chem. Soc.* **1987**, *109*, 3646; *Acta Crystallogr. Sect. C.* **1988**, *44*, 981; *J. Chem. Soc. Dalton Trans.* **1989**, 185; *Inorg. Chem.* **1988**, *27*, 3118.

[8] [MnCd(egta)] · $8H_2O$: white needles: $0.48 \times 0.17 \times 0.08$ mm^3, Enraf-Nonius CAD4 diffractometer, $M_r = 687.78$, monoclinic, space group $P2_1/c$ with $a = 15.47(3)$, $b = 9.633(9)$, $c = 18.86(3)$ Å, $\beta = 108.2(1)°$, $V = 2671$ Å^3 and $Z = 4$ ($\rho_{calcd} = 1.710$ g cm^{-3}; $Mo_{K\alpha}$ radiation, $\lambda = 0.71073$ Å, $\mu = 13.234$ cm^{-1}), structure solved by direct methods and successive Fourier difference synthesis, refinement of 328 variables with anisotropic thermal parameters, $R(F) = 0.063$ and $R_w(F) = 0.083$, 2477 absorption corrected reflections with $I \geq 3\sigma(I)$. Further details of the crystal structure determination may be obtained from the Fachinformationszentrum Karlsruhe, Gesellschaft für wissenschaftlich-technische Information mbH, W-7514 Eggenstein-Leopoldshafen 2 (FRG), on quoting the depository number CSD-56895, the names of the authors, and the journal citation.

[9] M. E. Lines, *J. Phys. Chem. Solids.* **1970**, *31*, 101.

[10] J. J. Borrás-Almenar, R. Burriel, E. Coronado, D. Gatteschi, C. J. Gómez-García, C. Zanchini, *Inorg. Chem.* **1991**, *30*, 947–950.

The Seven-Component Reaction**

By *Alexander Dömling* and *Ivar Ugi**

Dedicated to Professor Friedrich Asinger on the occasion of his 90th birthday

One-pot reactions that form products from at least three different starting materials and incorporate substantial portions of these reagents are termed multicomponent reactions (MCR). This name includes reactions involving at least three different functional groups, some of which may, however, be parts of the same reagent molecule. In general, the MCR are sequences of bimolecular reaction steps that proceed according to the zipper principle, that is, each reaction step is prerequisite for the following stage. The best known examples of MCR are the α-aminoalkylations,[1] to which belong, for example, the Mannich condensation,[2] the Bucherer–Bergs reaction,[3] and formally also the one-pot synthesis of α-ferrocenylalkylamines,[4] as well the Passerini and Ugi reaction (four-component condensation, 4CC).[5] A more recent example of an MCR is the Pauson–Khand reaction.[6]

MCR offer substantial advantages over other synthesis reactions, because most often they use less of the reagents and save time and effort.

In the five-component condensation of primary amines, aldehydes, carbon dioxide, alcohols, and isocyanides to form α-acylaminocarbonamides[7] the highest number of different components were condensed. This reaction is a 4CC in which one of the components, the alkyl carboxylate, is synthesized from two starting materials, alcohol and carbon dioxide.

What is the highest number of different starting materials that can be involved in an MCR?[8] In our opinion a MCR with more than seven reaction partners is scarcely feasible.

Through a combination of an Asinger condensation,[9] whose α-mercaptoaldehyde component is formed from an α-haloaldehyde and SH^-, and a 4CC with a monoalkyl carboxylate according to Scheme 1, it is possible to condense seven different starting materials (7CC) to afford **8** in 43% yield (see Experimental Procedure). Initially in this reaction,

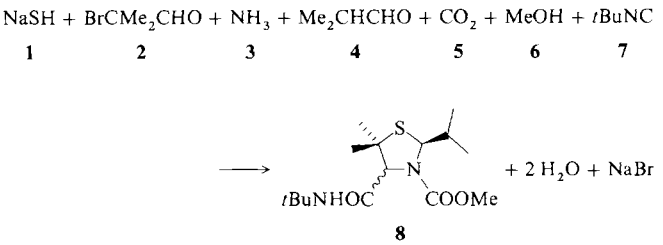

Scheme 1. Stoichiometry of the 7CC.

9 is formed from sodium hydrogen sulfide (**1**) and α-bromoisobutyraldehyde (**2**) and reacts further with ammonia (**3**) and isobutyraldehyde (**4**) in an Asinger condensation to furnish **10**. Compound **11** is formed in an equilibrium with carbon dioxide (**5**)[10] and methanol (**6**). The thiazoline **10** is protonated by **11** to yield **12**, that together with **13** adds to *tert*-butylisocyanide (**7**) to form the α-adduct **14**, which rearranges to **8** by an O to N migration (see Experimental Procedure and Scheme 2).

An analogous 7CC affording **15** (see Experimental Procedure) is possible in 18% yield with the seven components **1**–**3**, **5**, ferrocenaldehyde, ethyl isocyanoacetate, and ethanol.

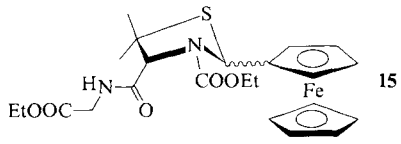

15

Table 1. Conditions and results of the syntheses of **8** and **15**.

Product	Conversion [%] [a]	Yield [%] [b]	Diastereomeric ratio [c]	Solvent [d]	*p* [bar]
8	70	43	2:1	MeOH	16
15	58	18	14:9	EtOH	48

[a] Based on unchanged Asinger product (determined from the ^{1}H NMR spectrum of the reaction mixture). [b] Pure substance after flash chromatography. [c] Determined from the ^{1}H NMR spectrum of the reaction mixture. [d] Alcoholic component.

[*] Prof. Dr. I. Ugi, Dipl.-Chem. A. Dömling
Organisch-chemisches Institut I der Technischen Universität München
Lichtenbergstrasse 4, D-W-8046 Garching (FRG)

The diastereomeric ratios determined by GC-MS analysis and ^{1}H NMR spectroscopy of the crude mixture (Table 1) are low, in accord with the suggested reaction sequence (Scheme 2). The relative configuration of the two stereocenters could not be determined. We assume from the mechanism, however, that the substituents of the major diastereoisomer in 2- and 4-positions are *trans* to each other.

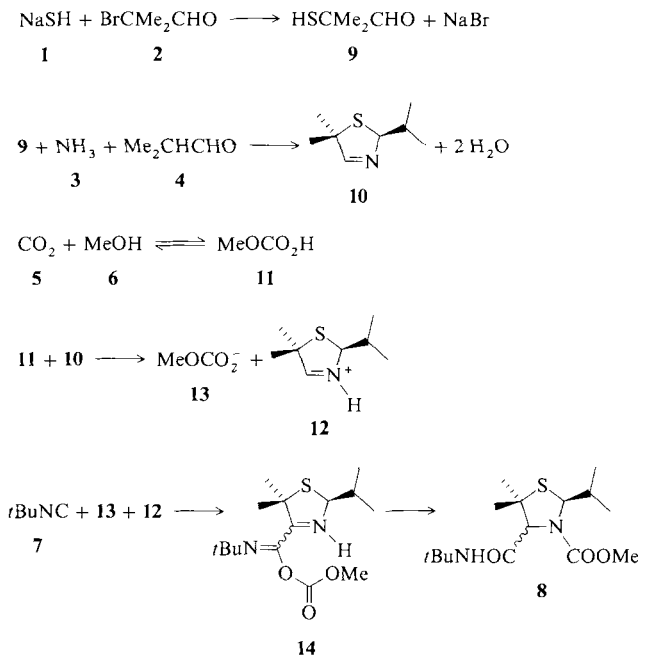

Scheme 2. Mechanism of the 7CC.

Further studies are in progress to extend the seven-component reaction to oxazole,[12] imidazole, 1,3-thiazine, 1,3-oxazine, and 1,3-pyrimidine ring systems.

Experimental Procedure

General procedure for a 10 mmol batch: To a solution of anhydrous sodium hydrogen sulfide (0.56 g) in alcohol (50 mL) at -10 °C are added α-bromoisobutyraldehyde (1.51 g) and aldehyde (10 mmol), and ammonia is bubbled through the solution for 15 min. This solution was treated with isocyanide (10 mmol) and stirred for 6 days under the pressure of CO_2 given in Table 1. As workup the alcohol was removed, the residue was taken up in ethyl acetate (20 mL), washed with 20 mL water, the organic phase was separated off and dried with magnesium sulfate, and the solvent was removed in vacuum. The residue was separated by flash chromatography with hexane/ethyl acetate as eluent.

Selected physical data of the major diastereomers: **8**: colorless powder, m.p. = 148 °C. ^{1}H NMR ($CDCl_3$, 360 MHz): δ = 0..92 (d, 3H, J = 6.89 Hz), 0.95 (d, 3H, J = 6.64 Hz), 1.34 (s, 9H), 1.41 (s, 3H), 1.62 (s, 3H), 2.67–2.72 (m, 1H), 3.68 (s, 3H), 4.1 (s, 1H), 5.17 (d, 1H, J = 5.49 Hz), 5.45 (s, br, 1H); ^{13}C NMR ($CDCl_3$, 90 MHz): δ = 17.5, 20.5, 26.7, 28.7, 32.5, 33.4, 51.4, 52.7, 71.7, 77.1, 156.2, 169.0. MS (CI): m/z 317 (MH^+). IR (KBr): $\tilde{\nu}$ [cm^{-1}] = 1728(s), 1662(s).

15: yellow powder, m.p. = 160 °C (decomp.). ^{1}H NMR ($CDCl_3$, 360 MHz): δ = 1.18 (tr, 3H, J = 7.10 Hz), 1.30 (tr, 3H, J = 7.13 Hz), 1.46 (s, 3H), 1.68 (s, 3H), 4.0–4.28 (m, 13H, –Fc, twice CH2), 4.33 (s, 1H), 4.53 (s, 1H), 4.71 (s, 1H), 6.40 (m, 2H); ^{13}C NMR ($CDCl_3$, 90 MHz): δ = 14.1, 14.3, 24.7, 33.5, 41.0, 61.5, 61.9, 63.6, 67.8, 68.9, 69.0, 71.7, 75.9, 88.5, 154.9, 166.8, 169.6. MS (CI): m/z 503 (MH^+). IR (KBr): $\tilde{\nu}$ [cm^{-1}] = 1761(s), 1700(s, br). Correct C,H,N analysis for **8** and **15**.

Received: December 2, 1992 [Z 5720IE]
German version: *Angew. Chem.* **1993**, *105*, 634

[1] H. Hellmann, G. Opitz, *α-Aminoalkylierungen*, Verlag Chemie, Weinheim, **1960**.
[2] C. Mannich, I. Krösche, *Arch. Pharm. (Weinheim, Ger.)* **1912**, *250*, 647.
[3] H. Bergs, Ger. Pat. 566094, **1929**; *Chem. Abstr.* **1933**, *27*, 1001; H. T. Bucherer, W. Steiner, *J. Prakt. Chem.* **1934**, *140*, 291.
[4] R. Herrmann, I. Ugi, *Tetrahedron* **1981**, *27*, 1001.
[5] M. Passerini, *Gazz. Chim. Ital.* **1921**, *51*(II), 126, *ibid.* **1921**, *51* (II), 181; I. Ugi, S. Lohberger, R. Karl in *Comprehensive Organic Synthesis: Selectivity for Synthetic Efficiency, Vol. 2* (Eds.: B. M. Trost, C. H. Heathcock), Pergamon, Oxford, **1991**, p. 1083.
[6] I. U. Khand, G. R. Knox, P. L. Pauson, W. R. Watts, *J. Chem. Soc. Chem. Commun.* **1971**, 36; N. E. Schore, *Org. React.* **1990**, *40*, 1.
[7] I. Ugi, C. Steinbrückner, *Chem. Ber.* **1961**, *94*, 2802; E. Haslinger, *Monatsh. Chem.* **1978**, *109*, 749.
[8] Multicomponent reactions are difficult to access by computer. See, however, the reviews "Multicomponent One-Pot Annulations Forming Three to Six Bonds", G. H. Posner, *Chem. Rev.* **1986**, *86*, 831, and "Sequential Transformations in Organic Chemistry—Synthesis Strategy with a Future", L. F. Tietze, U. Beifuss, *Angew. Chem.* **1993**, *105*, 137; *Angew. Chem. Int. Ed. Engl.* **1993**, *32*, 131.
[9] F. Asinger, M. Thiel, *Angew. Chem.* **1958**, *70*, 667; F. Asinger, H. Offermanns, *Angew. Chem.* **1967**, *79*, 953; *Angew. Chem. Int. Ed. Engl.* **1967**, *6*, 907.
[10] Eine aktuelle Anwendung von CO_2 in der Organischen Chemie: G. Zadel, E. Breitmaier, *Angew. Chem.* **1992**, *104*, 1070; *Angew. Chem. Int. Ed. Engl.* **1992**, *31*, 1035.
[11] K. C. Baczko, *Gmelin Handbuch der Anorganischen Chemie, Kohlenstoff Teil C3: Verbindungen*, Verlag Chemie, Weinheim, **1973**.
[12] M. Weber, J. Jakob, J. Martens, *Liebigs Ann. Chem.* **1992**, 1.

Tetranuclear Cuboidal and Hexanuclear Prismatic Iron–Sulfur–Nitrosyl Clusters**

By *Michael J. Scott* and *Richard H. Holm**

Homometallic $[Fe_4(\mu_3\text{-}S)_4]$ and heterometallic $[MFe_3(\mu_3\text{-}S)_4]$ cubane-type clusters and the cuboidal $[Fe_3(\mu_3\text{-}S)(\mu_2\text{-}S)_3]$ cluster are now familiar entities in iron–sulfur chemistry and biochemistry.[1] $[MFe_3S_4]$ clusters provide the best current simulations of the *immediate* coordination environments of Mo and V atoms in the corresponding cofactors of nitrogenase.[1, 2] However, cuboidal clusters with the inverted core atom population $[Fe_4(\mu_3\text{-}S)_3]$ and its heterometal analogues $[MFe_3(\mu_3\text{-}S)_3]$ assume new significance in view of the Kim–Rees model of the FeMo-cofactor of the nitrogenase from *Azotobacter vinelandii*, which consists of the cuboidal units $[Fe_4S_3]$ and $[MoFe_3S_3]$ bridged by two μ_2-S atoms and a third unidentified atom in an assembly of trigonal pseudosymmetry.[3] Recognizing that the only structurally authenticated example of $[Fe_4S_3]$ is found in Roussin's black anion $[Fe_4S_3(NO)_7]^-$ and noting an unpublished report of a related Fe_4Se_3 species,[4–7] we have explored certain tetranuclear Fe clusters with nitrosyl and sulfido ligands **1**–**5**.

$[Fe_4S_3(NO)_7]^-$	**1**	$[Fe_4S_3(NO)_4(PPh_3)_3]$	**4**
$[Fe_4S_4(NO)_4]$	**2**	$[Fe_4S_3(NO)_4(PPh_3)_3]^+$	**5**
$[Fe_4S_4(NO)_4]^-$	**3**	$[Fe_6S_6(NO)_6]^{2-}$	**6**

In reaction (a), electron-precise **2**[8] in refluxing dichloromethane is rapidly converted to **4**. The structure of **4**

$$[Fe_4S_4(NO)_4]\ (\mathbf{2}) + 4Ph_3P \longrightarrow [Fe_4S_3(NO)_4(PPh_3)_3]\ (\mathbf{4}) + Ph_3PS \qquad (a)$$

[*] Prof. R. H. Holm, M. J. Scott
Department of Chemistry, Harvard University
Cambridge, MA 02138 (USA)

[**] This work was supported by National Institutes of Health (Grant GM 28856; X-ray equipment was obtained through NIH Grant 1 S10 RR 02247).

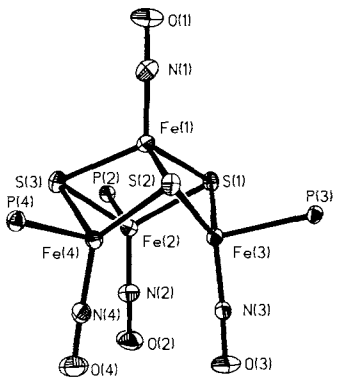

Fig. 1. The structure of **4** (phenyl groups omitted, 30% probability ellipsoids). Selected interatomic distances [pm] and angles [°]: Fe(1)-Fe(2) 257.1(2), Fe(1)-Fe(3) 261.4(2), Fe(1)-Fe(4) 262.8(2), Fe(2)-Fe(3) 277.1(2), Fe(2)-Fe(4) 278.0(2), Fe(3)-Fe(4) 267.8(2), Fe(1)-S 224.3(17), Fe_b-S 221.4(7), Fe-P 224.8(5), S-Fe(1)-S 105.5(16), S-Fe(1)-N(1) 113.2(7), Fe(1)-S-Fe_b 71.5(7), Fe_b-S-Fe_b 76.6(18), S-Fe_b-S 107.5(14), S-Fe_b-N 124(6), S-Fe_b-P 95.7(20), N-Fe_b-P 98.1(5), Fe(1)-N(1)-O(1) 177.9(7), Fe_b-N-O 177.0(6). Except for the unique angle, data involving P, S, and N atoms are mean values under idealized trigonal symmetry (Fe_b = Fe2–Fe4).

(Fig. 1)[9a] demonstrates that desulfurization of the initial $[Fe_4S_4]^{4-}$ core leads to cuboidal $[Fe_4S_3]^{4-}$;[10] **4** has idealized C_{3v} symmetry with basal Fe–Fe distances in the 2.678(2)–2.780(2) Å range and basal–apical (to Fe1) distances of 2.571(2)–2.628(2) Å. In dichloromethane, electron-rich **4** exhibits two reversible ($i_p/i_a \approx 1$) one-electron oxidation steps at 0.00 and +1.03 V vs. saturated calomel electrode (SCE). Reaction (b) afforded the $[Fe_4S_3]^{3-}$ monocation cluster **5** in isolable form. Reaction of **4** with 0.5 equivalents of I_2 also gave **5**, but as a solvated salt **[5][I]** owing to partial conversion of **5** to **1** over longer reaction times than that of reaction (b). In **[5][I]** and **[5][PF_6]**

$$\underset{\mathbf{4}}{[Fe_4S_3(NO)_4(PPh_3)_3]} + NOPF_6 \longrightarrow \underset{\mathbf{[5][PF_6]}}{[Fe_4S_3(NO)_4(PPh_3)_3][PF_6]} + NO \qquad (b)$$

(Fig. 2),[9b,c] the stereochemistry of the cation core is nearly C_{3v}. Analogous to the clusters **2** and **3**,[8] comparative structures allow qualitative identification of the electroactive molecular orbital. The Fe–Fe distances to the apical Fe1 atoms in **4** and **5** are only slightly altered. The most significant change upon oxidation occurs in the basal (Fe_b) atom separations which decrease by 7–19 pm, resulting in a more nearly regular Fe_4 tetrahedron in **5**. Consequently, the HOMO of **4** has considerable antibonding character amongst the three basal Fe atoms.

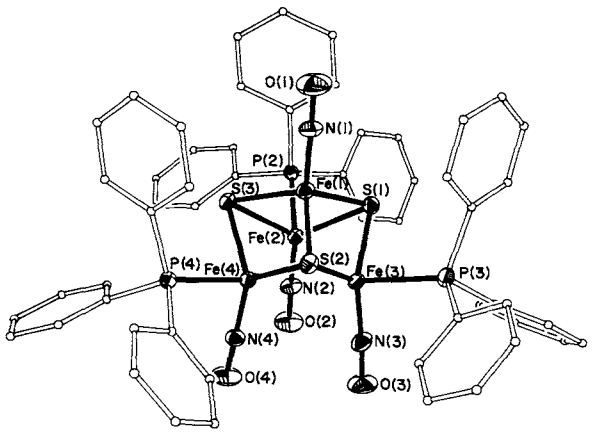

Fig. 2. The structure of **5** in the solvated **[5][I]** salt (30%) probability ellipsoids). Selected interatomic distances [pm]and angles [°]: Fe(1)-Fe(2) 258.8(2), Fe(1)-Fe(3) 260.6(2), Fe(1)-Fe(4) 258.7(2), Fe(2)-Fe(3) 260.6(2), Fe(2)-Fe(4) 262.2(2), Fe(3)-Fe(4) 259.0(2), Fe(1)-S 224.0(9), Fe_b-S 220.6(9), Fe-P 228.0(6), S-Fe(1)-S 103(2), S-Fe(1)-N(1) 113.6(3), Fe(1)-S-Fe_b 71.4(4), Fe_b-S-Fe_b 72.4(7), S-Fe_b-S 107.4(9), S-Fe_b-N 125.4(17), S-Fe_b-P 92.3(4), N-Fe_b-P 98(3). Data involving P, S, and N atoms are mean values under idealized trigonal symmetry (Fe_b = Fe2–Fe4). Phenyl group orientations in this cluster and **4** are similar. The structure of **5** in this compounds as in the PF_6^- salt are essentially identical.

In addition to its oxidative reactions, **4** is an immediate precursor to another cluster type by treatment with excess Ph_3P in DMF at 80 °C [Eq. (c)]. The cluster salt was precipitated by ether addition; the mononuclear species was obtained from the filtrate and identified by its IR spectrum[11] (THF, $\tilde{\nu}$ [cm^{-1}] = 1721, 1677). In the presence of Et_4NCl, pure $[Et_4N]_2$**[6]** could be isolated directly upon addition of ether.[12] The structures of this compound and $[Fe(dmf)_6]$**[6]** demonstrate the existence of the prismane dianion **6** (Fig. 3),[9e,f,13] stereochemically analogous to $[Fe_6S_6L_6]^{2-}$ and $[Fe_6S_6L_6]^{3-}$.[14] Cluster **6** is the first example of this

$$2\underset{\mathbf{4}}{[Fe_4S_3(NO)_4(PPh_3)_3]} \longrightarrow [Fe(NO)_2(PPh_3)_2] + [Fe(dmf)_6][Fe_6S_6(NO)_6] \qquad (c)$$
$$\mathbf{[Fe(dmf)_6][6]}$$

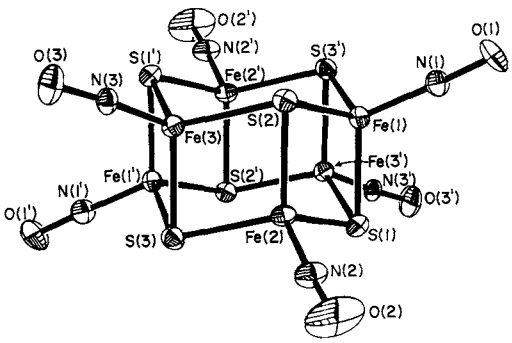

Fig. 3. The structure of **6** as its Et_4N^+ salt (30% probability ellipsoids); Selected interatomic distances [pm] and angles [°]: Fe(1)-Fe(2) 266.3(2). Fe(1)-Fe(3)' 265.6(2), Fe(2)-Fe(3) 265.9(2), mean Fe-S 222.1(5), mean Fe-N 166(1), mean Fe-N-O 176(1); within the Fe_3S_3 cyclohexane-type ring mean values are S-Fe-S 113.2(9), Fe-S-Fe 111.9(8); within the Fe_2S_2 rhombuses mean values are S-Fe-S 106.3(2) and Fe-S-Fe 73.6(2). Primed and unprimed atoms are related by an inversion center.

architecture with L ≠ RS^-, RO^-, or halide. The $[Fe_6S_6]^{8-}$ core in **6** is compressed relative to those in other species of this type; the Fe–Fe and Fe–S distances are about 0.1 and 0.05 Å shorter, respectively. The most remarkable property of **6** is the formation of an extensive electron transfer series. Four sequential reversible reductions are observed in the interval −0.7 to −1.7 V, and a quasi-reversible ($i_{pa}/i_{pc} < 1$), probable two-electron oxidation step near 0 V (Fig. 4). The relatively large potential difference between the second and third reductions is suggestive of an intervening structural change. In contrast to **6** prismatic $[Fe_6S_6]^{4+}$ and $[Fe_6S_6]^{3+}$ clusters exhibit at most a three-membered redox series.[14]

Clusters **1**, **4**, and **5** provide the initial entry to cuboidal $[Fe_4S_3]$ chemistry, albeit significantly modulated by nitrosyl ligation. The latter, with its attendant π-electron reservior potential, low oxidation state stabilization, and enhancement of metal–metal bonding, is undoubtedly responsible for these features: 1) *reductive* desulfurization of the cluster core (**2** → **4**); 2) the reductive five-membered electron transfer series **6** ⇌ $Fe_6S_6(NO)_6]^{6-}$; 3) small or irregular ^{57}Fe

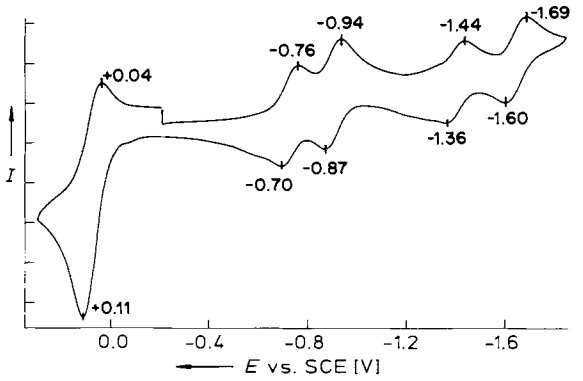

Fig. 4. Cyclic voltammogram of **6** in acetonitrile solution using a scan rate of 50 mVs^{-1} and a Pt working electrode; peak potentials vs. SCE are indicated. For the five redox steps, $E_{1/2} = +0.07$, -0.73, -0.90, -1.40, and -1.64 V.

isomer shift responses to core oxidation state changes at parity of coordination ($[FeS_3(NO)]$);[15] 4) large $\tilde{\nu}_{NO}$ responses to these changes in the oxidation states as in the comparisons **2**/**3**, (1788/1787(m), 1725(vs) cm^{-1}), **2**/**6** (1788/1698 cm^{-1}), and **4**/**5** (Experimental Procedure in dichloromethane). Although dimensionally similar to cofactor clusters,[2] the foregoing species are obviously not models of them. However, they may be synthetic precursors to $[Fe_4S_3]$ clusters with physiologically realistic oxidation levels by oxidative removal of NO ligands with retention of core structure. Such reactions are currently under investigation.

Experimental Procedure

All procedures were carried out under a pure dinitrogen atmosphere with freshly degassed solvents; the FAB-MS matrix was 3-nitrobenzyl alcohol.

4:**2**[8] (5.00 g, 10.6 mmol) and Ph_3P (11.1 g, 42.4 mmol) were refluxed in dichloromethane for 3 h. The precipitate was collected, washed with cold dichloromethane (2 × 50 mL), hexane, and ether which afforded 7.20 g (55%) of product as a black microcrystalline solid. IR (CH_2Cl_2) $\tilde{\nu}$[cm^{-1}] = 1757(s), 1730(vs), 1695(m). FAB-MS: *m/z* 1226(**5**).

[5][1]:**4** (50 mg, 0.041 mmol) in 15 mL of dichloromethane was treated with solid I_2 (6.0 mg, 0.024 mmol). The reaction mixture was stirred for 30 min and 70 mL of ether was added dropwise. One hour after the addition of I_2 the conversion of **4** to **5** was complete (by IR spectroscopy); at longer times peaks of **1** grow in. The solution was stored at 0 °C overnight (ca. 15 h). Single crystals of black **[5][1]** · $0.5CH_2Cl_2$ · $0.5Et_2O$ were isolated in moderate yield. IR (CH_2Cl_2) $\tilde{\nu}$[cm^{-1}] = 1801(m), 1782(vs), 1738(m).

[5][PF_6]:**4** (175 mg, 0.143 mmol) in 10 mL of dichloromethane was treated with solid $NOPF_6$ (25 mg, 0.14 mmol). The reaction mixture was stirred for 30 min and 60 mL of ether was added dropwise. The precipitate was collected and washed with ether which afforded 87 mg (44%) of product as a black microcrystalline solid. IR (CH_2Cl_2), $\tilde{\nu}$[cm^{-1}] = 1803(m), 1781(vs), 1735(m). FAB-MS: *m/z* 1226 (**5**).

[Et_4N]$_2$[6]:**4** (1.00 g, 0.815 mmol) and Ph_3P (0.428 g, 1.63 mmol) in 25 mL of DMF were heated at 80 °C for 12 h, and the solution was filtered. Et_4NCl (0.135 g, 0.815 mmol) was added to filtrate followed by dropwise addition of 300 mL of ether. The precipitate was collected, washed with CH_2Cl_2 (3 × 20 mL) and ether (2 × 20 mL), and was dried in vacuo to yield 0.242 g (56%) of black microcrystals. IR (MeCN), $\tilde{\nu}$[cm^{-1}] = 1698(vs). FAB-MS: *m/z* 707 ($[Fe_6S_6(NO)_6]^-$).

Received: December 8, 1992 [Z 5737 IE]
German version: *Angew. Chem.* **1993**, *105*, 621

[1] R. H. Holm, *Adv. Inorg. Chem.* **1992**, *38*, 1.
[2] B. K. Burgess, *Chem. Rev.* **1990**, *90*, 1377.
[3] J. Kim, D. C. Rees, *Science* **1992**, *257*, 1677.
[4] A. R. Butler, C. Glidewell, M.-H. Li, *Adv. Inorg. Chem.* **1988**, *32*, 335.
[5] C. T.-W. Chu, L. F. Dahl, *Inorg. Chem.* **1977**, *16*, 3245.
[6] C. Glidewell, R. J. Lambert, M. E. Harman, M. B. Hursthouse, *J. Chem. Soc. Dalton Trans.* **1990**, 2685.
[7] L. L. Nelson, Ph.D. Thesis, University of Wisconsin-Madison, 1981; *Diss. Abstrs.* **1981**, *42/08B*, 3258. Our preparation of **4** is similar to that described here for $[Fe_4Se_3(NO)_4(PPh_3)_3]$.
[8] C. T.-W. Chu, F. Y.-K. Lo, L. F. Dahl, *J. Am. Chem. Soc.* **1982**, *104*, 3409.
[9] Crystallographic data (T = 243 K): a) **4** · $2CH_2Cl_2$, $P2_1/c$, $a = 12.277(3)$, $b = 19.835(3)$, $c = 25.113(5)$ Å, $\beta = 110.37(2)°$, $V = 6016(2)$ Å^3, $Z = 4$, 4669 unique reflections, $R(R_w) = 0.0506(0.0491)$; b) **[5][1]** · $0.5CH_2Cl_2$ · $0.5Et_2O$, $P\bar{1}$, $a = 12.274(4)$, $b = 16.414(6)$, $c = 20.373(7)$ Å, $\alpha = 80.65(3)$, $\beta = 79.30(3)$, $\gamma = 75.44(3)°$, $V = 3875(2)$ Å^3, $Z = 2$, 6087 unique reflections, $R(R_w) = 0.0623(0.0581)$; c) **[5][PF_6]** · $2CH_2Cl_2$, $P2_1/n$, $a = 12.540(3)$, $b = 29.268(6)$, $c = 19.367(4)$ Å, $V = 6863(3)$ Å^3, $Z = 4$, 9023 unique reflections, $R(R_w) = 0.0871(0.0916)$; d) $[Fe(dmf)_6][3]_2$, monoclinic, space group $P2_1/c$, $a = 16.991(5)$, $b = 17.269(4)$, $c = 17.834(4)$ Å, $\beta = 90.72(2)°$ $Z = 4$; e) $[Fe(dmf)_6]$**[6]**, $P\bar{1}$, $a = 8.920(2)$, $b = 10.985(3)$, $c = 11.972(4)$ Å, $\alpha = 95.23(2)$, $\beta = 97.49(2)$, $\gamma = 105.84(2)°$, $Z = 1$; f) $(Et_4N)_2$**[6]**, $C2/c$, $a = 17.569(4)$, $b = 10.880(2)$, $c = 18.734(5)$ Å, $\beta = 91.55(2)°$, $V = 3580(2)$ Å^3, $Z = 4$, 1286 unique reflections, $R(R_w) = 0.0469(0.0377)$. Data were collected on a Nicolet P3F diffractometer using $Mo_{K\alpha}$ radiation; for unique reflections $F_0^2 > 3\sigma F_0^2$. The structures d) and e) were solved but not fully refined. Further details of the crystal structure investigations are available on request from the Director of the Cambridge Crystallographic Data Centre, 12 Union Road, GB-Cambridge CB21EZ (UK), on quoting the full journal citation.
[10] Inasmuch as clusters **1**–**6** contain linear Fe-NO groups, we adopt the $[NO]^+$ formalism in approximating Fe oxidation states.
[11] C. B. Ungermann, K. G. Caulton, *J. Am. Chem. Soc.* **1976**, *98*, 3862.
[12] In contrast, the system **2**/2Ph_3P in DMF at 80 °C does not undergo core rupture, yielding $[Fe(DMF)_6][3]_2$ which was identified by crystallography. [9d].
[13] This cluster has been mentioned in an abstract; the method of synthesis was not given: J. C. K. Ma, L. F. Dahl, *Abstrs. 201st American Chemical Society Meeting*, Atlanta, 1991, INOR 502.
[14] a) M. G. Kanatzidis, W. R. Hagen, W. R. Dunham, R. K. Lester, D. Coucouvanis, *J. Am. Chem. Soc.* **1985**, *107*, 953; b) M. G. Kanatzidis, A. Salifoglou, D. Coucouvanis, *Inorg. Chem.* **1986**, *25*, 2460, and references therein; c) W. Saak, G. Henkel, S. Pohl, *Angew. Chem.* **1984**, *96*, 153; *Angew. Chem. Int. Ed. Engl.* **1984**, *23*, 150.
[15] δ, ΔE_Q (mms^{-1}, 77 *K*): **4** ($Fe^{+0.5}$), 0.20, 1.07; **6** ($Fe^{+0.67}$), 0.26, 0.40; **5** ($Fe^{+0.75}$), 0.13, 0.37 (70%), 0.22, 1.50 (30%); **2** (Fe^{1+}), 0.20, 1.47. See also ref. [8] and D. Sedney, W. M. Reiff, *Inorg. Chim. Acta* **1979**, *34*, 231. Isomer shifts (δ) are referenced to Fe metal at rooom temperature.

Chiral Phosphinoaryldihydrooxazoles as Ligands in Asymmetric Catalysis: Pd-Catalyzed Allylic Substitution**

By *Peter von Matt* and *Andreas Pfaltz**

Palladium-catalyzed allylic substitution is a versatile, widely used process in organic synthesis,[1] and the development of efficient enantioselective catalysts for this reaction is an important goal of current research in this area.[2, 3] It has been shown that chiral phosphane ligands can induce substantial enantiomeric excesses in Pd-catalyzed reactions of racemic or achiral allylic substrates with nucleophiles.[2a–g] Recently, promising results have also been obtained with chiral bidentate nitrogen ligands.[2h, 3] We have found that palladium complexes of azasemicorrins **1** or methylenebis(dihydrooxazoles) **2** are effective catalysts for the enantioselective allylic alkylation of **5** or related substrates with dimethyl malonate (with **1** (R = $CH_2OSitBuMe_2$), **6a** was obtained in 95% *ee*).[3b] Analogous 1,3-dialkyl-2-propenyl acetates **7**, on the other hand, react very slowly and with poor enantioselectivity. Herein, we report a new class of ligands, chiral 2-(2-phosphinoaryl)dihydrooxazoles of type **3**, which overcome this limitation. With palladium complexes of these readily available ligands, high yields and remarkable enantioselectivities could be realized in allylic alkylations of aryl- and alkylsubstituted allyl acetates.

[*] Prof. A. Pfaltz, Dipl.-Chem. P. von Matt
Institut für Organische Chemie der Universität
St. Johanns-Ring 19, CH-4056 Basel (Switzerland)

[**] This work was supported by the Swiss National Science Foundation and F. Hoffmann-La Roche AG, Basel.

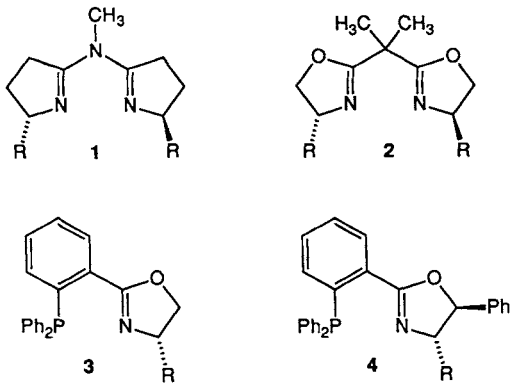

a R = CH_3
b R = CH_2Ph
c R = *i*Pr
d R = Ph
e R = *t*Bu

R = CH_2OSi*t*$BuMe_2$

2-(2-Phosphinophenyl)dihydrooxazoles such as **3**[4] or **4** can be easily prepared in two steps from 2-bromobenzonitrile (1. BuLi; Ph_2PCl; 2. amino alcohol, $ZnCl_2$, PhCl, reflux[5]; 10–30% overall yield). An alternative route involves dihydrooxazole formation from benzonitrile and an amino alcohol, followed by orthometallation with BuLi[6] and subsequent reaction with Ph_2PCl (**3c**: 35% overall yield). Starting from commercially available optically active amino alcohols, a variety of differently substituted enantiomerically pure ligands is readily accessible.[7] The corresponding allylpalladium(II) complexes, which we used as catalysts, were generated in situ from $[\{Pd(\mu\text{-}C_3H_5)Cl\}_2]$ and the corresponding ligands (1.3 equiv/[Pd]).[8]

The complexes derived from ligands **3** and **4** were found to be effective catalysts for allylic alkylations with stabilized carbanions. Under standard conditions[8] (2 mol% of catalyst and a mixture of *N,O*-bis(trimethylsilyl)acetamide (BSA)[2a] and catalytic amounts of KOAc as base[3b]) racemic 1,3-diphenyl-2-propenyl acetate **5** reacts smoothly with dimethyl malonate or acetylacetone affording optically active substitution products [Eq. (a), Table 1]. The phenyl

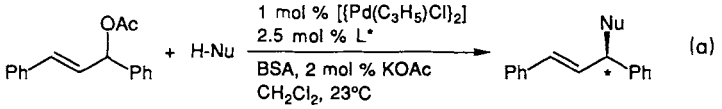

(a)

rac-**5**

(−)-(*S*)-**6a**
(+)-(*S*)-**6b**
(+)-(*R*)-**6c**

a: H-Nu = H-CH(COOMe)$_2$
b: H-Nu = H-CH(COMe)$_2$
c: H-Nu = H-C(NHAc)(COOEt)$_2$

derivative **3d** proved to be the optimal ligand for this substrate. After a remarkably short reaction time of 1 h at room temperature (c(**5**) = 0.3 M), the products (−)-**6a** and (+)-**6b** were isolated in essentially quantitative yields with enantiomeric excesses of 99% and 97%, respectively. These values compare favorably to the selectivities obtained with other ligands (**6a**/**b**: 48/96% *ee* with ferrocenyl phosphanes,[2e] 90/63% *ee* with chiraphos,[2e] 30/90% *ee* with BINAP;[2e] nitrogen ligands:[2h, 3]). The reaction with diethyl acetaminomalonate is slower but, after 3–4 d at 23 °C, also affords the desired product (+)-**6c** with excellent enantioselectivity and in essentially quantitative yield.

Table 2 summarizes the results obtained for the reaction of 1,3-dialkyl-2-propenyl acetates **7** with dimethyl malonate

Table 1. Enantioselective allylic alkylation of *rac*-**5** with (phosphinoaryldihydrooxazole)Pd catalysts according to Equation (a).[8] The ligands **3** and **4** are designated as L*.

L*	*ee* [%] (Yield) [a] (−)-(*S*)-**6a** [b]	*ee* [%] (Yield) [a] (+)-(*S*)-**6b** [b]	*ee* [%] (Yield) [a] (+)-(*R*)-**6c** [c]
3a	89 (98)	84 (98)	77 (97)
3b	97 (97)	93 (95)	91 (99)
3c	98 (98)	92 (98)	96 (94)
3d	99 (99) [d]	97 (98) [e]	97 (98) [f]
3e	95 (94)	94 (96)	96 (99)
4	85 (85)	75 (80)	67 (99)

[a] The *ee* values were determined by HPLC with chiral columns (**6a**: Daicel Chiralcel OD, hexane/*i*PrOH 99:1; **6b**: Daicel Chiralcel OJ, hexane/*i*PrOH 88:12; **6c**: Daicel Chiralcel OJ, hexane/*i*PrOH 4:1 → 1:1). Yields [%] refer to purified products after column chromatography. [b] (*S*)-Configuration according to the $[\alpha]_D$ values given in ref. [2c]. [c] The assignment of (*R*)-configuration is based on the sign of optical rotation of the corresponding dimethyl ester [2e]. [d] $[\alpha]_D = -18.4$ (c = 1.1, EtOH, 23 °C). [e] M.p. 48 °C; $[\alpha]_D = +9.3$ (c = 1.3, EtOH, 23 °C). [f] M.p. 97 °C; $[\alpha]_D = +50$ (c = 1.0, EtOH, 23 °C).

[Eq. (b)]. Enantioselective allylic alkylations have not been reported yet for this class of substrates.[9] Here, ligand **3e**

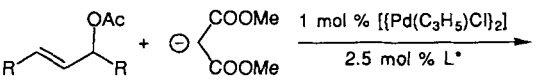

(b)

rac-**7a-c**

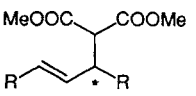

a: R = Me, **b**: R = *n*Pr, **c**: R = *i*Pr

(−)-**8a-c**

Table 2. Enantioselective allylic alkylation of *rac*-**7a–c** with dimethyl malonate and (phosphinoaryldihydrooxazole)Pd catalysts [a] according to Equation (b).

L*	*ee* [%] (Yield) (−)-**8a** [b]	*ee* [%] (Yield) (−)-**8b** [c]	*ee* [%] (Yield) (+)-**8c** [c]
3a	56 (95)	53 (61)	93 (91)
3b	54 (75)	63 (71)	92 (92)
3c	59 (99)	56 (72)	94 (88)
3d	50 (97)	49 (51)	89 (93)
3e	71 (96) [d]	69 (96) [e]	96 (88) [f]
4	46 (85)	59 (93)	89 (97)

[a] **7a/b** → **8a/b**: $H_2C(COOMe)_2$ (3 equiv), BSA (3 equiv), KOAc (2 mol%), CH_2Cl_2, 23 °C, 4 d [8]; **7c** → **8c**: $NaHC(COOMe)_2$ (1.5 equiv), DMF, 65 °C, 2 d. Yields [%] refer to purified products after column chromatography. [b] The *ee* values were deteremined by GC with a chiral column (octakis(3-*O*-butyryl-2,6-di-*O*-pentyl)-γ-cyclodextrin in OV 1701-vinyl). [c] The enantiomeric excess was determined by ^1H NMR spectroscopy ($CDCl_3$/0.25 equiv $[Eu(hfc)_3]$; splitting of the signals for the methoxy groups). [d] $[\alpha]_D = -19.8$ (c = 1.1, $CHCl_3$, 23 °C). [e] $[\alpha]_D = -9.1$ (c = 1.6, $CHCl_3$, 23 °C). [f] $[\alpha]_D = -19.9$ (c = 1.7, $CHCl_3$, 23 °C).

with a *tert*-butyl group at the stereogenic center gave the best enantioselectivities. The dimethyl and di-*n*-propyl derivatives **7a** and **7b**, respectively, reacted with dimethyl malonate under mild conditions, affording the expected products (−)-**8a/b** in high yields with about 70% *ee*. The diisopropyl derivative **7c** was found to be much less reactive (< 20% conversion under these conditions). However, under more vigorous conditions with $NaCH(COOMe)_2$ in DMF at 65 °C, **8c** was formed in good yield and high enantiomeric purity.

At present, no simple mechanistic rationale for the observed enantioselectivity can be offered. Compared to analogous reactions with C_2-symmetric ligands of type **1** or

2, which may be rationalized in a straightforward manner,[3e] the situation here is more complex. With non-symmetric phosphinoaryldihydrooxazoles, two diastereomeric allyl palladium intermediates must be considered, and in addition to steric interactions, electronic effects may play a role as well (differing *trans*-influence of the coordinating N and P atom; see, e.g., ref. [1d]).

Further studies, exploring the scope of these promising catalysts and the mechanism of enantioselection, are in progress. We are also examining the use of phosphinoaryldihydrooxazoles in other metal-catalyzed reactions.

Received: December 14, 1992 [Z 5748 IE]
German version: *Angew. Chem.* **1993**, *105*, 614

[1] a) J. Tsuji, I. Minami, *Acc. Chem. Res.* **1987**, *20*, 140; b) B. M. Trost, T. R. Verhoeven, in *Comprehensive Organometallic Chemistry, Vol. 8* (Eds.: G. Wilkinson, F. G. A. Stone, E. W. Abel), Pergamon, Oxford, **1982**, pp. 799–938; c) B. M. Trost, *Acc. Chem. Res.* **1980**, *13*, 385; d) C. G. Frost, J. Howarth, J. M. J. Williams, *Tetrahedron: Asymmetry*, **1992**, *3*, 1089.

[2] a) B. M. Trost, D. J. Murphy, *Organometallics* **1985**, *4*, 1143; b) P. R. Auburn, P. B. Mackenzie, B. Bosnich, *J. Am. Chem. Soc.* **1985**, *107*, 2033; P. B. Mackenzie, J. Whelan, B. Bosnich, *ibid.* **1985**, *107*, 2046; c) T. Hayashi, A. Yamamoto, T. Hagihara, Y. Ito, *Tetrahedron Lett.* **1986**, *27*, 191; T. Hayashi, A. Yamamoto, Y. Ito, E. Nishioka, H. Miura, K. Yanagi, *J. Am. Chem. Soc.* **1989**, *111*, 6301; T. Hayashi, *Pure Appl. Chem.* **1988**, *60*, 7; d) Y. Okada, T. Minami, Y. Sasaki, Y. Umezu, M. Yamaguchi, *Tetrahedron Lett.* **1990**, *31*, 3905; Y. Okada, T. Minami, Y. Umezu, S. Nishikawa, R. Mori, Y. Nakayama, *Tetrahedron Asymmetry* **1991**, *2*, 667; e) M. Yamaguchi, T. Shima, T. Yamagishi, M. Hida, *Tetrahedron Lett.* **1990**, *31*, 5049; *Tetrahedron Asymmetry* **1991**, *2*, 663; f) M. Sawamura, H. Nagata, H. Sakamoto, Y. Ito, *J. Am. Chem. Soc.* **1992**, *114*, 2586; g) B. M. Trost, D. L. Van Vranken, *Angew. Chem.* **1992**, *104*, 194; *Angew. Chem. Int. Ed. Engl.* **1992**, *31*, 228; B. M. Trost, D. L. Van Vranken, C. Bingel, *J. Am. Chem. Soc.* **1992**, *114*, 9327, B. M. Trost, L. Li, S. D. Guile, *ibid.* **1992**, *114*, 8745; h) A. Togni, *Tetrahedron Asymmetry* **1991**, *2*, 683; i) review: G. Consiglio, R. M. Waymouth, *Chem. Rev.* **1989**, *89*, 257 and ref. [1d].

[3] a) D. Müller, G. Umbricht, B. Weber, A. Pfaltz, *Helv. Chim. Acta* **1991**, *74*, 232; b) U. Leutenegger, G. Umbricht, C. Fahrni, P. von Matt, A. Pfaltz, *Tetrahedron* **1992**, *48*, 2143; c) A. Pfaltz, *Acc. Chem. Res.* **1993**, *26*, in press.

[4] Systematic name: 2-[2-(diphenylphosphino)phenyl]-4,5-dihydrooxazole.

[5] H. Witte, W. Seeliger, *Liebigs Ann. Chem.* **1974**, 996.

[6] A. I. Meyers, E. D. Mihelich, *J. Org. Chem.* **1975**, *40*, 3158; H. W. Gschwend, A. Hamdan, *ibid.* **1975**, *40*, 2008.

[7] P. von Matt, G. Koch, A. Pfaltz, unpublished results.

[8] For a representative procedure, see ref. [3b].

[9] For analogous allylic aminations, see ref. [2c].

Asymmetric Synthesis and Highly Diastereoselective *ortho*-Lithiation of Ferrocenyl Sulfoxides. Application to the Synthesis of Ferrocenyl Derivatives with Planar Chirality**

By *François Rebière, Olivier Riant, Louis Ricard,* and *Henri B. Kagan**

There are only a few convenient ways to prepare enantiomerically pure ferrocenyl compounds like **2** with planar chirality. The most popular method, based on the pioneering work of Ugi et al.,[1] is the resolution of (1-ferrocenylethyldimethylamine and its subsequent *ortho*-lithiation (92% *de*). This approach has been widely used, for example in the preparation of chiral mono- and diphosphanes with the ferrocene skeleton.[2a, b] A useful asymmetric synthesis of (1-ferrocenylethyl)dimethylamine was described in 1990 by asymmetric reduction of a ferrocenyl imine.[2c] We present here an alternate route to ferrocenyl compounds with planar chirality which is based on an efficient asymmetric synthesis of ferrocenylsulfoxides **1** and avoids a resolution step (Scheme 1).

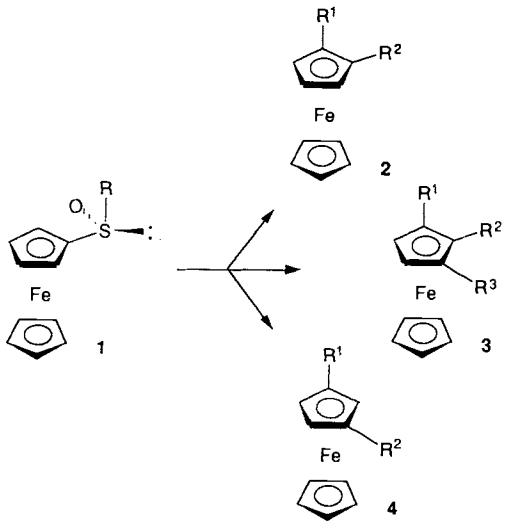

Scheme 1. Possible syntheses of ferrocenyl derivatives with planar chirality from chiral ferrocenyl sulfoxides **1**.

We recently devised a general method for the synthesis of sulfoxides with very high enantiomeric excesses.[3] In this "sulfite route" an enantiomerically pure cyclic sulfite (S_C,R_S)-**5**[4] was converted into a sulfinate which was then transformed into a sulfoxide (Scheme 2). Enantiomerically pure *tert*-butylsulfinate (S_C,S_S)-**6** could thus be prepared in 70% yield. We found that the reaction of **6** with ferrocenyllithium (conveniently obtained from ferrocene and *tert*-butyllithium[5]) gave *tert*-butylferrocenyl sulfoxide **1a** ($[\alpha]_D = +339$ ($c = 0.8$, $CHCl_3$), m.p. 156–157 °C) in 75% yield. This compound must have (S_S) configuration in analogy to the previously established configuration of sulfinate **6**.[3] It has been found that attack of organometallic compounds on **6** gives sulfoxides with full inversion of the configuration at sulfur.[3] The X-ray structure of sulfoxide **11** (vide infra) fully confirms this assignment. We could not detect traces of the enantiomer of **1a** by ^{1}H NMR spectrosopy using (3,5-dinitrobenzoyl)(1-phenylethyl)amine as a solvating agent.[6] Moreover, the specific rotation remained unchanged after recrystallization. It seems clear that sulfoxide **1a** is enantiomerically pure as were the other sulfoxides previously prepared by the sulfite method. Using the oxidant system we previously described,[7] cumene hydroperoxide (1 equiv) in the presence of 1 equivalent of the combination $Ti(OiPr)_4/(S,S)$-DET/H_2O (1:2:1) (DET = diethyl tartrate), we converted *tert*-butyl ferrocenyl sulfide **9** into sulfoxide **1a**. Flash chromatography on silica gel afforded sulfoxide (+)-**1a** (90% *ee*) in 55% yield. The (*S*) configuration is also predicted by the scheme of asymmetric induction that we had proposed[7] when the ferrocene group is viewed as an arene unit. The sulfite route is superior here to asymmetric oxidation for synthetic purposes.

Sulfoxide **1a** was easily deprotonated with one equivalent of *n*BuLi in THF at 0 °C to give **7**. Subsequent treatment

[*] Prof. Dr. H. B. Kagan, Dr. F. Rebière, Dr. O. Riant
Laboratoire de Synthèse Asymétrique (URA CNRS n° 1497)
Institut de Chimie Moléculaire d'Orsay
Université Paris-Sud, F-91405 Orsay (France)
Dr. L. Ricard
Laboratoire de Chimie du Phosphore et des Eléments de Transition
DCPH, Ecole Polytechnique
F-91128 Palaiseau (France)

[**] This work was supported by the CNRS, the Ministery of Research and Technology (fellowship to F. R.) and the Ministery of Education (fellowship to O. R.).

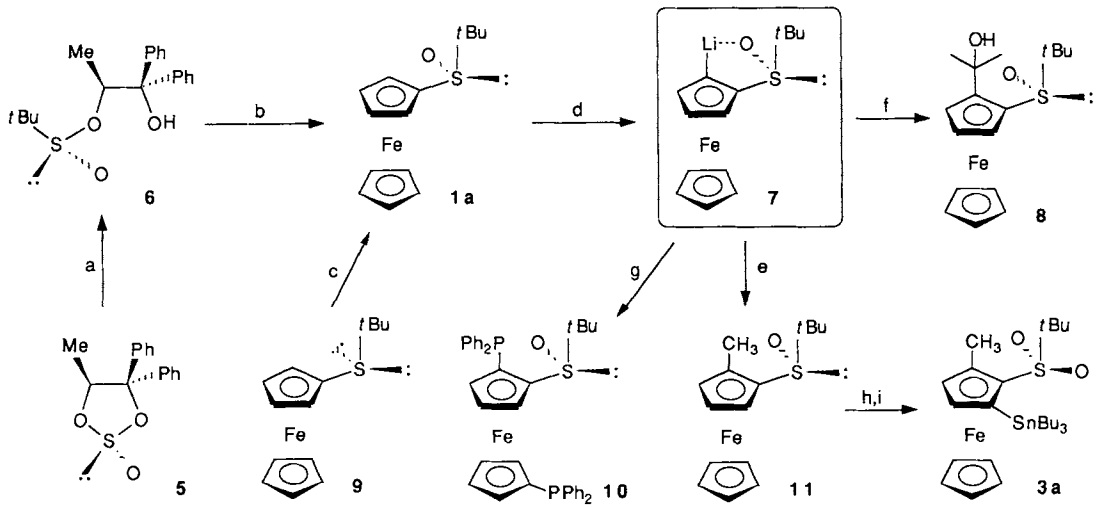

Scheme 2. Asymmetric synthesis of chiral ferrocene **1a** and its diastereoselective *ortho*-functionalization. a: *t*-BuMgCl, THF, −78 °C (75%). b: 2 Equiv ferrocenyllithium, THF (80%). c: $Ti(OiPr)_4$/(*S,S*)-DET/H_2O (1:2:1), cumene hydroperoxide, CH_2Cl_2, −20 °C (55%, 90% *ee*). d: 1.1 Equiv *n*BuLi, THF, 0 °C → room temperature (RT). e: CH_3I (80%). f: Acetone (85%). g: 1) 1 Equiv *n*BuLi, THF, 0 °C → RT; 2) Ph_2PCl (80%). h: Magnesium monoperoxyphthalate (MMPP), EtOH, 0 °C → RT (95%). i: 1) 1 Equiv *n*BuLi, THF, −20 °C; 2) nBu_3SnCl (51% from **1a**).

with methyl iodide at 20 °C gave *tert*-butyl (2-methylferrocenyl) sulfoxide **11** in 80% yield. Only traces of the minor diastereomer were detected by ^1H NMR spectroscopy (*de* > 96%). Crystallization in cyclohexane led to sulfoxide **11** which was suitable for X-ray analysis.[8] Figure 1 shows the (*S*) configuration at sulfur, as expected from the reaction mechanism, and the (*S*) configuration for the planar chirality.[9] It is also apparent that the *tert*-butyl group prefers the

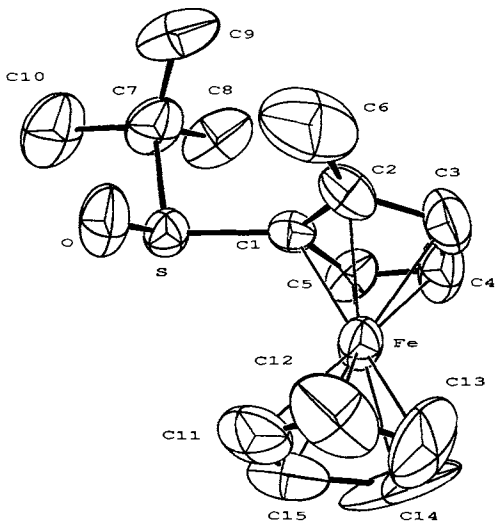

Fig. 1. Crystal structure of **11** (ORTEP, ellipsoids at the 50% probability level). Selected distances [Å], and bond and torsion angles [°] (the numbers in parentheses are estimated standard deviations in the last digits): S-O 1.492(6), S-C1 1.777(6), S-C7 1.860(7), C2-C6 1.54(1), C1-C5 1.371(9), C11-C15 1.36(1); O-S-C1 109.6(3), C1-C2-C6 129.1(8), O-S-C7 107.9(4), C1-S-C7 101.3(3); C7-S-C1-C2 93.51(70), O-S-C1-C2 −20.17(71).

anti orientation with respect to the iron atom, forcing the oxygen substituent to face the (pro-*S*) *ortho* position (even though this is occupied by a methyl group). The *ortho*-lithio compound **7** reacts with many electrophiles to give a large range of chiral ferrocenes. For example, ferrocenyl alcohol **8** was obtained by condensation with acetone (85% yield) ($[\alpha]_D = -29$ ($c = 0.8$, $CHCl_3$)). Deprotonation of **1a** with two equivalents of *n*BuLi followed by quenching with two equivalents of $ClPPh_2$ at room temperature gave diphosphanosulfoxide **10** in 80% yield ($[\alpha]_D = +437$ ($c = 0.5$, $CHCl_3$)).

We previously prepared (*R*)-ferrocenyl *p*-tolyl sulfoxide **1b** by the reaction of ferrocenyllithium with (+)-(R_S,1*S*) menthyl *p*-tolylsulfinate.[5] First attempts at the *ortho*-substitution of **1b** by the sequential addition of *n*BuLi at 0 °C and an electrophile had given a mixture of products. We found recently that the selective deprotonation was cleanly achieved by lithium diisopropylamide (LDA) at −78 °C in THF (Scheme 3). Quenching by trimethylsilyl chloride and tri-

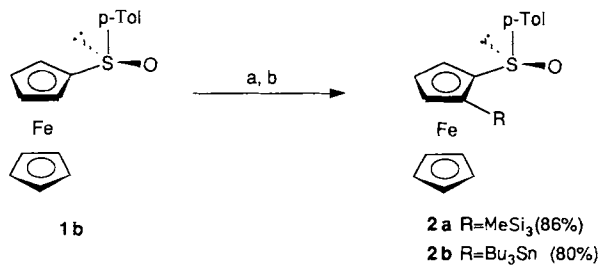

Scheme 3. Diastereoselective *ortho*-lithiation (≥98% *de*) of (*R*)-**1b**. a: LDA, THF, −78 °C. b: RCl.

butylstannyl chloride gave **2a** and **2b**, respectively, in high yield and with a very high diastereomeric excess (≥98%).[10] We tentatively propose that the ferrocenyl unit in **2a** and **2b** has an (*S*) configuration. Based on the assumption of the preferred conformation of **1b**, in which the *p*-tolyl group is *anti* to the iron atom (similar to the conformation of **11** shown in Fig. 1), the observed diastereoselectivity in the lithiation arises from the *ortho*-directing effect of the sulfinyl group.

We are currently investigating the catalytic properties of metal complexes with diphosphane **10** as a ligand. We are also trying to replace the sulfoxide group with other functional groups or remove it completely to set up a general route to enantiomerically pure ferrocenes with planar chirality (Scheme 1).[12, 13, 18]

Experimental Procedure

11: To a solution of (*S*)-**1a** (290 mg, 1 mmol) in dry THF (10 mL) at 0 °C was added dropwise *n*BuLi (0.7 mL of a 1.6 M solution, 1.1 mmol) under argon. The dark solution was stirred at 0 °C for 15 min and 2 h at room temperature. The mixture was cooled to 0 °C and iodomethane (120 μL, 2 mmol) was injected. The reaction mixture was stirred at room temperature for 1 h, then quenched with water, and extracted with diethyl ether. Pure **11** (270 mg, 80%) was isolated as an orange solid after flash chromatography on silica (cyclohexane/EtOAc 1:1) and recrystallized from cyclohexane ($[\alpha]_D = +274$ ($c = 1.5$, $CHCl_3$), m.p. = 104–106 °C).

2a: (*R*)-**1b** (87% *ee*) ($[\alpha]_D = -257$ ($c = 0.46$, $CHCl_3$)) was prepared in 75% yield according to ref. [5] but with a limited amount of ferrocenyllithium (1.0 equiv) at −35 °C in order to prevent the in situ racemization of **1b** (P. Diter, unpublished results). (*R*)-**1b** was recrystallized from hexane/cyclohexane (3:1) until the specific rotation ($[\alpha]_D = -295$ ($c = 0.3$, $CHCl_3$)) was constant. To a solution of (*R*)-**1b** (648 mg, 2 mmol) in dry THF (15 mL) was added dropwise LDA (1.2 mL of a 2 M solution, 2.4 mmol) at −78 °C under argon causing the formation of a light brown precipitate. The suspension was stirred for 15 min at this temperature before treatment with Me_3SiCl (380 μL, 3 mmol). After 10 min of stirring at −78 °C and warming to room temperature over 1 h, the reaction mixture was quenched with 2 N aqueous sodium hydroxide solution and extracted with diethyl ether. The pure sulfoxide **2a** was isolated as a bright orange solid (680 mg, 86%) after flash chromatography on silica (cyclohexane/diethyl ether 7:3). ($[\alpha]_D = +333$ ($c = 0.88$, $CHCl_3$). The enantiomeric excess of **1b** and **2a** (≥ 99%) was determined by HPLC on a chiral column (OD-H, Daicel Co.).

Received: September 1, 1992 [Z 5549 IE]
German version: *Angew. Chem.* **1993**, *105*, 644

[1] D. Marquarding, H. Klusacek, G. Gokel, P. Hoffmann, I. Ugi, *J. Am. Chem. Soc.* **1970**, *92*, 5389.
[2] a) T. Hayashi, M. Kumada, *Acc. Chem. Res.* **1982**, *15*, 395; T. Hayashi, T. Mise, M. Fukushima, M. Kagotani, N. Nagashima, Y. Hamada, A. Matsumoto, S. Kawakami, M. Konishi, K. Yamamoto, M. Kumada, *Bull. Soc. Chim. Jpn.* **1980**, *53*, 1138; b) M. Sawamura, H. Hamashima, Y. Ito, *Tetrahedron Asymmetry* **1991**, *2*, 593; c) D. M. David, L. A. P. Kane-Maguire, S. G. Pyne, *J. Chem. Soc. Chem. Commun.* **1990**, 888.
[3] F. Rebière, O. Samuel, L. Ricard, H. B. Kagan, *J. Org. Chem.* **1991**, *56*, 5991.
[4] Sulfite **5** can be obtained in two steps from ethyl (*S*)-lactate [3, 5] and is also commercially available at Aldrich Co.
[5] F. Rebière, O. Samuel, H. B. Kagan, *Tetrahedron Lett.* **1990**, *31*, 3121.
[6] M. Deshmukh, E. Duñach, S. Jugé, H. B. Kagan, *Tetrahedron Lett.* **1984**, *25*, 3467; Erratum *ibid.* **1985**, *26*, 402.
[7] S. H. Zhao, O. Samuel, H. B. Kagan, *Organic Syntheses* **1989**, *68*, 49 and references therein.
[8] Crystals of **11** ($C_{15}H_{20}FeOS$) were grown at room temperature from cyclohexane solution. Data were collected at 23 ± 1 °C on an Enraf-Nonius CAD4 diffractometer. The crystal structure was solved and refined using the SDP package from Enraf-Nonius. The compound crystallizes in space group $P2_12_12_1$; $a = 10.049(1)$, $b = 11.362(1)$, $c = 13.298(1)$ Å, $V = 1518.30(39)$ Å^3; $Z = 4$; $\rho_{calc} = 1.332$ g cm^{-3}; $Mo_{K\alpha}$ radiation ($\lambda = 0.71073$ Å), graphite monochromator; $\mu = 11.1$ cm^{-1}; $F(000) = 640$. A total of 2502 unique reflections were recorded in the range $2° < 2\theta < 60°$ of which 1187 were considered as unobserved ($F^2 > 3.0\sigma(F^2)$), leaving 1315 for solution and refinement. The structure was solved by direct methods, yielding a solution for iron, sulfur, and the Me and Cp carbon atoms. The hydrogen atoms were included as fixed contribution in the final stages of least-squares refinement; anisotropic temperature factors were used for all other atoms. A non-Poisson weighting scheme was applied with a *p*-factor equal to 0.08. $R = 0.049$, $R_w = 0.078$, G.O.F. = 1.62. The analysis confirms the (*S*) configuration at sulfur (agreement factors for the enantiomeric structure: $R = 0.054$, $R = 0.085$, G.O.F. = 1.755). Further details of the crystal structure investigation are available on request from the Director of the Cambridge Crystallographic Data Centre, 12 Union Road, GB-Cambridge CB21EZ (UK), on quoting the full journal citation.
[9] For nomenclature of planar chirality see K. Schlögl, *Top. in Stereochem.* **1967**, *1*, 39.
[10] Determined by ^{1}H NMR spectroscopy (*p*-tolyl Me group). For comparison, the epimer of **2a** was prepared by the method described in ref. [11] for inversion of configuration at the sulfur of sulfoxides.
[11] C. R. Johnson, D. McCants, Jr., *J. Am. Chem. Soc.* **1965**, *87*, 5404.
[12] For example, oxidation of **11** provides the sulfone which is activated for deprotonation and stannylation on the second *ortho* position. In that way *tert*-butyl [1-methyl-5-(tributylstannyl)-ferrocenyl]sulfone **3a** prepared (Scheme 2; D. Guillaneux, O. Riant, H. B. Kagan, unpublished results). Desulfonylation should provide enantiomerically pure (*S*)-**4** (R^1 = Me, $R^2 = Bu_3Sn$) [13].
[13] Reductive cleavage for replacing sulfinyl or sulfonyl groups by hydrogen atoms is a well-known process, for example see refs. [14, 15]. The substitution of vinyl and aryl sulfoxides is less common, but still possible, especially when the reaction is catalyzed by a transition metal complex [16, 17].
[14] M. Hudlicky, *Reductions in Organic Chemistry*, Ellis Horwood Limited and J. Wiley and Son, Chichester, **1984**, p. 88, and references therein.
[15] T. Y. Luh, Z. J. Ni, *Synthesis* **1990**, 89, and references therein.
[16] J. L. Fabre, M. Julia, J. N. Verpeaux, *Tetrahedron Lett.* **1982**, *23*, 2469.
[17] N. Furukawa, T. Shibutani, K. Matsumura, H. Fujihara, S. Oae, *Tetrahedron Lett.* **1986**, *27*, 3899.
[18] A related diastereoselective *ortho*-lithiation of chromium arene complexes has been recently described [19, 20].
[19] Y. Kondo, J. R. Green, J. Ho, *J. Org. Chem.* **1991**, *56*, 7199.
[20] J. Aubé, J. A. Heppert, M. L. Milligan, M. J. Smith, P. Zenk, *J. Org. Chem.* **1992**, *57*, 3563.

A New Type of Hexanuclear Iron(III) Hydroxo(oxo) Cluster

By *Charlie J. Harding, Richard K. Henderson,* and *Anne K. Powell**

In recent years the interest in oxo/hydroxo-bridged iron(III) compunds has increased because of their importance in natural systems. The hydrolytic polymerization of Fe^{III} compounds is recognised as a central feature in natural iron mineralization processes.[1–3] In aqueous solution Fe^{III} salts rapidly form a mixture of insoluble hydroxo(oxo) minerals, collectively described as "$Fe(OH)_3$", once the pH exceeds a value of 3. However, chelating ligands can slow or suppress this hydrolysis, offering the possibility of trapping intermediate oligomeric hydroxo(oxo) species. Many of the oligomeric iron(III) hydroxo(oxo) compounds previously reported, and most recently reviewed by K. S. Hagen,[4] have been prepared in nonaqueous solvents from precursors such as the trinuclear "basic iron carboxylates" $[Fe_3(\mu_3\text{-}O)(RCOO)_6(L)_3]^+$ (e.g. R = H, Cl, CH_3, C_6H_5, *t*Bu; L = H_2O, py), because of the ready hydrolysis of iron(III) compounds and the formation of thermodynamically stable "$Fe(OH)_3$" in aqueous media. As a result the oxo-bridged iron(III) centers of such compounds often have carboxylato bridges as well.[5–8] However, as was recently reported from this laboratory for the interaction of Fe^{3+} with the polycarboxylato ligand "heidi" (H_3heidi = $N(CH_2COOH)_2(CH_2CH_2OH)$), the polyiron hydroxo(oxo) compounds formed in aqueous solution display core structures in which only oxo and hydroxo bridges bind the iron centers together.[9] A related structure was found for an octanuclear iron(III) compound reported by Wieghardt et al., which has an $[Fe_8(\mu\text{-}O)_2(\mu\text{-}OH)_{12}]^{8+}$ core and was prepared by the hydrolysis of Fe^{III}/tacn (tacn = 1,4,7-triazacyclononane) in the absence of carboxylate ions.[10]

Here we report the preparation, isolation, and magnetic properties of a new type of hexanuclear iron(III) hydroxo(oxo) cluster anion in **1** and **2**, which is formed in aqueous

$M_4[Fe_6(\mu_3\text{-}O)_2(\mu_2\text{-}OH)_6(ida)_6] \cdot n H_2O$ **1**, M = Na; **2**, M = K

$H_2ida = HN(CH_2COOH)_2$

solution in the presence of the tridentate iminodiacetato ligand ida^{2-}. A single-crystal X-ray structure determination

[*] Dr. A. K. Powell, R. K. Henderson
School of Chemical Sciences, University of East Anglia
Norwich, NR4 7TJ (UK)
Dr. C. J. Harding
Department of Chemistry, The Open University
Walton Hall, Milton Keynes, MK7 6AA (UK)

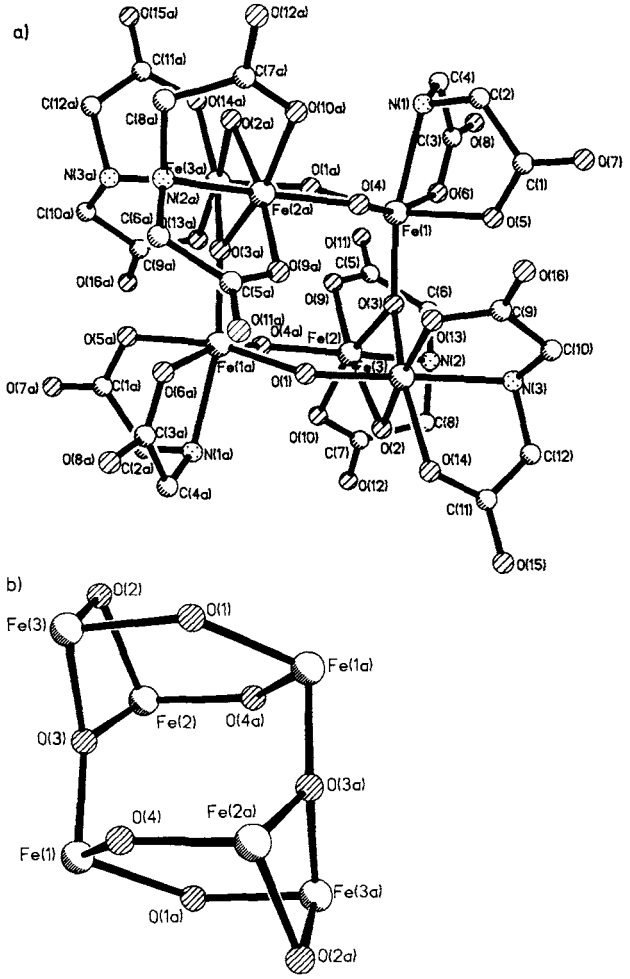

Fig. 1. The structures of a) the anion in **1**, b) the $[Fe_6(\mu_3\text{-}O)_2(\mu_2\text{-}OH)_6]^{8+}$ core of this anion.

of the sodium salt reveals that the anion in **1** (Fig. 1a) contains an $[Fe_6(\mu_3\text{-}O)_2(\mu_2\text{-}OH)_6]^{8+}$ core (Fig. 1b) with a structure unlike that observed for the three hydroxo(oxo)-hexairon compounds **3**–**5** previously reported (the curves in the formulas represent μ_2-carboxolato ligands).[6–8] Those

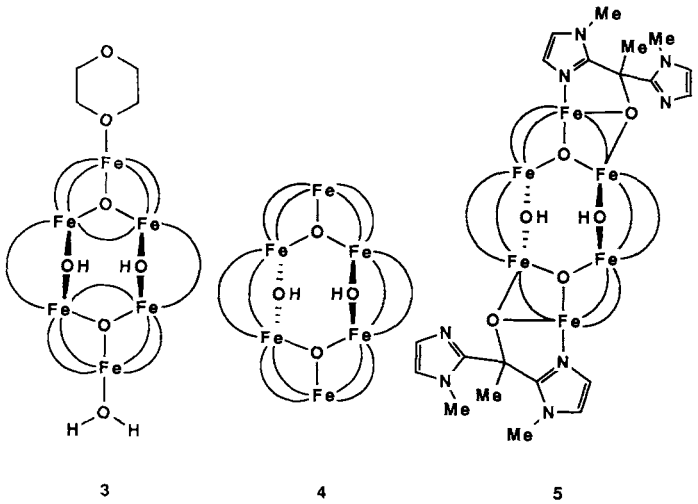

3 4 5

clusters are all derived from further reactions of basic iron carboxylate trimers in nonaqueous solvents, which result in two trimer units joining together by carboxylato and hydroxido bridges. Our new hexamer **1** is different for several reasons: firstly it is synthesized directly in an aqueous environment without the formation of intermediate trimer units, and secondly, none of the hydroxido bridges are supported by any other bridging ligand. As a result there are ten close iron–iron separations in **1** less than 3.7 Å, two more than in **3**–**5** (Fig. 2). The two other known types of Fe^{III} hexanuclear clusters form in methanolic solutions, and their iron centers are connected by alkoxido rather than hydroxido bridges.[11]

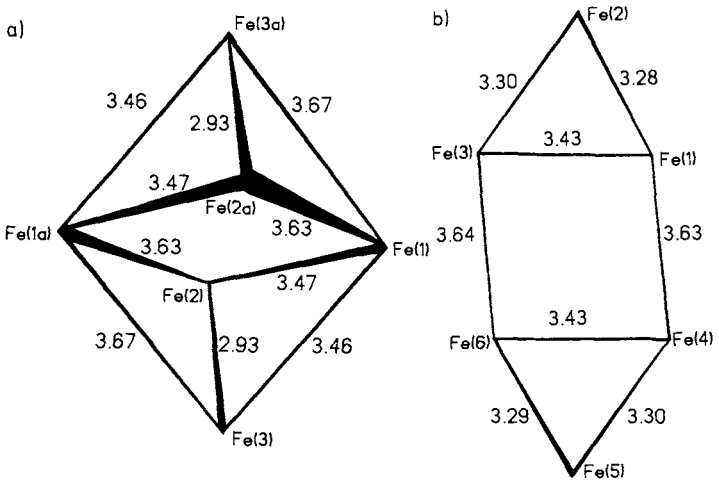

Fig. 2. Comparison of the iron–iron distances in **1** (a) and **3** (b).

The X-ray structure determination[12] of **1** shows that in the anion each iron center is octahedral and has a facially coordinated tridentate ida^{2-} ligand, and one μ_3-oxo and two μ_2-hydroxo bridges. In compounds **3**–**5**, the four central octahedral iron centers are coordinated by one μ_3-oxo and one μ_2-hydroxo bridge, and four other supporting ligands. The core of **1**, by analogy with compounds **3**–**5**, can be regarded as consisting of two μ_3-oxo-bridged Fe_3 triangles defined by Fe(1), Fe(2), Fe(3), O(3), and Fe(1a), Fe(2a), Fe(3a), O(3a). These triangles are in two parallel planes; the apical iron of one triangle (Fe(1)) is connected to the base iron atoms of the triangle opposite (Fe(2a) and Fe(3a)) by two intertrimer μ_2-hydroxo bridges. The two remaining μ_2-hydroxo bridges can be described as intratrimer bridges across the bases of the two triangles between Fe(2) and Fe(3), and Fe(2a) and Fe(3a). These μ_2-hydroxo bridges are in the same plane as the iron atoms of each triangle formed with O(3) or O(3a); the angles Fe(2)-O(2)-Fe(3) and Fe(2)-O(3)-Fe(3) (ideally 120°) are 95.7(5)° and 97.8(5)°, respectively. Consequently Fe(2) and Fe(3) are only 2.934 Å apart, whereas the Fe(1)–Fe(2) and Fe(1)–Fe(3) distances are 3.470 and 3.459 Å, respectively. In other words, the triangles cannot be described as equilateral, unlike in the classic basic iron carboxylate compounds.[13]

In contrast, compounds **3**–**5** possess structures that are derived from two μ_3-oxo-bridged trimers of the basic iron carboxylate type. These Fe_3 triangles are joined by two μ_2-hydroxo bridges and two or four carboxylato bridges to give an essentially planar hexanuclear framework. In **3** the two μ_2-hydroxo bridges are on the same side of this plane,[6] in **4** and **5** on opposite sides.[7,8]

Alternatively, the geometry of the iron core of **1** can be described in terms of two Fe_4 butterfly structures that share the atoms Fe(1) and Fe(1a) at the tips of the wings as illustrated in Figure 2a. Besides the ten Fe–Fe distances < 3.7 Å

in **1**, there are three further interactions <4.7 Å (Fe(1)–Fe(1a) = 4.51 Å, Fe(2)–Fe(3a) = Fe(2a)–Fe(3) = 4.66 Å); the next shortest distance in **3** (Fig. 2b) is between Fe(3) and Fe(4) at 4.76 Å.

The magnetic susceptibilities of **1** and **2** measured against temperature show the same behavior. The effective magnetic moment per iron atom, μ_{eff}/Fe, of **1** increases from 4.02 μ_B at room temperature to a maximum value of 4.81 μ_B at 5 K. (Fig. 3) The variation of χ and μ are parallel in **1** and **2**; the χ_m values are about 6% higher for **1**. The coincidence of the data for **1** and **2** seems to rule out monomeric impurities which can cause large increases in χ_m and μ at low temperatures in compounds that interact antiferromagnetically. Therefore the variation observed is a property of the hexameric ion. This is especially important at low temperature, where a sharp increase in μ is observed.

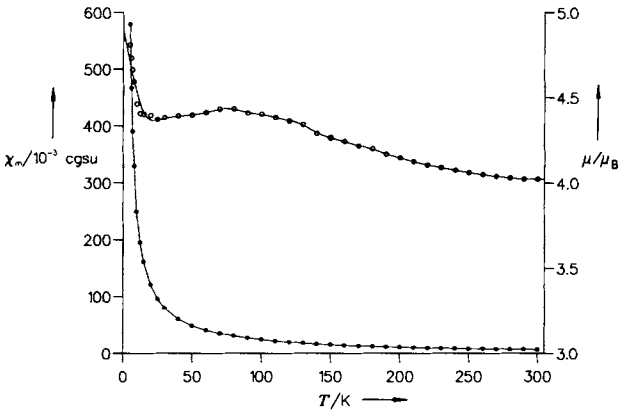

Fig. 3. The variation of the magnetic behavior of **1** between 5 K and 300 K. Upper curve: the fitted curve through the experimentally determined μ values (open circles). Lower curve: experimentally determined χ_m values. χ_m(S.I.) = χ_m(cgsu) $\times 4\pi \times 10^{-6}$ m^3 mol^{-1}.

The interpretation of magnetic data for Fe^{III} hexamers is certainly difficult.[8] The large number of possible pairwise interactions leads to the phenomenon of spin frustration. In our hexamers the high-temperature value of μ of 4 μ_B/Fe clearly shows that antiferromagnetic coupling occurs. If the structure is viewed as two trimers, the sharp rise in μ at low temperatures could be explained by intertrimer ferromagnetic exchange. A similar explanation is given by Hagen[11c] for the hexanuclear compound $[Fe_6(\mu_4\text{-}O)(\mu\text{-}OH)_8(OR)_4(tren)_2\}]^{2+}$ (tren = 2,2′,2″-triaminotriethylamine), although the room-temperature value of μ of 3.55 μ_B/Fe indicates a larger antiferromagnetic exchange than in our system.

Compounds such as **1** and **2** are precursors for mineralized iron(III) compounds (e.g. the core of ferritin) and may be representative of the speciation of iron in the "low molecular weight iron pool". The hexanuclear hydroxo(oxo)iron(III) clusters in **1** and **2** not only illustrate a new structural type, they also give rise to unusual magnetic properties. The interpretation of these properties will lead to advances in understanding the interactions in small anion-bridged cluster compounds.

Experimental Procedure

Compound **1**, $n = 14.5$, is prepared by the addition of a solution of H_2ida (7.5 mmol) and NaOH (17.5 mmol) in water (10 mL) to a solution of $FeCl_3$ (2.5 mmol) in water (10 mL) giving a clear dark red solution of pH ca. 7.5. Solid **1** can be obtained by slow evaporation of the aqueous solution. However, as **1** is very soluble, the addition of excess ethanol is preferable for its isolation. Crystals of **1** suitable for X-ray diffraction were obtained from a water/ethanol mixture. Correct C,H,N,Fe,Na analysis.

Compound **2**, $n = 12$, is synthesized in the same way as **1** with KOH (17.5 mmol) instead of NaOH. Correct C,H,N,Fe,K analysis.

Received: September 24, 1992
Revised version: January 2, 1993 [Z 5595 IE]
German version: *Angew. Chem.* **1993**, *105*, 583

[1] W. Schneider, *Chimia* **1988**, *42*, 9.
[2] *Iron Biominerals* (Eds.: R. B. Frankel, R. P. Blakemore), Plenum, New York, **1991**.
[3] W. Schneider, B. Schwyn in *Aquatic Surface Chemistry* (Ed.: W. Stumm), Wiley Interscience, New York, **1987**, p. 167.
[4] K. S. Hagen, *Angew. Chem.* **1992**, *104*, 1036; *Angew. Chem. Int. Ed. Engl.* **1992**, *31*, 1010.
[5] S. J. Lippard, *Angew. Chem.* **1988**, *100*, 353; *Angew. Chem. Int. Ed. Engl.* **1988**, *27*, 344, and references therein.
[6] W. Micklitz, S. J. Lippard, *Inorg. Chem.* **1988**, *27*, 3067.
[7] N. V. Gérbéléu, A. S. Batsanov, G. A. Timko, Yu. T. Struchkov, K. M. Indrichan, G. A. Popovich, *Dokl. Akad. Nauk SSSR* **1987**, *293*, 364.
[8] D. F. Harvey, C. A. Christmas, J. K. McCusker, P. M. Hagen, R. K. Chadha, D. N. Hendrickson, *Angew. Chem.* **1991**, *103*, 592; *Angew. Chem. Int. Ed. Eng.* **1991**, *30*, 598; J. K. McCusker, C. A. Christmas, P. M. Hagen, R. K. Chadha, D. F. Harvey, D. N. Hendrickson, *J. Am. Chem. Soc.* **1991**, *113*, 6114.
[9] S. L. Heath, A. K. Powell, *Angew. Chem.* **1992**, *104*, 191; *Angew. Chem. Int. Ed. Engl.* **1992**, *31*, 191.
[10] K. Wieghardt, K. Pohl, I. Jibril, G. Huttner, *Angew. Chem.* **1984**, *96*, 66; *Angew. Chem. Int. Ed. Engl.* **1984**, *23*, 77.
[11] a) K. Hegetschweiler, H. Schmalle, H. M. Streit, W. Schneider, *Inorg. Chem.* **1990**, *29*, 3625; b) K. Hegetschweiler, H. Schmalle, H. M. Streit, V. Gramlich, H.-U. Hund, I. Erni, *ibid.* **1992**, *31*, 1299; c) K. S. Hagen, V. S. Nair, *ibid.* **1992**, *31*, 4048.
[12] Crystal data: $C_{24}H_{65}Fe_6N_6Na_4O_{46.5}$, $M_r = 1608.87$, triclinic, space group $P\bar{1}$, $a = 11.381(4)$, $b = 14.897(6)$, $c = 18.788(8)$ Å, $\alpha = 96.30(3)$, $\beta = 90.48(3)$, $\gamma = 108.79(3)°$, $V = 2994(2)$ Å^3, $Z = 2$, $\rho_{calc} = 1.785$ g cm^{-3}, $Mo_{K\alpha}$ radiation (graphite monochromator), $\lambda = 0.71073$ Å, $\mu = 1.555$ mm^{-1}, $F(000) = 1646$, 6491 observed reflections with $F > 4.0\,\sigma(F)$, 11003 independent reflections were collected at 22 °C in an $(\omega - 2\theta)$ scan. A semiempirical absorption correction was applied. The structure was solved by a Patterson synthesis to locate the iron atoms and refined with full-matrix least-squres using the SHELXTL package. Refinement converged with $R = 0.0816$ (unit weights). The unit cell contains two identical independent hexameric anions with their centers of mass located on the inversion centers (0, 0, 0) and (0.5, 0.5, 0.5). The unit cell contained 29 water molecules matching the microanalysis; six disordered water molecules (site occupancy factor of 0.5) link the two hexameric anion cores through a network of hydrogen-bonded sodium cations. Further details of the crystal structure investigation are available on request from the Director of the Cambridge Crystallographic Data Centre, 12 Union Road, GB-Cambridge, CB2 1EZ, UK, on quoting the full journal citation.
[13] R. D. Cannon, R. P. White, *Prog. Inorg. Chem.* **1988**, *36*, 195.

E/*Z* Diastereoselective Enzymatic Hydrolysis of Esters and Diesters**

By *Tanja Schirmeister* and *Hans-Hartwig Otto**

Porcine liver esterase (PLE, E.C. 3.1.1.1) has been used frequently over the last few years for the enantioselective hydrolysis of *meso*- and prochiral diesters as well as for racemic monoesters.[1] The diastereoselectivity of this enzyme was studied among others on cyclopropane derivatives.[2] The ester groups in compounds which contain other labile structure elements could also be hydrolyzed,[3] such as those in β-lactams.[4] However, to our knowledge, there are no reports about enzymatic saponifications of *E*/*Z* diastereomeric monoesters and *E*/*Z* diastereotopic diesters. We report here for the first time about such hydrolyses exem-

[*] Prof. Dr. H.-H. Otto, Pharmacist T. Schirmeister
Pharmazeutisches Institut der Universität
LS Pharmazeutische Chemie
Hermann-Herder-Strasse 9, D-W-7800 Freiburg (FRG)

[**] This work was supported by the Fonds der Chemischen Industrie.

plified by compounds of the type **1**, mono- and dicarboxylates with an azetidine-3-ylide unit in an α position. These

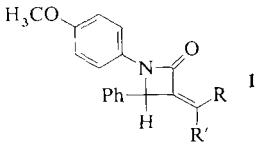

1

compounds cannot be hydrolyzed by conventional methods, since they are stable towards acids, and bases cause a retro-aldol reaction. The hydrolysis described here is therefore the method of choice, even more so since the free acids may be valuable intermediates in the synthesis of antibiotics, and since the method is also applicable for a great number of further arylidene and alkylidene malonates.[16]

The *Z*-positioned ester group in the diester **1**[5] is hydrolyzed selectively with PLE (experiment 1, Table 1). Experiments with other commonly used hydrolases failed with the exception of esterase from rabbit liver. The configuration was determined by a comparison of the chemical shifts in the ^{1}H NMR spectra.[5] The hemiester cannot be reacted further with PLE, however, the hydrolysis to the dicarboxylic acid is achieved with aqueous NaOH at room temperature (experiment 12). The diastereomeric compounds of experiments 4–11 revealed that the *Z* isomers are considerably better substrates for PLE. The acids of the *Z* isomers were obtained selectively from diastereomeric mixtures when the reaction was interrupted after the consumption of the equivalent amount of NaOH (pH-stat method).[6] The reaction course can be followed by thin-layer chromatography (TLC) (silica gel 60, cyclohexane/ethyl acetate/formic acid 49 : 49 : 2) because of the different R_F values of the substrates and products. The hydrolysis of the *E* isomers could not be achieved successfully; the reaction stops after the conversion of several percent (experiments 3, 5, 7, 9, 11). The product could only be isolated from experiments 7 and 9. No reaction was observed in experiment 11.

Table 1. Comparison of the enzymatic hydrolysis of the substrates **1** under the same conditions (see Experimental Procedure).

Experiment no.	**1** R	R'	*t* [h] [a]	Conversion [%] [a]	Product R	R'
1	COOEt	COOEt	72	100	COOH	COOEt
2	COOEt	Me	26	100	COOH	Me
3	Me	COOEt	168	11	Me	COOH [b]
4	COOMe	Me	48	100	COOH	Me
5	Me	COOMe	144	5	Me	COOH [b]
6	COOEt	H	21	100	COOH	H
7	H	COOEt	192	14	H	COOH
8	COOMe	H	18	100	COOH	H
9	H	COOMe	216	13	H	COOH
10	COOMe	Ph	312	100	COOH	Ph
11	Ph	COOMe	219	0	Ph	COOH
12	COOH	COOEt	240	0	COOH	COOH [c]

[a] Reaction time, average values from three or four experiments. [b] Conversions determined by consumption of NaOH. [c] Product (b.p. 131–133 °C, decomp) is obtained by hydrolysis with 0.1 N NaOH (2 h, 25 °C) in over 90% yield.

Evidently, the size of the group R' plays a role in the different reaction times necessary for the complete hydrolysis of the *Z* isomers under the same conditions. This assumption is also confirmed by a comparison of the achieved maximum conversions of the *E* isomers. Thus, the reaction rate decreases with the increasing size of the substituent (H > CH_3 > COOR > Ph). Another influence on the reaction rate is the varying solubility of the substrates. The very poor solubility of the substrates in water was a big problem at the beginning of our investigations.

Although it has been shown that many enzymes are still active in organic solvents,[7] the use of *nonpolar* solvents, apart from a few exceptions,[8] for reactions with hydrolases remained limited to esterifications and transesterifications. The addition of *polar* solvents for the better solubilization of the substrates is only possible to a certain degree without decreasing the activity of the enzymes, in particular for PLE. Thus, hydrolysis occurred for the substrates we used with addition of dimethylsulfoxide,[9] acetone,[4b] EtOH, *t*BuOH, dioxane, or THF; however, only conversions of up to approximately 15% could be achieved.[10] Only following the use of aqueous surfactant-buffer systems, that is by insertion of the substrate molecules into micelles, could all substrates be dissolved sufficiently. Nonionic surfactants were used since these have a high acid–base stability and do not denature proteins.[11] The choice of surfactant did not influence the reaction rate for similar micelle concentrations.[12]

Experimental Procedure

Substrate **1** (0.25 mmol) was dissolved under vigorous stirring by slow dropwise addition of 0.1 M phosphate surfactant buffer (pH 8.0), 0.07 M surfactant Triton X 100 (for other surfactants depending on molecular weight, critical micelle concentration (CMC), and aggregation number N_a 0.009–0.15 M) [13]. Thereafter PLE suspension 200 μL (= 1380 U mmol^{-1})[14] (for experiment 10, however, 500 μL = 3460 U mmol^{-1}) was added. The temperature (32 °C) and pH value were kept constant (pH-stat method, 0.1 N NaOH). After the reaction (see Table 1), the reaction mixture was brought to pH 2 with 2 N HCl and extracted with dichloromethane. The organic phase was dried with sodium sulfate and the solvent was removed under vacuum. The degree of conversion could be determined from the ^{1}H NMR spectrum of the residue. For the isolation, the organic phase was extracted with saturated $NaHCO_3$ solution, acidified (pH 2) with concentrated HCl, and extracted again with dichloromethane. The organic phase was washed several times with water (pH 2) to remove [15] the surfactant completely. After the organic phase had been dried and the solvent had been removed the residue was recrystallized from ethanol/petroleum ether. The separation of phases during the extractions was accelerated by centrifugation (10 min, 7000 U min^{-1}). Yields of up to 85% were obtained. The following surfactants were used: Nonidet P 40 (Fluka), Triton X 100, Brij 35, Pluronic F 68, Myrj 45 (Sigma).

Received: September 24, 1992 [Z 5596 IE]
German version: *Angew. Chem.* **1993**, *105*, 613

[1] E. J. Toone, M. J. Werth, J. B. Jones, *J. Am. Chem. Soc.* **1990**, *112*, 4946–4952; Li-Ming Zhu, M. C. Tedford, *Tetrahedron* **1990**, *46*, 6587–6611.
[2] M. Schneider, N. Engel, H. Boensmann, *Angew. Chem.* **1984**, *96*, 52–54; *Angew. Chem. Int. Ed. Engl.* **1984**, *23*, 64–66.
[3] J. A. Jongejan, J. A. Duine, *Tetrahedron Lett.* **1987**, *28*, 2767–2768; U. Burger, D. Erne-Zellweger, C. Mayerl, *Helv. Chim. Acta* **1987**, *70*, 587–592.
[4] a) M. Ohno, M. Otsuka, *Org. React.* **1989**, *37*, 13; b) Y. Shim, J. Shim, Y. Cho, K. Kim, *Bull. Korean. Chem. Soc.* **1989**, *10*, 33–34.
[5] S. Gürtler, H.-H. Otto, *Arch. Pharm. (Weinheim, Ger.)* **1989**, *322*, 105–109.
[6] a) As an equivalent of the *E* value described in ref. [6b], for the compounds from the experiments 4 and 5, an "E" value was calculated according to the formula: "*E*" = ln ([*Z*]/[Z_0]) / ln ([*E*]/[E_0]) = 186 as a measurement for the diastereoselectivity. PLE showed a specific activity of 0.17 U mg^{-1}; b) C. Chen, Y. Fujimoto, G. Girdaukas, C. Sih, *J. Am. Chem. Soc.* **1982**, *104*, 7294-7299.
[7] A. Klibanov, *Acc. Chem. Res.* **1990**, *23*, 114–120.

[8] H. Akita, Y. Enoki, H. Yamada, T. Oishi, *Chem. Pharm. Bull.* **1989**, *37*, 2876–2878.
[9] F. Björkling, J. Boutelje, S. Gatenbeck, K. Hult, T. Norin, P. Szmulik, *Bioorganic Chemistry* **1986**, *14*, 176–181.
[10] 10–15% of polar cosolvent only leads to a small decrease in the activity of the enzymes; however, this is not sufficient for the dissolution of the substrates. With 50% and more the substrates are dissolved sufficiently; however, the enzymes are denatured or precipitated.
[11] U. Pfüller, *Mizellen – Vesikel – Mikroemulsionen*, Springer, Berlin, **1986**, pp. 33–35.
[12] Micelle concentration = surfactant concentration × aggregation number^{-1} ($[M] = [C] \times N_a^{-1}$).
[13] Ref. [11], pp. 26–28.
[14] Based on the standard ethyl butyrate. PLE obtained from Fluka, 10 mg mL^{-1}, 140–180 U mg^{-1}.
[15] J. Salcedo, R. Hernandez, H. Celis, *Anal. Biochem.* **1983**, *132*, 324–327; see also [11], pp. 168–169.
[16] T. Schirmeister, H.-H. Otto, unpublished results.

Reduction of Geminal Dihalocyclopropanes with Lithium 4,4′-Di-*tert*-butylbiphenyl; Cyclopropyl Derivatives of Dilithiomethane and 1,2-Dilithioethane; Inferences Regarding the Intermediate Carbenoids

By *Cornelis P. Vlaar*, and *Gerhard W. Klumpp**

While alkyllithium compounds **1**[1] including 1,*n*-dilithioalkanes ($n \geq 4$) are common and thoroughly studied, only few geminal (**2**) and vicinal (**3**) dilithium compounds have been reported and their chemistry is largely terra incognita.[2] Repulsion between neighboring like charges in **2** and **3** is expected to lead to increased energies.[3] Accordingly,

$R^1R^2R^3CLi$ **1** $\quad R^1R^2CLi_2$ **2** $\quad R^1R^2LiC\text{-}CLiR^3R^4$ **3**

formation of **2** and **3** is found to be difficult,[4] and they decompose very easily.[5] Access to **2** and **3** is also restricted by a serious methodological limitation: the easiest route to organolithium compounds, RHal → RLi, proceeds in two steps for these compounds; only rarely can the second step providing **2** and **3** compete with the α- and β-elimination of LiHal from the intermediate α- and β-halolithium compounds.[6] The reduction of geminal dihalides with four equivalents of lithium 4,4′-di-*tert*-butylbiphenyl (LiDBB) at −80 °C (Scheme 1) can lead to compounds of types **2** (**2**-LiHal [Eq.(3)]) and **3**. **3**-LiHal is formed by the dimerization of **4** [Eq.(4)] or the reaction of $R^1R^2CLiHal$–LiHal with **2**-LiHal [Eq.(5)]. As an extension of our previous studies[7] we have subjected dihalonorcaranes (**5a,b**) and related compounds to LiDBB. Besides the expected products **7** and **8**, a new compound of type **3**, **9**-LiCl was found. This derivative of labile cyclopropylmethyllithium[8] is remarkably stable. First conclusions on the aggregation of carbenoids $R^1R^2CLiHal$–LiHal [Scheme 1, Eq.(1)] could be drawn from the observed dependence of the ratio (**7** + **8**):**9** on the reaction conditions.

To a stirred solution of 0.2 mmol **5a** (**5b**) in 10 mL diethyl ether at −95 °C was added by syringe 2 mL of a 0.45 M solution of LiDBB in THF. The reagent was allowed to flow slowly down the inner surface of the reaction vessel, which was maintained at −95 °C. After 5 min at the temperature given in Table 1, the reaction was quenched by addition of MeOD. The product mixture obtained after aqueous workup was analyzed by gas chromatography. Based on their respective deuterolysis (protonolysis) products (7-deuterio- and 7,7-dideuterionorcarane, and compounds **10** and **12**[9]) lithium compounds of types **7**–**9** and dilithium compound **11**, formed from **9** upon warming, were identified. In addition alkyne **15** arising from **11** via **14** was obtained. The results are listed in Table 1.

$$R^1R^2CHal_2 + 2\,LiDBB \longrightarrow R^1R^2CLiHal\text{-}LiHal + 2\,DBB \quad (1)$$

$$R^1R^2CLiHal\text{-}LiHal + LiDBB \longrightarrow \underset{\mathbf{4}}{(R^1R^2CLi)^{\cdot}\text{-}LiHal} + LiHal + DBB \quad (2)$$

$$\mathbf{4} + LiDBB \longrightarrow \underset{\mathbf{2}\text{-LiHal}}{R^1R^2CLi_2\text{-}LiHal} + DBB \quad (3)$$

$$2\,\mathbf{4} \longrightarrow \underset{\mathbf{3}\text{-LiHal}}{R^1R^2CLi\text{-}CLiR^1R^2\text{-}LiHal} \quad (4)$$

$$\mathbf{2}\text{-LiHal} + R^1R^2CLiHal\text{-}LiHal \longrightarrow \mathbf{3}\text{-LiHal} \quad (5)$$

Scheme 1. DBB = 4,4′-di-*tert*-butylbiphenyl. The structures of the compounds listed here are unknown. However, it is well established that organolithium compounds are modified by lithium halide[7c, 13, 16]. This is expressed here and in the text by the addition of -LiHal (no stoichiometry is implied) to the formulas and compound numbers or by expressions such as "lithium compounds of type..." Several proposed structures are discussed in the text.

Table 1. Reduction of **5a** and **5b** with LiDBB. The yields [%] of the lithium compounds of types **7**–**9** and other compounds are based on analysis by gas chromatography (internal standard: *n*-decane) after deuterolysis[a].

Run	**5a,b** Y	*T* [°C]	Additive [b]	**7** [c]	**8** [c]	**9** [d]	Other cmpds. yield [%]
1	Cl	−95		1 [e]		9	**6a**, 50
2	Cl	−75		6 [e]		71	
3	Cl	−75	5 [f] TMEDA [g]	14 [e]		50	
4	Cl	−65	5 [f] PMDTA [h]	31 ± 3	6 ± 3	13	
5	Cl	−65	2 [f] TMTAN [i]	52 ± 3	9 ± 3	15	
6	Cl	−40 [j]		8 [e]		72	
7	Cl	−30		14 [e]		60	
8	Cl	−75		0		39 [k]	**10** (Y = H), 11 [l]; **13**, 7
9	Cl	0		11 [e]		11	**11**, 58
10	Cl	25 [m]		1 < [e]		0	**12** (Y = H), 11; **15**, 48
11	Br	−95		25	8	25	
12	Br	−95	5 [f] TMEDA [g]	40 ± 3	8 ± 3	2	
13	Br	−95 [n]		24	55	1 <	

[a] All detected components are listed. The material missing from the mass balance cannot be accounted for. [b] Added to **5a,b**. [c] From the ratio of 7,7-dideuterio- and 7-deuterionorcarane obtained by ^{1}H NMR spectroscopy. [d] According to ^{1}H NMR spectroscopy only dideuterated material was present. [e] Sum of **7** and **8**. The deuterium distribution could not be determined precisely by ^{1}H NMR spectroscopy. [f] Equivalents, based on **5a** (**5b**). [g] TMEDA: *N,N,N′,N′*-tetramethylethylenediamine. [h] PMDTA: *N,N,N′,N″,N″*-pentamethyldiethylenetriamine. [i] TMTAN: *N,N′,N″*-trimethyl-1,4,7-triazacyclononane. [j] After the usual reaction time the reaction mixture was cooled to −90 °C, and a cold solution of *t*BuCl in THF was added until the color changed from blue to red. Deuterolysis followed. [k] Dimethylsulfate was added. The reaction mixture was allowed to warm to room temperature and subjected to aqueous workup. Yield of 7,7′-dimethyl-7,7′-dinorcarane. [l] Origin unknown. [m] Quenched with MeOH after 2.5 h. [n] Inverse addition. A solution of **5b** was added to 8 equiv LiDBB.

Run 1 shows that **5a** is initially transformed into carbenoid **6a**-LiCl, which at −95 °C reacts very slowly with LiDBB. At −75 °C (Run 2) **6a**-LiCl is converted completely into a mixture of lithium compounds of types **7**, **8**, and **9** [(**7** + **8**):**9** ≈ 1:12]. When a polydentate nitrogen base such as TMEDA, PMDTA, and TMTAN (for abbreviations see footnotes [g]–[i] in Table 1) is added to the starting solution of **5a** (Runs 3–5), the ratio (**7** + **8**):**9** inverts to a value of

[*] Prof. Dr. G. W. Klumpp, Drs. C. P. Vlaar
Scheikundig Laboratorium Vrije Universiteit
De Boelelaan 1083, NL-1081 Hv Amsterdam (The Netherlands)

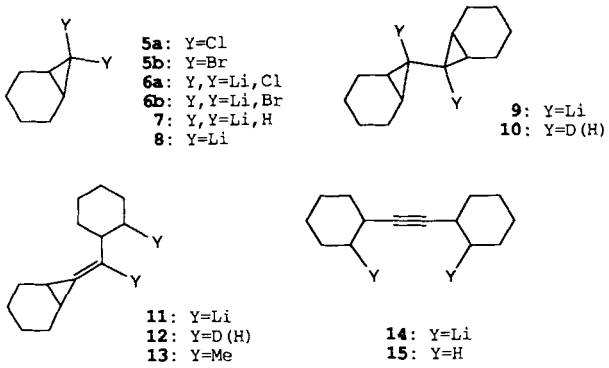

approximately 4:1 (**7**:**8** ≈ 5:1). These Lewis bases cleave aggregates of organolithium compounds in the order of activity TMEDA < PMDTA < TMTAN.[12] Their influence on the ratio (**7** + **8**):**9** may be explained most simply by the assumption that in the presence of PMDTA and TMTAN complexes **16** of the monomeric carbenoid **6a** are reduced by LiDBB to the corresponding α-lithioradicals **17**. The dominant reaction of **17** is hydrogen abstraction to give lithium compounds of type **7**. Only to a minor degree does LiDBB

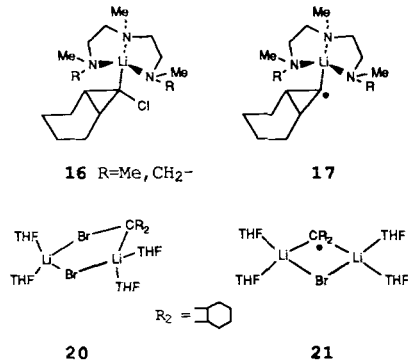

reduction of **17** lead to dilithium compounds of type **8**. For the reactions conducted without PMDTA and TMTAN (Runs 2(6) and 7–9) we propose a dimer of type **18** (Scheme 2) as the simplest aggregate of **6a**-LiCl that could lead predominantly to **9**-LiCl (and in Runs 9 and 10, to **11** and **14**). The proposal is based on the following assumptions: 1) **6a**-LiCl has structure **19**, which corresponds to the one calculated for CH_2LiF–LiF.[13] 2) In line with the common structural relationship between Li_2X_2 and Li_4X_4 systems (X = C, O, Hal),[14] two units of **19** combine to give aggregate **18**. In Run 6 the unreacted LiDBB was destroyed by addition of *t*BuCl before deuterolysis. No change in the composition of the product mixture was observed (cf. Run 2). This excludes the possibility that the reaction with the fourth equivalent of LiDBB takes place only after the addition of the first equivalent of electrophile. Therefore, processes A [Scheme 1, Eqs.(2),(4)] and B [Scheme 1, Eqs.(2),(3),(5)] shown in Scheme 2 are proposed as possible paths for the transformation of **18** into **9**-LiCl.[15]

Whereas cyclopropylmethyllithium rearranges into 4-lithiobutene already at −70 °C, **9**-LiCl is persistent at this temperature. As shown in Run 7, it is stable even at −30 °C in THF for several minutes. The reasons for the slower ring opening of **9**-LiCl are not known, but may be related to the bonding in (aggregated) 1,2-dilithioethane derivatives.[3b] After 5 min at 0 °C most of **9**-LiCl had rearranged to **11**-LiCl (Run 9, see also the formation of **13** in Run 8). When the reaction temperature is kept at 25 °C for a longer time (Run 10), only **12** and alkyne **15** are isolated in the ratio 1:5.

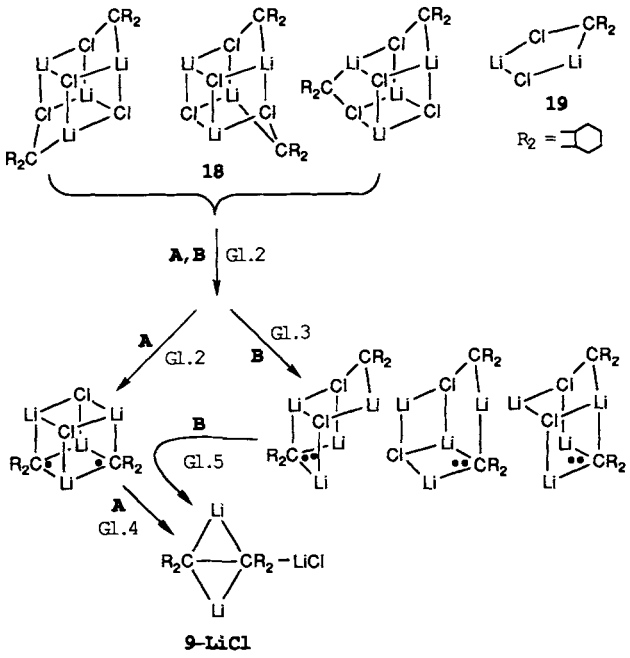

Scheme 2. For clarity, the complexation of lithium by THF is not shown. The representation of **9**-LiCl is based on the structure found for **3** ($R^1 = R^2 = R^3 = R^4 = SiMe_3$) (Sekiguchi et al.[4b]).

In Runs 11 and 12 the proportion of **7** + **8** is higher than in Runs 2 and 3. This suggests that the less stable[16] α-bromolithium compounds **5b**-LiBr (possible structure in THF: **20**, see ref.[13]) have a lower tendency toward aggregation than their chloro analogues **5a**-LiCl. Support of our hypothesis that compounds **7** and **8** arise from monomeric carbenoid presursors is provided by Run 13. When **5b** is added to an excess of LiDBB, **20** should be trapped by reduction to **21** before dimerization can take place. The α-lithio radical **21** is probably more stable and therefore less aggressive than **17**. Besides the product of hydrogen abstraction, **7**-LiBr, it forms the dilithium compound **8**-LiBr predominantly.

Several other geminal dihalocyclopropanes were examined under the conditions of Run 2(11). The deuterolysis results indicate that the reaction of 8,8-dichlorobicyclo[5.1.0]octane produces homologues of **7**-LiCl, **8**-LiCl, and **9**-LiCl in yields of 8, 22, and 31%, respectively. 1,1-Dibromo-2,2,3,3-tetramethylcyclopropane might lead to a carbenoid with greater steric hindrance and a reduced tendency toward dimerization. Accordingly it forms only traces (<1%) of the 1,2-dilithioethane derivative. After the reaction mixture was worked up with dimethylsulfate, pentamethylcyclopropane (20%) and hexamethylcyclopropane (47%) were obtained. For some obscure reason cyclopropylmethyltin was the sole product (20%) obtained from the reaction of 1,1-dibromocyclopropane after workup with trimethyltin chloride. However, the reaction of a 1:1 mixture of 1,1-dibromocyclopropane and **5a** yielded among other

products the 7-lithio-7-(1-lithiocyclopropyl)norcarane corresponding to **9**.

Received: October 22, 1992 [Z 5648 IE]
German version: *Angew. Chem.* **1993**, *105*, 599

[1] J. L. Wardell in *Comprehensive Organometallic Chemistry*, Vol. 1 (Eds.: G. Wilkinson, F. G. A. Stone, E. W. Abel), Pergamon Press, Oxford, **1982**, p. 43; B. J. Wakefield, *The Chemistry of Lithium Compounds*, Pergamon Press, Oxford, **1974**.

[2] a) Review: A. Maercker, M. Theis, *Top. Curr. Chem.* **1987**, *138*, 1–61. b) For **2** see literature review in [3a].

[3] a) N. J. R. van Eikema Hommes, P. von R. Schleyer, Y.-D. Wu, *J. Am. Chem. Soc.* **1992**, *114*, 1146–1151. b) See also: A. J. Kos, E. D. Jemmis, P. von R. Schleyer, R. Gleiter, U. Fischbach, J. A. Pople, *ibid.* **1981**, *103*, 4996–5002; A. Streitwieser, Jr., *Acc. Chem. Res.* **1984**, *17*, 353–357.

[4] a) Difficulties (or incomplete reactions) in the formation of **2** see J. R. Baran, Jr., R. J. Lagow, *J. Am. Chem. Soc.* **1990**, *112*, 9415–9416; H. Kawa, J. W. Chinn, Jr., R. J. Lagow, *J. Chem. Soc. Chem. Commun.* **1984**, 1664–1665. b) Compounds **3** form relatively easily only under the influence of carbanion-stabilizing factors (I. Sethson, D. Johnels, T. Lejon, U. Edlund, B. Wind, A. Sygula, P. W. Rabideau, *J. Am. Chem. Soc.* **1992**, *114*, 593–955, and references therein; A. Sekiguchi, T. Nakanishi, C. Kabuto, H. Sakurai, *ibid.* **1989**, *111*, 3748–3750; I. Murata, T. Nakawaza, M. Kato, T. Tatsuoka, Y. Sugihara, *Tetrahedron Lett.* **1975**, 1647–1650; A.-D. Schlüter, H. Huber, G. Szeimies, *Angew. Chem.* **1985**, *97*, 406–407; *Angew. Chem. Int. Ed. Engl.* **1985**, *24*, 404–405) or if the addition of Li to double bonds leads to a reduction of ring strain (C. P. Vlaar, unpublished results). The preparation of the parent compound $H_2LiC-CLiH_2$ by the addition of lithium to ethylene at $-180\,^{\circ}C$ requires highly reactive lithium vapor (N. J. R. van Eikema Hommes, F. Bickelhaupt, G. W. Klumpp, *Angew. Chem.* **1988**, *100*, 1100–1107; *Angew. Chem. Int. Ed. Engl.* **1988**, *27*, 1083–1084).

[5] LiH elimination from **2**: ref.[2a] pp.28–29; LiH elimination from **3**: ref. [7a]. Ether cleavage by **2**, see refs.[7b,d].

[6] P. M. Warner, S.-C. Chang, N. J. Koszewski, *J. Org. Chem.* **1985**, *50*, 2605–2606.

[7] a) N. J. R. van Eikema Hommes, F. Bickelhaupt, G. W. Klumpp, *Recl. Trav. Chim. Pays-Bas* **1987**, *106*, 514–515; b) N. J. R. van Eikema Hommes, F. Bickelhaupt, G. W. Klumpp, *Tetrahedron Lett.* **1988**, *29*, 5237–5240; c) N. J. R. van Eikema Hommes, F. Bickelhaupt, G. W. Klumpp, *J. Chem. Soc. Chem. Commun.* **1991**, 438–440; d) C. P. Vlaar, G. W. Klumpp, *Tetrahedron Lett.* **1991**, *32*, 2951–2952.

[8] T. Lansbury, V. A. Pattison, W. A. Clement, J. D. Sidler, *J. Am. Chem. Soc.* **1964**, *86*, 2247–2251.

[9] Authentic **10** (Y = H) was prepared by the oxidative coupling of *exo*-7-lithionorcarane with $CuBr_2$. ^1H NMR ($CDCl_3$, TMS): $\delta = 1.75$ (m, 4H), 1.52 (m, 4H), 1.12 (m, 8H), 0.51 (m, 4H), 0.42 (m, 2H); ^{13}C NMR ($CDCl_3$, TMS): $\delta = 25.04$, 23.56, 21.49, 14.88. (The *endo,endo* diastereomer of **10** was prepared in the same way from *endo*-7-lithionorcarane.) Authentic **12** (Y = H) was obtained from the adduct of 7-lithio-7-trimethylsilylnorcarane and cyclohexanecarbaldehyde by treatment with *t*BuOK [10]. ^1H NMR ($CDCl_3$, TMS): $\delta = 5.63$ (d, $^3J(H,H) = 7$ Hz, 1H), 2.12 (m, 1H), 1.8–1.1 (m, 20H); ^{13}C NMR ($CDCl_3$, TMS): $\delta = 129.93$, 123.16, 40.35, 32.96, 26.15, 26.12, 26.08, 23.26, 23.11, 21.38, 21.09, 12.83, 11.36.

[10] T. Hiyama, A. Kanakura, Y. Morizawa, H. Nozaki, *Tetrahedron Lett.* **1982**, *23*, 1279–1280.

[11] K. M. Nicholas, J. Siegel, *J. Am. Chem. Soc.* **1985**, *107*, 4999–5001. ^1H NMR ($CDCl_3$, TMS): $\delta = 2.30$ (m, 2H), 1.72 (m, 8H), 1.36 (m, 12H); ^{13}C NMR ($CDCl_3$, TMS): $\delta = 84.37$, 33.07, 28.89, 26.14, 25.84.

[12] See for example: G. Fraenkel, A. S. Chow, W. R. Winchester, *J. Am. Chem. Soc.* **1990**, *112*, 6190–6198.

[13] C. Rohde, T. Clark, E. Kaufmann, P. von R. Schleyer, *J. Chem. Soc. Chem. Commun.* **1982**, 882–884.

[14] W. N. Setzer, P. von R. Schleyer, *Adv. Organomet. Chem.* **1985**, *24*, 353–451.

[15] Under our reaction conditions 7,7'-binorcarylidene did not react to give **9**.

[16] J. Villiéras, M. Rambaud, B. Kirschleger, R. Tarhouni, *Bull. Soc. Chim. Fr.* **1985**, 837–843.

$[Tc_6X_8]$ Clusters in ternary Technetium Chalcogenides**

By *Welf Bronger,* Martin Kanert, Markus Loevenich, Dieter Schmitz,* and *Klaus Schwochau*

Octahedral structural units composed of six niobium, tantalum, molybdenum, or tungsten atoms have been known for more than four decades. The anions X which surround these M_6 octahedra as a first coordination sphere reveal two different configurations: the $[M_6X_{12}]$ cluster in which the X atoms coordinate the M_6 octahedron over the edges, and the $[M_6X_8]$ cluster in which the M_6 octahedron is coordinated by X atoms over its faces. The former composition occurs preferably in niobium and tantalum compounds and the latter in molybdenum and tungsten compounds. In the crystalline solid, the clusters are generally linked to one another through M atoms by anionic bridges.

The corresponding rhenium clusters whose existence was previously discussed in the sixties[1] were established for the first time in 1978 in ternary sulfides such as $Na_4Re_6S_{12}$.[2] $[Re_6S_8]$ clusters are found as the characteristic structural units which are bridged by additional S atoms or S_2 groups to build anionic frameworks. The alkali metal ions occupy vacancies which have suitable sulfur coordination spheres.

Are there analogous technetium clusters? To answer this question we have investigated the preparation and structural characterization of ternary technetium chalcogenides and the results of our findings are described herein.

The syntheses of the desired compounds were carried out in a radiochemical laboratory at the Institut für Nuklearchemie des Forschungszentrums Jülich. The technetium isotope ^{99}Tc was utilized, which among the long-lived nuclides is the only one accessible in weighable quantities through the induced fission of ^{235}U with thermal neutrons. ^{99}Tc decays with β^- emission ($t_{1/2} = 2.12 \times 10^5$ a, $E_{max} = 0.29$ MeV). Technetium and its compounds were handled in Plexiglass boxes which retain β radiation to the most part.

We have successfully prepared the ternary technetium chalcogenides **1**–**6**. The sulfides were synthesized by heating

$K_4Tc_6S_{12}$	$K_4Tc_6Se_{12}$	$Rb_4Tc_6S_{13}$	$Rb_4Tc_6Se_{12}$	$Cs_4Tc_6S_{13}$	$Cs_4Tc_6Se_{13}$
1	**2**	**3**	**4**	**5**	**6**

alkali metal carbonates, elemental technetium, and sulfur under an argon atmosphere at 800 °C for about 8 h. Well-formed, black, shiny crystals were obtained by extracting the cooled melt with water and ethanol. The synthesis of the selenides was achieved in an analogous manner under a hydrogen atmosphere. During attempts to produce sulfur compounds under a hydrogen stream, a new type of cluster compound was obtained; the structure determination is currently in progress.

All six chalcogenides are isolated phase-pure and crystallize with monoclinic cells in the space group $C2/c$. The lattice constants are listed in Table 1; compounds with the same composition are isostructural. Single crystal structure deter-

[*] Prof. Dr. W. Bronger, Dipl.-Chem. M. Kanert,
Dipl.-Chem. M. Loevenich, Dr. D. Schmitz
Institut für Anorganische Chemie der Technischen Hochschule
Prof.-Pirlet-Strasse 1, D-W-5100 Aachen (FRG)
Prof. Dr. K. Schwochau
Institut für Nuklearchemie des Forschungszentrums Jülich GmbH

[**] This work was supported by the Deutsche Forschungsgemeinschaft and the Fonds der Chemischen Industrie. We would like to thank Prof. Dr. G. Stöcklin for his hospitality and assistance at the Institut für Nuklearchemie des Forschungszentrums Jülich.

Table 1. Dimensions of the monoclinic unit cells (space group $C2/c$) for the ternary technetium chalcogenides **1**–**6**. The lattice constants as determined from Guinier photographs are given in Å and degrees (standard deviations in parentheses).

Compound	a	b	c	β
$K_4Tc_6S_{12}$ **1**	16.463(4)	9.667(3)	11.841(2)	91.40(2)
$K_4Tc_6Se_{12}$ **2**	17.165(2)	10.019(2)	12.301(2)	91.42(1)
$Rb_4Tc_6S_{13}$ **3**	9.745(2)	16.595(4)	13.913(3)	99.83(2)
$Rb_4Tc_6Se_{12}$ **4**	17.640(4)	10.092(1)	12.464(1)	91.30(1)
$Cs_4Tc_6S_{13}$ **5**	9.983(1)	17.120(4)	13.643(3)	100.68(1)
$Cs_4Tc_6Se_{13}$ **6**	10.275(2)	17.826(3)	14.161(4)	100.89(2)

minations[3] show that $[Tc_6X_8]$ clusters are found in both structure types as the structural units (Fig. 1). The six technetium atoms form in each case nearly regular octahedra; their average dimensions are given in Table 2. The eight chalcogen atoms are found over the octahedral faces. The resulting cube is again nearly regular (Table 2). The Tc_6 octahedron of every $[Tc_6X_8]$ unit is linked in all three directions in space to neighboring octahedra through additional X atoms or X_2 groups. The alkali metal ions are inserted in suitable interstices found within the anionic framework, whereby allowances are obviously made for the spatial requirement of the cations through a variation of the bridges linking the $[Tc_6X_8]$ units. The construction of the framework for the potassium compounds **1** and **2** is accomplished by connecting the $[Tc_6X_8]$ clusters through four X and two X_2 bridges each, according to the scheme $K_4[Tc_6X_8]X_{4/2}(X_2)_{2/2}$ (Fig. 2). In contrast, the larger interstices of the cesium compounds **5** and **6** are made possible through the formation of only two X but four X_2 bridges between adjacent $[Tc_6X_8]$ units, so that the formula $Cs_4[Tc_6X_8]X_{2/2}(X_2)_{4/2}$ results (Fig. 3).

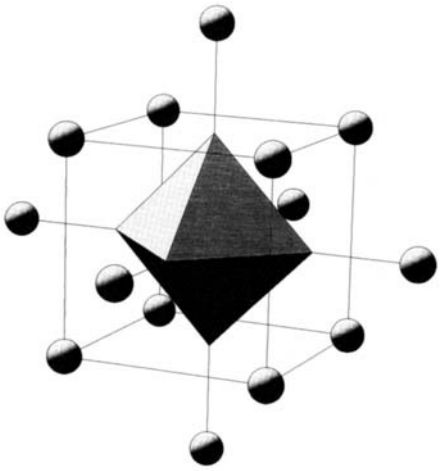

Fig. 1. The $[Tc_6X_8]$ structural unit and bridging chalcogen atoms.

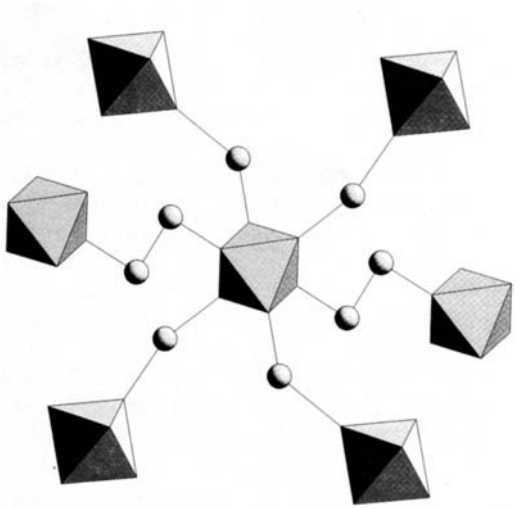

Fig. 2. Linkage of Tc_6 octahedra within the framework structure $\{[Tc_6X_8]X_{4/2}(X_2)_{2/2}\}^{4-}$. The X_8 cubes surrounding the Tc_6 octahedra were omitted for clarity.

Accordingly, in the structure of **4**, due to the relatively large selenium atoms, linkage through four Se^{2-} and two Se_2^{2-} bridges is sufficient to create the required space for the Rb^+ ions to be inserted, whereas in the sulfide **5**, two S^{2-} and four S_2^{2-} bridges are necessary. In the corresponding rhenium compounds, some of which are isostructural with the technetium compounds presented here, we observed an analogous trend.[4–8]

Table 2. Average values of comparable interatomic distances d [Å] and angles [°] (the real values are within the specified interval) [a].

	$K_4Tc_6S_{12}$ **1**	$Rb_4Tc_6S_{13}$ **3**	$Cs_4Tc_6S_{13}$ **5**	$K_4Tc_6Se_{12}$ **2**	$Rb_4Tc_6Se_{12}$ **4**	$Cs_4Tc_6Se_{13}$ **6**
$\bar{d}$(Tc-Tc)	2.61 ± 0.02	2.60 ± 0.02	2.61 ± 0.02	2.64 ± 0.02	2.65 ± 0.02	2.64 ± 0.02
$\bar{d}$(Tc-X^i)	2.39 ± 0.03	2.38 ± 0.03	2.39 ± 0.03	2.51 ± 0.03	2.51 ± 0.05	2.50 ± 0.02
$\bar{d}_{Tc}$-X^a)	2.476 ± 0.002	2.47 ± 0.03	2.47 ± 0.08	2.62 ± 0.03	2.623 ± 0.005	2.59 ± 0.06
$\bar{d}$(X^a-X^a)	2.110 [b]	2.03 ± 0.05	2.10 ± 0.03	2.403 [b]	2.427 [b]	2.39 ± 0.03
$\bar{d}$(X^i-X^i)	3.37 ± 0.03	3.36 ± 0.05	3.37 ± 0.06	3.54 ± 0.04	3.55 ± 0.07	3.54 ± 0.07
$\bar{\theta}$(Tc-Tc-Tc)	60.0 ± 0.7	60.0 ± 0.9	60.0 ± 0.8	60.0 ± 0.6	60.0 ± 0.5	60.0 ± 0.9
$\bar{\theta}$(X^i-X^i-X^i)	90.0 ± 1.5)	90.0 ± 1.6)	90.0 ± 1.5)	90.0 ± 1.6)	90.0 ± 1.9	90.0 ± 1.3

[a] X^i: chalcogen atoms within the $[Tc_6X_8]$ units, X^a: chalcogen atoms bridging Tc_6 clusters. [b] In the $A_4Tc_6X_{12}$ compounds the X^a atoms composing the X_2 bridges occupy special positions, so that the values listed here represent real distances rather than the average.

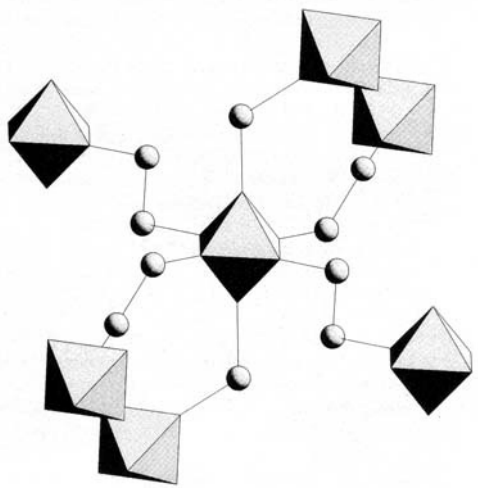

Fig. 3. Linkage of Tc_6 octahedra within the framework structure $\{[Tc_6X_8]X_{2/2}(X_2)_{4/2}\}^{4-}$. The X_8 cubes surrounding the Tc_6 octahedra were omitted for clarity.

Until now, the existence of $[M_6X_8]$ clusters in technetium chemistry was not shown conclusively. Structural entities

described as $\{[Tc_6Br_5]Br_6\}^{2-}$ anions appear to be structurally related.[9, 10] Here it is assumed that the five bromide ions are statistically distributed over the eight positions of the X_8 cube. However, the analytically determined composition, which points to a mixed-valent compound, contradicts the observed magnetism and high symmetry of the Tc_6 octahedron (see the following section).

In the ternary technetium chalcogenides we have presented here, technetium is found in each case in a +3 oxidation state, which indicates that there are 24 valence electrons per Tc_6 unit. According to MO calculations all the bonding states are occupied to give a stable electron configuration.[11] This is in accordance with the observation that all the Tc_6 octahedra are nearly regular, that is a collective Jahn–Teller effect does not occur.[12] The magnetic behavior is also in agreement with this. All six compounds reveal down to low temperatures nearly temperature-independent susceptibilities from -490 to $-665 \times 10^{-6}\ cm^3 mol^{-1}$. After diamagnetic correction [13] a weak temperature-independent paramagnetism is found; such paramagnetism is often observed in cluster compounds.[14–16]

Received: November 13, 1992 [Z 5682 IE]
German version: *Angew. Chem.* **1993**, *105*, 597

[1] H. Schäfer, H. G. Schnering, *Angew. Chem.* **1964**, *76*, 833.
[2] M. Spangenberg, W. Bronger, *Angew. Chem.* **1978**, *90*, 382; *Angew. Chem. Int. Ed. Engl.* **1978**, *17*, 368.
[3] Data collection with an Enraf–Nonius CAD 4 four circle diffractometer. Absorption correction according to the ψ scan technique. $K_4Tc_6S_{12}$: 9882 measured reflections ($Ag_{K\alpha}$, $2\theta_{max} = 48°$), 1648 symmetry-independent reflections with $F_o^2 > 3\sigma(F_o^2)$, $R = 0.031$, $R_w = 0.037$; $K_4Tc_6Se_{12}$: 13337 measured reflections ($Mo_{K\alpha}$, $2\theta_{max} = 60°$), 1593 symmetry-independent reflections with $F_o^2 > 3\sigma(F_o^2)$, $R = 0.031$, $R_w = 0.038$; $Rb_4Tc_6S_{13}$: 7410 measured reflections ($Ag_{K\alpha}$, $2\theta_{max} = 48°$), 1013 symmetry-independent reflections with $F_o^2 > 3\sigma(F_o^2)$, $R = 0.073$, $R_w = 0.090$; $Rb_4Tc_6Se_{12}$: 7246 measured reflections ($Ag_{K\alpha}$, $2\theta_{max} = 48°$), 880 symmetry-independent reflections with $F_o^2 > 3\sigma(F_o^2)$, $R = 0.044$, $R_w = 0.062$; $Cs_4Tc_6S_{13}$: 14430 measured reflections ($Mo_{K\alpha}$, $2\theta_{max} = 60°$), 1464 symmetry-independent reflections with $F_o^2 > 3\sigma(F_o^2)$, $R = 0.045$, $R_w = 0.059$; $Cs_4Tc_6Se_{13}$: 19761 measured reflections ($Mo_{K\alpha}$, $2\theta_{max} = 60°$), 1713 symmetry-independent reflections with $F_o^2 > 3\sigma(F_o^2)$, $R = 0.039$, $R_w = 0.052$. Further details of the crystal structure investigations may be obtained from the Fachinformationszentrum Karlsruhe, Gesellschaft für wissenschaftlich-technische Information mbH, D-W-7514 Eggenstein-Leopoldshafen 2 (FRG) on quoting the depository number CSD-56879, the names of the authors, and the journal citation.
[4] W. Bronger, M. Spangenberg, *J. Less. Common Met.* **1980**, *76*, 73.
[5] W. Bronger, H.-J. Miessen, P. Müller, R. Neugröschel, *J. Less Common. Met.* **1985**, *105*, 303.
[6] W. Bronger, H.-J. Miessen, R. Neugröschel, D. Schmitz, M. Spangenberg, *Z. Anorg. Allg. Chem.* **1985**, *525*, 41.
[7] W. Bronger, T. Schuster, *Z. Anorg. Allg. Chem.* **1990**, *587*, 74.
[8] W. Bronger, M. Loevenich, D. Schmitz, T. Schuster, *Z. Anorg. Allg. Chem.* **1990**, *587*, 91.
[9] V. I. Spitzin, S. V. Kryntchkov, M. S. Grigoriev, A. F. Kuzina, *Z. Anorg. Allg. Chem.* **1988**, *563*, 136.
[10] S. V. Kryntchkov, A. F. Kuzina, V. I. Spitzin, *Z. Anorg. Allg. Chem.* **1988**, *563*, 153.
[11] B. E. Bursten, F. A. Cotton, G. G. Stanley, *Isr. J. Chem.* **1980**, *19*, 132.
[12] W. Bronger, J. Fleischhauer, H. Marzi, G. Raabe, W. Schleker, T. Schuster, *J. Solid State Chem.* **1987**, *70*, 29.
[13] A. Weiss, H. Witte, *Magnetochemie*, Verlag Chemie, Weinheim, **1973**.
[14] A. Simon, H.-G. von Schnering, H. Schäfer, *Z. Anorg. Allg. Chem.* **1967**, *355*, 295.
[15] C. Perrin, M. Sergent, F. Le Traon, A. Le Traon, *J. Solid State Chem.* **1978**, *25*, 197.
[16] W. Bronger, H.-J. Miessen, *J. Less Common Met.* **1982**, *83*, 29.

Asymmetric Synthesis of α-Amino Acids and N-Protected α-Amino Aldehydes by Addition of Chiral Vinyl Anions to Sulfonylimines**

By *Manfred Braun** and *Kersten Opdenbusch*

The diversity of methods for the synthesis of α-amino carboxylic acids at our disposal today is based on only a few fundamental concepts. In addition to enzymatic procedures, these include, in particular, asymmetric hydrogenation of dehydroamino acids, alkylation of chiral glycine enolates, electrophilic and nucleophilic amination, addition of C nucleophiles to imino esters, and nucleophilic addition of CO_2H equivalents to chiral imines.[1] Herein we report for the first time on the stereoselective addition of chiral $^{\ominus}CO_2H$ and $^{\ominus}CHO$ synthons to prochiral sulfonylimines, providing access to nonracemic α-amino acids and the N-protected α-amino aldehydes, which are valuable synthetic building blocks (Scheme 1).

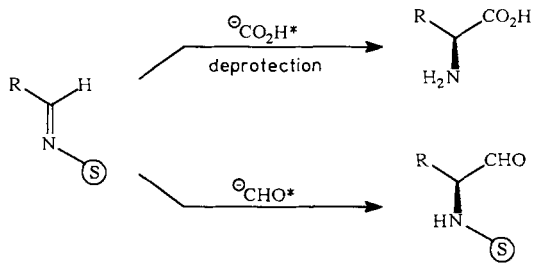

Scheme 1. Ⓢ: protecting group.

The dibromoolefin (*S*)-**1**, readily accessible from *S*-ethyl lactate in three steps, is converted into the vinyl anion **2** (*E*:*Z* > 99:1) by stereoselective bromine/lithium exchange with *n*-butyllithium (Scheme 2).[2] Subsequent addition of the mesityl sulfonylimines **3** at −110°C resulted mainly in the

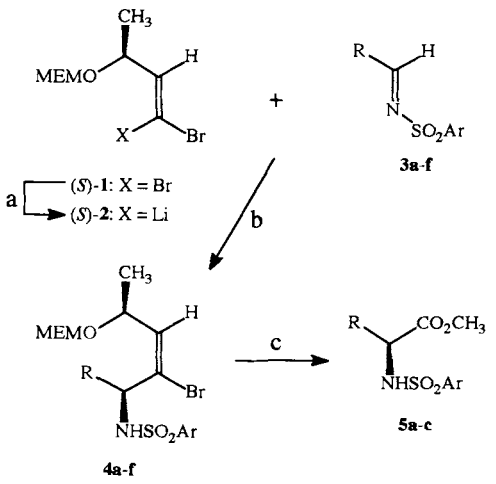

Scheme 2. Diastereoselective coupling of the dibromoolefin (*S*)-**1** with sulfonylimines **3** and cleavage of the adducts **4a–c**. a) *n*BuLi, Et_2O. b) THF. c) O_3, CH_2Cl_2, CH_3OH. Thex = $C(CH_3)_2CH(CH_3)_2$, Ar = 2,4,6-$(CH_3)_3C_6H_2$, MEM = $CH_2OCH_2CH_2OCH_3$. R see Table 1.

[*] Prof. Dr. M. Braun, Dipl.-Chem. K. Opdenbusch
Institut für Organische und Makromolekulare Chemie der Universität
Universitätsstrasse 1, D-W-4000 Düsseldorf (FRG)

[**] This work was supported by the Deutsche Forschungsgemeinschaft, the Fonds der Chemischen Industrie, and BASF AG (chemical donations). In this paper the introduced designation "sulfonylimine" is used for *N*-alkylidene sulfonamides

adducts **4**, whose diastereomeric excesses (*de*) and chemical yields are given in Table 1.[3] After column chromatography

Table 1. Adducts **4** prepared by addition of the vinyl anion **2** to mesityl sulfonylimines **3**.

Compound **3**–**4**	R	Yield [%] [a] **4**	(*de*) [%] [b] **4**
a	C_6H_5	62	92
b	4-$CH_3OC_6H_4$	63	92
c	4-(ThexMe$_2$SiO)C_6H_4	54	92
d	$(CH_3)_2CHCH_2$	20	94
e	$(CH_3)_2CH$	40	94
f	$(CH_3)_3C$	52	96

[a] Yields of products purified by column chromatography. [b] Each determined in the crude product by NMR spectroscopy.

of the adducts **4** the excess diastereomers are obtained with > 98% *de* each. The aryl-substituted imines **3a, b** were produced by heating a mixture of mesityl sulfonamide and the dimethyl acetal of the corresponding arylaldehyde.[4a] In contrast, the imines **3c–f** are prepared from the reaction of mesityl sulfonamide with thionyl chloride and the subsequent reaction of the *N*-sulfinyl arylsulfonamide Ar-$SO_2N{=}S{=}O$ formed with the corresponding aldehyde in the presence of boron trifluoride etherate.[4b] However, the sulfonylimines **3d** and **3e** derived from isobutyraldehyde and 3-methylbutanal, respectively, cannot be obtained free from the corresponding tautomeric enamine; thus, lower chemical yields are obtained for the adducts **4d** and **4e** (cf. Table 1; spectroscopic data of **4a–f** see Table 2).

Table 2. Characteristic spectroscopic data of the compounds **4a–f** and **12a–c**.

4a: ^{1}H NMR (300 MHz, $CDCl_3$, TMS int.): δ = 1.03 (d, J = 6.3 Hz, 3H, CH(O-)CH_3), 2.29 (s, 3H, ArCH_3), 2.65 (s, 6H, ArCH_3), 3.32 (s, 3H, OCH_3), 3.42–3.68 (m, 4H, OCH_2CH_2O), 4.35–4.45 (qd, J_q = 9.1 Hz, J_d = 6.3 Hz, 1H, CH(O-)CH_3), 4.65 (s, 2H, OCH_2O), 5.47 (d, J = 9.2 Hz, NH), 5.62 (d, J = 9.2 Hz, CH(N-)), 5.93 (d, J = 9.0 Hz, 1H, BrC=CH), 6.94–7.42 (m, 7H, ArH); (*R,S*)-diastereomer: 1.18 (d, J = 6.3 Hz, 3H), 6.04 (d, J = 9.0 Hz, 1H)

4b: ^{1}H NMR (300 MHz, $CDCl_3$, TMS int.): δ = 1.03 (d, J = 6.2 Hz, 3H, CH(O-)CH_3), 5.90 (d, J = 9.2 Hz, 1H, BrC=CH); (*R,S*)-diastereomer: 1.10 (d, J = 6.2 Hz, 3H), 6.01 (d, J = 9.2 Hz, 1H)

4c: ^{1}H NMR (300 MHz, $CDCl_3$, TMS int.): δ = 1.05 (d, J = 6.3 Hz, 3H, CH(O-)CH_3), 5.90 (d, J = 9.2 Hz, 1H, BrC=CH); (*R,S*)-diastereomer: 6.02 (d, J = 9.3 Hz, 1H)

4d: ^{1}H NMR (300 MHz, $CDCl_3$, TMS int.): δ = 1.18 (d, J = 6.3 Hz, 3H, CH(O-)CH_3), 5.69 (d, J = 9.4 Hz, 1H, BrC=CH); (*R,S*)-diastereomer: 5.80 (d, J = 9.4 Hz, 1H)

4e: ^{1}H NMR (300 MHz, $CDCl_3$, TMS int.): δ = 1.02 Hz (d, J = 6.2 Hz, 3H, CH(O-)CH_3), 5.80 (d, J = 9.5 Hz, 1H, BrC=CH); (*R,S*)-diastereomer: 5.85 (d, J = 9.5 Hz, 1H)

4f: ^{1}H NMR (300 MHz, $CDCl_3$, TMS int.): δ = 1.18 (d, J = 6.2 Hz, 3H, CH(O-)CH_3), 5.93 (d, J = 9.1 Hz, 1H, BrC=CH); (*R,S*)-diastereomer: 6.00 (d, J = 9.1 Hz, 1H)

12a: ^{1}H NMR (300 MHz, $CDCl_3$, TMS int.): δ = 1.29 (s, 3H, CH_3), 1.31 (s, 3H, CH_3), 2.24 (s, 3H, ArCH_3), 2.45 (s, 6H, ArCH_3), 3.62 (s, 3H, OCH_3), 4.59 (d, J = 4.5 Hz, 1H, CH(O-)), 5.19 (d, J = 4.5 Hz, CH(N-)), 6.84 (s, 2H, ArH), 7.31 (m, 5H, ArH)

12b: ^{1}H NMR (300 MHz, $CDCl_3$, TMS int.): δ = 0.92 (d, J = 7.0 Hz, 3H, CH(CH_3)$_2$), 1.03 (d, J = 7.1 Hz, 3H, CH(CH_3)$_2$), 1.18 (s, 3H, CH_3), 1.24 (s, 3H, CH_3), 1.55 (m, 1H, CH(CH$_3$)$_2$), 2.31 (s, 3H, ArCH_3), 2.69 (s, 6H, ArCH_3), 3.66 (s, 3H, OCH_3), 4.21 (dd, J_1 = 3 Hz, J_2 = 2.5 Hz, 1H, CH(N-)), 4.43 (d, J = 2.5 Hz, 1H, CH(O-)), 6.98 (s, 2H, ArH)

12c: ^{1}H NMR (300 MHz, $CDCl_3$, TMS int.): δ = 0.99 (s, 9H, C$(CH_3)_3$), 1.18 (s, 3H, CH_3), 1.24 (s, 3H, CH_3), 2.30 (s, 3H, ArCH_3), 2.72 (s, 6H, ArCH_3), 3.70 (s, 3H, OCH_3), 4.10 (d, J = 2.0 Hz, 1H, CH(N-)), 4.55 (d, J = 2.0 Hz, 1H, CH(O-)), 6.97 (s, 2H, ArH)

The ozonolysis of the bromoolefins **4a–c** in methanol/dichloromethane[5] leads directly to the N-protected amino acid methyl esters **5a–c** (70 to 80%). These can be converted into the free amino acids as exemplified by **5a**: saponification (LiOH, CH_3OH, H_2O) and subsequent cleavage of the sulfonamide protecting group with sodium naphthalenide in 1,2-dimethoxyethane at −40° C[6] affords phenylglycine in 78% yield (*ee* > 98%).

To obtain the N-protected amino aldehydes **8a–c** first the adducts **4a, e, f** are again lithiated (*tert*-butyllithium, THF) under bromine/lithium exchange. The dilithium compounds **6a–c** formed can then be protonated to give the *Z* alkenes **7a–c**, whose ozonolysis after workup with dimethyl sulfide affords the aldehydes **8a–c** in almost quantitative yields (Scheme 3). The MEM-protected lactaldehyde **9** formed at

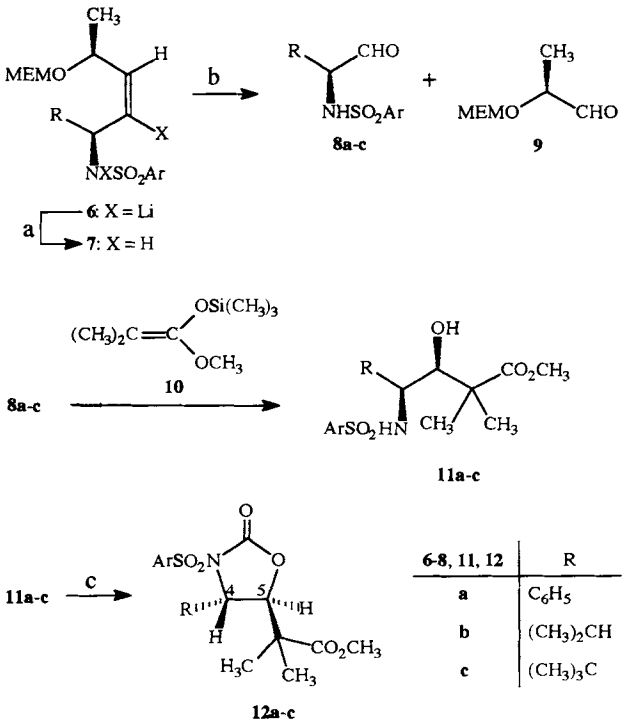

Scheme 3. Synthesis and diastereoselective Mukaiyama reaction of the N-protected amino aldehydes **8**. a) NH_4Cl, H_2O. b) O_3, CH_2Cl_2, $(CH_3)_2S$. c) $COCl_2$, toluene, pyridine or Et_3N.

the same time is condensed under high vacuum (10^{-4} Torr/25° C) in a trap cooled with liquid nitrogen and can be reused for the synthesis of the dibromoolefin **1**.[2] Under these conditions a racemization of the remaining N-protected amino aldehyde **8a–c** can be largely suppressed. Starting from the *R*-dibromoolefin **1**[2] obtained from *R*-2-methypropyl lactate, analogous sequences lead to the enantiomeric *N*-sulfonylated amino aldehydes *ent*-**8** or to the esters *ent*-**5**.

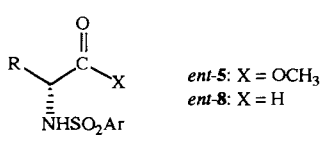

To test the applicability of the N-protected amino aldehydes **8a–c** as a starting material for further stereoselective

C–C couplings,[7] they were allowed to react with the ketene silyl acetal **10** in the presence of titanium tetrachloride ("Mukaiyama–aldol reaction"[8]). The *syn*-configurated adducts **11a–c** (72–76% yield based on **7**) are formed with a remarkable stereoselectivity (*de* > 98%), which can be interpreted as arising from a chelate-controlled reaction.[9] The relative configuration of the β-hydroxy esters **11a–c** is determined by its conversion into the oxazolidinones **12a–c** ($COCl_2$, pydridine, toluene). In the ^1H NMR spectra of **12a–c** the coupling constant (4.5 Hz) of the protons H4 and H5 allows an unambiguous assignment of the *trans* configuration (Table 2).[11, 12] Furthermore, ^1H NMR shift experiments with [Eu(hfc)$_3$][12] indicate an enantiomeric excess of the heterocycles **12a–c** of 93–96%.[13] The optical purity of **12a–c** lies only slightly below the diastereomeric excess of the corresponding purified adducts **4a, e, f**, which shows that the *N*-sulfonylated amino aldehydes **8** retain their configurations under the conditions of their formation, isolation, and conversion in the Mukaiyama reaction. However, as expected, heating the aldehydes **8** leads to racemization. The addition of the chiral vinyl anions (*S*)- and (*R*)-**2** to sulfonylimines **3** allows, in particular, an easy access to arylglycines[14] and N-protected arylglycine aldehydes with high enantioselectivity. In the latter case the mesityl sulfonyl protecting group proves to be an efficient stereoregulating element for nucleophilic additions to the aldehyde group.

Received: November 28, 1992 [Z 5710IE]
German version: *Angew. Chem.* **1993**, *105*, 595

[1] Reviews: R. M. Williams, *Synthesis of Optically Active α-Amino Acids*, *Vol. 7*, Pergamon, Oxford, **1989**; J. Mulzer, H.-J. Altenbach, M. Braun, K. Krohn, H.-U. Reissig, *Organic Synthesis Highlights*, VCH, Weinheim, **1991**, pp. 300–305; D. Seebach, R. Imwinkelried, T. Weber in *Modern Synthetic Methods, Vol. 4* (Ed.: R. Scheffold), Springer, Berlin, **1986**, pp. 125–259; U. Schöllkopf, *Pure Appl. Chem.* **1983**, *55*, 1799–1806; Tetrahedron Symposium-in-Print: α-Amino Acid Synthesis (Ed.: M. J. O'Donnell), *Tetrahedron* **1988**, *44*, 5253–5614.

[2] H. Mahler, M. Braun, *Tetrahedron Lett.* **1987**, *28*, 5145–5148; *Chem. Ber.* **1991**, *124*, 1379–1395.

[3] The corresponding tolyl sulfonylimines have considerably lower diastereoselectivities: H. Mahler, dissertation, Universität Düsseldorf, **1989**.

[4] a) J. Lichtenberger, J.-P. Fleury, B. Barette, *Bull. Soc. Chim. Fr.* **1955**, 669–680; G. Tosolini, *Chem. Ber.* **1961**, *94*, 2731–2737; b) G. Kresze, R. Albrecht, *Angew. Chem.* **1962**, *74*, 781–782; *Angew. Chem. Int. Ed. Engl.* **1962**, *1*, 595–596; R. Albrecht, G. Kresze, B. Mlakar, *Chem. Ber.* **1964**, *97*, 483–489.

[5] Compare K. Griesbaum, H. Keul, *Angew. Chem.* **1975**, *87*, 748–749; *Angew. Chem. Int. Ed. Engl.* **1975**, *14*, 716.

[6] S. Ji, L. B. Gortler, A. Waring, A. Battisti, S. Bank, W. D. Closson, *J. Am. Chem. Soc.* **1967**, *89*, 5311–5312.

[7] Compare J. Jurzac, A. Golebiowski, *Chem. Rev.* **1989**, *89*, 149–164.

[8] Compare T. Mukaiyama, *Org. React.* **1982**, *28*, 203–331.

[9] M. T. Reetz, *Angew. Chem.* **1984**, *96*, 542–555; *Angew. Chem. Int. Ed. Engl.* **1984**, *23*, 556–569; M. T. Reetz, M. W. Drewes, A. Schmitz, *ibid.* **1987**, *99*, 1186–1188 and **1987**, *26*, 1141–1143; M. T. Reetz, *ibid.* **1991**, *103*, 1559–1573 and **1991**, *30*, 1531–1546.

[10] The diastereomeric (at C3) product is formed in addition to **11a** from the aldol reaction with the lithium enolate of methyl isobutyrate in the ratio 8:1 in favor of the chelate-controlled compound. The coupling constant $J(^4H, ^5H)$ for *cis*-configurated **12a** is 6.8 Hz.

[11] S. Futagawa, T. Inui, T. Shiba, *Bull. Chem. Soc. Jpn.* 1973, *46*, 3308-3310; D. H. Rich, E. T. O. Sun, *J. Med. Chem.* **1980**, *23*, 27-33; D. J. Kempf, *J. Org. Chem.* **1986**, *51*, 3921-3926.

[12] [Eu(hfc)$_3$] = tris[3-(heptafluoropropylhydroxymethylene)-*d*-camphorato]-europium (purchased from Aldrich).

[13] In the presence of [Eu(hfc)$_3$] the resonance frequencies of the protons H4 and H5 of the enantiomeric compound *ent*-**12a** are shifted to higher and those of the compounds *ent*-**12b, c** to lower fields.

[14] D. A. Evans, D. A. Evrard, S. D. Rychnovsky, T. Früh, W. G. Whittingham, K. M. DeVries, *Tetrahedron Lett.* **1992**, *33*, 1189-1192; R. H. Williams, J. A. Hendrix, *Chem. Rev.* **1992**, *92*, 889-917.

Structures of Classical Reagents in Chemical Synthesis: $(n\text{BuLi})_6$, $(t\text{BuLi})_4$, and the Metastable $(t\text{BuLi} \cdot Et_2O)_2$**

By *Thomas Kottke* and *Dietmar Stalke**

Alkyllithium compounds are particularly important in synthetic chemistry as deprotonating and substituting reagents and as catalysts in polymerization.[1, 2] As long ago as 1917, Schlenk and Holtz reported the first synthesis of alkyllithium compounds;[3] in 1963 the first solid-state structural analysis of a substance of this class, namely tetrameric ethyllithium, was achieved by Dietrich.[4] Subsequently, numerous RLi compounds have been characterized by X-ray structure investigations.[5–12] The degree of oligomerization of the compounds of this class most commonly used in synthesis, *n*BuLi and *t*BuLi, have long been established by cryoscopic and spectroscopic measurements. In hydrocarbons *n*BuLi is hexameric[13–16] and *t*BuLi is tetrameric;[17–20] in donor solvents a lower degree of aggregation is preferred.[21–23] Until now, however, no information about the crystal structures of *t*BuLi and of donor-free *n*BuLi have been available. This is probably due to the fact that these compounds (especially *t*BuLi) are pyrophoric and that *n*BuLi is an oil at room temperature. Herein we describe the crystallization and the X-ray single-crystal structures[24] of donor-free *n*BuLi and *t*BuLi and also of the metastable adduct of *t*BuLi with one equivalent of diethyl ether.

For the crystallization, a temperature was chosen at which the nearly saturated solutions could be prepared; this should be as low as possible to avoid phase transitions during low temperature data collection (here: −90 °C). The limiting values taken into account were the melting point of *n*BuLi (−76 °C according to reference [1]; the melting point of the crystals investigated here, however, was −34(2) °C) and the temperature at which decomposition of $t\text{BuLi} \cdot Et_2O$ might occur (−40 °C[25] and −35 °C[26] for $t\text{BuLi} \cdot Et_2O$). To achieve a gradual and controlled crystallization, all solutions were prepared at −80 °C. The crystallization period was extended to one week by redissolving crystals formed initially, thus leaving a small number of nucleation sites in the solution. This technique appears to increase the probability of forming single crystals suitable for X-ray crystallography.[27] During the preparation of crystals for data collection (selecting and mounting a crystal and transporting it to the diffractometer) the temperature of a sample never exceeded −45 °C. This was facilitated by using apparatus developed for mounting crystals at low temperatures.[28] Thus the crystals could be kept at −60 °C on the polarization microscope slide, and then transferred to the diffractometer with a portable liquid nitrogen evaporator (see also ref. [29]). The use of inert gas Schlenk techniques and sealing with inert oil[28] were necessary to prevent the extremely oxygen and moisture-sensitive crystals from reacting with air.

All three compounds are discrete aggregates and no interactions between oligomers were found such as have been observed, for example, in the solid-state structure of MeLi (the shortest Li–C distance between two oligomeric units is 382 pm found in *n*BuLi; in MeLi it is 252 pm[5]). The framework of *n*BuLi consists of six Li atoms in a trigonal anti-prismatic (distorted octahedral) conformation (approximately D_{3d} symmetry) with six short (241.3(3)–243.7(3), average

[*] Dr. D. Stalke, T. Kottke
Institut für Anorganische Chemie der Universität
Tammannstrasse 4, D-W-3400 Göttingen (FRG)

[**] This work was supported by the Deutsche Forschungsgemeinschaft and the Fonds der Chemischen Industrie.

242.9 pm), and six long (289.8(3)–297.0(3), average 293.9 pm) Li–Li distances (Fig. 1). Analogous to cyclohexyllithium,[8] isotypic cyclopentyllithium,[12] and a lithiomethylcyclopropane derivative,[10] six faces of the octahedron are each capped by a single *n*Bu unit; two almost equilateral (and opposite) triangular faces with the longest edges remain unoccupied. Each α-carbon atom is coordinat-

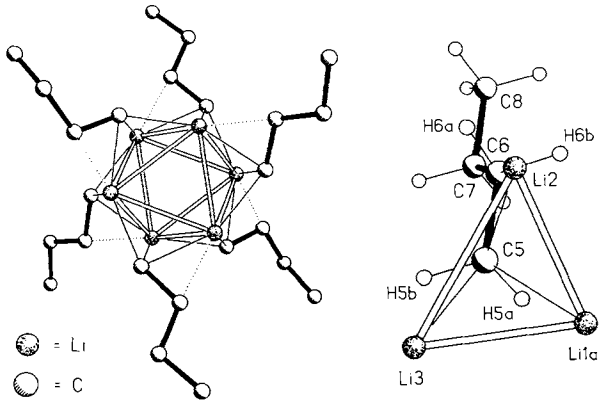

Fig. 1. Left: Crystal structure of *n*BuLi. Right: The projection perpendicular to one of the Li triangles of the distorted octahedron with a coordinated *n*Bu group. Selected bond lengths [pm] and angles [°] (average values): C_α–C_β 153.3(2), C_β–C_γ 152.1(5), C_γ–C_δ 150.5(6); C_α-C_β-C_γ 117.4(5), C_β-C_γ-C_δ 113.7(1).

ed to two Li atoms positioned at the corners of one of these (noncapped) triangles through short bonds (213.7(3)–217.5(3), average 215.9 pm), whereas the bond to the Li atom at the corner of the opposite triangle is significantly longer (226.2(3)–227.7(3), average 227.0 pm). Hence, the *n*Bu moieties do not lie centrally over the isosceles Li triangles but are shifted to one edge (Fig. 1 right). As a result of this, short distances occur between the β-C atoms and the Li atoms, which may be interpreted as electrostatic interactions (Li–C distance: 228.0(3)–229.5(3), average 228.7 pm; though they are in the range of the longer Li–C_α bonds). At the same time this conformation has short Li–H_α and Li–H_β distances (Fig. 1 right: 204(2) pm for Li3–H5b and 203(2) pm for Li2–H6a). The hydrogen atoms at the α–C and β–C atoms are arranged staggered with respect to the nearest Li atom. In conclusion, *n*BuLi shows similar structural characteristics to the cyclic alkyllithium compounds mentioned above. Even in the complex (*n*BuLi · LiO*t*Bu)$_4$ remarkably short Li–C_β distances are observed (234(1) pm[30]). Apparently a fourfold coordination of the Li atoms by including β–C atoms is preferred in spite of the elongation of a Li–C_α bond.

*t*BuLi consists of tetrameric units of almost T_d symmetry (Fig. 2) in the crystal. The asymmetric unit is made up of 4.5 tetramers; one tetramer is crystallographically generated through a twofold axis. Each face of the Li_4 tetrahedron is capped by a *t*Bu group such that the (terminal) Me groups are eclipsed with respect to the corresponding Li atoms of the (within the standard deviation) equilateral triangles (Fig. 2 right). This conformation again involves comparatively short Li–C_β distances (227.5(8)–256.6(9), average 237.4 pm). Thus, the structure of *t*BuLi is essentially different from that of MeLi in which the hydrogen atoms of the Me groups (in contrast to the conformation of C_β atoms in *t*BuLi) are staggered relative to the Li atoms.[6] As in *n*BuLi Li–C_β interactions may participate in determining the conformation of *t*BuLi, especially since the β-C atoms would

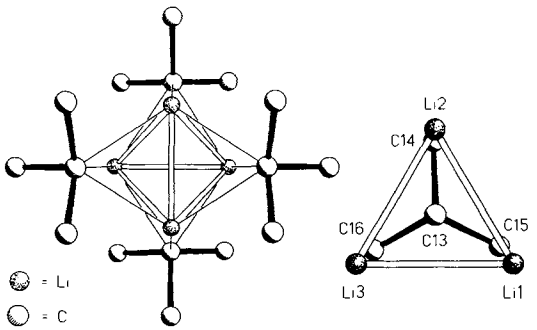

Fig. 2. Left: Crystal structure of *t*BuLi. Right: The projection perpendicular to one of the Li triangles of the tetrahedron with coordinated *t*Bu group. Selected bond lengths [pm] and angles [°] (minimum/maximum/average): C_α–C_β 150.9(5)/157.9(9)/153.4; C_β-C_α-C'_β 104.1(4)/108.5(5)/105.9, Li-C_α-Li' 62.1(4)/66.7(4)/64.9.

preferentially be staggered for steric reasons. The Li-C_α bond lenghts (214.7(17)–237.0(14), average 224.6 pm) are in the range of the values observed in similar compounds, while the Li–Li distances in *t*BuLi (238.3(9)–243.1(8), average 241.2 pm) are significantly shorter (Li–Li and Li–C [pm] in EtLi:[4] 255 and 225, respectively, in MeLi:[6] 256 and 227, respectively). The relatively large variation of the C–C and Li–C distances in *t*BuLi is caused by disorders of the *t*Bu groups.

*t*BuLi · Et_2O is a dimer which is generated crystallographically from the monomeric unit through a twofold axis (Fig. 3). The central four-membered ring consisting of two

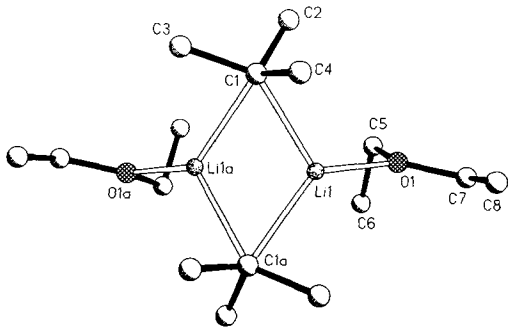

Fig. 3. Crystal structure of (*t*BuLi · Et_2O)$_2$. Selected bond lengths [pm] and angles [°]: Li1–C1 217.4(6), Li1–C1a 219.4(6), Li1–O1 194.0(5); Li1-C1-Li1a 63.6(2), C1-Li1-C1a 110.7(2).

Li and two bridging α–C atoms of the *t*Bu groups is strongly distorted about the Li–Li axis (the angle between the planes Li1–C1–Li1a and Li1–C1a–Li1a is 29.1(4)°), which is consistent with the steric demand of the Et_2O molecules and the *t*Bu groups. This steric hindrance provides a possible explanation for the absence of a second donating Et_2O molecule per Li atom as postulated for *t*BuLi in ether.[26] In connection with this it should be noted that solutions of *t*BuLi in ether are stable even with a large excess of ether (Et_2O:*t*BuLi ≈ 6:1) over a wider temperature range (up to about −40 °C), as observed in NMR studies.[26]

Experimental Procedure

All three compounds were prepared starting with commercially available solutions (in hexane or pentane); solvent was removed from these solutions under vacuum.

*n*BuLi: To *n*BuLi (2.9 g, 46 mmol), constantly stirred at −80 °C, precooled pentane was added dropwise until a homogeneous solution was obtained (ca. 20 mL). After one week at −90 °C colorless blocks crystallized with a melting point of −34(2) °C.

*t*BuLi: *t*BuLi (2.2 g, 34 mmol) was treated as described for *n*BuLi (ca. 18 mL pentane added). Crystallization over one week yielded colorless elongated blocks.

(*t*BuLi · Et_2O)$_2$: From various pentane/Et_2O ratios the best results were obtained by first adding 5 mL pentane and then 12 mL Et_2O (each precooled to −60 °C) dropwise to solid *t*BuLi (2.2 g, 34 mmol) at −80 °C. At −90 °C colorless blocks with a melting point of −38(2) °C were formed from the pale yellow solution.

Received: December 7, 1992 [Z 5732 IE]
German version: *Angew. Chem.* **1993**, *105*, 619

[1] B. J. Wakefield, *The Chemistry of Organolithium Compounds*, Pergamon, Oxford, **1974**.
[2] L. Brandsma, H. D. Verkruijsse, *Preparative Polar Organometallic Chemistry, Vol. 1*, Springer, Berlin, **1987**.
[3] W. Schlenk, J. Holtz, *Ber. Dtsch. Chem. Ges.* **1917**, *50*, 262.
[4] H. Dietrich, *Acta Crystallogr.* **1963**, *16*, 681.
[5] E. Weiss, E. C. A. Lucken, *J. Organomet. Chem.* **1964**, *2*, 197.
[6] E. Weiss, G. Hencken, *J. Organomet. Chem.* **1970**, *21*, 265.
[7] R. Zerger, G. Stucky, *J. Chem. Soc. Chem. Commun.* **1973**, 44.
[8] R. Zerger, W. Rhine, G. Stucky, *J. Am. Chem. Soc.* **1974**, *96*, 6048.
[9] H. Köster, D. Thoennes, E. Weiss, *J. Organomet. Chem.* **1978**, *160*, 1.
[10] A. Maercker, M. Bsata, W. Buchmeier, B. Engelen, *Chem. Ber.* **1984**, *117*, 2547.
[11] P. A. O'Neil, W. Clegg, contribution to the 14th crystallographic meeting (ECM14), **1992**, Enschede, The Netherlands.
[12] D. Hoffmann, P. von R. Schleyer, D. Stalke, unpublished results.
[13] D. Margerison, J. P. Newport, *Trans. Faraday Soc.* **1963**, *59*, 2058.
[14] I. Craubner, *Z. Phys. Chem.* **1966**, *51*, 225.
[15] H. L. Lewis, T. L. Brown, *J. Am. Chem. Soc.* **1970**, *92*, 4664.
[16] T. L. Brown, *Adv. Organomet. Chem.* **1965**, *3*, 365.
[17] M. Weiner, G. Vogel, R. West, *Inorg. Chem.* **1962**, *1*, 654.
[18] L. D. McKeever, R. Waack, *J. Chem. Soc. Chem. Commun.* **1969**, 750.
[19] W. M. Scowell, B. Y. Kimura, T. G. Spiro, *J. Coord. Chem.* **1971**, *1*, 107.
[20] W. McLean, P. T. Murray, R. C. Jarnagin, *J. Chem. Phys.* **1978**, *69*, 2715.
[21] D. Seebach, R. Hässig, J. Gabriel, *Helv. Chim. Acta* **1983**, *66*, 308.
[22] J. F. McGarrity, C. A. Ogle, *J. Am. Chem. Soc.* **1984**, *107*, 1805.
[23] W. Bauer, W. R. Winchester, P. von R. Schleyer, *Organometallics* **1987**, *6*, 2371.
[24] Crystallographic data: data collection on a Stoe-Siemens AED four-circle diffractometer with graphite-monochromated $Mo_{K\alpha}$ radiation. Structure solution with direct methods (G. M. Sheldrick, *Acta Crystallogr. Sect. A* **1990**, 467), full-matrix least-squares refinement on F^2 (SHELXL-92) *R* values: $R1 := \sum|F_o^2 - F_c^2|/\sum F_o$, $wR2 := (\sum w(F_o^2 - F_c^2)^2/\sum w(F_o^2)^2)^{0.5}$. **1**: *n*-$C_4H_9Li$, space group $P2_1/c$; $Z = 12$, $a = 1023.3(1)$, $b = 1676.3(2)$, $c = 836.3(1)$ pm, $\beta = 95.638(9)°$, $V = 1.4277(3)$ nm^3, $\rho_{calcd} = 0.894$ Mg m^{-3}; 4894 reflections, 1876 unique observed ($I > 2\sigma(I)$), were measured at −120 °C; the non-hydrogen atoms were refined anisotropically, all hydrogen atoms were located by difference fourier synthesis and free isotropically refined. $R1 = 0.0423$, $wR2 = 0.1097$ (all data) for 236 parameters and 36 restraints. **2**: *t*-C_4H_9Li, space group $C2/c$; $Z = 144$; $a = 7535.6(6)$, $b = 1382.6(1)$, $c = 1707.8(1)$, $\beta = 96.153(4)°$, $V = 17.690(2)$ nm^3; $\rho_{calcd} = 0.866$ Mg m^{-3}; 21225 reflections, 5617 unique observed ($I > 2\sigma(I)$), were measured at −93 °C; the non-hydrogen atoms were refined anisotropically, the hydrogen atoms were refined at calculated positions by using a riding model. $R1 = 0.0693$, $wR2 = 0.1823$ (all data) for 978 parameters and 468 restraints. **3**: $C_8H_{19}LiO$, space group $C2/c$; $Z = 8$; $a = 1068.4(8)$, $b = 1356.4(9)$, $c = 1427.4(13)$ pm, $\beta = 95.47(8)°$, $V = 2.059(3)$ nm^3; $\rho_{calcd} = 0.891$ Mg m^{-3}; 3843 reflections, 1114 unique observed ($I > 2\sigma(I)$), were measured at −120 °C; the non-hydrogen atoms were refined anisotropically, the hydrogen atoms were refined on calculated positions by using a riding model. $R1 = 0.0729$, $wR2 = 0.1871$ (all data) for 116 parameters and 42 restraints. Further details of the crystal structure investigations are available on request from the Director of the Cambridge Crystallographic Data Centre, 12 Union Road, GB-Cambridge CB2 1EZ, by quoting the full journal citation.
[25] P. D. Bartlett, S. Friedman, M. Stiles, *J. Am. Chem. Soc.* **1953**, *75*, 1771.
[26] T. F. Bates, M. T. Clarke, R. D. Thomas, *J. Am. Chem. Soc.* **1988**, *110*, 5109.
[27] A. McPherson, in *Preparation and Analysis of Protein Crystals*, Wiley Interscience, New York, **1982**.
[28] T. Kottke, D. Stalke, *J. Appl. Crystallogr.* **1993**, in press.
[29] M. Veith, W. Frank, *Chem. Rev.* **1988**, *88*, 81.
[30] M. Marsch, K. Harms, L. Lochmann, G. Boche, *Angew. Chem.* **1990**, *102*, 334; *Angew. Chem. Int. Ed. Engl.* **1990**, *102*, 308.

Enantioselective Catalytic Addition of Functionalized Dialkylzinc Compounds to β-Stannylated Aldehydes: A Convenient Preparation of Chiral β- and γ-Functionalized Secondary Alcohols**

By *Walter Brieden, Roswitha Ostwald*, and *Paul Knochel**

Recently we described a general method for the preparation of dialkylzinc compounds of the type **2** from the corresponding alkyl iodides **1**.[1] These functionalized organozinc reagents proved to be extremely useful for the catalytic asymmetric addition to aldehydes in the presence of the chiral catalyst **3**.[1, 2]. The method allows an easy access to polyfunctional secondary alcohols **4** in both enantiomeric forms with excellent enantioselectivity.[2m] Unfortunately, as we

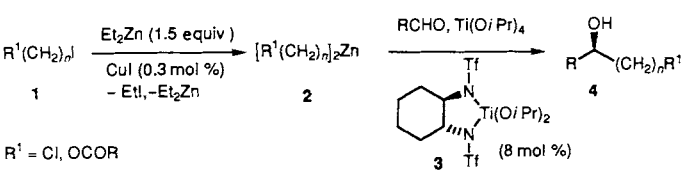

tried to extend this reaction to functionalized aldehydes bearing, for example, an oxygen functionality in the γ-position, stoichiometric amounts of the catalyst **3** were necessary.[1] In addition, acceptable chemical yields could only be obtained with *unfunctionalized* diorganozinc compounds **1**. We report now that this problem does not arise if β-stannylated aldehydes such as **5**[3] or **6**,[4] are used, and that with these aldehydes polyfunctionalized alcohols are readily accessible, which, in a second step, can be converted into polyoxygenated molecules.

The aldehydes **5** and **6** react readily under mild conditions (−35 to −25 °C, 16 h for **5a**, **b** and −60 to −50 °C, 2 h for **6**) with the functionalized diorganozinc compounds **2**, and afford good to excellent yields (67–89%) and enantioselectivities (90–97% *ee*)[5] of the stannylated alcohols **7**–**9** (Table 1). All reactions have been performed with a catalytic amount of **3** (ca. 8 mol%). Remarkably, the presence of an ester or halide functionality does not interfere in these reactions, even if the ester group is relatively close to the metal center (γ position), as is the case in the formation of **9f**. This method allows a one-step enantioselective synthesis of the

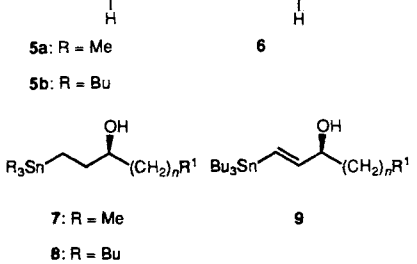

5a: R = Me
5b: R = Bu
6
7: R = Me
8: R = Bu
9

[*] Prof. Dr. P. Knochel, Dr. W. Brieden, R. Ostwald
Fachbereich Chemie der Universität
Hans-Meerwein-Strasse, D-W-3550 Marburg (FRG)

[**] This work was supported by the donors of the Petroleum Research Fund, administrated by the American Chemical Society, the Fonds der Chemischen Industrie, and the Deutsche Forschungsgemeinschaft (Sonderforschungsbereich 260). We thank Dr. U. Klar and Dr. D. Ventur (Schering AG) for a generous gift of Me_2SnCl_2 and Bu_3SnH.

allylic alcohol **9b** (88% yield, 92% *ee*), a building block for the preparation of prostaglandins and leucotrienes.[6] The alcohols **7**–**9** can be readily destannylated and thus open the way to several important classes of functionalized alcohols.

Table 1. Stannylated secondary alcohols of type **7**–**9**, obtained by the catalytic asymmetric addition of $[R^1(CH_2)_n]_2Zn$ **2** to the aldehydes **5** and **6**.

5/**6**	$R^1(CH_2)_n$ in **2**	**7**–**9**	Yield [%] [a]	*ee* value [%]	$[\alpha]_D^{20}$ [b]
5a	Et	**7a**	89	93	+3.1
5a	octyl	**7b**	80	97	−0.74
5b	octyl	**8a**	82	93	−1.0
5b	$(CH_2)_4OAc$	**8b**	85	93	−1.8
5b	$(CH_2)_5OAc$	**8c**	81	92	−1.4
5b	$(CH_2)_4Cl$	**8d**	79	95	−2.0
6	Et	**9a**	87	90	−0.30
6	pentyl	**9b**	88	92	−0.21
6	octyl	**9c**	72	90	−0.23
6	$(CH_2)_5OAc$	**9d**	75	91	−0.15
6	$(CH_2)_4Cl$	**9e**	69	95	−1.75
6	$(CH_2)_3OCOtBu$	**9f**	67	90	−1.50

[a] The reported yields are yields of isolated analytically pure product with the expected spectroscopic data (^1H NMR, ^{13}C NMR, IR and MS). [b] The optical rotations were measured in benzene.

The treatment of **8a** with *n*-BuLi (3 equiv, THF, −25 °C, 12 h) provides the γ-lithiated lithium alcoholate **11** (R^1 = Li) in good yields (Scheme 1). The deuterolysis of **11** gives the deuterated alcohol **13** (83% yield, degree of deuteration > 95%) and its iodolysis leads to 1-iodo-3-undecanol **14** (72%). However, because of the low reactivity of **11**, which may be due to the chelation of the γ-lithium atom with the OLi group,[7] this compound only reacted with a few electrophiles. The conversion of **8a** to the methoxyethoxymethyl (MEM) ether **10** allows the preparation of the reactive organolithium compound **12**, which reacts with benzaldehyde leading to the 1,4-diol derivative **15** as a 1:1 mixture of two diastereoisomers (75%). Interestingly, the transmetallation of **12** with the THF-soluble copper salt CuCN · 2 LiCl[8] affords a copper reagent (20 °C, 5 min), which reacts in good yield with various electrophiles. The benzoylation of **12** is of particular interest, providing the homoaldol product **16** (83%). The allylation of the copper derivative of **12** with ethyl α-(bromomethly)acrylate[9] gives the unsaturated ester **17** (84%), whereas its reaction with 1-iodohexyne furnishes the acetylenic ether **18** (74%). Finally, the unsaturated ketone **19** (81%) is accessible by an addition–elimination sequence with the copper derivative of **12** and 3-iodo-2-cyclohexen-1-one.[10] These reactions demonstrate that the chiral stannylated alcohol derivatives **10** can be used for the preparation of a variety of polyfunctionalized secondary alcohols in optically active form.[11]

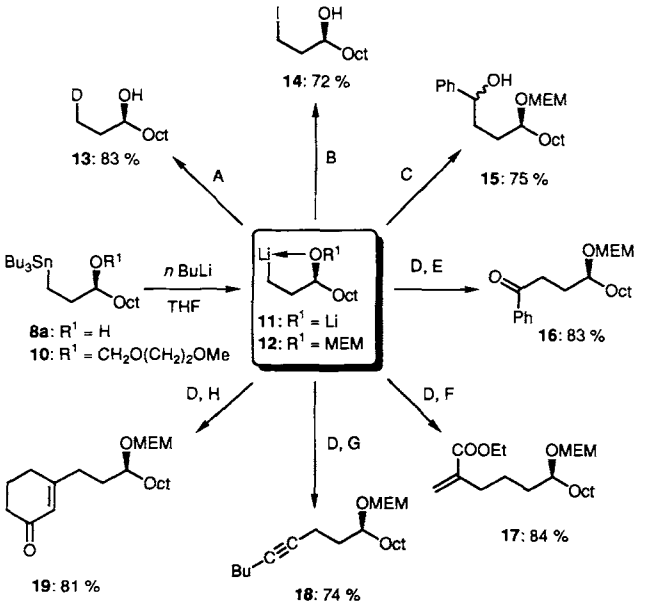

Scheme 1. A: D_2O, −25 °C; B: 1) $MgBr_2$; 2) I_2, −25 °C; C: PhCHO (2 equiv), −25 °C; D: CuCN · 2 LiCl (2 equiv), −20 to 20 °C; E: PhCOCl (2.5 equiv), −25 °C, 1 h; F: Ethyl α-(brommethyl)acrylate (3 equiv), −25 °C, 0.5 h, G: 1-Iodohexyne (2.5 equiv), −25 °C, 8 h; H: 3-Iodo-2-cyclohexen-1-one (2.5 equiv), −25 °C, 1 h.

The unsaturated alcohols **9** are versatile intermediates and lead to a range of interesting *polyfunctional* alcohols. After acylation of **9c**, the resulting acetate **21a** reacts with benzoyl chloride in the presence of bis-(dibenzylideneacetone)-palladium $[Pd(dba)_2]$ (2.5 mol%)[12] and tri-*o*-furylphosphane (5 mol%)[13] to give the γ-acetoxy ketone **20a** in 90% yield ($[\alpha]_D^{20}$ = − 8,5). Similarly, the reaction of **21b** with cyclohexanecarbonyl chloride furnishes the ketone **20b** (83%; *E*/*Z* ratio ca. 9:1). Thus, our method provides a highly enantioselective entry to nonracemic γ-alkoxy-α,β unsaturated carbonyl derivatives of type **20** which are useful building blocks in organic synthesis and are known to add various nucleophiles with excellent diastereoselectivity.[14] An iodolysis of the alcohol **9b** (I_2, ether, 20 °C, 5 h)[15] affords the iodide **22**[6] in excellent yield (98%, $[\alpha]_D^{20}$ = + 4,0).

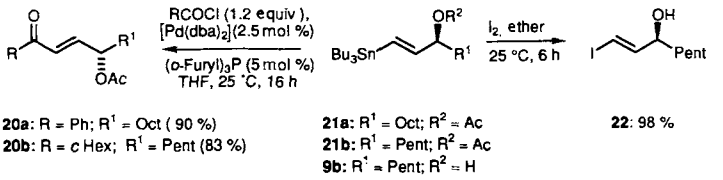

20a: R = Ph; R^1 = Oct (90 %)
20b: R = *c*Hex; R^1 = Pent (83 %)

21a: R^1 = Oct; R^2 = Ac
21b: R^1 = Pent; R^2 = Ac
9b: R^1 = Pent; R^2 = H

22: 98 %

In summary we have shown that the catalytic enantioselective addition of dialkylzinc compounds to the stannylated aldehydes **5** and **6** affords chiral alcohols, which, after standard transformations of the carbon–tin bond, leads to chiral polyfunctional alcohols.

Experimental Procedure

A 100 mL three-neck flask equipped with an argon inlet, a thermometer, and a septum cap was charged with dry toluene (3 mL), $Ti(OiPr)_4$ (3.8 mL, 13 mmol), and (1*R*,2*R*)-1,2-bis-(trifluorosulfonamido)cyclohexane (0.2 g, 0.53 mmol). The reaction was heated to 40–45 °C for 0.5 h, and then cooled to −60 °C. Bis(4-chlorobutyl)zinc (ca. 15 mmol; prepared from 1-chloro-4-iodobutane (8.20 g, 38 mmol, 50 °C, 16 h) [1], Et_2Zn (6.0 mL, 59 mmol), and a catalytic amount of CuI (20 mg, 0.11 mmol) were dissolved in dry toluene (16 mL) and added to the cooled reaction mixture. After a few minutes the aldehyde **5b** (1.96 g, 5.65 mmol) was added. The reaction mixture was stirred for 16 h at −35 °C (2 h at −60 °C for **6**) and was worked up in the usual way. The crude oil was purified by flash chromatography (hexane:ether 4:1), which afforded the pure alcohol **8d** as a colorless oil (1.97 g, 79%, $[\alpha]_D^{20}$ = 2.0 (*c* = 8.95, C_6H_6). In the case of the aldehyde **6**, an excess of only two equiv of $[R^1(CH_2)_n]_2Zn$ was required.

Received: December 10, 1992 [Z 5742 IE]
German version: *Angew. Chem.* **1993**, *105*, 629

[1] M. J. Rozema, S. AchyuthaRao, P. Knochel, *J. Org. Chem.* **1992**, *57*, 1956–1958.
[2] The catalyst **3** has been used in the addition of diethylzinc to unfunctionalized aldehydes: a) M. Yoshioka, T. Kawakita, M. Ohno, *Tetrahedron Lett.* **1989**, *30*, 1657–1660; b) H. Takahashi, T. Kawakita, M. Yoshioka, S. Kobayashi, M. Ohno, *ibid.* **1989**, *30*, 7095–7098; c) H. Takahashi, T. Kawakita, M. Ohno, M. Yoshioka, S. Kobayashi, *Tetrahedron* **1992**, *48*, 5691–5700. For other Ti-catalyzed enantioselecitve additions of R_2Zn to aldehydes, see: d) A. K. Beck, B. Bastani, D. A. Plattner, W. Petter, D. Seebach, H. Braunschweiger, P. Gysi, L. LaVecchia, *Chimia* **1991**, *45*, 238–244; e) B. Schmidt, D. Seebach, *Angew. Chem.* **1991**, *103*, 100–101; *Angew. Chem. Int. Ed. Engl.* **1991**, *30*, 99–101; f) D. Seebach, L. Behrendt, D. Felix, *ibid.* **1991**, *103*, 991–992 and **1991**, *30*, 1008–1009; g) B. Schmidt, D. Seebach, *ibid.* **1991**, *103*, 1383 and **1991**, *30*, 1321; h) J. L. v.d. Busssche-Hünnefeld, D. Seebach, *Tetrahedron* **1992**, *48*, 5719–5730. For excellent reviews concerning the asymmetric addition of diethylzinc to aldehydes: i) D. A. Evans, *Science* **1988**, *240*, 420–426; j) R. Noyori, M. Kitamura, *Angew. Chem.* **1991**, *103*, 34–55; *Angew. Chem. Int. Ed. Engl.* **1991**, *30*, 49–70; k) K. Soai, S. Niwa, *Chem. Rev.* **1992**, *92*, 833–856; l) R. O. Duthaler, A. Hafner, *ibid.* **1992**, *92*, 807–852; m) Both (*1R*,*2R*) as well as (*1S*,*2S*)-1,2-diaminocyclohexane are readily available by a resolution with (*R*,*R*) or (*S*,*S*) tartaric acid respectively: F. Galsbol, P. Steenbol, B. Sondergaard-Sorensen, *Acta Chem. Scand.* **1972**, *26*, 3605–3611.
[3] Y. Ueno, M. Ohta, M. Okawara, *Tetrahedron Lett.* **1982**, *23*, 2577–2580.
[4] a) P. A. Wender, S. McN. Sieburth, J. J. Petraitis, S. K. Singh, *Tetrahedron* **1981**, *37*, 3967–3975; b) I. Beaudet, J.-L. Parrain, J.-P. Quintard, *Tetrahedron Lett.* **1991**, *32*, 6333–6336; c) I. Marek, A. Alexakis, J. F. Normant, *ibid.* **1991**, *32*, 6337–6340; d) B. H. Lipshutz, E. L. Ellsworth, S. H. Dimock, D. C. Reuter, *ibid.* **1989**, *30*, 2065–2068; e) H. Imanieh, D. McLeod, P. Quayle, Y. Zhao, *ibid.* **1992**, *33*, 405–408.
[5] The enantiomeric excess (*ee* value) was determined by converting the alcohols to the corresponding mandelic esters with (*S*)-(+)-*O*-acetylmandelic acid ($[\alpha]_D^{28} = +153$ ($c = 2$, CH_3COCH_3)), and examining these by ^1H NMR (300 and 500 MHz spectra). The esters derived from the racemic alcohols were prepared in all cases: D. Parker, *J. Chem. Soc., Perkin Trans. 2* **1983**, 83–88.
[6] a) R. Noyori, M. Suzuki, *Angew. Chem.* **1984**, *96*, 854–882; *Angew. Chem. Int. Ed. Engl.* **1984**, *23*, 847–876; b) M. Suzuki, A. Yanagisawa, R. Noyori, *J. Am. Chem. Soc.* **1990**, *107*, 3348–3349; c) Y. Morita, M. Suzuki, R. Noyori, *J. Org. Chem.* **1989**, *54*, 1785–1787; d) R. Noyori, S. Suga, K. Kawai, S. Okada, M. Kitamura, *Pure Appl. Chem.* **1988**, *60*, 1597–1606; e) P. W. Collins, C. J. Jung, A. Gasiecki, R. Pappo, *Tetrahedron Lett.* **1978**, 3187–3190; f) R. F. Newton, D. P. Reynolds, *J. Chem. Soc. Perkin Trans. 1* **1983**, 683–685; g) B. H. Lipshutz, E. L. Ellsworth, *J. Am. Chem. Soc.* **1990**, *112*, 7440–7441; h) K. A. Babiak, J. R. Behling, J. H. Dygos, K. T. McLaughlin, J. S. Ng, V. J. Kalish, S. W. Kramer, R. L. Shone, *J. Am. Chem. Soc.* **1990**, *112*, 7441–7442; i) Review: F. Sato, Y. Kobayashi, *Synlett* **1992**, 849–857.
[7] Similar low reactivities of organolithium compounds bearing a OLi group in close proximity to the metal have been observed: a) B. Mudryk, T. Cohen, *J. Am. Chem. Soc.* **1991**, *113*, 1866–1867; b) B. Mudryk, T. Cohen, *J. Org. Chem.* **1991**, *56*, 5760–5761.
[8] P. Knochel, M. C. P. Yeh, S. C. Berk, J. Talbert, *J. Org. Chem.* **1988**, *53*, 2390–2392.
[9] J. Villieras, M. Rambaud, *Synthesis* **1982**, 924–926.
[10] E. Piers, I. Nagakura, *Synth. Commun.* **1975**, *5*, 193–201.
[11] All reactions were performed with the racemic tin derivatives **8a** and **10** which are readily available by the addition of octylmagnesium iodide to **5b**. However, the absence of racemization during these transformations was demonstrated in the following case: The lithium reagent **11** prepared from **8a** (93% *ee*) was treated with an excess of Me_2SiCl, and afforded after acidic workup 1-trimethylsilyl-3-decanol (79% yield, 93% *ee*; $[\alpha]_D^{20} = -4.0$ ($c = 6.69$, C_6H_6)).
[12] a) Y. Takahashi, T. Ito, S. Sakai, Y. Ishii, *J. Chem. Soc. Chem. Commun.* **1970**, 1065–1066; b) M. F. Rettig, P. M. Maitlis, *Inorg. Synth.* **1977**, *17*, 134–137; c) G. Mignani, F. Leising, R. Meyrueix, H. Samson, *Tetrahedron Lett.* **1990**, *31*, 4743–4746; d) Y. Tamaru, H. Ochiai, T. Nakamura, Z. Yoshida, *ibid.* **1986**, *27*, 955–958; e) E. Negishi, V. Bagheri, S. Chatterjee, F.-T. Luo, J. A. Miller, A. T. Stoll, *ibid.* **1983**, *24*, 5181–5184.
[13] a) J. K. Stille, *Angew. Chem.* **1986**, *98*, 504–519; *Angew. Chem. Int. Ed. Engl.* **1986**, *25*, 508–524; b) V. Farina, S. R. Baker, D. A. Behigni, S. I. Hauck, C. Sapinoe, *J. Org. Chem.* **1990**, *55*, 5833–5847; c) V. Farina, B. Krishnan, *J. Am. Chem. Soc.* **1991**, *113*, 9585–9595; d) V. Farina, G. P. Roth, *Tetrahedron Lett.* **1991**, *32*, 4243–4246.
[14] a) Y. Yamamoto, Y. Chounan, S. Nishii, T. Ibuka, H. Kitahara, *J. Am. Chem. Soc.* **1992**, *114*, 7652–7660; b) Review: T. Ibuka, Y. Yamamoto, *Synlett* **1992**, 769–777.
[15] G. A. Tolstikov, M. S. Miftakhov, N. A. Danilova, Y. L. Verl'der, *Synthesis* **1986**, 496–499.

Transfer Hydrogenation and Deuteration of Buckminsterfullerene C_{60} by 9,10-Dihydroanthracene and 9,9′,10,10′[D_4]Dihydroanthracene**

By *Christoph Rüchardt,* Matthias Gerst, Jochen Ebenhoch, Hans-Dieter Beckhaus, Eleanor E. B. Campbell, Ralf Tellgmann, Helmut Schwarz, Thomas Weiske,* and *Stephan Pitter*

Since the discovery and characterization of buckminsterfullerene C_{60} many attempts have been made at its derivatization.[1] The hydrogenated fullerenes $C_{60}H_x$ have been the subject of numerous, mostly theoretical publications,[2] which led to the conclusion that initially an exothermic 1,2-addition of hydrogen takes place. Only from the Birch reduction of C_{60}[3] could a homogeneous product $C_{60}H_{36}$ be isolated after thin-layer chromatography (TLC); however, the electron impact (EI) mass spectra indicated the presence of a second component with the empirical formula $C_{60}H_{18}$. At the time it was not possible to decide whether the $C_{60}H_{18}$ (not isolated) was a product of the Birch reduction or a pyrolysis product of $C_{60}H_{36}$.

We have now found that buckminsterfullerene C_{60} can be converted quantitatively into two hydrogenation products, $C_{60}H_{36}$ or $C_{60}H_{18}$, in a reproducible way with the new method of transfer hydrogenation[4, 5] recently described by us. The method is also suitable for the synthesis of $C_{60}D_{18}$ and $C_{60}D_{36}$. Since the first step of this reaction is a molecule-induced radical formation[6] by H addition, C_{60} is a particularly suitable candidate for the reaction because of its "radical sponge" properties.[7]

If C_{60} is heated to 350°C with 120-fold molar excess of dihydroanthracene (DHA) in a glass ampoule sealed under a nitrogen atmosphere, the H transfer to C_{60} can be followed from the changes in color. The initially dark violet melt, probably dissolved C_{60} in DHA, turns rust-brown, ruby-red, orange, yellow, and finally colorless within a few minutes. After the mixture had been cooled to room temperature (after ca. 30 min), the ampoule opened, and the anthracene derivatives sublimed off at 60–110°C (0.2 Torr), a white, solid product **A** ($C_{60}H_{36}$) could be isolated.[8] If the reaction time at 350°C is increased to 24 h, the degree of hydrogenation decreases accompanied by a darkening of the color and the formation of a second product **B** ($C_{60}H_{18}$), which likewise could be isolated.[8] In addition, C_{60} itself can again be identified. If the reaction is carried out in a sealed ESR tube at about 350°C, it is possible to record ESR spectra of the intermediary 9-hydroanthryl radicals. Correspondingly, deuterated products **C** and **D** are obtained from 9,9′,10,10′-[D_4]dihydroanthracene (degree of deuteration of the methylene protons of DHA 95%) after longer reaction times.

[*] Prof. Dr. C. Rüchardt, Dipl-Chem. M. Gerst, J. Ebenhoch, Dr. H.-D. Beckhaus
Institut für Organische Chemie und Biochemie der Universität Albertstrasse 21, D-W-7800 Freiburg (FRG)
Dr. E. E. B. Campbell, R. Tellgmann
Fakultät für Physik der Universität Freiburg und Freiburger Materialforschungszentrum
Prof. Dr. H. Schwarz, Dr. T. Weiske
Institut für Organische Chemie der Technischen Universität Berlin
Dipl.-Chem. S. Pitter
Institut für Anorganische Chemie der Universität Heidelberg

[**] Bimolecular radical formation through H transfer, Part 3. This work was supported by the Deutsche Forschungsgemeinschaft and the Fonds der Chemischen Industrie. We thank Prof. Dr. F. Diederich, ETH Zürich for samples of pure C_{60}, and Dr. W. Deck, Dipl.-Chem. R. Neuber, and Dipl.-Chem. A. Meissner for ^1H NMR and FT-IR spectra, and Prof. Dr. H. Grützmacher for stimulating discussions.

The homogeneous composition of the products is revealed by the clear separation by TLC and by field desorption mass spectra.[8] Figure 1 shows that the mass spectra, which were recorded by different methods, vary considerably in the amount of information they provide. The EI and the FD mass spectra can be interpreted most clearly.

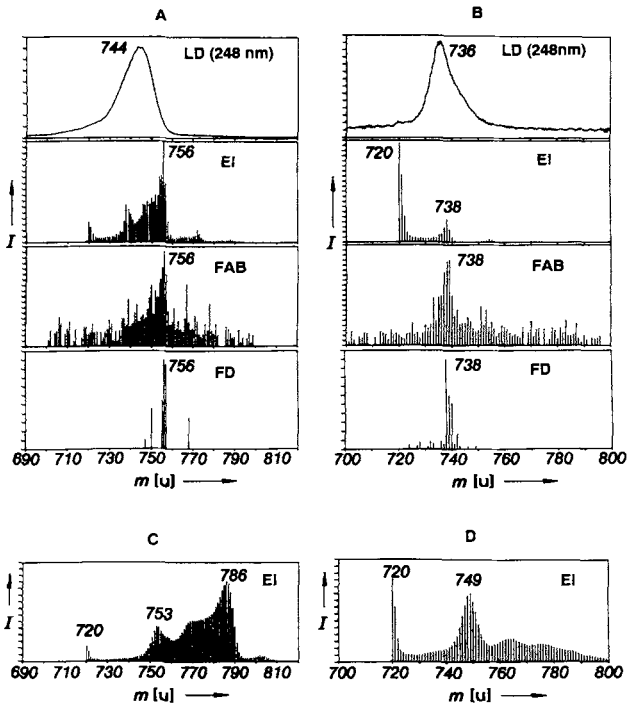

Fig. 1. Mass spectra of the products **A**, **B**, **C**, and **D** recorded with different techniques (see text). I = intensity in arbitrary units, m = mass in atomic mass units.

In the EI (70–100 eV, heating rate 5–100 $K s^{-1}$), FAB (Ar, 8 keV, matrix: *o*-nitrobenzyl alcohol), and FD spectra (field voltage 4 kV) the M^+ peak was always found and the M^{2+} peak was observed sometimes ($C_{60}H_{36}$, $C_{60}D_{36}$, and $C_{60}H_{18}$, $C_{60}D_{18}$, respectively[9]); in the laser desorption (LD) mass spectra (λ = 308 and 254 nm)[10] masses that were too small were observed. The reason for the shift is not yet known, but it seems to be due to the ionization steps in the LD experiment. The common feature of the EI mass spectra is the fragmentation in the spectrometer with the loss of H and D, respectively down to C_{60}. For the products **A** and **C** more intense mass peaks occur with the degree of substitution $x = 18$. Similar spectra but with more lines at higher masses through H and D addition, respectively, are obtained with the FAB method, whereas the FD spectra show almost only the M^+ peak. With the mass spectra of the products **C** and **D** it could be shown that the derivatives **A** and **B** really are hydrogenated fullerenes and not the oxides $C_{60}O_xH_y$, because the molecular weight increased accordingly with the degree of substitution.

The ^{1}H NMR spectra of $C_{60}H_{36}$ in $CDCl_3$, CD_2Cl_2, [D_6]benzene, and [D_8]THF at 25°C as well as in [D_6]dimethylsulfoxide (DMSO) at 25–100°C showed a broad group of signals between δ = 2.5 and 4.2 with three distinct maxima at δ = 3.3, 3.7, and 4.0.[3] In the originally clear solutions a precipitate formed after one hour at the most, in spite of an inert gas atmosphere.

In the FT-IR spectrum of **A** (KBr) bands were detected at $\tilde{\nu}$ = 2913(s), 2850(s), 1733(w), 1606(w), 1511(w), 1257(m), 1198(m), 1169(m), 1076(w), and 745(w) cm^{-1}. These bands could be clearly assigned to **A** following a comparison of the IR spectra with those of the starting materials. The bands of the C–H vibrations between $\tilde{\nu}$ = 2850 and 2920 cm^{-1} were clearly visible, whereas the bands at $\tilde{\nu}$ = 1511 and 1606 cm^{-1} indicate C=C bonds; for product **B** (KBr), the C–H bands, among others, were situated at $\tilde{\nu}$ = 2854(s), 2897(s), and 2925(s) cm^{-1}. The deuterated product **C** (KBr) showed, among others, a broad band at $\tilde{\nu}$ = 2128 cm^{-1}, characteristic for C–D vibrations. In the UV spectrum an absorption at λ = 230 nm was measured for **A** (CH_2Cl_2).

When **A** and **B** were heated they both showed a darkening of color at temperatures above 200°C, but no melting point up to 260°C. Both substances were dehydrogenated quantitatively to C_{60} (LD-MS) at 550°C within 15 min in ampoules sealed under an inert gas atmosphere. The chemical dehydrogenation of **A** with the H acceptors α-methylstyrene and anthracene was also successful (evidence of cumene from gas chromatography as well as LD-MS evidence of **B** and C_{60}). Evidently, the cage structure of C_{60} was retained during the reductions to give **A** and **B**. Consequently, the formation of the product **B**, which has a lower degree of hydrogenation (50%) than **A** with longer reaction time, can be understood as a dehydrogenation of **A** by the coproduct anthracene. From this reaction, among other products, the inert 1,2,3,4-tetrahydroanthracene is formed.

So far all attempts to obtain ESR spectra of the radical anions of the hydrogenated and deuterated fullerenes **A**–**D** by reduction (potassium in dimethoxyethane) have failed.[11] This indicates that there are only discrete double bonds present in $C_{60}H_{36}$, as expected from previous experiments on transfer hydrogenation[4, 5] and the Birch reduction.[3] Figure 2 depicts a probable structure of $C_{60}H_{36}$ minimized according to MM2 calculations (H_s = 159.91 kcal mol^{-1}, $\Delta H^0_{f,g}$ = 333.63 kcal mol^{-1}).

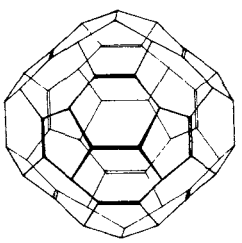

Fig. 2. Possible structure of $C_{60}H_{36}$.

Recent experiments reveal that 1,4-cyclohexadiene is also suitable for the transfer hydrogenation from C_{60} to $C_{60}H_{36}$ (LD-MS). The hydrogenation of C_{60} with DHA is superior to the Birch reduction as a synthetic method because of its simple execution (exactly reproducible), control to give $C_{60}H_{18}$ *or* $C_{60}H_{36}$, and the possibility of deuteration. It seems possible that further fullerenes may be synthesized with other H donors,[5, 12] and different degrees of hydrogenation.

Received: December 10, 1992 [Z 5741 IE]
German version: *Angew. Chem.* **1993**, *105*, 609

[1] a) H. Schwarz, *Angew. Chem.* **1992**, *104*, 301–305; *Angew. Chem. Int. Ed. Engl.* **1992**, *31*, 293–297, and references therein; b) F. Diederich, Y. Rubin, *ibid.* **1992**, *104*, 1123–1146 and **1992**, *31*, 1101–1124, and references therein.

[2] a) M. Saunders, *Science* **1991**, *253*, 330–331; b) G. E. Scuseria, *Chem. Phys. Lett.* **1991**, *176*, 423–427; T. Guo, G. E. Scuseria, *ibid.* **1992**, *191*, 527–532; c) D. A. Dixon, N. Matsuzawa, T. Fukunaga, F. N. Teppe, *J. Phys. Chem.* **1992**, *96*, 6107–6110; d) N. Matsuzawa, D. A. Dixon, T. Fukunaga, *ibid.* **1992**, *96*, 7594–7604.

[3] R. E. Haufler, J. Conceicao, L. P. F. Chibante, Y. Chai, N. E. Byrne, S. Flanagan, M. M. Haley, S. C. O'Brien, C. Pan, Z. Xiao, W. E. Billups, M. A. Ciufolini, R. H. Hauge, J. L. Margrave, L. J. Wilson, R. F. Curl, R. E. Smalley, *J. Phys. Chem.* **1990**, *94*, 8634–8636.
[4] C. Rüchardt, M. Gerst, M. Nölke, *Angew. Chem.* **1992**, *104*, 1516–1518; *Angew. Chem. Int. Ed. Engl.* **1992**, *31*, 1523–1525.
[5] M. Gerst, C. Rüchardt, *Chem. Ber.* **1993**, in press.
[6] W. A. Pryor, L. D. Iasswell, *Adv. Free Radical Chem.* **1975**, *5*, 27–99; J. A. K. Harmony, *Methods Free Radical Chem.* **1974**, *5*, 101–176; W. A. Pryor in *Organic Free Radicals* (*ACS Symp. Ser. 69*) (Ed.: W. A. Pryor), American Chemical Society, Washington, D.C., **1978**, p. 33–63.
[7] a) P. J. Krusic, E. Wasserman, P. N. Keizer, J. R. Morton, K. F. Preston, *Science* **1991**, *254*, 1183–1185; J. R. Morton, K. F. Preston, P. J. Krusic, S. A. Hill, E. Wasserman, *J. Phys. Chem.* **1992**, *96*, 3576–3578; b) C. N. McEwen, R. G. McKay, B. S. Larsen, *J. Am. Chem. Soc.* **1992**, *114*, 4412–4414; c) D. Schröder, D. K. Böhme, T. Weiske, H. Schwarz, *Int. J. Mass Spectrom. Ion Proc.* **1992**, *116*, R13–R21; d) S. Petrie, G. Javahery, J. Wang, D. K. Böhme, *J. Am. Chem. Soc.* **1992**, *114*, 6268–6269.
[8] According to TLC (silica gel, solvent mixture CH_2Cl_2:*n*-hexane 1:3, staining in an iodine chamber) for **A** a spot was found at $R_f = 0.35$, for **B** a spot at $R_f = 0.15$, in addition to small initial spots.
[9] The degree of deuteration of 95% of the [D_4]DHA leads to the main components $C_{60}D_{30}H_6$ and $C_{60}D_{11}H_7$.
[10] G. Ulmer, E. E. B. Campbell, R. Kühnle, H.-G. Busmann, I. V. Hertel, *Chem. Phys. Lett.* **1991**, *182*, 114–119.
[11] A highly resolved ESR spectrum, produced by eight and four differently coupling protons, was caused by traces of an impurity, which also occurred in the sublimate in higher concentrations after the workup.
[12] Also for the reaction of C_{70} with DHA several hydrogenated products could be identified in the LD-MS, which are being examined more closely at present.

Synthesis and Structure of Tetrasilylgermane, $Ge(SiH_3)_4$, and Other Silylgermanes**

By *Thomas Lobreyer, Heinz Oberhammer,* and *Wolfgang Sundermeyer**

Amorphous alloy or mixed semiconductors (a-SiGe:H, a-SiC:H) seem to be particularly suitable for a more efficient use of the various spectral ranges of sunlight and thus for an increase of the energy yielded from thin-film solar cells.[1] The mixtures of SiH_4/GeH_4 and SiH_4/CH_4 used for the plasma-enhanced chemical vapor deposition (PE-CVD) so far have not led to a satisfactory optoelectronic film quality over the total relevant energy range because of the different deposition behavior of GeH_4, CH_4, and SiH_4.[2] A significant improvement of the films is expected from such chemical compounds, in which some of the bonds of the amorphous network of the alloy semiconductor are already formed within the molecule. Thus, silylgermanes of the composition $GeH_n(SiH_3)_{4-n}$ ($n = 0-3$) would be suitable process gases for the deposition of a-SiGe:H mixed-semiconductor films. We report herein on the first synthesis of tetrasilylgermane and other silylgermanes.

In the reaction of monosilane and monogermane with dispersed alkali metals we observed[3,4] that SiH_4 reacts with sodium to give discrete sodium silylsilanides $NaSiH_n(SiH_3)_{3-n}$ ($n = 0-3$).[5] The first experiments aimed at explaining the mechanism of the Si–Si bond formation, which occurs with the evolution of hydrogen, were carried out with monogermane, in order to investigate the build-up reaction with a view to a possible Si–Ge coupling. If GeH_4 is introduced into the freshly prepared solution of the sodium silylsilanides in diglyme, kept at 100°C, a vigorous evolution of hydrogen and the loss of SiH_4 is observed. Surprisingly, the typical signals[6] of the negatively charged central Si atoms in the ^{29}Si NMR spectrum disappear. In contrast, only three signals, which are shifted to slightly higher field in comparison to the signals of the sodium silanides, occur for the SiH_3 substituents at $\delta = -88.1$, -84.9, and -79.3. These can be assigned to the novel sodium silylgermanides $NaGeH_n(SiH_3)_{3-n}$ ($n = 2,1,0$), **1a–c**.

This is confirmed, in particular, by the subsequent reaction of **1a–c** with methyl *p*-toluenesulfonate (*p*-$TosCH_3$), whose products, the methylsilylgermanes **2a**,[7] **2b**, and **2c**,[5] were isolated by preparative gas chromatography. Methylsilanes as subsequent products of the sodium silanides, which possibly did not react with GeH_4, could not be detected. Further studies aimed at explaining the reaction mechanism of the two formation reactions are currently in progress. The silylation of the sodium silylgermanides **1a–c** with silyl nonafluorobutanesulfonate, $C_4F_9SO_3SiH_3$, about which we reported recently,[3] has proven to be particularly interesting for the synthesis of Si–Ge-containing process gases. Depending on the content of **1a–c** in the solution from this reaction the silylgermanes $GeH_n(SiH_3)_{4-n}$ ($n = 2,1,0$) **3a–c** are obtained in good yields.

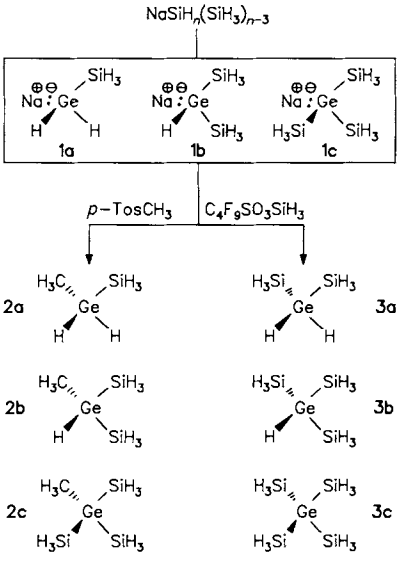

Our interest was intitally centered on the symmetrically built $Ge(SiH_3)_4$ (**3c**), which could be isolated in a two-step synthesis after purification by preparative gas chromatography in a yield of 47% (together with **3a** (15%)[8] and **3b** (24%)) as a clear, pyrophonic liquid which melts at −54°C and boils at 86.6°C/193 Torr. The vapor pressure curve was recorded for the CVD. The curve is described by $\lg p = -1348\,T^{-1} + 6.02$ (measured over the range of 28.9°C/36 Torr to 86.6°C/193 Torr). Both the proton-coupled ^{29}Si NMR spectrum (Fig. 1) and the mass spectrum clearly prove the existence of **3c**; the coupling of the Si atoms with the neighboring H atoms results in a quartet at $\delta = -85.18$ ($^1J_{Si,H}$) 203.75 Hz), which is split by the other nine protons to a deciplet ($^3J_{H,H}$) = 3.66 Hz).

[*] Prof. Dr. W. Sundermeyer, Dipl.-Chem. T. Lobreyer
Anorganisch-chemisches Institut der Universität
Im Neuenheimer Feld 270, D-W-6900 Heidelberg 1 (FRG)
Prof. Dr. H. Oberhammer
Institut für Physikalische und Theoretische Chemie
der Universität Tübingen

[**] This work was supported by the Bundesministerium für Forschung und Technologie (project no. 0328980 A) and the Fonds der Chemischen Industrie. We thank Degussa AG, Messer-Griesheim AG, and BASF AG for chemicals, and Dr. R. Geist, and M. Steiner and O. Walter for recording the mass spectra and the ^{29}Si NMR spectra, respectively.

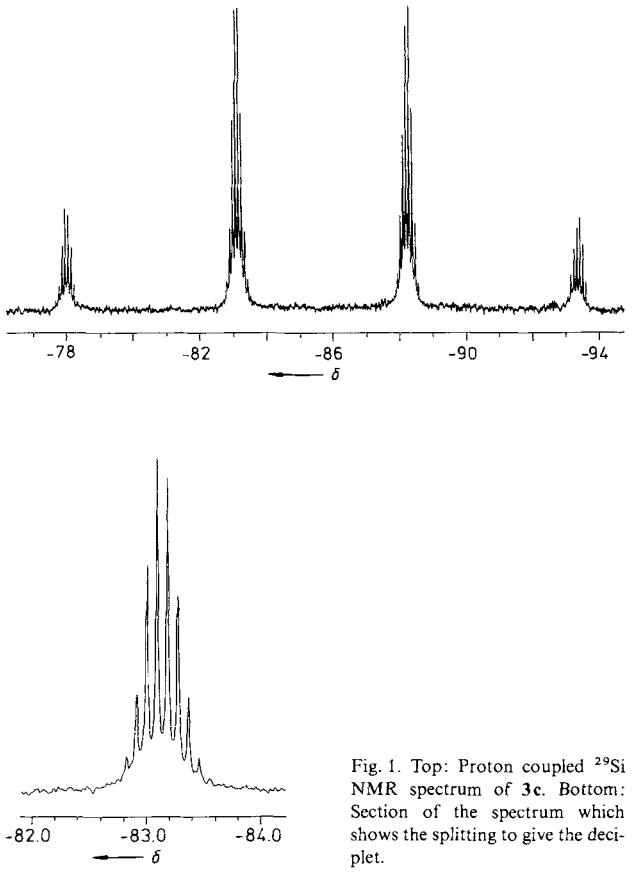

Fig. 1. Top: Proton coupled ^{29}Si NMR spectrum of **3c**. Bottom: Section of the spectrum which shows the splitting to give the deciplet.

The structure of $Ge(SiH_3)_4$ in the gas phase was determined by electron diffraction analysis.[9] The molecule has the expected T_d symmetry, and the silyl groups can rotate almost freely. The structure is depicted in Figure 2. The Ge–

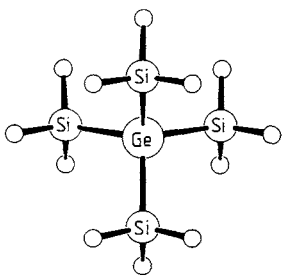

Fig. 2. Molecular structure of $Ge(SiH_3)_4$ **3c** in the gas phase (Distances [Å] and angles [°], limits of error are 3σ values) Ge–Si 2.370(1), Si–H 1.497(7); H–Si–H 106.8(11).

Si bond length (2.370(1) Å) is slightly longer than in $CH_3Ge(SiH_3)_4$ (2.366(2) Å[5]) and is in agreement (within the limits of error) with the value reported for H_3GeSiH_3 (2.357(20) Å[10]).

Experimental Procedure

1a–c: In a reactor fitted with a hollow stirrer (to intensify the contact between the gas and the dispersion) and a baffle plate (to break up the vortex and allow better dispersion) [3], sodium (10 g, 0.44 mol) was dispersed in diglyme (500 mL) at 100°C and allowed to react with monosilane, which was added continuously, to give sodium silanides of the composition $NaSiH_n(SiH_3)_{3-n}$ (n = 0–3) [5]. After 3 h monosilane was replaced, without interrupting the inflow of gas, by monogermane, which was added for 50 min under the same reaction conditions. The hydrogen, which was formed throughout the whole reaction escaped into a cold trap (−196°C), in which monosilane formed at the same time was trapped; this monosilane could be reused. After the reaction was interrupted the reddish solution formed was filtered through a G4 frit. The solution contained a mixture of silylgermanides $NaGeH_n(SiH_3)_{3-n}$ (n = 0–2) with a total yield of 70% (based on the amount of sodium used).

2a–c: In a 500 mL flask filled with nitrogen and fitted with a septum and a cold trap, methyl p-toluenesulfonate (30 g, 104 mmol), dissolved in diglyme (100 mL), was quickly added dropwise with a syringe to the solution containing **1a–c** (150 mL, 87 mmol) at −50°C. The completely decolored suspension formed was stirred for 10 min at −50°C. This was then allowed to warm to room temperature, during which time the volatile reaction products were trapped under vacuum in the cold trap (−196°C) and the mixture of substances was purified by fractionating condensation. The isolation of **2a–c** was achieved by preparative gas chromatography [11].

3a–c: The solution containing **1a–c** (150 mL, 87 mmol) was allowed to react with freshly prepared silyl nonafluorobutanesulfonate [3] (29.7 g, 90 mmol) in a 500 mL flask filled with nitrogen and fitted with a septum and a cold trap at −50°C. The suspension formed remained pale yellow. After removal of the cooling bath the volatile products were condensed under vacuum into the cold trap (−196°C) and separated from the monosilane formed by fractionating condensation. The isolation of **3a–c** was achieved by preparative gas chromatography [11].

2b: Yield 25%; ^1H NMR (90 MHz, C_6D_6): δ = 0.30 (d, 3H, $^3J(H,H)$ = 4.39 Hz, CH_3), 3.17 (m, 1H, GeH), 3.41 (d, 6H, $^1J(Si,H)$ = 197.8 Hz, $^3J(H,H)$ = 3.66 Hz, SiH_3); ^{29}Si NMR (17.75 MHz, C_6D_6): δ = −91.47; IR (gas): $\tilde{\nu}$[cm^{-1}] = 2993.9 w, 2926.5 w, 2156.0 vs, 2148.3 vs, 2030.7 vs, 937.2 m, 896.7 m, 890.0 m, 872.6 m, 866.8 vs, 808.0 m, 677.9 m, 671.1 m, 667.3 m; MS (70 eV): *m/z* 154–141 ($CGeSi_2H_x$), 140–126 ($GeSi_2H_x$), 124–110 ($CGeSiH_x$), 107–98 ($GeSiH_x$), 76–70 (GeH_x), 32–28 (SiH_x).

3b: Yield 24%; ^1H NMR (90 MHz, C_6D_6): δ = 2.20 (m, 1H, $^3J(H,H)$ = 4.15 Hz, GeH), 3.47 (d, 9H, $^1J(Si,H)$ = 204.10 Hz, SiH_3); ^{29}Si NMR (17.75 MHz, C_6D_6): δ = −90.40; IR (gas): $\tilde{\nu}$[cm^{-1}] = 2163.7 vs, 2030.7 s, 964.2 s, 952.7 s, 903.5 s, 863.0 vs, 668.3 s, 662.4 s; MS (70 eV): *m/z* 170–154 ($GeSi_3H_x$), 140–126 ($GeSi_2H_x$), 108–98 ($GeSiH_x$), 77–72 (GeH_x), 32–28 (SiH_x).

3c: Yield 47%; ^1H NMR (90 MHz, C_6D_6): δ = 3.57 (s, 12H, $^1J(Si,H)$ = 203.75 Hz, $^3J(Si,H)$ = 3.66 Hz, SiH_3); ^{29}Si NMR (17.75 MHz, C_6D_6): δ = −85.18 (qdec); IR (gas): $\tilde{\nu}$[cm^{-1}] = 2161.8 vs, 2155.1 vs, 2149.3 vs, 963.3 w, 952.7 w, 930.5 w, 860.1 vs, 84.0 w; MS (70 eV): *m/z* 190–182 ($GeSi_4H_x$), 170–154 ($GeSi_3H_x$), 138–126 ($GeSi_2H_x$), 107–98 ($GeSiH_x$), 79–72 (GeH_x), 32–28 (SiH_x).

Received: December 11, 1992 [Z 5743 IE]
German version: *Angew. Chem.* **1993**, *105*, 587

[1] G. H. Bauer, *Statusbericht Photovoltaik BMFT*, **1990**, *25*, 1–14.
[2] R. D. Plättner, W. W. Krühler, *Statusbericht Photovoltaik BMFT*, **1990**, *26*, 1–15.
[3] T. Lobreyer, J. Oeler, W. Sundermeyer, *Chem. Ber.* **1991**, *124*, 2405–2410 and references therein.
[4] T. Lobreyer, J. Oeler, W. Sundermeyer, DOS 4139113.6 (28. November 1991/03. June 1993), Degussa AG.
[5] T. Lobreyer, J. Oeler, W. Sundermeyer, H. Oberhammer, *Chem. Ber.* **1993**, *126*, in press.
[6] F. Fehér, M. Krancher, *Z. Naturforsch. B*, **1985**, *40*, 1301–1305.
[7] M. D. Sefcik, M. A. Ring, *J. Am. Chem. Soc.* **1973**, *95*, 5168–5173.
[8] K. M. Mackay, S. T. Hosfield, S. R. Stobart, *J. Chem. Soc. A* **1969**, 2937–2942.
[9] The electron diffraction intensities were recorded with a gas diffractograph KD-G2 at two camera distances (25 and 50 cm), with an accelerating potential of about 60 kV. The temperature of the sample vessel was 3°C, and that of the inlet nozzle 10°C. The photographic plates were interpreted with the usual methods (H. Oberhammer, W. Gombler, H. Willner, *J. Mol. Struct.* **1981**, *70*, 273) and intensities in the s ranges 2–18 and 8–35 Å^{-1} were used for the structure determination. The vibrational amplitudes (Ge–Si = 0.058(2) Å, Si···Si = 0.182(8) Å) indicate deformation vibrations of very low frequency for the $GeSi_4$ framework, which were found experimentally at 84 cm^{-1}. Vibrational corrections for interatomic distances were calculated by using a diagonal force field, which was derived from the vibrational amplitudes (f(Ge–Si) = 1.5 mdyn Å^{-1} and f(Si–Ge–Si) = 0.2 mdyn Å^{-1}).
[10] A. P. Cox, R. Varma, *J. Chem. Phys.* **1967**, *46*, 2007.
[11] Gas chromatography: Perkin Elmer F 21; packed column, support Chromosorb W, 25% SE-30, thermal conductivity detector (detector temperature 150°C), column oven temperature 30–120°C.

On the Strength of the C–H···O Hydrogen Bond and the Eclipsed Arrangement of the Methyl Group in a Tricyclic Orthoamide Trihydrate**

By *Juan J. Novoa,* Pere Constans,*
and *Myung-Hwan Whangbo**

In the thousands of compounds whose crystal structures have been determined by X-ray or neutron diffraction the conformation about the C_{sp^3}–CH_3 bonds is staggered. The only exception was reported for a crystalline trihydrate of tricyclic orthoamide **1** (i.e., **1** · $3H_2O$), in which the conformation about the C_{sp^3}–CH_3 bond is nearly eclipsed (N-C-C-H dihedral angle of 8.0°).[1, 2] Since in a single crystal of *anhydrous* **1** the conformation about the C_{sp^3}–CH_3 bond is staggered, the eclipsed arrangement in **1** · $3H_2O$ is attributed to the three C–H···O hydrogen bonds between the methyl group of **1** and the three water molecules surrounding **1**.[1] (In the schematic representation **2** the H···O contacts are represented by dashed lines. In addition to the C–H···O hydrogen bond, each water molecule makes a O–H···N hydrogen bond with one of the nitrogen atoms of an adjacent molecule **1**.)

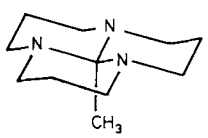

1

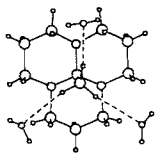

2

To explain this striking observation, Seiler et al.[1] carried out theoretical evaluations of the rotational barrier of the methyl group in **1** and the energy of the C–H···O hydrogen bond. Their ab initio SCF calculations for CH_3–$C(NH_2)_3$ (with the N lone pair antiperiplanar (*app*) to the C–CH_3 bond, structural parameters from the crystallographic study) show the staggered conformation to be more stable than the eclipsed by 5.52 kcal mol^{-1}. Thus, the minimum strength of each of the three C–H···O hydrogen bonds in **1** · $3H_2O$ must be about 1.8 kcal mol^{-1} to produce the eclipsed conformation (under the implicit assumption that the energies of the C(methyl)–H···O hydrogen bonds are additive). On the basis of their MP2-level calculations on model complexes CH_4···OH_2 and CH_4···OH_2···NH_3, Seiler et al.[1] concluded that the C–H···O hydrogen bond has this strength. In this evaluation, however, the basis set superposition errors[3] (BSSEs) were not corrected. According to our recent study,[4] the energy of the C–H···O hydrogen bond is at most 0.59 kcal mol^{-1} (based on MP2-level calculations for CH_4···OH_2 with a near Hartree–Fock limit (NHFL) basis set), and the large values reported by Seiler et al.[1] (1.45–1.94 kcal mol^{-1}) are due mainly to the BSSEs. Consequently, the explanation for the eclipsed conformation about the C_{sp^3}–CH_3 bond of **1** · $3H_2O$ remains a challenge to theoreticians, which prompted us to carry out systematic theoretical calculations aimed at understanding this unusual observations.

To estimate the rotational barrier for the methyl group of **1**, ab initio 6-31 + +G** SCF calculations were performed for the model compounds CH_3–$C(NH_2)_3$ and CH_3–$C[N(CH_3)_2]_3$ (with the N lone pair *app* to the C–C bond) with full geometry optimizations. These calculations show that the staggered conformation is more stable than the eclipsed by 5.44 kcal mol^{-1} in CH_3–$C(NH_2)_3$, and by 5.48 kcal mol^{-1} in CH_3–$C[N(CH_3)_2]_3$. These values are very close to that estimated by Seiler et al.[1] In addition, ab initio 6-31 + +G** SCF calculations for CH_3–CH_3 predict a rotational barrier of 2.98 kcal mol^{-1}, in good agreement with experiment. As already pointed out by Seiler et al., therefore, the rotational barrier of the methyl group in **1** is 5.4–5.5 kcal mol^{-1}, and this barrier should be overcome in **1** · $3H_2O$ by the stabilization energy associated with the three C–H···O hydrogen bonds.

The most accurate estimate of the energy of the C–H···O hydrogen bond, 0.59 kcal mol^{-1}, is based on the model CH_4···OH_2 in which one methane hydrogen atom forms a C–H···O hydrogen bond.[4] In **1** · $3H_2O$ all three hydrogen atoms of the methyl group participate in C–H···O hydrogen bonds. Thus, one might speculate that the energy of the C–H···O hydrogen bonding in **1** · $3H_2O$ is enhanced by a cooperative effect of the three C–H···O bonds of the methyl group. To test this hypothesis, we carried out MP2 calculations on the model compounds CH_4···OH_2, CH_4···$(OH_2)_2$ and CH_4···$(OH_2)_3$, whose geometries were chosen to have one, two, and three C–H···O hydrogen bonds, respectively.[5] According to our previous study of CH_4···OH_2,[4] use of diffuse functions is crucial in reducing the BSSEs. Our 6-31 + +G** MP2 calculations show that after correction of the BSSEs by the counterpoise method,[6] the energies of the hydrogen-bonding in CH_4···OH_2, CH_4···$(OH_2)_2$, and CH_4···$(OH_2)_3$ are 0.37,[7] 0.61, and 0.86 kcal mol^{-1}, respectively. Thus, the total energy of the hydrogen bonds of CH_4···$(OH_2)_n$ (n = 2, 3) is not larger but rather somewhat smaller than the value predicted by n times the C–H···O hydrogen-bond energy of CH_4···OH_2. Our 6-31 + +G** MP2 calculations for CH_4···OH_2···NH_3 (geometry of the C–H···O–H···N arrangement as found in **1** · $3H_2O$) show that the energy of the C–H···O hydrogen bond in CH_4···OH_2···NH_3 is 0.52 kcal mol^{-1} after BSSE correction; this is larger than that of CH_4···OH_2 by about 40% (0.52 vs. 0.37 kcal mol^{-1}). Thus, even if C–H···O–H···N hydrogen bonding is assumed to increase the energy of the C–H···O hydrogen bond by about 40%, the stabilization energy expected from the three C–H···O hydrogen bonds in **1** · $3H_2O$ (roughly $2.5 = 3 \times 0.59 \times 1.4$ kcal mol^{-1}) is much smaller than the rotational barrier of the methyl group in **1**.

Another estimate of the stabilization energy for the three C–H···O hydrogen bonds in **1** · $3H_2O$ was made by determining the rotational barriers of the methyl groups in **1** and **1** · $3H_2O$ (the three H_2O molecules were arranged around **1** as in crystalline **1** · $3H_2O$) on the basis of semiempirical AM1 SCF-MO calculations.[8] (AM1 calculations for CH_3–$C(NH_2)_3$ give a rotational barrier of 2.62 kcal mol^{-1}, which is about 2.8 kcal mol^{-1} lower than the ab initio value.) For the rigid rotation of the methyl group based on the experimental geometries, AM1 calculations show that the staggered conformation about the C_{sp^3}–CH_3 bond is more stable than the eclipsed by 1.53 kcal mol^{-1} in **1**, and by 0.27 kcal mol^{-1} in **1** · $3H_2O$. Namely, the three C–H···O hydrogen bonds in **1** · $3H_2O$ provide the stabilization energy of about 1.3 kcal mol^{-1}. The latter suggests a stabilization energy of about 1.8 kcal mol^{-1} for crystalline **1** · $3H_2O$ if we allow for

[*] Prof. J. J. Novoa, P. Constans
Departamento de Quimica Fisica
Universidad de Barcelona
E-08028 Barcelona (Spain)
Prof. M.-H. Whangbo
Department of Chemistry
North Carolina State University
Raleigh, NC 27695-8204 (USA)

[**] Work at North Carolina State University was supported by the U.S. Department of Energy, Office of Basic Energy Sciences, Division of Materials Science, under Grant DE-FG05-86ER45259. J. J. N. thanks DGICYT PB89-0268 and NATO for financial support.

a 40% increase as a result of the cooperative C–H···O–H···N hydrogen bonding effect. This estimate is consistent with the results of our ab initio calculations.

In the above estimates of the stabilization energy associated with the three C–H···O hydrogen bonds in $\mathbf{1} \cdot 3H_2O$, possible crystal effects were not taken into consideration. To remedy this situation, we calculated the energies of crystalline $\mathbf{1} \cdot 3H_2O$ by employing empirical atom–atom potentials.[9] The structure found in the crystal and the hypothetical structure resulting from it when the conformation about the C_{sp^3}–CH_3 bond is made staggered by rigid rotation are of interest. Our atom–atom potential calculations employed the potential parameters of Williams and Houpt[10] and those of Mirsky.[11] The Madelung energy was calculated by employing the point charges of the atoms that best simulate the electrostatic potentials[12] of **1** and H_2O calculated by the AM1 method. In addition to the usual atom–atom potential terms,[10, 11] the C–H···O hydrogen bond potentials of Cox et al.[13] were employed to calculate the energies of the C–H···O hydrogen bonds for all the H···O contacts shorter than 2.7 Å. Our calculations show that the energy of the interaction between one methyl group and the rest of the crystal is more favorable for the eclipsed than for the staggered arrangement by 2.97 kcal mol^{-1} with the the parameters of Williams and Houpt, and by 1.87 kcal mol^{-1} with the parameters of Mirsky. These values are comparable with the stabilization energies estimated by the present ab initio and AM1 calculations on model compounds.

To maintain the eclipsed arrangement about the C_{sp^3}–CH_3 bond of $\mathbf{1} \cdot 3H_2O$, the stabilization energy associated with the three C–H···O hydrogen bonds of each methyl group should be larger than 5.4–5.5 kcal mol^{-1}, but all our calculations suggest that this energy does not exceed 3 kcal mol^{-1}. Our results do not support the explanation of Seiler et al.[1] for the eclipsed conformation of $\mathbf{1} \cdot 3H_2O$ and lead us to wonder why an eclipsed arrangement is found about the C_{sp^3}–CH_3 bond of $\mathbf{1} \cdot 3H_2O$. It is possible that the observed structure of $\mathbf{1} \cdot 3H_2O$ is not a global but a local energy minimum. It is noted that organic conducting salts often have different phases with identical chemical compositions.[14]

Received: September 14, 1992
Revised version: November 13, 1992 [Z 5572 IE]
German version: *Angew. Chem.* **1993**, *105*, 640

[1] P. Seiler, G. R. Weisman, E. D. Glendening, F. Weinhold, V. B. Johnson, J. D. Dunitz, *Angew. Chem.* **1987**, *99*, 1216; *Angew. Chem. Int. Ed. Engl.* **1987**, *26*, 1175.
[2] P. Seiler, J. D. Dunitz, *Helv. Chim. Acta* **1989**, *72*, 1125.
[3] B. Liu, A. D. McLean, *J. Chem. Phys.* **1989**, *91*, 2348, and references therein.
[4] J. J. Novoa, B. Tarron, M.-H. Whangbo, J. M. Williams, *J. Chem. Phys.* **1991**, *95*, 5179.
[5] The C–H bond of each C–H···O bond was aligned along the bisecting line of the H-O-H angle of H_2O for $CH_4 \cdots OH_2$, $CH_4 \cdots (OH_2)_2$, and $CH_4 \cdots (OH_2)_3$. The C_{2v} and C_{3v} point group symmetries were assumed for $CH_4 \cdots (OH_2)_2$ and $CH_4 \cdots (OH_2)_3$, respectively. All fragment geometries were fixed.
[6] S. F. Boys, F. Bernardi, *Mol. Phys.* **1970**, *19*, 553.
[7] With the same geometrical constraints, the MP2 calculations with a NHFL basis set gave 0.52 kcal mol^{-1} for the C–H···O bond energy in $CH_4 \cdots OH_2$ [4].
[8] M. J. S. Dewar, E. G. Zoebisch, E. F. Healey, J. J. P. Stewart, *J. Am. Chem. Soc.* **1985**, *107*, 3902.
[9] For a recent review, see A. J. Pertsin, A. I. Kitaigorodsky, *The Atom-Atom Potential Method*, Springer, Berlin, **1987**.
[10] D. E. Williams, D. J. Houpt, *Acta Crystallogr. Sect. B* **1986**, *42*, 286.
[11] K. Mirsky, *Acta Crystallogr. Sect. A* **1976**, *32*, 199.
[12] J. J. P. Stewart, Quantum Chemistry Program Exchange, p. 455.
[13] S. R. Cox, L.-Y. Hsu, D. E. Williams, *Acta Crystallogr. Sect. A* **1981**, *37*, 293.
[14] For a review, see: J. M. Williams, H. H. Wang, T. J. Emge, U. Geiser, M. A. Beno, P. C. W. Leung, K. D. Carlson, R. J. Thorn, A. J. Schultz, M.-H. Whangbo, *Prog. Inorg. Chem.* **1987**, *35*, 51.

Structural Variations Observed in the $[Bi(O_2CCF_3)_4Ph]^{2-}$ Anion: Selective Cation–Anion Interactions through Hydrogen Bonds**

By *Steven R. Breeze* and *Suning Wang**

Hydrogen bonds are known to play an essential role in determining the shape and function of molecules,[1] and their influence on the structures of solids is widely recognized.[2] The controlled assembly of molecules by hydrogen bonding is a frequently used strategy in the synthesis of supramolecules and inorganic precursor compounds for solid-state materials.[3] However, systematic examinations on the effect of hydrogen bonds on the geometry and stability of inorganic complexes are scarce. We report here on the anionic bismuth complex $[Bi(O_2CCF_3)_4Ph]^{2-}$, whose solid-state structure can be dramatically influenced by interactions with its counterion by the formation of hydrogen bonds.

The reaction of $BiPh_3$ with trifuoroacetic acid and *N,N,N',N'*-tetramethyl-1,3-propanediamine (tmpda) in a 1:4:1 ratio produced **1** in good yield. The anion in com-

$[Me_2NH(CH_2)_3NHMe_2][Bi(O_2CCF_3)_4Ph]$ **1**

pound **1** displays an cuplike structure[4] in the solid state as shown in Figure 1. The Bi^{3+} ion is coordinated by one carbon atom of the phenyl group and four oxygen atoms of the acetate ligands with normal bond lengths and a square-pyramidal geometry. The lone pair of electrons probably occupies the vertex of the octahedron. The bismuth atom is 0.27 Å above the O1-O3-O1'-O3' plane. Compound **1** has a twofold proper rotation axis; the diammonium cation is disordered over this axis. The most unusual feature of the anion is the orientation of the four trifluoroacetato ligands—they

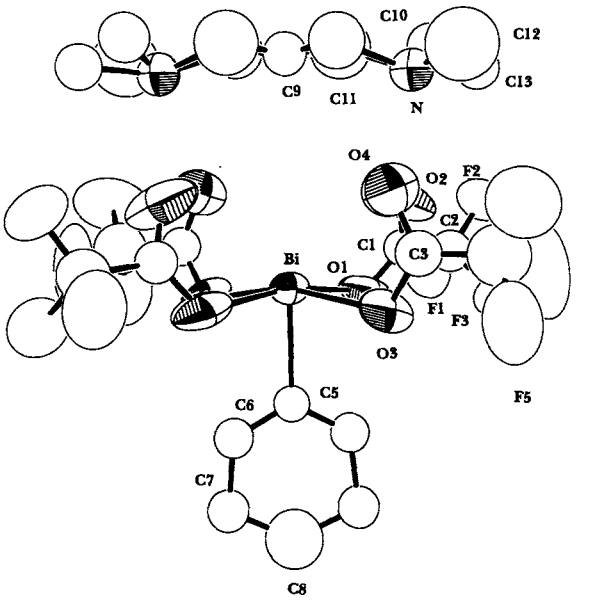

Fig. 1. Crystal structure of **1**; ellipsoids at the 50% probability level. Selected distances [Å] and angles [°]: Bi-O1 2.38(3), Bi-O3 2.42(2), Bi-C5 2.28(4); O1-Bi-O1' 169(1), O3-Bi-O3' 165(1).

[*] Prof. Dr. Suning Wang, S. R. Breeze
Department of Chemistry and Biochemistry
University of Windsor, Windsor, Ontario, N9B 3P4 (Canada)

[**] This work was supported by the Natural Sciences and Engineering Research Council of Canada.

all point up to form a cuplike shape. One would expect these acetato ligands to orient away from each other to minimize the repulsion between the negatively charged oxygen centers. We believe that this unusual orientation of the acetato ligands is caused by the interactions between the diammonium cations and the trifluoroacetato ligands through hydrogen bonds. The N–O2 and N–O4 distances, (2.82(4) and 3.01(4) Å, respectively) are comparable to the sum of van der Waals radii (3.05 Å) and indicative of weak hydrogen bonds.[5] Although the positions of the protons were not located by the X-ray diffraction experiment, we believe that they are bonded to the nitrogen atoms of the diamine and form hydrogen bonds to the oxygen atoms of the acetato ligands, since the amine is a much stronger Lewis base than the trifluoroacetato ligand. The C1-O2···N and C3-O4···N angles are 173(3) and 139(3)°, respectively. The two protons act as a "glue" to hold the four oxygen atoms and two nitrogen atoms together. In addition to the hydrogen bonds, the perfect match of the shape of the diammonium cation to that of the $[Bi(O_2CCF_3)_4Ph]^{2-}$ anion also appears to play an important role. For example, the largest separations between the oxygen atoms of the acetato ligands in the anion of **1** are 5.62(3) Å for O2···O2′ and 5.51(3) Å for O4···O4′, which are comparable to the N···N separation (4.92(3) Å) of the tmpda cation. When the tmpda cation in **1** was replaced by the tetramethylethylenediammonium (tmeda) cation, in which the span between the two ammonium groups is one CH_2 group shorter than that of tmpda (N···N = 3.67(7) Å), a dramatic structural change was observed, as is evident in Figure 2.[4]

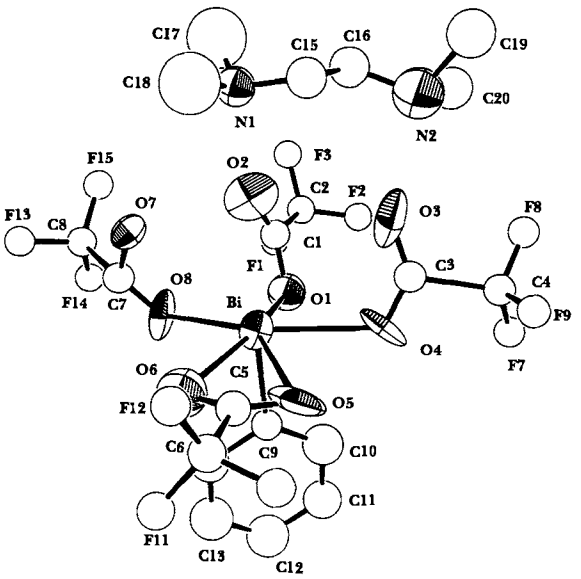

Fig. 2. Crystal structure of **2**; ellipsoids at the 50% probability level. Selected distances [Å] and angles [°]: Bi-O1 2.62(3), Bi-O4 2.50(4), Bi-O5 2.59(4), Bi-O6 2.34(4), Bi-O8 2.32(3), Bi-C9 2.20; O1-Bi-O4 71(1), O1-Bi-O8 71(1), O8-Bi-O6 87(1), O6-Bi-O5 52(1), O5-Bi-O4 78(1).

In contrast to **1** in compound **2** three of the four acetato ligands point up with respect to the phenyl ring; the fourth

$[Me_2NH(CH_2)_2NHMe_2][Bi(O_2CCF_3)_4Ph]$ **2**

acetato ligand chelates the Bi^{3+} ion and is in the equatorial plane. The five oxygen atoms coordinated to the bismuth center are coplanar, and the bismuth atom is 0.23 Å above the plane. The dihedral angle between the equatorial plane and the phenyl ring is 92.4°. Therefore, the coordination sphere of the Bi^{3+} ion could be described as pentagonal-pyramidal. Although such coordination geometry is uncommon for bismuth, it has been observed in some antimony compounds.[6] The ammonium groups are hydrogen-bonded to O2 and O3 only, as indicated by the N1–O2 and N2–O3 distances, 2.72(6) and 2.61(7) Å, respectively. The span between the two ammonium groups in tmeda in **2** is apparently too short for the formation of hydrogen bonds to all four oxygen atoms of the acetato ligands. Consequently, the $[Bi(O_2CCF_3)_4Ph]^{2-}$ anion no longer has a cuplike shape.

The effect of the shape of the diammonium cation on hydrogen bonds and the geometry of the $[Bi(O_2CCF_3)_4Ph]^{2-}$ anion can be further illustrated by the structure[4] of **3**.

$[Me_2NHCH_2CH(OH)CH_2NHMe_2][Bi(O_2CCF_3)_4Ph]$ **3**

Compound **3** was obtained in good yield by the reaction of $BiPh_3$ with trifluoroacetic acid and 1,3-bis(dimethylamino)-2-propanol (bdmap) in a 1:4:1 ratio. The bdmap diammonium cation in **3** is very similar to tmpda in **1** except that the middle CH_2 group in the tmpda is replaced by a CH(OH) group. Crystals of **3** are isomorphous with those of **1**. The structure of the anion in **3** (Fig. 3) resembles that of **1**—a cuplike structure—except that this "cup" is no longer empty, but hosting an OH group. The two ammonium groups are

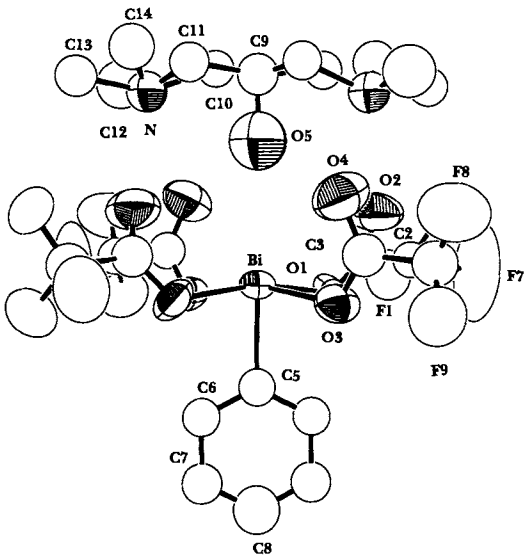

Fig. 3. Crystal structure of **3**; ellipsoids at the 50% probability level. Selected distances [Å] and angles [°]: Bi-O1 2.39(1), Bi-O3 2.40(1), Bi-C5 2.26(3); O1-Bi-O1′ 168.2(7), O3-Bi-O3′ 165.5(7).

hydrogen-bonded to the four oxygen atoms of the acetato ligands in a similar fashion as found in **1** (N–O2 = 2.76(2), N–O4 = 3.26(3) Å). The OH group shares its proton with the four oxygen atoms of the acetato ligands, as evidenced by the distances of O5–O2 = 3.19(2), O5–O4 = 3.03(2) Å. The suitable size of the cavity in the anion and the formation of hydrogen bonds between the OH group and the acetato oxygen atoms are apparently responsible for enclosure of the OH group. However, they are not the dominating factors in determining the cuplike shape of the anion, since **1** has a

similar structure to that of **3** and no OH group. We believe that hydrogen-bonding interactions between the ammonium group and the acetato ligands in **3** play a critical role in shaping the molecule as they do in **1**. Bi^{III} complexes are known to display versatile structural features in the solid state as a result of the presence of a lone pair of electrons.[6-9] However, the structural variations of the $[Bi(O_2CCF_3)_4Ph]^{2-}$ anion observed in compounds **1**–**3** are unprecedented and can only be explained by selective cation–anion interactions through hydrogen bonds. Such phenomena could also exist in other inorganic complex systems. The hydrogen bonds between the cation and anion appear to influence the stability of bismuth complexes in this system. For example, the neutral compound $Bi(O_2CCF_3)_2Ph$ could not be isolated due to its poor stability,[9] whereas the compounds described here with the $[Bi(O_2CCF_3)_4Ph]^{2-}$ anion were obtained readily in the presence of aliphatic diamines. Furthermore, compounds **1** and **2** are stable in solution for days while **3** decomposes rapidly upon dissolution. Further investigation of these cation-dependent salts is in progress.

Experimental Procedure

1: $BiPh_3$ (200 mg, 0.45 mmol) was dissolved in 15 mL of THF. 0.14 mL (1.87 mmol) of trifluoroacetic acid was added to the solution. After the reaction mixture was stirred for 1 h, 78 mg (0.45 mmol) of tmpa was added. After 1 h the solution was concentrated to about 5 mL, and hexane was added to crystallize the product. The colorless crystals of **1** were collected after 24 h (250 mg, 0.26 mmol, 63% yield). Correct C,H,N analysis. ^1H NMR ([D$_6$]acetone): δ = 2.52 (m, CH_2, 2H), 3.07 (s, CH_3, 12H), 3.47 (t, CH_2, 4H), 7.37 (m, CH, 1H), 7.91 (m, CH, 2H), 8.90 (m, CH, 2H).

Compounds **2** and **3** were obtained by the similar procedure. Satisfactory C,H,N analysis for **2**, correct C,H,N analysis for **3**. 1H NMR ([D$_8$]acetone) for **2**: δ = 3.16 (s, CH_3, 12H), 3.98 (s, CH_2, 4H), 7.38 (m, CH, 1H), 7.92 (m, CH, 2H), 8.86 (m, CH, 2H); for **3**: δ = 3.14 (s, CH_3, 12H), 3.42 (q, CH, 2H), 3.53 (q, CH, 2H), 4.88 (m, CH, 1H), 7.39 (m, CH, 1H), 7.90 (m, CH, 2H), 8.88 (m, CH, 2H).

Received: October 14, 1992 [Z 5626 IE]
German version: *Angew. Chem.* **1993**, *105*, 605

[1] [1] G. A. Jeffery, W. Saenger, *Hydrogen Bonding in Biological Structures*, Springer, New York, **1991**.

[2] W. C. Hamilton, J. A. Ibers, *Hydrogen Bonding in Solids*, Benjamin, New York, **1968**; A. F. Wells, *Structural Inorganic Chemistry*, 4th ed., Clarendon, Oxford, **1975**.

[3] S. Wang, S. J. Trepanier, J. C. Zheng, Z. Pang, M. J. Wagner, *Inorg. Chem.* **1992**, *31*, 2118–2127; J.-M. Lehn, *Angew. Chem.* **1990**, *102*, 1347; *Angew. Chem. Int. Ed. Engl.* **1990**, *29*, 1304.

[4] Crystal data: **1**, $C_{21}H_{25}BiF_{12}O_8N_2$, M_r = 870.42, monoclinic, space group $C2/c$, a = 9.161(5), b = 16.617(6), c = 19.94(1) Å, β = 94.12(5)°, V = 3027 Å^3, Z = 4, ρ_{calc} = 1.90 g cm^{-3}; **2**, $C_{20}H_{23}BiF_{12}O_8N_2$, M_r = 856.41, orthorhombic, space group $Pna2_1$, a = 26.117(9), b = 13.176(4), c = 8.644(2) Å, V = 2974(2) Å^3, Z = 4, ρ_{calc} = 1.91 g cm^{-3}; **3**, $C_{21}H_{25}BiF_{12}O_9N_2$, M_r = 886.42, monoclinic, space group $C2/c$, a = 9.242(6), b = 16.53(1), c = 19.840(6) Å, β = 93.69(4)°, V = 3025(3) Å^3, Z = 4, ρ_{calc} = 1.95 g cm^{-3}. Colorless single crystals of **1**–**3** were obtained from THF by slow diffusion of hexane at 23 °C. The crystals were mounted on glass fibers and sealed from air with epoxy glue. Data were collected over the range $2° < 2\theta < 48°$ for all compounds on a Rigaku AFC6-S diffractometer ($Mo_{K\alpha}$ radiation, 50 kV, 35 mA, graphite monochromator). All data were processed on a VAX workstation 3520 by using the TEXSAN crystallographic package (version 5.0) and corrected for Lorentz-polarization effects. Empirical absorption corrections were applied for all crystals. The position of the *Bi* atom in all structures was determined by direct methods. The refinements converged at final R and R_w values of 0.082 and 0.087 for **1** (150 variables and 970 reflections), 0.072 and 0.072 for **2** (170 variables and 1190 reflections), 0.057 and 0.054 for **3** (152 variables and 1054 reflections), ($F_0^2 \geq 3\sigma(F_0^2)$), respectively. The high R factors for **1** and **2** were caused by the poor quality of the crystals which showed severe twinning problems. In all compounds the CF_3 groups displayed varied degrees of disorders which could also contribute to the poor quality of the structure determinations of **1** and **2**. The positions of hydrogen atoms in **2** were calculated. Their contributions were included in the final structural factors calculation. Further details of the crystal structure investigations may be obtained from the Fachinformationszentrum Karlsruhe, Gesellschaft für wissenschaftlich-technische Information mbH, D-W-7514 Eggenstein-Leopoldshafen 2 (FRG) on quoting the depository number CSD-56897, the names of the authors, and the journal citation.

[5] J. Emsley, *Chem. Soc. Rev.* **1980**, *9*, 91–124.

[6] C. A. McAuliffe in *Comprehensive Coordination Chemistry, Vol. 3* (Eds.: G. Wilkinson, R. D. Gillard, J. A. McCleverty), Pergamon, Oxford, **1987**, pp. 237–298.

[7] M. C. Massiani, R. Papiernik, L. G. Hubert-Pfalzgraf, J. C. Daran, *J. Chem. Soc. Chem. Commun.* **1990**, 301–302.

[8] E. Asato, W. L. Drissen, R. A. G. de Graaff, F. B. Hulsbergen, J. Reedijk, *Inorg. Chem.* **1991**, *30*, 4210–4218.

[9] D. H. R. Barton, B. Charpiot, E. T. H. Dau, W. B. Motherwell, C. Pascard, *Helv. Chim. Acta* **1984**, *67*, 586–599.

Novel Triselenidotantalum Halfsandwich Complexes**

By *Kazuyuki Tatsumi*,* *Hiroyuki Kawaguchi*, and *Kazuhide Tani*

The chemistry of soluble transition metal selenides is of interest to both material scientists and coordination chemists.[1] Selenides of electron-deficient group 4 and 5 transition metals are rare, however, because of the propensity of chalcogenides to form insoluble polymers. Recently, solid-state reactions[2] and unusual hydrothermal syntheses[3] provided an interesting series of early transition metal selenides. If these reactions are to be conducted at room temperature and in solution, a solubilizing coligand such as C_5Me_5(Cp*) must be employed. In exploring the chemistry of tantalum selenides with organic ligands we have discovered the novel triselenido halfsandwich complexes **1** and **2**.

$[Cp^*Ta(Se)_3Li_3Cl(thf)_3]$ **1**
$[Cp^*Ta(Se)_3Li_2(tmeda)_2]$ **2**

tmeda = *N*,*N*,*N*′,*N*′-tetramethylethylenediamine

Reaction of $[Cp^*TaCl_4]$ and 4–5 equiv "Li_2Se_2"[4a] in THF under argon gave an orange solution. Removal of the solvent in vacuo, extraction of the resulting orange solid residue with benzene, and recrystallization from THF/hexane afforded **1** as yellow crystals in 43% yield.[5a] In contrast, the analogous reaction of $[Cp^*TaCl_4]$ with 4–5 equiv "Li_2Se"[4b] in THF gave a deep-red solution from which **1** could not be isolated. The LiCl unit in **1** could be removed by treatment with excess tmeda in toluene to produce **2** as yellow crystals in 86% yield.[5b] The highly hygroscopic and

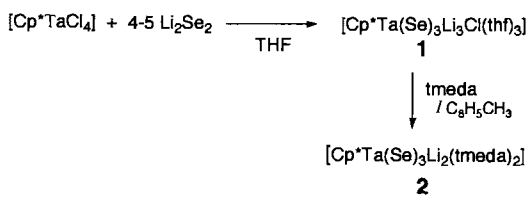

[*] Prof. Dr. K. Tatsumi, H. Kawaguchi, Prof. Dr. K. Tani
Department of Chemistry, Faculty of Engineering Science
Osaka University
Toyonaka, Osaka 560 (Japan)

[**] This research was supported in part by the Asahi Glass Foundation.

moderately air-sensitive complexes **1** and **2** were characterized by spectroscopy and X-ray structure analysis. Sharp ^{1}H NMR resonances in the expected range for Cp* indicate that **1** and **2** are diamagnetic, consistent with the d^0 electronic configuration of the tantalum center.

The molecular structures of **1** and **2** are shown in Figures 1 and 2, respectively.[6] The most important feature of these first organometallic compounds with three monoselenide anions is the common $[Cp^*Ta(Se)_3]^{2-}$ unit. There are no

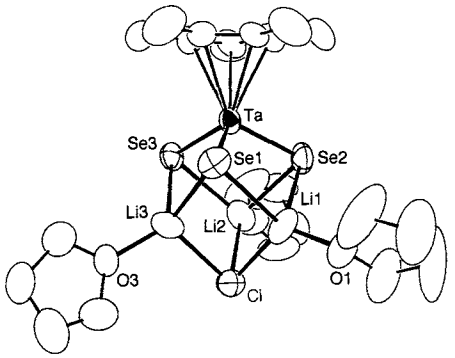

Fig. 1. Molecular structure of **1** (thermal ellipsoids at the 30% probability level). Selected bond lengths [Å]: Ta-Se1 2.406(2), Ta-Se2 2.395(2), Ta-Se3 2.407(2), Se1-Li1 2.64(2), Se1-Li3 2.64(5), Se2-Li1 2.54(4), Se2-Li2 2.57(3), Se3-Li2 2.62(3), Se3-Li3 2.59(4), Cl-Li1 2.38(3), Cl-Li2 2.36(3), Cl-Li3 2.39(4).

well-characterized examples of soluble tantalum selenides, and the $[TaSe_4]^{3-}$ ion is found only in extended solid-state structures. Examples of molecules with isostructural $[Cp^*Ta(E)_3]^{2-}$ units are limited to the hexagonal-prismatic cluster $[\{Cp^*Ta(S)_3Li_2(thf)_2\}_2]$ (**3**)[7] (E = S) and the trioxorhenium complex $[Cp^*Re(O)_3]$ (E = O).[8, 9] Group 5 metal selenides that have been structurally characterized include $[Cp'_2V_2Se_5]$ (Cp' = C_5H_4Me)[10] and $[Cp_3Nb_3(Se)_3(Se_2)Cl_2]$.[11]

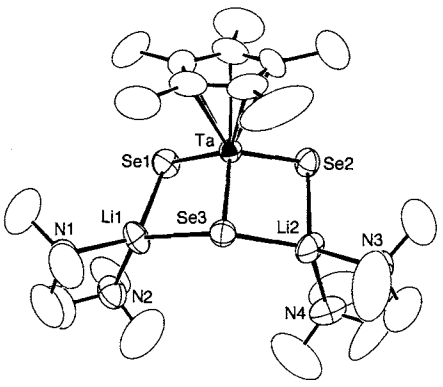

Fig. 2. Molecular structure of **2** (thermal ellipsoids at the 50% probability level). Selected bond lengths [Å] and angles [°]: Ta-Se1, 2.389(2); Ta-Se2, 2.384(2); Ta-Se3, 2.441(2); Se1-Li1, 2.60(3); Se2-Li2, 2.55(3); Se3-Li1, 2.56(3); Se3-Li2, 2.54(3); Se1-Li1-Se3, 94.7(8); Se2-Li2-Se3, 97.1(9).

In **1**, three Li atoms are bound to the $[Cp^*TaSe_3]$ fragment and each bridges two selenido ligands. A Cl atom caps the Li atoms, completing the $TaSe_3Li_3Cl$ cubane framework. Each Li atom is also bound to a THF molecule. The three Ta–Se distances are nearly the same, and the Cl atom is approximately equidistant from three Li atoms. Since all the bond lengths within the cubane core fall in a relatively narrow range (2.36–2.64 Å), the geometry is close to ideal except for the somewhat large Se-Ta-Se angles (103.68(7)–103.87(7)°). In comparison, the sulfur analogue $[Cp^*Ta(S)_3Li_3Cl(tmeda)_2(\mu\text{-tmeda})]$ (**4**) has an open cubane core.[7b] As the Li atoms in **4** are coordinated by tmeda instead of THF, two edges (a Li–S bond and a Li–Cl bond) are missing from the cubane core, probably because of the preferred tetrahedral coordination of the Li atoms.[12]

The two lithium atoms in **2** bridge two selenido ligands and are further coordinated by two nitrogen atoms of the tmeda ligands. The structure of **2** is less symmetrical than that of **1** because of the missing LiCl unit. The Se1-Ta-Se2 angle opens up to 106.26(8)°; the other Se-Ta-Se angles are 103.63(5)° and 104.54(6)°. The Ta–Se3 bond is longer than the Ta–Se1(Se2) bond by 0.05 Å.

The average Ta–Se bond lengths of 2.403 Å (**1**) and 2.405 Å (**2**) are slightly longer than that in $K_3[TaSe_4]$ (2.368 Å),[2d] but they are significantly shorter than the sum of the ionic radii of Ta^V and Se^{2-} (2.62 Å).[13] On the other hand, the Raman spectra of **1** and **2** exhibit bands at 265 cm^{-1} and 263 cm^{-1}, respectively, arising from Ta–Se stretching vibrations, which are at higher frequencies than the A_1 mode stretch (249 cm^{-1}) of $[TaSe_4]^{3-}$.[14] These observations indicate some Ta–Se π bonding in **1** and **2**.

Compounds **1** and **2** are readily soluble in THF, whereas they decompose gradually in acetonitrile to form red precipitates. Although the crystals of **1** are hardly soluble in nonpolar solvents, those of the tmeda adduct **2** are soluble in benzene and toluene. In THF, both **1** and **2** form yellow solutions that exhibit a UV/VIS absorption band at 341 nm. The sulfur analogues **3** and **4** form light-yellow solutions in THF that absorb at 302 nm and 301 nm. The lowest energy bands are assigned to charge-transfer transitions from orbitals of the chalcogenide lone pair to the lowest vacant d orbital of tantalum. The sulfide-to-selenide red shift (0.46 eV) is comparable to the difference in the first ionization potentials of these chalcogens (0.59 eV).[15]

Our synthesis of **1** and **2** provides a convenient entry to soluble tantalum selenides. The lithium cations bound to the selenium atoms may be easily replaced by suitable heteroelements to form a variety of heteronuclear selenide clusters.

Received: November 5, 1992 [Z 5666 IE]
German edition: *Angew. Chem.* **1993**, *105*, 627

[1] a) D. Fenske, J. Ohmer, J. Hachgenei, K. Merzweiler, *Angew. Chem.* **1988**, *100*, 1300; *Angew. Chem. Int. Ed. Engl.* **1988**, *27*, 1277; b) *Superconductivity in Ternary Compounds I* (Eds.: O. Fischer, M. B. Maple), Springer, Berlin, **1982**; c) M. A. Ansari, J. A. Ibers, *Coord. Chem. Rev.* **1990**, *100*, 223; d) S. C. Lee, R. H. Holm, *Angew. Chem.* **1990**, *102*, 868; *Angew. Chem. Int. Ed. Engl.* **1990**, *29*, 840; e) T. Saito, N. Yamamoto, T. Nagase, T. Tsuboi, K. Kobayashi, T. Yamagata, H. Imoto, K. Unoura, *Inorg. Chem.* **1990**, *29*, 764.

[2] a) C.-N. Chau, R. W. M. Wardle, J. A. Ibers, *Inorg. Chem.* **1987**, *26*, 2740; b) D. Kang, J. A. Ibers, *ibid.* **1988**, *27*, 549; c) S. Schreiner, L. E. Aleandri, D. Kang, J. A. Ibers, *ibid.* **1989**, *28*, 393; d) M. Latroche, J. A. Ibers, *ibid.* **1990**, *29*, 1503; e) Y.-j. Lu, J. A. Ibers, *ibid.* **1991**, *30*, 3317; f) A. C. Sutorik, M. G. Kanatzidis, *J. Am. Chem. Soc.* **1991**, *113*, 7754.

[3] a) J.-H. Liao, M. G. Kanatzidis, *J. Am. Chem. Soc.* **1990**, *112*, 7400; b) *Inorg. Chem.* **1992**, *31*, 431.

[4] a) "Li_2Se_2" was made from the stoichiometric reaction of Li metal with elemental Se in liquid ammonia. The liquid ammonia was evaporated off under a flow of dry oxygen-free Ar to give a reddish-brown powder. Before it was used, this powder was washed a few times with THF to give a flesh colored powder. The Se/Li ratio of the red THF washings is presumably higher than in "Li_2Se_2", and the resulting flesh-colored powder most likely contains Li_2Se. b) "Li_2Se" was prepared as white powder from the reaction of Li and Se_8 (16:1) in liquid ammonia.

[5] All manipulations were carried out under an argon atmosphere with dry solvents. Complexes **1** and **2** gave satisfactory elemental analysis. a) $[Cp^*Ta(Se)_3Li_3Cl(thf)_3]$ **1**: yellow crystals; ^{1}H NMR (270 MHz, $[D_8]$THF, 30 °C): δ = 2.40 (s, Cp*); UV/VIS (THF): $\lambda_{max}(\varepsilon)$ = 341 nm

(19000); Raman (crystals): $\tilde{\nu} = 265\ cm^{-1}$ (s, Ta = Se). b) [Cp*Ta(Se)$_3$Li$_2$(tmeda)$_2$] **2**: yellow crystals; ^{1}H NMR (270 MHz, C_6D_6, 30 °C): $\delta = 2.51$ (s, 15H, Cp*), 2.34 (s, 24H, $(CH_3)_2NCH_2CH_2N(CH_3)_2$), 2.15 (s, 8H, $(CH_3)_2NCH_2CH_2N(CH_3)_2$); UV/VIS (benzene): $\lambda_{max}(\varepsilon) = 341$ nm (21000); Raman (crystals): $\tilde{\nu} = 263\ cm^{-1}$ (s, Ta = Se).

[6] A single crystal of **1** or **2** was mounted in a thin-walled glass capillary and sealed under Ar. Reflection data were measured on a Rigaku AFC5R diffractometer at ambient temperature using the ω-2θ scan technique. The intensity data were corrected for Lorentz and polarization effects, and empirical absorption corrections were applied. The structure was solved and refined by using a TEXSAN program package. a) Crystal data for **1**, monoclinic, $P2_1/n$ (No. 14), $a = 8.681(2)$, $b = 16.600(9)$, $c = 21.817(5)$ Å, $\beta = 90.29(2)°$, $V = 3144(2)$ Å^3, $Z = 4$, $\varrho_{calc} = 1.744\ g\,cm^{-3}$, $2\theta_{max}(Mo_{K\alpha}) = 50.1°$. The structure was solved by direct methods and was refined to $R = 0.051$ and $R_w = 0.056$ by the full-matrix least-squares method for 2961 observed reflections with $I > 3.0\,\sigma(I)$ (298 variables, GOF = 2.03). b) Crystal data for **2**, orthorhombic, $Pna2_1$ (No. 33), $a = 23.484(5)$, $b = 9.949(2)$, $c = 13.676(2)$ Å, $V = 3195(2)$ Å^3, $Z = 4$, $\varrho_{calc} = 1.661\ g\,cm^{-3}$, $2\theta_{max}(Mo_{K\alpha}) = 50.8°$. The structure was solved by the Patterson method and was refined to $R = 0.034$ and $R_w = 0.043$ using the full-matrix least squares method for 2407 observed reflections with $I > 3.0\,\sigma(I)$ (288 variables, GOF = 1.83). Further details of the crystal structure investigations may be obtained from the Fachinformationszentrum Karlsruhe, Gesellschaft für wissenschaftlich-technische Information mbH, D-W-7514 Eggenstein-Leopoldshafen 2 (FRG), on quoting the depository number CSD-56887, the name of the authors, and the journal citation.

[7] a) K. Tatsumi, Y. Inoue, A. Nakamura, R. E. Cramer, W. VanDoorne, J. W. Gilje, *J. Am. Chem. Soc.* **1989**, *111*, 782; b) K. Tatsumi, Y. Inoue, H. Kawaguchi, M. Kohsaka, A. Nakamura, R. E. Cramer, W. VanDoorne, G. J. Taogoshi, P. N. Richmann, *Organometallics* **1993**, *12*, in press.

[8] a) W. A. Herrmann, R. Serrano, H. Bock, *Angew. Chem.* **1984**, *96*, 364; *Angew. Chem. Int. Ed. Engl.* **1984**, *23*, 383; c) J. Okuda, E. Herdtweck, W. A. Herrmann, *Inorg. Chem.* **1988**, *27*, 1254.

[9] A. H. Klahn-Oliva, D. Sutton, *Organometallics* **1984**, *3*, 1313.

[10] A. L. Rheingold, C. M. Bolinger, T. B. Rauchfuss, *Acta Crystallogr. Sect. C* **1986**, *42*, 1878.

[11] D. Fenske, P. G. Maué, *Z. Naturforsch. B* **1989**, *44*, 531.

[12] K. Gregory, P. von R. Schleyer, R. Snaith, *Adv. Inorg. Chem.* **1991**, *37*, 47.

[13] R. D. Shannon, *Acta Crystallogr. Sect. A* **1976**, *32*, 751.

[14] a) A. Müller, K. H. Schmidt, K. H. Tytko, J. Bouwma, F. Jellinek, *Spectrochim. Acta Part A* **1972**, *28*, 381; b) A. Müller, E. Diemann, R. Jostes, H. Bögge, *Angew. Chem.* **1981**, *93*, 957; *Angew. Chem. Int. Ed. Engl.* **1981**, *20*, 934.

[15] C. E. Moore, *Atomic Energy Levels*, National Bureau of Standards, Washington, **1949**.

$[Cr(CO)_5PCl_3]$—A P_1 Building Block for the Formation of Complexes with *cyclo*-P_x Ligands ($x = 3, 5$)**

By *Manfred Scheer,* Gabriele Friedrich*, and *Kay Schuster*

Coordination compounds with "naked" P_x ligands ($x > 2$) are obtained mainly from white phosphorus and the corresponding metal complex fragment.[1] Only two references of P–P bond-forming reactions starting from PX_3 (X = Cl, Br), in which P_2 ligands are formed, have been reported, namely the formation of $[Co_2(CO)_6(\mu,\eta^2\text{-}P_2)]$[4] and $[Co_2(CO)_6\{(\mu,\eta^2\text{-}P_2)(ML_n)_2\}]$ ($ML_n = M(CO)_5$, $CpMn(CO)_2$; M = Cr, W).[5]

Thus, we were surprised to find that from $[Cr(CO)_5PCl_3]$ and $K[MoCp^x(CO)_3]$ (Cp^x = Cp, Cp′, Cp″; Cp′ = η^5-C_5H_4-*t*Bu, Cp″ = η^5-1,3-C_5H_3tBu$_2$) [Eq. (a)] the main products formed were the complexes **1a–c** which contained *cyclo*-P_3 ligands. If $K[FeCp''(CO)_2]$ is used, the pentaphosphaferrocene derivative **3** is formed [Eq. (b)].

$$[Cr(CO)_5PCl_3] + K[MoCp^x(CO)_3] \xrightarrow[-KCl,\ -[Cr(CO)_6],\ -[MoCp^x(CO)_3]_2]{-78\,°C,\ THF} \mathbf{1a}, Cp^x = Cp;\ \mathbf{1b}, Cp^x = Cp';\ \mathbf{1c}, Cp^x = Cp'' \quad (a)$$

$$[Cr(CO)_5PCl_3] + K[FeCp''(CO)_2] \xrightarrow[-KCl,\ -[Cr(CO)_6],\ -[\{FeCp''(CO)_2\}_2]]{-78\,°C,\ THF} \mathbf{3} \quad (b)$$

According to the results of ^{31}P NMR spectroscopic investigations on the crude reaction mixtures, complexes **1a–c**, which have MoP_3 frameworks, are formed as the main products (**1a, b**: 92%, **1c**: 70%) as shown in (a). The only by-products are the Mo_2P_2 complexes **2a–c** and $[Mo_2Cp''_2(CO)_2(\mu,\eta^2\text{-}P_2)_2]$. Because the oxidized product

$[Mo_2Cp^x_2(CO)_4(\mu,\eta^2\text{-}P_2)]$ **2a**, Cp^x = Cp; **2b**, Cp^x = Cp′; **2c**, Cp^x = Cp″

$[\{Mo(CO)_3Cp^x\}_2]$ is formed in large amounts workup by column chromatography is necessary, leading to a loss in yield. The isolated yields amount to approximately 25% and are thus greater than that reported for $[MoCp^x(CO)_2(\eta^3\text{-}P_3)]$ (Cp^x = Cp, Cp*; Cp* = η^5-C_5Me_5).[6] The pentaphosphaferrocene derivative **3** was formed in 30% yield together with $[FeCp''(CO)_2PCl_2]$ ($\delta(^{31}P) = 369.2$). Compound **3** is isolated after sublimation in 10% yield.

The complexes formed are yellow (**1**), orange (**2**), and green (**3**) crystalline solids, which are sparingly soluble in *n*-pentane but readily soluble in CH_2Cl_2, benzene, and THF. Their properties and spectroscopic data (Table 1) are similar to those of isostructural compounds, which were prepared with other Cp^x ligands by the cothermolysis of P_4 with $[\{MCp^x(CO)_2\}_2]$ (M = Mo; Cp^x = Cp, Cp*;[6] M = Fe, Cp^x = Cp*[7]).

Table 1. Selected spectroscopic data of the compounds **1–4**.

$^{31}P\{^1H\}$ NMR (32.438 MHz, H_3PO_4 ext., 301 K, C_6D_6): **1a**: $\delta = -351.0$ (s); **1b**: −347.5 (s); **1c**: −348.9 (s); **2c**: −57.7 (s); **3**: 165.7 (s); **4**: 207.9 (s). – ^{13}C NMR (50.31 MHz, 301 K): **3**: $\delta = 30.38$ (s, CH_3), 31.51 (s, tert-C), 70.32 (s), 72.08 (s), 109.78 (s). – ^{1}H NMR (200.17 MHz, C_6D_6, 301 K): **1a**: $\delta = 4.20$ (s); **1b**: 0.90 (s, 9H), 4.32 (m, 2H), 4.41 (t, 2H, J(HH) = 2.0 Hz); **1c**: 0.97 (s, 18H), 4.52 (d, 2H), 4.87 (t, 1H); **2c**: 1.26 (s, 18H), 5.15 (t, 1H), 5.23 (d, 2H); **3**: 0.99 (s, 18H), 3.61 (d, 2H), 3.63 (t, 1H, J(HH) = 0.5).

IR (*n*-hexane): **1a**: $\tilde{\nu}$(CO)[cm^{-1}] = 1997 (s), 1941 (s); **1b**: 1999 (m), 1944 (m); **1c**: 1995 (s), 1937 (s); **2c**: 1983 (s), 1922 (s), 1902 (m), 1853 (w); **4**: 2077 (m), 2013 (m, sh), 1967 (vs, br).

EI-MS (70 eV, 150 °C): **1a**: *m/z* 312 (M^+, 38%), 256 ($M^+ - 2CO$, 100); **1b**: 368 (M^+, 46), 340 ($M^+ - CO$, 38), 312 ($M^+ - 2CO$, 100); **1c**: 424 (M^+, 25), 396 ($M^+ - CO$, 20), 368 ($M^+ - 2CO$, 96); **2c**: 724 (M^+, 5), 612 ($M^+ - 4CO$, 30); **3**: 388 (M^+, 100), 326 ($M^+ - P_2$, 97), 62 (P_2, 56); **4**: 588 (M^+, 28), 558 ($M^+ - CO$, 5), 551 ($M^+ - Cl$, 8), 446 ($M^+ - 5CO$, 15).

[*] Dr. M. Scheer,[+] G. Friedrich, Dipl.-Chem. K. Schuster
Institut für Allgemeine und Anorganische Chemie der Universität
Weinbergweg 16, D-O-4050 Halle (Saale) (FRG)

[+] Present address:
Department of Chemistry, Chemistry Building Indiana University
POB 242, Bloomington, IN 47405 (USA)

[**] This work was supported by the Deutsche Forschungsgemeinschaft, the Fonds der Chemischen Industrie, and the Deutsche Akademische Austauschdienst. We thank Prof. Dr. O. J. Scherer for his support of this work.

The influence of the $[Cr(CO)_5]$ complex fragment on the reactions (a) and (b) is of decisive importance. If these reactions are carried out starting from noncomplexed PCl_3, the percentage of P_2 derivatives formed increases considerably, and in the case of the reaction of PCl_3 with Cp″Mo complexes, **2c** is afforded as the main product. In the corresponding reaction (b) **3** is no longer formed. Thus, the pentacarbonylchromium(0) unit supports the multiple P–P linkage in the coordination sphere of transition metals. Assumptions that metallaphosphaacetylenes of the type $L_nM{\equiv}P$[8] ($ML_n = [Cr(CO)_n]$ ($n = 3-5$) or $[MCp^x(CO)_n]$, M = Mo or Fe ($n = 3$ or 2)) are intermediates of reactions (a) and (b) were not confirmed by experiments. If the reaction (a) is carried out at various temperatures (−78°C, −40°C, 25°C) in the presence of 2,3-dimethylbutadiene, the same products are formed as from the corresponding reactions without dimethylbutadiene. Thus, a greater importance must be attached to the description of the formation pathway of a stepwise P–P linkage through di- and triphosphorus compounds. The ability of the $[Cr(CO)_5]$ complex fragments to abstract CO,[9] leading to the formation of $[Cr(CO)_6]$ and thus to the production of $[MoCp^x(CO)_2]$ or [FeCp″] units is also of decisive importance. The results of the reaction of $[Cr(CO)_5PCl_3]$ with $Na_2[Cr_2(CO)_{10}]$ indicate P–P bond formation since, in addition to $[\{Cr(CO)_5\}_2PCl]$,[10] the diphosphane **4** is obtained as the main product [Eq. (c)].

$$3[Cr(CO)_5PCl_3] + 2Na_2[Cr_2(CO)_{10}] \xrightarrow[-[Cr(CO)_6]\ -[\{Cr(CO)_5\}_2PCl]\ -4NaCl]{-78\,^\circ C,\ THF} [\{Cr(CO)_5\}Cl_2PPCl_2\{Cr(CO)_5\}] \quad (c)$$

4

The yellow microcrystalline compound **4** is sparingly soluble in *n*-pentane but readily soluble in CH_2Cl_2, toluene, and THF. Compound **4** is stable in air for a limited period but should be stored in the dark under an inert gas atmosphere. The spectroscopic data of **4** (Table 1) are in accordance with those given by Fritz et al., who prepared **4** by electrochemical reduction of $[Cr(CO)_5PCl_3]$.[11]

Further investigations starting from $[Cr(CO)_5PCl_3]$ have shown that P_x ligands are also formed by reactions with other transition metallates. Furthermore, this method of synthesis also appears to be applicable to the heavier homologues of Group 15.

Experimental Procedure

1–3: $K[MCp^x(CO)_n]$ (M = Mo: Cp^x = Cp, Cp′, Cp″, $n = 3$; M = Fe: Cp^x = Cp″, $n = 2$) (3.75 mmol) was added to a solution of $[Cr(CO)_5PCl_3]$ (1.25 mmol) (prepared from $[Cr(CO)_5(thf)]$ and PCl_3 at room temperature) in THF (15 mL) and cooled to −78°C. The solution turned red. It was stirred for one hour at this temperature and then slowly allowed to warm up to room temperature. The solvent was then removed under vacuum and the residue was taken up in benzene (15 mL). Subsequently, KCl was filtered off and the solvent was again removed under vacuum.

For the workup of the molybdenum complexes the solid was taken up in CH_2Cl_2 (15 mL) and adsorbed onto silica gel (10 cm^3). This mixture was dried under vacuum and then applied to a column (silica gel, 35 × 2.5 cm). The *cyclo*-P_3 complexes **1a–c** were eluted as yellow fractions with *n*-hexane or *n*-hexane/toluene (2:1). After recrystallization from *n*-pentane these fractions precipitated in the form of yellow needles (**1a**: 30 mg (23%), m.p. 125°C; **1b**: 43 mg (22%), m.p. 112°C; **1c**: 60 mg (26%), m.p. 98°C). With *n*-hexane/toluene (1:1) **2a–c** were obtained as a mixture with $[\{MoCp^x(CO)_2\}_2]$. Compound **2c** could be isolated from this mixture by recrystallization from *n*-pentane in the form of orange crystals (15 mg; 4%).

To isolate the green needlelike crystals of **3**, the *n*-pentane extract from the reaction mixture was evaporated to dryness and sublimed at 120°C/10^{-4} Torr (**3**: 25 mg (10%), m.p. 115–118°C).

4: $[Cr(CO)_5PCl_3]$ (6 mmol) was allowed to react with $Na_2[Cr_2(CO)_{10}]$ (1.7 g, 4 mmol) as described above and then worked up. The residue was suspended in *n*-pentane (30 mL), transferred to a frit and extracted with hot *n*-pentane until the filtered extracts were colorless. 0.6 g of a mixture of **4** and $[Cr(CO)_6]$ was recrystallized from this solution at 5°C. This mixture was filtered and the solid dried. The chromium hexacarbonyl was sublimed off at 40°C/10^{-3} Torr, leaving microcrystalline, yellow **4** (0.55 g, 30%). The filtrate contained $[\{Cr(CO)_5\}_2PCl]$ as the main component.

Received: November 12, 1992 [Z 5678 IE]
German version: *Angew. Chem.* **1993**, *105*, 641

[1] Reviews: M. Scheer, E. Herrmann, *Z. Chem.* **1990**, *30*, 41-55; O. J. Scherer; *Angew. Chem.* **1990**, *29*, 1137-1155; *Angew. Chem. Int. Ed. Engl.* **1990**, *29*, 1104-1122. Furthermore, for example, M^IP_5 (M^I = Li, K) [2] and $[(C_5Me_5)P]_3$ [3] were used as starting materials.

[2] M. Baudler, T. Etzbach, *Angew. Chem.* **1991**, *103*, 590–591; *Angew. Chem. Int. Ed. Engl.* **1991**, *30*, 580–582.

[3] P. Jutzi, R. Kross, *Chem. Ber.* **1988**, *121*, 1399–1401.

[4] A. Vizi-Orosz, G. Palyi, L. Marko, *J. Organomet. Chem.* **1973**, *60*, C25–C26.

[5] H. Lang, L. Zsolnai, G. Huttner, *Angew. Chem.* **1983**, *95*, 1017; *Angew. Chem. Int. Ed. Engl.* **1983**, *22*, 976–977; *Angew. Chem. Suppl.* **1983**, 1463–1476.

[6] O. J. Scherer, H. Sitzmann, G. Wolmershäuser, *J. Organomet. Chem.* **1984**, *268*, C9–C12; *Acta Crystallogr. Sect. C* **1985**, *41*, 1761–1763; *Angew. Chem.* **1985**, *97*, 358–360; *Angew. Chem. Int. Ed. Engl.* **1985**, *24*, 351–353.

[7] O. J. Scherer, T. Brück, *Angew. Chem.* **1987**, *99*, 59; *Angew. Chem. Int. Ed. Engl.* **1987**, *26*, 59; O. J. Scherer, T. Brück, G. Wolmershäuser, *Chem. Ber.* **1988**, *121*, 935–938.

[8] Indications of the possible existence of metallaphosphaacetylenes are found in: M. H. Chisholm, K. Folting, J. W. Pasterczyk, *Inorg. Chem.* **1988**, *27*, 3057–3058; G. Becker, W. Becker, R. Knebl, H. Schmidt, U. Hildenbrand, M. Westerhausen, *Phosphorus Sulfur* **1987**, *30*, 349–352; P. Binger in *Multiple Bonds and Low Coordination in Phosphorus Chemistry* (Eds.: M. Regitz, O. J. Scherer) Thieme, Stuttgart, **1990**, p. 100.

[9] Compare with M. Scheer, C. Troitzsch, P. G. Jones, *Angew. Chem.* **1992**, *104*, 1395–1397; *Angew. Chem. Int. Ed. Engl.* **1992**, *31*, 1377–1379.

[10] Preparation see ref. [5].

[11] H. P. Fritz, T. Schöttle, *J. Organomet. Chem.* **1984**, *265*, 175–187.

Novel V^{III} Complexes with a Central $[V_3(\mu_3\text{-}S)(\mu\text{-}S_2)_3]^+$ or $[V_2(\mu\text{-}O)(\mu\text{-}SPh)_2]^{2+}$ Unit**

By *Norman S. Dean, Kirsten Folting, Emil Lobkovsky,* and *George Christou**

There are two main reasons for our continuing interest in V–S and V–O chemistry. Firstly, the mechanistic details behind the conversion of vanadyl impurities in crude oil into polymeric V^{III} sulfides during hydrodemetallation (HDM) and hydrodesulfurization (HDS) in the processing of crude oil is not understood.[1] Oxo-bridged V^{III} compounds and multinuclear V^{III}–S aggregates are likely intermediates in the early and late stages, respectively, of this transformation. Secondly, the comparison of V–S chemistry with the much better explored Mo–S chemistry is instructive. Despite the many similarities, V–S chemistry is proving sufficiently different from Mo–S chemistry that the study of the former is not a routine extension of the latter. In this report we describe two new structural types for vanadium compounds and contrast them with Mo compounds.

Treatment of $[V(SPh)_2(bpy)_2]PF_6$ (bpy = 2,2′-bipyridine) with four equivalents of sulfur in hot MeCN gives a dark

[*] Prof. Dr. G. Christou, N. S. Dean, Dr. K. Folting, Dr. E. Lobkovsky
Department of Chemistry and Molecular Structure Center
Indiana University
Bloomington, IN 47405 (USA)

[**] This work was supported by the Office of Basic Energy Sciences, Division of Chemical Sciences, U.S. Department of Energy (Grant DE-FG02-87ER13702).

green solution from which complex **1**[2, 16] can be isolated in 35–40% yield. The structure of the cation of **1** (Fig. 1) consists of a $[V_3(\mu_3\text{-}S)]$ unit with three edge-bridging $\eta^2:\eta^2:\mu\ S_2^{2-}$ groups and three chelating bipyridine ligands.

$[V_3S_7(bpy)_3]PF_6 \cdot 2MeCN$ **1**

The asymmetrically bridging S_2^{2-} units are found to have one longer (ave. 2.479 Å) and one shorter (ave. 2.372 Å) bond to each V atom; the longer V–S bonds are to the sulfur atoms that are almost coplanar with the V_3 triangle (Fig. 1). The idealized symmetry is C_{3v}, and the metals have the rare coordination number 7. Complex **1** is the first vanadium compound with a central $[M_3S(S_2)_3]$ unit,[3] although a complex with a $[V_3(\mu_3\text{-}S)(\mu\text{-}S)_3]$ framework is known.[4] Several complexes with a central $[Mo_3S(S_2)_3]$ unit have been characterized,[5] but none analogous to **1** with terminal bipyridine groups have been reported. The $[M_3E(S_2)_3]$ framework is also known for M = W, E = S[6] and M = Ti, E = O.[7]

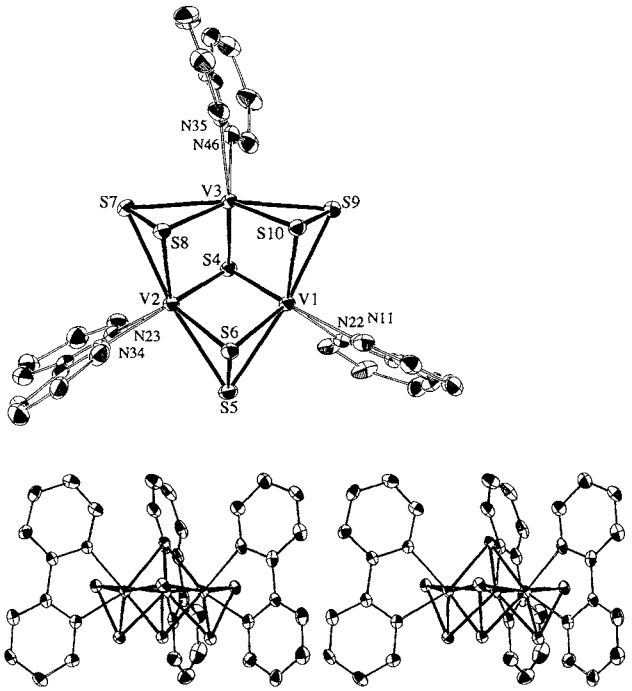

Fig. 1. ORTEP representation and stereoview of the cation of complex **1** (ellipsoids at the 50% probability level). Selected interatomic distances [Å] and angles [°]: V1-V2 2.770(1), V1-V3 2.767(1), V2-V3 2.750(1), S5-S6 2.040(2), S7-S8 2.034(2), S9-S10 2.032(2), V1-S4 2.329(2), V1-S5 2.470(2), V1-S6 2.381(2), V1-S9 2.483(2), V1-S10 2.354(2), V1-N11 2.204(4), V1-N22 2.210(4), V2-S4 2.329(2), V2-S5 2.497(2), V2-S6 2.361(2), V2-S7 2.467(2), V2-S8 2.392(2), V2-N23 2.183(4), V2-N34 2.189(4), V3-S4 2.314(2), V3-S7 2.484(2), V3-S8 2.357(2), V3-S9 2.473(2), V3-S10 2.386(2), V3-N35 2.181(4), V3-N46 2.190(4); V2-V1-V3 59.56(3), V1-V2-V3 60.17(3), V2-V3-V1 60.27(3), V1-S4-V2 72.97(5), V1-S4-V3 73.15(5), V2-S4-V3 72.63(5), V1-S5-V1 67.80(4), V1-S6-V2 71.49(5), V1-S9-V3 67.88(4), V1-S10-V3 71.44(5), V2-S7-V3 67.49(4), V2-S8-V3 70.76(5).

The V^{III} and Mo^{IV} units are isoelectronic. In analogy to the Mo complexes, **1** is diamagnetic in both the solid state and in solution, exhibiting a sharp ^1H NMR spectrum in CD_3CN. An EHMO calculation on the model system $[V_3S_7(NH_3)_6]^+$ also supports a diamagnetic nature for **1**. The calculated HOMO is a filled *e* set with metal–metal bonding character which is composed primarily (≈70%) of metal d orbitals. The LUMO of a_2 symmetry lies 1.3 eV above the HOMO and is composed (≈80%) of an antibonding combination of metal d orbitals.

The cyclic voltamogram of **1** in MeCN displays a reversible one-electron oxidation at −0.47 V (vs. Fc/Fc^+). The oxidized species, generated by controlled potential electrolysis, shows no EPR signal at 298 K or 77 K. On cooling to 5 K a broad, ill-defined EPR signal in the region $g \approx 2$ is observed. This behavior indicating rapid relaxation is consistent with the oxidized species being in a ^2E state, as suggested by the EHMO calculation, with low-lying excited states arising from the expected Jahn–Teller distortion. Coupling of the electron to all three vanadium nuclei would also contribute to further broadening of the EPR signal.

Hydrolysis of a solution of $NEt_4[V(Me_2bpy)(SPh)_4]$ (Me_2bpy = 4,4′-dimethylbipyridine) by adventitious H_2O in the MeCN solvent gave small amounts of the green complex **2**.[8, 16] The complex can be synthesized rationally and

$[V_2O(SPh)_4(Me_2bpy)_2]$ **2**

in adequate yield (40–50%) by controlled hydrolysis of a mixture of $[VCl_3(thf)_3]$, NaSPh, and Me_2bpy in THF. The structure of **2** (Fig. 2) consists of two face-sharing octahedra; the bridging ligands are an oxo and two PhS^- groups. The

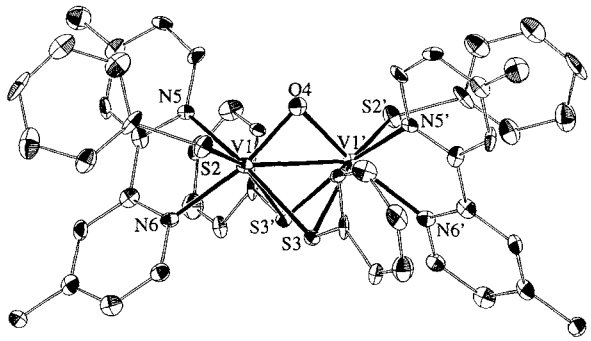

Fig. 2. ORTEP representation of complex **2** (ellipsoids at the 50% probability level). Primed and unprimed atoms are related by a crystallographic C_2 axis. Selected distances [Å] and angles [°]: V1-V1′ 2.579(3), V1-S2 2.394(3), V1-S3 2.432(2), V1-S3′ 2.493(3) V1-O4 1.841(6), V1-N5 2.152(6), V1-N6 2.184(7); V1-O4-V1′ 88.9(3), V1-S3-V1′ 63.15(8).

central $[M_2(\mu\text{-}O)(\mu\text{-}SPh)_2]^{2+}$ unit is unique for vanadium and extremely rare for any other metal; it has been found only in two Mo^{VI} dimers in a highly unsymmetrical form.[9] An M_2 unit bridged by hydroxo and bis-thiolato ligands is found in $[Cp_2Cl_3Mo_2(OH)(SMe)_2]$,[10] and a few examples of sulfido/bisthiolato bridged units are known.[11] The confacial bioctahedral arrangement is new for V^{III}–O compounds, in which the singly bridged $[V\text{-}O\text{-}V]^{4+}$ unit is common[12] and in general linear (or nearly so). In $[V_2O(OAc)_2(tacn)_2]^{2+}$ (tacn = 1,4,7-triazacyclononane) the V-O-V unit is bent with an angle of 130.2°.[13] The V···V distance in **2** (2.579(3) Å) is shorter than in **1** and comparable with that in **3** (2.60 Å) (edt = ethane-1,2-dithiolate).[14]

$[V_2(edt)_4]^{2-}$ **3**

EHMO calculations on the model complex $[V_2O(SH)_4(NH_3)_4]$ suggest the presence of a V–V single

bond in **2** in analogy to **3**. This is also supported by the acute V1-S3-V1′ angle ($\approx 63°$). The small magnetic moment of the complex ($\approx 0.6\ \mu_B$/V) is thus taken as indicating the coupling of the remaining two electrons by bridge-mediated antiferromagnetic exchange interactions (again in analogy to **3**) to give a singlet ground state and a triplet excited state. Thus, **2** is a rare example of a V^{III} compound with a V–V bond.[14, 15]

In summary, V–S chemistry continues to be the source of interesting new structural types and new V^{III} compounds with V–V bonds and/or strong interactions. The described work emphasizes both the similarities and differences between V and Mo chemistry. The framework of complex **1** is both structurally and electronically analogous to that of a well-known class of Mo–S compounds, whereas **2** has no exact structural or electronic Mo counterparts.

Experimental Procedure

1: Sulfur (0.128 g, 4.00 mmol) was added to a solution of $[V(SPh)_2(bpy)_2](PF_6)$ [17] (0.722 g, 1.00 mmol) in MeCN (35 mL), and the solution was heated to 65° for 2–3 h. The initial dark red color gradually changed to dark green and a tan precipitate formed. The solution was filtered and the filtrate volume reduced by 50%. After the addition of Et_2O (30 mL), storage of the solution at 0 °C overnight resulted in the precipitation of **1** as a green powder (0.12 g, 37% yield).

2: $[VCl_3(thf)_3]$ (0.711 g, 2.00 mmol), NaSPh (0.798 g, 6.00 mmol), and Me_2bpy (0.368 g, 2.00 mmol) were dissolved with stirring in THF (40 mL). Water (0.018 mL, 1.0 mmol) was added after 1 h, causing the solution to rapidly change color from red/purple to a dark green. After a further hour the solution was filtered and the filtrate volume reduced to 10 mL. Et_2O (40 mL) was added to precipitate **2** as a dark green powder (0.380 g, 41.2% yield).

Received: October 14, 1992 [Z 5625 IE]
German version: *Angew. Chem.* **1993**, *105*, 623

[1] a) B. G. Silbernagel, R. R. Mohan, G. H. Singhal, *ACS Symp. Ser.* **1984**, *248*, 91; b) B. G. Silbernagel, *J. Catal.* **1979**, *56*, 315; c) S. Asaoka, S. Nakata, C. Takeuchi, *ACS Symp. Ser.* **1987**, *344*, 275; d) M. Rose-Brussin, D. Moranta, *Appl. Catal.* **1984**, *11*, 85; e) P. C. H. Mitchell, C. E. Scott, J. P. Bonelle, J. G. Grimblot, *J. Chem. Soc. Faraday Trans. 1* **1985**, *81*, 1047.

[2] Correct C,H,N analysis for **1**. Crystal data: $C_{30}H_{24}N_6S_7V_3PF_6 \cdot 2CH_3CN$, triclinic, $P\bar{1}$, $T = -156$ °C, $a = 12.438(2)$, $b = 14.468(2)$, $c = 11.528(2)$ Å, $\alpha = 91.40(1)$, $\beta = 90.39(1)$, $\gamma = 85.09(1)°$, $V = 2066.18$ Å^3, $Z = 2$, $6° \le \theta \le 45°$. 533 refined parameters, 4546 unique reflections with $F > 3\sigma(F)$; $R = 0.0450$, $R_w = 0.0468$.

[3] $[V_3S(S_2)_3\{S_2CN(iBu)_2\}_3]$ and $[V_3S(S_2)_3\{S_2CN(iBu)_2\}_3]^-$ are mentioned in a conference abstract: S. G. Novick, E. I. Stiefel, H. H. Murray, *Abstracts of Papers, 4th Chemical Congress of North America, New York*, American Chemical Society, Washington D.C., **1991**; INOR 372. The metal centers in these compounds are in different oxidation states (2 V^{IV}, V^{III} and V^{IV}, 2 V^{III}) than in complex **1**.

[4] J. K. Money, J. C. Huffman, G. Christou, *Inorg. Chem.* **1988**, *27*, 507.

[5] a) J. Marcoll, A. Rabenau, D. Mootz, H. Wunderlich, *Rev. Chim. Miner.* **1974**, *11*, 607; b) A. Müller, S. Pohl, M. Dartmann, *Z. Naturforsch. B* **1979**, *34*, 434; c) H. Keck, W. Kuchen, J. Mathow, B. Meyer, D. Mootz, H. Wunderlich, *Angew. Chem.* **1981**, *93*, 1019; *Angew. Chem. Int. Ed. Engl.* **1981**, *20*, 975; d) T. R. Halbert, K. McGauley, W. H. Pan, R. S. Czernuszewicz, E. I. Stiefel, *J. Am. Chem. Soc.* **1984**, *106*, 1849; e) P. Klingelhöfer, U. Müller, C. Friebel, J. Pebler, *Z. Anorg. Allg. Chem.* **1986**, *543*, 22; f) V. P. Fedin, Y. V. Mironov, A. V. Virovets, N. V. Podberezskaya, V. Ye. Fedorov, *Polyhedron* **1992**, *11*, 2083.

[6] a) V. P. Fedin, M. N. Sokolov, O. A. Geras'ko, B. A. Kolesov, V. Ye. Fedorov, A. V. Mironov, D. S. Yufit, Yu. L. Slovohtov, Yu. T. Struchkov, *Inorg. Chim Acta* **1990**, *175*, 217; b) V. P. Fedin, M. N. Sokolov, K. G. Myakishev, O. A. Geras'ko, V. Ye. Fedorov, J. Macicek, *Polyhedron* **1991**, *10*, 1311.

[7] U. Müller, V. Krug, *Angew. Chem.* **1988**, *100*, 277; *Angew. Chem. Int. Ed. Engl.* **1988**, *27*, 293.

[8] Correct C,H,N analysis for **2**. Crystal data: $C_{48}H_{44}N_4OS_4V_2 \cdot OC_4H_8$, monoclinic, $C2/c$, $a = 16.954(3)$, $b = 15.969(2)$, $c = 18.830(3)$ Å, $\beta = 107.96(1)°$, $V = 4849.49$ Å^3, $Z = 4$, $6° \le 2\theta \le 50°$. 291 refined parameters, 2115 unique reflections with $F > 3\sigma(F)$; $R = 0.0644$, $R_w = 0.0646$.

[9] a) J. R. Dilworth, B. D. Neaves, P. Dahlstrom, J. Hyde, J. A. Zubieta, *Trans. Met. Chem.* **1982**, *7*, 257; b) K. Yamanouchi, J. E. Enemark, J. W. McDonald, W. E. Newton, *J. Am. Chem. Soc.* **1977**, *99*, 3529.

[10] C. Couldwell, B. Meunier, K. Prout, *Acta Crystallogr. Sect. B.* **1979**, *35*, 603.

[11] a) P. M. Boorman, K. A. Kerr, V. D. Patel, *J. Chem. Soc. Dalton Trans.* **1981**, 506; b) T. E. Wolf, J. M. Berg, K. O. Hodgson, R. B. Frankel, R. H. Holm, *J. Am. Chem. Soc.* **1979**, *101*, 4140.

[12] a) P. Chandrasekhar, P. H. Bird, *Inorg. Chem.* **1984**, *23*, 3677; b) J. K. Money, K. Folting, J. C. Huffman, G. Christou, *ibid.* **1987**, *26*, 944; c) J. A. Jensen, G. S. Girolomi, *ibid.* **1989**, *28*, 2114; d) G. Christou, D. Heinrich, J. K. Money, J. R. Rambo, J. C. Huffman, K. Folting, *Polyhedron* **1988**, *8*, 1723; e) P. Knopp, K. Wieghardt, B. Nuber, J. Weiss, W. S. Sheldrick, *Inorg. Chem.* **1990**, *29*, 363; f) S. G. Brand, N. Edelstein, C. J. Hawkins, G. Shalimoff, M. R. Snow, E. R. T. Tiekink, *ibid.* **1990**, *29*, 434; g) Y. Zhang, R. H. Holm, *ibid.* **1990**, *29*, 911.

[13] a) K. Wieghardt, M. Köppen, B. Nuber, J. Weiss, *J. Chem. Soc. Chem. Commun.* **1986**, 1530; b) M. Köppen, G. Fresen, K. Wieghardt, R. M. Llusar, B. Nuber, J. Weiss, *Inorg. Chem.* **1988**, *27*, 721.

[14] a) R. W. Wiggins, J. C. Huffman, G. Christou, *J. Chem. Soc. Chem. Commun.* **1983**, 1314; b) D. Szeymies, B. Krebs, G. Henkel, *Angew. Chem.* **1983**, *95*, 903; *Angew. Chem. Int. Ed. Engl.* **1983**, *22*, 885; c) J. R. Dorfman, R. H. Holm, *Inorg. Chem.* **1983**, *22*, 3179.

[15] a) O. A. Rajan, M. McKenna, J. Noordik, R. C. Haltiwanger, M. Rakowski-Dubois, *Organometallics* **1984**, *3*, 831; b) S. Gambarotta, M. Mazzanti, C. Floriani, M. Zehnder, *J. Chem. Soc. Chem. Commun.* **1984**, 1116; c) J. Darkwa, J. R. Lockmeyer, P. D. W. Boyd, T. B. Rauchfuss, A. L. Rheingold, *J. Am. Chem. Soc.* **1988**, *110*, 141.

[16] Further details of the crystal structure investigations may be obtained from the Fachinformationszentrum Karlsruhe, Gesellschaft für wissenschaftlich-technische Information mbH, D-W-7514 Eggenstein-Leopoldshafen 2 (FRG), on quoting the depository number CSD-56 896, the names of the authors, and the journal citation.

[17] N. S. Dean, G. Christou, unpublished.

The First Unsolvated Chelate and Cubane-Type Barium Complexes: Effective Compounds for the Sol–Gel Process

By *Sushil K. Pandey, Alexander Steiner, Herbert W. Roesky,** and *Dietmar Stalke*

Dedicated to Professor Ulrich Wannagat on the occasion of his 70th birthday

Cyclophosphazenes[1] are an important class of compounds employed as precursors in polymer chemistry.[2] Little is known on the chemistry of these compounds, in particular of cyclophosphazenes with Ba–N bonds. To our knowledge, no phosphazene–barium compounds have been reported to date. Before 1990,[3] molecular barium amides were totally unknown. We were particularly interested in these compounds because they can serve as precursors in the synthesis of complex oxides, which are used in high-temperature superconductors.[4] The metal oxide hydrates can be prepared by the sol–gel process.

We report here on the first unsolvated chelate and cubane-type barium complexes, which were prepared from barium bis(trimethylsilyl)amide.[5] Chelate complex **3** was prepared quantitatively from the reaction of amide **1** with **2**[6] (mol ratio 1:2) in *n*-hexane at 25 °C with elimination of $HN(SiMe_3)_2$. Compound **3** is a white, moisture-sensitive, nonvolatile solid. When **3** was heated to 110 °C at 0.01 bar it decomposed to **2** ($\delta(^{31}P) = 18.5$) and further decomposition products in low yield. Single crystals suitable for X-ray crystallography were obtained by storing a supersaturated solu-

[*] Prof. Dr. H. W. Roesky, Dr. S. K. Pandey, Dipl.-Chem. A. Steiner, Dr. D. Stalke
Institut für Anorganische Chemie der Universität
Tammannstrasse 4, D-W-3400 Göttingen (FRG)

[**] This work was supported by the Deutsche Forschungsgemeinschaft and the Fonds der Chemischen Industrie. S. K. P. thanks the Alexander-von-Humboldt Stiftung for a stipend.

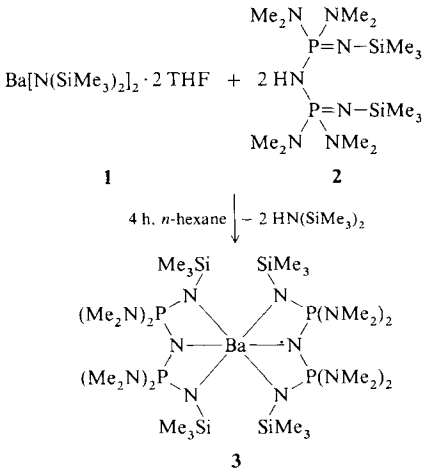

3

tion of **3** in toluene at 0 °C for two days and then at ambient temperature another two days.

Figure 1 shows the crystal structure of **3**. The monomeric compound contains a central six-coordinate barium atom located in the two planes defined by the almost planar backbones of the two tridentate phosphazene ligands. These two planes are perpendicular with respect to one another. Ba1 is surrounded by N1, N3, N4, and N6 in a tetrahedral fashion and linearly coordinated to N2 and N5. The distances from Ba1 to N2 and N5 are shorter (276 pm) than those to the silyl-substituted N atoms (285 pm). These distances are comparable to those observed in dimeric barium bis(trimethylsilyl)amide derivatives[5] with both bridging and terminal amido groups. There the distances between Ba and the bridging N atoms are longer, the distances to the terminal N atoms are shorter than those in **3**.

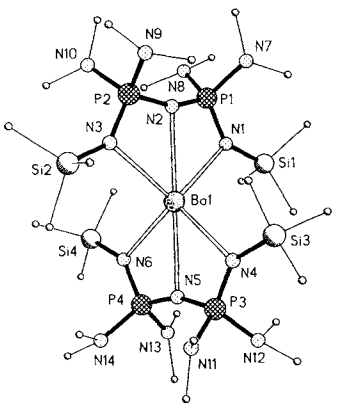

Fig. 1. Crystal structure of **3**. Selected bond lengths [pm] and angles [°] (ave.): Ba1-N1, N3, N4, N6 285, Ba1-N2, N5 276, P-NP 158, P-NSi 155, N-Si 168; P-N-P 158, N-P-N 108, Si-N-P 141.

Compound **5** was obtained from the reaction of amide **1** and the acyclic monosilylated ligand **4**[6] (mol ratio 1:1) in *n*-hexane at 25 °C. The reaction mechanism leading to the formation of heterocubane **5** can be described as follows: In a first step a lower-coordinated monocyclic intermediate is formed, which is stabilized in a second step by elimination of one equivalent of bis(trimethylsilyl)amine and simultaneous oligomerization [Eq. (a)].

$$4\,\mathbf{1} + 4\,H_2NP(NMe_2)_2NP(NMe_2)_2NSiMe_3 \xrightarrow{6\text{ h, }n\text{-hexane}} \underset{\mathbf{4}}{} \xrightarrow[-\,8\,HN(SiMe_3)_2]{} [\{BaNP(NMe_2)_2NP(NMe_2)_2NSiMe_3\}_4]$$

5

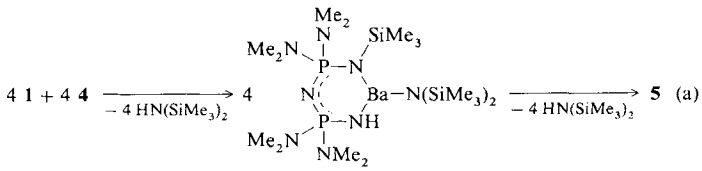

Compound **5** is a white, moisture-sensitive solid, which is extremely soluble in organic solvents. Single crystals suitable for X-ray crystallography were obtained by storing a saturated solution of **5** in *n*-hexane at 0 °C for a week. Compound **5** is tetrameric (Fig. 2), and the backbone of the structure consists of a barium–nitrogen heterocubane. Veith reports similar cagelike structures with main group elements.[7] The phosphazene ligands have different modes of coordination; two are tetradentate, the other two are tri- or pentadentate, (Fig. 3a–d). In all cases, the imido nitrogen atoms occupy four of the corners of the cubane and, thus, coordinate to three barium atoms (Ba–N: 271 pm (ave.); 259.4 to 283.1 pm), whereas each silylamido nitrogen atom coordinates to one barium atom (Ba–N: 290 pm (ave.); 286.8 to 297.9 pm). The other donor sites are occupied by either dimethylamino nitrogen atoms and solely phosphorus-bound nitrogen atoms. The barium atoms thus exhibit different coordination numbers (Ba1 and Ba4: 6, Ba3: 7, Ba2: 5). The coordination gap at Ba2 is filled by a close contact to a trimethylsilyl group of another tetrameric unit (Ba2–C: 334 pm).[8]

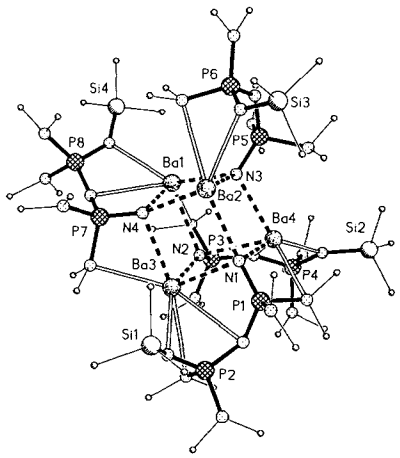

Fig. 2. Crystal structure of **5**. Bond lengths [pm] in the Ba–N cubane: Ba1-N2 274.3(6), Ba1-N3 267.9(6), Ba1-N4 283.1(6), Ba2-N1 266.6(7), Ba2-N3 261.8(6), Ba2-N4 262.4(7), Ba3-N1 272.3(7), Ba3-N2 259.4(6), Ba3-N4 275.6(6), Ba3-N1 282.5(6), Ba4-N2 280.6(6), Ba4-N3 267.1(6).

The formation of the Ba_4N_4 cluster is particularly surprising and gives reason to expect more new results. The compounds presented here may find interesting applications in high-tech material development. Sol–gel investigations on **3** and **5** have already given promising results in the preparation of metal oxide precursors. A white gel, consisting of $Ba(OH)_2 \cdot xH_2O$, can be easily prepared by hydrolysis of a

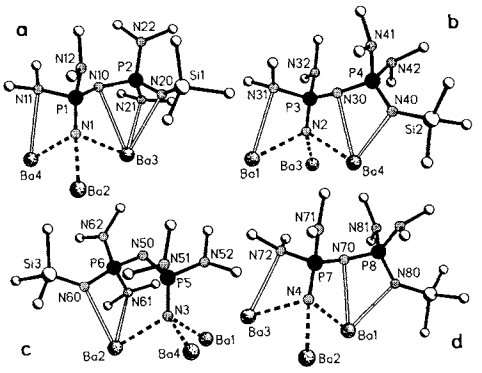

Fig. 3. Representation of the different coordination modes of the four phosphazene ligands **a**–**d** in **5**. Selected bond lengths [pm] and angles [°]: **a**: N1-P1 153.7(7), P1-N10 159.7(7), N10-P2 158.8(8), P2-N20 153.9(7), Ba4-N11 304.5(7), Ba3-N10 313.8(7), Ba3-N20 297.9(7), Ba3-N21 307.3(7); N1-P1-N10 120.3(4), P1-N10-P2 134.5(5), N10-P2-N20 120.7(4); **b**: N2-P3 154.4(6), P3-N30 159.7(7), N30-P4 156.6(7), P4-N40 156.9(7), Ba1-N31 304.1(6), Ba4-N30 293.8(7), Ba4-N40 286.8(6); N2-P3-N30 117.8(3), P3-N30-P4 158.6(5), N30-P4-N40 109.4(3); **c**: N3-P5 154.8(7), P5-N50 161.0(7), N50-P6 157.8(7), P6-N60 158.5(6), Ba2-N60 288.7(6), Ba2-N61 315.3(7); N3-P5-N50 122.8(3), P5-N50-P6 128.0(4), N50-P6-N60 121.9(3); **d**: N4-P7 155.3(7), P7-N70 160.4(7), N70-P8 157.1(7), P8-N80 157.6(7), Ba3-N72 291.5(7), Ba1-N70 291.2(7), Ba1-N80 287.4(6); N4-P7-N70 118.1(3), P7-N70-P8 155.0(5), N70-P8-N80 109.7(3).

solution of the barium compounds in toluene with water in methanol or ethanol.

Experimental Procedure

3: A solution of 1.5 g (3.5 mmol) of **2** in 20 mL *n*-hexane was added dropwise to a solution of 1.0 g (1.7 mmol) of **1** in 20 mL *n*-hexane. The reaction mixture was stirred at ambient temperature for 4 h. A pale yellow solution was obtained. After evacuation of all volatile compounds the spectroscopically pure compound was obtained in quantitative yield. Further purification can be achieved by recrystallization in *n*-hexane at 0 °C. M.p. 220 °C; ^{1}H NMR ($CDCl_3$, TMS ext.): $\delta = 0.1$ (s, 36H, $SiMe_3$), 2.5 (d, $J = 10.7$ Hz, 48H, NMe_2); ^{31}P NMR ($CDCl_3$, 85% H_3PO_4 ext.) $\delta = 5.2$ (s); ^{29}Si NMR (*n*-hexane/$CDCl_3$) $\delta = 7.1$ (s); IR (nujol): $\tilde{\nu}$[cm^{-1}] = 1284b, 1256s, 1100s, 1063s, 979vs, 857s, 826s, 740s, 719s, 671m, 626m, 503vs; MS(EI): *m/z* 990 (M^+, 20%), 564 (M^+ minus one ligand, 100%); satisfactory C,H,N analysis for $C_{28}H_{84}N_{14}P_4Si_4Ba$ (990.41).

5: A solution of 1.0 g (2.8 mmol) of **4** in 20 mL *n*-hexane was added dropwise to a solution of 1.7 g (2.8 mmol) of **1** in 20 mL *n*-hexane and stirred at ambient temperature for 6 h. A clear, pale yellow solution was obtained. After evacuation of all volatile compounds the white, foamy product remained in the reaction vessel (quantitative yield). M.p. 110 °C; ^{1}H NMR (C_6D_6, TMS ext.): $\delta = 0.4$ (s, 36H, $SiMe_3$), 2.5–2.7 (m, 96H, NMe_2); ^{31}P NMR (C_6D_6, 85% H_3PO_4 ext.) $\delta = 9.8$ (d), 26.4 (d); IR (nujol): $\tilde{\nu}$[cm^{-1}] = 1305s, 1244m, 1172s, 1080m, 969vs, 933m, 854s, 817s, 747m, 505vs; MS(EI): *m/z* 247 (M^+ minus two ligands; 50%), 355 (ligand; 100%).

Received: October 16, 1992 [Z 5632 IE]
German version: *Angew. Chem.* **1993**, *105*, 625
Publication delayed on authors' request

[1] H. W. Roesky, K. V. Katti, U. Seseke, M. Witt, E. Egert, R. Herbst, G. M. Sheldrick, *Angew. Chem.* **1986**, *98*, 447–448; *Angew. Chem. Int. Ed. Engl.* **1986**, *25*, 477–478; H. W. Roesky, K. V. Katti, U. Seseke, H. G. Schmidt, E. Egert, R. Herbst, G. M. Sheldrick, *J. Chem. Soc., Dalton Trans.* **1987**, 847–849; K. V. Katti, H. W. Roesky, M. Rietzel, *Inorg. Chem.* **1987**, *26*, 4032–4035; K. V. Katti, U. Seseke, M. Witt, H. W. Roesky, *Phosphorus Sulfur Relat. Elem.* **1987**, *30*, 421–423; R. Hasselbring, H. W. Roesky, M. Noltemeyer, *Angew. Chem.* **1992**, *104*, 613–615; *Angew. Chem. Int. Ed. Engl.* **1992**, *31*, 601–603.

[2] H. W. Roesky, M. Lücke, *Angew. Chem.* **1989**, *101*, 480–481; *Angew. Chem. Int. Ed. Engl.* **1989**, *28*, 493.

[3] M. F. Lappert, P. P. Power, A. R. Sanger, R. C. Srivastava, *Metal and Metalloid Amides*, Ellis Horwood, Chichester, **1980**; K. F. Tesh, T. P. Hanusa, J. C. Huffman, *Inorg. Chem.* **1990**, *29*, 1584–1586.

[4] L. G. Hubert-Pfalzgraf, *New J. Chem.* **1987**, *11*, 663–675; K. G. Caulton, L. G. Hubert-Pfalzgraf, *Chem. Rev.* **1990**, *90*, 969–995.

[5] B. A. Vaartstra, J. C. Huffman, W. E. Streib, K. G. Caulton, *Inorg. Chem.* **1991**, *30*, 121–125.

[6] R. Hasselbring, Dissertation, Universität Göttingen, **1992**.

[7] M. Veith, *Chem. Rev.* **1990**, *90*, 3–16.

[8] Crystal data of **3**: $C_{28}H_{84}N_{14}Si_4P_4Ba$, $M_r = 990.67$, monoclinic, soace group $P2_1/n$, $a = 1359.3(3)$, $b = 2076.2(3)$, $c = 2271.9(4)$ pm, $\beta = 98.62(3)^\circ$, $V = 6.339(2)$ nm^3, $Z = 4$, $\varrho_{calcd} = 1.038$ Mgm^{-3}, $F(000) = 2088$, $\lambda = 71.073$ pm, $T = -120$ °C, $\mu(Mo_{K\alpha}) = 0.832$ mm^{-1}. Data were collected on a Stoe-Siemens-AED diffractometer. Intensities of a rapidly cooled crystal with dimensions $0.4 \times 0.3 \times 0.2$ mm in an oil drop were collected by the $2\theta/\omega$ method in the range of $8^\circ \leq 2\theta \leq 45^\circ$. Of a total of 8447 reflections 8303 were independent and corrected for absorption. 8289 reflections were observed with $F_o > 4\sigma(F_o)$. The *R*1 values are $R_1 = \sum||F_o| - |F_c||/\sum F_o = 0.082$ ($F > 4\sigma F$) and $wR2 = [\sum w(F_o^2 - F_c^2)^2/\sum wF_o^4]^{1/2} = 0.254$ (all data) for $w^{-1} = \sigma^2(F_o^2) + (g_1 \cdot P)^2 + g_2 \cdot P$ with $P = (F_o^2 + 2F_c^2)/3$ and $g_1 = 0.114$, $g_2 = 56.843$. The relatively high *R*-value can be explained by a rotational disorder both of the Me_3Si and the Me_2N groups. All carbon atoms in **3** were refined in two positions with half occupancy. In addition, a disordered *n*-hexane molecule is present in the cell. **5**: $C_{44}H_{132}N_{28}Si_4P_8Ba_4$, $M_r = 1963.19$, triclinic, space group $P\bar{1}$, $a = 1630.3(6)$, $b = 1689.8(6)$, $c = 1875.2(7)$ pm, $\alpha = 71.30(2)$, $\beta = 82.46(2)$, $\gamma = 79.98(2)^\circ$, $V = 4.803(3)$ nm^3, $Z = 2$, $\varrho_{calcd} = 1.389$ Mgm^{-3}, $F(000) = 2034$, $\lambda = 71.073$ pm, $T = -120$ °C, $\mu(Mo_{K\alpha}) = 1.845$ mm^{-1}. Data were collected on a Stoe-Siemens-AED diffractometer. Intensities of a rapidly cooled crystal with dimensions $0.3 \times 0.3 \times 0.2$ mm in an oil drop were collected by the $2\theta/\omega$ method in the range of $8^\circ \leq 2\theta \leq 45^\circ$. Of a total of 16839 reflections 12579 were independent and corrected for absorption, and 12568 were observed with $F_o > 4\sigma(F_o)$. The *R*-values are $R1 = 0.044$ ($F > 4\sigma F$) and $wR2 = 0.121$ (all data); $g_1 = 0.059$, $g_2 = 16.630$. Both structures were solved with direct methods (SHELXS-90) [9] and refined by full-matrix least-squares on F^2 with all data (SHELXL-92) [10]. All non-hydrogen atoms were refined anisotropically. The hydrogen atoms were positioned with an ideal geometry and their positions calculated by using a riding model. Further details of the crystal structure investigations are available on request from the Director of the Cambridge Crystallographic Data Centre, 12 Union Road, GB-Cambridge CB2 1EZ (UK), by quoting the full journal citation.

[9] G. M. Sheldrick, *Acta Crystallogr. Sect. A*, **1990**, *46*, 467–473.

[10] G. M. Sheldrick, *SHELXL-92* University of Göttingen, Göttingen **1992**.

Diastereo- and Enantioselective Synthesis of 2-Substituted 3-Trialkylstannylcyclohexanones by Michael Addition of Trialkylstannyllithium to Cyclohexenone SAMP Hydrazone**

By *Dieter Enders,* Klaus-Jürgen Heider,* and *Gerhard Raabe*

Organotin compounds have been shown to be valuable building blocks for the construction of complex organic molecules.[1] The 1,4-addition of trialkylstannyllithium to α,β-unsaturated carbonyl compounds described by Still et al.[2] is a simple and efficient entry to functionalized tetraorganostannanes. In this reaction the enolate formed as an intermediate can be trapped by protons to give the simple adducts, and by alkyl iodides to give the *anti* tandem adduct stereoselectively.[2, 3] In the reactions with enones and trialkylsilylchloride silylenolethers are obtained,[4] and additions to aldehydes provide the aldol products.[5] The trialkylstannylketones formed are homoenolate equivalents[6] and can be easily converted into interesting synthetic building blocks, for example, 1,3-diols and dihydroxyketones,[7] cyclopropanes,[5, 8] enones,[9] unsaturated macrolides,[10] isoxazolines,[11] bicyclo[3.1.0]hexanes,[12] and spiroacetals.[13]

[*] Prof. Dr. D. Enders, Dipl.-Chem. K.-J. Heider, Dr. G. Raabe
Institut für Organische Chemie der Technischen Hochschule
Professor-Pirlet-Strasse 1, D-W-5100 Aachen (FRG)

[**] This work was supported by the Fonds der Chemischen Industrie. We thank Degussa AG, Schering AG, BASF AG, Bayer AG, and Hoechst AG for gifts of chemicals.

In the Michael addition of trialkylstannyl metal compounds[14] or trialkylstannylcuprates[15] to α,β-unsaturated ketones and the subsequent reaction with alkyl iodides, the *trans* products containing two new stereogenic centers are formed diastereoselectively. Until now optically active 3-trialkylstannylketones have only been prepared by diastereoselective addition to enantiomerically pure cyclohexenones.[15a, b, 16]

We report here for the first time on the regio-, diastereo-, and enantioselective synthesis of 2-substituted 3-trialkylstannylcyclohexanones. The key step is the Michael addition of trialkylstannyllithium to cyclohexenone SAMP or RAMP hydrazone, (*S*)-**3** and (*R*)-**3**, respectively, which are readily available from (*S*)- or (*R*)-1-amino-2-methoxymethylpyrrolidine (SAMP (*S*)-**2** or RAMP (*R*)-**2**, respectively) and cyclohexenone in 90% yield (Scheme 1).

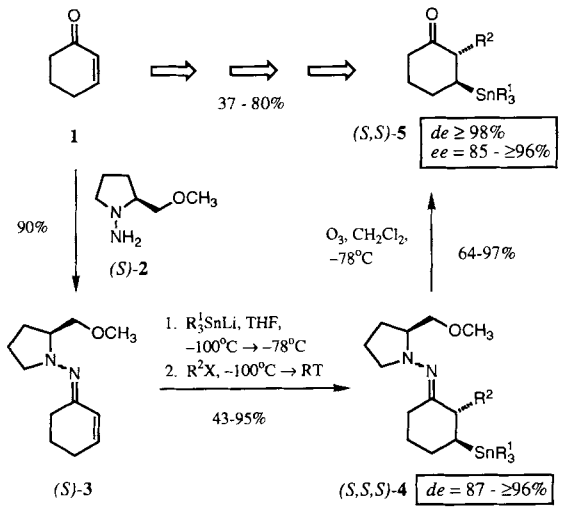

Scheme 1. Diastereo- and enantioselective synthesis of 2-substituted *trans*-3-trialkylstannylcyclohexanones (*S,S*)-**5**. RT = room temperature.

In tetrahydrofuran at −100 °C trimethylstannyllithium and tributylstannyllithium add to (*S*)-**3** regioselectively at the 4-position.[17] Trapping the resulting azaenolate with a saturated solution of ammonium chloride leads to the simple adducts (*S,S*)-**4a** and (*S,S*)-**4b** in only modest diastereomeric excess (*de* = 42–44%), whereas the *trans* tandem adducts (*S,S,S*)-**4c–h** with equatorial substituents are obtained in very good diastereomeric excess (*de* = 87–≥96%) in the reaction with alkyl iodides or bromides (Table 1). In this regard addition of trimethylstannyl anions gives poorer chemical yields (43–82%) and better induction (*de* = 44–≥96%) than the addition of tributylstannyl anions (yields 94–97%, *de* = 42–87%). In the case of 2-alkyl-3-trimethylstannylcyclohexanone SAMP hydrazones the isomer formed in excess can be enriched by chromatography.

The stannylated hydrazones **4** are subsequently converted to 3-trialkylstannylketones **5** by oxidative cleavage with ozone in very good yield without epimerization and racemization (64–93%, *de* ≥ 98%, *ee* = 42–≥96%). Ketones **5a–e** separate as colorless oils and ketones **5f–h** as colorless solids that can be recrystallized from ethanol, *n*-hexane, or diethyl ether.

When *para*-bromobenzylbromide is used as electrophile the bromine atom of (*S,S,S*)-**4a** is exchanged for a trimethylstannyl group in a side reaction. In addition to (*S,S,S*)-**4h** (43%) the stannylated product (*S,S,S*)-**4i** is obtained in a yield of 22% [Eq.(1)]. The conjugate addition of cyano-

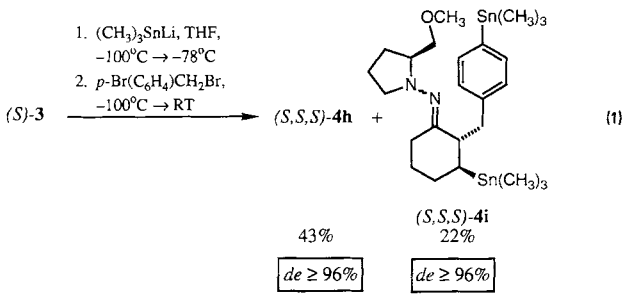

(tributylstannyl)methylcuprate[15c] as nucleophile to (*S*)-**3** and trapping of the resulting azaenolate with methyl iodide leads, after oxidative cleavage, to the Michael–Michael adduct (*S,S,S,R*)-**6** as the major product (yield 75%, *de* ≥ 75%), together with the simple tandem adduct (*S,S*)-**4d** (yield 16%, *de* ≥ 98%, *ee* = 88%) [Eq.(2)]

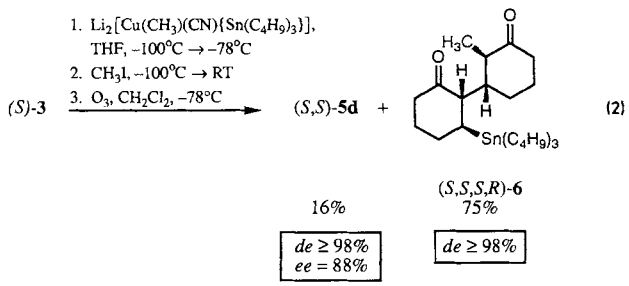

Table 1. 2-Substituted 3-trialkylstannylcyclohexanones **5** prepared by asymmetric Michael addition.

4/5	R^1	R^2	Yield **4** [%] (**3** → **4**)	*de* **4** [a] [%]		Yield **5** [%] (**3** → **5**)	$[\alpha]_D^{25}$ (*c*, $CHCl_3$)	*de* **5** [b] [%]	*ee* **5** [c] [%]	
a	CH_3	H	72	44	(*S,S*)	63	−75.0 (1.23)	–	44	(*S*)
b	nC_4H_9	H	97	42	(*S,S*)	86	− 55.4 [d]	–	42	(*S*)
c	CH_3	CH_3	77	≥96	(*S,S,S*)	73	−154.9 (0.89)	≥98	≥96	(*S,S*)
c [e]	CH_3	CH_3	68	≥96	(*R,R,R*)	66	+156.2 (0.89)	≥98	≥96	(*R,R*)
d	n-C_4H_9	CH_3	95	87	(*S,S,S*)	88	−104.0 [d]	≥98	85 [f]	(*S,S*)
e	n-C_4H_9	C_2H_5	94	87	(*S,S,S*)	60	− 94.9 (1.56)	≥98	87	(*S,S*)
f	CH_3	$CH_2CO_2CH_3$	82	90/94 [g]	(*S,S,S*)	79	− 69.9 (0.43)	≥98	93 [h]/≥96 [h,i]	(*S,S*)
g	CH_3	$(C_6H_5)CH_2$	75	≥96 [g]	(*S,S,S*)	73	−155.1 (1.01)	≥98	≥96	(*S,S*)
h	CH_3	p-$Br(C_6H_4)CH_2$	43 [j]	≥96	(*S,S,S*)	41	−122.7 (0.60)	≥98	≥96	(*S,S*)

[a] Determined by ^{13}C NMR spectroscopy (absolute configuration in parentheses). [b] Determined by ^1H NMR spectroscopy. [c] The value for *ee* corresponds to the *de* value for hydrazone **4** (absolute configuration in parentheses). [d] Neat. [e] RAMP used as chiral auxiliary. [f] Determined by ^{19}F NMR spectroscopy after reduction to the alcohol and esterification to the MTPA ester (see text). [g] After chromatography. [h] Measured by ^1H NMR shift experiment with $[Eu(hfc)_3]$. [i] After crystallization from ethanol. [j] Contains 22% **4i** as by-product.

The enantiomeric excess of **5f** was determined from its ^{1}H NMR spectrum with [Eu(hfc)$_3$] (hfc = tris[3-(heptafluoropropyl(hydroxymethylene-*d*-camphorato]) and that of **5c–e** and **5g,h** from the ^{19}F NMR spectra of the MTPA esters (MTPA = 3,3,3-trifluoro-2-methoxy-2-phenylpropionic acid), obtained by diastereoselective reduction with potassium tri-*sec*-butylhydroborate (K-Selectride)[18] to the (*S,S,S*)-2-alkyl-3-trialkylstannylcyclohexanol derivatives[19] and subsequent reaction with MTPA-Cl.[20] The racemic reference compounds were obtained by addition of the tin nucleophiles to cyclohexenone. The enantiomeric excesses determined in this fashion are in good agreement with the diasteromeric excesses obtained from ^{13}C NMR spectra at the stage of the hydrazone. Assignment of the absolute configurations (2*S*,3*S*) and (2*R*,3*R*) are based on X-ray crystal analyses of the compounds **5f**[21] and **5g**[22] (Fig. 1) obtained by tandem addition to (*S*)-**3**, and by circular dichroism (CD) measurements.[16a] All the 3-trialkylstannylketones **5** prepared with SAMP as auxiliary show a negative Cotton effect at $\lambda = 300$ nm, whereas the RAMP auxiliary leads to stannylketones with a positive Cotton effect.

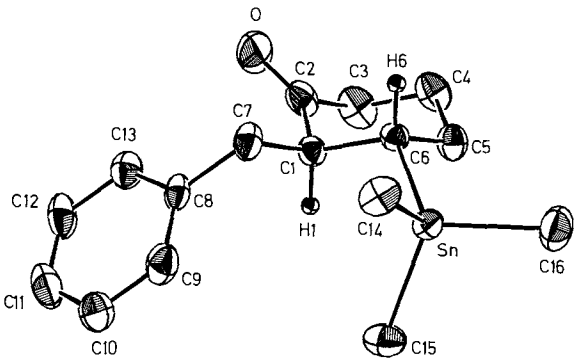

Fig. 1. Crystal structure of **5g**[22] (ORTEP[24], ellipsoids with 30% probability).

To our knowledge this is the first report of the asymmetric Michael addition of tin nucleophiles and provides a diastereo- and enantioselective entry to both enantiomeric series of *trans*-2-alkyl-3-trimethylstannylcyclohexanones.[25] Initial results show that this process can also be applied to open-chain α,β-unsaturated aldehyde SAMP hydrazones.

Experimental Procedure

A commercial 1.5 N solution of *n*-butyllithium in *n*-hexane (3 mL) was concentrated to dryness under vacuum. The residual yellow oil was dissolved in 4 mL anhydrous THF at 0 °C under inert gas, and 4.5 mmol hexaalkyldistannane (degassed under high vacuum or distilled) was added. After 15 min (hexabutyldistannane) or 2 h (hexamethyldistannane), the solution was cooled to −100 °C, and after a further 10 min 3 mmol (*S*)-3 was added dropwise. After the suspension was allowed to warm up to −78 °C over 3 h, an intensely yellow solution was obtained and stirred at this temperature for 2 h. At −100 °C a solution of 6 mmol electrophile in 4 mL THF was slowly added dropwise. The resulting solution was allowed to warm to room temperature within 15 min. The volatile components were condensed under vacuum into a trap cooled in liquid nitrogen, the residue was taken up in diethyl ether, washed with water and saturated NaCl solution, dried over magnesium sulfate, and concentrated to dryness. The crude product obtained can be used directly for the ozonolysis. The 3-trialkylstannyl SAMP hydrazones (*S,S,S*)-**4** were purified by column chromatography (silica gel, petroleum ether/diethyl ether 5:1 + 5% triethylamine).

Ozone was passed through a solution of (*S,S,S*)-**4** in dichloromethane at −78 °C until no more hydrazone could be detected by thin-layer chromatography (silica gel, petroleum ether/diethyl ether 5:1). After the excess ozone was driven off by a stream of argon, the reaction mixture was allowed to warm up, the solvent removed, and the product (*S,S*)-**5** purified by column chromatography (silica gel, petroleum ether/diethyl ether 20:1).

Received: November 26, 1992 [Z 5706 IE]
German version: *Angew. Chem.* **1993**, *105*, 592

[1] a) M. Pereyre, J.-P. Quintard, A. Rahm, *Tin in Organic Synthesis*, Butterworths, London, **1987**; b) P. G. Harrison, *Chemistry of Tin*, Blackie, Glasgow, **1989**; c) I. Omae, *J. Organomet. Chem. Libr.* **1989**, *21*, 1–355; d) *Organotin Compounds in Organic Synthesis* (Ed.: Y. Yamamoto) *Tetrahedron* **1989**, *45*, 909–1230.

[2] a) W. C. Still, *J. Am. Chem. Soc.* **1977**, *99*, 4836–4838; b) W. C. Still, A. Mitra, *Tetrahedron Lett.* **1978**, 2659–2662.

[3] Diastereoselective alkylation of 3-tributylstannylester enolates: G. J. McGarvey, J. M. Williams, *J. Am. Chem. Soc.* **1985**, *107*, 1435–1437.

[4] W. C. Still, *J. Am. Chem. Soc.* **1977**, *99*, 4186–4187.

[5] a) T. Sato, M. Watanabe, E. Murayama, *Tetrahedron Lett.* **1986**, *27*, 1621–1624; b) T. Sato, M. Watanabe, T. Watanabe, Y. Onoda, E. Murayama, *J. Org. Chem.* **1988**, *53*, 1894–1899.

[6] a) B. L. Chenard, *Tetrahedron Lett.* **1986**, *27*, 2805–2808; b) H. Ahlbrecht, P. Weber, *Synthesis* **1989**, 117–120; H. Ahlbrecht, P. Weber, *ibid.* **1992**, 1018–1025; c) Homoenolate dianions of secondary 3-tributylstannylamides: R. Goswami, D. E. Corcoran, *Tetrahedron Lett.* **1982**, *23*, 1463–1466.

[7] M. Ochiai, S. Iwaki, T. Ukita, Y. Matsuura, M. Shiro, Y. Nagao, *J. Am. Chem. Soc.* **1988**, *110*, 4606–4610.

[8] a) D. D. Davis, R. L. Chambers, H. T. Johnson, *J. Organomet. Chem.* **1970**, *25*, C13–C16; b) I. Fleming, C. J. Urch, *ibid.* **1985**, *285*, 173–191.

[9] a) Substituted α,β-unsaturated ketones: ref.[2a]; b) γ,β-unsaturated ketones: ref.[4]; c) γ,δ- and other unsaturated carbonyl compounds: M. Ochiai, T. Ukita, Y. Nagao, E. Fujita, *J. Chem. Soc. Chem. Commun.* **1984**, 1007–1008; M. Ochiai, T. Ukita, Y. Nagao, E. Fujita, *ibid.* **1985**, 637–638; M. Ochiai, S. Iwaki, T. Ukita, Y. Nagao, *Chem. Lett.* **1987**, 133–136; M. Ochiai, T. Ukita, S. Ikawi, Y. Nagao, E. Fujita, *J. Org. Chem.* **1989**, *54*, 4832–4840; K. Nakatani, S. Isoe, *Tetrahedron Lett.* **1985**, *26*, 2209–2212; J. E. Baldwin, R. M. Adlington, J. Robertson, *Tetrahedron* **1989**, *45*, 909–922.

[10] a) G. H. Posner, E. Asirvatham, K. S. Webb, S.-S. Jew, *Tetrahedron Lett.* **1987**, *28*, 5071–5074; b) G. H. Posner, K. S. Webb, E. Asirvatham, S.-S. Jew, A. Degl'Innocenti, *J. Am. Chem. Soc.* **1988**, *110*, 4754–4762.

[11] H. Nishiyama, H. Arai, T. Ohki, K. Itoh, *J. Am. Chem. Soc.* **1985**, *107*, 5310–5312.

[12] L. Plamondon, J. D. Wuest, *J. Org. Chem.* **1991**, *56*, 2066–2075, 2076–2081.

[13] M. G. O'Shea, W. Kitching, *Tetrahedron* **1989**, *45*, 1177–1186.

[14] a) Tributylstannylmagnesium chloride: J.-C. Lahournere, J. Valade, *J. Organomet. Chem.* **1971**, *33*, C7–C10; b) Review of Trialkylstannyllithium compounds: T. Sato, *Synthesis* **1990**, 259–270; c) Trimethylstannylsodium: H. G. Kuivila, G. H. Lein, *J. Org. Chem.* **1978**, *43*, 750–751; d) Triphenylstannylpotssium: R. J. P. Corriu, C. Guerin, *J. Organomet. Chem.* **1980**, *197*, C19–C21.

[15] a) E. Piers, H. E. Morton, J. M. Chong, *Can. J. Chem.* **1987**, *65*, 78–87, and references therein; E. Piers, R. D. Tillyer, *J. Org. Chem.* **1988**, *53*, 5366–5369; b) B. H. Lipshutz, S. Sharma, D. C. Reuter, *Tetrahedron Lett.* **1990**, *31*, 7253–7256; c) A. C. Oehlschlager, M. W. Hutzinger, R. Aksela, S. Sharma, S. M. Singh, *ibid.* **1990**, *31*, 165–168; S. Sharma, A. C. Oehlschlager, *J. Org. Chem.* **1991**, *56*, 770–776; d) S. Sharma, A. C. Oehlschlager, *Tetrahedron* **1991**, *47*, 1177–1184.

[16] a) Hudec, *J. Chem. Perkin Trans. 1* **1975**, 1020–1023; b) E. Piers, J. Y. Roberge, *Tetrahedron Lett.* **1991**, *32*, 5219–5222.

[17] 1,4-Addition of trimethylsilyllithium to cyclohexenone dimethylhydrazone: P. F. Hudrlik, A. M. Hudrlik, T. Yimenu, M. A. Waugh, G. Nagendrappa, *Tetrahedron* **1988**, *44*, 3791–3803.

[18] H. C. Brown, S. Krishnamurthy, *J. Am. Chem. Soc.* **1972**, *94*, 7159–7161.

[19] In the reduction with lithium aluminum hydride the (1*R*,2*S*,2*S*)-cyclohexanols are obtained with low diastereomeric excesses. See also: G. Wickham, H. A. Olszowy, W. Kitching, *J. Org. Chem.* **1982**, *47*, 3788–3793.

[20] J. A. Dale, D. L. Dull, H. S. Mosher, *J. Org. Chem.* **1969**, *34*, 2543–2549.

[21] A crystal of suitable quality formed in diethyl ether at −20 °C. The compound crystallizes in the orthorhombic space group $P2_12_12_1$ (no. 19) $a = 6.637(1)$, $b = 9.480(2)$, $c = 23.977(2)$ Å. A cell volume of 1508.7 Å^3, $Z = 4$, and $M_r = 333.0$, leads to a density of $\rho_{calc} = 1.466$ g cm^{-3}. Total number of electrons per unit cell $F(000) = 672$. Enraf-Nonius CAD4 four-circle diffractometer, graphite monochromator, $\Omega/2\theta$-scans, 20 °C, $Mo_{K\alpha}$ radiation ($\lambda = 0.71069$ Å), $\mu = 16.91$ cm^{-1}. A total of 3432 unique reflections were recorded ($+h+k+l$, $-h-k-l$ Friedel pairs), of which 3183 were observed ($I > 2\sigma(I)$), $R_m = 0.016$, $\sin\theta/\lambda_{max} = 0.649$. The structure was solved by the heavy-atom method (XTAL3.0[23]). Hydrogen atom positions were calculated. A total of 146 parameters were refined, $R = 0.046$ ($R_w = 0.044$). The maximum residual electron density was 1.3 e Å^{-3}. $X_{abs} = -0.04(6)$.

[22] Suitable crystals formed at −20 °C in diethyl ether. The substance crystallizes in the orthorhombic space group $P2_12_12_1$ (no. 19) $a = 7.645(1)$, $b = 16.255(3)$, $c = 13.078(1)$ Å. The cell volume of 1625.2 Å^3, $Z = 4$, and $M_r = 351.1$, leads to a density of $\rho_{calc} = 1.435$ g cm^{-3}. Overall number of electrons per unit cell $F(000) = 712$. Enraf-Nonius CAD4 four-circle diffractometer, graphite monochromator, $\Omega/2\theta$-scans, 0 °C, $Mo_{K\alpha}$ radiation ($\lambda = 0.71069$ Å), $\mu = 15.66$ cm^{-1}. A total of 3679 independent reflections were recorded ($\pm h + k + l$), of which 3524 were observed ($I > 2\sigma(I)$), $R_m = 0.027$, $\sin\theta/\lambda_{max} = 0.649$. The structure was solved by the heavy-atom method (XTAL3.0 [23]). Some of the hydrogen atom positions could be located, the remainder were calculated. A total of 164 parameters were refined. $R = 0.025$ ($R_w = 0.030$). The maximum residual electron density was 0.3 e Å^{-3} and $X_{abs} = -0.03(3)$. Further details of the crystal structure investigation may be obtained from the Fachinformationszentrum Karlsruhe, Gesellschaft für wissenschaftlich-technische Information GmbH, D-W-7514 Eggenstein-Leopoldshafen 2 (FRG) on quoting the depository number CSD-56952, the names of the authors, and the journal citation.

[23] S. R. Hall, J. M. Stewart, *XTAL3.0 Reference Manual*, Universitities of Western Australia und Maryland, **1990**.

[24] C. K. Johnson, Report ORNL-3794, Oak Ridge National Laboratory, Oak Ridge, Tennessee, **1965**.

[25] All compounds gave correct elemental analyses and spectra (^{1}H NMR, ^{13}C NMR, IR, UV) in agreement with their structures.

Molecular Tweezers with a Hydrocarbon Skeleton and Convergent Carboxyl Groups

By *Ralf Güther*, *Martin Nieger*, and *Fritz Vögtle**

As preorganized, acyclic host compounds "molecular tweezers" are distinguished by convergent functional groups that can "grasp" guest molecules.[1] To date only a few types of compounds have been reported to be efficient molecular tweezers; those prepared by Rebek et al. are the best known.[2] We have been trying for a number of years[1c, g] to utilize the characteristic features of cyclophane building blocks for the convergent arrangement of functional groups.[3] By linking two suitable cyclophane frameworks we have now been able to preorganize the functional groups so precisely that they are directly opposite each other when the guest molecule is enclosed (Fig. 1). The stereochemistry of [3.3]- and particularly [2.2]metacyclophanes offer interesting possibilities, which we will describe here.

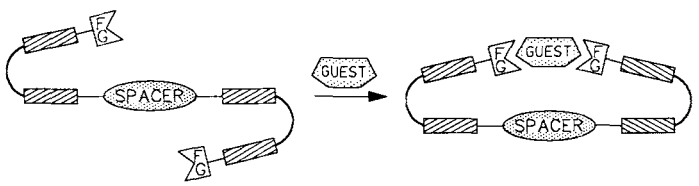

Fig. 1. Schematic representation of host–guest recognition with the new type of tweezer compounds (FG = functional group).

The double dithia[3.3]metacyclophane **5**, which has a stiff diyne bridge holding the two halves apart, exists exclusively in the double *syn* conformation shown in Figure 2, in which the two carboxyl groups are forced to face each other. Compound **5** was prepared in the following manner: 3,5-Dimethylbromobenzene and 3,5-dimethylbenzoic acid were converted into 2,11-dithia[3.3]metacyclophane **1** in a few steps.[5] Subsequent palladium-catalyzed ethynylation (a in Scheme 1) furnished the trimethylsilyl(TMS)-protected cyclophane **2**. The TMS groups were cleaved (b) to give **3**, and coupling of the alkyne moieties (c) led to diyne **4**, which could be hydrolyzed with trifluoroacetic acid (d) to yield **5**.

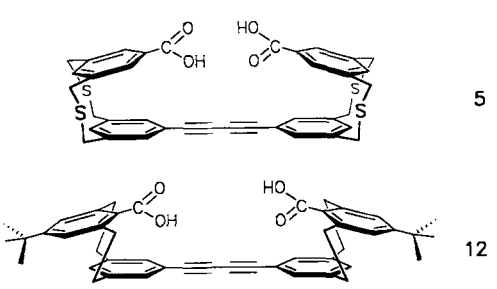

Fig. 2. Target molecule **5** based on the stereochemistry of [3.3]metacyclophanes with proven *syn* conformation of the [3.3]phane units; target molecule **12** based on the stereochemistry of [2.2]metacyclophanes with fixed *anti* conformation of the [2.2]phane units.

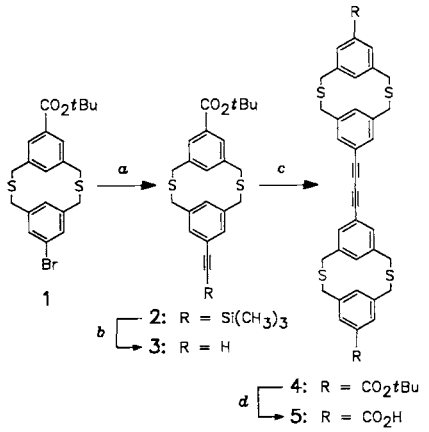

Scheme 1. Synthesis of **5**. a) Trimethylsilylacetylene/[$(Ph_3P)_2PdCl_2$]/CuI, triethylamine, 8 h at 80 °C, 90%; b) K_2CO_3, abs. methanol, 5 h at room temperature (RT), 92%; c) CuCl/$CuCl_2$, pyridine, 5 d at RT, 66%; d) CF_3COOH, 30 min at RT, > 90%.

Figure 2 also shows the rigidly fixed, "double" [2.2]metacyclophane **12** in the *anti* conformation, which was prepared as follows (the *tert*-butyl groups proved to be essential for increased solubility):[1g] 2,6-Dimethylaniline and 5-*tert*-butyl-1,3-dimethylbenzene were converted into dithia[3.3]metacyclophane **6**[5] in a few steps. Oxidation (a in Scheme 2) led to sulfone **7**, subsequent vacuum pyrolysis (b) provided [2.2]metacyclophane **8**. Palladium-catalyzed ethynylation (c) furnished the TMS-protected cyclophane **9**; the TMS groups were cleaved (d) to provide **10**, which could be coupled directly giving diyne **11**. Hydrolysis of the methyl ester groups in the interior of the cyclophane, which are blocked by the adjacent methylene groups, was possible only with LiI in pyridine.[7] In addition to the target molecule **12**, the monocarboxylic acid **13** was also always obtained.

Figure 3 shows the X-ray structure of the crystalline diester tweezer compound **11**.[8] It can be seen that both [2.2]metacyclophane units are in the desired *anti* conformation but twisted 180° to each other about the diyne axis. Since the molecule can twist freely about this axis in solution, the desired conformation in which the two functional groups face each other is possible.[9]

The molecular recognition possible with the two new types of tweezer compounds was tested first with diamines as guest

[*] Prof. Dr. F. Vögtle, Dipl.-Chem. R. Güther
Institut für Organische Chemie und Biochemie der Universität
Gerhard-Domagk-Strasse 1, D-W-5300 Bonn 1 (FRG)
Dr. M. Nieger
Institut für Anorganische Chemie der Universität Bonn

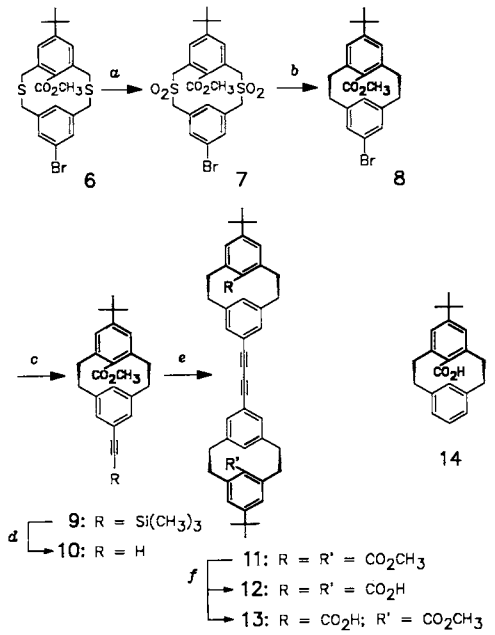

Scheme 2. Synthesis of **12** and **13** (reference compound **14** is shown on the right). a) H_2O_2/glacial acetic acid, benzene, 8 h at 60 °C, > 90%; b) Δ (pyrolysis), 87%; c) trimethylsilylacetylene/$[(Ph_3P)_2PdCl_2]$/CuI, triethylamine, 8 h at 70 °C, 26%; d) K_2CO_3, abs. methanol, 5 h at RT, > 90%; e) CuI, triethylamine, 6 h at 80 °C, 58%; f) LiI, abs. pyridine, 8 d reflux, 27%.

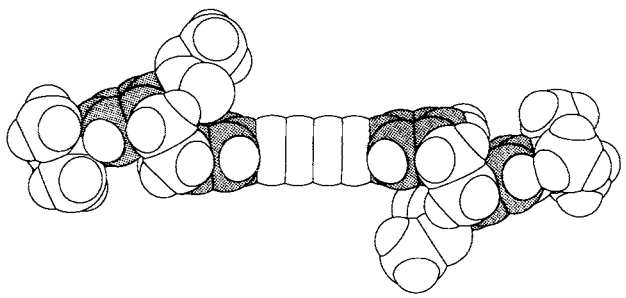

Fig. 3. X-ray structure of diester **11** with two *anti*-[2.2]metacyclophane units. The linearity of the diacetylene spacer is evident.

compounds. When 1,4-diazabicyclo[2.2.2]octane (DABCO, **15**) or piperazine (**16**) (Fig. 4) was added to a suspension of either of the host compounds **5** or **12** in trichloromethane, the mixture dissolved completely at a host–guest ratio of 1:1. In ^{1}H NMR experiments the signals of the protons of the guest, which are shifted to lower fields because of the magnetic anisotropy of the triple bonds, are not observed in the spectrum of the reference host compound **14** with DABCO (shifts of the signals as a result of proton transfers between the tweezer molecules **5** and **12** with DABCO and piperazine

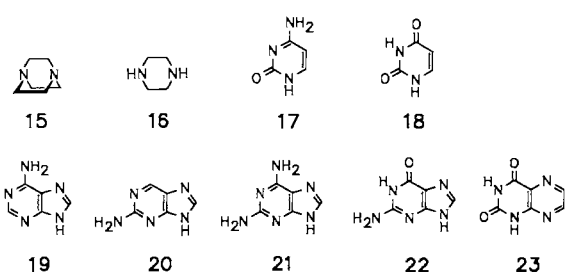

Fig. 4. List of the guest compounds examined.

Table 1. Physical data for **4**, **5**, **11**, **12**, and **13**.

4: M.p. > 300 °C. ^{1}H NMR (400 MHz, $CDCl_3$): δ = 1.58 (s, 18H; $OC(CH_3)_3$), 3.72 (s, 8H; CH_2), 3.77 (s, 8H, CH_2), 6.97 (d, ^4J(H,H) = 1.5 Hz, 4H; Ar-H), 7.00 (t, ^4J(H,H) = 1.5 Hz, 2H; Ar-H), 7.12 (t, ^4J(H,H) = 1.5 Hz, 2H; Ar-H), 7.47 (d, ^4J(H,H) = 2 Hz, 4H; Ar-H); ^{13}C NMR (100.62 MHz, $CDCl_3$): δ = 28.21 ($6CH_3$), 37.42 ($4CH_2$), 37.52 ($4CH_2$), 73.93 ($2C_q$), 80.98 ($OC(CH_3)_3$), 81.12 ($2C_q$), 121.83 ($2C_q$), 128.27 (4CH), 131.12 (4CH), 132.23 (2CH), 132.41 ($2C_q$), 134.99 (2CH), 137.14 ($4C_q$), 137.45 ($4C_q$), 165.20 (2CO). MS (70 eV): *m/z* 790.2297 ($M^{\oplus}$, 1%, $C_{46}H_{46}O_4S_4$, calc.: 790.2279)

5: M.p. > 300 °C. ^{1}H NMR (400 MHz, [D_5]pyridine): δ = 3.82 (s, 8H; CH_2), 3.92 (s, 8H; CH_2), 7.07 (d, ^4J(H,H) = 1.5 Hz, 4H; Ar-H), 7.15 (t, ^4J(H,H) = 1.5 Hz, 2H; Ar-H), 7.34 (t, ^4J(H,H) = 1.5 Hz, 2H; Ar-H), 8.05 (d, ^4J(H,H) = 2 Hz, 4H; Ar-H); ^{13}C NMR (62.89 MHz, [D_5]pyridine): δ = 37.50 ($4CH_2$), 37.85 ($4CH_2$), 74.44 ($2C_q$), 81.92 ($2C_q$), 121.88 ($2C_q$), 124.28 (2CH), 129.28 (4CH), 131.37 (4CH), 132.86 (2CH), 138.16 ($4C_q$), 138.42 ($6C_q$), 168.64 (2CO). MS (70 eV): *m/z* 678.1022 ($M^{\oplus}$, 1%, $C_{38}H_{30}O_4S_4$, calc.: 678.1027)

11: M.p. 276 °C. ^{1}H NMR (400 MHz, $CDCl_3$): δ = 1.36 (s, 18H; $C(CH_3)_3$), 2.21 (ddd, ^2J(H,H) = 13 Hz, ^3J(H,H) = 5 Hz, ^3J(H,H) = 12 Hz, 4H; CH_2), 3.02 (m, 8H; CH_2), 3.21 (ddd, ^2J(H,H) = 13 Hz, ^3J(H,H) = 5 Hz, ^3J(H,H) = 12 Hz, 4H; CH_2), 3.39 (s, 6H; OCH_3), 3.67 (t, ^4J(H,H) = 1.5 Hz, 2H; Ar-H_i), 7.20 (s, 4H; Ar-H), 7.22 (d, ^4J(H,H) = 1.5 Hz, 4H; Ar-H); ^{13}C NMR (62.89 MHz, $CDCl_3$): δ = 31.26 ($6CH_3$), 34.62 ($2C_q$), 37.77 ($4CH_2$), 41.23 ($4CH_2$), 50.97 ($2OCH_3$), 73.30 ($2C_q$), 82.21 ($2C_q$), 120.22 ($2C_q$), 124.69 (4CH), 130.54 (4CH), 133.04 ($2C_q$), 135.62 (2CH), 136.93 ($4C_q$), 143.35 ($4C_q$), 155.26 ($2C_q$), 165.29 (2CO). MS (70 eV): *m/z* 690.3719 ($M^{\oplus}$, 100%, $C_{48}H_{50}O_4$, calc.: 690.3709)

12: M.p. > 300 °C. ^{1}H NMR (250 MHz, [D_5]pyridine/$(CH_3)_4Si$): δ = 1.39 (s, 18H; $C(CH_3)_3$), 2.33 (ddd, ^2J(H,H) = 13 Hz, ^3J(H,H) = 5 Hz, ^3J(H,H) = 12 Hz, 4H; CH_2), 3.12 (m, 8H; CH_2), 3.89 (ddd, ^2J(H,H) = 13 Hz, ^3J(H,H) = 5 Hz, ^3J(H,H) = 12 Hz, 4H; CH_2), 4.01 (t, ^4J(H,H) = 1.5 Hz, 2H; Ar-H_i), 5.45 (br, 2H; CO_2H), 7.40 (s, 4H; Ar-H), 7.55 (d, ^4J(H,H) = 1.5 Hz, 4H; Ar-H); ^{13}C NMR (62.89 MHz, [D_5]pyridine/$(CH_3)_4Si$): δ = 31.36 ($6CH_3$), 34.73 ($2C_q$), 38.06 ($4CH_2$), 41.77 ($4CH_2$), 74.16 ($2C_q$), 83.99 ($2C_q$), 120.41 ($2C_q$), 125.03 (4CH), 131.49 (4CH), 135.36 ($2C_q$), 136.60 (2CH), 137.92 ($4C_q$), 144.17 ($4C_q$), 154.96 ($2C_q$), 167.53 (2CO). MS (70 eV): *m/z* 662.3384 ($M^{\oplus}$, 22%, $C_{46}H_{46}O_4$, calc.: 662.3396)

13: M.p. 288 °C. ^{1}H NMR (250 MHz, $CDCl_3$): δ = 1.35, 1.37 (s, 18H; $C(CH_3)_3$), 2.22, 2.26 (m, 4H; CH_2), 3.03, 3.05 (m, 4H; CH_2), 3.27 (m, 2H; CH_2), 3.42 (s, 3H; OCH_3), 3.48 (m, 2H; CH_2), 3.69, 3.72 (t, ^4J(H,H) = 1.5 Hz, 2H; Ar-H_i), 7.20, 7.21 (s, 4H; Ar-H), 7.28, 7.35 (d, ^4J(H,H) = 1.5 Hz, 4H; Ar-H); ^{13}C NMR (62.89 MHz, $CDCl_3$): δ = 31.24, 31.28 ($6CH_3$), 34.66 ($2C_q$), 37.82 ($4CH_2$), 41.29 ($4CH_2$), 50.99 (OCH_3), 73.09, 73.81 ($2C_q$), 82.10, 82.70 ($2C_q$), 120.18, 120.44 ($2C_q$), 124.74, 124.81 (4CH), 130.55, 130.78 (4CH), 131.82, 133.02 ($2C_q$) 135.64, 136.09 (2CH), 136.92, 137.03 ($4C_q$), 143.44, 144.73 ($4C_q$), 155.31, 155.77 ($2C_q$), 165.23, 169.50 (2CO). MS (70 eV): *m/z* 676.3568 ($M^{\oplus}$, 63%, $C_{47}H_{48}O_4$, calc.: 676.3553)

can thus be discounted almost completely). The host compound and DABCO crystallize out of trichloromethane as a 1:1 complex, as ^{1}H NMR and FAB mass spectra prove; the latter shows an intense peak for the 1:1 complex. No indications were given for formation of a 1:2 complex.

We also investigated the host properties of tweezer molecule **12** towards pyrimidine and purine bases (Fig. 4). Using the method described in ref.[10], we found distinctive selectivities in the host–guest recognition. 2,6-Diaminopurine (**21**) is bound more tightly (higher association constants) than adenine (**19**) or 2-aminopurine (**20**). The preference of guest **21** can be explained by its higher basicity and the better spatial complementarity between the host and guest as a result of the additional amino group. The association constants K_{assoc} of the complexes formed by **12** and 2,6-diaminopurine (**21**) and adenine (**19**) determined from the increase in solubility are $6.6(\pm 1.4) \times 10^4$ and $4.1(\pm 1.5) \times 10^4$ M^{-1}, respectively. Given a choice between uracil (**18**) and cytosine (**17**) host **12** shows a preference for uracil, $K_{assoc} = 1.4(\pm 0.6) \times 10^4$ M^{-1} (no definite host–guest effects were observed within experimental limitations with 2-aminopurine (**20**), cytosine (**17**), guanine (**22**), and 2,4-dihydroxypteridine (**23**)). In accord with this successful proof of the host properties of the tweezer compounds, no association was observed when **12** was replaced by the simple cyclophane **14**,[12] "half" of the molecular tweezers (Fig. 5).

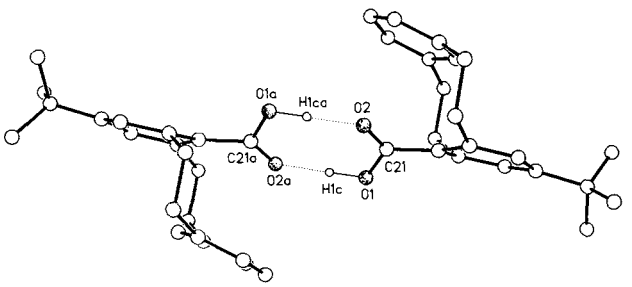

Fig. 5. X-ray structure of the reference compound **14** ("half of the tweezers"). The carboxyl groups are not separated by a spacer and form a dimer, as expected[14], by hydrogen bonding.

The 1:1 composition of the host–guest complexes of **12** and the high association constants suggest that the guest molecules are bound, as planned,[3] by hydrogen bonds in the noncollapsible molecular niche between the two functional groups. Remarkably, in earlier investigations of host compounds for nucleobases, for example tri- and bis(catechol) macrocycles,[10b-d] the same order of bonding strengths was found for this type of guest.

In conclusion, these tweezer molecules, the first constructed from cyclophanes, are strongly binding and selective hosts. The synthesis of other molecular tweezers of this type with various spacers, other functional groups, and with more than two convergent fixed functions appears to be worthwhile.

Experimental Procedure

11: Compound **10** (121 mg, 0.35 mmol) and copper(I) iodide (100 mg, 0.52 mmol) were dissolved in degassed triethylamine (30 mL) under inert gas and heated at 80 °C for 6 h. After the reaction mixture had cooled, the solvent was distilled off under vacuum and the residue purified by chromatography ($R_f = 0.76$; SiO_2, particle size 60–100 μm, dichloromethane/petroleum ether 40–60 (1:1)) to give colorless crystals (70 mg, 58%).

12/13: Compound **11** (69 mg, 0.1 mmol) was dissolved in anhydrous pyridine (30 mL), treated with anhydrous lithium iodide (403 mg, 3 mmol), and heated at reflux for 8 d. The solvent was distilled off under vacuum and the residue taken up in trichloromethane (20 mL) and 2N HCl (20 mL) and extracted repeatedly with trichloromethane. The combined organic phases were washed three times with 6N HCl and dried over Na_2SO_4. The solvent was removed under vacuum and the residue purified by flash chromatography (SiO_2, particle size 30–60 μm, trichloromethane/methanol (50:1)). Fraction 1 ($R_f = 0.45$): 36 mg (53%) monocarboxylic acid **13**; fraction 2 ($R_f = 0.22$); 18 mg, biscarboxylic acid **12**.

Received: December 12, 1992 [Z 5749 IE]
German version: *Angew. Chem.* **1993**, *105*, 647

[1] a) J. McKenna, J. M. McKenna, D. W. Thornthwaite, *J. Chem. Soc. Chem. Commun.* **1977**, 809; b) C. W. Chen, H. W. Whitlock, *J. Am. Chem. Soc.* **1978**, *100*, 4921; c) R. Leppkes, F. Vögtle, *Angew. Chem.* **1981**, *93*, 404; *Angew. Chem. Int. Ed. Engl.* **1981**, *20*, 396; d) M. Irie, M. Kato, *J. Am. Chem. Soc.* **1985**, *107*, 1024; e) S. C. Zimmerman, C. M. VanZyl, *ibid.* **1987**, *109*, 7894; f) J. C. Adrian, Jr., C. S. Wilcox, *ibid.* **1989**, *111*, 8055; g) F. Vögtle, H. Koch, K. Rissanen, *Chem. Ber.* **1992**, *125*, 2129; h) see ref. [2].

[2] a) J. Rebek, Jr., L. Marshall, R. Wolak, J. McManis, *J. Am. Chem. Soc.* **1984**, *106*, 1170; b) J. Rebek, Jr., B. Askew, M. Killoran, D. Nemeth, F.-T-Lin, *ibid.* **1987**, *109*, 2426; c) Review: J. Rebek, Jr., *Angew. Chem.* **1990**, *102*, 261; *Angew. Chem. Int. Ed. Engl.* **1990**, *29*, 245.

[3] See "Conformation Design": R. W. Hoffmann, *Angew. Chem.* **1992**, *104*, 1147; *Angew. Chem. Int. Ed. Engl.* **1992**, *31*, 1124.

[4] The *syn* conformation of **5** is supported by its ^{1}H NMR spectra and is typical of dithia[3.3]metacyclophanes: F. Vögtle, *Cyclophan-Chemie*, Teubner, Stuttgart, **1990**; *Cyclophane Chemistry*, Wiley, Chichester, **1993**, in press. Exceptions: J. Breitenbach, R. Hoss, M. Nieger, F. Vögtle, *Chem. Ber.* **1992**, *125*, 255.

[5] The syntheses of the simple metacyclophane building blocks **1** and **6** will be reported elsewhere.

[6] Rigid *anti* conformation of [2.2]metacyclophanes: a) F. Vögtle, P. Neumann, *Angew. Chem.* **1972**, *84*, 75; *Angew. Chem. Int. Ed. Engl.* **1972**, *11*, 73; *Cyclophanes, I, II* (Eds.: P. M. Keehn, S. M. Rosenfeld), Academic Press, New York, London, **1983**; b) F. Diederich, *Cyclophanes*, The Royal Society of Chemistry, Cambridge, **1991**.

[7] U. Lüning, C. Wangnick, K. Peters, H. G. von Schnering, *Chem. Ber.* **1991**, *124*, 397. Other methods were not successful.

[8] Crystal structure analysis of **11**[13]: colorless crystals, space group $P2_1/c$ (No. 14); $a = 8.966(1)$, $b = 24.374(7)$, $c = 8.947(1)$ Å, $\beta = 104.79(1)°$; $V = 1901(1)$ Å^3, $Z = 2$; $\rho_{calc} = 1.21$ g cm^{-1}; $Mo_{K\alpha}$ ($\lambda = 0.717073$ Å); $\mu(Mo_{K\alpha}) = 0.07$ mm^{-1}; $F(000) = 740$; $T = 193$ K; crystal dimensions: $0.10 \times 0.35 \times 0.45$ mm^3; Enraf–Nonius CAD4 diffractometer; $4° < 2\theta < 45°$; 2752 measured, 2482 unique reflections, 1294 of which with $|F| > 3\sigma(F)$. The structure was solved by direct methods and refined with SHELXTL-Plus (264 parameters): $R = 0.084$ ($R_w = 0.080$, $w^{-1} = \sigma^2(F) + gF^2$, $g = 0.0010$), all non-hydrogen atoms anisotropic, H atoms located by difference electron density determinations and refined with a riding model. The *tert*-butyl group is disordered [s.o.f. (site occupation factor) (C18, C19, C20) = 0.62(2)]. An extinction correction was conducted.

[9] According to a computer model of **12** based on the X-ray data of **11** the distance between the carboxyl oxygen atoms is ca. 10 Å; for a comparison, the corresponding distance in Rebek's system (acridine spacer with Kemp's tricarboxylic acid) is ca. 8.5 Å[2b].

[10] a) K. A. Connors, *Binding Constants. The Measurement of Molecular Complex Stability*, Wiley, New York, **1987**; b) C. Seel, F. Vögtle, *Angew. Chem.* **1991**, *103*, 433; *Angew. Chem. Int. Ed. Engl.* **1991**, *30*, 442; c) R. Hoss, F. Vögtle, *J. Chem. Soc. Chem. Commun.* **1992**, 1584; d) R. Hoss, F. Vögtle, *Chem. Ber.* **1993**, in press.

[11] Because of the low solubility of host compound **12**, the measurements of the increase in solubility were conducted only with a host concentration of 1×10^{-5} M. Thus the resulting uncertainty in the UV spectroscopic determination of the association constants is within the given order of magnitude. The synthesis of better soluble tweezer compounds with the same basic structure is the goal of current work.

[12] Crystal structure analysis of **14**[13]: colorless crystals, space group $P\bar{1}$ (No. 2); $a = 11.719(2)$, $b = 11.889(2)$, $c = 13.408(3)$ Å, $\alpha = 106.90(2)$, $\beta = 105.01(2)$, $\gamma = 91.72(2)°$; $V = 1715(1)$ Å^3, $Z = 4$; $\rho_{calc} = 1.19$ g cm^{-1}; $Mo_{K\alpha}$ ($\lambda = 0.717073$ Å); $\mu(Mo_{K\alpha}) = 0.08$ mm^{-1}; $F(000) = 664$; $T = 293$ K; crystal dimensions: $0.5 \times 0.6 \times 0.7$ mm^3; Siemens R3m/V diffractometer; $3° < 2\theta < 50°$; 6289 measured, 6013 unique reflections, 4735 of which with $|F| > 3\sigma(F)$. The structure was solved by direct methods and refined with SHELXTL-Plus (420 parameters): $R = 0.079$ ($R_w = 0.091$, $w^{-1} = \sigma^2(F) + gF^2$, $g = 0.0010$), all non-hydrogen atoms anisotropic, H atoms located by difference electron density determinations and refined with a riding model. The disordered *tert*-butyl group [s.o.f.(C18, C19, C20) = 0.49(1)] was refined isotropically. An extinction correction was conducted.

[13] Further details of the crystal structure investigation may be obtained from the Fachinformationszentrum Karlsruhe, Gesellschaft für wissenschaftlich-technische Information mbH, D-W-7514 Eggenstein-Leopoldshafen 2 (FRG) on quoting the depository number CSD-56894, the names of the authors, and the journal citation.

[14] See crystalline inclusion complex of host compounds with carboxyl groups: a) E. Weber, *J. Mol. Graphics*, **1989**, *7*, 12; b) I. Csöregh, O. Gallardo, E. Weber, S. Finge, C. Reutel, *Tetrahedron: Asymmetry*, **1992**, *3*, 1555.

Structure and Symmetry of the Benzene Cation**

By *Reiner Lindner, Hiroshi Sekiya, Bernhard Beyl,* and *Klaus Müller-Dethlefs**

The structure and symmetry of the benzene molecule, already a theme of early research in organic chemistry, was not completely clarified until recently, despite many attempts. In particular, the symmetry of the equilibrium structure in the electronic ground state has continually stimulated discussion.[1, 2] Only a few years ago Ermer[1] made clear that although D_{6h} symmetry was compatible with many experi-

[*] Dr. K. Müller-Dethlefs, Dipl.-Phys. R. Lindner, Dr. H. Sekiya,[+]
Dipl.-Phys. B. Beyl
Institut für Physikalische und Theoretische Chemie der Technischen Universität München
Lichtenbergstrasse 4, D-W-8046 Garching (FRG)

[+] Permanent address: Institute of Advanced Material Study
Kyushu University, Fukuoka (Japan)

[**] This work was supported by the Commission of the European Community (contract no. SC1-CT90-462-(BRMD)). H. S. thanks the Alexander von Humboldt Foundation for a one year research fellowship, 1991–1992.

mental results and ab initio calculations, D_{3h} symmetry cannot be definitely rejected. D_{6h} symmetry for the electronic ground state $S_0\,^1A_{1g}$ of benzene was proved only with the help of microwave spectra with completely resolved rotational lines (of singly and doubly deuterated benzene) *in the gas phase*, since an analysis of these clearly rules out D_{3h} symmetry.[3] Also for the first excited state $S_1\,^1B_{2u}$, the speculation on a deviation from the hexagonal, planar structure was finally convincingly ended by high-resolution spectroscopy in the gas phase, in this case by Doppler-free rotationally resolved fluorescence-excitation spectra of the $S_1 \leftarrow S_0$ transition.[4]

The perturbation of the π electron system by the removal of an electron to form the benzene cation is expected to cause a deviation from the structure and symmetry of the neutral molecule. Reduction to threefold symmetry is conceivable, which would correspond to a "localization" of the double bonds, either to D_{3h} in which the planar structure is maintained, or to C_{3v} and a chairlike structure similar to the chair conformation of cyclohexane. However, an in-plane symmetry reduction to D_{2h} is also feasible, as can be concluded from theoretical considerations.[5] The analysis of Rydberg series converging to the electronic ground state of the cation, and also of photoelectron spectra, point more towards the maintenance of a planar structure in the cation.[6] Nevertheless, the ground-state geometry cannot be deduced exactly because of the poor resolution of conventional photoelectron (PE) spectroscopy. In this communication, completely rotationally resolved ZEKE (*ze*ro *k*inetic *e*nergy) PE spectra are presented for the first time; through an analysis of these spectra, the symmetry group and structure of the cation could be determined.

In the neutral ground state S_0 of the benzene molecule the π electronic configuration is $(a_{2u})^2(e_{1g})^4$ and thus $^1A_{1g}$. On the transition to the cation an electron is removed from a degenerate bonding e_{1g} orbital. The resulting ionic ground state D_0 is degenerate ($^2E_{1g}$). The Jahn–Teller coupling that accompanies the electronic degeneracy causes a distortion along a non-totally symmetric normal coordinate that lifts the degeneracy.[7, 8] Model calculations therefore predict a D_{2h} symmetry for the cation for which there are three equivalent structures.[5] This distortion to D_{2h} can be detected experimentally in a matrix at low temperatures. The ESR spectra of $C_6H_6^+$ in a freon matrix indicate an increased spin density at C1 and C4 at 4.2 K but an equivalent spin density at 100 K.[9] Thus the question arises whether the D_{2h} structure is *static* and destabilized at higher temperatures by collisions with the matrix or whether a *dynamic* D_{2h} structure is stabilized by the matrix lattice. For weak Jahn–Teller coupling the stabilization energy for the distorted symmetry is smaller than the zero point energy of the Jahn–Teller active mode. Isolated—that is, under collision-free conditions—the three equivalent D_{2h} structures of the cation would dynamically interconvert rapidly, and the ground state of the cation would still be described in the D_{6h} symmetry group.[10] For strong Jahn–Teller coupling the cation would spend much time in one of the three structures, and would therefore be described in D_{2h}.

Rotationally resolved photoelectron spectroscopy as described in this paper allows an unambiguous structure determination. The symmetry of the cation can be deduced from the rotational transitions that occur, together with group theoretical considerations. The knowledge of the structure and the symmetry of the isolated benzene cation is desirable not only for testing quantum mechanical model calculations; it also has a not inconsiderable fundamental importance for organic chemistry.

As the usual methods of ion spectroscopy, such as laser-induced fluorescence, are not applicable to the benzene cation because of the extremely low fluorescence yields, the rotationally resolved PES offers an attractive alternative method. In the past few years the ZEKE-PE technique has established itself as a high-resolution spectroscopic method ($0.2-0.4\ cm^{-1} \approx 25-50\ \mu eV$) for molecular ions,[11–14] and recently has also been applied in studies of microsolvation of larger molecular clusters.[15, 16] ZEKE-PE spectroscopy of molecules and the ZEKE photodetachment of anions[17] are now recognized spectroscopic methods in chemistry.[18–20] For larger molecules combination with a supersonic molecular beam is particularly suitable. The intense cooling of the internal degrees of freedom in this case leads to significantly increased selectivity of excitation and to less complicated spectra.

The benzene molecule is an oblate symmetric rotor, whose rotational energy is described in the first approximation by the two constants B and C and the quantum numbers J and K. The quantum number J describes the total angular momentum of the molecule, K its projection along a quantization direction fixed with respect to the molecule, namely the principal axis. In a vibronically or electronically degenerate state, the influence of the vibronic or electronic angular momentum on the rotational energy must also be taken into account. This Coriolis coupling is described by the constant ζ_{eff}.[8]

The benzene molecules are ionized in a two-photon, two-color process via the first electronically excited state $S_1 6^1$ as intermediate resonance (the symbol 6^1 here represents a vibrational state in which the normal vibrational mode ν_6 is excited with one quantum). The first laser selects a rovibronic state in $S_1 6^1$ and from this state the second laser ionizes the molecule. Depending on the symmetry of the intermediate state, different rovibronic states of the ion are populated. The conservation of the symmetry of the nuclear spin wavefunction on transition, and the symmetry selection rules and rules for coupling of angular momenta severely restrict the number of possible transitions. From the assignment of the transitions and the rotational progressions that occur, the symmetry and structure of the cation can be deduced.

Figure 1 shows the spectra for the transitions from the intermediate states $S_1 6^1$ ($J' = 1$, $K' = 1, +l$) and $S_1 6^1$ ($J' = 2$, $K' = 2, +l$); the rotational states in $S_1 6^1$ are assigned according to ref. [24b]. The most notable feature is the appearance of progressions in the total angular momentum quantum number N^+ (without electron spin) of the ionic core. For transitions between bound states the selection rules $\Delta J = 0, \pm 1$ and $\Delta K = 0, \pm 1$ are valid. Here, however, on transition from a bound to an unbound state the leaving electron can compensate for the angular momentum by vector coupling depending on the partial wavefunction type (s, p, d,...), thus enabling higher rotational angular momentum changes.[21, 22]

A model to explain the observed transitions was formed on considering the following: Starting from the rovibronic symmetry of the intermediate state the symmetry of the final state that can be reached in a one-photon transition is determined. The symmetry of this state is dictated by the rovibronic symmetry of the ion core and the symmetry of the leaving electron. Since the symmetry of the nuclear spin wavefunction is not changed by the transition, the rovibronic symmetry of the ion core, and therefore also the symmetry of the leaving electron is fixed. From the correlation of the symmetry group of the cation with the group $D_{\infty h}$ the partial wavefunction type of the electron is obtained and thereby the possible rotational states of the ion core.[22] Those transi-

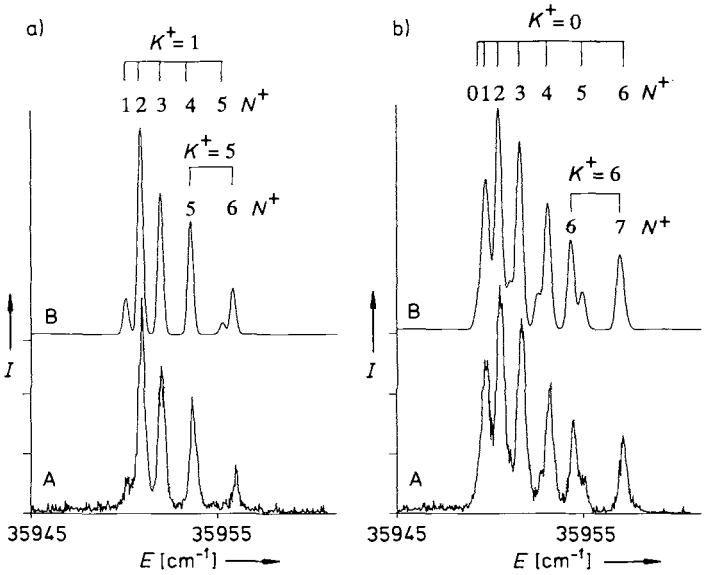

Fig. 1. Recorded (A) and simulated ZEKE spectra (B) of the transitions $D_0\,^2E_{1g} \leftarrow S_1\,6^1\,^1E_{1u}$ ($J'=1$, $K'=1$, + l) (a) and $D_0\,^2E_{1g} \leftarrow S_1\,6^1\,^1E_{1u}$ ($J'=2$, $K'=2$, + l) (b). Gaussian bands with a width of 0.3 cm^{-1} (FWHM) were assumed for the simulation. The intensities I of the ZEKE signals were taken from the spectra. E = energy of the ionizing laser.

tions for which the partial wavefunctions of the ZEKE electron correlate with symmetries that are allowed in a purely electronic transition are expected to be the strongest. For D_{6h} symmetry of the benzene cation, that is the symmetry species e_{2g} with partial wavefunctions $|l=2, \lambda=2\rangle$, $|l=4, \lambda=2\rangle$, and $|l=4, \lambda=4>$ (λ is the projection of the orbital angular momentum l of the ZEKE electron on the principal axis). Analogously one obtains for D_{3h} the species e' with the additional partial wavefunction $|l=1, \lambda=1\rangle$ and for D_{2h} the species $a_g + b_{1g}$ with the additional partial wavefunction $|l=0, \lambda=0\rangle$. In all three cases only the lowest electron angular momentum partial waves from s to g are considered. A determination of the symmetry of the cation is thus possible through the assignment of the rotational transitions in the ZEKE spectrum. On the basis of the above-mentioned model, all the lines are consistent with the assumption of D_{6h} symmetry. None of the intense lines expected from the additional partial wavefunctions for D_{3h} or D_{2h} are observed in the spectra. In the electronic ground state the benzene cation may thus be described as having D_{6h} symmetry. The conclusion is therefore that the stabilization by Jahn–Teller distortion is smaller than the energy of the zero point vibration, and the reduction in symmetry induced by the distortion has therefore no influence on the observed rotational transitions.

With ten rotational states in the P and R branches of the intermediate resonance $S_1\,6^1$ as initial state, 44 lines could be assigned in the ZEKE PE spectrum. This enabled a fit of rotational constants of the benzene cation by the method of least squares.[23] The standard deviation of 0.034 cm^{-1} represent only an eighth of the line width and are an indication of the good quality of the fit. In Table 1 these constants and also the values for the ground state S_0 and the intermediate resonance state $S_1\,6^1$ of the neutral molecule are listed.[24] A comparison of the ground state constants of the neutral and the ionized molecule reveals that the benzene ring is only marginally influenced by the removal of an electron. In particular the values of the rotational constant C, corresponding to the moment of inertia about the axis perpendicular to the ring, are almost identical.

Table 1. Spectroscopic constants for the ground state $S_0\,^1A_{1g}$ and the excited state $S_0\,6^1\,^1E_{1u}$ (Γ_{ev}) of benzene and the ground state $D_0\,^2E_{1g}$ of the cation, for a fit without the restriction $C = B/2$.

	S_0 [24]	$S_1\,6^1$ [24]	D_0 [a]
B [cm^{-1}]	0.18977389	0.1817904	0.18912 ± 0.00056
C [cm^{-1}]	0.0948637	0.0908482	0.09494 ± 0.00022
ζ_{eff}	0	−0.57873	0.4534 ± 0.0065

[a] This work.

A slight contraction or expansion of the ring on ionization is compatible with the error limits. The deviation from the planarity condition $C = B/2$ lies within the error limits for the rotational constants of the cation. This is consistent with the determined symmetry D_{6h}, which requires a planar structure. The rotational constants were therefore also fitted under the assumption of planarity, and the constants obtained thus were given preference. These values are given in Table 2 and contrasted with the results of an ab initio calculation.[5]

Table 2. Spectroscopic constants for the benzene cation in the ground state $D_0\,^2E_{1g}$, for a fit with the restriction $C = B/2$, and, for comparison, the values derived from the bond lengths obtained in an ab initio calculation.

	D_0 [a]	Calculation [5]
B [cm^{-1}]	0.18956 ± 0.00034	0.18844
C [cm^{-1}]	0.09478 ± 0.00017	0.09422
ζ_{eff}	0.4543 ± 0.0066	–

[a] This work.

The pairs of values suggest a stretching of the ring bonds, which agrees with the intuitive expectation of what happens when an electron is removed from a bonding orbital. The experimentally obtained stretching of approximately 0.1% is, however, about a factor 5 smaller than that predicted by theory. The strength of the bond in the benzene molecule is apparently affected less by the removal of one of the four e_{1g} electrons than previously assumed. An exact statement on the lengths of the C–C and the C–H bonds will only be possible after additional measurements on the perdeuterated benzene C_6D_6.

Experimental Procedure

The principle of the ZEKE PE spectroscopy relies on the extraction of electrons from the ionization volume with an electrical pulse temporally delayed from the ionization process. Two slightly different variations of the method are in present use. In the first, free electrons with a vanishingly small kinetic energy are detected. In the second, which is applied here, high-lying, long-lived Rydberg states that have a lifetime in the µs range because of their high principal quantum number ($n > 150$) are ionized by a delayed field, and the extracted electrons are detected resolved in time (*P*ulsed *F*ield *I*onization, PFI). An exact description of the method may be found in refs. [13, 25]. An energy resolution of about 0.25 cm^{-1} is achieved in the PFI–ZEKE measurements reported here.

Benzene vapor (Aldrich, 99%) with a vapor pressure of approximately 70 mbar pulsed together with 4 bar argon as carrier gas (Messer-Griesheim, 4.5) was expanded through a piezovalve (nozzle diameter 500 µm) into a vacuum. The central region of the supersonic molecular beam obtained thus was skimmed with a cone-shaped skimmer before entering the ionization and extraction volume. The laser system for the ionization of the benzene molecule (1 + 1′ resonance-enhanced two-photon two-color ionization) comprises two dye lasers (Lumonics HD-500) pumped by a Nd:YAG laser (Continuum NY-82/20). The two laser beams pass through the ionization chamber antiparallel and intercept the molecular beam there. The photoelectrons are accelerated in the direction of the detectors by means of an extraction pulse delayed in time relative to the light pulse and are detected there, resolved in time (Fig. 2). The dependence of

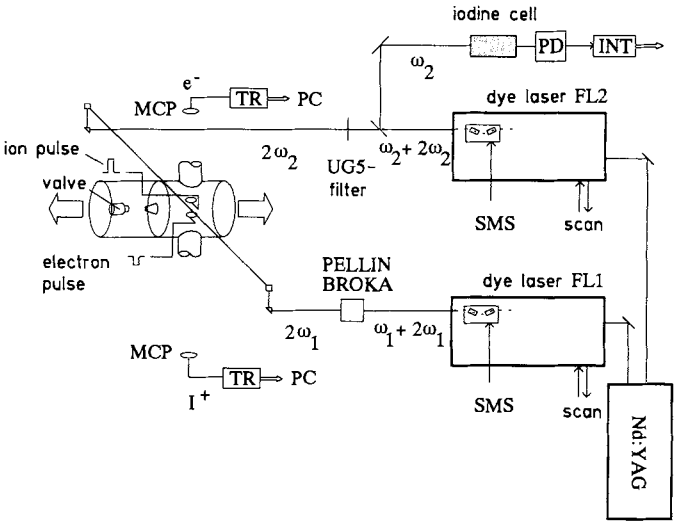

Fig. 2. Diagram of the experimental setup: MCP, multichannel plates; TR, transient recorder; PC, dedicated computer HP QS/20; PD, photodiode; INT, integrator; SMS, control of the stepping motor for frequency-doubling crystal.

the detected ZEKE signal on the laser wavelength gives information on the rovibronic states of the ionized molecule.

Received: November 16, 1992 [Z 5687 1E]
German version: *Angew. Chem.* **1993**, *105*, 631

[1] O. Ermer, *Angew. Chem.* **1987**, *99*, 791–793; *Angew. Chem. Int. Ed. Engl.* **1987**, *26*, 782.
[2] R. Janoschek, *Angew. Chem.* **1987**, *99*, 1332; *Angew. Chem. Int. Ed. Engl.* **1987**, *26*, 1298.
[3] M. Oldani, R. Widmer, G. Grassi, A. Bauder, *J. Mol. Struct.* **1988**, *190*, 31–40.
[4] a) E. Riedle, J. Pliva, *Chem. Phys.* **1991**, *152*, 375–389; b) personal communication by E. Riedle (Garching).
[5] K. Raghavachari, R. C. Haddon, T. A. Miller, V. E. Bondybey, *J. Chem. Phys.* **1983**, *79*, 1387–1395.
[6] A. W. Potts, W. C. Price, D. G. Streets, T. A. Williams, *Faraday Discuss. Chem. Soc.* **1972**, *54*, 168–181.
[7] H. A. Jahn, E. Teller, *Proc. R. Soc. London A* **1937**, *161*, 220.
[8] G. Herzberg, *Molecular Spectra and Molecular Structure, Vol. III*, Van Nostrand, Princeton, USA, **1966**.
[9] M. Iwasaki, K. Toriyama, K. Nunome, *J. Chem. Soc. Chem. Commun.* **1983**, 320–322.
[10] S. R. Long, J. T. Meek, J. P. Reilly, *J. Chem. Phys.* **1983**, *79*, 3206–3219.
[11] K. Müller-Dethlefs, M. Sander, E. W. Schlag, *Z. Naturforsch. A* **1984**, *39*, 1089–1091.
[12] W. Habenicht, G. Reiser, K. Müller-Dethlefs, *J. Chem. Phys.* **1991**, *95*, 4809–4820.
[13] K. Müller-Dethlefs, E. W. Schlag, *Annu. Rev. Phys. Chem.* **1991**, *42*, 109–136.
[14] D. Rieger, G. Reiser, K. Müller-Dethlefs, E. W. Schlag, *J. Phys. Chem.* **1992**, *96*, 12–14.
[15] G. Reiser, O. Dopfer, R. Lindner, G. Henri, K. Müller-Dethlefs, E. W. Schlag, S. D. Colson, *Chem. Phys. Lett.* **1991**, *181*, 1–4.
[16] O. Dopfer, G. Lembach, T. G. Wright, K. Müller-Dethlefs, *J. Chem. Phys.*, in press.
[17] R. Metz, S. Bradforth, D. Neumark, *Adv. Chem. Phys.* **1992**, *81*, 1–61.
[18] E. R. Grant, M. G. White, *Nature* **1991**, *354*, 249–250.
[19] G. Drechsler, *Nachr. Chem. Tech. Lab.* **1992**, *40*, 20–22.
[20] *Römpp Chemie Lexikon*, 9. Aufl. (Eds.: J. Falbe, M. Regitz), Thieme, Stuttgart, **1992** (Entry ZEKE-Spektroskopie).
[21] H. Rudolph, V. McKoy, S. N. Dixit, *J. Chem. Phys.* **1989**, *90*, 2570–2574.
[22] K. Müller-Dethlefs, *J. Chem. Phys.* **1991**, *95*, 4821–4839.
[23] We wish to thank E. Riedle (Garching) for helpful cooperation in the development of the fitting program for ZEKE transitions.
[24] a) M.-L. Junttila, J. L. Domenech, G. T. Fraser, A. S. Pine, *J. Mol. Spectrosc.* **1991**, 147, 513–520; b) E. Riedle, T. Knittel, T. Weber, H. J. Neusser, *J. Chem. Phys.* **1989**, *91*, 4555–4563. c) The rotational constants for the $S_1 6^1$ state listed in Table 1 have been slightly adjusted from those in [24 b], by taking into account the more accurate values for the S_0 state from [24 a]: E. Riedle, as yet unpublished results.
[25] G. Reiser, W. Habenicht, K. Müller-Dethlefs, E. W. Schlag, *Chem. Phys. Lett.* **1988**, *152*, 119–123.

A New Atropisomeric Molecular Structure for Efficient Enantiodifferentiation**

By *Edwin Weber,** *Konstantinos Skobridis, Andreas Wierig, Stavroula Stathi, Luigi R. Nassimbeni,* and *Margaret L. Niven*

Axial chiral structural elements are extremely interesting for the construction of optically active auxiliaries (reagents, catalysts) for efficient asymmetric syntheses and the resolution of racemates.[1] Important examples of this class contain a biaryl unit, often the atropisomeric group 2,2′-substituted 1,1′-binaphthyl.[2] Recently chiral alcohols bearing bulky substituents (but not the characteristic biaryl unit) have proved themselves for the same purpose.[3]

We report here on the synthesis, optical resolution, structure, and potential applications of the atropisomeric compound **1** that combines the two structural characteristics

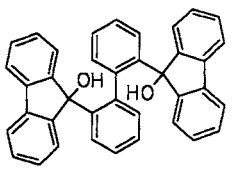

1

(biaryl unit and bulky alcohol group), which is therefore a promising reagent for enantiodiscrimination of organic com-

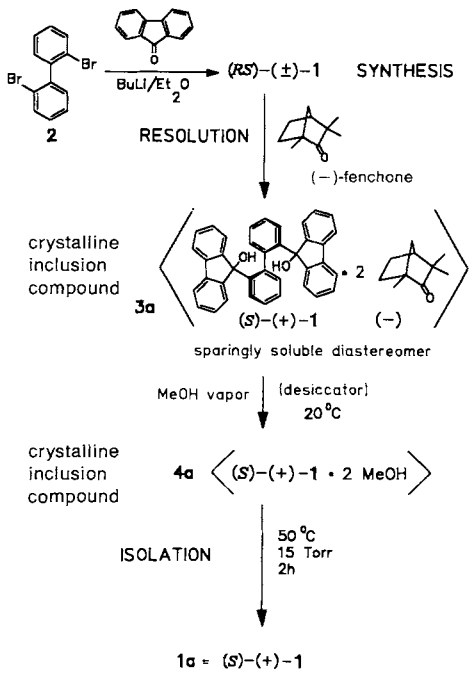

Scheme 1. (+)-Fenchone affords **1b** (= (*R*)-(−)-**1**) analogously.

[*] Prof. Dr. E. Weber,[+] Dr. K. Skobridis, Dipl.-Chem. A. Wierig, Dipl.-Chem. S. Stathi
Institut für Organische Chemie and Biochemie der Universität
Gerhard-Domagk-Strasse 1, D-W-5300 Bonn-1 (FRG)
[+] New address:
Institut für Organische Chemie der Technischen Universität Bergakademie
Leipziger Strasse 29, D-O-9200 Freiberg/Sachsen (FRG)
Prof. Dr. L. R. Nassimbeni, Dr. M. L. Niven
Department of Chemistry
University of Cape Town (South Africa)

[**] This work was supported by the Deutsche Forschungsgemeinschaft (SFB 334) and the Fonds der Chemischen Industrie.

pounds for a wide variety of applications. This prediction is further supported by the favorable properties of the fluorene group for the formation of crystalline inclusion compounds.[4] Remarkably, chiral auxiliaries of the diol type have not before incorporated the 9-fluorenyl group, which has excellent shielding potential through its large surface area.

Racemic **1** was obtained in 70% yield by lithiation (*n*Bu-Li/Et_2O) of 2,2'-dibromobiphenyl (**2**) and subsequent reaction with fluorenone (Scheme 1).[5] In order to resolve **1**, it was recrystallized from naturally occurring (−)-fenchone. The crystals that form are a 1:2 inclusion complex between (*S*)-(+)-**1** (=**1a**) and (−)-fenchone (the sparingly soluble diastereomer **3a**).

The absolute configuration (*S*) of the host **1a** was confirmed by X-ray structural analysis[6] of the inclusion complex **3a** by using the known configuration of the guest (−)-fenchone (Fig. 1). The host molecule has a conformation

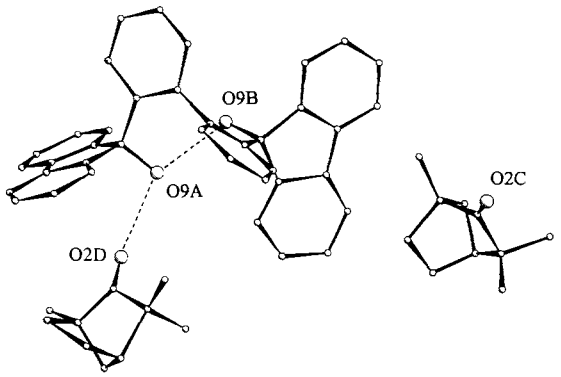

Fig. 1. Crystal structure of **3a** [**1a**·(−)-fenchone (1:2)]. For clarity the hydrogen atoms are omitted. Dashed lines specify hydrogen bonds.

characterized by an orthogonal twisting at the central biphenyl unit (torsional angle C10A-C11A-C11B-C10B = 89(2)°C). The fluorene units are also orthogonal to each other, and each fluorene unit is perpendicular to the phenyl ring to which it is bound. An intramolecular hydrogen-bond contact exists between the hydroxyl groups (O9A···O9B = 2.783 Å). In addition, one of the hydroxyl groups (O9A) forms a hydrogen bond to one of the two fenchone molecules (O9A···O2D = 2.756 Å). The other fenchone molecule in the 1:2 complex has no specific contacts and is situated between the host molecules in a lattice interstice (Fig. 2). Apparently this provides favorable conditions for a good fit between the particular enantiomers **1a** and (−)-fenchone in the crystalline inclusion complex **3a**.

The release of the optically pure host compound **1a** from the complex **3a** is not trivial. High temperatures must be avoided because of the potential racemization of **1a**. However, at low temperatures (−)-fenchone cannot be removed. We therefore used the following indirect route: Initially the firmly bound complex was exposed to an atmosphere saturated with MeOH vapor to exchange (−)-fenchone for MeOH. The new 1:2 inclusion complex with MeOH (**4a**) was dried in vacuum (50°C, 15 Torr) to conveniently afford the pure optically active host compound **1a**. The optical purity of **1a** was confirmed by HPLC on an Okamoto column. Compound **1a** has an optical rotation $[\alpha]_D^{20}$ of 334.2 (c = 0.5 in $CHCl_3$) and displays a positive Cotton effect at 269 nm. The racemization barrier for atropisomeric rearrangement **1a** → **1b** [= (*R*)-(−)-**1**] was determined to be 24 kcal mol^{-1}.[7]

The antipode **1b** was obtained by a similar process on use of (+)-fenchone instead of (−)-fenchone. The release of **1b** from the very soluble (and therefore isolable only with difficulty) diastereomeric inclusion complex **3b** [=**1b**·(−)-fenchone (1:2)] that is present in the mother liquor after crystallization of **3a**, is not as worthwhile.

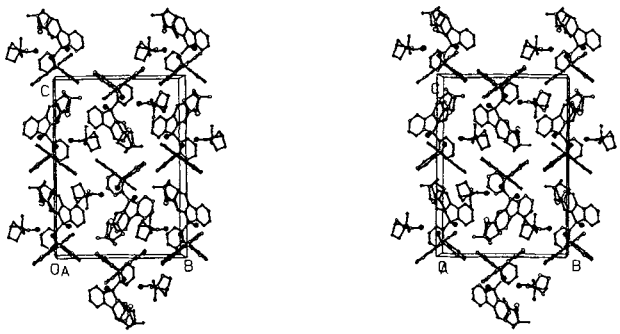

Fig. 2. Packing of **3a** [**1a**·(−)-fenchone (1:2)] in the crystal (stereoview). The hydrogen-bonded oxygen atoms are indicated as filled circles.

Compounds **1a** and **1b** (like racemic **1**) form inclusion complexes efficiently on crystallization with many organic amines and ketones, as well as with other classes of compounds, and form well-defined clathrates with 1:2 stoichiometry.[8] On separate use of **1a** or **1b**, the clathrate formation is enantioselective; for example, 3-methylpiperidine is included with *ee* > 99%, 2-methylpiperidine with *ee* = 40%, and 2-methylcyclohexanone with *ee* = 52%. On heating the isolated crystals of the inclusion complex, the freed guest compound distills off in optically active form, even on preparative scale. A reasonable assumption, therefore, is that **1a** and **1b** can also be used for resolution of racemates of other substances (such as chiral building blocks) by cocrystallization.

If the solid host substance is exposed to an atmosphere saturated with a racemic guest compound, enantioselective sorption takes place. Thus the chances that **1a** (and **1b**) may be developed as chemical sensors for enantioselection are good.[9] Applications as chiral catalysts—for example, in the addition of Grignard reagents to ketones[10a] or of alkylzinc compounds to aldehydes[10b]—or as chiral auxiliaries (aluminum hydride or borohydride reagents)[1, 2a] and NMR shift reagents[11] also seem possible.[12]

Since **1** can be modified in a variety of ways, for example by introducing substituents or varying the bridge, a broad use of this new atropisomeric molecular framework in enantiodifferentiation is expected.

Experimental Procedure

Racemic **1** [5]: A solution of *n*BuLi (53.1 mL, 85 mmol, 1.6N in *n*-hexane) was added slowly under argon at 0°C to 2,2'-dibromobiphenyl [13] (10.5 g, 38 mmol) in dry diethyl ether (70 mL). After the reaction mixture had been stirred for another 2 h at the same temperature, a solution of fluorenone (13.8 g, 77 mmol) in dry diethyl ether was added dropwise within 0.5 h. The mixture was stirred for a further 2 h at room temperature, heated at reflux for 15 h, and subsequently hydrolyzed (NH_4Cl solution). The major portion of the product precipitated and was isolated by filtration. The ethereal phase was separated

off, dried ($MgSO_4$), and evaporated to dryness in vacuum. Methanol was added to the oily residue, which caused more product to precipitate. Yield: 13.8 g (70%). M.p. 292–294 °C (phase change at 248–250 °C) [5]. IR (KBr): $\tilde{\nu}$[cm^{-1}] = 3650 (OH), 3110 (Ar), 1205, 1120, 1060 (C-O, OH), 780, 750, 740 (Ar). ^{1}H NMR (200 MHz, $CDCl_3$): δ = 4.12, 4.13 (2s, 2H; OH), 6.60 (dd, ^3J(H,H) = 8 Hz, ^4J(H,H) = 1.2 Hz, 2H; ArH), 7.05 (dt, ^3J(H,H) = 7.8 Hz, ^4J(H,H) = 2 Hz, 2H; ArH), 7.15–7.55 (m, 16H; ArH), 7.65–7.75 (m, 4H; ArH); ^{13}C NMR (250 MHz, $CDCl_3$): δ = 152.45, 150.68, 142.15, 140.57, 140.15, 139.37, 132.44, 129.37, 129.08, 128.98, 128.59, 128.37, 127.07, 126.20, 125.16, 124.87, 120.44, 119.89, 87.29. MS: m/z 514.1930 (M^+). Correct C,H analysis.

Resolution of **1**: Racemic **1** (10 g, 19.5 mmol) were dissolved in (−)-fenchone (120 mL) with heating. In an open flask colorless crystals of **3a**, the 1:2 inclusion complex between **1a** and (−)-fenchone, formed at room temperature within 1–2 days. These were isolated, washed with petroleum ether (40–60°), and dried. Yield: 70–90%, m.p. >150 °C (decomp.). Thereafter the crystals were exposed to an atmosphere saturated with MeOH in a desiccator at room temperature overnight. The included (−)-fenchone was completely exchanged for MeOH. The methanol was removed from this 1:2 inclusion complex (**4a**) by heating in vacuum (2 h, 50 °C, 15 Torr). Yield: 70–90%, colorless powder, m.p. 150–160 °C (racemization occurs); $[\alpha]_D^{20}$ = 334.2 (c = 0.5 in $CHCl_3$). Spectroscopic data conform to racemic **1**. The use of (+)-fenchone in the same procedure yielded **1b**.

Received: November 7, 1992 [Z 5670 IE]
German version: *Angew. Chem.* **1993**, *105*, 616

[1] D. Seebach, *Angew. Chem.* **1990**, *102*, 1363; *Angew. Chem. Int. Ed. Engl.* **1990**, *29*, 1320.

[2] a) R. Noyori, M. Kitamura, *Mod. Synth. Methods* **1989**, *5*, 115; R. Noyori, *Chem. Soc. Rev.* **1989**, *18*, 187; b) F. Toda, *Top. Curr. Chem.* **1987**, *140*, 43; c) E. Weber in *Inclusion Compounds, Vol. 4 (Key Organic Host Systems)* (Eds.: J. L. Atwood, J. E. D. Davies, D. D. MacNicol), Oxford University Press, Oxford, **1991**, Chapter 5.

[3] a) A. K. Beck, B. Bastani, D. A. Plattner, W. Petter, D. Seebach, H. Braunschweiger, P. Gysi, L. La Vecchia, *Chimia* **1991**, *45*, 238, and references therein; b) F. Toda in *Inclusion Compounds, Vol. 4 (Key Organic Host Systems)* (Eds.: J. L. Atwood, J. E. D. Davies, D. D. MacNicol), Oxford University Press, Oxford, **1991**, Chapter 4; c) E. Weber, C. Wimmer, A. L. Llamas-Saiz, C. Foces-Foces, *J. Chem. Soc. Chem. Commun.* **1992**, 733; see also *Chem. Ind. (London)* **1992**, 364.

[4] E. Weber, N. Dörpinghaus, I. Csöregh, *J. Chem. Soc. Perkin Trans. 2* **1992**, 2167; I. Csöregh, E. Weber, N. Dörpinghaus, *J. Chem. Soc. Chem. Commun.* **1992**, 110.

[5] Cf. G. Wittig, W. Schoch, *Justus Liebigs Ann. Chem.* **1971**, *749*, 38.

[6] Crystal data for **3a** [**1a**·(−)-fenchone (1:2)]: $C_{38}H_{26}O_2 \cdot (C_{10}H_{16}O)_2$, M_r = 819.1, space group $P2_12_12_1$ (no. 19), a = 11.717(3), b = 16.859(3), c = 22.960(6) Å, V = 4535(2) Å^3, Z = 4, ρ_{calcd} = 1.20 gcm^{-3}, $F(000)$ = 1752, $\mu(Mo_{K\alpha})$ = 0.684 cm^{-1}, crystal dimensions 0.30 × 0.32 × 0.45 mm. 4458 independent reflections, 1765 observed ($|F| > 2\sigma|F|$), Enraf-Nonius CAD4 diffractometer, T = 298 K, $\omega/2\theta$ scan, θ_{max} = 25°. Isotropic refinement of all non-hydrogen atoms, full-matrix least-squares method, (SHELX 76), R = 0.111, R_w = 0.115 [$w = (\sigma^2F + 0.001\ F^2)^{-1}$] for 269 parameters. The unfavorable reflections:parameters ratio that is caused by the poor crystal quality did not allow an anisotropic refinement of the atom positions and results in the relatively high R value. Further details of the crystal structure investigation may be obtained from the Fachinformationszentrum Karlsruhe, Gesellschaft für wissenschaftlich-technische Information mbH, D-W-7514 Eggenstein-Leopoldshafen 2 (FRG) on quoting the depository number CSD-57125, the names of the authors, and the journal citation.

[7] E. L. Eliel, *Stereochemie der Kohlenstoffverbindungen*, Verlag Chemie, Weinheim, **1966**, p. 39ff.

[8] E. Weber, K. Skobridis, C. Wimmer, *GIT Fachz. Lab.* **1992**, *36*, 740; L. J. Barbour, S. A. Bourne, M. R. Caira, L. R. Nassimbeni, E. Weber, K. Skobridis, A. Wierig, *Supramol. Chem.*, in press.

[9] F. L. Dickert, *Chem. Unserer Zeit* **1992**, *26*, 138; K. Cammann, U. Lemke, A. Rohen, J. Sander, H. Wilken, B. Winter, *Angew. Chem.* **1991**, *103*, 519; *Angew. Chem. Int. Ed. Engl.* **1991**, *30*, 516.

[10] a) B. Schmidt, D. Seebach, *Angew. Chem.* **1991**, *103*, 1383; *Angew. Chem. Int. Ed. Engl.* **1991**, *30*, 1321; b) B. Weber, D. Seebach, *ibid.* **1992**, *104*, 96 and **1992**, *31*, 84.

[11] a) F. Toda, R. Toyotaka, H. Fukuda, *Tetrahedron: Asymmetry* **1990**, *1*, 303; b) C. von dem Bussche-Hünnefeld, A. K. Beck, U. Lengweiler, D. Seebach, *Helv. Chim. Acta* **1992**, *75*, 438.

[12] We thank Prof. D. Seebach, ETH Zürich, for fruitful discussions.

[13] H. Gilman, B. J. Gaj, *J. Org. Chem.* **1957**, *22*, 447.

One-Flask Synthesis of Propargylic Alcohols from Organolithium Reagents, *N,N*-Disubstituted Amides, and Acetylenes**

By *Jih Ru Hwu,* Gholam Hosein Hakimelahi, Fung Fuh Wong,* and *Chun Chieh Lin*

Dedicated to Professor Alex Nickon on the occasion of his 65th birthday

Two-step synthetic sequences following standard methods often require two individual reactions. Method 1 in Scheme 1 shows an example in which a nucleophile :Nu is treated with the reagent RX to give :X and NuR in the first reaction. After being isolated, the intermediate NuR is allowed to react with nucleophile :L (from other source) to give the desired product in the second reaction. These two reactions could be combined into one by use of the "counterattack strategy"[1] (method 2), in which the reagent RL is first attacked by :Nu to give NuR and :L. The leaving group :L then counterattacks the intermediate NuR in situ to afford the desired product. Use of this method can simplify chemical transformations and minimize manipulations. With these advantages in mind we developed method 3, another type of efficient method that also combines two reactions.

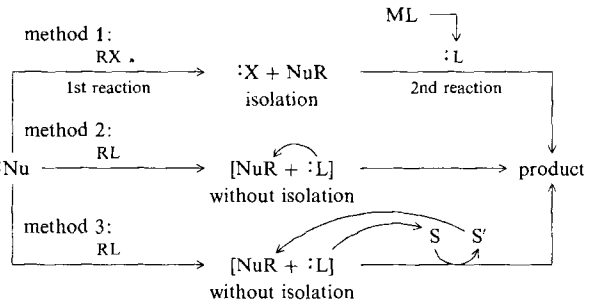

Scheme 1. Comparison of synthetic methods 1–3; 1 = traditional method, 2 = counterattack method, 3 = pseudo-counterattack method.

The first step in method 3, analogous to that in method 2, is the reaction between :Nu and RL to give NuR and the leaving group :L. This leaving group then reacts with compound S to generate an active species S', which subsequently attacks the intermediate NuR in situ. Because :L does not counterattack NuR directly as in method 2, we may refer to the compound RL as a "pseudo-counterattack reagent". Herein we report a novel way to synthesize propargylic alcohols by this "pseudo-counterattack strategy".

In our new, one-flask synthesis (Scheme 2) an organolithium reagent, an amide (also the solvent), and phenylacetylene were used to prepare the desired propargylic alcohols in 74–93% yields (Table 1). Propargylic alcohols can be used in the synthesis of the ω chain in prostaglandins[2] and for the preparation of pheromone components.[3] To obtain a high yield by this new method, we found it crucial to add the

[*] Prof. J. R. Hwu, F. F. Wong, C. C. Lin
Organosilicon and Synthesis Laboratory
Department of Chemistry, National Tsing Hua University
Hsinchu, Taiwan 30043 (Republic of China)
Prof. G. H. Hakimelahi
Organosilicon and Synthesis Laboratory
Institute of Chemistry, Academia Sinica (Republic of China)

[**] This research was supported by the National Science Council of the Republic of China (Grants NSC 82-0208-M007-072 and NSC 82-0208-M-001-126) and Academia Sinica.

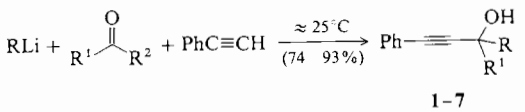

1-7

Scheme 2. Preparation of propargylic alcohols from organolithium reagents, amides, and phenylacetylene.

organolithium reagent to the solution of phenylacetylene in the appropriate amide. Inverse addition often led to low yields.

Table 1. One-flask synthesis of propargylic alcohols from organolithium reagents, *N,N*-disubstituted amides, and phenylacetylene at room temperature (see Scheme 2).

Entry	R	R^1	R^2	Product	Yield [%]
1	*n*Bu	H	NMe_2	**1**	90
2	*n*Bu	H	NEt_2	**1**	87
3	*n*Bu	H	$N(iPr)_2$	**1**	87
4	*n*Bu	H	$N(-(CH_2)_4-)$	**1**	90
5	*n*Bu	H	$N(-(CH_2)_5-)$	**1**	93
6	*n*Bu	Me	NMe_2	**2**	85
7	*n*Bu	*n*-$C_{11}H_{23}$	NEt_2	**3**	82
8	Me	Me	NMe_2	**4**	74
9	Ph	H	NMe_2	**5**	86
10	Ph	H	$N(-(CH_2)_4-)$	**5**	93
11	Ph	*n*-$C_{11}H_{23}$	NEt_2	**6**	90
12 [a]	Et	H	$N(iPr)_2$	**7**	71

[a] Grignard reagent EtMgBr was used instead of an organolithium reagent.

The mechanism of this reaction is shown in Scheme 3 for *n*BuLi, *N,N*-diisopropylformamide, and phenylacetylene. In the first step *N,N*-diisopropylformamide is attacked by *n*BuLi to give the stable intermediate valeraldehyde. The $(iPr)_2N^-$ anion formed from the amide reacts with phenylacetylene to generate the nucleophile lithium phenylacetylide. This acetylide attacks the intermediate valeraldehyde in situ to afford the desired propargylic alcohol **1**. Thus, in the entire transformation, *N,N*-diisopropylformamide can be considered a pseudo-counterattack reagent (Scheme 1).

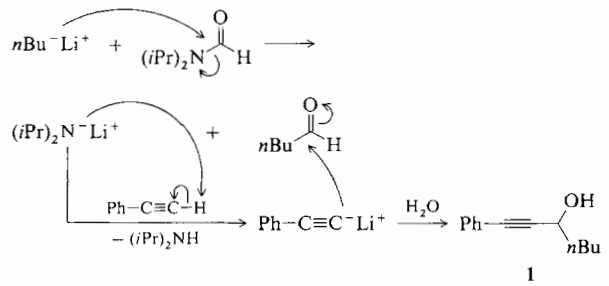

1

Scheme 3. Reaction mechanism of the new pseudo-counterattack method. *N,N*-diisopropylformamide functions as a pseudo-counterattack reagent synthetic method.

Smith et al.[4] reported a method for the preparation of α-hydroxy- and α-oxoamides by treating aldehydes, ketones, or esters with diisopropylcarbamoyl lithium, which is generated from *N,N*-diisopropylformamide and an alkyllithium reagent. The alkyllithium reagent functions as a base removing the formyl proton from *N,N*-diisopropylformamide. A mixed-solvent system of Et_2O, THF, and pentane is employed. In our method, the alkyllithium reagent acts as a nucleophile and replaces a dialkylamino group in the amide substrate. We believe that the different roles played by the organolithium reagents in these two methods arise, in part, from solvent effects. In our method the amide serves both as a substrate for the organolithium reagent and as the solvent. These polar aprotic solvents may enhance the nucleophilicity of an organolithium reagent by complexation.[5] Thus nucleophilic addition prevails over deprotonation. To reconfirm this point, we carried out a control experiment by treating *n*BuLi with *N,N*-dimethylformamide at 25 °C. The expected product, valeraldehyde, was isolated in 98% yield after 10 min. The yield gradually dropped to 0% within 1.5 h because of the instability of valeraldehyde in the presence of the base $LiNMe_2$ generated in situ.

The results in Table 1 (entries 1–7) indicate that many *N,N*-disubstituted amides can be employed in the newly developed method, including *N,N*-dimethyl-, *N,N*-diethyl- and *N,N*-diisopropylformamide, 1-formylpyrrolidine, 1-formylpiperidine, *N,N*-dimethylacetamide, and *N,N*-diethyldodecanamide. Although a number of organolithium reagents gave propargylic alcohols in good to excellent yields, Grignard reagents often gave inconsistent results. The best yield we ever obtained was 71% for propargylic alcohol **7**, which came from the reaction of EtMgBr with *N,N*-diisopropylformamide and phenylacetylene (entry 12).

Phenylacetylene was the most suitable alkyne, providing the desired propargylic alcohols (**1**–**7**) in 71–93% yields. 1-Hexyne and 1-octyne reacted with *N,N*-diisopropylformamide and *n*BuLi to afford the corresponding propargylic alcohols undec-6-yn-5-ol and tridec-6-yn-5-ol, respectively, in yields of only 30–33%. The difference in yield may be related to the acidity of the terminal acetylenic proton: phenylacetylene is more acidic than alkylacetylenes by about two pK units.[6] Inefficient proton transfer from an alkylacetylene to $(iPr)_2N^-$ generated in situ allows the latter species to enolize the aldehyde intermediates.

Experimental Procedure

Representative procedure: To a stirred solution containing *N,N*-diisopropylformamide (1.5 mL) and phenylacetylene (141 mg, 1.37 mmol, 1.0 equiv) was added *n*BuLi (1.4 M, 0.856 mL, 1.37 mmol, 1.0 equiv). After being stirred at room temperature under an atmosphere of nitrogen for 3 h, the reaction mixture was diluted with water, neutralized with 10% HCl, and extracted with Et_2O three times. The combined ethereal extracts were washed with water and brine, then dried over $MgSO_4$, filtered, and concentrated under reduced pressure. The residue was chromatographed on a column packed with silica gel to give 1-phenylhept-1-yn-3-ol (**1**) as a pale yellow oil in 87% yield (224 mg, 1.19 mmol).

Spectroscopic data for **1** [7]: ^{1}H NMR (300 MHz, $CDCl_3$, 25 °C): δ = 0.96 (t, ^3J(H,H) = 7.2 Hz, 3H, CH_3), 1.38–1.56 (m, 4H), 1.80–1.88 (m, 2H), 2.18 (br, 1H; OH), 4.63 (t, ^3J(H,H) = 6.6 Hz, 1H; C≡CCH), 7.31–7.35 (m, 3H; PhH), 7.45–7.48 (m, 2H; PhH); ^{13}C NMR ($CDCl_3$, 75 MHz, 25 °C): δ = 13.75, 22.16, 27.16, 37.45, 62.92, 84.80, 90.27, 122.84, 128.43, 128.51, 131.85; IR (neat): $\tilde{\nu}$[cm^{-1}] = 3358 (OH), 2223 (C≡C), 1601 (C=C), 1028 (C–O). **2** [8]: ^{1}H NMR: δ = 0.97 (t, ^3J(H,H) = 7.3 Hz, 3H; CH_3), 1.38–1.45 (m, 2H), 1.54–1.63 (m, 2H), 1.59 (s, $OCCH_3$), 1.75–1.81 (m, 2H), 2.15 (s, 1H; OH), 7.32–7.34 (m, 3H; PhH), 7.43–7.47 (m, 2H; PhH); ^{13}C NMR: δ = 13.79, 22.60, 26.73, 43.38, 68.58, 83.25, 93.00, 122.96, 128.38, 131.81; IR (neat): $\tilde{\nu}$[cm^{-1}] = 3381 (OH), 2208 (C≡C), 1584 (C=C), 1142 (C–O). **3**: ^{1}H NMR: δ = 0.91 (t, ^3J(H,H) = 6.6 Hz, 3H; CH_3), 0.97 (t, ^3J(H,H) = 7.2 Hz, 3H; CH_3), 1.24–1.76 (m, 26H), 2.11 (br, s, 1H; OH), 7.32–7.34 (m, 3H; PhH), 7.43–7.46 (m, 2H; PhH); ^{13}C NMR: δ = 13.82, 22.45, 22.69, 24.11, 26.32, 29.15, 29.38, 29.42, 29.63, 31.39, 31.72, 41.71, 41.99, 42.09, 42.11, 71.57, 84.21, 92.42, 123.13, 128.26, 128.35, 131.82; IR (neat): $\tilde{\nu}$[cm^{-1}] = 3408 (OH), 2203 (C≡C), 1599 (C=C), 1248 (C–O). **4** [9]: ^{1}H NMR: δ = 1.66 (s, 6H; $2CH_3$), 2.37 (br, s, 1H; OH), 7.32–7.34 (m, 3H; PhH), 7.44–7.47 (m, 2H; PhH); ^{13}C NMR: δ = 31.23, 65.45, 82.03, 93.78, 122.82, 128.18, 128.33, 131.74; IR (neat): $\tilde{\nu}$[cm^{-1}] = 3367 (OH), 2208 (C≡C), 1598 (C=C), 1158 (C–O). **5** [10]: ^{1}H NMR: δ = 2.54 (d, ^3J(H,H) = 4.9 Hz, 1H; OH), 5.70 (d, ^3J(H,H) = 4.9 Hz, 1H; C≡CCH), 7.26–7.51 (m, 8H; PhH), 7.63 (d, ^3J(H,H) = 7.4 Hz, 2H; PhH); ^{13}C NMR: δ = 64.06, 89.76, 122.58, 126.88, 128.46, 128.57, 128.74, 128.84, 129.03, 131.95, 140.84; IR (neat): $\tilde{\nu}$[cm^{-1}] = 3367 (OH), 2223 (C≡C), 1589 (C=C), 1029 (C–O). **6**: ^{1}H NMR: δ = 0.89 (t, ^3J(H,H) = 7.1 Hz, 3H; CH_3), 0.98–2.14 (m, 20H), 2.48 (s, 1H; OH), 7.22–7.48 (m, 6H; PhH), 7.48–7.52 (m, 2H; PhH), 7.72 (d,

^3J(H,H) = 7.7 Hz, 2H; PhH); ^{13}C NMR: δ = 13.81, 22.43, 24.51, 28.83, 29.13, 29.27, 29.34, 29.40, 31.38, 31.70, 45.38, 73.67, 85.90, 91.79, 122.91, 125.68, 125.86, 127.78, 127.91, 128.47, 131.90, 145.19; IR (neat): $\tilde{\nu}$[cm^{-1}] = 3409 (OH), 2218 (C≡C), 1599 (C=C), 1039 (C–O). 7 [10, 11]: ^{1}H NMR: δ = 1.09 (t, ^3J(H,H) = 7.4 Hz, 3H; CH_3), 1.72–1.91 (m, 2H), 2.12 (br. s, 1H; OH), 4.57 (t, ^3J(H,H) = 6.5 Hz, 1H; C≡CCH), 7.21–7.34 (m, 3H; PhH), 7.43–7.48 (m, 2H; PhH); ^{13}C NMR: δ = 9.23, 30.77, 64.13, 84.91, 89.98, 122.82, 128.48, 128.72, 131.87; IR (neat): $\tilde{\nu}$[cm^{-1}] = 3355 (OH), 2224 (C≡C), 1598 (C=C), 1102 (C–O).

Received: November 6, 1992 [Z 5667 IE]
German version: *Angew. Chem.* **1993**, *105*, 591

[1] a) J. R. Hwu, B. A. Gilbert, *Tetrahedron* **1989**, *45*, 1233; b) J. R. Hwu, *J. Org. Chem. (Shanghai)* **1992**, *12* (Supplement), 56; c) J. R. Hwu, T. Lee, B. A. Gilbert, *J. Chem. Soc. Perkin Trans. 1* **1992**, 3219.
[2] a) R. Noyori, M. Suzuki, *Angew. Chem.* **1984**, *96*, 854; *Angew. Chem. Int. Ed. Engl.* **1984**, *23*, 847; b) J. Rokach, J. Adams, *Acc. Chem. Res.* **1985**, *18*, 87; c) M. Suzuki, A. Yanagisawa, R. Noyori, *J. Am. Chem. Soc.* **1988**, *110*, 4718; d) S. Torii, H. Okumoto, F. Akahoshi, T. Kotani, *ibid.* **1989**, *111*, 8933.
[3] a) R. G. Vogt in *Pheromone Biochemistry* (Eds.: G. D. Prestwich, G. J. Blomquist), Academic Press, New York, **1987**; b) W. C. Sun, G. D. Prestwich, *Tetrahedron Lett.* **1990**, *31*, 801; c) W. C. Sun, C. S. Ng, G. D. Prestwich, *J. Org. Chem.* **1992**, *57*, 132.
[4] A. S. Fletcher, K. Smith, K. Swaminathan, *J. Chem. Soc. Perkin Trans. 1* **1977**, 1881.
[5] F. A. Carey, R. J. Sundberg, *Advanced Organic Chemistry, Part A*, 3rd ed., Plenum, New York, **1990**, p. 237.
[6] A. Streitwieser, Jr., D. M. E. Reuben, *J. Am. Chem. Soc.* **1971**, *93*, 1794.
[7] M. R. Golse, M. A. Liermain, *Bull. Soc. Pharm. Bordeaux* **1962**, *101*, 3; [*Chem. Abstr.* **1963**, *58*, 4451].
[8] M. N. Rybakova, *Uch. Zap. Permsk. Gos. Univ. im A. M. Gor'kogo* **1970**, *207*, 278; [*Chem. Abstr.* **1972**, *76*, 24821p].
[9] B. Tomek, J. Gabriel, CS-A 148737 (Cl. C 07c), **1973**; [*Chem. Abstr.* **1973**, *79*, 136485a].
[10] A. Arcadi, S. Cacchi, F. Marinelli, *Tetrahedron* **1985**, *41*, 5121.
[11] H. C. Brown, G. A. Molander, S. M. Singh, U. S. Racherla, *J. Org. Chem.* **1985**, *50*, 1577.

Vanadium Phosphate Framework Solid Constructed of Octahedra, Square Pyramids, and Tetrahedra with a Cavity Diameter of 18.4 Å**

By *Victoria Soghomonian, Qin Chen, Robert C. Haushalter,* and Jon Zubieta**

The intense contemporary interest in the chemistry of vanadium oxide phosphate (V-P-O) compounds reflects the catalytic relevance of the V-P-O system[1, 2] and the astonishing structural variability of the networks of connected vanadium and phosphorus polyhedra that are found in these compounds.[3–10] This structural diversity is associated in part with the ability of vanadium–oxygen compounds to form tetrahedral, square-pyramidal, and octahedral coordination polyhedra and to build larger aggregates by condensation of polyhedra through shared oxygen atoms.[11] Our objective has been the preparation of V-P-O framework solids that encapsulate organic guests to produce large cavities or tunnels. After the organic template is removed by ion exchange or thermal methods, the solid may sorb substrate molecules in a size- and shape-selective fashion.[12] We have exploited hydrophobic/hydrophilic interactions to fashion materials with segregated polar and nonpolar cavities[13] and introduced lower valent vanadium sites into the V-P-O networks to reduce the polarity of the framework and to disrupt the tendency to form the lamellar backbones so common to $MO(PO_4)$ networks.[14] Our efforts have now culminated in the isolation of the unique V-P-O phase **1**.

$(H_3NCH_2CH_2NH_3)_2(H_3NCH_2CH_2NH_2)[V^{III}(H_2O)_2\text{-}(V^{IV}O)_8(OH)_4(HPO_4)_4(PO_4)_4(H_2O)_2]\cdot 2H_2O$ **1**

The hydrothermal reaction of V_2O_5, vanadium metal, ethylenediamine, methylphosphonic acid, and phosphoric acid gave blue crystals of **1** in 80% yield.[15] X-ray structural analysis of **1**[16] revealed a complex three-dimensional structure with a large cavity occupied by the organic cations (Fig. 1). Compound **1** is constructed from corner-sharing

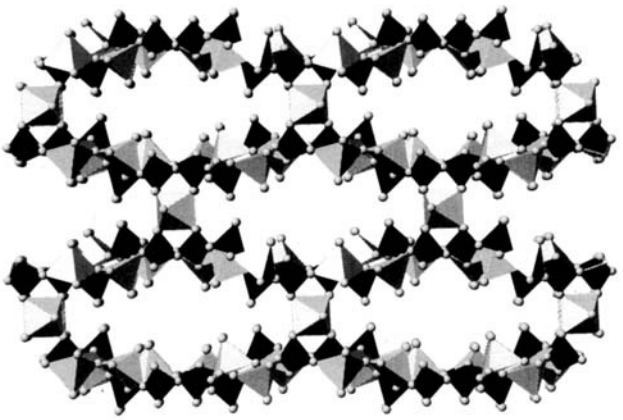

Fig. 1. A view of the structure of **1** down the crystallographic *b* axis showing the elliptically shaped tunnels which have an atom-to-atom diameter of 18.4 Å.

V^{IV} square pyramids, V^{III} octahedra,[17] and PO_4^{3-} and HPO_4^{2-} tetrahedra and displays a number of structural motifs common to V-P-O phases. There are two types of binuclear V^{IV} units in the V^{IV}-P-O lamellar framework: $[V_2(\mu_2\text{-}PO_4)_2]$ and $[V_2(\mu\text{-}OH)(\mu_2\text{-}PO_4)]$ groups.[18] As these motifs alternate within the V^{IV}-P-O planes, {V-O-V} units are found rather than the $\{V\text{-}O\text{-}V\}_\infty$ chains more generally observed in V-P-O phases.

The overall structure may be described as undulating layers constructed of corner-sharing (through a μ^2-OH group) V^{IV} square pyramids and HPO_4^{2-} and PO_4^{3-} tetrahedra connected by V^{III} octahedra. The fundamental building blocks of the layers are domed rings made up of eight polyhedra: four VO_5 square pyramids, and two HPO_4^{2-} and two PO_4^{3-} tetrahedra (Fig. 2 top). These rings are amphiphilic; the four less polar vanadyl groups are on one side of the plane defined by the V and P atoms and four P–O groups are on the opposite side (Fig. 2 bottom). Two of these four P–O groups are strongly polar P–OH groups, the other two are bound to interlamellar diaqua V^{III} center. Each ring exhibits the V=O and P–OH groups in an *anti* orientation and is surrounded by six other rings. In two of the neighboring rings the V=O groups are oriented up and the P–OH groups down along the *b* axis (V=O up/P–OH down); the other four rings have the arrangement V=O down/P–OH up. Within each layer, strips

[*] Prof. J. Zubieta, V. Soghomonian, Dr. Q. Chen
Department of Chemistry
Syracuse University
Syracuse, NY 13244 (USA)
Dr. R. C. Haushalter
NEC Research Institute
4 Independence Way
Princeton, NJ 08540 (USA)

[**] The work at Syracuse University was supported by a grant from the National Science Foundation to J. Z. (CHE9119910).

formed from rings with V=O up/P–OH down alternate with parallel strips with V=O down/P–OH up. The two types of rings in the parallel strips are offset from one another by 0.5 *b*. This up–down connectivity of the domed rings gives rise to the undulations in the layers and large holes (diameter ca. 6.2–7.2 Å atom to atom) within the layers.

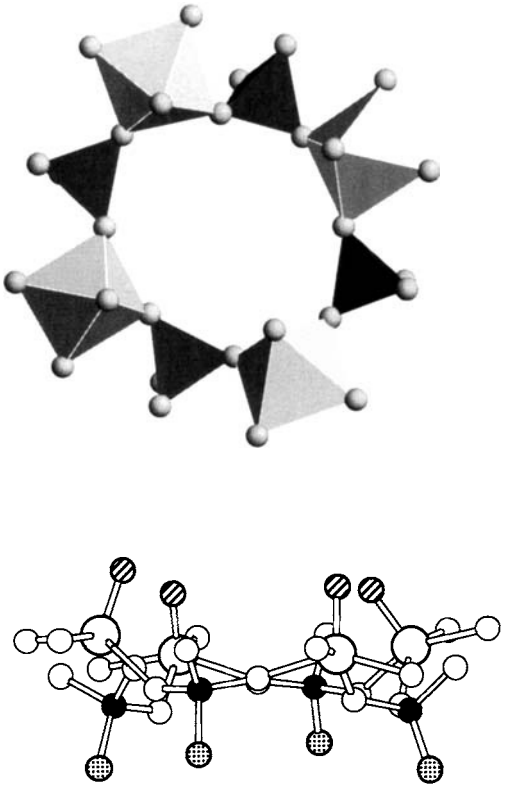

Fig. 2. The ring building block in **1** constructed from eight polyhedra. Top: View perpendicular, and bottom: View parallel to the plane of the ring. Note in the bottom picture that the less polar V=O groups lie on one face of the ring (striped circles) and the more polar P–O groups (stippled circles) on the opposite face. The largest circles are V atoms, the black circles are P atoms.

The three-dimensional structure is formed by the connection of these layers through $V^{III}(H_2O)_2$ centers. These V^{III} atoms serve to produce elliptical cross sections in the large cavities by drawing together the polar regions of the layer while the nonpolar regions of the layers are pushed away from the organic cations. The V^{III}–V^{III} distance of the long axis of the elliptical channels, 18.4 Å, is the same as length of the unit cell along *c*. The polar NH_3+ ends of the organic cations and the water of crystallization are situated within the cavities so as to maximize hydrogen-bonding interactions with the polar P–OH and $V(H_2O)_2$ portions of the framework; the less polar carbon backbones of the organic templates are associated with the V=O groups.

As was found in the case of the microporous molybdenum phosphates,[12] hydrophilic/hydrophobic interactions appear to be an important factor in determining how this type of mixed organic–inorganic compound can crystallize. In compound **1** a potentially labile aqua ligand occupies an incipient vacant coordination site within a micropore. Although we have not yet performed experiments to study the sorption properties of **1**, such microporous oxides displaying shape-selective access to a transition element side could prove useful.[12]

The successful incorporation of a relatively large organic template into a V-P-O solid phase described in this work demonstrates several emerging themes in the development of synthetic routes to such designed materials.[12] Since the structures adopted by V-P-O phases are dependent on the templates employed, hydrophobic/hydrophilic interactions can exploited in the self-assembly of the frameworks by proper choice of templating inorganic and organic cations. Incorporation of both inorganic and organic cations into the V-P-O framework induces segregation of polar and nonpolar regions with the production of large incipient void volumes. When reduced vanadium centers are introduced, specifically V^{III}, a framework with reduced polarity is created. The octahedral (oxo-deficient) geometry preferred by V^{III} leads to a more flexible connectivity, which dramatically extends the structural chemistry of the system. Finally, when the V/P ratio is increased above 1.0, the relative vanadyl (V=O) content of the structure is enhanced. Since M=O moieties are considerably less polar than P–O groups, the tendency of solids rich in M=O units to encapsulate organic templates should be enhanced.

Received: November 2, 1992 [Z 5659 IE]
German version: *Angew. Chem.* **1993**, *105*, 601

[1] G. Centi, F. Trifiro, J. R. Ebner, V. M. Franchetti, *Chem. Rev.* **1988**, *88*, 55.
[2] B. L. Hodnett, *Catal. Rev. Sci. Eng.* **1985**, *27*, 373.
[3] G. Huan, J. W. Johnson, A. J. Jacobson, E. W. Corcoran, Jr., D. P. Goshorn, *J. Solid State Chem.* **1991**, *93*, 514, and references therein.
[4] K. H. Lii, L. F. Mao, *J. Solid State Chem.* **1992**, *96*, 436, and references therein.
[5] a) A. Patter, A. R. Saple, R. Y. Kelken, *J. Chem. Soc. Chem. Commun.* **1991**, *356*, and references therein; b) C. Montes, M. E. Davis, B. Murray, M. Narayana, *J. Phys. Chem.* **1990**, *94*, 6425.
[6] $[Zn_2VO(PO_4)_2]$: K. H. Lii, H. J. Tsai, *J. Solid State Chem.* **1991**, *90*, 291; $[Cs_2V_3P_4O_{17}]$: K. H. Lii, Y. P. Wang, S. L. Wang, *ibid.* **1989**, *80*, 127; $[K_2V_3P_4O_{17}]$: K. H. Lii, H. J. Tsai, S. L. Wang, *ibid.* **1990**, *87*, 396; $[A_2VOP_2O_7]$ (A = Cs, Rb): K. H. Lii, S. L. Wang, *ibid.* **1989**, *82*, 239; $[AVP_2O_7]$ (A = Li–Cs): K. H. Lii, Y. P. Wang, Y. B. Chen, S. L. Wang, *ibid.* **1990**, *86*, 143, and references therein; $[NaVOPO_4]$: K. H. Lii, C. H. Li, T. M. Chen, S. L. Wang, *Z. Kristallogr.* **1991**, *197*, 67; $[RbV_3P_3O_{13+x}]$: K. H. Lii, C. S. Lee, *Inorg. Chem.* **1990**, *29*, 3298.
[7] $[A_{0.5}VOPO_4] \cdot xH_2O$ (A = Na, $x = 2.0$; A = K, $x = 1.5$): S. L. Wang, H. Y. Kang, C. Y. Cheng, K. H. Lii, *Inorg. Chem.* **1991**, *30*, 3496; $[K_2(VO)_2P_3O_9(OH)_3] \cdot 1.125\,H_2O$: K. H. Lii, H. J. Tsai, *ibid.* **1991**, *30*, 446; $[K_2(VO)_3(HPO_4)_4]$: *J. Solid State Chem.* **1991**, *91*, 331.
[8] $[LiVOPO_4]$: A. V. Lavrov, V. P. Nikolaev, G. G. Sadikov, M. A. Porai-Koshits, *Sov. Phys. Dokl. (Engl. Transl.)* **1982**, *27*, 680.
[9] $[NH_4(VO)(HPO_4)]$: K. H. Lii, N. S. Wu, B. R. Chen, *J. Solid State Chem.* **1992**, *97*, 283.
[10] $[Ca_2V(PO_4)(HPO_4)_2] \cdot H_2O$ and $[Ca_2V(PO_4)(P_2O_7)]$: K. H. Lii, N. S. Wen, C. C. Su, B. R. Chen, *Inorg. Chem.* **1992**, *31*, 439; $[Cs_3V_3P_{12}O_{36}]$: A. V. Lavrov, V. P. Nikolaev, G. G. Sadikov, M. Ya, *Sov. Phys. Dokl. (Engl. Transl.)* **1981**, *26*, 631; $[CsV_2P_3O_{16}]$: B. Klinert, M. Z. Jansen, *Z. Anorg. Allg. Chem.* **1988**, *567*, 87; $[Na_3V_2P_3O_{12}]$: C. Delmar, R. Olazcuage, F. Cherkaoui, R. Brochu, G. LeFlen, *C. R. Seances Acad. Sci. Ser. C* **1978**, *287*, 169.
[11] A. Müller, M. T. Pope, *Angew. Chem.* **1991**, *103*, 56; *Angew. Chem. Int. Ed. Engl.* **1991**, *30*, 34.
[12] R. C. Haushalter, L. A. Mundi, *Chem. Mater.* **1992**, *4*, 31.
[13] $K_4(Me_2NH_2)[V_{10}O_{10}(OH)_4(PO_4)_7(H_2O)_2] \cdot 4\,H_2O$: V. Soghomonian, Q. Chen, R. C. Haushalter, J. Zubieta, C. J. O'Connor, *Science*, in press.
[14] $K_2[(V^{IV}O)_2V^{III}(PO_4)(H_2PO_4)(H_2O)_2]$: R. C. Haushalter, C. J. O'Connor, M. Thompson, Z. Wang, J. Zubieta, *Inorg. Chem.*, in press; $K[V^{IV}OV^{III}(HPO_4)_3(H_2O)_2]$: *ibid.*, in press.
[15] The reaction of V_2O_5, V (−325 mesh), $CH_3PO_3H_2$, H_3PO_4, $H_2N(CH_2)_2NH_2$, and H_2O in a mol ratio of 0.95:1:2.79:7.33:6.73:1056.5 for 4 d at 200 °C in a 23 mL Teflon-lined Parr acid digestion bomb (30% fill volume) gaves two products. Phosphate **1** formed as dark blue, diamond-shaped plates in over 80% yield (based on total V), while the amorphous white product was formed in less than 20% yield. We were unable to optimize these reaction conditions to reduce the amount of the side product.
[16] **1**: Monoclinic, space group $P2_1/n$ with $a = 14.313(3)$, $b = 10.151(2)$, $c = 18.374(4)$ Å, $\beta = 90.39(2)°$, $V = 2669.5(10)$ Å^3, $Z = 2$, $\rho_{calc} = 2.086$ g cm^{-3}, $\mu(Mo_{K\alpha}) = 20.4$ cm^{-1}, $R = 0.0565$ for 2084 reflections with $2\theta < 45°$ and $I < 3\sigma(I)$ (248 parameters); Rigaku AFC5S diffractometer, graphite monochromator. The structure was solved by using the direct-methods routine of the SHELXTL program package. One of the $(H_3NCH_2CH_2NH_3)^{2+}$ ions exhibits disorder of one of the terminal NH_3

 © VCH Verlagsgesellschaft mbH, W-6940 Weinheim, 1993 0570-0833/93/0404-0611 $ 10.00+.25/0

groups over two positions; the disorder was modelled by fixing the N-population parameters at each site as 0.75 and 0.25, respectively. The other organic cations were disordered at the inversion centers and modelled as rigid groups with C–C distances of 1.48(2) Å and C–N distances of 1.41(2) Å. The disorder of the groups is evident in the large thermal parameters associated with these cations. Such behavior is not uncommon in structures of this type since the cations reside in large cavities and possess considerable freedom of motion. All other parameters are unexceptional. Hydrogen atom positions could not be located on the final difference Fourier maps. Hydrogen atoms, excluding those of the phosphate OH groups, which have not been introduced either in calculated or observed positions, were placed in their calculated positions and constrained to ride on their associated carbon or nitrogen atoms. Further details of the crystal structure investigation may be obtained from the Fachinformationszentrum Karlsruhe, Gesellschaft für wissenschaftlich-technische Information mbH, D-W-7514 Eggenstein-Leopoldshafen 2 (FRG) on quoting the depository number CSD-56810, the names of the authors, and the journal citation.

[17] The oxidation state assignments of the vanadium centers are consistent with the observed geometries and with valence sum calculations. I. D. Brown, K. K. Wu, *Acta Crystallogr.* **1976**, *B32*, 1957.

[18] D. Beltran-Porter, P. Amoros, R. Ibanez, E. Martinez, A. Beltran-Porter, *Solid State Ionics*, **1989**, *32/33*, 57.

Photochemical Carboxylation of Cubanes**

By *A. Bashir-Hashemi**

Dedicated to Professor Harold Hart

Multiple functionalization of the cubane framework has remained a formidable synthetic task requiring the sequential introduction and stepwise manipulation of substituents.[1] *ortho*-Metalation of amidocubanes[2] has until now been the method of choice for the synthesis of the polycarboxylcubanes.[3] In this communication we report a new methodology for introducing one or more carboxyl groups selectively on the cubane skeleton.

Fifty years ago, Kharasch and Brown reported the photochemical reaction of cyclohexane with oxalyl chloride to give cyclohexane carboxylic acid.[4] This little-known reaction has had limited synthetic application since rearrangements of the radical intermediates result in lower yields of the desired products.[5] By virtue of the cubane geometry, the cubyl radical **1** is an exception.[6] The cubane skeleton constrains the tertiary bridgehead radical to a pyramidal structure. Both hydrogen abstraction and β-scission in this species are unfavorable because these processes lead to intermediates of even higher energy, such as cubene **2**,[7] or **3**, a radical which is exceptionally strained because it is also a bridgehead alkene. Related reports indicate that the cubyl radical has been generated at high temperatures without rearrangement.[6] Also, the observation that cubane can be polyiodinated by means of radical reactions[8] supports the view that photochemical carboxylation of the cubane skeleton could be synthetically useful.

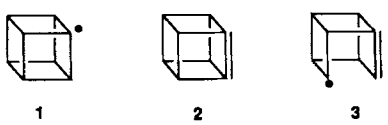

1 **2** **3**

Indeed, the reaction of commercially available 1,4-dimethoxycarbonylcubane (**4**)[9] with oxalyl chloride under irradiation from a sunlamp for 6 h produced,[10] after esterification with MeOH, 1,2,4-trimethoxycarbonylcubane (**5**) in 72% yield.[11]

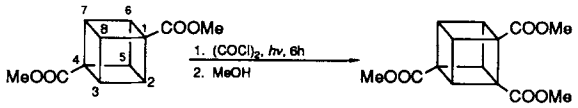

4 **5**

Extension of the reaction time to 48 h led to formation of 1,2,4,7-tetramethoxycarbonylcubane (**6**) in 55% yield and the pentacarboxylated derivative **8** in which chlorocarbonylation of the 1,2,4,6-tetrasubstituted precursor **7** occurred at the positions adjacent to only one of the methoxycarbonyl groups. The ^{1}H NMR spectrum of compound **8** shows only one resonance for the three identical cubyl protons at $\delta = 4.64$. The formation of isomer **7** was observed after 10 h of irradiation. Other isomers of tetra- or pentasubstituted cubanes in which chlorocarbonylation had occurred at positions *ortho* to two carbonyl groups were absent.

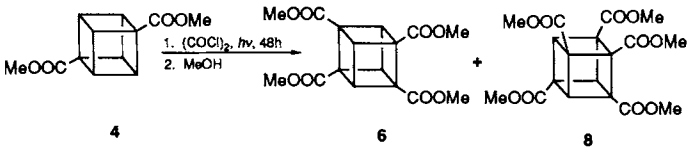

4 **6** **8**

These observations indicate a remarkable degree of regioselectivity which results from the reduced reactivity of the C–H bonds adjacent to the carbonyl groups. Therefore, it was predicted that the initial photochemical carbonylation of methoxycarbonylcubane (**9**) should occur at the β and γ positions since α positions would be deactivated by the electronic effect of the methoxycarbonyl group. Statistical considerations (three β positions as compared to one γ position) favor the formation of the 1,3 isomer **10**[12] as the dominant product.

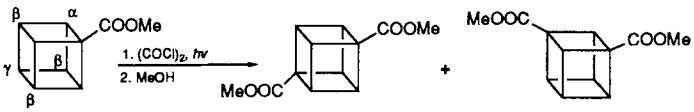

9 **4** **10**

The photochemical chlorocarbonylation of **9** with oxalyl chloride was followed by ^{1}H NMR spectroscopy. In the spectra recorded after 6, 18, and 36 h, the formation of 1,3- and 1,4-disubstituted cubanes and their transformation to higher substituted cubanes was monitored. After 36 h the 1,3,5-trisubstituted **11** had been converted into the 1,3,5,7-tetrasubstituted cubane **12**. Minor amounts of compounds **6′** and **7′**, which originated from the 1,4-disubstituted intermediate **4′**, were also detected.

[*] Dr. A. Bashir-Hashemi, Sr. Scientist
GEO-CENTERS
762 Rt. 15 South
Lake Hopatcong, NJ 07849 (USA)

[**] Drs. G. Doyle, T. Axenrod, and J. R. Hardee are thanked for their contributions and N. Gelber and Dr. T. H. Chen for their technical assistance. Useful discussions with Prof. P. E. Eaton are greatly appreciated. This research was supported by Armament Research, Development, and Engineering Center (ARDEC).

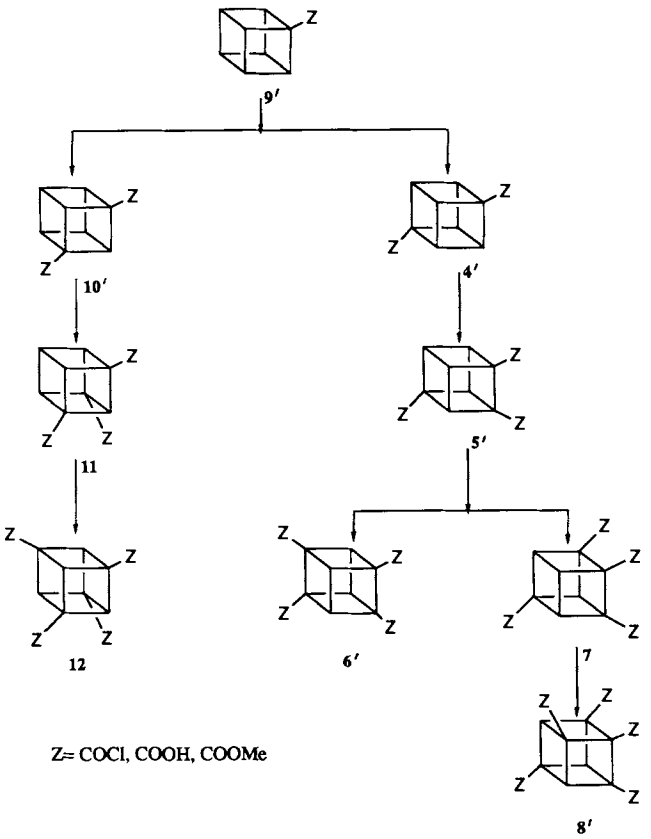

On a preparative scale, the irradition of cubane carboxylic acid **9** (with H instead of Me) (1.0 g) with oxalyl chloride (20 mL) in a quartz flask with a Rayonet photochemical reactor (1849 Å–2537 Å) for 4 h produced, after hydrolysis, **12** (Z = COOH) in 60% yield. In contrast, the original synthesis of the T_d-symmetric tetracarboxylic acid **12** by *ortho*-metalation required multiple synthetic steps.[1]

In conclusion, a simple and efficient photochemical procedure for the direct carboxylation of cubane has been demonstrated. In contrast to *ortho*-metalation, this methodology places the new functionalities at remote sites (β and γ) and makes possible the synthesis of a wide range of cubanes.

Received: October 26, 1992 [Z 5652 IE]
German version: *Angew. Chem.* **1993**, *105*, 585

[1] P. E. Eaton, *Angew. Chem.* **1992**, *104*, 1447; *Angew. Chem. Int. Ed. Engl.* **1992**, *31*, 1421; H. Higuchi, I. Ueda in *Carbocyclic Cage Compounds: Chemistry and Applications* (Eds.: E. J. Osawa, O. Yonemitsu), VCH, New York, **1992**, pp. 217–244.

[2] P. E. Eaton, G. Castaldi, *J. Am. Chem. Soc.* **1985**, *107*, 724; A. Bashir-Hashemi, *ibid.* **1988**, *110*, 7234.

[3] P. E. Eaton, G. T. Cunkle, G. Marchioro, R. M. Martin, *J. Am. Chem. Soc.* **1987**, *109*, 948; P. E. Eaton, H. Higuchi, R. Millikan, *Tetrahedron Lett.* **1987**, *28*, 1055; P. E. Eaton, C.-H. Lee, Y. Xiong, *J. Am. Chem. Soc.* **1989**, *111*, 8016; A. Bashir-Hashemi, H. L. Ammon, C. S. Choi, *J. Org. Chem.* **1990**, *55*, 416; J. C. Bottaro, P. E. Pennwell, R. J. Schmitt, *ibid.* **1991**, *56*, 1306; G. Castaldi, R. Colombo, P. Allegrini, *Tetrahedron Lett.* **1991**, *32*, 2173; P. E. Eaton, Y. Xiong, J. P. Zhou, *J. Org. Chem.* **1992**, *57*, 4277.

[4] M. S. Kharasch, H. C. Brown, *J. Am. Chem. Soc.* **1940**, *62*, 454; *ibid.* **1942**, *64*, 329.

[5] P. K. Freeman, F. A. Raymond, J. C. Sutton, W. R. Kindley, *J. Org. Chem.* **1968**, *33*, 1448; K. B. Wiberg, V. Z. Williams, Jr., *ibid.* **1970**, *35*, 369; D. E. Applequist, T. Saski, *ibid.* **1978**, *43*, 2399.

[6] P. E. Eaton, T. W. Cole, Jr., *J. Am. Chem. Soc.* **1964**, *86*, 962; T.-Y. Luh, L. M. Stock, *J. Org. Chem.* **1978**, *43*, 3271; R. M. Moriarty, J. S. Khosrowshahi, R. S. Miller, J. Flippen-Andersen, R. Gilardi, *J. Am. Chem. Soc.* **1989**, *111*, 8943; K. Hassenrück, J. G. Radziszewski, V. Balaji, G. S. Murthy, A. J. McKinley, D. E. David, V. M. Lynch, H.-D. Martin, J. Michl, *ibid.* **1990**, *112*, 873; D. A. Hrovat, W. T. Borden, *ibid.* **1990**, *112*, 875, P. E. Eaton, J. Tsanaktsidis, *ibid.* **1990**, *112*, 876; E. W. Della, G. M. Elsey, N. J. Head, J. C. Walton, *J. Chem. Soc. Chem. Commun.* **1990**, 1589; P. E. Eaton, Y. C. Yip, *J. Am. Chem. Soc.* **1991**, *113*, 7692; J. C. Walton, *Chem. Soc. Rev.* **1992**, *2*(12), 105.

[7] P. E. Eaton, M. Maggini, *J. Am. Chem. Soc.* **1988**, *110*, 7230.

[8] D. S. Reddy, M. Maggini, J. Tsanaktsidis, P. E. Eaton, *Tetrahedron Lett.* **1991**, *31*, 805.

[9] Available from Enichem (Italy).

[10] Under these reaction conditions no evidence for the formation of seco-cubanes was found. See P. E. Eaton, R. Millikan, *Org. Chem.* **1990**, *55*, 2823; A. Bashir-Hashemi, P. R. Dave, H. L. Ammon, T. Axenrod, *Tetrahedron Lett.* **1990**, *31*, 4835.

[11] In a typical reaction, a stirred solution of cubane **4** (1.0 mmol) in 10 mL of oxalyl chloride in a Pyrex flask was irradiated with a General Electric 275-W sunlamp, held approximately 12 cm from the reaction flask. The temperature of the reaction mixture was kept at 30–40 °C. After the irradiation period was complete, excess oxalyl chloride was removed, and the acid chlorides were converted into methyl esters by treatment with methanol. The formation of each intermediate was verified by comparison of the esterified product with authentic samples [1, 3]. See also: T. Axenrod, B. Liang, A. Bashir-Hashemi, P. R. Dave, D. S. Reddy, *Magn. Reson. Chem.* **1991**, *29*, 88. – New compounds were fully characterized.

[12] J. C. Barborak, L. Watts, R. Pettit, *J. Am. Chem. Soc.* **1966**, *88*, 1328.

2,2′-Bipyrimidineoxalatocopper(II) Complexes: From the Mononuclear Complex to the 2D Sheetlike Polymer**

By *Giovanni De Munno, Miguel Julve,* Francesco Nicolo', Francesc Lloret, Juan Faus, Rafael Ruiz,* and *Ekkehard Sinn*

The preparation and chemistry of oxalato transition metal complexes, we restrict ourselves here to Cu^{II} complexes, have been thoroughly investigated.[1] The coordination modes of the oxalato (ox) ligand are well characterized both in solution[2] and in the solid state.[3] Polynuclear bischelate oxalato complexes have attracted the interest of magnetochemists in the last fifteen years[3, 4] because of their remarkable ability to transmit electronic effects between paramagnetic centers separated from each other by more than 5 Å. In fact, oxalato-bridged Cu^{II} complexes provided the first examples of complexes with orbital reversal[5] and tunable exchange interactions.[6] The possibility of tuning the singlet–triplet energy gap (J) between 0 and $-386\ cm^{-1}$ in dinuclear μ-oxalatocopper(II) complexes by varying the terminal ligands is a very striking result.[6]

2,2′-Bipyrimidine (bpym) can also act as a bidentate[7] or a bisbidentate[8] ligand. Strong antiferromagnetic coupling has been achieved between Cu^{II} ions separated by more than 5.5 Å in bpym-bridged Cu^{II} complexes (J ranges from -236

[*] Prof. M. Julve, Dr. F. Lloret, Prof. J. Faus, R. Ruiz
Departament de Química Inorgànica
Facultat de Química de la Universitat de València
Dr. Moliner 50, E-46100-Burjassot, València (Spain)
Prof. G. De Munno
Dipartimento di Chimica, Università della Calabria
I-87030 Arcavacata di Rende, Cosenza (Italy)
Dr. F. Nicolo'
Dipartimento di Chimica e Struttura Moleculare, Università di Messina
Messina (Italy)
Prof. E. Sinn
School of Chemistry, University of Hull
Kingston upon Hull, HU67RX (UK)

[**] This work was supported by the Spanish DGICYT (Project PB91-0807-602-01) and the Italian Ministero dell'Università e della Ricerca Scientifica e Tecnologica. R. R. thanks the Conselleria de Cultura, Educació i Ciència for a doctoral grant.

to $-191\ cm^{-1}$).[8b,c] The exchange coupling in both oxalato- and bpym-bridged complexes was explained with a simple orbital model by the large σ in-plane overlap of the $d_{x^2-y^2}$ magnetic metal orbitals through the oxalato or bpym bridge.[6, 8b, 9]

We tried to prepare the mononuclear mixed-ligand complex [Cu(bpym)(ox)], intending to use it as a "complex ligand" to obtain homo- and heteropolymetallic species with exchange interactions. Our first attempts resulted in the isolation and structural characterization[10] of the novel mononuclear complex **1** as well as the polymeric compound **2**.

$[Cu(bpym)(ox)(H_2O)_2] \cdot 5H_2O$ **1**
$[Cu_2(bpym)(ox)_2] \cdot 5H_2O$ **2**

The crystal structure of **1** is composed of neutral $[Cu(bpym)(ox)(H_2O)_2]$ units and uncoordinated water molecules. The copper atom is hexacoordinate (Fig. 1); two nitrogen atom of bpym and two oxygen atoms of the oxalato ligand are found in the equatorial plane, whereas the two axial positions are occupied by oxygen atoms of aqua ligands. The bonds between the copper center and the equatorial atoms (2.002(6)–1.934(6) Å) are shorter than those to the axial oxygen atoms (average 2.529(7) Å), as expected for a six-coordinate Cu^{II} complex. The equatorial atoms N(1), N(2), O(1), O(2) are almost coplanar, and the copper atom is only 0.020(1) Å out of the equatorial mean plane in the direction of the O(5) atom. The oxygen atoms of the five waters of crystallization are reasonably close together (2.742–2.913 Å) indicating the existence of medium-strength hydrogen bonds.

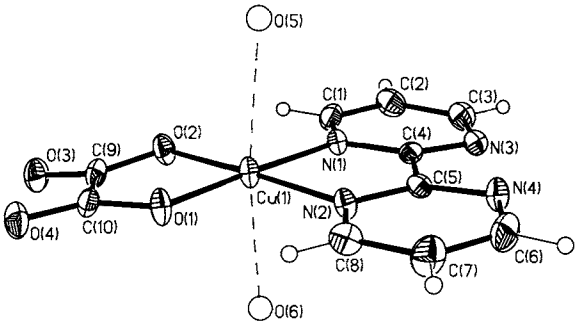

Fig. 1. Molecular structure of **1** (ellipsoids at the 30% probability level) with the atom numbering. Selected distances [Å] and angles [°] with standard deviations in parentheses: Cu(1)-O(1) 1.934(6), Cu(1)-O(2) 1.936(5), Cu(1)-N(1) 2.002(6), Cu(1)-N(2) 1.976(6), Cu(1)-O(5) 2.554(7), Cu(1)-O(6) 2.503(7); O(1)-Cu(1)-O(2) 85.5(2), O(1)-Cu(1)-N(1) 176.7(2), O(1)-Cu(1)-N(2) 95.1(2), O(1)-Cu(1)-O(5) 97.8(2), O(1)-Cu(1)-O(6) 93.4(2), O(2)-Cu(1)-N(1) 97.9(2), O(2)-Cu(1)-N(2) 177.3(3), O(2)-Cu(1)-O(5) 91.5(3), O(2)-Cu(1)-O(6) 89.8(3), N(1)-Cu(1)-N(2) 81.5(3), N(1)-Cu(1)-O(5) 83.2(2), N(1)-Cu(1)-O(6) 86.6(3), N(2)-Cu(1)-O(5) 91.0(3), N(2)-Cu(1)-O(6), 87.6 [13].

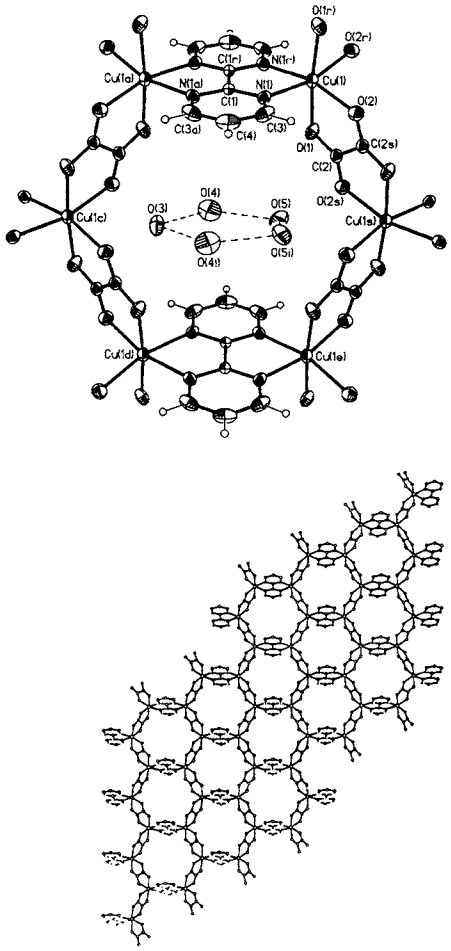

Fig. 2. Crystal structure of **2** (ellipsoids at the 30% probability level). Top: Hexameric repeating unit showing the atom numbering and the inclusion of water molecules. Bottom: View of a sheet of **2** perpendicular to the *xy* plane (hydrogen atoms and water molecules have been omitted for clarity). Selected distances [Å] and angles [°] with standard deviations in parentheses: Cu(1)-O(1) 2.076(3), Cu(1)-O(2) 2.086(3), Cu(1)-N(1) 2.129(3); O(1)-Cu(1)-O(2) 79.7(1), O(1)-Cu(1)-N(1) 97.0(1), O(2)-Cu(1)-N(1) 95.2(1), O(1)-Cu(1)-O(1r) 173.8(1), O(2)-Cu(1)-O(1r) 96.0(1), N(1)-Cu(1)-O(1r) 87.8(1), O(2)-Cu(1)-O(2r) 94.6(1), N(1)-Cu(1)-O(2r) 164.9(1) (symmetry code: (r) $1-x, y, -z$) [14].

The crystal structure of **2** is made up of parallel sheets each consisting of an infinite hexagonal array of copper atoms bridged by bisbidentate oxalato and bpym ligands; the copper atom exhibits a six-coordinate CuN_2O_4 chromophore (Fig. 2). A lengthening of the Cu–O and Cu–N equatorial distances is observed in **2** with respect to **1**: their average values increase from 1.989(6) and 1.935(6) Å in **1** to 2.129(3) and 2.086(3) Å in **2**. In contrast the Cu–O axial distances decrease remarkably (average values 2.076(3) and 2.529(6) Å in **2** and **1**, respectively). As a consequence of these geometrical variations, the coordination environment at the copper center does not show significant octahedral distortion. As shown in Figure 2, this two-dimensional polymer extending in the *xy* plane is formed by the repetition of almost circular rings. The intraring Cu···Cu distances are 5.680(1) [Cu(1)···Cu(1a)], 5.406(1) [Cu(1)···Cu(1s)], 9.559(2) [Cu(1)···Cu(1c)], 9.445(2) [Cu(1)···Cu(1e)], 11.022(2) [Cu(1)···Cu(1d)] and 10.942(2) [Cu(1c)···Cu(1s)] Å. These layers are stacked by graphite-like interactions between bpym rings of different layers; the C(4)···C(4′) distance [(′) $= 1-x, y, -1-z$] is 3.839 Å. The five disordered water molecules accomodated in each hole of the sheetlike polymer are linked together by means of hydrogen bonds to form a planar ring.[15] In each water ring at the center of the cavity the O(4) atom is linked by hydrogen bonds to the equivalent O(4′) atoms (2.59(2) Å for O(4)···O(4′)) of the rings in the cavities above and below, resulting in columns of H_2O rings inserted in the channels delimited by the cavities along the *z* direction. These hydrogen bonds, directed almost along the *z*-axis, dictate the crystal packing in that direction more strongly than the above-mentioned intralayer hydrogen bonds. Furthermore, the water cluster is attached to the wall of the channel by hydrogen bonds between each O(3) atom and two equivalent O(2) atoms of the adjacent layers (2.936(6) Å for O(3)···O(2)).

The temperature dependence of the magnetic susceptibility per Cu^{II} ion of complex **2** between 4.2 and 300 K is indica-

tive of a relatively weak antiferromagnetic interaction. At room temperature the value of χ_M (per mol of Cu^{II}) is 1.20×10^{-3} cm^3 mol^{-1}. Upon cooling χ_M increases until a sharp maximum is achieved at 16 K, then it decreases. Heat capacity measurements reveals no three-dimensional magnetic order for **2** on the low-temperature side of the curve down to 2 K (absence of λ-type peak). Thus the susceptibility maximum arises from two-dimensional magnetic interactions. It is not possible to fit the experimental data satisfactorily with one-dimensional models. This result is not surprising because the magnetic orbitals of Cu^{II} in **2** can be described in principle by both $d_{x^2-y^2}$ and d_{z^2} orbitals, indicating a possible exchange pathway through both oxalato and bpym bridging ligands. Moreover, the different efficiency of these bridges in transmitting exchange coupling would lead to an alternating magnetic plane. This last assumption is supported by the fact that the observed magnetic behavior cannot be reproduced by a model of a regular two-dimensional hexagonal array. The lack of a theoretical law for an alternating magnetic plane precludes a correct analysis of the magnetic data of such a new material.

Experimental Procedure

1: 2,2'-Bipyrimidine (0.158 g, 1 mmol) dissolved in a minimum amount of ethanol was added to an aqueous solution (80 mL) containing $Cu(NO_3)_2 \cdot 3H_2O$ (0.242 g, 1 mmol) yielding a blue-green solution. Solid sodium oxalate (0.134 g, 1 mmol) was added slowly with stirring and gentle warming. The solvents were allowed to evaporate at room temperature over several days to give blue hexagonal crystals of **1** which were filtered off and dried on filter paper. **1** provided a correct elemental analysis (C, H, N, Cu).

2: A solution of $Cu(NO_3)_2 \cdot 3H_2O$ (0.060 g, 0.25 mmol) in a minimum amount of water was added to an aqueous solution (100 mL) of **1** (0.436 g, 1 mmol). Slow evaporation of the resulting green solution gave cubic green crystals of **2** after a few days, and a mixture of crystals of **1** and **2** when the solution was allowed to evaporate nearly to dryness. **2** provided a correct elemental analysis (C, H, N, Cu).

Received: October 24, 1992 [Z 5642 IE]
German version: *Angew. Chem.* **1993**, *105*, 588

[1] K. V. Krisnamurthy, G. M. Harris, *Chem. Rev.* **1961**, *61*, 213.
[2] I. Castro, J. Faus, M. Julve, A. Gleizes, *J. Chem. Soc. Dalton Trans.* **1991**, 1937, and references therein.
[3] O. Kahn, *Angew. Chem.* **1985**, *97*, 837; *Angew. Chem. Int. Ed. Engl.* **1985**, *24*, 834; H. Oshio, U. Nagashima, *Inorg. Chem.* **1992**, *31*, 3295; A. Gleizes, M. Julve, M. Verdaguer, J. A. Real, J. Faus, X. Solans, *J. Chem. Soc. Dalton Trans.* **1992**, 3209.
[4] Y. Pei, Y. Journaux, O. Kahn, *Inorg. Chem.* **1989**, *28*, 100; H. Okawa, N. Matsumoto, H. Tamaki, Communication presented at the 29th I.C.C., Switzerland **1992**.
[5] J. J. Girerd, M. Verdaguer, O. Kahn, *Inorg. Chem.* **1980**, *19*, 274; M. Verdaguer, A. Michalowicz, J. J. Girerd, N. Alberding, O. Kahn, *ibid.* **1980**, *19*, 3271.
[6] M. Julve, M. Verdaguer, O. Kahn, A. Gleizes, M. Philoche-Levisalles, *Inorg. Chem.* **1984**, *23*, 3808.
[7] I. Castro, M. Julve, G. De Munno, J. A. Real, F. Lloret, J. Faus, *J. Chem. Soc. Dalton Trans.* **1992**, 1739, and references therein.
[8] a) G. Brewer, E. Sinn, *Inorg. Chem.* **1985**, *24*, 4580; b) M. Julve, G. De Munno, G. Bruno, M. Verdaguer, *ibid.* **1988**, *27*, 3160; c) M. Julve, M. Verdaguer, G. De Munno, J. A. Real, G. Bruno, *ibid.*, in press.
[9] S. Alvarez, M. Julve, M. Verdaguer, *Inorg. Chem.* **1990**, *29*, 4500.
[10] X-ray structure analyses: Siemens R3m/V automatic diffractometer, $Mo_{K\alpha}$, $\lambda = 0.71073$ Å, graphite monochromator, 298 K. Data collection, solution and refinement: ω-2θ, standard Patterson methods with subsequent Fourier recycling, SHELXTL-PLUS [11]. **1**: $C_{10}H_{20}N_4CuO_{11}$ ($M_r = 435.6$), orthorhombic, space group $P2_12_12_1$, $a = 6.544(2)$, $b = 13.838(4)$, $c = 19.319(7)$ Å, $V = 1749.4(10)$ Å^3, $Z = 4$, $\rho_{calcd.} = 1.655$ g cm^{-3}, $\mu = 13.1$ cm^{-1}, 2θ range 3–50°, crystal size $0.35 \times 0.38 \times 0.20$ mm^3, $F(000) = 900$. 1803 unique reflections, and 1475 assumed as observed with $I > 3\sigma(I)$. Refinement of 199 variables with anisotropic thermal parameters for all non-hydrogen atoms (except the oxygen atoms of water molecules) gave $R(F_o) = 0.0525$, $R_w(F_o) = 0.0613$ and $S = 1.49$ with $w^{-1} = \sigma^2(F_o) + 0.002395(F_o)^2$. **2**: $C_{12}H_{16}N_4Cu_2O_{13}$ ($M_r = 551.4$), monoclinic, space group $C2/m$, $a = 9.445(2)$, $b = 16.622(3)$, $c = 6.202(1)$ Å, $\beta = 101.4(1)$°, $V = 954.6(3)$ Å^3, $Z = 2$, $\rho_{calcd.} = 1.918$ g cm^{-3}, $\mu = 23.1$ cm^{-1}, 2θ range 3–55°, crystal size $0.34 \times 0.19 \times 0.23$ mm^3, $F(000) = 556$. 1147 unique reflections, and 981 assumed as observed with $I > 3\sigma(I)$. Ψ-scan absorption correction was applied (max. and min. transmission factors 0.355/0.472) [12]. Refinement of 86 variables with anisotropic thermal parameters for all non-hydrogen atoms gave $R(F_o) = 0.0420$, $R_w(F_o) = 0.0470$ and $S = 1.67$ with $w^{-1} = \sigma^2(F_o) + 0.001000(F_o)^2$. The space group of **2** cannot be uniquely determined from the systematic absences, which only indicate the presence of a *C*-centered cell; the choice is between the acentric *C*2 or *Cm* groups and the centric *C*2/*m* one. The latter was favored by the intensities statistics, and consequently the structure solution and refinement were carried out in the centrosymmetric space group. The analysis of the residual electronic density in a final difference-Fourier map revealed three distinct peaks (two, O(4) and O(5), in general positions and one, O(3), in special position on a twofold axis), which could be interpreted as crystallization water molecules. The elemental analysis indicated a 5:2 ratio between the crystallization water and copper. Five oxygen atoms of the water molecules may be obtained by applying the twofold axis operation to the three peaks, while 10 positions are obtained when also the mirror operation is also applied. Then, we tried to refine the structure in *C*2 and *Cm*, but all our attempts gave worse results with large correlations between atomic positional parameters. Therefore, the refinement was completed in *C*2/*m* by assuming a disordered disposition of the water molecules in which 10 half oxygen atoms are arranged as two staggered five-membered rings. Further details of the crystal structure investigations are available on request from the Fachinformationszentrum Karlsruhe, Gesellschaft für wissenschaftlich-technische Information mbH, D-W-7514 Eggenstein-Leopoldshafen 2 (FRG), on quoting the depository number CSD-56958, the names of the authors, and the journal citation.
[11] SHELXTL PLUS, Version 3.4, Siemens Analytical X-Ray Instruments Inc., Madison, WI, 1989.
[12] A. C. T. North, D. C. Philips, F. S. Mathews, *Acta Crystallogr. Sect. A* **1968**, *24*, 351.
[13] Bond lengths and angles in the bpym and oxalato ligands are in agreement with those reported in the literature. Although the pyrimidyl rings of bpym are planar, the ligand as a whole is not planar (the dihedral angle between the six-membered pyrimidyl rings is 4.4(3)°). The oxalato ligand is quite planar; the maximum deviation from the mean plane is 0.077(7) Å at O(2). The dihedral angle between the mean planes of the bpym and oxalato ligands is 7.1(2)°. The O–C bond lengths of oxalate occur in two sets (1.281(9) and 1.267(9) Å for O(2)–C(9) and O(1)–C(10), and 1.248(10) and 1.212(12) Å for O(3)–C(9) and O(4)–C(10)) as a result of its bidentate coordination to copper.
[14] The bpym and oxalato ligands are planar and form a dihedral angle of 99.4(1)°. The O–C bond lengths in the oxalato ligand in **2** are all identical (1.242(4) Å) on account of its quasi-symmetrical bischelating coordination to copper.
[15] The disorder is such that two sets of five half oxygen atoms are arranged as a ten-membered ring (O···O separation ca. 1.4 Å) formed by two staggered pentagons. For clarity, only one set of five atoms is shown in the top picture in Figure 2, where it should be noted that O(3) lies on the twofold axis. The five water molecules are almost planar (the largest deviation from the mean plane is 0.07(1) Å. The dihedral angle between this plane ant that of bpym is 15.7(2)°.

Reaction Tuning in Zeolites: An in situ MAS NMR Study of Acetaldehyde on HZSM-5**

By *Eric J. Munson* and *James F. Haw**

Zeolites have found widespread use in the petroleum industry as catalysts, for example, for the catalytic cracking of vacuum gas oil into gasoline[1] and the conversion of methanol to gasoline on zeolite HZSM-5.[2, 3] A relatively recent application of zeolites is as solid catalysts in synthetic organic chemistry.[4–6] One advantage of zeolites over conventional homogeneous catalysts is that the pores of the zeolite can act as tiny microreactors that dictate the maximum size of the reagent and product molecules. In addition,

[*] Prof. Dr. J. F. Haw, E. J. Munson
Department of Chemistry, Texas A & M University
College Station, TX 77843 (USA)

[**] We thank the National Science Foundation (Grant CHE-8918741) for financial support of this work. E. J. M. is a fellow of the American Chemical Society Division of Analytical Chemistry sponsored by Eastman Chemical Company.

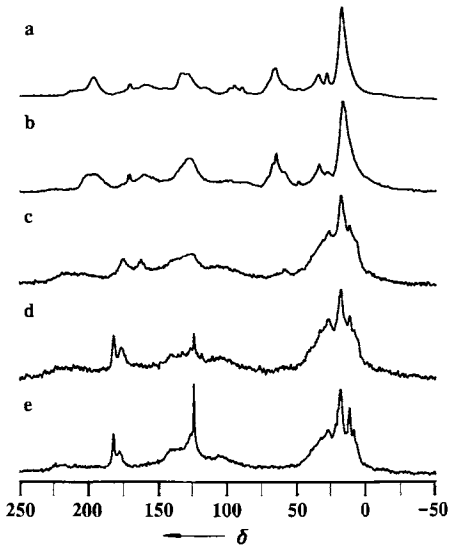

Fig. 1. ^{13}C MAS NMR spectra of [1,2-^{13}C]acetaldehyde on HZSM-5. a) 298 K; b) 20 min at 353 K; c) 20 min at 433 K; d) 20 min at 473 K; e) 10 min at 523 K. Complex aldol reactions occurred at low temperatures; CO ($\delta = 184$) and CO_2 ($\delta = 126$) formed at 523 K.

a number of zeolites with acidic, basic, or redox centers are available. We demonstrate here that the reactions of acetaldehyde in zeolite HZSM-5 can be tuned to give different products depending on whether water and/or oxygen are coabsorbed in the catalyst.

These reactions were carried out inside sealed zirconia rotors that were heated in an NMR probe to temperatures up to 523 K; the products were detected by using solid-state NMR with magic-angle spinning (MAS).[7–10] Figure 1 shows ^{13}C MAS NMR spectra of [1,2-^{13}C]acetaldehyde as it was heated to 523 K on zeolite HZSM-5. Following adsorption at 298 K (Fig. 1a) almost all of the acetaldehyde condensed to form a complex mixture of products. After heating to 433 K, these products began to crack, and CO ($\delta = 184$) and CO_2 ($\delta = 126$) were formed at 523 K.

As shown in Figure 2, absorption of water moderated the activity of the catalyst and permitted the selective conversion

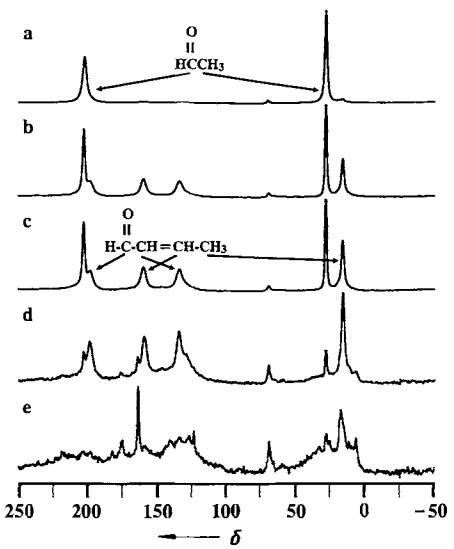

Fig. 2. ^{13}C MAS NMR spectra of [1,2-^{13}C]acetaldehyde on HZSM-5 that had been saturated with water. a) 298 K; b) 10 min at 353 K; c) 30 min at 353 K; d) 20 min at 393 K; e) 20 min at 433 K. Crotonaldehyde ($\delta = 199, 160, 135$, and 19) was produced selectively at 353–393 K.

of acetaldehyde (which was stable at 298 K) to crotonaldehyde at 353–393 K. This product was stable up to ca. 433 K. One way to view the effect of the coadsorbed water is that it reduces the acidity of the strong acid sites of HZSM-5 to that of the less acidic hydronium-ZSM-5; this affects the acid-catalyzed aldol reaction. The environment in the zeolite is still acidic, as reflected in the moderate downfield shifts of the signals of C-1 and C-3.[11] The selective formation of crotonaldehyde from acetaldehyde on basic zeolite NaZSM-5 in a flow reactor was previously reported in the patent literature by Dessau.[12]

Moderating the acidity of HZSM-5 by coadsorption of water also permitted other selective reactions. In the presence of water *and* oxygen, [1,2-^{13}C]acetaldehyde was converted to [1,2-^{13}C]acetic acid in high yields as verified by both the ^{13}C chemical shifts (Fig. 3) and the $^{1}J_{C,C}$ coupling constant of 56 Hz.[13] A separate control experiment con-

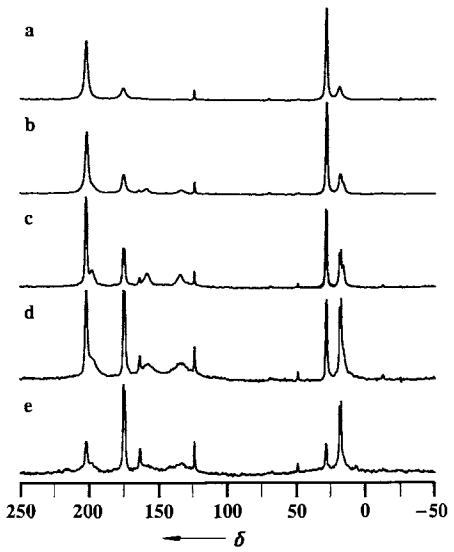

Fig. 3. ^{13}C MAS NMR spectra of [1,2-^{13}C]acetaldehyde and oxygen on HZSM-5 that had been saturated with water. a) 1 h at 298 K; b) 10 h at 298 K; c) 10 min at 393 K; d) 30 min at 393 K; e) 10 min at 433 K. The major product was acetic acid ($\delta = 176$ and 21). A small amount of crotonaldehyde also formed.

firmed that acetic acid is unreactive on the zeolite under these conditions. The oxidation of aldehydes to carboxylic acids by molecular oxygen is a well-characterized reaction in solution,[14] and provided that the acidity is tuned by coadsorption of water, it is the predominant reaction in HZSM-5 under these conditions.

This study has shown that the product selectivity of organic synthetic reactions in zeolites can be tuned by coadsorbates. This effect must be kept in mind when the solvent or other reaction conditions for organic synthesis with zeolite catalysts are selected.

Experimental Procedure

HZSM-5 was obtained from UOP Corporation and [1,2-^{13}C]acetaldehyde from Cambridge Isotopes. The protocol for the experiment depicted in Figure 1 is described in ref. [8]. For the experiments in Figures 2 and 3, the catalyst was first heated at 393 K for 1 h under vacuum and subsequently exposed to water vapor until saturation. The catalyst then packed into a glass ampule in a dry-box, attached to a vacuum line, and evacuated to 10^{-2} Torr. After adsorption of acetaldehyde with or without oxygen, the ampule was sealed to ensure sample integrity and placed into a zirconia rotor in which the reactions and NMR studies were conducted.

^{13}C NMR spectra were acquired on a modified Chemagnetics CMC-200 spectrometer operating at 50.06 MHz and with a MAS frequency of 3–4.5 kHz. Single-pulse ^{13}C excitation (Bloch decay) with proton decoupling (pulse delay = 1 4 s, 100 400 transients) was used to obtain the spectra presented in this contribution.

Received: October 28, 1992 [Z 5655 IE]
German version: *Angew. Chem.* **1993**, *105*, 643

[1] C. N. Satterfield, *Heterogeneous Catalysis in Practice*, McGraw-Hill, New York, **1980**, pp. 151–179.
[2] C. D. Chang, *Hydrocarbons from Methanol*, Marcel Dekker, New York, **1983**.
[3] C. D. Chang, A. J. Silvestri, *J. Catal.* **1977**, *47*, 249–259.
[4] W. Hölderich, M. Hesse, F. Näumann, *Angew. Chem.* **1988**, *100*, 232; *Angew. Chem. Int. Ed. Engl.* **1988**, *27*, 226–246. See also J. M. Thomas, *ibid.* **1988**, *100*, 1735 and **1988**, *27*, 1673.
[5] W. F. Hölderich, H. van Bekkum in *Introduction to Zeolite Science and Practice* (Eds.: H. van Bekkum, E. M. Flanigen, J. C. Jansen), Elsevier, Amsterdam, **1991**, pp. 631–726.
[6] J. Weitkamp in *Catalysis and Adsorption by Zeolites* (Eds.: G. Öhlmann, H. Pfeifer, R. Fricke), Elsevier, Amsterdam, **1991**, pp. 21–46.
[7] J. F. Haw, B. R. Richardson, I. S. Oshiro, N. D. Lazo, J. A. Speed, *J. Am. Chem. Soc.* **1989**, *111*, 2052–2058.
[8] E. J. Munson, D. B. Ferguson, A. A. Kheir, J. F. Haw, *J. Catal.* **1992**, *136*, 504 509.
[9] M. A. Anderson, J. Klinowski, *J. Am. Chem. Soc.* **1990**, *112*, 10–18.
[10] Y. Xu, C. P. Grey, J. M. Thomas, A. K. Cheetham, *Catal. Lett.* **1990**, *4*, 251 260.
[11] D. Farcasiu, A. Ghenciu, G. Miller, *J. Catal.* **1992**, *134*, 118–125.
[12] R. Dessau, (Mobil Oil Corp.), USA 5026919, **1991**.
[13] G. A. Gray, P. D. Ellis, D. D. Traficante, G. E. Maciel, *J. Magn. Reson.* **1969**, *1*, 41 54.
[14] S. A. Maslov, E. A. Blyumberg, *Russ. Chem. Rev.* **1976**, *45*, 155–167.

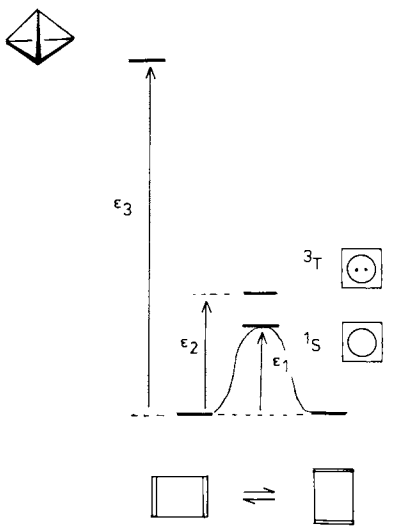

Scheme 1. Schematic energy diagram for the valence isomerization of cyclobutadiene.

Aza- versus Phospha-Substitution in Cyclobutadiene: A Theoretical Evaluation of Bonding Properties

By *Wolfgang W. Schoeller** and *Thilo Busch*

While the chemistry and bonding properties of cyclobutadiene (**1**) have been explored in detail,[1, 2] studies on analogous aza compounds are rare and on phospha compounds completely lacking. Regitz et al.[3a–c] recently reported on the synthesis and structural investigation of monoazacyclobutadiene (azete). Suitable precursors for the synthesis of phosphacyclobutadiene have been prepared in the past few years as well.[4] We determined the structures and energies of the parent compound **1** and the aza and phospha analogues by quantum chemical calculations at the MCSCF level[5] and report our results here. Our investigations may serve as a basis for understanding the effect of Group 5 element substitution on the structure and bonding in **1**.

Cyclobutadiene (**1**) adopts a rectangular geometry with localized π bonds.[6] The following aspects of its chemistry are important (Scheme 1):
a) the valence isomerization of rectangular **1** through a square (open-shell) singlet transition state (^1S), as determined by the energy barrier ε_1;
b) a low-lying triplet state with a small energy separation (ε_2) with respect to the singlet ground state, since cyclobutadiene is an antiaromatic cyclic conjugated π system. The triplet state of **1** lowest in energy (^3T) adopts a square geometry;
c) the energy difference (ε_3) between **1** and its structural isomer tetrahedrane.

We investigated these aspects of the analogous heterocyclobutadienes. These π systems are expected to adopt trapezoidal geometries. We also studied the total energy (ΔE) of fragmentation of the tetrahedranes (e.g., T_d-$C_4H_4 \rightarrow 2\,C_2H_2$).

In the two extreme cases all of the CH groups of **1** are replaced by the heteroatoms P or N to give cyclic P_4 and cyclic N_4, respectively. The former structure corresponding to white phosphorus should be particularly stable, whereas cyclic N_4 is expected to fragment readily to give two N_2 molecules. Consequently, the effect of mono- and disubstitution of **1** on the stability of the corresponding tetrahedranes is of particular interest. The ground state geometries of the structures examined are shown in Figure 1 and their energies

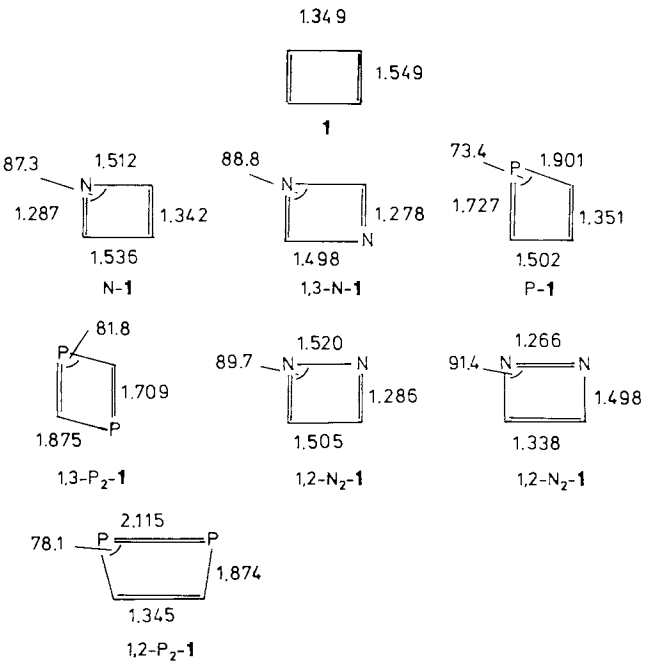

Fig. 1. Bonding parameters of cyclobutadiene and some of its aza and phospha analogues; bond lengths in Å units, bond angles in °.

[*] Prof. Dr. W. W. Schoeller, T. Busch
Fakultät für Chemie der Universität
Postfach 8640, D-W-4800 Bielefeld (FRG)

are listed in Table 1. Positive values (in kcal mol^{-1}) refer to endothermic and negative values to exothermic energies.

For the parent compound **1** the calculated energy barrier for valence isomerization proceeding through the open-shell singlet state (ε_1, Table 1) is slightly higher than the value determined experimentally by Maier et al. (6.6 kcal mol^{-1}).[7] The energy difference is on the order of the expected zero-point vibrational energy, which was not explicitly accounted for in our work, and which may slightly lower the energy barrier ε_1, as was shown for cyclobutadiene.[8] In general, valence isomerization in the phospha derivatives is more facile than in the aza derivatives, since the PC double bond is weaker than the NC double bond.[9] In other words, the delocalization of the π electrons benefits from the weaker double bonds. The energy barrier decreases further with increasing phospha substitution and is almost zero for the P_4 cyclobutadiene ($\varepsilon_1 = 1.7$ kcal mol^{-1}). Thus it can be expected that the phosphacyclobutadienes react preferentially as biradicals rather than as olefinic compounds. Concomitant with the weak double bond localization is the decreased singlet–triplet energy separation (ε_2). Nevertheless for all phosphacyclobutadienes the triplet state is always above the singlet state in energy. In contrast, aza substitution in **1** causes an increase in the energy barrier (ε_1) for valence isomerization. 1,3-Diazacyclobutadiene can be considered a "push–pull"[6] cyclobutadiene; its singlet ground state is stabilized relative to that of **1**. Its valence isomerization proceeds through a nonplanar transition structure with C_{2v} symmetry (see Table 1).

Table 1. Relative energy values (in kcal mol^{-1}) of cyclobutadiene and some of its aza and phospha analogues at the MCSCF level.

Compound	Symmetry [a]	ε_1	ε_2	ε_3	ΔE [b]
1	D_{2h} (D_{4h})	8.4	14.8	36.4	−27.2
N-**1**	C_s (C_{2v})	12.1	18.9	30.1	−54.9
1,3-N_2-**1**	C_{2h} (C_{2v})	18.9 (12.8) [c]	26.9	36.1	−93.2
P-**1**	C_s (C_{2v})	7.2	7.4	13.6	−1.5
1,3-P_2-**1**	C_{2h} (D_{2h})	3.1	8.2	−11.8	−21.5
P_4-**1**	D_{2h} [d] (D_{4h}) [d]	1.7	6.8	−47.2	−26.0

[a] Symmetry in parentheses refers to transition state geometries for valence isomerization. [b] Values for fragmentation of the (substituted) tetrahedranes into (from top to bottom) 2 C_2H_2, C_2H_2 + HCN, 2 HCN, C_2H_2 + HCP, 2 HCP, and 2 P_2, respectively. [c] Value in parentheses is relative to the dipolar nonplanar transition state. [d] Planarity was assumed.

The 1,2-diazacyclobutadienes are higher in energy than their 1,3 isomers, the isomer with two C=N bonds (1,2-N_2-**1**) by 12.1 kcal mol^{-1} and the other isomer with one N=N and one C=C bond (1,2-N_2-**1'**) by 22.5 kcal mol^{-1} (at the MRCI/MCSCF level). In contrast, only one 1,2-diphosphacyclobutadiene having a P=P and a C=C double bond (1,2-P_2-**1**) is stable. Relative to its 1,3 isomer it is 10.6 kcal mole^{-1} lower in energy.

Cyclobutadiene (**1**) and its aza analogues are all lower in energy than the corresponding tetrahedranes (ε_3, Table 1), and their tendency to fragment (ΔE) increases with increasing aza substitution. In addition to the data in Table 1 it should be noted that the fragmentation of triazatetrahedrane and tetrazatetrahedrane into HCN + N_2 and 2 N_2, respectively, is exothermic ($\Delta E = -135.9$ and -191.0 kcal mol^{-1}, respectively). This indicates that their corresponding cyclobutadiene derivatives once generated would also easily undergo retro-[2 + 2] addition. For the azete only flash pyrolysis (700 °C, 5×10^{-6} mbar) leads to retrocyclization.[3b,c] Similar behavior has been observed for cyclobutadienes.[1] In contrast, the introduction of phosphorus rather than nitrogen to **1** makes the tetrahedrane isomers more stable.[10,11] 1,3-Diphosphacyclobutadiene is already less stable than its corresponding tetrahedrane isomer. Our results indicate that the heterocyclobutadienes are interesting targets for matrix isolation studies.[12]

Received: May 11, 1992
Revised version: December 14, 1992 [Z 5338 IE]
German version: *Angew. Chem.* **1993**, *105*, 635

[1] G. Maier, *Angew. Chem.* **1974**, *86*, 491–505; *Angew. Chem. Int. Ed. Engl.* **1974**, *13*, 425–438; *ibid.* **1988**, *100*, 317–341; **1988**, *27*, 309–332. This review summarizes the relevant literature prior to 1988.

[2] T. Bally, S. Masamune, *Tetrahedron* **1980**, *36*, 343–370; earlier work on cyclobutadiene is summarized in M. P. Cava, M. J. Mitchell, *Cyclobutadiene and Related Compounds*, Academic Press, New York, **1967**.

[3] a) U.-J. Vogelbacher, M. Regitz, R. Mynott, *Angew. Chem.* **1986**, *98*, 835–836; *Angew. Chem. Int. Ed. Engl.* **1986**, *25*, 842–843; b) U.-J. Vogelbacher, M. Ledermann, T. Schach, G. Michels, U. Hees, M. Regitz, *ibid.* **1988**, *100*, 304–305 and **1988**, *27*, 272–273; c) M. Ledermann, M. Regitz, K. Angermund, P. Binger, C. Krüger, R. Mynott, R. Gleiter, I. Hyla-Kryspin, *ibid.* **1988**, *100*, 1616–1618 and **1988**, *27*, 1559–1561; d) G. Maas, M. Regitz, R. Rahm, J. Schneider, P. J. Stang, C. M. Crittell, *J. Chem. Soc. Chem. Commun.* **1990**, 1456–1457; e) U. Hees, U.-J. Vogelbacher, G. Michels, M. Regitz, *Tetrahedron* **1989**, *45*, 3115–3130; f) U. Hees, M. Ledermann, M. Regitz, *Synlett* **1990**, *7*, 401–403; g) U. Hees, J. Schneider, O. Wagner, M. Regitz, *Synthesis* **1990**, *9*, 834–840; h) G. Maas, R. Rahm, F. Krebs, M. Regitz, P. J. Stang, C. M. Crittell, *Chem. Ber.* **1991**, *124*, 1661–1665; i) for a status report see M. Regitz, *Nachr. Chem. Tech. Lab.* **1991**, *39*, 9–13.

[4] a) P. Binger in *Multiple Bonds and Low Coordination in Phosphorus Chemistry* (Eds.: M. Regitz, O. Scherer), Thieme, Stuttgart, **1990**, pp. 90–111; b) B. Breit, U. Bergsträsser, G. Maas, M. Regitz, *Angew. Chem.* **1992**, *104*, 1043–1046; *Angew. Chem. Int. Ed. Engl.* **1992**, *31*, 1055–1058.

[5] a) All the quantum chemical calculations were carried out at the ab initio double-ζ level with polarization functions at the heavy atoms. The corresponding basis sets were constructed from Huzinaga type functions (S. Huzinaga, *Approximate Atomic Functions. II*, Technical Report, The University of Alberta, Edmonton, Alberta, Canada, **1971**) as follows: C, N: (9,5) in the contraction [5, 4 × 1/3, 2 × 1]; P: (11,7) in the contraction [5, 6 × 1/4, 3 × 1]; H: (4) [3,1]. One set of polarization functions was added to the heavy atoms: ζ_d for C,N, and P = 0.8, 0.95, and 0.5, respectively. The MCSCF [5b], MRCI [5c], and CEPA-1 calculations were carried out with the MOLPRO program systems [5d]. MCSCF wave functions were used in the geometry optimization with inclusion of the full π space. Corrections for higher excitations were performed with the Davidson procedure [5e]. The frozen core approximation was applied in the MCSCF and MRCI calculations. The accuracy of optimization is $\lesssim 10^{-7}$ Hartree. After optimization each point on the potential energy surface was refined by the MRCI calculations with the MCSCF wavefunction given as reference. Further investigations indicate that the lone pairs (on P, N) have no effect on the equilibrium geometries. This was tested by inclusion of these electron pairs in the active space of the MCSCF treatment and reoptimization. For the configuration interaction all of the singly and doubly excited configurations with respect to the MCSCF wavefunction were considered; the inner shells were not correlated. For the tetrahedrane structures (calculations of ε_3) we utilized RHF-optimized geometries in an MCSCF calculation, in which the active space consisted of four orbitals, to obtain the reference wavefunction for the subsequent MRCI calculation. Perfect closed-shell systems result for the tetrahedranes, as evident from the expansion coefficients of the MSCF wavefunction. For the computations of the ΔE values the CEPA-1 electron correlation approach was utilized, based on the RHF geometries of the tetrahedranes and their fragments C_2H_2, HCN, HCP, N_2, and P_2. b) H. J. Werner, W. Meyer, *J. Chem. Phys.* **1980**, *73*, 2342–2356; c) H. J. Werner, P. J. Knowles, *J. Chem. Phys.* **1988**, *89*, 5803–5814; d) MOLPRO-91, program version by P. J. Knowles and H. F. Werner; e) S. R. Langhoff, E. R. Davidson, *Intern. J Quantum Chem.* **1973**, *7*, 759–777.

[6] W. T. Borden, *Diradicals*, Wiley, New York, **1982**, pp. 1–72. This article reviews the most important theoretical work on cyclobutadiene.

[7] G. Maier, R. Wolf, H.-O. Kalinowski, *Angew. Chem.* **1992**, *104*, 764–766; *Angew. Chem. Int. Ed. Engl.* **1992**, *31*, 738–740.

[8] R. Janoschek, J. Kalcher, *Intern. J. Quantum Chem. Quantum Chem. Symp.* **1990**, *38*, 653–664.

[9] W. W. Schoeller in ref. [4a], Table 1.

[10] For a detailed analysis of the energy differences between P_4 (T_d), P_8 (O_h), and P_2 see a) R. Ahlrichs, S. Brode, C. Ehrhardt, *J. Amer. Chem. Soc.* **1985**, *107*, 7260–7264; b) G. Trinquier, J.-P. Daudey, N. Komiha, *J. Amer. Chem. Soc.* **1985**, *107*, 7210–7212.

[11] In addition to the values of ε_3 and ΔE listed in Table 1 for **1** and its mono- and disubstituted derivatives the following quantities (in kcal mol^{-1}) were obtained (at MP4/6-311g(2d,p)//MP2/6-31g(d) level): **1** 31.7 (ε_3), −27.3 (ΔE); N-**1** 26.2, −55.5; 1,3-N_2-**1** 29.1, −90.0; P-**1** 9.3, −3.2; 1,3-P_2-**1** −17.3, −18.3. 1,2,3-N_3-**1** -135.3 (ΔE); N_4-**1** -188.5; 1,2,3-P_3-**1** -29.4; P_4-**1** −39.5. These values are in good accord with the results of the more involved MCSCF calculations (see Table 1). The calculations were conducted with the GAUSSIAN 90 set of programs (M. J. Frisch, M. Head-Gordon, G. W. Trucks, J. B. Foresman, H. B. Schlegel, K. Raghavachari, M. A. Robb, J. S. Binkley, C. Gonzalez, D. J. Defrees, F. J. Fox, R. A. Whiteside, R. Seeger, C. F. Melius, J. Baker, R. L. Martin, L. R. Kahn, J. J. P. Stewart, S. Topiol, J. A. Pople, Gaussian Inc., Pittsburgh, PA, **1990**).

[12] We have computed the IR spectra of **1** and its mono- and disubstituted derivatives, as they have the best prospects for experimental verification. The vibrational analyses were performed within the harmonic approximation at MP2/6-31G* level. Details of the computed spectra are available on request and we will comment on them only briefly here. For example, an inversion center in **1** and its 1,3-heteroderivatives simplifies the expected IR spectra. For **1** seven IR-active bands [12a] and for 1,3-P_2-**1** six IR-active bands [12b] are predicted. For P-**1** the situation is more complicated since it has no inversion center. Here all 15 vibrations are IR-active. a) For **1** these values are in excellent agreement with experiment [1] (values in cm^{-1}): 559 (b_{3u}), 750 (b_{2u}), 1081 (b_{1u}), 1293 (b_{2u}), 1619 (b_{1u}), 3281 (b_{2u}), 3300 (b_{1u}). b) For 1,3-P_2-**1** (values in cm^{-1}): 275 (a_u), 581 (b_u), 672 (a_u), 946 (b_u), 1168 (b_u), 3267 (b_u).

BOOKS

This section contains book reviews and a list of new books received by the editor. Book reviews are written by invitation from the editor. Suggestions for books to be reviewed and for book reviewers are welcome. Publishers should send brochures or (better) books to the Book Editor, Dr. Gerhard Karger, Redaktion Angewandte Chemie, Postfach 101161, D-W-6940 Weinheim, Federal Republic of Germany. The editor reserves the right of selecting which books will be reviewed. Uninvited books not chosen for review will not be returned.

Book Reviews

Kirk/Othmer Encyclopedia of Chemical Technology. Vol. 1: A to Alkaloids. Vol. 2: Alkanolamines to Antibiotics (Glycopeptides). 4th Edition. (Series editor: *J. J. Kroschwik.*) Edited by *M. Howe-Grant.* Wiley, Chichester. Vol. 1: 1991. XXII, 1087 pp., hardcover £ 135.00.—ISBN 0-471-52669-X; Vol. 2: 1992. XXVIII, 1018 pp., hardcover £ 135.00.—ISBN 0-471-52670-3

In September 1991 a new edition of "Kirk/Othmer" started to appear from the publishers John Wiley and Sons. The fourth edition of this standard Encyclopedia of Chemical Technology will consist of 27 volumes (25 on topics in alphabetical order, together with a supplementary volume and a keyword index), which is one more than in the third edition. Up to now Volumes 1 and 2 have appeared. The rest are to follow at three-monthly intervals, so that the entire work should be completed by the end of 1998.

Volume 1 (33 articles) extends from "Ablative Materials" to "Alkaloids", and Volume 2 (27 articles) from "Alkanolamines" to "Antibiotics". Scanning through the articles it is evident that the new Kirk/Othmer continues the excellent tradition of earlier editions. The contributions have again been written by acknowledged experts, and despite this (or perhaps because of it) they can be understood even by the interested non-specialist. The literature citations are carefully chosen and very up-to-date; some of the articles even cite sources as recent as 1991.

The choice of topics reflects recent progress in science and technology. For example, separate articles are now dedicated to key technologies such as "Advanced Ceramics" (for electronic and engineering components), to developing fields with high growth potential such as "Antiaging Agents", and to technologies that have increased in importance such as "Aeration" (in biotechnology and effluent treatment). On the other hand product areas that have stagnated or become less important (e.g., acetylene, anthraquinone derivatives) have now been relegated to subsections. Other articles have been revised and updated. A high standard of treatment has been maintained throughout. This applies not only to bulk commodity products but also to products in the middle or at the end of the value-added chain. Thus, on the one hand new developments in large-scale processes such as the production of cyclohexanol by addition of water to cyclohexene, or of adipic acid from butadiene as a cheap feedstock, and on the other hand advances in specialized areas, for example the synthesis of special amines such as *tert*-butylamine, where the Ritter reaction is being replaced by the more environmentally acceptable direct catalytic amination of isobutene, are treated with equal thoroughness.

The articles that are concerned not with products but with basic science (e.g., absorption and adsorption), with working techniques (e.g., analytical methods), or with environmental topics (e.g., atmospheric pollution) also reflect the latest knowledge. For example, in the article on "Air Pollution" we find not only data from measurements in 1990 and values for the ozone-depleting potential and greenhouse-effect potential of important atmospheric pollutants, but also an informative section on "Indoor Air Pollution", which puts this topic into perspective without playing down the risks. Whereas in "Ullmann" the topics of a more fundamental nature are treated in a separate series, in the new Kirk/Othmer these are integrated into the main volumes.

Unlike previous editions this new edition consistently uses SI units in the tables and figures (although in the text the American units are occasionally added in parentheses—not surprisingly, some conversion errors have crept in here, but on the whole these are comparatively rare).

Some of the articles contain many abbreviations, which can be rather troublesome. Headings such as "UOP MRU–ORU Processes" (Vol. 1, p. 593) convey hardly anything to the reader who wants to find information quickly. On encountering a sentence such as "The related simple design concepts of WES, WUB, and LUB for constant-pattern adsorption are discussed later" (Vol. 1, p. 540, "Adsorption Dynamics"), the reader who is new to the subject but wants to find out more will be deterred rather than encouraged to read on, especially as the meaning of WES, WUB, and LUB can only be discovered by first turning back to page 517 (for

LUB) then further on (!) to page 564 (for WES and WUB). On the other hand, in cases where abbreviations are listed at the end of an article, when one no longer needs them, it is simply a waste of space (e.g., "IARC", Vol. 1, p. 310, and "ADI", Vol. 2, p. 578.

In the articles concerned with products one finds that the information given in the section "Economic Aspects" in each case varies greatly in the amount of detail and sometimes in quality. For example, under "Ammonia", "Adipic Acid", and "Acrylonitrile" one finds a considerable amount of information about production capacities, consumption, and market growth, not only for the USA but also for Europe and Asia. In contrast, under "Anthraquinones" (Vol. 2, p. 811) the section "Economic Aspects" gives only one quantitative item, the price. Under "Alkyl Phenols" (Vol. 2, p. 128) the "Economic Aspects" amount to no more than a breakdown of the production costs, and under "Amino Resins and Plastics" (Vol. 2, p. 635) they consist essentially of a list of manufacturers occupying nearly half a page. Here the work could certainly have been improved by some systematization and unification of treatment, like that found in the corresponding sections of "Ullmann".

However, despite the few shortcomings the new Kirk/Othmer, like its predecessors, is a work of reference in the top rank worldwide, and it is essential to every scientific and technical library as a complementary work to "Ullmann".

Friedbert Nees
BASF Aktiengesellschaft
Ludwigshafen (FRG)

Computational Chemistry. Structure, Interactions and Reactivity. (Series: Studies in Physical and Theoretical Chemistry.) Edited by *S. Fraga*. Elsevier, Amsterdam, 1992. Part A: XXXII, 744 pp., Part B: XIX, 661 pp., hardcover HFl 995.00.—ISBN 0-444-88512-9

This two-volume work of altogether more than 1400 pages is the result of the efforts of 111 authors. More than half of these are Spanish; moreover, the make-up of nationalities in the rest is significant, as it is dominated by countries such as Argentina, Cuba, and Mexico. Thus the work is in effect a literary demonstration by the Hispanic countries. The editor has exercised little, if any, control over the authors, and has also succumbed to the temptation of assuming that one can never have too much content and variety. It therefore comes as no surprise to find that the majority of the 52 chapters have turned out to be neither "computational" nor "chemistry". It is not possible here, nor even necessary, to describe in detail and evaluate all the chapters. Instead this review will offer some general comments on the contributions, will identify those chapters that are in the nature of a general overview of a particular topic, and will discuss the extent to which they present results relating to theories that are described.

Unfortunately a good many of the authors seem unable (or unwilling) to present review articles of general interest such as one expects to find in a book of this kind. These authors assume that their own work and very individual views will be of interest to the reader, and they give numerous references to their own publications. For example, in the report on excited states of simple molecules it is not clear why one should want to systematically calculate the excited states of molecules with two, three, and four atoms. Who is interested in this apart from the author? What is sadly missing here is a review of the current situation in theoretical photochemistry. Another example is the article on configurational interaction, which is in fact very well written, but leaves one at the end wondering what it all adds up to. What are the capabilities and limitations of the computational methods described? To discuss such methods without including the sets of basis functions is like having a vessel without a bottom. Moreover, the article fails to give any experimental results, and without these one cannot evaluate the theories. The authors of a chapter on basis sets have even managed to discuss the topic entirely in verbal terms, giving neither basis sets nor any results derived from them. One also feels regret for what is missing in the chapter on molecular integrals based on Slater functions, in which the final climax is a closely printed list of pointless integral formulas. A chapter entitled "Geometries, Energies and Molecular Properties" includes, in addition to the properties mentioned here, calculations of dipole and quadrupole moments, field gradients, and electron densities for many molecules such as H_2O, NH_3, CH_4, C_6H_6, etc., with six basis sets in each case. However, the 19 enormous tables amount to nothing more than a large occupational therapy exercise, as the discussion of the basis set dependence at the Hartree–Fock level, without taking into account electron correlations, has long since ceased to be of interest to anyone. Regrettably, this antiquated article is not an isolated example; to conclude these adverse comments the prize for this must go to Cuba for the contribution on "Approximate Methods for Polyatomic Systems", in which a whole group of authors introduces the reader to the basic equations of the elementary Hartree–Fock theory and to the NDO approximation—and this in 1992!

The transition from the barren wastes to the more worthwhile contributions is smooth. A chapter on photoelectron spectroscopy contains not only an up-to-date account of the theory but also many examples, in which different methods of calculation are compared with each other and with experimental results. The literature on this topic is extensively reviewed. In this respect one should also mention the article by Moccia which is an introduction to calculations on multiphoton processes, including a detailed account of the theory and of methods of calculation together with results. Leaving the area of spectroscopy the reader's attention may be caught, for example, by a chapter on solvent effects in reacting systems. The theories of the self-consistent reaction field are clearly described, but unfortunately their applications are only indicated sketchily. This situation could quickly change, as these methods are already included in the latest versions of readily available program packages. The reader concerned with applications will also certainly appreciate the analysis of the concepts of basicity and acidity using reliable ab-initio calculations. This excellent article is hidden away under the rather uninformative title "Organic Molecules". The chapter by Smeyers on "Non-Rigid Molecules" meets the criteria for a good and easily understandable review article. The applications described are mainly to calculations on IR spectra of systems with internal rotation. The contribution by Strausz et al. on the Wolff rearrangement of α-diazoketones is worth mentioning as a classic example of the application of modern ab-initio methods of calculation to a chemical problem. Ventura gives an excellent review of chemical reactivity, with a pithy discussion in which formulas are kept to a minimum; the aspects covered range from the energy hypersurface through modern quantum chemical methods of calculation to reaction dynamics, concluding with kinetics and thermodynamics. The concise style continues in the section on applications, without leaving out any of the essentials. The examples chosen range from gas phase reactions to enzyme reactions. This very informative review,

which does not overload the reader with irrelevant details, is one of the highlights of the two volumes, as also is the account by Barthelat and Durand of the theory of the effective Hamiltonian operator. Such operators provide the theoretical basis for calculations on heavy atoms, and consequently their importance can hardly be overstated. Such a readable and full account of this topic is unlikely to be found elsewhere.

Other topics treated in these two volumes include mathematical fundamentals, atomic scattering experiments, biochemistry, quantum electrodynamics, NMR spectroscopy, statistical mechanics, models of liquids, superconductivity, crystal physics, and metallurgy. However, these topics are so far removed from the title of the work that it is not possible to review them here. Paradoxically, in contrast to this one searches in vain for contributions on modern semiempirical methods of calculation. It is unfortunate that readers interested in computational chemistry will have to load their bookshelves with so much ballast in order to have access to the few articles that are relevant.

Rudolf Janoschek
Institut für Theoretische Chemie
der Universität Graz (Austria)

Photodissociation of Simple Molecules in the Gas Phase. By *H. Sato*. Bunshin, Tokyo, 1992. V, 158 pp., paperback Yen 1100.—ISBN 4-89390-092-7-C3543-P1100E

For some years now H. Sato of Mi'e University has been monitoring the literature on photodissociation processes of small molecules in the gas phase, and at annual intervals people interested in this field have received from him a booklet listing publications during the past year. All these references covering the years from 1970 to 1991 have now been collected together into a book. This is the period that has seen the laser become firmly established as a tool for photolytic studies and analysis. The book consists of two tables, together with an associated list of over 1000 references. Altogether the compilation covers about 280 simple molecules and more than 70 van der Waals molecules. Recently the survey has also included organometallic compounds that are of importance in chemical vapor deposition studies. The structure of the tables is very simple, with entries listing the initial molecular species, the photolyzing wavelength (or generating source), method used to identify the breakdown fragments, and final products, as well as the literature citation and a few brief comments. The entries are arranged according to the initial species.

This is not a textbook, nor is it a monograph along the lines of H. Okabe's book *Photochemistry of Small Molecules*. As Okabe notes in the foreword, it has more in common with the much costlier spectroscopic data collection *Constants of Diatomic Molecules*, by Huber and Herzberg. It is a book to refer to when one is setting out to photolyze a new molecule and wishes to find out what relevant work has been published recently. Thus it is intended for the active researcher, for whom it can be thoroughly recommended. In my own laboratory the booklets that were its forerunners have proved invaluable when planning experiments. I would like to have these data available on a floppy disk, which should also make it possible to search according to reaction products.

According to the publishers, the price, including postage, is \$ 17.50 in the USA and \$ 19.50 in Europe. I have just learnt from Dr. Sato that Supplement VI of his collection "Photodissociation of Simple Molecules in the Gas Phase" has been published in *Research Reports of the Faculty of Engineering, Mi'e University*, Vol. 17, December 1992.

Friedrich Stuhl
Fakultät für Chemie
der Universität Bochum (FRG)

Entropy Analysis. An Introduction to Chemical Thermodynamics. By *N. C. Craig*. VCH Publishers, New York/VCH Verlagsgesellschaft, Weinheim, 1992. XI, 208 pp., hardcover DM 72.00.—ISBN 1-56081-539-6/3-527-89539-6

This book aims to provide students in their first semester with an introduction to thermodynamics along new lines. The author sets out to develop the fundamental laws of thermodynamics from a global perspective instead of the usual system-orientated viewpoint. As the title of the book indicates, the treatment focuses on entropy as the key variable, since the first law (the conservation of energy) can be regarded as being automatically fulfilled from the global standpoint. The book consists of ten chapters and an appendix. After an introduction the author deals with the fundamental principles of thermodynamics (the first law, the concept of enthalpy, the second law), then with their application to heat engines, the molecular significance of entropy, applications to chemical reactions (the definition of the Gibbs energy, chemical equilibria, electrochemical reactions), and the interconversion between different forms of energy. Each chapter ends with a detailed summary of its contents. The appendix consists of four sections. The first short one (three pages) discusses the relationship between the global and system-orientated approaches to thermodynamics. Two further sections contain examples to illustrate the interpretation of the proposed concepts from the molecular (microscopic) point of view. The last section consists of 30 pages of tables listing standard enthalpies and entropies of formation and Gibbs energies, and specific heats of the elements and of more than a thousand compounds, mostly inorganic.

The global approach chosen here undoubtedly has advantages in some parts of the subject. For example, it is found that beginners often have great difficulty with problems where, in order to apply the second law, one has to combine the "system" and the "surroundings" to form a new "supersystem". The global approach avoids the complications associated with systems that are not closed. Also the description of irreversible processes is simplified. The introduction of the molecular significance of entropy at an early stage is a welcome feature.

However, the author incurs a penalty for his approach, since for each process he has to consider a number of systems, each with its own internal energy. The first law takes the form:

$$\Delta U_{\text{total}} = \Delta U_{\sigma} + \Delta U_{\theta} + \Delta U_{\text{wt}} + \ldots = 0$$

in which the suffix σ denotes the reacting system under consideration, θ denotes a heat reservoir system, and wt a mechanical system. These systems are illustrated by diagrams. The processes that are analyzed involve an exchange of energy between the partial systems. However, in physical terms this compartmentalization often breaks down; to take the simple case of an exothermic reaction in solution, the latter is also the heat reservoir. This is an abstract idea that the beginner will not always find easy. The fundamental difference between the internal energy as a state function on the one hand, and on the other hand the concepts of work

 © *VCH Verlagsgesellschaft mbH, W-6940 Weinheim, 1993* *0570-0833/93/0404-0621 \$ 10.00+.25/0*

input and heat introduced or removed, which are not state functions, does not clearly emerge. The concepts of work and heat are replaced by the energies of the mechanical system and of the heat reservoir system, respectively. For the relationship between the two approaches one has to go to the appendix. It seems very doubtful whether the approach adopted here will really help the student to gain a deeper understanding of thermodynamics and apply it to practical situations later on.

The avoidance of using the methods of differential and integral calculus will certainly be helpful to first-semester students, who do not usually have a sufficient mathematical background at this stage. However, by the second semester at the latest, a more exact mathematical formulation becomes essential; the usual level of thermodynamics lecture courses in Germany at this stage goes beyond that of the book. In many cases, therefore, the student will then need to switch to a different approach, and there is a risk that the earlier simplifications will become a hindrance to a deeper understanding.

Within the intended scope of the book, the treatment is, on the whole, rigorous. Nevertheless, it seemed to this reviewer that in some places the author makes statements, in anticipation of later discussions, that could be misunderstood. Although these are later corrected when the topics are treated in detail, there is a risk that by then the reader has the misconceptions so firmly in his or her head that it is difficult to correct them. For example, the statement in Chapter 4 (p. 42) that entropy is a measure of disorder is inappropriate in relation to the subsequent more detailed treatment in Chapter 6. In Chapter 3 reference is made to the heat capacity of the thermal reservoir before the specific heat c_p has been defined. Also the short section on "the molecular basis of the reaction enthalpy" is not very helpful.

There are many exercise problems at the end of each chapter, sometimes with hints on the method of solution. The consistent use of SI units throughout is a good feature. The high price of the book will deter students from buying it, especially since it scarcely goes far enough to cover the first semester of study.

Friedrich Temps
Institut für Physikalische Chemie
der Universität Göttingen (FRG)

Organic Synthesis with Oxidative Enzymes. By *H. L. Holland.* VCH Verlagsgesellschaft, Weinheim, 1992. XI, 463 pp., hardcover DM 168.00.—ISBN 3-527-27956-3

Biocatalysis techniques are increasingly developing as attractive alternatives to well established conventional chemical methods for many chemical transformations. This applies also to oxidations, as is impressively shown by H. L. Holland in this book. The applications of oxidoreductases in organic synthesis are summarized here in ten chapters, each plentifully illustrated with formula schemes and supported by a comprehensive and up-to-date bibliography (up to May 1990). Although alcohol dehydrogenases can also be used oxidatively, these are not covered. The book is intended for organic chemists who wish to learn about the capabilities of oxidative biotransformations and their use on a preparative scale. Some of these can be performed using isolated enzymes, which are even commercially available in a few cases, but the majority of the transformations described are only possible by using whole cells, i.e. living microorganisms. Although this whole cell technology has already been established in industry for several decades, e.g. for the hydroxylation of steroids, its applications to organic syntheses in other fields has so far been minimal compared with the use of isolated biocatalysts. One reason for this is that up to now the majority of oxidases have been difficult or impossible to obtain in active form together with the necessary cofactors and activators. A second reason is that many organic chemists still feel a great aversion and reluctance to use methods that are "too biological", and are therefore not very amenable to being controlled and—even more importantly—rationalized. Mindful of this obstacle to getting started, Holland has followed his introductory chapter, in which he describes the basic mechanisms of enzymic catalysis by mono- and dioxygenases, peroxidases, and also reductases, with a chapter on general laboratory techniques for performing biotransformations. In this he describes briefly how one goes about obtaining the microorganism needed for the purpose, and then how the actual transformation is carried out.

The following seven chapters present the current state of the art regarding the most important organic biotransformations. Chapter 3 describes hydroxylations at saturated carbon atoms; the main emphasis is on steroids and terpenes, but also included are hydroxylations at the benzylic position in a wide variety of arenes, and applications to *N*-dealkylations. Chapter 4 deals with oxidations of unsaturated CC bonds, describing biocatalytic epoxidations of olefins and arenes, and the currently very interesting conversion of aromatic hydrocarbons to enantiomerically pure *cis*-dihydrodiols as useful synthetic building blocks. Chapter 5 is concerned with biocatalytic Baeyer–Villiger oxidations, and Chapter 6 with oxidations at heteroatoms such as nitrogen and sulfur to give *N*-oxides, sulfoxides, sulfones, etc. Chapter 7 describes the conversion of CC single bonds to double bonds, with special reference to steroids and fatty acids, then in the following chapter the author collects together all the reactions that cannot be categorized under the previous headings. These include, for example, the oxidative coupling of phenols and their oxidation to quinones, and the biocatalytic breakdown of alkyl chains. In the penultimate chapter, which is very long in keeping with its importance, Holland describes reductive biotransformations, including the enzymic removal of hydroxy groups and halogens, the reduction of sulfoxides to sulfides and of *N*-oxides to amines, and especially the conversion of isolated double bonds and α,β-unsaturated carbonyl compounds to the corresponding saturated hydrocarbons. Lastly, Chapter 10 contains a survey of the many different types of enzyme-catalyzed syntheses described in the foregoing chapters, and with this as the theme the author gives advice, especially for the non-specialist, regarding criteria for identifying a suitable microorganism to perform a particular conversion. After also discussing the possibility of applying genetic engineering methods, the book ends with a brief, but optimistic, review of future prospects.

H. L. Holland has produced here a book that sets new standards. He informs the reader expertly, comprehensively, and without unnecessarily lengthy detail, about the capabilities and range of applications of the various biocatalysts described. He has wisely resisted the temptation to view his special subject through rose-colored spectacles and praise it to the skies. In every case he presents a critical evaluation, indicates perspectives, and points out examples where biocatalysis offers no advantages compared with conventional methods. In accordance with his self-imposed task of addressing organic chemists and helping them to make decisions and overcome fears, whenever possible Holland gives topical examples illustrating how the products from biosyn-

theses can be used in subsequent organic syntheses (e.g., as in the dioxygenases and the Baeyer–Villiger oxidation).

The book can be recommended unreservedly both for the specialist in academia or industry who wants detailed information and for the synthetic chemist who is keen to learn about these methods but has little previous knowledge. It is likely to earn a place as a standard work in the bioorganic literature.

Karlheinz Drauz, Herbert Waldmann
Degussa AG, Hanau
Institut für Organische Chemie und Biochemie
der Universität Bonn (FRG)

Salt Effects in Organic and Organometallic Chemistry. By *A. Loupy* and *B. Tchoubar*. VCH Verlagsgesellschaft, Weinheim/VCH Publishers, New York, 1992. XVI, 315 pp., hardcover DM 164.00.—ISBN 3-527-28025-1/0-89573-954-2

We have all met these problems! A reaction fails to proceed at the necessary rate, or does not give the desired selectivity. One obvious way around this kind of everyday problem is to change the solvent. It is less well known that reaction rates, equilibria, and regio- and stereoselectivities can be dramatically altered by adding chemically inert salts. Specific salt effects, i.e. those that depend not only on the concentration and charge of the ions but also on the chemical nature of the salt, have not yet been accepted into the preparative chemist's armory to any significant extent. Probably one reason for this is that the relevant information is widely scattered throughout the literature and has not previously been collected together. This monograph on salt effects in organic and organometallic chemistry by the French authors Loupy and Tchoubar is probably the first of its kind, and its dust-cover promises a gold-mine of information, experience, and ideas. Does the book live up to this claim? Yes, to a large extent it does.

After a brief introduction to the classification of salt effects, the authors describe the effects of salts on the rates of substitution and addition reactions. This is followed by a survey of how the regio- and stereochemical course of a reaction can be influenced by adding salts. Lastly the book deals with the effects of salts on the positions of equilibria, and discusses the importance of salt effects in organometallic chemistry. This last part is much shorter than the book's title leads one to expect. The work ends with an appendix summarizing some of the general concepts used in the foregoing chapters (e.g., the classification of solvents, hard and soft acids and bases).

This monograph is an English translation of the book published in France in 1988 under the same title. Regrettably, the opportunity to update it by including recent developments has been allowed to pass, and thus in general the literature references only extend up to 1988; a few papers from the period 1988–1990 are mentioned only in the appendix. There are very few factual errors (e.g., Eqn. 7–94 on p. 270), and those that have crept in scarcely affect the meaning. The salt effect referred to on page 175, namely the effect of adding a cuprate to a chiral Michael acceptor, is correctly described but is shown for the wrong stereoisomer. The subject index of only five pages is of little help when one is looking for specific subject areas (instead the reader should refer to the very detailed list of contents), and there is no author index (an omission that has unfortunately become too common nowadays). If these shortcomings could be remedied in a new edition it would considerably improve the book's usefulness.

The authors have been largely successful in their efforts to achieve a useful organization of the information contained in well over a thousand publications. In describing the effects observed they have mainly avoided including mathematical derivations. In view of the large mass of data it is hardly surprising that occasionally the guiding theme is lost and gives way to a mere list of observations. However, this is not a disadvantage insofar as it has enabled the authors to include some related areas that would otherwise have been left out. The extensive sections on salt effects in regio- and stereoselective reactions are likely to be especially useful; chemists working on these topics will find here a wealth of stimulating ideas, and they may well find it worthwhile to buy a personal copy. Libraries, despite their tight budgets, cannot afford to be without the book.

Norbert Krause and *Robert Wagner*
Institut für Organische Chemie
der Technischen Hochschule Darmstadt (FRG)

Hydrogen Bonding in Biological Structures. By *G. A. Jeffrey* and *W. Saenger*. Springer, Berlin, 1991. XIV, 569 pp., hardcover DM 198.00.—ISBN 3-540-50839-2

In the living world of biomolecules hydrogen bonds are the most important of all noncovalent bond types. They play an essential role in the formation of biological macromolecules such as the globular proteins and the DNA double helix, and in the mechanism of enzyme-substrate recognition. This area of study is the subject of a new monograph by G. A. Jeffrey and W. Saenger, which places special emphasis on the geometrical aspects.

The first part begins with a short historical survey, followed by an account of the characteristics and functions of hydrogen bonding. The authors describe the possible types of geometries and effects on the molecular structure, cooperativity, ordering, and statistics, and discuss experimental and computational methods for studying these effects.

In the second part the patterns of intra- and intermolecular hydrogen bonding in small molecules are discussed on the basis of available structural data. In particular the authors consider hydrogen bonding in alcohols and saccharides, which often form crystal structures with extended cooperative networks. This is followed by detailed discussions of the structures of purines and pyrimidines and the possible base pairings in these compounds, and of the crystal structures of nucleosides and nucleotides. There is also a short section on amino acids.

Part 3 of the book is concerned with hydrogen bonding in biological macromolecules. The structures of oligosaccharides and cyclodextrins are discussed very thoroughly, leading to general conclusions about cooperativity and dynamics in extended hydrogen-bonded networks. A further section deals with internal hydrogen bonding in proteins, describing the types of geometries and patterns that are found. The flexibility of protein molecules and their hydrogen bonds has been investigated by hydrogen–deuterium exchange experiments. Nucleic acids and their possible base pairings are also discussed from the standpoint of hydrogen bonding. There is also a section on protein–nucleic acid recognition mechanisms.

Part 4 is concerned mainly with aggregates formed by water molecules. First the authors introduce the models used to

describe water, ice, clathrates, and the hydrate and layer hydrate compounds formed by small molecules. They then go on to discuss the hydration of proteins and nucleic acids, describing in detail the arrangement of water molecules on the surfaces of these macromolecules, and the formation of water clusters in the region of the transition to the bulk solvent.

Taken as a whole this is a comprehensive standard work on hydrogen bonding in biological systems. However, owing to the difficulty of obtaining data for hydrogen atoms in large structures the main emphasis is on small molecules such as saccharides and nucleic acid bases, for which adequate structural data are available. The energies of hydrogen bonds are difficult to analyze, and consequently they are not treated to any significant extent here. The same also applies to entropy effects, such as are involved in the stabilization of structures by hydration. The schemes and tables contain a wealth of experimentally determined structural data, and the discussions in the text are supported throughout by clear diagrams. The introductions to the individual chapters give sufficient information to ease the way for readers new to the subject. The author's aim was certainly not to write a short compendium on the subject, but nevertheless the book contains a wealth of useful information not only for the specialist but also for the reader with more general interests, and this will ensure that it appeals to a wide readership.

Ulrich Abele and *Georg E. Schulz*
Institut für Organische Chemie und Biochemie
der Universität Freiburg (FRG)

Rapid Reactions in Solution. By *H. Strehlow*. VCH Verlagsgesellschaft, Weinheim/VCH Publishers, New York, 1992. XIV, 341 pp., hardcover DM 176.00.—ISBN 3-527-28260-2/1-56081-126-9

Any student or researcher who has needed to find out about fast reactions will know that since the publication in 1964 of Edward Caldin's book *Fast Reactions in Solution* there has been no more recent treatment of the methods and results of this area of research. This book by Hans Strehlow now fills that gap.

In the language of chemists, "rapid" reactions are those with time-scales in the range from nanoseconds to several seconds. Although even faster processes in the femtosecond range can nowadays be studied, and there is speculation concerning what information of interest to the chemist this can yield, such processes are not the subject of this book. As Strehlow emphasizes in his introduction, the investigator concerned with the dynamics of chemical processes is not primarily interested in obtaining numerical values of rate constants with the highest possible accuracy; instead the aim is to elucidate reaction mechanisms and to observe and characterize the elementary steps in complex systems. Strehlow has set out to provide the investigator, by means of examples of applications, with as comprehensive an understanding as possible, so that he or she can choose the most suitable method for a given problem. Reading the book is certainly not enough by itself to reach that goal, but it provides a firm basis for more detailed discussions with the experts, of whom Strehlow is indisputably one of the most competent. He has used nearly all the methods himself, has been involved in their development in some cases, and he and his research group at the Max-Planck-Institut in Göttingen have made numerous contributions to the understanding of reactions in solution.

The subject matter is arranged according to the various methods, beginning with flow techniques, which have now developed to the point where they can be applied even to reactions in the microsecond range. Then relaxation methods and NMR techniques are both treated at some length. The book ends by describing flash photolysis and pulse radiolysis methods. The area with which Strehlow is most closely associated is electrochemistry, as might be guessed from the fact that the modern and highly successful NMR methods are given only about the same amount of space as polarography, a highly specialized method limited to homogeneous reactions. From this it can be seen that the author is concerned to present the methods in a way that reflects their historical development. Regrettably, fluorescence quenching is only briefly mentioned under the heading of "Other Methods". In recent years this technique has yielded much valuable information, especially in colloid chemistry; the technology is now highly developed, and advances in the theoretical understanding of fluorescence quenching in compartmentalized systems (extension of the Perrin theory) have led to new ways of interpreting the data.

Many of the applications chosen as examples belong to the early investigations that yielded basic information about the elementary steps of proton transfer, metal complex formation, and enzyme–substrate interactions; most of the systems discussed here are those that have been extensively studied by the author's own group. However, developments of other kinds have not been ignored. An example of these is fluctuation analysis, which has become important in membranes research and other areas. Nevertheless, Strehlow's book contains few examples of applications in biophysical chemistry, or references to such work.

Strehlow introduces the theoretical aspects in a way that reveals him to be an outstanding teacher who can explain the principles clearly and understandably. The introduction to the kinetics of micelle formation is a prime example of how the discussion of a simplified system can serve to prepare the reader for a more abstract formulation. Likewise the introduction to NMR methods, where the Bloch equations and the relationships based thereon are of special interest for applications in physical chemistry, is excellent from a learning standpoint—my students have already had much amusement from the illustration of the spin-echo experiment. The occasional cartoons are probably even more effective in contributing to a better understanding. Moreover, the book shows evidence of careful editorial planning, with a clear layout.

The book is accompanied by a floppy disk containing computation programs. This may be useful to many readers, but nowadays many statistical and graphics programs are widely available, and most research groups whose work involves relaxation curves or correlation functions already have the "Discrete" program installed in their computer systems so that exponential functions can be fitted to data.

Many scientists working in this field are members of the "Discussion Group on Fast Reactions in Solution" run by the Royal Society (London), and attend the Group's annual discussion meeting. One of the founder members of this Group was Edward Caldin, who is also still an active participant in these annual discussions, and at this year's meeting I talked with him about Strehlow's book. He reacted quite spontaneously by saying "I am delighted that my book has been replaced by Professor Strehlow's book, which I

have read and greatly admire." I can certainly endorse that view.

Georg Ilgenfritz
Institut für Physikalische Chemie
der Universität Köln (FRG)

Carbocyclic Cage Compounds: Chemistry and Applications. (Series: Methods in Stereochemical Analysis. Series editor: *A. P. Marchand.*) Edited by *E. Osawa* and *O. Yonemitsu.* VCH Verlagsgesellschaft, Weinheim/VCH Publishers, New York, 1992. XIV, 409 pp., hardcover DM 168.00. – ISBN 3-527-27933-4/0-89573-728-0.

This is the third major work on carbopolycyclic compounds to appear within the last four years. Whereas Haufe and Mann (*Chemistry of Alicyclic Compounds,* **1989**; see *Angew. Chem.* **1991**, *103*, 111; *Angew. Chem. Int. Ed. Engl.* **1991**, *30*, 1191) approach the subject in a systematic way, the multiauthor volume edited by Olah (*Cage Hydrocarbons,* **1990**) and the book reviewed here are unstructured collections of review articles in a style similar to that of *Chemical Reviews*. The latter journal did in fact include an issue in 1989 containing 17 reviews on the same subject area. Despite this there is little overlapping of the contents, which gives an indication of the wide-ranging nature and high level of activity in polycycles chemistry.

We learn from the preface that this book arose from a series of symposia on cage compounds that took place in Japan in the 1980s, extending to the beginning of the 1990s. As one might expect from this, the articles vary considerably in their breadth of subject matter, length, readability, up-to-dateness, and so on. Nevertheless, most of the older contributions appear to have been revised to bring them up to date, so that in general the articles take into account work published up to 1989, with a few references to publications in 1990 and 1991. A lamentable exception is Chapter 11 in which, out of about 110 references, the most recent are one from 1981, two from 1982, and one from 1983.

The subtitle should be regarded with caution. Anyone who expects to find applications of cage compounds in fields other than chemistry will be disappointed. Apart from a mention in the preface, applications are only seriously addressed in the last chapter (solar energy storage). It is a sad commentary on the present situation regarding support for basic research that it is felt necessary and realistic to justify it by citing potential applications of doubtful validity; here, for example, research on cubane is justified by dubious references to possibilities for explosives or pharmaceuticals.

Most of the book's contents are concerned with down-to-earth organic chemistry. In Chapter 1 A. P. Marchand gives a very readable review of the use of cage compounds as intermediates in organic synthesis, and as rigid structures within which reactive intermediates that could not exist otherwise may be prepared, observed, or identified from the stable products that result from them. The reaction schemes are clear and well annotated, a virtue not shared by some of the other articles.

Chapter 2 (K. Naemura) deals with cage compounds that are highly symmetrical but nevertheless chiral (an example is D_3-trishomocubane). Many of the schemes show several structural formulas together, identified only by numbers, which necessitates much turning of pages and spoils the clarity of the presentation.

Chapter 3 (H. W. Kroto and D. R. M. Walton) is a short one on "Postfullerene Organic Chemistry", and is rather out of place here in several respects. Firstly, the aromatic C_{60} soccerball structure (according to the preface a "fantastic superstar", which rather misleadingly appears in several copies, sadly shrunken, on the front cover) is fundamentally different from the small saturated molecules treated in the rest of the book. Secondly, this article consists not so much of research results as of speculations about possible synthetic routes to individual fullerenes (at the time when this chapter was written the flood of publications on C_{60} chemistry was only just beginning).

Chapter 4 (F. Matsuda and H. Shirahama) on "Natural Products Chemistry in Three Dimensions" discusses the observation that unsaturated macrocycles often adopt a preferred conformation in which the plane of a double bond is perpendicular to the plane of the macrocycle, with important consequences for the reactivity. Chapters 5 (propellanes, Y. Tobe), 6 (cyclophanes derived from vinyl arenes, J. Nishimura), 7 (prismanes, G. Mehta and S. Padma – very lucid and worth reading), 8 (cubanes, H. Higuchi and I. Ueda), and 9 (bishomocubanes, W. L. Dilling) review recent developments in the chemistry of these compound classes, with the emphasis in each case on the work of the authors.

In Chapter 10 C. Ganter describes in detail the elegant methods and results of his cartography of "Adamantaneland". Chapter 11 (J. Fournier and B. Waegell) discusses the reflex and anti-reflex effects, which are concerned with the influence of axial substituents at the 3- and 5-positions on the conformations of cyclohexanones. In Chapter 12 T. Miyashi, Y. Yamashita, and T. Mukai give a concise description of photochemical methods for synthesizing cage compounds, and the photochemical reactions that these undergo in the presence of electron transfer catalysts. Lastly, Chapter 13 (K. Hirao, A. Yamashita, and O. Yonemitsu) discusses the problems that still remain to be overcome in trying to apply a simple reaction (norbornadiene$\rightleftharpoons$quadricyclane) on a technical scale.

The overall impression from these articles is of thoroughly sound contributions to the field. The rather nonsensical statement "Asymmetry is a necessary but insufficient criterion for a chiral molecule to have a nonsuperposable enantiomer" (p. 62) is, fortunately, not typical. When dimethyldioxirane is wrongly described as "dimethyldioxolane" (p. 241) and Meldrum's acid (isopropylidene malonate) as a "glutaric acid derivative" (p. 280), one might well excuse these as no more than minor slips. Unfortunately there are also some annoying errors in the formula diagrams. For example, in pagodane (p. 36) two bonds are missing from the "waist" of the molecule, the stick projection of the C_{60} football on page 98 is not successful, and in the alleged conformational equilibrium shown at the top of page 324 the two formulas actually represent a pair of constitutional isomers. The repeated appearance of certain topics, such as 2 + 2-photocycloaddition and the Favorsky ring contraction, was probably unavoidable. I would have preferred a more definite continuity of theme in several of the articles, and even throughout the book.

The technical quality (typography, binding, etc.) is good, and the number of printing errors is acceptably small. Libraries and specialists in the field should buy the book, but most other chemists are unlikely to wish to do so, in view of its specialized nature and the fact that parts of it are no longer completely up-to-date.

Christoph Rücker
Institut für Organische Chemie und Biochemie
der Universität Freiburg (FRG)

The Synthesis of Insect Pheromones, 1979–1989. (Series: The Total Synthesis of Natural Products, Vol. 9. Series editor: *J. ApSimon.*) By *K. Mori.* Wiley, Chichester, 1992. IX, 534 pp., hardcover, £ 98.00.—ISBN 0-471-55189-9

Insect pheromones, a group of natural products that modify insect behavior, have attracted the attention of many synthetic chemists during the last two decades because of their importance in biology, ecology, and biological plant protection. In this volume of over 500 pages on the synthesis of insect pheromones, Kenji Mori single-handedly and skillfully reviews the literature on the subject for the years 1979–1989, and describes in detail an enormous variety of new methods, as well as variations and improvements on already known methods. It is intended as a continuation from an article by the same author that appeared in Volume 4 of this series "The Total Synthesis of Natural Products". As one of the most successful and best known synthetic pheromone chemists, Mori can justly be described as the guru of pheromone synthesis, especially in the area of chiral and enantiomeric compounds. Understandably, therefore, a considerable part of the book is concerned with enantioselective methods of synthesis.

Probably every pheromone chemist of this period is represented in the literature references, of which there are over 1200. These cover all the leading international and national journals, but also include some publications in rather unusual journals that are not easily accessible to most readers. A very impressive feature of the book is the formula schemes, which probably account for a high proportion of the work that has gone into the book; the author makes a special point of thanking his colleagues in Tokyo for their help in preparing them. With over 1000 (!) formula schemes the volume is a picture-book of pheromone synthesis and a striking example of the art of clear presentation. The book is an especially valuable resource for the chemist who needs a quick survey of all the existing synthetic methods for particular pheromone structures, and wants to avoid too much laborious reading of descriptions of syntheses.

However, the volume also deserves careful reading. After a brief summary of the most important monographs and reviews on pheromones research during the period covered, which is almost a tabulation in its format, there follows a short introduction (Chapter 2) describing general synthetic and analytical methods. Chapters 3 onwards deal with actual syntheses. The chapters are arranged according to structural types, starting with hydrocarbons then continuing through alcohols, esters, etc., up to heterocyclic pheromones containing nitrogen and sulfur. However, any desired compound can easily be located by means of a molecular formula index at the end of the book. Alternatively the reader can look up a given pheromone-producing insect species in the usual way by using the contents list.

As a result of the above arrangement of subject matter, the first half of the book is mainly concerned with the sex attractants that have relatively simple structures, and are produced by butterflies and moths. This is followed in the second half of the book by the more complex pheromones produced by other insect species. Altogether the syntheses of 260 pheromones are described and illustrated by formula schemes. The text relating to a particular synthesis is only one or two sentences in most cases, usually giving just the key reaction and the starting materials. However, the amount of detail in the formula schemes fully makes up for the brevity of the text. In each case the relationship to the insect that produces the substance is explained, and sometimes details of the analysis and structure determination are given; often also the biological activity of the compound is described. For some optically active chiral pheromones the relationship between absolute configuration and biological activity is briefly discussed. The question of stereobiology is considered from a more general standpoint in the final chapter.

To sum up, this book is essential reading for synthetic organic chemists, and is an excellent work of reference that no laboratory involved with pheromones should be without.

Otto Vostrowsky
Institut für Organische Chemie
der Universität Erlangen-Nürnberg (FRG)

Data Fitting in the Chemical Sciences. By *P. Gans.* XII, 258 pp., hardcover £ 29.95.—ISBN 0-471-93412-7

This book explains the mathematical fundamentals of the most commonly used methods of data fitting. In view of the growing use of microcomputers and program libraries in the recording and presentation of data, the book should prove a valuable aid, as it contains a critical survey of the use of statistical methods and the limitations of the various mathematical techniques. The introductory chapter begins by describing an example to illustrate the need for a model as a basis for interpreting experimental data and presenting results. Chapter 2 is concerned with experimentally measured quantities, errors in data, and the propagation of errors. The author uses an example to illustrate the difference between random and systematic errors, pointing out that only random errors can be handled by statistical methods. The following two chapters deal in turn with linear and nonlinear least-squares fitting methods. The author also describes the derivation of the formulas that are used in most application programs, so that the interested reader can follow these through to their final form. Although not every chemist is as familiar as P. Gans is with the matrix notation used, the treatment of some simple examples helps the reader to feel more at ease with the otherwise tedious mathematical derivations. Chapters 5 and 6 deal with the empirical and theoretical models needed for the interpretation or presentation of experimental data. Here the author first considers the limiting conditions affecting the model parameters that are to be determined. This is followed by a discussion of methods for controlling experiments so as to improve the quality of the data. Here the author again makes a special point of warning the reader about systematic errors that cannot be analyzed by statistical methods: "Sometimes a factor may be unsuspected until after the experiment has been performed and the data analyzed. In that case it is better to repeat the experiments with that factor under control than to try to extract information from flawed data." Chapter 6 addresses the question of when it is appropriate to use least-squares fitting methods, and suggests criteria for deciding, on the basis of the statistical properties of the experimental data, whether a model can be rejected. Here it is repeatedly emphasized that, even under the best statistical conditions, one can never prove the correctness of a model.

The second half of the book is devoted to some special types of data fitting problems. Chapter 7 is concerned with the representation of data by polynomials and with smoothing and differentiation methods. Chapter 8 deals with the fitting of data to spline functions, single and multiple exponential functions, Gaussian and Lorentzian functions, trigonometric functions, and surface functions. Chapter 9 summarizes those aspects of the Fourier transformation that are relevant to data fitting. Chapter 10 treats a special topic

with which the author has been concerned in the past, the application of statistical methods to potentiometric titration. The book ends with an appendix consisting of seven short sections, which include definitions of the most important terms used in statistics and brief explanations of matrix algebra, partial differentiation, the calculation of expectation values, and various minor mathematical theorems.

The author has set out to describe the processes of data compilation and analysis that take place inside the "black box" (the microcomputer and associated application programs), and in particular to draw attention to the problems and difficulties of data handling. The reader is specifically warned about the possible pitfalls that await the inexperienced user when data are interpreted with the help of such a "black box". The book fulfills this task very well, and it should be of considerable value to all who use microcomputers and application programs for statistical data analysis. I can recommend it unreservedly for such readers.

Horst Hippler
Institut für Physikalische Chemie
der Universität Göttingen (FRG)

Spectrochemical Analysis by Atomic Absorption and Emission. By *L. H. J. Lajunen*. The Royal Society of Chemistry, London, 1992. XII, 242 pp., paperback £ 18.50.—ISBN 0-86186-873-8

This book, which is intended for students and teachers of analytical chemistry, describes the state of knowledge in atomic spectroscopy in the early 1990s. Following a short historical sketch and a general explanation of the terms used, the fundamental theory is presented. This forms the basis for a clearly understandable description of various analytical techniques, ranging from flame atomic absorption spectroscopy (flame-AAS) through graphite furnace AAS (GFAAS) and other AAS methods, inductively coupled plasma atomic emission spectroscopy (ICP-AES), and ICP-mass spectrometry (ICP-MS), to atomic fluorescence spectroscopy. For each technique the basic instrumentation is described first, followed by the capabilities, problems, and ways of solving them. The lengths of the chapters reflect the relative importance of the different methods. Thus the most extensive chapters are those on the three most important routine techniques, namely flame-AAS, graphite furnace AAS, and plasma-AES. Also included, however, are short descriptions of recently developed techniques such as ICP-MS and the different types of sample introduction systems used (although here the book does not go into much detail, and also some small errors have crept in, such as an incorrect figure showing a mass spectrum on page 197).

A very positive feature of the book is that the author does not waste time on trivia but concentrates on important relationships and an overall view, though without neglecting the problems. For example, a separate chapter is devoted to sample preparation, ranging from sample acquisition through digestion techniques to methods of separation and enrichment. The clear presentation of the material is also greatly helped by the detailed and well-arranged list of contents and the many figures (148) and tables (46), which both support and amplify the information in the text. To round off the book there is a section in which the different atomic spectroscopy methods are summarized and compared, together with a list of books for further reading and of the most important relevant journals.

The book can be recommended for everyone who wishes to learn about the capabilities and limitations of analysis by atomic spectroscopy. It is especially suitable for students with interests in analytical chemistry, for whom it offers a clearly understandable and thorough grounding in modern atomic spectroscopy. It is to be hoped that it will reach a wide readership, as it covers a broad range of subject matter in a very readable form.

Ralf Meinke
Institut für Anorganische Chemie
der Universität Hannover (FRG)

New Books
see next page

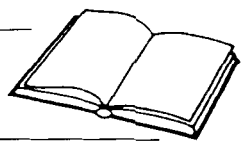

New Books

Industrial Organic Pigments. Production, Properties, Applications. By **W. Herbst, K. Hunger**. VCH Verlagsgesellschaft, Weinheim, **1993**. 630 pp., hardcover, DM ca. 280.—ISBN 3-527-28161-4

Zeolite, Clay, and Heteropoly Acid in Organic Reactions. By **Y. Izumi, K. Urabe, M. Onaka**. VCH Verlagsgesellschaft, Weinheim, **1992**. 166 pp., hardcover, DM 128.—ISBN 3-527-29011-7

Electrochemical and Electrocatalytic Reactions of Carbon Dioxide. Edited by **B. P. Sullivan, K. Krist, H. E. Guard**. Elsevier, Amsterdam, **1993**. 299 pp., hardcover, $ 212.50.—ISBN 0-444-88316-9

Chemical Vapor Deposition. Principles and Applications. Edited by **M. L. Hitchman, K. F. Jensen**. Academic Press, London, **1993**. 677 pp., hardcover, £ 75.—ISBN 0-12-349670-5

Diplom- und Doktorarbeit. Anleitungen für den naturwissenschaftlich-technischen Nachwuchs. By **H. F. Ebel, C. Bliefert**. VCH Verlagsgesellschaft, Weinheim, **1993**. 219 pp., paperback, DM 39.—ISBN 3-527-30003-1

Kinetic Theory and Irreversible Thermodynamics. By **B. C. Eu**. Wiley, Chichester, **1992**. 732 pp., hardcover, £ 67.—ISBN 0-471-61524-2

Biotechnology, Vol. 2. Genetic Fundamentals and Genetic Engineering. Edited by **H.-J. Rehm, G. Reed**. VCH Verlagsgesellschaft, Weinheim, **1993**. 880 pp., hardcover, single volume price DM 490.–, subscription price DM 390.—ISBN 3-527-28312-9

Biofilms – Science and Technology (Proc. NATO Adv. Study Inst., Alvor, Portugal, May 18-29, 1992). Edited by **L. F. Melo, T. R. Bott, M. Fletcher, B. Capdeville**. Kluwer, Dordrecht, Netherlands, **1993**, 728 pp., hardcover, Dfl. 385.—ISBN 0-7923-2022-0

Magnetic Resonance of Carbonaceous Solids. Edited by **R. E. Botto, Y. Sanada**. American Chemical Society, Washington, DC, **1992**. 678 pp., hardcover, $ 149.95.—ISBN 0-8412-1866-8

Measurement Challenges in Atmospheric Chemistry. Edited by **L. Newman**. American Chemical Society, Washington, DC, **1992**. 424 pp., hardcover, $ 94.95.—ISBN 0-8412-2470-6

Liquid-Crystal Polymers, Edited by **N. A. Platé** (Series: Specialty Polymers, Series Editor: **J. M. C. Cowie**). Plenum Press, New York, **1993**, 438 pp, hardcover, $ 110.—ISBN 0-306-44219-1

Handbook on Semiconductors. Completely revised and enlarged edition. Vol 1: Basic Properties of Semiconductors, Series editor: **T. S. Moss**, Editor of volume 1: **P. T. Landsberg**, Elsevier Science Publishers B. V., Amsterdam, **1992**, 1204 pp., hardcover, Dfl. 595.—ISBN 0-444-88855-1

Aufgaben zur technischen Chemie. By **P. Kripylo, K. Pilchowski, W. Pritzkow**. Verlag für Grundstoffindustrie, Leipzig, **1992**. 226 pp., hardcover, DM 48.—ISBN 3-342-00636-6

Ring-Opening Polymerization. Mechanisms, Catalysis, Structure, Utility. Edited by **D. J. Brunelle**. Hanser Verlag, München, **1993**. 361 pp., hardcover, DM 188.—ISBN 3-446-16293-3

Advances in Chemical Physics. Edited by **I. Prigogine**. Wiley, Chichester, **1993**. 744 pp., hardcover, £ 136.—ISBN 0-471-54018-8

Physical Methods of Chemistry Vol IXA. Investigations of Surfaces and Interfaces – Part A. Edited by **B. W. Rossiter, R. C. Baetzold**. Wiley, Chichester, **1993**. 516 pp., hardcover, £ 98.—ISBN 0-471-54406-X

Natural and Synthetic Sweet Substances. By **A. Krutosiková, M. Uher**. Ellis Horwood, Chichester, **1992**. 223 pp., hardcover, $ 81.—ISBN 0-13-612805-X

Biocatalysts in Organic Synthesis. Studies in Organic Chemistry, 46. By **J. Halgas**. Elsevier, Amsterdam, **1992**. 334 pp., hardcover, $ 180.– ISBN 0-444-98698-7

Characterization of Materials. By **J. B. Wachtman**. Butterworth Heinemann, Stoneham, USA, **1992**. 480 pp., hardcover, $ 74.95.—ISBN 0-7506-9215-4

Thermal Analysis – Techniques & Applications. Edited by **E. L. Charsley**. Royal Society of Chemistry, Cambridge, **1992**. 296 pp., hardcover, £ 45.—ISBN 0-85186-375-2

Handbook on Semiconductors, Vol. 1. Basic Properties on Semiconductors. Edited by **T. S. Moss**. Elsevier, Amsterdam, **1992**. 1060 pp., hardcover, $ 372.—ISBN 0-444-88855-1

Time-Resolved Macromolecular Crystallography. Edited by **D. W. J. Cruickshank, J. R. Helliwell, L. N. Johnson**. Oxford University Press, Oxford, **1992**. 334 pp., hardcover, £ 35.—ISBN 0-19-855781-7

Organischer Metallschutz. Entwicklung und Anwendung von Beschichtungsstoffen. Edited by **J. Ruf**. Vincentz, Hannover, **1993**. 844 pp., hardcover, DM 169.—ISBN 3-87870-320-1

Wärmeübertragung. Berechnungen mit dem PC. Edited by **J. M. Chawla, G. Wiskot**. VDI, Düsseldorf, **1992**. 286 pp., paperback, DM 128.—ISBN 3-18-400949-1

Mathematik für Chemiker. 4. überarbeitete Auflage. Edited by **G. Just, D. Oelschlägel**. Deutscher Verlag für Grundstoffindustrie, Leipzig, **1993**. 236 pp., hardcover, DM 36.– ISBN 3-342-00632-3

Modern Perspectives in Inorganic Crystal Chemistry, Vol. 382. Edited by **E. Parthé**. Kluwer, Dordrecht, The Netherlands, **1992**. 292 pp., hardcover, Dfl 180.—ISBN 0-7923-1954-0

Organic Superconductors (Including Fullerenes). Synthesis, Structure, Properties and Theory. Edited by **J. M. Williams et al**. Series Editor: **R. N. Grimes**. Prentice Hall, New Jersey, **1992**. 400 pp., hardcover, $ 91.10.—ISBN 0-13-640566-5

Chemical Hardness. (Structure and Bonding, Vol. 80). Edited by **K. Sen, D. M. P. Mingos**. Series Editors: **J. M. Clarke, J. B. Goodenough, J. A. Ibers et al.** Springer, Heidelberg, **1993**. 268 pp., hardcover, DM 228.—ISBN 3-540-56091-2

Foamglas. Industrial Insulation Handbook. Editions Technip, Paris, **1992**. 512 pp., hardcover, FF 590.—ISBN 2-930049-00-6

Lipid Analysis: A Practical Approach. Edited by **R. J. Hamilton, S. Hamilton**. Oxford University Press, Oxford, **1992**. 330 pp., hardcover, £ 35.—ISBN 0-19-963098-4

Electron Paramagnetic Resonance of d Transition Metal Compounds, Vol. 16. Edited by **F. E. Mabbs, D. Collison**. Elsevier, Amsterdam, **1992**. 1326 pp., hardcover, Dfl 995.—ISBN 0-444-89852-2

Second Supplements to the 2nd Edition of Rodd's Chemistry of Carbon Compounds, Vol. 1 – Part C. Edited by **M. Sainsbury**. Elsevier, Amsterdam, **1992**. 388 pp., hardcover, Dfl 365.—ISBN 0-444-89758-5

Second Supplements to the 2nd Edition of Rodd's Chemistry of Carbon Compounds, Vol. II – Parts A & B (Partial). Edited by **M. Sainsbury**. Elsevier, Amsterdam, **1992**. 544 pp., hardcover, Dfl 515.—ISBN 0-444-89844-1

Advances in Mass Spectrometry. Edited by **P. J. Kistemaker, N. M. M Nibbering**. Elsevier, Amsterdam, **1992**. 950 pp., hardcover, Dfl 450.—ISBN 0-444-88871-3

Out of the Crystal Maze. Chapters from the History of Solid-State Physics. Edited by **L. Hoddeson, E. Braun, J. Teichmann, S. Weart**. Oxford University Press, Oxford, **1992**. 720 pp., hardcover, £ 50.—ISBN 0-19-505329-X

Registered names, trademarks, etc. used in this journal, even when not marked as such, are not to be considered unprotected by law.

© VCH Verlagsgesellschaft mbH, D-W-6940 Weinheim, 1992. – Printed in the Federal Republic of Germany by Konrad Triltsch Druck- und Verlagsanstalt Würzburg.

All rights reserved (including those of translation into foreign languages). No part of this issue may be reproduced in any form — by photoprint, microfilm, or any other means — nor transmitted or translated into a machine language without written permission from the publishers. Only single copies of contributions, or parts thereof, may be made for personal use. This journal was carefully produced in all its parts. Nevertheless, authors, editors, and publisher do not warrant the information contained therein to be free of errors. Readers are advised to keep in mind that statements, data, illustrations, procedural details, or other items may inadvertently be inaccurate.

Valid for users in the USA: The appearance of the code at the bottom of the first page of an article (serial) indicates the copyright owner's consent that copies of the article may be made for personal or internal use, or for the personal or internal use of specific clients. This consent is given on the condition, however, that the copier pay stated per-copy fee through the Copyright Clearance Center, Inc. (CCC), for copying beyond that permitted by Sections 107 or 108 of the U.S. Copyright Law. This consent does not extend to other kinds of copying, such as copying, for general distribution, for advertising or promotional purposes, for creating new collective works, or for resale. For copying from back volumes of this journal see 'Permissions to Photo-Copy: Publisher's Fee List' of the CCC.

Editorial office: Postfach 10 11 61, D-W-6490 Weinheim, Federal Republic of Germany, Telephone (06201) 606 315, Telex 465 516 vchwh d, Telefax (06201) 606 328, E-Mail Z16@DHDURZ2 in Earn Bitnet.

Editor: *Peter Gölitz*

Associate editors: *N. A. Compton, R. H. Schmidt-Radde, K. J. Schneider*. **Book editor:** *G. Karger*. **Editorial assistant:** *E. Schweikart*

Publishers: VCH Verlagsgesellschaft mbH. (Managing Directors: *Hans Dirk Köhler, Dr. Karlheinz Köpfer*). Pappelallee 3, D-W-6940 Weinheim, Federal Republic of Germany.

Advertising office (Advertising Manager: *N. Schippel*): Postfach 10 11 61, D-W-6940 Weinheim, Federal Republic of Germany. Telephone (0 62 01) 606 312, Telefax (0 62 01) 606 328.

ANGEWANDTE CHEMIE
International Edition in English
Volume 32 · Number 5
May 1993
Pages 629–766

Capillary Electrophoresis: Methods and Scope

New Analytical Methods (44)

By Heinz Engelhardt,* Wolfgang Beck, Jörg Kohr, and Thomas Schmitt

Capillary electrophoresis is a new analytical technique that has seen a great upswing in recent years, because this adaptation of electrophoresis may be automated and simple, direct quantification is possible. As in conventional electrophoresis, samples with a large range of molecular weights, from inorganic ions to biopolymers such as DNA and proteins, can be separated. Uncharged molecules can also be separated when micelle-forming detergents are added to the buffer; the distribution mechanism that then comes into play increases the separation efficiency of this micellar electrokinetic chromatography. Chiral additives such as cyclodextrins make the separation of enantiomers possible. The rapid increase in the popularity of capillary electrophoresis is reflected in instrument sales and the growing number of scientific publications dealing with the method, and it seems that the future of this technique is assured.

1. Introduction[**]

Analytical separation methods such as chromatography and electrophoresis have played an important role in the determination of the composition of complex biological, environmentally relevant, and industrial samples. Gas-liquid chromatography (GLC) and high-performance liquid chromatography (HPLC) allow the separation, identification, and quantification of the components of complex mixtures in a very short time. The combination of the high-performance separation systems with sensitive, selective, and specific detectors, such as UV/VIS diode array detectors (DAD), mass spectrometers, and Fourier transform infrared (FTIR) spectrometers makes it possible to identify the separated substances unequivocally. Development in instrumentation is so far advanced that chromatographic analysis is now almost fully automated.

The areas of application of GLC and HPLC are clearly defined by the demands made by the analytical method on the sample. In view of the vast number of nonvolatile compounds it is not surprising that HPLC is today the most widely used separation technique with a continuing high growth rate. (The market for HPLC instruments is at present growing at over 10% per year.) Problems always arise with HPLC when polar and ionogenic (and in particular basic) samples or biopolymers are to be analyzed rapidly and efficiently. This is an inherent problem of chromatography with stationary phases based on silica gel. Although phases are now available for which such problems are hardly noticeable (polymer-based stationary phases have not been applied widely because of their swelling capacity, lower efficiency, and limited pressure stability), the development of a technique for the separation of ionogenic substances still requires great skill and a detailed knowledge of the multifarious sorption and exchange processes involved.

[*] Prof. Dr. H. Engelhardt, Dipl.-Chem. W. Beck, Dipl.-Chem. T. Schmitt
Institut für angewandte physikalische Chemie der Universität
D-W-6600 Saarbrücken 11 (FRG)
Dr. J. Kohr
Lonza AG, CH-3930 Visp (Switzerland)

[**] Frequently used abbreviations: CE = capillary electrophoresis, CGE = capillary gel electrophoresis, EC = electrochromatography, EOF = electroosmotic flow, GLC = gas-liquid chromatography, HPLC = high-performance liquid chromatography, IEF = isoelectric focusing, ITP = isotachophoresis, MEC = micellar electrokinetic chromatography, RSD = relative standard deviation, SDS = sodium dodecylsulfate.

 © VCH Verlagsgesellschaft mbH, W-6940 Weinheim, 1993 0570-0833/93/0505-0629 $ 10.00+.25/0

Charged particles migrate at different rates in solution under the influence of an electric field. In the first half of the century the terms "electrophoresis" or "electrical transportation" were introduced for this behavior.[1-4] Differences in the rate of migration can have two causes: either the molecules have different charges and are thus accelerated to different extents by the applied field, or the migrations of the molecules are slowed down to differing degrees as a result of their individual frictional resistances. In the simplest case the separation of a solution of an electrolyte can be carried out in a tube, since here no interactions with a stationary phase can occur. In practice, however, distortions of the substance zones occur on account of differing densities of the electrolyte and convection currents originating from the transport of Joule heat to the capillary wall. In classical electrophoresis, as introduced by Tiselius,[5] gels or strips of paper impregnated with solutions of electrolytes are used to reduce the distortions arising from convection. In addition, frictional resistance introduced for macromolecules with low charge differences increases the separation efficiency. Polyacrylamide gel electrophoresis (PAGE) makes possible the efficient separation of DNA molecules and proteins. The separation performance can be optimized by varying the degree of cross-linking of the gels. Gel electrophoresis can be used for direct determination of the molecular weight of proteins denatured by sodium dodecyl sulfate (SDS). In this case the separation is due solely to the hindrance of the migration by the gel (in the absence of a gel all proteins denatured by SDS would migrate at almost equal rates).

Classical electrophoresis (with gels or paper) unfortunately has two significant disadvantages. Firstly, quantitative analysis is possible only with reflection measurements; proteins must first be dyed, and the results are subject to considerable errors. Secondly, the voltage gradient that can be applied across the gel bed is limited. Since the heat evolved increases with the square of the voltage, efficient cooling is necessary to prevent the gel from drying out. The time required for an analysis using a gel bed 10 cm in length can thus be as much as several hours. The advantage with respect to modern automated separation processes is that several separations can be carried out simultaneously in one gel by using separate tracks; the sample throughput is thus greatly increased. In

Heinz Engelhardt

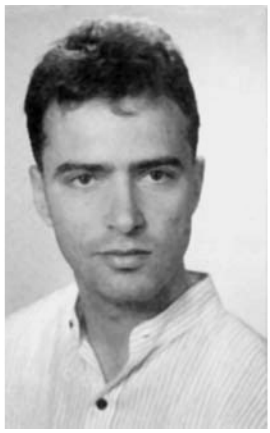

Wolfgang Beck

Jörg Kohr

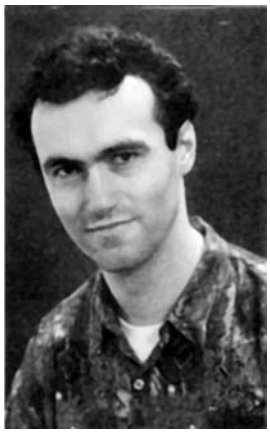

Thomas Schmitt

Heinz Engelhardt, born in Nuremberg in 1936, studied chemistry at the University of Erlangen-Nuremberg and gained his doctorate in 1965. He was a postdoctoral fellow at Northeastern University in Boston in 1969–1970. In 1971 he obtained his "Habilitation" in analytical organic chemistry, and in that year accepted a chair at the University of the Saarland, where he is currently Professor of Applied Physical Chemistry. Engelhardt has published more than 130 papers on chromatography and is the author of the book "Hochdruck-Flüssigkeits-Chromatographie", which was also published in English, Russian, and Chinese. He is editor of several journals, chairman of the Arbeitskreis Chromatographie of the Gesellschaft Deutscher Chemiker (GDCh), and a member of the board of the Subdivision of Analytical Chemistry of the GDCh. In 1992 he obtained the Dal Nogare Award and in 1993, the A. J. P. Martin Award of the Chromatographic Society of Great Britain.

Wolfgang Beck was born in 1964 in Fürth/Bavaria and studied chemistry at the University of the Saarland from 1985 to 1990. In his diploma thesis with H. Engelhardt he synthesized and characterized HPLC stationary phases for the separation of chiral compounds. Since 1990 he has been working towards his doctorate. His work deals with the improvement of detection methods and the optimization of UV detection, diode array detection, and indirect UV detection.

Jörg Kohr, born in 1963 in Saarlouis/Saarland, studied chemistry at the University of the Saarland (diploma 1989) and received his doctorate in 1992 for his research with H. Engelhardt on the application of polymer-coated quartz capillaries in capillary electrophoresis.

Thomas Schmitt was born in 1964 in Quierschied/Saar and studied chemistry from 1985 to 1991 at the University of the Saarland. His diploma thesis dealt with the separation of DNA restriction fragments by capillary gel electrophoresis. Since 1991 he has been working towards his doctorate in Saarbrücken on the separation of chiral compounds by capillary electrophoresis.

addition, the flatbed method readily allows two-dimensional (2D) operation in which different separation mechanisms are employed. The excellent separation performance of 2D gel electrophoresis in protein analysis will be mentioned here only briefly.

2. Principles of Capillary Electrophoresis

Various attempts have been made to reduce convection currents in free electrolytes when open tubes are used, for example, by rotating the tube about its axis.[6] The use of thin capillaries, either of glass[6, 7] or Teflon,[8] with an internal diameter between 200 and 500 μm was found to be successful. Quartz capillaries[9–12] with internal diameters of 25–200 μm made it possible to carry out highly efficient separations of proteins and dansyl amino acids. The negative influence of thermally induced convection was greatly reduced with these capillaries because of the relatively large surface to volume ratio. Quartz capillaries of the type used in GLC make it possible to use detectors for the on-line detection of the separated substances within the capillary. In the second half of the 1980s the simplicity of the apparatus required led to an increased interest in capillary electrophoresis (CE), often referred to as capillary zone electrophoresis (CZE). Since in all separations the substances are injected as discrete zones at the beginning of the capillary and the components of the samples migrate as discrete zones, we shall refer to this simple case simply as capillary electrophoresis (CE).

The basic construction of a CE apparatus is shown schematically in Figure 1. The thin quartz capillary (25–100 μm

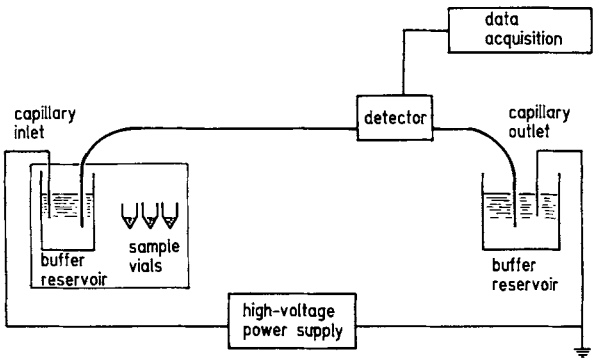

Fig. 1. Schematic diagram of a CE apparatus.

in diameter), 20 to 100 cm in length, bridges the two buffer vessels, between which a voltage of up to about 30000 V is applied. A relatively small "slug" of the sample (a few nL!) is introduced at the anodic end of the capillary. This is done by replacing the buffer vessel by a sample vial; in other words, the end of the capillary is dipped into the sample solution. The advantages and disadvantages of the various methods of sample introduction are discussed in detail in Section 3 "Apparatus".

The migration of the sample is induced by the applied voltage. The electrophoretic migration is always accompanied by an electroosmotic flow (EOF) of a certain magnitude, which contributes in a passive manner to the transport of the sample zones but not to their separation. This EOF depends strongly on the pH value of the buffer and the surface properties of the capillary. It can be so large that not only neutral molecules but even negative ions are transported to the detector, that is, in the opposite direction to that of their electrophoretic migration. Since in most buffers dissociation of silanol groups leads to the presence of negative charges at the surface of the quartz capillaries, in turn inducing positive charges in the vicinity of the surface, the EOF is directed towards the cathode; thus the detector is usually positioned near the cathode. The EOF helps in the transport of the sample zones to the detector, so that when the EOF is sufficiently large anions can also be transported to the cathode. The result of a separation of cationic, anionic, and neutral substances by means of CE is shown in Figure 2. Under these conditions all uncharged molecules migrate with the same velocity, that of the EOF, and cannot be separated, whereas the separation of the ions is possible because of their differing electrophoretic mobilities.

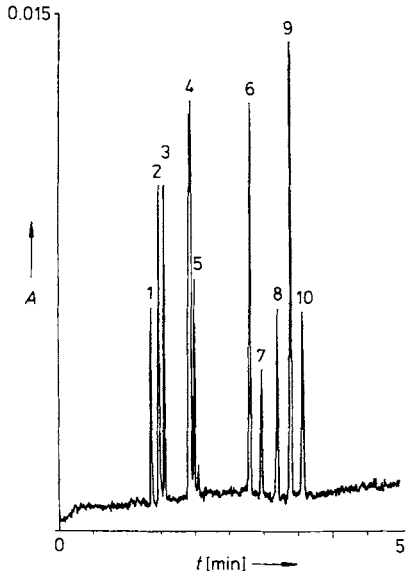

Fig. 2. Demonstration of a separation of positive and negative ions using capillary electrophoresis. Conditions capillary: L (length) = 30/37 cm, ID (inner diameter) = 75 μm; buffer: 33 mM borate, pH 9.5; field: E = 350 Vcm^{-1}, UV detection at 214 nm. Sample: 1 = trimethylphenylammonium bromide, 2 = histamine, 3 = 4-aminopyridine, 4 = benzyl alcohol, 5 = phenol, 6 = syringaldehyde, 7 = 2-(*p*-hydroxyphenyl)acetic acid, 8 = benzoic acid, 9 = vanillic acid, 10 = *p*-hydroxybenzoic acid.

Apart from this simplest form of CZE in which the separation depends only on mobility differences, numerous variations have been introduced: in capillary gel electrophoresis (CGE) the capillary is filled with a gel; the electrophoretic migration of macromolecules is influenced by the gel matrix, leading to a separation according to molecular size. Uncharged molecules can be separated by means of micellar electrokinetic chromatography (MEC). When detergents are added to the buffer, the neutral molecules are distributed between the buffer and the micelles according to their hydrophobic properties. Since a distribution process is involved, this is a chromatographic technique. The separation is due to the mobility of the micelles, which are generally negatively charged. In the case of isoelectric focusing (IEF) the separa-

tion is carried out in a pH gradient, which is formed in the electric field when ampholytes are added to the buffer. Of less importance is electrochromatography (EC), in which HPLC stationary phases are used and the transport of the samples is brought about only by the electroosmotic flow. Finally we should mention the oldest capillary separation technique, isotachophoresis (ITP), which has recently become more important because of its use in CE for sample concentration.

2.1. Electrophoretic Migration

An increase in voltage and consequently an increase in the field strength E leads to an increase in the electrophoretic migration velocity u of the ions and thus to a faster analysis. The applied voltage decreases over the total length L_{tot} of the capillary. The velocity and hence the electrophoretic mobility μ is determined from the time t the sample stays in the capillary between sampling (usually at the anodic end of the capillary) and detection, and the effective capillary length L_{eff}. With commercial equipment the capillary length between detection window and capillary end (usually the cathodic end) can be between 5 and 20 cm. This additional length must be considered when determining mobilities. The correlation between these values is given by Equation (1). A single ion experiences an accelerating force K_B [Eq. (2)],

$$\mu = \frac{u}{E} = \frac{L_{eff}}{Et} = \frac{L_{eff} L_{tot}}{Ut} \quad (1)$$

$$K_B = zFE \quad (2)$$

F is the Faraday constant (96 500 C mol^{-1}) and z the effective charge of the ion. This force is opposed by the frictional force K_R, which is approximated by Stokes' Law [Eq. (3)]; η is the dynamic viscosity [Pa s] and r the Stokes radius [cm].

$$K_R = 6\pi\eta r \quad (3)$$

The electrophoretic migration velocity u is thus defined by Equation (4). Electrophoretic separations are possible only

$$u = \frac{zFE}{6\pi\eta r} \quad (4)$$

when the ions have different mobilities. The effective charge equals the formal charge minus the charge contribution of the surrounding oppositely charged *rigid* double layer.[14] During the migration the ion takes this fraction of the double layer with it and thus migrates more slowly than expected on the basis of its formal charge. This is known as the electrophoretic effect and is greatest for a thin *diffuse* double layer surrounding the ion. This characteristic double layer can be calculated by Debye–Hückel theory, and its thickness is inversely proportional to the square root of the electrolyte concentration. It can be shown that the effective ionic charge, and thus the migration velocity, decreases with increasing ionic strength.

In the case of large molecules with radii greater than the thickness of the double layer, their mobility is independent of their size (provided that they have similar compositions);[14] this makes the electrophoretic separation of large molecules more difficult, as the migration rate of DNA molecules and proteins denatured by SDS is identical in pure electrolytes. Separation can only be achieved when the migration is influenced by sieve effects (e.g. in gels) or exclusion effects.

2.2. Electroosmotic Flow

While electrophoresis is responsible for the separation of molecules with differing mobilities, electroosmosis causes a flow of the buffer solution in the electric field. In most cases the electrophoretic migration of the ions in CE is reinforced by the electroosmotic flow (EOF), which depends on the distribution of the charges in the vicinity of the capillary surface. Almost every surface carries charges; in the case of quartz capillaries these are negative and induced by dissociation of the silanol groups. The surface charges are balanced by corresponding opposite charges in the buffer. In a quartz capillary this double layer, shown schematically in Figure 3, is dominated by positive ions arranged in a static and a diffuse layer at the surface. If a field is applied parallel to the

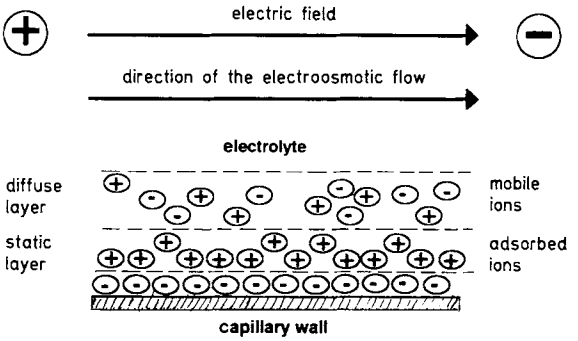

Fig. 3. Schematic diagram of the charge distribution at the capillary surface.

surface, the counterions in the mobile layer are pulled parallel to its axis along with the liquid in the capillary. Thus for quartz capillaries the induced EOF is in the direction of the cathode. An extremely flat piston-shaped flow profile results. This leads to considerably less band broadening than obtained with hydrodynamic flow with applied pressure, for which a parabolic Hagen–Poisseuille flow profile is observed, which depends strongly on the radius of the capillary and the flow velocity. In capillaries packed with glass beads or silica gel particles the EOF should be independent of the particle diameter of the packing material and should lie in the same direction as in the empty capillary. It is thus theoretically possible to use either very small particles (1 μm or less in diameter) or long columns in a chromatographic separation. The procedure known as electrochromatography (EC) is thus a subject of increasing interest,[15] since it should combine the selectivity of HPLC with the separation efficiency of CE. By using nonporous particles it is possible to eliminate the contribution to the band broadening caused by diffusion within the pores.

The magnitude of the EOF can be described simply by the Helmholtz equation [Eq. (5)]. It is inversely proportional to

$$\mu = \frac{\varepsilon E \zeta}{4 \pi \eta} \tag{5}$$

the viscosity η of the electrolyte and proportional to its dielectric constant ε, to the applied field strength E, and to the number of charges at the capillary wall (and thus to ζ, the "zeta potential" they induce). In the case of quartz capillaries the EOF decreases with the concentration of the electrolyte and the amount of organic components added, and increases with the degree of dissociation of the silanol groups at the surface; in other words, it increases with increasing pH. The pH dependence of the EOF for quartz capillaries and the corresponding reproducibility of the mobility is shown in Figure 4. The largest variations occur at intermediate pH values in the vicinity of the pK value of silicic acid. The deviations can be reduced, however, by increasing the conditioning time following a change in the pH value of the buffer; the hysteresis effects are then decreased. For reproducible analyses conducted with untreated capillaries the rinsing and conditioning times following a change in the buffer must be standardized; this can reduce hysteresis effects in the EOF.[16]

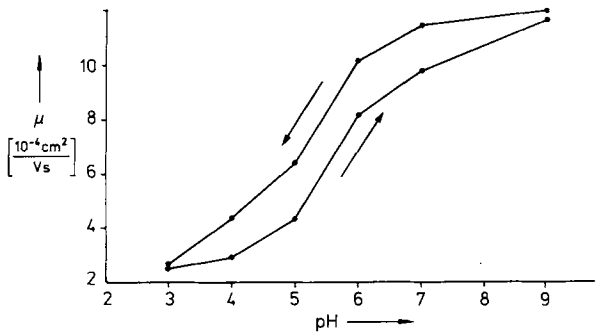

Fig. 4. pH Dependence of the electroosmotic flow μ. Conditions: capillary: $L = 40/47$ cm, $ID = 75$ μm; buffer: 10 mM phosphate; neutral marker: benzyl alcohol; $E = 425\ \mathrm{Vcm^{-1}}$.

Electroosmotic flow is observed for all electrophoretic separation techniques, since surface charges can never be completely eliminated. On the one hand it can lead to a convective mixing of the electrophoretic zones, while on the other it plays an important role in the transport of the zones through the capillary. In capillary electrophoresis the detector is generally situated near the cathode because of the omnipresent EOF. Since anions are also transported to the cathode when the velocity of their electrophoretic migration is less than the EOF, it is possible to separate cations and anions in one single analysis. In other CE techniques (e.g. in MEC) the EOF is used solely for the transport of the (in part uncharged) samples to the detector. The capillary surface can be chemically modified to control, eliminate, and even reverse the EOF. Measuring the magnitude of the EOF is the single means of determining changes at the capillary surface, for example, the irreversible adsorption of components of the sample. All other methods for the characterization of the surface fail because of the very low surface area ($< 10\ \mathrm{cm^2}$). Surface-modified capillaries show hardly any hysteresis effects when the buffer is changed, and because of the reduced adsorption they are extremely well suited for the analysis of proteins (see Section 4.2.2 "Chemically Modified Capillaries").

The addition of long-chain cationic detergents such as cetyltrimethylammonium salts, which are adsorbed at the silanol groups of the surface, makes a reversal of the EOF possible.[17] A detergent double layer is formed in which the positive charges are arranged in the direction of the electrolyte. Capillaries thus coated can be used for the separation of rapidly migrating inorganic ions.[18]

2.3. Band Broadening

The main contribution to band broadening in capillary chromatography is that due to the Hagen–Poiseuille flow profile. This contribution increases with the square of the diameter of the capillary and is inversely proportional to the diffusion coefficient of the sample in the electrolyte (Aris–Taylor equation or mass transfer term of the Golay equation[19]). Because of the slow radial diffusion in liquids the flow profile is not balanced, and capillary liquid chromatography is thus not possible with capillaries > 50 μm in diameter. The diffusion coefficients of samples in gases are larger by a factor of 10^4, however, and the parabolic flow profile is rapidly balanced out by radial diffusion. Capillary gas chromatography is thus a highly efficient separation technique. Since in CE the flow profile is piston-shaped as a result of the electroosmotic flow, the contribution of the flow profile to band broadening can be neglected, and only the longitudinal diffusion term must be taken into account.

The band broadening H can be calculated from Equation (6), where D is the diffusion coefficient of the sample in

$$H = \frac{2D}{u} = \frac{2D}{\mu E} \tag{6}$$

the electrolyte. Using the relation $H = L/N$ we can calculate the number of theoretical plates from Equation (7). U is the

$$N = \frac{\mu U}{2D} \tag{7}$$

voltage, which decreases along the length L of the column. It should be mentioned that the mobility μ of the ions is a combination of the electrophoretic mobility μ_{ep} and the electroosmotic mobility μ_{eo}. The number of plates increases with increasing voltage and decreasing diffusion coefficients of the samples (in contrast to HPLC, where the number of plates decreases rapidly with decreasing diffusion coefficients). Giddings[14] showed that at room temperature and across a wide range this relationship can be reduced to Equation (8). When voltages between 100 and 50000 V are em-

$$N = 20\ z\ U \tag{8}$$

ployed for the separation of ions with effective charges z between 1 and 10, it is possible to achieve up to 10 million

theoretical plates per meter. In this respect CE is clearly superior to HPLC. The mathematical expressions derived for chromatography have been adapted for the description of the band broadening in CE and can as such also be used to describe transport phenomena in the capillary. It should be mentioned, however, that in chromatography samples are always transported through the detector (after elution from the column and the consequent dilution) with the same velocity. In CE with on-column detection the migration rate of the samples at the detector window can vary. A comparison of the number of theoretical plates is thus not completely valid.

The high numbers of theoretical plates predicted have indeed been realized for the analysis of DNA molecules in gel-filled capillaries.[20] However, DNA molecules are a special case, since they do not interact with the capillary surface because of their negative charges. Such high numbers of plates have not yet been achieved for separations of proteins, although up to 500000 plates per meter have been obtained with coated capillaries. A slight degree of adsorption at the surface leads to local changes in the EOF and thus to a distortion of the piston-shaped profile. In addition, any adsorption leads to a decrease in mass transfer. The mass transfer term of the Golay equation can no longer be neglected, and the band broadening increases.

As mobility and the EOF increase with increasing voltage, the analysis time can be decreased. Because the sample spends less time in the column, band broadening decreases and the number of plates increases. When the voltage is increased, however, the buffer solution warms due to Joule heating. Heat transport occurs solely across the capillary wall, and a radial temperature (and thus viscosity) gradient is built up at right angles to the electrophoretic migration.[21, 22] Cooling the capillary increases the temperature gradient, but this is necessary in order to avoid degassing and local overheating. Viscosity differences between the center of the capillary and the capillary wall lead to migration differences, and thus to band broadening and loss of resolution.

The negative influence of this radial temperature gradient can only be reduced by reducing the inner diameter of the capillary. In a cylindrical tube the temperature difference between the center and the wall of the capillary increases with the square of the capillary diameter. This is the reason for the use of extremely narrow capillaries (diameter 25–100 μm) in CE. However, a decrease in the capillary diameter implies a reduction in the length of the light path and thus in the detection sensitivity (Lambert–Beer Law). Alternatively, Joule heating can also be reduced by reducing the buffer concentration and/or using buffers with lower ionic conductivity.

The reduction in the conductivity of the buffer is subject to limits. If there is a large difference between the conductivity in the buffer and sample zones, the induced local variations in the electrical field will lead to distortion of the zones and thus to a decrease in the separation efficiency. If the conductivity in the sample zone is greater than that in the carrier electrolyte, the diminished resistance will lead to a reduction in the field strength. The molecules at the maximum sample concentration will thus migrate more slowly than at the flanks of the peak. This leads to an extreme distortion of the zones, with a slow increase and a rapid falloff (leading). When conductivity in the buffer is greater than in the sample zone, peaks with a high degree of tailing are observed. Symmetrical peaks are obtained only when the conductivities are identical. The buffer concentration must thus be adjusted for the given separation problem (dissociation and mobility of the samples). In addition, mobility differences between sample ions and buffer ions can lead to isotachophoretic effects, which generally result in triangular peak forms that may cause integration problems.

The buffer concentration can be varied only within narrow limits. An increase in the buffer concentration leads to more Joule heating, which can be compensated for by lowering the voltage. This, however, increases the time required for the analysis and thus the time the sample spends in the capillary. As a result the increase in the longitudinal diffusion leads to a greater band broadening. In the optimization of the separation efficiency in CE it is thus necessary to take into account the influence of Joule heating, the conductivity differences between samples zones and electrolytes, and the detection sensitivity that can be achieved, in order to obtain high resolution with short analysis times.

3. Apparatus

Commercial capillary electrophoresis instruments have been available since 1988, and the number of suppliers is increasing. The various instruments are quite similar, since the actual separation system is very simple. Slight differences are found in the way in which the sample is introduced and in the number and type of detectors offered. We have no intention of surveying the market but intend to emphasize the typical requirements made on the various components of the apparatus.

3.1. Voltage Source

The voltage should be adjustable within the range from -30 to $+30$ kV and should remain constant at the value required. In addition it is useful to be able to adjust the voltage and current separately. When the voltage, or better the current, is monitored during the analysis it may be possible to localize any problems that may occur. In commercial instruments the high-voltage source shuts off automatically when the analysis compartment is opened to prevent accidents due to high voltage. Similar precautions must be taken when an apparatus is constructed in the laboratory.

3.2. Sample Introduction

The most difficult problem in capillary electrophoresis is reproducible sample introduction. The sample zone must be kept small to avoid band broadening; this requires the injection of very small sample volumes in the range 5–50 nL.[23–25] Excessively large sample volumes rapidly lead to peak distortions and loss of resolution.[26, 27] To meet these extreme requirements and for the manipulation of such small sample volumes, miniaturized[28, 30] and automated sample introduction[29–31] is indispensable. Reproducible introduc-

Table 1. Types of injection used in capillary electrophoresis.

	Electrokinetic injection	Hydrostatic injection	Hydrodynamic injection	Injection by sample splitting
Injection by	electric field	siphoning effect	pressure or vaccum	electrical sample splitter and split-flow systems
Automatization	yes	yes	yes	no
Smallest sample volume	$<10\,\mu L$ (multiple injection)	$<10\,\mu L$ (multiple injection)	$\approx 10\,\mu L$ (multiple injection)	$>10\,\mu L$ by dosing capillary or HPLC syringe (no multiple injection)
Discrimination effects with sample introduction	yes	no	no	yes (for electrical splitters) no (for flow split systems)
RSD values	4.1% (from ref. [30])	<2.9% (from refs. [30, 33])	2–3% (experimentally found)	<3% (ideal case for electrical splitter) (from ref. [34]) ≈2% (for split flow systems) (from ref. [35])

tion of the small sample volumes is an important requirement for quantitative analysis with acceptable standard deviations. The most important types of sample injection used in various commercial instruments are summarized in Table 1.

3.2.1. Electrokinetic Injection

In this injection method the sample vial into which the capillary dips is connected to the voltage source; a voltage is applied for a short interval causing the components of the sample to migrate into the separation capillary. The amount Q of the sample depends on the magnitude of the applied voltage U_i, the time t_i during which the voltage is applied, and the mobility of the components of the sample according to Equation (9),[30] where c is the concentration of the sample

$$Q = \frac{(\mu_p + \mu_{eo})\,\pi r^2 U_i t_i c}{8\eta L} \tag{9}$$

in the solution. This relationship makes clear the problem of this method of injection—the discrimination between sample components of differing mobilities. The electrical resistance of the sample solution (the ionic strength) relative to that of the electrolyte solution also affects the reproducibility of the procedure.[32] A relative standard deviation (RSD) of 4.1% for peak area measurements has been determined for automatic electrokinetic sample introduction.[30] In general it is possible to improve the reproducibility of quantitative analysis greatly by using an internal standard, as is the case for all procedures which are accompanied by problems with sample introduction (e.g. capillary gas chromatography).

3.2.2. Hydrostatic Injection

This method takes advantage of a difference in level between the buffer reservoir and the sample vial for the introduction of small sample volumes; the sample solution is introduced into the capillary by siphoning. The sample volume introduced depends on the difference in levels (generally 5–10 cm), the time, and the hydrodynamic properties (viscosity η, density ρ) of the electrolyte solution. Density and viscosity differences between the sample and the electrolyte solution can thus be neglected. The amount of sample introduced can be calculated by using Equation (10). The amount injected

$$Q = \frac{\rho g \pi r^4 \Delta h t_i c}{8\eta L} \tag{10}$$

thus depends only on the difference in levels and the injection time. Injection times of several seconds are normally used, and the level difference must be adjusted accordingly. Manual injection leads to poor reproducibility in quantification (RSD 10%), while with automatic, computer-aided injection RSDs of 2%[30] or better[33] can be achieved.

3.2.3. Pressure Injection

In this method the sample is injected by applying a pressure difference between the sample vial and the end of the capillary; to achieve this the pressure is either increased in the sample vial or reduced at the end of the capillary. These two possibilities also make it easy to rinse the capillary with fresh buffer solutions. The amount of sample introduced is calculated from Equation (11) and depends only on the pressure difference and the injection time. This is the most commonly used technique in commercial instruments. According to our experience the RSD lies between 2 and 3%; it can be reduced to below 1% when an internal standard is used.

$$Q = \frac{\Delta p \pi r^4 t_i c}{8\eta L} \tag{11}$$

3.2.4. Sample Splitters

Splitting systems analogous to those used in capillary gas chromatography have also been described for CE sample introduction; we can distinguish between electrical and hydrodynamic splitting systems. In the case of the electrical sample splitter (Fig. 5) the junction with the separation capillary is situated at the center of the dosage capillary. Since the field strengths applied to the two capillaries are unequal, the sample moves within two different current circuits; the splitting ratio is determined by the ratio of the two currents

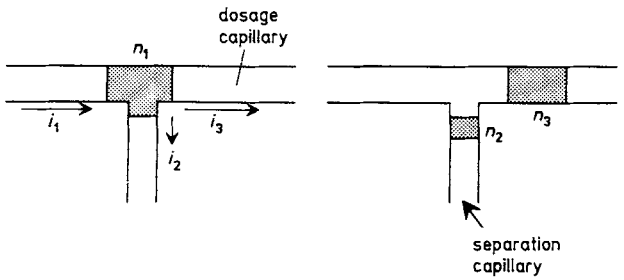

Fig. 5. Schematic diagram of an electric sample splitter. i_1, i_2, and i_3 denote the currents in the corresponding sections of the capillary; n_1 is the amount of sample prior to sample splitting, n_2 the amount introduced, and n_3 the remainder. Left: during sample splitting. Right: after the sample is split.

in the capillaries. The RSD for this method has been reported to be $<3\%$.[34] In the hydrodynamic splitting system an HPLC syringe is used to introduce the sample volume into a T-piece. The splitting ratio is determined by the ratios of diameter and length of the separation capillary and overflow capillary.[35] An RSD of approximately 2% has been reported for this technique, which requires, however, relatively large sample volumes. Other splitting systems, some of which use HPLC pumps,[36] have been described, but they have not provided better reproducibility.

3.2.5. Reproducibility of Sample Introduction

The reproducibility of sample introduction is influenced by a number of factors. Conductivity differences between the separation electrolyte and the sample solution,[37] large differences in the concentrations of the various components of the sample[33] and their electrophoretic mobilities,[38] and differences in the sample matrix[32] all affect the reproducibility. CE is the method of choice, however, when only very small sample volumes are available, for example, in the analysis of ions in drops of rainwater.[39] In commercial, automated instruments miniaturization of sample introduction is so advanced that a sample volume of 3 μL suffices for several injections.

The problems with the reproducibility of sample introduction in CE are due to the small pressure differences and short injection times required. When larger volumes are injected, the efficiency of the separation rapidly decreases. Attempts have therefore been made to introduce larger volumes and to sharpen the zones prior to the actual separation. This can be done by making use of isotachophoresis effects (ITP) prior to the actual CE separation, as will be described in Section 4.6. Samples may also be concentrated by means of transient increases in the field strength. This can be carried out most easily when a water "plug" is injected into the capillary prior to the actual sample introduction ("sample stacking").[40] The voltage decrease across the "nonconductor" water is so great that the following sample zone is concentrated in the much larger field present there. Enrichment factors of up to 100 have been achieved.

3.3. Thermostatting

The main purpose of thermostatting is to remove Joule heat. Both air and liquid thermostats are used in commercial instruments and allow the temperature to be controlled in the range from 15 to roughly 60 °C. For most applications intensive air cooling suffices.[41] The influence of temperature on efficiency and selectivity is at present still a subject of discussion.One reason for this is that in commercial instruments only the capillary (or sections thereof) is thermostatted, while the buffer reservoir is not always kept at the same temperature as the capillary. It has been shown, however, that for the separation of DNA fragments in gel-filled capillaries the actual separation performance decreases with increasing temperature, although the relative migrations, in other words the selectivity of the separations, can be increased.[42]

3.4. Capillaries

Polyimide-coated quartz capillaries 25 to 100 μm in diameter are generally used in CE. In principle glass or plastic capillaries could be used, though these are not sufficiently transparent in the short-wave UV range. The polyimide layer of the quartz capillaries must be removed at the site of the detector either mechanically or by burning off before the capillary is coated or used.[13] Capillaries with UV-transparent coatings have recently become available. Untreated and unmodified capillaries are used for most applications. The quartz capillaries obtained from different suppliers differ with respect to the precision and constancy of their internal diameter as well as to the treatment of the inner surface and the optical transmission in the lower wavelength region. It is thus advisable to treat new capillaries with 1 M NaOH prior to their initial use in order to obtain complete hydroxylation of the surface.

Surface modification of the capillaries can be carried out with the same methods described for the modification of silica gels for the preparation of stationary phases for HPLC or for coating capillary columns for gas chromatography. As already mentioned, changes in the EOF can be used to characterize modified capillary surfaces; characterization by gas-chromatographic techniques has also been described.[43] The advantages and disadvantages of modified capillaries and gel-filled capillaries will be discussed in combination with the various separation techniques for which they are used.

3.5. Detection

Detection is still the greatest technical problem in CE. Because of the short cell length (mean capillary diameter) the demands made on the detectors with respect to sensitivity, noise, stray light effects, etc. are extremely high. Nevertheless, modified UV detectors designed for HPLC are most frequently used. Detection is carried out directly in the capillary in order to avoid efficiency loss due to peak broadening outside the capillary. Typical bandwidths of the zone in the capillary are around 5 mm ($N = 500000$), which corresponds to a volume of 10 nL (for a 50 μm capillary). These extremely small volumes are also the reason for the mass sensitivity, which has often been referred to as astounding. The world record at present is a reported detection limit of 300 molecules with a signal-to-noise ratio of 3:1[44] for derivatized

amino acids detected by laser-induced fluorescence. Although concentration sensitivity is more important for routine use, it is restricted by the short absorption path (mean capillary diameter!). UV Detection in CE gives concentration limits that are 30 to 100 times lower than those in HPLC.[45] In the case of irradiation at right angles to the capillary axis the limit depends on the detector noise and the effective cell length, which is lower than the nominal value (the inner diameter of the capillary). Stray light effects due to inefficient focusing (light from the capillary wall!) and nonideal cylindrical capillary geometry[46] increase the background noise; these effects can be largely eliminated by optimization of the optics (slit, lens, etc.). The detector most often used is a UV detector with a fixed or variable wavelength. In spite of the short path length it is also possible to record UV spectra with sensitive diode array detectors[47,48] (see Fig. 14).

Samples that do not absorb in the UV can be detected with commercial instruments by means of indirect UV detection.[18,49-53] An electrolyte that absorbs in the UV whose mobility is similar to that of the sample to be separated is added to the buffer or is used as a buffer component. Because of the necessity for electroneutrality the amount of added electrolyte must be less where the sample migrates (displacement mechanism). As a result the buffer has a higher transmission, and a negative peak, as shown schematically in Figure 6, is recorded. Examples are given in Sections 4.1.4 and 4.2.1 in the description of ion analysis (Figs. 12 and 17). The detection sensitivity in indirect UV detection depends on the molar extinction coefficient of the added UV-absorbent background electrolyte and corresponds to that of normal UV absorption.[54]

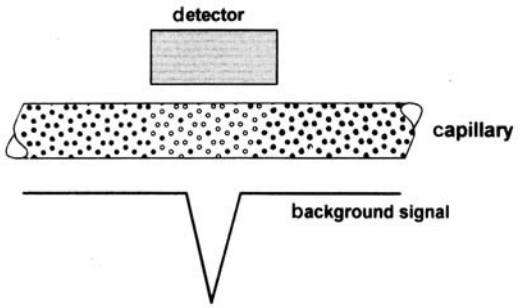

Fig. 6. Principle of indirect UV detection. • = UV-absorbing buffer ions; ○ = ionic sample components that are not UV absorbing.

In addition to UV detectors, fluorescence detectors have also recently become commercially available. The main difference between the two is the light source. Besides the usual deuterium and xenon flashlamps, much more complex laser systems are on the market. Since in the latter the excitation lies in visible range, samples must be derivatized accordingly. Indirect fluorescence detection is also possible and should become universally applicable when suitable fluorophores without quenching effects become available.[55-57]

Conductivity detection and other electrochemically based techniques appear promising but are as yet not commercially available. As a highlight we should mention the trace analysis of alkali metal and alkaline earth ions directly in the capillary by using microelectrodes.[58] The problem with conductivity detection is that the conductivity in the zone containing the substance to be analyzed is only slightly higher than that of the electrolyte. Suppression techniques for the reduction of the buffer conductivity such as those used in HPLC cannot be applied here. Conductivity detection in CE has already been described by a number of workers.[59-64] It has, for example, been possible by using amperometric detection to analyze neurotransmitters in nerve cells directly; the separation was carried out in 5 μm capillaries.[65-68]

Because of the low flow rates (100 nL min^{-1}), coupling CE with mass spectrometry also appears feasible. The main problem is that the transition from the capillary to the ion source, where high vacuum is necessarily present, must be constructed in such a way that the eluent is not sucked out of the capillary. A pressure drop of 1 bar leads to a linear flow velocity of 1 cm s^{-1} when applied to a capillary 1 m in length and with an internal diameter of 50 μm. The laminar parabolic flow profile thus induced would lead to a noticeable loss of efficiency; a "protective flow" must thus be applied around the capillary prior to ionization. Electrospray MS permits mass spectrometric detection of biopolymers by multiple ionization.[69-72]

Other detection methods (Raman spectroscopy[73] and measurements of on-line radioactivity,[74] circular dichro-

Table 2. Detection methods in capillary electrophoresis.

Detection method	Detection limits absolute amount [mol]	concentration [mol/l]	Typical applications	Remarks
UV absorption	10^{-15}–10^{-13}	10^{-7}–10^{-4}	aromatic compounds, proteins, nucleic acids, ...	standard detection in CE (available in all commercial instruments)
Indirect UV absorption	10^{-16}–10^{-13}	10^{-8}–10^{-4}	metal ions, amines, organic and inorganic ions, sugars	possible with commercial instruments
Fluorescence	10^{-18}–10^{-13}	10^{-9}–10^{-4}	derivatized amino acids, DNA, peptides, proteins	derivatization necessary for many samples
Laser-induced fluorescence	10^{-21}–10^{-17}	10^{-13}–10^{-7}	DNA fragments, derivatized amino acids	lasers are still very expensive (use in VIS and near-UV)
Indirect fluorescence	10^{-16}–10^{-14}	10^{-7}–10^{-5}	alcohols, amines, anions, cations, sugars	only a few applications described
Amperometry	10^{-16}–10^{-14}	10^{-8}–10^{-6}	reducible or oxidizable substances, e.g., neurotransmitters	capillaries with inner diameters up to 2 μm can be used
Conductometry	10^{-18}–10^{-16}	10^{-7}–10^{-5}	ionic samples, e.g., metal ions, amines, carboxylic acids	changing capillaries is difficult
Potentiometry	10^{-19}	10^{-8}	alkali metal and alkaline earth ions; selective detection by ion-selective microelectrodes	use and preparation of microelectrodes difficult
Mass spectrometry	10^{-17}	10^{-8}	proteins, peptides, drug monitoring	interfaces commercially available, coupling with automated systems possible
On-line radioactivity measurements	10^{-18}–10^{-16}	10^{-10}–10^{-8}	^{32}P and ^{14}C in biochemically relevant compounds	good detection sensitivity using stop-flow systems

ism,[75] refractive index,[76] and capillary vibration[77]) have been described in the literature. It is not possible at present to estimate their suitability for routine use.

The limits of detection for the most frequently used detection systems are listed in Table 2. It is clear that excellent mass sensitivities can be achieved because of the small volumes involved. The concentration sensitivities lie in the range of those found for HPLC.

Chromophores can naturally be introduced into non-UV-active and nonfluorescing samples prior to the separation by using the standard derivatization reagents. Special reagents for electrophoresis that permit the simultaneous introduction of charges are a topic of discussion.[78-81]

4. Separation Techniques in Capillary Electrophoresis

4.1. Capillary Electrophoresis in Uncoated Capillaries

4.1.1. The Influence of the pH Value

The influence of the pH value on the transport of samples to the detector has two causes. Firstly, as already mentioned, a separation based on electrophoretic migration is dominated more or less by the EOF, whose magnitude is determined by the dissociation of the surface silanol groups. Secondly, the mobility of the ions is determined by their degree of dissociation in the carrier electrolyte and thus by its pH value. The separation can therefore be optimized by changing the pH value and the buffer. In the case of weak electrolytes the greatest migration differences, in other words the highest selectivities, are obtained when the pH value of the buffer lies between the pK_s values of the sample components, as is already known from classical electrophoresis. Nondissociated samples migrate through the capillary at the velocity of the EOF. As has been shown, the EOF also depends on the pH value and the other properties of the electrolyte, in particular on its ionic strength. The dependence of the EOF on the pH value in quartz capillaries is shown in Figure 4.

The possibilities provided by the combination of electrophoretic migration and EOF can be demonstrated on nucleotides. The EOF is directed towards the cathode, and the nucleotides migrate to the anode; triphosphates are the fastest because of their high charge. Even at high pH values (pH > 10) the EOF does not suffice to transport the triphosphates to the detector at the cathode. If the electrophoretic mobilities of the mono- and diphosphates are lower than the EOF, they will be transported to the detector and will reach it at different times. The separation of this type of sample is shown in Figure 7. Under these experimental conditions the vector component of the EOF is insufficient to transport the triphosphates, which migrate to the anode compartment. The triphosphates can be analyzed by reversing the polarity, while the di- and monophosphates are driven by the EOF in the opposite direction. The mobility can be varied by the addition of ion pair-forming substances in such a manner that all the nucleotides can be separated in one run.[82] The separation of anions with greatly different mobilities in one single analysis is also possible when the EOF is reversed by surface modification and simultaneous field reversal (see Fig. 16).

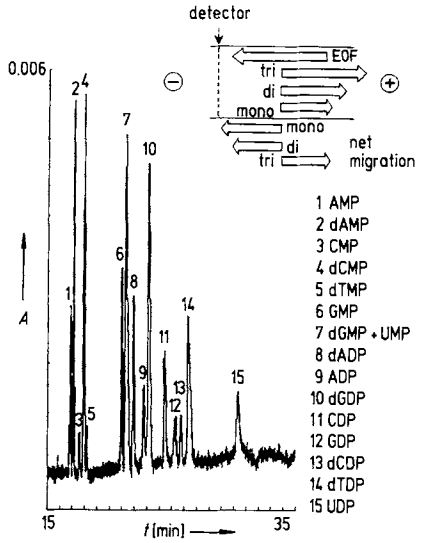

Fig. 7. Separation of mono- and dinucleotides with an untreated capillary. Conditions: capillary: $L = 75$ cm, $ID = 75$ μm, buffer: 100 mM CAPS (3-(cyclohexylamino)-1-propanesulfonic acid), pH 10.5; field: $E = 200$ V cm^{-1}, $I = 35$ μA; sample concentration: 100–250 mM. Trinucleotides migrate faster to the anode and cannot be detected.

4.1.2. The Influence of Ionic Strength

The lower the ionic strength, the lower the Joule heating of the electrolyte. On the other hand, the differences in the conductivity between the sample zone and the carrier electrolyte should be negligible. The larger the ionic strength of the electrolyte, the lower the EOF.

The influence of the ionic strength on the EOF and the mobility of the ions is shown in Figure 8a. In all cases the current is held constant. The neutral marker (benzyl alcohol) is eluted after about 15 minutes at a concentration of 100 mM,

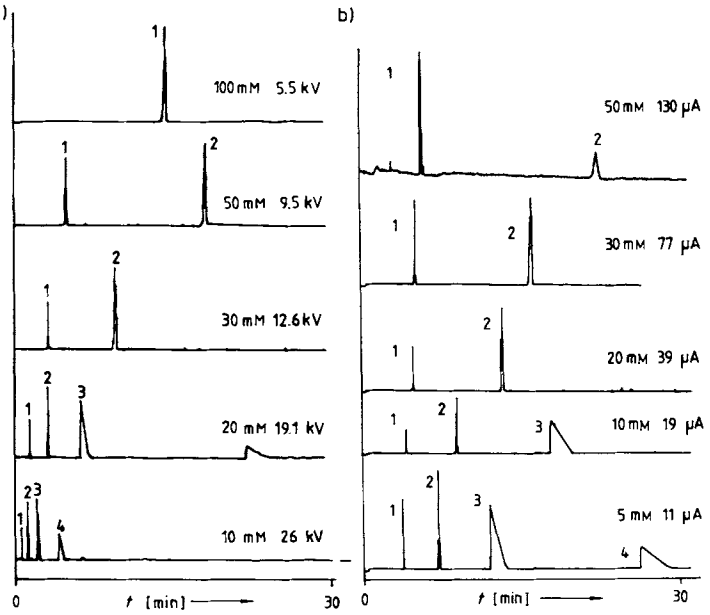

Fig. 8. Dependence of the EOF on the ionic strength of the buffer. Conditions: capillary: $L = 44$ cm, $ID = 75$ μm; buffer: borate solutions of various concentrations, pH 9.5; a) constant current (100 μA); b) constant field (230 V cm^{-1}). Sample: 1 = benzyl alcohol, 2 = benzoic acid, 3 = benzene-1,2-dicarboxylic acid, 4 = benzene-1,3,5-tricarboxylic acid.

while the carboxylic acids which migrate to the anode are not eluted. If the ion concentration is reduced to 20 mM the separation is complete after about 20 minutes, at 10 mM after 5 minutes. The analysis time is determined here by the size of the EOF, since the effective sample migration is almost independent of the buffer concentration. Because of their lower mobility with respect to the borate ions of the buffer, the di- and tricarboxylic acids migrate as asymmetrical peaks with tailing. Such triangular peaks are always observed when the mobility difference between the carrier electrolyte and the sample is too great.[8] Samples with mobilities greater than that of the buffer ion exhibit leading. Symmetrical peaks, and thus high numbers of theoretical plates, are obtained only when the mobilities of the sample and carrier electrolyte are equal. Analogous effects are observed when a constant voltage is used, as shown in Figure 8b. Comparison of Figures 8a and 8b clearly demonstrates the advantages of low buffer concentrations and high possible voltages: the analysis time can be reduced tremendously (Fig. 8a). Thus low buffer concentrations and high field strength are optimal.

Figure 9 shows the influence of the buffer concentration on the band broadening H of samples with different mobilities. Low band-broadening and high separation performance are observed for the neutral marker benzyl alcohol (breakthrough of the zone with EOF) and for the only weakly dissociated *p*-hydroxybenzoic acid even at a low buffer concentration (50 mM). At this buffer concentration the band broadening for the di- and tricarboxylic acids is intolerably high. Even at higher buffer concentrations the band broadening is not as low as that obtained for nondissociated or weakly dissociated samples.

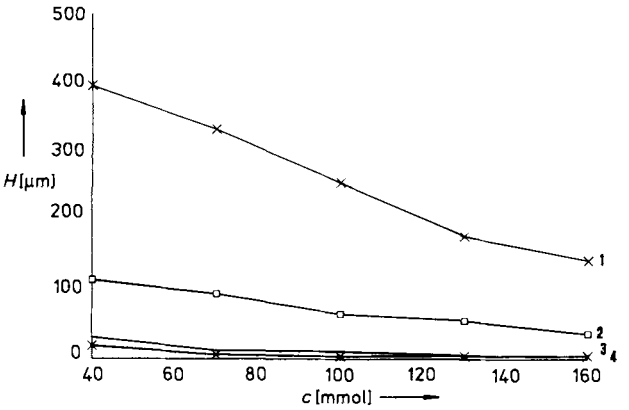

Fig. 9. Influence of the buffer concentration on the band width H. Conditions: capillary: L = 50/54 cm, ID = 50 µm; buffer: borate solutions of various concentrations, pH 8.5; field: E = 560 Vcm^{-1}; UV detection at 214 nm. Sample: 1 = benzene-1,3,5-tricarboxylic acid, 2 = benzene-1,2-dicarboxylic acid, 3 = *p*-hydroxybenzoic acid, 4 = benzyl alcohol.

4.1.3. Choice of the Buffer

Several factors must be taken into consideration when choosing the buffer. As shown above, the mobilities must be equal in order to obtain a high separation performance. The concentrations of the buffer ions should be greater than the concentration of the ions in the sample solution; this also leads to sharply defined, symmetrical zones. However, high ionic strength implies a high current density for a given voltage gradient, and thus an increase in Joule heating. These effects can be simply measured in the form of deviations from Ohm's law, as shown in Figure 10 for two buffer systems and capillaries with different inner diameters. The advantage of organic buffers, which have low conductivities, can clearly be seen. Even for the thicker capillary Ohm's law is obeyed throughout the whole range for the buffer 3-(cyclohexylamino)-1-propanesulfonic acid (CAPS), while with the same capillary and a borate buffer the range of linearity only extends up to 10 kV. The advantages of the thinner capillaries for heat transport can also be seen for the borate buffer; it is still possible to work at 25 kV with the 50 µm capillary. It is also possible to achieve shorter analysis times, since these are inversely proportional to the applied field strength.

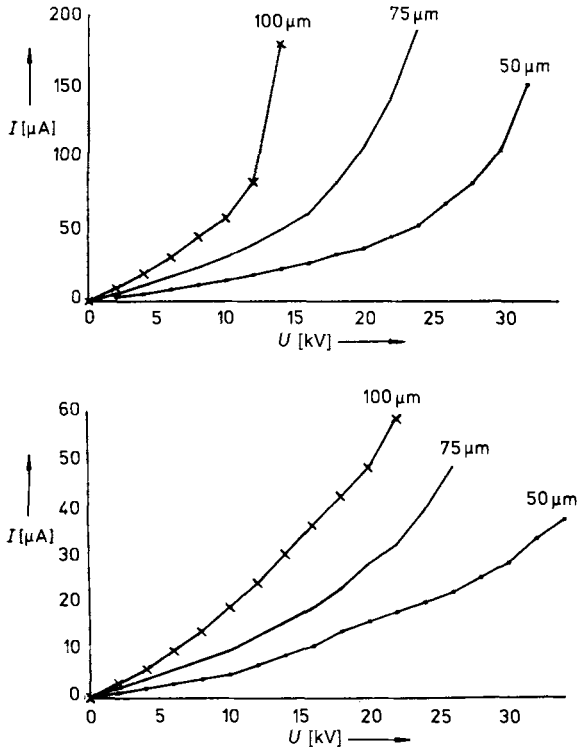

Fig. 10. Current–voltage dependence as a function of the capillary diameter and the buffer concentration. Top: buffer: 20 mM borate, pH 9.5. Bottom: buffer: 25 mM CAPS, pH 11.0.

4.1.4. Areas of Application

Electrophoresis in uncoated capillaries is the standard technique particularly suitable for the separation of small molecules with permanent charges. Thus it is possible to separate aliphatic and aromatic carboxylic acids, sulfonic acids, amino acids, phenols, nucleotides, and amines without great difficulty. A good survey of recent applicatons is available in the two articles written by Kuhr.[83, 84] An example of a separation of sugars and sugar acids is shown in Fig-

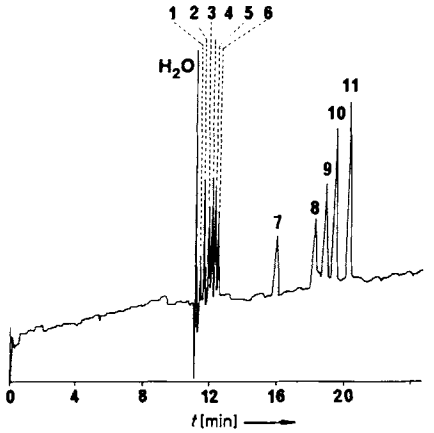

Fig. 11. Separation of carbohydrates by CZE. Conditions: capillary: $L = 100/122$ cm, $ID = 50$ μm; buffer: 6 mM sorbate, pH 12.1; field: $E = 203$ Vcm^{-1}, $I = 13$ μA; $T = 30$ °C; UV detection at 256 nm; CE instrument: ABI model 270A. Sample: 1 = raffinose, 2 = 2-deoxy-D-ribose, 3 = galactose, 4 = glucose, 5 = rhamnose, 6 = mannose, 7 = *N*-acetylneuraminic acid, 8 = gluconic acid, 9 = galacturonic acid, 10 = glucuronic acid, 11 = mannuronic acid (from ref. [85]).

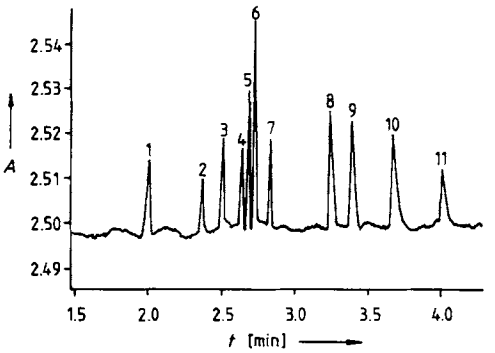

Fig. 12. Separation of metal ions, amines, and amino alcohols (indirect UV detection). Conditions: capillary: $L = 50/58$ cm, $ID = 75$ μm; buffer: 5 mM imidazole, pH 4.5; field: $E = 430$ Vcm^{-1}, $I = 9$ μA. Sample: 1 = NH_4^+, K^+, 2 = Na^+, 3 = dimethylamine, 4 = Ca^+, 5 = trimethylamine, 6 = Mg^{2+}, 7 = Li^+, 8 = diethylamine, 9 = triethylamine, 10 = diethanolamine, 11 = triethanolamine. Sample concentrations: 1–3 ppm (from ref. [51]).

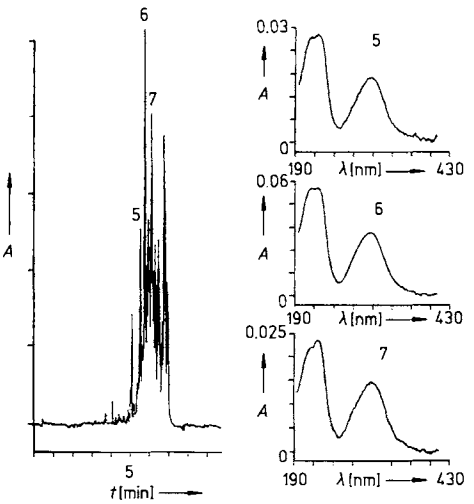

Fig. 13. Separation of tannic acids and their characterization (diode array detection). Spectra are shown for the marked peaks. Conditions: capillary: $L = 50/80$ cm, $ID = 75$ μm; buffer: 50 mM borate, pH 9.5; field: $E = 375$ Vcm^{-1}, $I = 32$ μA. Detection: Perkin Elmer LC-480.

ure 11;[85] Figure 12 shows the separation of cations and lower aliphatic amines with indirect UV detection. Imidazole is used here as both an electrolyte component and a UV absorber.[51] Figure 13 shows the CE of a natural tannin mixture. The separation of charged molecules with relatively large hydrophobic residues can be improved by the addition of SDS, as is demonstrated in Figure 14a with aromatic sulfonic acids. The resolution of the fast migrating components is only possible in the presence of SDS; the migration of the letter acids is, as expected, not influenced by the SDS. The scope for the optimization of CE separations by adding detergents will be discussed in detail in Section 4.5, which deals with micellar electrokinetic chromatography. The per-

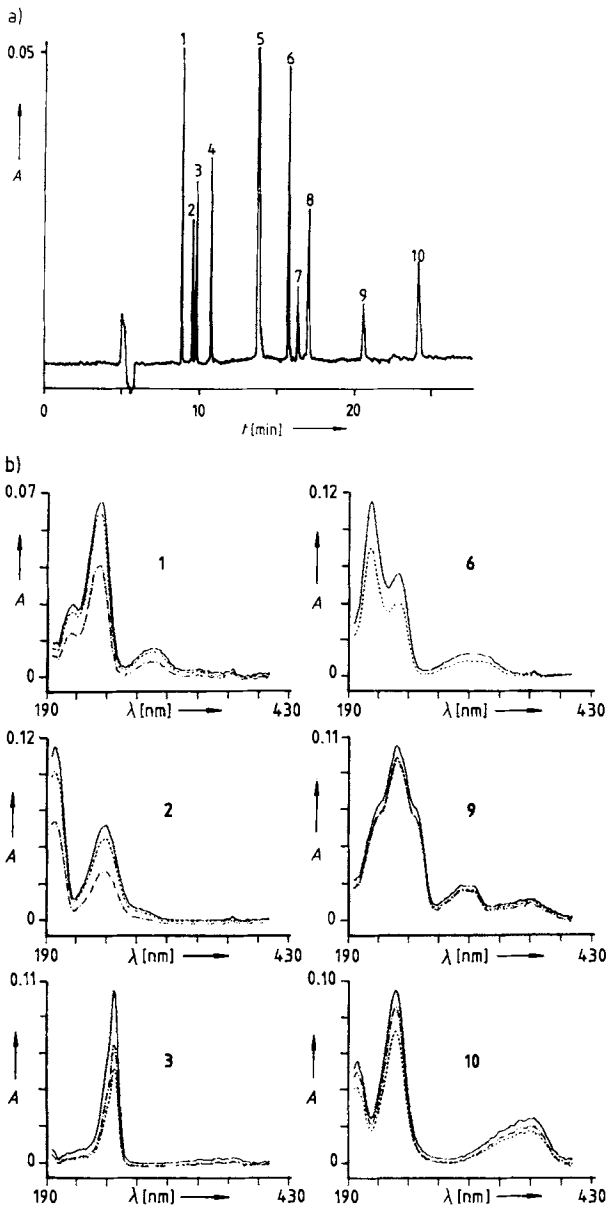

Fig. 14. Separation of aromatic sulfonic acids and their characterization (diode array detection). a) Conditions: capillary: $L = 50/80$ cm, $ID = 75$ μm; buffer: 59 mM borate, 50 mM SDS, pH 9.5; field: $E = 310$ Vcm^{-1}, $I = 39$ μA. Sample: 1 = 2-naphthylamine-6-sulfonic acid, 2 = sulfanilic acid, 3 = benzenesulfonic acid, 4 = anthracene-2-sulfonic acid, 5 = 1-naphthylamine and 2-methylnaphthylene, 6 = 1-hydroxymethyl-2-naphthol-6-sulfonic acid, 7 = 2-naphthol-6-sulfonic acid, 8 = R-acid, 9 = G-acid, 10 = H-acid. b) Spectra for the given components. Detection was carried out using a Perkin Elmer LC-480 adapted for capillary electrophoresis.

formance of diode array detectors (DAD) in capillary electrophoresis is also demonstrated in Figures 13 and 14b. Purity determination by means of UV spectra recorded at the peak maxima and (for overlapping peaks) at the points of inflection is possible even for the sharp, narrow peaks obtained in CE; Figure 14b shows the overlap observed for the on-line UV spectra of the acids.

4.2. Capillary Electrophoresis in Surface-Modified Capillaries

The EOF can be controlled by chemical modification or dynamic coating of the capillary surface. The possibility of the absorption of sample components at the capillary surface is simultaneously reduced and the reproducibility of the analysis improved. Surface-modified capillaries are, for example, absolutely necessary for the analysis of proteins.

4.2.1. Dynamically Modified Capillaries

The simplest method of modifying the surface of quartz capillaries is to add to the buffer solution a component which will be preferentially adsorbed by the surface silanol groups. The resulting layer influences the EOF and also reduces the absorption due to hydrophobic or electrostatic repulsion.

As shown in Figure 15, the use of cationic detergents leads to the formation of a double layer in which the positive charges are directed towards the interior of the capillary; the EOF is reversed as a result. This technique also permits the

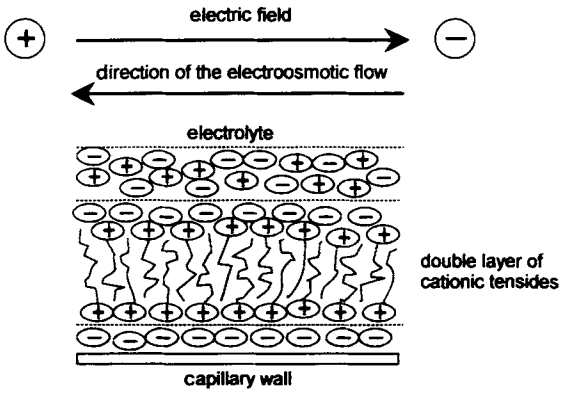

Fig. 15. Schematic representation of EOF reversal induced by cationic detergents.

separation of rapidly migrating anions when the field is also reversed,[117] as is shown schematically in Figure 16; this should be compared with the case demonstrated in Figure 7, in which the EOF is directed towards the cathode and the rapidly migrating triphosphates migrate to the anode. It was possible to detect the latter by means of polarity reversal, though the slowly migrating anions were no longer observed. If the EOF is also reversed, both rapidly and slowly migrating anions can be detected and determined in one single analysis. Figure 17 demonstrates this for the analysis of inorganic and organic anions in the ppm range with indirect UV

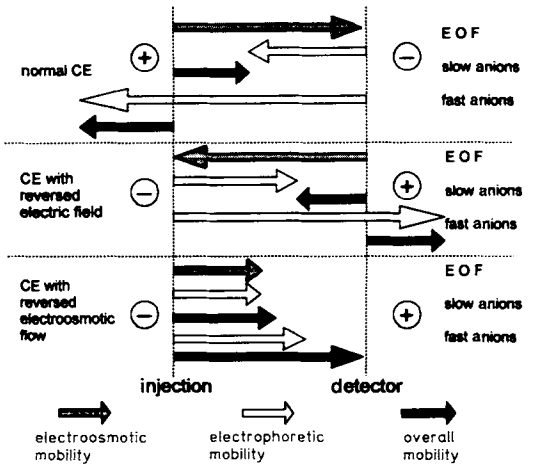

Fig. 16. Migration of ions with normal and with reversed EOF.

detection. Chromate is used as the UV absorber,[118] and the capillary is coated with cetyl trimethylammonium bromide, for example. Care must be taken that the critical micellar concentration is not exceeded when the detergent is present.

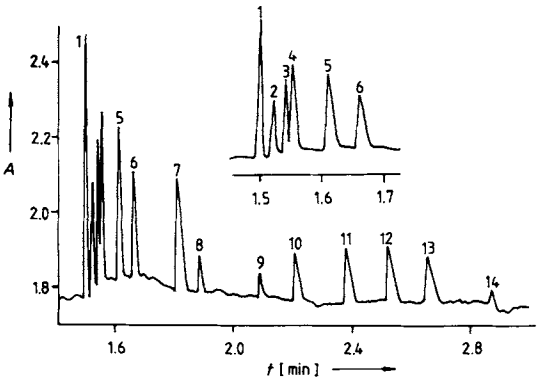

Fig. 17. Separation of inorganic and organic anions. Conditions: capillary: $L = 42/50$ cm, $ID = 75$ μm; buffer: 5 mM chromate, 0.5 mM hexadecyltrimethylammonium bromide (dynamic coating), pH 8.1; field: $E = 600$ Vcm^{-1}. Sample: 1 = bromide, 2 = chloride, 3 = sulfate, 4 = nitrite, 5 = nitrate, 6 = azide, 7 = fluoride, 8 = phosphate, 9 = carbonate, 10 = acetate, 11 = propionate, 12 = butyrate, 13 = valeriate, 14 = D-gluconate.

Positive surface charges are also used in the separation of proteins. The adsorption of cationic proteins is hindered by the electrostatic repulsion achieved either by adding detergents[92] or by coating the capillary surface with ethylene imine, which can also be cross-linked at the surface.[108] A high number of theoretical plates is achieved, and symmetrical peaks are observed for basic proteins. When lower polyamines are added to the buffer[90] the adsorption of proteins at the capillary surface can be reduced. The efficiencies are high, though the field strength must be kept low because of the high intrinsic conductivity of the buffer. Since the EOF is also decreased, the analysis times are relatively high. Figure 18 shows, as an example, the separation of standard proteins. Table 3 lists the separation systems generally used for the separation of proteins in uncoated capillaries.

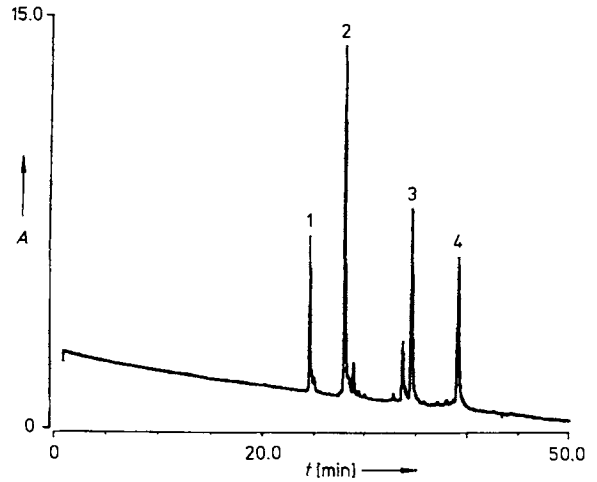

Fig. 18. Separation of basic proteins in an untreated capillary. Conditions: capillary: Polymicro, $L = 55/75$ cm, $ID = 50$ μm; buffer: 50 mM phosphate, 40mM 1,3-diaminopropane, 20mM K_2SO_4, pH 3.5; field: $E = 200$ Vcm^{-1} (from refs. [90, 113]). Sample: 1 = cytochrome C, 2 = lysozyme, 3 = ribonuclease, 4 = chymotrypsinogen.

Table 3. Protein separations with buffer additives in an uncoated capillary.

Buffer [a]	c [mM]	pH	pI	N [$\times 10^3$ m^{-1}]	Ref.
tricine/KCl	10/20	8.3	5–7	500	[86]
CHES/K_2SO_4/EDTA	100/250/1	9.0	5–11	100	[87]
phosphate/betaine/K_2SO_4	40/2000/100	6.7	9–11	300	[88]
phosphate/sultone	100/1000	7.0	5–11	300	[89]
1,3-diaminopropane/K_2SO_4	40/20	3.5	9–11	300	[90]
phosphate/BRIJ 35	10/10 ppm	7.0	3–11	100	[91]
phosphate/FC 134	50/100 ppm	7.0	7–11	300	[92]
borate/SDS	100/0.5%	10.0	4–6	?	[93]

[a] Abbreviations: tricine = *N*-[2-hydroxy-1,1-bis(hydroxymethyl)ethyl]glycine, CHES = 2-(cyclohexylamino)ethanesulfonic acid, BRIJ 35 = polyethyleneglycol lauryl ether, FC 134 = Fluorad (fluorine-containing cationic detergent; 3M Company, St. Paul, MN (USA)).

4.2.2. Chemically Modified Capillaries

The techniques developed for gas chromatography (polymer coating) and methods used for the modification of silica gel surfaces (silylation reactions, surface polymerization) have been applied to the modification of capillaries for use in electrophoresis. Table 4 contains a list of the most important coating methods, and their main areas of application, and the stability ranges of the coatings. The greatest limitation of the coatings prepared by silanization is their limited stability at higher pH values, a fact which is painfully well known from HPLC. The disadvantage of polymer coatings is their extreme hydrophobicity, which has led to the widespread use of such phases for protein separation in the presence of nonionic or zwitterionic[91] detergents. As already mentioned, the coating and its stability can be most easily characterized by the reduction or constancy of the EOF.

In analogy to classical electrophoresis, acrylamide coatings have often been used for the separation of proteins by CE;[16, 103–105] these coatings are often described as "linear acrylamide". Figure 19 shows the separation of the same standard proteins as in Figure 18 with a polyacrylamide-coated capillary. In spite of the considerably reduced EOF it

Table 4. Survey of capillary coating methods.

Functionality	pH range	Applications	Ref.
Conventional Coatings			
trimethylsilyl-	7	small molecules	[94]
trimethylsilyl-	9	MEC	[95]
RP-C8 [a]	9	proteins	[96]
RP-C18 [b]	9	proteins	[96, 97]
polyethylenglycol-	3–5	proteins	[98]
diol-	3–5	proteins	[94, 99]
[3-(2,3-epoxypropoxy)propyl]-trimethoxysilane [c]	5	proteins	[100]
maltose	3–7	proteins	[99]
pentafluoroaryl-	7	proteins	[101]
α-lactalbumin	8	proteins	[102]
Polymer coatings			
linear polyacrylamide	2–8	proteins	[16, 103, 104]
	(to 10) [d]	IEF	[105, 106]
		DNA fragments	[107]
polyethylenimine	3–11	proteins	[108]
1-vinyl-2-pyrrolidine	2–6	proteins	[100]
poly(methylglutamate)	7	proteins	[109]
polymethylsiloxane (OV1)	7	MEC	[110, 111]
polyethyleneglycol	7	MEC	[110, 111]
polysiloxane/β-cyclodextrin	7	chiral separations	[112]

[a] RP-C8 = *n*-octylsilyl. [b] RP-C18 = *n*-octadecylsilyl. [c] Also commercially available as "glycidoxypropylsilane". [d] Stability range given in ref. [105] or highest pH used in measurements.

is possible to work at normal field strengths, so that the separation is complete after about 5 minutes. A further advantage of coated capillaries lies in the greater constancy and reproducibility of the EOF. A disadvantage is their reduced stability at high pH values (pH > 7). The use of ionic coatings[108, 113] can in addition lead to a pH-independent flow or to a reversal of the EOF.

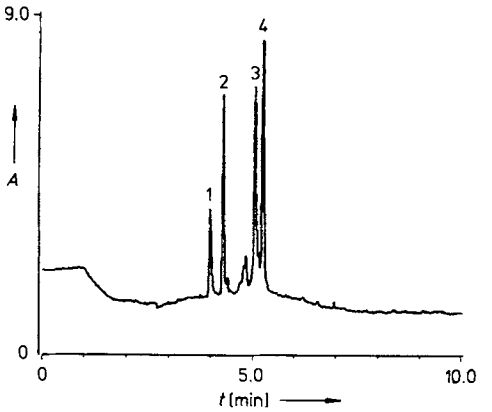

Fig. 19. Separation of basic standard proteins in a capillary coated with linear polyacrylamide. Conditions: capillary: $L = 31/48$ cm; buffer: 30 mM citrate, pH 3.0; field: $E = 410$ Vcm^{-1}. Sample: 1 = cytochrome C, 2 = lysozyme, 3 = ribonuclease A, 4 = chymotrypsinogen [$c = 0.2$ mg mL^{-1}].

As shown in Figures 18 and 19, the separation of proteins can be carried out successfully with both dynamically and permanently coated capillaries. Apart from the general remarks made here, no conclusion as to the advantages and disadvantages of the two separation techniques is possible at present.

Apart from protein separation, the main area of application of coated capillaries is in micellar electrokinetic chromatography (MEC), where the EOF must be reduced to

obtain long residence times in the capillary.[100, 111] When gel-filled capillaries are used, the EOF must be eliminated by capillary coatings in order to keep the gel stationary. Enantiomers could be separated with a capillary coated with a polysiloxane containing cyclodextrin groups,[112] although interactions with the capillary surface otherwise always lead to extreme losses in efficiency.

4.3. Isoelectric Focusing (IEF)

In classical electrophoresis, IEF is a highly efficient separation process, and it can also be used for the determination of the isoelectric points of proteins. A pH gradient is established along the separation pathway in an ampholyte-stabilized gel.[114] In this pH gradient a protein migrates only as long as it is charged and stops at the pH value corresponding to its isoelectric point (pI). The ampholytes are either added to the buffer or covalently bound to the gel.[115–118] This is necessary for the stabilization of the pH gradient because of the relatively long analysis times. The pH gradient is established before the sample is introduced by applying a voltage. Stabilizing gels are not required for the transfer of IEF in the capillary; however, the EOF must be reduced or completely eliminated in order to allow formation of the pH gradient.[119–122] This can be done either by coating the capillary surface or by increasing the viscosity of the buffer solution by adding highly viscous polymers (e.g. hydroxymethylcellulose).[123] The latter is particularly useful, since IEF requires the use of very high pH values.

In contrast to flatbed IEF, in CE the formation of the pH gradient in the capillary and the focusing of the proteins is carried out in one step. The capillary is filled with the solution of the samples in the ampholyte mixture; dilute sodium hydroxide is introduced into the capillary at the anode side and phosphoric acid at the cathode side. A high current flows when the voltage is first applied. The end of the focusing is evident by the reduction in the current to a constant low value. After the sample has been focused (and thus separated) in the capillary, it must be transported to the detector. This is generally carried out by exchanging the cathode electrolyte for a NaOH–NaCl solution, which destroys the pH gradient, mobilizes the focused proteins, and allows their transport to the detector.[124] Since the focusing occurs throughout the whole capillary, also between the detector and the cathode, proteins with extremely high pI values cannot be detected by this method. This can be prevented by filling the capillary with NaOH beyond the detection site. An example demonstrating the scope of IEF in capillaries is shown in Figure 20.

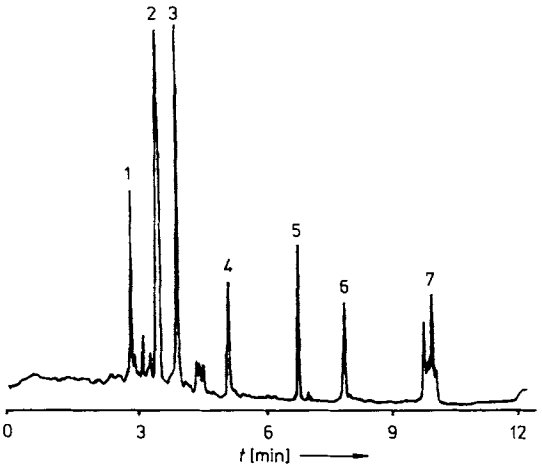

Fig. 20. Isoelectric focusing of a protein standard mixture (pI 5.1–7.5). Conditions: capillary: $L = 12$ cm, $ID = 25$ mm, coated capillary; buffer: Bio-Lyte ampholyte, pH 3–10 (catholyte: 0.01 M phosphoric acid, anolyte: 0.02 M NaOH); mobilization with 0.08 M NaCl and 0.02 M NaOH; voltage for focusing and mobilization: 7 kV; UV detection at 280 nm (0.1 AUFS) (Application Note 31, BioRad). Sample: 1 = human hemoglobin C, 2 = human hemoglobin A, 3 = equine myoglobin, 4 = equine myoglobin (minor band), 5 = human carbonic anhydrase, 6 = bovine carbonic anhydrase, 7 = β-lactoglobulin B.

4.4. Capillary Gel Electrophoresis (CGE)

The enormous growth in popularity of capillary electrophoresis and the introduction of commercial instruments were induced by the American Human Genome Project. DNA fragments from sequencing reactions, restriction fragments, etc. have been separated almost solely by CGE.[20, 125, 126] Of the various types of gels used in classical flatbed gel electrophoresis, acrylamide,[127] agarose,[128, 130] and cellulose[129] are generally used as the matrix in CGE. The prerequisite for the stability of the gel in the capillary is the complete elimination of the EOF. This can be achieved by coating or chemically modifying the capillary wall.[103, 104] Initially the gel was often cross-linked with the surface coating during the polymerization in the capillary.[20, 131] The selectivity of the gels was varied by changing the ratio of the acrylamide monomer concentration (% T) to the concentration of the cross-linker (% C). The remarkable separation performance of these capillaries is demonstrated in Figure 21.[132, 133] The number of theoretical plates amounts to several million and increases with increasing migration time.[133] This apparent contrast to the situation in chromatography shows that apparently only the longitudinal diffusion contributes to the band broadening, and that at least for CGE Equation (6) correctly describes the dependence of the number of plates on the diffusion coefficient.

In practice these fixed gels had some disadvantages. They dried out very rapidly at the ends of the capillary (bubble formation) and were thus of no further use. An exchange of the buffer in the capillaries was either impossible or required a great deal of time. The thermal stability of such gels was also poor, and commercial applications could not be realized. The preparation of these capillaries requires a great deal of skill in the modification of the surface and, in particular, in carrying out the polymerization in the capillary.[132, 134]

These problems can be avoided when the capillary is filled with a solution of a high molecular weight, water-soluble polymer instead of polymerizing cross-linked gels directly in the capillary.[135, 136] "Linear polyacrylamide" (0% C) is also used for this purpose.[42] The polymers are introduced into the buffer reservoir, and the capillaries are filled by the application of pressure. The EOF must, of course, also be eliminated, so that the gel remains stationary in the capillary during the separation; any flow reduces the efficiency of the separation. The selectivity of very high molecular weight "linear gels" (e.g. 12% T) is similar to that of cross-linked gels

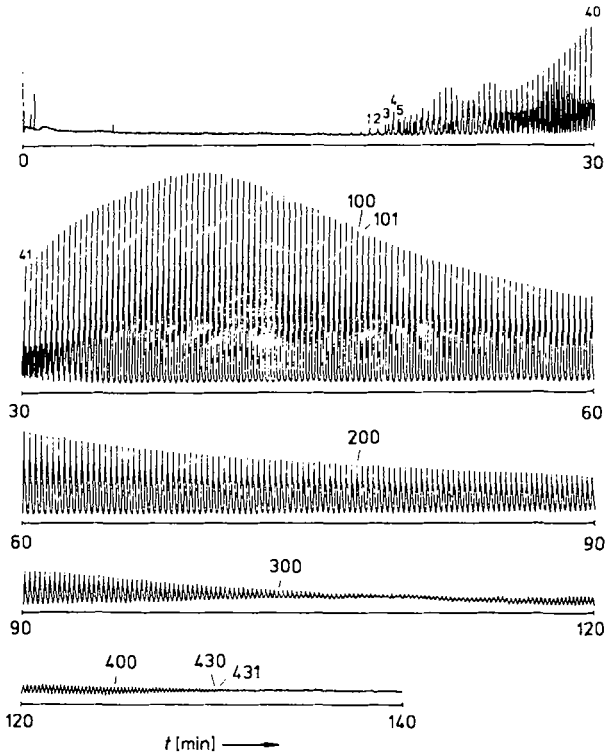

Fig. 21. Separation of poly(uridine-5'-phosphate). Conditions: capillary: L_{eff} = 45 cm, ID = 100 μm; gel: polyacrylamide 6% T, 5% C; buffer: 0.1 M Tris/0.25 M boric acid/7 M urea; field: E = 300 Vcm^{-1}, I = 12 μA; injection: 5000 V, 2 s; UV detection at 260 nm (taken from ref. [132]).

polymerized in the capillary. Figure 22 shows the separation of restriction fragments (PBR 322) in a capillary filled with "linear gel" (3% T, 0% C).[137] Here the number of theoretical plates is greater than 600000 plates per meter. At such high plate numbers the capillaries should not be coiled, since this reduces the efficiency.[138] As already mentioned, the separation of DNA fragments in gels is temperature dependent. As a comparison between Figures 22 and 23 (the same separation carried out at 20 and 50 °C) shows, the selectivity increases with temperature, particularly for higher molecular

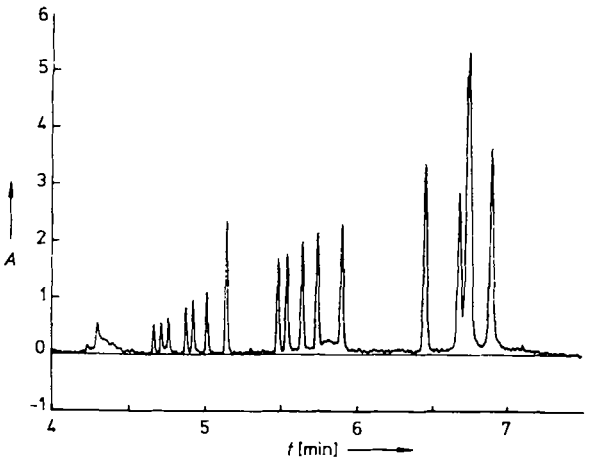

Fig. 22. Separation of DNA restriction fragments with "liquid gels". Conditions: capillary: L = 20/27 cm; buffer: 100 mM Tris-borate buffer, pH 8.3, 3% (w/v) linear polyacrylamide, capillary coated with linear polyacrylamide; field: E = 300 Vcm^{-1}; UV detection at 254 nm, T = 20 °C. Sample: pBR 322 Hae III restriction fragments. Apparatus: Pace System, Beckman Instruments.

weight fragments, and the separation improves although the number of plates decreases with increasing temperature. Theory and practice agree here, too. Apart from linear polyacrylamides, hydroxyethylcellulose has also been used successfully for the separation of restriction fragments.[135, 139]

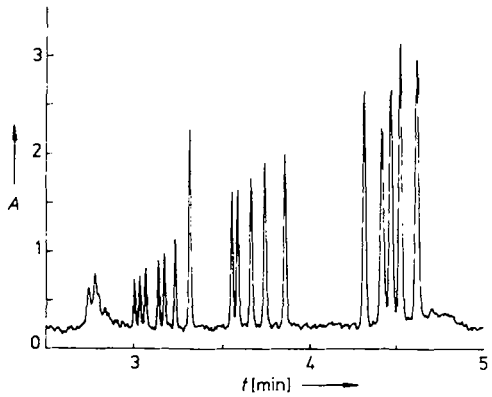

Fig. 23. Temperature influence on the separation of DNA restriction fragments. Conditions as in Figure 22; T = 50 °C.

CGE has been used almost solely for the separation of DNA fragments. The sensitive detection of proteins in gel-filled capillaries at low wavelengths (< 230 nm) in the UV is not possible, as acrylamides are not optically transparent below 250 nm; cellulose derivatives should be useful here. Interactions between the proteins and the gels may also play a role, since until now only the successful separation of proteins denatured with SDS in gel-filled capillaries has been described.[138, 140, 141] Only laser-induced fluorescence has been used for detection in the DNA sequencing, because the amounts of sample available are very small; the limit of detection lies at 10^{-11} M.

4.5. Micellar Electrokinetic Chromatography (MEC)

In CE any uncharged molecules present are eluted between the cations and the anions and are not separated. The addition of anionic detergents to the buffer (SDS is generally used) leads to the formation of micelles around the uncharged molecules; since the micelles carry a negative charge, they migrate to the anode.[142, 143] If the capillaries are not coated, and the EOF is larger than the rate of migration of the micelles, they will also be transported to the detector at the cathode. In this case the effective rate of migration of the sample components is equal to the vector sum of the electrophoretic migration to the anode and the electroosmotic velocity. Since micelles always migrate with almost the same rate, the separation is due to the distribution of the uncharged molecules between the buffer solution and the interior of the micelles; this is shown schematically in Figure 24. Chromatography is indeed the correct term here, as the mechanism leading to the separation of the uncharged molecules is based on a distribution equilibrium. In the case of ions this distribution process is superimposed on the actual electrophoretic migration.

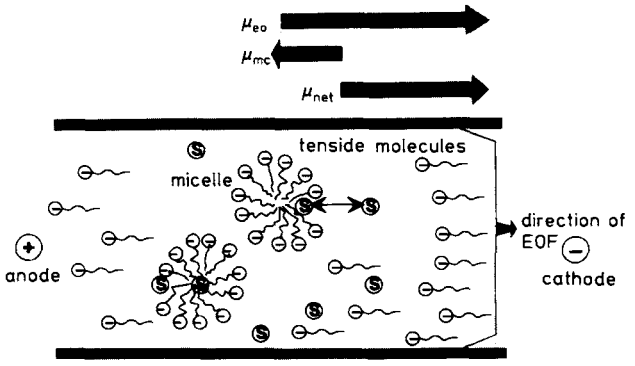

Fig. 24. Schematic representation of micellar electrokinetic chromatography (MEC). S = sample components. μ_{eo} = electroosmotic mobility, μ_{mc} = micelle mobility; μ_{net} = net mobility.

Optimization strategies for the MEC method will be demonstrated below with the example of the separation of fluorenylmethyloxycarbonyl (Fmoc) derivatives of amino acids. The separation of eleven Fmoc amino acids is shown in Figure 25. Because of the relatively large contribution made by the neutral derivatizing reagent, which is the same for all the samples, the electrophoretic mobility of the derivatives is very similar and almost no separation is observed. The addition of SDS to the buffer leads to a much better separation of the Fmoc amino acids (Fig. 26) under otherwise identical conditions. The addition of an organic component to this buffer can lead to a further improvement in the separation. The separation shown in Figure 27 was carried out under conditions identical to those in Figure 26 but with methanol added to the buffer. This additive has an influence on the distribution equilibrium of the sample between the buffer and the micelles, changes the EOF, and affects the solubility of the sample in the buffer.[144]

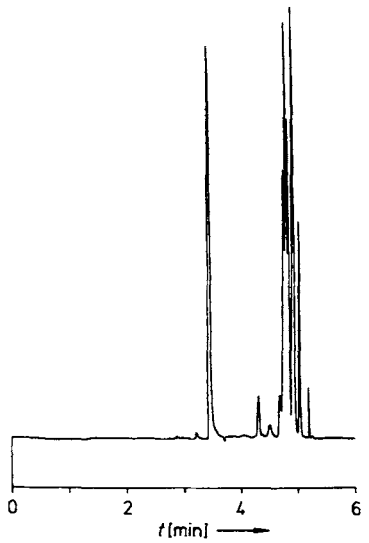

Fig. 25. Separation of eleven Fmoc amino acids by CZE. Conditions: capillary: Chrompack, L = 50/75 cm, ID = 50 μm; buffer: 50 mM borate, pH 9.5; field: E = 330 Vcm^{-1}; UV detection at 200 nm. Sample: Fmoc amino acids.

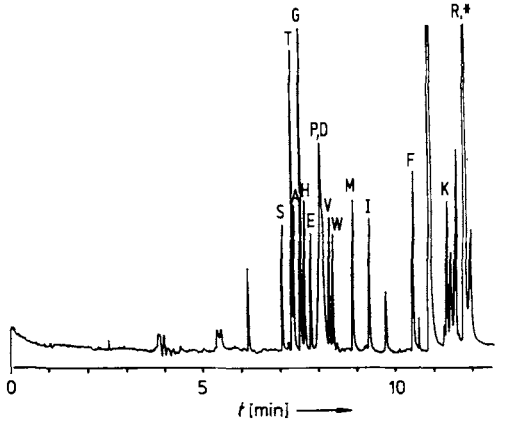

Fig. 26. Separation of 16 Fmoc amino acids by MEC. The peaks are identified by the one-letter-code for amino acids; * = system peak. Conditions: buffer: 50 mM borate, pH 9.5, 50 mM SDS; otherwise as in Figure 25.

Besides anionic detergents and organic solvents, neutral or charged components such as urea, zwitterions, and other sources of ion pairs may be added to the buffer. As the separation is based on distribution equilibria, it is naturally also temperature-dependent. Of course high concentrations of organic components cannot be used, since hardly any micelles will be formed. However, separation is still possible when the concentration of the detergent is in the submicellar range. It was possible to separate chiral compounds by adding chiral components such as alkylated amino acid derivatives and cyclodextrins to the SDS-containing buffer.[145-147] Such a system was also used to separate polycyclic aromatic hydrocarbons by MEC.[148] High concentrations of urea and cyclodextrins were used to improve the solubility of the aromatic compounds in the aqueous buffer. A typical example of the application of MEC for the separation of neutral molecules is shown in Figure 28. Since the variations with respect to both the samples to be separated and the organic additives to the aqueous buffer system appear to be unlimited, MEC is an extremely versatile technique. A very

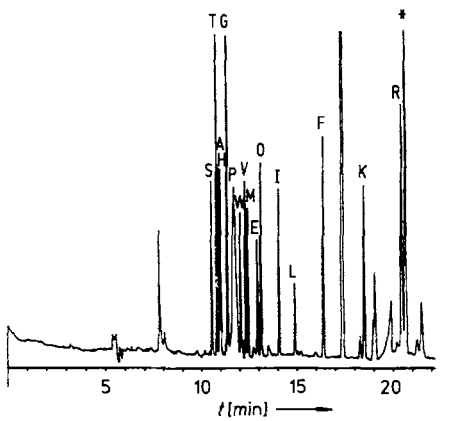

Fig. 27. Separation of 16 Fmoc amino acids by MEC with methanol as buffer additive. For peak identification see Figure 26. Conditions: buffer: 50 mM borate, pH 9.5, 50 mM SDS, 10% methanol (v/v); otherwise as in Figure 25.

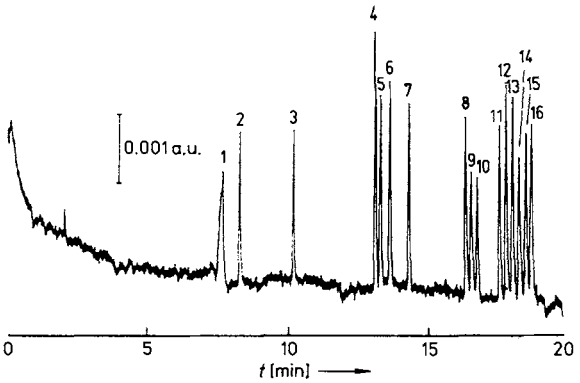

Fig. 28. Separation of phenols by MEC. Conditions: capillary: $L = 65$ cm, $ID = 50$ µm; buffer: 1 mmol SDS in 20 mM borate-phosphate buffer, pH = 7.0; field: $E = 300$ Vcm^{-1}, $I = 28$ µA; UV detection at 270 nm, $T \approx 25$ °C. Sample: 1 = water, 2 = acetylacetone, 3 = phenol, 4 = *o*-cresol, 5 = *m*-cresol, 6 = *p*-cresol, 7 = *o*-chlorophenol, 8 = *m*-chlorophenol, 9 = *p*-chlorophenol, 10 = 2,6-xylenol, 11 = 2,3-xylenol, 12 = 2,5-xylenol, 13 = 3,4-xylenol, 14 = 3,5-xylenol, 15 = 2,4-xylenol, 16 = *p*-ethylphenol (from ref. [142]). a.u. = absorption units fall scale.

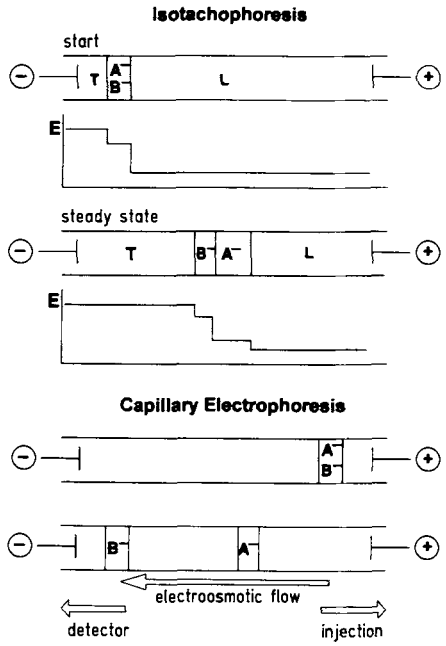

Fig. 29. Schematic comparison of ITP and CZE.

recent monograph[149] provides an excellent survey of its wide range of applications.

4.6. Isotachophoresis (ITP)

While the electrophoretic separation techniques with capillaries that we have described so far correspond to elution chromatography (discontinuous sample introduction, constant eluent composition, different rates of migration for the sample components), ITP[150] corresponds to displacement chromatography. In both cases all the components of the sample migrate with the same velocity. ITP was described many years ago and was at that time carried out in Teflon tubes. The method did not find wide use as an analytical technique because of the problems associated with the selection of suitable electrolytes. In ITP the sample is introduced between two electrolytes of different ionic mobility; these must be chosen in such a way that they limit the mobility range of the components of the sample. In general the lead electrolyte has the highest and the terminating electrolyte the lowest mobility of all the migrating ions. All ions with the same charge migrate at an equal rate when the stationary state is achieved.[151, 152] This is shown schematically in Figure 29 and compared with the potential variation in CE. For ITP the field strength is different in each zone but constant within each zone; the field jumps suddenly at the zone boundary. Thus in ITP only ions with the same charge are separated. The concentration dependence of the sample zones can be described by a square-wave function. As in displacement chromatography, the zones follow one another directly. A step-shaped signal is obtained when a conductivity detector is used.

ITP has been used mainly for the separation of inorganic ions and of organic carboxylic acids. The method is not widely used because of detection problems and the difficulty of finding suitable electrolytes for samples of unknown composition. One specific problem is that the separation of proteins and other complex mixtures requires suitable spacers, electrolytes with migration rates between those of the sample components, for better separation of the zones. Because suitable spacers are not available, ITP has hardly been used in bioanalytical work. Like displacement chromatography, ITP causes dilute samples to be concentrated and is thus useful as a concentration process prior to a CE separation.[153–156] Problems arising from the dosage of relatively large volumes of dilute samples can thus be overcome. The concentration step can be carried out directly in the separation capillary used for CE. A short zone of the lead electrolyte is introduced into the capillary filled with the separation electrolyte; then the sample is injected. Sample volumes

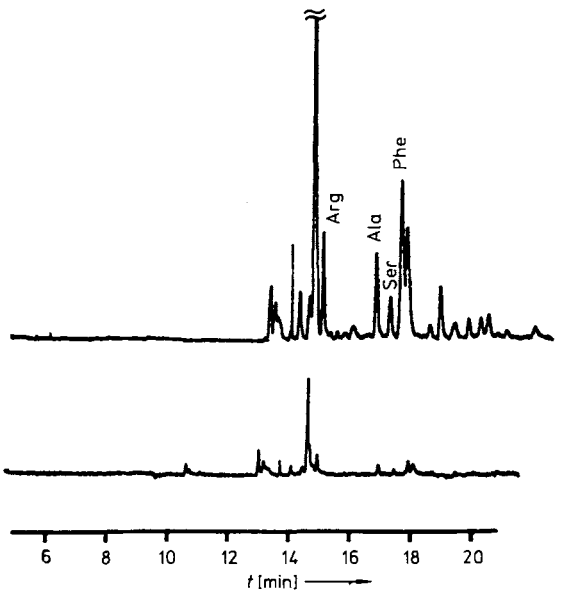

Fig. 30. Isotachophoresis for sample enrichment in CZE. Lower electropherogram: fluoresceinisothiocyanate (Fitc)-derivatized amino acids (without enrichment by ITP), injection: 2 s/5 kV, separation voltage 25 kV. Upper electropherogram: coupling of an ITP capillary to the CZE capillary. Voltage in ITP: 10 kV, in CZE: 25 kV, injection and sample as above, detection: laser-induced fluorescence at 488/514 nm (from ref. [153]).

in the μL range can be applied. The normal electrolyte is then introduced as a terminating electrolyte. The enrichment takes place in the direction of the lead electrolyte with enrichment factors of up to 100.[153, 156] It has been shown that with proteins the addition of ammonium acetate to the sample solution[157] can have the same effect; the acetate ion acts as the lead electrolyte. The coupling of two instruments, ITP for enrichment and CE for separation, each with a UV detector, has also been described.[153] When the enriched ITP zone reaches the first detector, the system is switched over to CE separation. The enrichment and subsequent CE separation achieved by such an arrangement is demonstrated in Figure 30.

4.7. Electrochromatography (EC)

Band broadening in HPLC results primarily from the parabolic flow profile and diffusion into and out of the pores of the stationary phase. Attempts have been made to reduce this contribution to band broadening by reducing the particle diameter; this reduction is opposed by the high pressure drop required. In the ideal case the EOF is independent of the particle diameter of the material used to pack the capillaries. In addition the piston-shaped flow profile of the EOF leads us to expect high separation performance. It thus appears possible in principle to combine the high selectivity of HPLC with the efficiency of CE by using packed columns.[21, 158] The separation principles and stationary phases used are those of HPLC, but the transport of ionic components is due to electric migration. Extremely small nonporous particles (1 μm in diameter) are used in order to reduce the contribution of the sorption process to band broadening. The favorable theoretical predictions for this technique have not yet been verified experimentally. The reduced plate heights achieved are not much better than those attained in HPLC.[15] One reason for this is the detection problem: in CE detection is carried out directly through the separation capillary; this is no longer possible when packed columns are used. Thus the problems known from micro-HPLC resulting from the coupling of the detector to the separation capillary also occur here.

5. Outlook

The separation systems discussed above based on electric migration are summarized in Table 5. The technique most often used is certainly CE in uncoated or surface-modified quartz capillaries (open tubes). Neutral molecules can also be separated in this system when a micelle-forming agent is added.

CE has several advantages over classical electrophoresis:
- extremely high separation efficiency,
- simple on-line detection and quantification,
- simple operation,
- short analysis times,
- simple automation,
- low consumption of buffers.

The advantages compared with HPLC are
- the high separation efficiency,
- the rapid establishment of equilibrium when the analytical conditions are changed,
- short analysis times,
- low consumption of buffers,
- minimal sample preparation (suspensions can be injected directly).

The disadvantages of CE lie in
- the use of UV detectors because of their low concentration sensitivity,
- the poor reproducibility and control of the electroosmotic flow,
- the adsorption of the analytes at the surface of the capillary, which is always accompanied by a loss of efficiency.

Commercial instruments, some already second-generation, are presently available for the routine CE analysis. This is also reflected in the nature of publications appearing, where practice-oriented papers are slowly outnumbering those describing theory and methods. Whereas in 1990 only 225 papers were listed under the heading "capillary electrophoresis" in the review volume of *Analytical Chemistry*[83] (more than half of these dating from 1988/89), the literature survey for the two following years[84] contains 523 publications. It was not our intention when compiling this article to provide a complete literature survey, but to give an objective overview (although personal preferences have certainly played a part)

Table 5. Separation systems driven by an electric field in a capillary.

Capillary zone electrophoresis	Capillary gel electrophoresis	Micellar electrokinetic chromatography	Electro-chromatography	Isotachophoresis in capillaries	Isoelectric focusing in capillaries
modified/ unmodified capillaries	modified and gel-filled capillaries	unmodified capillaries	packed capillaries	unmodified capillaries	modified/ unmodified capillaries
EOF controlled/ uncontrolled	EOF suppressed	with EOF	with EOF	with EOF	EOF suppressed/ very low
separation by electrophoretic migration; influence of EOF	separation by electrophoretic migration with sieve effect; no EOF	separation by electrophoretic migration and distribution of the sample between micelle and buffer; influence of EOF	separation by interaction with a stationary phase (LC separation system); EOF functions as pump	separation by electrophoretic migration; influence of EOF	separation according to the isoelectric point of the sample; mobilization of the sample zone towards detector not necessary when small EOF present
many applications for small and large charged molecules	separation according to molecular size of DNA molecules and SDS-denatured proteins	wide application range for small, neutral, and charged molecules	application range as for HPLC (no practical use so far)	limited application range sample preconcentration technique for CE	separation of zwitterionic samples according to their pI values

of the current scope and limiations of CE. CE complements the established separation techniques, HPLC and GC; its advantages are found in situations where the latter reach their limits, that is, in the separation of polar and ionogenic, low molecular weight materials and in the analysis of proteins and other biopolymers.

As the history of the development of the established separation techniques has shown, method-oriented publications are typically followed by those dealing with applications in various areas. The tendency of the analytical chemist to test as many separations as possible with the new technique can also be observed here. Even polycyclic aromatic hydrocarbons have been separated with CE; however, we make no comment as to whether this is a worthwhile application (see Section 4.5). Further developments are possible by coupling CE with other separation techniques and with spectroscopic techniques, in particular mass spectrometry.

The first monographs and collected editions dealing with CE have appeared or been announced.[159, 160]

Our own work in this area has been supported by the Deutsche Forschungsgemeinschaft, the Fonds der Chemischen Industrie, and by graduate scholarships provided by the Saarland to J. Kohr and T. Schmitt. We thank friends and colleagues for an intensive and fruitful exchange of ideas. T. Schmitt thanks Prof. B. L. Karger, Northeastern University, Boston, for allowing him to carry out experimental work in his laboratories. We also thank Beckman and Millipore for providing us with instruments.

Received: September 16, 1992 [A 904 IE]
German version: *Angew. Chem.* **1993**, *105*, 659
Translated by Prof. Dr. T. N. Mitchell, Dortmund (FRG)

[1] P. König, *Actas Trab. Congr. Sud. Am. Chim. III Congr. Rio de Janeiro*, **1937**, *2*, 334. See also *Arch. Pathol.* **1939**, *192*, 271.
[2] G. Berraz, *An. Asoc. Quim. Argent.* **1943**, *31*, 96.
[3] T. Wieland, *Angew. Chem.* **1950**, *62*, 31.
[4] E. L. Durrum, *J. Am. Chem. Soc.* **1950**, *72*, 2943.
[5] A. Tiselius, *Trans. Faraday Soc.* **1937**, *33*, 527.
[6] S. Hjerten, *Chromatogr. Rev.* **1967**, *9*, 122–219.
[7] R. Virtanen, *Acta Polytech. Scand. Chem. Incl. Metall. Ser.* **1974**, *123*, 1.
[8] F. E. P. Mikkers, F. M. Everaerts, T. P. E. M. Verheggen, *J. Chromatogr.* **1979**, *169*, 11.
[9] J. W. Jorgenson, K. D. Lukacs, *J. Chromatogr.* **1981**, *218*, 209.
[10] J. W. Jorgenson, K. D. Lukacs, *Anal. Chem.* **1981**, *53*, 1298.
[11] J. W. Jorgenson, K. D. Lukacs, *HRC & CC J. High. Resolut. Chromatogr. Chromatogr. Commun.* **1981**, *4*, 230.
[12] J. W. Jorgenson, K. D. Lukacs, (*Winston-Salem, N.C.*) *Clin. Chem.* **1981**, *27*, 1551.
[13] J. A. Lux, U. Häusig, G. Schomburg, *J. High. Resolut. Chromatogr.* **1990**, *13*, 373–374.
[14] J. C. Giddings, *Unified Separation Science*, Wiley, New York, **1991**.
[15] J. H. Knox, I. H. Grant, *Chromatographia* **1991**, *32*, 317–328.
[16] J. Kohr, H. Engelhardt, *J. Microcolumn Sep.* **1991**, *3*, 491–495.
[17] X. Huang, J. A. Luckey, M. J. Gorden, R. N. Zare, *Anal. Chem.* **1989**, *61*, 767.
[18] W. R. Jones, P. Jandik, *J. Chromatogr.* **1991**, *546*, 445.
[19] J. C. Giddings, *Dynamics of Chromatography, Part I: Principles and Theory*, Dekker, New York, **1965**.
[20] A. Guttman, A. S. Cohen, D. N. Heiger, B. L. Karger, *Anal. Chem.* **1990**, *62*, 137.
[21] J. H. Knox, *Chromatographia* **1988**, *26*, 329.
[22] R. J. Nelson, A. Paulus, A. S. Cohen, A. Guttman, B. L. Karger, *J. Chromatogr.* **1989**, *480*, 111–127.
[23] M. J. Sepaniak, R. O. Cole, *Anal. Chem.* **1987**, *59*, 472.
[24] M. J. Sepaniak, R. O. Cole, *Anal. Chem.* **1987**, *59*, 1470.
[25] M. J. Sepaniak, R. O. Cole, *Anal. Chem.* **1988**, *60*, 617.
[26] X. Huang, W. Coleman, R. Zare, *J. Chromatogr.* **1989**, *480*, 95.
[27] T. Tsuda, K. Nomura, G. Nakagawa, *J. Chromatogr.* **1983**, *264*, 385.
[28] H. F. Yin, S. R. Motsch, J. A. Lux, G. Schomburg, *J. High. Resolut. Chromatogr.* **1991**, *14*, 282.
[29] S. Honda, S. Iwasa, S. Fujiwara, *J. Chromatogr.* **1987**, *404*, 313.
[30] D. J. Rose, J. W. Jorgenson, *Anal. Chem.* **1988**, *60*, 642–648.
[31] H. Schwarz, M. Melera, R. Brownlee, *J. Chromatogr.* **1989**, *480*, 129.
[32] X. Huang, M. J. Gordon, R. A. Zare, *Anal. Chem.* **1988**, *60*, 375.
[33] M. E. Schwartz, Waters Division of Milipore, Poster PT-44, 3rd Int. Symp. High Perform. Capillary Electrophoresis, San Diego, CA (USA), **1991**.
[34] M. Deml, F. Foret, P. Bocek, *J. Chromatogr.* **1985**, *59*, 320.
[35] J. Tehrani, R. Macomber, L. Day, *J. High. Resolut. Chromatogr.* **1991**, *14*, 10.
[36] T. Tsuda, R. N. Zare, *J. Chromatogr.* **1991**, *559*, 103.
[37] D. Burton, M. Sepaniak, M. Maskavinec, *Chromatographia* **1986**, *21*, 583.
[38] X. Huang, J. A. Lucky, M. J. Gordon, R. N. Zare, *Anal. Chem.* **1989**, *61*, 766.
[39] K. Bächmann, T. Groh, I. Haumann, K.-H. Steeg, S. Engelmann in *Conference Report, 11th Königsteiner Chromatographietagen 1991*, GIT-Verlag, Darmstadt, **1991**, p. 76.
[40] D. S. Burgi, R. L. Chien, *J. Microcolumn Sep.* **1991**, *3*, 199–202.
[41] W. Beck, H. Engelhardt in *Conference Report, 11th Königsteiner Chromatographietagen 1991*, GIT-Verlag, Darmstadt, **1991**, p. 40.
[42] B. L. Karger, lecture at the 3rd Int. Symp. High Perform. Capillary Electrophoresis, San Diego, CA, **1991**.
[43] J. A. Lux, H. Yin, G. Schomburg, *J. High. Resolut. Chromatogr.* **1990**, *13*, 145.
[44] D. Y. Chen, H. P. Swerdlow, H. R. Harke, J. Z. Zhang, N. J. Dovichi, *J. Chromatogr.* **1991**, *559*, 237–246.
[45] H. Engelhardt in *Conference Report, 11th Königsteiner Chromatographietagen 1991*, GIT-Verlag, Darmstadt, **1991**, p. 12.
[46] G. Bruin, G. Stegeman, A. Van Asten, X. Xu, J. Kraak, H. Poppe, *J. Chromatogr.* **1991**, *559*, 163–181.
[47] J. Lindevogel, P. Sandra, L. C. Verhagen, *J. High. Resolut. Chromatogr.* **1990**, *13*, 295.
[48] S. Kobayashi, T. Udea, M. Kikumoto, *J. Chromatogr.* **1989**, *480*, 179.
[49] J. Romano, P. Jandik, W. R. Jones, P. E. Jackson, *J. Chromatogr.* **1991**, *546*, 411.
[50] F. Foret, S. Fanali, A. Nardi, P. Bocek, *Electrophoresis (Weinheim, Fed. Repub. Ger.)* **1990**, *11*, 780.
[51] W. Beck, H. Engelhardt, *Chromatographia* **1992**, *33*, 313.
[52] G. Bondoux, P. Jandik, W. Jones, *J. Chromatogr.* **1992**, *602*, 79–88.
[53] M. Koberda, M. Konkowski, P. Youngberg, W. Jones, A. Weston, *J. Chromatogr.* **1992**, *602*, 235–240.
[54] P. Jandik, W. R. Jones, *J. Chromatogr.* **1991**, *546*, 431.
[55] T. Garner, E. S. Yeung, *Anal. Chem.* **1991**, *62*, 2198.
[56] L. Gross, E. S. Yeung, *Anal. Chem.* **1990**, *62*, 427.
[57] E. S. Yeung, W. G. Kuhr, *Anal. Chem.* **1991**, *63*, 275A.
[58] C. Haber, I. Silvestri, S. Röösli, W. Simon, *Chimia*, **1991**, *45*, 117.
[59] F. E. P. Mikkers, F. M. Everaerts, T. P. E. M. Verheggen, *J. Chromatogr.* **1979**, *169*, 11.
[60] M. Ackermans, F. M. Everaets, J. L. Beckers, *J. Chromatogr.* **1991**, *549*, 335.
[61] X. Huang, R. Zare, *Anal. Chem.* **1991**, *63*, 2193.
[62] X. Huang, R. Zare, *Anal. Chem.* **1991**, *63*, 2193.
[63] X. Huang, R. Zare, S. Sloss, A. Ewing, *Anal. Chem.* **1991**, *63*, 189.
[64] X. Huang, T. Pang, M. Gorden, R. Zare, *Anal. Chem.* **1987**, *59*, 2747.
[65] R. A. Wallingford, A. G. Ewing, *Anal. Chem.* **1988**, *60*, 258.
[66] C. Engstrom-Silverman, A. G. Ewing, *J. Microcolumn Sep.* **1991**, *3*, 141.
[67] A. G. Ewing, A. Wallingford, T. Olefirowicz, *Anal. Chem.* **1989**, *61*, 292A–294A, 296A, 298A, 300A–303A.
[68] R. A. Wallingford, A. G. Ewing, *Anal. Chem.* **1988**, *60*, 1972–1975.
[69] J. Loo, H. R. Udseth, R. Smith, *J. Mikrocol. Sep.* **1989**, *1*, 5, 225.
[70] L. Hernandez, J. Escalona, N. Joshi, N. Guzman, *J. Chromatogr.* **1991**, *559*, 183–196.
[71] R. Smith, H. Udseth, C. Barinaga, C. Edmonds, *J. Chromatogr.* **1991**, *559*, 197–208.
[72] J. A. Loo, H. K. Jones, H. Udseth, R. Smith, *J. Microcolumn Sep.* **1989**, *1*, 5, 223.
[73] C. Chen, M. Morris, *Appl. Spectrosc.* **1988**, *42*, 515–518.
[74] S. Pentoney Jr., R. Zare, *Anal. Chem.* **1989**, *61*, 1643.
[75] P. Christensen, E. Yeung, *Anal. Chem.* **1989**, *61*, 1344–1347.
[76] C. Chen, T. Demana, S. Huang, M. Morris, *Anal. Chem.* **1989**, *61*, 1593.
[77] J. Wu, T. Odake, T. Katimori, T. Sawada, *Anal. Chem.* **1991**, *63*, 2216.
[78] S. Honda, S. Iwase, A. Makino, S. Fujiwara, *Anal. Biochem.* **1989**, *176*, 73–77.
[79] S. Wu, N. Dovichi, *J. Chromatogr.* **1989**, *480*, 141–156.
[80] J. Green, J. Jorgenson, *HRC & CC J. High. Resolut. Chromatogr. Chromatogr. Commun.* **1984**, *7*, 529–531.
[81] B. W. Wright, G. A. Roos, R. D. Smith, *J. Microcolumn Sep.* **1989**, *1*, 85–89.
[82] D. Perrett, G. Ross, Poster M4 at the 4th Int. Symp. High Perform. Capillary Electrophoresis, Amsterdam, **1992**.
[83] W. G. Kuhr, *Anal. Chem.* **1990**, *63*, 403R–414R.
[84] W. G. Kuhr, *Anal. Chem.* **1992**, *64*, 389R–407R.

[85] A. E. Vorndran, P. J. Oefner, H. Scherz, G. K. Bonn, *Chromatographia* **1992**, *33*, 163–168.
[86] H. H. Lauer, D. McManigill, *Anal. Chem.* **1986**, *58*, 166–170.
[87] J. S. Green, J. W. Jorgenson, *J. Chromatogr.* **1989**, *478*, 63–70.
[88] M. Bushey, J. Jorgenson, *J. Chromatogr.* **1989**, *480*, 301–310.
[89] J. A. Bullock, L. C. Yuan, *J. Microcolumn Sep.* **1991**, *3*, 241–248.
[90] Waters Application Note 1991, Waters Division of Millipore.
[91] J. K. Towns, F. E. Regnier, *Anal. Chem.* **1991**, *63*, 1126–1132.
[92] A. Emmer, M. Jansson, J. Roerade, *J. Chromatogr.* **1991**, *547*, 544–550.
[93] E. Kenndler, K. Schmidt-Beiwl, *J. Chromatogr.* **1991**, *545*, 397–402.
[94] J. Jorgensen, K. Lukacs, *Science* **1983**, *222*, 266–272.
[95] A. Balchumas, M. Sepaniak, *Anal. Chem.* **1987**, *59*, 1466–1470.
[96] A. Dougherty, C. Woolley, D. Williams, D. Swaile, R. Cole, M. Sepaniak, *J. Liq. Chromatogr.* **1991**, *14*, 907–921.
[97] M. Sepaniak, D. Swaile, A. Powell, R. Cole, *J. High. Resolut. Chromatogr.* **1990**, *13*, 679.
[98] G. Bruin, J. Chang, R. Kuhlman, K. Zegers, J. Kraak, H. Poppe, *J. Chromatogr.* **1989**, *471*, 429–436.
[99] G. Bruin, R. Huisden, J. Kraak, H. Poppe, *J. Chromatogr.* **1989**, *480*, 339–349.
[100] R. McCormick, *Anal. Chem.* **1988**, *60*, 2322–2328.
[101] S. Swedberg, *Anal. Biochem.* **1990**, *185*, 51–56.
[102] Y.-F. Maa, K. Hyver, S. Swedberg, *J. High Resolut. Chromatogr.* **1991**, *14*, 65.
[103] S. Hjerten, *J. Chromatogr.* **1985**, *347*, 191–197.
[104] S. Hjerten, K. Ellenbring, F. Kilar, J. Liao, *J. Chromatogr.* **1987**, *403*, 47–61.
[105] K. Cobb, V. Dolnik, M. Novotny, *Anal. Chem.* **1990**, *62*, 2478–2483.
[106] M. Strege, A. Lagu, *Anal. Chem.* **1991**, *63*, 1233–1236.
[107] C. Bolger, M. Zhu, R. Rodriguez, T. Wehr, *J. Liq. Chromatogr.* **1991**, *14*, 895–906.
[108] F. Regnier, J. Towns, *J. Chromatogr.* **1990**, *516*, 69–78.
[109] D. Bentrop, J. Kohr, H. Engelhardt, *Chromatographia* **1991**, *32*, 171–178.
[110] S. Terabe, H. Utsumi, K. Otsuka, T. Ando, T. Inonata, S. Kuze, Y. Hanaoka, *J. High. Resolut. Chromatogr. Chromatogr. Commun.* **1986**, *9*, 666.
[111] J. Lux, H. Yin, G. Schomburg, *J. High Resolut. Chromatogr.* **1990**, *13*, 145.
[112] S. Mayer, V. Schurig, *J. High. Resolut. Chromatogr.* **1992**, *15*, 129–131.
[113] J. Kohr, Dissertation, Universität des Saarlandes, **1992**.
[114] P. C. Righetti, *Isoelectric Focusing: Theory, Methodology and Applications*, Elsevier, Amsterdam, **1983**.
[115] P. G. Righetti, *Immobilized pH Gradients: Theory and Methodology*, Elsevier, Amsterdam, **1990**.
[116] P. G. Righetti, *Sep. Purif. Methods* **1975**, *4*, 23.
[117] B. J. Radola in *Isoelectric Focusing* (Ed.: N. Catsimpoolas), Academic Press, New York, **1976**, p. 119ff.
[118] A. Chrambach, N. Y. Nguyen in *Electrokinetic Separation Methods* (Eds.: P. G. Righetti, C. J. van Oss, J. W. Vanderhoff), Elsevier, Amsterdam, **1979**, pp. 337–368.
[119] S. Hjerten, *J. Chromatogr.* **1985**, *347*, 191.
[120] S. Hjerten, J. L. Liao, *Protides Biol. Fluids* **1986**, *34*, 727.
[121] S. Hjerten, K. Ellenbring, F. Kilar, J. L. Jiao, A. J. C. Chen, C. J. Siebert, M. D. Zhu, *J. Chromatogr.* **1987**, *403*, 47.
[122] F. Kilar, S. Hjerten, *Electrophoresis* (*Weinheim, Fed. Repub. Ger.*) **1989**, *10*, 23.
[123] J. R. Mazzeo, I. S. Krull, *Anal. Chem.* **1992**, *63*, 2852.
[124] R. Nelson, A. S. Cohen, R. S. Rush, B. L. Karger, Beckman Application Data, Separation of Proteins by IEF Capillary Electrophoresis, **1991**.
[125] L. M. Smith, *Nature* **1991**, *349*, 812–813.
[126] A. S. Cohen, D. R. Najarian, B. L. Karger, *J. Chromatogr.* **1990**, *516*, 49.
[127] A. S. Cohen, D. R. Najarian, B. L. Karger, *J. Chromatogr.* **1990**, *516*, 59–60.
[128] P. Bocek, A. Chrambach, *Electrophoresis* (*Weinheim, Fed. Repub. Ger.*) **1992**, *13*, 18–31.
[129] M. Strege, A. Lagu, *Anal. Chem.* **1991**, *63*, 1233.
[130] S. R. Motsch, M. H. Kleemiss, G. Schomburg, *J. High. Resolut. Chromatogr.* **1991**, *14*, 628.
[131] D. N. Heiger, A. S. Cohen, B. L. Karger, *J. Chromatogr.* **1990**, *516*, 33.
[132] H. F. Yin, J. A. Lux, G. Schomburg, *J. High. Resolut. Chromatogr.* **1990**, *13*, 625.
[133] H. F. Yin, M. H. Kleemiss, J. A. Lux, G. Schomburg, *J. Microcolumn Sep.* **1991**, *3*, 331.
[134] J. A. Lux, H. F. Yin, G. Schomburg, *J. High Resolut. Chromatogr.* **1990**, *13*, 437.
[135] S. Nathakarnkitkool, P. J. Öfner, G. Bartsch, M. A. Chin, G. K. Bonn, *Electrophoresis* (*Weinheim, Fed. Repub. Ger.*) **1992**, *13*, 18–31.
[136] J. Sudor, F. Foret, P. Bocek, *Electrophoresis* (*Weinheim, Fed. Repub. Ger.*) **1991**, *12*, 1056–1058.
[137] T. Schmitt, Diplomarbeit, Universität des Saarlandes, **1991**.
[138] S. Wicar, M. Vilanchek, A. Belenkii, A. S. Cohen, B. L. Karger, *J. Microcolumn Sep.* **1992**, *4*, 339.
[139] M. Strege, A. Lagu, *Anal. Chem.* **1991**, *63*, 1233–1236.
[140] K. Ganzler, K. S. Greve, A. S. Cohen, B. L. Karger, A. Guttman, N. C. Cooke, *Anal. Chem.* **1992**, *64*, 2665.
[141] A. S. Cohen, B. L. Karger, *J. Chromatogr.* **1987**, *397*, 409–417.
[142] S. Terabe, K. Otsuka, K. Ichikawa, A. Tsuchiya, T. Ando, *Anal. Chem.* **1984**, *56*, 111–113.
[143] S. Terabe, K. Otsuka, T. Ando, *Anal. Chem.* **1985**, *57*, 834–841.
[144] A. G. Ewing, A. Wallingford, *Adv. Chromatogr.* **1989**, *29*, 1.
[145] S. Terabe, M. Shibata, Y. Miyashita, *J. Chromatogr.* **1989**, *480*, 403.
[146] K. Otsuka, S. Terabe, *J. Chromatogr.* **1990**, *515*, 221–226.
[147] A. Dobashi, T. Ono, S. Hard, J. Yamaguchi, *Anal. Chem.* **1989**, *61*, 1984.
[148] S. Terabe, Y. Miyashita, O. Shibata, E. Barnhaut, C. Alexander, B. Patterson, B. L. Karger, K. Hosoya, N. Tanaka, *J. Chromatogr.* **1990**, *516*, 23–31.
[149] J. Vindevogel, P. Sandra, *Introduction to MEC* in *Chromatographic Methods*, Hüthig, Heidelberg, **1992**.
[150] Conference Report: 7th Int. Symp. on CE and ITP (*J. Chromatogr.* **1991**, *545*, 2).
[151] *New Directions in Electrophoresis*, (Eds.: J. W. Jorgenson, N. Philips), (*ACS Symp. Ser.* **1987**, *33*).
[152] *Analytical Isotachophoresis*, (Eds.: P. Bocek, M. Deml, P. Gebauer, V. Dolnik, B. J. Radola), VCH Publishers, New York, **1988**.
[153] D. S. Steghehuis, H. Irth, U. R. Tjaden, J. Van der Greef, *J. Chromatogr.* **1991**, *538*, 393–402.
[154] D. Kaniansky, J. Marak, *J. Chromatogr.* **1990**, *498*, 191.
[155] V. Dolnik, K. A. Cobb, M. Novotny, *J. Microcolumn Sep.* **1990**, *2*, 127.
[156] L. Krivankova, F. Foret, P. Bocek, *J. Chromatogr.* **1991**, *545*, 307.
[157] B. L. Karger, lecture at the 16th Int. Symp. Column Liq. Chromatogr. Baltimore (USA), **1992**.
[158] J. H. Knox, I. Grant, *Chromatographia* **1987**, *24*, 135–143.
[159] N. Guzman, *Capillary Electrophoresis*, Dekker, in press.
[160] S. F. Y. Li, *Capillary Electrophoresis* (*J. Chromatogr. Libr.* **1992**, *52*).

The Coordination Chemistry of Multidentate Isocyanide Ligands

By F. Ekkehardt Hahn*

In spite of the excellent ligation properties of isocyanides, until a few years ago there was only a small number of known multidentate ligands of this type. One of the reasons for this lack of interest, when compared to monodentate isocyanides, was the linear arrangement of the M–C≡N–R group, which usually inhibits the formation of mononuclear chelate complexes and leads to the formation of multinuclear or polymeric metal complexes. In these, the multidentate ligand acts in a monodentate fashion towards each metal atom. Only recently has a series of polyisocyanides with large ligand backbones been synthesized successfully. Bidentate isocyanides can bridge two metal atoms or react to give chelates with only one metal center. Tripodal ligands form mono- or binuclear complexes, in which the largest organometallic rings observed to date occur (up to 36 atoms). This class of ligands promises to be interesting for the synthesis of stable, diagnostically important technetium complexes of the type $[Tc(CNR)_6]^+$. There also appear to be applications for tripodal isocyanides in catalysis. A facial, chiral $Cr(CNR^*)_3$ unit might be able to catalyze the hydrogenation or isomerization of prochiral double bonds. It is even possible to bind triisocyanides with suitable backbones to carbonyl trimetal clusters, thereby stabilizing them, or making selective cluster formation possible. Coordinated isocyanides can be transformed readily into carbene ligands, which, in the future, could lead to complexes with polycarbene ligation.

1. Introduction

The almost simultaneous discovery of isocyanides by Gautier[1] and Hoffmann[2] more than one hundred years ago posed a series of interesting questions for chemists of the time. Was it indeed possible that in the case of the newly synthesized ethylisocyanide, in contrast to the known propionitrile, "the carbon of the ethyl group is soldered to the molecule by attachment to the nitrogen"?[1b] and could the carbon be present in these compounds in the divalent state? It was probably not the "very uncomfortable odor"[3] of volatile isocyanides, described by one of the discoverers, which hindered further investigations, but rather the fact that these compounds were only accessible by the difficult and frequently low-yield transformation of metal cyanides with alkyl iodides.[4] Only the fundamental work by Ugi et al.[5] regarding the dehydration of formamides with phosgene led to a convenient and versatile method for the synthesis of isocyanides[4] and opened the door for the study of these interesting compounds and their metal complexes.[6]

Today, an almost countless number of isocyanides is known, some of which have significant synthetic potential. An example are the alkylisocyanides, which can be α-metalated, and have been shown to be synthons for α-metalated primary amines.[7] However, even today simple isocyanides such as isocyanogen[8a] and diisocyan[8b] are a challenge for the synthetic chemist. A further simple isocyanide that is difficult to prepare is ethynyl isocyanide (**1**),[9] which has been shown to exist in interstellar space.[10] A number of isocyanides with fluorinated side chains[11] or even naturally occurring isocyanides have since become known, for example, the antibiotic xanthocillin (**2**),[12] or (±)-9-isocyanopupukeanane (**3**), for which an X-ray structure analysis[13] and a total synthesis[14] have been performed.

Isocyanides have also achieved importance in coordination and organometallic chemistry. Their excellent ligation properties, as well as the wide potential for substitution at the side chain, have led to a substantial chemistry of isocyanide metal complexes.[6] Coordinated isocyanides can be transformed into carbenes[15] (even hexacarbene complexes are possible[15a]) and can be used for forming C–C bonds.[16] Trichloromethylisocyanide complexes[17] and anionic transition metal complexes of isocyanides[18] have been prepared and shown to have valuable synthetic applications. Even the structure of an isocyanide deprotonated at the α-carbon atom has been characterized by X-ray crystallography.[19] The use of monodentate isocyanide ligands shows great promise in medical diagnostic applications. For instance, hexaisocyanide complexes of the monochromatic γ emitter ^{99m}Tc **4**[20] are very useful for radiological diagnoses because of the excellent radiophysical properties of this technetium isotope,[21] in particular, for the imaging of blood flow in the heart.[22]

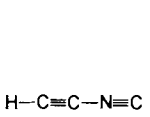

1

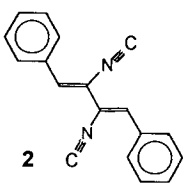

2

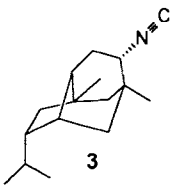

3

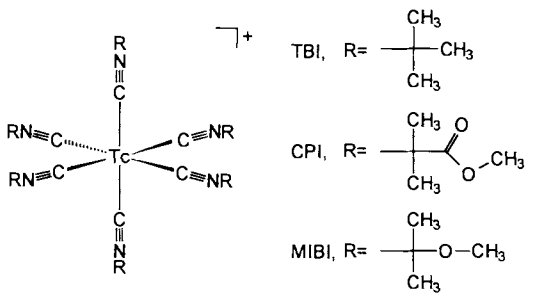

4

[*] Prof. Dr. F. E. Hahn
Institut für Anorganische und Analytische Chemie der Freien Universität
Fabeckstrasse 34–36, D-W-1000 Berlin 33 (FRG)

The reactivity and coordination chemistry of multidentate isocyanides are relatively unexplored, in comparison with the corresponding knowledge about monodentate isocyanide ligands. This is unfortunate insofar as multidentate ligands are expected to exhibit special properties, for instance the chelate effect. For multidentate isocyanides, however, the rigid linear M–C≡N–R unit usually prohibits the formation of chelates and leads instead to di- or multinuclear metal complexes **5**. In these complexes, the multidentate isocyanide ligand functions only as a monodentate base towards each metal atom. Only ligands with a sufficiently large number of atoms in the backbone between the isocyanide groups satisfy the stereochemical requirements for the formation of chelate complexes **6**.

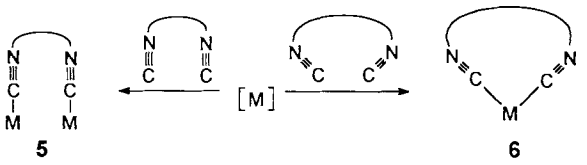

5 **6**

Model studies with rhodium complexes of bidentate aliphatic isocyanide ligands[23, 24] have shown that at least seven methylene groups between the isocyanide functionalities are necessary for chelate formation. The reasons for this special situation become clear when the structural parameters of an ethylenediamine complex (**7**) are compared with those of two *cis*-oriented isocyanide units in an octahedral or square-planar complex (**8**; Scheme 1).

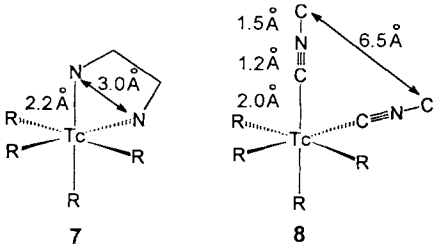

7 **8**

Scheme 1. Selected bond lengths in ethylenediamine and isocyanide technetium complexes (average values). Left: in the $Tc(H_2NCH_2CH_2NH_2)_2$ unit of *trans*-$[TcO_2(en)_2]^+$ [25]; right: in the $[Tc(CN\text{-}t\text{Bu})_4(bpy)]^+$ ion [26].

If ideal geometry is assumed, the distance between the nitrogen atoms in **7** is about 3.0 Å, whereas in the isocyanide complex **8** the carbon atoms that need to be linked for chelate formation are separated by more than 6.5 Å. Even when a nonideal geometry (C-Tc-C < 90°) is assumed, the distance to be bridged is still about 6 Å. The necessity of a large number of atoms in the backbone between two isocyanide functionalities leads to large chelate rings (a 12-membered ring would form in a chelate complex with 1,7-heptanediisocyanide), which in turn diminishes the chelate effect. This sterically unfavorable situation is the reason for the underdeveloped state of the coordination chemistry of multidentate, potentially chelating, isocyanide ligands.

However, recently there has been an increase in the interest in coordination compounds with polyisocyanide ligands. Apart from the academic interest in the formation of chelate complexes despite the mentioned steric obstacles, other aspects related to the application of this chemistry have surfaced. For instance, for the complexation of ^{99m}Tc, chelating isocyanide ligands are an interesting alternative to the currently employed monodentate ligands.

Furthermore, there are potential applications for tripodal triisocyanide ligands in organic synthesis. Labile [(arene)Cr-$(CO)_3$] complexes **9** (arene = naphthalene, phenanthrene) are effective catalyst precursors for hydrogenation[27] and isomerization[28] reactions. The catalytically active $Cr(CO)_3$ fragment **10a**, which has three open coordination sites, is generated by the dissociation of the arene ligand from **9**. In spite

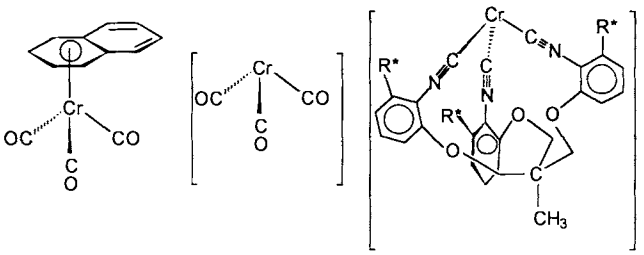

9 **10a** **10b**

of a number of attempts to obtain a chiral CrL_3 fragment corresponding to $Cr(CO)_3$,[29] it has so far been impossible to prepare a chiral catalyst. To achieve high catalyst activity,

F. Ekkehardt Hahn was born in Jena in 1955. He studied chemistry up to the Vordiplom (1978–1981) at the Technischen Universität (TU) Berlin, and thereafter he was awarded a Fullbright travel grant and continued his studies at the University of Oklahoma (Prof. J. J. Zuckermann). After obtaining his Master of Science he returned to Berlin in 1982, where he completed his Diplom in 1983 and his dissertation in 1985 on the synthesis and X-ray structures of organolanthanide compounds with Prof. H. Schumann. From 1985–88 he was a postdoctoral fellow with Prof. K. N. Raymond at the University of California, Berkeley (initially with a NATO research fellowship). 1988–1990 he completed his habilitation at the TU Berlin with studies on the use of technetium complexes for radiodiagnostic applications. In 1991 he was appointed Privatdozent and awarded a Karl Winnacker fellowship. Since March 1992 he has been a Professor of Inorganic Chemistry at the Freien Universität Berlin. His main areas of research are the development of multidentate ligands and their use for the selective complexation of technetium, gadolinium, and copper, as well as the organometallic chemistry of isocyanides and carbenes.

the ligands of the CrL_3 units must be good π acids and be facially oriented. These conditions should be fulfilled by complexes of chiral-substituted tripodal triisocyanides **10b**, in which the function and positions of the three facial CO groups in **10a**[30] are assumed by the linked isocyanide units.

2. Bidentate Isocyanide Ligands

The coordination compounds of bidentate isocyanide ligands can be separated into three general categories. The first contains multinuclear complexes without direct metal–metal interactions between the complexed metal atoms. The second category encompasses those metal complexes in which the bidentate isocyanide ligand bridges two metals in such a fashion that direct metal–metal interactions are possible after complexation by the ligands, and the third category comprises mononuclear chelate complexes with diisocyanide ligands.

2.1. Binuclear and Polymeric Complexes without Metal–Metal Interactions

The bidentate, "rigid" isocyanides 1,3-phenyldiisocyanide, 2,4-tolyldiisocyanide, or 4,4'-diphenylmethanediisocyanide employ bent bridges to link the metal atoms. These ligands react with $[\{Rh(CO)_2Cl_2\}_2]$, yielding two-dimensional, insoluble coordination polymers $[Rh(bridge)_2Cl \cdot xH_2O]_n$ (Fig. 1) with an interlayer distance between 3.21 and 3.36 Å. The

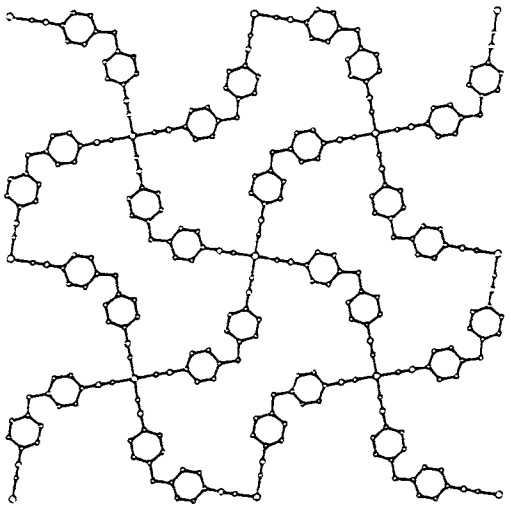

Fig. 1. Structural model of the two-dimensional, layer-type coordination polymer $[Rh(4,4'\text{-diphenylmethanediisocyanide})_2Cl \cdot H_2O]_n$ [31].

term template polymerization has been coined to describe this type of reaction.[31] When 1,4-phenyldiisocyanide or 4,4'-biphenyldiisocyanide are used as ligands, linearly bridged coordination polymers can be obtained.[32] The reaction of the linear ligand 1,4-phenyldiisocyanide with metallamacrocycles such as tetrabenzylphorphyrin iron, yields linear dimers, trimers, and polymers.[33] These polymers are formed by the use of the two axial coordination sites at the metal center. Compounds of this type were developed in the hope of obtaining one-dimensional polymers with cofacial π systems for semiconductor applications.

By using appropriate starting materials, bidentate phenyldiisocyanide ligands can also be used to prepare monomeric complexes. For instance, 1,4-phenyldiisocyanide reacts with two equivalents of $[Et_4N]^+[W(CO)_4(PR_3)Cl]^-$ to give the binuclear complex $[(CO)_4(PR_3)W\text{–}CNC_6H_4NC\text{–}W(CO)_4(PR_3)]$.[34] The reaction of 1,2-phenyldiisocyanide, which has only recently become available in good yields,[35] with $[ClAuSMe_2]$ affords the binuclear complex $[C_6H_4(NC\text{–}AuCl)_2]$.[36] A completely different path to binuclear diisocyanide-bridged complexes has been reported by D. Lentz et al. They found that, when heated, $[(CO)_5Cr(CN\text{–}CF{=}CF_2)]$ dimerizes to give the 1,2-substituted hexafluorocyclobutane complexes **11a,b** (Scheme 2).[37]

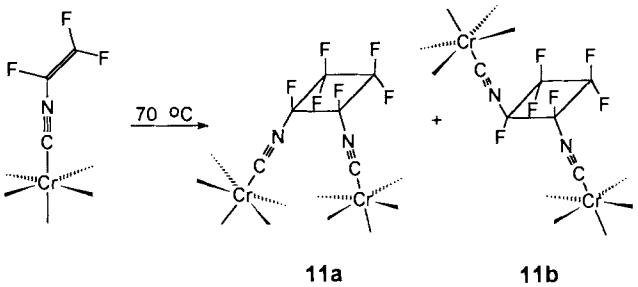

Scheme 2. Dimerization of $[(CO)_5Cr\{CNC(F){=}CF_2\}]$.

A multitude of other [M-CN-R-NC-M] complexes of type **5** with different metals and bridging groups R, are known.[6] Their complete enumeration here, however, would exceed the scope of this survey.

2.2. Bidentate Complexes with Metal–Metal Interactions

Tetra(arylisocyanide)rhodium(I) complexes aggregate in solution to give higher oligomers with $Rh^I\text{–}Rh^I$ bonds.[38] This leads to the possibility of a two-center oxidative addition. To investigate this aspect in more detail, bridged $Rh^I\text{–}Rh^I$ complexes of type **12** with four diisocyanide ligands (with 1,3-propanediisocyanide **13**[39] and 2,5-dimethylhexane-2,5-diisocyanide **14** as ligands) were synthesized and structurally characterized.[40]

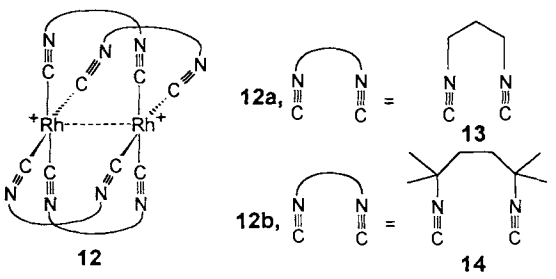

The ligand geometry was chosen so that chelate formation with a single metal atom was impossible, but that a Rh–Rh'

unit could be "clamped" together. Despite the increase in the length of the bridge between the isocyanide functionalities in **14** compared to **13**, the Rh–Rh distances in **12a** (3.242(1) Å) and **12b** (3.262(1) Å) are nearly identical. The expected interaction between the two Rh^{I} centers is confirmed by the Rh–Rh distance, the dark blue color of **12a**, and by the fact that CH_3I is oxidatively added, forming yellow $[Rh_2(\mathbf{13})_4(CH_3)(I)]^{2+}$. The reaction of **12a** with HCl yields a similar complex, which, upon irradiation (546 nm, 12 M HCl) forms the yellow Rh_2^{II} complex **15** and one equivalent of H_2. While the importance of this photoinduced redox reaction was recognized immediately, the storage of solar energy by using **12a** is still a long way away.[41] The X-ray crystal structure of **15**, which is more readily obtained by the oxidation of **12a** with Cl_2, confirms the expected shortening of the Rh–Rh distance in comparison to that in **12a,b** to 2.837(1) Å; the structure of **15** is built from two square-pyramidal $Rh^{II}C_4Cl$ units.[42]

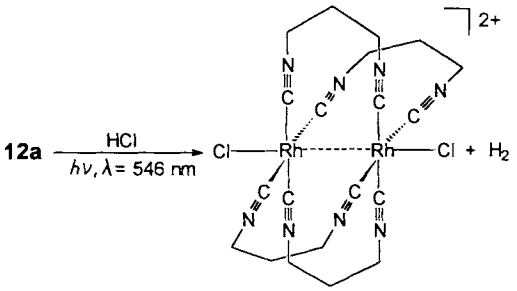

15

The span width of the diisocyanide ligand was further increased by the use of 1,8-*p*-menthanediisocyanide **16**. This ligand also forms a rhodium complex of type **12**, but with a large (4.479(2) Å) Rh–Rh separation.[43] The more interesting reaction is that of **16** with divalent transition metals. In the binuclear Pd^{II} complex **17**[44] the metal–metal distance is large enough for Cl^- or Br^-, but not the larger thiocyanate, to be inserted. Iodine is also not inserted in the Pd–Pd bond, but reacts with **17** to give the doubly bridged complex **18**.

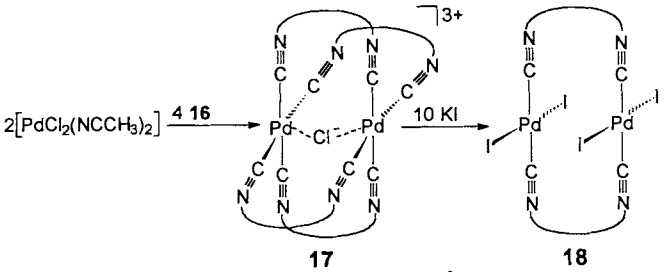

17 **18**

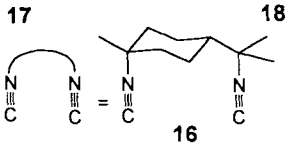

16

Halides are also inserted in the reaction of NiX_2 (X = Cl, Br) with **16**.[45] In the binuclear rhodium(I) or iridium(I) complexes of **16** this is not the case, even though structurally they are in a position to do so. This observation is most likely due to the lower charge compared to Ni^{II} or Pd^{II} complexes.[44]

2.3. Chelate Complexes with Diisocyanide Ligands

The isocyanides presented in Sections 2.1 and 2.2 do not fulfill the structural requirements for the coordination of both CN groups to a single metal center. As early as 1978, a number of research groups began work on the problem of whether diisocyanides can be constructed in such a manner as to allow the formation of mononuclear chelate complexes. Early model studies gave indications that 1,7-heptanediisocyanide should be capable of this coordination behavior.[23] The formed metallacycle would then be 12-membered. The first experiments led to the postulation of compounds of type **19**, in which two diisocyanide ligands form a square-planar Rh^{I} chelate complex. When present in suitable concentrations the metal complexes aggregate in solution to give oligomers, as has also been observed for mononuclear complexes of the type $[Rh(CNR)_4]^+$.[38] Chelate formation was proposed based on geometric considerations and the electronic spectra of the compounds.[23]

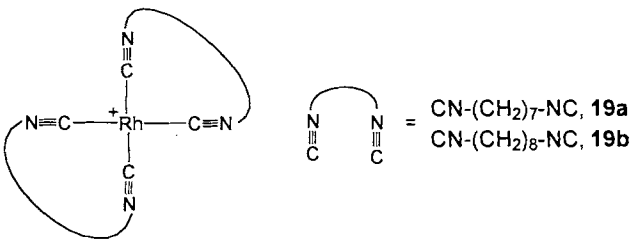

19

Another early report deals with substitution reactions on complexes of type **19b**.[24] One of the bidentate diisocyanide ligands in **19b** can be substituted by PPh_3 or $Ph_2PCH_2CH_2PPh_2$, leading to phosphane-substituted chelate complexes with only one coordinated bidentate diisocyanide.[24] So far, it has not been possible to characterize one of these complexes by X-ray structure analysis.

The first unambiguous proof for the formation of chelate complexes by bidentate diisocyanides was provided by R. J. Angelici et al. in 1982 by using aromatic diisocyanides. The ligands **20a** and **20b** have eight atoms between the isocyanide groups (roughly equivalent to the eight methylene groups in **19b**). They were prepared by etherification of the correspond-

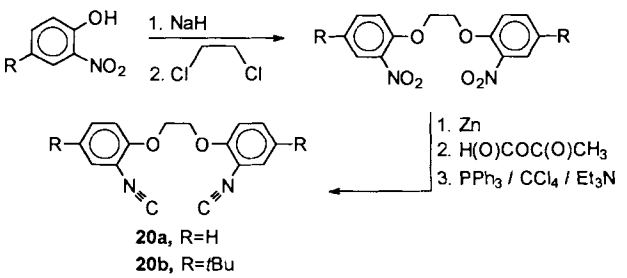

20a, R=H
20b, R=*t*Bu

ing nitrophenols with 1,2-dichloroethane, reduction and formylation of the nitro group, and finally dehydration of the obtained diformamides.[46]

The trimethylsiloxy-substituted compounds **20c** and **20d** were prepared by an interesting variation of this synthesis. First, two 4-hydroxybenzoxazole units were linked by an ethylene (**20c**) or trimethylene (**20d**) group. The isocyanide functionalities were deprotected by lithiation and subsequent silation of the benzoxazole oxygen atom.[47] The use of $ClSiMe_3$ led to exclusive silation of the oxygen atom. The reverse reaction (Si–O cleavage with KF) for coordinated 2-siloxyphenylisocyanides leads to carbene complexes in high yields, by a nucleophilic attack of the oxygen atom at the isocyanide nitrogen atom (see Section 3.4).

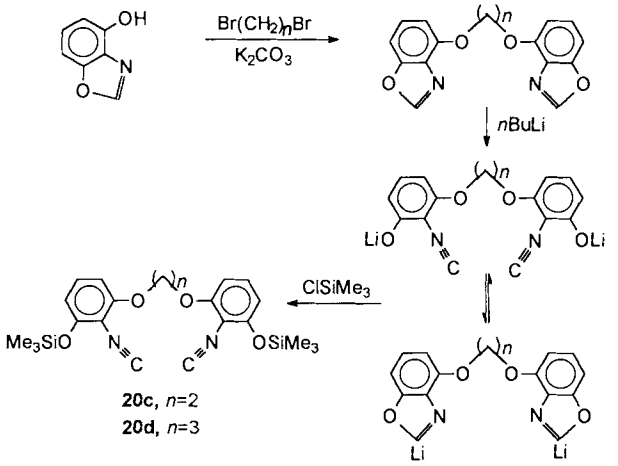

The reaction of **20b** with $[\{Rh(cod)Cl\}_2]$, followed by anion exchange with $NaBPh_4$, leads in good yield (81%) to crystalline $[Rh(\mathbf{20b})_2]BPh_4 \cdot 1.5\,CH_3CN$.[48] The X-ray structure analysis shows that the Rh^I ion is surrounded in a square-planar fashion by two chelating ligands (Fig. 2).[47] The 13-membered chelate rings formed in this complex are among the largest known for organometallic compounds. In solution the Rh complex forms oligomers, while in the crystal two cations form a dimer with a Rh^I–Rh^I distance of 3.384 Å.[48]

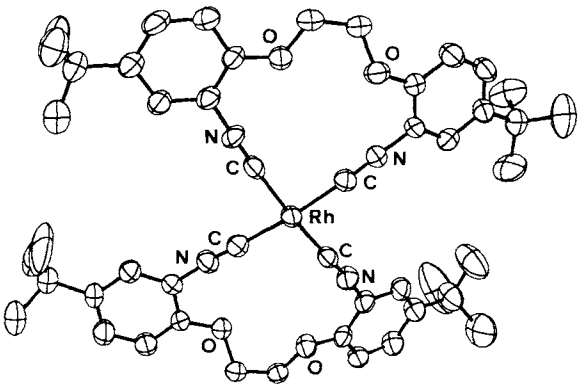

Fig. 2. Molecular structure of the cation in $[Rh(\mathbf{20b})]BPh_4 \cdot 1.5CH_3CN$ [47]. The Rh^I ion is in a square-planar environment.

Analogous, but crystallographically uncharacterized cationic Rh^I complexes are formed with the ligand **20a**.[48] Ligand **20c** does not form chelates, but binuclear cations with four diisocyanide bridges $[Rh_2(\mathbf{20c})_4]^{2+}$, which are structurally equivalent to complex **12**. In a rigid chelate complex, it is probably impossible to arrange the sterically demanding trimethylsiloxy groups in a noninterfering manner. In contrast the slightly bigger ligand **20d** forms monomeric Rh^I chelate complexes. In this case, the trimethylsiloxy groups inhibit the formation of oligomers in solution.

Ligand **20a** can be used to obtain complexes like $[(CO)_4M(\mathbf{20a})]$ (M = Cr, Mo, W),[46] as well as *cis* and *trans* isomers of $[Fe(\mathbf{20a})_2Cl_2]$.[49] Even though these complexes have not been structurally characterized, a multitude of spectroscopic data in addition to the proven ability of **20b** for chelate formation makes the likelihood that these compounds are also chelate complexes very high.

Even a reduction in the number of atoms in the backbone between the isocyanide groups still allows chelate complex formation. While **20a–c** have eight and **20d** even nine atoms in the backbone, **21** has only seven atoms between the isocyanide groups. This is approximately equivalent to seven methylene groups and corresponds to the smallest proposed potentially chelating diisocyanide so far.[23]

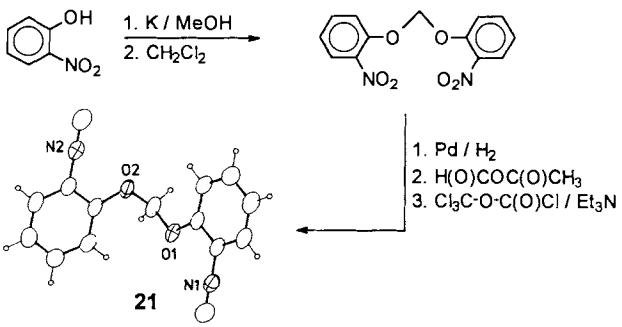

Compound **21** was obtained in 45% yield by the etherification of two equivalents of *o*-nitrophenol with dichloromethane,[50] reduction of the nitro group by Pd/H_2, formylation of the resulting amine, and finally dehydration of the diformamide according to the method of Ugi et al.[51] The X-ray structure analysis of the free ligand shows no abnormalities. The bond lengths in the phenoxyisocyanide groups ($d(C{\equiv}N)$ = 1.150(3) and 1.153(3) Å) correspond to those found in monodentate phenylisocyanides.[52]

In analogy to **20a,b**, **21** reacts with $[(C_7H_8)M(CO)_4]$ (C_7H_8 = norbornadiene, M = Cr,Mo) to form the chelates **22**.[51] The evidence for the formation of mononuclear chelate complexes includes the good solubility in dichloromethane,

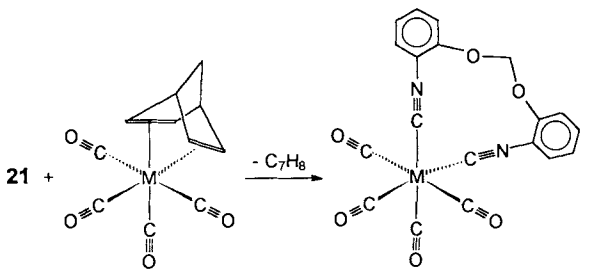

the appearance of the molecular ion in the mass spectrum, as well as spectroscopic data. The IR spectra are very similar to those of [(CO)$_4$M(**20a**)].[46] The spectrum of **22a** exhibits fewer than the four allowed CO absorption bands, but the broadness and intensity of bands at lower wavenumbers make the overlap of two absorption bands in this region quite probable. A similar situation is found with *cis*-[(CO)$_4$M(CN-*p*-tol)$_2$] (M = Cr, Mo; tol = tolyl).[53] Furthermore, two CN absorption bands are found for **22**, while only one is expected for a binuclear complex [{(CO)$_5$M}$_2$**22**].

3. Tridentate Isocyanide Ligands

Until the beginning of the 1990s, almost nothing was known about the synthesis or the coordination chemistry of triisocyanides. Such ligands could in principle have either linear topology such as **23** or a tripodal topology such as **24**. A report describing the synthesis of a linear triisocyanide was published in 1990. The ligand was obtained by coupling of α-metalated diphenylmethylisocyanide[7] with 1,3-dibromopropane.[54] The coordination chemistry of this ligand has not yet been explored.

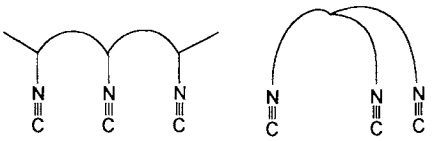

23 **24**

Tripodal isocyanides were unknown until 1990, with the exception of a few compounds that did not act as tripods.[5b, 55] However, more recently, the synthesis of a number of such ligands has been completed.[56–64] They exhibit an interesting coordination chemistry and are, in some instances, capable of forming mononuclear chelate complexes despite the linear M–C≡N–R unit in the metal complex. In some cases this leads to very large organometallic rings. Also a triangular M_3 plane in carbonyl trimetal clusters like [$Os_3(CO)_{12}$] can be bridged. The coordination chemistry of tripodal triisocyanides will be presented in the following sections.

3.1. Chelate Complexes with Tripodal Aromatic Triisocyanide Ligands

The driving force for the development of chelating tripodal aromatic triisocyanides was the search for new ligands for the complexation of ^{99m}Tc. In the first successful synthesis three *o*- or *m*-nitrophenol units were linked with tris-(3-chloropropyl)amine by a Williamson etherification. This backbone topology had been successful in the synthesis of tricatechol ligands,[65, 66] while neither tris(2-chloroethyl)amine nor tris-(4-chlorobutyl)amine are suitable for backbone construction due to their tendency for ring formation. The obtained trinitro compounds can be transformed into the tripodal aromatic triisocyanides **25**[56, 57] and **26**[58] by reduction of the nitro

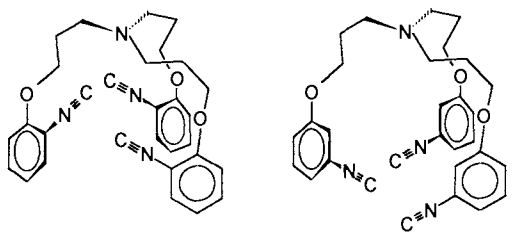

25 **26**

groups to primary amines, subsequent formylation, and dehydration according to Ugi et al.[5]

The crucial question was then whether these triisocyanides could indeed form chelate complexes. One possible problem is the formation of three 18-membered rings in a facial complex with **25** as a ligand while a complex with **26** would even contain three 20-membered rings. Ligands **25** and **26** were allowed to react with [(C_7H_8)M(CO)$_3$] (C_7H_8 = cycloheptatriene, M = Cr, Mo, W) in dichloromethane. These reactions proceed by the facile replacement of the cycloheptatriene ligand by the tripodal triisocyanide, forming the complexes **27** and **28** in 69–87% yield.[56, 58] Attempts to obtain crystalline samples of **27c** and **28** led to an interesting observation. Compound **28** crystallizes from dichloromethane as well-formed rhombuses, which can be recrystallized as often as needed from this solvent. In contrast, the complexes **27a–c** do not crystallize readily from dichloromethane. Once crystals (of, for example, **27c**) have formed, however, they do not redissolve, and their combustion analyses show marked deviations from calculated values for *fac*-[(CO)$_3$W(**25**)]. To explain these deviations, X-ray crystal structure determinations of **27c** and **28** were undertaken. The results indicate that facial chelate complexes have formed with both ligands (Fig. 3). The 18- and 20-membered rings obtained thereby were at that time the largest of their kind known for organometallic compounds.

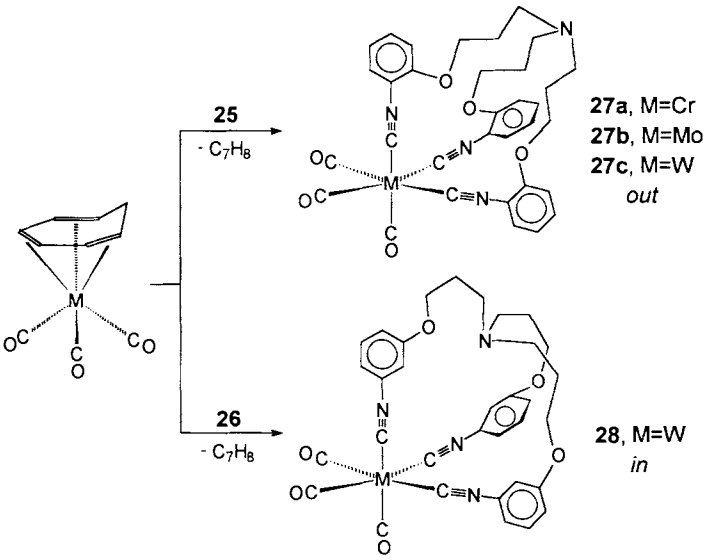

The main difference between **27c** and **28** is the conformation and configuration of the central nitrogen atom of the ligand backbone. In **27c** the nitrogen atom is protonated and the unit is present in the *out* configuration. Most likely, in-

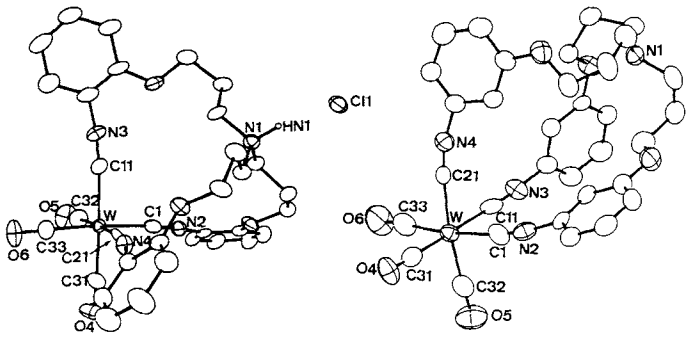

27c·HCl, *out* **28**, *in*

Fig. 3. Molecular structures of the chelate complexes **27c** · HCl and **28**.

version at the nitrogen is inhibited by the coordination of the ligand to the metal atom. Hence, the nitrogen atom is fixed in the *out* configuration and is subsequently protonated by HCl—which is either present as solvent impurities or formed by dichloromethane cleavage—to form the hydrochloride **27c** · HCl. Complexes **27a,b** behave similarly and are assumed to have analogous structures. In the soluble complex **28** the central nitrogen atom adopts the *in* conformation and remains unprotonated.

Analogous bond lengths and angles in **27c** and **28** are identical within error limits. The C≡N bond lengths are longer than in uncoordinated ligands such as **21** (Table 1), due to π back bonding in the metal complex. The IR spectra

Table 1. Selected structural parameters of tripodal triisocyanides and their metal complexes.

Cmpd.	Bond length [Å] [a]				Bond angle [°] [a]			Ref.
	M-CN	M-CO	N≡C	C≡O	M-C-N	M-C-O	C-N-C	
27c · HCl	2.114	1.984	1.167	1.167	172.9	176.9	171.7	[58]
27d	2.10	2.01	1.18	1.16	175	177	169	[59]
28	2.098	1.994	1.159	1.169	173.7	177.9	165.1	[58]
33	2.098	1.994	1.160	1.157	177.4	178.1	172.3	[61]
35			1.135				176.6	[56]
37b	2.129	1.996	1.154	1.154	172.1	177.6	174.1	[60]
38a	2.123	1.993	1.160	1.158	171.6	177.9	173.7	[60]
38b	2.13	1.99	1.15	1.16	177	177	171	[61]

[a] Average values.

of **27a–c**, which are not substantially different, exhibit the expected A_1 and E bands for complexes with C_{3v} symmetry. These bands are found in the same energy range as in complexes of the type *fac*-[$(CO)_3$W(aromatic isocyanide)$_3$].[53, 67] The *m*-substituted ligand in **28** is a weaker σ donor, but a better π acceptor than the *o*-substituted ligand in **27a–c** (see Table 2). This substitution dependence of IR spectra of aromatic isocyanides was already mentioned by Ugi et al.[5a]

The protonation of the ligands in **27** and the unfavorable solubility of the formed hydrochlorides led to the development of tripodal, aromatic triisocyanides that have a methine group which cannot be protonated as the central group in the backbone.[61] The key step in the synthesis of **30** was the formation of the trichloride **29**.

The reaction of **30** with [(C_7H_8)W$(CO)_3$] leads to a soluble chelate complex (see Table 2).[61] Attempts to obtain this

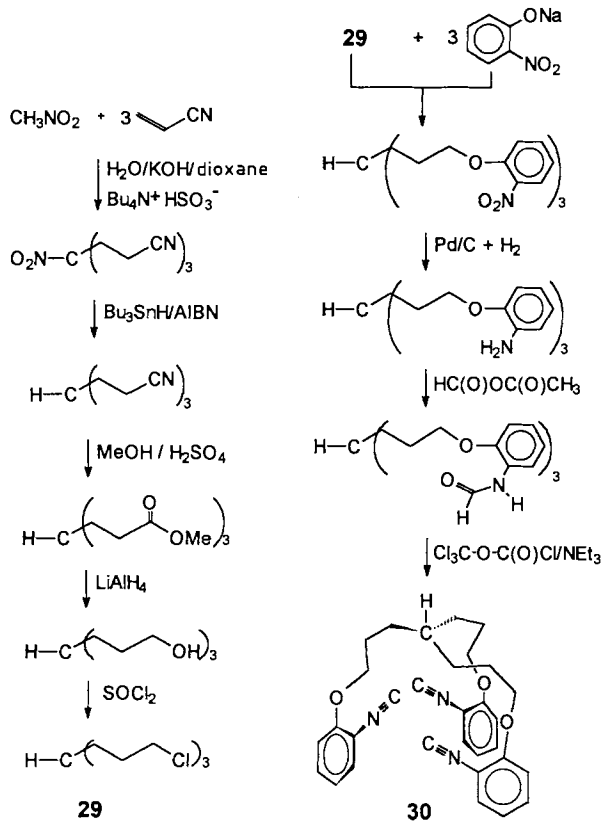

compound in crystalline form have so far been unsuccessful. Therefore it could not be determined whether the methine group is in the *in* or *out* configuration. The ^{13}C NMR spectrum (Fig. 4), however, is very informative in this regard. The doubling of all signals indicates that the reaction leads to a mixture of *in*-**31a** and *out*-**31b** configurational isomers

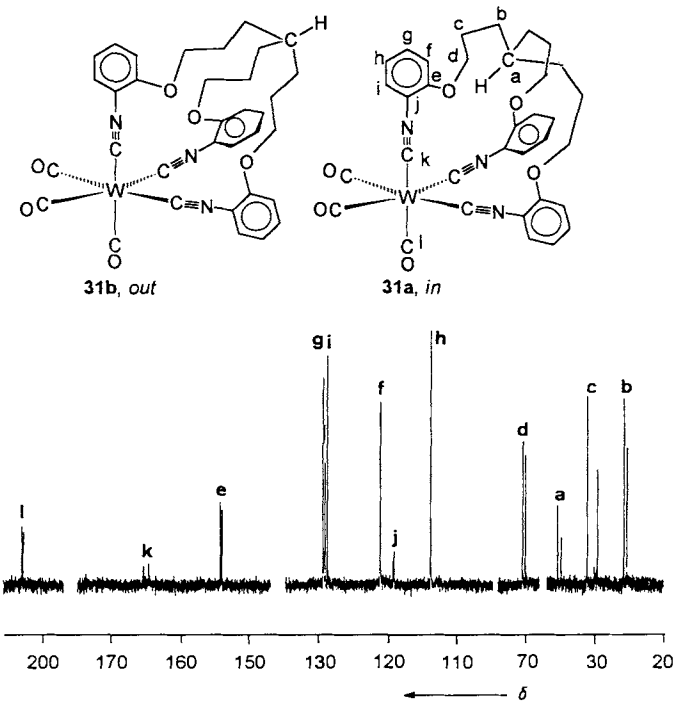

Fig. 4. ^{13}C NMR spectrum of a 5:3 mixture of complexes **31a** and **31b**.

(5:3 ratio). The *in* isomer is easily identifiable in the ^{1}H NMR spectrum by a septet for the proton of the central methine shifted downfield to $\delta = 2.50$. This is due to the penetration by the proton on the central carbon atom a into the deshielding region of the anisotropy cones of the C≡N bonds (see Section 3.2). Attempts at separating the isomers chromatographically have so far been unsuccessful.

The results obtained led to the synthesis of ligand **32** (see Table 2).[61] This ligand also contains a bridgehead carbon atom which cannot be protonated, and the number of atoms in the backbone is reduced. The methyl substituent at the bridgehead was introduced to sterically encumber the formation of *in* isomers in order to obtain homogeneous, crystallizable samples of *out* isomers.

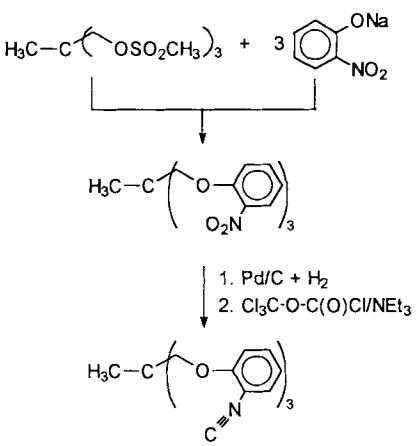

32

The reaction of **32** with $[(C_7H_8)W(CO)_3]$ in dichloromethane leads indeed to the soluble complex *fac*-$[(CO)_3W(\mathbf{32})]$ **33** in good yield. The X-ray structure analysis of **33** confirms the formation of the desired chelate complex (Fig. 5, see Table 1).[61] The decrease in the number of backbone atoms between the isocyanide functionalities from thirteen to nine has apparently no effect on the chelating ability. The introduction of the methyl group at the central carbon atom successfully inhibited the formation of *in* isomers, forcing an exclusive *out* configuration.

Apparently, tripodal triisocyanides are very well suited for the preparation of facial chelate complexes. The configuration or conformation of the central backbone atom can be influenced by the ligand design. The size of the ligand backbone can be varied over a broad range without appreciably affecting either the ligand's ability for chelate formation or the linear geometry of the M–C≡N–R unit (see Table 1).

In some instances, it was found that during complex formation, small amounts (5–7%) of higher oligomers were isolated along with the desired monomeric products. During the course of the preparation of **27c** it was possible to separate a dimer in 5% yield from the main product by fractional crystallization and to characterize this species by X-ray structure analysis. In *fac,fac*-$[\{(\mathbf{25})W(CO)_3\}_2] \cdot 2HCl \cdot 2CH_2Cl_2$ **(27d)** (Fig. 6), the two $W(CO)_3$ units are bridged by two ligands **25**.[59] Each ligand binds to one metal atom through two of its isocyanide groups, while the third isocyanide group bridges to the other metal atom. This creates a chelate ring composed of 36 atoms, which is, to the best of our knowledge, the largest one of its kind in organometallic compounds. The central nitrogen atoms of both ligands are protonated and adopt the *out* configuration. The positions of the hydrogen atoms on the central backbone atoms were not determined.

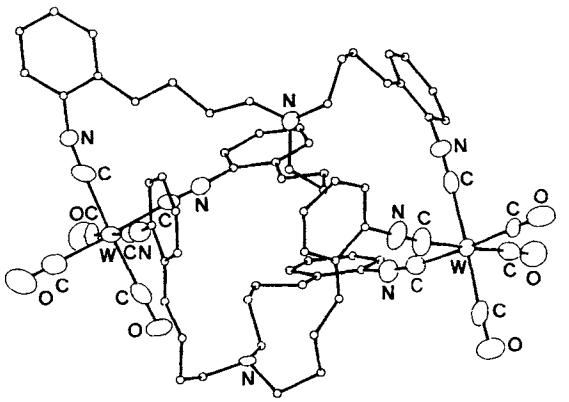

27d

Fig. 6. Molecular structure of *fac,fac*-$[\{(\mathbf{25})W(CO)_3\}_2] \cdot 2HCl \cdot 2CH_2Cl_2$; the O atoms attached to the phenyl rings in **25** are not differentiated from the C atoms in the ligand backbone. The solvent and HCl molecules are omitted for clarity [59].

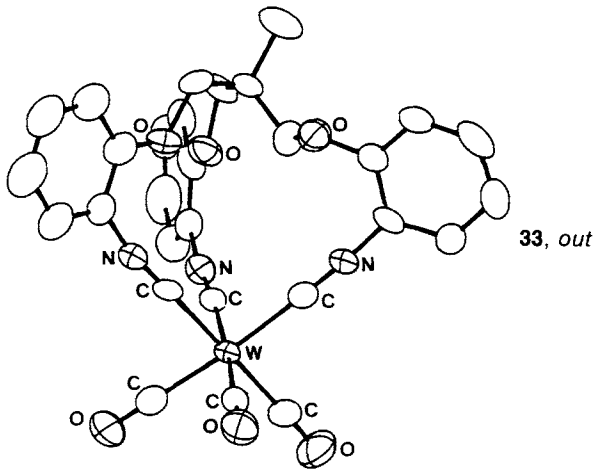

33, *out*

Fig. 5. Molecular structure of *out*-$[(CO)_3W(\mathbf{32})]$ **33**.

Preliminary investigations showed that homoleptic complexes of the type *fac*-$[Cr(\mathbf{32})_2]$ **34** can be obtained by the reaction of the tripodal ligand with bisnaphthalenechromium.[68] The bright red compound **34** was isolated in 60% yield (Table 2).[69] Cr(0) complexes with six monodentate aliphatic isocyanide ligands have already been obtained from bisnaphthalenechromium in analogous ways.[68] The classic method for the synthesis of hexaisocyanidechromium(0) compounds using chromium(II) acetate[70] leads with **32** to higher oligomers, whose molecular structures have so far not been elucidated.[69]

The reaction of **25** with $^{99m}TcO_4^-$ leads to the incorporation of ^{99m}Tc into the ligand. In this case, the ligand is present in large excess and acts as the reducing agent as well as the complexing agent. This behavior was observed previously in

Table 2. Selected spectroscopic data of tripodal triisocyanides and their metal complexes.

Cmpd.	IR: $\tilde{\nu}$[cm^{-1}] [a]		^{13}C NMR: δ		Ref.
	N≡C	C≡O	N≡C	C≡O	
25	2118		167.6 s, br.		[58]
26	2113		164.0 s, br.		[58]
27a · HCl	2140, 2078	1949, 1885	[b]		[58]
27b · HCl	2138, 2079	1940, 1888	[b]		[58]
27c · HCl	2137, 2068	1933, 1878	[b]		[58]
28	2135, 2052	1950, 1900	161.6	204.4	[58]
30	2123		[c]		[61]
31a	2132, 2068	1931, 1872	164.4	202.9	[61]
31b	like **31a**		165.2	202.7	[61]
32	2126		167.4		[61]
33	2142, 2079	1937, 1892	162.7	203.7	[61]
34	1943 vs, br.		[c]		[69]
35	2148		156.4 (t, ^1J(N,C) = 5.6 Hz)		[56]
36	2148		156.1 (t, ^1J(N,C) = 5.6 Hz)		[60]
37a	2162, 2120	1933,1859	151.0	206.6	[60]
37b	2167, 2122	1930, 1849	150.8	206.6	[60]
38a	2160, 2115	1932, 1854	151.8	207.4	[60]

[a] All IR spectra in KBr. [b] Insoluble. [c] Not observed.

the synthesis of hexaisocyanide complexes with monodentate isocyanide ligands.[71] The technetium(I) complex of **25** is assumed to have a structure analogous to that of the complex of **34**.[57] It is so far unclear whether the coordinated ligands are protonated on the backbone nitrogen atom, or if the complex is a monocationic $^{99m}Tc^I$ compound.

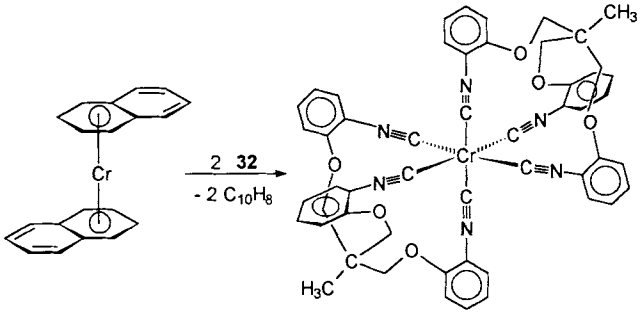

34, *out*

3.2. Chelate Complexes with Tripodal Aliphatic Triisocyanide Ligands

Further experiments were carried out to investigate if it is possible to prepare complexes with aliphatic triisocyanides. It was also of interest to determine the mimimum number of atoms in the backbone of the ligand necessary for chelate formation. For these purposes, the ligand **35** was prepared by the dehydration of 3,3',3''-nitrilotripropionamide[72] (Fig. 7).[56] At room temperature **35** is a viscous oil, which can be crystallized from methanol at low temperatures. Its X-ray structure, the first to be determined for a saturated aliphatic triisocyanide, shows a molecule with C_3 symmetry. The length of the N≡C bond (1.135(3) Å) determined by X-ray crystallography is significantly shorter than the N≡C bond lengths in aliphatic isocyanides determined by using electron diffraction.[73] The reasons behind the differences in these results, as well as the necessary corrections, have been

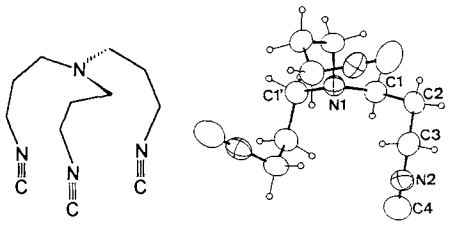

35

Fig. 7. Schematic representation and molecular structure of ligand **35**.

discussed, for example, in the case of 1,4-phenyldiisocyanide.[52a]

The ^{1}H NMR spectrum of the ligand **35** shows $^2J(^{14}N,^1H)$ and $^3J(^{14}N,^1H)$ coupling with the isocyanide nitrogen atom.[56] This has been described previously for aliphatic isocyanides.[74] The ^{13}C NMR spectrum also shows coupling between the isocyanide nitrogen atom and the neighboring carbon atoms.[56, 75] All coupling with the isocyanide nitrogen atom disappears upon complex formation, an important aid for the identification of metal complexes with isocyanide ligands.

Unfortunately, this aid cannot be used in the investigation of the product of the reaction of **35** with $[(C_7H_8)W(CO)_3]$, as the formed complex is too insoluble. The IR spectrum of this product, however, indicates at least local C_{3v} symmetry (Table 2). This observation and the elemental analysis[56] indicated that higher, insoluble oligomers were formed.[58] However, protonation of the ligand, as observed during the formation of **27c** (see Fig. 3) cannot be ruled out conclusively, even though the product is free of chloride.

To eliminate the factors that might cause the insolubility of complexes containing **35**, the ligand **36** was prepared with an all carbon backbone.[60] This ligand cannot be protonated at the central methine group and it allows the investigation of the coordination chemistry of aliphatic, tripodal triisocyanides with a small number of backbone atoms. The backbones of the ligands **35** and **36** are nearly identical and, in the case of chelate formation, would lead to the smallest rings (12 atoms) observed so far.

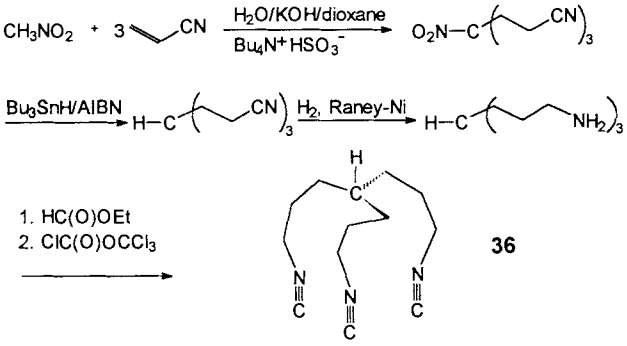

36

The ^{1}H NMR spectrum of **36** (Fig. 8 top) shows the previously mentioned ^2J(N,H) coupling for the CH_2 protons neighboring the isocyanide functionalities. The signal of the proton of the methine group overlaps with that of the methylene group B at $\delta = 1.45$. The reaction of **36** with $[(C_7H_8)$-

$Cr(CO)_3$] in dichloromethane yields the highly soluble complex *fac*-[$(CO)_3$Cr(**36**)] (**37a**) (see Table 2). The multiplicity of the signal of the methylene group D in the ^{1}H NMR spectrum of **37a** has been reduced from a triplet of triplets in the free ligand to the expected triplet by the coordination of the isocyanide group. The methine signal is strongly shifted downfield to $\delta = 2.43$. This allows the distinction between the two configurational isomers (*in* and *out*, Fig. 8 bottom). The downfield shift can only be explained by the presence of the *in* isomer, as only then can the proton of the methine group penetrate the deshielding region of the anisotropy cones of the N≡C bonds.

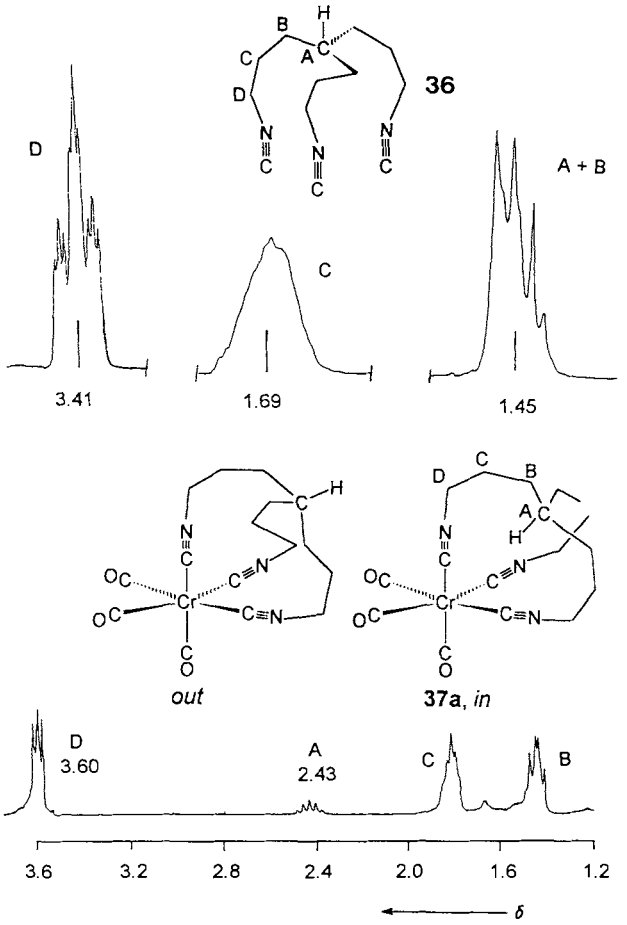

Fig. 8. ^{1}H NMR spectrum of **36** and its tricarbonylchromium complex **37a**.

The structure analysis of the isostructural complex *fac*-[$(CO)_3$W(**36**)] (**37b**) shows that the above assumptions are correct (Fig. 9, see Table 1). All three ligand branches coordinate to the same tungsten atom, which leads to the formation of 12-membered chelate rings. The central methine group adopts the *in* configuration.[60]

The structure analysis of **37b** shows that aliphatic, tripodal triisocyanides with only seven atoms between the isocyanide functionalities are also capable of forming chelate complexes. Hence it should be possible to obtain monomeric chelate complexes with the nitrogen-containing ligand **35**. This ligand indeed reacts with [(C_7H_8)W$(CO)_3$] under high dilution conditions to yield *fac*-[$(CO)_3$W(**35**)] (**38a**), which was characterized by X-ray diffraction (Fig. 9, Table 1).[60] Apparently

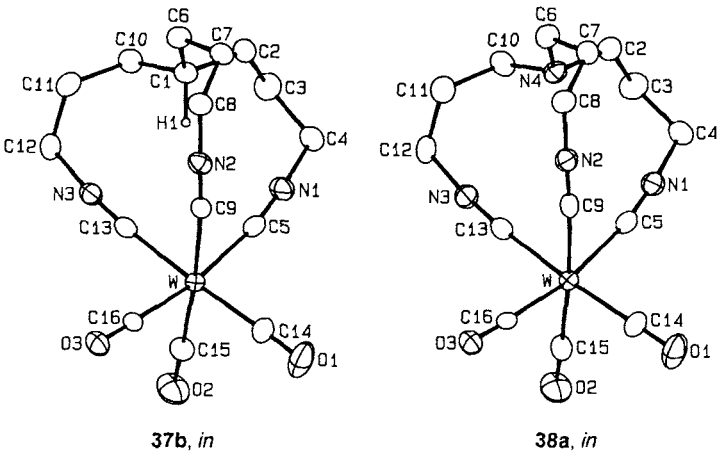

Fig. 9. Molecular structures of **37b** (left) and **38a** (right).

the formation of larger oligomers is favorable at higher concentrations, leading to the previously described insoluble compounds.[58] This assumption is supported by the isolation of the dimeric species *fac,fac*-[{$(CO)_3$W(**35**)}$_2$] (**38b**), which is formed in small amounts (ca. 5%) during the preparation of **38a**.[61] The structure of **38b** (Fig. 10) shows two $W(CO)_3$ units bridged by two ligands **35**. As was the case for **27d** (see Fig. 6) each ligand coordinates one metal center with two isocyanide groups, while the third isocyanide branch forms the bridge to the other metal atom. The nitrogen atom in the backbone of the complexes **27c** · HCl and **27d** are protonated and in the *out* configuration, while in **38a** and its dimer **38b** the nitrogen atoms are not protonated and exhibit the *in* conformation.

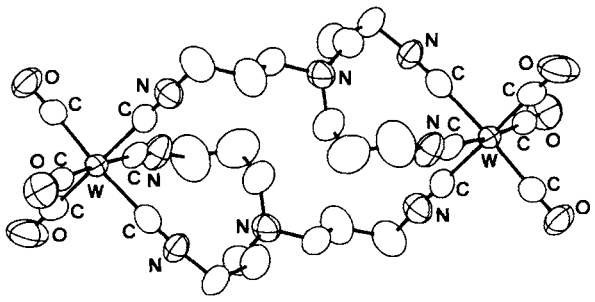

Fig. 10. Molecular structure of the dimer *fac,fac*-[{[$N(CH_2CH_2CH_2NC)_3$]-$W(CO)_3$}$_2$] **38b**.

The IR spectra of the monomeric complexes **37a,b** and **38a** (see Table 2) are in accordance with those found for complexes with monodentate aliphatic isocyanides like *fac*-[$(CO)_3$W-$(CNR)_3$].[76] The spectra indicate that **35** and **36** are better σ donors and weaker π acceptors than aromatic triisocyanides such as **25**, **26**, **30**, or **32**. The M–CN and M–CO bond lengths, however, are only mildly affected by this (Table 1). Apparently the structural parameters reflect the electronic conditions much less accurately than the IR spectra.

It is noteworthy that the triisocyanides **32**, **35**, and **36** with fewer backbone atoms do not cause any larger deviations

from the linearity of the M-C-N or C-N-C angles than were observed for ligands with larger backbones. This occurs despite the fact that isocyanide complexes are known which are bent at the nitrogen atom.[77] This means that a large ligand backbone, with many atoms between the isocyanide functionalities, is not absolutely necessary for chelate formation.

3.3. Reactions with $[M_3(CO)_{12}]$ Clusters

Low molecular weight carbonyl metal clusters act as catalysts and, in some instances, can serve as model systems for the investigation of reaction sequences on catalytically active metal surfaces.[78] One prerequisite for these studies is cluster stability (that is, the lack of any propensity for decomposition into smaller fragments). This condition is not fulfilled particularly in carbonyl clusters of the first transition metal series, since the M–M bonds there are generally weak. One method for the stabilization of clusters lies in bridging the metal atoms with multidentate ligands. Many clusters have trimetallic planes bridged by main group elements.[79] Other clusters are reinforced by tridentate phosphane[80a–c] or arene[80d] ligands. As early as 1980 an attempt was made to bridge a triangular plane in clusters of the type $[M_3(CO)_{12}]$ (M = Fe, Ru, Os) with triisocyanide ligands, making use of the fact that their properties are similar to carbon monoxide.[55] The ligand prepared for this purpose, *cis,cis*-1,3,5-cyclohexanetriisocyanide, proved unsuitable. Even though in form A (CN axial) the three isocyanide carbon atoms form an equilateral triangle with an edge length of about 2.5 Å, the ligand assumes the unfavorable form B (CN equatorial), in contrast to the analogous triamine.[81]

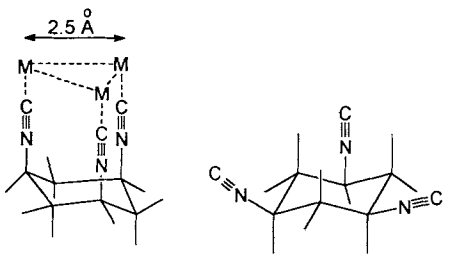

A B

The tripodal ligands presented in Sections 3.1 and 3.2 do not have this type of conformational problem. They do not, however, possess an ideal topology, since they react with trimetal clusters by chelating only one metal atom, thereby destroying the cluster framework. The ideal ligand would be a tailor-made triisocyanide with a small enough backbone to preclude chelate formation with a single metal atom. The ligand **39**, developed nearly simultaneously by two research groups,[62, 63] fulfills these requirements. If the isocyanide groups are parallel, the distance between the isocyanide carbon atoms is calculated to be 2.55 Å, assuming an angle of 109° at the quaternary carbon atom and a C–CH_2 distance of 1.54 Å. When further considering that the M–C≡N–CH_2 unit can deviate from linearity, it becomes apparent that **39** should be able to bridge trimetallic planes in $[M_3(CO)_{12}]$ clusters (M = Fe, d(M–M) = 2.69, 2.55 Å;[82] M=Ru, d(M–M) = 2.848 Å;[83] M = Os, d(M–M) = 2.881 Å[84]).

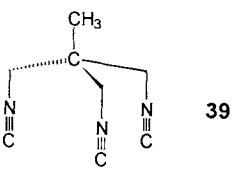

39

It proved indeed possible to obtain the bridged clusters **40a** (yield 55%) and **40b**[62] by allowing **39** to react with $[Os_3(CO)_{10}(NCCH_3)_2]$.[85] Compared to the starting material, the X-ray crystal structure of **40a** shows a nearly unchanged Os_3 frame (d(Os–Os) = 2.896 Å) and almost linear Os–C≡N and C≡N–CH_2 angles (ca. 170°). The reaction of **40a** with Me_3NO/MeCN and another equivalent of **39** yields the bicapped cluster **40b**.

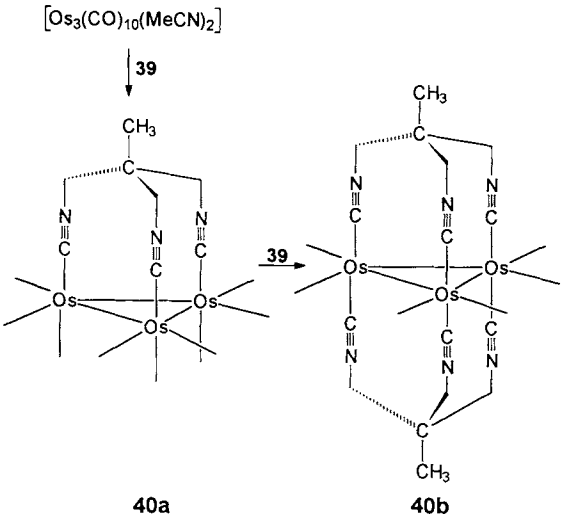

40a **40b**

The stability of metal–metal bonds in $[M_3(CO)_{12}]$ clusters increases in the order Fe < Ru < Os. For the Os clusters, and, in a more limited way, for the Ru clusters, substitutions of the CO groups are possible without causing cluster fragmentation. The corresponding triiron clusters are significantly less stable. While ruthenium and osmium pentacarbonyl react quickly to give the corresponding dodecacarbonyls, iron pentacarbonyl is more stable than $[Fe_3(CO)_{12}]$. Therefore a different path was chosen for the synthesis of $M_3(CO)_9$ (M = Fe, Ru) units bridged by **39**.[63, 64] In the first step, **39** was ligated to three mononuclear metal carbonyls according to the method of Hieber.[63, 86] The IR spectrum of thus obtained **40c** indicates that the isocyanide groups occupy the axial position on the iron atoms, displaying C_{3v} symmetry.[87] Apart from the shift of the C≡N absorption band in the IR spectrum, the coordination of the isocyanide groups to a metal center can be identified by the downfield shift of the resonance signal for the methylene group in the ^{1}H NMR spectrum ($\Delta\delta$ = 0.22–0.31).[63]

Upon irradiation (high-pressure mercury lamp), highly diluted solutions of **40c** evolve CO, and the slightly yellow reaction mixture turns dark green within 10 minutes. Preliminary analyses indicate the formation of a triisocyanide-bridged cluster which also contains bridging CO ligands.

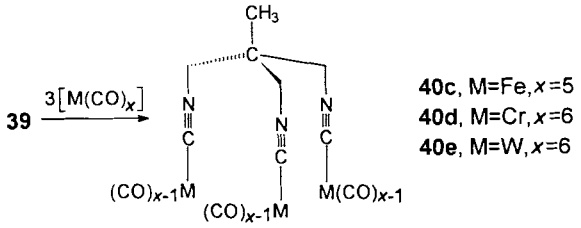

This cluster, however, fragments very readily, during which a transformation of the triisocyanide ligand is observed as well. This sensitivity has so far precluded a structure analysis. The high reactivity of this triiron cluster is not surprising when considering that the reaction of $[Fe_3(CO)_{12}]$ with MeNC results in cluster fragmentation as soon as more than two CO groups have been replaced.[88]

An interesting property of **39** is the possibility not only to coordinate each isocyanide group separately, but also to different metals (Fig. 11).[64] In this way it is possible for **39** to coordinate one, two, or three $Cr(CO)_5$ fragments to form the complexes **40f–h**. The structure of **40f** (Fig. 11) provides the unique opportunity to compare the N≡C bond lengths of coordinated and free isocyanide functions in the same molecule. Even though the IR absorption band of the coordinated isocyanide group is shifted 45 cm^{-1} to higher energies in comparison with the free isocyanide groups, the bond lengths of all three groups are identical within error limits. Apparently the coordinated isocyanide functionality acts only as σ donor. The complexes **40g** and **h** containing two and three $Cr(CO)_5$ units, respectively, were identified by the downfield shift of the signal for the protons of the methylene group in the ^1H NMR spectrum.[64]

This downfield shift also permitted the identification of complexes with different carbonyl metal fragments. The complex $[H_3CC(CH_2NC)\{CH_2NC\text{-}W(CO)_5\}\{CH_2NC\text{-}Cr(CO)_5\}]$ was characterized by the three signals of the methylene groups at $\delta = 3.45$ (H_2C-NC), 3.70 (H_2C-NC-$Cr(CO)_5$), and 3.91 (H_2C-NC-$W(CO)_5$).[61] It is thus possible to obtain the starting materials for clusters containing different transition metal atoms by preparing correspondingly coordinated triisocyanide ligands such as **39**. The formation of metal–metal bonds can then be initiated by irradiation, as for the triiron complex, or by other methods (oxidation or reduction of the carbonyl metal unit). The most prominent advantage of this method is that the desired cluster can be preformed by using stable mononuclear carbonyl isocyanide metal units.

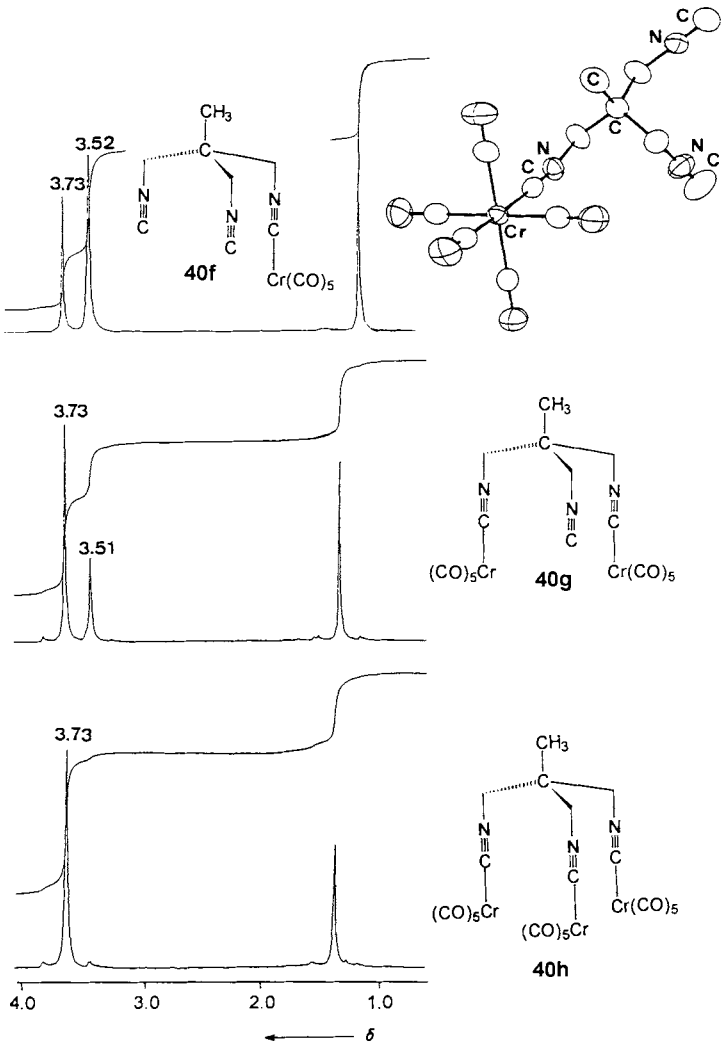

Fig. 11. ^1H NMR spectra of the complex $[CH_3\text{-}C(CH_2NC)_x\{CH_2NCCr(CO)_5\}_{3-x}]$ ($x = 0, 1, 2$) and the molecular structure of $[CH_3\text{-}C(CH_2NC)_2\{CH_2NCCr(CO)_5\}]$ **40f**.

3.4. Experiments for the Construction of Polyisocyanides by Template Synthesis

After it had been shown that tripodal isocyanides of varying backbone sizes have the ability to form chelate complexes, an attempt was made to prepare such ligands by template synthesis from monodentate isocyanides already bound to a metal center. A promising starting material for such reactions is coordinated β-hydroxyphenylisocyanide (**41a**). It should be possible to link three of these ligands, when facially coordinated to a metal center, by using the three hydroxyl groups and a suitable tripodal linker. In this way, novel as well as previously described ligands with an ether bridge could be obtained (Scheme 3).

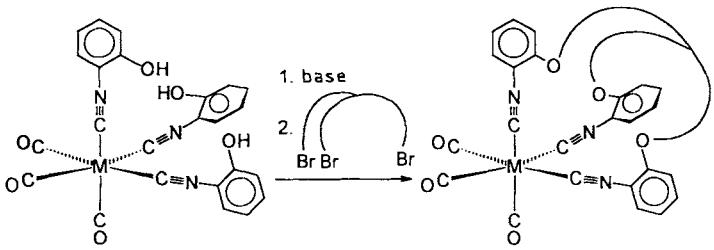

Scheme 3. Construction of tripodal ligands by template synthesis.

Free **41a** is not stable, however, but quantitatively cyclizes to form benzoxazole **41b**.[89] Benzoxazole can be deprotonated by strong bases, such as *n*BuLi. The open ring formed can then be stabilized by regiospecific silylation at the oxygen atom using trimethylchlorosilane, forming β-trimethylsiloxyphenylisocyanide **41c**.[90] With trimethyltin chloride instead exclusively the stannylated benzoxazole **41d** is formed.[90]

In order to study possible alkylations according to Scheme 3, **41c** was allowed to react with $[W(CO)_5(thf)]$,[91]

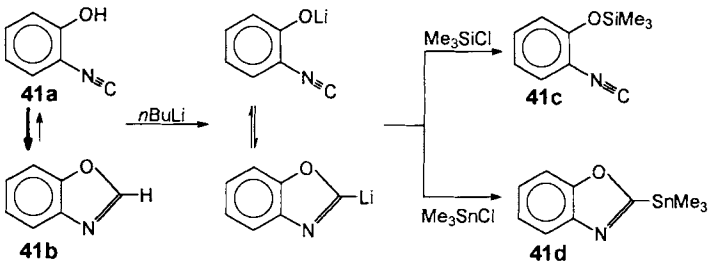

which yielded complex **42a** (Fig. 12).[61] It is known that aliphatic β-hydroxyalkylisocyanides like $HOCH_2CH_2NC$ can be stabilized by coordination to electron-rich $(CO)_5M$ fragments (M = Cr, Mo, W).[92] Coordination to late transition metals (Pt^{2+}, Pd^{2+}, Au^+), however, leads to the rapid formation of carbene complexes with cyclic oxazolidine-2-ylidene ligands. This reaction proceeds by an intramolecular

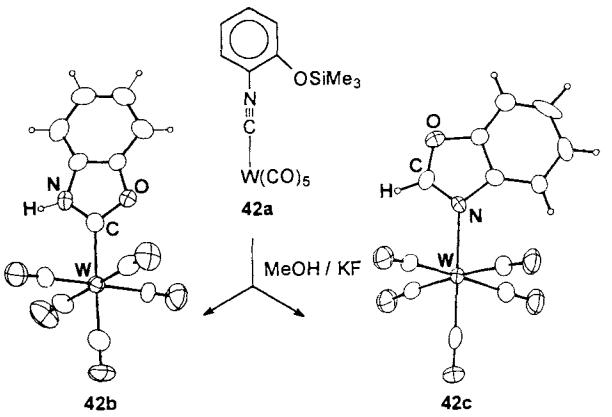

Fig. 12. Molecular structures of (dihydrobenzoxazole-2-ylidene)pentacarbonyltungsten **42b** and (benzoxazole)pentacarbonyltungsten **42c**.

nucleophilic attack of the hydroxy group on the isocyanide, which is activated due to the lack of $(d \rightarrow p)\pi$ back bonding.[93] A stabilization of the isocyanide carbon atom by tungsten(0) was expected for the complex formed by the cleavage of the trimethylsilyl protecting group from **42a**. The silyl group is indeed removed readily by stirring **42a** in methanol in the presence of a catalytic amount of KF.[94] Surprisingly, the product of this Si–O bond cleavage is not the expected $(CO)_5W$ complex with coordinated β-hydroxyphenylisocyanide, but a mixture of the heterocarbene complex **42b**, with coordinated dihydrobenzoxazole-2-ylidene, and the complex **42c** with N-coordinated benzoxazole[95] (Fig. 12).[61] The carbene formation by intramolecular nucleophilic attack on the isocyanide carbon atom was therefore not prevented by the relatively electron-rich tungsten(0) center. Apparently, in addition to the stabilization provided by metal–ligand back bonding (**A**) and by the $(p \rightarrow p)\pi$ bonds of the heteroatoms (**B**), the aromaticity of the carbene ligand (**C**) makes a crucial contribution to the thermodynamic stability of the complex (Scheme 4). This stabilization cannot occur with aliphatic β-hydroxyisocyanides, which are stabilized at W^0.

These assumptions are also supported by a comparison of the structural parameters of **42b** and **42c**. The $W–C_{carbene}$ distance in **42b** (2.185(10) Å) is in the range found for corresponding bonds in other $(CO)_5W$–C(carbene) complexes.[96] The bond lengths in the heterocarbene ring of **42b** are, as expected for an arene, rather similar (from 1.329(14) to 1.399(13) Å). In the N-coordinated benzoxazole ring of **42c**, however, one finds clearly distinguishable single and double bonds (e.g., $d(N–C_{CH}) = 1.271(10)$, $d(N–C_{Ph}) = 1.397(10)$ Å). Analogous behavior has been observed for (dihydrobenzoxazole-2-ylidene)tetracarbonyl iron, which has been structurally characterized.[61]

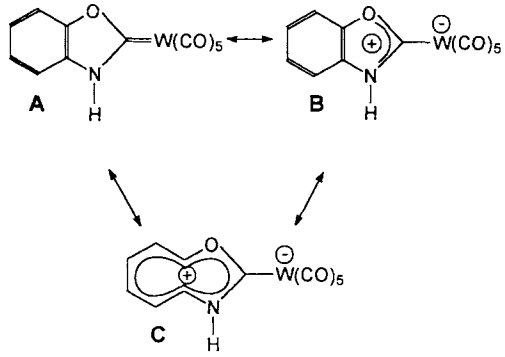

Scheme 4. Resonance structures for (dihydrobenzoxazole-2-ylidene)pentacarbonyltungsten.

It appears that template syntheses using coordinated β-hydroxyphenylisocyanide are not feasible due to the cyclization of the coordinated ligand. There is, however, the possibility to alkylate the nitrogen atom of the formed dihydrobenzoxazole-2-ylidene ligands. The N-bound proton in **42b** is readily removed by bases, enabling subsequent electrophilic alkylation of this nitrogen atom.[97] After deprotonation by NaH, **42b** reacts with MeI or $H_2C=CHCH_2Br$ to form the complexes **42d** and **42e**, respectively (Fig. 13).[61]

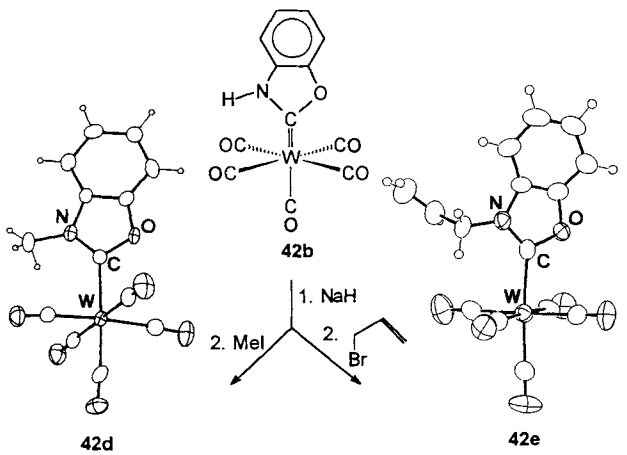

Fig. 13. Molecular structure of (*N*-methyldihydrobenzoxazole-2-ylidene)pentacarbonyltungsten **42d** and (*N*-allyldihydrobenzoxazole-2-ylidene)pentacarbonyltungsten **42e**.

Complex **42e** can be further transformed thermally to give the olefin–carbene complex **42f**. Such complexes are assumed to be of great importance for catalytic processes.[96d, 97, 98] Complex **42f** can be characterized unambiguously by the

changes in the ^{1}H NMR spectrum. The coordination of the allylic double bond causes an upfield shift, especially for the olefinic methylene protons ($\delta = 2$). The resonance signals for the protons of the N-bound methylene group are also diastereotopically split by the coordination of the double bond.

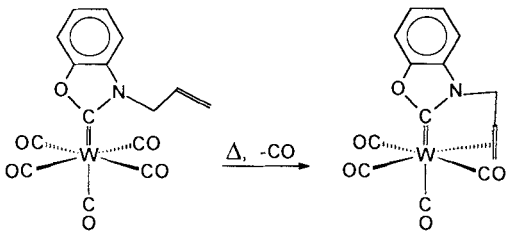

42e **42f**

4. Tetradentate Isocyanide Ligands

Up to now, only a few tetraisocyanides are known. The synthesis of the cyclic, aliphatic isocyanide **43** was reported in 1981.[99] It was postulated that this ligand forms mononuclear complexes with a number of transition metals. In this case, very small chelate rings would have to form. From the molecular structure of the $[Rh(\mathbf{20b})]^+$ cation (see Fig. 2), it appears that linking two ligand molecules **20b** by an ethylene bridge should be difficult. The formation of mononuclear, planar metal complexes, in which all four isocyanide functionalities of a single **43** ligand are coordinated to the same metal, therefore appears to be unlikely.

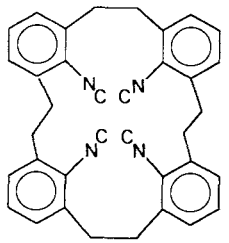

43

The synthesis of tetraisocyanides is possible starting from the triisocyanides described in Sections 3.1 and 3.2. If, during the synthesis of **29**, the reductive elimination of the ligand backbone nitro group is not performed, subsequent reduction of this group together with the aromatic nitro functionalities to primary amines leads, after formylation and dehydration, to a tetraisocyanide.[61] Assuming the *in* configuration at the central carbon atom, such ligands are capable of occupying four coordination sites in trigonal-bipyramidal complexes. Only a large ligand backbone, however, allows the transition from O_h (octahedral) to C_{3v} symmetry (trigonal bipyramid) in a metal complex. The coordination chemistry of the only known linear tetraisocyanide has not yet been explored.[54]

5. Summary and Outlook

As is the case in all new areas of research, the investigation of metal complexes of polyisocyanides is currently dominated by the coordination chemistry and the search for synthetic pathways leading to new ligands and complexes. Tripodal triisocyanide ligands are especially characterized by a rich and varied coordination chemistry. Most notable is the fact that the formation of mononuclear chelate complexes is possible with rather different ligands. The composition of the ligand backbone (nitrogen or carbon as central atom) as well as its size can be varied over a wide range. The work with tripodal ligands indicates that, starting from the results of structural analyses, it is possible to influence the structural parameters of the complexes substantially by altering the ligand design.

The future will bring the development of ligands with different backbones, maybe even tetradentate ligands. The investigation of the reactions of coordinated polyisocyanides is also only at its very beginning. The preparation of siloxy-substituted tripodal triisocyanide ligands can be envisioned. After coordination to a metal atom, it then should be feasible to transform these compounds by Si–O bond cleavage and subsequent intramolecular carbene formation into previously nearly unknown polycarbene ligands.[100] The preparation of facial chromium complexes, $[CrL_3^*]$ (L_3^* = chiral-substituted tripodal triisocyanide), should lead to interesting catalytic reactions. Finally, the use of triisocyanides in the preparation of $^{99m}Tc^I$ complexes for medical diagnostic purposes cannot be overlooked. Multidentate ligands, in contrast to their monodentate analogues, raise the possibility of linking the ligands to a molecule with high biospecificity. This, in turn, would influence the in vivo distribution of the subsequently formed technetium isocyanide complexes.

I wish to extend my gratitude to my graduate students for their enthusiastic cooperation. Dr M. Tamm deserves special mention for the synthesis of the tripodal triisocyanides and their metal complexes. I wish to thank Professor H. Schumann for always providing me with support during my habilitation, during which time a large number of the described complexes were prepared. Professor E. P. Künding receives my thanks for bringing the interesting problems of the catalysis with chromium carbonyls and isocyanides to my attention. Past and present support of our work by the Deutsche Forschungsgemeinschaft, the Graduate College "Synthese und Strukturaufklärung niedermolekularer Verbindungen" at the Technischen and the Freien Universität Berlin, as well as the Fonds der chemischen Industrie is gratefully acknowledged. A doctoral fellowship from the BASF AG for Dr. M. Tamm was especially appreciated. Financial support for our work with technetium was provided by the Institut für Diagnostikforschung (a subsidiary of the Schering AG) at the Freien Universität Berlin.

Received: September 22, 1992 [A 903 IE]
German version: *Angew. Chem.* **1993**, *105*, 681

[1] a) A. Gautier, *Liebigs Ann. Chem.* **1867**, *142*, 289–294; b) *ibid.* **1868**, *146*, 119–124; c) *ibid.* **1869**, *149*, 155–161; d) *ibid.* **1869**, *149*, 29–35.

[2] a) A. W. Hofmann, *Liebigs Ann. Chem.* **1867**, *144*, 115–120; b) *ibid.* **1868**, *146*, 107–19.

[3] There are differing reports regarding the smell and the physiological properties of isocyanides. While Gautier describes the smell of—probably impure—ethylisocyanide as very uncomfortable and unbearable [1b], Hoffmann reports that vapors of phenylisocyanide leave a bitter taste on the tongue and create "especially in the throat an asphyxiating effect". [2a] Other groups report that pure compounds do not have unpleasant smells (cf. H. Lindemann, L. Wiegrebe, *Ber. Dtsch. Chem. Ges.* **1930**, *63*, 1650–6, in particular, p. 1655). Volatile alkylisocyanides like

MeNC or EtNC have indeed an unpleasant smell, while higher or alkylisocyanides with substituted side chains are practically free of any smell. Polyisocyanides are in general not volatile and are free of smell. In a study by the Bayer AG the toxic effect of isocyanides was tested. It was found that—with some exceptions—mice could tolerate doses of 500–5000 mg per kg body weight (cf. reference [67b] in [5b]).

[4] Reviews on synthetic methods for isocyanides: C. Grundmann, *Methoden Org. Chem. (Houben Weyl)* 4th ed. **1952–1985**, *vol.* E5, pp. 1611–1658.

[5] a) I. Ugi, R. Meyr, *Chem. Ber.* **1960**, *93*, 239–248; b) Review: I. Ugi, U. Fetzner, U. Eholzer, H. Knupfer, K. Offermann, *Angew. Chem.* **1965**, *77*, 492–504; *Angew. Chem. Int. Ed. Engl.* **1965**, *4*, 472–484; see also [4].

[6] Reviews: W. P. Fehlhammer, *Nachr. Chem. Tech. Lab.* **1982**, *30*, 187–189; E. Singleton, H. E. Oosthuizen, *Adv. Organomet. Chem.* **1983**, *22*, 209–130; P. M. Treichel, *ibid.* **1973**, *11*, 21–86.

[7] U. Schöllkopf, *Angew. Chem.* **1977**, *89*, 351–360; *Angew. Chem. Int. Ed. Engl.* **1977**, *16*, 339–348.

[8] a) S. J. Goede, F. J. J. de Kanter, F. Bickelhaupt, *J. Am. Chem. Soc.* **1991**, *113*, 6104–6107; b) G. Maier, H. P. Reisenauer, J. Eckwert, C. Sierakowski, T. Stumpf, *Angew. Chem.* **1992**, *104*, 1287–1289; *Angew. Chem. Int. Ed. Engl.* **1992**, *31*, 1218–1220.

[9] M. Krüger, H. Dreizler, D. Preugschat, D. Lentz, *Angew. Chem.* **1991**, *103*, 1674–1676; *Angew. Chem. Int. Ed. Engl.* **1991**, *30*, 1644–1646.

[10] K. Kawaguchi, M. Ohishi, S.-I. Ishikawa, N. Kaifu, *Astrophys. J.* **1992**, *386*, L51–L53.

[11] a) D. Lentz, K. Graske, D. Preugschat, *Chem. Ber.* **1988**, *121*, 1445–1447; b) D. Lentz, B. Pötter, R. Marschall, I. Brüdgam, J. Fuchs, *Chem. Ber.* **1990**, *123*, 257–260.

[12] D. Britton, W. B. Gleason, M. Glick, *Cryst. Struct. Commun.* **1981**, *10*, 1497–1500.

[13] B. J. Burreson, P. J. Scheuer, J. Finer, J. Clardy, *J. Am. Chem. Soc.* **1975**, *97*, 4763–4764.

[14] E. J. Corey, M. Behforouz, M. Ishiguro, *J. Am. Chem. Soc.* **1979**, *101*, 1608–1609; H. Yamamoto, H. L. Sham, *ibid.* **1979**, *101*, 1609–1611.

[15] a) U. Plaia, H. Stolzenberg, W. P. Fehlhammer, *J. Am. Chem. Soc.* **1985**, *107*, 2121–2122; b) W. P. Fehlhammer, K. Bartel, U. Plaia, A. Völkl, A. T. Liu, *Chem. Ber.* **1985**, *118*, 2235–2254; c) D. J. Doonan, A. L. Balch, *Inorg. Chem.* **1974**, *13*, 921–927.

[16] a) A. C. Filippou, C. Völkl, W. Grünleitner, P. Kiprof, *Angew. Chem.* **1990**, *102*, 224–226; *Angew. Chem. Int. Ed. Engl.* **1990**, *29*, 207–209; b) E. M Carnahan, S. J. Lippard, *J. Am. Chem. Soc.* **1990**, *112*, 3230–3231; c) J. Wu, P. E. Fanwick, C. P. Kubiak, *ibid.* **1988**, *110*, 1319–1321; d) D. Lentz, I. Brüdgam, H. Hartl, *Angew. Chem.* **1984**, *96*, 511–512; *Angew. Chem. Int. Ed. Engl.* **1984**, *23*, 525–526. e) F. A. Cotton, S. A. Duraj, W. J. Roth, *J. Am. Chem. Soc.* **1984**, *106*, 6987–6993.

[17] G. Beck, W. P. Fehlhammer, *Angew. Chem.* **1988**, *100*, 1391–1394; *Angew. Chem. Int. Ed. Engl.* **1988**, *27*, 1344–1347.

[18] J. E. Corella II, R. L. Thompson, N. J. Cooper, *Angew. Chem.* **1992**, *104*, 55–57; *Angew. Chem. Int. Ed. Engl.* **1992**, *31*, 83–84.

[19] B. Ledig, M. Marsch, K. Harms, G. Boche, *Angew. Chem.* **1992**, *104*, 80–81; *Angew. Chem. Int. Ed. Engl.* **1992**, *31*, 79–80.

[20] a) M. J. Abrams, A. Davison, A. G. Jones, C. E. Costello, H. Pang, *Inorg. Chem.* **1983**, *22*, 2798–2800.

[21] Review: M. Molter, *Chem. Ztg.* **1979**, *103*, 31–52.

[22] a) R. J. English, J. Kozlowski, S. S. Tumeh, B. L. Holman, *J. Nucl. Med. Technol.* **1987**, *15*, 138–143; b) A. G. Jones, M. J. Abrams, A. Davison, J. W. Brodack, A. K. Toothaker, S. J. Adelstein, A. I. Kassis, *J. Nucl. Med. Biol.* **1984**, *11*, 225–234.

[23] K. Kawakami, M. Okajima, T. Tanaka, *Bull. Chem. Soc. Jpn.* **1978**, *51*, 2327–2329.

[24] P. Yaneff, J. Powell, *J. Organomet. Chem.* **1979**, *179*, 101–113.

[25] M. E. Kastner, M. J. Lindsay, M. J. Clarke, *Inorg. Chem.* **1982**, *21*, 2037–2040.

[26] L. A. O'Connell, J. Dewan, A. G. Jones, A. Davison, *Inorg. Chem.* **1990**, *29*, 3539–3547.

[27] M. Sodeoka, M. Shibasaki, *J. Org. Chem.* **1985**, *50*, 1149–1150.

[28] M. Sodeoka, H. Yamada, M. Shibasaki, *J. Am. Chem. Soc.* **1990**, *112*, 4906–4911.

[29] A. F. Cunningham Jr., E. P. Kündig, *J. Org. Chem.* **1988**, *53*, 1823–1825.

[30] R. Dabard, G. Jaouen, G. Simonneaux, M. Cais, D. H. Kohn, A. Lapid, D. Tatarsky, *J. Organomet. Chem.* **1980**, *184*, 91–101.

[31] A. Efraty, I. Feinstein, L. Wackerle, F. Frolow, *Angew. Chem.* **1980**, *92*, 649–650; *Angew. Chem. Int. Ed. Engl.* **1980**, *19*, 633–634.

[32] a) I. Feinstein-Jaffe, F. Frolow, L. Wackerle, A. Goldman, A. Efraty, *J. Chem. Soc. Dalton Trans.* **1988**, 469–476; b) A. Efraty, I. Feinstein, F. Frolow, *Inorg. Chem.* **1982**, *21*, 485–488.

[33] M. Hanack, S. Deger, A. Lange, *Coord. Chem. Rev.* **1988**, *83*, 115–136.

[34] J. S. Rommel, J. B. Weinrach, D. S. Grubisha, D. W. Bennett, *Inorg. Chem.* **1988**, *27*, 2945–2949.

[35] Y. Ito, A. Ohnishi, H. Ohsaki, M. Murakami, *Synthesis* **1988**, 714–715.

[36] W. P. Fehlhammer, W. Finck, *J. Organomet. Chem.* **1991**, *414*, 261–270.

[37] D. Lentz, D. Preugschat, unpublished results; D.Lentz, Freie Universität Berlin, personal communication.

[38] K. R. Mann, J. G. Gordon II, H. B. Gray, *J. Am. Chem. Soc.* **1975**, *97*, 3553–3555.

[39] N. S. Lewis, K. R. Mann, J. G. Gordon II, H. B. Gray, *J. Am. Chem. Soc.* **1976**, *98*, 7461–7463.

[40] K. R. Mann, J. A. Thich, R. A. Bell, C. E. Coyle, H. B. Gray, *Inorg. Chem.* **1980**, *19*, 2462–2468.

[41] a) K. R. Mann, N. S. Lewis, V. M. Miskowski, D. K. Erwin, G. S. Hammond, H. B. Gray, *J. Am. Chem. Soc.* **1977**, *99*, 5525–5526; b) I. S. Sigal, K. R. Mann, H. B. Gray, *ibid.* **1980**, *102*, 7252–7256.

[42] K. R. Mann, R. A. Bell, H. B. Gray, *Inorg. Chem.* **1979**, *18*, 2671–2673.

[43] K. R. Mann, *Cryst. Struct. Commun.* **1981**, *10*, 451–457.

[44] C.-M. Che, F. H. Herbstein, W. P. Schaefer, R. E. Marsh, H. B. Gray, *Inorg. Chem.* **1984**, *23*, 2572–2575.

[45] W. L. Gladfelter, H. B. Gray, *J. Am. Chem. Soc.* **1980**, *102*, 5909–5910.

[46] R. J. Angelici, M. H. Quick, G. A. Kraus, D. T. Plummer, *Inorg. Chem.* **1982**, *21*, 2178–2184.

[47] D. T. Plummer, B. A. Karcher, R. A. Jacobson, R. J. Angelici, *J. Organomet. Chem.* **1984**, *260*, 347–362.

[48] M. L. Winzenburg, J. A. Kargol, R. J. Angelici, *J. Organomet. Chem.* **1983**, *249*, 415–428.

[49] J. A. Kargol, R. J. Angelici, *Inorg. Chim. Acta* **1983**, *68*, 127–130.

[50] A. Klausener et al. in *Methoden Org. Chem. (Houben Weyl)* 4th ed. **1952–1991**, vol. E14a/1, pp. 12–13.

[51] F. E. Hahn, M. Tamm, P. Hein, unpublished results.

[52] a) M. Colapietro, A. Domenicano, G. Portalone, I. Torrini, I. Hargittai, G. Schultz, *J. Mol. Struct.* **1984**, *125*, 19–32; b) V. B. Carter, D. Britton, W. B. Gleason, *Cryst. Struct. Commun.* **1977**, *6*, 543–548.

[53] J. A. Connor, E. M. Jones, G. K. McEwen, M. K. Lloyd, J. A. McCleverty, *J. Chem. Soc. Dalton Trans.* **1972**, 1246–1253.

[54] M. G. Hill, M. C. Comstock, K. R. Mann, *J. Org. Chem.* **1990**, *55*, 4950–4951.

[55] R. A. Michelin, R. J. Angelici, *Inorg. Chem.* **1980**, *19*, 3853–3856.

[56] F. E. Hahn, M. Tamm, *Angew. Chem.* **1991**, *103*, 213–215; *Angew. Chem. Int. Ed. Engl.* **1991**, *30*, 203–205.

[57] F. E. Hahn, M. Tamm, A. Dittler-Klingemann, R. Neumeier, *Chem. Ber.* **1991**, *124*, 1683–1686.

[58] F. E. Hahn, M. Tamm, *Organometallics* **1992**, *11*, 84–90.

[59] F. E. Hahn, M. Tamm, *J. Organomet. Chem.* **1990**, *398*, C19–C21.

[60] F. E. Hahn, M. Tamm, *Angew. Chem.* **1992**, *104*, 1218–1221; *Angew. Chem. Int. Ed. Engl.* **1992**, *31*, 1212–1214.

[61] F. E. Hahn, M. Tamm, unpublished results; M. Tamm, dissertation, Technische Universität Berlin, **1992**.

[62] E. C. Constable, B. F. G. Johnson, F. K. Khan, J. Lewis, P. R. Raithby, P. Mikulcik, *J. Organomet. Chem.* **1991**, *403*, C15–C18.

[63] F. E. Hahn, M. Tamm, *J. Organomet. Chem.* **1991**, *410*, C9–C12.

[64] F. E. Hahn, M. Tamm, *Chem. Ber.* **1992**, *125*, 119–121.

[65] F. E. Hahn, S. Rupprecht. *Chem. Ber.* **1991**, *124*, 481–486.

[66] F. E. Hahn, S. Rupprecht, *J. Chem. Soc. Chem. Commun.* **1991**, 224–225.

[67] F. A. Cotton, F. Zingales, *J. Am. Chem. Soc.* **1961**, *83*, 351–355.

[68] E. P. Kündig, P. L. Timms, *J. Chem. Soc. Dalton Trans.* **1980**, 991–995.

[69] F. E. Hahn, M. Tamm, E. P. Kündig, unpublished results.

[70] a) L. Malatesta, A. Sacco, S. Ghielmi, *Gazz. Chim. Ital.* **1952**, *82*, 516–521; b) G. J. Essenmacher, P. M. Treichel, *Inorg. Chem.* **1977**, *16*, 800–806.

[71] A. G. Jones, A. Davison, J. Kronauge, M. J. Abrams (Harvard College and Massachusetts Institute of Technology) EP 213945 [*Chem. Abstr.* **1987**, *17*, 92826c].

[72] F. E. Hahn, M. Tamm, R. Weimann, J. Pickardt, *Acta Crystallogr. Sect. C* **1990**, *46*, 1567–1569.

[73] a) For CF_3NC: D. Christen, K. Ramme, B. Haas, H. Oberhammer, D. Lentz, *J. Chem. Phys.* **1984**, *80*, 4020–4024; b) For CH_3NC: L. Halonen, I. M. Mills, *J. Mol. Spectrosc.* **1978**, *73*, 494–502.

[74] I. D. Kuntz, Jr., P. von R. Schleyer, A. Allerhand, *J. Chem. Phys.* **1961**, *35*, 1533–1534.

[75] I. Morishima, A. Mizuno, T. Yonezawa, *J. Chem. Soc. Chem. Commun.* **1970**, 1321–1322.

[76] R. B. King, M. S. Saran, *Inorg. Chem.* **1974**, *13*, 74–78.

[77] J.-M. Bassett, D. E. Berry, G. K. Barker, M. Green, J. A. K. Howard, F. G. A. Stone, *J. Chem. Soc. Dalton Trans.* **1979**, 1003–1011.

[78] Review: E. L. Muetterties, M. J. Krause, *Angew. Chem.* **1983**, *95*, 135–148; *Angew. Chem. Int. Ed. Engl.* **1983**, *22*, 135–148.

[79] Reviews: a) RP-bridged clusters: G. Huttner, K. Knoll, *Angew. Chem.* **1987**, *99*, 765–783; *Angew. Chem. Int. Ed. Engl.* **1987**, *26*, 743–760; b) Sulfur-bridged carbonylosmium clusters: R. D. Adams, *Polyhedron* **1985**, *4*, 2003–2025; c) H. Vahrenkamp, *Adv. Organomet. Chem.* **1983**, *22*, 169–208.

[80] a) J. J. de Boar, J. A. van Doorn, C. Masters, *J. Chem. Soc. Chem. Commun.* **1978**, 1005–1006; b) J. T. Mague, C. L. Lloyd, *Organometallics* **1992**, *11*, 26–34; c) A. Stützer, P. Bissinger, H. Schmidbaur, *Chem. Ber.* **1992**, *125*, 367–372; d) Review: H. Wadepohl, *Angew. Chem.* **1992**, *104*, 253–268; *Angew. Chem. Int. Ed. Engl.* **1992**, *31*, 247–262.

[81] J. E. Sarneski, A. T. McPhail, K. D. Onau, L. E. Erickson, *J. Am. Chem. Soc.* **1977**, *99*, 7376–7378.

[82] C. H. Wei, L. F. Dahl, *J. Am. Chem. Soc.* **1966**, *88*, 1821–1822.

[83] R. Mason, A. I. M. Rae, *J. Chem. Soc. A* **1968**, 778–779.
[84] E. R. Corey, L. F. Dahl, *Inorg. Chem.* **1962**, *1*, 521–526.
[85] B. F. G. Johnson, J. Lewis, D. A. Pippard, *J. Chem. Soc. Dalton Trans.* **1981**, 407–412.
[86] W. Hieber, D. von Pigenot, *Chem. Ber.* **1956**, *89*, 193–201.
[87] F. A. Cotton, R. V. Parish, *J. Chem. Soc.* **1960**, 1440–1446.
[88] S. Grant, J. Newman, A. R. Manning, *J. Organomet. Chem.* **1975**, *96*, C11–C12.
[89] a) J. P. Ferris, F. R. Antonucci, R. W. Trimmer, *J. Am. Chem. Soc.* **1973**, *95*, 919–920; b) R. R. Fraser, T. S. Mansour, S. Savard, *Can. J. Chem.* **1985**, *63*, 3505–3509.
[90] P. Jutzi, U. Gilge, *J. Organomet. Chem.* **1983**, *246*, 159–162.
[91] W. Strohmeier, F.-J. Müller, *Chem. Ber.* **1969**, *102*, 3608–3612.
[92] W. P. Fehlhammer, K. Bartel, B. Weinberger, U. Plaia, *Chem. Ber.* **1985**, *118*, 2220–2234.
[93] a) W. P. Fehlhammer, K. Bartel, U. Plaia, A. Völkl, A. T. Liu, *Chem. Ber.* **1985**, *118*, 2235–2254; b) U. Plaia, H. Stolzenberg, W. P. Fehlhammer, *J. Am. Chem. Soc.* **1985**, *107*, 2171–2172; c) W. Beck, W. Weigand, U. Nagel, M. Schaal, *Angew. Chem.* **1984**, *96*, 377–378; *Angew. Chem. Int. Ed. Engl.* **1984**, *23*, 377–378.
[94] W. P. Fehlhammer, H. Hofmeister, H. Stolzenberg, B. Boyadjiev, *Z. Naturforsch. B* **1989**, *44*, 419–428.
[95] W. Beck, C. Weis, J. Wieczorek, *J. Organomet. Chem.* **1971**, *30*, 89–96.
[96] a) J.-C. Daran, Y. Yeannin, *Acta Crystallogr. Sect. B* **1980**, *36*, 1392–1395; b) O. S. Mills, A. D. Redhouse, *Angew. Chem.* **1965**, *77*, 1142–1143; *Angew. Chem. Int. Ed. Engl.* **1965**, *4*, 1082; c) C. P. Casey, T. J. Burkhardt, C. A. Bunnell, J. A. Calabrese, *J. Am. Chem. Soc.* **1977**, *99*, 2127–2133; d) C. P. Casey, N. W. Vollendorf, K. J. Haller, *J. Am. Chem. Soc.* **1984**, *106*, 3754–3764.
[97] L. Zanatto, R. Bertani, R. A. Michelin, *Inorg. Chem.* **1990**, *29*, 3265–3268.
[98] a) F. Volantron, O. Eisenstein, *J. Am. Chem. Soc.* **1986**, *108*, 2173–2179; b) C. P. Casey, A. J. Shusterman, N. W. Vollendorf, K. J. Haller, *ibid.* **1982**, *104*, 2417–2423; c) C. Alvarez, A. Pacreau, A. Parlier, H. Rudler, J.-C. Daran, *Organometallics* **1987**, *6*, 1057–1064; d) C. Alvarez Toledano, H. Rudler, J.-C. Daran, Y. Jeannin, *J. Chem. Soc. Chem. Commun.* **1984**, 574–576; e) C. Alvarez Toledano, A. Parlier, H. Rudler, J.-C. Daran, Y. Jeannin, *ibid.* **1984**, 576–578.
[99] Y. Ito, K. Kobayashi, N. Seko, T. Saegusa, *Heterocycles* **1981**, *16*, 181.
[100] a) H. Werner, B. Weber, O. Nürnberg, J. Wolf, *Angew. Chem.* **1992**, *104*, 1105–1107; *Angew. Chem. Int. Ed. Engl.* **1992**, *31*, 1025–1027; b) W. A. Herrmann, D. Mihalios, K. Öfele, P. Kiprof, F. Belmedjahed, *Chem. Ber.* **1992**, *125*, 1795–1799.

Sequence-Specific Recognition and Modification of Double-Helical DNA by Oligonucleotides

By Nguyen T. Thuong and Claude Hélène*

Dedicated to Professor Charles Sadron on the occasion of his 90th birthday

Nucleic acids can be selectively recognized by a large number of natural and synthetic ligands. Oligonucleotides provide the highest specificity of recognition. They can bind to a complementary single-stranded sequence by forming Watson–Crick hydrogen bonds. They can also recognize the major groove of double-helical DNA at specific sequences by forming Hoogsteen or reverse Hoogsteen hydrogen bonds with purine bases of the Watson–Crick base pairs, resulting in a triple helix. Triple-helix formation through oligonucleotide binding to DNA is a sequence-specific interaction involving primarily homopurine · homopyrimidine sequences in the double-helical target. Extending the range of recognition sequences remains a challenge to chemists. Both thermodynamic and kinetic parameters for triplex formation have been determined. These parameters indicate, for example, that triple-helix formation is a much slower process than duplex formation. Nuclease-resistant oligonucleotides synthesized with the α-anomers of nucleosides (instead of the natural β-anomers) also form triple helices with double-stranded DNA. Triple-helix-forming oligonucleotides can be modified, for example, by attaching DNA intercalating agents to enhance their binding affinity. They may also be modified with reagents that induce irreversible reactions in their target sequence upon chemical or photochemical activation. Thus, artificial nucleases can be developed with very high sequence specificity on megabase-size DNA. Furthermore, triple-helix-forming oligonucleotides can be used to selectively control gene expression. When bound to the regulatory region(s) of specific genes they may prevent activation (or repression) of transcription. When binding occurs near or downstream from the transcription initiation site, elongation of the transcript may be inhibited. Therefore, the potential exists for developing new gene-blocking agents with therapeutic applications in the treatment of gene disorders.

1. Introduction

The recognition of specific nucleic acid sequences has been the subject of a large number of studies over many years. This interest arises from the early observation that gene expression in all living organisms is controlled by regulatory proteins that bind to specific sequences on single- or double-stranded nucleic acids. During the last ten years, resolution of the X-ray crystallographic structures of several nucleic acid–protein complexes has provided details of the molecular interactions involved in protein–nucleic acid recognition.[1] Despite these advances and the study of model systems[2] we are not yet in a position to predict the oligopeptide sequence that will recognize any given nucleic acid sequence.

Nucleic acids, especially double-stranded DNA, bind a large number of naturally occurring and synthetic ligands, such as antibiotics or antitumor agents. For example, intercalating agents insert their aromatic rings between two adjacent base pairs of double-helical DNA.[3] Minor groove-binding ligands have also been reported to alter biological processes that involve DNA as a substrate.[4] Until very recently there was no ligand available with a high enough selectivity to recognize a single sequence in double-helical DNA within a living cell. The size of the DNA genome in living organisms ranges from a few million base pairs in bacteria (4.5×10^6 in *Escherichia coli*, the bacterium that colonizes the intestinal tract in humans) to a few billion in higher (eukaryotic) systems (about 3×10^9 base pairs in human DNA, which is not the largest genome among all living organisms).[5] Viruses, which after infection rely on the host cell for multiplication, have smaller genomes consisting of either single- or double-stranded ribo- or deoxyribonucleic acids (RNA or DNA). For example, the genetic information (genome) of the human immunodeficiency virus (HIV) is contained within a single-stranded RNA chain of about 9200 ribonucleotides.[6]

In order for a ligand to recognize a single sequence in a nucleic acid it should interact with a number of nucleotides or base pairs; this number depends on the size of the targeted nucleic acid (Fig. 1). The minimum number of base pairs that must be recognized in a bacterium such as *E. coli* (4.5×10^6 base pairs) is about 11, while that in a human cell (3×10^9 base pairs) is approximately 17.[7] These estimations are based on a statistical distribution of base pairs in the DNA genome and an equal number of A · T and G · C base pairs. More sophisticated calculations can be done by using additional parameters such as the nearest neighbor frequencies, which have been determined for many organisms.[7]

The only nucleic acid binding ligands known to date that can achieve such a high degree of specificity are nucleic acids themselves. Since the discovery of the DNA double-helical

[*] Prof. C. Hélène
Laboratoire de Biophysique
Muséum National d'Histoire Naturelle
INSERM U.201–CNRS URA 481
43 rue Cuvier, F-75231 Paris Cedex 05 (France)
Telefax: Int. code +(1) 40793705
Dr. N. T. Thuong
Centre de Biophysique Moléculaire, CNRS
F-45071 Orléans Cedex 02 (France)

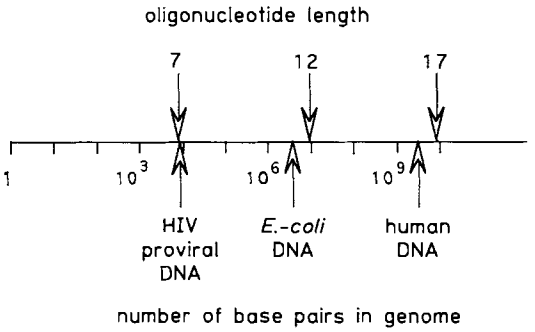

Fig. 1. The required length an oligonucleotide should be in order to recognize a unique DNA sequence in the genome of a living organism has been calculated, assuming a random distribution of base pairs and a fraction of A · T (G · C) base pairs equal to 0.5. There are four possibilities (A, T, G, or C) for each nucleotide position. Due to the complementarity of base pairs (A opposite T, G opposite C) in double-stranded DNA, there are $4^n/2$ different sequences of n base pairs for odd values of n and $4^n/2 + 4^{n/2}/2$ for even values of n [195]. When single-stranded DNA or RNA is the target and, for a site size of n nucleotides, there are 4^n distinguishable sequences. In higher (eukaryotic) organisms, the fraction of A · T base pairs is about 0.6. The nearest neighbor frequency is also known, which allows more detailed calculations to be performed (see ref. [7]). For example, the sequence $^{5'}CG^{3'}$ (but not $^{5'}GC^{3'}$) is underrepresented in eukaryotic genomes (about five times less frequent than calculated on a statistical basis). Sequences containing only C and G with several $^{5'}CG^{3'}$ sequences will have less probability of being found in eukaryotic DNA than sequences rich in A and T. The genome of *E. coli* (4.5×10^6 base pairs) and of human beings (3×10^9 base pairs) is indicated together with that of HIV. The genetic information of HIV is carried by a single-stranded RNA, but following infection, this RNA is reverse transcribed into double-stranded DNA which integrates into the DNA of the infected cell. A minimum length of about 17 bases is therefore required to recognize a unique sequence within the proviral DNA once it is integrated in the genome of the infected cell.

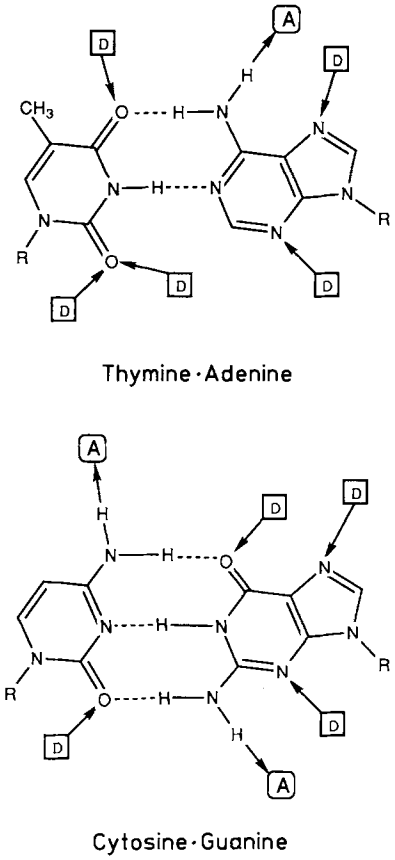

Fig. 2. Watson–Crick base pair formation. Hydrogen bond donor (D) and acceptor (A) sites within both the major and the minor groove are indicated (taken from ref. [2]).

structure in 1953,[8] the Watson–Crick model of base pair formation has provided the code for recognition of any single-stranded nucleic acid sequence. Two hydrogen bonds allow the recognition of adenine (A) by thymine (T) or uracil (U), and three hydrogen bonds are involved in recognition of guanine (G) by cytosine (C) (Fig. 2). Due to these selective recognition rules it is possible to design an oligonucleotide that will recognize any base sequence on a single-stranded nucleic acid target. The isomorphism of purine · pyrimidine

Nguyen Thanh Thuong left Vietnam in 1950, at the age of twenty, came to France, and studied chemistry at Ecole Superieure de Chimie de Mulhouse from 1954 to 1958. In 1960, he received his doctorate in chemistry under the supervision of P. Chabrier in Paris. Until 1978 he worked as an organic chemist in industry, then joined the Centre de Biophysique Moléculaire (CNRS) in Orléans. His fields of interest are the synthesis and application of modified oligonucleotides in molecular biology.

Claude Hélène was born in 1938. After graduating from the Ecole Normale Supérieure de Saint-Cloud, he received his Ph.D. in 1966 from the University of Paris. In 1967 he moved to the Centre de Biophysique Moléculaire, a CNRS Institute, in Orleans as a CNRS researcher. In 1974 he became Director of this institute. In 1976 he was appointed as Professor to the Chair of Biophysics at the Muséum National d'Histoire Naturelle in Paris, where he created a new INSERM and CNRS research unit in 1980. Since 1990 he has also been a Scientific Director at Rhône-Poulenc. In 1988 he was elected a full member of the French Academy of Sciences. Claude Hélène has been involved early on in studies on nucleic acid excited states and photochemistry, and on protein (peptide)–nucleic acid interactions. During the last ten years, he has developed new approaches in the field of antisense and antigene oligonucleotides.

base pairs ensures that there is no major distortion of the phosphodiester backbones of a double helix (the two chains wrap around each other in a regular way). Hydrogen bonding interactions between purines and/or pyrimidines other than A · T(U) or G · C are possible, but the distortion of the backbone introduces an energy penalty that leads to rejection of such interactions in a (perfect) double helix. However, under certain circumstances some base pairs such as G · T ("wobble" base pair) can be accommodated within a double helix. The high fidelity of DNA replication, which ensures that genetic information is not lost during cell division, requires a highly sophisticated proofreading process, thereby eliminating erroneous bases introduced by the enzymatic replication machinery.[9]

It has long been recognized that nucleic acid base pairs of double-helical DNA retain hydrogen bonding capabilities in both the minor and major groove of the double helix. These capabilities may be exploited for sequence-specific recognition (see Fig. 2).[2] A few years after the discovery of the DNA *double helix* structure,[8] it was shown that a *triple helix* could be formed by polynucleotides.[10] Two chains of the polyribonucleotide poly(rU) are able to simultaneously bind to one chain of poly(rA). This was the starting point for a number of studies, showing that double helices containing only purines in one chain could bind a third polynucleotide containing only pyrimidines (e.g., poly(dCT) binding to poly(dGA) · poly(dCT)) or only purines (e.g., poly(dG) binding to poly(dG) · poly(dC)) (Fig. 3).[11-13] The hydrogen bonding interactions involved in triple-helix formation are often referred to as Hoogsteen hydrogen bonds. Hoogsteen discovered that in cocrystals of adenine and thymine derivatives a hydrogen bonding pattern different from that of Watson–Crick base pairs was present.[14] These hydrogen bonds are involved when a (third) strand of poly(dT) binds to a Watson–Crick-paired poly(dA) · poly(dT) double helix.

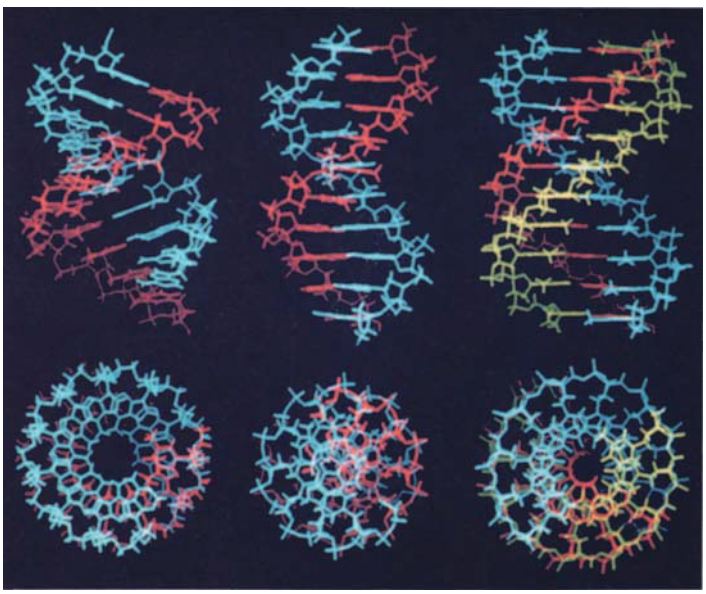

Fig. 3. Model of A-DNA (left), B-DNA (center), and triple-helical DNA (right). End-on views of the structures are shown below. The A- and B-DNA structures were obtained from the atomic coordinates given by Arnott et al. [208]. The triple helix structure was obtained by energy minimization [63] starting from the structure obtained by X-ray diffraction of poly(dA) · 2poly(dT) fibers [50]. In this triple-helical structure, the third strand contains only pyrimidines, which are hydrogen bonded to the purine strand of the double helix according to the Hoogsteen hydrogen bonding mode in Figure 5. The third strand runs parallel to the Watson–Crick purine strand. Other possible triple-helical structures are discussed in the text.

The interest in triple helices was recently rekindled when it was shown that:

1) Mirror-repeat homopurine · homopyrimidine sequences of circular double-stranded DNA could adopt a new structure, called H-DNA, under superhelical stress.[15-17] This structure arises from the concomittant formation of a triple helix and a single-stranded loop (Fig. 4) within superhelical circular DNA.

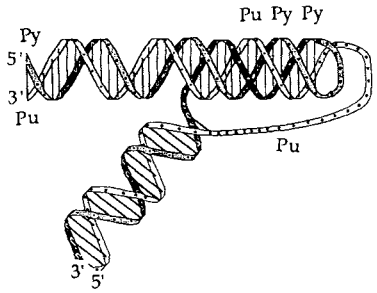

Fig. 4. Structure of H-DNA formed when a mirror-repeat polypurine · polypyrimidine sequence is subjected to supercoiling constraints within circular DNA. Half of the polypyrimidine strand folds back on the pu · py double helix to form a py × pu · py triple helix, and the corresponding complementary half of the polypurine sequence becomes single-stranded. Alternatively, the polypurine sequence can fold back on the pu · py double helix to form a pu × pu · py triple helix and a polypyrimidine single strand (adapted from ref. [16]).

2) Short oligonucleotides could bind to the major groove of double-helical DNA by forming a local triple helix through sequence-specific Hoogsteen hydrogen bond formation.[18-20, 99]

This review will focus mainly on triple-helix formation by short oligonucleotides bound to double-helical DNA. New information has been accumulating during the last few years on the structure, thermodynamics, and kinetics of such interactions. The possibility of designing a new generation of sequence-specific regulators of gene expression based on DNA recognition by triple-helix-forming oligonucleotides has a great deal of interest in the chemistry and biology of oligonucleotide analogues. We have called this approach the "antigene" strategy[21] (a specific gene being the target of a triple-helix-forming oligonucleotide) by analogy with the "antisense" strategy (where the oligonucleotide is targeted to a single-stranded "sense" nucleic acid, such as a messenger RNA (mRNA) or a viral RNA, through formation of Watson–Crick base pairs). Several recent reviews on the antisense strategy have been published,[22-25] and this aspect of oligonucleotide chemistry and biology will not be dealt with in the present review, except when similar chemical modifications have been introduced in both the antigene and antisense approaches.

2. Triple-Helix Formation by Oligonucleotides

2.1. Base Triplets

As stated in the introduction, triple-helix formation relies upon hydrogen bonding interactions between bases in the

third strand and purines already engaged in Watson–Crick hydrogen bonding to pyrimidines. Figure 5 shows the base triplets that could be formed with natural bases.[21] Several features are of importance:

1) All base triplets in Figure 5 involve two hydrogen bonds with the purines of the A · T and G · C base pairs.

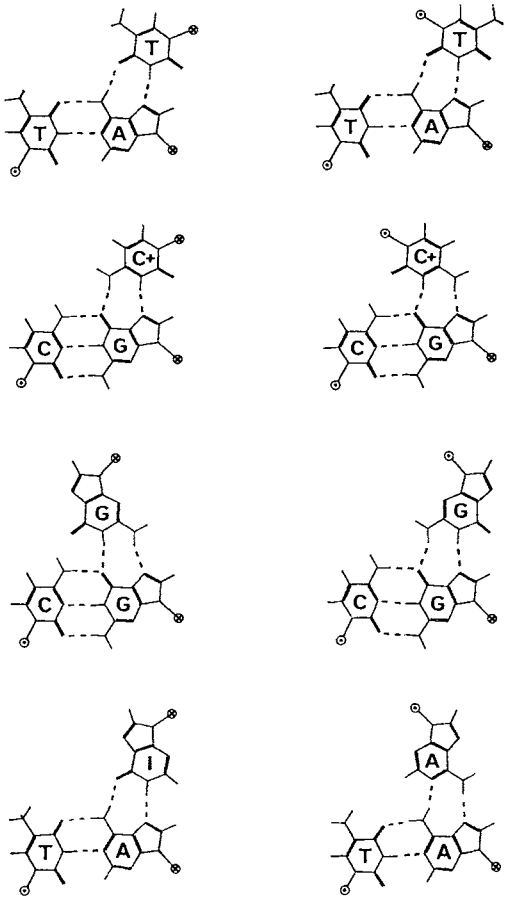

Fig. 5. Base triplets formed by Watson–Crick A · T and G · C base pairs with T, protonated C (C^+), G, A, and I. If bases in the third strand are in the *anti* conformation with respect to the sugar ring, the triplets in the left column correspond to a parallel orientation of the third strand with respect to the homopurine sequence of the DNA target, while those in the right column correspond to the reverse orientation. For the T × A · T triplets, the one on the left corresponds to the Hoogsteen hydrogen bonding pattern, whereas the one on the right corresponds to reverse Hoogsteen (see text). Some of these base triplets have been found in the crystal structures of transfer RNAs [26, 27] [e.g. G × G · C (reverse Hoogsteen bonds) and A × A · U]. Of course, many other possibilities exist where a single hydrogen bond is formed by the base in the third strand with any of the bases in the Watson–Crick base pairs. The structures of the base triplets shown in this figure were obtained from energy-minimized triple helices of ten identical base triplets (see ref. [63]).

2) In order to form two hydrogen bonds with G in a G · C base pair, cytosine must be protonated. The pK value of isolated deoxycytidine is 4.3, but the apparent pK is raised in oligonucleotides and multistranded nucleic acids due to their polyanionic character. Homopyrimidine oligonucleotides can form stable triple helices at acidic pH but, as expected, their stability decreases as the pH increases. However, the pH dependence is affected by the distribution of cytosines within the oligonucleotide sequence. Adjacent cytosines will create an unfavorable situation due to electrostatic repulsions between protonated rings.

3) All base triplets involving T, C, or G in the third strand may adopt two isomeric configurations. One series (left-hand side of Fig. 5) correspond to the hydrogen bonding scheme discovered by Hoogsteen in cocrystals of A and T,[14] and will be referred to as *Hoogsteen base triplets*. The other series (right-hand side on Fig. 5) involves a 180° rotation of the base in the third strand, and will be referred to as *reverse Hoogsteen base triplets*. Adenine in the third strand can adopt only a single configuration for the formation of two hydrogen bonds. The resulting A × A · T base triplet belongs to the reverse Hoogsteen category. Inosine can form two Hoogsteen hydrogen bonds with A · T base pairs (I × A · T).

4) One important parameter in designing oligonucleotides that bind to the major groove of double-helical DNA is the isomorphism of base triplets. When the C-1′ atoms of the Watson–Crick base pairs are fixed, the position of the C-1′ atom of the nucleotide in the third strand depends on the base triplet (Fig. 6). Only two triplets T × A · T and

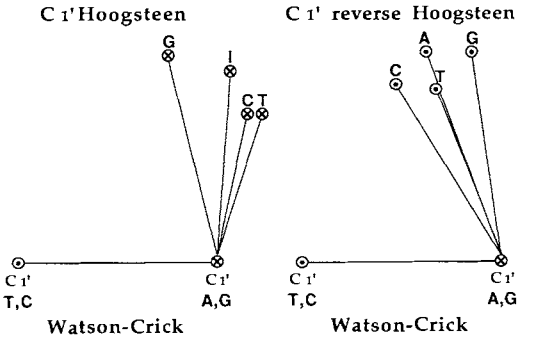

Fig. 6. Isomorphism of base triplets. The C1′ atoms of the three nucleotides belonging to each triplet are shown, with the C1′ atoms of the Watson–Crick base pair T · A or C · G located at a fixed position. The C1′ atoms of the nucleotide in the third strand are shown in either the Hoogsteen mode of hydrogen bonding (left column of Fig. 5) or in the reverse Hoogsteen mode (right column of Fig. 5).

C^+ × G · C are isomorphous. Other combinations lead to a distortion of the backbone(s) of the triple helix in order to minimize the effects of non-isomorphism. Hence, triple helix stability will be reduced when several steps along the triple helix are distorted.

2.2. Orientation of the Third Strand

Accoding to Figure 5, triple helix-forming oligonucleotides can be synthesized from naturally occurring nucleosides. The bases in the third strand bind to the purine bases in the target DNA through hydrogen bonds. To avoid the distortion of the oligonucleotide backbone that would result from switching from one strand of the double helix to the other, triple helices preferentially form at homopurine · homopyrimidine sequences of DNA (i.e. all purines in the target sequence belong to the same strand of the double helix).

As stated previously (Fig. 6), only two base triplets (T × A · T and C^+ × G · C) are isomorphous when Hoogsteen hydrogen bonds are involved. Thus, triple-helix-forming oligonucleotides containing only pyrimidines (T and C)

have been the subject of the majority of recent studies.[21] However, despite the backbone distortion that results from the heteromorphism of other base triplets, oligonucleotides other than those containing only pyrimidines are able to form triple helices with homopurine · homopyrimidine sequences of DNA. Oligonucleotides containing either G and T,[28, 29] G and A,[30, 31] or G, T, and C[32] have been shown to form triple helices. The formation of purine × purine · pyrimidine triplets was also shown to occur with either intramolecularly folded oligonucleotides,[33–35] polynucleotides with repeating units,[36, 37] or polypurine · polypyrimidine sequences in supercoiled plasmids.[38–40]

With all nucleotides in the *anti* conformation,[*] Hoogsteen hydrogen bonds lead to a parallel orientation of the third strand with respect to the homopurine target strand. Reverse Hoogsteen hydrogen bonding corresponds to an antiparallel orientation. If nucleotides in the third strand adopt the *syn* conformation, these orientations are reversed.

The orientation of third-strand oligonucleotides has been verified in several different ways:

1) For oligonucleotides which have a symmetrical base sequence (i.e. when the same base sequence is read in the 5′ → 3′ and 3′ → 5′ directions), attachment to particular positions of a cleaving reagent such as Fe-EDTA[**][19, 30] or a photocross-linking reagent[18, 41] has allowed direct determination of the orientation from an analysis of the location of the cleavage or cross-linking sites (cleavage at cross-linked sites was achieved with alkaline treatment[18, 41]).

2) For asymmetrical sequences optical melting curves (determinations with optical methods),[42] footprinting,[60, 122] or gel retardation experiments[29, 98] carried out with sequences of opposite polarities were used to determine which of the two orientations was bound to the target DNA.

In all cases, the orientation was found to obey the rules presented above. Oligopyrimidines bind in a parallel orientation with respect to the homopurine strand of the target DNA sequence.[18, 19, 41, 42] Oligopurines bind in an antiparallel orientation.[30] For oligonucleotides containing G and T the orientation was originally proposed to be parallel to the homopurine sequence[28] but later shown to be antiparallel.[29]

The intrinsic stability of T × A · T and G × G · C base triplets favors the Hoogsteen mode of hydrogen bonding. However, the energy penalty associated with the distortion of the backbone imposed by the non-isomorphism of these two triplets is less important for the reverse Hoogsteen configuration (Fig. 6). Therefore it might be surmised that the orientation of an oligonucleotide containing G and T should depend on the number of TpG and GpT steps in the third strand. This prediction has been experimentally verified.[43]

An oligonucleotide containing T, C, and G [$d(T_4CT_4G_6)$] was shown to bind in a parallel orientation with respect to the homopurine sequence.[32] In this complex six adjacent G × G · C Hoogsteen triplets formed together with Hoogsteen T × A · T and C^+ × G · C base triplets.

2.3. Extension of Recognition Sequences for Triple-Helix Formation

Triple-helix formation requires a homopurine · homopyrimidine sequence in the target DNA. A non-natural deoxynucleotide (1-(2-deoxy-β-D-ribofuranosyl)-4-(3-benzamidophenyl)imidazole) was recently shown to bind both T · A and C · G Watson–Crick base pairs when incorporated in an oligopyrimidine.[215] Although this derivative does not discriminate T · A from C · G base pairs, it allows triple helix formation at oligopurine sequences interrupted by one pyrimidine. It remains a challenge to design oligonucleotides that will recognize mixed purine/pyrimidine sequences. Recent work has shown that alternate-strand triple-helix formation can be achieved in different ways. Formation of this structure allows the recognition of a mixed sequence in which homopurine sections alternate on the two strands of DNA.

2.3.1. *Oligonucleotides with Opposite Polarities*

Two homopyrimidine oligonucleotides that bind in a parallel orientation with respect to the homopurine sequence of duplex DNA can be linked to each other at their 3′ or 5′ ends.[44–46] Different linkers have been described which allow simultaneous binding of the homopyrimidine oligonucleotides to adjacent purine tracts on alternate strands of the DNA duplex in parallel but opposite orientations (see **1**).

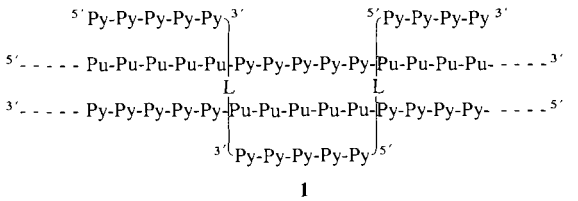

1

A 3′-3′-oligodeoxynucleotide **2** containing two pyrimidine sequences flanking a 1,2-dideoxy-D-ribose was synthesized on a support **3**, in which the first nucleoside was attached to the CPG through its 5′-hydroxyl group. After the first pyrimidine oligomer in the 5′-3′ direction was assembled by using nucleoside-5′-phosphoramidites **4**, the linker residue was introduced in the opposite orientation through its 3′-phosphoramidite **5**. The second pyrimidine sequence was then assembled in the usual 3′-5′ direction through the classical nucleoside-3′-phosphoramidites.[44]

[*] The fundamentals of the structure of nucleic acids and their building blocks are described in biochemistry textbooks. See for example, D. Voet, J. G. Voet, *Biochemistry*, Wiley, **1990**, Chapter 28.

[**] Abbreviations used in this review: Ac: acetyl, amP: 2-aminopurine-9-β-D-2′-deoxyribofuranoside (**17a**), Acr: 2-methoxy-6-chloro-2-methoxyacridine, bp: base pair, B: nucleic base, B′: N-protected nucleic base, Bz: benzoyl, Cm: 2′-*O*-methylpseudoisocytidine (**14a**), CPG: controlled pore glass, DMT: dimethoxytrityl, dNu: 2′-deoxyribonucleoside, Dr: daunorubicine, EDTA: ethylenediaminetetraacetic acid, Elli: ellipticine, Et: ethyl, Etd: ethidium, Ibu: isobutyryl, *i*Pr: isopropyl, Me: methyl, MODA: 6-methyl-8-oxo-2′-deoxyadenosine, MPPO: methylpyrroporphyrin XXI, Phe: phenacyl, OP: orthophenanthroline, P1: 5-amino-1-(2′-deoxy-β-D-ribofuranosyl)-3-methyl-1*H*-pyrazolo[4,3-*d*]pyrimidine-7-one, p: phosphate, pAr: arylphosphate, ps: thiophosphate, psR: phosphorothioester, Pf: proflavine, PNA: polyamide nucleic acid, Pso: psoralen, Pyr: pyridocarbazole, Z × Y · X: a base triplet where base Z is located in the third strand and Y · X is the Watson–Crick base pair (× represents Hoogsteen or reverse Hoogsteen hydrogen bonds, · represents Watson–Crick hydrogen bond).

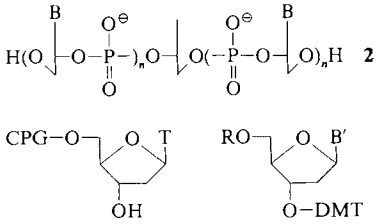

2

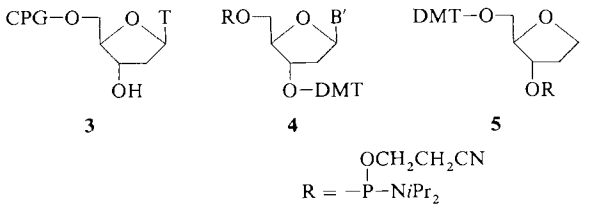

3 **4** **5**

With an analogous approach and the phosphoramidite of 1,3-propanediol (**6**), pyrimidine oligonucleotides with a 3′-3′- or a 5′-5′-internucleotide junction (**7** or **8**, respectively) were synthesized.[45] The latter were assembled from the classical support **9** (the first nucleotide is attached to CPG through its 3′-hydroxyl group) in the opposite direction to that described above. Similarly, by using the H-phosphonate of the

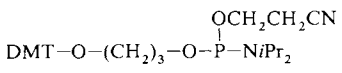

6

d-5′PypPyp- - - - -Py3′p-$(CH_2)_3$-p3′PypPyp- - - - -Py5′ **7**

d-3′PypPyp- - - - -Py5′[p$(CH_2)_3$]$_3$p5′PypPyp- - - - -Py3′ **8**

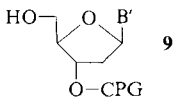

9

linkers **10**, **11a**, and **11b**, pyrimidine 3′-3′-linked oligonucleotides were obtained,[46] and shown to bind to alternate strands on double-helical DNA fragments.

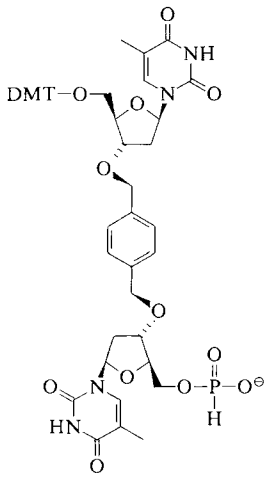

10: *p*-d-ribose dimer

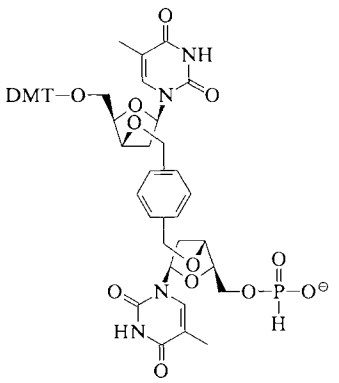

11a: *p*-d-xylose dimer
11b: *o*-d-xylose dimer

2.3.2. *Oligonucleotides with the Same Polarity*

One can take advantage of the different orientations that third-strand oligonucleotides adopt, depending on the nature of the base triplets involved in triple-helix formation. This should allow oligonucleotides containing only natural 3′-5′ phosphodiester linkages to simultaneously bind both strands of double-helical DNA by switching from one homopurine sequence to another. Sun et al.[43] have shown that the orientation of oligonucleotides containing G and T depends on the number of GpT and TpG steps. Consequently an oligonucleotide containing G and T can be designed to recognize adjacent purine tracts on alternate strands of the duplex. Beal and Dervan[47] have used the opposite orientations of pyrimidine and purine oligonucleotides bound to a homopurine sequence of duplex DNA to design a mixed-sequence oligonucleotide capable of forming an alternate-strand triple helix. The structures depend on whether the target site is 5′-(purine)$_m$(pyrimidine)$_n$-3′ or 5′-(pyrimidine)$_m$(purine)$_n$-3′. The former requires a pyrimidine domain and a purine domain linked by a 3′-5′ phosphodiester, while the latter requires that the third strand has at least two nucleotides as a linker at the site of crossover in the major groove.[47]

2.3.3. *Oligonucleotides Made from α- and β-Oligomers with the Same Polarity*

The reverse orientation of the pyrimidine oligo-α-nucleotide third strand with respect to that of the corresponding β-oligomer[122] (Section 3.3 for α-oligodeoxynucleotides) can be used to construct another set of molecules which are able to bind adjacent homopurine sequences on alternate DNA strands (see **12**). An oligo-α-deoxynucleotide covalent-

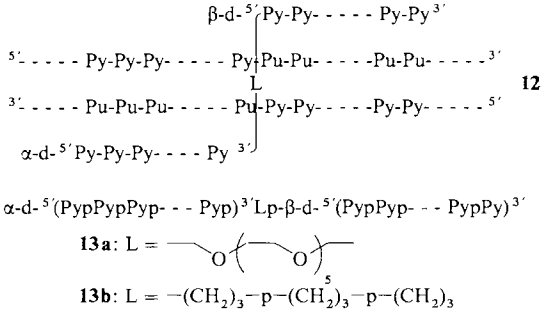

12

13a: L =

13b: L = $-(CH_2)_3-p-(CH_2)_3-p-(CH_2)_3$

ly linked to a β-oligomer of the same polarity through either a hexaethylene glycol **13a** or a 1,3-propanediol derivative **13b** were readily synthesized by using the classical solid support **9** and 3′-phosphoramidites of α- and β-deoxynucleosides (V. Roig, N. T. Thuong, unpublished results).

2.4. Structure of Triple Helices

There is no crystal structure yet available for short triple-stranded oligonucleotides which gives a detailed description of the conformation of all nucleotide units in the three strands. Fiber diffraction data are available on polynucleotide structures.[48–51] Triple-helical complexes (either intra- or intermolecular) are the subject of intensive studies by NMR techniques.[52–58] Based on fiber diffraction data it was concluded that the triple-stranded structure poly(dT) × poly(dA) · poly(dT) had a large axial rise per base

triplet with the three strands forming a 12-fold helix of the A-family all containing C3′-*endo* furanose rings. In contrast, two-dimensional ^{1}H NMR studies of a 31-base DNA oligonucleotide, which folds to form a stable intramolecular triplex at acidic pH, have shown that most of the triplex sugars are close to the C2′-*endo* conformation.[54] However, stacking interactions between the purines in an intermolecular complex containing 11 base triplets have suggested that the oligopurine strand exhibits an A-helical base stacking conformation.[52] A molecular dynamics (MD) simulation of the DNA triplex, $d(TC)_5 \cdot d(GA)_5 \cdot d(TC)_5$ has also revealed considerable deviation from the fiber diffraction model.[59]

An assignment of nonexchangeable protons for an intramolecular triple helix with seven base triplets has been proposed on the basis of three-dimensional homonuclear NOESY–TOCSY ^{1}H NMR spectroscopic studies.[58] Exchangeable protons have also been identified for both Watson–Crick and Hoogsteen hydrogen-bonded protons.[52–54] Cytosine and protonated cytosine involved in $C^+ \times G \cdot C$ base triplets can also be distinguished. Future NMR experiments will certainly give more detailed information on local conformations within the triple helix and their sequence dependence.

Conformational changes in DNA induced by triple-helix formation have been characterized by the change in reactivity of bases toward chemical or photochemical reagents. Cleavage by a copper–phenanthroline chelate has been used to obtain a footprint of the triple-helix-forming oligonucleotide on the DNA double helix.[60] The region covered by the oligonucleotide was protected, whereas a strong enhancement of cleavage was observed on the purine-rich strand at the triplex–duplex junction on the 3′-side of the homopyrimidine oligonucleotide. A strong binding site for an ellipticine derivative was detected at the triplex–duplex junction on the 5′-side of the pyrimidine oligonucleotide.[61] Intercalation of ethidium or acridine derivatives at this same junction induces a conformational change that is detected by the hypersensitivity to diethylpyrocarbonate (EtO_2C-O-CO_2Et).[62] Psoralen derivatives (5- or 8-methoxypsoralen) exhibit enhanced reactivity under UV-B irradiation, forming a cross-link between the two duplex strands at the duplex–triplex junction, provided there is a 5′ TpA 3′ sequence (M. Takasugi, C. Hélène, unpublished results). This increased photochemical reactivity was related to enhanced intercalation of the psoralen ring at the triplex–duplex junction.

Molecular modeling and energy minimization studies have also shown that triple-helix formation induces conformational changes, notably at the duplex–triplex junctions.[63, 64] Experimental evidence for bending has been provided by recent electrophoretic mobility studies on DNA fragments containing a triple helix site at different positions.[64] A slight retardation of mobility was observed, which was maximized when the triple-helical region was centrally located. However, similar experiments carried out by Maher et al.[65] showed that DNA restriction fragments carrying a triple-helical region exhibited permutation-dependent acceleration of the mobility rather than retardation in a manner consistent with DNA stiffening rather than bending at the duplex–triplex junction. It can be predicted that triple-stranded DNA helices exhibit a reduced flexibility as compared to a double helix due to the higher radial charge density and the additional constraints arising from the presence of a third strand. Bending at the junction should also occur due to changes in helical parameters of the duplex within the triple-helical region. Energy minimization studies show that bending occurs toward the minor groove at the 5′-junction and toward the major groove at the 3′-junction.[64] In addition, bending is expected to depend on the nucleotide sequence at and near the duplex–triplex junctions.

A conformational distortion in the DNA duplex induced by triplex formation was detected in the regulatory region of human *papilloma* virus type II.[66] Hypermodification by chemical reagents such as dimethylsulfate, diethylpyrocarbonate, and osmium tetroxide were observed at bases flanking the triplex-forming region. An increased accessibility to chemical probes was interpreted as being due to a bend in the DNA duplex at the triplex–duplex junction. As shown by energy minimization studies, the bend induced by intermolecular triple helix formation depends on the sequence at the junction.[64] It is therefore expected that reactivity toward chemical probes will also be sequence-dependent. Clearly, more experimental data is needed to clarify the conformational changes that are expected to occur at and near a triple helix site.

Changes in DNA conformation induced by triple helix formation are also revealed by UV-photofootprinting. Following UV irradiation, adjacent pyrimidines form both pyrimidine dimers (with a cyclobutane ring involving the C5 and C6 carbon atoms on each pyrimidine) and 6,4-photoadducts (with a single bond between the two pyrimidines). The formation of 6,4-photoadducts is prevented by triple helix formation, both in pyrimidine × purine · pyrimidine[67] and purine × purine · pyrimidine[68] triplexes.

Uranyl-mediated photocleavage of phosphodiester bonds has also been used to probe the accessibility of phosphates in the triple helix.[69] Reduced accessibility was found on the purine strand, especially at its 5′-end, whereas enhanced cleavage was observed near the 3′-end of the pyrimidine strand when only $T \times A \cdot T$ triplets were involved.

2.5. Specificity of Triple-Helix Formation

The specificity of triple-helix formation has been probed by different techniques. Dervan et al.[19, 70, 71] used Fe-EDTA attached to a thymine base of the third strand to cleave the target DNA at the specific site of triple-helix formation. This method gives only qualitative information on the extent of binding but allows for a rapid comparison of sequence selectivity. A recent report[206] has shown that the affinity cleavage reaction can be made quantitative. A second method relies upon spectroscopic studies, in which "optical melting curves" are recorded and analyzed according to a two-state (all-or-none) model describing the dissociation of the third strand from the double helix.[72, 73] The precision of thermodynamic measurements from UV melting curves is often limited by the difficulty in obtaining good base lines before and after the melting process. The difference in stability introduced by mismatches has been estimated to be 3.2–4.0 kcal mol^{-1} per mismatch in one study[73] and to range

from 1.8 kcal mol^{-1} for the less destabilizing G × G · C non-canonical triplet to 5.9 kcal mol^{-1} for the most destabilizing C × T · A mismatch in another study.[72] The energy difference between canonical and non-canonical base triplets was estimated to vary between 3 and 6 kcal mol^{-1} from the superhelical density that is required to induce the transition to the triplex H-DNA structure in plasmids.[75] Polyacrylamide gel electrophoresis (PAGE) was also used to investigate base sequence specificity,[74] but no quantitative data on differences in triplex stability were reported. Footprinting techniques using, for example, DNase I or Cu–phenanthroline as cleaving reagents could also be used to analyze sequence specificity of triplex formation.

It should be emphasized that the change in stability due to a mismatch in a triple-helical structure depends on many parameters among which are: the nature of the mismatch, the nearest neighbors flanking the mismatch in the triplex sequence, the pH if one of the base triplets involves protonation of a cytosine (or an adenine in a A × G · C triplet[76]), the ionic strength, and the presence of ligands. Therefore one should be careful in drawing general conclusions from a study where only one set of conditions is used.

Griffin and Dervan[70] observed similar stabilities for the G × T · A and the canonical T × A · T triplet by affinity cleavage experiments. However, this holds true only when the G × T · A triplet is flanked by T × A · T triplets on both sides. The presence of C$^+$ × G · C triplets as nearest neighbors destabilizes this interaction.[71, 72] The G × T · A triplet within intramolecular triplexes was extensively studied by NMR,[76, 77] and was shown to involve a single hydrogen bond between the $NH_2(2)$ proton of G and the C = O(4) group of T. This result was consistent with that proposed on the basis of energy minimization and molecular modeling studies.[72] The structure and stability of X × G · C mismatches in the third strand of intramolecular triplexes was also studied by NMR.[78] The hydrogen-bonding scheme proposed for the G × G · C triplet was again identical to that obtained by energy minimization.[72] This scheme (with a single hydrogen bond) is different from that shown in Figure 5 for G × G · C triplets, in which two hydrogen bonds are formed. This difference probably reflects the backbone distortion due to the lack of base triplet isomorphism when a G × G · C triplet is flanked by two T × A · T triplets in a parallel orientation (Hoogsteen mode). The hydrogen-bonding scheme of Figure 5 is appropriate when adjacent guanines recognize a tract of adjacent G · C base pairs in the double helix.

As yet, only a little data is available on mismatch effects in purine × purine · pyrimidine triple helices.[30] For pyrimidine × purine · pyrimidine triplexes guidelines are emerging for choosing the base in the third strand that will give the highest stability when a purine · pyrimidine Watson–Crick base pair in duplex DNA is replaced by a pyrimidine · purine base pair (i.e. when a homopurine tract is interrupted by a pyrimidine).[63, 71, 72] Mismatches in the duplex itself may lead to enhanced stability.[63] For example, an A · C mismatch in the double helix forms a T × A · C triplet which is more stable than the canonical base triplet T × A · T.

Sequence-selective recognition of homopurine · homopyrimidine sequences within long molecules of duplex DNA was first reported in plasmids of a few thousand base pairs, where a single cut was observed when the triplex-forming oligonucleotide was equiped with either Fe-EDTA[19] or Cu–phenanthroline.[79] With Fe-EDTA as a cleaving reagent, Strobel et al. showed that a triplex-forming 18mer oligomer was able to cut the DNA of bacteriophage λ at a single position within the 48 502 base pair genome,[80] and that a 20mer recognized and cleaved a single site inserted in chromosome III of the yeast *Saccharomyces cerevisiae*, which contains 3.4×10^5 base pairs.[81] Dervan et al. then developed an elegant strategy to cleave long DNA sequences at a single site.[82, 83] They used a triplex-forming oligonucleotide that overlapped a methylation/restriction site. These are sites which are recognized by both endonucleases and methylases. When the sequence is first methylated (e.g. on adenines), the endonuclease is no longer able to cleave. *Eco*RI, *Msp*I, *Hae*III, *Taq*I, *Alu*I, and *Hpa*II methylase/endonucleases recognize symmetric sequences that contain two or three contiguous purines or pyrimidines which may overlap a triplex site. An oligonucleotide recognizing a homopurine · homopyrimidine sequence which overlaps a methylase recognition site prevents methylation at this site, while all other sites are methylated. When the endonuclease partner is added, only the unmethylated site is cleaved; the others are protected by methylation. The technique developed with triplex-forming oligonucleotides is similar to that described by Szybalsky et al.[84, 85] which they called the "Achilles heel" cleavage technique. In this technique a DNA-binding protein (e.g. the lac repressor) is used to protect a DNA sequence from being methylated. The restriction endonuclease then cleaves selectively this protected site.

These results show the high selectivity of triple helix formation in long DNA molecules (chromosomes) and the possible development of triple-helix-forming oligonucleotides for use in gene mapping on intact chromosomes. The possibility of using a degenerate oligonucleotide pool to screen for potential binding and cleavage sites on cosmid clones of chromosomes extends the potentiality of the technique to DNA regions which have not yet been sequenced.[83]

2.6. Thermodynamics and Kinetics of Triple-Helix Formation

Several studies have been devoted to the determination of thermodynamic parameters for Hoogsteen hydrogen bond formation by oligopyrimidines. The ΔH values were obtained from UV melting curves,[42, 73, 86, 89] change in T_m with DNA concentration,[87] differential scanning calorimetry (DSC),[86, 88, 89] and kinetic measurements.[91] The systems that were studied include those containing either three different strands,[87, 89, 91] a Watson–Crick duplex hairpin structure binding a "Hoogsteen oligopyrimidine",[42] or a single-stranded oligopurine bound to an oligopyrimidine with the formation of both Watson–Crick and Hoogsteen hydrogen bonds.[86] The reactions were analyzed according to a two-state model for the transition from triplex to duplex + single strand[42, 87, 88, 91] or to three single strands.[86] Only values obtained from DSC measurements do not rely on a model for the triplex-to-duplex reaction. ΔH

values calculated for different sequences are given in Table 1. The lowest value (2 kcal mol^{-1} per base triplet) has been obtained from calorimetric measurements.[89] However, these authors report van't Hoff ΔH values obtained from optical melting curves or DSC shape analysis that are about three times higher than the calorimetric enthalpy. In another study the van't Hoff and DSC values were nearly identical within experimental error.[86] Clearly, more data are required to obtain a reliable picture of the thermodynamic properties of triple helices, but the results presently available show that triple helices are less stable than double helices. The stability is expected to depend on the base-triplet sequence, the nature (charge) and concentration of cations, and, in the case of cytosine-containing third strands, on pH. The enthalpy of cytidine protonation was estimated to be -2.8 ± 0.3 kcal mol^{-1}.[42]

Table 1. Thermodynamic parameters for the transition from triplex to duplex.

Sequence of third strand (5′ → 3′)	ΔH [kcal mol^{-1}]	ΔS [cal mol^{-1} K^{-1}]	Ref.
CTTCCTCCTCT [a]	84 ± 5	234 ± 15	[42]
CTTCCTCCTCT [b]	65 ± 7 [c]	187 ± 19 [c]	[86]
	57 ± 6 [d]	181 ± 18 [d]	[86]
CCTCTCCTCCCT [e]	80	243	[73]
T_{10} [f]	23.3 ± 0.9	56 ± 3	[87]
$C_3T_4C_3$ [f]	42 ± 4	120 ± 14	[87]
$T_5CTCTCTCTCT$ [g]	30.4 ± 2	97.6 ± 7	[89]
$T_3C_2TC_2TC_2TCT_2CT_2CT_6$ [h]	112 ± 6	350 ± 20	[91]

[a] From melting curves (pH 6). [b] pH 6, $\overset{*}{C}$ is 5-methylcytosine. [c] From $1/T_m$ vs. $\ln C_T$ (where C_T is total third-strand concentration). [d] From DSC curves. [e] From UV melting curves, pH 5.0. [f] From $1/T_m$ vs. $\ln C_T$, pH 5.5. [g] From DSC, pH 6.5. [h] From kinetic measurements, pH 6.8.

Kinetic measurements have shown that triple-helix formation is a slower process than double-helix formation.[90, 91] Maher et al.[90] used an *Ava* I restriction endonuclease assay to measure rate constants for the association (pseudo-first order) and for the dissociation (first order) of a triple helix formed by a 21mer containing 5-methylcytosines and a 21 bp double-stranded target within a 6.4 kbp plasmid. Depending on the reaction conditions (salt concentration and pH), k_{ass} values ranged from 8×10^2 to 2.2×10^3 M^{-1} s^{-1} and k_{diss} values from 2.4×10^{-4} to 2.2×10^{-5} s^{-1}. The equilibrium constant (for the association) ranged from 3.3×10^6 to 10^8 M^{-1} depending on salt and pH conditions. The association rate was about three orders of magnitude slower than that of double helices. Increasing the pH led to a large increase in the dissociation rate and a small reduction in the association rate. The presence of Mg^{2+} ions increased the association rate.

Rougée et al.[91] made the observation that in many cases the thermal dissociation (heating) curve, as measured by UV spectroscopy, was shifted toward higher temperatures than the association (cooling) curve. This hysteresis was used to carry out a complete kinetic analysis of triplex formation involving a 21mer oligopyrimidine bound to a double-helical DNA fragment with 21 base pairs. The association constant ranged from 13 to 300 M^{-1} s^{-1} at 15 °C and pH 6.8, when the NaCl concentration was increased from 20 to 300 mM in the absence of Mg^{2+} ions. The reaction rate was greatly increased in the presence of Mg^{2+} ions. The dissociation constant (1.5×10^{-6} s^{-1}) was independent of NaCl concentration. A mismatch X × A · T (X ≠ T) in the center of the triple helix had no effect on the association rate but induced a large increase in the dissociation rate constant (from 1.5×10^{-6} s^{-1} for the canonical T × A · T triplet, to 2×10^{-3} s^{-1} for the more destabilizing C × A · T mismatch). The activation energy for association was found to be negative. These results were explained by a "nucleation-zipping model" in which three to five base triplets constitute the nucleus. The effect of different salts points to the importance of multivalent cations in the stabilization of triple helices, through an increase of the association rate constant. Monovalent cations have the same effect at higher concentrations in the absence of multivalent cations. In the presence of divalent cations (e.g. Mg^{2+}), monovalent cations may decrease the extent of triplex formation through their inhibitory effect on multivalent cation-binding to DNA.

Kinetic studies, and especially the observation that the rate of triple helix formation is slow, have implications for the development of oligonucleotides for use in controlling gene transcription or replication. If the oligonucleotide must compete with a protein or an enzyme for binding to a specific sequence on DNA, kinetic phenomena might become the limiting factor in competition experiments.

2.7. Cooperative Binding of Oligonucleotides to Duplex DNA

The binding of two contiguous oligonucleotides on a single-stranded template is a cooperative phenomenon because of stacking interactions between base pairs at the junction of the two oligonucleotides. The same situation occurs when two homopyrimidine oligonucleotides bind to two adjacent homopurine · homopyrimidine sequences on duplex DNA.[92] Two oligonucleotides which do not bind to adjacent sequences can be made to bind cooperatively if the 3′-end of one oligonucleotide and the 5′-end of the other one are elongated by two complementary sequences that can form Watson–Crick base pairs.[93] These two additional sequences act as dimerization domains. When two oligonucleotides are bound adjacent to each other on a DNA template, they may be ligated by either a phosphodiester[94, 95] or a pyrophosphate[95] linkage. The 5′-terminal phosphate of one of the oligonucleotides can be activated with BrCN, imidazole, and $NiCl_2$ to form a phosphodiester bond with the 3′-OH of the adjacent oligonucleotide.[94] Alternatively, 1-(1-dimethylaminopropyl)-3-ethylcarbodiimide hydrochloride may be used as a condensing agent.[95]

Two double-helical DNA fragments can be brought in juxtaposition upon binding to a triple-helix-forming oligonucleotide, which can form Hoogsteen hydrogen bonds with the terminal sequences of the two DNA fragments.[96, 97] Upon chemical activation by *N*-cyanoimidazole, the proximal 3′-hydroxyl and 5′-phosphate termini undergo covalent ligation on one or both strands.[96] The same reaction may be achieved when the oligonucleotide binds to alternate strands to juxtapose the duplex termini into a triple-helical complex.[97]

3. Enhancement of Triplex Stability by Oligonucleotide Modifications

3.1. Base Modifications

Modified bases have been introduced into triple-helix-forming oligonucleotides either to improve binding under physiological conditions or to extend the range of recognition sequences. Replacement of cytosine by 5-methylcytosine was shown to stabilize the triple helix made by polynucleotide chains polyd(CT) × polyd(GA) · polyd(CT) at pH values up to 8.[100] Similarly, 5-methylcytosine was introduced into triple-helix-forming oligonucleotides and shown to extend the pH range over which a triplex was formed with a homopurine · homopyrimidine sequence of duplex DNA.[101, 102, 128] Thermodynamic analysis showed that stabilization is mainly due to entropic effects arising from the formation of a "spine" of hydrophobic methyl groups carried by thymine and 5-methylcytosine in oligopyrimidines.[102] Substitution of 5-bromouracil for thymine also extends triple helix stability towards higher pH, and combination of both substitutions (Br^5U and m^5C) strongly increased the cleavage efficiency of oligonucleotides tethered to Fe-EDTA at higher pH values.[101]

Oligonucleotides containing 5-bromouracil, 5-methylcytosine, and 5-bromocytosine can easily be constructed from the commercially available deoxyribonucleoside-3′-phosphoramidites. However, protonation of the nitrogen atom N(3) of cytosine is still required to form the triplex, which is markedly destabilized with increasing pH when it contains contiguous $C^+ \times G \cdot C$ triplets.

To overcome this limitation, oligonucleotides containing the nucleoside couples (dT, dG),[29, 32, 43] (dA, dG),[30, 31] [dT, 2′-*O*-methylpseudoisocytidine (**14**) (Cm)],[103] [dT, 6-methyl-8-oxo-deoxyadenosine (**15a**) (MODA)],[105] [dT, 8-oxo-deoxyadenosine (**15b**)],[106] [dT, P1 (**16**)][107] (Fig. 7), and [damP (**17**), dG] were constructed. 2′-Deoxyxanthosine and 2′-deoxyinosine have also been introduced into oligonucleotides.[104]

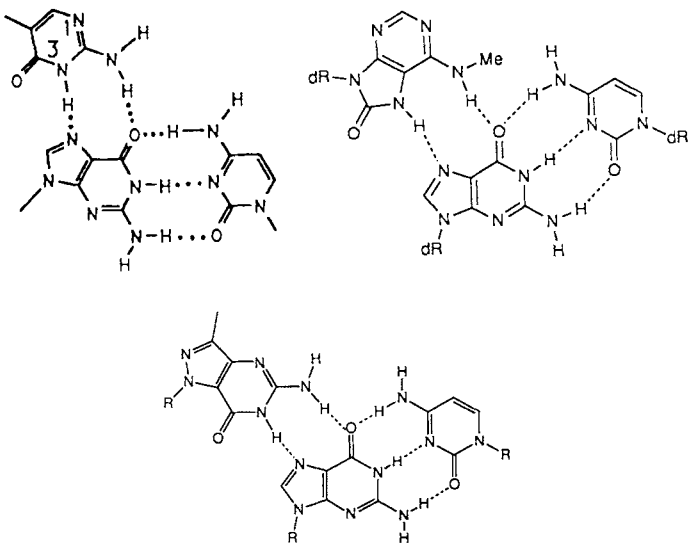

Fig. 7. Base triplets formed by modified bases with G · C base pairs of DNA. Top left: pseudoisocytidine (**14**) [103]; top right: MODA (**15**) [105] (The same hydrogen bonding scheme applies to 8-oxoadenine [106]); bottom: nucleoside P1 (**16a**) [107]. In contrast to cytosine, these modified bases do not require protonation to form two hydrogen bonds (see Fig. 5).

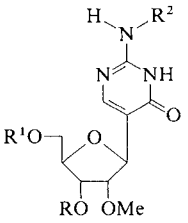

14a: R, R^1, R^2 = H (Cm)

14b: R = $-P(OCH_2CH_2CN)-NiPr_2$, R^1 = DMT, R^2 = Ac

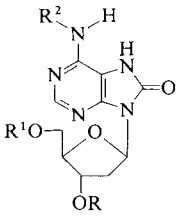

15a: R, R^1 = H, R^2 = CH_3 (MODA)

15b: R, R^1, R^2 = H

15c: R = $-P(O^\ominus)(=O)-H$, R^1 = DMT

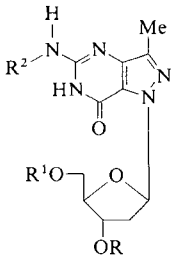

16a: R, R^1, R^2 = H (P_1)

16b: R = $-P(OCH_2CH_2CN)-NiPr_2$, R^1 = DMT, R^2 = Ibu

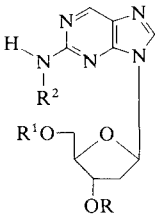

17a: R, R^1, R^2 = H (amP)

17b: R, R^1 = 4-NO_2-Bz, R^2 = Bz

17c: R = $-P(OCH_2CH_2CN)-NiPr_2$, R^1 = DMT, R^2 = Bz

Incorporation of Cm **14a** into a pyrimidine oligomer was achieved through its phosphoramidite **14b**, which was obtained in a seven-step synthesis from pseudoisocytidine.[103] In its neutral form, Cm can form two hydrogen bonds (Hoogsteen configuration) with guanine of a G · C base pair (Fig. 7 top left). In contrast to cytidine no protonation is required.

Oligonucleotides containing MODA **15a** were assembled by using the 3′-H-phosphonate derivative **15c**.[105] The nucleoside **15a** was prepared from N^6-methyl-2′-deoxyadenosine by bromination and subsequent displacement of the bromide in the 8-position with acetate, which was then removed by methanolysis.[105] 8-Oxo-2′-deoxyadenosine (**15b**) was also introduced into oligonucleotides through the phosphoramidite[106] of the 8-methoxyadenine derivative. These two derivatives (**15a** and **15b**) can form two hydrogen bonds with G in a G · C base pair, without the need for protonation (Fig. 7 top right).

The deoxyribonucleoside P1 **16a** was synthesized in five steps by construction of the heterocyclic ring and subsequent incorporation into pyrimidine oligodeoxyribonucleotides through its phosphoramidite **16b**.[107] This modified nucleotide can form two hydrogen bonds with G of a G · C base pair (Fig. 7).

Purine oligonucleotides consisting of dG and 2-aminopurine-9β-D-2′-deoxyribofuranoside (**17a**, amP) were assembled by using the phosphoramidite **17c** (V. Roig, N. T. Thuong, unpublished results). Compound **17c** was obtained from **17b**, which was prepared by a transglycosylation reac-

tion using 3′-5′-di-*O*-(4-nitrobenzoyl)thymidine as a glycosyl donor, and subsequent separation of the anomers.

Among the couples of base triplets [(T × A · T, C^+ × G · C), (T × A · T, G × G · C), (A × A · T, G × G · C), (T × A · T, Cm × G · C), (T × A · T, MODA × G · C), (T × A · T, P_1 × G · C), and (amP × A · T, G × G · C)] used to form triple helices, only (T × A · T, C^+ × G · C), (T × A · T, Cm × G · C), and (amP × A · T, G × G · C) are isomorphous couples (see Figs. 5–7). In contrast to cytosine, which must be protonated to form two hydrogen bonds with guanine of G · C Watson–Crick base pairs, the modified bases Cm, MODA, 8-oxoadenine, and P1 were shown to recognize G · C base pairs in a pH-independent manner.

3.2. Backbone Modifications

When deoxyribose is replaced by ribose a stabilization of intermolecular triple helices is observed.[210, 214] Pyrimidine oligo*ribo*nucleotides bind more strongly to duplex DNA than corresponding oligo*deoxyribo*nucleotides. 2′-OMe derivatives bind more strongly than unsubstituted oligoribonucleotides.[210, 214]

Incorporation of phosphorothioate groups into polynucleotides has been shown to have a dramatic effect on triplex formation: poly[d(TC)] · poly[d(sGsA)] spontaneously dismutates to a triplex at pH 8, whereas poly[d(sTsC)] · poly(d(GA)] could not form a triplex.[108] As shown with poly[d(GA)] · 2poly[d(sTC)] and poly[d(sGA)] · 2poly-[d(TC)],[108] a phosphorothioate 5′ to a purine increases the T_m of the triplex while at a position 5′ to a pyrimidine it decreases the T_m.

Formation of a triple helix involves strong electrostatic repulsion between the negatively charged partner strands. Metal ions play an important role in the stability of triple helices. Reducing the negative charge of the third strand by introducing neutral backbones is an attractive possibility to enhance triple-helix stability. However, with methylphosphonate backbones, there is no evidence for triplex stabilization. On the contrary, triplex formation was not detected between $d(A)_{19}$ and $d(T)_{19}$ when either strand was replaced by a methylphosphonate strand.[109] Furthermore, triplex formation between $d(CT)_8$ and $d(AG)_8$ in which the pyrimidine strand consisted of methylphosphonates required a lower pH than the phosphodiester analogue.[110] However, in both of these two examples, one of the Watson–Crick strands contained a methylphosphonate backbone. Therefore any conclusion must await data in which only the third strand carries methylphosphonate groups. It should be kept in mind that methylphosphonate groups exist in two diastereoisomeric forms and that 2^n diastereoisomers are present in an oligomer containing *n* such linkages. It is expected that the stereochemistry at the phosphorus atom plays an important role on triple helix formation and stability.

Oligomers with neutral analogues of dinucleoside phosphodiester linkages **18** were synthesized in order to form triple helices with duplex DNA under physiological salt conditions.[111] The incorporation of each analogue linkage was achieved by using the *N*-benzoyl-5-methyl-2′-deoxycytidine-thymidine (5-MeC-T) dimer protected at the 5′-end with dimethoxytrityl (DMT) and derivatized at the 3′-end with a H-phosphonate salt. The methylphosphonate dinucleoside **19a** was obtained by using the 5′-dimethoxytrityl-deoxyribonucleoside-3′-methylphosphonic imidazolide. Reaction of dinucleoside H-phosphonate with carbon tetrachloride in

d-$^{5'}$TpCpTpC^{Me}-TpC^{Me}-TpC^{Me}-TpC^{Me}-TpTpTpT$^{3'}$ **18**

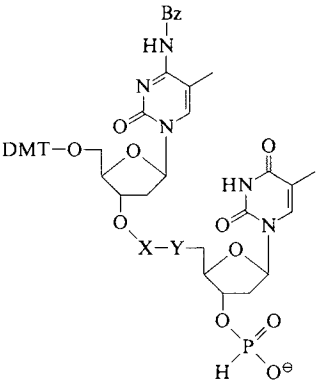

19a: X–Y = Me–P(=O)–O (*R,S*-methylphosphonate)

19b: X–Y = NH–$(CH_2)_2$–OMe–P(=O)–O (*R,S*-methoxyethylphosphoramidate)

19c: X–Y = CH_2–O (formacetal)

19d: X–Y = CH_2–S (thioformacetal)

the presence of methoxyethylamine led to the precursor of the dinucleoside phosphoramidate **19b**. The precursor of the formacetal dinucleoside **19c** was generated from a 3′-trialkylsilyl-thymidine and a 5′-dimethoxytrityl-deoxynucleoside-3′-methyl thioacetal, activated with *N*-bromosuccinimide. In an analogous manner to the preparation of the formacetal dimer, the thio analogue **19d** was obtained starting from the 5′-thio analogue. The formacetal linkage is suitable for sequence-specific triple-helix formation, whereas oligonucleotides with thioformacetal, methylphosphonate, and methoxyethylamidate linkages exhibited reduced affinity for duplex DNA.[111]

Oligomers with a neutral polyamide backbone (**20**, PNA) were designed by replacing the deoxyribose-phosphodiester linkage of DNA by an oligomer of aminoethylglycine.[112] PNA was constructed with a standard peptide-coupling procedure. The BOC-protected pentafluorophenyl ester of the thymine monomer **21** was synthesized by condensation of the BOC-aminoethylglycine with the pentafluorophenyl ester of thymine acetic acid. PNA binds more strongly to single-stranded complementary sequences than normal oligonucleotides. A 2:1 (PNA:DNA) stoichiometry was obtained. This might hold only for pyrimidine–PNA which is able to form triplexes rather than duplexes, through both Watson–Crick and Hoogsteen hydrogen bonding interactions.

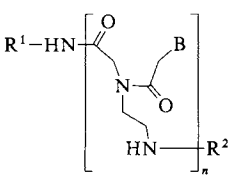

20: R^1 = Lys–NH_2
R^2 = H or acridine derivative

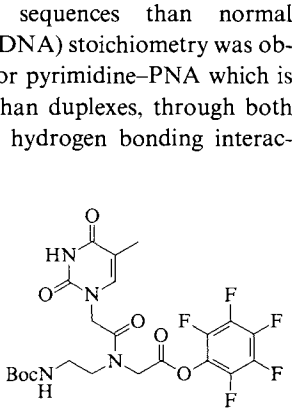

21

PNA also binds to double-stranded DNA by a strand-displacement reaction.[112] In this reaction, the double helix is

locally disrupted and the PNA binds to its complementary strand. This strand displacement reaction is reminiscent of the reaction catalyzed by the Rec A protein from *E. coli*, which allows one polynucleotide chain to invade a double helix containing a homologous sequence to form a D-loop, in which one of the Watson–Crick strands is displaced and replaced by the invading polynucleotide chain.[152–158] If the results obtained with PNA containing only one (T) or two (C and T) bases can be extrapolated to any base sequence, then new possibilities will be open to bind PNAs to any base pair sequence of DNA. This would relieve the constraints that presently limit triple helix formation by oligodeoxynucleotides to homopurine · homopyrimidine sequences of DNA.

3.3. Triplex Formation by α-Oligonucleotides

Natural nucleic acids are constructed with the β-anomers of nucleotide units **22**. It is possible to synthesize the α-anomers **23**[113–116] and subsequently build α-oligonucleotides, in which all units have the α-configuration. These α-oligomers are resistant to both endo- and exonucleases.[115–117]

β-D-deoxyribonucleotides **22** α-D-deoxyribonucleotides **23**

a: B = thymine, **b**: B = cytosine, **c**: B = adenine, **d**: B = guanine, **e**: B = 2-aminopurine, **f**: B = 5-methylcytosine

Pyrimidine α-D-deoxyribonucleosides **23a,b**[118a] can be obtained by an anomerization reaction, while purine α-D-deoxyribonucleosides **23c,d**[118a] and **23e**[118b] were synthesized by a transglycosylation procedure using pyrimidine β-D-deoxyribonucleosides as the glycosyl donor. 5-Methyl-2′-deoxy-α-cytidine **23f** was prepared by activation of the C(4) position of α-thymidine followed by aminolysis.[122]

Starting from α-deoxyribonucleosides, the assembly of the oligo-α-deoxyribonucleotide chain was achieved by adaptation of either the phosphotriester method in solution[114–116] or the phosphoramidite method on solid support.[119–121] The efficiency of the coupling reaction was similar to that obtained for the synthesis of oligo-β-deoxyribonucleotide derivatives. Oligo-α-deoxyribonucleotides containing either 5-methylcytosine (**23f**)[122] or 2-aminopurine (**23e**) (V. Roig, N. T. Thuong, unpublished results) were constructed by using phosphoramidite building blocks.

α-Oligomers bearing an acridine derivative, through a phosphodiester linkage at either their 3′- (**24a**) or 5′-ends (**25a**), were first synthesized in solution.[115,123] The latter (**25a**)[121] and the psoralen derivative **25b** were readily obtained from the phosphoramidites **28a** and **28b** by the solid-phase procedure. With the previously described thiophosphate method,[133–136] oligo-α-deoxynucleotides covalently linked at either their 3′- (**26**) or 5′-ends (**27**) to either acridine, psoralen, orthophenanthroline, azidoproflavine, proflavine, or *para*-azidophenacyl derivatives were obtained (see Fig. 9).[18,41,124]

α-d-$(Nup)_nR$ **24** R-α-d-$(pNu)_n$ **25**

α-[$(Nup)_nNu$]psR **26** Rsp-α-d-[$(Nup)_nNu$] **27**

a: R = (Acr)–NH–$(CH_2)_5$–, **b**: R = (Pso)–O–$(CH_2)_6$–

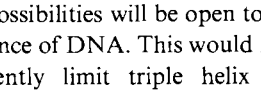

28a: R = (Acr)–NH–$(CH_2)_5$–
28b: R = (Pso)–O–$(CH_2)_6$–

The binding of α-oligonucleotides to double-stranded DNA was investigated by different techniques, including cross-linking to the target sequence,[18,41,124] absorption spectroscopy,[122] and inhibition of restriction enzyme cleavage.[122] Only oligopyrimidine sequences have been tested for triple helix formation. The orientation of the α-strand with respect to the homopurine · homopyrimidine sequence of duplex DNA depends on the sequence. An α-oligomer containing only thymine was bound in a parallel orientation with respect to the poly(dA) sequence of the target duplex as was the oligonucleotide synthesized with the β-anomers.[18,41] In contrast, α-oligonucleotides containing T and C were bound in an antiparallel orientation with respect to the homopurine sequence of the target.[122] The change in orientation induced by cytosines in the α-strand was explained as a consequence of triple helix stabilization due to formation of isomorphous base triplets. According to energy minimization studies, α-oligo(dT) and α-oligo(dC) prefer to bind in a parallel orientation with respect to the oligo(dA) and oligo(dG) strands, respectively, of the target duplex and engage in reverse Hoogsteen hydrogen bonding interactions.[125] As shown previously (Fig. 5), $T \times A \cdot T$ and $C^+ \times G \cdot C$ base triplets are not isomorphous in the reverse Hoogsteen configuration, but are isomorphous in the Hoogsteen configuration. The net result is that an α-oligonucleotide containing both C and T prefers to bind in an antiparallel orientation in order to avoid the distortion of the backbone that would occur in the parallel orientation. It may be expected that the orientation will depend not only on the number of cytosines in the α-oligonucleotide but also on their distribution within the sequence.

Triple helices formed by α-oligonucleotide binding to natural DNA are slightly less stable than those formed by their β-analogues. However, they can be stabilized by intercalating agents attached to the ends of the α-oligomer.[122] Since an α-oligopyrimidine containing both C and T binds in the reverse orientation as compared to a β-oligonucleotide, an intercalating agent attached to the 3′-end of the α-oligomer will intercalate at the 5′-pyrimidine-purine-3′ step of the duplex–triplex junction, as does an intercalating agent attached to the 5′-end of a β-oligonucleotide. An α-oligonucleotide–psoralen conjugate can be cross-linked under UV irradiation to its target site, provided there are cross-linkable thymines in the vicinity of the triplex–duplex junction (C. Giovannangeli, C. Hélène, unpublished data). The nuclease resistance of α-oligonucleotides make these compounds attractive for development as regulators of gene transcription in vivo.

3.4. Oligonucleotides Covalently Linked to Intercalating Agents

Intercalating agents attached to either the 5′- or 3′-end(s) of oligonucleotides were originally developed in order to increase the affinity of antisense oligonucleotides toward their complementary single-stranded sequence.[126, 127] The same strategy was applied to triple helix-forming oligonucleotides with the expectation that an intercalator attached to one (or both) end(s) of such an oligonucleotide would intercalate at the triplex–duplex junction. In support of this strategy, an oligopyrimidine–intercalator conjugate strongly stabilized the triple helix formed upon binding of the oligomer to duplex DNA.[128, 129] Fluorescence and molecular modeling studies showed that intercalation was strongly favored on the 5′-side of the third-strand oligonucleotide, since the intercalating agent recognizes a 5′-pyrimidine–purine-3′ sequence at the duplex–triplex junction (Fig. 8). Such a sequence is known to be a strong intercalation site for many polycyclic aromatic molecules.[3] The same conclusion was drawn for oligonucleotides carrying a psoralen derivative attached to the 5′-end.[130]

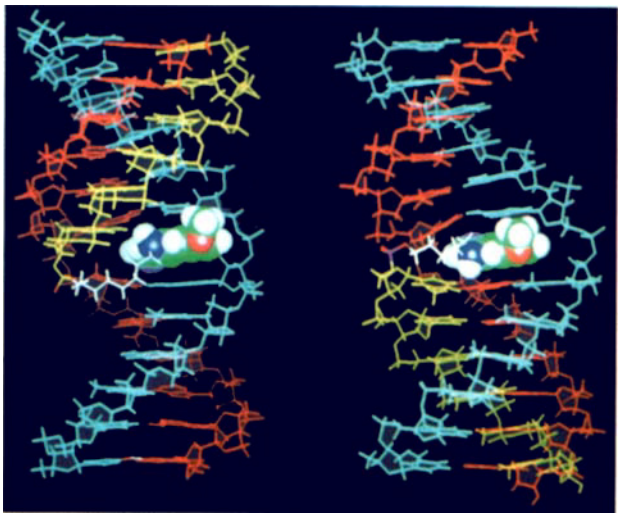

Fig. 8. Molecular models of triple helices formed by oligonucleotide–intercalator conjugates and double-helical DNA. The intercalating agent is 9-amino-6-chloro-2-methoxyacridine tethered either through a pentamethylene linker to the 5′-phosphate (right) or through a nonaethylene linker to the 3′-phosphate (left) of the triplex-forming oligonucleotide (in light green). The acridine derivative is shown intercalated between the last base triplet of the triple helix and the first base pair of the duplex at the duplex–triplex junction (see ref. [209]).

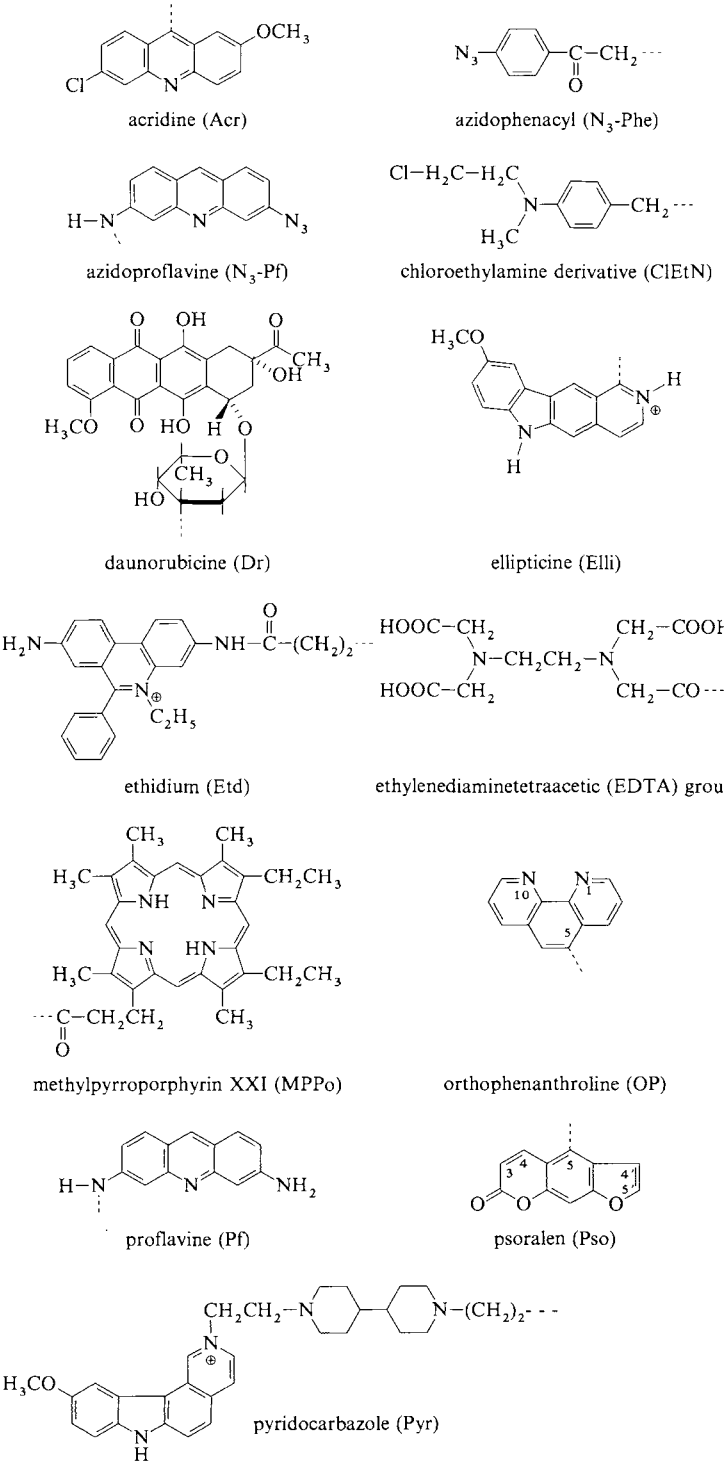

Fig. 9. Structure of different ligands tethered to triple-helix-forming oligonucleotides. The dashed line indicates the site of attachment to the linker (see text and ref. [134]).

3.4.1. Incorporation of Conjugate Groups during the Assembly of Oligonucleotides

The direct incorporation of the conjugate group (see Fig. 9) during the assembly of the oligomers generally involves the following steps: 1) Introduction of a functional group such as a hydroxy group and appropriate protection of the other functional groups not engaged in the coupling reaction. 2) A coupling reaction providing protection to the oligonucleotide conjugates. 3) Use of conditions for the removal of the protecting group (unblocking) which do not affect the conjugated oligomers.

Oligodeoxynucleotides carrying an acridine derivative (9-amino-6-chloro-2-methoxyacridine) at either the 3′- (**29a**) or 5′-end (**30a**) were first synthesized in solution by using the phosphotriester method by coupling the hydroxy group of the acridine derivative **31a** with either the 3′-arylphosphodiester **32** or 5′-arylphosphodiester **33** of the protected oligonucleotide.[126, 127] Unblocking of the nucleic acid bases was carried out by treatment with sodium hydroxide in order to avoid cleavage of the 9-aminoacridine bond. By this

method, an EDTA moiety was tethered to the 3′-phosphate of the oligomer **29b** through the trimethylester of the EDTA derivative **31b**. In the same way, an acridine and an EDTA group were respectively attached to the 3′- and 5′-ends of oligothymidylates.[131]

d-$(Nup)_n$-R **29** R-d-$(pNu)_n$ **30**

a: R = (Acr)–NH–$(CH_2)_5$
b: R = (EDTA)–NH–$(CH_2)_6$
c: R = (Pso)–O–$(CH_2)_6$

(Acr)–NH–$(CH_2)_5$–OH **31a** (EDTA-Me_3)–NH–$(CH_2)_6$–OH **31b**

DMTd-$(Nu'p)_n$ **32** d-(pNu')-Bz **33**

Solid-phase preparation of oligonucleotides attached through their 5′-ends to either an intercalator **30a** or a photoreactive group **30c** was easily achieved by condensing the phosphoramidite derivative of either an acridine **28a** or psoralen **28b** with the 5′-hydroxy group of an oligonucleotide still fixed to the solid support.[132, 181]

3.4.2. *Incorporation of Conjugate Groups into Unblocked Oligonucleotides*

This strategy involves the introduction of appropriate functional groups in the two unprotected moieties, followed by their specific coupling, thereby providing the conjugated oligodeoxyribonucleotide. Many systems can be used by introducing functional groups into the oligodeoxyribonucleotides, including phosphate, phosphorothioate, amine, thiol, carboxy, and *cis*-diol groups. Among these systems, the *S*-alkylation reaction of the phosphorothioate group by substituted alkyl halides was extensively used to prepare conjugated oligonucleotides utilized in the study of the triple helix.

Introduction of a thiophosphate group at either the 3′- (**34**) or 5′-end (**35**) of the oligonucleotide can be achieved either by the phosphotriester method in solution or through the phosphoramidite on solid phase. Modification of the 5′-end with a phosphorothioate group was easily achieved by condensing bis(cyanoethyl)-*N*,*N*-diisopropylamidophosphite (**36**) activated by tetrazole with the 5′-hydroxy group of the protected oligomer assembled either in solution[133] or on solid support,[134] followed by a sulfurization step. The 5′-thiophosphate group can be unblocked in oligonucleotides by reaction with NH_4OH. Introduction of the thiophosphate group on the 3′-end by solid-phase synthesis involved attachment of the nucleoside through its 3′-(2-cyanoethylthiophosphate) to a solid support by a dithiodiethyl bridge **37**. The latter may be easily obtained by using the dithiodiethanol-derivatized solid phase **38** and the classical nucleoside-3′-cyanoethyl phosphoramidite, and replacing the oxidation step with a sulfurization step. After assembly of the oligonucleotide chains, the 3′-thiophosphate was unblocked and released from the support by treatment with an aqueous solution of dithiothreitol and NaOH.[135, 136] Condensation of the thiophosphate-containing oligonucleotides **34** and **35** with halogenoalkyl ligands, RX, **39**, yields the phosphorothioester of the conjugated oligonucleotides, **40** and **41**, respectively (see Fig. 9 for the nature of R).[133, 134, 136] With the methods described above, an oligothymidylate covalently linked to an acridine at its 3′-phosphate and to orthophenanthroline at its 5′-end (**42**) was synthesized.[159]

Recently the nucleophilicity of the phosphorothioate was also used to conjugate the binuclear platinum II **43** to the 5′-end of oligodeoxynucleotides.[167] Phosphorylation of either 4-(*N*-2-chloroethyl-*N*-methylamino)benzylamine[137] or the amino derivative of ethidium[138] with an oligonucleotide containing a terminal phosphate led to the phosphoramidate oligomers, **44a** and **44b**, respectively.

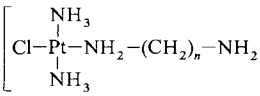

43

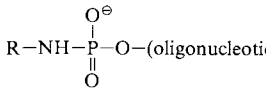

44a: R = *p*-[$(ClCH_2CH_2)(CH_3)N$]$C_6H_4CH_2$
44b: R = Etd

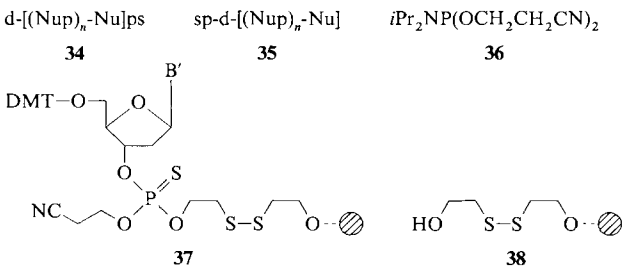

d-[$(Nup)_n$-Nu]ps **34** sp-d-[$(Nup)_n$-Nu] **35** $iPr_2NP(OCH_2CH_2CN)_2$ **36**

37 **38**

39: R–X = (Acr)–NH–$(CH_2)_5$–Br, (Dr)–NH–(CO)–$(CH_2)_n$–Br, (Elli)–NH–$(CH_2)_3$–NH–(CO)–$(CH_2)_n$–Br, (N_3Phe)–Br, (N_3Pf)–$(CH_2)_n$–Br, (OP)–NH–(CO)–$(CH_2)_n$–Br, (Pf)–$(CH_2)_n$–Br, (Pso)–O–$(CH_2)_2$–I, (Pyr)–Br

d-[$(Nup)_n$-Nu]psR **40** Rsp-d-[$(Nup)_n$-Nu] **41**

(OP)–(NH)–(CO)–CH_2–sp–CH_2–$C(CH_3)_2$–CH_2–p–$(Tp)_8$–$(CH_2)_5$–NH–(Acr)

42

4. Triple-Helix Ligands

Multivalent cations favor triplex formation at neutral pH. It was mentioned in Section 2.6 that Mg^{2+} ions strongly stabilized py × pu · py triple helices, and it seems that Mg^{2+} or other divalent cations are absolutely necessary for the formation of such triple helices.[17] Polyamines such as spermine and spermidine strongly stabilize triple helices.[19, 128, 139] The concentration of polyamine in the nucleus of eukaryotic cells is in the millimolar range. Therefore triple helices might be stabilized in the cell nucleus. This

potential might be important for the natural regulation of certain genes through intramolecular H-DNA formation as well as for the artificial control of gene expression by triple helix-forming oligonucleotides.

It was of interest to establish whether some well-known ligands of the DNA double helix could also bind to a triple helix. Spectroscopic studies of the classical DNA intercalator ethidium bromide have shown that it does intercalate into triple helices.[140, 141] Ethidium binding to poly(dA) · 2poly(dT) shifts the transition from triplex to duplex + single strand toward higher temperatures.[140] This appears to be due to the low affinity of ethidium for the double helix, poly(dA) · poly(dT), which exists in solution in a nonstandard conformation. The binding of ethidium to short triplex sequences containing both T × A · T and C^+ × G · C base triplets induces a decrease of the temperature for the triplex-to-duplex transition and an increase of that for the duplex-to-single strand transition.[141] This result shows that for the sequence investigated in this study, ethidium binds more strongly to the duplex than to the triplex structure. Energy minimization studies have shown that ethidium, which is a positively charged cation, prefers to bind between T × A · T base triplets to avoid electrostatic repulsion with the positively charged C^+ × G · C base triplet.[142]

Minor groove-binding ligands of double-helical DNA such as netropsin and a distamycin analogue have been shown to bind to triplex structures formed by either polynucleotides poly(dA) · 2poly(dT)[143a] or short oligonucleotides $(dT)_6 \cdot (dA)_6 \cdot (dT)_6$.[143b] In both cases, the ligand binds to the triplex structure without dissociation of the third strand. However, netropsin thermally destabilizes the triplex state, while it stabilizes the corresponding duplex.[143]

The only triple helix-specific ligands reported until now are benzopyridoindole derivatives (Fig. 10),[144] which according to Mergny et al. lead to a strong stabilization of triplexes. The melting temperature of the triplex-to-duplex

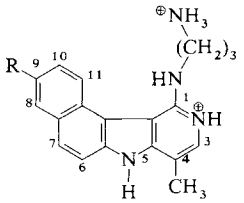

Fig. 10. General structure of benzo[*e*]pyridoindole derivatives which bind to and stabilize triple helices (see ref. [144]). The derivative in which R = OCH_3 gives the best stabilization of the triple helix.

transition was increased by up to 20 K. The stabilization was shown to depend on the base triplet sequence with a strong preference for T × A · T triplets. This dependency is due to the electrostatic repulsion which occurs when the positively charged ligand is close to positively charged C^+ × G · C base triplets. The results of energy transfer experiments have suggested an intercalation of the benzopyridoindole ring between adjacent base triplets. The stabilization provided by these compounds for a triplex formed on the β-lactamase gene of *E. coli* enhanced the inhibitory effect of the triple helix-forming oligonucleotide on transcription by *E. coli* RNA polymerase. It was also reported that upon UV irradiation covalent adducts were formed with the target strand at very low drug concentrations. These studies open the way to designing better ligands for triple helices and to synthesizing oligonucleotide–ligand conjugates that have a high selectivity and strong affinity for duplex DNA sequences.

5. Triple-Helix Formation on a Single-Stranded Nucleic Acid Target

5.1. Recognition of a Polypurine Sequence through both Watson–Crick and Hoogsteen Hydrogen Bonds

In the preceding discussion, triple-helix formation involved a duplex DNA target, which is recognized by an oligonucleotide, thus providing the third strand. In intramolecular triplexes (H-DNA) formed from polypurine · polypyrimidine sequences, one of the strands folds back on the double helix to form a triple helix.[15–17, 145] Therefore, it should be possible to form a triple helix on a single-stranded DNA fragment. Since in both pu × pu · py and py × pu · py triple helices the third strand binds to the purine strand of the Watson–Crick double helix, a single-stranded homopurine sequence can be chosen as a target. Two approaches have been described thus far:

1) A polypyrimidine sequence may be chosen such that half will form Watson–Crick base pairs, while the other half will form Hoogsteen hydrogen bonds to the Watson–Crick duplex.[86, 146] This configuration is possible because the Watson–Crick and Hoogsteen polypyrimidine sequences are antiparallel in a py × pu · py triple helix (**45**). The linker be-

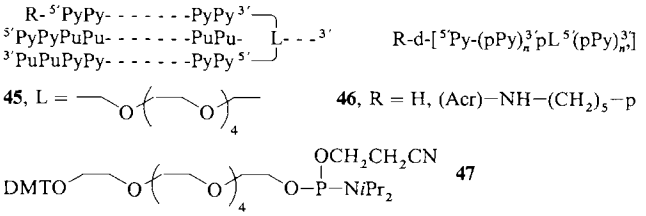

tween the two polypyrimidine sequences may be a non-nucleotidic chain, such as hexaethylene glycol (**45**, **46**),[146] or a short sequence of three to five nucleotides (C. Giovannangeli, C. Hélène, unpulished results). A similar situation was described by Xodo et al.[86] in the study of triplex formation between a short oligopurine (11mer) and a longer polypyrimidine sequence (24mer) that resembled a H-DNA structure. The hexaethylene glycol oligonucleotides **45** and **46** could be prepared with automatic synthesizers from the phosphoramidite **47**.

2) The Watson–Crick and Hoogsteen polypyrimidine sequences may be incorporated into a circular molecule (as in **48**) by using two short loops (optimum length of five nucleotides) to connect the two polypyrimidine sequences.[147, 148]

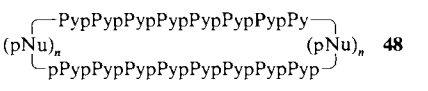

Cyclization of linear 5′-phosphorylated oligomers was achieved by a chemical method (BrCN/imidazole/Ni^{2+}), in which short complementary single-stranded DNA templates were used to bring the free 3′-OH and activated 5′-phosphate moities adjacent to each other.

In both approaches, the linear or cyclic polypyrimidine oligonucleotides recognize the polypurine sequence by forming both Watson–Crick and Hoogsteen hydrogen bonds (Fig. 11). Adenines are thus recognized by four hydrogen bonds and guanines by five hydrogen bonds. For example, the 16 nucleotide sequence investigated by Giovannangeli et al.,[146] which is part of the HIV genome, contains nine adenine and seven guanine bases. Therefore, the polypyrimidine ligand is able to form 71 hydrogen bonds with its target. The discrimination of mutant targets, which differ by a single base, is very high as compared to a complementary antisense oligonucleotide, since both Watson–Crick and Hoogsteen hydrogen bonding is perturbed.

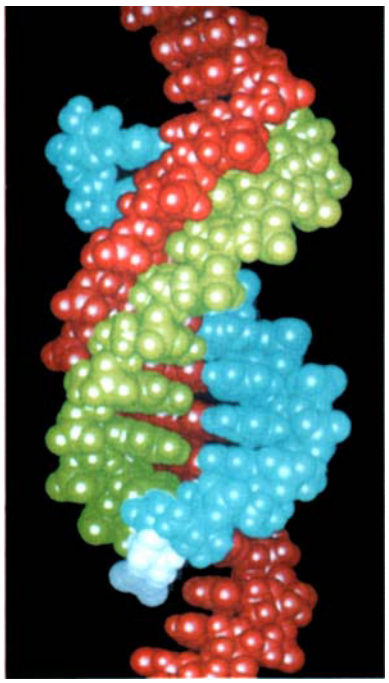

Fig. 11. Space-filling model of a triple helix formed by a single-stranded oligopurine target (red) with a chimeric oligonucleotide consisting of two polypyrimidine sequences attached to each other through a hexaethyleneglycol linker (white). The linker can also be made of an oligonucleotide [211]. One of the polypyrimidine sequence (blue) forms Watson–Crick base pairs with the target, whereas the second forms Hoogsteen base pairs (green) (see ref. [146]). The 3′- and 5′-ends of the polypyrimidine chimeric oligonucleotide can be joined together to generate a circular oligomer [147, 148].

The cyclic oligonucleotides with optimized loops bind with higher affinity to a polypurine target than linear oligomers which contain the same bases.[148] This has been attributed to the entropic benefit of preorganization in the cyclic molecule. Reactive groups can be attached at one or both ends of the linear oligomers. For example, it was shown that attachment of an intercalating agent to the 5′-end of **45** strongly stabilized the triplex structure, provided the Watson–Crick portion of the oligomer was extended by one or two base pairs.[146] The intercalating agent may be made reactive toward the target sequence. We have recently shown that a psoralen derivative attached to the 5′-end of the Hoogsteen strand can be cross-linked to both the target purine and the Watson–Crick pyrimidine strands, thereby "locking" the triplex structure in place. Replication of such irreversibly blocked templates is inhibited.[211] We have called these molecules "oligonucleotide clamps".[211]

5.2. Binding of Oligonucleotides to the Single-Stranded Region which Results from the Formation of Intramolecular Triplexes (H-DNA)

A mirrored polypurine · polypyrimidine sequence of double-helical circular DNA can undergo a transition to form an intramolecular triplex, thereby relaxing some of the constraints imposed by supercoiling.[15–17] During this process, either half of the polypurine sequence folds back on the double helix to form a pu × pu · py triple helix, in which approximately half of the polypyrimidine sequence becomes single-stranded, or half of the polypyrimidine sequence folds back to form a py × pu · py triple helix, in which half of the polypurine sequence becomes single-stranded (Fig. 4). In both cases, an oligonucleotide may be designed to be complementary to the single-stranded sequence. Oligomer binding has been observed in vitro[149, 150] and in vivo[149] and has been shown to favor H-DNA formation by trapping the single-stranded portion of the DNA.[150]

A similar model was proposed to describe effects observed during in vivo transcription of the polypurine-containing strand of the immunoglobulin A (IgA) switch region in a supercoiled plasmid.[151] Nascent RNA transcripts remain associated with their template through RNase H-sensitive, RNA–DNA hybrids, which stabilize an intramolecular triplex and result in the formation of stable, less supercoiled conformers of the plasmid.

6. RecA-Mediated Formation of Three-Stranded Structures

General genetic recombination involves the exchange of genetic information between homologous sequences carried by two chromosomes. A key step in recombination is the alignment and pairing of homologous DNA sequences. Recombinases, such as the RecA protein of *E. coli*, bind cooperatively to single-stranded oligonucleotides. In the presence of homologous double-stranded DNA, they induce the formation of a synaptic complex in which three strands of DNA are associated with recA proteins.[152–155] When a supercoiled circular DNA is used as a substrate, deproteinization of the synaptic complexes leads to the formation of joint molecules, in which the single-stranded oligonucleotide is still bound to the supercoiled DNA. Linearization of the DNA by a restriction endonuclease which relieves the constraints associated with supercoiling, releases the oligonucleotide. When long single-stranded DNA fragments are used instead of short oligonucleotides (and ATP is used instead of non-hydrolyzable ATPγS) strand exchange can take place, for example between a circular single strand and linear duplex DNA.[153, 154]

In the presence of the non-hydrolyzable ATP analogue, 5′-(γ-thio)ATP (ATPγS) and ADP, RecA protein can pair a short single-stranded 15mer with duplex DNA.[155] However, a homology of only eight bases is sufficient to form such synaptic complexes. Association of the oligonucleotide with duplex DNA survives the removal of RecA protein provided that the length of shared homology is at least 26 base pairs.[155] The structure of these three-stranded complexes is not yet known. One strand of duplex DNA can be displaced to form a D-loop, but an alternative structure in which all three strands are hydrogen bonded has been proposed.[152] It should be noted that there is a fundamental difference between the triple helices discussed in the remaining sections of this review and the RecA-mediated three-stranded complexes. This difference resides in the orientation of the third strand. In triple helices [both intramolecular (H-DNA) and intermolecular], the third strand has an opposite polarity with respect to the Watson–Crick strand of the identical base sequence, whereas in RecA-mediated three-stranded complexes the third (invading) strand has the same polarity as the Watson–Crick strand of identical sequence.

RecA-mediated formation of three-stranded complexes can be used to introduce site-specific lesions in duplex DNA. An oligonucleotide having a psoralen group on the furan ring was used to form a joint molecule with a homologous sequence of duplex DNA in the presence of RecA.[156] Upon UV irradiation, the psoralen was further cross-linked (pyrone side) to a thymine in the complementary strand of the oligonucleotide. Since psoralen cross-linking requires correct positioning of the double bonds which react to form the cyclobutane ring, this result suggests that the oligonucleotide was bound to its complementary sequence through Watson–Crick base pairs. Oligonucleotides of at least 50 residues in length were necessary to observe 50% efficiency of the cross-linking reaction. These complexes were further used to study the mechanism of cross-link repair by *E. coli* ABC excinuclease.[156]

A homologous joint formed by an oligonucleotide with duplex DNA in the presence of RecA was shown to inhibit transcription initiation when the oligonucleotide was homologous to a promoter region and to prevent transcription elongation when it was bound downstream from the promoter.[157] RecA-mediated formation of three-stranded complexes inhibits cleavage by restriction enzymes and methylation by associated methylases when the oligonucleotide covers a restriction site. This observation has been used to develop a new strategy (called RARE for "RecA-assisted restriction endonuclease" cleavage) to make single cuts in long DNA fragments and chromosomes.[158] When a three-stranded complex is formed, methylation is inhibited at this particular site, but takes place at other methylase recognition sites. Upon subsequent addition of the corresponding restriction endonuclease, only the non-methylated site is cleaved. This technique is similar in its principle to the "Achilles heel" method developed by Koob and Szybalsky[84,85] and to that described by Strobel and Dervan,[81–83] which uses triple helix-forming oligonucleotides. However the RARE procedure offers a more general approach, since any double-stranded sequence can be "invaded" by a third strand in the presence of RecA.

7. Sequence-Specific Modifications of DNA

7.1. Sequence-Specific Cleavage of Duplex DNA by Triple-Helix-Forming Oligonucleotides Tethered to Active Reagents

Sequence-specific triple-helix formation by oligodeoxynucleotides has led to the development of artificial nucleases that are able to cleave DNA at specific sites. Under physiological conditions, direct cleavage can be achieved by attaching to the oligonucleotide a reagent capable of generating reactive species, such as hydroxyl radicals, upon *chemical* activation. This strategy has been used with metal complexes, such as Fe-EDTA[19,30,80,81,131] or copper–phenanthroline.[79,159] Alternatively, cleavage can be induced by *photochemical* activation of an aromatic group such as an ellipticine derivative.[61,160] The yields of these reactions are usually low, except with copper–phenanthroline, for which 70% cleavage of double-stranded DNA was reported.[79] The attachment of intercalating agents such as phenanthroline or ellipticine was described in Section 3.4. Oligonucleotides with an EDTA group at the C(5) position of dU were assembled on solid phase via the 3′-phosphoramidite derivative **49c** of the modified nucleoside **49b**. Compound **49b** was obtained by conversion of 2′-deoxyuridine into the amino derivative **49a**, which was acylated with an (EDTA triethylester) hydroxysuccinimide ester.[204]

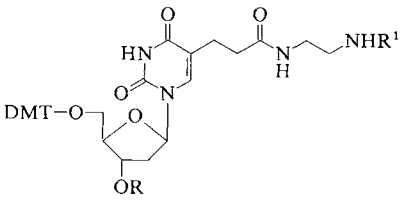

49a: R, R^1 = H
49b: R = H, R^1 = (EDTA-Et_3)
49c: R = $-P(OCH_2CH_2CN)-NiPr_2$, R^1 = (EDTA-Et_3)

Rather than attaching a chemical reagent to one end of the triplex-forming oligonucleotide, it is also possible to attach an enzyme.[203] An oligonucleotide–staphylococcal nuclease adduct cleaves plasmid DNA with a 75% yield at a specific site. By using two target sequences on the same DNA molecule, it is possible to excise DNA fragments. Even though cleavage by the nuclease does not occur at a single phosphodiester bond, the fragments can be used in cloning studies.[203]

Diffusible reagents, such as OH• radicals, which are generated within one of the double helix grooves, are expected to yield an asymmetric distribution of cleavage patterns on opposite strands. In Figure 12 top a cylindrical projection of the sugar–phosphate backbone of "standard" B-DNA is shown. If one assumes that OH• radicals are generated in the center of one of the grooves, they will attack the deoxyriboses according to their distance distribution. Faster reaction is expected at sugars located in a direction perpendicular to the *groove* axis and not to the *helix* axis. When the reactive sites are plotted on a linear representation of DNA with

arrow lengths proportional to an estimated reactivity, their distribution is clearly asymmetric (Fig. 12 bottom). Cleavage sites are shifted toward the 3'-end when OH• radicals are produced within the minor groove and toward the 5'-end when they are produced in the major groove.

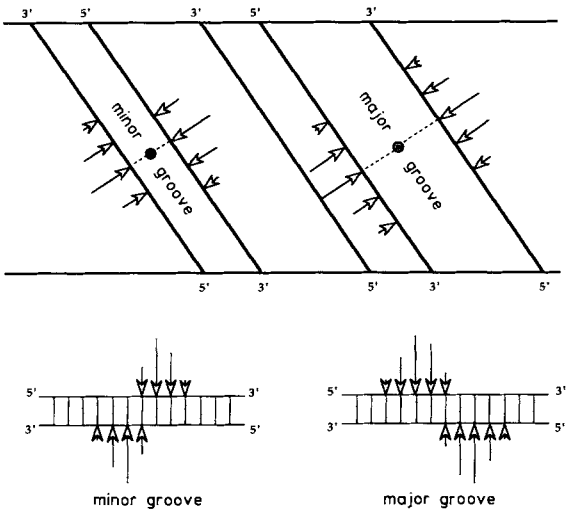

Fig. 12. Asymmetric distribution of the cleavage sites on the two DNA strands generated by a diffusible species (e.g., OH• radicals) within the major or minor groove of the DNA double helix. The upper portion shows a schematic cylindrical projection of the sugar–phosphate backbone of the B-form of DNA [201]. The cylinder was cut open, spread on a flat surface and viewed from the outside. If reactive species (e.g., OH• radicals) are generated in the center of a groove (dot within a circle) they will react the most with sugars which are closest in space (in a direction perpendicular to the groove axis). They do *not* belong to the nucleotides of the same base pair. Reactivity (cleavage) will be related to distance, as shown by the arrows on the cylindrical projection and, in the bottom portion of the figure, on a linear representation of the double helix. The two "waves" of cleavage sites on each strand reveal an asymmetric distribution. They are shifted to the 3'-side when cleavage occurs in the minor groove and to the 5'-side when cleavage occurs in the major groove. The actual location, amplitude, and distribution of the cleavage sites depend on the position of the OH• radical-generating species with respect to the double helix of DNA.

The cleavage patterns observed with Fe-EDTA linked at C(5) of a pyrimidine nucleoside of an oligonucleotide show that this probe is located in the major groove of duplex DNA.[19] When site-specific cleavage with copper–phenanthroline was analyzed the cleavage patterns were found to be shifted to the 3'-side on opposite strands. This indicates that cleavage takes place in the minor groove.[79, 205] Different linkers were used to tether phenanthroline to the triplex-forming oligonucleotide. The results showed that cleavage was due to phenanthroline intercalated at the triplex–duplex junction. Intercalation brought the two nitrogen atoms of phenanthroline into the minor groove where copper chelation occurred, leading to the production of the oxidative species in the presence of a reducing agent (3-mercaptopropionic acid). Therefore binding of the oligonucleotide in the major groove together with phenanthroline intercalation at the triplex–duplex junction, targeted the cleavage reaction to the minor groove, leading to the characteristic asymmetric distribution of cleavage sites to the 3'-side on opposite strands (Fig. 13). Site-specific cleavage occurred at higher temperatures and pH values than anticipated on the basis of the stability of the oligonucleotide–DNA triple helix. The intercalation model provides an explanation for these observations. Oligonucleotide binding to the major groove and copper binding to intercalated phenanthroline in the minor groove should lock the complex in place, with phenanthroline acting as a bridge connecting the two grooves.

7.2. Cross-Linking of Oligonucleotides with Double-Helical DNA

Indirect cleavage of duplex DNA may occur after covalent bond formation between a reactive group tethered to a third-strand oligonucleotide and nucleotides of the target DNA, followed by cleavage of the phosphodiester bonds at the cross-linked sites under alkaline conditions. This method was used by Le Doan et al.[18] and Praseuth et al.[41] to demonstrate sequence-specific triplex formation with both β- and α-oligonucleotides by using azidoproflavine and azidophenacyl, respectively, to photo-induce cross-linking of the oligonucleotides to their target sequence (Fig. 9).

Oligonucleotides covalently linked to alkylating agents, such as *N*-2-chloroethyl-*N*-methylaminobenzylamide, were also shown to cross-link with specific DNA sequences and to undergo site-specific cleavage under alkaline conditions.[161, 162, 164–166] This alkylation is specific for the N(7) position of guanines as is that induced by other reagents,

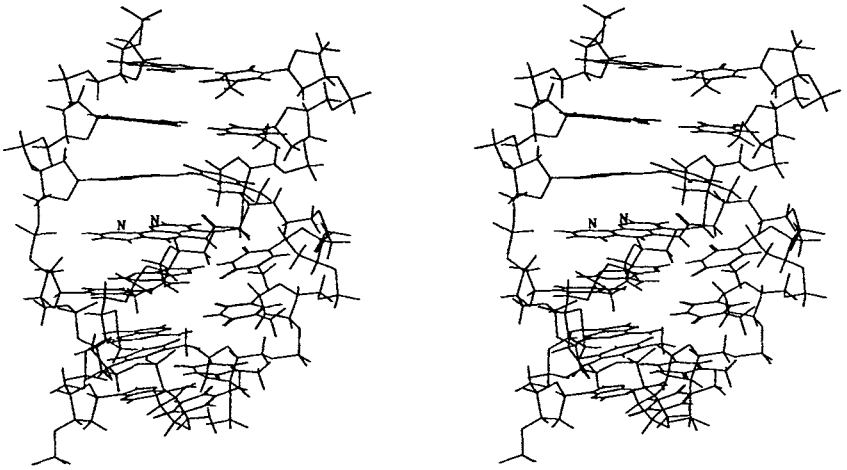

Fig. 13. Stereodiagram of phenanthroline intercalation at the triplex–duplex junction. Three base pairs (top) and three base triplets (bottom) are shown. The 5'-phosphate of the third-strand oligonucleotide is linked through a hexamethylene linker to 5-amino-1,10-phenanthroline. The third strand is bound to the major groove, to where it also brings the linker tethered to phenanthroline. When phenanthroline intercalates, the two nitrogen atoms point into the minor groove, where copper chelation and cleavage take place.

such as N^4,N^4-ethano-5-methyldeoxycytidine (**50**)[163] and thymidine (**51**) with an *N*-bromoacetyl group attached by a

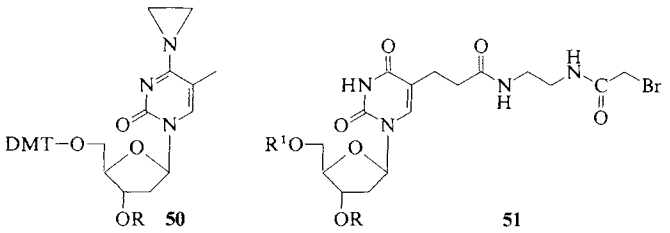

50 **51**

linker to the C(5) position of the pyrimidine ring.[162, 166] Treatment under alkaline conditions results in depurination of the alkylated guanine, followed by β-elimination reactions which result in backbone cleavage and the emergence of 5′- and 3′-phosphate termini with an efficiency of about 95%. In all these reactions, the cross-linking reagent can only react with one of the two DNA strands. The resulting cleavage is therefore limited to one strand. However, two alkylating oligonucleotides can be engineered in such a way as to bind to adjacent inverted sites on double-helical DNA and to alkylate at single guanine positions on opposite strands. If the two alkylated guanines are separated by a few base pairs, the two single-strand breaks can lead to single-site double-strand cleavage of long DNA fragments with an efficiency of up to 90%, as recently demonstrated in a yeast chromosome.[166]

Cross-linking of oligonucleotides with a double-stranded DNA target was also observed with a binuclear platinum derivative **43**.[167] One of the Pt centers was allowed to react with a 5′-phosphorothioate of the oligonucleotide, and the second Pt center formed a covalent adduct with guanines in the target sequence.

7.3. Sequence-Specific Cross-Linking of the Two Strands of Double-Helical DNA by Psoralen–Oligonucleotide Conjugates

Psoralens have been used for many years as photoactive probes of DNA and RNA structures, as photoactive drugs against dermatological diseases such as psoriasis, and as tools for studying the mechanisms of mutagenesis and repair processes.[168] Upon UV irradiation, they react with thymines in DNA, and when intercalation occurs at 5′TpA3′ sites they form a cross-link between the two DNA strands by reacting with the two thymines on opposite strands. Cross-linking involves a [2 + 2] cycloaddition between the 5,6 double bond of the thymine and the 3,4 (pyrone) and/or 4′,5′ (furan) double bonds of psoralen. Structural studies carried out by using NMR spectroscopic techniques have concluded that the psoralen ring at the cross-linked site is oriented with the C(8) position in the minor groove and with a *cis-syn* configuration for each of the adducts.

Triple-helix formation involves binding of the oligonucleotide in the *major* groove. Therefore, in order to bring a psoralen to a 5′TpA3′ site with the appropriate orientation necessary to form a cross-link between the two DNA strands, the psoralen ring should be attached to the oligonucleotide through its C(5) position (see Fig. 9). Experiments with several sequences as targets for the psoralen–oligonucleotide conjugates showed that sequence-specific cross-linking of the two DNA strands could be achieved with a high yield, provided a 5′TpA3′ step is located at the junction between the triplex and duplex structures[130, 202] (Fig. 14). Recent experiments have shown that a psoralen–oligonucleotide conjugate is able to find its site-specific target within the three billion base pairs of human DNA (C. Giovannangeli, L. Perrouault, C. Hélène, unpublished results). The target sequence was carried by the proviral DNA of HIV, which was integrated as a single copy into one of the chromosomes of a chronically infected human cell line.

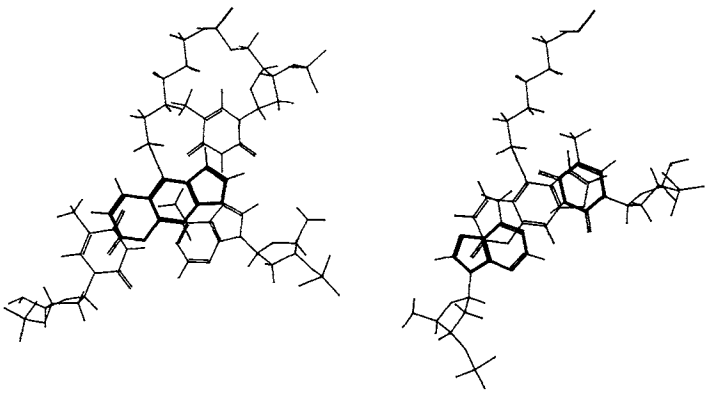

Fig. 14. Energy-minimized structures of an oligonucleotide–psoralen conjugate. The psoralen is attached to the 5′-end of a triplex-forming oligonucleotide and intercalates at the triplex–duplex junction. This figure shows the psoralen ring stacked over the last base triplet of the triple helix (T × A · T) (left) and below the first base pair (T · A) of the duplex (right). Only one position of the psoralen ring is shown, with the furan ring oriented toward the first thymine of the duplex region (the sequence at the duplex–triplex junction is $^{5'}$TpA$^{3'}$). The two reactive double bonds of psoralen [4′,5′-(furan side) and 3,4-(pyrone side)] are close to the 5,6 double bonds of the two thymines that react to form cyclobutane units, leading to a cross-link between the two strands of DNA (see ref. [130] and [202]).

The psoralen ring may a priori adopt two orientations at its intercalation site by rotating 180° around the C(5)–O bond. However, the psoralen derivative at the cross-linked site was shown to be predominantly oriented with its furan side bound to the purine-rich strand.[130] This preferential orientation reflects both the difference in binding energy of the two rotamers and the difference in photochemical reactivity. The second parameter seems to be more important, since the furan ring positioned in close proximity to the homopurine sequence yields an appropriate orientation for the two reactive double bonds of psoralen with respect to the double bonds of the two thymines on opposite strands (Fig. 14).

8. Gene Control by Triplex-Forming Oligonucleotides

The formation of a local triple-helical structure arising from the binding of an oligonucleotide to a specific sequence on the DNA double helix can affect gene expression in several ways (see Fig. 15 for a schematic representation of inhibitory processes in the case of transcription):

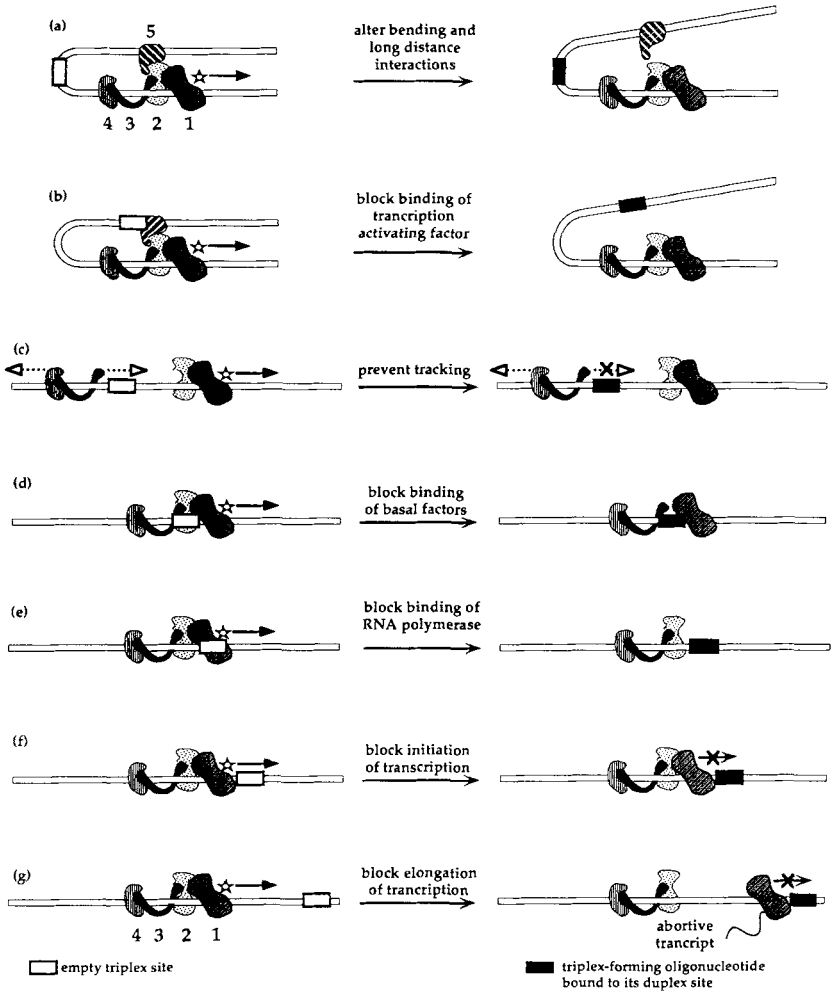

Fig. 15. Schematic representation of different mechanisms by which triple-helix-forming oligonucleotides can block transcription. The transcription machinery involves RNA polymerase and associated factors, activating factors that bind upstream in the promoter region, and activators that bind to enhancer sequences at long distance from the RNA polymerase binding site and act through folding of the double helix. The arrow indicates the direction of transcription, and the star denotes the transcription start site. The open box represents the unoccupied triplex site and the filled box represents the triple helix formed on duplex DNA. Proteins are schematically represented: RNA polymerase (1) with associated basal factors (2) interacting with transcription activating factors, which can bind either within the same promoter region (3,4)—either directly or after sliding along the promoter sequence—or at a long distance and interact with the transcription machinery through folding of the DNA duplex (5). The triple-helix forming oligonucleotide can thus: a) alter bending of the DNA, thereby preventing long distance interactions between enhancer-bound proteins and the transcription machinery; b) block binding of activators, which act either through long distance interactions, or through factors bound next to the RNA polymerase complex (not shown); c) block tracking of transcription factors which bind to an enhancer sequence far away from the promoter and slide along the DNA to contact the polymerase machinery, as shown recently for late T4 genes [172]; d) block binding of basal factors (polypeptides associated with the protein that carries the enzymatic (polymerizing) activity); e) prevent binding of the polypeptide chain (RNA polymerase) which carries the polymerizing activity; f) prevent initiation of transcription upon binding downstream but in contact with the transcription machinery; g) block elongation of transcription when bound within the transcribed region of the gene. Other mechanisms, such as recruiting triple helix-binding proteins that might perturb the fine tuning of interactions between all protein factors involved in the transcription machinery or perturbing the structure of nucleosomes bound upstream or downstream of the promoter region, are not shown. Perturbation of chromatin structure may alter transcription (see ref. [173] for a review).

1) The triplex-forming oligonucleotide can overlap the recognition and binding sites of one of the components of the transcription or replication machinery.[169-173, 196] Competition for binding to the same site is expected to exert a direct effect on the biological process (Fig. 15b,d,e).

2) The DNA conformational change which has been demonstrated to occur upon triplex formation[60-69] may perturb the binding of protein factors and/or enzymes. The perturbation of the double helix extends outside the oligonucleotide binding site, and medium-range effects on protein binding can therefore be expected. Long-range effects may also occur due to triplex-induced bending, change in bending, and/or stiffening of the DNA double helix. These types of conformational perturbations might alter through-space interactions between, for example, two transcription factors bound to different regions of the DNA or may modify the distribution of nucleosomes within the chromatin structure (Fig. 15a,c).

3) A triplex-forming oligonucleotide bound immediately downstream of RNA polymerase attached to its promoter site might prevent initiation of transcription. Inhibition might also occur when an oligonucleotide binds close enough to DNA polymerase at an origin of replication (Fig. 15f).

4) An oligonucleotide bound to DNA might act as a "roadblock" for the transcription or replication enzymes (Fig. 15g). It is likely that short oligonucleotides will not be strong enough ligands to stop the enzymatic machinery once it is launched on the DNA. This phenomenon is reminiscent of antisense oligodeoxynucleotides, which do not prevent translation when bound to the coding sequence of a mRNA, unless ribonuclease H cleaves the target mRNA at the oligodeoxynucleotide binding site. Ribosomes moving along a mRNA will displace a bound oligonucleotide in the same way that they unfold secondary structures in mRNA. Only irreversible reactions, induced by either RNase H or chemical reagents attached to the oligonucleotide, will be able to stop the translation of ribosomes. A similar situation is expected for replication or transcription. Only an irreversible reaction induced at the oligonucleotide binding site is expected to stop the DNA processing enzymes.

The mechanisms described thus far rest upon *inhibition* of an enzymatic process acting on DNA as a template. The binding of an oligonucleotide to the major groove of DNA with the formation of a local triple helix might also lead to an *activation* of the enzymatic process. There are numerous accounts of activating factors, which act positively on transcription, but there are also negatively regulating protein factors that upon binding to a gene control region decrease the efficiency of transcription.[171] Preventing the binding of such factors by triple helix-forming oligonucleotides will relieve their inhibitory effects. Alternatively, changes in DNA

and/or chromatin structure might also enhance the efficiency of transcription and/or replication.[173]

The aforementioned discussion refers only to transcription and replication, two biological processes involving DNA as a matrix, for which there are published reports on the effects of triplex-forming oligonucleotides. However, there are other biological phenomena in which enzymatic systems use DNA as a matrix. For example, DNA repair might be affected by triplex-forming oligonucleotides. The enzymatic machineries responsible for DNA repair have to recognize defects in the DNA double helix arising from either replication errors (mismatches) or damage induced in DNA by exogenous influences (radiation, chemicals, drug metabolites, etc).[9] If the altered site in the double helix is close to, or overlaps a triplex-binding site, then DNA repair might be affected. Other processes, such as recombination, modulation of DNA supercoiling by topoisomerases, and alterations in chromatin superstructure,[173] may be altered by triplex-forming oligonucleotides as well. In addition there might be proteins which specifically bind triple-helical structures within cells.[179] They could stabilize both intramolecular (H-DNA) and intermolecular (oligonucleotide-directed) triple helices.

8.1. Inhibition of Restriction Enzyme Binding and Cleavage

Restriction enzymes and methylases provide interesting tools for demonstrating that triplex-forming oligonucleotides can inhibit protein binding to specific DNA sites.[174–176] Several examples have been described in previous sections. This strategy was used to induce site-specific cleavage of long DNA fragments including chromosomes (see Section 2.5). A triplex-forming oligonucleotide can protect a restriction site from methylation by the corresponding methylase; unprotected sites are methylated. When the restriction enzyme is then added to this partially modified DNA only the protected site is cleaved.[82, 83] Most of the experiments described to date deal with overlapping recognition sites [i.e. the triplex-forming site overlapped (by one or more base pairs) the enzyme recognition site]. However, longer range effects might be observed due to the conformational change induced by triplex formation.

8.2. Inhibition of Eukaryotic Transcription Factor Binding In Vitro

There are several examples described in which oligonucleotide-directed triple-helix formation prevents transcription factor binding. Oligonucleotides containing C and T,[65, 174, 182] G and T,[28, 185–187] and G and C[183] have been used to inhibit transcription factors from binding to specific sites in the promoter regions of several genes. In a few cases, the resulting inhibition of transcription has been documented both in vitro[28, 65, 182] and in cell cultures.[182, 185, 187] Intramolecular triplexes (H-DNA) may also play a similar role. For example, a poly(dG) · poly(dC) sequence was placed at the 5′-end of a thymidine kinase promoter in mouse LTK$^-$ cells.[184] Formation of a triplex (with G × G · C base triplets) was proposed to inhibit binding of a *trans*-activating factor that stimulates transcription when the (dG · dC) tract is double-stranded.

Maher et al. have examined the effects of triple helix-forming oligonucleotides in an eukaryotic (*Drosophila*) cell-free transcription system.[65] Homopurine · homopyrimidine sequences were inserted in various configurations relative to the binding sites of the *trans*-activating factor Sp1 in eukaryotic promoters. Promoter- and oligonucleotide-specific repression of basal transcription was observed in the absence of Sp1. These effects were ascribed to the alteration in DNA flexibility arising from triple helix formation at the promoter region. However, other mechanisms, such as inhibition of DNA tracking (Fig. 15c) may modify the appropriate interactions of activators or basal factors with RNA polymerase by preventing sliding along the DNA double helix. Transcription inhibition by triplex-forming oligonucleotides required the preassembly of triple-helical complexes prior to addition of nuclear extracts. This result might arise from activities present in the nuclear extracts which might decrease DNA accessibility, and/or trap or hydrolyze the oligonucleotide, thereby decreasing its free concentration. We have shown that nuclear extracts contain nuclease activities that hydrolyze oligonucleotides which are not tightly bound to either proteins or DNA. Addition of the *trans*-activating factor Sp1 after the triplex-forming oligonucleotides did not cause derepression, independently of whether Sp1 binding sites overlapped the triple helix sites or not. These results suggest that transcription control could be exerted by triplex-forming oligonucleotides that bind at sites which *do not* overlap known protein binding sites.

8.3. Inhibition of Transcription Initiation and Elongation In Vitro

In 1968 Morgan and Wells[177] demonstrated that transcription of polynucleotide duplexes in which all purines were on the same strand (poly[d(T · C)] · poly[d(G · A)] or poly(dA) · poly(dT)) was inhibited when a third strand RNA (poly[r((U · C)] or poly(rU)) was added prior to addition of RNA polymerase from *E. coli*.

An oligonucleotide bound immediately downstream of *E. coli* RNA polymerase was shown to inhibit transcription of the β-lactamase gene.[181] The triplex-forming site was adjacent to the binding site of RNA polymerase on the β-lactamase promoter, as evidenced by DNase I footprinting experiments. Upon addition of nucleoside triphosphates, transcription did not start immediately when the oligonucleotide was bound. A delay was observed that could be related to the lifetime of the triplex. Dissociation of the oligonucleotide allowed RNA polymerase to initiate transcription. Triple helices can be strongly stabilized by a benzo[*e*]pyridoindole derivative.[144] In the presence of such a ligand, the effect of the triplex-forming oligonucleotide on transcription initiation at the β-lactamase promoter was observed at much lower concentrations of the oligonucleotide. Inhibition was made irreversible when a psoralen–oligonucleotide conjugate was used to cross-link the oligonucleotide with its target sequence following UV irradiation.[181]

An oligonucleotide bound far downstream from the transcription initiation site of a DNA carrying a eukaryotic Pol II promoter was shown to transiently arrest transcription until the oligonucleotide was displaced by RNA polymerase moving along its template.[180] A polymerase complex stalled near a triple helix seems to mediate triple helix dissociation. The oligonucleotide acted as a "roadblock" only when it was cross-linked to its target site.[180] Transcription initiation by T7 RNA polymerase has been inhibited by oligonucleotide-directed triple-helix formation at a site overlapping the polymerase-specific promoter.[207]

8.4. Inhibition of Transcription In Vivo

There have been few reports clearly demonstrating that oligonucleotide-induced effects on transcription inside cells occurred as a result of triplex formation and inhibition of *trans*-activating factors. Postel et al.[185] provided evidence for binding of a triplex-forming oligonucleotide to the *myc* gene by showing that a DNase I-hypersensitive site was masked by the oligonucleotide in cell nuclei. We have used the gene encoding the α subunit of the interleukin 2 receptor (IL2Rα) to demonstrate triplex-specific effects[182, 212, 213]. The target sequence within the promoter of the IL2Rα gene overlaps the recognition site for a transcription factor (NFκB), which strongly activates transcription. A mutant of the target sequence was constructed which could not bind a triplex-forming 15mer oligonucleotide. In transfected cells, whereas the wild-type (natural sequence) gene was inhibited by the 15mer oligonucleotide, the mutant gene was not. This result clearly demonstrated that triplex formation was a prerequisite for the inhibitory effect of the oligonucleotide. In this system, we made use of oligonucleotides carrying either an intercalating agent at the 5′-end (an acridine derivative), which could strongly stabilize the triple-helical structure,[212] or a psoralen derivative which could photo-induce a cross-link between the two strands of DNA at the oligonucleotide binding site.[213] In the latter case, analysis of the target DNA after irradiation of the cells showed that the cross-link was indeed formed at the expected oligonucleotide site within irradiated cells.[213] Chemical probes, such as $KMnO_4$, DMS, and OsO_4/pyridine, can be used in living cells: They might allow the characterization of intermolecular triplexes by in vivo footprinting, as demonstrated recently for intramolecular H-DNA in bacteria.[188]

In several studies, an inhibitory effect on gene transcription of oligonucleotides expected to form triple helices was observed, even though it was not directly demonstrated that inhibition resulted from triple-helix formation. The IL2Rα gene promoter in T-lymphocytes and the HIV-1 promoter region in acutely or chronically infected cells were chosen as targets. A decrease in mRNA synthesis was observed in both cases.[186, 187]

8.5. Inhibition of DNA Replication

Triplex-forming oligonucleotides might prevent the replication machinery from moving through the oligonucleotide binding site. However, it is more likely that the oligonucleotide–DNA complex will be dissociated when replication progresses. An irreversible reaction induced at the oligonucleotide binding site should bring more efficient inhibitory effects.

The binding of an oligonucleotide to an origin of replication might prevent assembly of the replication machinery and therefore inhibit initiation of the biological process. An oligonucleotide–intercalator conjugate targeted at the origin of replication of SV 40 was shown to inhibit viral DNA replication in CV 1 cells.[189] However, there are mechanisms other than triplex formation which might explain these results, as discussed in the original report. There is as yet no other data available on replication inhibition when duplex DNA is used as a template. However, with single-stranded DNA as a template we have recently shown that a chimeric oligonucleotide carrying both the Watson–Crick and Hoogsteen sequences can block replication by T7 DNA polymerase by forming a triple helix on the single-stranded target.[211]

In other experiments in which single-stranded DNA was used as a template for either *E. coli* (Klenow fragment) or *Thermus aquaticus* (Taq) DNA polymerase, replication was shown to stop in the middle of polypurine (or polypyrimidine) tracts.[190] This result was ascribed to the formation of pu × pu · py or py × pu · py triple helices, because of the folding of the second half of the polypurine (or polypyrimidine) tract on the double helix formed by the template and its replicated complementary strand. Such inhibition of replication was relieved when a single-strand binding protein was preincubated with the template.[190]

8.6. Detection of Triple-Stranded Structures within Cells

A monoclonal antibody for triplex DNA was produced by immunizing mice with poly[d(T^mC)] · poly[d(GA)] · poly[d($^mC^+T$)], which forms a stable triple helix under physiological conditions.[192] Binding of this antibody to metaphase chromosomes and interphase nuclei was observed by immunofluorescent microscopy of mouse myeloma cells, which had been fixed in methanol/acetic acid.[192] Immunopositive regions corresponding to condensed chromatin rings were also observed in fixed polytene chromosomes of *Chironomus tentans* and *Drosophila melanogaster*.[193] The abundance of polypurine · polypyrimidine sequences in the DNA of eukaryotes[198, 199] makes it likely that H-DNA (intramolecular triplexes) can form under topological constraints.[178] There is as yet no report on the immunological detection of intermolecular triplexes within living cells.

9. Summary and Outlook

The demonstration[18–20] that short oligonucleotides can form sequence-specific complexes with double-stranded DNA has opened a new field of investigations. Binding occurs in the major groove of the double helix and each base pair is recognized by two hydrogen bonds. Even though triple helix stability is less than that of a double helix, the specificity is at least as good as that of double-helical complexes. Single sites can be recognized in the genomic DNA of

higher organisms, which has opened new possibilities for sequence-specific cleavage of individual chromosomes at a limited number of sites. Oligonucleotide-directed triple helix formation can also be used to fish out double-stranded DNA sequences from a complex mixture.[191]

Triple-helix formation was originally limited to target sequences in which all purines belonged to the same strand. As shown in this review, the range of recognition sequences has been extended, but it still remains a challenge to organic chemists to design new base analogues able to read all four base pairs (A · T, T · A, G · C, C · G). Strand displacement reactions [e.g. with polyamide nucleic acids (PNAs)[112] or by recombinase-mediated reactions][155-158] might represent alternatives to triple-helix formation, which are not limited by the variety of base pair sequences they are able to recognize.

Many genes possess polypurine · polypyrimidine stretches, which appear to be over-represented in the genome of higher organisms.[198-200] Therefore, triple-helix-forming oligonucleotides offer new possibilities of controlling gene expression at the gene level. There are usually only two copies of each gene in a diploid cell. This characteristic might be an advantage in comparison with other targets for oligonucleotides, such as mRNA sequences which are present in large numbers within cells. The "antigene strategy",[21] which targets the oligonucleotide to the gene itself, is therefore an attractive alternative to the "antisense strategy",[22, 194] which targets the oligonucleotide to the mRNAs rather than to the gene.[197]

A fair amount of chemistry is being devoted to improving stability, selectivity, and range of recognition sequences of triple helix-forming oligonucleotides. Some of the problems facing the in vivo use of antigene oligonucleotides are similar to those encountered with antisense oligonucleotides. These problems include stability in biological media, cell uptake, intracellular distribution, pharmacokinetics. The synthesis of oligonucleotide analogues and the study of their physicochemical and biological properties provide the basic principles and the concepts for the development of a new family of therapeutic agents.

We wish to thank all our collaborators whose work is referred to in this review. We also thank Dr. Daniel Pilch for careful reading and comments, and Catherine Alvarez for typing the manuscript. Work in our laboratories has been supported by Rhône-Poulenc.

Received: October 22, 1992 [A 901 IE]
German version: *Angew. Chem.* **1993**, *105*, 697

[1] T. Steitz, *Q. Rev. Biophys.* **1990**, *23*, 205–280; S. Harrison, *Nature* **1991**, *353*, 715–719.
[2] C. Hélène, G. Lancelot, *Prog. Biophys. Mol. Biol.* **1982**, *39*, 1–68.
[3] S. Neidle, H. M. Berman, *Prog. Biophys. Mol. Biol.* **1983**, *41*, 43–66; B. C. Baguley, *Anti-Cancer Drug Design* **1991**, *6*, 1–35.
[4] C. Zimmer, U. Wähnert, *Prog. Biophys. Mol. Biol.* **1986**, *47*, 31–112; C. Bailly, J. P. Hénichart, *Bioconjugate Chem.* **1991**, *2*, 379–393.
[5] B. Lewin, *Genes*, Wiley, New York, **1983**.
[6] S. Wain-Hobson, P. Sonigo, O. Danes, S. Cole, M. Alizon, *Cell*, **1985**, *40*, 9–17.
[7] C. Hélène, J. J. Toulmé in *Oligodeoxynucleotides: Antisense Inhibitors of Gene Expression* (Ed.: J. S. Cohen), McMillan Press, London, **1989**, pp. 137–172.
[8] J. D. Watson, F. H. C. Crick, *Nature* **1953**, *171*, 737–738.
[9] M. Radman, R. Wagner, *Annu. Rev. Genet.* **1986**, *20*, 523; R. S. Lahne, K. G. Au, P. Modrich, *Science* **1989**, *245*, 160–164.
[10] G. Felsenfeld, D. Davies, A. Rich, *J. Am. Chem. Soc.* **1957**, *79*, 2023.
[11] G. Felsenfeld, H. T. Miles, *Annu. Rev. Biochem.* **1967**, *36*, 407–448.
[12] A. M. Michelson, J. Massoulié, W. Guschlbauer, *Prog. Nucleic Acids Res. Mol. Biol.* **1967**, *6*, 83–141.
[13] R. D. Wells, D. A. Collier, J. C. Hanvey, M. Shimizu, F. Wohlrab, *FASEB J.* **1988**, *2*, 2939–2949.
[14] K. Hoogsteen, *Acta Crystallogr.* **1959**, *12*, 822–823.
[15] S. M. Mirkin, V. I. Lyamichev, K. V. Drushlyak, V. N. Dobrynin, S. A. Filippov, M. D. Frank-Kamenetskii, *Nature* **1987**, *330*, 495–497.
[16] H. Htun, J. E. Dahlberg, *Science* **1989**, *243*, 1571–1576.
[17] Y. Kohwi, T. Kohwi-Shigematsu, *Proc. Natl. Acad. Sci. USA* **1988**, *85*, 3781–3785.
[18] T. Le Doan, L. Perrouault, D. Praseuth, N. Habhoub, J. L. Decout, N. T. Thuong, J. Lhomme, C. Hélène, *Nucleic Acids Res.* **1987**, *15*, 7749–7760.
[19] H. E. Moser, P. B. Dervan, *Science* **1987**, *238*, 645–650.
[20] V. I. Lyamichev, S. M. Mirkin, M. D. Frank-Kamenetskii, C. R. Cantor, *Nucleic Acids Res.* **1988**, *16*, 2165–2178.
[21] C. Hélène, *Anti-Cancer Drug Design* **1991**, *6*, 569–584.
[22] C. Hélène, J. J. Toulmé, *Biochim. Biophys. Acta* **1990**, *1049*, 99–125.
[23] E. Uhlmann, A. Peyman, *Chem. Rev.* **1990**, *90*, 543–584.
[24] U. English, D. H. Gauss, *Angew. Chem.* **1991**, *103*, 629–646; *Angew. Chem. Int. Ed. Engl.* **1991**, *30*, 613–629.
[25] S. T. Crooke, *Annu. Rev. Mol. Toxicol.* **1992**, *32*, 329.
[26] A. Jack, J. E. Ladner, A. Klug, *J. Mol. Biol.* **1976**, *108*, 619–649.
[27] G. L. Quigley, A. H. J. Wang, N. C. Seeman, F. L. Suddath, A. Rich, J. L. Sussman, S. H. Kim, *Proc. Natl. Acad. Sci. USA* **1975**, *72*, 4866–4870.
[28] M. Cooney, G. Czernuszewicz, E. H. Postel, S. J. Flint, M. E. Hogan, *Science* **1988**, *241*, 456–459.
[29] R. H. Durland, D. J. Kessler, S. Gunnell, M. Duvic, B. M. Pettitt, M. E. Hogan, *Biochemistry* **1991**, *30*, 9246–9255.
[30] P. A. Beal, P. B. Dervan, *Science* **1991**, *251*, 1360–1363.
[31] D. S. Pilch, C. Levenson, R. H. Shafer, *Biochemistry* **1991**, *30*, 6081–6087.
[32] C. Giovannangeli, M. Rougée, T. Montenay-Garestier, N. T. Thuong, C. Hélène, *Proc. Natl. Acad. Sci. USA*, **1992**, *89*, 8631–8635.
[33] I. Radhakrishnan, C. de los Santos, D. J. Patel, *J. Mol. Biol.* **1991**, *221*, 1403–1418.
[34] F. M. Chen, *Biochemistry* **1991**, *30*, 4472–4479.
[35] S. D. Jayasena, B. H. Johnston, *Biochemistry* **1992**, *31*, 320–327.
[36] C. Mark, D. Thiele, C. Schneider, W. Guschlbauer, *Nucleic Acids Res.* **1978**, *5*, 1979–1996.
[37] A. G. Letai, M. A. Palladino, E. Fromm, V. Rizzo, J. R. Fresco, *Biochemistry* **1988**, *27*, 9108–9112.
[38] T. Kohwi-Shigematsu, Y. Kohwi, *Nucleic Acids Res.* **1991**, *15*, 4267–4271.
[39] J. Bernués, R. Beltran, J. M. Casasnovas, F. Azorin, *EMBO J.* **1989**, *8*, 2087–2094.
[40] D. Michel, G. Chatelain, Y. Herault, G. Brun, *Nucleic Acids Res.* **1992**, *20*, 439–443.
[41] D. Praseuth, L. Perrouault, T. Le Doan, M. Chassignol, N. Thuong, C. Hélène, *Proc. Natl. Acad. Sci. USA* **1988**, *85*, 1349–1353.
[42] G. Manzini, L. E. Xodo, D. Gasparotto, F. Quadrifoglio, G. A. van der Marel, J. H. van Boom, *J. Mol. Biol.* **1990**, *213*, 833–843.
[43] J. S. Sun, T. de Bizemont, G. Duval-Valentin, T. Montenay-Garestier, C. Hélène, *C.R. Acad. Sci. Paris, Ser. III* **1991**, *313*, 585–590.
[44] D. A. Horne, P. B. Dervan, *J. Am. Chem. Soc.* **1990**, *112*, 2435–2437.
[45] A. Ono, C. N. Chen, L. S. Kan, *Biochemistry* **1991**, *30*, 9914–9921.
[46] B. C. Froehler, T. Terhorst, J. P. Shaw, S. N. McCurdy, *Biochemistry* **1992**, *31*, 1603–1609; S. McCurdy, C. Moulds, B. Froehler, *Nucleosides Nucleotides* **1991**, *10*, 287–290.
[47] P. A. Beal, P. B. Dervan, *J. Am. Chem. Soc.* **1992**, *114*, 4976–4982.
[48] S. Arnott, P. J. Bond, *Nature New Biol.* **1973**, *244*, 99–101.
[49] S. Arnott, E. Selsing, *J. Mol. Biol.* **1974**, *88*, 509–521.
[50] S. Arnott, P. J. Bond, E. Selsing, P. J. C. Smith, *Nucleic Acids Res.* **1976**, 2459–2470.
[51] J. Lourdes Campos, J. A. Subirana, *J. Biomol. Struct. Dyn.* **1991**, *8*, 793–800.
[52] C. de los Santos, M. Rosen, D. Patel, *Biochemistry* **1989**, *28*, 7282–7289.
[53] P. Rajagopal, J. Feigon, *Nature* **1989**, *339*, 637–640.
[54] V. Sklenar, J. Feigon, *Nature* **1990**, *345*, 836–838.
[55] D. S. Pilch, C. Levenson, R. H. Shafer, *Proc. Natl. Acad. Sci. USA* **1990**, *87*, 1942–1946.
[56] M. M. W. Mooren, D. E. Pulleyblank, S. S. Wijmenga, M. J. J. Blommers, C. W. Hilbers, *Nucleic Acids Res.* **1990**, *18*, 6523–6529.
[57] R. Macaya, E. Wang, P. Schultze, V. Sklenar, J. Feigon, *J. Mol. Biol.* **1992**, *225*, 755–773.
[58] I. Radhakrishnan, D. J. Patel, *Biochemistry* **1992**, *31*, 2514–2523.
[59] C. A. Laughton, S. Neidle, *J. Mol. Biol.* **1992**, *223*, 519–529.
[60] J. C. François, T. Saison-Behmoaras, C. Hélène, *Nucleic Acids Res.* **1988**, *16*, 11431–11440.
[61] L. Perrouault, U. Asseline, C. Rivalle, N. T. Thuong, E. Bisagni, C. Giovannangeli, T. Le Doan, C. Hélène, *Nature* **1990**, *344*, 358–360.
[62] D. Collier, J. L. Mergny, N. T. Thuong, C. Hélène, *Nucleic Acids Res.* **1991**, *19*, 4219–4224.

[63] J. S. Sun, J. L. Mergny, R. Lavery, T. Montenay-Garestier, C. Hélène, *J. Biomol. Struct. Dyn.* **1991**, *9*, 411–424.
[64] J. Chomilier, J. S. Sun, D. A. Collier, T. Montenay-Garestier, C. Hélène, R. Lavery, *Biophys. Chem.* **1992**, *45*, 143–152.
[65] L. J. Maher III, P. B. Dervan, B. J. Wold, *Biochemistry* **1992**, *31*, 70–81.
[66] D. A. Hartman, S. R. Kuo, T. R. Broker, L. T. Chow, R. D. Wells, *J. Biol. Chem.* **1992**, *267*, 5488–5494.
[67] V. I. Lyamichev, M. D. Frank-Kamenetskii, V. N. Soyfer, *Nature* **1990**, *344*, 568–570.
[68] V. I. Lyamichev, O. N. Voloshin, M. D. Frank-Kamenetskii, V. N. Soyfer, *Nucleic Acids Res.* **1991**, *19*, 1633–1638.
[69] P. E. Nielsen, *Nucleic Acids Res.* **1992**, *20*, 2735–2739.
[70] L. C. Griffin, P. B. Dervan, *Science* **1989**, *245*, 967–971.
[71] L. L. Kiessling, L. C. Griffin, P. B. Dervan, *Biochemistry* **1992**, *31*, 2829–2834.
[72] J. L. Mergny, J. S. Sun, M. Rougée, T. Montenay-Garestier, F. Barcelo, J. Chomilier, C. Hélène, *Biochemistry* **1991**, *30*, 9791–9798.
[73] R. W. Roberts, D. M. Crothers, *Proc. Natl. Acad. Sci. USA* **1991**, *88*, 9397–9401.
[74] K. Yoon, C. A. Hobbs, J. Koch, M. Sardaro, R. Kutny, A. L. Weis, *Proc. Natl. Acad. Sci. USA* **1992**, *89*, 3840–3844.
[75] B. P. Belotserkovskii, A. G. Veselkov, S. A. Filippov, V. N. Dobrynin, S. M. Mirkin, M. D. Frank-Kamenetskii, *Nucleic Acids Res.* **1990**, *18*, 6621–6624.
[76] E. Wang, S. Malek, J. Feigon, *Biochemistry* **1992**, *31*, 4838–4846.
[77] I. Radhakrishnan, X. Gao, C. de los Santos, D. Live, D. J. Patel, *Biochemistry* **1991**, *30*, 9022–9030.
[78] R. F. Macaya, D. E. Gilbert, S. Malek, J. S. Sinsheimer, J. Feigon, *Science* **1991**, *254*, 270–274.
[79] J. C. François, T. Saison-Behmoaras, C. Barbier, M. Chassignol, N. T. Thuong, C. Hélène, *Proc. Natl. Acad. Sci. USA* **1989**, *86*, 9702–9706.
[80] S. A. Strobel, H. E. Moser, P. B. Dervan, *J. Am. Chem. Soc.* **1988**, *110*, 7927–7929.
[81] S. A. Strobel, P. B. Dervan, *Science* **1990**, *249*, 73–75.
[82] S. A. Strobel, P. B. Dervan, *Nature* **1991**, *350*, 172–174.
[83] S. A. Strobel, L. A. Doucette-Stamm, L. Riba, D. E. Housman, P. B. Dervan, *Science* **1991**, *254*, 1639–1642.
[84] M. Koob, E. Grimes, W. Szybalski, *Science* **1988**, *241*, 1084–1086.
[85] M. Koob, W. Szybalsky, *Science* **1990**, *250*, 271–273.
[86] L. E. Xodo, G. Manzini, F. Quadrifoglio, *Nucleic Acids Res.* **1990**, *18*, 3557–3564.
[87] D. S. Pilch, R. Brousseau, R. H. Shafer, *Nucleic Acids Res.* **1990**, *18*, 5743–5750.
[88] J. Ohms, T. Ackermann, *Biochemistry* **1990**, *29*, 5237–5244.
[89] G. E. Plum, Y. W. Park, S. F. Singleton, P. B. Dervan, K. J. Breslauer, *Proc. Natl. Acad. Sci. USA* **1990**, *87*, 9436–9440.
[90] L. J. Maher III, P. B. Dervan, B. J. Wold, *Biochemistry* **1990**, *29*, 8820–8826.
[91] M. Rougée, B. Faucon, J. L. Mergny, F. Barcelo, C. Giovannangeli, T. Montenay-Garestier, C. Hélène, *Biochemistry* **1992**, *31*, 9269–9278.
[92] S. A. Strobel, P. B. Dervan, *J. Am. Chem. Soc.* **1989**, *111*, 7286–7287.
[93] M. D. Distefano, J. A. Shin, P. B. Dervan, *J. Am. Chem. Soc.* **1991**, *113*, 5901–5902.
[94] K. J. Luebke, P. B. Dervan, *J. Am. Chem. Soc.* **1989**, *111*, 8733–8735.
[95] N. G. Dolinnaya, O. V. Pyatrauskene, Z. A. Shabarova, *FEBS Lett.* **1991**, *284*, 232–234.
[96] K. J. Luebke, P. B. Dervan, *J. Am. Chem. Soc.* **1991**, *113*, 7447–7448.
[97] K. J. Luebke, P. B. Dervan, *Nucleic Acids Res.* **1992**, *20*, 3005–3009.
[98] R. G. Shea, P. Ng, N. Bischofberger, *Nucleic Acids Res.* **1990**, *18*, 4859–4866.
[99] M. T. Sarocchi-Landousy, B. L. Haas, W. Guschlbauer, *Biochemistry* **1977**, *16*, 5414–5420.
[100] J. S. Lee, M. L. Woodsworth, L. J. P. Latimer, A. R. Morgan, *Nucleic Acids Res.* **1984**, *12*, 6603–6614.
[101] T. J. Povsic, P. B. Dervan, *J. Am. Chem. Soc.* **1989**, *111*, 3059-3061.
[102] L. E. Xodo, G. Manzini, F. Quadrifoglio, G. A. van der Marel, J. H. van Boom, *Nucleic Acids Res.* **1991**, *19*, 5625–5631.
[103] A. Ono, P. O. P. Ts'o, L. S. Kan, *J. Am. Chem. Soc.* **1991**, *113*, 4032–4033; *J. Org. Chem.* **1992**, *57*, 3225–3230.
[104] M. Shimizu, H. Inoue, E. Ohtsuka, *Nucleic Acids Symp. Ser.* **1991**, *25*, 141 - 142.
[105] S. H. Krawczyk, J. F. Milligan, S. Wadwani, C. Moulds, B. C. Froehler, M. D. Matteucci, *Proc. Natl. Acad. Sci. USA* **1992**, *89*, 3761–3764.
[106] P. S. Miller, P. Bhan, C. D. Cushman, T. L. Trapane, *Biochemistry* **1992**, *31*, 6788–6793.
[107] J. S. Koh, P. B. Dervan, *J. Am. Chem. Soc.* **1992**, *114*, 1470–1478.
[108] L. J. P. Latimer, K. Hampel, J. S. Lee, *Nucleic Acids Res.* **1989**, 1549–1561.
[109] L. Kibler-Herzog, B. Kell, G. Zon, K. Shinozuka, S. Mizan, W. D. Wilson, *Nucleic Acids Res.* **1990**, *18*, 3545–3555.
[110] D. E. Callahan, T. L. Trapane, P. S. Miller, P.O.P. Ts'o, L. S. Kan, *Biochemistry* **1991**, 1650–1655.
[111] M. Matteucci, K. Y. Lin, S. Butcher, C. Moulds, *J. Am. Chem. Soc.* **1991**, 7767–7768.
[112] P. E. Nielsen, M. Egholm, R. H. Berg, O. Buchardt, *Science* **1991**, *254*, 1497–1500; M. Egholm, O. Buchardt, P. E. Nielsen, R. H. Berg, *J. Am. Chem. Soc.* **1992**, *114*, 1895–1897. See also: C. Meier, J. W. Engels, *Angew. Chem.* **1992**, *104*, 1039; *Angew. Chem. Int. Ed. Engl.* **1991**, *31*, 1008.
[113] U. Sequin, *Helv. Chim. Acta* **1974**, *57*, 68–81.
[114] F. Morvan, B. Rayner, J. L. Imbach, D. K. Chang, J. W. Lown, *Nucleic Acids Res.* **1986**, *14*, 5019–5035.
[115] N. T. Thuong, U. Asseline, V. Roig, M. Takasugi, C. Hélène, *Proc. Natl. Acad. Sci. USA* **1987**, *84*, 5129–5133.
[116] F. Morvan, B. Rayner, J. L. Imbach, S. Thenet, J. R. Bertrand, J. Paoletti, C. Malvy, C. Paoletti, *Nucleic Acids Res.* **1987**, *15*, 3421–3437.
[117] C. Cazenave, M. Chevrier, N. T. Thuong, C. Hélène, *Nucleic Acids Res.* **1987**, *15*, 10507–10521.
[118] a) T. Yamaguchi, M. Saneyoshi, *Chem. Pharm. Bull.* **1986**, *32*, 1441–1450; b) R. Kurfürst, Ph.D. Thesis, Orleáns, **1990**.
[119] N. T. Thuong, M. Chassignol, *C.R. Acad. Sci. Paris, Ser. II* **1987**, *305*, 1527–1530.
[120] F. Morvan, B. Rayner, J. P. Leonetti, J. L. Imbach, *Nucleic Acids Res.* **1988**, *16*, 833–847.
[121] N. T. Thuong, M. Chassignol, *Tetrahedron Lett.* **1988**, *29*, 5905–5908.
[122] J. S. Sun, C. Giovannangeli, J. C. François, R. Kurfürst, T. Montenay-Garestier, U. Asseline, T. Saison-Behmoaras, N. T. Thuong, C. Hélène, *Proc. Natl. Acad. Sci. USA* **1991**, *88*, 6023–6027.
[123] J. S. Sun, U. Asseline, D. Rouzaud, T. Montenay-Garestier, N. T. Thuong, C. Hélène, *Nucleic Acids Res.* **1987**, *15*, 6149–6158.
[124] D. Praseuth, M. Chassignol, T. Takasugi, T. Le Doan, N. T. Thuong, C. Hélène, *J. Mol. Biol.* **1987**, *196*, 939–942.
[125] J. S. Sun, R. Lavery, *J. Mol. Recognition* **1992**, *5*, 93–98.
[126] U. Asseline, N. T. Thuong, C. Hélène, *C.R. Acad. Sci. Paris, Ser. III* **1983**, *297*, 369–372.
[127] U. Asseline, M. Delarue, G. Lancelot, F. Toulmé, N. T. Thuong, T. Montenay-Garestier, C. Hélène, *Proc. Natl. Acad. Sci. USA* **1984**, *81*, 3297–3301; U. Asseline, F. Toulmé, N. T. Thuong, M. Delarue, T. Montenay-Garestier, C. Hélène, *EMBO J.* **1984**, *3*, 795–800.
[128] J. S. Sun, J. C. François, T. Montenay-Garestier, T. Saison-Behmoaras, V. Roig, N. T. Thuong, C. Hélène, *Proc. Natl. Acad. Sci. USA* **1989**, *86*, 9198–9202.
[129] D. A. Collier, N. T. Thuong, C. Hélène, *J. Am. Chem. Soc.* **1991**, *113*, 1457–1458.
[130] M. Takasugi, A. Guendouz, M. Chassignol, J. L. Decout, J. Lhomme, N. T. Thuong, C. Hélène, *Proc. Natl. Acad. Sci. USA* **1991**, *88*, 5602–5606.
[131] M. Boidot-Forget, M. Chassignol, M. Takasugi, N. T. Thuong, C. Hélène, *Gene* **1988**, *72*, 361–371.
[132] N. T. Thuong, M. Chassignol, *Tetrahedron Lett.* **1988**, *29*, 5905–5908.
[133] N. T. Thuong, M. Chassignol, *Tetrahedron Lett.* **1987**, *28*, 4157–4160.
[134] N. T. Thuong, U. Asseline in *Oligonucleotides and Analogues* (Ed.: F. Eckstein), IRL Press, Oxford, **1991**, Chapter 12.
[135] U. Asseline, N. T. Thuong, *Tetrahedron Lett.* **1988**, *29*, 2521–2524.
[136] U. Asseline, E. Bonfils, R. Kurfürst, M. Chassignol, V. Roig, N. T. Thuong, *Tetrahedron* **1992**, *48*, 1233–1254.
[137] D. G. Knorre, V. V. Vlassov, *Prog. Nucleic Acids Res. Mol. Biol.* **1985**, *32*, 292–322.
[138] L. Z. Benimetskaya, N. V. Bulychev, A. L. Kozionov, A. A. Koshkin, A. V. Lebedev, S. Yu Novozhilbbv, M. I. Stockmann, *Bioorg. Khim.* **1988**, *14*, 48–57.
[139] K. J. Hampel, P. Crosson, J. S. Lee, *Biochemistry* **1991**, *30*, 4455–4459.
[140] P. V. Scaria, R. H. Shafer, *J. Biol. Chem.* **1991**, *266*, 5417–5423.
[141] J. L. Mergny, D. Collier, M. Rougée, T. Montenay-Garestier, C. Hélène, *Nucleic Acids Res.* **1991**, *19*, 1521–1526.
[142] J. S. Sun, R. Lavery, J. Chomilier, K. Zakrzewska, T. Montenay-Garestier, C. Hélène, *J. Biomol. Struct. Dyn.* **1991**, *9*, 425–436.
[143] a) Y. W. Park, K. J. Breslauer, *Proc. Natl. Acad. Sci. USA* **1992**, *89*, 6653–6657; b) K. Umemoto, M. H. Sarma, J. Luo, R. H. Sarma, *J. Am. Chem. Soc.* **1990**, *112*, 4539–4545.
[144] J. L. Mergny, G. Duval-Valentin, C. H. Nguyen, L. Perrouault, B. Faucon, M. Rougée, T. Montenay-Garestier, E. Bisagni, C. Hélène, *Science* **1992**, *256*, 1681–1684.
[145] S. C. Harvey, J. Luo, R. Lavery, *Nucleic Acids Res.* **1988**, *16*, 11795–11809.
[146] C. Giovannangeli, T. Montenay-Garestier, M. Rougée, M. Chassignol, N. T. Thuong, C. Hélène, *J. Am. Chem. Soc.* **1991**, *113*, 7775–7777.
[147] E. T. Kool, *J. Am. Chem. Soc.* **1991**, *113*, 6265–6266.
[148] G. Prakash, E. T. Kool, *J. Am. Chem. Soc.* **1992**, *114*, 3523–3527.
[149] D. Michel, G. Chatelain, Y. Herault, G. Brun, *Nucleic Acids Res.* **1992**, *20*, 439–443.
[150] B. P. Belotserkovskii, M. M. Krasilnikova, A. G. Veselkov, M. D. Frank-Kamenetskii, *Nucleic Acids Res.* **1992**, *20*, 1903–1908.
[151] M. E. Reaban, J. A. Griffin, *Nature* **1990**, *348*, 342–344.
[152] P. Hsieh, C. S. Camerini-Otero, R. D. Camerini-Otero, *Genes Dev.* **1990**, *4*, 1951–1963.
[153] B. J. Rao, M. Dutreix, C. M. Radding, *Proc. Natl. Acad. Sci. USA* **1991**, *88*, 2984–2988.

[154] B. J. Rao, B. Jwang, M. Dutreix, *Biochimie* **1991**, *73*, 363–370.
[155] P. Hsieh, C. S. Camerini-Otero, R. D. Camerini-Otero, *Proc. Natl. Acad. Sci. USA* **1992**, *89*, 6492–6496.
[156] S. Cheng, B. Van Houten, H. B. Gampert, A. Sancar, J. E. Hearst, *J. Biol. Chem.* **1988**, *263*, 15110–15117.
[157] E. I. Golub, D. C. Ward, C. M. Radding, *Nucleic Acids Res.* **1992**, *20*, 3121–3125.
[158] L. Ferrin, R. D. Camerini-Otero, *Science* **1991**, *254*, 1494–1497.
[159] J. C. François, T. Saison-Behmoaras, M. Chassignol, N. T. Thuong, C. Hélène, *J. Biol. Chem.* **1989**, *264*, 5891–5898.
[160] T. Le Doan, L. Perrouault, U. Asseline, N. T. Thuong, C. Rivalle, E. Bisagni, C. Hélène *Antisense Res. and Develop.* **1991**, *1*, 43–54.
[161] O. S. Fedorova, D. G. Knorre, L. M. Podust, V. F. Zarytova, *FEBS Lett.* **1988**, *228*, 273–276.
[162] T. J. Povsic, P. B. Dervan, *J. Am. Chem. Soc.* **1990**, *112*, 9428–9430.
[163] J. P. Shaw, J. F. Milligan, S. H. Krawczyk, M. Matteucci, *J. Am. Chem. Soc.* **1991**, *113*, 7765–7766.
[164] E. B. Brossalina, E. N. Demchenko, V. V. Vlassov, S. V. Mamaev, *Antisense Res. Dev.* **1991**, *1*, 229–242.
[165] D. G. Knorre, V. V. Vlassov, *Genetica* **1991**, *85*, 53–63.
[166] T. J. Povsic, S. A. Strobel, P. B. Dervan, *J. Am. Chem. Soc.* **1992**, *114*, 5934–5941.
[167] E. S. Gruff, L. E. Orgel, *Nucleic Acids Res.* **1991**, *19*, 6849–6854.
[168] G. D. Cimino, H. B. Gamper, S. T. Isaacs, J. E. Hearst, *Annu. Rev. Biochem.* **1985**, *54*, 1151–1193.
[169] M. Ptashne, A. A. F. Gann, *Nature* **1990**, *346*, 329–331.
[170] C. C. Thompson, S. L. Mcknight, *Trend Genet.* **1992**, *8*, 232–236.
[171] R. Weinmann, *Gene Expression* **1992**, *2*, 81–91.
[172] D. R. Herendeen, G. A. Kassavetis, E. P. Geiduschek, *Science* **1992**, *256*, 1298–1303.
[173] G. Felsenfeld, *Nature* **1992**, *355*, 219–224.
[174] L. J. Maher III, B. J. Wold, P. B. Dervan, *Science* **1989**, *245*, 725–730.
[175] J. C. François, T. Saison-Behmoaras, N. T. Thuong, C. Hélène, *Biochemistry* **1989**, *28*, 9617–9619.
[176] J. C. Hanvey, M. Shimizu, R. D. Wells, *Nucleic Acids Res.* **1989**, *18*, 157–161.
[177] A. R. Morgan, R. D. Wells, *J. Mol. Biol.* **1968**, *37*, 63–80.
[178] T. L. Davis, A. B. Firulli, A. J. Kinniburgh, *Proc. Natl. Acad. Sci. USA* **1989**, *86*, 9682–9686.
[179] R. Kiyama, R. D. Camerini-Otero, *Proc. Natl. Acad. Sci. USA* **1991**, *88*, 10450–10454.
[180] S. L. Young, S. H. Krawczyk, M. D. Matteucci, J. J. Toole, *Proc. Natl. Acad. Sci. USA* **1991**, *88*, 10023–10026.
[181] G. Duval-Valentin, N. T. Thuong, C. Hélène, *Proc. Natl. Acad. Sci. USA* **1992**, *89*, 504–508.
[182] M. Grigoriev, D. Praseuth, P. Robin, A. Hemar, T. Saison-Behmoaras, A. Dautry-Varsat, N. T. Thuong, C. Hélène, A. Harel-Bellan, *J. Biol. Chem.* **1992**, *267*, 3389–3395; C. Hélène, N. T. Thuong, A. Harel-Bellan, *Ann. N.Y. Acad. Sci., Antisense Strategies*, **1992**, *660*, 27–36.
[183] J. E. Gee, S. Blume, R. C. Snyder, R. Ray, D. M. Miller, *J. Biol. Chem.* **1992**, *267*, 11163–11167.
[184] Y. Kohwi, T. Kohwi-Shigematsu, *Genes Dev.* **1991**, *5*, 2547–2554.
[185] E. H. Postel, S. J. Flint, D. J. Kessler, M. E. Hogan, *Proc. Natl. Acad. Sci. USA* **1991**, *88*, 8227–8231.
[186] F. M. Orson, D. W. Thomas, W. M. McShan, D. J. Kessler, M. E. Hogan, *Nucleic Acids Res.* **1991**, *19*, 3435–3441.
[187] W. M. McShan, R. D. Rossen, A. H. Laughter, J. Trial, D. J. Kessler, J. G. Zendegui, M. E. Hogan, F. M. Orson, *J. Biol. Chem.* **1992**, *267*, 5712–5721.
[188] P. Karlovsky, P. Pecinka, M. Vojtiskova, E. Makaturova, E. Palecek, *FEBS Lett.* **1990**, *274*, 39–42.
[189] F. Birg, D. Praseuth, A. Zerial, N. T. Thuong, U. Asseline, T. Le Doan, C. Hélène, *Nucleic Acids Res.* **1990**, *18*, 2901–2908.
[190] N. Baran, A. Lapidot, H. Manor, *Proc. Natl. Acad. Sci. USA* **1991**, *88*, 507–511.
[191] T. Ito, C. L. Smith, C. R. Cantor, *Proc. Natl. Acad. Sci. USA* **1992**, *89*, 495–498.
[192] J. S. Lee, G. D. Burkholder, L. J. P. Latimer, B. L. Haug, R. P. Braun, *Nucleic Acids Res.* **1987**, *15*, 1047–1061.
[193] G. D. Burkholder, L. J. P. Latimer, J. S. Lee, *Chromosoma* **1991**, *101*, 11–18.
[194] C. Hélène, *Eur. J. Cancer* **1991**, *27*, 1466–1471.
[195] P. B. Dervan, *Science* **1986**, *232*, 464–471.
[196] J. P. Landers, T. C. Spelsberg, *CRC Crit. Rev. Eukaryotic Gene Expression* **1992**, *2*, 19–63.
[197] J. M. Chubb, M. E. Hogan, *Trends Biotechnol.* **1992**, *10*, 132–136.
[198] A. M. Beasty, M. J. Behe, *Nucleic Acids Res.* **1988**, *16*, 1517–1528.
[199] M. J. Behe, *Biochemistry* **1987**, *26*, 7870–7875.
[200] H. Manor, B. S. Rao, R. G. Martin, *J. Mol. Evol.* **1988**, *27*, 96–101.
[201] J. Aymami, M. Coll, C. A. Frederick, A. H. J. Wang, A. Rich, *Nucleic Acids Res.* **1989**, *17*, 3229–3245.
[202] C. Giovannangeli, N. T. Thuong, C. Hélène, *Nucleic Acids Res.* **1992**, *20*, 4275–4281.
[203] D. Pei, D. R. Corey, P. G. Schultz, *Proc. Natl. Acad. Sci. USA* **1990**, *87*, 9858–9862.
[204] G. B. Dreyer, P. B. Dervan, *Proc. Natl. Acad. Sci. USA* **1985**, *82*, 447–450.
[205] D. S. Sigman, *Biochemistry* **1990**, *29*, 9097–9105.
[206] S. F. Singleton, P. B. Dervan, *J. Am. Chem. Soc.* **1992**, *114*, 6957–6965.
[207] L. J. Maher III, *Biochemistry* **1992**, *31*, 7587–7595.
[208] S. Arnott, R. Chandrasekharan, D. L. Birdsall, A. G. W. Leslie, R. L. Ratliff, *Nature* **1980**, *283*, 743.
[209] T. Montenay-Garestier, J. S. Sun, J. Chomilier, J. L. Mergny, M. Takasugi, U. Asseline, N. T. Thuong, M. Rougée, C. Hélène in *Molecular Basis of Specificity in Nucleic Acid-Drug Interactions* (Ed.: B. Pullman, J. Jortner), Kluwer Acad. Publ., Amsterdam, **1990**, pp. 275–290.
[210] C. Escudé, J. S. Sun, T. Garestier, M. Rougée, C. Hélène, *C.R. Acad. Sci. Paris, Ser. III*, **1992**, *315*, 521–525.
[211] C. Giovannangeli, N. T. Thuong, C. Hélène, *Proc. Nat. Acad. Sci. USA*, **1993**, in press.
[212] M. Grigoriev, D. Praseuth, A. L. Guieysse, P. Robin, N. T. Thuong, C. Hélène, A. Harel-Bellan, *C.R. Acad. Sci. Paris, Ser. III, Life Sciences*, **1993**, in press.
[213] M. Grigoriev, D. Praseuth, A. L. Guieysse, P. Robin, N. T. Thuong, C. Hélène, A. Harel-Bellan, *Proc. Nat. Acad. Sci. USA*, **1993**, in press.
[214] M. Shimizu, A. Konishi, Y. Shimada, H. Inoue, E. Ohtsuka, *FEBS Letters*, **1992**, *302*, 155–158.
[215] L. C. Griffin, L. L. Kiessling, P. A. Beal, P. Gillespie, P. B. Dervan, *J. Am. Chem. Soc.* **1992**, *114*, 7976–7982.

The Marcus Inverted Region from Theory to Experiment

By *Günter Grampp**

At first the theoretical papers of the 1992 Nobel Prize winner R. A. Marcus were not regarded by the experimentalists as the challenge they actually represented. From the very first publication on electron transfer reactions in May 1956,[1] which contains statements on the dependence of the free energy of activation of such reactions on the participating ions or molecules, their charges, and the solvent, they had the opportunity to put these theoretical predictions to the test. But even the paper on the Marcus cross correlation,[2] a easy-to-apply equation that should predict the rate constants of any redox process from the individual electron self-exchange reactions, attracted little attention from the experimenters.

The most spectacular theoretical prediction, however, applied to the relation between the free energy of activation ΔG^* and the free energy of reaction ΔG^0 of an electron transfer reaction,[**] and postulates the existence of a "Marcus inverted region". This unusual kinetic behavior and its experimental verification is the theme of this highlight.

Two quantities play an important role in every chemical reaction: the free energy of activation ΔG^* and the free energy of reaction ΔG^0. The latter determines whether the reaction is endergonic ($\Delta G^0 > 0$), thermoneutral ($\Delta G^0 = 0$), or exergonic ($\Delta G^0 < 0$). The rate constant of an electron transfer reaction is derived from the usual approach according to Equation (1).

$$k_{et} = A \exp(-\Delta G^*/RT) \tag{1}$$

To compare the experimentally determined rate constants with those calculated from Equation (1), theory must make sound statements on the composition of the free energy of activation ΔG^* and the preexponential factor A. The Marcus theory does both in a form that can be tested by experiment.

Of crucial importance is the reorganizational energy λ (Fig. 1); it describes the required rearrangement of the system of reactants and solvation shell necessary for electron transfer. For the same coordinates of the nuclei, the starting system (R) is differentiated from the final system (P, see Fig. 1) by the energy contribution λ. The reorganization energy λ has two components, the internal reorganization energy λ_i that accounts for the change in the bond lengths and bond angles on electron transfer, and the external reorganization energy λ_o that comprises the energy for the required rearrangement of the solvent shell [Eq. (2)]. The

$$\lambda = \lambda_i + \lambda_o \tag{2}$$

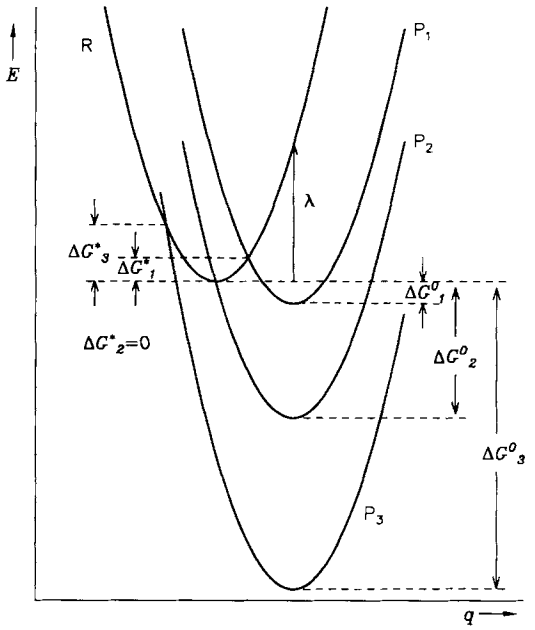

Fig. 1. The potential energies E of the reactants (R) and the products (P_1–P_3) of three systems with different free energies of reaction ΔG^0, as a function of the nuclear configuration q. 1: Exergonic reaction with $|\Delta G_1^0| > 0$ and $\Delta G_1^* > 0$; 2: exergonic reaction with $|\Delta G_2^0| = \lambda$ and $\Delta G_2^* = 0$; 3: $|\Delta G_3^0| > \lambda$ and $\Delta G_3^* > 0$ (Marcus inverted region).

influence of the solvent is described by purely physical properties, namely its refractive index n and its dielectric constant ε_s as combined in the Pekar factor $\gamma = (1/n^2 - 1/\varepsilon_s)$. This means that, in contrast to correlations that rely on empirical solvent parameters, the slope and intercept of graphs of $\lg k_{et}$ versus γ have a physical meaning.[3] The original Marcus theory did not consider dynamic solvent effects, but was later extended to include them.[4]

With Equation (1) and purely algebraic arguments a relationship between the free energy of activation ΔG^* and the free energy of reaction ΔG^0 can be established [Eq. (3)]. This

$$\Delta G^* = \frac{\lambda}{4}\left(1 + \frac{\Delta G^0}{\lambda}\right)^2 \tag{3}$$

is the famous Marcus equation that is strongly contrary to all chemical intuition because of the quadratic dependence of the free energy of activation on the free energy of reaction.

From experience we know that ΔG^* and therefore also the rate constant k of a reaction depend on ΔG^0,[5] and as a result, a number of "linear free energy relatonships" have been formulated that all involve the proportionality expressed in Equation (4). Thus in the beginning the Marcus

$$\lg k \sim -\Delta G^* \sim \Delta G^0 \tag{4}$$

theory had difficulty in gaining acceptance. While the elementary principles, for example that the electron transfer

[*] Priv.-Doz. Dr. G. Grampp
Institut für Physikalische und Theoretische Chemie
der Universität Erlangen-Nürnberg
Egerlandstrasse 3, D-W-8520 Erlangen (FRG)
Telefax: Int. code + (9131)85-8307

[**] The Marcus free energy of activation ΔG^* is related to the classical free energy of activation ΔG^+ of Eyring by the following relation: $\Delta G^+ = \Delta G^* - RT\ln(c^* h N_L A/RT)$. That k_{et} is a second order rate constant in Equation (1) is taken into account in the units of concentration c^* (mol L^{-1}). A = preexponential factor.

 © VCH Verlagsgesellschaft mbH, W-6940 Weinheim, 1993 0570-0833/93/0505-0691 $ 10.00+.25/0

can take place only between isoenergetic states as a consequence of the first law of thermodynamics, were accepted as a matter of course, the implications of Equation (3) appeared obscure to chemists. A close examination of this equation shows that it predicts a decrease in the rate constants with increasing exergonicity, a direct result of the quadratic relationship between ΔG^* and ΔG^0. For a long time experimental confirmation of this phenomenon, which was described by the phrase "Marcus inverted region", was sought intensively. The experimenters soon realized that only for photoinduced electron transfer reactions or for radiochemically generated energetic systems would a reaction have large enough exergonicity to display this behavior.

There are, however, several kinetic studies that show unambiguously that the rate constants of strongly exergonic *inter*molecular electron transfer reactions in solution approach a limiting value k_{diff}, which is the value for diffusion-controlled reactions (Fig. 2). The classic papers of Rehm and Weller[6] on fluorescence quenching by electron transfer have proved this conclusively.

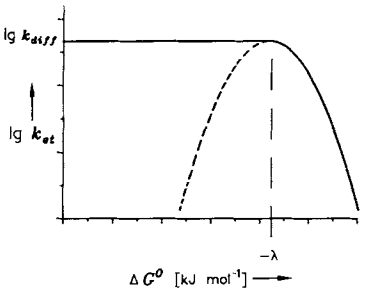

Fig. 2. The logarithm of the rate constants k_{et} of an electron transfer reaction, as function of the free energy of reaction ΔG^0. The solid line represents Rehm–Weller behavior and the broken line the Marcus inverted region. The maximum of this curve lies at $\Delta G^0 = -\lambda$.

This immense discrepancy between Marcus theory and experiment justifiably caused some skeptical comments in the beginning.[7] The breakthrough for the Marcus theory with regard to the inverted region was made about twenty years after its publication. The first occurrence of an inverted region was observed by J. J. Miller and the late G. L. Closs in a pulse radiolysis induced *intra*molecular electron transfer reaction.[8a] Through a skilful linking of donor and acceptor units by a rigid part of the molecule, the spacer, they could achieve a fixed reaction distance between the two units. Biphenyl served as donor and several aromatic hydrocarbons or quinones as acceptors. Even conformers with axial and equatorial units bound to the spacer were studied.[8b] By variation of the donor and acceptor units, a really phenomenal synthetic achievement, the ΔG^0 values were varied by means of the individual redox potentials to reach the inverted region. A convincing decrease in the rate constants k_{et} was found for values of $|\Delta G^0| > \lambda$.

Since then the existence of the inverted region has been proved conclusively for a series of molecules with bridged donor/acceptor units. Porphyrins were coupled to quinones and the reaction distance between the donor and the acceptor was varied. Remarkable achievements in synthesis were made to prepare diverse saturated six-membered ring systems as bridging units between the donor unit 1,4-dimethoxynaphthalene and acceptor unit dicyanoethylene.[10] Electron transfer reactions in proteins over large distances[11] likewise show the effect, as do photoinduced reactions in organic glasses[12] or the melts of aromatic hydrocarbons.[13] An inverted region has also been detected in inorganic transition metal complexes for the *intra*molecular electron transfer between two ligands.[14]

All examples mentioned thus far, and only a few have been selected, have in common the *intra*molecular electron transfer step. In contrast, up to now Rehm–Weller behavior has been found for all charge separation reactions described by the rate constant k_{et} in Scheme 1.

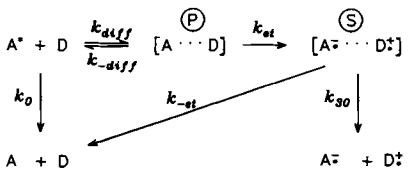

Scheme 1. Mechanism of a charge separation reaction between donor D and acceptor A. Ⓟ = precursor complex, Ⓢ = successor complex.

This finding invites further investigations on the precursor complex Ⓟ. One must distinguish here between contact ion pairs and solvent-separated ion pairs. Interested readers are referred to reference [15]. Without expanding on the structural differences of these loose complexes, it should be mentioned that combination reactions between the components of these species have certain similarities with intramolecular electron transfer. For example, the diffusion of the reaction partners to one another, which forms the precursor complex Ⓟ in bimolecular reactions, is redundant. Moreover, the distances between the reacting centers are more or less fixed.

As a result it was also possible to find the Marcus inverted region for charge recombinations, for example, for the electron back transfer (rate constant k_{-et}, Scheme 1). Unambiguous experimental proof was found for the existence of the inverted region for the electron back transfer from photoexcited singlet states of preformed radical ion pairs comprising 9,10-dicyano- or 2,6,9,10-tetracyanoanthracene as acceptor and a large number of aromatic hydrocarbons as donor.[16]

This electron back transfer took place from radical ion pairs derived from excited singlet states. Always present as competing reaction is the separation into the free solvatied ions $A^{\bullet -}$ and $D^{\bullet +}$, represented by the rate constant k_{30} ($\triangleq k_{diff}$) (Scheme 1).

In 1989 Russian authors studied the electron back transfer for radical ion pairs in the triplet state and likewise found an inverted effect. Through the use of a solvent with a low dielectric constant ε_s, the diffusion of the components of the radical ion pair away from each other was hindered.

Relatively few publications deal with both the electron transfer reactions discussed above, namely, the charge separation (k_{et}) and the electron back transfer (k_{-et}), in the same system. A new paper by Gray et al. concerns exactly this problem. Through fluorescence quenching experiments the authors succeeded in measuring the rate constant k_{et} of the forward reaction for triplet states of the iridium complex

$[\{Ir(1,5\text{-cyclooctadiene})(\mu\text{-pyrazolyl})\}_2]$ $(= Ir_2)$ with *N*-alkylpyridinium salts (py^+) as donors.[18] Whereas for the forward reaction formulated in Equation (5) the diffusion-

$$^3Ir_2 + py^+ \xrightarrow{k_{et}} Ir_2^{\bullet+} + py^{\bullet} \quad (5)$$

controlled limiting value in the strongly exergonic region is almost achieved (Rehm–Weller behavior), the electron back transfer reaction described in Equation (6) shows distinctly the inverted behavior of Marcus.

$$Ir_2^{\bullet+} + py^{\bullet} \xrightarrow{k_{et}} Ir_2 + py^+ \quad (6)$$

We found exactly the same situation for a purely organic redox system. The forward reaction proceeding from triplet states of the dye thionine with different aromatic hydrocarbons and amines as donors according to Equation (7) clearly

$$^3Th^+ + D \xrightarrow{k_{et}} [Th^{\bullet} \cdots D^{\bullet+}] \quad (7)$$

demonstrated Rehm–Weller characteristics, which has been known for a long time,[19] while the electron back transfer reaction [Eq. (8)] lies just as clearly in the Marcus inverted region.[20]

$$^3[Th^{\bullet} \cdots D^{\bullet+}] \xrightarrow{k_{-et}} Th^+ + D \quad (8)$$

The actual reasons for the different reaction behaviors is still topic of theoretical studies. Several models have been proposed only to be rejcted again. For instance, models that take into account quantum mechanical tunneling for the Marcus inverted region were developed, but they could not satisfactorily explain the quantitative differences between Rehm–Weller and Marcus behavior.[21] Energetically low-lying electronically excited states were thought to explain the absence of the Marcus inverted region for charge separation reactions, as was the dielectric saturation of the solvent molecules in the first solvent coordination sphere.[22] It was also noted that the electron transfer in intermolecular and intra- or pseudo-intramolecular back transfer reactions can also take place for other reaction distances.[23]

All these models are extremely difficult to test by experiment. So the occurrence or absence of the Marcus inverted region is still a field for wide-ranging theoretical deliberation. Interested readers are referred to a recent review.[24]

Nevertheless it can be categorically stated that all the predictions of the Marcus theory on the kinetics of electron transfer have been fully verified,[25] and they also contain explanations for such complex phenomena as the charge separation on photosynthesis, chemiluminescence, the collection of solar energy, and electron penetration reactions. Therefore the justification of the Royal Swedish Academy of Sciences for the award of the Nobel prize for Chemistry to R. A. Marcus in 1992 was singularly apt when they declared that it is a realistic theory.

German version: *Angew. Chem.* **1993**, *105*, 724

[1] R. A. Marcus, *J. Chem. Phys.* **1956**, *24*, 966.
[2] R. A. Marcus, *Discuss. Faraday Soc.* **1960**, *29*, 21.
[3] G. Grampp, W. Jaenicke, *Ber. Bunsenges. Phys. Chem.* **1991**, *95*, 904.
[4] a) H. Sumi, R. A. Marcus, *J. Chem. Phys.* **1986**, *84*, 4894; b) H. Heitele, *Angew. Chem.* **1993**, *105*, 378; *Angew. Chem. Int. Ed. Engl.* **1993**, *38*, 359.
[5] F. Scandola, V. Balzani, G. B. Schuster, *J. Am. Chem. Soc.* **1981**, *103*, 2519.
[6] a) D. Rehm, A. Weller, *Ber. Bunsenges. Phys. Chem.* **1969**, *73*, 834; b) *Isr. J. Chem.* **1970**, *8*, 256.
[7] N. Sutin, *J. Phys. Chem.* **1986**, *90*, 3465.
[8] a) J. R. Miller, L. T. Calcaterra, G. L. Closs, *J. Am. Chem. Soc.* **1984**, *106*, 3047; b) G. L. Closs, J. R. Miller, *Science* **1988**, *240*, 440.
[9] a) M. R. Wasielewski, M. P. Niewczyk, W. A. Svec, E. B. Pewitt, *J. Am. Chem. Soc.* **1985**, *107*, 1080; b) M. P. Archev, V. P. Y. Gadzekpo, J. R. Bolton, J. A. Schmidt, A. C. Weedon, *J. Chem. Soc. Faraday Trans. 2* **1986**, *82*, 2305; c) M. D. Irvine, R. J. Harrison, G. S. Beddard, P. Leighton, J. K. M. Sanders, *Chem. Phys.* **1986**, *104*, 315.
[10] N. S. Hush, M. N. Paddon-Row, E. Cotsaris, H. Oevering, J. W. Verhoeven, M. Heppner, *Chem. Phys. Lett.* **1985**, *117*, 8.
[11] a) J. R. Miller, G. McLendon, *J. Am. Chem. Soc.* **1985**, *107*, 7781; b) G. McLendon, *Acc. Chem. Res.* **1988**, *21*, 160.
[12] J. R. Miller, J. V. Beitz, R. K. Huddeston, *J. Am. Chem. Soc.* **1984**, *106*, 5057.
[13] K. Kemnitz, *Chem. Phys. Lett.* **1988**, *152*, 305.
[14] P. Chen, R. Duesing, D. K. Graff, T. J. Meyer, *J. Phys. Chem.* **1991**, *95*, 5850.
[15] J. Mattay, M. Vondenhof, *Top. Curr. Chem.* **1991**, *159*, 217.
[16] a) I. R. Gould, D. Ege, S. L. Mattes, S. Farid, *J. Am. Chem. Soc.* **1987**, *109*, 3794; b) I. R. Gould, J. E. Moser, B. Armitage, S. Farid, *ibid.* **1989**, *111*, 1917; c) I. R. Gould, D. Ege, J. E. Moser, S. Farid, *ibid.* **1990**, *112*, 4290; d) F. Lewitzka, H.-G. Löhmannsröben, *Z. Phys. Chem. (Munich)* **1990**, *169*, 181.
[17] P. P. Levin, P. F. Pluzhnikov, V. A. Kuzmin, *Chem. Phys.* **1989**, *137*, 331.
[18] T. M. McCleskey, J. R. Winkler, H. B. Gray, *J. Am. Chem. Soc.* **1992**, *114*, 6935.
[19] U. Steiner, G. Winter, *Chem. Phys. Lett.* **1978**, *55*, 364.
[20] G. Grampp, G. Hetz, *Ber. Bunsenges. Phys. Chem.* **1992**, *96*, 198.
[21] R. A. Marcus, P. Siders, *J. Am. Chem. Soc.* **1981**, *103*, 748.
[22] a) T. Kakitani, N. Mataga, *Chem. Phys.* **1985**, *93*, 381; b) *J. Phys. Chem.* **1987**, 91, 6277.
[23] a) G. Greiner, P. Pasquini, R. Weiland, H. Orthweiss, H. Rau, *J. Photochem. Photobiol. A*, **1990**, *51*, 179; b) M. Tachiya, S. Murata, *J. Phys. Chem.* **1992**, *96*, 8441.
[24] P. Suppan, *Top. Curr. Chem.* **1992**, *163*, 95.
[25] R. A. Marcus, *Angew. Chem.* **1993**, *105*, No. 8; *Angew. Chem. Int. Ed. Engl.* **1993**, *32*, No. 8 (Nobel lecture).

 © *VCH Verlagsgesellschaft mbH, W-6940 Weinheim, 1993* *0570-0833/93/0505-0693 $ 10.00+.25/0*

Absolute Asymmetric Synthesis by Irradiation of Chiral Crystals

By *Gerd Kaupp** and *Michael Haak*

The formation of enantiopure optically active biomolecules is an important chapter in the history of evolution. The physical phenomena which can generate and augment asymmetry[1] have been known for a long time. However, since 1975[2] there are also crystal chemical solutions of the problem, which moreover can be used in asymmetric synthesis. When achiral molecules crystallize in chiral space groups and the irradiation of the crystals leads to chiral products, one speaks justly and correctly of "absolute" asymmetric synthesis. For this, the use of chiral agents and thus also the "crystal-selecting" human hand must be dispensed with, even though the latter is useful for syntheses.

Absolute asymmetric [2 + 2] photodimerizations of achiral compounds in crystals have been known since 1982.[3] Compound **1** (Scheme 1) crystallizes in the chiral space group $P2_1$. Crystals of **1** obtained from the melt and from ethanol on irradiation give either (+)- or (−)-**2** with enantiomeric excesses (*ee* values) of 0 to 95% and higher. The result varies from crystallization batch to crystallization batch; however, 100% *ee* of the (+)- and the (−)-enantiomer **2** were also obtained.[3] This confirms that the photoreaction occurs *stereospecifically* (lattice-controlled or topochemical) and that in the batches with lower optical yields the preceding crystallization leads to mixtures of left- and right-handed chiral crystals. Many asymmetric syntheses of this kind occur with considerably lower optical yields (e.g. <7% *ee*[3]), or they are dependent on the conversion.[3] This is, however, not surprising, even when only crystals of a single chirality are present, because studies by atomic force microscopy (AFM)[4] have shown that photodimerizations proceed from the surface to the interior of the crystal, during which extensive molecular regroupings (on the scale of the lattice constants) take place. The degree of the obtainable stereoselectivities clearly depends on the various mechanisms which are involved in those processes.[4]

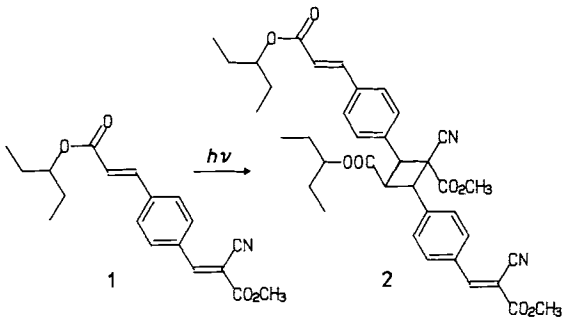

Scheme 1. **1** is *achiral*, but forms chiral crystals, which upon irradiation form *chiral* **2**.

The fact that relatively often spontaneous asymmetric crystallization of achiral compounds occurs with the formation of either right- or left-handed crystals is the result of autoseeding with the first crystal formed.[3, 5] Thus, in favorable cases all of the supersaturated solution yields only crystals of one chirality (analogously from melts), which, of course, cannot be predetermined. The chirality can only be influenced by manual seeding with selected crystals.

Enantioselective syntheses with achiral molecules in host crystals constructed from chiral molecules[6] belong as little to absolute asymmetric syntheses as do intramolecular photoreactions (di-π-methane rearrangement or γ-H transfer) following the manual selection of enantiomorphic crystals[7a] or after seeding with such crystals.[8] However, Scheffer, Trotter et al.[7b] developed further their highly selective di-π-methane rearrangement of diisopropyl dibenzobarrelenedicarboxylate to give the dibenzosemibullvalene derivative (quantitative *ee* at conversions of a few percent) into an absolute asymmetric synthesis, and Sakamoto et al.[9] have recently found another intramolecular absolute asymmetric synthesis by irradiation of crystals of achiral **3** (Scheme 2), which also crystallize in the chiral space group $P2_12_12_1$. Optically active **4** is obtained after photolysis of **3** without external seeding for the crystallization. In seven of ten crystallizations from hexane the (+)-enantiomer **4** predominated, in three cases the (−)-enantiomer **4**. The optical yields (10% *ee* at 0 °C, 75% chemical yield) can be improved by reducing the temperature (40% *ee* at −40 °C, 70% yield; no reaction at −78 °C; however, formation of racemic **4** in solution also at −78 °C). This is again a reminder of the necessity of the formation of a new phase by the product, which is accompanied by extensive molecular transports (on the scale of the crystal lattice constants) in all known cases.[4] Evidently, as a result of these, the chiral conformers **3** have—as in solution—the opportunity for racemization and further conformational alterations. Nevertheless, the chirality advantage given by the crystal is retained partly. Although, in principle, it is not necessary for the action of an asymmetric crystal environment that the molecules are arranged as uniform chiral conformers, it is essential for the helical compound **3**[9] that the one enantiomorphic type of crystal contains the molecules **3** in the right-handed helix (*P*), the other in the left-handed helix (*M*).[10]

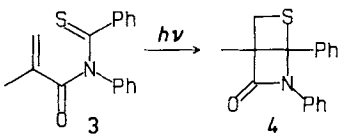

Scheme 2. **3** is *achiral*, but forms chiral crystals, which upon irradiation form *chiral* **4**.

As long as the absolute configuration of the products (e.g. **2** or **4**) and of the enantiomorphic crystals has not been determined, usually those leading to (+)-products are designated as (+)-crystals and vice versa. Without knowledge of the absolute configurations there is also no correlation between the chirality of the crystal and the helicity of the lat-

[*] Prof. Dr. G. Kaupp, Dipl.-Chem. M. Haak
FB 9 – Organische Chemie I der Universität
Postfach 2503, D-W-2900 Oldenburg (FRG)
Telefax: Int. code + (441)798-3409

tice-frozen conformer. To elucidate the principle we arranged the unit cell ($P2_12_12_1$) of **3** with the left-handed helix arbitrarily as left handed. Compound (1*R*,4*S*)-**4** [(−) or (+)] is formed unavoidably from the left-handed helix **3**. Correspondingly, (1*S*,4*R*)-**4** must be formed from the enantiomorphic crystal arranged in the right-handed way. This is represented in Figure 1 on the basis of optimized geometries from semiempirical PM3 calculations. Regardless of whether the adoption of the configurations agrees with reality, it thus becomes clear that the spontaneous asymmetric crystallization determines the chirality of the excess enantiomer **4** exclusively. The energetically most favorable conformer of **3** (Fig. 1; *M* or *P*) is 13 kcal mol^{-1} less stable than **4** according to our calculations,[11] and thus it should show optimal reactivity. According to the X-ray structure analysis,[9] in the crystal the pitch of the helix is reduced. This is evident from the significantly shortened distances between the reactive centers: the semiempirical calculated distances S-1/C-6 and C-2/C-5 in **3** are 4.33 and 3.26 Å, respectively, (where the numbers refer to the sequence of atoms in the chain starting from S);[11] in contrast, in the crystal they were determined to be 3.59 and 3.11 Å, respectively.[9] This compression also contributes to the selectivity of the crystal photolysis.

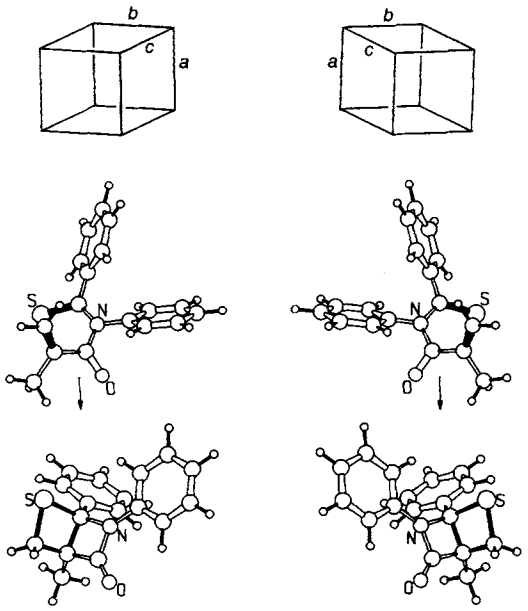

Fig. 1. Top: $P2_12_12_1$ unit cell ($a = 9.535(2)$, $b = 9.782(2)$, $c = 16.428(3)$ Å) of **3**, left- and right-handed arrangement; middle: left-handed (*M*) and right-handed helix (*P*) of **3** where *M* and *P* are descriptors for helicity (*M* = minus and *P* = plus); bottom: (1*R*,4*S*)-**4** and (1*S*,4*R*)-**4**.

Absolute asymmetric synthesis by irradiation of chiral crystals,[10] now extended to intramolecular reactions, supports the assumption of the prebiotic origin of natural chirality. The chemical mechanisms here appear to be so conclusive and efficient that they should in any case be retained besides the complicated physical interpretations.[1] It must be remembered that of the 230 space groups 65 are chiral and that of these $P2_12_12_1$ and $P2_1$ belong to the five most frequent in the organic crystals.

Regardless of these fundamental findings a wide field has opened up for efficient asymmetric syntheses by approved photochemical reactions. Far too little attention has been paid to the phenomenon of the spontaneous asymmetric crystallization to date, with the result that the step to the polarimeter or the use of chiral NMR shift reagents after the photolysis has mostly not been taken; otherwise without doubt many a supposed racemate would have turned out to be optically active.[12]

German version: *Angew. Chem.* **1993**, *105*, 727

[1] *Origins of Optical Activity in Nature* (Ed.: D. C. Walker), Elsevier, New York, **1979**.

[2] B. S. Green, M. Lahav, G. M. J. Schmidt, *Mol. Cryst. Liq. Cryst.* **1975**, *29*, 187-200. Bromination of manually selected enantiomorphic single crystals of 4',4'-dimethylchalcone to give optically active products (K. Penzien, G. M. J. Schmidt, *Angew. Chem.* **1969**, *81*, 628; *Angew. Chem. Int. Ed. Engl.* **1969**, *8*, 608) is incorrectly termed "absolute asymmetric synthesis".

[3] L. Addadi, J. van Mil, M. Lahav, *J. Am. Chem. Soc.* **1982**, *104*, 3422-3429; Recent example: M. Hasegawa, Y. Hashimoto, *Mol. Cryst. Liq. Cryst.* **1992**, *219*, 1-15; Review: V. Ramamurthy, K. Venkatesan, *Chem. Rev.* **1987**, *87*, 433-481.

[4] G. Kaupp, *Angew. Chem.* **1992**, *104*, 606-609 and 609-612; *Angew. Chem. Int. Ed. Engl.* **1992**, *31*, 592-595 and 595-598.

[5] J. M. McBride, R. L. Carter, *Angew. Chem.* **1991**, *103*, 298-300; *Angew. Chem. Int. Ed. Engl.* **1991**, *30*, 293-295.

[6] T. Fujiwara, N. Nauba, K. Hamada, F. Toda, K. Tanaka, *J. Org. Chem.* **1990**, *55*, 4532-4537.

[7] a) S. V. Evans, M. Garcia-Garibay, N. Omkaram, J. R. Scheffer, J. Trotter, F. Wireko, *J. Am. Chem. Soc.* **1986**, *108*, 5648-5650; b) J. Chen, J. R. Scheffer, J. Trotter, *Tetrahedron* **1992**, *48*, 3251-3274; there also absolute configuration of starting conformer and of product.

[8] A. Sekine, K. Hori, Y. Okashi, M. Yagi, F. Toda, *J. Am. Chem. Soc.* **1989**, *111*, 697-699.

[9] M. Sakamoto, N. Hokari, M. Takahashi, T. Fujita, S. Watanabe, I. Iida, T. Nishio, *J. Am. Chem. Soc.* **1993**, *115*, 818.

[10] Also among the intramolecular asymmetric reactions [7,8] known to date chiral conformations must occur.

[11] PM3 according to J. J. P. Stewart (*J. Comput. Chem.* **1989**, *10*, 209) with Spartan version 2.0 from Wavefunction, Inc., Irvine, CA, USA on an IBM RS6000 H32 Workstation calculated with complete geometry optimization. The best boat conformation of **3** (rotation about the C-4/C-5 bond) is only about 0·6 kcal mol^{-1} less stable than the helix. Representation of the molecules with Schakal 92/AIX-UNIX version from E. Keller, Universität Freiburg, on an IBM RS6000.

[12] Editorial note: After this paper had been received, another solid-state photochemical asymmetric synthesis was reported: A. L. Roughton, M. Muneer, M. Demuth, I. Klopp, C. Krüger, *J. Am. Chem. Soc.* **1993**, *115*, 2085-2087.

Ordered Molecular Arrays as Templates: A New Approach to the Synthesis of Mesoporous Materials

By *Peter Behrens** and *Galen D. Stucky*

During the past decade, physicists have discovered a new world in mesoscopic systems, in which classical models collide with quantum effects. It is a world in which electronic transport becomes a coherent process and any change in phase leads to a macroscopic change in conductance. Similarly, small changes in atomic structure or externally applied electromagnetic fields can cause large changes in absorption edges, polarization, optical transparency, and general nonlinear response. Using electrooptic interconnects in this dimension offers the possibilities of decreasing processing times in optical computers, increasing our capabilities to manipulate and store visual images, and a host of other potential applications.

The physicist's and engineer's approach to the mesoscopic world[1] has been by way of molecular beam epitaxy (MBE) and atomic layer epitaxy (ALE) on substrates with an ordered two-dimensional lattice to fabricate ultra-thin (monolayer) semiconductor epitaxial layers. Quantum wires in which carriers and electronic wave functions have only one degree of freedom can be formed in the MBE approach by corrugation of quantum layers or by lateral structuring, but are still a challenge below diameters of about 100 Å.

The chemist's interest in the mesoscopic world has been equally intense, based on a long-held recognition that ultimately all materials and living organisms have their origins in the collective assembly of a small number of atoms or molecules. Whether it be the beginning of life, crystallization, or the natural formation of a complicated biological nanocomposite like a sea shell, the inherent future properties such as shape, mechanical strength, color, conductivity, etc. of an extended structure are established very early as the molecules or atoms assemble and make the critical transition from few units with nanoscale dimensions to mesoscopic arrays. It is at this metamorphosis that macroscopic collective properties are defined and have their birth.

Two chemical approaches to the micro- and mesophase manipulation of atoms and molecules have been most extensively used. The first, in which considerable progress has been made, is the assembly of microcluster atomic arrays. Examples include small chunks of metal[2a] that are solubilized and protected by a coating of ligands, such as $[HNi_{38}Pt_6(CO)_{48}]^{5-}$[2b] and $[Au_{55}(PPh_3)_{126}]^{6+}$[2c] as well as the use of competitive core cluster growth and surface capping (which terminates the cluster growth) of semiconductor clusters.[3] A limitation has been the difficulty in subsequently ordering these clusters into three-dimensional supramolecular lattices.

A second approach has been to use two-dimensional, structure-directing surfaces and three-dimensional porous media for molecular recognition. The chemical growth from solution of superlattice layered structures, giving a periodic array of planes of atoms or molecules with confinement in one dimension (perpendicular to the expitaxial grown layers) has been beautifully developed by the research groups of Mallouk, Marks, and Katz for applications such as enantioselective synthesis and nonlinear optical devices.[4] The separation of the layers in these nanophase materials is generally less than 20 Å.

Microporous phases with three-dimensional framework structures are now routinely synthesized by using molecular units or hydrated alkali or alkaline earth cations as templates. Their well-defined pore structures and pore sizes (3 to 13 Å) reflect the template dimensions. Chronologically the development of this microporous synthesis chemistry has evolved from zeolites that possess crystalline aluminosilicate frameworks to pure silicate phases, and more recently to compounds that exhibit similar framework structures but have compositions in which Al and/or Si are substituted by other elements such as Be, B, Ga, Ge, Zn, and P. The aluminosilicate and silicate microporous solids have found extensive application in the fields of ion exchange (consider the use of zeolite A as water softener in detergents), desiccation, sorption (e.g., gas separation and purification), and catalysis. Especially for the latter two applications, the geometric restrictions imposed by the porous framework are of importance in differentiating between molecules of different size (size exclusion from intraporous sorption); and in the selectivity of starting materials, transition states, and products of catalytic processes ("shape-selective catalysis").[5]

In the last five years, new applications of the precisely defined void structure of zeolite-type microporous solids have been envisaged. In an approach to "supramolecular architecture"[6] and "nanoscale inclusion chemistry"[7] based not on molecular ensembles but on extended solid state structures, they serve as a versatile host medium for assembling and maintaining controlled microstructures of quantum dots and wires,[8] organic molecules and polymers,[9] metal carbonyls and organometallic molecules,[8d, 10] redox systems and electron-transport chains,[11] as well as nanosize reaction vessels.[12a] This type of host–guest chemistry results in synthetic nanocomposite materials that can be described as "expanded" metals and semiconductors, stabilized arrays of aligned molecules or spatially organized redox systems for which applications in optoelectronics,[8a, 8b] nonlinear optics,[9a, 9b] optical data storage and image processing[8a] (for example by spectral hole burning),[9c] and enzyme mimicking[12b] are conceivable.

There has been a growing interest in the extension of the microporous molecular sieve synthesis and applications to mesoscopic dimensions. Typical areas for the application of mesoscopic zeolite-type structures are in separation (e.g., protein separation and selective adsorption of large organic molecues from waste waters) and catalysis (e.g., processing of tar sand and of the high distillates of crude oils to valuable low-boiling products). Another is in the supramolecular as-

[*] Dr. P. Behrens
Fakultät für Chemie der Universität
Postfach 5560, D-W-7750 Konstanz (FRG)
Telefax: Int. code + (7531)88-3898
Prof. Dr. G. D. Stucky
University of California, Santa Barbara, CA (USA)

 © VCH Verlagsgesellschaft mbH, W-6940 Weinheim, 1993 0570-0833/93/0505-0696 $ 10.00+.25/0

sembly of molecular arrays and polymers for electronic and optical applications.

Although there have been numerous attempts to carry over the crystallinity and the well-defined pore structure of zeolites to the mesoporous regime, the direct synthesis of three-dimensional mesoporous[13] materials containing cages and channels with access pores greater than 13 Å has until now been unsuccessful. Other routes to mesoporous solids such as forming pillars of layered compounds have been investigated.[14–16] Although mesoporosity was observed in some of the systems investigated, the pore size distribution was broader than in microporous zeolites.

The usual technique for preparing zeolites is the hydrothermal treatment of aluminosilicate gels or solutions containing metal (alkali or alkali earth) or organic ions (e.g., tetraalkylammonium ions) or molecules (e.g., amines). First progress towards enlarging the pore sizes in zeolite-type compounds was achieved by changing the composition of the gel from that of an aluminosilicate. This led to the discovery of the aluminophosphate VPI-5,[17] a one-dimensional channel structure with channel diameters of ≈13 Å, and of the gallophosphate cloverite,[18] featuring a cavity with a diameter of about 30 Å. Although the windows are about 13 Å at their widest point, their effective kinetic diameter is much smaller because of the clover-leaf shape of the opening.

The ions and molecules present in the hydrothermally treated gel act as templates during its crystallization; that is, they direct the formation of a specific zeolite framework and are usually occluded in the voids of the crystallizing solids. Even today this template effect is not fully understood. One proposal is that the template molecules change the chemistry of the crystallizing gel. Organic templates, on the other hand, may also act merely as "void fillers", preventing the crystallization of thermodynamically more stable dense phases. One obvious way to zeolites with larger pores is the use of large molecular organic templates, which should give large voids. This approach was, of course, followed by many laboratories but over a long period has not led to a definite claim of a mesoporous structure.

Recently, researches of Mobil Oil Company[19, 20] used a new concept in the synthesis of porous material which at long last has led to the first synthesis of mesoporous structures. The templating agent is no longer a single, solvated, organic molecule or metal ion, but rather a self-assembled molecular array. This template leads to mesoporous zeolites with adjustable pore sizes between 16 and >100 Å, covering well the mesoporous range of greatest interest. These compounds, named MCM-41 (MCM stands for Mobil's Composition of Matter), possess a hexagonal arrangement of parallel channels which can be directly visualized by a transmission electron microscope.[20] The arrangement of pores is very regular, and the pore size distribution measured by absorption is nearly as sharp as that of conventional zeolites.[19, 20b] A structural model of an MCM-41 material is given in Figure 1.

Kresge et al.[20a] and Beck et al.[20b] propose that a liquid crystal templating mechanism is operative in the synthesis of their mesoporous materials. Typically, the templates they use are quaternary ammonium ions $C_nH_{2n+1}(CH_3)_3N^+$, which are also useful as surfactants in detergents. These ions are known to form micelles in aqueous solutions (Fig. 2). In a

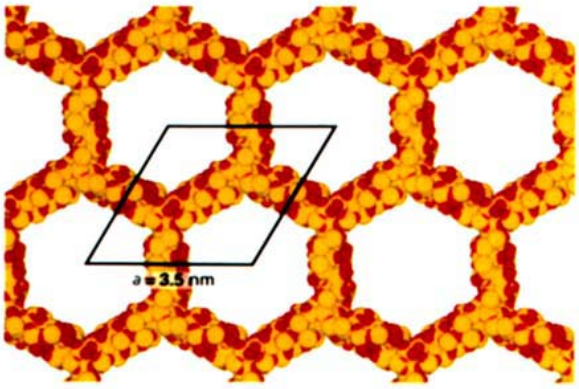

Fig. 1. Schematic representation of the structure of a MCM-41 phase with an interpore distance of ≈35 Å, amorphous wall structure, and hexagonal pores.

picture similar to the recently proposed "can-and-cement" model of the crystallization of microporous zeolites,[21] these template molecules are assumed to be ordered in the aqueous gel; during crystallization, the silicate or aluminosilicate solution present between the template assemblies becomes the "walls" of the porous solid. Different types of order have

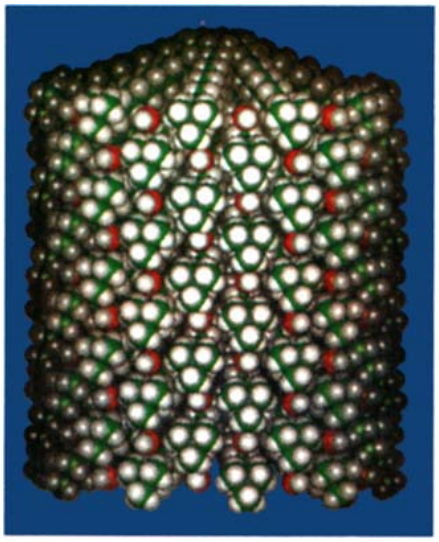

Fig. 2. Schematic representation of the exterior surface of a cylindrical micelle. The ends of the micelle cylinder are probably best visualized as hemispherical.

been found in surfactant–water liquid crystals, including lamellar, hexagonal, and cubic phases.[22] Accordingly, MCM-41 materials, which have a hexagonal arrangement of mesoporous channels are templated by the hexagonal phase. Strong support for the liquid crystal template mechanism comes from the discovery of cubic and layered crystallization products[20, 23] that possibly are templated by the cubic and lamellar liquid crystal phases. According to the templating mechanism, the alkyl chain length n influences the pore size of the MCM-41 material. For example, for $n = 12$, 14 or 16 the pore size is 30 Å, 34 Å, and 38 Å, respectively.[19, 20]

Communications may be submitted in English *or* in German. Further details regarding the submission of communications can be found in the "Notice to Authors" reproduced in the January issue of the journal. Copies thereof may be obtained from the editorial office upon request.

Formation and Complex Stabilization of a New Chainlike Phosphazene Anion by Co^{II}-Assisted Oxidative Scrambling of $[N(PPh_2)_2]^-$**

By *Jochen Ellermann,* Jörg Sutter, Falk A. Knoch,* and *Matthias Moll*

Dedicated to Professor Heinrich Nöth on the occasion of his 65th birthday

The linear phosphazene cation **1**[1] has a great synthetic potential and is particularly suitable for the preparation of cyclometallaphosphazenes.[2, 3] We report now on the formation of the similar phosphazene anion **2** whose sequence of atoms is reversed and its complexation to give a novel spirocyclic cobaltaphosphazene.

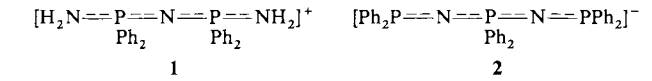

1 **2**

Surprisingly, when anhydrous cobalt(II) chloride is treated with lithium bis(diphenylphosphino)amide (**3**)[4–6] in the molar ratio 1:2 in boiling toluene, no complex **4** is formed [Eq. (a)], but in accordance with Equation (b) the red-black spirocyclic cobaltaphosphazene **5**[7] is obtained with the scrambling of the P-N-P ligand in **3**. As shown by the crystal

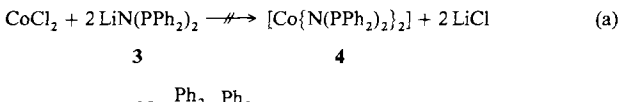

3 **4** (a)

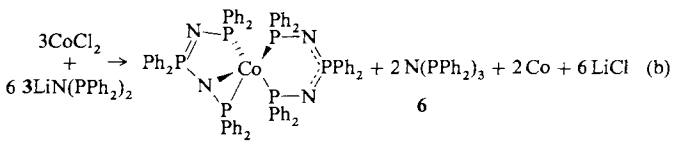

5 **6** (b)

structure analysis (Fig. 1) this spirocycle contains three rings of different sizes, that is, in **5**, **2** acts both as a bidentate P ligand and as tridentate P and N chelating ligand. In addition to **5**, tris(diphenylphosphino)amine **6**[8–10] and cobalt metal are formed. Cobalt(0) and **5** could be isolated almost quantitatively in the amounts expected according to Equation (b).

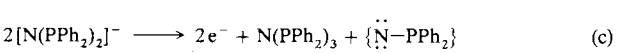

6 **7** (c)

Consequently, it is assumed that the anion of **3** is oxidized to give **6** with the formation of the nitrene **7** according to Equation (c), whereas cobalt(II) chloride is reduced to cobalt metal. The intermediate **7** is trapped by a further anion of **3** with the formation of **2**, which then coordinates the remaining cobalt(II) to give **5**.

The cobalt(II) ion contained in **5** has a distorted coordination polyhedron in the solid state, which can be considered as a N1-capped CoP_4 tetrahedron or as a distorted tetragonal pyramid with an apical P3 and a N1-P1-P4-P6 base (Fig. 1).[11] As expected both forms lead to a d^7 low-spin electronic state.[12]

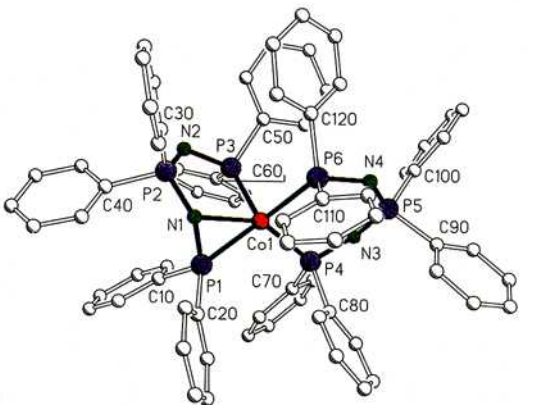

Fig. 1. Crystal structure of **5** (without the H atoms). Important distances [pm] and angles [°]: Co1-P1 217.4(1), Co1-P3 234.2(2), Co1-P4 220.6(1), Co1-P6 231.9(1), Co1-N1 221.2(3), P1-N1 165.3(3), P2-N1 163.6(3), P2-N2 158.1(4), P3-N2 165.9(3), P4-N3 162.6(3), P5-N3 159.5(3), P5-N4 158.9(3), P6-N4 162.3(3); P1-Co1-P3 99.6(1), P1-Co1-P4 106.4(1), P3-Co1-P4 110.8(1), P1-Co1-P6 144.8(1), P3-Co1-P6 101.4(1), P4-Co1-P6 92.1(1), P1-Co1-N1 44.3(1), P3-Co1-N1 86.0(1), P4-Co1-N1 149.6(1), P6-Co1-N1 109.7(1), Co1-P1-N1 69.1(1), N1-P2-N2 117.1(2), Co1-P3-N2 106.4(1), Co1-P4-N3 118.0(1), N3-P5-N4 119.0(1), Co1-P6-N4 120.5(1), Co1-N1-P1 66.7(1), Co1-N1-P2 110.5(2), P1-N1-P2 125.6(2), P2-N2-P3 117.9(2), P4-N3-P5 123.4(2), P5-N4-P6 129.2(2).

The P–N bond lengths all lie between the values of P–N single (177 pm) and P–N double bonds (156 pm),[13] as they occur in phosphazenes. The bonds P2–N2 (158.1 pm), P5–N3 (159.5 pm), and P5–N4 (158.9 pm) are mainly of double bond character, whereas the distances P2–N1 (163.6 pm), P1–N1 (165.3 pm), P3–N2 (165.9 pm), P4–N3 (162.6 pm), and P6–N4 (162.3 pm) correspond rather to bond lengths between single and double bonds.

The UV/VIS spectrum of **5** (solvent: toluene) is very similar to those of comparable cobalt(II) complexes in which the central atom is in a tetragonal-pyramidal environment.[14, 15] One weak and two intense absorptions at 15850 ($^2A_1 \rightarrow {}^2B_2$),[16] and 21250 ($^2A_1 \rightarrow {}^2E$) and 26750 ($^2A_1 \rightarrow {}^2B_1$) cm^{-1}, respectively, are observed (the assignments are tentative).

[*] Prof. Dr. J. Ellermann, Dipl.-Chem. J. Sutter, Dr. F. A. Knoch, Dr. M. Moll
Institut für Anorganische Chemie der Universität Erlangen-Nürnberg
Egerlandstrasse 1, D-W-8520 Erlangen (FRG)

[**] Chemistry of polyfunctional molecules, Part 110. This work was supported by the Fonds der Chemischen Industrie, Hoechst AG, and Riedel de Haen AG. We thank Prof. Dr. D. Sellmann for the support of X-ray structure analysis. – Part 109: J. Ellermann, F. A. Knoch, K. J. Meier, M. Moll, *J. Organomet. Chem.* **1992**, *428*, C44–C51.

Experimental Procedure

All operations were carried out under a nitrogen atmosphere in dry, N_2-saturated solvents. Compound **3** was prepared according to refs. [5,6]. Anhydrous $CoCl_2$ was purchased from Merck-Schuchardt, Hohenbrunn near Munich.

To a suspension of **3** (7.625 g, 19.49 mmol) in toluene (75 mL), anhydrous $CoCl_2$ (1.265 g, 9.74 mmol) was added. After the mixture had been heated and stirred under reflux for 5 h, elemental magnetic cobalt and LiCl precipitated from the dark red reaction mixture. The mixture was filtered and the filtrate concentrated to a fifth of its volume. Compound **5**, which precipitated as a red-black, crystalline solid, was purified by recrystallization from hot toluene. Finally, it was dried in vacuo for 48 h. Yield: 3.67 g (92%). Single crystals of **5** were obtained by layering a saturated solution of **5** in CH_2Cl_2 with *n*-pentane at room temperature. Correct elemental analysis (C,H,N,P,Co); decomposition at 227 °C. ^1H NMR (270 MHz, CD_2Cl_2): $\delta = 8.51$ (s, 32H; C_6H_5), 7.70 (s, 4H; C_6H_5), 7.37 (s, 12H; C_6H_5), 2.95 (br. s, 12H; C_6H_5) [12]; $^{13}C\{^1H\}$ NMR (67.94 MHz, CD_2Cl_2): $\delta = 131.0$ (s, C-*ortho*; C_6H_5), 128.2 (s, C-*para*; C_6H_5), 127.2 (s, C-*meta*; C_6H_5), 119.5 (br s, C-*ipso*; C_6H_5) [12]; $^{31}P\{^1H\}$ NMR (109.38 MHz, CD_2Cl_2; H_3PO_4): $\delta = -150$ (s, half-value width 125 ppm) [12]. IR (KBr): $\tilde{\nu}$ [cm^{-1}] [17] = 3070 w–m, 3051 m [ν(CH)], 1584 m, 1478 m–s, 1432 s [ν(CC)], 1303 m [δ(CH)], 1192 vs, 1170 s [ν(P = N)]; 1132 vs [P-sens. q, P^V] [18], 1093 s [P-sens. q, P^{III}] [18], 1046 m–s [ν(P=N)], 1026 m [δ(CH)], 997 m [C_6H_5-ring vibration.]; 807 s [ν(PN)]; 735 s [γ(CH)]; 714 m–s [P-sens. r, P^V] [18], 693 vs [Φ(CC)] [18], 676 m–s [ν(PN)], 568 m, 552 m–s [γ(P-N-P)], 537 s [P-sens. y, P^V] [18], 515 s, 490 m–s [P-sens. y, P^{III}] [18], 427 m [P-sens. t, P-C_6H_5] [18]; 368 m, br [δ(NP_2)]. FD-MS: *m/z* 1225 (M^+).

The LiCl was extracted with THF from the above-mentioned residue of LiCl and pyrophoric cobalt metal and determined qualitatively. After the remaining crude cobalt was dried it weighed 362 mg (6.14 mmol; corresponding to 63% of the amount of Co used) and the content of pure Co was determined complexometrically to be 98.5% after transformation into $CoSO_4$. Identification of **6**: The volatile components of the combined filtrates of **5** were removed under vacuum. The pale brown residue was eluted with toluene (25 mL) and the solution was layered with *n*-pentane (35 mL), leading to a crystal conglomerate of colorless, clear, square crystals of **6**, which were embedded in a microcrystalline thin layer of **5**. Crystals of **6** were removed mechanically, separated, and analyzed [10].

Received: November 12, 1992 [Z 5679 IE]
German version: *Angew. Chem.* **1993**, *105*, 763

[1] D. L. Herring, C. M. Douglas, *Inorg. Chem.* **1964**, *3*, 428.
[2] H. W. Roesky, K. V. Katti, U. Seseke, M. Witt, E. Egert, R. Herbst, G. M. Sheldrick, *Angew. Chem.* **1986**, *98*, 447; *Angew. Chem. Int. Ed. Engl.* **1986**, *25*, 477.
[3] K. V. Katti, H. W. Roesky, M. Rietzel, *Inorg. Chem.* **1987**, *26*, 4032.
[4] H. Schmidbaur, F. E. Wagner, A. Wohlleben-Hammer, *Chem. Ber.* **1979**, *112*, 496.
[5] J. Ellermann, M. Lietz, *Z. Naturforsch. B* **1980**, *35*, 64.
[6] A. Schmidpeter, F. Steinmüller, W. S. Sheldrick, *Z. Anorg. Allg. Chem.* **1989**, *579*, 158.
[7] According to replacement nomenclature: 1.1.3.3.5.5.7.7.9.9.11.11-dodecaphenyl-2.4.8.10-tetraaza-6-cobalta-1.3.5.7.9.11-hexaphospha-6-spirotricyclo[5.3.1.$0^{6,8}$]undecane.
[8] J. Ellermann, W. Wend, *J. Organomet. Chem.* **1985**, *281*, C29–C32.
[9] J. Ellermann, E. Köck, H. Zimmermann, M. Gomm, *Acta Crystallogr. Sect. C* **1987**, *43*, 1795.
[10] A correct C,H,N elemental analysis was obtained for the white crystals of **6**. On the basis of MS, $^1H\{^{31}P\}$ NMR, $^{31}P\{^1H\}$ NMR, and IR spectra (KBr) (3 ν(PN): 873 (w–m), 841 (s), 828 (s) cm^{-1}) compound **6** is identical with a sample of $N(PPh_2)_3$ prepared by a different route [8] and characterized by X-ray crystallography [9]. The IR spectrum allows a rapid and clear distinction from the isomeric Ph_2P–P(Ph)=N–PPh_2; ν(P=N): 1160 (s) cm^{-1}. See also: H. Nöth, L. Meinel, *Z. Anorg. Allg. Chem.* **1967**, *349*, 225; H. Schmidbaur, S. Lauteschläger, F. H. Köhler, *J. Organomet. Chem.* **1984**, *271*, 173.
[11] Crystal structure analysis of **5**: red-black, prismatic single crystals with the dimensions 0.4 × 0.4 × 0.3 mm obtained from CH_2Cl_2/*n*-pentane and measured at 293 K. Triclinic, space group $P\bar{1}$; $Z = 2$; $a = 1289.4(5)$, $b = 1317.1(6)$, $c = 2036.0(8)$ pm, $\alpha = 82.86(3)$, $\beta = 82.10(3)$, $\gamma = 63.44(3)°$, $V = 3.040(3)$ nm^3, $\rho_{calcd} = 1.34$ gcm^{-3}; ω scan, $3.0 < \omega < 30°\,min^{-1}$, $3° < 2\theta < 54°$ ($Mo_{K\alpha}$, $\lambda = 71.073$ pm, graphite monochromator). Of 13428 independent reflections 7247 have $F < 4\sigma(F)$. SHELXTL-PLUS, direct methods, anisotropic refinement of the non-hydrogen atoms, the positions of the hydrogen atoms of the phenyl groups were taken from the difference Fourier synthesis and retained in the refinement, hydrogen atoms with fixed isotropic temperature factor. $R = 0.037$, $R_w = 0.033$. Further details of the crystal structure investigation may be obtained from the Fachinformationszentrum Karlsruhe, Gesellschaft für wissenschaftlich-technische Information mbH, D-W-7514 Eggenstein-Leopoldshafen 2 (FRG) on quoting the depository number CSD-320581, the names of the authors, and the journal citation.
[12] Magnetic moment: $\mu_{eff} = 2.39(\pm 0.15)$ μ_B. The paramagnetism of the cobalt(II) ion, corresponding to an unpaired electron, leads to paramagnetic shifts and line broadening in the NMR spectra (see Experimental Procedure), which make an interpretation more difficult.
[13] N. N. Greenwood, A. Earnshaw, *Chemistry of the Elements*, Pergamon Press, Oxford, **1984**, p. 627.
[14] G. Dyer, D. W. Meek, *J. Am. Chem. Soc.* **1967**, *89*, 3983.
[15] J. Ellermann, W. H. Gruber, *Z. Anorg. Allg. Chem.* **1969**, *364*, 55.
[16] The band assignment assumes an ideal C_{4v} symmetry and refers to the orbital and energy level diagram given in ref.[14].
[17] Abbreviations: vs = very strong, s = strong, m = medium, w = weak, br = broad.
[18] Designation according to D. H. Whiffen, *J. Chem. Soc.* **1956**, 1350.

Hypothetical Carbon Modifications Derived from Zeolite Frameworks**

By *Reinhard Nesper,* Karlheinz Vogel,* and *Peter E. Blöchl**

Dedicated to Professor Hartmut Bärnighausen on the occasion of his 60th birthday

The discovery of fullerene modifications of carbon, in particular C_{60}, and their laboratory-scale production have stimulated a large number of theoretical and experimental investigations.[1,2] Interest in the potential of carbon to form new, exotic structures with surprising physical properties has grown. Recent studies[3–8] have concentrated on graphite-related materials such as fullerenes, graphitic microtubules, and negatively curved graphitic carbon—compounds composed of sp^2-hybridized C atoms. Surprisingly, only few reports on modifications with sp^3-hybridized C atoms have appeared.[9] Such compounds are likely to exhibit a structural variety rivaling that of the graphite-related materials that are currently attracting a great deal of attention. The stability of the C–C single bond is manifested in diamond; its bond energy is only 0.02 eV per atom less than that of graphite. Compounds made up of tetrahedral building blocks such as group 14 elements (C, Si, Ge, Sn, Pb) as well as solid H_2O and SiO_2 are known for their complex structural chemistry. The existence of amorphous silicon and carbon and of crystalline and glassy silicates indicates the enormous structural variety and kinetic stability of arrangements of these building blocks.

We investigated ordered carbon modifications with sp^3 C atoms which are derived from structures found in nature, namely zeolites.[10] Zeolite frameworks consist of tetracoordinated $MO_{4/2}$ units (M = Si, Al, etc.). Formal replacement of each $MO_{4/2}$ unit by one carbon atom and appropriate rescaling provides the desired model structures. We took all known zeolite structures[10] into account but have omitted those containing three- and four-membered rings. Six candidates remained for further investigation.

In order to determine the energetic stability of these six carbon allotropes we performed electronic structure calculations. We used the ab initio molecular dynamics method of

[*] Prof. Dr. R. Nesper, Dr. K. Vogel
Laboratorium für Anorganische Chemie der Eidgenössischen Technischen Hochschule
Universitätstrasse 6, CH-8092 Zürich (Switzerland)
Telefax: Int. code + (1)252-8935
Dr. P. Blöchl
IBM Research Division, Zurich Research Laboratory
Säumerstrasse 4, CH-8803 Rüschlikon (Switzerland)

[**] This work was supported by the Schweizerische Nationalfonds zur Förderung der wissenschaftlichen Forschung.

Car and Parrinello[11] based on the local density approximation (LDA)[12] in combination with the projector-augmented (plane) wave (PAW) method developed by one of us (P.E.B.).[20] The PAW method overcomes the well-known problems in the application of the pseudopotential method to first-row and transition metal elements by expanding the electronic wave functions in augmented plane waves. It has been successfully applied to several systems such as small and large molecules and surfaces,[13] and the solid-state systems here. The accuracy of the PAW method is comparable to that of state-of-the-art pseudopotential and linear augmented plane wave methods. The Car–Parrinello technique was used here to optimize the trial structures without imposing symmetry or other constraints.

In the present study we used augmented plane waves up to a kinetic energy of 25 Ry (1 Ry = 13.605804 eV). An increase to 35 Ry provided the same results. Our calculations are based on supercells for which the product of the number of atoms and the number of reciprocal lattice points k (N (atoms) × N(k-points)) is between 92 and 136. Table 1 contains selected calculated energies for the zeolite-derived carbon modifications.

Table 1. Hypothetical carbon modifications. The columns contain the designation, the structure type, the energy difference ΔE [eV] in cohesive energy per atom relative to diamond, and the LDA band gaps E_G [eV].

Modification	Structure type	ΔE	E_G
C_{DIA}	diamond	0.00	4.21
C_{MTN}	zeolite ZSM-39	0.07	3.26
C_{MEP}	melanophlogite	0.09	3.96
C_{BIK}	bikitaite	0.21	3.14
C_{MTT}	zeolite ZSM-23	0.27	3.68
C_{TON}	zeolite Theta-1	0.34	3.28
C_{FER}	ferrierite	0.49	2.50

The energy–volume dependence is shown in Figure 1. All but one of the structures investigated are energetically favored over C_{60}, which according to LDA calculations[6] and experiment[14] is higher in energy than diamond by 0.42 eV and 0.38 eV per atom, respectively. C_{MEP} and C_{MTN} have the

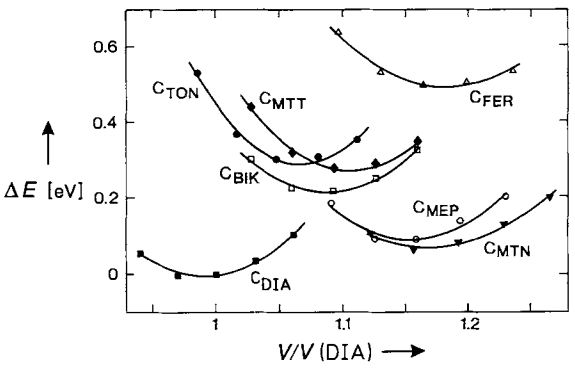

Fig. 1. Energy–volume diagram of hypothetical carbon modifications. Energy differences and volumes are given per C atom and scaled relative to diamond. V (DIA) refers to the experimentally determined volume of diamond.

lowest energies ever calculated for any hypothetical carbon modifications.[3–7] In the following discussion we will concentrate on these two compounds.

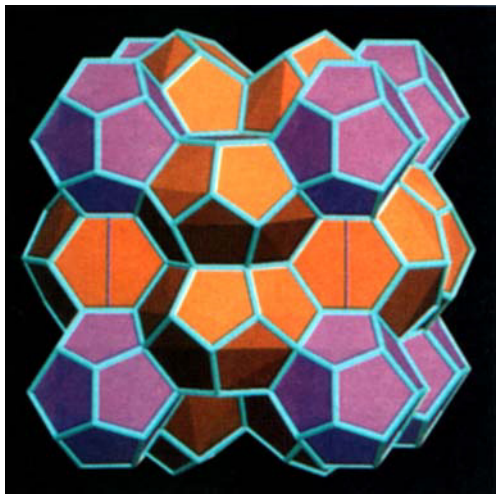

Fig. 2. Structure of C_{MEP}, which correspouds to the clathrate I structure (purple: C_{20} pentagonal dodecahedra, orange: C_{24} cages.)

C_{MEP} and C_{MTN} correspond to the well-known clathrate I and clathrate II structures, respectively (Figs. 2 and 3), which are found in a number of isoelectronic compounds like $[As_8Ge_{38}]I_8$,[15] $[Ge_{46-x}I_x]I_8$ with $x = 8/3$,[16] and $Na_x[Si_{136}]$ with $x = 3-11$.[17][*] Both structures are space-

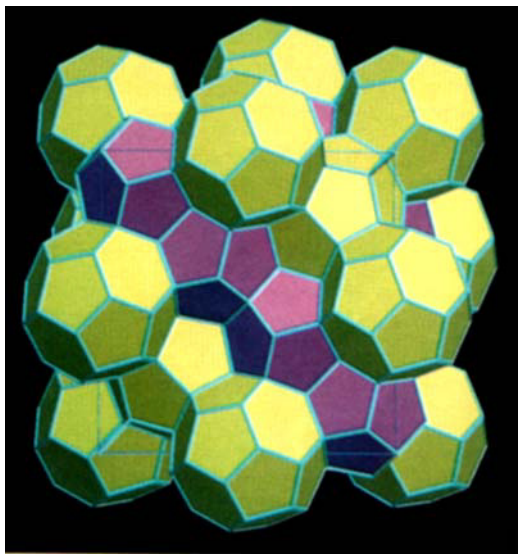

Fig. 3. Structure of C_{MTN}, which corresponds to the clathrate II structure. The large C_{28} cages (yellow) form a superdiamond framework, the pentagonal dodecahedra C_{20} (purple) a supertetrahedron.

filling arrangements of face-sharing fullerene-like cages with twelve pentagons and zero, two, or four hexagons. It is interesting that the structural patterns in C_{MEP} and C_{MTN} are similar to those in the fullerenes despite the grossly different bonding (sp^3 vs. sp^2 hybridization). In these polymeric allotropes the minimal difference between the bond angle in a

[*] Framework atoms in brackets; the counterions I^- and Na^+ occupy the voids.

five-membered ring (108°) and in an ideal tetrahedron (109.47°) accounts for the stability. An ideal structure composed of sp^3 C atoms would therefore contain solely face-sharing pentagonal dodecahedra. However, as it is impossible to build an infinite structure from pentagonal dodecahedra alone, six-membered rings are required even though they introduce greater ring strain. With this general building principle, namely face-sharing fullerene-like cages, it is possible to construct a large class of polymorphic solids that are expected to be similar in energy to the ones we have studied. Recently Guo et al. proposed structures for transition metal carbide clusters forming face-sharing pentagonal dodecahedra.[18] The structures of C_{MEP} and C_{MTN} can be considered extensions of these clusters to bulk structures (cf. Figs. 2,3).

C_{MTN} and C_{MEP} exhibit large band gaps that are even 6 and 23% smaller than that of diamond. (These numbers should be taken with a grain of salt as the LDA does not in principle allow the prediction of excitation energies. Trends, however, are usually well reproduced.) These hypothetical carbon modifications have a number of interesting characteristics. The large cages might accommodate interstitial dopant atoms providing a means to engineer their electronic and optical properties. The nearest-neighbor distances for the interstitial sites within the various fullerene-like cages are 207 and 255 pm for C_{MTN} and 215 and 223 pm for C_{MEP}, compared to 153 pm in diamond. The first value always refers to the nearest-neighbor distance in pentagonal dodecahedron. The average volume per atom is increased by about 15% over diamond but considerably less than in graphite (153%) and in solid C_{60} (205%).

We expect C_{MTN} and C_{MEP} to exhibit high mechanical stability once they are formed, as a result of their low energy difference compared to C_{DIA}, the large energy required to break a C–C bond, and the three-dimensional linkage of the network C atoms.

Currently we are investigating whether the new structures can be identified in the products formed by the Krätschmer process. High-pressure experiments on C_{60} are being performed as well.[19] An alternate synthetic route would the epitaxial growth of these solids on, for example, the carbide clusters of Guo et al.[18]

Received: May 19, 1992
Revised version: February 1, 1993 [Z 5361 IE]
German version: *Angew. Chem.* **1993**, *105*, 786

[1] H. W. Kroto, J. R. Heath, S. C. O'Brien, R. F. Curl, R. F. Smalley, *Nature* **1985**, *318*, 162.
[2] W. Krätschmer, L. D. Lamb, K. Fostiropoulos, D. R. Huffman, *Nature* **1990**, *347*, 354.
[3] T. Lenosky, X. Gonze, M. Teter, V. Elser, *Nature* **1992**, *355*, 333.
[4] D. Vanderbilt, J. Tersoff, *Phys. Rev. Lett.* **1992**, *68*, 511.
[5] M. O'Keeffe, G. B. Adams, O. F. Sankey, *Phys. Rev. Lett.* **1992**, *68*, 2325.
[6] G. B. Adams, O. F. Sankey, J. B. Page, M. O'Keeffe, D. A. Drabold, *Science* **1992**, *256*, 1792.
[7] S. J. Townsend, T. J. Lenosky, D. A. Muller, C. S. Nichols, V. Elser, *Phys. Rev. Lett.* **1992**, *69*, 921.
[8] N. Hamada, S. Sawada, A. Oshiyama, *Phys. Rev. Lett.* **1992**, *68*, 1579.
[9] R. L. Johnston, R. Hoffmann, *J. Am. Chem. Soc.* **1989**, *111*, 810; R. Biswas, R. M. Martin, R. J. Needs, O. H. Nielsen, *Phys. Rev. B* **1987**, *35*, 9559; *ibid.* **1984**, *30*, 3210; M. T. Yin, *ibid.* **1984**, *30*, 1773.
[10] W. M. Meier, D. H. Olson, *Atlas of Zeolite Structure Types*, Butterworths, London, **1987**. The carbon modifications are designated by C_{ABC}, where ABC refers to the notation of the corresponding zeolite.
[11] R. Car, M. Parrinello, *Phys. Rev. Lett.* **1985**, *55*, 2471.
[12] We used the results of D. M. Ceperly and B. J. Alder (*Phys. Rev. Lett.* **1980**, *45*, 566) for the homogeneous electron gas in the parametrization of J. P. Perdew and A. Zunger (*Phys. Rev. B* **1981**, *10*, 5048).
[13] A. J. Fisher, P. E. Blöchl, *Phys. Rev. Lett.*, submitted.
[14] H.-D. Beckhaus, C. Rüchardt, M. Kao, F. Diederich, C. S. Foote, *Angew. Chem.* **1992**, *104*, 69; *Angew. Chem. Int. Ed. Engl.* **1992**, *31*, 63.
[15] H. Menke, H. G. von Schnering, *Naturwissenschaften* **1972**, *59*, 420.
[16] R. Nesper, J. Curda, H. G. von Schnering, *Angew. Chem.* **1986**, *98*, 369; *Angew. Chem. Int. Ed. Engl.* **1986**, *25*, 350.
[17] C. Cros, M. Pouchard, P. Hagenmuller, *C. R. Hebd. Seances Acad. Sci* **1965**, *260*, 4764; *J. Solid State Chem.* **1970**, *2*, 570.
[18] B. C. Guo, K. P. Kerns, A. W. Castleman, *Science* **1992**, *255*, 1411; B. C. Guo, S. Wei, J. Purnell, S. Buzza, A. W. Castleman, *ibid.* **1992**, *256*, 515; S. Wei, B. C. Guo, J. Purnell, S. Buzza, A. W. Castleman, *ibid.* **1992**, *256*, 818.
[19] M. Wörle, K. Syassen, R. Nesper, unpublished.
[20] P. E. Blöchl, *Phys. Rev. B*, submitted.

Self-Assembly, Structure, and Spontaneous Resolution of a Trinuclear Triple Helix from an Oligobipyridine Ligand and Ni^{II} Ions**

By *Roland Krämer, Jean-Marie Lehn,* André De Cian*, and *Jean Fischer*

Double-helical metal complexes, termed helicates, have been shown to form by the spontaneous assembly of oligo-2,2′-bipyridine (bpy) strands and metal ions that favor tetrahedral coordination geometry, such as Cu^{I} and Ag^{I}.[1–3] Complexes containing from two to five metal centers, that is, di- to pentahelicate species, have been obtained thus.[1–4]

Helicate formation is a self-organization process[5] displaying positive cooperativity.[6] It results from the tetrahedral coordination imposed by each $Cu(bpy)_2^+$ site and from the design of the ligands. These two features constitute, respectively, the recognition event and the molecular steric "instruction" that lead to the preferential generation of double-helical structures. In the general context of programmed supramolecular systems,[1] helicate formation may be described as the result of the reading by metal ions of the molecular information stored in the oligo(bpy)strands following a tetrahedral coordination algorithm.[5, 7]

A number of double helical complexes involving other ligand molecules and presenting two metal centers have been reported.[8–13] When the ligand contains two[14–17] or three[17] terpyridine units, double-helical complexes with two or three octahedral metal centers, respectively, may be obtained.

The steric information contained in the oligo(bpy)strands yielding double helicates resides in the disposition of the nitrogen sites and in the 6,6′-disubstitution of the bpy units.[1–7] The latter hinders the binding of metal ions that prefer octahedral coordination geometry, which would be expected to yield triple helicates. This might, however, become possible through a slight modification of the steric instruction by shifting from a 6,6′- to a 5,5′-disubstitution. We now report that the trinuclear triple-helical complex **1** is indeed formed spontaneously by self-assembly from three 5,5′-disubstituted tris(bpy) strands **5** and three Ni^{II} ions.

A triply bridged dinuclear Fe^{II} complex of a bis(bpy) ligand[18] and probably also a related bis(Fe^{II}) complex possess triple-helical features.[12] A triple-helical arrangement has been assigned to dinuclear Fe^{III} complexes of tripodal ligands on the basis of NMR and circular dichroism (CD) data.[19]

[*] Prof. Dr. J.-M. Lehn, Dr. R. Krämer
Laboratoire de Chimie Supramoléculaire
Institut Le Bel, Université Louis Pasteur
4, rue Blaise Pascal, F-67000 Strasbourg (France)
Telefax: Int. code + (88) 41-1020
Prof. Dr. J. Fischer, Dr. A. DeCian
Laboratoire de Cristallochimie et de Chimie Structurale
Institut Le Bel, Université Louis Pasteur, Strasbourg

[**] This work was supported by the CNRS (URA 422 and URA 424). R. K. thanks the Deutscher Akademischer Austauschdienst for a post-doctoral research fellowship. We thank Dr. Masayuki Takahashi and Matthias John for help with circular dichroism measurements.

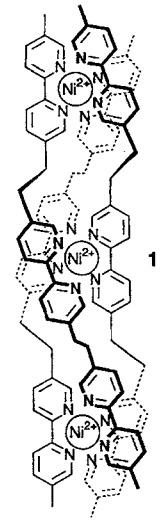

1

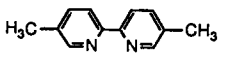

2

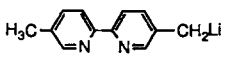

3

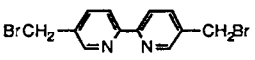

4

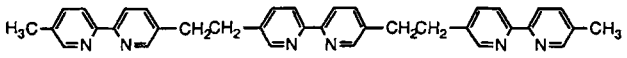

5

Recently, the self-assembly and the triple-helical structure of a dinuclear Co^{II}[13, 20] complex has been described. The present species **1** represents the first triple helicate containing three metal centers.

The tris(bpy) strand **5**[21] was easily accessible in 71% yield by the reaction of monolithiated 5,5′-dimethylbipyridine **3** (obtained by treating **2**[22] with BuLi in THF) with 5,5′-bis(bromomethyl)bipyridine **4**.[23] Reaction of **5** with $NiSO_4$ gave a pink complex, which was isolated as the perchlorate salt $[(\mathbf{5})_3Ni_3](ClO_4)_6$, whose composition was determined by FAB^+ mass spectroscopy and microanalysis. Its UV/VIS spectrum exhibited absorptions at wavelengths similar to those of $[Ni(5,5'\text{-dimethylbipyridine})_3]^{2+}$, but the extinction coefficients were about three times larger.[24] The proton NMR spectrum of the helicate showed very broad signals between $\delta = 5$ and $\delta = 160$, consistent with that of the mononuclear Ni^{II} complex mentioned above.[25]

The structure of $\mathbf{1}(ClO_4)_6$ was determined by X-ray crystallography (Fig. 1).[26] It consists of $[(\mathbf{5})_3Ni_3]^{6+}$ ions in which three strands of ligand **5** are wrapped around each other and held together by three Ni^{II} ions forming a trinuclear triple-helical complex, a trihelicate $^3\mathscr{H}$, as represented schematically by **1**.

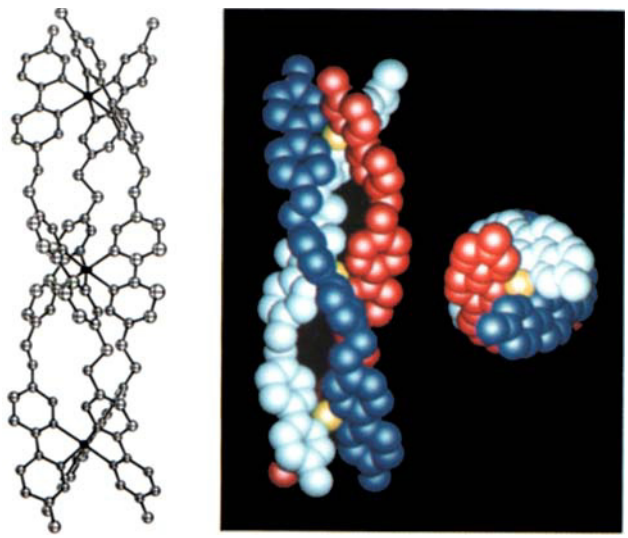

Fig. 1. ORTEP representation of the crystal structure of the self-assembled trinuclear triple helical Ni^{II} complex **1** (left); CPK representations along and perpendicular to the axis of the three metal ions (right).

The helical features of the triple helicate **1** are defined by several parameters. The angle of twist, that is, the angle of rotation of the helix, between two successive Ni centers is about 75° and approximately 149° between the first and third Ni center. This means that a full turn of the helix would involve 5.8 metal centers. Since the Ni ··· Ni distance is 8.6 Å, the helical pitch (length per turn) is about 41 Å. The solid-state structure is, however, not a regular triple helix of D_3 symmetry. It has a C_2 axis perpendicular to the NiNiNi axis and passing through the middle of central C–C bond of the central bpy of one strand; the other two strands are interconverted by this axis. The radius of the circumscribed cylinder measures approximately 5.3 Å. The total length of the triple helix is about 28 Å (distance between the carbon atoms of the terminal CH_3 groups). The C-CH_2-CH_2-C dihedral angle of 158° is much closer to the *trans* than to the *gauche* form. The triple helix **1** is therefore rather elongated, displaying a looser twist than the double helix of nucleic acids and even more so than the cuprohelicates (pitch about 30–35 Å[27] and 12 Å, respectively).[1] In view of this extended structure there is no significant stacking overlap between the bpy groups of two successive Ni centers. One may note that triple helical species are also found in proteins such as collagen,[28] in nucleic acids,[27] and in supramolecular liquid crystals.[29]

The three Ni centers of **1** are so aligned that the structure is linear, whereas the cuprotrihelicate showed a slight bend.[1] The Ni^{II} ions present octahedral coordination with Ni–N distances of 2.04–2.12 Å.

The unit cell contains two complexes **1** and twelve perchlorate counterions. Each species **1** is located in a special position of the space group $C2$. The helices are parallel to each other with their axes perpendicular to the a,b plane of the unit cell. They are arranged in layers in which each helix **1** is

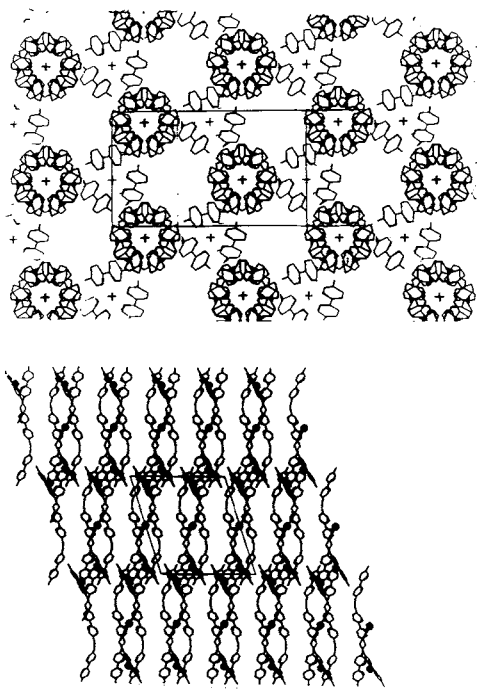

Fig. 2. Hexagonal packing of triple helical species **1** viewed along the axis of the helices with the a and b axes respectively horizontal and vertical in the plane of the figure (top); view of the packing in a plane perpendicular to the top view, showing the layers of helices **1** and the channels present in the structure (bottom).

located at the center of a hexagon of six surrounding helices; the distance between neighboring axes is 13.5 Å (Fig. 2). The layers of helices are stacked along the *c* axis and are shifted along the *a* axis; the projection of the fourth layer perpendicular to the *a*, *b* plane coincides with the first layer. This arrangement creates channels parallel to the *c* axis of the unit cell and tilted by about 19° with respect to the axis of the helices. These channels contain the anions which are partly disordered.[26]

The *C*2 space group of the crystals indicated that they were chiral, which suggested that they contained only one of the two triple-helical enantiomers, either right-handed or left-handed. Several single crystals were selected, and their solutions were subjected to circular dichroism measurements. They showed optical activity, displaying circular dichroism curves of the two opposite types (Fig. 3). Thus, crystallization of the trihelicate **1** $(ClO_4)_6$ occurs with spontaneous resolution, a remarkable feature not presented by the cuprohelicates,[1, 2] where helicity induction has been attained by introducing chiral centers into the oligo(bpy) strand.[30]

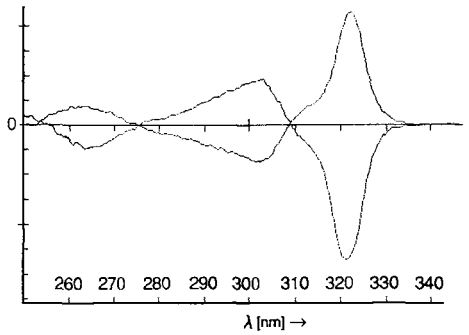

Fig. 3. Circular dichroism curves measured for individual single crystals of **1**$(ClO_4)_6$ in acetonitrile/water (9/1) at room temperature; positive and negative curves of different amplitudes were obtained for different crystal; the ordinates are proportional to molecular ellipsicities; in the present case the curve with negative Cotton effect was recorded for a solution that was 4.5 times more concentrated than that giving a positive Cotton effect.

However, when a number of crystals of **1**$(ClO_4)_6$ were examined, the circular dichroism $\Delta\varepsilon_{323}$ values were not constant but varied from -178 to $+659\ M^{-1}cm^{-1}$. A few presented no optical activity.[31a] A value $\Delta\varepsilon_{308} = -406.6$ has been reported for the $[Ni(bpy)_3](ClO_4)_2 \cdot 2H_2O$ complex.[31b] These variations in $\Delta\varepsilon$ were not due to racemization in solution, since the maximal loss of optical activity of **1**$(ClO_4)_6$ was 23% in 24 hours. Thus, **1** is much more stable against racemization than optically active $[Ni(bpy)_3]^{2+}$.[32] Therefore, the spontaneous resolution was only partial, and apparently each crystal contained different amounts of species of left- and right-handed helicity. This behavior may be attributed to microtwinning of the chiral crystals, each being composed of domains of opposite helicity.[33] Experiments are underway to determine the optical purity of these crystals and the optical properties of the pure enantiomers.

The present results demonstrate the spontaneous formation of a trinuclear triple helix by self-assembly from three ligand molecules and three metal ions. They also represent a successful application of molecular programming[5–7] to the spontaneous but directed generation of desired supramolecular architectures.

In the self-assembly of helicates, three main features that bear structural information determining the nature and shape of the helical species formed may be distinguished: 1) the precise structure of the *binding site*; it determines in particular the ability to coordinate metal ions with a given geometry the number of strands bound; 2) the *spacer* separating the binding sites; as pointed out earlier[1] it must favor interstrand over intrastrand binding, and it influences the tightness of the helix (its pitch) through the rotation of one metal center with respect to the next one; 3) most importantly the *configuration of the coordination centers* determines whether the structure is indeed of helical nature; helicity implies that all metal centers have the same screw sense (see also ref. [30]). As a corollary, helicity induction requires the introduction of elements of asymmetry.[30]

The programme containing these information features is molecular and linear; its operation is supramolecular and takes place through the reading of the information according to the coordination algorithm of the metal ion. More generally, self-assembly may involve interactions other than metal ion coordination, such as hydrogen bonding, stacking, or donor–acceptor effects as found in proteins,[28] nucleic acids,[27] liquid crystals,[29] and molecular complexes.[36]

Further developments involve the investigation of variations in ligand structure on the features of double and triple helicates, the determination of their physico-chemical (thermodynamic, kinetic, electrochemical, photochemical) properties, the exploration of the coordination chemistry of the ligand strands (for instance with cubic metal ions). Beyond these systems lies the investigation of processes involving several ligands and metal ions, that is, multicomponent self-assembly.[37]

Experimental Procedure

5: Lithium diisopropylamide was prepared by addition of butyllithium (7.2 mmol, 1.6 M solution in hexane) to diisopropylamine (1.05 mL, 7.43 mmol) in dry THF (20 mL) under argon at -78 °C. This solution was added slowly by canula to 5,5′-dimethyl-2,2′-bipyridine (**2**)[22] (1.33 g, 7.22 mmol) in dry THF (20 mL) at -78 °C. The dark reddish brown reaction mixture was allowed to reach 0 °C. 5,5′-Bis(bromomethyl)-2,2′-bipyridine (**4**)[23] (408 mg, 1.18 mmol) in THF (30 mL) was added dropwise with stirring within about 40 minutes. Stirring at 0 °C was continued for 30 min, and then water (20 mL) was added to quench the reaction. THF was removed in vacuum, and the yellow precipitate filtered off, suspended in MeOH (50 mL), and filtered off again. The remaining solid was recrystallized from chloroform/methanol. The white, microcrystalline powder was vacuum-dried (50 °C, 3 h). Yield 470 mg (71%). M.p. 275–278 °C. FAB$^+$: *m/z* 549.2 $[M + H^+]^+$. ^{1}H NMR ($CDCl_3$): $\delta = 8.6$–8.3 (m, 12H; bpy-H), 7.8–7.6 (m, 6H; bpy-H), 3.06 (s, 8H; CH_2), 2.43 (s, 6H; CH_3). Correct C, H, N analysis.

$[(\mathbf{5})_3Ni_3](ClO_4)_6$, **1**$(ClO_4)_6$: **5** (60.0 mg, 0.109 mmol) was suspended in 80 mL of an ethanol/water mixture /1/1) and heated under reflux. The ligand was partially dissolved by addition of 0.5 M H_2SO_4 (0.40 mL). After 15 minutes stirring, $NiSO_4 \cdot 6H_2O$ (28.7 mg, 0.109 mmol) in 3 mL water was added dropwise. At the end of the addition, a clear, almost colorless solution was obtained. Heating at reflux was continued for 15 h. Some drops of a saturated $LiClO_4$ solution were added to the hot reaction solution, which was then kept at 5 °C for several hours. The pink precipitate was filtered off, washed with water, and redissolved in acetonitrile (40 mL). Water (24 mL) was added, and the pink solution was allowed to stand in an open beaker. After several days, a gel had formed that contained pink crystals. Water (30 mL) was added with shaking and the liquid was decanted from the crystals. These were successively washed with water, ethanol, and ether, and air dried. Yield 36 mg (38%). FAB$^+$: *m/z* 2317.2 $[M - ClO_4^-]^+$, 2218.4 $[M - 2ClO_4^- + e^-]^+$, 2120.4 $[M - 3\ ClO_4^- + 2e^-]^+$. UV/VIS: λ_{max} [nm] (ε) 258 (113000), 308 (152000), 320 (164000), 525 (53). Correct C, H, N analysis for **1** $(ClO_4)_6 \cdot 12H_2O$.

Received: December 30, 1992 [Z 5783 IE]
German version: *Angew. Chem.* **1993**, *105*, 764

[1] J.-M. Lehn, A. Rigault, J. Siegel, J. Harrowfield, B. Chevrier, D. Moras, *Proc. Natl. Acad. Sci. USA* **1987**, *27*, 2565.
[2] J.-M. Lehn, A. Rigault, *Angew. Chem.* **1988**, *100*, 1121; *Angew. Chem. Int. Ed. Engl.* **1988**, *27*, 1095.
[3] T.-M. Garrett, U. Koert, J.-M. Lehn, A. Rigault, D. Meyer, J. Fischer, *J. Chem. Soc. Chem. Commun.* **1990**, 557.

 © VCH Verlagsgesellschaft mbH, W-6940 Weinheim, 1993 0570-0833/93/0505-0705 $ 10.00+.25/0

[4] J.-M. Lehn, J.-P. Sauvage, J. Simon, R. Ziessel, C. Piccini-Leopardi, G. Germain, J.-P. Declercq, M. Van Meersche, *Nouv. J. Chim.* **1987**, *7*, 413.
[5] J.-M. Lehn, *Angew. Chem.* **1990**, *102*, 1347; *Angew. Chem. Int. Ed. Engl.* **1990**, *29*, 1304.
[6] A. Pfeil, J.-M. Lehn, *J. Chem. Soc. Chem. Commun.* **1992**, 838; T.-M. Garrett, U. Koert, J.-M. Lehn, *J. Phys. Org. Chem.* **1992**, *5*, 529.
[7] J.-M. Lehn in *Perspectives in Coordination Chemistry*, (Eds. A. F. Williams, C. Floriani, A. E. Merbach), VHCA, Basel/VCH, Weinheim, **1992**, p. 447.
[8] G. Struckmeier, U. Thewalt, J.-H. Fuhrhop, *J. Am. Chem. Soc.* **1976**, *98*, 278.
[9] M. Barley, E. C. Constable, S. A. Corr, R. C. S. McQueen, J. C. Nutkins, M. D. Ward, M. G. B. Drew, *J. Chem. Soc. Dalton Trans.* **1988**, 2655.
[10] C. Piguet, G. Bernardinelli, A. F. Williams, *Inorg. Chem.* **1989**, *28*, 2920.
[11] K. Potts, *Bull. Soc. Chim. Belg.* **1990**, *99*, 741.
[12] M.-T. Youinou, R. Ziessel, J.-M. Lehn, *Inorg. Chem.* **1991**, *30*, 2144.
[13] C. Piguet, C. Bernardinelli, B. Boyquet, A. Quattropani, A. F. Williams, *J. Am. Chem. Soc.* **1992**, *114*, 7440.
[14] E. C. Constable, M. D. Ward, D. A. Tocher, *J. Am. Chem. Soc.* **1990**, *112*, 1256.
[15] E. C. Constable, R. Chotalia, *J. Chem. Soc. Chem. Commun.* **1992**, 64.
[16] J. D. Crane, J.-P. Sauvage, *New J. Chem.* **1992**, *16*, 649.
[17] J. Hall, J.-M. Lehn, unpublished.
[18] B. R. Serr, K. A. Andersen, C. M. Elliott, O. P. Anderson, *Inorg. Chem.* **1988**, *27*, 4499.
[19] J. Libman, Y. Tor, A. Shanzer, *J. Am. Chem. Soc.* **1987**, *109*, 5880.
[20] A. F. Williams, C. Piguet, G. Bernardinelli, *Angew. Chem.* **1991**, *103*, 1530; *Angew. Chem. Int. Ed. Engl.* **1991**, *30*, 1490.
[21] A ligand related to **5** (containing CH_2OCH_2 units between the bpy groups) has been obtained earlier by another route: Y. He, J.-M. Lehn, unpublished.
[22] W. H. F. Sasse, C. P. Whittle, *J. Chem. Soc.* **1961**, 1347; G. M. Badger, W. H. F. Sasse, *ibid.* **1956**, 616.
[23] F. Ebmayer, F. Vögtle, *Chem. Ber.* **1989**, *122*, 1725; A. D. Hamilton, H.-D. Rubin, A. Bocarsly, *J. Am. Chem. Soc.* **1984**, *106*, 7255.
[24] $[Ni(5,5'\text{-dimethylbipyridine})_3](ClO_4)_2$ was prepared analogously to $[Ni(5,5'\text{-dimethylbipyridine})_3]Cl_2$ [25]. UV/VIS Specrum in $MeCN/H_2O$ (/1): λ_{max} [nm] (ε) = 255 (43500), 304 (47000), 316 (44000), 520 (10).
[25] M. Wicholas, R. S. Drago, *J. Am. Chem. Soc.* **1968**, *90*, 6946.
[26] (a) X-ray structure analysis of **1** $(ClO_4)_6$ ($C_{108}H_{96}N_{18}O_{24}Cl_6Ni_3$), M_r = 2418.9; pink crystals ($0.30 \times 0.25 \times 0.20$ mm^3). The first cell determined was trigonal with a = 24.594 Å, α = 31.90°; a careful check of intensities related by the C_3 axis showed a very high discrepancy (>25%) for a number of strong and medium reflections, therefore **1** $(ClO_4)_6$ was assumed to be monoclinic, space group $C2$ with a = 23.418(4), b = 13.518(3), c = 24.598(4) Å, β = 108.52(2)°, V = 7383.8 Å^3, Z = 2, ϱ_{calcd} = 1.088, $F(000)$ = 2496, μ = 5.471 cm^{-1}. Most of the crystals (obtained by slow evaporation of acetonitrile/water solutions) exhibited cracks either in the mother liquor or within a few minutes in air. One crystal free of cracks was selected and mounted on a rotation free goniometer head. In the attempt to find an orientation matrix and to collect data on an Enraf–Nonius diffractometer (graphite monochromator, $Mo_{K\alpha}$ radiation, λ = 0.70930 Å) at −100 °C, the crystal showed no diffraction power after 12 hours and exhibited cracks. Therefore, data were collected at room temperature ($\theta/2\theta$ scans, $4 < 2\theta < 60°$). Three standard intensities showed a decay of 34% during data collection and were corrected with a linear time-dependent function. Semiempirical absorption corrections based on ψ curves of four reflections were applied. At this stage, data was analyzed for the presumed presence of a C_3 axis; data were transformed by assuming a trigonal cell, and intensities were averaged. The overall $R_{int}(I)$ factor was 0.24, by far higher then normally expected, and therefore the monoclinic system was retained. The systematic absences hkl ($h + k = 2n + 1$) together with E statistics and Nz test suggested space group $C2$ or Cm. With Z = 2, the cation **1** must lie on a special position of the space group; the only possibility is a twofold axis; therefore the true space group is $C2$. The structure was solved by a combination of Patterson, difference Fourier, and full least-squares methods with the Enraf–Nonius Molen/Vax package [26b] (F refinements, $w = 1/\sigma^2, \sigma^2(F^2) = \sigma^2_{counts} + (pI)^2, p$ = 0.08). One anion is well resolved; for the second, only the chlorine atom was found, and the third could not be located (this ClO_4^- anion is probably disordered in the channels of the structure). An attempt was made to determine the absolute configuration by comparing xyz and $-x-y-z$ refinements, but the differences are very small and gave no clear answer. Microtwinning [35] or lamellar twinning [36] are not excluded. $R(F)$ = 0.105, $Rw(F)$ = 0.134 for 2721 reflections having $I > 3\sigma(I)$ and 599 variables. Maximum residual electron density = 0.8 eÅ^{-3}. Further details of the crystal structure investigation are available on request from the Director of the Cambridge Crystallographic Data Center, 12 Union Road, GB-Cambridge CB2 1EZ (UK), on quoting the full journal citation. Crystals of **1** $(PF_6)_6[Ni(N_6C_{36}H_{32})_3]^{6+} \cdot 6PF_6^-$ were also analyzed by using CuKα graphite monochromated radiation on a Philips PW 1100/16 machine at room temperature. This complex is isostructural with **1** $(ClO_4)_6$, a = 23.454(4), b = 13.535(3), c = 24.619(4) Å, β = 108.45(2)°. The number of usable data was too low, and the results were worse than those for **1** $(ClO_4)_6$. b) B. A. Frenz "The Enraf-Nonius CAD4-SDP" in *Computing in Crystallography* (Eds.: H. Schenk, R. Olthof-Hazekamp, H. Van Koningveld, G. C. Bassi), Delft University Press, **1978**, pp. 64–71.
[27] W. Saenger, *Principles of Nucleic Acid Structure*, Springer, Heidelberg, **1984**.
[28] G. E. Schulz, R. H. Schirmer, *Principles of Protein Structure*, Springer, Heidelberg, **1979**.
[29] C. Fouquey, J.-M. Lehn, A.-M. Levelut, *Adv. Mater.* **1990**, *5*, 254.
[30] W. Zarges, J. Hall, J.-M. Lehn, C. Bolm, *Helv. Chim. Acta* **1991**, *74*, 1843.
[31] (a) For CD measurements crystals of **1**$(ClO_4)_6$ were chosen on inspection with a polarizing microscope. CD spectra were taken in $MeCN/H_2O$ 9/1 within two hours after dissolution of the crystal. The concentration of the solution was determined by measuring the absorbance at 320 nm. (b) J. Ferguson, C. J. Hawkins, N. A. P. Kane-Maguire, H. Lip, *Inorg. Chem.* **1969**, *8*, 771.
[32] $[Ni(bpy)_3]Cl_2$ looses half of its optical activity in about 15 minutes in aqueous solution at room temperature, see: G. T. Morgan, F. H. Burstall, *J. Chem. Soc.* **1931**, 2213.
[33] Related cases of twinning in chiral crystals have been reported, for instance, in helicenes [34] and in other cases [35]. We thank Prof. J. D. Dunitz for a discussion of these features.
[34] B. S. Green, M. Knossow, *Science* **1981**, *214*, 795; R. H. Martin, M. J. Marchant, *Tetrahedron* **1974**, *30*, 343.
[35] A. Karrer, J. D. Dunitz, *Acta Cryst.* **1987**, *A43*, 430.
[36] D. Philip, J. F. Stoddart, *Synlett* **1991**, 445.
[37] P. Baxter, J.-M. Lehn, A. DeCian, J. Fischer, *Angew. Chem.* **1993**, *105*, 92; *Angew. Chem. Int. Ed. Engl.* **1993**, *32*, 69.

Formation of Interwoven 2-D Networks by the Spontaneous Strict Self-Assembly of $[\{M(CO)_3(\mu_3\text{-}OH)\}_4]$ (M = Mn, Re) and Complementary Angular Spacer Molecules**

By *Steven B. Copp, S. Subramanian,* and *Michael J. Zaworotko**

Predictable self-assembly of supramolecular species by directed covalent or noncovalent bonding is one of the great challenges and opportunities that faces modern chemistry.[1] Nature, with very limited tools, is replete with simple yet elegant examples of self-assembly. Synthetic chemistry, however, has thus far only offered tantalizing suggestions that the limits of synthesis, given the diverse range of tools at our disposal, are perhaps set only by imagination. In this context, symmetry and functionality at the molecular level are not only exploitable but critically important facets of self-assembly.[1, 2] Diamond, ice, and KH_2PO_4 are three well-known[3] examples of how the shape and inherent ability of a moiety to self-assemble can influence the three-dimensional (3-D) solid-state structure; in ice and KH_2PO_4 this is a consequence of noncovalent bonding. It is therefore perhaps surprising that it has only recently been realized that appropriately tetrafunctionalized organic molecules with S_4 symmetry can also self-assemble[4, 5] and generate aesthetically pleasing superdiamondoid 3-D networks, sometimes with open architecture.[4c, d, 5] An alternate and potentially more versatile approach to the construction of 3-D supramolecular architecture is the cocrystallization of complementary molecular components, in other words a "strict self-assembly".[6] This approach has already been demonstrated for 1-D and 2-D structures,[7–9] and we recently extended it to superdiamondoid networks by employing $[\{M(CO)_3(\mu_3\text{-}OH)\}_4]$ (**1**,

[*] Dr. M. J. Zaworotko, S. B. Copp, Dr. S. Subramanian
Department of Chemistry
Saint Mary's University
Halifax, Nova Scotia, B3H3C3 (Canada)
Telefax: Int. code + (902)420-5261

[**] Manifestations of Noncovalent Bonding in the Solid State, Part 4. This work was supported by the NSERC, Canada. Part 3: S. Subramanian, M. J. Zaworotko, *Can. J. Chem.*, in press.

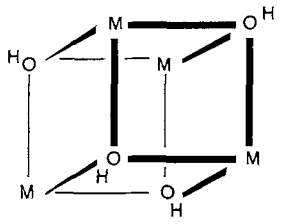

1: M = $Mn(CO)_3$; **2**: M = $Re(CO)_3$

M = Mn[10]; **2** M = Re[11]), cubanelike molecules with T_d or close to T_d symmetry and four rigid hydrogen-bond donors (Fig. 1), and linear difunctional hydrogen-bond acceptor molecules.[12] We explored the generality and versatility of strict self-assembly based upon T_d molecules by exploiting nonlinear spacer groups with **1** and **2** in order to generate 2-D hydrogen-bonded networks of varying but predictable levels of interpenetration and openness.

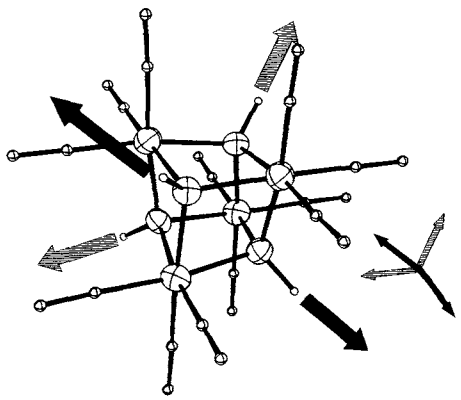

Fig. 1. Perspective view (ORTEP) of a molecule of **1** or **2**. The μ_3-OH groups are oriented (large arrows) towards the vertices of a tetrahedron.

Complex **1** cocrystallizes from acetonitrile with excess 1,3-diaminopropane[13] (DAP) or hexamethylenetetrammine[14] (HMTA) to afford the 2-D "chicken-wire" networks $(\mathbf{1} \cdot 2\,DAP)_n$ and $(\mathbf{1} \cdot 1.5\,HMTA)_n$, respectively. The structure of $(\mathbf{1} \cdot 2\,DAP)_n$ shown in Figure 2 reveals how two independent DAP molecules bridge adjacent molecules of **1** through OH···N hydrogen bonds (O···N separations range from 2.702(7) to 2.782(9)Å). The DAP molecules adopt W conformations and facilitate separations of 10.26 and 11.73 Å between the cubes. The different separations reflect the orientations of the nitrogen lone pairs within the DAP molecules. The space within the network is large enough to hold one ordered acetonitrile molecule per molecule of **1**. The structure of $(\mathbf{1} \cdot 1.5\,HMTA)$ is dramatically different. Since HMTA should be capable of acting as a tetrafunctional H-bond acceptor, a diamondoid network is anticipated when it is cocrystallized with **1** in a 1:1 ratio. However, the solid obtained from the 1:1 cocrystallization has 1.5 molecules of HMTA per molecule of **1**, presumably because HMTA is too small to simultaneously accomodate four molecules of **1**. Two types of HMTA molecules are found in the structure, both of which engage in only two hydrogen bonds: two-thirds of the molecules (i and ii, Fig. 3) are in the tetrameric species $(\mathbf{1} \cdot HMTA)_4$ with N···O distances of 2.863(14) and 2.773(12)Å, respectively; the remainder (iii, Fig. 3) bridge adjacent tetramers (N···O 2.931(13)Å) to form a sheet of 2-D "chicken wire" in the *ab* plane with large cavities. Two

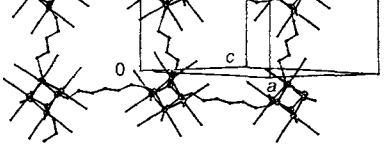

Fig. 2. Perspective view of the "chicken-wire" solid-state structure adopted by $\mathbf{1} \cdot 2\,DAP$. Carbonyl ligands and CH_2 hydrogen atoms are omitted for clarity in this and subsequent figures.

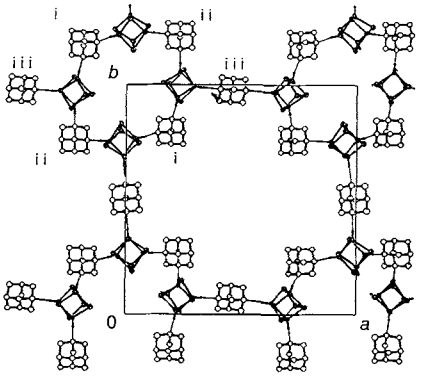

Fig. 3. View onto the *ab* plane in $\mathbf{1} \cdot 1.5\,HMTA$ showing the "chicken-wire" network of the tetrameric units. Crystallographic twofold axes pass through the HMTA molecules.

disordered acetonitrile molecules lie within the tetramer, which, as evident from Figure 4, is thus a type of cavitand. The open spaces in the network are filled by adjacent sheets.

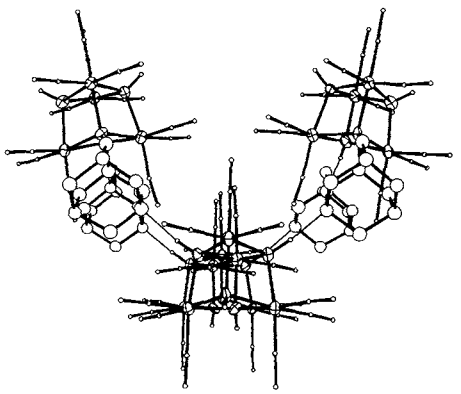

Fig. 4. Perspective view of $[\mathbf{1} \cdot HMTA]_4$. Two disordered solvent molecules are located inside the cavity of the tetramer.

Cocrystallization of **2** with two equivalents of 4,4'-dipyridine (dipy) from methanol/CH_3CN affords colorless crystals of the three-component network $(\mathbf{2} \cdot 2\,dipy \cdot 2\,MeOH)_n$.[15] The methanol molecules are integral components of the resulting hydrogen-bonded network and profoundly influence its structure by acting as angular bridges between molecules

of dipy and **2** (MeOH $\cdots$ dipy, O $\cdots$ N = 2.714(13)Å; μ_3-OH $\cdots$ O(H)Me, O $\cdots$ O = 2.560(10)Å). A 3-D structure is thereby precluded but hydrogen bonding between **2** and the other end of each dipy molecule (μ_3OH $\cdots$ dipy, O $\cdots$ N = 2.606(11)Å) sustains an open 2-D network with large intercube separations of 15.75Å (Fig. 5). The resulting cavities

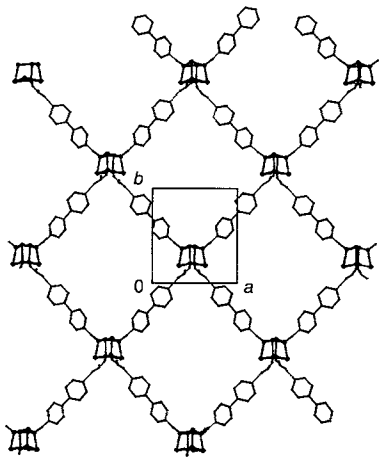

Fig. 5. Perspective view (ORTEP) of one of the two independent 2-D networks of **2** · 2 dipy · MeOH. Alternate cells are occupied in the crystallographic *ab* plane.

are filled by self-inclusion of a second identical but independent network, affording what is to our knowledge a novel[16] doubly interwoven carpetlike structure (Scheme 1).

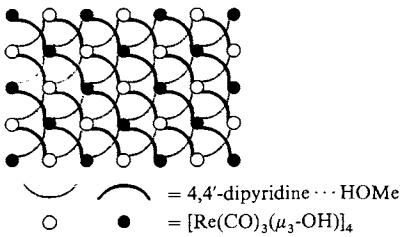

Scheme 1. Schematic representation of the interwoven structure of **2** · 2 dipy · 2 MeOH.

In summary, strict self-assembly of **1** or **2** and complementary multifunctional hydrogen-bond acceptor or acceptor/donor molecules leads to aesthetically pleasing supramolecular 2-D or 3-D compounds that are manifestations of directed noncovalent bonding and are therefore predictable,[17] controllable, and readily crystallized. The key to predictability in such networks appears to be quite simple: restrict the geometry and number of strong H-bond donor/acceptor moieties present in each component. The salient feature here is that in principle the concepts are general and should apply to a diverse range of structurally similar (Scheme 2)[17] or even dissimilar[18] components.

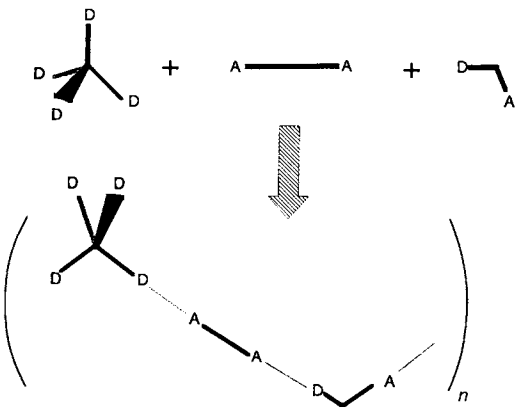

Scheme 2. Schematic representation of the general approach to construction of 2-D networks from three complementary molecular components. D = Hydrogen-bond donor; A = hydrogen-bond acceptor.

Received: December 18, 1992 [Z 5760/5761IE]
German version: *Angew. Chem.* **1993**, *105*, 755

[1] G. M. Whitesides, J. P. Mathias, C. T. Seto, *Science* **1991**, *254*, 1312.
[2] a) P. L. Anelli, P. R. Ashton, R. Ballardini, V. Balzani, M. Delgado, M. T. Gandolfi, T. T. Goodnow, A. E. Kaifer, D. Philp, M. Pietraszkiewicz, L. Prodi, M. V. Reddington, A. M. Z. Slawin, N. Spencer, J. F. Stoddart, C. Vicent, D. J. Williams, *J. Am. Chem. Soc.* **1992**, *114*, 193, and references therein; b) P. R. Ashton, G. R. Brown, N. S. Isaacs, D. Giuffrida, F. H. Kohnke, J. P. Mathias, A. M. Z. Slawin, D. R. Smith, J. F. Stoddart, D. J. Williams, *ibid.* **1992**, *114*, 6330, and references therein, c) J.-M. Lehn, *Angew. Chem.* **1990**, *102*, 1347; *Angew. Chem. Int. Ed. Engl.* **1990**, *29*, 1304, and references therein.
[3] L. Pauling, *The Nature of the Chemical Bond*, 2nd, Cornell Univ. Press, Ithaca, New York, **1948**.
[4] a) O. Ermer, *J. Am. Chem. Soc.* **1988**, *110*, 3747; b) O. Ermer, A. Eling, *Angew. Chem.* **1988**, *100*, 856; *Angew. Chem. Int. Ed. Engl.* **1988**, *27*, 829; c) O. Ermer, L. Lindenberg *Chem. Ber.* **1990**, *123*, 1111; d) O. Ermer, L. Lindenberg, *Helv. Chim. Acta* **1991**, *74*, 825.
[5] M. Simard, D. Su, J. D. Wuest, *J. Am. Chem. Soc.* **1991**, *113*, 4696.
[6] J. S. Lindsey *New J. Chem.* **1991**, *15*, 153.
[7] J.-M. Lehn, M. Mascal, A. DeCian, J. Fischer, *J. Chem. Soc. Chem. Commun.* **1990**, 479.
[8] a) S. J. Geib, S. C. Hirst, C. Vicent, A. D. Hamilton, *J. Chem. Soc. Chem.* Commun. **1991**, 1283; b) F. Garcia-Tellado, S. J. Geib, S. Goswami, A. D. Hamilton, *J. Am. Chem. Soc.* **1991**, *113*, 9265.
[9] J. A. Zerkowski, C. T. Seto, G. M. Whitesides, *J. Am. Chem. Soc.* **1992**, *114*, 5473.
[10] a) M. Herberhold, F. Wehrmann, D. Neugebauer, G. Huttner, *J. Organomet. Chem.* **1978**, *152*, 329; b) M. D. Clerk, M. J. Zaworotko, *J. Chem. Soc. Chem. Commun.* **1991**, 1607.
[11] M. Herberhold, G. Süss, *Angew. Chem.* **1975**, *87*, 710; *Angew. Chem. Int. Ed. Engl.* **1975**, *14*, 700.
[12] **1** and **2** cocrystallize with two equivalents of a wide range of linear difunctional hydrogen-bond acceptors to generate diamondoid networks. For example, 1,4-diaminobenzene, 1,2-diaminoethane, and 4,4'-dipyridyl generate two-, three- and fourfold interpenetrated diamondoid networks, respectively: a) S. B. Copp, S. Subramanian, M. J. Zaworotko, *J. Am. Chem. Soc.* **1992**, *114*, 8719. b) S. B. Copp, S. Subramanian, M. J. Zaworotko, unpublished results.
[13] a) Crystals were grown from hot acetonitrile, decompose at ca. 200 °C, and are insoluble in aprotic organic solvents under ambient conditions. IR (KBr)[cm^{-1}]: ν_{OH} = 2859(s); ν_{CO} = 2013(s), 1904(s). Space group $P2_1/n$ (No. 14, nonstandard), a = 17.2454(16), b = 10.2592(8), c = 19.7952(20)Å, β = 101.384(12)°, V = 3343.3(5)Å^3; ρ_{calcd} = 1.57 gcm^{-3} for Z = 4; 2178 (out of 3205) observed ($I > 3\sigma I$, 2θ 2–40°) reflections afforded R = 0.038, R_w = 0.041. OH, CH_3, and one set of NH_2 hydrogen atoms were located by inspection of the difference Fourier map and fixed. CH_2 hydrogen atoms were fixed in calculated positions (d_{C-H} = 1.08 Å); one set of NH_2 hydrogen atoms could not be located. Intramolecular distances and angles were observed to be within expected ranges. b) Further details of the crystal structure investigation are available on request from the Director of the Cambridge Crystallographie Data Centre, 12 Union Road, GB-Cambridge CB2 1EZ (UK), on quoting the full journal citation.
[14] Crystals were grown from hot chloroform, decompose at ca. 150 °C, and are insoluble in aprotic organic solvents. IR (KBr) [cm^{-1}]: ν_{OH} = 3314(s), 2964(s); ν_{CO} = 2019(s), 1929(s). Space group $P4_22_12$ (No. 94), a = 21.4558(18), c = 15.5713(23), V = 7168.3(12)Å^3; ρ_{calcd} = 1.67 g cm^{-3}; 2133 (out of 3001) observed ($I > 3\sigma I$, 2θ 2–40°)) refelctions afforded R = 0.043, R_w = 0.040. Hydrogen atoms were calculated (OH, CH_2) and fixed during least-squares refinement. The enantiomorph was fixed by using Friedel equivalents and the Rogers method. The solvent molecules were observed to be disordered. Refinement of all solvent atoms as carbon with site occupancy as a variable gave two molecules of solvation. All intramolecular distances and angles were observed to be within expected ranges. See also ref. [13b].
[15] Crystals are insoluble in aprotic organic solvents, even hot acetonitrile, become opaque at ca. 150 °C, but show no other signs of decomposition

below 250 °C. IR (KBr)[cm^{-1}]: ν_{OH} = 2744(s); ν_{CO} = 2011(s), 1915(s). Space group $P2/c$ (No. 13), a = 10.5407(10), b = 11.6973(10), c = 17.868(3)Å, β = 94.37(4)°, V = 2196.7(4)Å^3; ρ_{calcd} = 2.31 gcm^{-3} for Z = 2; 2876 (out of 3873) observed ($I > 3\sigma I$) reflections afforded R = 0.033, R_w = 0.038. Hydrogen atoms were calculated (CH) or located by inspection of the difference Fourier map and fixed during least-squares refinement. All intramolecular distances and angles were observed to be within expected ranges. In the absence of MeOH a fourfold superdiamondoid network that enclathrates two molecules of acetonitrile per molecule of **1** or **2** is obtained (see ref. [12]). See also ref. [13b].

[16] Four independent, folded, nonplanar, interpenetrating networks as a consequence of self-assembly were observed in benzene-1,3,5-tricarboxylic acid: a) D. J. Duchamp, R. E. Marsh, *Acta Crystallogr. Sect. B* **1969**, *25*, 5; b) F. H. Herbstein, *Top. Curr. Chem.*, **1987**, *140*, 107.

[17] Whereas the structure of **1** · 1.5 HMTA is the result of serendipity and is unlikely to be general, the molecular "chicken-wire" type structure observed for **1** · 2 DAP is reproducible (**1** · 2 diacetone alcohol) and molecular "carpet" structures with the same dimensions as **2** · 2 dipy · 2 MeOH can be obtained with *n*-BuOH and *i*-PrOH. M. J. Zaworotko, S. B. Copp, S. Subramanian, unpublished results.

[18] As noted by a referee the networks reported herein are not the only hydrogen-bonded networks that can be generated from organometallic molecules that are multifunctional hydrogen-bond donors. For example, $[(Me_3Sn)_4Fe(CN)_6] \cdot 2H_2O$ forms infinite networks when its bound water molecules form hydrogen bonds to bridging water (U. Behrens, A. K. Brimah, R. D. Fischer, *J. Organomet. Chem.*, **1991**, *411*, 325) or dioxane (M. Adam, A. K. Brimah, R. D. Fischer, L. Xing-Fu, *Inorg. Chem.*, **1990**, *29*, 1597) molecules. The hydrogen-bonded chains are crosslinked by covalent Lewis acid–base interactions.

Ca_3AuN: A Calcium Auride Subnitride**

By *Jürgen Jäger, Dagmar Stahl, Peter C. Schmidt,* and *Rüdiger Kniep**

Dedicated to Professor Dietrich Mootz on the occasion of his 60th birthday

Recently with $NaBa_3N$[1] a new subnitride was presented that crystallizes in the hexagonal Perowskite structure (like for example, $CsNiCl_3$[2]) and that is characterized by "spatial separation" of ionic and metallic bonding components. By drawing on the crystal chemistry of the alkali metal suboxides[3] under consideration of the electronegativities of nitrogen, barium, and sodium, the bonding in $NaBa_3N$ is described as follows:[1] $Na^+Ba_3^{2+}N^{3-} \cdot 4e^-$; results of band structure calculation are in accord with these concepts.

In the course of our investigations into ternary and quaternary nitrides with elements of the 11 th group of the periodic system, we have now prepared the compound Ca_3AuN. The product, which according to X-ray powder studies contains one phase (blue-violet crystals of cubic habit with a metallic luster), was obtained as follows: calcium (shot) and gold (wire) were placed in the molar ratio 3:1 in a corundum crucible and heated at a rate of 200 K h^{-1} to 950 °C in a quartz reaction tube under argon, exposed at this temperature to a stream of nitrogen (1 atm) for 24 h, and finally cooled to room temperature at 6 K h^{-1}. In the Ca–Ag–N system an intermediate phase with a brassy luster was obtained in this way;[4] the ductility and perfect cleavability of the layered crystals have as yet prevented a structure determination. The nitridocuprates known today[5] are all shiny black crystals, thin layers of which appear red and transparent.

Ca_3AuN[6] crystallizes in the cubic perowskite structure (Fig. 1). This structural type also occurs in the ternary nitrides Ca_3XN (X = P, As, Sb, Bi, Ge, Sn, Pb),[7] which in agreement with the results of band structure calculations,[8] have the ionic formula $Ca_3^{2+}X^{3-}N^{3-}$. Nitrogen in these compounds is surrounded by an octahedron of calcium atoms; the NCa_6 octahedra share corners and are linked into a three-dimensional framework $^3_\infty[NCa_{6/2}]$. In the crystal structure of Ca_3AuN, calcium and gold together form a cubic face-centered arrangement. The Ca–N bond lengths of 241.1 pm are approximately equal to those in α-Ca_3N_2 (245.1(2)–248.2(2) pm[9]). The Ca–Ca distances (340.9 pm) are shorter than in the metal (394 pm[11]), while the Ca–Au distances (340.9 pm) correspond to the sum of the radii of Ca and Au in the metals (341 pm[11]).

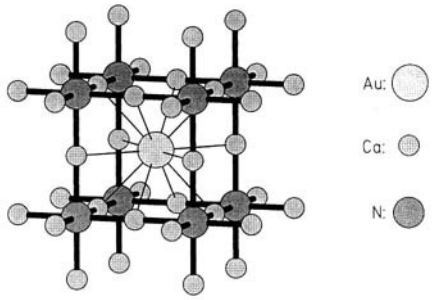

Fig. 1. Section of the crystal structure of Ca_3AuN.

Since the electronegativities[12] of gold (2.54) and nitrogen (3.04) are larger than that of calcium (1.0), the following simple model of the chemical bond in Ca_3AuN can be deduced: $Ca_3^{2+}Au^-N^{3-} \cdot 2e^-$. This agrees with the concept of the chemical bond in $NaBa_3N$,[1] and results in an overall metallic character for Ca_3AuN. The picture was also verified by the results of the band structure calculations according to the ASW method (ASW = *a*ugmented *s*pherical *w*ave).[13] The quantum mechanical calculations in this investigation were not restricted to Ca_3AuN, but to provide suitable comparison, were extended to CsAu[15] (an ionic auride) and Al_2Au[16] (an intermetallic phase with metallic character). Ca_3AuN is shown to have energetically low-lying, filled N 2p and Au 6s and Au 5d bands, while the Fermi level lies in a broad band with Au 6p and Ca character. In Figure 2 the dependence of the charge densities for gold on the radius of

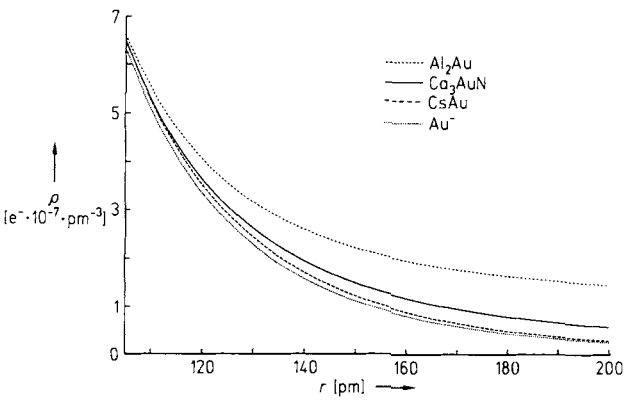

Fig. 2. Dependence of the charge densities at gold on the radius around its central position in the compounds Al_2Au, Ca_3AuN, and CsAu.

[*] Prof. Dr. R. Kniep, Dipl.-Ing. J. Jäger, Dipl.-Ing. D. Stahl
Eduard-Zintl-Institut der Technischen Hochschule Darmstadt
Hochschulstrasse 10, D-W-6100 Darmstadt (FRG)
Fax: Int. code + (6151)16-4073
Prof. Dr. P. C. Schmidt
Institut für Physikalische Chemie der Technischen Hochschule Darmstadt

[**] This work was supported by the Deutsche Forschungsgemeinschaft and the Fonds der Chemischen Industrie. R.K. thanks Prof. A. Simon, Stuttgart, for useful discussions.

its central position is depicted for the compounds Al_2Au, Ca_3AuN, and CsAu. The spherically averaged charge density for Au in CsAu corresponds very well to that for a "free Au^-". In Al_2Au the electron density approaches a high value at large distances from the Au core, characteristic for metallic bonds. The curve for the electron density at gold in Ca_3AuN suggests the presence of an auride.

Received: January 16, 1993 [Z 5814 IE]
German version: *Angew. Chem.* **1993**, *105*, 738

[1] P. E. Rauch, A. Simon, *Angew. Chem.* **1992**, *104*, 1505; *Angew. Chem. Int. Ed. Engl.* **1992**, *31*, 1519.
[2] G. N. Tishchenko, *Trans. Inst. Kristallogr. Akad. Nauk USSR* **1955**, *11*, 93.
[3] A. Simon, *Struct. Bonding (Berlin)* **1979**, *36*, 81.
[4] Part of a thesis in progress (J. Jäger) at the Technische Hochschule Darmstadt: molar ratio Ca:Ag = 1:1; indexing of the X-ray powder diagram: tetragonal (a = 487, c = 813 pm) or hexagonal (a = 543, c = 813 pm).
[5] J. Jäger, R. Kniep, *Z. Naturforsch. B* **1992**, *47*, 1290.
[6] Crystal structure determination of Ca_3AuN: Space group $Pm3m$; a = 482.15(5), Z = 1; ρ_{calcd} = 4.91 g cm^{-3}; Ca in 3*c* (0, 0.5, 0.5), Au in 1*a* (0, 0, 0), N in 1*b* (0.5, 0.5, 0.5); R = 0.015; 54 independent observed reflections ($F \geq 2\sigma(F)$); Philips PW-1100 diffractometer; 2θ range between 5 and 60°; $Mo_{K\alpha}$ radiation. Further details of the crystal structure investigation may be obtained from the Fachinformationszentrum Karlsruhe, Gesellschaft für wissenschaftlich-technische Information mbH, D-W-7514 Eggenstein-Leopoldshafen 2 (FRG) on quoting the depository number CSD-56978 the names of the authors, and the journal citation.
[7] M. Y. Chern, D. A. Vennos, F. J. DiSalvo, *J. Solid State Chem.* **1992**, *96*, 415.
[8] D. A. Papaconstantopoulos, W. E. Pickett, *Phys. Rev. B* **1992**, *45*, 4008.
[9] P. Höhn, *Ternäre und quaternäre Nitridometallate: Verbindungen in den Systemen Lithium-Erdalkalimetall-Übergangsmetall-Stickstoff*, Dissertation, Technische Hochschule Darmstadt, **1993**. Redetermination of the crystal structure of α-Ca_3N_2 [10]: Space group *Ia*3; a = 1147.41(2) pm, Z = 16, Ca in 48*e* (0.34604(4), 0.11756(5), 0.10989(5)), N1 in 24*d* (0.4615(3), 0, 1/4) and N2 in 8*b* (1/4, 1/4, 1/4); R = 0.020; 367 independent observed reflections; STOE Stadi-4 diffractometer; 2θ range between 3 and 60°; $Mo_{K\alpha}$ radiation.
[10] Y. Laurent, J. Lang, M. Th. Le Bihan, *Acta Crystallogr. Sect. B.* **1968**, *24*, 494.
[11] W. B. Pearson, *The Crystal Chemistry and Physics of Metals and Alloys*, Wiley-Interscience, New York **1972**, p. 151.
[12] L. Pauling, *The Nature of the Chemical Band*, 3rd ed., Cornell University Press, Ithaca, NY (USA), **1960**
[13] A. R. Williams, J. Kübler, C. D. Glatt, *Phys. Rev. B* **1979**, *19*, 6094. The ASW method is based on the local density function approximation and uses the atomic sphere approximation (ASA). In the ASA the crystal is divided into overlapping spheres. The parameters were chosen as in [14].
[14] P. C. Schmidt, D. Stahl, B. Eisenmann, R. Kniep, V. Eyert, J. Kübler, *J. Solid State Chem.* **1992**, *97*, 93.
[15] M. Kogachi, S. Ishibata, *J. Jpn. Inst. Met.* **1983**, *47*, 912.
[16] M. E. Straumanis, K. S. Chopra, *Z. Phys. Chem. N.F.* **1964**, *42*, 344.

(η^1-tpMn, η^5-tpCr) → (η^1-tpCr, η^5-tpMn) Thiophene (tp) Conversion due to Bimetallic Activation: A Novel Metal-Exchange Reaction**

By *Thomas A. Waldbach, Petrus H. van Rooyen,* and *Simon Lotz**

Reactions of thiophenes (tp) in transition metals complexes are currently a topic of great interest. A variety of coordination modes of thiophene in mono-, bi-, and trimetallic complexes are known and were recently reviewed.[1] Much of the work in this field centers around studies on mechanisms that may be of importance in the hydrodesulfurization of petroleum[2] and in materials with optical or conducting properties.[3] Thiophene, activated by coordination to transition metals, is a very versatile reagent and undergoes many interesting reactions, such as the insertion of transition metals into the C–S bond,[4] dimerization,[5] intermolecular silyl transfer,[6] intramolecular interconversion of η^1-sulfur and η^2-olefin isomers of [Cp*(CO)$_2$Re(benzol[b]tp)],[7] and the remarkable reactions of the two isomeric forms of [Cp*Ir(2,5-Me$_2$tp)] with iron carbonyls[8] and acetylenes.[9] Here we extend this list of novel reactions and report a metal exchange, facilitated by a η^1:η^5-bridging tp ligand, in an activated heterobimetallic complex.

A solution of [(η^5-2-LiC$_4$H$_3$S)Cr(CO)$_3$],[10] prepared by treating *n*-BuLi (10% excess) in THF with [(η^5-tp)Cr(CO)$_3$][11] at −50 °C, was stirred with one equivalent of [Mn(CO)$_5$X] (X = Br, Cl) for 1 h at −90 °C and 0.5 h at room temperature. The reaction mixture was dried under vacuum, and the residue chromatographed in dichloromethane/hexane (1:1) on silica gel. Slow evaporation of the solvent from the first orange band give crystals of the novel complex **2** in about 10% yield. In addition to the main product **2**, apart from [(η^5-tp)Cr(CO)$_3$], [Mn$_2$(CO)$_{10}$], and a polar intractable residue, a second orange product of very different polarity was also collected and afforded **1** in even

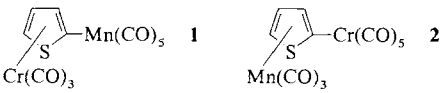

1 **2**

lower yield (<2%). Higher yields of **1** (10%) were obtainable by shorter reaction times, lower temperatures, and faster column chromatography.

When crystals of complex **1** were dissolved in polar solvents such as acetone and THF, they spontaneously underwent a metal exchange process to afford the thermodynamically favored compound **2**. The conversion of **1** into **2** was studied by ^{1}H NMR spectroscopy. Intensity measurements reveal that a pure sample of **1** (15 mg) converts almost quantitatively (>85%) into **2** at 30 °C in deuterated acetone over a period of 24 h. The spectra show only signals for **1** or **2** (>99%), which indicates a conversion with no side products. Factors contributing to this facile process include a very labile π-coordinated tp ligand on Cr(CO)$_3$, labile carbonyl ligands on the Mn(CO)$_5$ fragment, the formation of a relatively strong tp–Mn σ bond, solvents with coordinating properties (e.g., THF), and a driving force towards the thermodynamically favored product. However, this irreversible conversion was inhibited in dichloromethane, and analytically pure crystals of both **1** and **2** could therefore be obtained from dichloromethane/hexane mixtures. A novel intramolecular flip of the tp ligand is postulated as mechanism for the metal exchange. Whereas **1** inserts CO to form the stable complex **3**, no reaction was observed for **2** in a CO atmosphere. The complexes were fully characterized by elemental analysis and IR, ^{1}H NMR, ^{13}C NMR, and mass spectra; these data[12] support our formulations of **1** and **2**.

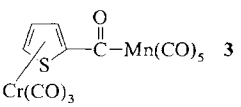

3

The patterns of the bands associated with the carbonyl vibrations in the IR spectrum of **1** are typical for independent Cr(CO)$_3$ and Mn(CO)$_5$ moieties. The tp ligand in **1** places more electron density on the chromium atom than in the precursor [Cr(η^5-tp)(CO)$_3$],[11] which is reflected by the

[*] Prof. S. Lotz, T. A. Waldbach, P. H. van Rooyen
Department of Chemistry, University of Pretoria
Pretoria 0002 (South Africa)

[**] π-Heteroatom Complexes, Part 1. This work was supported by the Foundation for Research and Development, Pretoria.

shift of the carbonyl frequencies to lower wavenumbers. Although overlapping in the IR spectrum of **2** hampered unique assignments, it can be seen that the $Cr(CO)_5$-fragment displays vibrational frequencies lower than those observed for $[Cr(CO)_5I]$, but higher than those found for $[Cr(CO)_5I]^-$.[13] The ^1H NMR spectra of **1** and **2** show the expected three nonequivalent resonances for the tp protons, with different chemical shifts and coupling constants. The reduction of electron density on the tp ring on going from **1** to **2** is reflected in the spectra by a downfield shift for the protons of **2**. Conclusive spectral evidence for the structural assignment of the bimetallic compounds **1** and **2** are found in their ^{13}C NMR spectra. The broad signal associated with $Mn(CO)_5$ at $\delta = 208$ and the chemical shift for the $Cr(CO)_3$ unit of $\delta = 238$ in **1** is absent in the spectrum of **2**. Instead, a broad signal for the $Mn(CO)_3$ fragment at $\delta = 219$ and two resonances at $\delta = 218$ (*cis*-CO) and 222 (*trans*-CO), typical for $Cr(CO)_5$ fragments, are observed; this is in good agreement with values reported in literature.[14] The relatively high value for the *ipso*-carbon when bonded to chromium may indicate some carbene character in this bond (Scheme 1).

X-ray diffraction studies were performed on suitable crystals of **1** and **2**, obtained by recrystallization from dichloromethane/hexane mixtures. The compounds **1** (orange) and **2** (yellow) crystallized in different space groups.[15] The solid state conformations are essentially identical (Fig. 1 and 2), but with some important differences in the bond distances. The distance between the Mn atom and the center of the tp ring in **2** is 1.720(5) Å, significantly shorter than the distance of 1.850(3) Å observed for the Cr center in **1**. The bond

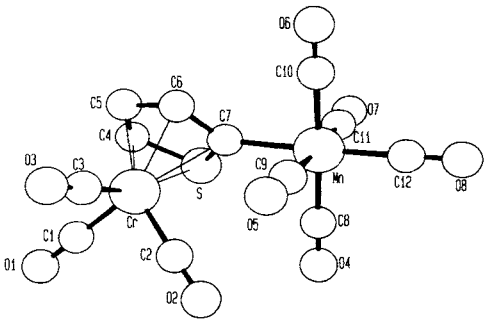

Fig. 1. Crystal structure of **1**. Selected distances [Å] and angles [°]: Cr-tp(center) 1.850(3), Mn-C7 2.079(2), Cr-S 2.381(1), Cr-C4 2.198(3), Cr-C5 2.218(3), Cr-C6 2.228(3), Cr-C7 2.289(2), S-C4 1.723(3), S-C7 1.764(2), C4-C5 1.371(4), C5-C6 1.428(4), C6-C7 1.390(3), C4-C5-C6 111.8(3), C5-C6-C7 115.5(3), C6-C7-S 107.6(2), C7-S-C4 93.3(1), S-C4-C5 111.7(2), S-C7-Mn 122.0(1), C6-C7-Mn 129.7(2).

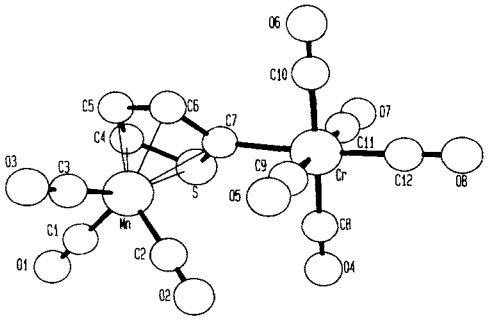

Fig. 2. Crystal structure of **2**. Selected distances [Å] and angles [°]: Mn-tp(center) 1.720(5), Cr-C7 2.112(4), Mn-S 2.330(1), Mn-C4 2.131(4), Mn-C5 2.150(4), Mn-C6 2.252(3), Mn-C7 2.299(4), S-C4 1.729(4), S-C7 1.768(4), C4-C5 1.399(6), C5-C6 1.472(5), C6-C7 1.485(5), C4-C5-C6 115.3(4), C5-C6-C7 109.3(3), C6-C7-S 109.7(3), C7-S-C4 94.5(2), S-C4-C5 110.0(4), S-C7-Cr 122.0(2), C6-C7-Cr 127.7(3).

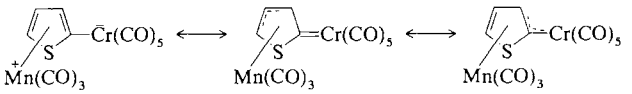

Scheme 1. Resonance structures of **2**.

lengths of the bridging tp ligand in **1** are typical for η^5-coordinated thiophene ligands: the C4–C5 and C6–C7 distances are clearly shorter than the C5–C6 distance. In contrast, the corresponding C6–C7 distance in **2** is equal to the C5–C6 bond length, which compares with normal $C(sp^2)$–$C(sp^2)$ single bond distances (1.48 Å).[16] Both allylic resonance structures (Scheme 1) are therefore plausible for **2**. The short $Cr(\eta^1)$–C7 bond (2.112(4) Å) in **2** is comparable to values recorded for aminocarbene complexes of chromium[17] and supports the ^{13}C NMR data in indicating some carbene character for C7.[14]

Ligand exchange reactions from the coordination sphere of a complex form the basis of most reactions in organometallic chemistry. By contrast, the exchange of metal atoms each from their own ligand environment to that of the other involves the breaking and making of many bonds and is, as far as we are aware, unprecedented in the literature for simple organometallic compounds. Furthermore, after this $\eta^1 \rightleftarrows \eta^5$ conversion of metal bonding was realized, the displacement of the chromium atom in [(η^5-thiophene)$Cr(CO)_3$] by manganese within the fixed ligand environment became an attractive possibility. The stability of **2** is remarkable, and initial efforts to displace the $Cr(CO)_5$ fragment by a ligand and protonate the thiophene ligand to afford the target compound $[(\eta^5\text{-tp})Mn(CO)_3]^+$ failed. Treatment of **2** with HBF_4 under CO atmosphere and at elevated temperatures afforded an unstable intermediate, which displayed an additional carbonyl frequency at 1658 cm^{-1} in the infrared spectrum, and immediately converts back to **2** during workup.

In conclusion, we report the first example of a metal exchange reaction which we believe will have wider application. Further studies are directed towards investigating the mechanism and kinetics of the exchange process, extending the range of transition metals participating in metal exchange, deducing optimum conditions for the promotion of the exchange process, and expanding the concept to other compounds with cyclic heterodiene and cyclopentadienyl ligands. The above example clearly demonstrates the importance of ligand activation by transition metals in heterobimetallic complexes.

Received: December 4, 1992 [Z 5727 IE]
German version: *Angew. Chem.* **1993**, *105*, 795

[1] R. J. Angelici, *Coord. Chem. Rev.* **1990**, *105*, 61–76; T. B. Rauchfuss, *Prog. Inorg. Chem.* **1991**, *39*, 259–329; D. L. Kershner, F. Basolo, *Coord. Chem. Rev.* **1987**, *79*, 279–292.

[2] R. J. Angelici, *Acc. Chem. Res.* **1988**, *21*, 387–394; D. A. Lesch, J. W. Richardson, Jr., R. A. Jacobson, R. J. Angelici, *J. Am. Chem. Soc.* **1984**, *106*, 2901–2906; L. Dong, S. B. Duckett, K. F. Ohman, W. D. Jones, *ibid.* **1992**, *114*, 151–160.

[3] J. Roncali, *Chem. Rev.* **1992**, *92*, 711–738; H. S. Nalwa, *Appl. Organomet. Chem.* **1991**, *5*, 349–377; O. A. Patil, A. J. Heeger, F. Wudl, *Chem. Rev.* **1988**, *88*, 183–200.

[4] J. Chen, L. M. Daniels, R. J. Angelici, *J. Am. Chem. Soc.* **1990**, *112*, 199–204; S. Luo, A. E. Ogilvy, T. B. Rauchfuss, A. L. Rheingold, S. R. Wilson, *Organometallics* **1991**, *10*, 1002–1009.

[5] R. M. Chin, W. D. Jones, *Angew. Chem.* **1992**, *104*, 340–341; *Angew. Chem. Int. Ed. Engl.* **1992**, *31*, 357–358.

[6] M. S. Loft, D. A. Widdowson, T. J. Mowlem, *Synlett* **1992**, *2*, 135–136.

[7] M.-G. Choi, R. J. Angelici, *Organometallics* **1992**, *11*, 3328–3334.

[8] J. Chen, L. M. Daniels, R. J. Angelici, *J. Am. Chem. Soc.* **1991**, *113*, 2544–2552.

[9] J. Chen, R. J. Angelici, *Organometallics* **1992**, *11*, 992–996.
[10] M. N. Nefedova, V. N. Setkina, D. N. Kursanov, *J. Organomet. Chem.* **1983**, *244*, C21–C23.
[11] E. O. Fischer, K. Öfele, *Chem. Ber.* **1958**, *91*, 2395–2399.
[12] **1**: IR (CH_2Cl_2) Mn(CO)$_5$: $\tilde{\nu}$[cm^{-1}] = 2130 (m), 2075 (w), 2038 (vs), 2021 (s); Cr(CO)$_3$: 1947 (s), 1856 (s, br); ^{1}H NMR (300 MHz, $CD_3C(O)CD_3$, 10 °C): δ = 6.16 (dd, ^3J = 3.53 Hz, ^4J = 0.73 Hz, 1H; H5), 5.98 (dd, ^3J = 3.53, 3.07 Hz, 1H; H6 or H4), 5.94 (dd, ^3J = 3.07 Hz, ^4J = 0.75 Hz, 1H; H6 or H4); ^{13}C NMR (75.43 MHz, $CD_3C(O)CD_3$, 10 °C): δ = 235 (Cr*C*O), 208 (Mn*C*O), 112 (*C*7), 109, 97, 96 (*C*4–6); MS (70 eV): *m/z* (%) 413 (11) [M^+ − H]; R_f = 0.60; correct C,H analysis for $CrMnC_{12}H_3SO_8$. **2**: IR (CH_2Cl_2): $\tilde{\nu}$[cm^{-1}] = 2065 (m), 2044 (vs), 1992 (m), 1977 (m), 1924 (s); ^{1}H NMR (300 MHz, $CD_3C(O)CD_3$, 10 °C): δ = 7.11 (d, ^3J = 3.58 Hz, 1H; H6 or H4), 6.78 (t, ^3J = 3.20 Hz, 1H; H5), 6.50 (d, ^3J = 2.94 Hz, 1H; H6 or H4); ^{13}C NMR (75.43 MHz, $CD_3C(O)CD_3$ 10 °C): δ = 218 (*cis*-Cr*C*O), 222 (*trans*-Cr*C*O), 219 (Mn*C*O), 164 (*C*7), 109, 103, 102 (*C*4–6); MS (70 eV): *m/z* (%) 414 (8) [M^+]; R_f = 0.71; correct C,H analysis for $CrMnC_{12}H_3SO_8$.
[13] E. Lindner, H. Behrens, *Spectrochim. Acta* **1967**, *A23*, 3025.
[14] B. E. Mann, *Adv. Organomet. Chem.* **1974**, *12*, 135–213.
[15] Enraf-Nonius CAD4 diffractometer, T = 297 K, $Mo_{K\alpha}$ radiation (λ = 0.7107 Å), graphite monochromator, $3 < \theta < 30°$. Crystal data for **1**: $C_{12}H_3O_8SCrMn$, M_r = 414.15, monoclinic, $P2_1/c$, a = 13.120(1), b = 6.842(1), c = 16.885(2) Å, β = 93.32(1)° (based on 25 reflections with $18 < \theta < 20°$), V = 1513.1(2) Å^3, Z = 4, ρ_{calcd} = 1.85 g cm^{-3}, $F(000)$ = 816, μ = 1.65 mm^{-1}. 4881 unique reflections measured, 3511 were considered observed ($|I| > 3\sigma|I|$). All the non-hydrogen atoms were refined anisotropically, and the hydrogen atoms were included in the refinement in calculated positions, riding on their associated heavy atoms but with the isotropic thermal parameters free to refine independently. 212 parameters were refined: R_w = 0.044 (R = 0.056) using σ^{-2} (F_{obs}) weights. Interchanging the two metal atoms in the structure resulted in R_w = 0.050 (R = 0.064). Crystallographic data for **2**: $C_{12}H_3O_8SCrMn$, M_r = 414.15, triclinic, $P\bar{1}$, a = 7.155(1), b = 8.586(1), c = 12.338(2) Å, α = 80.97(1), β = 86.84(1), γ = 82.67(6)° based on 25 reflections with $16 < \theta < 17°$), V = 742.0(2) Å^3, Z = 2, ρ_{calcd} = 1.81 g cm^{-3}, $F(000)$ = 408, μ = 1.68 mm^{-1}. 4312 unique reflections measured, 3572 considered as observed ($|I| > 3\sigma|I|$). All the non-hydrogen atoms were refined anisotropically, and the hydrogen atoms were included in the refinement in experimentally determined positions with the isotropic thermal parameters also free to refine independently. 220 parameters were refined: R_w = 0.029 (R = 0.038) using σ^{-2} (F_{obs}) weights. Interchanging the two metal atoms in the structure resulted in a R_w of 0.039 (R = 0.047). Further details of the crystal structure investigation are available on request from the Director of the Cambridge Crystallographic Data Centre, 12 Union Road, GB-Cambridge, CB2 1EZ (UK), on quoting the full journal citation.
[16] J. March, *Advanced Organic Chemistry*, Wiley, New York, **1988**, p. 19.
[17] U. Schubert in *Transition Metal Carbene Complexes* (Eds.: U. Schubert, H. Fischer, P. Hofmann, K. Weiss, K. H. Dötz, F. R. Kreißl), Verlag Chemie, Weinheim, **1983**, pp. 94–96.

A Novel Synthesis of Pyrrole-2-carboxylic Acid Derivatives by Ring Transformation of 1,2-Thiazolium Salts through Sulfur Extrusion

By *Andreas Rolfs* and *Jürgen Liebscher**

Attention has been directed recently toward pyrrole-2-carboxylic acid derivatives as lead structures for the development of effective anticonvulsants,[1] but these compounds have long been important as analgesics and antiinflammatory agents as well.[2, 3] These types of pyrroles are also employed in the synthesis of natural products and analogous compounds such as porphyrins,[4] oligopyrroles,[5] and nucleosides.[6] Derivatives of pyrrole-2-carboxylic acid have been prepared, for example, by ring-closing reactions and ring transformations, often with restrictions on the substitution pattern.[7] We report here on an efficient route to pyrrole-2-carboxylates and -nitriles based on a novel ring transformation of substituted 2-methyl-1,2-thiazolium salts by sulfur extrusion.

When 2-alkoxycarbonylmethyl- or 2-cyanomethyl-1,2-thiazolium salts **1** were heated in polar solvents in the presence of base, the pyrrole-2-carboxylic acid derivatives **5** formed spontaneously (Method A, see Experimental Procedure and Table 1). The sulfur atom of the 1,2-thiazole ring

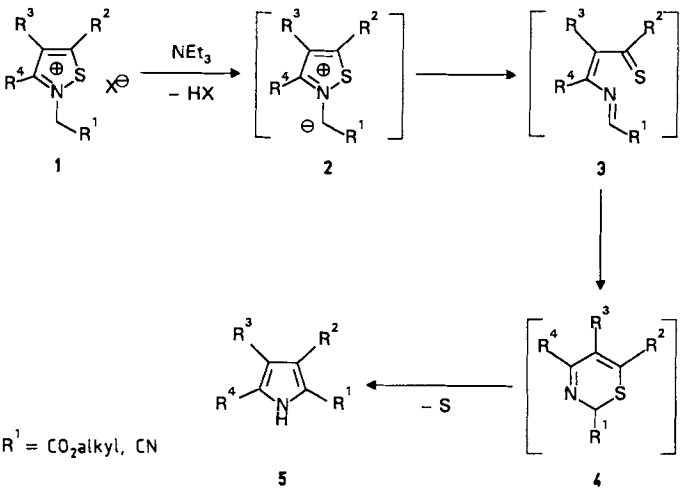

Table 1. 1*H*-Pyrroles **5a**–**5k**, synthetic method (see Experimental Procedure), and yields.

Cmpd.	R^1	R^2	R^3	R^4	Method	Yield [a] [%]
5a	CO_2CH_3	C_6H_5	C_6H_5	H	A	86.7 (C)
5b	CO_2CH_3	C_6H_5	H	C_6H_5	A	84.5 (R)
5c	CO_2CH_3		2-$CH_3C_6H_4$	H	A	91 (C)
5d	$CO_2C_2H_5$		4-FC_6H_4	H	A B	81.4 (R) 80.0 (R)
5e	CO_2CH_3		4-ClC_6H_4	H	A	92 (C)
5f	CO_2CH_3	NHC_6H_5	C_6H_5	CH_3	A	100 (R)
5g	CO_2CH_3	SCH_3	4-ClC_6H_4	H	A	72.3 (C)
5h	CN	NHC_6H_5	C_6H_5	CH_3	B	82.1 (C)
5i	CO_2CH_3	NHC_6H_5	$CO_2C_2H_5$	CH_3	B	73.1 (R)
5j	CO_2CH_3	4-ClC_6H_4	H	H	B	68 (C) [b]
5k	$CO_2C_2H_5$		4-ClC_6H_4	H	B	79.8 (R)

[a] Purification by column chromatography (C) or recrystallization (R). [b] Thermally sensitive.

was extruded to give elemental sulfur, which could be easily removed from products **5**. In the presumed course of the reaction initial deprotonation of the exocyclic methyl group leads to zwitterion **2**. Electrocyclic ring opening of **2** could provide the 3-alkylidenaminoprop-2-enethiocarbonyl compound **3**, and subsequent ring closure could give the ring-expanded 1,2-dihydro-1,3-thiazine **4**. Compound **4** is then converted to pyrrole **5** by a further deprotonation and extrusion of sulfur, as was shown by R. R. Schmidt in related work.[8] In connection with this proposed mechanism it should be mentioned that the net transformation proceeds much more readily for thiazolium salts with electron-donating substituents (R^2 = NR'_2, SCH_3) than for those with aryl groups (R^2 = aryl).

[*] Prof. Dr. J. Liebscher, Dipl.-Chem. A. Rolfs
Fachbereich Chemie der Humboldt-Universität
Hessische Strasse 1-2, D-O-1040 Berlin (FRG)
Telefax: Int. code + (30)2846-8343

Very high yields of 1*H*-pyrroles **5** were often obtained. In addition, the choice of substituents is not restricted, which allowed us to prepare a series of previously unknown pyrroles **5** (Table 2). The substituents R^1, however, must be sufficiently electron-withdrawing for the reaction to succeed. In the reactions of 2-benzyl-1,2-thiazolium salts and 2-alkyl-1,2-thiazolium salts **1** (R^1 = phenyl, or H and alkyl, respectively) either no reaction was observed or the corresponding 1,2-thiazoles were obtained in the presence of strong bases by dealkylation. Treatment of the 2-(4-nitrobenzyl)-1,2-thiazolium salt **1** (R^1 = 4-$NO_2C_6H_4$, R^2 = morpholino, R^3 = 4-ClC_6H_4, R^4 = H) with triethylamine gave the deprotonation product **6** (Table 2).

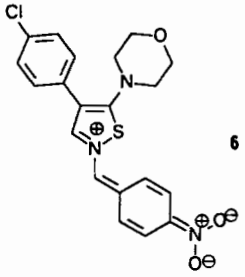

6

Since alkylations of 1,2-thiazoles are not particularly smooth, the 1,2-thiazolium salts **1** were obtained by oxidative cyclization[9] of enaminothiocarbonyl compounds **7**.[10] Products with various substituents R^2–R^4 other than those listed for the compounds in Table 1 can be prepared from the appropriate precursors **7**. The synthesis of starting material **1** and the further ring transformation to the pyrrole-2-carboxylic acid derivatives **5** can often be combined in a one-pot process (Method B).

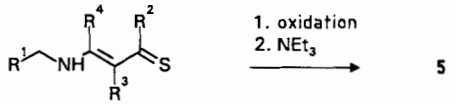

5

7, R^1 = CO_2alkyl, CN

The ring transformation with sulfur extrusion described here provides a general principle for the preparation of hetarylcarboxylates and -nitriles. Initial investigations with 2-alkoxycarbonylmethyl- and 2-cyanomethyl-1,2,4-thiadiazolium salts demonstrate that imidazole-2-carboxylic acid derivatives can be synthesized analogously.

Experimental Procedure

Method A: To a stirred solution of 10 mmol 1,2-thiazolium salt **1** in 50 mL methanol was added 12 mmol triethylamine in 5 mL methanol. The solution was briefly heated to reflux or was heated for 5 min at reflux (**1a** and **1b**). When the reaction mixture was allowed to cool and pyrrole **5** precipitated, it was filtered off and dissolved in dichloromethane, sulfur removed by filtration, and the crude product recrystallized. Alternatively, the product was purified by column chromatography on silica gel (eluent *n*-hexane/ethyl acetate).

Method B: 10 mmol Enaminothiocarbonyl compound **7** was oxidized by treatment with 10 mmol triethylamine and 10 mmol iodine (**6i**, **6j**) or bromine (**6d**, **6h**) or with 11 mmol H_2O_2 (**6k**) in 50 mL ethanol, chloroform, or methanol. After the oxidation was complete 12 mmol triethylamine in 5 mL methanol was added dropwise, and the reaction mixture was stirred and heated briefly at reflux. The workup was analogous to that in Method A.

Table 2. Selected physical data for compounds **5a**–**5k** [a].

5a: M.p. 125–126 °C (CH_3OH/H_2O); ^{1}H NMR ($CDCl_3$): δ = 3.72 (s, 3H; CH_3), 7.31–7.06 (11H; arom. H, -CH=), 9.23 (br, 1H; NH); ^{13}C NMR ($CDCl_3$): δ = 51.3 (CH_3), 119.59 (C2-pyrrole), 120.45 (C5-pyrrole), 126.04 (C-*para*), 126.77 (C4-pyrrole), 126.85 (C-*para*), 127.55, 128.12, 128.28, 130.70 (C-*ortho*, C-*meta*), 129.39 (C3-pyrrole), 134.12 (C-*ipso*), 134.39 (C-*ipso*), 161.56 (C=O); IR (KBr): $\tilde{\nu}$[cm^{-1}] = 1665 (C=O); MS: *m/z* 277 ($M^{\oplus}$; 54%), 245 ($M^{\oplus}$ – CH_3OH; 100).

5b: M.p. 179 °C (CH_3OH), ref. [11]: M.p. 182 °C ($CHCl_3$).

5c: M.p. 138 °C (Et_2O, *n*-hexane); ^{1}H NMR ($CDCl_3$): δ = 2.23 (s, 3H; CH_3), 2.95 (m, 4H; 2 × NCH_2), 3.64 (m, 4H; 2 × OCH_2), 3.86 (s, 3H; OCH_3), 6.64 (d, *J* = 3.4 Hz, 1H; -CH=), 7.19 (s, 4H; arom. H), 8.82 (br, 1H; NH); ^{13}C NMR ($CDCl_3$): δ = 20.65 (CH_3), 51.12 (OCH_3), 52.09 (NCH_2), 67.51 (OCH_2), 112.35 (C4-pyrrole), 119.63 (C2-pyrrole), 121.41 (C5-pyrrole), 125.19, 127.40, 129.65, 131.57, 135.01 (C-*ipso*), 137.36 (C-*ortho*), 142.49 (C3-pyrrole), 160.31 (C=O); IR (KBr): $\tilde{\nu}$[cm^{-1}] = 1710 (C=O); MS: *m/z* 300 ($M^{\oplus}$; 53%), 285 ($M^{\oplus}$ – CH_3; 21), 269 ($M^{\oplus}$ – CH_3O; 100).

5d: M.p. 183.5–185.5 °C (C_2H_5OH); ^{1}H NMR ($CDCl_3$): δ = 1.39 (t, *J* = 7.1 Hz, 3H; CH_3), 3.09 (m, 4H; 2 × NCH_2), 3.72 (m, 4H; 2 × OCH_2), 4.36 (q, *J* = 7.1 Hz, 2H; CH_2), 6.84 (d, *J* = 3.55 Hz, 1H; -CH=), 6.92–7.59 (4H; arom. H), 8.90 (br, 1H; NH); MS: *m/z* 318 ($M^{\oplus}$; 19%), 274 ($M^{\oplus}$ – C_2H_4O; 13), 213 (52), 29 ($C_2H_5^{\oplus}$; 100).

5e: M.p. 191–193 °C (CH_3OH); MS: *m/z* 320 ($M^{\oplus}$; 15%), 289 ($M^{\oplus}$ – OCH_3; 11), 261 ($M^{\oplus}$ – CO_2CH_3; 23), 15 ($CH_3^{\oplus}$; 100).

5f: M.p. 163–165 °C (CH_3OH); ^{13}C NMR ($CDCl_3$): δ = 12.88 (CH_3), 51.03 (OCH_3), 109.19 (C4-pyrrole), 116.30 (C2-pyrrole), 116.77 (C-*ortho*-aniline), 119.62 (C-*para*-aniline), 125.91 (C-*para*), 128.02 (C-*meta*), 128.20 (C-*meta*-aniline), 128.72 (C-*ortho*), 131.34 (C5-pyrrole), 134.07 (C3-pyrrole), 134.35 (C-*ipso*), 143.62 (C-*ipso*-aniline), 161.68 (C=O); IR (KBr): $\tilde{\nu}$[cm^{-1}] = 1675 (C=O).

5g: M.p. 176 °C (C_2H_5OH); ^{1}H NMR ($CDCl_3$): δ = 2.41 (s, 3H; SCH_3), 3.93 (s, 3H; OCH_3), 7.02 (d, *J* = 3.15 Hz, 1H; -CH=), 7.34 (d, *J* = 8.9 Hz, 2H; arom. H-*ortho*), 7.53 (d, 2H; arom. H-*meta*), 9.34 (br, 1H; NH).

5h: M.p. 189–190 °C ($CHCl_3$); IR (KBr): $\tilde{\nu}$[cm^{-1}] = 2210 (C≡N).

5i: M.p. 162–163 °C (C_2H_5OH); ^{1}H NMR ($CDCl_3$): δ = 1.15 (t, *J* = 7.1 Hz, 3H; CH_3), 2.52 (s, 3H; CH_3), 3.62 (s, 3H; OCH_3), 4.14 (q, *J* = 7.1 Hz, 2H; CH_2), 6.85–7.20 (5H; arom. H), 7.62 (s, 1H; NH), 9.98 (br, 1H; NH-pyrrole).

5j: M.p. 93–95 °C (CH_3OH); ^{1}H NMR ($CDCl_3$): δ = 3.77 (s, 3H; CH_3), 6.32 (t, *J* = 2.75 Hz, 1H; -CH=, C4-pyrrole), 6.93 (t, *J* = 2.75 Hz, 1H; -CH=, C5-pyrrole), 7.30 (d, *J* = 8.8 Hz, 2H; arom. H-*ortho*), 7.50 (d, 2H; arom. H-*meta*), 9.31 (br, 1H; NH); ^{13}C NMR ($CDCl_3$): δ = 51.29 (CH_3), 112.31 (C4-pyrrole), 117.80 (C2-pyrrole), 122.12 (C5-pyrrole), 127.84 (C-*meta*), 130.69 (C-*ortho*), 130.94 (C3-pyrrole), 132.77 (C-*ipso*), 133.57 (C-*para*), 161.37 (C=O); IR (KBr): $\tilde{\nu}$[cm^{-1}] = 1675 (C=O).

5k: M.p. 234–236 °C (acetone); ^{1}H NMR ($CDCl_3$): δ = 1.37 (t, *J* = 7.1 Hz, 3H; CH_3), 2.29 (s, 3H; NCH_3), 2.43 (m, 4H; 2 × NCH_2), 3.10 (m, 4H; 2 × NCH_2), 4.35 (q, *J* = 7.1 Hz, 2H; OCH_2), 6.82 (d, *J* = 3.6 Hz, 1H; -CH=), 7.30 (d, *J* = 8.8 Hz, 2H; arom. H-*ortho*), 7.47 (d, 2H; arom. H-*meta*), 8.78 (br, 1H; NH); MS: *m/z* 347 ($M^{\oplus}$; 5.4%), 318 ($M^{\oplus}$ – C_2H_5; 4.4), 43 ($C_2H_5N^{\oplus}$; 100).

6: M.p. 254–255 °C ($CHCl_3/CH_3OH$); ^{1}H NMR (300 MHz, $CDCl_3$): δ = 3.53–3.79 (m, 4H; CH_2-morph.), 3.93 (m, 2H; CH_2-morph.), 4.37 (m, 1H; CH-morph.), 4.69 (m, 1H; CH-morph.), 7.25 (s, 1H; -CH=), 7.35 (d, *J* = 8.6 Hz, 2H; arom. H-*ortho*-4-ClC_6H_4), 7.53 (d, 2H; arom. H-*meta*-4-ClC_6H_4), 7.93 (d, *J* = 8.75 Hz, 2H; arom. H-*ortho*-4-$NO_2C_6H_4$), 8.28 (d, 2H; arom. H-*meta*-4-$NO_2C_6H_4$), 8.37 (s, 1H; -CH=); MS: *m/z* 415 ($M^{\oplus}$; 11%), 330 ($M^{\oplus}$ – C_4H_7NO; 27), 86 ($C_4H_8NO^{\oplus}$; 100).

[a] ^{1}H NMR spectra measured at 80 MHz, ^{13}C NMR spectra at 300 MHz, MS at 70 eV; all compounds provided correct elemental analyses.

Received: December 21, 1992 [Z 5765 IE]
German version: *Angew. Chem.* **1993**, *105*, 797

[1] J. Liebscher, A. Knoll, A. Rolfs, A. Ushmajew, D. Lohmann, G. Faust, E. Morgenstern, P. Scharfenberg: "3-Aminopyrrole, Verfahren zu ihrer Herstellung und ihre Verwendung als Arzneimittel"; EP-OS 0431 371 (12. June 1991); *Chem. Abstr.* **1991**, *115*, 92063s.

[2] J. B. Doherty, M. N. Chang, C. P. Dorn: "Nonsteroidal compounds as antiinflammatory and analgesic agents"; EP-OS 72 013 (16 February 1983); *Chem. Abstr.* **1983**, *99*, 22311y.

[3] G. G. Massaroli: "Pyrrole-3-carboxylic acids with central analgesic activity"; DE 3415 321 (13 May 1985); *Chem. Abstr.* **1986**, *104*, 19507h.

[4] N. Ono, K. Sugi, T. Ogawa, *Chem. Express* **1991**, *11*, 6, 869–872.
[5] A. Gossauer, W. Hirsch, *Justus Liebigs Ann. Chem.* **1974**, 1496–1513.
[6] E. A. Meade, L. B. Townsend, *Bioorg. Med. Chem. Lett.* **1991**, 111–114.
[7] G. P. Bean in *Chemistry of Heterocyclic Compounds, Vol. 48, Part 1* (Ed.: R. A. Jones), Wiley, New York, **1990**, pp. 107–159, 241–252.
[8] R. R. Schmidt, *Angew. Chem.* **1975**, *87*, 603–638; *Angew. Chem. Int. Ed. Engl.* **1975**, *14*, 581.
[9] D. L. Pain, B. J. Peart, K. R. H. Wooldridge in *Comprehensive Heterocyclic Chemistry, Vol. 6* (Ed.: K. T. Potts), Pergamon, **1984**, p. 166.
[10] Compounds **7** were prepared by the reaction of glycine esters with 3-aminothioacrylic acid amides (J. Liebscher, B. Abegaz, *Synthesis* **1982**, *9*, 769–771), with 1,2-dithiolium salts (G. Duguay, C. Metayer, H. Quiniou, *Bull. Soc. Chim.* **1974**, 2853), with α-mercapto-α'-formylstilbene (M. Pulst, S. Steingrüber, E. Kleinpeter, *Z. Chem.* **1977**, *17*, 93–94), with (2-chlorovinyl)methylenammonium salts (J. Liebscher, H. Hartmann, *ibid.* **1974**, *14*, 189–190), with 3-hydroxy-thioacrylic acid amides (J. Goerdeler, A. Laqua, D. Lindner, *Chem. Ber.* **1974**, *107*, 3518–3532), and by the reaction of enamines with phenylisothiocyanates (J. Goerdeler, A. Laqua, C. Lindner *ibid.* **1974**, *107*, 3518–3532).
[11] K. W. Law, T.-F. Lai, M. P. Sammes, A. R. Katrizky, T. C. W. Mak, *J. Chem. Soc. Perkin Trans. 1* **1984**, 111–118.

Molecular Recognition of Hexaaqua Transition Metal(II) Ions**

By *Ulf Auerbach, Claudia Stockheim, Thomas Weyhermüller, Karl Wieghardt,** and *Bernhard Nuber*

Dedicated to Professor Heinrich Nöth on the occasion of his 65th Birthday

The significance of noncovalent interactions in the molecular recognition of molecules in solution for biological receptors and for supramolecular assemblies is undisputed. Sterically favorable hydrophobic (e.g. stacking of aromatic building blocks) and hydrophilic interactions (hydrogen bonds) are decisive for the stereognostic properties of molecular assemblies.[1] The term "coordination in the second coordination sphere" is defined by Stoddart et al.[2] as the noncovalent bonding of molecular units to the first coordination sphere of a transition metal complex. This concept is traced back to Werner.[3] The bonding of crown ethers is particularly well documented, for example in the second coordination sphere of ammine complexes through the formation of several N–H···O bonds.[4] In contrast, cyclodextrins[5a] and calix[4]arenes[5b] have so-called hydrophobic pockets, into which complexes with hydrophobic ligands can be inserted. We have now observed that octahedral neutral complexes with a *cis*-trisphenolato metal(III) structural unit can bind hexaaqua transition metal(II) ions in the second coordination sphere with a certain degree of selectivity.

Recently we reported that the ligand 1,4,7-tris(5-*tert*-butyl-2-hyroxybenzyl)-1,4,7-triazacyclononane (LH_3) forms exceptionally stable complexes LM^{III} **1**–**3** with Cr^{III}, Fe^{III}, and Co^{III} ions.[6] These compounds are very soluble in all organic solvents. The three coordinated, *cis*-positioned phenolato oxygen atoms in **1**–**3** still have basic properties, as shown by their reaction with aqueous $HClO_4$ in CH_3OH. In this case twofold O–H···O bridged dinuclear complexes of the type $[(LH)_2M^{III}_2](ClO_4)_2 \cdot 2H_2O$ are formed.[6] This residual basicity of the O donor atoms can also be used for the formation of complexes.

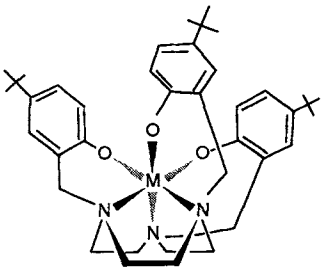

1: M = Cr
2: M = Fe
3: M = Co

The reaction of **3** in acetone with the hexaaqua metal(II) cations $[M^{II}(OH_2)_6](ClO_4)_2$ in the ratio 2:1 leads to the crystalline, trinuclear complexes **4**, **5a**, and **6**–**8**. If

$$2\,\mathbf{3} + [M^{II}(OH_2)_6](ClO_4)_2 \xrightarrow{(CH_3)_2CO} \underset{\mathbf{4-8}}{[(LCo^{III})_2M^{II}](ClO_4 \cdot 2(CH_3)_2CO}$$

$$2\,\mathbf{3} + [Fe^{III}(OH_2)_6](ClO_4)_3 \longrightarrow \underset{\mathbf{5b}}{[(LCo^{III})_2Fe^{III}](ClO_4)_2 \cdot 2(CH_3)_2CO}$$

Scheme 1. **4**: M = Mn; **5a**: M = Fe; **6**: M = Co; **7**: M = Ni; **8**: M = Zn.

$[Fe^{III}(OH_2)_6](ClO_4)_3$ is used, red crystals of **5b** are obtained (Scheme 1). Figure 1 shows the structure of the dication in crystals of **5a**.[7] They are doubly face-sharing, trinuclear

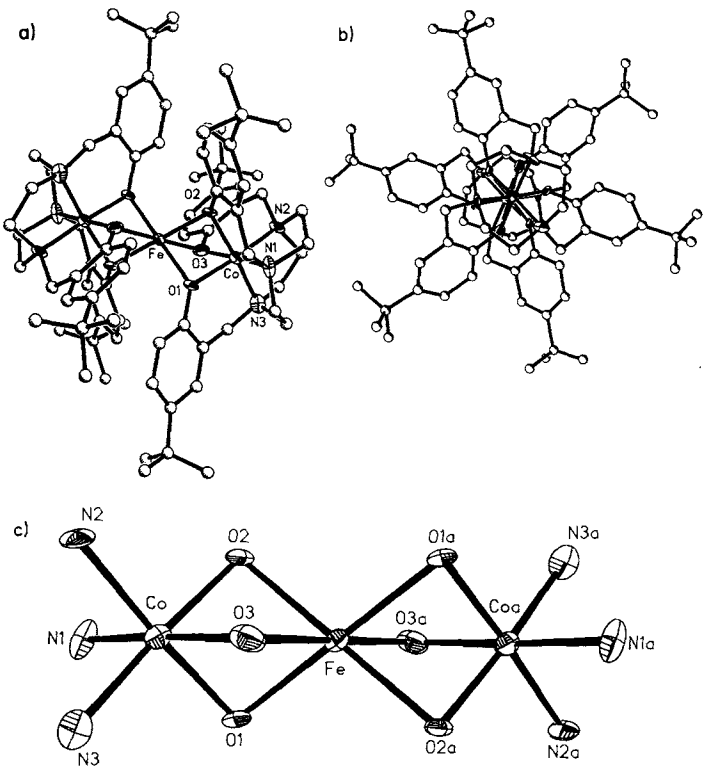

Fig. 1. Structure of the cation in **5a**: a) side view; b) view in the direction of the CoFeCo axis; c) representation of the first coordination sphere of the cation. Selected bond lengths [Å] in **5a** and in parentheses for **5b**: Co-O 1.93(1), 1.91(1), 1.94(1), (1.95(2), 1.92(1), 1.93(1)); Co-N 1.96(2), 1.97(2), 1.97(2), (1.95(2), 1.90(2), 1.95(2)); Fe-O 2.07(1), 2.06(1), 2.13(1), (2.03(2), 2.02(1), 2.02(2)).

[*] Prof. Dr. K. Wieghardt, Dr. U. Auerbach, Dipl.-Chem. C. Stockheim, Dipl.-Chem. T. Weyhermüller
Lehrstuhl für Anorganische Chemie I der Universität
Postfach 10 21 48, D-W-4630 Bochum (FRG)
Telefax: Int. code +(234)700-2001
Dr. B. Nuber
Anorganisch-chemisches Institut
Im Neuenheimer Feld 270, D-W-6900 Heidelberg (FRG)

[**] This work was supported by the Fonds der Chemischen Industrie.

cations, in which the six oxygen atoms of the phenolate groups of the two LCo^{III} units are bound to the Fe^{II} ion. Thus, complex **3** is a tridentate ligand, which is coordinated twice in the *first* coordination sphere of the central Fe^{II} ion. The structure of the trication in **5b** is analogous,[7] but with a central Fe^{III} ion.

Interestingly, **1** and **2** do not react under the same reaction conditions to give the above-mentioned complex type. The basicity of the O atoms in **1** and **2** is reduced due to the stronger Lewis acidic character of $Cr^{III}(t_{2g}^3)$ and the high-spin Fe^{III} ion ($t_{2g}^3e_g^2$) in comparison to the low-spin Co^{III} center (t_{2g}^6) in **3**,[6] and is not sufficient to force the substitution of the aqua ligands of the $[M^{II}(OH_2)_6]^{n+}$ ions. If excess $Na[BPh_4]$ is added to a solution of **1** or **2** and $[M^{II}(OH_2)_6](ClO_4)_2$ (2:1) in acetone, crystals of **9**–**16** precipitate (Scheme 2).

$$2\,\mathbf{1}\text{ or }2\,\mathbf{2} + [M^{II}(OH_2)_6](ClO_4)_2 \xrightarrow[(CH_3)_2CO]{Na[BPh_4]} [(LM^{III})_2\{M^{II}(OH_2)_6\}][BPh_4]_2 \cdot 4(CH_3)_2CO$$

9–**16**

Scheme 2. **9**: M^{II}/M^{III} = Mn/Cr; **10**: M^{II}/M^{III} = Co/Cr; **11**: M^{II}/M^{III} = Ni/Cr; **12**: M^{II}/M^{III} = Zn/Cr; **13**: M^{II}/M^{III} = Mn/Fe; **14**: M^{II}/M^{III} = Co/Fe; **15**: M^{II}/M^{III} = Ni/Fe; **16**: M^{II}/M^{III} = Zn/Fe.

Figure 2 shows the structure of the cation in crystals of **16**.[7] The central hexaaqua metal(II) ion is bound through six O–H ··· O contacts to two LFe^{III} neutral molecules; each coordinated H_2O molecule thus forms a hydrogen bond to a phenolate oxygen atom. Thus, chelate complex formation in the *second* coordination sphere of the $[M^{II}(OH_2)_6]^{2+}$ ion is achieved. In addition, the four H_2O molecules in equatorial positions are each bound to one acetone solvent molecule through a weak O–H ··· O contact. The structures of **13** and **9** are analogous to that of **16**.[7] The average Cr–O, Fe–O, Mn–O, and Zn–O distances in **9**, **13**, and **16** correspond to those in the neutral complexes **1** and **2**[6] as well as to those in the salts of the hexaaqua metal(II) cations $[Mn(OH_2)_6]^{2+}$ and $[Zn(OH_2)_6]^{2+}$.[8]

Interestingly, the reaction of $[Cu(OH_2)_6](ClO_4)_2$ with **1** or **2** does *not* lead to the crystallization of products of the type **9**–**16**. The reason for this may be the stretched octahedral structure of $[Cu(OH_2)_6]^{2+}$ (Jahn–Teller distortion), which prevents the double formation of three equivalent O–H ··· O contacts with **1** or **2**. This means that the complex formation in the second coordination sphere leads to a certain selectivity, which is influenced by differing stereochemical details of the $[M^{II}(OH_2)_6]^{2+}$ ions.

We have tested this selectivity qualitatively as follows: the products, which crystallized from reaction solutions and contained **1**, and an equimolar mixture of two different $[M^{II}(OH_2)_6]^{2+}$ ions were analyzed with regard to their divalent metal ion content. The results are summarized in Table 1. From these results it follows that the $[Zn(OH_2)_6]^{2+}$ ion is bound with the greater selectivity (4:1) when in competition with the $[Mn(OH_2)_6]^{2+}$ ion, whereas the $[Co(OH_2)_6]^{2+}$ ion shows hardly any selectivity preference over the $[Ni(OH_2)_6]^{2+}$ ion (1:1). Consequently, the formation of **10** and **11** is favored in Co/Mn and Ni/Mn solutions, respectively. Since the results of the selection experiments in Table 1 are consistent with each other, the possibility that different solubility products of the salts feign this selectivity is unlikely (it is assumed to be the same for all complexes). The crystalline products do not consist of a mixture of two

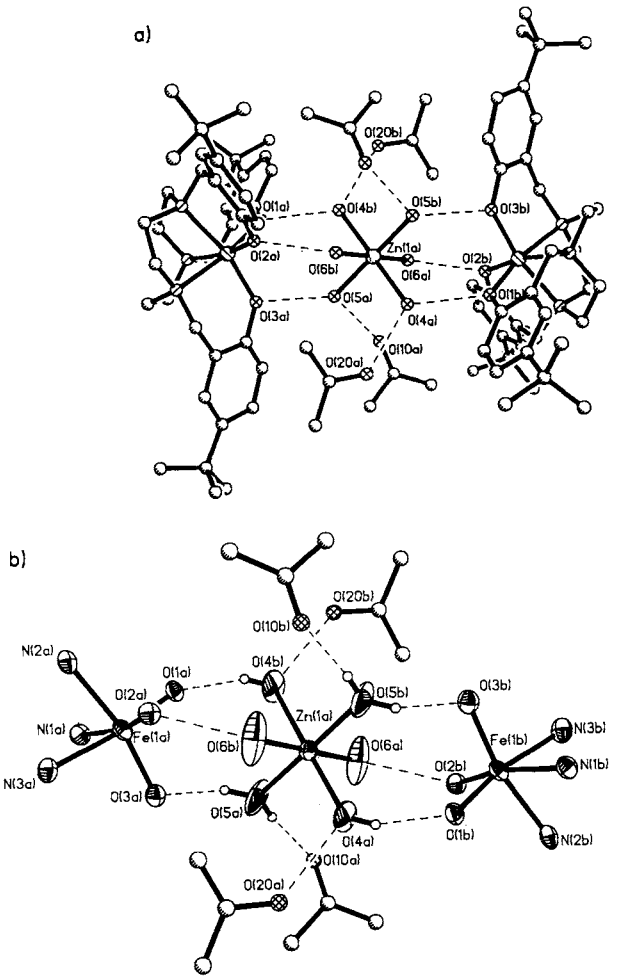

Fig. 2. Structure of $[(LFe)_2\{Zn(OH_2)_6\}]^{2+}$ in **16**: a) overall view of the cation; b) first coordination sphere. The structures of **9** and **11** are analogous. Selected bond lengths [Å] in **16** and in parentheses for **9** and **13**: Fe-O 1.938(7), 1.940(7), 1.921(7), (Cr-O 1.95(1), 1.96(1), 1.95(1); Fe-O 1.930(8), 1.940(8), 1.939(9)); Fe-N 2.212(9), 2.206(9), 2.221(9), (Cr-N 2.10(2), 2.10(1), 2.11(2); Fe-N 2.22(1), 2.19(1), 2.21(1)); Zn-O 2.09(1), 2.081(9), 2.04(1), (Mn-O 2.16(1), 2.19(1), 2.20(1); Mn-O 2.172(9), 2.17(1), 2.196(9)); O1 ··· O4 2.72(1), (2.74; 2.69(1)); O2 ··· O6 2.66(1), (2.68; 2.73(1)); O3 ··· O5 2.62(1), (2.72; 2.68(1)); O5 ··· O(20) 2.81(2), (not found; 2.99(2)); O5 ··· O(10) 2.68(1), (not found; 3.00(2)).

kinds of crystal, but of uniform mixed crystals (homeomorphy).

Thus complexes **9** and **12** are the extremes regarding the stability of the compounds **9**–**12** in solution; **9** is more un-

Table 1. Selectivity experiments [a]. The composition of the solutions ($[M^1(OH_2)_6]^{2+}$:$[M^2(OH_2)_6]^{2+}$ (1:1)) is compared to that of the crystalline products [b].

Solution		Products	
$[M^1(OH_2)_6]$	$[M^2(OH_2)_6]$	M^1 [c]	M^2 [c]
$[Zn(OH_2)_6]^{2+}$	$[Ni(OH_2)_6]^{2+}$	48	52
$[Zn(OH_2)_6]^{2+}$	$[Mn(OH_2)_6]^{2+}$	87	13
$[Ni(OH_2)_6]^{2+}$	$[Mn(OH_2)_6]^{2+}$	83	17
$[Co(OH_2)_6]^{2+}$	$[Mn(OH_2)_6]^{2+}$	80	20
$[Co(OH_2)_6]^{2+}$	$[Mn(OH_2)_6]^{2+}$	80	20
$[Co(OH_2)_6]^{2+}$	$[Ni(OH_2)_6]^{2+}$	47	53

[a] Reaction solution: 1.0 mmol **1** as well as 0.25 mmol each of $[M^1(OH_2)_6](ClO_4)_2$ and $[M^2(OH_2)_6](ClO_4)_2$ in 50 mL acetone, 0.20 g $Na[BPh_4]$. [b] The metal content M^1, M^2 was determined by atomic absorption spectroscopy. [c] The sum of the components [%] of both divalent cations in the crystalline products is 100%.

stable than **12**. Structural reasons for this tendency can be found from the X-ray structure analyses of **9**, **13**, and **16**. In these structures the O–H ··· O distances between the phenolate oxygen atoms and the aqua ligands are 2.72 (**9**), 2.70 (**13**), and 2.68 Å (**16**). The O ··· O distances within one triangular face of the octahedron, in whose corners are situated the phenolate oxygen atoms, are on average in **9**: 2.82, in **13**: 2.89, and in **16**: 2.89 Å, whereas this distance for the surface of the $[M^{II}(OH_2)_6]^{2+}$ octrahedron, which is bound through O–H ··· O contacts to **1** or **2** is in **9**: 3.07, in **13**: 3.07, and in **16**: 2.88 Å. From this it can be concluded that the triangular faces involving the oxygen atoms which lie opposite each other in **16** are better matched with respect to their size than those in **9** and **13**, and thus **16** is more stable in solution. The effects are small and different bond strengths of the O–H ··· O interactions, a result of the differences in basicity of the phenolate and water oxygen atoms, may be a further factor.

We are at present investigating the possibility of binding complexes of the type **1** and **2** with different O ··· O distances and residual basicity of the O atoms to a polymer, in order to achieve the separation and selective enrichment of $[M^{II}(OH_2)_6]^{2+}$ ions in aqueous solutions in very small concentrations.

Experimental Procedure

The synthesis of complexes **1**, **2**, and **3** was recently described [6]. Synthesis of the complexes **4**, **5a**, **6**–**8** and **5b**: To a solution of **3** (1.0 mmol) in acetone (50 mL) was added the hexaaquametal(II) perchlorate $[M(OH_2)_6](ClO_4)_2$ (0.60 mmol) (M = Mn, Fe, Co, Ni, Zn) under exclusion of air at 20 °C. After the mixture had been stirred for 30 min and subsequently filtered, $NaClO_4 \cdot H_2O$ (0.10 g) was added and half of the solvent was removed on a rotary evaporator. Red crystals of the desired complex grew within 12 h (≈75% yield). **5b** was prepared analogously with $[Fe(OH_2)_6](ClO_4)_3$ (0.60 mmol). Temperature-independent magnetic moments (80–295 K; Faraday method): **4**: 5.9, **5**: 5.5, **6**: 4.8, **7**: 3.1 μ_B; **8**: diamagnetic; **5a**: 5.9 μ_B.

Synthesis of the complexes **9**–**16**: To a solution of **1** or **2** (1.0 mmol) in acetone (50 mL) was added $[M(OH_2)_6](ClO_4)_2$ (0.60 mmol) (each of M = Mn, Co, Ni, Zn) at 20 °C and stirred. After the mixtures had been stirred for 30 min, $Na[BPh_4]$ (0.20 g) and ethanol (15 mL) were added to the clear solutions. From these solutions crystals precipitated in an open vessel (≈70% yield) after approximately 3–5 d. From temperature-dependent (4.2–295 K) magnetic susceptibility measurements it followed that the spins in **9**–**11**, and **13**–**15** were weakly coupled in an intramolecular antiferromagnetic manner. Temperature-independent magnetic moments of 3.8 μ_B/Cr and 5.9 μ_B/Fe were found for **12** and **16**. All complexes gave satisfactory elementary analyses (C, H, N, metal).

Received: December 7, 1992 [Z57341E]
German version: *Angew. Chem.* **1993**, *105*, 735

[1] The term "stereognostic" was coined recently: T. S. Francyk, K. R. Czerwinski, K. N. Raymond, *J. Am. Chem. Soc.* **1992**, *114*, 8138.

[2] D. R. Alston, P. R. Ashton, T. H. Lilley, J. F. Stoddart, R. Zarzycki, A. M. Z. Slawin, D. J. Williams, *Carbohydr. Res.* **1989**, *192*, 259.

[3] A. Werner, *Z. Anorg. Chem.* **1983**, *3*, 267; *Ber. Dtsch. Chem. Ges.* **1912**, *45*, 121.

[4] a) J. F. Stoddart, R. Zarzycki in *Cation Bindung by Macrocycles* (Eds.: Y. Inoue, G. W. Gokel), Dekker, New York, **1990**, p. 631. b) D. R. Alston, A. M. Z. Slawin, J. F. Stoddart, D. J. Williams, R. Zarzycki, *Angew. Chem.* **1987**, *99*, 697; *Angew. Chem. Int. Ed. Engl.* **1987**, *26*, 693.

[5] a) A. Harada, Y. Hu, S. Yamamoto, S. Takahashi, *J. Chem. Soc. Dalton Trans.* **1988**, 729; b) J. L. Atwood, G. W. Orr, F. Hamada, R. L. Vincent, S. G. Bott, K. D. Robinson, *J. Am. Chem. Soc.* **1991**, *113*, 2760.

[6] U. Auerbach, T. Weyhermüller, K. Wieghardt, B. Nuber, E. Bill, C. Butzlaff, A. X. Trautwein, *Inorg. Chem.*, **1993**, 32, 508.

[7] Crystal structure analyses: The structures of **5a**, **5b**, **9**, **13**, and **16** were determined by X-ray crystallography with $Mo_{K\alpha}$ radiation. The intensities of **5a** and **16** were measured at 163 K, those of the other compounds at 295 K. The diffraction behavior of all crystals was limited; above $2\theta = 45°$ only a few reflections were observed ($I \geq 2.5\sigma(I)$). In all structures problems arose due to the disorder of the butyl groups, which could not be resolved satisfactorily. In **5b**, **9**, and **13** the positions of several acetone solvent molecules could not be determined precisely, because they left the crystal assembly during the measurement. These problems, which are impounded still further by slightly disordered ClO_4^- and BPh_4^- anions, led to relatively poor *R* values. In **16** it was possible to localize several of the positions of the H atoms in the O–H ··· O bridges. Crystal data **5a**: $a = 21.744(4)$, $b = 16.751(3)$, $c = 26.586(5)$ Å, $\beta = 91.13(3)°$; space group $C2/c$; $Z = 4$; $\mu(Mo_{K\alpha}) = 0.60\ mm^{-1}$; 7806 possible reflections, of which 3130 independent, observed ($F \geq 3.0\sigma(F)$); 434 parameters; $R = 0.14$; $R_w = 0.14$. **5b**: $a = 27.03(1)$, $c = 33.81(4)$ Å; space group $R\bar{3}$ (no. 148); $Z = 9$; $\mu(Mo_{K\alpha}) = 0.64\ mm^{-1}$; 6989 possible reflections, of which 2604 independent, observed; 237 parameters; $R = 0.11$; $R_w = 0.10$. **9**: $a = 14.221(3)$, $b = 27.080(7)$, $c = 17.671(4)$ Å, $\beta = 98.33(2)°$; space group $P2_1/n$ (no. 14); $Z = 2$; $\mu(Mo_{K\alpha}) = 0.30\ mm^{-1}$; 14079 possible reflections, of which 5824 independent, observed; 644 parameters; $R = 0.15$, $R_w = 0.13$; **13**: $a = 14.256(4)$, $b = 27.066(7)$, $c = 17.706(5)$ Å, $\beta = 97.87(2)°$; space group $P2_1/n$ (no. 14); $Z = 2$; $\mu(Mo_{K\alpha}) = 0.35\ mm^{-1}$; 11533 possible reflections, of which 6290 independent, observed; 658 parameters; $R = 0.099$; $R_w = 0.096$. **16**: $a = 13.972(3)$, $b = 27.128(5)$, $c = 17.757(4)$ Å, $\beta = 96.76(3)°$; space group $P2_1/n$ (no. 14); $Z = 2$; $\mu(Mo_{K\alpha}) = 0.46\ mm^{-1}$; 11709 possible reflections, of which 5545 independent, observed; ($I \geq 2.0\sigma(I)$); 707 parameters; $R = 0.11$, $R_w = 0.11$. Further details of the crystal structure investigations may be obtained from the Fachinformationszentrum Karlsruhe, Gesellschaft für wissenschaftlich-technische Information mbH, D-W-7514 Eggenstein-Leopoldshafen 2 (FRG) on quoting the depository number CSD-56999, the names of the authors, and the journal citation.

[8] The Mn–O distance in $[Mn(OH_2)_6][Th(NO_3)_6] \cdot 2H_2O$ is 2.18 Å: H. Montgomery, R. V. Chastain, E. C. Lingafelter, *Acta Crystallogr.* **1966**, *20*, 731. The Zn–O distance in $K_2[Zn(OH_2)_6](SO_4)_2$ is 2.08 Å: J. Whitnall, C. H. L. Kennard, J. Nimmo *Cryst. Struct. Commun.* **1975**, *4*, 717.

The P4-Phosphazene Base as Part of a New Metal-Free Initiator System for the Anionic Polymerization of Methyl Methacrylate**

By *Thomas Pietzonka* and *Dieter Seebach**

Anionic polymerization of activated olefins, for which methacrylate is a prototype, leads to products having high molecular weights ($M_n > 10000\ g\,mol^{-1}$) and narrow polydispersities ($M_w/M_n < 1.3$) if either metal-free systems[1,2] or metals with a very bulky ligand sphere are used[3–7] and if the chain-initiating step[8] is irreversible. As counterions large ("soft") cations such as Bu_4N^+ or $(Me_2N)_3S^+$ are preferred. In the protonated form of the P4-phosphazene base **1** developed by Schwesinger and Schlemper[9] the positive charge is delocalized over 17 (!) positions, causing the base to be unusually reactive.[10] As **1** forms an extremely soft cation, we have now checked its ability to catalyze anionic polymerizations.

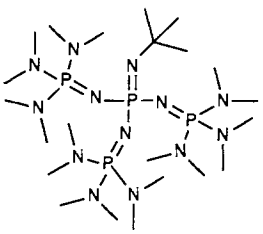

1

We found that methyl methacrylate (MMA, **2**) may be polymerized in high yields in different solvents at various temperatures with the P4 base **1**. The initiating system was prepared by treating small amounts of ethyl acetate with P4

[*] Prof. Dr. D. Seebach, Dr. T. Pietzonka
Laboratorium für Organische Chemie
der Eidgenössischen Technischen Hochschule
ETH-Zentrum
Universitätstrasse 16, CH-8092 Zürich (Switzerland)

[**] Part of the Ph.D. thesis of Thomas Pietzonka, Dissertation number 10000, ETH Zürich, **1992**.

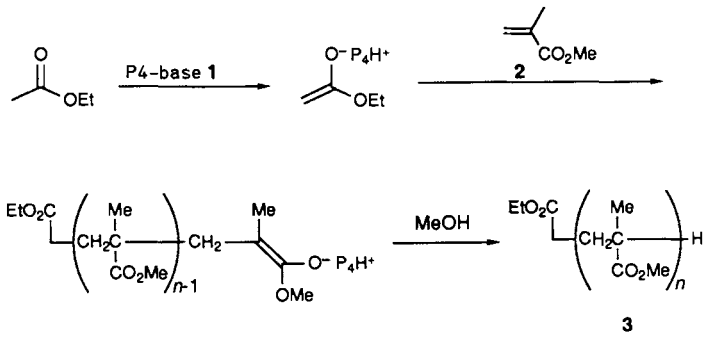

base. Monomer **2** was continuously added and the reaction quenched after 30 minutes by addition of methanol.

All of the prepared poly(methyl methacrylate)s show molecular weights of $M_n > 10000\ g\,mol^{-1}$,[11] whereas their polydispersities D (M_w/M_n)[11] strongly depend on the reaction conditions; polymerizations carried out in hexane gave broadly distributed mixtures of polymers, whereas in the more polar THF smaller D-values were observed, down to 1.11 (Table 1).

Table 1. Average molecular weights and polydispersities D of poly(methyl methacrylate)s obtained with P4 base/ethyl acetate (EA) as initiator [11]. RT = room temperature.

Expt	Conditions	Molar ratio EA:P4:MMA	$M_n$theor [kg mol^{-1}]	M_n [kg mol^{-1}]	M_w [kg mol^{-1}]	D
1	toluene/RT	1:1:76	7.5	10.5	18.4	1.80
2	hexane/RT	1:1:85	8.4	17.2	35.8	1.82
3	THF/−78 °C	1:1:55	5.5	44.3	101.5	2.29
4	THF/RT	1:1.1:126	11.0	12.2	14.9	1.22
5	THF/60 °C	1:1.1:126	11.0	15.2	16.9	1.11
6	THF/60 °C	1:1.1:378	35.0	22.2	26.3	1.18
7	THF/60 °C	0:1.0:161	16.1	33.0	68.0	2.05

In experiments 1–3 (Table 1) the molecular weights achieved were clearly higher than the ones calculated from the initiator:monomer ratio. Obviously not all of the P4 molecules **1** initiated a chain. For polymerizations in which THF was used as solvent both the $M_n$theor: M_n ratio and the dispersity D strongly depended on the reaction temperature. At −78 °C broadly distributed polymers with too high molecular weights were isolated. At elevated temperatures (experiments 4–6) the determined molecular weights correspond well to those calculated, showing that under these reaction conditions the P4 base is able to initiate an anionic polymerization efficiently. The most narrowly distributed polymers were obtained in THF solution at 60 °C (experiments 5 and 6, Table 1). In contrast to anionic polymerizations with metal-bearing initiators, which lead predominantly to isotactic diads,[13] all poly(methyl methacrylate)s formed in THF contain approximately 80% syndiotactic diads.[12] Preliminary experiments have shown that other monomers, for instance ethyl acrylate, can also be polymerized by using the P4/ethyl acetate initiator system. The polymerization even takes place without addition of ethyl acetate, but the polydispersity of the polymer increases (experiment 7, Table 1).

Further optimizations of this new anionic polymerization with emphasis on the influence of monomer and solvent purity are in progress. Special attention is paid to the question if the polymer prepared with the P4 base is "living", in other words, whether block copolymers with different monomers can be prepared.

Experimental Procedure

Polymerization of MMA with the P4 base: Into an oven-dried 100 mL, two-neck, round-bottomed flask, fitted with a serum cap, were introduced 50 mL of THF and 45 μL (0.49 mmol) of ethyl acetate under argon. At reaction temperature a solution of 325 mg (0.34 mmol) P4 base **1** in 0.2 mL of THF was added, followed by dropwise addition of 20 mL (190 mmol) of methyl methacrylate (**2**) within 20 minutes. The reaction mixture was stirred for 0.5 h, quenched by addition of 1 mL of methanol, and concentrated to dryness. The residue was dissolved in a minimum of THF and precipitated by addition of the resulting solution to 200 mL of MeOH. The solvent was decanted and the residue dried under high vacuum at 50 °C until its weight remained constant to give 16.4 g (87%) PMMA with $M_n = 22200\ g\,mol^{-1}$, $D = 1.18$ [11] as a colorless, brittle powder. ^{1}H NMR (200 MHz, C_6D_5Cl, 80 °C): $\delta = 1.3$ (br. s, CH_3 (syndiotactic triad)), 1.4 (br. s, CH_3 (heterotactic triad)), 1.5 (br. s, CH_3 (isotactic triad)), 2.0–2.5 (br. m, CH_2), 3.7 (br. s, OCH_3) (a commercial sample was used as a reference, see also ref. [12]).

Received: December 18, 1992 [Z 5756 IE]
German version: *Angew. Chem.* **1993**, *105*, 741

[1] One of the classical chain-terminating reactions is the so-called back-biting, in the case of MMA an intramolecular Claisen condensation, which occurs in the presence of metal cations such as Li^+ or Na^+, and which leads to low molecular weight polymers: M. Morton: *Anionic Polymerisation, Principles and Practice*, Academic Press, New York **1983**.
[2] M. T. Reetz, R. Ostarek, *J. Chem. Soc. Chem. Commun.* **1988**, 213.
[3] O. W. Webster, W. R. Hertler, D. Y. Sogah, W. B. Farnham, T. V. RajanBabu, *J. Am. Chem. Soc.* **1983**, *105*, 5706; O. W. Webster, W. R. Hertler, D. Y. Sogah, G. M. Cohen, *Macromolecules* **1987**, *20*, 1473.
[4] T. Adachi, H. Sugimoto, T. Aida, S. Inoue, *Macromolecules* **1992**, *25*, 2280.
[5] D. G. H. Ballard, R. J. Bowles, D. M. Haddleton, S. N. Richards, R. Sellens, D. L. Twose, *Macromolecules* **1992**, *25*, 5907.
[6] S. K. Varshney, R. Jérôme, P. Bayard, C. Jacobs, R. Fayt, P. Teyssié, *Macromolecules* **1992**, *25*, 4457.
[7] H. Yasuda, M. Furo, H. Yamamoto, *Macromolecules* **1992**, *25*, 5115.
[8] M. T. Reetz, T. Knauf, U. Minet, C. Bingel, *Angew. Chem.* **1988**, *100*, 1422; *Angew. Chem. Int. Ed. Engl.* **1988**, *27*, 1373.
[9] R. Schwesinger, H. Schlemper, *Angew. Chem.* **1987**, *99*, 1212; *Angew. Chem. Int. Ed. Engl.* **1987**, *26*, 1167. R. Schwesinger, *Nachr. Chem. Tech. Lab.* **1990**, *38*, 1214.
[10] T. Pietzonka, D. Seebach, *Chem. Ber.* **1991**, *124*, 1837; *Angew. Chem.* **1992**, *125*, 1543; *Angew. Chem. Int. Ed. Engl.* **1992**, *31*, 1481.
[11] Determined by gel permeation chromatography (GPC) and comparison with an polystyrene standard and low-angle laser light scattering (LALLS) experiments. We thank O. Keiser for the help with the GPC analysis of the polymers and M. Colussi for the LALLS measurements.
[12] Determined by analysis of the NMR spectra: F. A. Bovey, *High Resolution NMR of Macromolecules*, Academic Press, New York, **1972**. H. G. Elias, *Makromoleküle*, 5th ed., Hüthig & Wepf, Basel, **1990**.
[13] H. Yuki, K. Hatada, *Adv. Polym. Sci.* **1979**, *31*, 1; M. T. Reetz, *Angew. Chem.* **1988**, *100*, 1028; *Angew. Chem. Int. Ed. Engl.* **1988**, *27*, 994.

Reduction of a Tetraaryldigallane to Afford a Radical Anion with Ga–Ga Multiple Bonding Character**

By *Xiaoming He, Ruth A. Bartlett, Marilyn M. Olmstead, Karin Ruhlandt-Senge, Bradley E. Sturgeon,* and *Philip P. Power**

Organometallic complexes of heavier main group 3 elements of types **1a**,[1] **1b**,[2] and **1c**[3] have recently been prepared in good yield. These interesting compounds feature

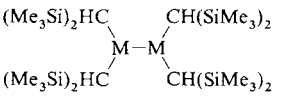

1a, M = Al
1b, M = Ga
1c, M = In

[*] Prof. P. P. Power, X. He, R. A. Bartlett, Dr. M. M. Olmstead, Dr. K. Ruhlandt-Senge, B. E. Sturgeon
Department of Chemistry
University of California
Davis, CA 95616 (USA)
Telefax: Int. code + (916)752-8995

[**] This work was supported by the National Science Foundation and the Petroleum Research Fund.

metal–metal single bonds between the three-coordinate metal centers. Parallel studies have shown that closely related boron compounds can be synthesized by using bulky alkyl or aryl substituents.[4–6] In addition, the reduction of tetraaryldiboranes afforded diborane dianions of types **2**[7]

$[Mes_2BBPhMes]^{2-}$ **2** (Mes = 2,4,6-$Me_3C_6H_2$)

$[Me_2NPhBBPhNMe_2]^{2-}$ **3**

and **3**,[8] which had B–B double bonds that are analogous to C–C double bonds in substituted ethenes. In view of the facility with which the reductions to **2** or **3** occurred, it was decided to attempt to extend this chemistry to aryl derivatives of the heavier members of the group. In this paper some preliminary results concerning the reduction of a tetraaryldigallane are now described.

Tetraaryldigallane **4** was synthesized by the reaction of four equivalents of TripMgBr with $Ga_2Cl_4 \cdot 2$ dioxane. Its structure features a Ga–Ga bond length of 2.515(3) Å and a

$Trip_2GaGaTrip_2$ **4**
Trip = 2,4,6-$iPr_3C_6H_3$

Ga–C distance of 2.008(7) Å. Moreover, there is a torsion angle of 43.8° between the two GaC_2 planes. The Ga–Ga bond length in **4** is similar to that in **1b** (2.541(1) Å[2]); however, the latter compound has an almost planar central Ga_2C_4 unit.

The treatment of a solution of **4** in diethyl ether with an excess of lithium powder affords a dark ochre solution. When [12]crown-4 is added crystals of salt **5** can be obtained. The X-ray crystal structure of **5** (Fig. 1)[9] shows that the

$[Li([12]crown\text{-}4)_2]^+ \left[\begin{array}{c} Trip \quad\quad Trip \\ \diagdown \quad\quad \diagup \\ Ga{=}Ga \\ \diagup \quad\quad \diagdown \\ Trip \quad\quad Trip \end{array} \right]^{\bullet -}$ **5**

neutral precursor **4** has been singly reduced to give the radical anion $[Trip_2Ga{=}GaTrip_2]^{\bullet -}$. This reduction produces dramatic structural changes. The Ga–Ga distance is shortened to 2.343(2) Å, and the torsion angle between the GaC_2 planes is decreased to 15.5°. There is also a slight lengthening in the Ga–C bonds to approximately 2.038(2) Å. The decrease of the Ga–Ga distance by 0.17 Å and the closure of the torsion angle are consistent with the formation of a one-electron π bond between the galliums. In this respect, **5** is analogous to the corresponding boron radical anions $[B_2R_4]^{\bullet -}$ which were generated in solution.[10] The Ga–Ga distance in **5** is the lowest reported to date; the shortest Ga–Ga distance previously known, 2.388(5) Å, was observed in $Ga_2[I_3Ga\text{-}GaI_3]$.[12] The difference in the Ga–Ga distances in **4** and **5** represents a shortening of almost 7%. This value is comparable to the 8–9% difference between single and double bond lengths in the heavier main group elements.

The presence of an unpaired electron in the $[Trip_2Ga\text{-}GaTrip_2]^{\bullet -}$ radical anion is manifested in broad, paramagnetically shifted resonances in the ^1H NMR spectrum. In addition, THF solutions of **5** at room temperature show a strong EPR signal[12] (Fig. 2). This signal is complex since gallium has two major isotopes (^{69}Ga and ^{71}Ga) both with $I = 3/2$, which exist in an approximately 60:40 ratio. A preliminary analysis of the spectrum reveals couplings of approximately 354. and 439. mT between the unpaired electron and the ^{69}Ga and ^{71}Ga nuclei. These values are consistent with the location of the unpaired electron in a π orbital. Although the crystals of **5** appear black, they are dark brown-red in transmitted light. A UV/VIS absorption spectrum displays bands at 360 and 900 nm that are attributable to the radical anion in **5**. Work on **5** and related compounds is continuing.[13]

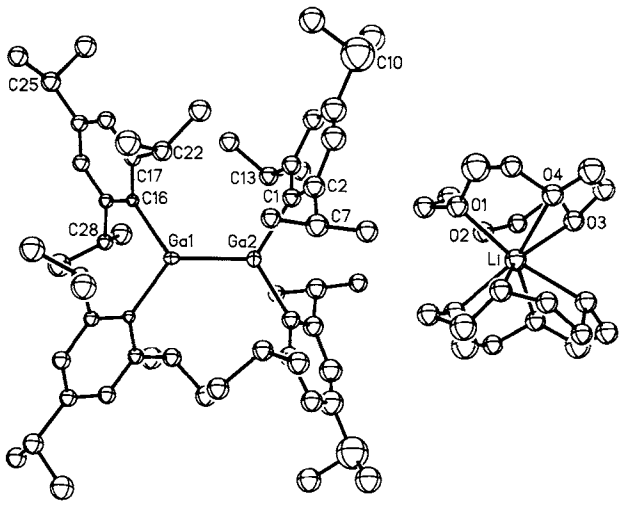

Fig. 1. Crystal structure of **5**. H atoms are omitted for clarity. Bond lengths [Å] and angles [°]: Ga1-Ga2 2.343(2), Ga1-C16 2.036(8), Ga2-C1 2.039(10), Li-O(ave.) 2.36(5); C1-Ga2-C1a 117.4(6), Ga1-Ga2-C1 121.3(3), C16-Ga1-C16a 111.5(5), Ga2-Ga1-C16 124.2(2).

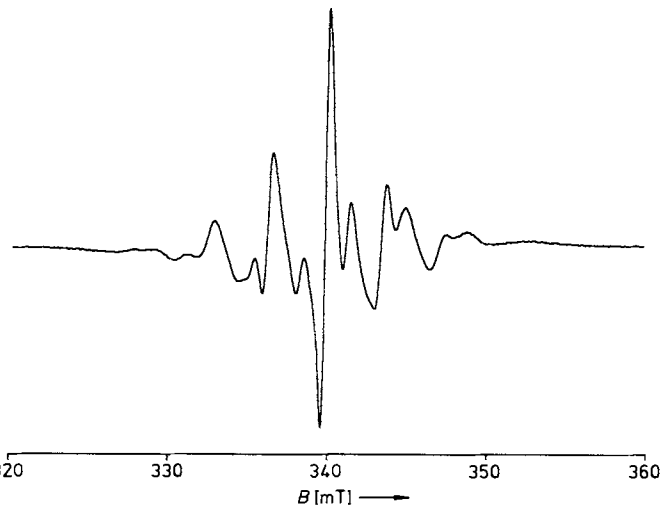

Fig. 2. A plot of the EPR spectrum of **5** in THF at ca. 25 °C. The complexity of the signal is due to coupling to different isotopic pairs of gallium isotopes ($I = 3/2$), which are present in the following percentages: $^{69}Ga/^{71}Ga$ ca. 48%; $^{69}Ga/^{69}Ga$ ca. 36%; $^{71}Ga/^{71}Ga$ ca. 16%.

Experimental Procedure

4: Under anaerobic and anhydrous conditions, 250 mL of 0.105 M diethyl ether solution (26.25 mmol) of TripMgBr was added dropwise to $Ga_2Gl_4 \cdot 2$ dioxane (3.0 g, 6.54 mmol), suspended in diethyl ether (50 mL) and cooled in a dry ice/acetone bath. Stirring was continued for 3 h at this temperature and a further 10 h with cooling by an ice/salt mixture. Filtration and removal of the solvents under reduced pressure gave a yellow-green semisolid residue which was taken up in hexane (250 mL). Filtration, concentration to approximately 50 mL, and storage at 20 °C for 20 h afforded **4** as yellow crystals in 83% yield (5.2 g). M.p. 113–115 °C.

5: A solution of **4** (2 g, 2.1 mmol) in diethyl ether (50 mL) was added to a suspension of lithium powder (0.1 g, 14.4 mmol) in diethyl ether (20 mL) with

cooling in a dry ice/acetone bath. Stirring was continued for 2 h during which time the solution turned dark blue-green. The reaction mixture was warmed to approximately $-10\,^{\circ}C$ in an ice/salt bath and stirred for a further 3 h. Filtration of the now dark-ochre solution was followed by the addition of [12]crown-4 (0.7 mL, 4.2 mmol). The solution was concentrated to ca. 15 mL and stored at -20 C for 48 h to furnish **5** as black crystals in 80% yield (2.2 g) which gave a satisfactory C,H analysis. M.p. 128–129 °C.

Received: December 7, 1992 [Z 5735IE]
German version: *Angew. Chem.* **1993**, *105*, 761

[1] W. Uhl, *Z. Naturforsch. B* **1988**, *43*, 1113.
[2] W. Uhl, M. Layh, T. Hildenbrand, *J. Organomet. Chem.* **1989**, *364*, 289.
[3] W. Uhl, M. Layh, W. Hiller, *J. Organomet. Chem.* **1989**, *368*, 139.
[4] W. Biffar, H. Nöth, H. Pommerening, *Angew. Chem.* **1980**, *92*, 63; *Angew. Chem. Int. Ed. Engl.* **1980**, *19*, 56.
[5] K. Schlüter, A. Berndt, *Angew. Chem.* **1980**, *92*, 64; *Angew. Chem. Int. Ed. Engl.* **1980**, *19*, 57.
[6] A. Moezzi, M. M. Olmstead, R. A. Bartlett, P. P. Power, *Organometallics*, **1992**, *11*, 2383.
[7] A. Moezzi, M. M. Olmstead, P. P. Power, *J. Am. Chem. Soc.* **1992**, *114*, 2715.
[8] A. Moezzi, R. A. Bartlett, P. P. Power, *Angew. Chem.* **1992**, *104*, 1075; *Angew. Chem. Int. Ed. Engl.* **1992**, *31*, 1082.
[9] Crystal data for **5** at 130 K with $Mo_{K\alpha}$ radiation ($\lambda = 0.71069$ Å): $a = 13.109(2)$, $b = 45.182(9)$ Å, tetragonal, space group $P4_12_12$, $Z = 2748$ reflections ($I > 3\sigma(I)$), $R = 0.071$. Further details of the structure may be obtained from the Fachinformationszentrum Karlsruhe Gesellschaft für wissenschaftlich-technische Information mbH, D-W-7514, Eggenstein-Leopoldshafen 2 (FRG) on quoting the depository number CSD-56944, the names of the authors, and the journal citation.
[10] H. Klusik, A. Berndt, *Angew. Chem.* **1981**, *93*, 903; *Angew. Chem. Int. Ed. Engl.* **1981**, *20*, 870.
[11] G. Gerlach, W. Hönle, A. Simon, *Z. Anorg. Allg. Chem.* **1982**, *486*, 7.
[12] The EPR spectrum was recorded on a Bruker ER-200 spectrometer operating at a frequency of 9.47 Hz with a microwave power of 2 mW, a modulation amplitude of 0.125 mT, and a scan time of 200 s.
[13] After the submission of this paper, we learned from a reviewer that two other groups (those of K. Pörschke and W. Uhl) have synthesized the radical anion $[R_2AlAlR_2]^{\cdot-}$ ($R = CH(SiMe_3)_2$, Al–Al = 2.53 Å) which is closely related to **5**. These results have since been published: C. Pluta, K.-R. Pörschke, C. Krüger, K. Hildenbrand, *Angew. Chem.* **1993**, *105*, 451; *Angew. Chem. Int. Ed. Engl.* **1993**, *32*, 388; W. Uhl, A. Vester, W. Kaim, J. Poppe, *J. Organomet. Chem.* **1993**, in press. In our laboratory we have also succeeded in isolating $[Trip_2AlAlTrip_2]^{\cdot-}$ which has an Al–Al distance of 2.470(2) Å. An account of this work will be published separately.

5-Dimethylamino-5′-nitro-2,2′-bithiophene—a New Dye with Pronounced Positive Solvatochromism**

By *Franz Effenberger** and *Frank Würthner*

Dedicated to Professor Emanuel Vogel and Professor Klaus Hafner on the occasion of their 65th birthdays

All the significant findings on solvent parameters, their determination, and their respective advantages and disadvantages on application in very diverse reactions have been soundly summarized by C. Reichardt.[1] According to this information the solvatochromism of special compounds, which is easily quantified by UV/VIS spectroscopy, is particularly suitable for the empirical determination of solvent parameters. Of the many types of compounds studied, three have proved to be particularly good models for this purpose because of their pronounced solvatochromic properties: a) the Z values of Kosower obtained from the solvent-dependent (intermolecular) charge-transfer (CT) transitions in pyridinium compounds,[2] b) the $E_T(30)$ values of Dimroth, Reichardt, et al. obtained from the longest wavelength UV/VIS absorption of pyridinium N-phenoxides[3] and c) the π^* values of Taft, Kamlet, et al. derived from the long-wavelength absorption of benzene and styrene derivatives containing both donor and acceptor substituents.[4]

The Z values have a disadvantage over the $E_T(30)$ values: in solvents of higher polarity the CT transition overlaps with the strong $\pi \rightarrow \pi^*$ absorption, which restricts the range of application considerably. Another advantage of the $E_T(30)$ values over the Z values is the enormous width of the absorption region covered by the solvatochromism, which in addition is largely in the visible spectrum. A disadvantage of the $E_T(30)$ values is that the phenolates used for their determination are strongly basic. $E_T(30)$ values are therefore not available for solvents with high acidity. To a certain extent this disadvantage can be compensated for by the use of more weakly basic pyridinium N-phenoxides.[5] Because of the specific interactions of protic and Lewis acidic solvents with the phenolate group, the $E_T(30)$ values of these solvents are not a general measure for the solvent polarity.[6] These specific solvation effects[3, 8] occur in all betaine dyes that display negative[7] solvatochromism because of their negatively charged phenolate group in the electronic ground state. Dyes displaying positive[7] solvatochromism show smaller specific interactions and are therefore generally better suited for the description of solvent polarity parameters in terms of unspecific electrostatic interactions.

As hitherto no universally applicable positive solvatochromic dye was known,[9] Kamlet and Taft defined an "averaged" π^* scale from the solvatochromic behavior of seven standard and about forty auxiliary compounds. Although this scale in essence reproduces the stabilization of the excited state by electrostatic interactions correctly, in contrast to the $E_T(30)$ and Z scales it has no clear, well-understood reference process as basis.[10] In addition, the tabulation of other solvents or solvent mixtures proved troublesome.

In the context of studies on conjugated polyenes[11] and oligothiophenes[12] containing donor and acceptor substituents, we have prepared several amino- and nitro-substituted oligothiophenes that display exceptionally strong solvatochromic properties. Here we report on the solvato-

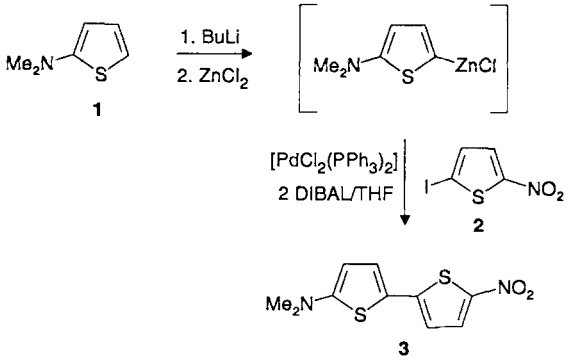

Scheme 1. 1) **1** and BuLi in *n*-hexane/THF; 2) addition to $ZnCl_2$ in THF; 3) addition of Zn-metalated **1** and **2** in THF to 5 mol% $[PdCl_2(PPh_3)_2]$/2 DIBAL (diisobutylaluminium hydride, 1 M in *n*-hexane) in THF, 3 h at room temperature.

[*] Prof. Dr. F. Effenberger, Dipl.-Chem. F. Würthner
Institut für Organische Chemie der Universität
Pfaffenwaldring 55, D-W-7000 Stuttgart 80 (FRG)
Telefax: Int. code + (711)685-4269

[**] This work was supported by the Deutsche Forschungsgemeinschaft (SFB 329) and the Fonds der Chemischen Industrie. We thank Prof. W. Liptay, Mainz, for his program SOLVDEPE, Dr. R. Wortmann and Mr. P. Krämer for the EFISH and electrooptical absorption measurements, and Ms. S. Henkel for the crystal structure determination.

chromic behavior of 5-dimethylamino-5'-nitro-2,2'-bithiophene (**3**) and its suitability for the establishment of a π^* scale that is based on only *one* model compound and whose absorption wavelengths lie in the easily detectable visible spectral range.

Bithiophene **3** was synthesized by a transition metal catalyzed coupling reaction[13] from the aminothiophene **1** and 2-iodo-5-nitrothiophene (**2**) according to Scheme 1 and is obtained in pure form as violet crystals (m.p. 176–177 °C). It is readily soluble in all organic solvents and displays unusually large solvatochromic shifts, which extend almost over the whole visible range, from $\lambda = 466$ nm (*n*-hexane) to $\lambda = 597$ nm (formamide/water) (Fig. 1).

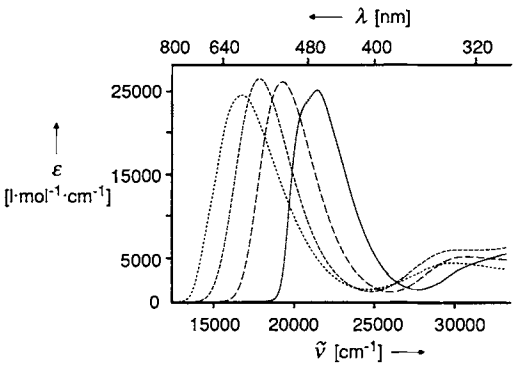

Fig. 1. UV/VIS absorption spectrum of **3** (4×10^{-5} M) in *n*-hexane (——), THF (– – –), dimethylsulfoxide (----), and formamide/water (1:1) (·····).

The X-ray structure analysis[14] shows that bithiophene **3**—in contrast to comparable biphenyl derivatives[15]—is almost completely planar; therefore conjugation is not reduced by twisting of the end groups and the thienyl system or of the thienyl groups themselves (Fig. 2). A further indication of the good electron delocalization in **3** is the distinct equalization of the C–C bond lengths within both thiophene units. As a result the electron distribution in **3** resembles that of merocyanines.[16]

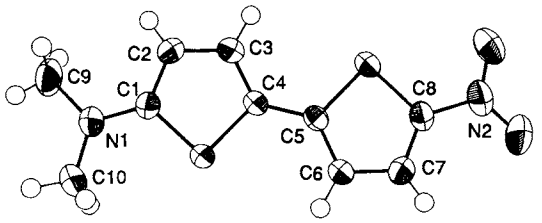

Fig. 2. Crystal structure of **3** (ORTEP projection). Selected distances [Å]: C1–N1 1.356(3), C1–C2 1.383(4), C2–C3 1.402(3), C3–C4 1.372(3), C4–C5 1.438(2), C5–C6 1.385(3), C6–C7 1.399(3), C7–C8 1.363(4), N2–C8 1.417(3); bond angles [°]: C9-N1-C10 120.2; dihedral angle [°]: Me_2N-thienyl 4.5, thienyl-thienyl 3.7, thienyl-NO_2 2.1.

The large electronic interaction between the two end groups is not only evident in the pronounced solvatochromism, but also in other physical properties that suggest that the donor- and acceptor-substituted oligothiophenes could find application in nonlinear optics.[17] According to EFISH measurements, the static hyperpolarizability of the donor- and acceptor-substituted bithiophenes is almost twice as large as that of the corresponding biphenyls. The agreement between these experimentally determined hyperpolarizabilities and the values calculated from solvatochromic data for this class of compounds is excellent.[12]

The electrooptic absorption measurements[12b] showed that the change in dipole moment on electronic excitation is oriented parallel to the transition dipole and is constant over the whole CT band. Thus the entire long-wavelength absorption band of **3** arises from a single electronic transition.

Table 1. Physical molecular properties of 5-dimethylamino-5'-nitro-2,2'-bithiophene (**3**) and 4-dimethylamino-4'-nitrobiphenyl (DNB) [12b].

Measured quantities	**3**	DNB
dipole moment in the ground state μ_g [D] [a]	7.95	6.72
dipole moment in the excited state μ_e [D] [b]	22	24
hyperpolarizability β_z (1064 nm) [esu] [c]	318×10^{-30}	89×10^{-30}
static hyperpolarizability β_0 [esu] [d]	54×10^{-30}	33×10^{-30}
absorption maximum λ_{max} (*n*-hexane) [nm]	466	375
absorption maximum λ_{max} (formamide) [nm]	577	420
extinction coefficient ε_{max} [$L\,mol^{-1}\,cm^{-1}$] [e]	25000	20000
oscillator strength *f* [e]	0.46	0.47

[a] According to Debye–Guggenheim–Smith (in benzene). [b] Electrooptical absorption measurements. [c] EFISH measurement, reference quartz $d_{11} = 1.2 \times 10^{-9}$ esu. [d] Calculated according to the two-level model from EFISH data (1064 nm). [e] In *n*-hexane, $f = 4.32 \times 10^{-9} \int \varepsilon d\tilde{\nu}$.

Prompted by these physical quantities, we examined the solvatochromic properties of **3** by recording its absorption spectrum in three aliphatic, eleven dipolar-aprotic, seven aromatic, five chlorinated, and six protic solvents.

Solvatochromism can either be described empirically[1–8] or be based on physical properties which quantify the solvent effect on the absorption behavior.[18] For **3** an excellent correlation ($r = 0.9923$) is established with the solvent function defined by dielectric constant ε and the refractive index n_D according to the method of Liptay for the 13 aliphatic and dipolar–aprotic solvents (excluding dioxan).[18, 19] The aromatic solvents and dioxan deviate substantially from the regression line, because their large quadrupole moments cannot be described by the macroscopic solvent parameters ε and *n*. The empirical representation of the solvent polarity by suitable molecules like **3**, however, encompasses all operative effects on the molecular microscopic level.

Since the π^* scale was set up with dyes that do not enter into specific interactions with dipolar-aprotic solvents, it is not surprising that a very good correlation between the absorption wavenumbers of **3** and the π^* values of the relevant solvents was obtained [Eq. (a)].

$$\tilde{\nu}_{max}(\mathbf{3}) = 21\,166\ cm^{-1} - 3323\ cm^{-1} \cdot \pi^* \quad (r = 0.9979) \quad (a)$$

In aromatic and in chlorinated hydrocarbons the absorption transitions of **3** occur at shorter wavelengths than calculated on the basis of the π^* values according to Equation (a). Kamlet, Taft, et al. have introduced a correction parameter δ for these solvents to account for the different contributions of the polarization and dispersion forces[4, 20] [Eq. (b)];

$$\tilde{\nu}_{max}(\mathbf{3}) = 21\,126\ cm^{-1} - 3337\ cm^{-1} \cdot (\pi^* - 0.1 \cdot \delta) \quad (r = 0.9936) \quad (b)$$

$\delta = 0$ for aliphatic and dipolar–aprotic solvents, 0.5 for chlorinated aliphatic solvents, and 1 for aromatic solvents (and dioxan). When the correction term $d \cdot \delta$ is taken into account for a *d* value of -0.1 for the bithiophene **3**, we also obtained

a very good correlation between the absorption wavelengths and the known π^* values including those for all the chlorinated and aromatic solvents we studied (Fig. 3).

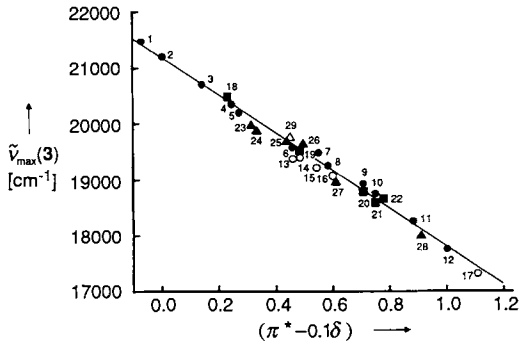

Fig. 3. Correlation of the absorption wavenumbers with the π^* scale according to Taft, Kamlet et al. and including the correction term δ. Aliphatic and dipolar-aprotic solvents (●) [1 *n*-hexane, 2 cyclohexane, 3 triethylamine, 4 dibutyl ether, 5 diethyl ether, 6 butyl acetate, 7 ethyl acetate, 8 THF, 9 acetone, 10 acetonitrile, 11 DMF, 12 DMSO]; protic solvents (○) [13 *n*-butanol, 14 2-propanol, 15 ethanol, 16 methanol, 17 formamide]; chlorinated solvents (■) [18 CCl_4, 19 trichloroethylene, 20 chloroform, 21 1,2-dichloroethane, 22 dichloromethane]; aromatic solvents (▲) [23 mesitylene, 24 *p*-xylene, 25 toluene, 26 benzene, 27 chlorobenzene, 28 nitrobenzene]. 29 Dioxan (Δ) was treated like an aromatic solvent ($\delta = 1$); for formamide and chloroform the π^* values were taken from ref. [4a].

Thus in terms of Equation (b), reliable π^* values can be determined simply and fast with only *one* indicator dye, because bithiophene **3**, in contrast to the indicator dyes used till now,[4] fulfills *all* criteria for establishing solvent parameters: namely, good spectral sensitivity, absorption in the visible range in which all solvents are transparent, high intensity of the CT transition not masked by other electronic transitions, and good solubility in all organic solvents.

Received: December 11, 1992 [Z 5747 IE]
German version: *Angew. Chem.* **1993**, *105*, 742

[1] a) C. Reichardt, *Solvents and Solvent Effects in Organic Chemistry*, 2nd ed., VCH, Weinheim, **1988**; b) C. Reichardt, *Angew. Chem.* **1979**, *91*, 119–131; *Angew. Chem. Int. Ed. Engl.* **1979**, *18*, 98–110.

[2] a) E. M. Kosower, *An Introduction to Physical Organic Chemistry*, Wiley, New York, **1968**; b) E. M. Kosower, *J. Am. Chem. Soc.* **1958**, *80*, 3253–3260.

[3] a) K. Dimroth, C. Reichardt, T. Siepmann, F. Bohlmann, *Justus Liebigs Ann. Chem.* **1963**, *661*, 1–37; b) C. Reichardt, *Chem. Soc. Rev.* **1992**, 147–153.

[4] a) M. J. Kamlet, J.-L. M. Abboud, R. W. Taft, *J. Am. Chem. Soc.* **1977**, *99*, 6027–6038; b) M. J. Kamlet, J.-L. M. Abboud, M. H. Abraham, R. W. Taft, *J. Org. Chem.* **1983**, *48*, 2877–2887.

[5] M. A. Kessler, O. S. Wolfbeis, *Chem. Phys. Lipids* **1989**, *50*, 51–56.

[6] a) R. W. Taft, M. J. Kamlet, *J. Am. Chem. Soc.* **1976**, *98*, 2886–2894; b) *J. Chem. Soc. Perkin Trans. 2* **1979**, 1723–1729.

[7] Positive (negative) solvatochromism: bathochromic (hypsochromic) shifts of the absorption band with increasing solvent polarity.

[8] a) S. Hünig, O. Rosenthal, *Justus Liebigs Ann. Chem.* **1955**, *592*, 161–179; b) L. G. S. Brooker, A. C. Craig, D. W. Heseltine, P. W. Jenkins, L. L. Lincoln, *J. Am. Chem. Soc.* **1965**, *87*, 2443–2450.

[9] The merocyanine dye of Brooker et al. upon which the χ_R scale is based [8 b] does have a long-wavelength absorption band with pronounced solvatochromism, but here, too, specific interactions with protic solvents lead to an additional bathochromic shift that is not caused by the solvent polarity.

[10] See ref. [1a], p. 403.

[11] a) F. Effenberger, H. Schlosser, P. Bäuerle, S. Maier, H. Port, H. C. Wolf, *Angew. Chem.* **1988**, *100*, 274–277; *Angew. Chem. Int. Ed. Engl.* **1988**, *27*, 281–284; b) F. Effenberger, H. C. Wolf, *New J. Chem.* **1991**, *15*, 117–123; c) C. Bubeck, F. Effenberger, L. Häußling, D. Neher, C.-P. Niesert, H. Ringsdorf, *Adv. Mater.* **1992**, *4*, 413–416.

[12] a) F. Würthner, Dissertation, Univ. Stuttgart, **1993**; b) F. Würthner, F. Effenberger, R. Wortmann, P. Krämer, *Chem. Phys.*, in press.

[13] a) M. Kumada, *Pure Appl. Chem.* **1980**, *52*, 669–679; b) V. N. Kalinin, *Synthesis* **1992**, 413–432.

[14] a) G. M. Sheldrick, *SHELXS 86*, Univ. Göttingen, **1986**; b) C. K. Johnson, *ORTEP-II, A Fortran Thermal Ellipsoid Plot Program for Crystal Structure Illustrations*, Oak Ridge, TN, USA, **1971**. c) Further details of the crystal structure investigation may be obtained from the Fachinformationszentrum Karlsruhe, Gesellschaft für wissenschaftlich-technische Information mbH, D-W-7514 Eggenstein-Leopoldshafen 2 (FRG) on quoting the depository number CSD-57065, the names of the authors, and the journal citation.

[15] a) J. Zyss, I. Ledoux, M. Bertault, E. Toupet, *Chem. Phys.* **1991**, *150*, 125–135; b) G. Casalone, A. Gavezzotti, M. Simonetta, *J. Chem. Soc. Perkin Trans. 2* **1973**, 342–345.

[16] a) S. Dähne, *Chimia* **1991**, *45*, 288–296; b) M. Klessinger, *Chem. Unserer Zeit* **1978**, *12*, 1–10.

[17] a) D. J. Williams, *Angew. Chem.* **1984**, *96*, 637–651; *Angew. Chem. Int. Ed. Engl.* **1984**, *23*, 690–704; b) J. Simon, P. Bassoul, S. Norvez, *New J. Chem.* **1989**, *13*, 13–21.

[18] a) W. Liptay, *Angew. Chem.* **1969**, *81*, 195–206; *Angew. Chem. Int. Ed. Engl.* **1969**, *8*, 177–188; b) W. Liptay, *Z. Naturforsch. A* **1965**, *20*, 1441–1471.

[19] W. Liptay, *Program SOLVDEPE*, English version, Univ. Mainz, **1992**. The correlation analysis was performed by neglecting the dispersion term and the polarizability of **3** in the spherical Onsager model.

$$\tilde{\nu} = \tilde{\nu}_{gas} - \frac{1}{hc_0}\mu_g \Delta\mu f - \frac{1}{2hc_0}\Delta\mu^2 f'$$

f = permittivity function $f_{(\varepsilon)} = \frac{1}{4\pi\varepsilon_0 a^3}\frac{2(\varepsilon-1)}{(2\varepsilon+1)}$

f' = polarizability function $f_{(n)} = \frac{1}{4\pi\varepsilon_0 a^3}\frac{2(n^2-1)}{(2n^2+1)}$

[20] R. W. Taft, J.-L. M. Abboud, M. J. Kamlet, *J. Am. Chem. Soc.* **1981**, *103*, 1080–1086.

Protonation of Phenyl(trimethylsilyl)acetylene: A Surprisingly Weak Stabilization of a Carbocation by a β-Trimethylsilyl Group**

By *A. Jerry Kresge** and *John B. Tobin*

Carbocations are strongly stabilized by β-trimethylsilyl substituents:[1] effects amounting to several tens of kcal mol^{-1} have been calculated[2] and observed[3] in the gas phase, and an acceleration by a factor of 10^{12} has been determined for a reaction in solution;[4] β-silyl-substituted carbocations have also been observed directly quite recently and their stability has been assessed by NMR spectroscopy.[5] We were surprised, therefore, to find that the β-trimethylsilyl substituent in phenyl(trimethylsilyl)acetylene (**1**) speeds up the protonation of this substance to give the phenyl β-trimethylsilylvinyl cation (**2**) [Eq. (a)] by a factor of only 300.

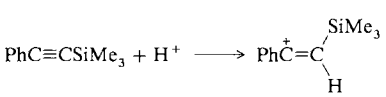

(a)

1 **2**

Phenyl(trimethylsilyl)acetylene is converted cleanly into acetophenone by moderately concentrated aqueous perchloric acid (45 wt%); during which phenylacetylene can be detected as an intermediate. The first stage of this reaction may therefore be formulated as the protodesilylation [Eq. (b)]; the phenylacetylene so produced is then hydrated more slow-

[*] Prof. A. J. Kresge, Dr. J. B. Tobin
Department of Chemistry, University of Toronto
Toronto, Ontario M5S 1A1 (Canada)

[**] This work was supported by the Natural Sciences and Engineering Research Council of Canada and the donors of the Petroleum Research Fund administered by the American Chemical Society.

ly by the well-known acid-catalyzed reaction to give acetophenone [Eq. (c)].

$$PhC{\equiv}CSiMe_3 + H^+ \xrightarrow[-H^+]{H_2O} PhC{\equiv}CH + HOSiMe_3 \quad (b)$$

$$PhC{\equiv}CH \xrightarrow[H_2O]{H^+} PhC(OH)=CH_2 \longrightarrow PhCCH_3 \quad (c)$$

Although the UV spectra of **1** and phenylacetylene are quite similar, there is a difference in the region $\lambda = 250$–260 nm, and this can be used to monitor the protodesilylation spectroscopically. Conveniently measurable rates are obtained for the acid concentrations 10–40 wt% aqueous $HClO_4$. The reaction is first-order, and the rate constants increase sharply with increasing acidity. These rate constants give a good linear correlation when treated by the Cox–Yates method[6] by using the X_0 acidity function.[7] This correlation provides the catalytic coefficient for dilute solution $k_H^+ = (8.93 \pm 0.35) \times 10^{-5}\ M^{-1} s^{-1}$. Comparison of rates of reaction in 0.79 M perchloric acid in H_2O and D_2O also gives the isotope effect $k_H^+/k_D^+ = 1.79 \pm 0.06$. This isotope effect is characteristic of a process that involves rate-determining hydron transfer (hydron = H^+, D^+, or T^+) from the hydronium ion to a carbon base.[8] Similar isotope effects have been obtained for the hydration of other acetylenes,[9] a reaction known to occur by rate-determining protonation of the acetylenic carbon atom to give a vinyl cation.[9, 10] The slope of the present Cox–Yates correlation is also similar to that obtained for the hydration of other acetylenes.[9b, 11] The accumulated evidence thus indicates that the protodesilylation of **1** likewise occurs by rate-determining proton transfer to acetylenic carbon atom [Eq. (a)]; this step is then presumably followed by rapid nucleophilic displacement of the trimethylsilyl group from the vinyl cation **2** [Eq. (d)].

$$PhC^+(H)=C(SiMe_3) \xrightarrow[-H^+]{H_2O} PhC{\equiv}CH + HOSiMe_3 \quad (d)$$

2

Since the rate-determining steps for the hydration and protodesilylation of acetylene are the same, an assessment of the cation-stabilizing effect of β-trimethylsilyl substituents can be made by comparing the rate of the protodesilylation of **1** with the rate of hydration of phenylacetylene. Use of $k_H^+ = 2.86 \times 10^{-7}\ M^{-1} s^{-1}$ for phenylacetylene[9b] then leads to an acceleration of the reaction by a factor of 312 ± 16, which is equivalent to a β-silyl stabilization, relative to hydrogen, of $\Delta\Delta G^{\neq} = 3.4$ kcal mol^{-1}. This value is very much smaller than the large stabilization energies, ranging from 20 to 50 kcal mol^{-1}, which have been calculated[2] and observed[3] for the β-silyl effect in the gas phase, as well as the stabiliztion energy of 17 kcal mol^{-1} observed in solution for the solvolysis of a cyclohexyl substrate with optimal conformation.[4] The present $\Delta\Delta G^{\neq}$ value is similar, however, to the β-silyl stabilization energy found for proton addition to ethyl β-trimethylsilylvinyl ether in aqueous solution (2.9 kcal mol^{-1})[12] [Eq. (e)]. In that case the low stabilization energy was attributed to a nonoptimum transition state geometry **3**, in which the dihedral angle θ between the C–$SiMe_3$ bond and the vacant p orbital of the positively charged carbon atom deviates significantly from the value, $\theta = 0$, required for the maximum hyperconjugative interaction of this bond with the cationic center; this caused a considerable reduction of the hyperconjugative component of the stabilization, which constitutes the major part of the β-silyl effect.[2, 4]

$$Me_3SiCH{=}CHOEt + H^+ \longrightarrow Me_3SiCH_2\overset{+}{C}HOEt \quad (e)$$

This dihedral angle does have its optimum value in the transition state of the present reaction (**4**) inasmuch as the C–$SiMe_3$ bond and the vacant p orbital lie in the same plane throughout the protonation process and consequently $\theta = 0$. In the present case, however, another angle, that between the C–$SiMe_3$ bond and the adjacent C–C bond, designated ϕ in structure **5**, has a value that is probably far from optimal. Hyperconjugative interaction will be maximum when the C–$SiMe_3$ bond and the vacant cationic p orbital are parallel and $\phi = 90°$ but, as protonation of the acetylenic carbon atom takes place, this angle begins with an initial-state value of $\phi =$ is 180° and then reaches a final-state value of only $\varphi = 120°$ in the fully formed vinyl cation. In the transition

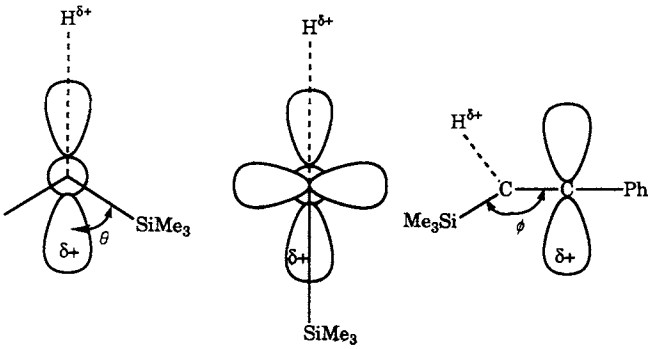

3 **4** **5**

state, this angle will of course be considerably greater than $\varphi = 120°$; and that will lead to a sizeable reduction in the hyperconjugative interaction, consistent with the weak β-silyl effect found here. This analysis implies that substantially stronger β-silyl effects should be observed in systems, such as solvolysis of vinyl substrates, where a near-optimum value of ϕ is already present in the reaction's initial state.

Received: December 2, 1992 [Z 5722 IE]
German version: *Angew. Chem.* **1993**, *105*, 748

[1] Recent reviews: Y. Apeloig in *The Chemistry of Organic Silicon Compounds*, *1*, (Eds.: S. Patai, Z. Rappoport), Wiley, New York, **1989**, p. 57; J. B. Lambert, *Tetrahedron*, **1988**, *46*, 2677.
[2] S. G. Wierschke, J. Chandrasekhar, W. L. Jorgensen, *J. Am. Chem. Soc.* **1985**, *107*, 1496; M. R. Ibrahim, W. L. Jorgensen, *ibid.* **1989**, *111*, 819; Y. Apeloig, M. Karni, A. Stanger, H. Schwarz, T. Drewello, G. Czekay, *J. Chem. Soc. Chem. Commun.* **1987**, 989; K. A. Nguyen, M. S. Gordon, G. Wang, J. B. Lambert, *Organometallics* **1991**, *10*, 2798.
[3] D. Hajdasz, R. Squires, *J. Chem. Soc. Chem. Comm.* **1988**, 1212; X. Li, J. A. Stone, *J. Am. Chem. Soc.* **1989**, *111*, 5586; G. A. McGibbon, M. A. Brook, J. K. Terlouw, *J. Chem. Soc. Chem. Comm.* **1992**, 360.
[4] J. B. Lambert, G. Wang, R. B. Finzel, D. H. Teramura, *J. Am. Chem. Soc.* **1987**, *109*, 7838.
[5] H.-U. Siehl, F.-P. Kaufmann, Y. Apeloig, V. Brande, D. Danovich, A. Berndt, N. Stamatis, *Angew. Chem.* **1991**, *103*, 1546; *Angew. Chem. Int. Ed. Engl.* **1991**, *30*, 1479; G. K. S. Prakash, V. P. Reddy, G. Rasul, J.

Casanova, G. A. Olah, *J. Am. Chem. Soc.* **1992**, *114*, 3076; H.-U. Siehl, F.-P. Kaufmann, *ibid.* **1992**, *114*, 4937.
[6] R. A. Cox, K. Yates, *J. Am. Chem. Soc.* **1978**, *100*, 3861; R. A. Cox, *Acc. Chem. Res.* **1987**, *20*, 27.
[7] R. A. Cox, K. Yates, *Can. J. Chem.* **1981**, *59*, 2116; A. J. Kresge, H. J. Chen, G. L. Capen, M. F. Powell, *ibid.* **1983**, *61*, 249.
[8] J. R. Keeffe, A. J. Kresge in *Techniques of Chemistry, Vol. VI Investigation of Rates and Mechanisms of Reactions*, 4th ed. (Ed. C. F. Bernasconi), Wiley, New York, **1986**, Part 1, Chapter XI.
[9] a) W. Drenth, H. Hogeveen, *Recl. Trav. Chim. Pays-Bas* **1960**, *79*, 1002; E. J. Stamhuis, W. Drenth, *ibid.* **1963**, *82*, 385; D. S. Noyce, M. A. Matesich, M. D. Schiavelli, P. E. Peterson, *J. Am. Chem. Soc.* **1965**, *87*, 2295; D. S. Noyce, M. D. Schiavelli, *ibid.* **1968**, *90*, 1023. b) N. Banait, M. Hojatti, P. Findlay, A. J. Kresge, *Can. J. Chem.* **1987**, *65*, 441.
[10] R. W. Bott, C. Eaborn, D. R. M. Walton, *J. Chem. Soc.* **1965**, 384; D. S. Noyce, M. D. Schiavelli, *J. Am. Chem. Soc.* **1968**, *90*, 1020.
[11] Y. Lucchini, G. Modena, *J. Am. Chem. Soc.* **1990**, *112*, 6291.
[12] A. J. Kresge, J. B. Tobin, *J. Phys. Org. Chem.* **1991**, *4*, 587.

New Chiral Porphyrins—Syntheses and Molecular Recognition of Amino Acid Esters

By *Yasuhisa Kuroda,* Yusuke Kato, Takuji Higashioji,* and *Hisanobu Ogoshi**

Synthetic chiral porphyrins have attracted much interest as model compounds for the chiral environments of heme proteins.[1] We report herein a new synthetic route to chiral porphyrins and their chiral recognition behavior. Since the required synthetic building blocks are achiral atropisomeric tetraarylporphyrins with *ortho*-substituted phenyl groups and simple bridging reagents, the route is suitable for the preparation of a series of chiral porphyrins for the systematic investigation of molecular recognition properties. Our synthetic scheme is based on the following strategy (Fig. 1).

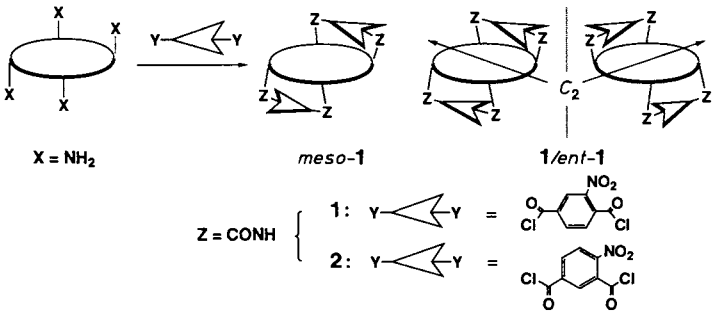

Fig. 1. Schematic representation of the synthesis of chiral porphyrins.

When the $\alpha,\alpha,\beta,\beta$ atropisomers of tetraarylporphyrins are doubly bridged with an unsymmetric, difunctionalized reagent, a mixture of a *meso* porphyrin and a pair of enantiomeric porphyrins with a C_2 symmetry axis parallel to the porphyrin plane may result,[2] which may be separated by chromatography. For example, the reaction of $\alpha,\alpha,\beta,\beta$-tetrakis(*ortho*-aminophenyl) porphyrin with nitroterephthaloloyl chloride in THF gave two doubly bridged porphyrins, *meso*-**1** and **1**/*ent*-**1**, which could be purified by silica gel chromatography.[3] The product with the larger R_f value on a silica gel TLC plate was further resolved into the enantiomers **1** and *ent*-**1** on a chiral HPLC column. The chirality of these products is clearly demonstrated by their circular dichroism (CD) spectra, which show completely symmetric Cotton effects in the region of the Soret bands. The analogous reaction with 4-nitroisophthaloyl chloride gave, following chromatographic separation, *meso*-**2** and **2**/*ent*-**2**; the enantiomers could be separated again by HPLC.[4] All compounds were characterized by ^{1}H NMR spectroscopy and fast atom bombardment mass spectrometry (FAB-MS).

In spite of the slight difference between the bridging positions of **1** (*para*) and **2** (*meta*), the topological structures of these porphyrins were expected to be quite different; the angles between planes of the porphyrin and the bridging benzene units in **1** and **2** are predicted by calculations to be approximately 0° and 70–80°, respectively (see Fig. 2).[5]

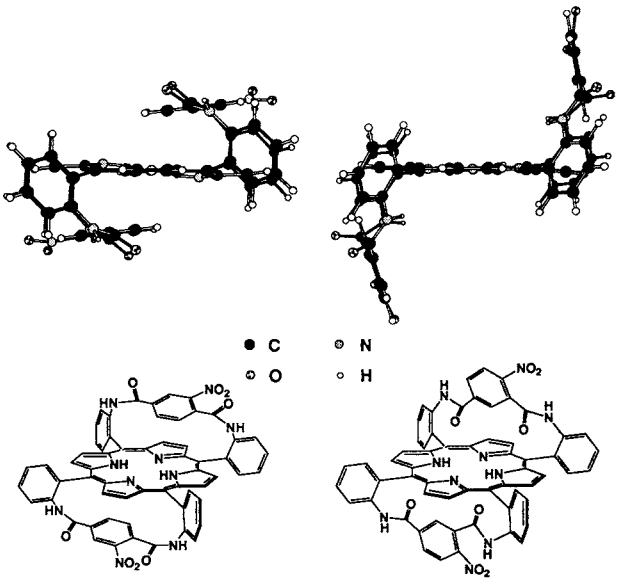

Fig. 2. Ball-and-stick molecular models of one each of the sets of enantiomers **1**/*ent*-**1** (left) and **2**/*ent*-**2** (right) (see ref. [5]).

We attempted to evaluate the chiral recognition abilities of **1** and **2** by determining the association constants of the adducts formed by their Zn complexes and amino acid methyl esters.[6] Titration experiments indicate that various types of amino acid methyl esters form 1:1 complexes with **1**-Zn and **2**-Zn (Table 1). The following interesting aspects of the molecular recognition are clear: a) coordination of the amino acid to *meso*-**1**-Zn is hindered significantly compared with that to TPP-Zn, by the benzene bridge; b) in contrast, *meso*-**2**-Zn shows a high affinity for amino acids, while the affinity for corresponding simple amines is low; c) the chiral porphyrins **2** and *ent*-**2** show significant chiral recognition for amino acids.

Upon complex formation, the ^{1}H NMR signals of the protons of the amino acid ester exhibit upfield shifts that are dependent on their distance from the amino group. For example, valine shows upfield shifts of $\Delta\delta$ = 6.2, 2.2, 2.2, and 0.9 for C_α-H, C_β-H, CH_3 (*i*Pr), and CH_3 (ester), respectively. The electronic spectra of these Zn porphyrins also show a clear redshift of the Soret bands (ca. 8 nm) upon addition of the amino acid, while the corresponding uncomplexed porphyrins do not. These observations strongly indicate coordination of the amino group on the Zn atom. Comparison of association constants for amino acids esters and the corresponding amines strongly indicates that the methoxycar-

[*] Prof. Dr. Y. Kuroda, Prof. Dr. H. Ogoshi, Y. Kato, T. Higashioji
Department of Synthetic Chemistry
Kyoto University
Sakyo-ku, Kyoto 606 (Japan)
Telefax: Int. code +(75)753-4979

Table 1. Association constants K_a for the adducts of Zn porphyrin complexes and amino acid esters [a].

Substrate HCR^1R^2-NH_2	TPP-Zn	*meso*-**1**-Zn	*meso*-**2**-Zn	K_a [M^{-1}] [b] (+)-**2**-Zn [c]	(−)-**2**-Zn [c]
$R^1 = CO_2Me$ [d]					
$R^2 = Ph$	2100 (100)	–	8800 (300)	7000 (300)	11000 (1000)
$R^2 = PhCH_2$	2600 (100)	900 (100)	10000 (500)	2800 (200)	15000 (1000)
$R^2 = 3,4\text{-}(OMe)_2C_6H_3CH_2$	2500 (100)	1100 (100)	14000 (500)	5400 (500)	24000 (600)
$R^2 = (CH_3)_2CH$	2000 (100)	–	14000 (500)	3900 (100)	22000 (800)
$R^1 = H$					
$R^2 = Ph$	3700 (100)	–	2300 (200)	2300 (100)	–
$R^2 = 3,4\text{-}(OMe)_2C_6H_3CH_2$	13000 (500)	–	4100 (100)	4100 (100)	–
$R^2 = (CH_3)_2CH$	5900 (200)	–	2200 (100)	1700 (100)	–

[a] In $CHCl_3$, at 15 °C. [b] No statistical correction for the plane symmetry of (+)-**2** and (−)-**2** was applied. Standard deviations are given in parentheses. [c] Absolute configurations of these enantiomeric porphyrins were not determined. The signs (+) and (−) are based on the CD spectra in the Soret region (see ref. [4]). [d] All amino acids used in this work have L configuration.

bonyl group participates in the attractive interaction between **2**-Zn and the substrate. This attractive interaction is best explained by a hydrogen bond between the carbonyl oxygen atom of the amino acid ester and amide hydrogen atom of **2**-Zn; upon coordination of the amino group to the Zn atom these two atoms are only 1.9 Å apart. This hydrogen bonding is confirmed by the observation in the ^1H NMR titration experiments that two signals for amide NH protons shift upon addition of valine methyl ester from $\delta = 6.76/7.34$ to 7.45/7.65. Existence of the hydrogen bond is further supported by a result from preliminary IR spectroscopic measurements: upon addition of the amino acid, the NH stretching bond of the amide groups in **2**/*ent*-**2**-Zn, originally observed 3403 cm^{-1}, shifts to 3305 cm^{-1}; this can be explained by the formation of a NH···O hydrogen bond.[7]

Since chiral recognition logically requires at least a *spatially oriented* three-point interaction, the observed chiral recognition for amino acid esters suggests that there is a significant difference between the hydrogen-bonding abilities of the two amide groups at the 1- and 3-positions of the bridging benzene ring in **2**/*ent*-**2**-Zn. Thus, the amino acid receptor **2**/*ent*-**2**-Zn utilizes three kinds of interactions: coordination of the Zn atom, hydrogen bonding, and steric repulsion. Interestingly, these three interactions correspond to three characteristic elements of amino acids: the amino group (coordination), the carboxyl group (hydrogen bonding), and the side chain (steric repulsion).

The new synthetic route to chiral porphyrins reported here is expected to be widely applicable for various structural variations. Preliminary studies on chiral recognition show that, in contrast with chiral crown ethers,[8] chiral porphyrins differentiate between neutral amino acid esters.

Received: October 13, 1992
Revised version: January 14, 1993 [Z 5622 IE]
German version: *Angew. Chem.* **1993**, *105*, 774

[1] a) J. T. Groves, R. S. Myers, *J. Am. Chem. Soc.* **1983**, *105*, 5791; b) D. Mansuy, P. Battioni, J.-P. Renaud, P. Guerin, *J. Chem. Soc. Chem. Commun.* **1985**, 155; c) H. Ogoshi, K. Saita, K. Sakurai, T. Watanabe, H. Toi, Y. Aoyama, Y. Okamoto, *Tetrahedron Lett.* **1986**, *27*, 6365; d) Y. Aoyama, K. Saita, H. Toi, H. Ogoshi, Y. Okamoto, *ibid.* **1987**, *28*, 4853; e) B. Boitrel, A. Lecas, E. Rose, *J. Chem. Soc. Chem. Commun.* **1989**, 349; f) S. O'Malley, T. Kodadek, *J. Am. Chem. Soc.* **1989**, *111*, 9116; g) K. Konishi, T. Sugino, T. Aida, S. Inoue, *ibid.* **1991**, *113*, 6487; h) Y. Naruta, F. Tani, N. Ishihara, K. Maruyama, *ibid.* **1991**, *113*, 6865.

[2] If the α,α,α,α-atropisomer is doubly bridged, other chiral porphyrins may be obtained in which the C_2 symmetry axis is perpendicular to the porphyrin plane.

[3] Very similar reactions of the α,α,α,α-atropisomer with isophthaloyl chloride and 5-nitroisophthaloyl dichloride have been reported; the products were, however, not chiral. See, a) J. P. Collman, R. R. Gagne, C. A. Reed, T. R. Halbert, G. Lang, W. T. Robinson, *J. Am. Chem. Soc.* **1975**, *97*, 1427; b) J. P. Collman, J. I. Brauman, J. P. Fitzgerald, P. D. Hampton, Y. Naruta, T. Michida, *Bull. Chem. Soc. Jpn.* **1988**, *61*, 47.

[4] HPLC conditions and CD data: HPLC: column/solvent/separation factor α/resolution factor R_s: CD spectra: $[\theta]$ $M^{-1}cm^{-1}$ (λ [nm]): **1**/*ent*-**1**: YMC, A-K43/CH_2Cl_2-EtOH (97:3)/1.64/1.57; $\pm 2.0 \times 10^3$ (434); **2**/*ent*-**2**: Daicel, Chiralcel OD/hexane:EtOH (1:1)/2.98/1.98; $\pm 5.8 \times 10^2$ (424).

[5] These angles were estimated from MO calculations (AM1 in MOPAC Version 6.02, J. J. P. Stewart, *QCPE Bull.* **1989**, *9*, 10) and molecular mechanics calculations using Dreiding-I force field (NMRgraf, Molecular Simulations, Inc).

[6] a) Y. Aoyama, T. Uzawa, K. Saita, Y. Tanaka, H. Toi, H. Ogoshi, *Tetrahedron Lett.* **1988**, *29*, 5271; b) Y. Aoyama, A. Yamagishi, M. Asagawa, H. Toi, H. Ogoshi, *J. Am. Chem. Soc.* **1988**, *110*, 4076; *ibid.* **1990**, *112*, 3145.

[7] L. J. Bellamy, *The Infra-red Spectra of Complex Molecules*, Wiley, New York, **1958**, pp. 203–233, 252–255.

[8] a) E. B. Kyba, K. Kenji, L. R. Sousa, M. G. Siegel, D. J. Cram, *J. Am. Chem. Soc.* **1973**, *95*, 2692; b) S. C. Peacock, L. A. Domeier, F. C. A. Gaeta, R. C. Helgeson, J. M. Timko, D. J. Cram, *ibid.* **1978**, *100*, 8190, and references therein.

The Synthesis and Ab Initio Structure Determination of $Zn_4O(BO_3)_2$, a Microporous Zincoborate Constructed of "Fused" Subunits of Three- and Five-Membered Rings**

By *William T. A. Harrison,** *Thurman E. Gier,* and *Galen D. Stucky*

Substitution of boron for aluminum and/or silicon in zeolite molecular sieves has long been a topic of interest.[1–3] A rare example of complete boron substitution for both Si and Al is provided by "boralite", $Zn_4O(BO_2)_6$,[4] a direct topological analogue of the aluminosilicate sodalite-type framework found in, for example, $Na_4OH(AlSiO_4)_3$.[5] In general, however, boron atoms, which usually substitute for aluminum atoms, have only been introduced into aluminosilicate molecular sieves in small quantities, although the technological implications of such doping reactions are extremely important, as in the boron/MFI zeolite.[6]

[*] Dr. W. T. A. Harrison
Department of Chemistry, University of Houston
Houston, TX 77204-5641 (USA)
Telefax: Int. code +(713)743-2787
Dr. T. E. Gier, Prof. Dr. G. D. Stucky
Department of Chemistry, University of California
Santa Barbara, CA 93106-9510 (USA)

[**] This work was supported in part by the Office of Naval Research and the National Science Foundation (Grant No. DMR 9208511). We thank Dr. V. I. Srdanov (UCSB) for carrying out the powder-second-harmonic-generation test.

We describe here one result of our exploratory syntheses in the area of zincoborates that complements the rapidly growing family of zincophosphate and related (Be/Zn)(P/As) molecular sieves,[7, 8] consisting of framework elements from groups 2, 12, and 15 of the periodic table. $Zn_4O(BO_3)_2$ is a novel neutral-framework material containing micropores, built up from "fused", vertex-sharing tetrahedral ZnO_4 and triangular BO_3 units. Several other zincoborate compounds are known,[9] but none are similar to the phase described herein.

The final atomic coordinates for $Zn_4O(BO_3)_2$ are listed in Table 1, selected geometrical data in Table 2. $Zn_4O(BO_3)_2$

Table 1. Atomic coordinates and isotropic temperature factors for $Zn_4O(BO_3)_2$. Rhombohedral, $R\bar{3}c$, $a = 9.9115(4)$ Å, $\alpha = 48.602(1)°$.

Atom	W [a]	x	y	z	U_{iso} [Å^2]
Zn(1)	12*f*	0.6408(2)	0.6925(2)	0.0794(2)	0.007(1)
B(1)	6*e*	0.728(2)	0.772	1/4	0.005 [b]
O(1)	12*f*	0.5854(8)	0.8045(7)	0.2181(8)	0.007(2)
O(2) [c]	6*e*	0.396(2)	3/4	0.104	0.018(4)
O(3)	4*c*	0.7986(4)	0.7986	0.7986	0.013(4)

[a] Wyckoff-site notation. [b] Not refined. [c] Fractional site occupancy = 5/6.

Table 2. Selected bond lengths [Å] and angles [°] for $Zn_4O(BO_3)_2$ [a].

Bond lengths		Bond angles	
Zn(1)-O(1)	1.906(5)	O(1)-Zn(1)-O(1)′	106.2(3)
Zn(1)-O(2)	1.962(5)	O(1)-Zn(1)-O(3)	112.1(4)
Zn(1)-O(1)′	1.926(5)	O(1)′-Zn(1)-O(3)	110.2(2)
Zn(1)-O(3)	1.962(2)	O(1)-Zn(1)-O(2)	110.1(3)
B(1)-O(1) × 2	1.435(5)	O(1)′-Zn(1)-O(2)	111.2(2)
B(1)-O(2)	1.367(7)	O(2)-Zn(1)-O(3)	107.2(3)
		O(1)-B(1)-O(1)′	120.1(8)
		O(1)′-B(1)-O(2)	119.9(4)
		O(1)-B(1)-O(2)	120.0(4)

[a] The crystallographically distinct atom is primed.

has a three-dimensional structure built up from five atoms per asymmetric unit (1 Zn, 1 B, 3 O), forming vertex-sharing tetrahedral ZnO_4 and triangular BO_3 subunits, which enclose small, elongated cavities (Fig. 1) and a three-dimen-

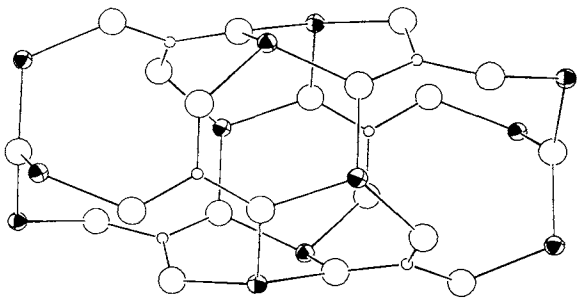

Fig. 1. ORTEP plot of the cage configuration in $Zn_4O(BO_3)_2$ viewed perpendicular to [111], showing the fused three- and five-membered rings. B: small empty circles; Zn: filled circles; O: large empty circles. Atom radii are arbitrary.

sional network of channels (Fig. 2). These channels propagate in the crystallographic [100], [010], and [001] directions; their estimated diameter is 3.5 Å. Each oxygen atom is bound to three neighbors—two zinc atoms and one boron

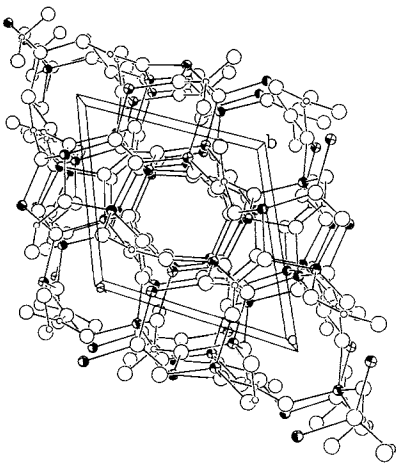

Fig. 2. ORTEP plot of the unit cell of $Zn_4O(BO_3)_2$ viewed down [100], showing the one-dimensional channels. B: small, empty circles, Zn: filled circles; O: large empty circles. Atom radii are arbitrary.

atom for O(1) and O(2) (Fig. 3), and three zinc atoms for O(3) (Table 1). The following average bond lengths [Å] and angles [°] were determined: d(Zn–O) = 1.939(3), d(B–O) = 1.412(4), θ (O–Zn–O) = 109.5(2), and θ (O–B–O) = 120.0(4). The Zn/B/O connectivity in $Zn_4O(BO_3)_2$ results in oxygen-bridged "three-membered" rings (Fig. 3) and "five-membered" rings of nodal (Zn and B) atoms that surround the central cage, although the oxygen atoms in these rings are all three-coordinate as noted above, in contrast to the typical twofold T–O–T′ (T = tetrahedron) connectivity in tetrahedral molecular sieve structures. The connectivity in these fused rings is Zn–B–Zn and Zn–B–Zn–B–Zn, respectively, ignoring oxygen atoms; in other words, each ring contains a Zn–O–Zn linkage, but no B–O–B links. Extending Smith's zeolite-cage nomenclature scheme[18] to this new type of connectivity would result in an 18-nodal-atom cage with the designation $3^6 5^4$ (six three-membered rings and four five-membered rings). These cages are aligned in the crystallographic [111] direction and interlinked, resulting in a three-dimensional microporous network.

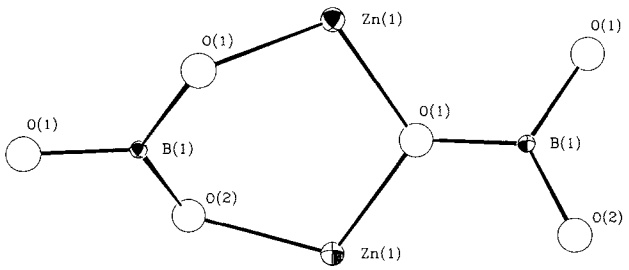

Fig. 3. Detail of the "three-membered" ring in $Zn_4O(BO_3)_2$ built up from tetrahedral ZnO_4 and trigonal-planar BO_3 groups. Selected bond lengths [Å] (standard deviations) in parentheses): Zn(1)-O(1) 1.906(5), Zn(1)-O(1)′ 1.926(5), Zn(1)-O(2) 1.962(5), B(1)-O(1) 1.435(5), B(1)-O(2) 1.367(7).

In summary, we have prepared and characterized a new, neutral-framework zincoborate structure containing a novel network of small channels and cavities. Typically, the product was a powder, but the crystal structure could be elucidated by ab initio methods from laboratory X-ray data, indicating the power of current diffraction software techniques. Further synthetic work is now in progress to determine if other novel, open structures containing tricoordinate

boron atoms as framework species can be prepared. The presence of oxygen-atom vacancies in the framework is also notable, and may facilitate substitution reactions with the Zn/B/O framework itself.

Experimental Procedure

Synthesis: The hydrothermal reaction (sealed teflon pouch, 200 °C, 4 d, pH ca. 8.5) of 3.814 g of borax ($Na_2B_4O_7 \cdot 10H_2O$), 3.440 g of 4 M NaOH solution, 6.43 g of $Zn(NO_3)_2$, and 10 mL of water resulted in a highly crystalline, white powder, which could be indexed "by hand" on a rhombohedral basis with approximate lattice constants of $a = 9.910$ Å and $\alpha = 48.62°$ (hexagonal setting: $a \approx 8.160$ Å, $c \approx 26.156$ Å). The systematic absences of the powder data (rhombic setting: *hhl*, $l = 2n$; *hhh*, $h = 2n$) indicated space groups $R3c$ or $R\bar{3}c$, and no extra lines were left unindexed. The powder was tested for nonlinear optical activity by a powder-second-harmonic-generation (PSHG) test [10] which gave a null response, indicating that the material probably crystallizes in centrosymmetric space group. The space group $R\bar{3}c$ (No. 167) was thus assumed for this material and confirmed by the successful course of the structure refinement. Thermogravimetric analysis indicated no weight loss for this material below 600 °C.

Structure Determination: The crystal structure of $Zn_4O(BO_3)_2$ was solved by ab initio methods from laboratory X-ray powder data [11,12,13]. High-resolution data were collected for a flat-plate sample of $Zn_4O(BO_3)_2$ over 12 h on a Scintag PAD-X automated diffractometer (θ-θ geometry, $16° < 2\theta < 100°$, step-size 0.02°). Optimal estimates of the individual reflection intensities were extracted by a profile-fitting method invented by Pawley [14] and developed by Le Bail [15]. The appropriate "profile" parameters were refined by least-squares fitting, and the intensities themselves (with respect to the $Cu_{K\alpha 1}$ wavelength) were optimized by an iterative procedure [15] using the program GSAS [16]. A total of 186 structure-factor-moduli ($F_{hkl} > 0$) were obtained from the data and corrected for Lorentz, polarization, and multiplicity effects, the maximum possible number of F_{hkl} values observable within the $(\sin\theta)/\lambda$ limit was 230. These F_{hkl} values were used to develop a direct-methods solution (software: SHELXS-86 [17]; 335 triplet-phase-relations, 7 negative-quartet-phase-relations generated) for the crystal structure of $Zn_4O(BO_3)_2$. Careful examination of the direct methods results indicated a plausible tetrahedral fragment (eventually atoms Zn(1) and O(1)), and the model was developed further by placing the two remaining tetrahedral vertices about the center of this fragment and assuming reasonable Zn–O bond distance/angle parameters. These two ZnO_4 vertices (O(2) and O(3)) were both evidently on crystallographic special positions (see Table 1) and were constrained as such. These four atomic positions were used as the starting model for a conventional Rietveld refinement against the X-ray powder data. The Rietveld refinement (program: GSAS) progressed smoothly, and profile and atomic parameters were progressively added to the model as variables in the normal way. A five-parameter pseudo-Voigt function was used to describe the X-ray line-shape and the variation of its width as a function of the scattering angle; a correction for preferred orientation (direction [111]) was allowed to vary during the refinement. At the end of the initial refinement, a difference Fourier synthesis identified one distinct peak at roughly (0.74, 0.75, $\frac{1}{4}$) which was a chemically reasonable site for a boron atom. Bond-length restraints were applied to this B-atom site (d(B–O) = 1.43(2) Å) to assure a stable convergence of the positional parameters of the boron atom. Assuming full occupancy for all five atom sites results in a unit-cell stoichiometry of $Zn_{12}B_6O_{22}$ whose charge does not balance (apparent charge = −2). Because no extra-framework sites were apparent from Fourier maps, the fractional occupancy factors for the oxygen atoms were refined. Those for O(1) and O(3) refined to values near to unity (1.00(2) and 1.08(3), respectively), while that of O(2) refined to a value of 0.84(2). The fractional occupancy of O(2) was then fixed at 0.833, and those for O(1) and O(3) were set to 1.0, giving a charge-neutral unit-cell content of $Zn_{12}B_6O_{21}$ or $Zn_4O(BO_3)_2$. Refining this model resulted in a satisfactory convergence to final agreement values of $R_p = 0.109$ and $R_{wp} = 0.142$, as defined in Table 3. Further details of the crystal structure investigation may be obtained from the Fachinformationszentrum Karlsruhe, Gesellschaft für wissenschaftlich-technische Information mbH, D-W-7514 Eggenstein-Leopoldshafen 2 (FRG) on quoting the depository number CSD-56997, the names of the authors, and the journal citation.

Table 3. Crystallographic data for $Zn_4O(BO_3)_2$.

empirical formula	$Zn_4O_7B_2$
M_r	384.37
crystal form	white powder
crystal system	rhombohedral
$a = b = c$ [Å]	9.9115(4)
$\alpha = \beta = \gamma$ [°]	48.602(1)
V [Å^3]	502.61
Z	3
space group	$R\bar{3}c$ (No. 167)
T [°C]	25(1)
$\lambda(Cu_{K\alpha})$ [Å]	1.54178
ρ_{calc} [g cm^{-3}]	3.81
refinement method	X-ray Rietveld refinement
software	GSAS
extinction correction	none applied
absorption correction	none applied
data range	$16 \le 2\theta \le 100°$
number of data	4198 powder data points
parameters (reflections)	31 (191)
R_p [a]	0.109
R_{wp} [b]	0.142

[a] $R_p = \sum|y_o - Cy_c|/\sum|y_o|$. [b] $R_{wp} = [\sum w(y_o - Cy_c)^2/\sum wy_o^2]^{1/2}$; C is a scaling factor.

Received: November 30, 1992 [Z 5715 IE]
German version: *Angew. Chem.* **1993**, *105*, 788

[1] R. Szostak, *Molecular Sieves. Principles of Synthesis and Identification*, Van Nostrand Reinhold, New York, **1989**.
[2] D. W. Breck, *Zeolite Molecular Sieves*, Wiley, New York, **1974**.
[3] M. Taramasso, G. Perego, B. Notari, in *Proc. 5th Int. Conf. Zeolites* (Ed.: L. V. Rees), Heyden, Philadelphia, p. 205.
[4] P. Smith-Verdier, S. Garcia-Blanco, *Z. Kristallogr.* **1980**, *151*, 175.
[5] S. Luger, J. Felsche, P. Fischer, *Acta Crystallogr. Sect. C* **1987**, *43*, 1.
[6] D. S. Santilli, S. I. Zones, in *Synthesis of Microporous Materials: Vol. 1: Molecular Sieves* (Eds.: M. L. Occelli, H. E. Robson), Van Nostrand Reinhold, New York, **1992**, p. 373.
[7] G. Harvey, W. M. Meier, in *Zeolites: Facts, Figures, Future: Studies in Surface Science and Catalysis, Vol 49* (Eds.: P. A. Jacobs, R. A. van Santen) Elsevier, Amsterdam, p. 411.
[8] T. E. Gier, G. D. Stucky, *Nature* **1991**, *349*, 508; W. T. A. Harrison, T. E. Gier, K. L. Moran, J. M. Nicol, H. Eckert, G. D. Stucky, *Chem. Mater.* **1991**, *3*, 27; T. M. Nenoff, W. T. A. Harrison, T. E. Gier, G. D. Stucky, *J. Am. Chem. Soc.* **1991**, *113*, 378; W. T. A. Harrison, T. E. Gier, G. D. Stucky, *J. Mater. Chem.* **1991**, *1*, 153; T. E. Gier, W. T. A. Harrison, G. D. Stucky, *Angew. Chem.* **1991**, *103*, 1191; *Angew. Chem. Int. Ed. Engl.* **1991**, *103*, 1169. W. T. A. Harrison, T. E. Gier, T. E. Martin, G. D. Stucky. *J. Mater. Chem.* **1992**, *2*, 175; W. T. A. Harrison, T. M. Nenoff, M. M. Eddy, T. E. Martin, G. D. Stucky. *ibid.* **1992**, *2*, 1127. W. T. A. Harrison, T. E. Gier, G. D. Stucky. *Zeolites* **1993**, in press.
[9] Seven Zn/B/O phases are included in the JCPDS Powder Diffraction File, with card numbers: 9-107, 9-153, 24-1438, 27-983, 27-1487, 37-1486 and 39-1126.
[10] J. P. Dougherty, S. K. Kurtz, *J. Appl. Crystallogr.* **1976**, *9*, 145.
[11] A. Le Bail, G. Ferey, P. Amoros, D. Beltran-Porter, *Eur. J Solid State Inorg. Chem.* **1989**, *26*, 419.
[12] M. A. Lafontaine, A. Le Bail, G. Ferey, *J. Solid State Chem.* **1990**, *85*, 220.
[13] A. K. Cheetham, A. P. Wilkinson, *J. Phys. Chem. Solids.* **1991**, *52*, 1199.
[14] G. S. Pawley, *J. Appl. Crystallogr.* **1981**, *14*, 357.
[15] A. Le Bail, H. Duroy, J. L. Fourquet, *Mater. Res. Bull.* **1988**, *23*, 447.
[16] A. C. Larson, R. B. Von Dreele, R. B. GSAS User Guide, Los Alamos National Laboratory, Los Alamos, New Mexico 87545, USA, **1985–1991**.
[17] G. M. Sheldrick, SHELXS-86 User Guide, Universität Göttingen, **1986**.
[18] J. V. Smith, *Chem. Rev.* **1988**, *88*, 149.

Synthesis of the Mono(Dewar Benzene) Isomer of [1.1]Metacyclophane**

By *Geerlig W. Wijsman, Daniël S. van Es, Willem H. de Wolf,* and *Friedrich Bickelhaupt**

Small, strained cyclophanes with nonplanar benzene rings are of great interest because of their unusual structure and reactivity. In this respect the question of the extent of aromaticity in such compounds is particulary important.[1–3] In the series of simple metacyclophanes the borderline for stability at room temperature is found between [4]metacyclophane

[*] Prof. Dr. F. Bickelhaupt, Drs. G. W. Wijsman, D. S. van Es, Dr. W. H. de Wolf
Scheikundig Laboratorium, Vrije Universiteit
De Boelelaan 1083, NL-1081 HV Amsterdam (The Netherlands)

[**] This research was supported by the Stichting Scheikundig Onderzoek in Nederland (SON) and the Nederlandse Organisatie voor Wetenschappelijk Onderzoek (NWO) (G. W. W.).

(**1a**), which can only be trapped as a short-lived intermediate,[1,4] and [5]metacyclophane (**1b**).[1,5] In contrast, [2.2]metacyclophane (**2b**)[6,7] is much more stable and was first reported almost one hundred years ago. We were interested in investigating whether [1.1]metacyclophane **2a**, the smallest compound in this series, can be synthesized ; **2a** can be considered a [5]metacyclophane derivative, but it may be more strained than **1b** because of the additional rigidity imparted by the aromatic ring in the bridge. Although we have not yet been successful in synthesizing **2a**, we report here on a crucial step en route: the preparation of the also quite strained mono(Dewar benzene) isomer **3** (systematic name: tetracyclo[9.1.1.1^{5,9}.0^{3,12}]tetradeca-2,5,7,9(14),11(13)-pentaene) and some of its reactions.

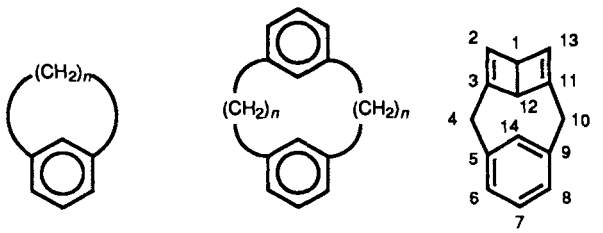

1a: $n = 4$
1b: $n = 5$

2a: $n = 1$
2b: $n = 2$

3

In analogy to the successful syntheses of the [*n*]metacyclophanes **1**,[1,4,5] we attempted to prepare **2a** by the fourfold elimination of HX from bispropellane **4**, which in turn was obtained in three steps: Birch reduction of **6**[8] gave **7**, subsequent conversion provided dichloride **8**, and double addition of bromochlorocarbene yielded **4**.

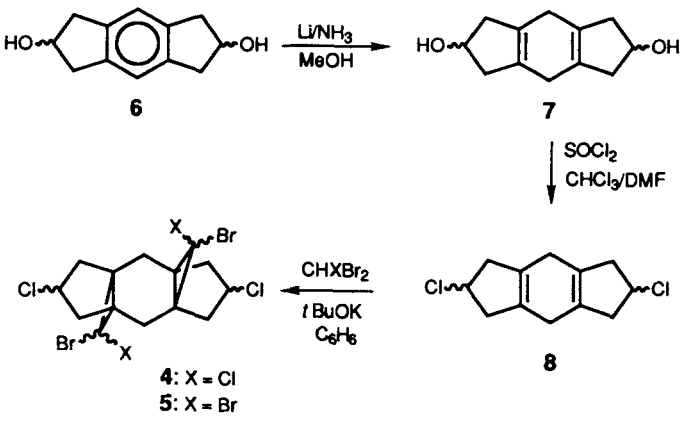

4: X = Cl
5: X = Br

Compounds **4**–**8** are mixtures of stereoisomers. In the analogous reaction of **8** with dibromocarbene to furnish **5**, one of the stereoisomers was isolated in crystalline form; its structure was determined by X-ray crystallography[9] to be that of **5a** (the tetrabromo analogue of **4a**). It was thus possible to assign the structures of the other isomers of **5**, and also of **4**, by comparison of the ^{1}H NMR spectra.

When a solution of the isomeric mixture **4** in DMSO was treated with potassium *tert*-butoxide at room temperature, compounds **9a,b** and **3** were formed in addition to a yellow polymer. Unfortunately, purification of the slightly stable metacyclophane **3** was quite difficult. Various methods of purification were attempted; **3** was finally obtained only 80% pure by column chromatography and recrystallization. It has not yet been possible to remove the remaining **9a,b**. The structure of **3** as a Dewar benzene isomer of the expected **2a** was established by NMR spectroscopy, mass spectrometry, and its chemical transformations.

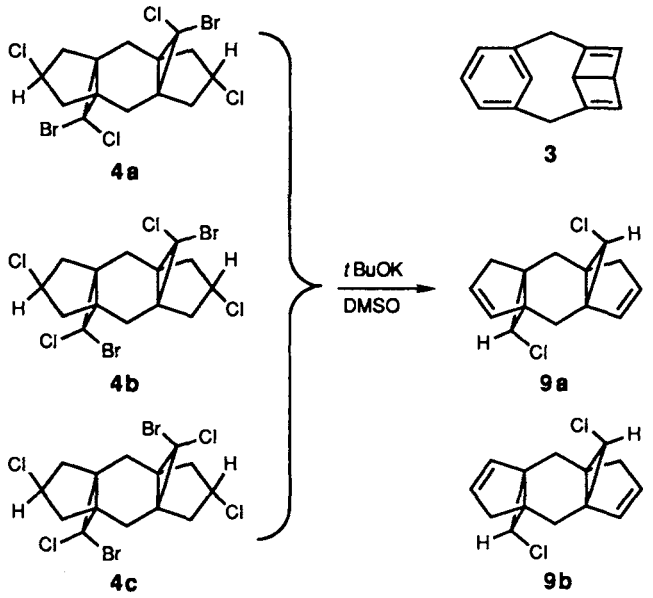

The ^{1}H NMR signals (400 MHz, [D$_8$]THF) are especially instructive for the structure determination of **3**; the chemical shifts of the signals indicate the presence of a 1,3-disubstituted benzene ring ($\delta = 7.14$ and 6.82, $^3J(H,H) = 7.3$ Hz, A_2B system; $\delta = 7.24$, br. s) with a normal aromatic ring current, a Dewar benzene ($\delta = 5.88$, 3.38, 2.13!), and a benzylic methylene bridge ($\delta = 4.03$, 2.95, $^2J(H,H) = 16.5$ Hz, AB system). The ^{1}H NOE and ^{13}C NMR spectra are also in accord with the proposed structure. The signal of H12 on the Dewar benzene unit ($\delta = 2.13$) is very informative. Its unusual chemical shift can be explained by the strong shielding of the aromatic ring, which proves that the central eight-membered ring occurs in the chair–boat conformation (Scheme 1). This

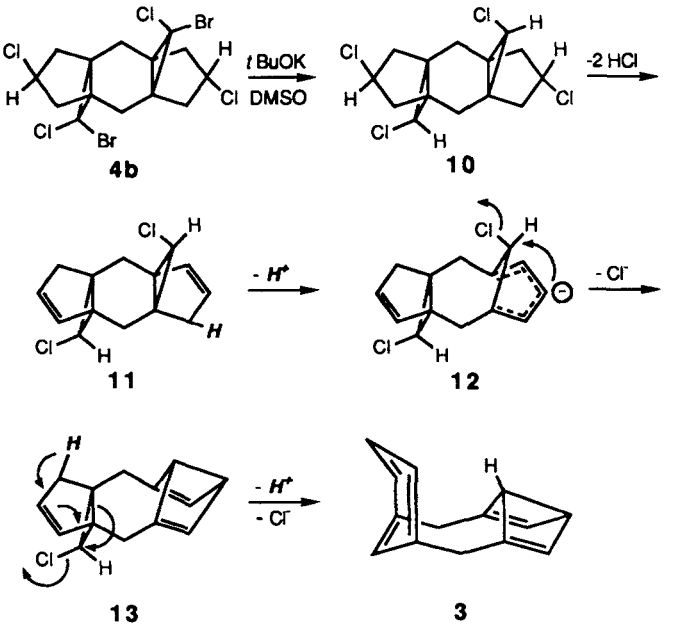

Scheme 1. Postulated reaction sequence for the formation of **3**.

is expected because of the *trans* orientation of the two cyclopropane rings in compound **4**. Interestingly, this conformation plays a minor role in simple [5]metacyclophanes of type **1**, as the crown conformation is usually more stable.[1]

Although the unexpected formation of **3** is not completely understood, the general mechanism can be outlined based on studies of small [*n*]metacyclophanes[1] (Scheme 1). We believe the stereoisomer **4b** to be the most likely precursor for **3** on the basis of the following mechanistic and stereochemical considerations. The reduction of the bromo function in **4b** to give **10** is certainly the initial and fastest step in the reaction sequence;[10] this step must be postulated for the formation of **3** but can also be deduced directly from the structures of **9a,b**. Subsequent double elimination of HCl leads to **11** (or to the regioisomer corresponding to **9b**). Abstraction of an allylic proton and (probably simultaneous) electrocyclic ring opening then provides **12**. Finally, intramolecular S_N2-type substitution with the *anti* chlorine atom as the leaving group generates the Dewar benzene portion of **13**. This sequence has a perfect analogy in the formation of 2,6-tetramethylene(Dewar benzene).[11] In this way the central ring, in **4b** originally a six-membered ring, is expanded into a seven-membered ring in **13**. The conditions are then met for the aromatization of the propellane system of **13** to give **3**, a step known from the formation of [5]metacyclophane (**1b**). The *syn* position of the chlorine atom relative to the five-membered ring is important for the smooth transformation.[1,4]

The high strain energy of **3** is evident from its reactivity. The compound is not stable at room temperature for very long. The strain in **3**, as in **1b**,[1,12] is reduced when the compound serves as a diene in Diels–Alder reactions (Scheme 2). This reaction proceeds very quickly with strong

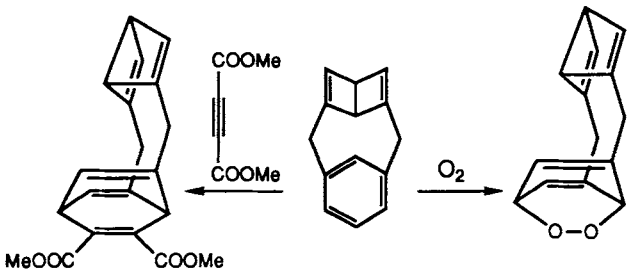

14 **3** **15**

Scheme 2. Diels–Alder reactions with **3** as the diene.

dienophiles like maleic anhydride and tetracyanoethene; the reaction with dimethyl acetylenedicarboxylate lasted about one day and provided adduct **14**, which was isolated in pure form and characterized by NMR spectroscopy and high-resolution mass spectrometry (HRMS). Compound **3** reacts with the oxygen in air to give endoperoxide **15**. Although the reaction is accelerated by irradiation, it is not certain if sensitization plays a role.

We have tried to aromatize the Dewar benzene portion of **3** thermally and photochemically in order to obtain the parent compound **2a**; these experiments have not been successful so far but have led to polymeric products.

Experimental Procedure

Compounds **7**[13] and **8**[14] were prepared according to known methods.

4: To a cooled (0 °C) solution of **8** (0.45 g, 2.0 mmol) and $CHBr_2Cl$ (2.46 g, 12 mmol) in anhydrous benzene (20 mL) under nitrogen was added *t*BuOK (1.33 g, 12 mmol) over 0.5 h. The reaction mixture was stirred for another 1 h and then poured into a cold water/ether mixture. The resulting precipitate which was removed by filtration was composed primarily of stereoisomers **4a–c**. The organic phase was treated again with $CHBr_2Cl$ and *t*BuOK. A standard workup provided a total of 547 mg **4** (1.14 mmol, 57%), probably a mixture of all ten possible stereoisomers of **4**. **4a–c**: ^{1}H NMR (400 MHz, $CDCl_3$): δ = 4.29 (m, 2H; CHCl), 3.01–2.87 (m, 4H), 2.48–2.24 (m, 4H), 2.22 (s, 4H (**4c**)), 2.18 (AB system, 4H, δ_A = 2.23, δ_B = 2.13; ^2J(H,H) = 14 Hz (**4b**)), 2.15 (s, 4H (**4a**)); HR-MS: $C_{14}H_{14}{}^{79}Br^{81}Br^{35}Cl_3{}^{37}Cl$ ($M^{+\cdot}$) calcd.: *m/z* 483.8167, found: *m/z* 483.816 ± 0.002.

3: To a solution of **4** (173 mg, 0.36 mmol) in anhydrous DMSO (35 mL) at room temperature under nitrogen was added *t*BuOK (3.6 mmol) over 3 h. The reaction mixture was stirred for another 0.5 h and then poured into cold water/pentane. The aqueous phase was extracted with pentane five times. The combined pentane phases were washed with water, dried ($MgSO_4$), concentrated, and chromatographed (Al_2O_3, activity II-III eluting with pentane). **9a,b** could not be removed by chromatography but could be partially removed by multiple recrystallizations from pentane. **3**: ^{1}H NMR (400 MHz, [D_8]THF): δ = 7.24 (br. s, 1H; H 14), 7.14 (t, ^3J(H,H) = 7.3 Hz, 1H; H7), 6.82 (d, ^3J(H,H) = 7.3 Hz, 2H; H6/8), 5.88 (br. s, 2H; H 2/13), 3.49 (AB system: δ_A = 4.03, δ_B = 2.95, ^2J(H,H) = 16.5 Hz, 4H; H4/10), 3.38 (br. s, 1H; H1), 2.13 (br. s, 1H; H12); ^{13}C NMR (50.29 MHz, [D_8]THF): δ = 161.5 (s; C3/11), 149.1 (d, J(C,H) = 155 Hz; C14), 143.3 (s; C5/9), 131.1 (d, J(C,H) = 170 Hz; C2/13), 129.2 (d, J(C,H) = 160 Hz; C7), 125.3 (d, J(C,H) = 161 Hz; C6/8), 54.7 (d, J(C,H) = 152 Hz; C12), 42.4 (d, J(C,H) = 156 Hz; C1), 37.7 (t, J(C,H) = 129 Hz, C4/10); HR-MS: $C_{14}H_{12}$ ($M^{+\cdot}$) calcd.: *m/z* 180.0939, found: *m/z* 180.092 ± 0.001.

Diels–Alder reactions: The reactions were conducted in an NMR tube. A solution of **3** in $CDCl_3$ was treated with a small excess of the dienophile, and the reaction was followed by ^{1}H NMR spectroscopy. Products **14** and **15** could be purified by column chromatography (silica gel or alumina, eluting with pentane/ether). **14**: ^{1}H NMR (400 MHz, $CDCl_3$): δ = 6.59 (ddd, ^3J(H,H) = 5.6 Hz, ^4J(H,H) = ^4J(H,H) = 2 Hz, 2H), 6.49 (d, J(H,H) = 2 Hz; 2H(Dewar benzene)), 4.83 (t, ^3J(H,H) = 5.6 Hz, 1H), 4.73 (t, ^4J(H,H) = 2 Hz, 1H), 3.79 (s, 3H; Me), 3.76 (s, 3H; Me), 3.60 (m, 1H), 3.49 (m, 1H), 3.13 (AB system with a further coupling: δ_A = 3.26 (d), δ_B = 3.00 (br. s), ^2J(H,H) = 15.8 Hz, ^4J(H_A,H) = 2 Hz, 4H); ^{13}C NMR (50.29 MHz, $CDCl_3$): δ = 166.2 (s), 166.0 (s), 156.1 (s), 153.3 (s), 147.5 (s), 145.6 (s), 139.0 (d, J(C,H) = 172 Hz), 136.1 (d, J(C,H) = 175 Hz), 56.3 (d, J(C,H) = 145 Hz), 52.2 (q, J(C,H) = 147 Hz), 52.1 (d, J(C,H) = 147 Hz), 52.0 (q, J(C,H) = 147 Hz), 48.1 (d, J(C,H) = 145 Hz), 43.4 (d, J(C,H) = 161 Hz), 33.0 (t, J(C,H) = 129 Hz); HR-MS: $C_{20}H_{18}O_4$ ($M^{+\cdot}$) calcd.: *m/z* 322.1205, found: *m/z* 322.121 ± 0.001.

15: ^{1}H NMR (400 MHz, $CDCl_3$): δ = 6.62 (ddd, ^3J(H,H) = 5.7 Hz, ^4J(H,H) = ^4J(H,H) = 2 Hz, 2H), 6.48 (d, ^4J(H,H) = 2 Hz; 2H(Dewar benzene)), 5.11 (t, ^3J(H,H) = 5.7 Hz, 1H), 4.95 (br. s, 1H), 3.62 (m, 1H), 3.56 (br. s, 1H), 3.16 (AB system with a further coupling: δ_A = 3.39 (d), δ_B = 2.93 (br. s), ^2J(H,H) = 16.3 Hz, ^4J(H_A,H) = 2 Hz, 4H); ^{13}C NMR (50.29 MHz, $CDCl_3$): δ = 154.6, 151.7, 140.2, 131.5, 79.6, 72.1, 52.1, 43.7, 32.9; HR-MS: $C_{14}H_{12}O_2$ ($M^{+\cdot}$) calcd.: *m/z* 212.0837, found: *m/z* 212.084 ± 0.001.

Received: January 7, 1993 [Z 5800 IE]
German version: *Angew. Chem.* **1993**, *105*, 739

[1] F. Bickelhaupt, *Pure Appl. Chem.* **1990**, *62*, 373, and references therein.
[2] Y. Tobe, A. Takemura, M. Jimbo, T. Takahashi, K. Kobiro, K. Kakiuchi, *J. Am. Chem. Soc.* **1992**, *114*, 3479, and references therein; F. Bockisch, H. Dreeskamp, T. von Haugwitz, W. Tochtermann, *Chem. Ber.* **1991**, *124*, 1831, and references therein.
[3] L. W. Jenneskens, E. N. van Eenige, J. N. Louwen, *New J. Chem.* **1992**, *16*, 775, and references therein; T. J. Lee, J. E. Rice, R. B. Remington, W. D. Allen, H. F. Schaefer III, *Chem. Phys.* **1988**, *123*, 1, and references therein; F. Bockisch, J. C. Rayez, D. Liotard, B. Duguay, *J. Comput. Chem.* **1992**, *13*, 1047.
[4] G. B. M. Kostermans, P. van Dansik, W. H. de Wolf, F. Bickelhaupt, *J. Am. Chem. Soc.* **1987**, *109*, 7887.
[5] J. W. van Straten, W. H. de Wolf, F. Bickelhaupt, *Tetrahedron Lett.* **1977**, 4667.
[6] M. Pellegrin, *Rec. Trav. Chim.* **1899**, *18*, 457.
[7] P. M. Keehn, S. M. Rosenfeld, *Cyclophanes, Vol 1*, Academic Press, New York, **1983**.
[8] L. Trøgen, U. Edlund, *Acta Chim. Scand. Ser. B* **1979**, *33*, 109.
[9] We thank Dr. A. L. Spek, Rijksuniversiteit Utrecht, for communicating these unpublished results.
[10] The reduction of the bromo function in 1,1-bromohalocyclopropanes with *t*BuOK in DMSO appears to be a general reaction; G. W. Wijsman, unpublished.
[11] L. A. M. Turkenburg, J. W. van Straten, W. H. de Wolf, F. Bickelhaupt, *J. Am. Chem. Soc.* **1980**, *102*, 3256.
[12] L. A. M. Turkenburg, P. M. L. Blok, W. H. de Wolf, F. Bickelhaupt, *Angew. Chem.* **1982**, *94*, 291; *Angew. Chem. Int. Ed. Engl.* **1982**, *21*, 298.
[13] P. W. Rabideau, *Tetrahedron* **1989**, *45*, 1579.
[14] G. A. C. Gough, H. King, *J. Chem. Soc.* **1928**, 2436.

A Sulfide-Linked Oligonucleotide Analogue with Selective Hybridization Properties**

By *Bin Meng, Stephen H. Kawai, Daguang Wang, George Just,* Paul A. Giannaris,* and *Masad J. Damha**

Dedicated to Professor Jean Jacques on the occasion of his 75th birthday

In response to the instability of DNA and RNA oligomers in vivo as well as problems regarding cellular uptake, a great deal of recent work has been devoted to the development of nucleic acid analogues for use as specific inhibitors of gene expression (the antisense strategy).[1] In addition to oligonucleotides bearing modified phosphodiester groups, a number of antisense systems in which the phosphate group is replaced altogether have been described.[2] Apart from evaluating the suitability of antisense systems as potential therapeutics, the study of their DNA and RNA hybridization properties addresses the fundamental question of the role played by the backbone (sugar–phosphate units in natural strands) in the formation and stabilization of nucleic acid helices.

Our research in the antisense field has focused on oligonucleotide analogues in which phosphodiester groups are replaced by dialkyl sulfide linkages.[3] We chose this modification as it is stable and nonhydrolyzable, and because examination of models suggested that binding to complementary oligonucleotide targets would not be disrupted. In work previously carried out in our laboratory, DNA strands incorporating internucleoside dialkyl sulfides were synthesized and shown to possess enhanced stability towards nuclease degradation. These sulfide-containing strands also exhibited cooperative binding to both fully natural DNA and RNA.[4]

Here, we describe the preparation of a mixed ribo–deoxyribo dinucleoside analogue **11** in which the two furanoses are linked through a thioether group, and the successful incorporation of this compound into DNA. In evaluating the effect of this modification on complexation with complementary natural nucleic acids (DNA, RNA), we were surprised by the marked selectivity of the system for RNA.

Phosphoramidite **9** was synthesized from the 3′-deoxy-3′-(2-hydroxyethyl)ribofuranosylthymine derivative **1**[5] as outlined in Scheme 1. The oxidative removal of the *p*-methoxyphenyl group was effected by treatment with ceric ammonium nitrate (CAN), and followed by mesylation of the resulting alcohol **2**, which afforded the 5′-end of the dimer in 74% yield. The coupling of mesylate **3** and thionucleoside **4**[5] was carried out in *N,N*-dimethylformamide (DMF) employing cesium carbonate (84% yield). The solvent was deoxygenated by saturation with nitrogen over 20 min; this was necessitated by the otherwise rapid oxidation of the thiol to the disulfide under basic conditions. The deacetylation of **5** by ammonia cleanly gave diol **6** in 97% yield. The 5′-hydroxyl function was then selectively protected[6] by a dimethoxytrityl (DMTr) group, and immediately following, the 2′-*O*-acetate group required during the subsequent solid-phase synthesis was reintroduced with acetic anhydride to yield **7** (76% yield). The 3′-silyl ether was cleaved with tetra-*n*-butylammonium fluoride (94%), and the resulting alcohol **8** was treated with 2-cyanoethyl-*N,N*-diisopropylchlorophosphoramidite under standard conditions[7] to yield (68%) the appropriately activated dimer **9** (mixture of P-isomers) for incorporation into DNA.

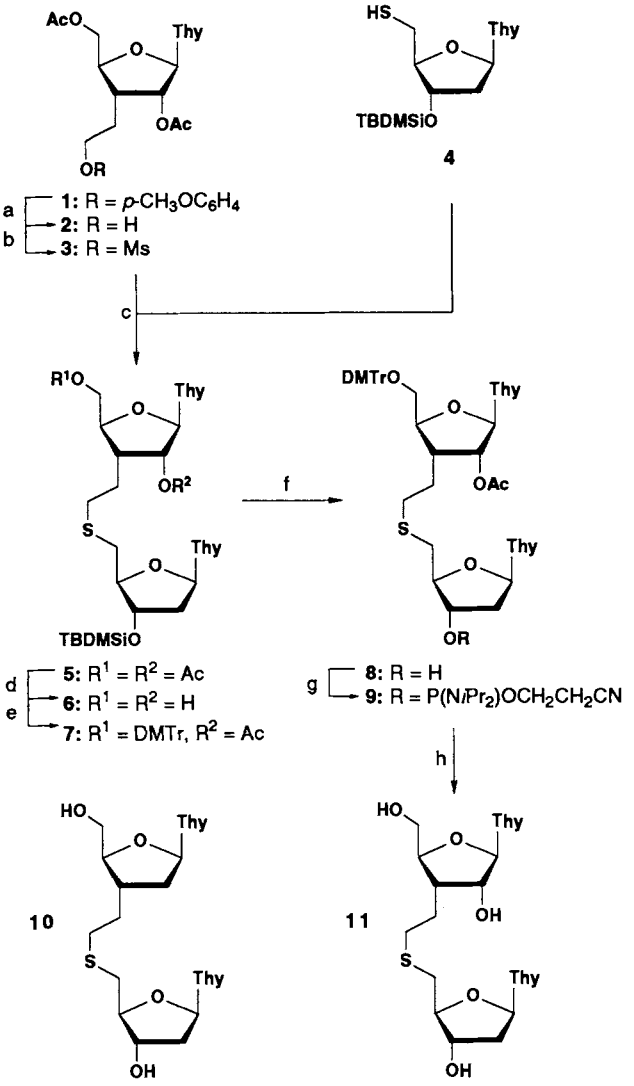

Scheme 1. Synthesis of phosphoramidite **9**. TBDMSi = *tert*-butyldimethylsilyl. a) CAN/H_2O/MeCN, 0 °C, 30 min (76%); b) MsCl/Et_3N/CH_2Cl_2, 1 h (97%); c) Cs_2CO_3/DMF (84%); d) NH_3/MeOH, 0 °C, 11 h (97%); e) DMTrCl/Et_3N/pyridine, 8 h then Ac_2O (62 equiv) (76%); f) nBu_4NF/THF, 1 h (94%); g) $iPr_2NP(Cl)OCH_2CH_2CN$/Et_3N/CH_2Cl_2, 6 h (72%); h) from **8**, OPC: TFA/MeCN/H_2O then NH_4OH/H_2O.

To confirm that the internucleoside sulfide linkages are stable to enzymatic degradation, triol **11** (prepared from **8** by cleavage of the DMTr group with trifluoroacetic acid (TFA) and deacetylation with ammonium hydroxide during purification with an oligonucleotide purification cartridge (OPC)) was subjected to a number of nucleases. Incubation of **11** with SVPDE, nuclease S_1, nuclease P_1, and CSPDE did to result in any modification of the dimer.[8]

The modified DNA dodecamer **12** (Fig. 1), which incorporates three sulfide-linked ribofuranosylthymine-thymidine dimers **11** ($T_S^{OH}T$), was synthesized by the phosphoramidite method[9] by using standard solid-phase techniques.[10] A fifth bottle containing a 0.08 M solution of **9** in acetonitrile was attached to the DNA synthesizer, and the reaction time

[*] Prof. G. Just, Prof. M. J. Damha, B. Meng, Dr. S. H. Kawai, D. Wang, P. A. Giannaris
Department of Chemistry, McGill University
801 Sherbrooke St. W., Montreal, Quebec, H3A 2K6 (Canada)

[**] This work was supported by the Natural Sciences and Engineering Research Council of Canada and the Ministère de l'éducation du Québec (FCAR). We are grateful to Prof. O. A. Mamer (McGill University Biomedical Mass Spectrometry Unit) for the measurement of mass spectra.

 © VCH Verlagsgesellschaft mbH, W-6940 Weinheim, 1993 0570-0833/93/0505-0729 $ 10.00+.25/0

for the tetrazole-mediated coupling of **9** to the growing chain was increased to 10 min. To verify that the sulfides incorporated into the strand are not converted to the sulfoxide or sulfone during the oxidation step of the cycle, a sample of the sulfide dimer was stirred in the reagent I_2/pyridine/THF/H_2O for 15 minutes (30 times longer in the synthetic cycle). Thin-layer chromatography of a mixture of sulfoxide and sulfone dimers obtained with buffered Oxone reagent ($2KHSO_5 \cdot KHSO_4 \cdot K_2SO_4$) clearly demonstrated that no oxidation had taken place. The fully natural DNA strands **13** and **14**, as well as RNA dodecamer **15**, were also prepared by standard solid-phase methods.[11]

mixed oligomer **12**: G C G T_S^{OH}T T_S^{OH}T T_S^{OH}T G C T
DNA oligomer **13**: G C G T T T T T T G C T
DNA oligomer **14**: A G C A A A A A A C G C
RNA oligomer **15**: r(A G C A A A A A A C G C)

Fig. 1. Sequences of oligomers **12**–**15** shown in 5′ to 3′ direction. $T_S^{OH}T$ denotes the sulfide-linked dimers.

The results of thermal denaturation studies[12] are summarized in Table 1. The data clearly indicates that the strands containing $T_S^{OH}T$ dimers can discriminate between complementary DNA and RNA over a wide range of salt concentrations. As expected, cooperative binding between unmodified DNA strands **13** and **14**, and between **13** and natural RNA oligomer **15**, was observed with melting temperatures (T_m) of 55 °C and 52 °C (100 mM NaCl), respectively. In the case of hybridization between the sulfide-containing oligomer **12** and RNA **15**, a melting temperature of 34 °C was measured at the same salt concentration. This corresponds to a decrease in T_m of 6.3 K per sulfide-substitution and indicates that, while weakening the complexation to targeted RNA, the modification still allows for good cooperative binding. However, in the case of complexation between modified oligomer **12** and DNA dodecamer **14**, no cooperative transition was observed over a wide range of salt concentrations.

Table 1. Melting temperatures T_m [°C] and hypochromicities (in parentheses) [a].

c (NaCl) [mM]	**13/14**	**13/15**	**12/14**	**12/15**
10	47 (24)		[b]	19 (10)
100	55 (24)	52 (24)	[b]	34 (10)
210	58 (24)		[b]	39 (12)
910	65 (24)		[b]	40 (12)

[a] Thermal denaturation was carried out in phosphate buffer (pH 7.0) at the indicated NaCl concentrations. Curves were obtained by recording the absorbance at 260 nm (average of 30 readings) at 1 min intervals between 5 and 80 °C and at a rate of 0.5 °C min^{-1}. [b] No observable T_m.

This selectivity is also clearly demonstrated by native-gel hybridization. Mixtures of the complementary oligomers **12** and DNA **14**, **12** and RNA **15**, DNA **13** and DNA **14**, and DNA **13** and RNA **15** were incubated in 30% sucrose solutions containing 10 mM magnesium chloride and then applied to separate lanes of a polyacrylamide gel containing no urea. Oligomers **12** through **15** were also applied individually. After electrophoresis (4 °C/18 h/5 mA) the gel showed bands corresponding to duplexes DNA **13**/DNA **14** and DNA **13**/RNA **15**, as well as that formed between **12** and RNA **15**. Moreover, this latter band migrated much more slowly than either **13**/**14** or **13**/**15**, reflecting the lower charge (three fewer phosphate groups) of the complex **12**/**15**. In contrast, the lane containing the mixture of **12** and DNA **14** showed only the two bands corresponding to the unassociated single strands.

This selectivity exhibited by **12** for RNA is quite surprising; only a few oligonucleotide analogues exist that can discriminate between DNA and RNA, and these systems are very different from the natural structures.[13] DNA is known to be much more flexible than RNA, which manifests itself in the fact that double helices of the latter usually form A-type helices whereas duplex DNA is polymorphic.[14] Thus, one would expect that any modified system that binds to RNA should also complex to DNA. Efforts are presently underway to gain an understanding of this selectivity.

Experimental Procedure

5: Cesium carbonate (549 mg, 1.68 mmol) was suspended in dry, deoxygenated DMF (9 mL), and a solution containing **3** (505 mg, 1.17 mmol) and **4** (479 mg, 1.29) in DMF (14 mL) was added under nitrogen. The reaction mixture was stirred for 1 h, the solvent evaporated, and the residue extracted with dichloromethane and washed with aqueous bicarbonate and water. Chromatography of the crude material over silica gel (1:2.5 EtOAc/hexanes) afforded sulfide **5** (84%). – ^{1}H NMR (300 MHz, $CDCl_3$): δ = 0.092 (s, 6H; $SiMe_2$), 0.90 (s, 9H, *t*Bu), 1.60–1.80 (m, 2H; ^{5}H1″), 1.92, 1.93 (2s, 6H; 2 × 5-Me), 2.10, 2.15 (2s, 6H; 2 × CO-Me), 2.18–2.26 (m, 2H, ^{3}H2′), 2.41–2.51 (m, 1H; ^{5}H3′), 2.51–2.70 (m, 2H; ^{5}H2″), 2.75 (A of ABX, 1H; ^{3}H5′A), 2.78 (B of ABX, 1H; ^{3}H5′B), 3.94 (q, 1H; ^{5}H4′), 4.10 (dt, 1H; ^{3}H4′), 4.28–4.37 (m, 3H; ^{3}H3′, ^{5}H5′), 5.45 (d, 1H; ^{5}H2′), 5.61 (s, 1H; ^{5}H1′), 6.21 (t, 1H; ^{3}H1′), 7.30, 7.56 (2s, 2H; 2 × H6), 9.01 (br s, 2H; 2 × NH); J(^{5}H1′, ^{5}H2′) = 0 Hz, J(^{3}H1′, ^{3}H2′) = 6.6, J(^{5}H2′, ^{5}H3′) = 6.0, J(^{5}H3′, ^{5}H4′) = 7.5, J(^{3}H3′, ^{3}H4′) = 4.5, J(^{3}H4′, ^{3}H5′A) = 5.7, J(^{3}H4′, ^{3}H5′B) = 4.9, ^2J(^{3}H5′A, ^{3}H5′B) = –13.8; ^{13}C NMR (75.4 MHz, $CDCl_3$) δ = 11.11 (2 × 5-Me), 17.12 (Si-*C*-Me_3), 20.22, 20.32 (2 × CO-*Me*), 24.31 (^{5}C1″), 25.21 (Si-Me_2, Si-C-*Me*$_3$), 30.50 (^{5}C2′), 33.49(^{3}C5′), 39.87 (^{3}C2′), 40.16 (^{5}C3′), 62.88 (^{5}C5′), 73.01 (^{3}C3′), 76.67 (^{5}C2′), 81.69, 84.54, 85.18 (^{3}C1′, 2 × C4′), 91.27 (^{5}C1′), 110.25, 110.70 (2 × C5), 135.35, 135.62 (2 × C6), 149.82, 150.10 (2 × C2), 163.79, 163.87 (2 × C4), 169.21, 169.94 (2 × *C*O-Me); FAB-MS glycerol/NBA (nitrobenzyl alcohol)): *m/z* 725 (MH^+, 7.5%), 599 (MH^+ – ThyH, 52), 473 (MH^+ – 2 ThyH, 12), 399 (33), 341 (57), 295 (17), 213 (100).

8: FAB-MS: *m/z* 871 (MH^+, 59%), 745 (MH^+ – ThyH, 28), 551 (MH^+ – DMTrOH, 87); HRMS (FAB, glycerol): *m/z* calcd. for $C_{45}H_{50}N_4O_{12}S$: 870.31459, found: 870.31421.

9: FAB-MS: *m/z* 1072 (MH^+, 10%), 946 (MH^+ – ThyH, 8), 853 (MH^+ – $iPr_2NP(OH)OCH_2CH_2CN$, 5), 768 (MH^+ – DMTr, 9) 551 (16), 457 (100); ^{31}P NMR (81.0 MHz, $CDCl_3$) δ = 148.94, 149.31.

12–**15**: DNA oligomers were synthesized with an Applied Biosystems DNA/RNA synthesizer (model 381A) employing amidine-protected phosphoramidites and LCAA-CPG (LCAA = long-chain alkyl amine, CPG = controlled pore glass) bearing 3′-terminal deoxyribonucleosides. Oligomers were prepared on a 1.0 μmol scale employing the standard synthesis cycle. In the case of **12**, a 0.08 M solution of **9** was attached to a fifth port on the synthesizer and the coupling time increased to 10 min from the standard 60 s. The coupling efficiency of **9** was routinely >98% as monitored by the release of the DMTr cation. RNA oligomer **15** was prepared by standard means.

Received: November 1, 1992 [Z 5674 IE]
German version: *Angew. Chem.* **1993**, *105*, 733

[1] U. Englisch, D. H. Gauss, *Angew. Chem.* **1991**, *103*, 629; *Angew. Chem. Int. Ed. Engl.* **1991**, *30*, 613; E. Uhlmann, A. Peyman, *Chem. Rev.* **1990**, *90*, 544; B. J. Dolnick, *Biochem. Pharm.* **1990**, *40*, 671; *Oligonucleotides: Antisense Inhibitors of Gene Expression (Top. Mol. Struct. Biol. 12)* (Ed.: J. S. Cohen), MacMillan Press, London, **1989**.

[2] M. Engholm, O. Buchardt, P. E. Nielson, R. H. Berg, *J. Am. Chem. Soc.* **1992**, *114*, 1895; See also "Highlight": C. Meier, J. W. Engels, *Angew. Chem.* **1992**, *104*, 1039; *Angew. Chem. Int. Ed. Engl.* **1992**, *31*, 1008; E. M. Huie, M. R. Kirshenbaum, G. L. Trainor, *J. Org. Chem.* **1992**, *57*, 4569; B. Musicki, T. S. Widlanski, *Tetrahedron Lett.* **1991**, *32*, 1267; M. Matteucci, *Nucleosides Nucleotides* **1991**, *10*, 231; J. F. Cormier, K. K. Ogilvie, *Nucleic Acids Res.* **1988**, *16*, 4583; E. P. Stirchak, J. E. Summerton, D. D. Weller, *J. Org. Chem.* **1987**, *52*, 4202.

[3] Sulfide-linked *bis*-homonucleosides have been reported: Z. Huang, K. C. Schneider, S. A. Benner, *J. Org. Chem.* **1991**, *56*, 3869.

[4] A sulfide-containing DNA oligomer of the same sequence as **12** that incorporates T_ST dimers **10** was found to exhibit cooperative binding to *both* natural DNA **14** and RNA **15**. T_m values of 32 and 30 °C, respectively, were

obtained at 100 mM NaCl. S. H. Kawai, D. Wang, P. A. Giannaris, M. J. Damha, G. Just, *Nucl. Acids Res. 21*, in press.
[5] S. H. Kawai, D. Wang, G. Just, *Can. J. Chem.* **1992**, *70*, 1573. S. H. Kawai, J. Chin, G. Just, *Carbohydr. Res.* **1991**, *211*, 245.
[6] G. H. Hakimelahi, Z. A. Proba, K. K. Ogilvie, *Can. J. Chem.* **1982**, *60*, 1106.
[7] M. J. Gait, *Oligonucleotide Synthesis: A Practical Approach*, IRL Press, Oxford, **1984**.
[8] SVPDE = snake venom phosphodiesterase, CSPDE = calf spleen phosphodiesterase; triol **11** was incubated with enzyme at 37 °C for 36 h, after which time the digests were analyzed by HPLC. Under identical conditions, T_pT was completely degraded to monomers.
[9] M. H. Caruthers, *Science* **1985**, *230*, 281.
[10] After cleavage from the support and base-deprotection, the oligomers were detritylated and purified by reverse-phase chromatography with OPC (Applied Biosystems) cartridges. RNA oligomer **15** was purified on 16% PAGE and desalted by reverse-phase chromatography (C18 Sep-Pack, Waters).
[11] N. Usman, K. K. Ogilvie, M. Y. Jians, R. J. Cedergren, *J. Amer. Chem. Soc.* **1987**, *109*, 7845.
[12] T_m values are reported as the intersection of the absorbance versus temperature curve and the midpoint between the upper and lower linear sloping base lines.
[13] *enantio*-DNA (oligo-L-dA) was shown to complex complementary RNA, but not DNA: S. Fujimori, K. Shudo, Y. Hashimoto, *J. Amer. Chem. Soc.* **1990**, *112*, 7436. 2',5'-Linked oligo-RNA binds RNA selectively over DNA: M. J. Damha, P. A. Giannaris, unpublished results. A carbamate-linked morpholino-nucleoside oligomer binds DNA selectively over RNA: E. P. Stirchak, J. E. Summerton, D. D. Weller, *Nucleic Acids Res.* **1989**, *17*, 6129).
[14] W. Saenger, *Principles of Nucleic Acid Structure*, Springer, New York, **1988**, Chaps. 9-11.

Synthesis of the First Stable 2-Chromaoxetane and its Homologues via α-Phosphonio(methylidene) Complexes of Hexavalent Chromium, Molybdenum, and Tungsten**

By *Jörg Sundermeyer,** *Klaus Weber*, and *Hans Pritzkow*

The synthesis of stable organochromium(VI) compounds appeared for a long time to be an inaccessible goal. Only recently have there been promising attempts[1] in this area of research in organometallic chemistry. However, till now neither the synthesis of an alkylidenechromium(VI) complex nor the isolation of 2-chromaoxetanes, that is, of four-membered ring compounds with an oxa-2-metallacyclobutane skeleton have been reported. 2-Metallaoxetanes have been discussed as short-lived intermediates in oxo transfer reactions from reactive oxo complexes such as OsO_4, CrO_2Cl_2, or oxo(porphyrinato) species to olefins.[2] Although these organometallic intermediates have a surprisingly high thermodynamic stability according to quantum mechanical calculations,[3] the synthesis and structural characterization of the electron-deficient metallacycles with a metal center in the highest oxidation state (d^0 electron configuration) remained a particular challenge.[4, 5] These four-membered ring compounds appear to be predestined to decompose into a thermodynamically particularly stable oxo complex and an olefin.[5] We now report on the synthesis and characterization of the first Cr^{VI} complex **1a** containing a formal Cr–C double bond and on the unusual cycloaddition reaction of **1a** and its heavier homologues **1b,c** with diphenyl ketene, which affords the stable compounds **2a–c** containing 2-metallaoxacyclobutane frameworks.

Only recently we proposed higher valent α-phosphonio(methylidene) complexes of molybdenum, tungsten, and rhenium, amongst them also tetrahedral complexes of the type $[M(=NtBu)_2(=CHPPh_3)_2]$ (M = Mo, W), in which four multiple bonds, two each to an anionic carbon and nitrogen atom, are present.[6] Complexes of this type have very reactive (because strongly polar) metal–carbon bonds, which even react spontaneously with thermodynamically stable molecules like CO and CO_2, a reactivity that is typically lacking for the d^0 alkyl- and aryloxo and alkyl- and arylimido complexes of the sixth and seventh group. Surprisingly, $[Cr(=NtBu)_2Cl_2]$,[7] the relatively easily reducible *tert*-butylimido derivative of chromyl chloride, can also be transformed into the hitherto unknown α-phosphonio(methylidene)chromium(VI) complexes through the transylidation reaction with two equivalents of the ylides $R_3P=CH_2$ (R = alkyl, aryl) (see Scheme 1). The example presented here

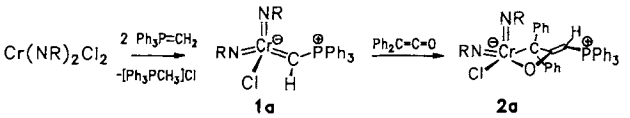

Scheme 1. Synthesis of **1a** and **2a**. R = *t*Bu.

(**1a**) is isoelectronic to the hitherto unknown alkylidene complexes of formally hexavalent chromium containing the binding unit $[Cr=CHSiR_3]$. Compound **1a** displays significant spectroscopic characteristics of alkylidene complexes; for instance, the NMR signals of the metal-bound α-CH function are shifted downfield ($\delta_C = 200.1$, $\delta_H = 11.84$) relative to the signals of the free, unmetalated phosphorus ylide $Ph_3P=CH_2$ ($\delta_c = -4.2$, $\delta_H = 0.77$).[8] The pronounced Cr–C double bond character is also reflected in the high barrier for rotation about this bond axis, which renders the signals of the *tert*-butylimido groups inequivalent at the low-temperature limit (Scheme 2). The free energy of activation for the hindered rotation was calculated from the coalescence temperature of these signals in the variable-temperature ^1H NMR spectra. The value of $\Delta G^{\ddagger}_{(336K)} = 75\ kJ\,mol^{-1}$ ($17.9\ kcal\,mol^{-1}$) lies within the range of $\Delta G^{\ddagger} = 15$–$18\ kcal\,mol^{-1}$ determined for the alkylidene molybdenum and tungsten complexes of the Schrock type.[9]

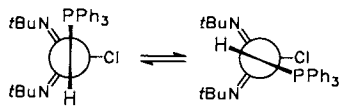

Scheme 2. Newman projection of two conformations obtained by rotation about the Cr–C bond.

Compound **1a**, like the derivatives of the heavier homologues **1b** (M = Mo) and **1c** (M = W), can be used as complex-modified C-nucleophiles for selective C–C coupling or C–O cleavage reactions. Phosphorus ylides that are not sub-

[*] Dr. J. Sundermeyer, Dipl.-Chem. K. Weber
Institut für Anorganische Chemie der Universität
Am Hubland, D-W-8700 Würzburg (FRG)
Telefax: Int. Code +(931)888-4605
Dr. H. Pritzkow
Anorganisch-chemisches Institut der Universität
Im Neuenheimer Feld 270, D-W-6900 Heidelberg (FRG)

[**] Organometallic Imido Complexes—Higher Valent Derivatives of the d-Metal Acids, Part 7. This work was supported by the Fonds der Chemischen Industrie, the Deutsche Forschungsgemeinschaft, and the Universitätsbund Würzburg. We thank Prof. Dr. H. Werner for his kind support and the company H. C. Starck, Berlin, for gifts of chemicals. Part 6: J. Sundermeyer, J. Putterlik, H. Pritzkow, *Chem. Ber.* **1993**, *126*, 289-296.

stituted by a metal do not typically undergo such reactions. Thus carbon monoxide and isonitriles insert diastereoselectively to form η^2-acyl or iminoacyl complexes (Scheme 3) that were characterized by crystallography,[10] whereas for lactones a C–O bond in the ring is cleaved.[11]

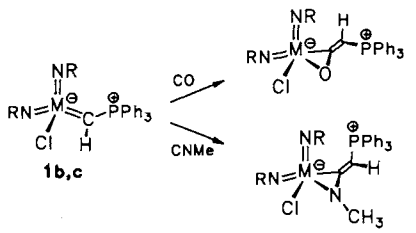

Scheme 3. Insertion of CO and CNR into **1b** and **1c**.

We present here the result of the reaction with diphenyl ketene as an unusual example of the reactivity of **1a–c**. In all three reactions neither the expected product of the usual [2 + 2] cycloaddition **B** (see Scheme 4) nor the resonance-stabilized enolate complex **C**, conceivably formed by a simple insertion reaction, was isolated. Instead on the evidence of the typical ^{183}W satellites in the ^{13}C NMR spectrum of **2c**, a bond between the CPh_2 unit and the tungsten center can be deduced without doubt. The lack of a typical ν(C=O) stretching band in the IR spectrum of the spectroscopically almost identical products **2** (Table 1) suggested that the common structural element must be an [M-O-C-C] four-membered ring with an exocyclic α-phosphonio(methylidene) unit. This assumption was confirmed by the determination

Table 1. Selected spectroscopic data of the complexes **2**. The NMR spectra of **2a** were recorded in CD_2Cl_2 at 190 K, those of **2b,c** in C_6D_6 at 298 K.

	2a	**2b**	**2c**
^{1}H NMR			
δ_{CH-P} ($^1J_{PH}$)	4.14 (22.0)	4.23 (23.5)	4.30 (23.0)
^{13}C NMR			
δ_{CH-P} ($^1J_{PC}$)	56.7 (101.7)	58.5 (98.6)	61.8 (100.9)
δ_{MOC}	193.9	196.7	196.1
δ_{MC} ($^3J_{PC}$)	68.0 (8.6)	68.4 (8.6)	69.7 (7.1)
^{31}P NMR			
δ_P	16.9	16.0	15.4
IR (KBr)			
ν_{C-O} (vs)	1492	1488	1484
ν_{P-C} (vs)	860	860	855
$\nu_{M=N-C}$ (vs)	1200/1236	1204/1248	1242/1289

of the single-crystal structure of **2b** (Fig. 1). The metal atom of **2b** lies at the center of a distorted square-pyramidal coordination polyhedron and is part of a four-membered metallacycle that forms one edge of the base. The four-membered ring is folded along the O–C2 vector by 39.6°. Another structural characteristic is the trigonal-planar coordination of the carbocationic center C1 (sum of the angles 359.6°), whose charge is compensated by the + M effects of the O atom and the conjugated carbanionic center C3. The C1–O distance is comparable to the corresponding distance in enols. In contrast to the characteristics of the d^0-2-metallaoxetane [Mo(NAr)(O*t*Bu)$_2$(η^2-(*O*,*C*)OCH(C_6F_5)CH*t*Bu)], a rather unstable complex at 25 °C reported only recently by Schrock et al.,[5] the bond lengths determined here for **2b** indicate a stabilization of the four-membered ring, which is expressed in the resonance form **D** (Scheme 4). Since

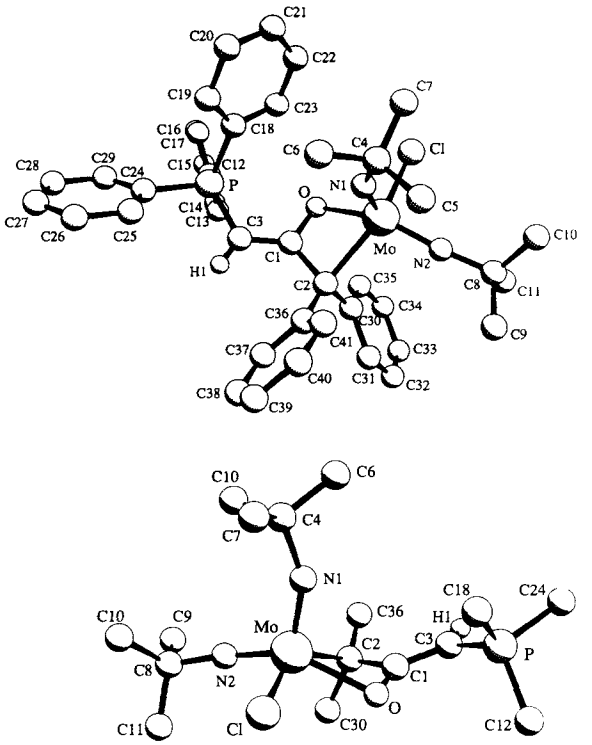

Fig. 1. Schakal representation of the molecular structure of **2b**. For clarity in the view shown at the bottom, only the *ipso* C atoms of the five phenyl groups are shown. Selected Bond lengths [Å] and angles [°]: Mo-N1 1.737(2), Mo-N2 1.732(3), Mo-Cl 2.390(2), Mo-C2 2.277(4), Mo-O 2.162(2), O-Cl 1.312(5), C1-C2 1.492(4), C1-C3 1.367(5), C3-P 1.734(3); Mo-N1-C4 152.4(2), Mo-N2-C8 173.4(3), N1-Mo-N2 109.6(1), N1-Mo-C2 105.2(1), N2-Mo-C2 101.3(1), N1-Mo-O 103.2(1), N1-Mo-Cl 103.6(1), Mo-O-C1 91.4(1), O-C1-C2 110.7(2), Mo-C2-C1 82.6(2), C2-Mo-O 62.6(1), O-C1-C3 121.4(2), C2-C1-C3 127.5(3); dihedral angles: P-C3-C1-C2 167.4, P-C3-C1-O −4.1.

2b does not tend to decompose thermally into $[Ph_3PCH{=}C{=}Ph_2]^+[MoO(NtBu)_2Cl]^-$, it would be an interesting challenge also to attempt the synthesis of 2-metallaoxetane by addition of a polarized [C=C] bond of an allenylphosphonium ion to a polar, nucleophilic [M=O] function.

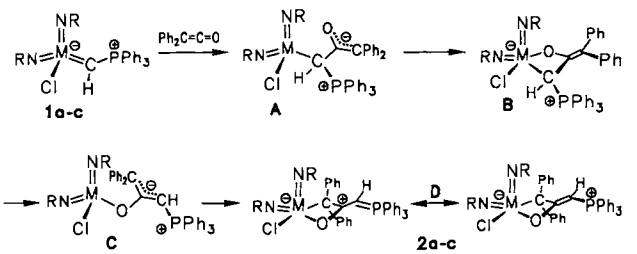

Scheme 4. Plausible mechanism for the formation of **2a–c** and their resonance forms. R = *t*Bu.

The complexes **2** show a stereochemically dynamic behavior in solution. Low-temperature NMR studies on **2a–c** confirm that axial and basal imido functions exchange rapidly. Even at 190 K the equivalence of these ligands observed in the ^{1}H and ^{13}C NMR spectra cannot be lifted.

A plausible mechanism for the formation of **2a–c** seems to be a nucleophilic attack of the α-C atom in **1a–c** on the

ketene, followed by rearrangement of the betain-like oxallyl intermediate **A** to the zwitterionic enolate species **C**, although none of the intermediates could be isolated or detected by spectroscopic methods (Scheme 4). Crucial for the next M–C bond linkage accompanied by reorganization of the 2-metallaoxetane framework is the formation of the exocyclic, planar α-phosphoniomethylene unit. The reactivity pattern presented here is not restricted to reactive ketenes, but is possible with almost all CO_2 derivatives, including the parent compound, the relatively inert CO_2 itself.[10]

Experimental Procedure

1a: A solution of $[Cr(=NtBu)_2Cl_2]$ [7] (1.00 g, 3.8 mmol) in toluene (50 mL) under an inert atmosphere (argon) at −78 °C was treated with $Ph_3P{=}CH_2$ (2.08 g, 7.5 mmol). After slow warming to room temperature (2 h), the deep violet suspension was stirred for a further 2 h and then filtered through a glass frit covered with dried Celite. After washing the precipitated $[Ph_3P{-}CH_3]Cl$ with toluene, the filtrate was concentrated to 10 mL under reduced pressure and layered with *n*-hexane (30 mL). At −30 °C the dark violet, finely crystalline product precipitated. It was washed with *n*-pentane (20 mL), and any remaining solvent was removed under high vacuum ($<10^{-3}$ mbar). Yield: 1.67 g (93%), m.p. 64 °C (decomp.).

2a–c: **1a**, **1b**, or **1c** (1 mmol) was dissolved in THF (20 mL) and treated with diphenyl ketene (190 μL, 1.1 mmol) at −90 °C. After warming to room temperature (1 h) the mixture was stirred for another 60 min and then filtered over a glass frit covered with dried Celite. The filtrate was concentrated to 5 mL under reduced pressure. After layering with *n*-pentane (20 mL), the crystalline products **2a–c** precipitate. Suitable single crystals of **2b** were grown from methylcyclohexane/THF. **2a**: orange crystals, 75%, decomp. >75 °C; **2b**: beige crystals, 90%, decomp. >119 °C; **2c**: light beige crystals, 95%, decomp. >151 °C.

Received: December 10, 1992 [Z 5740IE]
German version: *Angew. Chem.* **1993**, *105*, 751

[1] $[Cr(=NtBu)_2(mesityl)_2]$ and its chemistry: M. B. Hursthouse, M. Motevalli, A. C. Sullivan, G. Wilkinson, *J. Chem. Soc. Chem. Commun.* **1986**, 1398–1399; A. C. Sullivan, G. Wilkinson, M. Motevalli, M. B. Hursthouse, *J. Chem. Soc. Dalton Trans.* **1988**, 53–60; $[(\eta^5\text{-}C_5H_5)Cr(=NtBu)_2Br]$ and its chemistry: N. Meijboom, C. J. Schaverien, A. G. Orpen, *Organometallics* **1990**, *9*, 774–782; $[(\eta^5\text{-}C_5Me_5)Cr(=O)_2\text{-}Me]$: S.-K. Noh, R. A. Heintz, B. S. Haggerty, A. L. Rheingold, K. H. Theopold, *J. Am. Chem. Soc.* **1992**, *114*, 1892–1893.

[2] K. B. Sharpless, A. Y. Teranishi, J.-E. Bäckvall, *J. Am. Chem. Soc.* **1977**, *99*, 3120–3128; reviews: K. A. Jørgensen, B. Schiøtt, *Chem. Rev.* **1990**, *90*, 1483–1506; B. Meunier, *ibid.* **1992**, *92*, 1411–1456.

[3] A. K. Rappé, W. A. Goddard III, *J. Am. Chem. Soc.* **1980**, *102*, 5115–5117; A. K. Rappé, W. A. Goddard III, *ibid.* **1982**, *104*, 3287–3294.

[4] S. C. Ho, S. Hentges, R. H. Grubbs, *Organometallics* **1988**, *7*, 780–782.

[5] G. C. Bazan, R. R. Schrock, M. B. O'Regan, *Organometallics* **1991**, *10*, 1062–1067.

[6] J. Sundermeyer, K. Weber, O. Nürnberg, *J. Chem. Soc. Chem. Commun.* **1992**, 1631–1633.

[7] A. Danopoulos, W.-H. Leung, G. Wilkinson, B. Hussain-Bates, M. B. Hursthouse, *Polyhedron* **1990**, *9*, 2625–2634.

[8] Selected spectroscopic data of **1a**: ^1H NMR (400 MHz, C_6D_6, 25 °C): $\delta = 1.05$ (s, 9H, $NCMe_3$), 1.59 (s, 9H, $NCMe_3$), 7.02–7.15, 7.59–7.64 (m, 15H, PPh_3), 11.84 (d, 1H, $^2J(PH) = 7.6$ Hz, Cr=CH-P); ^{13}C NMR (100.6 MHz, C_6D_6, 25 °C): $\delta = 31.70$ (s, $NCMe_3$), 31.86 (s, $NCMe_3$), 72.26 (s, $NCMe_3$), 73.03 (s, $NCMe_3$), 128.75 (d, $^3J(PC) = 11.9$ Hz, *m*-C_{Ph}), 129.64 (d, $^1J(PC) = 87.5$ Hz, *i*-C_{Ph}), 132.09 (d, $^4J(PC) = 2.7$ Hz, *p*-C_{Ph}), 134.04 (d, $^2J(PC) = 9.9$ Hz, *o*-C_{Ph}), 200.14 (d, $^1J(PC) = 35.7$ Hz, Cr=CH-P); ^{31}P NMR (161.9 MHz, C_6D_6, 25 °C): $\delta = 20.8$; IR(KBr): $\tilde{\nu} = 3056$ w ($C\text{-}H_{ar}$), 2964, 2916 vs (C-H), 1480 m, 1436 vs, 1352 m ($C(CH_3)_3$), 1235 s, 1215 vs, 1204 vs (Cr=N-C), 1100 vs, 1020 m, 996 m, 904 vs (P-C), 804 m, 752 s, 716 s, 688 vs, 512 vs, 460 w, 432 w, 382 w, 348 w cm^{-1}. Correct elemental analysis for **1a** und **2a–c**.

[9] Review: R. R. Schrock, W. E. Crowe, G. C. Bazan, M. DiMare, M. B. O'Regan, M. H. Schofield, *Organometallics* **1991**, *10*, 1832–1843.

[10] J. Sundermeyer, K. Weber, H. Pritzkow, unpublished; J. Sundermeyer, K. Weber, Poster P8, *3rd International Conference on the Chemistry of the Early Transition Metals*, Brighton, **1992**.

[11] J. Sundermeyer, K. Weber, H. Werner, N. Mahr, G. Bringmann, O. Schupp, *J. Organomet. Chem.* **1993**, *444*, C37–C40.

[12] Crystal structure of **2b**: $C_{41}H_{44}ClMoN_2OP$, $M_r = 743.18$, triclinic, space group $P\bar{1}$ (no. 2), $a = 12.295(2)$, $b = 12.610(2)$, $c = 15.415(3)$ Å, $\alpha = 97.74(1)$, $\beta = 103.17(1)$, $\gamma = 117.62(1)°$, $Z = 2$, $V = 1980.2(6)$ Å^3, $\rho_{calcd} = 1.25$ g cm^{-3}, crystal size $0.3 \times 0.3 \times 0.2$ mm, $\mu = 4.1$ cm^{-1}. Intensity measurements: Syntex R3 diffractometer, $Mo_{K\alpha}$ radiation, ω scan, $2\theta_{max} = 50°$, 6956 reflections measured of which 5449 observed ($I > 2\sigma_I$), empirical absorption correction. Structure determination: solution with Patterson and difference Fourier sytheses. Non-hydrogen atoms were refined anisotropically, H atoms isotropically, methyl H atoms were introduced as part of a rigid group. $R = 0.040$, $R_w = 0.042$ ($w = 1/\sigma_F^2$, 548 parameters, residual electron density 0.3 e Å^{-3}. All calculations were performed with the programs SHELX76 and SHELX86 [13]. Further details of the crystal structure investigation may be obtained from the Fachinformationszentrum Karlsruhe, Gesellschaft für wissenschaftlich-technische Information mbH, D-W-7514 Eggenstein-Leopoldshafen 2 (FRG) on quoting the depository number CSD-56950, the names of the authors, and the journal citation.

[13] G. M. Sheldrick, SHELX76, *Program for Crystal Structure Determination*, University of Cambridge, **1976**; SHELXS86, Universität Göttingen, **1986**.

Titanium-Catalyzed Epoxy–Hydroxylation of Allylic Alcohols: A Convenient Diastereoselective Synthesis of Epoxy Diols**

By *Waldemar Adam** und *Bernd Nestler*

The titanium(IV)-catalyzed epoxidation of allylic alcohols by *tert*-butyl hydroperoxide (TBHP) represents a convenient route to synthetically valuable epoxy alcohols.[1] When allylic hydroperoxides are employed as substrates,[2] which are readily accessible through the ene reaction of singlet oxygen with olefins, the olefins are converted into epoxy alcohols without the need of a separate oxygen atom donor. In this direct epoxy–hydroxylation of olefins the allylic hydroperoxide generated in situ serves a double role; namely, it first acts as an oxygen donor, and after oxygen transfer the resulting allylic alcohol functions as an acceptor. We report here that this useful methodology can be extended to the direct epoxy–hydroxylation of the chiral allylic alcohol **1a** (Scheme 1) to afford the highly regio- and diastereoselective epoxy diol **4a**, for which the hydroperoxy homoallylic alcohol **2a**[3] is a key intermediate. The advantage of this epoxy–hydroxylation is that up to four successive chiral centers can

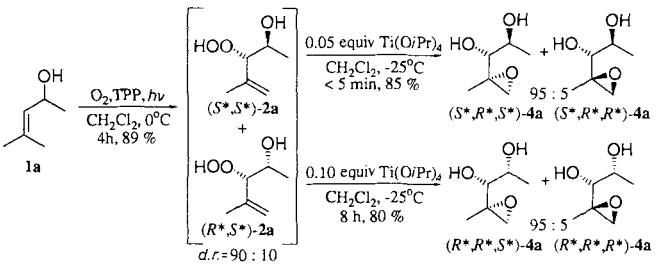

Scheme 1. Stereoselective transformation of the allylic alcohol **1a** into the epoxy diol **4a**. TPP = tetraphenylporphyrin. The asterisks on *R* and *S* indicate that they are relative configurations.

be constructed with predictable configuration, as illustrated for the allylic alcohol **1b** [Eq. (a)].

The fast rate with which the epoxidation proceeds is remarkable, especially since α, β-unsaturated diols are general-

[*] Prof. Dr. W. Adam, Dipl.-Chem. B. Nestler
Institut für Organische Chemie der Universität
Am Hubland, D-W-8700 Würzburg (FRG)
Telefax: Int. code +(931)888-4606

[**] This work was supported by the Deutsche Forschungsgemeinschaft (SFB 347: Selektive Reaktionen Metall-aktivierter Moleküle) and the Fonds der Chemischen Industrie.

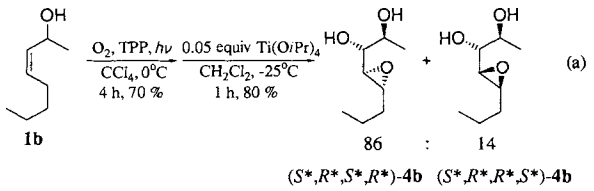

ly poor substrates for titanium metal-assisted epoxidations.[4] For example, when the epoxidation of the allylic diol (*S**,*S**)-**3a** (not shown), derived from the hydroperoxide (*S**,*S**)-**2a**, was attempted with TBHP in the presence of $Ti(OiPr)_4$, even after three days no epoxy diol **4a** was observed although ten times as much catalyst was employed as in the direct transformation of the hydroperoxide (*S**,*S**)-**2a**.

This large difference in reactivity can be rationalized in terms of the proposed mechanism[5] for such metal-catalyzed reactions (Scheme 2). The first steps consist of reversible formation of the complex **I**, in which both the allylic substrate **3** (AOH, oxygen acceptor) and the hydroperoxide **2** (AOOH, oxygen donor) are bound to the titanium by successive ligand exchanges. Irreversible oxygen transfer in this "loaded complex" **I** then yields the coordinated epoxide **4**. A favorable kinetic feature is the fact that the hydroperoxide **2** (AOOH) is converted by oxygen atom transfer directly in the coordination sphere of the titanium to the allylic substrate **3** (AOH). Hence only replacement of epoxy diol **4** (EOH) by ligand exchange with fresh hydroperoxide **2** (AOOH) is necessary to regenerate the loaded complex **I** and thereby complete the catalytic cycle. For the tridentate hydroperoxide **2** such exchange is expected to be fast, but if the epoxidation of diol **3** is performed with TBHP instead of hydroperoxide **2** as oxygen donor, the bidentate TBHP is ineffective in substituting the tridentate epoxy diol **4** and, as expected, the titanium(IV)-catalyzed epoxidation is slower than the direct transformation of hydroperoxide **2**. Moreover, since small amounts of $Ti(OiPr)_4$ are usually employed in such conversions with TBHP, it is reasonable to assume that all coordination sites of the catalyst are occupied by the bidentate diol **3a** (**II** in Scheme 2), and formation of the loaded complex **I** should, therefore, be significantly more difficult.

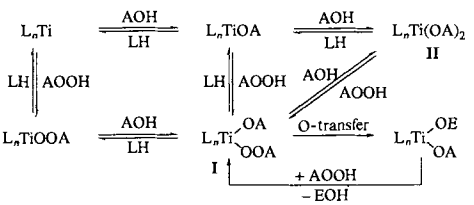

Scheme 2. Proposed mechanism[5] for metal-catalyzed epoxidations. AOH = vinylic diol **3**, AOOH = hydroperoxide **2**, EOH = epoxy diol **4**.

The substantial rate difference observed in the epoxy–hydroxylation of the diastereomeric hydroperoxy alcohols (*S**,*S**)-**2a** and (*R**,*S**)-**2a** is of mechanistic interest and of use for synthesis. Whereas only minutes sufficed for complete reaction when (*S**,*S**)-**2a** was treated with catalytic amounts of $Ti(OiPr)_4$, the diastereomer (*R**,*S**)-**2a** required hours under comparable conditions (Scheme 1); nonetheless, in both cases the epoxy diols were obtained with high diastereoselectivity (*d.r.* = 95:5). Presumably the allylic alcohols (*S**,*S**)-**3a** and (*R**,*S**)-**3a** are bound with unequal strength at the titanium metal site in the loaded complex **I**. Indeed, this was confirmed through control experiments. After the addition of an equimolar amount of $Ti(OtBu)_4$ to a solution of (*S**,*S**)-**3a**, the signals of the CHO*H* protons in the ^1H NMR spectrum completely vanished. This implies that (*S**,*S**)-**3a** was completely coordinated to the metal. In contrast, under identical conditions only small amounts of (*R**,*S**)-**3a** were bound to titanium, as indicated by the fact that the corresponding CHO*H* resonance signals remained unchanged, that is, they correspond to those in the free diol. These different abilities for coordination of both diastereomers (*S**,*S**)-**3a** and (*R**,*S**)-**3a** apparently arise from unfavorable steric interactions between the isopropenyl and the methyl group, which occur for the (*R**,*S**)-configurated diol (structure **A**) but not for the (*S**,*S**)-configurated diol (structure **B**).

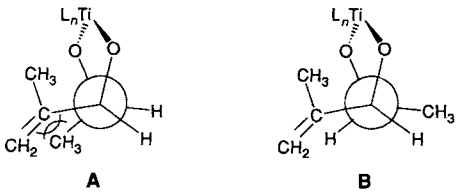

Besides these mechanistic implications, the different reactivity of the diastereomeric hydroperoxides in the titanium(IV)-catalyzed epoxy–hydroxylation is also significant for synthesis. For example, for the kinetic resolution of diastereomeric mixtures of **2a**, the latter are conveniently obtained through the photooxygenation of the chiral allylic alcohol **1a** (Scheme 1). Thus, the allylic alcohol **1a** was transformed diastereoselectively to the epoxy diols (*S**,*R**,*S**)- and (*S**,*R**,*R**)-**4a** (*d.r.* = 95:5) in a one-pot, two-step process simply by adding catalytic amounts of $Ti(OiPr)_4$ to the photooxygenated solution of allylic alcohol **1a** and stopping the reaction after complete consumption of the hydroperoxide (*S**,*S**)-**2a**.

In summary, chiral allylic alcohols can be converted efficiently and diastereoselectivity to epoxy diols by photooxygenation and subsequent titanium(IV)-catalyzed oxygen transfer. In the case of allylic alcohol **1a** as substrate, three successive chiral centers are constructed with predictable configuration, while for substrate **1b** even a total of four chiral centers are fixed. Use of enantiomerically pure allylic alcohols should make optically active epoxy diols accessible, which should in turn serve as useful building blocks in asymmetric synthesis. Significant for mechanistic understanding and preparative applications is the finding that tridentate hydroperoxides are necessary as effective oxygen atom donors in the titanium(IV)-catalyzed epoxidation of bidentate vinylic diols.

Experimental Procedure

To a solution of (*S**,*S**)-**2a** (264 mg, 2.00 mmol) in CH_2Cl_2 (4 mL) was introduced $Ti(OiPr)_4$ (29 μL, 5 mol%) at −25 °C in the presence of molecular sieves (4 Å). After 5 min the reaction mixture was diluted with diethyl ether (4 mL), and water (0.1 mL) was added under vigorous stirring. The mixture was stirred for an additional 30 min, then the solvent was evaporated (18 Torr, 20 °C) and the residue **immediately** purified by column chromatography on silica gel by elution with diethyl ether. This afforded **4a** [(*S**,*R**,*S**):(*S**,*R**,*R**) = 95:5] (224 mg, 85%) as colorless plates, m.p. 71–72 °C.

Received: December 3, 1992 [Z 5725 IE]
German version: *Angew. Chem.* **1993**, *105*, 767

[1] a) T. Itoh, K. Jitsukawa, K. Kaneda, S. Teranishi, *J. Am. Chem. Soc.* **1979**, *101*, 159–169; b) E. D. Mihelich, *Tetrahedron Lett.* **1979**, 4729–4732; c) B. E. Rossiter, T. R. Verhoeven, K. B. Sharpless, *ibid.* **1979**, 4733–4736; d) V. S. Martin, S. S. Woodard, T. Katsuki, Y. Yamada, M. Ikeda, K. B. Sharpless, *J. Am. Chem. Soc.* **1981**, *103*, 6237–6240; e) M. G. Finn, K. B. Sharpless in *Asymmetric Synthesis, Vol. 5* (Ed.: J. D. Morrison), Academic Press, Orlando, FL, USA, **1985**, p. 247.

[2] a) W. Adam, A. Griesbeck, E. Staab, *Tetrahedron Lett.* **1986**, *27*, 2839–2842; b) W. Adam, S. Kömmerling, E.-M. Peters, K. Peters, H. G. von Schnering, M. Schwarm, E. Staab, A. Zahn, *Chem. Ber.* **1988**, *121*, 2151–2155; c) W. Adam, M. Braun, A. Griesbeck, V. Lucchini, E. Staab, B. Will, *J. Am. Chem. Soc.* **1989**, *111*, 203–212.

[3] W. Adam, B. Nestler, *J. Am. Chem. Soc.* **1992**, *114*, 6549–6550.

[4] a) S. Takano, Y. Iwabuchi, K. Ogasawara, *J. Am. Chem. Soc.* **1991**, *113*, 2786–2787; b) *Synlett* **1991**, 548–550.

[5] S. S. Woodard, M. G. Finn, K. B. Sharpless, *J. Am. Chem. Soc.* **1991**, *113*, 106–113.

Epoxidation of 2-Methyl-3-phenylbenzofurans with Dimethyldioxirane: A Novel Reversible Valence Isomerization between Labile Benzofuran Epoxides and Quinone Methides, their Rearrangement, Methanolysis, and Cycloaddition Chemistry**

By *Waldemar Adam,* Lazaros Hadjiarapoglou, Karl Peters,* and *Markus Sauter*

2,3-Dimethylbenzofuran epoxides are rather labile compounds[1] which readily rearrange even at about $-20\,^{\circ}C$ by a 1,3-hydrogen migration with the participation of the 3-methyl group to afford mixtures of the hemiacetals and their ring-opened phenols [Eq. (a)]. Other substituents, for example, a 3-phenyl instead of the 3-methyl group, should facilitate the elucidation of the chemistry of these novel benzofuran epoxides. Indeed, epoxidation of the 2-methyl-3-phenylbenzofurans **1** with dimethyldioxirane afforded the expected epoxides **2** or their valence isomeric quinone methides **3** quantitatively, which could be characterized by NMR spectroscopy at $-25\,^{\circ}C$. From the chemical transformations (Scheme 1) it becomes evident that the benzofuran epoxides **2** and the quinone methides **3** coexist through the unprecedented reversible valence isomerization **2** ⇌ **3**.

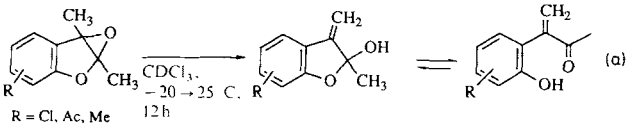

Reaction of the benzofuran **1a**[2] with dimethyldioxirane (in acetone)[3] at -70 to $-20\,^{\circ}C$ afforded within 4 h quantitatively the hitherto unknown epoxide **2a**. The solvent was removed by distillation at $-25\,^{\circ}C$ to afford **2a** as a red oil. The ^1H NMR [methyl group at $\delta = 1.73$ (s, 3H)] and ^{13}C NMR spectroscopic data (singlets at $\delta = 70.6$ and 96.4) confirm unequivocally the epoxide structure of **2a**. Since the epoxide **2a** itself contains no chromophore to absorb in the visible region, the red color is assigned to the quinone methide **3a**, present in the product mixture by valence isomerization of the epoxide; however, insufficient amounts of **3a** are formed to permit IR and NMR spectroscopic detection. This isomerization is analogous to that of furans to *cis*-enediones, when the former are oxidized with *meta*-chloroperbenzoic acid (MCPBA)[4] or dimethyldioxirane.[5] A related, but irreversible valence isomerization was reported[6] in the rearrangement of 2*H*-chromenes into oxabenzobicyclohexenes.

In solution, the epoxide **2a** is stable at room temperature for at least 24 h, but exposure for more than three days to ambient temperature led to total decomposition into a complex, intractable mixture which consisted of many products. In contrast, heating the epoxide **2a** in the presence of catalytic amounts (ca. 0.1 mol%) of tetraethylammonium bromide in acetone at 40 °C for 8 h yielded benzofuran-2-one **4a** nearly quantitatively.[7]

Reaction of the epoxide **2a** with methanol at 20 °C gave the hemiacetal **5a** (*d.r.* = 50:50) within 30 min, which was isolated in 76% yield after column chromatography as colorless needles (m.p. 102–102.5 °C, Et_2O/petroleum ether).[8] Unlike the corresponding hemiacetals derived from the 3-methyl-substituted benzofuran epoxides,[1, 12] **5a** does not undergo ring opening to give its tautomer **5'a**.

An unexpected reaction of the epoxide **2a** was its cycloaddition with tetracyanoethylene (TCNE) to afford the benzofurofuran **6a** in 96% yield (colorless needles, m.p. 183–184 °C, Et_2O/petroleum ether).[8] The epoxide **2a** reacts with an excess of ethyl vinyl ether at room temperature in two hours to give the adduct **7a**, the product of an inverse Diels–Alder reaction; **7a** was isolated in 86% yield after distillation of the solvent and column chromatography (colorless powder, m.p. 72–73 °C, Et_2O/petroleum ether). Compounds **6a** and **7a** were characterized by X-ray structure analysis (Fig. 1).[9]

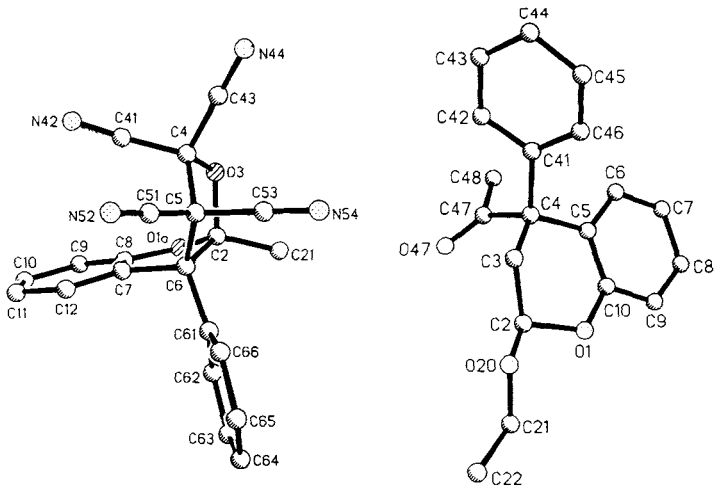

Fig. 1. Crystal structures of the benzofurofuran **6a** (left) and the benzopyran **7a** (right) (ORTEP).

In contrast to **1a**, the reaction of the benzofuran **1b**[10] with dimethyldioxirane did not yield the expected epoxide **2b**, but instead the quinone methide **3b** was obtained quantitatively as a dark red solid. The structure assignment is based on NMR spectroscopic data measured at $-30\,^{\circ}C$. The most characteristic signals in the ^1H NMR spectrum are

[*] Prof. Dr. W. Adam, Dr. L. Hadjiarapoglou, Dipl.-Chem. M. Sauter
Institut für Organische Chemie der Universität
Am Hubland, D-W-8700 Würzburg (FRG)
Telefax: Int. code +(931)888-4606
Dr. K. Peters
Max-Planck-Institut für Festkörperforschung
D-W-7000 Stuttgart 80 (FRG)

[**] This work was supported by the Deutsche Forschungsgemeinschaft (SFB 172: "Molekulare Mechanismen kanzerogener Primärveränderungen") and the Fonds der Chemischen Industrie.

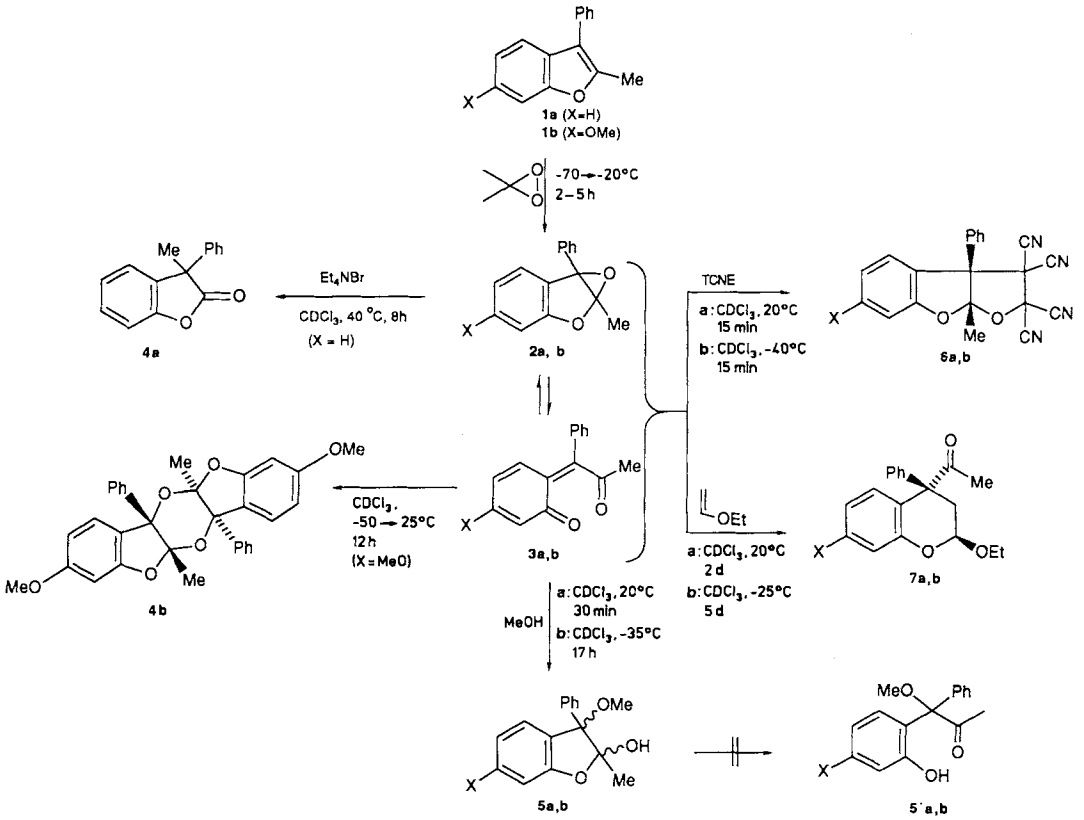

Scheme 1. Rearrangement, methanolysis, and cycloaddition chemistry of the benzofuran epoxide **2** and the quinone methide **3**.

those of the methyl group at $\delta = 2.20$ (s, 3H) and of the olefinic proton 2-H at $\delta = 5.70$ (d, $J = 1.6$ Hz, 1H), and in the ^{13}C NMR spectrum those of the acetyl group at $\delta = 28.0$, of the cyclohexadienone carbonyl atom at $\delta = 185.1$, and of the carbonyl atom of the acetyl group at $\delta = 203.9$. These data are in accord with those of known quinone methides.[11]

Presumably the formation of quinone methide **3b** is facilitated by the +M effect of the 6-methoxy group, which stabilizes the intermediate benzylic cation derived from the cleavage of the bond between the epoxide oxygen and the C-3 atom. That the resulting 1,3 dipole is a reasonable intermediate is supported by the fact that on warming the quinone methide **3b** from −30 to 20 °C over 5–10 h, dimerization to the 1,4-dioxane derivative **4b** (colorless solid, m.p. 276–277 °C) was observed.[8] Compound **4b** exhibits the molecular peak at *m/z* 508 in the mass spectrum, and due to its symmetry (C_i), one set of signals is displayed in the ^1H and ^{13}C NMR spectra. Although not even traces of epoxide **2b** can be observed by NMR spectroscopy at low temperature, it is hard to conceive how the quinone methide **3b** dimerizes into **4b** without passing through the ring-opened 1,3 dipolar structure of epoxide **2b**.

Methanolysis of the quinone methide **3b** led, like the epoxide **2a**, exclusively to attack at the benzylic position to yield the adduct **5b** as a pale yellow oil in 83% yield (*d.r.* = 43:57).[8] Also the reaction between the quinone methide **3b** and TCNE at −40 °C gave the 1,3 dipolar cycloadduct **6b** in 78% yield (colorless needles, m.p. 127–128 °C, Et_2O/petroleum ether).[8] Finally, the reaction of the quinone methide **3b** with ethyl vinyl ether led to the benzopyran **7b**, which is extremely sensitive towards moisture and, therefore, no satisfactory elemental analysis could be obtained; however, the spectroscopic data of the [4 + 2] cycloadduct **7b** are very similar to those of **7a**.

This unusual set of mutual reactions of the benzofuran epoxide **2a** and the quinone methide **3b** (Scheme 1), that is, they both give the epoxide trapping products **5a,b** with methanol, both afford the 1,3 dipolar cycloadducts **6a,b** with TCNE, and both lead to the inverse Diels–Alder adducts **7a,b** with ethyl vinyl ether, speaks for the reversible valence isomerization **2** ⇌ **3**. These results account for the previously reported difficulty in observing labile benzofuran epoxides.[12]

Received: December 8, 1992 [Z 5736 IE]
German version: *Angew. Chem.* **1993**, *105*, 769

[1] W. Adam, J. Bialas, L. Hadjiarapoglou, M. Sauter, *Chem. Ber.* **1992**, *125*, 231–234.
[2] G. Cardillo, R. Cricchio, L. Merlini, *Tetrahedron* **1971**, *27*, 1875–1883.
[3] W. Adam, J. Bialas, L. Hadjiarapoglou, *Chem. Ber.* **1991**, *124*, 2377.
[4] K. P. Manfredi, P. W. Jennings, *J. Org. Chem.* **1989**, *54*, 5186–5188.
[5] B. M. Adger, C. Barett, J. Brenan, M. Anthony, M. C. Kervey, R. W. Murray, *J. Chem. Soc. Chem. Commun.* **1991**, 1061–1062.
[6] A. Padwa, A. Au, G. A. Lee, W. Owens, *J. Am. Chem. Soc.* **1976**, *98*, 3555-3564.
[7] A. Padwa, A. Au, W. Owens, *J. Org. Chem.* **1978**, *43*, 303–310.
[8] For all stable new compounds satisfactory elemental analyses ($\Delta < 0.5\%$) were obtained and the labile products gave consistent spectral data.
[9] X-ray structural analysis of benzofurofuran **6a**, monoclinic, $P2_1/c$, $a = 1732.9$ (5), $b = 1311.3$ (4), $c = 702.3$ (2) pm, $\beta = 97.60$ (2)°, $\varrho_{calcd} = 1.244\ g\,cm^{-3}$, $Z = 4$; 2792 unique reflections were observed, $R = 0.057$, $R_w = 0.050$; X-ray structural analysis of benzopyran **7a**, triclinic, $P\bar{1}$, $a = 1174.1$ (3), $b = 1477.4$ (5), $c = 1042.2$ (3) pm, $\alpha = 90.85$ (3), $\beta = 91.82$ (2), $\gamma = 76.05$ (2)°, $Z = 4$, $\varrho_{calcd} = 1.330\ g\,cm^{-3}$, 4593 unique reflections were observed, $R = 0.055$, $R_w = 0.043$. Further details of the crystal structure investigations may be obtained from the Fachinformationszentrum Karlsruhe, Gesellschaft für wissenschaftlich-technische Information mbH, D-W-7514 Eggenstein-Leopoldshafen 2, (FRG), on quoting the depository number CSD-56882, the names of the authors, and the journal citation.
[10] R. Royer, C. Hudry, *Bull. Soc. Chim. Fr.* **1961**, 939-943.
[11] M. Benson, L. Jurd, *Org. Magn. Reson.* **1984**, *22*, 86–89.
[12] W. Adam, H. Hadjiarapoglou, T. Mosandl, C. Saha-Möller, D. Wild, *J. Am. Chem. Soc.* **1991**, *113*, 8005–8011.

S_N2 Reaction versus Electron Transfer in the Oxygen Transfer by Dimethyldioxirane to Nitrogen Heteroarenes**

By *Waldemar Adam** and *Dieter Golsch*

Dimethyldioxirane (DMD), especially in acetone,[1] has been developed into an effective but mild reagent for the oxidation of π bonds, heteroatoms, and even σ bonds.[2] While most of these oxygen atom transfer reactions appear to take place by direct substitution (S_N2) on the dioxirane peroxide bond by the nucleophile, more complex electron-transfer (ET) activity has been implicated (Scheme 1) particularly for substrates with low oxidation potentials.[3]

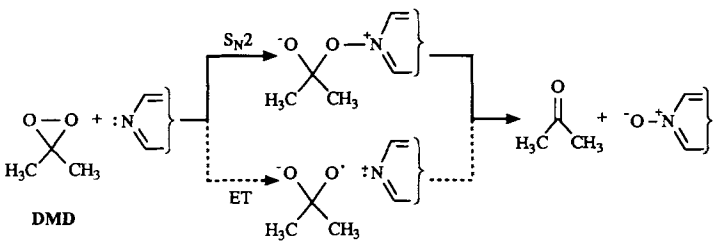

Scheme 1.

The purpose of the present mechanistic study was to probe for ET involvement in the heteroatom oxidation of nitrogen heteroarenes by comparing the relative rates and regioselectivities of DMD oxygen transfer with those of CH_3I methylation. The S_N2 behavior of CH_3I is well defined, for which electronic and steric factors play their usual role.[4] For the heteroarenes examined herein, a clear-cut S_N2 rather than ET mechanism applies in the nitrogen lone pair oxidation by DMD.

The results of the comparative reactivities are best appreciated in the log k_{rel}(DMD) versus log k_{rel}(MeI) plot in Figure 1, for which a good straight line ($y = -0.54 + 1.38\,x$) with a correlation coefficient $r = 0.977$ was obtained. For

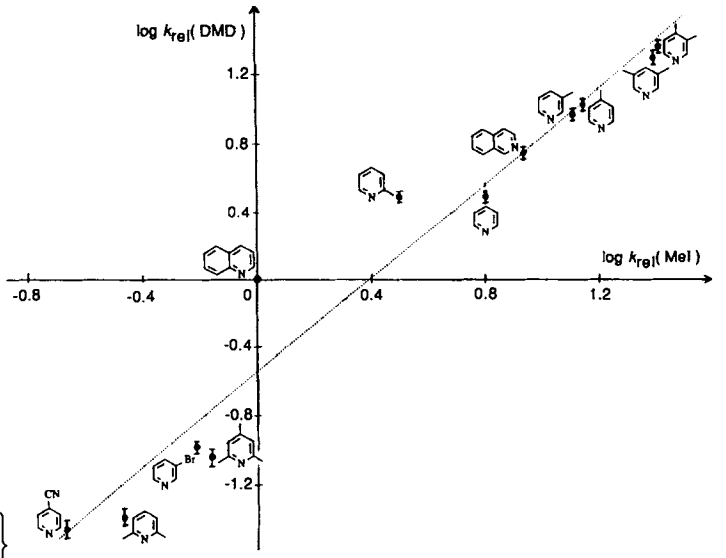

Fig. 1. Plot of log k_{rel}(DMD) versus log k_{rel}(MeI); values are taken from Table 1.

this purpose the acetone solutions of DMD (ca. 0.1 M)[1] were prepared according to our modified procedure,[5] which is more convenient than previous preparations.[1, 6] The relative rate constants k_{rel}(DMD) (Table 1) were determined by competition experiments with quinoline as reference substrate. The constants k_{rel}(MeI) (Table 1) were determined from literature data (they were extrapolated from related data under diverse conditions and normalized relative to quinoline as reference substrate).

Despite the fact that the k_{rel}(MeI) values came from various sources and had to be extrapolated, their correlation with the k_{rel}(DMD) data (Fig. 1) is quite good, especially if one keeps in mind the set of diverse structure types employed in this correlation. This result clearly speaks for a S_N2 mechanism in the oxygen transfer to the nitrogen atom of these heteroarenes.

Table 1. Relative rate constants for oxygen transfer by DMD [k_{rel}(DMD)] and for methylation by CH_3I [k_{rel}(MeI)], pK_a values and ionization potentials [$E_{IP adiab.}$ and E_{IP}(N:)] for heteroarenes and for their *N*-oxides [E_{IP}(NO)] all in eV.

Entry	Substrate	k_{rel}(DMD) [a]	k_{rel}(MeI) [b]	pK_a [c]	E_{IP}(adiab.) [d]	E_{IP}(N:) [e]	E_{IP}(NO) [f]
1	4-pyridine carbonitrile	0.0352 ± 0.0035	0.214 [7b]	1.48 [8a]	10.40	10.30 [10a]	8.95
2	2,6-lutidine	0.0415 ± 0.0042	0.340 [7d]	6.77 [7d]	8.85	9.30 [10b]	–
3	2,4,6-collidine	0.0923 ± 0.0092	0.693 [7d]	7.48 [7d]	8.90	9.20 [10a]	–
4	3-bromopyridine	0.104 ± 0.0050	0.613 [7b]	2.84 [7d]	9.75	–	–
5	quinoline	1.00	1.00 [7a]	4.93 [8b]	8.64	9.20 [10c]	8.00
6	pyridine	3.12 ± 0.12	6.33 [7a–d]	5.17 [7d]	9.33	9.60 [10a]	8.78
7	2-picoline	3.12 ± 0.12	2.99 [7c]	5.97 [7d]	9.02	9.50 [10a]	8.21
8	isoquinoline	5.59 ± 0.28	8.63 [7a,b]	5.46 [8b]	8.53	9.40 [10c]	7.98
9	3-picoline	9.34 ± 0.47	12.9 [7b,c]	5.68 [7d]	8.93	9.49 [10d]	8.20
10	4-picoline	10.6 ± 0.53	13.7 [7b,c]	6.02 [7d]	9.03	9.50 [10a]	8.12
11	3,5-lutidine	19.7 ± 1.2	25.0 [7b]	6.14 [7d]	9.25	9.52 [10a]	–
12	3,4-lutidine	23.0 ± 1.4	26.6 [7b]	6.52 [7d]	9.15	9.46 [10a]	–

[a] Determined by competition experiments with quinoline as reference substrate. [b] Relative to quinoline ($k = 0.800 \times 10^{-4}\ M^{-1}s^{-1}$). [c] At 20 °C in H_2O. [d] Adiabatic ionization of the π-electron system; all in ref. [9b] except entry 1 (ref. [9a]). [e] Lone pair ionization; all in ref. [9b] except entry 1 (ref. [9a]). [f] Ionization potential of the corresponding *N*-oxide.

Since a direct correlation exists between nucleophilicity and pK_a of the nitrogen base, the log k_{rel}(DMD) data were plotted against the pK_a values of the heteroarenes (Table 1). This appeared particularly attractive since accurate pK_a data are available under a consistent set of experimental conditions for the aromatic nitrogen bases examined here; how-

[*] Prof. Dr. W. Adam, Dipl.-Chem. D. Golsch
Institut für Organische Chemie der Universität
Am Hubland, D-W-8700 Würzburg (FRG)
Telefax: Int. code +(931)888-4606

[**] This work was supported by the Deutsche Forschungsgemeinschaft (SFB 347: "Selektive Reaktionen Metall-aktivierter Moleküle") and the Fonds der Chemischen Industrie.

ever, such a plot gave a much poorer correlation ($r = 0.398$). In hindsight this is not too surprising because the pK_a values do not reflect the steric factors that result from methyl or benzo substitution in the proximity of the nitrogen heteroatom, which can hinder the oxygen transfer by the dioxirane. By excluding such sterically encumbered substrates (Table 1, entries 2, 3, 5, 7), again an excellent correlation is observed ($y = -2.47 + 0.59\,x$; $r = 0.994$). Therefore, the principal reason why the $\log k_{rel}$(DMD) versus $\log k_{rel}$(MeI) plot for all twelve substrates correlates much better ($r = 0.977$) than that for the $\log k_{rel}$(DMD) versus pK_a plot ($r = 0.398$) is that oxygen transfer by DMD and methylation by CH_3I are subject to similar steric factors. Furthermore, if a straight line is calculated for the $\log k_{rel}$ values of DMD versus those of MeI in the case of the eight sterically unhindered pyridines, the best correlation is obtained ($y = -0.59 + 1.38\,x$; $r = 0.999$).

How good, however, is the correlation of the relative rate constants of DMD [$\log k_{rel}$(DMD)] with the ionization potentials of these heteroarenes? The plot of $\log k_{rel}$(DMD) against the adiabatic ionization potentials E_{IP}(adiab.), that is the energy of the ionization out of the π-electron system of the heteroarene, was unsatisfactory even for the eight sterically unhindered pyridines ($r = 0.830$). All twelve pyridines together again gave a much poorer correlation ($r = -0.399$).

If electron transfer is responsible for the oxidation of the nitrogen heterorenes by DMD, then one should choose ionization potentials which measure the removal of an electron out of the lone pair of the nitrogen atom, [E_{IP}(N:)]. Again, a plot of $\log k_{rel}$(DMD) versus E_{IP}(N:) gave a very bad correlation ($r = -0.213$). Consequently, these reactivity data confirm a S_N2 and not an ET mechanism for the oxidation of nitrogen heteroarenes by dimethyldioxirane. Like methylation by methyl iodide, oxygen transfer by DMD is also subject to electronic *and* steric factors in the heteroarene.

Another criterion for the differentiation of the S_N2 and the ET mechanism is the comparison of the regioselectivities for the DMD oxidation and CH_3I methylation of heteroarenes with several nitrogen sites. An impressive selection of regioselectivities is illustrated in Scheme 2.

Since *N*-oxides have substantially lower ionization potentials (by ca. 1 eV) than the corresponding *N*-heteroarenes (Table 1), when ET would apply, the second oxygen transfer should proceed even more readily than the first. Therefore, one would expect both 1,7- and 4,7-phenanthroline to give the appropriate dioxides with an excess of DMD. Indeed, the 7-monoxide of the 1,7-isomer and the 4,7-dioxide of the 4,7-isomer were obtained.

This is analogous to CH_3I, for which *N*,*N*'-dimethylation of 4,7-phenanthroline takes place readily, while only *N*-monomethylation can be achieved with the 1,7-isomer.[11] The *peri* hydrogen atom at C-10 obstructs the approach of the two electrophiles CH_3I and DMD and therewith prevents S_N2 attack at N-1.

Still more revealing are the results of the DMD oxidations of the three regioisomeric dimethylaminopyridines (Scheme 2). The *para* isomer gives exclusively the corresponding pyridine-*N*-oxide and the *ortho* isomer exclusively the dimethylamino-*N*-oxide. This selectivity is identical to the *N*-methylation by CH_3I.[12] In contrast the *meta* isomer behaves in a more complicated manner; while DMD afforded a 17:83 mixture of the pyridine-*N*-oxide and dimethylamino-*N*-oxide (Scheme 2), *N*-methylation by CH_3I is reported[12] to take place exclusively at the pyridine nitrogen atom, and a peroxy acid oxidizes the dimethylamino nitrogen preferentially.[12] Thus, for the *meta* isomer there exists a substantial differentiation between these three electrophiles, of which DMD displays intermediate behavior between *N*-methylation by CH_3I and *N*-oxidation by RCO_3H. Presumably steric factors are responsible for the control of the preferred S_N2 attack by the electrophile. That also electronic factors may play a role, is reflected in nicotine as substrate (Scheme 2). All three reagents exclusively attack the pyrrolidine nitrogen, as would be expected for the higher nucleophilicity of this aliphatic nitrogen atom.[13]

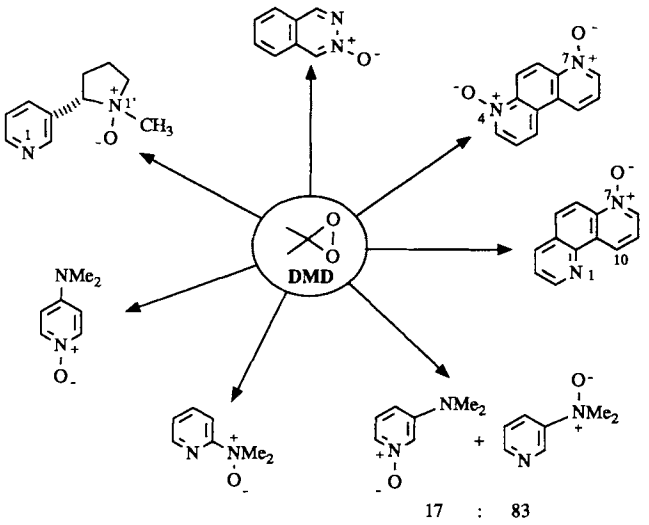

Scheme 2. Regioselective oxidations of bidentate nitrogen heteroarenes by DMD.

In summary, comparison of the relative rates of the DMD oxidation of nitrogen heteroarenes with those of methylation by methyl iodide reveals that the S_N2 mechanism rather than electron transfer applies for the DMD oxidation. This is particularly evident from the poor correlation between the relative rate constants of oxygen transfer by DMD and the ionization potentials E_{IP}(adiab.) and E_{IP}(N:). Also the regioselectivities of the DMD oxidation of bidentate nitrogen heteroarenes are consistent with S_N2 attack on the peroxide bond of the dioxirane, controlled by the usual steric and electronic factors.

Received: December 19, 1992 [Z 5763 IE]
German version: *Angew. Chem.* **1993**, *105*, 771

[1] R. W. Murray, R. Jeyaraman, *J. Org. Chem.* **1985**, *50*, 2847–2853.
[2] a) R. W. Murray in *Modern Models of Bonding and Delocalization* (Eds.: J. F. Liebman, A. Greenberg), VCH Publ., New York, **1988**, p. 311; b) W. Adam, R. Curci, J. O. Edwards, *Acc. Chem. Res.* **1989**, *22*, 205–211; c) R. W. Murray, *Chem. Rev.* **1989**, *89*, 1187–1201; d) R. Curci, *Adv. Oxygenated Processes* **1990**, *2*, 1; e) W. Adam, R. Curci, L. Hadjiarapoglou, R. Mello in *Organic Peroxides* (Ed.: W. Ando), Wiley, Chichester, England, **1992**, p. 221; f) W. Adam, L. Hajiarapoglou, *Top. Curr. Chem.*, in press.
[3] a) R. W. Murray, M. K. Pillay, R. Jeyaraman, *J. Org. Chem.* **1988**, *53*, 3007–3011; b) R. Mello, F. Ciminale, M. Fiorentino, C. Fusco, T. Prencipe, R. Curci, *Tetrahedron Lett.* **1990**, *31*, 6097–6100; c) W. Adam, S. E. Bottle, R. Mello, *J. Chem. Soc. Chem. Commun.* **1991**, 771–773; d) W. Adam, G. Asensio, R. Curci, M. E. González-Núñez, R. Mello, *J. Am. Chem. Soc.* **1992**, *114*, 8345–8349.
[4] P. B. D. De La Mare, B. E. Swedlund in *The Chemistry of the Carbon-Halogen Bond, Part 1* (Ed.: S. Patai), Wiley, London, **1973**, p. 407.
[5] W. Adam, J. Bialas, L. Hadjiarapoglou, *Chem. Ber.* **1991**, *124*, 2377.
[6] a) W. Adam, Y.-Y. Chan, D. Cremer, J. Gauss, D. Scheutzow, M. Schindler, *J. Org. Chem.* **1987**, *52*, 2800–2803; b) W. Adam, L. Hadjiarapoglou, A. Smerz, *Chem. Ber.* **1991**, *124*, 227–232.

[7] a) J. Packer, J. Vaughan, E. Wong, *J. Am. Chem. Soc.* **1958**, *80*, 905–907; b) A. Fischer, W. J. Galloway, J. Vaughan, *J. Chem. Soc.* **1964**, 3596–3599; c) A. Dondoni, G. Modena, P. E. Todesco, *Gazz. Chim. Ital.* **1961**, *91*, 613–619; d) K. Clarke, K. Rothwell, *J. Chem. Soc.* **1960**, 1885–1895.
[8] a) I. R. Bellobono, M. A. Monetti, *J. Chem. Soc. Perkin Trans. 2*, **1973**, 790–793; b) A. Albert, J. N. Phillips, *J. Chem. Soc.* **1956**, 1294–1304.
[9] a) *Beilstein, Handbook of Organic Chemistry, E. V. Vol. 22*, Springer, Heidelberg, **1990**; b) *ibid. Vol. 20*, **1989**.
[10] a) B. G. Ramsey, F. A. Walker, *J. Am. Chem. Soc.* **1974**, *96*, 3314–3316; b) E. Heilbronner, V. Hornung, F. H. Pinkerton, S. F. Thames, *Helv. Chim. Acta* **1972**, *55*, 289–301; c) F. Brogli, E. Heilbronner, T. Kobayashi, *ibid.* **1972**, *55*, 274–288; d) L. Klasinc, I. Kovak, M. Scholz, G. Kluge, *Croat. Chem. Acta* **1978**, *51*, 43–53.
[11] S. Hünig, J. Groß, E. F. Lier, H. Quast, *Justus Liebigs Ann. Chem.* **1973**, 339–358.
[12] R. Frampton, C. D. Johnson, A. R. Katritzky, *Justus Liebigs Ann. Chem.* **1971**, *749*, 12–15.
[13] a) J. D. Phillipson, S. S. Handa, *Phytochemistry* **1975**, *14*, 2683–2690; b) J. I. Seeman, J. F. Whidby, *J. Org. Chem.* **1976**, *41*, 3824–3826.

$[(\overset{\frown}{PP})_2RhH]$ and $[(\overset{\frown}{PP})_2Rh][O_2CH]$ Complexes as Models for the Catalytically Active Intermediates in the Rh-Catalyzed Hydrogenation of CO_2 to HCOOH**

By *Thomas Burgemeister, Fritz Kastner,* and *Walter Leitner**

The hydrogenation of CO_2 to formic acid is an interesting approach to the chemical exploitation of CO_2.[1, 2] We reported recently that up to 1150 moles of formic acid per mole of rhodium may be obtained under the conditions summarized in Scheme 1 by using catalyst **1c**, generated in situ from $[\{Rh(cod)Cl\}_2]$ ($c_{Rh} = 1.35 \times 10^{-3}$ M) and dppb[3] (dppb: Rh = 1.2).[4] At about the same time, Nicholas and Tsai published the results of their investigations on the hydrogenation of CO_2 in THF with the ionic complex $[Rh(PPhMe_2)_3(nbd)][BF_4]$ (**2**) as catalyst.[5] After activation of **2** with hydrogen, 64 moles of formic acid were formed per mole rhodium per day under more drastic conditions (p = 100 atm, T = 40 °C).

$$H_2 + CO_2 \underset{\mathbf{1a\text{–}d}}{\overset{\text{DMSO, NEt}_3}{\rightleftharpoons}} HCO_2H$$

Scheme 1. Rhodium-catalyzed hydrogenation of CO_2 to formic acid. Conditions: p = 40 atm, T = 297 K, and t = 18 h. The catalyst **1** is generated in situ from $[\{Rh(cod)Cl\}_2]$ (**A**) (c(Rh) = 10^{-2} M) and a bidentate phosphane ($\overset{\frown}{PP}$: Rh = 1.2). **1a**: **A** + dppe, 13 mol HCO_2H per mol Rh; **1b**: **A** + dppp, 185; **1c**: **A** + dppb, 210; **1d**: **A** + dippe, 205 mol HCO_2H per mol Rh.

In the course of our efforts to optimize in situ catalysts of type **1**, we established that the catalytic activity was influenced greatly by the steric and electronic properties of the phosphane ligand (see Scheme 1). Approximately the same tendency was observed for the rhodium-catalyzed transfer-hydrogenation with formates.[6] In this communication, we report preliminary investigations with the model complexes **3**[7] and **4** that should contribute to our understanding of these phenomena on a molecular level.

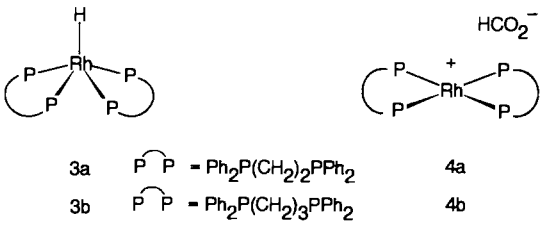

3a $\overset{\frown}{P\ P}$ = $Ph_2P(CH_2)_2PPh_2$ **4a**
3b $\overset{\frown}{P\ P}$ = $Ph_2P(CH_2)_3PPh_2$ **4b**

The conformity of our model complexes with the actual active species in the catalytic cycle is emphasized by the fact that model **3b** may likewise be used as catalyst for the hydrogenation of CO_2 in DMSO. Under the conditions described in Scheme 1, 30 moles of formic acid per mole of **3b** were formed within 16 hours. The large difference in activity between **3b** and **1b** can be attributed to the different ligand-to-metal ratio, because a comparable reduction in activity is observed for the in situ system **1c** upon raising the ligand-to-metal ratio to 2:1 (as in **3b**). The 18e complex **3b** is, of course, far less reactive than a coordinatively unsaturated, hypothetical intermediate [(dppp)RhH]. Depending on the ligand, complexes of type $[(\overset{\frown}{PP})RhH]$ form clusters of formula $[\{(\overset{\frown}{PP})Rh(\mu\text{-}H)\}_x]$, which probably exist in equilibrium with the corresponding monomers under the above catalytic conditions.[8] The supposition that such fragments are the catalytically active intermediates in the hydrogenation of CO_2 in DMSO is supported by the observation that the catalytic activity (200 cycles in 18 hours) of [(dippe)Rh-(η^3-C_4H_7)], which gives rise to $[\{(dippe)Rh(\mu\text{-}H)\}_2]$ under H_2-pressure[8b] is almost identical to that of the in situ catalyst **1d**. On the other hand, not even half as many catalytic cycles as for **1c** were observed for the cationic complex $[(dppb)Rh(nbd)][CF_3SO_3]$ (83 moles of formic acid per mole of rhodium within 18 hours). From the latter observation, it appears improbable that the hydrogenation of CO_2 to formic acid under our reaction conditions proceeds according to the mechanism described by Nicholas et al.[5]

Complex **3b** reacts at room temperature in DMSO, under 1 atm CO_2, to give complex **4b** quantitatively in less than thirty minutes. The reaction is accompanied by a change in the color of the solution from red to yellow, and may be monitored by ^1H NMR spectroscopy, through the disappearance of the hydride ligand signal at $\delta = -10.51$ (dq, J(H,Rh) = 8 Hz, J(H,P) = 19 Hz) and concomitant growth of a signal for the formyl proton at δ = 8.55. A protonation of complex **4b** prior to insertion of CO_2 by residual water in $[D_6]$DMSO[9] is not observed, owing to the low basicity of the dppp ligand. If, upon completion of the transformation of **3b** into **4b**, the carbon dioxide atmosphere is replaced by hydrogen, the solution virtually decolorizes, and a high-field signal ($\delta = -8.66$, dm, $J(H,P_{trans}) = 138$ Hz, J(H,Rh) = 12 Hz $\approx J(H,P_{cis})$) is observed in the ^1H NMR spectrum, characteristic of the cation $[(dppp)_2Rh(H)_2]^+$.[10] The integration of the NMR signals is consistent with the formulation $[Rh(dppp)_2(H)_2][HCO_2]$ **5**. After about 30 minutes, **3b** and **5** can be observed in a ratio of 1:1 in the solution, and

[*] Dr. W. Leitner
Institut für Anorganische Chemie der Universität
Universitätsstrasse 31, D-W-8400 Regensburg (FRG)
New address
Max-Planck-Gesellschaft
Arbeitsgruppe CO_2-Chemie an der Universität Jena
Lessingstrasse 12, D-O-6900 Jena (FRG)
Dr. T. Burgemeister, F. Kastner
Zentrale Analytik der Naturwissenschaftlichen Fakultät IV der Universität Regensburg
Abteilung für NMR-Spektroskopie

[**] CO_2 Activation, Part 2. This work was supported by the Fonds der Chemischen Industrie (Liebig-Stipendium for W. L.). We thank Degussa AG for a gift of hydrated rhodium(III) chloride. Part 1: [4a]. $\overset{\frown}{PP}$ = bidentate phosphane.

hence every step of the catalytic cycle depicted in Scheme 2 for the hydrogenation of CO_2 to formic acid can be detected by ^1H NMR spectroscopy.

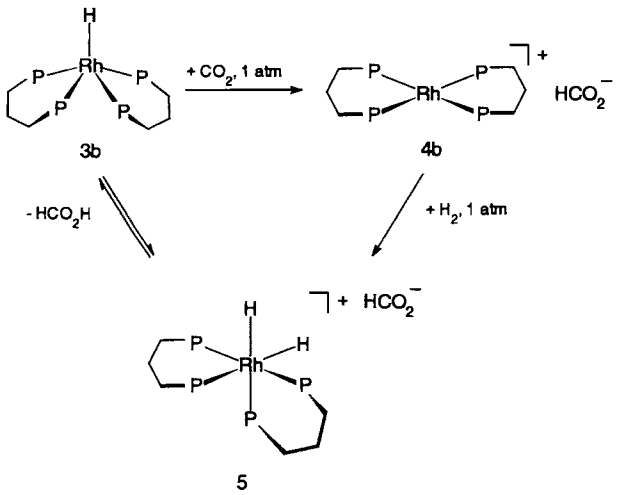

Scheme 2. Intermediates determined by ^1H NMR spectroscopy in the hydrogenation of CO_2 to formic acid, with the complex **4b** as catalyst ([D$_6$]DMSO, 297 K).

The reaction of **3a** with CO_2, carried out in suspension owing to its insolubility in DMSO, produces a yellow solution in which no formate can be detected by ^1H NMR spectroscopy. Complex **4a** is, however, obtained in good yield from the reaction of [(dppe)Rh(acac)] with HCO_2H in THF in the presence of a further equivalent of dppe. The analogous synthesis of **4b** is only successful if performed at $-40\,^\circ C$. While **4a** is also accessible through reaction of [(dppe)$_2$RhCl] with KO_2CH in acetone under reflux, the analogous reaction with [(dppp)$_2$RhCl] gives **3b** in over 80% yield under the same conditions. Here, the intermediate formation of **4b** may be observed by ^1H NMR spectroscopy, and the liberated CO_2 detected through clouding of an aqueous $Ba(OH)_2$ solution.

It is apparent from the NMR data that the complexes **4** undergo complete dissociation in [D$_6$]DMSO. This distinguishes them from previously characterized formatorhodium complexes,[5, 11] as well as from the related complexes [(iPr$_3$P)$_2$Rh(O$_2$CCR$_3$)],[12] in which the carboxylate group is coordinated to the metal through at least one of the two oxygen atoms, even in solution.

The influence of the chelate ring size on the propensity of the formate group towards C–H activation that is apparent from the above described reactivities of **4a** and **4b** reflects the different catalytic activities of in situ systems **1a** and **1b**. This influence can be quantified according to the rate of $^{13}CO_2/^{12}CO_2$ exchange ([D$_6$]DMSO, $T = 297$ K, 1 atm $^{13}CO_2$), because the characteristic signal of the HCO_2^- group in the ^1H NMR spectrum ($\delta = 8.55$) is split into a doublet (J(H,C) = 172 Hz) upon incorporation of $^{13}CO_2$. The half-life for the incorporation of $^{13}CO_2$ into **4a** is thus determined to be 7.5 hours, in contrast to a mere 8 minutes for **4b**.

This tendency is also observed for H/D exchange in the formyl position. Under an atmosphere of D_2, incorporation of deuterium is already quantitative for **4b** after 15 minutes, but is only 25% complete after 64 hours for **4a**. From the data available it is not possible to decide whether the poor catalytic activity of the dppe complex arises from relatively slow H_2 cleavage[10] or from low reactivity towards CO_2.

In contrast to the related nickel complex [(cy$_3$P)$_2$Ni(H)(O$_2$CH)],[13] H/D exchange is *faster* than CO_2 exchange for **4b**. One possible explanation is that CO_2 remains in the coordination sphere of the rhodium center directly after decarboxylation,[14] and thus not every C–H bond cleavage leads to CO_2 exchange. It is also conceivable that the activation of the formyl group is strongly accelerated following oxidative addition of H_2 or D_2 to **4b**.

The results described herein provide the first unambiguous experimental proof that CO_2 is inserted into the M–H bond of a neutral rhodium complex.[11, 15, 16] This reaction has been shown by quantum mechanical calculations to be a potential elementary step in the rhodium-catalyzed hydrogenation of CO_2,[17] and has already been established experimentally for other metals.[18] The most important consequence of this study is, however, the fact that starting from complexes of type **3**, every step of the catalytic cycle for the rhodium-catalyzed hydrogenation of CO_2 to formic acid can be monitored by ^1H NMR spectroscopy, and that the influence of the ligands on the reactivity of the resulting intermediates **4** relates directly to their influence on the catalytic activity of the corresponding in situ systems. Thus, we have an efficient model at our disposal, in which the influence of steric and electronic properties of a phosphane ligand on the catalytic activity of a metal center may be studied systematically. In this way, we hope to be somewhat closer to an understanding of those effects vital for rational catalyst design.

Experimental Procedure

All manipulations were performed under exclusion of atmospheric oxygen. The complexes and ligands used were prepared according to known procedures. High-pressure experiments were accomplished as described elsewhere [4a]. NMR studies were carried out on a Bruker AC250 spectrometer.

4a: To a solution of [(nbd)Rh(acac)] (180 mg, 0.61 mmol) in THF (20 mL) was added dppe (492 mg, 1.23 mmol), and the mixture heated to boiling. A yellow solid separated within 30 min. After cooling to room temperature, dry formic acid (30 µL, 0.79 mmol) was added, and the mixture stirred for 30 min. The color of the precipitate faded slightly. To complete the precipitation, pentane (20 mL) was added. Following filtration, washing with pentane, and thorough drying under high vacuum, **4a** was obtained (490 mg, 85%) in analytically pure form. ^1H NMR ([D$_6$]DMSO, 250 MHz): $\delta = 8.55$ (s, 1H, HCO_2^-), 7.38 (m, 8H, *para*-H), 7.24 (m, 32H, *meta*, *ortho*-H), 2.20 (br.m, 8H, P-CH$_2$-); $^{31}P\{^1H\}$ NMR ([D$_6$]DMSO, 101 MHz): $\delta = 58.8$ (d, J(Rh,P) = 133 Hz).

4b: Preparation was as described for **4a**, but with the addition of formic acid and workup at $-40\,^\circ C$. ^1H NMR ([D$_6$]DMSO, 250 MHz): $\delta = 8.55$ (s, 1H, HCO_2^-), 7.18 (m, 40H, Ph), 2.39 (br.m, 8H, P-CH$_2$-), 1.81 (br.m, 4H, -CH$_2$-); $^{31}P\{^1H\}$ NMR ([D$_6$]DMSO, 101 MHz): $\delta = 9.1$ (d, J(Rh,P) = 133 Hz); $^{13}C\{^1H\}$ NMR ([D$_6$]DMSO, 63 MHz): $\delta = 164.7$ (s; gated decoupling: d, J(H,C) = 171.7 Hz, HCO_2^-).

Received: November 2, 1992 [Z 5660 IE]
German version: *Angew. Chem.* **1993**, *105*, 781

[1] a) A. Behr, *Carbon Dioxide Activation by Metal Complexes*, VCH, Weinheim, **1988**; b) *Enzymatic and Model Carboxylation and Reduction Reactions for Carbon Dioxide Utilization* (*NATO ASI Ser. C* **1990**, *314*).

[2] a) A. Behr, *Angew. Chem.* **1988**, *100*, 681; *Angew. Chem. Int. Ed. Engl.* **1988**, *27*, 661; b) I. S. Kolomnikov, T. V. Lysak, *Russ. Chem. Rev. (Engl. Transl.)* **1990**, *59*, 344; c) D. Walther, *Nachr. Chem. Tech. Lab.* **1992**, *40*, 1214.

[3] The following abbreviations and acronyms are used: $\overset{\frown}{PP}$ = two monodentate ligands or one bidentate chelate ligand in which phosphorus is the donor atom; dppe = 1,2-bis(diphenylphosphino)ethane; dppp = 1,3-bis(diphenylphosphino)propane; dppb = 1,4-bis(diphenylphosphino)butane; dippe = 1,2-bis(diisopropylphosphino)ethane; cod = 1,5-cyclooctadiene; nbd = 2,5-bicyclo[2.2.1]heptadiene (norbornadiene); DMSO = dimethylsulfoxide.

[4] a) E. Graf, W. Leitner, *J. Chem. Soc. Chem. Commun.* **1992**, 623; b) W. Leitner, *GIT Fachz. Lab.* **1992**, *36*, 912.

[5] J.-C. Tsai, K. M. Nicholas, *J. Am. Chem. Soc.* **1992**, *114*, 5117.

[6] a) H. Brunner, W. Leitner, *Angew. Chem.* **1988**, *100*, 1231; *Angew. Chem. Int. Ed. Engl.* **1988**, *27*, 1180; b) W. Leitner, J. M. Brown, H. Brunner, *J. Am. Chem. Soc.* **1993**, *115*, 152.

[7] A. Sacco, R. Ugo, *J. Chem. Soc.* **1964**, 3274.
[8] a) M. D. Fryzuk, W. E. Piers, F. W. B. Einstein, T. Jones, *Can. J. Chem.* **1989**, *67*, 883; b) M. D. Fryzuk, T. Jones, F. W. B. Einstein, *Organometallics* **1984**, *3*, 185.
[9] T. Yoshida, T. Okano, Y. Ueda, S. Otsuka, *J. Am. Chem. Soc.* **1981**, *103*, 3411.
[10] B. R. James, D. Mahajan, *Can. J. Chem.* **1979**, *57*, 180.
[11] T. Yoshida, D. L. Thorn, T. Okano, J. A. Ibers, S. Otsuka, *J. Am. Chem. Soc.* **1979**, *101*, 4212.
[12] M. Schäfer, J. Wolf, H. Werner, *J. Chem. Soc. Chem. Commun.* **1991**, 1341.
[13] D. J. Darensbourg, P. Wiegreffe, C. G. Riordan, *J. Am. Chem. Soc.* **1990**, *112*, 5759.
[14] a) J. C. Calabrese, T. Herskovitz, J. B. Kinney, *J. Am. Chem. Soc.* **1983**, *105*, 5914; b) L. Dahlenburg, C. Prengel, *Organometallics* **1984**, *3*, 934.
[15] The formation of **4a** from the reaction of **3a** with CO_2 in CH_3CN is postulated on the basis of ^{31}P NMR data [16a]. Under these conditions, we obtained a yellow powder whose ^1H NMR and IR spectra are not identical to those of **4a**, but which nonetheless allowed the formation of a carbonato or hydrogencarbonato complex to be inferred. The ^{31}P NMR spectra of these compounds and of **4a** show, upon complete dissociation, only the signal of $[(dppe)_2Rh]^+$ and are therefore identical.
[16] a) S. Slater, J. H. Wagenknecht, *J. Am. Chem. Soc.* **1984**, *106*, 5367; b) S. Krogsrud, S. Komiya, T. Ito, J. A. Ibers, A. Yamamoto, *Inorg. Chem.* **1976**, *15*, 2798.
[17] a) A. Dedieu, C. Bo, F. Ingold in [1a], p. 23–42; b) C. Bo, A. Dedieu, *Inorg. Chem.* **1989**, *28*, 304.
[18] a) L. S. Pu, A. Yamamoto, S. Ikeda, *J. Am. Chem. Soc.* **1968**, *90*, 3896; b) S. Komiya, A. Yamamoto, *Bull. Chem. Soc. Jpn.* **1976**, *49*, 784; c) D. J. Darensbourg, M. Y. Darensbourg, L. Y. Goh, M. Ludvig, P. Wiegreffe, *J. Am. Chem. Soc.* **1987**, *109*, 7539; d) J. R. Pugh, M. R. M. Bruce, B. P. Sullivan, T. J. Meyer, *Inorg. Chem.* **1991**, *30*, 86.

Can Single-Chain Perfluoroalkylated Amphiphiles Alone Form Vesicles and Other Organized Supramolecular Systems?**

By *Marie-Pierre Krafft, Françoise Giulieri,* and *J. G. Riess**

The formation of bilayers and vesicles usually requires bicaudal (double chain) amphiphiles, which can be either natural or synthetic.[1, 2] On the other hand, single-chain amphiphiles at concentrations higher than the critical micellar concentration tend normally to aggregate into micelles which may be spherical, cylindrical, or plate-shaped.[3] In the latter case lamellar mesophases can form but only at very high concentrations (> 50 % w/v).

When dilute dispersions are considered, the formation of bilayers and vesicles from single-chain amphiphiles (i.e. amphotropic behavior) requires an element of order to promote the alignment of the molecules in bilayers and to maintain molecular packing.[3] Such order can be brought about through steric interactions. Rigid amphiphiles have thus been reported to form vesicles when they possess a rodlike segment inserted between the polar head and the hydrophobic chain (typically biphenyl, azobenzene, or diphenylazomethine moieties).[4] Rigid coamphiphiles like cholesterol are also used to obtain stable vesicles.[5] Order can also be brought about by intermolecular associations, including those resulting from electrostatic forces (pairing of oppositely charged amphiphiles),[6] hydrogen bonding,[7] or polymerization.[8]

[*] Prof. J. G. Riess, Dr. M.-P. Krafft, F. Giulieri
Unité de Chimie Moléculaire, associée au CNRS
Université de Nice-Sophia Antipolis
Faculté des Sciences, F-06108 Nice Cedex 2 (France)
Telefax: Int. code + 93529020

[**] This work was supported by the Centre National de la Recherche Scientifique. The authors are grateful to the Centre Commun de Microscopie Appliquée (CCMA, Prof. G. Nicaise, S. Pagnotta, J. P. Laugier) of the Université de Nice-Sophia Antipolis for assistance.

We investigated whether lamellar phases, vesicles, and, more generally speaking, organized supramolecular systems could be obtained from a single pure monocaudal nonrigid amphiphile by reinforcing the *hydrophobic interactions* in the surfactant film through the use of a highly perfluorinated tail, without recourse to classical steric effects or intermolecular associations.

For this purpose we prepared a linear "perfluoroalkylated" amphiphile (F-alkyl-PC) **1** phosphocholine derivative[9] and its hydrocarbon analogue **2**, and examined their dispersions in water with a view to assessing the effect of the fluorinated chain on supramolecular organization.

$C_8F_{17}C_2H_4OP(O)_2^-OC_2H_4N^+(CH_3)_3$ **1**
$C_{10}H_{21}OP(O)_2^-OC_2H_4N^+(CH_3)_3$ **2**

We report here that in contrast to its hydrocarbon analogue, F-alkyl-PC **1** forms stable organized supramolecular systems even in very dilute aqueous dispersions, without the need of secondary additives (Scheme 1). Depending on the conditions of preparation, various organized systems, significantly different in morphology, including stacked bilayers, vesicles, globules, and long fibers are observed.

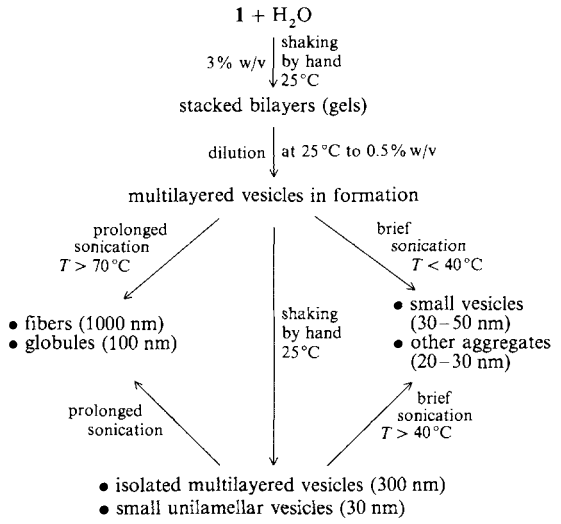

Scheme 1. Organized supramolecular systems formed by **1**.

Dispersions of F-alkyl-PC have been prepared by hydrating the thin-layered compound with distilled water for 15 min at room temperature, followed by gentle shaking by hand. Depending on the concentration, clear to slightly turbid gels with viscoelastic properties were obtained. These gels display a consistency ranging from gelatin-like (1–3 % w/v) to glass-like (> 6 % w/v). They remain stable at room temperature for over 12 months without any sedimentation, crystallization, or phase separation. The gels can even be heat-sterilized (121 °C, 15 min, 15 Nm^{-2}) without apparent modification.

Investigation of such gels (3 % w/v) by transmission electron microscopy (TEM)[10] shows that they consist uniformly of stacked bilayers (Fig. 1). The lamellar structure of these assemblies is supported by optical polarization microscopy which visualizes the characteristic defects of the bilayers called "maltese crosses" and "oily strikes".[11] The lamellar structure is further supported by proton-decoupled ^{19}F NMR spectroscopy which shows a significant decrease of the linewidth of all resonance signals when temperature increases (e.g. from ca. $\Delta\nu_{1/2} = 400$ Hz at 10 °C to ca. 70 Hz at 70 °C

 © VCH Verlagsgesellschaft mbH, W-6940 Weinheim, 1993 0570-0833/93/0505-0741 $ 10.00+.25/0

for the CF_3CF_2 resonance signal), indicating a mesophase transition. Complete melting of the F-alkyl chain occurs in the liquid phase over an unusually large temperature range (30–60 °C), in line with our previous observations on liposomes of glycerophosphocholines with two perfluorinated alkyl groups.[12]

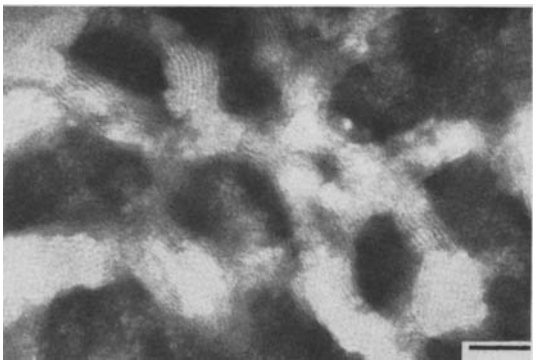

Fig. 1. TEM (negative staining) of a dispersion (3% w/v, shaken by hand at room temperature) of **1**. The length of the bar corresponds to 50 nm.

When the gels are diluted with water to a final concentration of 0.5% w/v, then gently shaken by hand for 1 min at room temperature, the constitution of multilayered vesicles "in formation" is observed. This is comparable to what occurs during the formation of liposomes from a coarse dispersion of phospholipids. When this dispersion is shaken by hand for a longer period, *isolated* multilayered vesicles are obtained, as shown by TEM micrographs (Fig. 2). Their sizes were evaluated by laser light scattering spectroscopy (LLSS), which showed large aggregates (300 nm, 40%) in addition to smaller aggregates (30 nm, 60%). The latter may consist either of micelles or of small vesicles and are not visible with TEM.

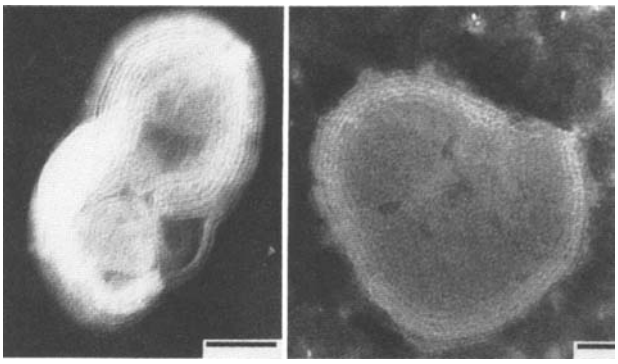

Fig. 2. TEM of isolated multilayered vesicles in a dilute dispersion (0.5% w/v) of **1** after gentle shaking by hand at room temperature. The length of each bar corresponds to 50 nm.

Brief sonication of the multilayered vesicle-containing dispersions at 40 °C or below (Scheme 1) (sonifier: Branson B30, titanium probe, 4 min, dial 5, pulse 50) led to the formation of small bilayered vesicles, which could be observed by TEM. Long aggregates were also present on the micrographs, and we suspect these to be fragments of lamellae, precursors of the vesicles.[13] LLSS measurements did not allow the distinction between the small vesicles and the long aggregates, and indicated only the presence of small particles of about 30 nm in diameter. After one month at room temperature, no significant evolution of sizes was detected by LLSS.

When the multilamellar vesicle-containing dispersions (0.5% w/v) are sonicated at a temperature at which the F-alkyl chain is completely fluid (i.e. above 70 °C when no further decrease of the linewidth of the ^{19}F NMR resonance signals is observed), two populations of aggregates of distinct morphologies are formed: globules and fibers. Their sizes have been evaluated on electron micrographs to be about 100 nm in diameter for the globules and about 1000 nm in length for the fibers. Since repulsion forces between bilayers usually increase with temperature,[14] we can suppose that at 70 °C bilayers dissociate to form inversed-phase microdomains stabilized by hydrophobic interactions. The globules may thus consist of closely packed assemblies of inverse micelles stabilized in water by a monolayer belt.[15] The fibers may be a one-dimensional extension of the spherical inverted structure.

Preliminary stability studies show that the fibers slowly grow, within a few weeks at room temperature, into a superstructure consisting of assembled fibers. This superstructure (several μm long) can be observed by contrast-phase optical microscopy. It is noteworthy that for the assemblies with perfluorinated alkyl chains reported here no crystallization was observed, even after a month, while limited lifetime is usual for fibrous aggregates.[16]

The strong tendency towards aggregation evidenced for the single-chain F-alkylated phosphocholine is in sharp contrast with the behavior of its hydrocarbon analogue **2** whose dispersions remain fluid, like water, even at concentrations up to 30% w/v. No evidence of liquid crystal formation has been detected in such solutions by polarization microscopy. In addition no aggregates have been imaged by TEM. LLSS measurements only showed the presence of micelle-sized aggregates (3–5 nm). The line width of the NCH_3 resonance signal in the ^1H NMR spectra (3 Hz) is also consistent with the formation of isolated micelles. Under the same conditions a far less well-resolved spectrum is obtained for the F-alkylated amphiphile **1**, with a NCH_3 line width of about 10 Hz. These results show that the dispersions of **2** only consist of fluid micelles, even when its concentration is increased to 30% w/v.

The formation of organized systems—multilayered and unilamellar vesicles, globules and fibers—by an F-alkylated phosphocholine, when compared to the inability of its hydrocarbon analogue to form anything more organized than micelles, establishes that a single F-alkyl chain can be sufficient to induce the alignment of amphiphilic molecules in bilayers. One major component of this driving force is likely to arise from the strongly hydrophobic interactions of the F-alkyl chains, endowing the molecule with a *strong* amphotropic (lyotropic + thermotropic) behavior. It also means that the tendency toward organization because of such hydrophobic effects overcomes the low intermolecular interactions between F-alkylated chains.

The geometry of the amphiphile may also contribute to the development of supramolecular aggregation properties.[17] Conically shaped surfactants (typically single-chain ones) tend to form micelles more easily, whereas cylindrically shaped ones prefer to assemble in bilayers. The bulkiness of the F-alkylated chain can therefore also be one of the factors which confers to the amphiphile the cylindral shape propitious to the formation of bilayers and vesicles.

Much attention has been focused on the influence of entropy on interactions in both natural and synthetic membranes; there is, however, a scarcity of suitable model mem-

branes; which may have hindered the understanding of the aggregation behavior. The single-chain systems reported here and the unique aggregation properties induced by perfluorinated chains may help provide insight into interactions between amphiphilic surfaces.

Received: November 30, 1992 [Z 5713 IE]
German version: *Angew. Chem.* **1993**, *105*, 783

[1] H. Eibl, *Angew. Chem.* **1984**, *96*, 247–262; *Angew. Chem. Int. Ed. Engl.* **1984**, *23*, 257–271.
[2] T. Kunitake, Y. Okahata, *J. Am. Chem. Soc.* **1977**, *99*, 3860–3861.
[3] H. Ringsdorf, B. Schlarb, J. Venzmer, *Angew. Chem.* **1988**, *100*, 117–162; *Angew. Chem. Int. Ed. Engl.* **1988**, *27*, 113–158.
[4] T. Kunitake, Y. Okahata, M. Shimomura, S. Yasunami, K. Takarabe, *J. Am. Chem. Soc.* **1981**, *103*, 5401–5413.
[5] J. A. Bouwstra, H. E. J. Hofland, G. S. Gooris, H. E. Jundginger in *Emulsions – A Fundamental and Practical Approach* (Ed.: J. Sjöblom), Kluwer, Dordrecht, **1992**, pp. 227–238.
[6] H. Fukuda, K. Kawata, H. Okuda, *J. Am. Chem. Soc.* **1990**, *112*, 1635–1637.
[7] W. R. Hargreaves, D. W. Deamer, *Biochemistry* **1978**, *17*, 3759–3768.
[8] R. Benz, W. Prass, H. Ringsdorf, *Angew. Chem.* **1982**, *94*, 388–389; *Angew. Chem. Int. Ed. Engl.* **1982**, *21*, 368–369; *Angew. Chem. Suppl.* **1982**, 869–880.
[9] M.-P. Krafft, J. P. Rolland, P. Vierling, J. G. Riess, *New J. Chem.* **1990**, *14*, 869–875.
[10] A drop of the dispersion was applied for 1 min on a carbon-coated grid, dried with filter paper, then stained for 1 min with phosphotungstic acid (2%, pH adjusted at 7), according to R. R. C. New in *Liposomes: A Practical Approach* (Ed.: R. R. C. New), University Press, Oxford, **1990**, p. 140. The samples were observed by using a Philips microscope (CM 12) at 80 KV under a magnification of 30000 to 60000.
[11] Observations were made on thin layers of dispersions with a polarizing microscope (Olympus BHS) between crossed polarizer and analyser, according to J. R. Bellare, H. T. Davis, W. G. Miller, G. E. Scriven, *J. Colloid Interface Sci.* **1990**, *136*, 305–326.
[12] C. Santaella, P. Vierling, J. G. Riess, *Angew. Chem.* **1991**, *103*, 584–586; *Angew. Chem. Int. Ed. Engl.* **1991**, *30*, 567–568; J. G. Riess, C.Santaella, P. Vierling, *Jorn. Commun. Com. Esp. Deterg.* **1991**, *22*, 157–171.
[13] R. B. Pansu, B. Arrio, J. Roncin, J. Faure, *J. Phys. Chem.* **1990**, *94*, 796–801.
[14] J. Marra, J. N. Israelachvili, *Biochemistry* **1985**, *24*, 4608–4621.
[15] Y. Murakami, J. I. Kikuchi, T. Takaki, K. Uchimura, *J. Am. Chem. Soc.* **1985**, *107*, 3373–3374.
[16] J. Fuhrhop, P. Schnieder, J. Rosenberg, E. Boekema, *J. Am. Chem. Soc.* **1987**, *109*, 3387–3390.
[17] J. N. Israelachvili, D. J. Mitchell, B. W. Ninham, *Biochim. Biophys. Acta* **1977**, *470*, 185–201.

Investigations of the Structure and Kinetics of Intermediates in Proton-Induced Alkylidyne–Isocyanide Ligand Coupling Reactions**

By *Cecilia M. Bastos, Nancy Daubenspeck,* and *Andreas Mayr**

Dedicated to Professor Herbert D. Kaesz on the occasion of his 60th birthday

Proton-induced alkylidyne–isocyanide coupling reactions[1, 2] belong to a class of coupling reactions whose general features are well understood.[3] However, mechanistic details of this type of transformation are much less well defined. The immediate coupling precursors are assumed to be N-protonated alkylidyne isocyanide metal complexes,[1, 2] but it was also found that the preferred site of protonation in these complexes is the alkylidyne carbon atom.[2] This paper is concerned with the structural effects of protonation of alkylidyne isocyanide complexes and with the mechanism of the methanol-catalyzed transformation of $C_{(alkylidyne)}$-protonated alkylidyne isocyanide metal complexes into aminoacetylene metal complexes.

The cationic alkylidene complexes **2a–e** precipitate when complexes **1a–c**[4] are protonated in ether with trifluoromethanesulfonic acid or tetrafluoroboric acid [Eq. (a)]. The

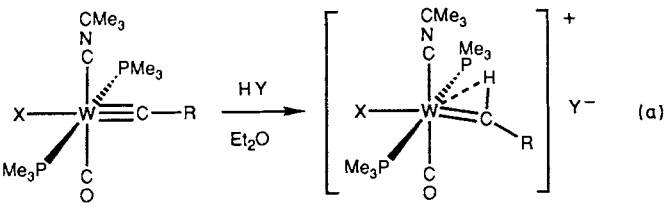

(a)

1

a: R = Ph, X = Cl
b: R = Ph, X = I
c: R = Me, X = Cl

2

a: R = Ph, X = Cl, Y = CF_3SO_3
b: R = Ph, X = Cl, Y = BF_4
c: R = Ph, X = I, Y = CF_3SO_3
d: R = Ph, X = I, Y = BF_4
e: R = Me, X = Cl, Y = CF_3SO_3

molecular structures of complexes **1a** (Fig. 1) and **2b** (Fig. 2) were determined by X-ray crystallography.[5] The bonding parameters of **1a** are as expected for a Fischer-type alkylidyne complex.[6] The structural changes associated with the

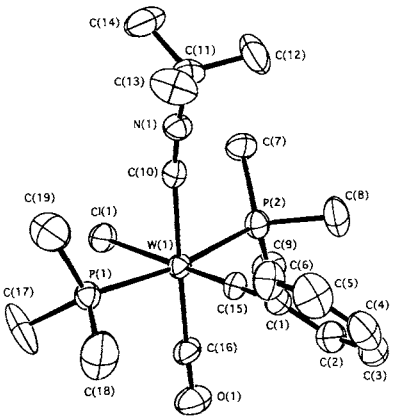

Fig. 1. Molecular structure of **1a**. Selected bond lengths [Å] and angles [°]: W(1)-C(15) 1.82(1), W(1)-C(10) 2.16(1), W(1)-C(16) 1.98(1), W(1)-Cl(1) 2.572(3), W(1)-P(1) 2.480(3), W(1)-P(2) 2.490(3), C(15)-C(1) 1.44(1); W(1)-C(15)-C(1) 179.3(8), C(10)-W(1)-C(15) 89.7(4), C(15)-W(1)-C(16) 89.2(4), P(1)-W(1)-P(2) 168.64(9), Cl(1)-W(1)-C(10) 90.4(3), Cl(1)-W(1)-C(15) 179.2(3), Cl(1)-W(1)-C(16) 90.7(3).

protonation of the alkylidyne carbon are clearly visible in the superimposition of the two structures (Fig. 3). The protonated alkylidyne ligand in **2b** is shifted from the coordination site, which it would occupy in an ideal octahedral coordination polyhedron, apparently to optimize the agostic interaction between the metal center and the formed C–H bond.[7] The plane of the alkylidene ligand is oriented roughly diagonally to the coordination axes of the adjacent ligands, such that the C15–H30 bond is oriented towards the isocyanide

[*] Prof. A. Mayr, Dr. C. M. Bastos, N. Daubenspeck
Department of Chemistry
State University of New York at Stony Brook
Stony Brook, NY 11794-3400 (USA)
Telefax: Int. code +(516) 632-7960

[**] This work was supported by the National Science Foundation (CHE 8921564 and CHE 9000884). We thank Raju Subramanian and Prof. Stephen A. Koch for the X-ray crystallographic studies and Prof. Albert Haim for helpful discussions.

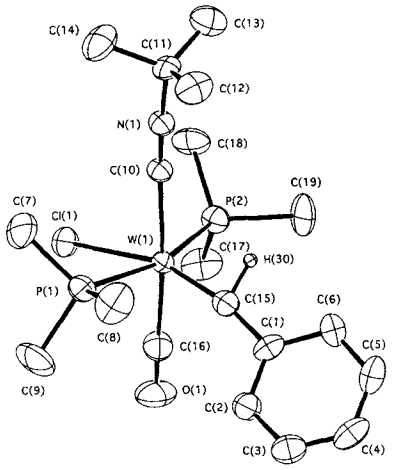

Fig. 2. Molecular structure of the cation of **2b**. Selected bond lengths [Å] and angles [°]: W(1)-C(15) 1.88(1), W(1)-C(10) 2.17(1), W(1)-C(16) 2.03(1), W(1)-Cl(1) 2.449(3), W(1)-P(1) 2.520(3), W(1)-P(2) 2.513(3), C(15)-C(1) 1.46(1), C(15)-H(30) 1.17(8), W(1)-H(30) 1.88(8); W(1)-C(15)-C(1) 167.8(8), C(10)-W(1)-C(15) 103.3(4), C(15)-W(1)-C(16) 81.3(4), P(1)-W(1)-P(2) 163.1(1), Cl(1)-W(1)-C(10) 91.9(3), Cl(1)-W(1)-C(15) 161.5(3), Cl(1)-W(1)-C(16) 83.4(3), W(1)-C(15)-H(30) 72(4).

ligand and the phenyl substituent towards the carbonyl ligand.

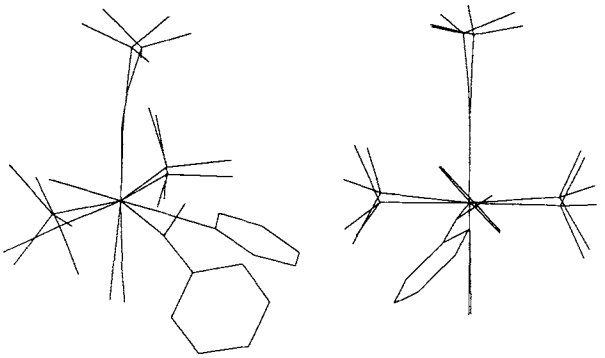

Fig. 3. Two views of the superimposed structures of **1a** and **2b**.

Complexes **2a–e** are moderately thermally stable in dry CH_2Cl_2. However, in the presence of small amounts of methanol, they isomerize cleanly into the aminoacetylene complexes **3** [Eq. (b)], which were isolated and characterized spectroscopically (see Experimental Procedure). The relative orientation of the ligands X and Y in complexes **3** was not established. The isomerization reactions are pseudo-first-order in complexes **2**. Observed rate constants or relative rates are listed in Table 1. The dependency of the reaction rate of

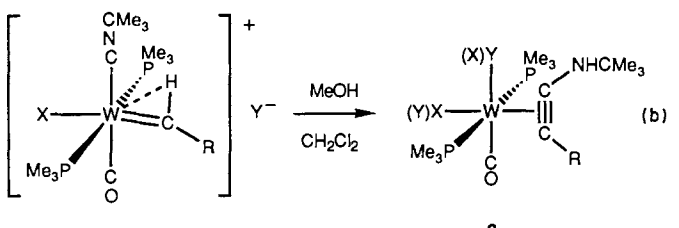

2a,c-e **3**

a: R = Ph, X = Cl, Y = CF_3SO_3
b: R = Ph, X = I, Y = CF_3SO_3
c: R = Ph, X = I, Y = BF_4
d: R = Me, X = Cl, Y = CF_3SO_3
e: R = Me, X = Cl, Y = Cl
f: R = Me, X = Cl, Y = 4-Me-$C_6H_4SO_3$

Table 1. Rate constants k [s^{-1}] or relative rates v for the transformation of complexes **2** into complexes **3** in CH_2Cl_2. [MeOH] = 1.97×10^{-1} M.

2	Y	X	R	k/v
2a	CF_3SO_3	Cl	Ph	6.5×10^{-4}
2c	CF_3SO_3	I	Ph	1.1×10^{-3}
2d	BF_4	I	Ph	3.2×10^{-4}
2e	CF_3SO_3	Cl	Me	7.3×10^{-5}
2f [a]	Cl	Cl	Me	<1 min [b]
2g [a]	$CH_3C_6H_4SO_3$	Cl	Me	<5 min [b]

[a] See Experimental procedure. [b] To completion.

complex **2a** on the concentration of methanol follows saturation kinetics.[8] These results imply the reversible formation of an adduct between **2a** and methanol. To probe the mechanism of this reaction further, the dependency of the reaction rate on several variables was tested: a) The rate shows little dependence on the nature of the coordinated halide ligand X. b) The reaction is significantly slower when the substituent (R) on the alkylidene carbon atom is changed from a phenyl group to a methyl group. c) The rate depends very strongly on the nature of the counterion Y^-, increasing with the nucleophilicity of Y^-.

Proton-induced alkylidyne–isocyanide coupling reactions have previously been proposed to proceed via N-protonated alkylidyne isocyanide metal complexes, that is alkylidyne (aminomethylidyne)metal complexes of type **A**, as the immediate coupling precursors.[1, 2] In the related coupling of two isocyanide ligands,[9, 10] bis(aminomethylidyne)metal complexes **B** are firmly established as intermediates. Filippou et al. synthesized stable complexes of type **B** by sequential addition of electrophiles (alkylation) to two isocyanide ligands and demonstrated that the coupling of the two aminomethylidyne ligands is induced by the addition of nucleophiles.[11] If we accept the assumption that the protonation of the isocyanide ligands also in reaction (b) brings about the activation of the coupling reaction, then the mechanism must involve a reversible step in which a proton in the alkylidene–methanol adduct is transferred to the isocyanide ligand. We propose that methanol acts as the proton transfer agent.

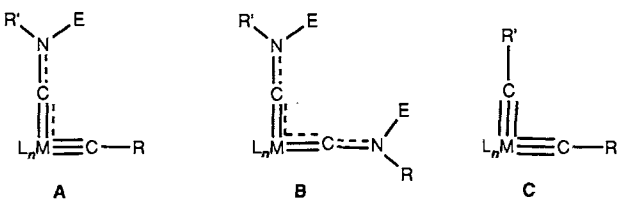

Scheme 1. Postulated proton transfer mechanism.

A possible mechanism for the proton transfer is shown in Scheme 1.[12] The C15–N1 distance of 4.12 Å found in the structure of **2a** even suggests that a C···H···O···H···N hydrogen-bonded arrangement of alkylidene ligand, methanol, and isocyanide ligand may participate in the proton transfer step. The slower rate of reaction of the methyl-substituted complex **2e**, compared to that of **2a**, would be explained by a lower equilibrium concentration of **5** for **2e**, due to an increased basicity of the alkylidene carbon atom in **2e**. The strong dependency of the rates of the nucleophilicity of the anions Y^- indicates that the actual coupling step is induced by nucleophilic attack of Y^- at intermediate **5**.[13] The alternative to this step would be spontaneous coupling of the alkylidyne and aminomethylidyne ligands in **5** and trapping of the formed aminoacetylene complexes by Y^-. In this case a much smaller anion dependency would be anticipated.[14]

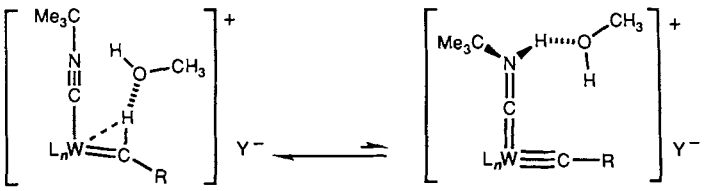

4 **5**

The results, therefore, support the assumption of discrete alkylidyne(aminomethylidyne)metal complexes **A** as intermediates in proton-induced alkylidyne–isocyanide coupling reactions. In the formal coupling of two alkylidyne ligands[15] discrete bis(alkylidyne) complexes **C** were not postulated as intermediates, since such species would be expected to be very unstable.[16, 17] The observation of alkylidene–isocyanide coupling in complexes **2** in the presence of the "non-nucleophilic" ions $CF_3SO_3^-$ and BF_4^- shows clearly how strongly the alkylidyne (aminomethylidyne) intermediates **A** are activated for coupling. Recently Lippard et al. reported evidence for similar intermediates in the silyl halide–induced coupling of siloxymethylidyne and carbonyl ligands.[18]

Experimental Procedure

All kinetics experiments were performed under argon and under rigorously anhydrous conditions. The reaction vessel was immersed in a constant temperature bath at 20.0 ± 0.1 °C. The reactions were monitored by IR spectroscopy, by measuring the absorbance of the carbonyl band of the alkylidene complexes **2**.

2a: Complex **1a** (0.107 g, 0.19 mmol) was dissolved in ether (5 mL), the solution was cooled to −78 °C, and CF_3SO_3H (20 mL, 0.226 mmol, 1.2 equiv) was added. A yellow precipitate formed almost quantitatively upon warming to 0 °C. The mixture was centrifuged, the supernatant decanted, and the product was washed with ether (2 × 5 mL) and dried under vacuum. The complexes **2b–e** were obtained in an analogous way with the appropriate acid.

Spectroscopic data: The IR spectra were measured in CD_2Cl_2, the NMR spectra in CD_2Cl_2. The first $\tilde{\nu}$ values given in the IR data refer to $\nu(CNCMe_3)$, the second to $\nu(CO)$. The ^1H NMR data give the δ value for the C(*H*)R proton, the ^{13}C NMR data for the corresponding *C*(H)R carbon atom.

2a: IR: $\tilde{\nu}$[cm^{-1}] = 2189, 1993; ^1H NMR (−30 °C): $\delta = -3.2$; ^{13}C NMR (−30 °C): $\delta = 230.8$ (J(C,H) = 67 Hz). **2b**: IR: $\tilde{\nu}$[cm^{-1}] = 2189, 1993; ^1H NMR ($CDCl_3$): $\delta = -2.57$; ^{13}C NMR ($CDCl_3$): $\delta = 230.4$ (J(C,H) = 72 Hz). **2c**: IR: $\tilde{\nu}$[cm^{-1}] = 2186, 1987. **2d**: IR: $\tilde{\nu}$[cm^{-1}] = 2188, 1987; ^1H NMR (−30 °C, $CDCl_3$): $\delta = -3.01$; ^{13}C NMR: $\delta = 230.2$ (J(C,H) = 77 Hz). **2e**: IR: $\tilde{\nu}$[cm^{-1}] = 2185, 1992; ^1H NMR: $\delta = -2.53$; ^{13}C NMR: $\delta = 241.7$ (J(C,H) = 73 Hz).

3: An aliquot of one of the complexes **2a,c–e** (0.075–0.15 mmol) was dissolved in CH_2Cl_2 (1 mL). Then methanol (8 μL, 1.97×10^{-1} mmol) was added. Aliquots were taken at regular time intervals, and the IR spectra were recorded at room temperature. In a series of experiments with complex **2a** the methanol concentration was varied from 6.9×10^{-2} to 9.8×10^{-1} M. In two sets of experiments equivalent amounts of NEt_4Cl (**2f**) and $NEt_4(4\text{-}CH_3C_6H_4SO_3)$ (**2g**) were added to **2e** before methanol addition. The kinetics for **2b** were not measured.

Spectroscopic data: The IR data refer to ν(CO), the ^{13}C NMR data to $\delta(RCCNHCMe_3)$. IR: $\tilde{\nu}$[cm^{-1}] = 1947 (**3a**, **3b**), 1946 (**3c**), 1939, 1917(**3d**), 1924 (**3e**), 1931 (**3f**); ^{13}C NMR: $\delta = 209.1$, 206.8 (**3a**, **3b**), 210, 209, 203, 201 (two isomers of **3c**), 212.5, 210.5 (**3d**), 206, 200 (**3e**), 207.5, 206.5 (**3f**).

Received: November 23, 1992 [Z 5696 IE]
German version: *Angew. Chem.* **1993**, *105*, 793

[1] A. C. Filippou, W. Grünleitner, *Z. Naturforsch. B* **1989**, *44*, 1023.
[2] A. Mayr, C. M. Bastos, *J. Am. Chem. Soc.* **1990**, *112*, 7797.
[3] A. Mayr, C. M. Bastos, *Prog. Inorg. Chem.* **1992**, *40*, 1.
[4] a) A. Mayr, M. F. Asaro, M. A. Kjelsberg, K. S. Lee, D. Van Engen, *Organometallics* **1987**, *6*, 432; b) C. M. Bastos, Ph.D. Thesis, State University of New York at Stony Brook, **1991**.
[5] X-ray quality crystals of **1a** were obtained by slow cooling of a hot saturated solution of the complex in hexane. Crystal data for **1a**: $C_{19}H_{32}ClOP_2NW$, $M = 562.65$, $P1$ (no. 2), $a = 11.5645(6)$, $b = 11.6849(8)$, $c = 9.8517(6)$ Å, $\alpha = 108.838(5)$, $\beta = 100.921(5)$, $\gamma = 89.095(5)°$, $V = 1235.7(3)$ Å^3, $Z = 2$, $\rho_{calcd} = 1.512$ g cm^{-3}, $\mu(Mo_{K\alpha}) = 50.16$ cm^{-1}, 5348 unique observed data, $2\theta < 53.9°$, $R = 0.039$, $R_w = 0.041$. X-ray quality crystals of **2b** were obtained by slow diffusion of ether into a concentrated solution of **2b** in CH_2Cl_2. Crystal data for **2b**: $C_{19}H_{33}BClF_4OP_2NW$, $M = 659.53$, $P2_1/n$ (no. 14), $a = 13.834(3)$, $b = 13.647(7)$, $c = 14.597(7)$ Å, $\beta = 94.68(3)°$, $V = 2747(3)$ Å^3, $Z = 4$, $\rho_{calcd} = 1.595$ g cm^{-3}, $\mu(Mo_{K\alpha}) = 45.44$ cm^{-1}, 4574 unique observed data, $2\theta < 48.0°$, $R = 0.037$, $R_w = 0.043$. All intensity measurements were made at room temperature, using graphite-monochromated $Mo_{K\alpha}$ radiation ($\lambda = 0.71069$ Å), and a variable-rate, ω-2θ scan technique. Empirical absorption corrections were applied. (For **2b**, the intensities of three reflections, which were measured after every 60 min of X-ray exposure time, declined by 27.40%. A linear correction factor was applied.) The structures were solved by direct methods and refined by full-matrix least squares. All calculations were performed with the TEXRAY programs. Further details of the crystal structure investigations may be obtained from the Fachinformationszentrum Karlsruhe, Gesellschaft für wissenschaftlich-technische Information mbH, D-W-7514 Eggenstein-Leopoldshafen 2 (FRG), on quoting the depository number CSD-57032, the names of the authors, and the journal citation.
[6] G. Huttner, A. Frank, E. O. Fischer, *Isr. J. Chem.* **1977**, *15*, 133.
[7] The bonding parameters of the alkylidene ligand in **2b** are similar to those in the structures of two related neutral complexes a) $[W(CHCMe_3)Cl_2(CO)(PMe_3)_2]$: J. H. Wengrovius, R. R. Schrock, M. R. Churchill, H. J. Wassermann, *J. Am. Chem. Soc.* **1982**, *104*, 1739; b) $[W(CHPh)Cl_2(CO)(PMe_3)_2]$: A. Mayr, M. F. Asaro, M. A. Kjelsberg, K. S. Lee, D. Van Engen, *Organometallics* **1987**, *6*, 432.
[8] A plot of $1/k_{obs}$ versus 1/[MeOH] for **2a** is linear (intercept = 368 *s*; slope = 247 sM).
[9] E. M. Carnahan, S. J. Lippard, *J. Chem. Soc. Dalton Trans.* **1991**, 699.
[10] A. C. Filippou, W. Grünleitner, *J. Organomet. Chem.* **1990**, *393*, C10.
[11] A. C. Filippou, W. Grünleitner, C. Völkl, P. Kiprof, *Angew. Chem.* **1991**, *103*, 1188; *Angew. Chem. Int. Ed. Engl.* **1991**, *19*, 1167.
[12] Deprotonation of the alkylidene ligand, presumably the slowest step in any mechanism for the equilibration of species such as **4** and **5**, is very rapid. The rate of H–D exchange between **2b** and CH_3OD is too fast to be measured by conventional spectroscopic methods.
[13] An increase of the concentration of Y^-, $Y = CF_3SO_3$ ($NEt_4CF_3SO_3$), led to a decrease of the reaction rate of **2a**. It is assumed that adduct formation between methanol and added $NEt_4CF_3SO_3$ reduces the effective concentration of methanol.
[14] R. G. Wilkins, *Kinetics and Mechanisms of Reactions of Transition Metal Complexes*, VCH, Weinheim, **1991**.
[15] a) G. A. McDermott, A. Mayr, *J. Am. Chem. Soc.* **1987**, *109*, 580; b) A. Mayr, C. M. Bastos, N. Daubenspeck, G. A. McDermott, *Chem. Ber.* **1992**, *125*, 1583.
[16] a) C. N. Wilker, R. Hoffmann, O. Eisenstein, *Nouv. J. Chim.* **1983**, *7*, 535; b) R. Hoffmann, C. N. Wilker, S. J. Lippard, J. L. Templeton, D. C. Brower, *J. Am. Chem. Soc.* **1983**, *105*, 146.
[17] D. C. Brower, J. L. Templeton, D. M. P. Mingos, *J. Am. Chem. Soc.* **1987**, *109*, 5203.
[18] J. D. Protasiewicz, A. Masschelein, S. J. Lippard, *J. Am. Chem. Soc.* **1993**, *115*, 808.

Transition-Metal-Substituted Volatile Alanes, Gallanes, and Indanes: Synthesis and Structure**

By *Roland A. Fischer,* Joachim Behm, Thomas Priermeier,* and *Wolfgang Scherer*

Transition-metal-substituted alanes, gallanes, and indanes have so far attracted little attention. Their instability and tendency to disproportionate prevent their isolation in a pure form and make their chemistry appear fruitless.[1] These particular compounds, however, possibly possess a high industrial potential: they might be suitable as single-source precursors for the chemical vapor deposition of bimetallic thin films such as β-CoGa.[2, 3] We have now begun the systematic development of this type of compound with the aim of achieving volatility and defined pyrolysis to yield the pure metal phase by structural modification of the molecular precursor.[4]

The synthesis of stable complexes with a metal ratio of 1:1 is not easy. From the syntheses of **1**–**12** (Scheme 1, Table 1) it is seen that tetracarbonylcobaltate does *not* react with $[(CH_3)_3SiCH_2]_2InCl$ to give the expected CoIn complex, an analogue of the stable CoGa compound **5**,[4] but rather it reacts with the elimination of trialkylindium to give **13** (Fig. 1).[5] The remarkable feature of the structure of **13** is

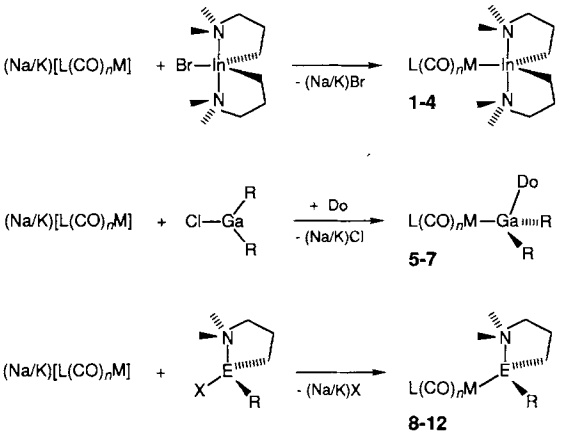

Scheme 1. Syntheses of complexes **1**–**12**.

Table 1. The complexes **1**–**12**.

Cmpd.	M	L	*n*	R	Do
1	Fe	Cp	2	-	-
2	Mn	CO	4	-	-
3	Co	CO	3	-	-
4	Ni	Cp	1	-	-
5	Co	CO	3	CH_2tBu	THF
6	Co	CO	3	H	NMe_3
7	Mn	CO	4	H	NMe_3
8 [a]	Co	PPh_3	3	Cl	-
9 [a]	Fe	Cp	2	Et	-
10 [b]	Fe	Cp	2	CH_2tBu	-
11 [b]	Co	PMe_3	3	CH_2tBu	-
12 [b]	Ni	Cp	1	CH_2tBu	-

[a] E = Ga. [b] E = Al.

[*] Dr. R. A. Fischer, Dr. J. Behm, Dipl.-Chem. T. Priermeier
Dipl.-Chem. W. Scherer
Anorganisch-chemisches Institut der Technischen Universität München
Lichtenbergstrasse 4, D-W-8046 Garching (FRG)
Telefax: Int. code +(89) 3209-3473

[**] Organo-Group 13 Metal Complexes of the d-Block Elements, Part 6. This work was supported by the Deutsche Forschungsgemeinschaft (habilitation grant for R. A. F.). We thank Prof. W. A. Herrmann for his support. - Part 5: R. A. Fischer, J. Behm, E. Herdtweck, *J. Organomet. Chem.* **1992**, *437*, C29–C34.

$[\{(CO)_4Co\}_2In(CH_2SiMe_3)(thf)]$ **13**

the distorted tetrahedral environment of the indium atom. The sum of the angles (354°) about the In atom, which involve Co1, Co2, and C2, indicates an almost planar environment. If alkyl groups such as *tert*-butyl or methyl are found at the indium atom, an undesired symmetrization occurs, giving compounds of the type $[\{L(CO)_nM\}_3In]$.

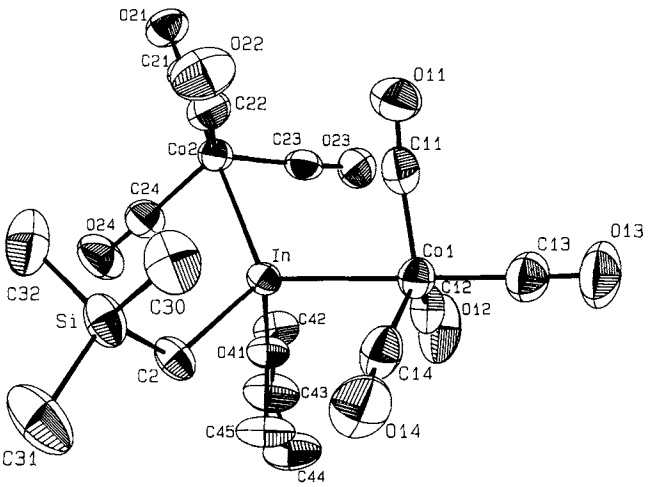

Fig. 1. Crystal structure of **13** (ORTEP). Selected bond lengths [pm] and angles [°]: In-Co1 263.83(4), In-Co2 263.03(4), In-O41 233.9(2), In-C2 216.8(3); Co1-In-Co2 117.17(1), Co1-In-O41 104.67(5), Co1-In-C2 118.30(8), Co2-In-O41 97.31(4), Co2-In-C2 118.63(8), O41-In-C2 92.42(8). The In atom lies 34.7 pm above the plane Co1, Co2, O41.

The only dialkylindium complexes known to date to be resistant to exchange are *cis*-$[L_2PtInR_2]$ (L_2 = $Cy_2P(CH_2)_2PCy_2$, Cy = *cyclo*-C_6H_{11}; R = CH_2SiMe_3)[6] and *fac*-$[(Me_3P)_3(Et)(H)IrInEt_2]$,[7] however, these are *not* volatile. The FeIn complex **1** (Fig. 2[5]) and its Mn, Co, and Ni analogues **2**–**4** (Scheme 1) owe their combination of stability *and* volatility to two chelating 3-dimethylaminopropyl groups which shield the In center. With the very long In–N3 and In–N4 distances, which vary by approximately 10 pm, and a clearly nonlinear N-In-N arrangement (angle N3-In-N4 = 155.4(2)°), the trigonal-bipyramidal environment of the In atom in **1** is unusually strongly deformed. If the Fe complex fragment is replaced by an electronegative bromide substituent, the resulting structure has identical In–N distances, approximately 10 and 20 pm shorter than those in **1**, and a linear N-In-N arrangement.[8] EHMO calculations on similar systems[9] indicate that the reason for these differences may be an electron transfer from the d-block metal into σ^*(In–N) orbitals. Photolysis of **1** in daylight leads to **14**. The In–N bond of the alkylindium complex fragment

$[(\mu\text{-CO})(\mu\text{-InR})\{(Cp(CO)Fe_2\}_2]$ **14**, R = $(CH_2)_3NMe_2$

($In[(CH_2)_3NMe_2]$ isolobal with CH_2) in the Fe_2In complex **14** no longer participates in the electron system of the d-

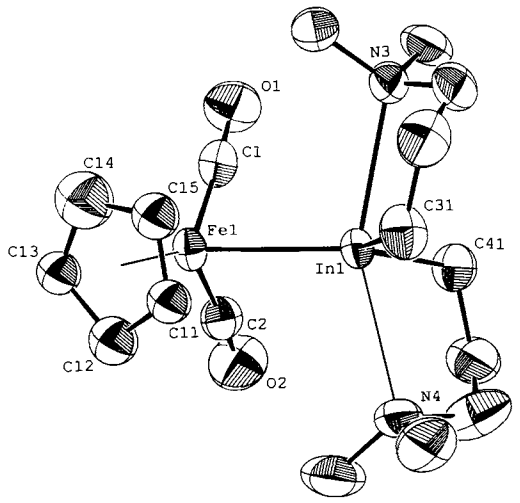

Fig. 2. Crystal structure of 1 (ORTEP). Selected bond lengths [pm] and angles [°]: Fe-In 263-93(8), Fe-Cl 173.3(7), Fe-C2 175.7(7), In-N3 264.3(5), In-N4 272.6(5), In-C31 220.7(6), In-C41 219.5(6), C1-Fe-In 84.4(2), C2-Fe-In 85.9(2), C1-Fe-C2 89.2(3), Fe-In-N3 101.7(8), Fe-In-N4 102.9(2), Fe-In-C31 123.6(2), Fe-In-C41 117.4(2), N3-In-N4 155.4(2), C31-In-C41 119.0(3), Fe-Cp 175.1.

block metals on symmetry grounds and is shortened to 239.2(6) pm.[5] Similarly, the σ(Co–Ga) bonds also react sensitively to variation of the substituents. The shortest Co–Ga distance known so far is found in **8** (237.8 pm) (Fig. 3).[5]

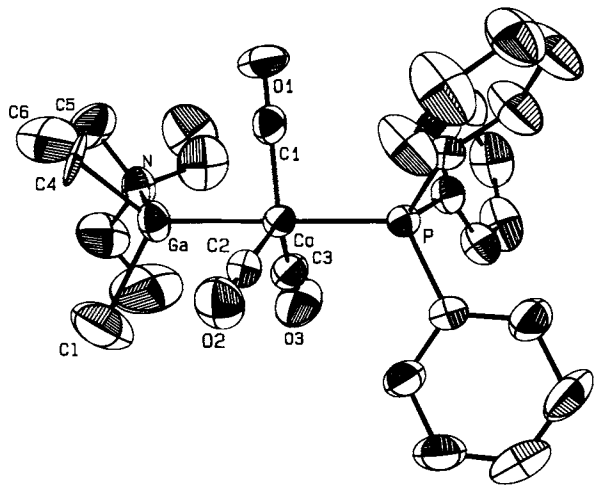

Fig. 3. Crystal structure of **8** (ORTEP). Selected bond lengths [pm] and angles [°]: Co-Ga 237.78(4), Ga-C1 217.6(1), Ga-N 217.2(3), Ga-C4 201.8(2), Co-P 220.02(8); Ga-Co-P 175.56(3), Ga-Co-C1 84.39(8), Ga-Co-C2 83.50(8), Ga-Co-C3 83.65(9), Co-Ga-C1 114.50(3), Co-Ga-N 116.93(6), Co-Ga-C4 120.20(7).

The exchange of the chlorine substituent in **8** for a methyl group (**8**-Me) extends the Co–Ga bond length to 249.7(3) pm.[5] The upper limit for σ(Co–Ga) distances seems to be about 260 pm.[4]

Intramolecular adduct formation or the use of sterically demanding groups are proven means for the preparation of organometallic compounds of Group 13 elements with unusual properties.[6, 8] Thus, the existence of the H_2Ga complexes **6** and **7** is particularly surprising, especially when one considers how little success has been achieved despite the intensive search for analogous compounds with H_2B units.[10] In the ^{1}H NMR spectra of **6** and **7** one broad Ga–H resonance signal is found at δ = **5**–**6**, which has the appropriate intensity ratio to that of the donor ligand NMe_3. The $2A_1 + E$ (splitting) pattern characteristic for $LM(CO)_4$ complexes with C_s symmetry for **6** is, as expected, shifted to higher wavenumbers by approximately 10 cm^{-1}, in comparison with the analogous alkyl compound **5**.[4] Compounds **6** and **7** start to decompose at about 80 °C in a sealed NMR tube, which leads to the liberation of the donor ligand, Ga deposition, H_2 evolution, and the formation of [E(M-$(CO)_n)_3$]. An attack at the carbonyl ligands does not occur! Correspondingly, the otherwise typical L_nM-Co-Al coordination is, in the Fe, Co, and Ni complexes **10**, **11**, and **12**, obviously suppressed in favor of hitherto unknown aluminum d-block metal bonds. Since single crystals suitable for X-ray structure analysis have not yet been obtained, the proposal for the structure is based on the complete agreement of the spectroscopic data of **10**–**12** with those of the formally analogous Ga complexes **8** and **9**. The chiral environment of the Al center and the occurrence of a chelate structure are manifested in the magnetic nonequivalence of all the ring protons of the metallacycle, the methylene protons of the neopentyl group, and the two methyl groups at the N atom. In the ^{13}C NMR spectrum of the FeAl complex **10** two sharp resonance signals for the diastereotopic carbonyl groups occur at δ = 219.5 and δ = 219.2; these have the same intensity. The existence of an $L(CO)_3$Co-Al unit is confirmed for **11**, for example, also by the $A_1 + E$ pattern in the IR spectrum, which is analogous to that of the structurally characterized complex **9**; from −90 to +150 °C the CO ligands in **11** are equivalent. The ^{31}P NMR resonance signal of **11** lies within the expected range (δ = 9.0), likewise the ^{27}Al NMR resonance signals for the complexes **10**–**12** at δ = 200(±15). Even the replacement of the bromine substituent in BrH_2AlNMe_3 by strong organometallic nucleophiles is possible without CO attack, and leads, by the elimination of the alkali metal bromide, to a product soluble in toluene, which we are investigating at present. Based on the complexes **1**–**12** the unexploited chemistry of the highly reactive d-block metal–Group 13 metal bond can now be developed.[11]

Experiments confirming the unexpected all-round suitability of *undecomposed volatile* complexes—depending on their structure at −10 to +100 °C and 10^{-1} to 10^{-3} mbar—for the chemical vapor deposition of intermetallic films such as β-CoGa and ε-NiIn, are described in the following communication.[3]

Experimental Procedure

1: Under argon (using a U-shaped tube fitted with a frit [4]) Na[Cp-$(CO)_2$Fe]·0.5 THF (2.35 g, 10 mmol) and $BrIn\{(CH_2)_3NMe_2\}_2$ (3.67 g, 10 mmol) [8] were mixed together in THF at −10 to + 25 °C. After the mixture had been stirred for 30 min the solvent was removed under vacuum. The product was extracted with *n*-pentane and crystallized at −78 °C (yellow crystals, 3.95 g, 85% yield). **2**–**13** were accessible in an analogous way.

Selected physical data: **6**: colorless needles (*n*-pentane), m.p. −15 °C (decomp > 40 °C, sublimation at −10 °C, 10^{-3} Torr). ^{1}H NMR (399.78 MHz, [D$_8$]toluene, 25 °C, TMS): δ = 1.92 (s, 9 H, NCH_3), 5.36 (s, br, 2 H, GaH); ^{13}C NMR (100.5 MHz, [D$_8$]toluene, 25 °C, TMS): δ = 49.5 (q, NCH_3), 205.1 (s, CoCO). IR [12]: $\tilde{\nu}$[cm^{-1}] = 2074 st, 2006 st, 1978 sst, 1964 sst (ν(CO)). Correct C, H, N analysis. **11**: white microcrystalline powder (*n*-pentane), m.p. 35 °C (sublimation at 60 °C, 10^{-3} Torr). δ = 0.66 (d, 1H, ^1J(H,H) = 14.1 Hz, $AlCH_2$), 0.68–0.76 (ABCD, 1H, $AlCH_2CH_2$), 0.79–0.88 (ABCD, 1H, $AlCH_2CH_2$), 0.95 (d, 1H, ^1J(H,H) = 14.1 Hz, $AlCH_2C$), 1.09 (d, 9H, ^2J(P,H) = 8.5 Hz, PCH_3), 1.29 (s, 9H, CCH_3), 1.64–16.8 (ABCD, 1H, $AlCH_2CH_2$), 1.79–1.83 (ABCD, 1H, $AlCH_2CH_2$), 2.06 (s, 3H, NCH_3), 2.06–2.10 (ABCD, 1H, NCH_2CH_2), 2.27 (s, 3H, NCH_3), 2.35–2.40 (ABCD, 1H, NCH_2CH_2); ^{13}C{^{1}H} NMR (100.5 MHz, C_6D_6, 25 °C, TMS): δ = 11.4 (br, $AlCH_2CH_2$), 22.5 ($AlCH_2CH_2$), 32.2 ($AlCH_2C$), 34.8 (CCH_3), 34.9 (br, $AlCH_2C$), 47.5 (NCH_3), 47.7 (NCH_3), 65.0 (NCH_2), 205.8 (d, ^1J(P,C) = 8 Hz, CoCO); ^{27}Al{^{1}H} NMR (104.14 MHz, [D$_8$]toluene, 25 °C, $Al(NO_3)_3/H_2O$ ext.) δ = 198 ($\nu_{1/2}$ = 4340 Hz); ^{31}P{^{1}H} NMR (161.9 MHz, [D$_8$]toluene,

$-80\,^{\circ}C$, 85% H_3PO_4 ext.): $\delta = 9.0$. IR (*n*-pentane): $\tilde{\nu}[cm^{-1}] = 1922$ sst, 1903 sst (ν(CO)). EI-MS (70 eV): m/z 403 (M^+, 3%). Correct elemental analysis.

Received: December 24, 1992 [Z 5774 1E]
German version: *Angew. Chem.* **1993**, *105*, 776

[1] S. K. Boocock, S. G. Shore in *Comprehensive Organometallic Chemistry. Vol. 6* (Eds.: G. Wilkinson, F. G. A. Stone, E. W. Abel), Pergamon, Oxford, **1982**, p. 947ff.

[2] Y.-J. Chen, H. D. Kaesz, Y. K. Kim, H.-J. Müller, R. S. Williams, Z. Xue, *Appl. Phys. Lett.* **1989**, *55*, 2760–2762.

[3] R. A. Fischer, W. Scherer, M. Kleine, *Angew. Chem.* **1993**, *105*, 778; *Angew. Chem. Int. Ed. Engl.* **1993**, *32*, 748.

[4] R. A. Fischer, J. Behm, *Chem. Ber.* **1992**, *125*, 37–42.

[5] Crystal structure investigations [$Mo_{K\alpha}$]: **13**, triclinic, $P\bar{1}$ (no. 2); $a = 932.1(2)$, $b = 1054.2(2)$, $c = 1257.7(3)$ pm; $\alpha = 80.19(2)$, $\beta = 80.55(2)$, $\gamma = 85.05(2)^{\circ}$; $Z = 2$; $\rho_{calcd} = 1.706\ g\,cm^{-3}$; $R = 0.039$ ($R_w = 0.025$) for 3804 independent reflections. **1**, monoclinic, $P2_1/c$ (no. 14); $a = 1329.1(3)$, $b = 978.4(2)$, $c = 1524.8(3)$ pm; $\beta = 95.53(1)^{\circ}$; $Z = 4$; $\rho_{calcd} = 1.526\ g\,cm^{-3}$; $R = 0.032$ ($R_w = 0.039$) for 2800 independent reflections. The ring C atoms C11–C15 are disordered. **8**, triclinic, $P\bar{1}$ (no. 2); $a = 927.1(2)$, $b = 1147.0(3)$, $c = 1416.1(4)$ pm; $\alpha = 85.12(2)$, $\beta = 85.23(2)$, $\gamma = 75.21(2)^{\circ}$; $Z = 2$; $\rho_{calcd} = 1.433\ g\,cm^{-3}$; $R = 0.066$ ($R_w = 0.059$) for 4114 independent reflections. C4 and C6 are disordered. Further details of the crystal structure investigations may be obtained from the Fachinformationszentrum Karlsruhe, Gesellschaft für wissenschaftlich-technische Information mbH, D-W-7514 Eggenstein-Leopoldshafen 2 (FRG) on quoting the depository number CSD-56977, the names of the authors, and the journal citation. The structures of **4**, **8**-Me, **9**, and **14** will be published at a later date.

[6] R. A. Fischer, J. Behm, *J. Organomet. Chem.* **1991**, *413*, C10–C14.

[7] D. L. Thorn, R. L. Harlow, *J. Am. Chem. Soc.* **1989**, *111*, 2575–2580.

[8] H. Schumann, F. H. Görlitz, T. D. Seuss, W. Wassermann, *Chem. Ber.* **1992**, *125*, 3–7; H. Schumann, U. Hartmann, W. Wassermann, *Polyhedron* **1990**, *9*, 353–362; H. Schumann, U. Hartmann, A. Dietrich, J. Pickardt, *Angew. Chem.* **1988**, *100*, 1119–1120; *Angew. Chem. Int. Ed. Engl.* **1988**, *27*, 1077–1078.

[9] L. M. Clarkson, N. C. Norman, L. J. Farrugia, *Organometallics* **1991**, *10*, 1286–1292; A. E. Reed, P. von R. Schleyer, *J. Am. Chem. Soc.* **1990**, *112*, 1434–1445.

[10] J. D. Basil, A. A. Aradi, N. K. Bhattacharyya, N. P. Rath, C. Eigenbrot, T. P. Fehlner, *Inorg. Chem.* **1990**, *29*, 1260–1270.

[11] **1**–**12** undergo complex insertion reactions (insertion of, for example, chalcogens (S, Se, Te) and pnictogens (P, As) into the d-block metal–Group 13 metal bond) and show a very promising photochemistry (cf. the transformation of **1** into **14**).

[12] The localization of the $\nu(GaH_2)$ vibration in the IR spectra of **6** and **7** is still not clear due to the overlapping carbonyl bands. Deuteration experiments are in progress.

β-CoGa and ε-NiIn Films from Organometallic Single-Source Precursors: Ligand-Control of the Film Composition**

By *Roland Fischer*,* *Wolfgang Scherer*, and *Matthias Kleine*

Thin-film heterostructures such as CoGa on GaAs produced by molecular beam epitaxy are currently the subject of intensive study.[1] These materials could become essential as new Ohmic contacts or Schottky barriers. For example, they could serve as Gate metallizations for metal semiconductor field-effect transistors (MESFETs) for the construction of ultralarge-scale integrated circuits (ULSIs).[2] Starting from *two* separate precursors, the chemical gas-phase epitaxy of β-CoGa on GaAs(100) has been achieved.[3] The deposition of such bimetallic materials from single-source precursors is particularly advantageous when all the factors essential for the layering process are incorporated into the molecular structure of the precursor and thus, only pressure and temperature remain as regulating parameters.[4] The transition-metal-substituted alanes, gallanes, and indanes **1**–**6** (Fig. 1),[5] about whose suitability for chemical vapor deposition of intermetallic films we report here, come close to this property profile.

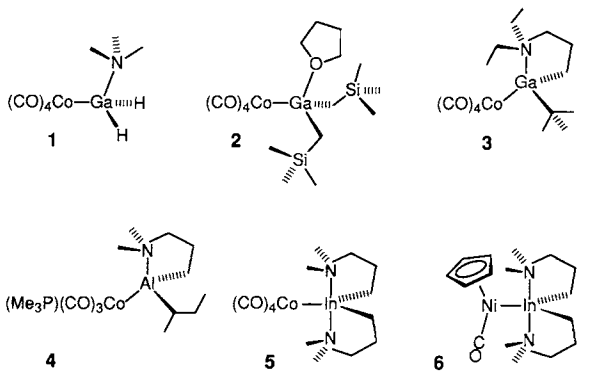

Fig. 1. Volatile transition-metal-substituted alanes, gallanes, and indanes [5].

The vapor pressure of the CoIn system **5**, which is 0.020(5) mbar (tensiometric[6]) at 20 °C is exemplary for this group of compounds. For the chemical vapor deposition (CVD) a horizontal hot-walled reactor was used. Complexes **1**–**6** were sublimed at 2.5×10^{-3} mbar from a thermostated reservoir directly into the reaction zone preheated to 200–400 (±10) °C,[7] and pyrolyzed there. Carrier gases were not used. Volatile by-products were collected in a cold trap (−196 °C). The analysis of the highly adhesive, metallic, polycrystalline films[8] (Table 1) deposited on various substrates (growth rate ca. $1\,\mu m\,h^{-1}$), and of the gaseous by-products[9] showed that the degradation of the precursors occurs according to Scheme 1.

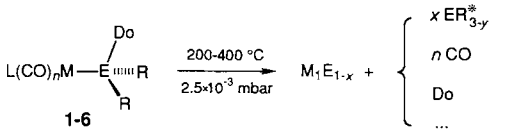

Scheme 1. Degradation reactions of the precursors **1**–**6** to give intermetallic phases. (L = CO, Cp, PMe_3; $n = 1$–3; M = Co, Ni; E = Al, Ga, In; $0 \geq x \geq 1$; R* = alkyl, then $y = 0$; R* = Cp, then $y = 2$; "..." denotes cleaved, volatile organic ligands or ligand fragments [9]).

Table 1. Results of the analytical characterization of the thin films deposited from the precursors **1**–**6** according to Scheme 1 [8,9].

Precursor	M	E	$T_{substrate}$ (±10 °C)	M/E (±0.05)	x (±0.05)	atom % C (±0.2)	atom % O (±0.2)	atom % H (±0.2)
1	Co	Ga	200	1.0	0.0	2	1	2
2	Co	Ga	350	2.1	0.50	3	1	2
3	Co	Ga	250	2.2	0.55	12	1	11
3	Co	Ga	300	1.5	0.32	5	2	4
3	Co	Ga	350	1.1	0.05	4	2	4
4	Co	Al	300	2.0	0.50	4	3	3
5	Co	In	250	1.0	0.0	1	1	4
6	Ni	In	250	2.9	0.70	1	1	2
6	Ni	In	350	1.1	0.05	1	1	1

[*] Dr. R. A. Fischer, Dipl.-Chem. W. Scherer, Dipl.-Chem. M. Kleine
Anorganisch-chemisches Institut der Technischen Universität München
Lichtenbergstrasse 4, D-W-8046 Garching (FRG)
Telefax: Int. code +(89) 3209-3473

[**] This work was supported by the Deutsche Forschungsgemeinschaft (habilitation grant for R. A. F.). We thank Prof. W. A. Herrmann and Prof. F. Baumgärtner for their support.

The 1:1 metal ratio of the precursors is *not* necessarily reproduced in the films. Thus, from the degradation of **2** approximately half of the gallium is found as $Ga(CH_2SiMe_3)_3$ (which is stable to pyrolysis) in the cold trap. The discharge of the Group 13 metal proved to be a general effect. For a given substrate temperature this process is controlled by the ligands at both metal centers, as shown, for example, by the comparison of **2** and **3**.[10] Since **1**–**6** sublime without decomposition, and the pressure in the system is low, we assume surface reactions are the explanation for this occurrence. According to mass spectrometric findings[11] the lowest energy and probably favored first steps in the degradation of the molecule are the cleavage of the donor ligand at the Group 13 metal and the breaking of the intermetallic bond. Thereafter, competition between ligand fragmentation and ligand reorganization plays a role. The latter may, in certain cases, lead to thermally stable organometallic compounds of Group 13 elements, which then desorb. Thus, it is understandable that the deposition of CoGa from a 1:1 mixture of $GaEt_3$ and $[Cp(CO)_2Co]$ at 250–300 °C and 1010 mbar (laminar flow reactor) afforded cobalt-rich, metastable α-Co_xGa_{1-x} films ($x \geq 0.41$). Only a tenfold excess of the gallium precursor compensates for its inefficient pyrolysis and leads—mass transport limited—to β-CoGa films.[3] However, the vacuum degradation of single-source precursors to yield a thin film is controlled kinetically[12] and offers the interesting possibility of adjusting the composition of the film through regulation of the temperature alone. If the formation of thermally stable organometallic compounds of Group 13 elements during the growth of the film is negligible, the limiting value M/E = 1 is already reached at very low temperatures. This is particularly the case for **1** and **5**.[10] Thus, the instability of gallane prevents a discharge of gallium for **1**, in sharp contrast to the related complex $[(CO)_5MnSiH_3]$, in which the silane is a potentially stable leaving group.[13] However, not only the substituents at the Group 13 metal are involved in the degradation process, the ligands at the d-block metal are also important. Whereas **5** affords Co_1In_1 films exclusively, the closely related NiIn precursor **6** gives, depending on the substrate temperature, films with a NiIn ratio of 2.9 to 1.1. The determining factor for this is the extent of Cp transfer to the In atom, leading to the formation of [CpIn], which leaves the reaction chamber. The ligand control of the composition of the film is an aspect that in future should be considered when CVD experiments are carried out. This is particularly true when, during heterogeneous pyrolysis, a part of the ligand sphere takes part in reorganization processes, and is bound *unfragmented* in the form of stable, volatile by-products.[14]

The suitability of CO ligands for CVD precursors is disputed. There is the danger of CO dissociation and thus, of the contamination of the film with C and O. We found, however, that the films were surprisingly low in impurities (Table 1, Fig. 2). Typical values are 1–4 atom% C and ≤1 atom% O (N, P could not be detected). The best conductivities (about 100 $\mu\Omega$cm) are close to the literature values.[15] The residual C content seems to stem from hydrocarbon ligands, since high C contents appear together with high H contents (EA[8]), whereas contaminations with O are only influenced by the leak velocity and the manipulation of the samples. The degradation of the precursors in the plasma-enhanced CVD experiment is remarkably less selective, leading to considerably higher $(CH)_x$ portions in the bimetallic films.[16]

The identity of the phases of the films corresponds to the binary phase diagram of the respective combination of metals. β-CoGa, for example, consists of 34.4% Ga to 57.8% Ga at 25 °C.[17] All CoGa films obtained proved to be single-phase β-CoGa with a dominant [110] reflection.[18] In the Co/In system only $CoIn_2$ and $CoIn_3$ are stable.[19] CoIn films deposited from **5** show reflections which are attributed to these phases.[18] The phase diagrams of other interesting alloys such as Co/Al, Ni/Ga, and Ni/In are more complex, and the homogeneity regions are narrower. Thus, it is very difficult to obtain single-phase films. We have achieved this for the first time with NiIn films deposited from **6** at 350 °C. The complete indexed X-ray diffractogram[18] (Fig. 3) contains only reflections of the hexagonal ε-NiIn phase,[20] a potential epitactic contact metal for GaAs and InP.[2] These results are encouraging for the further development of single-source precursors for bimetallic films.

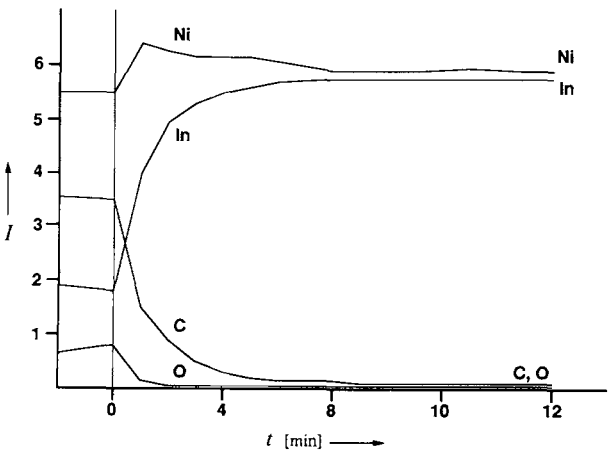

Fig. 2. Depth profile (Auger electron spectroscopy) of a film deposited on GaAs(100) $Ni_{0.52}In_{0.48}$ (see Table 1, last entry) from **6** at 350 °C. The signal intensity I (peak to peak ratio in arbitrary units) is plotted against the sputter time t (argon ions) for the Auger lines: Ni, LMM at 848 eV; In, MNN at 404 eV; C, KLL at 272 eV, and O, KLL at 504 eV.

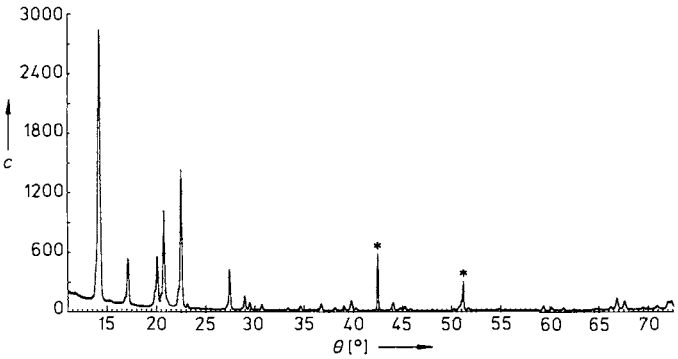

Fig. 3. X-ray powder diffractogram [18] of the $Ni_{0.52}In_{0.48}$ film from Figure 2 in the range 11° ≤ θ ≤ 73° (abscissa). The most intense reflection [*hkl*], θ value (relative intensity %): [101], 14.22° (100); [110], 17.09° (7); [111], 20.05° (6); [002], 20.74° (11); [201], 22.49° (18); [112], 27.39° (5). The reflections marked with * stem from the GaAs substrate. c = counting rate.

Experimental Procedure

The precursor reservoir of the reactor fueled with substrates and conditioned 24 h at ≤ 5×10^{-6} Torr and 250 °C was filled with substance (0.5–1.0 g) under argon at 25 °C. After the reservoir had been cooled to −30 °C, the deposition zone was warmed up to the desired substrate temperature under continuous

vacuum. After the vacuum had stabilized the reservoir temperature was regulated slowly up to a system pressure of about 2.5×10^{-3} mbar and deposition was carried out for about 5–6 h.

Received: December 24, 1992 [Z 5775 IE]
German version: *Angew. Chem.* **1993**, *105*, 778

[1] T. C. Kuo, T. W. Kang, K. L. Wang, *J. Cryst. Growth* **1991**, *111*, 996–1002; T. C. Kuo, K. L. Wang, R. Arghvani, T. George, T. L. Lin, *J. Vac. Sci. Technol. B* **1992**, *10*, 1923–1927.

[2] D. A. Baugh, A. A. Talin, R. S. Williams, T.-C. Kuo, K. L. Wang, *J. Vac. Sci. Technol. B* **1991**, *9*, 2154–2156; M. Tanaka, N. Ikarashi, H. Sakakibara, K. Ishida, T. Nishinaga, *Appl. Phys. Lett.* **1992**, *60*, 835–837.

[3] F. Maury, A. A. Talin, H. D. Kaesz, R. S. Williams, *Chem. Mater.* **1993**, *5*, 84–89.

[4] A. N. McInnes, M. B. Power, A. R. Barron, *Chem. Mater.* **1992**, *4*, 11–14, and references therein.

[5] R. A. Fischer, J. Behm, T. Priermeier, W. Scherer, *Angew. Chem.*, **1993**, *105*, 776; *Angew. Chem. Int. Ed. Engl.* **1993**, *32*, 746.

[6] D. F. Shriver, M. A. Drezdzon, *The Manipulation of Air-Sensitive Compounds*, 2nd ed. Wiley, New York, **1986**, pp. 168–176.

[7] A temperature range of 300 ± 50 °C is of interest for commercial applications [1–3].

[8] The films deposited on borosilicate glass, quartz, Si(100), GaAs(100), InP(100), KBr disks, and stainless steel were characterized by: Auger electron spectroscopy (AES; Perkin–Elmer Phi 595, initial irradiation 3 keV, intensity 0.20 μA), scanning electron microscopy (SEM), energy-dispersive X-ray spectroscopy (EDX), X-ray powder diffractometry [18], classical combustion analysis according to Pregl (EA; yield of ca. 20–50 mg film by dissolving the KBr substrates in water or by quenching of the reaction reaction tube) as well as by atomic absorption spectroscopy (AAS) after the dissolution of the film in HNO_3. Quantitative AES and EDX data were calibrated against AAS and EA values and against standard samples ($Co_{0.50}Ga_{0.50}$). A significant variation of the composition over the layered surface (ca. 3.5 cm^2) and layer thickness (0.2 μm to ca. 6–7 μm) was not present (AES, EDX).

[9] The trapped volatile by-products were fractionated under high vacuum, isolated, and characterized (^1H, ^{13}C NMR; IR; GC/IR/MS; AAS). The percentage of Group 13 metal discharged was determined quantitatively (AAS) by acidic hydrolysis. The liberation of CO was confirmed by GC/IR. The spectrum of the organic by-products, depending on the precursors, is dominated by olefins such as isobutene, 3-dimethylaminopropene (and isomers thereof), or cyclopentadiene. The donor ligands trimethylamine and tetrahydrofuran from **1** or **2** are deposited without fragmentation. The trimethylsilylmethyl groups in **2** afford a mixture consisting mainly of tetramethylsilane, trimethylsilane, 1,2-bis(trimethylsilyl)ethane, and ethyltrimethylsilane.

[10] If halide groups are present at the Group 13 metal, as in the complex $[(CO)_4CoGaCl_2(thf)]$, the composition of the films is constant only above 500 °C [3,15].

[11] R. A. Fischer, J. Behm. *Chem. Ber.* **1992**, *125*, 37–42; R. A. Fischer, J. Behm, T. Priermeier, *J. Organomet. Chem.* **1992**, *429*, 275–285.

[12] G. B. Stringfellow, *Organometallic Vapor Phase Epitaxy*, Academic Press, New York, **1989**, pp. 141–208.

[13] G. T. Stauf, P. A. Dowben, N. M. Boag, L. M. De La Graza, S. L. Dowben, *Thin Solid Films* **1988**, *156*, 327–334.

[14] J. A. Glass, Jr., S. S. Kher, J. T. Spencer, *Chem. Mater.* **1992**, *4*, 530–538; R. Kumar, F. R. Fronczek, A. W. Maverick, W. G. Lai, G. L. Griffin, *ibid.* **1992**, *4*, 577–582; S. L. Cohen, M. Liehr, S. Kasi, *J. Vac. Sci. Technol. A* **1992**, *10*, 863–868.

[15] Y.-J. Chen, H. D. Kaesz, Y.-K. Kim, H.-J. Müller, R. S. Williams, Z. Xue, *Appl. Phys. Lett.* **1989**, *55*, 2760–2762.

[16] For the plasma-induced CVD, a vertical parallel plate flow reactor was used (60 W, 13.56 MHz, 78 cm^2 electrode surface area, self-bias) at about 0.1 mbar. The purely thermal deposition of intermetallic phases from **3**–**6** was achieved with the use of carrier gases (N_2, H_2) in the same reactor, and leads to crystalline films, which are currently under investigation.

[17] K. M. Wunsch, E. Wachtel, *Z. Metallkd.* **1982**, *73*, 311-315.

[18] X-ray diffraction pattern: Huber–Guinier diffractometer 653; Ge monochromator ($\lambda = 154.056$ pm); data accumulation with 10 s scan time and 0.005° step width (step-scanning method) in the grazing incidence (6°) for flat preparations; θ values calibrated against Si (internal). Selected data: β-CoGa [2,3,15], deposited at 350 °C from **3** on borosilicate glass: space group: $Pm\bar{3}m$ (no. 221); $a = 287.68(1)$ pm; $V = 23.8$ pm^3; the most intense reflections: [*hkl*], θ value (relative intensity %): [110], 22.32° (100); [200], 32.40° (7); [211], 40.96° (10). ε-NiIn [20], deposited from **6** on GaAs(100) at 350 °C: crystal system: hexagonal; $a = 524.37(5)$, $c = 435.09(5)$ pm, $V = 103.60$ pm^3; for the most intense reflections see Figure 3.

[19] J.-D. Schöbel, H. H. Stadelmaier, *Z. Metallkd.* **1970**, *61*, 342-343.

[20] E. Hellner, *Z. Metallkd.* **1950**, *41*, 401, 401-409. See also: Joint committee on Powder Diffraction Standard (JCPDS-File), card number 7-178.

Models for the Photosynthetic Reaction Center—Synthesis and Structure of Porphyrin Dimers with *cis*- and *trans*-Ethene and Skewed Hydroxymethylene Bridges**

By *Mathias O. Senge, Kevin R. Gerzevske, M. Graça H. Vicente, Timothy P. Forsyth,* and *Kevin M. Smith**

Dedicated to Professor Emanuel Vogel on the occasion of his 65th birthday

Covalently linked porphyrin dimers are of continuing interest as biomimetic models of the photosynthetic reaction center.[1] They serve as models for studying charge separation, exciton transfer, and other spectroscopic characteristics of the "special pair" in the bacterial reaction center.[2] To facilitate such studies the geometry of the subunits in a dimer must be known, and preferably the relative arrangement of the subunits should be varied to study effects of interplanar separation and spatial arrangement, for example, on the photophysical parameters. Herein we report the preparation and structural characterization of three bisporphyrins with different macrocycle arrangements: cofacial, extended linear, and skewed "gable-type" macrocycle orientations.

Of special interest are cofacial (face-to-face) porphyrin dimers which have considerable overlap of the π-electron systems and thus mimic the situation in vivo more closely than linear arrays. Although a number of such compounds has been prepared, their synthesis is laborious and plagued with low yields.[3–5] In general such compounds can be prepared only by linking two porphyrins with two or more bridging units ("strapping")[4] or by using rigid bridging units such as biphenylenediyl, anthracenediyl,[5] or 1,2-phenylene[6] which force the subunits into a cofacial arrangement. Tetrapyrroles linked by flexible bridging units such as CH_2-CH_2 invariably lead to the formation of dimers with extended structures.[7]

Recently it was shown that the titanium-induced reductive coupling (McMurry reaction)[8] of 5-formylporphyrins **2**, which are easily derived from octaethylporphyrin (OEP) **1**, provides convenient access to CH=CH bridged bisporphyrins.[9] For thermodynamic reasons this reaction should lead to the *trans* isomer **4**. However, spectroscopic data indicate[9] that when the Ni formylporphyrin **2b** is used, a mixture of *cis* and *trans* isomers results.

The coupling of **2b** proceeds in about 50% yield to give the ethene-bridged bis(porphyrinato)nickel(II) complex. After 1 h reaction time several signals for the *meso* protons were observed in the ^1H NMR spectrum (Fig. 1b), and UV/VIS spectroscopy indicated the presence of two compounds. Two of the NMR signals for the *meso* protons were identical with those obtained for **4b**, which was prepared by the reaction sequence shown in Scheme 1.[10]

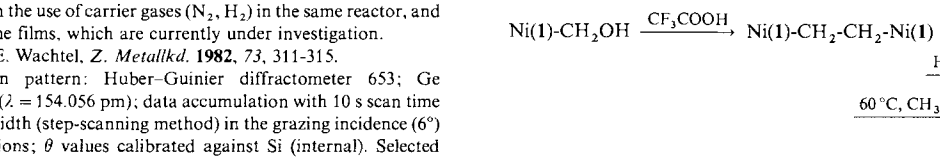

Scheme 1. Synthesis of **4b**. acac = acetylacetonate.

[*] Prof. Dr. K. M. Smith, Dr. M. O. Senge, K. R. Gerzevske, Dr. M. G. H. Vicente, T. P. Forsyth
Department of Chemistry
University of California, Davis, CA 95616 (USA)

[**] This work was supported by the National Science Foundation (CHE-90-01381) and the Deutsche Forschungsgemeinschaft (Se543/1-1). We thank Prof. G. V. Ponomarev (Moscow) for stimulating discussions.

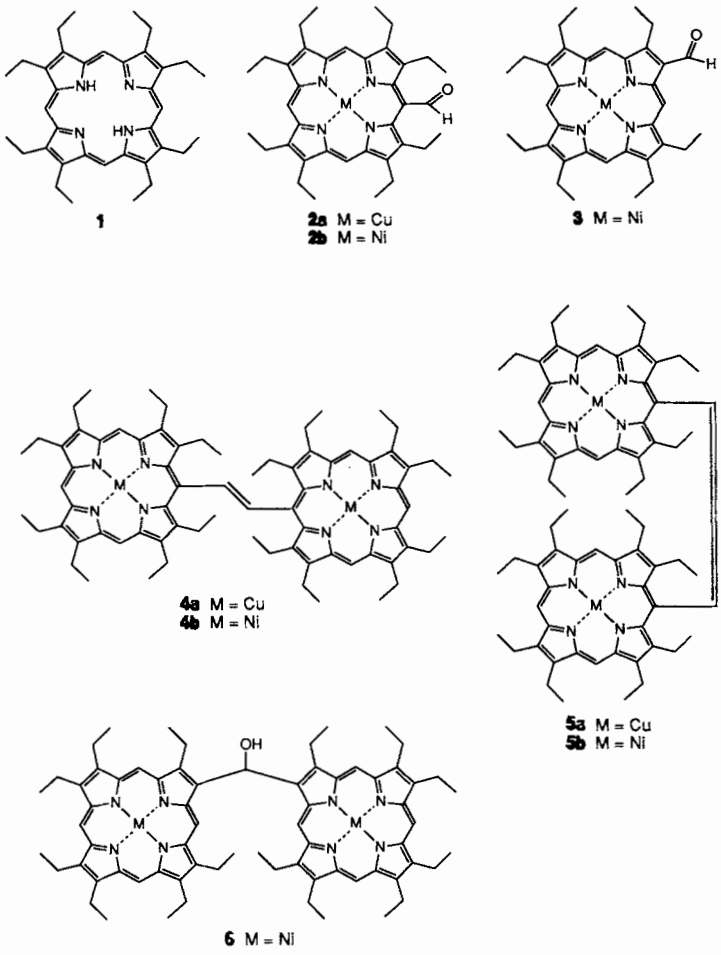

A variable-temperature NMR study in $[D_2]$1,1,2,2-tetrachloroethane showed broadening and subsequent disappearance of two of the signals for the *meso* protons above 120 °C.

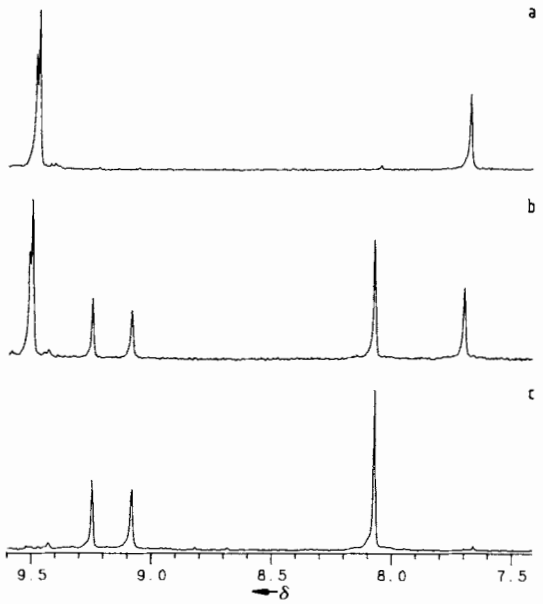

Fig. 1. ^{1}H NMR spectra of the Ni^{II} porphyrin dimers in $[D_2]$1,1,2,2-tetrachloroethane; region for the *meso* protons. a) Spectrum of **4b**, identical with the one obtained after heating the sample from spectrum b) for 1 h at 120 °C; b) spectrum of the product mixture from the coupling of **2b** after 1 h reaction time; c) spectrum of **5b**. For assignments of the signals see ref. [12].

The remaining NMR signals (Fig. 1a) were identical with those obtained for the *trans* isomer prepared according to the method of Ponomarev and Shul'ya.[10]

The results of the NMR studies can thus be interpreted as indicating the conversion of the *cis* compound **5b** into the *trans* compound **4b**. This process is irreversible, possibly because of the slightly acidic solvent used which led to acid-catalyzed formation of the thermodynamically more stable *trans* isomer. Likewise, heating **5b** in $[D_2]$1,1,2,2-tetrachloroethane at 120 °C for roughly 12 h resulted in complete conversion to **4b**. A similar conversion was observed after prolonged irradiation. However, treatment with acid at room temperature led to no changes. A variable-temperature NMR study of the pure *trans* dimer **4b** showed only broadening of the peaks arising from the *meso* protons.

After evaporation of the NMR sample containing **4b**, brown crystals were obtained from CH_2Cl_2/CH_3OH. Preliminary X-ray data show clearly the *trans* configuration of the bridging CH=CH unit and an extended linear array of the porphyrins with coplanar orientation of the macrocycle planes.[11] The structure closely resembles that obtained for a CH_2-CH_2 bridged Ni^{II}(OEP) dimer.[7a] This allowed a correct assignment of the NMR and UV/VIS data of the *trans* compound **4b**.[12] The situation was much simpler for the related copper(II) compounds. Coupling of **2a** led to formation of the dimer in about 70% yield. After column

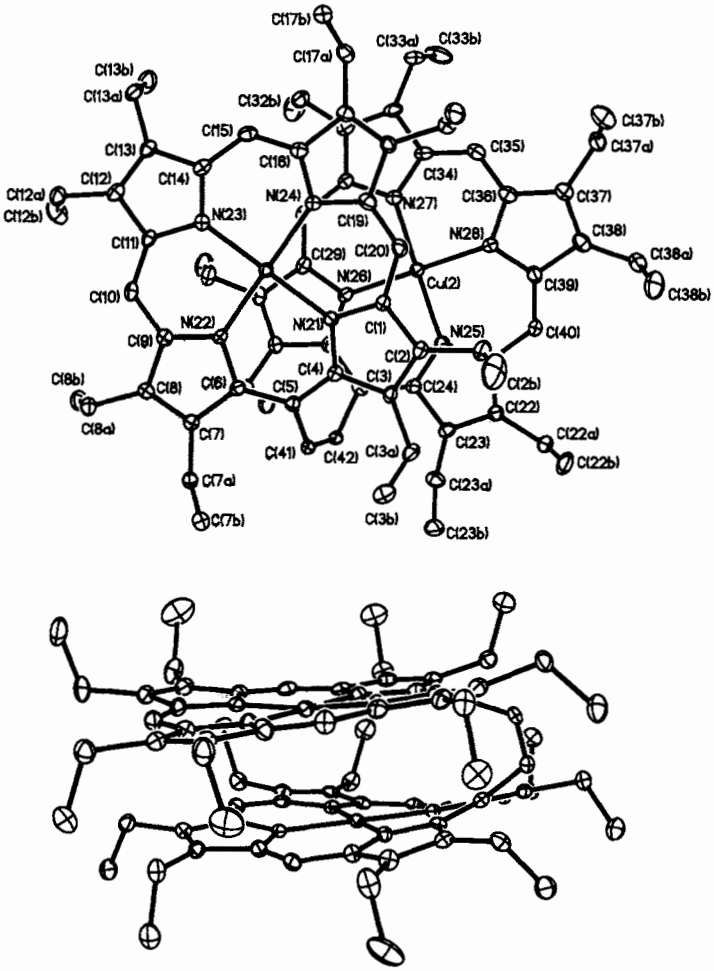

Fig. 2. The crystal structure of **5a**. Ellipsoids are drawn at the 40% occupancy level. Top: Top view; bottom: side view. Selected bond lengths [Å] and angles [°]: C(5)-C(41) 1.489(7), C(41)-C(42) 1.327(7), C(42)-C(25) 1.489(6), C(5)-C(41)-C(42) 121.9(4), C(25)-C(42)-C(41) 123.8(4).

chromatography and crystallization from CH_2Cl_2/CH_3OH, a single compound (**5a**) was obtained which displayed sharp UV/VIS absorption maxima at 393 and 568 nm. The crystal structure analysis[13, 14] (Fig. 2) indicate the predominant formation of the *cis* ethene-bridged bisporphyrin **5a**. Thus this type of system is readily accessible.

The *trans* dimer **4a** is insoluble in most organic solvents and was thus easily separated from the *cis* dimer **5a** during chromatography; **4a** remained on top of the column used for purification, while **5a** was cleanly eluted. By analogy the formation of both isomers in the dimerization of **2b** leads to two sets of signals for the *meso* protons. The unexpected formation of a *cis* bisporphyrin from **2b** and its predominant formation from **2a** appear to indicate strong π–π stacking of the two halves of the dimer prior to final formation of the alkene bond.

The strong overlap of the π-electron systems deduced from the crystal structure indicates that porphyrin–porphyrin aggregation plays a significant role in stabilizing the cofacial macrocycle arrangement. The two macrocycles are almost parallel; the angle between the two planes of the four nitrogen atoms is 1.9°. If the bridging double bond alone were to influence the geometry of the dimer, an arrangement with larger angles between the planes would have been expected. The short mean separation of the two planes by 3.36 Å can thus be explained only by aggregation forces that bring the two macrocycles into the observed cofacial conformation. This value is close to those reported for other cofacial dimers, for example, 3.43 Å in a 1,2-phenylene-bridged[6b] and 3.45 Å in a biphenylenediyl-bridged bisporphyrin,[5a] and 3.52 Å in "Cu_2-hexyldiporphyrin-7".[4a] The Cu–Cu separation in **4a** is 4.63 Å, which, together with a slip angle of 43.9°, leads to a lateral shift of the metal centers by 3.21 Å. These quantities have been used by Scheidt and Lee[15] to classify the degree of porphyrin aggregation. On this basis, the present dimer falls into the middle range of this type of interaction. The geometry of the bisporphyrin with its lateral displacement of the two macrocycles resembles closely the arrangement predicted by Abraham et al.[16] on the basis of NMR studies for the aggregation of metalloporphyrins in solution. The displacement of the macrocycles clearly results from electrostatic interactions between the metal centers and the aromatic ring system. The signals of the *meso* protons of the *cis* dimer **5b** are shifted upfield up to $\Delta\delta = 1.5$. This indicates a shielding effect in the stacked porphyrin array in solution similar to that observed in the crystal structure. The UV/VIS spectra show generally a blueshifted Soret band for the *cis* dimer (393 nm) compared to that of the *trans* dimer (414 nm) indicating excitonic interaction. Similar results were obtained for a 1,2-phenylene-bridged dimer by Osuka et al.[6b] No changes were observed in NMR spectra recorded below −80 °C. This indicates that the two halves of the bisporphyrins oscillate against each other and that only an averaged structure is observed on the NMR timescale.

The use of the McMurry reaction also allows a further variation in the geometry of the dimers obtained. If instead of a *meso*-formyl-substituted a β-formyl-substituted porphyrin (**3**) is used, the reaction proceeds not by formation of a connecting HC=CH unit but rather by loss of one of the formyl groups and formation of a hydroxymethylene-bridged dimer **6**. The crystal structure analysis of **6** (Fig. 3) shows that this type of dimer has a skewed arrangement of the two porphyrin rings.[14, 17] The two planes through the nitrogen atoms of the porphyrins form an angle of 77.3°. The macrocycle conformation in the two subunits is quite different. While the *meso* carbon atoms in the macrocycle with Ni(1) show an average deviation from planarity of 0.35 Å,

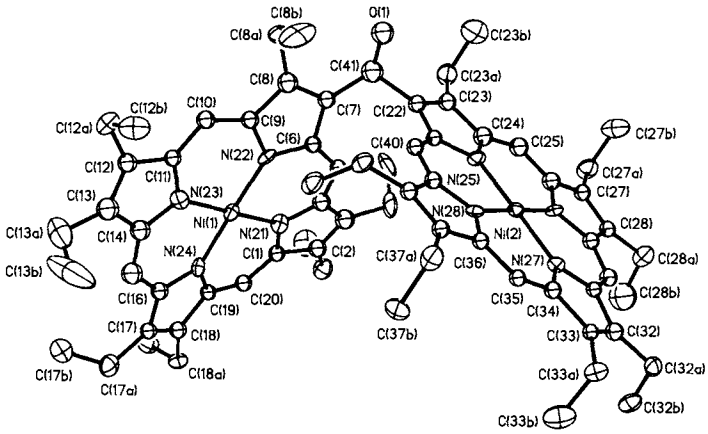

Fig. 3. The crystal structure of **6**. Ellipsoids are drawn at the 40% occupancy level. Selected bond lengths [Å] and angles [°]: C(7)-C(41) 1.54(2), C(22)-C(41) 1.55(2), C(41)-O(1) 1.32(2), C(7)-C(41)-C(22) 113(1), C(7)-C(41)-O(1) 116(1), C(22)-C(41)-O(1) 110(1).

those of the ring with Ni(2) show deviations of only 0.1 Å. A similar situation prevails in the crystal structure of **5a**: in one ring the *meso* carbon atoms are displaced on average by 0.05 Å, while in the other displacements of 0.36 Å are observed. These results might have implications for influencing the conformational flexibility[18] in tightly packed porphyrin arrays.

A simple variation of the position of the formyl group in the starting material thus allows the formation of two dimer types with very distinct geometric features. In addition, when the starting complex **2** has the appropriate metal ion, cofacial bisporphyrins **5** with *cis* double bonds can be prepared, which can be easily converted to the *trans* compounds **4**. This makes possible further studies on the dependence of photophysical parameters and catalytic properties on the relative geometrical arrangement of the porphyrin subunits.

Received: December 9, 1992 [Z 5738 IE]
German version: *Angew. Chem.* **1993**, *105*, 745

[1] Reviews: M. R. Wasilewski in *Chlorophylls* (Ed.: H. Scheer), CRC Press, Boca Raton, FL, USA, **1991**, p. 269; D. Gust, T. A. Moore, *Top. Curr. Chem.* **1991**, *159*, 103.

[2] H. Michel, O. Epp, J. Deisenhofer, *EMBO J.* **1986**, *5*, 2445; T. O. Yeates, H. Komiya, A. Chirino, D. C. Rees, J. P. Allen, G. Feher, *Proc. Natl. Acad. Sci. USA* **1988**, *85*, 7993.

[3] J. P. Collman, P. S. Wagenknecht, N. S. Lewis, *J. Am. Chem. Soc.* **1992**, *114*, 5665; J. P. Collman, J. E. Hutchison, M. A. Lopez, R. Guilard, *ibid.* **1992**, *114*, 8066.

[4] a) M. H. Hatada, A. Tulinsky, C. K. Chang, *J. Am. Chem. Soc.* **1980**, *102*, 7116; b) R. Karaman, T. C. Bruice, *J. Org. Chem.* **1991**, *56*, 3470; T. H. Tran-Thi, J. F. Lipskier, P. Maillard, M. Momenteau, J.-M. Lopez-Castillo, J.-P. Jay-Gerin, *J. Phys. Chem.* **1992**, *62*, 1073; c) J. P. Collman, A. O. Chong, G. B. Jameson, R. T. Oakley, E. Rose, E. R. Schmittou, J. A. Ibers, *J. Am. Chem. Soc.* **1981**, *103*, 516.

[5] a) J. P. Fillers, K. G. Ravichandran, I. Abdalmuhdi, A. Tulinsky, C. K. Chang, *J. Am. Chem. Soc.* **1986**, *108*, 417; b) A. Osuka, T. Nagata, K. Maruyama, *Chem. Lett.* **1991**, 481.

[6] a) H. Meier, Y. Kobuke, S.-i. Kugimiya, *J. Chem. Soc. Chem. Commun.* **1989**, 923; b) A. Osuka, S. Nakajima, T. Nagata, K. Maruyama, K. Toriumi, *Angew. Chem.* **1991**, *103*, 579; *Angew. Chem. Int. Ed. Engl.* **1991**, *30*, 582; c) T. Nagata, A. Osuka, K. Maruyama, *J. Am. Chem. Soc.* **1990**, *112*, 3054.

[7] a) P. B. Hitchcock, *J. Chem. Soc. Dalton Trans.* **1983**, 2127; b) M. O. Senge, H. Hope, K. M. Smith, *J. Chem. Soc. Perkin Trans. 2* **1993**, 11.

[8] J. E. McMurry, T. Lectka, J. G. Rico, *J. Org. Chem.* **1989**, *54*, 3748; J. E. McMurry, *Chem. Rev.* **1989**, *89*, 1513.

[9] M. G. H. Vicente, K. M. Smith, *Synlett* **1990**, 579; *J. Org. Chem.* **1991**, *56*, 4407.

[10] G. V. Ponomarev, A. M. Shul'ya, *Chem. Heterocycl. Comp. (Engl. Transl.)* **1986**, *22*, 228; *ibid.* **1988**, *24*, 276.

[11] Crystal structure analyses of the *trans* dimers proved to be very difficult. Due to the insolubility of **4a** and **4c** no crystals were obtained for the Cu

and Zn complexes; likewise we have not yet been able to grow crystals of **4d**. Brown cubes of **4b** were obtained from $CHCl_3/CH_3OH$. $C_{74}H_{88}N_8Ni_2 \cdot 2CHCl_3$, triclinic, space group $P\bar{1}$, $a = 10.286(1)$, $b = 12.812(2)$, $c = 14.775(2)$ Å, $\alpha = 104.64(1)$, $\beta = 108.46(1)$, $\gamma = 95.66(1)°$, $V = 1752.8(7)$ Å^3; data collection at 126 K with $Cu_{K\alpha}$ radiation. The structure solution revealed all atoms including two $CHCl_3$ molecules of solvation and clearly showed the *trans* configuration of the connecting double bond. However, refinement below $R = 0.19$ was not possible due to systematic twinning problems.

[12] Characterization of the Ni^{II} *cis* and *trans* dimers: **4b**: m.p. > 300 °C; UV/VIS (CH_2Cl_2): λ_{max}[nm](ε) = 414 (1.599×10^5), 488 (30400), 530 (20740), 566 (22760). ^1H NMR (300 MHz, $CDCl_3$, 25 °C): $\delta = 9.50$ (s, 2H, *meso*), 9.48 (s, 4H, *meso*), 7.66 (s, 2H, CH=CH), 3.88 (m, 16H, CH_2), 3.76 (q, 8H, CH_2), 3.37 (m, br, 8H, CH_2), 1.83, 1.82 (t, 12H each, CH_3), 1.75 (t, 12H, CH_3), 1.02 (t, 12H, CH_3). **5b**: m.p. > 300 °C; UV/VIS (CH_2Cl_2): λ_{max}[nm](ε) = 393 (1.682×10^5), 435 (12190), 568 (14650). ^1H NMR (300 MHz, $CDCl_3$, 25 °C): $\delta = 9.30$, 9.05 (s, 2H each, *meso* and CH=CH), 8.06 (s, 4H, *meso*), 4.03, 3.84, 3.75, 3.57, 3.47, 2.89 (m, 4H each, CH_2), 2.60 (s, 8H, CH_2), 1.83 (m, 12H, CH_3), 1.43–1.53 (m, 24H, CH_3), 0.67 (t, 12H, CH_3). The *cis* and *trans* isomers can easily be separated based on solubility properties.

[13] Crystal structure data of **5a** (crystallized from CH_2Cl_2/CH_3OH): $C_{74}H_{88}N_8Cu_2$, $M_r = 1216.6$, monoclinic, space group $P2_1/n$, $a = 19.208(7)$, $b = 14.672(5)$, $c = 24.170(7)$ Å, $\beta = 111.15(3)°$, $V = 6352(4)$ Å^3, $Z = 4$; $\rho_{calcd} = 1.271$ Mg m^{-3}; $\mu(Mo_{K\alpha}) = 0.718$ mm^{-1}. Data collection on a Siemens R3m/V diffractometer at 130 K with $Mo_{K\alpha}$ radiation ($\lambda = 0.71073$ Å) and a graphite monochromator; crystal size: $0.52 \times 0.32 \times 0.21$ mm. Patterson synthesis, refinement by least-squares on $|F|$, all atoms refined with anisotropic thermal parameters, H atoms incorporated using a riding model, $R = 0.056$, $wR = 0.064$, $S = 1.22$; 8040 reflections observed with $F > 5.0\,\sigma(F)$, $2\theta_{max} = 55°$ [14].

[14] Further details of the crystal structure investigations may be obtained from the Fachinformationszentrum Karlsruhe, Gesellschaft für wissenschaftlich-technische Information mbH, D-W-7514 Eggenstein-Leopoldshafen 2, on quoting the depository number CSD-57206, the name of the authors, and the journal citation.

[15] W. R. Scheidt, Y. J. Lee, *Struct. Bonding (Berlin)* **1987**, *64*, 1.

[16] R. J. Abraham, F. Eivazi, H. Pearson, K. M. Smith, *J. Chem. Soc. Chem. Commun.* **1976**, 698; *ibid.* **1976**, 699.

[17] Crystal structure data of **6** (crystallized from CH_2Cl_2/CH_3OH): $C_{69}H_{80}N_8O \cdot CH_2Cl_2$, $M_r = 1255.7$, monoclinic, space group $C2/c$, $a = 40.31(2)$, $b = 14.997(7)$, $c = 21.954(11)$ Å, $\beta = 108.60(4)°$, $V = 12579(10)$ Å^3, $Z = 8$; $\rho_{calcd} = 1.305$ Mg m^{-3}; $\mu(Mo_{K\alpha}) = 0.735$ mm^{-1}. Data collection on a a Syntex $P2_1$ diffractometer at 130 K with $Mo_{K\alpha}$ radiation ($\lambda = 0.71073$ Å) and a graphite monochromator; crystal size: $0.35 \times 0.22 \times 0.11$ mm. Patterson synthesis, refinement by least-squares on $|F|$, only metal, nitrogen, and side chain atoms were refined with anisotropic thermal parameters, H atoms incorporated using a riding model, one ethyl group and the hydroxyl group were disordered, $R = 0.122$, $wR = 0.120$, $S = 1.45$; 5146 reflections observed with $F > 2.0\,\sigma(F)$, $2\theta_{max} = 48°$ [14].

[18] K. M. Barkigia, L. Chantranupong, K. M. Smith, J. Fajer, *J. Am. Chem. Soc.* **1988**, *110*, 7566; M. O. Senge, *J. Photochem. Photobiol. B:* **1992**, *16*, 3.

Separation of Diastereomers by Distillation—A New Procedure for the Synthesis of Optically Active Heterocyclic Carboxylic Acids

By *Elke Fritz-Langhals**

In the conventional preparation of optically active carboxylic acids by resolution, the racemic carboxylic acids are treated with an optically active amine, and the resulting diastereomeric salts are separated by fractional crystallization. This standard method has also been used for the isolation of the optically active heterocyclic carboxylic acids **1a–d**. The resolution of 2-tetrahydrofurancarboxylic acid **1a** (X = O, $n = 1$), for example, has been performed with brucine, cinchonidine,[1] quinine,[2] and the optically active amines 4-bromo- and 4-chloro-1-phenylethylamine,[3] which are not commercially available. The yields are moderate or low, however, especially when products of high optical purity are required. Moreover, since the isolation of the second enantiomer from the mother liquor presents considerable difficulties, a second optically active amine is necessary. The resolutions of analogous heterocyclic carboxylic acids such as 2-tetrahydrothiophenecarboxylic acid **1b** (X = S, $n = 1$)[2, 4] and 2-tetrahydropyrancarboxylic acid **1c** (X = O, $n = 2$)[2] suffer from similar complications.

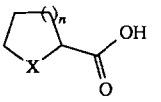

1a: X = O, $n = 1$; **1b**: X = S, $n = 1$
1c: X = O, $n = 2$; **1d**: X = S, $n = 2$

The disadvantages of classical resolution prevent the preparation of larger amounts of optically pure compounds and restrict the possibility of applications of optically active heterocyclic carboxylic acids in pharmaceuticals such as Terazosin, a vasodilator,[6] and as building blocks for liquid crystals.[7] The isolation of *both* enantiomers in *one* step would be particularly desirable. We wondered if instead of the differences in solubilities of diastereomeric compounds, the differences in boiling points could be used for simple preparative separations. For this purpose we linked the previously mentioned racemic heterocyclic carboxylic acids with various optically active amino acid esters with an amide bond. The resulting diastereomeric carboxylic acid amides **2** (Table 1) displayed unusually large differences in boiling points of up to 7 K, thus allowing separation by distillation.

Table 1. Separation of diastereomers (*R,S*)-**2** and (*S,S*)-**2** by distillation.

	Diastereomers **2**						
2	R	R′	t_r [a]	B.p. [b]	Type/*l* [c]	*de* [%] [d]	Yield [%] [e]
2a	$CH(CH_3)_2$	CH_3	1. 16.68	98	PC/1	>99 (*R,S*)	80
			2. 17.58	103	PC/1	>99.5 (*S,S*)	49
2a′	CH_3	C_2H_5	1. 16.68	103	SBC/1	>99 (*R,S*)	80
			2. 17.28	107	SBC/1	98 (*S,S*)	81
2a″	$CH_2CH(CH_3)_2$	CH_3	1. 18.57	108	SBC/1	99.8 (*R,S*)	87
			2. 19.07	115	SBC/1	95.1 (*S,S*)	53
2b	$CH(CH_3)_2$	CH_3	1. 21.06	110	PC/0.4	91 (*R,S*)	34
			2. 22.19	ca. 130 [f]	PC/0.4	68 (*S,S*)	46
			1. 21.06	ca. 103	PC/0.6	70 (*R,S*)	83
			1. 21.06	110	SBC/1	>99.9 (*R,S*)	60
2c	$CH(CH_3)_2$	CH_3	1. 18.62	77	SBC/1	78 (*R,S*)	54
			2. 19.08	82	SBC/1	80 (*S,S*)	45
2d	$CH(CH_3)_2$	CH_3	1. 21.82	134	SBC/1	96	11
			1. 21.82	ca. 131 [f]	SBC/1	90	72
			2. 23.13	ca. 138 [f]	SBC/1	68	44

[a] GC retention time on Carbowax 20M, 25 m quartz capillary, heated from 70–230 °C at a rate of 8 °C min^{-1}. [b] Boiling point [°C] at a pressure of ca. 0.01 Torr. [c] Type of column: PC: packed column 5 cm in diameter packed with 4 mm glass spirals, reflux ratio ca. 5:1 to 10:1; SBC: spinning-band column, reflux ratio ca. 20:1. Length *l* in m. [d] Diastereomeric excess obtained in preparative separation; the absolute configuation (in parentheses) was assigned after hydrolysis of the optically enriched diastereomer by comparison with the literature values for the optical rotations. [e] Refers to one diastereomer. [f] Pressure ca. 0.05 Torr.

For example, the acid chloride derivative **3a** of racemic 2-tetrahydrofurancarboxylic acid **1a** was treated with (*S*)-valine methyl ester (*ee* > 99 %[8]) to provide the diastereomeric amides **2a** (X = O, $n = 1$, R = $CH(CH_3)_2$, R′ = CH_3) (Scheme 1), and these were separated by distillation through a 1 m packed column (Table 1). Acidic hydrolysis of the two fractions "(*R,S*)" and "(*S,S*)" gave the two enantiomers of **1a** without racemization. (*S*)-Valine may also be recovered

[*] Dr. E. Fritz-Langhals
Consortium für Elektrochemische Industrie GmbH
Zentrale Forschung der Wacker-Chemie GmbH
Zielstattstrasse 20, D-W-8000 München 70 (FRG)

without significant loss of optical purity (*ee* > 96.6%). This simple separation providing both enantiomers in high yield and optical purity can be performed in the laboratory easily with amounts between 0.5 and 1 kg per run.

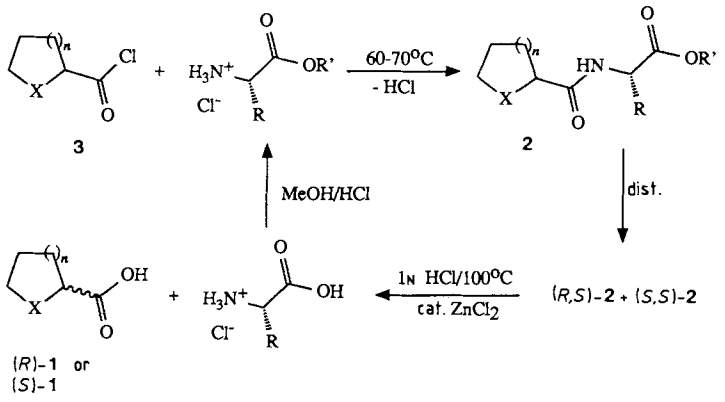

Scheme 1.

As shown in Table 1, the methyl and ethyl esters of (*S*)-alanine and (*S*)-leucine can be used instead of (*S*)-valine derivatives. Besides the heterocyclic carboxylic acids **1a–c** previously known in optically active form, the two enantiomers of 2-tetrahydrothiopyrancarboxylic acid **1d** (X = S, $n = 2$) could be isolated by this procedure. Of course, the optical purity achieved by the separation of diastereomers can be improved by increasing the reflux ratio and the number of theoretical plates. The effort required for the distillation can be estimated from the difference in the GC retention times.

In contrast to the amides described here, the diastereomeric esters prepared from heterocyclic carboxylic acids and various optically active alcohols[9] have minimal boiling point differences (< 1 K). This illustrates that in analogy to resolution by fractional crystallization, various derivatives must be tested to determine whether they are suitable for separation by distillation. In contrast to the traditional method, however, simple GC analysis of the product mixture gives a quick and reliable assessment of the separation, as the difference in the retention times reflects the difference in boiling points.

Experimental Procedure

Heterocyclic carboxylic acid amides **2**: To a stirred suspension of 0.98 mol (*S*)-amino acid ester hydrochloride[10] in 350 mL toluene heated at 50–70 °C was added dropwise 0.89 mol heterocyclic carboxylic acid chloride **3** (obtained from carboxylic acids **1a**, **1b**[4a], **1c**[11], or **1d**[12] by reaction with thionyl chloride). The reaction mixture was stirred and heated at this temperature until the evolution of HCl had ceased (ca. 20 h). The reaction mixture was washed with water and distilled. Representative yields: **2a** 94%, **2a″** 87%, **2b** 79%, **2c** 80%, **2d** 73% (R = $CH(CH_3)_2$, R′ = CH_3). The diastereomeric pairs were separated by distillation, see Table 1.

(*R*)-**1a**: A mixture of 100 g (0.437 mol) (*R,S*)-**2a** (diastereomer ratio (*R,S*):(*S,S*) = 98.7:1.3) and 3 g (22 mmol) $ZnCl_2$ in 400 mL 1 M HCl was heated at 100 °C for 4 d. The reaction mixture was concentrated to dryness and the residue extracted with methyl *tert*-butyl ether (MTBE). The filtered MTBE extract was distilled giving 36 g (78%) (*R*)-**1a** with b.p. 83 °C/0.3 Torr (ref.[10] b.p. 97–100 °C/1.05 Torr); $[\alpha]_D^{27} = +33.3$ ($c = 1.23$, $CHCl_3$; ref.[1]: −30.1 ($c = 1.21$, $CHCl_3$) for the (*S*) enantiomer), $[\alpha]_D^{23} = +33.5$, $[\alpha]_D^{27} = +35.1$ ($c = 1.07$, $CHCl_3$; ref.[1]: +30.4 ($c = 1.01$, $CHCl_3$)). For the determination of enantiomer ratio the product was reduced with $LiAlH_4$ to give the tetrahydrofurfurylalcohol which was then analyzed by gas chromatography[13]. The ratio found was *R*:*S* = 98.7:1.3. The residue filtered off the MTBE phase consisting of (*S*)-valine hydrochloride was dried in vacuo and weighed (43 g, 70% recovery). For the determination of the optical purity of the recovered valine a portion was treated with methanol/HCl and trifluoroacetic anhydride and then analyzed by gas chromatography (Chiral-XE-60-S-Val). The enantiomer ratio found was *S*:*R* = 98.3:1.7.

Received: December 12, 1992 [Z 5750 IE]
German version: *Angew. Chem.* **1993**, *105*, 785

[1] P. C. Bélanger, H. W. R. Williams, *Can. J. Chem.* **1983**, *61*, 1383–1386.
[2] O. Červinka, O. Bajanzulyn, A. Fábryová, A. Šačkus, *Collect. Czech. Chem. Commun.* **1986**, *51*, 404–407.
[3] H. Nodaira, O. Osada, M. Kondo, A. Takebayashi, JP-P 01 216 962, **1989**, *Chem. Abstr.* **1990**, *112*, 158 037h.
[4] a) G. Claeson, H.-G. Jonsson, *Ark. Kemi* **1967**, *26*, 247–257; b) G. Stork, A. F. Kreft III, *J. Am. Chem. Soc.* **1977**, *99*, 3851–3853.
[5] a) H. Merz, K. Stockhaus, H. Wick, *J. Med. Chem.* **1977**, *20*, 844–846; b) V. Valenta, J. Holubek, E. Svátek, V. Miller, M. Vlková, M. Protiva, *Collect. Czech. Chem. Commun.* **1987**, *52*, 2534–2544.
[6] Reviews: a) D. Descours, D. Festal, J. M. Leger, A. Carpy, *Helv. Chim. Acta* **1991**, *74*, 1757–1763; b) Z. L. Chang, J. F. Bauer, *Anal. Profiles Drug Subst.* **1991**, *20*, 693–727; c) S. Titmarsh, J. P. Monk, *Drugs* **1987**, *33*, 461–477.
[7] W. Hemmerling, H.-R. Dübal, C. Escher, G. Illian, Y. Inoguchi, I. Müller, M. Murakami, D. Ohlendorf, R. Wingen (Hoechst AG) DE-A 3 827 600, **1990**, *Chem. Abstr.* **1990**, *113*, P06 578m.
[8] (*S*)-Valine was obtained from Degussa. The optical purity of the methyl ester was determined by gas chromatography[13] after it had been converted into the trifluoroacetate.
[9] Menthyl, bornyl, fenchyl, and 2-butyl 2-tetrahydrofurancarboxylates and a number of (*S*)-lactates were examined.
[10] a) K. Freudenberg, W. Kuhn, I. Bumann, *Ber. Dtsch. Chem. Ges.* **1930**, *63*, 2380–2390; b) R. Schwyzer, B. Iselin, H. Kappeler, B. Riniker, W. Rittel, H. Zuber, *Helv. Chim. Acta* **1958**, *41*, 1272.
[11] D. J. Pasto, M. P. Serve, *J. Am. Chem. Soc.* **1965**, *87*, 1515–1521.
[12] a) D. M. Roush, E. M. Prie, L. K. Templeton, D. H. Templeton, C. H. Heathcock, *J. Am. Chem. Soc.* **1979**, *101*, 2971–2981; b) G. B. Brown, C. W. H. Partridge, *ibid.* **1944**, *66*, 839; c) H. T. Clarke, E. R. Taylor, *Organic Syntheses, Collective Volume I*, 2nd ed., Wiley, New York, **1941**, pp. 115–116.
[13] Chiral-XE-60-S-Val, 50 m, quartz capillary (Chromopak, Munich).

An Ab Initio MO Study on Stabilizing Interactions in Dinuclear Zr/Al Complexes with a Planar Tetracoordinate Carbon Center**

By *Rolf Gleiter,* Isabella Hyla-Kryspin, Shuqiang Niu,* and *Gerhard Erker*

In their seminal work, Hoffmann et al. considered the possibility of stabilizing planar methane.[1] They concluded that the distortion of tetrahedral methane to the square-planar CH_4 isomer leaves only six electrons available to form four C–H bonds and a doubly occupied 2p orbital at the carbon center (Scheme 1). This high-energy structure can be stabilized by σ-donor and π-acceptor substituents X. These thoughts were substantiated by Schleyer et al. by ab initio calculations.[2] Only a few structures have been determined so far in which a carbon atom is surrounded by four substituents in a single plane.[3]

Scheme 1.

[*] Prof. Dr. R. Gleiter, Dr. I. Hyla-Kryspin, S.Niu
Organisch-chemisches Institut der Universität
Im Neuenheimer Feld 270, D-W-6900 Heidelberg (FRG)
Telefax: Int. code + (6221) 564205
Prof. Dr. G. Erker
Organisch-chemisches Institut der Universität
Corrensstrasse 40, D-W-4400 Münster (FRG)

[**] This research was supported by the Volkswagen-Stiftung, the Deutsche Forschungsgemeinschaft (SFB 247), the Fonds der Chemischen Industrie, and BASF AG.

Prompted by the experimental work of Erker et al.[4] on zirconocene complexes such as **1** we present here a theoretical model based on ethylene. Bending a $=CH_2$ unit of ethylene into a T-shape (Fig. 1) stabilizes the C–C σ orbital but destabilizes two C–H σ orbitals (denoted as P^+ and P^-).

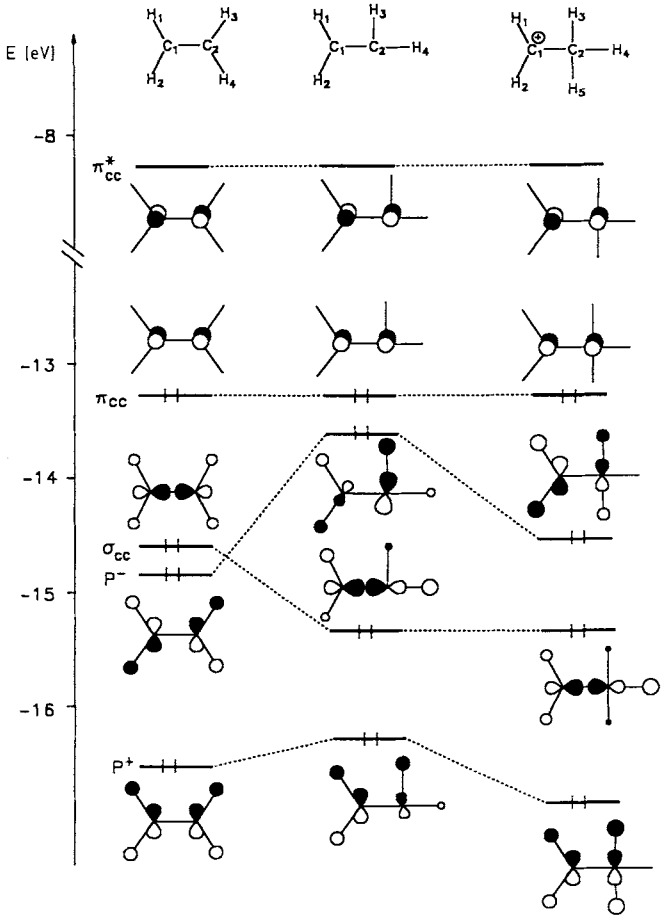

Fig. 1. Correlation diagram for the protonation of distorted T-shaped ethylene.

As a result this distorted ethylene is about 2 eV higher in energy than the normal structure. When a suitable σ-acceptor orbital is offered (e.g. the 1s orbital of a proton, Fig. 1) the highest occupied σ MO may be stabilized considerably. Further stabilization may be achieved by introducing an additional π-acceptor substituent. A group that fulfills both conditions is a d^0 zirconocene fragment, as it provides both σ- and π-accepting energy levels.[5]

Our previous investigations on the nature of agostic interactions of alkenyl moieties bound to a Cp_2ZrX (**2**) or a Cp_2Zr^+ (**3**) fragment, respectively, have shown that in the case of **2** a specific combination of steric and electronic effects must be met[6] for an agostic interaction, whereas in the case of **3** electronic factors dominate.[7]

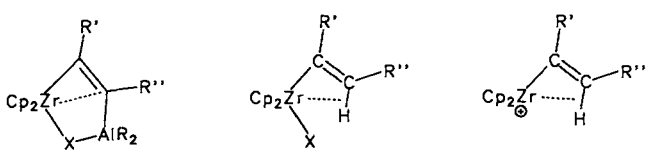

1a: X=H
1b: X=Cl

2

3

To test our qualitative arguments presented for a distorted ethylene molecule as a model for constructing complexes containing planar tetracoordinate carbon and to probe the acceptor and donor capabilities of a $ZrCp_2$ moiety we have carried out model calculations on the neutral dimetallic complexes **4**–**8**.

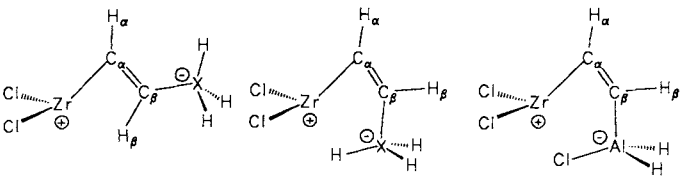

4: X=Al
5: X=B

6: X=Al
7: X=B

8

The calculations were carried out with the Gaussian 86 program[8] using STO-3G basis sets for all atoms (**4**–**7**)[9] and a split valence basis set for Zr[10] in the case of **8**. In addition we also carried out Extended Hückel (EH) calculations[11] on these systems using standard parameters for all atoms.[12] In our model calculations we replaced the Cp groups of the real molecules by chloro ligands which has been shown in other studies to provide a good theoretical substitute for the actual bent metallocene system.[13]

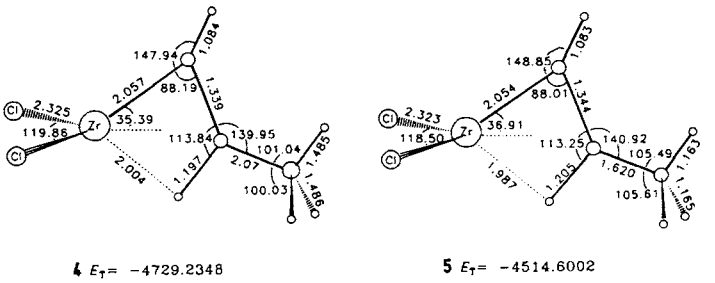

4 E_T= -4729.2348

5 E_T= -4514.6002

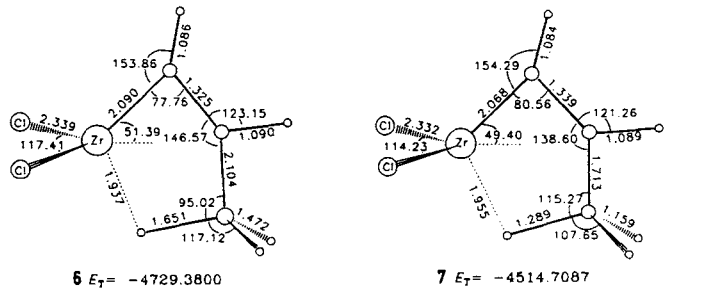

6 E_T= -4729.3800

7 E_T= -4514.7087

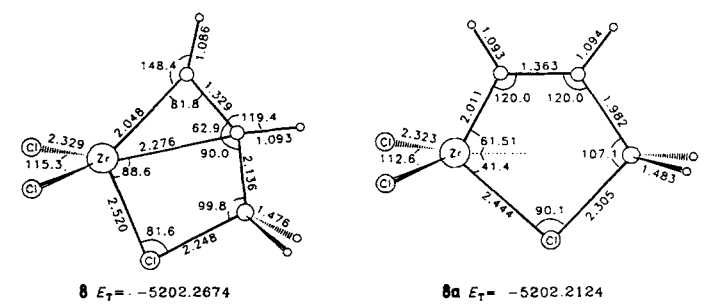

8 E_T= -5202.2674

8a E_T= -5202.2124

Fig. 2. Geometrical parameters and total energies [Hartree] for **4**–**8**.

 © VCH Verlagsgesellschaft mbH, W-6940 Weinheim, 1993 0570-0833/93/0505-0755 $ 10.00+.25/0

The fully optimized geometries of **4**–**8** are shown in Figure 2. The "inside" structures **6** and **7** were found to be more stable than the "outside" congeners **4** and **5** by 91 and 68 kcal mol^{-1}, respectively. The geometrical parameters calculated for **6**–**8** are remarkably close to those reported from X-ray investigations on **1**.[4]

The geometry optimization under the constraint that both olefinic carbon atoms maintain normal sp^2 hybridization but leaving all other parameters relaxed, leads to the "standard structures" **6a**–**8a**. As an example, we have depicted the constrained structure of **8a** at the bottom of Figure 2. The standard structures are 46.4 (**6a**), 47.5 (**7a**), and 34.0 (**8a**) kcal mol^{-1} less stable than **6**–**8**. In order to find out why the geometries of structures **6**–**8** are preferred, we calculated the differences in the overlap populations ΔOP and the differences in the electron densities Δq of **6**–**8** and **6a**–**8a** (Table 1). An analysis of the data shows that the structures

Table 1. Differences in the overlap populations (ΔOP) and in the electron densities (Δq) of fully optimized (**6**–**8**) and standard structures (**6a**–**8a**).

	ΔOP			
Structure	Zr-C_β	C_β-H_β	C_β-Al/B	Zr-Al/B
6–**6a**	0.2129	−0.0002	−0.1549	0.0585
7–**7a**	0.1332	−0.0023	−0.1235	0.0901
8–**8a**	0.1981	0.0022	−0.1459	0.0597

	Δq* [a]				
Structure	Zr	C_α	C_β	H_β	Al/B
6–**6a**	+0.17	−0.10	+0.03	−0.04	−0.01
7–**7a**	+0.10	−0.07	+0.10	−0.05	−0.10
8–**8a**	+0.49	−0.06	+0.04	−0.01	−0.15

[a] Positive sign of Δq means an increase in the electron density

with the square-planar carbon atom (**6**–**8**) are stabilized by a strong Zr–C_β bonding interaction and to lesser extent by Zr–Al/B interactions. This can be visualized by comparison of the contour plots of the HOMO-1 of **8** and the HOMO of its congener **8a** (Fig. 3). The MO plots are based on EH calculations on **8** with application of experimental X-ray structure data, and on **8a** with sp^2-hybridized C_α and C_β.[14] It is evident that there is a strong σ-bonding interaction between the 4d orbital at Zr and the 2p orbital at C_β in **8**. This interaction is absent in **8a**. Our analysis shows furthermore that any direct $\pi(C_\beta)$–d_π(Zr) interaction is negligible, although some Zr–C_α π interaction may be present.[3, 4]

To conclude we can say that the planar tetracoordinate geometry at the C_β center of **1** is based on electronic effects. It is not stabilized by additional (C_β–Zr) delocalization of the olefinic π electrons or the good donor properties of *both cis* metal substituents. The major factors contributing to its stabilization are the "in-plane" σ-acceptor property of the Zr center which stabilizes the high-lying P$^-$ MO of the distorted ethylene, and the good donor properties of C_α, Al, and R″.

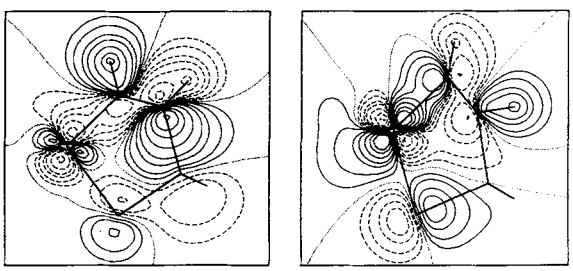

Fig. 3. Contour plots of the HOMO of **8a** (standard structure, left), and the HOMO-1 of **8** (planar structure, right). The values of the contour lines are ± 0.01, ± 0.02, ± 0.04, ± 0.06, ± 0.10, ± 0.22, ± 0.30.

Received: December 11, 1992 [Z 5744IE]
German version: *Angew. Chem.* **1993**, *105*, 753

[1] R. Hoffmann, R. W. Alder, C. F. Wilcox Jr. *J. Am. Chem. Soc.* **1970**, *92*, 4992; R. Hoffmann *Pure Appl. Chem.* **1971**, *28*, 181.
[2] J. B. Collins, J. D. Dill, E. D. Jemmis, Y. Apeloig, P. von R. Schleyer, R. Seeger, J. A. Pople, *J. Am. Chem. Soc.* **1976**, *98*, 5419;
[3] Reviews: G. Erker, *Nachr. Chem. Tech. Lab.* **1992**, *40*, 1099; G. Erker *Comments Inorg. Chem.* **1992**, *13*, 111.
[4] G. Erker, R. Zwettler, C. Krüger, R. Noe, S. Werner *J. Am. Chem. Soc.* **1990**, *112*, 9620; G. Erker, M. Albrecht, S. Werner, M. Nolte, C. Krüger, *Chem. Ber.* **1992**, *125*, 1953; G. Erker, M. Albrecht, C. Krüger, S. Werner *Organometallics* **1991**, *10*, 3791; G. Erker, M. Albrecht, C. Krüger, S. Werner, P. Binger, F. Langhauser *ibid.* **1992**, *11*, 3517; M. Albrecht, G. Erker, M. Nolte, C. Krüger *J. Organomet. Chem.* **1992**, *427*, C1; G. Erker, M. Albrecht, C. Krüger, S. Werner *J. Am. Chem. Soc.* **1992**, *114*, 8531; A. D. Horton, A. G. Orpen *Angew. Chem.* **1992**, *104*, 912; *Angew. Chem. Int. Ed. Engl.* **1992**, *31*, 876.
[5] J. W. Lauher, R. Hoffmann *J. Am. Chem. Soc.* **1976**, *98*, 1729.
[6] G. Erker, R. Zwettler, C. Krüger, R. Schlund, I. Hyla-Kryspin, R. Gleiter *J. Organomet. Chem.* **1988**, *346*, C15; G. Erker, R. Zwettler, C. Krüger, I. Hyla-Kryspin, R. Gleiter *Organometallics* **1990**, *9*, 524; I. Hyla-Kryspin, R. Gleiter, C. Krüger, R. Zwettler, G. Erker *Organometallics* **1990**, *9*, 517.
[7] R. Gleiter, I. Hyla-Kryspin, S. Niu, G. Erker, unpublished.
[8] M. J. Frisch, J. S. Binkley, H. B. Schlegel, K. Raghavachari, C. F. Melius, R. L. Martin, J. J. P. Stewart, F. W. Bobrowicz, C. M. Rohlfing, L. R. Kahn, D. J. Defrees, R. Seeger, R. A. Whiteside, J. D. Fox, E. M. Fleuder, J. A. Pople, GAUSSIAN 86, Carnegie Mellon Quantum Chemistry Publishing Unit, Pittsburgh, PA **1984**.
[9] W. J. Hehre, L. Radom, P. von R. Schleyer, J. A. Pople, *Ab initio Molecular Orbital Theory*, Wiley, **1986**; S. Huzinaga, J. Andzelm, M.Klobukowski, E. Radzio-Andselm, Y. Sakai, H. Tatewaki, *Gaussian Basis Sets For Molecular Calculations*, Elsevier, Amsterdam, **1984**.
[10] K. D. Dobbs, W. J. Hehre *J. Comput. Chem.* **1987**, *8*, 880.
[11] R. Hoffmann, W. N. Lipscomb *J. Chem. Phys.* **1962**, *36*, 2179; **1962**, *37*, 2872; R. Hoffmann, *ibid.* **1963**, *39*, 1397.
[12] R. H. Summerville, R. Hoffmann *J. Am. Chem. Soc.* **1976**, *98*, 7240; K. Tatsumi, A. Nakamura, P. Hofmann, P. Stauffert, R. Hoffmann *ibid.* **1985**, *107*, 4440.
[13] N. Koga, K. Morokuma *Chem. Rev.* **1991**, *91*, 823 and references therein; H. Kawamura-Kuribayashi, N. Koga, K. Morokuma *J. Am. Chem. Soc.* **1992**, *114*, 2359; L. A. Castonguay, A. K. Rappé *J. Am. Chem. Soc.* **1992**, *114*, 5832.
[14] EH calculations predict that **8** is 13.9 kcal mol^{-1} more stable than **8a**.

Phosphinidenetantalum(v) Complexes of the Type [(N_3N)Ta=PR] as Phospha-Wittig Reagents (R = Ph, Cy, *t*Bu; $N_3N = (Me_3SiNCH_2CH_2)_3N$)**

By *Christopher C. Cummins, Richard R. Schrock,** and *William M. Davis*

We wish to report that terminal phosphinidene complexes of the type [(N_3N)Ta=PR] (R = Ph, *c*-C_6H_{11}(Cy), *t*Bu; $N_3N = (Me_3SiNCH_2CH_2)_3N$) are readily prepared and, furthermore, that these complexes react smoothly with aldehydes to generate phosphaalkenes. Phosphaalkenes[1, 2] stabilized either by conjugation[3] or by sterically demanding substitu-

[*] Prof. Dr. R. R. Schrock, C. C. Cummins, Dr. W. M. Davis[+]
Department of Chemistry
Massachusetts Institute of Technology
Cambridge, MA 02139 (USA)
Telefax: Int. code +(617) 253-7670

[+] X-ray structure analysis.

[**] This work was supported by the National Science Foundation (Grant CHE 91 22827). C.C.C. thanks the National Science Foundation for a Predoctoral Fellowship. — The term phosphinidene complex is used here instead of that recommended by IUPAC, λ^3-phosphanediyl complex.

ents[4] have previously been prepared by silicon migration[3] or dehydrohalogenation;[4] Mathey et al. have developed a phospha-Wittig reaction that produces phosphaalkenes stabilized by $M(CO)_5$ (M = Cr, W) complexation.[5] The utilization of terminal phosphinidene complexes as phospha-Wittig reagents has not been described previously, perhaps in part because complexes containing the required M=PR linkage are extremely rare;[6] known examples[7-10] employ quite bulky substituents (e.g. the "supermesityl" (2,4,6-$tBu_3C_6H_2$) group) at phosphorus. Transient phosphinidene complexes of low-valent transition metals have been generated,[11] but these are electrophilic at phosphorus, much in the same manner as Fischer carbenes are electrophilic at carbon; we sought a nucleophilic phosphinidene complex.[12] Recently we reported the synthesis of a series of trigonal-monopyramidal complexes in which the presence of an empty coordination site is sustained by a ligand of the N_3N type,[13, 14] and we reasoned that the pocket formed by the three "upright" R_3Si substituents would be effective at stabilizing a nucleophilic phosphinidene unit.

Addition of $TaCl_5$ and $Li_3(N_3N)$[14] powders to ether at $-78\,^{\circ}C$ resulted in formation of $[(N_3N)TaCl_2]$ (**1**), a yellow crystalline solid, which was isolated in 32% yield by crystallization from ether after removal of LiCl [Eq. (1), see Table 1

$$Li_3(N_3N) + TaCl_5 \xrightarrow[-3\,LiCl]{Et_2O,\ -78\ to\ 25\,^{\circ}C} \underset{\mathbf{1}}{[(N_3N)TaCl_2]} \qquad (1)$$

for NMR data for the new compounds]. The molecule is apparently fluxional[15] since the three arms of the N_3N ligand are equivalent on the NMR timescale. Treatment of dichloride **1** with two equivalents of LiPHR[16] afforded the corresponding phosphinidene complexes **2** in good yield [Eq. (2)]. At present there is no evidence to indicate whether

$$\underset{\mathbf{1}}{[(N_3N)TaCl_2]} + 2\,LiPHR \xrightarrow[-2\,LiCl,\ -H_2PR]{Et_2O,\ -40\ to\ 25\,^{\circ}C} [(N_3N)Ta{=}PR] \qquad (2)$$

2a, R = Ph
2b, R = Cy
2c, R = *t*Bu

the TaP multiple bond is formed by dehydrohalogenation, with the second equivalent of phosphide acting as the base, or alternatively by α-proton abstraction from a bis(phosphide) complex;[17] when one equivalent of LiPHPh was slowly added to a solution of **1**, a mixture of **2a** and unreacted **1** was obtained.

The NMR spectra (^1H, ^{13}C, and ^{31}P; Table 1) of phosphinidene complexes **2** support the proposed formulation as follows: 1) the presence of one phosphorus atom per tantalum center is indicated by doublet splitting (J_{CP}) of two of the carbon resonances attributed to the N_3N ligand; 2) the phosphinidene ^{31}P signal is observed at low field, as expected;[18] 3) the ^{31}P signal for each phosphinidene complex is somewhat broad (**2a**, $\Delta\nu_{1/2} = 105$ Hz; **2b**, 140 Hz; **2c**, 205 Hz), consistent with local threefold symmetry at tantalum and consequent quadrupolar broadening by ^{181}Ta[19] (> 99% natural abundance[20]); 4) the three arms of the N_3N ligand are equivalent on the ^{13}C and ^1H NMR timescales.

A single-crystal X-ray diffraction study[21] of **2b** confirmed the proposed structure of phosphinidene complexes **2** (Fig. 1).

Table 1. NMR data for tantalum complexes **1**–**3** and phosphaalkenes **4** [a].

Cmpd.	^1H	^{13}C	^{31}P
1	3.849 (t, CH_2) 2.500 (t, CH_2) 0.409 (s, $SiMe_3$)	65.86 (CH_2) 55.76 (CH_2) 2.17 ($SiMe_3$)	
2a[b]	7.842 (t, Ph, *ortho*) 7.158 (m, Ph, *meta*) 6.911 (t, Ph, *para*) 3.519 (t, CH_2) 2.193 (t, CH_2) 0.608 (s, $SiMe_3$)	158.98 (d, $^1J_{PC}$ = 19.7, Ph) 134.81 (s, Ph) 128.17 (d, J_{PC} = 9.0, Ph) 127.43 (d, J_{PC} = 4.8, Ph) 54.68 (s, CH_2) 51.50 (d, $^3J_{PC}$ = 7.8, CH_2) 5.49 (d, $^4J_{PC}$ = 4.2, $SiMe_3$)	175.1
2b	3.513 (t, CH_2) 2.153 (t, CH_2) 3.432 (m, 1H, Cy) 2.401 (m, 2H, Cy) 1.754 (m, 4H, Cy) 1.426 (m, 1H, Cy) 1.152 (m, 3H, Cy) 0.614 (s, $SiMe_3$)	61.52 (d, $^1J_{PC}$ = 26.3, Cy) 53.73 (s, NCH_2) 51.20 (d, $^3J_{PC}$ = 7.3, NCH_2) 35.79 (d, J_{PC} = 5.9, Cy) 27.97 (d, J_{PC} = 8.1, Cy) 26.23 (s, Cy) 6.35 (d, $^4J_{PC}$ = 2.7, $SiMe_3$)	209.8
2c	3.498 (t, CH_2) 2.149 (t, CH_2) 1.673 (d, $^3J_{PH}$ = 11.6, *t*Bu) 0.593 (s, $SiMe_3$)	60.34 (d, $^1J_{PC}$ = 24.7, PC) 53.64 (s, CH_2) 51.23 (d, $^3J_{PC}$ = 7.6, CH_2) 34.22 (s, $C(CH_3)_3$) 6.33 (d, $^4J_{PC}$ = 3.3, $SiMe_3$)	227.3
3	3.313 (t, CH_2) 2.145 (t, CH_2) 0.479 (s, $SiMe_3$)	53.72 (CH_2) 48.80 (CH_2) 2.27 ($SiMe_3$)	
4a	8.660 (d, $^2J_{PH}$ = 24.6, P=CH) 1.161 (d, $^3J_{PH}$ = 10.2, P*t*Bu) 1.132 (d, $^4J_{PH}$ = 1.8, C*t*Bu)	194.73 (d, $^1J_{PC}$ = 48.3, P=C) 38.05 (d, $^2J_{PC}$ = 12.2, $CCMe_3$) 32.16 (d, $^1J_{PC}$ = 34.2, $PCMe_3$) 31.03 (d, $^3J_{PC}$ = 12.9, $CCMe_3$) 30.42 (d, $^2J_{PC}$ = 11.5, $PCMe_3$)	275.0
4b[c]	9.014 (d, $^2J_{PH}$ = 25.2, P=CH) 7.639 (m, 2H, Ph) 7.366 (m, 3H, Ph) 1.248 (d, $^4J_{PH}$ = 2.4, *t*Bu)	200.85 (d, $^1J_{PC}$ = 40.8, P=C) 142.80 (d, $^1J_{PC}$ = 43.5, Ph) 131.61 (d, J_{PC} = 15.2, Ph) 129.50 (s, Ph) 128.74 (d, J_{PC} = 5.3, Ph) 39.03 (d, $^2J_{PC}$ = 15.6, CMe_3) 30.89 (d, $^3J_{PC}$ = 12.0, CMe_3)	221.7
4c[d]	9.073 (d, $^2J_{PH}$ = 23.7, P=CH) 4.497 (m, 2H, C_5H_4) 4.125 (m, 2H, C_5H_4) 3.978 (s, 5H, C_5H_5) 1.192 (d, $^3J_{PH}$ = 9.9, *t*Bu)	175.96 (d, $^1J_{PC}$ = 41.7, P=C)	272.5

[a] Spectra recorded in C_6D_6 at 25 °C unless otherwise stated; coupling constants in Hz. [b] ^{13}C NMR spectrum recorded in CD_2Cl_2. [c] Spectra of **4b** recorded in CD_2Cl_2. [d] Complete ^{13}C NMR data not available for **4c** because of its facile dimerization.

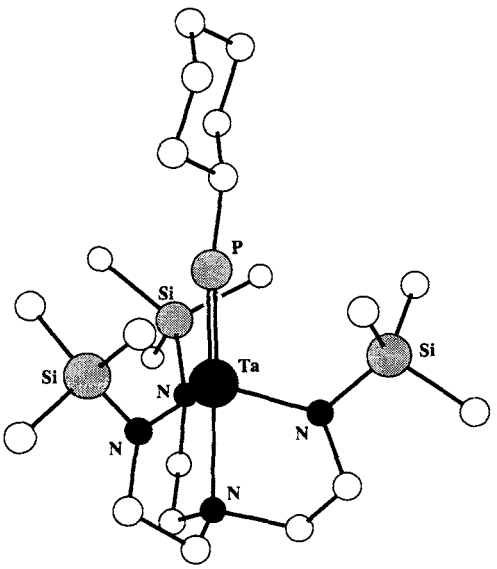

Fig. 1. Crystal structure of **2b**.

Multiple bonding between Ta and P is indicated by the short TaP distance of 2.145(7) Å (the sum of covalent radii for Ta and P is 2.44 Å[22]); this is expected, as symmetry considerations permit formation of a pseudo-triple bond for the approximately linear phosphinidene unit. Inspection of the structure suggests that stabilization of the reactive Ta=P linkage is a result of its location within the pocket afforded by the surrounding $SiMe_3$ substituents. These groups shield the Ta=P bond, but Ta is still accessible through the three clefts between the arms of the N_3N ligand, and access to P is also possible because of its relatively small organic sub-

stituent. This combination of structural features results in stable phosphinidene complexes (**2a** was heated in C_6D_6 solution for 12 h at 100 °C with no observable decomposition) that react readily with appropriate small substrates.

Aldehydes react smoothly with **2** to provide the stable oxotantalum complex[23–25] **3** and the corresponding phosphaalkene **4** (Scheme 1). Formation of the phosphaalkene in this manner is reminiscent of the olefination of carbonyl compounds as mediated by high-valent tantalum alkylidene complexes.[26] The reaction is likely to proceed via a four-membered metallacycle,[27] and it would be interesting to know what role the amine donor plays in either the formation or destruction of this postulated metallacycle.[28] Simple phosphaalkenes are stable when substituted with bulky groups, whereas with smaller substituents they are prone to dimerize or oligomerize;[1, 2] the following set of experiments illustrates that phosphinidene complexes **2** are capable of producing, in a synthetically useful manner, both stable and reactive phosphaalkenes.

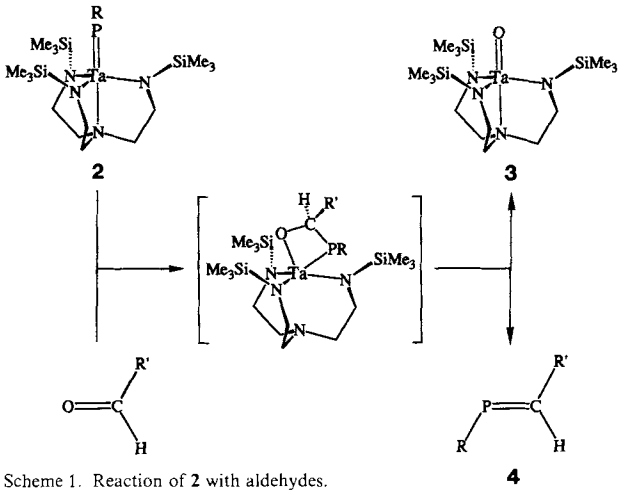

Scheme 1. Reaction of **2** with aldehydes.

The reaction between pivalaldehyde and [(N_3N)Ta=P*t*Bu] (**2c**) was relatively slow (complete after 7 h at 95 °C; 0.05 mol L^{-1} of each reagent) but proceeded smoothly to provide phosphaalkene **4a** (Scheme 2) and **3**; **4a** was previously prepared by a two-step synthesis requiring 11 weeks.[29] Phosphaalkenes such as **4a** are readily identified by their characteristic low-field ^{31}P and ^{13}C chemical shifts and diagnostic $^1J_{CP}$ coupling[1, 2] (Table 1); the $^2J_{PH}$ coupling can be useful in distinguishing the *E* (depicted) and the *Z* isomers.[30, 31] In the reaction between [(N_3N)Ta=PPh] (**2a**) and pivalaldehyde (25 °C; 0.05 mol L^{-1} of each reagent) the new phosphaalkene **4b** (Scheme 2) was produced quantitatively (according to ^1H NMR) in less than 5 minutes. After [(N_3N)Ta=O] (**3**) was removed by filtration through alumina, **4b** was isolated in pure form as a nonvolatile oil. When [(N_3N)Ta=P*t*Bu] (**2c**) was treated with ferrocenealdehyde (FcCHO)[32], the resulting red color indicated formation of phosphaalkene **4c**, which is stable for short periods at 25 °C but ultimately dimerizes to 1,3-diphosphetane **5** (Scheme 2).[33] Yellow-orange **5** was obtained in pure form by filtration of an ethereal solution through alumina; it formed as a single diastereomer. The reaction of **2a** with FcCHO resulted in the rapid generation of [(N_3N)Ta=O] (**3**), but phosphaalkene **4d** (Scheme 2) was too unstable to be observed at 25 °C. However, **4d** was trapped efficiently in the presence of cyclopentadiene (20 equiv) as Diels–Alder adduct **6**;[34] the adduct was an approximately 1:1 mixture of two diastereomers, the result of two possible modes of addition of the *E* phosphaalkene **4d** to cyclopentadiene. One diastereomer of **6** (Scheme 2) was isolated in pure form by filtration through alumina and subsequent crystallization from pentane at −40 °C.

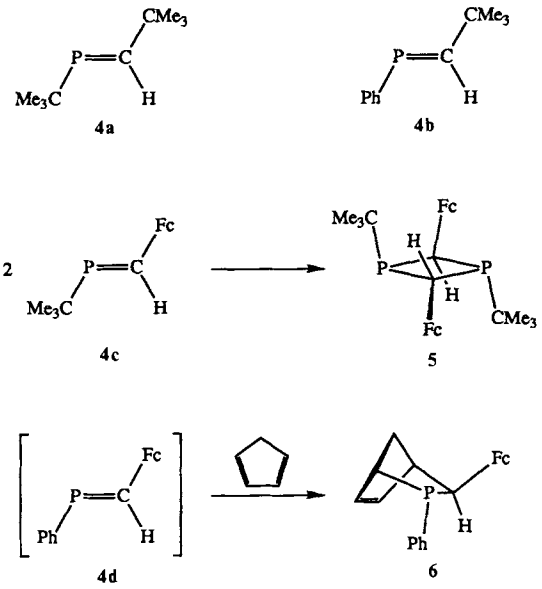

Scheme 2. Phosphorus-containing products.

With the ready isolation of cycloadducts such as **6**, it becomes clear that [(N_3N)Ta=PR] complexes could be useful for the one-pot synthesis of many phosphaalkenes or molecules derived from phosphaalkenes, by sequential phospha-Wittig and cycloaddition reactions. The phospha-Wittig reaction with [(N_3N)Ta=PR] (**2**) contrasts with (and is complementary to) the related reaction decribed by Mathey[5] in that the phosphaalkene products are *not* complexed to a low-valent transition metal, but are produced in the free state, with attendent differences in stability and reactivity. It is also significant that complexes **2** are the first stable phosphinidene complexes of a d^0 transition metal.[35] By comparing the bond energies of the C=O (173 kcal mol^{-1})[36] and P=C (approximately 110 kcal mol^{-1})[37–38] linkages, it may be estimated that the Ta=O bond energy is at least 63 kcal mol^{-1} greater than the Ta=P bond energy, consistent with the well-known[24] oxophilicity of tantalum. Mathey has noted[5] that the diagonal relationship between carbon and phosphorus leads to a strong similarity in the chemistry of these elements. We intend to investigate whether tantalum phosphinidene complexes catalyze metathesis reactions of phosphaalkenes, by analogy with olefin metathesis.[39]

Experimental Procedure

General: Satisfactory elemental analyses (C, H, N) were obtained for complexes **1**, **2a**, **2c**, **3**, and **6**. All operations were performed with inert-atmosphere techniques and appropriately dried and degassed solvents. Unless otherwise stated, procedures were carried out at 25 °C.

1: $TaCl_5$ powder (6.246 g, 17.437 mmol) and Li_3(N_3N) powder (6.636 g, 17.437 mmol) were added to 300 mL of ether that was stirred at −78 °C under Ar. The reaction mixture was allowed to warm to 25 °C over 5 h and subsequently stirred for 19 h. LiCl was removed by filtration through a bed of celite, and the reaction mixture was concentrated to ca. 20 mL and chilled to −40 °C for 12 h. The yellow crystalline product was then collected by filtration, washed with 5 mL of cold ether, and dried in vacuo (3.425 g, 5.600 mmol, 32%).

2a: A pale yellow solution of LiPHPh (1.260 g, 10.860 mmol, 2.1 equiv) in 250 mL of ether was chilled to −40 °C, and **1** (3.163 g, 5.172 mmol) was added with stirring; the color changed to deep burgundy and then to yellow-gold over a period of 10 min. The reaction mixture was stirred overnight at 25 °C, at which point LiCl was removed by filtration through a bed of celite. The solvents were removed in vacuo, and the yellow residue was washed with 100 mL of pentane, collected by filtration, and dried in vacuo to yield **2a** (2.920 g, 4.501 mmol, 87%) as a yellow powder. **2a** may be obtained readily in crystalline form by chilling a concentrated ether solution to −40 °C. **2b** and **2c** were prepared similarly, except that they are more soluble than **2a** in pentane, and therefore were crystallized from pentane at −40 °C.

4b: A stirred solution of **2a** (1.274 g, 1.964 mmol) in 15 mL of dichloromethane was treated with pivalaldehyde (254 mg, 2.946 mmol). After 3 h the solvent was removed in vacuo, the residue was extracted with 10 mL of ether, and the extract was filtered through a 1.5 cm plug of basic alumina in a 30 mL sintered glass frit. The plug was then washed with 50 mL of additional ether. The ether was removed from the filtrate in vacuo to give **4b** as a nonvolatile oil (291 mg, 1.633 mmol, 83%) that was > 95% pure by NMR (^{1}H, ^{13}C, and ^{31}P).

Reveived: December 18, 1992 [Z 5762IE]
German version: *Angew. Chem.* **1993**, *105*, 758

[1] R. Appel, *Multiple Bonds and Low Coordination in Phosphorus Chemistry* (Eds.: M. Regitz, O. J. Scherer), Thieme, Stuttgart, **1990**, pp. 157–219.
[2] R. Appel, F. Knoll, I. Ruppert, *Angew. Chem.* **1981**, *93*, 771; *Angew. Chem. Int. Ed. Engl.* **1981**, *20*, 731.
[3] G. Becker, *Z. Anorg. Allg. Chem.* **1976**, *423*, 242.
[4] T. A. van der Knaap, T. C. Klebach, F. Visser, F. Bickelhaupt, *Tetrahedron* **1984**, *40*, 765.
[5] F. Mathey, *Acc. Chem. Res.* **1992**, *25*, 90.
[6] A. H. Cowley, A. R. Barron, *Acc. Chem. Res.* **1988**, *21*, 81.
[7] P. B. Hitchcock, M. F. Lappert, W.-P. Leung, *J. Chem. Soc. Chem. Commun.* **1987**, 1282.
[8] R. Bohra, P. B. Hitchcock, M. F. Lappert, W.-P. Leung, *Polyhedron* **1989**, *8*, 1884.
[9] A. H. Cowley, B. Pellerin, J. L. Atwood, S. G. Bott, *J. Am. Chem. Soc.* **1990**, *112*, 6734.
[10] E. Niecke, J. Hein, M. Nieger, *Organometallics* **1989**, *8*, 2290; this communication describes terminal aminophosphinidene complexes (M = Mo, W) generated in situ.
[11] F. Mathey, *Angew. Chem.* **1987**, *99*, 285; *Angew. Chem. Int. Ed. Engl.* **1987**, *26*, 275.
[12] A discussion of electrophilic and nucleophilic complexes with terminal phosphinidene ligands is given in ref. [1], pp. 38–45.
[13] C. C. Cummins, J. Lee, R. R. Schrock, W. M. Davis, *Angew. Chem.* **1992**, *104*, 1510; *Angew. Chem. Int. Ed. Engl.* **1992**, *31*, 1501.
[14] C. C. Cummins, R. R. Schrock, W. M. Davis, *Organometallics* **1992**, *11*, 1452.
[15] F. A. Cotton, G. Wilkinson, *Advanced Inorganic Chemistry*, 5th ed., Wiley, New York, **1988**, pp. 1318–1323.
[16] H. V. R. Dias, P. P. Power, *J. Am. Chem. Soc.* **1989**, *111*, 144.
[17] Z. Hou, D. W. Stephan, *J. Am. Chem. Soc.* **1992**, *114*, 10088.
[18] A ^{31}P NMR shift of $\delta = 193.0$ is given for a linear phosphinidene [9], whereas bent phosphinidenes have ^{31}P NMR signals in the range $\delta =$ 666.1 to 799.5 [7,8].
[19] S. M. Socol, S. Lacelle, J. G. Verkade, *Inorg. Chem.* **1987**, *26*, 3221.
[20] *NMR and the Periodic Table* (Eds.: R. K. Harris, B. E. Mann), Academic Press, New York, **1978**.
[21] Structure of **2b**. Data were collected at −72 °C on an Enraf-Nonius CAD-4 diffractometer with $Mo_{K\alpha}$ radiation (graphite monochromator). A total of 3900 reflections were collected to a 2θ value of 54.9°. An empirical absorption correction was applied. The structure was solved by a combination of Patterson and difference Fourier techniques. Carbon and nitrogen atoms were refined isotropically due to absorption problems; the heavier atoms were refined anisotropically. Due to disorder, the cyclohexyl moiety was modeled as a rigid group. The final cycle of full-matrix least-squares refinement was based on 2375 observed reflections ($I > 3.00\sigma(I)$) and 128 variable parameters and converged (largest parameter shift was less than 0.01 times its esd) with $R = 0.065$ and $R_w = 0.064$. A final difference Fourier map showed no chemically significant features. Crystal data are $a = 19.754(2)$, $b = 11.862(1)$, $c = 12.993(1)$ Å, V = 3044.4(8) Å^3, space group $Pna2_1$, $Z = 4$. Further details of the crystal structure investigation may be obtained from the Fachinformationszentrum Karlsruhe, Gesellschaft für wissenschaftlich-technische Information mbH, D-W-7514 Eggenstein-Leopoldshafen 2 (FRG), on quoting the depository number CSD-57068, the names of the authors, and the journal citation.
[22] L. Pauling, *The Nature of the Chemical Bond*, 3rd ed., Cornell University Press, New York, **1960**.
[23] A. van Asselt, B. J. Burger, V. C. Gibson, J. E. Bercaw, *J. Am. Chem. Soc.* **1986**, *108*, 5347.
[24] D. R. Neithamer, R. E. LaPointe, R. A. Wheeler, D. S. Richeson, G. D. Van Duyne, P. T. Wolczanski, *J. Am. Chem. Soc.* **1989**, *111*, 9056.
[25] G. Parkin, J. E. Bercaw, *J. Am. Chem. Soc.* **1989**, *111*, 391.
[26] R. R. Schrock, *J. Am. Chem. Soc.* **1976**, *98*, 5399.
[27] G. C. Bazan, R. R. Schrock, M. B. O'Regan, *Organometallics* **1991**, *10*, 1062.
[28] An X-ray structural determination on $[(N_3N)TaCH_3(\eta^1\text{-}O_3SCF_3)]$ showed that the tertiary amine moiety is distant from Ta (2.536 Å) compared with the corresponding parameter for **2b** (2.36(2) Å); C. C. Cummins, R. R. Schrock, W. M. Davis, unpublished results.
[29] E. Niecke, E. Symalla, *Chimia* **1985**, *39*, 320.
[30] R. Appel, J. Menzel, F. Knoch, P. Volz, *Z. Anorg. Allg. Chem.* **1986**, *534*, 100.
[31] M. Yoshifuji, K. Toyota, N. Inamoto, *Tetrahedron Lett.* **1985**, *26*, 1727.
[32] D. E. Bublitz, K. L. Rinehart, Jr., *Org. React.* **1969**, *17*, 1.
[33] For a discussion of 1,3-diphosphetanes see ref. [1], p. 162, and references therein.
[34] For a discussion of [4 + 2] cycloadditions involving phosphaalkenes see ref. [1], p. 163–166, and references therein
[35] Ref. [17] gives evidence for a transient Zr^{IV} phosphinidene complex.
[36] L. Pauling, *General Chemistry*, 3rd ed., Freeman, San Francisco, **1970**, p. 913.
[37] M. W. Schmidt, P. N. Truong, M. S. Gordon, *J. Am. Chem. Soc.* **1987**, *109*, 5217.
[38] P. von R. Schleyer, D. Kost, *J. Am. Chem. Soc.* **1988**, *110*, 2105.
[39] R. R. Schrock, *Acc. Chem. Res.* **1990**, *23*, 158.

Bromine Azide—Determination of the Molecular Structure by Electron Diffraction in the Gas Phase**

By *Magdolna Hargittai,* Inis C. Tornieporth-Oetting,* Thomas M. Klapötke,* Maria Kolonits,* and *István Hargittai**

The experimental determination of the molecular structure of halogen azides XN_3 (X = F, Cl, Br, I) is particularly hindered, since all XN_3 compounds are explosive substances.[1–4] Nevertheless many azides have been structurally characterized: HN_3[5] and FN_3[6] by microwave (MW) spectroscopy, F_3CN_3 by a combined analysis of electron diffraction (ED) and MW spectroscopy[7] ClN_3 by MW spectroscopy,[8] IN_3 by X-ray crystallography of single crystals,[9] and H_3CN_3 by ED.[10] Recently quantum mechanical ab initio calculations have increased knowledge on the structures of halogen azides. For example ab initio calculations were carried out at a high level for HN_3,[11] FN_3,[7, 11] ClN_3,[11] BrN_3,[11] IN_3,[9, 11] and $I_2N_3^+$.[12] Prior to this work there were no reports of structural data for BrN_3 and IN_3 determined by gas-phase experiments. Since, on the basis of available structural information for halogen azides, the structure parameters for BrN_3 could be predicted with high accuracy, the experimental determination of the molecular structure was an interesting challenge.

[*] Prof. Dr. M. Hargittai, M. Kolonits
Structural Chemistry Research Group
of the Hungarian Academy of Sciences,
Eötvös University, H-1431 Budapest, PO Box 117 (Hungary)
Priv.-Doz. Dr. T. M. Klapötke, Dr. I. C. Tornieporth-Oetting
Institut für Anorganische und Analytische Chemie
der Technischen Universität
Strasse des 17. Juni 135, D-W-1000 Berlin 12 (FRG)
Telefax: Int. code + (30) 314-21 106
Prof. Dr. I. Hargittai
Institute of General and Analytical Chemistry
Budapest Technical University
and Hungarian Academy of Sciences, H-1521 Budapest (Hungary)

[**] This research was supported by the Hungarian National Scientific Research Foundation (OTKA, No. 2103), the Fonds der Chemischen Industrie, the Deutsche Forschungsgemeinschaft (KL 636/2-2), the Bundesministerium für Bildung und Wissenschaft (Graduiertenkolleg: Synthese und Strukturaufklärung niedermolekularer Verbindungen) and the German-Hungarian (TU Berlin, TU Budapest) partnership.

The crucial problem was to produce the bromine azide vapor and direct it into the electron diffraction apparatus safely. Finally, BrN_3 was synthesized according to Equation (a) (see Experimental Procedure).

$$Br_2 + NaN_3 \text{ (excess)} \xrightarrow{1\,h,\ 20\,^\circ C} BrN_3 + NaBr \qquad (a)$$

The electron diffraction intensities from experiments for the two camera distances used are shown in Figure 1. The radial distribution obtained from the 50 cm camera distance is shown in Figure 2.

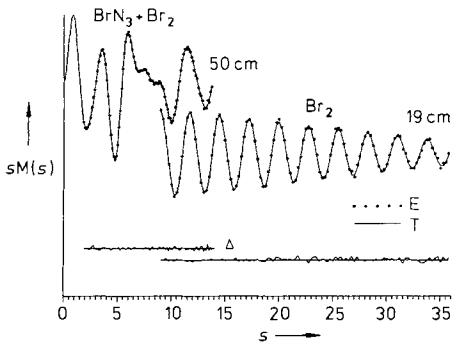

Fig. 1. Electron diffraction intensities from the molecular beam of the gaseous product from the reaction of bromine and sodium azide. Conditions: 60 kV electrons, sample container at −78 °C, nozzle at room temperature. The data, which were determined with a camera distance of 50 cm, were best approximated by a model of 73% BrN_3 and 27% Br_2. The data, which were determined with a camera distance of 19 cm, could be approximated by bromine alone. $M(s)$ = molecular intensity, $s = (4\pi/\lambda)\sin(\theta/2)$ in $Å^{-1}$.

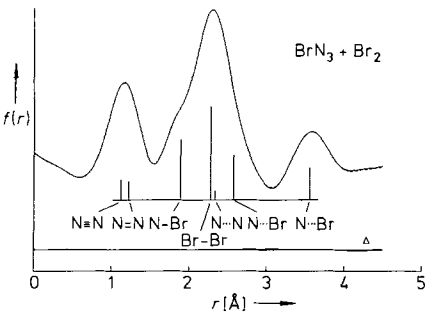

Fig. 2. Radial distribution $f(r)$ obtained from the electron diffraction intensities of the data from the experiment with a camera distance of 50 cm (cf. Fig. 1). The heights of vertical bars are roughly proportional to the relative weights of the contributions of internuclear distances r to electron scattering.

The experiment with a camera distance of 50 cm was carried out with sufficient BrN_3 to elucidate its structure with the assumption of some of the parameters. The two N–N bond lengths could not be refined independently from one another so their difference was constrained from the MP2 MO calculations.[11] The mean amplitudes of vibration were calculated by a normal coordinate analysis. The results of the structural analysis are summarized in Table 1. Although the structure parameters obtained experimentally generally agree with those of the HF MO calculation, the distances determined from the MP2 calculation seem to be too large. This effect is not unexpected, because the equilibrium bond length (the result of the computation, r_e) should always be smaller than the experimentally determined thermal average bond length (r_g).[13] The calculated difference of the two N–N bond lengths is probably much better determined than the individual bond lengths. The BrN_3 molecule has a *trans*

Table 1. Bond lengths r_g [Å] and bond angles [°] of BrN_3 determined by electron diffraction (ED) [a, b] and ab initio calculations for comparison [11].

	ED	HF/6-31G(d,p) [c]	MP2/6-31G(d,p) [d]
$(N\text{-}N)_{mean}$	1.180 ± 0.003	1.171	1.211
ΔN-N	0.102 [e]	0.146	0.102
N2-N3	1.129 ± 0.022	1.098	1.160
N1-N2	1.231 ± 0.022	1.244	1.262
Br-N	1.899 ± 0.006	1.896	1.923
N-N-N	170.7 ± 2.4	174.2	171.4
Br-N-N	109.7 ± 1.1	109.1	108.5

[a] The azide content of the sample was found to be 73 ± 1%, the Br–Br distance in Br_2 was determined to be $r_g(Br\text{–}Br) = 2.284 \pm 0.005$ Å. [b] Estimated total errors [23], indicated as error limits, include $\sqrt{2}$ times the least-squares standard deviation, a systematic error of 0.2%, and an uncertainty introduced by a change of 0.044 Å (the difference between the HF and MP2 all electron calculations, see ref. [11]) in the assumed ΔN-N value. [c] All electron HF MO calculation [11]. [d] All electron MP2 MO calculation [11]. [e] Assumed from the MP2 calculation [11].

configuration for which the Br–N bond lengths and the mean N–N bond lengths, as well as the Br-N-N and the N-N-N bond angles are determined with relatively high precision (Scheme 1). These structure parameters are consistent with those of other halogen azides. Quite recently the structure of the isoelectronic BrNCO was determined by MW spectroscopy.[14] This contains a NCO chain, which is slightly bent away (ca. 8°) from the Br atom (cf. BrN_3, 9°). In BrNCO the Br–N distance was found to be 1.862 Å, just slightly shorter than that in BrN_3 (1.899 Å). The angle at the bromine-carrying nitrogen atom, however, in BrNCO is significantly larger than the corresponding Br-N-N angle in BrN_3 (117.99 vs. 109.7°).

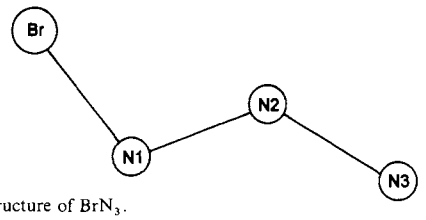

Scheme 1. Molecular structure of BrN_3.

Although halogen azides can be handled more readily in solution, preparations for the pure compounds have been described.[15–18] In a separate experiment we synthesized BrN_3 on a preparative scale in order to grow single crystals of BrN_3.[19] However, this has so far been unsuccessful, which is mainly due to the fact that BrN_3 always explodes during the liquid/solid phase transition.

Experimental Procedure

At −196 °C bromine (0.25 g, 1.56 mmol) was placed in a glass tube (diameter 4 mm) and sodium azide (0.13 g, 2.00 mmol) was layered over it. The glass tube was then warmed to −10 °C and placed into the container of the nozzle system of the electron diffraction apparatus. A modification of a previously described nozzle system built for very volatile substances was used [20]. The flow of vapor was regulated by a needle valve. The sample container was first recooled to −196 °C and evacuated. The sample was then warmed to 0 °C and allowed to react for 1 h at room temperature with the needle valve closed. In the most successful experiment (50 cm camera distance) the valve was gradually opened during electron diffraction.

Setting the nozzle system to the 19 cm camera distance, we experienced that only bromine escaped from the reaction mixture. In another experiment the sample was allowed to warm to 0 °C with the needle valve left open. After 20 minutes the electron diffraction patterns were recorded and they proved to originate predominantly from bromine.

Caution: Bromine azide is explosive[21] and very sensitive to phase transitions and pressure changes! In one experiment the NaN_3 was compacted on the

frozen Br_2 to make it more difficult for bromine to escape. This sample exploded and the (PTFE) container was blown apart. When the surface of the cold trap was cleaned there was also a small explosion.

Received: December 23, 1992 [Z 5768 IE]
German version: *Angew. Chem.* **1993**, *105*, 773

[1] D. E. Milligan, M. E. Jacox, *J. Chem. Phys.* **1964**, *40*, 2461.
[2] F. Raschig, *Ber. Dtsch. Chem. Ges.* **1908**, *41*, 4194.
[3] D. A. Spencer, *J. Chem. Soc.* **1925**, *127*, 217.
[4] A. Hantzsch, M. Schümann, *Ber. Dtsch. Chem. Ges.* **1900**, *33*, 522.
[5] B. P. Winnewisser, *J. Mol. Spectrosc.* **1980**, *82*, 220.
[6] D. Christen, H. G. Mack, G. Schatte, H. Willner, *J. Am. Chem. Soc.* **1988**, *110*, 707.
[7] K. O. Christe, D. Christen, H. Oberhammer, C. J. Schack, *Inorg. Chem.* **1984**, *23*, 4283.
[8] R. L. Cook, M. C. L. Gerry, *J. Chem. Phys.* **1970**, *53*, 2525.
[9] P. Buzek, T. M. Klapötke, P. von R. Schleyer, I. C. Tornieporth-Oetting, P. S. White, *Angew. Chem.* **1993**, *105*, 289; *Angew. Chem. Int. Ed. Engl.* **1993**, *32*, 275.
[10] D. W. W. Anderson, D. W. H. Rankin, A. Robertson, *J. Mol. Struct.* **1972**, *14*, 385.
[11] M. Otto, S. D. Lotz, G. Frenking, *Inorg. Chem.* **1992**, *31*, 3647.
[12] I. C. Tornieporth-Oetting, P. Buzek, P. von R. Schleyer, T. M. Klapötke, *Angew. Chem.* **1992**, *104*, 1391; *Angew. Chem. Int. Ed. Engl.* **1992**, *31*, 1338.
[13] M. Hargittai, I. Hargittai, *Int. J. Quant. Chem.* **1992**, *44*, 1057.
[14] K. D. Hensel, M. E. Lam, M. C. L. Gerry, H. Willner, *J. Mol. Spectrosc.* **1992**, *151*, 184.
[15] K. Dehnicke, *J. Inorg. Nucl. Chem.* **1965**, *27*, 809.
[16] K. Dehnicke, *Angew. Chem.* **1967**, *79*, 253; *Angew. Chem. Int. Ed. Engl.* **1967**, *6*, 240.
[17] a) K. Dehnicke, *Angew. Chem.* **1976**, *88*, 612; *Angew. Chem. Int. Ed. Engl.* **1976**, *15*, 553; b) K. Dehnicke, *Adv. Inorg. Chem. Radiochem.* **1983**, *26*, 169.
[18] K. Dehnicke, *Angew. Chem.* **1979**, *91*, 527; *Angew. Chem. Int. Ed. Engl.* **1979**, *18*, 500.
[19] IR (gas, 2 Torr, 20 °C, 10 cm): 3170 w ($\nu_1 + \nu_2$), 2282 m (2 ν_2), 2038 vs (ν_1; ν-N_3, asym.), 1156 s/1143 s (ν_2; ν-N_3, sym.), 688 m/676 m (ν_3; ν-BrN), 460 w/445 w (ν_4; δ-N_3).
[20] I. Hargittai, J. Hemádi, J. Tremmel, *Jenaer Rundschau* **1968**, *13*, 3. See also J. Tremmel, I. Hargittai in *Stereochemical Applications of Gas-Phase Electron Diffraction, Part A.* (Eds.: I. Hargittai, M. Hargittai), VCH, New York, **1988**, Chapter 6.
[21] ΔH_f^0 (BrN_3, g) = +90 kcal mol^{-1}; estimated from: ΔH_f^0 (Br, g) = 26.8 kcal mol^{-1}, ΔH_f^0 (N_3, g) = +105.0 kcal mol^{-1} [12,22] and BE (N-Br) = 42 kcal mol^{-1} (from: BE(N-Br) = 0.5[BE(N_2) + BE(Br_2)] + 23.2($\chi_N - \chi_{Br}$)^2). BE = bond energy.
[22] D. A. Johnson, *Some Thermodynamic Aspects of Inorganic Chemistry*, Cambridge University Press, Cambridge, **1982**.
[23] M. Hargittai, I. Hargittai, *J. Chem. Phys.* **1973**, *59*, 2513.

Phosphane (PH_3) in the Biosphere**

By *Günter Gassmann** and *Dietmar Glindemann*

Synthetic phosphane (PH_3) is an industrial product and used in the form of metal phosphides as insecticides and as dopant gas in electronic chip manufacture.[1] Mineral phosphides are only known from meteorites in the form of schreibersite.[2] Biogenic phosphane has been detected and described a few times since the beginning of this century.[3] These early reports of biogenic phosphane formation in Nature have been questioned until recently.[4] In 1988, Hungarian scientists succeeded in detecting biogenic phosphane in sewage sludge[5] and they predicted its ubiquitous occurrence in the hydrosphere. This prediction was confirmed recently, when phosphane was detected in harbor sludge and marine sediments.[6] In these cases phosphane occurred together with methane, confirming reports from as early as 1929.[7] This points to an obligatory correlation between methanogenesis and the reduction of phosphate to phosphane in Nature. The global production of biogenic methane is estimated to be 500 million metric tons per year,[8] of which 100 million metric tons originate from bovine rumens. If methanogenesis and the reduction of phosphate to phosphane are correlated as indicated above, measurable amounts of phosphane must be expected in the biosphere.

To test the hypothesis that CH_4 and PH_3 production occurs together, we searched for phosphane in various sources including the feces of cattle. In the fresh pats from grazing cattle we detected phosphane in nanogram quantities. Phosphane was also found in the content of rumen, gut, and manure of freshly slaughtered cattle. Interestingly, the phosphane concentration increases along the course of digestion, with highest values in the excretion products (Table 1, entries 1–4).

Table 1. PH_3 in the digestive tract of cattle, and in the feces and manure of cattle and swine.

Entry	Origin	PH_3 [ng kg^{-1}]
1	rumen (of cattle)	2.9 ± 0.1
2	gut (of cattle)	5.1 ± 1.1
3	cow pat	9.0 ± 0.1
4	cattle manure	13.9 ± 5.4
5	colon (of swine)	103.0 ± 4.5
6	manure (of swine)	964.1 ± 11.7

If measurable amounts of phosphane are present in the intestinal tract of a herbivore, higher concentrations should be expected in the gut content of an omnivore, even if less methane will be formed. The higher phosphate contents of the food could yield larger amounts of phosphane. Our results on the feces of pigs are listed in Table 1 (entries 5 and 6). Humans consume phosphate-rich food like meat, sausage, cheese spread, and soft drinks. Consequently, we expected to find phosphane in their feces. We examined the feces of a baby (milk diet), of an eight-month-old weaned toddler (mixed diet), of an adult vegetarian, and of a married couple (identical mixed diet), and found the phosphane quantities given in Table 2.

Table 2. PH_3 content of the feces of man.

Entry	Origin	PH_3 [ng kg^{-1}]
1	baby (4.5 months old; milk diet)	not detectable
2	toddler (8.5 months old; mixed diet)	162.1 ± 11.7
3	vegetarian	12.7 ± 1.7
4	married couple (husband; mixed diet)	81.0 ± 17.3
5	married couple (wife; mixed diet)	81.2 ± 16.4

Due to their phosphate-rich food omnivores are expected to show a high phosphane production. Thus, we examined two species of predatory fish, plaice and cod. In cod we found an age-dependent phenomenon. While immature cod showed no phosphane in their guts, mature cod had detectable phosphane concentrations in their intestinal tracts (Table 3;

[*] Dr. G. Gassmann, D. Glindemann
Biologische Anstalt Helgoland
Zentrale Hamburg
Notkestrasse 31, D-W-2000 Hamburg 52 (FRG)

[**] This work was supported in part by the Bundesministerium für Forschung und Technologie. – According to the IUPAC rules for nomenclature both phosphine and phosphane is permitted for PH_3; however, the second name is recommended. See *Nomenclature of Inorganic Chemistry* (Ed.: G. J. Leigh), Blackwell Scientific Publ., Oxford, **1990**.

Table 3. PH_3 in the intestinal tract of fish.

Entry	Origin	PH_3
1	cod (immature)	not detectable($n = 23$)
2a	cod (mature)	5.4 ± 0.2 pg/individual
2b	cod (mature)	69.1 ± 4.6 pg/individual[12]
3	plaice	138.0 ± 45.0 fg/individual($n = 46$)

entries 1, 2a, b). In contrast, phosphane is generally present in plaice at much lower concentrations (Table 3; entry 3).

Although our study is only based on a few examples, the results strongly suggest that biogenic phosphane is formed in the biosphere wherever methanogenic conditions prevail. In order to confirm the biogenic origin of phosphane, "fecult" experiments were carried out with two different phosphane-free culture media. Inoculants were 250 mg human feces with a phosphane content of 3 pg. Inoculated media and blanks (500 cm^3) were incubated anaerobically at 36 °C for 6 and 14 days, respectively. As shown in Table 4 and Figure 1, the phosphane and diphosphane contents rise 8500- and 31 000-fold, respectively. This experiment convincingly demonstrates the existence of a biological system which produces phosphane and diphosphane.

Table 4. Formation of PH_3 and P_2H_4 in an anaerobic mixed bacterial culture.

Entry	Origin	PH_3	P_2H_4
		[ng kg^{-1}]	
1	blank A	0.0	0.0
2	"fecult" medium A (6 days)	14.7 ± 0.1	0.5 ± 0.1
3	"fecult" medium A (14 days)	0.3 ± 0.1	186.7 ± 22.0
4	blank B	0.0	0.0
5	"fecult" medium B (6 days)	51.2 ± 14.4	0.6 ± 0.1
6	"fecult" medium B (14 days)	0.0	24.0 ± 5.2

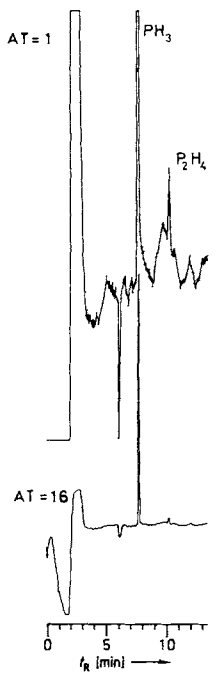

Fig. 1. Gas chromatogram of a gas sample (10 cm^3 from 1150 cm^3) of "fecult" medium A (6 days; 50 cm^3 from 500 cm^3) with phosphorus-selective thermionic detection. Separation (retention time $t_R = 7.60$ min and 10.17 min, respectively) and determination of 55.2 pg PH_3 (peak height 4342 mm at attenuation (AT) = 1) and 398 fg P_2H_4 (peak height 32 mm at AT = 1). Analytical column (0.35 mm internal diameter): 5 m CPWax-57CB + 10 m Poraplot-Q + 50 m CPWax-57CB. Helium as carrier gas at 100 kPa; oven temperature 40 °C isothermal. The detection limit of phosphane is 70 fg (Hewlett-Packard 5890 II-NPD).

The confirmation of phosphane production in the biosphere sheds new light on various issues. The ignition of methane by the autoignition of diphosphane provides the basis for a biogenic ignition mechanism, which Wolfe[9] claimed as an explanation for the legendary fire-breathing dragon (if it ever existed). Likewise it offers a plausible explanation for the phenomenon of lights over swampy grounds or cemeteries (ignis fatuus or will-o'-the-wisp; cf.[2]).

For the first time, it is now possible to evaluate the participation of phosphane in the global biogeochemical cycle of phosphorus. Devai et al.[5] showed that biogenic phosphane accompanies the methane production in a sewage sludge digester (Imhoff Tank). In this system the ratio of phosphane to methane is 0.0035 vol%. The extrapolation of this value based on a global biogenic methane production of 500 million tons, reveals the potential for the formation of 40 000 metric tons of biogenic phosphane per year.

A very important aspect of phosphane formation in the biosphere is the toxicity of phosphane. It is genotoxic to human lymphocytes in concentrations of a few nanograms per liter culture medium.[10] The biogenesis of phosphane in the human intestinal tract may be the factor which is responsible for the increased risk of cancer in carnivores and omnivores in comparison with vegetarians.[11] The involvement of phosphane biogenesis for human cancer epidemiology deserves to be investigated more closely[13].

Experimental Procedure

Sampling of feces (15–150 g) was carried out in the field (Table 1; entry 3), at farms around Hamburg (Table 1; entries 4, 6), in the slaughter house in Hamburg (Table 1; entries 1, 2, 5), in the Pediatric Hospital in Hamburg-Altona (Table 2; entries 1, 2). Other samples were taken from members of this institute (Table 2; entries 3–5). Fish were caught by the German research vessel "HEINCKE" (Table 3; entries 1–3). The phosphane content was determined in the laboratory or aboard the research vessel within one hour of sampling. Because of a shortage of mature cod specimens, only two single measurements are given in Table 3. Because of the difficulty in determining the exact weight of the intestinal tract of fish on board ship, the phosphane content was related to the individual. Experiments with living vertebrates were not carried out.

The "fecult" experiments were performed in 500 cm^3 glass bottles equipped with rubber caps. The sterile, anaerobic culture medium for "fecult" A contained (per dm^3) 5 g bactopeptone, 2.5 g bacto yeast extract, 5 g D-(+)-glucose, 10 g KH_2PO_4, 0.4 g $(NH_4)_2Fe(SO_4)_2 \cdot 6H_2O$, 1 g $CaSO_4 \cdot 2H_2O$, and 2 g $MgSO_4 \cdot 7H_2O$. "Fecult" B corresponds to medium A, but bactopeptone was replaced by 200 cm^3 meat extract from 50 g fresh beef. 250 mg human feces with a known phosphane content (3 pg) was used as inoculum. Anaerobicity was controlled by the addition of resazurine. The culture bottles were pressurized with nitrogen to 100 kPa. Aliquots of the liquid phase (50 cm^3) were withdrawn with a gas-tight syringe after 6 and 14 days, and digested under alkaline conditions as reported elsewere [6]. The phosphane content was determined immediately after digestion.

Received: January 8, 1993 [Z 5801 IE]
German version: *Angew. Chem.* **1993**, *105*, 749

[1] World Health Organization, *Phosphine and Selected Metal Phosphides (Environmental Health Criteria 73)*, Geneva, **1988**.
[2] G. E. Hutchinson in *The Biology of Phosphorus* (Ed.: L. J. Wolterink), Michigan State College Press, **1951**, p. 1–35.
[3] W. Kulka, *Zentralbl. Bakteriol. Parasitenkd. Infektionskrankh. Hyg. Abt. 1* **1912**, *61*, 336–344; H. K. Barrenscheen, H. A. Beckh-Widmanstetter, *Biochem. Z.* **1923**, *140*, 279–283; K. J. Rudakov, *Zentralbl. Bakteriol. Parasitenkd. Infektionskrankh. Hyg. Abt. 2* **1927**, *70*, 202–214; W. P. Iverson, *Nature* **1968**, *217*, 1265–1267.
[4] R. J. P. Williams in *Phosphorus in the Environment: Its Chemistry and Biochemistry* (Ciba Found. Symp.), Elsevier, Oxford, **1978**, 95–116.
[5] I. Devai, L. Felföldy, I. Wittner, S. Plosz, *Nature* **1988**, *333*, 343–345.
[6] G. Gassmann, F. Schorn, *Naturwissenschaften* **1993**, *80*, 78–80; G. Gassmann, F. Schorn, unpublished results.
[7] K. J. Rudakow, *Zentralbl. Bakteriol. Parasitenkd. Infektionskrankh. Hyg. Abt. 2* **1929**, *79*, 229–245.
[8] B. Hileman, *Chem. Eng. News* **1992**, *70* (no. 6) 26–28.

[9] R. S. Wolfe, *Adv. Microb. Physiol.* **1971**, *6*, 109.
[10] V. F. Garry, J. Griffith, T. J. Danzl, R. L. Nelson, E. B. Whorton, L. A. Krueger, J. Cervenka, *Science* **1989**, *246*, 251–255.
[11] J. Chang-Claude, R. Frentzel-Beyme, U. Eilber, *Epidemiology* **1992**, *3*, 395–401; G. Johansson, *Effects of a shift from a mixed diet to a lactovegetarian diet on some colon cancer associated characteristics*, Karolinska Institute, Stockholm, **1990**.
[12] This species of cod displays an abnormal growth, as large as a fist, on its kidney in addition to its relatively high intestinal phosphane content. This phenomenon is not rare in mature cod. A possible connection between the phosphane content and the abnormal growth will be investigated in more detail during future expeditions.
[13] Phosphane is a relatively stable compound. The half-life period (5–28 h) depends on the concentration of $OH^{\bullet}$ radicals in ambient air. The amphoteric chemical properties of phosphane imply an unchanged exhalation of phosphane in cases of poisoning by metal phosphides. Oxidized derivatives such as hypophosphite, phosphite, and phosphate are urinal excretion products (cf. [1]).

$[Cp^*TaS_3\{Rh(cod)\}_2]$ and $[Cp^*TaS_3\{RuH(PPh_3)_2\}_2]$: A New Class of Heterometallic TaM_2 Clusters

By *Kazuyuki Tatsumi,* Hiroyuki Kawaguchi, Yoshihisa Inoue, Akira Nakamura, Roger E. Cramer,** and *James A. Golen*

We recently reported the synthesis of the trisulfidotantalum complexes **1**.[1] An important feature of these molecules is that the lithium cations are bound directly to the sulfido

$[\{Cp^*TaS_3Li_2(thf)_2\}_2]$ **1a**

$[\{Cp^*TaS_3Li_2(dme)\}_2]$ **1b**

$[Cp^*TaS_3Li_2(tmeda)_2]$ **1c**

$[\{Cp^*TaS_3Li_3Cl(tmeda)\}_2(\mu\text{-tmeda})]$ **1d**

$Cp^* = C_5Me_5$, dme = 1,2-dimethoxyethane, tmeda = *N,N,N',N'*-tetramethylethylenediamine

ligands. Thiometalates such as $[MoS_4]^{2-}$, $[WS_4]^{2-}$, $[VS_4]^{3-}$, and $[ReS_4]^-$ are known to react with various metal halides to give a multitude of heterometallic clusters,[2–6] often comprised of linear arrays of metal atoms. We hoped that complexes **1** would serve as starting materials for the synthesis of rare organotantalum clusters.[6b] In fact, complexes **1** were found to react smoothly with $[\{RhCl(cod)\}_2]$ (cod = 1,5-cyclooctadiene) and $[RuH(Cl)(PPh_3)_3]$ to give the trinuclear clusters **2** and **3**. These reactions and the structures of the resulting clusters are described here.

[*] Prof. Dr. K. Tatsumi, H. Kawaguchi
Department of Chemistry, Faculty of Engineering Science
Osaka University
Toyonaka, Osaka 560 (Japan)
Telefax: Int. code +(6)857-3952
Prof. Dr. R. E. Cramer
Department of Chemistry
University of Hawaii at Manoa
Honolulu, HI 96822 (USA)
Y. Inoue, Prof. Dr. A. Nakamura
Department of Macromolecular Science, Faculty of Science
Osaka University
Toyonaka, Osaka 560 (Japan)
Prof. Dr. J. A. Golen
Department of Chemistry
University of Massachusetts, Dartmouth
North Dartmouth, MA 02747 (USA)

$[Cp^*TaS_3\{Rh(cod)\}_2]$ **2**

$[Cp^*TaS_3\{RuH(PPh_3)_2\}_2]$ **3**

Treatment of **1a** with two equivalents of $[RhCl(cod)]_2$ in THF at 50 °C yielded a dark brown solution, from which we isolated **2** as yellow-brown crystals. Analogously, the reaction of **1a** with four equivalents of $[RuH(Cl)(PPh_3)_3]$ in THF (2 h, 50 °C) afforded cluster **3** as reddish-brown crystals. Use of **1b–1d** instead of **1a** in the above reactions also gave clusters **2** and **3**. The $TaRh_2$ cluster **2** is freely soluble in nonpolar organic solvents, while crystals of **3** are only slightly soluble in hexane and benzene. Both compounds are somewhat air- and moisture-sensitive and also diamagnetic. These clusters were fully characterized by NMR, IR, and Raman spectroscopy, elemental analysis, and X-ray structure analysis.

The molecular structure of **2**[7] shown in Figure 1 consists of a Cp^*TaS_3 half-sandwich unit and two Rh(cod) complex fragments, and has virtual but not crystallographically imposed mirror symmetry. The central Cp^*TaS_3 unit assumes

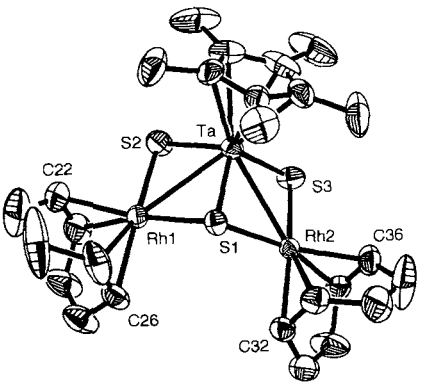

Fig. 1. Molecular structure of **2** (thermal ellipsoids at the 50% level). Selected distances [Å] and angles [°]: Ta-Rh1, 2.982(1); Ta-Rh2, 2.953(1); Ta-S1, 2.307(1); Ta-S2, 2.279(1); Ta-S3, 2.274(1); Rh1-S1, 2.364(1); Rh1-S2, 2.347(2); Rh2-S1, 2.366(1); Rh2-S3, 2.354(1); Rh1-Ta-Rh2, 84.4(1); S1-Rh1-S2, 98.4(1); S1-Rh2-S3, 98.5(1); Ta-S1-Rh1, 79.3(1); Ta-S2-Rh1, 80.3(1); Ta-S1-Rh2, 78.4(1); Ta-S3-Rh2, 79.3(1).

a slightly distorted three-legged piano stool structure, in which the S_3 plane is parallel (179.7°) to the plane of the Cp* ring. Each Rh atom is bound to two sulfido ligands and S1 bridges the Rh atoms. The Ta, S1, S2, and Rh1 atoms are coplanar (maximum deviation, 0.005 Å), as are Ta, S1, S3, and Rh2 (maximum deviation, 0.087 Å). The two double bonds in the cod ligand are perpendicular to the corresponding RhS_2Ta plane. The mean Ta–Rh distance of 2.968 Å suggests a dative bond between d^8 Rh and d^0 Ta, a conclusion which is supported by the expansion of the S-M-S angles and concomitant contraction of the M-S-M angles within the M_2S_2 quadrilaterals. There is no direct bonding between the Rh atoms (3.983(1) Å). The S2-Ta-S3 angle (106.4(1)°) is slightly larger than the S1-Ta-S2 (102.1(1)°) and S1-Ta-S3 (102.6(1)°) angles. Compared to the other Ta–S bonds the Ta–S1 bond is 0.03 Å longer as a result of binding two Rh centers; the Rh–S1 distances are also increased (0.012 Å, 0.017 Å).

In the temperature-dependent ^1H NMR spectra of **2** in $[D_8]$toluene the olefinic protons of the η^4-cod ligands give rise to three peaks $\delta = 5.63$, 5.44, and 5.23 at −90 °C with the intensity ratio of 1:2:1. The intensity of the central peak must be due to an accidental overlap of two resonances (or

the chemical shifts of the two signals are so close that they are not resolved even at −90 °C). As the temperature is raised, the two outside peaks broaden and merge with the central peak above the coalescence temperature of approximately −60 °C. This broad signal then becomes increasingly sharp up to 30 °C ($\delta = 5.24$).[8] We think that the η^4-cod ligands rotate around the Ta–Rh bond axes in solution. The solid-state NMR spectrum shows the four olefinic protons to be nonequivalent. The analysis of the variable-temperature ^{1}H NMR spectra will be reported in detail elsewhere.[9]

In the molecular structure of **3**[10] (Fig. 2) the two $Ru(H)(PPh_3)_2$ complex fragments are unsymmetrically coordinated to the Cp^*TaS_3 unit. Three sulfido ligands link

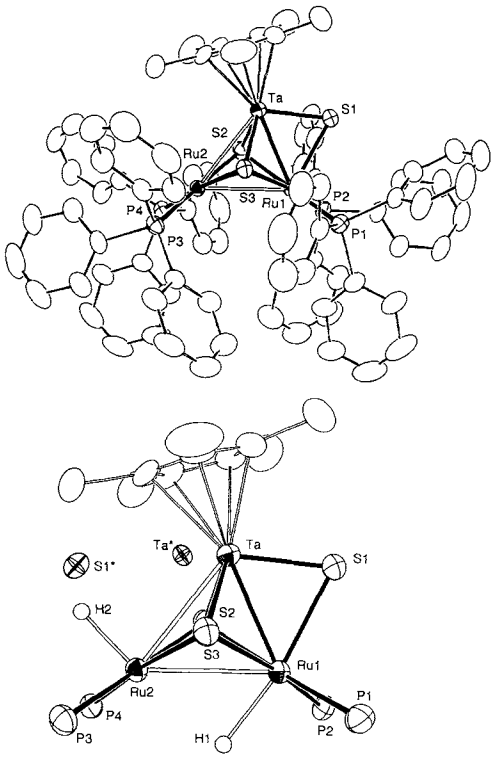

Fig. 2. Molecular structure of **3** (thermal ellipsoids at the 50% level). The entire molecule (top) and its main frame with hydride positions (bottom) are shown. The molecule is disordered with the occupancy factors of 0.9 and 0.1; Ta* and S1* belong to the minor configuration. Selected distances [Å] and angles [°]: Ta-S1, 2.258(4); Ta-S2, 2.333(3); Ta-S3, 2.301(2); Ru1-S1, 2.521(4); Ru1-S2, 2.498(4); Ru1-S3, 2.455(3); Ru1-P1, 2.343(4); Ru1-P2, 2.349(3); Ru2-S2, 2.403(3); Ru2-S3, 2.385(3); Ru2-P3, 2.301(2); Ru2-P4, 2.299(3); Ru1-H1, 1.93(3); Ru2-H2, 1.70(3); S1-Ta-S2, 96.5(1); S2-Ta-S3, 92.4(1); S1-Ta-S3, 99.1(1); Ta-S1-Ru1, 68.7(1); Ta-S2-Ru1, 68.0(1); Ta-S3-Ru1, 69.2(1); Ta-S2-Ru2, 82.4(1); Ta-S3-Ru2, 83.5(1); S2-Ru1-S3, 84.9(1); P1-Ru1-P2, 98.8(1); S2-Ru2-S3, 88.6(1); P3-Ru2-P4, 97.5(1); Ru1-S2-Ru2, 75.6(1); Ru1-S3-Ru2, 76.7(1).

Ru1 to the Ta atom, while two sulfido ligands bridge Ru2 and Ta. As a consequence, the Ta–Ru1 distance is short (2.703(4) Å) and the Ta–Ru2 distance is very long (3.119(5) Å), in contrast to the equilateral $TaRh_2$ triangle in **2**. The Ta–S bonds of two μ_3-sulfur atoms S2 and S3 are elongated by 0.075 and 0.043 Å relative to the Ta–S1 bond. Conversely, the Ru1–S1 bond is somewhat longer than the Ru1–S2(S3) bonds. The Ru-bound phosphane ligands are situated *trans* to the μ_3-sulfido ligands. Although determination of the positions of hydrogen atoms from X-ray data alone is difficult, we nonticed a distinct peak on the Fourier map in each Ru coordination sphere, which could be assigned to terminal hydrido ligands. The corresponding structure is shown at the bottom of Figure 2; the Ru2–H1 (2.40 Å) and Ta–H2 (3.33 Å) distances are too long to invoke bonding interactions. When these hydrido ligands are included, the coordination geometry at Ru1 is distorted octahedral, whereas the geometry at Ru2 is square-pyramidal. The difference in coordination number results in longer Ru1–S (mean, 2.491 Å) and Ru1–P (mean, 2.346 Å) bonds relative to the corresponding Ru2–S (mean, 2.394 Å) and Ru2–P (mean, 2.300 Å) bonds. The Ru1–Ru2 (3.004(5) Å) and Ta–Ru2 distances are long. However, expansion of the S-M-S angles and contraction of the M-S-M angles within each M_2S_2 quadrilateral suggests that weak metal–metal bonding is present. It is interesting that the coordinatively unsaturated Ru2 center does not strongly interact with either the Ta or Ru1 atom.

The $^{31}P\{^1H\}$ NMR spectrum of **3** in [D$_8$]THF shows two singlets at $\delta = 43.7$ and 49.8. In the hydrido region two triplets of equal intensity were detected at $\delta = -15.0$ ($J_{PH} = 13.0$ Hz) and −24.6 ($J_{PH} = 35.5$ Hz).[11] These observations provide evidence for the *cis* (or facial) disposition of a hydrido and two phosphane ligands at each of two chemically different Ru centers, and prove that neither of the hydrido ligands bridge two Ru atoms. The NMR results are entirely consistent with the solid-state structure shown in Figure 2; this configuration was found by NMR to be rigid up to 60 °C.

The synthesis of these $TaRh_2$ and $TaRu_2$ clusters demonstrates that the $Cp^*TaS_3Li_2$ unit in complexes **1** can serve as a convenient precursor for organoheteronuclear clusters. There are two important aspects in this cluster formation: 1) the reactions proceed smoothly under mild conditions so that the labile ligands such as cod and H remain bound and are incorporated into the clusters; 2) the two metal centers, each coordinated to such a ligand, are in close proximity, and we may expect the two metal centers to cooperate for substrate activation.

Experimental Procedure

All operations and manipulations were carried out under an argon atmosphere, and the solvents were dried before use.

2: A solution of $[\{RhCl(cod)\}_2]$ (0.14 g, 0.28 mmol) in THF was added to a solution of **1a** (0.21 g, 0.14 mmol). The resulting reddish-brown solution was warmed to 50 °C and stirred for 2 h. After removal of the solvent in vacuo, the residue was extracted with benzene (10 mL), which upon evaporation left a dark-brown solid of **2** in nearly quantitative yield. Recrystallization from hexane gave yellow-brown crystals suitable for X-ray diffraction (45% yield). Satisfactory C,H,S-analysis. Raman (crystals): $\tilde{\nu}[cm^{-1}] = 432$(m), 315(m); ^{1}H NMR (100 MHz, C_6D_6): $\delta = 2.01$ (s(br), 16H, cod(methylene)), 2.19 (s, 15H, Cp*), 5.39 (s(br), 8H, cod(olefin)).

3: A solution of **1a** (0.11 g, 0.096 mmol) in THF (10 mL) was added to a slurry of $[RuH(Cl)(PPh_3)_3]$ (0.36 g, 0.40 mmol) in THF. The resulting suspension was warmed to 50 °C with stirring for 2 h, whereupon a clear reddish-brown solution was obtained. The solvent was removed and the residue extracted with benzene (20 mL). Recrystallization from THF/hexane gave reddish-brown crystals of **3** in 44% yield. Satisfactory C,H-analysis. Raman (crystals): $\tilde{\nu}[cm^{-1}] = 446$(w); ^{1}H NMR (400 MHz, [D$_8$]THF): $\delta = 7.0-7.3$ (m, 60H, PPh_3), 2.01 (s, 15H, Cp*), −15.0 (t, $J_{PH} = 13.0$ Hz, 1H, Ru-*H*), −24.6 (t, $J_{PH} = 35.5$ Hz, 1H, Ru-*H*); $^{31}P\{^1H\}$ NMR (21.35 MHz, [D$_8$]THF, 95% H_3PO_4 external standard): $\delta = 49.8$ (s, 2P), 43.7 (s, 2P).

Received: January 18, 1993 [Z 5817 IE]
German version: *Angew. Chem.* **1993**, *105*, 791

[1] a) K. Tatsumi, Y. Inoue, A. Nakamura, R. E. Cramer, W. VanDoorne, J. W. Gilje, *J. Am. Chem. Soc.* **1989**, *111*, 782; b) K. Tatsumi, Y. Inoue, H. Kawaguchi, M. Kohasaka, A. Nakamura, R. E. Cramer, W. VanDoorne, G. J. Taogoshi, P. N. Richmann, *Organometallics* **1993**, *12*, 352.

[2] a) E. Diemann, A. Müller, *Coord. Chem. Rev.* **1973**, *10*, 79; b) A. Müller, S. Sarkar, *Angew. Chem.* **1977**, *89*, 748; *Angew. Chem. Int. Ed. Engl.* **1977**, *16*, 705; c) A. Müller, H. Bögge, U. Schimansi, *J. Chem. Soc. Chem. Commun.* **1980**, 91; d) A. Müller, E. Krickemeyer, H. Bögge, *Z. Anorg. Allg. Chem.* **1987**, *554*, 61.

[3] a) J. C. Huffman, R. S. Roth, A. R. Siedle, *J. Am. Chem. Soc.* **1976**, *98*, 4340; b) J. K. Stalick, A. R. Siedle, A. D. Mighell, C. R. Hubbard, *ibid.* **1979**, *101*, 2903; c) J.-M. Manoli, C. Potvin, F. Sécheresse, *J. Chem. Soc. Chem. Commun.* **1982**, 1159; d) C. Potvin, J.-M. Manoli, F. Sécheresse, S. Marzak, *Inorg. Chem.* **1987**, *26*, 4370; e) P. Klingelhöfer, U. Müller, *Z. Anorg. Allg. Chem.* **1988**, *556*, 70.

[4] a) D. Coucouvanis, *Acc. Chem. Res.* **1981**, *14*, 201, and references therein.; b) D. Coucouvanis, E. D. Simhon, N. C. Baenzinger, *J. Am. Chem. Soc.* **1980**, *102*, 6644; c) D. Coucouvanis, N. C. Baenzinger, E. D. Simhon, P. Stremple, D. Swenson, A. Kostikas, A. Simopoulos, V. Petrouleas, V. Papaefthymiou, *ibid.* **1980**, *102*, 1732; d) J. W. McDonald, G. D. Friesen, W. E. Newton, *Inorg. Chim. Acta* **1980**, *46*, L79.

[5] a) K. E. Howard, T. B. Rauchfuss, A. L. Rheingold, *J. Am. Chem. Soc.* **1986**, *108*, 297; b) K. E. Howard, T. B. Rauchfuss, S. R. Wilson, *Inorg. Chem.* **1988**, *27*, 3561; c) K. E. Howard, J. R. Lockemeyer, M. A. Massa, T. B. Rauchfuss, S. R. Wilson, X. Yang, *ibid.* **1990**, *29*, 4385.

[6] a) Y. Do, E. D. Simhon, R. H. Holm, *Inorg. Chem.* **1985**, *24*, 4635; b) Recently tetrathiometalates $[MS_4]^{3-}$ of Nb and Ta were prepared and were found to give $[MFe_2S_4Cl_4]$ clusters. S. C. Lee, R. H. Holm, *J. Am. Chem. Soc.*, **1990**, *112*, 9654.

[7] Crystal structure analysis of **2** [10]: single crystal with dimensions $0.2 \times 0.4 \times 0.6$ mm^3, monoclinic space group $C2/c$, $a = 33.29(1)$, $b = 12.047(2)$, $c = 13.711(3)$ Å, $\beta = 90.50(2)°$, $V = 5498(2)$ Å^3, $Z = 8$, $\rho_{calcd} = 2.016$ Mg m^{-3}. Data collection with a Nicolet R3m/V diffractometer; $Mo_{K\alpha}$ radiation, 2θ scans, $2\theta = 4-60°$, 8842 measured reflections, 8055 independent, 7469 observed ($F_o > 1.0\,\sigma F_o$), empirical absorption correction based on azimuthal scans. Solution and refinement with the Nicolet SHELXTL PLUS package (direct methods); all non-hydrogen atoms were refined anisotropically and hydrogen atoms were put at calculated positions with a fixed isotropic U value; full matrix, refined parameters 283, $R = 0.0347$ and $R_w = 0.0474$, GOF = 0.96, maximum residual electron density 0.90 and -0.75 eÅ^3.

[8] The full width at half-height ($v_{1/2}$) of the olefinic proton resonance at 30 °C is 8 Hz, and the coupling with the Rh nuclei was not detected. The corresponding resonance for $[\{Rh(cod)Cl\}_2]$ in C_6D_6 at room temperature comes at $\delta = 4.40$ with $v_{1/2} = 10$ Hz (100 MHz).

[9] K. Tatsumi, H. Kawaguchi, K. Tani, R. E. Cramer, J. W. Gilje, T. T. Bopp, unpublished.

[10] Crystal structure analysis of **3**: single crystal with dimensions $0.2 \times 0.2 \times 0.3$ mm^3, triclinic space group $P\bar{1}$, $a = 12.84(1)$, $b = 14.21(2)$, $c = 21.620(9)$ Å, $\alpha = 81.5(1)$, $\beta = 74.5(1)$, $\gamma = 75.2(1)°$, $V = 3663(2)$ Å^3, $Z = 2$, $\rho_{calcd} = 1.565$ Mg m^{-3}. Data collection with a Rigaku AFC5R diffractometer; $Mo_{K\alpha}$ radiation, ω-2θ scan, $2\theta = 4-50.1°$, 13157 measured reflections, 13098 independent, 9953 observed ($I > 3.0\,\sigma I$), empirical absorption correction based on azimuthal scans. Solution and refinement with the TEXSAN package of Molecular Structure Corporation (direct methods); all non-hydrogen atoms except for the THF solvent molecule were refined anisotropically and hydrogen atoms were put at calculated positions; full matrix, refined parameters 1064, $R = 0.0331$ and $R_w = 0.0424$, GOF = 1.63, maximum residual electron density 1.05 and -0.82 eÅ^3. The molecule is disordered with major and minor occupancies of 0.9 and 0.1. In the minor configuration (see Fig. 2 bottom), S1* bridges Ta* and Ru2 instead of Ta and Ru1; the Ta*–Ru2 distance is 2.619(4) Å while the Ta*-Ru1 distance is longer at 3.206(5) Å. Due to its low occupancy, we were only able to locate two atoms, Ta* and S1*, of the minor configuration. This structure was solved twice with different crystals, once in Osaka and once in Honolulu. The Osaka results, which are slightly more accurate, are those reported here. Very similar disorder was found in both crystals. Further details of the structure analysis for **2** and **3** may be obtained from the Fachinformationszentrum Karlsruhe, Gesellschaft für wissenschaftlich-technische Information mbH, D-W-7514 Eggenstein-Leopoldshafen 2 (FRG), on quoting the depository number CSD-57031, the names of the authors, and the journal citation.

[11] The resonance of the hydrido ligand in $[RuH(Cl)(PPh_3)_3]$ appears at $\delta = -17.75$ with $J_{PH} = 26$ Hz in CD_2Cl_2. P. S. Allman, B. R. McGarvey, G. Wilkinson, *J. Chem. Soc. (A)*, **1968**, 3143.

BOOKS

This section contains book reviews and a list of new books received by the editor. Book reviews are written by invitation from the editor. Suggestions for books to be reviewed and for book reviewers are welcome. Publishers should send brochures or (better) books to the Book Editor, Dr. Gerhard Karger, Redaktion Angewandte Chemie, Postfach 101161, D-W-6940 Weinheim, Federal Republic of Germany. The editor reserves the right of selecting which books will be reviewed. Uninvited books not chosen for review will not be returned.

Book Reviews

Molecular Dynamics Simulation. Elementary Methods. By *J. M. Haile*. Wiley, Chichester, 1992. XI, 489 pp., hardcover £ 47.50.—ISBN 0-471-81966-2

This book by J. M. Haile gives the information that is promised by the title. After an introductory chapter on the philosophy of computer simulation, it introduces classical dynamics and the fundamental principles of computer simulation of dynamics in Chapter 2. The next topic is simulation of systems consisting of hard spheres (Chapter 3). Simulation techniques for systems with continuous potential energy functions are treated in the next two chapters: finite-difference methods and soft-sphere systems. The last two chapters discuss methods for determining static properties (Chapter 6) and dynamic properties (Chapter 7) of a simulated system. There are 13 appendices containing background material, examples of computer programs, and other useful information. The book also contains a bibliography of books and articles on the subject.

The book is a useful addition to the literature on computer simulation of atomic and molecular systems. It gives a thorough and practical explanation of the basics of molecular dynamics simulation. Since each chapter contains a separate list of references, the interested reader has easy access to more advanced literature. Each chapter also contains a number of exercises which offer the opportunity to obtain insight by practical work. The book reads easily and illustrates the theory with graphs and results from simulations where possible. Moreover, it treats a number of topics, such as reliability of trajectories and results, propagation of errors, equilibration, and sampling problems, that are often only briefly mentioned in other texts on the subject.

To those who are seriously interested in dynamic computer simulation techniques I can recommend reading this neat and well-written book.

Wilfred F. van Gunsteren
Laboratorium für Physikalische Chemie
der Eidgenössischen Technischen Hochschule
Zürich (Switzerland)

New Books

Electron Microprobe Analysis, 2nd Edition. Edited by **S. J. B. Reed.** Cambridge University Press, Cambridge, **1993.** 326 pp., hardcover, £ 45.—0-521-41956-5

Analytiker Taschenbuch, Bd. 11. Edited by **R. Rorsdorf, W. Fresenius, and H. Günzler.** Springer, Heidelberg, **1993.** 258 pp., hardcover, DM 98.—ISBN 3-540-55487-4

Charge Transfer Photochemistry of Coordination Compounds. By **O. Horváth, and K.L. Stevenson.** VCH, New York/Weinheim, **1993.** 464 pp., hardcover, $ 98.-/DM 238.-.—ISBN 1-56081-564-7/3-527-89564-7

Concise Encyclopedia of Materials Characterization. Edited by **R.W. Cahn, and E. Lifshin.** Pergamon Press Ltd., Oxford, **1992.** 670 pp., hardcover, £ 150.-.—ISBN 0-08-040603-3

Electron Microprobe Analysis, 2nd Edition. Edited by **S.J.B. Reed.** Cambridge University Press, Cambridge, **1993.** 326 pp., hardcover, £ 45.-.—ISBN 0-521-41956-5

Reagent Chemicals. (American Chemical Society Specifications). American Chemical Society, Washington, **1993.** 806 pp., hardcover, $ 149.95.—ISBN 0-8412-2502-8

Encyclopedia of Chemical Technology, Vol. 5. Edited by **J.I. Kroschwitz, M. Howe-Grant.** Wiley, New York, **1993.** 1072 pp., hardcover, $ 150.-.—ISBN 0-471-52673-8

Fourier Transform Raman Spectroscopy. Instrumentation and Chemical Applications. By **P. Hendra, C. Jones, G. Warnes.** Ellis Horwood, New York, **1991.** 311 pp., hardcover, $ 90.50.—ISBN 0-13-327032-7

Modern NMR Spectroscopy. A Guide for Chemists. By **J.K.M. Sanders, B.K. Hunter.** Oxford University Press, Oxford, **1993.** 314 pp., paperback, £ 23.50.—ISBN 0-19-855567-9

Principles of Electrochemistry. By **J. Koryta, J. Dvorák, L. Kavan.** Wiley, Chichester, **1993.** 486 pp., paperback, £ 24.95.—ISBN 0-471-93838-6

Biochemische Methoden zur Schadstofferfassung im Wasser. Möglichkeiten und Grenzen. Edited by **Fachgruppe Wasserchemie in der GDCh.** VCH Verlagsgesellschaft mbH, Weinheim, **1993.** 174 pp., hardcover, DM 130.-.—ISBN 3-527-28551-2

Materials Fundamentals of Molecular Beam Epitaxy. By **J.Y. Tsao.** Academic Press, London, **1992.** 301 pp., paperback, £ 37.-.—ISBN 0-12-701625-2

Sulphones in Organic Synthesis. (Tetrahedron Organic Chemistry Series, Vol. 10). By **N.S. Simpkins.** Pergamon Press, Oxford, **1993.** 381 pp., paperback, £ 30.-.—ISBN 0-08-040284-4

Progress in Heterocyclic Chemistry, Vol. 4. Edited by **H. Suschitzky, E.F.V. Scriven.** Pergamon Press, Oxford, **1992.** 295 pp., hardcover, £ 60.-.—ISBN 0-08-040612-2

Chemistry. The Experience. By **A. Ratcliffe.** Wiley, Chichester, **1993.** 219 pp., paperback, £ 21.50.—ISBN 0-471-57707-3

A Scientist's and Engineer's Guide to Workstations and Supercomputers. By **R.H. Landau, P.J. Fink, Jr.** Wiley, Chichester, **1992.** 390 pp., paperback, £ 34.95.—ISBN 0-471-53271-1

Chromatography of Polymers. Characterization by SCE and FFF. Edited by **T. Provder.** American Chemical Society, Washington, **1993.** 338 pp., hardcover, $ 94.95.—ISBN 0-8412-2625-3

Chemical Sciences Graduate School Finder 1992–1993. American Chemical Society, Washington, **1992.** 600 pp., paperback, $ 44.95.—ISBN 0-8412-2522-2

Organische Chemie. Chemie-Basiswissen II. By **H.P. Latscha, H.A. Klein.** Springer, Berlin, **1993.** 661 pp., paperback, DM 48.-.—ISBN 3-540-56341-5

Methodologie Pour l'Extrapolation des Procédés Chimiques. By **J.-P. Euzen, P. Trambouze, J.-P. Wauquier.** Éditions Technip, Paris, **1993.** 250 pp., hardcover, FF 375.—ISBN 2-7108-0635-5

The Fullerenes. Edited by **H.W. Kroto, J.E. Fischer, D.E. Cox.** Pergamon Press, Oxford, **1993.** 314 pp., hardcover, £ 29.95.—ISBN 0-08-0421520

Mathematik in der Chemie. By **K. Jug.** Springer, Berlin, **1993.** 311 pp., paperback, DM 48.-.—ISBN 3-540-55771-7

Dictionary of Substances and their Effects (DOSE), Vol 1. Edited by **M. Richardson.** Royal Society of Chemistry, Cambridge, **1992.** hardcover, £ 180.-.—ISBN 0-85186-381-0

Biosensor Design and Application. Edited by **P.R. Mathewson, J.W. Finley.** American Chemical Society, Washington, **1992.** 202 pp., hardcover, $ 54.95.—ISBN 0-8412-2494-3

Isotope Effects in Gas-Phase Chemistry. Edited by **J.A. Kaye.** American Chemical Society, Washington, **1992.** 438 pp., hardcover, $ 97.95.—ISBN 0-8412-2471-4

Mixed Surfactant Systems. Edited by **P.M. Holland, D.N. Rubingh.** American Chemical Society, Washington, **1992.** 451 pp., hardcover, $ 99.95.—ISBN 0-8412-2468-4

Homogeneous Transition Metal Catalyzed Reactions. Edited by **W.R. Moser, D.W. Slocum.** American Chemical Society, Washington, **1992.** 625 pp., hardcover, $ 139.95.—ISBN 0-8412-2007-7

Biosensors. Theory and Applications. By **D.G. Buerk.** Technomic, Basel, **1993.** 221 pp., hardcover, SFr. 187.-.—ISBN 0-87762-975-7

Determination of Electronic and Optical Properties. (Physical Methods of Chemistry, Vol. 8). Edited by **B.W. Rossiter, R.C. Baetzold.** Wiley, Chichester, **1993.** 531 pp., hardcover, £ 105.-.—ISBN 0-471-54407-8

Catalysis and Surface Characterisation. Edited by **T.J. Dines, C.H. Rochester, J. Thomson.** Royal Society of Chemistry, Cambridge, **1992.** 292 pp., hardcover, £ 47.50.—ISBN 0-85186-335-3

Surfactants in Lipid Chemistry: Recent Synthetic, Physical, and Biodegradative Studies. Edited by **J.H.P. Tyman.** Royal Society of Chemistry, Cambridge, **1992.** 183 pp., hardcover, £ 39.50.—ISBN 0-85186-395-7

An Introduction to the Management of Laboratory Data. By **C.N. Hegarty.** Royal Society of Chemistry, Cambridge, **1992.** 588 pp., hardcover, £ 85.-.—ISBN 0-85186-219-5

Fundamental Principles of Polymeric Materials. By **S.L. Rosen.** Wiley, Chichester, **1993.** 420 pp., hardcover, £ 41.95.—ISBN 0-471-57525-9

Biodegradable Polymers and Plastics. Edited by **M. Vert, J. Feijin, A. Albertsson, G. Scott, E. Chiellini.** Royal Society of Chemistry, Cambridge, **1992.** 302 pp., hardcover, £ 45.-.—ISBN 0-85186-207-1

Fundamentals of Nuclear Magnetic Resonance. By **J.W. Hennel, J. Klinowski.** Longman, Harlow, Great Britain, **1993.** 288 pp., paperback, £ 22.50.—ISBN 0-582-06703-0

Current Trends in Sonochemistry. Edited by **G.J. Price.** Royal Society of Chemistry, Cambridge, **1992.** 184 pp., hardcover, £ 39.50.—ISBN 0-85186-365-5

Registered names, trademarks, etc. used in this journal, even when not marked as such, are not to be considered unprotected by law.

© VCH Verlagsgesellschaft mbH, D-W-6940 Weinheim, 1992. – Printed in the Federal Republic of Germany by Konrad Triltsch Druck- und Verlagsanstalt Würzburg.

All rights reserved (including those of translation into foreign languages). No part of this issue may be reproduced in any form — by photoprint, microfilm, or any other means — nor transmitted or translated into a machine language without written permission from the publishers. Only single copies of contributions, or parts thereof, may be made for personal use. This journal was carefully produced in all its parts. Nevertheless, authors, editors, and publisher do not warrant the information contained therein to be free of errors. Readers are advised to keep in mind that statements, data, illustrations, procedural details, or other items may inadvertently be inaccurate.

Valid for users in the USA: The appearance of the code at the bottom of the first page of an article (serial) indicates the copyright owner's consent that copies of the article may be made for personal or internal use, or for the personal or internal use of specific clients. This consent is given on the condition, however, that the copier pay stated per-copy fee through the Copyright Clearance Center, Inc. (CCC), for copying beyond that permitted by Sections 107 or 108 of the U.S. Copyright Law. This consent does not extend to other kinds of copying, such as copying, for general distribution, for advertising or promotional purposes, for creating new collective works, or for resale. For copying from back volumes of this journal see 'Permissions to Photo-Copy: Publisher's Fee List' of the CCC.

Editorial office: Postfach 10 11 61, D-W-6490 Weinheim, Federal Republic of Germany, Telephone (06201) 606 315, Telex 465 516 vchwh d, Telefax (06201) 606 328, E-Mail Z16@DHDURZ2 in Earn Bitnet.

Editor: *Peter Gölitz*

Associate editors: *N. A. Compton, R. H. Schmidt-Radde, K. J. Schneider.* **Book editor:** *G. Karger.* **Editorial assistant:** *E. Schweikart*

Publishers: VCH Verlagsgesellschaft mbH. (Managing Directors: *Hans Dirk Köhler, Dr. Karlheinz Köpfer*), Pappelallee 3, D-W-6940 Weinheim, Federal Republic of Germany.

Advertising office (Advertising Manager: *N. Schippel*): Postfach 10 11 61, D-W-6940 Weinheim, Federal Republic of Germany, Telephone (0 62 01) 606 312, Telefax (0 62 01) 606 328.

ANGEWANDTE CHEMIE
International Edition in English
Volume 32 · Number 6
June 1993
Pages 767–922

Superelectrophiles**

By George A. Olah*

In memory of Hans Meerwein

Electrophiles that are capable of further interaction (coordination, solvation) with strong Brønsted or Lewis acids can be activated in this way. The resulting enhancement of their reactivity is great compared to that of their parent compounds under conventional conditions and indicates superelectrophile formation (i.e., electrophiles with doubly electrodeficient (dipositive) nature whose reactivity substantially exceeds that of their parent electrophiles). As representative examples the protolytic or electrophilic activation of the following electrophiles in superacidic and related strongly electrophilic media is discussed: oxonium, carboxonium, sulfonium, selenonium, and telluronium ions; acyl cations; protonated CO, CO_2, COS, and carbonic and thiocarbonic acids; heteroatom-substituted carbocations (and some of their boron analogs); halonium ions; azonium (including nitronium) and carbazonium ions. Emphasis is placed on both experimental chemical investigations and theoretical treatment of the involved systems. As prototypes for protolytically activated onium ions, the protohydronium dication (diprotonated water) and its sulfur analogue, the protosulfonium dication, are of particular significance. The protoacetyl and protoformyl dication (diprotonated carbon monoxide), diprotonated carbonic acid and carbon dioxide, diprotonated hydrogen cyanide and nitriles, as well as the protonitronium dication —among others—and their emerging chemistry are discussed as examples of superelectrophiles.

1. Introduction and General Concepts

Electrophiles are reagents that take up electrons in their reactions and thus are electron acceptors; that is, they are electron-deficient compounds.[1, 2] The statement attributed to Rundle that "there are no electron-deficient compounds, only theory-deficient chemists" may have reflected the view of the 1950s, but since that time much has happened to improve our understanding. The proton is the ultimate electrophile, having no electron at all. In the condensed state, however, no "naked" proton can exist, and it is always solvated (associated). Trivalent carbocations are similarly highly electron-deficient electrophiles, although they tend to compensate partially for their electron deficiency by either intra- or intermolecular interactions. The better stabilized the species (e.g. a carboxonium ions or acyl cation) the less electron-deficient it is.

Over the course of 35 years my research group has studied and continues to investigate long-lived electrophilic intermediates. These include carbocations,[3] acyl cations, carboxonium ions, several onium ions[4] including oxonium, sulfonium, halonium,[5] nitronium, and azonium ions, as well as other electron-deficient species. Our studies generally uti-

[*] Prof. Dr. G. A. Olah
Loker Hydrocarbon Research Institute
University of Southern California
University Park, Los Angeles, CA 90089 (USA)

[**] Chemistry in Superacid. Part 11. Presented in part as the LeBel Lectures, University of Strasbourg (France) in May 1991, and at the Symposium on "Carbocations, Carboxonium and Onium Ions", Loker Hydrocarbon Research Institute in January 1992.

 © VCH Verlagsgesellschaft mbH, W-6940 Weinheim, 1993 0570-0833/93/0606-0767 $ 10.00+.25/0

lized superacidic media like the essential low-nucleophilicity environments,[6] since long-lived, highly electron-deficient (i.e., acidic) species in the condensed state can only exist in such environments. Our studies resulted in what is now generally referred to as *superacidic, stable-ion chemistry* and the chemistry of stable carbocations.[3, 6] Thousands of publications from around the world have contributed and are continuing to contribute to this very active field.

During our studies on superacidic systems we made observations which indicated that superacids, besides being highly ionizing, low-nucleophilicity media, in some instances were also capable of additional unexpected activation of electrophiles by further protolytic (or electrophilic) interaction (coordination, solvation). In 1975 we first reported[7] that in superacidic media the acetyl cation (CH_3CO^+) and nitronium ion (NO_2^+) display highly enhanced reactivity indicative of their protolytic (protosolvated) activation[*] through the dications, $CH_3\overset{+}{C}=\overset{+}{O}H$ and NO_2H^{2+}. Later we found similar indications for the protoformyl dication ($HCOH^{2+}$, diprotonated CO). In 1986 we described studies relating to the protohydronium dication (H_4O^{2+})[8] and subsequently the tetrahydridosulfonium dication, H_4S^{2+}[9]. In 1989 we published a brief review on protonated (protosolvated) onium ions (onium dications).[10] The overall concept and significance of these studies, however, has as yet aroused relatively little response or even interest in the broader chemical community. This is probably because our studies were considered of highly specialized nature involved generally in somewhat exotic superacidic systems. Not unlike most chemists' attitude towards mass spectrometric, gas-phase ion chemistry, superacidic chemistry is still frequently viewed as a field where surprising (even "magic") observations can be made, which do not necessarily relate to "real" chemistry.

Electrophilic solvation (or protosolvation) of electrophiles such as onium, carboxonium, and related ions involves their further interaction with Lewis or Brønsted superacids. Such interaction of these ions with superacid systems can in the limiting case lead to extremely reactive de facto dications, although electrophilic assistance by the strong acids through polarized donor–acceptor interactions should have similar effect. Electrophilic activation can play a significant role in Friedel–Crafts and superacid-catalyzed reactions, as well as in solid-acid-catalyzed systems and even in enzymatic reactions. This review centers on this emerging field and calls attention to the general significance of protolytic/electrophilic activation and the role of superelectrophiles, that is, electrophiles of doubly electron-deficient (dipositive) nature whose reactivity greatly exceeds that of their parent compounds in aprotic or conventional acidic media. The definition is arbitrary, as is that of superacids, but describes the remarkably enhanced reactivity of activated, dipositive electrophiles.

As already emphasized, in the condensed state the ultimate electrophile, the proton, cannot exist in its "free" form, but will interact with any electron donor present in its environment. We shall nevertheless use "H^+" as a shorthand depiction throughout this review for simplicity. Furthermore, in the condensed state cations must be balanced by appropriate anions (counter- or gegenions). Again for simplicity we shall not reflect on the effect of counterions (ion pairing, dissociation, etc.). None of these limitations exist, of course, in the gas phase. For example in mass spectrometric and related studies, free ions (including H^+) and their reactions can be readily investigated. The differences between gaseous molecule–ion reactions and condensed-state chemistry are well recognized. The present discussion will primarily emphasize the behavior of electrophiles in the condensed state, and the ways they can be activated. Only occasional comparison with gas-phase behavior of electron-deficient ions will be made. This will be the case particularly when considering the results of theoretical, quantum mechanical calculations, which are increasingly used as a powerful tool in chemistry. These calculations usually still relate only to idealized gas-phase conditions. Whereas such calculations give much insight into the nature of reactive electrophilic intermediates and their reactions, by necessity they neglect ion–pair interactions, clustering, solvation, etc., although recently efforts have been made to include solvent effects (for example, in Pople's GAUSSIAN 92 program).

An impressive and ever expanding number of new gas-phase techniques, including mass spectrometric methods under relatively high pressure,[11] allows experimental study of interactions between ions and neutral molecules that include some association (clustering). Ion–molecule equilibria that were studied in the gas phase include those of $H_3O^+(H_2O)_n$ and $CH_5^+(CH_4)_n$, in which twenty or more neutral molecules

[*] In protosolvation the interaction between the heteroatom and the second proton is not as strong as in protonation, but is sufficient to form a superelectrophile.

Georg Olah was born in 1927 and educated in Budapest, Hungary. He moved in 1957 first to Canada and then to the USA with the Dow Chemical Company. Since 1977 he has been Director of the Loker Hydrocarbon Research Institute and Distinguished Professor of Organic Chemistry at the University of Southern California, Los Angeles. He is a member of the US National Academy of Sciences, a Foreign Member of the Italian Academia dei Lincei, and an Honorary Member of the Hungarian Academy of Sciences. He received Honorary Doctorates from the University of Durham (England), the University of Munich, and his alma mater, the Technical University of Budapest. He is the recipient of many awards including the American Chemical Society Awards in Petroleum Chemistry, Creative Work in Synthetic Organic Chemistry, and the Roger Adams Award. His research interests are in the area of synthetic and mechanistic organic chemistry, reactive intermediates (carbocations), superacids, and hydrocarbon chemistry. He has published close to 1000 scientific papers, holds 100 patents, and authored or co-authored 15 monographs.

associate with the ionic center. In a way these conditions are similar to solvation, though, of course, the number of associated molecules is very limited.

Acid–base interactions are at the heart of our understanding of chemistry. The concept of acidity and basicity and its broader application in electrophile–nucleophile interactions represents the core of what is considered heterolytic (ionic) chemistry. These concepts are too well known to be repeated here. It should be pointed out, however, that for too long the assumed fundamental differences between gas-phase and condensed-state chemistry hindered our understanding of the underlying general concepts and their logical application to develop new insights into related chemistry.

The concepts of acidity were originally developed in solution chemistry and are primarily still related to aqueous systems. "Strong" mineral acids are H_2SO_4, HCl, HNO_3, etc. These acids span only a relatively limited range of acidities. It has generally been assumed that gas-phase studies on the "free" proton and its reactions has little to offer to our understanding of condensed-phase chemistry.

Since the early sixties the development of superacids opened up new vistas in condensed-state chemistry and helped to narrow, but not to eliminate, the gap between gas-phase and condensed-state chemistry.[6]

Superacids were arbitrarily defined as acids stronger than 100% sulfuric acid (in case of Brønsted acids, by Gillespie[6b]) or $AlCl_3$ (in case of Lewis acids, by us[6a]). The logarithmic Hammett acidity (H_0) scale was extended from -12 for 100% H_2SO_4, to -25 in the case of some "magic acids" (fluoroantimonic or related acid systems). As in the condensed state the proton is always solvated; in a superacid system based, for instance, on HF, HSO_3F, etc. protonated cations (in the examples, H_2F^+ and $H_2SO_3F^+$) are present in conjunction with their counterions. Indeed significant differences (including steric and chemical) were observed for different protocations under nonexchanging conditions. In superacidic systems, the anions are generally associated through fluorine bridges to form oligomeric anions. This helps to delocalize the negative charge and thus to enhance the proton donor ability of the systems. This also takes place in solid, polymeric superacids, such as Nafion-H.

Superacids and their electrophilic chemistry was comprehensively reviewed,[6] and readers are referred to these reviews.

Protonation (protosolvation) or the related Lewis acid complexation (alkylation) of electrophiles capable of undergoing further interaction results in doubly electron-deficient, dicationic superelectrophiles that are substantially different from the large spectrum of dications formed by conventional depletion of electrons from neutral molecules (or atoms).

Carbodications are of increasing significance both in solution and in gas-phase chemistry. Their structural properties have been addressed in recent reviews.[12, 13] These reviews focus on organic dications that are observable under superacidic, stable-ion conditions or detectable in the gas phase by charge-stripping mass spectrometry. They also illustrate that the rigorous bonding topology that applies to carbodications is quite different from the building-block methodology that is used for neutral molecules.[14]

Besides protonation/alkylation of nonbonded electron pairs of onium ions, carboxonium ions, and the like (see later sections) it is also possible to form geminal onium dications (**1**) by protonating/alkylating covalent bonds in these ions or in certain carbocations. Typcial examples include diprotonated methane,[15] and diprotonated hetero-substituted methanes (**2**).[16]

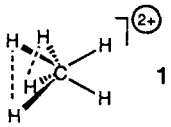

1

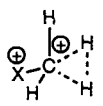

2, X=NH_3, OH_2, HN_2 etc.

The former has two three-center two-electron (3c–2e) bonds to attach the six hydrogens to the carbon atom of methane. The latter includes the protonation of a nonbonded electron pair on the heteroatom as well as a 3c–2e bond.

To appreciate the viability of doubly charged species it is instructive to recall that as far back as 1933 Pauling predicted kinetic stability for the dicationic dimer of helium.[17a] He_2^{2+} is isoelectronic with the hydrogen molecule. Coulomb explosion studies and theoretical calculations support this prediction.[17b] A activation barrier of 33.2 kcal mol^{-1} has been calculated for its exothermic (by 200 kcal mol^{-1}) dissociation. Possibly even more impressive is that the He^+–He^+ bond distance of 0.741 Å is 0.037 Å shorter than the H–H bond in hydrogen. This establishes that the bonding interaction in the dication is strong enough to counter the substantial electrostatic charge–charge repulsion.

2. Oxonium Dications

To assess the scope of electrophilic or protolytic activation we first address the extent to which further alkylation or protonation of heteroatoms in onium ions is possible. In these cases the heteroatom's nonbonded electron pairs bind the proton (as in the protonation of ammonia). The question then arises whether heteroatoms with several lone pairs can undergo second protonation despite strong charge–charge repulsion.

2.1. Alkyloxonium Dications

Alkyloxonium ions are formally derived from the parent hydronium ion H_3O^+ by substituting one, two, or all three hydrogen atoms with alkyl groups (i.e., ROH_2^+, R_2OH^+, R_3O^+). These are referred to as primary, secondary, or tertiary oxonium ions; those containing hydrogen atoms are termed acidic oxonium ions.

Alkyl cations observed as long-lived stable species in superacidic media[18] are extremely powerful alkylating agents. Alkyloxonium ions are significantly stabilized by alkyl substituents.[14] Meerwein salts, such as the trimethyl and triethyl oxonium ions R_3O^+ with various counterions such as SbF_6^-, BF_4^-, $SbCl_6^-$ and PF_6^-, are excellent alkylating agents for nucleophiles containing heteroatoms but are not capable of C-alkylating aromatic or aliphatic compounds. In conjunction with strong protic acids, such as FSO_3H, CF_3SO_3H, or FSO_3H:SbF_5 (Magic Acid), however, they were found to alkylate aromatics readily. For example, ben-

zene and toluene have been methylated and ethylated with trimethyl- and triethyloxonium salts in the presence of Magic Acid.[19] The methylation of toluene gave an isomer distribution (60% *ortho*-, 11% *meta*-, and 21% *para*-xylene) typical of an aromatic substitution reaction with a reactive electrophilic reagent. The protolytic activation of trialkyloxonium ions points to a protonation (protosolvation) of the nonbonded electron pair of the oxygen atom, which enhances the electrophilicity of the alkyl groups (see Scheme 1). Lewis acid complexation has a similar effect.

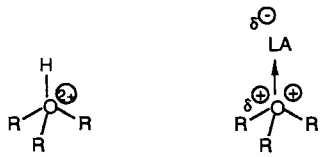

Scheme 1. Activation of oxonium ions by protonation or by Lewis acids (LA).

Theoretical calculations were carried out to determine the energies of water, methanol, dimethyl ether, and the trimethyloxonium ions, as well as of their mono- and diprotonated forms and the related proton affinities (see Table 1).[20a]

The diprotonated acidic methyloxonium ions $MeOH_3^{2+}$ and $Me_2OH_2^{2+}$ are thermodynamically unstable and dissociate to the monoprotonated ions and a proton, but the kinetic barriers to deprotonation are significant. In the case of H_4O^{2+} this amounts to about 39 kcal mol^{-1}. These data relate to isolated molecules in the gas phase; in superacidic solutions clustering of the dipositive ions with their precursors could aid the stabilization by greatly facilitating delocalization of excess charge.

The optimized structures for mono- and diprotonated (methylated) oxonium ions for all species for which potential energy minima were found (intermediates) are depicted in Scheme 2.

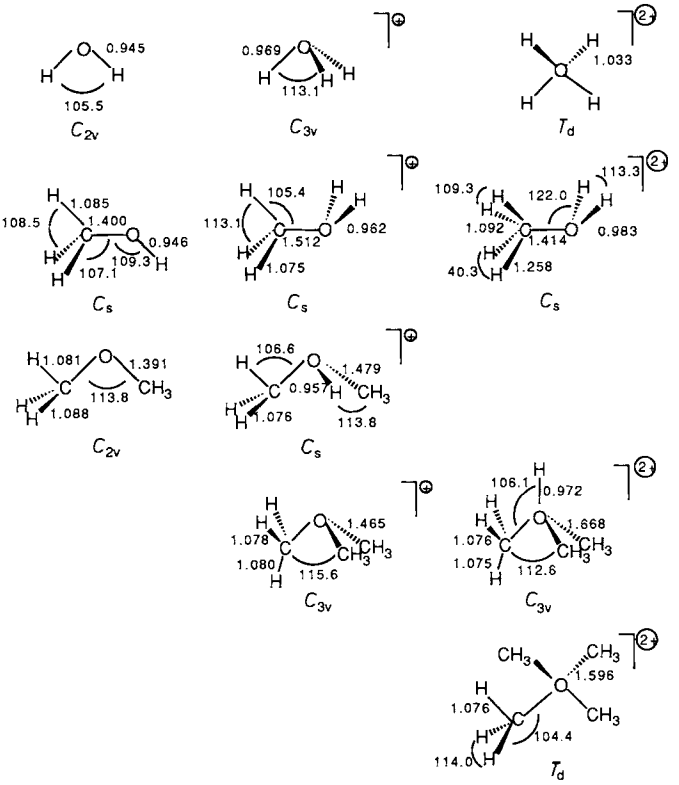

Scheme 2. HF/6-31G* optimized structures of H_2O, MeOH, Me_2O, and Me_3O^+, as well as of the most stable isomers of their mono- and diprotonated or methylated derivatives (bond lengths in Å, angles in degrees).

Table 1. Absolute energies E [Hartree] [a] with zero-point energies [kcal mol^{-1}] [20b] in parentheses [b], proton affinities PA [kcal mol^{-1}] [a] in the gas phase [20c, d], and enthalpies from isodesmic equations [kcal mol^{-1}] [20e] [a] (determined with the G2 method) for the protonatable and protonated molecules and ions discussed in this review.

Base B	E_B	E_{BH^+}	$E_{BH^{2+}}$	1st PA		2nd PA	calcd	
				calcd	exp.	calcd	ΔH_1^{iso}	ΔH_2^{iso}
H_2O	−76.19596 (12.9)	−76.47382 (20.6)	−76.38558 (25.7)	168.1	166.5	−58.9	0.0	0.0
	[−76.33205] [c]	[−76.59193] [c]	[−76.49330] [c]	(164.6) [c]		(−60.4) [c]		
MeOH	−115.34495 (31.0)	−115.64418 (38.5)	−115.59182 (41.7)	181.8	181.9	−34.6	−13.4	−22.5
Me_2O	−154.50207 (48.3)	−154.81314 (55.7)	−154.84654 (64.3) [d]	189.3	192.1	9.5 [d]	−20.8	−67.8 [d]
			−154.82683 (59.9) [d]					
Me_3O^+	−193.98172 (73.0)	−194.02561 (72.9)	–	29.1	–	–	–	−82.9
HCHO	−114.16527 (16.3)	−114.44283 (24.6)	−114.40516 (30.1)	167.4	171.7	−27.7	0.0	0.0
CH_3CHO	−153.34284 (33.5)	−153.64287 (41.3)	−153.64380 (46.0)	182.0	186.6	−2.6	−14.1	−24.2
$(CH_3)_2CO$	−192.52161 (50.4)	−192.83541 (57.8)	−192.86592 (62.3)	191.0	196.7	15.8	−22.7	−42.8
HCOOH	−189.23823 (20.8)	−189.52656 (28.3)	−189.53034 (33.6)	174.9	178.8	−1.5	−6.8	−26.0
CH_3COOH	−228.41544 (37.5)	−228.72008 (44.7)	−228.74990 (49.8)	185.4	190.2	15.1	−17.0	−42.3
CO	−113.01803 (3.1)	−113.25354 (10.2)	−113.13663 (14.2)	142.2	141.9	−75.9	26.4	49.0
	[−113.17749] [c]	[−113.39965] [c]	[−113.34039] [c]		(140.9) [c]		(−69.3) [c]	
H_2CO_3	−264.29462 (19.9)	−264.59336 (31.4)	−264.61027 (36.3)	185.4	190.2	15.1	−17.0	−42.3
CO_2	−188.10220 (7.1)	−188.30729 (12.9)	−188.24468 (16.5)	177.4	–	7.2	−13.3	−34.3
H_2S	−398.78821 (9.2)	−399.06253 (16.3)	−399.01724 (21.4)	166.5	170.2	−32.0	0.0	0.0
	[−398.93073] [c]	[−399.19796] [c]	[−399.15060] [c]	(169.2) [c]		(−28.2) [c]		
MeSH	−437.95235 (27.8)	−438.24988 (34.4)	−438.23706 (38.8) [d]	181.6	187.4	−18.4 [d]	−14.6	−10.4 [d]
	−438.26575 (36.9) [d]							
Me_2S	−477.12066 (45.7)	−477.43700 (52.1)	−477.49478 (61.2) [d]	193.6	200.6	19.4 [d]	−26.4	−51.5 [d]
	−477.45799 (56.0) [d]							
Me_3S^+	−516.62408 (69.4)	−516.69001 (74.4)	–	37.9	–	–	–	−69.8

[a] Calculation on the MP2/6-31G*//HF/6-31G* level. [b] Calculation on the HF/6-31G* level. [c] These values are from Gaussian-2 (G2) calculations. [d] Calculations on the MP2/6-31G*//MP2/6-31G* level.

Acid-catalyzed alkylation of aromatics with alcohols is widely used. Whereas tertiary (and secondary) alcohols react with relative ease by a carbocationic mechanism, alkylation with primary alcohols is generally achieved only in case of more reactive aromatics, and even then under forcing conditions.

Monoprotonation of methanol under superacidic, stable-ion conditions gives the methyloxonium ion as a stable, well-defined oxonium ion [Eq. (1)].

(1)

The methyloxonium ion reacts with nucleophiles by proton transfer or displacement analogous to nucleophilic S_N2 substitutions to yield methylated products. It is significant that in superacidic media, or with solid superacids, methylation of aromatics is greatly facilitated.[21] This might reflect activation through further protonation (protosolvation) of the nonbonded electron pair of the oxygen atom, as shown in Equation (2). Alternatively, methanol, which readily undergoes intermolecular dehydration under acidic conditions to give dimethyl ether, then forms dimethyloxonium ion $(CH_3)_2OH^+$ and, on further protonation, a superelectrophilic methylating agent [Eq. (3)].

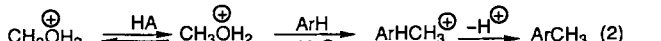

(2)

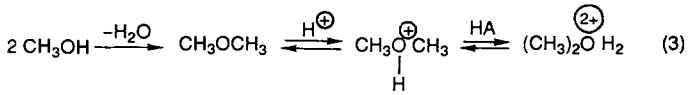

(3)

The methyloxonium ion $MeOH_2^+$ in superacidic media also readily undergoes ionic hydrogenation to give methane.[22] As cleavage to the methyl cation (CH_3^+) is improbable for energetic reasons, the reaction is best interpreted as proceeding through a superelectrophilic protonated methyloxonium dication (Scheme 3).

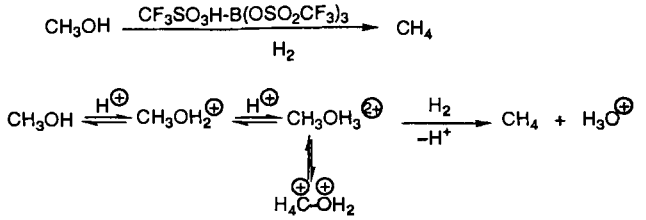

Scheme 3. Ionic reduction of methanol to yield methane in superacids and a plausible pathway for this reaction.

As shown by the theoretical calculations, diprotonation of methanol in the gas phase gives preferentially the O,C-protonated dication $^+CH_4OH_2^+$. In solution, however, contribution from the O,O-protonated form is possible [Eq. (4)].

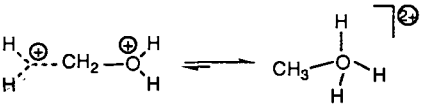

(4)

When methanol (or dimethyl ether) reacts with superacids (either HF–SbF_5, FSO_3H–SbF_5 or TaF_5, NbF_5, etc.) under forcing conditions (100–300 °C), self-condensation occurs. When reacting methanol (or trimethyl phosphate) with phosphorus pentoxide or polyphosphoric acid, at 190 °C, Pearson detected C_3–C_9 alkanes as well as toluene and C_8–C_{10} aromatics.[23] He suggested electrophilic methylation of methanol, but this is expected only on oxygen and would give dimethyl ether. In superacids methanol is completely protonated; there is no evidence for any deprotonation equilibrium. It is possible that under these conditions it is the methyloxonium ion $CH_3OH_2^+$ which undergoes methylation at a C-H bond (Scheme 4). The active methylating agent is considered to be a superelectrophilic methylating agent formed in the system.

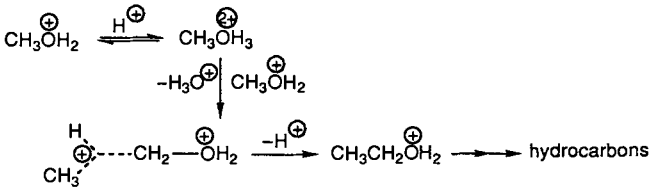

Scheme 4. Probable mechanism for the self-condensation of methanol in superacids.

Once the first C–C coupling is achieved, protonated ethanol will readily yield the observed hydrocarbon products (by further alkylation or through dehydration to ethylene, which is known to react further by acid-catalyzed electrophilic chemistry). Dimethyl ether can react in a similar way to methanol (Scheme 5).

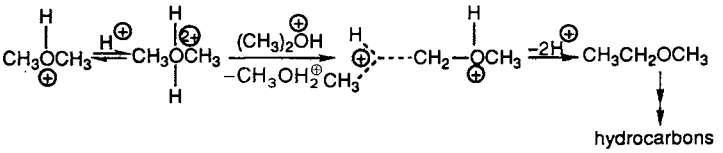

Scheme 5. Mechanism for the self-condensation of dimethyl ether in superacids.

Similar activation is possible in the carbonylation of dimethyl ether (or methanol) to methyl acetate [Eq. (5)] in superacidic (HF–BF_3) solution.[24] The methyloxonium ion does not normally react with CO, unless activated by superacids to yield a superelectrophilic dication.

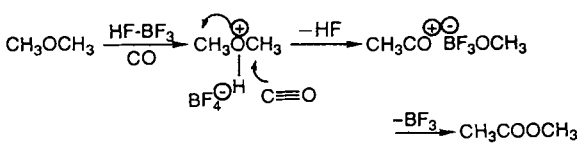

(5)

2.2. Protohydronium Dication (Diprotonated Water)

In understanding the chemistry of protonated (protosolvated) alkyloxonium ions, the parent tetrahydridooxonium dication H_4O^{2+} (protohydronium dication, diprotonated water) is of fundamental significance.

The existence of protonated water, H_3O^+ (hydronium ion), was first postulated in 1907.[25] Its preeminent role in acid-catalyzed reactions in aqueous media was first realized in the acid–base theory of Brønsted and Lowry.[26] Direct evidence for the hydronium ion in solution and in the solid state came mainly from IR,[27] Raman,[28] and neutron diffraction studies.[29] The gaseous ion was observed in mass spectrometric studies.[30] In superacid solution the hydronium ion was shown to be extremely stable by ^1H and ^{17}O NMR spectroscopy.[6, 31–33] In fact, Christe has isolated hydronium ion salts with a variety of counterions such as SbF_6^-, AsF_6^-, and BF_4^-.[34] All of the available experimental and high-level ab initio theoretical data support a tetrahedral geometry for the hydronium ion (Scheme 6).[33, 35, 36]

Scheme 6. Structures of H_3O^+ and H_4O^{2+}.

Gold et al. prepared long-lived isotopic hydronium ions such as H_3O^+, H_2DO^+, and HD_2O^+ in HSO_3F:SbF_5–D_2O/SO_2ClF solutions and characterized them by ^1H and ^2H NMR spectroscopy without exchange.[31a, c]

Subsequently, we demonstrated that in even stronger superacidic media (HF/DF–SbF_5 with increasing amounts of SbF_5) hydrogen/deuterium exchange of isotopic hydronium ions including $D_2H^{17}O^+$ and $DH_2^{17}O^+$ with superacids can be monitored by ^{17}O NMR spectroscopy.[37a] The acidity of the FSO_3H–SbF_5 (1:1) system (H_0) is about -21, whereas H_0 for the 1:1 mixture of HF and SbF_5 is estimated at -25. Two mechanisms are possible for the observed H/D exchange (Scheme 7): a) deprotonation–protonation equilibria involving the neutral molecules and the monocations or b) protonation–deprotonation equilibria involving monocations exchanging H and D through OH_4^{2+} dications. Because H/D exchange occurs only at the highest acidities (i.e., with HF/DF–SbF_5 but not with HSO_3F/DSO_3F–SbF_5) and no deprotonation to form water is feasible in these systems, the results suggest that isotopic exchange takes place via isotopomeric H_4O^{2+}. Under extremely strongly acidic conditions the remaining nonbonded electron pair of the oxygen atom of H_3O^+ apparently also undergoes a protolytic interaction.

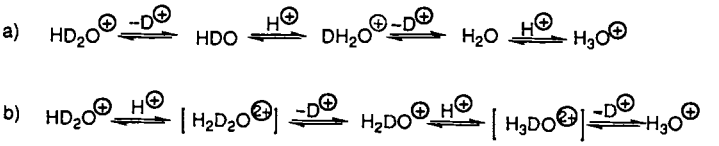

Scheme 7. Two possible mechanisms for H/D exchange for water in superacids.

To evaluate the structure and stability of the H_4O^{2+} dication, ab initio calculations have been carried out.[37] The H_4O^{2+} dication is isoelectronic with H_4N^+, CH_4, and BH_4^-, all known to have tetrahedral geometries. At the HF/6-31G* level, the structure with T_d symmetry corresponds to an energy minimum but not the planar D_{4h} form (Table 2). Apparently the double positive charge can be adequately accommodated in the tetrahedral structure to prevent spontaneous fragmentation. It should be recalled that in H_3O^+ the oxygen is negatively charged, the positive charge being essentially on the hydrogen atoms.

Thermodynamically H_4O^{2+} is unstable towards deprotonation to H_3O^+ by 59.8 kcal mol^{-1} (HF/6-31G*) (see Table 2), although it has significant kinetic stability (deprotonation barrier 39.4 kcal mol^{-1}). These energies remain nearly the same when valence electron correlation interactions are included in the calculation: the deprotonation energy for H_4O^{2+} becomes -52.9 kcal mol^{-1}, the activation barrier 43.9 kcal mol^{-1} (MP4SDTQ/6-31G**//HF/6-31G*). The planar H_4O^{2+} structure is 94.6 kcal mol^{-1} less stable than the tetrahedral. The heat of formation of H_4O^{2+} is estimated as 557 kcal mol^{-1} from $\Delta H_f^0(H_3O^+) =$ 139 kcal mol^{-1} and $\Delta H_f^0(H^+) = 365.2$ kcal mol^{-1}, the calculated heat of deprotonation.

More recently calculations[20a] using the GAUSSIAN-2 method made the deprotonation favorable by -61.9 kcal mol^{-1} and lowered the activation energy slightly to 38.2 kcal mol^{-1}. The proton affinity calculated for 298 K at the same level is 60.4 kcal mol^{-1}. These data support the previous studies and conclusions reached for an associative mechanism of the H/D exchange of H_3O^+ in superacidic media.

Although the activation energy for the deprotonation of H_4O^{2+} is substantial, it may be affected by tunneling. Within a range of 5 kcal mol^{-1} below the classical barrier (considered to be the maximum deprotonation barrier of H_4O^{2+},

Table 2. Absolute energies [Hartree] and relative energies [kcal mol^{-1}] in parentheses for H_4O^{2+} and H_3O^+ calculated on different levels of theory.

	Symmetry		3-21G// 3-21G	6-31G*// 6-31G*	Based on 6-31G*-geometry HF/6-31G**	MP2/6-31G**	MP3/6-31G**	MP4SDTQ/6-31G**
H_4O^{2+}	T_d	energy minimum	−75.80958 (0.0)	−76.19498 (0.0)	−76.22033 (0.0)	−76.42139 (0.0)	−76.42910 (0.0)	−76.43474 (0.0)
$H_3O^+\cdots H^+$	transition state for proton loss		−75.73475 (47.0)	−76.13220 (39.4)	−76.15110 (43.4)	−76.35243 (43.4)	−76.35841 (44.4)	−76.36474 (43.9)
H_4O^{2+}	D_{4h}	planar	−75.67607 (83.8)	−76.05481 (88.0)	−76.07569 (90.8)	−76.27164 (93.7)	−76.27911 (94.1)	−76.28400 (94.6)
H_3O^+	C_{3v}	(at higher level)	−75.89123 (−51.2)	−76.28934 (−59.2)	−76.31005 (−56.3)	−76.50583 (−53.0)	−76.51394 (53.2)	−76.51902 (−52.9)

namely the "bare" Born-Oppenheimer barrier + zero-point energy for the transition state), the reaction rate was calculated to change sharply from 10^9 to 10^3. Similarly, the calculated H/D isotope effect (through a dissociative mechanism, that is, cleavage into H^+/D^+ and H_3O^+) only becomes substantial directly below the classical threshold. Since, in general, any tunneling effect for the deprotonation is small, it was concluded that the kinetic stability of H_4O^{2+} is indeed significant.

Despite this kinetic stability of H_4O^{2+}, calculations show that the protonation of H_3O^+ is thermodynamically unfavorable; however, it must be recognized that the calculational data referred to dilute gas-phase conditions and thus do not fully relate to condensed-state conditions. Solvation or clustering effects may have a major influence. In particular in small dications, solvation tends to diminish the effect of charge-charge repulsion, and thus could bring H_4O^{2+} into a thermodynamically more accessible region. Superacid solutions of H_3O^+ could be highly structured. Thus, the H_4O^{2+} protons might be shared by more than one H_3O^+ in a dynamic fashion (Scheme 8).

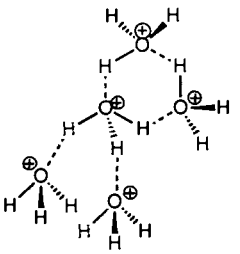

Scheme 8. Possible stabilization of H_4O^{2+} by H_3O^+ ions in superacids.

3. Carboxonium Dications (Diprotonated/Alkylated Carbonyl Compounds)

Carboxonium ions were first studied by Meerwein. They are highly stabilized compared to alkyl cations.[17] Their behavior reflects both their oxonium and carbenium ion nature, though the former predominates (Scheme 9). This de-

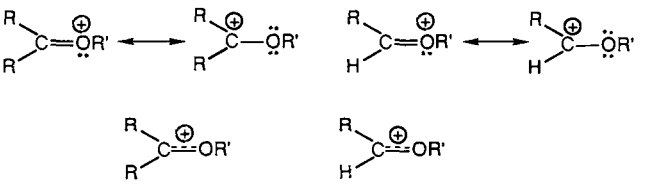

Scheme 9. Top: Resonance structures of protonated/alkylated ketones and aldehydes. Bottom: Formulation as delocalized carbenium ions. R' = H, alkyl, aryl.

piction of delocalized carboxonium ions is fully warranted by their physical (spectroscopic) properties and chemical behavior. Carboxonium ions, according to Perst's classification,[14a,b] can be acidic or neutral and regarded as carbenium ions in which the carbocationic center bears hydroxy or alkoxy (aryloxy) substituents (Scheme 9). Depending on the number of oxygen atoms attached to the carbocationic center the carboxonium ions are primary, secondary, and tertiary (Scheme 10).

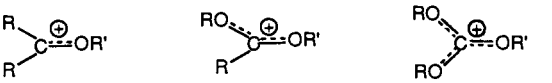

Scheme 10. Primary, secondary, and tertiary carboxonium ions. R' = H, alkyl.

Carboxonium ions are ambident electrophiles and can react either by transferring the ligand attached to oxygen (H, alkyl, or aryl group) to a nucleophile Y^- or by addition of the nucleophile to the carbocationic center (Scheme 11).

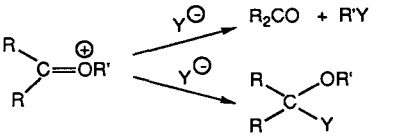

Scheme 11. Carboxonium ions as ambident electrophiles.

The carbocationic nature of carboxonium ions is limited by strong delocalization resulting from contributions of the oxonium forms. This restricts the reactions at the carbocationic center to those with efficient nucleophiles.

Acidic carboxonium ions tend to be efficient proton transfer agents. Nucleophilic attack at the carbocationic center has been observed only rarely (see below), and results primarily in rearrangement reactions in strong acid solutions. However, the carbocationic reactivity of carboxonium ions can greatly be enhanced by their protosolvation (protonation) in superacidic solutions.

Trivalent carbocations (carbenium ions) have long been recognized as efficient hydride abstractors that generate, for example, related carbocations from tertiary isoalkanes [Eq. (6)]. In contrast, carboxonium ions, being weaker electrophiles, show no hydride abstracting ability with isoalkanes when they react in aprotic solvents (SO_2 or SO_2ClF).

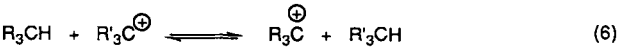

(6)

Brouwer and Kiffen,[38] however, observed that both protonated acetaldehyde and acetone readily reacted in 9:1 mixtures of HF and SbF_5 or HF and BF_3 with isobutane to give the *tert*-butyl cation. (The proposed reaction mechanisms are shown in Scheme 12).

Brouwer and Kiffin stated that "The hydride transfer from an alkane molecule to a hydroxycarbonium ion to form an alkylcarbenium ion and an alcohol molecule is thermodynamically a very unfavorable reaction. The equilibrium of this reaction as such would lie completely to the side of the starting compounds. It is the high degree of the protonation of the alcohol that renders the hydride transfer thermodynamically possible."

It is now apparent, based on the low carbocationic reactivity of the methylcarboxonium ($CH_3CH{=}\overset{+}{=}OH$) and dimethylcarboxonium ($(CH_3)_2C{=}\overset{+}{=}OH$) ions and thermodynamic considerations, that the observed hydride transfer re-

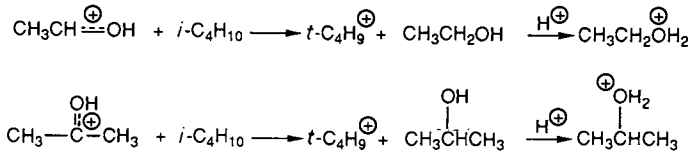

Scheme 12. Initially proposed mechanism for the hydride abstraction from isobutane by acetaldehyde or acetone in superacids.

actions in solutions containing an excess of superacid were indeed induced by superelectrophilic diprotonated acetaldehyde or acetone, respectively, and not by the monoprotonated species (Scheme 13).

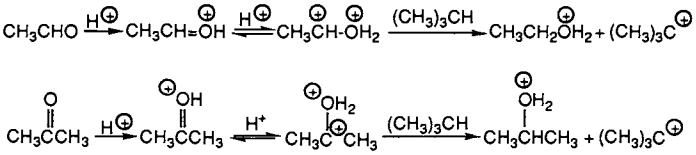

Scheme 13. More likely mechanism for the hydride abstraction of Scheme 12, involving dications.

The reactions with diprotonated superelectrophiles are thermodynamically favored, and protonated alcohols are formed directly in the hydride transfer reaction (not by subsequent protonation of neutral alcohols). The diprotonated carbonyl compounds act as extremely reactive superelectrophiles.

Protonated formaldehyde reacts similarly [Eq. (7)]. We observed[39] that when monomeric formaldehyde was treated with a 3:1 mixture of HF and SbF_5 or HSO_3F and SbF_5 (containing some HF) in SO_2ClF solution at -78 to $-40\,^{\circ}C$, protonated fluoromethanol $FCH_2OH_2^+$ was obtained. It was suggested at the time that the reaction proceed-

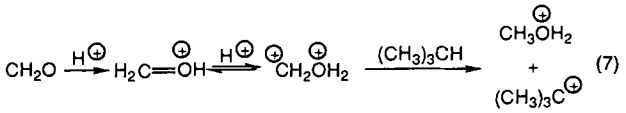

(7)

ed with formation of fluoromethanol, which was subsequently protonated [Eq. (8)]. Analogously, the reaction with HCl gave protonated chloromethanol $ClCH_2OH_2^+$.[40]

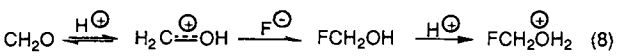

(8)

It now seems possible that the process involves the more reactive superelectrophilic diprotonated (protosolvated) formaldehyde on reaction with F^- at the carbon, which has greatly enhanced carbocationic properties. This would give the stable protonated fluoromethanol directly. Furthermore, formaldehyde is readily reduced to the methyloxonium ion (and subsequently to methane) under ionic hydrogenation conditions even at room temperature,[22] while monoprotonated formaldehyde is considered to have too weak a carbocationic nature to be able to account for the reactions (Scheme 14).

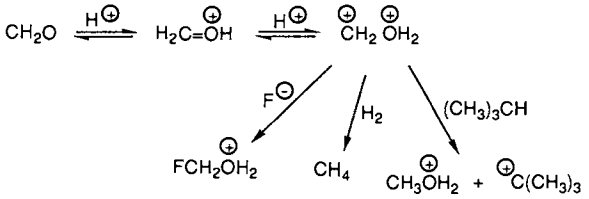

Scheme 14. Reactions with formaldehyde in superacidic media.

The diprotonation of the carbonyl compounds, formaldehyde, acetaldehyde, and acetone, was also studied by MO theoretical calculations (see Table 1).[20] Diprotonation is increasingly favored along the series from formaldehyde through acetaldehyde to acetone. The optimized structures of the neutral and mono- and diprotonated species are shown in Scheme 15.

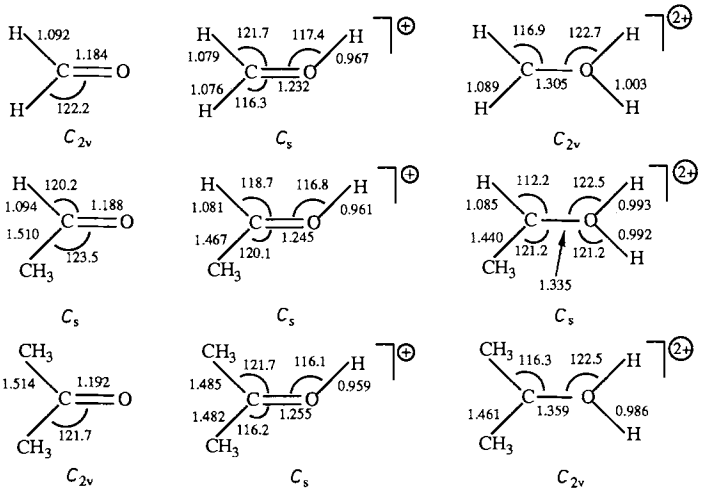

Scheme 15. Optimized structures (HF/6-31G*) of neutral and mono- and diprotonated formaldehyde, acetaldehyde, and acetone.

Krivdin, Facelli, et al.[41] recently also carried out a theoretical study of the protonation of acetone and calculated NMR chemical shifts and coupling constants for the mono- and diprotonated species. Experimentally no diprotonated acetone could be observed (by NMR). This is, however, not unexpected, as its equilibrium concentration should be very low and fast exchange with the monoprotonated form difficult to freeze out.

4. Protonated (Lewis Acid Complexed) Acyl Dications

Acyl cations are relatively weak electrophiles. This is easily understood, since their structure is predominantly that of a linear carboxonium ion (Scheme 16).[42] In their reactions with suitable nucleophiles, such as π-arenes or heteroatom donor nucleophiles, the readily polarizable linear acylium ions undergo displacement of a π-electron pair to oxygen,

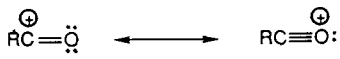

Scheme 16. Resonance structures of acyl cations. The predominant structure is on the right.

bending the ion. The empty p orbital that develops as a result on the carbocationic center enables the reaction to proceed. As example, the acetylation of benzene is depicted in Scheme 17.

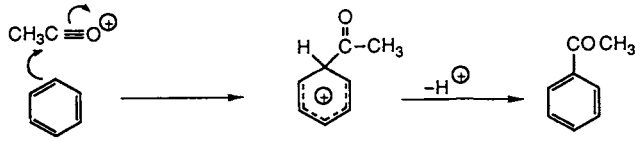

Scheme 17. Acetylation of benzene as an example of the nucleophilic attack of an acyl cation on an arene.

The lack of reactivity of acyl cations such as the acetyl cation with deactivated arenes or weakly electron-donating, saturated hydrocarbons is therefore not unexpected. However, under strongly acidic conditions such reactions including superelectrophilic activation of the acetyl cation are greatly enhanced. For instance, Friedel–Crafts type acetylation of benzene and chlorobenzene with acetyl hexafluoroantimonate ($CH_3CO^+SbF_6^-$) is enhanced when using superacidic CF_3SO_3H as solvent instead of the relatively weak CF_3CO_2H. Shudo[43] found that short reaction times (15–30 min) gave high (78–81%) yields in CF_3SO_3H, whereas even 10 to 50 times longer reaction times gave only less than 1–8% yield in CF_3CO_2H.

Brouwer and Kiffen[44a] have reported the hydride transfer from isobutane to the acetyl cation generated from acetic acid in excess HF–BF_3. We,[44b] on the other hand, showed that such a reaction does not occur with isolated acetylium salts in aprotic solvents such as SO_2, SO_2ClF, AsF_3, and CH_2Cl_2. Further, the hydride abstraction from isobutane by the acetyl cation is endothermic by 8.5 kcal mol^{-1} (in the gas phase). In all probability, therefore, the reaction proceeds by protonation (protosolvation) of the acetyl cation by the superacidic HF–BF_3 system (Scheme 18).

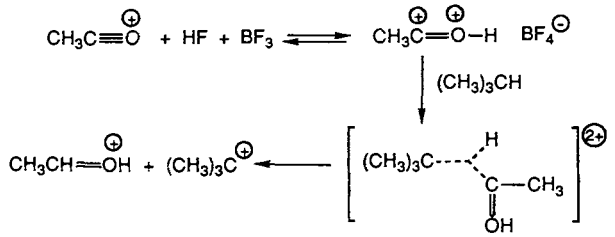

Scheme 18. Probable mechanism of the hydride transfer between CH_3CO^+ and $(CH_3)_3CH$ in HF–BF_3.

The superelectrophilic protoacetyl dication has not been observed by NMR spectroscopy. In the IR spectrum of the acetyl cation in superacids, however, a shift in the carbonyl stretching frequency is observed. Theoretical calculations have shown that the structure CH_3COH^{2+} corresponds to the global minimum. This agrees with charge-stripping mass spectrometric studies in which the $C_2H_4O^{2+}$ dication has been observed.[45] Interestingly, the isomer protonated at the C-H bond, $^+CH_4{-}C^+{=}O$, is only 24.6 kcal mol^{-1} less stable than the O-protonated acetyl cation. The isoelectronic analogue of $C_2H_4O^{2+}$ is diprotonated diazomethane ($CH_4N_2^{2+}$), which has also been studied theoretically.

Apart from Brønsted acid activation, the acetyl cation (and other acyl ions) can also be activated by Lewis acids. While the 1:1 CH_3COX–AlX_3 Friedel–Crafts complex is inactive for the isomerization of alkanes, a complex with a two equivalents of AlX_3 was found by Vol'pin et al.[46,47] to be extremely reactive in the isomerization of saturated hydrocarbons and other electrophilic reactions [Eq. (9)].

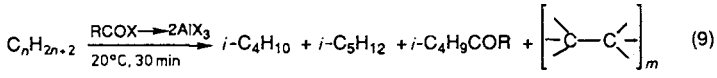

(9)

Vol'pin calls the $CH_3COCl \cdot 2AlCl_3$ complex an aprotic superacid. The results indicate that the acetyl cation is highly activated by further O-complexation with a second molecule of AlX_3 (the equivalent of protonation or protosolvation) (Scheme 19).

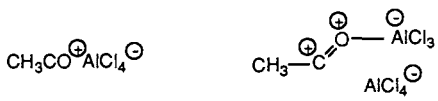

Scheme 19. Left: the Friedel–Crafts complex; right: the aprotic superacid complex.

Alternatively, the ionization of acetyl chloride with excess $AlCl_3$ can involve bidentate interaction (Scheme 20).

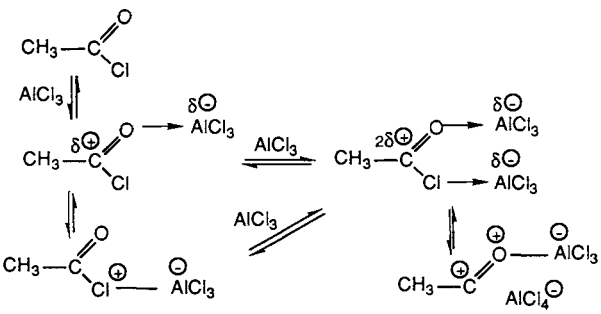

Scheme 20. Activation of acetyl chloride by bidentate coordination to $AlCl_3$.

5. Diprotonated Carboxylic Acids

Acetic acid (and other carboxylic acids) become protonated in superacids to form stable, observable (by NMR) carboxonium ions. Cleavage to related acyl cations is observed by raising the temperature of the solutions. In an excess of the superacid a diprotonation equilibrium can play a role in the ionization process [Eq. (10)].[42]

Protonation of formic acid in superacids leads, after the formation of the parent carboxonium ion at low temperature, to the generation of CO; the formyl cation is not ob-

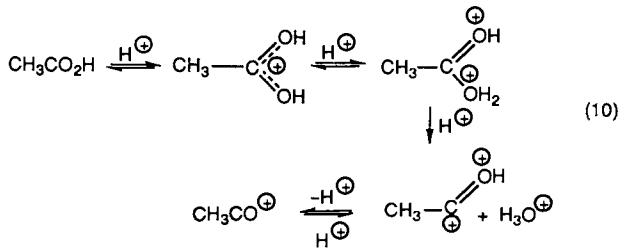

(10)

served by NMR (see Section 7). A diprotonation equilibrium may be again involved [Eq. (11)].

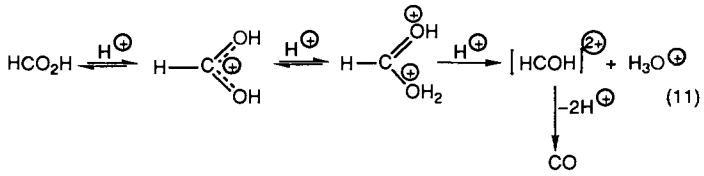

(11)

The protonation and diprotonation of formic and acetic acid was also studied theoretically (see Table 1).[40] In Scheme 21 the optimized structures of neutral and protonated and diprotonated acetic acid are compared.

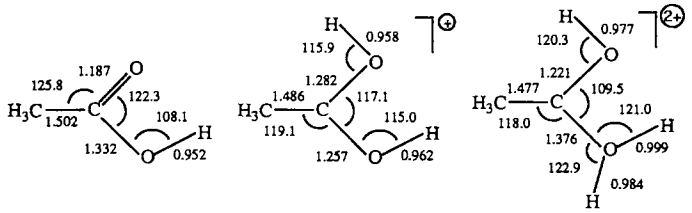

Scheme 21. Calculated structures of neutral and mono- and diprotonated acetic acid that correspond to minima on the potential energy surface.

6. Diprotonated Esters

The acid-catalyzed hydrolysis of esters [Eq. (12)] is assumed to involve an equilibrium between intermediates protonated at the carbonyl and the ether oxygen atom. The

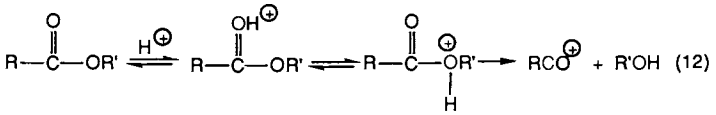

(12)

latter leads to cleavage of the acyl–oxygen bond. When R′ is capable of forming a sufficiently stabilized carbocation, the alkyl–oxygen bond is ruptured [Eq. (13)].

Whereas esters protonated at the carbonyl oxygen atom have been observed and studied under stable-ion conditions,[6] the isomeric acyloxonium ions were proposed to be

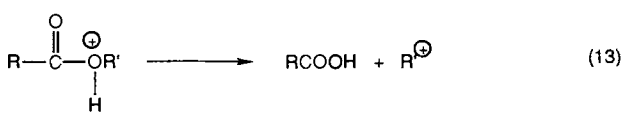

(13)

intermediates, however, without structural (spectroscopic) evidence. In the presence of nucleophiles they were assumed to react rapidly to yield their cleavage products.

In superacidic solution where esters are completely protonated, their protolysis can be considered to involve diprotonation, as shown in case of methyl acetate. In superacids the carbonyl-protonated ester does not show any deprotonation equilibrium, but there can be an equilibrium with the diprotonated form [Eq. (14)]. Similar behavior is indicated in the

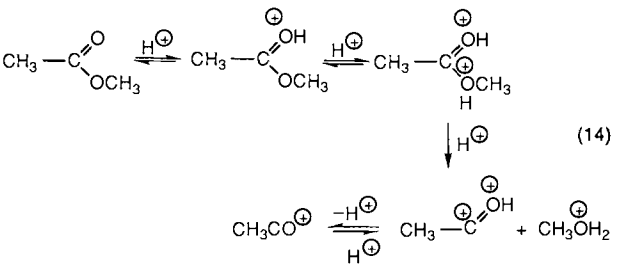

(14)

methylation with the powerful methyl fluoride–antimony pentafluoride complex [Eq. (15)].

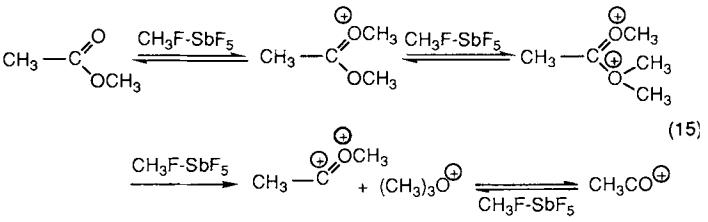

(15)

7. Diprotonated Carbon Monoxide (Protoformyl Dication)

C-Protonation of carbon monoxide leads to the formyl cation (HCO^+). O-Protonation leading to the isoformyl cation (^+COH) is energetically less favored. The formyl and isoformyl cations are stable in the gas phase, and the latter was also detected in interstellar space.[48] Neither ion has been observed in superacidic solutions by NMR where most other acyl cations are stable and readily studied.[42]

The failure to observe the static formyl cation by ^1H NMR in superacid solutions, even at low temperatures, is now recognized to be due to fast intermolecular exchange resulting from a second protonation from the protoformyl dication (diprotonated carbon monoxide).[49] ^{13}C NMR studies do show an exchanging formyl cation system.

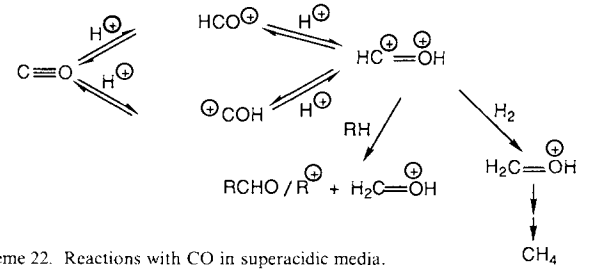

Scheme 22. Reactions with CO in superacidic media.

The existence of diprotonated carbon monoxide can also explain the observed high reactivity of carbon monoxide in superacidic media (Scheme 22). With saturated hydrocarbons both carbonylation and formylation was observed. Adamantane, for example, reacts under pressure of CO to yield 1-adamantane-carboxaldehyde along with the 1-carboxylic acid and 1-alcohol [Eq. (16)].[50] The latter two products are the expected Koch–Haaf products produced through the bridgehead 1-adamantyl cation (formed by hydride abstraction).

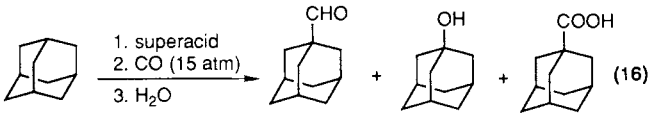

(16)

The yield of 1-adamantanecarboxaldehyde increased from 9.1 to 14.5 to 21% along the series CF_3SO_3H, CF_3SO_3H–$B(OSO_2CF_3)_3$, and CF_3SO_3H–SbF_5. The increase in yield with increasing acidity supports direct formylation of the adamantane C-H bond by the formyl cation or more probably by its more reactive protosolvated dicationic form [Eq. (17), where $E^+ = HCO^+$ or $HCOH^{2+}$]. As with the

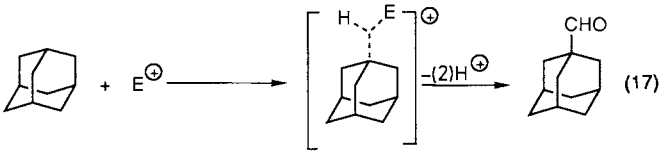

(17)

acetyl cation (see Section 4), the linear formyl monocation itself would not be reactive enough to attack C-H σ bonds. An alternative pathway for the formation of 1-adamantanecarboxaldehyde could be hydride abstraction from excess adamantane by the 1-adamantanoyl cation (or its protosolvated form) formed in the Koch reaction. This was ruled out by labeling studies with 1,3,5,7-tetradeuterioadamantane, which showed no significant deuterium incorporation into the CHO group.[50]

The suggested de facto formylating agent is either the protosolvated formyl cation or the protoformyl dication present in equilibrium in the superacidic system. Protosolvation of the formyl cation can render it highly reactive. In fact in the aromatic formylation[51] of toluene (T) and benzene (B) with CO in the strongly superacidic HF–SbF_5 medium at −95 °C gave a low k_T/k_B rate ratio of 1.6 and increased proportion of *ortho* substitution. On the other hand, with less acidic HF–BF_3 the k_T/k_B ratio at 0 °C was 860; the *para*-substituted product was predominant. In the former case the de facto formylating species must be highly activated[52] because it does not significantly discriminate between toluene and benzene.

The formylation of arenes such as benzene and toluene with HCOF and excess BF_3 showed a substrate selectivity of $k_T/k_B = 36$ and also gave increased *ortho* substitution.[51] Complexation of the formyl cation to a Lewis acid ($H\text{-}\overset{+}{C}{=}O \rightarrow BF_3$) can explain the data. When the formyl cation forms a complex with excess Lewis acid, it is more reactive than the parent cation or the 1:1 HCOF · BF_3 complex, similar to Vol'pin's RCOCl · $2AlCl_3$ systems.[46, 47]

Protonation of carbon monoxide to either the formyl or isoformyl cation is exothermic. The formyl cation was calculated to be more stable than the isoformyl ion by 38 kcal mol^{-1}. The calculated rearrangement barrier of 36 kcal mol^{-1} (MP3/6-31G**)[53, 54] suggests that the isoformyl cation, once formed, should be a relatively long-lived species. There are also significant kinetic barriers to deprotonation (Scheme 23).

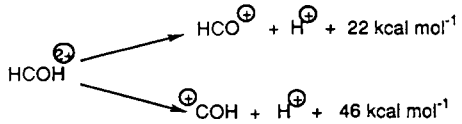

Scheme 23. Reaction energies for the deprotonation of the formyl dication.

Theoretical calculations at the MP2/6-31G*//HF/6-31G* level gave the values shown in Table 1 for the energies for mono- and diprotonated CO and the corresponding proton affinities and isodesmic enthalpies. The optimized structures (calculated at the HF/6-31G* level) are shown in Scheme 24.

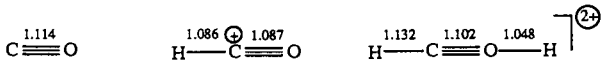

Scheme 24. Optimized structures of neutral and mono- and diprotonated CO, each with $C_{\infty v}$ symmetry.

Theoretical calculations support the kinetic stability of the protoformyl dication,[53] which has also been observed by mass spectrometry.[55] The dication with its very short C–O bond distance of 1.102 Å has a deprotonation barrier of more than 20 kcal mol^{-1}.

8. Protonated and Diprotonated Carbonic Acid and Carbon Dioxide

Carbonic acid has specific importance in nature. The equilibria of carbon dioxide and water [combined in Eq. (18)] and their significance are well recognized. Although carbon-

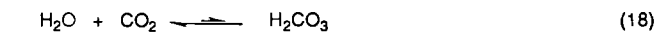

(18)

ates are among the most abundant minerals on earth, carbonic acid is difficult to observe spectroscopically in its free form. Only an NMR spectrum of its ether complex $H_2CO_3 \cdot Et_2O$ has been reported.[56]

Protonated carbonic acid in superacidic media is remarkably stable.[57] It can be obtained by simply dissolving carbonates or hydrogen carbonates in FSO_3H–SbF_5 (or other superacids). The solutions decompose only at around 0 °C to give hydronium ions and carbon dioxide [Eq. (19)]. The SbF_6^- salt of $H_3CO_3^+$ can even be isolated.

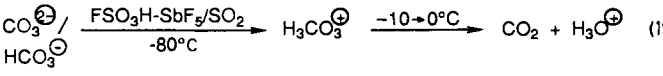

(19)

The close analogy between protonated carbonic acid and the guanidinium ion explains its stability. Both are highly resonance stabilized (Scheme 25).

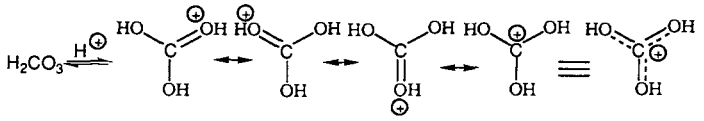

Scheme 25. Resonance structures for protonated carbonic acid.

The guanidinium ion undergoes further protonation in superacid solution, and the dication was observed in such media by NMR spectroscopy. Protonated carbonic acid can also readily undergo a second protonation to $H_4CO_3^{2+}$.[58] Theoretical calculations reveal the similarity between diprotonated guanidine and diprotonated carbonic acid, but due to more rapid proton exchange (Scheme 26), $H_4CO_3^{2+}$ has not yet been observed as a static dication by NMR spectroscopy.

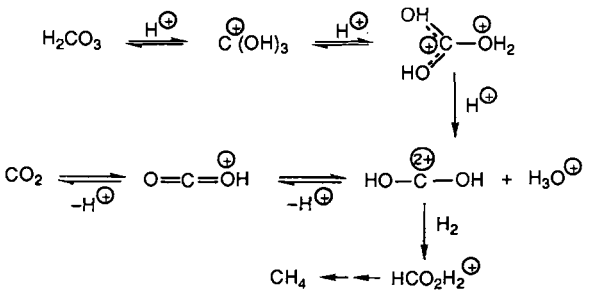

Scheme 26. Equilibria of protonated and diprotonated carbonic acid and their reactions.

The observation that carbonic acid in superacidic media can act as a carboxylating agent[57] under certain circumstances and readily undergoes ionic reduction to methane is significant, as it points to the intermediacy of protonated (diprotonated) carbon dioxide (Scheme 26). The protolytic cleavage of carbonic acid, which leads to carbon dioxide, also implicates protonated and diprotonated CO_2, that is, $O{=}C{=}OH^+$ and $HO{=}C{=}OH^{2+}$, respectively. Koch and Schwarz were the first to study $CO_2H_2^{2+}$ by ab initio molecular studies.[59]

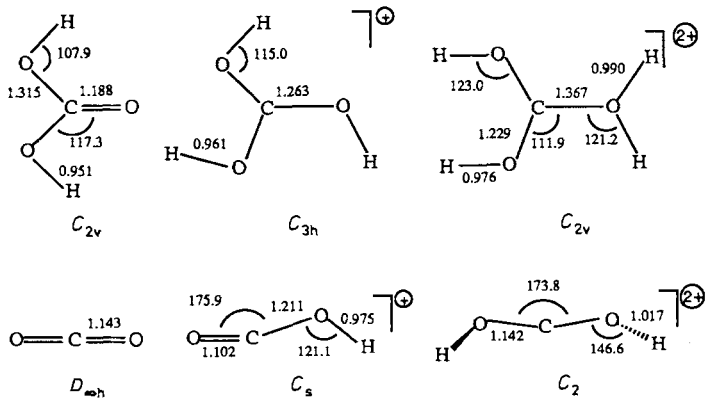

Scheme 27. Optimized structures of carbonic acid and carbon dioxide in neutral and mono- and diprotonated form.

Our calculations of the energies of mono- and diprotonated carbonic acid and carbon dioxide as well as their proton affinities are shown in Table 1. Optimized structures calculated at the HF/6-31G* level are depicted in Scheme 27. Protonation and diprotonation of carbon dioxide bends the molecule somewhat and thus results in the formation of reactive carboxylating agents.

Protonated and diprotonated carbonic acid and carbon dioxide may also have implications in biological carboxylation processes. Although behavior in highly acidic solvent systems cannot be extrapolated to in vivo conditions, related multidentate interactions at enzymatic sites are possible.

The boron analogue of diprotonated carbonic acid is protonated boric acid [Eq. (20)], which Attina, Cacace, and Ricci studied in the gas phase.[60]

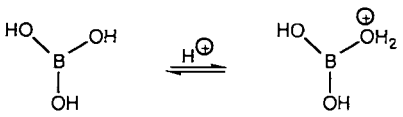

(20)

In solution chemistry the facile reaction of boric acid[61] or trimethyl borate[59] with HF or fluorosulfuric acid containing HF to give boron trifluoride is indicative of a pathway via protonated boric acid (or trimethyl borate). Though boric acid is only a weak Lewis acid, its reactivity toward nucleophiles such as F^- is greatly enhanced by protonation (Scheme 28).

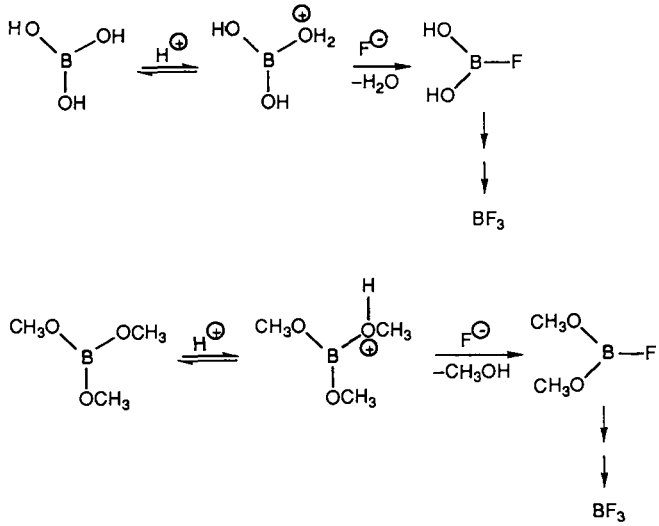

Scheme 28. Enhancement of the nucleophilicity of boric acid and trimethylborate by protonation.

9. Sulfonium, Selenonium, and Telluronium Dications

Similarly to oxonium ions, sulfonium ions also undergo protonation (protosolvation) in superacids to produce sulfur-based superelectrophiles [Eq. (21)]. The parent sulfoni-

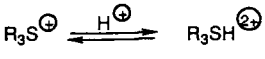

(21)

um ion is the trihydridosulfonium ion (H_3S^+), that is, protonated H_2S. The ion has been characterized in the superacidic medium FSO_3H–SbF_5/SO_2 at low temperature by ^1H NMR spectroscopy.[62] It is also well known in the gas phase and was studied by mass spectrometric techniques. Christe[63] has isolated $H_3S^+SbF_6^-$ as a white crystalline solid at low temperatures. It reacts with water to liberate H_2S. The pyramidal nature of the sulfonium ion **3** was substantiated by vibrational spectroscopy.[63]

3 **4**

Similarly to the hydronium ion,[37] the hydrogen atoms of the sulfonium ion also exchange with deuterium in superacids. The H^+/D^+ exchange of H_3S^+ and its isotopomers has been followed by ^1H NMR spectroscopy.[64] Compared to the FSO_3H/SO_2 system, the H^+/D^+ exchange rate is considerably enhanced in the more acidic 4:1 mixtures of FSO_3H and SbF_5/SO_2 and further enhanced in the even more acidic 1:1 mixtures of FSO_3H and SbF_5/SO_2.

Again, two mechanisms are possible for this hydrogen–deuterium exchange in superacids (Scheme 29): a deprotonation/deuteration equilibrium in which hydrogen sulfide is reprotonated/redeuterated by the acid system and a protonation/deuteration of the isotopomeric sulfonium ions to their dications (for example, **4**) and subsequent dedeuteration/deprotonation.

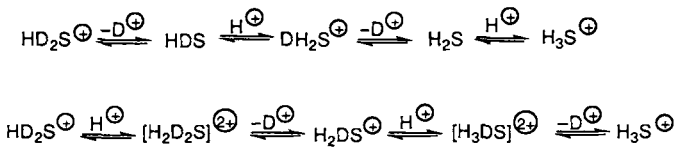

Scheme 29. Possible mechanisms for H/D exchange of H_2S in superacids.

The observed isotopic exchange does not per se permit unequivocal differentiation between the two mechanisms. However, the increased exchange rate observed with increase in the acid strength of the Magic Acid system (from 4:1 to 1:1) supports the mechanism involving H_4S^{2+}. The H_0 value of the 1:1 system is -21.5, that of the 4:1 system about -18. The alternative mechanism would be expected to show the opposite influence because dissociation of H_3S^+ would be facilitated by decreasing acidity. Furthermore, H_3S^+ shows no indication of any deprotonation equilibrium in superacid solution (according to NMR studies).

To probe the structure and stability of H_4S^{2+}, ab *initio* theoretical calculations were carried out with Pople's GAUSSIAN programs. The isoelectronic first-row species, BH_4^-, CH_4, NH_4^+,[65] the discussed H_4O^{2+} cation, along with the second-row species AlH_4^-, SiH_4, and PH_4^+,[66] and the isoelectronic H_4S^{2+} cation[67] are all expected to be tetrahedral. Indeed, at the HF/6-31G* level of theory the structure of diprotonated hydrogen sulfide having T_d symmetry corresponds to a minimum on the potential energy surface.

Although H_4S^{2+} is thermodynamically unstable toward deprotonation by 59.2 kcal mol^{-1}, it has significant kinetic stability because the activation energy is calculated to be 25.2 kcal mol^{-1}. The heat of formation is estimated to be 584 kcal mol^{-1}. The S–H bond distance in the tetrahedral structure is 1.396 Å. H_4S^{2+} should be obtained more readily by protonation of H_3S^+ than H_4O^{2+} by protonation of H_3O^+ [Eq. (22)]. The larger size of the sulfur atom may help

(22)

to accommodate the additional charge better. Again it must be pointed out that these calculational data refer to isolated gas-phase conditions under which protonation of H_3S^+ is not thermodynamically favored. Association (clustering) may also play an important role in the condensed phase and could give a very structured dication-like species with C_{3v} symmetry in superacidic solution (Scheme 30).

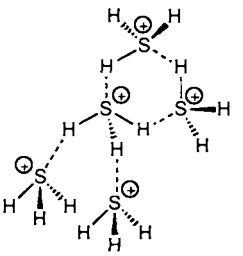

Scheme 30. Possible stabilization of H_4S^{2+} ions by H_3S^+ ions in superacids.

Calculations have also been carried out on the planar SH_4^{2+} dication. This D_{4h} structure is less stable than its T_d isomer by 245 kcal mol^{-1}. This energy difference is surprisingly larger than its counterpart for H_4O^{2+} (94.6 kcal mol^{-1}). Despite its high thermodynamic instability, planar H_4S^{2+} represents a local minimum on the potential energy surface.[68] Surprisingly, the S–H bond distances in planar H_4S^{2+} (1.379 Å) are 0.017 Å shorter than in the tetrahedral isomer.

Whereas tetrahedral H_4S^{2+} may be viewed as diprotonated H_2S, planar H_4S^{2+} represents dioxidized sulfurane (H_4S).

Trialkylsulfonium ions are, at best, weak alkylating agents. They do not alkylate aromatic hydrocarbons. Laali et al., however, found[69] that similar to their oxonium analogues in the presence of superacids trialkylsulfonium ions are greatly activated and alkylate arenes with ease [Eq. (23)]. Protic activation of the sulfonium ions via their dications is indicated.

(23)

Theoretical calculations on the series of methylsulfonium ions and dications were carried out[20a] to determine their energies and their related proton affinities (Table 1). Diprotonated sulfanes are shown to be considerably more stable than their oxo analogues. The optimized structures for all species located at minima are depicted in Scheme 31.

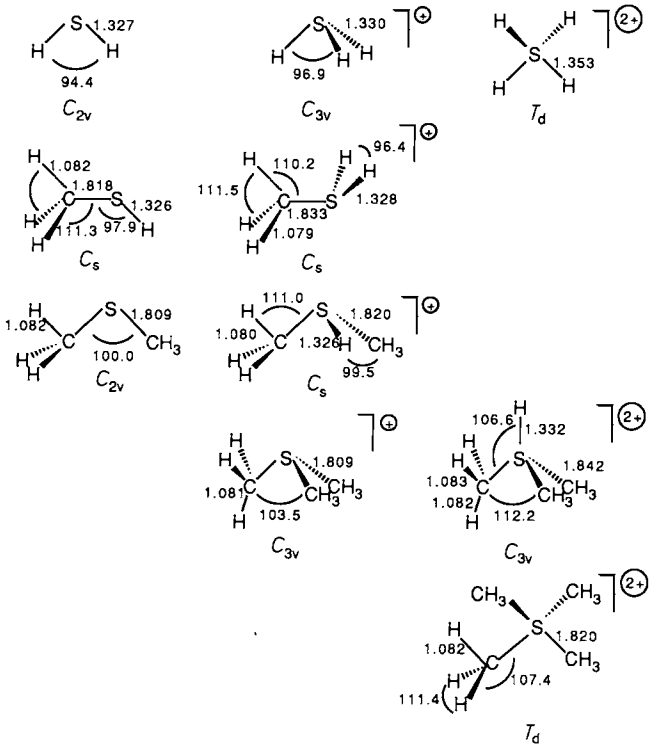

Scheme 31. HF/6-31g* optimized structures of the most stable isomers of neutral sulfur-containing bases and their mono- and diprotonated and mono- and dialkylated ions.

Radom[68] reported a theoretical study of the tetrahydridoselenonium dication, SeH_4^{2+}. No experimental studies are, however, thus far available.

Laali et al. have studied[69] the superacid-catalyzed alkylation of arenes with trialkylselenonium and telluronium ions. In analogy to previously discussed alkylations with trialkyloxonium and sulfonium ions (see Section 3 and above), they concluded that further protonation to the related onium dications activates them, allowing alkylation of arenes to occur [Eq. (24), X = Se, Te].

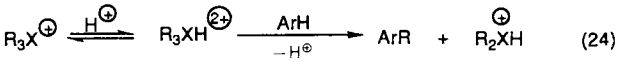

(24)

10. Diprotonated/Dialkylated Thiocarbonyl Compounds, Thiocarboxylic Acids, Thiocarbonic Acid, and Carbonyl Sulfide

Thioketones are protonated in superacids and were studied by ^{13}C NMR spectroscopy.[70] Further protonation by excess superacid as formulated in Equation (25) is indicated by their enhanced activity in electrophilic reactions.

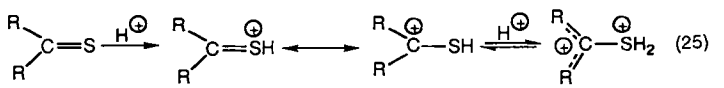

(25)

Thiocarboxylic acids like their oxygen analogues form stable protonated ions in superacidic media[71] (Scheme 32).

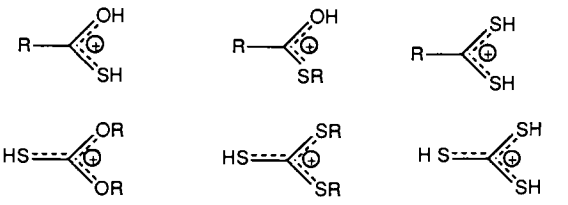

Scheme 32. Resonance-stabilized monoprotonated thiocarboxylic and thiocarbonic acids and their esters.

Thiocarbonates are also readily protonated in superacid to protonated thiocarbonic acid (**5**),[72] which is also formed through the cleavage of dialkylthiocarbonates. There is an

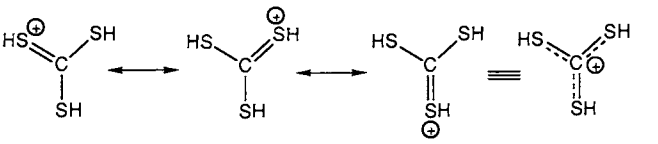

5

indication that diprotonated thiocarbonic acid present in a preequilibrium with its monocation is eventually cleaved at somewhat elevated temperatures to give carbon disulfide [Eq. (26)]. The protolytic cleavage proceeds consecutively through di- and monoprotonated carbon disulfide.

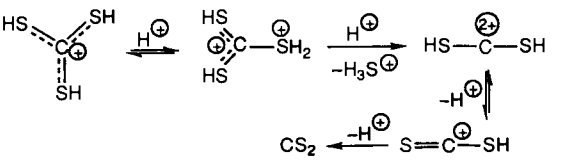

(26)

Protonation of carbon disulfide and carbonyl sulfide in superacids is accompanied by ready oxidation. However, COS was methylated by the CH_3F–SbF_5 complex and found to be a very reactive electrophilic thiocarboxylating agent for arenes[73] [Eq. (27)].

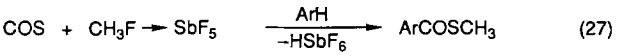

(27)

11. Protonated/Alkylated Dialkylhalonium Dications

In the presence of acid catalysts haloalkanes become alkylating agents. In 1877 Friedel and Crafts discovered the catalytic effect of anhydrous aluminium trichloride in alkylation reactions (Friedel–Crafts reaction).[74] The mechanism of the reaction is today understood to involve coordination of a nonbonded electron pair in the halogen atom of R–X:, giving either a polarized donor–acceptor complex or an alkylcarbenium ion pair (depending on the nature of the alkyl halide, the Lewis acid, and the reaction medium) [Eq. (28)].

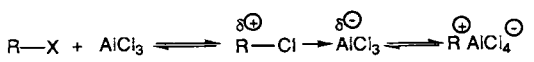

(28)

Use of an excess of a powerful Lewis acid halide such as SbF_5 in low nuleophilicity solvent systems (SO_2, SO_2ClF, etc.) provides stable alkyl cations as persistent, long-lived species.[75, 76] In contrast, when an excess of the haloalkane is used, self-alkylation leads to the formation of dialkylhalonium ions, which have even been isolated as stable salts [Eq. (29), X = Cl, Br, I].

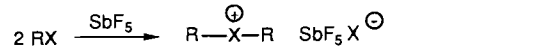

(29)

Fluoroalkanes do not give dialkylfluoronium ions, because of the high electronegativity of fluorine. Instead a C–H (or C–C) bond is alkylated. Fluoromethane, for example, undergoes alkylative self-condensation according to Equation (30).[77]

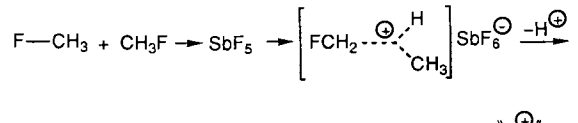

(30)

Halomethanes represent a rather special case. As the "bare" methyl cation is energetically extremely unfavorable, no persistent methyl cation has been observed in superacidic media. Instead polarized donor–acceptor complexes or dimethylhalonium ions are formed. Dimethylhalonium ions in superacidic media show extremely enhanced reactivity. This behavior is apparently caused by protolytic (electrophilic) activation involving the nonbonded electron pair of the halogen atom (Scheme 33).

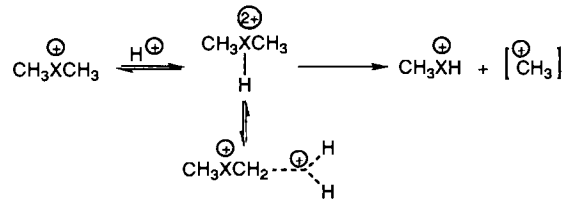

Scheme 33. Possible explanation for the strong enhancement of the reactivity of methylations with halomethanes in superacids.

When the dimethylbromonium ion reacts with the isotopomeric CD_3F–SbF_5 complex, methyl interchange is observed, which indicates that an intermediate superelectrophile $(CH_3)_3Br^{2+}$ is formed by further methylation on the bromine atom [Eq. (31)].[59]

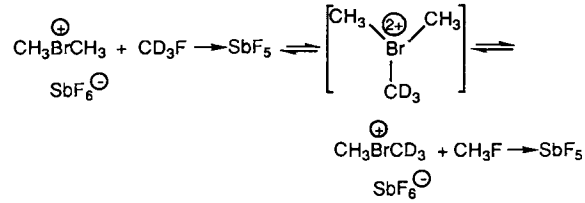

(31)

12. Protonated or Lewis Acid Complexed Halocarbenium Dications and Their Analogues

Not only onium and carboxonium ions, but also certain heteroatom-substituted carbocations are protolytically activated in superacids.

Trivalent alkyl cations (trialkylcarbenium ions) R_3C^+ with a sextet of electrons at the carbocationic carbon are strong Lewis acids and powerful electrophiles. The formal electron deficiency at the carbocationic centers is, however, decreased by interaction with attached electron donor ligands. These can be not only π-donors (such as arenes, vinyl groups, etc. acting through conjugative interactions) or n-donors (such as halogen, oxygen, nitrogen, or sulfur atoms acting through n–p back donation), but also σ-donors (such as alkyl or cycloalkyl groups acting through hyperconjugative C–H or C–C bond delocalization). Only in the case of the methyl cation CH_3^+ are such stabilizing interactions absent. CH_3^+ is thus the ultimate electrophilic alkyl cation, which explains why in the condensed state it is not observed in its "free" form (at least with such spectroscopic methods as NMR or IR). Most other alkyl cations can be observed as stable, long-lived species in superacidic media, although primary or secondary alkyl cations readily rearrange to their more stable tertiary (or secondary) isomeric ions. The reader is referred to reviews about stable carbocations for further information.[3, 6, 78]

In 1972 I suggested[79] that carbocations can be divided into two limiting categories: trivalent carbocations, of which CH_3^+ is the parent ion, and five (or higher) coordinate ions, of which the methonium ion CH_5^+ may be considered the parent. The former are frequently called classical ions and the latter nonclassical.

The protonation of methane to form CH_5^+ was studied theoretically and experimentally, including by ESCA spectroscopy.[80] The diprotonation of methane to form CH_6^{2+} has also been studied.[81] Schmidbaur et al. were able to isolate a pentakis(triphenylphosphanaurio)methonium salt analogous to CH_5^+ [Eq. (32), HMPA = hexamethylphosphoric triamide] and determined its crystal structure.[82a] A salt related to CH_6^{2+} (**1**) has also been obtained.[82b]

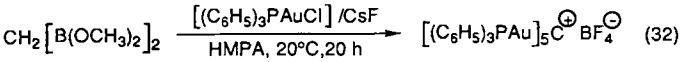

(32)

The CH_4^+ radical cation is the parent molecular ion in mass spectrometry studies of methane. Our theoretical calculations first revealed its planar structure.[83a] Stahl, Schwarz, Vogel et al.[83b] studied the gas-phase CH_4^+, CH_4^{2+}, and CH_5^{2+} ions by experimental and ab initio molecular orbital investigations. The planar CH_4^{2+} dication was also investigated theoretically by Radom.[83c]

It is informative to recall the parent C_1 carbocations CH_2^{2+}, CH_3^+, CH_4^+, CH_4^{2+}, CH_5^+, CH_6^{2+} and their preferred structures (Scheme 34). CH_5^+ and CH_6^{2+} are accessible by protonating and diprotonating methane. Loss of H_2 from CH_6^{2+} gives CH_4^{2+}, and the radical ion CH_4^+ is generated by electron loss from methane. The CH_2^{2+} dication was investigated in the gas phase and theoretically.[84] Formation of its substituted analogues is indicated in superacid systems.

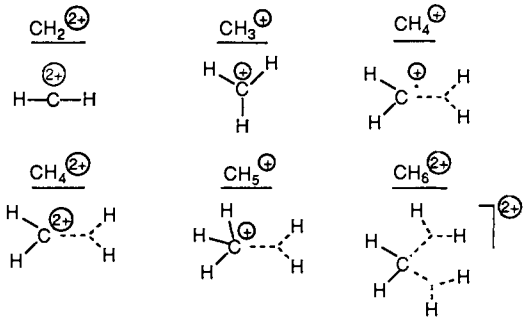

Scheme 34. The most stable structures of C_1 carbocations.

Whereas, as mentioned before, the free methyl cation CH_3^+ is not observable in solution chemistry, its alkyl- or halogen-substituted analogues, such as $(CH_3)_2CH^+$, $(CH_3)_3C^+$, $(CH_3)_2CX^+$, $CH_3CX_2^+$, and CX_3^+ (X = Cl, Br, I), have been prepared and studied as stable ions in superacidic media. If the neighboring groups can be affected by further protolytic (or electrophilic) interaction, the electron deficiency of the carbocationic center becomes more pronounced, which results in enhanced superelectrophilic reactivity.

Trihalomethyl cations CX_3^+ (X = Cl, Br, I), characterized by NMR spectroscopy in superacidic media,[85,86] are substantially resonance-stabilized by back-donation from the nonbonded electron pairs of the halogen atoms (Scheme 35).

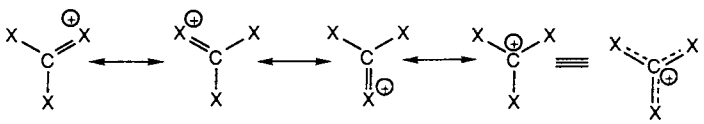

Scheme 35. Resonance structures of the trihalomethyl cation.

The significant delocalization deduced from their ^{13}C NMR spectra results in their being only moderately active electrophiles. The chemical shift for CCl_3^+ is $\delta = 236$, deshielded by 159 ppm from $HCCl_3$, whereas $C^+(CH_3)_3$ is deshielded by some 320 ppm from $HC(CH_3)_3$.

Bach et al. found that $CCl_4/AlCl_3$ is an extremely reactive hydride abstracting and ionic chlorinating system for adamantane.[87a] Use of the CCl_4/HF–SbF_5 system (and in related superacids) greatly enhances the reactivity of hydride abstraction from hydrocarbons to form carbocations as shown by Sunko et al.[87b] Sommer et al. reported similar activation in the carbonylation of propane.[87c] A similar reactivity was also observed for dichloromethane (or dibromomethane) and chloroform.[87e]

As CCl_3^+ is only a weak electrophile according to ^{13}C NMR results for the stable ion, these results are difficult to interpret on the basis of initial formation of CCl_3^+ alone. In order to explain the unexpected reactivity it is suggested that the CCl_3^+ ion formed by ionization of CCl_4 with $AlCl_3$ or SbF_5 can further coordinate with excess Lewis acids (or the related conjugate protic acids), forming a superelectrophile (Scheme 36).

Cleavage of the Cl_2CClH^{2+} dication can even give the incipient CCl_2^{2+} dication, an even more reactive superelectrophile. This dication would promote extremely facile intermolecular hydride transfer giving the $HCCl_2^+$ ion, which itself could then react further (Scheme 37).

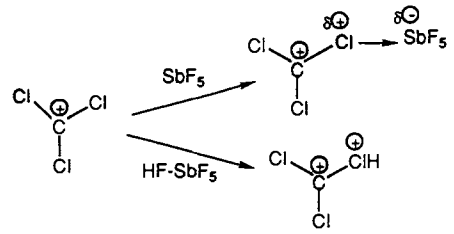

Scheme 36. Proposed activation of CCl_3^+ by Lewis acids or superacids.

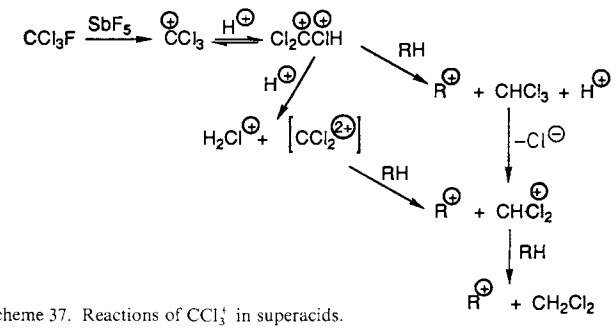

Scheme 37. Reactions of CCl_3^+ in superacids.

Chloroform and dichloromethane (or its fluorine exchange product, CH_2F_2) were observed as by-products of the reactions. It is possible, however, that protolytic ionization of chloroform, formed in the first hydride transfer reaction can account for CH_2Cl_2 formation.

The boron analogue for CCl_2^{2+} is BCl_2^+. Ionization (or donor–acceptor complexation) of BCl_3 with strong Lewis acids produces a superelectrophilic analogue. This is involved in the Friedel–Crafts reaction of BCl_3 with arenes (Scheme 38).[88]

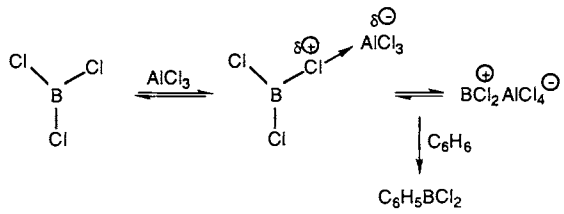

Scheme 38. Friedel-Crafts borylation of arenes.

The aluminum analogue, anhydrous aluminum trichloride, is the most widely used Friedel–Crafts catalyst.[89a] Its activity is generally assigned to the Lewis acidity of its monomeric form, although it has long been recognized that it is dimeric up to 440 °C except in strongly coordinating solvents.[89a] This doubly halogen-bridged dimer is, however, catalytically inactive, because both aluminum atoms are four coordinate. As the dissociation energy for the reaction $Al_2Cl_6 \rightleftharpoons 2\,AlCl_3$ is 29 ± 1 kcal mol^{-1}, it is more reasonable to postulate that dimeric Al_2Cl_6 undergoes less energetic opening of only one of the chlorine bridges at a time [Eq. (33)].

The resulting monobridged Al_2Cl_6 contains a tricoordinate electron-deficient aluminum atom. In the limiting case it ionizes to $AlCl_2^+AlCl_4^-$. Al_2Cl_6 may consequently act as a

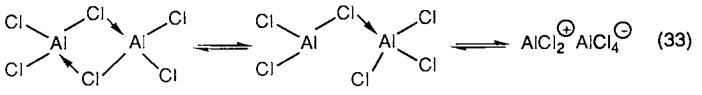

(33)

strong Lewis acid and readily coordinates with haloalkanes or other suitable electron donor reagents [Eq. (34)].

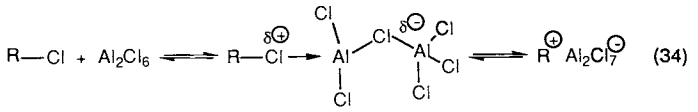

(34)

Superacidic antimony pentafluoride (and related Lewis acid fluorides) are known to be associated, but as in **6**, only through monofluorine bridges.[89a]

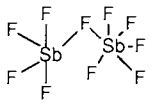

6

Mukaiyama found[89b] that highly efficient catalytic Friedel-Crafts acylation reactions and Beckmann rearrangements can be carried out with $GaCl_3$–$AgClO_4$ and $SbCl_5$–$AgClO_4$, which are assumed to give ionic $GaCl_2^+ClO_4^-$ and $SbCl_4^+ClO_4^-$. Highly polarized donor–acceptor complexes would, however, be similarly active.

In the hydroboration reaction of olefins with diborane, the $B_2H_6 \rightleftharpoons 2BH_3$ equilibrium is assumed. It is again possible that opening of just one of the hydrogen bridges, according to Equation (35) can account for the electrophilic reactivity of diborane in some cases. This is particularly valid

(35)

in the absence of ether (or other complexing agents). Hurd's early work showed that not only ethylene, but benzene and even methane react with diborane at elevated temperatures and without side reactions with solvents to give boronated by-products.[90a] Silanes were later also shown to react with diborane.[90b]

When $(CH_3)_2CCl_2$ is ionized in SbF_5-containing superacids[86] $(CH_3)_2CCl^+$ is formed. This system converts alkanes extremely efficiently. The ion is thus probably activated by superelectrophilic solvation or even by incipient superelectrophilic $(CH_3)_2C^{2+}$ dication formation (Scheme 39). The reaction sequence of Scheme 40 is accordingly proposed for the reaction with isobutane.

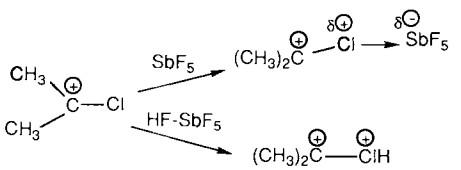

Scheme 39. Activation of $(CH_3)_2CCl^+$ by Lewis acids or superacids.

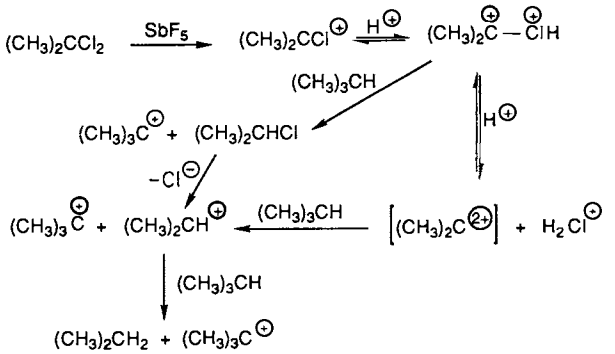

Scheme 40. Proposed reaction sequence for the superacid-catalyzed reaction of $(CH_3)_2CCl_2$ with isobutane.

Sommer et al. observed that Br^- or Br_2 added to superacid HF–SbF_5 solutions greatly accelerated the carbonylation of alkanes such as propane.[87d] They proposed the formation of a "Br^+" ion (called a "superelectrophile"), which abstracted a hydride ion from propane prior to carbonylation. However, there is no evidence for monoatomic Br^+ in solution. As we and Houk showed,[91] even if it existed, its triplet form would be preferred over the singlet, and it would give unselective carbonylation of propane, in contradiction of the experimental findings. It is more probable that further protolytic activation of H_2Br^+ or Br_2^+H (as well as Br_3^+) explains the increased reactivity towards hydrocarbons. Reports, notably by Gold et al.[92a] and Kramer,[92b] called attention to the high acidity of liquid HBr in solvents such as SO_2ClF.[92c] Further protolytic equilibrium [Eq. (36)] is possible in excess superacid and would explain some of the unexpected results.

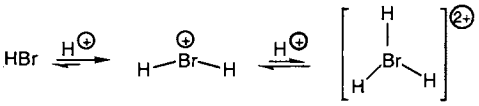

(36)

As discussed by Lowry and Richardson,[93] the *leveling effect* means that "no acid stronger than the conjugate acid of the solvent can exist in appreciable concentration in that solvent". Thus in aqueous solution no acid stronger than H_3O^+ can exist, in HSO_3F none stronger than $H_2SO_3F^+$, in HBr none stronger than H_2Br^+, etc. However, in excess superacids in which "bases" are completely monoprotonated, equilibria with their diprotonated "bases", i.e. H_4O^{2+}, $H_3SO_3F^{2+}$, H_3Br^{2+}, are possible.

In an alternative pathway for Sommer's bromine-assisted carbonylation of propane in superacids[87c,d] the bromocarbonyl cation forms as intermediate. Halocarbonyl cations (XCO^+, X = Cl, Br, I) have recently been prepared under stable-ion conditions as long-lived species at low temperatures [Eq. (37)] and were characterized by ^{13}C NMR spectroscopy.[87e] The bromocarbonyl cation itself, however,

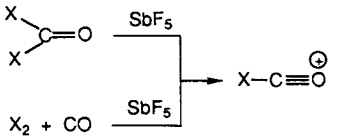

(37)

may not be reactive enough to influence the reaction. Further activation by coordination with protic or Lewis superacids can convert it into a superelectrophile that is highly reactive and that reacts selectively with the C–H bond of propane to yield the 2-carbonylated product [Eq. (38)].

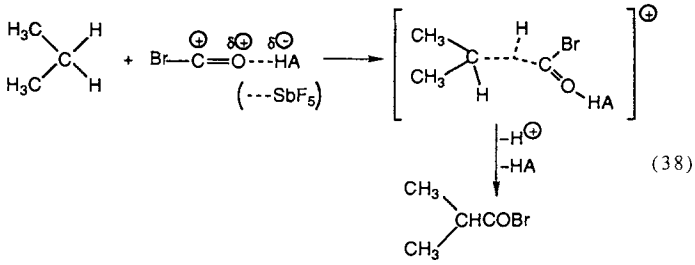

(38)

13. Dicationic Nitrogen-Containing Systems

Substituted nitromethanes react with benzene in superacidic trifluoromethanesulfonic acid (TFSA) to give the corresponding oximes in high yields [Eq. (39)].[94a] In this

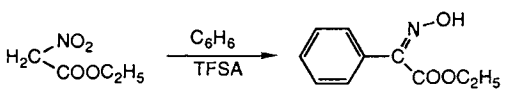

(39)

reaction, O,O-diprotonation of the nitro group was invoked by Shudo to explain the remarkable reactivity (Scheme 41).

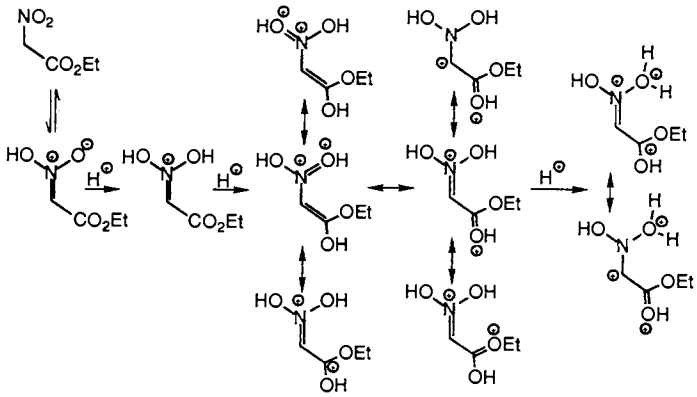

Scheme 41. Multiple protonation of ethyl nitroacetate and important resonance structures for the cations.

α,β-Unsaturated nitroolefins also react with benzene in TFSA. Dicationic O,O-diprotonated nitroolefins were suggested as reaction intermediates [Eq. (40)].[94b] Shudo et al. have exploited these reactions to carry out highly interesting organic transformations.[95, 96]

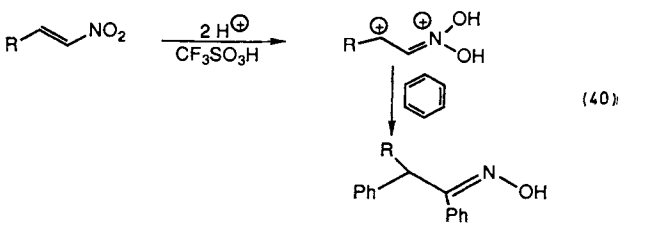

(40)

Other heteroatom-substituted carbocations[97] are also activated by superacids. α-Nitro and α-cyanocarbenium ions, $R_2C^+NO_2$ or R_2C^+CN, are thought to undergo O- or N-protonation, respectively, which greatly enhances the electrophilicity of the carbocationic centers [Eq. (41) and (42)].

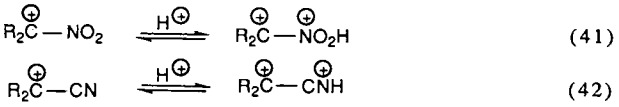

(41)

(42)

The acid-catalyzed reaction of hydrogen cyanide and nitriles with aromatic hydrocarbons (Gattermann and Houben-Hoesch reactions, respectively) are well known. The generally accepted mechanism includes N-protonation of HCN or the nitriles to form the corresponding nitrilium ions. Meerwein first studied protonated nitriles as BF_4^- salts,[14b] and we were able to protonate HCN in superacids [Eq. (43), R = H, alkyl].[6, 14b] The resonance-stabilized nitrilium ions show only limited iminocarbenium ion nature and accordingly are only mildly electrophilic agents.

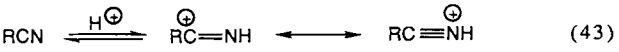

(43)

In order to explain the experimentally observed high reactivity of HCN and alkyl nitriles under superacidic conditions, Shudo reported[98] results of studies that indicate that in the Gattermann reactions, diprotonated HCN is involved as the de facto reagent. Accordingly, the mechanism of the Gattermann reaction in superacids can be depicted as in Equation (44).

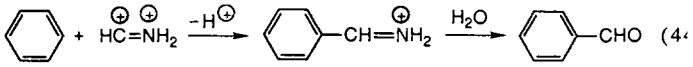

(44)

N,N-diprotonated HCN was first suggested by Schwarz's studies (Scheme 42a).[99] For the Houben–Hoesch reaction

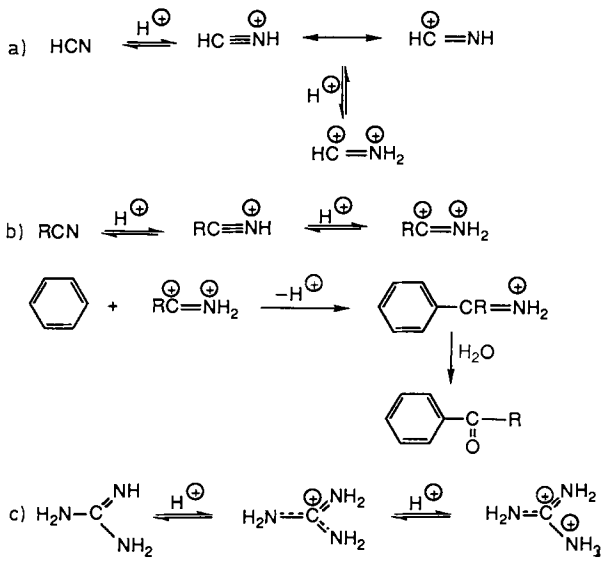

Scheme 42. Protonation/deprotonation equilibria for a) HCN, b) RCN, and c) guanidine. Under b) a mechanism for the Houben-Hoesch reaction is also proposed.

in superacids Shudo similarly suggested that N,N-diprotonated nitriles are the de facto reagents (Scheme 42b).

Guanidine was also found to undergo diprotonation in superacids (Scheme 42c); the dication was observed (by NMR spectroscopy) as a stable species.[100] Diprotonated guanidine and its derivatives are similar to the diprotonated carbonic acids discussed in Section 8. Theoretical calculations indicate that methanimine, too, can give a stable diprotonated intermediate [Eq. (45)].[59] Formamidine can similarly undergo diprotonation [Eq. (46)].

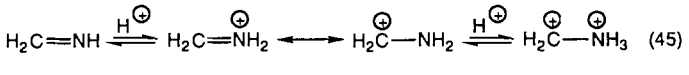

(45)

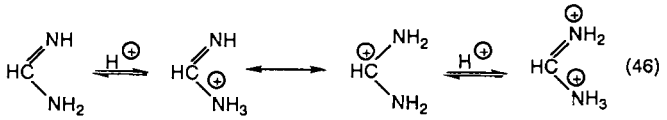

(46)

The protonation of diazomethane was shown experimentally to take place either on nitrogen or carbon.[101] Presumably in superacids interconversion goes through a diprotonated form [Eq. (47)] and not through a deprotonation–reprotonation reaction (for which there is no evidence).

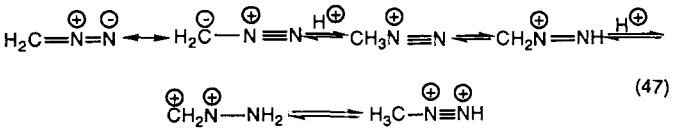

(47)

The protonation of hydrazoic acid was shown in our investigations to give the aminodiazonium ion, $H_2NN_2^+$.[102] Subsequent cleavage liberates N_2 probably assisted by protosolvation.

14. Diprotonated Nitric Acid and the Protonitronium Dication

Protonation of nitric and nitrous acid is of substantial interest because of subsequent cleavage to the nitronium and nitrosonium ion.[103] The pioneering studies go back to Hantzsch and Ingold, who made the now generally accepted proposal that the initial protonation of nitric acid yields the nitracidium ion,[103] that is, nitric acid protonated at the hydroxy group [Eq. (48)].

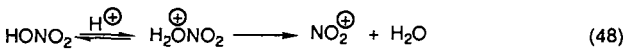

(48)

The ready cleavage of the nitracidium ion to the nitronium ion involves practically no barrier. This is considered to be a consequence of its structure, which can be described as a nitronium ion solvated by water. More recent theoretical calculations, however, indicate that the stable form of protonated nitric acid is that of the dihydroxynitrosonium ion. Its cleavage to the nitronium ion in excess of superacid could thus proceed by diprotonation [Eq. (49)].[104]

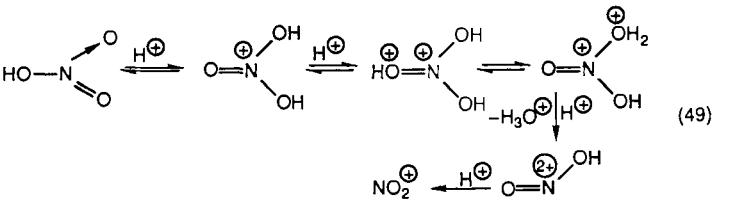

(49)

Nitronium salts such as $NO_2^+BF_4^-$ were introduced by us as highly reactive nitrating agents. They are generally used in aprotic solvents, for instance nitromethane, sulfolane (= *S,S*-dioxotetrahydrothiophene), or dichloromethane.[103] A large variety of arenes can be nitrated with excellent yields.

Highly deactivated arenes such as *meta*-dinitrobenzene are, however, not nitrated under these conditions. In contrast in superacidic FSO_3H solution, nitronium salts nitrate *meta*-dinitrobenzene to form 1,3,5-trinitrobenzene in 70% yield.[105] Similarly, $NO_2^+BF_4^-$ does not nitrate deactivated nitrofluorobenzenes in sulfolane solution, but in superacidic TFSA efficient nitration takes place.[106] Whereas nitronium salts show no reactivity towards methane in aprotic media, the reaction takes place, albeit in low yield, in FSO_3H to give nitromethane.[107] These data indicate that the nitronium ion is activated by the superacidic media. To explain the highly increased reactivity of the nitronium ion, it has been proposed[107, 110] that the linear nitronium ion, despite being a positively charged species, can undergo protonation (protosolvation) to the protonitronium dication (NO_2H^{2+}), an extremely reactive superelectrophile. The linear nitronium ion $O{=}N^+{=}O$ has neither a vacant atomic orbital on nitrogen nor a low-lying molecular orbital. Its electrophilic potential is mainly due to its polarizability when interacting with π-donor aromatic nucleophiles. In contrast to a reactive arene, a strongly deactivated arene is too weak an electron donor to bring about such polarization. A "reactive" nitronium ion should be bent and have a developing p orbital on nitrogen. The driving force for the formation of such a reactive nitronium ion is the ability of the nonbonded electron pairs on the oxygen atoms to coordinate with the strong protic acid in the nitrating system.

Simonetta's lower level calculation[108] on the assumed protonitronium dication did not locate a minimum. Recent high-level ab initio calculations, however, show that NO_2H^{2+} is an energy minimum (Scheme 43).[104]

The protonitronium dication, an analogue of nitrous acid, is characterized by quite short N–O1 (1.055 Å) and N–O2

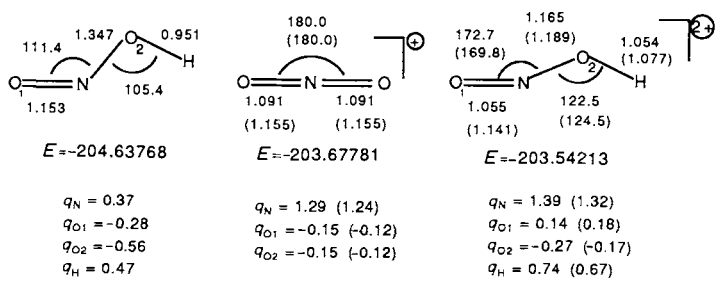

Scheme 43. Geometries (bond lengths in Å, bond angles in degrees), energies (in Hartrees), and partial charges q calculated by ab initio methods for nitrous acid, the nitronium ion, and the protonitronium dication (at the 6-31G*//6-31G* level and in parentheses at the MP2/6-31G**//MP2/6-31G** level).

(1.165 Å) bonds. The shorter N–O1 bond distance is caused by the strong interaction of (formally) doubly occupied p_y and p_z orbitals of the oxygen atom with the empty orbitals of the nitrogen atom, thereby generating incipient triple-bond character in the N–O1 bond, whereas the shorter N–O2 bond is due to the interaction of an empty p_y orbital of nitrogen with an occupied p_y orbital of the hydroxyl oxygen, causing the double-bond character of N–O2 bond. This interaction is also reflected in the O-N-O bond angle (170°) of NO_2H^{2+} which is much larger than that in HNO_2 (111°). In other words lone-pair–bond-pair repulsion in HNO_2 makes the O-N-O angle closer to the tetrahedral angle.

Although the protonitronium dication is substantially more energetic than the nitronium ion, the deprotonation barrier was calculated to be 17 kcal mol^{-1}. It should be mentioned again that calculated results refer to the gas phase, while in superacidic solvents dications can be stabilized through delocalization of excess charge by solvation or clustering. Instead of complete dication formation, however, protosolvation can also account for activation.[109]

15. Bidentate and Multidentate Activation of Electrophiles over Solid Superacids and Relevance to Catalytic and Enzymatic Systems

The discussion of superelectrophiles has centered on the activation of electrophiles in superacidic solution. However, superacidic systems are not limited to solution chemistry. Solid superacids, possessing both Brønsted and Lewis acid sites, are increasing in significance. They range from supported or intercalated systems, to highly acidic perfluorinated resinsulfonic acids (such as Nafion-H and its analogues), to certain zeolites (such as H-ZSM-5). A more detailed discussion of these systems is beyond the scope of this paper, and reviews are available.[6] One of the major difficulties in characterizing solid acids is the accurate determination of their acidity. The most frequently used methods are based on kinetic rather than thermodynamic measurements. These can give data on catalytic activity of the solid acids, but not necessarily on their thermodynamic acidities. Also the extrapolation of results of measurements based on assumed analogies with solution equilibria studies is questionable, for instance in the determination of H_0 and related acidity functions.[110] Spectroscopic studies, frequently based on surface acid–base interactions, calorimetric measurements, and recently solid-state NMR methods including ^{1}H MAS NMR studies of zeolites have started to change the picture.[111]

Solid acids such as Nafion-H or HZSM-5 possess superacidic properties. In order to explain how these acidic solids can sometimes display remarkable activity, for example in allowing the catalytic transformations of extremely low nucleophilicity alkanes (even methane), a reappraisal of the activity at the acid sites of such solid acids is expedient.

Nafion-H is known to contain acidic SO_3H groups clustered together (Fig. 1). H-ZSM-5, which also displays superacidic activity, was found by Haag et al.[112] to isomerize and alkylate alkanes readily (H_2 was formed as the protolytic by-product in stoichiometric amounts). In the zeolite, active Brønsted and Lewis acid sites are again in close proximity (approximately 2.5 Å) (Scheme 44).

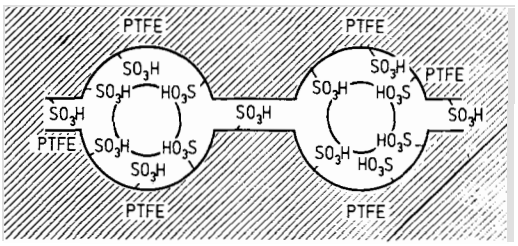

Fig. 1. Sketch of a perfluorinated resinsulfonic acid similar to Nafion-H, showing clustering of SO_3H groups; PTFE = poly(tetrafluoroethylene).

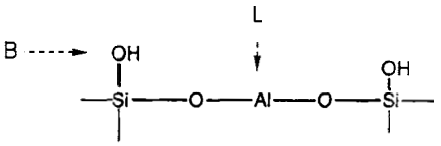

Scheme 44. Brønsted (B) and Lewis acid sites (L) in zeolites

It is not unreasonable to suggest that in these (and other) solid superacid catalyst systems, bi- or multidentate interaction forming highly reactive intermediates is possible. This amounts to the solid-state equivalent of protosolvation (protonation) discussed previously for solution systems.

Nature is able to perform its own transformations in ways which chemists have only started to understand. At enzymatic sites many significant transformations take place which are acid catalyzed (in a generalized sense electron-deficient metal-ion-catalyzed processes can also be included). Because the unique geometry at enzymatic sites frequently makes bi- and multidentate interactions possible, the principles discussed throughout this paper may also help improve our understanding of some enzymatic processes.

16. Conclusions and Significance

The discussion throughout this article has emphasized the increasing body of experimental observations and related theoretical calculations which show that a variety of electrophiles capable of further interaction (coordination) with Brønsted or Lewis superacids can be greatly activated by them. Examples are onium and carboxonium ions, acyl cations, halonium, azonium, carbazonium ions, and even certain substituted carbocations and the like. This activation produces *superelectrophiles*, that is, electrophiles of doubly electron-deficient (dipositive) nature whose reactivity (Scheme 45, top) significantly exceeds that of their parent monocations under conventional reaction conditions. Superelectrophiles are highly reactive intermediates. They are the de facto *reactive intermediates* of many electrophilic reactions in superacidic systems (including those involving solid

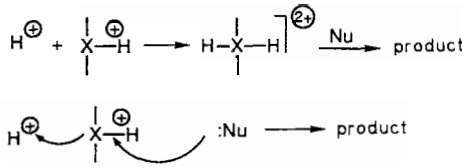

Scheme 45. Activation by superacids. Top: formation of a dication; bottom: electrophilic assistance.

superacids) and should be differentiated from energetically low-lying, much *more stable intermediates*, which frequently are observable and even isolable but not necessarily reactive without further activation.

It should be recognized, however, that some of the observed superelectrophilic reactions may also proceed with only "electrophilic assistance" by the superacids without forming distinct dipositive intermediates (Scheme 45, bottom). This may be the case in reactions with suitable nucleophiles, such as π-donor arenes and olefines or substrates containing n-donor heteroatoms, but not necessarily with weak σ-donor alkanes or highly deactivated π systems. Protosolvolytic (electrophilic) activation of electrophiles referred to throughout this article should be considered in this context.

Examples of superelectrophiles studied so far and their parent monocations are listed in Scheme 46.

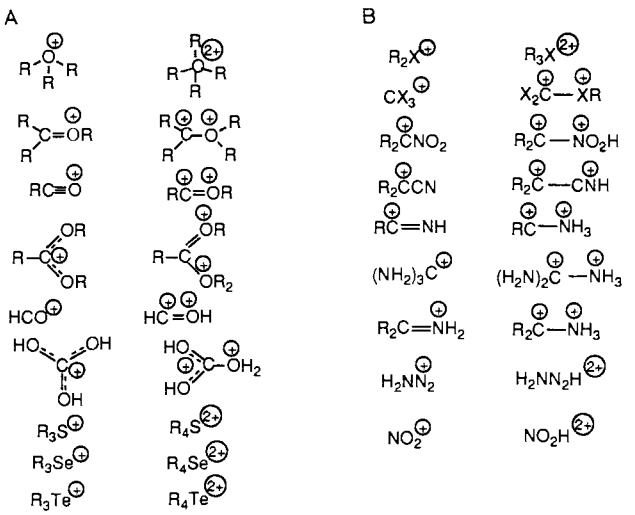

Scheme 46. Examples of superelectrophiles and the electrophiles from which they are derived. A: R = H, alkyl, Lewis acid. B: X = Cl, Br, I; R = H, alkyl. In each group the parent electrophiles are in the left column.

I am grateful to all my collaborators listed in the references who contributed so much to the development of the chemistry discussed in this review. Particularly, I would like to acknowledge the contribution of Professor G. K. S. Prakash to our joint efforts over the years in the chemistry of superacidic and stable-ion systems. Financial support of our work was provided by the National Science Foundation, the National Institutes of Health, the Office of Naval Research, and the Loker Hydrocarbon Research Institute.

Received: April 27, 1992 [A 902 IE]
German version: *Angew. Chem.* **1993**, *105*, 805

[1] J. March, *Advanced Organic Chemistry*, 3rd ed., Wiley, New York, **1985**, p. 179.
[2] G. A. Olah, K. Wade, R. E. Williams, *Electron Deficient Boron and Carbon Clusters*, Wiley-Interscience, New York, **1991**, and references therein.
[3] G. A. Olah, *Angew. Chem.* **1973**, *85*, 183; *Angew. Chem. Int. Ed. Engl.* **1973**, *12*, 173; *Carbocations and Electrophilic Reactions*, Verlag Chemie, Weinheim, **1973**/Wiley, New York, **1974**, and references therein.
[4] G. A. Olah, A. M. White, D. H. O'Brien, *Chem. Rev.* **1970**, *70*, 561.
[5] G. A. Olah, *Halonium Ions*, Wiley-Interscience, New York, **1975**.
[6] a) G. A. Olah, G. K. S. Prakash, J. Sommer, *Superacids*, Wiley-Interscience, New York, **1985**, and references therein; b) R. J. Gillespie, *Acc. Chem. Res.* **1968**, *1*, 202.
[7] G. A. Olah, A. Germain, H. C. Lin, D. A. Forsyth, *J. Am. Chem. Soc.* **1975**, *97*, 2928.
[8] G. A. Olah, G. K. S. Prakash, M. Barzaghi, K. Lammertsma, P. von R. Schleyer, J. A. Pople, *J. Am. Chem. Soc.* **1986**, *108*, 1062.
[9] G. A. Olah, G. K. S. Prakash, M. Marcelli, K. Lammertsma, *J. Phys. Chem.* **1988**, *92*, 878.
[10] G. A. Olah, G. K. S. Prakash, K. Lammertsma, *Res. Chem. Intermed.* **1989**, *12*, 141.
[11] a) H. M. Hogg, P. Kabarle, *J. Chem. Phys.* **1965**, *43*, 449; b) H. M. Hogg, R. N. Hanes, P. Kabarle, *J. Am. Chem. Soc.* **1966**, *88*, 2838; c) P. Kabarle, *Annu. Rev. Phys. Chem.* **1977**, *28*, 445; d) *Gas Phase Chemistry*, *Vol. 2* (Ed.: M. T. Bowers), Academic Press, Orlando, FL, USA, **1979**.
[12] G. K. S. Prakash, T. N. Rawdah, G. A. Olah, *Angew. Chem.* **1983**, *95*, 356; *Angew. Chem. Int. Ed. Engl.* **1983**, *22*, 390.
[13] K. Lammertsma, P. von R. Schleyer, H. Schwarz, *Angew. Chem.* **1989**, *101*, 1313; *Angew. Chem. Int. Ed. Engl.* **1989**, *28*, 1321.
[14] a) H. Perst, *Oxonium Ions in Organic Chemistry*, Verlag Chemie, Weinheim, **1971**; b) in *Carbonium Ions, Vol. 5* (Eds.: G. A. Olah, P. von R. Schleyer), Wiley-Interscience, New York, **1976**; c) G. A. Olah, D. H. O'Brien, A. M. White, *Chem. Rev.* **1970**, *70*, 561 and references therein; in *Carbonium Ions, Vol. 4* (Eds.: G. A. Olah, P. von R. Schleyer), Wiley-Interscience, New York, **1973**.
[15] a) M. Guihas, A. G. Brenton, H. J. Beynon, M. Raberenovic, P. von R. Schleyer, *J. Chem. Soc. Chem. Commun.* **1985**, 210; *J. Phys. B* **1984**, *17*, L605; b) K. Lammertsma, M. Barzaghi, G. A. Olah, J. A. Pople, P. von R. Schleyer, M. Simonetta, *J. Am. Chem. Soc.* **1985**, *105*, 5258.
[16] K. Lammertsma, *J. Am. Chem. Soc.* **1984**, *106*, 4619.
[17] a) L. Pauling, *J. Chem. Phys.* **1933**, *1*, 56; b) J. F. Babb, M. L. Du, *Chem. Phys. Lett.* **1990**, *167*, 273.
[18] a) G. A. Olah, 44th Reaction Mechanism Conference, Brookhaven, NY, USA, **1962**; b) G. A. Olah, W. S. Tolgyesi, S. J. Kuhn, M. E. Moffat, I. J. Bastien, E. B. Baker, *J. Am. Chem. Soc.* **1963**, *85*, 1328; c) G. A. Olah, E. B. Baker, J. E. Evans, W. S. Tolgyesi, J. S. McIntyre, I. J. Bastien, *ibid.* **1964**, *86*, 1360.
[19] G. A. Olah, J. R. De Member, Y. K. Mo, J. J. Svoboda, P. Schilling, J. A. Olah, *J. Am. Chem. Soc.* **1974**, *96*, 884.
[20] a) N. Hartz, R. Golam, G. A. Olah, *J. Am. Chem. Soc.*, **1993**, *115*, 1277; b) zero point vibrational energies at the HF/6-31G*//HF/6-31G* level were scaled by a factor of 0.8929; c) proton affinities of the reaction $B + H^+ \rightarrow BH^+$ have been calculated from the following formula:

$$PA = -\Delta H_{298} = -\Delta E_0^{elec} - \Delta ZPE + 5/2\,RT$$

The ΔE_0^{elec} term includes all electronic effects, the term ΔZPE is the difference in zero point energies for B and BH^+, and the final term is the temperature correction. All of the calculations are reported here for a temperature of 300 K (D. A. Dixon, A. Komornicki, W. P. Kraemer, *J. Chem. Phys.* **1984**, *81*, 3603); d) experimental proton affinities have been taken from S. G. Lias, F. J. Liebman, R. D. Levin, *J. Phys. Chem. Ref. Data* **1984**, *13*, 695; e) ΔH_1^{iso} are the enthalpies of the following isodesmic reactions: $B: + H_2XH^+ = BH^+ + H_2X$. ΔH_2^{iso} are the enthalpies of the isodesmic reactions: $BH^+ + H_2XH_2^{2+} = BH_2^{2+} + H_2XH^+$. X = O for the oxygen series, X = C=O for the carboxonium series, X = S for the sulfur series.
[21] J. Kaspi, D. D. Montgomery, G. A. Olah, *J. Org. Chem.* **1978**, *43*, 3147.
[22] G. A. Olah, A.-H. Wu, *Synlett* **1990**, 599.
[23] D. E. Pearson, *J. Chem. Soc. Chem. Commun.* **1974**, 397.
[24] A. Bagno, J. Bukala, G. A. Olah, *J. Org. Chem.* **1990**, *55*, 4384.
[25] A. Hantzsch, K. S. Caldwell, *Z. Phys. Chem.* **1907**, *58*, 575; H. Goldschmidt, O. Udby, *ibid.* **1907**, *60*, 728.
[26] a) J. N. Brønsted, *Recl. Trav. Chim. Pays-Bas* **1923**, *42*, 718; J. N. Brønsted, *J. Phys. Chem.* **1926**, *30*, 777; b) T. M. Lowry, *Trans. Faraday Soc.* **1924**, *20*, 13; *Chem. Ind. (London)* **1923**, 1048.
[27] D. E. Bethell, N. Sheppard, *Chem. Phys.* **1953**, *21*, 1321; C. C. Ferisso, D. F. Horning, *ibid.* **1955**, *23*, 1464; P. A. Giguere, *Rev. Chim. Miner.* **1966**, *3*, 627; M. Fourmier, J. C. R. Roziere, *C. R. Seances Acad. Sci. Ser. C* **1970**, *270*, 729.
[28] a) R. C. Taylor, G. L. Vidale, *J. Am. Chem. Soc.* **1956**, *78*, 5999; b) P. A. Giguere, C. Madec, *Chem. Phys. Lett.* **1976**, *37*, 569, and references therein.
[29] J. O. Lundgren, J. M. Williams, *J. Chem. Phys.* **1973**, *58*, 788; J. O. Lundgren, R. Tellgren, I. Olovsson, *Acta Crystallogr. Sect. B* **1978**, *34*, 2945.
[30] a) P. Kebarle, R. M. Haynes, J. G. Colling, *J. Am. Chem. Soc.* **1967**, *89*, 5753; b) A. W. Castelman, Jr., I. N. Tang, H. R. Munkelwitz, *Science* **1971**, *173*, 1025.
[31] a) V. Gold, J. L. Grant, K. P. Morris, *J. Chem. Soc. Chem. Commun.* **1976**, 397, and references therein; b) G. A. Olah, G. K. S. Prakash, J. Sommer, *Superacids*, Wiley-Interscience, New York, **1985**, and references therein; c) for more recent acidity measurements see V. Gold, K. Laali, K. P. Morris, L. Z. Zdunek, *J. Chem. Soc. Perkin Trans. 2* **1985**, 859.
[32] G. D. Mateescu, G. M. Benedikt, *J. Am. Chem. Soc.* **1979**, *101*, 3959.
[33] G. A. Olah, A. L. Berrier, G. K. S. Prakash, *J. Am. Chem. Soc.* **1982**, *104*, 2373.
[34] K. O. Christe, C. K. Schack, R. D. Wilson, *Inorg. Chem.* **1975**, *14*, 2224.
[35] M. C. R. Symons, *J. Am. Chem. Soc.* **1980**, *102*, 3982.
[36] a) R. R. Rodwell, L. Radom, *J. Am. Chem. Soc.* **1981**, *103*, 2865; b) R. A.

Whiteside, M. J. Frisch, J. A. Pople, *The Carnegie-Melon Quantum Chemistry Archive*, 3rd ed., **1983**.
[37] a) G. A. Olah, G. K. S. Prakash, M. Barzaghi, K. Lammertsma, P. von R. Schleyer, J. A. Pople, *J. Am. Chem. Soc.* **1986**, *108*, 1032; b) W. Koch, N. Heinrich, H. Schwarz, F. Maquin, D. Stahl, *Int. J. Mass. Spectrom. Ion Processes* **1985**, *67*, 305.
[38] D. M. Brouwer, A. A. Kiffen, *Recl. Trav. Chim. Pays-Bas* **1973**, *92*, 809.
[39] G. A. Olah, G. D. Mateescu, *J. Am. Chem. Soc.* **1971**, *93*, 781.
[40] G. A. Olah, S. H. Yu, *J. Am. Chem. Soc.* **1975**, *97*, 2793.
[41] L. B. Krivdin, S. V. Zinchenko, G. A. Kalabin, J. C. Facelli, M. F. Tufno, R. H. Contreras, A. Yu. Denisov, O. A. Gavrilyuk, V. I. Mamatyuk, *J. Chem. Soc. Faraday Trans.* **1992**, *88*, 2459.
[42] G. A. Olah, A. Germain, A. M. White in *Carbonium Ions, Vol. 5* (Eds.: G. A. Olah, P. von R. Schleyer), Wiley-Interscience, New York, **1976**, p. 2049–2133, and references therein.
[43] K. Shudo, lecture at the Loker Hydrocarbon Research Institute Symposium, University of Southern California, Los Angeles, January 1992.
[44] a) D. M. Brouwer, A. A. Kiffen, *Recl. Trav. Chim. Pays-Bas* **1973**, *92*, 689, 809, 906; b) G. A. Olah, A. Germain, H. C. Lin, D. A. Forsyth, *J. Am. Chem. Soc.* **1975**, *97*, 2928.
[45] W. Koch, G. Frenking, H. Schwarz, F. Maquin, D. Stahl, *Int. J. Mass Spectrom. Ion Processes* **1985**, *63*, 59.
[46] a) I. S. Akhrem, A. V. Orlinkov, L. V. Afanaseva, M. E. Vol'pin, *Dokl. Acad. Nauk SSSR* **1988**, *298*, N1 107; b) M. Vol'pin, I. Akhrem, A. Orlinkov, *New J. Chem.* **1989**, *13*, 771.
[47] M. E. Vol'pin, I. S. Akhrem, *Proc. Fifth Int. Symp. Rel. Homogeneous Heterogeneous Catal.* (Novosibirsk), VNU Science Press NV, Utrecht, **1986**, p. 136.
[48] P. W. Hartland, N. D. Kim, S. A. H. Petrie, *Aust. J. Chem.* **1989**, *43*, 9.
[49] G. A. Olah, A. Germain, H. C. Lin, D. A. Forsyth, *J. Am. Chem. Soc.* **1975**, *97*, 2928.
[50] a) O. Farooq, M. Marcelli, G. K. S. Prakash, G. A. Olah, *J. Am. Chem. Soc.* **1988**, *110*, 864; b) H. Koch, W. Haaf, *Angew. Chem.* **1960**, *72*, 628.
[51] G. A. Olah, F. Pelizza, S. Kobayashi, J. A. Olah, *J. Am. Chem. Soc.* **1976**, *98*, 296.
[52] G. A. Olah, K. Dunne, Y. K. Mo, P. Szilagyi, *J. Am. Chem. Soc.* **1972**, *94*, 4200.
[53] a) M. W. Wong, B. F. Yates, R. H. Nobes, L. Radom, *J. Am. Chem. Soc.* **1987**, *109*, 3181; b) W. J. Bouma, L. Radom, *ibid.* **1983**, *99*, 5484; c) P. N. L. Summers, J. Tyrrell, *ibid.* **1977**, *99*, 3960; d) P. Cremaschin, M. Simonetta, *Theor. Chim. Acta* **1971**, *43*, 351.
[54] W. J. Hehre, L. Radom, P. von R. Schleyer, J. A. Pople, *Ab Initio Molecular Orbital Theory*, Wiley-Interscience, New York, **1986**.
[55] D. Stahl, F. Maquin, *Chem. Phys. Lett.* **1984**, *106*, 531.
[56] a) G. Gattow, V. Gerevath, *Angew. Chem.* **1965**, *77*, 132; *Angew. Chem. Int. Ed. Engl.* **1965**, *4*, 149; b) A. G. Galinos, A. A. Carotti, *J. Am. Chem. Soc.* **1961**, *83*, 752.
[57] G. A. Olah, A. M. White, *J. Am. Chem. Soc.* **1967**, *90*, 1884.
[58] G. A. Olah et al., unpublished results.
[59] W. Koch, H. Schwarz, *Chem. Phys. Lett.* **1986**, *125*, 443.
[60] M. Attina, F. Cacace, A. Ricci, presented at the Congress of the Italian Chemical Society 1990 in San Benedetto del Tronto.
[61] W. Kwasnik in *Handbuch der Präparativen Anorganischen Chemie, Vol. 1* (Ed.: G. Brauer), Enke, Stuttgart, **1975**, p. 234.
[62] G. A. Olah, D. H. O'Brien, C. U. Pittman, Jr., *J. Am. Chem. Soc.* **1967**, *89*, 2996.
[63] K. O. Christe, *Inorg. Chem.* **1975**, *14*, 2230.
[64] G. A. Olah, G. K. S. Prakash, M. Marcelli, K. Lammertsma, *J. Phys. Chem.* **1988**, *92*, 878.
[65] M. B. Krogh-Jespersen, J. Chandrasekhar, E. U. Würthwein, J. B. Collins, P. von R. Schleyer, *J. Am. Chem. Soc.* **1980**, *102*, 2263.
[66] D. B. Adams, *J. Chem. Soc. Faraday Trans. 2* **1977**, *73*, 991.
[67] H. F. Prest, W.-B. Tzeng, M. J. Brom, C.-Y. Ng, *J. Am. Chem. Soc.* **1983**, *105*, 7531.
[68] a) L. Radom, unpublished results; b) S. A. Pope, I. H. Hillier, M. F. Guest, *Faraday. Symp. Chem. Soc.* **1984**, *19*, 1.
[69] K. Laali, H. Y. Chen, R. J. Gerzina, *J. Org. Chem.* **1987**, *52*, 4126.
[70] G. A. Olah, T. Nakajima, G. K. S. Prakash, *Angew. Chem.* **1980**, *92*, 837; *Angew. Chem. Int. Ed. Engl.* **1980**, *19*, 811.
[71] G. A. Olah, A. M. White, D. H. O'Brien, *Chem. Rev.* **1970**, *70*, 561, and references therein.
[72] G. A. Olah, A. Ku, A. M. White, *J. Org. Chem.* **1969**, *34*, 1827.
[73] G. A. Olah, M. R. Bruce, F. L. Clouet, *J. Org. Chem.* **1981**, *46*, 438.
[74] a) *Friedel-Crafts and Related Reactions, Vols. 1–4* (Ed.: G. A. Olah), Wiley-Interscience, New York, **1963–1965**; b) G. A. Olah, *Friedel-Crafts Chemistry*, Wiley-Interscience, New York, **1973**.
[75] G. A. Olah, J. R. DeMember, *J. Am. Chem. Soc.* **1969**, *91*, 2113.
[76] Siehe [5], and references therein.
[77] G. A. Olah, J. R. DeMember, R. H. Schlosberg, *J. Am. Chem. Soc.* **1969**, *91*, 2112.
[78] G. A. Olah, *Chem. Scr.* **1981**, *18*, 97.
[79] G. A. Olah, *J. Am. Chem. Soc.* **1972**, *94*, 808.
[80] G. A. Olah, G. K. S. Prakash, R. E. Williams, L. D. Field, K. Wade, *Hypercarbon Chemistry*, Wiley-Interscience, New York, **1987**.
[81] a) K. Lammertsma, G. A. Olah, M. Barzaghi, M. Simonetta, *J. Am. Chem. Soc.* **1982**, *104*, 6851; b) K. Lammertsma, M. Barzaghi, G. A. Olah, J. A. Pople, P. von R. Schleyer, M. Simonetta, *ibid.* **1983**, *105*, 5258.
[82] a) F. Scherbaum, A. Grokmann, B. Huber, C. Krüger, H. Schmidbaur, *Angew. Chem.* **1988**, *100*, 1602; *Angew. Chem. Int. Ed. Engl.* **1988**, *27*, 1544; b) F. Scherbaum, A. Grokmann, G. Müller, H. Schmidbaur, *ibid.* **1989**, *101*, 464 and **1989**, *28*, 463.
[83] a) G. A. Olah, G. Klopman, *Chem. Phys. Lett.* **1971**, *11*, 604; b) D. Stahl, F. Maquin, T. Gäumann, H. Schwarz, P. W. Carrupt, P. Vogel, *J. Am. Chem. Soc.* **1985**, *107*, 5049; c) M. W. Wang, L. Radom, *ibid.* **1989**, *111*, 1155.
[84] K. Lammertsma, *Rev. Chem. Intermed.* **1988**, *9*, 141, and references therein.
[85] G. A. Olah, L. Heiliger, G. K. S. Prakash, *J. Am. Chem. Soc.* **1989**, *111*, 8020.
[86] G. A. Olah, Y. K. Mo in *Carbonium Ions, Vol. 5* (Eds.: G. A. Olah, P. von R. Schleyer), Wiley-Interscience, New York, **1976**, p. 2135–2262, and references therein.
[87] a) R. D. Bach, R. C. Badger, *Synthesis* **1979**, 529; b) H. Vancik, K. Percac, D. E. Sunko, *J. Am. Chem. Soc.* **1990**, *112*, 7418; c) J. Sommer, lecture at the Loker Hydrocarbon Research Institute Symposium, University of Southern California, Los Angeles, January 1992; J. Sommer, J. Bukala, S. Rouba, R. Graff, A. Ahlberg, *J. Am. Chem. Soc.*, submitted; d) S. Delavarenne, M. Simon, M. Fauconet, J. Sommer, *J. Chem. Soc. Chem. Commun.* **1989**, 1049; J.-C. Culman, M. Simon, J. Sommer, *ibid.* **1990**, 1098; J. Sommer, J.-C. Culman, S. Delavarenne, M. Fauconet, M. Simon, *Actual. Chim.* **1991**, 55; J. Bukala, J.-C. Culman, J. Sommer, *J. Chem. Soc. Chem. Commun.*, in press; e) G. K. S. Prakash, J. W. Bausch, G. A. Olah, *J. Am. Chem. Soc.* **1991**, *113*, 3203; f) G. A. Olah, A. Wu, O. Farooq, *J. Org. Chem.* **1989**, *54*, 1463; G. A. Olah, O. Farooq, Q. Wang, A. Wu, *ibid.* **1990**, *55*, 1224; G. A. Olah, Q. Wang, *Synthesis*, in press.
[88] BCl_2^+ have not yet been observed directly, but analogues with strong electron-donating groups such as $[tmpBN(CH_3)_2]^+$ as substituents were reported. H. Nöth, R. Staudigl, *Angew. Chem.* **1981**, *93*, 830; *Angew. Chem. Int. Ed. Engl.* **1981**, *20*, 794.
[89] a) G. A. Olah, *Friedel-Crafts Chemistry*, Wiley-Interscience, New York, **1973**; b) T. Harada, T. Ohno, S. Kobayashi, T. Mukaiyama, *Synthesis* **1991**, 1216.
[90] a) D. T. Hurd, *J. Am. Chem. Soc.* **1948**, *70*, 2053; b) G. A. Olah, L. D. Field, K. Lammertsma, D. Pacquin, K. Suemmerman, *Nouv. J. Chim.* **1983**, *7*, 279.
[91] Y. Li, X. Wang, F. Jensen, K. Houk, G. A. Olah, *J. Am. Chem. Soc.* **1990**, *112*, 3922.
[92] a) J. Emsley, V. Gold, M. J. B. Jais, L. Z. Zdunek, *J. Chem. Soc. Perk in Trans. 2* **1982**, 881; J. Emsley, V. Gold, M. J. B. Jais, *J. Chem. Soc. Chem. Commun.* **1979**, 1961; b) G. M. Kramer, *J. Org. Chem.* **1975**, *40*, 298, 302; c) No reliable H_0 measurements are yet available for neat, anhydrous HBr. In 1 M anhydrous sulfolane solution it was reported, however, to be a stronger acid than H_2SO_4, but weaker than FSO_3H or $HClO_4$: R. W. Alder, G. R. Chalkey, M. C. Whiting, *Chem. Commun.* **1966**, 405.
[93] T. H. Lowry, K. S. Richardson, *Mechanism and Theory in Organic Chemistry*, 2nd ed., Harper-Row, New York, **1981**, p. 230.
[94] a) T. Ohwada, N. Yamagata, K. Shudo, *J. Am. Chem. Soc.* **1991**, *113*, 1364; b) K. Okabe, T. Ohwada, T. Ohta, K. Shudo, *J. Org. Chem.* **1989**, *54*, 733.
[95] T. Ohwada, T. Ohta, K. Shudo, *Tetrahedron* **1987**, *43*, 297.
[96] M. Yato, T. Ohwada, K. Shudo, *J. Am. Chem. Soc.* **1990**, *112*, 5341.
[97] For a review see X. Creary, *Chem. Rev.* **1991**, *91*, 1625.
[98] a) M. Yato, T. Ohwada, K. Shudo, *J. Am. Chem. Soc.* **1991**, *113*, 691; b) K. Shudo et al., personal communication.
[99] W. Koch, N. Heinrich, H. Schwarz, *J. Am. Chem. Soc.* **1986**, *108*, 5400.
[100] G. A. Olah, A. M. White, *J. Am. Chem. Soc.* **1963**, *85*, 2642.
[101] J. F. McGarrity, D. P. Cox, *J. Am. Chem. Soc.* **1983**, *105*, 3961.
[102] A. Mertens, K. Lammertsma, M. Arvanaghi, G. A. Olah, *J. Am. Chem. Soc.* **1983**, *105*, 5657.
[103] G. A. Olah, R. Malhotra, S. C. Narang, *Nitration: Methods and Mechanisms*, VCH, New York, **1989**, and references therein.
[104] G. A. Olah, G. Rasul, R. Aniszfeld, G. K. S. Prakash, *J. Am. Chem. Soc.* **1992**, *114*, 5608.
[105] G. A. Olah, H. C. Lin, *Synthesis* **1974**, 444.
[106] G. A. Olah, K. Laali, G. Sanford, *Proc. Natl. Acad. Sci. USA* **1992**, *89*, 6670.
[107] G. A. Olah, A. Germain, H. C. Lin, D. Forsyth, *J. Am. Chem. Soc.* **1975**, *97*, 3928.
[108] P. Cremaaschin, M. Simonetta, *Theor. Chim. Acta* **1974**, *34*, 175.
[109] NO_2H^{2+} was recently also observed experimentally in mass spectrometric studies: T. Weiske, W. Koch, H. Schwarz, *J. Am. Chem. Soc.*, submitted.
[110] K. Tanabe, *Solid Acids and Bases*, Academic Press, New York, **1970**.
[111] a) E. M. Arnett, R. A. Haaksma, B. Chawla, M. H. Healy, *J. Am. Chem. Soc.* **1986**, *108*, 4888; b) P. Batamack, C. Doremieux-Morin, J. Fraissard, *Catal. Lett.* **1991**, *11*, 119.
[112] W. O. Haag, R. H. Dessau, Int. Catalaytic Congress, Berlin, **1984**, II. 105.

Transition Metal Complexation of σ Bonds

By Robert H. Crabtree*

The first σ complexes were found in the 1960s and 1970s, but they did not attract more than passing attention. Only now are we beginning to recognize their key role in the chemical reactions of σ bonds, and this has encouraged more detailed study. In contrast with the more familiar π-donor complexes such as M–(CH_2=CH_2) and complexes like M–NH_3, in which the lone pair of electrons on the N atom is bound to the metal atom, in a σ complex an X–H group binds to the transition metal atom; the X–H σ-bonding electron pair acts as a 2e donor to give an (X-H)-M type complex. Dihydrogen complexes (X = H) are one important group of σ complexes. C-H-M complexes (X = R_3C) with an agostic C-H-M interaction have not only been found in the ground state but also implicated in the transition states of many important organometallic transformations such as Ziegler–Natta catalysis and sigma bond metathesis. The importance of X–H bond activation will encourage continued growth in this field.

1. Introduction

An electrophile E^+ can react with an X–H bond to give a σ complex **1**, in which the X–H bond acts as a 2e donor. **1a** and **1b** show two common ways of representing **1**. Coordination to E^+ alters the chemical properties of the X–H bond and can activate it either for nucleophilic attack at X or deprotonation [Eq. (1)]. In many cases adduct **1** is not

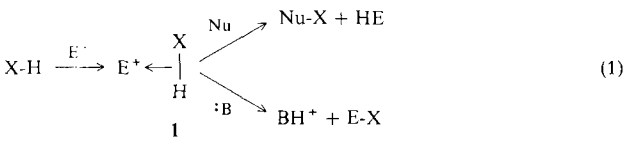

(1)

1

stable enough to be isolable in the condensed phase. For example, the gas-phase species H_3^+ (**2**, H–H = 0.88 Å),[1] the adduct of H_2 and a proton, is too strong an acid to exist in solution.

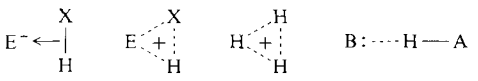

1a **1b** **2** **3**

The X–H bond is always coordinated side-on to E^+, as in **1**, in sharp contrast to the linear structure **3** (HA = acid, B = base).

Since **1** is a two-electron system, only the Ψ_1 molecular orbital, which bonds over all three centers, is filled (Fig. 1a). This three center, two-electron (3c-2e) bond therefore leads to a closed structure. In contrast, **3** is a four-electron system, and so Ψ_2 must be filled. As this molecular orbital has an antibonding interaction on one side of the triangle, formation of a linear structure is preferred. Sometimes steric effects or the conformation of the molecule prevent a 3c-2e bond from adopting its preferred geometry, and an "open" or canted side-on arrangement is adopted.

Main group elements often form bridged hydrides (e.g. B_2H_6) and alkyl complexes (e.g. $(LiMe)_4$), and even in carbon chemistry, several isolable cations with 3c-2e bonds are now known.[2] The prospects for isolating main group dihydrogen complexes have been examined theoretically.[3]

If the electrophile is a transition metal ion then the HX(σ) → M bond is much the same as in H_3^+ (Fig. 1b); however, the d_π electrons on the metal can now strengthen the M–(HX) interaction by backbonding into the HX σ* orbital (Fig. 1c). Modest backbonding accounts for the sta-

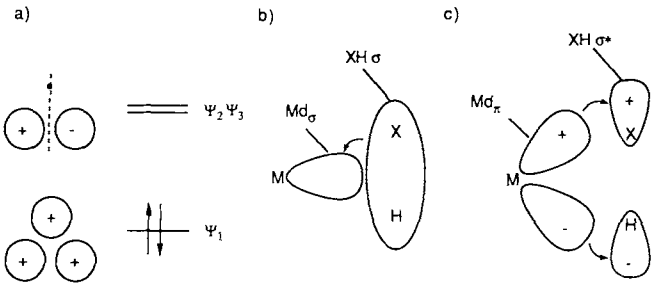

Fig. 1. The bonding picture for a σ complex. a) In H_3^+ only the totally symmetric orbital Ψ_1, which bonds over all three centers, is occupied. Occupation of Ψ_2 would lead to the opening of one edge of the triangle (nodal plane marked as a dotted line). b) In an M-(H-X) complex the electrons of the X–H σ bond are donated to an empty metal d_σ orbital. This resembles the totally symmetric Ψ_1 orbital in H_3^+ and is analogous to the binding of the lone pair on NH_3 to a metal atom. c) Electron density from the M(d_π) orbital is donated to the XH σ* orbital (back-donation). This resembles $M(d_\pi) \rightarrow CO(\pi^*)$ back-donation and is unique to a transition metal σ complexes. An isolable complex must have some backbonding, but strong back-donation leads to cleavage of the X–H bond by oxidative addition to give an X-M-H complex.

bility of many σ complexes, but strong backbonding can lead to X–H bond scission in the process known as oxidative addition to give compounds of the type X-M-H as shown in Equation (2).

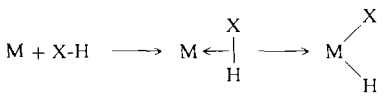

(2)

In complexes with weak backbonding, the length of X–H bond is similar to that in free X–H. The acidity and electrophilicity of XH can be strongly enhanced, however, because σ bonding reduces the electron density in the X–H unit. Stronger back-donation can lead to σ complexes with elongated X–H bonds and reduced electrophilicity of the X–H group.

[*] Prof. Dr. R. H. Crabtree
Yale Chemistry Department
New Haven, CT 06511-8118 (USA)

The strength of the M–(HX) interaction is also affected by the energy of the X–H σ and σ* orbitals. The more basic X–H systems (e.g., Si–H compounds) have higher lying σ orbitals which lead to enhanced M–(HX) σ bonding. Weaker X–H bonds such as M–H bonds will have lower energy σ* orbitals, leading to enhanced π back-donation. As expected from this analysis, M-H-M and Si-H-M complexes are almost always strongly bound, and the X–H bond is substantially stretched relative to the free state.

Perhaps one of the most striking examples of a σ complex is the dihydrogen complex **4**[4] (cy = cyclohexyl) synthesized by Kubas et al., which was one of the most significant recent

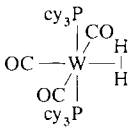

4

discoveries in inorganic chemistry. The formation of **4** was proved by NMR spectroscopy and neutron diffraction methods; its slow reversible equilibration [Eq. (3)] with complex **5**, the product of oxidative addition, was studied by NMR spectroscopy.

$$\underset{\mathbf{4}}{[W(H{-}H)(CO)_3(Pcy_3)_2]} \rightleftharpoons \underset{\mathbf{5}}{[W(H)_2(CO)_3(Pcy_3)_2]} \qquad (3)$$

If complex **4** is regarded as being derived from $(CO)_3(Pcy_3)_2W + H{-}H$, then it must be considered a σ complex. This is appropriate because the H–H distance in **4** (0.82 Å by neutron diffraction) is little changed from its value in free H_2 (0.74 Å). Since the H–H bonds in most H_2 complexes are not stretched, it is not surprising that the activation energy for loss of H_2 (more generally XH) is not usually large. Facile loss of XH can be important in applications to catalysis, for example, because the resulting coordinatively unsaturated intermediates may be very reactive.

We can also look at σ complexes as being derived from the classical adduct $[L_nM(X)(H)]$ in which an attractive interaction between X and H causes these two ligands to approach one another. This description is more appropriate for "stretched" σ complexes in which the X–H distance is substantially longer than in the free XH molecule. Such stretched complexes with H_2 ligands are known but are most common with Si–H ligands. Eisenstein et al.[5] have shown how hydrido ligands even in classical dihydrides of type $[L_nMH_2]$ have a mutually attractive interaction not present in CH_4.[5b] Attractive interactions between ligands are likely to facilitate reactions such as reductive elimination and insertion, reactions in which two ligands must approach each other to reach the transition state. Factors that stabilize a complex like **6** should also stabilize the transition state for oxidative addition and reductive elimination [Eq. (4)] and lower the activation energy. This helps explain the special facility of these reactions in transition metal complexes.

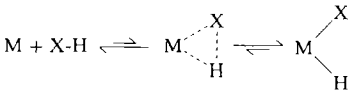

(4)

6

Some other transition metal σ complexes, for example, with B–H, Si–H, and C–H bonds, were known before 1970. As early as 1960, Nöth and Hartwimmer[6] prepared the Ti^{III} complex $[Cp_2Ti(H_2BH_2)]$ and proposed an M-H-B bridged structure based on IR data. Kaesz, Dahl, et al. were the first to prove B-H-M bridging crystallographically in $[Mn_3(CO)_{10}(H)(B_2H_6)]$, which has one Mn-H-Mn and six B-H-Mn bridges.[7]

While boranes commonly have B-H-B bridges, analogous structures are not found in silanes and alkanes; the first C-H-M and Si-H-M systems thus were particularly noteworthy. Ibers et al.[8] drew attention to a close CH···M contact of 2.6 Å in $[RuCl_2(PPh_3)_3]$ but preferred not to infer any special attractive interaction; similar effects were seen in other compounds.[9] In 1968, Trofimenko[10] proposed a CH···M interaction in **7** (R = H) based on the high-field signal in the C-*H* NMR spectrum ($\delta = -2.4$) and evidence in the IR spectrum of a weak C–H bond (ν(CH) = 2664, 2704 cm^{-1}). Cotton et al.[11a] confirmed the C-H-Mo bridge in **7** (R = Ph) by X-ray crystallography and proposed the now-standard 3c–2e bonding model. The fluxionality of complex **7** was studied by NMR spectroscopy and an estimated activation energy of 17–20 kcal mol^{-1} was associated with the M–HC binding energy.[11b] A complex analogous to **7** with a B-H-M bridge was also prepared.[11c] In related work Perutz, Poliakoff, Turner, et al. presented strong evidence from IR spectroscopy for the binding of CH_4 to $M(CO)_5$ (M = Cr, Mo, W) in a methane matrix.[12]

The first silane σ complex (**8**) was formed from R_2SiH_2 and $[Re_2(CO)_{10}]$. When R is methyl, the coupling constant J(R,Si-*H*) in the ^1H NMR spectrum is reduced from 4.2 Hz in the free silane to 1.5 Hz in the complex.[13a] The first mononuclear silane σ complex was mentioned at an Ameri-

Robert H. Crabtree, born in London in 1948, was an undergraduate at Oxford with Dr. M. L. H. Green and a graduate student at Sussex University with Prof. J. Chatt. He then spent four years at the CNRS Natural Products Lab at Gif with Dr. H. Felkin. He has been at Yale since 1977 and since 1985 as Full Professor. He won the Organometallic Chemistry prizes of the Royal Society of Chemistry (1990) and the American Chemistry Society (1993) and is the author of an organometallic chemistry text.

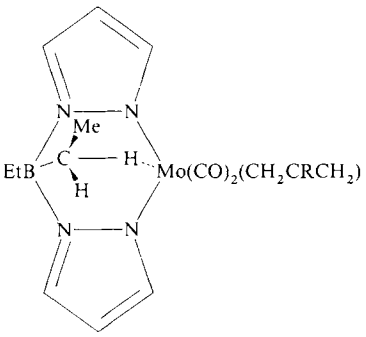

7

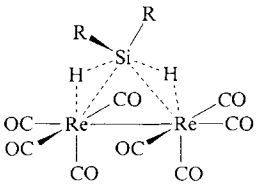

8

can Chemical Society meeting and reported in 1970 only as a news item in *Chemical & Engineering News*.[13b] One reason that the field did not develop significantly at that time may have been the misconception that such relatively weak M–(XH) interactions as found in **7** would not have usefully large effects on the reactivity of the X–H bond.

Starting in the early 1980s, the activity in the area of C–H activation led to renewed interest in compounds with C-H-M bridges. In their 1983 review, Brookhart and Green[14] directed attention to C-H-M systems, which they named agostic. During the same period, Schubert et al.[15] carefully defined the chemistry and structure of a homologous series of Si-H-M systems which they also examined with neutron diffraction.

With the identification of σ complexes the three-part structure of modern coordination chemistry is complete. The field started with Werner's studies of complexes with lone pair donors such as NH_3. The recognition of π-donor complexes in the 1950s led to the development of organometallic chemistry. The recent developments in the studies of σ complexes have been encouraged by the current interest in σ-bond activation.

2. Dihydrogen Complexes

In spite of their relatively recent discovery, dihydrogen complexes are prototypes of σ complexes. Reviews by Kubas,[4b] myself,[16] and especially by Jessop and Morris[17] report work from over 300 papers. Dihydrogen or (η^2-H_2) complexes are sometimes called nonclassical as opposed to classical hydrido complexes, which have terminal M–H bonds only. The strength of M→(H_2) backbonding largely determines if [$L_nM(H)_2$] or [$L_nM(H_2)$] is formed (Fig. 1). Morris proposed that in the IR spectrum of [$L_nM(N_2)$] a $\nu(N_2)$ band in the range 2060–2160 or 2180 cm^{-1} indicates that the L_nM complex fragment has a π-basic character appropriate for forming [$L_nM(H_2)$].

It is not always easy to differentiate between $M(H)_2$ and M(η^2-H_2) complexes. Neutron diffraction studies are difficult and only five structures have been published. Determining the position of an H_2 ligand may or may not be possible in X-ray structure analyses. Spectroscopic methods are therefore of key importance in characterization. Kubas[18] identified the absorption at 2800 cm^{-1} in the IR spectrum of **4** as the "$\nu(H_2)$" stretch; for free H_2, $\nu(H_2)$ is observed at 4000 cm^{-1} (Raman). Unfortunately, Raman studies on H_2 complexes have not been successful because the complexes decomposed under laser irradiation even when exceptional precautions were taken.[19] The coupling constant ^1J(H,D) of 32 Hz in the ^{1}H NMR of the HD analogue of **4** was a most convincing piece of spectroscopic evidence, since the coupling constant for free HD is 43 Hz, and for the classical H-M-D complexes <1 Hz. The neutron diffraction study of **4** gave a separation r(H–H) of 0.82 Å, but librational motion of the H_2 ligand may make this value too short. The distance r(H–H) of 0.86 Å determined by solid-state NMR is probably more accurate.[20]

Before 1984, many undetected H_2 complexes had certainly been made. In most cases, protonation of a metal hydride gives an H_2 complex, at least as an intermediate. This complex often loses H_2 and undergoes further reactions to form a stable compound. In 1971, Aresta et al.[21] reported the synthesis of "[$FeH_4(PR_3)_3$]"; they were obviously puzzled by an unexpected IR band at 2380–2400 cm^{-1} which disappeared on loss of H_2 and formation of [$FeH_2L(PR_3)_3$] (L = N_2 or vacancy). We were able to reassign the complex as [$FeH_2(H_2)(PR_3)_3$] in 1986 on the basis of T_1 measurements (NMR spectroscopy);[22] this result was later confirmed by neutron diffraction experiments [r(H–H) = 0.82(1) Å].[23]

The T_1 method we proposed for identifying (η^2-H_2) complexes[24] is often useful. Two protons that are close together (<1 Å) relax very rapidly primarily by the dipole–dipole (DD) mechanism. Thus T_1 for the spin of the H_2 ligand in the ^{1}H NMR spectrum can be very short. T_1 is a function not only of structure of the complex but is also dependent on the magnetic field strength of the spectrometer and on molecular motion (temperature and solvent). We found that the complicating factor of molecular motion in solution could be removed by studying the temperature dependence of T_1. Unless the moment of inertia of the molecule is too small (e.g., $[ReH_9]^{2-}$), a minimum T_1 value, denoted T_1(min) can be found at a readily accessible temperature, usually between −80 and 20 °C. Since T_1(min) scales with spectrometer field, the field used must be cited. Although T_1 values determined at arbitrary temperatures cannot be compared with each other, T_1(min) values may be compared even for compounds with different moments of inertia.

The interpretation of the resulting T_1(min) value went through several improvements with time. We argued that in a dihydrogen complex the relaxation of the spins of the closely spaced pair of H_2 protons should be dominated by DD relaxation. We showed[25] that the calculated contribution to DD relaxation from all possible pairs of H ligands in a structurally characterized series of complexes was in reasonable agreement with experiment. Morris et al.[26a] pointed out that if the H_2 ligand is rapidly spinning, the rate of relaxation should fall to 25% of the static value. The assumption of a freely rotating H_2 ligand resulted in substantially better agreement. Since much of the activation energy for M–(H_2) rotation must be due to backbonding in the M–(H_2) bond, which must be small for an η^2-H_2 ligand, fast rotation is consistent with the bonding scheme of Figure 1. Eckert et al. measured the activation energy for the rotation of the H_2 ligand in [$MH(H_2)\{P(CH_2CH_2PPh_2)_3\}$]$BPh_4$ by inelastic neutron scattering.[26b] This is indeed small but higher for M = Fe (1.82 kcal mol^{-1}) than for M = Ru (1.36 kcal mol^{-1}), as previously proposed by Morris on the basis of the T_1 values and the higher lability of the Ru com-

plex, even though Ru is normally considered to be more π-basic.[26c]

The T_1(min) value for $[ReH_7(PPh_3)_2]$ is lower than for most classical hydrides but higher than for most nonclassical species, which led us to propose[22] that this and related species "might...constitute an intermediate group". This seemed to be contradicted by the neutron diffraction structure of $[ReH_7(dppe)]$ (dppe = $Ph_2PCH_2CH_2PPh_2$) determined by Howard et al.,[27] which showed it to be a classical heptahydride. Since the T_1 value for the dppe complex is 13% less than that predicted from the structure (assuming only H–H dipole–dipole relaxation), additional contributions to spin relaxation had to be present. Cotton et al.[28a] suggested several possibilities. Halpern et al.,[28b] Bakhumutov et al.,[28c] and our own group[29a] attributed the additional contribution to spin relaxation to metal–hydrogen DD relaxation. It is now clear that for Re, Nb, V, Mn, Co, and Ta, the M–H DD contribution, easily calculated assuming normal M–H distances, must be subtracted from the observed T_1(min) value to make the data comparable with those from hydrido complexes of other metals. Once corrected in this way, a short T_1(min) value (<40 ms at 250 MHz) denotes a nonclassical structure and a long T_1(min) (>100 ms) a classical structure; for intermediate values a distinction cannot be made, however.[29b]

The story took an unexpected turn when Howard, Koetzle, et al.[30] found that in **9** one H_2 unit has an unprecedented r(H–H) of 1.357 Å (neutron diffraction, Fig. 2). This distance was much longer than those in the previously reported H_2 complexes and supported the existence of an intermediate group between classical hydrides and "normal" H_2 complexes—stretched H_2 complexes. There was some initial question as to whether **9** really is an H_2 complex, but there is good evidence that it is. Complex **9** does not adopt the tricapped trigonal-prismatic structure found for all known classical nine-coordinate polyhydrido complexes (including $[ReH_7(dppe)]$), but has the dodecahedral coordination expected for an eight-coordinate complex (the midpoint of the stretched H_2 ligand is considered one of the coordination positions). Molecular mechanics calculations[31] show that the smallest separation between nonbonded hydrogen atoms in strained organic structures is 1.7 Å. Finally, the T_1 value of **9** is best interpreted if the H_2 ligand is assumed to be rapidly rotating about the M–(H_2) axis, as expected for H_2 complexes but not classical hydrides. Morris et al.[17] suggested a r(H–H) range of 1.1–1.6 Å as appropriate for stretched H_2 complexes. $[ReH_7L_2]$ complexes analogous to **9** may be borderline cases as was emphasized by the HF-SCF theoretical studies of Hay et al. on the complex with L = PH_3, which suggested that the classical form is only 2–4 kcal mol^{-1} more stable than the nonclassical one. PH_3 is a better donor ligand than PAr_3 (Ar = aryl) and should therefore stabilize the classical form.[32]

$[ReH_7\{P(p\text{-}C_6H_4CH_3)_3\}_2]$ **9**

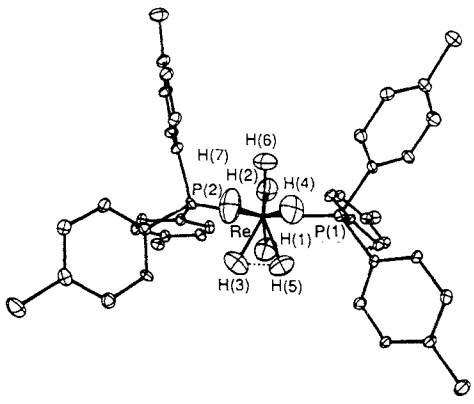

Fig. 2. The structure of the first stretched H_2 complex **9** (obtained by neutron diffraction). The H3–H5 distance in the H_2 ligand is 1.357 Å. The view is approximately aligned along the pseudo-S_4 axis of the dodecahedron. The unlabeled atoms are the carbon atoms of the tolyl groups (from ref. [30]).

One reason that the stretched H_2 ligand in **9** was so unexpected is that the previously known hydrides with structures on the borderline between classical and nonclassical (**4**/**5**, **10**/**11**, **12**/**13**)[33] have two tautomers in solution, one classical, the other nonclassical but with a normal (i.e. unstretched) H–H distance. As the activation energies are sufficiently large, 16 kcal mol^{-1} for reaction (3), 11.2 kcal mol^{-1} for reaction (5), and 11.6 kcal mol^{-1} for reaction (6), the two forms can be distinguished by NMR spectroscopy at low temperature. It has generally been thought that the activation barrier is due to cleavage of the H_2 bond. Now it seems far more likely that the energy barrier arises from the rearrangement of the heavy ligands, and that the hydrido ligands in the classical forms are not *cis* to each another but as shown in Equation (5) for **10** → **11**. This picture is also consistent with the absence of a kinetic isotope effect for reaction (3)[34a] and Morokuma's RHF study[34b] of the oxidative addition of H_2 to the $Pt(PH_3)_2$ complex fragment. The H–H distance in the transition state was calculated to be only 0.77 Å, but the P-Pt-P angle decreases from 180° to 130°.

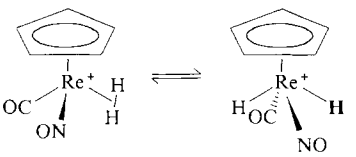

(5)

10 **11**

$[ReH_4(CO)L_3]^+ \rightleftharpoons [ReH_2(H_2)(CO)L_3]^+$ (6)

12 **13**

If there were little or no change in the positions of the heavy ligands, the equilibration of classical and nonclassical forms might be very fast on the NMR timescale, which could complicate physical studies and characterization. In this case, the coupling constants J(H,D) and J(H,P) should be temperature- and perhaps solvent-dependent. Such behavior was found for *trans*-$[Os(H_2)H(depe)_2]^+$ (depe = $Et_2PCH_2CH_2PEt_2$) which may therefore be a candidate for fast equilibration.[35a]

An interesting illustration of the importance of the positions of the heavy atoms is the solid-state chemistry of a complex synthesized by Bianchini et al. Crystalline $[Co(PP_3)(N_2)]^+$ undergoes reversible substitution of the N_2 ligand for H_2, but two different isomers of the product can be formed, classical or nonclassical, depending on the coun-

terion. X-ray studies of the BPh_4^- salt show that formation of the classical dihydride requires considerable rearrangement of the geometry around Co. This rearrangement is presumably favored by packing effects in this salt. In contrast, when PF_6^- is used as the counterion, the nonclassical H_2 complex is formed. In solution the H_2 complex is always formed, whatever the counterion.[36]

Several other stretched H_2 complexes are now known (Table 1). Their properties are intermediate between those of H_2 complexes with normal H–H separations and classical hydrides. For example, $[ReH_5(H_2)L_2]$ ($L = P(p\text{-tolyl})_3$) loses H_2 when warmed to 60 °C, while the classical hydride $[ReH_7L_2]$ (L_2 = dppe) survives intact to >120 °C. H_2 complexes with normal H–H separations tend to lose H_2 at much lower temperatures; however, there are as yet no unstretched H_2 complexes in the $[ReH_7L_2]$ series for a direct comparison. Unlike normal H_2 complexes whose pK_a would be expected to be no higher than 15, the stretched H_2 complex $[ReH_7(PPh_3)_2]$ requires a very strong base such as *n*BuLi for deprotonation.[32]

Table 1. Selected structural and NMR data for some stretched dihydrogen complexes.

Complex	H-H [Å]	Method [a]	^1J(H,D)	Ref.
$[Re(H_2)H_5\{P(p\text{-}MeC_6H_4)_3\}_2]$	1.357	nd	–	[30]
	1.35	T_1	–	[37b]
$[Re(H_2)H_5\{P(p\text{-}CF_3C_6H_4)_3\}_2]$	1.24	T_1	–	[37b]
$[Re(H_2)H_5\{P(p\text{-}MeOC_6H_4)_3\}_2]$	1.42	T_1	–	[37b]
$[Os(en)_2(H_2)(OAc)]^+$	1.34	nd	1.6	[38a]
$[Os(en)_2(H_2)(Br)]^+$	–	–	2.3	[38a]
$[Os(en)_2(H_2)(Cl)]^+$	–	–	7.2	[38a]
$[Os(en)_2(H_2)(MeCN)]^{2+}$	–	–	17.9	[38a]
$Ni(H_2)$	1.41	[b]	–	[38b]

[a] Method used to determine the H–H distance. nd = neutron diffraction, T_1 (NMR spectroscopy). [b] Theoretical value determined by CMD-CI calculations.

Unstretched H_2 complexes do not show a very large change in T_1(min) or ^1J(H,D) when the electronic properties of the metal center are altered by changing the ligands. We found that the exchange of $L = PMe_2Ph$ for $P(OCH_2)_3CEt$ or CO in $[RuH(H_2)L(triphos)]^+$ (triphos = $PhP(CH_2CH_2PPh_2)_2$) had only a small effect on these parameters.[37a] Stretched H_2 complexes are much more sensitive to electronic effects. The T_1(min) values for a series of $[Re(H_2)H_5\{P(p\text{-}XC_6H_4)_3\}_2]$ complexes vary with the electron donor/acceptor properties of X in a way that suggests that the strongest donor group, OMe, leads to a lengthening of $r(H\cdots H)$ to 1.42 Å and the strongest acceptor group, CF_3, causes a shortening to 1.24 Å.[37b]

A remarkable series of stretched H_2 complexes was prepared recently by Taube et al.[38a] In the complex ions $[Os(en)_2(H_2)(X)]^{n+}$ the coupling constant ^1J(H,D) varies greatly: the complex with X = OAc, $n = 1$ [r(H–H) = 1.34 Å by neutron diffraction] has a ^1J(H,D) value of 1.6 Hz; the complex with X = MeCN, $n = 2$, a value of 17.9 Hz. This J(H,D) value of 1.6 Hz is much less than that found for normal H_2 complexes (12–34 Hz), but the acetonitrile complex has a coupling constant within the normal range. We now need to know how the chemical and physical properties of the H_2 ligand vary with r(H–H).

A useful review of theoretical work has been published by Burdett, Eisenstein, et al.[39] Theoretical studies by Siegbahn et al. suggest that the binding energy in $[Ni(H_2)]$, with an $H\cdots H$ distance of 1.41 Å, is as much as 9.5 kcal mol^{-1} with respect to Ni and H_2. Figure 3 shows how the $H\cdots H$ bond energy for two free H atoms changes with distance according to Kolos and Wolniewicz.[38c,d] A surprisingly large proportion of the H–H bond energy is retained at long distances (e.g. about 50% at 1.35 Å).

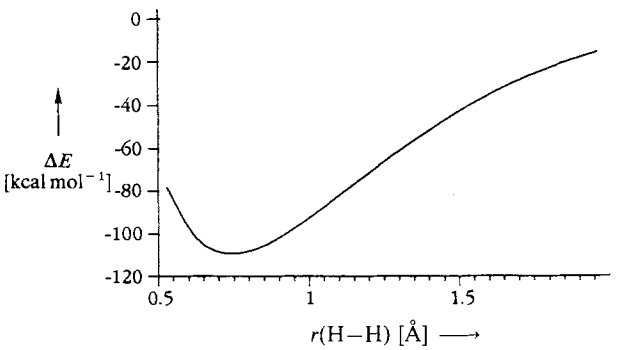

Fig. 3. The potential energy curve for two isolated H atoms according to the calculations of Kolos and Wolniewicz (from ref. [38c,d]).

Strong $H\cdots H$ interactions are probably involved in quantum exchange coupling. Heinekey et al.[40a] were very surprised to find that in the ^1H NMR spectrum of $[Cp^*IrH_3]^+$ the hydride resonances showed very temperature-dependent second-order signals. Attempts to analyze these in the usual way provided apparent H,H′ coupling constants that were unusually large and extremely temperature dependent. For example, for the Ir complex with $L = AsPh_3$, J_{app} changed from 376 Hz at 176 K to 570 Hz at 189 K. A neutron diffraction study showed that all the $H\cdots H$ distances are >1.67(1) Å and are therefore essentially nonbonding.[40b] Heinekey, Zilm, et al.[40b] and Weitekamp et al.[40c] suggested that the exchange effect is due to abnormal motion of the MH_3 unit which brings the H and H′ atoms unusually close together. Rotational tunneling of an H_2 complex has also been considered as possibly responsible for the exchange effects.[40d] The observation that the effect is quenched in the deuterated complex $[Cp^*LIr(D)(H)(D)]^+$ is consistent with quantum mechanical exchange effects being responsible, because the H and D nuclei are not identical particles. The effects can be very large. For example, for the complex with L = CO, J_{app} can approach 20000 Hz.[40e] The required close approach of the H and H′ atoms may be favored if a complex of the type $[Cp^*IrLH(H_2)]^+$ is not too far removed in energy from the ground state. Eisenstein et al. found another type of attractive interaction in $[FeH_2(H_2)(PEt_2Ph)_3]$ between the terminal Fe–H bond and the H_2 ligand in the same molecule. The major contribution to the interaction was attributed to the electron donation of the M–H(σ) to the H–H(σ^*) molecular orbital and was thought to be responsible for the conformation of the H_2 ligand and to contribute to the activation energy for the rotation of the H_2 ligand.[23]

An H_2 ligand probably bridges the two metalloporphyrin groups in the isolable complex [L(OEP)Ru(H_2)Ru(OEP)L] (L = *tert*-butyl-5-phenylimidazole, OEP = octaethylpor-

phyrin; $J(H,D) = 15$ Hz).[41] A species of this sort may be involved in reaction (7) in which two monohydrido complexes eliminate H_2.

$$2[(thf)(OEP)Ru\text{-}H] + 2THF \longrightarrow 2[(thf)_2(OEP)Ru] + H_2 \quad (7)$$

Polyhydrides are a rich source of dihydrogen complexes; Lin and Hall[42a] reported calculations at the MP2 level on a number of these compounds. They found that the nonclassical form is favored for $[MH_6L_2]^+$, $[MH_7L_2]$, and $[RuH_6L_2]$, while the classical form is favored for $[WH_4L_4]$, $[ReH_5L_3]$, $[ReH_4L_4]^+$, $[MoH_4L_4]$, and $[OsH_5L_3]$ (L = PH_3; M = Rh, Ir). The heptahydrides are as yet unknown, but would be interesting synthetic targets. Calculations on cyclopentadienylpolyhydrido complexes[42b] showed that the strongly donating Cp ligand favors formation of classical hydrides. Only for the unknown complex $[CpRh(CO)H_3]^+$ (related to Heinekey's system mentioned above) was an H_2 complex the most stable tautomer. Trispyrazolylborate, as a poorer donor ligand, may be more suitable for forming nonclassical structures such as $[\{HB(3,5\text{-}Me_2pz)_3\}Rh(H_2)H_2]$ (Me_2pz = dimethylpyrazolyl) (T_1 (min) = 42 ms at 400 MHz) prepared by von Philipsborn, Venanzi, et al.[43]

Burdett et al.[44] suggested that polyhydrido complexes best described as containing H_3 or H_n ligands may exist, but none has yet been found. Distinguishing securely between a ground state H_3 complex and its possible tautomeric forms, such as $MH(H_2)$ and MH_3, is difficult. As early as 1961, Lipscomb et al.[45a] suggested that the three *endo* hydrogen atoms in $[B_{11}H_{14}]^-$ might be arranged in the form of an equilateral triangle with short H–H distances. The X-ray structure analysis,[45b] NMR spectroscopic studies in solution and in the solid state, and theoretical studies[46] all suggest that the H ··· H distances are all entirely nonbonding (r(H–H) > 1.7 Å) and that the structural units with the *endo* H atoms consist of two BHB bridges and one terminal BH unit.

We obtained evidence for an H_3 complex in a simple "reaction" of a nonclassical polyhydride, the fluxional proton exchange between $M(H_2)$ and the M–H positions.[33c] The very fluxional classical hydride **12** (L = PMe_2Ph) is in slow equilibrium with the nonclassical tautomer **13** [Eq. (8)]. We

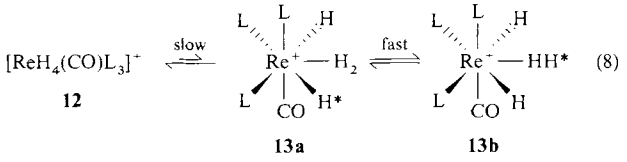

12 **13a** **13b** (8)

found that site exchange between the terminal hydrides and the H_2 ligand in **13** (**13a** → **13b**) has a significantly (1.7 kcal mol^{-1}) larger energy barrier than that for conversion between the two tautomers **12** and **13**. Thus the exchange in **13** does not proceed via the classical isomer **12**: if hydrogen exchange is not dissociative with respect to the H_2 ligand, it must be associative. After excluding other associative pathways, we were left with a mechanism in which one terminal hydride approaches the H_2 ligand, and the resulting transition state or intermediate with an H_3 ligand leads to exchange [Eq. (9)]. Since we were not able to observe

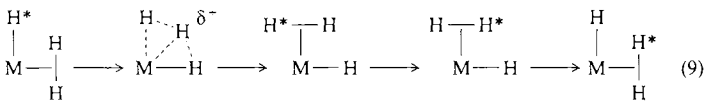

(9)

decoalescence of the signals of the classical isomer by low-temperature ^{1}H NMR spectroscopy, we assume that the barrier to site exchange is also lower than that for interchange of the two tautomers. If this is true, the most likely exchange path for the classical isomer is one in which the terminal hydrido ligands do not associate to form an H_2 ligand. Theoretical work[47] for the related complex $[Fe(H_2)H(PH_3)_4]^+$ supports the idea of an open, allyl-like η^3-H_3 complex as a transition state for fluxional exchange in **13**. Although H_3^+ itself is cyclic, at least one bond of the three-membered ring is cleaved upon binding to a metal atom as a result of back-donation. A plausible interpretation[24] of a transition state with an open H_3 unit is the transfer of a protonic H atom of an H_2 complex to the hydridic H atom of a terminal M–H group. This fluxional process is also the simplest example of a sigma bond metathesis reaction [Eq. (10)] for which the four-center transition state shown has been widely accepted. The chemistry of Equation (8) suggests that the σ complex of Equation (10) (M = Re) is a likely precursor to this transition state.

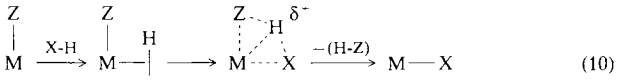

(10)

A very simple reaction of H_2 complexes is loss of H_2. This generates a two-electron vacancy at the metal center which allows a ligand such as the substrate for a catalytic reaction to bind. The complexes $[MH_4L_3]$ (M = Fe, Ru, Os; L = tertiary phosphane) all have the same stoichiometry, but the Fe and Ru complexes are very much more labile and more catalytically active for a variety of reactions, including alkane activation. Our T_1 data suggested that the Fe and Ru complexes have H_2 ligands, while the Os complex is a classical hydride;[22] this proposal was supported by neutron diffraction studies on the Fe and Os complexes.[23] Some H_2 complexes are so labile that a substantial pressure of H_2 is required for their preparation in significant quantities. A good example is the Cr analogue of **4**, which has been studied by IR and NMR spectroscopic methods under 60 atm H_2 pressure. When the magnetization corresponding to the $Cr(H_2)$ resonance was inverted, the recovery of the original magnetization follows a biexponential curve. The faster process reflects the short T_1 (min) of 10 ms, the slower is a result of slow exchange with free H_2 in solution; the activation energy for loss of H_2 extracted from the data is 12.7 (±1) kcal mol^{-1}.[48] A catalyst for alkyne hydrogenation is formed from $[RuH(H_2)\{PhP(CH_2CH_2PPh_3)_3\}]^+$ after initial loss of H_2.[49]

Heterolytic cleavage of the coordinated H_2 ligand to give a metal hydride and a proton is an important reaction for H_2 complexes. The H_2 ligand in $[IrH(H_2)(bq)(PPh_3)_2]^+$ (bq = 7,8-benzoquinolinato) is kinetically more acidic than the Ir–H group, although they must have the same pK_a.[44] Heinekey et al. described an interesting equilibrium in which

14 and **15** only slowly interconvert.[50a] The equilibrium [Eq. (11)] lies on the side of **14**, which has a pK_a of 17.5 in

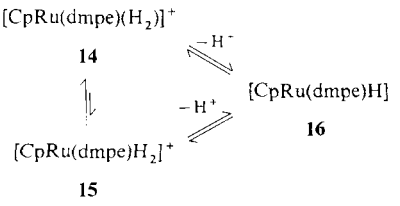

(11)

acetonitrile. In a case like this, thermodynamics requires that the less abundant compound be the most acidic, because the two tautomers share the same conjugate base. Although the dihydrogen complex is the weaker acid thermodynamically, it alone is capable of protonating the conjugate base **16** at a significant rate (according to saturation transfer in NMR spectroscopic studies).[49] The same data also imply that the terminal hydrido ligand of **16**, rather than the metal center, is the kinetically preferred site for protonation. Similarly, $[CpRu(H_2)(PPh_3)_2]^+$ is formed on protonation of the neutral hydride, but the complex irreversibly rearranges to the classical isomer on warming.[50a]

Morris et al. looked at the effect of the R group on the position of the tautomeric equilibrium and the pK_a in $[CpRuH_2(R_2PCH_2CH_2PR_2)]^+$. The change from R = *p*-$C_6H_4CF_3$ to R = Me causes the pK_a to increase from 4.5 to 10. This is a substantial shift and correlates well with the oxidation potential of $[CpRuH(R_2PCH_2CH_2PR_2)]$, which becomes easier to oxidize, and the position of tautomeric equilibrium, which moves to favor the classical isomer.[35b] Attack of D^+ on the metal atom in $[Cp_2WH_2]$ would be expected to give the classical complex $[Cp_2WH_2D]^+$. The deuterido ligand should be positioned between the two hydrido ligands, because this is the position of the M lone pair. The distribution of the isotopic label found in the product led Parkin and Bercaw to invoke protonation at M–H to give a rapidly spinning HD complex as intermediate, followed by irreversible oxidative addition of the η^2-HD ligand.[50b]

Heinekey et al.[51] and Morris et al.[52] both showed that the thermodynamic acidity of free H_2 (pK_a ca. 35)[53] can be dramatically enhanced when bound as a σ complex; the pK_a values of H_2 σ complexes are in the range of roughly 10 to −2 (water scale).[54] The acidity enhancement is comparable[55] to that produced by forming the radical cation $XH^{\cdot+}$ and greatly exceeds the acidity enhancement caused by binding XH to a metal through a lone pair on X. For example, when H_2O is bound to a divalent metal cation in the usual way through a lone pair on the O atom the acidity is typically enhanced by only about 6 pK units. Morris[56] showed how the acidity of $[L_nM(H_2)]$ complexes can be estimated from the π-donor ability of the L_nM complex fragment, which is in turn estimated from Lever's[57] electrochemical parameters for the L_nM group.

We have seen that as M–H_2 binding gets stronger, as in the stretched H_2 complexes, the acidity of H_2 complexes tends to decrease. For d^0 complexes, in contrast, higher acidity is expected because back-donation is absent, but the strength of M–H_2 binding will be small for the same reason. No d^0 dihydrogen complexes have been isolated to date; however, a labile complex between Cp_2^*Eu and H_2 has been inferred from its ^1H NMR spectrum.[58] This leads to the apparent paradox that the activation of the ligand is large when the binding is weak and vice versa.

Hydrogenolysis of d^0 alkyl complexes is usually rapid, as in the sigma bond metathesis reaction (12) (R = alkyl). Al-

$$[Cp_2ZrRCl] + H_2 \longrightarrow [Cp_2ZrHCl] + RH \quad (12)$$

though oxidative addition cannot occur in a d^0 system, an allowed alternative is the formation of an H_2 complex. The acidity of the bound H_2 ligand should be sufficient to allow protonation of the alkyl group, which is strongly basic. A mechanism with an H_2 complex as an intermediate would explain the inverse isotope effect k_{H_2}/k_{D_2} of 0.85 in the hydrogenolysis of the alkyl ligand in $[Cp_2^*Zr(CH_2tBu)Cl]$,[59] if a preequilibrium involving H_2 or D_2 coordination favored D_2, as can be the case in H_2 complexes.[60]

The metal centers in most H_2 complexes are d^6 and have octahedral coordination, but d^8, d^4, and d^2 complexes such as $[Co(H_2)P(CH_2CH_2PPh_2)_3]^+$,[61a] $[ReH_2(H_2)(CO)(PMe_2Ph)_3]^+$, and $[Re(H_2)H_5(PAr_3)_2]$ are known. In a d^0 polyhydrido complex the metal center has no lone pairs, and so the M–H bond must be protonated. At −80 °C, we find that the classical hydride $[WH_6(L_3)]$ (L_3 = PhP-$(CH_2CH_2PPh_2)_2$, T_1(min) at 250 MHz = 103 ms) is protonated reversibly in solution to give "$[WH_7(L_3)]^+$", which only loses H_2 on heating to −20 °C. The product, $[WH_{7-2x}(H_2)_x(L_3)]^+$ has a short T_1(min) value of 21 ms [Eq. (13)]. If $x = 0$ the permitted oxidation state for W would

$$[WH_6(L_3)] + H^+ \longrightarrow [WH_{(7-2x)}(H_2)_x(L_3)]^+ \quad (13)$$

be exceeded, and $x = 1$ is unlikely because a d^0 system cannot backbond and so would not be expected to give a stable H_2 complex. Thus the most reasonable formulations have $x = 2$ or 3.[62]

Direct protonation of an M–H unit was also evident for the d^6 complex [Cp*FeH(dppe)] examined by Lapinte et al. At −80 °C protonation gives the dihydrogen complex (T_1(min) at 300 MHz = 7 ms), but at −40 °C this complex irreversibly rearranges to the classical tautomer (T_1(min) at 300 MHz = 175 ms) [Eq. (14)].[63]

$$[Cp^*FeH(dppe)] \xrightarrow{H^+,\ -80\ ^\circ C} [Cp^*Fe(H_2)(dppe)]^+ \xrightarrow{-40\ ^\circ C} [Cp^*Fe(H)_2(dppe)]^+ \quad (14)$$

A reaction involving net heterolysis of dihydrogen is D_2/H^+ isotope exchange [Eq. (15)]. This seems to be very effi-

$$D_2 + ROH \rightleftharpoons HD + ROD \quad (15)$$

cient when the complex has an M–(H_2) arrangement as in $[Ru(H_2)(OEP)(thf)]$,[64] or a *cis*-$MH(H_2)$ arrangement as in $[IrH(H_2)(bq)(PPh_3)_2]^+$;[65] the classical hydrides studied were inactive. In the Ru complex, the metal center appears to increase the acidity of the H_2 ligand sufficiently so that it can directly exchange with the protons in solution. The mechanism proposed for the reaction of the Ir complex is shown in Equation (16). The role of the H_2 ligand seems simply to be to dissociate to allow D_2 access to the metal center. Once D_2

$$MH(H_2) \xrightarrow{D_2} MH(D_2) \longrightarrow MD(HD) \xrightarrow[-HD]{ROH}$$
$$MD(ROH) \longrightarrow MH(ROD) \xrightarrow{D_2} MH(D_2) + ROD \quad (16)$$

is coordinated, fluxional exchange leads to deuteration of the terminal site. Subsequent binding of the protic solvent then leads to exchange between the deuterido ligand and the bound solvent. Sterically less demanding solvents like MeOH are found to bind more strongly and to show reduced catalytic activity relative to sterically demanding solvents like *tert*-BuOH; the former probably tend to prevent the D_2 from binding to the metal by direct competition for the site at the metal.

Reversible electrochemical one-election oxidation is shown by $[Os(H_2)(NH_3)_5]^{2+}$[66a] and $[Re(H_2)Cl(PMe_2Ph)_4]$,[66b] but these complexes decompose on oxidation. The reduction of protons to H_2 has been studied in connection with the nickel-containing enzyme, hydrogenase.[67a] Electrochemical reduction of a number of Ni^{II} precursors such as **17** in protic medium leads to the evolution of H_2.[67b] Because the reaction is first order in nickel, the two

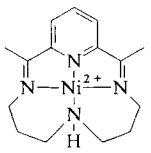

17

electron-transfer steps and the two protonation steps seem to occur on a single metal center. A $Ni^{II}(H_2)$ complex seems the most plausible immediate precursor from which H_2 is lost in this reaction [Eq. (17)].[67b] If this is the case in hydrogenase, as has been suggested,[67c] σ complexes may have biological significance.

$$Ni\text{-}L \xrightarrow{e^-} (Ni\text{-}L)^- \xrightarrow{H^+} H\text{-}Ni\text{-}L \xrightarrow{e^-,H^+} (H_2)\text{-}Ni\text{-}L \xrightarrow{-H_2} Ni\text{-}L \quad (17)$$

3. Alkane Complexes and Agostic C-H-M Systems

In its σ complexes the C–H bond is more weakly bound than is H_2 in H_2 complexes, perhaps because the C–H bond is slightly less basic and much more hindered than the H–H bond in dihydrogen ligands. There are many isolable H_2 complexes but for the moment no analogues for coordinated methane or other alkanes. For C-H-M complexes to be isolable the C–H bond must be part of a ligand L that is already strongly bound to the metal center, in which case, the chelate effect favors the binding.

The first evidence for alkane complexes[12] came from low-temperature studies of photochemically generated $M(CO)_5$ complex fragments (M = Cr, Mo, W) in an alkane or alkane/rare gas matrix. In early work, H_2 complexes were identified in studies on very similar complex fragments in H_2 matrices.[68]

Alkane complexes also appear to be intermediates in certain reactions. Moore, Bergman, et al.[69a] identified $[CpRh(CO)(H\text{–}CH_2tBu)]$ as an intermediate in the gas-phase photolysis of $[CpRh(CO)_2]$ in the presence of CMe_4. The energy of the Rh–alkane bond is at least 5 kcal mol^{-1}, and the subsequent reaction to give $[CpRh(CO)(H)(CH_2tBu)]$ has an activation energy of approximately 4.5 kcal mol^{-1} at $-100\,^{\circ}C$. In other studies,[69b] short-lived alkane and related complexes with M–alkane bond energies in the range of 7–11 kcal mol^{-1} have been detected. In complexes with coordinated CH_3F, however, an M–F bond seems more likely than a (C-H)-M bond.

Bergman et al.,[69c] Norton et al.,[70] and Heinekey et al.[71] all reported on complexes (**18**–**20**) in which isotope exchange between α-C–H and M–H sites in an alkyl hydride is faster than reductive elimination of alkane [Eq. (18)].

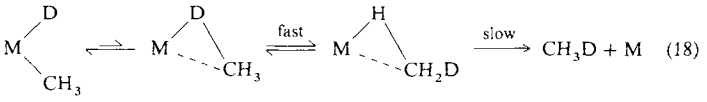

$$\xrightarrow{\text{slow}} CH_3D + M \quad (18)$$

18–**20** (M = Cp*Ir(PMe_3), **18**; Cp_2W, **19**; Cp_2Re^+, **20**)

Bergman first proposed that an alkane σ complex is involved. Complexes **18** and **20**[69c, 71] show an inverse kinetic isotope effect (k_H/k_D = 0.5 (Ir), 0.8 (Re)) for reductive elimination, which is also consistent with a preequilibrium involving an alkane σ complex before loss of alkane. The alkane complex is sufficiently long lived so the metal atom can coordinate interchangeably to different C–H bonds and reversibly undergo oxidative addition. A smiliar isotope exchange in $[Ir(PPh_3)_2D(CH_2CHDtBu)(solvent)_2]^+$,[72] could proceed by the same pathway; however, in this case an alternative mechanism involving rapid α-elimination via a carbene intermediate [IrHD(=CHCHD*t*Bu)] is possible because of the coordinative lability of the ligated solvent molecule.

Agostic complexes of type **21** are often recognized in X-ray studies. Although the hydrogen atom is not always well located, its position can sometimes be inferred from the po-

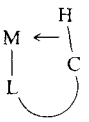

21

sitions of the heavy atoms. Neutron diffraction studies show that the C–H bond is not greatly elongated (bound, 1.13–1.19 Å; unbound, 1.1 Å) by the interaction. In early work on complexes with weak agostic interactions, it was not clear whether the C–H bond just happened to be close to the metal atom or whether there was a genuine attraction. Complex **7** was the first to show a very short separation and therefore an unambiguously attractive interaction. We compared[73a] a series of structures of C-H-M complexes to determine the kinetic pathway for {C–H} + M → {C-M-H} by the method of Bürgi and Dunitz.[73b] The C–H bond approaches the metal atom end-on, resulting in a strong M–H interaction; the C–H bond then rotates bringing the carbon atom close to the metal center (Fig. 4). In all cases the C-H-M unit is bent with canted side-on coordination of C–H as expected from the bonding scheme of Figure 1. The transition state suggested in our work[73a] resembles that found in RHF calculations by Morokuma et al.[74a] for addition of CH_4 to [RhCl-

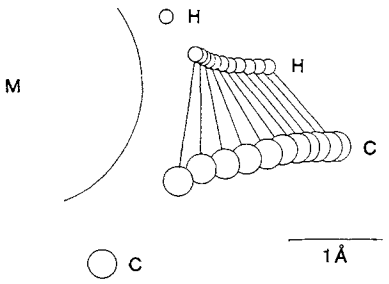

Fig. 4. A kinetic pathway for the reaction M + C–H → C-M-H as deduced from a series of structures of agostic complexes (from ref. [73]).

$(PH_3)_3$]. A methane complex was also identified as an intermediate in the heterolytic C–H activation of CH_4 with $L_nTi{=}NH$ to give $[L_nTi(Me)NH_2]$.[74b] As might be expected, a metal center capable of binding H_2 as a σ complex can often bind other X–H groups [Eq. (19)].

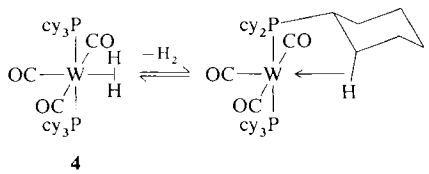

4 (19)

Apart from crystallography, NMR spectroscopy is most useful for detecting C-H-M bridges. In the complex the $^{13}C,H$ coupling constant $^1J(^{13}C,H)$ is reduced by up to 50% relative to the uncomplexed ligand (free, ca. 125 Hz, bound 60–120 Hz), just as $^1J(H,D)$ is reduced by about the same amount in unstretched H_2 complexes (free, 43 Hz, bound 22–33 Hz). The signal of the agostic H atom normally appears upfield from tetramethylsilane, and in this respect resembles a metal-bound rather than a C-bound H atom. Unfortunately, interpretation of the NMR spectrum is often complicated by dynamic processes. For example, an agostic CH_3 group will normally rotate so rapidly that each proton is in the bridging site for one-third of the time. From the value of the resulting averaged $^1J(C,H)$ coupling constant an agostic methyl group cannot be securely distinguished from an unbound methyl group; the upfield shift of the agostic CH_3 group is also reduced by two-thirds.

Shapley et al.[75a] showed that Isotopic Perturbation of Resonance (IPR) in NMR spectroscopy[75b] is very useful in such a case. The methyl group is partially deuterated and the isotope shifts for CH_2D and CHD_2 are measured. The different zero-point energies of the two C–H(D) bonds lead to a substantial enrichment of H atoms in the bridging site. Assuming that bridging and terminal ligands have a significant chemical shift difference $\Delta\delta$, as is usually the case, the averaged resonance for the isotopomers will show a temperature-dependent shift relative to the CH_3 signal. Since any process, such as oxidative addition, that causes the symmetry of the CH_3 to be lowered will in general also lead to an IPR effect, interpretation requires care. IR studies show the expected shift of the C–H band to lower energy upon complexation, consistent with bond weakening. The typical frequency range observed for alkane σ complexes is $\nu(C{-}H) = 2250{-}2800\ cm^{-1}$.

Agostic complexes can be on the mechanistic pathway in organometallic reactions such as alkene insertion [Eq. (20)]

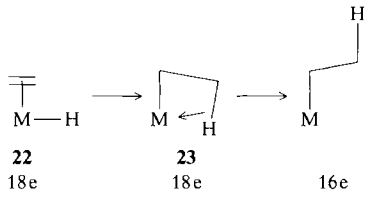

22 18e **23** 18e 16e (20)

or CO insertion.[76a] Morokuma et al.[74c] found a β-agostic transition state for alkene insertion in $[Rh(CO)_2(PH_3)(C_2H_4)H]$, for example. Sometimes an alkene hydrido complex like **22** is the ground state of the system, sometimes the agostic alkyl complex **23** is, as in the case of $[Cp^*Co(C_2H_4)(CH_2CH_2{-}H)]^+$.[76b] Brookhart et al. proposed that a metal center at which **22** and **23** readily interconvert should also be suitable for the much rarer alkene insertion into metal–alkyl bond, a reaction which proceeds readily in the closely related species $[Cp^*Co\{P(OMe)_3\}(CH_2CH_2{-}H)]^+$, which is an alkene polymerization catalyst [Eq. (21)].[77] An α-agostic alkyl complex was proposed[14]

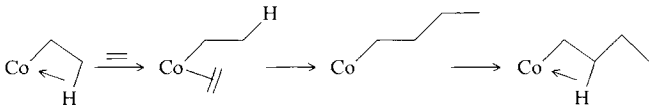

(21)

[Co = $Cp^*Co\{P(OMe)_3\}$]

as being the intermediate that undergoes insertion in Ziegler–Natta alkene polymerization catalysts. If so, the agostic binding may rotate the methyl group towards the alkene and so prepare it for insertion [Eq. (22)]. Direct evi-

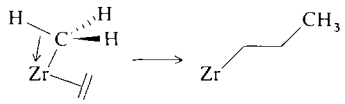

(22)

dence for this has now been obtained by Brintzinger et al.[78a] and by Bercaw et al.[78b] in an experiment originally conceived by Grubbs et al.[78c] in which the stereochemistry of the insertion is different if C–H or C–D is involved in the agostic binding. If an isotope effect is found, agostic transition states are indicated. α-Agostic alkyl complexes such as $[Cl_2(Me_3P)_2(C_2H_4)Ta\{CH(\eta{-}H)tBu\}]$ are now well known.[78d] Canty[79a] found that loss of ethane from $[Pd(bpy)Me_3I]$ (bpy = bipyridine) requires loss of I^- and proposed that formation of an agostic bond helps the methyl group rotate and start bond formation with the adjacent methyl group. GVB calculations by Low and Goddard[79b] on ethane loss from MMe_2 (M = Pd, Pt) also implicate a methyl group rotation in the transition states, the structures of which resemble those of known, stable agostic complexes. Shapley et al. identified an agostic Os_3 complex **21** that was in equilibrium with its tautomer **22** [Eq. (23)].[75]

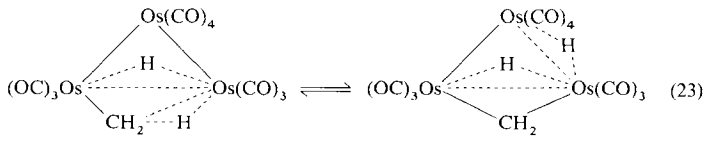

(23)

Albéniz et al.[80] found the set of equilibrating tautomers in Equation (24), which shows that the coordinated σ bond tends to form *trans* to a ligand with a strong trans effect, in this case the aryl group. The activation energy for exchange

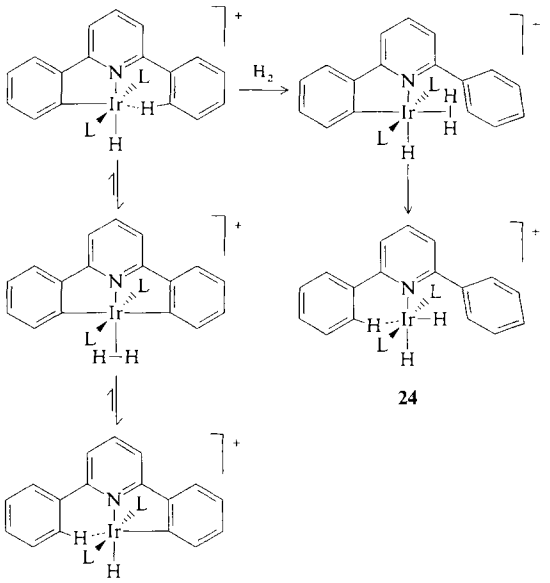

(24)

24

was only 12.3 kcal mol^{-1}. The H_2 complex depicted is a possible intermediate.[80] In the presence of excess H_2, the C–H group was displaced and a conventional H_2 complex was formed. With longer reaction times, this complex undergoes hydrogenolysis to give **24**, perhaps by the pathway of Equation (24).

Gladysz et al. invoked agostic intermediates to account for the migration of the metal atom from one enantioface to the other in a variety of alkene complexes of the type $[Cp(NO)(PR_3)Re(alkene)]^+$.[81] Since the metal atom does not dissociate and the alkene ligand does not undergo stereochemical or isotope scrambling, the metal must bind to a C–H bond as it passes across the alkene plane.

As for H_2 complexes, the d^6 configuration is the most common for agostic M-(C-H) complexes. d^0 Complexes show short M···C contacts as are found in a number of crystal structures of complexes of f-block elements. $[Cp''_2Yb]$ and $[Cp''_2Eu]$ ($Cp'' = (1,3\text{-}Me_3Si)_2C_5H_3$) are rare examples from the lanthanide group.[82] In the Eu complex the Eu···C separation is 3.09 Å, whereas the normal Eu–C bond length is 2.7 Å. Actinide complexes more commonly show agostic M-(C-H) bonds. In $[Cp^*_2Th(CH_2tBu)_2]$ one α-CH bond on each neopentyl ligand is bent back towards the metal forming Th-C-H angles of 84.4° and 87.1° (determined by neutron diffraction).[83a] Many other examples are known, but in some cases the complexes may not be truly agostic; instead alkyl groups may be semibridging leading to structures reminiscent of that of $[Me_2Al(\mu\text{-}Me)_2AlMe_2]$, in which the C–H bonds are thought not to be involved in coordination. Here, the 3c-2e bond involves the two Al and the C atom only.[83b] Examples of d^0 transition metal complexes include the α- and β-agostic $[Ti(\eta^2\text{-}CH_3)(dmpe)Cl_3]$ and $[Ti(\eta^3\text{-}CH_2CH\text{–}H)(dmpe)Cl_3]$,[84a] and the α-agostic alkylidene complex $[Cp_2ClTa{=}C\text{–}H(tBu)]$.[84b]

Weak C–H···M attractions were identified by Albinati, Pregosin, et al.[85] in a number of late transition metal complexes. The H···M distances are in the range 2.3–2.5 Å. In the ^1H NMR spectra of these complexes the resonances are not shifted upfield and the $^1J(C,H)$ values are not reduced as in complexes with normal agostic interactions. Since the square-planar coordination geometry of the d^8 metal is almost undistorted by the approach of the C–H bond perpendicular to this plane, these complexes must represent a very early stage of C–H···M bridge formation.

By analogy with H_2 complexes the C–H bond becomes more acidic on binding. For example, the pK_a (water scale) of the agostic CH group in **25** is 14.[55,86]

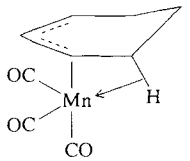

25

Reaction (25) is especially interesting since deprotonation gives a metal alkyl complex. In the starting complex a C–H bond on a remote, unactivated portion of an alkyl chain is

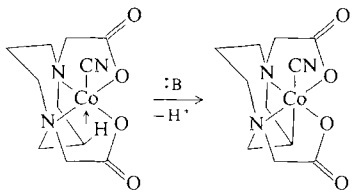

(25)

sufficiently acidified to be deprotonated by methoxide ion.[87] The degree of C-*H*-M acidification is probably comparable to that for the $M(H_2)$ case.

The selectivity order for alkane reactions is usually tertiary > secondary > primary, because both the tertiary radical (homolytic cleavage) and the tertiary carbonium ion (heterolytic cleavage) are more stable than the corresponding secondary or primary species. If a σ complex were involved in the alkane reaction, we might expect more facile deprotonation relative to the free alkane, but the order of selectivity would not be tertiary > secondary > primary. Deprotonation of the agostic complex **21** is certainly more facile than deprotonation of an alkane. If the C atom involved in the agostic bond is tertiary, then the required side-on coordination and formation of the σ complex is strongly disfavored as a result of steric effects. Even for simple complexes of type M–R very few examples are known with tertiary R groups.

Shilov et al. carried out ground-breaking studies on Pt^{II} catalyzed H/D exchange in alkanes [Eq. (26)] which proceed

$$C_6H_{12} \xrightarrow{PtCl_4^{2-},\ D^+} C_6H_{12-x}D_x \qquad (26)$$

by heterolytic C–H activation and are not selective for tertiary sites. Several examples of the proposed alkylplatinum intermediates were isolated.[89] An alkane complex would be an attractive intermediate for this heterolysis, but none has been directly detected.

The selectivity in reactions of alkanes with cobalt(III) acetate also deviates from the normal order tertiary > secondary > primary.[90] **26** shows the selectivity pattern (% at-

tack at each position shown) for oxidation of 2-methylpentane. Here we have a very electrophilic metal ion which is at

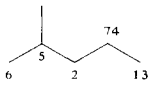

26

the same time a powerful 1e oxidizing agent. The large kinetic isotope effect observed indicates that C–H bond breaking is important in the transition state. The data was interpreted in terms of an outer sphere, 1e oxidation of the alkane in a preequilibrium process, followed by rate-determining deprotonation of the $RH^{\bullet+}$ radical cation. The mechanistic work in this area was carried out long before σ complexes or proton-coupled electron transfer (PCET, shown in Eq. (27),

$$C\text{–}H + B \rightarrow C^{\bullet} + BH^{+} + e^{-} \quad (27)$$

B = base, C–H = bond in RH)[91] were recognized. PCET can take place when a substrate RH cannot lose an electron directly, but concerted deprotonation and oxidation is favorable. Alkanes are very difficult either to deprotonate or to oxidize, but as we discussed in more detail elsewhere,[92] PCET in an alkane complex is consistent with the kinetic data and is chemically reasonable. PCET should be considered whenever alkane oxidation occurs with an abnormal selectivity pattern.

4. B-H-M and Al-H-M Complexes

Since B-H-B bridges are already known in neutral boranes, it is no surprise that B-H-M complexes are also very stable and have been known for a long time. BH_4^- forms many such complexes, for example, $[Ti(HBH_3)_2(H_2BH_2)(PMe_3)_2]$, $[Cp_2Zr(H_2BH_2)_2]$, and $[Hf(H_3BH)_4]$; AlH_4^- behaves similarly.[14b, 93]

As methane complexes have not been characterized by crystallography, some idea of the structure of M-H–CH_3 complexes can be gained from M-H–BH_3^-, although the strength of the BH_4–M interaction is much greater. In $[FeH(dppe)_2(\eta^2\text{-H–}BH_3)]$ the B-H-M bond angle is surprisingly large (162°).[94]

5. Si-H-M and Sn-H-M Complexes

A substantial series of σ complexes of silanes are known, many of which were carefully characterized by Schubert et al.[95] using neutron diffraction. In general, their structures more closely resemble those of oxidative addition products than those of σ complexes with an unstretched Si–H bond. This is also evident in the ^1H NMR spectrum: the percentage reduction in $^1J(Si,H)$ is much greater than for $M(H_2)$ or C-H-M complexes. In $[(MeCp)Mn(HSiPh_3)(CO)_2]$, for example, the coupling constant $^1J(Si,H)$ is 65 Hz compared to approximately 200 Hz for free $HSiPh_3$.[96] The greater basicity of the Si–H bond relative to H–H and C–H bonds probably makes the Si–H unit a better σ donor. Since the Si–H bond is weaker than H–H and C–H bonds, the Si–H σ* orbital is more accessible and the Si–H unit is therefore a better π acceptor. Si···H distances in the range 1.7–1.85 Å are common (Si–H bond 1.48 Å, sum of the van der Waals radii 3.1 Å). These silane adducts with stretched Si–H bonds are not particularly reactive and do not lose silane or undergo nucleophilic attack at the silicon atom.

If a change in the ligands or silane substituents causes a buildup of negative charge on the metal atom or of positive charge on the Si atom, the increased back-donation to the Si–H σ* orbital causes the extent of oxidative addition to increase. Like stretched H_2 complexes, these silane complexes are very sensitive to electronic effects. The best indicators of the extent of oxidative addition are noted by Schubert et al.:[97] the coupling constant $J(Si,H)$, which decreases with advancing oxidative addition, the Mn–Si distance, which increases, and the $\Delta H^{\neq}$ value for dissociation of silane, which decreases. Table 2 shows some of the NMR and structural data for the Mn complexes $[(C_5H_4Me)Mn(CO)L(HSiR_3)]$. The ease of dissociative loss of silane in $[(C_5H_4Me)Mn(CO)_2(H\text{–}SiR_3)]$ follows the order $SiCl_3 \ll SiPh_3 < SiHEt_2$, as expected on the premise that the complex with the least stretched Si–H bond should lose silane most easily.[95]

Table 2. Data for $[(MeC_5H_4)Mn(CO)L(H\text{–}SiR_3)]$ reflecting the extent to which oxidative addition of silane has advanced (from ref. [95]).

L	R_3	r(Mn-Si) [Å]	J(Si-H) [a] [Hz]	J(Si-Mn-H) [b] [Hz]
CO	HPh_2	2.364(2)	205.2	63.5
CN(*t*Bu)	HPh_2	–	194.1	57.5
$P(OPh)_3$	HPh_2	–	199	45
$P(p\text{-}ClC_6H_4)_3$	HPh_2	–	196	46.5
PPh_3	HPh_2	–	191	43
$P(p\text{-}MeC_6H_4)_3$	HPh_2	–	191	44.5
PMe_3	HPh_2	2.327(1)	188	38
CO	Cl_3	2.254(1)	–	54.8
PMe_3	Cl_3	–	–	20 [c]

[a] Coupling constant of the uncomplexed Si–H bond. [b] Coupling constant of the complexed Si–H bond. [c] Oxidative addition in this complex must be very advanced or even complete.

The crystal structures of the same series of Mn complexes suggest that the main change as the oxidative addition proceeds is a decrease in r(Mn–Si) rather than a change in r(Mn–H) or r(Si–H). This led Schubert to propose a reaction trajectory for oxidative addition in which the H atom of the Si–H unit approaches the metal center, and the Si–H unit then pivots so as to bring the Si atom up to the metal. This agrees with the trajectory we postulated later for the interaction of a C–H bond with a metal atom,[73] and with theoretical work.[98a] EH calculations carried out by Saillard, Schubert, et al.[98b] on $[CpMn(CO)_2(H\text{–}SiH_3)]$ are consistent with the bonding scheme in Figure 1. The Si–H overlap integral falls from 0.74 in the free Si–H bond to only 0.24 for Mn-Si-H, consistent with their being stretched σ complexes. The Si–H distances in the complexes in Table 2 are roughly 20% greater than Si–H distances in free sp^3-Si–H bonds; in comparison, the H–H bond in **4** is only 11% longer and typical agostic C–H bonds are <10% longer. Yang determined the energy of the coordination of an Si–H unit to the $CpMn(CO)_2$ complex fragment by photoacoustic calorimetry. Electron-donating R groups on silicon destabilize the adduct as do bulky SiR_3 groups, although the steric effect is

first evident at a cone angle of 135°.[99] In contrast, the binding energy of silanes to the $Cr(CO)_5$ complex fragment is strengthened by the presence of electron-releasing groups on Si. One explanation is that since the Cr fragment is predominantly a σ acid and not a π base, the basicity of the Si–H group is the controlling factor.[100] Thus, it is probable that the complexes $[(R_3Si–H)Cr(CO)_5]$ are unstretched.

Several di- and polynuclear silane σ complexes are known, of which **27** is of particular interest. As d^1 centers the Ti

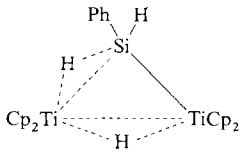

27

atoms are not very effective at backbonding, and the Si–H distances in **27** are only 7% longer than in the free silane, although the coupling constant J(Si,H) does show a substantial decrease on binding (from 148 Hz to 58 Hz for the terminal Si–H bond). The original tetrahedral geometry at the Si atom is also largely retained as opposed to the more distorted geometry at the Si atom in $[CpMn(CO)_2(H–SiR_3)]$. These observations indicate that **27** is an unstretched σ complex, rare for a silane.

The reactions of complexes **28** suggest that these are unstretched silane complexes. The silane is very easily dis-

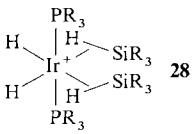

28

placed, consistent with a small extent of oxidative addition in **28**. The silane is also extremely sensitive to nucleophiles; **28** is the most efficient catalyst known for silane alcoholysis [Eq. (28)]. Mechanistic studies were consistent with the

$$R_3SiH + R'OH \longrightarrow R_3SiOR' + H_2 \qquad (28)$$

sequence shown in Scheme 1. Although the pathways via the silane σ complex and the oxidative addition product are kinetically indistinguishable, the spectroscopic data for **28** is much more consistent with a bis(silane)iridium(III) complex, at least for the resting state.[101] The electrophilicity induced

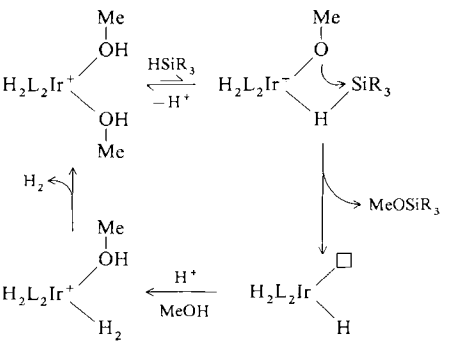

Scheme 1. The proposed mechanism of silane alcoholysis catalyzed by $[IrH_2(PPh_3)_2(H–SiR_3)_2]^+$ (from ref. [101]). □ = vacancy.

in the X–Y bond by binding to the metal atom and forming a σ complex is evident in this catalytic system as a large enhancement in the susceptibility of the system to nucleophilic attack at Si, rather than as an enhancement of proton acidity, no doubt because a free Si–H bond has a positive partial change on the silicon atom and a partial negative charge on the H atom.

Alternative formulations for **28** (L = PR_3) such as $[Ir(H)(SiR_3)(H–SiR_3)(H_2)L_2]^+$ and $[Ir(SiR_3)_2(H_2)_2L_2]^+$ could be ruled out from the long T_1(min) values. For a related Os complex, however, the T_1(min) value of 17 ms at 200 MHz indicates that the dihydrogensilyl tautomer $[Os(H_2)SiR_3(CO)L_2]$ dominates.[102a] The factors that govern this type of equilibrium are not yet understood. A clear-cut example of an unstretched silane complex $[\{(C_6H_{11})PSiH(mesityl)\}_3Cr(CO)_3]$ (J(Si,H) = 136 Hz, r(Si–H) = 1.52(4) Å, r(Cr–Si) = 2.616(1) Å, r(Cr–H) = 1.75(5) Å) has now been reported.[102b]

We were surprised to find that in contrast with other seven-coordinate complexes, $[ReH_2(SiPh_3)(CO)(PMe_2Ph)_3]$ is not fluxional by ^1H NMR spectroscopy.[103] An X-ray study showed a distorted geometry for the heavy atoms. Later we were able to crystallize $[ReH_6(SiPh_3)(PPh_3)_2]$, a complex first obtained by Ephritikhine, and show by X-ray and neutron diffraction that four H···Si distances are short (2.12–2.45 Å), although not as short as in $[CpMn(CO)_2(H–SiR_3)]$.[104] The presence of attractive interligand interactions was confirmed in theoretical work of Lin and Hall, which also showed that the P···H distances were rather shorter than normal (2.56 Å).[105] These interligand interactions may be responsible for the unusual fluxional properties of $[ReH_2(SiPh_3)(CO)(PMe_2Ph)_3]$.

Si-H-M intermediates have been proposed as the immediate precursors to the four-center transition state in sigma bond metathesis reactions.[106]

Schubert et al.[107] showed how Sn–H bonds behave as donors in σ complexes. For example, $[(C_5H_4Me)Mn(HSnPh_3)(CO)_2]$ has a Sn···H distance of 2.16 Å and $^1J(^{119}SnH)$ is 270 Hz; in comparison the values for the uncomplexed Sn–H bond are 1.6 Å and 1500–1800 Hz. This suggests that Sn–H bond in σ complexes tends to be even more stretched than the Si–H bond in the analogous complexes.

6. P-H-M and S-H-M Complexes

A σ complex with an agostic P–H bond **29** was reported by Pregosin, Albinati, et al.[108] as the protonation product of the corresponding neutral bis(μ-phosphanido) complex.

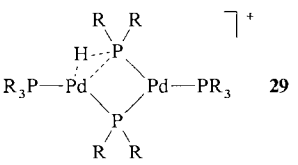

29

Four distinct signals for the R_2P groups are seen in the NMR spectrum, and instead of the normal J(P,H) values for terminal P–H bonds of 322–324 Hz, the μ-H atom has a J(P,H)

value of 151 Hz. NOE data suggest an r(P–H) of 1.9 Å. Since the location of the H atom is not easy to determine, it is quite possible that similar complexes lie unrecognized in the literature.

$[(PhS)Fe(CO)_3(PEt_3)]^-$ is protonated at $-80\,^\circ C$ to give as the kinetic adduct a complex assigned as $[(\eta^2\text{-PhS–H})Fe(CO)_3(PEt_3)]$, a σ complex with an S–H bond. It irreversibly converts to the classical hydrido complex $[PhSFeH(CO)_3(PEt_3)]$ on warming.[109]

7. M-H-M and M-H-M′ Complexes

M-H-M complexes have been known for a long time, are of great importance in structural chemistry, and can be considered σ complexes of an M–H bond. The bridging hydride ligand does not seem to be particularly reactive, and as befits a σ complex, the M-H-M unit is always bent.[110] Venanzi et al.[111] exploited the synthetic consequences of the σ-bond concept by synthesizing a series of new M-H-M complexes from the reaction of various metal hydrides (18e) with coordinatively unsaturated metal complex fragments (16e) [Eq. (29)]. M-H-M complexes are usually stretched in the

$$[L_nM-H] + [M'L'_n] \longrightarrow [L_nM-H-M'L'_n] \qquad (29)$$

sense that the distance from M to the bridging H atom is usually substantially longer than to a terminal H atom. Possible exceptions are complexes with a weakly π-basic M′ atom such as Cu^+, but no neutron diffraction structures are available on any of these complexes yet.

The extension of reaction (29) to cases in which M′ is Cu^+, Ag^+, and $Au(PPh_3)^+$ produced some interesting heterobimetallic hydrido clusters.[112] A number of complexes are known in which Au-H-M bridges are present, for example, **30**.[113] The structure of **30** (R = Ph) is shown on the left side

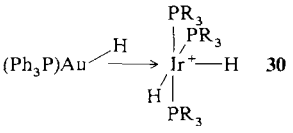

30

of Figure 5; the P–Au and H–Ir vectors point to the center of the Au-H-Ir triangle, as befits a 3c-2e bond. The Au–H1/H2 bonds are fluxional and can be rationalized by the transfer of $(AuPPh_3)^+$ between the two Ir–H sites, in close analogy to the η^3-H_3 intermediate suggested for fluxional H atoms in M(H)(H_2) complexes. $[MeC(CH_2PPh_2)_3MH_3]$ (M = Rh, Ir) reacts with one and two $AuPPh_3^+$ groups to give MAu and MAu_2 hydrido complexes, respectively.[114] These are part of a series extending from the analogous H_2 complexes such as $[(H_2)IrH_2(PR_3)_3]^+$[115a] to the M-H-M complexes like $[(dppe)Rh(\mu\text{-}H)_2IrH_2(PR_3)_2]$ reported by Venanzi, Albinati, et al.[111] The structure of an interesting Au_4 complex with H bridges is shown in Figure 5 left.[116]

Both Caulton et al.[115b] and Venanzi et al.[114b] looked at the reactions of polyhydrides with Ag^+ and Cu^+ ions (M'^+). The structures of the products tend to contain M'_3 triangles or M'_6 octahedra (Fig. 6). Cu···Cu distances in

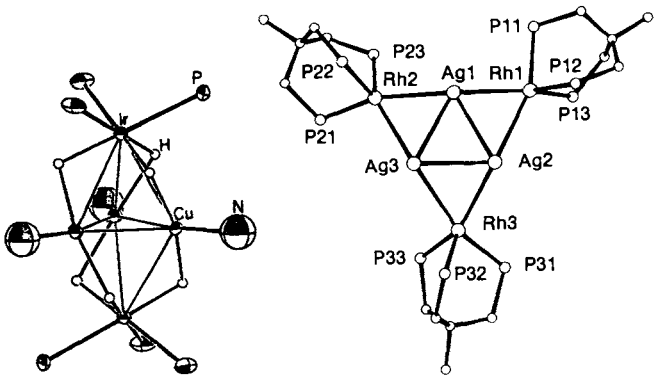

Fig. 6. The X-ray crystal structures of $[\{(MeCN)Cu\}_3\{(\mu\text{-}H)_3Ir(PMe_2Ph)_3\}_2]^{3+}$ (left) and $[Ag_3\{(\mu\text{-}H)_3Rh(PPh_2CH_2)_3CMe\}_3]^{3+}$ (right) cations. The hydrido ligands were not located in the Ag_3Rh_3 structure (from refs. [114b, 115b]).

$[\{(MeCN)Cu\}_3\{(\mu\text{-}H)_3Ir(PMe_2Ph)_3\}_2]$ are typically 2.6 Å and can clearly be interpreted as bonding. The interactions in some of these complexes are more complicated than simple σ complexation, and direct M′–M′ bonds are also possible.[117] $[H_{24}Cu_6Re_4(PPh_3)_8]^{2+}$ is an unusual hydride-rich cluster but the locations of the H atoms are as yet not known.[115c] Although the terminal $(AuPPh_3)^+$ complex fragment can formally replace H^+ in many hydrido complexes, replacing a μ-H ligand by the gold complex fragment does not always lead to a similar structure; an example where the structure is retained upon substitution is shown in **31** and **32**.[118] The Au_3 complex **33** would be isolobal with

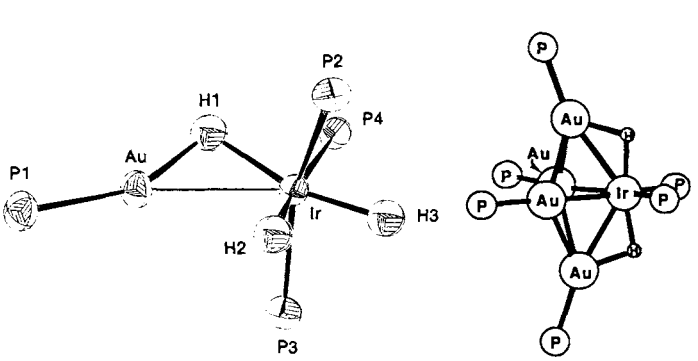

Fig. 5. Left: The X-ray crystal structure of $[(PPh_3)Au(\mu\text{-}H)IrH_2(PPh_3)_3]^+$. Note how the P1–Au and H3–Ir vectors point to the center of the Ir-Au-H^1 triangle (from ref. [113]). Right: The X-ray crystal structure of $[\{(PPh_3)Au\}_4(\mu\text{-}H)_2Ir(PPh_3)_2]^{3+}$ (from ref. [116]).

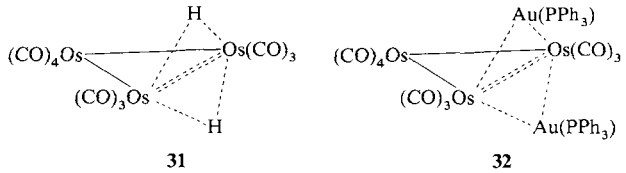

31 **32**

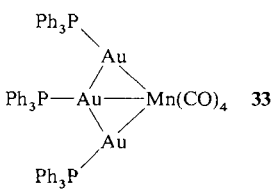

33

an as yet unknown trihydrogen analogue.[119] Albinati, Venanzi, et al. proposed that the bonding is not simply of the

σ type but that direct $M(d_\pi) \rightarrow Au(p)$ interactions may also contribute.[120]

8. Can X–Y σ Complexes Exist if X ≠ H, Y ≠ H?

For strong complexation in X–Y σ complexes, one of the two atoms X or Y must be a H atom. If X or Y has a lone pair or the ligand has an X–H bond, then these will bind preferentially to the metal atom. In $[IrH_2(PPh_3)_2(IMe)_2]^+$ the MeI ligand can bind to the Ir atom without the C–I bond breaking.[121] Crystallographic studies show, however, that the I atom binds to the Ir center through its lone pair. Since the C–I σ bond is not involved, these are not σ complexes. An enhancement of the electrophilicity of the MeI ligand is certainly observed, but it is much more modest than in σ complexes; only a strong nucleophile like an enamine can attack MeI, but not a weak one like MeOH. A main group compound like $Me_2Al(\mu\text{-}Me)_2AlMe_2$, is a σ complex of an Al–C bond, but similar bridges are not seen in transition metals.

In a few complexes the X–Y bond of the ligand (X,Y ≠ H) is very close to the metal atom. For example, **34**[122] has short nonbonded Ir···C distances of 2.80 and 3.39 Å. On heating, the complex rearranges by the Green–Eilbracht[123] reaction, which corresponds to the oxidative addition of a C–C bond, to give **35** [Eq. (30)]. Unlike the analogous reactions of C-H-M complexes in which the activation energy is low, heating at 150 °C is required for the rearrangement of **34**.

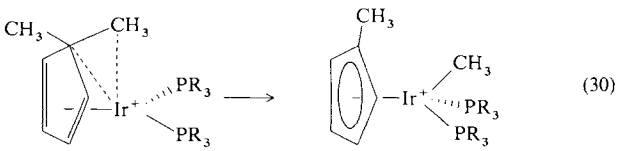

(30)

34 **35**

Another remarkable class of clusters of the type $[M\{Au(PPh_3)\}_n]$, including $[Pt\{Au(PPh_3)\}_8]^{2+}$ (**36**), was reported by Steggerda.[124] In these complexes the Au···Au distances of 2.8–3.15 Å are very short (2.67 Å in Au metal). In the isolobal polyhydrido complexes a pair of H ligands interacts, but here all the Au atoms, not just a pair, interact because they are essentially close packed around the Pt atom. It is still not clear if complexes like **34** and **36** can be described as σ complexes. Pignolet et al. recently reported that **36** catalyzes very rapid (one turnover per second for the solid) isotope exchange in H_2/D_2 mixtures and has proposed that $M(H_2)$ and M-H-Au complexes are reactive intermediates.[125]

9. Complexes with Three-Center, Four-Electron X-H-M Bridges

Some complexes with X-H-M bridges are not σ complexes, as shown by Brammer et al.[126] These bridges resemble conventional hydrogen bonds and are considered 3c-4e interactions. Their distinguishing characteristics are: 1) the X-H-M group is linear and not bent; 2) on complex formation the signal of the bridging hydrogen atom moves to low field in the ^1H NMR spectrum rather than high field; 3) the bridge can form even if the metal atom has an 18e configuration, in contrast to a σ complex. The open or linear geometry as in H_3^- (**37**) is characteristic of a 3c-4e interaction, while the

$[H{-}H{-}H]^-$ **37**

closed, triangular, or side-on arrangement is characteristic of a σ interaction as in H_3^+ (**2**).[127]

The X-H-M bridge is essentially a hydrogen bond, since X is usually an electronegative atom (N atom), an electronegative group, or a carbon-bearing electronegative substituent. A careful neutron diffraction study of $[Et_3NH][(Co(CO)_4)]$ at 15 K shows that the Co···H distance is 2.613 Å, close to but somewhat less than the sum of the van der Waals radii (ca. 3 Å), and just within the range of M···H distances (1.8–2.8 Å) found in agostic systems. The N–H distance in this complex is 1.054 Å, somewhat longer than the average distance (1.033 Å by neutron diffraction) in free R_3NH^+ ions; the N–H···Co angle is 180°. The $[Co(CO)_4]^-$ ion has a distorted tetrahedral symmetry; three OC-Co-CO angles open up by about 6° to give an approximately C_{3v} arrangement. The ^1H NMR signal of the bridging proton is at $\delta = 8.31$ in C_6D_6, a chemical shift very different from those of agostic complexes. Other similar examples but with a smaller M···H separations are known, for example, in $[Pt\text{-}Br(C_{10}H_6NMe_2)(C_{10}H_6NMe_2)]$ $r(Pt\cdots H) = 2.11$ Å.[128]

10. Characteristics of σ Complexes

Structures **38**–**40** are three possible representations of $[L_nM(HX)]$ complexes. Their relative importance is likely to depend on the electronegativity of L_nM, X, and H. Normally, the L_nM fragment will be the most electropositive and **38** will be dominant. Structure **40** gives the H atom its enhanced acidity, but its significance decreases when the L_nM complex fragment is a better donor (and therefore more electropositive) or when the X atom becomes more electropositive (as in SiHM complexes). Structure **39** ($X = SiR_3$) gives unstretched Si-H-M complexes their enhanced sensitivity to nucleophilic attack at the Si atom with the M–H unit as leaving group.

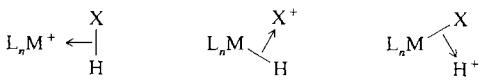

38 **39** **40**

All σ complexes have a closed or bent structure appropriate for a 3c-2e bond. For the XY group to bind, the metal must be coordinatively unsaturated in order to be able to accept the electron pair of the XY σ bond. So far, one of the two atoms, X or Y, has to be a H atom. This allows the close approach of the X–H bond to the metal atom and back-donation into the XH σ* orbital. Two extreme structures can be distinguished: unstretched σ bond complexes in which the X–Y bond is weakened only a little relative to free XY, and stretched σ complexes in which the structure more closely resembles the product of the oxidative addition of the XY

ligand to the metal atom with some attractive interaction between the X and Y atoms. Depending on the XY unit, the unstretched (e.g. XY = H_2, CH) or the stretched (e.g., XY = SiH, SnH) σ complexes are more common. In the unstretched σ complexes, the electrophilic character of the XY unit is greatly enhanced. In $M(H_2)$ and C-H-M complexes, this is reflected by the enhanced acidity of the H atom. In SiH complexes, the result is enhanced sensitivity to nucleophilic attack at the Si atom. In these ways, σ complexation provides a powerful method for X–Y bond activation.

11. Conclusion

Although σ complexation is a widespread phenomenon, this area of research is still at an early stage of development. Patterns are now emerging as different classes of σ complexes are compared. Although the M–(XY) binding energies are often low, σ binding can have a large effect on the chemistry of the X–Y bond. σ Complexes are often intermediates or transition states in reactions such as oxidative addition and alkene insertion, and the added stabilization contributes to lowering the activation energy for the reactions. σ Complexation also provides a way to stabilize what would otherwise be coordinatively unsaturated species. σ Complexes are intermediates in reactions in which the enhanced electrophilicity of the X–Y bond induced by binding activates the bond for nucleophilic attack. σ Complexation allows a metal to activate a σ bond without oxidative addition by sigma bond metathesis. For a metal with a d^2 or higher configuration this merely provides an alternative pathway to oxidative addition, but for d^0 systems, oxidative addition is not possible. Our understanding of the role of σ complexation in chemistry is still in a primitive state.

I would like to thank Professors M. L. H. Green, O. Eisenstein, J. W. Faller, J. H. Prestegard, R. H. Morris, D. M. Heinekey, M. Saunders, and K. W. Zilm for helpful discussions. I thank the Centre National de la Recherche Scientifique for financing a visit to the Laboratoire de Chimie Théorique at Orsay, where this review was written, the National Science Foundation for funding our research in this area, and my successive co-workers, Maryellen Lavin, Douglas Hamilton, Ana Albéniz, Xiao-Liang Luo, and Demetrius Michos, who have contributed most of the ideas in our work.

Received: August 25, 1992 [A 906 IE]
German version: *Angew. Chem.* **1993**, *105*, 828

[1] S. C. Foster, A. R. W. McKellan, J. R. Peterkin, J. K. G. Watson, F. S. Pan, M. W. Crofton, T. Oka, *J. Chem. Phys.* **1986**, *84*, 91–96.
[2] J. E. McMurry, T. Lectka, *Acc. Chem. Res.* **1992**, *25*, 47–53; G. A. Olah, G. K. S. Prakash, R. E. Williams, L. D. Field, K. Wade, *Hypercarbon Chemistry*, Wiley, New York, **1987**.
[3] C. A. Nicolaides, E. D. Simandiras, *Chem. Phys. Lett.* **1992**, *196*, 213–219.
[4] a) G. J. Kubas, R. R. Ryan, B. I. Swanson, P. J. Vergamini, H. J. Wasserman, *J. Am. Chem. Soc.* **1984**, *100*, 451–452; b) G. J. Kubas, *Acc. Chem. Res.* **1988**, *21*, 120–128.
[5] a) S. A. Jackson, O. Eisenstein, *J. Am. Chem. Soc.* **1990**, *112*, 7203–7207. b) This is related to the fact that $[L_nM^{N-2}(H_2)]$ and $[L_nM^N(H_2)]$ can be of comparable stability, but $C^{IV}H_4$ is very much more stable than $H_2C^{II}(H_2)$.
[6] R. Nöth, R. Hartwimmer, *Chem. Ber.* **1960**, *93*, 2238.
[7] H. D. Kaesz, W. Fellman, G. R. Wilkes, L. F. Dahl, *J. Am. Chem. Soc.* **1965**, *87*, 2753–2755.
[8] S. J. LaPlaca, J. A. Ibers, *Inorg. Chem.* **1965**, *4*, 778–783.
[9] N. A. Bailey, J. M. Jenkins, R. Mason, B. L. Shaw, *Chem. Commun.* **1965**, 267; K. W. Muir, J. A. Ibers, *Inorg. Chem.* **1970**, *9*, 440–447; D. M. Roe, P. M. Bailey, K. Moseley, P. M. Maitlis, *J. Chem. Soc. Chem. Commun.* **1972**, 1273.
[10] S. Trofimenko, *J. Am. Chem. Soc.* **1968**, *90*, 4754–4755.
[11] a) F. A. Cotton, T. LaCour, A. G. Stanislowski, *J. Am. Chem. Soc.* **1974**, *96*, 754–760; b) F. A. Cotton, A. G. Stanislowski, *ibid.* **1974**, *96*, 5074–5082; c) F. A. Cotton, M. Jeremic, A. Shaver, *Inorg. Chim. Acta* **1972**, *6*, 543–551.
[12] M. A. Graham, R. N. Perutz, M. Poliakoff, J. J. Turner, *J. Organomet. Chem.* **1972**, *34*, C34–C36; M. Poliakoff, J. J. Turner, *J. Chem. Soc. Dalton Trans.* **1974**, 2276; R. N. Perutz, J. J. Turner, *J. Am. Chem. Soc.* **1975**, *97*, 4791–4800.
[13] a) J. K. Hoyano, W. A. G. Graham, *J. Am. Chem. Soc.* **1969**, *91*, 4568; b) W. A. G. Graham, M. J. Bennett, *Chem. Eng. News* **1970**, *48* (24), 75; W. A. G. Graham, *J. Organomet. Chem.* **1986**, *300*, 81–91.
[14] a) M. Brookhart, M. L. H. Green, *J. Organomet. Chem.* **1983**, *250*, 395–408; b) M. Brookhart, M. L. H. Green, L. L. Wang, *Prog. Inorg. Chem.* **1988**, *36*, 1–124.
[15] U. Schubert, K. Ackermann, B. Worle, *J. Am. Chem. Soc.* **1982**, *104*, 7378–7380; U. Schubert, K. Bahr, J. Müller, *J. Organomet. Chem.* **1987**, *327*, 357–363.
[16] R. H. Crabtree, *Acc. Chem. Res.* **1990**, *23*, 95–101.
[17] P. J. Jessop, R. H. Morris, *Coord. Chem. Rev.* **1992**, *121*, 155–284.
[18] G. J. Kubas, *J. Less Common Metals* **1991**, *173*, 475–81.
[19] B. Chase, W. Griffith, R. H. Crabtree, unpublished.
[20] K. W. Zilm, R. A. Merrill, M. W. Kummer, G. J. Kubas, *J. Am. Chem. Soc.* **1986**, *108*, 7837–7839.
[21] M. Aresta, P. Gioannoccaro, M. Rossi, A. Sacco, *Inorg. Chim. Acta* **1971**, *5*, 115–118.
[22] R. H. Crabtree, D. G. Hamilton, *J. Am. Chem. Soc.* **1986**, *108*, 3124–3125.
[23] L. S. Van der Sluys, J. Eckert, O. Eisenstein, J. H. Hall, J. C. Huffman, S. A. Jackson, T. F. Koetzle, G. J. Kubas, P. J. Vergamini, K. G. Caulton, *J. Am. Chem. Soc.* **1990**, *112*, 4831–4841.
[24] R. H. Crabtree, M. Lavin, L. Bonneviot, *J. Am. Chem. Soc.* **1986**, *108*, 4032–4037.
[25] X.-L. Luo, R. H. Crabtree, *Inorg. Chem.* **1990**, *29*, 2788–2791.
[26] a) K. A. Earl, G. Jia, P. A. Maltby, R. H. Morris, *J. Am. Chem. Soc.* **1991**, *113*, 3027–3039; b) J. Eckert, A. Albinati, R. P. White, C. Bianchini, M. Peruzzini, *Inorg. Chem.* **1992**, *31*, 4241; c) M. T. Baustista, E. P. Capellani, S. D. Drouin, R. H. Morris, C. T. Schweitzer, A. Sella, J. Zubkowski, *J. Am. Chem. Soc.* **1991**, *113*, 4876.
[27] J. A. K. Howard, S. A. Mason, F. C. Diamond, S. Crennell, P. A. Keller, J. L. Spencer, *J. Chem. Soc. Chem. Commun.* **1988**, 1502.
[28] a) F. A. Cotton, R. L. Luck, *J. Am. Chem. Soc.* **1989**, *111*, 5757; *Inorg. Chem.* **1989**, *28*, 6–8, 2181–2186; F. A. Cotton, R. L. Luck, D. Root, R. A. Walton, *Inorg. Chem.* **1990**, *29*, 43–47; b) P. J. Desrosiers, L. Cai, Z. Lin, R. Richards, J. Halpern, *J. Am. Chem. Soc.* **1991**, *113*, 4173–4184; c) D. G. Gusev, A. B. Vymenits, V. I. Bakhmutov, *Inorg. Chem.* **1991**, *30*, 3116–3118.
[29] a) X.-L. Luo, J. A. K. Howard, R. H. Crabtree, *Magn. Reson. Chem.* **1991**, *29*, S89–93; X.-L. Luo, H. Liu, R. H. Crabtree, *Inorg. Chem.* **1991**, *30*, 4740–4742. b) These arise largely because stretched H_2 complexes have much lower H···H relaxation than normal H_2 complexes because the effect falls off with r^6(H–H).
[30] L. Brammer, J. A. K. Howard, O. Johnson, T. F. Koetzle, J. L. Spencer, A. M. Stringer, *J. Chem. Soc. Chem. Commun.* **1991**, 241–242.
[31] M. Saunders, Yale University, personal communication, **1991**.
[32] G. R. Haynes, R. L. Martin, P. J. Hay, *J. Am. Chem. Soc.* **1992**, *114*, 28–36.
[33] a) G. J. Kubas, C. J. Unkefer, B. I. Swanson, E. Fukushima, *J. Am. Chem. Soc.* **1986**, *108*, 7000–7009; b) M. S. Chinn, D. M. Heinekey, N. G. Payne, C. D. Sofield, *Organometallics* **1989**, *8*, 1824–1826; F. M. Conroy-Lewis, S. J. Simpson, *J. Chem. Soc. Chem. Commun.* **1986**, 506–507; *ibid.* **1987**, 1675–1676; G. Jia, R. H. Morris, *J. Am. Chem. Soc.* **1991**, *113*, 875–883; c) X.-L. Luo, R. H. Crabtree, *ibid.* **1990**, *112*, 6912–6920.
[34] a) K. Zhang, A. A. Gonzalez, C. D. Hoff, *J. Am. Chem. Soc.* **1989**, *111*, 3627–3632; b) K. Kitaura, S. Obara, K. Morokuma, *J. Am. Chem. Soc.* **1981**, *103*, 2891.
[35] a) K. A. Earl, G. Jia, P. A. Maltby, R. H. Morris, *J. Am. Chem. Soc.* **1991**, *113*, 3027–3039; b) G. Jia, R. H. Morris, *ibid.* **1991**, *113*, 875–883.
[36] C. Bianchini, C. Mealli, M. Peruzzini, F. Zanobini, *J. Am. Chem. Soc.* **1992**, *114*, 5905–5906.
[37] a) D. Michos, X.-L. Luo, R. H. Crabtree, *Inorg. Chem.* **1992**, *31*, 4245–4250; b) D. Michos, X.-L. Luo, J. A. K. Howard, R. H. Crabtree, *ibid.* **1992**, *31*, 3914–3916.
[38] a) T. Hasegawa, Z. Li, S. Parkin, R. McMullan, H. Taube, 29th ICCC, Lausanne, **1992**, Abstract P575; b) M. R. A. Blomberg, P. E. M. Siegbahn, *J. Chem. Phys.* **1983**, *78*, 986–987; c) W. Kolos, L. Wolniewicz, *ibid.* **1964**, *41*, 3663–3673; d) J.-F. Riehl, Dissertation, Orsay, **1991**.
[39] J. K. Burdett, O. Eisenstein, S. A. Jackson in *Transition Metal Hydrides* (Ed.: A. Dedieu), VCH, Weinheim, **1991**, p. 149.
[40] a) D. M. Heinekey, N. G. Payne, G. K. Schulte, *J. Am. Chem. Soc.* **1988**, *110*, 2303–2305; b) K. W. Zilm, D. M. Heinekey, J. M. Millar, N. G. Payne, P. Demou, *ibid.* **1989**, *111*, 3088–3089; D. M. Heinekey, J. M.

Millar, T. F. Koetzle, N. G. Payne, K. W. Zilm, *ibid.* **1990**, *112*, 909–919; c) D. H. Jones, J. A. Labinger, D. P. Weitekamp, *ibid.* **1989**, *111*, 3087–3088; d) H. H. Limbach, G. Scherer, M. Maurer, B. Chaudret, *Angew. Chem.* **1992**, *104*, 1414–1418; *Angew. Chem. Int. Ed. Engl.* **1922**, *31*, 1369–1372; e) D. M. Heinekey, University of Washington, personal communication, **1992**.

[41] J. P. Collman, J. E. Hutchinson, P. S. Wagenknecht, N. S. Lewis, M. A. Lopez, R. Guilard, *J. Am. Chem. Soc.* **1990**, *112*, 8206–8208.

[42] a) Z. Lin, M. B. Hall, *Inorg. Chem.* **1992**, *31*, 4262–4265; b) *Organometallics* **1992**, *11*, 3801–3804.

[43] U. E. Bucher, T. Lengweiler, D. Nanz, W. von Philipsborn, L. M. Venanzi, *Angew. Chem.* **1990**, *102*, 573–574, *Angew. Chem. Int. Ed. Engl.* **1990**, *29*, 548–549.

[44] J. K. Burdett, M. R. Pourian, *Organometallics* **1987**, *6*, 1684–1691.

[45] a) E. B. Moore, L. L. Lohr, W. N. Lipscomb, *J. Chem. Phys.* **1961**, *35*, 1329–1334; b) T. D. Getman, J. A. Krause, S. G. Shore, *Inorg. Chem.* **1988**, *27*, 2398–2399.

[46] A. R. Siedle, X.-L. Luo, L. Wisniewski, K. W. Zilm, E. Clot, P. Maitre, O. Eisenstein, unpublished.

[47] F. Maseras, M. Duran, A. Lledós, J. Bertrán, *J. Am. Chem. Soc.* **1992**, *114*, 2922–2928.

[48] J. M. Millar, R. V. Kastrup, M. T. Melchior, I. T. Horvath, C. D. Hoff, R. H. Crabtree, *J. Am. Chem. Soc.* **1990**, *112*, 9643–9645.

[49] C. Bianchini, C. Bohanna, M. A. Esteruelas, P. Frediani, A. Meli, L. A. Oro, M. Peruzzini, *Organometallics* **1992**, *11*, 3837–3844.

[50] a) M. S. Chinn, D. M. Heinekey, *J. Am. Chem. Soc.* **1990**, *112*, 5166–5175; b) G. Parkin, J. E. Bercaw, *J. Chem. Soc. Chem. Commun.* **1989**, 255–257.

[51] M. S. Chinn, D. M. Heinekey, *J. Am. Chem. Soc.* **1987**, *109*, 5865–5867.

[52] G. Jia, R. H. Morris, *Inorg. Chem.* **1990**, *29*, 581–582.

[53] E. Buncel, B. Menon, *J. Am. Chem. Soc.* **1977**, *99*, 4457–4461.

[54] S. S. Kristjansdottir, J. R. Norton in *Transition Metal Hydrides* (Ed.: A. Dedieu), VCH, Weinheim, **1992**, Chap. 9.

[55] O. B. Ryan, M. Tilset, V. D. Parker, *J. Am. Chem. Soc.* **1990**, *112*, 2618–2626.

[56] R. H. Morris, *Inorg. Chem.* **1992**, *31*, 1471–1478.

[57] A. B. P. Lever, *Inorg. Chem.* **1990**, *29*, 1271–1285; *ibid.* **1991**, *30*, 1980–1985.

[58] S. P. Nolan, T. J. Marks, *J. Am. Chem. Soc.* **1989**, *111*, 8538–8540.

[59] F. Wochner, H. H. Brintzinger, *J. Organomet. Chem.* **1986**, *309*, 65–75.

[60] A. A. Gonzalez, C. D. Hoff, *Inorg. Chem.* **1989**, *28*, 4295–4297.

[61] C. Bianchini, C. Mealli, A. Meli, M. Peruzzini, F. Zanobini, *J. Am. Chem. Soc.* **1988**, *110*, 8725.

[62] X. L. Luo, D. Michos, R. H. Crabtree, *Inorg. Chem.* **1993**, *32*, 1370–1375.

[63] P. Hamon, L. Toupet, J.-R. Hamon, C. Lapinte, *J. Organomet. Chem.* **1992**, *428*, 49–58.

[64] J. P. Collman, P. S. Wagenknecht, R. T. Hembre, N. S. Lewis, *J. Am. Chem. Soc.* **1990**, *112*, 1294–1295.

[65] A. C. Albéniz, D. M. Heinekey, R. H. Crabtree, *Inorg. Chem.* **1991**, *30*, 3632–3635.

[66] a) W. D. Harman, H. Taube, *J. Am. Chem. Soc.* **1990**, *112*, 2261–2263; b) F. A. Cotton, R. L. Luck, *Inorg. Chem.* **1989**, *28*, 2181–2186.

[67] a) J. R. Lancaster, *The Bioinorganic Chemistry of Nickel*, VCH, Weinheim, **1988**; b) L. E. Efros, H. H. Thorn, G. W. Brudvig, R. H. Crabtree, *Inorg. Chem.* **1992**, *21*, 1722–1732; Resolution of **17** does not lead to a Ni^{I} species rather to a $Ni^{II}L^{\bullet+}$ species; c) R. H. Crabtree, *Inorg. Chim. Acta* **1986**, *125*, L7.

[68] M. A. Graham, R. N. Perutz, M. Poliakoff, J. J. Turner, *J. Organomet. Chem.* **1972**, *34*, C34–C36; R. N. Perutz, J. J. Turner, *J. Am. Chem. Soc.* **1975**, *97*, 4791–4796; S. P. Church, F.-W. Grevels, H. Hermann, K. Schaffner, *J. Chem. Soc. Chem. Commun.* **1985**, 30; R. K. Upmacis, M. Poliakoff, J. J. Turner, *J. Am. Chem. Soc.* **1986**, *108*, 3645–3651; R. L. Sweany, *ibid.* **1986**, *108*, 6986–6991; R. L. Seveany in *Transition Metal Hydrides* (Ed.: A. Dedieu), VCH, Weinheim, **1991**, pp. 65–101.

[69] a) E. P. Wasserman, C. B. Moore, R. G. Bergman, *Science* **1992**, *255*, 315–318; b) C. E. Brown, Y. Ishikawa, P. A. Hackett, D. M. Rayner, *J. Am. Chem. Soc.* **1990**, *112*, 2530–2536; G. K. Yang, K. S. Peters, V. Vaida, *Chem. Phys. Lett.* **1986**, *125*, 566–568; J. K. Klassen, M. Selke, A. A. Sorensen, *J. Am. Chem. Soc.* **1990**, *112*, 1267–1268; c) R. A. Periana, R. G. Bergman, *ibid.* **1986**, *108*, 7332–7346.

[70] R. M. Bullock, C. E. L. Headford, S. E. Kegley, J. R. Norton, *J. Am. Chem. Soc.* **1985**, *107*, 727–729.

[71] G. L. Gould, D. M. Heinekey, *J. Am. Chem. Soc.* **1989**, *111*, 5502–5504.

[72] a) M. J. Burk, M. P. McGrath, R. H. Crabtree, *J. Am. Chem. Soc.* **1988**, *110*, 620. b) However, the intermediacy of an alkane complex cannot be excluded.

[73] a) R. H. Crabtree, E. M. Holt, M. E. Lavin, S. M. Morehouse, *Inorg. Chem.* **1985**, *24*, 1986–1992; b) H. B. Bürgi, J. Dunitz, *Acc. Chem. Res.* **1983**, *16*, 153–161.

[74] a) N. Koga, K. Morokuma, *Chem. Rev.* **1991**, *91*, 823–842; b) T. R. Cundari, *J. Am. Chem. Soc.* **1992**, *114*, 10557–10563; c) N. Koga, K. Kitaura, S. Obara, K. Morakuma, *ibid.* **1985**, *107*, 7109–7112.

[75] a) R. B.Calvert, J. R. Shapley, *J. Am. Chem. Soc.* **1978**, *100*, 7726–7727; *ibid.* **1977**, *99*, 5225–5226; b) M. Saunders, M. H. Jaffe, P. Vogel, *ibid.* **1971**, *93*, 2558–2559.

[76] a) N. Koga, K. Morokuma in *Transition Metal Hydrides* (Ed.: A. Dedieu), VCH, Weinheim, **1991**, pp. 185–233; b) M. Brookhart, W. Lamanna, M. B. Humphrey, *J. Am. Chem. Soc.* **1982**, *104*, 2117–2126.

[77] G. F. Schmidt, M. Brookhart, *J. Am. Chem. Soc.* **1985**, *107*, 1443–1444.

[78] a) H. Krauledat, H. H. Brintzinger, *Angew. Chem.* **1990**, *102*, 1459–1460; *Angew. Chem. Int. Ed. Engl.* **1990**, *29*, 1412–1413; b) W. E. Piers, J. E. Bercaw, *J. Am. Chem. Soc.* **1990**, *112*, 9406–9407; c) L. Clawson, J. Soto, S. L. Buchwald, M. L. Steigerwald, R. H. Grubbs, *ibid.* **1985**, *107*, 3377–3378; d) J. D. Fellman, R. R. Schrock, D. D. Traficante, *Organometallics* **1982**, *1*, 481–484.

[79] a) A. J. Canty, *Acc. Chem. Res.* **1992**, *25*, 83; b) J. Low, W. A. Goddard, *Organometallics* **1986**, *5*, 609.

[80] A. C. Albéniz, G. K. Schulte, R. H. Crabtree, *Organometallics* **1992**, *11*, 242–249.

[81] T. S. Peng, J. A. Gladysz, *J. Am. Chem. Soc.* **1992**, *114*, 4174–4181.

[82] P. B. Hitchcock, J. A. K. Howard, M. F. Lappert, S. Prashkar, *J. Organomet. Chem.* **1992**, *437*, 177–189, and references therein.

[83] a) J. W. Bruno, G. M. Smith, T. J. Marks, C. K. Fair, A. J. Schultz, J. M. Williams, *J. Am. Chem. Soc.* **1986**, *108*, 40–56; b) T. D. Tilley, R. A. Andersen, A. Zalkin, *ibid.* **1982**, *104*, 3725–3727; H. Mauermann, P. N. Swepston, T. J. Marks, *Organometallics* **1985**, *4*, 200–202.

[84] a) Z. Dawoodi, M. L. H. Green, V. S. B. Mtetwa, K. Prout, *J. Chem. Soc. Chem. Commun.* **1982**, 1410; b) R. R. Schrock, *Acc. Chem. Res.* **1979**, *12*, 98–104.

[85] A. Albinati, P. S. Pregosin, F. Wombacher, *Inorg. Chem.* **1990**, *29*, 1812–1817; F. Neve, M. Ghedini, A. Crispini, *Organometallics* **1992**, *11*, 3324–3327.

[86] S. S. Kristjansdottir, A. E. Moody, R. T. Weberg, J. R. Norton, *Organometallics* **1988**, *7*, 1983–1987.

[87] W. E. Broderick, K. Kanamori, R. D. Willett, J. I. Legg, *Inorg. Chem.* **1990**, *30*, 3875–3881; K. Kanamori, W. E. Broderick, R. F. Jordan, R. D. Willett, J. I. Legg, *J. Am. Chem. Soc.* **1986**, *108*, 7122–7124.

[88] A. E. Shilov, *The Activation of Saturated Hydrocarbons by Transition Metal Complexes*, Riedel, Dordrecht, **1984**.

[89] L. A. Kushch, V. V. Lavrushko, Y. S. Misharin, A. P. Moravskii, A. E. Shilov, *Nouv. J. Chim.* **1983**, *7*, 729–733.

[90] J. Hanotier, P. Cameron, M. Hanotier-Bridoux, P. de Radzitsky, *J. Chem. Soc. Perkin Trans. 2* **1972**, 2247–2252; J. Hanotier, M. Hanotier-Bridoux, *J. Mol. Catal.* **1981**, *12*, 133–147.

[91] T. J. Meyer, *J. Electrochem. Soc.* **1984**, *131*, 221C; H. H. Thorp, J. E. Sarneski, G. W. Brudvig, R. H. Crabtree, *J. Am. Chem. Soc.* **1989**, *111*, 9249–9250.

[92] J. E. Sarneski, R. H. Crabtree, unpublished.

[93] B. D. James, M. G. Wallbridge, *Prog. Inorg. Chem.* **1970**, *11*, 99–231.

[94] R. Bau, H. S. H. Yuan, M. V. Baker, L. D. Field, *Inorg. Chim. Acta* **1986**, *114*, L27–L28.

[95] U. Schubert, *Adv. Organomet. Chem.* **1990**, *30*, 151–187; U. Schubert, J. Müller, H. G. Alt, *Organometallics* **1987**, *6*, 469–472.

[96] K. Colomer, R. J. P. Corriu, C. Manzin, A. Vioux, *Inorg. Chem.* **1982**, *21*, 368–373.

[97] U. Schubert, G. Scholz, J. Müller, K. Ackermann, B. Wörle, R. F. D. Stansfield, *J. Organomet. Chem.* **1986**, *306*, 303–326.

[98] a) J.-Y. Saillard, R. Hoffmann, *J. Am. Chem. Soc.* **1984**, *106*, 2006–2026; b) H. Rabaa, J.-Y. Saillard, U. Schubert, *J. Organomet. Chem.* **1987**, *330*, 397–413.

[99] D. M. Hester, J. Sun, A. W. Harper, G. K. Yang, *J. Am. Chem. Soc.* **1992**, *114*, 5234–5240.

[100] S. Zhang, G. R. Dobson, T. L. Brown, *J. Am. Chem. Soc.* **1991**, *113*, 6908–6926.

[101] X.-L. Luo, R. H. Crabtree, *J. Am. Chem. Soc.* **1989**, *111*, 2527–2535.

[102] a) M. A. Esteruelas, L. A. Oro, C. Valero, *Organometallics* **1991**, *10*, 462–466; b) M. Driess, M. Reisgys, H. Pritzkow, *Angew. Chem.* **1992**, *104*, 1514–1516; *Angew. Chem. Int. Ed. Engl.* **1992**, *31*, 1510–1513.

[103] X.-L. Luo, G. K. Schulte, P. Demou, R. H. Crabtree, *Inorg. Chem.* **1990**, *29*, 4268–4273.

[104] X.-L. Luo, D. Baudry, P. Boydell, M. Nierlich, M. Ephritikhine, R. H. Crabtree, *Inorg. Chem.* **1990**, *29*, 1511–1517.

[105] D. Lin, M. B. Hall, *Inorg. Chem.* **1991**, *30*, 2569–2572.

[106] H.-G. Woo, J. F. Walzer, T. D. Tilley, *J. Am. Chem. Soc.* **1992**, *114*, 7047–7055; K. I. Gell, B. Posin, J. Schwartz, G. M. Williams, *J. Am. Chem. Soc.* **1982**, *104*, 1846–1855.

[107] U. Schubert, E. Kunz, B. Harkers, J. Willnecker, J. Meyer, *J. Am. Chem. Soc.* **1989**, *111*, 2572–2574; H. Piana, U. Kirchgassner, U. Schubert, *Chem. Ber.* **1991**, *124*, 743–756, and references therein.

[108] A. Albinati, F. Lianza, M. Pasquali, M. Sommovigo, P. Leoni, P. S. Pregosin, H. Rüegger, *Inorg. Chem.* **1991**, *30*, 4690–4692.

[109] M. Y. Darensbourg, W. F. Liaw, C. G. Riordan, *J. Am. Chem. Soc.* **1989**, *111*, 8051–8052.

[110] R. Bau, R. G. Teller, S. W. Kirtley, T. F. Koetzle, *Acc. Chem. Res.* **1979**, *12*, 176–183.

[111] A. Musco, R. Nägli, L. M. Venanzi, A. Albinati, *J. Organomet. Chem.* **1982**, *228*, C15.

[112] I. D. Salter, *Adv. Organomet. Chem.* **1989**, *29*, 249–343.
[113] H. Lehner, D. Matt, P. S. Pregosin, L. M. Venanzi, *J. Am. Chem. Soc.* **1982**, *104*, 6825–6827.
[114] a) A. Albinati, F. Demartin, P. Jamser, L. F. Rhodes, L. M. Venanzi, *J. Am. Chem. Soc.* **1989**, *111*, 2115–2125; b) F. Bachechi, L. M. Venanzi, *ibid.* **1985**, *107*, 1760–1761.
[115] a) L. F. Rhodes, K. G. Caulton, *J. Am. Chem. Soc.* **1985**, *107*, 259–260; b) T. H. Lemmen, J. C. Huffman, K. G. Caulton, *Angew. Chem.* **1986**, *109*, 267–269; *Angew. Chem. Int. Ed. Engl.* **1986**, *25*, 262–264; L. F. Rhodes, J. C. Huffman, K. G. Caulton, *J. Am. Chem. Soc.* **1985**, *107*, 1759–1760; c) L. F. Rhodes, R. L. Bansemer, K. Folting, J. C. Huffman, K. G. Caulton, *Inorg. Chem. Acta* **1992**, *191*, 31–34.
[116] B. D. Alexander, A. M. Mueting, L. H. Pignolet, *Inorg. Chem.* **1990**, *29*, 1313–1319.
[117] D. G. Evans, D. M. P. Mingos, *J. Organomet. Chem.* **1982**, *232*, 171–191.
[118] K. Burgess, B. F. G. Johnson, D. A. Kaner, J. Lewis, P. R. Raithby, S. N. A. B. Syed-Mustaffa, *J. Chem. Soc. Chem. Commun.* **1983**, 455–457, and references therein.
[119] J. E. Ellis, R. A. Faltynek, *J. Am. Chem. Soc.* **1977**, *99*, 1801.
[120] A. Albinati, H. Lehner, L. M. Venanzi, M. Wolfer, *Inorg. Chem.* **1987**, *26*, 3933–3939.
[121] M. J. Burk, B. Segmuller, R. H. Crabtree, *Organometallics* **1987**, *6*, 2241–2246.
[122] R. H. Crabtree, R. P. Dion, D. J. Gibboni, D. V. McGrath, E. M. Holt, *J. Am. Chem. Soc.* **1986**, *108*, 7222–7727.
[123] F. W. C. Benfield, M. L. H. Green, *J. Chem. Soc. Dalton Trans.* **1974**, 1325–1332; P. Eilbracht, *Chem. Ber.* **1980**, *113*, 2211–2218, and references therein.
[124] J. J. Bour, R. P. F. Kanters, P. P. Schlebos, J. J. Steggerda, *Recl. Trav. Chim. Pays-Bas* **1988**, *107*, 211–220; R. P. F. Kanters, P. P. Schlebos, W. P. Bosman, H. J. Behm, J. J. Steggerda, *Inorg. Chem.* **1988**, *27*, 4034–4037.
[125] M. A. Aubart, L. H. Pignolet, *J. Am. Chem. Soc.* **1992**, *114*, 7901–7903.
[126] L. Brammer, J. M. Charnock, P. L. Coggin, R. J. Goodfellow, A. G. Orpen, T. F. Koetzle, *J. Chem. Soc. Dalton Trans.* **1991**, 1789–1798; L. Brammer, M. C. McCann, R. M. Bullock, R. K. McMullan, P. Sherwood, *Organometallics* **1992**, *11*, 2339–2345.
[127] T. A. Albright, J. K. Burdett, M. H. Whangbo, *Orbital Interactions in Chemistry*, Wiley, New York, **1985**, p. 98.
[128] I. C. M. Wehman-Ooyevaar, D. M. Grove, H. Kooiman, P. van der Sluis, A. L. Spek, G. van Koten, *J. Am. Chem. Soc.* **1992**, *114*, 9916.

Solid-State Chemistry with Nonmetal Nitrides

By Wolfgang Schnick*

Among the nonmetal nitrides, the polymeric binary compounds BN and Si_3N_4 are of particular interest for the development of materials for high-performance applications. The outstanding features of both substances are their thermal, mechanical, and chemical stability, coupled with their low density. Because of their extremely low reactivity, boron and silicon nitride are hardly ever used as starting materials for the preparation of ternary nitrides, but are used primarily in the manufacture of crucibles or other vessels or as insulation materials. The chemistry of ternary and higher nonmetal nitrides that contain electropositive elements and are thus analogous with the oxo compounds such as borates, silicates, phosphates, or sulfates was neglected for many years. Starting from the recent successful preparation of pure P_3N_5, a further binary nonmetal nitride which shows similarities with Si_3N_4 with regard to both its structure and properties, this review deals systematically with the solid-state chemistry of ternary and higher phosphorus(v) nitrides and the relationship between the various types of structure found in this class of substance and the resulting properties and possible applications. From the point of view of preparative solid-state chemistry the syntheses, structures, and properties of the binary nonmetal nitrides BN, Si_3N_4, and P_3N_5 will be compared and contrasted. The chemistry of the phosphorus(v) nitrides leads us to expect that other nonmetals such as boron, silicon, sulfur, and carbon will also participate in a rich nitride chemistry, as initial reports indeed indicate.

1. Introduction

Nitrogen, the main component of the atmosphere, is omnipresent. The lightest element in the fifth main group plays an important role in chemical compounds, in particular in the oxidation states v and III (NO_3^- and NO_2^-, respectively) as well as −III (NH_3, $-NH_2$, −NH−, and $\gtrless$N−). The oxidation state of nitrogen in the nitrides is also −III; only a few hundred nitrides have so far been characterized, although for example the neighboring element oxygen has been shown to form more than ten thousand oxides. In spite of this relatively small number, the nitrides include some extremely useful compounds: silicon nitride, Si_3N_4, has become an important nonoxidic material, whose applications range from ceramic turbochargers to integrated semiconductor modules.[1, 2] Because of its unusually high thermal conductivity ($285\,Wm^{-1}K^{-1}$[3]), aluminum nitride is predestined for use as a substrate material in semiconductor manufacture. Boron nitride is used as a high-temperature crucible material, as a lubricant (hexagonal (*h*)-BN), and in the abrasives sector (cubic (*c*)-BN). In recent years *h*-BN has also become increasingly important in the manufacture of composite materials.

The extreme stability of the substances, which are used as high-performance ceramics, is due in part to the strengths of the bonds joining the constituent elements; a second important factor is the presence of highly crosslinked structures in the solid state. When the electronegativity difference is only small, heteronuclear bonds with a high degree of covalent character are formed. The high chemical, thermal, and mechanical stability of nitridic materials such as silicon nitride or boron nitride results from the interplay of these two factors: extremely strong bonds between the elements and the presence of highly crosslinked covalent structures.

Besides these two criteria, the extremely high bond energy of N_2 (941 $kJmol^{-1}$) as a possible decomposition product of the nitrogen compounds is also of importance when discussing the thermal stability of nitridic materials. Compared with the corresponding oxides, the thermal dissociation of many nitrides with evolution of N_2 (for the oxides O_2, bond energy: 499 $kJmol^{-1}$) occurs at much lower temperatures. Thus, the elimination of N_2 from Si_3N_4 occurs at atmospheric pressure at about 1900 °C, while SiO_2 can be heated to over 2000 °C without any noticeable decomposition. Aluminum nitride decomposes above about 1800 °C, while the extrapolated boiling point of Al_2O_3 is about 3000 °C.

The affinity of most elements for oxygen is larger than that for nitrogen, thus the bond energies for element–oxygen bonds are generally higher than those of the corresponding element–nitrogen bonds (single bond energies: Si–O = 444, Si–N = 335; P–O = 407, P–N = 290 $kJmol^{-1}$[4]). Similarly the bond enthalpies of the oxides are significantly higher than those of the corresponding nitrides ($\Delta H_f^0(SiO_2) = -911$, $^1/_3[\Delta H_f^0(Si_3N_4)] = -248$; $^1/_2[\Delta H_f^0(B_2O_3)] = -637$, $\Delta H_f^0(BN) = -254$; $^1/_2[\Delta H_f^0(Al_2O_3)] = -838$, $\Delta H_f^0(AlN) = -318\,kJmol^{-1}$[5]), although a quantitative comparison is difficult because of their differing compositions.

The formation of oxides is thus an important side reaction in the syntheses of nitrides. Thus, the preparation of nitrides in a pure state requires the complete exclusion of oxygen and water. This precondition has certainly previously played an important role in hindering a detailed investigation of nitrides.

Among the theoretically possible binary main group element nitrides with nitrogen in the oxidation state −III and the electropositive elements in the maximum oxidation state corresponding to their group number, many are either nonexistent or have until now not been obtained in a pure

[*] Prof. Dr. W. Schnick
Laboratorium für Anorganische Chemie der Universität
Postfach 101251, D-W-8580 Bayreuth (FRG)
Telefax: Int. code (921)55-2535

and well-defined form because of their low stability (Fig. 1). Li_3N exhibits an unusually high tendency for formation; the reaction between lithium metal and molecular nitrogen starts at room temperature and atmospheric pressure without any additional activation. In contrast, there is no reliable evidence for the existence and stability of analogous compounds of the heavier alkali metals. Apparently in the nitrides M_3N (M = Na, K, Rb, Cs) the high formal charge of the nitride ion (N^{3-}) and the unfavorable molar ratio of cations to anions (3:1) make it impossible to form a stable ionic structure in which the electrostatic, coordinative, and lattice-energetic requirements of a stable solid material are fulfilled. For the alkaline earth metals, binary nitrides with the composition M_3N_2 are, however, known for all the elements.

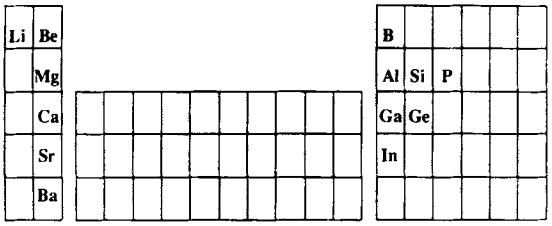

Fig. 1. Binary nitrides are only known for a fraction of the main group elements in the maximum oxidation state corresponding to their group numbers.

In contrast to the ionic structures of the nitrides of lithium and the alkaline earth metals, the decreasing electronegativities from the third group onwards lead to the formation of compounds with more covalent character (e.g. BN, AlN, Si_3N_4). As the group number increases, the heavier homologues in their highest oxidation state show a clearly decreasing tendency to form stable binary nitrides: In the third main group TlN is "missing", while in the neighboring group tin and lead form no stable nitrogen compounds with the expected stoichiometry M_3N_4.[6] This trend continues up to the sixth main group; here no compounds with the composition $M^{VI}N_2$ (M = S, Se, Te) are known. In some cases the instability of the element–nitrogen bond appears to be responsible for the nonexistence of the corresponding binary nitrides. Thus stable molecular compounds of antimony(v) and nitrogen are only formed when the basicity of the nitrogen atoms is decreased by electron-withdrawing groups or by mesomeric effects,[7] a requirement which is hardly realizable in the speculative compound Sb_3N_5. In the case of other main group elements (e.g. carbon and sulfur) the reasons for the hitherto nonexistence of corresponding binary nitrides (C_3N_4 and SN_2) appear to be more complex or to be due to preparative problems.

The binary nonmetal nitrides BN, Si_3N_4, and P_3N_5 will be main subjects of the following discussion. These are the only nonmetal nitrides so far studied in detail in which the electropositive elements have the maximum possible oxidation state corresponding to their group number. The syntheses, structure, and properties of BN and Si_3N_4 were described many years ago. However, both compounds had been studied because of their application in the area of high-performance materials. Because of preparative difficulties, pure phosphorus(v) nitride has only recently been obtained. Although P_3N_5 is thermodynamically appreciably less stable than BN or Si_3N_4, it has still been possible to develop a multifaceted solid-state chemistry of the phosphorus(v) nitrides. This success has provided the impetus for a further systematic search for new ternary and higher nonmetal nitrides.

2. The Binary Nonmetal Nitrides BN, Si_3N_4, and P_3N_5

Binary nitrides form the basis for the syntheses of ternary or higher nonmetal nitrides containing electropositive elements. Innumerable methods for the preparation of these compounds are known; however, only a limited number of these procedures which afford pure, well-defined products can be readily carried out under laboratory conditions. Such methods must be applied when the binary nitrides are to be used in the syntheses of new compounds.

2.1. Boron Nitride BN

Within the family of known ceramic materials boron nitride has the lowest density ($\varrho = 2.27\ g\,cm^{-3}$). It is colorless in the pure state and sublimes at about 2330 °C under a nitrogen pressure of one atmosphere.[8] Its decomposition

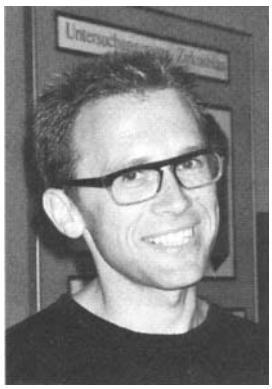

Wolfgang Schnick, born in 1957 in Hannover, studied chemistry at the Universität Hannover and received his doctorate there in 1986, having worked with Martin Jansen on alkali metal ozonides. After a postdoctoral year with Albrecht Rabenau at the Max-Planck-Institut für Festkörperforschung in Stuttgart he moved to the Universität Bonn. His habilitation in the field of inorganic chemistry was completed at the beginning of 1992. His particular interest within the area of preparative solid-state chemistry lies with the nitrides; his work is mainly concerned with their preparation and characterization, and the determination of the relationship between structures and properties. A further main area of interest involves the preparation of new types of compounds which can potentially be used as ceramic materials, ionic conductors, pigments, and catalysts. In 1989 Wolfgang Schnick was awarded the Benningsen–Foerder Prize of Nordrhein-Westfalen and in 1992 he received a Heisenberg scholarship from the Deutsche Forschungsgemeinschaft. In addition, he obtained a "Dozentenstipendium" from the Fonds der Chemischen Industrie and the Academy Prize of the Göttinger Akademie der Wissenschaften. Since 1993 he has been a Professor of Inorganic Chemistry at the Universität Bayreuth.

vapor pressure (N_2) is 1.6 Pa at 1900 °C and 573 Pa at 2300 °C,[8] while under a high nitrogen pressure (50 MPa) boron nitride melts at about 3300 °C.[9] Its thermodynamic data are also known.[8, 10] Boron nitride is isoelectronic with elemental carbon and, like the latter, occurs in several modifications. Hexagonal boron nitride (*h*-BN, α-BN) is the most stable form under normal conditions. It is analogous to graphite in that it contains planar layers of condensed six-membered $[B_3N_3]$ rings (d(B–N) = 145 pm). In contrast to carbon (staggered stacking) these layers are stacked directly above each other, so that the boron atoms of one layer are in direct contact with the nitrogen atoms of the neighboring layers (d(B···N) = 333 pm). Under normal conditions the cubic (*c*-BN, β-BN) and hexagonal (γ-BN) forms of boron nitride with zinc blende- and wurtzite-type structures, respectively, are metastable.[8]

Many procedures for the preparation of boron nitride have been suggested.[10] Exceptionally pure products are obtained from the reactions of boron trichloride BCl_3 with NH_3 or N_2/H_2 at temperatures below 1300 °C, or by microwave discharge.[10, 11] Oxygen-free boron nitride can also be prepared from the reaction of $K[BH_4]$ with NH_4Cl at temperatures up to 1050 °C.[10] A number of industrial methods for the synthesis of boron nitride are also known, although they do not always afford pure products. These include the reactions of oxygen-containing boron compounds such as B_2O_3 or $B(OH)_3$ with nitriding compounds such as urea, biuret ($NH(CONH_2)_2$), dicyandiamide, or melamine and the carbothermal reduction of B_2O_3 with carbon and nitrogen at 1800 to 1900 °C.[10] The reaction of alkaline earth metal cyanamides ($CaCN_2$, $SrCN_2$, $BaCN_2$) with boric acid $B(OH)_3$ leads to mixtures of *h*-BN and the corresponding borates and cyanides.[10, 12] The direct nitridation of elemental boron can also be carried out at temperatures above 1200 °C; however, this process is of neither industrial nor preparative importance.[10, 11] Chemical vapor deposition (CVD) of boron nitride has been attempted starting from a large number of volatile, molecular boron compounds, which are particularly suitable for the formation of amorphous or crystalline thin films or fine powders.[8] Several boron-containing polymers have also been used as precursors for BN.[13] Under typical laboratory conditions most processes afford *h*-BN, which is either amorphous or has a strongly disordered crystalline structure; these can, however, be converted to a regular crystalline state by suitable thermal aftertreatment.[8, 10] The conversion of hexagonal (α-BN) to cubic (β-BN) boron nitride at high pressures and temperatures is favored when Li_3BN_2 or Mg_3BN_3 are used.[14]

2.2. Silicon Nitride Si_3N_4

Silicon nitride is at present the most important nitridic material in the area of high-performance applications[15] because of its great hardness (Vickers hardness = 1400–1700 MNm^{-2}), its high mechanical strength (up to about 1300 °C), and its low density ($\varrho = 3.2\ g cm^{-3}$). Pure Si_3N_4 decomposes above about 1900 °C. Crystalline silicon nitride exists in two polymorphous modifications (α-Si_3N_4, β-Si_3N_4); in both cases the structures consist of topologically similar three-dimensional networks composed of corner-sharing SiN_4 tetrahedra (d(Si–N) ≈ 174 pm (mean value))[16] (Fig. 2). The two modifications differ only slightly in their lattice energies (difference ≈ 1.3 %[17]); the heat of conversion has been estimated to be about 30 $kJ mol^{-1}$.[17] Because of this small difference in stability the two phases can coexist. The proportion of the α-modification increases as the temperature at which the Si_3N_4 is prepared decreases. The reconstructive phase transition (above 1650 °C) only takes place in the direction α-Si_3N_4 → β-Si_3N_4; the reverse reaction appears to be kinetically hindered.

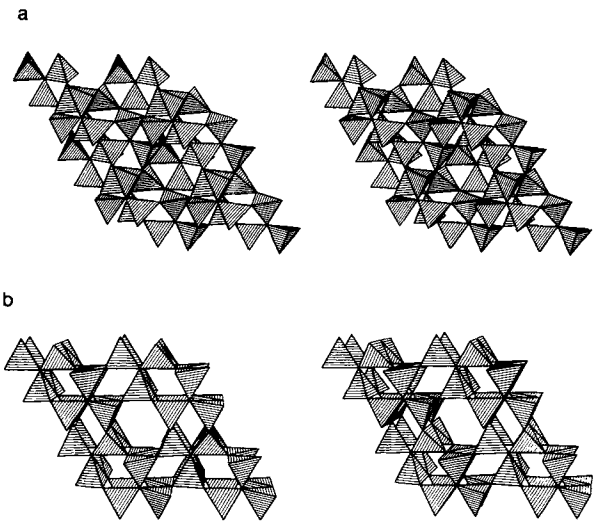

Fig. 2. Crystal structures of α-Si_3N_4 (a) and β-Si_3N_4 (b) (stereoscopic representation looking along [001]). The SiN_4 tetrahedra are shown as closed polyhedra.

Three methods for the preparation of pure silicon nitride are of particular importance and are also used industrially: the direct nitridation of elemental silicon,[15, 18–21] the carbothermal reduction of silicon dioxide under a nitrogen or ammonia atmosphere,[15, 22–26] and the ammonolyses of $SiCl_4$ or SiH_4.[15, 27–31] The ammonolysis reactions are particularly suitable for preparative purposes; they lead initially to amorphous and relatively undefined silicon diimide $Si(NH)_2$, which is converted at temperatures above about 900 °C to amorphous Si_3N_4 and above about 1300 °C to α-Si_3N_4.[15, 27–29, 32]

2.3. Phosphorus(v) Nitride P_3N_5

In contrast to the well-studied nitrides BN and Si_3N_4, very little reliable information on the synthesis, structure, and properties of P_3N_5 was available for a long time. Thus, phosphorus(v) nitride is only mentioned in passing in Allcock's monograph on phosphorus–nitrogen compounds,[33] while it takes up only a few lines in Corbridge's thousand-page book on phosphorus compounds.[34]

In principle it should be possible to prepare P_3N_5 by methods analogous to those used for BN and Si_3N_4. However, neither the direct nitridation of elemental phosphorus in low-pressure plasma[35] nor the simple ammonolysis of molecular phosphorus compounds such as PCl_5, P_4S_{10}, $(PNCl_2)_3$, $(PN(NH_2)_2)_3$, or $SP(NH_2)_3$[36–42] lead to the formation of pure, crystalline, and well-defined phosphorus(v)

nitride. Such attempts lead in fact to amorphous products that in some cases still contain chlorine, sulfur, or hydrogen; these generally have a very large surface area and cannot be characterized further. The main problem in the synthesis of pure crystalline P_3N_5 is that this nitride is much less thermally stable than BN or Si_3N_4; thus, decomposition with evolution of nitrogen occurs above about 850 °C [Eq. (1)].

$$2\,P_3N_5 \longrightarrow 6\,PN + 2\,N_2 \longrightarrow 3\,P_2 + 5\,N_2 \quad (1)$$

Brown undefined amorphous phosphorus(III) nitride is formed in this reaction; thus, in contrast to the situation for boron or silicon nitride it is not possible to remove impurities (such as H, Cl or S) simply by raising the temperature and thereby obtaining monophasic P_3N_5. The preparation of pure crystalline P_3N_5 starting from molecular phosphorus compounds is thus a tightrope walk between incipient thermal decomposition and sufficient activation of the P–N bonds (cleavage and reformation) for the construction of an ordered crystalline solid via amorphous polyphosphazene intermediates.[43] Since thermal activation alone is insufficient, the necessary P–N bond breaking and formation must be supported by chemical means.

The ammonolysis of PCl_5 or $(PNCl_2)_3$ using NH_4Cl rather than NH_3 at temperatures below 800 °C indeed leads to the formation of colorless, microcrystalline compact P_3N_5 that is hydrogen- and chlorine-free [Eqs. (2), (3)]. It seems likely that the HCl present, which in pure form decomposes P_3N_5 at higher temperatures with the formation of volatile products, leads to the reversible and reconstructive formation of crystalline P_3N_5.[43]

$$(PNCl_2)_3 + 2\,NH_4Cl \xrightarrow{780\,^\circ C,\ 2d} P_3N_5 + 8\,HCl \quad (2)$$

$$3\,PCl_5 + 5\,NH_4Cl \xrightarrow{780\,^\circ C,\ 2d} P_3N_5 + 20\,HCl \quad (3)$$

According to IR, EXAFS, ED, HRTEM, and ^{15}N and ^{31}P solid-state MAS NMR spectroscopic studies,[*] phosphorus(v) nitride P_3N_5 has a three-dimensional network, consisting of corner-sharing PN_4 tetrahedra (d(P–N) = 160 pm).[43] The solid, formulated as ${}^3_\infty[P^{[4]}_3N^{[3]}_2N^{[2]}_3]$, contains two types of nitrogen atom in a molar ratio of 2:3, which are linked to three and two phosphorus atoms, respectively.[43] Because of a stacking disorder in P_3N_5 demonstrated by HRTEM,[43] it has so far not been possible to carry out a complete single-crystal X-ray structural analysis. However, recently, completely ordered single crystals of P_3N_5 have been obtained.[43]

3. Ternary and Higher Phosphorus(v) Nitrides

The combination of the two elements phosphorus and nitrogen is isosteric with a corresponding combination of silicon and oxygen. This fact stimulated the systematic study of the siloxanes (typical building block: $-R_2Si-O-SiR_2-$)[44,45] in analogy to the isosteric phosphazenes (typical building block: $-R_2P=N-PR_2=$). Wide-ranging systematic investigations of the chemistry of molecular P–N compounds have led to the discovery of a very large number of well-characterized monomeric, oligomeric, and polymeric phosphazenes; these can contain diverse substituents R (such as F, Cl, Br, NH_2, NR_2, CF_3, N_3, NCS, NCO). It has proved possible not only to synthesize chain-like and cyclic phosphazenes of widely varying molecular size but also to cross-link such units to give polymeric materials with exactly tailored properties.[33,34,46] In contrast to the phosphazenes, the siloxanes are, however, much less readily accessible; thus, the systematic investigation of this class of compounds has taken place only relatively recently.[44,45]

The situation is completely opposite in the case of the corresponding Si–O and P–N solid-state compounds. While a large group of preparatively readily accessible Si–O compounds (silicates, silicon dioxide)[47] is known which also includes a number of naturally occurring species (e.g. quartz, pyroxene, amphibole, kaolinite, pyrophillite, mica, feldspar), there were only a few indications of the possible existence of analogous P–N compounds.[48,49] The analogy between silicon oxides (silicates) and phosphorus(v) nitrides is, however, not so close as the isostericity between molecular siloxanes and phosphazenes discussed previously, in which in each case a molar ratio of Si:O = P:N = 1:1 is involved. The consideration of typical silicate building blocks and the corresponding phosphorus–nitrogen isosteres shows the formal charge to be different in each case: SiO_4^{4-}/PN_4^{7-}, $Si_3O_9^{6-}/P_3N_9^{12-}$, SiO_2/PN_2^-. When these charges are compensated in ternary compounds by cations of electropositive elements (e.g. alkali metals or alkaline earth metals), we can expect that mainly covalent P–N substructures as well as contacts between nitrogen and the cations with clearly ionic character will be formed. Thus, in spite of their differing overall composition the phosphorus(v) nitrides should contain P–N substructures which have isosteric analogues within the silicate family.

For a long time it proved impossible to prepare phosphorus(v) nitrides in a pure crystalline form, and no reliable information existed on the structure and properties of particular compounds. The greatest problem was that pure P_3N_5 was not available as a starting material for the preparation of such compounds. Thus, the development of a route to well-defined phosphorus(v) nitride (see Section 2.3) was a basic precondition for the systematic study of ternary and higher phosphorus(v) nitrides containing electropositive elements.

3.1. Alkali Metal and Alkaline Earth Metal Phosphorus(v) Nitrides

Ternary phosphorus(v) nitrides derived from metals should be accessible from the corresponding binary nitrides. The analogy with oxo chemistry suggests that a reaction between an "acidic" nonmetal nitride (P_3N_5) and a "basic" metal nitride should be successful. For various reasons the quasibinary Li_3N/P_3N_5 system appeared to be particularly suitable for the systematic study of the ternary phosphorus(v) nitrides: Among the alkali metals only lithium forms a binary nitride with the composition M_3N (M = Li, Na, K,

[*] EXAFS = extended X-ray absorption fine structure, ED = electron diffraction, HRTEM = high-resolution transmission electron microscopy, MAS = magic angle spinning.

Rb, Cs). Lithium nitride is readily available from its constituent elements;[50] in addition its thermodynamic stability is sufficient to permit reactions with phosphorus(v) nitride to be carried out in the temperature range 600–850 °C.

The quasibinary Li_3N/P_3N_5 system has so far afforded four lithium phosphorus(v) nitrides, which have been prepared in a pure form and characterized both structurally and with respect to their properties: Li_7PN_4,[51] $Li_{12}P_3N_9$,[52, 53] $Li_{10}P_4N_{10}$,[54] and $LiPN_2$[55] can in each case be prepared in solid-state reactions between stoichiometric amounts of the binary nitrides Li_3N and P_3N_5 [Eqs. (4)–(7)]. A crucial factor

$$7\,Li_3N + P_3N_5 \xrightarrow[\text{W crucible, } N_2 \text{ atm.}]{620\,^\circ C,\ 4d} 3\,Li_7PN_4 \quad (4)$$

$$4\,Li_3N + P_3N_5 \xrightarrow[\text{W crucible, } N_2 \text{ atm.}]{750\,^\circ C,\ 5d} Li_{12}P_3N_9 \quad (5)$$

$$10\,Li_3N + 4\,P_3N_5 \xrightarrow[\text{W crucible, } N_2 \text{ atm.}]{720\,^\circ C,\ 5d} 3\,Li_{10}P_4N_{10} \quad (6)$$

$$Li_3N + P_3N_5 \xrightarrow[\text{W crucible, } N_2 \text{ atm.}]{800\,^\circ C,\ 4d} 3\,LiPN_2 \quad (7)$$

in these reactions is the choice of the crucible material, since at the temperatures used lithium nitride reacts with all the standard materials. Pure tungsten metal is particularly suitable for the crucibles for these reactions, since under the reaction conditions used the interior of the crucible is passivated by a layer of tungsten nitride, which, when all the experimental parameters (temperature, reaction time, particle size of the Li_3N used) are optimized, prevents a further attack on the crucible to give Li_6WN_4.

Besides reactions between the binary nitrides, it is also possible to react the lithium phosphorus(v) nitrides themselves with Li_3N or P_3N_5 to obtain the corresponding ternary phases [Eqs. (8)–(11)].

$$2\,Li_3N + LiPN_2 \xrightarrow[\text{W crucible, } N_2 \text{ atm.}]{620\,^\circ C,\ 14d} Li_7PN_4 \quad (8)$$

$$2\,Li_3N + 4\,LiPN_2 \xrightarrow[\text{W crucible, } N_2 \text{ atm.}]{700\,^\circ C,\ 5d} Li_{10}P_4N_{10} \quad (9)$$

$$6\,P_3N_5 + 10\,Li_7PN_4 \xrightarrow[\text{W crucible, } N_2 \text{ atm.}]{630\,^\circ C,\ 10d} 7\,Li_{10}P_4N_{10} \quad (10)$$

$$3\,Li_3N + 3\,LiPN_2 \xrightarrow[\text{W crucible, } N_2 \text{ atm.}]{770\,^\circ C,\ 5d} Li_{12}P_3N_9 \quad (11)$$

The lithium phosphorus(v) nitrides are obtained from these syntheses as colorless powders or transparent single crystals. The sensitivity of the compounds towards hydrolysis increases with increasing lithium content and their thermal stability decreases. While $LiPN_2$ is stable up to about 900 °C and is hardly affected by moist air or water, Li_7PN_4 decomposes above 650 °C and is hydrolyzed by water in a violent reaction. The two other ternary compounds $Li_{12}P_3N_9$ and $Li_{10}P_4N_{10}$ take up an intermediate position in both respects, decomposing above about 780 °C and being somewhat sensitive towards hydrolysis.

All the lithium phosphorus(v) nitrides referred to have an ionic structure consisting of Li^+ ions and complex P–N anions. The common structural features are the PN_4 tetrahedra, which can be linked in different ways through common vertices: Li_7PN_4 contains "isolated" $[PN_4]^{7-}$ ions (mean P–N bond length = 171 pm), which are isoelectronic with orthosilicate $[SiO_4]^{4-}$ and orthophosphate $[PO_4]^{3-}$ building blocks. In the cubic unit cell of Li_7PN_4, the complex anions are arranged in a manner analogous to the β-tungsten type (A15) (Fig. 3), while the Li^+ ions are tetrahedrally coordinated by the nitrogen atoms of the PN_4 tetrahedra. The crystal structure of Li_7PN_4 can be considered as an anti-fluorite type. Thus, the nitrogen atoms adopt a distorted cubic close packing, in which Li^+ ions and phosphorus atoms occupy all the tetrahedral holes in an ordered manner.[51]

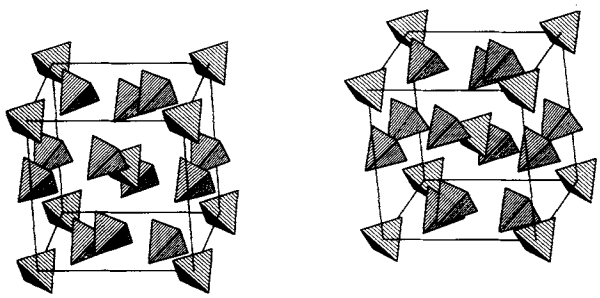

Fig. 3. Unit cell of Li_7PN_4 (stereoscopic representation). The PN_4 tetrahedra are shown as closed polyhedra; for the sake of clarity the Li^+ ions are not shown [51].

At the quasibinary Li_3N/P_3N_5 intersection, $LiPN_2$ is found as the compound with the lowest lithium content. PN_4 tetrahedra are again the characteristic building blocks of the P–N substructure. However, because of the molar ratio P:N = 1:2 they are not isolated but form a three-dimensional infinitely linked network $^3_\infty[PN_{4/2}^-]$, which is topologically equivalent to and isoelectronic with β-cristobalite (SiO_2) (d(P–N) = 164.5(7) pm, $\sphericalangle$ P-N-P = 123.6(8)°[55]). Compared with the C9 type (the idealized β-cristobalite structure), $LiPN_2$ is clearly distorted; all the PN_4 tetrahedra are rotated by an angle $\varphi = 34.2°$ about their axes of inversion. According to O'Keeffe and Hyde,[56] a distortion of this type starting from a filled variant of the C9 type ($\varphi = 0°$) leads, by a continuous transformation, to the chalcopyrite type ($\varphi = 45°$), a superstructural variant of zinc blende. Thus, the crystal structure of $LiPN_2$ (Fig. 4) can also be explained on the basis of the concept of sphere packing: Li^+ ions and phosphorus atoms systematically occupy half of the tetrahedral holes in a distorted cubic closest packing of nitrogen atoms in an ordered manner. The Li^+ ions and phosphorus

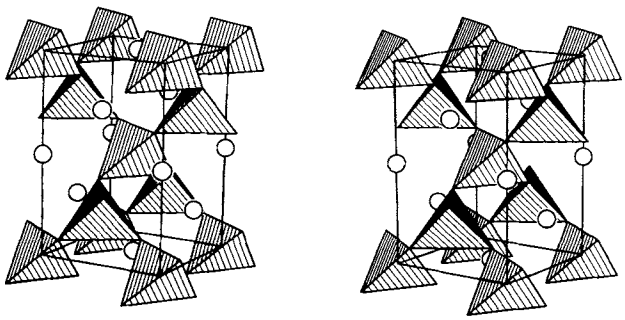

Fig. 4. Crystal structure of $LiPN_2$ (stereoscopic representation). The PN_4 tetrahedra, which are condensed at all their vertices, are shown as closed polyhedra, the Li^+ ions as open circles [55].

atoms in $LiPN_2$ and Li_7PN_4 appear not to be influenced by the significantly different bonding situations of P and N on the one hand or of Li and N (mainly covalent and ionic, respectively), on the other; thus, it is surprising to find such extreme structural similarities.

Within the quasibinary Li_3N/P_3N_5 system, Li_7PN_4 and $LiPN_2$ are the two ternary compounds with the highest and lowest lithium content, respectively. Their anionic P–N substructures $[PN_4]^{7-}$ and $^3_\infty[PN_{4/2}^-]$ are isosteric analogues of orthosilicate and silicon dioxide, respectively; these two Si–O compounds have the lowest and highest degree of condensation of SiO_4 tetrahedra, respectively. In analogy with the large family of silicate structures, it appeared appropriate to search for phosphorus(v) nitrides with an intermediate degree of condensation of corner-sharing PN_4 tetrahedra, which are perhaps similar to the chain or layer silicates.

Two further ternary compounds within the Li_3N/P_3N_5 system, Li_4PN_3 and $Li_5P_2N_5$, have both been prepared in a pure state and structurally characterized. In comparison with Li_7PN_4 and $LiPN_2$, both of these lithium phosphorus(v) nitrides have an intermediate lithium content. We thus expected to find an intermediate degree of condensation of the corner-sharing PN_4 tetrahedra. In fact Li_4PN_3, in analogy to the cyclotrisilicate $[Si_3O_9]^{6-}$, contains complex anions with three corner-sharing PN_4 tetrahedra,[52, 53] and thus the formula for this lithium phosphorus(v) nitride is $3(Li_4PN_3) = Li_{12}P_3N_9$. The cyclic anions exist in a chair conformation (Fig. 5).

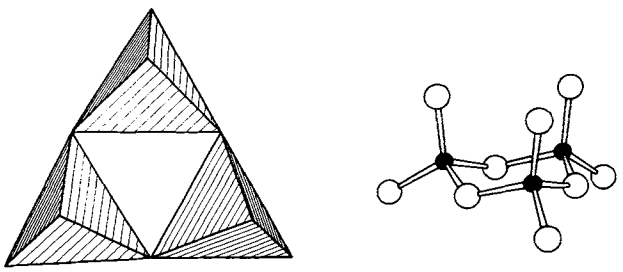

Fig. 5. Cyclotrisilicate-like $[P_3N_9]^{12-}$ ions (chair form) in $Li_{12}P_3N_9$ [52,53].

Since the molar ratio of phosphorus to nitrogen in $Li_5P_2N_5$ is 2:5, the analogy with the silicates leads us to expect either layer-type arrangements (silicate example: $Ba[Si_2O_5]$)[57] or double rings (example: $[Ni(H_2N(CH_2)_2NH_2)_3]_3[Si_6O_{15}] \cdot 26H_2O$[58]) consisting of corner-sharing PN_4 tetrahedra. In fact this lithium phosphorus(v) nitride contains complex $[P_4N_{10}]^{10-}$ ions, which are thus the first nitrido analogue of molecular phosphorus(v) oxide P_4O_{10} (Fig. 6).[54] As in molecular P_4O_{10}, and in agreement with the assumption of higher double bond or polar bond character, the bonds to the terminal atoms are clearly shorter than those to the bridging atoms (P_4O_{10}: $d(P–O_{term}) = 141–151$, $d(P–O_{br}) = 153–160$ pm;[59] $[P_4N_{10}]^{10-}$: $d(P–N_{term}) = 158$, $d(P–N_{br}) = 168$ pm[54]).

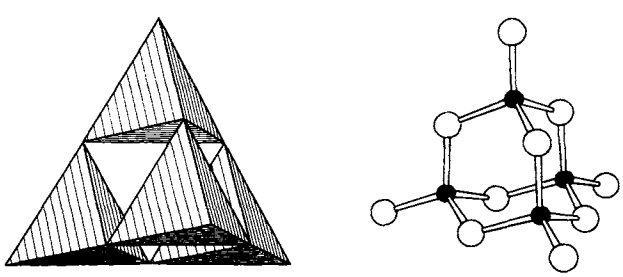

Fig. 6. Structure of the $[P_4N_{10}]^{10-}$ ion in $Li_{10}P_4N_{10}$. The complex anion has T_d symmetry in the solid and a regular tetrahedral structure [54].

There is a close relationship between the $[P_4N_{10}]^{10-}$ cage and the cagelike double rings in the silicates.[58] Thus both the $[P_4N_{10}]^{10-}$ ions and the $[Si_6O_{15}]^{6-}$ double rings are composed of "dreier"[*] rings. An $[Si_4O_{10}]^{4-}$ building unit isosteric with the $[P_4N_{10}]^{10-}$ ion, which represents the smallest possible cage built up of corner-sharing SiO_4 tetrahedra, has so far not been observed.

In the solid state, the complex anions in $2(Li_5P_2N_5) = Li_{10}P_4N_{10}$ have ideal T_d symmetry; the ten nitrogen atoms form an almost undistorted section from cubic closest packing. In comparison with the situation in molecular phosphorus(v) oxide, a much more favorable packing of the complex building units is attained in the solid state; molecular P_4O_{10}, like urotropine, has a distorted body-centered structure (with respect to the center of gravity of the molecule),[60] while the packing of the $[P_4N_{10}]^{10-}$ units is derived from the cubic face-centered zinc blende-type structure.[54] In the solid the neighboring $[P_4N_{10}]^{10-}$ ions, which themselves have an almost completely regular tetrahedral structure, are arranged in a manner such that they face each other with their triangular surfaces parallel and rotated by 60° (Fig. 7).

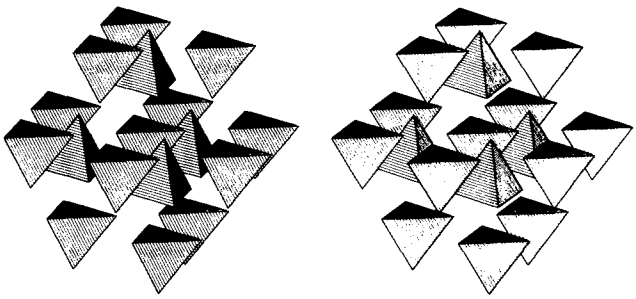

Fig. 7. Packing of the $[P_4N_{10}]^{10-}$ ions in the solid state (stereoscopic representation).

The extension of this packing principle to a three-dimensional infinite solid leads to the formation of "free" layers, which extend in all directions in space because of the cubic symmetry of the crystal (Fig. 7): The lithium ions occupy these layers. Because of the topology of the complex anions in $Li_{10}P_4N_{10}$, the packing described for the solid does not permit the relatively high number of cations ($Li^+:[P_4N_{10}]^{10-} = 10:1$) to be coordinated in a uniform manner by the nitrogen atoms. The Li^+ ions are coordinated either in a trigonal planar manner, tetrahedrally, or with a distorted octahedral nitrogen environment; the molar ratio of these arrangements is 6:1:2. The remaining ten per cent of the lithium ions are distributed with disorder on a site with

[*] The term "dreier" ring was coined by Liebau [47] and is derived from the German word drei, which means three; however, a dreier ring is not a three-membered ring, but a six-membered ring comprising *three* tetrahedral centers and *three* electronegative atoms (cf. Figs. 5 and 6). Similar terms exist for rings comprising four, five, and six tetrahedral centers (and the corresponding number of electronegative atoms), namely "vierer", "fünfer", and "sechser" rings, respectively.

higher multiplicity. Lattice-energy and point-potential calculations[61] confirm that in the highly symmetric packing of the complex anions in $Li_{10}P_4N_{10}$ only a proportion of the cations can be accommodated in positions with deep potential wells (tetrahedrally and octahedrally coordinated Li^+ ions). Only flat potential wells are available for the remaining cations, these leading in part to intrinsic disorder.

In all these lithium phosphorus(v) nitrides the Li–N contact distances determined $d(Li–N) = 192–224$ pm) are approximately equal to the sum of the ionic radii and increase as expected with the increasing coordination number of the cations. When the electronegativity differences $\Delta\chi$ between lithium and nitrogen ($\Delta\chi = 2.0$) and between phosphorus and nitrogen ($\Delta\chi = 1.0$) are taken into account, a simple Pauling-type estimate[62] leads us to expect P–N substructures with predominantly covalent bond character (78% covalent). The interactions between lithium and nitrogen should in contrast be predominantly (63%) ionic. A systematic study of the lithium–phosphorus(v) nitrides is also of interest because the covalent and polarizable P–N substructures in these compounds, in combination with their ionic Li–N contacts, should lead to a considerable mobility of the Li^+ ions in the solid state, so that they could form a new class of ionic conductors. Impedance-spectroscopic measurements on $LiPN_2$ and Li_7PN_4[63] (Fig. 8) confirm this prediction. The solid state Li^+ ion conductivities determined are,

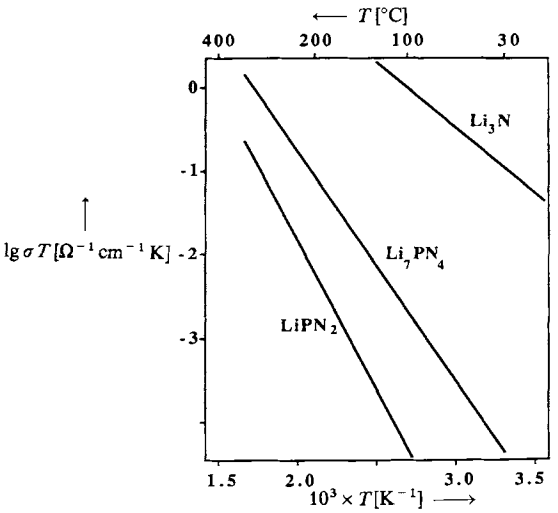

Fig. 8. Temperature dependence of the Li^+ ion conductivities in Li_3N, $LiPN_2$, and Li_7PN_4 [63].

however, lower than the extremely high conductivities of binary Li_3N,[50] which arise on the one hand from an appreciable doping with hydrogen according to the formula $Li_{3-x}H_xN$, and on the other from the unusual crystal structure of lithium nitride. Li_7PN_4 has a higher conductivity and a lower activation energy than $LiPN_2$ (Table 1). This difference between the two lithium phosphorus(v) nitrides can be understood on the basis of the crystal structures, the coordination of the Li^+ ions, and the number of charge carriers available in the solid state: In both Li_7PN_4 and $LiPN_2$ all cations are coordinated tetrahedrally by nitrogen, the observed contact distances Li–N being identical on average

Table 1. Specific Li^+ ion conductivities and activation energies of Li_3N, Li_7PN_4, and $LiPN_2$.

	σ_{400K} [$\Omega^{-1}cm^{-1}$]	E_a [kJ mol^{-1}]	Ref.
Li_3N	4.0×10^{-3}	24	[50]
Li_7PN_4	1.7×10^{-5}	47	[51, 63]
$LiPN_2$	6.9×10^{-7}	59	[55, 63]

(Li_7PN_4: 209 pm; $LiPN_2$: 209 pm).[51, 55] The number of charge carriers available for ionic conductivity is, however, much higher in Li_7PN_4. Thus, Li_7PN_4, because of its composition, contains much more lithium; in addition the anti-fluorite crystal structure (identical with a defect CsCl type) has a large number of interstitial sites which are available for ionic conduction. $LiPN_2$, in contrast, has a closely packed structure (chalcopyrite type, identical to a zinc blende modification). In this case no interstitial sites of comparable geometry are available. A diffusion of the Li^+ ions in the solid state is thus considerably hindered in $LiPN_2$, which results in a higher activation energy and a conductivity lower than that of Li_7PN_4.[63]

$Li_{10}P_4N_{10}$ contains structural features which lead us to expect a high mobility of the Li^+ ions in the solid: the symmetrical packing of the $[P_4N_{10}]^{10-}$ ions leads to the formation of free layers which permeate the solid in all directions. The intrinsic disorder of the cations in this compound, the fact that the Li^+ ions most probably occupy broad, shallow potential wells, and the coordination modes of a fraction of the Li^+ ions which are particularly favorable for ionic conduction (trigonal planar) are all factors which would favor a high Li^+ ionic conductivity in the solid.[53, 54]

The lithium phosphorus(v) nitrides discussed above contain either discrete complex P–N anions (Li_7PN_4, $Li_{12}P_3N_9$, $Li_{10}P_4N_{10}$) or a three-dimensional network of PN_4 tetrahedra($LiPN_2$). In the silicate family, the cyclosilicates are less stable than the corresponding chainlike compounds. Hard cations (e.g. Li^+, Mg^{2+}) increase this effect, while soft cations (e.g. Ca^{2+}, K^+) stabilize the rings.[47] The replacement of the monovalent Li^+ ions by bivalent alkaline earth metal ions while the P:N ratio is kept at 1:3 leads, in contrast to the observations made for the silicates, to a surprising result: A solid-state reaction between the corresponding amounts of the binary nitrides Ca_3N_2 and P_3N_5 [Eq. (12)] affords a ternary alkaline earth phosphorus(v) nitride of the composition Ca_2PN_3.

$$2\,Ca_3N_2 + P_3N_5 \xrightarrow[\text{W crucible, } N_2 \text{ atm.}]{800\,^\circ C,\ 4d} 3\,Ca_2PN_3 \qquad (12)$$

While "dreier" rings are present in $Li_{12}(PN_3)_3 = Li_{12}P_3N_9$, the alkaline earth phosphorus(v) nitride contains infinite chains $^1_\infty[PN_2N^{4-}_{2/2}]$ of corner-sharing PN_4 tetrahedra (Fig. 9).[64] The "zweier" chain found here has an extreme stretching factor $f_s = 1.0$, as found, for example, in the chain silicate $CaMn[Si_2O_6]$.[47, 65] As well as the calcium compound, a magnesium phosphorus(v) nitride Mg_2PN_3 is also known[66] whose crystal structure is an ordered wurtzite variant. More recent studies[67] indicate that this phosphorus(v) nitride also contains infinite "zweier" chains made up of corner-sharing PN_4 tetrahedra.

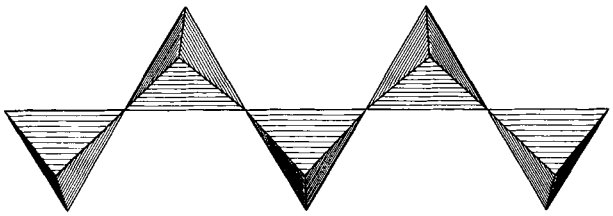

Fig. 9. Infinite "zweier" chains of corner-sharing PN_4 tetrahedra in Ca_2PN_3 [64].

3.2. Phosphorus(v) Nitride Imides and P–N Sodalites

The first intermediate in the ammonolysis of phosphorus pentachloride could in principle be the corresponding pentaamide $P(NH_2)_5$. In fact, however, condensation reactions occur when only a fraction of the chlorine atoms have been replaced by NH_2 groups; these lead to the formation of oligocyclo- and polyphosphazenes.[68] Product formation is influenced both by the reaction temperature and the ratio of NH_3 to PCl_5, so that either chlorine-rich compounds, such as $[NPClNH_2]_x$, or completely substituted compounds, such as $[NP(NH_2)_2]_x$, are obtained. It was postulated that the final product of substitution and condensation reactions in the ammonolysis of PCl_5 was a polymeric compound $^3_\infty[PN_{2/2}(NH_2)_{2/2}] \triangleq HPN_2$.[69–71] However, it is in fact found that the reaction of phosphorus pentachloride and ammonia leads to a vast number of different oligomeric and polymeric phosphazenes; thus, a homogeneous reaction product HPN_2 is not formed. The compound HPN_2 can, however, be obtained in a pure crystalline form from the heterogeneous ammonolysis of pure phosphorus(v) nitride under pressure [Eq. (13)]. A particularly useful procedure[72] involves the in situ preparation of the ammonia required, starting from the corresponding amounts of ammonium chloride and magnesium nitride [Eq. (14)].

$$P_3N_5 + NH_3 \xrightarrow{580\ °C,\ 14d} 3\ HPN_2 \quad (13)$$

$$Mg_3N_2 + 6\ NH_4Cl \xrightarrow{400\ °C} 8\ NH_3 + 3\ MgCl_2 \quad (14)$$

Like $LiPN_2$, phosphorus(v) nitride imide HPN_2 has a network structure $^3_\infty[PN^-_{4/2}]$ consisting of PN_4 tetrahedra linked through all four vertices by corner-sharing. This structure can be derived from the isosteric β-cristobalite-type (d(P–N) = 160 pm, $\sphericalangle$ P-N-P = 130°[72]); the hydrogen atoms are covalently bonded to one half of the nitrogen atoms of the P–N skeleton.[72]

A second phosphorus(v) nitride imide, HP_4N_7,[73] can be obtained by reacting the required amounts of P_3N_5 and ammonium chloride in sealed quartz ampoules [Eq. (15)].

$$4\ P_3N_5 + NH_4Cl \xrightarrow{820\ °C,\ 14d} 3\ HP_4N_7 + HCl \quad (15)$$

Equation (16) shows that the removal of one molecule of ammonia from four formula units of HPN_2 leads mathematically to the formation of HP_4N_7. It is unfortunately not possible to carry out this reaction preparatively, since the thermal decomposition of HPN_2 cannot be halted at the stage of HP_4N_7.

$$4\ HPN_2 \xrightarrow[-NH_3]{} HP_4N_7 \quad (16)$$

There appears to be a close structural relationship between the two phosphorus(v) nitride imides. Thus, HP_4N_7 can be regarded as a shear structure variant of HPN_2. As shown above, the structure of HP_4N_7 results from the elimination of one nitrogen atom (as NH_3) from four formula units of HPN_2; two of the remaining nitrogen atoms of the P–N skeleton then saturate the valences at the phosphorus atom. With respect to the β-cristobalite-like P–N substructure $^3_\infty[P^{[4]}N^{[2]}_{4/2}{}^-]$ in HPN_2, a fraction (two sevenths) of the nitrogen atoms in HP_4N_7 must form three P–N bonds according to the formula $^3_\infty[P^{[4]}_4N^{[2]}_5N^{[3]}_2{}^-]$.[73]

The ternary phosphorus(v) nitrides so far discussed that incorporate electropositive elements (hydrogen, alkali metals, or alkaline earth metals) mainly contain P–N structural elements with isosteric analogues in the silicate family. It thus seemed appropriate to treat Si–O compounds of particular interest, such as framework silicates and zeolites, as structural models for the preparation of new phosphorus(v) nitrides.

The importance of zeolites as catalysts, molecular sieves, adsorbents, and ion exchangers has increased considerably in recent years. The properties that render them so useful are based particularly on the characteristic topology of their tetrahedral skeletal structures, which have the general composition TO_2 (T = Si, Al).[74] By exchanging aluminum or silicon for other elements such as B, P, Ga, Ge, As, Sb, Ti, Zr, Hf, Fe, Cr, it proved possible to tailor the catalytic properties of zeolites in a manner favorable for certain applications.[74, 75] Substitution in the anion substructure of the framework, for example by replacing oxygen by other electronegative elements, has, in contrast, been almost completely neglected. It appeared to us that the preparation of nitrido zeolites should be particularly interesting in view of the possibility of obtaining desirable material properties (stability) and modifying the chemical properties of the zeolites (basicity).

The synthesis of a zeolite-like framework structure $^3_\infty[PN^-_{4/2}]$ is possible[76] when, for the in situ preparation of ammonia in the high-pressure ammonolysis of P_3N_5, Zn_3N_2 rather than Mg_3N_2 is treated with ammonium chloride [Eq. (17)]. The reaction then proceeds quantitatively to afford $Zn_5H_4[P_{12}N_{24}]Cl_2$ [Eq. (18)]. Analogously to HPN_2, a

$$Zn_3N_2 + 6\ NH_4Cl \xrightarrow{400\ °C} 8\ NH_3 + 3\ ZnCl_2 \quad (17)$$

$$4\ P_3N_5 + 4\ NH_3 + ZnCl_2 \xrightarrow{640\ °C} Zn_5H_4[P_{12}N_{24}]Cl_2 + 8\ HCl \quad (18)$$

phosphorus(v) nitride is formed, with a molar ratio P:N = 1:2, while at the same time zinc and chlorine are incorporated into the solid through gaseous $ZnCl_2$, which is volatile under the experimental conditions. A complete exchange of the hydrogen atoms in the product obtained is possible in a subsequent reaction with additional $ZnCl_2$ in which HCl is liberated [Eq. (19)].

$$Zn_5H_4[P_{12}N_{24}]Cl_2 + 2\ ZnCl_2 \xrightarrow{700\ °C,\ 3d} Zn_7[P_{12}N_{24}]Cl_2 + 4\ HCl \quad (19)$$

In $Zn_7[P_{12}N_{24}]Cl_2$ phosphorus and nitrogen form a sodalite-like three-dimensional network $^3_\infty[PN_{4/2}^-]$ of PN_4 tetrahedra which are linked through all four vertices by corner-sharing. (d(P–N) = 163.7 pm, ∢ P-N-P = 126°; Fig. 10).

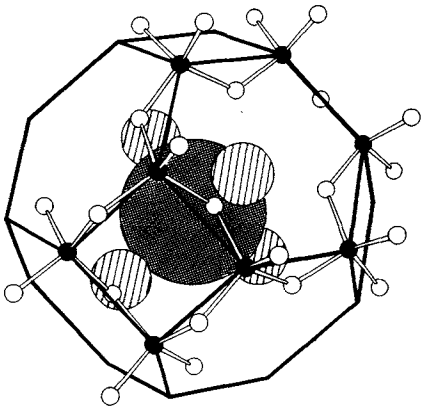

Fig. 10. Section of the crystal structure of $Zn_7[P_{12}N_{24}]Cl_2$. The zeolite-like β-cage made up of condensed $[P_4N_4]$ and $[P_6N_6]$ rings is shown. P: black, N: white, Cl: gray, Zn: striped. The size of Zn^{2+} and Cl^- corresponds to their respective ionic radii [76].

While in HPN_2 and $LiPN_2$, as in β-cristobalite, only three-dimensionally bonded $[P_6N_6]$ rings are found, the sodalite-like skeleton also contains $[P_4N_4]$ rings. The two types of rings together form truncated octahedra (β cages), which are typical building units of sodalites and zeolites. Situated at the center of each β-cage is a chloride ion, in a tetrahedral environment of Zn^{2+} ions. Besides the Zn–Cl contact (260 pm), the metal cations have contact with three nitrogen atoms of the P–N skeleton (d(Zn–N) = 196 pm). According to the formula $Zn_7[P_{12}N_{24}]Cl_2$, there is a statistical defect occupancy (occupancy factor 7/8) at the Zn position. A fraction of the Zn^{2+} ions can be replaced by two protons each, which in turn are covalently bonded to nitrogen atoms of the P–N skeleton. The P–N sodalite has a phase width of $Zn_{(7-x)}H_{2x}[P_{12}N_{24}]Cl_2$ ($0 \le x \le 2$). By starting from a material with a lower metal content $Zn_6H_2[P_{12}N_{24}]Cl_2$, it is possible to prepare a chlorine-free phosphorus(v) nitride $Zn(PN_2)_2$ by elimination of HCl [Eq. (20)]; the structure of the product is highly distorted and it is no longer crystalline.[73, 77] It is, however, probable that this compound possesses a three-dimensional network structure of corner-sharing PN_4 tetrahedra containing $[P_4N_4]$ and $[P_6N_6]$ rings.[73, 77]

$$Zn_6H_2[P_{12}N_{24}]Cl_2 \xrightarrow{800\ °C,\ 3d} 6\ Zn(PN_2)_2 + 2\ HCl \qquad (20)$$

The synthetic method described previously is not suitable for the preparation of modified P–N sodalites containing other metal cations, (e.g. alkaline earth metals, transition metals, lanthanides). On the one hand, it requires that the corresponding binary metal nitride M_3N_2 be both existent and stable, while on the other, the metal chloride MCl_2 formed in the reaction with NH_4Cl must have a certain minimum volatility.

P–N Sodalites $M_5H_4[P_{12}N_{24}]Cl_2$ (M = Zn, Co, Ni) can also be obtained remarkably easily by reacting corresponding amounts of the metal chloride MCl_2, hexachlorocyclotriphosphazene $(PNCl_2)_3$, and ammonium chloride [Eq. (21)]. This reaction is carried out in sealed ampoules,

$$5\ MCl_2 + 4\ (PNCl_2)_3 + 12\ NH_4Cl \xrightarrow{700\ °C,\ 2d} M_5H_4[P_{12}N_{24}]Cl_2 + 44\ HCl \qquad (21)$$

and the batch size is limited by the amount of HCl formed. An alternative procedure involves the use of a molecular phosphorus component in which the chlorine atoms are completely replaced by amino groups $[\{PN(NH_2)_2\}_3]$ [Eq. (22)]; in this case the product is the hydrogen-free P–N sodalite $M_7[P_{12}N_{24}]Cl_2$.[77]

$$7\ MCl_2 + 4\ (PN(NH_2)_2)_3 \xrightarrow{700\ °C,\ 2d} M_7[P_{12}N_{24}]Cl_2 + 12\ NH_4Cl \qquad (22)$$

A particularly elegant method for the preparation of P–N sodalites modified in various ways is the simple reaction between phosphorus(v) nitride imide HPN_2 and the corresponding metal halide MX_2 [Eq. (23)], which affords compounds with a large number of different metal cations and halide ions (e.g. M = Mg, Cr, Mn, Fe, Co, Ni, Cu, Zn, Pb; X = Cl, Br).[73, 77]

$$5\ MX_2 + 12\ HPN_2 \xrightarrow{700\ °C,\ 2d} M_5H_4[P_{12}N_{24}]X_2 + 8\ HX \qquad (23)$$

By using the methods described above it has been possible to obtain a wide variety of P–N sodalites. As well as divalent cations such as Mg^{2+}, Zn^{2+}, Mn^{2+}, Co^{2+}, Ni^{2+}, Cu^{2+}, Pb^{2+}, trivalent cations such as Cr^{3+}, Fe^{3+}, and even monovalent cations such as Cu^+ can be incorporated. In all cases phase widths are observed in which a fraction of the metal ions can be replaced by the corresponding number of hydrogen atoms, which are then covalently bonded to nitrogen atoms of the P–N skeleton.[73, 77]

The P–N sodalites exhibit remarkable properties: They are thermally stable up to about 800 °C (in a nonoxidizing atmosphere) and are inert towards all common solvents as well as hot acids and alkalis. Of particular interest is the fact that, depending on the metal cation present, some P–N sodalites are intensely colored (blue (Co, Ni), brown (Fe), dark green (Cr)), which suggests that they may find a use as pigments.

3.3. Silicon Phosphorus(v) Nitride $SiPN_3$

With respect to the development of new high-performance phosphorus(v) nitride ceramic materials it appears attractive to look at purely covalent ternary compounds containing both phosphorus and a second electropositive element, the latter being able to form a stable nitride which is a known ceramic material (BN, AlN, Si_3N_4). Earlier attempts to prepare ternary nitrides in the system Si–P–N or B–P–N starting from the binary nitrides were unsuccessful because of the low self-diffusion coefficient of these substances and the fact that the binary nitrides do not melt congruently.

Silicon phosphorus(v) nitride $SiPN_3$ is, however, available from the molecular precursor **D** in which the required structural element ≡Si–N=P≡ is already preformed (Scheme 1).

Compound **D** can be obtained in a three-step synthesis starting from bis(trimethylsilyl) azane ("hexamethyldisilazane") **A** and proceeding via the intermediates **B** and **C**. Low temperature ammonolysis of **D**, followed by removal of the ammonium chloride formed and pyrolysis in a stream of ammonia, leads to $SiPN_3$.[78]

$$(CH_3)_3Si{-}NH{-}Si(CH_3)_3 \xrightarrow{SiCl_4} Cl_3Si{-}NH{-}Si(CH_3)_3 \xrightarrow{Cl_2,\ -40\,^\circ C}$$

A **B**

$$Cl_3Si{-}N(Cl){-}Si(CH_3)_3 \xrightarrow{PCl_5} Cl_3Si{-}N{=}PCl_3 \xrightarrow[2.)\ NH_3,\ 800\,^\circ C]{1.)\ NH_3,\ -70\,^\circ C} SiPN_3$$

C **D**

Scheme 1.

Silicon phosphorus(v) nitride has a three-dimensional network structure of corner-sharing alternating PN_4 and SiN_4 tetrahedra. Analogous to the isosteric compounds Si_2N_2O[79] and Si_2N_2NH,[80] the crystal structure of $SiPN_3$ is derived from a defect wurtzite modification. It contains two-dimensional infinitely linked layers of condensed six-membered $[Si_3N_3]$ rings in a boat form; half of the silicon atoms in the rings are replaced by phosphorus atoms. The $^2_\infty[(Si/P)_3N_3]$ layers, which are arranged parallel to each other in the crystal, are linked through bridging nitrogen atoms which saturate the remaining free valences at phosphorus and silicon (Fig. 11).[78] $SiPN_3$ decomposes above about

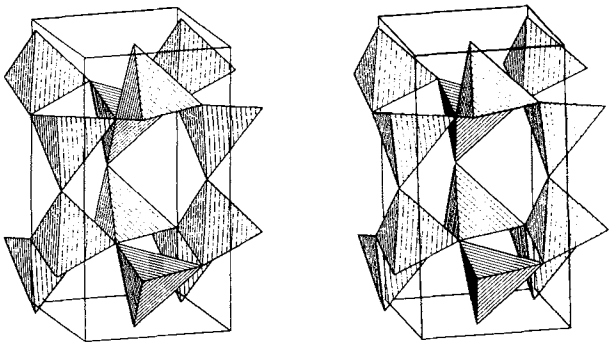

Fig. 11. Crystal structure of $SiPN_3$ (stereoscopic representation). The SiN_4 and PN_4 tetrahedra are shown as closed polyhedra [78].

1000 °C to give Si_3N_4 and gaseous phosphorus (P_4), which acts as an oxygen scavenger. After 3 h at 1400 °C the decomposition product is pure α-Si_3N_4, which acts as a nucleus for crystallization. Calcination of commercially available amorphous Si_3N_4 by the addition of small amounts of $SiPN_3$ gives pure crystalline Si_3N_4 with a low oxygen content and a high content of α-Si_3N_4, which is preferred for sintering processes.[78]

4. Ternary Boron Nitrides

Very few ternary boron nitrides have so far been prepared. The dimorphic lithium boron nitride Li_3BN_2[81-83] and the analogous sodium compound Na_3BN_2[84] have been studied in detail and structurally characterized. Magnesium boron nitride Mg_3BN_3[85] is also known; like Li_3BN_2 it has a catalytic effect on the conversion of hexagonal (*h*-BN) to cubic boron nitride (*c*-BN) under high-temperature/high-pressure conditions.[14] A more complex cerium boron nitride $Ce_{15}B_8N_{25}$ has also been described.[86] Besides Na_3BN_2, these ternary compounds are obtained by reacting the corresponding binary nitrides at temperatures between 800 °C (α-Li_3BN_2) and 1480 °C ($Ce_{15}B_8N_{25}$). Since binary sodium nitride as a starting material for the preparation of Na_3BN_2 does not exist, a procedure for the preparation of this compound had to be devised in which Na_3N is a formal intermediate. The reaction of a mixture of elemental sodium and sodium azide has proved suitable [Eq. (24)]. Under the reaction conditions the otherwise unstable alkali metal nitride appears to react instantaneously to give the required product.[84]

$$2\,Na + NaN_3 + BN \xrightarrow[1000\,^\circ C,\ 15\ min]{\text{Belt apparatus, } 4\,GPa} Na_3BN_2 + N_2 \quad (24)$$

The ternary boron nitrides so far characterized contain only "isolated" B–N anions rather than condensed structural units. Thus, Li_3BN_2 and Na_3BN_2 are constructed of alkali metal cations and linear, symmetrical units NBN^{3-}. The complex anion has 16 valence electrons and is thus isoelectronic with CO_2, NCO^-, CNO^-, N_2O, N_3^-, CN_2^{2-}, C_3^{4-}[87,88] and CBN^{4-}.[89] The relatively short B–N bond length (134 pm[82-84]) can be explained on the basis of either a considerable degree of double bond character or a polar bond; this result is in agreement with spectroscopic studies.[81] The two dimorphic modifications of Li_3BN_2 differ in particular in a reorientation of the linear $[BN_2]^{3-}$ ions; all the Li^+ ions in β-Li_3BN_2 (isostructural with Na_3BN_2) are almost tetrahedrally coordinated by nitrogen atoms, while in α-Li_3BN_2 they are in part linearly coordinated.[82,83]

Unexpectedly, Mg_3BN_3 also contains linear $[BN_2]^{3-}$ ions, the structure in fact is $[(Mg^{2+})_3(BN_2^{3-})(N^{3-})]$; the "isolated" N^{3-} ions have no direct contact with boron atoms.[85] A trigonal planar anion $[BN_3]^{6-}$ (d(B–N) = 146 pm), isoelectronic with orthoborate $[BO_3]^{3-}$, was found in $Ce_{15}B_8N_{25}$; again "isolated" N^{3-} ions are also present, which are octahedrally surrounded by cerium atoms.[86] The remarkably short Ce–Ce distances (d(Ce–Ce) $\geq$ 363 pm) indicate the presence of metal-metal bonds as well as the presence of a mixed-valency compound according to $[(Ce^{4+})_6(Ce^{3+})_9(BN_3^{6-})_8(N^{3-})]$.[86]

5. Ternary Silicon Nitrides

In spite of many attempts it has so far been possible to prepare only a few ternary silicon nitrides containing electropositive elements in a pure form and to characterize them both structurally and with respect to their properties. The isotypic compounds $MSiN_2$ (M = Be, Mg, Mn, Zn) with the same valence electron concentration (VEC) of 4[90] can be considered as ternary substitution variants of aluminum nitride (AlN).[91-97] Their preparation in pure form is possible by solid-state reactions of the corresponding binary nitrides [Eq. (25)] or, in the case of the manganese com-

pound, by reacting Si_3N_4 with elemental manganese in an ammonia atmosphere [Eq. (26)].[94]

$$Mg_3N_2 + Si_3N_4 \xrightarrow[N_2]{1200\,^\circ C} 3\,MgSiN_2 \quad (25)$$

$$3\,Mn + Si_3N_4 + 2\,NH_3 \xrightarrow{1050\,^\circ C} 3\,MnSiN_2 + 3\,H_2 \quad (26)$$

In the solid state these compounds contain three-dimensional infinite network structures with SiN_4 tetrahedra linked through all four vertices by corner-sharing, which forms condensed $[Si_6N_6]$ twelve-membered rings (d(Si–N) = 174–180 pm, $\sphericalangle$ Si-N-Si = 122° in $MgSiN_2$[96]). Together with the metal cations these lead to a wurtzite-like structure.

$LiSi_2N_3$[98] and the structurally very similar silicon nitride imide Si_2N_2NH[80] have defect wurtzite structures. The lithium compound can be obtained by reacting stoichiometric amounts of the binary nitrides (100 h, 1000 °C). Crystalline silicon nitride imide[80] is obtained from silicon and ammonia under ammonothermal conditions by using potassium amide as a mineralizer [Eq. (27)].

$$2\,Si + 3\,NH_3 \xrightarrow[6\,kbar\,NH_3]{550/600\,^\circ C,\ 120\,h} Si_2N_2NH + 4\,H_2 \quad (27)$$

Analogous to Si_2N_2O and $SiPN_3$ (see Section 3.3), $LiSi_2N_3$ and Si_2N_2NH consist of two-dimensional infinite, parallel layers of condensed $[Si_6N_6]$ twelve-membered rings in a boat form, which are linked together by bridging nitrogen atoms (d(Si–N) = 171–176 pm). In Si_2N_2NH the hydrogen atoms are covalently bonded to the bridging nitrogen atoms, while in $LiSi_2N_3$ the Li^+ ions occupy free tetrahedral sites in the defect wurtzite structure. Silicon nitride imide (like silicon diimide $Si(NH_2)_2$, which has so far only been obtained in an undefined amorphous form) is an intermediate in the industrial preparation of Si_3N_4 from the ammonolysis of silicon tetrachloride. It decomposes above about 1050 °C with elimination of ammonia to give Si_3N_4.[80]

Lanthanum silicon nitride $LaSi_3N_5$ is obtained by reacting the binary nitrides under pressure (1830 °C, 270 bar N_2);[99] the reaction of Si_3N_4 with La_2O_3 (2000 °C, 50 bar N_2) also affords the compound as single crystals.[100] As for all ternary silicon nitrides which have so far been characterized, $LaSi_3N_5$ has a three-dimensional network structure with SiN_4 tetrahedra linked through all four vertices by corner-sharing. The solid contains "dreier", "vierer", "fünfer", and "sechser" (six-, eight-, ten-, and twelve-membered) rings with alternating silicon and nitrogen atoms. According to the molar ratio Si:N = 3:5, two-fifths of the nitrogen atoms are bonded to three silicon atoms (d(Si–N) = 173–181 pm), while the remainder (three-fifths) have only two silicon atoms as directly bonded neighbors (d(Si–N) = 162–173 pm). Lanthanum is coordinated by a total of nine nitrogen atoms of the Si–N substructure (d(La–N) = 244–312 pm).[100]

Besides the compounds mentioned above, the existence of further ternary silicon nitrides such as Li_2SiN_2, Li_5SiN_3, and Li_8SiN_4 has been postulated, although it has so far not been possible to obtain exact structural data for these compounds or to determine their composition unequivocally.[101–104] Studies of the quasibinary Li_3N/Si_3N_4 system have also produced some evidence for the existence of ternary lithium silicon nitrides with ionic conducting properties in the solid state.[105] A number of different phases was also identified in the Be_3N_2/Si_3N_4 system.[106, 107]

A number of germanium compounds isotypic with the corresponding silicon nitrides mentioned above are also known.[49, 93, 94, 97, 101, 103, 108]

6. Special Cases: Carbon and Sulfur

In agreement with the quantification of the Van-Arkel-Ketelaar triangle as described by Allen,[109, 110] the nonmetals carbon, sulfur, or selenium (which are more electronegative than boron, silicon, or phosphorus) form binary nitrides which exhibit a clear preference for molecular structures. These binary nitrogen compounds in low oxidation states are often discrete molecules with homonuclear bonds (e.g. $(CN)_2$, S_4N_4, S_4N_2, S_5N_6[111]), though some polymeric compounds are also known (e.g. $(CN)_x$ and $(SN)_x$). Carbon and sulfur in the maximum oxidation state corresponding to their group number (IV and VI, respectively) have so far not provided any indication of the existence of the binary nitrides C_3N_4 and SN_2, respectively. Although ab initio calculations indicate that a hypothetical binary carbon nitride with a β-Si_3N_4-like structure should have an unusual mechanical stability,[112, 113] no compound of the composition C_3N_4 has until now been prepared in a pure defined form.[114–116]

The cyanamides can, however, formally be considered as ternary carbon(IV) nitrides ($M^I_2CN_2$, M = Li, Na, K, Ag, Tl; $M^{II}CN_2$, M^{II} = Ca, Sr, Ba, Zn, Pb) which contain the linear anion CN_2^{2-} with 16 valence electrons.[117–120] Lithium cyanamide can be prepared from lithium carbide and lithium nitride in molten lithium [Eq. (28)], though the separation of the product from lithium metal is preparatively difficult.[117, 118] Pure Li_2CN_2 can be obtained easily on a preparative scale from the reaction between lithium nitride and melamine in a molar ratio of 1:2 [Eq. (29)].[121]

$$Li_2C_2 + 4\,Li_3N \xrightarrow[Li\ melt]{530\,^\circ C,\ 150\,h} 2\,Li_2CN_2 + 10\,Li \quad (28)$$

$$(NCNH_2)_3 + 2\,Li_3N \xrightarrow{650\,^\circ C} 3\,Li_2CN_2 + 2\,NH_3 \quad (29)$$

Alkali metal hydrogen cyanamides ($NaHCN_2$, $Na_4H_2(CN_2)_3$[122, 123]) and crystalline cyanamide (H_2CN_2[124, 125]) have been prepared and structurally characterized. The reaction of dicyandiamide with cesium carbonate leads to cesium dicyanamide $Cs[(CN)_2N]$, which in the solid state contains the bent pentaatomic anion $N{\equiv}C{-}\ddot{N}{-}C{\equiv}N^-$.[126]

In the case of sulfur(VI) no ternary or higher nitrides have so far been obtained. The only compound worthy of mention here is the sulfur(IV) compound K_2SN_2, which in the solid state contains the bent anion SN_2^{2-} isosteric with SO_2.[127] Exact structural data are, however, not yet available for this compound.

7. Outlook and Future Prospects

Numerous new publications, not only in the area of nonmetal nitrides, make it clear that nitride chemistry is still only in its infancy[128] and that many fascinating results can be expected. As shown by the results of systematic studies on the phosphorus nitrides, nonmetal nitrides have the potential for the development of novel solids with interesting properties; these can be either related to the technically, industrially, and economically important sulfates, phosphates, and silicates, or may be completely novel. In contrast to oxygen, nitrogen affords an extension of the structural scope, since covalent bonds can be formed not only to two, but also to three or even four neighboring atoms.[129] The synthesis of nitrido zeolites according to the structural model provided by the zeolites appears particularly attractive with respect to desirable material properties and the modification of known compounds. However, the extended structural possibilities offered by nitrogen lead us to expect that completely new types of structures should also be possible.

Regardless of the possible applications of such compounds as ceramic materials, ionic conductors, catalysts, or pigments, the systematic exploration of new nonmetal nitrides will close a large gap in the chemistry of the main group elements.

My grateful thanks are due to my co-workers Ute Berger, Verena Schultz-Coulon, Jan Lücke, and Martin Volkmann for their tenacity, their inspiration, and their enthusiasm during our pleasant and fruitful cooperation in the area of the phosphorus nitrides. I should like to thank the Deutsche Forschungsgemeinschaft, the Fonds der Chemischen Industrie, and the Ministerium für Wissenschaft und Forschung des Landes Nordrhein-Westfalen for their generous financial support. I am particularly indebted to Monika Schmitt for her understanding, her support, and for many stimulating suggestions.

Received: October 6, 1992 [A 907 IE]
German version: *Angew. Chem.* **1993**, *105*, 846

[1] C. Boberski, R. Hamminger, M. Peuckert, F. Aldinger, R. Dillinger, J. Heinrich, J. Huber, *Angew. Chem. Adv. Mater.* **1989**, *101*, 1592; *Angew. Chem. Int. Ed. Engl. Adv. Mater.* **1989**, *28*, 1560; *Adv. Mater.* **1989**, *1*, 378.
[2] G. Petzow, *Ber. Bunsenges. Phys. Chem.* **1989**, *93*, 1173.
[3] G. A. Slack, *J. Phys. Chem. Solids* **1987**, *48*, 641.
[4] A. F. Hollemann, E. Wiberg, *Lehrbuch der Anorganischen Chemie*, de Gruyter, Berlin, **1985**, p. 139.
[5] G. H. Aylward, T. J. Findlay, *Datensammlung Chemie*, Verlag Chemie, Weinheim, **1975**, p. 80ff.
[6] A few reports of the preparation of tin nitride have been published, but in all cases the samples obtained could not be clearly characterized: a) R. S. Lima, P. H. Dionisio, W. H. Schreiner, *Solid State Commun.* **1991**, *79*, 395; b) R. G. Gordon, D. M. Hoffman, U. Riaz, *Chem. Mater.* **1992**, *4*, 68; c) L. Maya, *Inorg. Chem.* **1992**, *31*, 1958.
[7] W. Neubert, H. Pritzkow, H. P. Latscha, *Angew. Chem.* **1988**, *100*, 298; *Angew. Chem. Int. Ed. Engl.* **1988**, *27*, 287.
[8] R. T. Paine, C. K. Narula, *Chem. Rev.* **1990**, *90*, 73.
[9] V. L. Vinogradov, A. V. Kostanovskii, *High Temp. (Engl. Transl.)* **1991**, *29*, 901.
[10] a) A. Meller, *Gmelin Handbuch der Anorganischen Chemie, Boron Compounds, 1st Suppl. Vol. 2*, Springer, Berlin, **1980**, p. 1; b) *ibid. 2nd Suppl. Vol. 1*, **1983**, p. 20; c) *ibid. 3rd Suppl. Vol. 3*, **1988**, p. 1, and references therein.
[11] Yu. I. Krasnokutskii, S. N. Ganz, V. D. Parkhomenko, *J. Appl. Chem. USSR (Engl. Transl.)* **1976**, *49*, 307.
[12] S. Podsiadlo, J. Orzel, *Pol. J. Chem.* **1984**, *58*, 323.
[13] a) M. G. L. Mirabelli, L. G. Sneddon, *Inorg. Chem.* **1988**, *27*, 3271; b) D. Seyferth, W. S. Rees, Jr., *Chem. Mater.* **1991**, *3*, 1106; c) L. Maya, H. L. Richards, *J. Am. Ceram. Soc.* **1991**, *74*, 406.
[14] a) C. Hohlfeld, *J. Mater. Sci. Lett.* **1989**, *8*, 1082; b) M. Kagamida, H. Kanda, M. Akaishi, A. Nukui, T. Osawa, S. Yamaoka, *J. Crystal Growth* **1989**, *94*, 261; c) S. Nakano, H. Ikawa, O. Fukunaga, *J. Am. Ceram. Soc.* **1992**, *75*, 240.
[15] H. Lange, G. Wötting, G. Winter, *Angew. Chem.* **1991**, *103*, 1606; *Angew. Chem. Int. Ed. Engl.* **1991**, *30*, 1579.
[16] M. Billy, J.-C. Labbe, A. Selvaray, *Mater. Res. Bull.* **1983**, *18*, 921.
[17] R. Grün, *Acta Crystallogr. Sect. B* **1979**, *35*, 800.
[18] G. Schwier, G. Nietfeld, *Werkstoffe und Konstruktion* **1988**, *2*, 149.
[19] G. Schwier, G. Nietfeld, *Sprechsaal*, **1988**, *121*, 174.
[20] G. Boden, S. Klemm, K. Quaritsch, *Silikattechnik* **1987**, *38*, 161.
[21] G. Boden, R. Irmisch, G. Himpel, T. Reetz, *Sprechsaal* **1989**, *122*, 224.
[22] Y. Tuohino, R. Laitinen, K. Torkell in *Proc. 3rd Int. Conf. Powder Proc. Sci.* (Eds.: G. L. Messing, S. Hirano, H. Hausner), American Ceramic Society, Westerville, USA, **1989**, p. 337ff.
[23] K. Komeya, H. Inoue, *J. Mater. Sci.* **1975**, *10*, 1243.
[24] H. Inoue, K. Komeya, A. Tsuge, *J. Am. Ceram. Soc.* **1982**, *65*, 205.
[25] M. Mori, H. Inoue, T. Chirai in *Progress in Nitrogen Ceramics* (Eds.: F. L. Riley), Nijhoff, Den Haag, **1983**, p. 149ff.
[26] T. Ishii, A. Sano, I. Imai in *Silicon Nitride-1* (Eds.: S. Somiya, M. Mitomo, M. Yoshimura), Elsevier, London, **1990**, p. 59ff.
[27] M. Blix, W. Wirbelauer, *Ber. Dtsch. Chem. Ges.* **1903**, *36*, 4220.
[28] O. Glemser, P. Naumann, *Z. Anorg. Allg. Chem.* **1959**, *298*, 134.
[29] K. S. Mazdiyasni, C. M. Cooke, *J. Am. Ceram. Soc.* **1973**, *56*, 628.
[30] S. Prochazka, C. Greskovich, *Am. Ceram. Soc. Bull.* **1987**, *57*, 579.
[31] W. M. Shen (Union Carbide), EP-B 365295, **1989**, *Chem. Abstr.* **1990**, *113*, P11030n.
[32] Y. Kohtoku in *Silicon Nitride-1* (Eds.: S. Somiya, M. Mitomo, M. Yoshimura), Elsevier, London, **1989**, p. 71ff.
[33] H. R. Allcock, *Phosphorus-Nitrogen Compounds*, Academic Press, New York, **1972**, p. 288.
[34] D. E. C. Corbridge, *Phosphorus - An Outline of its Chemistry, Biochemistry, and Technology*, Elsevier, Amsterdam, **1990**, p. 120.
[35] S. Vepřek, Z. Iqbal, J. Brunner, M. Schärli, *Philosoph. Mag. B* **1981**, *43*, 527.
[36] J. Cremer, H. Harnisch (Hoechst AG), DE-A 2608018, **1977**; *Chem. Abstr.* **1978**, *88*, 9160b.
[37] J. Cremer, E. Joerchel, H. Harnisch (Hoechst AG), DE-A 2516915, **1976**; *Chem. Abstr.* **1977**, *86*, 57574v.
[38] A. Stock, *Ber. Dtsch. Chem. Ges.* **1906**, *39*, 1967.
[39] A. Stock, B. Hoffman, *Ber. Dtsch. Chem. Ges.* **1903**, *36*, 314.
[40] A. M. Ficquelmont, *C. R. Hebd. Seances Acad. Sci.* **1935**, *200*, 1045.
[41] H. Jacobs, R. Kirchgässner, *Z. Anorg. Allg. Chem.* **1990**, *581*, 125.
[42] W. Schnick, *Z. Naturforsch. B* **1989**, *44*, 942.
[43] W. Schnick, J. Lücke, unpublished results.
[44] U. Wannagat, G. Bogedain, A. Schervan, H. C. Marsmann, D. J. Brauer, H. Bürger, F. Dörrenbach, G. Pawelke, C. Krüger, K. H. Claus, *Z. Naturforsch. B* **1991**, *46*, 931.
[45] U. Wannagat, D. Burgdorf, H. Bürger, G. Pawelke, *Z. Naturforsch. B* **1991**, *46*, 1039.
[46] H. R. Allcock, *Chem. Rev.* **1972**, *72*, 315.
[47] F. Liebau, *Structural Chemistry of Silicates*, Springer, Berlin, **1985**.
[48] E. V. Borisov, E. E. Nifant'ev, *Russ. Chem. Rev. (Engl. Transl.)* **1977**, *46*, 842.
[49] N. E. Brese, M. O'Keeffe, *Struct. Bonding (Berlin)* **1992**, *79*, 307.
[50] A. Rabenau, *Solid State Ionics* **1982**, *6*, 277.
[51] W. Schnick, J. Lücke, *J. Solid State Chem.* **1990**, *87*, 101.
[52] W. Schnick, *Phosphorus Sulfur Silicon Relat. Elem.*, in press.
[53] W. Schnick, U. Berger, unpublished results.
[54] W. Schnick, U. Berger, *Angew. Chem.* **1991**, *103*, 857; *Angew. Chem. Int. Ed. Engl.* **1991**, *30*, 830.
[55] W. Schnick, J. Lücke, *Z. Anorg. Allg. Chem.* **1990**, *588*, 19.
[56] M. O'Keeffe, B. G. Hyde, *Acta Crystallogr. Sect. B* **1976**, *32*, 2923.
[57] K. F. Hesse, F. Liebau, *Z. Kristallogr.* **1980**, *153*, 33.
[58] Y. Smolin, *Sov. Phys. Crystallogr. (Engl. Transl.)* **1970**, *15*, 23.
[59] M. Jansen, B. Lüer, *Z. Kristallogr.* **1986**, *177*, 149.
[60] M. Jansen, M. Möbs, *Z. Kristallogr.* **1982**, *159*, 283.
[61] R. Nesper, (ETH-Zürich), personal communication.
[62] L. Pauling, *The Nature of the Chemical Bond*, Cornell University Press, Ithaca New York, **1960**, p. 97ff.
[63] W. Schnick, J. Lücke, *Solid State Ionics* **1990**, *38*, 271.
[64] W. Schnick, V. Schultz-Coulon, *Angew. Chem.* **1993**, *105*, 308; *Angew. Chem. Int. Ed. Engl.* **1993**, *32*, 280.
[65] R. L. Freed, D. R. Peacor, *Am. Mineral.* **1967**, *52*, 709.
[66] R. Marchand, Y. Laurent, *Mater. Res. Bull.* **1982**, *17*, 399.
[67] W. Schnick, V. Schultz-Coulon, unpublished results.
[68] A. Schmidpeter, C. Weingand, F. Hafner-Roll, *Z. Naturforsch. B* **1969**, *24*, 799.
[69] H. Schiff, *Justus Liebigs Ann. Chem.* **1857**, *101*, 299.
[70] W. Couldridge, *J. Chem. Soc.* **1888**, *53*, 398.
[71] C. Gerhardt, *Ann. Chim. Phys.* **1846**, *18*, 188.
[72] W. Schnick, J. Lücke, *Z. Anorg. Allg. Chem.* **1992**, *610*, 121.
[73] J. Lücke, dissertation Universität Bonn, **1993**.
[74] J. V. Smith, *Chem. Rev.* **1988**, *88*, 149.

[75] W. Hölderich, M. Hesse, F. Näumann, *Angew. Chem.* **1988**, *100*, 232; *Angew. Chem. Int. Ed. Engl.* **1988**, *27*, 226.
[76] W. Schnick, J. Lücke, *Angew. Chem.* **1992**, *104*, 208; *Angew. Chem. Int. Ed. Engl.* **1992**, *31*, 213.
[77] W. Schnick, J. Lücke, M. Volkmann, unpublished results.
[78] H. P. Baldus, W. Schnick, J. Lücke, U. Wannagat, G. Bogedain, *Chem. Mater.* in press.
[79] I. Idrestedt, C. Brosset, *Acta Chem. Scand.* **1964**, *18*, 1879.
[80] D. Peters, H. Jacobs, *J. Less-Common Met.* **1989**, *146*, 241.
[81] J. Goubeau, W. Anselment, *Z. Anorg. Allg. Chem.* **1961**, *310*, 248.
[82] H. Yamane, S. Kikkawa, H. Horiuchi, M. Koizumi, *J. Solid State Chem.* **1986**, *65*, 6.
[83] H. Yamane, S. Kikkawa, M. Koizumi, *J. Solid State Chem.* **1987**, *71*, 1.
[84] J. Evers, M. Münsterkötter, G. Oehlinger, K. Polborn, B. Sendlinger, *J. Less-Common Met.* **1990**, *162*, L17.
[85] H. Hiraguchi, H. Hashizume, O. Fukunaga, A. Takenaka, M. Sakata, *J. Appl. Crystallogr.* **1991**, *24*, 286.
[86] J. Gaude, P. L'Haridon, J. Guyader, J. Lang, *J. Solid State Chem.* **1985**, *59*, 143.
[87] H. J. Meyer, *Z. Anorg. Allg. Chem.* **1991**, *593*, 185.
[88] W. Jeitschko, R. Pöttgen, *Inorg. Chem.* **1991**, *30*, 427.
[89] H. J. Meyer, *Z. Anorg. Allg. Chem.* **1991**, *594*, 113.
[90] E. Parthé, *Crystal Chemistry of Tetrahedral Structures*, Gordon and Breach, New York, **1964**, p. 3ff.
[91] P. Eckerlin, A. Rabenau, H. Nortmann, *Z. Anorg. Allg. Chem.* **1967**, *353*, 113.
[92] P. Eckerlin, *Z. Anorg. Allg. Chem.* **1967**, *353*, 225.
[93] J. David, Y. Laurent, J. Lang, *Bull. Soc. Fr. Mineral. Cristallogr.* **1970**, *93*, 153.
[94] M. Maunaye, R. Marchand, J. Guyader, Y. Laurent, J. Lang, *Bull. Soc. Fr. Mineral. Cristallogr.* **1971**, *94*, 561.
[95] M. Wintenberger, R. Marchand, M. Maunaye, *Solid State Commun.* **1977**, *21*, 733.
[96] M. Wintenberger, F. Tcheou, J. David, J. Lang, *Z. Naturforsch. B* **1980**, *35*, 604.
[97] T. Endo, Y. Sato, H. Takizawa, M. Shimada, *J. Mater. Sci. Lett.* **1992**, *11*, 424.
[98] J. David, Y. Laurent, J. P. Charlot, J. Lang, *Bull. Soc. Fr. Mineral. Cristallogr.* **1973**, *96*, 21.
[99] C. E. Holcombe, L. Kovach, *Am. Ceram. Soc. Bull.* **1981**, *60*, 546.
[100] Z. Inoue, M. Mitomo, N. Ii, *J. Mater. Sci.* **1980**, *15*, 2915.
[101] R. Juza, H. H. Weber, E. Meyer-Simon, *Z. Anorg. Allg. Chem.* **1953**, *273*, 48.
[102] J. Lang, J. P. Charlot, *Rev. Chim. Miner.* **1970**, *7*, 121.
[103] J. David, J. P. Charlot, J. Lang, *Rev. Chim. Miner.* **1974**, *11*, 405.
[104] A. T. Dadd, P. Hubberstey, *J. Chem. Soc. Dalton Trans.* **1982**, 2175.
[105] H. Yamane, S. Kikkawa, M. Koizumi, *Solid State Ionics* **1987**, *25*, 183.
[106] I. C. Huseby, H. L. Lukas, G. Petzow, *J. Am. Ceram. Soc.* **1975**, *58*, 377.
[107] T. M. Shaw, G. Thomas, *J. Solid State Chem.* **1980**, *33*, 63.
[108] R. Marchand, Y. Laurent, J. Guyader, P. L'Haridon, P. Verdier, *J. Eur. Ceram. Soc.* **1991**, *8*, 197.
[109] L. C. Allen, *J. Am. Chem. Soc.* **1989**, *111*, 9003.
[110] L. C. Allen, *J. Am. Chem. Soc.* **1992**, *114*, 1510.
[111] J. D. Woollins, *Non-Metal Rings, Cages and Clusters*, Wiley, New York, **1988**, p. 96ff.
[112] A. Y. Liu, M. L. Cohen, *Science* **1989**, *245*, 841.
[113] A. Y. Liu, M. L. Cohen, *Phys. Rev. B.* **1990**, *41*, 10727.
[114] H. X. Han, B. J. Feldman, *Solid State Commun.* **1988**, *65*, 921.
[115] L. Maya, L. A. Harris, *J. Am. Ceram. Soc.* **1990**, *73*, 1912.
[116] L. Maya, D. R. Cole, E. W. Hagaman, *J. Am. Ceram. Soc.* **1991**, *74*, 1686.
[117] M. G. Down, M. J. Haley, P. Hubberstey, R. J. Pulham, A. E. Thunder, *J. Chem. Soc. Chem. Commun.* **1978**, 52.
[118] M. G. Down, M. J. Haley, P. Hubberstey, R. J. Pulham, A. E. Thunder, *J. Chem. Soc. Dalton Trans.* **1978**, 1407.
[119] K. M. Adams, M. J. Cooper, M. J. Sole, *Acta Crystallogr.* **1964**, *17*, 1449.
[120] M. J. Cooper, *Acta Crystallogr.* **1964**, *17*, 1452.
[121] U. Berger, W. Schnick, unpublished results.
[122] M. G. Barker, A. Harper, P. Hubberstey, *J. Chem. Res. Synop.* **1978**, 432.
[123] A. Harper, P. Hubberstey, *J. Chem. Synop.* **1989**, 194.
[124] B. H. Torrie, *J. Raman Spectrosc.* **1992**, *23*, 465.
[125] B. H. Torrie, R. Von Dreele, A. C. Larson, *Mol. Phys.* **1992**, *76*, 405.
[126] P. Starynowicz, *Acta Crystallogr. Sect. C* **1991**, *47*, 2198.
[127] M. Herberhold, W. Ehrenreich, *Angew. Chem.* **1982**, *94*, 637; *Angew. Chem. Int. Ed. Engl.* **1982**, *21*, 633; *Angew. Chem. Suppl.* **1982**, 1346.
[128] Compare for example a) K. Dehnicke, J. Strähle, *Angew. Chem.* **1992**, *104*, 978; *Angew. Chem. Int. Ed. Engl.* **1992**, *31*, 955; b) F. J. DiSalvo, *Science* **1990**, *247*, 649.
[129] See for example the coordination and bonding situation in SiO_2 and Si_3N_4, P_2O_5 and P_3N_5 or B_2O_3 and BN.

Molecular Machines: How Motion and Other Functions of Living Organisms Can Result from Reversible Chemical Changes

By Dan W. Urry*

Certain model proteins dramatically fold and become more ordered on raising the temperature. When the temperature is raised to drive folding and assembly, these model proteins can lift weights and perform work; they can produce motion. The temperature of warm-blooded animals, however, is kept constant. Therefore, motion cannot result from a change in temperature. In this case, a free energy change, caused, for example, by an increase in the concentration of a chemical, can lower the temperature at which the protein folding and assembly transition occurs from above to below physiological temperature. Raising the concentration of a chemical isothermally has indeed been shown to result in motion and the efficient performance of work. These model proteins and the mechanism they reveal provide insight into the molecular basis for diverse biological functions; they are models for the molecular machines that comprise the living organism, and they provide a new class of materials for both medical and nonmedical applications.

1. Introduction

A molecular machine, commonly an assembly of polymeric molecules, is a structural fabrication that can convert energy from one form or location to another. Living organisms represent the synergistic integration of functionally diverse molecular machines made of a single class of polymers, the proteins.

The living organism is capable many types of energy conversions, specifically free energy transductions, which are responsible for its existence. The functions of living organisms involve Gibbs free energy changes caused, for instance, by changes in mechanical force and/or length, changes in temperature and/or the extent of order, changes in pressure and/or volume, changes in chemical potential and/or numbers of a chemical species, changes in the oxidative state and/or numbers of electrons of chemical moieties, or by changes due to the absorption of light or other electromagnetic radiation. When free energy in one of the above forms is available to the correct protein construct (i.e., a specific molecular machine), the free energy can be converted or transduced by the appropriate protein into any one of the other forms.

While the molecular machines of living organisms are functionally diverse, a common molecular mechanism could be responsible for the many paired free energy transductions required for life.[1] The purpose of this review is to elucidate such a mechanism and to impart a sense of understanding of the underlying molecular processes.

Perhaps because in the words of Albert Szent-Gyorgyi,[2] "Motion has always been looked upon as the index of life," our elucidation of the molecular process can begin by considering how motion can occur. But we also start with motion, because it can be the direct result of the folding and assembly or the unfolding and disassembly of protein constructs, and because the underlying mechanism for diverse free energy transductions can be seen most directly in a simple, visual assay in which this reversible folding and assembly of specific model proteins results in motion. These model proteins can be referred to as elastic protein-based polymers, as they derive from repeating sequences found in the mammalian elastic protein, elastin.

The repeating sequences and designed modifications thereof are polymerized into high molecular weight polymers; hence the name elastic protein-based polymers or simply elastomeric polypeptides. Most fundamental is that these repeating sequences fold and/or self-assemble into more highly ordered structures when the temperature is raised in water. This increase in order of the polypeptide with increase in temperature is referred to as an inverse temperature transition, and the temperature at which the folding occurs is indicated as T_t. It is in learning the rules whereby these molecules fold and assemble on raising the temperature (and thereby in learning how to control the temperature T_t for the folding transition) that insight into diverse free energy transductions can be gained.

Significantly, *in warm-blooded animals temperature is not raised to achieve the transition for folding and assembly; rather the temperature at which the folding and assembly occur is lowered from above to below physiological temperatures.* This is referred to as the ΔT_t mechanism. In this way, the free energy input required to lower the transition temperature becomes the free energy of contraction for useful mechanical work. When the free energy input involves a change in the concentration of a chemical and the folding results in a contraction, this is called chemomechanical transduction; it is chemically elicited motion. The efficiency of this mechanism, which utilizes shifting the temperature of inverse temperature transitions to achieve chemomechanical transduction, appears to be an order of magnitude more efficient than mechanisms involving charge–charge interactions or protein denaturation (see Section 7). Furthermore, all of the six free energy changes noted above have now been shown to employ the ΔT_t mechanism to drive folding and assembly. Thus a common mechanism could underlie the diverse molecular machines of living organisms.

[*] Prof. Dr. D. W. Urry
Laboratory of Molecular Biophysics
The University of Alabama at Birmingham
VH300
Birmingham, AL 35294-0019 (USA)
Telefax: Int. code + (205)934-4256

 © VCH Verlagsgesellschaft mbH, W-6940 Weinheim, 1993 0570-0833/93/0606-0819 $ 10.00+.25/0

With a rationale for the design of model proteins and a practicable mechanism, both considered in some detail below, it becomes possible to mimic biological processes, and this area of biomimetics provides many challenges for applications both medical and nonmedical ranging from tissue reconstruction to robotics.

2. Model Proteins that Increase Order on Increasing the Temperature

2.1. Polypeptides that Crystallize from Water on Raising the Temperature

A polypeptide with a correct balance of apolar (hydrophobic) and polar moieties can be soluble in water at low temperature and yet, on raising the temperature, it can separate out. Such a polypeptide is *cyclo*(Val-Ala-Pro-Gly-Val-Gly)$_2$, that is, a cyclic analogue of the repeating hexapeptide of elastin, (VAPGVG)$_n$. In fact, *cyclo*(VAPGVG)$_2$ crystallizes on raising the temperature and dissolves on lowering the temperature (see Fig. 1).[3] Because a crystal is the epitome of order, molecules that go from a random distribution in solution to a discretely ordered crystal are molecules that increase order on raising the temperature.

2.2. Polypeptides that Self-Assemble into Fibers on Raising the Temperature

Removing the essentially neutral alanine residue (being neither apolar nor polar) from the hexapeptide (VAPGVG), gives the pentapeptide (VPGVG). This is the most prominent repeating sequence in elastin, occurring more than eleven times in a single sequence, that is, (VPGVG)$_{11}$.[4-6] High

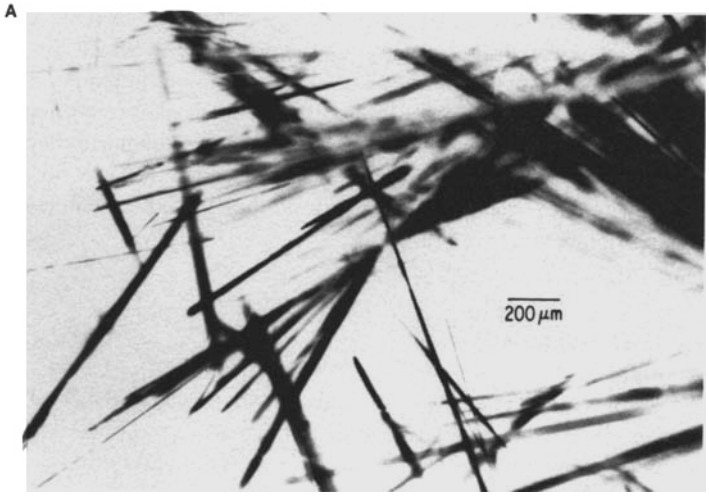

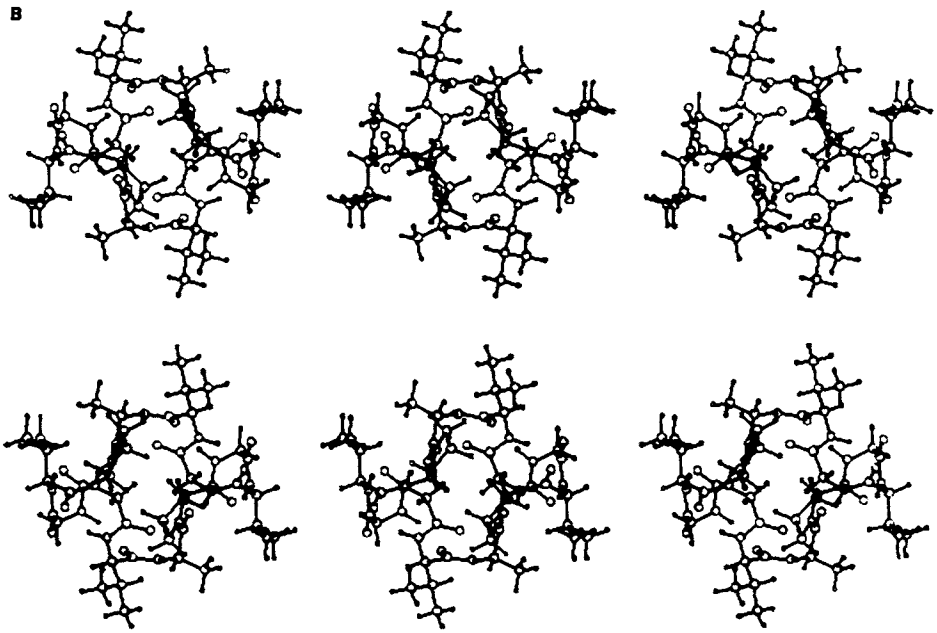

Fig. 1. A) Crystals of *cyclo*(VAPGVG)$_2$, which form on raising the temperature and dissolve on lowering the temperature (from reference [3]). B) Working model of the structure of *cyclo*(VAPGVG) based on NMR data and molecular mechanics and dynamics calculations. Top: view of one side; bottom: view of the other side (from reference [14]). In each row are stereo-pairs: the right-hand pair are for cross-eye viewing and the left-hand pair for wall-eye viewing. The structure is characterized by internal hydrogen bonds and externally directed aliphatic side chains.

Dan W. Urry, born in 1935, obtained his B.A. in medical biology at the University of Utah, Salt Lake City, and graduated with a Ph.D. in Physical Chemistry under H. Eyring in 1964. After a postdoctorate fellowship at Harvard University, he worked at the University of California in Berkeley, and the University of Chicago before moving to the University of Alabama at Birmingham, where since 1970 he has been Director of the Laboratory of Molecular Biophysics and Professor of Biochemistry and, in addition since 1979, Professor of Physiology and Biophysics. The honors conferred upon him include the Wright A. Gardner Award 1991 and the selection as Scientist of the Year 1988 by the Research and Development Magazine. He is member of the editorial boards of several journals and has published over 400 papers. His main research interests are protein structure and function, structures and applications of protein-based polymers, biomolecular materials, the channel mechanism of ion transport, and the ΔT_t mechanism of energy conversion.

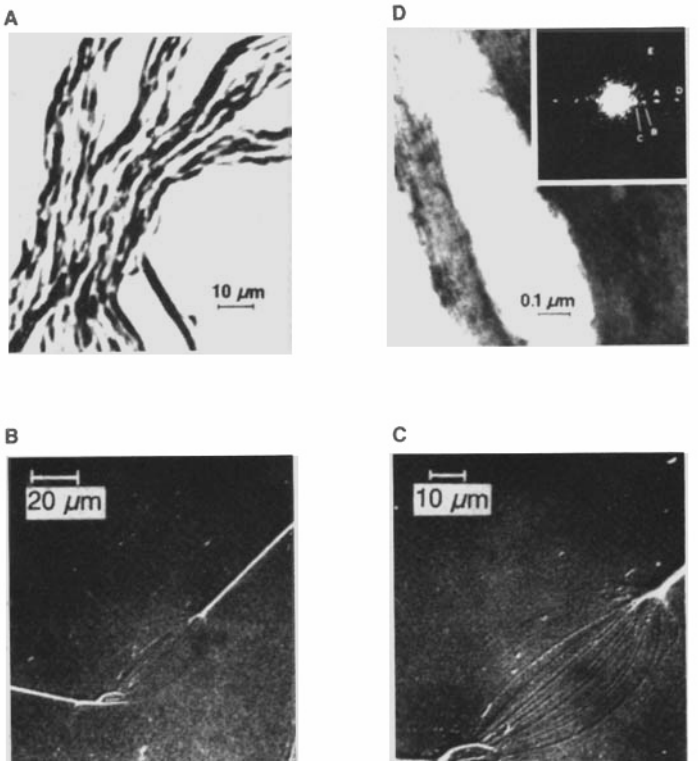

Fig. 2. Self-assembly of poly[f_x(VPGVG),f_x(VPGXG)] into anisotropic fibers (X = Glu, Lys; $0.1 \leq f_x \leq 0.2$). A water-soluble carbodiimide was used to cross-link the Glu and Lys side chains during initial aggregation [10]. A) Light micrograph (without staining and using only the form birefringence for contrast) showing the formation of fibers several microns in diameter (from reference [9]). B) and C) Scanning electron micrographs after aluminum coating of a single fiber (two to three microns in diameter) that splays out into many parallel fibrils and coalesces back into the same sized fiber (from reference [10]). D) Transmission electron micrograph of negatively stained fibrils, showing that they comprise filaments about 5 nm in diameter aligned parallel to one another (from reference [11]). Inset: optical diffraction of negatively stained nascent aggregates of poly(VPGVG), showing a dominant meridional reflection near 5 nm and diagonal reflection indicative of an underlying helical structure (from reference [87]).

molecular weight protein-based polymers of this repeat, poly(VPGVG), are also soluble in water below 25 °C. On raising the temperature above 25 °C, they aggregate and undergo a phase transition to a viscoelastic state that is about 50% peptide and 50% water by weight.[7] If the nascent aggregates are caught on a carbon-coated grid and negatively stained, transmission electron microscopy shows them to comprise 5 nm wide filaments with a supercoiled or twisted substructure.[8] Under conditions where chemical cross-linking can occur, this protein-based polymer can be seen, by light microscopy, to have self-assembled into several micron diameter fibers (Fig. 2A).[9] By scanning electron microscopy the fibers are seen to be made up of parallel aligned fibrils (Fig. 2B and C), and by transmission electron microscopy and negative staining the fibrils are seen to arise from the association of 5 nm diameter filaments (Fig. 2D).[7, 10, 11] This protein-based polymer self-assembles into anisotropic fibers on raising the temperature.

2.3. Basis for the Inverse Temperature Behavior

The cyclopentadecapeptide, *cyclo*(VPGVG)$_3$, has a conformation that is nearly identical to that of poly(VPGVG);[12] it also aggregates on raising the temperature, and its crystal structure is about one-fourth water by weight; the water forms hydrophilic channels within the stacks of cyclopentadecapeptides but no water is present between molecules (Fig. 3).[13] Also, its crystal structure exhibits six hydrophobic rods. The hydrophobic rods are formed by apolar side chains, and they run parallel to each stack of molecules such that the intermolecular interactions are dominated by contacts between hydrophobic side chains. The molecular structure of *cyclo*(VAPGVG)$_2$ thus also appears to be one where the more polar peptide moieties are buried and the more apolar (hydrophobic) side chains are at the exterior for hydrophobic contacts when forming the crystal on raising the temperature (see Fig. 1B).[14]

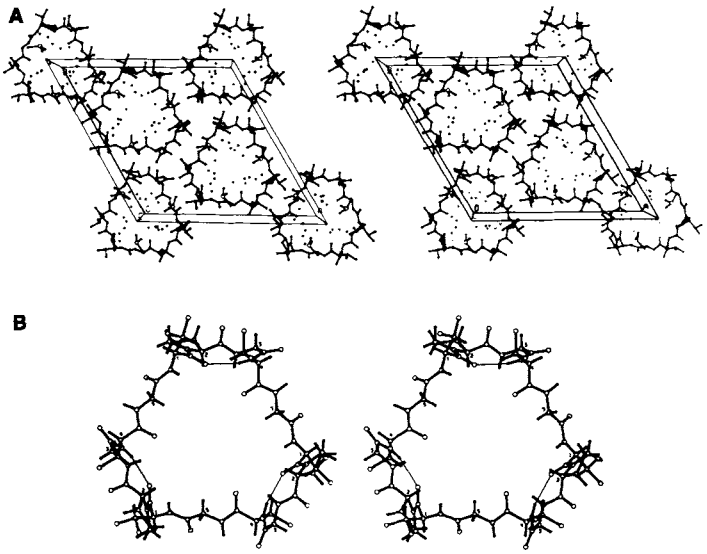

Fig. 3. *Cyclo*(VPGVG)$_3$: A) Stereo-pair view (cross-eye) of the crystal structure showing that intermolecular contacts are dominated by association of hydrophobic side chains and that the substantial amount of water in this aggregated state is within the threefold symmetric stacks of molecules. B) Molecular structure in stereo-pair view (cross-eye) showing the β-turns on end and suspended segments connecting the β-turns (from reference [13]). This has been shown to be the same conformation with only slight torsional angle changes in the backbone as the helical poly(VPGVG); that is, it corresponds to the cyclic conformation of the linear poly(VPGVG) [12].

These molecules are characterized in their aggregated or crystalline states by hydrophobic association. Before aggregation the hydrophobic side chains are surrounded by water, and the water molecules abutting apolar moieties have been shown in the crystal structure of alkane gas hydrates and in the crystal structure of the protein crambin to be arranged as pentagons. In the methane gas hydrate, twelve such pentagons enclose a methane molecule, that is, a pentagonal dodecahedran (Fig. 4A).[15] In crambin, pentagons of water are seen adjacent to the aliphatic side chain of leucine (Fig. 4C).[16]

Hydrophobic hydration, which is most explicitly exemplified in the pentagonal arrays of water molecules, is a favorable exothermic process; the enthalpy of hydration, ΔH(hydration), is negative. Solubility in water is limited, however, because of the limiting Gibbs free energy of solvation given by the expression, ΔG(hydration) = ΔH(hydration) $- T\Delta S$(hydration). In this case the entropy of hydra-

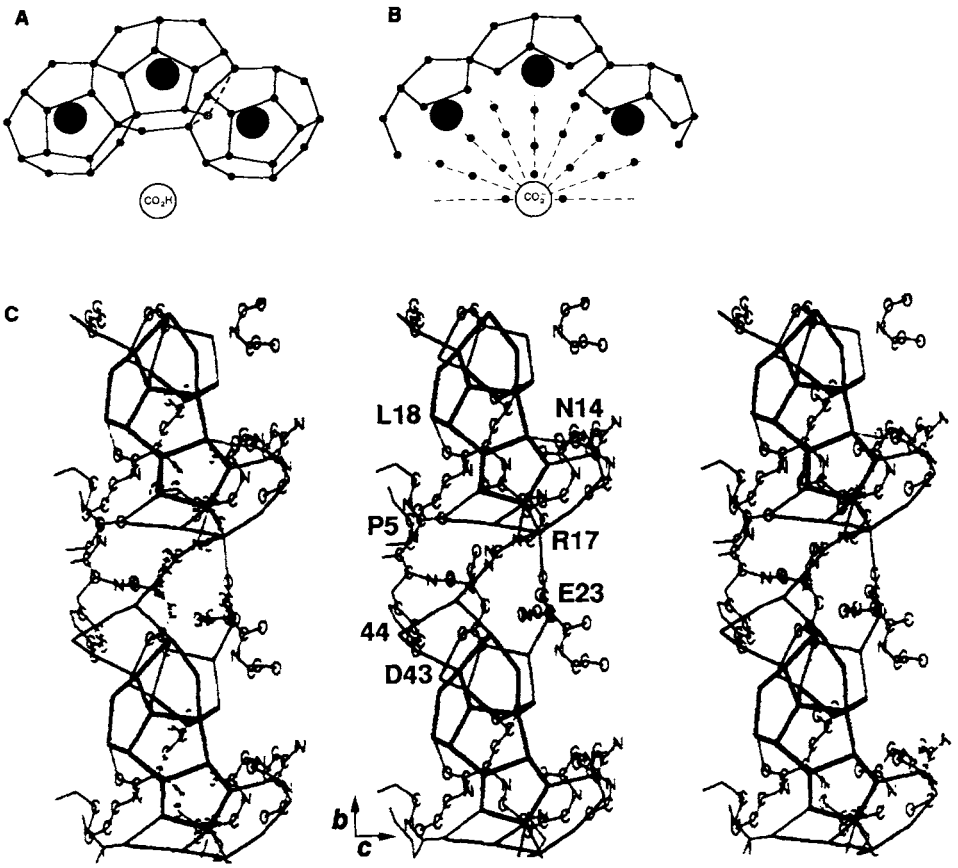

Fig. 4. Examples of the pentagonal arrangement of water molecules associated with hydrophobic residues. A) Crystal structure of alkane gas hydrates surrounded by water molecules arranged into pentagons. About twelve pentagons surround the alkane. (From reference [15].) These are the more ordered water molecules surrounding hydrophobic moieties that become less ordered bulk water when the hydrophobic moieties associate. B) A carboxylate group destructuring the pentagonal arrays as it forms its own hydration shells. ●: hydrophobic moieties; ○: polar (e.g., ionizable) groups; • oxygen atom of a water molecule. C) Stereo-pairs of a section of the crystal structure of crambin showing the pentagonal arrangements of water molecules, for example, adjacent to the leucine-18 (L18) side chain (from reference [16]).

tion, ΔS(hydration), is negative due to the increase in order of the water.[17-19] Accordingly, on raising the temperature of these protein-based polymers in water, the more ordered water surrounding the hydrophobic moieties becomes less ordered bulk water; this positive entropy change is larger in magnitude than the negative entropy change that arises because the polypeptide part of the system becomes more ordered. It is the unique structuring and destructuring of water molecules relative to hydrophobic hydration and dehydration that is responsible for these polypeptides exhibiting increased order on increasing the temperature, and it is all in keeping with the second law of thermodynamics.

With regard to energy conversion, the perturbations that interfere with or assist the water structuring around hydrophobic moieties such as the carboxyl and carboxylate of Figure 4A and B become the free energy changes that drive polypeptide folding or unfolding.

3. Motion (Contraction) Due to Thermally Driven Folding

Numerous physical studies indicate[20,21] that poly(VPGVG) folds into a dynamic helical structure by optimizing intramolecular hydrophobic contacts. The folded state, a β-spiral also known as state II, is given in Figure 5A along with an extended structure, state I, in Figure 5B.[22]

These deductions at the molecular level can be tested on a macroscopic scale. By γ-irradiation cross-linking of poly(VPGVG) in state II, an elastomeric matrix is formed. The matrix is designated as X^{20}-poly(VPGVG), signifying that a 20 Mrad dose of cobalt-60 radiation was used.

This matrix swells in water below 20 °C, and it contracts to less than one-half its extended length on raising the temperature to 40 °C.[1] This is a macroscopic counterpart of the thermally driven folding of poly(VPGVG). On attaching a weight at 20 °C, the elastic matrix stretches; on raising the temperature to 40 °C, it contracts and lifts the weight (Fig. 6). This is thermally driven contraction; it is the conversion of thermal energy into useful mechanical work or thermomechanical transduction (that is, thermal energy⇌mechanical work). The elastic cross-linked matrix is a heat-driven molecular machine.

In general, the proteins of living organisms do not function as heat-driven molecular machines. Most commonly they function as chemically driven molecular machines. How then might this mechanism become more relevant to biological function? The answer lies in determining the chemical means whereby the temperature of the folding and assembly transition can be changed or controlled. For example, if the temperature of the folding transition is above physiological temperature, then the model protein will be unfolded at 37 °C. But if by a chemical means, the temperature T_t of the folding transition can be lowered to below 37 °C, then the model protein should be folded at physiological temperature. By the process of chemically changing or controlling the temperature at which the folding transition occurs, it becomes possible to have a chemically driven molecular machine. In what follows, the means of chemically and otherwise changing the temperature of the folding transition are reviewed.

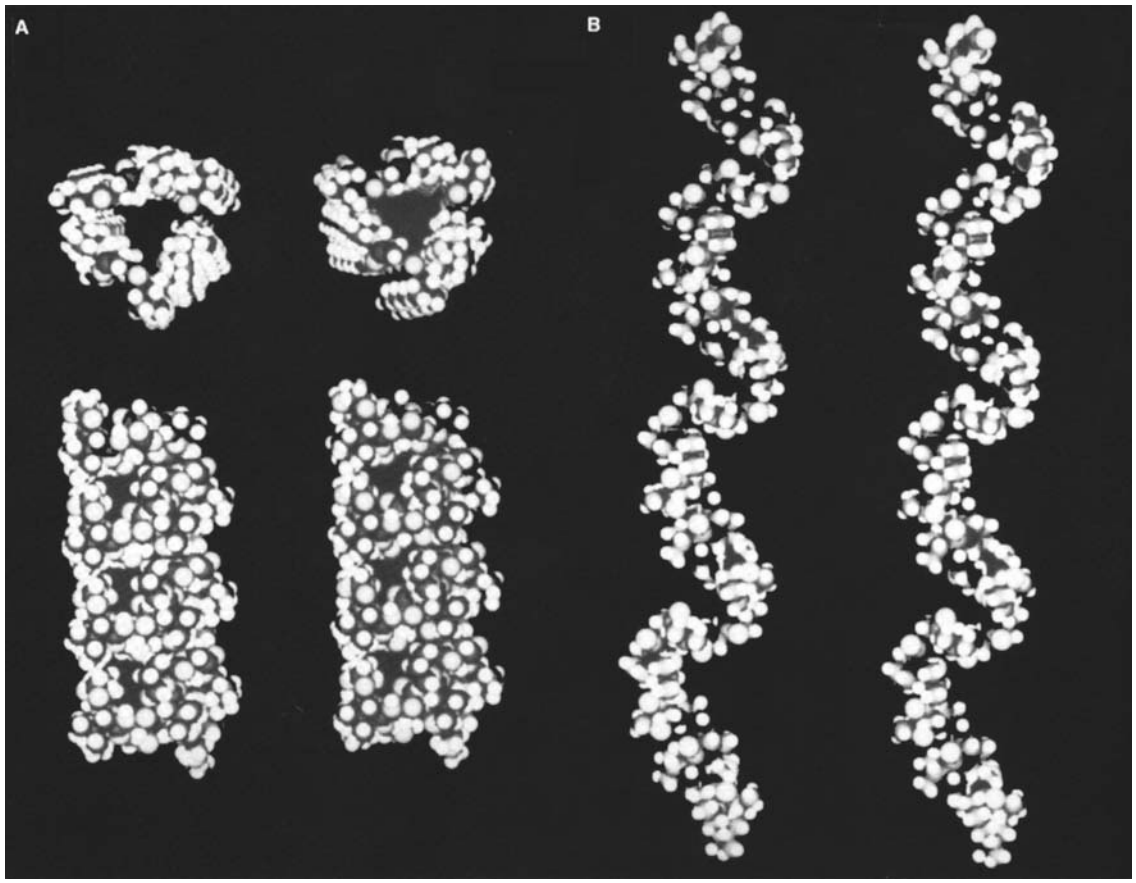

Fig. 5. Stereo-pairs (cross-eye views) of the molecular structure of poly(VPGVG). A) The β-spiral structure has approximately three pentamers per turn. Contacts between the turns of the β-spiral involve the Val-$^1\gamma$-CH_3 group of repeat i with the Pro-β-CH_2 group of repeat $(i + 3)$. The view along the spiral axis (top) shows the space for water inside the spiral, as within the stacks of *cyclo*$(VPGVG)_3$ molecules represented in Figure 3A. The side view (bottom) depicts the linear helical conformation that corresponds to the conformation of the cylic isomer in Figure 3. B) An extended state in which the interturn hydrophobic contacts have been disrupted and where the hydrophobic moieties would be surrounded by more highly ordered water as in Figure 4 (from reference [22]).

4. Deliberate Change in the Temperature T_t at which Folding Occurs

The chemical parameters that can change the value of T_t may be grouped as intrinsic and extrinsic. Intrinsic to the class of model proteins of 50000 Da molecular weight or greater are 1) the concentration of polypentapeptide itself, 2) changes in the amino acid composition within the polypentapeptide, 3) changes in the degree of ionization of functional side chains controlled by changes in pH, 4) the phosphorylation of side chains such as serine by enzymes called kinases, 5) the oxidation or reduction of a prosthetic group attached to the model protein either electrically, chemically, or enzymatically, and 6) photochemical reactions of attached chromophores. With awareness of the concentration effect and of certain conformational restrictions, the effect of changing the amino acid composition on the value of T_t can be determined. The result is a hydrophobicity scale based for the first time directly on the hydrophobic folding and assembly process of interest. The extrinsic chemical parameters are the effects 1) of salts and 2) of organic solutes. There are already examples for each of the above intrinsic and extrinsic variables including, most recently, that of photochemical reactions. Another extrinsic variable, pressure, has also been found to change the value of T_t. It may also be noted that there is a dependence on chain length that becomes significant at lower molecular weights where shorter chain lengths result in higher values of T_t.

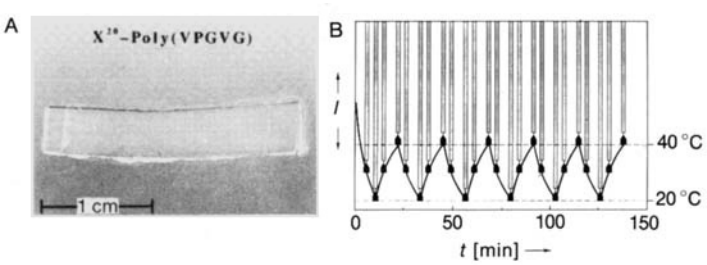

Fig. 6. A) Elastomeric strip of X^{20}-poly(VPGVG). B) A series of thermally driven contraction/relaxation cycles of lifting and lowering a weight. The contraction is the visible macroscopic result of hydrophobic folding and assembly as the temperature is raised. (From reference [35].)

4.1. Intrinsic Chemical Changes

The chemical equivalent of raising the temperature in molecular systems that exhibit inverse temperature transitions is chemically lowering the transition temperature T_t at which the folding occurs.

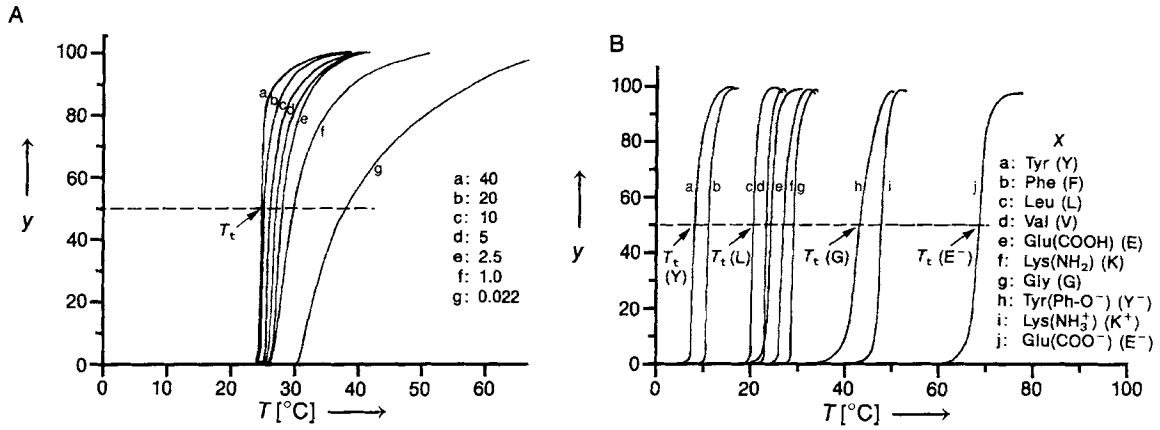

Fig. 7. TPτ profiles for aggregation of poly[f_v(VPGVG),f_x(VPGXG)]. Turbidity (y[%]) is monitored at 300 nm. A) Concentration dependence of T_t for $f_v = 1$, that is, for poly(VPGVG). The concentrations for a–g are given in mg mL^{-1} (from reference [7]). B) Composition dependence of TPτ for $f_x = 0.2$ (from reference [1]). The change in T_t with composition is the basis for a new hydrophobicity scale (see Fig. 8 and Table 1).

4.1.1. *Effect of Concentration*

When the concentration of poly(VPGVG) is increased, the temperature of the inverse temperature transition decreases till a high concentration limit is reached at about 40 mg mL^{-1}.[7] In Figure 7A are given a series of temperature profiles for turbidity formation (TPτ curves) in which the temperature for the onset of turbidity decreases and the steepness of the curve increases as the concentration is increased to the high concentration limit. For this high-concentration limit the temperature T_t of the inverse temperature transition is the temperature at which 50% of the normalized turbidity is obtained. Accordingly, this is the concentration that was used for comparing polypentapeptides of different compositions, and this effect should be kept in mind when examining each of the other means of changing the value of T_t.

4.1.2. *Effect of Composition*

The general formula for the polypentapeptide can be written as poly[f_v(VPGVG),f_x(VPGXG)] where f_v and f_x are mole fractions ($f_x + f_v = 1$), and X is any of the naturally occurring amino acid residues or chemical modifications thereof. A series of TPτ curves are given in Figure 7B for $f_x = 0.2$.[1] Again T_t is defined as the temperature for half-maximal turbidity. As may be seen by plotting f_x versus T_t for all of the naturally occurring amino acid residues (Fig. 8),[23] residues more hydrophobic than Val (Ile(I), Phe(F), etc.) lower the temperature of the transition, whereas less hydrophobic residues like Ala(A), Gly(G) and polar residues like Asp(COO$^-$)(D$^-$) or Lys(NH$_3^+$)(K$^+$) raise the temperature of the transition (i.e., raise the value of T_t). The plots are essentially linear. Therefore, on extrapolating the linear plots to $f_x = 1$, values of T_t are obtained that give an index of relative hydrophobicity. These values are given in Table 1.[23]

4.1.3. *Effect of Changing the Degree of Ionization by Changing the pH*

A very effective means of raising the value of T_t is to increase the degree of ionization α of an amino acid residue such as Asp(COO$^-$), Lys(NH$_3^+$), or Glu(COO$^-$). The most potent in this respect is the Glu (E) residue (see Table 1 and Figs. 7B and 8). With $f_x = 0.2$ the transition temperature in water is too high to measure (greater than 80 °C). On addi-

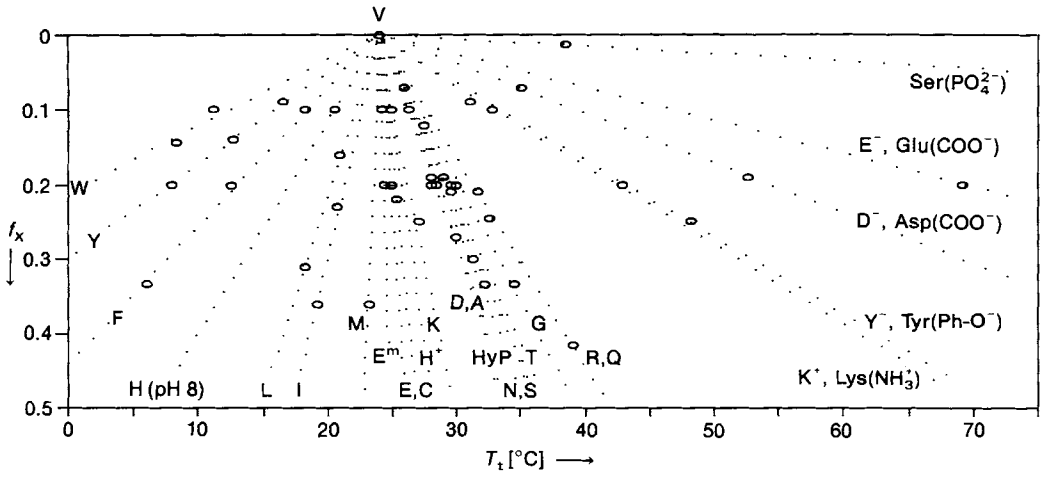

Fig. 8. Plots of T_t for poly-[f_v(VPGVG),f_x(VPGXG)] in phosphate-buffered saline as a function of f_x, at small f_x. At such low X content the plots are essentially linear, and the relative values can be compared for a reference composition (see Table 1). (From reference [23].)

Table 1. Temperature of the inverse temperature transition, T_t for poly[f_x(VPGVG),f_x(VPGXG).

Amino acid X	T_t [°C]	Correlation coefficient
Lys(NMeN, red.) [a]	−130	1.000
Trp (W)	−90	0.993
Tyr (Y)	−55	0.999
Phe (F)	−30	0.999
His (pH 8) (H)	−10	1.000
Pro (P)	(−8)	[b]
Leu (L)	5	0.999
Ile (I)	10	0.999
Met (M)	20	0.996
Val (V)	24	[c]
Glu($COOCH_3$) (E^m)	25	1.000
Glu(COOH) (E)	30	1.000
Cys (C)	30	1.000
His (pH 4) (H^+)	30	1.000
Lys(NH_3) (K)	35	0.936
Asp(COOH) (D)	45	0.994
Ala (A)	45	0.997
HyP	50	0.998
Asn (N)	50	0.997
Ser (S)	50	0.997
Thr (T)	50	0.999
Gly (G)	55	0.999
Arg (R)	60	1.000
Gln (Q)	60	0.999
$Lys(NH_3^+)$ (K^+)	120	0.999
Tyr(Ph-O) (Y)	120	0.996
Lys(NMeN, ox.) [a]	120	1.000
Asp(COO) (D)	170	0.999
Glu(COO) (E)	250	1.000
Ser(PO_4^{2-})	1000	1.000

[a] NMeN represents *N*-methylnicotinamide pendant on a lysyl side chain, i.e., *N*-methylnicotinate attached by amide linkage to the ε-NH_2 of lysine. The reduced state is *N*-methyl-1,6-dihydronicotinamide residue. [b] Calculated. [c] Serves as reference substance.

tion of 0.15 N NaCl the value of T_t for $\alpha = 1$ (i.e., Glu(COO^-) is 69 °C, which is shifted from 24 °C for $\alpha = 0$, that is, Glu(COOH). For the extrapolated reference state of $f_x = 1$, the value for Glu(COO^-) is 250 °C and for Glu(COOH) is 30 °C (see also Fig. 18).

4.1.4. *Effect of Phosphorylation of a Serine Side Chain*

The most potent means (on a per mole pentamer basis) yet found for changing the value of T_t is phosphorylation.[124] It is some four times more potent than the Glu(COO^-) perturbation. For the extrapolated reference state of $f_x = 1$, the value for Ser(PO_4^{2-}) is greater than 1000 °C. While electrostatic interactions have in the past been given as the explanation for the prominent use in biology of phosphorylation/dephosphorylation in changing protein structure to achieve function, the present mechanism provides a more potent explanation in aqueous systems. This will be discussed in Section 8.1.1.

4.1.5. *Effect of Electrochemical or Chemical Reduction of a Prosthetic Group*

Reduction of a chemical moiety could be expected to change the value of T_t for the protein-based polymer to which it is bound. Recent results have demonstrated that the electrochemical reduction of *N*-methylnicotinamide (NMeN), pendant on a lysine side chain, very significantly lowers the value of T_t for the polymer. For poly[0.73(GVGVP),0.27(GK(NMeN)GVP)] T_t was 48 °C and on partial reduction became 31 °C (Fig. 9A). When extrapolated to $f_x = 1$, the oxidized state would give 120 °C for T_t, and with the assumption of complete reduction, the electrochemically reduced state expected to yield the 6-hydroxy-*N*-methyl-1,4,5,6-tetrahydronicotinamide would give 37 °C for T_t. If conversion in the experiment were not complete, the value of T_t would be lower. The present best estimate places the value below 0 °C. The UV absorption spectra corresponding to the TPτ curve of Figure 9A are given in Figure 9B (Urry, Hayes, Gowda, and Harris, unpublished results).

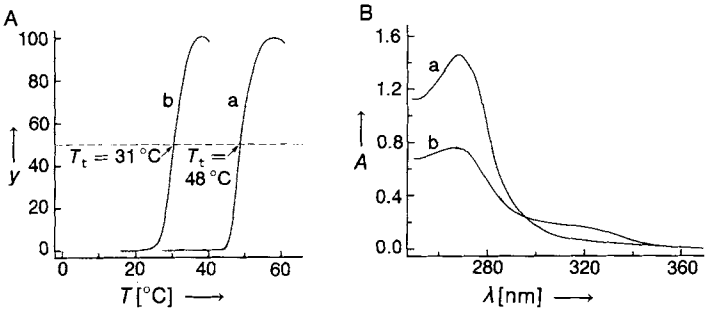

Fig. 9. A) Dependence of T_t on redox state of the *N*-methylnicotinamide residue in poly[0.73(GVGVP),0.27(GK(NMeN)GVP)]. At a concentration of 10 mg mL^{-1}, T_t is 48 °C when oxidized (a), and 31 °C when reduced at −1.8 V for 30 min in a carbonate/KCl buffer system at pH 9. B) Absorption spectra corresponding to the curves in A, after the samples were diluted by 50% with buffer.

Chemical reduction with dithionite has been found to reduce T_t from 49 °C to 9 °C for an estimated 60% reduction based on the absorption spectra for *N*-methyl-1,6-dihydronicotinamide. Extrapolating to $f_x = 1$ gives for the oxidized state the same T_t value as in the electrochemical experiment of 120 °C and for the reduced state a value of −130 °C. The ΔT_t of 250 °C for this NMeN redox couple is slightly larger than the ΔT_t of 220 °C for the Glu(COOH)/Glu(COO^-) chemical couple.[125]

4.1.6. *Effect of Photochemical Reactions*

It was also anticipated, and has now been confirmed, that photochemical reactions would change the hydrophobicity or polarity of a photoreactive side chain or chromophore attached to an amino acid side chain. As the photoproducts can be quite varied, some reactions could be expected that would raise the value of T_t whereas others might decrease it. This will be an interesting feature to pursue. In the results obtained to date (K. Heimbach, T. Parker, and D. W. Urry, unpublished data) photochemical reaction of a spiropyran attached by ester linkage to a Glu residue causes a decrease in the value of T_t, and photochemical reaction of an attached cinnamic acid moiety causes a dark reversible increase in T_t.

4.2. Extrinsic Chemical Changes

Many extrinsic chemical perturbations of salts and organic solutes have now been identified that change the temperature of the inverse temperature transition. In both categories some raise the value of T_t while others lower it.

4.2.1. Effects of Adding Salts

The first demonstrated salt effect was that of sodium chloride, which lowers the value of T_t 14 °C N^{-1} (i.e., gram equivalent per liter).[26] NaBr is less effective in lowering T_t whereas NaI and NaSCN cause small increases. The salts with the most potent effect on a normality basis are those with multivalent anions such as the carbonates, sulfates, and phosphates. A number of these salt effects are shown in Figure 10A. All have the potential of being used for chemically driven folding or, as in the case of the few that raise T_t, for chemically driven unfolding.

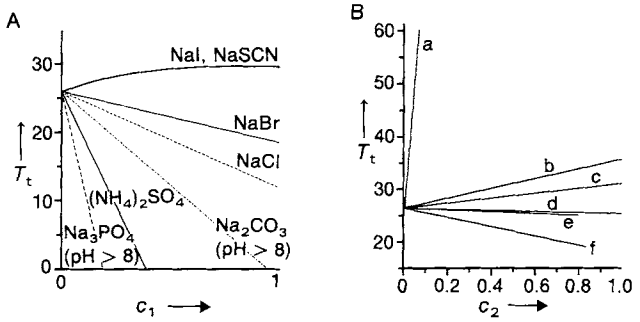

Fig. 10. Influence of salts (A, adapted from reference [35]) and organic solutes (B, unpublished data) on T_t for poly(VPGVG). c_1 = salt concentration in N. c_2 = concentration of organic solute in M. a: sodium dodecyl sulfate; b: guanidinium chloride; c: urea; d: ethylene glycol; e: glycerol; f: trifluoroethanol.

4.2.2. Effects of Organic Solutes

As seen in Figure 10B, the effects of organic solutes appear to be more variable than those of salts, and a few are even biphasic. Organic solutes in order of decreasing potency for raising T_t are sodium dodecylsulfate (600 °C mol^{-1} at 0.1 M), guanidine hydrochloride (12 °C mol^{-1} at 0.3 M), urea (5.5 °C mol^{-1} at 0.3 M), and Triton X-100, which is biphasic (22 °C mol^{-1} at 0.3 M). Organic solutes that lower T_t are ethylene glycol, trifluoroethanol (−11 °C mol^{-1} at 0.4 M), trifluoracetic acid, and glycerol (−2.2 °C mol^{-1} at 0.4 M). Dimethyl sulfoxide and ethylene glycol (at very low concentrations) are biphasic, which increases the value of T_t at lower concentrations and progressively lowers the value of T_t at higher concentrations.

4.3. Another Extrinsic Change: Pressure

Increases in pressure will also raise the value of T_t [27] and will do so most effectively if aromatic residues such as Phe(F), Tyr(Y), and Trp(W) are present (Fig. 11). The effect occurs because the volume occupied per water molecule is less when the water molecules are more ordered around aromatic moieties than in bulk water. This means that application of pressure could be used to drive unfolding, and the release of pressure could bring about folding.

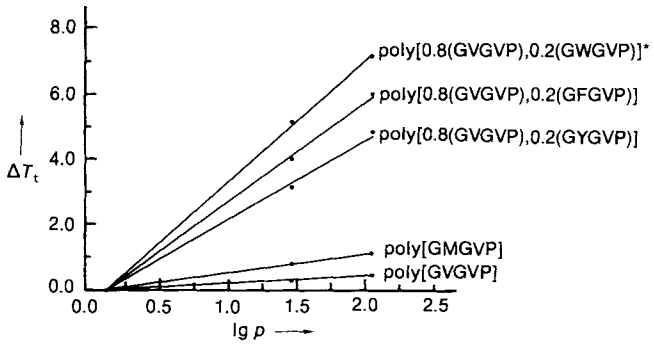

Fig. 11. The effect of pressure on T_t. The data is plotted according to the Clausius–Clapeyron equation. The change in transition temperature ΔT_t is plotted versus lg p (p in atm); the slope is thus $p\Delta V/\Delta S$. By using differential scanning calorimetry data to evaluate $\Delta S(=\Delta H/T)$, the volume changes can be calculated. (From reference [27].)

4.5. A Unifying Basis for Diverse Energy Conversions: The ΔT_t Mechanism

The ΔT_t mechanism is currently under investigation to determine just how ubiquitous it is. Many intrinsic and extrinsic chemical changes have now been shown to change the temperature at which the inverse temperature transition (the temperature of the hydrophobic folding and assembly transition) occurs. These are the initial, necessary demonstrations of feasibility in properly designed elastic protein-based polymers before conditions can be developed for working with a viscoelastic phase that has been made into a suitable cross-linked elastic matrix. Several chemical energy inputs and pressurization energy can result in contraction of the elastic materials with the performance of useful mechanical work, and it can be argued that an even more diverse set of energy conversions will be possible. This discussion and the categorization of the energy conversions will be introduced by a brief review of the development of the ΔT_t mechanism.

It was first observed that polypeptides or model proteins with the correct balance of apolar (hydrophobic) and polar moieties became more ordered on raising the temperature. This process was called an inverse temperature transition. For some of the polypeptides the inverse temperature transition was seen to be a reversible phase transition with the formation of a more dense, polypeptide-rich, viscoelastic phase on raising the temperature. When the viscoelastic phase was cross-linked, elastic matrices were formed which, on raising the temperature past the inverse temperature transition, would contract and in doing so could lift weights that were a thousand times the dry weight of the matrix. These matrices could thus perform useful mechanical work on raising the temperature. Such elastic matrices may be called zero-order molecular machines of the inverse temperature transition (T_t) type.

Next, having demonstrated that varying the composition of the protein-based polymer systematically altered the transition temperature, it was anticipated that changing the de-

gree of ionization of a functional side chain in the polypeptide (an intrinsic chemical change) would change the temperature at which the inverse temperature transition occurred, because this varies the composition without synthesis of a new polymer. It was further anticipated that the cross-linked viscoelastic phase of such a polypeptide would exhibit an isothermal pH-driven contraction capable of doing useful mechanical work. This was observed.[28] In general, such an elastic matrix (in which chemical energy or any other energy source could change the temperature of the inverse temperature transition and thereby cause contraction enabling useful mechanical work to be performed) will be called a first-order molecular machine of the T_t type. The work performed is the direct result of hydrophobic folding and assembly. The energy conversions now directly demonstrated to be feasible, indirectly argued as occurring, or proposed as possible by the ΔT_t mechanism are summarized in Figure 12. The T_t-type

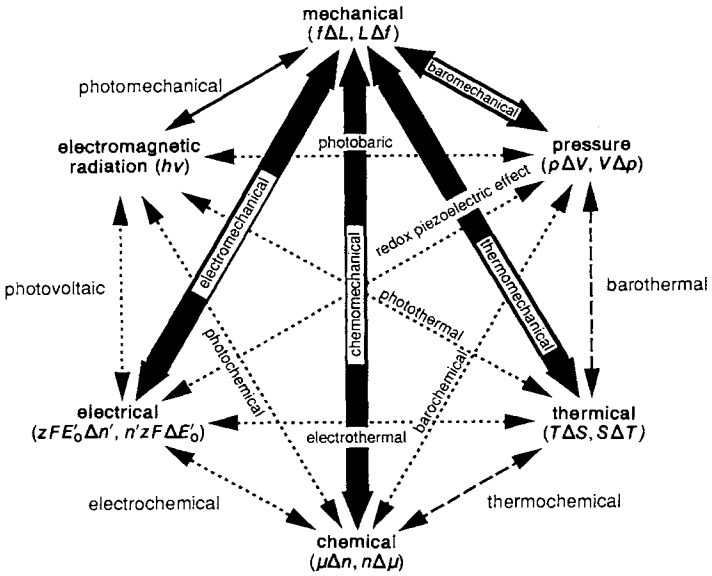

Fig. 12. Demonstrated and putative energy conversions with molecular machines of the T_t type. The bold arrows indicate the energy conversions that have been observed with the elastic protein-based matrices. Photomechanical energy conversion is inferred from photoreduction of nicotinamide [90] and, for example, from photoisomerism of a cinnamic acid chromophore attached to a side chain. To our knowledge these arrows include all energy conversions that can occur in the living organism, and all appear possible by T_t-type molecular machines.

first-order energy conversions are those with arrows directly terminating at the mechanical apex. Those already demonstrated are depicted as broad arrows; the one for which the shift in T_t has been demonstrated in a suitably designed polypeptide prior to cross-linking is indicated by the solid line; those for which there is indirect data are indicated by the dashed arrows; and those which are as yet hypothetical are given as the dotted arrows.

The arrows indicating energy conversions not ending at the mechanical apex will be considered second-order energy conversions of the T_t type. Though they utilize the hydrophobic folding and assembly capacity of the elastic matrix, mechanical work is not one of the pair of energies being interconverted.

5.1. First-Order Molecular Machines of the T_t Type

5.1.1. Conversion of Chemical Energy into Mechanical Work

The capacity chemically to change the temperature T_t at which the folding and assembly transition occurs implies that conversion of chemical energy into mechanical work can occur isothermally, that is, under the homoiothermic conditions of warm-blooded animals.

5.1.1.1. Proton-Driven Contraction

This ΔT_t mechanism was first demonstrated for chemomechanical transduction. The demonstration utilized the γ-irradiation cross-linked matrix, X^{20}-poly[0.8(VPGVG),0.2-(VPGEG)], shown above Figure 13A. First, however, the conditions under which thermally driven contraction occur were examined. At low pH (2.2), this matrix in phosphate-buffered saline (0.15 N NaCl, 0.01 M phosphate) begins to contract as the temperature is raised above 20 °C. This thermally driven contraction is complete by 40 °C. At a higher pH (4.5), thermally driven contraction does not begin until near 45 °C. By the ΔT_t mechanism, it should be possible to maintain the temperature at 37 °C and lower the pH to drive contraction. This does occur, as seen in Figure 13A. Raising the concentration of protons converts the Glu(COO^-) residue to Glu(COOH), and the matrix at 37 °C contracts picking up a weight.[28] The cross-linked Glu-containing matrix converts chemical energy into mechanical work; it is a chemically driven molecular machine, that is, chemical energy ↔ mechanical work.

5.1.1.2. Salt-Driven Contraction

As shown in Figure 10A, addition of NaCl lowers the value of T_t for poly(VPGVG) by 14 °C N^{-1}. Even the change from pure water to 0.15 N NaCl at 25 °C results in quite significant contractions.[29] Figure 13B shows a series of salt-driven contractions and relaxations of the X^{20}-poly(VPGVG) elastic matrix shown. Accordingly, an extrinsic chemical change can be used to drive contraction and to perform useful mechanical work. Any salt capable of changing the value of T_t may be expected to drive contraction, including those shown in Figure 10A.

When the protein-based polymer contains a charged moiety such as a Glu(COO^-) residue, the sensitivity of T_t to salt concentration is an order of magnitude greater in the low concentration range (Luan and Urry, unpublished data). When the polymer concentration is 40 mg mL^{-1}, this increased effect is observed between 0 and 0.2 N. Above this concentration of salt, the coefficient is again near 15 °C N^{-1}. The effect arises presumably from the weak ion-pairing of the salt's sodium cation with the carboxylate anion of the protein-based polymer. In this case a smaller chemical energy change could be expected to perform a given amount of chemical work. The comparison of the efficiency of the charge–charge repulsion mechanism and the ΔT_t mechanism is discussed in the following without considering this increased sensitivity.

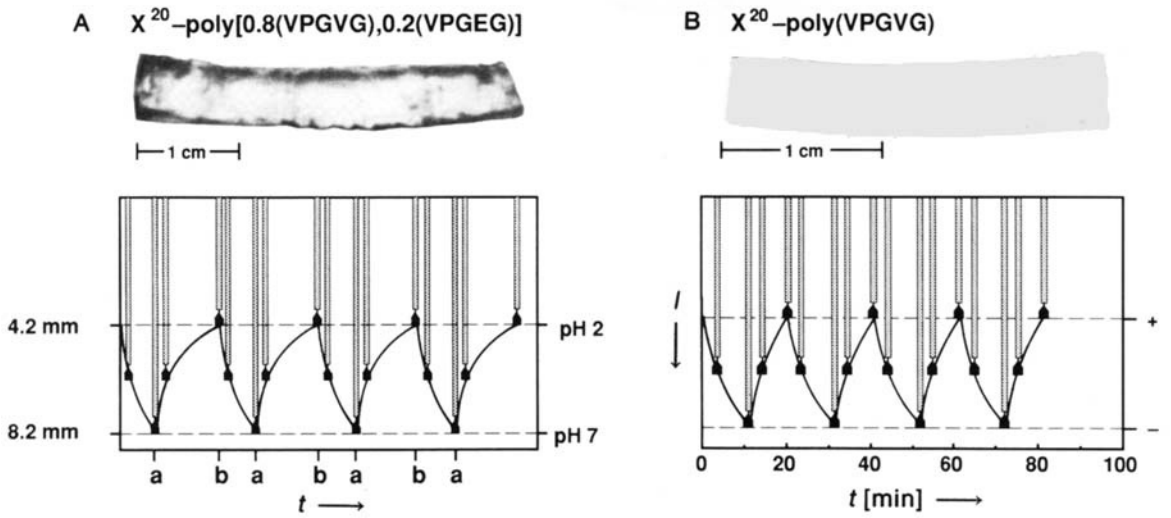

Fig. 13. A) A strip of cross-linked, Glu-containing elastic matrix, here X^{20}-poly[0.8(VPGVG),0.2(VPGEG)] as proton-driven molecular machine. At low pH the length of the strip of elastic matrix with a weight attached was 4.2 mm; on raising the pH the strip extended lowering the weight (b, neutralization); when the pH was lowered (by addition of acid at a) the strip contracted lifting the weight. This proton-driven molecular machine can be operated through many cycles. (From reference [35].) B) A strip of cross-linked poly(VPGVG) as salt-driven molecular machine. The strip is extended in the absence of salt. Addition of salt causes a contraction, and the the weight is lifted. This cycle can be repeated for days without any loss in the extent of contraction. Run in reverse, that is, providing the mechanical energy of stretching, this molecular machine could be used for desalination. (From reference [35].) + : salt present. – : no salt present.

5.1.1.3. Reduction-Driven Contraction

With a 20 Mrad cross-linked *N*-methylnicotinamide containing elastic matrix, X^{20}-poly[0.73(GVGVP),0.27(GK-(NMeN)GVP)], partial reduction by dithionite has now been observed to lower the temperature range over which thermally driven contraction occurs. Accordingly, at a temperature of 40 °C the matrix contracts when dithionite is added and picks up a weight. Thus, contraction driven by chemical reduction has now been observed.[30] Since reduction may also be carried out electrochemically this may be termed electromechanical transduction as indicated in Figures 12 and 14.

5.1.2. Conversion of Pressurization Energy into Mechanical Work

In Section 4.3, pressure was noted as another variable, extrinsic to the polypeptide, that could change the value of T_t, particularly in protein-based polymers containing aromatic residues. From the increase in T_t as the pressure was increased and the experimental heat divided by the transition temperature, it was calculated that a water molecule in bulk water occupies a greater volume than a water molecule in the solvent sphere surrounding the most hydrophobic moieties (the aromatic moieties such as those of the Phe(F), Tyr(Y) and Trp(W) residues).[27] At the appropriate temperature and at elevated pressure the elastic matrix suspending a weight will be extended, and the aromatic moieties will be surrounded by the more ordered, denser water. On releasing the pressure, the more ordered water molecules convert to bulk water as the model protein hydrophobically folds, thereby contracting and performing the mechanical work of lifting the weight. This baromechanical transduction has now been observed.[31] At the appropriate temperature, the properly designed elastic matrix is a pressure-responsive molecular machine.

In this example of a molecular machine capable of free energy transduction, the interconverting Gibbs free energies are the products of the intensive variable of mechanical force and the extensive variable of distance the weight is moved against the force of gravity and of the intensive variable of pressure and the extensive variable of change in volume.

5.2. Second-Order Molecular Machines of the T_t type

As an example of a T_t-type second-order energy conversion, consider a swollen matrix of unfolded polypeptides containing both an oxidized component of a redox couple, for example *N*-methylnicotinamide, and the charged moiety of a chemical couple, for example (COO^-), in which the composition of the protein-based polymer is such that T_t is just above the operating temperature. Under these circumstances, either lowering the pH to convert the COO^- into COOH or reduction of the nicotinamide, the oxidized prosthetic group (redox couple), would lead to hydrophobic folding and assembly. If the oxidized prosthetic group were reduced, then the resulting folding would be expected to shift the pK_a of the carboxyl moiety, and under the proper conditions the chemical result would be an uptake of protons (a decrease in proton chemical potential). If, on the other hand, the pH were lowered and the carboxylate anion were protonated, the electrochemical potential of the oxidized prosthetic group would be expected to shift in favor of reduction and the electrical result could be the uptake of electrons. Either of these scenarios could be designated as electrochemical transduction as the arrow connecting the electrical and chemical apices in Figure 12 indicates. Both would utilize the hydrophobic folding, but the energy produced or the work performed would not be mechanical in nature. The elastic

matrix so designed to achieve electrochemical transduction would be in our designation a second-order molecular machine of the T_t type.

Equivalent scenarios could be described for other T_t-type second-order energy conversions such as photochemical, photovoltaic, thermochemical, that is, for any of the pairwise energy conversions not including the mechanical apex of Figure 12.

There are, therefore, many energy conversions that may be considered to arise from the basic ΔT_t mechanism. Future studies will be directed toward designing protein-based polymers, and the suitable experimental apparatus and conditions for each, with which to demonstrate these energy conversions. To our knowledge these include all of the energy conversions which occur in living organisms. The effectiveness and efficiency of the ΔT_t mechanism for each interesting energy conversion will need to be established. By the process of natural selection living organisms probably would evolve to utilize the most efficient mechanism for energy conversion that is available to its composition.

A summary of the ΔT_t mechanism of free energy transduction is given in Figure 14 for zero-order and first-order molecular machines of the T_t types.

6. Physical Basis for ΔT_t-Type Energy Conversions

The physical basis for the ΔT_t mechanism of energy conversion resides in changing hydration within the system. For the conversion of chemical energy into mechanical work by means of intrinsic chemical changes, the basis is the competition for hydration between hydrophobic and more polar moieties (for example, between Val side chains and the carboxylate anion) that are both part of the same amphiphilic polymer with constraints on the distance between them. As this distance can be changed only by changes in the folded state of the polymer, control can be exercised over the folding/unfolding process.

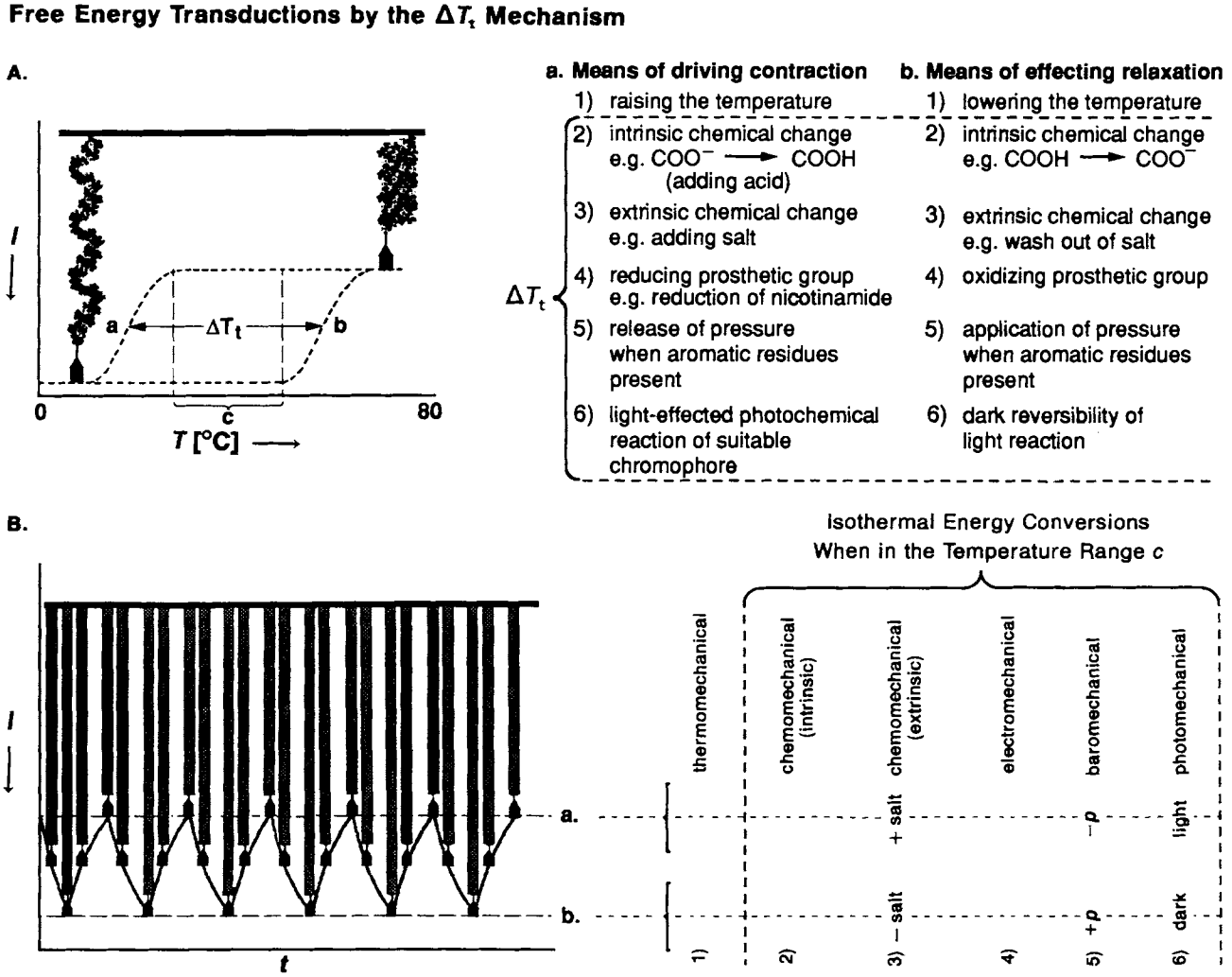

Fig. 14. Summary and present state of the development of the ΔT_t mechanism. A) Left: Schematic illustration of the β-spiral of poly(VPGVG) in extended (unfolded) state at low temperature and contracted (folded) state at elevated temperature. The temperature range over which the transition occurs is designated as ΔT_t; the temperature range over which maximal contraction can be achieved is indicated by c. Right: the list of conditions that can influence T_t. B) Left: Schematic illustration of an elastic protein-based model reversibly undergoing contraction and relaxation when in the temperature range c. Right: The energy conversions of items 1)–6) of A that achieve contraction, and the conditions required for them. The photochemical reaction can either raise or lower the value of T_t; both have been observed.

6.1. When Hydrophobic Hydration Dominates in Amphiphilic Polymers

When hydrophobic hydration dominates in amphiphilic polymers such as proteins, in our view the prevalence of the more ordered water structure surrounding the hydrophobic species results in an inadequate water structure for the hydration of charged species. The free energy of hydration of the charged species is less favorable (higher), and ionization is less probable. This is seen experimentally as a hydrophobicity-induced increase in the pK_a.

The protein-based polymer poly[0.8(VPGVG),0.2-(VPGEG)] in water at 37 °C has a pK_a of 4.6; the more hydrophobic poly[0.8(IPGVG),0.2(IPGEG)] under the same conditions has a pK_a of 6.0.[32] With correct design of primary structure even greater shifts can be seen.

Deliberate changes in the nanometer range can result in extraordinary pK_a shifts. Schematic representations of the β-spirals of the poly(GVGVP) and pentapeptides that differ from poly(GVGVP) by the introduction of Glu(E) and Phe(F) residues are given in Figure 15. In the polypeptide in

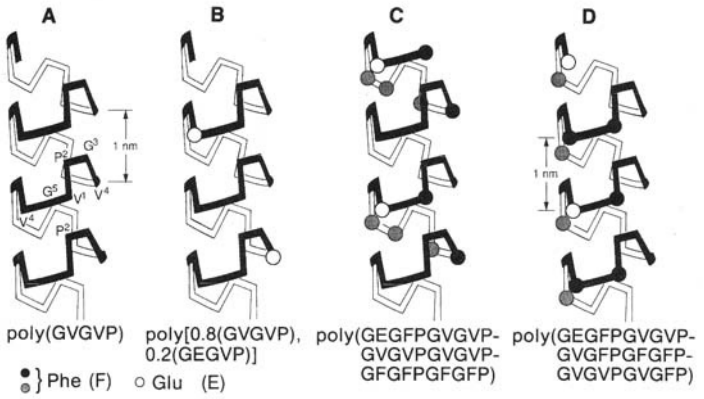

Fig. 15. Schematic representations of the β-spiral structure of polypeptides. A) Poly(GVGVP). B) Random incorporation of Glu(E) residues in 20% of the poly(GVGVP) pentamers. C) The polytricosapeptide, poly(GEGFPGVGVPGVGVPGVGVPGFGFPGFGFP), in which the Phe(F) residues are in a fixed relationship to the Glu(E) residue. D) The polytricosapeptide, poly(GEGFPGVGVPGVGFPGFGFPGVGVPGVGFP), in which the particular folding of the β-spiral with three pentamers per turn provides an optimal arrangement of the Phe residues around the Glu residue. (From reference [33].)

Figure 15D, the Phe(F) residues are optimally arranged around the Glu(E) residue. Figure 16 depicts the acid–base titration curves for the polymers in Figure 15 (I, IV, and V) as well as those of two other polymers (II and III) consisting of the same pentamers as those in Figure 15C and D, respectively, but the pentamers are randomized.[33] Thus, the Phe(F) residues are optimally placed for the β-spiral structure in polymer V, which results in a remarkable pK_a for Glu(E) at 20 °C in water of 8.1, a shift from a pK_a value of 4.3 for polymer I under these conditions. It is the proximity of the aromatic (phenyl) side chains surrounded by the more ordered water molecules that make hydration of the COO^- moiety in polymer V so unfavorable.

An estimate of the repulsive Gibbs free energy of hydration can be obtained from the chemical potential μ of the protons required to maintain the Glu side chain at 50% ionization. As $\mu = RT\ln a$ where a is activity, $\mu = RT\ln[H^+]$, since at the low proton concentrations, activity is equivalent to concentration. Rewriting with the logarithm to the base 10 (lg) gives $\mu = 2.3\,RT\lg[H^+]$, but as $pH = -\lg[H^+]$, the chemical potential becomes $\mu = -2.3\,RT\,pH$. The change in proton chemical potential $\Delta\mu$ required to maintain the Glu side chain at 50% ionization (that is, at its pK_a), is simply $\Delta\mu = -2.3\,RT\Delta pK_a$. Since $R = 1.987\ cal\,mol^{-1}\,K^{-1}$, RT at 20 °C (293 K) is 582 $cal\,mol^{-1}$, a ΔpK_a of −3.8 (4.3−8.1) requires a $\Delta\mu$ of 5 $kcal\,mol^{-1}$.

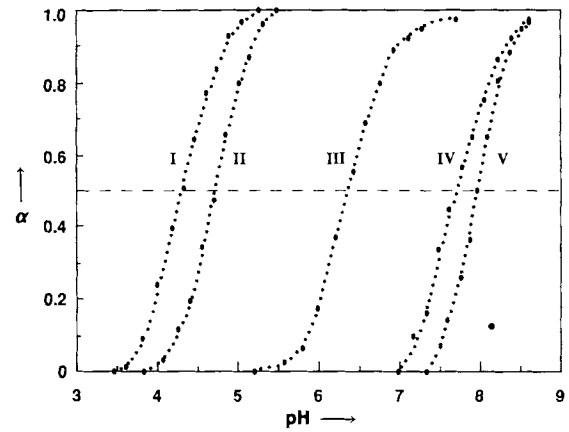

Fig. 16. Structure-dependent pK_a shifts induced by hydrophobicity, demonstrated by the resolved acid–base titration curves for polymers B–D of Figure 15 (I, IV, and V, respectively), as well as for an isomer each of IV and V (II and III, respectively), which were synthesized by direct polymerization of the pentamers and not by the polymerization of the tricosamers. (From reference [33].) α = degree of ionization.

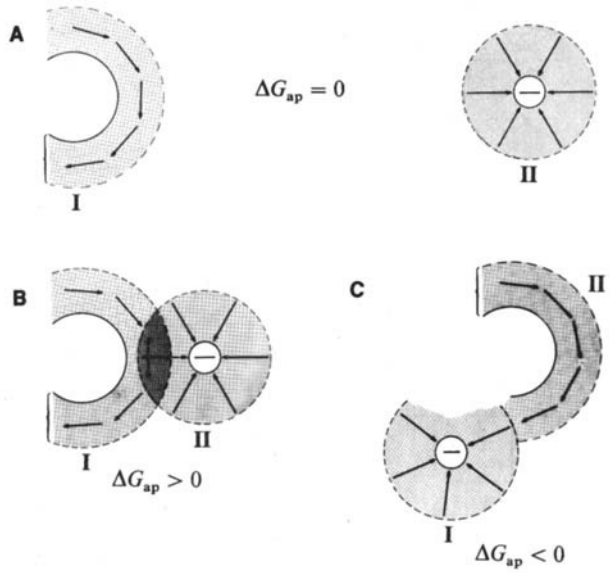

Fig. 17. Relationship between the distance from charged species to hydrophobic moiety and ΔG_{ap} for hydration-mediated apolar–polar interactions. The water molecules are represented as dipole moment vectors. The water vector is tangential to the surface of the hydrophobic moiety (I), whereas it points directly at the negatively charged moiety (II). A) When the hydrophobic and polar species are far apart, there is no interaction. Each receives its full free energy of hydration. B) When the hydration shells overlap, there is a loss of free energy of hydration and ΔG_{ap} is positive. This can give rise to the hydrophobicity-induced pK_a shifts when the apolar moieties dominate. As the charged species form, there is a destructuring of the hydrophobic hydration sphere. C) For special orientations of apolar and polar moieties in which water molecules can simultaneously serve both hydration spheres, ΔG_{ap} is negative. This can be seen in the crystal structure of crambin (Fig. 4C). (From reference [34].)

This is the hydration-mediated apolar–polar repulsive free energy, ΔG_{ap}, which drives unfolding on ionization of the carboxyl group. An attempt to depict ΔG_{ap} is shown in Figure 17.[34] With the aspartic acid residue Asp(D) in place of the glutamic acid residue Glu(E) in polymers I(A) and V(D) of Figures 15 and 16, the pK_a values are 3.9 and 10.1, respectively, giving a ΔG_{ap} of 8.3 kcal mol^{-1}. This is the largest pK_a shift yet observed in a designed model protein (Urry, Gowda, Perry, Parker, Jing, Harris, unpublished results).

6.2. When Ionic Hydration Dominates in Amphiphilic Polymers

In our view, in this case the more ordered water molecules surrounding the hydrophobic moieties are substantially disrupted by the orientation of water molecules to hydrate the proximal charged moieties. With loss of the more structured water surrounding the hydrophobic moieties, there is no longer the Gibbs free energy as driving force for the inverse temperature transition, that is, for the hydrophobic folding. Therefore, the polymer unfolds.

Recall that the hydration of hydrophobic moieties is exothermic (ΔH(hydration) is negative). Since the hydrophobic hydration is structured (that is, the less ordered bulk water becomes the more ordered water of hydrophobic hydration), ΔS(hydration) is negative. Because $-T\Delta S$(hydration) is therefore positive and of a magnitude similar to the negative ΔH(hydration), solubility is limited. In the polymer, solubility reflects the presence of the unfolded state and insolubility of the hydrophobic-containing species the presence of the folded state. Folding and unfolding of the polymer arises when the relative magnitudes of the two terms are changed. When the charged species is present, there would be less of the structured water surrounding the hydrophobic moiety; ΔS(hydration) for the transition would be smaller, and a higher temperature T would be required before $-T\Delta S$(hydration) dominates. Therefore, T_t would increase with increase in numbers of charged species.

That the temperature of the transition increases with increased degree of ionization α is clearly shown in Figure 18.[35] Corresponding with increase in degree of ionization and increase in T_t, the heat required to destructure the more structured water around hydrophobic moieties is seen to decrease (Fig. 19).[36] When there are less than two COO^- moieties per hundred residues, the endothermic heat required to drive the transition is reduced almost to one-fourth. In our interpretation, the hydration of the two COO^- moieties formed in a hundred residues effectively destroyed some three-fourths of the more ordered structure of the water that had surrounded the hydrophobic moieties.

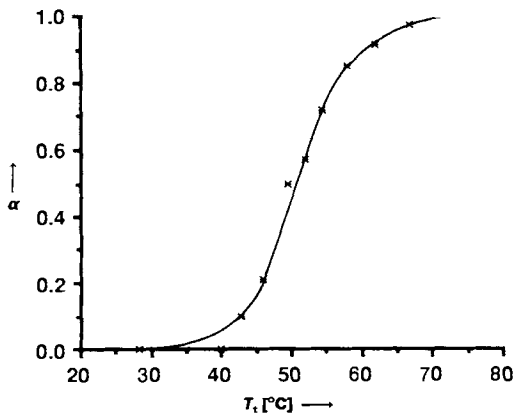

Fig. 18. Dependence of T_t on degree of ionization α for poly[0.8(VPGVG),0.2(VPGEG)] in 0.15 N NaCl. The acid–base titration was carried out at 37 °C. (From reference [35].)

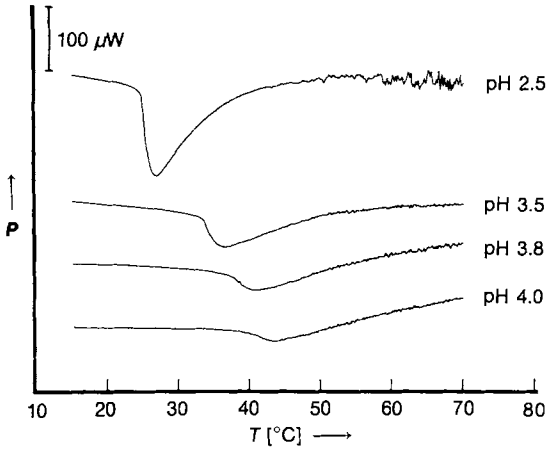

Fig. 19. Differential scanning calorimetry scans of poly[0.8(VPGVG), 0.2(VPGEG)] in water at several pH values. At pH 2.5 when essentially all Glu residues are present as COOH, the endothermic heat required to destructure the waters of hydrophobic hydration is 0.97 kcal per mol^{-1} pentamer. As the pH is raised producing more COO^- moieties, the temperature of the transition increases, consistent with the data in Figure 18, and importantly, the endothermic heat of the transition decreases. By the time there are less than 2 COO^- groups per 100 residues (pH 4.0), the heat required to destructure the waters of hydrophobic hydration is reduced to 0.27 kcal per mol^{-1} pentamer (from reference [36]). P = heat flow; a negative peak represents an endothermic process, a positive peak an exothermic process.

The T_t hydrophobicity scale of Table 1 shows that there is essential continuity from the most hydrophobic residues, Trp(W), to the most polar moiety, PO_4^{2-}. Charged species provide more extreme examples of the competition for hydration. Qualitatively, however, the same argument can be applied whenever an intrinsic chemical change to a more polar moiety results in an increase in the value of T_t.

7. Relative Efficiencies for Converting Chemical Energy into Mechanical Work (Motion)

Much is known about muscle contraction in terms of the sliding filament model in which actin filaments slide past myosin rods,[37] and a third elastic filament, titin, is probably important in the assembly process.[38] Nonetheless, there is considerable controversy about the source of force development. The prevalent swinging cross-bridge theory is being challenged by proposed length changes and force development in the myosin rods in one school[39] and in the actin filament in another.[40] Also, the calculation of efficiency requires more than merely the consideration of the ATP consumed at the filaments; the ATP equivalents required to achieve the important calcium ion concentration changes must also be considered.

It is possible to compare efficiencies of model systems. The charge–charge repulsion mechanism, represented by polymethacrylic acid, and the salt-dependent collapse of the collagen structure can be compared with phenomena observed with protein-based polymers. A measure of efficiency η can be the mechanical work achieved, which is the product of the force f and the displacement ΔL, divided by the chemical energy $\Delta\mu \cdot \Delta n$ expended in performing the work, where $\Delta\mu$ is the change in chemical potential discussed above and Δn is the change in number of moles for the intrinsic change. For example, Δn can be the number of moles of carboxylate groups (COO^-) changed to acid groups (COOH). The expression for efficiency therefore can be written as Equation (a).

$$\eta = \frac{f\Delta L}{\Delta\mu\Delta n} \qquad \text{(a)}$$

Fortunately, polymethacrylic acid (**1**) utilizes the same ($COOH/COO^-$) chemical couple as the protein-based polymer, poly[0.8(VPGVG),0.2(VPGEG)]. Also, the cross-linked matrices of both can contract to about one-half their extended length and can lift weights that are a thousand times greater than their dry weight. The numerators $f\Delta L$ are thus similar in magnitude.[41–43] Where the difference occurs is in the chemical energy required to achieve that work.

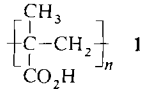

1

For polymethacrylic acid, extension due to charge–charge repulsion is achieved when 50 to 60% of the carboxyl groups are converted to COO^-, and the collapse of the extended state to achieve contraction is complete by 0 to 10% ionization.[41–43] Thus some 40 carboxylate groups must be protonated per 200 backbone atoms for complete contraction. For X^{20}-poly[0.8(VPGVG),0.2(VPGEG)], only 4 carboxylates per 300 backbone atoms need to be protonated for complete contraction. Thus, the Δn is more than ten times larger for the polymethacrylic acid system. Also, the change in the chemical potential $\Delta\mu$ of protons required to achieve any particular degree of ionization is greater for the charge–charge repulsion case (polymethacrylic acid) as shown in Figure 20.[1] The change in proton chemical potential to go from 50–60% to 0–10% ionization is some 2 pH units for polymethacrylic acid because of the negative cooperativity of the titration curve.[1,42] For the protein-based polymer, the titration curve exhibits positive cooperativity, and the change of only a fraction of a pH unit achieves the required change in degree of ionization. This comparison is summarized in Scheme 2. The conversion of chemical energy into mechanical work is thus over ten times more efficient for the ΔT_t mechanism than for the charge–charge repulsion mechanism.

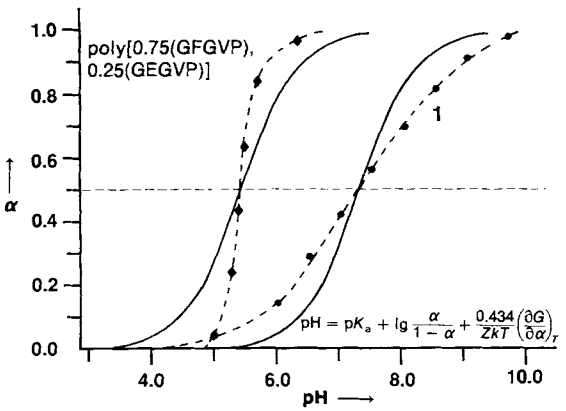

Fig. 20. Acid–base titration curves for poly[0.75(GFGVP),0.25(GEGVP)], which is steeper than the reference curve (solid line), and of polymethacrylic acid (**1**), which is less steep than the reference curve. The reference curves are calculated from the first two terms of the equation (bottom right). Whether the curve is steeper than the reference curve depends on the sign of $(\partial G/\partial\alpha)_T$, which is positive for apolar–polar repulsion and negative for the charge–charge repulsion. (From reference [1].)

η_{cc} = efficiency of charge–charge repulsion mechanism (as exemplified by polymethacrylic acid)
w: $\Delta L \approx 0.5$; $f \approx 1000 \times$ dry weight
Δn: > 40 ($COO^- \rightarrow COOH$) per 200 backbone atoms
$\Delta\mu$: ($\Delta\alpha \approx 0.6 \rightarrow \Delta pH \approx 2.0$) ≈ 2.8 kcal mol^{-1}

η_{ap} = efficency of apolar–polar repulsion free energy mechanism (as exemplified by X^{20}-poly[4(VPGVG),(VPGEG)])
w: $\Delta L \approx 0.5$; $f \approx 1000 \times$ dry weight
Δn: < 4 ($COO^- \rightarrow COOH$) per 300 backbone atoms
$\Delta\mu$: ($\Delta\alpha \approx 0.8 \rightarrow \Delta pH \approx 0.7$) ≈ 0.94 kcal mol^{-1}

Result: $\frac{\eta_{ap}}{\eta_{cc}} > 10$

Scheme 1. Comparison of the efficiency of chemomechanical transductions. For the definition of η see Equation (a) and the explanatory text.

It may be noted that just as polymethacrylic acid can be used as a model for charge–charge interaction, polymers such as poly(*N*-isopropylacrylamide) have been found to display inverse temperature transitions referred to as lower critical solution temperatures (LCST). For an extensive review, see Schild.[44] Related properties were observed because of the proper balance of apolar and polar moieties, but a ΔT_t-type of mechanism was not recognized, perhaps because of the more limited control of composition.

Complete salt-driven contraction can readily be achieved in X^{20}-poly(VPGVG) on going from 0 to 1 N NaCl, and even a change from 0 to 0.15 N NaCl can drive very effective contractions.[28] For contraction in collagen, special salts are required, such as LiBr and NaSCN, and urea. These solutes lower the temperature at which denaturation occurs. For LiBr, the best characterized case, the low concentration limit was 0 to 0.3 N, and the high concentration limit was 11.25 N.[45] Again, the change in chemical potential required to drive contraction was over an order of magnitude greater in the collagen model.

8. The ΔT_t Mechanism and Insight into Diverse Biological Penetralia

In the foregoing sections, the effect of changing proton concentrations and the equivalent of changing the p*K*a of a protonatable functional moiety provided ready illustrations of the ΔT_t mechanism. That proton gradients are a fundamental commodity in living organisms is well appreciated.

For example, in the Stryer encyclopedic biochemistry text it is emphasized that "...proton gradients are a central interconvertible currency of free energy in biological systems".[46a] In fact, Stryer shows that proton gradients are equivalent to each of the free energy apices of Figure 12 except the one involving pressure.[46b]

8.1. The ΔT_t Mechanism in Protein Folding and Assembly

In the ΔT_t mechanism decreasing proton concentration, for example, increases the number of polar COO^- groups, which in our interpretation destructures the more ordered water surrounding hydrophobic moieties, thereby removing the driving force for hydrophobic folding. Here an equivalence is drawn between the polar COO^- group and the even more polar phosphate group, PO_4^{2-}. As the phosphate group is several times more polar on the T_t-hydrophobicity scale (see Table 1), it is reasonable in the thylakoid membrane of chloroplasts that "...about three protons flow through the CF_1–CF_0 complex per ATP synthesized..."[47] ATP is adenosine triphosphate, the most generally recognized energy currency in living organisms, which is commonly used to phosphorylate proteins to activate them. ADP, adenosine diphosphate, is formed in the process.

8.1.1. Effect of Phosphorylation on an Elementary Depiction of Protein Folding

To depict the ΔT_t mechanism in protein folding, a clam-shaped globular protein is considered that can be in either of two states, open or closed (Fig. 21A). The conditions are such that the temperature for the inverse temperature transition T_t is below the working temperature. Therefore, the equilibrium lies on the side of the hydrophobically folded, closed state. When opened, the hydrophobic moieties become surrounded by more highly ordered water molecules; this is unfavorable as the system is above the transition temperature. On phosphorylation of the hydroxyl group near the cleft, the tendency of the negative phosphate group for hydration is so strong that it prevents the formation of the more ordered water around the sufficiently proximal hydrophobic moieties. The temperature for the hydrophobic transition is raised above the working temperature, and the equilibrium is now shifted to the open state.

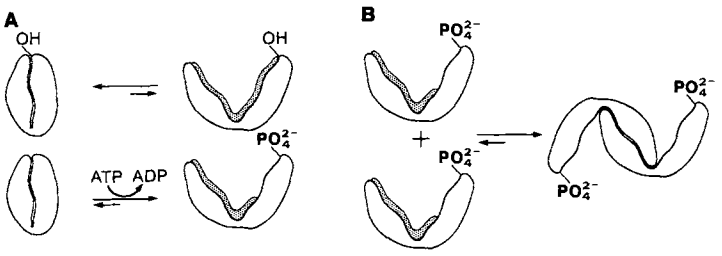

Fig. 21. A) Phosphorylation-driven unfolding illustrated for a hypothetical clam-shaped globular protein. Before phosphorylation the equilibrium lies on the left-hand side; after phosphorylation with ATP it lies on the right-hand side at the same temperature. For details see text. B) Phosphorylation-driven dimerization; for details see Section 8.1.3. The dotted region represents areas of hydrophobic hydration in A and B. (From reference [1].)

The effect of phosphorylation on T_t has been demonstrated with the elastic protein-based polymer, poly[30(IPGVG),(RGYSLG)],[24] where RGYSLG is a cyclic AMP-dependent protein kinase site from the enzyme, lysozyme.[48,49] In the buffer system for the kinase, T_t of the test polymer is 18 °C as shown in Figure 22. On introduction of the protein

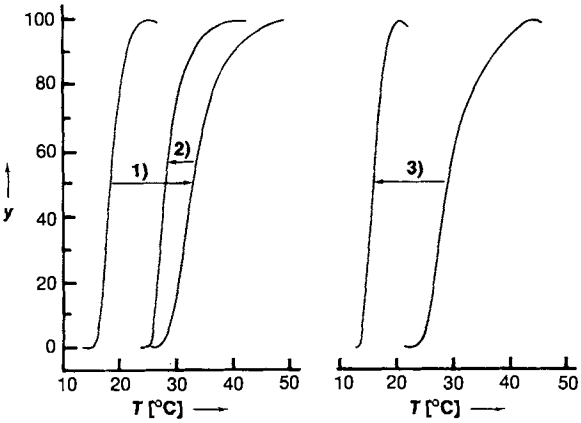

Fig. 22. Effect of protein kinase phosphorylation of the serine unit in RGYSLG on the temperature of the inverse temperature transition T_t in poly[30(IPGVG),(RGYSLG)]. 1) Protein kinase phosphorylation; 2) protonation, pH 7.3 → 2.0; 3) dephosphorylation by phosphatase (from reference [24]). y = % turbidity.

kinase and ATP, about 50% of the Ser residue of RGYSLG becomes phosphorylated, and the temperature of the hydrophobic folding and assembly transition is raised to 32 °C.[24] Thus at an intermediate temperature of 25 °C, one phosphate in three hundred residues would cause the unfolding of the elastic protein-based polymer. The formation of four COO^- moieties per hundred residues raised the transition temperature by 40 °C in poly[0.8(IPGVG),0.2(IPGEG)].[50] In terms of the hydrophobicity scale of Table 1, some four COO^- groups are equivalent to one phosphate group, and this is consistent with a ratio of three to four protons per phosphorylation, as in the case of the thylakoid membrane of chloroplasts.[43]

8.1.2. Heat-Shock Proteins, Chaperonins, and Biology's Modulation of Hydrophobic Folding

When *E. coli* bacteria are subjected to an abrupt increase in temperature, their response is to produce a set of proteins called heat-shock proteins (hsp). Consistent with the stabilization of hydrophobic folding on an increase in temperature, the hsp are uniquely involved in facilitating the transportation and folding of proteins in which hydrophobic associations are paramount. In terms of inverse temperature transitions and the ΔT_t mechanism, an increase in temperature would increase hydrophobic folding and could shift folding equilibria such that proteins could become trapped in nonfunctional, hydrophobically interacted states. This has brought to light a set of homologous proteins, called chaperonins,[51] from other organisms that function to assist protein folding by ATP modulation of hydrophobic association.

A complex process of modulating hydrophobic associations is the transport of proteins encoded in the cell nucleus

through the lipid bilayer of the outer mitochondrial membrane and the insertion of the properly folded state into the lipid layer of the inner mitochondrial membrane.[52, 53] The 70 kDa chaperonins, which provide that function, are released upon ATP hydrolysis. Presumably, phosphorylation disrupted the hydrophobic association. That phosphorylation indeed modulates the hydrophobic associations is more apparent in a series of chaperonin-assisted protein systems in which hydrophobic folding is directly implicated.

In the denaturation and refolding of protein or in the folding of a protein after its synthesis, the functional protein is understood to be the thermodynamically favored state of the protein.[54] Proteins, however, can become trapped in metastable states. Metastable hydrophobic associations with transition temperatures well below physiological temperatures could occur, and in our view the role of chaperonins is to tend these more hydrophobic domains of proteins until the appropriate circumstances are at hand when the more hydrophobic domains may form proper associations. The studies of Landry and Gierasch suggest that chaperonin 60 binds to the hydrophobic aspects of an α-helix from the enzyme rhodanese.[55] Studying T4-lysozyme interaction with chaperonin 70, Matsumura et al. [56] conclude that the preference is for interaction with aliphatic residues; the propensity for interaction is proportional to the likelihood of the residue being buried in the hydrophobic interior of the protein.

There is evidence that the associations of chaperonins with difficult-to-fold proteins is dominantly hydrophobic in nature, as well as good evidence that association is controlled by ATP hydrolysis, for example by phosphorylation. In a review Lorimer[51] states that "...The formation of native Rubisco (dimeric ribulose biphosphate carboxylase) from the binary chaperonin 60–Rubisco complex requires the presence of chaperonin 10 and MgATP.[57, 58] The hydrolysis of ATP appears necessary because nonhydrolyzable analogs do not support the reaction..." and later "...Of particular interest is the striking similarity between the structures of muscle actin (375 residues) and the ATPase fragment (386 residues) of chaperone 70.[59] This has prompted the intriguing idea that both proteins may share a similar mechanism for coupling the hydrolysis of ATP to the association–dissociation of protein–protein complexes". And finally Lorimer concludes in the abstract of the review, "Although this permits the mechanism of ATP hydrolysis to be understood at the atomic level, the manner in which this is coupled to folding, assembly, or release of the target protein remains obscure". The present review should remove that obscurity. ATP hydrolysis, for example phosphorylation, influences folding and assembly by removing of the thermodynamic driving force for hydrophobic association as depicted in Figure 21A.

The protein constructs can be such that phosphorylation disrupts or promotes hydrophobic folding and assembly, as shown in Section 8.1.3.

8.1.3. Elementary Depictions of Protein Assembly

The most obvious depiction of the effect of phosphorylation on hydrophobic assembly, the assembly/disassembly of a filament, is shown in Figure 23. The protein subunits, which do not have multiple conformations available, are capped on each end with hydrophobic surfaces that can be disrupted by phosphorylation. When the protein can exist in

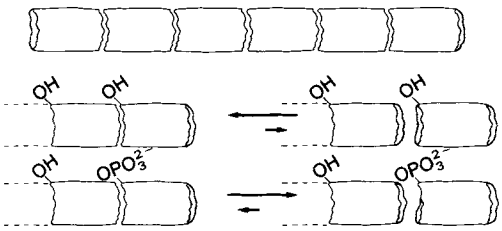

Fig. 23. Representation of the modulation of filament assembly by globular proteins capable of only a single conformation. Top: The ends of the globular proteins are hydrophobic; assembly (center) would therefore be the result of an inverse temperature transition. Phosphorylation is shown to shift the equilibrium away from filament formation, that is, phosphorylation leads to dissociation (bottom). This is the most elementary case. Often conformational changes occur such that phosphorylation can also lead to association as shown in Figure 24. (From reference [88].) The shaded areas represent a shell of clathrate water.

two states, open or closed, as shown in Figure 21A, additional possibilities exist. Even in the phosphorylated state there is still hydrophobic surface that is covered with more ordered water of hydrophobic hydration. As shown in Figure 21B, when the residual functional hydrophobic surfaces of the open state are complementary, phosphorylation can drive hydrophobic dimerization. With more complex structures having different conformational states available and more complex surfaces, filament formation, for example, could be driven by phosphorylation. Thus, as in microtubule growth and shortening,[60–62] the binding of GTP, an analog of ATP, could cause an unfolding and exposure of hydrophobic surfaces favoring tubule growth, whereas the conversion to the less polar GDP with but two phosphates could result in the formation of more stable dimers which would dissociate and cause a shortening of the tubule.

8.2. A Prototypic Sliding Filament Model of a T_t-type Molecular Machine

Instead of the hydrophobic folding depicted in Figure 5, a pair of filaments each with a hydrophobic surface could be responsible for the shortening process of contraction. This is equivalent to the straightening of the clam-shaped globular protein of Figure 21 to form a rod or filament as shown in Figure 24. Under conditions for optimizing hydrophobic overlap of two such rods, the structure on the upper right would be obtained. Due to hydrophobic hydration shown at the upper left, efforts to slide one rod or filament past the other would meet a resistance. The equilibrium would lie on

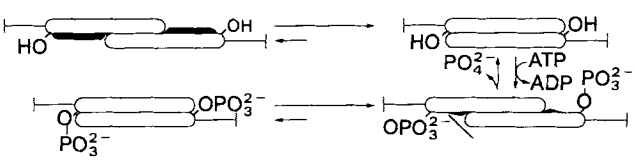

Fig. 24. Phosphorylation-driven extension in a prototypic sliding filament model. See text for discussion. (From reference [1].)

the side of maximal overlap, the contracted state. If the two filaments were phosphorylated as indicated in the lower part of Figure 24, sliding could occur with formation of an extended or relaxed state. Each filament could comprise different proteins, and even multiple proteins; cross-bridges could occur with complex hydrophobic interactions between filaments. However, the basis for interaction between filaments could be the ATP modulation of hydrophobic association, as crudely depicted in Figure 24. It would be a first-order molecular machine of the T_t type.

8.3. First-Order Molecular Machines of the T_t Type: Stretched Extracellular Matrix Causing Intracellular Chemical Response

The elastic protein-based polymeric matrix X^{20}-poly[0.8(VPGVG),0.2(VPGEG)], provides a direct demonstration that stretching of the elastic matrix can result in a chemical response. As shown in Figure 25, when this matrix is not under tension, the pK_a was determined by acid–base titration to be 3.99.[63] On application of the small force of 1 g to stretch the matrix, the pK_a increased to 4.84. At an intermediate pH of 4.5, the effect of stretching would be to take up protons as the chemically induced response of stretching.

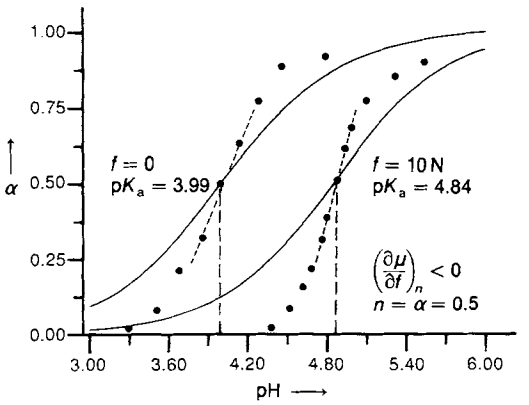

Fig. 25. Stretch-induced pK_a shift in X^{20}-poly[0.8(VPGVG),0.2(VPGEG)]. The solid curves are the reference curves as in Figure 20. The effect of an increase in force f is a decrease in the chemical potential μ of the protons required to maintain the elastic matrix at 50% ionization. Thus $(\partial\mu/\partial f)n$ is negative; the sign is exactly the opposite of that for the charge–charge repulsion mechanism, as seen in Figure 20. This defines the new mechanism. Of particular importance is the fact that the effect of the stretching (i.e. the increase in mechanical force) can be a chemical response. See the text for further details. Another feature to note in the data is that both before and after stretching the curves are steeper than the curve calculated from the first two terms of the equation in Figure 20. This positive cooperativity is due to the apolar–polar repulsive free energy of hydration. (From reference [63].)

As shown in Figures 15 and 16, with the appropriate design of the protein-based polymer the initial pK_a could be as high as 8 and stretching would raise the pK_a further. If, for example, the pK_a were 7 and the matrix were stretched to give a pK_a of 8, at physiological pH the effect would be the uptake of protons. By changing the functional group to that of a Lys residue, the direction of the shift would be reversed and the effect would be the release of protons. Thus the design of the stretchable matrix can determine the response that occurs in this mechanochemical transduction.

The increase in pK_a of a $COOH/COO^-$ chemical couple that occurs on stretching results, in our view, from the stretching of the hydrophobically folded matrix, which causes exposure of hydrophobic groups. Around these an ordered structure of water forms. Though there is more water in the matrix, it is unsuited for hydration of the polar COO^- moiety, and the free energy of this species increases as evidenced by the increase in pK_a. Similarly, the free energy of a peptide bearing a bound phosphate group could be expected to increase on stretching; accordingly, dephosphorylation would be a more likely response. It should even be possible to drive phosphorylation of another species by this increase in free energy of the phosphate. As a test of this, stretching of the X^{20}-poly[30(IPGVG),(RGYS(PO_4^{2-})LG)] matrix should drive the protein kinase reaction backwards and achieve phosphorylation of ADP. This test of the ΔT_t mechanism will be attempted once technical difficulties are overcome.

A clear picture is now emerging that in living cells tensional forces (stretching of the extracellular matrix to which the cells are attached) can signal intracellular chemical responses.[64] This is thought to involve receptors in the cell membrane, called integrins, which bind at specific attachment sites to proteins in the extracellular matrix. One such cell attachment sequence is the celebrated GRGDSP sequence of fibronectin, where RGD is the key sequence[65–69] to which fibroblasts and other cells attach. A related sequence in the protein laminin is a preferred site for endothelial cell attachment, which utilizes the vitronectin receptor as opposed to the fibronectin receptor.[70]

The attachment of a cell to a stretchable matrix is illustrated in Figure 26. The specific matrix is represented as X^{20}-poly[20(GVGVP),(GRGDSP)] to which cells have been shown to attach, spread, and grow to confluence.[71] In the natural tissue the attachment would be to proteins in the extracellular matrix where stretching can occur to the extent characteristic of the tissue. As depicted in Figure 26 a cell is attached to its matrix by means of two integrins within the cell membrane. Between the two attachment sites are cytoskeletal (muscle-like) fibers that contract relative to the

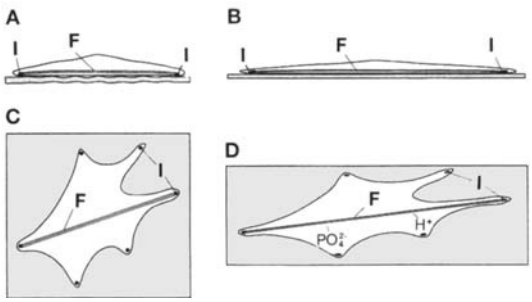

Fig. 26. Effect of stretching of a cell attached to an elastic substrate. A) Cross-section of a cell attached to the elastic matrix X^{20}-poly[20(GVGVP),(GRGDSP)] (shaded) as substrate by means of integrins (I), which bind to its cell attachment sites GRGDSP. Cytoskeletal fibers (F) contract between integrins and cause some buckling of the substrate. B) Cross-section of the elastic matrix when stretched. C) Top view of A. D) Top view of B. The tension in the cell is due to the stretching of the elastic matrix to which it is attached. The physical result is that the cytoskeletal fibers become stretched, and the integrins possibly also become deformed. For further details see text.

matrix causing some buckling. When the matrix is stretched, the cytoskeletal fibers are stretched, and the integrin itself could be deformed (shown by conversion from a spherical to an ellipsoidal shape). Since, as seen in Figure 25, stretching of X^{20}-poly[4(VPGVG),(VPGEG)] causes a chemical response, so too could stretching of the cellular components. Ingber states in his review[64] that "...mechanical stimuli can alter many cell functions, including ion transport, release of chemical second messengers, protein syntheses, secretion, and even expression of specific genes". In this way a cell can respond appropriately to maintain or remodel a tissue to meet the demands placed on it by the physical role that it must fill. Much earlier Glagov et al. showed that vascular wall cells (e.g., smooth muscle cells), when attached to purified internal elastic lamina of aorta and stimulated by subjection to cyclic stretching, produce the macromolecular components required of a vascular extracellular matrix.[72-74]

The stimulus for a cell to function in a manner appropriate to the tissue in which it resides could be provided by a first-order molecular machine of the T_t type. A tensional force could give rise to increased exposure of hydrophobic surfaces to effect a change in proton concentration with all of its possible ramifications.[46] As noted above, it could effect a more direct transferral of a phosphate moiety to activate a number of possible responses, or it could effect a release of Ca^{2+}, etc.

8.4. Second-Order Molecular Machines of the T_t Type: Oxidation of Food as Cells' Energy Source

Chemical energy arises from changes in chemical potential, that is, from concentration changes or concentration gradients. When thinking of chemical energy in food, one means the oxidation of the food giving rise to carbon dioxide, water, and energy, commonly viewed in terms of heat. But the oxidation of food results in the reduction of certain prosthetic groups, which in giving up their electrons to oxygen generate a concentration gradient of protons. This gradient in turn results in the formation of ATP, a more flexible, equivalent energy currency in living organisms (see Stryer[46a] for a general reference). This is called oxidative phosphorylation, and it involves the electron transport chain, a series of proteins with prosthetic groups that can be reduced and oxidized.

In Section 5.2 was given an example of a second-order molecular machine of the T_t type in which either the reduction of a nicotinamide moiety would result in proton uptake, or the protonation of a carboxylate group in an uptake of electrons. In the electron transport chain, the oxidation of a reduced nicotinamide or of a reduced flavine residue gives rise to proton release on one side of a cell membrane to produce a proton concentration gradient. In the second-order molecular machine of the T_t type of the proper design, oxidation of a reduced nicotinamide residue could result in the release of a proton. If that were done in the appropriate circumstance, as in the inner membrane of a mitochondrion, and the release were between the inner and outer membrane, this could generate a proton concentration gradient capable of production of ATP by phosphorylation of ADP. Again, the nature of the competition between polar and apolar moieties for hydration in macromolecules capable of inverse temperature transitions could explain another important free energy conversion of living organisms.

8.5. Medical Relevance to Elastin Fiber Formation and Pathology

Elastin is perhaps most noteworthy for its capacity to provide tissues with their required elasticity without contributing greatly to pathological and associated disease states. This is particularly true in view of the findings that it has a low turnover in the body. The half-life for elastin, as determined by three independent methods, is of the order of 70 years or more![75, 76] This implies a remarkable durability particularly in the aortic arch and thoracic aorta, where in that period of time the elastic fibers will have undergone some 2 billion demanding stretch/relaxation cycles.

There is indeed failure, however, from chronic processes such as a very slow pathological calcification but also sometimes from catastrophic occurrences, as in the dissecting aortic aneurysm. In the lung, which is chronically exposed to oxidizing and other toxic atmospheres, elastic fiber destruction can be severe resulting in pulmonary emphysema, which is responsible for more than 100000 deaths per year in the U.S. alone.

8.5.1. A New Perspective on Pulmonary Emphysema

Pulmonary emphysema is usually described as a biochemical process without a significant biophysical component. The biochemical process is characterized by decreased antiprotease activity allowing for proteolytic digestion and fragmentation of elastin fibers in the lung. In the genetic anomaly of deficiencies in α_1-antiproteases, pulmonary emphysema is the focal disease process, and it is generally thought that the primary process results from unchecked proteolytic digestion of elastin; but why does the primary disability occur in the lungs and not in the arteries where the demand for elastic function is so stringent?

On the basis of the ΔT_t mechanism, the primary insult can be the oxidation of the hydrophobically folded and assembled elastin fibers and the toxic reactions that result in more polar moieties, which lead to an increase in the value of T_t above physiological temperature and the unfolding of the protein. It would then be the partially unfolded protein that is susceptible to proteolytic digestion; otherwise, why would the lung be the tissue most notably affected by the genetic defect and why would this happen in a protein otherwise remarkable for its resistance to proteolytic degradation as evidenced by its long half-life for turnover even under demanding circumstances? That oxidants cause elastin fiber unfolding has been demonstrated in an experiment with an O_2^--generating system and hydrogen peroxide.[77] These oxidants can be released by a human macrophage attacking an airborne particulate in the lung and as a consequence also damage the elastic fibers by oxidation.

8.5.2. Absence of Elastin Fibers in Scar Tissue

In the wound repair response, the activity of prolyl hydroxylase is markedly elevated in order to hydroxylate the

prolyl residues of nascent collagen as required for the formation of a strong connective tissue. The same enzyme hydroxylates the prolyl residues of nascent elastin, but this raises its T_t above physiological temperatures, and elastin fibers do not form. This explains the paucity of elastin fibers in scar tissue.[77]

9. Biomimetics and Applications of Elastic Protein-Based Polymers

What has, in fact, been described while demonstrating the ΔT_t mechanism of free energy transduction is a new class of biomaterials. From the knowledge developed while detailing the T_t-based hydrophobicity scale and the numerous means of controlling the value of T_t, the new class of biomaterials can be designed for an extraordinarily diverse set of applications, both medical and nonmedical. At present there are twenty U.S. patents and patents pending, and additional patent coverage is being sought in Europe and the Far East. To date, only the earlier patents have been cited in the literature, and thus the new developments of this laboratory constitute the state of the art.

The medical applications under development include the use of the elastomeric matrices as a barrier for the prevention of adhesions following surgery and other trauma, the development of cell attachment matrices aimed at tissue reconstruction, and drug delivery using all the means of controlling T_t. The latter implies converting many free energies to useful mechanical work for releasing drugs as well as for controlling rates of their degradation. In nonmedical applications the concept of drug delivery can be extended to controlled pesticide release; in the general area of robotics the materials can simultaneously be sensor and actuator, utilizing the many forms of free energy transduction which can each be designed for diverse conditions—where chemomechanical transduction could occur, high efficiency, high sensitivity, and enzymatic specificity are anticipated. Also, the elastic matrix, being predominantly entropic in nature, is extraordinarily durable. As with the natural elastic fiber, which is a predominantly entropic elastomer having a half-life in the body of some seventy years,[75, 76] it has the potential to sustain billions of stretch–relaxation cycles.

9.1. Medical Applications

For use in the body a material must be biocompatible. For poly(GVGVP) and its cross-linked elastic matrix, X^{20}-poly(GVGVP), this has been determined. The series of recommended biological tests that have been utilized (the results are given in parentheses) include 1) the test for the Ames mutagenicity (nonmutagenic), 2) the cytotoxicity–agarose overlay (nontoxic), the tests for 3) acute systemic toxicity (nontoxic), and 4) intracutaneous toxicity (nontoxic), 5) muscle implantation (favorable), the tests for 6) acute intraperitoneal toxicity (nontoxic), 7) systemic antigenicity (nonantigenic), 8) dermal sensitization—the Magnusson and Kligman maximization method (nonsensitizing), and 9) pyrogenicity (nonpyrogenic), 10) Lee–White clotting study (normal clotting time), and 11) the in vitro hemolysis test (nonhemolytic). "Thus, this new elastomeric polypeptide biomaterial...exhibits an extraordinary biocompatibility".[78]

This degree of biocompatibility takes on added significance in view of the complications that have arisen with the use of silicon and polyurethane (for example, approval for use in breast implants has recently been withdrawn, etc.) and in view of the sensitization and allergenic responses to implants made of treated natural protein.

9.1.1. Prevention of Post-Surgical Adhesions

In the United States and Europe in the 60 million operations per year a potential postoperative complication is the formation of adhesions. The outcome of many of these could be improved with a material that would prevent or reduce the incidence of unwanted adhesions. The elastic protein-based polymers (in this context referred to as bioelastic materials) are being tested for efficacy in preventing adhesions in three different animal models: in the rat as a contaminated peritoneal model, in the rabbit eye in connection with strabismus and retinal surgical procedures, and in the calf for the use of the total artificial heart as a bridge to heart transplantation.

The studies are most advanced in the contaminated peritoneal model.[79] In 29 control animals adhesions formed, whereas with use of X^{20}-poly(GVGVP) sterilized with ethylene oxide gas, 80% of 29 animals showed insignificant adhesions (59% no adhesions, and 21% grade 1 adhesions). An example of a grade 1 adhesion is shown in Figure 27 in which the small sheet of X^{20}-poly(GVGVP) is seen against the abdominal wall, and a small band of adhesion is seen to have grown around the optically transparent matrix and attached to a loop of bowel.[80] No fibrous capsule had encased the bioelastic material as is usual for a foreign material; there is no inflammation of the abdominal wall where contact has been maintained for two weeks; and the adhesion is weak and can be detached with a light pull.[79]

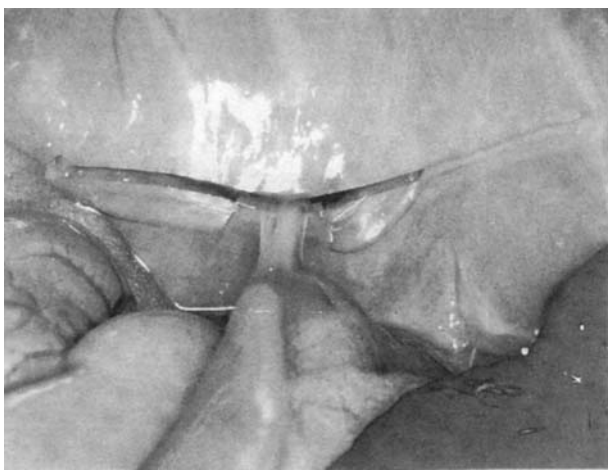

Fig. 27. View of the abdomen in which a sheet of X^{20}-poly(GVGVP) around which a strip of adhesion has grown lies against the abdominal wall. See text for discussion. (From reference [80].)

9.1.2. Cell Attachment Matrices and Tissue Reconstruction

While the simple matrix, X^{20}-poly(GVGVP), provides very poor support for cell attachment, inclusion of the cell attachment sequence, GRGDSP, as noted in Section 8.3, results in a matrix in which the cells can not only attach but can also spread and grow to confluence.[71,81] Shown in Figure 28 on the bioelastic matrix, X^{20}-poly[n(GVGVP), (GRGDSP)] (*n* ranges from 20 to 100), are low-density platings of bovine aortic endothelial cells (A) and *ligamentum nuchae* fibroblasts (B) that have grown to confluence at three days (C and D, respectively).

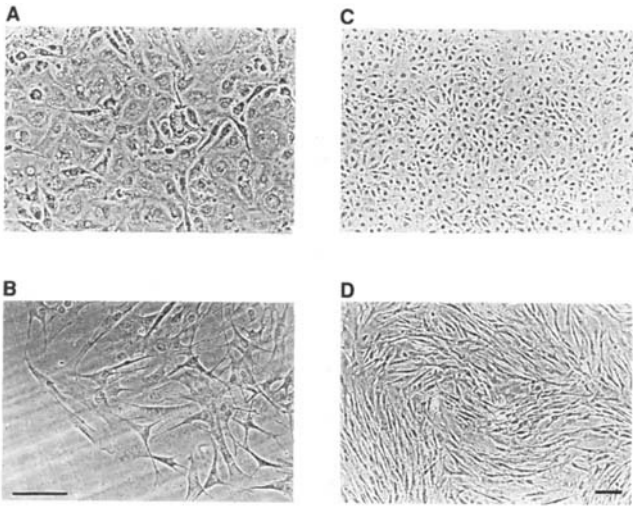

Fig. 28. Cell growth on the elastic matrices, X^{20}-poly[*n*(GVGVP),(GRGDSP)] (*n* is in the range of 20 to 100). A and C: bovine aortic endothelial cells: B and D *ligamentum nuchae* fibroblasts. In A and B the cells were plated at high density. In C and D they were plated at low density (1×10^4 cells per mL) and then allowed to grow to confluence over a period of three days. The cells are seen to adhere, spread, and grow to confluence. (From reference [71].) The bars in B and D represent 100 μm.

Recall the discussion in Section 6.1 in relation to Figure 26 in which a stretched extracellular matrix causes intracellular responses, and cells so stimulated produce the requisite macromolecules to sustain the applied forces. Based on this concept, the approach with the bioelastic materials is to design a biocompatible cell attachment matrix that can serve as a temporary functional scaffolding while being remodeled into a natural tissue appropriate for sustaining the stresses of its tissue site of function.

9.1.3. Drug Delivery

The opportunity of controlling T_t in bioelastic matrices offers the challenge of utilizing a most effective means to achieve a particular drug-delivery regimen.[82,83] Chemical clocks can be introduced with designed half-lives, which would initiate a contraction or a swelling to effect drug release. For example, depending on the sequence in which it is found, the carboxamide of asparagine, Asn(N), in phosphate-buffered saline will hydrolytically cleave to form aspartic acid, Asp(D).[84] At physiological pH, this conversion of a carboxamide to a carboxylate anion could then effect the change in T_t just as effectively as raising the pH.

One use of carboxamide ($CONH_2$) breakdown to carboxylate (COO^-) is illustrated in Figure 29 where the rate of drug release from a doped, homogenous slab depends on the half-life of the asparagine (Asn(N)) or glutamine (Gln(Q)) carboxamide.[82] Sequences containing the N or Q residues can be chosen so that the half-lives range from days to decades.[84] Additionally, linkages that have different rates of hydrolytic cleavage can be placed in the backbone of the protein-based polymer. In a series of recently synthesized protein-based polymers, half-lives ranging from days to tens of days have been obtained under conditions in which the half-life of the control, poly(GVGVP) or X^{20}-poly(GVGVP), appears to be in the range of many years.[83]

Given the many means of achieving the useful mechanical work of drug delivery depicted in Figure 12 (i.e., the set of arrows ending at the mechanical apex), an optimal means of delivery can probably be found for every situation. The delivery vehicle could be designed to release drugs in response to the chemical abnormality of the diseased tissue to be treated. And the delivery vehicle would degrade into amino acids and a sensor, which itself could be an amino acid or a natural prosthetic group.

The capacity to sense the altered chemistry of the diseased state and to respond with drug delivery has been called the diagnostic–therapeutic pair. In the case of specially designed elastic protein-based polymers, bioelastic materials, the first-order molecular machine could function by using the chem-

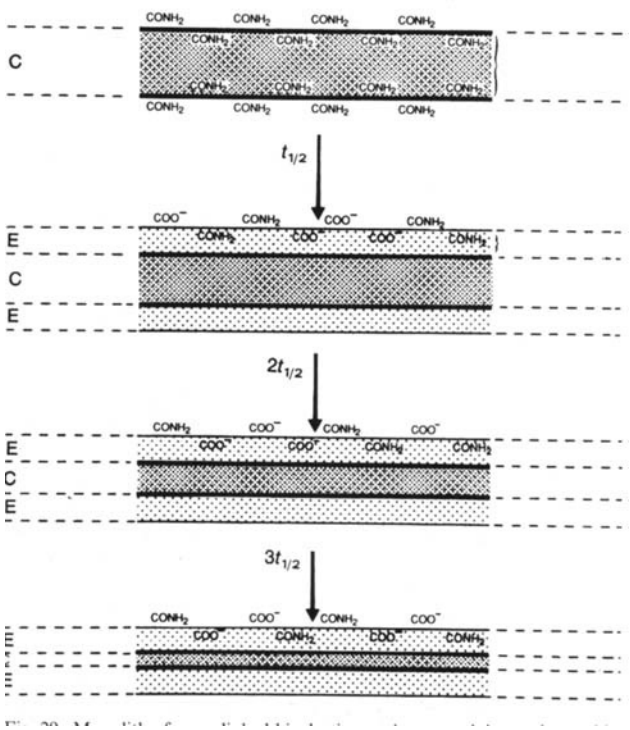

Fig. 29. Monolith of cross-linked bioelastic matrices containing carboxamide moieties from asparagine and glutamine residues (C). At the aqueous interface the $CONH_2$ groups hydrolytically cleave to yield carboxylates, which increases the T_t of the surface layer and causes its volume to swell to 10 times its original size (E). This allows, for example, for diffusional release of drug that had previously been doped in the slab. The rate at which the surface layer swells and the drug is released depends on the half-life $t_{1/2}$ of the Asn or Glu carboxamide; this can be controlled by the sequence in which it is placed. (From reference [89].)

ical energy provided by the difference in the chemical concentration of a substance in the diseased state to trigger the mechanical response that releases the drug. Since a change in the redox state can be used to drive a contraction or a swelling (see Section 5.1.1.3), such a system, if coupled to a redox enzyme such as glucose oxidase or glucose reductase, could utilize changed glucose concentrations to bring about release of the therapeutic agent. This approaches the ultimate objective of drug delivery, which by Pitt and Schindler's definition is "...to develop delivery systems which respond to the biochemical need for the drug, comparable to the way the human body exercises control over releases and distribution of its own endogenous biological agents".[85]

9.2. Nonmedical Applications

9.2.1. Biomimetics

Biomimetics may be considered the technique of mimicking or utilizing biological materials and processes. The purpose could be to obtain a substance with the *strength* of spider drag-line silk, or the *durability* of the biological elastomer, or the *toughness* of a composite ceramic represented by a seashell, or the special aqueous *adhesiveness* of the mussel protein glue. It could be used to design prosthetic materials as *temporary functional scaffoldings* for tissue reconstruction, as discussed in Section 9.1.2 for a medical application. Or it could be employed to obtain molecular machines with the *miniaturization* of the flagellar rotary motor, with the *efficiency* for energy conversion as in chemomechanical transduction (Section 7), with the *specificity* introduced by enzymes, with *reliability* to undergo many cycles of use, with the *sensitivity* of a channel function elicited by the stimulus of a chemical, light, a pressure change, etc., or with a *uniqueness* to utilize new sources of energy.

9.2.2. Reversible Mechanochemical Engines

In the McGraw-Hill *Concise Encyclopedia of Science and Technology*,[86] an engine is defined as "a machine designed for the conversion of energy into useful mechanical motion". When useful mechanical motion or work is performed by a first-order molecular machine of the T_t type, the machine is a reversible molecular engine. When the source of energy is chemical, the first-order molecular machine can be a reversible mechanochemical engine. These mechanochemical engines can use any of the intrinsic or extrinsic chemical concentration changes noted in Sections 4.1 and 4.2 to perform useful mechanical work. At one extreme, an engine could use the chemical concentration differences between fresh (river) water and sea water to drive a turbine. At another extreme, it could use specific enzyme sites to assay for specific enzyme activities. On the other hand, since the ΔT_t mechanism is reversible, mechanical work could be the energy input for chemical separations (e.g., desalination). These reversible mechanochemical engines are as diverse as the chemical energy inputs that can change the temperature T_t of the inverse temperature transition.

9.2.3. Transducers

A transducer is defined by Webster's *International Dictionary* as "a device actuated by power from one system and supplying power in the same or any other form to a second system...." The units of power are energy per unit time. Thus, the molecular machines of the T_t type, capable of the energy conversions depicted in Figure 12, could be called molecular transducers of the T_t type. The processes themselves have regularly been referred to as free energy transductions.

When the device operates on the principle of the elastomeric bands of Figure 13, it would be a low-power transducer because of the relatively long time to half contraction (on the order of minutes), but as with an elastomeric band the energy stress could be supplied over a period of time at fixed length, and then the snap-back of an elastomeric band on removal of the tension can be seen with response times of a fraction of a second. Also, with improvement in fabrication, the time constant of the elastomeric band construct could be shortened. Higher power molecular transducers of the T_t type require different concepts, such as the sliding filament design of Figure 24. This design would not be dependent on the slower folding and unfolding required for the transition from one structural state to another in Figure 5. The response time in striated muscle, a sliding filament device, is on the scale of fractions of a second. A similar time constant would be applicable to the flagellar rotary motor of bacteria.

As in the integration of the diagnostic–therapeutic pair into a single device to be used in drug delivery, here the integration of sensor and actuator into a single device is envisaged for applications in robotics.

9.2.4. Superabsorbents

The elastomeric sheets or viscoelastic materials normally consist of about 50% water by weight in their contracted or coacervate state, and they can be lyophilized to form dry paper-like or even Styrofoam-like states. When swollen, however, they can contain more than 90% water by weight. Accordingly, the materials are potential superabsorbents which could be triggered by any of the means for controlling the transition summarized in Figure 12; that is, these superabsorbent devices present an unusual control over the transition to the superabsorbent state.

Having discussed esoteric, perhaps even heady, devices this review can end at the opposite extreme with a more down-to-earth application, that of a biodegradable diaper. Consider the properties it could have: a capacity to absorb liquids ten times its own weight, a thermal control element where liquid would be drawn from warmer to cooler temperatures, a pressure response which could convert water to more dense states rather than squeeze it out as in a sponge, and a capacity to decompose within a selected period of time and in minutes with only mild chemical treatment.

10. Summary and Outlook

10.1. Summary

A series of model proteins has been studied which exhibits an increase in intramolecular and intermolecular order on increasing the temperature. This phenomenon is called an inverse temperature transition and the temperature at which it occurs is designated as T_t. The increase in order within the protein arises because the more ordered water molecules surrounding the hydrophobic moieties become less ordered bulk water as folding and assembly occurs, which is characterized by intra- and intermolecular contacts involving hydrophobic moieties. On cross-linking, elastomeric matrices are formed in which the inverse temperature transition is seen as a contraction capable of doing the useful mechanical work of lifting a weight against the gravitational force.

By carefully changing the amino acid composition of the model protein, the temperature T_t can be changed in a regular manner allowing a hydrophobicity scale to be developed for all of the natural amino acids. It is then seen that there are many ways of changing the value of T_t. Chemical changes in the model protein, such as changing the degree of ionization of a side chain, phosphorylating and dephosphorylating a serine side chain, or reducing an attached redox moiety (e.g., a nicotinamide) dramatically change the value of T_t, as do adding salts or organic solutes to the medium. Changing the pressure also changes the value of T_t.

Next, it is appreciated that lowering T_t from above to below a working temperature is equivalent to raising the temperature from below to above T_t. Thus, for the cross-linked matrices, all means of lowering the value of T_t become means for isothermally driving contraction and the performance of useful work. This means that the elastic matrices have become molecular machines capable of converting one form of free energy into another. With the inclusion of photochemical reactions, which has just been demonstrated, there are six forms of free energy that could be interconverted by the ΔT_t mechanism. The intensive variables for these free energies are mechanical force, temperature, pressure, chemical potential, electrochemical potential, and electromagnetic radiation. To our knowledge, these include all the free energy conversions of living organisms. Proteins that can carry out these energy conversions could be considered molecular machines. A device that operates by thermally driven contraction (folding) on raising the temperature is called a zero-order molecular machine of the T_t type. The other energy conversions resulting in contraction are called first-order molecular machines of the T_t type. Those energy conversions not involving mechanical force are called second-order molecular machines of the T_t type. While these conversions utilize the hydrophobic folding transition, mechanical force, the direct result of folding, is not one of the intensive variables involved. Thus, the ΔT_t mechanism is a unifying basis for diverse energy conversions.

The physical basis for the ΔT_t-type energy conversions is described as arising out of the competition of apolar (hydrophobic) and polar moieties for waters of hydration in polymers in which there are constraints on the distances between the moieties. An analysis is presented which shows that the ΔT_t mechanism for conversion of chemical energy into mechanical work is an order of magnitude more efficient than the charge–charge repulsion mechanism in aqueous systems.

It is then anticipated that, under the pressure of natural selection, living organisms would have evolved to utilize the most efficient mechanism available to its composition. Accordingly, this mechanism provides new insight into many not so readily explained biological processes. The correlation between the central role of phosphorylation in protein mechanisms and phosphorylation as the most dramatic chemical perturbation for changing the value of T_t is considered more than coincidental.

Finally, the potential medical applications of the new biomaterials that these elastic protein-based model proteins represent are considered. Discussions of applications include the prevention of postsurgical adhesions, tissue reconstruction, and drug delivery. And the potential of these materials as reversible mechanochemical engines and transducers is discussed briefly.

10.2. Outlook

The outlook challenges both basic research and applied research. There is the challenge to demonstrate each of the energy transductions of Figure 12 by designing the appropriate protein-based polymer and the requisite apparatus with which to study the energy conversion. There is the need to quantitate the apolar–polar free energies of repulsion for ionization of each relevant amino acid residue, to evaluate the effects of naturation/denaturation and purification, as well as of solutes on the hydrophobic folding and assembly process, to quantitate hydrophobic domain size and intensity for independence of hydrophobic domain folding and assembly, and to quantitate hydrophobicity-enhanced charge–charge interactions. There is also the need to study protein structure and function with the foregoing perspective. Specific questions might be: does phosphorylation (or ionization) of amino acid residues with shifted pK_a values disrupt hydrophobic associations?

The emergence of a new material is naturally associated with the search for applications. When the material appears capable of performing the many free energy transductions involving all of the intensive variables of mechanical force, temperature, pressure, chemical potential, electrochemical potential, and electromagnetic radiation, the number of opportunities increase. When the basic material is biocompatible and appears to function on the same principles as proteins, the number of potential medical applications alone becomes extraordinarily large. When the basic material is essentially ignored by the body but can be modified by introducing cell attachment sites, specific enzyme sites, natural chemical clocks, enzyme prosthetic groups, etc., to fill specifically defined functional roles, the opportunities seem limited only by the resources with which to pursue them. This capacity to start with an innocuous elastic protein-based polymer capable of exhibiting an inverse temperature transition and then to design-in any of many possible functions or combinations of functions provides exciting challenges for the future. In all of this there is the pleasure of turning concepts into molecular machines of practical value.

I wish to acknowledge the many members of the Laboratory of Molecular Biophysics, past and present, who have contributed so extensively to the work reviewed here. This research was supported in part by contract N00014-89-J-1970 from the Department of the Navy, Office of Naval Research, and by grant HL-29578 from the National Institutes of Health.

Received: August 17, 1992 [A 905 IE]
German version: *Angew. Chem.* **1993**, *105*, 859

[1] D. W. Urry, *Prog. Biophys. Mol. Biol.* **1992**, *57*, 23–57.
[2] A. Szent-Györgyi, *Acta Physiol. Scand.* **1945**, *9*, 1–116.
[3] D. W. Urry, M. M. Long, H. Sugano, *J. Biol. Chem.* **1978**, *253*, 6301–6302.
[4] L. B. Sandberg, N. T. Soskel, J. B. Leslie, *N. Engl. J. Med.* **1981**, *304*, 566–579.
[5] L. B. Sandberg, J. B. Leslie, C. T. Leach, V. L. Torres, A. R. Smith, D. W. Smith, *Pathol. Biol.* **1985**, *33*, 266–274.
[6] H. Yeh, N. Ornstein-Goldstein, Z. Indik, P. Sheppard, N. Anderson, J. C. Rosenbloom, G. Cicila, K. Yoon, J. Rosenbloom, *Collagen Relat. Res.* **1987**, *7*, 235–247.
[7] D. W. Urry, T. L. Trapane, K. U. Prasad, *Biopolymers* **1985**, *24*, 2345–2356.
[8] D. W. Urry in *Methods in Enzymology* (Eds.: L. W. Cunningham, D. W. Frederiksen), Academic Press, New York, **1982**, pp. 673–716.
[9] D. W. Urry, *Ultrastruct. Pathol.* **1983**, *4*, 227–251.
[10] D. W. Urry, K. Okamoto, R. D. Harris, C. F. Hendrix, M. M. Long, *Biochemistry* **1976**, *15*, 4083–4089.
[11] D. W. Urry, M. M. Long in *Elastin and Elastic Tissue* (*Adv. Exp. Med. Biol.* **1977**, *79*). pp. 685–714.
[12] D. W. Urry, T. L. Trapane, H. Sugano, K. U. Prasad, *J. Am. Chem. Soc.* **1981**, *103*, 2080–2089.
[13] W. J. Cook, H. M. Einspahr, T. L. Trapane, D. W. Urry, C. E. Bugg, *J. Am. Chem. Soc.* **1980**, *102*, 5502–5505.
[14] C.-H. Luan, N. R. Krishna, D. W. Urry, *Int. J. Quantum Chem. Quantum Biol. Symp.* **1990**, *17*, 145–159.
[15] M. V. Stackelberg, H. R. Müller, *Naturwissenschaften* **1951**, *38*, 456.
[16] M. M. Teeter, *Proc. Natl. Acad. Sci. USA* **1984**, *81*, 6014–6018.
[17] J. T. Edsall, H. A. McKenzie, *Adv. Biophys.* **1983**, *16*, 53–183.
[18] H. S. Frank, M. W. Evans, *J. Chem. Phys.* **1945**, *13*, 507–532.
[19] W. Kauzmann, *Adv. Protein Chem.* **1959**, *14*, 1–63.
[20] D. W. Urry, *J. Protein Chem.* **1988**, *7*, 1–34.
[21] D. W. Urry in *Molecular Conformation and Biological Interactions* (Eds.: P. Bararam, S. Ramaseshan), Indian Acad. Sci., Bangalore, India, **1991**, pp. 555–583.
[22] D. W. Urry, *Polym. Mater. Sci. Eng.* **1990**, *62*, 587–593.
[23] D. W. Urry, D. C. Gowda, T. M. Parker, C.-H. Luan, M. C. Reid, C. M. Harris, A. Pattanaik, R. D. Harris, *Biopolymers* **1992**, *32*, 1243–1250.
[24] A. Pattanaik, D. C. Gowda, D. W. Urry, *Biochem. Biophys. Res. Commun.* **1991**, *178*, 539–545.
[25] D. W. Urry, L. C. Hayes, D. C. Gowda, C. M. Harris, R. D. Harris, *Biochem. Biophys. Res. Commun.* **1992**, *188*, 611–617.
[26] C.-H. Luan, T. M. Parker, K. U. Prasad, D. W. Urry, *Biopolymers* **1991**, *31*, 465–475.
[27] D. W. Urry, L. C. Hayes, D. C. Gowda, T. M. Parker, *Chem. Phys. Lett.* **1991**, *182*, 101–106.
[28] D. W. Urry, B. Haynes, H. Zhang, R. D. Harris, K. U. Prasad, *Proc. Natl. Acad. Sci. USA* **1988**, *85*, 3407–3411.
[29] D. W. Urry, R. D. Harris, K. U. Prasad, *J. Am. Chem. Soc.* **1988**, *110*, 3303–3305.
[30] D. W. Urry, L. C. Hayes, D. C. Gowda, C. M. Harris, S. Q. Peng, R. D. Harris, unpublished results.
[31] D. W. Urry, L. C. Hayes, T. M. Parker, R. D. Harris, *Chem. Phys. Lett.* **1993**, *201*, 336–340.
[32] D. W. Urry, S. Q. Peng, T. M. Parker, *Biopolymers* **1992**, *32*, 373–379.
[33] D. W. Urry, D. C. Gowda, S. Q. Peng, T. M. Parker, R. D. Harris, *J. Am. Chem. Soc.* **1992**, *114*, 8716–8717.
[34] D. W. Urry, C. Sandorfy in *Drug and Anesthetic Effects on Membrane Structure and Function (Adv. Membr. Fluid. 5)*, **1991**, pp. 91–131.
[35] D. W. Urry, C.-H. Luan, B. A. Cox, "Proteins I: Structure, Hydrophobicity, Elasticity and Energy Conversion" in *Treatise on Bioelectrochemistry: Biomacromolecules, Vol. 4* (Ed.: G. Lenaz), Bologna, Italy, in press.
[36] D. W. Urry, C.-H. Luan, R. D. Harris, K. U. Prasad, *Polym. Prepr. Am. Chem. Soc. Div. Polym. Chem.* **1990**, *31*, 188–189.
[37] R. Cooke, *CRC Crit. Rev. Biochem.* **1986**, *21*, 53–118.
[38] J. Trinick, *Curr. Opin. Cell Biol.* **1991**, *3*, 112–119.
[39] G. H. Pollack, *Muscles & Molecules: Uncovering the Principles of Biological Motion*, Ebner & Sons, Seattle, WA, USA, **1990**.
[40] C. E. Schutt, U. Lindberg, *Proc. Natl. Acad. Sci. USA* **1992**, *89*, 319–323.
[41] A. Katchalsky, S. Lifson, I. Michaeli, M. Zwick in *Size & Shape of Contractile Polymers: Conversion of Chemical & Mechanical Energy* (Ed.: A. Wasserman), Pergamon, New York, **1960**, pp. 1–40.
[42] A. Katchalsky, *J. Polym. Sci.* **1951**, *7*, 393–412.
[43] W. Kuhn, B. Hargitay, A. Katchalsky, H. Eisenberg, *Nature* **1950**, *165*, 514–516.
[44] H. G. Schild, *Prog. Polym. Sci.* **1992**, *17*, 163–249.
[45] I. Z. Steinberg, A. Oplatka, A. Katchalsky, *Nature* **1966**, *210*, 568–571.
[46] a) L. Stryer, *Biochemistry*, 3rd ed., Freeman, New York, **1988**; b) ref. [46a], p. 423.
[47] Ref. [46a], p. 529.
[48] D. C. Phillips in *Lysozyme* (Eds.: E. F. Osserman, R. E. Canfield, S. Beychok), Academic Press, New York, **1974**, pp. 9–30.
[49] B. E. Kemp, E. Benjamini, E. G. Krebs, *Proc. Natl. Acad. Sci. USA* **1976**, *73*, 1038–1042.
[50] D. W. Urry, D. K. Chang,. H. Zhang, K. U. Prasad, *Biochem. Biophys. Res. Commun.* **1988**, *153*, 832–839.
[51] G. H. Lorimer, *Curr. Opin. Struct. Biol.* **1992**, *2*, 26–34.
[52] U. C. Manning-Krieg, P. E. Scherer, G. Schatz, *EMBO J.* **1991**, *10*, 3273–3280.
[53] P. J. Kang, J. Ostermann, J. Schilling, W. Neupert, E. A. Craig, N. Pfanner, *Nature* **1990**, *348*, 137–143.
[54] C. B. Anfinsen, *Science* **1973**, *181*, 223.
[55] S. J. Landry, L. Gierasch, *Biochemistry* **1992**, *30*, 7359–7362.
[56] M. Matsumura, W. J. Becktel, B. J. Matthews, *Nature* **1988**, *334*, 406–410.
[57] P. Goloubinoff, J. T. Christeller, A. A. Gatenby, G. H. Lorimer, *Nature* **1989**, *342*, 884–889.
[58] P. V. Viitanen, T. H. Lubben, J. Reed, P. Goloubinoff, D. P. O'Keefe, G. H. Lorimer, *Biochemistry* **1991**, *29*, 5665–5671.
[59] K. M. Flaherty, D. B. McKay, W. Kabsch, K. C. Holmes, *Proc. Natl. Acad. Sci. USA* **1991**, *88*, 5041–5045.
[60] T. Mitchison, M. Kirschner, *Nature* **1984**, *312*, 237.
[61] M. Kirschner, T. Mitchison, *Cell* **1986**, *45*, 329.
[62] R. A. Walker, E. T. O'Brien, N. K. Pryer, M. F. Soboeiro, W. A. Voter, H. P. Erickson, E. D. Salomon, *J. Cell. Biol.* **1988**, *107*, 1437–1488.
[63] D. W. Urry, S. Q. Peng, L. Hayes, J. Jaggard, R. D. Harris, *Biopolymers* **1990**, *30*, 215–218.
[64] D. Ingber, *Curr. Opin. Cell Biol.* **1991**, *3*, 841–848.
[65] E. Ruoslahti, M. D. Pierschbacher, *Science* **1987**, *238*, 491–497.
[66] C. A. Buck, A. F. Horwitz, *Annu. Rev. Cell. Biol.* **1987**, *3*, 179–205.
[67] M. J. Humphries, *J. Cell. Sci.* **1990**, *97*, 585–592.
[68] E. Ruoslahti, *J. Clin. Invest.* **1991**, *87*, 1–5.
[69] M. D. Pierschbacher, E. Ruoslahti, *Nature* **1984**, *309*, 30–33.
[70] M. D. Pierschbacher, E. Ruoslahti, *J. Biol. Chem.* **1987**, *262*, 17294.
[71] A. Nicol, D. C. Gowda, D. W. Urry, *J. Biomed. Mater. Res.* **1992**, *26*, 393–413.
[72] D. Y. M. Leung, S. Glagov, M. B. Mathews, *Exp. Cell Res.* **1977**, *109*, 285–298.
[73] D. Y. M. Leung, S. Glagov, M. B. Mathews, *Science* **1976**, *191*, 475–477.
[74] H. Holinsky, S. Glagov, *Circ. Res.* **1964**, *14*, 400–413.
[75] J. T. Powell in *The Cause and Management of Aneurysms* (Eds.: R. M. Greehalgh, J. A. Marrick), W. B. Saunders, London, **1990**, pp. 89–96.
[76] R. B. Rucker, D. Tinker, *Int. Rev. Exp. Pathol.* **1977**, *17*, 1–44.
[77] D. W. Urry, *J. Protein Chem.* **1988**, *7*, 81–114.
[78] D. W. Urry, T. M. Parker, M. C. Reid, D. C. Gowda, *J. Bioact. Compat. Polym.* **1991**, *6*, 263–282.
[79] L. D. Hoban, M. Pierce, J. Quance, I. Hayward, A. McKee, D. C. Gowda, D. W. Urry, T. Williams, *J. Surg. Res.* **1993**, in press.
[80] D. W. Urry, A. Nicol, D. C. Gowda, L. D. Hoban, A. McKee, T. Williams, D. B. Olsen, B. A. Cox, Biotechnology Polymers: Medical, Pharmaceutical and Industrial Applications in *Conferences in Print Series* (Eds.: C. G. Gebelein), Technomic, Lancaster, Pa, USA, **1993**, in press.
[81] A. Nicol, D. C. Gowda, D. W. Urry, *J. Vasc. Surg.* **1991**, *13*, 746–748.
[82] D. W. Urry in *Cosmetic and Pharmaceutical Applications of Polymers* (Eds.: C. G. Gebelein, T. C. Cheng, V. C. Yang), Plenum, New York, **1991**, pp. 181–192.
[83] D. W. Urry, D. C. Gowda, C. Harris, R. D. Harris, B. A. Cox, *Polym. Prepr. Am. Chem. Soc. Div. Poly. Chem.* **1992**, *33*, 84–85.
[84] A. B. Robinson, *Proc. Natl. Acad. Sci. USA* **1974**, *71*, 885–888.
[85] C. G. Pitt, A. Schindler in *Progress in Contraceptive Delivery Systems* (Eds.: E. Hafez, W. Van Os), MTP (Kluwer, Lancaster, Great Britain) **1980**, pp. 17–46.
[86] *McGraw-Hill Concise Encyclopedia of Science and Technology*, 2nd ed., McGraw-Hill, **1989**, p. 711.
[87] D. Volpin, D. W. Urry, I. Pasquali-Rochetti, L. Gotte, *Micron* **1976**, *7*, 193–198.
[88] D. W. Urry in *Protein Folding: Deciphering the Second Half of the Genetic Code* (Eds.: L. Gierasch, J. King), Am. Assoc. Sci., Washington, DC, **1990**, pp. 63–71.
[89] D. W. Urry, *Polym. Mater. Sci. Eng.* **1990**, *63*, 329–336.
[90] K. Kalyanasundaram, T. Colassis, R. Humphry-Baker, P. Savarino, E. Barni, E. Pelizzetti, M. Grätzel, *J. Am. Chem. Soc.* **1989**, *111*, 3300–3311.

Conjugated Enediynes—An Old Topic in a Different Light

By *Rolf Gleiter** and *Detlef Kratz*

If *Angewandte Chemie* had published "Highlights" twenty years ago, the topic of this article would certainly have been addressed then. The most recent reports from the research groups led by Nicolaou,[1] Diederich, [2] Vollhardt,[3] and Myers[4] prove that the chemistry of conjugated enediynes continues to flourish. What is more remarkable, however, is the difference in the goals of the investigations of enediynes then and now. Twenty years ago the syntheses of new $4n$ and $(4n + 2)$ π-electron systems and tetrahedranes were the main points under consideration; today's motivation for examining these compounds comes from natural products chemistry and from interest in new modifications of carbon.

Biologically Active Anticancer Antibiotics: Nicolaou et al. were not only the first to complete the synthesis of the anticancer antibiotic calicheamycin γ_1,[1a, d] indeed a preparative masterpiece, they also contributed to the understanding of the mode of action of the aglycon (**1**) responsible for the DNA cleavage.[1b, c] The incorporation of the enediyne unit in the ten-membered ring of the aglycon enhances the reactivity of the already labile planar 6 π-electron system; after activation by attack of a nucleophile, the triple bonds are even closer together and ring closure to give a 1,4-diradical (Bergman cyclization)[5] is induced. For the systematic study of the mechanism of DNA cleavage cyclodeca-3-ene-1,5-diyne (**2**) was prepared as the most strained member of a series of monocyclic conjugated enediynes; because of the short transannular distance between the triple bonds (d = 3.25 Å in **1**), its cyclization via the 1,4-diradical **3** to give tetralin (**4**) proceeds even at 50 °C. By determining the structures of a number of model compounds Nicolaou et al. were able to predict whether an enediyne would undergo Bergman cyclization at room temperature, and thus be a potential anticancer drug. The transannular separation of the triple bonds serves as the decisive parameter; in compounds in which $d < 3.2$–3.31 Å, spontaneous Bergman cyclizations can be expected.

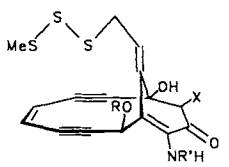

1

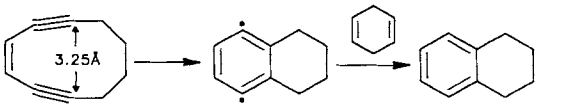

2 3 4 (55%)

Kinetics and Mechanism: First evidence that cyclization of conjugated enediynes proceeds via 1,4-didehydrobenzene intermediates like **6** was reported by Bergman et al. about twenty years ago[5] in an elegant study of the dideuterated parent compound, *cis*-hexa-3-ene-1,5-diyne (**5**). Recently, the same research group examined an expanded system, (*Z*,*Z*)-deca-3,7-diene-1,5,9-triyne (**7**), and proved that the analogous double cycloaromatization gives rise to 2,6-didehydronaphthalene (**9**),[6] which is isolated as naphthalene (**10**) after H abstraction from the solvent. The cyclizations of both **5** and **7** are first-order reactions. The rearrangement of **5** to give deuterated benzene proceeds almost quantitatively at 190 °C in dilute solution and has an activation energy of 32 kcal mol^{-1}. In contrast, the reaction of **7** (at 190 °C) provides naphthalene in only 10% yield.

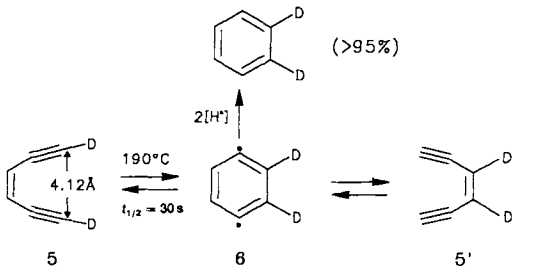

5 6 5'

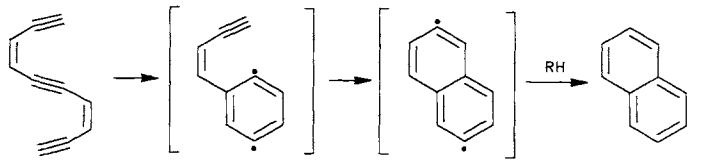

7 8 9 10 (10?

New Aromatic and Antiaromatic π Systems: A logical connection can be made here to the recently published work of Myers and Finney,[4] in which the extremely unstable 1,2,6,7-tetradehydro[10]annulene (**19**), which can be handled only at temperatures below −40 °C, also rearranges to give naphthalene as the stable, final product. The synthesis of the new [10]annulene is outlined in Scheme 1. Key steps include the Pd-catalyzed Heck coupling of **11** and **12** to give **13**, the chain extension by means of a Wittig reaction to furnish **16**, and the Cr^{II}-catalyzed ring closure to provide **18**. This last reaction proceeds in 40% yield, which is quite remarkable for a ring closure forming a ten-membered cycle.

The cyclization of the aromatic ten-membered ring compound **19** does not proceed by cisoid ring formation analogous to the reactions of **5** and **7** but by "diagonal" reaction to give the diradical 1,5-didehydronaphthalene (**20**),

[*] Prof. Dr. R. Gleiter, Dr. D. Kratz
Organisch-chemisches Institut der Universität
Im Neuenheimer Feld 270, D-W-6900 Heidelberg (FRG)
Telefax: Int. code + (6221) 56-4205

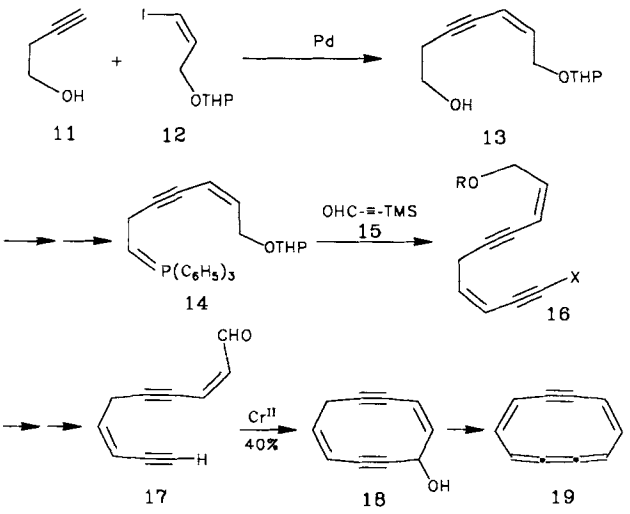

Scheme 1. THP = tetrahydropyran.

which reacts further by hydrogen abstraction to afford naphthalene. Considering that the "reactants" (alkyne and cumulene units) in **19** are held apart by approximately 3 Å by the allylic bridge, it is not so surprising that **19** undergoes the fastest diradical cycloaromatization reaction observed to date with an activation energy of only 16.4 kcal mol^{-1}.

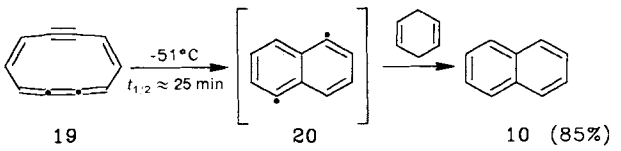

Interestingly, the activation energy for the formation of the diradical from the cumulene subunit in neocarcinostatin is close to that for **19**. This lends further support for the proposed mechanism of DNA cleavage by neocarcinostatin via an *anti*-configurated diradical. This type of ring formation corresponds to the analogous reaction of the nonisolable diyne **21** which can be trapped as the polycondensed aromatic compound zethrene (**22**)[7a, b] in what can be considered to be the "diagonal" version of the Bergman cyclization.

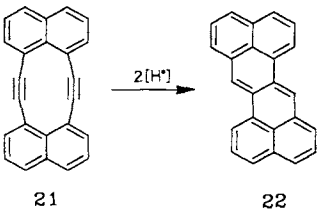

Orientation-Dependent Reactions of Triple Bonds: At this point we digress to briefly review some of the original studies of conjugated diynes and enediynes and pay tribute to the "Highlights" of 25 years ago. As early as 1956 Cram et al. reported attempts at cyclizing two parallel triple bonds to give a cyclobutadiene derivative.[8] Compounds with other connectivities of triple bonds as a function of orientation (yielding tetrahedrane or leading to linear *cis*- or *trans*-butadiene structures, see Scheme 2) were examined later by E. Müller et al., H. Staab et al., and H. W. Whitlock et al.[9–11] Progress in this field was achieved especially when the two C≡C bonds were attached to a rigid framework or built into a cycle, which fixed the bonds not only sterically but also held them closer together. The reactivity was increased as a result. In addition to these studies we should mention the work of Sondheimer et al.[12] and Eglinton, Raphael, et al.[13] which focused primarily on the relation between the aromaticity/antiaromaticity of these compounds and the number of π electrons in the cycle.

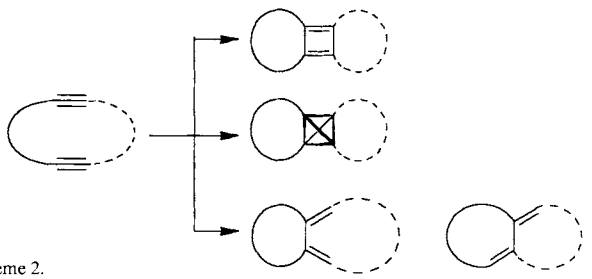

Scheme 2.

New Acyclic π Systems and [*n*]Phenylenes: Vollhardt et al. have extended the series of open-chain diyne compounds originally studied with the syntheses of persubstituted arenes with alkynyl substituents, for example, hexaethynylbenzene (**23**)[14] and more recently hexabutyldiynylbenzene (**24**).[3]

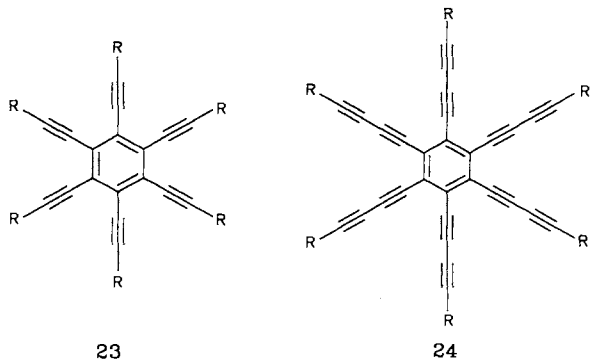

Scheme 3. **23**: $\lambda_{max} = 335$ nm; R = H, $SiMe_3$. **24**: $\lambda_{max} = 375$ nm; R = $Si(iPr)_3$.

The syntheses of these and related compounds is based on the multiple Heck couplings of the appropriate terminal alkyne with hexabromo- or hexaiodobenzene. There is no unequivocal evidence for delocalization of the electrons in the "in-plane" π orbitals of the six triple bonds similar to the apparent conjugation of the electrons in the benzene rings π MOs and those of the substituents. However, the redshift ($\Delta\lambda_{max} = 50$ nm) of all UV bands of the 54 π electron system of **24** relative to those arising from the 30 π electron system in **23** is striking. Arenes with *o*-ethynyl substituents may undergo multiple, simultaneous cyclization induced by transition metals to give polycycles such as [3]phenylene.[14b] It remains to be seen whether reaction of **24** will lead to the

synthesis of [6]phenylene (antikekulene), as Vollhardt has predicted. In contrast to the previously mentioned ring closures of enediynes via diradicals, reactions providing the [*n*]phenylenes, catalyzed by transition metal complexes such as $[CpCo(CO)_2]$, are typical trimerization reactions of triple bonds.

Diacetylenes and Poly(enediyne)s: For polymer chemists on the lookout for new materials, polymeric enediyne compounds continue to be of interest. The synthesis of these compounds relies on the solid-state intramolecular 1,4-addition of diacetylenes **25** to give poly(diacetylene)s **26**.[15a] The

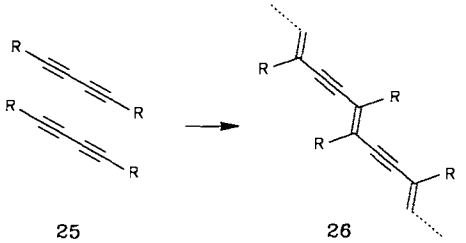

25 26

conjugated backbone of double and triple bonds in these compounds allows the extended delocalization of the π electrons, and as a result these compounds have interesting optical properties and absorb visible light.[15b,c] To better understand the spectroscopic properties of these one-dimensional poly(enediyne)s, the *cis*- and *trans*-linked oligomers **27** and **28** were prepared;[16,17] due to the improved solubility rela-

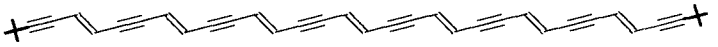

27 (λ_{max} = 454 nm)

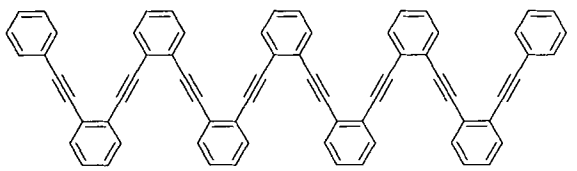

28 (λ_{max} = 388 nm)

tive to that of the polymers, these compounds could be characterized. The Pd-catalyzed Heck reaction of haloarenes and terminal alkynes was systematically applied, and because of the high yields of the individual reaction steps, sufficient amounts of the new oligomers were obtained. Compounds **27** and **28** each contain eight triple bonds, but whereas **28** has 70 conjugated π electrons and is only slightly colored (λ_{max} = 388 nm), the *trans*-substituted oligomer **27** has only 30 conjugated π electrons and is yellow (λ_{max} = 454 nm). This observation can be explained by the greater capacity of double bonds (compared to the π bonds of benzene) to contribute to delocalization. The two oligomers have similar thermal properties; investigations with DSC (differential scanning calorimetry) show that a strongly exothermic reaction takes place at higher temperatures (**27**: 204 °C; **28**: 286 °C), which produces black solids. Compounds **27** and **28** could serve as potential precursors for one- and two-dimensional graphite-like band structures; *inter*molecular reaction of **27** and domino-like *intra*molecular cyclization of **28** could lead to polyacenes or the previously mentioned [*n*]phenylenes, respectively. In this context, the all-*Z* isomer of **27** (**7** is a partial structure) would be a worthwhile target.

Graphite-like Structures: The extrapolation of the one-dimensional enediyne chains into two- and three-dimensional networks leads to the theoretically interesting graphite-related compounds proposed by Hoffmann, Kertesz, et al.[18] Recent work by Diederich et al. has brought the realization of these fascinating modifications of carbon one step closer.[19] Rational variations in the synthesis allowed the preparation of the silyl-protected derivatives (**29b–d**) of the cross-conjugated enediyne compound tetraethynylethylene (**29a**).[19c] The unprotected $C_{10}H_4$ compound could serve as a precursor for polymeric *peri*-naphthalene or naphthalene, though in this case double Bergman cyclization would be required, yielding 1,4,5,8-tetradehydronaphthalene, which would then undergo fourfold H abstraction to give **10**. The highly reactive cross-conjugated hydrocarbon **29a** polymerizes upon isolation. This feature is also common to compounds **2**, **5**, **7**, and **19**, and these compounds can only be obtained in dilute solution at low temperatures. Because of the high C/H ratio in the monomers one may assume that the resulting black polymers, which have not yet been characterized, have properties similar to those of graphite.

Diederich's goal is to systematically construct mono- and polycyclic units of the target carbon modification from the partially protected enediynes **29b–d**. Oxidative Hay coupling of the unprotected triple bonds leads to the cyclic derivatives of [12]annulene and [18]annulene, **30** and **31**,[2] respectively, or to open-chain compounds such as **32**,[19b] depending on the substrate employed. The extent of conjugation in **32** can be estimated by comparison of its UV/Vis spectrum (λ_{max} = 432 nm) with that of linear **27** (λ_{max} = 454 nm). As expected, the absorptions of the cyclic compounds are shift-

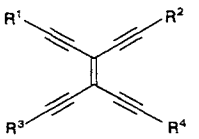

29a-d

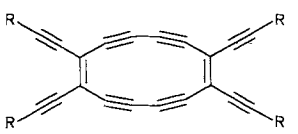

30 (λ_{max} = 680 nm)

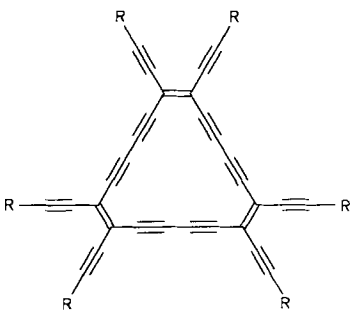

31 (λ_{max} = 480 nm)

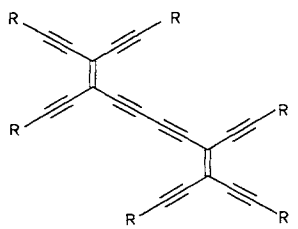

32 (λ_{max} = 432 nm)

Scheme 4. **29a**: $R^1 = R^2 = R^3 = R^4 = H$. **29b**: $R^1 = R^2 = Si(iPr)_3$, $R^3 = R^4 = H$. **29c**: $R^1 = R^3 = Si(iPr)_3$, $R^2 = R^4 = H$. **29d**: $R^1 = R^2 = R^3 = Si(iPr)_3$, $R^4 = H$.

ed to longer wavelengths as was already observed for the corresponding unsubstituted annulenes.[12] It is hoped that unusual modifications of carbon can be constructed from these intermediates after deprotection and renewed coupling of their terminal triple bonds. We hope that the synthesis of further intriguing enediynes will be reported in the near future.

German version: *Angew. Chem.* **1993**, *105*, 884

[1] a) K. C. Nicolaou, C. W. Hummel, E. N. Pitsinos, M. Nakada, A. L. Smith, K. Shibayama, H. Saimoto, *J. Am. Chem. Soc.* **1992**, *114*, 10083; b) K. C. Nicolaou, G. Zuccarello, C. Riemer, V. A. Estevez, W.-D. Dai, *ibid.* **1992**, *114*, 7360; c) K. C. Nicolaou, A. Liu, Z. Zeng, S. McComb, *ibid.* **1992**, *114*, 9276; d) K. C. Nicolaou, W.-M. Dai, *Angew. Chem.* **1991**, *103*, 1453; *Angew. Chem. Int. Ed. Engl.* **1991**, *30*, 1387.

[2] J. Anthony, C. B. Knobler, F. Diederich, *Angew. Chem.* **1993**, *105*, 437; *Angew. Chem. Int. Ed. Engl.* **1993**, *32*, 406.

[3] R. Boese, J. R. Green, J. Mittendorf, D. L. Mohler, K. P. C. Vollhardt, *Angew. Chem.* **1992**, *104*, 1643; *Angew. Chem. Int. Ed. Engl.* **1992**, *31*, 1643.

[4] A. G. Myers, N. S. Finney, *J. Am. Chem. Soc.* **1992**, *114*, 10986.

[5] a) R. R. Jones, R. G. Bergman, *J. Am. Chem. Soc.* **1972**, *94*, 660; b) R. G. Bergman, *Acc. Chem. Res.* **1973**, *6*, 25.

[6] K. N. Bharucha, R. M. Marsh, R. E. Minto, R. G. Bergman, *J. Am. Chem. Soc.* **1992**, *114*, 3120.

[7] a) R. H. Mitchell, F. Sondheimer, *Tetrahedron* **1970**, *26*, 2141; b) H. A. Staab, J. Ipaktschi, A. Nissen, *Chem. Ber.* **1971**, *104*, 1182.

[8] D. J. Cram, N. L. Allinger, *J. Am. Chem. Soc.* **1956**, *78*, 2518.

[9] E. Müller, J. Heiss, M. Sauerbier, D. Streichfuss, R. Thomas, *Tetrahedron Lett.* **1968**, 1195.

[10] a) H. A. Staab, H. Mack, E. Wehinger, *Tetrahedron Lett.* **1968**, 1465; b) J. Ipaktschi, H. A. Staab, *ibid.* **1967**, 4403.

[11] H. W. Whitlock, J. K. Reed, *J. Org. Chem.* **1969**, *34*, 875.

[12] W. H. Okamura, F. Sondheimer, *J. Am. Chem. Soc.* **1967**, *89*, 5991.

[13] O. M. Behr, G. Eglinton, A. R. Galbraight, R. A. Raphael, *J. Chem. Soc.* **1966**, 3614.

[14] a) R. Diercks, J. C. Armstrong, R. Boese, K. P. C. Vollhardt, *Angew. Chem.* **1986**, *98*, 270; *Angew. Chem. Int. Ed. Engl.* **1986**, *25*, 268; b) R. Diercks, K. P. C. Vollhardt, *ibid.* **1986**, *98*, 268 and **1986**, *25*, 266.

[15] a) G. Wenz, M. A. Miller, M. Schmidt, G. Wegner, *Macromolecules* **1984**, *17*, 837; b) A. D. Nava, M. Thakur, A. E. Tonelli, *ibid.* **1990**, *23*, 3055; c) R. J. Butera, B. Simic-Glavaski, J. B. Lando, *ibid.* **1990**, *23*, 199.

[16] R. H. Grubbs, D. Kratz, *Chem. Ber.* **1993**, *126*, 149.

[17] F. Wudl, S. P. Bitler, *J. Am. Chem. Soc.* **1986**, *108*, 4685.

[18] R. Hoffmann, T. Hughbanks, M. Kertesz, P. H. Bird, *J. Am. Chem. Soc.* **1983**, *105*, 4831; R. H. Baugham, H. Eckhardt, M. Kertesz, *J. Chem. Phys.* **1987**, *87*, 6687.

[19] a) F. Diederich, Y. Rubin, *Angew. Chem.* **1992**, *104*, 1123; *Angew. Chem. Int. Ed. Engl.* **1992**, *31*, 1101; b) A. M. Boldi, J. Anthony, C. B. Knobler, *ibid.* **1992**, *104*, 1270 bzw. **1992**, *31*, 1240; c) Y. Rubin, C. B. Knobler, F. Diederich, *ibid.* **1991**, *103*, 708 and **1992**, *30*, 695.

Light from Silicon—Renaissance of Siloxene and Polysilane?**

By *Christian Zybill** and *Vesselinka Petrova-Koch**

In crystalline silicon c-Si radiative recombination processes are only possible in limited amounts (quantum yields of ca. 10^{-4}%) as a result of the indirect band gap(s) $E_{g,\,ind.}$. Since, because $E_{g,\,ind.} = 1.11$ eV, the luminesence[1] does not lie in the visible spectral region, this semiconductor, otherwise so frequently used in microelectronics, is not suitable for optoelectronic applications. A solution is offered by the qualitative alteration of the Si band structure during the transfer to nanocrystalline structural units in the "quantum size regime" (i.e the range in which the size of the particles influences the physical and chemical properties) or by use of luminescent silicon molecular compounds.

The luminescence described here of porous silicon is caused essentially by emission from quantized states in the crystallite interior as well as from energetically low-lying states on the crystallite surface.

Since 1990, the scientific interest on the subject of "light from silicon" has increased exponentially. The reason for this was the observation[2a] of a red to green photoluminescence from nanoporous silicon, which is even visible to the naked eye at room temperature and has a quantum yield of several percent. This is comparable with the luminescence from GaAs, the most frequently used material for optoelectronic applications at present.

Thus, the luminescence–quantum yield of porous silicon is five orders of magnitude greater than that of c-Si. (Fig. 1, the scale of the intensity of the photoluminescence extends over six orders of magnitude). Furthermore, it was shown[2b–d] that the luminescence from the band (ca. 0.3 eV wide) can also be excited electrically; however, the quantum yields of the electroluminescence (10^{-3}%) are still relatively low. Thus, this result can be considered as a first step in the direction of optoelectronic building blocks based on silicon.

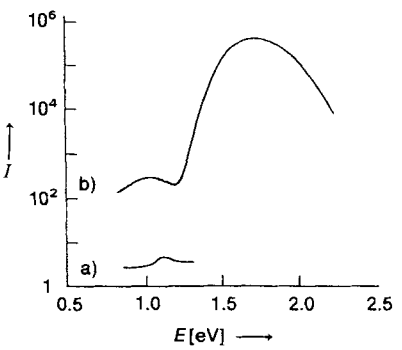

Fig. 1 The photoluminescence spectrum of porous silicon at 300 K (b) compared with that of c-Si (a) [12c]. The intensity I of the luminescence ($I = h\nu = \hbar\omega$ [eV]) extends over six orders of magnitude (Excitation: $\hbar\omega_L = 2.6$ eV = 500 mN cm^{-2}).

[*] Dr. C. Zybill
Anorganisch-chemisches Institut der Technischen Universität München
Lichtenbergstrasse 4, D-W-8046 Garching (FRG)
Dr. V. Petrova-Koch
Physik-Department der Technischen Universität München, E16
J. Franck-Strasse 1, D-W-8046 Garching (FRG)

[**] We wish to thank Prof. Dr. H. Schmidbaur, Prof. Dr. S. Vepřek, and Prof. Dr. F. Koch for valuable suggestions. Dr. E. Hartmann and Dipl.-Phys. M. Enachescu provided us with a 3D STM image of porous silicon.

Porous silicon is generally prepared by anodic etching of c-Si wafers in HF.[3] Investigations with transmission electron microscopy (TEM)[4a] and X-ray diffraction[4b] show that a self-organized nanostructure is thus formed (for a growth model see [5]). In the case of luminous porous silicon, it could be established empirically that crystallites with diameters of less than 50 Å are present. The form of these aggregates is, however, at present still under debate; quantum wires[2a] as well as so-called quantum dots and a quantum sponge have been proposed.[4a] It is, however, clear that these samples have an extremely large inner surface of several hundred m^2 per cm^3. This means that every tenth to hundredth(!) silicon atom is a surface atom. The inner surface is, after the preparation, initially passivated with hydrogen (SiH_x), which can be removed by thermal aftertreatment,[2d] UV irradiation,[6a] the use of electron beams,[6b] or by air oxidation (formation of a SiO_2 surface as dielectric matrix).

A fundamental electronic property of this new silicon modification discovered by Lehmann and Gösele (Fig. 2) is the blue shift of the UV absorption edge by several hundred meV[5, 6c] in comparison to that of c-Si. This effect is greater than that observed, for example, for amorphous silicon a-Si:H. The blue shift of the absorption edge[6c, 9] can only be a result of quantum size effects on the energy states in the crystallite interior. By effective mass and tight binding calculations of the state density of porous silicon this effect can be confirmed quantitatively.[7]

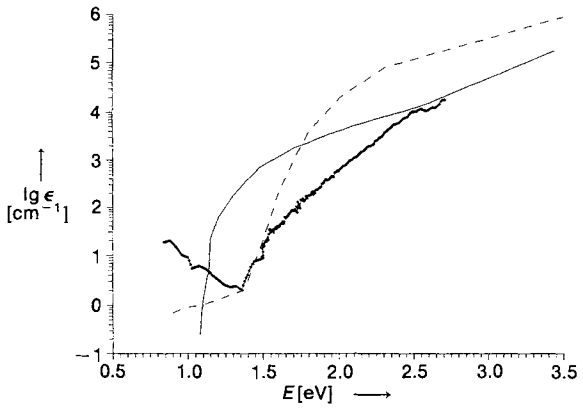

Fig. 2. The absorption edge of porous silicon (···) compared with that of c-Si (—) and that of a-Si:H (- -) according to [6c]. ε = absorption coefficient.

The most interesting electronic property of porous silicon is its photoluminescence. The mechanism of the photoluminescence is very complex, and separate experimental results appear at first to be contradictory. In the initial phase of the investigations this fact has led to the assumption of up to 13 hypotheses, which, however, can be based on three theoretical models. The first group includes models that ascribe the luminescence to recombination processes from quantum states in the interior of quantum wires[2a] or quantum dots.[2c] The second approach is completely different and is based on the assumption that luminescent molecules such as polysilanes[8a] or siloxenes are found on the inner surface of porous silicon.[8b] Besides these two extreme points of view, more recently several hypotheses were proposed and summarized to give a third model.[6c] This considered, above all, discrete, energetically low-lying states on the crystallite surface (surface states) together with quantized states in the crystallite interior. As a result of new important experimental findings this third polycausal approach has become more and more likely.

The following experimental results speak against the second approach, namely that silicon-containing molecular compounds are present on the surface of porous silicon:

- An important counterargument is that the luminescence quantum yield of porous silicon and that of thermally oxidized (O_2) porous silicon (transformation of the hydrogenated SiH_x surface into an oxidized SiO_2 surface) are almost identical.[9a] As is generally known, a surface film from SiO_2 shows, however, no red luminescence.[9b] A convincing counterargument is also that nanocrystalline Si layers[9c] deposited by CVD and thermally oxidized with O_2 as well as Si crystallites dispersed in ethylene glycol and oxidized show similar luminescence behavior.[9d]
- On resonance excitation satellite bands are observed within the luminescence band, which confirm a moment-conserving phonon participation in the optical transitions.[9e] These results are clearly in accord with the occurrence of recombination processes from energy states in the crystallite interior, but do not mean that siloxenes or polysilanes do not participate in luminescence processes.

Now let us consider the proof for energy states on the crystallite surface (model 3). Discrete surface states of lower energy can play an important role in recombination processes, and a series of experimental results can only be understood by the occurrence of such surface states:

- Raman spectroscopic studies on porous silicon show the Si–Si vibrational modes typical for small crystallites at 510–520 cm^{-1}. Furthermore, a broadened Si–Si vibrational band shifted to 480 cm^{-1} is observed by IR spectroscopy (which is more sensitive to the surface), which can be explained by reconstruction of the Si–Si bonds on the crystallite surface. This surface reconstruction similarly leads to a broadening of the Si–H vibrational band in porous silicon in comparison with that of an ideal Si–H vibrational mode.[9f]
- On the crystallite surfaces considerable quantities of "dangling bonds" (very stable Si radicals) can be detected by ESR,[10a] ODMR (optical detection of magnetic resonance), and SDPC (spin-dependent photo-conduction) measurements.[10b] This also agrees with a significant absorption below 1.11 eV in the spectrum of porous silicon, which can only be explained by the existence of deep crystal defects in the band gap. The concentration of Si radicals (dangling bonds), determined by ESR measurements, for samples with optimal luminescence is 10^{16} cm^{-3}; a value which in turn is higher than that for amorphous a-Si:H. The spin density of porous silicon is increased up to 10^{19} cm^{-3} by degradation processes; the luminescence yield of these samples is inversely proportional to the spin density.
- Furthermore, the UV absorption edge of porous silicon changes significantly on saturation of the samples with H_2 (reaction of the radicals with the formation of Si–H bonds). The crystallite size remains unchanged. This is in agreement with the existence of discrete states on the crystallite surface, as discussed in reference [6c].

- Also "tight binding" calculations (which only consider the interactions with the nearest neighbors) confirm the occurrence of surface states (in the form of a reconstruction of the crystallite surface), which lie energetically lower than the quantum states of the crystallites.[11]
- In addition, a red shift of the luminescence is observed on low-temperature oxidation (with constant crystallite size) or on aftertreatment of porous silicon, for example with propanol.[12a]
- Finally, there is a great similarity between the time-resolved photoluminescent behavior of porous silicon and that of a-Si:H.[9b] In amorphous silicon radiative recombination occurs—as proven—through so-called flat localized states ("Urbach tail").

A more exact analysis of the time-, temperature-, and wavelength-dependence of the luminescence behavior of porous silicon shows that several mechanisms are active.

Apart from the above-mentioned luminescence band, porous silicon shows two further bands (Fig. 3). The band 2

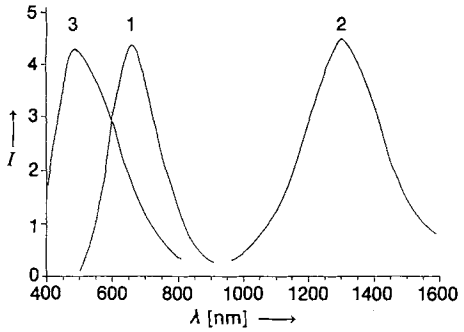

Fig. 3. Schematic representation of the three luminescence bands of porous silicon observed so far: 1: the red bands with slow decay times [2a,9e], 2: the IR band, which was first observed at 4.2 K [12b], and 3: the green-blue band [9e,12d] with rapid decay times.

lies in the region 0.8–1.2 eV [12b, c] and was already observed in 1984 in photoluminescence investigations at 4.2 K, which in the meantime has been almost forgotten. Furthermore, by photoluminescence spectroscopy with different retardation times an additional luminescence band 3 at 2.3–2.5 eV was observed.[12d, e] A special property of this band in the blue region is its extremely rapid decay time (10 ns or less in contrast to a few μs for the luminesence of band 1). It could be shown that also the rapid decay of the luminescence of the band 3 is intrinsic for porous silicon.[12e] Model approaches[6c, 13] provide preliminary explanations for the rapid luminescence (in the range of ns). However, for a better understanding of the three luminescence processes, especially of the latter two mentioned, still many investigations are necessary. All three observed luminescence channels can be of practical significance.

Silicon-containing molecular compounds—siloxenes and polysilanes: What are siloxenes? A siloxene is a layered polymer of $Si_6H_3(OH)_3$. Characteristic for siloxene is probably the partial retention of Si–Si bonds in Si_6 rings, which are saturated by hydrogen substituents and linked together.

Siloxene is prepared by a topochemical hydrolysis reaction from $CaSi_2$, which in all probability also has a layered structure of Si_6 rings. Siloxene samples were described about 130 years ago by Wöhler,[14a] and later by Hönigschmidt[14b] and Kautsky.[14c, d] The structural model with Si_6 rings, proposed by Kautsky and Hengge, was further refined by Weiss et al., who carried out X-ray structural investigations; however, the model has still not been completely proven since to date no suitable single crystals have been obtained.[14e]

A detailed investigation of the photoluminescence properties of siloxenes is mainly the result of work by Hengge.[14f, g] Renewed, intensive investigations and quantum mechanical calculations[15] on siloxenes have been in progress for about two years. The most important experimental result obtained is the observation of a luminescence quantum yield in the percent range, which is comparable to that of porous silicon,[16] and it is this behavior that has led to the renaissance of siloxene research.

Generally, the prepared siloxene samples are polycrystalline and undergo slow hydrolytic decomposition in the air. For siloxene samples that were annealed at temperatures of up to 400 °C, however, luminescence intensity (for shift of the peak position) remains almost unchanged.[12a]

These results show that despite structural rearrangements the luminescence is retained. The cause of the luminescence of siloxenes as well as the structure of these compounds (do in fact only Si_6 rings occur or are there also larger silicon clusters present?) are by no means completely explained. The question must be posed whether the luminescence from siloxenes cannot also be ascribed to a nanostructure comparable to porous silicon.

Indeed, based on preliminary investigations by SAXS (small angle X-ray scattering), in siloxene structural domains of the size of 15–20 Å can be proven.[17] These contradictory results certainly require further intensive reseach, including a possible examination of the structure of the radiative samples.

Furthermore, polysilanes are of interest as an additional class of molecular model compounds. For example, from the pioneering work by West on cyclohexasilanes, it is known that these form relatively stable radical anions and cations ($g = 2.0044$, dodecamethylcyclohexasilane, UV spectrum: $\lambda_{max} = 248$ nm, $\varepsilon_0 = 5400$, $\lambda_{max} = 256$ nm (sh), $\varepsilon_0 = 1100$), in which, according to results from ESR spectroscopy, the SOMO (semi-occupied molecular orbital) is delocalized over the whole Si_6 skeleton.[18] According to investigations by Miller, Michl et al. polysilanes also show luminescence already at 293 K, albeit at 340 and 450 nm (excitation wavelength = 390 nm) with some astonishingly high quantum yields up to 70% and with a lifetime in the 0.1 ns range for the shortwave band. The mechanism of the luminescence of long-chain polysilanes has been studied in detail.[19]

Considering the complex set of questions that still need to be answered, there is a significant overlap of molecular chemistry and solid-state physical problems, which can only be resolved by intensive cooperative work of chemists and physicists in this area.

Although the single models in future may require some modification, one thing is certain: Both porous silicon and nanocrystalline silicon in dielectric matrix, as well as silicon-containing molecular compounds such as siloxene and polysilane luminesce with similar quantum yields to GaAs!

The specific applications for which these materials are suitable will be shown by future developments.

German version: *Angew. Chem.* **1993**, *105*, 887

[1] In this article the term (photo)luminescence is used exclusively; that is, no distinction is made between fluorescence and phosphorescence.

[2] a) L. T. Canham, *Appl. Phys. Lett.* **1990**, *57*, 1046; b) A. Richter, P. Steiner, F. Kozlowski, W. Lang, *IEEE Electron Device Lett.* **1991**, *12*, 691; c) N. Koshida, H. Koyama, *Appl. Phys. Lett.* **1992**, *60*, 347; d) V. Petrova-Koch, A. Kux, F. Müller, T. Muschik, F. Koch, V. Lehmann, *Mater. Res. Soc. Symp. Proc.* **1992**, *283*, in press.

[3] A. Uhlir, *Bell Syst. Tech. J.* **1956**, *35*, 333.

[4] a) V. Lehmann, H. Cerva, *Mater. Res. Soc. Symp. Proc.* **1992**, *256*, 2; b) V. Lehmann, B. Jobst, T. Muschik, A. Kux, V. Petrova-Koch, *Jpn. J. Appl. Phys.*, **1993**, *32*, 23.

[5] V. Lehmann, U. Gösele, *Appl. Phys. Lett.* **1991**, *58*, 856.

[6] a) R. T. Collins, M. A. Tischler, J. H. Stathis, *ibid.* **1992**, *61*, 1649; b) J. Christen, V. Petrova-Koch, V. Lehmann, T. Muschik, A. Kux, M. Grundmann, D. Blomberg, *21st ICPS, Beijing, August* **1992**; c) F. Koch, V. Petrova-Koch, T. Muschik, A. Nikolov, V. Gavrilenko, *Mater. Res. Soc. Symp. Proc.* **1992**, *283*, 197.

[7] S. Y. Ren, J. D. Dow, *Phys. Rev. B: Condens. Matter* **1992**, *45*, 6492.

[8] a) S. Prokes, O. J. Glembocki, V. M. Bermudez, R. Kaplan, L. E. Friedersdorf, P. C. Searson, *Phys. Rev. B: Condens. Matter* **1992**, *45*, 1378. b) M. S. Brandt, H. D. Fuchs, M. Stutzmann, J. Weber, M. Cardonga, *Solid State Commun.* **1992**, *81*, 307.

[9] a) V. Petrova-Koch, T. Muschik, A. Kux, B. K. Meyer, F. Koch, V. Lehmann, *Appl. Phys. Lett.* **1992**, *61*, 943; b) T. Muschik, V. Petrova-Koch, V. Lehmann, B. K. Meyer, F. Koch, unpublished results; c) M. Rückschloss, B. Landkammer, O. Ambacher, S. Veprek, *Mater. Res. Soc. Symp. Proc.* **1992**, *283*, 65. d) K. A. Littau, P. J. Szajowski, A. J. Müller, A. R. Kortan, L. E. Brus, *J. Phys. Chem.* **1993**, *97*, 1224; e) P. D. Calcott, K. J. Nash, L. T. Canham, M. J. Kane, D. Brumhead, *J. Phys. Cond. Matter* **1993**, *5*, L91; f) G. S. Hiyashi, Y. Y. Chabal, G. W. Trucks, K. Raghavachari, *Appl. Phys. Lett.* **1990**, *56*, 656.

[10] a) H. Linke, P. Omling, B. K. Meyer, V. Petrova-Koch, T. Muschik, V. Lehmann, *Mater. Res. Soc. Symp. Proc.* **1992**, *283*, 251; b) M. S. Brandt, M. Stutzmann, *Appl. Phys. Lett.* **1992**, *61*, 2569.

[11] V. Gavrilenko, P. Vogl, F. Koch, *Mater. Res. Soc. Symp. Proc.* **1992**, *283*, 431.

[12] a) A. Kux, F. Müller, F. Koch, *Mater. Res. Soc. Symp. Proc.* **1992**, *283*, 311; b) C. Pickering, M. I. J. Bealöe, D. J. Robbins, P. J. Pearson, R. Greef, *J. Phys. C: Solid State Phys.* **1984**, *17*, 6535; c) M. Stutzmann, J. Weber, M. S. Brandt, H. D. Fuchs, M. Rosenbauer, P. Deak, A. Höpner, A. Breitschwerdt, *DPG-Frühjahrsber.*, Regensburg, **1992**; d) A. V. Adrianov, P. I. Kovalev, V. B. Shuman, I. D. Yaroshetskii, *JETP Lett.* **1992**, *56*, 236; e) V. Petrova-Koch, T. Muschik, D. I. Kovalev, F. Koch, V. Lehmann, *Mater. Res. Soc. Symp. Proc.* **1992**, *283*, 179.

[13] S. B. Zhang, Chin-Yuyeh, A. Zunger, Materials Research Society meeting in Boston, December **1992**, conference abstracts.

[14] a) F. Wöhler, *Liebigs Ann. Chem.* **1863**, *127*, 264; b) O. Hönigschmid, *Monatsh. Chem.* **1909**, *30*, 509; c) H. Kautsky, *Z. Anorg. Allg. Chem.* **1921**, *117*, 209; d) Kolloid-Z. **1943**, *102*, 1; e) A. Weiss, G. Beil, H. Meyer, *Z. Naturforsch. B* **1980**, *35*, 25–30. f) E. Hengge, *Chem. Ber.* **1962**, *95*, 645, 648; g) E. Hengge, K. Pretzer, *ibid.* **1963**, *96*, 470.

[15] D. Deak, M. Rosenbauer, M. Stutzmann, J. Weber, M. S. Brandt, *Phys. Rev. Lett.* **1992**, *69*, 2531.

[16] "Siloxene" samples luminesce typically in the spectral range of 700–740 nm; the position of the emission maximum is a function of the pronounced substituent effects as well as of the preparation process. In the work from Weiss et al. [14e], in particular, the intercalation of solvent molecules between the layers is studied.

[17] H. Franz, V. Petrova-Koch, T. Muschik, V. Lehmann, J. Peisl, *Mater. Res. Soc. Symp. Proc.* **1992**, *283*, 133.

[18] R. West in *Comprehensive Organometallic Chemistry* (Eds.: G. Wilkinson, F. G. A. Stone, E. W. Abel), Pergamon, **1982**.

[19] J. Michl, J. W. Downing, T. Karatsu, A. J. McKinley, G. Poggi, G. Wallraff, R. D. Miller, *Pure Appl. Chem.* **1988**, *60*, 959.

Models for Peptide Receptors

By *Hans-Jörg Schneider**

The development of selective host compounds for reversible binding of peptides is one of the most interesting fields in biomimetic chemistry. The topic is of importance for the understanding of molecular recognition mechanisms including those in proteins, for analytical methods, which incorporate sensor technology, and for the preparation of stereochemically pure peptides. The efficient preparation of peptides with a completely or partially "nonnatural" configuration[1] is a particularly attractive research area in medicinal chemistry because of the enormous diversity of biological activity of many oligopeptides. The therapeutically important stability of peptides against proteases, which often degrade the peptides, administered, for instance, as antibiotics, before they reach their target, can be significantly improved by the introduction of D-amino acids instead of L-amino acids.

In view of this importance and of the early success of the "chiral resolution machine" of Cram et al.,[2] which uses crown ethers containing bisnaphthyl units to separate amino acids, it is somewhat surprising that the selective complexation of peptides by organic host compounds has not yet been attempted on a very broad scale. The major noncovalent interactions for peptides have been analyzed by D. H. Williams et al. for the example of natural host vanomycin (**1**),[3] which binds the carboxylate terminus of Ala-Ala sequences of a peptidoglycan precursor compound (highlighted in boldface superimposed on the structural formula of **1**). A model limited predominantly to the carboxylate binding niche of this antibiotic was obtained by Hamilton et al.[4] in the form of compound **2**; the NMR spectrum of this model compound shows that a proton is transferred from bound

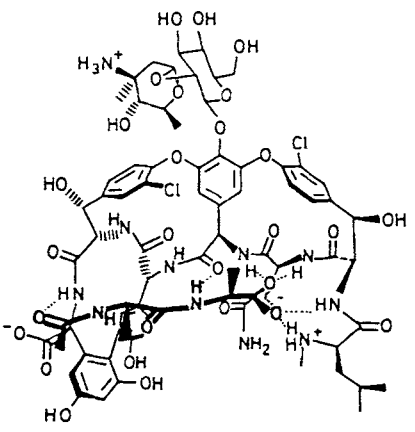

1

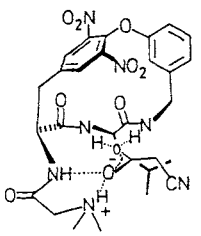

2

[*] Prof. H.-J. Schneider
Fachrichtung Organische Chemie der Universität
D-W-6600 Saarbrücken 11 (FRG)
Telefax: Int. code + (681)302-4105

carboxylic acids (e.g., the cyanoacetic acid superimposed on the structural formula of **2**) to its dimethylamino terminus.

Rebek et al. have developed systems like **3** from Kemp's acid and diaminonaphthalenes or *para*-phenylenediamine as spacer between the converging diimidelactam units. The energy difference for the binding of enantiomers of rigid diketopiperazines in systems with 2,6-dimethylnaphthalene as spacer can be up to 2.5 kcal mol^{-1},[5a] but for more flexible peptides (e.g., with *para*-phenylenamine as spacer) this reduces to about 0.5 kcal mol^{-1}.[5b] The association constants in chloroform are maximally $K = 4700\,\text{M}^{-1}$; in general they are smaller for imides than for amides.[5c] For normal amide groupings, the analysis of a large number of supramolecular associations in chloroform as solvent yields—in the absence of additional effects—a common binding energy of (1.2 + 0.2) kcal mol^{-1} or $K \cong 10\,\text{M}^{-1}$ for each hydrogen bond formed.[6]

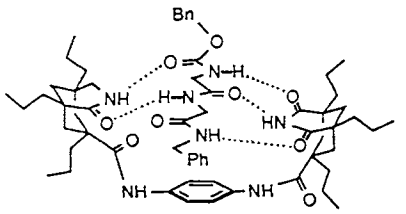

3

Crown ethers bearing amino acids as substituents were also used for the binding of peptides. Thus, according to Žinič et al.[7], the "lariate" ether **4** serves as "symporter" for the simultaneous binding of a potassium ion and a dipeptide carboxylate: for transport, enantiomer ratios sym_l/sym_d of 1.6 (for amino acid derivatives) are achieved. NMR measurements also show anisochronism, but binding constants for the associates have not yet been determined.

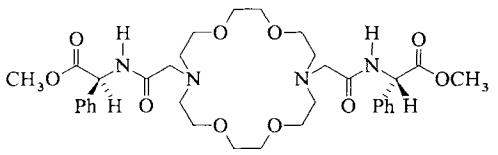

4

C. Still et al.[8] of Columbia University, New York, have been most intensely involved with the development of macrocyclic host compounds for the enantioselective complexation of peptides. Whereas the mono- and semicyclic receptors employed earlier, like **5** (X = SO_2),[8a] still show only relatively modest preferences of up to 80% *ee* between peptidic ammonium ions, not only because of their high conformational flexibility, $\Delta\Delta G$ values of over 3 kcal mol^{-1} have already been accomplished with the basketlike tricyclic model **6** (X = S).[8b] The host **6** binds Boc-protected peptides with the small NHMe end groups close to its phenyl rings. The L isomer is consistently preferentially bound; at the same time the host discriminates between side chains of Ala, Val, and Leu, for instance.

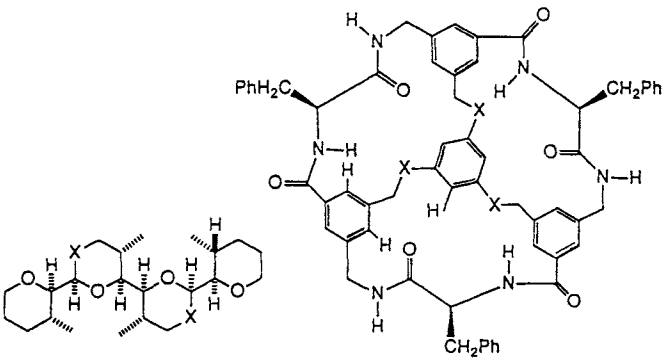

5 **6**

Most recently Still et al. have made a further breakthrough with the polycyclic receptor **7**,[8c] which not only displays similar enantioselectivities also for N-acylated and Boc-protected peptides, but also can be synthesized surprisingly easily: The condensation of Boc-protected (*R*,*R*)-1,2-diaminocyclohexane (H_2B) with pentafluorophenyl esters of trimesic acid ($A(OH)_3$) (Scheme 1) gives a 39% yield of the desired cyclooligomer **7**; even the treatment of the commercially available free diamine H_2B with trimesic acid trichloride ACl_3 affords in one step a yield of 13% that is still very acceptable when compared with many macrocyclizations! The bonding energies show a preference for L configurations,

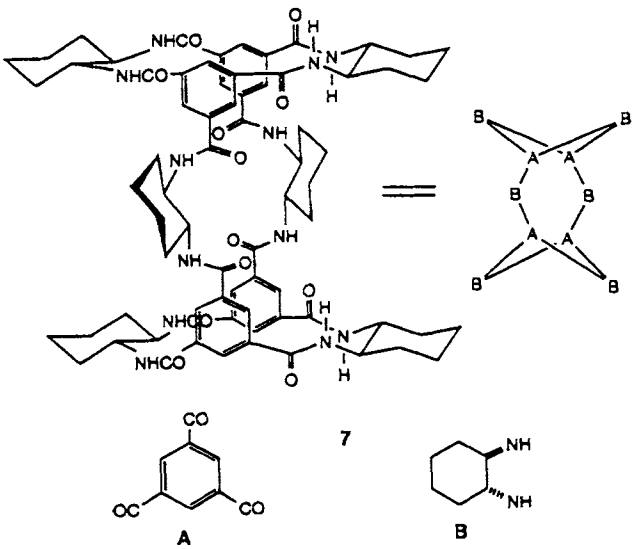

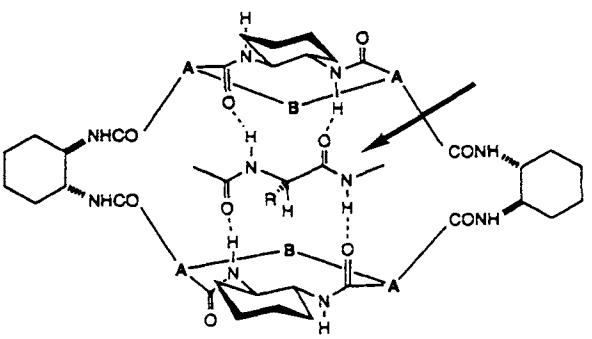

Scheme 1. Top: Structural formula and schematic representation of **7**; bottom: **7** with peptide guest (arrow).

which increases with the size of the side chain, for example, from 1.9 for Gly through 3.5 for Ala to 5.0 for Val (in each case in kcal mol^{-1} for the relevant *N*-acyl-NHMe-dipeptide in chloroform). One explanation for this could be that the side chain contributes significantly to the binding through van der Waals forces with the host's phenyl rings—on this subject, see the analyses of the binding of **1** by Williams et al.[3c]—or that the solvent molecule (chloroform) no longer finds space in the cavity next to, for example, the small glycine residue. The geometries of the complex were consistent with the results of force field simulations, and supported experimentally by the upfield shifts $\Delta\delta$ of the protons that are in contact with the host's phenyl rings, which are induced by the ring current (e.g., $\Delta\delta = 2.5$ for the valine methyl proton).

The possible applications of host compounds that are easy to synthesize, capable of immobilization, and able to separate peptides with over 99% *ee* are apparent. In what direction should future research go? Extension to larger peptides is desirable—although the system **7** binds even tripeptides very efficiently, the application of synthetic large-cavity complexes will probably reach a limit set by preparative considerations. The differentiation of the peptide termini, that is the direction of the sequence, might be achieved by the introduction of terminal anionic and/or cationic groups into the receptor. For preparative applications, receptors that can also be used on a larger scale for the separation of diastereomers would be welcomed. More difficult is the development of compounds that also function in aqueous medium. The rational design of new synthetic peptide receptors and antibiotics from them, as well as the efforts to understand biological systems will necessitate the increased application of physical and calculational methods. Finally the implementation of signalling functions—in the simplest case chromophoric elements—is a crucial step to turn the promising systems into actual receptors in the biological sense and to make them applicable for sensor technology.

German version: *Angew. Chem.* **1993**, *105*, 890

[1] See, for example, G. Jung, A. G. Beck-Sickinger, *Angew. Chem.* **1992**, *104*, 375; *Angew. Chem. Int. Ed. Engl.* **1992**, *31*, 367.

[2] D. J. Cram, J. M. Cram, *Acc. Chem. Res.* **1978**, *11*, 8.

[3] a) D. H. Williams, J. P. Waltho, *Pure Appl. Chem.* **1989**, *61*, 585; b) *Biochem. Pharmacol.* **1988**, *37*, 133; c) D. H. Williams, J. P. L. Cox, A. J. Doig, M. Gardner, U. Gerhard, P. T. Kaye, A. R. Lal, I. A. Nicholls, C. J. Salter, R. C. Mitchell, *J. Am. Chem. Soc.* **1991**, *113*, 7020, and references therein.

[4] A. D. Hamilton, N. Pant, A. V. Muehldorf, *Pure Appl. Chem.* **1988**, *60*, 533; N. Pant, A. D. Hamilton, *J. Am. Chem. Soc.* **1988**, *110*, 2002.

[5] a) K.-S. Jeong, A. V. Muehldorf, J. Rebek, Jr., *J. Am. Chem. Soc.* **1990**, *112*, 6144; b) M. Famulok, K.-S. Jeong, G. Deslongchamps, J. Rebek, Jr., *Angew. Chem.* **1991**, *103*, 880; *Angew. Chem. Int. Ed. Engl.* **1991**, *30*, 858; c) K.-S. Jeong, T. Tjivikuva, A. Muehldorf, G. Deslongchamps, M. Famulok, J. Rebek, Jr., *J. Am. Chem. Soc.* **1991**, *113*, 201; W. L. Jorgensen, D. L. Severance, *ibid.* **1991**, *113*, 209.

[6] H.-J. Schneider, R. K. Juneja, S. Simova, *Chem. Ber.* **1989**, *122*, 1211.

[7] a) M. Žinić, L. Frkanec, V. Škarić, J. Trafton, G. W. Gokel, *Supramol. Chem.* **1992**, *1*, 47; b) *J. Chem. Soc. Chem. Commun.* **1990**, 1726.

[8] a) G. Li, W. C. Still, *J. Org. Chem.* **1991**, *56*, 6964; b) J.-I. Hong, S. K. Namgoong, A. Bernardi, W. C. Still, *J. Am. Chem. Soc.* **1991**, *113*, 5111; c) S. S. Yoon, W. C. Still, *ibid.* **1993**, *115*, 823.

Tantalum(v) Phosphinidene Complexes as Phospha-Wittig Reagents**

By *Philip P. Power**

The report by Schrock et al.[1] describing the synthesis of tantalum phosphinidene complexes and their behavior as phospha-Wittig (or phosphinidene transfer) reagents will undoubtedly have a major impact in several areas of inorganic and organometallic chemistry. The title compounds, which have the formula **1**, R = Ph, *cyclo*-C_6H_{11}(Cy), or *t*Bu, are the first stable examples of electron-rich (or nucleophilic) phosphinidene complexes. In this manner, they are analogous to the Schrock-type carbenes,[2] and distinct from the transient phosphinidene complexes of low-valent transition metals.[3] The latter species contain an electrophilic phosphorus center and are thus analogous to the Fischer carbene complexes, which contain an electrophilic carbon center.[4] Stable phosphinidene transition metal complexes were originally reported by Lappert et al. in 1987,[5,6] but these and subsequent reports[7,8] employed large groups such as 2,4,6-*t*Bu$_3$C$_6$H$_2$ at the phosphorus center to ensure stability. In contrast, the new tantalum phosphinidene complexes **1** are stable with much smaller substituents at phosphorus such as Ph, Cy, and *t*Bu. In these tantalum complexes the stability has been ascribed to the use of the amido N_3N ligand. This trinegative, tetradentate amido ligand has enabled the isolation of some remarkable trigonal monopyramidal metal complexes with empty apical coordination sites.[9] When bound to tantalum, the ligand forms a protective pocket owing to the "upright" orientation of the three R_3Si substituents, yet, the ligand also permits access to the tantalum atom through the clefts between the arms of N_3N ligand. In addition, access to the phosphorus atom is possible owing to the relatively small organic substituents. Furthermore, the thermal stability of the complexes is such that

[(N$_3$N)Ta=PR] **1**

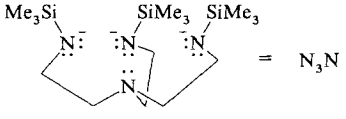

[*] Prof. P. P. Power
Department of Chemistry, University of California
Davis, CA 95616 (USA)
Telefax: Int. code + (916)752-8995

[**] The term phosphinidene is used here instead of the less common IUPAC term λ^3-phosphandiyl.

1, R = Ph can be heated for 12 h at 100 °C without observable decomposition.

The synthesis of the new complexes can be summarized by Equations (1) and (2). Phosphine elimination reactions similar to that in Equation (2) have been observed in silicon–phosphorus[10] and boron–phosphorus compounds.[11]

$$Li_3(N_3N) + TaCl_5 \xrightarrow[-3\,LiCl]{Et_2O,\ -78 \rightarrow -25\,^\circ C} [(N_3N)TaCl_2] \quad (1)$$

$$[(N_3N)TaCl_2] + 2\,LiPHR \xrightarrow[-2\,LiCl,\ -H_2PR]{Et_2O,\ -40 \rightarrow -25\,^\circ C} \underset{\mathbf{1}}{[(N_3N)Ta{=}PR]} \quad (2)$$

The structure of one of the new complexes, **1**, R=Cy (see Fig. 1), displays an almost linear Ta-P-C moiety and a short Ta–P distance of 2.145(7) Å. The ^{31}P NMR spectra of the complexes display low field signals between $\delta = 175.1$ and $\delta = 227.3$.

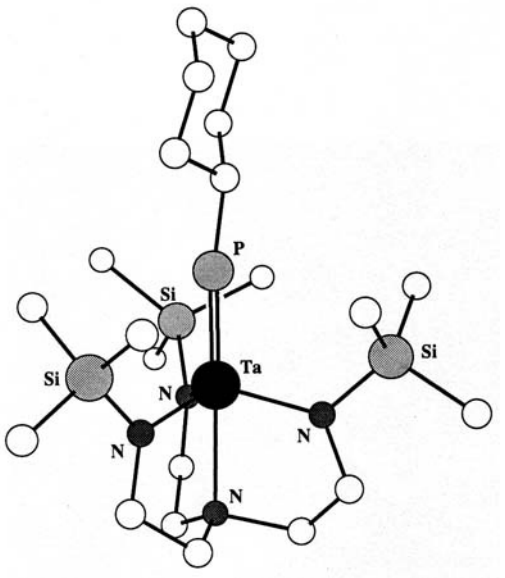

Fig. 1. Crystal structure of **1**, R = Cy.

The most remarkable characteristic of the new compounds concerns their reaction with various aldehydes [Eq. (3)] to give phosphaalkenes—a class of compounds first

$$[(N_3N)Ta{=}PR] + O{=}C\begin{matrix}R'\\H\end{matrix} \longrightarrow [(N_3N)Ta{=}O] + \begin{matrix}R'\\P{=}C\\R\quad H\end{matrix} \quad (3)$$

prepared by Becker in 1976.[12] This transformation, which proceeds under mild conditions, is analogous to the corresponding well-known reaction between tantalum alkylidene complexes and aldehydes to give alkenes.[13] It may proceed by a similar mechanism through a four-membered metallacycle.

The reaction is also quite notable in many other respects. For instance, it represents a new and general synthetic route to phosphaalkenes bearing a wide variety of phosphorus substituents. In addition, it is the first example of a transition metal reagent that metathesizes a heavier main group moiety under mild conditions. The close relationship between the reactions of tantalum alkylidene and tantalum phosphinidene complexes is yet another example of the so-called diagonal relationship between the chemistry of carbon and phosphorus.

It is probable that this new class of compounds can be extended to include the analogous arsinidene and stibinidene complexes, which when reacted with aldehydes could lead to a variety of arsa- and stibaalkenes, respectively. The alkylidene–phosphinidene relationship suggests that it may eventually be possible to obtain complexes with terminal phosphido M≡P ligands, either with tantalum or with the neighboring elements tungsten or molybdenum as the metal center.[14] Metathesis reactions[15] between these complexes and alkynes may give phosphaalkynes in an analogous manner.

German version: *Angew. Chem.* **1993**, *105*, 893

[1] C. C. Cummins, R. R. Schrock, W. M. Davis. *Angew. Chem.* **1993**, *105*, 758; *Angew. Chem. Int. Ed. Engl.* **1993**, *32*, 756.
[2] R. R. Schrock, *J. Am. Chem. Soc.* **1974**, *96*, 6796.
[3] F. Mathey. *Acc. Chem. Res.* **1992**, *25*, 90.
[4] E. O. Fischer, A. Maasböl. *Angew. Chem.* **1964**, *76*, 645; *Angew. Chem. Int. Ed. Engl.* **1964**, *3*, 580.
[5] P. B. Hitchcock, M. F. Lappert, W.-P. Leung, *J. Chem. Soc. Chem. Commun.* **1987**, 1282.
[6] R. Bohra, P. B. Hitchcock, M. F. Lappert, W.-P. Leung. *Polyhedron* **1989**, *8*, 1884.
[7] A. H. Cowley, B. Pellerin, J. L. Atwood, S. G. Bott, *J. Am. Chem. Soc.* **1990**, *112*, 6734.
[8] A. H. Cowley, A. R. Barron, *Acc. Chem. Res.* **1988**, *21*, 81.
[9] C. C. Cummins, J. Lee, R. R. Schrock, W. M. Davis. *Angew. Chem.* **1992**, *104*, 1510; *Angew. Chem. Int. Ed. Engl.* **1992**, *31*, 1501.
[10] G. Fritz, R. Uhlmann. *Z. Anorg. Allg. Chem.* **1978**, *442*, 95.
[11] H. V. R. Dias, P. P. Power. *J. Am. Chem. Soc.* **1989**, *111*, 114.
[12] G. Becker, *Z. Anorg. Allg. Chem.* **1976**, *423*, 242.
[13] R. R. Schrock. *J. Am. Chem. Soc.* **1976**, *98*, 5399.
[14] The coordinative stabilization of a phosphido-phosphinidene ligand was recently described by Scherer et al.: O. J. Scherer, R. Winter, G. Wolmershäuser, *J. Chem. Soc. Chem. Commun.* **1993**, 313.
[15] R. R. Schrock, *J. Organomet. Chem.* **1986**, *300*, 249.

 © *VCH Verlagsgesellschaft mbH, W-6940 Weinheim, 1993* *0570-0833/93/0606-0851 $ 10.00+.25/0*

Communications may be submitted in English *or* in German. Further details regarding the submission of communications can be found in the "Notice to Authors" reproduced in the January issue of the journal. Copies thereof may be obtained from the editorial office upon request.

Multinuclear Sandwich-type Complexes of Deprotonated β-Cyclodextrin and Copper(II) Ions**

By *Ralf Fuchs, Norbert Habermann,* and *Peter Klüfers**

In cyclodextrin chemistry "complexes" are usually host–guest complexes formed from the inclusion of a nonpolar molecule in the hydrophobic interior of a cyclodextrin torus[1] or several tori.[2] In contrast, metal complexes with cyclodextrins or with other carbohydrates as ligands are not well known.[3] The only metal complexes with large stability constants described so far are derivatives in which the cyclodextrin torus serves as a framework for attaching complexing functional groups.[4] But cyclodextrins themselves should also be capable of forming complexes, since simple polyols and monosaccharides form stable metal complexes in aqueous alkaline solution, in which they exist as multiply deprotonated polyolato ligands. Under these conditions copper(II) ions and diols form homoleptic bis{diolato(2−)}-cuprates in which the copper center has square-planar coordination.[5] We report here on our efforts at constructing multinuclear sandwich-type complexes from cyclodextrins in which two cyclodextrin tori are joined by copper(II) ions to form a double torus according to the strategy outlined in Scheme 1.

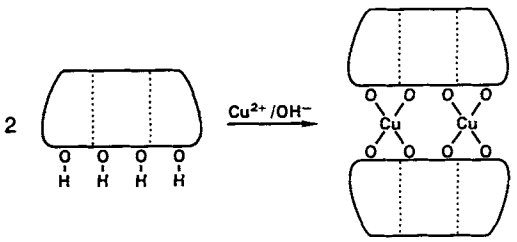

Scheme 1. Formation of multinuclear sandwich-type complexes from cyclodextrins and Cu^{2+}.

Aqueous alkaline solutions with copper(II) ions and cyclodextrins (at the time only poorly characterized) were described in 1927 by Messmer and later by Japanese authors.[6] Matsui et al.[6b] reported that a solution of β-cyclodextrin treated with an excess of NaOH takes up two mol equivalents of copper(II) hydroxide. When we used LiOH as the alkali metal hydroxide we could precipitate blue crystals with varying water content from similar solutions by adding ethanol. As described in the Experimental Procedure at the end of this communication, rhombic crystals of a water-rich form of compound **1** were obtained (**1a**, $x \approx 40$; water

$Li_{11}[Cu_4(\beta\text{-cdH}_{11.5})_2] \cdot x\,H_2O$ **1** β-cdH$_{21}$ = β-cyclodextrin

content determined by analysis). The blue crystals were examined by X-ray crystallography with an area detector.[7] The result of the structure analysis is seen in the figures: Figure 1 shows a homoleptic tetranuclear complex, in which two cyclodextrin tori line up such that their O2–O3 edges face each other and four copper ions are bound to oxygen atoms in distorted square-planar coordination geometry. In

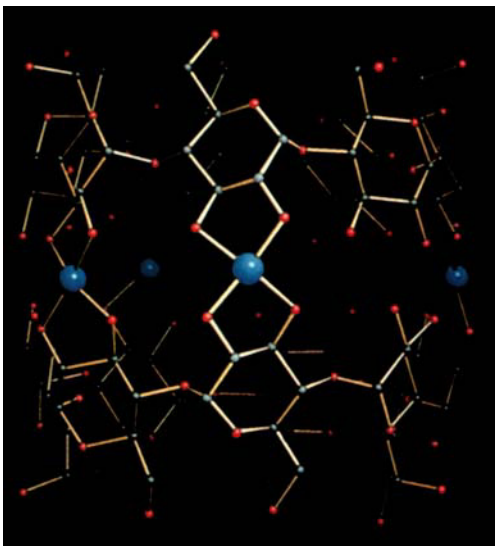

Fig. 1. Side view of the structure of the double torus in **1a**; blue: copper, red: oxygen, gray: carbon.

the double torus copper-bound anhydroglucose residues alternate with copper-free monomer units. As a result of the uneven number of ring members this alternation is not possible throughout the whole complex, but rather Cu-a and Cu-g are directly next to each other. In Figure 2 the double torus between these two copper atoms is cut open, unrolled, and shown from the outer side.

The depiction emphasizes a special feature of the complex not found in the complexes of simpler polyolates, namely, intramolecular hydrogen bonds. These can be inferred from the extent that the cyclodextrin rings were deprotonated: in the crystal structure of **1a** eleven lithium ions were localized per Cu_4 complex, which implies that each cyclodextrin ligand is deprotonated at least 9.5 times. The diolate groups bound to copper are doubly deprotonated according to findings on simple polyols. Thus the degree of deprotonation of each anhydroglucose unit not bound to copper is 1/2. Based on these values and the O–O distances in **1a**, a regular

[*] Prof. Dr. P. Klüfers, Dr. R. Fuchs, Dr. N. Habermann
Institut für Anorganische Chemie der Universität
Engesserstrasse, Gebäude 30.45, D-W-7500 Karlsruhe 1 (FRG)
Telefax: Int. code + (721)608-4290

[**] Polyol-Metal Complexes, Part 4. This research was supported by the Bundesministerium für Forschung und Technologie (grant no. 0319368A), Akzo AG, Wuppertal, and Wacker-Chemie, Munich (donation of cyclodextrin). – Part 3: [5a].

arrangement of nine isolated hydrogen bonds of type $O^- \cdots H-O$ can be deduced; these are represented in Figure 2 by dashed lines.

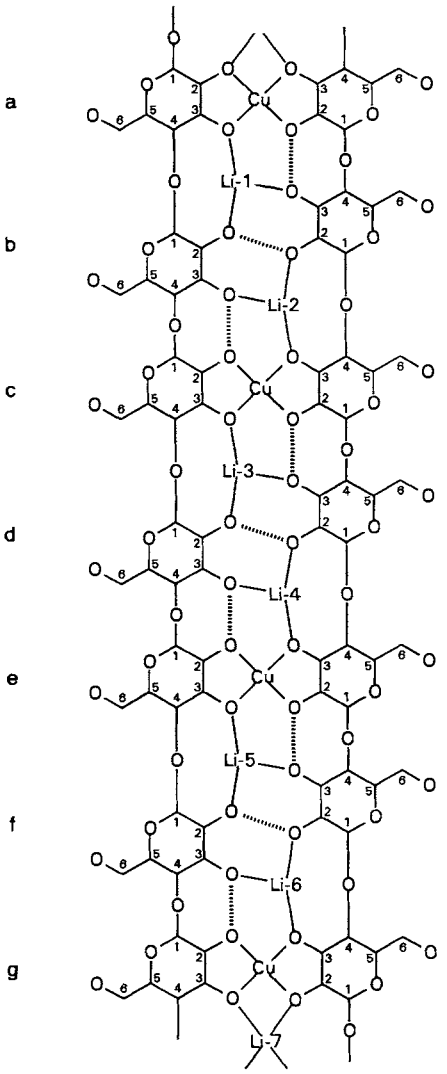

Fig. 2. Topology of the double torus and atomic labeling. All atoms except Li are labeled according to the formula A-*nm* (A = element symbol, *n* = position in the anhydroglucose ring, *m* = monomer unit (a–g in the left, a′–g′ in the right anhydroglucose strand)). O···O distances [pm] in $O^- \cdots H-O$ bonds in **1a**/**1b** (σ = 2 pm): O2a′-O3b′ 261/263, O2b-O2b′ 250/259, O3b-O2c 256/260, O2c′-O3d′ 256/261, O2d-O2d′ 247/254, O3d-O2e 257/267, O2e′-O3f′ 258/257, O2f-O2f′ 262/246, O3f-O2g 258/256.

When simple polyols and monosaccharides are treated with sufficient amounts of the alkali metal hydroxide and copper(II) salt, almost all of the polyol is converted into the deprotonated ligand. Thus it is not immediately evident why only four and not seven copper atoms are incorporated into our complex. We assume that the reason is the formation of intramolecular hydrogen bonds, which are possible for oligosaccharides like β-cyclodextrin but not for simple polyols or monosaccharides. The acidity of the nine protons in the hydrogen bonds is decreased, and deprotonation to give diolate(2−) ligands is apparently not possible under the given conditions.

Seven of the eleven lithium ions are found within the double torus of the tetracuprate complex ion. One of these lithium ions bridges the adjacent anhydroglucose pairs a and g, which are coordinated to copper ions; the other six lithium ions are each bound to three cyclodextrin O atoms in a regular pattern (Figs. 2 and 3). Seven water molecules are mounted in the polar middle of the cavity, which is hydrophobic up to the openings, forming a heptagon and completing the tetrahedral coordination environment of the lithium ions.

Other water molecules are bound to the water heptagon in **1a**. Figure 3 shows six positions, some not fully occupied, of these water molecules in the interior of the double torus; these water molecules have contact with water molecules on the exterior near the openings of the double torus.

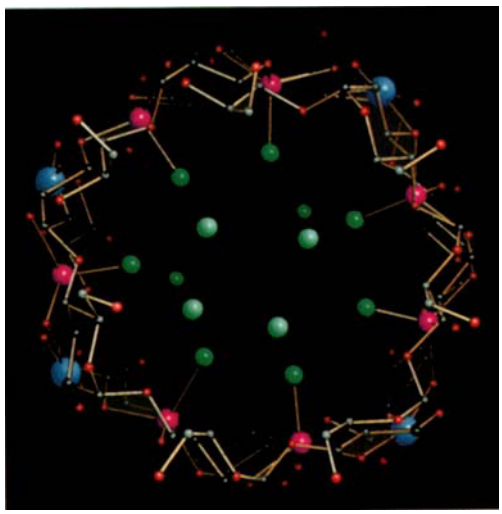

Fig. 3. View of the structure of the double torus in **1a** from the top; colors as in Fig. 1, violet: lithium, green: water.

A portion of the water of crystallization can be easily removed from **1a**. Upon warming to 70 °C (atmospheric pressure) the compound gives up two-thirds of its water content. A crystal of **1** containing less water (**1b**, $x \approx 25$; water content determined only by X-ray crystallography), which we obtained from a solution with a higher concentration of electrolytes, gives an idea of the dehydration process. Complex **1b** forms crystals with the same symmetry as and with cell parameters similar to those of crystals of **1a**. The structure analysis[7] shows the same $[Li_7(H_2O)_7Cu_4(\beta\text{-}cdH_{11.5})_2]^{4-}$ core as in **1a**; however, here the canals of water heptagons are empty, and no water molecules are found between the double tori. The apparently more tightly bound water molecules that form hydrogen bonds to most of the alkoxy O atoms and bring the coordination numbers of the latter to 4 are unaffected. In Figure 4 the double torus is somewhat compressed as a result of the dehydration but is essentially unchanged (see legend to Fig. 2). The packing of the double tori in the crystal resembles stacks of coins and facilitates the diffusion of the water molecules. The packing in **1b** is more dense; in **1a** the tori are surrounded by more water molecules and the stacking axis is tilted.

The metal-bridged cyclodextrin double torus described here could lead to new applications of cyclodextrins as enzyme models and as catalysts in their own right. A hydrophobic tube is found in both simple cyclodextrins and in **1**, although in **1** it is more functionalized. The hydrophobic cavity of the double torus is roughly 1.5 nm long and divided into two halves by a polar region in the middle. The polar region is formed from basic alkoxy units, which bind Lewis acidic centers of various strengths and hardnesses (Li^+,

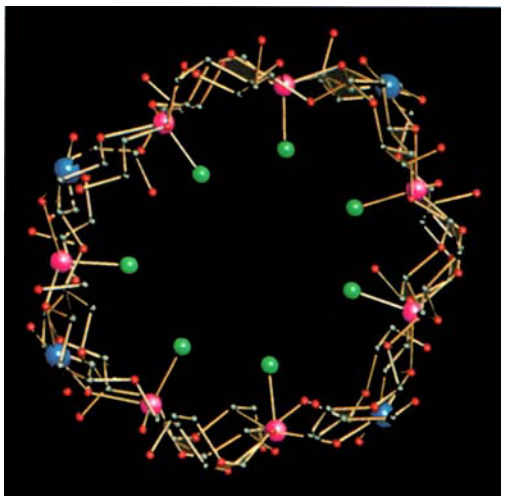

Fig. 4. View of the structure of the double torus in **1a**; colors as in Fig. 3.

Cu^{2+}); in addition, Cu^{2+} is a redox-active transition metal, and water is bound in precisely this region.

There is evidence that these units also exist in solution. Preliminary investigations of solvent equilibria indicate that simple polyols and monosaccharide derivatives form complexes with large stability constants in alkaline solution. At pH values above 11 even ethylenediamine is displaced from copper by diolate(2−) ligands; in amine-free solutions diolatocopper compounds form at pH ≈ 7.[8] We do not yet know, however, to what extent alkali metal cations associate with large, highly charged anions as in **1**.

Experimental Procedure

A solution of $Cu(OH)_2$ (0.97 g, 10 mmol), β-cyclodextrin (cyclomaltoheptaose; 5.68 g, 5 mmol), 8 mL H_2O, and 8 mL 5M LiOH (40 mmol LiOH) was sealed under N_2 and in the dark, and ethanol vapors were allowed to diffuse into the solution. Blue crystals formed within a few weeks; m.p. 205 °C (decomp after gradual dehydration). The crystal of **1a** examined by X-ray crystallography originated from this sort of sample; the elemental analysis indicates 3.6 instead of 4 Cu atoms and 13.2 instead of 11 Li atoms; in other words, **1a** is in a mixture with other complexes.

Received: December 24, 1992 [Z 5776 IE]
German version: *Angew. Chem.* **1993**, *105*, 895

[1] For an introduction see G. A. Jeffrey, W. Saenger, *Hydrogen Bonding in Biological Structures*, Springer, Berlin, **1991**, p. 309ff.

[2] J. F. Stoddart, *Angew. Chem.* **1992**, *104*, 860–862; *Angew. Chem. Int. Ed. Engl.* **1992**, *31*, 846–848.

[3] K. Burger, L. Nagy in *Biocoordination Chemistry* (Ed.: K. Burger), Ellis Horwood, Chichester, **1990**, pp. 236–283.

[4] A. W. Coleman, C.-C. Ling, M. Miocque, *Angew. Chem.* **1992**, *104*, 1402–1404; *Angew. Chem. Int. Ed. Engl.* **1992**, *31*, 1381–1383.

[5] a) M. Klaassen, P. Klüfers, *Z. Anorg. Allg. Chem.*, **1993**, *619*, 661–668; b) N. Habermann, M. Klaassen, P. Klüfers, *Chem. Ber.* **1992**, *125*, 809–814.

[6] a) E. Messmer, *Z. Phys. Chem.* **1927**, *126*, 369–416; b) Y. Matsui, T. Kurita, M. Yagi, T. Okayama, K. Mochida, Y. Date, *Bull. Chem. Soc. Jpn.* **1975**, *48*, 2187–2191.

[7] **1a**: $C_{84}H_{121}Cu_4Li_{11}O_{70}\cdot 40H_2O$, $M_r = 3301.981$; crystal of dimensions $0.20 \times 0.25 \times 0.30$ mm with stacking faults along [100], the packing direction of the cyclodextrin tori; $P2_12_12_1$; $a = 1918.2(3)$, $b = 2706.2(4)$, $c = 3575.4(9)$ pm; $V = 18560(6) \times 10^6$ pm^3; $Z = 4$, $\rho_{calcd} = 1.2214(4)$ g cm^{-3}; STOE-IPDS, $Mo_{K\alpha}$, $0 < \omega < 66°$ and $100 < \omega < 121°$ in steps of 1.1°, recording time 8 min per plate at a recording power of 1.5 kW (X-ray tube), $T = -60$ °C, 45569 reflections, of which 25140 were symmetry independent ($R = 0.052$), $\theta_{max} = 24°$; structure determination by direct (SHELXS) and Fourier methods (Beta-Test version of SHELXL-92), and subsequent refinement (full matrix) with SHELX-76; 10089 reflections with $I \geq 6\sigma(I)$, 917 parameters, $R = 0.103$, $R_w = 0.141$, $w^{-1} = \sigma^2(F) + 0.00166\,F^2$; $S = 1.09$. Because the quality of the data was unsatisfactory, the following limitations were applied: only Cu anisotropic; for the occupancy factors of the water O atoms only the values 1 (U in SHELXL-92 < 150 pm^2) and 0.5 (U > 150 pm^2) were differentiated; water content according to crystallography: 42 H_2O. – **1b**: $C_{84}H_{121}Cu_4Li_{11}O_{70}\cdot 25H_2O$, $M_r = 3031.753$; crystal of dimensions $0.08 \times 0.10 \times 0.11$ mm with stacking faults along [100]; $P2_12_12_1$; $a = 1613.4(12)$, $b = 2755.1(20)$, $c = 3323.5(33)$ pm; $V = 14773(21) \times 10^6$ pm^3; $Z = 4$, $\rho_{calcd} = 1.363(19)$ g cm^{-3}; STOE-IPDS, $Mo_{K\alpha}$, $0 < \omega < 360°$ in steps of 1.1°, recording time 45 min per plate at a recording power of 1.5 kW (X-ray tube), room temperature, 166289 reflections, of which 21930 were symmetry independent ($R = 0.043$), $\theta_{max} = 24°$; structure determination as for **1a**; 11026 reflections with $I \geq 4\sigma(I)$, 825 parameters, $R = 0.121$, $R_w = 0.110$, $w^{-1} = \sigma^2(F) + 0.00025\,F^2$. Further details of the crystal structure investigation may be obtained from the Fachinformationszentrum Karlsruhe, Gesellschaft für wissenschaftlich-technische Information mbH, D-W-7514 Eggenstein-Leopoldshafen 2 (FRG) on quoting the depository number CSD-56990, the names of the authors, and the journal citation.

[8] N. Habermann, P. Klüfers, unpublished.

The Self-Assembly of Catenated Cyclodextrins**

By *Dominique Armspach, Peter R. Ashton, Christopher P. Moore, Neil Spencer, J. Fraser Stoddart*, Trevor J. Wear,* and *David J. Williams*

Supramolecular chemistry[1] has paved the way for self-assembly processes[2] to be developed[3] for the construction of large, ordered, molecular and polymolecular arrays. Catenanes, rotaxanes, and knot compounds[4, 5] have been identified[3, 6] as prototypes for the development of a new synthetic methodology that will be necessary to attain nanometer-scale structures easily and efficiently. Following on from a reliance on covalent bonds[4] to direct the formation of mechanically interlocked molecular systems, the use of metal ion templates has produced[5] a wealth of novel catenanes, rotaxanes, and knots. The application of π-π stacking and edge-to-face interactions involving aromatic rings,[3, 6] along with hydrogen bonding,[7] to construct catenanes and rotaxanes has extended the potential of self-assembly as a synthetic paradigm into the field of organic chemistry. Concurrently with this activity on wholly synthetic systems, the cyclodextrins (CDs) have attracted a lot of attention[8] as building blocks in self-assembling rotaxanes[9] and polyrotaxanes,[10] usually in aqueous media but also quite recently[11] in organic solvents with chemically modified CDs. In 1958, Lüttringhaus, Cramer, Prinzbach, and Henglein[12] attempted to harness the weak noncovalent bonding forces that exist in water between α-CD and a series of substrates containing a hydroquinol ring etherified with, for example, two $(CH_2)_9CH_2SH$ groups in order to obtain, after oxidation, an α-CD catenated by macrocyclic disulfides. Although the experiment failed, it is important in the history of catenated compounds, because it was the first

[*] Prof. J. F. Stoddart, D. Armspach, P. R. Ashton, Dr. N. Spencer
School of Chemistry, University of Birmingham
Edgbaston, Birmingham B15 2TT (UK)
Telefax: Int. code + (21)414-3531
Dr. D. J. Williams
Chemical Crystallography Laboratory
Department of Chemistry
Imperial College, London (UK)
Dr. C. P. Moore, Dr. T. J. Wear
Kodak Limited
Headstone Drive, Harrow
Middlesex HA1 4TY (UK)

[**] This work was supported by the Science and Engineering Research Council and by Kodak Limited. We also thank Dr. Andrew Quick of the University of London Computing Centre for preparing the computer-aided ball-and-stick and space-filling representations of the [2]catenanes. These diagrams were produced with the Convex AVS Visualization Software.

reported attempt to synthesize such compounds. Now 35 years on, we have succeeded finally in catenating cyclodextrins. Here, we report the synthesis from *pure*[13] heptakis(2,6-di-*O*-methyl)-β-cyclodextrin (DM-β-CD, Fig. 1) of two [2]catenanes and two [3]catenanes as a mixture of isomers, the characterization of these novel compounds by FAB-MS and NMR spectroscopy, and the X-ray crystal structure of one of the [2]catenanes.

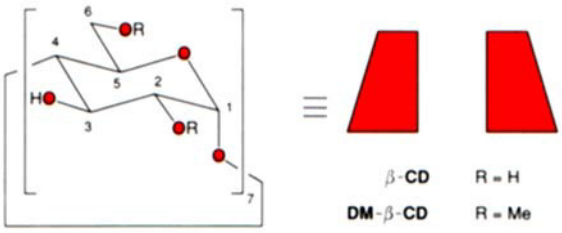

Fig. 1. Structural formula and schematic representation of β-CD and DM-β-CD.

Since we anticipated difficulties in the isolation of catenated CDs, we focussed our attention initially upon one of the methylated CD derivatives[13] that are known to exhibit good solubilities in organic solvents as well as in water. We chose DM-β-CD (Fig. 1), whose torus-shaped cavity is extended and more rigid than that of the parent β-CD, in order to enhance the binding of aromatic ring-containing substrates[14] through their hydrophobic interactions with DM-β-CD in aqueous solution. Since the diol **1**, based on a bitolyl unit (Scheme 1), forms a strong complex (see below) in aqueous solution with DM-β-CD, we investigated the reaction of the more nucleophilic diamine **2** (derived from **1**) under Schotten-Baumann[15] reaction conditions with terephthaloyl chloride (see Scheme 2). In this manner, we satisfied, as far as possible, the interrelated requirements of the substrate,[16] the reaction, and the media for efficient macrocyclization to afford catenated DM-β-CD derivatives in aqueous solution.

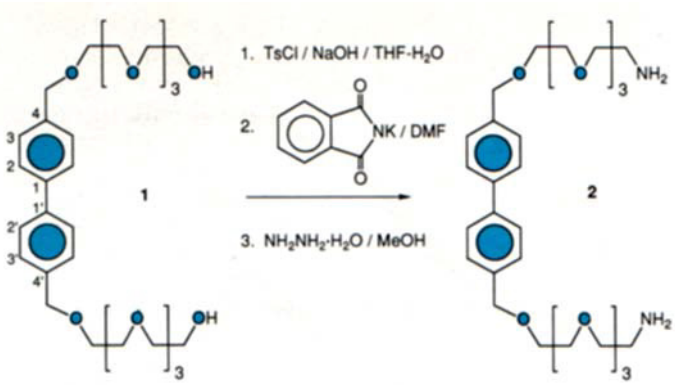

Scheme 1.

The binding properties of the diol **1** and the diamine **2** with both β-CD and DM-β-CD in D_2O were investigated by ^{1}H NMR spectroscopy at room temperature. Upfield chemical shift changes in the CDs,[17] particularly for H3 and H5, were accompanied by an upfield chemical shift change[17] for H2 and H2′ in the substrates. The 1:1 stoichiometries of the β-CD · **1** complex (deduced by probing H3 in β-CD and H2 and H2′ in **1**) and of the DM-β-CD · **2** complex (deduced by probing[18] OMe6 in DM-β-CD and H2 and H2′ in **2**) were confirmed[19] by the method of continuous variations (Job's plots). Through ^{1}H NMR spectroscopy it was also possible to obtain association constants (K_a) for the 1:1 complexes β-CD · **1** and DM-β-CD · **1** in D_2O. The K_a values[20] of $8900 \pm 500\ kg\,mol^{-1}$ and $41\,000 \pm 3000\ kg\,mol^{-1}$, respectively, augured well for our attempts to catenate CDs with synthetic macrocycles containing bitolyl units.

The diol **1** was converted into the diamine **2** by the Gabriel procedure (Scheme 1). The water-soluble inclusion complex, which is formed when equimolar amounts of DM-β-CD and

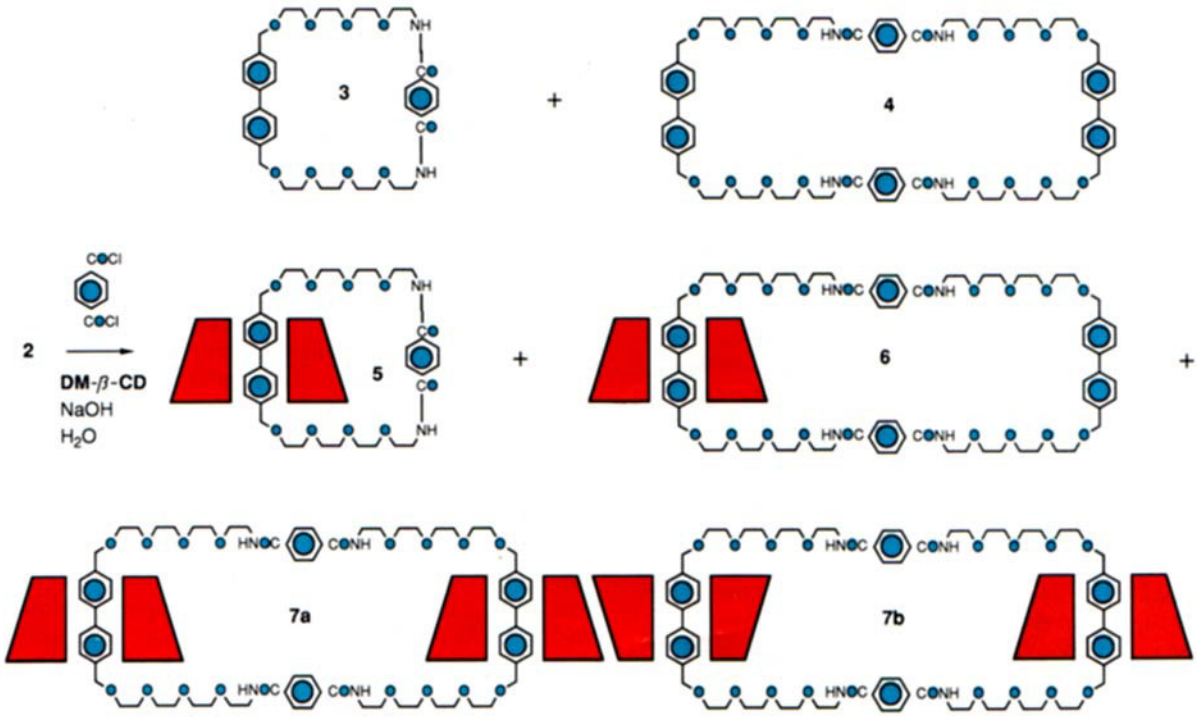

Scheme 2.

2 are dissolved in a large volume of 0.01 N NaOH solution, was treated with 1.1 equivalents of terephthaloyl chloride under sonication at 5 °C (Scheme 2). In addition to isolating the macrocycles **3** (12%, formed by intramolecular ring closure of a straight-chain intermediate) and **4** (3.5%, formed by intermolecular ring closure), the related two [2]catenanes **5** (3.0%) and **6** (0.8%), and the isomeric [3]catenanes **7a** and **7b** (1.1%, as an equimolar mixture) were characterized[21] following chromatography of the $CHCl_3$ extracts of the reaction mixture on silica gel. The relative yields of **3** and **4**, and of **5** and **6** indicate that, somewhat disappointingly, the macrocyclizations leading to catenane formation are inhibited[22] by the bound DM-β-CD component(s).

The solubility characteristics of these catenated CDs are quite unusual and distinctive. With the exception[23] of **6**, they are soluble in hydroxylic (e.g., H_2O and MeOH), halogenated (e.g., CH_2Cl_2 and $CHCl_3$), and aromatic hydrocarbon (e.g., C_6H_6 and MePh) solvents.

The positive ion FAB-MS of **5** and **6** are characteristic of [2]catenanes[24]: in addition to peaks for the molecular ions—often including bound sodium—fragmentation peaks are also observed for the component macrocyclic rings. For **5**, peaks are observed for $[M + Na]^+$, $[M + Na - \mathbf{3}]^+$, and $[M - \text{DM-}\beta\text{-D}]^+$, and for **6** for $[M + Na]^+$, $[M]^+$, $[M - \text{DM-}\beta\text{-CD}]^+$, and $[M + Na - \mathbf{4}]^+$. In the case of the [3]catenanes **7a** and **7b**, the presence of the derived [2]catenane **6**, after loss of one DM-β-CD ring is evident in the positive ion FAB-MS. Thus, peaks are observed for $[M + Na]^+$, $[M + Na - \text{DM-}\beta\text{-CD}]^+$, $[M - 2\,\text{DM-}\beta\text{-CD}]^+$, and $[M + Na - \mathbf{6}]^+$.

The ^{13}C NMR spectra of **5** and **6**, recorded in $CDCl_3$, show that the DM-β-CD component in both [2]catenanes retains its C_7 symmetry, that is, the expected eight signals are observed, in keeping with rapidly pirouetting synthetic macrocycles around the CD torus. However, the original C_{2v} symmetry of **3** and D_{2h} symmetry of **4** are lowered to local symmetries that are C_1 and C_2, respectively, under the influence of the chiral DM-β-CD rings that are rapidly circumrotating in both **5** and **6**. The outcome is a doubling in the number of ^{13}C NMR signals from 16 to 32 on going from **3** to **5** and from **4** to **6**. For example, the signals observed for the bitolyl methylene carbon atoms at $\delta = 72.9$ in both **3** and **4** are replaced by signals at $\delta = 72.5$ and 72.9 in **5** and at $\delta = 72.8$ and 72.9 in **6**. Also, in the ^{13}C NMR spectrum of **5**, the amide carbonyl carbon atoms give rise to two signals at $\delta = 167.0$ and 168.0, whereas they resonate as one signal at $\delta = 166.5$ in the ^{13}C NMR spectrum of **3**. The consequences of catenane formation upon the local symmetries of the synthetically derived ring components are also reflected in the ^1H NMR spectra of **5** and **6**. Most strikingly, the ^1H NMR spectrum of **5** in C_6D_6 solution (Fig. 2) reveals the imposed heterotopic character upon sets of aromatic protons within both the bitolyl and terephthaloyl units, as well as upon the bitolyl methylene groups within which each pair of protons display their expected diastereotopicities. These various topic relationships give rise to three AA′BB′ systems for the 12 aromatic protons and two AB systems for the four bitolyl methylene protons. The ^1H NMR spectrum of **5** was recorded at −60 °C in CD_2Cl_2 solution. Since no temperature dependence was observed, the synthetic macrocyclic component must either be located firmly in one position with respect to the DM-β-CD component, or it must still be circumrotating rapidly on the ^1H NMR time scale.[25] We suspect the latter circumstance prevails, since no temperature dependence was observed in the ^1H NMR spectrum of **6** when it was recorded at −60 °C in CD_2Cl_2 solution. This [2]catenane is perfectly constructed for a degenerate process

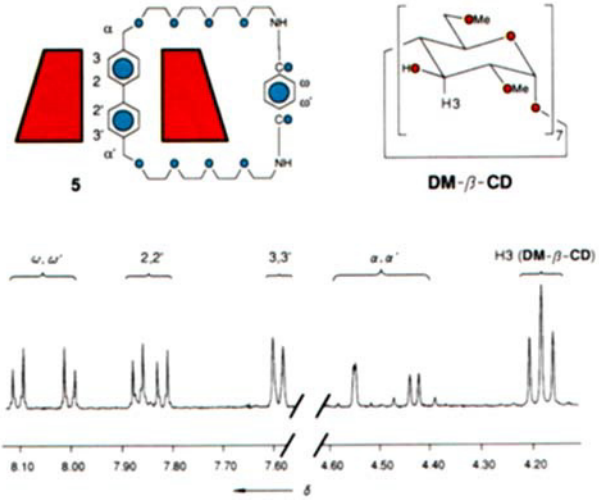

Fig. 2. A section of the ^1H NMR spectrum of the [2]catenane **5** recorded in C_6D_6 solution.

of exchange of the DM-β-CD ring to occur between the equivalent bitolyl units in the synthetic macrocyclic component. Yet it continues to display local C_2 symmetry down to −60 °C in CD_2Cl_2 solution where precipitation of **6** occurs, causing signals to broaden in the ^1H NMR spectrum. Both the ^1H and ^{13}C NMR spectra of **7**, recorded in $CDCl_3$, reveal the presence of two isomers, the head-to-head/tail-to-tail **7a** and head-to-tail/head-to-tail **7b**. In **7a**, the synthetic macrocyclic component has averaged D_2 symmetry (i.e., it behaves like **4**), whereas in **7b**, it has averaged C_2 symmetry (i.e., it behaves like **6**). The spectra are in accordance with these two symmetry types.[26] In addition, the presence of two sets of equal intensity signals for the DM-β-CD protons in the ^1H NMR spectrum of **7a**/**b** confirms the presence of an equimolar mixture of orientational isomers. Their separation is under investigation.[26]

After extensive trials with a wide range of different solvent systems, we obtained small, but well-formed, single crystals of the [2]catenane **5** suitable for X-ray crystallography.[27, 28] The crystal structure of **5** (Fig. 3) reveals that in the solid state the bitolyl unit of the macrocyclic bislactam component is positioned inside the DM-β-CD torus, and the planar bislactam residue lies against the outside. The phenylene rings in the bitolyl unit are nonplanar; the upper ring has a well-defined orientation, whilst the lower one is disordered and adopts two orientations, twisted by about 40° in either one or other direction with respect to the upper ring. As a consequence, the lower polyether strand adopts several different conformations, and that illustrated in Figure 3 represents one of many that can be fitted to the diffuse tube of electron density that appears in this region of the structure. The axis of the bitolyl unit is not inserted perpendicularly through the DM-β-CD torus, but is inclined by about 63° to the plane defined by the seven glycosidic oxygen atoms. Surprisingly, there is no hydrogen bonding between the polyether oxygen atoms and the hydroxyl groups on the upper rim of the cyclodextrin. Indeed, those oxygen atoms that lie over the upper rim of the DM-β-CD torus are directed *away* from the hydroxyl groups. The partial weight included H_2O molecules[*] lie within hydrogen-bonding distance of one of the amide nitrogen atoms. Apart from small perturbations in the orientations of the methoxyl groups on the upper and lower rims of the DM-β-CD component, the gross C_7 geometry of the cyclodextrin is retained.

[*] That is, not all the potential sites for water of crystallization are occupied in different molecules of the crystal.

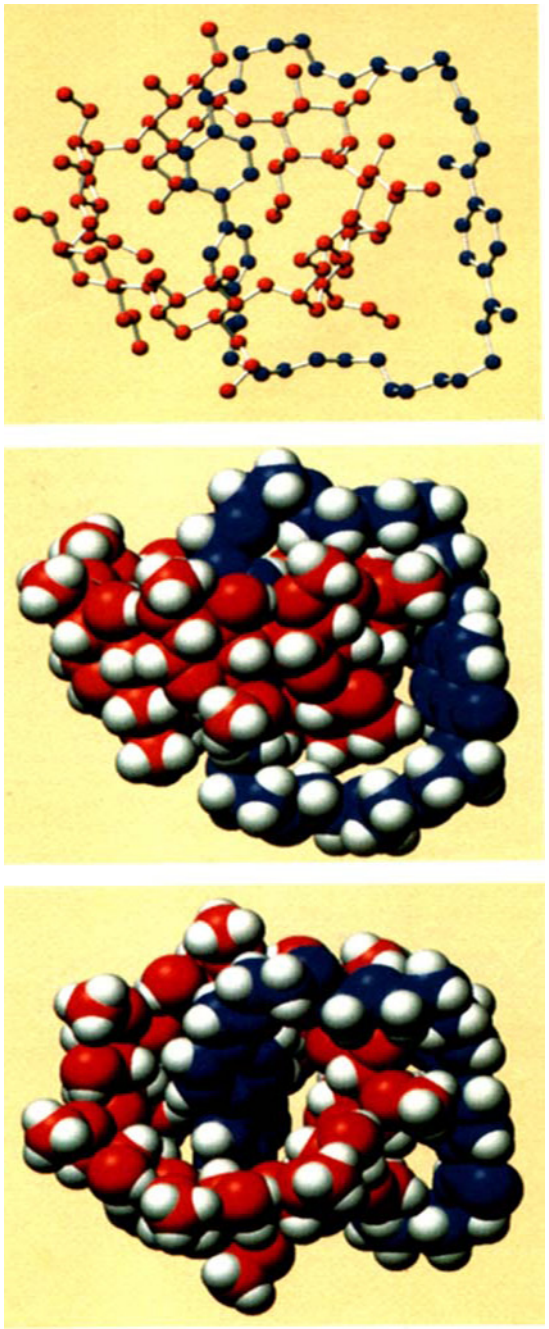

Fig. 3. Top: Structure of **5** in the crystal with the DM-β-CD component depicted in red and the macrocyclic bislactam component (**3**) in blue. Space-filling representations of the [2]catenane viewed from the side of the CD torus (center) and from above (bottom).

We can now anticipate the catenation of β-CD,[29] as well as the lower (α-CD) and higher (γ-CD) homologues—and their chemically modified derivatives—as a prelude to constructing compounds that function as molecular devices, which are soluble in water, in addition to a wide range of organic solvents.

Experimental Procedure

1: Reaction of 4,4′-bis(bromomethyl)biphenyl [30] (10.0 g, 0.029 mol) with the monosodium salt of tetraethyleneglycol—prepared in situ from tetraethylene glycol (160 mL, 1.10 mol) and sodium (2.7 g, 0.117 mol)—for 18 h at 60 °C gave the diol **1** as a colorless oil (12.5 g, 76%) after chromatography on SiO_2($CHCl_3$:MeOH 92:8); positive ion FAB-MS: *m/z* 567, 589, and 605 for $[M + H]^+$, $[M + Na]^+$, and $[M + K]^+$, respectively. ^1H NMR ($CDCl_3$): $\delta = 2.84$ (s; 2H), 3.57 (t, $J = 5.5$ Hz; 4H), 3.61–3.72 (m; 28H), 4.59 (s; 4H), 7.39 (d, $J = 8$ Hz; 4H), 7.54 (d, $J = 8$ Hz; 4H); ^{13}C NMR ($CDCl_3$): $\delta = 61.7$, 69.5, 70.3, 70.6 (× 2), 70.7 (× 2), 72.6, 73.0, 127.1, 128.3, 137.3, 140.3.

2: When the diol **1** (10.0 g, 17.6 mmol) was treated with *p*-toluene sulfonyl chloride (7.6 g, 40 mmol) and NaOH (2.0 g, 50 mmol) in 30 mL of THF-H_2O (2:1) for 4 h at 0 °C, the pure ditosylate (14.5 g) was obtained without further purification in 94% yield. Positive ion FAB-MS: *m/z* = 874 and 897 for $[M]^+$ and $[M + Na]^+$, respectively; ^1H NMR ($CDCl_3$): $\delta = 2.43$ (s; 6H), 3.57–3.72 (m; 28H), 4.16 (t, $J = 5.5$ Hz; 4H), 4.60 (s; 4H), 7.33 (d, $J = 8$ Hz; 4H), 7.41 (d, $J = 8$ Hz; 4H), 7.56 (d, $J = 8$ Hz; 4H), 7.79 (d, $J = 8$ Hz; 4H); ^{13}C NMR ($CDCl_3$): $\delta = 21.6$, 68.7, 69.2, 69.5, 70.5, 70.6 (× 3), 70.7, 73.0, 127.1, 128.0, 128.3, 129.8, 134.0, 137.3, 140.3, 144.8.

Reaction of the ditosylate (140 g, 16 mmol) with potassium phthalimide (6.9 g, 37.2 mmol) in DMF (100 mL) for 7 h at 90 °C afforded the pure diphthalimide as a colorless oil (12.1 g, 92%). Positive-ion FAB-MS: *m/z* 824 and 847 for $[M]^+$ and $[M + Na]^+$, respectively; ^1H NMR ($CDCl_3$): $\delta = 3.58$–3.69 (m; 24H), 3.73 (t, $J = 5.5$ Hz; 4H), 3.90 (t, $J = 5.5$ Hz; 4H), 4.59 (s; 4H), 7.40 (d, $J = 8$ Hz; 4H), 7.55 (d, $J = 8$ Hz; 4H), 7.70 (m; 4H), 7.83 (m; 4H); ^{13}C NMR ($CDCl_3$): $\delta = 37.3$, 67.9, 69.5, 70.1, 70.6 (× 2), 70.7 (× 2), 73.0, 123.2, 127.1, 128.2, 132.2, 133.9, 137.4, 140.2, 168.2.

Treatment of the diphthalimide (12.0 g, 14.5 mmol) with hydrazine hydrate (3.7 mL) in MeOH (250 mL) under reflux for 1 h gave the diamine **2** as a slightly yellowish oil (6.1 g, 75%) after chromatography on SiO_2 ($CHCl_3$:MeOH:NH_4OH 49:9:1). Positive ion FAB-MS *m/z* 565 and 587 for $[M + H]^+$ and $[M + Na]^+$, respectively; ^1H NMR ($CDCl_3$): $\delta = 2.80$ (bs; 4H), 3.52 (t, $J = 5.5$ Hz; 4H), 3.62–3.72 (m; 28H), 4.61 (s; 4H), 7.43 (d, $J = 8$ Hz; 4H), 7.58 (d, $J = 8$ Hz; 4H); ^{13}C NMR ($CDCl_3$): δ ($CDCl_3$) = 41.7, 69.6, 70.3, 70.6 (× 2), 70.7 (× 2), 73.0, 73.3, 127.1, 128.3, 137.3, 140.3.

3, **4**, **5**, **6**, **7a**/**b**: A solution of the diamine **2** (1.0 g, 1.8 mmol), *pure* [13] DM-β-CD (2.5 g, 1.9 mmol) and sodium hydroxide (200 mg, 5.0 mmol) in H_2O (500 mL) was sonicated for 2 h at room temperature. Powdered terephthatholyl chloride (405 mg, 2.0 mmol) was added whilst maintaining the temperature of the reaction below 5 °C. The suspension was sonicated for a further 2 h at room temperature. The reaction mixture was extracted with $CHCl_3$ (3 × 100 mL) and the combined organic layers were washed with 1 N sodium hydroxide solution and H_2O, and then dried ($MgSO_4$). Removal of the solvent in vacuo gave a colorless solid, which was purified by chromatography on SiO_2($CHCl_3$:MeOH 92:8) to afford four fractions. They were characterized as follows: Fraction 1, DM-β-CD; Fraction 2, the macrocyclic **3** (150 mg, 12%, m.p. 134–135 °C); positive ion FAB-MS: *m/z* 695 and 717 for $[M + H]^+$ and $[M + Na]^+$, respectively; ^1H NMR ($CDCl_3$): $\delta = 3.58$–3.72 (m; 32H), 4.55 (s; 4H), 7.24 (bt; 2H), 7.35 (d, $J = 8$ Hz; 4H), 7.41 (d, $J = 8$ Hz; 4H), 7.70 (s; 4H); ^{13}C NMR ($CDCl_3$): $\delta = 40.0$, 69.4, 69.8, 70.2, 70.5, 70.6, 70.7 (× 2), 72.9, 126.9, 127.2, 128.3, 136.8, 137.2, 140.0, 166.5; Fraction 3, which was purified further by preparative TLC on SiO_2 (CH_2Cl_2:MeOH 91:9) to afford (a) the macrocyclic **4** (45 mg, 3.5%, m.p. 148–149 °C); positive ion FAB-MS: *m/z* 1390 and 1412 for $[M + H]^+$ and $[M + Na]^+$, respectively; ^1H NMR ($CDCl_3$): $\delta = 3.56$–3.68 (m; 64H), 4.52 (s; 8H), 7.31 (bs; 4H), 7.34 (d, $J = 8$ Hz; 8H), 7.48 (d, $J = 8$ Hz, 8H), 7.84 (s; 8H); ^{13}C NMR ($CDCl_3$) $\delta = 39.9$, 69.4, 69.8, 70.2, 70.5 (× 2), 70.6 (× 2), 72.9, 127.0, 127.3, 128.3, 137.1, 137.2, 140.2, 166.7; (b) the catenane **5** (105 mg, 3%, m.p. 175–176 °C); positive ion FAB-MS: *m/z* 2049, 1353, and 695 for $[M + Na]^+$, $[M - 3 + Na]^+$, and $[M - DM\text{-}\beta\text{-}CD]^+$, respectively; ^1H NMR (C_6H_6): $\delta = 3.02$ (dd, $J = 3.5$; 10 Hz, 7H), 3.20–3.85 (m; 53H), 3.37 (s; 21H), 3.44 (s; 21H), 3.89 (ddd, $J = 2$, 4.5, 10 Hz; 7H), 4.18 (t, $J = 10$ Hz; 7H), 4.41, 4.45 (AB system, $J_{AB} = 13$ Hz; 2H), 4.54, 4.55 (AB system, $J_{AB} = 13$ Hz; 2H), 4.81 (d, $J = 3.5$ Hz; 7H), 5.30 (s; 7H), 7.46 (bt; 1H), 7.59 (d, $J = 8$ Hz; 4H), 7.82 (d, $J = 8$ Hz; 2H), 7.86 (bt; 1H), 7.87 (d, $J = 8$ Hz; 2H), 8.00 (d, $J = 8$ Hz, 2H), 8.11 (d, $J = 8$ Hz; 2H); ^{13}C NMR ($CDCl_3$): $\delta = 59.0$, 60.3, 70.4, 70.7, 73.3, 81.9, 83.3, 101.2 for the DM-β-CD component and 40.1, 40.3, 72.5, 72.9, 126.0, 126.4, 127.5, 127.7, 127.9, 128.0, 137.1, 137.5, 138.6 (× 2), 138.9, 140.1, 167.0, 168.0 for component **3**, excluding the 14 OCH_2 signals which overlap in the region 69.8–70.6; Fraction 4 was purified further by preparative TLC on SiO_2(CH_2Cl_2:MeOH 9:1) to afford (a) the catenane **6** (20 mg, 0.8%) as an amorphous solid; positive ion FAB-MS: *m/z* 2743, 2721, 1389, and 1353 for $[M + Na]^+$, $[M]^+$, $[M - DM\text{-}\beta\text{-}CD]^+$, and $[M + Na - \mathbf{4}]^+$, respectively; ^1H NMR ($CDCl_3$): $\delta = 3.23$ (dd, $J = 3.5$, 10 Hz; 7H), 3.30 (s; 21H), 3.59 (s; 21H), 3.29–3.74 (m; 92H), 3.89 (t, $J = 10$ Hz; 7H), 4.57 (s; 4H), 4.61 (s; 4H), 4.92 (d, $J = 3.5$ Hz; 7H), 5.06 (s; 7H), 7.16 (bt; 2H), 7.32 (bt; 2H), 7.38 (d, $J = 8$ Hz, 4H), 7.39 (d, $J = 8$ Hz; 4H), 7.52 (d, $J = 8$ Hz; 4H), 7.53 (d, $J = 8$ Hz; 4H), 7.83–7.93 (m; 8H); ^{13}C NMR ($CDCl_3$): $\delta = 58.9$, 60.3, 70.3, 70.6, 73.3, 82.1, 83.4, 101.2 for the DM-β-CD component and 39.9 (× 2), 72.8, 72.9, 126.7, 126.8, 127.3, 127.4, 128.0, 128.1, 137.0, 137.2, 137.4, 137.8, 139.8, 140.2, 166.6 (× 2) for component **4**, excluding the 14 OCH_2 signals which overlap in the region 69.6–70.7; (b) and the orientationally isomeric **7a** and **7b** as an equimolar mixture (39 mg, 1.1%); positive ion FAB-MS: *m/z* 4072, 2742, 1389, and 1353 for $[M + Na]^+$, $[M + Na - DM\text{-}\beta\text{-}CD]^+$, $[M - 2\,DM\text{-}\beta\text{-}CD]^+$, and $[M + Na - \mathbf{6}]^+$, respectively. Both ^1H and ^{13}C NMR spectroscopic data were consistent with the presence of approximately equal amounts of **7a** and **7b** in Fraction 4 (b). At present, attempts are being made to separate the isomers and characterize them fully [26]. Single crystals of

5, suitable for X-ray structural analysis [27, 28] have been grown by vapor diffusion of iPr_2O into an ethanolic solution of the [2]catenane.

Received: January 4, 1993 [Z 5796 IE]
German version: *Angew. Chem.* **1993**, *105*, 944

[1] J.-M. Lehn, *Angew. Chem.* **1988**, *100*, 91; *Angew. Chem. Int. Ed. Engl.* **1988**, *27*, 89; *ibid.* **1990**, *102*, 1347 and **1990**, *29*, 1304.

[2] J. F. Stoddart in Host-Guest Molecular Interactions: From Chemistry to Biology (*Ciba Found. Symp. 158*), Wiley, Chichester, **1991**, pp. 5–22; J. S. Lindsey, *New. J. Chem.* **1991**, *15*, 153; G. M. Whitesides, J. P. Mathias, C. T. Seto, *Science* **1991**, *254*, 1312; J. Rebek, Jr. in *Molecular Recognition: Chemical and Biochemical Problems II* (Ed.: S. M. Roberts), RSC Special Publication No. 111, Cambridge, **1992**, pp. 65–73.

[3] a) D. Philp, J. F. Stoddart, *Synlett* **1991**, 445; b) P. L. Anelli, N. Spencer, J. F. Stoddart, *J. Am. Chem. Soc.* **1991**, *113*, 5131; c) P. R. Ashton, C. L. Brown, E. J. T. Chrystal, T. T. Goodnow, A. E. Kaifer, K. P. Parry, A. M. Z. Slawin, N. Spencer, J. F. Stoddart, D. J. Williams, *Angew. Chem.* **1991**, *103*, 1055; *Angew. Chem. Int. Ed. Engl.* **1991**, *30*, 1039; d) P. L. Anelli, P. R. Ashton, R. Ballardini, V. Balzani, M. Delgado, M. T. Gandolfi, T. T. Goodnow, A. E. Kaifer, D. Philp, M. Pietraszkiewicz, L. Prodi, M. V. Reddington, A. M. Z. Slawin, N. Spencer, J. F. Stoddart, C. Vicent, D. J. Williams, *J. Am. Chem. Soc.* **1992**, *114*, 193; P. R. Ashton, D. Philp, N. Spencer, J. F. Stoddart, *J. Chem. Soc. Chem. Commun.* **1992**, 1124 and in *Molecular Recognition: Chemical and Biochemical Problems II* (Ed.: S. M. Roberts), RSC Special Publication No. 111, Cambridge, **1992**, pp. 51–63.

[4] G. Schill, *Catenanes, Rotaxanes and Knots*, Academic Press, New York, **1971**; D. M. Walba, *Tetrahedron* **1985**, *41*, 3161.

[5] C. O. Dietrich-Buchecker, J.-P. Sauvage, *Chem. Rev.* **1987**, *87*, 795; in *Bioorganic Chemistry Frontiers*, Vol. 2 (Ed.: H. Dugas), Springer, Berlin, **1991**, pp. 195–248; in *Supramolecular Chemistry* (Eds.: V. Balzani, L. De Cola), Kluwer, Dordrecht, **1992**, pp. 259–277.

[6] J. F. Stoddart, *Chem. Br.* **1991**, *27*, 714; *Chem. Aust.* **1992**, *59*, 576.

[7] Recently, a supramolecular self-assembly process, which also relies upon a combination of hydrogen bonding and π–π interactions with a template to form an interlocked ring systems, has resulted in the formation of a novel [2]catenane with identical rings in a one-pot double macropolycyclization reaction. See C. A. Hunter, *J. Am. Chem. Soc.* **1992**, *114*, 5303. Also, F. Vögtle, S. Meier, R. Hoss, *Angew. Chem.* **1992**, *104*, 1628; *Angew. Chem. Int. Ed. Engl.* **1992**, *31*, 1619.

[8] J. F. Stoddart, *Angew. Chem.* **1992**, *104*, 860; *Angew. Chem. Int. Ed. Engl.* **1992**, *31*, 846.

[9] H. Ogino, *J. Am. Chem. Soc.* **1981**, *103*, 1303; H. Ogino, K. Ohata, *Inorg. Chem.* **1984**, *23*, 3312; K. Yamanari, Y. Shimura, *Bull. Chem. Soc. Jpn.* **1983**, *56*, 2283; J. S. Manka, D. S. Lawrence, *J. Am. Chem. Soc.* **1990**, *112*, 2440; T. V. S. Rao, D. S. Lawrence, *ibid.* **1990**, *112*, 3614; D. L. Dick, T. V. S. Rao, D. Sukumaran, D. S. Lawrence, *ibid.* **1992**, *114*, 2664; R. Isnin, A. E. Kaifer, *ibid.* **1991**, *113*, 8188; R. S. Wylie, D. H. Macartney, *ibid.* **1992**, *114*, 3136.

[10] A. Harada, M. Kamachi, *J. Chem. Soc. Chem. Commun.* **1990**, 1322; *Macromolecules* **1990**, *23*, 2821; A. Harada, J. Li, M. Kamachi, *Nature* **1992**, *356*, 325; G. Wenz, B. Keller, *Angew. Chem.* **1992**, *104*, 201; *Angew. Chem. Int. Ed. Engl.* **1992**, *31*, 197; M. Born, H. Ritter, *Makromol. Chem. Rapid. Commun.* **1991**, *121*, 471.

[11] G. Wenz, E. van der Bey, L. Schmidt, *Angew. Chem.* **1992**, *104*, 758; *Angew. Chem. Int. Ed. Engl.* **1992**, *31*, 783.

[12] A. Lüttringhaus, F. Cramer, H. Prinzbach, F. M. Henglein, *Chem. Ber.* **1958**, *613*, 185.

[13] C. M. Spencer, J. F. Stoddart, R. Zarzycki, *J. Chem. Soc. Perkin Trans. 2* **1987**, 1323, and references therein.

[14] Preliminary ^{1}H NMR spectroscopic studies in D_2O established that compounds carrying two 2-[2-(2-hydroxyethoxy)ethoxy] groups with the substitution pattern of α,α' on *p*-xylene, 1,4 on benzene, and 1,5 and 2,6 on naphthalene did not form complexes with either β-CD or DM-β-CD. Although 4,4′-bis[2-[2-[2-(2-hydroxyethoxy)ethoxy]ethoxy]ethoxy]biphenyl does form a complex with β-CD and DM-β-CD, the corresponding diamine does not form catenated compounds with DM-β-CD under the same conditions as those described in Scheme 2 for the diamine **2** based on a bitolyl unit.

[15] J. F. King, R. Rathore, J. Y. L. Lam, Z. R. Guo, D. F. Klassen, *J. Am. Chem. Soc.* **1992**, *114*, 3028.

[16] The bitolyl and bislactam units in the macrocycles **3** and **4** confer a certain amount of rigidity which we believe is ultimately essential for the self-assembly of the catenated DM-β-CDs, **5**, **6**, and **7a**/**b**.

[17] When the 1:1 complexes β-CD · **1** and DM-β-CD · **1** are formed in D_2O at concentrations of 1.3×10^{-2} M, the $\Delta\delta$ values experienced by H3 (in both β-CD and DM-β-CD) and by H2 and H2′ (in **1**) are −0.17 and −0.20, respectively; that is, in this case the chemical shift changes are coincidentally the same for each complex.

[18] This experiment was carried out in 0.1 N NaOD/D_2O solution in order to maintain a constant pD of 13, at which **2** exists entirely as the diamine and DM-β-CD entirely as the heptaol. The Job's plot could not be obtained for β-CD and **2** under these conditions, since β-CD is partially deprotonated in 0.1 N NaOD/D_2O solution.

[19] K. A. Connors, *Binding Constants. The Measurement of Molecular Complex Stability*, Wiley, New York, **1987**.

[20] It can be shown (D. R. Alston, T. H. Lilley, J. F. Stoddart, *J. Chem. Soc. Chem. Commun.* **1985**, 1600) that for 1:1 complex formation, the observed chemical shift difference Δ between the free and complexed components, for an appropriate ^{1}H NMR probe, is dependent upon the concentration c of the 1:1 complex, according to equation, $\Delta = \Delta_0 - (\Delta/c)^{1/2}(\Delta_0/K_a)^{1/2}$, where Δ_0 is the chemical shift difference between the ^{1}H NMR probe in the fully formed 1:1 complex and in the free components. Measurements of the chemical shift differences for H3 in DM-β-CD at various concentrations and a subsequent plot of Δ against $(\Delta/c)^{1/2}$ gave rise to straight lines, which confirmed 1:1 complex formation. The K_a values were calculated directly from the slopes and the ordinate intercepts of these lines. Note that the K_a value for DM-β-CD · **2** has still to be determined.

[21] No acylation of DM-β-CD seems to take place during the Schotten-Baumann reaction. Polyamides were also produced during the course of the reaction between **2** and terephthaloyl chloride, but they could be separated easily from the desired products by the purification procedure described in the Experimental Procedure.

[22] However, it is conceivable that the formation of **3** and **4** is controlled by templates of sodium or hydrated sodium ions in the 0.01 N NaOH solution.

[23] The [2]catenane **6** is only sparingly soluble in H_2O and MeOH. Catenanes **5**, **6**, and **7a** and **b** are all soluble in Me_2CO but not at all in Et_2O.

[24] W. Vetter, E. Logemann, G. Schill, *Org. Mass. Spectrom.* **1977**, *12*, 351.

[25] Saturation transfer experiments involving H3 and H5 in the DM-β-CD component and the aromatic protons in the synthetic macrocyclic component support the view that in organic solvents both the bitolyl and terephthaloyl units occupy the cavity of the CD at different times.

[26] For example, the bitolyl methylene group in **7a** can be identified in the ^{1}H NMR spectrum ($CDCl_3$) as *one* singlet at $\delta = 4.62$, whereas *two* singlets are observed at $\delta = 4.59$ and 4.65 for these protons in **7b**. In common with the ^{1}H NMR spectrum of the [2]catenane **6**, the diastereotopicities of the bitolyl methylene protons are not evident. Since this communication was accepted for publication, separation of **7a** from **7b** has been achieved by using reverse-phase HPLC under conditions where **7b** is eluted ahead of **7a**.

[27] Crystal data for **5** · H_2O: orthorhombic, $a = 14.989(2)$, $b = 23.147(8)$, $c = 31.254(7)$ Å, $V = 10843$ Å^3, space group $P2_12_12_1$, $Z = 4$, $\varrho = 1.25$ g cm^{-3}, 4159 independent observed reflections with $[|F_o| > 3\sigma(|F_o|)$, $2\theta \leq 116°]$ refined to a current $R = 0.143$, $R_w = 0.138$ [28].

[28] Siemens P3/PC diffractometer, ω-scans, $Cu_{K\alpha}$ radiation (graphite monochromator). The structure was solved by direct methods and refined isotropically (there were too few observed data to permit meaningful anisotropic refinement). Further details of the crystal structure investigations can be obtained from the Cambridge Crystallographic Data Centre, 12 Union Road, Cambridge CB2 1EZ (UK) on quoting the full journal citation.

[29] D. Armspach, P. R. Ashton, C. P. Moore, N. Spencer, J. F. Stoddart, T. J. Wear, unpublished results.

[30] See [3c] and C. L. Brown, PhD Thesis, University of Sheffield, **1991**.

[W(CH)(dmpe)$_2$(*n*Bu)], a Complex with a Bent Methylidyne Ligand**

By *Joseph Manna, Steven J. Geib,* and *Michael D. Hopkins**

Among the extensive class of transition metal alkylidyne (or carbyne) complexes,[1] the parent derivatives—those bearing the methylidyne ligand (CH)—are underrepresented.[2–4] That these particular complexes are scarce is unfortunate, as it is only in the context of their structures, properties, and reactivity that the electronic and steric effects of the alkylidyne R groups of all other types of alkylidyne compounds can be fully judged. Although the reactivity of methylidyne complexes has been explored in some de-

[*] Prof. M. D. Hopkins, J. Manna, Dr. S. J. Geib
Department of Chemistry, University of Pittsburgh
Pittsburgh, PA 15260 (USA)
Telefax: Int. code + (412)624-8552

[**] This research was supported by the National Science Foundation, the Camille and Henry Dreyfus Foundation, the Alfred P. Sloan Foundation, and the David and Lucile Packard Foundation.

tail,[2-5] the only detailed X-ray crystallographic study of a compound with a terminal methylidyne ligand was unsuccessful due to disorder in the crystal.[6] As part of our studies of the electronic structures of alkylidyne complexes,[7] we have prepared and structurally characterized the methylidyne compound **1**. In addition to providing the first precise

$[W(CH)(dmpe)_2(n\text{Bu})]$ **1**

dmpe = $Me_2PCH_2CH_2PMe_2$

data for a methylidyne complex, compound **1** is significant in that it clearly illustrates that the molecular and electronic structure of the M≡C–H moiety can be strongly perturbed by the *trans* ancillary ligand, and because of the surprising observation that its methylidyne ligand is bent by nearly 20°.

Addition of *n*-butyllithium (1 equiv) to a pentane/toluene (4:1) solution of $[W(CH)(dmpe)_2(OTf)]$ (1 equiv; OTf = O_3SCF_3),[8] followed by workup and recrystallization from toluene at −40 °C, provides yellow **1** in 45% yield. Compound **1** was characterized by elemental analyses,[9] ^1H, ^{13}C, and ^{31}P NMR spectroscopy,[9] and X-ray crystallography.[10] The ^1H and ^{13}C NMR spectroscopic data for **1** are uniquely consistent with its formulation as an η^1-methylidyne complex. The ^1H and ^{13}C NMR signals of the methylidyne ligand are observed at $\delta = 6.01$ and $\delta = 244.9$, respectively, nearly identical to the positions of the corresponding signals in $[W(CH)(dmpe)_2Cl]$ (^1H, $\delta = 5.98$; ^{13}C, $\delta = 246$),[2b] and the splittings of the signals show that these nuclei are coupled to each other ($^1J_{C,H} = 121$ Hz), to tungsten ($^1J_{C,W} = 173$, $^2J_{H,W} = 67$ Hz), and to phosphorus. It is noteworthy, however, that the magnitudes of the couplings within the WCH unit are smaller than those of simple methylidyne compounds ($^1J_{C,H} = 130-150$, $^1J_{C,W} = 192-289$, $^2J_{H,W} = 79.6-90$ Hz),[2-4] as well as those of the Lewis acid adducts $[W(CH \cdot AlMe_3)(PMe_3)_3Cl]$ and $[W(CH \cdot AlMe_2Cl)(PMe_3)_3Cl]$ ($^1J_{C,H} = 129.4$ and 144.0, respectively, and $^2J_{H,W} = 83.5$ and 81.6 Hz, respectively).[2c] In fact, the value of $^1J_{C,H}$ for **1** is equal to that for the distorted methylidene complex $[W(CH_2)(PMe_3)_4I](OTf)$.[2c] These data suggest that the electronic structure of the W≡C–H core of **1** differs from those of previously reported methylidyne compounds; the differences between **1** and other compounds of the $[W(CH)L_4X]$ type can be traced directly to the presence of the strongly σ-donating *n*-butyl ligand in **1**.

The molecular structure of **1** was established by a single-crystal X-ray diffraction study (Fig. 1).[10] Although it is otherwise qualitatively similar to those of other *trans*-$[M(CR)L_4X]$ complexes,[1a,c,d] the structure of **1** is distinctive in two respects. First, the lengths of the W≡C (1.827(5) Å) and W–C (2.405(6) Å) bonds are longer than expected (cf. $d(W{\equiv}C) = 1.796(11)$ Å for $[W(CPh)(dmpe)_2Br]$ and $d(W{-}C) = 2.258(8)$ Å for $[W(CC\textit{t}Bu)(CH\textit{t}Bu)(CH_2\textit{t}Bu)(dmpe)]$),[7,11] since the *trans* influences of the methylidyne and *n*-butyl ligands are very strong. Although the above-mentioned W≡C distance does not lie outside of the range of known W≡C distances,[1a,c,d] it does, surprisingly, appear to be longer than that observed for the compositionally disordered Lewis acid adduct **2** ($x \approx 0.18$,

$[W(CH \cdot AlMe_{2-x}Cl_{1+x})(PMe_3)_3Cl]$ **2**

$d(W{\equiv}C) = 1.807(6)$ Å),[6] and is roughly equal to that found for the methylidene complex $[W(CH_2)(PMe_3)_4I](OTf)$

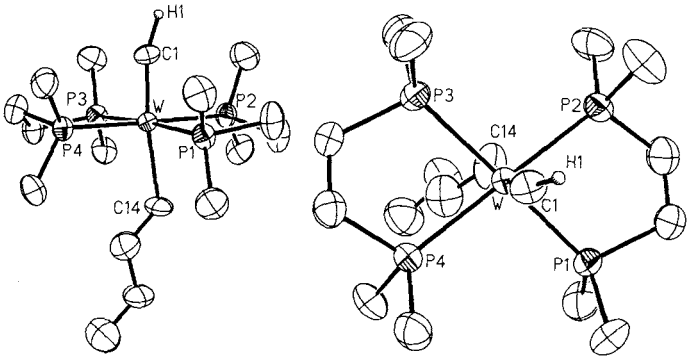

Fig. 1. Two views of the molecular structure of **1**. All hydrogen atoms except H1 have been omitted for clarity. Non-hydrogen atoms are represented by their thermal ellipsoids, which are drawn at the 50% probability level; the sphere for hydrogen is of arbitrary size. Selected bond lengths [Å] and bond angles [°]: W-C1 1.827(5), C1-H1 1.137(73), W-P1 2.436(2), W-P2 2.448(1), W-P3 2.452(2), W-P4 2.452(1), W-C14 2.405(6); W-C1-H1 162.3 (39), C1-W-C14 172.6(2), C1-W-P1 90.5(2), C1-W-P2 90.9(2), C1-W-P3 94.2(2), C1-W-P4 89.0(2), C14-W-P1 87.5(2), C14-W-P2 81.8(2), C14-W-P3 87.9(2), C14-W-P4 98.3(2), P1-W-P2 80.9(1), P2-W-P3 99.3(1), P3-W-P4 80.9(1), P4-W-P1 98.9(1).

(1.83(2) Å).[5c] Second, and more striking, is that the methylidyne ligand of **1** is decidedly bent (∢ W≡C–H = 162.3(39)°).[12] This result is unexpected in view of the fact that 70 of the 75 structurally characterized alkylidyne complexes possess M≡C–R bond angles greater than 170°; the bending for **1** is the largest yet observed.[1a,c,d] Remarkably, the methylidyne bond angle in **1** is comparable to that of **2** (163.8(44)°) (Scheme 1),[6] for which the bending of the W≡C–H linkage has been interpreted as being the result of the interaction between the methylidyne ligand and the aluminum center.

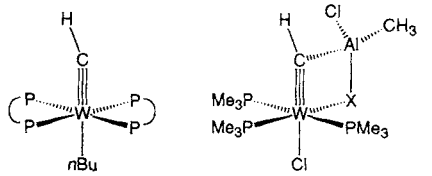

1
d(W≡C) 1.827 (5) Å
∢(W≡C–H) 162.3 (39)°

2
d(W≡C) 1.807 (6) Å
∢(W≡C–H) 163.8 (44)°
X = 0.82 CH_3, 0.18 Cl

Scheme 1. Comparison of the important structural data of **1** and **2**.

There are several possible explanations for the bending of the methylidyne ligand of **1**. The first stems from the observation that molecules of **1** are arranged in the crystal in a head-to-head fashion (Fig. 2). In this dimer, which is formed about a crystallographic center of inversion, there is significant interdigitation among the methylidyne ligands and dmpe methyl groups; the intermolecular distances between the methylidyne ligands ($d(W{\equiv}C\cdots C{\equiv}W) = 3.58$, $d(W{\equiv}C{-}H\cdots C{\equiv}W) = 3.02$, $d(W{\equiv}C{-}H\cdots H{-}C{\equiv}W) = 2.84$ Å) are 0.2–0.4 Å larger than the sums of the corresponding van der Waals radii ($2r_C = 3.4$, $r_C + r_H = 2.9$, $2r_H = 2.4$ Å). It is well known that C≡C–H bending force constants are small by comparison to those of C=C–H and C–C–H groups;[13] if W≡C–H bending force constants are also small, the bending of the methylidyne ligand may simply be a response to the forces of crystal packing, and specifically to the methylidyne ligand of the adjacent molecule. Arguing against this possibility, however, is the fact that the bending

of the methylidyne ligand results in even closer van der Waals contacts for H1 elsewhere in the dimer (d(H1 ··· H(dmpe)) = 2.41, 2.42, 2.68 Å); a smaller bend would seem to be required if avoidance of such contacts is the only important factor.

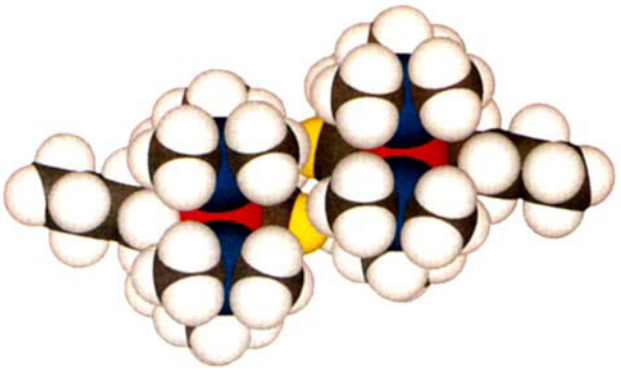

Fig. 2. Space-filling representation of the head-to-head docking of two molecules of **1** in the crystal. The hydrogen atoms of the methylidyne ligand are highlighted in yellow. Selected intermolecular distances [Å] and angles [°] between the methylidyne ligands: d(WC ··· CW) = 3.577, d(WCH ··· CW) = 3.023, d(WCH ··· HCW) = 2.842, ∢(W≡C ··· C) = 139.0.

A second possibility is that the methylidyne ligand of **1** is intrinsically bent. An ab initio theoretical study of the hypothetical ion $[Cr(CH)(CO)_5]^+$ specifically addressed the question of methylidyne bending, and found the linear geometry to be the most stable.[14] One difference, though, between the M≡C π orbitals of **1** and those of $[Cr(CH)(CO)_5{}^+]$ is that those of **1** are nondegenerate in the limiting C_{2v} symmetry imposed by the dmpe ligands (∢ PWP ≈ 81° and 99° within and between the dmpe ligands, respectively). Calculations by Hall et al. indicate that the slight (3°) tilting of the ethylidyne methyl group of $[Cr(CMe)(CO)_4Cl]$ induced by crystal-packing is responsible for the widely differing Cr–CO bond lengths found for this molecule (Δd(Cr–C) = 0.056 Å);[15] it is possible, in a reverse fashion, that the inequivalency of the W≡C π orbitals that arises from the asymmetry of the dmpe ligands results in the bending of the C–H bond. Alternatively, the W≡C–H linkage could be bent for electronic reasons related to the *trans n*-butyl ligand. It has been noted that the C–H coupling constants for methylidyne ligands are about 100 Hz smaller than those for alkynes, indicating that the methylidyne C–H bonds are derived from a hybrid orbital at the triply bonded carbon that has greater p-orbital character than a first-order sp hybrid orbital.[4] The methylidyne C–H coupling constant for **1** is smaller still, suggesting an even higher degree of p-orbital character in its C–H bond relative to those of other methylidyne complexes. While a bonding description for **1** based upon formal sp^2 hybridization at the multiply bonded carbon atom is clearly inappropriate, the bending of the methylidyne ligand may reflect partial double-bond character of the W≡C bond resulting from rehybridization to accommodate the strongly σ-donating *n*-butyl ligand *trans* to it; this would be consistent with the elongated W≡C bond.

Finally, it is interesting to consider the crystal structure of **1** in the context of the rich C–C bond-forming chemistry of alkylidyne complexes. These species react with alkynes to give metallacyclobutadienes, metallatetrahedranes, and cyclopentadienyl metal compounds, as well as alkyne polymerization and metathesis products.[1a–c] In addition, intramolecular alkylidyne–alkylidyne coupling reactions are observed for bis(alkylidyne) compounds,[16, 17] and are a key step in the reductive coupling of carbon monoxide.[16, 18] Electronic factors aside, it is reasonable to expect that these reactions should be more facile for methylidyne complexes than for other alkylidyne complexes, because of the minimal steric demands of the methylidyne ligand. Consistent with this hypothesis is the recent observation by Templeton et al. that $[Tp'M(CH)(CO)_2]$ (M = Mo, W; Tp' = $HB(3,4\text{-}Me_2C_3HN_2)_3$) spontaneously dimerizes to give the unique vinylidene-bridged species $[\{Tp'M(CO)_2\}_2(\mu\text{-}CCH_2)]$.[4] In light of this, a particularly intriguing possibility is that the head-to-head docking and the bent C–H bond of **1** in the solid state represent an early intermediate along the reaction coordinate for the intermolecular methylidyne–methylidyne coupling of **1**, this coupling being sterically arrested by interferences among the dmpe methyl groups.

Received: July 3, 1992
Revised version: February 8, 1993 [Z 5448 IE]
German version: *Angew. Chem.* **1993**, *105*, 897

[1] a) A. Mayr, H. Hoffmeister, *Adv. Organomet. Chem.* **1991**, *32*, 227; b) A. Mayr, *Comments Inorg. Chem.* **1990**, *10*, 227; c) H. Fischer, P. Hofmann, F. R. Kreissl, R. R. Schrock, U. Schubert, K. Weiss, *Carbyne Complexes*, VCH Publishers, New York, **1988**; d) W. A. Nugent, J. M. Mayer, *Metal-Ligand Multiple Bonds*, Wiley, New York, **1988**; e) H. P. Kim, R. J. Angelici, *Adv. Organomet. Chem.* **1987**, *27*, 51; f) M. A. Gallop, W. R. Roper, *ibid.* **1986**, *25*, 121.

[2] a) P. R. Sharp, S. J. Holmes, R. R. Schrock, M. R. Churchill, H. J. Wasserman, *J. Am. Chem. Soc.* **1981**, *103*, 965; b) S. J. Holmes, D. N. Clark, H. W. Turner, R. R. Schrock, *ibid.* **1982**, *104*, 6322; c) S. J. Holmes, R. R. Schrock, M. R. Churchill, H. J. Wasserman, *Organometallics* **1984**, *3*, 476.

[3] M. H. Chisholm, K. Folting, D. M. Hoffman, J. C. Huffman, *J. Am. Chem. Soc.* **1984**, *106*, 6794.

[4] G. M. Jamison, A. E. Bruce, P. S. White, J. L. Templeton, *J. Am. Chem. Soc.* **1991**, *113*, 5057.

[5] a) S. J. Holmes, R. R. Schrock, *J. Am. Chem. Soc.* **1981**, *103*, 4599; b) M. R. Churchill, H. J. Wasserman, *Inorg. Chem.* **1981**, *20*, 4119; c) M. R. Churchill, H. J. Wasserman, S. J. Holmes, R. R. Schrock, *Organometallics* **1982**, *1*, 766; d) A. J. Schultz, J. M. Williams, R. R. Schrock, S. J. Holmes, *Acta Crystallogr. Sect. C* **1984**, *40*, 590.

[6] M. R. Churchill, A. L. Rheingold, H. J. Wasserman, *Inorg. Chem.* **1981**, *20*, 3392.

[7] J. Manna, T. M. Gilbert, R. F. Dallinger, S. J. Geib, M. D. Hopkins, *J. Am. Chem. Soc.* **1992**, *114*, 5870.

[8] Prepared from $[W(CH)(dmpe)_2Cl]$ by a procedure analogous to that for $[W(CH)(PMe_3)_4(OTf)]$ [2c].

[9] NMR data for **1** (C_6D_6, 25 °C, J in Hz). ^{1}H NMR (300.13 MHz): δ = 6.01 (quin, ^2J(HW) = 67, ^3J(HP) = 4.1, 1H; W≡CH), 1.66 (br, 12H; PCH_3), 1.51 (m, 4H; PCH_2), 1.37 (br, 12H; PCH_3), 1.33 (m, 4H; PCH_2), 1.40 (m, 2H; $WCH_2CH_2CH_2CH_3$), 1.13 (m, 2H; $WCH_2CH_2CH_2CH_3$), 1.06 (t, 3H; $WCH_2CH_2CH_2CH_3$), −1.19 (m, 2H; $WCH_2CH_2CH_2CH_3$). ^{13}C NMR (75.46 MHz; assignments made by comparison with $^{13}C\{^1H\}$ NMR data): δ = 244.9 (d quin, ^1J(CH) = 121, ^1J(CW) = 173, ^2J(CP) = 13.4; W≡CH), 40.9 (t quin, ^1J(CH) = 117, ^3J(CP) = 5.6; $WCH_2CH_2CH_2CH_3$), 35.2 (m; PCH_2), 33.5 (t, ^1J(CH) = 125; $WCH_2CH_2CH_2CH_3$), 29.0 (m; PCH_3), 15.9 (m; PCH_3), 14.2 (q, ^1J(CH) = 123; $WCH_2CH_2CH_2CH_3$), 3.97(t quin, ^1J(CH) = 117, ^2J(CP) = 8.0; $WCH_2CH_2CH_2CH_3$). $^{31}P\{^1H\}$ (121.49 MHz): δ = 21.5 (s, ^1J(PW) = 271). Correct C,H analyses.

[10] Crystal data for $C_{17}H_{42}P_4W$: Triclinic, $P\bar{1}$, a = 9.198(2), b = 9.337(2), c = 15.084(2) Å, α = 82.55(2), β = 82.35(2), γ = 72.75(2)°, V = 1220.6(4) Å^3, Z = 2, ϱ_{calcd} = 1.508 g cm^{-3}, $\mu(Mo_{K\alpha})$ = 49.91 cm^{-1}, T = 224 K. The structure was solved by direct methods. All 3421 reflections measured ($4° < 2\theta < 46°$) were used in the refinement of the structure. A semiempirical absorption correction (XABS) and an extinction correction were applied to the data. All non-hydrogen atoms were located and refined anisotropically. The methylidyne hydrogen atom H1 appeared as a distinct feature in a Fourier difference map ($\Delta\rho$(H(1)) = 0.58 e Å^{-3}; $\sigma(\rho)$(average) = 0.20 e Å^{-3}) and was refined isotropically (U = 0.110(27) Å^2). Although there are larger difference peaks in the map than that for H1, these either lie near the tungsten center (d < 1.14 Å), and hence are attributable to noise associated with that atom, or, in one case, is the result of slight disorder within the *n*-butyl ligand (near C15). For this reason, and because of the well-behaved refinement of this atom, we believe the H1 peak to be genuine. All other hydrogen-atom positions were calculated (d(C–H) = 0.96 Å); R_F = 0.0298, R_{wF} = 0.0341, GOF = 0.94, δ/ρ = 1.08 e Å^{-3} (near W), data:parameter ratio = 16.8:1. Further details of the crystal structure investigation are available on request from the

Director of the Cambridge Crystallographic Data Centre, 12 Union Road, GB-Cambridge CB2 1EZ (UK), on quoting the full journal citation.
[11] M. R. Churchill, W. J. Youngs, *Inorg. Chem.* **1979**, *18*, 2454.
[12] Following the completion of this work, we reported (J. Manna, S. J. Geib, M. D. Hopkins, *J. Am. Chem. Soc.* **1992**, *114*, 9199) that [W(CH)(dmpe)$_2$(CCSiMe$_3$)] also appears to possess a bent methylidyne ligand ($\measuredangle$(W≡C–H = 164.4 (55)°), although the deviation from linearity is not as statistically significant as in the case of **1**. We are attempting to confirm these observations through neutron diffraction studies.
[13] E. B. Wilson, Jr., J. C. Decius, P. C. Cross, *Molecular Vibrations*, McGraw-Hill, New York, **1955**, p. 176.
[14] J. Ushio, H. Nakatsuji, T. Yonezawa, *J. Am. Chem. Soc.* **1984**, *106*, 5892.
[15] A. A. Low, M. B. Hall, *Organometallics* **1990**, *9*, 701.
[16] A. Mayr, C. M. Bastos, *Prog. Inorg. Chem.* **1992**, *40*, 1.
[17] A. C. Filippou, W. Grünleitner, C. Völkl, P. Kiprof, *Angew. Chem.* **1991**, *103*, 1188; *Angew. Chem. Int. Ed. Engl.* **1991**, *30*, 1167; H. G. Alt, *ibid.* **1991**, *103*, 1139 and **1991**, *30*, 1119, and references therein.
[18] R. N. Vrtis, S. J. Lippard, *Isr. J. Chem.* **1990**, *30*, 331.

Gaseous Mercury(IV) Fluoride, HgF_4: An Ab Initio Study**

By *Martin Kaupp** and *Hans Georg von Schnering*

The group 12 elements are usually considered to be main group rather than transition elements, since the completely filled $(n-1)$d shell does not participate in chemical bonding.[1, 2] Hence, the known chemistry of these elements is restricted to the M^{II} or lower oxidation states.[2] In general, the maximum achievable oxidation numbers increase from left to right within the first half of a given transition metal row (up to Mn^{VII}, Ru^{VIII}, and Os^{VIII}, respectively) but drop back in the second half. While the discovery of Cu^{IV} in Cs_2CuF_6[3a] and of Au^{V} in $CsAuF_6$[3b] have stimulated interest in group 12 elements exhibiting oxidation states beyond II, there is only one report of a short-lived, electrochemically generated Hg^{III} species in solution.[4]

The first four ionization potentials of Zn, Cd, and Hg (cf. Table 1) clearly show that mercury is the most likely candidate for the occurrence of oxidation states higher than II (which invariably involve d orbitals in bonding) within this group. At least in part this is due to relativistic effects which stabilize and contract the 6s orbital but destabilize and expand the 5d orbitals (spin-orbit coupling also splits the d levels).[5] Thus, ionization from d levels becomes easier and simultaneously sd hybridization is energetically more favorable with Hg than with Zn or Cd. The same effects are responsible for the great importance of the III or V oxidation states in gold chemistry compared to copper or silver[6].

Table 1. Ionization energies [eV] of the group 12 elements.

	I	II	III	IV
Zn exp. [a]	9.391	17.96	39.7	59.4
calcd. [b]	9.2	17.7	39.3	59.2
Cd exp. [a]	8.991	16.904	37.47	
calcd. [b]	8.8	16.6	37.2	53.4
Hg exp. [a]	10.43	18.751	34.2	
calcd. [b]	10.2	18.3	34.7	48.0

[a] Cf. ref. [15]. [b] This work: Averaged coupled pair functional results (cf., e.g. ref. [12b]) with quasirelativistic 20-valence-electron pseudopotentials [8e, 16] and 6s5p3d2f valence basis sets. No spin–orbit coupling has been considered.

[*] Dr. M. Kaupp, Prof. Dr. H. G. von Schnering
Max-Planck-Institut für Festkörperforschung
Heisenbergstrasse 1, D-W-7000 Stuttgart 80 (FRG)
Telefax: Int. code + (711)689-1562

[**] We thank Prof. Dr. H. Stoll and Dr. H. Borrmann for valuable discussions.

We have carried out high-level ab initio calculations, by using relativistic pseudopotentials, on the structure, stability, and vibrational frequencies of gaseous HgF_4. Our results strongly suggest it to be a viable molecular species. For comparison we have also studied KrF_2, one of the few known and well-characterized[7] endothermic fluorine compounds.

The structure of HgF_4 (in D_{4h} symmetry), optimized at the Hartree–Fock (HF),[8a] MP2,[8a, b] and QCISD levels[9, 10] of theory is shown in Figure 1. Harmonic vibrational frequency analysis at the HF level[8a] (see below) confirms the square-planar structure to be a minimum on the potential energy surface, in agreement with the expectations for a tetracoordinate low-spin $5d^8$ species,[1] and with previous results for the isoelectronic AuF_4^-.[6c]

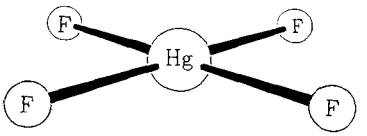

Fig. 1. Structure of HgF_4. Calculated Hg–F distances [Å] (D_{4h} symmetry): 1.886 (HF, cf. refs. [8a,b]); 1.962 (MP2, cf. refs. [8a,b]); 1.923 (MP2, with one additional f function at the metal); 1.904 (ANO–MP2, cf. refs. [8a,b, 9, 10]); 1.884 (ANO–QCISD, cf. refs. [9, 10]).

The results of large-scale ANO-QCISD and ANO-QCISD(T) calculations[9, 10] of the energies of several important reactions involving HgF_4 or KrF_2[11] are shown in Table 2. Experimental data for KrF_2 are also included. The most probable decomposition pathway for HgF_4 in the gas phase (at least at low concentrations) is the reductive elimination of F_2 [Table 2, Eq. (a)]. This reaction is slightly exothermic at the QCISD level ($\Delta E = -12.5\ kJ\,mol^{-1}$) but slightly endothermic ($\Delta H_0 = +11.6\ kJ\,mol^{-1}$) when contributions from connected triple excitations to the wavefunction (QCISD(T)) and zero point vibrational energy corrections (ZPE) are included. In contrast, loss of F_2 from KrF_2 [Table 2, Eq. (b)] is considerably exothermic ($\Delta H = -75.5\ kJ\,mol^{-1}$). Hence, the oxidation of (gaseous monomeric) HgF_2 by KrF_2 [Eq. (c)] also is remarkably exothermic ($\Delta H_0 = -94.2\ kJ\,mol^{-1}$).

Table 2. Reaction energies [kJ mol^{-1}] involving HgF_4 or KrF_2 [a].

Reaction	ZPE [b]	QCISD [c]	QCISD(T) [c]	exp.
(a) $HgF_4 \rightarrow HgF_2 + F_2$	−7.1	−12.5	+18.7	
(b) $KrF_2 \rightarrow Kr + F_2$	−3.8	−93.3	−75.5	−60.2 [d]
(c) $HgF_2 + KrF_2 \rightarrow HgF_4 + Kr$	+3.3	−80.8	−94.2	
(d) $F_2 \rightarrow 2\,F$	−7.1	+114.5	+142.9	+159.7
				(+154.2) [e,f]
(e) $KrF_2 \rightarrow Kr + 2\,F$	−10.9	+21.3	+67.4	+99.5 [d]
(f) $HgF_4 \rightarrow Hg + 4\,F$	−23.4	+562.2	+642.7	
(g) $HgF_2 \rightarrow Hg + 2\,F$	−9.2	+460.2	+481.2	
(h) $HgF_4 \rightarrow HgF_2 + 2\,F$	−14.2	+102.9	+161.6	

[a] Calculations at the QCISD-optimized structures. [b] Unscaled HF zero-point vibrational energy contributions. [c] Quadratic CI results [9, 10] without vibrational energy corrections. [d] Cf. ref. [7c]. [e] Cf. ref. [17]. [f] $D_e(D_0)$ values given.

At the ANO-QCISD(T) level of theory, the F_2 and KrF_2 atomization energies [Table 2, Eqs. (d) and (e)], which are quite demanding to calculate,[7d, 12] agree within about 17 and 40 kJ mol^{-1} to those values obtained from experiment (i.e. the average binding energies are underestimated by ca. 17 and 20 kJ mol^{-1}, respectively). The accuracy for the at-

omization energies of HgF_4 and HgF_2 [Eqs. (f) and (g)] is somewhat less certain as, for example, spin-orbit coupling was not included in the QCI calculations. Unfortunately no accurate experimental value for gaseous HgF_2 is available. However, the remaining correlation energy errors in HgF_4 will be larger than those in HgF_2 (as seen by the larger contribution of triple excitations to the average binding energy, cf. Table 2). Thus we probably *underestimate* rather than overestimate the stability of HgF_4 relative to HgF_2! Due to error compensation the F_2 elimination reactions will exhibit smaller errors than the atomization energies (in these reactions the number of electron pairs is kept constant). Indeed, the error in the QCISD(T) reaction energy for F_2 elimination from KrF_2 [Eq. (b)] is only about 19 kJ mol^{-1}. We estimate the error in the energy for oxidation of HgF_2 by KrF_2 [Eq. (c)] also to be below about 20–30 kJ mol^{-1}. A detailed account of the performance of various theoretical approaches, and of the influence of relativistic effects on the reaction energies, will be published elsewhere.[13]

The atomization energies given in Table 2 [Eqs. (e)–(g)] show that, while the average Hg–F binding energy in HgF_4 (ca. 160 kJ mol^{-1}) is considerably smaller than that in HgF_2 (ca. 240 kJ mol^{-1}), it is still significant and much larger than the average Kr–F binding energy in KrF_2 (50 kJ mol^{-1} [7c]). The two additional Hg–F bonds in HgF_4 together account for a gain of about 160 kJ mol^{-1} compared to $HgF_2 + 2$ F [Eq. (h)]. Thus, in the gas phase the formation of HgF_4 from HgF_2 and atomic fluorine also would be significantly exothermic. In the solid state HgF_2 will be favored by its lattice energy: Preliminary calculations indicate that there is no significant stabilization of HgF_4 by aggregation or anionic complexation.[13] We expect HgF_4 to be a rather volatile substance.

The results of the harmonic vibrational frequency analysis (at the HF level[8a]) for HgF_4 are listed in Table 3. Due to the high symmetry present, the IR and Raman spectra are expected to contain only four and three bands, respectively. Thus, it should be possible to identify HgF_4, if obtained, by means of vibrational spectroscopy (the wavenumbers calculated for HgF_2[14] are significantly different). In view of the good agreement between Hartree–Fock and experimental frequencies of HgF_2[14] and AuF_4^-,[6c] we expect a similar accuracy (ca. 10–20 cm^{-1}) in the calculated wavenumbers for HgF_4.

Table 3. Calculated harmonic vibrational wavenumbers for HgF_4 [a].

Symmetry	ω [cm^{-1}]	Character	IR [b]	Raman [b]
b_{2u}	179	out of plane	yes	no
A_{2u}	233	out of plane	yes	no
b_{2g}	252	in plane	no	yes
E_u	261	in plane	yes	no
b_{1g}	650	stretch	no	yes
A_{1g}	652	stretch	no	yes
E_u	721	stretch	yes	no

[a] Cf. ref. [8a]. [b] Infrared or Raman activity.

In conclusion, our calculations indicate that it should be possible to prepare and characterize (e.g. by matrix isolation spectroscopy) mercury(IV) fluoride. Even if decomposition into $HgF_2 + F_2$ [Eq. (a)] were slightly exothermic, the significant nuclear reorganization involved (two Hg–F bonds are broken and one F–F bond is formed), and the small reaction energy suggest a significant activation barrier for this reaction. Unfortunately, our attempts to obtain an accurate estimate for the barrier height have failed up to now. The wavefunction near the transition state has strong multireference character (i.e. large nondynamical electron correlation effects have to be considered), and the internal nuclear coordinates are strongly coupled (spin–orbit coupling may also complicate the situation).

The gas-phase reaction $HgF_2 + KrF_2 \rightarrow HgF_4 + Kr$ [Eq. (c)] is considerably exothermic. Perhaps, a solvent-based low-temperature variant of this reaction is a route into Hg^{IV} chemistry. The calculated vibrational frequencies should aid in the experimental characterization of HgF_4.

Received: January 29, 1993 [Z 5840 IE]
German version: *Angew. Chem.* **1993**, *105*, 952

[1] a) F. A. Cotton, G. Wilkinson, *Advanced Inorganic Chemistry*, 5th ed, Wiley, New York, **1988**; b) N. N. Greenwood, A. Earnshaw, *Chemistry of the Elements*, Pergamon, Oxford, **1984**.

[2] *Comprehensive Coordination Chemistry, Vol. 5* (Ed.: G. Wilkinson), Pergamon, Oxford, **1987**.

[3] a) W. Harnischmacher, R. Hoppe, *Angew. Chem.* **1973**, *85*, 590; *Angew. Chem. Int. Ed. Engl.* **1973**, *12*, 582; b) K. Leary, N. Bartlett, *J. Chem. Soc. Chem. Commun.* **1972**, 903.

[4] R. L. Deming, A. L. Allred, A. R. Dahl, A. W. Herlinger, M. O. Kestner, *J. Am. Chem. Soc.* **1976**, *98*, 4132.

[5] See for example: P. Pyykkö, *Chem. Rev.* **1988**, *88*, 563.

[6] a) P. Schwerdtfeger, *J. Am. Chem. Soc.* **1989**, *111*, 7261; b) P. Schwerdtfeger, M. Dolg, W. H. E. Schwarz, G. A. Bowmaker, P. D. W. Boyd *J. Chem. Phys.* **1989**, *91*, 1762. c) P. Schwerdtfeger, P. D. W. Boyd, S. Brienne, A. K. Burrell, *Inorg. Chem.* **1992**, *31*, 3481. See also ref. [5].

[7] See for example: a) F. Schreiner, J. G. Malm, J. C. Hindman, *J. Am. Chem. Soc.* **1965**, *87*, 25; b) W. Harshberger, R. K. Bohn, S. H. Bauer, *ibid.* **1967**, *89*, 6466. c) S. R. Gunn, *J. Phys. Chem.* **1967**, *71*, 2934. d) P. S. Bagus, B. Liu, H. F. Schaefer III, *J. Am. Chem. Soc.* **1972**, *94*, 6635, and references therein.

[8] a) Structure optimizations at the Hartree–Fock (HF) level and with second order Møller–Plesset perturbation theory (MP2, cf. ref. [8b]) as well as HF harmonic vibrational frequency analyses employed the Gaussian 90 and Gaussian 92 programs (cf. ref. [8c, d]). Mercury has been treated as a 20-valence-electron system, the 60 core electrons being replaced by an quasirelativistic multielectron-fit pseudopotential (ref. [8e]), as it is known that scalar relativistic effects have to be included to obtain reliable data for mercury systems (see, e.g., ref. [5]). Similar pseudopotentials have been used for Kr (8 valence electrons, ref. [8f]) and F (7 valence electrons, ref. [8g]). Contributions from spin-orbit coupling have not been considered in the present study. The HF and MP2 calculations employed an (8s7p5d)/[6s5p3d] GTO valence basis set for Hg (ref. [8e]), a (6s6p1d)/[4s4p1d] valence basis on Kr (ref. [8f]) and (5s5p1d)/[3s3p1d] including diffuse functions on F (ref. [8h]). b) Explanations of standard levels of ab initio theory including HF and MP2 may be found in: W. J. Hehre, L. Radom, P. von R. Schleyer, J. A. Pople, *Ab Initio Molecular Orbital Theory*, Wiley, New York, **1986**. c) Gaussian 90, Revision F, M. J. Frisch, M. Head-Gordon, G. W. Trucks, J. B. Foresman, H. B. Schlegel, K. Raghavachari, M. Robb, J. S. Binkley, C. Gonzalez, D. J. DeFrees, D. I. Fox, R. A. Whiteside, R. Seeger, C. F. Melius, J. Baker, L. R. Kahn, J. J. P. Stewart, S. Topiol, J. A. Pople, Gaussian, Inc., Pittsburgh, PA, **1990**. d) Gaussian 92, Revision A, M. J. Frisch, G. W. Trucks, M. Head-Gordon, P. M. W. Gill, M. W. Wong, J. B. Foresman, B. G. Johnson, H. B. Schlegel, M. A. Robb, E. S. Replogle, R. Gomperts, J. L. Andres, K. Raghavachari, J. S. Binkley, C. Gonzalez, R. L. Martin, D. I. Fox, D. J. DeFrees, J. Baker, J. J. P. Stewart, J. A. Pople, Gaussian, Inc., Pittsburgh PA, **1992**. e) D. Andrae, U. Häussermann, M. Dolg, H. Stoll, H. Preuss, *Theor. Chim. Acta* **1990**, *77*, 123. f) A. Nicklass, Diplom Thesis, Universität Stuttgart, **1990**. g) M. Dolg, Dissertation, Universität Stuttgart, **1989**. h) M. Kaupp, P. von R. Schleyer, H. Stoll, H. Preuss, *J. Am. Chem. Soc.* **1991**, *113*, 6012.

[9] For an explanation of the quadratic configuration interaction singles + doubles (QCISD) method and its extension by perturbation theoretical inclusion of triple excitations (QCISD(T)), see for example: J. A. Pople, M. Head-Gordon, K. Raghavachari, *J. Chem. Phys.* **1987**, *87*, 5968.

[10] a) QCISD and QCISD(T) calculations employed 8s7p5d2f, 6s6p5d3f, and 7s7p3d1f valence bases on Hg, Kr, and F, respectively, contracted in a general contraction scheme to 4s3p3d2f, 2s2p3d2f, and 3s3p2d1f. The contraction coefficients were obtained from the corresponding atomic natural orbitals (ANO, cf. ref. [10b]). All electrons outside the pseudopotential cores have been correlated. The QCI calculations used the MOLPRO92 (cf. ref. [10c]) and Gaussian (cf. ref. [8c, d]) programs. b) J. Almlöf, P. R. Taylor, *J. Chem. Phys.* **1987**, *86*, 4070. c) Ab initio program package MOLPRO by H.-J. Werner and P. J. Knowles. See for example: H.-J. Werner,

Adv. Chem. Phys. **1987**, *69*, 1 (cf. C. Hampel, K. Peterson, H.-J. Werner, *Chem. Phys. Lett.* **1992**, *190*, 1, and references therein, for the QCI program).
[11] The ANO–QCISD optimized (cf. ref. [9,10]) Kr–F bond length in KrF_2 is 1.873 Å, in good agreement with experiment (cf. ref. [7b]).
[12] See for example: a) G. E. Scuseria, T. P. Hamilton, H. F. Schaefer III, *J. Chem. Phys.* **1990**, *92*, 568; b) R. J. Gdanitz, R. Ahlrichs, *Chem. Phys. Lett.* **1988**, *143*, 413.
[13] M. Kaupp, H. Stoll, H. G. von Schnering, unpublished results.
[14] The HF harmonic vibrational frequencies for HgF_2: $\tilde{\nu}$[cm^{-1}] = 159 (Π_u), 577 (Σ_g), and 648 (Σ_u); experimental IR (matrix isolation) and Raman vibrational frequencies, $\tilde{\nu}$[cm^{-1}] = 170, 568, and 642, respectively (cf. A. Given, A. Loewenschuss, *J. Chem. Phys.* **1980**, *72*, 3809).
[15] C. E. Moore, *Ionization Potentials and Ionization Limits Derived from the Analysis of Optical Spectra (Natl. Stand. Ref. Data Ser. US Natl. Bur. Stand.* **1970**, *34*).
[16] M. Dolg, U. Wedig, H. Stoll, H. Preuss, *J. Chem. Phys.* **1987**, *86*, 866.
[17] M. W. Chase, C. A. Davies, J. R. Downey, Jr., D. J. Frurip, R. A. McDonald, A. N. Syverud, *J. Phys. Chem. Ref. Data Suppl.* **1985**, *14*, 635.

Reduced $[Fe_8S_6]$ Clusters: Binding Links between FeS and Active Centers of Iron-Sulfur Proteins**

By *Siegfried Pohl** and *Ulrich Opitz*

Iron–sulfur clusters form the active centers of a series of proteins. Their function is not only limited to the transfer of electrons, but they are also able to bind different substrates.[1, 2] The structural diversity of these Fe–S clusters, in particular, in the various nitrogenases and hydrogenases, is probably greater than that of the compounds known to date. This is also indicated by the first model of the FeMo cofactor of the nitrogenase of *Azotobacter vinelandii* based on an X-ray structure analysis by Kim and Rees.[3]

The wide spread of iron–sulfur clusters, their formation, probably at a very early stage of evolution, as well as their different ways of functioning gain additional significance in the light of a new theory from Wächtershäuser about the origin of life.[4, 5] Thus, a central role is played by the reaction of FeS with H_2S to give FeS_2 and H_2, which was recently reproduced under "geochemical" conditions in the laboratory.[6]

With $[Fe_8S_6I_8]^{4-}$ we have isolated the first Fe–S cluster, containing exclusively iron(II) centers (see Fig. 1). The $[Fe_8S_6]^{4+}$ cores of such clusters may not only serve as molecular models for the mentioned reduction of H^+ to H_2, but may also be suitable precursors for the modeling of active centers.

The iodo ligands, which cannot be described as biomimetic, seem to preclude the use of $[Fe_8S_6I_8]^{4-}$ as precursor for models of active centers of Fe–S proteins. However, under certain conditions the frequently used thiolato ligands are unsuitable for redox reactions, and this is probably not only valid in synthetic models. Thus, the distinct lack of cysteinyl ligands in the FeMo cofactor of *Azotobacter vinelandii* is striking.[3] Possibly also in Nature one reason for this lack of cysteinyl ligands is the avoidance of the formation of disulfide in multielectron processes such as N_2 reduction. Against this background, in synthetic model compounds iodide can in some cases be even more suitable than thiolate as a—for the occurring potentials—non-redox active ligand.

[*] Prof. Dr. S. Pohl, Dipl.-Chem. U. Opitz
Fachbereich Chemie der Universität
Postfach 25 03, D-W-2900 Oldenburg (FRG)
Telefax: Int. code + (441)798-3329

[**] This work was supported by the Deutsche Forschungsgemeinschaft and the Fonds der Chemischen Industrie.

Furthermore, the existence of Fe–S clusters raises the question of whether similar cluster fragments could not be (have been) present on FeS surfaces (e.g. mackinawite). Thus, in addition to the assumptions of Wächtershäuser,[5] electron transfer *and* substrate binding would be possible at such "active centers". The relatively simple reaction summarized in Equation (a) (non-stoichiometric) yields the octanu-

$$[Fe_4S_4I_4]^{2-} \xrightarrow[THF/CH_3CN]{[FeI_2(PR_3)_2]} [Fe_8S_6I_8]^{4-} \quad (a)$$

$PR_3 = PMePh_2$

clear Fe–S cluster as ammonium salt **1**, in the form of black prismatic crystals, which are stable in air for a short period.

$(PhCH_2NEt_3)_4\,[Fe_8S_6I_8]$ **1**

Formally, reaction (a) can be reduced to reaction (b). However, we have only obtained amorphous iron sulfide from reaction (b). Thus, an Fe^{II} excess seems favorable or even

$$2[Fe_4S_4I_4]^{2-} + 2PR_3 \longrightarrow [Fe_8S_6I_8]^{4-} + 2SPR_3 \quad (b)$$

necessary for the formation of the $[Fe_8S_6]$ cluster. Thus, for the optimized synthesis [Eq. (c)] (see also Experimental Procedure), an even greater Fe^{II} share is used. It is noteworthy

$$[Fe_4S_4I_4]^{2-} + 3FeI_2 + 3I^- + 4PMePh_2 \xrightarrow[THF/CH_3CN]{} 1/2[Fe_8S_6I_8]^{4-} + SPMePh_2 + 3[FeI_3PMePh_2]^- \quad (c)$$

that with only a slight variation of the reaction conditions and with identical stoichiometric ratios as for the preparation of **1** according to Equation (a) exclusively the hexanuclear cluster **2** is isolated.[7] Such a cluster with a slightly

$[Fe_6S_6I_2(PR_3)_4]$ **2**

different phosphane was previously characterized by Holm et al. a few years ago and was described as a "basket cluster".[8, 9] An X-ray structure analysis of **2** confirmed the identical construction.[10] Evidently, the formation of the $[Fe_8S_6]$ cluster occurs via the intermediate **2**. This hypothesis is supported by the reaction of **2** with $[FeI_3PR_3]^-$ in CH_2Cl_2, which also yields the octanuclear Fe–S cluster.[10] Reaction (d) shows, however, that **2** does not necessarily occur as intermediate.

$$[Fe_4S_4I_4]^{2-} \xrightarrow[THF/CH_3CN]{[Fe_2I_4(dppe)_2]} [Fe_8S_6I_8]^{4-} \quad (d)$$

$dppe = Ph_2PCH_2CH_2PPh_2$

The use of a bidentate phosphane ligand, which as a result of the distance of its coordinating centers should not be in the position to stabilize a compound analogous to **2**, nevertheless leads to the octanuclear Fe–S cluster according to (d), which can be isolated in the form of the salt **3** (see also Fig. 2), even if in significantly lower yield. Apparently, PR_3

$[Fe(dppe)(CH_3CN)_4]_2\,[Fe_8S_6I_8]$ **3**

is essential for the given reactions as a sulfur acceptor.[11] The formed phosphane sulfide can be easily separated. Thus, this route to $[Fe_8S_6]$ clusters is much more favorable and more unambiguous than the one described several years ago, which by using elemental iron led to the $[Fe_8S_6I_8]^{3-}$ anion.[12, 13]

Compounds **1** and **3** were characterized by X-ray structure analyses.[14] Both compounds contain $[Fe_8S_6I_8]^{4-}$ anions,

but with different cations. The cluster anion in **1** has crystallographic C_{4h} symmetry, whereas the anion of **3** lies on an inversion center. Possibly, the occupation of different crystallographic point groups is the reason why the extent of the observed tetragonal distortion of the Fe_8 cube in **1** and **3** is very different (Figs. 1 and 2). In **3** this distortion leads to differences in the Fe–Fe distances of on average almost 11 pm.

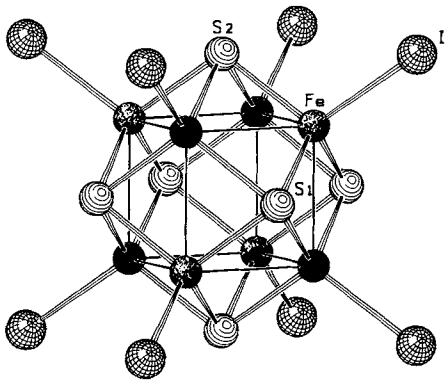

Fig. 1. Crystal structure of the anion of **1** (C_{4h} symmetry). Important distances [pm] and angles [°]: Fe-I 259.1(2), Fe-Fe 269.2(2) (eight distances) and 272.5(3) (four distances), Fe-S 231.3(3) and 232.6(3); Fe-S-Fe 107.8(1)–111.8(1) and 70.7(1)–72.2(1).

Rhombic dodecahedral $[M_8S_6]$ clusters such as in **1** and **3** were not only confirmed in other synthetic compounds such as $[Fe_8S_6I_8]^{3-}$,[12] $[Co_8S_6(SR)_8]^{4-}$,[15] $[Fe_3Ni_5S_6I_8]^{4-}$,[16] or $[Ni_8S_6Cl_2(PR_3)_6]$[17] (an inverse variant is $[Fe_6S_8(PR_3)_6]^{2+}$ [18]), but also observed in minerals such as the pentlandites,[19] bartonite,[20] or djerfisherite[21] (for the calculation of the electronic structure of $[M_8S_6]$ clusters see refs.[22, 23]).

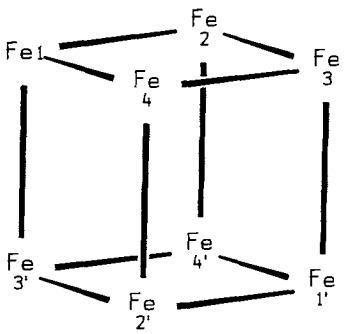

Fig. 2. Schematic representation of the Fe_8 cube in **3**. The cluster anion $[Fe_8S_6I_8]^{4-}$ is constructed as in **1**, and in **3** has C_i symmetry. Important distances [pm] and angles [°]: Fe1-Fe2 266.1(2), Fe2-Fe3 269.5, Fe3-Fe4 264.0, Fe4-Fe1 265.5, Fe1-Fe3' 276.1, Fe2-Fe4' 277.8.

According to preliminary investigations compound **1** reacts with elemental sulfur again to give the $[Fe_4S_4]$ cluster used as the starting material. In view of the reaction of FeS with H_2S, an almost analogous reaction seems to be of particular interest, that is the question of whether the cluster reacts according to Equation (e) with the formation of hydrogen. Similar is true for the reactions with thiols RSH. Such reactions are being carried out at present.

$$[Fe_8S_6I_8]^{4-} + 2H_2S \xrightarrow{?} 2[Fe_4S_4I_4]^{2-} + 2H_2 \qquad (e)$$

Experimental Procedure

All operations were carried out under a nitrogen atmosphere in dry, N_2 saturated solvents.

1: FeI_2 (0.928 g, 3 mmol), $(PhCH_2NEt_3)I$ (0.957 g, 3 mmol), $PMePh_2$ (0.801 g, 4 mmol), and $(PhCH_2NEt_3)_2[Fe_4S_4I_4]$ (1.234 g, 1 mmol) were dissolved in a mixture of THF and CH_3CN (1:1) (40 mL). The solution was kept at room temperature for six days. Then the solvent was removed and the residue was taken up in CH_3CN (40 mL). Insoluble material was separated by filtration and the solution was concentrated stepwise. After every step a fraction of **1** crystallized within two days. The solution was decanted each time, and the crystals were washed with CH_2Cl_2. After five steps a total of about 0.5 g (ca. 40%) **1** was obtained. Correct elemental analysis.

3: $[Fe_2I_4(dppe)_2]$ (1.416 g, 1 mmol) and $(PhCH_2NEt_3)_2[Fe_4S_4I_4]$ (1.234 g) were heated under reflux for a short time in a mixture of THF (40 mL) and CH_3CN (20 mL). After the mixture had cooled it was filtered and the precipitate formed was discarded. The solution was concentrated to 20 mL. After six days black, rod-like crystals of **3** were formed, which crystallized as $3 \cdot 2THF \cdot 2CH_3CN$. Yield: 0.1 g (ca. 6%). The high solvent content prevented exact quantitative analyses; however, we have always obtained a correct ratio of Fe:S:I.

Received: February 6, 1993 [Z 5854IE]
German version: *Angew. Chem.* **1993**, *105*, 950

[1] W. Kaim, B. Schwederski, *Bioanorganische Chemie*, Teubner, Stuttgart, **1991**, p. 135–149, and references therein.
[2] R. Cammack in *Advances in Inorganic Chemistry*, *Vol. 38* (Eds.: R. Cammack, A. G. Sykes), Academic Press, London, **1992**, p. 281–322, and references therein.
[3] J. Kim, D. C. Rees, *Science* **1992**, *257*, 1677; *Nature* **1992**, *360*, 553.
[4] G. Wächtershäuser, *Syst. Appl. Microbiol.* **1988**, *10*, 207.
[5] G. Wächtershäuser, *Prog. Biophys. Mol. Biol.* **1992**, *58*, 85.
[6] E. Drobner, H. Huber, G. Wächtershäuser, D. Rose, K. O. Stetter, *Nature* **1990**, *346*, 742.
[7] The ratio of $[Fe_4S_4I_4]^{2-}$ to $[FeI_2(PR_3)_2]$ is according to Equation (a) 1:2. If the solution is concentrated within one day, **2** crystallizes in approximately 70% yield; cf. Experimental Procedure for **1**.
[8] B. S. Snyder, M. S. Reynolds, I. Noda, R. H. Holm, *Inorg. Chem.* **1988**, *27*, 595; B. S. Snyder, R. H. Holm, *ibid.* **1988**, *27*, 2339; M. S. Reynolds, R. H. Holm, *ibid.* **1988**, *27*, 4494; B. S. Snyder, R. H. Holm, *ibid.* **1990**, *29*, 274.
[9] C. Chen, J. Cai, Q. Liu, D. Wu, X. Lei, K. Zhao, B. Kang, *Inorg. Chem.* **1990**, *29*, 4878.
[10] S. Pohl, U. Opitz, unpublished results.
[11] Phosphane sulfide could be detected by spectroscopy.
[12] S. Pohl, W. Saak, *Angew. Chem.* **1984**, *96*, 886; *Angew. Chem. Int. Ed. Engl.* **1984**, *23*, 907.
[13] According to ref. [12] amorphous mixtures of FeS and $(Et_4N)_3[Fe_8S_6I_8]$ are usually formed. The formation of crystals appears to be subject to coincidences, which can hardly be influenced.
[14] **1** tetragonal, $I4/m$, $a = 1635.5(2)$, $c = 1466.8(3)$ pm, $V = 3923.5 \times 10^6$ pm^3, $Z = 2$, $\rho_{calcd} = 2.051$ g cm^{-3}, $Mo_{K\alpha}$ radiation, $2\theta_{max} = 50°$, 1813 independent reflections, observed ($I > 2\sigma(I)$) 1275, number of variables 95, empirical absorption correction (ψ scan) $R = 0.052$, $R_w = 0.056$ (**1** is isotypic with the compound described in ref. [16] with the cluster $[Fe_3Ni_5S_6I_8]^{4-}$). **3** monoclinic, $P2_1/n$, $a = 1376.0(1)$, $b = 2387.9(3)$, $c = 1707.9(2)$ pm, $\beta = 102.37(2)°$, $V = 5481.5 \times 10^6$ pm^3, $Z = 4$, $\rho_{calcd} = 1.885$ g cm^{-3}, $Mo_{K\alpha}$ radiation, $2\theta_{max} = 48°$, 8634 independent reflections, observed ($I > 2\sigma(I)$) 5040, number of variables 501, empirical absorption correction (ψ scan) $R = 0.049$, $R_w = 0.044$. Programs: G. M. Sheldrick, SHELX-76, program for crystal structure determination, Cambridge, England, **1976**; SHELXTL-PLUS, Siemens; Drawing: E. Keller, SCHAKAL 88b, Freiburg, **1988**. Further details of the crystal structure investigation may be obtained from the Fachinformationszentrum Karlsruhe, Gesellschaft for wissenschaftlich-technische Information mbH, D-W-7514 Eggenstein-Leopoldshafen 2 (FRG) on quoting the depository number CSD-57055, the names of the authors, and the journal citation.
[15] G. Christou, K. S. Hagen, R. H. Holm, *J. Am. Chem. Soc.* **1982**, *104*, 1744; G. Christou, K. S. Hagen, J. K. Bashkin, R. H. Holm, *Inorg. Chem.* **1985**, *24*, 1010.
[16] W. Saak, S. Pohl, *Angew. Chem.* **1991**, *103*, 869; *Angew. Chem. Int. Ed. Engl.* **1991**, *30*, 881.
[17] D. Fenske, J. Hachgenei, *Angew. Chem.* **1985**, *97*, 684; *Angew. Chem. Int. Ed. Engl.* **1985**, *24*, 706.
[18] F. Cecconi, C. A. Ghilardi, S. Midollini, *J. Chem. Soc. Chem. Commun.* **1981**, 640; A. Agresti, M. Bacci, F. Cecconi, C. A. Ghilardi, S. Midollini, *Inorg. Chem.* **1985**, *24*, 689.
[19] V. Rajamani, C. T. Prewitt, *Can. Mineral.* **1973**, *12*, 178.
[20] H. T. Evans, Jr., J. R. Clark, *Am. Mineral.* **1981**, *66*, 376.
[21] B. S. Tani, *Am. Mineral.* **1977**, *62*, 817, and references therein.
[22] J. K. Burdett, G. J. Miller, *J. Am. Chem. Soc.* **1987**, *109*, 4081.
[23] G. G. Hoffman, J. K. Bashkin, M. Karplus, *J. Am. Chem. Soc.* **1990**, *112*, 8705.

Contrasting Structures of Pyramidal Carbocations and Their Silicon Analogues**

By *Eluvathingal D. Jemmis,* Govindan Subramanian, Bharatam V. Prasad, Seiji Tsuzuki,* and *Kazutoshi Tanabe*

Extension of the structure of *nido*-B_5H_9 (**1**) to the isoelectronic pyramidal carbocation $C_5H_5^+$ (**2**)[1] was "obvious".[1a,b] At the time the bridging hydrogen atoms of the basal B_4H_8 unit were eliminated to give the C_4H_4 unit in $C_5H_5^+$.[1a] In the meantime, derivatives of **2** have been synthesized.[2] Herein we present theoretical calculations on the homologous $Si_5H_5^+$ compound and on related compounds. These calculations suggest that the structures with bridging H atoms and not those isostructural to $C_5H_5^+$ (**2**) with terminal H atoms correspond to minima on each of the potential energy surfaces. If, however, for the structures with terminal H atoms the calculated negative vibrational frequencies are followed, more stable structures of lower symmetry are obtained.

The structures considered in this study are shown in Figure 1. In the classical isoelectronic analogues of **1**, namely **2**–**5**, the base of the pyramid is formed from a carbon square. The replacement of four BH_2 groups in **1** for SiH groups results in the structures **6**–**8**, when the terminal H atoms are retained, and the structures **9**–**11**, when the bridging H atoms are retained.[3]

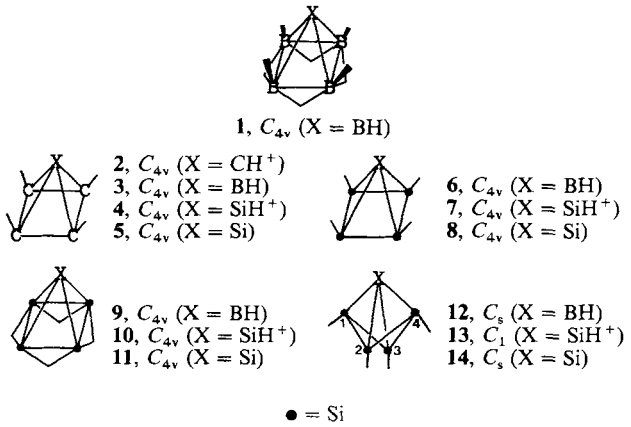

Fig. 1. Structures of B_5H_9 **1**, C_4H_4X (X = CH^+, BH, SiH^+, Si; **2**–**5**), and Si_4H_4X (X = BH, SiH^+, Si; **6**–**14**).

Geometries of **1**–**11** were initially optimized with imposed C_{4v} symmetry at the HF/6-31G* level[4a,b] by using the Gaussian 82[4c] and Gaussian 90[4d] series of programs. Frequency analysis at the same level showed that structures **1**–**3**, **5**, and **9**–**11** represent true minima (Table 1). The significance of electron correlation was examined by optimizing structures **6**–**14** further at the MP2/6-31G* level.[4e,f] Finally single-point calculations at the MP4SDTQ(fc)/6-31G* level[4g] were carried out on the HF/6-31G* optimized geometries of **6**–**14**. The total and relative energies obtained from these calculations are given in Table 1, and Tables 2 and 3 list the important structural parameters used in the discussion.[5]

The bonding in half-sandwich compounds has been well documented.[1b,6,7] The compatibility of the overlapping orbitals has been used to explain the distortion of the ring

Table 1. Absolute energies E [Hartree], relative energies E_{rel} [kcal mol^{-1}] [a], and unscaled zero-point energies ZPE [kcal mol^{-1}] of **1**–**14**.

Molecule (symmetry)	E HF/6-31G*	E_{rel}//HF/6-31G* HF	MP2	MP4 [b]	ZPE [c]
1 (C_{4v})	−128.57827 [d]				70.17
2 (C_{4v})	−191.86519				54.20
3 (C_{4v})	−178.95344				51.35
4 (C_{4v})	−442.90274				47.91 (2)
5 (C_{4v})	−442.59303				43.13
12 (C_s)	−1183.13069	0.00	0.00 [e]	0.00 [e]	32.27
6 (C_{4v})	−1183-12805	1.09	0.86	0.18	31.63 (3)
9 (C_{4v})	−1183.06782	39.26	36.77	29.75	32.06
13 (C_1)	−1447.15330	0.00	0.00 [f]	0.00 [f]	30.53
7 (C_{4v})	−1447.15265	−0.04	0.51	1.09	30.03 (2)
10 (C_{4v})	−1447.05546	60.13	56.41	47.17	29.10
14 (C_s)	−1446.79556	−0.00	0.00 [g]	0.00 [g]	25.15
8 (C_{4v})	−1446.78959	2.85	7.29	7.78	24.15 (3)
11 (C_{4v})	−1446.68554	68.10	69.11	62.74	24.10

[a] Includes zero-point energy correction scaled by 0.89. [b] Single-point MP4SDTQ (frozen core)/6-31G*//HF/6-31G* calculation. [c] Number of imaginary frequencies in parentheses. [d] From ref. [16]. [e] The corresponding E values are −1183.61280 and −1183.63766 Hartree. [f] The corresponding E values are −1447.62178 and −1447.63815 Hartree. [g] The corresponding E values are −1447.29079 and −1447.30726 Hartree.

Table 2. Selected bond lengths [Å] and angles [°] for **1**–**11** optimized at the HF/6-31G* level.

Molecule	[a]	[b]	[c]	[d]	[e]
1	1.811	1.702	1.181	1.179	−6.8 [f] 122.2 [g]
2	1.450	1.555	1.068	1.069	−6.7 [f]
3	1.449	1.641	1.174	1.069	−2.8 [f]
4	1.467	1.931	1.447	1.071	5.3 [f]
5	1.446	2.035	–	1.069	3.6 [f]
6	2.236	2.117	1.184	1.465	−19.2 [f]
7	2.273	2.414	1.458	1.458	−13.0 [f]
8	2.235	2.516	–	1.463	−12.6 [f]
9	2.585	2.105	1.186	1.679	114.7 [g]
10	2.821	2.435	1.456	1.676	119.2 [g]
11	2.652	2.506	–	1.668	115.0 [g]

[a] Ring atom–ring atom distance. [b] Ring atom–cap atom distance. [c] Cap atom–hydrogen atom distance. [d] Ring atom–hydrogen atom distance. [e] Positive value indicates that ring hydrogen atoms are bent away from the cap. [f] Ring centroid–ring atom–hydrogen atom angle. [g] Ring centroid (midpoint of the ring atom–ring atom distance)–bridging hydrogen atom angle.

Table 3. Selected bond lengths [Å] for **12**–**14** optimized at the HF/6-31G* level.

Bond [a]	**12**	**13**	**14**
Si1-Si2	2.231	2.276	2.262
Si2-Si4	2.231	2.307	2.262
Si4-Si3	2.326	2.276	2.309
Si3-Si1	2.326	2.250	2.309
Si1-X	2.006	2.501	2.352
Si2-X	2.254	2.533	2.759
Si3-X	2.006	2.337	2.352
Si4-X	2.463	2.533	2.836

[a] X = BH (**12**), SiH^+ (**13**), Si (**14**).

[*] Prof. E. D. Jemmis, G. Subramanian
School of Chemistry, University of Hyderabad
Central Univ. P. O., Hyderabad – 500134 (India)
Dr. B. V. Prasad
Department of Chemistry
University of Alabama at Birmingham
UAB Station, Birmingham, AL 35294 (USA)
Dr. S. Tsuzuki, Dr. K. Tanabe
National Chemical Laboratory for Industry
Tsukuba, Ibaraki, 305 (Japan)

[**] This work was supported by the Department of Science and Technology, New Delhi. E. D. J. thanks the Research School of Chemistry, Australian National University, for a fellowship during his visit, during which some of the calculations were carried out.

substituents from the carbocyclic pyramid base.[7a] Similar parallels are expected when the carbocyclic ring is replaced by the homologous silacyclic ring (Si_4H_4 as base). The Si–Si distances in the base in **6**–**8** (Table 2, second column) lie between the values for standard single (2.353 Å as calculated for disilane[8]) and double (2.129 Å as calculated for planar disilene[9]) bonds, which reflects the delocalization of the bonding electrons in the basal four-membered Si ring. A similar trend was observed in **2**.[7]

The silicon compounds **6**–**8**, however, were found to correspond to higher order stationary points (imaginary frequencies, see Table 1). This is because the Si_4 ring is larger than the C_4 ring (Table 2), which forces large Si–H out-of-plane bending to obtain optimum ring-cap overlap.[7] Hence caps with more diffuse orbitals[10] are required in order to reduce the out-of-plane bending of the ring substituents and increase the binding with the cap.

While the BH cap has the optimum interaction with a carbocycle, it is least favored for a silacycle (**6**). This is evident from the larger out-of-plane bending of the ring substituents (cf. **3** and **6**, Table 2, far right) and the exothermicities of the reactions (a) and (b) calculated at the HF/6-31G* level.

4 + **6** ⟶ **3** + **7** $-47.3\ \mathrm{kcal\,mol^{-1}}$ (a)

5 + **6** ⟶ **3** + **8** $-13.1\ \mathrm{kcal\,mol^{-1}}$ (b)

Even the orbitals of SiH^+ and Si are not sufficiently diffuse to allow optimum overlap with the four-membered Si ring (Table 1). Hence, these prefer puckered structures **12**–**14** with puckering angles of 29.5 (**12**), 0.9 (**13**), and 36.2° (**14**) (values calculated at the HF/6-31G* level) between Si1Si2Si3-Si2Si3Si4 planes. The Si–Si distances in the puckered structures **12**–**14** are not very different from those in structures **6**–**8** with C_{4v} symmetry (cf. entries in columns 2 and 3 of Table 2 with those in Table 3). The distortion from C_{4v} to C_s or C_1 symmetry (**6** → **12**, **7** → **13** and **8** → **14**) led to only marginal net gains in stabilization. Correlation diagrams show that the destabilization of σ-type orbitals is nearly equal to the stabilization gained by π-type orbitals. This is reflected in the relative stabilities of these isomers (Table 1). It is interesting to note, however, that these puckered structures of lower symmetry are not minima for pyramidal carbocations.[1b, 11]

In contrast, structures **9**–**11** obtained from **1** by retaining the bridging hydrogen atoms in the basal ring were found to be minima, though higher in energy than the structures **6**–**8** and **12**–**14** (Table 1). In these structures, the silicon atoms of the four-membered ring are divalent and participate in three-center two-electron bonding. Such structures with low valent silicon and bridging hydrogen atoms have been well documented.[3, 12] The Si–Si distances are appreciably longer than expected in hydrogen-bridged structures (2.585 Å in HSi-(μ-$H)_2$-SiH)[13]). Interestingly, the corresponding carbon compounds are not known. Although the Si_4 basal ring with the bridging hydrogen atoms in **9**–**11** is larger than that in **6**–**8** (Table 2), a cap with a less diffuse p-orbital (BH) is also a minimum (**9**). The stability of the structures **9**–**11** can be best explained by considering a tetrahedral environment around silicon with two hydrogen atoms in one plane and a lone pair orbital and the rehybridized p_π orbital in the other plane (Scheme 1). The lone pair orbitals, which lie in the plane of the Si_4 ring, orientate the π orbitals towards the cap. This enhances the overlap between the cap and the ring orbitals,[7] which is confirmed by the MO coefficients.

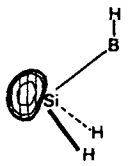

Scheme 1. Section of **9** showing the orbital of the lone pair.

In summary, the puckering in **12**–**14**, and the orientation of the rehybridized π orbitals in the bridged isomers **9**–**11** are the key factors responsible for the stability of the silicon analogues of **1**. Their structures are contrary to those expected and observed in **2** and its isostructural analogues **3**–**5**. Similar results have also been observed in silicon clusters.[14] A square pyramidal Si_5 cluster is calculated to be higher in energy than a trigonal bipyramidal structure, which is similar to the distorted structures discussed here. Furthermore, our results suggest that $Si_6H_6^{2+}$ may prefer geometries other than the pentagonal pyramidal structure, as observed for $C_6H_6^{2+}$.[15]

Received: December 29, 1992
Revised version: March 2, 1993 [Z 5786IE]
German version: *Angew. Chem.* **1993**, *105*, 921

[1] a) R. E. Williams, *Inorg. Chem.* **1971**, *10*, 210–214; b) W. D. Stohrer, R. Hoffmann, *J. Am. Chem. Soc.* **1972**, *94*, 1661–1668; c) R. E. Williams, *Progress in Boron Chemistry*, Pergamon, Oxford, England, **1970**, p. 51; d) R. Hoffmann, W. N. Lipscomb, *J. Chem. Phys.* **1962**, *36*, 2179–2195; e) W. N. Lipscomb, *Boron Hydrides*, W. A. Benjamin, New York, **1963**, p. 80; f) H. Schwarz, *Angew. Chem.* **1981**, *93*, 1046–1058; *Angew. Chem. Int. Ed. Engl.* **1981**, *20*, 991–1003; g) H. Kollmar, H. O. Smith, P. von R. Schleyer, *J. Am. Chem. Soc.* **1973**, *95*, 5834–5836; h) M. J. S. Dewar, R. C. Haddon, *ibid.* **1973**, *95*, 5836–5837; i) W. J. Hehre, P. von R. Schleyer, *ibid.* **1973**, *95*, 5837–5839; j) S. Yonda, Z. Yoshida, *Chem. Lett.* **1972**, 607–610; k) M. J. S. Dewar, R. C. Haddon, *J. Am. Chem. Soc.* **1974**, *96*, 255–256; l) J. Feng, J. Leszczynski, B. Weiner, M. C. Zerner, *ibid.* **1989**, *111*, 4648–4655; m) M. Saunders, H. A. Jimenez-Vazquez, *Chem. Rev.* **1991**, *91*, 375–397.

[2] a) S. Masamune, M. Sakai, H. Ona, A. J. Jones, *J. Am. Chem. Soc.* **1972**, *94*, 8956–8958; b) S. Masamune, *Pure Appl. Chem.* **1975**, *44*, 861–884; c) G. Maier, H. Rang, H. O. Kalinowski, *Angew. Chem.* **1989**, *101*, 1293–1295; *Angew. Chem. Int. Ed. Engl.* **1989**, *28*, 1232.

[3] a) E. D. Jemmis, B. V. Prasad, S. Tsuzuki, K. Tanabe, *J. Phys. Chem.* **1990**, *94*, 5530–5535; b) E. D. Jemmis, B. V. Prasad, P. V. A. Prasad, S. Tsuzuki, K. Tanabe, *Proc. Indian Acad. Sci. Chem. Sci.* **1990**, *102*, 107–115.

[4] a) P. C. Hariharan, J. A. Pople, *Theor. Chim. Acta* **1973**, *28*, 213–222; b) M. M. Francl, W. J. Pietoro, W. J. Hehre, J. S. Binkley, M. S. Gordon, D. J. DeFrees, J. A. Pople, *J. Chem. Phys.* **1982**, *77*, 3654–3665; c) J. S. Binkley, R. A. Whiteside, K. Raghavachari, R. Seeger, D. J. DeFrees, H. B. Schlegal, M. J. Frisch, J. A. Pople, L. R. Kahn, Gaussian 82, Carnegie-Mellon University, Pittsburg, PA, USA, **1982**; d) M. J. Frisch, M. Head-Gordon, G. W. Trucks, J. B. Foresman, H. B. Schlegal, K. Raghavachari, M. A. Robb, J. S. Binkley, C. Gonzalez, D. J. DeFrees, D. J. Fox, R. A. Whiteside, R. Seeger, C. F. Melius, J. Baker, R. L. Martin, L. R. Kahn, J. J. P. Stewart, S. Topiol, J. A. Pople, Gaussian 90, Gaussian Inc., Pittsburg, PA, USA, **1990**; e) C. Møller, M. S. Plesset, *Phys. Rev.* **1934**, *46*, 618–622; f) J. A. Pople, J. S. Binkley, S. Seeger, *Int. J. Quantum Chem. Symp.* **1976**, *10*, 1; g) R. Krishnan, J. A. Pople, *Int. J. Quantum Chem.* **1978**, *14*, 91–100.

[5] The geometric data obtained at the MP2/6-31G* level for **6**–**14** varied by about only 3% from the SCF results and are hence not included in the discussion.

[6] a) K. Wade, *Chem. Commun.* **1971**, 792–793; b) D. M. P. Mingos, *Nature (London) Phys. Sci.* **1972**, *236*, 99–102; c) W. W. Porterfield, M. E. Jones, K. Wade, *Inorg. Chem.* **1990**, *29*, 2919–2933; and references therein.

[7] a) E. D. Jemmis, P. von R. Schleyer, *J. Am. Chem. Soc.* **1982**, *104*, 4781–4788; b) E. D. Jemmis, *ibid.* **1982**, *104*, 7017–7020.

[8] W. J. Hehre, L. Radom, P. von R. Schleyer, J. A. Pople, *Ab initio Molecular Orbital Theory*, Wiley Interscience, New York, **1986**, p. 151.

[9] K. Krogh-Jesperson, *J. Phys. Chem.* **1982**, *86*, 1492–1495.

[10] The atomic radii or the optimized exponents in a basis set indicate the expected trend of the diffuse character of the orbitals (C < B < Si).

[11] a) V. I. Minkin, R. M. Minyaev, Yu. A. Zhdanov, *Nonclassical Structures of Organic Compounds*, Mir Publishers, Moscow, **1987**, p. 71; b) D. J. Wales, R. G. A. Bone, *J. Am. Chem. Soc.* **1992**, *114*, 5399–5406, and references therein.
[12] a) B. T. Luke, J. A. Pople, M.-B. Krogh-Jesperson, Y. Apeloig, M. Karni, J. Chandrasekhar, P. von R. Schleyer, *J. Am. Chem. Soc.* **1986**, *108*, 270–284; b) M. Bogey, H. Bolvin, C. Demuynck, J. L. Destombes, *Phys. Rev. Lett.* **1991**, *66*, 413–416; c) A. B. Sannigrahi, P. K. Nandi, *Chem. Phys. Lett.* **1992**, *188*, 575–583, and references therein; d) R. S. Grev, H. F. Schaefer III, J. Chem. Phys. **1992**, *97*, 7990–7998, and references therein; e) G. Trinquier, J.-C. Barthelat, *J. Am. Chem. Soc.* **1990**, *112*, 9121–9130.
[13] G. Trinquier, *J. Am. Chem. Soc.* **1990**, *112*, 2130–2137.
[14] a) K. Raghavachari, *J. Chem. Phys.* **1986**, *84*, 5672–5686; b) G. Pacchioni, J. Koutecký, *ibid.* **1986**, *84*, 3301–3310; c) T. Slee, L. Zhenyang, D. M. P. Mingos, *Inorg. Chem.* **1989**, *28*, 2256–2261.
[15] K. Krogh-Jesperson, *J. Am. Chem. Soc.* **1991**, *113*, 417–423, and references therein.
[16] M. Buhl, P. von R. Schleyer, *J. Am. Chem. Soc.* **1992**, *114*, 477–491.

(CHCl$_3$, $c = 0.8$)) were obtained in 68 and 62% yield, respectively (Scheme 1). Their IR, ^{1}H NMR, ^{13}C NMR, and mass spectra as well as the elemental analyses are consistent with the assigned structures.

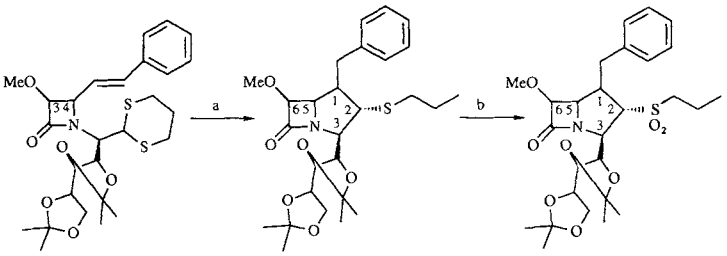

Scheme 1. a) 3.2 equiv Bu_3SnH, AIBN, toluene, 90 °C. b) *meta*-chloroperoxybenzoic acid (MCPBA), CH_2Cl_2, 20 °C.

The Use of Radical Cyclization in the Preparation of Substituted Methyl Carbapenem Antibiotic Precursors**

By *Josefa Anaya,* Derek H. R. Barton, Stephan D. Gero, Manuel Grande, Nieves Martin*, and *Catherine Tachdjian*

The pharmaceutical importance of β-lactam antibiotics with resistance to β-lactamase, such as theinamycin and other related compounds,[1] as well as the inhibition of human leukocyte elastase (HLE) by cephalosporins[2] and the remarkable properties of monocyclic β-lactams,[3] have provoked a continuing high level of interest in the chemical synthesis of β-lactams.

The potent antibacterial properties and the challenging chemical problems have made carbapenem-type compounds major synthetic objectives. Due to the chemical instability of the bicyclic ring system, the main synthetic strategies start with an appropriate monocyclic β-lactam with the correct configuration at C3 and C4. The second ring is then formed by manipulations at N1 and C4. The well-established methods that are employed are Wittig-type reactions, aldol condensations, and, in particular, insertion reactions via carbenoid-type intermediates.[4]

We report here the synthesis of 1,2,3,6-tetrasubstituted carbapenams and 1,3,6-trisubstituted carbapenems from the readily available[5] 1,3,4-trisubstituted azetidin-2-ones **1**, in which the five-membered ring is formed by radical cyclization.[6, 7] The starting monobactams we used were the 3α,4α and 3β,4β monobactams **1a** and **1b**, respectively.

Our first aim was to study the tin radical cyclization to **2a** and **2b** in an *exo*-trig process.[8] In contrast to C. Gutiérrez et al.,[9] we found that when the monobactams **1a** and **1b** were treated with tri-(*n*-butyl)stannane and 2,2′-azobis-(isobutyronitrile) (AIBN), the corresponding carbapenams **2a** ($[\alpha]_D = +3.4$ (CHCl$_3$, $c = 1$)) and **2b** ($[\alpha]_D = -13$ (CHCl$_3$, $c = 0.8$)) were obtained in 68 and 62% yield, respectively (Scheme 1). Their IR, ^{1}H NMR, ^{13}C NMR, and mass spectra as well as the elemental analyses are consistent with the assigned structures.

The relative configuration at C1 and C2, for both carbapenams has been deduced from the vicinal coupling constants of the hydrogen atoms H1 and H2. In the carbapenam **2a**, the *trans* orientation of the substituents at C1/C2, C2/C3, and C5/C1 was based on the large values for the coupling constants: $J_{1,2} = 10$, $J_{2,3} = J_{5,1} = 8$ Hz. This *trans* arrangement is only possible with the 1β,2α-substituted carbapenam **2a**, because C3 and C5 have the configuration 3β,5α. In the carbapenam **2b**, the coupling constants in the ^{1}H NMR spectrum ($J_{1,2} = 8$, $J_{2,3} = 4$ Hz) were in agreement with the calculated theoretical values[10] ($J_{1,2} = 6.6$, $J_{2,3} = 5.4$ Hz) for a *cis* and a *trans* arrangement of the protons H1/H2 and H2/H3, respectively. The *trans* arrangement of H5 and H1 ($J_{5,1} = 8$ Hz) was deduced from the stereochemical assignment in **2a**. The sulfone derivatives **3a** (m.p. 125 °C, $[\alpha]_D = +11$ (CHCl$_3$, $c = 0.8$)) and **3b** ($[\alpha]_D = -17$ (CHCl$_3$, $c = 0.7$)) were prepared in order to elucidate the absolute configuration at C1 and C2. An X-ray crystal structure determination of **3a** (Fig. 1) allowed the unequivocal assignment of the absolute configuration (1*R*,2*S*) to this compound, and consequently to its sulfide carbapenam precursor **2a**.[11]

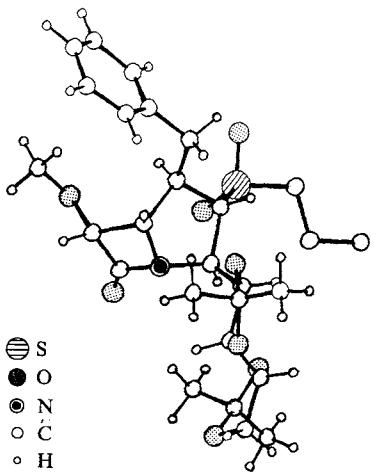

Fig. 1. Molecular structure of **3a**.

[*] Dr. J. Anaya, Prof. Dr. M. Grande, N. Martín
Universidad de Salamanca, Departamento de Química Orgánica
Facultad de Ciencias Químicas, Plaza de los Caídos, 1–5
E-37008 Salamanca (Spain)
Prof. Dr. D. H. R. Barton, Dr. C. Tachdjian
Department of Chemistry, Texas A & M University
Texas (USA)
Dr. S. D. Gero
Institut de Chimie des Substances Naturelles, C.N.R.S.
Gif sur Yvette (France)

[**] Penem is an abbreviation for the basic framework of unsaturated penicillins: 4-thia-1-azabicyclo[3.2.0]hept-2-en-7-one.

Conversion of the carbapenams **2a** and **2b** into the corresponding 1,3,6-trisubstituted carbapenems, unfortunately, was not possible; all attempts to remove the isopropylidene protecting groups in **2a**, **2b**, **3a**, and **3b** were unsuccessful. This failure prompted us to change our synthetic strategy to the synthesis of carbapenem systems from the monocyclic β-lactams **1a** and **1b**. A suitable approach might be the removal of the isopropylidene groups, then oxidative cleavage of the glycol units of the monobactams **1c** and **1d** (Scheme 2), and finally intramolecular cyclization to form the carbapenam ring. In this way we obtained the tetraol

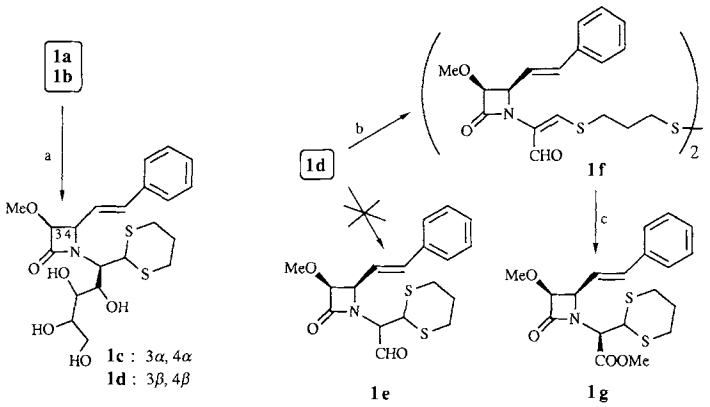

Scheme 2. a) CF_3COOH, MeOH, 20 °C. b) Ph_3BiCO_3, CH_3CN, reflux. c) MnO_2, NaCN, MeOH, 20 °C.

monobactam derivatives **1c** (m.p. 125 °C, $[\alpha]_D = +53.5$ (MeOH, $c = 0.85$)) and **1d** (m.p. 177 °C; $[\alpha]_D = -82$ (MeOH, $c = 1$)) in 82 and 90% yield, respectively. Classical methods for the oxidative cleavage of diols (sodium periodate, potassium permanganate, etc.) were carried out on compound **1d**, but these did not give the desired compound **1e**. Mild oxidants such as triphenylbismuth carbonate,[12] gave the disulfide **1f** in 85% yield. Several ways to regenerate the 1,3-dithiane ring system from **1f** were examined:[13] The methyl ester **1g** (m.p. 156 °C, $[\alpha]_D = -84$ ($CHCl_3$, $c = 0.7$)) was obtained by the use of manganese(IV) oxide and sodium cyanide in methanol,[14] however, in only 10% yield.

Finally, we found that our synthetic strategy to obtain 1,3,6-trisubstituted carbapenems from the monocyclic β-lactams **1** could be realized by using the silylated monobactam **1h** as an intermediate (Scheme 3). The silylated compound **1h** ($[\alpha]_D = -48$ ($CHCl_3$, $c = 1$)) was prepared in 70% yield from the monobactam **1d** and then transformed with tri-(*n*-butyl)stannane and AIBN into the carbapenam **2c** in 75% yield. The *cis* arrangement of the substituents at C1 and C2 for **2c** was assigned from the ^1H NMR data ($J_{1,2} = J_{5,1} = 8.2$, $J_{2,3} = 4$ Hz), which are in agreement with those reported for **2b**.

The carbapenam **2c** was converted into a mixture of aldehydes **4** and **5** by deprotection of the silyl groups and oxidative cleavage of the glycol units. The aldehydes **4** ($[\alpha]_D = -12$ ($CHCl_3$, $c = 1$)) and **5** ($[\alpha]_D = -32$ ($CHCl_3$, $c = 0.8$)) were obtained in 40 and 20% yield (based on **2c**), respectively, after column chromatography. The carbapenam **4** was transformed into the carbapenem **5** in 80% yield by treatment with MCPBA followed by thermolysis of the sulfoxide in refluxing toluene. Finally, the methyl ester carbapenem **6** ($[\alpha]_D = -26$ ($CHCl_3$, $c = 0.5$)) was prepared in 75% yield from **5**.[14]

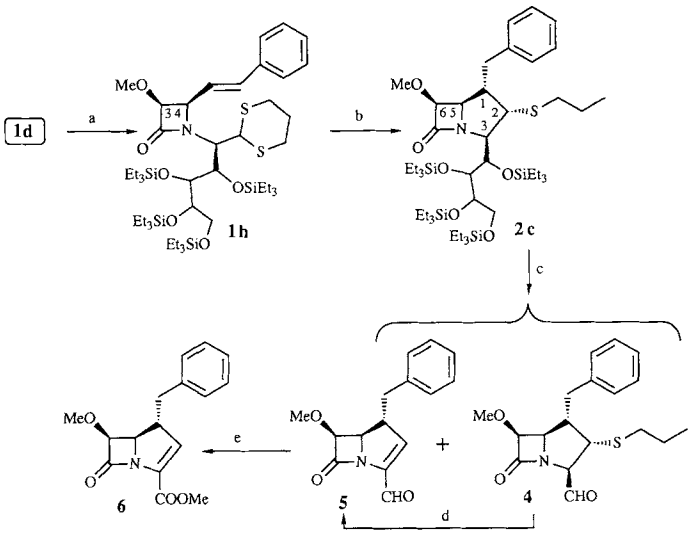

Scheme 3. a) Et_3SiCl, pyridine, 4-dimethylaminopyridine (catalyst), 20 °C. b) 3.2 equiv. Bu_3SnH, AIBN, toluene, 90 °C. c) Bu_4NF, THF, 0 °C; Ph_3BiCO_3, CH_3CN, reflux. d) MCPBA, CH_2Cl_2, 20 °C; toluene, reflux. e) MnO_2, NaCN, MeOH, 20 °C.

From the results reported here and those previously disclosed,[15] we have demonstrated that the synthetic strategy based on the use of *D*-glucosamine as chiral auxiliary in the Staudinger reaction[5] is an efficient and versatile approach for the synthesis of the most important types of β-lactams. Further studies on the application of these results in the synthesis of optically active carbapenems and carbacephems[16] are now underway.

Received: December 24, 1992 [Z 5773 IE]
German version: *Angew. Chem.* **1993**, *105*, 911

[1] J. S. Kahan, F. Kahan, R. Goegelman, S. A. Currie, M. Jackson, E. O. Stapley, A. K. Miller, D. Hendin, S. Mochales, S. Hernández, H. B. Woodruff, J. Birnbaum, *J. Antibiot.* **1979**, *32*, 1; K. Yamamoto, T. Yoshioka, Y. Kato, N. Shibamoto, K. Okamura, Y. Shimauchi, T. Ishikura, *ibid.* **1980**, *33*, 796.

[2] J. B. Doherty, B. M. Ashe, L. W. Argenbright, P. L. Barker, R. J. Bonney, G. O. Chandler, M. E. Dahlgren, C. P. Dorn, P. E. Finke, R. A. Firestone, D. Fletcher, W. K. Hagmann, R. Mumford, L. O'Grady, A. L. Maycock, J. M. Pisano, S. K. Shah, K. R. Thompson, M. Zimmerman, *Nature* **1986**, *322*, 192.

[3] R. A. Firestone, P. L. Barker, J. M. Pisano, B. M. Ashe, M. E. Dahlgren, *Tetrahedron* **1990**, *46*, 2255; W. K. Hagmann, K. R. Thompson, S. K. Shah, P. E. Finke, B. M. Ashe, H. Weston, A. L. Maycock, J. B. Doherty, *Bioorg. Med. Chem. Lett.* **1992**, *2*, 681.

[4] Recent reviews: T. Nagahara, T. Kametani, *Heterocycles* **1987**, *25*, 729; G. I. Georg in *Studies in Natural Product Chemistry, Vol. 4* (Ed.: A-ur. Rahman), Elsevier, Amsterdam, **1989**, p. 431; C. Palomo in *Recent Progress in the Chemical Synthesis of Antibiotics* (Eds.: G. Lukacs, M. Ohno), Springer, Berlin, **1990**, p. 565.

[5] D. H. R. Barton, A. Gateau-Olesker, J. Anaya-Mateos, J. Cléophax, S. D. Gero, A. Chiaroni, C. Riche, *J. Chem. Soc. Perkin Trans. 1* **1990**, 3211.

[6] M. D. Bachi, F. Frolow, C. Hoornaert, *J. Org. Chem.* **1983**, *48*, 1841; M. D. Bachi, A. De Mesmaeker, N. Stevenart-De Mesmaeker, *Tetrahedron Lett.* **1987**, *28*, 2637.

[7] Comprehensive reviews: D. P. Curran, *Synthesis* **1988**, 417; B. Giese, *Radicals in Organic Synthesis; Formation of Carbon-Carbon Bonds*, Pergamon, Oxford, **1986**; D. J. Hart, *Science* **1984**, *223*, 883; M. Ramaiah, *Tetrahedron* **1987**, *43*, 3541.

[8] D. L. J. Clive, G. J. Chittattu, V. Farina, W. A. Kiel, S. M. Menchen, C. G. Russell, A. Singh, C. K. Wong, N. J. Curtis, *J. Am. Chem. Soc.* **1980**, *102*, 4438; V. K. Yadav, A. G. Fallis, *Tetrahedron Lett.* **1988**, *29*, 1541.

[9] K. Schmidt, S. O'Neal, T. C. Chan, C. P. Alexis, J. M. Uribe, K. Losserner, C. G. Gutiérrez, *Tetrahedron Lett.* **1989**, *30*, 7301.

[10] C. A. G. Haasnoot, F. A. A. M. De Leeuw, C. Altona, *Tetrahedron* **1980**, *36*, 2783.
[11] The details of the X-ray crystal structure will be published elsewhere.
[12] D. H. R. Barton, S. D. Gero, C. D. Maycock, *J. Chem. Soc. Perkin Trans. 1* **1982**, 1541; D. H. R. Barton, J. P. Finet, W. B. Motherwell, C. Pichon, *Tetrahedron* **1986**, *42*, 5627.
[13] J. P. Danehy, W. E. Hunter, *J. Org. Chem.* **1967**, *32*, 2047; L. E. Overman, E. M. O'Connor, *J. Am. Chem. Soc.* **1976**, *98*, 771; M. D. D. Allen in *Organic Synthesis Collective Vol. 2* (Ed.: A. H. Blatt), Wiley, New York, **1943**, p. 580; H. C. Brown, P. M. Weissmann, N. M. Yoon, *J. Am. Chem. Soc.* **1966**, *88*, 1458.
[14] E. J. Corey, N. W. Gilman, B. E. Ganem, *J. Am. Chem. Soc.* **1968**, *90*, 5616.
[15] D. H. R. Barton, J. Anaya, A. Gateau-Olesker, S. D. Gero, *Tetrahedron Lett.* **1992**, *33*, 6641.
[16] R. N. Guthikonda, L. D. Cama, B. G. Christensen, *J. Am. Chem. Soc.* **1974**, *96*, 7585; R. A. Firestone, J. L. Fahey, N. S. Maciejiwicz, G. S. Patel, B. G. Christensen, *J. Med. Chem.* **1977**, *20*, 551.

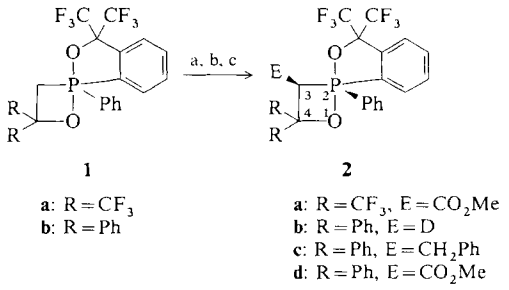

Scheme 1. a) 4 equiv *n*BuLi, THF, $-40\,^{\circ}C$, 2 h; b) E^{+}, $-40\,^{\circ}C \leq T \leq -30\,^{\circ}C$, 3 h; c) aqueous NH_4Cl solution, $-30\,^{\circ}C$.

Synthesis, Structure, and Thermolysis of a 3-Methoxycarbonyl-1,2 λ^5-oxaphosphetane**

By *Takayuki Kawashima,* Katsuhiro Kato,* and *Renji Okazaki**

The study of 1,2-oxaphosphetanes by NMR spectroscopy at low temperature has played an important role in elucidating the factors that influence the stereochemistry of the Wittig reaction.[1] These studies were carried out mainly on nonstabilized ylides, although a few examples of semistabilized ylides were also investigated.[2] By contrast, 1,2-oxaphosphetanes derived from stabilized ylides have so far not been observed.[1d, 3] Recently we succeeded in synthesizing isolable 1,2-oxaphosphetanes with a pentacoordinate P atom and Martin ligand.[4] We now report the synthesis, structure, and thermal reactivity of a 3-methoxycarbonyl-1,2 λ^5-oxaphosphetane, the first 1,2 λ^5-oxaphosphetane with a pentacoordinate P atom to be formally derived from a stabilized ylide.

4,4-Bis(trifluoromethyl)-1,2 λ^5-oxaphosphetane **1a**, prepared in 93% yield by the method previously reported for **1b**,[4] was treated with *n*BuLi and then with excess $ClCO_2Me$ in THF to give 3-methoxycarbonyl-4,4-bis(trifluoromethyl)-1,2 λ^5-oxaphosphetane **2a** as colorless needles in 54% yield (Scheme 1). The structure of **2a** is strongly supported by its ^{31}P ($\delta = -36.7$) and ^{19}F NMR spectra (two sets of doublets of quartets). In the ^1H NMR spectrum a doublet due to the methine proton is observed at $\delta = 5.25$ ($^2J_{(H,P)} = 25.8$ Hz). In the ^{13}C NMR spectrum, the signals for the quaternary C4 atom and the carbon atom of the carbonyl group occur at $\delta = 74.31$ (doublet of septets, $^2J_{(C,P)} = 13.8$ Hz, $^2J_{(C,F)} = 32.4$ Hz) and at $\delta = 162.92$ (d, $^2J_{(H,P)} = 6.5$ Hz), respectively. This is the first isolation and spectroscopic observation of a 1,2-oxaphosphetane with a carbonyl group at the C3 atom.

The X-ray crystallographic analysis of **2a** indicates that the P atom is in a distorted trigonal bipyramidal environment, in which two oxygen atoms are in the apical positions (Fig. 1).[5] The bond angle O1-P1-O2 deviates from linearity by 14.1(3)°; the P1–O1 bond (1.781(6) Å) is longer than the P1–O2 bond (1.716(6) Å). The lengths of the three equatorial bonds P1–C1, P1–C8, and P1–C16 are very similar. The dihedral angles O1-P1-C8-C7 and C7-O1-P1-C8 are −3.7(5) and 4.2(5)°, respectively, indicating that the four-membered ring is slightly puckered. This is one of the common structural features of 1,2-oxaphosphetanes reported previously.[4, 6]

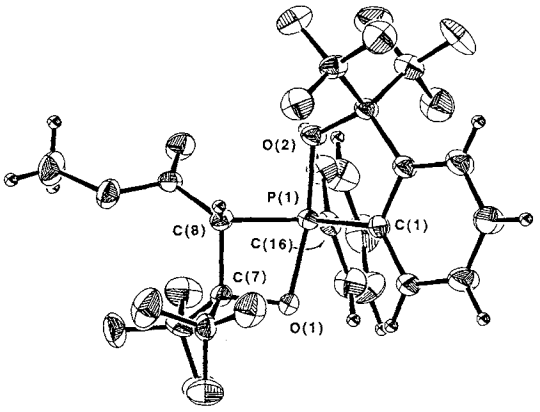

Fig. 1. Crystal structure of **2a** (ORTEP, the CH_3Cl is omitted for clarity). Selected bond lengths [Å] and bond angles [°]: P1-O1 1.781(6), P1-O2 1.716(6), P1-C1 1.805(9), P1-C8 1.823(9), P1-C16 1.823(9), C7-C8 1.55(1), O1-C7 1.40(1); O1-P1-O2 165.9(3), O1-P1-C8 75.5(3), P1-O1-C7 97.0(5), O1-C7-C8 97.0(7), P1-C8-C7 90.2(5), C1-P1-C8 125.0(4), C1-P1-C16 114.7(4), C8-P1-C16 119.8(4).

The phenyl group at the P atom in **2a** is *cis* to the methoxycarbonyl group, indicating that the methoxycarbonylation at the C3 atom occurred stereoselectively from the side of the phenyl group. This selectivity was also observed in the reactions of the lithium derivative **1b–Li**[7] with AcOD and $PhCH_2Br$, which gave **2b** (deuterated to 86%) and **2c**[8] (55%), respectively.

Compound **2a** was heated to about 70 °C under argon to give the olefin **3a** and the cyclic phosphinate **4** quantitatively. A kinetic study on the olefin formation from **2a** by ^{19}F NMR spectroscopy showed that the reaction was first order with respect to **2a**. The rate constants k of the reactions at 69.0 °C in the deuterated solvents [D_8]toluene (ε[9] = 2.38), [D_3]acetonitrile ($\varepsilon = 36.2$), and [D_6]dimethyl sulfoxide ($\varepsilon = 49$) were 8.36×10^{-6}, 1.22×10^{-4}, and $2.93 \times 10^{-4}\ s^{-1}$, respectively, showing a significant solvent effect for **2a** in comparison with that reported for **1b** (k(acetonitrile)/k(toluene) = 1.28).[4]

[*] Assoc. Prof. Dr. T. Kawashima, Prof. Dr. R. Okazaki, K. Kato
Department of Chemistry, Faculty of Science
The University of Tokyo
Hongo, Bunkyo-ku, Tokyo 113 (Japan)

[**] This work was partially supported by a Grant-in-Aid for Scientific Research on Priority Area of Organic Unusual Valency (No. 04217205, T. K.) and a Grant-in-Aid for Scientific Research (A) (No. 04403005, R. O.) from the Ministry of Education, Science, and Culture, Japan. We are grateful to Dr. N. Tokitoh, The University of Tokyo, for the determination of the X-ray structure of **2a**. We also thank Central Glass and Tosoh Akzo Co. Ltd. for gifts of fluorine compounds and alkyllithium compounds, respectively.

The parameters $\Delta H^{\neq} = 24.4 \pm 0.31$ kcal mol^{-1} and $\Delta S^{\neq} = -10.6 \pm 0.84$ cal mol^{-1} K^{-1} were estimated from the temperature dependence of the rate constants for the decomposition of **2a** in [D_8]toluene.[10] The rate constant at 200 °C of the olefin formation from **1a** was measured to be 1.12×10^{-5} s^{-1} in the same solvent, that for the decomposition of **2a** (calculated from the above-mentioned thermodynamic parameters) was 2.50×10^{-1} s^{-1}. This shows that **2a** decomposes about 22000 times faster than **1a**.

The introduction of a methoxycarbonyl group at the C3 position of **1a** did not lead to any noticeable structural change. However, the decomposition of **2a** with the formation of an olefin shows a significant solvent effect, and an acceleration of the rate of reaction in comparison with the decomposition of **1a** or **1b**. This indicates that the transition state for the decomposition of **2a** is more polar, and that negative charge generated on the C3 atom is stabilized by the electronic effect of the methoxycarbonyl group, thus the activation barrier for the olefin formation is lowered.[11]

Experimental Procedure

*n*BuLi (1.68 M solution of hexane, 3.6 mL, 4.0 equiv) was added to a solution of **1a** [12] (0.797 g, 1.50 mmol) in THF (7 mL) at −40 °C. After 2 h $ClCO_2Me$ (0.6 mL, 4.4 equiv, excess) was added to the mixture under argon. The reaction mixture was stirred at −40 to −30 °C for 3 h. After usual workup, the crude mixture was recrystallized from $CHCl_3$, and gave **2a** as colorless needles in 54.1% yield.

2a: M.p. 114–115 °C (decomp); correct elemental analysis for $C_{21}H_{13}F_{12}O_4P \cdot H_2O$; IR (KBr): $\tilde{\nu}$[cm^{-1}] = 1751 (C = O); high-resolution MS (70 eV): calcd. for $C_{21}H_{13}F_{12}O_4P$: *m/z* 588.0360, found 588.0357; ^{1}H NMR (500 MHz, $CDCl_3$, 27 °C, TMS): δ = 3.79 (s, 3H; OCH_3), 5.25 (d, ^2J(H,P) = 25.8 Hz, 1H; PC*H*), 7.42–7.49 (m, 3H; *p*, *m*-H of P-Ph), 7.70–7.79 (m, 3H; C*H*), 8.16 (dd, ^3J(H,P) = 15.3 Hz, ^3J (H,H) = 8.0 Hz, 2H; *o*-H of P-Ph), 8.42 (dd, ^3J(H,P) = 12.5 Hz, ^3J(H,H) = 7.3 Hz, 1H; C*H*); ^{13}C{^{1}H} NMR (125 MHz, $CDCl_3$, 27 °C, TMS): δ = 53.01 (s; OCH_3), 64.37 (d, ^1J(C,P) = 120.1 Hz; PCH), 74.31 (dsept, ^2J(C,P) = 13.8 Hz, ^2J(C,F) = 32.4 Hz; $CH_2C(CF_3)_2$), 82.72 (sept, ^2J(C,F) = 31.0 Hz; $C(CF_3)_2$), 121.82 (q, ^1J(C,F) = 287.5 Hz; $C(CF_3)$ (CF_3)), 122.24 (q, ^1J(C,F) = 286.4 Hz; $C(CF_3)$ (CF_3)), 122.32 (q, ^1J(C,F) = 286.7 Hz; $CH_2(CF_3)$ (CF_3)), 122.42 (q, ^1J(C,F) = 286.1 Hz; $CH_2(CF_3)$ (CF_3), 125.03 (d, ^3J(C,P) = 15.2 Hz; CH), 127.96 (d, ^3J(C,P) = 16.2 Hz; *m*-CH of P-Ph), 130.24 (d, ^1J(C,P) = 148.9 Hz; C), 130.66 (d, ^1J(C,P) = 147.7 Hz; C), 132.05 (d, ^3J(C,P) = 14.9 Hz; CH), 132.20 (d, ^4J(C,P) = 3.7 Hz, *p*-CH of P-Ph), 134.33 (d, ^4J(C,P) = 3.3 Hz; CH), 134.94 (d, ^2J(C,P) = 13.1 Hz; *o*-CH of PPh), 134.98 (d, ^2J(C,P) = 12.4 Hz; CH), 135.55 (d, ^2J(C,P) = 20.6 Hz; C), 162.92 (d, ^2J(C,P) = 6.5 Hz; C = O); ^{19}F NMR (84.25 MHz, $CDCl_3$, 27 °C, $FCCl_3$): δ = −78.11, −74.16 (q, ^4J(F,F) = 9.4 Hz), −76.54, −72.71 (q, ^4J(F,F) = 9.3 Hz); ^{31}P{^{1}H} NMR (36.23 MHz, $CDCl_3$, 27 °C, 85% H_3PO_4, external standard): δ = −36.7.

Received: December 4, 1992 [Z 5728 IE]
German version: *Angew. Chem.* **1993**, *105*, 941

[1] Recent examples: a) B. E. Maryanoff, A. B. Reitz, *Chem. Rev.* **1989**, *89*, 863; b) E. Vedejs, C. F. Marth, R. Ruggeri, *J. Am. Chem. Soc.* **1988**, *110*, 3940; c) B. E. Maryanoff, A. B. Reitz, *Phosphorus Sulfur* **1986**, *27*, 167; d) B. E. Maryanoff, A. B. Reitz, M. S. Mutter, R. R. Inners, H. R. Almond, Jr., R. R. Whittle, R. A. Olofson, *J. Am. Chem. Soc.* **1986**, *108*, 7664; e) A. B. Reitz, S. O. Nortey, A. D. Jordan, Jr., M. S. Mutter, B. E. Maryanoff, *J. Org. Chem.* **1986**, *51*, 3302.

[2] For a benzylidene ylide: W. J. Ward, Jr., W. E. McEwen, *J. Org. Chem.* **1990**, *55*, 493. Another example was reported in the reaction with $PhCOCF_3$ (ref. [1a]). For a vinylmethylene ylide: E. Vedejs, T. J. Fleck, *J. Am. Chem. Soc.* **1989**, *111*, 5861.

[3] E. Vedejs, T. Fleck, S. Hara, *J. Org. Chem.* **1987**, *52*, 4637.

[4] T. Kawashima, K. Kato, R. Okazaki, *J. Am. Chem. Soc.* **1992**, *114*, 4008.

[5] $C_{21}H_{13}F_{12}O_4P \cdot 0.5CHCl_3$, m = 647.97, crystal size 0.200 × 0.100 × 0.600 mm, monoclinic, space group *C*2/c, a = 20.883(6), b = 8.880(4), c = 27.210(8) Å, β = 93.86(2)°, V = 5035(5) Å^3, Z = 8, ϱ_{calcd} = 1.710 g cm^{-3}, R = 0.073, Rw = 0.075. Further details of the crystal structure investigation are available on request from the Director of the Cambridge Crystallographic Data Center, 12 Union Road, GB-Cambridge CB2 1EZ (UK), on quoting the full journal citation.

[6] G. Chioccola, J. J. Daly, *J. Chem. Soc. A* **1968**, *568*; F. Ramirez, C. P. Smith, J. F. Pilot, *J. Am. Chem. Soc.* **1968**, *90*, 6726; H. J. Bestmann, K. Roth, E. Wilhelm, R. Böhme, H. Burzlaff, *Angew. Chem.* **1979**, *91*, 945; *Angew. Chem. Int. Ed. Engl.* **1979**, *18*, 876.

[7] The lithium derivative **1b–Li** shows a ^{31}P NMR signal at δ = −28.2 at −40 °C; this indicates that here also the P atom is pentacoordinate. The signal is shifted to δ = 36.7 above −30 °C. The 3-methoxycarbonyl derivative **2d**, prepared from **1b–Li**, was observed by ^{31}P NMR spectroscopy (δ = −42.0), but decomposed to afford the corresponding olefin during purification by chromatography on SiO_2.

[8] Besides **2c**, the 3-butyl derivative (**2**: R = Ph; E = *n*Bu) was obtained in 14% yield as a minor product.

[9] Dielectric constants at 25 °C; C. Reichardt, *Solvents and Solvent Effects in Organic Chemistry*, 2nd ed., VCH, Weinheim, **1988**, p. 408.

[10] Rate constants: 8.36×10^{-6} s^{-1} (69.0 °C), 2.61×10^{-5} (80.0), 7.82×10^{-5} (90.0), 1.76×10^{-4} (100.0), and 4.96×10^{-4} (111.3).

[11] The present solvent effect is too small in comparison with those reported for the reactions involving a zwitterionic intermediate (ref. [9], p. 153). Pseudorotation was not observed experimentally. Therefore, we think the present results support a concerted but non-synchronous mechanism rather than a P–C bond heterolysis mechanism: H. J. Bestmann, *Pure Appl. Chem.* **1980**, *52*, 771.

[12] **1a**: M.p. 70–75 °C (decomp) (EtOH); ^{1}H NMR ($CDCl_3$): δ = 4.02 (dd, ^2J(H,P) = 23.6, ^2J(H,H) = 17.0 Hz, 1H; PC*H*H'), 4.32 (dd, ^2J(H,P) = 19.7, ^2J(H,H) = 17.0 Hz, 1H; PCH*H'*), 7.40–7.48 (m, 3H; *p*, *m*-H of P-Ph), 7.70–7.79 (m, 3H; C*H*), 7.98 (dd, ^3J(H,P) = 15.3, ^3J(H,H) = 7.2 Hz, 2H; *o*-H of P-Ph), 8.45 (dd, ^3J(H,P) = 13.0 Hz, ^3J(H,H) = 7.4 Hz, 1H; C*H*); ^{31}P NMR ($CDCl_3$): δ = −33.3; satisfactory ^{13}C and ^{19}F NMR spectra and correct O,H,N analyses were obtained.

UO_2^{2+}-Catalyzed Oligothioadenylate Synthesis with High Regio- and Stereoselectivity**

By *Masamitsu Shimazu, Kazuo Shinozuka,* and *Hiroaki Sawai**

Phosphorthioate analogues of oligonucleotides with a defined configuration at the phosphorous atom are of importance for the investigation of the stereochemical course of enzymatic reactions[1] and for the development of new chemotherapeutic drugs.[2] Among these analogues, 2′-5′-oligothioadenylates have been reported to possess effective anti-HIV activity[3] and to activate 2′-5′-oligoadenylate-dependent endoribonuclease (RNase L), inducing mRNA degradation.[4] Enzymatically, 2′-5′-oligothioadenylates with *Rp* configuration are produced from *Sp*-ATP$_\alpha$S by 2′-5′-oligoadenylate synthetase.[5] Synthesis of 2′-5′-oligothioadenylates with a variety of thiophosphoryl configurations has been accomplished by conventional phosphite triester[6] and hydrogenphosphonate approaches.[7] In 1989 we showed that UO_2^{2+} salts catalyze the polymerization of adenosine-5′-phosphoroimidazolide (ImpA) very efficiently in aqueous solution, yielding 2′-5′-oligoadenylates.[8] The use of adenosine-5′-thiophosphoroimidazolide (Imp(S)A) should make it possible to study the stereochemical features of the UO_2^{2+}-catalyzed polymerization and to prepare biologically active 2′-5′-oligothioadenylates. We report here that the UO_2^{2+} ion catalyst controls the oligomerization with remarkably high regio- and stereoselectivity.

Synthesis of adenosine-5′-thiophosphoazolide (Xp(S)A) was carried out as shown in Scheme 1. Adenosine was first thiophosphorylated[9] and then treated with imidazole (ImH) or benzimidazole (BzimH) to give adenosine-5′-thiophosphodiimidazolide. After alkaline hydrolysis with pyri-

[*] Prof. Dr. H. Sawai, M. Shimazu, Dr. K. Shinozuka
Department of Chemistry, Faculty of Engineering
Gunma University
Kiryu, Gunma 376 (Japan)

[**] This work was partially supported by a Grant-in-Aid for Scientific Research from the Ministry of Education, Science, and Culture, Japan, and by Aji no Moto Company. We thank Dr. Leslie E. Orgel for comments on the manuscript.

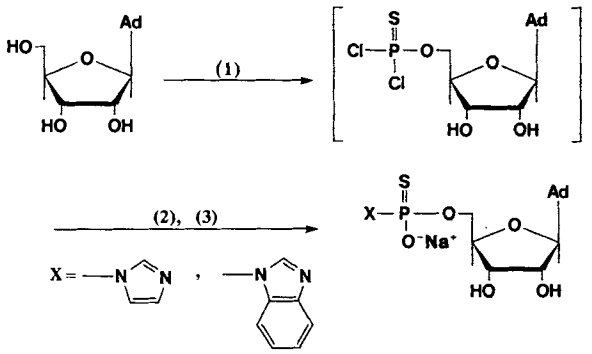

Scheme 1. Preparation of adenosine-5′-thiophosphorazolides (Xp(S)A). (1) $PSCl_3$ in $(EtO)_3PO$; (2) imidazole or benzimidazole; (3) weak alkaline hydrolysis.

dine/H_2O and purification by DEAE-Sephadex column chromatography, the resulting Imp(S)A or Bzimp(S)A was obtained as a nearly 1:1 diastereoisomeric mixture. The yields of Imp(S)A and Bzimp(S)A from adenosine were 30% and 19%, respectively. The *Rp* and *Sp* diastereomers of Bzimp(S)A were resolved by HPLC, and the configurations at thiophosphoryl group were determined by ^{31}P NMR spectroscopy[11] (Table 1).

Table 1. HPLC retention times t, ^{31}P chemical shifts, and stability toward SVPD (half-life $\tau_{1/2}$ at 37 °C) of the diastereomers of Bzimp(S)A and 2′-5′-$(p(S)A)_2$.

Compound	t [min] [a]	δ (^{31}P) [b]	$\tau_{1/2}$ [h]
Rp-Bzimp(S)A	44.1	61.43	–
Sp-Bzimp(S)A	44.8	60.33	–
Rp-$(p(S)A)_2^{2'-5'}$	19.0	56.49 [c]	8.5
Sp-$(p(S)A)_2^{2'-5'}$	−21.2	55.57 [c]	≫48.0 [d]

[a] HPLC retention time for a linear gradient of MeOH (2.4 → 51.2% in 60 min) in 10 mM triethylammonium acetate (TEAA), pH 7.3, flow rate 1.0 mL min^{-1}, ODS-silicagel column. [b] Measured at 36.44 MHz in 100 mM TEAA, pH 7.3, containing 50% D_2O. [c] The chemical shift for the thiophosphoryl group at the internucleotidyl bond. [d] No digestion directed by time indicated.

Oligomerization of Xp(S)A was carried out in a mixture of Xp(S)A (50 mM) and $UO_2(NO_3)_2$ (2 mM) in 0.2 M *N*-ethylmorpholine/HNO_3 buffer (pH 7.0) at 25 °C. According to HPLC analysis no more starting material was present in the reaction mixture after 5 days. The reaction products were isolated by HPLC, and their structures were ascertained by COSY ^1H NMR. The configuration of the thiophosphoryl group of the oligomers was determined by susceptibility toward snake venom phosphodiesterase (SVPD) digestion (half-life), retention time of reverse-phase HPLC, and ^{31}P chemical shift (Table 1). The *Rp* diastereomers had shorter retention times,[6,7] larger (δ ^{31}P) values,[11] and were more easily digested with SVPD than the corresponding *Sp* diastereomers.[1a,10]

Table 2 shows the yields of the oligomerization of the several azolides. The imidazolide with normal phosphoryl group, ImpA, yielded oligonucleotides up to the hexadecamer,[8] whereas chain elongation from Imp(S)A was significantly suppressed and the main products were 2′-5′-linked dimers and trimers. The 2′-5′-internucleotidyl bond was preferentially formed in all of the UO_2^{2+}-catalyzed polymerizations.

Figure 1a shows the HPLC elution profile of the reaction mixture obtained from Imp(S)A. Oligomers with *Rp* configurations were preferentially formed, although the starting Imp(S)A was a nearly 1:1 mixture of diastereomers. In order to achieve a better understanding of the stereoselectivity we carried out the oligomerization of the *Rp*- and *Sp*-Bzimp(S)A diastereoisomers both separately and as a mixture.

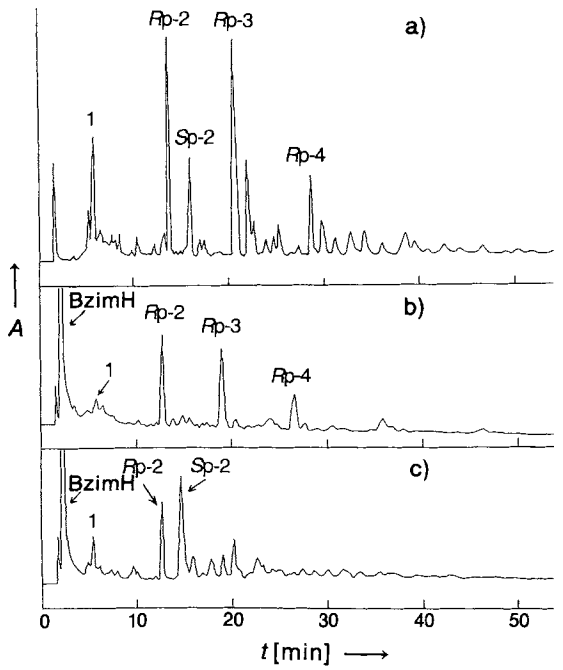

Fig. 1. HPLC profiles of oligothioadenylates obtained from the UO_2^{2+}-catalyzed oligomerization of (a) (*Rp*)- + (*Sp*)-Imp(S)A, (b) (*Sp*)-Bzimp(S)A and (c) (*Rp*)-Bzimp(S)A. 1, p(S)A; *Rp*-2: (*Rp*)-$(p(S)A)_2^{2'-5'}$; *Sp*-2: (*Sp*)-$(p(S)A)_2^{2'-5'}$; *Rp*-3: (*RpRp*)-$(p(S)A)_3^{2'-5',2'-5'}$; *Rp*-4: (*RpRpRp*)-$(p(S)A)_4^{2'-5',2'-5',2'-5'}$. Chromatography column: RPC-5 (250 × 4 mm); flow rate: 1.0 mL min^{-1}, elution: A → B (60 min), A: 2 mM TRIS acetate, pH 7.5 + 0.1 mM EDTA, B: 70 mM $NaClO_4$ + 2 mM TRIS acetate + 0.1 mM EDTA; detection: UV absorption at 260 nm.

HPLC profiles of the reaction mixtures are shown in Figures 1b and 1c. The *Sp* monomer (Fig. 1b) effectively promoted the formation of 2′-5′-oligomers up to the hexamer. These oligomers were digested easily with SVPD,[1a,10]

Table 2. UO_2^{2+}-catalyzed formation of 2′-5′-oligoadenylate analogues.

Substrate	Reaction time [days]	c (UO_2^{2+}) [mM]	HPLC yield of 2′-5′-oligoadenylate [%] monomer	*Rp* dimer	*Sp* dimer	*RpRp* trimer	tetramer	≥ pentamer
ImpA	4	1	0.1		6.0 [a]	12.8 [a]	10.7	30.9 [b]
(*Rp*)- + (*Sp*)-Imp(S)A	5	2	7.2	12.6	7.4	20.6	7.0	
(*Rp*)- + (*Sp*)-Bzimp(S)A	7	2	51.6	25.1	9.8	4.2		

[a] Phosphodiester linkage (no stereoisomer). [b] Oligomer up to hexadecamer.

which indicates that they were only *Rp* isomers. On the other hand, the main products from the *Rp* monomer (Fig. 1c) were 2′-5′-linked *Sp* and *Rp* dimers, and further chain elongation was not observed. It was ascertained by HPLC that the *Sp* monomer was consumed faster than the *Rp* monomer in the reaction. When the diastereoisomeric mixture of Bz-imp(S)A was used as a starting monomer, the oligomerization proceeded insufficiently and hydrolysis of the monomer predominated.

Our studies have thus shown that *Sp*-Bzimp(S)A leads to the 2′-5′-linked *Rp* oligomers in high yields, whereas *Rp*-Bz-imp(S)A also forms the *Sp* dimer. We thus propose that the oligomerization involves an inversion mechanism.

The available results lead to a working hypothesis for the course of UO_2^{2+}-catalyzed regio- and stereoselective oligomerization: Kainosho et al.[12] and Feldman et al.[13] reported that UO_2^{2+} forms a cluster-type complex with adenosine-5′-monophosphate, in which the phosphate group and 3′-hydroxy group coordinate to the UO_2^{2+} ion. We postulate that the stereoselective oligomerization takes place via similar types of complexes formed from the UO_2^{2+} ion and Xp(S)A (Fig. 2). The enhanced nucleophilicity of the 2′-hydroxy

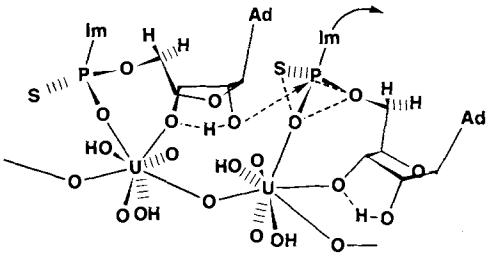

Fig. 2. Proposed stereochemical course of the UO_2^{2+}-catalyzed oligothioadenylate formation from (*Sp*)-adenosine-5′-thiophosphoroimidazolide (the protons of the ribose ring are omitted). The imidazole leaving group is oriented favorably with the incoming 2′-OH group in the complex. The *Rp* monomer also forms a complex with the UO_2^{2+} ion, but in this case the leaving and incoming groups are not oriented favorably with one another.

group is ascribed to a hydrogen-bonded ring in the anion of the coordinated state.[14] Sequential 2′-5′-internucleotidyl bond formation is likely to occur through attack of the 2′-hydroxy group of a coordinated Xp(S)A molecule at the thiophosphoryl group of the adjacently coordinated Xp(S)A molecule. The thiophosphoryl oxygen atom, but not the corresponding sulfur atom of the Xp(S)A, coordinate to the UO_2^{2+} ion, since sulfur is a weaker electron donor than oxygen toward the UO_2^{2+} ion.[15] The orientation of the thiophosphoryl monomers imposed by the coordination of the oxygen atom to the UO_2^{2+} ion allows a degree of stereoselectivity that is rarely encountered except in enzymatic reactions.

Suhadolnik et al.[3] reported that oligomers with *Rp* configuration reveal strong biological activities, for example the (*RpRp*)-trimer-5′-triphosphate inhibits HIV-1 reverse transcriptase.

2′-5′-oligothioadenylates with *Rp* configuration are preferentially formed in aqueous solution in the oligomerization catalyzed by UO_2^{2+} ions, without the need for protecting groups. The reaction is very useful, therefore, for the simple stereoselective synthesis of 2′-5′-linked oligothioadenylates.

Received: November 3, 1992,
Revised version: February 9, 1993 [Z 5662 IE]
German version: *Angew. Chem.* **1993**, *105*, 909

[1] a) F. Eckstein, *Angew. Chem.* **1983**, *95*, 431–447; *Angew. Chem. Int. Ed. Engl.* **1983**, *22*, 423–439; b) F. Eckstein, G. Gish, *Trends Biochem. Sci.* **1989**, *14*, 97–100; c) V. Mizrahi, R. N. Henrie, J. F. Marlier, K. A. Johnson, S. J. Benkovic, *Biochemistry* **1985**, *24*, 4010–4018.
[2] a) *Oligodeoxynucleotides, Antisense Inhibitors of Gene Expression* (Ed.: J. S. Cohen), Macmillan, London, **1989**; b) W. Gao, C. A. Stein, J. S. Cohen, G. E. Dutschman, Y.-C. Cheng, *J. Biol. Chem.* **1989**, *264*, 11521–11526; c) M. Matsukura, K. Shinozuka, G. Zon, H. Mitsuya, M. Reitz, J. S. Cohen, S. Broder, *Proc. Natl. Acad. Sci. USA* **1987**, *84*, 7706–7710; d) C. Majumder, C. A. Stein, J. S. Cohen, S. Broder, S. H. Wilson, *Biochemistry* **1989**, *28*, 1340–1346.
[3] a) H. C. Schroeder, R. J. Suhadolnik, W. Pfleiderer, R. Charubala, W. E. G. Mueller, *Int. J. Biochem.* **1992**, *24*, 55–63; b) R. J. Suhadolnik, B. Lebleu, W. Pfleiderer, R. Charubala, D. C. Montefiori, W. M. Mitchell, R. W. Sobol, S. W. Li, K. Kariko, N. L. Reichenbach, *Nucleosides Nucleotides* **1989**, *8*, 987–990; c) D. C. Montefiori, R. W. Sobol, S. W. Li, N. L. Reichenbach, R. J. Suhadolnik, R. Charubala, W. Pfleiderer, A. Modliszewski, W. E. Robinson, W. M. Mitchell, *Proc. Natl. Acad. Sci. USA* **1989**, *86*, 7191–7194.
[4] a) K. Kariko, R. W. Sobol, L. Suhadolnik, S. W. Li, N. L. Reichenbach, R. J. Suhadolnik, R. Charubala, W. Pfleiderer, *Biochemistry* **1987**, *26*, 7127–7135; b) G. Charachon, R. W. Sobol, C. Bisbal, T. Salehzada, M. Silhol, R. Charubala, W. Pfleiderer, B. Lebleu, R. J. Suhadolnik, *ibid.* **1990**, *29*, 2550–2556.
[5] C. Lee, R. J. Suhadolnik, *Biochemistry*, **1985**, *24*, 551–555.
[6] a) P. S. Nelson, C. T. Bach, J. P. H. Verheyden, *J. Org. Chem.* **1984**, *49*, 2314–2317; b) R. Charubala, W. Pfleiderer, *Nucleosides Nucleotides* **1987**, *6*, 513–516; c) R. Charubala, W. Pfleiderer, R. J. Suhadolnik, R. W. Sobol, *ibid.* **1991**, *10*, 383–388.
[7] C. Battistini, M. G. Brasca, S. Fustinoni, *Tetrahedron* **1992**, *48*, 3209–3226.
[8] H. Sawai, K. Kuroda, T. Hojo, *Bull. Chem. Soc. Jpn.* **1989**, *62*, 2018–2023.
[9] A. W. Murray, P. C. L. Wong, B. Friedrichs, *Biochem. J.* **1969**, *112*, 741–746.
[10] a) F. R. Byant, S. J. Benkovic, *Biochemistry* **1979**, *18*, 2825–2828; b) P. M. J. Burgers, F. Eckstein, *Proc. Natl. Acad. Sci. USA* **1978**, *75*, 4798–4800; c) B. Uznanski, W. Niewiarowski, W. J. Stec, *Tetrahedron Lett.* **1982**, *23*, 4289–4292; d) J. F. Marlier, S. J. Benkovic, *ibid.* **1980**, *21*, 1121–1124.
[11] a) P. J. Romaniuk, F. Eckstein, *J. Biol. Chem.* **1982**, *257*, 7684–7688; b) P. A. Bartlett, F. Eckstein, *ibid.* **1982**, *257*, 8879–8884; c) R. Cosstick, F. Eckstein, *Biochemistry* **1985**, *24*, 3630–3638.
[12] M. Kainosho, M. Takahashi, *Nucleic Acid Symp. Ser.* **1983**, *12*, 181–184.
[13] I. Feldman, K. E. Rich, *J. Am. Chem. Soc.* **1970**, *92*, 4559–4564.
[14] a) R. M. Izatt, L. D. Hansen, J. H. Rytting, J. J. Christensen, *J. Am. Chem. Soc.* **1965**, *87*, 2760–2761; b) G. I. Birnbaum, J. Giziewicz, C. P. Huber, D. Shugar, *J. Am. Chem. Soc.* **1976**, *98*, 4640–4644.
[15] a) W. W. Wendlandt, J. M. Bryant, *Science* **1956**, *123*, 1121; b) A. E. Comyns, *Chem. Rev.* **1960**, *60*, 115–146.

A Branched-Chain Nonacarbene with a Nonadecet Ground State: A Step Nearer to Superparamagnetic Polycarbenes

By *Nobuo Nakamura, Katsuya Inoue*, and *Hiizu Iwamura**

While ferromagnetism of transition metals and lanthanoids is ascribed to the macroscopic ordering of their 3d and 4f electron spins, respectively, the 2s and/or 2p electron spins of open-shell organic molecules can, in general, contribute only to paramagnetism due to their small magnetic moment (typically $S = 1/2$, $\mu_{eff} = 1.73\,\mu_B$). If an organic molecule acquires a huge magnetic moment, it might form a single magnetic domain and exhibit superparamagnetic behavior, such as pseudo-hysteresis. Even organic ferromagnets could be realized if ferromagnetic coupling between high-spin molecules in the solid were to occur. The basic principles leading to these molecules are based on the orthogonality of the singly occupied orbitals in space and on

[*] Prof. Dr. H. Iwamura, Prof. Dr. N. Nakamura, K. Inoue
Department of Chemistry, Faculty of Science
The University of Tokyo
Hongo, Bunkyo-ku, Tokyo 113 (Japan)

the topological symmetry.[1] Carbenes in triplet ground states are examples of the former,[2] and a Schlenk diradical $R_2C^{\cdot}$–m-C_6H_4–$^{\cdot}CR_2$ with the triplet ground state is a representative of the latter.[3] It is amply demonstrated by the one-dimensional poly(m-phenylenecarbenes) **1** that combination of these two concepts is effective in the construction of organic molecules with higher spin quantum numbers.[4] Extension of this system to the two-dimensional branched-chain hexacarbene **2** with a tridecet ground state ($S = 6$) has also been successful.[5] In order to ensure this branched-chain strategy for organic molecules with higher spin and to obtain information on any restriction which might arise in this approach, studies on higher homologues of the hexacarbene, **2**, are extremely important. In the present communication, the synthesis and magnetic properties of the nonacarbene **3** are reported.

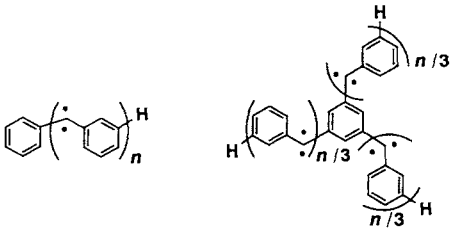

1 (n = 1 ~ 5) **2**, n = 6 **3**, n = 9

The synthetic route to the precursor of **3**, namely **4d**, via nonaketone **4b** is illustrated in Scheme 1. The diethylamine-catalyzed trimerization of the aryl ethynyl ketone served as a key step in the synthesis of 1,3,5-tris(aroyl)benzene.[5] The nonadiazo compound **4d** was purified by chromatography and characterized by IR, UV/VIS, and NMR spectroscopy.

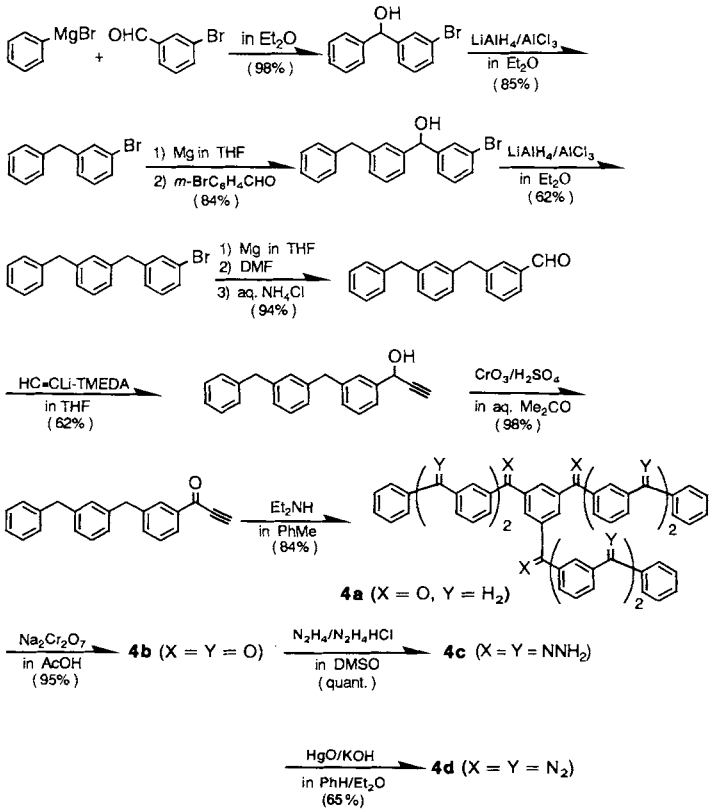

Scheme 1. Synthetic pathway for the nonadiazo compound **4d** via the nonaketone **4b** and the nonahydrazone **4c**.

The connectivity of the H and C atoms of **4b** was confirmed by H,H- and C,H-COSY spectra.

Photolysis of **4d** in 2-methyltetrahydrofuran (MTHF) glasses at 6.5 K in an X-band ESR spectrometer resulted in the appearance of strong, complex ESR signals centered at about 330 mT, which are characteristic of unoriented high-spin species. The shape of the signals and the position of the center of the signals were dependent on both the modulation amplitude and the scan direction of the main external field. This suggests considerable anisotropy of the principal axes of the zero-field tensor and slow relaxation.

UV light was introduced through a quartz light guide and used to photolyze a solution of **4d** in MTHF glasses in a quartz basket suspended in the superconducting solenoid (≤ 7 T) of an Oxford Faraday magnetic balance at 2 K. The magnetic measurements on **3** thus produced were performed in situ. The plots of magnetization M versus the applied magnetic field strength H at 2.1 and 10.0 K were analyzed in terms of the Brillouin function to give a spin quantum number $S = 9.0_0$ for **3**, a new record for a purely organic molecule (Fig. 1). When the external magnetic field was switched

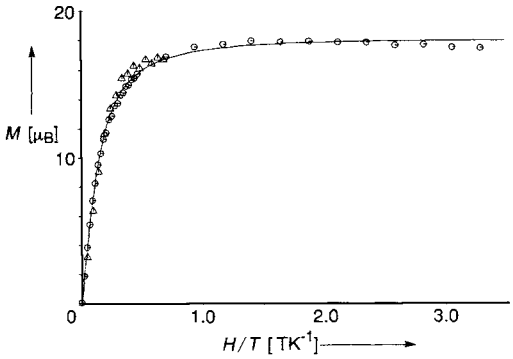

Fig. 1. Magnetization M of nonacarbene **3** in MTHF glasses at 2.1 K (o) and 10.0 K (Δ). Solid line corresponds to the theoretical curve of $S = 9$.

on and off by a SQUID magnetometer, the magnetization did not follow instantaneously, but required a half-life of about 30 min to recover at 5 K.

At least two prerequisites must be fulfilled for the observation of the $S = 9$ state of **3**: First the wavelength of the light must be in the range 400–480 nm, otherwise ESR signals due to triplet carbenes, quintet dicarbenes, and other high-spin species, are observed. Second the concentration of the sample should be < 1 mmol L^{-1}, otherwise the effective magnetic moment is lowered by about 15% at 2 K relative to that at 20 K, probably due to antiferromagnetic intermolecular interactions.

There are two important messages from this work. First the branched-chain pseudo-two-dimensional framework in **2** and **3** is appropriate for controlling its high-spin ground state, at least up to nonacarbene ($S = 9$) in **3**. Second, there are indications that the rotation of the principal axis of dipolar coupling and magnetization at cryogenic temperatures is hindered.

Experimental Procedure

1,3,5-Tris[3-((3-benzoyl)benzoyl)benzoyl]benzene (**4b**): 1,3,5-Tris[3-((3-benzyl)benzyl)benzoyl]benzene **4a**, obtained by trimerization of 1-[3-((benzyl)benzyl)phenyl]prop-2-yn-1-one, was oxidized with $Na_2Cr_2O_7 \cdot 2H_2O$ in acetic acid to give the nonaketone **4b** [6]. After chromatography on silica gel with hexane and dichloromethane **4b** was obtained in 95% yield. M.p. 118–119 °C; IR (Nujol): $\tilde{\nu}$[cm^{-1}] = 1690 (C=O); FAB-MS: m/z 1016.4 (M^+ + H, 14%), 1015.4 (M^+, 13).

1,3,5-Tris[diazo(3-(diazo(3-(diazo(phenyl)methyl)phenyl)methyl)phenyl)-methyl]benzene (**4d**): The nonaketone **4b** was converted to the corresponding nonahydrazone **4c** by the addition of anhydrous hydrazine and hydrazine hydrochloride in dimethyl sulfoxide (DMSO) at 90 °C. The nonahydrazone **4c** was then oxidized with HgO in a benzene/CH_2Cl_2 mixture in the presence of a 3 M solution of KOH in ethanol. The mixture was stirred for 7 days at room temperature. Filtration of the reaction mixture followed by concentration of the filtrate in vacuo left a deep wine-red oil, which was immediately chromatographed on alumina (Woelm neutral, activity IV) at 0 °C with hexane and benzene. This afforded the nonadiazo compound **4d** as a deep red oil in 65% yield. ^{1}H NMR (270 MHz, $CDCl_3$, 21 °C): $\delta = 7.43-6.85$ (m); IR(Nujol): $\tilde{\nu}$[cm^{-1}] = 2060; UV/VIS(MTHF): λ_{max}[nm](ε) = 520 (950).

Photolysis and magnetic measurement: A solution of about 20 μg of **4d** in 80 μL of MTHF in a quartz sample basket suspended in a superconducting solenoid was irradiated with UV light ($480 > \lambda > 400$ nm). The UV light was obtained by a combination of a Kenko B-390 band-path filter and an OCLI type B cold mirror. During the magnetic measurement the field gradient was kept constant at 5 Tesla m^{-1} while the main field was changed from 0 to 7 Tesla.

Received: January 18, 1993 [Z 5816 IE]
German version: *Angew. Chem.* **1993**, *105*, 900

[1] H. C. Longuet-Higgins, *J. Chem. Phys.* **1950**, *18*, 265.
[2] E. Wasserman, L. C. Snyder, W. A. Yager, *J. Chem. Phys.* **1964**, *41*, 1763.
[3] G. Kothe, K.-H. Denkel, W. Sümmermann, *Angew. Chem.* **1970**, *82*, 935; *Angew. Chem. Int. Ed. Engl.* **1970**, *9*, 906.
[4] I. Fujita, Y. Teki, T. Takui, T. Kinoshita, K. Itoh, F. Miko, Y. Sawaki, H. Iwamura, A. Izuoka, T. Sugawara, *J. Am. Chem. Soc.* **1990**, *112*, 4074, and references therein.
[5] N. Nakamura, K. Inoue, H. Iwamura, T. Fujioka, Y. Sawaki, *J. Am. Chem. Soc.* **1992**, *114*, 1484.
[6] ^{1}H NMR data (270 MHz, $CDCl_3$, 21 °C): $\delta = 8.41$ (s, 3H; 2,4, 6-H), 8.23 (t, ^4J(H,H) = 1.7 Hz, 3H, 2′-H), 8.14 (t, ^4J(H,H) = 1.7 Hz, 3H; 2″-H), 8.03 (d, ^3J(H,H) = 8.1 Hz, 3H; 6′-H), 8.00 (d, ^3J(H,H) = 8.1 Hz, 3H; 4′-H), 7.97 (d, ^3J(H,H) = 8.1 Hz, 6H; 4″,6″-H), 7.74 (d, ^3J(H,H) = 8.1 Hz, 6H; 2‴,6‴-H), 7.62 (t, ^3J(H,H) = 8.1 Hz, 3H; 5′-H), 7.57 (t, ^3J(H,H) = 8.1 Hz, 3H; 5″-H), 7.52 (t, ^3J(H,H) = 8.1 Hz, 3H; 4‴-H), 7.41 (t, ^3J(H,H) = 8.1 Hz, 6H; 3‴,5‴-H).

Monomeric Tris(η^2-pyrazolato)Lanthanoid Complexes with the Bulky 3,5-Di(*tert*-butyl)pyrazolato Ligand**

By *Joanna E. Cosgriff, Glen B. Deacon*, Bryan M. Gatehouse, Holger Hemling,* and *Herbert Schumann**

Dedicated to Professor Bruce West on the occasion of his 65th Birthday

Pyrazolate (pz) ions mainly behave as bridging ligands owing to the directional characteristics of the lone pairs on the nitrogen atoms,[1] but some f-block complexes have chelating η^2-pyrazolato ligands.[2–5] In all these complexes, the f-block metal atoms also have either cyclopentadienyl ligands[2, 3] or bridging pz ligands.[4, 5] No tris(η^2-pyrazolato) lanthanoid complexes have been reported; the simple [Ln-(pz)$_3$] complexes (Ln = Nd,[5] Yb[6]) have low solubility and are probably polymeric with only bridging pz groups, whilst [Nd(Me$_2$pz)$_3$(thf)] (Me$_2$pz$^-$ = 3,5-dimethylpyrazolate; thf = tetrahydrofuran) is dimeric with μ-Me$_2$pz and η^2-Me$_2$pz ligands and, unexpectedly, bridging THF ligands.[5] We now have used the bulky 3,5-di(*tert*-butyl)pyrazolato (tBu$_2$pz$^-$) ligand to give tris(η^2-pyrazolato)lanthanoid compounds as monomeric, petroleum ether-soluble [Ln(η^2-tBu$_2$pz)$_3$(thf)$_2$] complexes, the first metal complexes of any element with η^2-bound pyrazolate ions as the sole anionic ligands. The X-ray structure of the neodymium complex confirms the monomeric nature of the compounds.

Reaction of bis(pentafluorophenyl)mercury and 3,5-di(*tert*-butyl)pyrazole with an excess of lanthanoid metal in THF at room temperature gave the air- and water-sensitive complexes **1**–**4** (Ln = La (**1**), Nd (**2**), Gd (**3**), or Er (**4**)) in 36–55% yield [Eq. (a)].

$$2\,Ln + 3[Hg(C_6F_5)_2] + 6\,Ht\text{Bu}_2pz \xrightarrow{THF} \underset{\mathbf{1-4}}{2[Ln(t\text{Bu}_2pz)_3(thf)_2]} + 3\,Hg\downarrow + 6\,C_6F_5H \quad (a)$$

The mass spectra of **1**–**4** show mononuclear [Ln-(tBu$_2$pz)$_3^+$] parent ions, in contrast to the [Nd(Me$_2$pz)$_3$(thf)] complex,[5] which gives dinuclear ions and no [Nd-(Me$_2$pz)$_3^+$]. This result and the high solubility of **1**–**4** in petroleum ether infer monomeric structures, and this was established by the X-ray crystal structure of **2** (Fig. 1).[7]

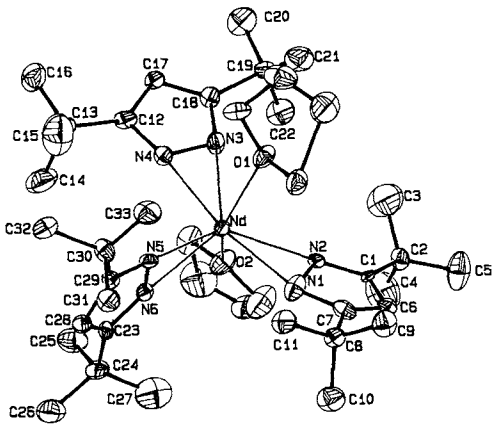

Fig. 1. Crystal structure of **2** (H atoms omitted for clarity). Selected distances [pm] and angles [°] (Cen 1, Cen 2, and Cen 3 denote the centers of the bonds N1-N2, N3-N4 and N5-N6, respectively): Nd-N1 243(1), Nd-N2 246(1), Nd-N3 241.8(8), Nd-N4 238.1(8), Nd-N5 249.2(9), Nd-N6 247.7(6), Nd-O1 247.5(6), Nd-O2 243.2(8), N1-N2 136(1), N3-N4 138(1), N5-N6 140(1); N1-Nd-N2 32.2(3), N3-Nd-N4 33.3(3), N5-Nd-N6 32.7(2), O1-Nd-O2 145.2(6), Cen1-Nd-Cen2 140.3(4), Cen2-Nd-Cen3 109.2(3), Cen1-Nd-Cen3 110.6(4), Cen1-Nd-O1 84.5(3), Cen1-Nd-O2 88.0(4), Cen2-Nd-O1 81.0(4) Cen2-Nd-O2 88.5(3), Cen3-Nd-O1 112.0(6), Cen3-Nd-O2 102.5(3).

Coordination of three η^2-(tBu$_2$pz) ligands and two THF ligands gives irregular eight coordination for the central Nd atom. The Nd–N distances (Fig. 1) increase from silimar to those for η^2-Me$_2$pz to near those for μ-Me$_2$pz in [{Nd-(η^2-Me$_2$pz)$_2$(μ-Me$_2$pz)(μ-thf)}$_2$] (**5**).[5] Although the elongation can be attributed to the steric demands of three η^2-tBu$_2$pz$^-$ ligands, the Nd–O distances are normal for Ln–O(thf) lengths.[11] A clearer picture of the stereochemistry around the neodymium center is obtained if the arrangement of oxygen atoms of the THF ligands and the mid points (Cen 1–Cen 3) of the N–N bonds is considered.[15] This arrangement is intermediate between a trigonal bipyramid

[*] Dr. G. B. Deacon, J. E. Cosgriff, Dr. B. M. Gatehouse
Chemistry Department, Monash University
Clayton, Victoria 3168 (Australia)
Telefax: Int. code +(613)565-4597
Prof. Dr. H. Schumann, Dipl.-Chem. H. Hemling
Institut für Anorganische und Analytische Chemie
der Technischen Universität
Strasse des 17 Juni 135, D-W-1000 Berlin 12 (FRG)

[**] Organoamido- and Aryloxo-lanthanoids, Part, and Organometallic Lanthanoid Compounds, Part 77. This work was supported by the Australian Research Council and an Australian Postgraduate Research Award for J. C., the Fonds der Chemischen Industrie and the Deutsche Forschungsgemeinschaft.—Part 5. G. B. Deacon, T. Feng, P. MacKinnon, R. H. Newnham, S. Nickel, B. W. Skelton, A. H. White, *Aust. J. Chem.*, **1993**, *46*, 387. Part 76. H. Schumann, M. Glanz, J. Winterfeld, H. Hemling, *J. Organomet. Chem.* **1993**, *445*, C1.

with O1 and O2 apical, and Cen 1, Cen 2, and Cen 3 in the equatorial positions (Cen 1, Cen 2, Cen 3, and Nd are coplanar, deviation $\leq 0.08(4)$ pm), and square pyramidal with Cen 3 apical, and transoid Cen 1, Cen 2, and O1, O2 relationships in the square plane (Nd 75.71(2) pm above the plane). In either case, the skeletal angles (Fig. 1) deviate considerably from those for regular arrangements. Although tBu$_2$pz is bridging in the only reported complex of this ligand [{Ni(tBu$_2$pz)(NO)}$_2$],[16] it is sufficiently bulky (cf. pz[5, 6] and Me$_2$pz[5]), in conjunction with the nondirectional ionic character of lanthanoid–ligand bonding, to promote formation of monomeric [Ln(η^2-pz)$_3$] complexes.

The petroleum ether-soluble compounds **1**–**4** are potential synthetic reagents of comparable utility to [Ln{N(SiMe$_3$)$_2$}$_3$] species[17] in protolytic ligand exchange reactions. To illustrate this, **6** [Odpp$^-$ = 2,6-diphenylphenolate; Eq. (b)] has been readily prepared from **2**. The high solubility of 3,5-di(*tert*-butyl)pyrazole in petroleum ether facilitates the separation of products.

$$\underset{\mathbf{2}}{[\mathrm{Nd}(t\mathrm{Bu_2pz})_3(\mathrm{thf})_2]} + 3\,\mathrm{HOdpp} \longrightarrow \underset{\mathbf{6}}{[\mathrm{Nd}(\mathrm{Odpp})_3(\mathrm{thf})_2]} + 3\,\mathrm{H}t\mathrm{Bu_2pz} \quad \text{(b)}$$

Experimental Procedure

Syntheses and characterization. All operations were carried out under a purified N_2 or Ar atmosphere. **1**: La powder (0.80 g, 5.7 mmol), [Hg(C_6F_5)$_2$] [18] (1.48 g, 2.8 mmol), and HtBu$_2$pz [19] (1.00 g, 5.5 mmol) were stirred together in THF (40 mL) at room temperature for 2 days. The reaction mixture was filtered and evaporated until solid deposited. Dissolution by warming and cooling to room temperature gave **1** (0.84 g, 55%) as a white powder. Correct C,H,La analyses. ^{1}H NMR (200 MHz, C_6D_6): δ = 1.13 (m, 8H, β-H(thf)), 1.39 (s, 54H, tBu), 3.25 (t, J = 6.5 Hz, 8H, α-H(thf)), 6.37 (s, 3H, H4(tBu$_2$pz)). MS (L = tBu$_2$pz): m/z 676 (NdL_3^+, 0.3%), 661 (NdL_3^+ – Me, 0.3%), 497 (NdL_2^+, 0.8%), 481 (NdL_2^+ – MeH, 0.9%), 180 (LH^+, 20%), 165 (LH^+ – Me, 100%). IR (Nujol/Fluorolube, strong bands only) $\tilde{\nu}$[cm^{-1}] = 2948, 2895, 2858, 1456, 1430, 1412, 1357, 1250, 1224, 1031, 1016, 993, 875, 787. After analogous preparations, **3** was isolated similarly, and **2** and **4** were obtained by evaporation of the filtered reaction mixture to dryness and crystallization of the residue from pentane/THF at –10 °C. The IR spectra of **2**–**4** were essentially identical with that of **1**, and their mass spectra showed features corresponding with those of **1**.

Reaction of **2** with HOdpp: A solution of **2**, prepared in situ from Nd powder (0.68 g, 4.7 mmol), [Hg(C_6F_5)$_2$] (0.74 g, 1.4 mmol), and HtBu$_2$pz (0.50 g, 2.8 mmol) in THF (40 mL) was filtered onto HOdpp (0.68 g, 2.8 mmol) and stirred briefly at room temperature. The blue solution was concentrated to about 8 mL, which resulted in deposition of light blue [Nd(Odpp)$_3$(thf)$_2$]. After addition of pentane the mixture was stirred to dissolve any HtBu$_2$pz and the blue solid was collected (0.78 g, 55%). The IR and mass spectra were in agreement with those of the authentic compound [20, 21]. Evaporation of the filtrate gave a white residue of HtBu$_2$pz (IR identification).

Received: January 26, 1993 [Z 5827 IE]
German version: *Angew. Chem.* **1993**, *105*, 906

[1] S.Trofimenko, *Chem. Rev.* **1972**, *72*, 497–509.
[2] C. W. Eigenbrot, K. N. Raymond, *Inorg. Chem.* **1981**, *20*, 1553–1556.
[3] C. W. Eigenbrot, K. N. Raymond, *Inorg. Chem.* **1982**, *21*, 2653–2660.
[4] H. Schumann, P. R. Lee, J. Loebel, *Angew. Chem.* **1989**, *101*, 1073–1075; *Angew. Chem. Int. Ed. Engl.* **1989**, *28*, 1033–1035.
[5] G. B. Deacon, B. M. Gatehouse, S. Nickel, S. N. Platts, *Aust. J. Chem.* **1991**, *44*, 613–621.
[6] G. Bielang, Doktor des Fachbereiches Chemie Thesis, University of Hamburg, 1979.
[7] **2**: Air-sensitive blue crystals, $C_{41}H_{73}N_6NdO_2$, M_r = 826.3, monoclinic, space group $P2_1$, a = 976.0(1), b = 1972.7(3), c = 1179.6(2) pm, β = 98.76(1)°, V = 2244.7(5) 10^{-30} m^3, z = 2, ρ_{calcd} = 1.222 g cm^{-3}, crystal 0.25 × 0.15 × 0.30 mm^3; Enraf-Nonius CAD-4 four-circle diffractometer, $Mo_{K\alpha}$ radiation 71.069 pm, graphite monochromator, (ω-2θ) scan, $1 \leq 2\theta \leq 49$°, at 165 K, 3671 independent reflections, 3265 observed ($F_o > 6\sigma(F_o)$) used in the refinement (SDP software package (data reduction) [8], SHELX76 [9]). 450 refined parameters, R = 0.0398, data corrected for Lorentz and polarization effects [10]. Non-hydrogen atoms refined with anisotropic thermal parameters. H positions calculated and refined isotropically with a common displacement factor ($U_{iso,H}$ = 0.111(8) Å^2). Further details of the crystal structure investigations may be obtained from the Fachinformationszentrum, Karlsruhe, Gesellschaft für wissenschaftlich-technische Information mbH, D-W-7514 Eggenstein-Leopoldshafen 2 (FRG) on quoting the depository number CSD-57054, the names of the authors and the journal citation.
[8] B. A. Frenz, Enraf, SDP-Plus Structure Determination Package, Version 3.0, Enraf-Nonius Delft, **1985**.
[9] G. M. Sheldrick, SHELX 76, Program for Crystal Structure Determination, University of Cambridge, **1976**.
[10] D. Walker, D. Stewart, *Acta Crystallogr. Sect. A* **1968**, *24*, 321–324.
[11] Subtraction of an ionic radius [12] of an eight-coordinate Nd^{3+} ion from the Nd–O distance gives 134 pm. This corresponds closely to the difference (134(5) pm) derived from Ln–O(thf) distances of organolanthanoid–THF complexes with coordination numbers 7–10 [13] and contrasts to the differences (149–159 pm) for THF complexes of bulky lanthanoid aryloxides [14].
[12] R. D. Shannon, *Acta Crystallogr. Sect. A* **1976**, *32*, 751–767.
[13] G. B. Deacon, P. I. MacKinnon, T. W. Hambley, J. C. Taylor, *J. Organomet. Chem.* **1983**, *259*, 91–97.
[14] G. B. Deacon, T. Feng, S. Nickel, M. I. Ogden, A. H. White, *Aust. J. Chem.* **1992**, *45*, 671–683.
[15] In η^2-pyrazolato–Ln coordination, the bond can be viewed as a nondirectional and ionic interaction between the N–N bond and the Ln^{3+} center.
[16] K. S. Chong, S. J. Rettig, A. Storr, J. Trotter, *Can. J. Chem.* **1979**, *57*, 3090–3098.
[17] For example: P. B. Hitchcock, M. F. Lappert, A. Singh, *J. Chem. Soc. Chem. Commun.* **1983**, 1499–1501.
[18] G. B. Deacon, R. N. M. Smith, *J. Org. Chem. USSR (Engl. Transl.)* **1982**, *18*, 1854–1855.
[19] J. Elguero, E. Gonzalez, R. Jacquier, *Bull. Soc. Chim. Fr.* **1968**, 707–713.
[20] G. B. Deacon, S. Nickel, P. MacKinnon, E. R. T. Tiekink, *Aust. J. Chem.* **1990**, *43*, 1245–1257.
[21] A band at 1069(s) cm^{-1} was inadvertently omitted from the reported spectrum [20].

Delocalization of Electrons in the Dodecahedrane Cage—A D_{2h}-Symmetrical 4c-3e Radical Cation as a Structural Borderline Case**

By *Klaus Weber, Horst Prinzbach,* Reto Schmidlin, Fabian Gerson,* and *Georg Gescheidt**

Dedicated to Professor Herbert Zimmermann on the occasion of his 65th birthday

The very special architecture of cage dienes **1** (7,8;12,19-bisseco-1,16-dodecahedradiene, pagodadiene) and **2** (1,16-dodecahedradiene)[1, 2] with their perfect *syn*-periplanar, parallel C=C bonds account for notable gradations in structure and energy:[3] the transannular distance d between the two π bonds (π,π distance) increases from 2.62 to 3.52 Å, the pyramidalization angle ϕ of the olefinic centers from 9.9 to 42.9°, and the diene strain (MM2) from 25.3 to 36.3 kcal mol^{-1}.[1–3]

Remarkable consequences of these differences are: **1** undergoes photochemical [2 + 2] cycloaddition, homoconjugate addition of bromine,[1] and, above all, facile one- and

[*] Prof. Dr. H. Prinzbach, Dipl.-Chem. K. Weber
Chemisches Laboratorium der Universität
Institut für Organische Chemie und Biochemie
Albertstrasse 21, D-W-7800 Freiburg (FRG)
Telefax: Int. code + (761) 203-2815
Dr. G. Gescheidt, Dipl.-Chem. R. Schmidlin, Prof. Dr. F. Gerson
Institut für Physikalische Chemie der Universität
Klingelbergstrasse 80, CH-4056 Basel (Switzerland)

[**] Applications of ENDOR Spectroscopy to Radical Cations in Freon Matrixes, Part 11. This research was supported by the Deutsche Forschungsgemeinschaft, the Fonds der Chemischen Industrie, BASF AG, and the Schweizerische Nationalfonds zur Förderung der wissenschaftlichen Forschung. We thank Prof. Dr. E. Haselbach and Prof. Dr. T. Bally, Universität Fribourg, Switzerland, for their help with the experiments with ^{60}Co irradiation, and Dr. P. Such, Bruker Analytische Messtechnik, Rheinstetten, for measuring ENDOR spectra above 35 MHz. – Part 10: A. Arnold, U. Burger, F. Gerson, E. Kloster-Jensen, S. P. Schmiedlin, *J. Am. Chem. Soc.*, in press.

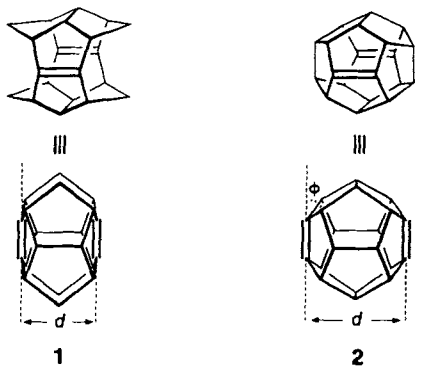

1 2

two-electron oxidations. In the resulting radical cation $\mathbf{1}^{\bullet+}$ and dication $\mathbf{1}^{2+}$ cyclic electron delocalization is effective (σ homoaromaticity).[4-6]

Of general importance is the question whether the ions $\mathbf{2}^{\bullet+}$ and $\mathbf{2}^{2+}$ derived from **2**, in which the π,π distance is much larger (ca. 3.5 Å), can still profit from transannular electron delocalization ($\mathbf{2a}^{\bullet+}$, $\mathbf{2b}^{\bullet+}$; $\mathbf{2a}^{2+}$, $\mathbf{2b}^{2+}$). The borderline situation of nonbonding π,π interactions[7] in **2** and in the radical cations and dications is emphasized by the fact that in contrast to reactions of **1**, direct irradiation of **2** and addition of bromine do not lead to the formation of transannular C–C bonds.[11]

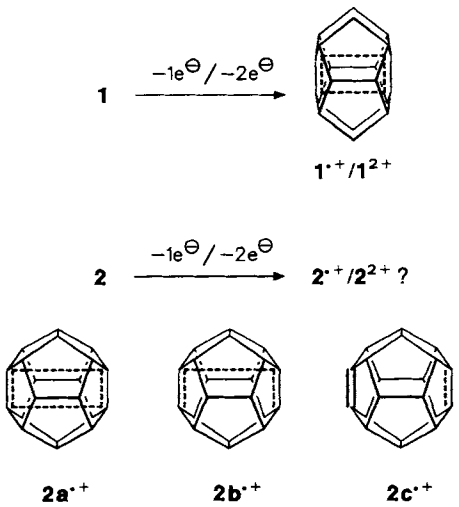

We report here on the preparation of the radical cation $\mathbf{2}^{\bullet+}$ and its characterization by ESR spectroscopy. The radical cation of the monoene $\mathbf{3}^{\bullet+}$ serves as a "localized" reference compound (cf. $\mathbf{2c}^{\bullet+}$). This study could be carried out because the unusually bent and highly reactive (towards O_2) olefins **2** ($\phi = 42.9°$) and **3** ($\phi = 43.5°$) are surprisingly thermally stable and isolable.

The first attempts at generating $\mathbf{2}^{\bullet+}$ and $\mathbf{3}^{\bullet+}$ in liquid phase in analogy to $\mathbf{1}^{\bullet+}$ (electrochemically, by reaction with $AlCl_3$ or tris(*p*-bromophenyl)ammonium hexachloroantimonate), failed;[13] however, the radical cations could be produced in Freon matrices by γ irradiation (^{60}Co source, 77 K, $CFCl_3$, $CF_2ClCFCl_2$ or CF_3CCl_3).[14] The ESR spectra of these rigid solutions of $\mathbf{2}^{\bullet+}$ (moss green) and $\mathbf{3}^{\bullet+}$ (colorless) exhibit pronounced *g* anisotropy in all matrices used ($g_1 = 1.9881$, $g_2 = 2.0039$, $g_3 = 2.0329$) and, accordingly, consist of three groups of equidistant lines (Fig. 1). For $\mathbf{2}^{\bullet+}$

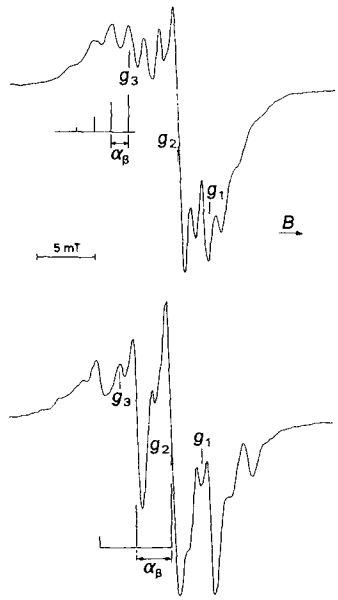

Fig. 1. ESR spectra of the radical cations $\mathbf{2}^{\bullet+}$ (top) and $\mathbf{3}^{\bullet+}$ (bottom).

with eight symmetry-equivalent β protons, the hyperfine coupling constant *a* has an average value of 1.45 ± 0.05 mT, while for $\mathbf{3}^{\bullet+}$ with four symmetry-equivalent β protons the average value is 3.10 ± 0.05 mT. These values are corroborated by ^1H ENDOR studies. All ENDOR signals are split into a parallel and a perpendicular component of a quasi-axial hyperfine tensor.[15] The parallel components of *a* throughout have larger absolute values than the perpendicular ones, a finding that indicates a positive sign of the coupling constants, as expected for β protons.[16]

The following relation can be applied to the coupling constants *a* of the β protons:[17] $a_\beta = B \cdot \rho \cdot \cos^2\theta$, where *B* is a proportionality factor, ρ the spin population on the adjacent π center, and θ the dihedral angle formed by the $2p_z$ axis at this center and the C–H_β bond. The factor *B* was estimated from the coupling constant of the methyl protons of tetramethylethene ($a_\beta = 1.72$ mT).[18] Since the methyl groups are freely rotating, the average value of $\cos^2\theta$ is 0.5; hence $B = 6.88$ mT. Based on this *B*-value and the experimentally determined coupling constants a_β, the dihedral angle θ for $\mathbf{2}^{\bullet+}$ is 23° ($\rho = 0.25$, spin population distributed evenly over four π centers) and for $\mathbf{3}^{\bullet+}$ is 18° ($\rho = 0.5$, spin population distributed evenly over two π centers). These dihedral angles are in good agreement with those calculated for $\mathbf{2a}^{\bullet+}$ and $\mathbf{3}^{\bullet+}$ ($\theta(\mathbf{2a}^{\bullet+}) = 19$, $\theta(\mathbf{3}^{\bullet+}) = 21°$; MMX[19] followed by UHF-AM1 calculations[20] for the radical cations). The agreement between the experimentally determined coupling constants and those from INDO calculations is equally good:[21] for $\mathbf{2a}^{\bullet+}$ 1.45 vs. 1.68 mT, for $\mathbf{3}^{\bullet+}$ 3.10 vs. 3.29 mT. Indeed, the SOMO of $\mathbf{2a}^{\bullet+}$ has the π_- character expected for the HOMO in the early stages of the "symmetry-forbidden" dimerization of two ethene molecules (Fig. 2).

In analogy to $\mathbf{1}^{\bullet+}$ ($a_\beta = 1.544$ mT), $\mathbf{2a}^{\bullet+}$ has a delocalized structure with D_{2h} symmetry on the hyperfine timescale. According to the UHF-AM1 calculations, the π,π distance in $\mathbf{2a}^{\bullet+}$ (3.53 Å) is almost unchanged relative to that in **2**; the pyramidalization ($\phi = 47.3°$) is more pronounced by ap-

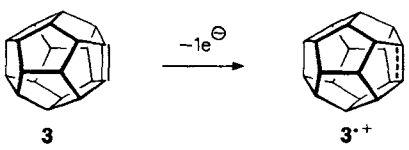

3 $\mathbf{3}^{\bullet+}$

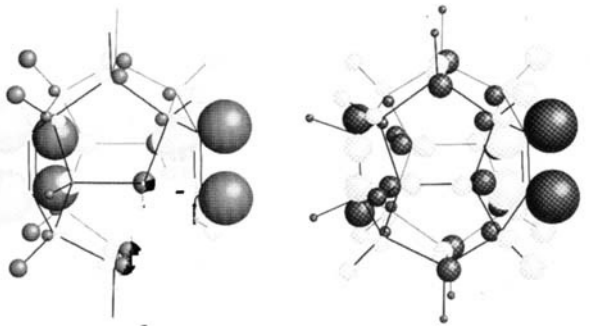

Fig. 2. Highest occupied molecular orbital (SOMO) of $2a^{\bullet+}$ (left) and $3^{\bullet+}$ (right).

proximately 4° (the rigidity of the dodecahedrane framework prevents the compression of the cage, as is possible in the bisseco reference pair $1/1^{\bullet+}$), and the olefinic bonds are somewhat longer (1.35 vs. 1.33 Å). In comparison, the change in pyramidalization between **3** and $3^{\bullet+}$ ($\phi = 51.3°$) is much larger and the olefinic bond becomes even longer (1.43 Å). The significantly weaker through-space homoconjugation[22] in $2a^{\bullet+}$ and the considerably greater strain energy ($E_{str}(2) = 105.3$, $E_{str}(1) = 73.9$ kcal mol^{-1}) are reflected in the markedly reduced persistence of $2a^{\bullet+}$ relative to $1^{\bullet+}$ (2 d at 293 K vs. 2 d at 77 K in Freon matrices, 1–2 h at temperatures above 110 K). Considering the coefficients in the SOMO of the radical cation, through-bond conjugation should be negligible. Photoelectron spectra and electrochemical measurements are anticipated to provide quantifiable experimental data on the interactions between the π bonds in **2**.[23]

Received: January 14, 1993 [Z 5807 IE]
German version: *Angew. Chem.* **1993**, *105*, 907

[1] W.-D. Fessner, H. Prinzbach, *The Pagodane Route to Dodecahedrane* in *Cage Hydrocarbons* (Ed.: G. A. Olah), Wiley, New York, **1990**, pp. 353–405; W.-D. Fessner, B. A. R. C. Murty, P. R. Spurr, R. Pinkos, J.-P. Melder, H. Fritz, H. Prinzbach, *Chem. Ber.* **1992**, *125*, 1697–1717; B. A. R. C. Murty, R. Pinkos, P. R. Spurr, W.-D. Fessner, G. Lutz, H. Fritz, D. Hunkler, H. Prinzbach, *ibid.* **1992**, *125*, 1719–1739.

[2] J.-P. Melder, R. Pinkos, H. Fritz, H. Prinzbach, *Angew. Chem.* **1990**, *102*, 105–109; *Angew. Chem. Int. Ed. Engl.* **1990**, *29*, 95–99.

[3] G. Szeimies in *Reactive Intermediates* (Ed.: R. A. Abramovitch), Plenum, New York, **1983**, Chap. 3, p. 299; P. M. Warner, *Chem. Rev.* **1989**, *89*, 1067; W. T. Borden, *ibid.* **1989**, *89*, 1095; W. Luef, R. Keese, *Top. Stereochem.* **1991**, 231.

[4] H. Prinzbach, B. A. R. C. Murty, W.-D. Fessner, J. Mortensen, J. Heinze, G. Gescheidt, F. Gerson, *Angew. Chem.* **1987**, *99*, 488–490; *Angew. Chem. Int. Ed. Engl.* **1987**, *26*, 457–458.

[5] D. Elsässer, K. Hassenrück, H.-D. Martin, B. Mayer, G. Lutz, H. Prinzbach, *Chem. Ber.* **1991**, *124*, 2863–2869.

[6] G. K. S. Prakasch, V. V. Krishnamurthy, R. Herges, R. Bau, H. Yuan, G. A. Olah, W.-D. Fessner, H. Prinzbach, *J. Am. Chem. Soc.* **1988**, *110*, 7764–7772; R. Herges, P. von R. Schleyer, M. Schindler, W.-D. Fessner, *ibid.* **1991**, *113*, 3649–3656.

[7] H.-D. Martin, B. Mayer, *Angew. Chem.* **1983**, *95*, 281–313; *Angew. Chem. Int. Ed. Engl.* **1983**, *22*, 283; R. Gleiter, W. Schäfer, *Acc. Chem Res.* **1990**, *23*, 369–375; R. Herges, Universität Nürnberg-Erlangen, personal communication; cf. the smallest π,π distance in *p*-cyclophanes (ca. 3.0 Å)[8], graphite (ca. 3.35 Å)[9], and aggregated porphyrins (3.2–3.6 Å)[10].

[8] K. Lonsdale, H. J. Milledge, K. V. Rao, *Proc. R. Soc. Londen A* **1960**, *255*, 82; H. Hope, J. Bernstein, K. N. Trueblood, *Acta Crystallogr.* **1972**, *16*, 1733.

[9] A. F. Holleman, E. Wiberg, *Lehrbuch der Anorganischen Chemie*, de-Gruyter, Berlin, **1985**, p. 701.

[10] C. A. Hunter, J. K. M. Sanders, *J. Am. Chem. Soc.* **1990**, *112*, 5525–5534.

[11] K. Weber, Dissertation, Universität Freiburg, **1993**; J.-P. Melder, R. Pinkos, H. Fritz, J. Wörth, H. Prinzbach, *J. Am. Chem. Soc.* **1992**, *114*, 10213–10231.

[12] K. Weber, H. Fritz, H. Prinzbach, *Tetrahedron Lett.* **1992**, *33*, 619–622.

[13] The dodecahedryl radical has not yet been observed directly (ESR, 170 K, cyclopropane): L.A. Paquette, D. R. Lagerwall, H.-G. Korth, *J. Org. Chem.* **1992**, *57*, 5413–5419.

[14] T. Shida, E. Hasselbach, T. Bally, *Acc. Chem. Res.* **1984**, *17*, 180–186; M. C. R. Symons, *Chem. Soc. Rev.* **1984**, *13*, 393.

[15] Depending on the type of matrix used, the sets of eight ($2^{\bullet+}$) and four ($3^{\bullet+}$) β protons give rise to single or several close-lying sets of ENDOR signals, indicating that the medium can cause a reduction in symmetry. For $2^{\bullet+}$, the signals appear between 32 and 38 MHz and correspond to $1/2\,a + \nu_H$, where a is the coupling constant in MHz and ν_H is the frequency of the free proton (14.56 MHz). (The corresponding signals for $1/2\,a - \nu_H$ between 3 and 9 MHz are too weak to be detected in the ENDOR system.) For $3^{\bullet+}$, the signals for both $1/2\,a + \nu_H$ and $1/2\,a - \nu_H$ are observed at 57–60 and 28–31 MHz, respectively. The average values of a are 41 MHz or 1.45 mT for $2^{\bullet+}$, and 87 Hz or 3.10 mT for $3^{\bullet+}$. Other signals associated with smaller couplings ($a < 13$ MHz or 0.46 mT) appear in the region from 9 to 22 MHz ($\nu_H \pm 1/2\,a$) for both radical cations. The assignment of these signals to more distant sets of equivalent protons is problematic. For information on the ENDOR technique: H. Kurreck, B. Kirste, W. Lubitz, *Electron Nuclear Double Resonance Spectroscopy of Radicals in Solution*, VCH, Weinheim, **1988**.

[16] A. Arnold, U. Burger, F. Gerson, E. Kloster-Jensen, S. P. Schmidlin, *J. Am. Chem. Soc.*, in press; F. Gerson *High Resolution ESR-Spektroscopy*, Verlag Chemie, Weinheim, **1971**.

[17] C. Heller, H. M. McConnell, *J. Chem. Phys.* **1960**, *32*, 1535–1539.

[18] T. Shida, Y. Egawa, H. Kubodera, T. Kato, *J. Chem. Phys.* **1980**, *73*, 5963–5970.

[19] PC Model, Version 430, Serena Software, Bloomington, IN, **1990–1991**.

[20] M. J. S. Dewar, E. G. Zoebisch, E. F. Healy, J. J. P. Stewart, *J. Am. Chem. Soc.* **1985**, *107*, 3902–3909.

[21] J. A. Pople, D. L. Beveridge, *Approximate Molecular Orbital Theory*, McGraw-Hill, New York, **1970**.

[22] D. Elsässer, Dissertation, Universität Düsseldorf, **1991**. We thank Prof. Dr. H.-D. Martin for this information.

[23] Investigations with Prof. Dr. H.-D. Martin, Dr. B. Mayer (Düsseldorf), and Prof. Dr. J. Heinze (Freiburg) are in progress.

Self-Assembly of a New Class of Tetranuclear Copper(I) and Silver(I) Complexes**

By *Raymond Ziessel** and *Marie-Thérèse Youinou**

Achieving spontaneous and selective formation of self-assembled systems is one of the major goals in supramolecular chemistry.[1, 2] Of recent interest is the formation of double- and triple-helical structures by complexation of two or three ligands twisted about metal ions lying on the helical axis.[3–5] It was recently demonstrated that one of the key points in the assembly of helicate structures is the subtle design of ligands with suitable spacers.[6] We have been particularly interested in the synthesis of oligomultidentate ligands in which the spacer groups are also capable of specific coordination of metal ions. To our knowledge, self-organization processes with ligands possessing two different types of complexation sites composed of a macrocyclic framework and complexing side-arms have not yet been studied. As a first step towards the specific complexation of different metal ions by a self-assembly process, we report herein on a novel ligand containing a bipyridine-based macrocycle with phenanthroline side-arms, and on the spontaneous formation of tetrameric copper(I) and silver(I) complexes of this hybrid ligand possessing double-helicate structures.

[*] Dr. R. Ziessel
Ecole Européenne des Hautes Etudes des Industries Chimiques
de Strasbourg
IPCMS, UMR n° 46
1, rue Blaise Pascal, F-67008 Strasbourg Cedex (France)
Dr. M.-T. Youinou
Laboratoire de Chimie des Métaux de Transition et de Catalyse
URA au CNRS n° 424, Institut Le Bel, Université Louis Pasteur
4, rue Blaise Pascal, F-67000 Strasbourg (France).

[**] This work was supported by the Centre National de la Recherche Scientifique.

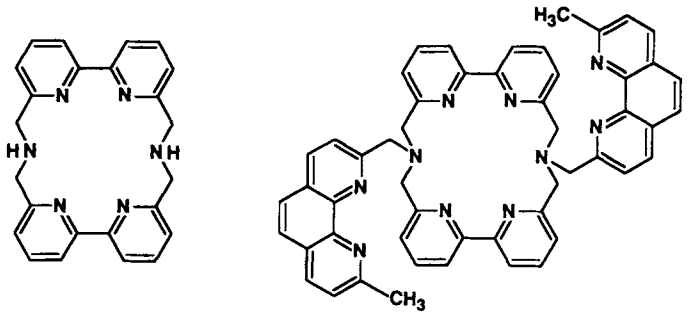

1 2

Ligand **2** was synthesized in 75% yield in a straightforward manner by reaction of 2-chloromethyl-9-methyl-1,10-phenanthroline[7] with macrocycle **1**[8] in anhydrous CH_3CN with triethylamine as base. 1,10-Phenanthroline (phen) groups were chosen as the pendant subunits since they favor specific binding with d^{10} metals and their rigidity serves to increase the stability of polymetallic systems. As expected, complexation of macrocycle **1** (1 equiv) with $[Cu(CH_3CN)_4]BF_4$ (1 equiv)[9] in degassed CH_2Cl_2/MeOH (1:1) under argon gave $[Cu(\mathbf{1})]BF_4$ (**3**) (Scheme 1; yield 67%, FAB^+-MS: m/z 456.9

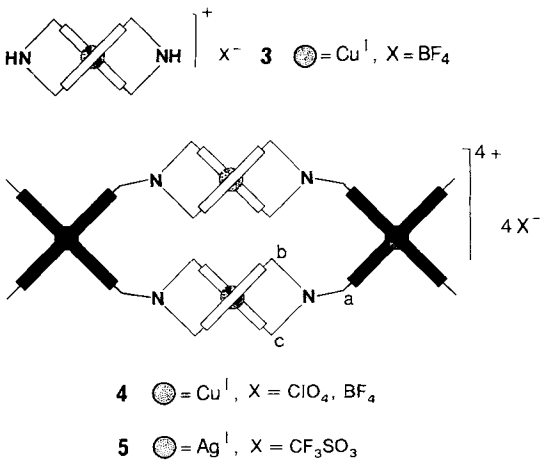

3 ○ = Cu^I, X = BF_4

4 ○ = Cu^I, X = ClO_4, BF_4

5 ○ = Ag^I, X = CF_3SO_3

Scheme 1. Proposed binding modes in complexes **3**–**5**. □ = bpy ■ = phen.

($M^+ - BF_4$), λ_{max} = 460.0 nm). In the ^1H NMR spectra of **3** in coordinating solvents such as $[D_3]$acetonitrile (oxygen-free), the broad signals observed can be explained in terms of a fast exchange process between ligand-coordinated Cu^I ions and solvated forms, for example, $[Cu(CH_3CN)_4]^+$; the equilibrium lies on the side of the ligated complex. This type of process does not occur in noncoordinating solvents such as CD_2Cl_2. Similar behavior was previously observed for flexible binuclear macrocyclic complexes.[10] The reaction of the novel ligand **2** with $[Cu(CH_3CN)_4]X$ (X = BF_4, ClO_4) in CH_3CN led instantaneously to an air-stable, deep-red complex which analyzed as the tetranuclear species $[Cu_4(\mathbf{2})_2]X_4$ (**4**) (Scheme 1, X = BF_4, yield 95%, FAB^+-MS: m/z 2128.4 ($M^+ - BF_4$), λ_{max} = 456.4 nm, ε = 11 800 L cm^{-1} mol^{-1}).

The well-defined ^1H NMR spectrum of **4** (Fig. 1 A) reveals that the two ligands **2** are equivalent and that the two halves of each ligand **2** are also equivalent. The signals of the methylene protons are split into three AB patterns (J_{AB} = 16.4, 11.3, 14.6 Hz; $\Delta\nu$ = 237.7, 191.1, 47.3 Hz) and shifted significantly upfield by $\Delta\delta \approx 1.5$ due to the shielding of either

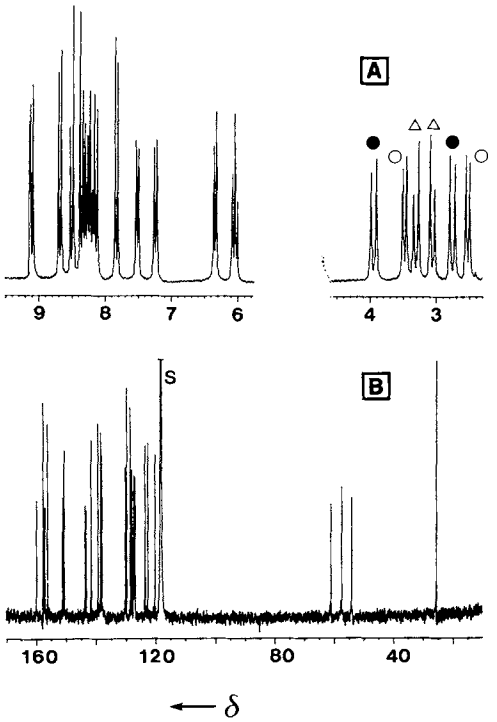

Fig. 1. NMR spectra of complex **4**, X = BF_4, in $[D_3]$acetonitrile. A) 200 MHz ^1H NMR; signals due to CH_3 and solvent molecules are omitted for clarity; Δ, ○, and ● denote the CH_2 AB systems. B) 50.3 MHz ^{13}C-{^1H} NMR (S = solvent).

the bpy or the phen subunits. The observation of the diastereotopic methylene protons (labeled a, b, c in Scheme 1) is certainly due to the chirality of the molecule,[4, 6] which is illustrated by the D_2-symmetric structure in Scheme 1. The ^{13}C NMR spectrum with its pattern of resonances including only 1 methyl, 3 methylene, and 22 signals of aromatic carbon atoms (Fig. 1 B) also confirms such a conclusion.

When a solution of **2** in CD_2Cl_2 was treated with successive aliquots (0.25 equiv) of $[Cu(CH_3CN)_4]BF_4$ in $[D_3]$acetonitrile, complex **4** formed spontaneously. Since this was the only species detected by ^1H NMR spectroscopy, even at a ligand to copper ratio of 2:1, this indicates a positive cooperativity in copper complexation, as previously observed in helicate formation.[11]

The X-ray structure analysis of the perchlorate derivative of **4**[12] shows that the complex contains $[Cu_4(\mathbf{2})_2]^{4+}$ ions and uncoordinated perchlorate ions. The structure of the complex cation is represented in Figure 2. The four coplanar copper(I) ions form a rhombus with sides of 7.133(2) Å and interior angles of 40.75(3)° and 139.25(5)°; two copper ions (Cu2 and Cu3) lie on the imposed C_2 axis of the molecule. Each copper(I) ion has distorted tetrahedral coordination. Cu1 (and Cu1′) is coordinated to four nitrogen atoms of two phen subunits belonging to two distinct ligands, whereas Cu2 and Cu3 are coordinated to nitrogen atoms of two bpy units of the same macrocycle. Each ligand wraps around two crystallographically independent copper(I) ions, and not surprisingly, the coordination about Cu1 and Cu3 have different distortions as a result of geometric demands of the macrocycle and the phen subunits (Fig. 2 A). As required by the C_2 symmetry of the structure, the phen subunits are arranged in a *cis* fashion, and the two bpy moieties of each macrocycle form a cross at Cu2 and Cu3, as represented in Scheme 1. The overall structure is best described as a double-stranded helicate (Fig. 2 B), as already suggested by the NMR data. However, in the solid state, a lowering of the symmetry of

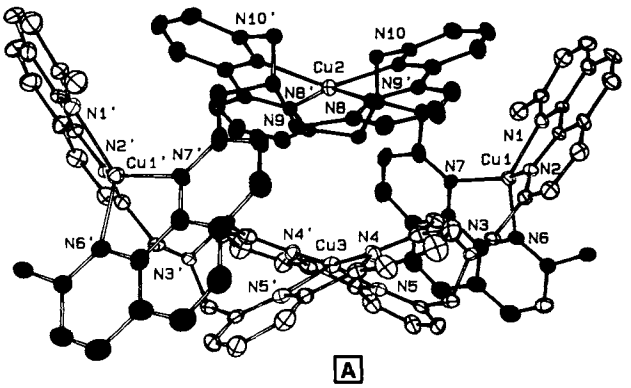

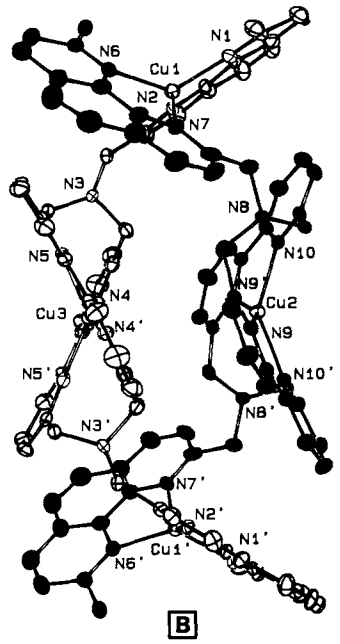

Fig. 2. A) X-ray crystal structure of the cation in **4** (ORTEP, ellipsoids at the 50% probability level). The hydrogen atoms are omitted for clarity. Selected distances [Å] and angles [°]: Cu1-Cu2 and Cu1-Cu3 7.133(2), Cu2-Cu3 4.966(3), Cu1-Cu1′ 13.372(3), Cu1-N1 2.03(1), Cu1-N2 2.017(9), Cu1-N6 2.05(1), Cu1-N7 1.999(9), Cu2-N9 and Cu2-N9′ 2.023(9), Cu2-N10 and Cu2-N10′ 2.174(9), Cu3-N4 and Cu3-N4′ 2.00(1), Cu3-N5 and Cu3-N5′ 2.24(1); Cu3-Cu1-Cu2 40.75(3), Cu1-Cu2-Cu1′ 139.25(5); N1-Cu1-N2 82.7(4), N6-Cu1-N7 83.3(4), N1-Cu1-N6 131.7(4), N2-Cu1-N7 134.6(4), N1-Cu1-N7 115.5(4), N2-Cu1-N6 116.4(4), N9-Cu2-N9′ 153.0(5), N10-Cu2-N10′ 142.0(5), N9-Cu2-N10′ and N9′-Cu2-N10 79.3(4), N9-Cu2-N10 and N9′-Cu2-N10′ 109.7(4), N4-Cu3-N4′ 159.8(6), N5-Cu3-N5′ 140.0(5), N4-Cu3-N5′ and N4′-Cu3-N5 78.6(4), N4-Cu3-N5′ and N4′-Cu3-N5 108.5(4). B) View of the cation in **4** showing the double-stranded helicate.

complex **4** is observed, although the symmetrical Cu_4 core is still maintained. The macrocyclic spacer (bpy · bpy) seems to favor self-assembly as long as the stereochemical demands of the Cu^I ions are satisfied. As recently described by one of us,[13] very few complexes are known in which four copper atoms each possessing a tetrahedral geometry are in a planar arrangement.[14]

The synthetic method that led to **4** was used in the preparation of the tetranuclear silver(I) complex. Mixing $AgCF_3SO_3$ (2 equiv) with ligand **2** (1 equiv) in CH_3CN/CH_2Cl_2 solution gave, after workup, white crystals of complex **5** (yield 70%, FAB^+-MS: m/z 2491.1 ($M^+ - CF_3SO_3$)). In the ^1H NMR spectrum three distinct AB patterns due to the CH_2 groups with upfield shifts of $\Delta\delta \approx 1.6$ are observed ($J_{AB} = 13.0, 15.1, 14.6$ Hz; $\Delta\nu = 14.1, 42.2, 199.7$ Hz) in analogy to complex **4**. Consequently a double-helical structure is also proposed for complex **5**. Physicochemical studies are currently in progress in order to gain more insight into this unusual self-assembly process.

Experimental Procedure

The synthesis and characterizations of **2** will be fully reported in due course.

Complex **4**, X = BF_4: To a stirred solution of macrocycle **2** (0.100 g, 0.124 mmol) in 15 mL anhydrous CH_2Cl_2 was added a solution of $[Cu(CH_3CN)_4]BF_4$ (0.081 g, 0.260 mmol) in 15 mL anhydrous CH_3CN at room temperature and under argon. During the addition the color of the solution instantaneously turned deep-red, indicating fast Cu^I complexation. After 12 h the solution was filtered over celite and evaporated to dryness. Slow diffusion of THF into a solution of the perchlorate salt in CH_3CN provided crystals of **4** suitable for X-ray analysis. (Yield for X = BF_4 95%.) UV/Vis (CH_3CN) λ_{max} [nm] (ε) = 456.4 (11800), 274.1 (117000), 225.8 (128800); ^1H NMR (200.1 MHz, [D$_3$]acetonitrile, 25 °C): δ = 9.10 (d, 4H, ^3J(H,H) = 8.4 Hz), 8.68 (d, 4H, ^3J(H,H) = 8.3 Hz), 8.50 (d, 4H, ^3J(H,H) = 8.9 Hz), 8.35 (d, 4H, ^3J(H,H) = 8.9 Hz), 8.28 (d, 4H, ^3J(H,H) = 7.5 Hz), 8.22 (t, 4H, ^3J(H,H) = 7.5 Hz), 8.13 (d, 4H, ^3J(H,H) = 8.4 Hz), 7.82 (d, 4H, ^3J(H,H) = 8.3 Hz), 7.51 (d, 4H, ^3J(H,H) = 7.2 Hz), 7.24 (d, 4H, ^3J(H,H) = 7.9 Hz), 6.34 (d, 4H, ^3J(H,H) = 7.5 Hz), 6.04 (t, 4H, ^3J(H,H) = 7.8 Hz), 3.35 (ABq, 8H, J_{AB} = 16.4 Hz, $\Delta\nu$ = 237.7 Hz), 3.19 (ABq, 8H, J_{AB} = 14.6 Hz, $\Delta\nu$ = 47.3 Hz), 3.00 (ABq, 8H, J_{AB} = 11.3 Hz, $\Delta\nu$ = 191.1 Hz), 2.19 (s, 12H); ^{13}C-{^1H} NMR (50.3 MHz, [D$_3$]acetonitrile, 25 °C): δ = 159.89, 157.68, 157.11, 156.25, 151.18, 150.70, 143.68, 143.35, 141.63, 139.38, 138.46, 138.05, 130.15, 129.75, 128.50, 128.03, 127.40, 127.13, 126.91, 123.57, 122.62, 120.19, 61.07, 57.45, 54.11, 25.48; MS (FAB^+ in mNBA (*meta*-nitrobenzyl alcohol) matrix): m/z 2128.4 ($M^+ - BF_4$, expected isotopic profile), 2041.1 ($M^+ - 2BF_4$), 1953.7 ($M^+ - 3BF_4$), 1021.1 ($M^{2+} - 2BF_4$), 933.1 ($M^+ - 2 - 2Cu - 4BF_4$), 869.3 ($M^+ - 2 - 3Cu - 4BF_4$), 725.1 ($M^+ - 2 - 4Cu - 4BF_4$), 661.1 ($M^+ - 2 - phen - 4Cu - 4BF_4$); MS (Electrospray ($ES^+$) in H_2O/CH_3CN 1:1, grammicidin as internal standard: m/z 1020.2 (2(**2**) + 2Cu + BF_4), 869.8 (2(**2**) + 2Cu), 651.9 (2(**2**) + 4Cu + BF_4), 467.1 (2(**2**) + 4Cu); correct C,H,N-analysis for $[C_{104}H_{84}N_{20}Cu_4](BF_4)_4$ (M_r = 2215.30).

Complex **5**: To a stirred solution of macrocycle **2** (0.100 g, 0.124 mmol) in 25 mL anhydrous CH_2Cl_2 was added a solution of $AgCF_3SO_3$ (0.080 g, 0.311 mmol) in 5 mL anhydrous CH_3CN at room temperature. After 8 h the solution was filtered over celite and evaporated to ca. 2–3 mL. Slow diffusion of Et_2O into the solution led to a white precipitate, which after recrystallization from CH_2Cl_2/hexane afforded complex **5** as light-sensitive microcrystals (yield 70%). UV/Vis (CH_3CN): λ_{max} [nm] (ε) = 302 (sh, 20700), 278.1 (52400), 231.3 (54000); ^1H NMR (200.1 MHz, [D$_3$]acetonitrile, 25 C): δ = 8.53 (d, 4H, ^3J(H,H) = 8.3 Hz), 7.99 (d, 4H, ^3J(H,H) = 8.3 Hz), 7.83 (d, 8H, ^3J(H,H) = 4.6 Hz), 7.72 (d, 4H, ^3J(H,H) = 8.9 Hz), 7.66 (d, 8H, ^3J(H,H) = 8.3 Hz), 7.60 (d, 4H, ^3J(H,H) = 7.1 Hz), 7.47 (d, 4H, ^3J(H,H) = 8.9 Hz, 7.38 (t, 4H, ^3J(H,H) = 4.6 Hz), 6.73 (d, 8H, ^3J(H,H) = 8.1 Hz), 3.99 (ABq, 8H, J_{AB} = 13.0 Hz, $\Delta\nu$ = 14.1 Hz), 3.58 (ABq, 8H, J_{AB} = 15.1 Hz, $\Delta\nu$ = 42.2 Hz), 3.02 (ABq, 8H, J_{AB} = 14.6 Hz, $\Delta\nu$ = 199.7 Hz), 3.00 (s, 12H); ^{13}C-{^1H} NMR (50.3 MHz, [D$_3$]acetonitrile, 25 °C): δ = 160.67, 160.34, 157.36, 155.99, 151.41, 151.07, 143.84, 143.02, 140.65, 140.04, 139.58, 138.03, 128.12, 127.37, 126.97, 126.12, 125.82, 125.02, 124.21, 123.78, 121.41, 121.12, 66.71, 63.87, 63.09, 28.18. MS (FAB^+ in mNBA as matrix): m/z 2493.1 ($M^+ - CF_3SO_3$, expected isotopic profile), 2344.1 ($M^+ - 2CF_3SO_3$), 2195.1 ($M^+ - 3CF_3SO_3$), 1171.0 ($M^{2+} - 2CF_3SO_3$), 1024.4 ($M^+ - 2 - 2Ag - 4CF_3SO_3$); MS ($ES^+$ in H_2O/CH_3CN 1:1): m/z 1171.9 (2(**2**) + 4Ag + $2CF_3SO_3$), 511.1 (2(**2**) + 4Ag), 707.2 (**2** − phen + Ag), 407.0 (2(**2**) − 2phen + 4Ag); correct C,H,N-analysis for $[C_{104}H_{84}N_{20}Ag_4](CF_3SO_3)_4$ (M_r = 2641.62).

Received: January 28, 1993 [Z 5836 IE]
German version: *Angew. Chem.* **1993**, *105*, 929

[1] J.-M. Lehn, *Angew. Chem.* **1990**, *102*, 1347–1362; *Angew. Chem. Int. Ed. Engl.* **1990**, *29*, 1304–1319, and references therein.
[2] J. S. Lindsey, *New J. Chem.* **1991**, *15*, 153–180.
[3] J.-M. Lehn, A. Rigault, J. Siegel, J. Harrowfield, B. Chevrier, D. Moras, *Proc. Natl. Acad. Sci. USA* **1987**, *84*, 2565–2569; J.-M. Lehn, A. Rigault, *Angew. Chem.* **1988**, *100*, 1121–1123; *Angew. Chem. Int. Ed. Engl.* **1988**, *27*, 1095–1097.
[4] A. F. Williams, C. Piguet, G. Bernardinelli, *Angew. Chem.* **1991**, *103*, 1530–1532; *Angew. Chem. Int. Ed. Engl.* **1991**, *30*, 1490–1492; C. Piguet, G. Bernardinelli, B. Bocquet, A. Quattropani, A. F. Williams, *J. Am. Chem. Soc.* **1992**, *114*, 7440–7451.
[5] M.-T. Youinou, R. Ziessel, J.-M. Lehn, *Inorg. Chem.* **1991**, *30*, 2144–2148.
[6] S. Rüttimann, C. Piguet, G. Bernardinelli, B. Bocquet, A. F. Williams, *J. Am. Chem. Soc.* **1992**, *114*, 4230–4237.
[7] G. R. Newkome, K. J. Theriot, V. K. Gupta, F. R. Fronczek, G. R. Baker, *J. Org. Chem.* **1989**, *54*, 1766–1769.
[8] G. R. Newkome, S. Pappalardo, V. K. Gupta, F. R. Fronczek, *J. Org. Chem.* **1983**, *48*, 4848–4851, and references therein.

[9] B. J. Hathaway, D. G. Holah, J. D. Poslethwaite, *J. Chem. Soc.* **1961**, 3215–3218.
[10] M.-T. Youinou, J. A. Osborn, J.-P. Collin, P. Lagrange, *Inorg. Chem.* **1986**, *25*, 453–461.
[11] A. Pfeil, J.-M. Lehn, *J. Chem. Soc. Chem. Commun.* **1992**, 838–840.
[12] X-ray structure analysis of **4**, perchlorate salt ($C_{104}H_{84}N_{20}O_{16}Cl_4Cu_4$), $M = 2265.9$; deep-red crystals ($0.150 \times 0.150 \times 0.120$ mm^3); monoclinic space group $C2/c$ with $a = 28.627(8)$, $b = 13.222(4)$, $c = 28.097(8)$ Å, $\beta = 91.96(2)^\circ$, $V = 10629.7$ Å^3, $Z = 4$, $\varrho_{calcd} = 1.416$ g cm^{-3}, $F(000) = 4640$, $\mu = 24.19$ cm^{-1}. A crystal of **4** suitable for X-ray structure analysis was selected on a cooled plate and mounted from the mother liquor. 6172 intensity data were collected on a Philips PW 1100/16 diffractometer at $-100\,^\circ$C with $Cu_{K\alpha}$ radiation $\lambda = 1.5418$ Å (Ni monochromator) ($\theta/2\theta$ scan, $6^\circ < 2\theta < 102^\circ$). The systematic absences together with the E statistics and the NZ test suggested the space group to be $C2/c$. Successful structure solution and refinement confirmed this choice. The structure was solved by a combination of Patterson, difference Fourier, and full matrix least-squares methods). The final conventional residuals were $R = 0.0696$ and $R_w = 0.0930$ for 3266 reflections having $I > 3\sigma(I)$ and 677 variables. Further details of the crystal structure investigation are available on request from the Director of the Cambridge Crystallographic Data Centre, 12 Union Road, Cambridge CB2 1EZ (UK), on quoting the full journal citation.
[13] M.-T. Youinou, N. Rahmouni, J. Fischer, J. A. Osborn, *Angew. Chem.* **1992**, *104*, 771–773; *Angew. Chem. Int. Ed. Engl.* **1992**, *31*, 733–735.
[14] a) R. G. Vranka, E. L. Amma, *J. Am. Chem. Soc.* **1966**, *88*, 4270–4271; b) A. M. Manotti Lanfredi, A. Tiripicchio, A. Camus, N. Marsich, *J. Chem. Soc. Chem. Commun.* **1983**, 1126–1128, and references therein.

Controlling Valence Tautomerism of Cobalt Complexes Containing the Benzosemiquinone Anion as Ligand**

By *David M. Adams, Andrea Dei, Arnold L. Rheingold,* and *David N. Hendrickson**

Several different types of transition metal complexes are electronically labile, where electronic degeneracy or near-degeneracy leads to vibronic interactions and an appreciable sensitivity to the environment. Electronic lability is characteristic of mixed-valence,[1] spin-crossover,[2] and valence-tautomeric[3] metal complexes. Electronically labile complexes have been indicated as potential building blocks for molecular electronic devices.[4] Small collections of these molecules could be expected to exhibit bistability; thus, as a result of an external perturbation they could be made to flip-flop between two states. In fact, polycrystalline samples of Fe^{II} spin-crossover complexes have been shown to exhibit bistability in the LIESST (light-induced excited spin state trapping) effect discovered by Gütlich et al.[5] When a polycrystalline spin-crossover complex is maintained at low temperatures (< 50 K), the whole crystalline sample can be interconverted between the stable low-spin state and the metastable high-spin state with photons of different wavelengths. The metastable high-spin state will remain indefinitely as long as the sample is kept below about 50 K. In this paper we will show that thermally driven bistability is possible for cobalt complexes that exhibit valence tautomerism.

Complexes of transition metal ions with the benzosemiquinone and catecholate anions as ligands have been described in terms of localized bonding.[3] One of the most intriguing aspects of these complexes is the thermally driven valence tautomerism that has been observed for some complexes in solution.[6] One cobalt complex[6] exists in solution in two valence tautomeric forms [Eq. (a)]. One complex consists of

$$[Co^{II}(bpy)(3,5\text{-dtbsq})_2] \rightleftharpoons [Co^{III}(bpy)(3,5\text{-dtbsq})(3,5\text{-dtbcat})] \quad (a)$$

Co^{II} with two benzosemiquinonate anions (3,5-dtbsq$^-$ = 3,5-di-*tert*-butylbenzosemiquinone anion) as ligands and a 2,2′-bipyridine (bpy) ligand, and the other of Co^{III} with one dtbsq and one catecholato (3,5-dtcat^{2-}) ligand. The room-temperature X-ray structure[6] of [Co^{III}(bpy)(3,5-dtbsq)-(3,5-dtbcat)] shows that the ligands are in two different oxidation states and that the metal is trivalent. In order to see if these valence tautomeric complexes exhibit bistability, we systematically changed the bipyridine ligand to other diiminium ligands. The goal was to find a compound that exhibits the $Co^{II} \leftrightarrow Co^{III}$ tautomeric transformation in the solid state.

A series of complexes with the composition [Co($\overset{\frown}{N\,N}$)(3,5-dtbsq)("3,5-dtbq")], where "3,5-dtbq" is either the benzosemiquinone anion or catecholate form of the ligand and the $\overset{\frown}{N\,N}$ diiminium ligand is 4,4′-diphenyl-2,2′-bipyridine (dpbpy), 4,4′-dimethyl-2,2′-bipyridine (dmbpy), 1,10-phenanthroline (phen, complex **1**), 2,2′-bipyrimidine (bpym), or 2,2′-bipyrazine (bpz, complex **2**), was prepared. Magnetic susceptibility

[Co(phen)(3,5-dtbsq)$_2$] **1** [Co(bpz)(3,5-dtbsq)$_2$] **2**

data for polycrystalline samples of the dpbpy, dmbpy, and bpy complexes show that they are Co^{III} complexes with one unpaired electron on the dtbsq ligand (μ_{eff} is 1.83–2.12 μ_B in the 100–300 K range). On the other hand, the phen, bpym, and bpz complexes have μ_{eff} values of 5.17, 5.03, and 4.38 μ_B, respectively, at 300 K. These three complexes are clearly [Co^{II}($\overset{\frown}{N\,N}$)(3,5-dtbsq)$_2$] complexes at 300 K in the solid state.

X-ray crystal structures were determined at 238 K for **1** · ($C_6H_5CH_3$)[7] and at 296 K for **2**.[8] Complex **2** has C_2 symmetry, in which the two equivalent dtbsq ligands have Co–O bond lengths of 2.046(4) and 2.057(4) Å, and Co–N distance is 2.130(4) Å. This is clearly a high-spin Co^{II} complex with two dtbsq ligands. For comparison, the Co–O bond lengths for the Co^{III} complex [Co(bpy)(3,5-dtbsq)(3,5-dtbcat)] range from 1.851(6) to 1.906(6) (Å) with Co–N lengths of 1.940(7) and 1.957(7) Å.[6] The fact that this bipyridine complex is a Co^{III} complex was established[6] by the bond lengths in the ligands, the presence of an intervalence charge-transfer electronic absorption band in the near-IR region associated with the mixed-valence ligand structure, and the observation of a relatively isotropic EPR signal for an organic radical. The X-ray structure of the phen complex **1** is shown in Figure 1. The two dtbsq ligands are not related by symmetry; the Co–O bond lengths of one are 2.004(4) and 2.011(4) Å and of the other are 2.002(4) and 1.987(4) Å. These values together with the average Co–N bond length (2.082 Å) suggest that **1** is intermediate between the Co^{II} and Co^{III} forms at 238 K. The values of C–O bond lengths for *o*-quinone-derived ligands are known[3] to reflect the oxidation state of the ligand: 1.29(1) Å for a coordinated benzosemiquinone anion and 1.35(1) Å for a catecholate ligand. In the case of the phen complex, one ligand has C–O lengths of 1.291(8) and 1.294(8) Å, and the other 1.302(7) and 1.305(7) Å. These two ligands appear to be dtbsq ligands. Perhaps at 238 K the phen complex has converted from high-spin Co^{II} into low-spin Co^{II}, and at lower temperatures it will finally experience the tautomeric shift to a Co^{III} complex.

[*] Prof. Dr. D. N. Hendrickson, D. M. Adams, Prof. A. Dei[+]
Department of Chemistry-0506
University of California at San Diego
La Jolla, CA 92093-0506 (USA)
Telefax: Int. code + (619)534-4864
Prof. Dr. A. L. Rheingold
Department of Chemistry, University of Delaware
Newark, DE 19716 (USA)
[+] On sabbatical leave from the Universitá di Firenze, Firenze (Italy).

[**] This work is supported by the U.S. National Science Foundation (CHE 9115286 to D.N.H.) and the U.S. National Institutes of Health (HL 13652 to D.N.H.).

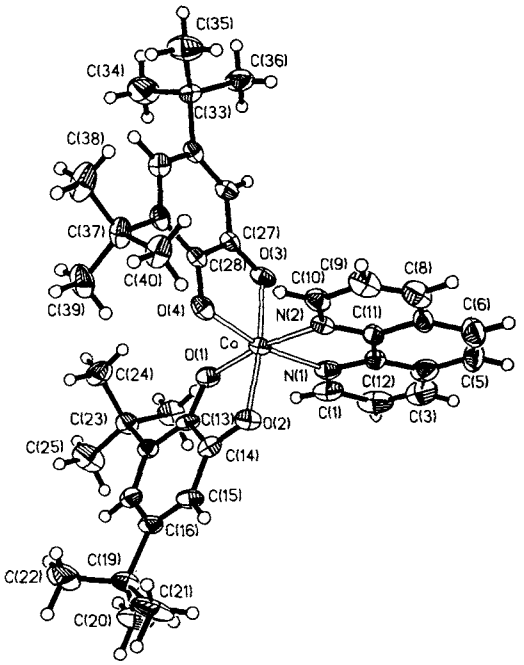

Fig. 1. Structure of $1 \cdot (C_6H_5CH_3)$ with atom labeling scheme. The toluene solvate molecule is not shown.

In the [Co(N N)(3,5-dtbsq)("3,5-dtbq")] series, three of the complexes are Co^{II} and three are Co^{III} tautomers in the solid state at room temperature. The variation in properties is understandable in view of the changes in reduction potentials[9] for the series of diiminium ligands: −2.40 V (dmbpy); −2.18 V (bpy); −2.04 V (phen); −1.80 (bpym); and −1.70 V (bpz). If the ligand is more easily reduced (i.e., has a more positive reduction potential), it can stabilize the Co^{II} form of the complex by accepting electron density into its π^* orbital. Variable-temperature electronic absorption spectra (320–820 nm) were run for all of the complexes dissolved in toluene. In solution they all show temperature-dependent spectra that indicate the presence of the valence tautomerism equilibrium as in Equation (a). The temperature dependence

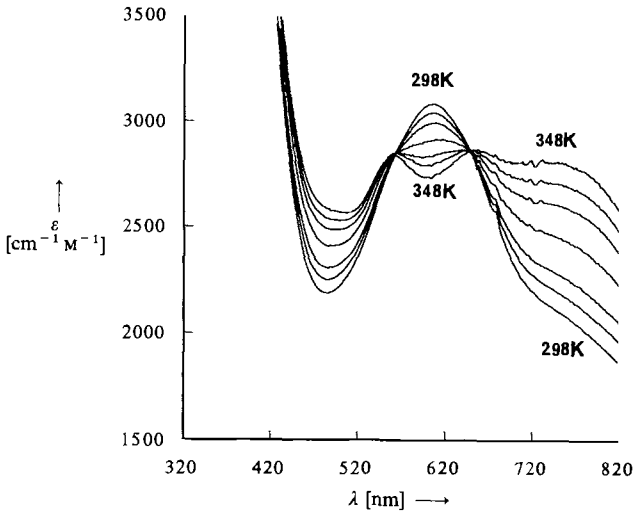

Fig. 2. Temperature dependence of the electronic absorption spectrum of a toluene solution of [Co(dpbpy)(3,5-dtbsq)(3,5-dtbcat)]; at $T = 298$, 303, 308, 318, 328, 338, and 348 K. The molar extinction coefficient ε is plotted versus wavelength λ.

of the electronic spectrum of [Co(dpbpy)(3,5-dtbsq)(3,5-dtbcat)] in toluene is shown in Figure 2. At room temperature there is a band at about 600 nm, which is characteristic of the Co^{III} form of the complex. As the temperature is increased to 333 K a band at about 770 nm increases in intensity; this band belongs to the Co^{II} form of the complex. The temperature at which there is approximately equal amounts of Co^{II} and Co^{III} complexes correlates well with the variation in redox potential of the diiminium ligand.

It is more difficult to find a complex which exhibits the valence tautomeric transformation in the solid state. We have now found the first example. In Figure 3 are shown magnetic susceptibility data for a polycrystalline sample of the cobalt–phen complex **1**. At low temperatures (< 200 K)

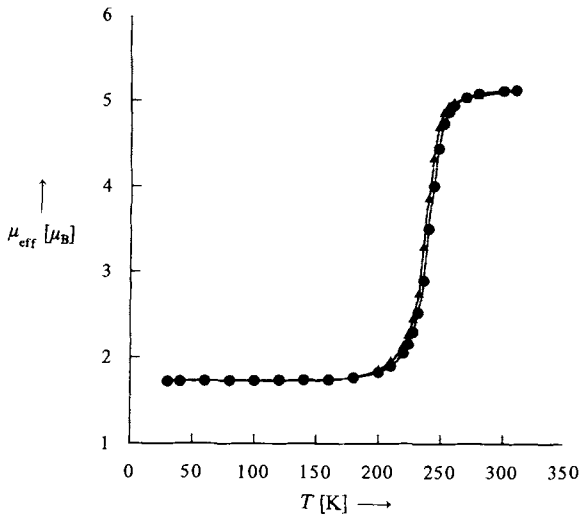

Fig. 3. Plot of effective magnetic moment per molecule μ_{eff} versus temperature T for a polycrystalline sample of $1 \cdot (C_6H_5CH_3)$. The sample was first cooled to 30 K, and measurements were carried out as T was increased (●). After the measurement was completed at 320 K, data were collected (▲) as the sample T was decreased to 30 K.

μ_{eff}/molecule is 1.7 μ_B, whereas above about 270 K the value is 5.1 μ_B. This complex undergoes a relatively abrupt transformation centered around approximately 240 K, which explains why the X-ray structure was done at 238 K. Thus, this complex is [Co^{III}(phen)(3,5-dtbsq)(3,5-dtbcat)] below 200 K and converts into [Co^{II}(phen)$(3,5\text{-dtbsq})_2$] above about 270 K. It is important to emphasize that it is very necessary to have the toluene solvate molecule present, for without it the complex does not undergo the transformation. The sensitivity to solvate molecules observed for this valence-tautomeric transformation is reminiscent of solvate sensitivities observed for spin-crossover[2] and mixed-valence[11] complexes.

The transformation seen for the Co–phen complex **1** (Fig. 2) is so abrupt that it probably involves a phase transition, which is somewhat substantiated by the small (ca. 5 K) hysteresis measured (see Fig. 3). The valence-tautomeric transformation $Co^{II} \rightarrow Co^{III}$ is entropy driven. At low temperatures in the Co^{III} complex an $S = 1/2$, ground state is thermally populated, whereas at high temperatures in the Co^{II} complex one $S = 5/2$, one $S = 1/2$, and two $S = 3/2$ states are thermally populated, because of weak Co^{II}–dtbsq exchange interactions.[10] Not only is there electronic entropy gain associated with the Co^{III}-to-Co^{II} conversion, but as the energy of the vibrations for the CoO_4N_2 modes in the

Co^{II} complex is higher, there is also a vibrational entropy gain. Efforts are ongoing to prepare several more complexes that exhibit the valence-tautomeric transformation in the solid state.

Experimental Procedure

The synthesis of [Co(phen)(3,5-dtbsq)$_2$] is given as a general scheme for preparation of cobalt complexes containing benzosemiquinone anions as ligands. All reactions were carried out under an inert atmosphere of Ar in Schlenkware with degassed reagent-grade solvents (Aldrich). The starting tetramer [Co$_4$(3,5-dtbsq)$_8$] was prepared by a published procedure [11], and a portion (0.646 g) suspended in 100 mL of methylcyclohexane. This reactant and the ligand phen (0.220 g in 100 mL of methylcyclohexane) were dissolved in their separate solutions by heating to 100 °C. The phen solution was then added dropwise over 30 min to the tetramer solution. After half the solution had been added, a purple microcrystalline precipitate was visible. After the addition was complete, the solution was stirred for an additional 30 min at 100 °C. Upon cooling, 0.700 g of a purple microcrystalline solid was filtered off. This solid was recrystallized by dissolving 0.200 g in 100 mL of toluene, filtering hot, and then slowly evaporating the solution under a steady flow of N_2 gas. All cobalt complexes gave good chemical analyses for C, H, N, and Co.

Received: January 25, 1993 [Z 5826 IE]
German version: *Angew. Chem.* **1993**, *105*, 954

[1] D. N. Hendrickson in *Mixed Valency Systems: Applications in Chemistry, Physics and Biology* (Ed.: K. Prassides), Kluwer, Dordrecht, **1991**, Chap. 5, pp. 67–90; H. G. Jang, R. J. Wittebort, Y. Kaneko, M. Nakano, M. Sorai, D. N. Hendrickson, *Inorg. Chem.* **1992**, *31*, 2265; M. S. Mashuta, R. J. Webb, J. K. McCusker, E. A. Schmitt, K. J. Oberhausen, J. F. Richardson, R. M. Buchanan, D. N. Hendrickson, *J. Am. Chem. Soc.* **1992**, *114*, 3815; R. J. Webb, T.-Y. Dong, R. K. Chadha, C. G. Pierpont, D. N. Hendrickson, *ibid.* **1991**, *113*, 4806.

[2] P. Gütlich, *Structure Bonding (Berlin)* **1981**, *44*, 83; P. Gütlich in *Chemical Mössbauer Spectroscopy* (Ed.: R. H. Herber), Plenum, New York, **1984**; C. N. R. Rao, *Int. Rev. Phys. Chem.* **1985**, *4*, 19; P. Gütlich, A. Hauser, *Coord. Chem. Rev.* **1990**, *97*, 1; E. König, *Prog. Inorg. Chem.* **1987**, *35*, 527.

[3] C. G. Pierpont, S. K. Larson, S. R. Boone, *Pure Appl. Chem.* **1988**, *60*, 1331; C. G. Pierpont, R. M. Buchanan, *Coord. Chem. Rev.* **1981**, *38*, 45.

[4] O. Kahn, J. Krobert, C. Jay, *Adv. Mater.* **1992**, *4*, 718; O. Kahn, J.-P. Launay, *Chemtronics* **1988**, *3*, 140; J.-P. Launay in *Molecular Electronic Devices II* (Ed.: F. L. Carter), Dekker, New York, **1987**.

[5] S. Decurtins, P. Gütlich, C. P. Köhler, H. Spiering, A. Hauser *Chem. Phys. Lett.* **1984**, *105*, 1; P. Gütlich, A. Hauser, *Pure Appl. Chem.* **1989**, *61*, 849.

[6] R. M. Buchanan, C. G. Pierpont, *J. Am. Chem. Soc.* **1980**, *102*, 4951.

[7] Crystal data for **1** · $C_6H_5CH_3$: $C_{40}H_{48}CoN_2O_4 \cdot C_7H_8$, monoclinic, $P2_1/c$, $a = 10.425(3)$, $b = 32.226(8)$, $c = 13.454(4)$ Å, $\beta = 111.39(2)°$, $V = 4208.6(18)$ Å^3, $Z = 4$, $\varrho_{calcd} = 1.218$ g cm^{-3}, $\mu(Mo_{K\alpha}) = 4.48$ cm^{-1}, $T = 238$ K. Of 4787 data collected (Siemens P4, $4° \le 2\theta \le 42°$), 4552 were independent, and 2879 were observed ($5\sigma F_0$). The Co atom was located by direct methods. All atoms were refined as in ref. [8]. $R(F) = 0.0489$, $R(wF) = 0.0629$ [12].

[8] Crystal data for **2**: $C_{36}H_{46}CoN_4O_4$, orthorhombic, $Ccc2$, $a = 16.233(6)$, $b = 26.894(10)$, $c = 8.472(2)$ Å, $V = 3698.6(13)$ Å^3, $Z = 4$, $\varrho_{calcd} = 1.181$ g cm^{-3}, $\mu(Mo_{K\alpha}) = 5.00$ cm^{-1}, $T = 296$ K. Of 1852 data collected (Siemens P4, $4° \le 2\theta \le 45°$), 1759 were independent, and 1307 were observed ($3\sigma F_0$). The noncentrosymmetric space group was chosen (instead of $Ccem$) as required by the placement of a chiral trischelate complex on a special position. The structure was solved intuitively by placing the Co atom in an arbitrary position on the twofold axis. The correctness of the reported hand was determined by the refinement of a multiplicative term (1.11(8)) for $\Delta F''$. All non-hydrogen atoms were refined with anisotropic thermal parameters, and hydrogen atoms were treated as idealized contributions. $R(F) = 0.0461$, $R(wF) = 0.0504$ [12]. SHELXTL-PC software (G. Sheldrick, Siemens, Madison, WI, USA).

[9] Y. Kawanishi, N. Kitamura, S. Tazuke, *Inorg. Chem.* **1989**, *28*, 2968–2975.

[10] M. W. Lynch, R. M. Buchanan, C. G. Pierpont, D. N. Hendrickson, *Inorg. Chem.* **1981**, *20*, 1038; A. Dei, D. Gatteschi, *Inorg. Chim. Acta* **1992**, *198–200*, 813.

[11] R. M. Buchanan, B. J. Fitzgerald, C. G. Pierpont, *Inorg. Chem.* **1979**, *18*, 3439.

[12] Further details of the crystal structures investigations are available from the Director of the Cambridge Crystallographic Data Centre, 12 Union Road, GB-Cambridge CB2 1EZ (UK), on quoting the complete journal citation.

Hydrogen Bonds as a Crystal Design Element for Organic Molecular Solids with Intermolecular Ferromagnetic Interactions**

By *Esteve Hernàndez, Montse Mas, Elies Molins, Concepció Rovira*, and *Jaume Veciana**

Ferromagnetism in purely organic molecular solids has attracted considerable interest in the last few years.[1] Up to now, only three open-shell organic molecules—free radicals or radical ions—exhibiting such a magnetic property in the solid state are known.[2] In order to obtain this cooperative property it is necessary not only to choose suitable open-shell molecules but also to orient them properly relative to each other in a three-dimensional network, because ferromagnetism is a three-dimensional phenomenon.[3] In these supramolecular organizations, the correct electronic mechanisms that give rise to the parallel, or ferromagnetic (FM), spin alignment between neighboring molecules along three (or two) directions of space must be established.[4] Appropriate structural modifications and chemical functionalizations of stable open-shell molecules represent a promising approach to supramolecular organizations[5] in which the natural predilection for antiparallel, or antiferromagnetic (AF), spin alignment is avoided.[1, 4] In fact, the use of *crystal design elements* provides one of the most direct ways to control the relative orientations of molecules[6] and, therefore, of their electronic interactions in crystalline and noncrystalline solids.[7] Hence, basic studies devoted to the control of crystal packings and, through them, the magnetic properties of organic molecular solids are in great demand.[5]

We report here an example of the nitronyl nitroxide free radical **1**,[8] in which hydrogen bonds have been used for the first time as a crystal design element to obtain a crystalline supramolecular organization showing intermolecular ferromagnetic interactions.

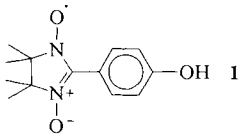

1

The study of the radical **1** seemed promising, because this compound combined a priori most of the structural and electronic prerequisites to show at least a short-range FM ordering of hydrogen-bonded molecules: 1) semiempirical molecular orbital (MO) calculations revealed strong electronic polarizations of NO and OH bonds ($N^{+0.09}$–$O^{-0.34}$ and $O^{-0.27}$–$H^{+0.24}$),[9] indicating that the NO groups could act as acceptors and the OH group as a donor in hydrogen bonds; 2) the noncollinear relative orientation of NO and OH groups, together with the strong directionality usually observed for hydrogen bonds,[7] could favor the formation in the solid state of a hydrogen-bonded network with a high dimensionality, and 3) MO calculations based on the UHF approximation[9] showed that **1** fulfilled most of the electronic requirements that were considered relevant for the

[*] Dr. J. Veciana, E. Hernàndez, M. Mas, Dr. E. Molins, Dr. C. Rovira
Institut de Ciència de Materials de Barcelona
Campus de la U.A.B., E-08193 Bellaterra (Spain)

[**] This work was supported by the Programa Nacional de Nuevos Materiales (C.I.C. y T., Grant No. MAT 91/0553). We thank Dr. B. Martínez (Laboratori de Propietats Elèctriques i Magnètiques. ICMAB) for magnetic measurements.

attainment[10] of FM couplings in molecular solids, either through the so-called McConnell I mechanism or the charge transfer mechanism involving frontier orbitals.[4, 11, 12]

Radical **1** was prepared by the reported method and was crystallized from toluene.[13] An X-ray structure determination revealed that it crystallizes with two crystallographically independent molecules A and B in the asymmetric unit, which are almost identical in structure (Fig. 1).[14] The

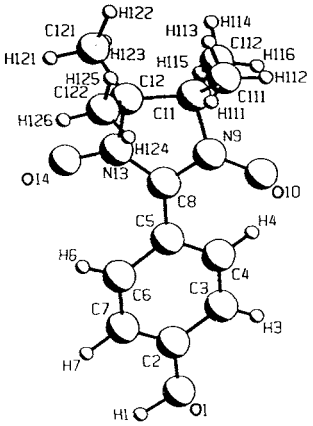

Fig. 1. Molecular structure of the conformer A of **1** showing the atomic numbering scheme. Selected interatomic distances [Å] and angles [°] (standard deviations in parentheses) [and for conformer B, in square brackets]: H1-O1 1.04(4) [1.08(4)], O1-C2 1.360(4) [1.368(4)], C5-C8 1.452(4) [1.445(4)], C8-N9 1.362(4) [1.330(4)], N9-O10 1.274(3) [1.289(3)], C8-N13 1.340(4) [1.360(4)], N13-O14 1.283(3) [1.275(3)]; O10-N9-C8 125.0(2) [126.1(2)], N9-C8-N13 107.3(2) [107.0(2)], C8-N13-O14 127.0(2) [126.5(2)], H1-O1-C2 116.(2) [107.(2)].

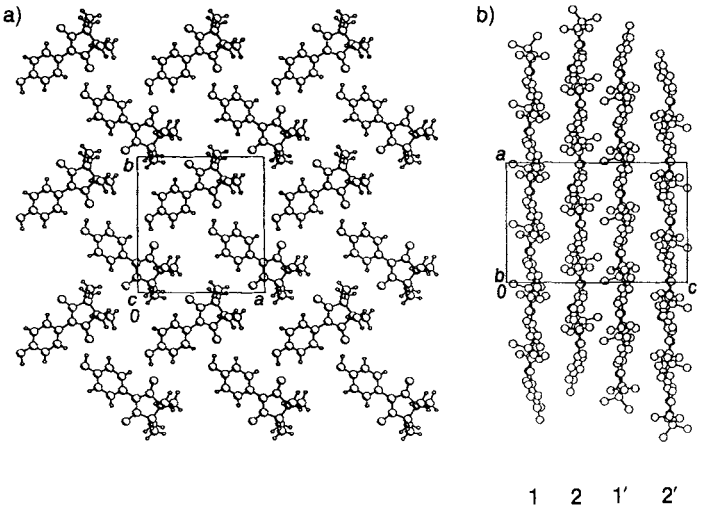

Fig. 2. Packing of radical **1** in the unit cell. a) 2-D hydrogen-bonded network of molecules with A conformation viewed along the c axis. b) Packing along the c axis. The 2-D networks labeled 1 comprise molecules with A conformation and those labeled 2 with B conformation. The 2-D network 1′ (and 2′) is related to network 1 (and 2) by the twofold screw axis parallel to the c axis. Selected hydrogen bond distances [Å] and angles [°] (standard deviations in parenthesis) of O-H···O and C-H···O types (unprimed and primed figures refer to molecular conformations A and B, respectively); symmetry code: (i) x,y,z; (ii) $-0.5+x,-y,z$; (iii) $-0.5+x,1-y,z$; (iv) $0.5+x,1-y,z$; (v) $0.5+x,-y,z$; all distances and angles fulfill the geometrical requirements of hydrogen bonds [7]): H1$^{(i)}$···O14$^{(ii)}$ 1.65(4), H(1′)$^{(i)}$···O(10′)$^{(iii)}$ 1.61(4), H(113)$^{(i)}$···O(10)$^{(iv)}$ 2.39(3), H(122)$^{(i)}$···O(10)$^{(iv)}$ 2.34(3), H(116′)$^{(i)}$···O(14′)$^{(v)}$ 2.61(4), H(121′)$^{(i)}$···O(14′)$^{(v)}$ 2.45(3), O(1)-H(1)$^{(i)}$···O(14)$^{(ii)}$ 165.(1); O(1′)-H(1′)$^{(i)}$-O(10′)$^{(iii)}$ 177.(5), C(111)-H(113)$^{(i)}$···O(10)$^{(iv)}$ 168.(3), C(121)-H(122)$^{(i)}$···O(10)$^{(iv)}$ 167.(2), C(112′)-H(116′)$^{(i)}$···O(14′)$^{(v)}$ 159.(3), C(121′)-H(121′)$^{(i)}$···O(14′)$^{(v)}$ 163(3).

phenyl rings in both molecules are almost coplanar with the OH groups, but form angles of 32.7(1) and 33.6(2)° with the plane of the α-nitronyl nitroxide O-N-C-N-O grouping. The crystal packing of radical **1** is shown in Figure 2. Unexpectedly only one of the two NO groups forms strong hydrogen bonds with the OH groups of neighboring molecules.[15] Such hydrogen bonds exist between molecules with identical conformations and give rise to zigzag chains along the a axis (see Fig. 2a). Each one of these chains meshes with the translationally related chains along the b axis. The meshing occurs through interactions between the O atoms of the free NO groups of one chain and the H atoms belonging to vicinal CH_3 groups of neighboring chains. Such C-H···O interactions have the crystallographic requirements to be considered as weak hydrogen bonds.[7] Moreover, spectroscopic evidence supports this description.[15] Thus, two-dimensional hydrogen bonded networks, parallel to the ab plane, are present in the crystal structure of **1** (see Fig. 2a). Such 2-D networks are, in addition, closely packed along the c axis with intermolecular contacts ranging from 3.5 to 4.0 Å (see Fig. 2b). The most relevant feature observed from all the short contacts of this densely packed structure is the absence of significant intermolecular overlaps between SOMOs, which are usually considered responsible for AF interactions in molecular solids.[4, 12] In fact, both within and between the 2-D molecular sheets only short contacts that are generally claimed as the origin of intermolecular FM interactions are observed.[16] Therefore, these local structural features suggest the possibility of FM interactions with distinct intensities along the three spatial axes.

The presence of three-dimensional magnetic interactions in **1** was supported by single-crystal electron spin resonance (ESR) experiments at room temperature. These experiments showed an exchange-narrowed single line with a pure Lorentzian line shape whatever the orientation of the crystal. This behavior is characteristic of exchange coupling in 3-D spin systems.[17] Static magnetic susceptibility data were collected on a SQUID magnetometer in the $1.8 \leq T \leq 250$ K temperature range at an applied magnetic field of 10 kOe for a 20 mg sample consisting of several crystals of **1**. Paramagnetic susceptibilities are shown in Figure 3. Above 5 K, the data obey the Curie–Weiss law, $\chi_p = C/(T-\theta)$, where $C = 0.379$ emu K mol^{-1} and $\theta = +0.8$ K. The high temperature value of $\chi_p T$ (0.37 emu K mol^{-1}) is close to that expected (0.376) for noninteracting $S = 1/2$ units, with $g = 2.006$. Below 50 K, $\chi_p T$ increases continuously with decreasing temperature, reaching 0.48 emu K mol^{-1} at 1.8 K. Such a large value is a clear indication of the existence of intermolecular FM interactions in **1**. Below 5 K, paramagnetic susceptibility data gradually deviate downwards from the Curie–Weiss curve (Fig. 3a) extrapolated from the data at high temperatures. A much better fit of the experimental data is obtained over the whole temperature range of 1.8–250 K with the theoretical curve (Fig. 3a) calculated from the ferromagnetic 1-D Heisenberg model[18] with an intrachain coupling of $J/k = +0.49$ K and $S = 1/2$. Therefore, this result suggests that the FM coupling within a chain is dominant. Unfortunately, the rest of the magnetic interactions in this spin system are too weak to be observable at temperatures higher than 1.8 K with this static technique.

The field dependence of the magnetization of **1** is also shown in Figure 3 at several temperatures, together with the theoretical curve for an ideal paramagnet with $S = 1/2$ and $g = 2.006$. It is clear that radical **1** magnetizes more rapidly than an ideal paramagnet and also that the magnetization curve is steeper when the temperature is lowered. This is

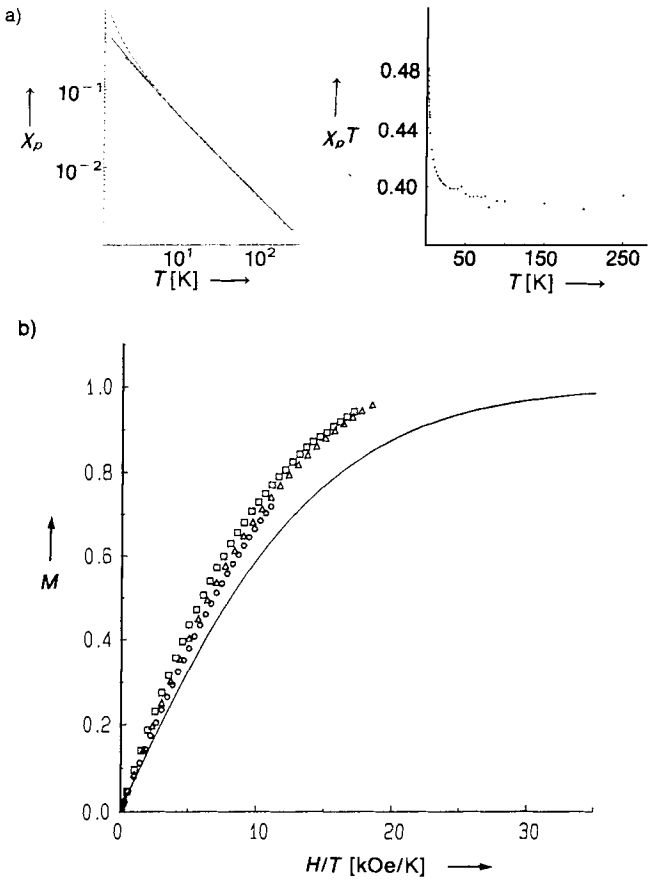

Fig. 3. a) Left: Temperature dependence of the paramagnetic susceptibility χ_p [emu mol^{-1}] of **1**. The dashed line represents the fit of the experimental data (see the text) to the Curie–Weiss law and the solid line the fit to the ferromagnetic 1-D Heisenberg model. Right: The plot of the product χ_pT[emu kmol^{-1}] versus T. b) Field dependence of the magnetization M [μ_B per molecule] of **1** at 2 (□), 3 (△), and 5 (○) K, measured in the applied magnetic field range $0.1 \leq H \leq 55$ kOe.

further evidence of the presence of intermolecular FM interactions in this spin system, which is in full agreement with the susceptibility results. The magnetic behavior described above is very similar to that recently reported for the β phase of an analogous nitronyl nitroxide bearing NO_2 substituents instead of the OH groups, which undergoes a transition to a bulk ferromagnetic ordered state below 0.65 K.[2a, 19] It is therefore important to extend the magnetic measurements with **1** at low temperatures to the mK region in order to determine the nature of all the operative intermolecular magnetic interactions and to check whether a long-range ferromagnetic ordering occurs. Such experiments are in progress.

We have shown above that the establishment of hydrogen bonds between open-shell molecules is a suitable strategy for preparing molecular solids with a high dimensional organization. Our work culminated in a case where ferromagnetic intermolecular interactions have been achieved.

Received: December 10, 1992 [Z 5745 IE]
German version: *Angew. Chem.* **1993**, *105*, 919

[1] Recent overviews: a) *Mol. Cryst. Liq. Cryst.* **1989**, *176*, 1–562; b) *Mater. Res. Soc. Symp. Proc.* **1990**, *173*, 3–92; c) *Molecular Magnetic Materials* (Eds.: D. Gatteschi, O. Kahn, J. S. Miller, F. Palacio), Kluwer, Dordrecht, **1991**.

[2] a) H. Tamura, Y. Nakazawa, D. Shiomi, K. Nozawa, Y. Hosokoshi, M. Ishikawa, M. Takahashi, M. Kinoshita, *Chem. Phys. Lett.* **1991**, *186*, 401; b) P.-M. Allemand, K. C. Khemani, A. Koch, F. Wudl, K. Holczer, S. Donovan, G. Grüner, J. D. Thompson, *Science* **1991**, *253*, 301; c) R. Chiarelli, A. Rassat, P. Rey, *J. Chem. Soc. Chem. Commun.* **1992**, 1081; A. Rassat, *Mol. Cryst. Liq. Cryst.*, in press.

[3] Ferromagnetism may be two-dimensional in some rather exceptional conditions, but it is never one-dimensional. See: R. L. Carlin, *Magnetochemistry*, Springer, Berlin, **1986**; F. Palacio in ref. [1c], pp. 1–34.

[4] For the different mechanisms of ferromagnetic couplings in molecular solids derived from free radicals see: a) H. Iwamura, *Adv. Phys. Org. Chem.* **1990**, *26*, 179; b) C. Kollmar, O. Kahn, *Acc. Chem. Res.*, in press.

[5] A. Caneschi, D. Gatteschi, L. Pardi, R. Sessoli, *Helv. Chim. Acta*, in press.

[6] Sometimes referred to as *crystal engineering tools*; substituents, chemical functions, and structural features giving rise to strong and directional intermolecular bonds such as hydrogen bonds, chlorine–chlorine bonds, etc.

[7] P. Dauber, *Acc. Chem. Res.* **1980**, *13*, 105; R. Taylor, O. Kennard, *ibid.* **1984**, *17*, 320; G. R. Desiraju, *Crystal Engineering: the Design of Organic Solids*, Elsevier, New York, **1989**; M. C. Etter, *Acc. Chem. Res.* **1990**, *23*, 120; J. A. Zerkowski, C. T. Seto, D. A. Wierda, G. M. Whitesides, *J. Am. Chem. Soc.* **1990**, *112*, 9025; M. C. Etter, *J. Phys. Chem.* **1991**, *95*, 4601.

[8] IUPAC name of **1**: 2-(4-hydroxyphenyl)-4,4,5,5-tetramethyl-4,5-dihydro-1*H*-imidazolyl-1-oxy-3-oxide.

[9] MO calculations were performed with the MOPAC Version 5.0 package (QCPE no. 581, J. J. P. Stewart, Department of Chemistry, Indiana University) with MNDO and AM1 methods.

[10] Such calculations revealed the presence of atoms with positive (NO groups) and negative (H atoms of the OH and CH_3 groups) electron spin densities, as well as a localization of the frontier orbitals in different spatial regions—the singly occupied molecular orbital (SOMO) is localized on both NO groups and the highest doubly occupied MO (HOMO) and the lowest unoccupied one (LUMO) mainly on the aromatic substituent.

[11] H. M. McConnell, *J. Chem. Phys.* **1963**, *39*, 1910.

[12] J. B. Goodenough, *Magnetism and the Chemical Bond*, Interscience, New York, **1963**, p. 167; H. M. McConnell, *Proc. R. A. Welch Found. Conf. Chem. Res.* **1967**, *11*, 144; K. Awaga, T. Sugano, M. Kinoshita, *Chem. Phys. Lett.* **1987**, *141*, 540.

[13] E. F. Ullman, J. H. Osiecki, D. G. B. Boocock, R. Darcy, *J. Am. Chem. Soc.* **1972**, *94*, 7049.

[14] Crystal data: $C_{13}H_{17}N_2O_3$, orthorhombic, $Pca2_1$, $a = 11.765(3)$, $b = 12.726(4)$, $c = 17.601(4)$ Å, $V = 2635(1)$ Å^3, $Z = 8$, $\varrho_{calcd} = 1.26$ g cm^{-3}; Enraf-Nonius CAD-4, $Mo_{K\alpha}$ ($\lambda = 0.7107$ Å), graphite monochromator; $T = 293 \pm 3$ K; measuring range: $2.0° < 2\theta < 50°$; 5023 measured reflections, 2647 unique reflections, 1978 reflections with $F > 1\sigma(F)$. The structure was solved by using direct methods (MULTAN82 package); the full matrix refinement on F (MoLEN package) converged at $R = 0.054$, $Rw = 0.044$. Further details of the crystal structure investigation are available on request from the Director of the Cambridge Crystallographic Data Centre, 12 Union Road, GB-Cambridge CB21EZ (UK), on quoting the full journal citation.

[15] The O–H and C–H stretching vibrations corresponding to the OH and CH_3 groups of radical **1** in the dilute solution (CCl_4) and solid state (KBr) IR spectra have striking differences. For both vibrations, when solid-state hydrogen bonds form their stretching frequencies decrease. See ref. [7].

[16] It is thought that short contacts between atoms with positive and negative spin densities as well as intermolecular overlaps between SOMO–HOMO and SOMO–LUMO lead to FM intermolecular interactions. See refs. [4, 11, 12].

[17] R. Kubo, *Lectures in Theoretical Physics*, Interscience, New York, **1959**, p. 120; A. Bencini, D. Gatteschi, *EPR of Exchange Coupled Systems*, Springer, Berlin, **1990**, p. 135ff.

[18] D. D. Swank, C. P. Landee, R. D. Willet, *Phys. Rev. B* **1979**, *20*, 2154.

[19] Y. Nakazawa, M. Tamura, N. Shirakawa, D. Shiomi, M. Takahashi, M. Kinoshita, M. Ishikawa, *Phys. Rev. B* **1992**, *46*, 8906.

A Two-Dimensional Ice with the Topography of Edge-Sharing Hexagons Intercalated between $CdNi(CN)_4$ Layers

By *Ki-Min Park, Reiko Kuroda,* and *Toschitake Iwamoto**

The topography of two-dimensional ice, that is, a two-dimensional network of H_2O molecules in the solid state, is related to the connection mode for O atoms participating in the network. The hydrogen-bonded network of the H_2O

[*] Prof. Dr. T. Iwamoto, Dr. K.-M. Park, Prof. Dr. R. Kuroda,
Department of Chemistry, College of Arts and Sciences
The University of Tokyo
Komaba, Meguro, Tokyo 153 (Japan)
Telefax: Int. code + (813)3485-2904

molecules in $Cd(H_2O)_2Ni(CN)_4 \cdot 4H_2O$ (**1**) consists of edge-sharing hexagons whose corners are three-connected O atoms, as has been revealed in its single-crystal structure. There are more H atoms than can be accounted for in the full formation of hydrogen bonding in the network.

A number of 2D ice-like networks have been found in "2D hydrates" or "hydrate intercalation compounds" with specific topography.[1] Typical networks seen for organic hydrates comprise edge-sharing pentagons enclosing diols or amines as guests:[2] the puckered edge-sharing pentagons in $(CH_3)_2C(OH)(CH_2)_2C(OH)(CH_3)_2 \cdot 4H_2O$[2d] consist of H_2O molecules and OH groups of the diol in a 2:1 ratio; the three- and four-connected O atoms (in a 2:1 ratio) form a hydrogen-bonded network in which all H atoms participate. In $[N(C_3H_7)_4]F \cdot 11H_2O$ both O and F atoms are at four-connected centers in the 2D network built of H_2O and F^- ions.[3] When a network of edge-sharing hexagons is built of H_2O molecules only, the O atoms should be three-connected, which leaves one of the H atoms or lone pairs out of the network formation at every O atom. The network in **1** has this type of 2D structure. The free protons and/or lone pairs may be expected to show the characteristic behavior of proton or electron transfer along the 2D network. Although the ligating and intercalated H_2O molecules in $[SnCl_2(H_2O)] \cdot H_2O$[4] appear to form a 2D network of edge-sharing tetragons and octagons whose corners are three-connected O atoms, the distance between the corners of the tetragons, that is, an edge of the octagon, is rather long (3.02(5) Å) for the hydrogen bond between two H_2O molecules.

Pale yellow single crystals of **1** were obtained unexpectedly from an aqueous solution containing $CdCl_2$, $K_2[Ni(CN)_4]$ and pn (1,2-diaminopropane), in an attempt to prepare the inclusion compound $[Cd(pn)Ni(CN)_4] \cdot 0.5$ guest.[5] As shown in Figure 1, the crystal has a double layer structure in

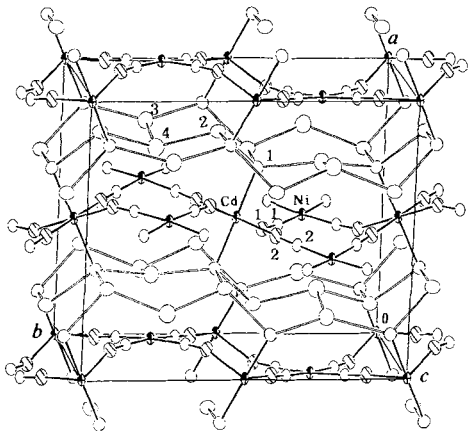

Fig. 1. A perspective view of $Cd(H_2O)_2Ni(CN)_4 \cdot 4H_2O$ along the *c* axis (50% probability for thermal ellipsoids whose sections are shown for Cd and Ni). The atomic numbering for C, N (hatched) and O is indicated by numeral only; the sequences are C2-N2-Cd-N1-C1-Ni for the metal complex network and Cd-O1-O2-O4-O3 for the water network. Atomic coordinates *x/a*, *y/b*, *z/c*: Cd, 0.5, 0.5, 0.5; Ni, 0.4335(1), 0.25, 0.0115(2); N1 0.4254(6), 0.3984(5), 0.2978(9); N2 0.4720(6), 0.3977(5), 0.7290(9); C1 0.4252(6), 0.3415(5), 0.1883(9); C2 0.4559(6), 0.3414(5), 0.8364(9); O1 0.6708(5), 0.4343(4), 0.4285(8); O2 0.8205(5), 0.5695(5), 0.5466(9); O3 0.7879(9), 0.75, 0.064(1); O4 0.7467(9), 0.75, 0.442(1).

which the puckered networks of $[CdNi(CN)_4]_\infty$ and of H_2O molecules are stacked alternately along the crystal's *a* axis.[6] The network of $[CdNi(CN)_4]_\infty$ extending along the *bc* plane is very similar to those observed for the host structures of $Cd[NH_2(CH_2)_nNH_2]Ni(CN)_4 \cdot x$ guest clathrates.[7]

Two H_2O molecules coordinate *trans* to each other at the Cd atom in the metal complex sheet; each of them participate in the hydrogen-bonded network of H_2O molecules intercalated between the sheets. As shown in Figures 1 and 2,

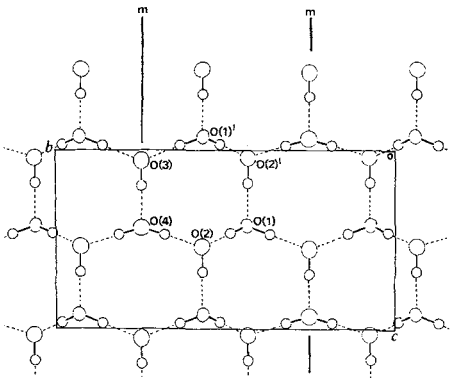

Fig. 2. Proposed hydrogen-bonding scheme for water molecules in edge-sharing H_2O hexagons extending along *bc* plane at $a \approx 3/4$. Positions of H atoms have been tentatively assigned according to the symmetry elements of the *Pnma* space group. O1' and O2' are generated by a 2_1 rotation followed by a translation of $-c/2$. m = mirror plane.

there are four kinds of crystallographically independent O atoms for the six water molecules in the formula unit: O1, the ligating oxygen, and O2 are on general positions, and O3 and O4 are on the mirror plane at $b = 3/4$. These O atoms are arranged with the usual O···O distances for hydrogen bonding from 2.821(9) to 2.86(2) Å, to form puckered networks of edge-sharing boat-shaped hexagons along the *bc* plane at $a \approx 1/4$. Those O-O-O angles bisected by the mirror plane at O3 (133.7(4)) and O4 (130.0(5)°) are considerably larger than the tetrahedral angle, whereas the others are within the range of 107.4(3) to 113.8(3)°. Viewed along the *a* axis, the hexagon with the larger angles is surrounded by six other smaller hexagons. A similar puckered network of edge-sharing boat-shaped hexagons is seen in the *ac* plane of hexagonal ice (I_h).

Since each edge of the edge-sharing hexagons is an O–H···O hydrogen bond, the structure requires nine of the H atoms and lone pairs of six H_2O molecules to participate in the hydrogen bond formation. There are, however, twelve H atoms and twelve lone pairs in total, of which two lone pairs are used in coordination bonds to the Cd atoms. If both H atoms of the ligating O1 participate in the hydrogen bond formation in the network, nine H atoms and nine lone pairs can be tentatively assigned according to the symmetry elements of the *Pnma* space group as shown in Figure 2. Three H atoms and one lone pair remain still unassigned.

The Ni–O3 distance of 2.81(1) Å suggests that a H atom on O3 is directed toward the $3d_{z^2}$ occupied orbital of the Ni^{2+} ion; the angles about O3 are not unreasonable for such an arrangement. A lone pair directed toward this center appears less probable because of the π-electron-rich environment in the vicinity of the Ni^{2+} ion coordinated to four CN^- ligands. The angles about O2 indicate that a H atom on O2 may be directed toward the opening in the mesh of the cyanometal complex network. Unfortunately we were unable to assign any signals in the final difference Fourier syntheses with highest electron density of 0.6 e $Å^{-3}$ to H atoms.

The puckered network of water molecules appears to be commensurate with that of the metal-containing layers in the structure of **1**. Recently $Fe(H_2O)_2Ni(CN)_4 \cdot 4H_2O$ was determined to be isomorphous to **1**.[8] The powder X-ray data

 © VCH Verlagsgesellschaft mbH, W-6940 Weinheim, 1993 0570-0833/93/0606-0885 $ 10.00+.25/0

for $Ni(H_2O)_2Ni(CN)_4 \cdot xH_2O$ ($x > 3$) (orthorhombic, $a = 12.20$, $b = 13.84$, and $c = 7.09$ Å, converted from reported values[9]) suggest that this compound is also isomorphous to the hydrate described here. Hence similar 2D networks of water molecules appear to be ubiquitous in $M(H_2O)_2Ni(CN)_4 \cdot 4H_2O$ (M a divalent cation in the last half of the first transition series) in the analogy with the Hofmann-type clathrates $M(NH_3)_2Ni(CN)_4 \cdot 2G$ (M: Mn, Fe, Co, Ni, Cu, Zn, or Cd; G: C_6H_6, $C_6H_5NH_2$, etc.).[7]

Received: January 22, 1993 [Z 5821IE]
German version: *Angew. Chem.* **1993**, *105*, 939

[1] G. A. Jeffrey in *Inclusion Compounds, Vol. 1* (Eds.: J. L. Atwood, J. E. D. Davies, D. D. MacNicol), Academic Press, London, **1984**, p. 135.
[2] a) D. Schwarzenbach, *J. Chem. Phys.* **1968**, *48*, 4134; b) H. S. Kim, G. A. Jeffrey, *ibid.* **1970**, *53*, 3610; c) G. A. Jeffrey, M. S. Shen, *ibid.* **1972**, *57*, 56; d) G. A. Jeffrey, D. Mastropaulo, *Acta Crystallogr. Sect. B* **1978**, *34*, 552.
[3] J. Lipkowski, R. Luboradzki, K. Udachin, Y. Dyadin, *J. Inclusion Phenom.* **1992**, *13*, 295.
[4] B. Kamenar, D. Grdenic, *J. Chem. Soc.* **1961**, 3954.
[5] K.-M. Park, T. Iwamoto, *J. Chem. Soc. Chem. Commun.* **1992**, 72.
[6] Crystal data for $CdNiC_4H_{12}N_4O_6$, $M = 383.27$; orthorhombic, *Pnma*, $a = 12.415(1)$, $b = 14.296(1)$, $c = 7.435(1)$ Å, $V = 1319.6(1)$ Å^3, $Z = 4$; $\varrho_{exp.} = 1.92(1)$, $\varrho_{calcd} = 1.93$ g cm^{-3}; Rigaku AFC5S, $Mo_{K\alpha}$ radiation, 2θ-ω scan in $4^\circ \leq 2\theta \leq 60^\circ$, block-diagonal least-squares method to refine all non-H atoms anisotropically to $R = 0.0447$ and $Rw = 0.0591$, GOF = 3.2536 for 92 parameters using 1600 reflections. Further details of the crystal structure investigation may be obtained from the Fachinformationszentrum Karlsruhe, Gesellschaft für wissenschaftlich-technische Information mbH, D-W-7514 Eggenstein-Leopoldshafen 2 FRG, on quoting the depository number CSD-57044, the names of the authors, and the journal citation.
[7] T. Iwamoto in *Inclusion Compounds, Vol. 5* (Eds.: J. L. Atwood, J. E. D. Davies, D. D. MacNicol), Oxford University Press, Oxford, **1991**, p. 177.
[8] T. Kitazawa, Toho University, personal communication.
[9] Y. Mathey, C. Mazieres, *Can. J. Chem.* **1974**, *52*, 3637.

Dimeric and Trimeric Aminoalanes with Inverse Bridging Functions

By *Christiane Klein, Heinrich Nöth,* Matthias Tacke,* and *Martina Thomann*

Dedicated to Dr. Wolfgang Fritsche on the occasion of his 65th birthday

Monomeric aminoalanes $AlX_n(NR_2)_{3-n}$ (X = H, Cl, Br, CH_3) have not been detected to date, because they are stabilized by the formation of cyclic dimers and trimers with an AlN framework, which includes μ-diorganoamino groups. Thus in the solid state Me_2NAlH_2 occurs as the trimer **1**[1] and Me_2NAlCl_2 as the dimer **2**, which contains a planar Al_2N_2 four-membered ring.[2] Not unexpectedly according to this scheme, steric factors influence the ring size. NMR data show that **3**, the dimer of $ClAl(NMe_2)_2$, also contains μ-dimethylamino groups besides terminal Me_2N groups that are *trans* to one another.[3] The dimer of $HAl(NMe_2)_2$ (**4**) is analogous to **3**.[4] The oligomerization of the aminoalanes can be kinetically suppressed, as the transition from dimeric $Al(NMe_2)_3$ (**5**) to monomeric $Al(NiPr_2)_3$[5] or $Al[(N(SiMe_3)_2]_3$ (**6**) shows. We hoped to obtain monomeric bis(diorganoamino)alanes and perhaps even monomeric mono(diorganoamino)alanes by the introduction of bulky R_2N groups.

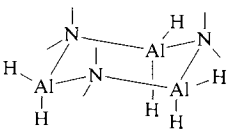

1

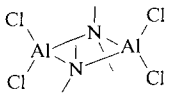

2

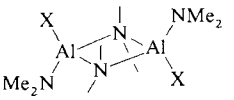

3, X = Cl
4, X = H
5, X = NMe_2

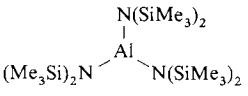

6

According to known procedures[7] the reaction of $AlH_3 \cdot NMe_3$ with 2,6-dimethylpiperidine [Eq. (1)] gave 2,6-dimethylpiperidinoalane (**7**) in 79% yield, which in contrast to the trimer Me_2NAlH_2,[1] exists as a *dimer*.[8, 9]

The trimeric 2,2,6,6-tetramethylpiperidinoalane **8** is readily formed from $LiAlH_4$ and 2,2,6,6-tetramethylpiperidinium chloride [Eq. (2)]. IR and NMR spectra confirm a μ-H-trialane structure.

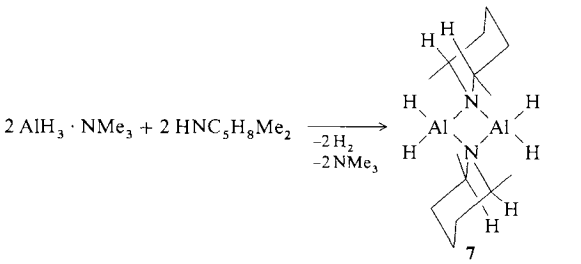

(1)

7

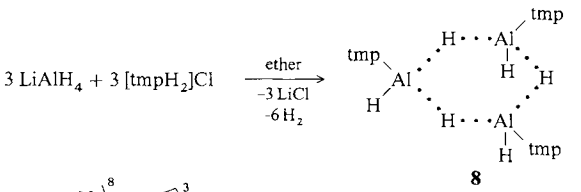

(2)

8

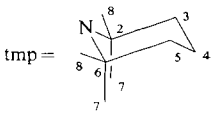

The presence of terminal 2,2,6,6-tetramethylpiperidino groups (tmp) is deduced from the position of the ^{13}C NMR signals,[10] which precludes the possibility of tetracoordinated nitrogen atoms. Because the signals for only one type of tmp group are observed, these must all be identical (all axial or equatorial for a chair conformation, or all *cis* for planar conformations of the ring).[11] The *cis* arrangement of the tmp groups indicated in the structural formula **8** follows from the IR spectrum, which shows three bands of approximately equal intensity in the region expected for Al–H stretching modes at 1863, 1834, and 1778 cm^{-1}. The first two are assigned to the in-phase and out-of-phase vibrational modes of the terminal Al–H groups. The broader band at longer wavelength is attributed to the vibrational mode of the Al_2H bridge. For an arrangement of the terminal H atoms in $(tmpAlH_2)_3$ with two *cis* and one *trans* H atom, three IR bands would be expected in the region of the terminal Al–H stretching vibrations.

The compound $(tmp_2AlH)_2$ **9** is obtained in a reaction according to Equation (3) in toluene at reflux. The replace-

[*] Prof. Dr. H. Nöth, Dipl.-Chem. C. Klein, Dr. M. Tacke, Dr. M. Thomann
Institut für Anorganische Chemie der Universität
Meiserstrasse 1, D-W-8000 München 2
Telefax: Int. code + (89)590-2451

[**] This work was supported by the Fonds der Chemischen Industrie and the Chemetall GmbH. M. Tacke thanks the DFG for a post-doctoral grant and Prof. Dr. A Oskam for time on a matrix apparatus.

ment of the hydride hydrogen atoms in **9** by tmp groups was not accomplished even after 16 h in the presence of a large excess of tmpH in boiling toluene. There is no μ-amino

$$2\,AlH_3\cdot NMe_3 + 4\,tmpH \xrightarrow[-2NMe_3]{-4H_2} \underset{\mathbf{9}}{\text{tmp}_2Al(\mu\text{-H})_2Al\text{tmp}_2} \quad (3)$$

group in **9**. Instead, as the X-ray structure analysis shows, a doubly H-bridged aminodialane is present. Characteristic for this compound, which is thermally stable at 255 °C, is the broad IR band at 1770 cm^{-1} that is assigned to the vibrational mode of the bridging H atoms. Since the ^{13}C NMR spectrum shows only a set of four signals, the rotation of the tmp groups about their Al–N bonds is not hindered.

The structural parameters[12] (Fig. 1) of **9** are in accord with an Al–Al interaction, because the Al–Al distance of 2.680(2) Å, though longer than in $(Me_2AlH)_2$ (2.62 Å),[13] is

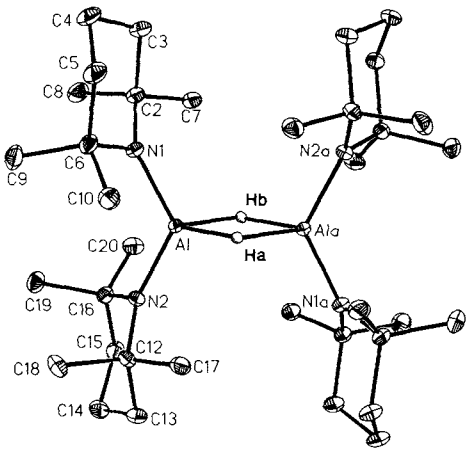

Fig. 1. Molecular structure of **9** *in the crystal. Ellipsoids represent 25% probability.* Selected bond lengths: Al-Ala 2.680(2), Al-N1 1.836(3), Al-N2 1.835(2), Al-Ha 1.68(2), Al-Hb 1.67(2). Selected bond angles [°]: Ha-Al-Hb 74.8(13), N1-Al-N2 126.9(1), Al-N1-C2 126.4(2), Al-N1-C6 116.5(2), Al-N2-C12 126.7(1), Al-N2-C16 116.4(1). The N atoms lie in the same plane as the C and Al atoms. Hydrogen atoms of the tmp groups have been omitted for clarity.

nevertheless only a little longer than the Al–Al distance of 2.660(1) Å in the dialane(4) $[(Me_3Si)_2CH]_4Al_2$.[14] The N-Al-N bond angle of 126.9(1)° is much wider than the tetrahedral angle and is certainly the result of the steric requirement of the tmp group, as confirmed by a comparison with the C-Al-C angle of 118.5(9)° and 117(1)° in $Me_2AlH_2AlMe_2$[13] or $Me_2AlMe_2AlMe_2$.[15] Also the lengthening of the Al···Al distance in **9** is probably attributable to these steric effects. The Al–N bond length in **9** is 1.835(3) Å. It is therefore somewhat longer than the Al–N bond in $Al[N(SiMe_3)_2]_3$ (1.78(2) Å), but distinctly shorter than the Al–N bonds of tetracoordinate Al and tetracoordinate N, for example in **7** (1.951(3) Å).

The Al–H distances in **9** of, on average, 1.68(2) Å are similar to those in $(Me_2AlH)_2$ (1.68(2) Å) and $[(Me_3C)_2AlH]_3$ (1.726(5) Å),[16] and are thus longer than in many hydridoaluminates (examples: $Li[AlH_4]$, 1.54–1.69(1) Å;[17,18] $Li[HAl(NMe_2)_3]$, 1.52(2) Å;[19] $Li[H_2Al\{N(SiMe_3)_2\}_2]\cdot 2OEt_2$, 1.55–1.62(2) Å or $Li[H_3AlN(SiMe_2)]\cdot OEt_2$ (1.58–1.62(2)).[20] This can be interpreted as an indication of an only weak association between the two monomeric $HAl(tmp)_2$ units in **9**, and therefore the formation of the monomers **10**[22] from **9** as depicted in Equation (4) should be possible.

$$\underset{\mathbf{9}}{(tmp_2AlH)_2} \longrightarrow \underset{\mathbf{10}}{2\,tmp_2AlH} \quad (4)$$

On evaporation of **9** in vacuum at 50 °C followed by condensation of the vapor together with a thousandfold excess of argon to form a matrix,[21] the IR spectrum (Fig. 2) show a

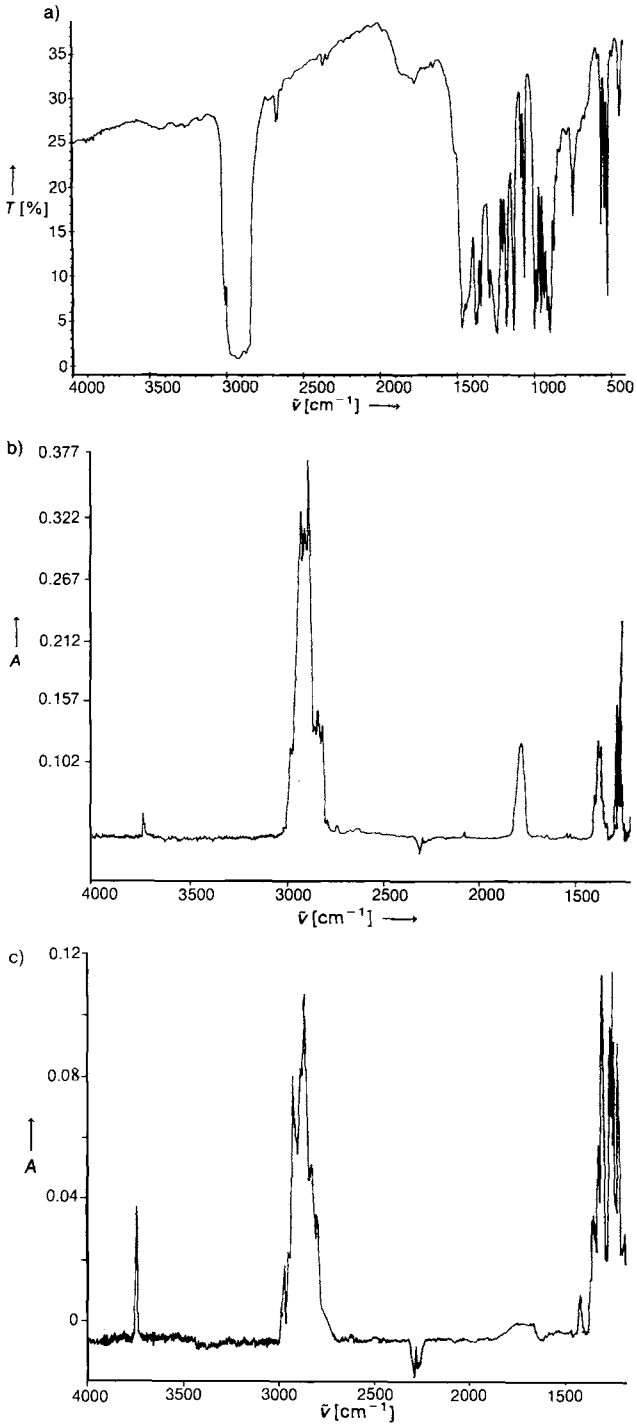

Fig. 2. IR spectra of monomeric (**10**) and dimeric tmp_2AlH (**9**). a) Before evaporation: **9** (recorded in Nujol over the range 4000–400 cm^{-1}. b) After evaporation of **9** and freezing of the vapor in an Ar matrix: **10** (absorption IR spectrum over the range 4000–1210 cm^{-1}). c) After evaporation of the Ar matrix. T = transmission, A = absorption (arbitrary units).

single, sharp band in the region of the Al–H stretching vibration at 1858 cm^{-1}, which is shifted by 88 cm^{-1} to higher wavenumbers relative to the corresponding band in **9**. This reflects the conversion of **9** to the monomeric $(tmp)_2AlH$ **10**.[22] On evaporation of the argon, **10** dimerizes again to **9**.

To our knowledge, **10** is thus the second alane of type $HAlX_2$ beside $HAlCl_2$[23] that has been characterized by IR spectroscopy. The ν(Al–H) frequency, shifted by 110 cm^{-1} to longer wavenumbers relative to that of $HAlCl_2$ (ν(Al–H) = 1968 cm^{-1}) is consistent with the smaller negative inductive effect of the amino group; the trend parallels the change in the B–H frequencies in the series $HBCl_2$, $HB(OR)_2$, and $HB(NR_2)_2$.[24]

Therefore **8** and **9** are the first examples of aminoalanes in which the amino groups are no longer in the role of bridging ligands. Rather, in the compounds $(tmp_nAlH_{3-n})_2$ ($n = 1, 2$) the inverse bridging function Al···H···Al, which is not predicted by chemical intuition, is present.

Experimental Procedure

7: 2,6-Dimethylpiperidine (10.8 mL) was added dropwise to a stirred solution of $AlH_3 \cdot NMe_3$ (3.59 g, 40 mmol) in toluene (30 mL) at −40 °C. Hydrogen evolution began at room temperature. After stirring for 12 h the solvent was removed under vacuum, and pure **7** remained. Single crystals of **7** were grown in a small volume of toluene. Yield: 4.45 g **7** (79%), m.p. 150 °C. ^{1}H NMR (C_6D_6) (270 MHz): δ = 1.16–1.37 (γ-CH_2), 1.38 (CH_3), 1.55–1.88 (β-CH_2), 3.46 (α-CH); ^{13}C NMR (100 MHz): δ = 22.09, 22.27 (C4), 30.61, 30.72 (C3, 5), 34.53 (CH_3), 51.21 (C2, 6); ^{27}Al NMR (70 MHz, standard $[Al(OH_2)_6]^{3+}$): δ = 145 (broad). IR: ν(Al-H) = 1828 cm^{-1}.

8: $LiAlH_4$ (1.0 g, 26 mmol) was suspended in ether (50 mL) and stirred. At −40 °C [tmpH$_2$]Cl (4.25 g) was added in portions. After stirring for 12 h the insoluble matter was separated, the ether removed from the solution under vacuum, and the residue sublimed at 60 °C under high vacuum. Yield: 1.3 g **8** (30%), decomp. > 280 °C; molar mass (in benzene): 528 g mol^{-1}; calculated for the trimer, 507. As yet no single crystals could be obtained from **8**. ^{1}H NMR (C_6D_6) (270 MHz): δ = 1.27 (γ-CH_2), 1.36 (CH_3), 1.55–1.76 (β-CH_2), 4.54 (AlH); ^{13}C NMR (100 MHz): δ = 18.52 (C4), 33.75 (C7, 8), 40.11 (C3, 5), 51.72 (C2, 6); ^{27}Al NMR (70 MHz): δ = 112; IR: ν(Al-H) range: (Nujol): $\tilde{\nu}$[cm^{-1}] = 1863, 1834, 1778; (toluene) 1867, 1850, 1797, 1734.

9: At −40 °C tetramethylpiperidine (15 mL) was added dropwise to a stirred solution of $AlH_3 \cdot NMe_3$ (3.31 g, 37 mmol) in toluene (30 mL). After the mixture had reached room temperature and the gas evolution had stopped, it was heated at reflux for 10 h. On cooling **9** precipitated. Yield: 3.5 g (31%). More **9** was obtained on reducing the volume of the solution. Decomp. > 255 °C. ^{1}H NMR (C_6D_6) (270 MHz): δ = 1.06 (CH_3, 12H), 1.25–1.55 (CH_2, 6H); ^{13}C NMR (100 MHz): δ = 18.81 (C4), 32.03 (C7, 8), 38.59 (C3, 5), 49.58 (C2, 6); ^{14}N NMR (14 MHz, $NaNO_3$): δ = −257; ^{27}Al NMR (70 MHz): δ = 135; IR: ν(Al-H) range: $\tilde{\nu}$[cm^{-1}]: 1770 (broad).

Received: September 17, 1992 [Z 5577 IE]
German version: *Angew. Chem.* **1993**, *105*, 923

[1] A. J. Downs, D. Duckworth, J. C. Machell, C. R. Pulham, *Polyhedron* **1992**, *11*, 1295–1304.
[2] A. Ahmed, W. Schwarz, H. Hess, *Acta Crystallogr. Sect. B* **1977**, *33*, 3574–3576.
[3] At room temperature only one ^{1}H NMR signal at δ = 2.44 is observed, but at −80 °C two are found. $\delta(^{27}Al)$ = 114.7 corresponds to a tetracoordinate Al atom. In solution, therefore, a Me_2N exchange takes place at room temperature; see also P. Wolfgardt, Dissertation, Universität München, **1975**; J. K. Ruff, *J. Am. Chem. Soc.* **1961**, *83*, 1798–1800.
[4] δ^1H = 2.69, 2.33 (1:1), δ^{27}Al = 127, δ^{14}N = −365 (v. broad), P. Wolfgardt, Dissertation, Universität München, **1975**.
[5] J. K. Ruff, *J. Am. Chem. Soc.* **1961**, *83*, 2835–2839.
[6] G. M. Sheldrick, W. S. Sheldrick, *J. Chem. Soc.* A **1969**, 2279–2282.
[7] J. K. Ruff, M. F. Hawthorne, *J. Am. Chem. Soc.* **1961**, *83*, 535–538.
[8] In contrast to $(Me_2NAlH_2)_3$ [1], Me_2NGaH_2 is dimeric: P. L. Baxter, A. J. Downs, D. W. H. Rankin, H. E. Robertson, *J. Chem. Soc. Dalton Trans.* **1985**, 807–814. The same holds for the "inverse" compounds Me_2ENH_2 (E = Al, Ga): L. V. Interrante, G. A. Siegel, M. Garbauskar, C. Hejna, G. A. Slack, *Inorg. Chem.* **1989**, *28*, 252–257; M. J. Almond, M. G. B. Drew, G. F. Jenkins, D. A. Rice, *J. Chem. Soc. Dalton Trans.* **1992**, 5–9.
[9] For **7** the following crystallographic data were determined: **3**: a = 16.055(3), b = 8.906(2), c = 11.886(2) Å, $\alpha = \beta = \gamma = 90°$, V = 1699.5(9) Å^3. The structure solution in the centrosymmetric orthorhombic space group *Ibam* gave a model with disorder of the dimethylpiperidino group. On consideration of the position of the ellipsoids the model did not fulfil the expected symmetry. The structure solution in the acentric space group *Iba2* did not remove this disorder and, similar to the refinement in *Ibam*, yielded unrealistic C–C distances. In principle the same was valid in monoclinic systems. Also at −80 °C the collected data provided no satisfactory structure solution. Thus only the dimeric nature of the compound was ascertained.
[10] If a μ-amino structure were present, $\delta(^{13}C)$ of the C atoms adjacent to N atoms (C2,6) should lie in the range δ = 58–64 (S. Weber, Dissertation, Universität München, **1983**; H. Nöth, S. Weber, *Z. Naturforsch. Teil B* **1983**, *38*, 1460–1465.
[11] J. Weidlein, U. Müller, K. Dehnicke, *Schwingungsfrequenzen 1, Hauptgruppenelemente*, Thieme, Stuttgart, **1981**.
[12] X-ray crystal structure of **9**: $C_{18}H_{38}N_2Al$, M_r = 308.5, a = 21.414(8), b = 7.945(2), c = 24.231(5) Å, β = 113.76(2)°, V = 3773(2) Å^3, space group $C2/c$, Z = 8, single crystal dimensions 0.32 × 0.2 × 0.65 mm^3, $Mo_{K\alpha}$ radiation, Siemens P4 diffractometer, ω scan, scan width 1.10°, 2θ range 3.0–50.0°, scan rate 2.5–29.3° min^{-1}, 3470 measured intensities, 2653 considered observed ($F > 3\sigma(F)$), structure solution with direct methods. R = 0.0473, R_w = 0.0722, SHELXTL PLUS PC program system, non-hydrogen atoms anisotropicic, hydrogen atoms isotropic. Bridging hydrogens were refined in position and with temperature factors u_i, all other H atoms in calculated sites with a riding model. Further details of the crystal structure investigation may be obtained from the Fachinformationszentrum Karlsruhe, Gesellschaft for wissenschaftlich-technische Information mbH, D-W-7514 Eggenstein-Leopoldshafen 2 (FRG) on quoting the depository number CSD-57170, the names of the authors, and the journal citation.[13] A. Almenningen, G. A. Anderson, F. R. Forgaard, A. Haaland, *Acta Chem. Scand.* **1972**, *26*, 2315–2321.
[14] W. Uhl, *Z. Naturforsch. B* **1988**, *43*, 1113–1118.
[15] A. Almeningen, S. Halvorsen, A. Haaland, *Acta. Chem. Scand.* **1971**, *25*, 1937–1945.
[16] W. Uhl, *Z. Anorg. Allg. Chem.* **1989**, *570*, 37–51.
[17] N. Skar, B. Post, *Inorg. Chem.* **1967**, *6*, 669–671; G. Linti, Dissertation, Universität München, **1990**, (low-temperature measurement).
[18] G. Linti, Dissertation, Universität München, **1990**.
[19] G. Linti, H. Nöth, P. Rahm, *Z. Naturforsch. B* **1988**, *43*, 1101–111.
[20] A. Heine, D. Stalke, *Angew. Chem.* **1992**, *104*, 941–942; *Angew. Chem. Int. Ed. Engl.* **1992**, *31*, 854–855.
[21] Matrix-Apparatur: G. Boxhoorn, A. Oskam, *Inorg. Chim. Acta.* **1978**, *29*, 243–248.
[22] $\delta(^{27}Al)$ of **9** dissolved in toluene remained almost unchanged on warming from 20 to 80 °C; that is, the monomerization observed in the gas phase is not detected with NMR methods. A molar mass determination of **9** in benzene was not performed for this reason.
[23] H. Schnöckel, *J. Mol. Struct.* **1978**, *50*, 275–280.
[24] L. Lynds, *Spectrochim. Acta* **1966**, *22*, 2123–2127; W. J. Lehmann, T. P. Onak, I. S. Shapiro, *J. Chem. Phys.* **1959**, *30*, 1215–1220; J. Goubeau, E. Bessler, D. Wolf, *Z. Anorg. Allg. Chem.* **1967**, *352*, 285–262.

CD Exciton Chirality Method: New Chromophores for Primary Amino Groups**

By *Dario Gargiulo, Guolin Cai, Norihiro Ikemoto, Nina Bozhkova, Joshua Odingo, Nikolina Berova,* and *Koji Nakanishi**

The circular dichroic (CD) exciton chirality method is a microscale procedure for determining the absolute configurations and conformations of compounds containing two or more chromophores.[1, 2] Hydroxyl groups are converted into various *para*-substituted benzoate groups, and other symmetric chromophores, which may or may not be identical. When two identical benzoate groups interact through space,

[*] Prof. K. Nakanishi, Dr. D. Gargiulo, Dr. G. Cai, Dr. N. Ikemoto, Dr. N. Bozhkova, J. Odingo, Prof. N. Berova
Department of Chemistry
Columbia University, New York, NY 10027 (USA)
Telefax: Int. code + (212) 932-8273

[**] This work was supported by National Institutes of Health (grants 34509 to KN and 5F32CA08972 to NI) and National Science Foundation (grant INT 90-15531 to KN, N. Berova).

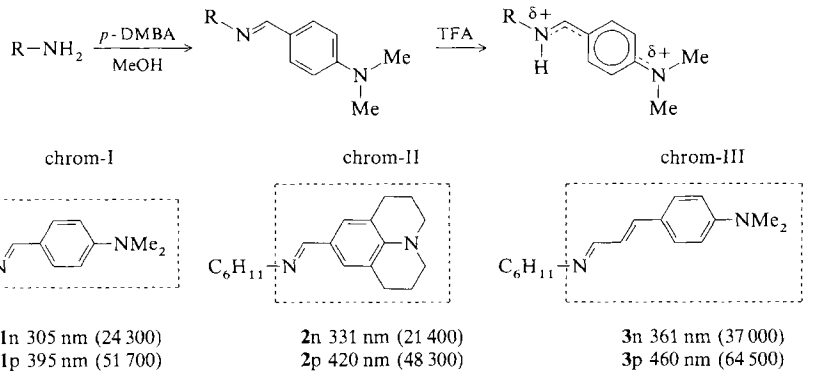

1n 305 nm (24 300)
1p 395 nm (51 700)

2n 331 nm (21 400)
2p 420 nm (48 300)

3n 361 nm (37 000)
3p 460 nm (64 500)

Scheme 1. Top: Neutral and protonated Schiff bases formed from a primary amine and *para*-dimethylaminobenzaldehyde (pDMBA). Bottom: Schiff bases from cyclohexylamine and pDMBA, julolidinecarbaldehyde [9], and *para*-dimethylaminocinnamaldehyde. The chromophoric groups are designated chrom-I, chrom-II, and chrom-III, respectively. The λ_{max} and ε values (in parentheses) for the neutral (n) and protonated (p) compounds were determined in acetonitrile for **1** and **2**, and in methanol for **3**. The Schiff base species were protonated by addition of trifluoroacetic acid (TFA) to the cell.

they give rise to CD curves split into a positive and a negative component (that is, they are bisignate) the signs of which are defined by the absolute orientation of the two electric transition moments. The CD curves of compounds containing two different chromophores, for example, methyl galactopyranoside-2,4-bis(*p*-bromobenzoate)-3,6-bis(*p*-methoxycinnamate), are complex and constitute a fingerprint of that compound. The finding that such characteristic CDs can be reproduced by pairwise summation of interacting chromophores is currently being applied to structural studies of oligosaccharides.[2, 3] Conventionally amino groups are also acylated and have been treated similarly to hydroxyl groups.[3–7]

In the following, we describe three chromophores that can be prepared selectively from primary amines in the presence of free hydroxyl groups (Scheme 1). The three aldehydes, *para*-dimethylaminobenzaldehyde,[8] julolidinecarbaldehyde,[9] and *para*-dimethylaminocinnamaldehyde,[8] all react readily under very mild conditions and afford the imines, chrom-I, chrom-II, and chrom-III, respectively, in high yields. Upon protonation these Schiff bases undergo drastic bathochromic shifts, and the extinction coefficients ε are intensified two- to threefold by formation of cyanine-type dyes.[10] Since the coupling of chromophores is approximately proportional to the absorption intensity, chromophores with intense absorptions increase the sensitivity of the method. Furthermore, chromophores absorbing at long wavelengths are important when samples themselves contain chromophoric groups or impurities whose absorbance bands may overlap with those of the chromophores and interfere with analysis.

The model chiral amines, (*R,R*)-(−)-1,2-diaminocyclohexane, the 1,3-diamine derived from kasugamycin,[11] and methyl-α-L-acosaminide were derivatized with the three aldehydes (Scheme 2),[12] and their UV/VIS[1] and CD spectra were recorded before and after protonation (Fig. 1, Table 1). The 1,3-diamine was converted directly into the bis(Schiff bases) **7** and **8** without protection of the hydroxyl groups. In the acosamine derivative **9**, chrom-III was used for amino derivatization, while ethyl *para*-methoxyphenylpentadienoate was employed to yield the chromophore (chrom-IV) for the hydroxyl group.

All derivatives displayed very strong CD bisignate curves (evident in the large *A* values in Table 1); the signs of the CD curves correctly represent the absolute sense of twist between the C–N and C–O bonds. In compounds containing chromophores I–III the *trans* configuration of the N=C bond and the *syn* orientation of the H_a and H_b hydrogen atoms in both the neutral and protonated species (see structures **4**–**6** in Scheme 2) result in parallel electric transition moments and C–N bonds. In chromophore IV also, the direction of the electric transition moment coincides with the direction of the original C–O bond.[13]

Note that this is unlike the cyanine dye reported earlier by us, and 2,4-hexadienylidenimine, in which sign reversal of

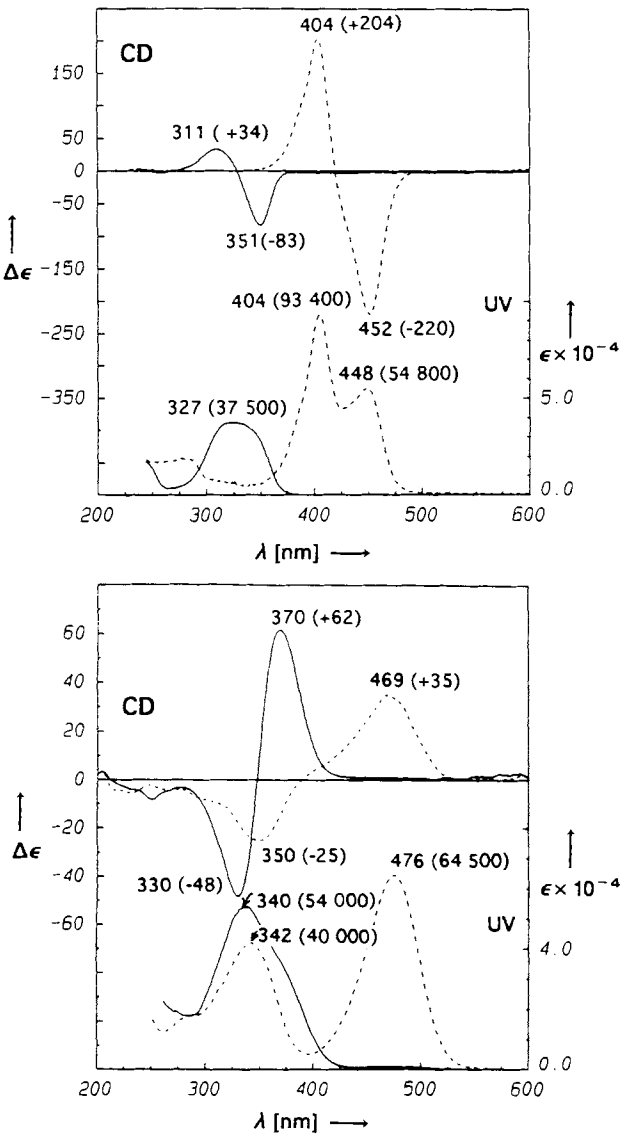

Fig. 1. UV/VIS and CD spectra: Top: neutral **5** (solid line) and protonated **5** (dashed line) in acetonitrile. Bottom: neutral **9** (solid line) and protonated **9** (dashed line). In the CD spectrum of **9** a bisignate couplet is still observed between the red-shifted protonated chrom-III and neutral chrom-IV. Above the CD curves, $\lambda_{ext}(\Delta\varepsilon)$ values are given. Above the UV bands, $\lambda_{max}(\varepsilon)$ values are given.

 © *VCH Verlagsgesellschaft mbH, W-6940 Weinheim, 1993* *0570-0833/93/0606-0889 $ 10.00+.25/0*

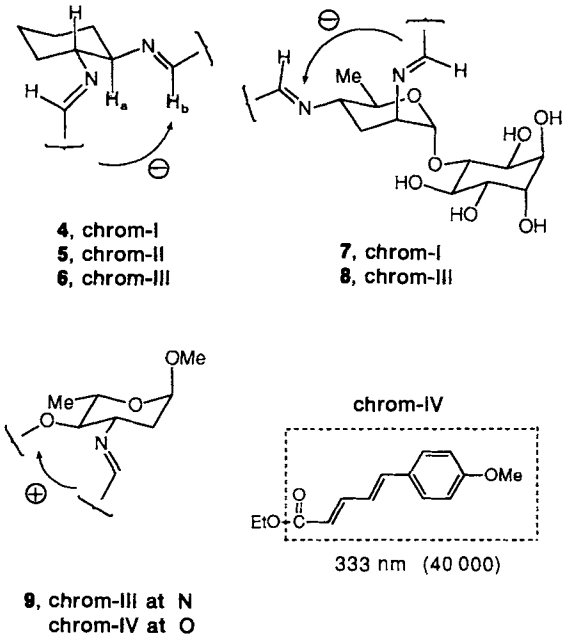

Scheme 2. Bis(Schiff base) derivatives of (*R,R*)-(−)-1,2-diaminocyclohexane (**4**–**6**), kasugamine (**7**, **8**) and L-acosamine (**9**). The braces indicate the position of the chromophoric groups. For the definitions of chrom-I, chrom-II, and chrom-III, see Scheme 1. The $\lambda_{max}(\varepsilon)$ of the chrom-IV source, ethyl *para*-methoxyphenylpentadienoate, was determined in methanol (synthesis of this ester: K. Nakanishi et al. unpublished). In the partial structure shown for the neutral **4**–**6**, the protons H_a and H_b are in *syn* orientation; the same conformation holds for the protonated species also (to be published).

the exciton couplet was observed because direction of the electric transition moment of the chromophore and C–N bond are not parallel.[10, 14, 15]

The UV/VIS and CD spectra of compounds **5** in their unprotonated and protonated forms are displayed in Figure 1 (top). The bisignate curves that reveal a negative Cotton effect are centered at the λ_{max} of the UV/VIS spectrum of the chromophores; protonation induces a red shift of about 100 nm in the absorption maximum and increases the *A* value from −117 to −424 (Table 1). As in the case of cyanine dyes,[10] the UV/VIS spectra of protonated species **4**, **5**, and **6** showed doubling of the signals due to exciton coupling between the red-shifted chromophores.[16]

Table 1. UV/VIS and CD data of neutral (n) and protonated (p) species **4**–**9**. The *A* values (amplitudes) are the differences ($\Delta\varepsilon$) of the two extrema of the split CD curves. A negative sign for *A* indicates that the Cotton effect at longer wavelengths has a negative sign and that at shorter wavelengths a positive sign. The reverse is true for a positive sign for *A*.

Cmpd.	λ_{max} (ε)	λ_{ext} ($\Delta\varepsilon$)	*A*	Solvent
4n	300 (43000)	332 (−83.1)/292 (+53.4)	−136	MeCN
4p	423 (53300)/387 (86100)	428 (−202.2)/386 (+190.4)	−392	MeCN
5n	327 (37500)	351 (−83.0)/311 (+33.6)	−117	MeCN
5p	448 (54800)/404 (93400)	452 (−220)/404 (+204.0)	−424	MeCN
6n	357 (63000)	383 (−70.2)/344 (+58.3)	−128	MeOH
6p	502 (71000)/451 (116000)	508 (−151.0)/448 (+144.0)	−295	MeOH
7n	325 (48000)	334 (−56.2)/294 (+26.6)	−83	MeCN
7p	411 (93800)	417 (−151)/383 (+110.0)	−261	MeCN
8n	368 (63000)	385 (−23.1)/348 (+15.5)	−39	MeOH
8p	484 (93000)	498 (−94.4)/450 (+84.4)	−178	MeOH
9n	340 (54000)	370 (+61.8)/330 (−48.2)	+110	MeOH
9p	342 (40000)/476 (64500)	469 (+35.0)/350 (−25.0)	+60	MeOH

In the presence of added water, the Schiff base and its protonated derivatives prepared from chrom-I hydrolyzed back to the starting amine and aldehyde; the protonated Schiff base hydrolyzed faster than its unprotonated counterpart.[17] The derivatives with chrom-III were relatively stable to hydrolysis.[18] Therefore, anhydrous conditions must be used during manipulation of the derivatives containing chrom-I, and this chromophore is recommended when recovery of the starting amine is desired.

Chromophores I–III are useful for microscale stereochemical assignments of compounds with primary amino groups because of 1) ease of preparation of Schiff bases and protonated Schiff bases, 2) the strong CD couplets lying at long wavelengths, and 3) possible recovery of the starting amine. Further studies on other natural products containing an amino group, especially those of biochemical significance, are underway.

Experimental Procedure

4n: A solution of (*R,R*)-1,2-diaminocyclohexane (4.2 mg, 0.037 mmol) and pDMBA (11.0 mg, 0.074 mmol) in anhydrous methanol (0.5 mL) was stirred for 12 h at room temperature in the presence of anhydrous Na_2SO_4. After filtration and concentration, the residue was dissolved in ethyl acetate with few drops of triethylamine, and hexane was added to precipitate the product as a white solid. Yield: 12.6 mg, 91% m.p., 148.5–149.5 °C, uncorrected (from EtOAc/*n*-hexane).

9n: A solution of methyl-α-L-acosaminide hydrochloride (2.0 mg, 0.010 mmol) and *para*-dimethylaminocinnamaldehyde (1.8 mg, 0.010 mmol) in anhydrous methanol (0.5 mL) was heated at reflux for 2.5 h in the presence of anhydrous Na_2SO_4. The reaction mixture was filtered, and the solvent evaporated. The residue was redissolved in dichloromethane and precipitated with hexane to yield the Schiff base hydrochloride (3.4 mg, 96%), which was then heated at reflux with 1-(5-(4-methoxyphenyl)-1-oxo-2,4-pentadienyl)-1*H*-1,2,4-triazole (5.6 mg, 0.020 mmol) and diazabicycloundecane (3.0 mg, 0.020 mmol) in anhydrous dichloromethane (2 mL) for 45 min. Flash chromatography (silica gel, 50% ethyl acetate/hexane, ca. 0.1% Et_3N) of the reaction mixture afforded bis-(Schiff base) **9**n as a yellow solid. Yield: 2.2 mg, 43%.

Received: January 13, 1993 [Z 5805 IE]
German version: *Angew. Chem.* **1993**, *105*, 913

[1] N. Harada, K. Nakanishi, *Circular Dichroic Spectroscopy-Exciton Coupling in Organic Stereochemistry*, University Science Books, Mill Valley, CA, USA, **1983**.
[2] M. Chang, H. V. Meyers, K. Nakanishi, M. Ojika, J. H. Park, M. H. Park, R. Takeda, J. T. Vázquez, W. T. Wiesler, *Pure Appl. Chem.* **1989**, *61*, 1193.
[3] W. T. Wiesler, N. Berova, M. Ojika, H. V. Meyers, M. Chang, P. Zhou, L.-C. Lo, M. Niwa, R. Takeda, K. Nakanishi, *Helv. Chim. Acta* **1990**, *73*, 509.
[4] M. Kawai, U. Nagai, M. Katsumi, *Tetrahedron Lett.* **1975**, 3165.
[5] G. L. Verdine, K. Nakanishi, *J. Chem. Soc. Chem. Commun.* **1985**, 1093.
[6] H. E. Smith, J. R. Neergaard, E. P. Burrows, F.-M. Chen, *J. Am. Chem. Soc.* **1974**, *96*, 2908.
[7] a) P. Zhou, N. Berova, K Nakanishi, M. J. Rohmer, *J. Chem. Soc. Chem. Commun.* **1991**, 256; b) P. Zhou, N. Berova, K. Nakanishi, M. Knani, M. J. Rohmer, *J. Am. Chem. Soc.* **1991**, *113*, 4040.
[8] These chromophores have been used for detection of amino compounds: a) H. Falter, K. Jayasimhulu, R. A. Day, *Anal. Biochem.* **1975**, *67*, 359; b) P. Baumann, N. Narasimhachari, *J. Chromatogr.* **1973**, *86*, 269.
[9] Preparation: Julolidine (2.0 g, 12 mmol) and $POCl_3$ (1.1 mL, 12 mmol) in dimethylformamide (5 mL) were heated for 2 h at 80–100 °C. The mixture was poured into ice water, neutralized with sodium acetate, and cooled to afford yellow crystals (1.65 g, 72%).
[10] a) D. Gargiulo, F. Derguini, N. Berova, K. Nakanishi, N. Harada, *J. Am. Chem. Soc.* **1991**, *113*, 7046; b) N. Berova, D. Gargiulo, F. Derguini, K. Nakanishi, N. Harada, *ibid.*, in press.
[11] Y. Suhara, K. Maeda, H. Umezawa, *Tetrahedron Lett.* **1966**, 1239.
[12] 1,2-Diaminocyclohexane was derivatized at room temperature with stoichiometric amounts of dimethylaminobenzaldehyde for 10 h and 2–3 days, for diamine concentrations of 10^{-2} and 10^{-3} M, respectively; in the case of dimethylaminocinnamaldehyde (chrom-III) the time was 3 h and 24 h, respectively, for the two concentrations.
[13] K.Nakanishi, M. Kuroyanagi, H. Nambu, E. M. Oltz, R. Takeda, G. L. Verdine, A. Zask, *Pure Appl. Chem.* **1984**, *56*, 1031.

[14] V. Buss, K. Kolster, B. Görs, *Tetrahedron Asymmetry* **1993**, *4*, 1.
[15] D. Gargiulo, N. Ikemoto, N. Bozhkova, J. Odingo, G. Cai, N. Berova, K. Nakanishi, unpublished results.
[16] The intensity ratio of the first and second absorption bands is dependent on the dihedral angle θ between the transition moments; when θ is larger than 90°, the first band at longer wavelengths is stronger, and vice versa. In the present case, θ is less than 90°: N. Harada, H. Uda, *J. Chem. Soc. Chem. Commun.* **1982**, 230.
[17] The CD of **4n** (10^{-5} M, 1% water in MeCN) disappeared after 48 h, while the UV of **4p** (ca. 10^{-5} M, 1% water in MeCN, 0.2% TFA) disappeared completely after 7 h at room temperature.
[18] In protonated compounds with chrom-III, it is necessary to measure the CD immediately after addition of TFA, because the N=C bond undergoes partial *trans* to *cis* isomerization with time. In contrast, with chrom-I and chrom-II neither the neutral nor the protonated derivatives isomerize. A detailed account of these aspects will be published shortly.

A New Form of Coordinated Carbon: A C_3 Chain That Is Anchored by a Transition Metal on Each End and Spanned by a Third**

By *Weiqing Weng, Atta M. Arif*, and *J. A. Gladysz**

Dedicated to Professor Wolfgang Beck on the occasion of his 60th birthday

Diverse forms of elemental carbon (C_x) have been incorporated into isolable polynuclear transition metal complexes.[1–3] These range from single carbon atoms sepulchered in metal clusters to unsupported C_1–C_4 chains that span two metals. Such species have been found to have promising catalytic and materials properties.[4] In particular, the pioneering efforts of Shriver et al. and Bradley established that unique reactivity is associated with cluster complexes with *exposed* carbon atoms.[1] We therefore sought to develop new approaches to polynuclear complexes containing unusual types of C_x fragments.

We recently demonstrated that "terminal" transition metal acetylide complexes [$L_nMC{\equiv}CH$] can be lithiated to give complexes containing C_2Li ligands ([$L_nMC{\equiv}C^-Li^+$], **I**).[5] These have proven to be valuable building blocks that can be derivatized by electrophiles in high yields. We sought to synthesize a trimetallic C_3 species—a heretofore unknown type of carbon adduct—via Fischer carbene complexes derived from binuclear carbonyl compounds (**II**), as sketched in Scheme 1.[6] Alkoxy groups have been abstracted from many Fischer carbene complexes by electrophiles to give either cationic or neutral carbyne complexes.[7] In the case of **II**, this would initially yield the C_3 species **III**, which could undergo further reaction because of the proximity of another metal (M″) to the electrophilic C≡M′ center.

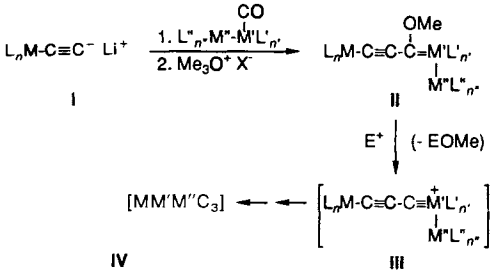

Scheme 1. Planned route to trimetallic C_3 complexes [MM′M″C_3].

The rhenium/lithium C_2 complex **1** was generated as reported earlier,[5] and sequentially treated with [$Re_2(CO)_{10}$] and $Me_3O^+BF_4^-$. Workup gave the alkynylcarbenetrirhenium complex **2** in 92% yield, as shown in Scheme 2. Complex

[{Re*}(C≡CLi)] **1**, {Re*} = (η^5-C_5Me_5)Re(NO)(PPh_3)

cis-[{Re*}(C≡C-C(OMe)=)Re(CO)$_4${Re(CO)$_5$}] **2**

2 was characterized by microanalysis, and NMR (^1H, ^{13}C, ^{31}P) and IR spectroscopy ($\nu_{C\equiv C}$ 2097 cm^{-1}).[8]

Many properties of **2** were similar to those of the dirhenium carbene complexes [RC(OR′)=Re(CO)$_4${Re(CO)$_5$}],[9] which had been analogously prepared by Fischer et al. earlier. The *cis* arrangement of ligands was established by ^{13}C NMR (−50 °C/C_7D_8; δ), which gave one signal for the four equivalent CO ligands of the Re(CO)$_5$ group (197), and four signals for the remaining types of CO ligands (201, 200, 196, 192; 1:2:1:1).[10] However, the C=Re ^{13}C NMR signal (240) was not as far downfield as those of the dirhenium

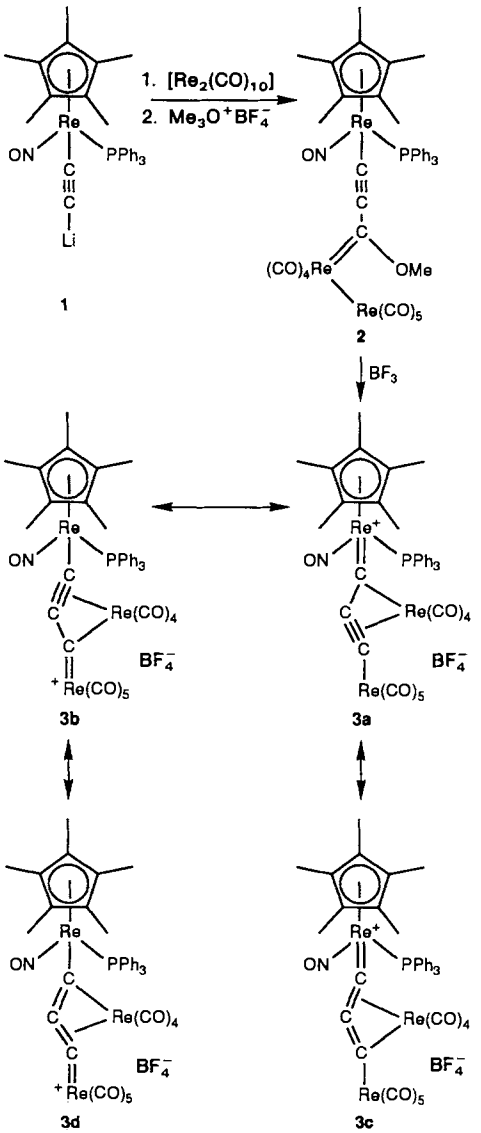

Scheme 2. Synthesis of Re_3C_3 complexes.

[*] Prof. Dr. J. A. Gladysz, Dr. W. Weng, Dr. A. M. Arif
Department of Chemistry
University of Utah
Salt Lake City, UT 84112 (USA)
Telefax: Int. code + (801) 581-8433

[**] We thank the Department of Energy for support of this research.

carbene complexes (318–377). Also, the ReC≡ signal (203, d, $J_{C,P}=14$ Hz) and the ν_{NO} band in the IR spectrum (1664 cm^{-1}) were intermediate between those of acetylide complexes [{Re*}(C≡CR)] (98–86, d, $J_{C,P}=16-18$ Hz; 1629–1637 cm^{-1}) and vinylidene complexes $[\{Re^*\}(=C=CHR)]^+BF_4^-$ (329, d, $J_{C,P}=10-11$ Hz; 1681–1698 cm^{-1}).[5a] These data suggest a significant contribution by a zwitterionic $^+Re=C=C=C(OMe)-Re^-$ resonance form to the structure of **2**.

Fischer found that the dirhenium carbene complexes reacted with Al_2X_6 to give cationic carbyne complexes $[(RC\equiv)Re(CO)_4\{Re(CO)_5\}]^+AlX_4^-$, which exhibited diagnostic downfield C≡Re ^{13}C NMR signals (e.g., at $\delta=356$).[9c] Thus, **2** was similarly treated with BF_3. A cationic C_3 complex (**3**) was isolated in 64% yield that gave a microanalysis and an ion in the FAB mass spectrum consistent with an analogous carbyne product. The ^{13}C NMR spectrum showed three signals that could be attributed to the C_3 fragment (297.1, d, $J_{C,P}=10$ Hz; 146.6, s; 95.1, s). However, the downfield resonance exhibited a P–C coupling constant characteristic of carbon bound to the cyclopentadienyl rhenium moiety.

Therefore, the crystal structure of **3** was determined. The result, shown in Figure 1, reveals **3** to be the novel

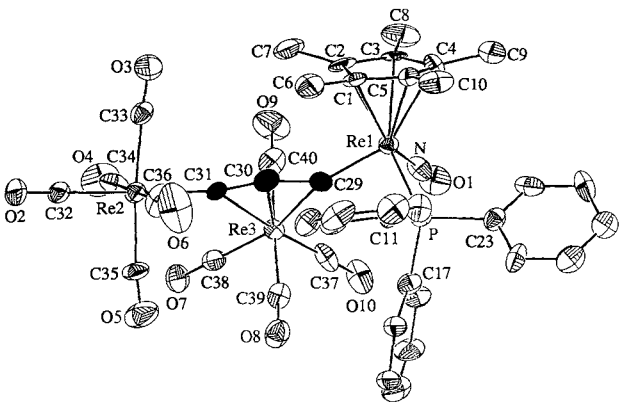

Fig. 1. Structure of the cation of **3**. Selected bond lengths [Å] and angles [°]: Re1-C29 1.94(3), C29-C30 1.41(6), C30-C31 1.28(5), C31-Re2 2.09(4), Re3-C29 2.24(3), Re3-C30 2.27(4), Re3-C31 2.43(4), Re1-P 2.440(9), Re1-N 1.73(3), Re1-C29-C30 140(3), C29-C30-C31 152(4), C30-C31-Re2 155(3).

rearrangement product $[\{Re^*\}(\mu\text{-}\eta^1:\eta^3:\eta^1\text{-}CCC)(Re(CO)_4)\{Re(CO)_5\}]^+BF_4^-$. Complex **3** contains a C_3 chain that is bent (152(4)°), anchored by rhenium atoms on each end, and spanned by a third rhenium. Several pathways for its formation are possible. We suggest that the linear C_3 complex $[\{Re^*\}(CCC)Re(CO)_4\{Re(CO)_5\}]^+BF_4^-$ is initially generated. One carbon terminus then bridges the $Re(CO)_4$ and $Re(CO)_5$ moieties, and the former migrates to the CCC π system.

Structurally, **3** can be viewed as a composite of two resonance forms with the Re=C–C≡C–Re backbones **3a** and **b**, as illustrated in Scheme 2. The pattern of Re–C and C–C bond lengths (Fig. 1) shows that **3a** dominates, consistent with the stronger donor properties of the Ph_3P-substituted rhenium atom. Indeed, the $Ph_3PRe=C$ bond length is identical to those in two cyclopentadienyl alkylidene complexes of the formula $[\{Re\}(=CRR')]^+X^-$.[11] Alternatively, **3** can be formulated with Re=C=C=C–Re backbones (**3c,d**). However, these resonance forms predict nearly equal carbon–carbon bond lengths.

We can identify only remote analogies between **3** and compounds that have been previously reported. For example, **3** can be considered a π-propargyl (η^3-RC≡C–CR′R″)[12] complex of $Re(CO)_4$, or an alkylidene-substituted variant (η^3-RC≡C–C=CR′R″),[13] in which all of the substituents on the C_3 core have been replaced by rhenium atoms. The physical and chemical properties of **2** and **3** are under investigation. Importantly, their visible spectra show unique intense absorptions.[14] Additional characteristics, and extensions of the methodology in Scheme 1, will be described in the near future.

Received: January 4, 1993 [Z 5797 IE]
German version: *Angew. Chem.* **1993**, *105*, 937

[1] a) J. S. Bradley, *Adv. Organomet. Chem.* **1983**, *22*, 1; b) P. L. Bodgan, C. Woodcock, D. F. Shriver, *Organometallics* **1987**, *6*, 1377, and references therein

[2] Selected references to carbide cluster compounds from 1992: a) C. J. Adams, M. I. Bruce, M. J. Liddell, B. W. Skelton, A. H. White, *J. Chem. Soc. Chem. Commun.* **1992**, 1314; b) M. H. Chisholm, C. E. Hammond, V. J. Johnston, W. E. Streib, J. C. Huffman, *J. Am. Chem. Soc.* **1992**, *114*, 7056; c) M. Akita, S. Sugimoto, M. Tanaka, Y. Moro-oka, *ibid.* **1992**, *114*, 7581; d) S. W. Simerly, S. R. Wilson, J. R. Shapley, *Inorg. Chem.* **1992**, *31*, 5146.

[3] Lead references to $[L_nM(C)_xM'L'_n]$ complexes: a) W. Beck, W. Knauer, C. Robl, *Angew. Chem.* **1990**, *102*, 331; *Angew. Chem. Int. Ed. Engl.* **1990**, *29*, 318; b) M. Etienne, P. S. White, J. L. Templeton, *J. Am. Chem. Soc.* **1991**, *113*, 2324; c) G. Koutsantonis, J. P. Selegue, *ibid.* **1991**, *113*, 2316; d) F. R. Lemke, D. J. Szalda, R. M. Bullock, *ibid.* **1991**, *113*, 8466; e) P. Binger, P. Müller, P. Philipps, B. Gabor, R. Mynott, A. T. Herrmann, F. Langhauser, C. Krüger, *Chem. Ber.* **1992**, *125*, 2209; f) P. J. Stang, R. Tykwinski, *J. Am. Chem. Soc.* **1992**, *114*, 4411; g) R. Crescenzi, C. L. Sterzo, *Organometallics* **1992**, *11*, 4301.

[4] a) Y. Izumi, T. Chihara, H. Yamazaki, Y. Iwasawa, *J. Chem. Soc. Chem. Commun.* **1992**, 1395; b) Y. Sun, N. J. Taylor, A. J. Carty, *Organometallics* **1992**, *11*, 4293, and references therein; c) J. Lewis, M. S. Khan, A. K. Kakkar, B. F. G. Johnson, T. B. Marder, H. B. Fyfe, F. Wittmann, R. H. Friend, A. E. Dray, *J. Organomet. Chem.* **1992**, *425*, 165.

[5] a) J. A. Ramsden, W. Weng, J. A. Gladysz, *Organometallics* **1992**, *11*, 3635; b) J. A. Ramsden, W. Weng, A. M. Arif, J. A. Gladysz, *J. Am. Chem. Soc.* **1992**, *114*, 5890.

[6] Reactions with mononuclear carbonyl complexes, and syntheses of bimetallic C_3 complexes, are reported separately: W. Weng, J. A. Ramsden, A. M. Arif, J. A. Gladysz, *J. Am. Chem. Soc.* **1993**, *115*, in press.

[7] H. Fischer in *Carbyne Complexes* (Eds.: H. Fischer, P. Hofmann, F. R. Kreißl, R. R. Schrock, U. Schubert, K. Weiss), VCH, Weinheim, **1988**, Chapter 1.

[8] a) Complete preparative, spectroscopic, analytical, and crystallographic details were given to the reviewers, and are available from the authors upon request. b) Further details of the crystal structure investigation may be obtained from the Fachinformationszentrum Karlsruhe, Gesellschaft für wissenschaftlich-technische Information mbH, D-W-7514 Eggenstein-Leopoldshafen 2 (FRG), on quoting the depository number CSD-57169, the names of the authors, and the journal citation.

[9] a) E. O. Fischer, E. Offhaus, J. Müller, D. Nöthe, *Chem. Ber.* **1972**, *105*, 3027; b) E. O. Fischer, T. L. Lindner, H. Fischer, G. Huttner, P. Friedrich, F. R. Kreißl, *Z. Naturforsch. B* **1977**, *32*, 648; c) E. O. Fischer, P. Rustemeyer, *J. Organomet. Chem.* **1982**, *225*, 265.

[10] Other *cis*-$[(L)Re(CO)_4Re(CO)_5]$ complexes give similar ^{13}C NMR patterns: a) W. Tam, M. Marsi, J. A. Gladysz, *Inorg. Chem.* **1983**, *22*, 1413; b) C. P. Casey, S. M. Neumann, *J. Am. Chem. Soc.* **1978**, *100*, 2544.

[11] J. J. Kowalczyk, A. M. Arif, J. A. Gladysz, *Chem. Ber.* **1991**, *124*, 729, and references therein.

[12] a) V. V. Krivykh, E. S. Taits, P. V. Petrovskii, Y. T. Struchkov, A. I. Yanovskii, *Mendeleev Commun.* **1991**, 103; b) C. P. Casey, T. L. Underiner, P. C. Vosejpka, J. A. Gavney, Jr., P. Kiprof, *J. Am. Chem. Soc.* **1992**, *114*, 10826; c) T.-M. Huang, J.-T. Chen, G.-H. Lee, Y. Wang *ibid* **1993**, *115*, 1170.

[13] a) J. Gotzig, H. Otto, H. Werner, *J. Organomet. Chem.* **1985**, *287*, 247; b) G. Jia, A. L. Rheingold, D. W. Meek, *Organometallics* **1989**, *8*, 1378; c) A. K. McMullen, J. P. Selegue, J.-G. Wang, *ibid.* **1991**, *10*, 3421; d) A. Hills, D. L. Hughes, M. Jimenez-Tenorio, G. J. Leigh, C. A. McGeary, A. T. Rowley, M. Bravo, C. E. McKenna, M.-C. McKenna, *J. Chem. Soc. Chem. Commun.* **1991**, 522; e) C. Bianchini, M. Peruzzini, F. Zanobini, P. Frediani, A. Albinati, *J. Am. Chem. Soc.* **1991**, *113*, 5453; f) L. D. Field, A. V. George, G. R. Purches, I. H. M. Slip, *Organometallics* **1992**, *11*, 3019.

[14] UV/VIS [nm] ($\varepsilon[M^{-1}cm^{-1}]$), CH_2Cl_2: **2**, 276 sh (21000), 304 (18000), 342 sh (14000), 464 (26000); **3**, 268 sh (22000), 300 sh (16000), 344 sh (12000), 432 (11000).

1-Iodoalkynes Can Also Be Dimerized: A New Head-to-Tail Coupling**

By *José Barluenga,* José M. González, Isidro Llorente,* and *Pedro J. Campos*

The oligomerization of alkynes by transition metals has been studied extensively.[1] Although linear dimerization is an attractive alternative, only a limited number of examples are known.[1, 2] A terminal alkyne is required for this reaction, and usually mixtures of dimers are formed. The current interest in selective dimerization of terminal alkynes[3] prompted us to investigate the reaction of readily available 1-iodoalkynes,[4] in which Ipy_2BF_4 (py = pyridine)[5] is used to mediate C–C bond formation.[6] In fact, when the starting alkyne was allowed to react with Ipy_2BF_4/HBF_4[7] in CH_2Cl_2, an unprecedent coupling of 1-iodoalkynes took place furnishing the corresponding head-to-tail dimers (Scheme 1).

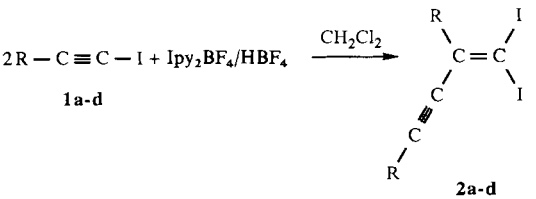

Scheme 1. Linear dimerization of 1-iodoalkynes catalyzed by Ipy_2BF_4/HBF_4. **1**, **2**: **a**, R = C_6H_5; **b**, R = 4-$CH_3C_6H_4$; **c**, R = 4-ClC_6H_4; **d**, R = 4-$CH_3OC_6H_4$.

A number of 1-iodoalkynes were examined, and so far the best results were obtained by employing aryl substituted alkynes and a 1:2 mol ratio of Ipy_2BF_4 to HBF_4. Alkynes **1** were converted quantitatively into 1,3-diaryl-4,4-diiodobutenyne, in the other words, into the head-to-tail dimers **2a–d**. Typically, the alkyne was added to a solution of one equivalent of Ipy_2BF_4 and two equivalents of HBF_4 in CH_2Cl_2 (Scheme 1). Once the reagents were mixed at low temperature (−80 °C), the reaction mixture was allowed to warm to room temperature over approximately 15 h. We found that different experimental conditions were required depending on the aromatic substituent. Thus, for instance, the reaction of **1c** required 35 hours for completion, while that of **1d** was complete in only 3 minutes. Conventional isolation and purification techniques afforded pure samples of the dimers **2**, which were characterized by spectroscopy (Table 1) and gave correct elemental analyses.

From a mechanistic point of view, the formation of the dimer should regenerate an equivalent amount of "I^+". In good agreement with this assumption, when we used a 3:1 mol ratio of iodoalkyne to Ipy_2BF_4 and then hydrolyzed the reaction mixture, we observed the presence of the dimer and iodinated ketone in the crude product.[8] The latter arises from the nucleophilic attack of water on the likely intermediate iodonium ion.[5a] If an appropriate excess of the starting alkyne were employed, the catalytic head-to-tail dimerization of 1-iodoalkynes by Ipy_2BF_4 should be possible (Scheme 2).

[*] Prof. Dr. J. Barluenga, Dr. J. M. González, I. Llorente
Departamento de Química Organometálica,
Universidad de Oviedo
E-33071 Oviedo (Spain)
Prof. Dr. P. J. Campos
Departamento de Química,
Universidad de La Rioja
E-26071 Logroño (Spain)

[**] The research in this paper was supported in part by the DGICYT Grant No. PB89-0538. We thank Prof. Pablo Bernad for his assistance in recording mass spectra, and the Spanish Ministerio de Educación y Ciencia for a graduate fellowship to I. Llorente.

Table 1. Selected spectroscopic data for dimers **2**. ^1H and ^{13}C NMR spectra were recorded at 300 MHz and 75 MHz, respectively.

2a: Oil; ^1H NMR ($CDCl_3$): δ = 7.5–7.2 (m); ^{13}C NMR ($CDCl_3$): δ = 29.1 (CI_2), 91.9, 97.6, 122.1, 127.9, 128.1, 128.2, 128,2, 128.7, 131.2, 140.8, 141.6; IR neat: $\tilde{\nu}$[cm^{-1}] = 2198 (C≡C); MS (70 eV): *m/z* 456 ($M^{\oplus}$, 35%), 202 ($M^{\oplus} - I_2$, 100).

2b: M.p. 85 °C; ^1H NMR ($CDCl_3$): δ = 7.38 (d, ^3J(H,H) = 8.3 Hz, 2H), 7.32 (d, ^3J = 8.3 Hz, 2H), 7.20 (d, ^3J = 7.9 Hz, 2H), 7.12 (d, ^3J = 7.9 Hz, 2H), 2.38 (s, 3H, Me), 2.32 (s, 3H, Me); ^{13}C NMR ($CDCl_3$): δ = 21.3, 21.6, 27.2 (CI_2), 91.5, 98.0, 119.4, 128.1, 129.1, 129.1, 131.3, 138.3, 138.4, 139.1, 142.1; IR (KBr): $\tilde{\nu}$[cm^{-1}] = 2197 (C≡C); MS (70 eV): *m/z* 484 ($M^{\oplus}$, 100%), 230 ($M^{\oplus} - I_2$, 76).

2c: M.p. 118 °C; ^1H NMR ($CDCl_3$): δ = 7.23–7.45 (m); ^{13}C NMR ($CDCl_3$): δ = 29.2 (CI_2), 92.4, 96.7, 120.7, 128.7, 128.7, 129.5, 132.6, 134.5, 135.1, 139.3, 140.6; IR (KBr): $\tilde{\nu}$[cm^{-1}] = 2201 (C≡C); MS (70 eV): *m/z* 528 ($M^{\oplus}$ + 4, 4), 526 ($M^{\oplus}$ + 2, 24), 524 ($M^{\oplus}$, 36%), 270 ($M^{\oplus} - I_2$, 100).

2d: M.p. 131 °C; ^1H NMR ($CDCl_3$): δ = 7.43 (d, ^3J = 8.6 Hz, 2H), 7.37 (d, ^3J = 8.6 Hz, 2H), 6.91 (d, ^3J = 8.6 Hz, 2H), 6.84 (d, ^3J = 8.6 Hz, 2H), 3.85 (s, 3H, OMe), 3.81 (s, 3H, OMe); ^{13}C NMR ($CDCl_3$): δ = 26.2 (CI_2), 55.2, 55.2, 91.1, 97.9, 113.6, 114.0, 114.6, 129.6, 133.0, 133.6, 141.8, 159.5, 160.1; IR (KBr): $\tilde{\nu}$[cm^{-1}] = 2193 (C≡C); MS (70 eV): *m/z* 516 ($M^{\oplus}$, 74%), 262 ($M^{\oplus} - I_2$, 100).

2e: Oil; ^1H NMR ($CDCl_3$): δ = 6.25 (m, 1H), 5.70 (m, 1H), 2.3–2.0 (m, 8H), 1.8–1.5 (m, 8H); ^{13}C NMR ($CDCl_3$): δ = 21.3, 21.6, 22.1, 22.5, 25.1, 25.8, 25.9 (CI_2), 26.7, 28.6, 88.0, 99.0, 120.6, 128.9, 136.3, 139.6, 144.7; IR (neat): $\tilde{\nu}$[cm^{-1}] = 3026, 2181 (C≡C); MS (70 eV): *m/z* 464 ($M^{\oplus}$, 9%), 210 ($M^{\oplus} - I_2$, 100).

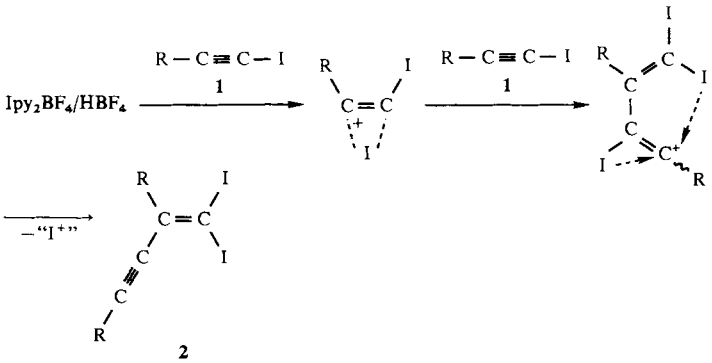

Scheme 2. Proposed mechanism for the catalytic dimerization of 1-iodoalkynes. The catalytic cycle depends on the liberation of "I^+".

We have been able to find conditions to for the successful coupling of 1-iodoalkynes using a catalytic amount of Ipy_2BF_4. The concentration of the iodinating reagent is a critical factor. Dilute (5×10^{-2} M) solutions of Ipy_2BF_4 in CH_2Cl_2 have proven to be valuable for the catalytic dimerization of **1a** and **1b**. Specifically, the reaction of the iodoalkyne and Ipy_2BF_4 in a mol ratio of 11:1 gave **2a** and **2b** in yields of 71 and 81%, respectively (yields of the pure isolated dimers based on the starting iodoalkyne). The reaction time was five days for **2a** and three days for **2b**. For the more reactive iodoalkyne **1d**, the concentration of the catalyst was lowered to 1×10^{-2} M. The reaction time was one hour, and the temperature was allowed to increase from −80 °C to −60 °C. Under these conditions **2d** was obtained in 77% yield. To explore the efficiency of this dimerization, we have also analyzed the reaction in the presence of larger excesses of iodoalkyne. Thus, for instance, when 50 mmol of **1d** was allowed to react for five hours with 1 mmol of Ipy_2BF_4 (2% with respect to the alkyne) and 2 mmol of acid under the previously described conditions, iodoalkyne **1d** was converted almost quantitatively into dimer **2d**.

This new reaction should be applicable to other iodoalkynes. In this context, we have found that 1-(1-cyclohexenyl)-2-iodoethyne (**1e**) can also be dimerized by reaction with Ipy_2BF_4/HBF_4 in CH_2Cl_2 (Scheme 3). Running the reaction

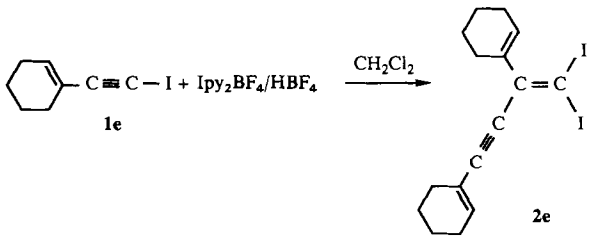

Scheme 3. Synthesis of a cross-conjugated (dienyl)enyne by the head-to-tail coupling of an iodoenyne.

at $-50\,^{\circ}C$ for 24 h, and using a 2×10^{-2} M solution of Ipy_2BF_4 and a 3:1 ratio of iodoalkyne to Ipy_2BF_4 gave a 32% yield of pure **2e**. Although these results are preliminary, this conversion of an iodoalkenyne suggests the feasibility of extending this reaction to other type of substrates. Studies on the optimization and further applications are at present in progress.

In short, a new catalytic protocol for dimerizing 1-iodoalkynes has been established. The strategy is based on the electrophilic character of iodine in Ipy_2BF_4/HBF_4 solutions. The reaction affords head-to-tail dimers with no evidence for the significant formation of other oligomers. The final products have an attractive functionality and could nicely compete with those derived from the transition metal coupling of alkynes.[9]

Received: December 21, 1992 [Z 5766 IE]
German version: *Angew. Chem.* **1993**, *105*, 928

[1] M. J. Winter in *The Chemistry of the Metal-Carbon Bond, Vol. 3* (Eds.: F. R. Hartley, S. Patai), Wiley, New York, **1985**, p. 259.
[2] P. A. Chaloner, *Handbook of Coordination Catalysis in Organic Chemistry*, Butterworths, London **1986**, p. 812.
[3] See for example: a) M. E. Thompson, S. M. Baxter, A. R. Bulls, B. J. Burger, M. C. Nolan, B. D. Santarsiero, W. P. Schaefer, J. E. Bercaw, *J. Am. Chem. Soc.* **1987**, *109*, 203–219; b) B. M. Trost, C. Chan, G. Ruhter, *ibid.* **1987**, *109*, 3486–3487; c) W. T. Boese, A. S. Goldman, *Organometallics* **1991**, *10*, 782–786; d) H. J. Heeres, J. H. Teuben, *ibid.* **1991**, *10*, 1980–1986; e) A. D. Horton, *J. Chem. Soc. Chem. Commun.* **1992**, 185–187.
[4] a) J. Barluenga, J. M. González, M. A. Rodríguez, P. J. Campos, G. Asensio, *Synthesis* **1987**, 661–662; b) A. Ricci, M. Taddei, P. Dembech, A. Guerrini, G. Seconi, *ibid.* **1989**, 461–463.
[5] a) For a study on the reactivity of Ipy_2BF_4 towards alkynes in the presence of nucleophiles see: J. Barluenga, M. A. Rodríguez, P. J. Campos, *J. Org. Chem.* **1990**, *55*, 3104–3106; b) A recent report: J. Barluenga, J. M. González, M. A. García-Martín, P. J. Campos, G. Asensio, *J. Chem. Soc. Chem. Commun.* **1992**, 1016–1017.
[6] J. Barluenga, J. M. González, P. J. Campos, G. Asensio, *Angew. Chem.* **1988**, *100*, 1604–1605; *Angew. Chem. Int. Ed. Engl.* **1988**, *27*, 1546–1547.
[7] HBF_4 was used as a 54% ethereal solution, which is commercially available from Merck. The acid protonates the two pyridine units, liberating "electrophilic iodine". Nucleophilic incorporation of pyridine into the substrate is thus avoided.
[8] Mixtures of the ketones $ArCOCHI_2$ and $ArCOCH_2I$ (Ar = aryl) are obtained. The longer the delay in performing the analysis, the higher the proportion of the latter ketone. Among other spectroscopic data, α,α-diiodo- and α-iodoketones have distinctive features in their ^1H NMR spectra. Monoiodo derivatives (CH_2I) show a singlet at $\delta \approx 4.3$, the corresponding diiodo derivatives (CHI_2) at $\delta \approx 6.5$.
[9] Concerning the functionality in the final products, two synthetic aspects deserve special attention. First, their potential applicability to the preparation of radialenes; see: H. Hopf, G. Maas, *Angew. Chem.* **1992**, *104*, 953–977; *Angew. Chem. Int. Ed. Engl.* **1992**, *31*, 931–954. Second, their usefulness in the preparation of unsaturated compounds having a high carbon content and a low hydrogen content; see, for instance, F. Diederich, Y. Rubin, *Angew. Chem.* **1992**, *104*, 1123–1145; *Angew. Chem. Int. Ed. Engl.* **1992**, *31*, 1101–1123. A. M. Boldi, J. Anthony, C. B. Knobler, F. Diederich, *ibid.* **1992**, *104*, 1270–1273 and **1992**, *31*, 1240–1242.

Ion-Spray Mass Spectrometry and High-Performance Liquid Chromatography—Mass Spectrometry of Synthetic Peptide Libraries**

By *Jörg W. Metzger, Karl-Heinz Wiesmüller, Volker Gnau, Jente Brünjes*, and *Günther Jung**

Dedicated to Professor Theodor Wieland on the occasion of his 80th birthday

Synthetic peptide libraries are composed of equimolar mixtures of immobilized or free peptides with defined length and sequence motifs which are gaining increasing interest for the screening for new lead structures (e.g. for antibiotics and enzyme inhibitors) and the investigation of ligand–receptor interactions.[1] Novel analytical tools are required for optimization of the synthesis and characterization of such complex mixtures.[2] In order to evaluate the potency of ion-spray (IS) mass spectrometry[3] for this purpose, we investigated a representative peptide library of 100 synthetic 48-component mixtures of octapeptides **1** (O defined, X un-

$$O_1O_2O_3O_4O_5X_1X_2X_3 \quad \mathbf{1}$$

defined positions, see Experimental Procedure) exhibiting the murine major histocompatibility complex (MHC) class I H2-K^b restricted sequence motif.[4] In addition, a second more complex library consisting of 24 576 nonapeptides **2**

$$X_1 - X_6OX_7X_8 \quad \mathbf{2}$$

representing the binding motif of the nonclassical murine MHC class I complex Qa-2^a[5] was analyzed. Such synthetic peptide mixtures resemble the isolated natural mixtures with defined length and "anchor amino acids" in defined positions.[4–6] These natural peptides originate from proteins processed within the cell and are presented in the MHC groove to cytotoxic T lymphocytes (CTL).[4, 7] Virus-specific CTL kill cells after recognition of MHC-bound foreign peptides processed, for example, from viral proteins.[8]

Peptides **1** and **2** were synthesized by solid-phase peptide synthesis on a multiple peptide synthesizer using Fmoc chemistry.[1, 6] The peptide mixtures **1** and **2** were obtained by treatment of the respective resins with trifluoroacetic acid followed by precipitation from diethyl ether. The monoisotopic relative molecular masses (RMM) of the 48 peptides **1** range between 1011.6 (octapeptide LNYRFSNV) and 1099.5 (octapeptide LNYRFEKM). Only 17 different mass values were obtained for these 48 peptides, since several peptides of the mixture are isobaric, that is, they have an identical molecular mass (± 0.1 u). As many as eight peptides (LNYRFTNL, LNYRFTNI, LNYRFSKL, LNYRFSQI, LNYRFSKI, LNYRFTQV, LNYRFTKV and LNYRFSQL) of this mixture, for example, have a RMM of 1039.6. The IS mass spectrum of **1** shows two groups of peaks with m/z values that correspond to the singly protonated molecular ions $[M + H]^+$ (m/z 1012.6–1100.5) and doubly proton-

[*] Prof. Dr. G. Jung, Dr. J. W. Metzger, Dr. K.-H. Wiesmüller, Dipl.-Chem. V. Gnau, Dipl.-Biol. J. Brünjes
Institut für Organische Chemie der Universität
Auf der Morgenstelle 18, D-W-7400 Tübingen (FRG)

[**] This work was supported by the Deutsche Forschungsgemeinschaft (SFB 323, Teilprojekt C-3 Metzger and Landesforschungsschwerpunkt Teilprojekt Jung).

ated molecular ions $[M + 2H]^{2+}$ (m/z 506.8–550.8) of the individual peptides (the region of the singly charged ions is depicted in Fig. 1). Multiple charges result from the protona-

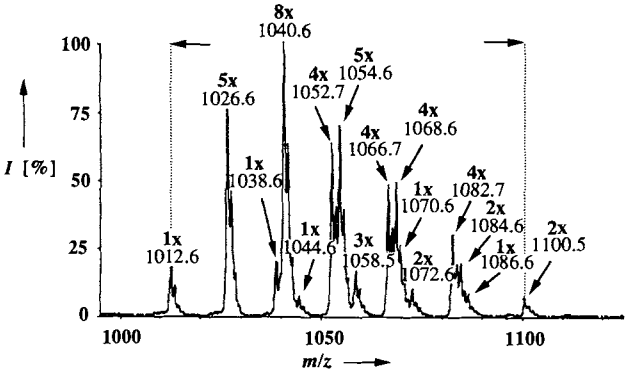

Fig. 1. IS mass spectrum of the 48-component peptide mixture **1** showing the region of the singly charged quasi-molecular ions (the m/z values of the smallest and largest peptides of the mixture are indicated by vertical dashed lines; peaks are labeled with the m/z value and the number isobaric peptides corresponding to this mass).

tion of the basic centers of the peptides.[9, 10] All peptides **1** contain at least two basic centers, the free N-terminus and the arginyl residue at position 4. Sixteen peptides of **1** have an additional positive charge located at the lysyl residue at position 7. Triply charged ions $[M + 3H]^{3+}$ of these peptides are observed between m/z 338.2 and 367.5. All m/z values expected for the $[M + H]^+$ ions of **1** can be found in the mass spectrum (Fig. 1). The absence of additional peaks in the mass spectrum is a strong hint that the mixture is free of possible by-products such as deletion peptides (masses lower than expected) and peptides containing noncleaved protecting groups (masses higher than expected).

Despite possible MS-related discrimination effects (e.g. due to the different basicity and hydrophilicity of the peptides) and the distribution of ion intensities to several charge states, the intensity distribution of the $[M + H]^+$ ions seems to reflect the number of isobaric peptides (Fig. 1) in the mixture.

Side products in peptide synthesis are easily detected by IS mass spectrometry and high-performance liquid chromatography combined with IS (HPLC-IS) mass spectrometry.[11, 12] In contrast to HPLC-UV detection, HPLC-IS mass spectrometry is capable of revealing the presence of

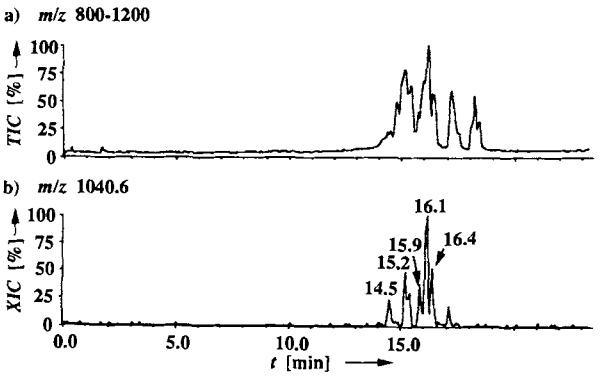

Fig. 2. HPLC-IS mass spectrum of **1**. a) Reconstructed total ion chromatogram (m/z 800–1200) and b) ion chromatogram of m/z 1040.6 corresponding to the monoisotopic $[M + H]^+$ ions of eight isobaric peptides of the mixture (TIC: total ion current; XIC: extracted ion current).

two or more peptides eluting at the same time. We used this on-line technique to confirm the presence of isobaric peptides in **1**. Mixture **1** was subjected to narrow-bore reversed-phase HPLC-IS mass spectrometry. After the gradient was optimized, the 48 peptides could be partially separated (see reconstructed total ion chromatogram; Fig. 2a). The ion chromatogram of m/z 1040.6 corresponding to the monoisotopic $[M + H]^+$ ions of eight different peptides shows five major peaks and indicates that three peptides coelute with other peptides with RMM 1039.6 (Fig. 2b). The mass spectra in the maxima of the five major peaks in the ion chromatogram of m/z 1040.6 show not only this ion but also further ions revealing other coeluting peptides (Fig. 3). Se-

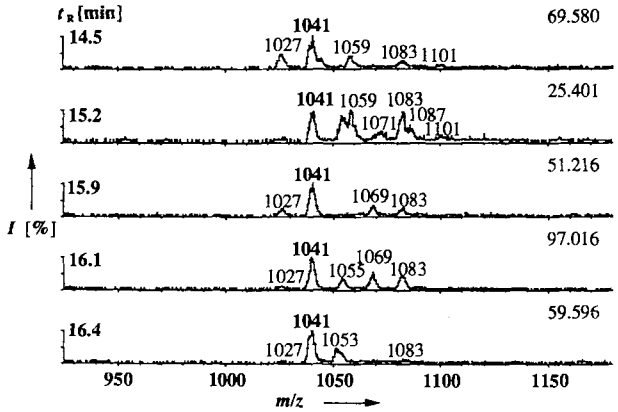

Fig. 3. IS mass spectra obtained in the peak maxima of the major peaks of the ion chromatogram of m/z 1040.6 (see Fig. 2b; t_R: retention time).

quence information on single peptides of **1** was obtained by tandem mass spectrometry (low-energy collison-induced dissociation).[13] When other isobaric peptides were present, on-line HPLC-MS/MS was used (data not shown).

Not only small peptide libraries can be analyzed by IS mass spectrometry. The IS mass spectrum of the 24576 nonapeptides of **2** (Fig. 4a) is very similar to the spectrum of the 48-component mixture **1** (cf. Fig. 1). Distinct peak groups corresponding to the singly protonated molecular ions are evident. The dashed vertical lines in the spectrum represent the m/z values expected for $[M + H]^+$ of the smallest (m/z 977.6, AITPVIHNI and corresponding isobaric peptides) and largest peptides (m/z 1179.5, EMNEIMHEF and corresponding isobaric peptides) of this mixture.

The number of isobaric peptides of **2** was calculated with a computer program and plotted versus the monoisotopic masses calculated for $[M + H]^+$ of these peptides (Fig. 4b). This representation is very similar to the IS mass spectrum of **2** (Fig. 4a). As in the case of the 48-component mixture, the observed intensity distribution of $[M + H]^+$ roughly reflects the number of isobaric peptides (see above) and therefore gives further information on the constituents of this mixture. A more detailed investigation of these quantitative aspects with defined mixtures of single purified peptides is in progress.

In summary, IS mass spectrometry alone or in combination with HPLC is a valuable tool for estimating the identity (for example the differentiation between hexa- and octapeptide libraries), composition, and purity of small and larger peptide mixtures. More detailed characterization of single peptides (i.e. sequence information) is possible only with mixtures consisting of a small number of peptides. According to our limited and preliminary experience with peptide

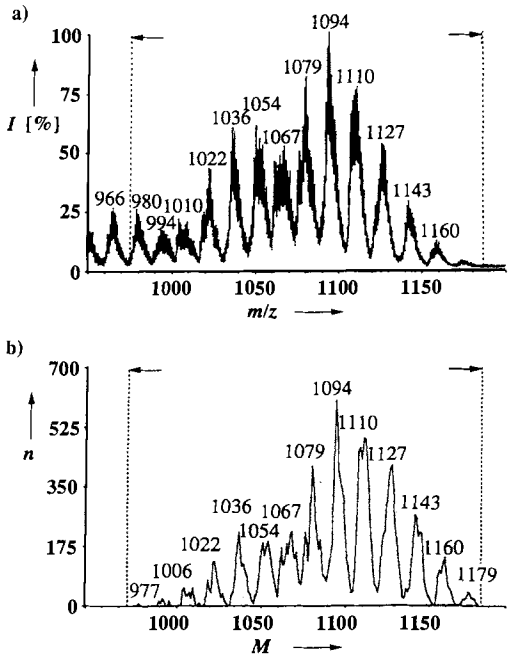

Fig. 4. a) IS mass spectrum of the synthetic nonapeptide library **2** consisting of 24575 components (region of the singly charged quasi-molecular ions; vertical dashed lines indicate calculated masses for the smallest and largest peptides of the mixture). b) Calculated number of isobaric peptides n of **2** vs. the monoisotopic molecular mass M of $[M + H]^+$ ions.

libraries in bio-assays, however, the construction of huge libraries seems to have restricted application.

Experimental Procedure

Peptide synthesis. The synthesis of 100 mixtures of octapeptides **1** (defined positions O_1: R,I,L,S,A; O_2: N; O_3: Y,P; O_4: R,D,E,K,T; O_5: F,Y; undefined positions X_1: T,I,E,S; X_2: N,Q,K and X_3: L,M,I,V) was performed by using premixed Fmoc-X_3-Wang resins (*p*-benzyloxybenzylalcohol–polystyrene cross-linked with 1% divinylbenzene) and the Fmoc/*t*Bu strategy. The moist resins were divided into equivalent amounts and coupled with amino acids X_2. The Fmoc protecting groups were removed and the resin-bound amino acids coupled with amino acids X_1. The amino acids were used in threefold excess; TBTU (*O*-benzotriazol-1-yl-*N*,*N*,*N*′,*N*′-tetramethyluronium tetrafluoroborate) was used for activation. Aliquots of the Fmoc–$X_1X_2X_3$ resin mixture were elongated to octapeptide mixtures on a multiple peptide synthesizer (SMPS 350, Zinsser Analytic, Frankfurt, FRG) (see ref. [1]). After cleavage of the peptide mixtures from the resins (trifluoroacetic acid/thioanisole/thiocresol 190:5:5, v:v:v) the synthetic 48-component mixture LNYRF$X_1X_2X_3$ was selected for mass spectrometric analysis.

Identical procedures were used for the synthesis and cleavage of the nonapeptide library **2** (defined position O: H; undefined positions X_1: A,E,K,Q; X_2: M,I,L,Q; X_3: L,I,N,T; X_4: D,E,K,P; X_5: V,I; X_6: M,I,L,K; X_7: E,Q,N,K; X_8: L,I,F.

IS mass spectrometry: Samples of the synthetic peptide mixtures (ca. 100 μg) were dissolved in methanol/1% formic acid (1:1, 1 mL). IS mass spectra were recorded on a triple-quadrupole mass spectrometer API III equipped with an ion-spray (nebulizer-assisted electrospray) source (Sciex, Thornhill, Ontario, Canada). The solutions were continuously infused with a medical infusion pump (Model 22, Harvard Apparatus, South Natick, USA) at a flow rate of 5 μL min^{-1}. Cesium iodide was used to calibrate quadrupoles Q_1 and Q_3. IS mass spectra were acquired at unit resolution by scanning from m/z 800 to 1200 with a step size of 0.1 Da and a dwell time of 10 ms. Five to eight spectra were summed. The potential of the spray needle was held at +4.9 kV. Spectra containing singly, doubly, and triply charged quasi-molecular ions were recorded at an orifice voltage of +60 V. A higher orifice voltage of +120 V was chosen to enhance the intensity of $[M + H]^+$ and to suppress the formation of multiply charged ions. The mass values above the (not centroided) mass peaks in the mass spectra (Figs. 1–4) correspond to the observed peak maxima. The observed intensities for the monoisotopic $[M + H]^+$ ions (calculated with C = 12.000) are higher than for the isotopic ^{13}C ions, which is in agreement with the natural isotope distribution calculated for the molecular peaks of the investigated peptides. Accuracy of mass assignment was ±0.1 u. Tandem mass spectrometry (collision-induced dissociation) was performed with argon as collision gas.

For on-line HPLC-MS an Applied Biosystems ABI 140A HPLC system and a narrow-bore column (Nucleosil C-18, 2 × 100 mm; 5 μm; Grom, Herrenberg, FRG) equipped with a precolumn (2 × 10 mm; same filling) at a flow rate of 200 μL min^{-1} were used. A linear gradient of 5 to 20% solvent B in 40 min was used (solvent A: 0.1% aqueous trifluoroacetic acid; solvent B: 0.1% trifluoroacetic acid in acetonitrile). The flow was split so that 40 μL min^{-1} entered the IS interface. A solution of 500 pmol of **1** in 5 μL of water was injected.

Computer program: A program for calculation of the molecular masses of the peptides and the number of isobaric peptides in libraries was designed, which generated all possible permutations within the peptide sequences as defined by the variable positions. The mass distribution was approximated by counting the number of different peptides within one atomic mass unit. In order to assist assignment of additional mass peaks in the IS mass spectrum corresponding to by-products, the expected masses for uncleaved protecting groups or deletion peptides can be calculated and displayed, too.

Received: September 17, 1992
Revised version: January 26, 1993 [Z 5723 IE]
German version: *Angew. Chem.* **1993**, *105*, 901

[1] G. Jung, A. G. Beck-Sickinger, *Angew. Chem.* **1992**, *104*, 375–391; *Angew. Chem. Int. Ed. Engl.* **1992**, *31*, 367–383.
[2] J. W. Metzger, K.-H. Wiesmüller, S. Stevanović, G. Jung in *Peptides 1992 (Proc. 22nd Eur. Pept. Symp. Interlaken, Schweiz, 1992)* (Eds.: C. Schneider, A. Eberle), Escom, Leiden, **1993**.
[3] A. P. Bruins, T. R. Covey, J. D. Henion, *Anal. Chem.* **1987**, *59*, 2642–2646.
[4] K. Falk, O. Rötzschke, S. Stevanović, G. Jung, H.-G. Rammensee, *Nature* **1991**, *351*, 290–296.
[5] O. Rötzschke, K. Falk, S. Stevanović, B. Grahovac, M. J. Soloski, G. Jung, H.-G. Rammensee, *Nature* **1993**, *361*, 642–644.
[6] S. Stevanović, K.-H. Wiesmüller, J. W. Metzger, A. G. Beck-Sickinger, G. Jung, *Bioorg. Med. Chem. Lett.* **1993**, *3*, 431–436.
[7] N. Zimmermann, O. Rötzschke, K. Falk, D. Rognan, G. Folkers, H.-G. Rammensee, G. Jung, *Angew. Chem.* **1992**, *104*, 928–931; *Angew. Chem. Int. Ed. Engl.* **1992**, *31*, 886–890.
[8] A. Townsend, H. Bodmer, *Annu. Rev. Immunol.* **1989**, *354*, 601–624.
[9] T. R. Covey, R. F. Bonner, B. I. Shushan, J. Henion, *Rapid Commun. Mass. Spectrom.* **1988**, *2*, 249–256.
[10] R. D. Smith, J. A. Loo, C. G. Edmonds, C. J. Barinaga, H. R. Udseth, *Anal. Chem.* **1990**, *62*, 882–899.
[11] A. Beck-Sickinger, G. Schnorrenberg, J. Metzger, G. Jung, *Int. J. Peptide Protein Res.* **1991**, *38*, 25–31.
[12] H. Dürr, A. G. Beck-Sickinger, G. Schnorrenberg, W. Rapp, G. Jung, *Int. J. Peptide Protein Res.* **1991**, *38*, 146–153.
[13] D. F. Hunt, J. R. Yates, J. Shabanowitz, S. Winston, C. R. Hauer, *Proc. Natl. Acad. Sci. USA* **1986**, *83*, 6233–6237.

$[P(MeNCH_2CH_2)_3N]$ as a Superior Catalyst for the Conversion of Isocyanates to Isocyanurates

By *Jian-Sheng Tang* and *John G. Verkade**

Triaryl isocyanurates are useful as activators for the continuous anionic polymerization and postpolymerization of ε-caprolactam to nylon-6 possessing a low unreacted monomer content and a highly stable melt viscosity.[1] Recently the superior thermal properties and hydrolytic stability of isocyanurate-based foams and plastics have generated considerable interest in the development of efficient isocyanate trimerization catalysts.[2] A wide variety of catalysts for the trimerization of aryl isocyanates to triaryl isocyanurates has been reported.[1, 3] Because impure triaryl isocyanurates are detrimental to the quality of nylon-6, much attention has been given to obtaining such activators in high purity.[1a] However, purification often results in substantial lowering of product yield, and attempts to increase the yield of trimer frequently require large amounts of catalyst, ex-

[*] Prof. J. G. Verkade, J.-S. Tang
Department of Chemistry, Iowa State University
Ames, IA 50011 (USA)
Telefax: Int. code + (515)294-0105

[**] This work was supported by the National Science Foundation.

tended reaction times, and vigorous conditions. Here we report on the superior properties of **1** as a unique catalyst for the trimerization of aryl isocyanates, and we present evidence for the catalytic pathway.

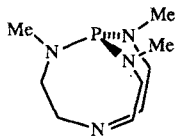

1

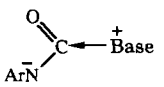

2

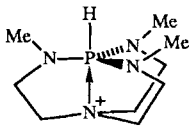

3

Because reported catalysts for the trimerization of isocyanates are typically Lewis bases, it has been proposed that their activity depends upon their basicity[4] and/or upon the stability of zwitterionic intermediates such as **2**.[3c, d] This suggests that a strong base capable of forming a stable zwitterionic intermediate could function as an efficient catalyst for the trimerization of aryl isocyanates. Recently we reported that **1** is an exceptionally strong base whose conjugate acid **3** has a pK_a of about 27 in DMSO,[5, 6] and that zwitterionic adducts such as **4** and **5** can be isolated.[7] The partial transannular bond in **4** was verified by an X-ray structure determination; the transannular distance between the bridgehead atoms in **4** (3.008 Å[7]) is intermediate between that presumed in **1** (ca. 3.35 Å[8]) and that measured in cation **3** (1.967 Å[7]). This distance in **4** is about 0.3 Å longer than that in its methylated derivative **6** (2.771 Å[7]), suggesting that the corresponding distance in **5** (ca. 2.5 Å; suitable crystals for X-ray crystallography could not be grown) is probably longer than in **7** (2.190 Å[7]).

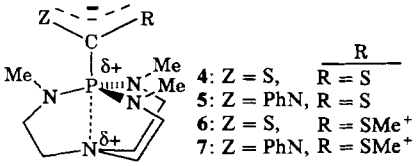

4: Z = S, R = S
5: Z = PhN, R = S
6: Z = S, R = SMe^+
7: Z = PhN, R = SMe^+

Trimers **8** and **9** can be synthesized in pure form (purity checked by thin-layer chromatography (TLC)) from the corresponding aryl isocyanates in respective yields of 97 and 99% and respective reaction times of 3 and 8 min at room temperature with only 0.33 mol% **1** as catalyst. By contrast, $P(NMe_2)_3$, an acyclic analogue of **1**, produces only a small yield of the cyclic dimer of phenyl isocyanate, even over an extended period of time. Catalyst **1** is also superior in comparison with the other catalysts previously described. Thus, for example, the conversion of phenyl isocyanate with Et_3N as a catalyst was reported to be complete at 100 °C but required 10% catalyst and a pressure of 800 MPa for 20 h;[3a, b] the reaction with $AsBu_3$ proceeded in 18 to 99% yield over 12–34 min, but the reaction is very sensitive to temperature.[3f] Moreover, criteria of purity were not addressed. While **1** is very soluble in organic solvents, benzene is best if a solvent is used for the reaction because the reagents are soluble and the product is insoluble. Thus simply washing the product with benzene provides **8** or **9**, pure by TLC, in nearly quantitative yield.

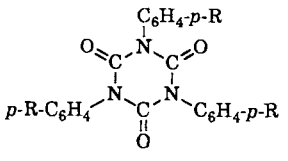

8: R = H
9: R = OMe

An electron-donating group on the aryl substituent of aryl isocyanates renders the carbonyl carbon atom less electrophilic, and hence makes trimerization more difficult, as has been shown for *p*-MeC_6H_4NCO.[3c, d] With **1** as the catalyst, we find that even a substrate with a *para*-methoxy substituent on the aryl ring can be trimerized in 99% yield upon extension of the reaction time to 8 min.

The reaction pathway shown in Scheme 1 is analogous to those proposed previously[3c, d, h] for other catalysts, although none of the zwitterionic catalyst–arylisocyanate adduct intermediates were detected previously. In our reaction with PhNCO with **1** as a catalyst, however, we observe a transient peak in the ^{31}P NMR spectrum (in C_6D_6) at $\delta = 29.46$ and a peak in the FAB mass spectrum at m/z 336.1 ($M + H$) for an isolated solid apparently containing an intermediate. With *p*-$MeOC_6H_4NCO$ a corresponding ^{31}P NMR signal is seen at $\delta = 29.23$ in C_6D_6. It is tempting to attribute these data in both cases to the corresponding intermediates **10**. The stability of adduct **5** (the sulfur analogue of **10**) to further reaction with PhNCS[7] can be ascribed to the diminished nucleophilicity of the PhN nitrogen atom and reduced electrophilicity of the PhNC carbon atom, induced by the less electronegative sulfur atom.

In the cyclodimerization of PhNCO, the equilibrium is reported to lie on the side of the starting material at higher temperatures,[9] and trimer formation is reported to be thermodynamically allowed from 0 to 850 K.[10] Thus the dimer/trimer ratio decreases with increasing temperature in the presence of the (weak) catalyst $P(NMe_2)_3$.[11] The much stronger catalytic action of **1** may be attributed to its substantial stabilizing influence on adducts **10** and **11** (Scheme 1), and particularly on **11**, which enables this adduct to nucleophilically attack the third ArNCO molecule.

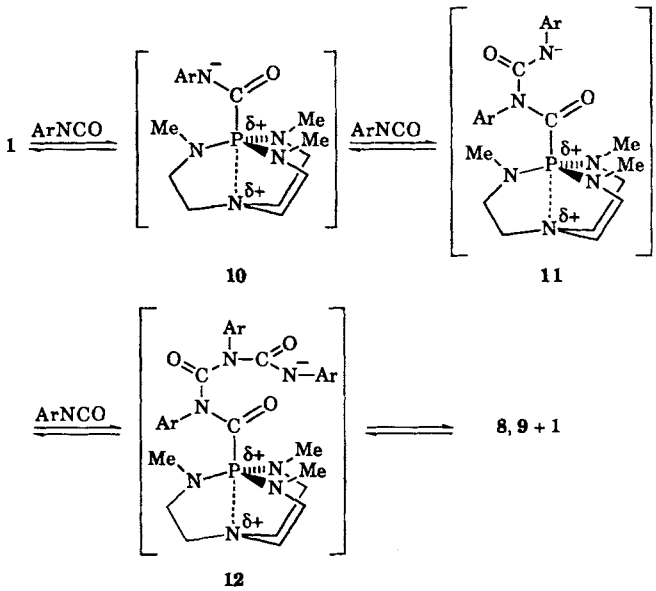

Scheme 1. Reaction pathway for the trimerization of ArNCO catalyzed by **1**.

The basicity of the nucleophilic nitrogen atom in **11** is undoubtedly enhanced by induction effects from the bridgehead nitrogen atom in the quasi- transannular bond shown to exist, for example, in **4**, **6**, and **7**.[7] It is reasonable to suppose that when intermediate **12** undergoes ring closure to

give the trimer, the resulting increased electron density on the PC carbon atom weakens the transannular bond, thereby facilitating departure of trimer and regeneration of the catalyst **1**, in which the transannular interaction is weakest.[7, 8] Strong support for the postulated flexibility of the transannular interaction in **1** (depending upon the phosphorus substituent) is the stepwise reduction of this distance over a series of eight compounds from 3.33 Å (which is essentially the sum of the P and N covalent radii) to 1.967 Å.[7]

Experimental Procedure

To a one-necked round-bottomed flask (250 mL, filled with N_2 and closed with a septum) containing a solution of **1** (0.11 g, 0.50 mmol) in dry benzene (10 mL) was added by syringe phenyl isocyanate (18.0 g, 99% pure, 150 mmol, Aldrich). After the mixture was stirred at room temperature for 3 min, the white precipitate that had very rapidly formed solidified into a mass within a few seconds. The solid was cooled to room temperature, dried under vacuum, ground to powder, stirred with 30 mL of dry benzene for 2 h, filtered in vacuo, washed again with 15 mL of dry benzene, and finally dried in vacuo to give 17.2 g (96.6%) of **8** (pure by ^{1}H NMR spectroscopy and TLC (silica gel, hexane:ether = 2:1, or $CHCl_3$, or $CHCl_3$:acetone = 50:1 as eluents)). M.p. (uncorrected) 279.0–279.5 °C (lit. 281–281.5 °C[1b]); ^{1}H NMR ($CDCl_3$): δ = 7.35–7.51 (m, C_6H_5); ^{13}C NMR (CD_3CN): δ = 128.21, 128.74, 129.16, 133.39, 148.46; HRMS (*m/z*): calcd and found for $C_{21}H_{15}N_3O_3$ 357.11134 (54, M^+); correct C,H,N-analysis.

The analogous reaction with *p*-$MeOC_6H_4NCO$ carried out over 8 min gave a 98.7% yield of **9** (pure by ^{1}H NMR spectroscopy and TLC (silica gel, same solvent systems as used for **8**)) after the product was washed with benzene (80 mL) and dried in vacuo at 50 °C. M.p. (uncorrected): 261.0–261.5 °C (lit. 261–2 °C[1b]); ^{1}H NMR ($CDCl_3$): δ = 3.81 (s, 9H, OCH_3), 6.96 (d, 4H, C_6H_4; $^3J_{HH}$ = 8.7 Hz), 6.27 (d, 4H, C_6H_4; $^3J_{HH}$ = 8.7 Hz); HRMS (*m/z*): calcd for $C_{24}H_{21}N_3O_6$, 447.14304. Found, 447.14358 (50, M^+).

To detect intermediates by ^{31}P NMR spectroscopy the reaction was carried out with 0.037 g (0.17 mmol) of **1** and 0.062 g (0.52 mmol) of PhNCO in 0.7 mL of C_6D_6, and with 0.057 g (0.26 mmol) of **1** and 0.094 g (0.79 mmol) of *p*-$MeOC_6H_4NCO$ in 0.7 mL of C_6D_6. When 0.08 g (0.7 mmol) of PhNCO was added by syringe to a solution of 0.1 g (0.5 mmol) of **1** in ether (10 mL), a colorless solid precipitated which was dried in vacuo to give 0.14 g of a colorless solid. ^{31}P NMR (CD_3CN): δ = 31.11, −9.35; MS (*m/z*, FAB): 336.1 (M + H, 10, 52) and 217.1 (M + H, 1, 100).

The analogous reaction with $P(NMe_2)_3$ (0.17 g, 1.0 mmol) was carried out in 45 mL of dry benzene with 11.9 g (0.10 mol) of PhNCO. The reaction mixture was heated at 60–70 °C for 5 d at 60–70 °C then left at room temperature for 10 h, whereupon a small amount of white precipitate appeared. The volatiles were removed under vacuum, the residue was stirred with 5 mL of benzene, and then the suspension was filtered, washed with acetonitrile (5 × 2 mL), and dried to give 0.48 g (4%) of cyclic dimer. M.p. 182–183 °C (lit. 175 °C[10]); ^{1}H NMR (CD_3CN): δ = 7.4–7.5 (m); HRMS (*m/z*): calcd for $C_{14}H_{10}N_2O_2$, 238.07423. Found, 238.07428 (3.5, M^+).

Received: December 30, 1992 [Z 57841E]
German version: *Angew. Chem.* **1993**, *105*, 934

[1] a) Z. Bukac, J. Sebenda (Ustav Makromol. Chem., CSAV Prag), CS-A 227247, **1985** (*Chem. Abstr.* **1986**, *105*, 173224r); b) *Chem. Prum.* **1985**, *35*, 361 (*Chem. Abstr.* **1984**, *103*, 123978c); c) J. Horsky, U. Kubanek, J. Marick, J. Kralicek, *ibid.* **1982**, *32*, 599 and (**1983**, *98*, 5459q).

[2] a) H. Ulrich, *J. Cell. Plast.* **1981**, *17*, 31; b) P. I. Kordemenas, J. E. Kresta, *Macromolecules* **1981**, *14*, 1434; c) D. K. Hoffmann, *J. Cell. Plast.* **1984**, *20*, 129.

[3] a) Y. Taguchi, I. Shubuya, M. Yasumoto, T. Tsuchiya, K. Yonemoto, *Bull. Chem. Soc. Jpn.* **1990**, *63*, 3486; b) Y. Taguchi, I. Shibuya (Agency of Industrial Sciences and Technology), HP-A 03109382, **1991** (*Chem. Abstr.* **1991**, *115*, 208022j); c) J. Mizuya, T. Yokozawa, T. Endo, *J. Polym. Sci. Part A Polym. Chem.* **1991**, *29*, 1545; d) T. Endo, J. Suike (Arokawa Chemical Industries, Ltd.), JP-A 01226878, **1989** (*Chem. Abstr.* **1990**, *112*, 77236v); e) K. Ashide (BP Chemicals Ltd.), EP-A 169708, **1986** (*Chem. Abstr.* **1987**, *107*, 134825j); f) F. R. Gubaidullin, M. I. Bakhitov, L. Sh. Zainutdinova, F. L. Kligman, R. G. Miftakhova (Kazan Chemical-Technological Institute), *SU-A* 1555328, **1990** (*Chem. Abstr.* **1990**, *113*, 78425p); g) D. Kermis, H. P. Mueller (Bayer AG), DE-A 3543925, **1987** (*Chem. Abstr.* **1987**, *107*, 176705a); h) W. Broda, E. V. Dehmlow, H.-J. Schulz, *Isr. J. Chem.* **1985**, *26*, 222; i) T. Endo, Y. Nambu (Asahi, Denka Kogyo, K. K.), EP-A 447074, **1991** (*Chem. Abstr.* **1992**, *116*, 41486v); j) H. J. Fabris, E. M. Mexey, H. Uelzmann (General Tire and Rubber Co.), US-A 3980594, **1976** (*Chem. Abstr.* **1976**, *85*, 193324v); k) E. A. Barsa, C. Conn (Upjohn Co.), US-A 4540781, **1985** (*Chem. Abstr.* **1985**, *104*, 89741d); l) I. Wakishima, Z. Kijima, *Bull. Chem. Soc. Jpn.* **1975**, *48*, 953; m) R. J. P. Corriu, G. f. Lanneau, V. D. Mehta, *Heteroatom Chem.* **1991**, *2*, 46; n) R. Richter, P. Müller, K. Wagner, *Angew. Makromol. Chem.* **1983**, *113*, 1.

[4] S.-W. Wong, K. Frisch, *J. Polym. Sci. Part A Polym. Chem.* **1986**, *24*, 2877.

[5] a) M. A. H. Laramay, J. G. Verkade, *Z. Anorg. Allg. Chem.* **1991**, *605*, 163; b) J. G. Verkade (Iowa State University), US-A 5051533, **1991** (*Chem. Abstr.* **1992**, *116*, 50379q).

[6] W. N. Olmstead, Z. Margolin, F. G. Bordwell, *J. Org. Chem.* **1980**, *45*, 3295. Herein is reported a more reliable value of 32.2 for the pK_a of *t*-BuOH in DMSO, which thus raises the pK_a of **3** to about 30.

[7] J.-S. Tang, M. A. H. Laramay, V. Young, S. Ringrose, R. A. Jacobson, J. G. Verkade, *J. Am. Chem. Soc.* **1992**, *114*, 3129.

[8] S.-K. Xi, H. Schmidt, C. Lensink, S. Kim, D. Wintergrass, L. M. Daniels, R. A. Jacobson, J. G. Verkade, *Inorg. Chem.* **1990**, *29*, 2214.

[9] R. G. Arnold, J. A. Nelson, J. J. Verbanc, *Chem. Rev.* **1957**, *57*, 59.

[10] T. A. Bykova, B. V. Lebedev, E. G. Kipanisova, E. N. Tarasov, T. N. Frenkel, V. A. Pankratov, S. V. Vinogradova, V. V. Korshak, J. Gen. Chem. USSR (*Engl. Transl.*) **1985**, 2303 (*Chem. Abstr.* **1984**, *100*, 86171z).

[11] M. I. Bakhitov, N. K. Emal'yanov, A. I. Tikhonova, I. G. Davletbaev, *Vysokomol. Soedin. Ser. B* **1983**, *25*, 830 (*Chem. Abstr.* **1984**, *100*, 86171z).

The Importance of the Rigidity of the Peptide Backbone for the Inhibitory Properties of BPTI Demonstrated by Semisynthetic Structural Variants**

By *Christian Groeger, Herbert R. Wenzel,* and *Harald Tschesche**

Proteinases play an essential role in metabolic processes. Their antagonists, the protein–proteinase inhibitors, block the action of proteinases in vivo, and this important control function makes them interesting as potential therapeutics.

Rational drug design requires detailed knowledge of all aspects of the mode of action of inhibitors; the results of investigations into the relationship between structure and function of naturally occurring inhibitors are the ideal basis for the development of new synthetic proteins with inhibitory properties.

Many proteinase inhibitors function as substrate analogues; therefore, besides a low dissociation constant of the corresponding enzyme-inhibitor complexes, the resistance to proteolysis (permanence) of the inhibitors against the target enzymes is essential.

In this paper we want to demonstrate with three semisynthetic "backbone" variants of the trypsin-kallikrein inhibitor BPTI (BPTI = basic pancreatic trypsin inhibitor = Kunitz trypsin inhibitor) from bovine organs, that a strong permanent trypsin inhibitor can be converted into a trypsin substrate by minor changes in the peptide backbone.

In contrast to the specificity-determining amino acid $P_1 = Lys^{15}$,[1] the P′ region of BPTI, ($P'_1 = Ala^{16}$, $P'_2 = Arg^{17}$, Fig. 1), can be replaced by a variety of residues without significantly reducing the anti-tryptic activity of the inhibitor.[2, 3] Even the complete removal of the side chains in this region is tolerated. Thus, the dissociation constant of the [Gly^{16},Gly^{17}] BPTI–trypsin complex is 2×10^{-12} M, only one order of magnitude higher than that of the native complex.

Since the influence of the side chains in this region is apparently small, it seemed instructive for further investiga-

[*] Prof. Dr. H. Tschesche, Dipl.-Chem. C. Groeger, Dr. H. R. Wenzel
Lehrstuhl für Biochemie der Universität
Fakultät für Chemie, D-W-4800 Bielefeld 1 (FRG)
Telefax: Int. code + (521)106-6146

[**] This work was supported by the Deutsche Forschungsgemeinschaft (Ts 8/24-2). We thank Werner Beck, Universität Tübingen, for recording the ion-spray mass spectra.

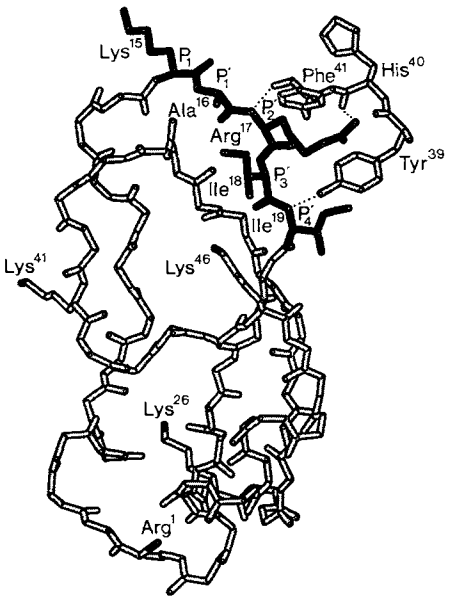

Fig. 1. A projection of the tertiary structure of the BPTI–trypsin complex [6] (section), residues Tyr^{39}, His^{40}, and Phe^{41} belong to trypsin. The P′ strand including side chains and the specificity-determining amino acid Lys^{15} as well as the N terminus and ε-amino groups of BPTI are shown in boldface. The dotted lines represent hydrogen bonds.

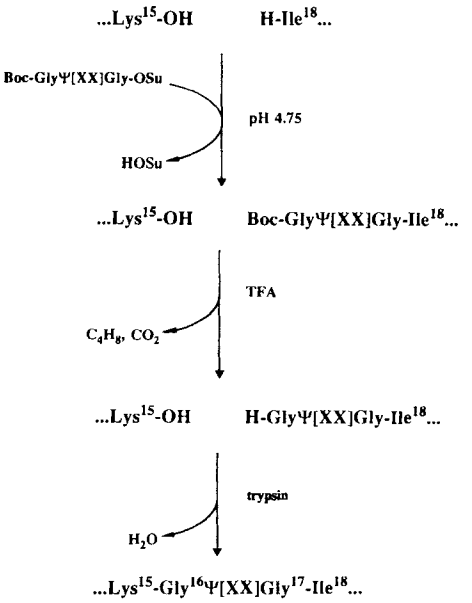

Scheme 1. The exchange of Ala^{16} and Arg^{17} by peptide analogues, (exemplified by a Boc-protected activated ester), starting from de(Ala^{16}-Arg^{17})-[*seco*-15/18]BPTI (XX = CH_2CH_2, CH_2NH, $COCH_2$). TFA = Trifluoroacetic acid.

tions into structure–function relationships to replace positions P′$_1$ and P′$_2$ with a series of peptide analogues derived from glycylglycine (Fig. 2). The introduction of the struc-

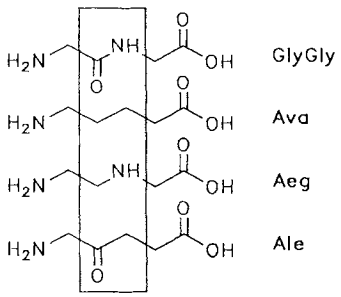

Fig. 2. Peptide analogues derived from glycylglycine. The box indicates the changed amide bond.

turally related building blocks 5-aminovalerianic acid (Ava), *N*-aminoethylglycine (Aeg), and 5-aminolevulinic acid (Ale), into the P′region of the inhibitor results in a complete or partial replacement of the P′$_1$–P′$_2$ amide bond with methylene groups. To introduce the building blocks, the P$_1$–P′$_1$ (Lys^{15}-Ala^{16}) bond in the reactive site of the inhibitor is cleaved with trypsin, and the amino acids Ala^{16} and Arg^{17} are removed with aminopeptidase K. This results in the formation of the inactive fragment de(Ala^{16}-Arg^{17})-[*seco*-15/18]BPTI.[4] The new N terminus at P′$_3$ = Ile^{18} can now be acylated by using the *N*-hydroxysuccinimide ester of Boc-Ava, (Boc = butoxycarbonyl), (Boc)$_2$-Aeg, and Z-Ale (Scheme 1).

Although the inhibitor fragment possesses a total of six potential sites for acylation (two N termini as well as ε-amino groups of four lysine residues, Fig. 1), the reaction can be carried out with a high degree of selectivity by controlling the pH value. For example, at a pH of 4.75, up to 25% of the product is monoacylated at Ile^{18}. After cleavage of the Boc or Z protecting group, the open Lys^{15}, Gly^{16}Ψ[XX]Gly^{17} bond is closed by using trypsin.[5]

Compared with [Gly^{16}-Gly^{17}]BPTI, [Ava$^{16-17}$]BPTI and [Aeg$^{16-17}$]BPTI have proved to be much weaker and, furthermore, temporary trypsin inhibitors; that is, they are degraded by the enzyme. The dissociation constants are about 2×10^{-9} and 7×10^{-9} M, respectively.

In contrast, the inhibitor [Ale$^{16-17}$]BPTI with a dissociation constant of 5×10^{-11} M is a strong and permanent inhibitor of trypsin.

A look at the subsite interactions[6] in the native BPTI–trypsin complex (Fig. 1) shows that the keto function of the P′$_1$–P′$_2$ amide bond is involved in neither intramolecular hydrogen bonds in BPTI nor intermolecular hydrogen bonds between BPTI and the enzyme. The NH group alone serves as donor for a hydrogen bond to the CO unit of Phe^{41} in trypsin and thus should contribute to the stability of the complex. The experiment shows, however, that [Aeg$^{16-17}$]BPTI has a slightly higher dissociation constant than [Ava$^{16-17}$]BPTI.

The good inhibitory properties and especially the resistance of the Ale derivative to breakdown by trypsin must be due to the restricted flexibilty of the bonding loop, because the keto function fixes four atoms in the same plane; the Ale derivative thus possesses some of the rigidity of [Gly^{16}-Gly^{17}]BPTI. A rigid binding region of the inhibitor means easier docking and a lower entropy loss[7] during complexation by the enzyme, which also leads to a higher affinity for the enzyme. At the same time the rigidity of the binding region explains the extremely slow proteolysis of the P$_1$–P′$_1$ peptide bond.[8]

In contrast, a flexible bonding loop, which additionally forms a hydrogen bond to the enzyme in the complexed state (Aeg derivative), leads to a much stronger reduction in degree of freedom than in a reaction with a loop with the same degree of flexibility that cannot form this bond (Ava derivative). Only the combined effects of backbone rigidity and hydrogen bond formation—as in [Gly^{16}-Gly^{17}]BPTI—result in the net energy gain for the complex formation, as shown by the lower dissociation constant of 2×10^{-12} M in contrast to the Ale derivative.

The structural variants of the peptide backbone of BPTI described here show that complementarity in the sense of a

perfect fit between enzyme and inhibitor is not as important as the rigidity of the peptide structure in the binding region. This rigidity is an absolute requirement for the proper function of the inhibitor as a permanent inhibitor.

Experimental Procedure

Ava·HCl was produced by acid hydrolysis of 2-piperidone. Aeg was synthesized from 1,2-diaminoethane and chloroacetic acid according to [9]. Ale·HCl was purchased from Merck. The addition of Boc or Z protecting groups and the esterification with hydroxysuccinimide were carried out according to standard procedures [10]. All derivatives and intermediates were characterized by ^{1}H NMR spectroscopy and mass spectrometry.

A general procedure for the synthesis of BPTI derivatives: De(Ala^{16}-Arg^{17})-[*seco*-15/18]BPTI (25 mg) (preparation see refs.[2,3]) was dissolved in bidistilled water (5 mL) and treated with a 30-fold molar excess of activated ester, dissolved in 1 mL of dioxane or dimethyl sulfoxide. The pH was maintained at 4.75 by addition of NaOH. After 4–5 h the solution was gel filtrated on Sephadex G-25, and the monoacylated product was separated by ion-exchange chromatography on CM Sepharose FF at pH 8.6 (NaCl gradient). The corresponding fractions were desalted on Sephadex G-25, and the protecting groups were cleaved with trifluoroacetic acid (15 min for Boc; 10 h for Z). The acid was removed under vacuum, and the residue taken up with the equivalent amount of bovine trypsin in Tris buffer pH 8. After 10 min the pH was lowered to 1.7 with dilute HCl, and the solution was subjected to gel filtration on Sephadex G-50 at pH 1.7. Finally, the inhibitor-containing fractions were repurified on CM Sepharose FF by ion-exchange chromatography, desalted on Sephadex G-25, and lyophilized. Yield: 0.5–2.5 mg, 2–10%. Ion-spray mass spectra of the synthesized inhibitor variants gave the expected molecular weights. The identity of the Aeg derivative was also confirmed by complete sequencing with the Edman degradation method. [Gly^{16}-Gly^{17}]BPTI was synthesized as described in [3].

Received: January 18, 1993 [Z 5838 IE]
German version: *Angew. Chem.* **1993**, *105*, 948

[1] H. Tschesche, *Angew. Chem.* **1974**, *86*, 21–40; *Angew. Chem. Int. Ed. Engl.* **1974**, *13*, 10–28.
[2] C. Groeger, H. R. Wenzel, H. Tschesche, *J. Protein Chem.* **1991**, *10*, 245–251.
[3] C. Groeger, H. R. Wenzel, H. Tschesche, *J. Protein Chem.* **1991**, *10*, 527–532.
[4] H. Jering, H. Tschesche, *Eur. J. Biochem.* **1976**, *61*, 453–463.
[5] U. Quast, J. Engel, E. Steffen, H. Tschesche, *Biochemistry* **1978**, *17*, 1675–1682.
[6] R. Huber, D. Kukla, W. Bode, P. Schwager, K. Bartels, J. Deisenhofer, W. Steigemann, *J. Mol. Biol.* **1974**, *89*, 73–101.
[7] R. J. Read, M. N. G. James in *Proteinase Inhibitors* (Eds.: A. J. Barrett, G. Salvesen), Elsevier, Amsterdam, **1986**, p. 323.
[8] W. R. Finkenstadt, M. A. Hamid, J. A. Mattis, J. Schrode, R. W. Sealock, D. Wang, M. Laskowski in *Bayer Symposium V. Proteinase Inhibitors* (Eds.: H. Fritz, H. Tschesche, L. J. Greene, E. Truscheit), Springer, Berlin, **1974**, S. 389–411.
[9] E. P. Heimer, H. E. Gallo-Torres, A. M. Felix, M. A. Ahmad, T. J. Lambros, F. Scheidl, J. Meienhofer, *Int. J. Peptide Protein Res.* **1984**, *23*, 203–211.
[10] M. Bodanszky, A. Bodanszky, *The Practice of Peptide Synthesis*, 1st ed., Springer, Berlin, **1984**, p. 12, 20, 125.

Synthesis and Complexation Studies of Neutral Anion Receptors

By *Suresh Valiyaveettil, Johan F. J. Engbersen, Willem Verboom*, and *David N. Reinhoudt**

The design and synthesis of receptor molecules for the selective complexation of ions has attracted much attention during the past two decades.[1] However, the number of host molecules for anions is very low compared to the number for cations. The reported host molecules contain either positively charged sites[2] or Lewis acid metal centers[3] to accomplish anion binding.[4]

In nature, the selective ion flow to and from the cell is regulated by ion-binding proteins that act as ion carriers and channels across the cell membrane. Quiocho et al.[5] have shown that the high specificity of phosphate transport by proteins is determined by extensive hydrogen bonding in the binding site. The phosphate binding site is formed by two similarly folded globular protein domains and is located in a cleft approximately 8 Å inside from the protein surface. Phosphate binding involves the formation of twelve hydrogen bonds, five from the main chain and seven from the side-chain residues.[5a]

In our attempts to mimic nature in the recognition of anions by the formation of multiple hydrogen bonds in three-dimensional arrangements, we have designed a new series of ligands with hydrogen-bond donor as well as acceptor sites. This strategy was based on the known structures of phosphate binding sites of proteins. In this communication we demonstrate that surprisingly strong anion binding can be achieved with relatively simple, neutral host molecules in which the H-bond donor and H-bond acceptor sites are present in a tetrahedral arrangement and interact with complementary groups on the anions. Since these receptor molecules are uncharged they are of particular interest as ionophores in membrane transport and for the introduction of anion selectivity in potentiometric membrane sensors.

The host molecules **1**, **2**, and **3**–**8** were synthesized starting from diethylenetriamine and tris(aminoethyl)amine, respectively, by reaction with the appropriate acid chlorides in the presence of triethylamine as base.[6] Compounds **1**–**8** were isolated in 70–90% yield after recrystallization from methanol, and were characterized by ^{1}H and ^{13}C NMR spectroscopy, mass spectrometry, and elemental analysis.

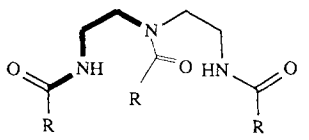

1 R = CH_2Cl
2 R = $(CH_2)_4CH_3$

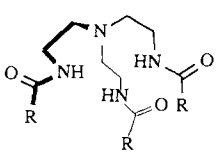

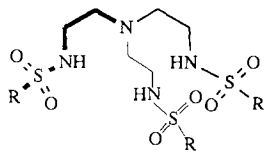

3 R = CH_2Cl
4 R = $(CH_2)_4CH_3$
5 R = C_6H_5
6 R = 4-$MeOC_6H_4$

7 R = 4-MeC_6H_4
8 R =

In ^{1}H NMR titration experiments of the ligands with $Bu_4N^+A^-$ ($A^- = H_2PO_4^-$, HSO_4^-, Cl^-) in chloroform, the NH signal of the ligands shifted $\Delta\delta \approx 1.5$–2.0 to lower field until a host–guest ratio of 1:1 was reached. No shift was observed in the NMR signal when the concentration of the anion was increased; however, in the titration with $H_2PO_4^-$ the NH signal shifted until a host–guest ratio of 1:2 was attained. These stoichiometries were confirmed by the characteristic $\delta(^{31}P)$ values for all host–guest complexes in acetonitrile upon addition of two equivalents of $Bu_4N^+H_2PO_4^-$. For example, the signal for ligand **8** showed a shift of $\Delta\delta = 0.345$ with one equivalent of $H_2PO_4^-$ and a further shift

[*] Prof. Dr. Ir. D. N. Reinhoudt, Dr. S. Valiyaveettil, Dr. J. F. J. Engbersen, Dr. W. Verboom
Laboratory of Organic Chemistry
University of Twente
P.O. Box 217, NL-7500 AE Enschede (The Netherlands)

of $\Delta\delta = 0.374$ with two equivalents. This host–guest complexation ratio of 1:2 was also reported by others and is attributed to dimerization of the $H_2PO_4^-$ ion by the formation of intermolecular hydrogen bonds.[7] The observed chemical shifts do not arise from proton transfer from $H_2PO_4^-$ and HSO_4^- to the ligands, since no shifts in the position of the CH_2N signal were observed in the ^1H NMR spectra of the complexes. Moreover, when ligands **1**–**8** were protonated by addition of *p*-toluenesulfonic acid or picric acid, a distinct downfield shift of the CH_2N signal of $\Delta\delta = 1.0-1.1$ was observed. The FAB^- mass spectra of the complexes of all the host molecules H with $Bu_4N^+A^-$ exhibit strong signals corresponding to $[HA^-]^-$ and $[HBu_4N^+A^-]^-$. The association constants (Table 1) for the complexation of ligands **1**–**8** with anions A^- (Bu_4N^+ as the counterion) were determined in acetonitrile by conductometry.[8]

Table 1. Association constants K [M^{-1}] for the reaction of **1**–**8** with the anions $H_2PO_4^-$, HSO_4^-, and Cl^- determined by conductometry [a].

	$H_2PO_4^-$	HSO_4^-	Cl^-
1	4700	36	96
2	870	65	63
3	6100	170	1740
4	280	31	290
5	870	56	100
6	510	73	190
7	3500	79	540
8	14200	38	1600

[a] Reactions in acetonitrile. The counterion in all cases was Bu_4N^+. Measurements were conducted at constant ionic strength with starting concentrations of **1**–**8** of 1–3 mM and of the salt of 0.9–1.1 mM. The concentrations of the salt and ligand were varied by dilution of the sample solution with a stock solution of the free salt. Initial concentrations were prepared by adding the appropriate amount of free ligand to 10 mL of the stock solution. The K values were determined with curve-fitting methods. The error is 5% for $K > 10^2\ M^{-1}$ and 10% for $K < 10^2\ M^{-1}$.

From this data it is clear that all ligands bind phosphate ions preferentially ($H_2PO_4^- > Cl^- > HSO_4^-$). The reference compound chloroacetamide was not complexed in these conductometric titrations. Ligand **8** shows highest affinity towards the phosphate ion, probably because of the increased electrophilicity of the sulfonamide NH group and preorganization of the binding sites by π-stacking interactions of the naphthyl groups.[9] The chloroacetamide derivatives **1** and **3** have a larger binding affinity than the caproamides **2** and **4**, which may be attributed to the higher polarization of the amide moieties in **1** and **3** caused by the inductive electron-withdrawing effect of the α-chloro substituents.

In conclusion, host molecules **1**–**8** show selective binding affinity towards anions exclusively by hydrogen-bond formation, and are thereby a unique mimic for anion-binding proteins. Although the association constants are not as high as those of the natural proteins, the simple structure of the models offers the possibility for synthetic manipulation. To achieve higher association constants and selectivities we are currently examining calixarenes and crown ether templates for organizing H-bond donor and acceptor binding sites for anions.

Experimental Procedure

The synthesis of **8** described is representative for the preparation of **1**–**8**: To a solution of tris(aminomethyl)amine (1.0 g, 6.8 mmol) and triethylamine (3.5 mL) in CH_2Cl_2 (100 mL) at 10 °C was added 2-naphthalenesulfonyl chloride (5.4 g, 23.9 mmol). The reaction mixture was stirred for 3 h, allowed to warm up to room temperature, stirred for another 3 h, and poured into water (200 mL). The aqueous layer was extracted with CH_2Cl_2 (2 × 100 mL). The combined organic layers were concentrated, and the resulting solid was recrystallized from methanol to give **8** in 84% yield. M.p. 127–128 °C; ^1H NMR (250 MHz, $CDCl_3$, 25 °C): δ = 8.48 (s, 3H, ArH), 7.9–7.7 (m, 12H, ArH), 7.5–7.6 (m, 6H, ArH), 6.28 (s, 3H, NH), 2.98 (t, 6H, CH_2), 2.56 (t, 6H, CH_2); ^{13}C NMR: δ = 136.5, 134.8, 132.1, 129.7, 129.4, 128.7, 128.5, 127.9, 127.4, 122.5 (ArC), 54.4 (CH_2NH), 40.9 (CH_2N); FAB MS (NBA matrix): m/z 717.1 ($M+1$); correct C,H,N analysis.

Received: December 12, 1992 [Z 5751 IE]
German version: *Angew. Chem.* **1993**, *105*, 942

[1] a) J.-M. Lehn, *Angew. Chem.* **1990**, *102*, 1347; *Angew. Chem. Int. Ed. Engl.* **1990**, *29*, 1304; b) H. J. Schneider, *ibid.* **1991**, *103*, 1419 and **1991**, *30*, 1417; c) F. P. Schmidtchen, A. Gleich, A. Schummer, *Pure Appl. Chem.* **1989**, *61*, 1535.

[2] a) B. Dietrich, J. Guilhem, J.-M. Lehn, C. Pascard, E. Sonveaux, *Helv. Chim. Acta* **1984**, *67*, 91; b) F. P. Schmidtchen, *J. Org. Chem.* **1986**, *51*, 5161; c) M. W. Hosseini, A. J. Blacker, J.-M. Lehn, *J. Am. Chem. Soc.* **1990**, *112*, 3896; d) P. D. Beer, J. W. Wheeler, A. Grieve, C. Moore, T. Wear, *J. Chem. Soc. Chem. Commun.* **1992**, 1225; e) G. Deslongchamps, A. Galán, J. de Mendoza, J. Rebek, Jr., *Angew. Chem.* **1992**, *104*, 58; *Angew. Chem. Int. Ed. Engl.* **1992**, *31*, 61.

[3] a) M. T. Blanda, J. N. Horner, M. Newcomb, *J. Org. Chem.* **1989**, *54*, 4626, and references therein; b) M. T. Reetz, C. M. Niemeyer, K. Harms, *Angew. Chem.* **1991**, *103*, 1515; *Angew. Chem. Int. Ed. Engl.* **1991**, *30*, 1472; c) X. Yang, C. B. Knobler, M. F. Hawthorne, *ibid.* **1991**, *103*, 1519 and **1991**, *30*, 1507; d) V. B. Chur, I. A. Tikhonova, A. I. Yanovskii, Yu. T. Struchkov, P. V. Petrovskii, S. Yu. Panov, G. G. Furin, M. E. Vol'pin, *J. Organomet. Chem.* **1991**, *418*, C29; e) P. D. Beer, J. Hodacova, S. E. Stokes, *J. Chem. Soc. Chem. Commun.* **1992**, 270; e) D. M. Rudkevich, W. P. R. V. Stauthamer, W. Verboom, J. F. J. Engbersen, S. Harkema, D. N. Reinhoudt, *J. Am. Chem. Soc.* **1992**, *114*, 9671.

[4] Pascal et al. synthesized a neutral host molecule which is claimed to bind a fluoride ion in its cavity; however, no evidence was given: R. A. Pascal Jr., J. Spergel, D. V. Engen, *Tetrahedron Lett.* **1986**, *27*, 4099.

[5] a) H. Luecke, F. A. Quiocho, *Nature* **1990**, *347*, 402; b) J. W. Pflugrath, F. A. Quiocho, *J. Mol. Biol.* **1990**, *200*, 163; c) J. L. Jacobson, F. A. Quiocho, *ibid.* **1988**, *204*, 783.

[6] The structure of our ligands is somewhat similar to that of the endo-tridentate podands developed by Potvin et al. However, these receptor molecules were designed for complexing Zn^{2+} ions mimicking the activity of carbonic anhydrase: R. Jairam, P. G. Potvin, *J. Org. Chem.* **1992**, *57*, 4136.

[7] L. S. Flatt, V. Lynch, E. V. Anslyn, *Tetrahedron Lett.* **1992**, *33*, 2785.

[8] The data obtained for the ^1H NMR chemical shifts in chloroform did not allow quantitative determination of the complexation constants, mainly because of the high association of the host and guest species in this moderately polar solvent and the relatively high concentrations required to obtain the NMR signals. In the conductometric experiments, however, complexation constants could be determined in the more polar solvent acetonitrile with much lower concentrations of host and guest molecules. Under these conditions the formation of only 1:1 host–guest complexes was observed.

[9] W. L. Jorgensen, D. L. Severance, *J. Am. Chem. Soc.* **1990**, *112*, 4768.

Electron Transfer-Catalyzed Diels–Alder Reactions with 2-Vinylindoles**

By *O. Wiest* and *E. Steckhan**

Electron Transfer (ET) is one of the most important elementary processes in chemistry.[1] During the last 15 years, mechanistic-theoretical investigations of ET reactions have made a great comeback, culminating in the award of the Nobel Prize for Chemistry to R. A. Marcus in 1992. In certain cases, reactions which proceed too slowly or not at all with neutral molecules can be effected by electron transfer. Thus, the [4 + 2] cycloaddition between two electron-rich

[*] Prof. Dr. E. Steckhan, Dipl.-Chem. O. Wiest
Institut für Organische Chemie und Biochemie der Universität
Gerhard Domagkstrasse 1, D-W-5300 Bonn 1 (FRG)

[**] This work was supported by the Deutsche Forschungsgemeinschaft (Ste 227/14-2), the Fonds der Chemischen Industrie, and the BASF AG. We thank Prof. Dr. G. P. Kreishman, University of Cincinatti, USA, for recording the NMR spectra.

substrates can be initiated by a one-electron oxidation of one of the components to its radical cation. After a cycloaddition at the radical cation stage, a back-electron transfer terminates the reaction sequence. The reaction is thus catalyzed by ET in the sense of a redox umpolung. The synthetic potential of these reactions has not until recently been investigated systematically.[2]

The importance of 2-vinylindoles as building blocks for indole alkaloids has been pointed out several times.[3] Compounds of the type **1** with a wide variety of substituents are easily accessible by using the method of Blechert et al. However, their use as 4π-electron components in Diels–Alder reactions is limited to very electron-deficient dienophiles, sometimes demanding drastic reaction conditions.[4]

We now report for the first time electron transfer-catalyzed Diels–Alder reactions of **1** with electron-rich dienophiles under mild reaction conditions and in good to moderate yields.

Based on our studies on the photoinduced electron transfer(PET)-catalyzed cycloadditions of indole,[5] we wanted to establish whether compounds of the type **1** react as dienes or dienophiles. Therefore, **1a** was allowed to react with 1,3-cyclohexadienes **2** under PET conditions. As PET sensitizers, triarylpyrylium salts such as **3** were used, since they have proven to be efficient electron transfer catalysts even in catalytic amounts.[2b, 5, 6] The cycloadduct **4a** is smoothly formed with **2a**, that is **1** reacted as a diene. If the chiral dienophile (5*R*)-**2b** is used, (*R*)-configurated **4b** is isolated as the only isomer. As a side reaction, the dimerization of the

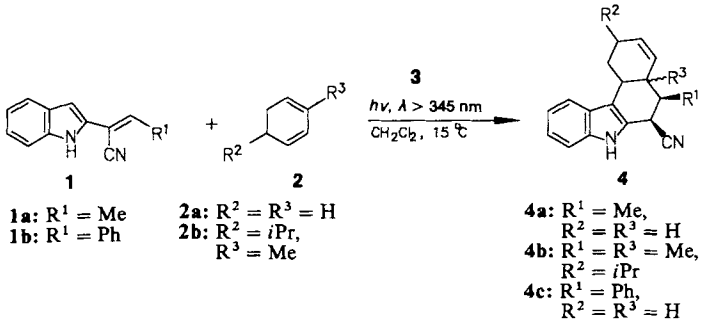

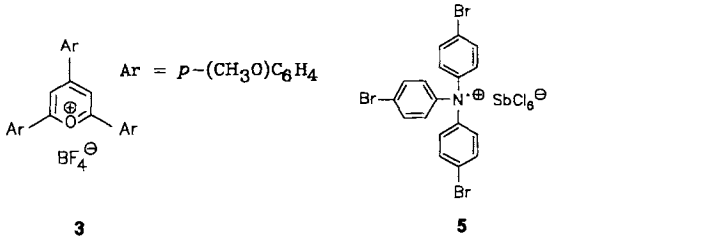

1,3-cyclohexadienes is observed, a reaction known[7] to be also catalyzed by PET. Alternatively, the reaction can be initiated by thermal ET with tris(4-bromphenyl)aminium hexachloroantimonate **5**.[8] However, lower yields are obtained in this case. The indole **1b** (Table 1) reacts in an analogous manner.

From previous investigations,[6] it was established that a cycloaddition can only take place if the oxidation potentials E_p (Ox) of the starting materials do not differ by more than 500 mV. Hence, styrenes **6** were chosen for further investigations because their oxidation potentials could be varied by suitable substitution over a wide range with negligible steric interference.

Table 1. Results of the ET-catalyzed Diels–Alder reaction of 2-vinylindoles **1** with 1,3-cyclohexadienes **2**.

Diene	Dienophile	Product	Yield [%]	*endo*/*exo*-Ratio
1a	**2a**	**4a**	61	2/1 [a]
1a	**2a**	**4a**	8	1.6/1 [a,b]
1a	**2b**	**4b**	33	only *endo*
1b	**2a**	**4c**	35	3.4/1 [a]

[a] Determined by gas chromatography in the crude product. [b] Thermal electron transfer with 10 mol% **5** (based on **1**).

Under PET conditions, the primary adduct **7** is aromatized by double dehydrogenation[9] to give the carbazole derivative **8**. If the reaction is performed under conditions

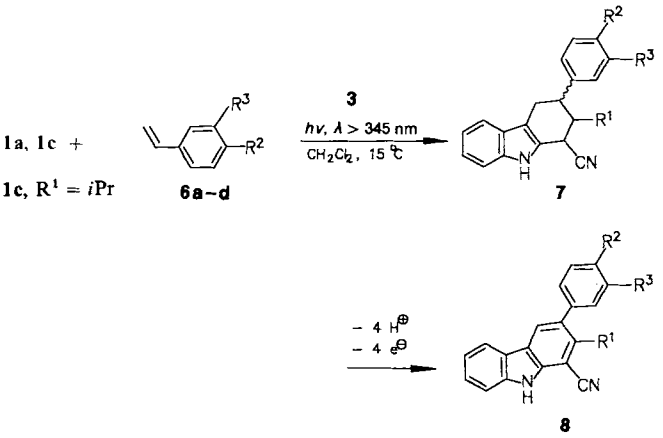

for thermal electron transfer, the *endo*/*exo* isomers of **7** are obtained in good yields. It can be seen from the results (Table 2) that the difference of the oxidation potentials determines the outcome of the reaction.

Table 2. Results of the ET-catalyzed Diels–Alder reaction of 2-vinylindoles **1** with substituted styrenes **6** and dependence on the difference of the oxidation potentials of the starting materials.

Diene	Dienophile	R^2	R^3	$\Delta Ep(Ox)$ [V]	Product	Yield [%]
1a	**6a**	OMe	H	0.17	**8a**	34
1a	**6a**	OMe	H	0.17	**7**	69 [a]
1a	**6b**	Me	H	0.55	–	– [b]
1a	**6c**	Cl	H	0.80	–	–
1c	**6d**	OMe	OMe	0.23	**8b**	24

[a] Thermal electron transfer with 10 mol% **5** (based on **1**). [b] Traces of the product detected by GC/MS.

Non-conjugated dienophiles such as 1-methoxycyclohexene do not react despite their suitable E_p(Ox) values. Therefore, we conclude that the intermediate stabilization of a benzyl or allyl radical plays a decisive role. Based on our experiences with the indole system[5, 10] and the preliminary results of mechanistic investigations,[11] the mechanism outlined in Scheme 1 for the reaction of the distonic radical cation formed by ET appears probable.

For the rearomatization of the indole system, the most likely mechanism is a thermal $[1_s,3_s]$ H shift followed by back-electron transfer. The $[1_s,3_s]$ H shift is symmetry forbidden for the neutral molecule, but not for the radical cation.[12] Shift reactions of this type have been well investigated by using spectroscopic[13] and theoretical[14] methods.

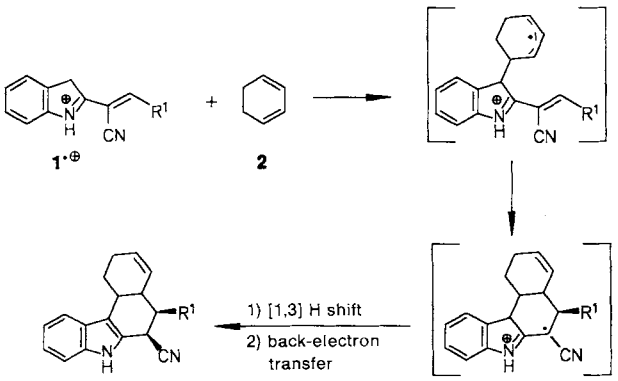

Scheme 1. Proposed mechanism of the ET-catalyzed [4 + 2] cycloaddition between **1** and **2**.

If the [1,3] H shift is prevented by suitable substitution (**9**) of the 2-vinylindole,[15] the double bond remains in the 1,9a-position of the tetrahydrocarbazole intermediate after back-electron transfer. Under the reaction conditions, in situ dehydrogenation takes place to give the highly substituted 4,4a-dihydrocarbazole **10** as the only product.[16]

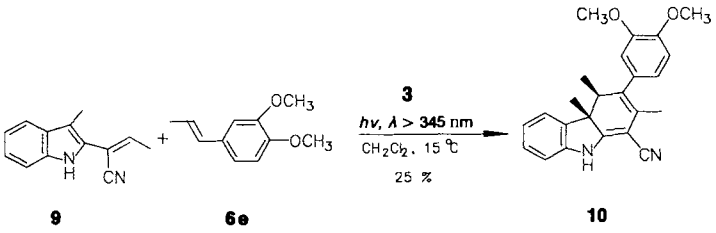

9 **6e** **10**

The reactions presented here open a new pathway for Diels–Alder reactions with 2-vinylindoles. The exact mechanism and the application of the reactions to the synthesis of indole alkaloids are currently under investigation.

Experimental Procedure

a) General procedure for PET-catalyzed reactions: Vinylindole **1** (0.5 mmol), dienophile **2** (0.7 mmol) or **6**, and **3** (0.02 mmol) were dissolved in anhydrous CH_2Cl_2 (50 mL), and the solution was degassed with argon in a Schlenk tube. The solution was irradiated in a water bath (15 °C) with a 450 W xenon lamp ($\lambda > 345$ nm). The pyrylium salt **3** was removed after the reaction with a short filtration column.

b) General procedure for the thermal electron transfer: Vinylindole **1** (0.5 mmol) and dienophile **2** (0.7 mmol) or **6** were dissolved in anhydrous CH_2Cl_2 (50 mL) and degassed with argon. The solution was cooled to 0 °C and a suspension of **5** (0.05 mmol) in CH_2Cl_2 (10 mL) was added dropwise.

For workup, in both cases the solvent was removed, and the residue was purified by chromatography. The *endo*/*exo* isomers were separated by HPLC (LiChrospher RP18-5, water/acetronitrile mixtures). All new compounds were identified spectroscopically. Regio- and stereochemistry were proven by two-dimensional NMR spectroscopy (COSY, HETCOR, NOESY), for example for **4b**: ^{1}H NMR (400 MHz, $CDCl_3$): $\delta = 8.04$ (br, 1H, H-7a), 7.65 (1H, d, $J = 7.8$ Hz, H-11), 7.33 (1H, d, $J = 8$ Hz, H-8), 7.18 (1H, t, $J = 7.8$ Hz, H-9), 7.09 (1H, t, $J = 8$ Hz, H-10), 5.71 (1H, d, $J = 10.8$ Hz, H-4), 5.66 (1H, d, $J = 10.8$ Hz, H-3), 3.93 (1H, d, $J = 4.9$ Hz, H-6), 2.99 (1H, m, H-11c) 2.36 (1H, m, H-1), 2.08 (1H, qd, $J = 6.8$ and 4.9 Hz, H-5), 1.94 (1H, ddd, $J = 12.6$, 9.7 und 2.9 Hz, H-1), 1.55 (2H, m, H-5, H-12), 1.36 (3H, d, $J = 6.8$ Hz, H-16), 1.18 (3H, s, H-15), 0.86 (3H, d, $J = 6.1$ Hz, H-12), 0.85 (3H, d, $J = 6.1$ Hz, H-14); ^{13}C NMR (100.6 MHz, $CDCl_3$): $\delta = 136.7$ (C-7a), 132.8 (C-3), 129.9 (C-4), 126.5 (C-6a), 125.6 (C-11a), 122.4 (C-9), 119.6 (C-10, C-11), 118.4 (C-17), 113.8 (C-11b), 111.2 (C-8), 39.5 (C-5), 38.6 (C-11c), 38.15 (C-2), 38.1 (C-4a), 31.5 (C-13), 30.9 (C-6), 26.8 (C-16), 26.03 (C-1), 19.9 (C-12), 19.5 (C-14), 14.2 (C-15); $[\alpha]_D^{23} = 94.5$ ($C = 0.49$ in CH_2Cl_2).

Received: January 18, 1993 [Z 5815 IE]
German version: *Angew. Chem.* **1993**, *105*, 932

[1] For reviews on this topic see for example a) L. Eberson, *Electron Transfer Reactions in Organic Chemistry*, Springer, Berlin, **1987**; b) J. Mattay, *Angew. Chem.* **1987**, *99*, 849–870; *Angew. Chem. Int. Ed. Engl.* **1987**, *26*, 825–846; c) *Photoinduced Electron Transfer Part A–D* (Eds.: M. Chanon, M. A. Fox), Elsevier, Amsterdam, **1988**.

[2] a) B. Harirchian, N. L. Bauld, *J. Am. Chem. Soc.* **1989**, *111*, 1826–1828; b) J. Mattay, *Synthesis* **1989**, 233–252; c) M. Schmittel, H. von Seggern, *Angew. Chem.* **1991**, *103*, 981–983; *Angew. Chem. Int. Ed. Engl.* **1991**, *30*, 999–1001; d) F. Müller, J. Mattay, *ibid.* **1992**, *104*, 207–208 and **1992**, *31*, 209–210.

[3] a) S. Blechert, *Liebigs Ann. Chem.* **1985**, 673–682; b) J. Wilkens, A. Kühling, S. Blechert, *Tetrahedron* **1987**, *43*, 3237–3246; c) U. Pindur, *Heterocycles* **1988**, *27*, 1253–1268; d) U. Pindur, L. Pfeuffer, *Chem. Ztg.* **1986**, *110*, 95–99.

[4] a) H. Schroers, dissertation, Universität Bonn, **1989**; b) J. Lévy, J. Sapi, J.-Y. Laronze, D. Royer, L. Toupet, *Synlett* **1992**, 601–602.

[5] a) A. Gieseler, E. Steckhan, O. Wiest, *Synlett* **1990**, 275–277; b) A. Gieseler, E. Steckhan, O. Wiest, F. Knoch, *J. Org. Chem.* **1991**, *56*, 1405–1411.

[6] a) J. Mlcoch, E. Steckhan, *Angew. Chem.* **1985**, *97*, 429–431; *Angew. Chem. Int. Ed. Engl.* **1985**, *24*, 412–414; b) J. Mlcoch, E. Steckhan, *Tetrahedron Lett.* **1987**, *28*, 1081–1084; c) M. Martiny, E. Steckhan, T. Esch, *Chem. Ber.*, in press.

[7] D. J. Bellville, D. D. Wirth, N. L. Bauld, *J. Am. Chem. Soc.* **1981**, *103*, 718–720.

[8] F. A. Bell, A. Ledwith, D. C. Sherrington, *J. Chem. Soc. C* **1969**, 2719–2720.

[9] Aromatization by simple dehydrogenation is known M. J. Climent, H. Garcia, S. Iborra, M. A. Miranda, J. Primo, *Heterocycles* **1989**, *29*, 115–121.

[10] O. Wiest, E. Steckhan, F. Grein, *J. Org. Chem.* **1992**, *57*, 4034–4037.

[11] Further mechanistic studies are in progress and will be published elsewhere.

[12] This [1,3] H shift was also observed on other systems: a) J. Delaunay, A. Orliac-Le Moing, J. Simonet, L. Toupet, *Tetrahedron Lett.* **1986**, *27*, 6205–6208; b) Ref. [6a].

[13] Review: H. Schwarz, *Top. Curr. Chem.* **1981**, *97*, 1–31.

[14] For a recent review see a) K. N. Houk, Y. Li, J. D. Evansek, *Angew. Chem.* **1992**, *104*, 711–739; *Angew. Chem. Int. Ed. Engl.* **1992**, *31*, 682–708; b) T. Clark, *J. Am. Chem. Soc.* **1987**, *109*, 6838–6840; c) Y. Hoppiliard, G. Bouchoux, *Org. Mass Spectrom.* **1982**, *17*, 534–536.

[15] T. Wirth, S. Blechert, *Synlett*, in press. We thank Dr. T. Wirth for a sample of **9**.

[16] The [4 + 2] cycloaddition of **9** and **6e** can be induced alternatively by potentiostatic electrolysis (undivided cell, working electrode: graphite, auxilary electrode: Pt, CH_3CN/CH_2Cl_2 1:1, 0.1 M $LiClO_4$, working potential 670 mV vs. $Ag/AgNO_3$). Thus, it is shown that the key intermediate of the reaction is the radical cation of **9**.

C–H Bond Addition to a V=NR Bond: Hydrocarbon Activation by a Sterically Crowded Vanadium System

By *Jan de With* and *Andrew D. Horton**

Electrophilic complexes whose central atom is a metal from Group 3 or 4, or an f-block element catalyze alkene polymerization[1] and activate C–H bonds;[1a, 2] the related vanadium chemistry has been hindered by the perceived instability of V^V complexes with σ-bound hydrocarbon ligands.[3] Recent reports of the highly reactive nature of M=NR bonds in coordinatively unsaturated imido complexes,[4] together with our development of a series of robust V^V complexes with bulky nitrogen ligands,[5] led us to attempt to synthesize three-coordinate imidovanadium complexes. We postulated that generation of **1** on thermolytic expulsion of R′–H from $[RN{=}V(NHR)_2R']$, would be facilitated by the small covalent radius and relatively labile na-

[*] Dr. A. D. Horton, J. de With
Koninklijke/Shell-Laboratorium, Amsterdam (Shell Research B.V.)
P.O. Box 3003, NL-1003 AA Amsterdam (The Netherlands)
Telefax: Int. code + (20) 630-8025

ture of M–C bonds for metals of the first transition series. Increased competition for the metal π-acceptor orbitals in bisimido complexes[6] was expected to lead to greater nucleophilicity of the imido N atom, and better polarization of C–H bonds. We report here the successful addition of a wide range of C–H bonds to a reactive V=N bond.

$[(RN=)_2V\text{–}NHR]$ ($R = tBu_3Si$) **1**

Crystalline complexes with σ-bound hydrocarbon ligands, stabilized by three bulky nitrogen ligands, were obtained in good yield in two steps from readily available $[RN=V(NHR)Cl_2]$[5] (Scheme 1). The presence of a plane of

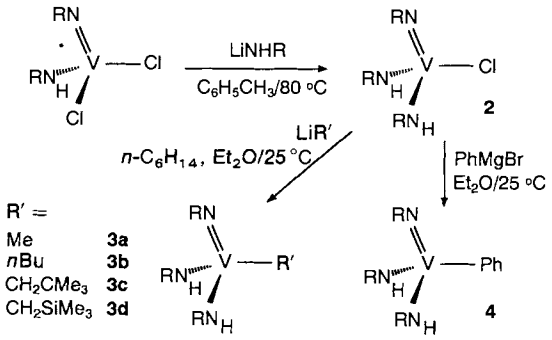

Scheme 1. Synthesis of sterically crowded hydrocarbylvanadium complexes. $R = tBu_3Si$.

symmetry in the monomeric pseudotetrahedral complexes is indicated by the observation of identical amido ligands and a single VCH_2 resonance signal in the ^1H NMR spectra of **3b–d** as well as **3e** and **6** (see Scheme 2). In line with previ-

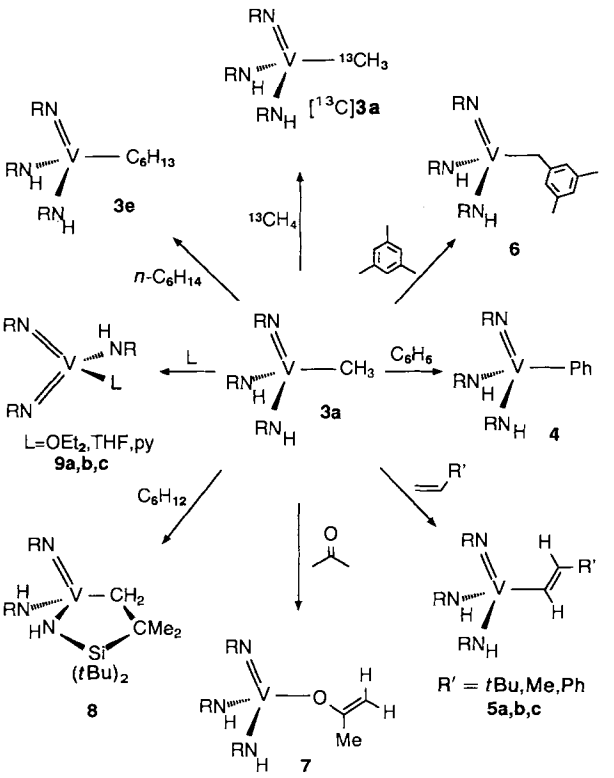

Scheme 2. Methane elimination reactions of **3a** (16 h, 80 °C; $R = tBu_3Si$; [^{13}C]**3a** formed in C_6D_{12} and **5a–c** and **7** formed in C_6H_{12}).

ous studies the ^{51}V NMR resonance signals for $[RN=V(NHR)_2R']$ show a clear upfield progression as the π-donating ability of the ligand R′ increases ($\delta(^{51}V)$: R′ = alkyl > alkenyl, Ph > Cl > OR).[3b, 5]

That the complexes **3** could activate C–H bonds was first confirmed by the clean formation of phenyl species **4** on thermolysis of the methyl compound **3a** in C_6H_6 (5 h at 80 °C). Reaction of **3a** at 80 °C with a range of substrates, either neat, or as solutions in inert cyclohexane, cleanly afforded activation products (Scheme 2) on a preparative scale. Other alkyl complexes exhibit similar C–H activation activity and no evidence was obtained for competitive, sterically demanding, β-H elimination reactivity for complexes containing β-hydrogen atoms (e.g. **3b**).

The formation of R′–H (rather than R′–D) on thermolysis of complexes **3** in C_6D_6 indicates that C–H activation does not occur by a simple sigma bond metathesis mechanism.[2] The intermediacy of unstable three-coordinate complex **1**, which may undergo C–H bond addition across one of the two V=N bonds, is strongly supported by the formation of Lewis base adducts **9a–c**, on thermolysis of complexes **3** in ether, THF, and pyridine/C_6D_{12}, respectively.

The clean first-order thermolysis of **3a** in C_6D_6, to give $[RN=V(NDR)_n(NHR)_{2-n}(C_6D_5)]$ ($n = 2$) via the observable intermediate with $n = 1$,[7] has been monitored by ^1H NMR spectroscopy and has allowed rate constants for CH_4 elimination at four temperatures in the range 60–90 °C to be obtained (e.g. $k = 11.4 \times 10^{-5}\ s^{-1}$ at 80 °C).[8] A significant rate enhancement for the first-row metal, compared to CH_4 elimination from $[(RNH)_3ZrMe]$, is found ($k_{Zr} = 10.6 \times 10^{-5}\ s^{-1}$ at 96.6 °C).[4a] The kinetic parameters determined from an Arrhenius plot are consistent with significant V–C bond breaking ($\Delta H^{\neq} = +123(8)\ kJ\,mol^{-1}$) in a late transition state, in which CH_4 formation is advanced ($\Delta S^{\neq} = +38(25)\ J\,K^{-1}$). Increased crowding in the precursor complexes, $[RN=V(NHR)_2R']$, appears to result in slightly more facile alkane expulsion, as shown by the relative reactivities with C_6D_6: **3d** > **3b** > **3a**.[9] Hydrocarbon elimination also appears to be more facile for complexes containing hydrocarbyl ligands bonded through an sp^2-carbon atom[4a] (e.g. **5**) than for those bonded through sp^3-carbon atoms,[10] although quantitative studies have not been carried out.

Selective formation of the *trans*-alkenyl complexes **5** from the reaction of **3a** with 1-alkenes, rather than the alternative *cis*-alkenyl or η^3-allyl complexes (for propene), is shown by the characteristic *trans*-$^3J_{H,H}$ coupling constant of 17 Hz (e.g. in **5a**). A clear preference for formation of the sterically, least crowded product is also seen in the selective activation of an sp^3 rather than an sp^2 C–H bond of 1,3,5-trimethylbenzene, as confirmed by the observation of resonance signals for the VCH_2 unit and those of three arene hydrogen atoms. Crystalline **5a** and **6** (but not **5b**, **c** or other $[RN=V(NHR)_2R']$ complexes) each show two sets of similar ^1H and ^{13}C NMR resonance signals. Restricted rotation about the metal–carbon bond, as previously observed in $[(RO)_3W(=O)(HC=CHtBu)]$,[11] may perhaps lead to two rotational isomers for sterically crowded **5a** and **6**. Formation of an *O*-enolatovanadium complex **7** on activation of an sp^3 C–H bond in acetone, rather than a less crowded α-metalated ketone species, reflects the greater affinity of the electrophilic V^V center for oxygen rather than carbon atoms.

The activation of alkanes by **3a** also shows a remarkable sensitivity to the steric environment of the C–H bonds: Methane and the primary C–H bonds of *n*-hexane react with **3a** to give alkyl species, whereas cyclohexane is inert. Intramolecular metalation of the NHR ligand leads in the lat-

ter case to a stable five-membered ring system in **8**. Achievement of the challenging goal of the activation of C–H bonds of CH_4 was confirmed by observation of the intense broad $V-^{13}CH_3$ resonance signal at $\delta = 32$ ($\Delta\nu_{1/2}$ 1000 Hz) in the product [^{13}C] **3a** obtained on pressurizing a C_6D_{12} solution of **3a** under $^{13}CH_4$ (10 bar; 4 h, 80 °C). The characteristic broad (plateau-like) nature of VCH_n signals is caused by a combination of unresolved coupling between the ^{13}C and ^{51}V nuclei ($I = 7/2$) and quadrupolar relaxation effects. ^{13}C incorporation was estimated at 80% by the formation of a 4:1 ratio of $^{13}CH_4$:$^{12}CH_4$ on thermolysis of the product in C_6D_6 in a sealed NMR tube.

The use of bulky nitrogen ligands has permitted the development of a family of thermally robust hydrocarbylvanadium(v) complexes, which show remarkable C–H bond activation by addition to a M=NR bond. The successful extension of such novel reactivity to a complex with a first-row transition metal,[4b, 12] in contrast to monomeric imido complexes containing coordinated Lewis bases which show no such activity,[8a, 13] is due to the sterically and electronically unsaturated nature of the proposed three-coordinate intermediate **1**. Although C–H activation with the V complexes **3** is somewhat more facile than with Zr complexes,[4a] the small size of the V^V ion hinders the activation of crowded cyclohexane. Attempts to isolate the intermediate **1** have so far been unsuccessful, but we have recently found that the labile nature of coordinated ether in **9a** allows this complex to act as a useful surrogate for **1** under mild conditions. The remarkable reactivity of **9a** will be reported elsewhere.[14]

Experimental Procedure

The products were characterized by ^{1}H, ^{13}C, and ^{51}V NMR spectroscopy, and, the crystalline products **2**, **3a–d**, **5a**, **7**, and **9a**, additionally by elemental analysis (C,H,N,Si,V). Yellow **2** and **3a** were obtained in 62 and 86% yield, respectively, as shown in the Scheme. Yellow **4** was obtained as shown in Scheme 1, or, more cleanly, by thermolysis of **3a** in C_6H_6 (Scheme 2); the complex decomposed on attempted crystallization from pentane. All thermolytic C–H activation reactions occurred quantitatively, as judged by ^{1}H NMR spectroscopy of the crude products; the high alkane solubility of the complexes frequently resulted in significantly lower isolated yields.

5a: A mixture of **3a** (0.41 g, 0.57 mmol) and *t*BuCH=CH_2 (0.37 mL, 2.87 mmol) in C_6H_{12} (10 mL) in a 25 mL autoclave was stirred at 80 °C for 16 h, and the solvent was then removed to afford a pure yellow product, which could be recrystallized from hexane. 1-Propene (5 bar) and styrene (5 equivalents) led analogously to **5b** and **5c**, respectively, which decomposed on attempted crystallization.

6, **8**: Heating a solution of **3a** in 1,3,5-trimethylbenzene or C_6H_{12} (16 h, 80 °C), followed by removal of the solvent, and crystallization from pentane or hexane, afforded red **6** and yellow **8**, respectively.

7: Treatment of **3a** with acetone (5 equivalents), analogous to the formation of **5a**, afforded pure yellow crystalline **7** (71% yield).

9a: Reaction of *n*BuLi (0.69 mmol) with **2** (0.48 g, 0.66 mmol) in hexane (20 mL) for 30 min at 25 °C, followed by removal of the solvent and extraction with hexane, afforded pure **3b**. Thermolysis of an Et_2O solution of **3b** (autoclave, 80 °C, 5 h), followed by removal of the solvent, afforded 0.39 g (85% overall yield) of spectroscopically pure red **9a**, which could be recrystallized from pentane. Selected ^{1}H NMR data (300 MHz, C_6D_{12}, 25 °C): **3a**: $\delta = 8.9$ (br, 2H; N*H*), 1.33 (s, 27H; CMe_3), 1.21 (s, 54H; CMe_3). **3b**: $\delta = 2.17$ (m, 2H; α-CH_2), 2.00 (m, 2H; β-CH_2), 1.19 (m, 2H, γ-CH_2), 0.79 (t, 3H; δ-CH_3). **4** (CD_2Cl_2): $\delta = 9.5$ (br, 2H; NH), 7.65 (m, 2H; Ph), 6.98 (m, 3H; Ph), 1.19 (s, 54H; CMe_3), 1.18 (s, 27H; CMe_3). **5a** [minor isomer]: $\delta = 7.36$ [7.09] (d, 1H; V*CH*=), 6.28 (br d, 1H; =*CH*(CMe$_3$)), 0.90 [0.88] (s, 9H; =CH(CMe_3)). **6** [minor isomer]: $\delta = 6.68$ [6.71] (s, 2H; *o*-H), 6.38 [6.30] (s, 1H; *p*-H), 3.36 [3.03] (br, 2H; VCH_2), 2.10 [2.08] (s, 6H; *Me*). **7**: $\delta = 4.30$, 3.95 (s, 1H; =CH_2), 1.81 (s, 3H; VOC(*Me*)=). **8**: $\delta = 8.4$, 8.0 (br, 1H; N*H*), 3.34 (br, d, 1H; VCH_2), 2.00 (s, 3H; CH_3), 1.50 (d, 1H; vCH_2), 1.33 (s, 27H; CMe_3), 1.28 (s, 3H; CH_3), 1.25 (s, 9H; CMe_3), 1.21 (s, 27H; CMe_3), 1.19 (s, 9H; CMe_3). **9a**: $\delta = 8.7$ (br, 1H; NH), 4.38 (q, 4H; CH_2CH_3), 1.25 (s, 81H; CMe_3). Selected ^{13}C NMR data (75.43 MHz, C_6D_{12}, 25 °C): **3a**: $\delta = 31.8$ (9C; CMe_3), 31.5 (18C; CMe_3), 25.5 (3C; CMe_3), 24.1 (6C; CMe_3). **4** (CD_2Cl_2): $\delta = 140.6$ (*m*-Ph), 126.3 (*o*-Ph), 125.8 (*p*-Ph). **5a**: $\delta = 156.6$ (d, ^1J(C,H) = 147 Hz, =*CH*(CMe$_3$)). **6** [minor isomer]: $\delta = 150.2$ [152.6] (*ipso*-Ph), 137.4 [137.0] (*m*-Ph), 127.3 [126.9] (*o*-Ph), 125.6 [124.5] (*p*-Ph), 21.5 (Me). **7**: $\delta = 167.6$ (VOC(Me)=), 92.3 (t, ^1J(C,H) = 158 Hz; =CH_2), 30.5 (VOC(Me)=). **8** (C_6D_6): $\delta = 33.8$ (VCH_2). **9** (CD_2Cl_2): $\delta = 73.5$ (CH_2CH_3), 12.8 (CH_2CH_3). Selected ^{51}V NMR data (78.86 MHz, C_6D_{12}, 25 °C; $\Delta\nu_{1/2}$ in Hz; $VOCl_3$: $\delta = 0$): **2**: $\delta = -34$ (370). **3a**: $\delta = 172$ (235). **3b**: $\delta = 264$ (290). **4** (CD_2Cl_2): $\delta = 81$. **5a**: $\delta = 99$ (220). **6** [minor isomer]: $\delta = 294$ [90] (310 [480]). **7**: $\delta = -229$ (180). **8**: $\delta = 449$ (1190). **9a**: $\delta = -65$ (1700).

Received: December 29, 1992 [Z 5787 IE]
German version: *Angew. Chem.* **1993**, *105*, 958

[1] a) R. F. Jordan, *Adv. Organomet. Chem.* **1991**, *32*, 325; b) X. Yang, C. L. Stern, T. J. Marks, *Organometallics* **1992**, *10*, 840; c) E. B. Coughlin, J. E. Bercaw, *J. Am. Chem. Soc.* **1992**, *114*, 7606; d) B. J. Burger, M. E. Thompson, W. D. Cotter, J. E. Bercaw, *ibid.* **1990**, *112*, 1566; e) G. Jeske, H. Lauke, H. Mauermann, P. N. Swepston, H. Schumann, T. J. Marks *ibid* **1985**, *107*, 8091.

[2] a) M. E. Thompson, S. M. Baxter, A. R. Bulls, B. J. Burger, M. C. Nolan, B. D. Santarsiero, W. P. Schaefer, J. E. Bercaw, *J. Am. Chem. Soc.* **1987**, *109*, 203; b) P. L. Watson, G. W. Parshall, *Acc. Chem. Res.* **1985**, *18*, 51.

[3] a) F. J. Feher, R. L. Blanski, *J. Am. Chem. Soc.* **1992**, *114*, 5886; b) D. D. Devore, J. J. Lichtenhan, F. Takusagawa, E. A. Maatta, *ibid.* **1987**, *109*, 7408; c) F. Preuss, H. Becker, J. Kaub, W. S. Sheldrick, *Z. Naturforsch. B* **1988**, *43*, 1195.

[4] a) C. C. Cummins, S. M. Baxter, P. T. Wolczanski, *J. Am. Chem. Soc.* **1988**, *110*, 8731; b) C. C. Cummins, C. P. Schaller, G. D. Van Duyne, P. T. Wolczanski, A. W. E. Chan, R. Hoffmann, *ibid.* **1991**, *113*, 2985; c) P. J. Walsh, F. J. Hollander, R. G. Bergman, *ibid.* **1988**, *110*, 8729; d) P. J. Walsh, A. M. Baranger, R. G. Bergman, *ibid.* **1992**, *114*, 1708; e) D. S. Glueck, J. Wu, F. J. Hollander, R. G. Bergman, *ibid.* **1991**, *113*, 2041; f) T. R. Cundari, *ibid.* **1992**, *114*, 10557.

[5] J. de With, A. D. Horton, *Organometallics* **1990**, *9*, 2207.

[6] a) Y.-W. Chao, P. A. Wexler, D. E. Wigley, *Inorg. Chem.* **1990**, *29*, 4592; b) D. P. Smith, K. D. Allen, M. D. Carducci, D. E. Wigley, *ibid.* **1992**, *31*, 1319; c) J. T. Anhaus, T. P. Kee, M. H. Schofield, R. R. Schrock, *J. Am. Chem. Soc.* **1990**, *112*, 1642.

[7] Consumption of **3a** was followed by ^{1}H NMR monitoring of the total CMe_3 integral for **3a** (amido and imido groups). Formation of [RN=V(NDR)$_n$(NHR)$_{2-n}$(C_6D_5)] ($n = 1, 2$) in C_6D_{12} solution is effectively zero order relative to the concentration of C_6D_6 for > 5 equivalents C_6D_6.

[8] The following rate constants for CH_4 elimination from [RN=V(NHR)$_2$$CH_3$] in C_6D_6 were obtained: $k \times 10^5 = 1.15$ (60 °C); 5.26 (70 °C); 11.4 (80 °C) 59.4 (90 °C) s^{-1}.

[9] Rough rate constants at about 25 °C for R'–H elimination from [RN=V(NHR)$_2$R'] in C_6D_6 (to give [RN=V(NDR)$_n$(NHR)$_{2-n}$(C_6D_5)] ($n = 1, 2$)) were obtained: $k \times 10^7 = 2.5$ (**3a**); 5.0 (**3b**); 9.0 (**3d**) s^{-1}.

[10] For example, solutions of the alkenyl complex **5a** in C_6D_{12} at 25 °C eliminate H_2C=CH(*t*Bu) with concomitant formation of [RN=V(NHR)$_3$] (40% conversion after 4 days). Similar hydrocarbon elimination from **4**, **5b**, **c** may be responsible for the decomposition observed during attempted crystallizations from alkane solutions.

[11] J. H. Freudenberger, R. R. Schrock, *Organometallics* **1986**, *5*, 398.

[12] After the completion of this work Wolczanski reported the generation of RN = Ti(OR)$_2$, which undergoes a range of addition reactions related to those discussed here: P. T. Wolczanski, 204th ACS National Meeting, Washington, D.C., USA, **1992**.

[13] a) J. E. Hill, R. D. Profilet, P. E. Fanwick, I. P. Rothwell, *Angew. Chem.* **1990**, *102*, 713; *Angew. Chem. Int. Ed. Engl.* **1990**, *29*, 664; b) R. D. Profilet, C. H. Zambrano, P. E. Fanwick, J. J. Nash, I. P. Rothwell, *Inorg. Chem.* **1990**, *29*, 4362; c) D. J. Arney, M. A. Bruck, S. R. Huber, D. E. Wigley, *ibid.* **1992**, *31*, 3755; d) Y. Bai, H. W. Roesky, M. Noltemeyer, M. Witt, *Chem. Ber.* **1992**, *125*, 825.

[14] J. de With, A. D. Horton, A. G. Orpen, *Organometallics*, in press.

Difluorodioxirane**

By *Antonio Russo* and *Darryl D. DesMarteau**

Dioxiranes are of theoretical and experimental interest as selective oxygenating agents.[1] All reported examples of dioxiranes are unstable at 22 °C as pure compounds and the

[*] Prof. Dr. D. D. DesMarteau, A. Russo[+]
Howard L. Hunter Chemistry Laboratory
Clemson University
Clemson, SC 29634-1905 (USA)
Telefax: Int. code + (803) 656-0627
[+] Permanent address: Ausimont, Via S. Pietro 50, I-20021 Bollate (Italy)

[**] This work was supported by Ausimont, Milan.

two most studied dioxiranes, dimethyldioxirane and methyl(trifluoromethyl)dioxirane, can only be isolated as solutions with the parent ketone. Difluorodioxirane (**1**) has been predicted to have a relatively high thermodynamic stability,[2] and based on the high thermal stability of the related difluorodiazirine,[3] **1** might be the most stable dioxirane. Compound **1** is claimed in a patent,[4] and as a possible intermediate in the pyrolysis of $CF_3O_2CF_3$[5] and in the reaction of $^3CF_2$ with O_2 in the presence of alkenes,[6] but it has never been isolated. Herein we report the synthesis and characterization of this rather stable molecule.

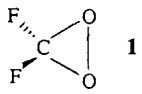

1

A potential route to **1** was envisioned by us to be the photochemical or thermal elimination of chlorine monofluoride from the unknown molecule $CF_2(OF)OCl$ (**2**). A potential route to compound **2** would be the oxidation of the anion $FOCF_2O^-$ by ClF. This anion could be generated in principle by the nucleophilic attack of fluoride ion on the unstable molecule FC(O)OF (**3**).[7]

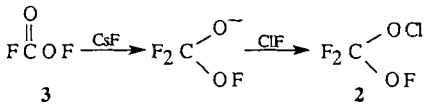

3 **2**

This idea was reinforced by the fact that **3** is converted to $CF_2(OF)_2$ (**4**) by reaction with elemental fluorine in the presence of CsF in a bomb.[7]

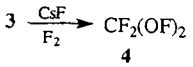

4

While **2** can indeed be prepared with an appropriate CsF catalyst,[8] it does not readily decompose into the desired compound **1**. However, in the process of refining the synthesis of **2**, in which the yields are highly variable (0–70%), we observed small amounts of an unusual low boiling product which we ultimately identified as difluorodioxirane (**1**). When this reaction was run in a flow system using a pelletized CsF catalyst, **1** became a major product (20–50%).

The mechanism for the formation of **1** was of interest since as stated previously, **2** is not a ready source of the dioxirane. At first we concluded that **1** might be formed by an intramolecular nucleophilic attack not involving ClF (Scheme 1 top). Under all conditions the reaction of **3** with CsF formed only COF_2 and O_2 as volatile products, and the presence of ClF was essential for the formation of **1**. When ClF was substituted by Cl_2 in this reaction, good yields of dioxirane **1** were also obtained. Since there are no examples of the oxidation of a perfluorinated alkoxide to a hypochlorite by Cl_2, this result further confirmed that **2** is not an intermediate in the formation of **1**. Similarly, the use of F_2 also gave **1**, however, only in low yield. We therefore propose the following electron transfer mechanism to explain the formation of **1** (Scheme 1 bottom).

The by-products in the reaction of **3** with CsF/ClF are CF_3OCl, COF_2, and O_2, whereas in the reaction with CsF/Cl_2 only COF_2 and O_2 are formed as by-products. With CsF/F_2, other products are CF_3OF, COF_2, O_2, and perhaps

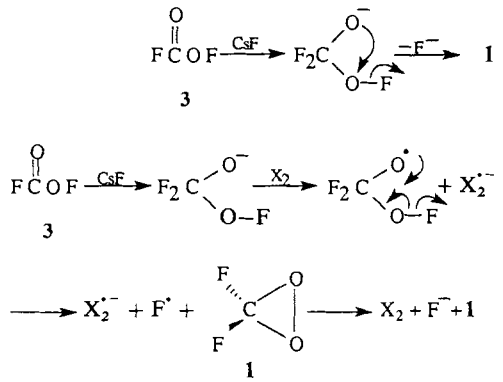

Scheme 1. Proposed reactions for the mechanism of the formation of **1**. Top: Intramolecular nucleophilic attack (rejected); bottom: Electron transfer; $X_2 = Cl_2$, ClF, F_2.

a small amount of **4**. The formation of CF_3OCl and CF_3OF arises from the known CsF-catalyzed oxidation of COF_2 by chlorine monofluoride and F_2, respectively.[9, 10]

Support for an intermediate $FOCF_2O^{\bullet}$ radical in the formation of **1** is evident in the reactions of **4** with alkenes. The latter has been shown to undergo cycloaddition with a variety of halogenated alkenes to give 1,3-dioxolanes.[11] In these reactions significant amounts of epoxides are observed under certain conditions. It is proposed that the dioxolanes arise via an $FOCF_2O^{\bullet}$ radical after initial F atom abstraction from **4** by excess alkene. Thus the epoxides in these reactions may arise from the formation of **1** as an intermediate by the cyclization of $FOCF_2O^{\bullet}$, and the subsequent reaction of **1** with the excess alkene.

The dioxirane structure **1** is significantly more likely than the alternative isomeric carbonyl oxide structure by theoretical calculations[6] and is consistent with our observed data and the reactivity of **1** towards alkenes. The IR spectrum of **1** is shown in Figure 1. Type A, B, and C bands are apparent

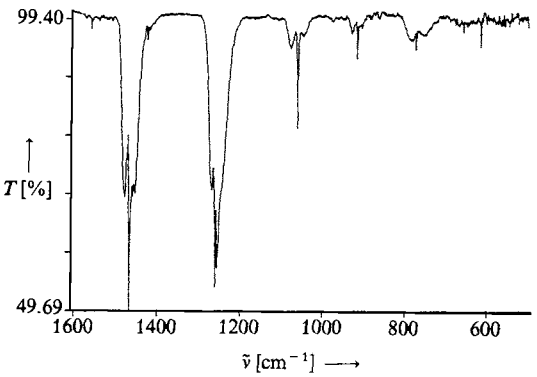

Fig. 1. The gas phase IR Spectrum of **1** (6 Torr).

as expected for the cyclic dioxirane with C_{2v} symmetry. In Table 1, the preliminary IR and Raman spectroscopic data for **1** are compared with the calculated values from Francisco and Williams.[12] The agreement for the observed nine fundamental vibrations is remarkably good. A detailed IR, Raman, and microwave investigation of **1** is in progress.

Difluorodioxirane is a pale yellow liquid below its boiling point of about −80 to −90 °C, and it exhibits a very low melting point (< −160 °C). Gas samples of pure **1** at 15 Torr and 22 °C show no decomposition after 12 h when moni-

Table 1. Calculated and experimentally determined vibrational frequencies for **1** in cm^{-1}.

Symmetry	Mode	Description	Calcd. [a]	IR [b]	Raman [c]
A_1	ν_1	CO stretch sym.	1543	1464 (vs)	
	ν_2	CF stretch sym.	1033	1061 (s)	1048
	ν_3	CF_2 scissor	761	772 (m)	712 (?)
	ν_4	OCO deform.	508	511 (vw)	
A_2	ν_5	CF_2 twist	406	-	416
B_1	ν_6	CF stretch. antisym.	1285	1259 (vs)	
	ν_7	CF_2 rocking	533	557 (w)	
B_2	ν_8	CO stretch. antisym.	964	911 (m)	
	ν_9	CF_2 wagging	637	617 (w)	624

[a] From ref. [12]. [b] In the gas phase. [c] Solution in $CFCl_3$.

tored in a glass IR cell. In contrast samples of **1** contaminated with small amounts of ClF are less stable under these conditions and significant amounts of the decomposition products COF_2 and O_2 are observed after 1 h. As expected **1** is a powerful oxidant and it readily transfers oxygen to alkenes, forming epoxides and COF_2 in high yield. With $CF_3CF=CF_2$, $F_2C=CFCl$, and $F_2C=CHF$ the respective epoxides are formed in >95% yield in the absence of solvent. With $CFCl_3$ as a solvent, similar results are observed. These are the first examples of the epoxidation of fluorinated alkenes by a dioxirane.

Experimental Procedure

1: In a typical reaction a mixture of equimolar amounts (0.5–2.0 mmol) of **3** and ClF at 23 °C were passed at reduced pressure through a Teflon FEP tube (35 cm × 1 cm outer diameter) containing 20 g of a pelletized CsF catalyst. The calculated flow rate of the mixture through the tube was 0.37 cm^3s^{-1}. The effluent exited into a trap cooled to −196 °C and under dynamic vacuum. The gases condensed at −196 °C were vacuum distilled several times through traps at −152 and −196 °C. This procedure gave **1** in the −196 °C trap, contaminated with small amounts of COF_2 and unreacted ClF. The unreacted ClF was separated from **1** by condensing excess SO_2 onto the mixture at −196 °C and allowing the sample to warm to about −100 °C. The ClF reacted with SO_2 to form SO_2ClF which was easily removed along with SO_2 by vacuum distillation through a −140 and −196 °C trap. **1**: M.p. < −160 °C/b.p. ≈ −80 to −90 °C; ^{19}F NMR (188 MHz, $CFCl_3$, 25 °C, CCl_4): $\delta = -29.9$ (s); IR (gas): see Table 1; Raman ($CFCl_3$, ca. −100 °C): see Table 1; MS (20 eV): *m/z* 82 ($M^{\oplus}$, trace), 66 ($CF_2O^{\oplus}$, 84), 50 ($CF_2^{\oplus}$, 4), 47 ($FCO^{\oplus}$, 100), 44 ($CO_2^{\oplus}$, 28), 32 ($O_2^{\oplus}$, 6), 28 ($CO^{\oplus}$, 10), 16 ($O^{\oplus}$, 3). The peak for the molecular ion in the MS was confirmed by selective ion monitoring.

The reactions of neat **1** (0.2 mmol) with CF_3CFCF_2 (0.5 mmol), CF_2CFCl (0.5 mmol), and CF_2CFH (0.5 mmol) were carried out in a 50 mL glass reactor by adding **1** and the alkene by vacuum transfer to the reactor at −196 °C. The mixture was then allowed to warm to 22 °C over 4 h and the products were identified by IR and NMR spectroscopy. Reactions of **1** in $CFCl_3$ (0.5 mL) were carried out on the same scale by mixing the alkene and $CFCl_3$ at 22 °C in the 50 mL reactor. The mixture was then cooled to −196 °C and **1** was added by vacuum transfer. The mixture was then warmed to 22 °C over 4 h and the solvent was removed by vacuum distillation. Yields of the respective epoxides in both reaction types were about 95% (determined by ^{19}F NMR spectroscopy). The epoxides were not separated from the excess alkene.

Received: December 7, 1992
Revised version: February 12, 1993 [Z 5730 IE]
German version: *Angew. Chem.* **1993**, *105*, 956

[1] a) R. W. Murray, *Chem. Rev.* **1989**, *89*, 1187; b) W. Adam, R. Curci, J. O. Edwards, *Acc. Chem. Res.* **1989**, *22*, 205.
[2] a) D. Cremer, T. Schmidt, J. Gauss, T. R. Radhakrishnan, *Angew. Chem.* **1988**, *100*, 431; *Angew. Chem. Int. Ed. Engl.* **1988**, *27*, 427; b) R. D. Bach, J. L. Andres, A. L. Owensby, H. B. Schlegel, J. J. W. McDowall, *J. Am. Chem. Soc.* **1992**, *114*, 7207.
[3] a) R. A. Mitsch, *J. Heterocycl. Chem.* **1966**, *3*, 245; *J. Org. Chem.* **1968**, *33*, 1847; b) M. D. Meyers, S. Frank, *Inorg. Chem.* **1966**, *5*, 1455.
[4] R. J. Talbott, P. J. Thompson (3M Co.), US-A 3632606, **1972**; *Chem. Abstr.* **1972**, *76*, P 99638.
[5] K. O. Christe, D. Plipovich, *J. Am. Chem. Soc.* **1971**, *93*, 51.
[6] M. Rahman, M. L. McKee, P. B. Shevlin, R. Sztyrbicka, *J. Am. Chem. Soc.* **1988**, *110*, 4002.
[7] R. L. Cauble, G. H. Cady, *J. Am. Chem. Soc.* **1967**, *89*, 5161.
[8] Details on the synthesis and properties of **2** will be reported separately.
[9] a) G. E. Gould, L. R. Anderson, D. E. Young, W. B. Fox, *J. Am. Chem. Soc.* **1969**, *91*, 1310; b) C. J. Schack, W. Maya, *ibid.* **1969**, *91*, 2902.
[10] M. Lustig, A. R. Pitochelli, J. K. Ruff, *J. Am. Chem. Soc.* **1967**, *89*, 2841.
[11] W. Navarrini, S. Fontana (Ausimont, SpA), EP-B 499157, **1992**; *Chem. Abstr.* **1992**, *117*, 236286h; *J. Fluorine Chem.* **1992**, *58*, 290; W. Navarrini, V. Tortelli, A. Zedda, *ibid.* **1992**, *58*, 143.
[12] J. S. Francisco, I. H. Williams, *Chem. Phys.* **1985**, *93*, 71.

Bis(*P*,*P*-di-*tert*-butyl-*N*-cyclohexylphosphinic amidato-*N*,*O*)nickel(II): Whether Planar or Tetrahedral—Both Isomers are Paramagnetic

By *Thomas Frömmel, Wilfried Peters, Hartmut Wunderlich,* and *Wilhelm Kuchen**

Dedicated to Professor Dietrich Mootz on the occasion of his 60th birthday

Complexes with tetracoordinated Ni^{II} are mostly planar, and more rarely tetrahedral. Occasionally, a ligand forms both structures, or in solution there is an equilibrium between the two isomers. This is true, as we have shown in previous work, also for the bidentate chelate ligands $[R_2P(S)NR']^-$, as they occur in complexes of the type **1**.[1] So far the diamagnetism and the lack of absorption bands in the electronic spectrum at wavelengths < 10000 cm^{-1} for the planar complexes, and paramagnetism ($\mu_{eff} \approx 3.0-3.4\ \mu_B$) for the tetrahedral complexes have been regarded as safe characteristics for the discrimination of the complexes. Whereas these assignment criteria, based on general experience, proved to be true in the case of **1**, they failed in the case of complex **2**. Complex **2** is paramagnetic in the solid state and shows an absorption at 7300 cm^{-1} in the powder spectrum: It contains, however, as the crystal structure determination showed, the exactly planar *trans*-NiN_2O_2 chromophore.[1]

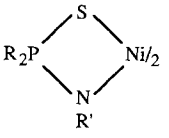

1

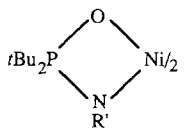

2–4

R = alkyl
R' = alkyl, phenyl

2, R' = *i*Pr
3, R' = *cyclo*-C_6H_{11}; **a**: olive-green, **b**: ink-blue
4, R' = *t*Bu

According to the synthetic route shown in Scheme 1 we have now been able to isolate olive-green (**3a**) and ink-blue (**3b**) crystals; the planar and tetrahedral isomers of the title complex **3**, respectively.[2] Complexes **3a** and **3b** precipitate

[*] Prof. Dr. W. Kuchen, Dipl.-Chem. T. Frömmel, Dr. W. Peters, Dr. H. Wunderlich
Institut für Anorganische Chemie und Strukturchemie der Universität
Universitätsstrasse 1, D-W-4000 Düsseldorf (FRG)
Telefax: Int. code + (211)311-2287

 © VCH Verlagsgesellschaft mbH, W-6940 Weinheim, 1993 0570-0833/93/0606-0907 $ 10.00+.25/0

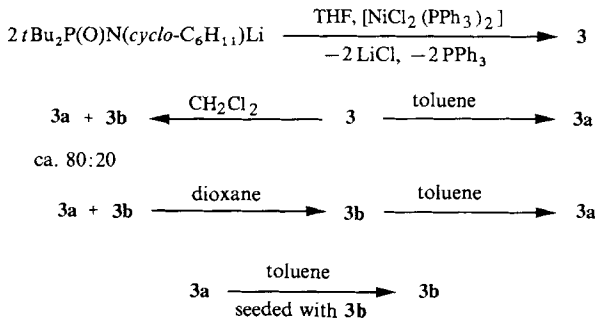

Scheme 1. Syntheses of the isomers **3a** (olive-green) and **3b** (ink-blue).

from the clear solutions of the complexes in the given solvents within a few days at 4 °C as well-formed crystals. Crystals of **3b** are obtained from a solution of **3a** after the addition of a few seed crystals.

Complexes **3a** and **3b** change slowly in air. In benzene they are monomeric. The ^{31}P NMR signal is, as for **2**, strongly shifted to higher field and both for **3a** and **3b** appears at $\delta = -813$ (CD_2Cl_2, 290 K). Both isomers exhibit identical magnetic properties: $\mu_{eff} = 3.3\ \mu_B$ (298 K), Curie–Weiss behavior between 280 and 80 K (solid state). The same magnetic moment was determined in CD_2Cl_2 at 293 K and Curie–Weiss behavior was observed between 293 and 190 K. Accordingly, the isotropic shift of the NMR signals (^1H, ^{31}P) in this temperature range is strictly linear with respect to T^{-1}.

The positions of the absorption bands in the powder spectra of **3a** and **3b** (Fig. 1, top) differ only slightly; however,

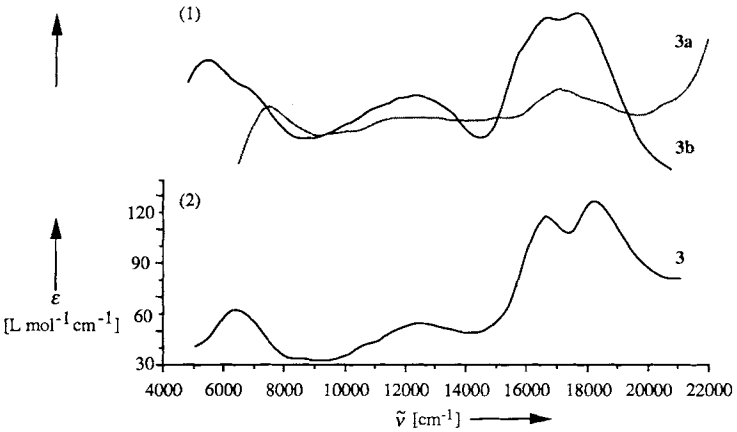

Fig. 1. 1) Powder spectra of **3a** and **3b** (in remission, $BaSO_4$ as standard); 2) solution spectra of **3** (toluene). I = intensity in arbitrary units.

with respect to the intensity of these bands the difference is considerable. The single-crystal transmission spectra[3] of both substances correspond to the powder spectra, and for **3b**, because of the lack of centrosymmetry in the tetrahedral complex, significantly more intense bands are observed. The latter statement is vindicated, since the structural investigation (see below) shows that crystals of **3a** and **3b** contain almost the same number of molecules per volume unit, and crystals of almost the same thickness were used for the recording of the spectra. It may also be mentioned, that the powder spectrum of **3a** is almost identical with that of the paramagnetic complex **2**, which is planar in the solid state.

The solution spectra of **3a** and **3b** (Fig. 1, bottom) did not vary whether they were recorded in toluene, CH_2Cl_2, or dioxane. These spectra are similar to the powder spectrum of **3b**, which corresponds to that of the tetrahedral thio complexes **1** (R = *t*Bu; R′ = *i*Pr, *cyclo*-C_6H_{11}),[1,4] whose powder and solution spectra are the same.[2] It can, therefore, be assumed that in solution at room temperature complex **3** is predominantly tetrahedral. The same is also valid for **2**, whose solution spectrum is almost superimposable with that of **3**, that is to say **2** does not remain planar in solution.[1]

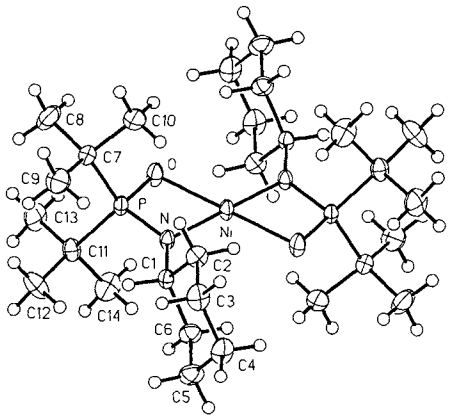

Fig. 2. Molecular structure of **3a** (ellipsoids drawn at 25% probability level) and atom designation [6]. The complex has $\bar{1}$-C_i symmetry with the Ni atom in the center of the symmetry. The H atoms are represented with a radius of 15 pm.

The crystal structure analysis (Fig. 2)[5] shows that the Ni atom in **3a** is exactly planar surrounded by two O and two N atoms (Ni–O 212.0(1) and Ni–N 190.0(1) pm). A higher coordination of the Ni atom by symmetry equivalent molecules can be excluded since the shortest distances to atoms of neighboring molecules are too large (Ni···H 476, Ni···C 548 pm). The O-Ni-N bond angle is 74.3(1)°, all the other angles at the Ni atom result from the centrosymmetry. The Ni-O-P-N four-membered ring is planar within 1.6 pm.

In contrast, the coordination of the Ni atom in **3b** is distorted tetrahedral (Fig. 3),[5] the most important bond angles being O-Ni-N 74.5(1), O-Ni-N′ 126.4(1), O-Ni-O′ 122.3(1), and N-Ni-N′ 140.6(1)°. The two planes through the

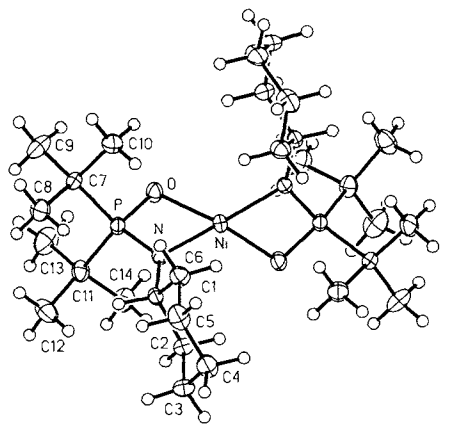

Fig. 3. Molecular structure of **3b**. The complex has 2-C_2 symmetry. Other information as in Figure 2.

atoms Ni,O,N and Ni,O′,N′ form an angle of 86.2°. It should be emphasized that the bond lengths Ni–O (205.9(2) pm) and Ni–N (194.5(2) pm) differ significantly from those of the planar complexes **2** and **3a**. To show the homogeneity of the

investigated crystalline material, an X-ray powder diffractogram of **3a** was recorded. The agreement between this and the diffraction pattern calculated from the single-crystal structure analysis was excellent; however, the X-ray powder diffractogram of **3a** showed large discrepancies with the one calculated for **3b**.[7, 8]

Once more the uniqueness of the $[t\mathrm{Bu_2P(O)NR'}]^-$ (R' = *i*Pr, *cyclo*-$\mathrm{C_6H_{11}}$) ligands is shown here: An apparently favorable combination of electronic and steric factors allows the formation of planar high-spin complexes of Ni^{II}. This is surprising, since for the analogous thio complexes **1** the tetrahedral coordination is preferred as the bulkiness of R' increases.[4] How great the influence of R' is on the properties of the complex is shown by the following preliminary results: According to the powder spectrum, complex **4** (R' = *t*Bu) is planar. Its μ_{eff} values vary from 1.7 (280 K) to 0.6 μ_B (80 K) (solid state) and suggest a spin-crossover between singlet and triplet state.

Experimental Procedure

Magnetic measurements were carried out according to Faraday (solid substance) and Evans (solution). ^{31}P NMR spectroscopy: Bruker AM 200 (81.026 MHz, CD_2Cl_2, 293 K, 85% H_3PO_4).

P,P-di-*tert*-butyl-*N*-cyclohexylphosphinic amide: 30% aqueous H_2O_2 (ca. 18 g) was slowly added to $t\mathrm{Bu_2PNH(cyclo\text{-}C_6H_{11})}$ [9] (160 mmol) in toluene (100 mL) and the mixture was stirred vigorously. After the exothermic reaction had subsided the organic phase was separated and the solvent was slowly evaporated at room temperature. The amide precipitated, generally in the form of colorless needles. Yield approximately 65%. Correct elemental analysis, m.p. 175 C, $\delta(^{31}P) = 54$ (toluene).

3 was prepared and handled under inert conditions. $t\mathrm{Bu_2P(O)NH(cyclo\text{-}C_6H_{11})}$ (19 mmol) in THF (25 mL) was treated with *n*-butyllithium (19 mmol, 1.6 M solution in hexane) and heated to reflux for a short time. The cooled solution was added to $[NiCl_2(PPh_3)_2]$ (9.63 mmol), and the resulting solution was stirred for 2 h at room temperature. Subsequently the solvent was removed under vacuum.

For the isolation of **3a** the residue was taken up in toluene (5 mL), centrifuged, and the clear solution obtained was kept at 4 °C. As a result olive-green crystals of **3a** precipitated slowly from the solution. Yield > 40%. Correct elemental analysis, m.p. 206 °C (decomp), molecular masses (cryoscopic in benzene): 550 (0.079 molal) 589 (0.085 molal).

For the isolation of **3b** the residue was taken up in CH_2Cl_2 (5 mL) and the solution was centrifuged. **3a** and **3b** precipitated from the solution as a mixture of olive-green and blue crystals, which was dissolved in the smallest amount of dioxane by mild heating. When the solution was left to stand mainly blue crystals of **3b** were obtained. If necessary, the latter process was repeated until the crystalline material was homogeneous. Yield > 40%. Correct elemental analysis, m.p. 193 °C (decomp).

Alternatively, a saturated solution of **3a** in toluene was allowed to react with a few seed crystals of **3b**. Ink-blue crystals of **3b** precipitated at 4 °C slowly in the course of several days.

Received: January 28, 1993 [Z 5837IE]
German version: *Angew. Chem.* **1993**, *105*, 926

[1] T. Frömmel, W. Peters, H. Wunderlich, W. Kuchen, *Angew. Chem.* **1992**, *104*, 632-633; *Angew. Chem. Int. Ed. Engl.* **1992**, *31*, 612-613, and references therein.

[2] Part of the planned dissertation of Dipl.-Chem. T. Frömmel, Universität Düsseldorf.

[3] We thank Dipl.-Chem. U. Rosellen and Dipl.-Chem. H. Mink, Institut für Theoretische Chemie der Universität Düsseldorf (Direktor Prof. Dr. H.-H. Schmidtke), for recording the single-crystal transmission spectra.

[4] A. Deeg, W. Kuchen, D. Langsch, D. Mootz, W. Peters, H. Wunderlich, *Z. Anorg. Allg. Chem.* **1991**, *606*, 119-132.

[5] **3a**: $C_{28}H_{58}N_2P_2O_2Ni$ (M_r = 575.4), space group $P\bar{1}$, a = 821.8(2), b = 1006.4(2), c = 1060.5(2) pm, α = 78.51(2), β = 76.33(2), γ = 79.04(2)°, V = 0.8257(1) nm³, Z = 1, ρ_{calcd} = 1.16 mg mm⁻³, μ = 0.71 mm⁻¹. Crystal size 0.3 × 0.35 × 0.4 mm³, Syntex-Siemens diffractometer $P2_1/P3$. 3815 symmetry independent reflections ($4 < 2\theta < 55°$, $Mo_{K\alpha}$, λ = 71.073 pm, graphite monochromator, ω: 2θ scan, 3028 observed reflections with $F > 4\sigma_F$). Solution and refinement [6]. $w^{-1} = \sigma_F^2 + 0.0004F^2$, 160 parameters, R = 0.034, R_w = 0.045 [8].-**3b**: space group *Pccn*, a = 1313.9(2), b = 1522.5(2), c = 1600.9(2) pm, V = 3.2026(6) nm³, Z = 4, ρ_{calcd} = 1.19 mg mm⁻³, μ = 0.73 mm⁻¹. Crystal size 0.4 × 0.5 × 0.7 mm³. 3660 reflections, of which 2164 observed, other information as for **3a**. 159 parameters, R = 0.033, R_w = 0.039 [8].

[6] SHELXTL PLUS Release 4.21/V, Siemens Analytical X-ray Instruments Inc.

[7] Guinier powder diffractometer G 600, (Huber, Rimsting (FRG)).

[8] Further details of the crystal structure investigation may be obtained from the Fachinformationszentrum Karlsruhe, Gesellschaft für wissenschaftlich-technische Information mbH, D-W-7514 Eggenstein-Leopoldshafen 2 (FRG) on quoting the depository number CSD-56976, the names of the authors, and the journal citation.

[9] W. Kuchen, D. Langsch, W. Peters, *Phosphorus, Sulfur, Silicon* **1990**, *54*, 55-61.

Control of the Linkage of Inorganic Fragments of V–O Compounds: From Cluster Shells as Carcerands via Cluster Aggregates to Solid-State Structures**

By *Achim Müller,** *Ralf Rohlfing, Erich Krickemeyer,* and *Hartmut Bögge*

Dedicated to Professor Heinrich Nöth on the occasion of his 65th birthday

The control of the linkage of fragments of inorganic complexes or molecules to form oligomers or infinite three-dimensional structures is of general interest, amongst other purposes, for the understanding of prebiotic processes and for the molecular engineering of materials; the laws governing these processes, however, are almost unknown. We can now show that the linking of $V^{n+}O_x$ polyhedra (tetrahedra, octahedra, and square pyramids) and the spin organization of the V centers in the aggregates under construction can be controlled over a wide range by predominantly anionic reagents (templates). Depending on the choice of these reagents, shell-like clusters (molecular containers, carcerands[11]) in which the directing agent is situated inside the cavity (**1**, **2a**, **3**, and **4**) or V–O aggregates in which the directing agent is positioned on the outer surface of the shell (**6**, **7**) are formed. The cluster anions of **2b** and **5** are transition forms of these two types and reveal novel host–guest systems and structural types. The results model fundamental processes that control the propensities for organization in material systems.[2]

$K_{10}[HV_{18}O_{44}(NO_3)] \cdot 14.5\,H_2O$ **1**

$(NEt_4)_6[HV_{22}O_{54}(SCN)]$ **2a**

$(NEt_4)_5(NH_4)_2[H_2V_{22}O_{54}(CH_3COO)] \cdot 7\,H_2O$ **2b**

$Na_{10}[H_2V_{18}O_{44}(H_2O)] \cdot 30\,H_2O$ **3**

$K_7[H_4V_{15}O_{40}(PO_4)] \cdot 10\,H_2O$ **4**

$Na_6[H_6V_{12}O_{30}F_2] \cdot 22\,H_2O$ **5**

$Na[V_2O_2(OH_2)_2(\mu\text{-}OH)(\mu\text{-}OH_2)(C_4O_4)_2] \cdot 6\,H_2O$ **6**

$K_2[H_6V_{10}O_{22}(CH_3COO)_6] \cdot 25\,H_2O$ **7**

The mixed valent (**1**–**5**, **7**) and reduced (**6**) vanadium–oxygen compounds were synthesized by reduction (**1**, **3**–**7**) of vanadate(V) or oxidation (**2a**,**b**) of vanadate(IV)/vanadate(V)

[*] Prof. Dr. A. Müller, Dipl.-Chem. R. Rohlfing, E. Krickemeyer, Dr. H. Bögge
Fakultät für Chemie der Universität
Postfach 100131, D-W-4800 Bielefeld 1 (FRG)

[**] This work was supported by the Deutsche Forschungsgemeinschaft and the Fonds der Chemischen Industrie.

species in water by controlling the type of linkage of the $V^{n+}O_x$ polyhedra by templates. The compounds were characterized by elemental analysis (including manganometric titration of the V^{IV} content, thermogravimetric determination of the water of crystallization, and ion-chromatographic determination of NO_3^-, PO_4^{3-}, and F^-), IR spectroscopy, single-crystal X-ray crystallography,[3] and determination of bond valence sums.[3]

The structures of the anions in the compounds **1**–**7** are depicted in Figure 1 (cagelike cluster shells (carcerands) containing templates in the center: type I), Figure 2 ("central" aggregates of clusters built up from $V^{n+}O_x$ polyhedra with terminal organic anions as ligands, that is, with a hydrophobic (screening) part as in squaric acid (3,4-dihydroxy-3-cyclobutene-1,2-dione): type II),[4] as well as in Figure 3. The structural types are shown schematically in Figure 4 and the number of the different $V^{n+}O_x$ polyhedra, the symmetry (point groups) of the V–O aggregates and the V^{IV}/V^V ratios are collated in Table 1. When the attractive type of interaction between the central nucleophilic anion or molecule (e.g. NO_3^- in **1**) and the electrophilic or Lewis acidic V^{n+} centers is weak, square pyramids are linked to form a carcerand[5] (**1**–**3**). If this interaction is strong, for instance when the anion bears a high charge (e.g., PO_4^{3-} in **4**), other polyhedra, primarily octahedra) also occur in the structures

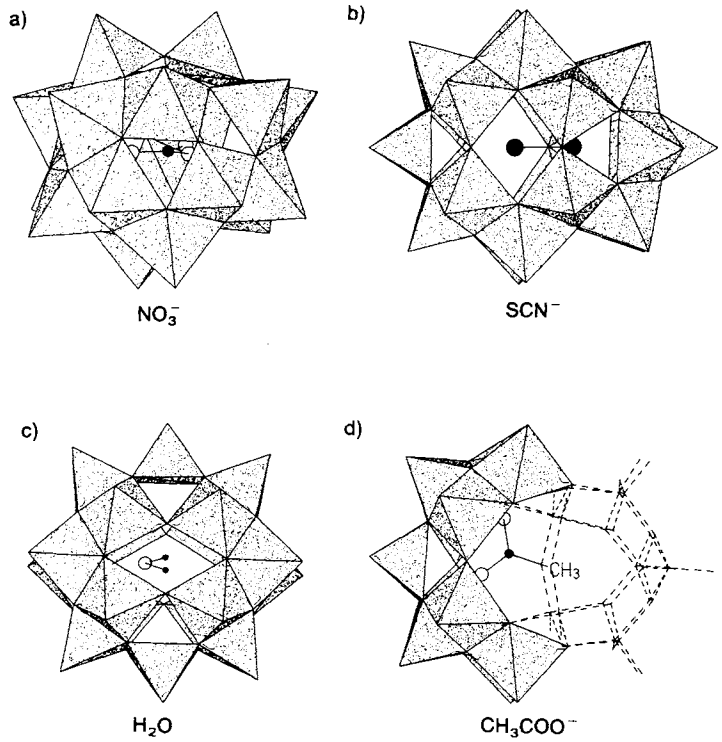

Fig. 1. Polyhedral representation of the anions of **1** (a), **2a** (b), **2b** (d; only one of the $V_{22}O_{54}$ half shells)), and **3**(c). The enclosed anions or molecules are given under the polyhedra for clarity. Selected distances [pm]: $V–O_{term}$ 156–163, $V–\mu_2$-O 171–193, $V–\mu_3$-O 178–212; special data for **1**: $V–\mu_2$-O(H) 195–196, N–O 120–129, $V\cdots O(NO)_2 > 278$, $O\cdots O(NO_2) > 274$; for **2a** S(CN)–S(CN) 209, $V\cdots S(CN) > 365$, $O\cdots S(CN) > 353$ (SCN^- disordered and CN not resolved); **2b**: C–O 124–130, C–C 147, $V\cdots O(CO) > 251$, $O\cdots O(CO) > 262$, $V\cdots C(O_2) > 344$, $O\cdots C(O_2) > 337$, $V\cdots C(H_3) > 398$, $O\cdots C(CH_3) > 359$; for **3**: $V–\mu_2$-O(H) 185–189, $V\cdots O(H_2) > 325$; $O\cdots O(H_2) > 314$, $O\cdots H(OH) > 279$ (exception: for the two O atoms of the shell that fix the H_2O molecule in the center by hydrogen bonds, $O\cdots O(H_2)$ 291–292 and $O\cdots H(OH) > 229$).

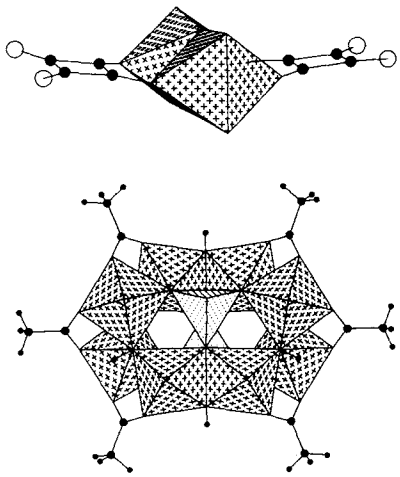

Fig. 2. Polyhedral representation of the anions of **6** (top) and **7** (bottom). Selected distances [pm]: $V–O_{term}$ 157–161, $V–\mu_2$-O(H) 194–199, V–O(C) 198–203; special data: for **6**: $V–O(H_2)_{term}$ 202–207, $V–\mu_2$-O(H_2) 236–240, C–O 121–131, C–C 142–148; for **7**: $V–\mu_3$-O 175–228, $V–\mu_3$O(H) 204–226, C–O 125–127, C–C 149–150.

(mainly formed by incorporating an atom of the template). In **5** the F^- ion is too small to be a guest in the cavity, but it creates a strong V–F interaction. In all cases, however, electronic influences can also play a role (see, for instance, the occurrence of VO_4 tetrahedra only in the case of V^V compounds. The salt **2b** includes a new type of host–guest cluster: the hydrophobic CH_3 group of the acetate anion hardly protrudes from one of the two $V_{22}O_{54}$ half-shells (see Fig. 1), and the carboxy group interacts relatively strongly with the V centers (refer to the relevant distances).

In particular, the following can be said of **1**–**7**: the structure of the anion of **4** is interesting, because three different VO_x polyhedra are present ($x = 4, 5, 6$), the special feature of the anion of **1** is the shell that is almost complementary to the central NO_3^- unit (but the C_2 axes of the shell and the NO_3^- ion do not coincide). The SCN^- ion in the anion of **2a**, which is situated disordered on the S_4 symmetry axis in the known $V_{22}O_{54}$ shell and therefore is formally located perpendicular to the smaller but topologically identical N_3^- ion in the similar $V_{18}O_{44}$ shell of $[H_2V_{18}O_{44}(N_3)]^{5-}$,[6] appears, as it were, to float within the carcerand (long V–(SCN) distances reveal extremely weak interactions). Whereas in the binuclear complex **6** two $V^{IV}O_6$ octahedra share edges, in **7** two sets of four edge-sharing $V^{IV}O_6$ octahedra are linked through two V^VO_4 tetrahedra in such a way that a novel double layer structure arises. Compound **5** has a structure

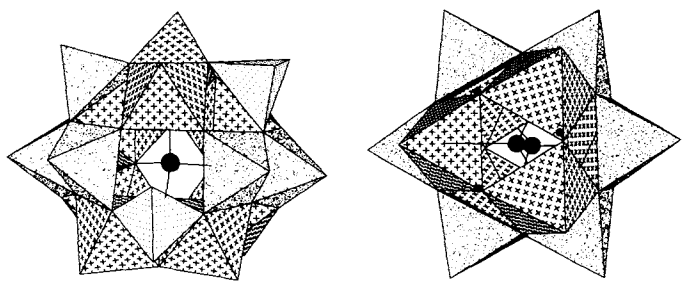

Fig. 3. Polyhedral representation of the anions of **4** (left) and **5** (right). Selected distances [pm]: $V–O_{term}$ 160–165, $V–\mu_2$-O(H) 181–205, $V–\mu_3$-O 181–213; special data: for **4**: $V–\mu_2$-O 169–204, P–O 152–155, V–O(PO_3) 218–230; for **5**: V–F 217–219, F···F 311 (octahedra indicated by crosses, square pyramids by random dots, and tetrahedra by regular dots).

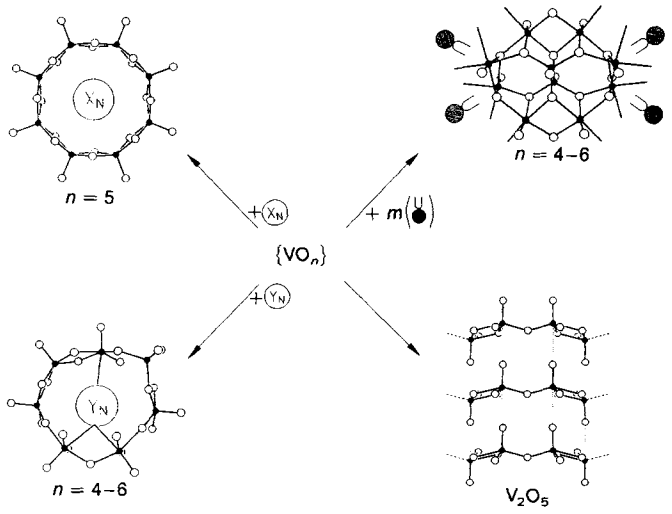

Fig. 4. Schematic representation of the possibilities for connecting VO_n units (n = coordination number; nucleophilic substrates: Y_N (strong) and X_N (weak); anionic substrate containing a hydrophobic part: ⌒).

Table 1. Structural types [a], VO_x polyhedral types, and the number of formal V^{IV}/V^{V} centers [b] of cluster anions in **1**–**7**.

	Type	V^{IV}/V^{V}	Octahedra	Square pyramids	Tetrahedra	Symmetry of the V-O-aggregate
1	I	12/6	-	18	-	C_2
2a	I	8/14	-	22	-	D_{2d}
2b	(II)	10/12	-	22	-	D_{2d}
3	I	14/4	-	18	-	D_{2h}
4	(I)	3/12	8 [c]	5	2 (V^{V})	C_1
5	(I)	10/2	6 [d] (V^{IV})	6	-	D_{3d}
6	II	2/-	2 [e] (V^{IV})	-	-	C_{2v}
7	II	8/2	8 [e] (V^{IV})	-	2 (V^{V})	C_{2h}

[a] I: Cagelike, containing a hydrophilic central template (guest) interacting weakly with the cluster shell; II: central cluster aggregate with the directing reagent containing a hydrophobic residue on the outside; (I): like I, but containing a hydrophilic central template and strong interactions; (II): like I, but with a central template containing a hydrophobic part (transition type between I and II). [b] Delocalized valence states, if not specifically designated otherwise. [c] One face-sharing and three edge-sharing pairs of octahedra. [d] Edge-sharing VO_5F octahedra. [e] Edge-sharing.

novel for the polyanion chemistry of transition metals.[7] It consists of two groups of three octahedra sharing edges as in a Keggin ion but with μ_3-F centers, linked through six square pyramids. Apparently the repulsion or direct contact of the F^- ions in the center ($F\cdots F = 311$ pm) determine the structure.

The topological and electronic diversity of vanadium–oxygen complexes is exceptional (compare also the many vanadium oxide minerals[8]). The pyramidal $O{=}V^{n+}O_4$ unit that dominates in the structural hierachy plays a central role. The manner of its linkage is directed by weak $O{=}V\cdots X$ interactions (X = nucleophile),[9–11] which result in molecular containers, but also in typical solid state structures as in V_2O_5[12] (O=V as nucleophile). A template principle underlies the formation and stacking of the V_2O_5 layers: layer $n+1$ forms on layer n through the weak $O{=}V\cdots O{=}V$ interactions. The distance d between the layers of 279.1 pm is correspondingly relatively large. The $O{=}V\cdots O{=}V$ interaction in V_2O_5 is apparently similar to that in the container compounds described here, though in these the weak repulsive interaction between the O=V groups influences the curvature of the shell. The interaction between the layers of the V_2O_5 lattice can also be compared with the $O{=}V(\text{shell})\cdots O{=}V(\text{cluster})$ interaction of the central $\{V_4O_4\}O_4$ cluster with the shell of the $[V_{34}O_{82}]^{10-}$ anion in $K_{10}[V_{34}O_{82}]\cdot 20H_2O$[13] ($V{=}O(\text{shell})\cdots O{=}V(\text{cluster}) > 254$ pm). Prerequisite for the presence of $O{=}V^{n+}O_4$ units in all cases is the relatively weak nucleophilicity and low basicity of the relevant centers of the directing agent (for example, in the case of the anions of strong acids like ClO_4^- and X^- (X = halogen), but also of H_2O and the O=V groups of a layer of V_2O_5). The V_2O_5 layer is stabilized, because the O=V groups of edge-sharing pyramids (with short V–V distances) are situated on different sides of the plane.

Experimental Procedure

1: A solution of KVO_3 (3.45 g, 25.0 mmol) in H_2O (50 mL) in a wide-necked Erlenmeyer flask (100 mL) covered with a watch glass was treated at 90 °C with N_2H_5OH (100%, 182 μL, 3.75 mmol) and maintained for 1 h at this temperature without stirring. Thereafter the pH of the dark brown solution was adjusted to about 8.0 with HNO_3 (65%) and held constant for 2 h by additions of more acid every 15 min. The solution was cooled to 20–25 °C after a further 3 h at 90 °C, and the precipitated black needles were filtered off after 1 day, washed with a little aqueous 2-propanol (50%) and air-dried. Yield: 1.6 g. IR (KBr): $\tilde{\nu}$ [cm^{-1}] = 1355(m, NO_3^-), 965(s, $V{=}O_{term}$), 815(w, NO_3^-), 700(s), 615(sh, V-O-V).

3–**7** were synthesized analogously by reduction of aqueous vanadate(v) solutions and subsequent addition of the anions PO_4^{3-} (**4**), F^- (**5**), $C_4O_4^{2-}$ (**6**), and CH_3COO^- (**7**) (instead of NO_3^- in **1**).

2a: A solution of NEt_4SCN (4.0 g, 21.2 mmol) in H_2O (100 mL) in a wide-necked Erlenmeyer flask (100 mL) covered with a watch glass was treated at 75 °C with freshly prepared $(NH_4)_8[H_9V_{19}O_{50}]\cdot 11H_2O$ [14] (0.83 g, 0.4 mmol) and maintained for 2–3 days at this temperature without stirring. The precipitated black crystals were filtered from the hot solution, washed with a small amount of cold H_2O, and air-dried. Yield: 0.5 g. IR (KBr): $\tilde{\nu}$[cm^{-1}]: 2040(m, SCN), 995(s, $V{=}O_{term}$), 835(m), 785(m), 705(s), 625(s, V-O-V).

2b was synthesized analogously in the presence of air from $(NH_4)_8[H_9V_{19}O_{50}]\cdot 11H_2O$ in the presence of CH_3COO^- (instead of SCN^- in **2a**).

Received: December 23, 1992 [Z 5772IE]
German version: *Angew. Chem.* **1993**, *105*, 916

[1] Cf. the definition of container and carcerand function in D. J. Cram, *Nature* **1992**, *356*, 29 and in F. Vögtle, *Supramolekulare Chemie*, 2nd ed., Teubner, Stuttgart, **1992**.

[2] The size of the clusters, the variation of the number of V^{IV}-(d^1) centers (spins), and their magnetic interaction (D. Gatteschi, L. Pardi, A. L. Barra, A. Müller, J. Döring, *Nature* **1991**, *354*, 463), as well as the size of the cavities can be influenced over a wide range (cf. the modeling of the cavities of zeolites: P. C. H. Mitchell, *ibid.* **1990**, *348*, 15). Furthermore, the cluster shells can be used as relatively inert matrices (with only small interactions) for anions of different sizes (A. Müller, E. Diemann, E. Krickemeyer, S. Che, *Naturwissenschaften* **1993**, *80*, 77).

[3] **1**: $P2_1/n$, $a = 1106.5(3)$, $b = 4618.0(14)$, $c = 1269.3(4)$ pm, $\beta = 113.56(2)$, $V = 5945(3)\times 10^6$ pm^3, $Z = 4$, $R = 0.075$ for 5055 independent reflections ($F_0 > 3\sigma(F_0)$). **2a**: $C2/c$, $a = 2072.6(8)$, $b = 2030.6(9)$, $c = 2417.6(9)$ pm, $\beta = 93.50(3)°$, $V = 10156(4)\times 10^6$ pm^3, $Z = 4$, $R = 0.118$ for 4558 independent reflections ($F_0 > 4\sigma(F_0)$); the R value is high, because of the disorder of the SCN^- ion in the center of the $V_{22}O_{54}$ shell). **2b**: $P\bar{1}$, $a = 1475.4(2)$, $b = 1505.1(2)$, $c = 1513.0(2)$ pm, $\alpha = 60.13(1)$, $\beta = 62.75(1)$, $\gamma = 87.00(1)$, $V = 2521.8(5)\times 10^6$ pm^3, $Z = 1$, $R = 0.039$ for 10684 independent reflections ($F_0 > 4\sigma(F_0)$). **3**: $P\bar{1}$, $a = 1202.7(2)$, $b = 1311.4(2)$, $c = 1347.1(1)$ pm, $\alpha = 114.93(1)$, $\beta = 93.21(1)$, $\gamma = 113.64(1)$, $V = 1699.2(3)\times 10^6$ pm^3, $Z = 1$, $R = 0.027$ for 7218 independent reflections ($F_0 > 4\sigma(F_0)$). The positions of the H atoms of the H_2O molecule were determined from difference Fourier maps according to a high-angle refinement and refined as riding on the relevant oxygen atoms with a fixed U value. **4**: $P2_1/n$, $a = 1251.2(2)$, $b = 1893.0(4)$, $c = 2062.0(3)$ pm, $\beta = 90.03(1)°$, $V = 4884.1(15)\times 10^6$ pm^3, $Z = 4$, $R = 0.050$ for 8558 independent reflections ($F_0 > 4\sigma(F_0)$). **5**: $P2_1/n$, $a = 1002.3(1)$, $b = 1267.0(2)$, $c = 1945.7(3)$ pm, $\beta = 100.33(1)°$, $V = 2430.8(5)\times 10^6$ pm^3, $Z = 2$, $R = 0.040$ for 3998 independent reflections ($F_0 > 4\sigma(F_0)$). The positions of the H atoms of the anion were determined from difference Fourier maps according to a high-angle refinement and refined as riding on the relevant O atoms with a fixed U value. **6**: Cc, $a = 1501.1(2)$, $b = 648.5(1)$, $c = 2032.3(3)$ pm, $\beta = 97.21(1)°$, $V = 1962.6(5)\times 10^6$ pm^3, $Z = 4$, $R = 0.097$ for 1722 independent reflections ($F_0 > 4.4\sigma(F_0)$). **7**: $P\bar{1}$, $a = 1021.4(2)$, $b = 1031.7(2)$, $c = 1558.5(3)$ pm, $\alpha = 78.12(1)$, $\beta = 78.66(1)$, $\gamma = 85.82(1)°$, $V = 1574.8(5)\times 10^6$ pm^3, $Z = 1$, $R = 0.040$ for 6402 independent reflections ($F_0 > 4\sigma(F_0)$). Measurements in the mother liquor.

The positions of the H atoms of the anion were determined from difference Fourier maps according to a high-angle refinement and refined as riding on the relevant O and C atoms with a fixed U value. The powder diagrams calculated from the single crystal data agree with those obtained from experiment. Further details of the crystal structure investigations may be obtained from the Fachinformationszentrum Karlsruhe, Gesellschaft für wissenschaftlich-technische Information mbH, D-W-7514 Eggenstein-Leopoldshafen 2 (FRG) on quoting the depository number CSD-56998, the names of the authors, and the journal citation. From the difference Fourier synthesis after a high-angle refinement, the following positions of the hydrogen atoms were determined crystallographically for **3**, **5**, and **7**: for **3** those of all water molecules (water of crystallization and the guest molecule); for **5** and **7** those of the anion, including the methyl protons of **7** (cf. Fig. **1**–**3**). Through the determination of the bond valence sums (I. D. Brown in *Structure and Bonding in Crystals, Vol. II* (Eds.: M. O'Keeffe, A. Navrotsky), Academic Press, New York, **1981**, p. 1) according to the equation $n = \exp[-(R-R_0)/B]$ (n is the bond valence, R = V-O distance in pm, $R_0 = 179$ pm, $B = 31.9$ pm), all protonated O atoms of the anions of **1**, **3**, **4**, and **6** were found by a characteristic lowering of the sum of the bond valences. Thus one μ_2-O(H) bridge is found for **1**, two for **3**, four for **4**, and one for **6**, which also has a μ_2-O(H_2) bridge (*trans* to $V{=}O_{term}$) and two terminal H_2O ligands (*trans* to μ_2-O(H) bridge). For the anions of **2a** and **2b** the protonations at the anion indicated by the equation followed from the charge balance. If not explicitly mentioned, the protonations occur at bridging O atoms.

[4] Anions of organic acids, that is, those with a hydrophobic residue, can function as terminal ligands to stabilize aggregates of $V^{n+}O_x$ polyhedra and screen these within the crystal lattice. (They adopt the function of the O=V groups in the container compounds.) Small or highly charged ligands such as F^- or PO_4^{3-} are not suitable, because they interact strongly with the V centers.

[5] After the isolation of the first host–guest compound of the V–O system with weak interaction and complementarity of the shell and the central spherical unit, the synthesis of $[H_2V_{18}O_{44}(N_3)]^{5-}$ and $[HV_{22}O_{54}(ClO_4)]^{6-}$ [6] were expected. However, an analysis of the cavities showed that, for example, in the $V_{18}O_{44}$ shell the incorporation of larger guests should also be possible (instead of the N_3^- ion, a NO_3^- ion, as in $[H_6V_{18}O_{44}(NO_3)]^{11-}$; unpublished results). This means that the space in this shell can also be used thus. (A container or carcerand function [1], of course, does not necessarily imply complementarity). A remarkable example of this is the compound **2a**. The size of the SCN^- ion hinders the isomorphous substitution of the topologically analogous N_3^- ion in the shell of $[H_2V_{18}O_{44}(N_3)]^{5-}$. Nevertheless control by the anionic template according to the argument in [6] is valid in all cases, because the size of the cluster shells always correlates with the size of the template. In the above-mentioned context the following results are particularly impressive for the control mechanism: 1. Shells of identical composition but different structures occur as a direct result of the dependence on the central anion (cf. O_{24} arrangement as rhombicuboctahedron in the $V_{18}O_{42}$ shell with central XY_4 or as the 14th archimedean body with a spherical guest like a halide ion: A. Müller, M. Penk, R. Rohlfing, E. Krickemeyer, J. Döring, *Angew. Chem.* **1990**, *102*, 927; *Angew. Chem. Int. Ed. Engl.* **1990**, *29*, 926, as well as [6]). 2. The central cubelike $\{V_4O_4\}O_4$ unit in $[V_{34}O_{82}]^{10-}$, which represents a section (though strongly distorted) of a cubic solid-state defect structure of the NaCl type, has almost a nucleation function for the genesis of the cluster shell [13]. One can talk of an "initiation–causality". It is also remarkable that all known cluster shells of type I can formally be derived from the V_2O_5 lattice [12] (e.g., the $V_{18}O_{44}$ and $V_{22}O_{54}$ shells (W. G. Klemperer, T. A. Marquart, O. M. Yaghi, *ibid.* **1992**, *104*, 51 and **1992**, *31*, 49), as well as the shell of $[V_{15}O_{36}Cl]^{6-}$ (A. Müller, E. Krickemeyer, M. Penk, H.-J. Walberg, H. Bögge, *ibid.* **1987**, *99*, 1060 and **1987**, *26*, 1045) and of **1**). (Some aspects of related host–guest chemistry are given in H. Reuter, *ibid.* **1992**, *104*, 1210 and **1992**, *31*, 1185, as well as in *Naturwiss. Rundschau* **1992**, *45*, 368.)

[6] A. Müller, E. Krickemeyer, M. Penk, R. Rohlfing, A. Armatage, H. Bögge, *Angew. Chem.* **1991**, *103*, 1720; *Angew. Chem. Int. Ed. Engl.* **1991**, *30*, 1674.

[7] However, a similar structure occurs in the $[(i\text{PrSn})_{12}O_{14}(OH)_6]^{2+}$ ion: H. Puff, H. Reuter, *J. Organomet. Chem.* **1989**, *373*, 173.

[8] H. T. Evans, Jr., J. S. White, Jr., *Mineral. Rec.* **1987**, *18*, 333; A. Müller, J. Döring, M. I. Khan, V. Wittneben, *Angew. Chem.* **1991**, *103*, 203; *Angew. Chem. Int. Ed. Engl.* **1991**, *30*, 210.

[9] In the carcerands with a centered anion the repulsive (O···anion) and attractive (V^{n+}···anion) forces are balanced (see also A. Müller, K. Hovemeier, R. Rohlfing, *Angew. Chem.* **1992**, *104*, 1214; *Angew. Chem. Int. Ed. Engl.* **1992**, *31*, 1192). This is plausibly demonstrated by the fact that in the compounds $(NEt_4)_2[V_4O_8(NO_3)(tca)_4]\cdot H_2O$ (D. D. Heinrich, K. Folting, W. E. Streib, J. C. Huffman, G. Christou, *J. Chem. Soc. Chem. Commun.* **1989**, 1411; tca = $C_4H_3SCOO^-$) and $[K\{V_4O_8(O_2CCH_2t\text{Bu})_4\}]\cdot[O_2CCH_2t\text{Bu}]\cdot 2\,t\text{BuCH}_2CO_2H$ (W. Priebsch, D. Rehder, M. von Oeynhausen, *Chem. Ber.* **1991**, *124*, 761) the $\{V_4O_{16}\}$ unit can complex a cation as well as an anion. Apparently more than four Lewis acidic V centers must be present to complex anions only.

[10] The type of linkage of the $O{=}V^{n+}O_4$ pyramids varies from weak, that is, linkage only through μ_2-O atoms according to the stoichiometry $\{(O{=}V)_1O_3\}_n$ of the Keggin type, to maximal, that is, linkage only through μ_3-O atoms according to the stoichiometry $\{(O{=}V)_3O_4\}_n$ of the extended $V_{18}O_{42}$ Keggin shell (M. T. Pope, A. Müller, *Angew. Chem.* **1991**, *103*, 56; *Angew. Chem. Int. Ed. Engl.* **1991**, *30*, 34). The molecular containers of type I, but also V_2O_5, with both μ_2-O and μ_3-O functions have on this scale an intermediate type of linkage, unpublished results.

[11] Cf. also M. T. Pope, *Nature* **1992**, *355*, 27.

[12] R. Enjalbert, J. Galy, *Acta Crystallogr. Sect. C* **1986**, *42*, 1467; A. F. Wells, *Structural Inorganic Chemistry*, 5th ed., Clarendon, Oxford, **1984**, p. 568.

[13] A. Müller, R. Rohlfing, J. Döring, M. Penk, *Angew. Chem.* **1991**, *103*, 575; *Angew. Chem. Int. Ed. Engl.* **1991**, *30*, 588.

[14] A. Müller, M. Penk, E. Krickemeyer, H. Bögge, H.-J. Walberg, *Angew. Chem.* **1988**, *100*, 1787; *Angew. Chem. Int. Ed. Engl.* **1988**, *27*, 1719.

Biosynthesis of Iridodials in the Defense Glands of Beetle Larvae (Chrysomelinae)**

By Michael Lorenz, Wilhelm Boland, and Konrad Dettner*

Cyclopentanoid natural products based on an iridoid structure are widespread in plants and insects.[1] In plants the iridoid glucosides, in particular, are of interest because some of these compounds exhibit pharmacological activity, while others are intermediates via secoiridoids in pathways leading to many alkaloids.[2] Thus, the biosynthesis of these compounds has been the subject of intensive investigation over the last 30 years. The key steps in the biosynthesis are the ω-hydroxylation of geraniol to 8-hydroxygeraniol and its further oxidation to 8-oxocitral. 8-oxocitral can be cyclized directly or after further transformations to the iridoid unit[2, 3] (analogous to Scheme 1). Additional oxidation and cyclization steps follow and lead to more than 1000 plant iridoids known today.[1, 4] In insects some volatile iridoids serve as pheromones,[5] while others such as **1**–**6** which are produced in defense glands serve as glues, insecticides, fixatives, or fumigants in defense secretions.[6]

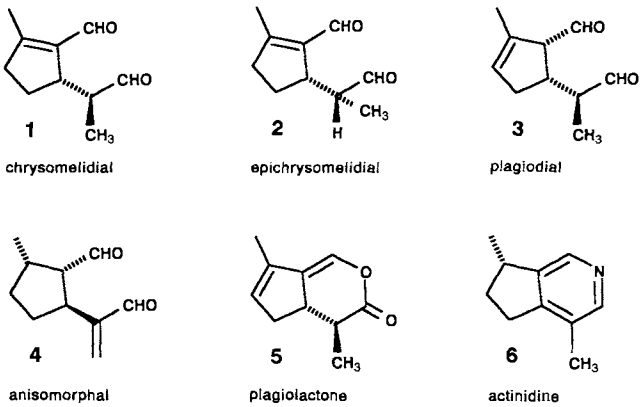

[*] Prof. Dr. W. Boland, Dr. M. Lorenz
Institut für Organische Chemie der Universität
Richard-Willstätter-Allee 2, D-W-7500 Karlsruhe (FRG)
Telefax: Int. code + (721)698-305
Prof. Dr. K. Dettner
Tierökologie II der Universität
Postfach 101252, D-W-8580 Bayreuth (FRG)

[**] This work was supported by the Deutschen Forschungsgemeinschaft (DFG) (SPP: Chemische Ökologie) and the Fonds der Chemischen Industrie.

The larvae of the leaf beetles *Phaedon cochleariae*, *Gastrophysa viridula*, and *Plagiodera versicolora* have nine pairs of glands which can be everted upon molestation. These are located on the meso or metathorax as well as on the first seven abdominal segments. A drop of a defense secretion appears at the gland openings, and for *P. cochleariae* and *G. viridula* this secretion consists mainly of chrysomelidial **1** and epichrysomelidial **2** as low molecular weight components[7] (see Fig. 1). In contrast, the glands of *P. versicolora* secrete

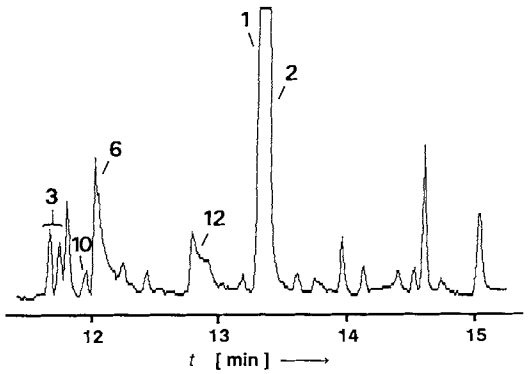

Fig. 1. Part of the gas chromatographic profile of volatile compounds from the defense secretion of *P. cochleariae* 24 h after the injection of [$^2H_5$]-**8** into the hemolymph. Elution conditions: RSL 300 (15 m × 0.32 mm) under programmed conditions (50 °C for 2 min, then at 10 °C min^{-1} to 200 °C); Finnigan Ion Trap ITD 800 as detector (scan range 35 → 250 Da sec^{-1}). Identified compounds: **1** = chrysomelidial, **2** = epichrysomelidial, **3** = plagiolactone and epiplagiolactone, **6** = actinidine, **10** = 1-nor[$^2H_5$]chrysomelidial, **12** = alkylindols.

the plagiodial **3** as well as the plagiolactone **5**, named after the insect itself.[7] While the biosynthesis of plant iridoids has been well-studied up to now there have been no detailed investigations into the biosynthesis of iridodials in insects. That the synthesis of iridodials in insects is part of terpene metabolism was established by the incorporation of [^{14}C]mevalonolactone into the dialdehyde anisomorphal **4** in the stick insect *Anisomorpha buprestoides*.[8] We report here that the biosynthesis of the iridodials **1**, **2**, and **3** in the larvae of the aforementioned beetles is, in principle, similar to the known plant metabolism but that the details reveal a surprising range of variations (see Scheme 1).

The experimental procedure was as follows: Aqueous solutions of deuterated precursors, (ca. 1 μL; 0.9% solution),[9] were injected into the hemolymph of 10 to 14-day-old larvae. About 4–36 h after the injection of the precursors, the animal is stimulated into secreting defense secretion from the everted glands. The resulting secretion was shown to contain [^{2}H]iridodials by using mass spectrometry.

The first traces of deuterated metabolites are detected as early as one hour after injection. Alternatively, the precursors can be fed to the larvae in the form of impregnated leaves; however, with this technique it took three days before significant incorporation could be detected. This experiment reveals that the larvae of the leaf beetles are able to take up plant precursors like geraniol or 8-hydroxygeraniol and to use them for the biosynthesis of iridoids. In order to obtain usable mass spectra from the minute quantities of [^{2}H]-metabolites present, 3-norprecursors of the types **7** and **8** were used; additional metabolic probes were labeled with deuterium at positions C1, C2, or C8.[9] The nor compounds allow a complete gas chromatographic separation of the metabolites and naturally occurring iridoids (Fig. 1). The experiments are based on the assumption that the synthetic 3-norprecursors are transformed in an analogous manner to the naturally occurring substrates. The appropiate reference substances, the 1-nor[^2H_n]chrysomelidials such as [$^2H_5$]-**10**, can be obtained by biomimetic reactions from the acyclic dialdehydes **9** by acid[10] or base[11] catalysis. Both variants yield 1-nor[$^2H_5$]chrysomelidial **10** without significant loss of deuterium at the C4 position of the precursor[12] (> 95% retention). This finding means that the mechanism of the acid-catalyzed cyclization (50% HCOOH)[10] of 8-oxocitral has to be partially modified. The base-induced cyclization of **9** (MeOH, 0.01 N NaOH, 10 min) is to be considered as a tandem-Michael addition starting by addition of H_2O or MeOH followed by cyclization and elimination of the conjugate base. In incubation experiments **7** and **8** were quickly converted by all three kinds of larvae into the corresponding 1-noriridodials, **10** and **11**, respectively. In addition, for *P. versicolora* and *G. viridula* the acyclic dialdehyde **9** was firmly established as an intermediate in the biosynthesis of **1** and **3**. This means that the biosynthesis of chrysomelidial **1** and plagiodial **3** in larvae of the aforementioned insects proceeds in an anologous manner to the biosynthetic sequence in plants (similar to Scheme 1). It can therefore be expected that both lifeforms possess similar enzymes.

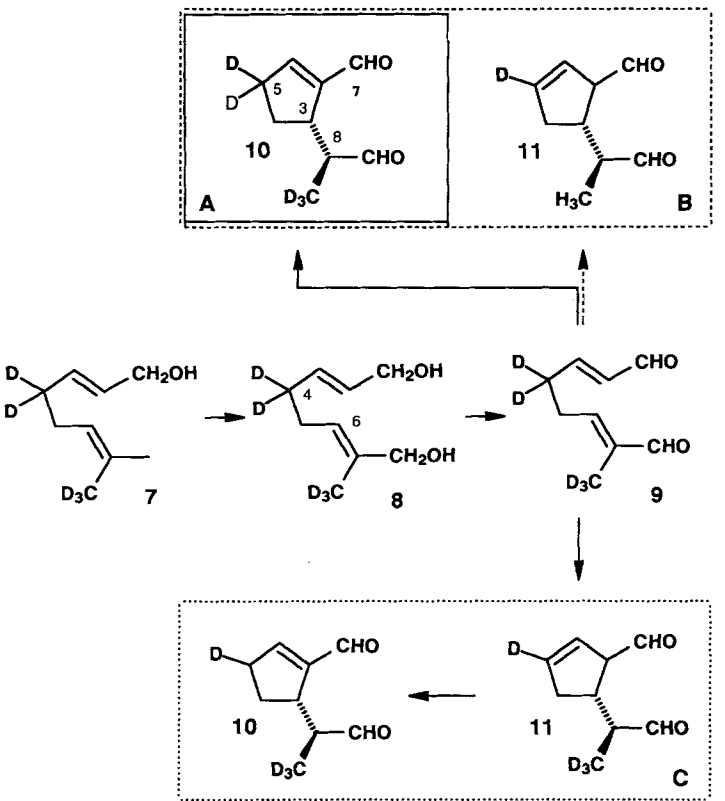

Scheme 1. The metabolism of deuterated 3-norgeraniols **7** and 3-nor-8-hydroxygeraniols **8** in different leaf beetle larvae. **A**, **B**, and **C** refer to the synthetic pathways of *G. viridula*, *P. versicolora*, and *P. cochleariae*, respectively.

However, the fate of the two deuterium atoms at position C4 in the precursors **7** and **8** also reveals differences in the biosynthetic pathways in the three leaf beetle larvae. Analogous to the biomimetic cyclizations the larvae of *G. viridula* convert **8**, (via **9**), into 1-nor[$^2H_5$]chrysomelidial **10** (Scheme 1, **A**) without loss of a deuterium atom from the C4 position of the precursor. The number of deuterium atoms at

C5 can be reliably determined from the mass spectra of **10** by using the base peak (*m/z* 69 corresponds to a fragment ion with C5–$^2H_2$; *m/z* 67 corresponds to C5–$^1H_2$).[12, 13] The deuterium at C2 in **8** is lost as expected; the deuterium on the aldehyde groups in **9** is not lost and thus rules out additional redox reactions on the way to **10** or **11**. The isomeric diol (6*Z*)-**8** is not metabolized.

When the larvae of *P. versicolora* are treated with the diol **8** and the resulting metabolites are subjected to analysis by mass spectrometry, the results indicate that two separate (Scheme 1, **B**) cyclases might be operating in the defense glands of this larva. The resulting 1-nor[$^2H_5$]chrysomelidial **10** has two deuterium atoms attached to C5, whereas the typical main product for this larva, 1-nor[$^2H_4$]plagiodial **11**, has lost one of the two hydrogen isotopes from the C4 atom of the precursor **8**. In addition, a 3-nor[$^2H_4$]plagiolactone corresponding to **5** has also only one deuterium atom attached to C5, which shows that it is derived from 1-nor-plagiodial **11**. Whether the lack of the methyl group of the nor precursor causes this kind of product distribution still needs to be examined. The two deuterium atoms attached to C5 of 1-nor[$^2H_4$]chrysomelidial **10** rule out the possibility that 1-nor[$^2H_4$]plagiodial **11** is first formed and that the thermodynamically more stable **10** is produced by isomerization of **11**.

Interestingly, the larvae of *P. cochleariae* have developed precisely this pathway (Scheme 1, **C**; see also Fig. 1). After the injection of **8** exclusively 1-nor[$^2H_4$]chrysomelidial **10** is found in their defense secretion. In **10**, one of the two enantiotopic deuterium atoms attached to C4 in the precursor is missing. The use of chiral (4*R*,5*S*)- or (4*S*,5*R*)-3-nor[4,5-$^2H_2$]geraniol of the type **7** (≥97% *ee* at C4) as precursor[9] leads to the enantiospecific removal of the C4-H_S hydrogen atom. Since the loss of a hydrogen atom from the C5 atom of the iridoid skeleton, regardless of the cyclization mechanism, determines the position of the ring double bond, for *P. cochleariae* it must be assumed that plagiodial **3** occurs as an intermediate on the way to chrysomelidial **1**. This finding is in formal accordance with the current theory of an acid-catalyzed cyclization[10] of 8-oxocitral to **1**. It can be supposed that the direct formation of **10** and **11** from a common intermediate of the cyclization occurs through the loss of a hydrogen atom from C2 and C5, respectively. Regardless of mechanistic aspects, it is, however, clear that in the course of evolution, at least within the genus Phaedonini (subfamily Chrysomelinae), two different pathways have been developed for synthesis of **1**. Further biogenetic studies on iridoid-producing larvae of the Phaedonini should make it possible to characterize members of this genus chemotaxonomically.

Received: December 17, 1992 [Z 5755 IE]
German version: *Angew. Chem.* **1993**, *105*, 904

[1] C. A. Boros, F. R. Stermitz, *J. Nat. Prod.* **1990**, *53*, 1055.
[2] L.-F. Tietze, *Angew. Chem.* **1983**, *95*, 840; *Angew. Chem. Int. Ed. Engl.* **1983**, *22*, 828.
[3] H. Inouye, S. Uesato, *Prog. Chem. Org. Nat. Prod.* **1987**, *50*, 169.
[4] S. R. Jensen, O. Kirk, B. J. Nielsen, *Phytochemistry* **1989**, *28*, 97.
[5] G. W. Dawson, D. C. Griffiths, N. F. Janes, A. Mudd, J. A. Picket, L. J. Wadhams, C. M. Woodcock, *Nature*, **1987**, *325*, 614.
[6] J. M. Pasteels, M. Rowell-Rahier, J.-C. Braekman, D. Daloze, *Biochem. Syst. Ecol.* **1984**, *12*, 395; K. Dettner, R. Fettköther, O. Ansteeg, R. Deml, C. Liepert, B. Petersen, E. Haslinger, W. Francke, *J. Appl. Entomol.* **1992**, *113*, 128; A. Hutz, K. Dettner, *J. Chem. Ecol.* **1990**, *16*, 2691.
[7] J. M. Pasteels, J. C. Braekman, D. Daloze, R. Ottinger, *Tetrahedron*, **1982**, *38*, 1891.
[8] J. Meinwald, G. M. Happ, J. Labows, T. Eisner, *Science* **1966**, *151*, 79.
[9] M. Lorenz, W. Boland, unpublished results.
[10] S. Uesato, Y. Ogawa, M. Doi, H. Inouye, *J. Chem. Soc. Chem. Commun.* **1987**, 1020.
[11] F. Bellesia, F. Ghelfi, U. M. Pagnoni, A. Pinetti, *Tetrahedron Lett.* **1986**, 381.
[12] A 1:1 mixture of 1-norchrysomelidial and 1-norepichrysomelidial [$^2H_5$]-**10** was obtained by boiling the dialdehyde [$^2H_5$]-**9** (0.15 g, 0.95 mmol) in 60% HCOOH for 1 h [10]. Chromatography on SiO_2 with hexane/Et_2O (3:7 v/v) yielded 63 mg (42%) [$^2H_5$]-**10**. MS (Finnigan, Ion Trap ITD 800, 70 eV): *m/z* 157 (M^+, 1.4%), 139(6), 138(5), 129(14), 128(6), 114(4), 113(4), 112(8), 111(15), 110(11), 109(6), 100(18), 99(13), 98(12), 97(29), 96(35), 95(36), 94(17), 93(12), 92(6), 85(7), 84(9), 83(19), 82(18), 81(18), 80(18), 79(16), 78(11), 71(9), 70(29), 69(100), 68(75), 67(43), 66(28), 65(11), 64(8), 59(12), 58(11), 57(9), 56(11), 55(11), 54(11), 53(15), 52(14), 46(12). High-resolution MS; calcd. for $C_9H_7{}^2H_5O_2$: 157.1151; found: 157.1182.
[13] According to high-resolution mass spectrometry (Finnigan MAT 90), the base peak for [$^2H_5$]-**10** (*m/z* 69) corresponds to a fragment ion of the structural formula $C_5H_5{}^2H_2^+$ and contains the C atoms of the ring; with the exception of a deuterium atom from the aldehyde group (C7) (cf. Scheme 1) no deuterium from the side chain is transferred to the ring during the fragmenation of **10**. This was confirmed by using reference substances of varying degrees and patterns of deuteration [9]. A hypothetical fragmentation scheme for iridodial is discussed in ref. [14].
[14] S. Uesato, Y. Ogawa, H. Ihouye, K. Saiki, M. H. Zenk, *Tetrahedron Lett.* **1986**, *27*, 2893.

Cage Extension to Clusters with Co_2/Co_3MoAs_6 Polyhedron Frameworks**

By *Michaela Detzel, Karl Pfeiffer, Otto J. Scherer,** and *Gotthelf Wolmershäuser*

Dedicated to Professor Heinrich Nöth on the occasion of his 65th birthday

The synthesis of molecules exclusively constructed from L_nM and naked E_n units (E = P, As, Sb, Bi) has developed into an unusually manifold area of research, particularly in recent times.[1] Little is known, however, about the reactivity of such complexes.[1]

The desired extension of Co_2/Co_3As_6 cage frameworks to nona- and decanuclear heteroatom clusters has now been achieved by allowing **1**[2] and **2**[2] (Cp* = η^5-C_5Me_5) to react with [Mo(CO)$_5$(thf)]. The respective products, **3** (violet crystals) and **4** (black crystals), are stable in air for a short period and dissolve scarcely in *n*-hexane, better in benzene and toluene, and easily in dichloromethane. The complexes are formed in satisfactory (**3**: 47%) and good (**4**: 74%) yields, respectively.

The X-ray structure analysis[3] shows that for **3** the trapezoidal face of the As_6 ligand in **1** which is still free is capped by the 12e$^-$ fragment [Mo(CO)$_3$], which, however, does not change the total number of the skeletal electron pairs (SEP). With 11 SEP, **1** belongs to the arachno type (n + 3) and **3** to the nido type (n + 2) of structure. The framework of the nonanuclear cluster **3** can be described as a stretched, triply capped trigonal As_4CoMo prism (Fig. 1), in which the three long edges are almost of the same length (As1 ··· As3 3.032, As4 ··· As6 3.023, Mo–Co1 3.030 Å; sum of the covalent radii according to Pauling: As–As = 2.42, Mo–Co = 2.46 Å). This leads to parallel triangular faces (dihedral angle 0.6°) and to six As–As bond lengths, whose average value is 2.47 Å. The framework of the Co_2MoAs_6 polyhedron of **3**

[*] Prof. Dr. O. J. Scherer, Dipl.-Chem. M. Detzel, Dr. K. Pfeiffer, Dr. G. Wolmershäuser[+]
Fachbereich Chemie der Universität
Erwin-Schrödinger-Strasse, D-W-6750 Kaiserslautern (FRG)
Telefax: Int. code + (631)205-3200

[+] X-ray structure analyses

[**] This work was supported by the Fonds der Chemischen Industrie.

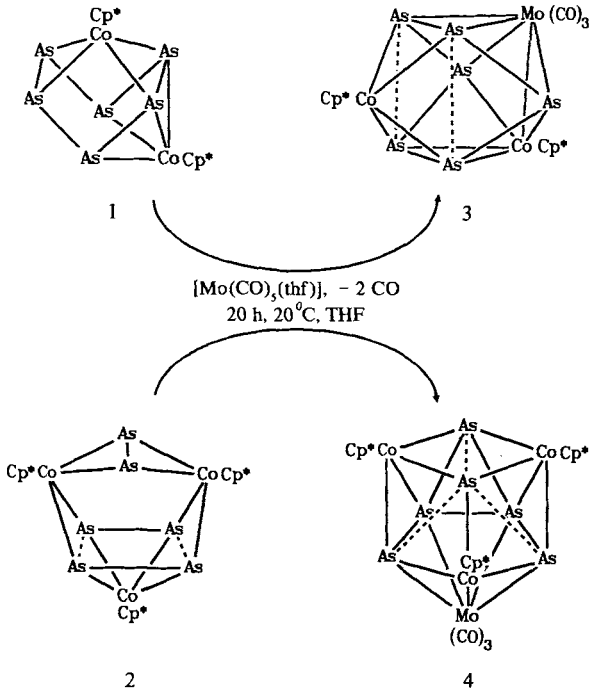

shows interesting parallels to the Bi_9^{5+} cluster ion **5**,[4] both with regard to the number of skeletal electrons (22, i.e. $n + 2 = 11$ SEP) and to the h/e ratio (h = average value of the three long edges of the prism, e = average value of the six edges of the triangles), which for **3** is 1.17 and for **5** is 1.15. In **5** (11 SEP) the occupation of the antibonding a_2'' orbital (HOMO) is responsible for the elongation of the trigonal prism;[4] in $B_9H_9^{2-}$ (10 SEP) this orbital is the LUMO.[5]

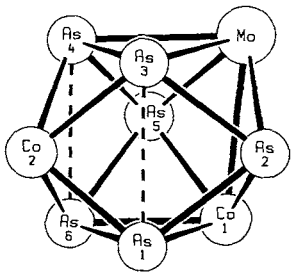

Fig. 1. Molecular structure of **3** without ligands. Selected distances [Å] and angles [°]: Co1-Mo 3.030(3), Co1-As1 2.518(3), Co1-As2 2.434(3), Co1-As5 2.426(3), Co1-As6 2.516(3), Co2-As1 2.364(3), Co2-As3 2.413(3), Co2-As4 2.412(3), Co2-As6 2.364(3), Mo-As2 2.588(2), Mo-As3 2.813(2), Mo-As4 2.817(3), Mo-As5 2.604(2), As1-As2 2.481(3), As2-As3 2.509(3), As3-As4 2.433(3), As4-As5 2.509(3), As1-As6 2.423(3), As5-As6 2.492(3), As1-As3 3.32, As4-As6 3.023, As2-As5 3.873; As1-As2-As3 74.8(1), As4-As5-As6 74.4(1), As2-As3-As4 106.4(1), As3-As4-As5 107.0(1), As2-As1-As6 107.0(1), As1-As6-As5 106.9(1); torsion angle As1,2,5,6/As2,3,4,5 78.6°.

^{1}H NMR investigations at different temperatures[6] show that the singlet for the Cp* ligands of **3** at room temperature splits into two separate signals for the Cp* ligands at Co1 and Co2 only at low temperature. These spectroscopic results indicate a rapid framework rearrangement often observed for nonanuclear clusters.[4]

The X-ray structure analysis[3] for the decanuclear heteroatom cluster **4** reveals a Co_3MoAs_6 polyhedron framework (Fig. 2a), which corresponds to a distorted sphenocorona[7] (Fig. 2b).[9] In comparison with the ideal polyhedron (Fig. 2b), the following important deviations are observed for the framework of **4** (Fig. 2a): a) The planar

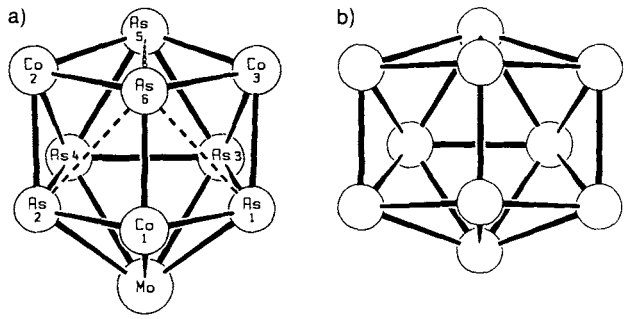

Fig. 2a) Molecular structure of **4** without ligands. Selected distances [Å] and angles [°]: Co1-Mo 2.933(3), Co1-As1 2.285(4), Co1-As2 2.286(3), Co1-As6 2.400(4), Co2-As2 2.407(4), Co2-As4 2.424(4), Co2-As5 2.315(4), Co2-As6 2.434(3), Co3-As1 2.422(4), Co3-As3 2.425(4), Co3-As5 2.309(4), Co3-As6 2.447(4), Mo-As1 2.667(3), Mo-As2 2.679(3), Mo-As3 2.714(3), Mo-As4 2.716(3), As1-As3 2.594(3), As2-As4 2.565(3), As3-As4 2.579(3), As3-As5 2.587(3), As4-As5 2.585(3), As1-As6 2.874, As2-As6 2.872, As5-As6 2.831; Co2-As5-Co3 110.1(1), Co2-As6-Co3 101.9(1), As5-Co2-As6 73.2(1), As5-Co3-As6 73.0(1), As1-Co1-As2 105.7(1), Co1-As2-As4 115.2(1), Co1-As1-As3 115.0(1), As1-As3-As4 101.4(1), As2-As4-As3 102.4(1). b) Sphenocorona; the ideal polyhedron was simulated by refinement of the structural model of **4** with suitable fixation of the bond lengths.

four-membered rings Co1, As2, Co2, As6, and Co1, As1, Co3, As6 (sum of the angles each 359.9°) are rhomboidally distorted, leading to an As···As diagonal distance of 2.87 Å (shown as a dashed line in Fig. 2a). b) In contrast to the five-membered ring As1, As2, As3, As4, Co1, (sum of the angles 539.7°; maximum deviation of the least-squares plane = 0.05 Å) the corresponding ring in sphenocorona is not planar (maximum deviation of the least-squares plane = 0.30 Å). c) The rhomboidally distorted, almost planar four-membered ring Co2, As5, Co3, As6 (sum of the angles 358.2°, fold angle 167.4°, As5···As6 2.83 Å) in **4** is contrasted by two neighboring three-membered rings (fold angle 159.9°) in the ideal polyhedron (Fig. 2b). The remaining five As–As bonds are almost identical in length (average 2.58 Å).

In spite of the Co_3MoAs_6 heteroatom cluster framework the asphericity[10] determined for **4** (23.4%) deviates only slightly from that of sphenocorona (18.9%[10]), a M_{10} polyhedron framework, which has so far not been found for transition metal clusters.[11] Compound **4**, however, shows a noteworthy structural parallel to gold clusters of the composition $[Au_{11}(PR_3)_7X_3]$.[11, 12] Inside the Au_{10} framework (cf. Fig. 2), consisting of ten triangles and three nonplanar quadrangles, is an interstitial gold atom, which obviously makes a significant contribution to the stability of the peripheral Au_{10} framework.[11, 12]

In contrast to the complexes **1**,[2] **2**,[2] and **3**, compound **4** shows no dynamic behavior as revealed by ^{1}H NMR studies.[6]

Experimental Procedure

3 [**4**]: To **1** [2] (81 mg, 0.094 mmol) [**2** (300 mg, 0.29 mmol) [2]] was added a solution of $[Mo(CO)_5(thf)]$, prepared by irradiation (90 min) (water-cooled 150 W mercury high-pressure lamp) of $[Mo(CO)_6]$ (240 mg, 0.091 mmol) in freshly distilled THF (50 mL). After the mixture had been stirred for 20 h at room temperature the reaction mixture was concentrated, adsorbed on to Al_2O_3 (ca. 1 g) (basic, 2% H_2O), and dried. In the purification by column chromatography (column 25 × 2.5 cm, packed with Al_2O_3/petroleum ether) with petroleum ether/toluene (1/1), exclusively **3** was eluted as an aubergine-colored [**4** as a dark brown] fraction. After the solvent had been removed **3** (47 mg, 47%) [260 mg, 74%, **4**] was obtained spectroscopically pure. Recrystallization was achieved by layering a concentrated solution of **3** [**4**] in dichloromethane with *n*-hexane at room temperature; **3** formed violet, hexagonal crystalline platelets [**4** dark brown to black crystal needles].

Received: January 21, 1993 [Z 5820 IE]
German version: *Angew. Chem.* **1993**, *105*, 936

[1] Most recent reviews: a) O. J. Scherer, *Angew. Chem.* **1990**, *102*, 1137–1155; *Angew. Chem. Int. Ed. Engl.* **1990**, *29*, 1104–1122; b) M. Scheer, E. Herrmann, *Z. Chem.* **1990**, *30*, 41–55; c) T. P. Fehlner, C. E. Housecroft, R. N. Grimes in *Inorganometallic Chemistry* (Ed.: T. P. Fehlner), Plenum, New York, **1992**, Chapters 2, 3, 6.
[2] O. J. Scherer, K. Pfeiffer, G. Heckmann, G. Wolmershäuser, *J. Organomet. Chem.* **1992**, *425*, 141–149.
[3] a) **3** monoclinic, $C2/c$ (no. 15); $a = 37.654(7)$, $b = 9.459(1)$, $c = 17.016(3)$ Å, $\beta = 105.772(8)°$, $Z = 8$, 3781 independent reflections ($Mo_{K\alpha}$; $2\theta_{max} = 48°$), of which 2805 observed with $I \geq 2\sigma(I)$; 316 parameters, $R(R_w) = 0.062(0.061)$. b) **4** monoclinic, $P2_1/n$, $a = 11.609(2)$, $b = 16.948(1)$, $c = 21.894(4)$ Å, $\beta = 99.16(1)°$, $Z = 4$, 5187 independent reflections ($Mo_{K\alpha}$; $2\theta_{max} = 48°$), of which 3369 observed with $I \geq 2\sigma(I)$; 267 parameters, $R(R_w) = 0.072(0.077)$. **4** contains about 1 disordered molecule CH_2Cl_2 per formula unit. One Cl atom occupies two different general positions (population ratio 0.6/0.4). c) Enraf-Nonius (CAD-4), $T = 298$ K, solution and refinement of the structures with the programs SHELXS-86, SHELX-76. Further details of the crystal structure investigations may be obtained from the Fachinformationszentrum Karlsruhe, Gesellschaft für wissenschaftlich-technische Information mbH, D-W-7514 Eggenstein-Leopoldshafen 2 (FRG) on quoting the depository number CSD-57030, the names of the authors, and the journal citation.
[4] J. D. Corbett, *Chem. Rev.* **1985**, *85*, 383–397, and references therein.
[5] M. E. O'Neill, K. Wade, *J. Mol. Struct.* **1983**, *103*, 259–269.
[6] ^{1}H NMR (400 MHz): **3** (C_7D_8, TMS ext.): δ (298 K) = 1.28 (s, 30H); δ (190 K) = 1.30 (s, 15H), 1.10 (s, 15H), $T_c = 231$ K, $\Delta G_{T_c} = 46 \pm 1$ kJ mol^{-1}; **4** (C_6D_6): δ (298 K) = 1.63 (s, 30H), 1.91 (s, 15H). IR (CH_2Cl_2, $\tilde{\nu}$(CO) [cm^{-1}]): **3**: 1931 (vs), 1857 (br, s), **4**: 1929 (vs), 1862 (br, s).
[7] The sphenocorona (Zalgaller polyhedron no. 86 [8]) has C_{2v} symmetry and consists of 10 vertices (2:4:2:2), 14 faces (12 equilateral triangles, 2 squares), and 22 edges.
[8] V. A. Zalgaller, *Seminars in Mathematics, Vol. 2 (Convex Polyhedra with Regular Faces)*, Consultants Bureau, New York, **1969**, pp. 1–92.
[9] Extensive discussion of the coordination number 10 in: D. L. Kepert, *Inorganic Stereochemistry*, Springer, Berlin **1982**, pp. 188-193.
[10] L. A. Aslanov, V. T. Markov, *Acta Crystallogr. Sect. A* **1989**, *45*, 661–671.
[11] D. M. P. Mingos, A. S. May in *The Chemistry of Metal Cluster Complexes* (Eds.: D. F. Shriver, H. D. Kaesz, R. D. Adams), VCH, Weinheim, **1990**, pp. 62–70.
[12] P. Bellon, M. Manassero, M. Sansoni, *J. Chem. Soc. Dalton Trans.* **1972**, 1481–1487.

Corrigendum

In the communication "The Seven-Component Reaction" by A. Dömling and I. Ugi (*Angew. Chem. Int. Ed. Engl.* **1993**, *32*, 563–564) structural formula **14** is incorrect. The correct formula is:

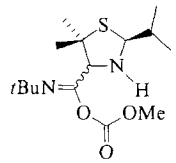

14

BOOKS

This section contains book reviews and a list of new books received by the editor. Book reviews are written by invitation from the editor. Suggestions for books to be reviewed and for book reviewers are welcome. Publishers should send brochures or (better) books to the Book Editor, Dr. Gerhard Karger, Redaktion Angewandte Chemie, Postfach 101161, D-W-6940 Weinheim, Federal Republic of Germany. The editor reserves the right of selecting which books will be reviewed. Uninvited books not chosen for review will not be returned.

Book Reviews

Perspectives in Coordination Chemistry. Edited by *A. F. Williams, C. Floriani*, and *A. E. Merbach*. VCH Verlagsgesellschaft, Weinheim/Verlag Helvetica Chimica Acta, Basel, 1992. XII, 486 pp., hardcover DM 148.00.—ISBN 3-527-28487-7/3-906390-02-0

It has now become common practice for the organizers of regular international conferences to ask the invited speakers to provide manuscripts, which are then published in collected form, either as a special section in one of the established journals or as a monograph. This procedure does not always ensure that the result is both up-to-date and of high quality from a scientific or publishing standpoint, since the manuscripts, often in camera-ready form and varying with regard to the care in their preparation, are in many cases not thoroughly checked before publication. However, this book, which contains about half of the main papers presented at the 29th International Conference on Coordination Chemistry (ICCC) in Lausanne in July 1992, demonstrates in an exemplary way that such "congress reports" can be produced so that they satisfy the needs of not only the editors, authors, and publisher, but also the consumers of scientific literature. The determination to make this high-quality book available within a very short time after the conference on which it is based has meant that not all the 23 articles could be published in the format of *Helvetica Chimica Acta*, but the camera-ready form in which the manuscripts were provided is of a quality that gives no grounds for complaint. Three of the articles (by Corbett, Cotton, and Shilov) have been reproduced directly from *Pure and Applied Chemistry*.

This collection of articles on "Perspectives in Coordination Chemistry" emphasizes the great diversity of the subject and its relevance to aspects of bioscience, materials science, and applications in fields such as industrial catalysis and

organic synthesis. Research on coordination chemistry shows a trend towards studying compounds of ever increasing complexity, with improvements in the reliability of synthesis through control of reactions proceeding alongside developments in analytical methods.

It is therefore not surprising that most of the articles in this volume are concerned with the area of "supramolecular structures", including clusters, with special attention not only to structure and chemical selectivity but also to physical and catalytic properties and the factors controlling them. Here it becomes evident that the intelligent design and skillful synthesis of complex organic ligands now plays a very important role. Mono- und polynuclear complexes with specially designed ligands are the subject of the contributions by Seel and Vögtle, Braunstein, Gatteschi et al., Hancock, Denti and Balzani et al., Hosseini, and Lehn. The related area of bioinorganic and relevant model systems is represented in articles by Fenton, Shilov, Luchinat et al., and R. J. P. Williams. Cluster formation and its coordinative aspects are also relevant to some current problems of solid-state chemistry, as shown in the articles by Dance, Corbett, Burdett, and Bürgi. The latter, in outlining the fascinating Bürgi–Dunitz concept, leads into studies of reaction mechanisms, which are represented in this volume by the articles by van Eldik and Ryabov. The role of solvents in relation to coordination compounds is discussed in articles by Burger and Enderby. Other aspects of coordination chemistry are treated in the articles on high-resolution optical spectroscopy (Güdel et al.), the δ bond (Cotton), and the reactivities of organometallic compounds (Carmona, Sanchez, et al.), while the special relevance to organic synthesis is discussed by Bäckvall et al.

There are, of course, differences in the nature and degree of complexity of the various contributions, varying from laboratory reports through informal essays to short reviews. For example, whereas Hancock's review of the size-selective complexation of metal ions by polydentate chelate ligands can be commended even to advanced students (cf. also a similar recent article in the *Journal of Chemical Education*), the article by Lehn suffers from the disadvantage of having no diagrams or structural formulas whatsoever, so that anyone who does not keep up with the details of published work on supramolecular structures will have the irksome task of referring to the cited papers to discover the structures of compounds such as helicates, carcerands, or speleands.

Altogether the book presents an up-to-date and representative overview of the current state of coordination chemistry, its many different aspects, and its future potential. Because of the central position that this subject occupies, linking such widely different areas as solid-state research, biochemistry, organic synthesis, and industrial catalysis, it is essential to learn something about it or to renew one's knowledge, even for nonspecialists.

Wolfgang Kaim
Institut für Anorganische Chemie
der Universität Stuttgart (FRG)

Chemistry. The Central Science. By *T. L. Brown, H. E. LeMay, Jr.*, and *B. E. Bursten*. Prentice Hall, Englewood Cliffs, NJ (USA), 1991. XXX, 1045 pp. (glossary and index 40 pp.), hardcover ca. DM 120.—ISBN 0-13-126210-6

This book provides a *first* text in chemistry for students at universities and colleges, and presents the core material typically followed at such institutions in the United States. Its aim is to help instructors to plan a coherent and well-organized course, and to give the students parallel material which amplifies, exemplifies, and illustrates the material they receive in lectures and classes.

The fifth edition of this text represents a considerable achievement. From the very beginning the authors convey the excitement and variety of their subject matter, while developing a very careful and rigorous presentation of concepts and material. Many beautiful color illustrations are one tool used to this end. But there is also a wealth of supplementary sections interspersed in the text. These are of three types; the "Chemistry at Work" sections introduce applications of the concepts being presented, those entitled "A Closer Look" tackle a topic more deeply and would enhance subsequent readings, and the "Historical Perspective" sections, which are rather fewer in number, give some sense of the way our fundamental chemical ideas evolved. These learning aids, together with an attractive and colorful layout, serve to complement the central text, which is the heart of the book. It is in the text itself that the thoughtfulness and craft of the authors is most evident. The presentation is lucid and easy to read. The organization and ordering of the introduction of ideas, concepts, and facts is very impressive and can hardly be faulted.

Any successful course book for instructors and pupils must contain good exercises, and "Chemistry. The Central Science" is no exception. Numerous problems at the end of each chapter help reinforce the material presented.

On the physical side of chemistry one can gain a clear idea of the level of the presentation by the mathematical knowledge presumed. The student needs to have mastered simple proportion; logarithms are used in presentation of pH and so forth, but there is a helpful appendix on them and on exponential notation. Differential calculus is not employed, so the treatment of rates, thermodynamics, and the Schrödinger equation is only descriptive. In the context of the British educational system, this places the book as one most likely to be useful to Advanced Level courses in schools, and as such would be a good addition to a school library. The coverage of descriptive inorganic and organic chemistry is less than that expected in most A-level syllabuses, so it would not serve as a central sixth-form text. However, it can be strongly recommended to chemistry teachers as an exemplary presentation of the core of the subject, and to prospective university students to reinforce their school work and whet their appetites for further study.

Jennifer Green
Inorganic Chemistry Laboratory
Oxford (United Kingdom)

Simple Views on Condensed Matter. (Series in Modern Condensed Matter Physics, Vol. 4.) By *P. G. de Gennes*. World Scientific, Singapore, 1992. X, 408 pp., paperback £ 25.00, hardcover £ 44.00.—ISBN 981-02-0910-X (paperback)/ 981-02-0909-6 (hardcover)

In 1992 Professor de Gennes was awarded the Nobel Prize for Physics in recognition of his numerous scientific achievements, which relate to a wide range of different phenomena. The great variety of his research activities and their importance to scientific progress resulted in many awards and honors, culminating finally in this Nobel Prize. All de Gennes' work up to now is contained in four books and over 350 scientific papers; to these is now added this new book "Simple Views on Condensed Matter", in which the author presents a personal selection of important publications. Thus it is not a textbook in the ordinary sense, but a collection of

interesting articles that have previously only appeared in specialist journals. It contains 40 articles, of which 13 are in French and the rest in English, and is divided into six chapters dealing with different areas of current interest. The first chapter is concerned with the basic principles of wave propagation and superconductivity in the solid state, and the second with phenomena in thermotropic liquid crystals. The latter materials show ordering phenomena like those in solid crystals, but are mobile like ordinary liquids, and consequently they have unusual optical properties. In liquid crystals one observes phenomena such as domain formation or dislocations that also occur in solids, and these analogies are especially emphasized here. The third chapter deals with the properties of flexible macromolecules, with the main emphasis on chain statistics, chain dynamics, conformational changes, and the different types of phase transformations. The topics covered also include modern methods of investigation such as low-angle neutron diffraction, which enables one to study chosen regions of a given molecule by the contrast variation technique. The fourth chapter is devoted to interfacial phenomena. The topics covered include adsorption by polymers, the stability of soap films, and the formation of emulsions and microemulsions. This is followed by a chapter on wetting and spreading; the topics treated in detail include the surface tension of solutions, melts, and solids, together with contact angles, film formation, and adhesion properties. The final chapter contains a detailed discussion of chirality phenomena, including studies of specific properties and interactions that are only found between enantiomers.

The publications reproduced here touch on many different topics, and are representative of the most important of de Gennes' areas of work. Many of the articles carry comments telling the reader about errors or new results. Much of the material presented is in such a form that it can serve as a source of rapid and up-to-date information, even without previous knowledge. Thus, readers whose interest is confined to one specific subject area will nevertheless profit from using the book. The chapters are of a high scientific standard, and contain interesting examples relating to many different aspects of condensed matter. The choice of topical subject matter will be of interest to a wide readership including chemists, physicists, engineers, and technologists. However, nonspecialists too will find this new book useful when they wish to learn more about new methods and modern insights. The articles contain many stimulating views and original ideas, and thus the book can be recommended most emphatically.

Heinz Rehage
Institut für Umweltanalytik
der Universität-Gesamthochschule Essen (FRG)

Geschichte der deutschen Großchemie. Entwicklung und Einfluss in Staat und Gesellschaft. By *W. Teltschik*. VCH Verlagsgesellschaft, Weinheim, 1992. XIV, 426 pp., hardcover DM 58.00.—ISBN 3-527-28444-3

The three largest chemical companies in the world are German-based; there is no other section of the German economy where a similar situation exists. Walter Teltschik, a chemist who has worked for many years in BASF, has set himself the task of describing the checkered history of German large-scale chemical industry in a book of a little over 400 pages.

The author makes an excellent and thorough job of covering the many developments that have occurred in nearly 130 years of industrial history and analyzing these in relation to the contemporary situation in the German state and in society. The book has been written with the benefit of much inside knowledge of the industry, supported by an extensive compilation of source material. Teltschik writes with a lively and engaging style. He enlivens the narrative with many quotations, while the passages containing statistics on production and consumption are kept agreeably brief or are relegated to the appendix. The clear division into subchapters with suitably informative titles and the inclusion of an excellent index section make the book a very useful reference source.

The first chapter, "Aufbruch" (beginnings), is especially successful. The author rightly honors Liebig and his chemist contemporaries as the originators of the German chemical industry, the successes of which he attributes (in later years also) mainly to the close and fruitful relationship between research in the universities and in industry. These successes eventually led to the German chemical industry gaining a dominant position in Europe. The three following chapters, entitled "Rückschläge" (setbacks), "Konzentration" (consolidation), and "Größenwahn" (megalomania), are excellent accounts of the splendors and miseries experienced by German chemical manufacturing during the years 1914 to 1945. The regeneration of the industry after World War II, at first hesitant then with near-explosive vigor, is also well described. Teltschik describes the great period of growth during the sixties under the title "Zügellosigkeit" (unbridled growth), the significance of which we can only appreciate with the wisdom of hindsight. The book concludes with the oil crisis and its effects ("Verunsicherung", i.e. uncertainty) and the recovery during the eighties ("Schubkräfte", thrusting forward); these chapters too are packed with absorbing accounts of the momentous events of those years.

In view of the wealth of topics covered, one is prompted to ask whether some important matters have received inadequate treatment. The description of the Fonds der Chemischen Industrie (Chemical Industry Research Fund of the FRG) as merely a provider of research scholarships fails to do it justice. In fact, since its formation in 1950 the Fonds has raised DM 370 million, mainly for the advancement of fundamental research, thereby making an important contribution to the high standard of research and teaching in German universities. It is an institution much envied in other countries. A further question concerns the objectivity of the presentation. The preface emphasizes the care that has been taken to present a balanced overall picture, but this does not mean that the author cannot have opinions. It is pleasing to find that Teltschik has not held back from making his own position clear when discussing people and events. This brings the text to life and stimulates the reader to examine his or her own position, whether in agreement or opposition.

The picture that Teltschik presents of Duisberg certainly invites disagreement. Much has been written about Duisberg, often in his praise. Teltschik takes an opposite view, showing as if through a magnifying lens the darker side of this historical figure, supported by quotations and accounts of events. To translate the key passage: "The rather mediocre chemist Duisberg had a predilection for long and pathetic speeches and knew how to present himself to advantage as the center of attention. His clever and energetic promotion of his idea of a 'community of interests' gained for him the status of a pioneering industrialist." Well! Another controversial passage appears near the end of the book, where Teltschik writes "The chemical industry remained an unloved child. However, even unloved children can earn attention through good behavior." However, it cannot be assumed that the reaction of the chemical industry to an exces-

sive amount of government legislation and regulation bordering on absurdity will always be one of docile adjustment. It is more likely that the affected manufacturing processes will be closed down or will be transferred, together with the associated research, to a country where the external constraints are more favorable. This has already started to happen in genetic engineering. I would therefore have preferred the book to end with an appeal to the legislators that, before enacting laws and regulations, they should ask themselves whether their proposals are sensible and feasible, and especially whether they are comparable with conditions in other countries.

In summary, this is a book well worth reading, and can be recommended not only for chemists but for everyone interested in the history of German industry.

Hans Rudolph
Krefeld (FRG)

Molecular Design of Electrode Surfaces. (Series: Techniques of Chemistry, Vol. 22. Series editors: *A. Weissberger, W. H. Saunders, Jr.*) Edited by *R. Murray*. Wiley, Chichester, 1992. XI, 427 pp., hardcover £ 105.00.—ISBN 0-471-55773-0

The title of this book sounds very promising, reflecting as it does the desire of every electrochemist to be able to prepare electrodes with tailored surface properties. However, even before opening it one suspects that it is concerned with chemically modified electrodes, then it at once becomes clear that the title describes the long-term aim and not the reality (yet). The subject of this multiauthor work edited by Royce Murray is in fact highly topical and is receiving much attention from electrochemists; this is the chemical modification of electrode surfaces with the aim of optimizing their catalytic properties. The idea is attractive, despite the fact that in practice there is often an inverse relationship between the stability of the modified surfaces and their efficiency for electron transfer.

The book begins with an introductory article by R. Murray on the wide variety of applications of modified electrodes, which are well documented here with 442 literature references. This is followed by a contribution by G. N. Salaita and A. T. Hubbard on the adsorption of organic molecules at well-defined single-crystal surfaces. The article mainly describes the authors' own ultra-high vacuum studies using low-energy electron diffraction (LEED) and electron energy loss spectroscopy (EELS), which impressively demonstrate that these methods can yield a wealth of detailed structural information about the adsorbed molecules. The third article, by J. S. Facci, is concerned mainly with Langmuir–Blodgett films; the examples are taken entirely from the author's work on C_{18}-ferrocene, which unfortunately fails to do justice to the highly interesting topic of Langmuir–Blodgett films. The next two articles deal with redox polymers. The first, by M. Majda, is mainly concerned with the transport mechanisms for electrons and positive charges in the polymer, while the second, by C. P. Andrieux and J.-M. Savéant, discusses catalytic reactions at electrodes coated with redox polymers. Chapter 6, by J. A. Bard and T. Mallonk, describes the chemical modification of electrode surfaces using microporous substances such as zeolites, and in Chapter 7 C. R. Leidner gives a short review of charge transport in polymers doped with metal complexes (mainly of Group VIII metals). In Chapter 8 N. Oyama and T. Ohsaka describe the use of voltammetry (mainly measuring current transients) to study charge transport, yielding information in the form of diffusion coefficients. The book ends with an article by C. R. Martin and L. S. van Dyke on material and charge transport in electronically conducting polymers (polyacetylene, polypyrrole, etc.).

The editor claims that this work is of special significance because it is the first to range over the whole field of modified electrodes, and after looking through it I am inclined to agree with that view. Royce Murray has not only been able to enlist a thoroughly competent team of authors, but has also assembled their contributions into a unified whole, giving a very good overview of this complex subject. However, this book is certainly not suitable as an introduction to modified electrodes for the newcomer, as it does not cover the fundamentals sufficiently for that, and the individual problems are mostly only treated very briefly (often with no more than a reference to the original papers). However, it gives an excellent overview of the different problem areas, the approaches to finding solutions, and the present state of research. The many literature references included in the individual chapters make this a valuable reference work. However, in this respect I found the index quite inadequate, as it is not very detailed. Moreover, for some of the words that I looked up (e.g. Prussian blue) the index led only to rather unimportant mentions in the text, whereas important ones were not listed. Nevertheless, considering the book as a whole, its purchase can be emphatically recommended for specialists and relevant libraries.

Dieter M. Kolb
Ableitung für Elektrochemie
der Universität Ulm (FRG)

Science and Practice of Liquid–Liquid Extraction, Vols. 1 and 2. (Oxford Engineering Science Series, Vol. 27. Series editors: *J. M. Brady, C. E. Brennen, A. L. Cullen, T. V. Jones, J. van Bladel, L. C. Woods* and *C. P. Wroth.*) Edited by *J. D. Thornton*. Clarendon Press, Oxford, 1992. Vol. 1: XVI, 603 pp., Vol. 2: XV, 436 pp., hardcover £ 60.00 each volume, £ 108.00 set.—ISBN 0-19-856236-5 (Vol. 1), 0-19-856237-3 (Vol. 2), 0-19-856178-4 (set)

Nine years after the publication of the *Handbook of Solvent Extraction*, edited by T. C. Lo, M. H. I. Baird, and C. Hanson, we now have a new work which collects together the latest knowledge of the science and technology of liquid–liquid extraction. Altogether there are 13 chapters, each reviewing a specific topic area.

Volume 1 is essentially concerned with the basic science of liquid–liquid extraction. Chapter 1 deals with the thermodynamics of the phase equilibria, with calculations to predict these equilibria, and with the choice of suitable solvents. The following chapter treats the basic theory of mass transfer and its application to exchange processes such as those occurring at the surfaces of jets and droplets (but omits to describe recent studies carried out in German-speaking countries on mass transfer in liquid–liquid systems). Chapter 3 summarizes work on the Marangoni effect, and its importance for mass transfer is examined in more detail in Chapter 4. The last of these five chapters on the basic science deals with the important subject of dispersion and coalescence. This is followed by three chapters on choosing apparatus and on design calculations. Chapter 6, on "Plug Flow Analysis", describes methods of calculation for "normal" counter-current extraction processes, and also for back-flow columns, for fractionating extraction processes using two solvents, and for crossflow and batch processes. Chapter 7 ("Axial Dispersion") describes the well-known residence time models, in-

cluding the relevant methods of measurement and their evaluation. Volume 1 ends with a further chapter on the design of extractors, and on choosing a design and layout using data from pilot experiments.

Volume 2 begins with four chapters on the application of liquid–liquid extraction methods in some special areas. Chapter 1 describes the use of reactive extraction techniques in metal refining. The basic principles and special extra conditions that apply to this field of application are first explained, then the processes currently used for individual metals or groups of metals are described. Chapter 2 is concerned with the reprocessing of nuclear fuel elements, beginning with a general introduction and a description of the different types of equipment, then going on to describe the processes currently used and possible future developments. However, it is questionable whether the details of the associated control technology and safety measures included at the end of this chapter are relevant to the main theme of the book. The following two chapters deal with applications of extraction technology in the pharmaceutical and food industries, with details of some special processes used, such as high-pressure extraction and the use of two-phase aqueous systems. The final chapter summarizes the various areas of application and indicates the directions in which these are now developing.

The work does not claim to be an introduction to the subject; instead the contributions by recognized experts are intended to summarize the current state of knowledge and to indicate topics for further research. The material is presented from a scientifically orientated standpoint, and is thus likely to be mainly of interest to engineers and chemists in universities and industrial research laboratories. The volumes give a good overview of the fundamental theory and some important areas of application of extraction processes. The comprehensive subject index makes it easy to locate information on special topics. There is some overlapping of subject matter between the individual contributions, but one can hardly expect that to be completely eliminated in a work of this kind. The fundamental theory is covered thoroughly and forms the basis for a treatment that emphasizes recent developments, including some unconventional ones, and this is therefore a valuable addition to the literature on liquid–liquid extraction.

Eberhard Aufderheide
Degussa
Antwerp (Belgium)

Selective Biocatalysis. A Synthetic Approach. By *L. Poppe* and *L. Novák*. VCH Verlagsgesellschaft, Weinheim, 1992. XII, 319 pp., hardcover DM 168.00.—ISBN 3-527-28372-2

Biotransformations in Organic Chemistry. By *K. Faber*. Springer, Berlin, 1992. IX, 319 pp., hardcover DM 128.00.—ISBN 3-540-55762-8

Methods based on enzyme catalysis have become firmly established in the standard repertoire of asymmetric synthesis techniques because of their high selectivities—in some instances serving to complement, in others to compete with, the conventional chemical methods of organic synthesis—as is documented by the almost exponential growth of the literature on new applications of enzymes for the preparation of chiral intermediates. Both methods based on fermentation and, more especially, the use of isolated enzymes, are benefiting from the continuing growth in the numbers of known enzyme types (now over 2500) and of those that are commercially available (over 350). The task of collecting together the huge wealth of reactions that can be performed, critically reviewing the possibilities, and presenting this information clearly in book form as a guide for synthetic chemists interested in applying these methods is a difficult one from several viewpoints. Firstly, this area of research is undergoing rapid development, and consequently by the time the book is printed the contents will no longer be completely up-to-date. Secondly, the resulting publication is in competition with a steadily growing number of review articles in the relevant specialist journals, which are usually read by synthetic chemists and can cover matters of detail from a more expert standpoint. The authors of the two monographs reviewed here have taken up this challenge, and have almost simultaneously produced works that cover the same topics and have also turned out to be very similar in content. Thus it is appropriate to compare them.

In both volumes a general introduction to the methods is followed by the main part in which enzyme-catalyzed (and also some selected yeast-mediated) transformations are treated in a hierarchical sequence. Some noticeable differences between the two treatments will be mentioned here. In the book by Poppe and Novák the discussion of some process-related problem areas (the characteristics, classification, kinetics, and immobilization of enzymes; the reaction medium; microbial transformations; the modification of biocatalysts; catalytic antibodies) is preceded by a detailed chapter of 40 pages on stereochemistry, in which the nomenclature, basic principles, and especially the classification of the different possible types of selectivity (diastereomeric, diastereotopic, enantiomeric, and enantiotopic) are defined. The latter system, although somewhat unconventional, serves as a very useful means of classifying the asymmetric reactions discussed in the main part of the book. However, the rigid arrangement according to types of biocatalysts means that specific chemical themes are scattered throughout widely separated chapters (e.g., hydrolysis by enzymes is treated in Chapter 3, by baker's yeast in Section 5.4, and by other microorganisms in Section 6.2.1). In contrast Faber, after a short introduction (probably based on a lecture manuscript), plunges straight into the main business and follows the general arrangement used in a successful earlier work with a similar title and subject (H. G. Davies, R. H. Green, D. R. Kelly, and S. M. Roberts, *Biotransformations in Preparative Organic Chemistry*, Academic Press, London, **1989**). In a less helpful arrangement, however, he treats the reversal of hydrolytic reactions in a separate chapter on "Special Techniques", in which the action of enzymes in organic solvents leading to the formation of esters, lactones, and amides is described. In both books the grouping together of basic principles and general features of the methods should help to prevent the contents from losing their usefulness too quickly as the more detailed material becomes outdated.

The main parts of both books provide the reader with what is promised by the title, namely a wealth of information with examples of reactions sensibly chosen from the synthetic organic chemist's viewpoint, i.e. with due regard to preparative usefulness (high chemical and optical yields). Both books place emphasis on hydrolytic and reductive transformations with their respective reverse reactions, which are at present the reaction types of greatest practical importance. The authors have made liberal use of figures and tables to present the material in a way that is textually and visually clear. Both monographs concentrate on "main-stream" preparative applications, and consequently some aspects of enzyme-catalyzed reactions are not treated as thoroughly as

one might wish (in particular Poppe and Novák devote a mere $11\frac{1}{2}$ pages to "Other Enzymes and Microorganisms", thus barely scratching the surface of this topic). However, the surveys are well written (apart from the minor faults mentioned below) and each chapter includes a comprehensive and up-to-date bibliography ("Poppe and Novák" contains 1660 citations altogether and "Faber" 1456, extending up to about mid-1991 in both cases), with references to the most important original papers and recent review articles. Scientists who keep up with the current literature will find few surprises here (though occasionally they may be surprised to find which publications are *not* cited), but they will appreciate the clearly presented comparisons. For others these books offer a rapid and detailed survey of the main areas of activity and new methodological developments in this highly topical and expanding field of research. Of the two books, "Poppe and Novák" is more in the nature of a scientific review, with a hierarchical arrangement of contents according to selectivity types which is best suited to the needs of the researcher. "Faber", on the other hand, has a more general approach based on types of transformations, with some of the character of a textbook, and didactic qualities that make some parts of it really enjoyable to read.

"Poppe and Novák" has been carefully edited, and only a few small isolated and unimportant errors are evident in the formula schemes (e.g., in Fig. 4.6. a the oxidizing and reducing agents have been interchanged) and in the Latin names of the microbe species (e.g., "*Penicillinum camamberti*" instead of *Penicillium camembertii*). That Faber has not been afraid to tackle the hard work of desktop publishing only becomes apparent on close examination of the book (actually on the imprint page), which accounts for the lower price. However, the risk involved in this has exacted a penalty, as careful reading unfortunately reveals a higher incidence of errors in formula diagrams (e.g., an extra OH group in Scheme 2.160, and a vinyl instead of an allyl substituent in Scheme 2.164), in the numbering of references, and in captions (e.g., Table 2.8), despite the fact that the author acknowledges the help of an internationally respected colleague in checking the work. In particular Chapter 2.1.4, "Hydrolysis and Formation of Phosphate Esters", contains many errors that need to be corrected, including inaccurate formulations (e.g., glucose-6-phosphate as an essential cosubstrate of dehydrogenases) and many incorrect statements (e.g., that carbohydrate *tri*phosphates are involved in glycosyl transfer reactions, that *phosphatases* are employed for the synthesis of phosphate esters, that kinases are a subgroup of *phosphatases*—could this misunderstanding be the reason for the inclusion of enzymic phosphorylations in Chapter 2.1 on "Hydrolytic Reactions"?—that nucleoside triphosphates are intrinsically *stable* in solution, and so on). Also the index (only 7 pages) is less than perfect with regard to completeness and conciseness of the entries.

Although Faber's book is more attractively priced and, for this reason especially, might help to fill a gap in the training of organic chemistry students, I have slight reservations about recommending it as a textbook to accompany a special lecture course. As a reference work for the desks of chemists engaged in research in this field "Poppe and Novák" seems more suitable, although the higher price may be an obstacle to individuals buying it. As the subject matter covered by each book alone is (rather surprisingly) considerably less than the sum of the two, chemical libraries should not hesitate to buy both.

Wolf-Dieter Fessner
Institut für Organische Chemie und Biochemie
der Universität Freiburg (FRG)

New Books
see next page

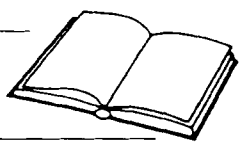

 © *VCH Verlagsgesellschaft mbH, W-6940 Weinheim, 1993* *0570-0833/93/0606-0921 $ 10.00+.25/0*

New Books

Inorganic Structural Chemistry. By **U. Müller**. Wiley, Chichester, **1993**. 264 pp., paperback, £ 14.95.—ISBN 0-471-93717-7

Glass-Fibre Databook. Compiled by **T.F. Starr**. Chapman & Hall, London, **1993**. 248 pp., paperback, £ 65.–.—ISBN 0-412-46280-X

Chemistry: The Study of Matter and Its Changes. By **J.E. Brady, J.R. Holum**. Wiley, Chichester, **1993**. 1109 pp., paperback, £ 22.95.—ISBN 0-471-59979-4

Re Organorhenium Compounds. Gmelin Handbook of Inorganic and Organometallic Chemistry. Edited by **A. Slawisch**. Springer, Berlin, **1992**. 259 pp., hardcover, DM 1.480.–.—ISBN 3-540-93659-9

Pb – Organolead Compounds. Gmelin Handbook of Inorganic and Organometallic Chemistry. Edited by **W. Petz**. Springer, Berlin, **1992**. 246 pp., hardcover, DM 1.410.–.—ISBN 3-540-93658-0

Mo Organomolybdenum Compounds. Gmelin Handbook of Inorganic and Organometallic Chemistry. Edited by **W. Petz, M. Winter**. Springer, Berlin, **1992**. 396 pp., hardcover, DM 2.218.–.—ISBN 3-540-93652-1

Ga Gallium. Gmelin Handbook of Inorganic and Organometallic Chemistry. Edited by **M. Mirbach, H. Demmer, M. Kotowski**. Springer, Berlin, **1992**. 320 pp., hardcover, DM 1.840.–.—ISBN 3-540-93657-2

Au Gold. Gmelin Handbook of Inorganic and Organometallic Chemistry. Edited by **R. Keim, G. Hönes, W. Huisl**. Springer, Berlin, **1992**. 348 pp., hardcover, DM 1.990.–.—ISBN 3-540-93655-6

Analytical Ultracentrifugation in Biochemistry and Polymer Science. Edited by **S.E. Harding, A.J. Rowe,** and **J.C. Horton.** Royal Society of Chemistry, Cambridge, **1992**. 630 pp., hardcover, £ 85.–.—ISBN 0-85186-345-0

Electron Paramagnetic Resonance of d Transition Metal Compounds. (Studies in Inorganic Chemistry, Vol. 16). By **F.E. Mabbs** and **D. Collison.** Elsevier, Amsterdam, **1992**. 1326 pp., hardcover, Dfl 995.–.—ISBN 0-444-89852-2

Aliphatic Compounds. (Second Supplements to the 2nd Edition of Rodd's Chemistry of Carbon Compounds, Vol. I). Edited by **M. Sainsbury.** Elsevier, Amsterdam, **1993**. 550 pp., hardcover, Dfl 490.–.—ISBN 0-444-89873-5

Catalytic Oxidations with Hydrogen Peroxide as Oxidant. (Catalysis by Metal Complexes, Vol. 9). Edited by **G. Strukul.** Kluwer, Dordrecht, The Netherlands, **1993**. 304 pp., hardcover, Dfl 210.–.—ISBN 0-7923-1771-8

Gene Regulation in Eukaryotes. By **E. Wingender**. VCH, Weinheim/New York, **1993.** 430 pp., hardcover, DM 178/$ 120.–.—ISBN 3-527-28460-5/1-56081-706-2

Einführung in die Physikalische Chemie. By **P.W. Atkins.** VCH, Weinheim, **1993**. 472 pp., paperback, DM 78.–.—ISBN 3-527-28027-8

Multiple Bonds between Metal Atoms. By **F.A. Cotton, R. A. Walton.** Oxford University Press, Oxford, **1993.** 787 pp., hardcover, £ 70.–.—ISBN 0-19-855649-7

Methods of Immunological Analysis, Vol. 1. Fundamentals. Edited by **R.F. Masseyeff, W.H. Albert, N.A. Staines.** VCH Weinheim/New York, **1993.** 715 pp., hardcover, DM 410.–/$ 265.–.—ISBN 3-527-27906-7/0-89573-902-X

Methods of Immunological Analysis, Vol. 2. Samples and Reagents. Edited by **W.H. Albert, N.A. Staines.** VCH, Weinheim/New York, **1993.** 591 pp., hardcover, DM 410.–/$ 265.–.—ISBN 3-527-27907-5/0-89573-903-8

Fire. By **H. Rossotti.** Oxford Science Publications, Oxford, **1993.** 288 pp., £ 19.95.—ISBN 0-19-855722-1

Encyclopedia of Materials Science and Engineering, Vol. 3. Supplementary. Edited by **R.W. Cahn FRS.** Pergamon Press, Oxford, **1993.** 2229 pp., hardcover, £ 250.–.—ISBN 0-08-040590-8

Supercritical Fluid Engineering Science. Fundamentals and Applications (ACS Symp. Ser. Vol. 514). Edited by **E.K. Kiran, J.F. Brennecke.** American Chemical Society, Washington, **1993.** 410 pp., hardcover, $ 98.95.—ISBN 0-8412-2513-3

Magnetic Resonance of Carbonaceous Solids. (Advances in Chemistry Series Vol. 229). Edited by **R.E. Botto, Y. Sanada.** American Chemical Society, Washington, **1993.** 664 pp., hardcover, $ 149.95.—ISBN 0-8412-1866-8

Carbohydrate Antigens. (ACS Symp. Ser. Vol. 519). Edited by **P.J. Garegg, A.A. Lindberg.** American Chemical Society, Washington, **1993.** 184 pp., hardcover, $ 49.95.— ISBN 0-8412-2531-1

Biocatalyst Design for Stability and Specificity. (ACS Symp. Ser. Vol. 516). Edited by **M.E. Himmel, G. Georgiou.** American Chemical Society, Washington, **1993.** 335 pp., hardcover, $ 98.95.—ISBN 0-8412-2518-4

Measurement Challenges in Atmospheric Chemistry. (Advances in Chemistry Series, Vol. 232). Edited by **L. Newman.** American Chemical Society, Washington, **1993.** 407 pp., hardcover, $ 94.95.—ISBN 0-8412-2470-6

Chemie und Geisteswissenschaften. Edited by **J. Mittelstraß, G. Stock**. Akademie Verlag, Berlin, **1992**. 340 pp., hardcover, DM 48.—ISBN 3-05-501604-1

How to Use Reverse-Phase HPLC. By **G. Szepesi**. VCH Verlagsgesellschaft mbH, Weinheim/New York, **1992**. 356 pp., hardcover, DM 168.–/$ 95.—ISBN 3-527-27939-3/0-89573-766-3

Perspectives in Medicinal Chemistry. Edited by **B. Testa, W. Fuhrer, E. Kyburz, R. Giger**. VCH Verlagsgesellschaft mbH/ Helvetica Chimica Acta, Weinheim/Basel, **1993**. 644 pp., hardcover, DM 225.—ISBN 3-527-28486-9/3-906390-04-7

Grundkurs Chemie. By **A. Arni.** VCH, Weinheim, **1993**. 354 pp., paperback, DM 48.—ISBN 3-527-29008-7

Organisch-chemisches Grundpraktikum. By **Th. Eicher, L.F. Tietze.** Thieme Verlag, Stuttgart, **1993.** 320 pp., paperback, DM 39.80.–ISBN 3-13-109601-2

Reproductive Toxicology. Edited by **M. Richardson.** VCH, Weinheim/New York, **1993**. 286 pp., hardcover, DM 195.–/$ 125.—ISBN 3-527-28561-x/1-56081-737-2

RP-HPLC für Anwender (Series: Die Praxis der instrumentellen Analytik. Series Editors: **U. Gruber, W. Klein**). By **W. Gottwald.** VCH, Weinheim, **1993.** 249 pp., paperback, DM 58.–ISBN 3-527-28518-0

Tierversuche in der Forschung. Denkschrift. A Publication of the **Deutsche Forschungsgemeinschaft.** VCH, Weinheim, **1993.** 93 pp., paperback, ca. DM 48.—ISBN 3-527-27209-7

Diplom- und Doktorarbeit. By **H.F. Ebel, C. Bliefert.** VCH, Weinheim, **1993.** 209 pp., paperback, DM 39.—ISBN 3-527-30003-1

Biotechnologie: Die Biologischen Grundlagen. By **M.D. Trevan, S. Boffey, K.H. Goulding, P. Stanbury.** Springer, Heidelberg, **1993**. 322 pp., paperback, DM 78.—ISBN 3-540-56191-9

Registered names, trademarks, etc. used in this journal, even when not marked as such, are not to be considered unprotected by law.

© VCH Verlagsgesellschaft mbH, D-W-6940 Weinheim, 1992. – Printed in the Federal Republic of Germany by Konrad Triltsch Druck- und Verlagsanstalt Würzburg.

All rights reserved (including those of translation into foreign languages). No part of this issue may be reproduced in any form — by photoprint, microfilm, or any other means — nor transmitted or translated into a machine language without written permission from the publishers. Only single copies of contributions, or parts thereof, may be made for personal use. This journal was carefully produced in all its parts. Nevertheless, authors, editors, and publisher do not warrant the information contained therein to be free of errors. Readers are advised to keep in mind that statements, data, illustrations, procedural details, or other items may inadvertently be inaccurate.

Valid for users in the USA: The appearance of the code at the bottom of the first page of an article (serial) indicates the copyright owner's consent that copies of the article may be made for personal or internal use, or for the personal or internal use of specific clients. This consent is given on the condition, however, that the copier pay stated per-copy fee through the Copyright Clearance Center, Inc. (CCC), for copying beyond that permitted by Sections 107 or 108 of the U.S. Copyright Law. This consent does not extend to other kinds of copying, such as copying, for general distribution, for advertising or promotional purposes, for creating new collective works, or for resale. For copying from back volumes of this journal see 'Permissions to Photo-Copy: Publisher's Fee List' of the CCC.

Editorial office: Postfach 10 11 61, D-W-6490 Weinheim, Federal Republic of Germany, Telephone (06201) 606 315, Telex 465 516 vchwh d, Telefax (06201) 606 328, E-Mail Z16@ DHDURZ2 in Earn Bitnet.

Editor: *Peter Gölitz*

Associate editors: *N. A. Compton, R. H. Schmidt-Radde, K. J. Schneider.* **Book editor:** *G. Karger.* **Editorial assistant:** *E. Schweikart*

Publishers: VCH Verlagsgesellschaft mbH. (Managing Directors: *Hans Dirk Köhler, Dr. Karlheinz Köpfer*), Pappelallee 3, D-W-6940 Weinheim, Federal Republic of Germany.

Advertising office (Advertising Manager: *N. Schippel*): Postfach 10 11 61, D-W-6940 Weinheim, Federal Republic of Germany, Telephone (0 62 01) 606 312, Telefax (0 62 01) 606 328.

ANGEWANDTE CHEMIE
International Edition in English
Volume 32 · Number 7
July 1993
Pages 923–1110

Methods for the Synthesis of μ-Hydrocarbon Transition Metal Complexes without Metal–Metal Bonds

By Wolfgang Beck,* Burkhard Niemer, and Michael Wieser

Dedicated to Professor Heinrich Nöth on the occasion of his 65th birthday

Transition metal complexes in which hydrocarbons serve as σ,σ-, σ,π-, or π,π-bound bridging ligands are currently of great interest. This review presents efficient and directed syntheses for such compounds, which often have very aesthetic structures. These reactions are among the most important reaction types in modern organometallic chemistry. They can be a useful aid for the synthesis of tailor-made compounds, for example, for models of catalytic processes and, specifically, for the construction of heterometallic compounds. We will discuss reactions of electrophilic complexes with nucleophilic ones, numerous transformations of (functionalized) hydrocarbons with metal complexes, the currently very topical complexes with bridging acetylide and carbide ligands, and organometallic polymers, which can be expected to have interesting and novel materials properties. Chisholm[1] has described the importance of these complexes as follows: "Central to the development of polynuclear and cluster chemistry are bridging ligands and central to organometallic chemistry are metal–carbon bonds. Thus bridging ligands hold a pivotal role in the development of dinuclear and polynuclear organometallic chemistry".

1. Introduction

Complexes incorporating hydrocarbons as bridges between metal atoms were known soon after the advent of modern organometallic chemistry. They are formed, for instance, by the reaction of metal carbonyls with alkynes[2] or by the dimerization of dicyclopentadienylrhodium.[3a] Cyclopolyenes such as cyclooctatetraene can act as bridges between two iron, cobalt, or platinum atoms.[3b] The synthesis of complexes with bridging polymethylene ligands from α,ω-dibromoalkanes and $[CpFe(CO)_2]^-$ was the first directed synthetic pathway.[4]

Why are complexes with hydrocarbon bridges of such great interest? They are models for intermediates in the Fischer–Tropsch process,[5] in the polymerization of alkenes[6a] and alkynes,[6b] and for unsaturated hydrocarbons chemisorbed on metal surfaces[7]—a first step during heterogeneous catalyses. It is possible to prepare in a directed way heterometallic species that can act as precursors for heterogeneous catalysts which incorporate different metals in stoichiometric proportions.[8] In addition, "early" and "late" transition metals, for example, zirconium and cobalt,[9] can be linked with hydrocarbon ligands. In organometallic polymers, unsaturated hydrocarbons can act as electronic bridges[10] ("molecular wires"[11]) between metal atoms. Electrochemical studies on compounds with bridging π ligands yield insights into the intramolecular electron transfer between two metal atoms.[12]

Due to the large number of currently known complexes with hydrocarbon bridges, this review cannot be complete; cluster compounds and polynuclear complexes with metal–metal bonds or supporting bridging ligands[9b, 13, 14] will be

[*] Prof. Dr. W. Beck, Dr. B. Niemer, Dipl.-Chem. M. Wieser
Institut für Anorganische Chemie der Universität
Meiserstrasse 1, D-80333 München (FRG)
Telefax: Int. code + (89)5902-451

 © VCH Verlagsgesellschaft mbH, D-69451 Weinheim, 1993 0570-0833/93/0707-0923 $ 10.00+.25/0

excluded for the most part. We will stress methods for the synthesis of μ-hydrocarbon complexes not having metal–metal bonds. Other reviews in the literature have organized these complexes according to compound type.[3, 15–17]

2. Reactions between Electrophilic and Nucleophilic Complexes

In general, complexes with bridging hydrocarbon ligands are formed in a predictable and unique fashion when organometallic nucleophiles are combined with corresponding electrophiles. In nearly all cases these are reactions of cationic and anionic complexes, yielding neutral products. Kochi coined the term "ion pair annihilation" for these in principle extremely simple reactions.[18] The reactions described in the following sections and the abbreviations used are summarized in Table 1.

Table 1. Overview of the reactions in Section 2[a].

Nucleophile	Electrophile	Section
$[L_m(OC)_nM]^-$	$[(\pi\text{-}Z)ML_n]^+$	2.1.
$[L_nM(Z)Nu]^-$	$[(\pi\text{-}Z)ML_n]^+/[ML_n]^+$	2.2.
$[L_nM(\pi\text{-}Z)]^-$	$[(\pi\text{-}Z)ML_n]^+$	2.3.
$[L_m(OC)_nM]^-$	$[(X\text{-}\pi\text{-}Z)ML_n]$	2.4.
$[L_nM(Z)]^-$	$[(X)ML_n]$	2.5.
$[L_nM]$ [19]	$[(X\text{-}Z)ML_n]$	2.6.

[a] $[L_mM(CO)_n]^-$ = carbonylmetalate ion, e.g., $[Re(CO)_5]^-$; M = metal; Z = hydrocarbon; Nu = nucleophilic substituent, e.g., S; X = halide; L = ligand; $[ML_n]^+$ denotes, e.g., $[Re(CO)_5]^+$; $[L_nM]$ denotes, e.g., $[(PPh_3)_2Pt]$; Cp = η^5-C_5H_5, Cp* = η^5-C_5Me_5; Fp = $[Fe(CO)_2Cp]$; Fp* = $[Fe(CO)_2Cp^*]$; Fc = ferrocenyl.

2.1. Reactions between Unsaturated Hydrocarbon Ligands in Cationic Metal Complexes and Carbonylmetalate Ions, and Redox Reactions

2.1.1. Addition Reactions

The addition of organic nucleophiles to unsaturated hydrocarbon ligands is one of the most investigated and important reactions in organometallic chemistry.[20] It has found broad application in organic synthesis[21] and is also a crucial step in industrial processes such as the Wacker process.[22]

The unsaturated hydrocarbon, for example, an olefin, is activated (becomes at least partially positively charged) by coordination to a transition metal atom and is thereby made susceptible to nucleophilic attack (Scheme 1). These reactions are characterized by high regio- and stereospecificity, which is also supported by theoretical studies.[20a, g, 23] Davies, Green, and Mingos formulated general, meanwhile well-established rules that predict that acyclic hydrocarbon ligands as well as those with an even number of coordinated carbon atoms (η^2, η^4...) are attacked preferentially (DGM rules: "even before odd" and "open before closed").

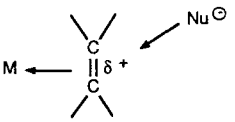

Scheme 1. Nucleophilic attack on a carbon atom activated by coordination.

The addition of organometallic nucleophiles (carbonylmetalate ions) to unsaturated hydrocarbon ligands in cationic complexes opened up a direct pathway to various compounds with hydrocarbon bridges.[24] The first example of this reaction type was found by us when $[CpM(CO)_3(\eta^2\text{-}C_2H_4)]^+$ (M = Mo, W) was allowed to react with $[Re(CO)_5]^-$.[25] This pathway to complexes like **1** with ethylene bridges has been briefly discussed by Ellis.[26] Interestingly, the $Cp(OC)_3M$ unit in complex **1** can be replaced by the stronger nucleophile $[Re(CO)_5]^-$.[27] Compound **2** can

$$[CpM(CO)_3(C_2H_4)]^+ + [Re(CO)_5]^- \longrightarrow [Cp(OC)_3MCH_2CH_2Re(CO)_5]$$
1

M = Mo, W

$$+ [Re(CO)_5]^- \quad - [CpM(CO)_3]^-$$

$$[(OC)_5Re(C_2H_4)]^+ + [Re(CO)_5]^- \longrightarrow [(OC)_5ReCH_2CH_2Re(CO)_5]$$
2

Wolfgang Beck was born in Munich in 1932 and completed his dissertation in 1960 with Professor W. Hieber at the Technische Hochschule in Munich. After his habilitation at the TH Munich in 1963, he accepted the offer of the chair for Inorganic and Analytical Chemistry at the University of Munich in 1968. He was awarded the Karl-Winnacker-Stipendium and the Chemiepreis der Akademie zu Göttingen. In 1977 he was a visiting professor at the University of Wisconsin in Madison. His research interests lie in coordination chemistry (metal complexes of pseudohalides and reactions of their coordinated ligands, metal complexes with biologically relevant ligands and of dyes) and organometallic chemistry.

Burkhard Niemer, born in Essen in 1962, studied chemistry from 1981 to 1987 at the Universities of Giessen and Munich. In 1990 he completed his dissertation under the supervision of Professor W. Beck on complexes with hydrocarbon bridges. After a stay with Professor H. D. Kaesz at the University of California, Los Angeles, he returned to Munich in 1992.

Michael Wieser was born in Munich in 1965 and studied chemistry from 1984 to 1990 at the Technische Universität and the University of Munich. He is currently a doctoral student with Professor W. Beck and working on the topic discussed in this review.

be obtained more directly by the reaction of $[(OC)_5Re(\eta^2\text{-}C_2H_4)]^+$ with $[Re(CO)_5]^-$.[28] The cationic rhenium ethylene complex can be prepared under very mild conditions (1 bar, room temperature) from $[(OC)_5Re]FBF_3$ and ethylene.[28, 29]

A number of μ-ethylene complexes could be prepared as outlined in Scheme 2. The cationic alkene complexes $[(OC)_5M(\eta^2\text{-}CH_2{=}CHR)]^+$ (M = Mn, Re), $[CpM(CO)_3(\eta^2\text{-}C_2H_4)]^+$ (M = Mo, W), $[(\eta^6\text{-}C_6H_6)Ru(PMe_3)_2(\eta^2\text{-}C_2H_4)]^+$[30] and the anionic species $[M(CO)_5]^-$ (M = Mn, Re), $[CpM(CO)_3]^-$ (M = Mo, W), and $[CpRu(CO)_2]^-$ were used for this purpose. In general, the μ-alkene complexes decompose upon heating with loss of the olefin and form dimetallic complexes with a M–M bond (compound **2** decomposes only at 140 °C!).

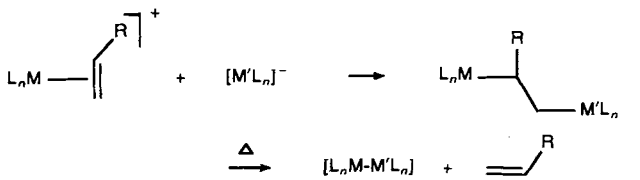

Scheme 2. Synthesis and decomposition of complexes with ethylene bridges.

The addition of $[Re(CO)_5]^-$ to the η^2-coordinated butadiene ligand in $[(OC)_5Re(\eta^2\text{-}H_2C{=}CHCH{=}CH_2)]^+$ gives as final product the stable μ-but-2-ene-1,4-diyl complex **3**.[31]

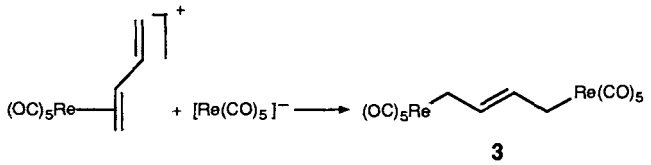

3

The use of cationic alkyne complexes as electrophiles leads to the formation of $\mu\text{-}\eta^1\text{:}\eta^1$-alkyne complexes (Scheme 3).[32] In contrast, molybdenum alkyne complexes in which the alkyne acts as a four-electron donor[33] react with $[Re(CO)_5]^-$ to give the heterodimetallatetrahedranes **4**.[34] When unsymmetrically substituted alkynes are used, it is thus possible to prepare chiral dimetallatetrahedranes with four different corner atoms. Two aspects of these reactions

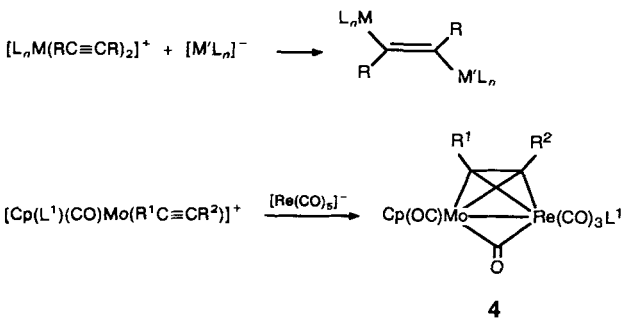

4

Scheme 3. Synthesis of $\mu\text{-}\eta^1\text{:}\eta^1$-alkyne complexes (top) and tetrahedranes (bottom) from alkyne complexes. R = COOMe, Me; $M'L_n$ = $Ru(CO)_2Cp$, $Re(CO)_5$, $Mn(CO)_5$; L_nM = $Cp(PMe_3)_2Ru$, etc.; L^1 = CO, PPh_3; R^1 = Me, Ph; R^2 = Me, Ph.

are remarkable: the elimination of CO from the $Re(CO)_5$ anion, which occurs under very mild conditions, and the migration of the ligand L^1 from Mo to Re. Analogous reactions were performed with $[Mn(CO)_5]^-$, $[CpW(CO)_3]^-$,[34b] and $[Ir(CO)_4]^-$.[35]

According to work by Green et al.,[36a] the $[CpFe(CO)_2]^-$ anion acts—in contrast to $[Re(CO)_5]^-$ and $[CpW(CO)_3]^-$—as a reducing agent towards the cationic molybdenum alkyne complex $[Cp(L)Mo(MeC{\equiv}CMe)_2]^+$. The products of the reaction are $[\{CpFe(CO)_2\}_2]$ and the 17-electron radical, $[CpMo(MeC{\equiv}CMe)_2]$,[36b] which yields dimers such as **5** with C_6 or C_8 bridges ("flyover" complexes, see also Section 2.1.2).

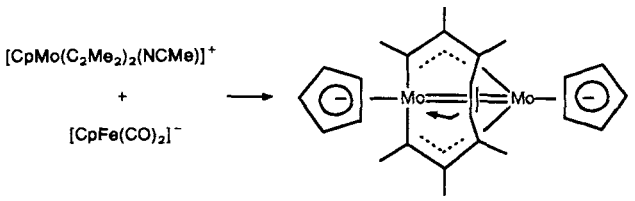

5

Organometallic nucleophiles, and especially $[Re(CO)_5]^-$, can be added to cationic complexes incorporating the following ligands: allyl,[37] η^4-diene,[38] trimethylenemethane,[38, 39] dienyl,[18, 39, 40] benzene,[41, 42] cycloheptatriene,[43] and tropylium.[38] In all cases, homo- and heterodimetallic complexes with σ,π-hydrocarbon bridges are formed (e.g. **6**–**8**). The first example of an addition of a carbonylmetalate ion to a *cyclic* hydrocarbon ligand (cycloheptatriene) was reported by Angelici et al.[43]

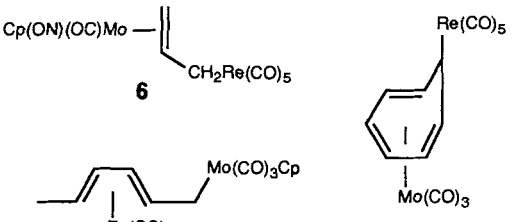

6 **7** **8**

The reaction of the chiral allyl complex $[CpMo(CO)(NO)(\eta^3\text{-}C_3H_5)]^+$ and $[M(CO)_5]^-$ (M = Mn, Re) proceeds as stereospecifically as with organic nucleophiles[44] to form *one* isomer (**6**, M = Re), a fact which is supported by theoretical calculations.[45]

The cation $[Cp^*Ir(\eta^2\text{-}C_2H_4)(\eta^3\text{-}C_3H_5)]^+$ can serve as a test compound for the DGM rules.[46] Contrary to these rules, $[Re(CO)_5]^-$ is added—presumably for steric reasons[46]—to the terminal carbon atom of the allyl ligand, forming **9**, which was characterized by X-ray crystallography.[47] The reaction of the Ir cation with organic nucleophiles leads to metallacyclobutanes by selective addition to the central carbon atom of the allyl ligand.[46]

The crystal structures show that the attack of the organometallic nucleophile on the π-bound hydrocarbon occurs always *exo* to the metal. Surprisingly, a MoRu complex with an $\eta^1\text{:}\eta^6$-cycloheptatriene bridge is also formed by the

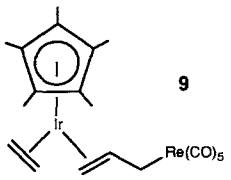

9

reaction of $[(\eta^7\text{-}C_7H_7)Mo(CO)_2Br]$ and $[Cp^*Ru(CO)_2]^-$. This reaction proceeds with an intermolecular CO transfer.[48] The $\mu\text{-}\eta^6\text{:}\eta^1\text{-}C_7H_7$ complexes have temperature-dependent NMR spectra, which suggests dynamic behavior in solution.[38, 48]

The adduct formed from $[(\eta^6\text{-}C_6H_6)Mn(CO)_3]^+$ and $[Re(CO)_5]^-$ gives an excellent example for fluxional behavior in organometallic compounds.[41, 42] We assume the transition state to be a benzene-bridged structure $[(OC)_3Mn^-(\mu\text{-}\eta^4\text{:}\eta^2\text{-}C_6H_6)Re^+(CO)_5]$ with 18 valence electrons on each metal atom. Such σ,π shifts are of great theoretical and practical interest owing to their role in homogeneous catalysis.[49] Alternatively, a transition state with a π,π-benzene bridge or a contact ion pair is also possible for the MnRe complex. Planar benzene bridges are known, for instance, in the dinuclear triple-decker complexes $[(CpV)_2(\mu\text{-}\eta^6\text{-}C_6H_6)]$[50] and $[(C_6H_3Me_3)_3Cr_2]$.[51] The formulation as contact ion pair also retains the noble gas configuration for both metal atoms.

$[Re(CO)_5]^-$ reacts with $[(\eta^5\text{-}C_6H_7)Ru(CO)_3]^+$, initially—in accord with the DGM rules—at the terminal carbon atom of the dienyl ligand. A subsequent transformation in solution, presumably an H migration, leads to the $\mu\text{-}\eta^1\text{:}\eta^4$-cyclohexadiene complex in which the $Re(CO)_5$ complex fragment is bound to a sp^2 carbon atom.[40]

Thiophene coordinated to a manganese atom is also activated towards the pentacarbonylrhenate ion. The reaction provides $[(OC)_3Mn(\mu\text{-}\eta^4\text{:}\eta^1\text{-}C_4H_4S)Re(CO)_5]$, in which the $Re(CO)_5$ complex fragment is attached to the carbon atom adjacent to the sulfur.[42] In the reaction of $[HFe(CO)_4]^-$ and $[HW(CO)_5]^-$ with $[(CO)_3Mn(C_4H_4S)]^+$, on the other hand, a hydride is added to the thiophene ligand.[52]

The extension of this synthetic strategy to organometallic dianions as nucleophiles leads to trinuclear heterometallic complexes with two hydrocarbon bridges (Scheme 4).

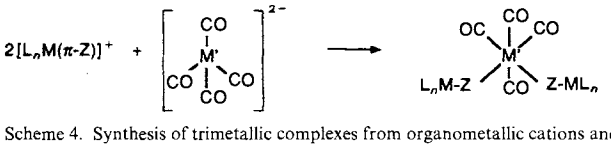

Scheme 4. Synthesis of trimetallic complexes from organometallic cations and carbonylmetalate dianions. Z = unsaturated hydrocarbon.

Complexes **10**–**17** were prepared by the reaction of $[Os(CO)_4]^{2-}$ or $[Ru(CO)_4]^{2-}$ with the cations $[(OC)_5Re(C_2H_4)]^+$, $[Cp(OC)(ON)Mo(C_3H_5)]^+$, $[Cp(OC)_2Mo(diene)]^+$, $[(OC)_3Fe(dienyl)]^+$, $[(OC)_3Mn(C_4H_4S)]^+$, $[(OC)_3Mn(C_6H_6)]^+$, $[(OC)_3M(C_7H_7)]^+$ (M = Cr, Mo).[53] In the same fashion, the cations $[(\eta^6\text{-}C_6H_6)(Me_3P)_2Ru(C_2H_4)]^{2+}$, $[Cp(OC)_2Re(C_3H_5)]^+$, $[(OC)_4M(C_3H_5)]^+$ (M = Fe, Ru),

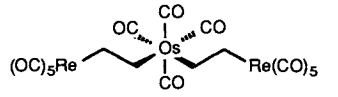

10

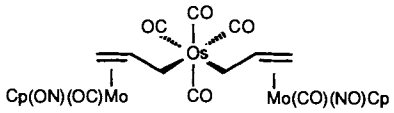

11

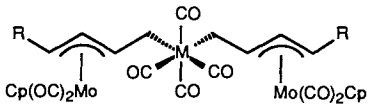

12 (M=Ru,Os; R=H,Me)

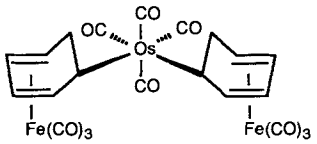

13

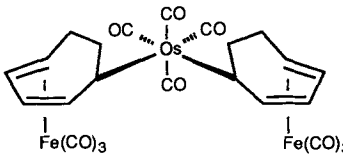

14

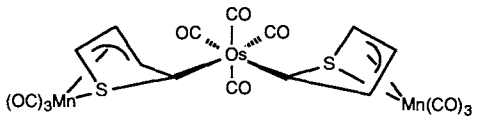

15

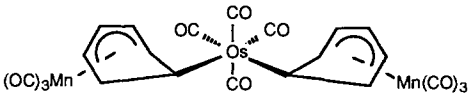

16

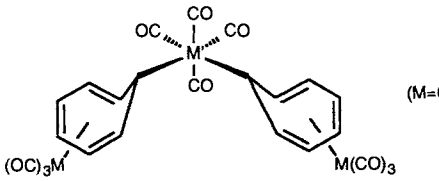

17 (M=Cr,Mo; M'=Ru,Os)

and $[Cp^*Ir(C_2H_4)(C_3H_5)]^+$ can be added twice to $[Os(CO)_4]^{2-}$.[47]

The $Re(CO)_5$ unit is isolobal with the methyl group. According to Hoffmann,[54] compound **10** can therefore also be termed 4-osma-1,7-dirhena-*n*-heptane. X-ray crystal structure determinations show that the hydrocarbon bridges on the Os atom always have a *cis* orientation in analogy to $[Me_2Os(CO)_4]$.[55] The carbon atoms bound to osmium in **13**–**15** are stereogenic. In solution it is possible to show that diastereomers are present, while in the crystal structures of **14** and **15** the carbon atoms that are σ-bound to osmium have the same configuration. Surprisingly, even the trinuclear complex **16** shows the fluxional behavior observed in solutions of $[(OC)_5Re(\mu\text{-}\eta^1\text{:}\eta^5\text{-}C_6H_6)Mn(CO)_3]$.

The pentanuclear complex **18** (4,5,6-triosma-1,9-dirhena-*n*-nonane), which has two ethylene bridges, forms when $[(OC)_5Re(\eta^2\text{-}C_2H_4)]^+$ is added to the trinuclear dianion

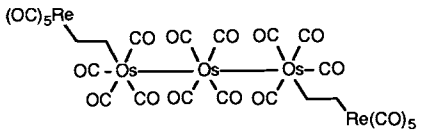

18

$[Os_3(CO)_{12}]^{2-}$, which in turn is prepared by deprotonation of the corresponding hydride.[56]

The reaction of the dianion $[Fe_2(CO)_8]^{2-}$ with the cationic rhenium ethylene complex leads, by insertion of CO into the Fe–C bond, to complex **19**, which has two bridging acyl ligands.[57] This is due to the lower stability of the Fe–C bond compared to its Os–C analogue. Similar complexes with organic substituents on the acyl-CO group have been described by Fischer et al.[58] and Kaesz et al.[59]

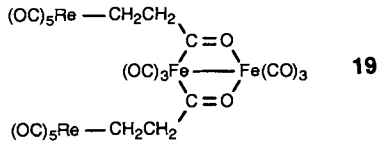

19

The use of highly reduced anions (Ellis compounds)[60] in reactions with cationic π complexes should, in principle, also lead to multinuclear complexes. However, the reaction of $[Ir(CO)_3]^{3-}$ with $[(OC)_5Re(\eta^2\text{-}C_2H_4)]^+$ yielded, under loss of ethylene, the linear, heterometallic, trinuclear hydrido complex $[(OC)_5Re{-}Ir(H)(CO)_3{-}Re(CO)_5]$ as the main product.[61] Attempts to crystallize this compound produced a crystal which, surprisingly, contained the chiral, trimetalated carbonate **20**, which exhibits a "windmill" structure.

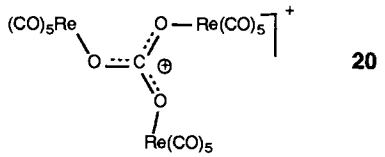

20

This compound can be regarded as a derivative of a trihydroxycarbenium ion[62] and could react with nucleophiles.[62c] The carbonate could be formed from CO_2 according to Equation (a).[63]

$$[Ir(CO)_3]^{3-} + 2\,CO_2 \longrightarrow [Ir(CO)_4]^- + CO_3^{2-} \qquad \text{(a)}$$

The organometallic nucleophiles $[Re(CO)_5]^-$ and $[Os(CO)_4]^{2-}$ are especially suited for the addition to π-coordinated hydrocarbons. These anions possess a relatively high degree of nucleophilicity,[27] and the metal–carbon σ bond formed is very stable.[64] Nearly constant metal–carbon σ bond lengths of 2.2–2.3 Å were found in the X-ray crystal structure determinations of a number of complexes. Scheme 5 summarizes the additions of carbonylmetalate ions to unsaturated hydrocarbon ligands in cationic complexes. Fischer et al.[65] studied the reactions of cationic carbyne complexes with carbonylmetalates; the addition of $[Co(CO)_4]^-$ to $[Cp(OC)_2Mn{\equiv}CR]^+$ afforded the complex $[Cp(OC)_2Mn{=}C(R){-}Co(CO)_4]$ with a carbyne bridge.

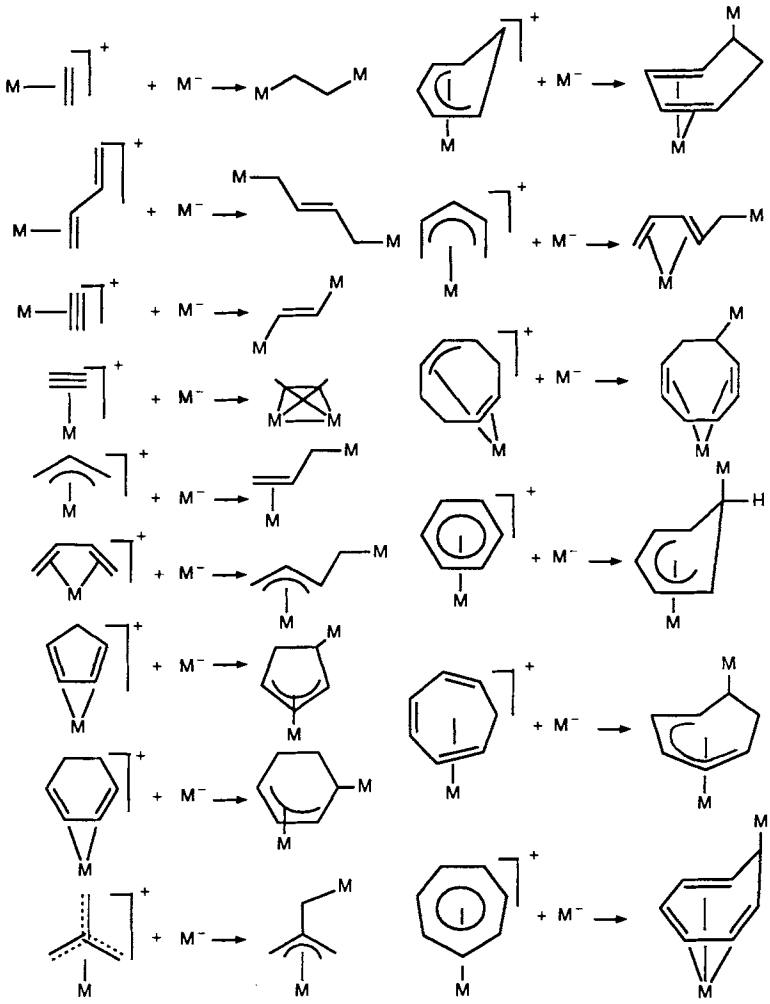

Scheme 5. Addition of organometallic nucleophiles M^- to π-bound hydrocarbons in cationic complexes.

2.1.2. Nucleophilic Addition or Electron Transfer between Cation and Anion? Redox Reactions

Evidence of electron transfer between cation and anion is found in many reactions. For instance, in reactions employing $[Re(CO)_5]^-$, $[Re_2(CO)_{10}]$ is often formed as a by-product; when $[Mn(CO)_5]^-$ is used, $[Mn_2(CO)_{10}]$ is actually the major product. The competition between nucleophilic addition and electron transfer has been particularly stressed by Kochi et al.[18] During the course of these reactions, 19- and 17-electron complexes can form, which can then combine to give the nucleophilic adduct, the C–C coupling product, or the dimer with a metal–metal bond (Scheme 6).

For instance, the reaction of $[(\eta^5\text{-hexadienyl})Fe(CO)_3]^+$ with $[CpMo(CO)_3]^-$ yields the heterometallic adduct **7**,

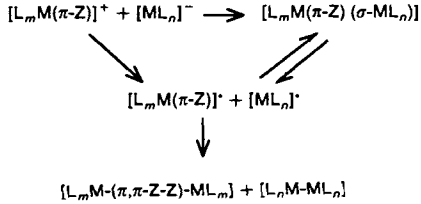

Scheme 6. Z = unsaturated hydrocarbon.

which decomposes thermally to the C–C coupling product **21** and dimer **22**.[18] After extensive studies, which included kinetic work, on the reaction between $[(\eta^5\text{-dienyl})Fe(CO)_3]^+$ and $[CpMo(CO)_3]^-$, Kochi concluded that nucleophilic addition is preferred over electron transfer (SET).[18]

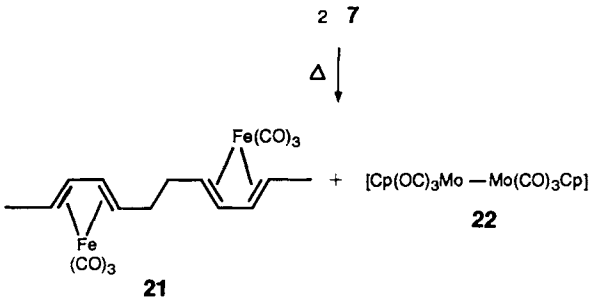

During the reaction of the tropylium complex $[(C_7H_7)Mo(CO)_3]^+$ with organometallic nucleophiles, the C–C coupling product is frequently observed.[25b, 38] These bis(cycloheptatrienyl) complexes can also be prepared from the cations by reduction with Zn, Cr^{II}, Na/Hg, and $NaC_{10}H_8$.[66]

In general, neutral 17-electron radicals preferentially dimerize with formation of a product with a metal–metal bond. In contrast, coupling reactions of 19-electron radicals that contain π ligands give rise to dimers with C–C coupled π ligands.[67] Examples include the dimerization of $[CpCo(\eta^5\text{-}C_7H_9)]$,[67] $[Cp_2Rh]$,[3a, 68] $[(\eta^5\text{-}C_8H_9)Fe(CO)_3]$,[69] $[(\eta^7\text{-}C_7H_7)M(CO)_3]$ (M = Cr, Mo, W),[25b, 66] and $[(\eta^6\text{-}C_6H_6)FeCp]$.[70] In the reduction of a cationic carbyne complex C–C coupling leads to the dinuclear bis(carbene) complex $[(OC)_5Cr{=}C(NEt_2){-}C(NEt_2){=}Cr(CO)_5]$.[71] The syntheses of the dimetallic complexes $[(OC)_3Mn(\mu\text{-}\eta^5{:}\eta^5\text{-}C_6H_6{-}C_6H_6)Mn(CO)_3]$ and $[(OC)_3Mn(\mu\text{-}\eta^4{:}\eta^4\text{-}C_6H_6{-}C_6H_6)Mn(CO)_3]^{2-}$ (**23**, by [2 + 2] cyclodimerization of coordinated benzene), were achieved by the reduction of $[(\eta^6\text{-}C_6H_6)Mn(CO)_3]^+$.[72a] The [2 + 2] cycloaddition of 16-electron osma- and ruthenacyclopentadiene leads to complex **24** and its "*trans*" isomer **25**.[72b] A Mn_2 complex with an $\eta^5{:}\eta^5$-dicyclohexadienyl bridge is formed as a by-product

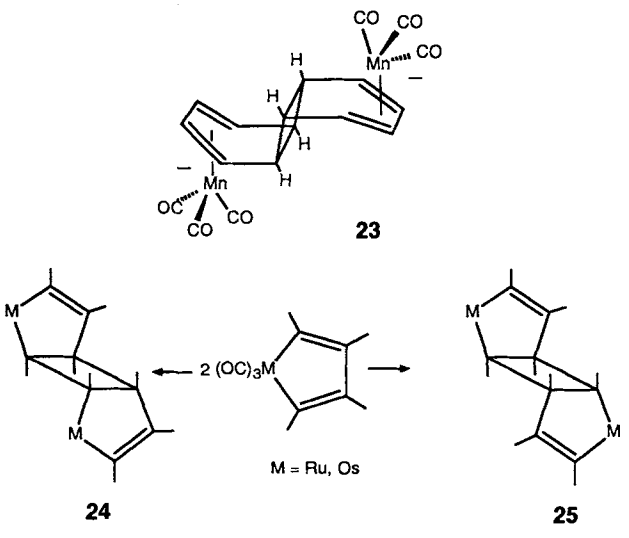

of the reaction between $[(OC)_3Mn\text{-}(\eta^6\text{-}C_6H_3Me_3)]^+$ and $AlMe_3$.[73] The 17-electron radical cations $[(\eta^4\text{-}C_8H_8)Fe(CO)_3]^+$[74] and $[CpFe(CO)_2CH_2C(R){=}CR_2]^+$[75] also undergo C–C coupling reactions.

The oxidation of $(\eta^4\text{-}C_8H_8)ML_n$ complexes yields the binuclear complexes $[M(\mu\text{-}\eta^5{:}\eta^5\text{-}C_8H_8{-}C_8H_8)M]^{2+}$ (M = $Fe(CO)_2P(OPh)_3$, $Fe(CO)_3$, RhCp, CoCp*) and other interesting products.[76] Geiger, Salzer, et al. observed especially remarkable structural changes in the cyclooctatetraene bridge during the (reversible) oxidation of the pseudo-triple-decker complexes $[(C_5R_5)M(\mu\text{-}C_8H_8)M(C_5R_5)]$ (M = Co, Rh, R = H, Me; Scheme 7).[77] Several bonding modes are

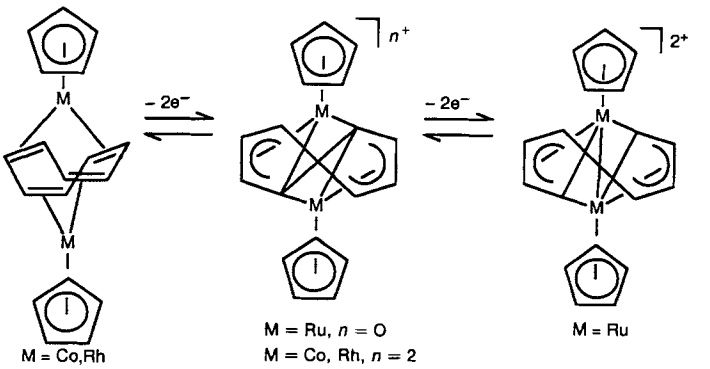

Scheme 7. Structural changes in the C_8H_8 ligand upon oxidation.

known for bridging cyclooctatetraene ligands.[78] Equally interesting is the oxidation of $[CpRu(\mu\text{-}C_8H_8)RuCp]$, which proceeds by insertion of both Ru atoms into a C–C bond of the cyclooctatetraene bridge to yield a so-called flyover complex.[79] Flyover complexes such as **5** may also be prepared by reducing cationic bis(alkyne) molybdenum complexes.[36b, 80] In attempted preparations of the sandwich complex $[CpV(C_8H_8)]$ from $C_8H_8^{2-}$, C–C coupling leads to three isomers of $[CpV(\mu\text{-}C_8H_8{-}C_8H_8)VCp]$.[81] A review article by Connelly comprehensively describes dimerizations of π-coordinated hydrocarbons induced by one-electron oxidations or reductions.[82]

The C–C coupling of two Cp ligands is achieved by lithiation of $[CpMn(CO)_3]$ and subsequent oxidation with $CuCl_2$.[83a] The reductive coupling of $[BrCCo_3(CO)_9]$ results in the linkage of two $[CCo_3(CO)_9]$ units by a C–C bond.[83b]

2.2. Reactions of Anionic Metal Complexes Containing a Nucleophilic Heteroatom Ligand with Coordinated Unsaturated Hydrocarbons or Organometallic Lewis Acids

In this section reactions following Scheme 8 are discussed.

Raubenheimer et al. were able to show that CS_2 adds to the anionic Fischer carbene $[(OC)_5Cr{=}C(OEt)CH_2]^-$ and that the CS_2 adduct can be alkylated at the sulfur atom.[84] Possible "alkylating agents" for Fischer carbene dithiolates

$$[L_nM(Z\text{-}Nu)]^- + [(Z)ML_n]^+ \longrightarrow [L_nM(Z\text{-}Nu\text{-}Z)ML_n]$$

Scheme 8. Nu = nucleophile.

include $[(OC)_5Re(\eta^2\text{-}C_2H_4)]^+$, $[CpW(CO)_3(\eta^2\text{-}C_2H_4)]^+$, and $[Cp(OC)(ON)Mo(\eta^3\text{-}C_3H_5)]^+$ or $[Re(CO)_5]^+$. Depending on whether one or two equivalents of base are employed, the di- or trimetallic complexes **26**–**29** are formed.[85, 86a]

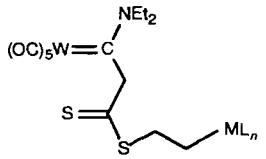

26: $ML_n = CpW(CO)_3$
27: $ML_n = Re(CO)_5$

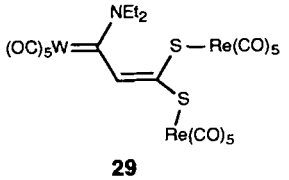

29

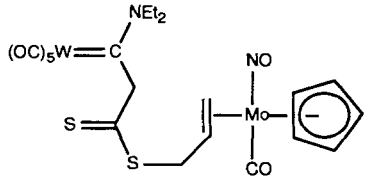

28

A further example for this type of reaction is the addition of the anionic thiocarbyne complex $[(HBpz_3)(OC)_2M(CS)]^-$ (M = Mo, W; pz = 3,5-dimethylpyrazol-1-yl)[87] to unsaturated hydrocarbons or to the metal atom in cationic complexes, giving rise to, for example, **30a,b**.[85, 86b] The use of cationic organometallic Lewis acids leads to rare[88] complexes like **30c–e** with thiocarbonyl bridges.[85, 86b]

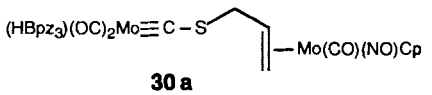

30a

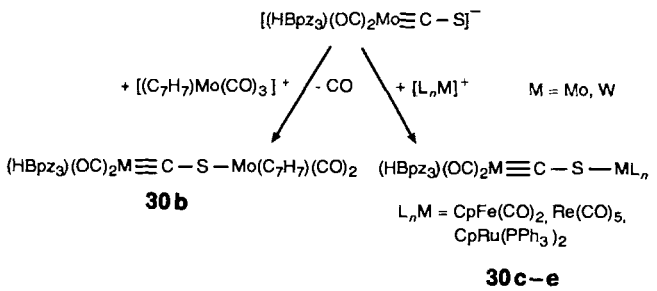

30b

L_nM = $CpFe(CO)_2$, $Re(CO)_5$, $CpRu(PPh_3)_2$

30c–e

The carboxylate ion $[Cp(OC)(Ph_3P)Fe{-}COO]^-$ can be "esterified" with the cationic ethylene complex $[(\eta^2\text{-}C_2H_4)Fe(CO)LCp]^+$, leading to $[Cp(OC)(Ph_3P)Fe{-}C(O){-}OCH_2CH_2{-}Fe(CO)(L)Cp]$, a complex with a carboxyethylene bridge.[89]

Adducts of tertiary diphosphanes and $[(OC)_3Cr(\eta^7\text{-}C_7H_7)]^+$ react with the cationic iron complex $[CpFe(CO)_2(thf)]^+$ to yield an FeCr complex with an η^6-$C_7H_7(Ph_2PCH_2CH_2CH_2PPh_2)$ bridge.[90]

2.3. C–C Coupling Reactions

C–C coupling of coordinated nucleophilic and electrophilic hydrocarbons enables the synthesis of numerous complexes with hydrocarbon bridges (Scheme 9).

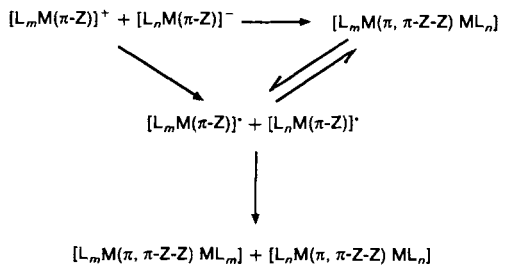

Scheme 9. Coupling of hydrocarbon ligands (Z) by C–C bond formation.

The first report on the C–C coupling of metal-coordinated hydrocarbons in cationic and anionic complexes was published by Kane-Maguire et al.[91] The addition of Li-ferrocene to the cyclohexadienyl ligand in $[(OC)_3Fe(\eta^5\text{-}C_6H_7)]^+$ leads to complex **31**. Other electrophilic and nucleophilic precursors, yielding, for instance, compounds **31**–**38**, are listed in Table 2.

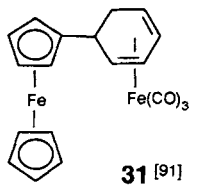

31 [91]

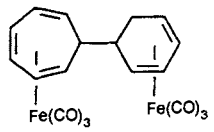

32 [96]

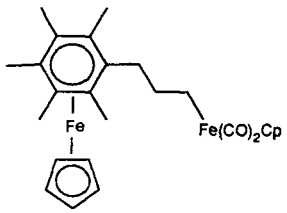

33 [97]

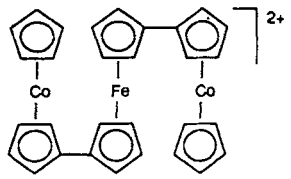

34 [100]

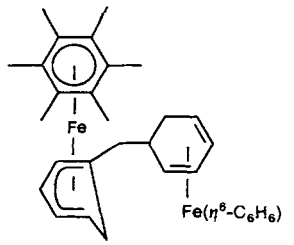

35 [102]

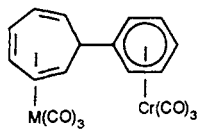

M=Cr,Mo

36 [108]

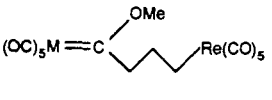

M=Cr,W

37 [106]

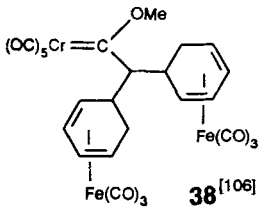

38 [106]

A large number of multinuclear complexes can be prepared from the anion of bis(tricarbonylchromium)diphenylmethane (Scheme 10).[109] The addition of the tropylium ion to tricarbonylcycloheptatrieneiron leads to polymeric complexes.[110]

Rosenblum et al. described C–C coupling reactions of σ-bound allyl ligands with cationic π complexes, for instance,

Table 2. C–C coupling reactions of metal-coordinated hydrocarbons.

Electrophile	Nucleophile	Ref.
$[(OC)_3Fe(cyclohexadienyl)]^+$	$[(OC)_3Fe(cyclohepta\text{-}1,3\text{-}diene\text{-}5,7\text{-}dione)]$	[92]
$[(\eta^5\text{-}C_5H_5)Fe(\eta^5\text{-}C_5H_4Br)]$	$[(OC)_3Mn(\eta^5\text{-}C_5H_4Li)]$	[93]
$[(\eta^6\text{-}C_6H_6)Cr(\eta^6\text{-}C_6H_5Cl)]$	$[(\eta^6\text{-}C_6H_6)Cr(\eta^6\text{-}C_6H_5Li)]$	[94]
$[(OC)_3M(cycloheptatrienyl)]^+$ M = (Cr, Mo, W)	$[(OC)_3Fe(cycloheptatrienyl)]^-$	[95]
$[(OC)_3Fe(cyclohexadienyl)]^+$	$[(OC)_3Fe(cycloheptatrienyl)]^-$	[96]
$[(OC)_2CpFe(C_2H_4)]^+$ $[(OC)_3FeCp]^+$	$[CpFe(\eta^5\text{-}C_6Me_5CH_2)]$	[97]
$[(OC)_2CpFe(=CHOMe)]^+$	$[CpFe(\eta^5\text{-}C_6Me_5CH_2)]$	[98a]
$[Fe_2(CO)_2Cp_2(\mu\text{-}CO)\text{-}(\mu\text{-}C\text{-}CH=CHOEt)]^+$	$[Fe_2(CO)_2Cp_2(\mu\text{-}CO)(\mu\text{-}C=CH_2)]$	[98b]
$[(OC)_3Fe(methoxycyclohexadienyl)]^+$	$[(OC)_2CpMo(cyanohexenyl)]^-$	[99]
$[Cp_2Co]^+$	$[(\eta^5\text{-}C_5H_5)Fe(\eta^5\text{-}C_5H_4Li)]$ $[(\eta^5\text{-}C_5H_4Li)_2Fe]$	[100]
$[(OC)_3M(cyclohexadienyl)]^+$ (M = Fe, Ru)	$[Cp_2Co]$ $[L_nRu(C_8H_8)]$	[101]
$[(C_6H_6)Fe(cyclohexadienyl)]^+$	$[(C_6Me_6)Fe\{C_6Me_5(=CH_2)\}]$	[102]
$[L_nM(\eta^5\text{-}C_5H_4)]$	$[L_nM(\eta^5\text{-}C_5H_4\text{-}C{\equiv}C\text{-}SnR_3)]$	[103]
$[(OC)_3Cr(RC_6H_4Cl)]$	$[(OC)_3Cr(C_6H_5Li)]$	[104]
$[(OC)_3M(cycloheptatrienyl)]^+$ (M = Cr, Mo, W)	$[FeC(O)CH_2]^-$ $[(OC)(Ph_3P)CpFeC(O)CH_2]^-$	[105]
$[(OC)_2CpFe(C_2H_4)]^+$ $[(OC)_5Re(C_2H_4)]^+$	$[(OC)_5M{=}C(OMe)CH_2]^-$ M = Cr, W	[106]
$[(CO)_3Fe(cyclohexadienyl)]^+$ $[(OC)_3M(cycloheptatrienyl)]^+$ (M = Cr, Mo, W)	$[(OC)_5Cr{=}C(OMe)CH]^{2-}$	[106b]
$[(OC)_3M(cycloheptatrienyl)]^+$ (M = Cr, Mo, W)	$[(OC)_3Mn(cycloheptatriene)]^-$ $[(OC)_3Mn(cyclooctatriene)]^-$ $[(OC)_3Mn(C_8H_8)]^-$	[107]
$[(OC)_3Mn(C_6H_6)]^+$ $[(OC)_3M(cycloheptatrienyl)]^+$ (M = Cr, Mo, W)	$[(OC)_3Cr(C_6H_5Li)]$ $[(OC)_3Cr(benzothiophene)]^-$ $[(OC)_3Cr(indene)]^-$ $[(OC)_3Cr(diphenylmethane)]^-$ $[(OC)_3Cr(fluorene)]^-$	[108]

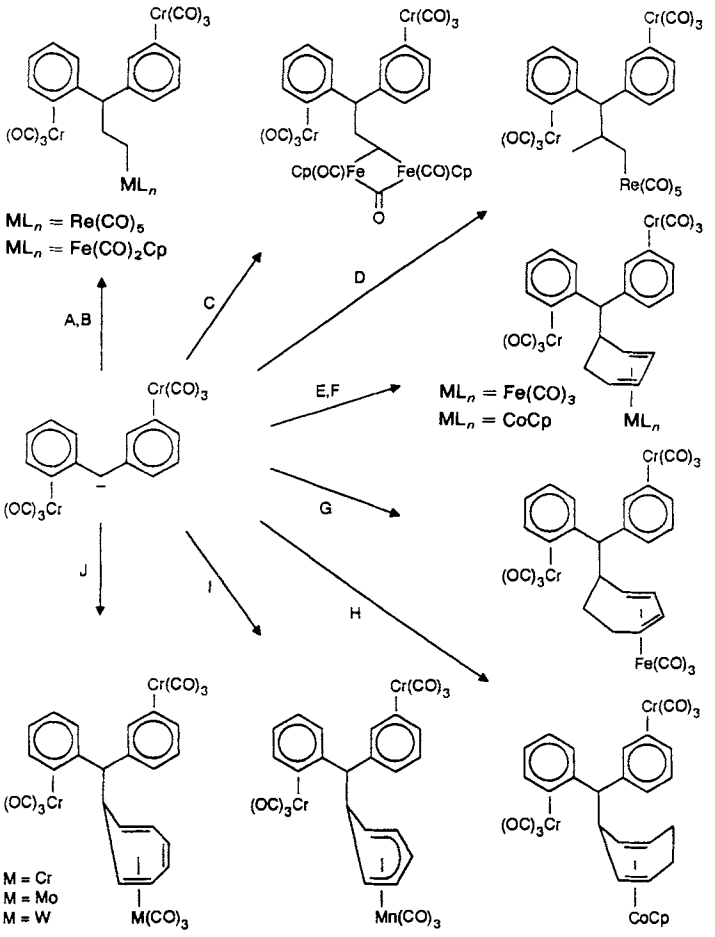

Scheme 10. A = $[(OC)_5Re(\eta^2\text{-}C_2H_4)]^+$, B = $[(OC)_2CpFe(\eta^2\text{-}C_2H_4)]^+$, C = $[Cp_2(OC)_2Fe_2(\mu\text{-}CO)(\mu\text{-}\eta^1{:}\eta^2\text{-}CH{=}CH_2)]^+$, D = $[(OC)_5Re(\eta^2\text{-}C_3H_6)]^+$, E = $[(OC)_3Fe(\eta^5\text{-}C_6H_7)]^+$, F = $[CpCo(\eta^5\text{-}C_6H_7)]^+$, G = $[(OC)_3Fe(\eta^5\text{-}C_7H_9)]^+$, H = $[CpCo(\eta^5\text{-}C_7H_9)]^+$, I = $[(OC)_3Mn(\eta^6\text{-}C_6H_6)]^+$, J = $[(OC)_3M(\eta^7\text{-}C_7H_7)]^+$ (M = Cr, Mo, W).

$[(OC)_2CpFe(C_2H_4)]^+$ and $[(OC)_3Fe(C_7H_7)]^+$.[111, 112] The cationic iron methylene complex $[Cp(OC)_2Fe{=}CH_2]^+$ adds to unsaturated σ-bound vinyl and allyl ligands to form dinuclear iron complexes.[112, 113] Cationic vinylidene complexes of iron or ruthenium as well as 2-ferrocenylpropene can dimerize or react with acetylide complexes.[114] In the same manner, (1,3-di(ferrocenyl)allyl)$^+$ can attack 2,4-bis(ferrocenyl)penta-1,3-diene.[115] A novel tricyclic dicarbene bridging two $Mn(CO)_2Cp$ units was obtained by Herrmann et al. by [2 + 2] cycloaddition of cyclopentadienylidene (prepared from diazacyclopentadiene)[116] in the presence of $[Mn(CO)_2Cp(thf)]$. Macomber et al. used α,β-unsaturated carbene complexes as electrophiles and were able to prepare numerous di- and even tricarbene complexes such as **39** by reactions with α-deprotonated carbene complexes.[117]

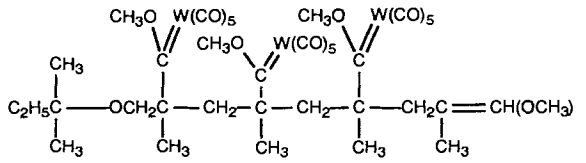

39

Transition metal complexes with aldehyde or ketone groups, for example, ferrocenylaldehyde, ferrocenylbis(aldehyde), [(2-formylnorbornadiene)RhCp], or $[(OC)_3Cr(acetophenone)]$, can act as electrophiles in reactions with anionic carbene complexes,[118] organometallic enolates,[119] or lithiated compounds like lithioferrocene or $[(OC)_3Cr\text{-}(C_6H_5Li)]$.[120] These lithiated species can also be employed in the Fischer carbene synthesis starting with metal carbonyls, allowing access to many dimetallic carbene or carbyne complexes.[121a]

When *p*-dilithium phenylene,[121c] *p*-dilithium biphenyl,[121d] or $o\text{-}C_6H_4(CH_2MgCl)_2$[121e] are used in the Fischer carbene or carbyne synthesis, complexes with bridging bis(carbene) and bis(carbyne) units such as $[(OC)_5W{=}C(OEt){-}p\text{-}C_6H_4{-}C(OEt){=}W(CO)_5]$, $[Br(OC)_4W{\equiv}C{-}p\text{-}C_6H_4{-}C{\equiv}W(CO)_4Br]$ are obtained directly.

A number of organometallic acid chlorides with the general formula $[L_nM(\eta^5\text{-}C_5H_4C(O)Cl)]$ undergo Friedel–Crafts acylation with ferrocene or $[(OC)_3ReCp]$.[122] The Wittig reaction can also be employed to couple two hydrocarbon ligands, for example, $[(OC)_3Fe(\eta^4\text{-}C_6H_7PR_3)]^+$ with $[(OC)_3Cr(\eta^6\text{-}C_6H_5C(O)H)]$ or $[(\eta^4\text{-}MeCH{=}CH{-}CH{=}CHCHO)Fe(CO)_3]$.[123] Two ferrocene molecules can be coupled by using acetals,[124] and two cobaltocene molecules can be linked by employing alkynes having electron-withdrawing groups.[125]

Dimetallic complexes can also be constructed by the [2 + 2] cycloaddition of one π- and one σ-bound alkyne ligand.[126] The [2 + 2] cycloaddition of cyclic alkadiynes to $[CpCo(CO)_2]$ leads, by formation of cyclobutadiene, to interesting superphane complexes[127] like **40**. During the reaction of $[Cp^*Rh(\eta^2\text{-}C_2H_4)_2]$ with thiophene, both a C–C coupling reaction and C–S bond cleavage in thiophene occur, giving rise to a dimetallic complex in which a $S(CH)_8S$ chain bridges two Cp*Rh units.[128]

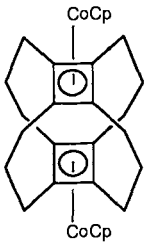

40

Other established methods in organic synthesis can be used to prepare μ-hydrocarbon complexes, for example, the McMurry reaction,[129] the Ullmann coupling of halocyclopentadienyl complexes,[130] the reaction of lithioferrocene[131] or anionic Fischer carbene complexes with dihalohydrocarbons[132a] or acid chlorides,[132b] the addition of $[(\eta^5\text{-}LiC_5H_4)Mn(CO)_3]$ to $[RC(O)C_5H_4Mn(CO)_3]$,[132c] and the condensation of ferrocenylaldehyde with acetone.[132d]

Trimethylstannylethynylcyclopentadienyl complexes react with iodo- and η^5-(1-iodovinyl)cyclopentadienyl complexes by C–C coupling to yield complexes $[L_nM(\eta^5\text{:}\eta^5\text{-}C_5H_4)CH{=}CH{-}C{\equiv}C(C_5H_4)M'L_n]$ and $[L_nM(\eta^5\text{:}\eta^5\text{-}C_5H_4)\text{-}C{\equiv}C(C_5H_4)M'L_n]$.[103, 133a] By reaction of $Bu_3SnC{\equiv}CSnBu_3$ with iodocyclopentadienyl complexes two Cp ligands can be coupled.[133b]

An interesting C–C coupling reaction of a CO ligand with olefin and diene ligands in titanium, zirconium, and hafnium complexes was observed by Erker et al. and expanded to a general synthetic approach (Scheme 11) for metallacyclic oxocarbene complexes.[9a, 134]

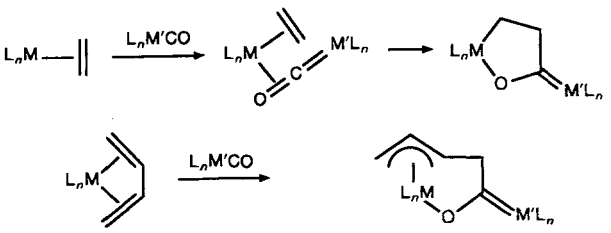

Scheme 11. M = Ti, Zr, Hf; M' = V, W, Fe, Co, Pt, etc.

The addition of the organometallic enolate $[Cp^*(Ph_3P)(ON)ReC(O)CH_2]^-$ to a CO ligand in cationic complexes yields interesting μ-malonyl complexes $[L_nM{-}C(O)CH_2C(O){-}ML_n]$ like **41**.[135]

Carbyne complexes of type $[Cp(CO)_2M{\equiv}C{-}R]$ (M = Mo, W) can be inserted into Pd–C bonds of palladacycles[136] in the same way as the isolobal alkynes (see Section 6).[14]

Finally, two unusual C–C coupling reactions should be mentioned: the reaction of an η^1-allenyl complex

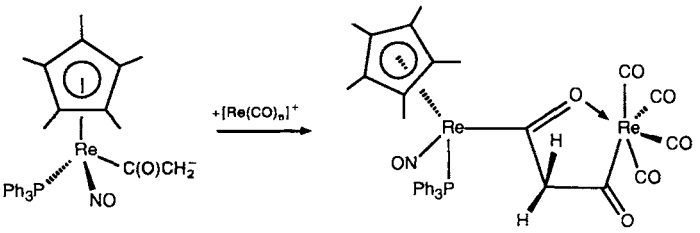

41

$[Cp(OC)_3W{-}CH{=}C{=}CH_2]$ with $[Fe_2(CO)_8(\mu\text{-}CH_2)]$ leads to a tungsten-substituted trimethylenemethane complex $[Cp(OC)_3W\{\mu\text{-}\eta^1\text{:}\eta^4\text{-}CHC(CH_2)_2\}Fe(CO)_3]$;[137] the photochemical reaction of a μ-vinylidenediplatinum complex with diphenylacetylene yields a complex with a $\eta^1\text{:}\eta^3$-butadiene bridge.[138] Redox reactions leading to C–C coupling are described in Section 2.1.2.

2.4. Nucleophilic Substitution of Halogen Atoms in Unsaturated Hydrocarbon Ligands by Carbonylmetalates

Arene(tricarbonyl)chromium complexes are among the most studied organometallic compounds. Stereo- and enantioselective nucleophilic substitution reactions have been investigated especially thoroughly.[139] Since 1988, Heppert et al.[121b, 140] and Hunter et al.[141] have obtained a series of complexes like **42** with bridging σ,π-arene ligands. These complexes are prepared by the substitution of the halogen atom in $[(C_6H_5X)(OC)_3Cr]$ complexes with the strongly nucleophilic organometallic anions $[Fe(CO)_4]^{2-}$, $[M(CO)_5]^{2-}$ (M = Cr, W), $[CpFe(CO)_2]^-$, and $[Cp^*Fe(CO)_2]^-$.

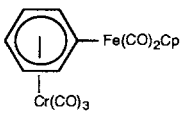

42

Less reactive carbonylmetalate ions like $[CpMo(CO)_3]^-$, $[CpNi(CO)]^-$, $[Mn(CO)_5]^-$, and $[Co(CO)_4]^-$ do not undergo this reaction.[140] As in the nucleophilic addition reactions discussed in Section 2.1, redox reactions compete with substitution. For instance, the reaction of $[(\eta^6\text{-}C_6H_5Cl)Cr(CO)_3]$ with $[M(CO)_5]^{2-}$ (M = Cr, W) proceeds by reductive dehalogenation and yields $[(\eta^6\text{-}C_6H_6)Cr(CO)_3]$. The use of $[CpFe(CO)_2]^-$ at low temperatures leads to the substitution product;[141] at higher temperatures, the SET reaction product is preferred.[140] Interestingly, it was not possible to replace the chlorine substituent in $[(OC)_3Cr(\mu\text{-}\eta^6\text{:}\eta^1\text{-}C_6H_4Cl)Fe(CO)_2Cp]$ with excess $[CpFe(CO)_2]^-$.[141] The reaction of $[(\eta^6\text{-}C_6H_4Cl_2)FeCp]^+$ and excess $[Re(CO)_5]^-$, on the other hand, yields the trimetallic complex $[CpFe(\mu\text{-}\eta^6\text{:}\eta^1\text{:}\eta^1\text{-}C_6H_4)\{Re(CO)_5\}_2]^+$ besides the monosubstituted product.[142] The Cl atom in $(\eta^6$-benzylchloride)chromium tricarbonyl can be replaced by $[Co(CO)_4]^-$.[142]

2.5. Reaction of Metal Complexes Containing an Anionic Hydrocarbon Ligand with Halo Complexes

Numerous σ,π-bridged complexes can be synthesized in a straightforward manner from lithiated arene complexes by

"umpolung". For instance, the reaction of lithioferrocene with halometal complexes leads to compounds of type **43** (Scheme 12).

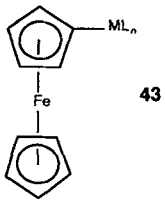

43

Scheme 12. ML_n = $CpFe(CO)_2$[143], $CpW(NO)_2$[144], $Mn(CO)_5$[143,145], $Ir(CO)(PPh_3)_2$[143], $CpM(CO)_3$ (M = Mo, W)[143], $Cp^*Ru(CO)_2$[146a], Cp_3U[146b], $V(C_5H_4Me)_2$[147].

The related half-sandwich compound $[Cp^*Ru(PMe_3)_2Fc]$ is formed from $[Cp^*Ru(PMe_3)_2CH_2tBu]$ and $[Cp_2Fe]$ by C–H bond cleavage.[148] When lithioferrocene is employed, trinuclear complexes can be prepared.[146] Lithiated di(benzene)chromium reacts with $[CpFe(CO)_2I]$ and $[(OC)_5ReI]$ in the same fashion, forming complexes with μ-η^6:η^1-arene bridges.[149] It was also possible to prepare compounds with bridges between early and late transition metal centers.[150] Complexes with a σ,π-C_5Cl_4 bridge can also be prepared, for example, $[(OC)_3Mn(\mu\text{-}\eta^5\text{:}\eta^1\text{-}C_5Cl_4)ML_n]$ (ML_n = $Re(CO)_5$, $Au(PPh_3)$, Cp_2TiCl, etc.).[151]

Lithiation of the dimetallic complex $[Cp(OC)_2Fe\text{-}(\mu\text{-}\eta^1\text{:}\eta^5\text{-}C_5H_4)Mn(CO)_3]$ with BuLi and subsequent reaction with $[Cp(CO)_2FeI]$ yields the corresponding trimetallic compound **44**.[152]

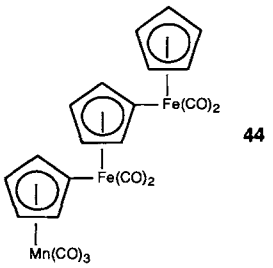

44

It is possible to coordinate metal complex fragments or Fe^{II} ions to the Cp rings of $[(OC)_3Mn(\eta^5\text{-}C_5H_4\text{–}CH_2\text{–}C_5H_4Li)]$[153] and $[(OC)_3Mn(\eta^5\text{-}C_6H_6\text{–}C_5H_4Li)]$[154] to form, for example, **45**. Rhodium, iridium,

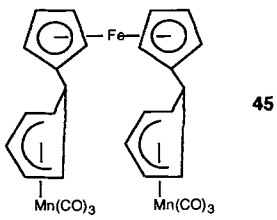

45

iron, and ruthenium complexes with η^3:η^4-cycloheptatrienyl bridges can be prepared from $[(OC)_3M(\eta^3\text{-}C_7H_7)]^-$ (M = Fe, Ru) and $[Rh(CO)_2Cl_2]_2$, $[\{(cod)RhCl\}_2]$ (cod = cyclooctadiene), or $[Ir(CO)_3Cl]$.[155]

The complex $[(\eta^5\text{-}C_6H_5Li)Cr(CO)_3]$ was used by Lotz et al. to prepare a number of benzene-bridged complexes[156] containing early and late transition metal atoms. A pseudo-triple-decker complex is formed from $[(\eta^6\text{-indene})(\eta^5\text{-indenyl})Re]^-$ and $[\{(cod)RhCl\}_2]$.[157]

Lithiated ethynylferrocene reacts with $[Cl_2Pt(PPh_3)_2]$ to give $[cis\text{-}(Ph_3P)_2Pt(C{\equiv}C\text{–}Fc)_2]$.[158] The tautomers with ketene bridges $[Cp^*(OC)_2Fe\text{–}C(=CH_2)\text{–}O\text{–}Zr(Cl)Cp_2]$ and $[Cp^*(OC)_2Fe\text{–}C(O)\text{–}CH_2\text{–}AuPPh_3]$ were obtained from the enolate $[Cp^*(OC)_2FeC(CH)_2O]^-$ and the corresponding chloro complexes.[159]

2.6. Oxidative Addition of Halogenated Hydrocarbons to Complexes with Metal Atoms in Low Oxidation States

An alternative route to complexes with σ,π-arene bridges is the oxidative addition of coordinated chlorobenzene to Pd^0 centers.[160, 161] The reaction of $[Pd(PR_3)_4]$ with $[CpFe(\eta^6\text{-}C_6H_5Cl)]^+$ and $[(OC)_3Cr(\eta^6\text{-}C_6H_5Cl)]$ yields complexes **46** and **47**, respectively. The CrPd compounds are intermediates in the Pd-catalyzed carbonylation of $[(\eta^6\text{-}C_6H_5Cl)Cr(CO)_3]$.[161]

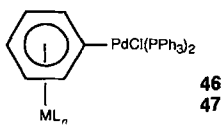

46: ML_n = $Cr(CO)_3$
47: ML_n = $[FeCp]^+$

Complexes of palladium and platinum with hydrocarbon bridges are prepared by double oxidative addition of $I(CH_2)_nI$ (n = 3–5)[162a] and of dibromoxylene to $[Me_2Pt(phen)]$ and $[Me_2M(bpy)]$ (M = Pd, Pt; phen = phenanthroline, bpy = bipyridine).[162b] *o*- and *p*-Bromobenzylbromide react with Ni^0 compounds to yield dinuclear nickel complexes with η^1:η^3-benzyl bridges.[162c] Isocyanide and carbon monoxide insert into the Ni–C σ bond of the products, leading to the formation of compounds **48** and **49**, among others.

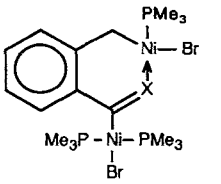

48: X = NR
49: X = O

μ-Acetylide complexes (see Section 7) can be prepared by the oxidative addition of $[(Ph_3P)_2Pt(Cl)(C{\equiv}CCl)]$ to a Pt^0 center.[151] The coordinated 2-chloroallyl ligand in $[Pt\{\eta^3\text{-}CH_2C(CH_2Cl)CH_2\}(PPh_3)_2]^+$ can be oxidatively added to Pt^0 complexes.[163] The resulting σ,π-allyl bridge is of the same type as the one found in the adduct of cationic trimethylenemethane complexes and carbonylmetalate ions.[38]

Oxidative addition can also be employed for the preparation of organometallic polymers.[164] The C–Br bond of 2-bromoethyl methacrylate can be added to the electron-rich dimethylplatinum complex $[PtMe_2(2,2'\text{-bipyridine})]$. The re-

sulting adduct can then be transformed by radical polymerization, with azobis(isobutyronitrile) (AIBN) as initiator, to the polyethylene derivative.

3. Addition of Lewis Acidic Complex Fragments to Free and Coordinated Unsaturated Hydrocarbons

A number of linear and cyclic polyenes can undergo addition of, for instance, two $[Fe(CO)_3]$, $[Fe(PMe_3)_3]$, $[Mn(CO)_2Cp]$, [CoCp], or $[Fe(CO)_2Cp]^+$[165] units to form complexes like **50a, b**.[165b] This opens up the possibility of forcing two organometallic complex fragments into close proximity. As a result of the intramolecular interactions between the metal atoms, these complexes should have different properties from those of the mononuclear analogues.[165b] Bis(arenetricarbonylchromium) complexes bridged by rigid polynorbornyl spacers show efficient through-bond coupling between the Cr atoms through 6.5 Å.[165c]

Many polymetallic arene complexes are known, for example, **50c**, which was obtained by the Fischer–Hafner method[166a] from $CrCl_3$, aluminum, $AlCl_3$, and phenylferrocene as arene.[166b] The same method allows the replacement of two Cp ligands in bis(ferrocene) by hexamethylbenzene.[166c]

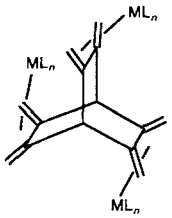

50a: $ML_n = Fe(PMe_3)_3$
50b: $ML_n = CoCp$

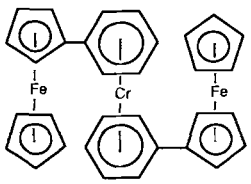

50c

In general, it is possible to bind the $Cr(CO)_3$ unit to compounds containing phenyl groups.[167] For instance, the reaction between $[Cr(CO)_6]$ and styrene yields $[(OC)_3Cr(styrene)]$,[168a] which can be irradiated to form the dimeric complex **51**.[168b] The complex $[(OC)_5Re{-}CH_2CH_2Ph]$ reacts with $[(OC)_3Cr(C_5H_5N)_3]$ and $Et_2O{\cdot}BF_3$ to form $[(OC)_5Re(\mu\text{-}\eta^1{:}\eta^6\text{-}CH_2CH_2C_6H_5)Cr(CO)_3]$.[169] An especially impressive example for a multinuclear complex with coordinated $Cr(CO)_3$ groups is the paracyclophane complex **52** synthesized by Elschenbroich et al.[170] Heterometallic compounds with $Cr(CO)_3$ complex fragments can be prepared by the reaction of $[(OC)_2CpFe(2\text{-}SC_4H_4)]$, $[(OC)_2CpFe(2\text{-benzofuran})]$, or $[(OC)_3Mn(\eta^5\text{-}C_5H_4Ph)]$ with $[Cr(CO)_6]$ or $[Cr(CO)_3(CH_3CN)_3]$.[171]

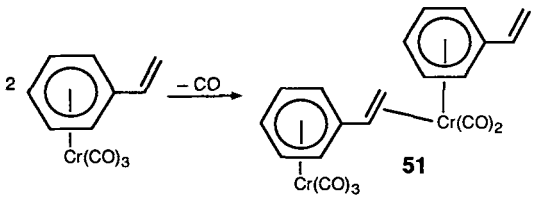

51

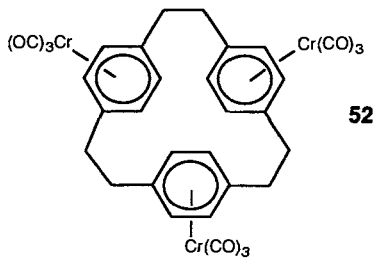

52

An important strategy for the synthesis of polydecker complexes is the addition of an unsaturated metal complex fragment to a π ligand of a sandwich compound (stacking reaction, Scheme 13).[172] Morrison et al. have used the Fischer–Hafner method (reaction of ferrocene with polyarenes in the presence of $AlCl_3$/Al) to bind $[FeCp]^+$ units to polyarenes.[173]

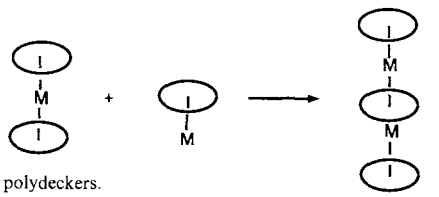

Scheme 13. Synthesis of polydeckers.

It was recently recognized that the $[Cp^*Ru]^+$ ion coordinates preferentially to arenes and polyarenes. This enables the preparation of interesting polynuclear compounds like **53–55** (see also Section 8).[174]

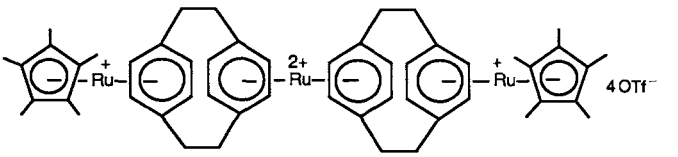

53

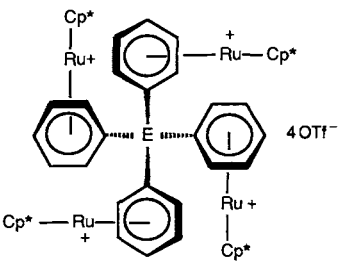

E = C, Si, Ge, Sn, Pb

54

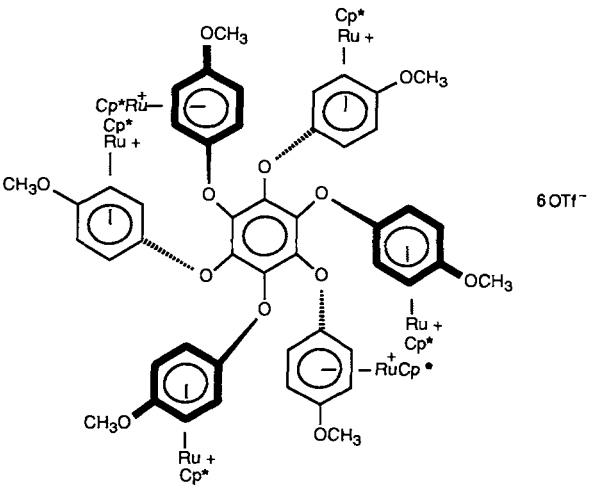

55

The $[Cp^*Ru]^+$ ion can bind twice to anthracene,[175] diphenylacetylene,[176] chrysene,[177] and diindenylruthenium (to give a tetradecker complex[178a]), as well as to indigo and its metal complexes.[178b] The Cp*Co group also adds to coordinated cyclopentadiene and cycloheptatriene[179, 180] to form triple-deckers like **56**. The $[Cp^*Ru]^+$ cation reacts with the half-sandwich complex $[Cp^*Ru(pentadienyl)]^+$ to form a complex with a ruthenabenzene bridge.[181]

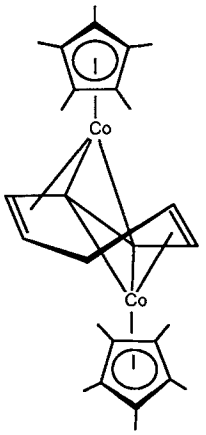

56

Fulvalene complexes with two different metal centers can be prepared by treating η^4-dihydrofulvalene complexes with substitutionally labile metal compounds (see Section 5).[182] The addition of the platinum(0) complex $[(Ph_3P)_2Pt]$ to the allene ligand in $[Cp(OC)(HPh_2P)Fe(CH_2{=}C{=}CH_2)]^+$ yields an FePt complex in which Fe is σ-bound to the central C atom of the $\eta^1{:}\eta^3$-allyl bridge.[183]

Kreiter et al.[184] examined photoreactions of $[M_2(CO)_{10}]$ (M = Mn, Re) with dienes, trienes, and allenes, and they were able to isolate a number of novel dinuclear complexes with bridging hydrocarbon ligands from the complicated reaction mixtures. Photoinduced [4 + 6] cycloaddition of conjugated dienes and bis(tricarbonylchromium)[μ-$\eta^6{:}\eta^6$-1,1′-bis(2,4,6-cycloheptatriene)] and bis(tricarbonylchromium)heptafulvalene complexes can also be used to prepare compounds with hydrocarbon bridges.[185]

Benzene and naphthalene can function as bridges between two or even three metal complex fragments.[7] Examples for the addition of a metal complex fragment to a σ-bound vinyl ligand can be found in the complexes with σ,π-vinyl bridges, $[(OC)_5Re(\mu\text{-}\eta^1{:}\eta^2\text{-}CH{=}CH_2)Fe(CO)_4]$,[186] $[(OC)_5Re(\mu\text{-}\eta^1{:}\eta^2\text{-}CH{=}CH_2)Re(CO)_5]^+$,[187a] and $[Fp(\mu\text{-}\eta^1{:}\eta^2\text{-}CH{=}CH_2)Fp]^+$ (Fp = $Cp(CO)_2Fe$).[187b] A large number of reports are found in the literature on μ-vinyl dimetallic complexes with a metal–metal bond[188] (Scheme 14) or a second supporting ligand.[189]

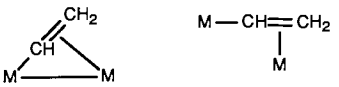

Scheme 14. Dimetallic μ-vinyl complexes.

During the course of their work on vinylidene complexes,[190] Werner et al. found that the $[Rh(Cl)L_2]$ unit can be added to the C=C bond in $[Cp(iPr_3P)Rh{=}C{=}CH_2]$.[191a] The highly reactive 14-electron species $[Rh(Cl)(PiPr_3)_2]$ coordinates to both C≡C bonds of 1,4-diethynylbenzene. The initially formed complex **57** (L = $PiPr_3$) rearranges to give the isomeric bis(vinylidene) complex **58**.[191b]

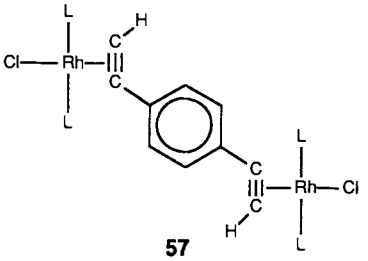

57

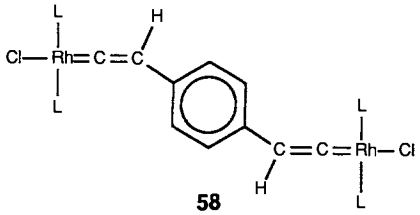

58

Following work by Wojcicki et al., a number of multinuclear compounds can be prepared from propargyl complexes $[L_nM{-}CH_2{-}C{\equiv}CR]$ and metal carbonyls.[192] Compound **59** is a σ,π-bridged complex without a metal–metal bond.

Polyynes and cyclopolyynes can undergo additions by several $[Co_2(CO)_6]$ units.[193a] Alkynyl-substituted Fischer carbene complexes react with $[Co_2(CO)_8]$ to form the trinuclear complex **60**, for example.[193b] The binding of $[Co_2(CO)_6]$ or $[Mo_2Cp_2(CO)_4]$ to $[Fc{-}CH{-}C{\equiv}C{-}C_3H_7]^+$ stabilizes the carbenium ion between two complex fragments.[194]

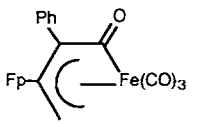

59

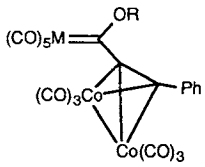

60

Numerous alkyne complexes are known in which the bridging alkyne ligand is σ,π-bound (Scheme 15).[195] Com-

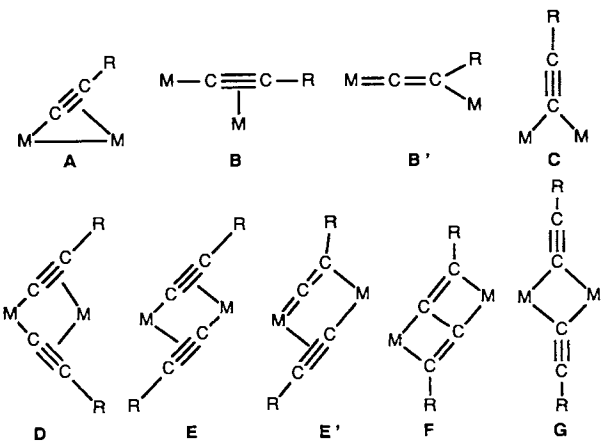

Scheme 15. Types of alkynyl complexes.

plexes **61** and **62** with σ,π-bound acetylide bridges (type **B**) were prepared by the reactions of the organometallic Lewis acid $[(OC)_5Re]^+$[196] with $[Cp(OC)_2Fe-C\equiv CR]$ and $HC\equiv CSiMe_3$, respectively.[197]

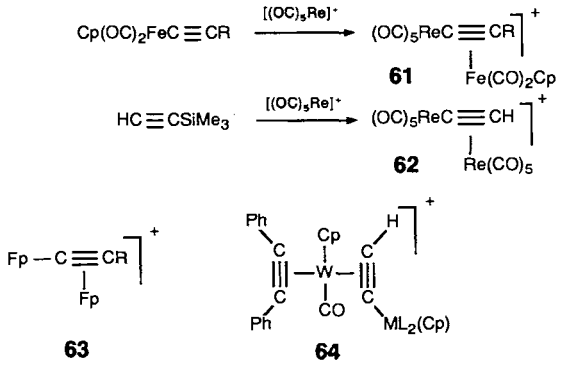

Selegue et al.[198] and Akita et al.[199] were able to synthesize the corresponding cationic σ,π-alkynyl complexes **63** and **64** (type **B**; Scheme 16). They obtained iron, ruthenium, and tungsten complexes by the addition of organometallic Lewis acids to σ-bound acetylide ligands. The X-ray crystal structures of **61**,[197b] **63**,[198], and **64**[199] prove the significance of the vinylidene structure **B'**. Interestingly, the diiron complex **63** shows fluxional behavior corresponding to a 1,2 proton shift.[199]

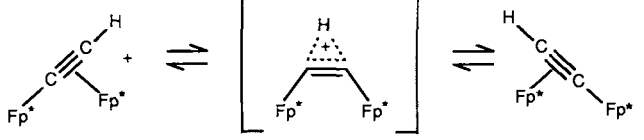

Scheme 16. Fluxional behavior of an Fe_2 complex.

The structure of $[(MeC_5H_4)Mn(CO)_2\{=C=C(H)-Fp^*\}]$, obtained from $[Fp^*-C\equiv C-H]$ and $[(MeCp)Mn(CO)_2(thf)]$, indicates zwitterionic contributions.[199b] The $[Pt(PPh_3)_2]$ complex fragment can be bound to the C≡C bond of the chloroethynyl complex $[Cl(Ph_3P)_2Pt-C\equiv C-Cl]$.[151] The σ-acetylide complex $[(dppe)(OC)_3Mn\ C\equiv CR]$ can add twice to Cu^+, Ag^+, and Au^+ ions.[200a]

Heterometallic complexes with two σ,π-acetylide bridges can be synthesized by using σ-bis(alkynyl) complexes. For instance, $[Cp_2Ti(C\equiv CR)_2]$ reacts as a type **D** chelating ligand with $FeCl_2$,[200b] $[Ni(CO)_4]$,[201] $[Co_2(CO)_8]$,[202] and $[(Ph_3P)_2Pt(C_2H_4)_2]$.[203] *cis*-$[M(C_6F_5)_2(thf)_2]$ (M = Pd, Pt) forms type **D** complexes with *cis*-$[Pt(C\equiv CR)_2L_2]$ (R = Ph, *t*Bu, $L_2 = 2PPh_3$, dppe, cod),[204a] while bridges of type **G** are obtained with $[TiCp_2(C\equiv CH\,tBu)_2]$.[204b] Complexes of type **E** can be prepared by the reaction of *cis*-$[Pt(C_6F_5)_2(C\equiv CR)_2]^{2-}$ (R = Ph, *t*Bu) and *cis*-$[M(C_6F_5)_2(thf)_2]$.[204a] In contrast, *cis*-$[(dppe)Pt(C\equiv CR)_2]$ and $[Rh_2Cl_2(CO)_4]$ react to yield a dinuclear compound with a single σ,π-acetylide bridge.[205]

Further complexes of type **E** are known for titanium,[206] iridium,[207] and zirconium.[208] The bonding in the latter species is best described by the participation of resonance structures of type **E** and **E'**. The reaction of $[(MeC_5H_4)_2TiCl_2]$ with $NaC\equiv CPh$ leads to an oxidative coupling of two acetylide ligands, forming complexes with type **F** bridges.[209, 210] A similar type **F** arrangement of phenylethynyl ligands was also found in a samarium complex.[211] Recently, variations in the conditions for the reaction of $[Me_2Si(C_5H_4)_2TiCl]_2$ with $LiC\equiv CPh$ made it possible to identify compounds of type **E**, **F**, and **G**.[212]

4. Substitution of Halogen or Triflate Substituents in Hydrocarbons by Nucleophilic Complexes

μ-Polymethylene complexes are among the oldest known compounds containing hydrocarbon bridges.[4, 17a] These compounds have been investigated primarily by the research groups led by King, Lindner, Moss, and Puddephatt and are models for hydrocarbons bound to the surface of metal catalysts.[5] They can generally be prepared with $n \geq 3$ from α,ω-dihalo compounds and carbonylmetalate ions (Scheme 17). Particularly useful starting materials were α,ω-bis(triflate) compounds,[213] as the triflate group is a much better leaving group than the halogen substituent. For instance, $[(OC)_5Mn(CH_2CH_2CH_2)Mn(CO)_5]$ was obtained by the bis(triflate) method.[213b] In contrast, the reaction of 1,3-dibromopropane with $Na[Mn(CO)_5]$ led to a cyclic carbene complex.[214]

$$X\text{-}(CH_2)_m\text{-}X + 2[L_nM]^- \xrightarrow[-2X^-]{} [L_nM\text{-}(CH_2)_m\text{-}ML_n]$$

Scheme 17. X = Br; $ML_n = FeCp(CO)_2$; $m = 3-6$ [4, 215, 216]. X = Br, I; $ML_n = RuCp(CO)_2$; $m = 1$, 3–10 [216–218]. X = Br, I; $ML_n = Co(DH)(pyridine)$; $m = 3-7$ [218b]. X = I, OSO_2CF_3; $ML_n = MoCp(CO)_3$, $CpW(CO)_3$; $m = 4$, 5, 10 [219, 220]. X = OSO_2CF_3, $ML_n = Mn(CO)_5$; $m = 2-6$, 10 [213, 216, 220]. X = OSO_2CF_3; $ML_n = Re(CO)_5$; $m = 2-5$, 10 [213a, 220, 221]. X = OSO_2CF_3; $ML_n = ReCp(NO)(PPh_3)$; $m = 3-5$, 8 [222].

The compounds $[L_nMCH_2C\equiv CCH_2ML_n]$ (ML_n = $Fe(CO)_2Cp$, $W(CO)_3Cp$) were obtained analogously. The iron complex can be oxidized to the butatriene complex **65**[223a] and can be employed as a building block for cluster synthesis.[223b]

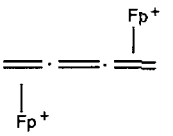

65

Heterometallic compounds of type **66** can be prepared from ω-iodoalkyl metal complexes by substituting a carbonylmetalate for the iodine group (Scheme 18).[224] This method also makes accessible the cobaltoxime complexes with hydrocarbon bridges $[py(DH)Co-R-Co(DH)py]$ ($R = (CH_2)_n$, $n = 4-8$; $CH_2C_6H_4CH_2$) from $[py(DH)Co(CH_2)_nCl]$, $(CH_2)_nBr_2$, or $C_6H_4(CH_2Br)_2$ and $[py(DH)Co]^-$[218b].

1,2-Dihaloalkanes and anionic transition metal complexes usually react to form ethylene and dimers with a metal–metal bond, while, in general, dihalomethane does not undergo such a reaction.[4, 214] An exception is its reaction with $[CpRu(CO)_2]^-$, which yields **67**.[217] The tetranuclear com-

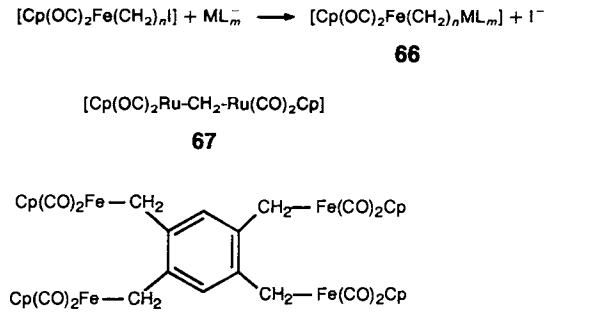

Scheme 18. Complex **66**: $n = 3$–6; ML_m = $CpMo(CO)_3$, $CpW(CO)_3$, $Re(CO)_5$, $Ru(CO)_2Cp$.

plex **68** was recently prepared in a corresponding fashion.[224c]

The dianions $[Fe(CO)_3L]^{2-}$,[225] $[CpRe(CO)_2]^{2-}$,[226] $[Ru(CO)_4]^{2-}$,[227a] $[Os(CO)_4]^{2-}$,[227b] and $[Os_2(CO)_8]^{2-}$[228] react with alkanediylbis(triflate) to form metallacycles such as **69a, b**. These reactions have been reviewed in the literature.[72b, 229]

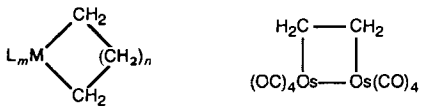

Of special interest is a type of complex with an unusual and rare ethylene bridge, which is perpendicular to the metal atoms. This complex is formed by the reaction of 1,2-dichloroethane with the dimer $[M_2X_6(PEt_3)_4]$ (M = Zr, Hf; X = Cl, Br).[230] A similar μ-η^2:η^2-ethylene bridge is also present in $[Cp^*Yb(\mu\text{-}C_2H_4)Pt(PPh_3)_2]$,[231a] $[(Cp_2^*Sm)_2(\mu$-η^2:η^4-RCH=CHPh)],[231b] and—in a distorted fashion—in $[(\mu\text{-}C_2H_4)(Cp_2Zr{-}Cl{-}AlEt_3)_2]$.[232] Hafnium complexes with alkanediyl bridges cannot be prepared by substitution of halogen substituents but rather by the reaction of $[Cp_2^*HfH_2]$ with α,ω-dienes (formally a double insertion of the olefin into the Hf–H bond).[233a] CO and SO_2 can be inserted into the metal–carbon bond of many μ-polymethylene complexes.[220, 233b]

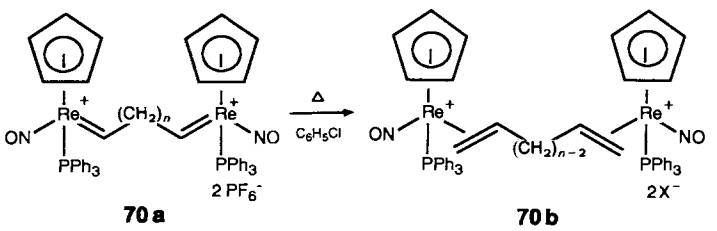

Abstraction of hydride from the μ-polymethylene complexes $[\{Cp(ON)(Ph_3P)Re\}_2(CH_2)_n]$ (n = 3, 4, 5, 8) leads to dicationic bis(carbene) complexes **70a**, which isomerize at higher temperatures to give the diene-bridged complexes **70b**.[222]

The trinuclear complex **71**, which can be oxidized to **72** with trityl salts, is formed when $[CpFe(CO)_2]^-$ is combined with the tris(sulfonate) $HC(CH_2OSO_2CH_3)_3$.[234]

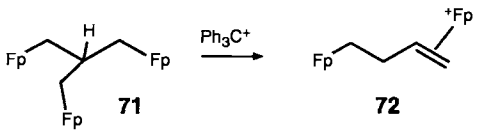

A large number of μ-hydrocarbon complexes can be prepared by allowing carbonylmetalate ions to react with cyclic dihalo or polyhalo compounds (octafluorocyclooctatetraene[236c]). The complexes **73**–**76** were prepared in this manner from the corresponding dihalo species and organometallic anions.[223a, 235, 236] Bis(triflates) with a THF framework

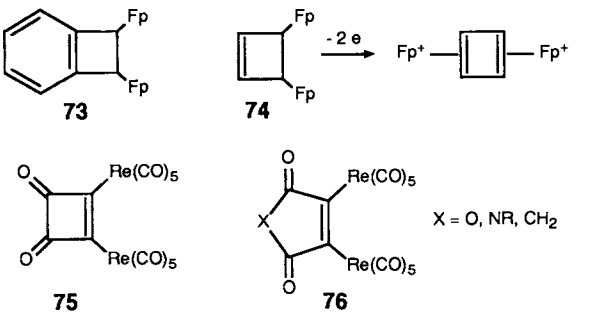

react with carbonylmetalate ions in the same fashion to yield hydrocarbon-bridged complexes.[236b] A series of homo- and heterometallic μ-η^1:η^1-ketene complexes $[L_nM{-}CH_2{-}C(O){-}M'L_n]$ was prepared by Akita et al. from metal-substituted acetylchlorides $[L_nM{-}CH_2C(O)Cl]$ and carbonylmetalate ions (examples of L_nM: Fp, $M'L_n = Mn(CO)_5$, Fp, Ni(CO)Cp).[237] Organometallic Lewis acids (e.g., Fp^+) can be added to the carbonyl oxygen atom of the ketene bridge.[237] The μ-ketene complexes are models for an important step in the Fischer–Tropsch process (Scheme 19).[5, 237] Seppelt et al. described the reactions of

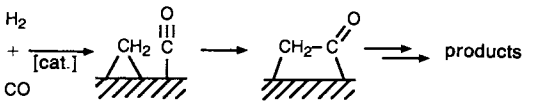

Scheme 19. μ-Ketene complexes as models for intermediates in the Fischer–Tropsch process.

difluoromalonyl dichloride with carbonylmetalate ions.[238] They were able to identify the complexes $[(OC)_5Mn{-}C(O){-}CF_2{-}C(O){-}Mn(CO)_5]$ and $[(OC)_5Mn{-}CF_2{-}C(O){-}Mn(CO)_5]$, among others.

Lentz et al. were able to obtain the (μ-η^1:η^1-difluoroethylenediyl) complex **77** by the reaction of $[Co(CO)_4]^-$ with difluorofumaric acid dichloride.[239] This reaction presumably proceeds via a bis(acyl) complex. We wanted to prepare a corresponding *trans*-bismetalated ethylene by the reaction of $[M(CO)_5]^-$ (M = Mn, Re) with fumaric acid dichloride. Unexpectedly, complexes **78** were formed.[240]

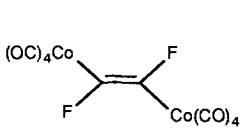

77

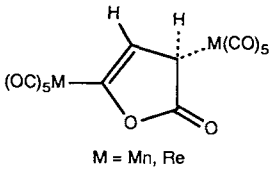

M = Mn, Re

78

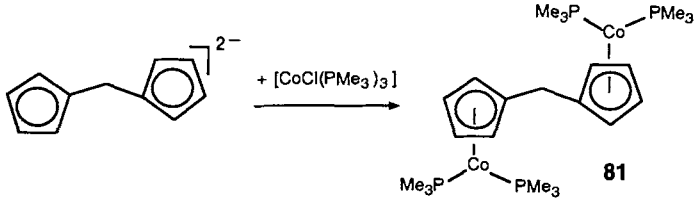

81

Decarbonylation of aroyl complexes often leads to complexes such as **79** with arene bridges. These have been the focus of recent studies, primarily by Hunter et al., on account of their potential as "electronic bridges".[214, 242]

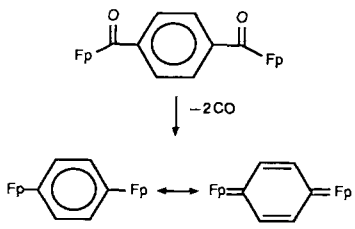

79

Quinoid structures have been suggested for the 1,4-dimetalated μ-phenylene complexes.[242a] Reactions with $[Cr(CO)_6]$ lead to complexes like **80** with σ,π-bridges (see Section 3).[242c]

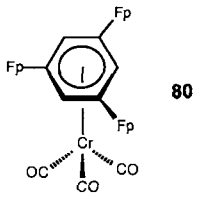

80

Electrochemical studies show that polymetalation of the arene ligand in $[(\eta^6\text{-}C_6H_6)Cr(CO)_3]$ leads to a stabilization of the corresponding radical cations.[242c] Numerous complexes of the type $[(OC)_3Cr(\mu\text{-}\eta^6\text{:}\eta^6\text{-}C_6H_5\text{–}C_6H_5)Cr(CO)_3]$, $[L_nM(\ \text{-}\eta^1\text{:}\eta^1\text{-}C_6R_4)ML_n]$, and $[(OC)_3Cr(\mu\text{-}\eta^6\text{:}\eta^1\text{-}C_6H_5)\text{-}ML_n]$ have been described in the literature.[165a, 166b, 167]

The decomposition of the μ-oxalyl complexes $[(OC)_5M\text{–}C(O)\text{–}C(O)\text{–}M(CO)_5]$ leads to the dimetal carbonyls $[(OC)_5M\text{–}M(CO)_5]$ (M = Mn, Re).[243] 1,8-Diferrocenylnaphthalene can be obtained from the reaction of 1,8-diiodonaphthalene with dilithioferrocene.[244]

5. Reactions of Dianionic Hydrocarbons with Metal Complexes

The reaction of dianionic hydrocarbons with halometal complexes can also lead to complexes with hydrocarbon bridges. Werner et al. used this method to synthesize homo- and heterometallic transition metal complexes containing a bis(cyclopentadienyl)methane bridge, for example, **81**.[245]

Bis(η^5-pentadienyl)-diruthenium complexes like **82** can be obtained by analogous methods.[246] Dilithiated 4,4'-dimethyl-2,2'-bipyridine and ferrocenecarbaldehyde can be used to synthesize redox-active ligand systems.[247] Complex **83** can be electrochemically polymerized to an electrochromic film.[247]

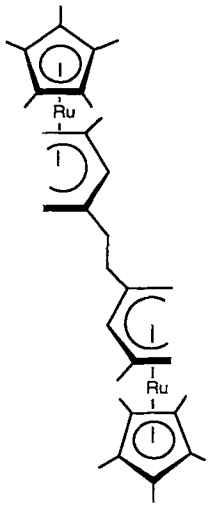

82

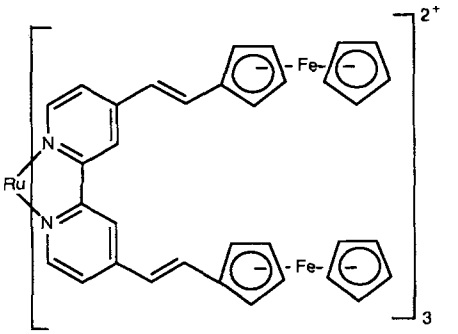

83

The homo- and heterodimetallic fulvalene complexes **84a**[83, 130, 131], studied primarily by Vollhardt et al.,[182] are currently of special interest. They can be obtained directly by the reaction of the fulvalene dianion with metal complexes.[248, 249] Fulvalene transition metal complexes **84b** with a cisoid arrangement and no metal–metal bond can be prepared in this manner as well.[248c]

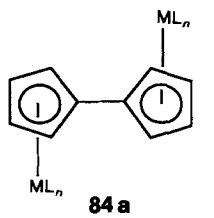

84a

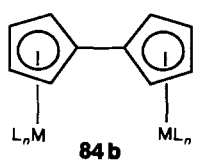

84b

A particularly elegant and selective synthetic method for heterometallic fulvalene complexes employs 3-cyclopentadienyl-2-cyclopentane-1-one as precursor.[182, 250] The reaction of 3,4-dimethylcyclopentanone with dilithioferrocene leads to cyclopentadienyl-substituted ferrocene; the lithium salt of the latter can be transformed into the triiron complex by reaction with $FeCl_2$.[251] Trinuclear heterometallic complexes with a fulvalene bridge, for example, 1,1'-di(nickelocenyl)ferrocene **85**[252] and numerous tercyclopentadienyl complexes like **86**,[253] have been reported as well. The synthesis and properties of bis(fulvalene)diiron ([0.0]-ferro-

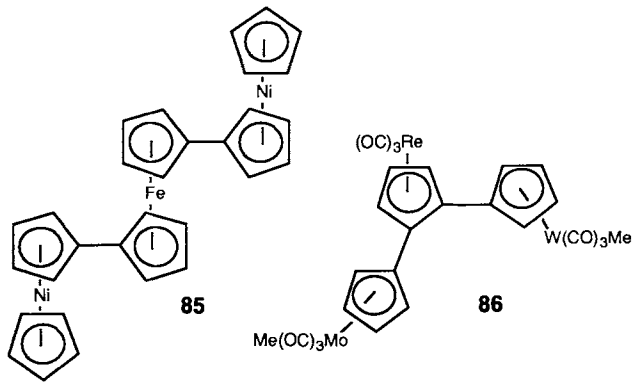

85 86

cenophane) and other [*m*,*m*]-metallocenophanes have recently been thoroughly reviewed.[249]

Why this special interest in fulvalene complexes? Cooperative effects between the metal centers are expected due to the spatial proximity of the metal atoms (even when a metal–metal bond is not present) and the high degree of electron delocalization in the fulvalene bridge.

The comprehensive synthetic and electrochemical studies by Astruc et al. regarding "electron storage" complexes (i.e. mixed-valence complexes) deserve special mention.[166c, 254, 255] For instance, the dicationic $Fe^{II}Fe^{II}$ complex **87** can be reversibly reduced to the corresponding $Fe^{I}Fe^{I}$ and $Fe^{0}Fe^{0}$ compounds.[166c] Electron transfer studies were also performed on di, tri, and tetrametallocenes[255b, 256, 257] and bis(fulvalene) complexes.[258] The dianions of pentalene,[259a] indacene,[259b] and tetraphosphafulvalene[259c] can be used in the same fashion as the fulvalene dianion in the construction of dimetallic complexes.

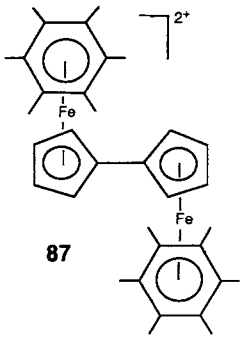

87

"Magnesium butadiene", MgC_4H_6, reacts with [Cp*La-(μ-Cl)$_2$K(dme)] (dme = dimethoxyethane) to yield a dilanthanum complex with a butadiene bridge, [Cp$^*_2$La(μ-η^1:η^3-C_4H_6)LaCp$^*_2$(thf)].[260a] The reaction of the di-Grignard compound [Cp$_2$M($CH_2MgBr)_2$] and [Cp$_2$M'Cl$_2$] (M, M' = Ti, Zr, Hf) leads directly to 1,3-dimetallacyclobutanes.[260b]

6. Insertion Reactions

The insertion of unsaturated hydrocarbons into metal–metal bonds to form complexes with hydrocarbon bridges is a relatively rare reaction type (Scheme 20). Examples include reactions of dimeric (oep)rhodium(II) complexes (oep = octaethylporphyrinato) with olefins.[261] By using kinetic methods, Halpern et al. were able to deduce a radical chain mechanism for this insertion.[261c] The μ-propene complex [(oep)Rh–$CH_2CH(CH_3)$–Rh(oep)] undergoes a dyotropic 1,2-exchange of the (oep)Rh groups.[262] The monomeric ruthenium porphyrin complex [(Ru(tmp)] (tmp = tetramesitylporphyrinato) reacts with acetylene by formal hydrocarbon insertion and formation of the binuclear complex [(tmp)Ru(μ-C_2H_2)Ru(tmp)].[263] NMR data indicate the presence of a μ-η^1:η^1-bis(carbene) complex.[263]

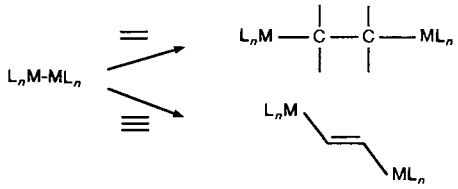

Scheme 20. Insertions of alkenes and alkynes into metal–metal bonds.

Corresponding reactions involving Co complexes (particularly $[Co(CN)_5]^{3-}$ and acetylenes) have been known for some time.[264] These complexes contain a *trans*-dimetallaethylene unit.[264] *cis*-Dimetalated olefins usually have a metal–metal bond or other bridging ligands.[72b, 265]

The insertion of tetrafluoroethylenes into the metal–metal bond of $[Co_2(CO)_8]$[266a] and [{(μ-SCH_3)Fe(CO)$_3$}$_2$][266b] leads to dinuclear complexes with a C_2F_4 bridge. At higher temperatures, these species rearrange to give complexes with carbene bridges. A 1,4-dimetallacyclohexane derivative is formed by the reaction of C_2F_4 with [Pt(cod)$_2$].[267]

Recently, the insertion of acetylene carboxylic acid esters into the Re–Re bond of [$Re_2(CO)_9(CH_3CN)$] was observed which led to the formation of [(OC)$_4$Re{*trans*-μ-η^1:η^2-RC=C(CO_2Me)}Re(CO)$_5$].[268]

The complexes [(R_3P)AuMe] (R = Me, Ph) react with F_3C–C≡C–CF_3 by means of insertion into the Au–Me bond, loss of ethane, and formation of the *cis* compounds [(R_3P)Au(CF_3)C=C(CF_3)Au(PR_3)].[269] A complex with an η^2:η^2-$C_2(CF_3)_2$ bridge is assumed as intermediate.[269b] In analogy to alkynes, isolobal[14, 54] carbyne complexes [Cp(OC)$_2$M≡C–R] (M = Mo, W) can be inserted into the Pd–C bond of metallacycles.[136] Isocyanides can also be inserted into the Pd–C bond of μ-acetylide palladium complexes.[270] According to work by Herberhold et al.,[271] the products of the insertion of chalcogens into the Li–C bond of lithiated cyclopentadienyl complexes can serve as starting materials for numerous multinuclear complexes with chalcogen bridges between the ring ligands.

7. Complexes with C_n Bridges

Complexes with acetylide bridges are a rapidly expanding class of materials. This type of complex can be prepared by several methods, which in principle have already been described: 1) from alkaline metal acetylides and alkyl complexes or metal halides, 2) from alkyne complexes having acidic protons and metal halides or alkyl complexes, 3) from cationic complexes containing σ,π-ethynyl bridges, 4) from

metal alkyls and acetylene, 5) from dihaloacetylene and carbonylmetalate ions, 6) from lithiated metal alkynes and metal halides, 7) by oxidative addition of dihaloacetylene, 1,3-diyne, or "$RC{\equiv}C^+$" to Pt^0, Rh^I, or Ir^I centers (Table 3).

Table 3. Dinuclear transition metal complexes containing a C_2 bridge. mes = mesityl.

Complexes with C_2 bridges	Starting materials	Ref.
$[Li_2(thf)_8V_2(\mu\text{-}C_2)(mes)_6]$	$[Li(thf)_4V(mes)_3R] + [Li_2C_2]$	[272]
$[Cp(OC)_3W{-}C{\equiv}C{-}W(CO)_3Cp]$	$[CpW(CO)_3Cl] + [Li_2C_2]$	[273]
$[(R_3P)Au{-}C{\equiv}C{-}Au(PR_3)]$	$[(R_3P)Au\text{-}C{\equiv}C\text{-}H] + [(P_3P)AuCl]$ /NaOEt	[274]
$[(Me_3P)_2(X)$-M$-C{\equiv}C-M(X)(PMe_3)_2]$ (M = Pd, Pt; X = Cl, I)	$[(Me_3P)_2M(C{\equiv}CH)_2] + [(Me_3P)_2MCl_2]$ /$HNEt_2$/CuCl	[275]
$[(OC)_5Re{-}C{\equiv}C{-}Re(CO)_5]$	$[(OC)_5Re(C{\equiv}CH)Re(CO)_5]BF_4$ /NaOEt	[197a, 276]
$[Cp^*(OC)_2Fe{-}C{\equiv}C{-}Fe(CO)_2Cp^*]$	$[Cp^*(OC)_2Fe(C{\equiv}CH)Fe$-$(CO)_2Cp^*]BF_4$/NaOMe	[199, 277]
$[Cp(Me_3P)_2Ru{-}C{\equiv}C{-}Zr(Cl)Cp_2]$	$[Cp(Me_3P)_2RuC{\equiv}CH] +$ $[Cp_2Zr(Cl)(CH_3)]$	[278]
$[Cp(\eta^2\text{-}Ph_2C_2)(OC)$-W$-C{\equiv}C-ML_2Cp]$ (M = Fe, Ru; L = PMe_3, $P(OMe)_3$, L_2 = dppe)	$[CpL_2M(C{\equiv}CH)W(CO)(Ph_2C_2)Cp]$ /KOtBu	[198]
$[Cp^*_2Sc{-}C{\equiv}C{-}ScCp^*_2]$	$2[Cp^*_2ScCH_3] + HC{\equiv}CH$	[279]
$[Cp(OC)_3Cr{-}C{\equiv}C{-}Cr(CO)_3Cp]$	$K[CpCr(CO)_3] + ClC{\equiv}CCl$	[280]
$[(OC)_5Mn{-}C{\equiv}C{-}Mn(CO)_5]$	$2Na[Mn(CO)_5] + I{-}C{\equiv}C{-}I$	[281]
$[Cp^*(ON)(Ph_3P)Re{-}C{\equiv}$ $C{-}Pd(Cl)(PEt_3)_2]$	$[Cp^*(ON)(Ph_3P)Re{-}C{\equiv}C{-}Li] +$ $[PdCl_2(PEt_3)_2]$	[282]
$[Cp^*(ON)(Ph_3P)Re{-}C{\equiv}$ $C{-}Rh(CO)(PPh_3)_2]$	$[Cp^*(ON)(Ph_3P)Re{-}C{\equiv}C{-}Li] +$ $[RhCl(CO)(PPh_3)_2]$	[282]
$(Ph_4P)_2[R{-}C{\equiv}C{-}$ $Au{-}C{\equiv}C{-}Au{-}C{\equiv}C{-}R]$	1. $[Au_2C_2] + 2\,KR/NH_3$fl. 2. $[Ph_4P]Cl$	[283]
$[Cl(R_3P)_2M{-}C{\equiv}C{-}M(PR_3)_2Cl]$	$[Cl(R_3P)_2M(C{\equiv}CCl)] +$ $[(C_2H_4)M(PR_3)_2]$	[284]
$[Cp(OC)_3W{-}C{\equiv}C{-}W(CO)_3Cp]$	$[Cp(OC)_2W(\mu\text{-}CO)(\mu$-$CH_2CO)W(CO)_2Cp]$	[285]
$[Cp_2(Me_3P)Ti{-}C{\equiv}C{-}Ti(PMe_3)Cp_2]$	$[Cp_2Ti(PMe_3)_2] +$ 2-methylene-1,1-diphenylcyclopropane or $[Cp_2TiCl_2] + Li_2C_2$	[286]
$[Cp(OC)_2Ru{-}C{\equiv}C{-}Ru(CO)_2Cp]$	$[Cp(OC)_2RuC{\equiv}CMe] +$ $[(t\text{BuO})_3W]_2$	[287]
$[(t\text{Bu}_3\text{SiO})_3Ta{=}C{=}C{=}$ $Ta(\text{OSi}t\text{Bu}_3)_3]$	$[(t\text{Bu}_3\text{SiO})_3Ta] + CO$	[288]
$[(t\text{BuO})_3W{\equiv}C{-}C{\equiv}W(\text{OtBu})_3]$	$[(t\text{BuO})_3W{\equiv}W(\text{OtBu})_3] +$ $[EtC{\equiv}C{-}C{\equiv}CEt]$	[289]

The H atom is made acidic by the π-coordination mode of the C≡CH ligand and can then be easily removed by bases (Scheme 21). This provides a direct way to μ-ethynediyl com-

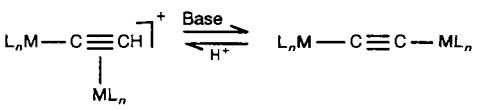

Scheme 21.

plexes.[197a, 199, 276–278] The cationic complex can be regenerated by addition of acid. When Me_3O^+ is used instead of an acid, the corresponding σ,π-propynyl complex can be obtained.[86a] The superhydride $K[BHEt_3]$ acts solely as base towards $[(OC)_5Re(\mu\text{-}\eta^1{:}\eta^2\text{-}C{\equiv}C{-}H)Re(CO)_5]^+$,[86a] while its addition to **88** leads—by attack of the hydride on the β carbon atom—to the μ-vinylidene complex **89**.[199]

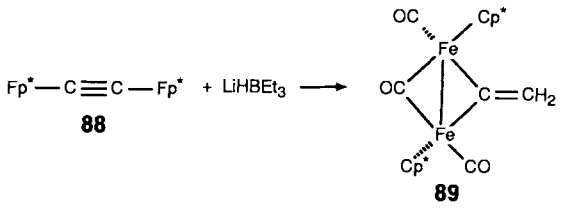

The formation of a W_2C_2 complex with an acetylide bridge from the ketene species $[Cp(OC)_2W(\mu\text{-}CO)(\mu\text{-}CH_2CO)W(CO)_2Cp]$ is unusual. The reaction proceeds by formal H_2O loss and intramolecular CO transfer.[285] Binger et al. described the reaction of $[Cp_2Ti(PMe_3)_2]$ with 2-methylene-1,1′-diphenylcyclopropane, which surprisingly also leads to a dititanium complex with an acetylide bridge.[286]

Of interest are the metathesis reactions between W≡W and C≡C[287, 289a–c] or C≡N[289d] triple bonds, leading to complexes like **90**. μ-Acetylide complexes are as suitable as alkynes[290a] and σ-alkynyl complexes $[L_nM{-}C{\equiv}C{-}R]$[290b] as building blocks for the synthesis of clusters.[292]

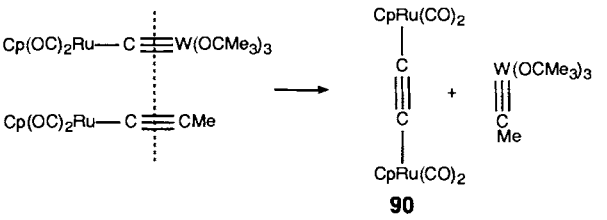

A μ-dicarbide tantalum complex with three cumulated double bonds is formed according to reaction (b) by CO

$$2[(t\text{Bu}_3\text{SiO})_3Ta] + CO \longrightarrow [(t\text{Bu}_3\text{SiO})_3Ta{=}O] + 1/2[\{(t\text{Bu}_3\text{SiO})_3Ta{=}C\}_2] \quad (b)$$

cleavage.[288] The cleavage of two C≡C bonds in 3,5-octadiyne leads to the complex $[\{(t\text{BuO})_3W{\equiv}C\text{-}\}_2]$.[289a]

The C–C distances in the bridging ligands of most of the complexes listed in Table 4 are only slightly different from the C–C bond lengths in acetylene, ethylene, and ethane (121, 134, 153 ppm, respectively). These complexes can

Table 4. Bond lengths in metal complexes with C_2 bridges.

Complexes	C-C [pm]	M-C [pm]	Ref.
$[(OC)_5Mn{-}C{\equiv}C{-}Mn(CO)_5]$	120.1(2)	201.1(2)	[281]
$[(OC)_5Re{-}C{\equiv}C{-}Re(CO)_5]$	120(3)	214(2)	[276b]
$[Cp(OC)_2Ru{-}C{\equiv}C{-}Ru(CO)_2Cp]$	119(1)	205(1)	[287]
$[Cp(OC)_3W{-}C{\equiv}C{-}W(CO)_3Cp]$	118(3)	217(2)	[285]
$[Cp^*_2Sc{-}C{\equiv}C{-}ScCp^*_2]$	122(1)	219.4(7)	[279]
$[Cp(Me_3P)_2Ru{-}C{\equiv}C{-}Zr(Cl)Cp_2]$	125(2)	199(1), 214(1)	[278b]
$[Cp(Me_3P)Ti{-}C{\equiv}C{-}Ti(PMe_3)Cp_2]$	125.3(2)	205.1(2)	[286]
$[Cl(Ph_3P)_2Pt{-}C{\equiv}C{-}Pt(PPh_3)_2Cl]$	125(2)	200(1)	[151]
$[(t\text{Bu}_3\text{SiO})_3Ta{=}C{=}C{=}Ta(\text{OSi}t\text{Bu})_3]$	137(4)	195(2)	[288]
$K_6[(NC)_5Co{-}(MeO_2C)C{=}C(CO_2Me){-}Co(CN)_5]$	133.3(5)	207.6(2)	[264]
$[Cp(Me_3P)_2Ru{-}(MeO_2C)C{=}C$-$(CO_2Me){-}Ru(CO)_2Cp]$	132(5)	216(3)	[32]
$[Cp(Me_3P)_2Ru{-}CH{=}CH{-}Zr(Cl)Cp_2]$	130(2)	209(2),218(2)	[278b]
$[(C_5H_4Me)_2(Cl)Zr{-}CH{=}CMe{-}Zr(Cl)Cp_2]$	132.8(5)	220.9(4) 229.6(4)	[290c]
$[(OC)_5Re{-}CH_2{-}CH_2{-}Re(CO)_5]$	152(2)	230(1)	[28]
$[Cp(Me_3P)_2Ru{-}CH_2{-}CH_2{-}Zr(Cl)Cp_2]$	149(1)	219(1), 228(1)	[278b]

therefore be regarded as dimetalated hydrocarbons, which is in agreement with the calculations for $[(OC)_5ReC_2Re(CO)_5]$ reported by Trogler et al.[276b] As is the case for the free hydrocarbons, an increase in the participation of the carbon s orbital leads to a decrease in the metal–C distance.[276b, 278b] The RuZr complexes **91** synthesized by Bullock et al. are the only known series with all three types of C_2 bridges, C≡C, C=C, and C–C.[278] These complexes are prepared from the corresponding alkynylruthenium complexes by reaction with the amidozirconium complex, by hydrozirconization with the Schwartz reagent $[Cp_2Zr(H)Cl]$, or by hydrozirconization of the vinylruthenium complex.

Agostic interactions between the Zr atom and the β hydrogen atom in **91b,c** have been proven by NMR spectroscopy.[278b] Hydrozirconization of alkenyl complexes

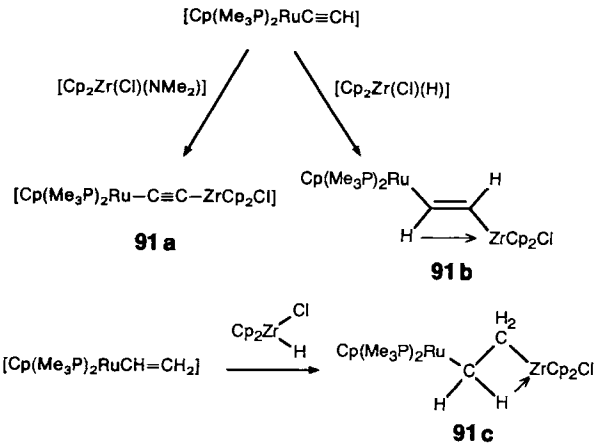

was first applied by Erker et al. for the synthesis of an ethylene-bridged dizirconium complex that also contained an agostic bond.[290c] Casey et al. used the Schwartz reagent for the hydrogenation of the carbene complex $[Cp(OC)_2Re{=}CHCH_3]$ (which is isolobal to an alkene). This reaction led to μ-alkylidene heterodimetallic complexes such as $[Cp(OC)_2Re(\mu\text{-}CHCH_3)Zr(Cl)Cp_2]$.[290d] In this context, the unusual Zr_2 complexes prepared by Orpen and co-workers are noteworthy.[291] They contain a type **C** alkyne bridge (see Scheme 15).

Attempts to prepare the μ-ethyne complex $[(OC)_5Re{-}C(H){=}C(H){-}Re(CO)_5]$ by proton abstraction from $[(OC)_5Re(\mu\text{-}\eta^1{:}\eta^2\text{-}CH{=}CH_2)Re(CO)_5]^+$ were not successful.[187]

CO, CO_2, and isocyanide can be inserted into the metal–carbon bond of complexes **91a,b**.[293]

Dimetallic complexes of type **92**, containing a bridging 1,3-butadiyne-1,4-diyl ligand, are known as well. They are prepared by the oxidative addition of HC≡C–C≡CH to $[Rh(Cl)(PiPr_3)_2]$,[294] by the reaction of $[CpL_2Fe{-}C{\equiv}C{-}C{\equiv}C{-}Li]$ and $[CpL_3MCl]$ (M = Mo, W),[295] or by the Pd-catalyzed reaction of $[Cp(OC)_2FeI]$ with $[Me_3Sn{-}C{\equiv}C{-}C{\equiv}C{-}SnMe_3]$.[296] Lappert et al.,[297a] Wrackmeyer et al.,[297b] and Brune et al.[298] have shown that vinyl, alkynyl, and aryl trimethylstannanes are especially suitable for the introduction of vinyl, alkynyl, and aryl ligands into metal complexes. Further examples of the application of these trimethylstannanes to the preparation of

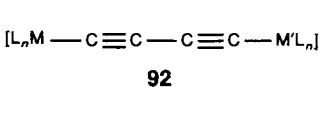

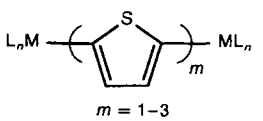

93a: $ML_n = Ru(CO)_2Cp$
93b: $ML_n = Pt(PBu_3)_2Cl$

94

complexes with bridging vinyl, acetylene, and *p*-phenylene ligands are described in the literature[133, 187, 298] and in Section 8. When 2,5-trimethylstannyl-substituted thiophenes and chloro complexes are employed, oligothiophene-bridged complexes **93** are formed, which are of interest due to the electrical conductivity of polythiophenes.[299]

Stang et al. discovered that alkynyl(phenyl)iodonium trifluoromethylsulfonate $[RC{\equiv}CIPh{\cdot}OSO_2CF_3]$ is a new, effective source of electrophilic alkynes $RC{\equiv}C^+$.[300a] The umpolung of the usual acetylene reactivity allows the preparation of σ-acetylide complexes in high yields.

The addition of bis(phenyliodonium)diyne bis(triflates) to chlororhodium complexes and Vaska-type iridium(I) complexes yields rod-shaped dicationic metal(III) complexes of type **92**.[300a] Similar complexes are formed from *p*-$HC{\equiv}C{-}C_6H_4{-}C{\equiv}CH$, NaOMe, and dichloroiron complexes.[300b] Cobalt clusters that are linked by a C≡C bridge are also known.[301]

Only a small number of μ-carbide complexes of type **94** are known to date (Scheme 22). They can be prepared by metathesis,[287, 302] radical reactions,[303] or by nucleophilic substitution.[304, 305] They are of interest as model systems for surface-bound carbide species.[5]

[(TPP)Fe=C=Fe(TPP)] [303]
$[(Me_3CO)_3W{\equiv}C{-}Ru(CO)_2Cp]$ [287,302]
[(pc)Fe=C=Fe(pc)] [303b]
$[(TPP)Fe{\equiv}C{-}Re_2(CO)_9]$ **95** [304]
$[(HB(pz)_3Mo{\equiv}C{-}Fe(CO)_2Cp]$ [305a]

Scheme 22. Known carbido complexes of type **94**. TPP = tetraphenylporphyrinato, pc = phthalocyaninato(2–), pz = 3,5-dimethylpyrazolyl.

Complex **95**[304] contains what is to the best of our knowledge the shortest metal–carbon bond known (Fe–C 160(1) pm) and can therefore be considered a metalated metal carbyne. Its preparation from the dichlorocarbene complex $[(TPP)Fe{=}CCl_2]$ and $[Re(CO)_5]^-$ proceeds presumably according to the reaction in Scheme 23. During the

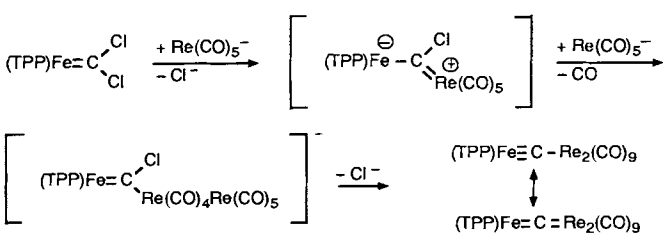

Scheme 23.

reaction of 1,3-dibromopropane and $[Mn(CO)_5]^-$, Casey also observed that the reaction does not proceed by substitution of the second bromine atom, but by the attack of an additional $[Mn(CO)_5]^-$ ion on the original metal center.[214b] When the carbonylmetalate ions $[Mn(CO)_5]^-$, $[Fe(CO)_4]^{2-}$, and $[Cr(CO)_5]^{2-}$ are employed, the corresponding compounds $[(TPP)Fe{=}C{=}ML_n]$ ($ML_n = Mn_2(CO)_9$, $Fe(CO)_4$, and $Cr(CO)_5$) are obtained.[86b, 304]

A novel synthetic pathway to μ-carbide complexes is found in the reaction of Lalor's halocarbyne complexes[305d] with platinum(0) complexes.[85, 86b] Compound **96**, which is prepared by this route, isomerizes at higher temperatures to give the carbide complex **97**. Less stable compounds can also be obtained with Ni^0 and Pd^0 complexes.[86b] A large number of heterodimetallacyclopropenes have been prepared by Stone et al. from Pt^0 compounds and arylcarbyne complexes (arylcarbynes are isolobal to alkynes).[14, 306]

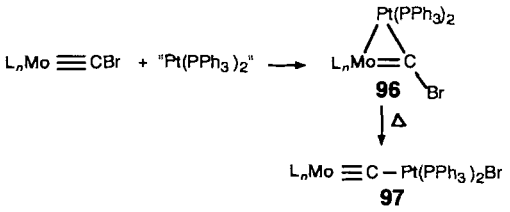

The elegant application by Gladysz et al. of the now-classical Fischer carbene and carbyne synthesis in a reaction sequence led to complexes with a novel type of C_3 carbon bridge (**98**).[307]

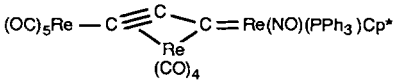

98

Templeton et al. reported the dimerization of the methylidyne complex $[tp'(OC)_2M{\equiv}CH]$ (M = Mo, W; tp' = $HB(3,5\text{-}Me_2C_3HN_2)_3$) to give the nonclassical μ-vinylidene complex **99**.[305b, c]

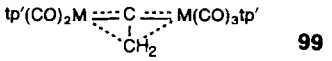

99

Complexes with C_{60} and C_{70} bridges have been synthesized, for example, the fullerenehexametal complexes $[\{(Et_3P)_2M\}_6C_{60}]$ (M = Pd, Pt)[308] and the diiridium complexes $[(R_3P)_2(Cl)(OC)IrC_nIr(CO)(Cl)(PR_3)_2]$ (n = 60, 70).[309a] Further transition metal compounds with bridging carbon ligands have been comprehensively reviewed recently by Diederich et al.[309b]

8. Organometallic Polymers with Hydrocarbon Bridges

Organometallic polymers, which are frequently obtained by the polymerization or copolymerization of monomers such as $[(\eta^6\text{-styrene})Cr(CO)_3]$ and $[(\eta^5\text{-}CH_2{=}CH{-}C_5H_4)Fe(CO)_2Me]$, are currently the subjects of intensive investigations.[310a] For instance, the polymerization of vinylferrocene—although first reported nearly 40 years ago[310b]—is still of active interest.[310c]

Studies of metal-containing polyenes and polyynes are quite topical because of the expected novel properties (rod-shaped molecules, liquid-crystal properties, nonlinear optical behavior, one-dimensional electrical conductivity) of these materials.[311] The first of these novel polymers **100** were obtained by Takahashi, Hagihara, et al.[312]

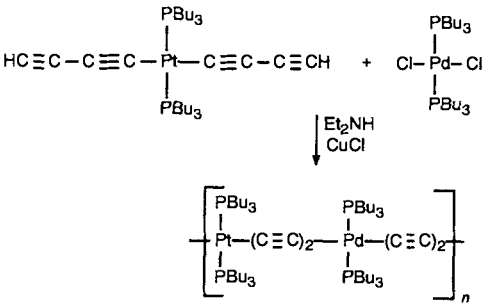

100

A general method for the preparation of polymers **101** and **102** is the stoichiometric reaction of dihalo complexes with bis(trimethylstannyl)diynes. Lewis et al. used this approach very successfully for the synthesis of oligomeric and polymeric μ-acetylide complexes.[313] The polymers obtained had an average molar mass of up to 200000. Using the same methodology, Lewis et al. prepared cross-linked Pt-containing polymers **103**.[314a] Polymers have also been obtained by reactions of $[(o,p\text{-}\eta^6\text{-}C_6H_4Cl)Cr(CO)_3]$ with $Me_3Sn{-}C{\equiv}C{-}SnMe_3$.[314b]

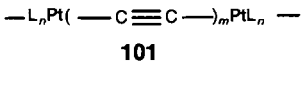

101

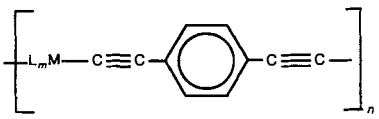

M = Ni, Pd, Pt, Fe, Rh **102**

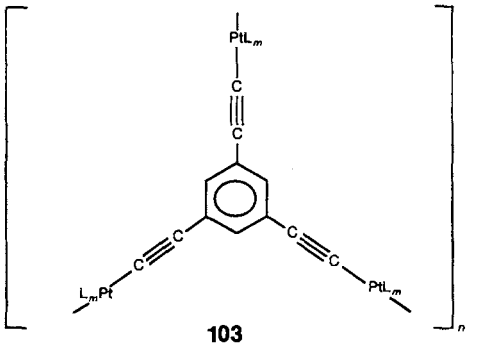

103

Polymer chains with metal-containing terminal groups are formed by the insertion of arylisocyanides (up to 100 times) into the Pd–C bond of the μ-acetylide complex

$[Cl(R_3P)_2Pd-C\equiv C-Pt(PR_3)_2Cl]$.[315] According to studies by Marder et al., terminal dialkynes react with $[Rh(PnBu_3)_4Me]$ to yield the corresponding polymers.[316] Hanack et al. reported layered (μ-acetylide)phthalocyaninatoiron complexes and described them as models for one-dimensional electrical conductors.[317]

Metallapolyynes with alkynyl and carbyne ligands $[-C\equiv M-C\equiv C-]_n$ are also of great interest.[318a] A corresponding monomer, the π-conjugated metallabutadiyne $[HC\equiv W(dmpe)_2(C\equiv C-H)]$, has been recently reported.[318b] The first reported organometallic polymer with arene bridges is **104**. This polymer is formed in the same

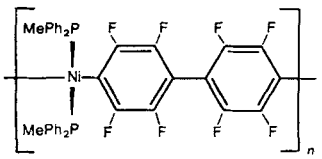

104

fashion as di- and trimetallic bis(methyldiphenylphosphine)nickel complexes containing tetra- and octafluoro-*p*,*p*′-biphenylene bridges: by the reaction of the corresponding organolithium compounds with bromonickel complexes.[319] Recent examples of ferrocene-containing polymers are polyferrocenyldisulfide[320] and polyferrocenylsilane.[321] Rosenblum et al. reported the Pd°-catalyzed synthesis of interesting face-to-face metallocene polymers from 1,8-diiodonaphthalene and dimetalated ferrocene or $CpCu\cdot SMe_2$.[244] The coordination of $M(CO)_3$ units (M = Cr, Mo) to the benzene rings of poly(*p*-phenylene) has also been reported.[322a] The oxidation of these molybdenum polymers increases their electrical conductivity.[322a] The same effect is observed in the ferrocene-containing polymer $[-Fc-CH=CH-(p\text{-}C_6H_4)-CH=CH-]_n$, which can be prepared by the Wittig reaction.[322b] Recently a conjugated polymer has been synthesized by metallacyclization of $[Cp\text{-}Co(PPh_3)_2]$ with 4,4′-diethynylbiphenyl.[322c]

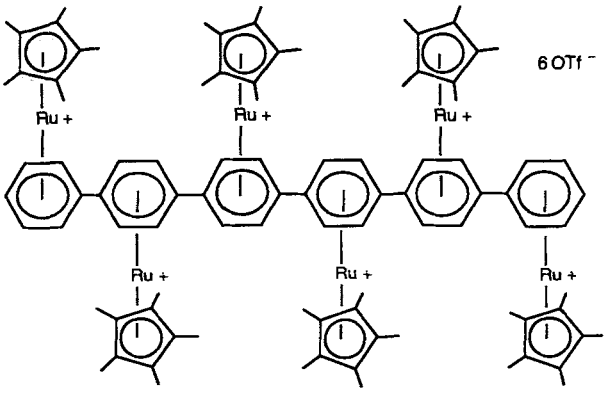

105

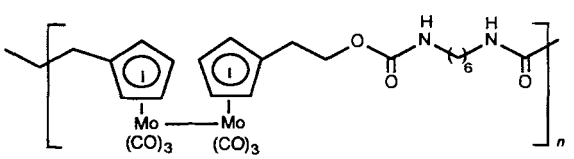

106

The $[Cp^*Ru]^+$ ion, which can be added to nearly all types of benzene rings (see Section 3), can serve as a building block for the construction of metal-containing organic solids having the desired shape (molecular engineering of solid-state materials).[174] An example of these interesting compounds is **105**. Metal-containing polyurethanes such as **106** are formed by the condensation of hexamethylenetriamine with β-hydroxyethyl-substituted cyclopentadienyliron and -molybdenum complexes.[323] The Mo–Mo bond in **106** can be cleaved photochemically.

9. Miscellaneous

The thermodynamically very stable diiron system $[Cp(OC)Fe(\mu\text{-}CO)(\mu\text{-}CR)Fe(CO)Cp]^+$ has significant synthetic potential. It has been used primarily by Casey et al.[324] for the synthesis of a large number of complexes with various hydrocarbon bridges. Reactions with the analogous Ru compound have been reported by Knox et al.[325] In general, the metal–metal bond remains intact in these reactions; however, hydride abstraction from the μ-alkylidenediiron complex $[\{Cp(OC)Fe\}_2(\mu\text{-}CO)(\mu\text{-}CHCH_2CH=CH_2)]$ is an exception. This reaction proceeds by cleavage of the metal–metal bond and yields, after a rearrangement, a μ-η^4:η^1-butadiene complex.[326] The formation of a C_3-bridged tetrairon complex from a methylidyne and a vinylidene complex is also of interest.[327] Tetrairon complexes with C_5 and C_7 bridges are known as well.[328] The cation **107**, an organometallic cyanine, could have interesting electron-transfer and nonlinear optical properties. In an unexpected fashion, Fehlhammer et al. obtained complex **108**, which has an N rather than a CH bridge.[329]

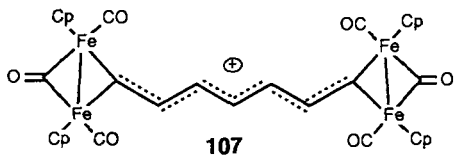

107

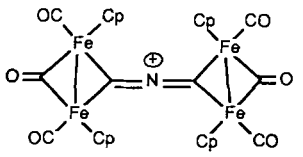

108

Complexes with bis(carbene) bridges are formed by Herrmann's diazo method[115] from bis(diazo) compounds and the coordinatively unsaturated metal complexes $[Cp(OC)_2Mn]$, $[Cp^*Rh(\mu\text{-}CO)_2RhCp^*]$, and $[(OC)_2CpMo\equiv MoCp(CO)_2]$.[330]

Zenneck exploited highly reactive intermediates from co-condensation reactions of metal vapors and arenes to prepare several multinuclear complexes (e.g., triple-decker complexes).[331] Dititanacyclobutane can be obtained by the thermolysis of 2-isopropyl-2-methyl-titanacyclobutane.[332a] Other dialkyl-substituted titanacyclobutanes combine with reactive Rh^{II}, Ir^{II}, Pd^{II}, and Pt^{III} complexes to yield, by loss of

olefin, μ-methylene heterodimetallic compounds $[Cp_2Ti(\mu\text{-}Cl)(\mu\text{-}CH_2)M(Cl)(L)Me]$ (M = Rh, Ir, Pd, Pt).[332b] TaIr complexes with two methylene bridges are formed by hydrogen abstraction from $[Cp_2Ta(CH_2)CH_3]$ with $[(\eta^5\text{-indenyl})Ir(CO)_2]$.[332c] Of interest is the formation of dimetallic complexes with a $\eta^5\text{:}\eta^5\text{-}Me_4C_5CH_2CH_2C_5Me_4$ bridge from tungstacyclobutadienes $L_nW{=}C(Me){-}C(Me){=}C(Me)$ and η^5-cyclopentadienyl complexes with a $-CH_2CH_2C{\equiv}CMe$ substituent.[332d] The metathesis reactions of Schrock carbene complexes and octatetraenes or 1,4-divinylbenzene produces bis(carbene) complexes, for example, $[L_nMo{=}CH{-}CH{=}CH{-}CH{=}CH{-}CH{=}ML_n]$.[333]

A complex with an $\eta^3\text{:}\eta^3$-1,3-butadiene bridge was found as the product of the reaction of a μ-dihydridorhodium(I) complex with butadiene.[334] The ethylene complex $[Cp_2(Me_3P)Zr(C_2H_4)]$ undergoes a novel reaction with cyclopropene; the ethylene ligand is protonated and subsequently a $\mu\text{-}\eta^1\text{:}\eta^2$-allenediyl complex is formed **109**.[335]

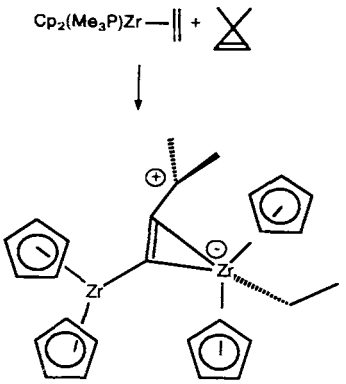

109

10. Outlook

Even though the selection of known complexes discussed in this review is certainly subjective, the wide array of multinuclear transition metal complexes with σ- or π-bound hydrocarbon bridges is evident. The reactions of carbonylmetalate ions with cationic π complexes clearly follow the isolobal principle.[14, 54] For instance, $[Re(CO)_5]^-$ acts like a carbanion and $[Re(CO)_5]^+$ like a carbenium ion, while the $[Re(CO)_5]$ unit acts like a methyl group. Cationic ethylene complexes such as $[(OC)_5Re(\eta^2\text{-}C_2H_4)]^+$ can be compared to carbenium ions, while μ-acetylide complexes like $[(OC)_5Re{-}C{\equiv}C{-}Re(CO)_5]$ behave like alkynes.

Since efficient syntheses are now available, it is important to investigate more closely the reactivity of these compounds and their applications. Can novel organic compounds be prepared with these complexes? One example is the synthesis of a novel polycycle by oxidation of **40** with Ce^{4+}.[127] The dimetallic iron complexes synthesized by Astruc et al.[254, 255] are interesting compounds for electron storage with electrochemical properties that may lead to application in electron transfer catalysis. Electrochemical investigations on heterodimetallic complexes might lead to new mixed-valence organometallic compounds.

Metal complexes with conjugated hydrocarbon bridges (double and triple bonds) or with donor and acceptor ligands are candidates for electrically conducting materials and for materials with second- and third-order nonlinear optical properties. These compounds have been only rarely studied as precursors for heterometallic catalysts. These applications appear to be attractive in the future. However, basic research, driven by scientific curiosity and independent of any potential application, should not be neglected.[336]

W. B. expresses his sincere thanks to the co-workers mentioned in the references for their exemplary efforts, their experimental and creative contributions, and the harmonious collaboration. The generous support of the Deutsche Forschungsgemeinschaft, the Fonds der Chemischen Industrie, Wacker Chemie, Munich, and DEGUSSA AG, Frankfurt, is gratefully acknowledged. We thank the following colleagues for valuable literature references and for providing us with unpublished manuscripts: Profs. D. H. Gibson, B. Angelici, M. Akita, D. A. Astruc, J. E. Bercaw. R. G. Bergman, R. M. Bullock, C. P. Casey, C. Elschenbroich, G. Erker, G. L. Geoffroy, J. A. Gladysz, J. A. Heppert, M. Herberhold, A. D. Hunter, C. G. Kreiter, E. Lindner, S. Lotz, J. R. Moss, A. Salzer, J. P. Selegue, J. Takats, J. L. Templeton, H. Werner, A. Wojcicki, U. Zenneck, Drs. P. Härter, and D. Wadepohl. We thank Dr. K. Sünkel for valuable discussions.

Received: February 12, 1993 [A 911 IE]
German version: *Angew. Chem.* **1993**, *105*, 969
Translated by Dr. Wolf Christian Wilisch, Pasadena, CA (USA)

[1] M. H. Chisholm, *Polyhedron* **1988**, *7*, 757–1077.
[2] A. A. Hock, O. S. Mills, *Proc. Chem. Soc.* **1958**, 233–234; W. Hübel, E. H. Braye, *J. Inorg. Nucl. Chem.* **1959**, *10*, 250–268, and references therein
[3] a) E. O. Fischer, H. Wawersik, *J. Organomet. Chem.* **1966**, *5*, 559–567; b) A. Nakamura, N. Hagihara, *Bull. Chem. Soc. Jpn.* **1960**, *33*, 425; F. A. Cotton, M. D. LaPrade, *J. Am. Chem. Soc.* **1968**, *90*, 2026–2031.
[4] R. B. King, *Inorg. Chem.* **1963**, *2*, 531–533.
[5] a) W. A. Herrmann, *Angew. Chem.* **1982**, *94*, 118–131; *Angew. Chem. Int. Ed. Engl.* **1982**, *21*, 117; b) C. Masters, *Adv. Organomet. Chem.* **1979**, *17*, 61–103.
[6] a) Gmelin Handbook of Inorganic Chemistry, *Organotitanium Compounds, Part 5, Springer*, **1990**, pp. 25–29, and references therein; b) G. Wilke, *Angew. Chem.* **1988**, *100*, 189–211; *Angew. Chem. Int. Ed. Engl.* **1988**, *27*, 185.
[7] Benzene and its derivatives as bridging ligands in transition metal complexes: H. Wadepohl, *Angew. Chem.* **1992**, *104*, 253–268; *Angew. Chem. Int. Ed. Engl* **1992**, *31*, 247–262.
[8] R. D. Adams, *Polyhedron* **1988**, *7*, 2251–2253, and references therein; J. R. Moss, M. L. Niven, E. E. Sutton, *Inorg. Chim. Acta* **1989**, *165*, 221–229.
[9] a) G. Erker, *Angew. Chem.* **1989**, *101*, 411–426; *Angew. Chem. Int. Ed. Engl.* **1989**, *28*, 397; b) D. W. Stephan, *Coord. Chem. Rev.* **1989**, *95*, 41–107.
[10] J. Li, A. D. Hunter, R. McDonald, B. D. Santarsiero, S. G. Bott, J. L. Atwood, *Organometallics* **1992**, *11*, 3050–3055.
[11] J.-M. Lehn, *Angew. Chem.* **1988**, *100*, 91–116; *Angew. Chem. Int. Ed. Engl.* **1988**, *27*, 89.
[12] a) M. Lacoste, H. Rabaa, D. Astruc, N. Ardoin, F. Varret, J.-Y. Saillard, A. Le Beuze, *J. Am. Chem. Soc.* **1990**, *112*, 9548–9557; b) D. Astruc, *Angew. Chem.* **1988**, *100*, 662–680; *Angew. Chem. Int. Ed. Engl.* **1988**, *27*, 643.
[13] M. H. Chisholm, *Polyhedron* **1988**, *7*, 757–1077; R. J. Puddephatt, *ibid.* **1988**, *7*, 767–773; R. M. Bullock, C. P. Casey, *Acc. Chem. Res.* **1987**, *24*, 167–173; A. Wojcicki, *Coordination Chemistry and Catalysis* (Ed.: J. J. Ziólkowski), World Publishing, **1988**, pp. 3–25.
[14] F. G. A. Stone, *Angew. Chem.* **1984**, *96*, 85–96; *Angew. Chem. Int. Ed. Engl.* **1984**, *23*, 89.
[15] μ-Methylene complexes with metal–metal bonds: W. A. Herrmann, *Proc. Appl. Chem.* **1982**, *54*, 65–82; *Adv. Organomet. Chem.* **1982**, *20*, 159–263; *Angew. Chem.* **1982**, *94*, 118–131; *Angew. Chem. Int. Ed. Engl.* **1982**, *21*,

117; *J. Organomet. Chem.* **1983**, *250*, 319–343; J. E. Hahn, *Prog. Inorg. Chem.* **1984**, *31*, 205–264.
[16] Comprehensive review of dinuclear μ-hydrocarbon complexes: J. Holton, M. F. Lappert, R. Pearce, P. I. W. Yarrow, *Chem. Rev.* **1983**, *83*, 135–201.
[17] a) μ-Polymethylene complexes: J. R. Moss, L. G. Scott, *Coord. Chem. Rev.* **1984**, 171–190; b) dinuclear complexes with saturated hydrocarbon bridges: C. P. Casey, J. D. Audett, *Chem. Rev.* **1986**, *86*, 339–352.
[18] R. E. Lehmann, J. K. Kochi, *Organometallics* **1991**, *10*, 190–202; J. K. Kochi, T. M. Bockman, *Adv. Organomet. Chem.* **1991**, *33*, 52–124.
[19] In the oxidative addition the complexes behave as Lewis acid and Lewis base; however, the metal complexes are generally very electron rich.
[20] a) S. G. Davies, M. L. H. Green, D. M. P. Mingos, *Tetrahedron* **1978**, *34*, 3047–3077; b) P. L. Pauson, *J. Organomet. Chem.* **1980**, *200*, 207–221; c) L. A. P. Kane-Maguire, E. D. Honig, D. A. Sweigart, *Chem. Rev.* **1984**, *84*, 525–543; d) R. C. Bush, R. J. Angelici, *J. Am. Chem. Soc.* **1986**, *108*, 2735–2746; e) J. P. Collmann, L. S. Hegedus, J. R. Norton, R. G. Finke, *Principles and Applications of Organotransition Metal Chemistry*, University Science Books, Mill Valley, **1987**; f) L. S. Hegedus, *The Chemistry of the Metal-Carbon Bond, Vol. 2*, Wiley Interscience, New York, **1985**; g) J.-E. Bäckvall, J. L. Davidson, St. G. Davies, M. L. H. Green, D. M. P. Mingos, J. A. S. Howell, P. Powell, *Reactions of Coordinated Ligands. Vol. 1*, Plenum, New York, **1986**; D. A. Sweigart, Y. K. Chung, E. D. Honig, T. J. Alavosus, W. A. Halpin, J. C. Williams, P. G. Williard, N. G. Connelly in *Organometallic Syntheses*, vol. 4 (Ed.: R. B. King), Elsevier, Amsterdam, **1988**; R. D. Pike, D. A. Sweigart, *Synlett* **1990**, 565–571.
[21] S. G. Davies, *Organotransition Metal Chemistry: Application to Organic Synthesis*, Pergamon, Oxford, **1982**.
[22] a) J. Smidt, W. Hafner, R. Jira, R. Sieber, J. Sedlmeier, A. Sabel, *Angew. Chem.* **1962**, *74*, 93–102; b) G. W. Parshall, *Homogeneous Catalysis*, Wiley, New York, **1980**.
[23] P. Sautet, O. Eisenstein, K. M. Nicholas, *Organometallics* **1987**, *6*, 1845–1849, and references therein.
[24] W. Beck, *Polyhedron* **1988**, *7*, 2255–2261; W. Beck, B. Niemer, J. Breimair, J. Heidrich, *J. Organomet. Chem.* **1989**, *372*, 79–83.
[25] a) W. Beck, B. Olgemöller, *J. Organomet. Chem.* **1977**, *127*, C45–C47; b) B. Olgemöller, W. Beck, *Chem. Ber.* **1981**, *114*, 867–876.
[26] J. E. Ellis, *J. Organomet. Chem.* **1975**, *86*, 1–56.
[27] R. E. Dessy, R. L. Pohl, R. B. King, *J. Am. Chem. Soc.* **1966**, *88*, 5121–5124; M. S. Corraine, C. K. Lai, Y. Zhen, M. R. Churchill, L. A. Buttrey, J. W. Ziller, J. D. Atwood, *Organometallics* **1992**, *11*, 35–40.
[28] K. Raab, U. Nagel, W. Beck, *Z. Naturforsch. B* **1983**, *38*, 1466–1476.
[29] W. Beck, K. Raab, *Inorg. Synth.* **1990**, *28*, 15–22.
[30] H. Werner, R. Werner, *Chem. Ber.* **1985**, *118*, 4543–4552.
[31] W. Beck, K. Raab, U. Nagel, W. Sacher, *Angew. Chem.* **1985**, *97*, 498–499; *Angew. Chem. Int. Ed. Engl.* **1985**, *24*, 505.
[32] J. Breimair, M. Steimann, B. Wagner, W. Beck, *Chem. Ber.* **1990**, *123*, 7–10.
[33] J. L. Templeton, *Adv. Organomet. Chem.* **1989**, *29*, 1–100.
[34] a) W. Beck, H.-J. Müller, U. Nagel, *Angew. Chem.* **1986**, *98*, 739–740; *Angew. Chem. Int. Ed. Engl.* **1986**, *25*, 734; b) H.-J. Müller, K. Polborn, M. Steimann, W. Beck, *Chem. Ber.* **1989**, *122*, 1901–1906.
[35] W. Knauer, Dissertation, Universität München, **1992**.
[36] a) M. Green, N. C. Norman, A. G. Orpen, *J. Am. Chem. Soc.* **1981**, *103*, 1269–1271; M. Green, N. C. Norman, A. G. Orpen, C. J. Schaverien, *J. Chem. Soc. Dalton Trans.* **1984**, 2455–2465; M. Green, N. K. Jetha, R. J. Mercer, N. C. Norman, A. G. Orpen, *ibid.* **1988**, 1843–1851; b) D. Pufahl, W. E. Geiger, N. G. Connelly, *Organometallics* **1989**, *8*, 412–415.
[37] H.-J. Müller, U. Nagel, W. Beck, *Organometallics* **1987**, *6*, 193–194.
[38] H.-J. Müller, U. Nagel, M. Steimann, K. Polborn, W. Beck, *Chem. Ber.* **1989**, *122*, 1387–1393, 2031.
[39] H.-J. Müller, W. Beck, *J. Organomet. Chem.* **1987**, *330*, C13–C16.
[40] B. Niemer, J. Breimair, B. Wagner, K. Polborn, W. Beck, *Chem. Ber.* **1991**, *124*, 2227–2236.
[41] B. Niemer, M. Steimann, W. Beck, *Chem. Ber.* **1988**, *121*, 1767–1769.
[42] B. Niemer, T. Weidmann, W. Beck, *Z. Naturforsch. B* **1992**, *47*, 509–516.
[43] R. C. Bush, R. A. Jacobson, R. J. Angelici, *J. Organomet. Chem.* **1987**, *323*, C25–C28.
[44] J. W. Faller, K.-H. Chao, *J. Am. Chem. Soc.* **1983**, *105*, 3893; *Organometallics* **1984**, *3*, 927–932.
[45] B. E. R. Schilling, R. Hoffmann, J. W. Faller, *J. Am. Chem. Soc.* **1979**, *101*, 592–598.
[46] J. B. Wakefield, J. M. Stryker, *J. Am. Chem. Soc.* **1991**, *113*, 7057–7059.
[47] S. Hüffer, W. Beck, unpublished results.
[48] R. L. Beddoes, E. St. Davies, M. Helliwell, M. W. Whiteley, *J. Organomet. Chem.* **1991**, *421*, 285–298.
[49] M. Tsutsui, A. Courtney, *Adv. Organomet. Chem.* **1977**, *16*, 241–282.
[50] K. Jonas, *Angew. Chem.* **1985**, *97*, 292–307; *Angew. Chem. Int. Ed. Engl.* **1985**, *24*, 295; K. Jonas, W. Rüsseler, K. Angermund, C. Krüger, *ibid.* **1986**, *98*, 904–905 and **1986**, *25*, 927; K. Jonas, W. Rüsseler, C. Krüger, E. Raabe, *ibid.* **1986**, *98*, 905–906 and **1986**, *25*, 928.
[51] W. M. Lamanna, W. B. Gleason, D. Britton, *Organometallics* **1987**, *6*, 1583–1584.
[52] a) D. A. Lesch, J. W. Richardson, Jr., R. A. Jacobson, R. J. Angelici, *J. Am. Chem. Soc.* **1984**, *106*, 2901–2906; b) R. J. Angelici, *Acc. Chem. Res.* **1988**, *21*, 387–394.
[53] a) W. Beck, B. Niemer, B. Wagner, *Angew. Chem.* **1989**, *101*, 1699–1701; *Angew. Chem. Int. Ed. Engl.* **1989**, *28*, 1705–1706; b) J. Breimair, B. Niemer, K. Raab, W. Beck, *Chem. Ber.* **1991**, *124*, 1059–1063; c) B. Niemer, J. Breimair, T. Völkel, B. Wagner, K. Polborn, W. Beck, *Chem. Ber.* **1991**, *124*, 2237–2244.
[54] R. Hoffmann, *Angew. Chem.* **1982**, *94*, 725–739; *Angew. Chem. Int. Ed. Engl.* **1982**, *21*, 711.
[55] F. L'Eplattenier, C. Pélichet, *Helv. Chim. Acta* **1970**, *53*, 1091–1099; W. J. Carter, J. W. Kelland, S. J. Okrasinski, K. E. Warner, J. R. Norton, *Inorg. Chem.* **1982**, *21*, 3955–3960.
[56] J. R. Moss, W. A. G. Graham, *Inorg. Chem.* **1977**, *16*, 75–79.
[57] J. Breimair, C. Robl, W. Beck, *Chem. Ber.* **1990**, *123*, 1661–1663.
[58] E. O. Fischer, V. Kiener, *J. Organomet. Chem.* **1970**, *23*, 215–223; *ibid.* **1972**, *42*, 447–457.
[59] a) C. E. Kampe, N. M. Boag, H. D. Kaesz, *J. Mol. Catal.* **1983**, *21*, 297–312; b) C. E. Kampe, H. D. Kaesz, *Inorg. Chem.* **1984**, *23*, 4646–4653.
[60] J. E. Ellis, *Adv. Organomet. Chem.* **1990**, *31*, 1–51; W. Beck, *Angew. Chem.* **1991**, *103*, 173–174; *Angew. Chem. Int. Ed. Engl.* **1991**, *30*, 168–169.
[61] J. Breimair, C. Robl, W. Beck, *J. Organomet. Chem.* **1991**, *411*, 395–404.
[62] a) D. Seebach, *Angew. Chem.* **1990**, *102*, 1363–1409; *Angew. Chem. Int. Ed. Engl.* **1990**, *29*, 1320; b) J. Ehrler, D. Seebach, *Liebigs Ann. Chem.* **1990**, 379–388. We thank Prof. H. Bock, Universität Frankfurt, for bringing this to our attention.
[63] See G. R. Lee, J. M. Maher, N. J. Cooper, *J. Am. Chem. Soc.* **1987**, *109*, 2956–2962.
[64] G. Al-Takhin, J. A. Connor, H. A. Skinner, *J. Organomet. Chem.* **1983**, *259*, 313–320.
[65] E. O. Fischer, J. K. R. Wanner, G. Müller, J. Riede, *Chem. Ber.* **1985**, *118*, 3311–3319; see also J. Chen, Y. Yu, K. Liu, G. Wu, P. Zheng, *Organometallics* **1993**, *12*, 1213–1220.
[66] J. D. Munro, P. L. Pauson, *J. Chem. Soc.* **1961**, 3475–3479; F. Zahedi, M. L. Ziegler, *Z. Naturforsch. B* **1979**, *34*, 918–920; H. Adams, N. A. Bailey, D. G. Willett, M. J. Winter, *J. Organomet. Chem.* **1987**, *333*, 61–69; W. D. Closson, P. Wriede, S. Bank, *J. Am. Chem. Soc.* **1966**, *88*, 1581–1583.
[67] W. E. Geiger, T. Gennett, G. A. Lane, A. Salzer, A. L. Rheingold, *Organometallics* **1986**, *5*, 1352–1359.
[68] N. El Murr, J. E. Sheats, W. E. Geiger, J. D. L. Holloway, *Inorg. Chem.* **1979**, *18*, 1443–1446.
[69] W. McFarlane, L. Pratt, G. Wilkinson, *J. Chem. Soc.* **1963**, 2162–2166.
[70] J.-R. Hamon, D. Astruc, P. Michaud, *J. Am. Chem. Soc.* **1981**, *103*, 758–766.
[71] E. O. Fischer, D. Wittmann, D. Himmelreich, D. Neugebauer, *Angew. Chem.* **1982**, *94*, 451–452; *Angew. Chem. Int. Ed. Engl.* **1982**, *21*, 444.
[72] a) R. L. Thompson, S. J. Geib, N. J. Cooper, *J. Am. Chem. Soc.* **1991**, *113*, 8961–8963; b) J. Takats, *Polyhedron* **1988**, *7*, 931–941.
[73] M. V. Gaudet, A. W. Hanson, P. S. White, M. J. Zaworotko, *Organometallics* **1989**, *8*, 286–293.
[74] N. G. Connelly, M. D. Kitchen, R. F. D. Stansfield, S. M. Whiting, P. Woodward, *J. Organomet. Chem.* **1978**, *155*, C34–C36.
[75] P. S. Waterman, W. P. Giering, *J. Organomet. Chem.* **1978**, *155*, C47–C50.
[76] R. P. Aggarwal, N. G. Connelly, B. J. Dunne, M. Gilbert, A. G. Orpen, *J. Chem. Soc. Dalton Trans.* **1991**, 1–9.
[77] J. Edwin, W. E. Geiger, A. Salzer, U. Ruppli, *J. Am. Chem. Soc.* **1987**, *109*, 7893–7894; J. Edwin, W. E. Geiger, *ibid.* **1990**, *112*, 7104–7112.
[78] J. H. Bieri, T. Egolf, W. von Philipsborn, U. Piantini, R. Prewo, U. Ruppli, A. Salzer, *Organometallics* **1986**, *5*, 2413–2425.
[79] W. E. Geiger, A. Salzer, J. Edwin, W. von Philipsborn, U. Piantini, A. L. Rheingold, *J. Am. Chem. Soc.* **1990**, *112*, 7113–7121; U. Kölle, *Angew. Chem.* **1991**, *103*, 970–972; *Angew. Chem. Int. Ed. Engl.* **1991**, *30*, 956.
[80] S. G. Bott, L. Brammer, N. G. Connelly, M. Green, A. G. Orpen, J. F. Paxton, C. J. Schaverien, S. Bristow, N. C. Norman, *J. Chem. Soc. Dalton Trans.* **1990**, 1957–1969; L. A. Brady, A. F. Dyke, S. E. Garner, S. A. R. Knox, A. Irving, S. M. Nicholls, A. G. Orpen, *ibid.* **1993**, 487–488.
[81] B. Bachmann, J. Heck, G. Meyer, J. Pebler, T. Schleid, *Inorg. Chem.* **1992**, *31*, 607–614.
[82] N. G. Connelly, *Chem. Soc. Rev.* **1989**, *18*, 153–185.
[83] a) A. N. Nesmeyanov, N. N. Sedova, Y. V. Volgin, Sazonova, *Izv. Akad. Nauk. SSSR Ser. Khim.* **1977**, *10*, 2353–2354; W. A. Herrmann, D. Andrejewski, E. Herdtweck, *J. Organomet. Chem.* **1987**, *319*, 183–195; b) G. H. Worth, B. H. Robinson, J. Simpson, *Organometallics* **1992**, *11*, 3863–3874.
[84] H. G. Raubenheimer, G. J. Kruger, H. W. Viljoen, *J. Chem. Soc. Dalton Trans.* **1985**, 1963–1966.
[85] W. Beck, J. Breimair, W. Knauer, T. Weidmann in *Transition Metal Carbyne Complexes*, (Ed.: F. R. Kreissl), Kluwer, Dordrecht, **1993**, pp. 189–199.
[86] a) T. Weidmann, Dissertation, Universität München, **1992**; b) W. Knauer, Dissertation, Universität München, **1992**.

[87] T. Desmond, F. J. Lalor, G. Ferguson, M. Parvez, *J. Chem. Soc. Chem. Commun.* **1984**, 75–77.
[88] B. D. Dombeck, R. J. Angelici, *J. Am. Chem. Soc.* **1974**, *96*, 7568–7569; S. Lotz, R. R. Pille, P. H. Van Rooyen, *Inorg. Chem.* **1986**, *25*, 3053–3057.
[89] D. H. Gibson, J. O. Franco, M. T. Harris, T.-S. Ong, *Organometallics* **1992**, *11*, 1993–1994.
[90] D. A. Brown, J. Burns, I. El-Gamati, W. K. Glass, K. Kreddan, M. Salama, D. Cunningham, T. Higgins, P. McArdle, *J. Chem. Soc. Chem. Commun.* **1992**, 701–702.
[91] L. A. P. Kane-Maguire, C. A. Mansfield, *J. Chem. Soc. Chem. Commun.* **1973**, 540–541.
[92] A. J. Birch, P. E. Cross, J. Lewis, D. A. White, S. B. Wild, *J. Chem. Soc. A* **1968**, 332–340.
[93] A. N. Nesmeyanov, N. N. Sedova, V. A. Sazanova, L. S. Borodina, *Dokl. Akad. Nauk. SSSR* **1972**, *207*, 617–620; *Dokl. Chem. (Engl. Transl.)* **1972**, *202/207*, 899–901.
[94] C. Elschenbroich, J. Heck, *Angew. Chem.* **1977**, *89*, 497–498; *Angew. Chem. Int. Ed. Engl.* **1977**, *16*, 479; C. Elschenbroich, J. Heck, W. Massa, M. Birkhahn, *Chem. Ber.* **1990**, *123*, 2321–2324.
[95] H. Airoldi, G. Deganello, G. Dia, P. Saccone, *Inorg. Chim. Acta* **1980**, *41*, 171–178.
[96] M. Moll, P. Würstl, H. Behrens, P. Merbach, *Z. Naturforsch. B* **1978**, *33*, 1304–1308.
[97] J.-R. Hamon, D. Astruc, E. Román, *J. Am. Chem. Soc.* **1981**, *103*, 2431–2433.
[98] a) V. Guerchais, *J. Chem. Soc. Chem. Commun.* **1990**, 534–536; b) C. P. Casey, M. S. Konings, K. J. Haller, *J. Organomet. Chem.* **1986**, *301*, C55–C58.
[99] A. J. Pearson, V. D. Khetani, *J. Chem. Soc. Chem. Commun.* **1986**, 1722–1774.
[100] K. E. Schwarzhans, W. Stolz, *Monatsh. Chem.* **1987**, *118*, 875–878; G. Ingram, P. Jaitner, K. E. Schwarzhans, *Z. Naturforsch. B* **1990**, *45*, 781–784.
[101] N. G. Connelly, A. G. Orpen, I. C. Quarmby, J. B. Sheridan, *J. Organomet. Chem.* **1986**, *299*, C51–C55.
[102] D. Astruc, D. Mandon, A. Madonik, P. Michaud, N. Ardoin, F. Varret, *Organometallics* **1990**, *9*, 2155–2164.
[103] C. L. Sterzo, J. K. Stille, *Organometallics* **1990**, *9*, 687–694; C. L. Sterzo, *ibid.* **1990**, *9*, 3185–3188.
[104] F. Rose-Munch, O. Bellot, L. Mignon, A. Semra, F. Robert, Y. Jeannin, *J. Organomet. Chem.* **1991**, *402*, 1–16.
[105] J. Breimair, M. Wieser, B. Wagner, K. Polborn, W. Beck, *J. Organomet. Chem.* **1991**, *421*, 55–64.
[106] a) J. Breimair, T. Weidmann, B. Wagner, W. Beck, *Chem. Ber.* **1991**, *124*, 2431–2434; b) C. Kelley, M. R. Terry, A. W. Kaplan, G. L. Geoffroy, N. Lugan, R. Mathieu, B. S. Haggerty, A. L. Rheingold, *Inorg. Chim. Acta* **1992**, *198–200*, 601–611.
[107] M. Wieser, K. Sünkel, C. Robl, W. Beck, *Chem. Ber.* **1992**, *125*, 1369–1373.
[108] J. Breimair, M. Wieser, W. Beck, *J. Organomet. Chem.* **1992**, *441*, 429–440.
[109] M. Wieser, K. Karaghiosoff, W. Beck, *Chem. Ber.*, **1993**, *126*, 1081–1089.
[110] P. McArdle, H. Sherlock, *J. Organomet. Chem.* **1976**, *116*, C23–C24.
[111] T. C. T. Chang, B. M. Foxman, M. Rosenblum, C. Stockmann, *J. Am. Chem. Soc.* **1981**, *103*, 7361–7362; A. Rosan, M. Rosenblum, J. Tancrede, *ibid.* **1973**, *95*, 3062–3064; J. C. Watkins, M. Rosenblum, *Tetrahedron Lett.* **1984**, *25*, 2097–2100; A. Sanders, T. Bauch, C. V. Magatti, C. Lorenc, W. P. Giering, *J. Organomet. Chem.* **1976**, *107*, 359–375.
[112] P. J. Lennon, A. Rosan, M. Rosenblum, J. Tancrede, P. Waterman, *J. Am. Chem. Soc.* **1980**, *102*, 7033–7038; T. W. Bodnar, A. R. Cutler, *Organometallics* **1985**, *4*, 1558–1565. Review: M. Rosenblum, *J. Organomet. Chem.* **1986**, *300*, 191–218.
[113] T. Bodnar, A. R. Cutler, *J. Organomet. Chem.* **1981**, *213*, C31–C36; M. Brookhart, J. R. Tucker, G. R. Husk, *J. Am. Chem. Soc.* **1983**, *105*, 258–264.
[114] A. Davison, J. P. Solar, *J. Organomet. Chem.* **1978**, *155*, C8–C12; N. Ye. Kolobova, V. V. Skripkin, G. G. Alexandrov, Yu. T. Struchkov, *ibid.* **1979**, *169*, 293–300; J. P. Selegue, *J. Am. Chem. Soc.* **1983**, *105*, 5921–5923; B. E. Boland-Lussier, R. P. Hughes, *Organometallics* **1982**, *1*, 635–639; L. Kollár, B. Floris, *J. Organomet. Chem.* **1992**, *441*, 117–123.
[115] E. G. Perevalova, A. N. Pushin, E. I. Klimova, Y. L. Slovokhotov, Y. T. Struchkov, *Organomet. Chem. USSR* **1989**, *2*, 745–749.
[116] W. A. Herrmann, K. Weidenhammer, M. L. Ziegler, *Z. Anorg. Allg. Chem.* **1980**, *460*, 200–206.
[117] a) D. W. Macomber, M.-H. Hung, A. G. Verma, R. D. Rogers, *Organometallics* **1988**, *7*, 2072–2074; b) D. W. Macomber, M.-H. Hung, P. Madhukar, M. Liang, R. D. Rogers, *ibid.* **1991**, *10*, 737–746; c) D. W. Macomber, M.-H. Hung, *J. Organomet. Chem.* **1989**, *366*, 147–154; d) D. W. Macomber, P. Madhukar, R. D. Rogers, *Organometallics* **1991**, *10*, 2121–2126.
[118] D. W. Macomber, P. Madhukar, R. D. Rogers, *Organometallics* **1989**, *8*, 1275–1282.
[119] S. Kamiyama, A. Kasahara, T. Izumi, I. Shimizu, H. Watabe, *Bull. Chem. Soc. Jpn.* **1981**, *54*, 2079–2082.
[120] A. A. Koridze, I. T. Chizhevsky, P. V. Petrovskii, E. I. Fedin, N. E. Kolobova, L. E. Vinogradova, L. A. Leites, V. G. Andrianov, Y. T. Struchkov, *J. Organomet. Chem.* **1981**, *206*, 373–391; L. M. Sandilands, C. J. L. Lock, R. Faggiani, N. Hao, B. G. Sayer, M. A. Quilliam, B. E. McCarry, M. J. McGlinchey, *ibid.* **1982**, *224*, 267–283.
[121] a) E. O. Fischer, F. J. Gammel, D. Neugebauer, *Chem. Ber.* **1980**, *113*, 1010–1019; E. O. Fischer, F. J. Gammel, J. O. Besenhard, A. Frank, D. Neugebauer, *J. Organomet. Chem.* **1980**, *191*, 261–282; E. O. Fischer, V. N. Postnov, F. R. Kreissl, *ibid.* **1982**, *231*, C73–C77; P. M. Fritz, J. Breimair, B. Wagner, W. Beck, *ibid.* **1990**, *426*, 343–350; b) J. A. Heppert, M. E. Thomas-Miller, P. N. Swepston, M. W. Extine, *J. Chem. Soc. Chem. Commun.* **1988**, 280–282; c) E. O. Fischer, W. Röll, N. H. T. Huy, K. Ackermann, *Chem. Ber.* **1982**, *115*, 2951–2964; d) N. Q. Dao, H. Ferrier, M. Jouan, E. O. Fischer, W. Röll, *J. Organomet. Chem.* **1984**, *275*, 191–207; e) N. H. T. Huy, P. Lefloch, F. Robert, Y. Jeannin, *ibid.* **1987**, *327*, 211–221; f) D. M. Anderson, G. B. Bristow, P. B. Hitchcock, H. A. Jassim, M. F. Lappert, B. W. Skelton, *J. Chem. Soc. Dalton Trans.* **1987**, 2843–2851.
[122] M. Cais (Technicon Research and Development Foundation Ltd), US-A 3138625, **1962/64**; *Chem. Abstr.* **1964**, *61*, 9530); W. P. Hart, D. Shihua, M. D. Rausch, *J. Organomet. Chem.* **1985**, *282*, 111–121; Y.-P. Wang, J. M. Hwu, *ibid.* **1990**, *399*, 141–147; N. J. Gogan, S. I. DeSilva, *Organometallics* **1990**, *9*, 1970–1972.
[123] P. Hackett, B. F. G. Johnson, J. Lewis, G. Jaouen, *J. Chem. Soc. Dalton Trans.* **1982**, 1247–1251; A. Hafner, J. H. Bieri, R. Prewo, W. von Philipsborn, A. Salzer, *Angew. Chem.* **1983**, *95*, 736–737; *Angew. Chem. Int. Ed. Engl.* **1983**, *22*, 713.
[124] V. I. Boev, A. V. Dombrovskii, *J. Org. Chim.* **1980**, *16*, 2098.
[125] (Denki Kagaku Kogyo) JP-A 58189164, November 4, 1983; *Chem. Abstr.* **1984**, *100*, 138962.
[126] K. Yasufuku, H. Jamazaki, *J. Organomet. Chem.* **1976**, *121*, 405–411.
[127] Review: R. Gleiter, *Angew. Chem.* **1992**, *104*, 29–46; *Angew. Chem. Int. Ed. Engl.* **1992**, *31*, 27; R. Gleiter, G. Pflästerer, B. Nuber, *J. Chem. Soc. Chem. Commun.* **1993**, 454–456.
[128] R. M. Chin, W. D. Jones, *Angew. Chem.* **1992**, *104*, 340–341; *Angew. Chem. Int. Ed. Engl.* **1992**, *31*, 357.
[129] J. Besancon, S. Szymoiak, C. Moise, *J. Organomet. Chem.* **1992**, *426*, 325–330; C. M. Adams, E. M. Holt, *Organometallics* **1990**, *9*, 980–986.
[130] a) M. D. Rausch, *J. Org. Chem.* **1961**, *26*, 1802–1805; A. N. Nesmeyanov, N. N. Sedova, Yu. T. Struchkov, V. G. Andrianov, E. N. Stakheeva, V. A. Sazonova, *J. Organomet. Chem.* **1978**, *153*, 115–122; b) C. LeVanda, K. Bechgaard, D. O. Cowan, U. T. Mueller-Westerhoff, P. Eilbracht, G. A. Candela, R. L. Collins, *J. Am. Chem. Soc.* **1976**, *98*, 3181–3187; D. R. Talham, D. O. Cowan, *Organometallics* **1987**, *6*, 932–937; T.-Y. Dong, T.-Y. Lee, H.-M. Lin, *J. Organomet. Chem.* **1992**, *427*, 101–110; E. W. Neuse, M. S. Loonat, *Transition Met. Chem.* **1981**, *6*, 260.
[131] A. Koray, M. Ertas, Ö. Bekaroglu, *J. Organomet. Chem.* **1987**, *319*, 99–101.
[132] a) D. W. Macomber, P. Madhukar, *J. Organomet. Chem.* **1992**, *433*, 279–285; b) D. C. O'Connor Salazar, D. O. Cowan, *ibid.* **1991**, *408*, 219–225; H. K. Sharma, F. Cervantes-Lee, K. H. Pannell, *ibid.* **1992**, *438*, 183–194; c) N. E. Kolobova, Z. P. Valueva, K. N. Anisimov, G. Z. Suleimanov, *Izv. Akad. Nauk SSSR Ser. Khim.* **1978**, 910; d) P. D. Harvey, J. G. Sharman, *Can. J. Chem.* **1990**, *68*, 223.
[133] a) C. L. Sterzo, *Organometallics* **1990**, *9*, 3185–3188; b) C. L. Sterzo, M. M. Miller, J. K. Stille, *ibid.* **1989**, *8*, 2331–2337; C. L. Sterzo, J. K. Stille, *ibid.* **1990**, *9*, 687–694.
[134] G. Erker, R. Pfaff, C. Krüger, S. Werner, *Organometallics* **1991**, *10*, 3559–3568; G. Erker, F. Sosna, R. Pfaff, R. Noe, C. Sarter, A. Kraft, C. Krüger, R. Zwettler, *J. Organomet. Chem.* **1990**, *394*, 99–112; G. Erker, B. Menjön, *Chem. Ber.* **1990**, *123*, 1327–1329; G. Erker, *Polyhedron* **1988**, *7*, 2451–2463; G. Erker, R. Lecht, F. Sosna, S. Uhl, Y.-H. Tsay, C. Krüger, H. Grondey, R. Benn, *Chem. Ber.* **1988**, *121*, 1069–1074; *Organometallics* (Eds.: A. de Meijere, H. tom Dieck), Springer, Heidelberg, **1987**, pp. 143–167; K. Mashima, K. Jyodoi, A. Ohyoshi, H. Takaya, *J. Chem. Soc. Chem. Commun.* **1986**, 1145–1146, *Organometallics* **1987**, *6*, 885–887, *Bull. Chem. Soc. Jpn.* **1991**, *64*, 2065–2076.
[135] J. M. O'Connor, R. Uhrhammer, A. L. Rheingold, D. L. Staley, R. K. Chadha, *J. Am. Chem. Soc.* **1990**, *112*, 7585–7598; J. M. O'Connor, R. Uhrhammer, A. L. Rheingold, D. M. Roddick, *ibid.* **1991**, *113*, 4530–4544.
[136] P. F. Engel, M. Pfeffer, J. Fischer, A. Dedieu, *J. Chem. Soc. Chem. Commun.* **1991**, 1274–1276.
[137] R. S. Keng, Y.-C. Lin, *Organometallics* **1990**, *9*, 289–291.
[138] E. Baralt, Ch. M. Lukehart, A. T. McPhail, D. R. McPhail, *Organometallics* **1991**, *10*, 516–520.
[139] See, for example M. F. Semmelhack, G. R. Clark, J. L. Harrison, Y. Thebtaranonth, W. Wulff, A. Yamashita, *Tetrahedron* **1981**, *37*, 3957–3965.
[140] J. A. Heppert, M. A. Morgenstern, D. M. Scherubel, F. Takusagawa, M. R. Shaker, *Organometallics* **1988**, *7*, 1715–1723; J. A. Heppert, M. E. Thomas-Miller, D. M. Scherubel, F. Takusagawa, M. A. Morgenstern, M. R. Shaker, *ibid.* **1989**, *8*, 1199–1206.

[141] G. B. Richter-Addo, A. D. Hunter, N. Wichrowska, *Can. J. Chem.* **1990**, *68*, 41–48.
[142] V. Galamb, G. Pályi, F. Ungváry, L. Marko, R. Boese, G. Schmid, *J. Am. Chem. Soc.* **1986**, *108*, 3344–3351.
[143] a) A. N. Nesmeyanov, L. G. Makarova und V. N. Vinogradova, *Izv. Akad. Nauk SSSR Ser. Khim* **1971**, 892 (*Chem. Abstr.* **1971**, *75*, 49290g); *ibid.* **1972**, 1600–1604 (and **1972**, *77*, 140255b); b) A. N. Nesmeyanov; L. G. Makarova, V. N. Vinogradova, *ibid.* **1973**, 2796–2798 (and **1974**, *80*, 96133w); *Bull. Acad. Sci. USSR. Div. Chem. Sci.* **1973**, 2731; c) K. H. Pannell, J. B. Cassias, G. M. Crawford, A. Flores, *Inorg. Chem.* **1976**, *15*, 2671–2675; d) A. G. Osborne, R. H. Whiteley, *J. Organomet. Chem.* **1979**, *181*, 425–437.
[144] M. Herberhold, H. Kniesel, L. Haumaier, A. Gieren, C. Ruiz-Pérez, *Z. Naturforsch. B* **1986**, *41*, 1431–1436.
[145] M. Herberhold, H. Kniesel, *J. Organomet. Chem.* **1987**, *334*, 347–358.
[146] a) M. Herberhold, W. Feger, U. Kölle, *J. Organomet. Chem.* **1992**, *436*, 333–350; b) M. Tsutsui, N. Ely, A. Gebala, *Inorg. Chem.* **1975**, *14*, 78–81.
[147] F. H. Köhler, W. A. Geike, P. Hofmann, U. Schubert, P. Stauffert, *Chem. Ber.* **1984**, *117*, 904–914.
[148] a) H. Lehmkuhl, R. Schwickardi, C. Krüger, G. Raabe, *Z. Anorg. Allg. Chem.* **1990**, *581*, 41–47; b) H. Lehmkuhl, *Pure Appl. Chem.* **1990**, *62*, 731–740.
[149] A. Agarwal, M. J. McGlinchey, T.-S. Tan, *J. Organomet. Chem.* **1977**, *141*, 85–97.
[150] K.-H. Thiele, C. Krüger, R. Boese, G. Schmid, T. Bartik, G. Pályi, *Z. Anorg. Allg. Chem.* **1990**, *590*, 55–64.
[151] K. Sünkel, U. Birk, Chemiedozententagung, **1993**, Dresden.
[152] T. Orlova, V. N. Setkina, P. V. Petrovskii, A. I. Yanovskii, A. S. Batsanov, Y. T. Struchkov, *Organomet. Chem. USSR* **1988**, *1*, 725–728.
[153] P. Härter, G. Boguth, E. Herdtweck, J. Riede, *Angew. Chem.* **1989**, *101*, 1058–1059; *Angew. Chem. Int. Ed. Engl.* **1989**, *28*, 1008.
[154] T.-M. Chung, Y. K. Chung, *Organometallics* **1992**, *11*, 2822–2826.
[155] A. Salzer, T. Egolf, W. von Philipsborn, *Helv. Chim. Acta* **1982**, *65*, 1145–1157; R. G. Ball, F. Edelmann, G.-Y. Kiel, J. Takats, R. Drews, *Organometallics* **1986**, *5*, 829–839; F. Edelmann, J. Takats, *J. Organomet. Chem.* **1988**, *344*, 351–356; F. Edelmann, G. Y. Kiel, J. Takats, A. Vasudevamurthy, M.-Y. Yeung, *J. Chem. Soc. Chem. Commun.* **1988**, 296–297.
[156] S. Lotz, M. Schindehutte, P. H. van Rooyen, *Organometallics* **1992**, *11*, 629–639; P. H. van Rooyen, M. Schindehutte, S. Lotz, *ibid.* **1992**, *11*, 1104–1111. A review on dimetallic σ,π-arene complexes will appear in *Adv. Organomet. Chem.* (S. Lotz, University of Pretoria, South Africa, personal communication).
[157] M. L. H. Green, N. D. Lowe, D. O'Hare, *J. Chem. Soc. Chem. Commun.* **1986**, 1547–1548.
[158] W. Weigand, Universität München, personal communication.
[159] I. Weinstock, C. Floriani, A. Chiesi-Villa, C. Guastini, *J. Am. Chem. Soc.* **1986**, *108*, 8298–8299.
[160] T. Aoki, Y. Ishii, Y. Mizobe, M. Hidai, *Chem. Lett.* **1991**, 615–618.
[161] V. Dufaud, J. Thivolle-Cazat, J.-M. Basset, R. Mathieu, J. Jaud, J. Waissermann, *Organometallics* **1991**, *10*, 4005–4015; J. F. Carpentier, F. Petit, A. Mortreux, V. Dufand, J.-M. Basset, J. Thivolle-Cazat, *J. Mol. Cat.* **1993**, *81*, 1–15.
[162] a) P. K. Monaghan, R. J. Puddephatt, *J. Chem. Soc. Dalton Trans.* **1988**, 595–599; J. D. Scott, R. J. Puddephatt, *Organometallics* **1986**, *5*, 1538–1544; b) A. J. Canty, A. A. Watson, *Inorg. Chim. Acta* **1988**, *154*, 5–7; c) J. Cámpora, E. Carmona, E. Gutiérrez, P. Palma, M. L. Poveda, C. Ruiz, *Organometallics* **1992**, *11*, 11–13; J. Cámpora, E. Gutiérrez, A. Monge, M. L. Poveda, E. Carmona, *ibid.* **1992**, *11*, 2644–2650.
[163] R. D. W. Kemmit, A. W. G. Platt, *J. Chem. Soc. Dalton Trans.* **1986**, 1603–1607.
[164] S. Achar, J. D. Scott, R. J. Puddephatt, *Organometallics* **1992**, *11*, 2325–2326.
[165] a) W. P. Fehlhammer, H. Stolzenberg in *Comprehensive Organometallic Chemistry, Vol. 4* (Eds.: G. Wilkinson, F. G. A. Stone, E. W. Abel), Pergamon, **1982**, pp. 513–613; F. Edelmann, K. J. Jens, U. Behrens, *Chem. Ber.* **1978**, *111*, 2895–2900; N. E. Kolobova, L. L. Ivanov, O. S. Zhvanko, *Izv. Akad. Nauk. SSSR Ser. Khim.* **1984**, 1667; K. Jonas, E. Diffense, D. Hobermann, *Angew. Chem. Suppl.* **1983**, 1005–1016; U. Hänisch, E. Tagliaferri, R. Roulet, P. Vogel, *Helv. Chim. Acta* **1983**, *66*, 2182–2190; b) F. H. Köhler, A. Steck, *J. Organomet. Chem.* **1993**, *444*, 165–177, and references therein; c) J. W. Merker, W. E. Geiger, M. N. Paddon-Row, A. M. Oliver, A. L. Rheingold, *Organometallics* **1992**, *11*, 4109–4116.
[166] a) E. O. Fischer, W. Hafner, *Z. Naturforsch. B.* **1955**, *10*, 665–668; b) A. N. Nesmeyanov, N. N. Zaitseva, L. P. Yur'eva, R. A. Stukan, *Izv. Akad. Nauk. SSSR Ser. Khim.* **1978**, 1420; c) M.-H. Desbois, D. Astruc, *Organometallics* **1989**, *8*, 1841–1847.
[167] R. Davis, L. A. P. Kane-Maguire in *Comprehensive Organometallic Chemistry, Vol.* 3 (Eds.: G. Wilkinson, F. G. A. Stone, E. W. Abel), Pergamon, **1982**, p. 1001 pp.
[168] a) I. U. Khand, C. A. L. Mahaffy, P. L. Pauson, *J. Chem. Res. Miniprint* **1978**, 4454–4455; b) A. N. Nesmeyanov, V. V. Krivykh, P. V. Petrovskii, V. S. Kaganovich, M. I. Rybinskaya, *J. Organomet. Chem.* **1978**, *162*, 323–342.
[169] V. S. Kaganovich, M. I. Rybinskaya, *Izv. Akad. Nauk SSSR Ser. Khim.* **1985**, 1644–1647; *Bull. Akad. Sci USSR Dir. Chem. Sci.* **1985**, 1503–1506.
[170] C. Elschenbroich, J. Schneider, M. Wünsch, J.-L. Pierre, P. Baret, P. Chautemps, *Chem. Ber.* **1988**, *121*, 177–183.
[171] N. E. Kolobova, L. V. Goncharenko, *Izv. Akad. Nauk. SSSR Ser. Khim.* **1979**, 900; T. E. Bitterwolf, *Polym. Mater. Sci. Eng.* **1983**, *49*, 368.
[172] See for example H. Werner, A. Salzer, *Synth. Inorg. Met. Org. Chem.* **1972**, *2*, 239–248; A. Salzer, H. Werner, *Angew. Chem.* **1972**, *84*, 949–950; *Angew. Chem. Int. Ed. Engl.* **1972**, *11*, 930–931; A. Salzer, T. Egolf, W. von Philipsborn, *J. Organomet. Chem.* **1981**, *221*, 351–360; W. Siebert, *Pure Appl. Chem.* **1988**, *60*, 1345–1348; V. Bockelheide, *ibid.* **1986**, *58*, 1–6; M. N. Boschkarer, I. L. Fedushkin, V. K. Cherkasov, H. Schumann, F. H. Görlitz, *Inorg. Chim. Acta* **1992**, *201*, 69–74.
[173] W. H. Morrison, Jr., E. Y. Ho, D. N. Hendricksen, *J. Am. Chem. Soc.* **1974**, *96*, 3603–3608.
[174] a) P. J. Fagan, M. D. Ward, J. C. Calabrese, *J. Am. Chem. Soc.* **1989**, *111*, 1698–1719; b) S. P. Nolan, K. L. Martin, E. D. Stevens, P. J. Fagan, *Organometallics* **1992**, *11*, 3947–3953.
[175] U. Kölle, M. H. Wang, *Organometallics* **1990**, *9*, 195–198.
[176] X. D. He, B. Chaudret, F. Dahan, Y.-S. Huang, *Organometallics* **1991**, *10*, 970–979.
[177] I. Chavez, M. Otero, E. Román, U. Müller, *J. Organomet. Chem.* **1992**, *427*, 369–378.
[178] a) A. R. Kudinov, P. V. Petrovskii, Y. T. Struchkov, A. I. Yanovskii, M. I. Rybinskaya, *J. Organomet. Chem.* **1991**, *421*, 91–115; b) A. Lenz, W. Beck, unpublished results.
[179] H. Wadepohl, W. Galm, H. Pritzkow, *Angew. Chem.* **1989**, *101*, 357–358; *Angew. Chem. Int. Ed. Engl.* **1989**, *28*, 345–347; H. Wadepohl, H. Pritzkow, *ibid.* **1987**, *99*, 132–134 and **1987**, *26*, 127.
[180] H. Wadepohl, W. Galm, H. Pritzkow, *Angew. Chem.* **1990**, *102*, 701–703; *Angew. Chem. Int. Ed. Engl.* **1990**, *29*, 686.
[181] H. W. Bosch, H.-U. Hund, D. Nietlispach, A. Salzer, *Organometallics* **1992**, *11*, 2087–2098.
[182] Review: P. A. McGovern, K. P. Vollhardt, *Synlett* **1990**, 493–500.
[183] M. R. Gregg, J. Powell, J. F. Sawyer, *J. Organomet. Chem.* **1988**, *352*, 357–366.
[184] C. G. Kreiter, W. Lipps, *Chem. Ber.* **1982**, *115*, 973–988; K.-H. Franzreb, C. G. Kreiter, *Z. Naturforsch. B* **1982**, *37*, 1058–1069; M. Leyendecker, C. G. Kreiter, *J. Organomet. Chem.* **1984**, *260*, C67–C70; C. G. Kreiter, M. Leyendecker, *ibid.* **1985**, *292*, C18–C20; C. G. Kreiter, M. Leyendecker, W. S. Sheldrick, *ibid.* **1986**, *302*, 35–46; *ibid.* **1986**, *302*, 217–234; C. G. Kreiter, W. Michels, R. Exner, *Z. Naturforsch. B* **1990**, *45*, 793–802.
[185] C. G. Kreiter, E. Michels, J. Kaub, *J. Organomet. Chem.* **1986**, *312*, 221–240; C. G. Kreiter, E. Michels, *ibid.* **1986**, *312*, 59–66.
[186] A. N. Nesmeyanow, M. I. Rybinskaya, L. V. Rybin, V. S. Kaganovich, *J. Organomet. Chem.* **1973**, 47, 1–32. Many early examples of dinuclear complexes with hydrocarbon bridges are listed in this article.
[187] a) P. Steil, W. Beck, F. G. A. Stone, *J. Organomet. Chem.* **1989**, *368*, 77–81; b) D. L. Lawrence, T. W. Bodnar, A. R. Cutler, *J. Organomet. Chem.* **1993**, *448*, 139–149.
[188] See for example C. P. Casey, P. C. Vosejpka, *Organometallics* **1988**, *7*, 934–936; I. Moldes, J. Ros, R. Mathieu, X. Solans, M. Font-Bardia, *J. Chem. Soc. Dalton Trans.* **1987**, 1619–1622; M. Rashidi, R. J. Puddephatt, *Organometallics* **1988**, *7*, 1636–1641; H. Suzuki, H. Omori, Y. Moro-Oka, *ibid.* **1988**, *7*, 2579–2581; S. A. R. Knox, *Pure Appl. Chem.* **1984**, *56*, 81–89.
[189] See for example G. Erker, K. Kropp, J. L. Atwood, W. E. Hunter, *Organometallics* **1983**, *2*, 1555–1561.
[190] H. Werner, R. Weinand, W. Knaup, K. Peters, H. G. von Schnering, *Organometallics* **1991**, *10*, 3967–3977.
[191] a) H. Werner, J. Wolf, G. Müller, C. Krüger, *J. Organomet. Chem.* **1988**, *342*, 381–398; b) H. Werner, T. Rappert, J. Wolf, *Isr. J. Chem.* **1990**, *30*, 377–384.
[192] A. Wojcicki, C. E. Shuchart, *Coord. Chem. Rev.* **1990**, *105*, 35–60; A. Wojcicki, *J. Cluster Sci.*, in press; C. E. Shuchart, G. H. Young, A. Wojcicki, M. Calligaris, G. Nardin, *Organometallics* **1990**, *9*, 2417–2420; G. H. Young, M. V. Raphael, A. Wojcicki, M. Calligaris, G. Nardin, N. Bresciani-Pahor, *ibid.* **1991**, *10*, 1934–1945; C. E. Schuchart, R. R. Willis, A. Wojcicki, *J. Organomet. Chem.* **1992**, *424*, 185–198, and references therein.
[193] a) C. E. Housecroft, B. F. G. Johnson, M. S. Khan, J. Lewis, P.R. Raithby, M. E. Robson, D. A. Wilkinson, *J. Chem. Soc. Dalton Trans.* **1992**, 3171–3178; Y. Rubin, C. B. Knobler, F. Diederich, *J. Am. Chem. Soc.* **1990**, *112*, 4966–4968; Y. Ito, M. Inouye, M. Murakami, M. Shiro, *J. Organomet. Chem.* **1990**, *385*, 399–408; b) A. Wienand, H.-U. Reissig, H. Fischer, D. Pflumm, C. Troll, *J. Organomet. Chem.* **1992**, *427*, C9–C14; L. Jordi, J. M. Moretó, S. Ricart, J. M. Vinas, M. Mejias, E. Molins, *Organometallics* **1992**, *11*, 3507–3510.
[194] C. Cordier, M. Gruselle, J. Vaisermann, L. L. Troitskaya, V. I. Bakhmutov, V. I. Solokov, G. Jaouen, *Organometallics* **1992**, *11*, 3825–3832.
[195] A. J. Carty, *Pure Appl. Chem.* **1982**, *54*, 113–130; A. J. Carty, A. A.

Cherkas, L. Randall, *Polyhedron* **1988**, *7*, 1045–1052, and references therein; R. Nast, *Coord. Chem. Rev.* **1982**, *47*, 89–124; E. Sappa, A. Tiripicchio, P. Braunstein, *Chem. Rev.* **1983**, *83*, 203–239; O. M. Abu Salah, M. I. Bruce, *J. Chem. Soc. Dalton Trans.* **1974**, 2302–2304; M. Ciriano, J. A. K. Howard, J. L. Spencer, F. G. A. Stone, H. Wadepohl, *ibid.* **1979**, 1749–1756; N. E. Kolobova, V. V. Skripkin, T. V. Rozantseva, Y. T. Struchkov, G. G. Aleksandrov, V. G. Andrianov, *J. Organomet. Chem.* **1981**, *218*, 351–359; A. T. Hutton, B. Shebanzadeh, B. L. Shaw, *J. Chem. Soc. Chem. Commun.* **1984**, 549–551; A. T. Hutton, C. R. Langrick, D. M. McEwan, P. G. Pringle, B. L. Shaw, *J. Chem. Soc. Dalton Trans.* **1985**, 2121–2130; S. P. Deraniyagala, K. R. Grundy, *Organometallics* **1985**, *4*, 424–426; M. Cowie, S. J. Loeb, *ibid.* **1985**, 852–857; G. A. Carriedo, D. Miguel, V. Riera, X. Solans, M. Font-Altaba, M. Coll, *J. Organomet. Chem.* **1986**, *299*, C43–C46; D. Seyferth, J. B. Hoke, D. R. Wheeler, *ibid.* **1988**, *341*, 421–437; G. Erker, W. Frömberg, R. Benn, R. Mynott, K. Angermund, C. Krüger, *Organometallics* **1989**, *8*, 911–920; P. N. V. P. Kumar, E. D. Jemmis, *J. Am. Chem. Soc.* **1988**, *110*, 125–131.

[196] W. Beck, K. Sünkel, *Chem. Rev.* **1988**, *88*, 1405–1421.

[197] a) M. Appel, J. Heidrich, W. Beck, *Chem. Ber.* **1987**, *120*, 1087–1089; b) P. M. Fritz, K. Polborn, M. Steimann, W. Beck, *ibid.* **1989**, *122*, 889–891.

[198] K. G. Frank, J. P. Selegue, *J. Am. Chem. Soc.* **1990**, *112*, 6414–6416.

[199] a) M. Akita, M. Terada, S. Oyama, Y. Moro-oka, Organometallics **1990**, *9*, 816–825; b) M. Akita, N. Ishii, M. Tanaka, Y. Moro-oka, *ibid.* in press.

[200] a) G. A. Carriedo, D. Miguel, V. Riera, X. Soláns, *J. Chem. Soc. Dalton Trans.* **1987**, 2867–2873; b) H. Lang, M. Herres, L. Zsolnai, W. Imhof, *J. Organomet. Chem.* **1991**, *409*, C7–C11.

[201] a) K. Yasufuku, H. Yamazaki, *Bull. Chem. Soc. Jpn.* **1972**, *45*, 2664; b) H. Lang, W. Imhof, *Chem. Ber.* **1992**, *125*, 1307–1311.

[202] H. Lang, L. Zsolnai, *J. Organomet. Chem.* **1991**, *406*, C5–C8.

[203] M. Ciriano, J. A. K. Howard, J. L. Spencer, F. G. A. Stone, W. Wadepohl, *J. Chem. Soc. Dalton Trans.* **1979**, 1749–1756.

[204] a) J. Forniés, M. A. Gómez-Saso, E. Lalinde, F. Martínez, M. T. Moreno, *Organometallics* **1992**, *11*, 2873–2883; b) J. R. Berenguer, L. R. Falvello, J. Fornies, E. Labinde, M. Tomas, *ibid.* **1993**, *12*, 6–7.

[205] A. T. Hutton, C. R. Langrick, D. M. McEwan, P. G. Pringle, B. L. Shaw, *J. Chem. Soc. Dalton Trans* **1985**, 2121–2130; S. W. Carr, P. G. Pringle, B. L. Shaw, *J. Organomet. Chem.* **1988**, *341*, 543–548.

[206] G. L. Wood, C. B. Knobler, M. F. Hawthorne, *Inorg. Chem.* **1989**, *28*, 382–388; U. Rosenthal, H. Görls, *J. Organomet. Chem.* **1992**, *439*, C36–C41.

[207] J. Müller, M. Tschampel, J. Pickardt, *J. Organomet. Chem.* **1988**, *355*, 513–524.

[208] G. Erker, W. Frömberg, R. Benn, R. Mynott, K. Angermund, C. Krüger, *Organometallics* **1989**, *8*, 911–920; N. Metzler, H. Nöth, *J. Organomet. Chem.*, in press.

[209] J. H. Teuben, H. J. De Liefde Meijer, *J. Organomet. Chem.* **1969**, *17*, 87–93.

[210] D. G. Sekutowski, G. D. Stucky, *J. Am. Chem. Soc.* **1976**, *98*, 1376–1382.

[211] W. J. Evans, R. A. Keyer, J. W. Ziller, *Organometallics* **1990**, *9*, 2628–2631.

[212] T. Cuenca, R. Gómez, P. Gómez-Sal, G. M. Rodriguez, P. Royo, *Organometallics* **1992**, *11*, 1229–1234.

[213] a) E. Lindner, M. Pabel, K. Eichele, *J. Organomet. Chem.* **1990**, *386*, 187–194; b) E. Lindner, M. Pabel, *ibid.* **1991**, *414*, C19–C21.

[214] a) R. B. King, *J. Am. Chem. Soc.* **1963**, *85*, 1922–1926; b) C. P. Casey, *J. Chem. Soc. Chem. Commun.* **1970**, 1220–1221; J.-A. M. Garner, A. Irving, J. R. Moss, *Organometallics* **1990**, *9*, 2836–2840.

[215] R. B. King, D. M. Braitsch, *J. Organomet. Chem.* **1973**, *54*, 9–14.

[216] M. Cooke, N. J. Forrow, S. A. R. Knox, *J. Organomet. Chem.* **1981**, *222*, C21–C24; *J. Chem. Soc. Dalton Trans.* **1983**, 2435–2440.

[217] Y. C. Lin, J. C. Calabrese, S. S. Wreford, *J. Am. Chem. Soc.* **1983**, *105*, 1679–1680.

[218] a) K. P. Finch, J. R. Moss, M. L. Niven, *Inorg. Chim. Acta* **1989**, *166*, 181–188; b) M. R. Domingo, A. Irving, Y.-H. Liao, J. R. Moss, A. Nash, *J. Organomet. Chem.* **1993**, *443*, 233–240; K. P. Finch, J. R. Moss, *ibid.* **1988**, *346*, 253–266; H. B. Friedrich, J. R. Moss, *Adv. Organomet. Chem.* **1991**, *33*, 235–290.

[219] H. Adams, N. A. Bailey, M. J. Winter, *J. Chem. Soc. Dalton Trans.* **1984**, 273–278.

[220] E. Lindner, M. Pabel, R. Fawzi, H. A. Mayer, K. Wurst, *J. Organomet. Chem.* **1992**, *435*, 109–121.

[221] S. F. Mapolie, J. R. Moss, *J. Chem. Soc. Dalton Trans.* **1990**, 299–305.

[222] C. Roger, T.-S. Peng, J. A. Gladysz, *J. Organomet. Chem.* **1992**, *439*, 163–175.

[223] a) T. E. Bauch, W. P. Giering, *J. Organomet. Chem.* **1978**, *144*, 335–349; b) M.-H. Cheng, H.-G. Shu, G.-H. See, S.-M. Peng, R.-S. Liu, *Organometallics* **1993**, *12*, 108–115.

[224] a) H. B. Friedrich, J. R. Moss, B. K. Williamson, *J. Organomet. Chem.* **1990**, *394*, 313–327; b) S. J. Archer, K. P. Finch, H. B. Friedrich, J. R. Moss, *Inorg. Chim. Acta* **1991**, *182*, 145–152; c) I. Ahmed, J. U. Ahmed, M. M. Karim, S. I. Sarder, S. S. Ullah, *Indian J. Chem.* **1992**, *31A*, 699–701.

[225] a) E. Lindner, E. Schauss, W. Hiller, R. Fawzi, *Angew. Chem.* **1984**, *96*, 727–728; *Angew. Chem. Int. Ed. Engl.* **1984**, *23*, 711; b) E. Lindner, E. Schauss, W. Hiller, R. Fawzi, *Chem. Ber.* **1985**, *118*, 3915–3931.

[226] E. Lindner, W. Wassing, *Organometallics* **1991**, *10*, 1640–1642.

[227] a) E. Lindner, R.-M. Jansen, H. A. Mayer, *Angew. Chem.* **1986**, *98*, 1000–1001; *Angew. Chem. Int. Ed. Engl.* **1986**, *25*, 1008; E. Lindner, R.-M. Jansen, H. A. Mayer, W. Hiller, R. Fawzi, *Organometallics* **1989**, *8*, 2355–2360; b) E. Lindner, R.-M. Jansen, W. Hiller, R. Fawzi, *Chem. Ber.* **1989**, *122*, 1403–1409.

[228] R. T. Hembre, C. P. Scott, J. R. Norton, *J. Am. Chem. Soc.* **1987**, *109*, 3468–3470.

[229] E. Lindner, *Adv. Heterocycl. Chem.* **1986**, *39*, 237–279; J. Takats, *J. Cluster Sci.*, in press.

[230] F. A. Cotton, P. A. Kibala, *Inorg. Chem.* **1990**, *29*, 3192–3196.

[231] a) C. J. Burns, R. A. Andersen, *J. Am. Chem. Soc.* **1987**, *109*, 915–917; b) W. J. Evans, T. A. Ulibarri, J. W. Ziller, *ibid.* **1990**, *112*, 219–223.

[232] a) H. Sinn, W. Kaminsky, *Adv. Organomet. Chem.* **1980**, *18*, 99–149; b) W. Kaminsky, J. Kopf, H. Sinn, H.-J. Vollmer, *Angew. Chem.* **1976**, *88*, 688–693; *Angew. Chem. Int. Ed. Engl.* **1976**, *15*, 629.

[233] a) J. E. Bercaw, J. R. Moss, *Organometallics* **1992**, *11*, 639–645; K. P. Finch, M. A. Gafoor, S. F. Mapolie, J. R. Moss, *Polyhedron* **1991**, *10*, 963–972; b) J. R. Moss, L. G. Scott, *J. Organomet. Chem.* **1989**, *363*, 351–370.

[234] M. Kobayashi, J. D. Wuest, *Organometallics* **1989**, *8*, 2843–2850.

[235] R. B. King, A. Efraty, W. C. Zipperer, *J. Organomet. Chem.* **1972**, *38*, 121–124.

[236] a) M. Schweiger, Dissertation, Universität München, **1988**, W. Beck, M. J. Schweiger, G. Müller, *Chem. Ber.* **1987**, *120*, 889–893; R. Gompper, E. Kottmair, *Z. Naturforsch. B* **1990**, *45*, 833–847; b) E. Lindner, M. Pabel, R. Fawzi, M. Steimann, *J. Organomet. Chem.* **1992**, *441*, 63–74, and references therein; c) R. P. Hughes, R. T. Carl, S. J. Doig, R. C. Hemond, D. E. Samkoff, W. L. Smith, L. C. Stewart, R. E. Davis, K. D. Holland, P. Dickens, R. P. Kashyap, *Organometallics* **1990**, *9*, 2732–2745; R. P. Hughes, S. J. Doig, R. C. Hemond, W. L. Smith, R. E. Davis, S. M. Gadol, K. D. Holland, *ibid.* **1990**, *9*, 2745–2753.

[237] M. Akita, A. Kondoh, T. Kazvahara, T. Takagi, Y. Moro-oka, *Organometallics* **1988**, *7*, 366–374; M. Akita, T. Kawahara, M. Terada, N. Kakinuma, Y. Moro-oka, *ibid.* **1989**, *8*, 687–693; M. Akita, A. Kondoh, Y. Moro-oka, *J. Chem. Soc. Dalton Trans.* **1989**, 1627–1630; M. Akita, H. Andoh, O. Mitani, T. Oku, Y. Moro-oka, *J. Mol. Cat.* **1989**, *56*, 107–116.

[238] W. Schulze, H. Hartl, K. Seppelt, *Angew. Chem.* **1986**, *98*, 189; *Angew. Chem. Int. Ed. Engl.* **1986**, *25*, 185.

[239] D. Lentz, D. Preugschat, *Angew. Chem.* **1990**, *102*, 308–310; *Angew. Chem. Int. Ed. Engl.* **1990**, *29*, 315.

[240] V. Weinrich, W. Beck, unpublished results.

[241] S. F. Mapolie, J. R. Moss, *Polyhedron* **1991**, *10*, 717–723.

[242] a) A. D. Hunter, A. B. Szigety, *Organometallics* **1989**, *8*, 2670–2679; b) A. D. Hunter, *ibid.* **1989**, *8*, 1118–1120; A. D. Hunter, J. L. McLernon, *ibid.* **1989**, *8*, 2679–2688, and references therein; R. Chukwu, A. D. Hunter, B. D. Santarsiero, *ibid.* **1991**, *10*, 2141–2152; R. Chukwu, A. D. Hunter, B. D. Santarsiero, S. G. Bott, J. L. Atwood, J. Chassaignac, *ibid.* **1992**, *11*, 589–597; c) A. D. Hunter, D. Ristic-Petrovic, J. L. McLernon, *ibid.* **1992**, *11*, 864–871; g) G. B. Richter-Addo, A. D. Hunter, *Inorg. Chem.* **1989**, *28*, 4063–4065.

[243] E. J. M. de Boer, J. de With, N. Meijboom, A. G. Orpen, *Organometallics* **1985**, *4*, 259–264.

[244] M.-T. Lee, B. M. Foxman, M. Rosenblum, *Organometallics* **1985**, *4*, 539–547; H. M. Nugent, M. Rosenblum, *J. Am. Chem. Soc.* **1993**, *115*, 3848–3849, and references therein.

[245] H. Werner, *Inorg. Chim. Acta* **1992**, *198–200*, 715–721; H. Werner, M. Treiber, A. Nessel, F. Linnert, P. Betz, C. Krüger, *Chem. Ber.* **1992**, *125*, 337–346.

[246] W. Weng, K. Kunze, A. M. Arif, R. D. Ernst, *Organometallics.* **1991**, *10*, 3643–3647.

[247] P. D. Beer, O. Kocian, R. J. Mortimer, *J. Chem. Soc. Dalton Trans.* **1990**, 3283–3288.

[248] a) C. J. Curtis, R. C. Haltiwanger, *Organometallics* **1991**, *10*, 3220–3226; b) M. D. Rausch, W. C. Spink, B. G. Conway, R. D. Rogers, J. L. Atwood, *J. Organomet. Chem.* **1990**, *383*, 227–252; c) P. Jutzi, J. Schnittger, B. Neumann, H.-G. Stammler, ibid. **1991**, *410*, C13–C19.

[249] U. T. Mueller-Westerhoff, *Angew. Chem.* **1986**, *98*, 700–716; *Angew. Chem. Int. Ed. Engl.* **1986**, *25*, 702; L. M. Alvaro, T. Cuenca, J. C. Flores, P. Royo, M. A. Pellinghelli, *Organometallics* **1992**, *11*, 3301–3306; T. J. Haas, U. T. Müller-Westerhoff, *Synth. React. Inorg. Met. Org. Chem.* **1991**, *22*, 227–245.

[250] A. P. Kahn, D. A. Newman, K. P. C. Vollhardt, *Synlett* **1990**, 141–142.

[251] H. Plenio, *Organometallics* **1992**, *11*, 1856–1859.

[252] H. Schottenberger, G. Ingram, D. Obendorf, R. Tessadri, *Synlett* **1991**, 905–907.

[253] R. Boese, R. L. Myrabo, D. A. Newman, K. P. C. Vollhardt, *Angew. Chem.* **1990**, *102*, 589–592; *Angew. Chem. Int. Ed. Engl.* **1990**, *29*, 549.

[254] D. Astruc, *Acc. Chem. Res.* **1986**, *19*, 377–383; D. Astruc, *Comments Inorg. Chem.* **1987**, *6*, 61.

[255] a) D. Astruc, *Tetrahedron* **1983**, *39*, 4027–4095; *Chem. Rev.* **1988**, *88*, 1189–1216; M. Lacoste, D. Astruc, M.-T. Garland, F. Varret, *Organometallics* **1988**, *7*, 2253–2255; M.-H. Desbois, D. Astruc, J. Guillin, F. Varret, A. X. Trautwein, G. Villeneuve, *J. Am. Chem. Soc.* **1989**, *111*, 5800–5809; M. Lacoste, H. Rabaa, D. Astruc, N. Ardoin, F. Varret, J.-Y. Saillard, A. Le Beuze, *ibid.* **1990**, *112*, 9548–9557; D. Astruc, M. Lacoste, L. Toupet, *J. Chem. Soc. Chem. Commun.* **1990**, 558–561; M.-H. Delville-Desbois, D. S. Brown, K. P. C. Vollhardt, D. Astruc, *J. Chem. Soc. Chem. Commun.* **1991**, 1355–1357; M.-H. Delville, M. Lacoste, D. Astruc, *J. Am. Chem. Soc.* **1992**, *114*, 8310–8311; S. Rittinger, D. Buchholz, M.-H. Delville-Desbois, J. Linarès, F. Varret, R. Boese, L. Zsolnai, G. Huttner, D. Astruc, *Organometallics* **1992**, *11*, 1454–1456; b) M. H. Delville, S. Rittinger, D. Astruc, *J. Chem. Soc. Chem. Commun.* **1992**, 519–520.

[256] P. Hudeczek, F. H. Köhler, *Organometallics* **1992**, *11*, 1773–1775.

[257] T.-Y. Dong, C.-C. Schei, M.-Y. Hwang, T.-Y. Lee, *J. Organomet. Chem.* **1991**, *410*, C39-C43. Review: W. E. Geiger, N. G. Connelly, *Adv. Organomet.* **1984**, *24*, 87–130.

[258] D. Obendorf, H. Schottenberger, C. Rieker, *Organometallics* **1991**, *10*, 1293–1297.

[259] a) E. E. Bunnel, L. Valle, N. L. Jones, P. J. Carroll, C. Barra, M. Gonzalez, N. Munoz, G. Visconti, A. Aizman, J. M. Manriguez, *J. Am. Chem. Soc.* **1988**, *110*, 6596–6598; b) W. L. Bell, C. J. Curtis, C. W. Eigenbrot, Jr., C. G. Pierpont, J. L. Robbins, J. C. Smart, *Organometallics* **1987**, *6*, 266–273; c) N. Maigrot, L. Richard, C. Charrier, F. Mathey, *Angew. Chem.* **1992**, *104*, 1082–1084; *Angew. Chem. Int. Ed. Engl.* **1992**, *31*, 1031–1032.

[260] a) A. Scholz, A. Smola, J. Scholz, J. Loebel, H. Schumann, K.-H. Thiel, *Angew. Chem.* **1991**, *103*, 444–445; *Angew. Chem. Int. Ed. Engl.* **1991**, *30*, 435; b) F. Bickelhaupt, *Angew. Chem.* **1987**, *99*, 1020–1035; *Angew. Chem. Int. Ed. Engl.* **1987**, *26*, 990.

[261] a) H. Ogoshi, J. Setsume, Z. Yoshida, *J. Am. Chem. Soc.* **1977**, *99*, 3869–3870; b) K. J. Del Rossi, B. B. Wayland, *J. Chem. Soc. Chem. Commun.* **1986**, 1653–1655; c) R. S. Paonessa, N. C. Thomas, J. Halpern, *J. Am. Chem. Soc.* **1985**, *107*, 4333–4335.

[262] B. B. Wayland, Y. Feng, S. Ba, *Organometallics* **1989**, *8*, 1438–1441.

[263] N. Rajapakse, B. R. James, D. Dolphin, *Can. J. Chem.* **1990**, *68*, 2274–2277.

[264] a) W. P. Griffith, G. Wilkinson, *J. Chem. Soc.* **1959**, 1629–1630; M. E. Kimball, J. P. Martella, W. C. Kaska, *Inorg. Chem.* **1967**, *6*, 414–416; b) P. S. Santos, K. Kawai, O. Sala, *Inorg. Chim. Acta* **1977**, *22*, 155–159; K. D. Grande, A. J. Kunin, L. S. Stuhl, B. M. Foxman, *Inorg. Chem.* **1983**, *22*, 1791–1794.

[265] a) See for example D. M. Hoffman, R. Hoffmann, *Organometallics* **1982**, *1*, 1299–1302; J. T. Mague, *Polyhedron* **1992**, *11*, 677–686; *Organometallics* **1986**, *5*, 918–926; R. W. Hilts, R. A. Franchuk, M. Cowie, *ibid.* **1991**, *10*, 304–316; M. Rashidi, G. Schoettel, J. J. Vittal, R. J. Puddephatt, *ibid.* **1992**, *11*, 2224–2228; b) M. R. Gagné, J. Takats, *ibid.* **1988**, 561–563; M. J. Burn, G. Yu, Kiel, F. Seils, J. Takats, J. Washington, *J. Am. Chem. Soc.* **1989**, *111*, 6850–6852.

[266] a) B. L. Booth, R. N. Haszeldine, P. R. Mitchell, J. J. Cox, *J. Chem. Soc. Chem. Commun.* **1967**, 529–530; b) J. J. Bonnet, R. Mathieu, R. Poilblanc, J. A. Ibers, *J. Am. Chem. Soc.* **1979**, *101*, 7487–7496.

[267] M. Green, A. Laguna, J. L. Spencer, F. G. A. Stone, *J. Chem. Soc. Dalton Trans.* **1977**, 1010–1016.

[268] R. D. Adams, L. Cheng, W. Wu, *Organometallics* **1992**, *11*, 3505–3507.

[269] a) C. M. Mitchel, F. G. A. Stone, *J. Chem. Soc. Chem. Commun.* **1970**, 1263–1264; b) J. A. J. Jarvis, A. Johnson, R. J. Puddephatt, *ibid.* **1973**, 373–374; A. Johnson, R. J. Puddephatt, J. L. Quirk, *J. Chem. Soc. Dalton Trans.* **1978**, 980–985.

[270] H. Ogawa, T. Joh, S. Takahashi, *J. Chem. Soc. Chem. Commun.* **1988**, 561–562.

[271] M. Herberhold, M. Biersack, *J. Organomet. Chem.* **1990**, *381*, 379–389; *ibid.* **1993**, *443*, 1–8; M. Herberhold, H.-D. Brendel, U. Thewalt, *Angew. Chem.* **1991**, *103*, 1664–1665; *Angew. Chem. Int. Ed. Engl.* **1991**, *30*, 1652–1654.

[272] G. Kreisel, P. Scholz, W. Seidel, *Z. Anorg. Allg. Chem.* **1980**, *460*, 51–55.

[273] N. A. Ustynyuk, V. N. Vinogradova, D. N. Kravtsov, Y. F. Orunenko, V. A. Piren, *Organomet. Chem. USSR* **1988**, *1*, 488.

[274] R. J. Cross, M. F. Davidson, A. J. McLennan, *J. Organomet. Chem.* **1984**, *265*, C37–C39; R. J. Cross, M. F. Davidson, *J. Chem. Soc. Dalton Trans.* **1986**, 411–414.

[275] H. Ogawa, T. Joh, S. Takahashi, K. Sonogashira, *J. Chem. Soc. Chem. Commun.* **1985**, 1220–1221; H. Ogawa, K. Onitsuka, T. Joh, S. Takahashi, Y. Yamamoto, H. Yamazaki, *Organometallics* **1988**, *7*, 2257–2260.

[276] a) W. Beck, B. Niemer, J. Breimair, J. Heidrich, *J. Organomet. Chem.* **1989**, *372*, 79–83; b) J. Heidrich, M. Steimann, M. Appel, W. Beck, J. R. Phillips, W. C. Trogler, *Organometallics* **1990**, *9*, 1296–1300.

[277] M. Akita, M. Terada, S. Oyama, S. Sugimoto, Y. Moro-oka, *Organometallics* **1991**, *10*, 1561–1568.

[278] a) R. M. Bullock, F. R. Lemke, D. J. Szalda, *J. Am. Chem. Soc.* **1990**, *112*, 3244–3245; b) F. R. Lemke, D. J. Szalda, R. M. Bullock, *ibid.* **1991**, *113*, 8466–8477.

[279] M. St. Clair, W. P. Schaefer, J. E. Bercaw, *Organometallics* **1991**, *10*, 525–527.

[280] N. A. Ustynyuk, U. N. Vinogradova, D. N. Kravtsov, *Organomet. Chem. USSR* **1988**, *1*, 45.

[281] J. A. Davies, M. El-Ghanam, A. A. Pinkerton, D. A. Smith, *J. Organomet. Chem.* **1991**, *409*, 367–376.

[282] A. Ramsden, W. Weng, A. M. Arif, J. A. Gladysz, *J. Am. Chem. Soc.* **1992**, *114*, 5890; J. A. Ramsden, W. Weng, J. A. Gladysz, *Organometallics* **1992**, *11*, 3635–3645.

[283] a) R. Nast, U. Kirner, *Z. Anorg. Allg. Chem.* **1964**, *330*, 311–316; b) R. Nast, P. Schneller, A. Hengefeld, *J. Organomet. Chem.* **1981**, *214*, 273–276.

[284] K. Sünkel, Universität München, personal communication.

[285] M.-C. Chen, Y.-J. Tsai, C.-T. Chen, Y.-C. Lin, T.-W. Tseng, G.-H. Lee, Y. Wang, *Organometallics* **1991**, *10*, 378–380.

[286] P. Binger, P. Müller, P. Philipps, B. Gabor, R. Mynott, A. T. Herrmann, F. Langhauser, C. Krüger, *Chem. Ber.* **1992**, *125*, 2209–2212.

[287] G. A. Koutsantonis, J. P. Selegue, *J. Am. Chem. Soc.* **1991**, *113*, 2316–2317.

[288] D. R. Neithammer, R. E. LaPointe, R. A. Wheeler, D. S. Richeson, G. D. Van Duyne, P. T. Wolczanski, *J. Am. Chem. Soc.* **1989**, *111*, 9056–9072.

[289] a) M. L. Listemann, R. R. Schrock, *Organometallics* **1985**, *4*, 74–83; b) K. G. Caulton, R. H. Cayton, M. H. Chisholm, J. C. Huffman, E. B. Lobkovsky, Z. Xue, *ibid.* **1992**, *11*, 321–326; c) T. M. Gilbert, R. D. Roger, *J. Organomet. Chem.* **1991**, *421*, C1–C5; d) M. H. Chisholm, K. Folting, J. C. Huffman, E. A. Lucas, *Organometallics* **1991**, *10*, 535–537.

[290] a) D. M. Hoffmann, R. Hoffmann, C. R. Fisel, *J. Am. Chem. Soc.* **1982**, *104*, 3858–3875; P. R. Raithby, M. J. Rosales, *Adv. Inorg. Radiochem.* **1985**, *29*, 169–247; E. Sappa, A. Tiripicchio, P. Braunstein, *Chem. Rev.* **1983**, *83*, 203–239; b) D.-K. Hwang, Y. Chi, S.-M. Peng, G.-H. Lee, *Organometallics* **1990**, *9*, 2709–2718; Y. Chi, H.-Y. Hsu, S.-M. Peng, G.-H. Lee, *J. Chem. Soc. Chem. Commun.* **1991**, 1023–1025, and references therein in [243]; c) G. Erker, W. Frömberg, K. Angermund, R. Schlund, C. Krüger, *ibid.* **1986**, 372–374; d) C. P. Casey, F. R. Askham, L. M. Petrovich, *J. Organomet. Chem.* **1990**, *387*, C31–C35.

[291] A. D. Horton, A. G. Orpen, *Angew. Chem.* **1992**, *104*, 912–914; *Angew. Chem. Int. Ed. Engl.* **1992**, *31*, 876–878.

[292] a) T. Weidmann, V. Weinrich, B. Wagner, C. Robl, W. Beck, *Chem. Ber.* **1991**, *124*, 1363–1368; b) G. A. Koutsantonis, J. P. Selegue, J.-G. Wang, *Organometallics* **1992**, *11*, 2704–2708; c) M. Akita, M. Terada, M. Tanaka, Y. Moro-oka, *ibid.* **1992**, *11*, 3468–3472; d) *ibid.* **1992**, *11*, 1825–1830.

[293] F. R. Lemke, D. J. Szalda, R. M. Bullock, *Organometallics* **1992**, *11*, 876–884; F. R. Lemke, R. M. Bullock, *ibid.*, **1992**, *11* 4261–4267.

[294] T. Rappert, O. Nürnberg, H. Werner, *Organometallics*, **1993**, *12*, 1359–1364; H. Werner, *Nachr. Chem. Tech. Lab.* **1992**, *40*, 435–444.

[295] A. Wong, P. C. W. Kang, C. D. Tagge, D. R. Leon, *Organometallics* **1990**, *9*, 1992–1994.

[296] R. Crescenzi, C. L. Sterzo, *Organometallics* **1992**, *11*, 4301–4305.

[297] a) C. J. Cardin, D. J. Cardin, M. F. Lappert, *J. Chem. Soc. Dalton Trans.* **1977**, 767–779; b) A. Sebald, C. Stader, B. Wrackmeyer, *J. Organomet. Chem.* **1986**, *311*, 233–242.

[298] T. Debaerdemaeker, C. Weisemann, H.-A. Brune, *J. Organomet. Chem.* **1988**, *350*, 91–99; R. Hohenadel, H.-A. Brune, *ibid.* **1988**, *350*, 101–108; C. Weisemann, G. Schmidtberg, H.-A. Brune, *ibid.* **1989**, *365*, 403–412; *ibid.* **1989**, *362*, 63–76; H.-A. Brune, R. Hohenadel, G. Schmidtberg, U. Ziegler, *ibid.* **1991**, *402*, 179–199.

[299] S. Kotani, K. Shiina, K. Sonogashira, *J. Organomet. Chem.* **1992**, *429*, 403–413; J. P. Selegue, K. Swarat, University of Kentucky, personal communication.

[300] a) P. J. Stang, C. M. Crittell, *Organometallics* **1990**, *9*, 3191–3193; P. J. Stang, R. Tykwinski, *J. Am. Chem. Soc.* **1992**, *114*, 4411–4412; b) L. D. Field, A. V. George, F. Laschi, E. Y. Malouf, P. Zanello, *J. Organomet. Chem.* **1992**, *435*, 347–356.

[301] G. H. Worth, B. H. Robinson, J. Simpson, *Organometallics* **1992**, *11*, 501–513; S. M. Elder, B. H. Robinson, J. Simpson, *J. Organomet. Chem.* **1990**, *398*, 165–176; B. F. G. Johnson, J. Lewis, P. R. Raithby, D. A. Wilkinson, *ibid.* **1991**, *408*, C9–C12.

[302] S. L. Latesky, J. P. Selegue, *J. Am. Chem. Soc.* **1987**, *109*, 4731–4733.

[303] a) D. Mansuy, J.-P. Lecomte, J.-C. Chottard, J.-F. Bartoli, *Inorg. Chem.* **1981**, *20*, 3119–3121; V. L. Goedken, M. R. Deakin, L. A. Bottomley, *J. Chem. Soc. Chem. Commun.* **1982**, 607–608; D. R. English, D. N. Hendrickson, K. S. Suslick, *Inorg. Chem.* **1983**, *22*, 367–368; b) G. Rossi, V. L. Goedken, C. Ercolani, *J. Chem. Soc. Chem. Commun.* **1988**, 46–47; E. N. Bakshi, C. D. Delfs, K. S. Murray, B. Peters, H. Homborg, *Inorg. Chem.* **1988**, *27*, 4318–4320; C. Ercolani, M. Gardini, V. L. Goedken, G. Pennesi, G. Rossi, U. Russo, P. Zanonato, *ibid.* **1989**, *28*, 3097–3099.

[304] W. Beck, W. Knauer, C. Robl, *Angew. Chem.* **1990**, *102*, 331–333; *Angew. Chem. Int. Ed. Engl.* **1990**, *29*, 293.

[305] a) M. Etienne, P. S. White, J. L. Templeton, *J. Am. Chem. Soc.* **1991**, *113*, 2324–2325; b) G. M. Jamison, A. E. Bruce, P. S. White, J. L. Templeton, *ibid.* **1991**, *113*, 5057–5059; c) G. M. Jamison, P. S. White, D. L. Harris, J. L. Templeton in *Transition Metal Carbyne Complexes* (Ed.: F. R.

Kreissl), Kluwer, Dordrecht, **1993**; d) T. Desmond, F. J. Lalor, G. Ferguson, M. Parvez, *J. Chem. Soc. Chem. Commun.* **1984**, 75–77.

[306] M. Green, J. A. K. Howard, A. P. James, C. M. Nunn, F. G. A. Stone, *J. Chem. Soc. Dalton Trans.* **1986**, 187–197; J. E. Goldberg, D. F. Mullica, E. Sappenfield, F. G. A. Stone, *ibid.* **1992**, 2495, and references therein; F. G. A. Stone, *Adv. Organomet. Chem.* **1990**, *31*, 53–89.

[307] W. Weng, A. A. Arif, J. A. Gladysz, *Angew. Chem.* **1993**, *105*, 937; *Angew. Chem. Int. Ed. Engl.* **1993**, *32*, 891; W. Weng, J. A. Ramsden, A. M. Arif, J. A. Gladysz, *J. Am. Chem. Soc.* **1993**, *115*, 3824–3825.

[308] P. J. Fagan, J. C. Calabrese, B. S. Malone, *Acc. Chem. Res.* **1992**, *25*, 98; P. J. Fagan, J. C. Calabrese, B. S. Malone, *J. Am. Chem. Soc.* **1991**, *113*, 9408–9409.

[309] a) A. L. Balch, J. W. Lee, C. Noll, M. M. Olmstead, *J. Am. Chem. Soc.* **1992**, *114*, 10984–10985; A. L. Balch, J. W. Lee, M. M. Olmstead, *Angew. Chem.* **1992**, *104*, 1400–1402; *Angew. Chem. Int. Ed. Engl.* **1992**, *31*, 1356–1358; b) F. Diederich, Y. Rubin, *ibid.* **1992**, *104*, 1123–1146 and **1992**, *31*, 1101.

[310] a) C. U. Pittman, C. E. Carraher, J. E. Sheats, M. D. Timken, M. Zeldin in *Inorganic and Metal-Containing Polymeric Materials* (Eds.: J. E. Sheats, C. E. Carraher, C. U. Pittman, M. Zeldin, B. Currell), Plenum, New York, **1989**, p. 1; C. U. Pittmann in *Comprehensive Organometallic Chemistry. Vol. 8* (Eds.: G. Wilkinson, F. G. A. Stone, E. W. Abel), Pergamon, **1982**, pp. 553–605; A. K. Saha, M. M. Hossein, *J. Organomet. Chem.* **1993**, *445*, 137–141; V. A. Sergeev, L. I. Vdovina, *Organomet. Chem. USSR* **1989**, *2*(1), 77–82; b) F. S. Arimoto, A. C. Havan, *J. Am. Chem. Soc.* **1955**, *77*, 6295–6297; c) S. Afeworki, P. K. Baker, O. L. Parri, C. D'Silva, *J. Organomet. Chem.* **1992**, *431*, 81–86.

[311] M. H. Chisholm, *Angew. Chem.* **1991**, *103*, 690–691; *Angew. Chem. Int. Ed. Engl.* **1991**, *30*, 673; H. S. Nalua, *Appl. Organomet. Chem.* **1991**, *5*, 349–377; A. M. Giroud-Godquin, P. M. Maitlis, *Angew. Chem.* **1991**, *103*, 370–398; *Angew. Chem. Int. Ed. Engl.* **1991**, *30*, 375–402; G. Frapper, M. Kertesz, *Inorg. Chem.* **1993**, *32*, 732–740, and references therein

[312] a) K. Sonogashira, S. Takahashi, N. Hagihara, *Abstr. 8th Int. Conf. Organomet. Chem.*, Kyoto, Japan, **1977**, 59; b) S. Takahashi, H. Monmoto, E. Murato, S. Kataoka, K. Sorogashira, N. Hagihara, *J. Polym. Sci. Polym. Chem. Ed.* **1982**, *20*, 565; c) T. Kaharu, H. Matsubara, S. Takahashi, *J. Mater. Chem.* **1991**, *1*, 145–146; d) N. Hagaihara, K. Sonogashira, S. Takahashi, *Adv. Polym. Sci.* **1980**, *41*, 149.

[313] a) S. J. Davies, B. F. G. Johnson, M. S. Khan, J. Lewis, *J. Chem. Soc. Chem. Commun.* **1991**, 187–188; b) M. S. Khan, S. J. Davies, A. K. Kakkar, D. Schwartz, B. Lin, B. F. G. Johnson, J. Lewis, *J. Organomet. Chem.* **1992**, *424*, 87–97, and references therein; c) J. Lewis, M. S. Khan, A. K. Kakkar, B. F. G. Johnson, T. B. Marder, H. B. Fyfe, F. Wittmann, R. H. Friend, A. E. Dray, *ibid.* **1992**, *425*, 165–176; d) S. J. Davies, B. F. G. Johnson, J. Lewis, M. S. Khan, *ibid.* **1991**, *401*, C43–C45; e) B. F. G. Johnson, A. K. Kakkar, M. S. Khan, J. Lewis, *ibid.* **1991**, *409*, C12–C14; f) S. J. Davies, B. F. G. Johnson, J. Lewis, P. R. Raithby, *ibid.* **1991**, *414*, C51–C53.

[314] a) M. S. Khan, D. J. Schwartz, N. A. Dasha, A. K. Kakkar, B. Lin, P. R. Raithby, J. Lewis, *Z. Anorg. Allg. Chem.* **1992**, *616*, 121; b) M. E. Wright, *Macromolecules* **1989**, *22*, 3256–3259.

[315] a) K. Onitsuka, H. Ogawa, T. Joh, S. Takahashi, Y. Yamamoto, H. Yamazaki, *J. Chem. Soc. Dalton Trans.* **1991**, 1531–1536; b) Onitsuka, T. Joh, S. Takahashi, *Angew. Chem.* **1992**, *104*, 893–894; *Angew. Chem. Int. Ed. Engl.* **1992**, *31*, 851–852.

[316] H. B. Fyfe, M. Mlekuz, D. Zargarian, N. J. Taylor, T. B. Marder, *J. Chem. Soc. Chem. Commun.* **1991**, 188–190.

[317] M. Hanack, S. Deger, A. Lange, *Coord. Chem. Rev.* **1988**, *83*, 115–136.

[318] a) T. P. Pollagi, J. Manna, T. C. Stoner, S. F. Geib, M. D. Hopkins, in *Transition Metal Carbyne Complexes*, (Ed.: F. R. Kreissl), Kluwer, Dordrecht, **1993**; b) J. Mana, S. J. Geib, M. D. Hopkins, *J. Am. Chem. Soc.* **1992**, *114*, 9199–9200.

[319] a) R. McDonald, K. C. Sturge, A. D. Hunter, L. Shilliday, *Organometallics* **1992**, *11*, 893–900; b) K. C. Sturge, A. D. Hunter, R. McDonald, B. D. Santarsiero, *ibid.* **1992**, *11*, 3056–3062.

[320] M. Herberhold, H.-D. Brendel, O. Nuyken, T. Pöhlmann, *J. Organomet. Chem.* **1991**, *413*, 65–78; P. F. Brandt, T. B. Rauchfuss, *J. Am. Chem. Soc.* **1992**, *114*, 1926.

[321] D. A. Foucher, B.-Z. Tang, I. Manners, *J. Am. Chem. Soc.* **1992**, *114*, 6246–6248.

[322] a) H. Funaki, K. Aramaki, H. Nishihara, *Chem. Lett.* **1992**, 2065–2068; b) S. I. Yaniger, D. J. Rose, N. P. McKenna, E. M. Eyring, *Macromolecules* **1984**, *17*, 2579; c) A. Ohkubo, K. Aramaki, H. Nishihara, *Chem. Lett.* **1993**, 271–274.

[323] a) S. C. Tenhaeff, D. R. Tyler, *Organometallics* **1991**, *10*, 473–482; b) *ibid.* **1991**, *10*, 1116–1123; c) *ibid.* **1992**, *11*, 1466–1473.

[324] C. P. Casey, P. J. Fagan, W. H. Miles, *J. Am. Chem. Soc.* **1982**, *104*, 1134–1136; C. P. Casey, E. A. Austin, Organometallics **1986**, *5*, 584–585; C. P. Casey, M. A. Gohdes, M. W. Meszaros, *ibid.* **1986**, *5*, 196–199; C. P. Casey, M. W. Meszaros, R. E. Colborn, D. M. Roddick, W. H. Miles, M. A. Gohdes, *ibid.* **1986**, *5*, 1879–1886; C. P. Casey, L. K. Woo, P. J. Fagan, R. E. Palermo, B. R. Adams, *ibid.* **1987**, *6*, 447–454; C. P. Casey, L. K. Woo, *J. Organomet. Chem.* **1987**, *328*, 161–168; C. P. Casey, E. A. Austin, A. L. Rheingold, *Organometallics* **1987**, *6*, 2157–2164; C. P. Casey, *Chem. Scr.* **1987**, *27*, 501–503; C. P. Casey, M. S. Konings, S. R. Marder, Y. Takezawa, *J. Organomet. Chem.* **1988**, *358*, 347–361; C. P. Casey, M. S. Konings, S. R. Marder, *ibid.* **1988**, *345*, 125–134; C. P. Casey, M. Crocker, P. C. Vosejpka, A. L. Rheingold, *Organometallics* **1989**, *8*, 278–282; C. P. Casey, P. C. Vosejpka, M. Crocker, *J. Organomet. Chem.* **1990**, *394*, 339–347.

[325] S. A. R. Knox, *Pure Appl. Chem.* **1984**, *56*, 81–89; M. J. Fildes, S. A. R. Knox, A. G. Orpen, M. L. Turner, M. J. Yates, *J. Chem. Soc. Chem. Commun.* **1989**, 1680–1682.

[326] C. P. Casey, M. S. Konings, M. A. Gohdes, M. W. Meszaros, *Organometallics* **1988**, *7*, 2103–2107.

[327] C. P. Casey, S. R. Marder, A. L. Rheingold, *Organometallics* **1985**, *4*, 762–766.

[328] C. P. Casey, M. S. Konings, S. R. Marder, *Polyhedron* **1988**, *7*, 881–902; W. P. Schaefer, J. M. Spotts, S. R. Marder, *Acta Crystallogr. Sect. C* **1992**, *48*, 811–814.

[329] W. P. Fehlhammer, A. Schröder, J. Fuchs, E.-U. Würthwein, *Angew. Chem.* **1992**, *104*, 604–606; *Angew. Chem. Int. Ed. Engl.* **1992**, *31*, 590.

[330] W. A. Herrmann, J. Plank, J. L. Hubbard, G. W. Kriechbaum, W. Kalcher, B. Koumbouris, G. Ihl, A. Schäfer, M. L. Ziegler, H. Pfisterer, C. Pahl, J. L. Atwood, R. D. Rogers, *Z. Naturforsch. B*, **1983**, *38*, 1392–1398.

[331] U. Zenneck, *Angew. Chem.* **1990**, *102*, 171–182; *Angew. Chem. Int. Ed. Engl.* **1990**, *29*, 138.

[332] a) K. C. Ott, R. H. Grubbs, *J. Am. Chem. Soc.* **1981**, *103*, 5922–5923; b) P. B. Mackenzie, K. C. Ott, R. H. Grubbs, *Pure Appl. Chem.* **1984**, *56*, 59–61; J. W. Park, P. B. Mackenzie, W. P. Schaefer, R. H. Grubbs, *J. Am. Chem. Soc.* **1986**, *108*, 6402–6404; F. Ozawa, J. W. Park, P. B. Mackenzie, W. P. Schaefer, L. M. Henling, R. H. Grubbs, *ibid.* **1989**, *111*, 1319–1327; c) M. J. Hostetler, R. G. Bergman, *J. Am. Chem. Soc.* **1990**, *112*, 8621–8623; M. J. Hostetler, M. D. Butts, R. G. Bergman, *Inorg. Chim. Acta* **1992**, *198-200*, 377–392; *J. Am. Chem. Soc.* **1993**, *115*, 2743–2752; d) J. F. Buzinkai, R. R. Schrock, *Inorg. Chem.* **1989**, *28*, 2837–2846.

[333] H. H. Fox, J.-K. Lee, L. Y. Park, R. R. Schrock, *Organometallics* **1993**, *12*, 759–768.

[334] M. D. Fryzuk, W. E. Piers, St. J. Rettig, *J. Am. Chem. Soc.* **1985**, *107*, 8259–8261.

[335] P. Binger, F. Langhauser, B. Gabor, R. Mynott, A. T. Herrmann, C. Krüger, *J. Chem. Soc. Chem. Commun.* **1992**, 505–506.

[336] See F. A. Cotton, *Chem. Eng. News* **1992**, *10*, 4–5.

The Role of Chemistry in the Development of Boron Neutron Capture Therapy of Cancer

By M. Frederick Hawthorne*

Dedicated to Professor Heinrich Nöth on the occasion of his 65th birthday

A therapeutic method that selectively destroys malignant cells in the presence of normal cells is a highly valued goal of oncologists and the possible salvation of cancer patients afflicted with some incurable forms of the disease. Selective cell destruction is, in principle, possible with a binary therapeutic strategy based upon the neutron capture reaction observed with the ^{10}B nucleus and a neutron of low kinetic energy (thermal neutron). This nuclear fission reaction produces both ^{4}He and $^{7}Li^{+}$ nuclei along with about 2.4 MeV of kinetic energy and weak γ-radiation. Since the energetic and cytotoxic product ions travel only about one cell diameter in tissue one may specify the cell type to be destroyed by placing innocent ^{10}B nuclei on or within only the doomed cells. This article describes the current status of chemical research aimed at the eventual adoption of this therapeutic method (boron neutron capture therapy or BNCT). The multidisciplinary nature of this research effort involves chemistry, biology, nuclear physics, medicine, and related specialties. Methods devised for bringing ^{10}B nuclei to tumor cells in therapeutic amounts are correlated with the structure of a generalized cell and the various cellular compartments available for boron localization. The synthesis methods employed for the creation of boron-containing biomolecules and drugs are presented along with representative data concerning their efficacy in tumor localization. The outlook for BNCT is especially bright at this time because of rapid developments in the fields of bioorganometallic chemistry, microbiology, immunology, and nuclear science, to name but a few. Very effective boron delivery vehicles have been demonstrated, and through the interaction of chemistry and biology these species are undergoing further improvement and evaluation of their suitability for BNCT.

1. Introduction

What would result if it were possible to selectively attach a nontoxic species **A** to cancer cells and, upon command, destroy only these malignant cells by converting their cell-bound **A** to a deadly cytotoxin through its activation with a second nontoxic reagent **B**? One would have created a *binary* method for cancer therapy characterized by greater selectivity, efficacy, and safety than the unitary, single agent, radiation and chemotherapy protocols commonly in use today. Most importantly, tumors now beyond any hope of long-term control could be destroyed. The key to this proposed binary therapy is the requirement that the innocent **A** and **B** species have a great propensity for mutual reaction and that the extremely energetic products of this reaction, **X** and **Y**, are confined to an extremely small volume by their very brief lifetimes. However, while **X** and **Y** exist they must function as efficient killers of cells. This binary process is described by the equations of Scheme 1, and an example of such a process, boron neutron capture therapy (BNCT), forms the subject of this article.

A + B $\longrightarrow$ **[AB]** $\longrightarrow$ **X + Y (short-lived cytotoxins)**

B + cell $\not\longrightarrow$

A + cell $\longrightarrow$ **A · cell (interactions specific to cancer cells)**

A · cell + B $\longrightarrow$ **[AB · cell]** $\longrightarrow$ **[(X + Y) · cell] (cell death)**

Scheme 1. A hypothetical binary cytotoxic reaction of two innocent reagents **A** and **B** to form the cell-killing reaction products **X** and **Y**. In BNCT, **A** represents a ^{10}B nucleus selectively emplaced in or on a malignant cell. **B** is a slow neutron, and **X** and **Y** represent high-energy $^{4}He^{2+}$ and $^{7}Li^{3+}$ ions.

[*] Prof. Dr. M. F. Hawthorne
Department of Chemistry and Biochemistry
University of California, Los Angeles
405 Hilgard Avenue, Los Angeles, CA 90024 (USA)

2. Boron Neutron Capture and Therapy

2.1. Historical Account of the Conceptualization of Boron Neutron Capture Theory

The rampant development of quantum mechanics, nuclear physics, and associated chemistry that occurred in the 1930s led James Chadwick[1] to the discovery of the neutron in 1932. Studies of the interactions of neutrons with a variety of materials uncovered the phenomenon of neutron scattering by elastic collisions[2] with atomic nuclei, especially the ubiquitous proton of the H atom. Capture of slow (or thermal) neutrons by certain nuclei was observed by Fermi,[3] and the disintegration of other specific nuclei by interaction with these thermal neutrons was observed by others, as well.[4] By 1935 a great mass of such experimental information had been collected; it was then clear that the ability of an atomic nucleus to capture a neutron was related not to the mass of the target nucleus, but to the actual structure of that nucleus. The concept of a characteristic effective cross-sectional area of a nucleus, expressed as units of 10^{-24} cm^2 (known as barn units), was introduced with this early work. The effective nuclear cross-section of boron for neutron capture was known to be exceptionally large, while boron's neighbors in the periodic table, nitrogen and carbon, exhib-

ited nuclear cross-sections that were comparatively quite small. An important 1935 paper by Taylor[5] described the capture of thermal neutrons by ^{10}B nuclei followed by the production of $^{4}He^{2+}$ (α-particles) and $^{7}Li^{3+}$. About 2 MeV of kinetic energy is distributed between these two heavy ion products. The translational range of the product ions was particularly short:[5] about 7.6 μm in photographic gelatin and 1.1 cm in air. Consequently, the lithium nucleus and the α-particle were short-lived, energetic products capable of doing immense local damage to organic materials through ionization processes. Thus, by 1936 the stage was set for the suggestion of the concept of boron neutron capture therapy (BNCT).

Gordon L. Locher of the Bartol Research Foundation of the Franklin Institute in Philadelphia, Pennsylvania, pointed out[6] in 1936 the potential medical applications of neutrons and boron neutron capture (BNC). His concept invoked the simple neutron capture reaction by boron for the basis of a binary therapeutic method as defined in Scheme 1. Accordingly, Locher's analogues of species **A** and **B** were the ^{10}B nucleus contained in a compound that specifically localizes in tumor and a thermal neutron, respectively. The energetic cytotoxic reaction products **X** and **Y** correspond to the α-particle and the lithium nucleus. The beauty of this proposal is the fact that no radioactive materials are involved and that the therapeutic process may be modulated by controlling the supply of neutrons to the tumor site.

The two necessary components of the boron neutron capture (BNC) process, a controllable source of low-energy neutrons with a usefully high flux and suitable boron compounds for concentration in tumors, were unknown in 1936, and Locher's concept was to remain prophetic until nuclear reactors were available to support an initial experimental test with thermal neutrons. This initial event did not occur until 1954 when Sweet, Farr et al.[7] attacked human brain tumors (glioblastoma multiforme) using ^{10}B-enriched borate as the ^{10}B target species in terminal patients at the Brookhaven National Laboratory (BNL) in cooperation with the Massachusetts General Hospital (MGH). These initial experiments will be discussed in Section 3.1. In these first examples, BNCT was applied to the problem of killing malignant glioma cells that remained at the tumor site following normal surgical procedures.

As expected from its potential medical applications, neutron capture therapy embraces a wide spectrum of scientific disciplines. The research literature pertinent to BNC and BNCT abounds with studies derived from such highly specialized fields as cell biology, nuclear science and engineering, radiation oncology, pathology, pharmacology, immunology, and others, in addition to chemistry. The present article is, however, restricted to topics at the interface of chemistry with these other disciplines, and it is written from the viewpoint of a chemist.

2.2. Rudimentary Aspects of BNCT

The correct description of the boron neutron capture reaction obtained with thermal neutrons (293 K $\triangleq$ 0.025 eV) is given in Scheme 2. The ^{11}B nucleus is incapable of undergoing a BNC reaction, whereas the effective nuclear cross-section of ^{10}B is 3837 barns. Table 1 presents the accepted nuclear cross-sections of the elements having unusually high values, as well as those elements of physiological importance commonly found in tissue. The ^{157}Gd nucleus has been considered as a target for neutron capture therapy due to its very high nuclear cross-section. However, the products of neutron capture are photons and Auger electrons of low energy. If ^{157}Gd can be placed in contact with DNA, double strand breaking may occur upon neutron capture.[8]

$$^{10}B + {}^{1}n_{th} \longrightarrow [^{11}B] \begin{cases} \nearrow {}^{4}He + {}^{7}Li + 2.79\ MeV \quad (6\%) \\ \searrow {}^{4}He + {}^{7}Li + 0.48\ MeV\ \gamma + 2.31\ MeV \quad (94\%) \end{cases}$$

Scheme 2. The two parallel nuclear fission reactions that occur upon capture of a slow (thermal) neutron, n_{th}, by a ^{10}B nucleus.

Two nuclides abundant in tissue (Table 1 A) stand out as participants in important neutron capture side-reactions

M. Frederick Hawthorne was born in 1928 in the state of Kansas. He entered the Missouri School of Mines and Metallurgy as a chemical engineering student in 1944. In 1947 he transfered to Pomona College and obtained his B.A. degree in 1949. In 1953 he completed his Ph.D. under Donald J. Cram at the University of California at Los Angeles (UCLA). After a year of postdoctoral research with George S. Hammond at Iowa State University, he accepted a position with the Rohm and Haas Co. in Huntsville, Alabama, in 1954, where he began his investigations in boron chemistry two years later. He was appointed Professor at the University of California, Riverside, in 1962. In 1969 he took up his present position as Professor of Chemistry (Inorganic) at UCLA. From that year he has been Editor-in-Chief of Inorganic Chemistry. Among his numerous awards are the American Chemical Society Award in Inorganic Chemistry (1973) and the Distinguished Service in the Advancement of Inorganic Chemistry Award (1988). He is a member of the U.S. National Academy of Sciences and the American Academy of Arts and Sciences. He was awarded an Honorary Ph.D. from Uppsala University in 1992 and is currently an Alexander von Humboldt Senior Scientist associated with Professor Nöth in Münich. He is a member of the Executive Committee of the International Society for Neutron Capture Therapy. His major research themes are centered about the use of boron clusters as building blocks in host-guest and supramolecular complexes, in homogeneous catalysis, as components of nanomechanical assemblies, and in the chemistry of BNCT biodelivery systems.

Table 1. Neutron capture cross-sections measured with thermal neutrons and natural isotopic abundances of physiologically important elements (A) and elements that display the greatest cross-sections, including ^{10}B (B) [a].

	Nuclide	Nuclear cross-section [Barn]	Natural abundance [%]
(A)	^{1}H	0.33	99.8
	^{12}C	3.4×10^{-3}	98.9
	^{14}N	1.8	99.6
	^{16}O	1.8×10^{-4}	99.8
	^{23}Na	0.43	100.0
	^{31}P	0.18	100.0
	^{32}S	0.53	95.0
	^{35}Cl	43	76.0
(B)	^{3}He	5.3×10^{3}	1.4×10^{-4}
	^{6}Li	9.4×10^{2}	7.5
	^{10}B	3.8×10^{3}	19.8
	^{113}Cd	2.0×10^{4}	12.2
	^{149}Sm	4.2×10^{4}	13.9
	^{155}Gd	6.1×10^{4}	14.8
	^{157}Gd	2.6×10^{5}	15.7
	^{235}U	5.8×10^{2}	7.2×10^{-1}

[a] Data taken from G. Friedlander, J. W. Kennedy, E. S. Macias, J. M. Miller, *Nuclear and Radiochemistry*, 3rd ed., John Wiley, New York, **1981**.

that occur during BNCT and thus contribute important doses of background radiation to the subject. These two neutron capture reactions play a role, not because of enhanced nuclear cross-sections of the target nuclei, but because of their very high concentrations in tissue. The neutron capture reactions[9b] of these nuclides, ^{1}H and ^{14}N, are detailed in Scheme 3. The passage of a neutron through hydro-

$$^{1}H + {}^{1}n_{th} \longrightarrow [^{2}H] \longrightarrow {}^{2}H + 2.23\ \text{MeV}\ \gamma$$

$$^{14}N + {}^{1}n_{th} \longrightarrow [^{15}N] \longrightarrow 0.63\ \text{MeV}\ p + {}^{14}C$$

Scheme 3. Neutron capture reactions involving ^{1}H and ^{14}N. Capture by ^{1}H releases high-energy γ-photons and a deuteron, whereas capture by ^{14}N yields an energetic proton and ^{14}C.

gen-rich media such as tissue results in the slowing and scattering of these neutrons by collisions with nuclei of the H atoms. Occasionally, a slowly moving neutron will be captured by such a proton to produce a deuteron accompanied by characteristic γ-radiation, which contributes to the total radiation dose. In another competing capture reaction, the nitrogen atoms available in tissue may capture a low-energy neutron and generate ^{14}C and a proton whose kinetic energy is 0.63 MeV. The kinetic energy imparted to the $^{7}Li^{3+}$ and $^{4}He^{2+}$ ions derived from the BNC reaction and that similarly associated with the proton and γ-photons produced as shown in Scheme 3 is transferred to the surrounding media. Since all of these energetic nuclear reaction products with the exception of the γ-photons, are heavy particles, this kinetic energy transfer is rapid and takes place along a very short path length. The rate of linear energy transfer (LET) of these particles is characteristically high; the immense energy of these reactions is therefore dissipated in a very small volume. As an example, the $^{7}Li^{3+}$ and $^{4}He^{2+}$ ions generated in the BNC reaction leave ionization tracks about 0.01 mm long or the equivalent of approximately one cell diameter. Thus, the high LET characteristic of particles produced by nuclear reactions that occur within tissue are especially lethal to affected cells because of the high density of deposited energy. Ideally, those cells that carry large numbers of ^{10}B nuclei are subject to destruction by BNC, while neighboring cells that are free of ^{10}B would be spared save for the contribution of the background $^{1}H(n,\gamma)^{2}H$ and $^{14}N(n,p)^{14}C$ reactions. In order to achieve this desired effect in BNCT, ^{10}B delivery should be as selective as possible to tumor tissue and should avoid normal tissue that will be subject to neutron irradiation. In addition, the actual concentration of ^{10}B in tumor must be sufficiently high to offer a localized binary therapeutic effect well above the background radiation dose delivered by the neutron capture processes of Scheme 3. The minimum ^{10}B concentration necessary for effective BNC has been repeatedly calculated and is generally accepted to be between 10 and 30 μg ^{10}B per g tumor depending upon the precise location of the ^{10}B with respect to vital components of the tumor cell structure. As the position of the ^{10}B nuclei is changed from the external cell wall to the cytoplasm to the nucleus of the cell, the required concentration of ^{10}B for effective BNCT decreases, as expected. Thus, if the ^{10}B is bound to the cell wall, 30 ppm or greater concentrations might be required, while if ^{10}B is localized within the nucleus of the tumor cell, a concentration of only 10 ppm or less might be required. Obviously, an additional factor is the steady state concentration of thermal neutrons in the targeted volume of tissue, since very low neutron intensities require proportionally longer irradiation times to produce the required number of BNC events for effective therapy. The quantification of the effective lethality of product particles or γ-radiation from neutron capture reactions is expressed in terms of their relative biological effectiveness (RBE) relative to γ-radiation. The RBE of particulate species or photons is expressed as the ratio of the energy dose of γ-radiation to the energy delivered by the particles or photons in question that accomplishes equivalent cell-killing or physiological damage to living tissue. While the precise values of RBE characteristic of commonly encountered particles and photons depend somewhat upon the conditions of the measurement, the heavy $^{7}Li^{3+}$ and $^{4}He^{2+}$ ions that arise from BNC have the commonly accepted (conservative) value of about 2.5 when taken together, (per neutron captured), although much higher values have been suggested. Similarly the products of the $^{14}N(n,p)^{14}C$ reaction are assigned an RBE of 2.7. Thermal (0.025 eV) neutrons themselves are relatively harmless (negligible RBE). The $^{1}H(n,\gamma)^{2}H$ reaction mainly contributes the energy of its characteristic γ-radiation (RBE of approximately 1.0) (Scheme 3). In practice, the total effective radiation dose delivered to a volume of tissue containing a fixed concentration of homogeneously distributed ^{10}B would be the sum of the energies delivered by each of the independent $^{1}H(n,\gamma)^{2}H$, $^{14}N(n,p)^{14}C$, and $^{10}B(n,a)^{7}Li$ reactions after multiplication by their respective RBE values. The ^{1}H and ^{14}N capture reactions obviously provide a radiation background upon which is superimposed the ^{10}B concentration-dependent (binary) BNC reaction.

The discussion thus far has centered upon the use of thermal neutrons as the applied neutron source, since their energy is sufficiently low for immediate nuclear capture to occur. However, the scattering of thermal neutrons as they encounter hydrogen atoms in tissue very seriously diminishes their availability at tumor sites located below the tissue surface.

Such deeply buried tumors can be addressed with BNCT by applying more energetic neutrons found in the 0.5 eV–1.0 keV region of the epithermal[10] range. Neutrons of this type are not sufficiently energetic to cause destructive ionization in tissue through hydrogen-recoil processes, but they are effectively slowed by continual encounters with H atoms in the media. These collisions are accompanied by the generation of heat, which is not destructive to tissue. However, as these epithermal neutrons pass through tissue, they will lose sufficient kinetic energy to become thermal neutrons and subject to capture by ^{10}B, ^{14}N, and ^{1}H nuclei. Thus, while directly applied thermal neutrons will give the maximum dose due to capture processes at the point of entry into tissue (zero depth), epithermal neutrons are not sufficiently slowed for effective capture until they have penetrated some distance into tissue.[10] This is the desired condition for noninvasive BNCT of deeply buried tumors.

Fast neutrons ($E > 10$ keV) are capable, through collision, of causing the ionization of hydrogen atoms from hydrogen-containing substrates, and in so doing, they create a severe type of radiation damage (hydrogen-recoil reaction).[11] This process is so biologically disruptive that an RBE as large as 5 has been suggested for fast neutrons.[12b] Fast neutrons are encountered as impurities in epithermal neutron beams, but they may be reduced in population by neutron beam moderation devices[13b] including specific band-pass filters. Whenever fast neutrons are present in a neutron beam used in BNCT, the effective radiation dose supplied by hydrogen recoil must be added to the total background dose supplied by the $^{1}H(n,\gamma)^{2}H$ γ-photons and the $^{14}N(n,p)^{14}C$ protons.

2.3. Neutron Sources for BNCT

2.3.1. Nuclear Reactors

As noted in Section 2.1, BNCT was conceptualized before a viable source of neutrons had been discovered. This restriction was lifted following the initial development of nuclear reactor technology in the 1940s, and Farr and Sweet could conduct the first clinical trials of BNCT with a thermal neutron beam in 1954.[7e] Epithermal beams have replaced thermal beams as the neutron source of choice for the reasons presented in Section 2.2.

It is currently believed that a dose (fluence) of 5×10^{12} epithermal neutrons per cm^2 will be required[14] for successful BNCT if every epithermal neutron is converted to a thermal neutron. To minimize the duration of patient exposure to the neutron source, reactors not less powerful than one megawatt would be required to achieve a clinically useful flux[14] of at least 10^9 neutrons per cm^2 per s. In addition, these epithermal neutron beams must be relatively free of both extraneous γ-photons and fast neutrons ($E > 10$ keV) and collimated to the greatest extent possible. Potentially, these therapeutic flux requirements could be met, in the United States alone, by approximately thirty-five nuclear reactors[15b] which could be modified for BNCT. Among the reactors of this type that have already been specifically dedicated for medical research are the Brookhaven Medical Research Reactor, the MIT (Massachusetts Institute of Technology) Research Reactor, the Georgia Institute of Technology Research Reactor, and the European Collaboration Reactor located at Petten, the Netherlands. The Power Burst Nuclear Reactor Facility located at the Idaho National Engineering Laboratory also has a reactor potentially capable of producing an intense therapeutic neutron beam if it were to be modified for BNCT research and therapy. The potential of epithermal neutron beams for the noninvasive therapy of internal tumors has yet to be fully realized; research efforts now underway promise the availability of such 1–1000 eV neutron beams with intensities of greater than 10^9 neutrons per cm^2 per s. The many interdependent variables that come into play in any actual BNCT experiment are the subject of extensive studies carried out by radiation physicists, radiation biologists, and nuclear reactor specialists, to name but a few. The interested reader is referred to the extensive work on computational modeling of BNCT radiation effects coupled with experimental verification exemplified by the pioneering work of Fairchild et al.[16b] at the Brookhaven National Laboratory, the work of Wheeler and Nigg et al.[17] at the Idaho National Engineering Laboratory, and Harling et al.[18] at MIT.

The fact remains that nuclear reactors are the only sources of thermal and epithermal neutrons available for research and clinical trials today. The limited number of potentially available reactors capable of clinical applications and the immobility of these reactors would limit the general usefulness of BNCT even if efficacious modalities for particular tumor types were developed. Consequently, the search for epithermal neutron beam sources other than nuclear reactors has begun.[19, 20]

2.3.2. Neutron Sources Other Than Nuclear Reactors

The development of BNCT as a generally available therapy depends upon securing a useful, safe, and relatively inexpensive epithermal neutron beam source that can be widely distributed in hospitals and medical centers located in populated urban areas. Research directed to this end is currently in progress.[19–21]

Collision of low energy protons, produced in an accelerator, with a lithuim target will produce epithermal neutrons. To secure epithermal neutrons for BNCT in this manner, proton currents would necessarily be high, and lithium target cooling problems would be severe. In addition, the high energy neutrons produced would require thermal moderation with materials such as D_2O. In an alternative procedure, the bombardment of heavy elements with high energy protons provides an array of neutrons whose energy distribution is generally richer in high energy neutrons than that observed in nuclear fission. These very energetic neutrons may be brought into the desired epithermal region through the use of moderating materials.

The synthetic nuclide, californium-252, is the only practical spontaneous neutron-emitter.[14, 22] This isotope has a half-life of 2.65 years. The neutron spectrum produced by ^{252}Cf decay is similar to that produced by a one megawatt nuclear reactor. Since it isotropically emits 2.3×10^6 neutrons per sec per μg, large (gram) quantities of this nuclide would be required to obtain the desired neutron

beam strength following thermal moderation and collimation, etc. The continual synthesis of large quantities of ^{252}Cf to fulfill the world's need of epithermal neutrons for BNCT would be a technically formidable and very expensive task, and, at the same time, would create a new set of international problems in nuclear safety and security.

The available sources of epithermal neutrons for BNCT based on the proton accelerator are now well understood in principle, and remaining problems are in the realm of engineering. Hopefully, these obstacles can be overcome, so that safe, economically viable neutron beams can become established in a variety of clinical settings.

2.4. Modeling BNCT for Clinical Applications

The interaction of the components of a specific neutron beam with the ^{10}B nuclei present in tumor, the normal tissues near the tumor, and the blood raise questions that must be answered before a complete BNCT system can be employed in actual therapy experiments. These questions concern the spatial distribution and effective dose (physical dose in rads × RBE = effective dose in rads or cGys) of each of the component radiation processes that came into play during the experiment and procedural matters such as choosing between a single-dose therapy mode versus the delivery of the required radiation dose in increments[10] (fractionation) with intervening time alotted for repair of radiation damage arising from low LET processes, principally γ-photon interactions. Since epithermal neutron beams are most desired because of their deeper tissue penetration, one must be able to quantify the effective dose contributed by the processes of Scheme 3 (γ-dose and nitrogen capture), fast neutron beam contaminant (H-recoil dose), and the $^{10}B(n,\alpha)^7Li$ capture reactions in both tumor (^{10}B tumor capture) and normal tissues (^{10}B tissue capture) as a function of depth and radial distance from the hypothetical neutron beam centerline.[10, 23] Precision is required in these calculations to avoid the delivery of a total effective dose to normal tissue that surpasses its ability to survive. The total effective dose that can be safely delivered to innocent tissues during tumor therapy limits the total effective dose that may be given to tumor. Blood and the vascularity associated with its distribution within the radiation volume present additional problems, which are now under scrutiny. As a general premise, one wishes to minimize the ^{10}B content of blood during therapy, and a high $^{10}B(tumor)/^{10}B(blood)$ concentration ratio is desired. However, in certain circumstances a tumor/blood concentration ratio for ^{10}B of unity is acceptable.[24] It is beyond the scope of this article to develop the reasons for, and the consequences of, these observations.

In order to approach the generalized problem of quantifying the effective radiation doses delivered to each point in the irradiated volume comprising normal tissues and tumor, use has been made of very refined microdosimetry measurements within phantom tissues during actual neutron beam irradiation. As an example, brain tumors (gliomas) have been popular subjects for study and consequently phantom human (and dog) heads have been constructed from acrylic polymers and provided with instruments for the determination of the effective doses from each of the various radiation sources encountered during neutron beam irradiation.[25] Due to the unique nature of each neutron beam employed, this procedure must be repeated for each beam in order to thoroughly characterize the flux and characteristics of its neutrons as well as the dose rate arising from indigenous γ-photon and fast neutron beam contaminants. After the complete characterization of the neutron beam and its interaction with tissue through the phantom procedure, one then employs these data using Monte Carlo methods for the description of neutron transport.[26] The resulting calculation of the therapeutic performance of defined concentrations of ^{10}B placed at various points within the phantom simulates the selective accretion of ^{10}B by tumor.[27] The concentration of ^{10}B simultaneously delivered to normal tissues within the radiation volume is usually assumed to be a definite fraction of the tumor ^{10}B concentration and to be homogenously distributed. Thus, a boron compound or boronated delivery system that provided a tumor/normal tissue selectivity factor of 10 would be assumed to be homogeneously distributed in normal tissue with a concentration of 2.5 μg ^{10}B per g tissue if the simultaneous tumor concentration were 25 μg ^{10}B per g. The performance of the therapeutic system is time-dependent, since each boron delivery system will have a characteristic biological half-life, and the concentration of ^{10}B in tumor, tissue, and blood will decrease with time.

Figure 1 is a graphical representation of the results of a typical BNCT simulation calculation supported by microdosimetry data obtained with a phantom human head.[28] The epithermal beam employed here is typical of those obtained from large multimegawatt reactors. Fast neutrons are present in the beam giving a significant H-recoil dose, while the beam is relatively free of significant γ-photon contamination. The beam port is 10 cm square. The hypothetical boron delivery system described above is used in the calculations; the concentration of ^{10}B in tumor and in tissue are 25 and 2.5 μg ^{10}B per g, respectively. The boron is assumed to be homogeneously distributed within both tumor and normal tissue. Blood is not treated as a separate tissue, but it is included in the normal tissue category. Recently, sophisticated treatments of expected damage rendered to the epithelial cells of the cranial capillaries due to the presence of ^{10}B in blood have been advanced.[24] The interesting result obtained is that sufficiently small capillaries with diameters similar to the 0.05 mm length of the ^{10}B fission fragment track are spared, because the effective ^{10}B concentration within them is reduced by their geometry and the simultaneous presence of the blood–brain barrier, which prevents the migration of the ^{10}B-containing species to positions behind the capillary endothelial cells. This effect can be incorporated into estimations of effective dose (rads × RBE) to normal tissue by using a reduced value for the RBE of the $^{10}B(n,\alpha)^7Li$ reaction in normal brain tissue that is 0.33 rather than 2.5. The higher value of the RBE was used in the construction of Figure 1, which represents the worst possible case for glioma therapy, but fairly approximates the results to be expected in the therapy of tumors located outside the cranium.

Curve C in Figure 1 (total effective dose rate to tumor) clearly shows a maximum at a depth of 2 cm. Normal tissue would also receive a maximum total effective dose rate near

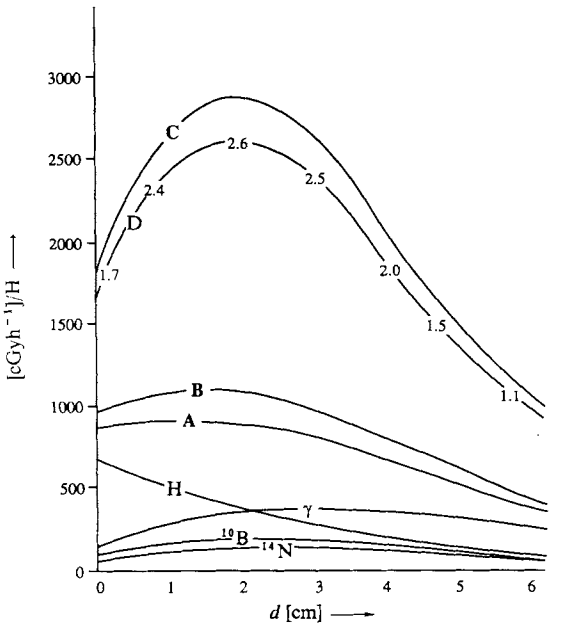

Fig. 1. Graphical display of the relative effective dose rate I of component energy imputs as a function of depth in tissue d, viewed on the centerline of a hypothetical epithermal neutron beam that impinges upon a human head. RBE values employed in these calculations were as follows: $^{10}B(n,\alpha)^7Li$ 2.5, $^{14}N(n,p)^{14}C$ 2.7, H (H-recoil from fast neutron-beam impurity) 5.0, and γ-photons contributed by $^1H(n,\gamma)^2H$, $^{10}B(n,\alpha)^7Li$, and beam impurity photons 1.0. The curves labeled ^{14}N, γ, and H refer to the contributions of the individual processes to the background radiation dose rate as a function of depth in tissue. The curve labeled ^{10}B is the contribution from 2.5 μg of ^{10}B per gram of tissue homogeneously distributed throughout normal tissue. Curve A is the sum of curves ^{14}N, γ, and H, while in curve B the dose rate provided by ^{10}B in normal tissue (Curve ^{10}B) is added. Curve C is the sum of the dose rate provided by 25 μg of ^{10}B per g of tissue homogeneously distributed in tumor and the background dose rate of curve A. The therapeutic gain (curve D) at any depth is obtained by dividing the dose rate of curve C by the maximum of curve B (1100 cGy h^{-1}). See the discussion for details.

2 cm in depth; thus, the total effective dose rate of approximately 1100 cGy h^{-1} in normal tissue would deliver the maximum allowable total effective dose for normal brain of about 1300 cGy (or 13 Gy) in approximately 71 minutes if the ^{10}B concentration remained unchanged throughout this irradiation period. Regardless of the tumor depth, the 71 minute irradiation period and the appropriate total effective dose rate for tumor (Curve C) would determine the total effective dose that could be given to the tumor site. For example, this dose is equal to 2200 cGy $\times$ 71/60 $\approx$ 2600 cGy at a tumor depth of 4 cm, while the corresponding value at 2 cm is 3500 cGy.

The efficacy attained in a particular BNCT experiment is defined as the dimensionless parameter known as therapeutic gain[27c] and defined as the total effective dose rate available to tumor at a specified depth (Curve C) divided by the maximum total effective dose rate delivered to normal tissue (Curve B). Thus the therapeutic gain at a depth of 2 cm is 2900 cGy h^{-1}/1100 cGy h^{-1} $\approx$ 2.6. At a tumor depth of 4 cm this value is 2200/1100 $\approx$ 2.0. In practice, therapeutic gain values less than 1.2, that is, at a depth greater than 5.5 cm in the example of Figure 1 (see Curve D), would probably not be considered to be useful. Since effective dose rates and exposure times must be computed prior to therapy, knowledge of the tumor's position must be accurately determined along with the concentration of ^{10}B in both tumor and normal tissue. These data, when combined with the biological half-life of the ^{10}B delivery system, permit dosimetric calculations to be made to determine the length of the neutron radiation period. The safety and convenience of the patient as well as the effect of ^{10}B loss from the tumor with time suggests that the beam exposure time must be minimized. Thus large reactors are required to provide the necessary optimized flux of greater than 10^9 epithermal neutrons per cm^2 per s. Calculations show that a single irradiation of 5×10^{12} thermalized[14] epithermal neutrons per cm^2 would provide the desired therapeutic dose.

Thermal neutron beams have not been treated in this article, since it is apparent that the analog of Figure 1 would contain total effective dose vs depth curves that have their maxima at the surface and decay rapidly with depth in tissue. While thermal neutron beams comparable in flux to the epithermal beam of Figure 1 provide therapeutic gain values greater than 2 at the surface, this parameter rapidly decreases to the useful limit of 1.2 at about 2 cm depth. These observations clearly support the need for epithermal neutron beams of high flux derived from a large nuclear reactor or an as yet unavailable proton accelerator discussed above (Section 2.3.2).

It is important at this point to compare the radiation damage mechanism of the $^{10}B(n,\alpha)^7Li$ process with that produced by the more conventional radiation source, γ-photons.[29] Conventional γ-photon doses of therapeutic significance result from an average of tens of thousands of γ-photon-initiated ionization tracks per cell, and stochastic principles do not apply since the γ-photons are presented to the tumor target cells in a homogeneous manner. On the other hand, BNC provides a therapeutic 10 Gy dose of about 25 high LET events per cell. Damage resulting from nonlethal doses of γ-photons is reparable with time, whereas the extreme damage per BNC event is not reparable, since heavy α and ^7Li fission products with a high LET are involved. The average number of BNC events per cell during a fixed exposure period will vary with the depth of the cell and the spatial distribution and concentration of ^{10}B nuclei within cells.[30] Since the ranges of the α and ^7Li fission products are short in tissue and comparable to one cell diameter, the response of individual cells will vary with intra- and intercellular distribution of ^{10}B and target cell geometry. Consequently, stochastic effects are of great importance in BNCT. If ^{10}B can be placed in or near a vital cellular component such as the nucleus, the number of BNC events required for cellular death is greatly reduced. ^{10}B that resides in the intercellular volume or on external cell walls is much less effective. Thus, the most highly prized boron compounds and associated delivery systems are those that enter the cell and bind to intracellular components. Furthermore, the visualization of boron within individual cells has great importance as an aid to boron compound design.

In addition to the heterogeneous nature of the ^{10}B distribution within and immediately surrounding individual tumor cells, additional heterogeneity introduced by the actual tumor morphology must be recognized. Large tumors are often characterized by a necrotic center that is poorly nourished surrounded by a vasculature that is capable of supplying nutrients for rapid peripheral tumor growth. This peripheral array of blood vessels is pressed into service as rapidly

as it can be created. As a consequence of this type of tumor growth and morphology, considerable macroscopic heterogeneity exists within the BNC target volume. The resulting gross inhomogeneity of ^{10}B distribution must be quantitatively evaluated and taken into account during therapy experiments and in the in vivo evaluation of new boron compounds and their associated delivery systems.

2.5. Methods of Analysis for Boron Pertinent to BNCT

Analytical methods for boron required for BNCT research, boron compound evaluation, and eventual clinical applications span a broad spectrum of useful and some not yet perfected procedures. These include the macroscopic and noninvasive estimation of ^{10}B concentrations in tumor and surrounding tissue with ^{10}B magnetic resonance imaging (MRI), which is under development, and the microscopic visualization of ^{10}B localization in tumor and tissue sections with α-track autoradiography. Intracellular boron distribution and quantification is another subject that has begun to yield important results. These and other related subjects are discussed in the following sections.

2.5.1. Noninvasive Macroscopic Estimation of ^{10}B Concentrations In Vivo

As pointed out above, safe and effective BNCT requires knowledge of the tumor's location, the concentrations of ^{10}B in tumor, blood, and normal tissues, and the rate at which the ^{10}B-containing species is eliminated from these biological compartments. Noninvasive methods for both tumor visualization and the determination of ^{10}B concentrations will be required. In principle, a chemically stable radiolabel having suitable characteristics for imaging and attached to a small fraction of the ^{10}B compound in question[31] could be employed, coupled with planar imaging as well as single photon emission computer tomography (SPECT) to visualize the compound in both primary and secondary metastatic tumors.[32] However, each double-labeled ^{10}B delivery system introduces complications and time constraints that are best eliminated.

Very recent research has explored the potential capability of NMR-active ^{11}B and ^{10}B nuclei in MRI and in the determination of the boron content of tumors loaded with the appropriate isotope. ^{1}H NMR imaging would be employed as an adjunctive modality. Continued development of this technique has achieved some success[33-36] with the more responsive ^{11}B nucleus, and the ^{10}B nucleus may prove to be useful in the near future. It may eventually be possible not only to locate tumors with $^{10}B/^{1}H$ MRI methods, but also to visualize in a quantitative fashion the local ^{10}B concentrations in tumor and normal tissue. These analytical methods would be noninvasive, relatively rapid, and involve the ^{10}B BNCT target nuclei as the signal-generating species. The reader is referred to the original literature[33-36] for the details of this developing technology.

2.5.2. Methods for the Macro and Micro Determination of Boron in Biological Samples

The need exists to determine accurately the concentration of boron present in biological research samples taken at biopsy and tissues obtained from animal biodistribution experiments. Such samples are often available in macroscopic quantities of 50 to 100 mg or more. Following the oxidative dissolution of weighed tissue samples, boron analysis of the aqueous sample is accomplished with the newly developed, inductively coupled or direct current plasma–atomic emission spectroscopy (ICP–AES[37] and DCP–AES,[38] respectively) methods. These AES methods determine boron in tissue reliably at levels of 1 ppm. Extension of this method to microscopic tissue samples of 1 mg obtained by needle biopsy is feasible with a modified sample preparation procedure.

An alternative to ICP-AES and DCP-AES for the analysis of biological samples utilizes the quantification of the prompt γ-photons emitted during thermal neutron capture by the ^{10}B present in the sample,[39-41] and comparison of the result with calibration measurements. This method requires a source of thermal neutrons and lacks the precision at low ^{10}B concentrations characteristic of the plasma–AES methods.

2.5.3. The Visualization and Microdosimetry of Boron in Biological Specimens

The discussion of the stochastic nature of the inter- and intracellular BNC processes in Section 2.4 pointed up the need for experimental methods capable of providing the spatial distribution of boron in tumor and surrounding tissue sections taken from experimental animals or humans at biopsy. The inhomogeneous structure of tumors makes such studies vital to the understanding of the effectiveness of candidate boron-containing compounds in reaching individual tumor cells in the tumor structure. The α-track autoradiography method[42, 43] is ideally suited for this purpose. The procedure involves the placement of very thin (6–10 μm) tissue sections upon nitrocellulose sheets followed by exposure of the array to a thermal neutron source. The high LET α and ^{7}Li products of the resulting $^{10}B(n,\alpha)^{7}Li$ reaction that are generated within the tissue sample sensitize the nitrocellulose for hydrolytic attack by strong aqueous base. Because of the limited track range of these particles and their high LET characteristics, individual neutron capture events are recorded and converted into visible tracks on the base-developed nitrocellulose film. Superposition of this track data upon that obtained from conventional optical representations of the same tissue section gives the relative density of ^{10}B nuclei with respect to the histology of the sample. By using calibration samples, this method can also be employed to obtain the ^{10}B concentration in tissue from track density data at ^{10}B concentrations as low as 1 μg per g sample.[44]

In addition to conventional histological samples taken from tumors, the α-track radiographic method has often been applied to whole-body cross sections of experimental mice and rats.

2.5.4. *Techniques for Imaging Boron on a Subcellular Scale*

The design of new boron-containing drugs and the elucidation of their associated tumor localization mechanisms could best be served if the movement and relative concentration of the drug within the targeted tumor cells could be followed in time-course experiments. The importance of such a capability to drug design derives from the fact that the most effective drugs will be those with the ability to enter tumor cells and bind with the cytoplasm, organelles, or even the nucleus. For example, if one were to synthesize a candidate DNA-binding boron system, it would be important to confirm this proposed intracellular targeting by direct observation of boron within the cell nucleus. At present, methods for such subcellular imaging have demonstrated their usefulness in specific examples and await further development.

The first method referred to here is the secondary-ion mass spectroscopic (SIMS) microscopy method,[45, 46] which may be applied to the quantitative determination of boron in single, freeze-fractured and dried, boron-containing cells taken from culture. This method has been applied to the imaging of cells targeted by efficacious boron drugs; it has a spatial resolution of 1 μm.

The second method is electron energy loss spectroscopic (EELS) imaging,[47] which employs elemental mapping with an analytical electron microscope or an energy-filtering transmission electron microscope. Preliminary results for boron with EELS have been reported,[48] but as in the case of the SIMS method, further development is required before this method of drug evaluation becomes generally useful.

3. Early Clinical Trials of BNCT and the Related Search for Suitable Boron-Containing Target Species

3.1. Initial Clinical Investigations (1951–1962)

The idea of actually applying Locher's binary BNCT concept[6] to medicine originated[49] with William H. Sweet, neurosurgeon at the Massachusetts General Hospital (MGH), Boston, and L. E. Farr, of the Brookhaven National Laboratory (BNL) Medical Department. Sweet and Farr proposed to improve the prognosis for brain tumor patients by employing BNCT to destroy the fibrils of residual tumor cells, which always remained following radical surgery to remove the accessible tumor.[50, 51] This procedure would remove the fibrils as foci for the reestablishment of the tumor. The life expectancy of patients with such malignant gliomas was usually less than six months, even with surgery. The fact that gliomas did not metastasize, the protection provided normal brain by the blood–brain barrier, and the resistance of these malignancies to all known forms of chemo- or radiotherapy made them excellent candidates for BNCT trials.

Earliest thoughts regarding the enhancement of distribution ratios for boron compounds in tumor and brain evolved from the concept that cerebral gliomas were accessible to the blood or "wet" side of the blood–brain barrier and would thus favor the uptake of hydrophilic species, while normal brain was relatively "dry" and less hydrophilic. Therefore, hydrophilic, nontoxic species were sought.[52]

Volunteer patients undergoing neurosurgical biopsy or resection were found to tolerate sodium borate ($Na_2B_4O_7$) in concentrations of up to 200 mg per kg body weight without severe side effects.[53] Biodistribution and time-course data indicated that shortly after intravenous injection of borate the concentration of boron in tumor was three times that found in normal brain and could be as high as 50 μg per g tumor. Boron was present in blood at concentrations as high, or higher, than those found in tumor.

Initial clinical trials were conducted by Farr and Sweet in 1954 with a thermal neutron beam from the Brookhaven Graphite Research Reactor and ^{10}B-enriched sodium borate on ten patients with glioblastoma multiforme.[54] Five patients received a single radiation dose, and five received multiple fractionated doses. No statistical prolongation of life was achieved. In 1959 the then new Brookhaven Medical Research Reactor was employed to treat sixteen more patients[55, 56] with ^{10}B-enriched borates as the target species. As before, no enhancement of survival times was observed, nor was α-particle-induced radiation damage observed in patients' brains at autopsy.

In the early 1960s the MGH/MIT Reactor, complete with a surgery located below a thermal beam port, became operational. Also during the 1950s and early 1960s, boron compounds were synthesized by several research groups and evaluated by Soloway et al.[57] of the MGH, who used murine models such as implanted ependymoblastomas for biodistribution experiments and time-course experiments. Many of the approximately 140 compounds evaluated by Soloway et al. were substituted phenylboronic acids (including 4-dihydroxyborylphenylalanine (BPA), which is of great interest today (see Section 7.9.1). During this same period the polyhedral borane anions $B_{10}H_{10}^{2-}$[58] and $B_{12}H_{12}^{2-}$[59] were discovered and their derivative chemistry extensively explored. In addition, the icosahedral carboranes[60] *closo*-1,2- and *closo*-1,7-$C_2B_{10}H_{12}$, were synthesized and derivatives prepared. The unusual kinetic stabilities of these polyhedral ions and carboranes immediately made them and their derivatives attractive candidates as BNCT target compounds. These developments coincided with the beginning of a new area of inorganic cluster chemistry. This subject is more fully described in Section 5.

Soloway evaluated the salt, $Na_2B_{10}H_{10}$, as a potential BNCT target species in animals and humans. Large quantities of $Na_2B_{10}H_{10}$ could be administered by intracarotid injection to humans (LD_{50} 1.0 g per kg in C3H mice) and later recovered and identified by ^{11}B NMR in urine specimens. In another experiment with CD1 Swiss mice[61] (male), the observed LD_{50} of $Na_2B_{12}H_{12}$ was 1025 ± 15 mg per kg body weight. Toxicity of the polyhedral ions was low, whereas the substituted phenylboronic acids often presented toxic reactions in animals.

Two boron compounds in ^{10}B-enriched form, 4-carboxyphenylboronic acid and $Na_2B_{10}H_{10}$ were chosen for a new set of human trials to be carried out at the MGH/MIT Reactor and MGH during 1961 and 1962. Eighteen patients[62] were subjected to a tumor "debulking" procedure, which removed extraneous tumor tissue and opened the skull for exposure to the poorly penetrating thermal neutron beam.

Two of these patients were given $Na_2{}^{10}B_{10}H_{10}$[*] by intracarotid injection, while sixteen received ^{10}B-enriched 4-carboxyphenylboronic acid. Patients were irradiated after reopening the craniotomy site. Again, no therapeutically useful effect was observed, and patients died between 10 days and 11.5 months post-irradiation. Neuropathological examination of patients at autopsy indicated radiation necrosis with vascular lesions of different types in the brains of 9 of 14 patients.[62] The cause of these effects was attributed to high concentrations of boron in blood at the time of neutron irradiation. Henceforth, it was thought to be desirable to employ boron reagents that were selectively accreted by tumor to ensure a mininal boron concentration in blood at the time of neutron irradiation. A second generation of candidate compounds were synthesized both by Soloway and by workers at the Du Pont Central Research Laboratory with this objective. For the most part these compounds were designed to function as tumoristatic alkylating agents or compounds capable of other covalent-bond-forming reactions with protein, and were based upon polyhedral borane anion[58, 59] and carborane[60] structures. The reader is referred to Sections 5.0 and 7.1 for a fuller description of these species. Of the compounds evaluated in biodistribution studies by Soloway for selective tumor accretion and effective clearance of the vasculature, the sodium salts of $B_{12}H_{11}SH^{2-}$ and 1,10-$B_{10}Cl_8(SH)_2^{2-}$ stood out,[61] but only the former salt was sufficiently nontoxic (LD_{50} in male CD1 Swiss mice was 73 ± 4 mg per kg body weight) to warrant further study. It was given the acronym BSH.

3.2. The Emergence of a BNCT in Japan: Hiroshi Hatanaka and $Na_2B_{12}H_{11}SH$

After spending several years at the MGH working with the BNCT team headed by Sweet, the neurosurgeon Hiroshi Hatanaka returned to Japan in 1968 and created a new chapter in the BNCT story. Hatanaka initiated a clinical trial with Japanese glioblastoma patients using ^{10}B-enriched BSH and primitive thermal neutron beams of low intenisty, which were available in the Tokyo area. The Shionogi Research Laboratories, Osaka, supplied $Na_2{}^{10}B_{12}H_{11}SH$ for these studies and synthesized the sodium salts of 1- and 2-$B_{10}H_9SH^-$ as alternatives (see Section 7.1).

The procedure developed in Japan was similar to that employed by Sweet in the 1961/1962 clinical trials. Patients with tumors near the periphery of the brain underwent a craniotomy followed by surgical debulking of the tumor mass. One to two weeks following this procedure the patients were given an intracarotid infusion of ^{10}B-enriched BSH at dosages between 30 and 80 mg per kg body weight delivered over one to two hours. Approximately twelve hours later, the cranium was opened and the surgical site exposed for thermal neutron irradiation. Only reactors of low flux were available (10^9 neutrons per cm^2 per sec), and irradiation times were of the order of three to five hours on a patient under remotely controlled anesthesia. Protection of the scalp was necessary to prevent radiation damage, since skin contained a moderate concentration of ^{10}B. Tumor samples taken at the time of irradiation indicated the presence of 13 to 60 μg ^{10}B per g tumor. The boron concentration in normal brain was not measured.[63] Because thermal neutrons were necessarily employed in these studies, penetration of the beam in tissue was less than 6 cm due to neutron scattering and attenuation.

Hatanaka's work has been published and widely discussed.[63–66] Noteworthy is the fact that no necrosis of the normal brain was observed, except in one atypical patient, who received an extraordinarily large neutron dose. This suggests that BSH was cleared from the blood before neutron irradiation commenced. However, recent work by Gavin et al.[24] suggests that the small diameter of the capillary vessels in normal brain coupled with the intact blood–brain barrier at all points other than tumor interfaces is the criterion for the blood-vessel-sparing mechanism, which effectively reduces the apparent boron concentration in blood. BSH is a small hydrophilic anion that does not cross the blood–brain barrier; its apparent inability to do so must also be related to its moderately strong complexation with high molecular weight proteins present in blood serum[67] that also do not penetrate the blood–brain barrier. This process was discussed above in Section 2.4. In general, the patients of Hatanaka fared well considering the deadly nature of their disease.[14] Of thirty-eight patients with Grade III and IV glioblastoma multiforme who were treated and twelve with tumors in the cerebral mantle less than 6 cm from the cortical surface, the reported mean survival was 44 months, and the median was about 26 months. Among them are several long term survivors: a man now 65 years old is alive and unaffected twenty years later; a 70-year-old woman and a 13-year-old girl also appear to be completely cured.

Hatanaka's results are remarkable, but they have stimulated some criticism within the medical community. The questions raised are centered about the consistency of data collection regarding patients and procedures, and the poor performance of the neutron beams that had to be employed. One must realize that Hatanaka demonstrated the efficacy of BNC in glioma therapy under conditions that were far from ideal. It is clear that thorough documentation could have been obtained if greater resources had been available.

The demonstration that BSH could be successfully applied as a target compound in the BNCT of glioblastoma multiforme has stimulated an international effort with this species as the centerpiece. Research groups located in the EC countries and others associated with the Idaho National Engineering Laboratory have initiated detailed pharmacokinetic studies of BSH with the aim of elucidating the mechanism responsible for its accretion in cerebral gliomas. Other studies pertain to the use of BSH in neutron irradiation experiments with large animals and its pharmacokinetics in humans. Clinical trials are being prepared in which the European consortium will employ the Petten reactor with BSH.

One complication in the use of BSH in therapy is the ease with which air-oxidation, perhaps catalyzed by traces of redox-active metal ions, takes place to form the disulfide dimer $[B_{12}H_{11}S]_2^{4-}$ and the corresponding oxodisulfide.[68, 69] Animal experiments have shown the former ion to be superior to BSH in tumor accretion,[70] but much more

[*] ^{10}B in constitutional formulas is used here to indicate that the compound contains 95–96% ^{10}B. See Section 5.1.

toxic. A blue, reactive radical is observed in acidified aqueous solutions of the disulfide ion.[68, 69] These oxidation reactions may be necessary in vivo to establish the presumed covalent coupling of BSH to cysteine residues. The reader is referred to Section 7.1 for futher information. These same reactions require tedious purification of BSH used for drug purposes. However, at the present time BSH is the only acceptable boron target compound that could be used today in clinical trials in Europe or the USA. As we shall see, other suitable target species are under rapid development, but BSH will probably remain as the baseline compound for clinical studies conducted in the immediate future.

4. Chemical Intermezzo

With the exception of certain of Hatanaka's patients, BNCT has thus far not proven to be an outright success. Aside from the rationale that relates the probable success of BNCT to the level of development of radiation oncology, the characteristics of available neutron beams, or the sophistication of dosimetry, the key to success was, and remains, the availability of nontoxic boron target compounds that selectively accumulate in neoplasms as opposed to normal tissues. The synthetic chemist encounters a major problem in the logical development of these useful neutron target species: the paucity of quantitative and even qualitative information pertaining to the chemical and biological differences between malignant and normal cells. Such information is vital, since these differences identify possible pathways for the selective uptake and retention of boron by tumor cells. However, two important areas of existing clinical practice make use of such tumor cell differentiation: chemotherapy and the radioimmunoimaging of tumors. Chemotherapeutic drugs are evaluated for their ability to kill cancer cells selectively without great concern for the concentration differences between malignant and neighboring normal tissues, since the effective differentiation between cancerous and normal cells is based upon disparate cell reproduction and metabolism rates. The precision of radioimmunoimaging techniques now available is possible, because radiopharmaceuticals, through their attachment to monoclonal antibodies, can differentiate between normal and tumor cells with such exquisite selectivity that high tumor-to-normal-cell concentration ratios are attained while the actual concentration of the radiopharmaceutical in tumor is miniscule.

Ideally practiced, BNCT requires even more demanding characteristics: the selectivity for tumor displayed by immunomediated radiopharmaceuticals coupled with concentrations of tumor-bound boron drugs greater than those used in chemotherapy and persisting in tumor for a period sufficient for effective neutron irradiation to be safely accomplished. Toxicity issues must also be controlled. Thus, the initial challenges to the chemist are: 1) identificaton of biodelivery (bioutilization) pathways that effectively differentiate between the targeted tumor and other tissues, and 2) design and synthesis of boron compounds that may be coupled to these biodelivery systems without serious compromise of biodelivery performance, but that maintain at least the lowest practical concentration of ^{10}B in tumor required for therapy (approximately 10^9 target atoms per cell). In addition, boron must accumulate in tumor, while its concentration in blood is simultaneously minimized. If these challenges can be met, the use of the blood–brain barrier to augment tumor cell differentiation is no longer necessary, and BNCT can be increased in scope to include malignancies other than cerebral gliomas. Thus, tumors such as melanoma, lymphoma, adenoma, sarcoma, and others, as well as their metastases, become candidate diseases for BNCT with epithermal neutron sources.

5. The Timely Discovery of Modern Borane Chemistry

The development of BNCT research beyond the level of effort seen in the 1950s is due to the discovery of new boron chemistry in the late 1950s and early 1960s that exceeded the greatest hopes of the chemists involved with the earliest clinical trials of BNCT. The discovery of whole new families of polyhedral borane derivatives that were stabilized by three-dimensional electron delocalization, and also capable of being incorporated into organic molecules as substituents, allowed the concept of BNCT to survive the early clinical trials that were conducted with inappropriate boron compounds and to progress to its present promising status.

These first aromatic polyhedral borane species to be discovered were the predicted icosahedral *closo*-$B_{12}H_{12}^{2-}$ ion[59] and the unpredicted *closo*-$B_{10}H_{10}^{2-}$ ion[58, 71] having the structure of a bicapped, square Archimedian antiprism. These ions were soon followed by the icosahedral *closo*-$C_2B_{10}H_{12}$ carborane isomers,[72, 73] which are isoelectronic and isostructural with the *closo*-$B_{12}H_{12}^{2-}$ ions. Other polyhedral anions of the general formula *closo*-$B_nH_n^{2-}$ were discovered, and the entire family with $n = 6$ through 12 became available.[74] Similarly, other *closo*-$C_2B_{n-2}H_n$ carboranes, likewise with $n = 6$ through 12, were synthesized.[75] These carborane molecules reacted with organic molecules, and isomers could be generated by movement of the polyhedral carbon atoms[72, 75] relative to each other over the polyhedral surface (polytopal rearrangements). Later research uncovered the corresponding *closo*-$CB_{n-1}H_n^-$ carborane series,[76, 77] whose members also form organic derivatives. Metallacarboranes in which one or more BH vertices of carboranes is replaced by a metal vertex were soon discovered,[78, 79] as were the corresponding metallaboranes.[80] The familial relationships of these and many other borane cluster derivatives have been integrated with chemical bond theory[81] and served as a generalized basis for the evolution of inorganic cluster chemistry[82] as a whole. The scope of modern boron chemistry extends far beyond the boundaries suggested here, and the interested reader is referred to specialized reviews of the many aspects of borane cluster chemistry.[83, 84] These seminal discoveries in inorganic and organometallic chemistry have made the search for effective BNCT compounds a feasible proposition, since these borane cluster compounds offered high boron content, excellent kinetic stabilities, and relatively simple derivativization for incorporation in organic molecules. Scheme 4 outlines several major features of borane cluster interconversions and some numbering conventions.

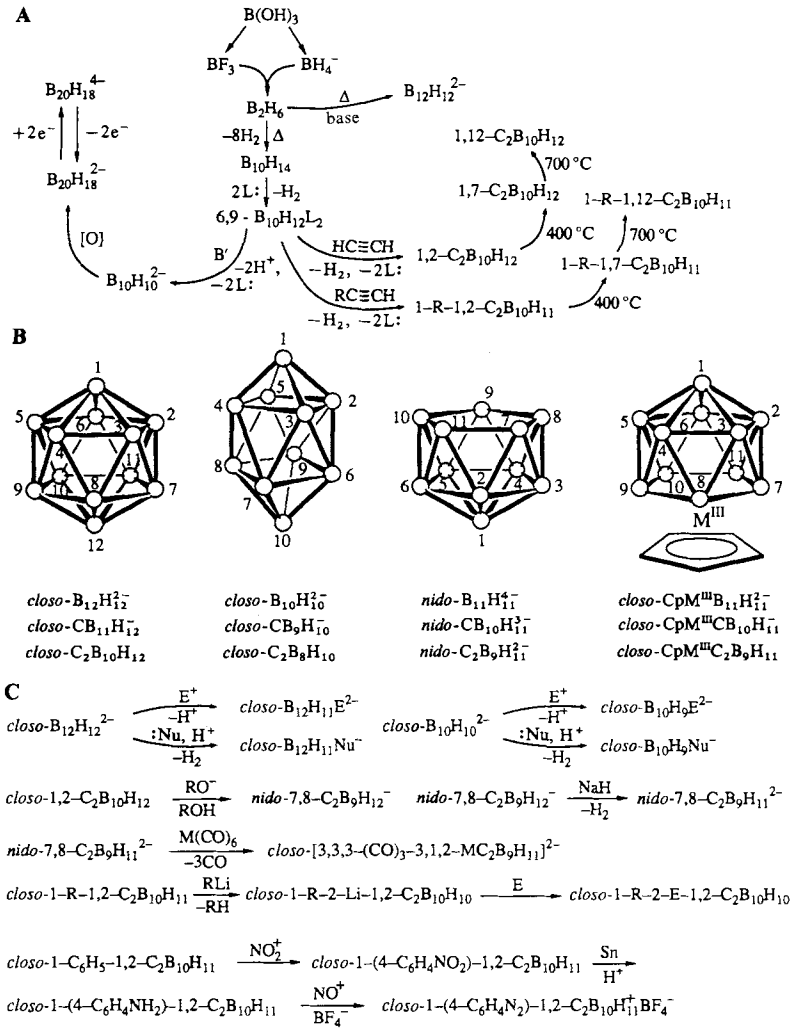

Scheme 4. An abbreviated presentation of some highlights of contemporary boron cluster chemistry of potential importance to BNCT. **A**: syntheses; **B**: structures; **C**: reactions. B′ = base, E = electrophile, :Nu = nucleophile, L: = ligand.

5.1. The Synthesis of ^{10}B-Enriched Species Required for BNCT

Scheme 4 is an abridged depiction of the familial relationship of the most accessible borane and carborane species that have been, or could be, employed in the synthesis of BNCT reagents. To achieve their full potential as ^{10}B delivery vehicles these building-block molecules must be enriched in the ^{10}B isotope. Enrichment to 95–96% ^{10}B is commonly employed, because the boric acid starting material is commercially available at this level of isotopic purity. In Scheme 4, diborane, $^{10}B_2H_6$, is the key intermediate for the synthesis of the three major families of ^{10}B-enriched borane derivatives: $^{10}B_{10}H_{10}^{2-}$, 1,2-$C_2{}^{10}B_{10}H_{12}$, and $^{10}B_{12}H_{12}^{2-}$ (see Scheme 4). Since the majority of the species that comprise the armamentarium of BNCT research may be derived from one of the three precursors described above, the requirement for ^{10}B-enrichment does not present difficulties, but considerable additional costs may arise from the purchase of commercially available ^{10}B-enriched compounds. The need for ^{10}B-enrichment should be considered in the design of synthesis routes for new compounds.

6. Classes of Boron Compounds and Bioutilization Pathways of Current Interest

Although it may be possible to administer boron-containing target species to animals and humans by oral or perilesional pathways, the majority of boron biodistribution data are collected following intravenous injection of the experimental compound. The diagram presented in Scheme 5

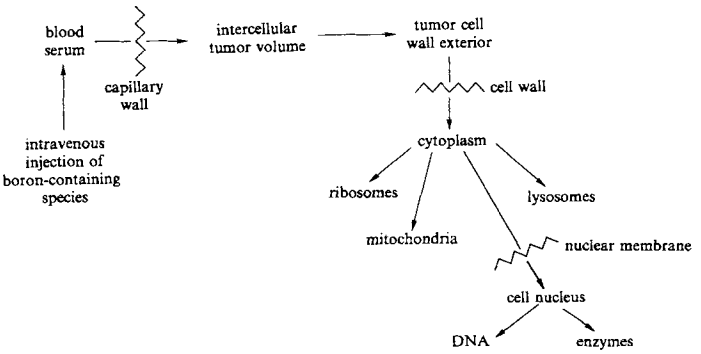

Scheme 5. A greatly simplified representation of the transport pathway required to bring a boron-containing species from the point of intravenous injection to the interior of a cell nucleus.

traces the possible pathway of a hypothetical boron-containing species as it approaches, binds, and later enters a tumor cell. As previously pointed out, the lethal potential of a ^{10}B nucleus increases markedly after entering the cell, and again after approaching the nucleus. Nuclear DNA is the target of greatest value, because in this case, only a single high LET neutron capture event within the DNA would be lethal to the cell.

The earliest attempts to correlate molecular structure and biodistribution of boron compounds[57] were concerned with cerebral gliomas, normal brain tissue, blood, and the influence of the blood–brain barrier. Now that tumors other than those related to the brain are under investigation as BNCT subjects, a wider variety of tumor morphological and metabolic features are considered in the development of new boron carriers.

Carrier species under investigation today for the delivery of boron to some particular locus of the targeted tumor cell may have been designed to enter a specific bioutilization pathway as a mimic of a known cellular constituent or metabolite. Other molecules, exemplified by monoclonal antibodies and their fragments, are selectively bound to tumor-cell receptor sites in the plasma membrane that are either overexpressed or uniquely expressed by tumor cells as opposed to normal cells. Such receptor-mediated molecules may be conjugated with boron-containing reagents and converted into very selective boron carriers. Small vesicles such as synthetic liposomes or modified low-density lipoproteins (LDLs), while not of molecular dimensions, may be employed as boron-carriers of a different type. Finally, some simple molecules such as porphyrins have proved to be useful for accumulation of boron in tumor (also termed boron localization), although the biological basis of this utility has not yet been clearly defined. Scheme 6 matches currently important boron-containing compounds with the biosynthesis of specific cellular components or the utilization of their characteristic receptors for BNCT. These items are found in the extracellular volume, the cell wall, the intracellular volume, and the cell nucleus.

6.1. A Brief Overview of Biodelivery Schemes

Molecular mimicry is employed in the design of compounds that may serve as boron-containing substitutes for molecules normally used in cell construction and metabolism. Species of this type have been employed, or proposed for use, in cellular phospholipid[85] and protein synthesis.[86] In addition, L-dopa surrogates[87] are under investigation for incorporation in melanin synthesis by melanotic melanoma cells.

Recent advances in nucleic acid chemistry have stimulated efforts to incorporate boron-containing base molecules, nucleosides, and nucleotides in target cell DNA or its precursors during biosynthesis.[88] The interaction of boron-containing "antisense" nucleotides and DNA ligands[89] with existing nuclear DNA molecules provides related avenues to the radiologically vulnerable nucleus.

Specialized molecules that, after attachment of boron-containing entities, bind with specific receptor sites of the tumor cell wall are also assumed, for the most part, to be endocytosed by the tumor cell. In some examples the receptor site is regenerated. This selective boron internalization process has broad scope and presents the capability of bringing a particular type of tumor cell under either successive or simultaneous attack by more than one type of receptor-specific boron carrier. An example would be two or more immunoglobulins targeted for different antigens which are

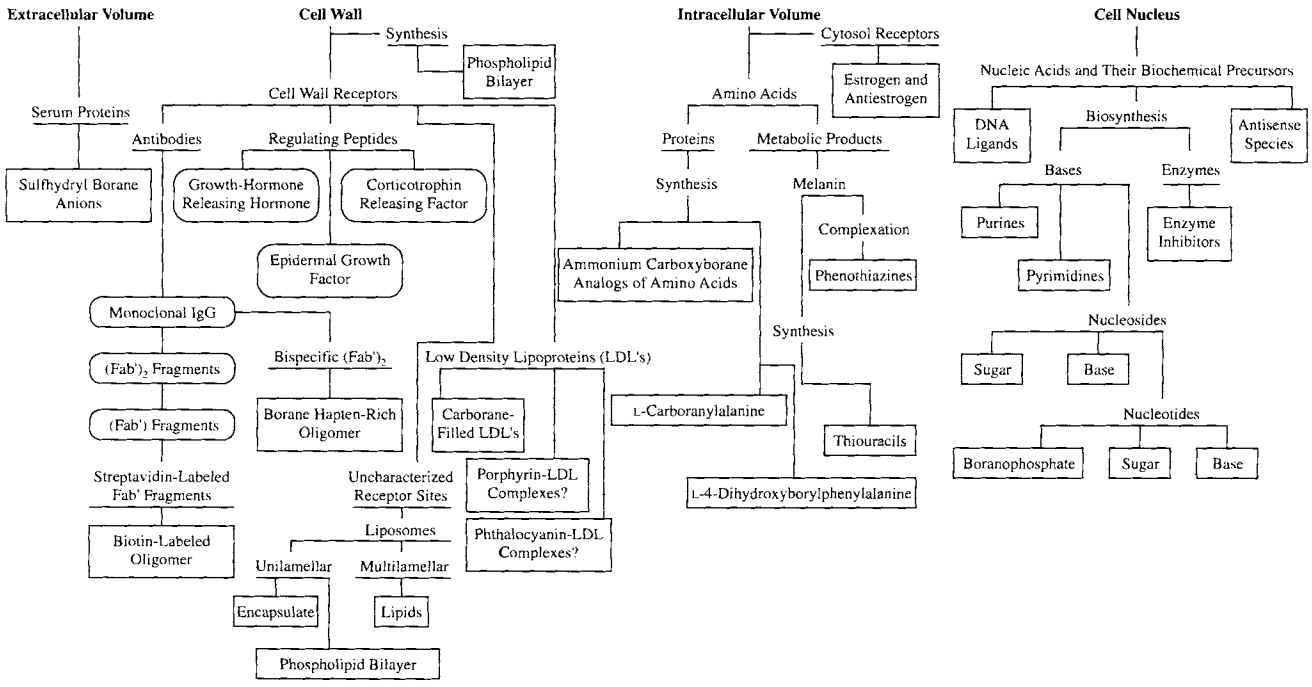

Scheme 6. A classification of boron-delivery vehicles based upon their method of incorporation into one of four biological compartments; extracellular volume, the cell wall, intracellular volume, and the cell nucleus. These assignments are subject to change as further progress is made. □: boron-containing species; ○: conjugate of a boron-containing reagent.

simultaneously expressed by the same tumor cell. The multiple attack, in principle, amplifies the effective concentration of ^{10}B nuclei associated with specific cell types.

The requirement of 10^9 B atoms per targeted cell for effective BNCT is difficult, but not impossible, to achieve by using individual molecules as the carrier species. However, organized aggregates of boron-rich molecules may enter delivery mechanisms specific to tumor cells and bring relatively huge quantities of boron to targeted cells with each delivery event. Such "supertanker" systems known at present are unilamellar liposomes[90] containing polyhedral borane anion solutes within the liposome's aqueous core and reconstituted LDLs in which the natural cholesteryl esters have been replaced with hydrophobic esters derived from carborane.[91] The reconstituted LDLs retain their ability to bind LDL receptor sites of tumor cells and become internalized through the still-functional apoprotein B-100 attached to the original LDL. Cell differentiation is observed, since compared to normal cells LDL receptor sites are extravagantly expressed on growing tumor cells. While the precise mechanisms responsible for selective liposome localization are presently unknown, receptor sites amenable to liposome binding and internalization must surely exist, since it is possible to observe fluorescent species[92] within tumor cells following their in vivo delivery by liposomes. Furthermore, the results obtained with boron-containing liposomes are understandable only if liposomes are selectively internalized by tumor cells. The liposome cell differentiation process is thought to be based upon the immature ad hoc vasculature unique to rapidly growing tumors. The capillaries present in such tumors will be permeable to very small liposomes (< 80 nm diameter), as observed, and allow their selective leakage into the tumor bed.[93] This size selection process may be amplified by more rapid endocytosis of liposomes bound to tumor cells than of liposomes bound to normal cells.

The porphyrin macrocycle is capable of highly selective incorporation into tumor cells in very high concentrations. Although a specific receptor-driven process appears to be responsible for these results, as in the case of liposomes, no discrete receptor sites have been identified. It is possible, however, that the LDL receptor sites serve porphyrin endocytosis through initial hydrophobic binding of the porphyrin derivatives in LDL vesicles and incorporation of the resulting LDL–porphyrin host–guest complex in the usual fashion.[94]

7. Boron-Containing Species and Their Delivery to Tumor Cells

Specific classes of boron-containing molecules and delivery vehicles are described below organized according to their targeted locations within the tumor cell in accord with Scheme 6. Interestingly, the progression of boron compound development actually follows the organization of Scheme 6, proceeding sequentially from left to right. Thus, as time passes chemists are brought ever closer to the tumor-cell nucleus and increasingly sophisticated chemistry. This is possible due to continued development of borane cluster chemistry and its close alliance with organic and bioorganic chemistry.

7.1. Species Localized in the Extracellular Volume

As pointed out in Sections 3.1 and 3.2, the serious consideration of BNCT for tumors other than cerebral gliomas is of relatively recent origin. The presence of the blood–brain barrier, which protects normal brain tissue from the entry of very hydrophilic species and which is degraded at the tumor site, provided a mechanism for tissue differentiation. Nontoxic and very hydrophilic boron compounds were sought, which would be localized in useful amounts in tumor.[57] With the level of sophistication of boron chemistry and related analytical methods of the early 1950s, no consideration could be given to the design of boron compounds specifically targeted for intracellular localization in tumor cells or other such niceties. In fact, the class of boron compounds most readily available at the time were the series of arylboronic acids evaluated by Soloway.[57] From a large number of candidates, ^{10}B-enriched 4-carboxyphenyl boronic acid was selected for use in clinical trials of 1959/1961 with terminal cancer patients, and DL-4-(dihydroxyboryl)phenylalanine (BPA), which is of current interest,[87] was set aside. In general, the relatively high toxicity and low boron content of the arylboronic acids make them less attractive than compounds that were to appear following the discovery of the boron chemistry described in Sections 3.1 and 5.0.

The characteristics of the $B_{10}H_{10}^{2-}$ and $B_{12}H_{12}^{2-}$ ions[58, 59] suggested that their sodium salts would have the hydrophilic properties then sought for BNCT. Evaluation of these salts in animals proved that they display low toxicity, are incapable of crossing the blood–brain barrier, and have promising characteristics with respect to tumor localization and blood clearance rates.[57] The $Na_2B_{10}H_{10}$ salt was employed in human trials (Section 3.1). Later work led to the synthesis of the polyhedral borane anion derivatives $B_{12}H_{11}SH^{2-}$[95, 69] and 1,10-$B_{10}Cl_8(SH)_2$.[96] The octachloro derivative proved to be too toxic for use, but the $B_{12}H_{11}SH^{2-}$ ion has gained notoriety as the well-known BSH ion. The thiol function was introduced in order to provide covalent disulfide bonding with thiol groups presented by serum and tumor proteins. It has been established that approximately 60% of injected $Na_2B_{12}H_{11}SH$ is weakly and noncovalently bound to serum proteins.[67] Neither free nor bound BSH crosses the intact blood brain barrier, although the tumor is accessible. Hatanaka's results in human glioma trials[63] and other results with humans[97] demonstrate that therapeutic quantities of BSH (> 20 ppm) are present in tumor, while low concentrations are simultaneously present in normal brain. Blood concentrations of boron are comparable to or higher than simultaneous tumor concentrations.

The thiol derivatives of the borane anions are potentially unstable with respect to air-oxidation. As an example, BSH is easily oxidized to the corresponding disulfide $B_{12}H_{11}SSB_{12}H_{11}^{4-}$ and its oxide $B_{12}H_{11}SS(O)B_{12}H_{11}^{4-}$,[68, 69] which has caused complications in product surety and analyses for its use as a drug. Acidified solutions of the disulfide rapidly turn blue, which indicates the presence of the radical

anion[68,69] $B_{12}H_{11}SH^-$ and/or a related radical dianion $B_{12}H_{11}\dot{S}^{2-}$.

The disulfide derived from BSH has been found to be taken up more efficiently than BSH itself by tumors in small animals.[98] Other in vitro data obtained by Fairchild et al. indicate that the disulfide, like BSH, is not taken up by the cell, but accumulates extracellularly.[99] Very recently Coderre et al. demonstrated[100] that the disulfide gave physically unrealistic RBE values of 1.1–1.4 for in vitro neutron irradiation experiments with 9L gliosarcoma cells. These results suggest that the radiation damage that leads to tumor death is actually extracellular and most likely located in the endothelial cells of the vasculature sustaining tumor metabolism. The precise mechanism of BNCT with BSH is, of course, unknown and will remain so until detailed pharmacokinetic studies are completed. Perhaps BSH becomes bound to the rich tumor vasculature at a fairly rapid rate, but leaves this compartment at a reduced rate as BSH is cleared from blood. At some time an optimal tumor/blood BSH ratio will be reached; neutron irradiation can then be carried out within the time window during which these conditions exist.

Shionogi Research Laboratories, Osaka, have synthesized two isomeric $B_{10}H_{10}^{2-}$ derivatives that correspond to BSH:[101] 1- and 2-$B_{10}H_9SH^{2-}$. Evaluation of these compounds is incomplete, but the $B_{10}H_{10}^{2-}$ framework probably offers no real advantage over $B_{12}H_{12}^{2-}$. Scheme 7 presents the synthesis of the $B_{12}H_{11}SH^{2-}$ ion and its more common reactions.

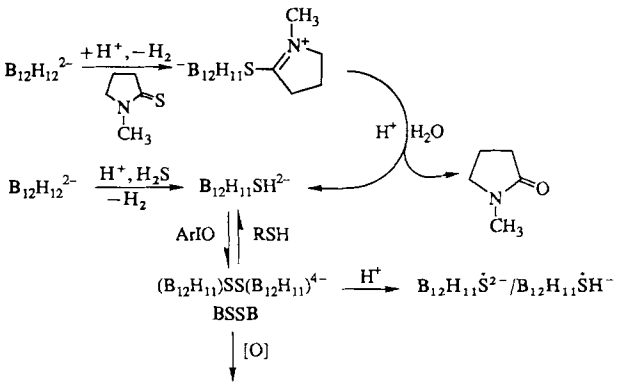

Scheme 7. A summary of $Na_2B_{12}H_{11}SH$ (BSH) syntheses and reactions. Ar = aryl.

7.2. Boron Localization Processes Utilizing Carborane Derivatives of Phospholipids as Constituents of Tumor Cell Walls

Scheme 6 suggests that boron can be delivered to tumor cells by mechanisms that selectively introduce boron-containing phospholipids as components of the plasma membrane bilayer of malignant cells. The accelerated rate of cell reproduction in tumor compared to that of normal tissue causes selective accretion of boron in tumor cells.

Carborane derivatives of phosphocholine glyceryl ethers have been proposed as boron carriers,[85] since it has been shown that naturally occuring lipid ethers such as **1** selectively accumulate in the plasma membrane of tumor cells giving attractive tumor/normal-tissue concentration ratios. In fact, 8–18% of the total phospholipid contained in the plasma membrane of cells grown in vitro can consist of the synthetic phopholipid ether **1**. Consequently, Lemmen and Werner[85] have synthesized DL-**2** with a 1,2-carboranyl group appended as shown. Results pertaining to the efficacy of **2** have not been reported.

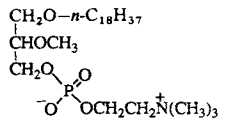

1

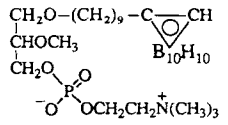

2

7.3. Boron Localization Through Selective Targeting of Antigens of the Tumor Cell Wall with Immunoglobulins

7.3.1. Boron-Conjugated Antibodies and Their Fragments as Boron Carriers

As suggested by Scheme 6, tumor cell walls carry a variety of receptor sites (antigens) for the recognition and binding of specific immunoglobulins. The existence of antigens which are specific to certain types of tumor cells or the overexpression of other antigens by tumor cells compared to normal cells allows the selective targeting of antigens in the tumor cell wall with the corresponding antibodies. Bale and Spar[102] first pointed out in 1967 that such tumor-targeted antibodies could probably be conjugated with suitable ^{10}B species and employed to deliver these boron atoms to the corresponding antigen sites of the tumor cell wall. The very selective immunoglobulin would then become the carrier of therapeutic quantities of boron. Since a maximum of about 10^6 antigenic sites of any one idiotype are present on each tumor cell and each malignant cell must carry about 10^9 ^{10}B atoms to achieve therapeutic levels, it is clear that each antigen-bound antibody must carry about 10^3 ^{10}B atoms. This assumes[103] that the equilibrium constant for antibody–antigen complexation is at least 10^9 M^{-1}. The fact that the binding constants associated with currently available antibodies can be as large as 10^{11} is encouraging. In addition, the observed internalization of antibody–antigen complexes on the cell surface offers hope that the boron delivered to the cell surface will actually move toward more effective regions of the cell, thus reducing the high density of boron atoms required if situated on the surface alone.[104] The simultaneous expression of several specific types of potentially useful antigenic sites by tumor cells suggests the possible use of "cocktails" of boron-conjugated antibodies, which would concurrently target several different antigens. This option effectively increases the total number of useful antigenic binding sites, which, in turn, could allow a reduction of the number of ^{10}B atoms required per antibody molecule.

These immunochemical guidelines could not be achieved until the early 1980s when Milstein and Köhler[105] developed hybridomas as a source of unlimited quantities of chemically homogeneous monoclonal IgG antibodies

(Mabs). Prior to this development, research workers hoping to employ immunoglobulins as boron delivery vehicles were restricted to the use of chemically heterogeneous polyclonal IgG antibodies tediously isolated from the sera of immunized animals.[106] Developments in genetic engineering have led to the essentially unlimited availability of a wide variety of antibody types such as IgG, $(Fab')_2$, and Fab' species, which may contain large segments of human immunoglobulin as well as customized functional groups for the directed conjugation of drugs, radioisotopes, and toxins. The humanized (chimeric) immunoglobulins offer a reduced risk of illiciting an unwanted immune response when administered to humans.[107] Figure 2 illustrates the general relationship of IgG Mabs and their $(Fab')_2$ and Fab' fragments, which may be obtained by enzymatic and chemical cleavage of parent IgG Mabs, or most conveniently, from engineered clones.

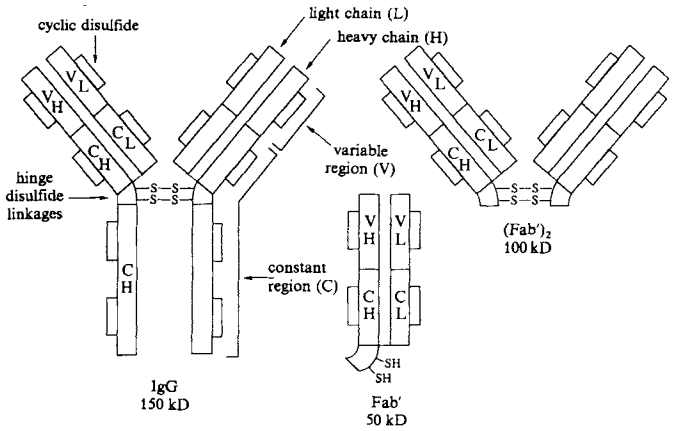

Fig. 2. Simplified representations of the immunoglobulins IgG, $(Fab')_2$, and Fab' and their structural relationships. Antigen binding occurs at the terminus of the VH and VL chains in each of the immunoglobulin types represented here. V_H and V_L chains are joined by S-S bonds represented by lines.

Scheme 8 diagrams the evolution of antibody conjugation and boron delivery methods as they have evolved with time. The initial investigation of boron-conjugation chemistry with model protein substrates such as bovine serum albumin and human γ-globulin was initiated nearly simultaneously in several laboratories in the 1970s. The initial chemical goal was the synthesis of useful boron-rich reagent molecules that contained nine to ten boron atoms each and displayed good reactivity for pendant ε-NH_2 or -SH groups of lysine and cysteine residues contained in the antibody structure.[108] Scheme 9 illustrates several representative examples of these early reagents together with others that were developed at a later date. Work of this sort progressed slowly with polyclonal IgG antibodies of various types and large protein molecules such as bovine serum albumin as model substrates.[109]

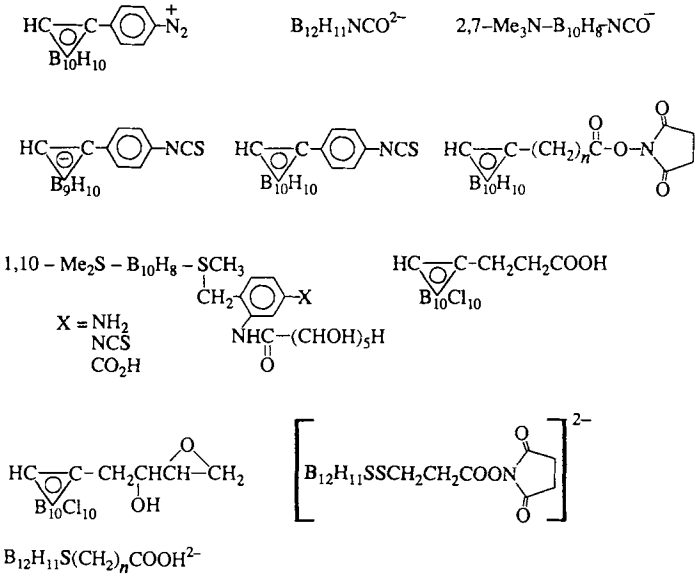

Scheme 9. Representative reagents investigated in past studies of immunoglobulin conjugation. Certain of these species are discussed elsewhere in this article. $n = 1-4$

The earliest attempt to demonstrate the feasibility of the antibody approach using polyclonal antibodies and simple conjugation reagents such as the diazonium salt **4** derived from 1-(4-aminophenyl)-1,2-carborane[110] (**3**) were seemingly successful. The diazonium salt **4** was conjugated with polyclonal antibodies directed against both human and murine histocompatibility antigens, and the conjugate employed for in vitro cell-killing of peripheral blood lymphocytes with a thermal neutron beam. Specific, antibody-directed cytotoxicity was observed, although the number of boron atoms attached to each antibody molecule was only of the order of 30 to 50 and these were of natural isotopic abundance (20% ^{10}B). In another experiment, identical cell-killing (30% survival after two minutes of radia-

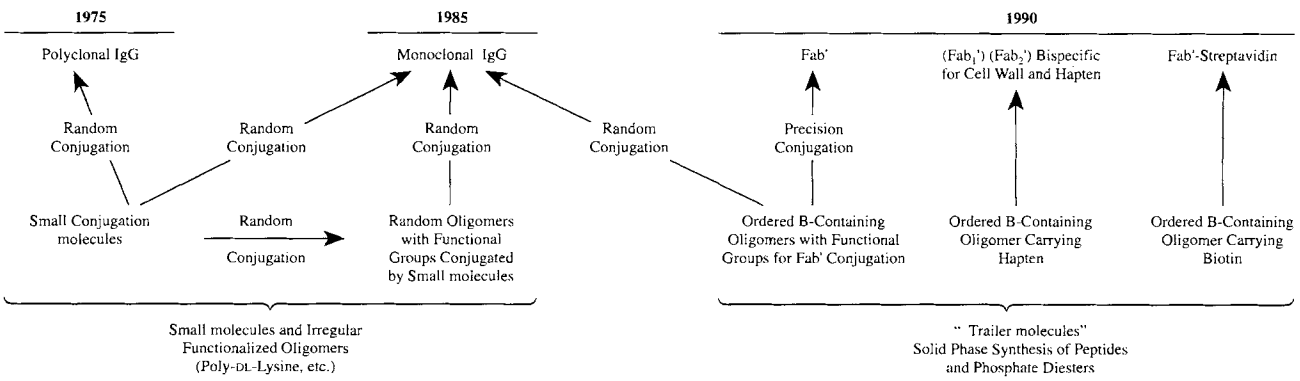

Scheme 8. The evolution of immunoglobulin conjugation methods to the discovery of highly specific bispecific antibodies potentially useful for the delivery of ^{10}B to tumor cells without resort to covalent conjugation.

tion) was observed with lymphocytes in contact with a solution of $K_2B_{10}H_{10}$ containing 2 μg of B per μL or 3.8×10^{-3} μg of B per μL conjugated to 1.9 μg antibody per μL (0.2% B of natural abundance). The efficacy of boron attached to antibody associated with the cell thus appears to be 500 times greater than when present in solution as $K_2B_{10}H_{10}$.

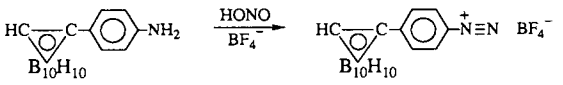

3 **4**

Later the diazonium salt **4** was conjugated with polyclonal caprine antibodies targeted at carcinoembryonic antigen (CEA). The conjugates, which contained up to eighty B atoms per antibody molecule, were employed in both in vitro[106a] and biodistribution studies with human colon tumor xenografts in golden hamsters.[106b] The results of these experiments demonstrated the immunological integrity of the boron conjugates, since good tumor localization was observed in the in vivo experiments. However, the injected dose of antibody conjugate was very low in all of these experiments and the boron content of the conjugate was relatively small. If attempts were made to increase the boron content of the antibody conjugates by increasing the extent of the conjugation reaction, the protein was denatured, precipitated, and lost immunoreactivity.[106, 111] In later work, reagents such as the anionic **5** were synthesized,[112] as well as other carborane derivatives of simple sugars[113] (for example **6**), in order to enhance the water solubility of the carborane derivative with hydrophilic groups. These attempts were unsuccessful.

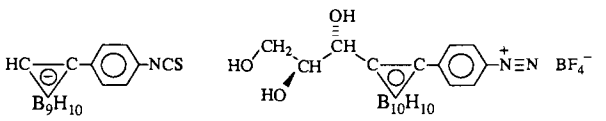

5 **6**

The complexity and heterogeneity of highly burdened antibody conjugates of either polyclonal or monoclonal origin led to the adoption of an alternative approach to boron-carrying Mabs having at least 10^3 B atoms per molecule. This new tactic recognized that large numbers of boron atoms might be attached to Mabs with minimal alteration of the Mab structure and function by connecting boron-rich oligomer molecules to only a few random sites on the Mab surface. For example, approximately five oligomer molecules carrying 200 boron atoms each might be randomly attached to available NH_2 or SH groups of the Mab and the resulting mixture of conjugates separated from unreacted Mab. As indicated in Scheme 8, this approach was first investigated in the early 1980s by several investigators.[114, 115] With the exception of the dextran-bridged systems of Gabel,[116] oligomeric boron-rich conjugation reagents were themselves randomly constructed species, prepared by reacting poly-DL-lysine[114] or poly-L-ornithine[115] with reagents such as DL-**7** or **8**. The chain lengths of the resulting conjugated oligomers were not known, and the number of unchanged NH_2 groups was variable. Further coupling of oligomers of this sort with Mabs of various idiotypes produced conjugated Mabs with average boron atom populations of 1×10^3–2×10^3. Unfortunately, the immunoreactivities of these conjugated Mabs were markedly lower than those of the parent Mabs. Also, time course experiments with mice proved the modified Mabs to be avidly bound to liver, whereas uptake by tumor was diminished. Recent studies with a starburst dendrimer bearing 48 amino groups as a substrate for reaction with DL-**7** gave similar results after conjugation with Mab.[117]

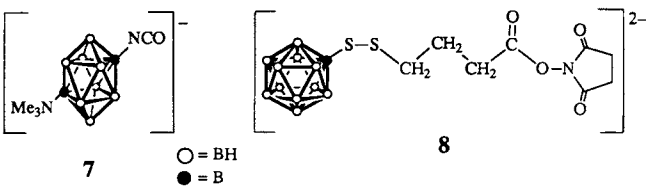

7 **8**

○ = BH
● = B

Contemporary with this approach through randomly constructed oligomers, we[118b, 119] began the investigation of precisely synthesized oligomeric peptides ("boron trailers") constructed from boron-rich α-amino acids using Merrifield's solid-phase synthesis method. Scheme 10 illustrates the amino acids employed in these studies:[120, 121] the hydrophobic *closo* species **9** and its ambiphilic *nido* derivative **10**. Scheme 11 depicts the synthesis of a fluorescence-labeled undecapeptide **11** from **9** and its conversion to the more hydrophilic structure **12** containing *nido* **10** residues. A similar fluorescence-labeled *nido* dipeptide **13** was prepared analogously. Random conjugation of **13** and **11** with anti-carcinoembryonic antigen IgG Mab T84.66 through active ester methods produced conjugated Mab molecules having an average of 63 and 490 boron atoms, respectively.[121] Biodistribution data were collected with nude mice bearing LS 174T xenografts and ^{125}I-labeled Mab conjugates. While the dipeptide conjugate gave biodistribution results that resembled those obtained with native Mab, the undecapeptide conjugate displayed greatly enhanced liver uptake and decreased tumor accretion. These observations[121] suggested that as the boron loading of the conjugate is increased the loss of circulating conjugate to liver effectively competes with localization in tumor. A smaller immunoglobulin

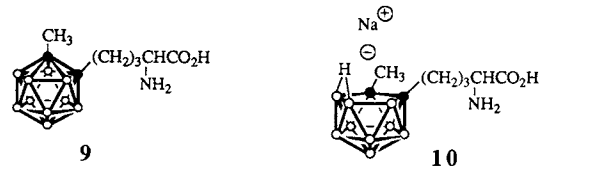

9 **10**

closo cage – very hydrophobic group

nido anion – hydrophilic or amphiphilic group

● C, ○ BH

Scheme 10. DL-**9** and one diastereomer of **10**, the amino acids employed in the synthesis of peptide oligomers used for antibody conjugation.

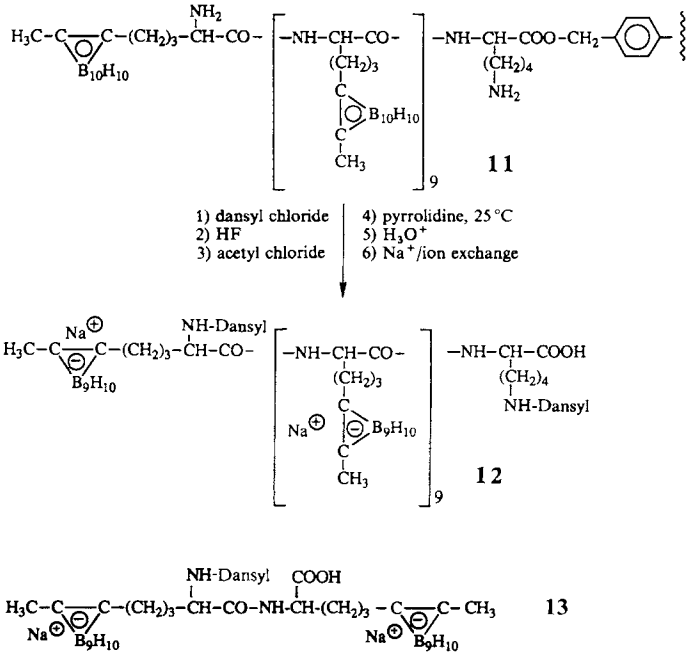

Scheme 11. The peptide **11** and its *nido* derivative **12**, prepared by solid-phase synthesis. Peptide **12** was conjugated with antibody, and the conjugate evaluated in biodistribution studies (see Section 7.3.1). In **12** and **13** dansyl (= 5-dimethylamino-1-naphthylsulfonyl) can be partly replaced by acetyl.

specifically labeled with a definite small number of hydrophilic oligomer reagent molecules would reduce the heterogeneity and complexity of the conjugate and perhaps lead to selective localization in tumor rather than in liver.[119]

The generalized Fab′ molecule depicted in Figure 2 represents a class of immunoglobulins that may be obtained from reductive cleavage of the two disulfide linkages in the hinge region of the corresponding $(Fab')_2$ species or possibly from engineered clones designed to express Fab′ or customized variants of its basic structure. The Fab′ derived from an IgG Mab having an antigen binding constant of $10^{11}\,M^{-1}$ might exhibit a binding constant of 10^{9}–$10^{10}\,M^{-1}$ and thus be useful as a carrier molecule. The two SH groups of each Fab′

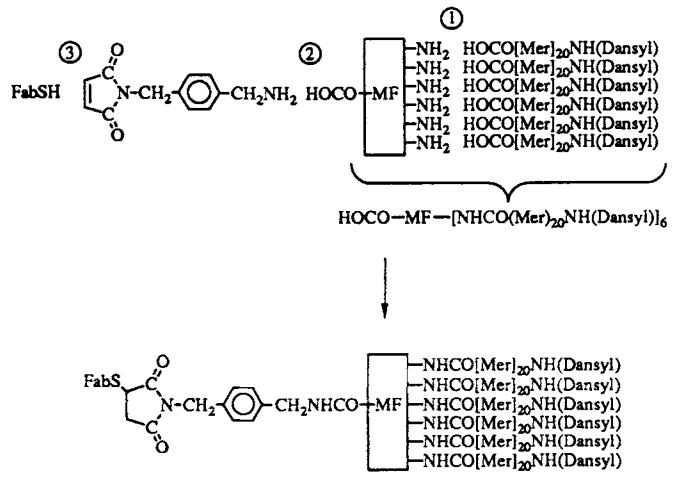

Scheme 12. Schematic representation of the assembly of a conjugate from Fab–SH and a linker molecule, a small lysine oligomer (manifold, MF) and boron-rich oligomers bearing fluorescent dansyl groups. The numerals indicate the order of assembly. Mer = repeating unit. The conjugate contains about 10^3 boron atoms.

molecule or the single SH group of a Fab–SH molecule may be employed for the conjugation[119] of arrays of precisely synthesized, boron-rich trailer molecules collected upon small precisely structured poly-L-lysine manifold molecules as shown in Scheme 12. Although the first trailer molecules such as **12** were diastereomeric mixtures of small amphiphilic peptides derived from DL-α-amino acids bearing anionic *nido*-carborane residues and fluorescent marker groups,[119–121] it is possible to assemble oligomers based upon the diphosphate esters of boron-rich diols[122] as shown in Scheme 13. The hydrophilic phosphate ester link-

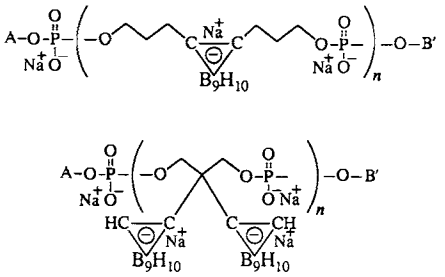

A = thymidine, B′ = $(CH_2)_6NH_2$, $n = 10$
A = biotin–C(O)NH$(CH_2)_6$, B′ = $(CH_2)_6NH_2$, $n = 20$
A = thymidine, B′ = $[CH_2CH(\text{fluorescein})CH_2OP(O)_2O(CH_2)_6NH_2]^-$, $n = 40$
A = $[\text{thymidine}OP(O)_2OCH_2CH(\text{fluorescein})CH_2]^-$, B′ = $(CH_2)_6SH$, $n = 50$

Scheme 13. An illustration of but a few of a myriad of possible structural motifs available through automated oligonucleotide methods for the synthesis of oligomeric boron-containing phosphate diesters.

age combined with anionic *nido*-carborane residues ensures hydrophilicity of the oligomeric reagents. The attractiveness of phosphate oligomers is further enhanced by their rapid automated synthesis with experimental procedures developed for DNA syntheses coupled with the ease with which UV-absorbent nucleoside residues, fluorescent marker groups, biotin, segments of polynucleotides, and terminal linker groups may be built into the oligomeric structure.[123] In one day it is possible to construct a phosphate trailer reagent, which could, in principle, contain many hundreds of boron atoms and be directly or indirectly linked to the SH functions of a Fab′ molecule.[119] Scheme 13 illustrates the structural scope of this new trailer chemistry and suggests a phosphate oligomer for linkage to Fab′ species through a suitable linker molecule. Research in this new area of chemistry is being actively pursued.

7.3.2. Binding of Boron and Hapten-Rich Oligomers to Cell Wall Antigen with Bispecific Antibodies and Other Host–Guest Interactions

Bispecific antibodies[124] such as the unsymmetrical $(Fab')_2$ species, $(Fab'_{nido})(Fab'_{CEA})$, offer the opportunity of binding a cell wall antigen, such as CEA, to a *nido*-carborane anion hapten group present in high concentration within a boron-rich hydrophilic trailer species. Immunochemical interactions of this sort would allow the concentration of large quantities of boron at cell wall antigenic sites without the use of covalent bonds. In practice the bispecific antibody would

be injected intravenously into the experimental tumor-bearing animal. Complexation of the Fab'_{CEA} segment of the bispecific antibody with CEA antigen sites ensues, the blood is cleared of excess circulating antibody, and then the boron- and hapten-rich trailer species is injected. Trailer-hapten-Fab'_{nido} binding occurs, and the selective (antigen-Fab'_{CEA})(Fab'_{nido}-hapten-trailer) bond formation process is completed. Scheme 14 illustrates the completed antigen complex. The boron-rich trailer molecule could contain an anionic *nido*-carborane-hapten group in each repeating unit and at least 10^3 boron atoms per trailer.

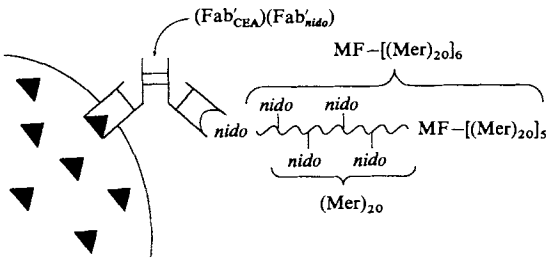

Scheme 14. The schematic representation of the use of a bispecific antibody (Fab'_{CEA})(Fab'_{nido}) for the simultaneous bonding of antigen of a tumor cell wall to boron- and *nido*-hapten-rich oligomer containing 10^3 boron atoms, similar to the manifold shown in Scheme 12.

The synthesis of a bispecific antibody of the type described here ultimately requires a source of the Fab'_{nido} fragment such as the parent IgG_{nido}. Such a Mab is now available from a murine hybridoma.[125] Scheme 15 illustrates the synthesis route for the bispecific antibody. Alternatively, this antibody might also be available from quadroma sources formed by gene fusion of available anti-CEA Mab and IgG_{nido} hybridomas.[126]

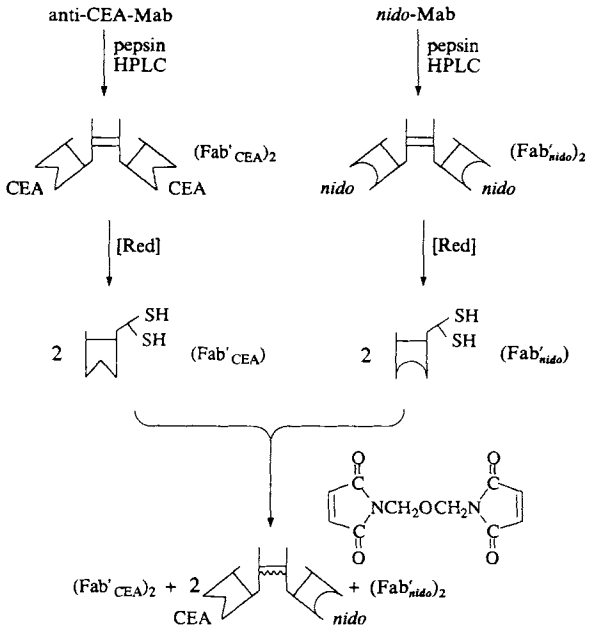

Scheme 15. The synthesis of a bispecific antibody from its IgG precursor molecules, anti-CEA–Mab and IgG_{nido}–Mab. Such a bispecific system is also illustrated in Scheme 14. [Red] = reduction.

A variant of the bispecific antibody concept is the application of the tightly associated streptavidin–$(biotin)_4$ complex.[127] In this instance Fab'_{CEA} is conjugated with two streptavidin molecules (one per SH group), and the experimental tumor-bearing animal injected intravenously. Following accretion of the Fab'_{CEA} at tumor and blood clearance, a boron-rich trailer species bearing a terminal biotin residue is administered in the same fashion. Ensuing in vivo complex formation would localize the boron-rich trailer molecule at antigenic sites occupied by Fab'_{CEA}. Recent progress toward the immunological approach to boron localization at tumors suggests that such delivery methods may eventually be useful with some tumor types. The use of antibody "cocktails" comprising mixtures of immunoglobulin carriers, each directed to a different antigen present on the same tumor cell, may be employed to enhance tumor boron concentrations. Difficulties such as tumor heterogeneity and uneven vasculaturization remain, but immunotransport methods may be combined with other completely different BNCT protocols.

7.4. Receptor-Mediated Bioregulatory Peptides as Boron Transport Vehicles

Related to the immunoglobulin carriage of boron to tumor cell antigens is the possible use of selected bioregulatory peptides as transport vehicles. The density of their receptor sites is far higher in tumor cell membranes than in normal cells.[128, 129] Although the actual number of such receptors present on each tumor cell may be as low as 10^4–10^5, receptors internalize their bound regulatory peptide and are regenerated. In effect, a pumping action exists for peptide internalization, which is itself regulated by the intracellular concentration of peptide. The useful rate of regeneration, coupled with the closer approach of internalized boron to the cell nucleus, lends validity to this boron delivery concept. Peptides such as epidermal growth factor (EGF)[128] and corticotropin-releasing hormone (CRH)[129] are candidate peptides having 53 and 41 amino acid residues, respectively. Both EGF and CRH are under evaluation as receptor-mediated boron delivery vehicles of relatively low molecular weight. EGF receptors are overexpressed by many human tumors found in the lung, breast, bladder, head, and neck. CRH is similarly targeted for pituitary tumors involving corticotrophic cells (Cushings disease). A third peptide of interest is growth hormone releasing hormone (GHRH), which, like CRH, is a pituitary-targeting peptide specific for somatotrophs (acromegaly) and composed of 40 amino acids. The successful application of CRH and GHRH delivery to BNCT of Cushing's disease and acromegaly would offer noninvasive procedures for these malignancies.

7.4.1. EGF Conjugation

Carlsson, Sjöberg et al.[128] and Barth, Carlsson et al.[130] have begun the investigation of EGF conjugation with primary carboranyl amines[131] such as **14** and its anionic *nido* analog **15** as well as (*R*)- and (*S*)-carboranylalanine (**16**).[86] Their conjugation procedure utilizes the coupling of dextran

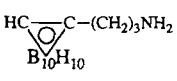

14

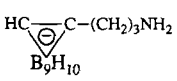

15

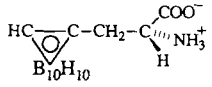

(*R*)-**16**

with the amino groups present in EGF and the amino groups of the amino carborane derivative, with 1-cyano-4-dimethylaminopyridinium tetrafluoroborate, as in Scheme 16, and provides relatively small conjugates (20–30 kD). They will be evaluated for boron delivery to glioma cells.

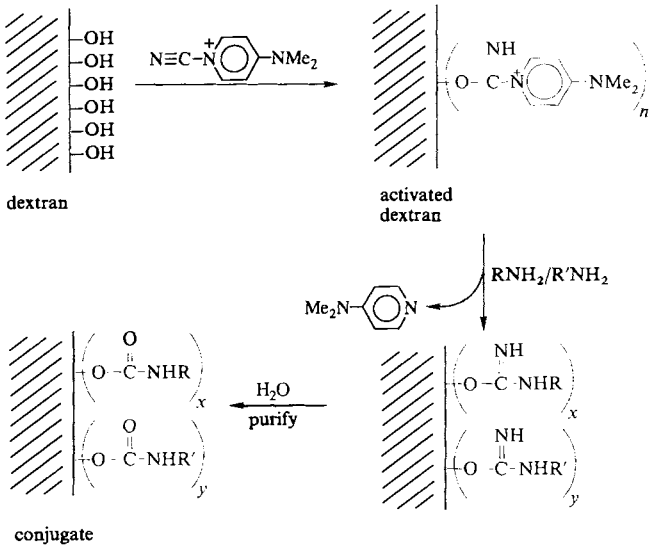

Scheme 16. Mechanism of the conjugation of EGF(RNH_2) with an amino-functionalized carborane derivative, $R'NH_2$ by means of dextran.

7.4.2. The Incorporation of Boron in CRH and GHRH Structures

CRH and GHRH are of similar size, but they differ with respect to their biologically important termini; CRH may be modified by the addition of an extraneous amino acid to its amino terminus without serious loss of corticotrophic cell activation.[129] GHRH may be similarly modified at its carboxyl terminus without significant loss of biological activity. Loriaux and Albertson et al.[129] have evaluated carborane-modified GHRH and ovine CRH species prepared by Chen et al.[132] CRH was synthesized with standard Merrifield solid-phase procedures except that the serine amino terminus was acylated with the carboranylacetic acid **17**. GHRH

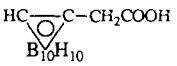

17

was modified at its carboxyl terminus by the addition of a lysine residue whose ε-amino group was acylated with **17**. Both the modified peptides evoked biological responses in vitro similar to that of the unmodified species.[129] Their efficacy of boron delivery remains to be determined. The boron content of the peptides could most reasonably be increased by the attachment of small boron trailer molecules rather than **17**. The size, charge, and hydrophobicity of the trailer will require careful selection to retain receptor recognition and binding by the conjugate.

7.5. Cell-Wall Receptor-Mediated Low-Density Lipoprotein (LDL) Vesicles as Boron Carriers

The LDL vesicle[133–135] illustrated in Figure 3 and briefly discussed in Section 6.1 comprises a phospholipid/cholesterol shell with a diameter of approximately 15–20 nm, filled with cholesteryl esters of long-chain alkyl carboxylic acids. Apoprotein B-100 is attached to the external

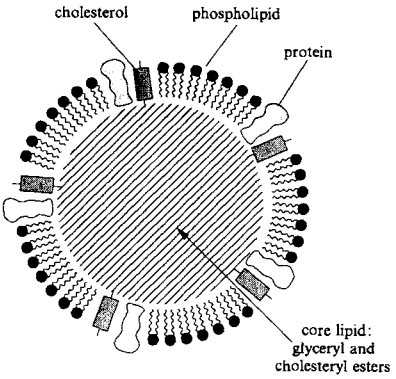

Fig. 3. A stylized cross-sectional view of a low-density lipoprotein vesicle filled with glyceryl and cholesteryl esters of fatty acids. The protein exposed on the vesicle surface responds to the LDL receptor sites present in the plasma membrane of cells.

surface of the vesicle and serves as a specific anchor for receptor sites located on the external cell walls of both malignant and normal cells. Receptor–LDL complexes are internalized by endocytosis, the LDL is degraded to cholesterol by lysosomes, and the receptor returns to the external cell wall. This pathway provides about 90% of the cholesterol necessary for cellular membrane synthesis.[136] Malignant cells are expected to utilize cholesterol (and LDLs) at a much higher rate than normal cells because of higher replication rates, and therefore to have correspondingly higher receptor turnover rates. This provides a basis for cellular differentiation and the targeting of tumor cells with boron if the cholesteryl esters of the LDL core are replaced with a boron-rich material. This concept was proposed by Kahl et al.,[91,137] who exploited it through the substitution of esters derived from fatty alcohols and carborane carboxylic acid, such as **18**, for the native cholesteryl esters[138] after removal of the latter material from harvested LDL vesicles by solvent extraction. The reconstituted boron-containing LDL vesicles contained approximately 12×10^3 boron atoms each.[91,137] Later work has shown[91b] that simple hydrophobic carborane derivatives such as 1-hexyl (**19**) or 2-propenyl (**20**) derivatives efficiently reconstitute LDL vesicles. In vitro evaluation of these novel boron carriers on CHO and V-79 Chinese hamster cells in conjunction with thermal neutron irradiation at the Brookhaven Medical Research Reactor established that boron was taken up intracellularly in concentrations as high as 240 μg boron per g cells.[91a] This will be recognized as a spectacular result!

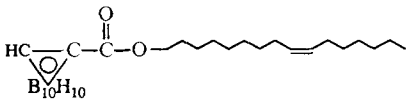

18

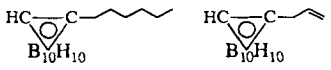

19 20

Kahl et al. have recently initiated biodistribution studies in small animals, but no results are available at this time.

7.6. LDL Complexes of Porphyrins and Phthalocyanines as Receptor-Mediated Boron Carriers

It has long been known that porphyrin, phthalocyanine, and related heterocyclic molecules have a propensity to localize in solid tumors and persist there in the long term. This property of porphyrins provides the basis of photodynamic therapy (PDT),[139] another binary therapeutic method that utilizes porphyrin derivatives localized in tumor as in situ photosensitizers for the production of singlet oxygen on irradiation with red light.[140] Candidate porphyrin derivatives that contain boron for BNCT purposes are also of interest for potential PDT applications. As pointed out in Section 6.1, the mechanism of this localization process or processes remains unknown, although the differentiation between uptake by normal and malignant tissues suggests that a receptor-mediated mechanism driven by very high turnover rates in tumor cells is involved. Porphyrins observed to be most effective in tumor localization are water soluble, amphiphilic species carrying hydrophobic substituents like BOPP (**23**). A plausible receptor-mediated mechanism might involve LDL vesicles,[94] which utilize their hydrophobic constituents to solvate and encapsulate circulating porphyrin. Rapid uptake of the porphyrin-loaded LDLs would then internalize the heterocycle.

The possible use of boron-containing porphyrins as BNCT agents has been explored from the early 1980s onward. Representative derivatives that have been synthesized are based upon tetraphenylporphyrin (e.g. BTPP (**21**))[141] and hematoporphyrin (e.g. VCDP (**22**)[142] and BOPP (**23**)).[143] The *nido*-7,8-$C_2B_9H_{11}^-$ residues present in **21** and **22** are necessary to lend water solubility to the array. Since the anionic *nido*-carboranyl substituent is an amphiphilic[119] rather than a hydrophilic substituent, this water-solubilizing tactic does not totally degrade the hydrophobic character of **21** and **22**. The porphyrin **23** would be expected to be more hydrophobic than **21** and **22**, since it contains four very hydrophobic *closo*-carboranyl groups,[144a] and only two hydrophilic carboxylate substituents enhance hydrophilic properties. The greater hydrophobicity of **23** may be a direct cause of its superior tumor localization and retention[144b,c] relative to **21** and **22**.

The biodistribution of **21**,[145] **22**,[142a,146] and **23**[143,147] was evaluated with a variety of murine tumor models. Tumor types included gliomas and melanomas. The porphyrin derivatives were administered by either intravenous or intraperitoneal injections. Although the boron localization data obtained in these experiments was dependent upon experimental details and the identity of the porphyrin derivative, all three compounds were taken up and retained for days, whereas **23** was retained for weeks. Concentrations of boron in liver were generally about twice that simultaneously observed in the tumor, and when measured, boron levels in spleen and kidney were also elevated. Boron cleared from blood with time. Injected doses of 25–50 mg B per kg body weight were often employed, and boron concentrations of 15 to 40 μg per g tumor were observed with carcinomas. Among porphyrin derivatives, **23**[147] provides the highest boron uptake by tumor combined with long retention times.

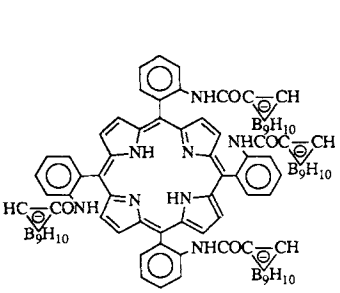

21 BTTP

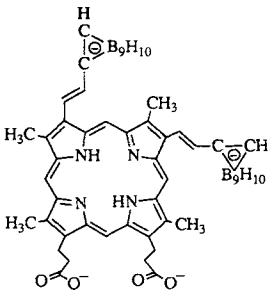

22 VCDP

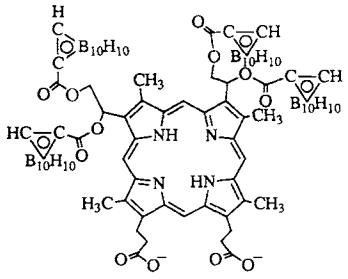

23 BOPP

Recent work with intracerebral glioma xenografts in CBA mice by Hill, Kahl et al.[148] proved that **23** injected intravenously or intraperitoneally (30 mg B per kg body weight) could be localized in glioma at concentrations greater than 20 μg B per g tumor, while the concentration in blood was less than half this value and in normal brain immeasurably low. Fluorescence studies with confocal laser scanning microscopy for **23** demonstrated that this compound was localized intracellularly and almost exclusively in organelles, both in vitro and in vivo. Density gradient ultracentrifugation studies proved these organelles to be mitochondria. It was calculated that this intracellular location of **23** could result in an up to tenfold reduction in the amount of boron required to achieve tumor necrosis by BNCT (2–3 μg B per g glioma). Porphyrin **23** is clearly an attractive candidate for a variety of tumors, and work pertinent to its adoption by the BNCT community is proceeding at a rapid pace.

Radiometal complexes of the phthalocyanines have been employed as diagnostic reagents, since they localize in tumors in a fashion reminiscent of porphyrins.[149] The sul-

fonated, water-soluble copper phthalocyanine has apparently been prepared by Soloway[149] through the reaction of 1-(4-aminophenyl)-*closo*-1,2-$C_2B_{10}H_{10}$ with copper tetra-(chlorosulfonyl)phthalocyanine followed by hydrolysis. No details on the purification, characterization, and efficacy of this species in tumor localization have yet been presented.

7.7. Synthetic Liposomes as Tumor-Differentiating "Supertankers" for Boron Delivery

In Sections 6.1 and 7.5, LDLs[91] and their cell wall receptors were discussed as potential systems for the delivery of boron in relatively large increments. Related to LDLs is the family of vesicles identified as synthetic unilamellar liposomes.[90] These liposomes consist of a phospholipid bilayer that forms a spherical shell surrounding an aqueous core. The liposomes that have been applied to BNCT have, for the most part, carried hydrophilic sodium salts of polyhedral borane anions as solutes in the aqueous center of the vesicle, although, in principle, the phospholipid bilayer could also carry dissolved lipophilic species. Small multilamellar liposomes having several discrete layers of phospholipids might be utilized with boron-containing lipids as constituents. Figure 4 presents a cross-sectional view of a typical unilamellar liposome on the right and details of the bilayer structure. The

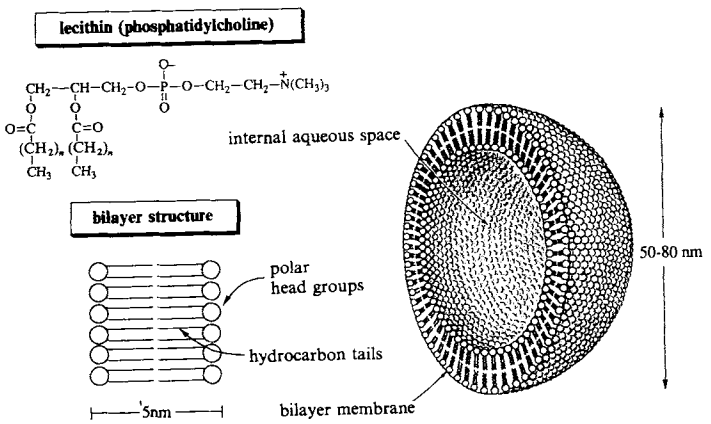

Fig. 4. Cross-sectional view of a liposome of the type found to be useful for boron delivery to tumors in mice. Synthetic phosphatidylcholine forms the bilayer membrane of these synthetic liposomes. Cholesterol is present in the bilayer, as well.

unilamellar liposomes employed for the localization of boron in tumor [90] range from 30–80 nm in diameter, and utilize cholesterol-rich bilayers of pure synthetic phospholipid to lend mechanical strength required for long-term circulation in the vascular system. Although the liposome shown in Figure 4 consists of a phospholipid having no net charge on its polar terminus, liposomes with net negative[150] or positive charges[151] can be prepared. Surface charge affects biodistribution and pharmacokinetics. As shown in Section 7.7.1, liposomes of the type employed for boron delivery are capable of excellent selective localization in a variety of tumors following intravenous injection. They have previously been employed as tumor-selective delivery vehicles for radiopharmaceuticals used in animal models[152] and in human diagnosis.[153] Unlike LDLs, synthetic liposomes carry no receptor-seeking appendages, although, as pointed out in Section 6.1, they are selectively internalized by tumor cells. This cellular differentiation process is believed to be due, at least to a large extent, to the immature and consequently abnormally porous vasculature of rapidly growing tumors.[93] The internalization process itself could arise by nonspecific endocytosis of the coated-pit → coated-vesicle type.[92, 154] Alternatively, LDL receptor sites may in some way be available to small liposomes and thereby provide a selective internalization pathway as in the case of LDLs themselves.

7.7.1. Unilamellar Liposomes

We have carried out extensive studies[90, 155] of unilamellar liposomes of the type illustrated in Figure 4 as boron delivery vehicles. Earlier results obtained by workers at Vestar, Inc. proved that liposomes of this type preferentially deliver their contents to tumor cells in animals and humans to provide levels of effector molecules in tumor five to ten times that of normal tissue, including blood.[151–153] Sodium salts of polyhedral borane anions based upon $B_{10}H_{10}^{2-}$, its oxidation product, n-$B_{20}H_{18}^{2-}$,[*] and their derivatives have provided water solutions (250–300 mM) of sodium salts with excellent hydrolytic stabilities, which were employed as the aqueous cores of 40–80 nm liposomes.[90, 155] These hyperosmotic vesicles proved to be generally stable; they can be stored for months and remain in circulation for 3–4 days. However, the stabilities observed in vivo were always a function of the identity of the solute present in the core. Biodistribution studies with many boron-containing liposomes of the type used here proved that liver and spleen (reticuloendothelial cells) accreted appreciable quantities of liposomes in competition with tumor. The initial liver-to-tumor boron concentration ratios were often about 2:1, but decreased with time. Blood always cleared with time, and tumor-to-blood boron ratios of 5:1 or higher were not uncommon when the concentration of boron in tumor was in the therapeutic range (20–40 μg B per μg tumor). Protocols exist for the suppression of liposome uptake by reticuloenthelial cells.[151] The effective toxicity of all compounds[90, 155] delivered by liposomes should be decreased as a result of encapsulation. Although detailed toxicity data is not yet available for the majority of the more interesting compounds studied, no acute effects have been observed in mice whose tumors acquire therapeutic levels of boron. The majority of the biodistribution work was accomplished with BALB/c mice bearing implanted EMT6 murine adenocarcinomas.[90, 155]

$Na_2B_{10}H_{10}$ was the first polyhedral borane anion to be encapsulated as outlined above.[90, 155] Time-course evaluation with low total injected boron doses (6 mg B per kg body weight) proved that although the $B_{10}H_{10}^{2-}$ ion was entering tumor, liver, and spleen, all of these tissues were cleared at similar rates, and boron was not retained in the tumor. BSH ($Na_2B_{12}H_{11}SH$, 7 mgB per kg body weight) gave essentially

[*] n here represents the "normal" isomer synthesized first and i its photoisomer.

the same result as that obtained with $Na_2B_{10}H_{10}$. These initial results suggested that in order to be effective the borane derivative must be capable of reaction with components of the cytoplasm such as the ubiquitous amino groups indigenous to intracellular proteins.

The interconversion of the isomeric n-$B_{20}H_{18}^{2-}$ (**24**)[157] and i-$B_{20}H_{18}^{2-}$ (**25**)[158] ions, depicted in Scheme 17, and their chemistry,[156] illustrated with **24** in Scheme 18,[90, 155] suggested their possible intracellular incorporation as shown in Scheme 19. The $B_{20}H_{18}^{2-}$ ions deliver twice as many boron

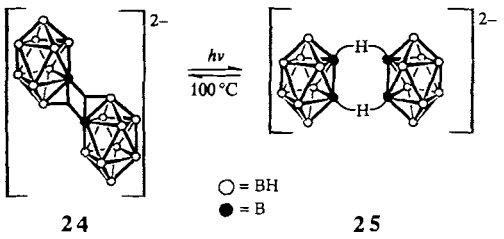

Scheme 17. Reversible interconversion of thermodynamically favored n-$B_{20}H_{18}^{2-}$ (**24**) and its less stable photoisomer, i-$B_{20}H_{18}^{2-}$ (**25**).

atoms per three ions as $Na_2B_{10}H_{10}$ thus increasing boron availability for the same osmotic stress on the liposome. Scheme 4 indicates the preferred synthesis[71] of $B_{10}H_{10}^{2-}$ from $B_{10}H_{14}$, which could be adapted to the synthesis of ^{10}B-enriched $B_{10}H_{10}^{2-}$ to serve as a precursor for a series of compounds including n- and i-$B_{20}H_{18}^{2-}$.

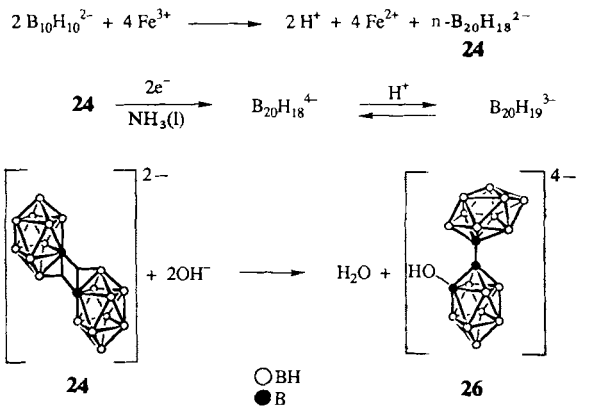

Scheme 18. The formation of n-$B_{20}H_{18}^{2-}$ (**24**) and its subsequent two-electron reduction to form e^2-$B_{20}H_{18}^{4-}$ (e = equatorial), which undergoes acid-catalyzed rearrangement to the ae and a^2 isomers (a = apical). The $B_{20}H_{19}^{3-}$ intermediates are observed, and the most stable a^2-$B_{20}H_{19}^{3-}$ isomer is easily isolated. The apical and equatorial positions of the component $B_{10}H_9^{2-}$ cages are joined by a normal two-election bond, which generates the three isomeric frameworks of $B_{20}H_{19}^{3-}$ and $B_{20}H_{18}^{4-}$. The *kinetically controlled reaction of* **24** *with* OH^- yields the 2-hydroxy isomer **26**, which is isoelectronic with ae-$B_{20}H_{18}^{4-}$.

As expected, liposomes containing Na_2(n-$B_{20}H_{18}$) (15 mg B per kg body weight) exhibited improved performance by increasing the quantity of boron available in a standard liposome dose. More significantly, the n-$B_{20}H_{18}^{2-}$ ion was retained by tumor, while other tissues were more rapidly cleared. The boron concentration in tumor was 24 μg B per g, and the tumor-to-blood ratio was 1.2:1 twenty-four hours after injection. These values changed to 3.3 μg and 14:1 after 48 h.

The more reactive photoisomer Na_2(i-$B_{20}H_{18}$) (11 mg B per kg body weight) was quite persistent. The boron concentration in tumor after 48 h (14 μg per g) was still 71% of the value at 6 h. During this period the tumor-to-blood concentration ratio increased to 12:1. Free Na_2(i-$B_{20}H_{18}$) in buffer was not retained when injected (11 mg B per kg body weight), but rapidly excreted; the tumor, blood, and liver concentrations of boron were only 1.9, 1.9, and 8.9 μg B per g, respectively, after 24 h. An experiment in which two injections of Na_2(i-$B_{20}H_{18}$)-containing liposomes (15 mg B per kg body weight injected at 0 and 24 h) were administered yielded similar results after 24 h. After the second injection and a total time of 48 h, the boron concentration in tumor was 27 μg B per g, and the tumor-to-blood concentraton ratio was 2.6:1. These are therapeutically useful values. The concentration of boron in the liver was about 60 μg B per g.

Evaluation of liposomes that contained derivatives of the isomeric $B_{20}H_{18}^{4-}$ ions provided the basis of new localization concepts. The isomeric hydrolysis products $B_{20}H_{17}OH^{4-}$[156a] of **24** (**26** in Scheme 18) or **25** are isoelectronic with the $B_{20}H_{18}^{4-}$ ions[159] produced by two-electron reduction of **24** or **25**. The potassium salt of **26** was evaluated for use in BNCT in the usual fashion and shown to be rapidly cleared from tumor as in the case of $Na_2B_{10}H_{10}$. However, $Na_3B_{20}H_{19}$[159] produced by protonation of a^2-$B_{20}H_{18}^{4-}$ (8 mg B per kg body weight) behaved differently. Nearly 30 μg B per g tumor was found after 6 h. Concentrations of boron in tumor decreased at a moderate rate, while concentrations in liver increased for 30 h. Boron levels in blood reached 7.5 μg B per g after 48 h, while the tumor concentration fell to 12 μg per g. These results preface the discovery of the most efficacious polyhedral borane anion yet evaluated.

The ammonia-substituted ae-$B_{20}H_{18}^{4-}$, $B_{20}H_{17}NH_3^{3-}$ (**27**, see Scheme 20) is similar to the parent anion except that an uncharged NH_3 molecule has been formally substituted for hydride ligand, thus reducing the ionic charge to −3. Evaluation of $Na_3B_{20}H_{17}NH_3$ in liposomes (11 mg B per kg body weight) produced spectacular results as shown in the time course plot of Figure 5.[160, 161] Even with the low injected dose employed, the boron concentration of 25 μg B per g

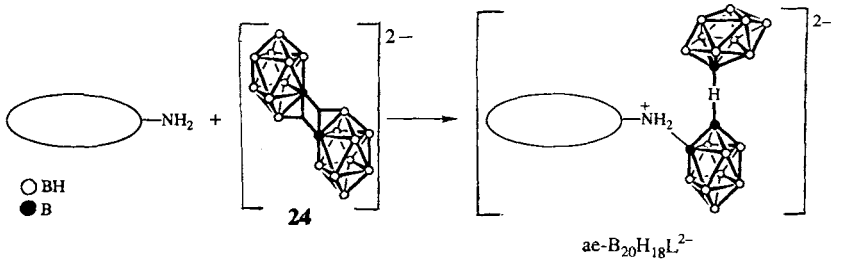

Scheme 19. Proposed reaction of an intracellular protein molecule, symbolized as ○–NH_2, with **24** to form an ae derivative. The i-$B_{20}H_{18}^{2-}$ isomer (**25**) would provide a similar, but more facile reaction.

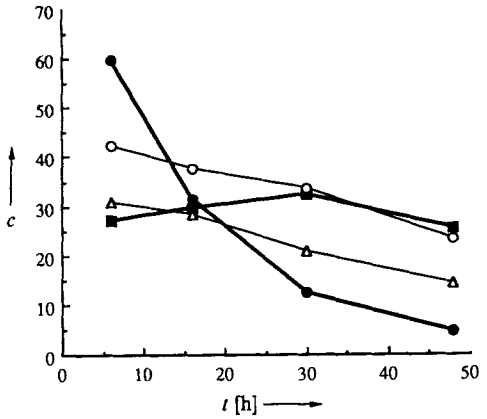

Fig. 5. Data from a time-course study on the distribution of liposomal $Na_3B_{20}H_{17}NH_3$ (**27**) in BALB/c mice bearing EMT6 mammary adenocarcinomas. c = boron concentration in tissue in μg per g. ● in blood, ■ in tumor, o in liver, Δ in spleen. The injected dose was 11 mg per kg body weight.

respectively. In fact, the boron concentration of tumor increases during the first 30 h and reaches a maximum of 35 μg per g. One plausible explanation of these results is based upon the possible intracellular two-electron oxidation of **27** to $B_{20}H_{17}NH_3^-$ (**28**) within tumor cells as shown in Scheme 20. The single negative charge of **28** would enhance

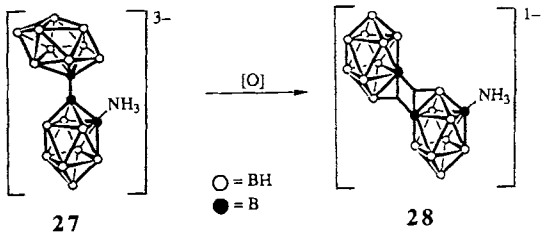

Scheme 20. Proposed intracellular oxidation of **27** to the very reactive, but hypothetical $B_{20}H_{17}NH_3^-$ (**28**), which should rapidly bind with intracellular protein. [O] = intracellular oxidation.

the electrophilicity of this ion compared to the $B_{20}H_{18}^{2-}$ ions, and could thus improve the intracellular bonding (see Scheme 19). In addition some other feature prevents the extensive uptake of **27** by liver and promotes the concomitant low final blood levels of boron. Extensive evaluation of **27** is underway, since its liposomes offer one of the most effective boron delivery systems yet described in small animals.

Another reactive polyhedral borane anion derivative has been recently described and evaluated for suitability for BNCT.[162] This species is 2-isocyanato-*closo*-$B_{10}H_9^{2-}$ (**29**)[163], whose isocyanate function is expected to form the corresponding urea derivative upon intracellular reaction with amino groups of protein as described in Scheme 21. Data from preliminary biodistribution studies with liposomes that contain the disodium salt of **29** (9 mg B per kg body weight) are presented in Figure 6 along with a comparable set of results obtained with $Na_2B_{10}H_{10}$ (6 mg B per kg body weight). These results prove that **29** is better retained by tumor, liver, and spleen than its unsubstituted parent, $Na_2B_{10}H_{10}$. One may conclude that the isocyanate function of **29** serves, as expected, by linking to intracellular protein.

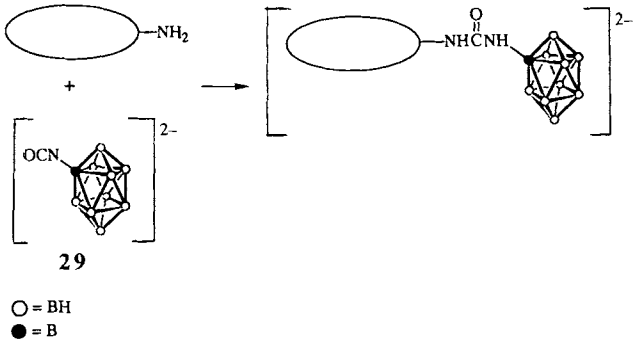

Scheme 21. Proposed reaction of **29** with an intracellular protein molecule ○-NH_2.

The synthesis and evaluation of liposomes containing other polyhedral anions that bear functional groups continues.

Although Moore et al.[164] reported the delivery of hydrophobic thiouracil derivatives of carborane (see Section 7.10.1) dissolved in lipid bilayer to murine melanoma xenografts on use of 100 nm phospholipid-supported liposomes, the efficacy of this procedure could not be deduced from the reported results except that high tumor selectivity was observed.

The simplicity, broad scope, and exciting preliminary results obtained with liposomes have established them as one of the most promising boron delivery methods yet devised.

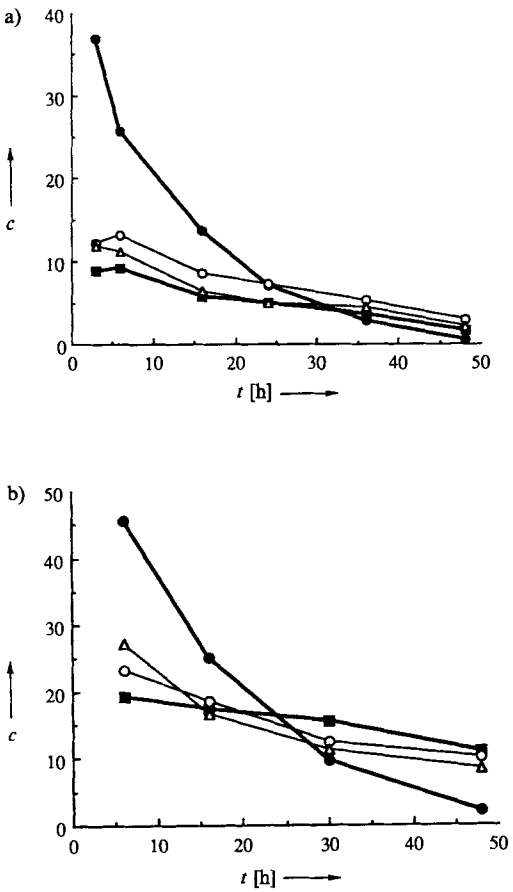

Fig. 6. Comparison of the distribution of liposomal $Na_2B_{10}H_{10}$ (a) and Na_2[2-OCN-$B_{10}H_9$] (b) from time-course studies on EMT6 mammary adenocarcinomas grown in BALB/c mice. The injected dose was 6 mg per kg body weight in a) and 9 mg per kg body weight in b). For explanation of other symbols, see Figure 5.

7.8. The Potential of Sex Hormone Receptors as Vehicles for the Delivery of Boron to the Cell Nucleus

Both breast and prostate cancer have predominant cell lines that depend upon the constant uptake of estrogen and dihydrotestosterone, respectively. These hormones become effective following complexation with their respective receptors present in the cytosol of the proper cell, followed by translocation of the resulting hormone–receptor complex to the chromatin within the cell nucleus. Both Hadd[165] and Kahl[166] have synthesized carborane derivatives of estradiol (**30** and **31**, among others). Hechter and Schwartz[167] used available data pertinent to receptor site densities to calculate the probable concentration of boron that could be obtained with receptors of this type. With efficacious hormone surrogates carrying one carborane cage per molecule (ten boron atoms) only about 0.015 μg B per g tissue could be delivered to chromatin in this fashion. The goal of 1–2 μg B per g tissue was thought to be reasonable, since the boron targets were placed in the cell nucleus.

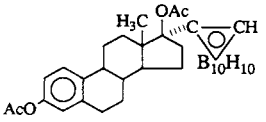

30

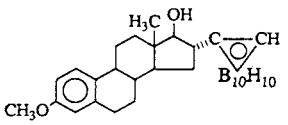

31

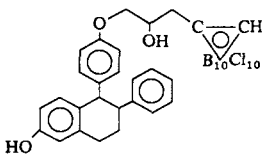

32

Work has apparently been abandoned with this aspect of selective boron delivery. However, Gabel et al.[168] synthesized a boron-rich analog, **32**, of the antiestrogen molecule U23 469-M that contained a decachlorocarborane substituent. This compound was taken up nonspecifically by ZR 75-1 breast cancer cells and partially inhibited the uptake of estradiol in these cells. The estimated 10^4–10^5 receptor sites available per cell are far less than the number required to achieve therapeutic levels of boron. This line of endeavor has been abandoned as well. Even though boron was placed within the cell nucleus, it has been impossible to approach the concentrations required for BNCT.

7.9. Boron-Containing Amino Acids as Prescursors in Protein Synthesis

Recent emphasis has been placed upon the evaluation of a variety of boron-containing amino acid derivatives that may carry boron to tumors by becoming incorporated in protein synthesis or metabolism within the rapidly growing tumor cell. L-4-Dihydroxyborylphenylalanine[87] has received particular attention. L-Carboranylalanine,[144a] an analog of phenylalanine, was only recently synthesized by improved methods.[86a, 86b] Spielvogel pioneered the synthesis of natural amino acid surrogates[169] in which a carbon atom has been replaced by an isoelectronic and isosteric boron atom having four valence electrons and a negative formal charge. These studies constitute one of the most dynamic areas of BNCT research currently under investigation.

7.9.1. Studies with L-4-Dihydroxyborylphenylalanine

Snyder et al.[170] first reported DL-4-dihydroxyborylphenylalanine (BPA (DL-**33**); see Scheme 23), which was subsequently examined in animals by Soloway in the 1950s and found to provide the most favorable tumor/brain selectivity (8.5:1) of all the boronic acids similarly screened at that time.[57] Interest in BPA as a BNCT target compound was dormant until Mishima et al.[87, 171] discovered its efficacy against B-16 melanoma in vitro and in hamsters bearing Greene's melanoma during neutron irradiation experiments[171] with ^{10}B-enriched **33**. Further work with Duroc pigs[171] and humans[172] afflicted with melanoma proved that ^{10}B-enriched DL- or L-**33**, was effective in BNCT and that primary lesions that were highly pigmented were destroyed. Because of the extremely low solubility of **33** in water, the compound was administered by perilesional injection (i.p.) or orally. Esterification of **33** with sugars improved its solubility.[173] This use of **33** against melanoma was developed by Mishima et al.[87] based upon the fact that the melanin pigment normally present in active melanoic neoplasms is synthesized from natural amino acids containing aromatic rings such as L-dopa, L-tyrosine, and L-phenylalanine. Presumably, this process involves 5,6-indolequinone as an intermediate. It was assumed[87, 171] that **33** would fall into this class of melanin precursors[174] and enter the characteristic melanin produced by intracellular melanosomes. Scheme 22 illustrates the biosynthesis of melanin. However, the insertion of **33** in this mechanism would require that the

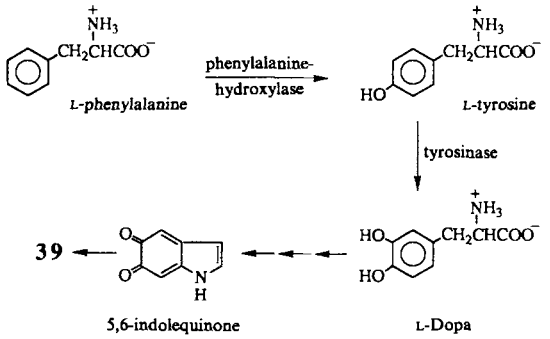

Scheme 22. The stepwise enzymatic oxidation of L-phenylalanine leading to the 5,6-indolequinone polymer melanin **39**. The structure of **39** has not been precisely determined.

4-dihydroxyboryl group be removed[175] prior to the formation of the quinone, presumably as boric acid. This loss of boric acid could occur through acid-catalyzed hydrolysis of the B–C bond or by oxidative cleavage of the C–B bond (Scheme 23). Migration of boric acid from the cell interior to the extracellular volume is a facile process that should preclude the accumulation of boron within tumor. The accre-

tion of therapeutic boron concentrations in melanomas (and other tumor types) is therefore likely to be due to another bioutilization process.

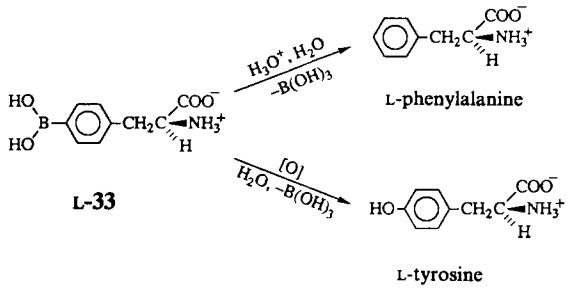

Scheme 23. Known reactions of L-33, which may occur in vivo and lead to the loss of boric acid.

Other experimental observations made with ion microscopy that shed light on this problem have been reported by Morrison et al.[46] These workers developed a cell-culture system for the study of drug uptake into a malignant, highly pigmented M-3 murine melanoma clonal strain. The pigment level (extent of melanization) could be matched, area for area, to ion intensities from superimposed photomicrographs and ion images by using the aryl-bound deuterium present in [D_4]-L-tyrosine and boron in DL-**33** as sources of the imaged ions. In any given area of the cell culture the increase in melanin concentration correlated linearly with an increase in deuterium concentration due to the uptake of tyrosine, a known melanin precursor (Scheme 22). The boron concentration did not change as melanin was produced; DL-**33** consequently does not deposit its boron in the melanin of developing melanoma cells.

Coderre et al. demonstrated that **33** is accreted by the weakly pigmented B-16 melanoma carried by C57BL mice.[176] This result suggests that **33** uptake, which according to other experiments favors the L-stereoisomer,[174] proceeds through active transport of the amino acid for purposes other than the synthesis of melanin. This is important to therapy since many forms of human melanoma are variably pigmented, and very dangerous metastases are not pigmented early in their development.

In addition, Coderre et al.[174] demonstrated that L-**33** was much more effective than its enantiomer against Harding–Passey melanoma, that oral administration of ^{10}B-enriched **33** achieved tumor concentrations of boron as high as 40 μg per g in BALB/c mice,[176] and that the growth inhibition of these tumors was directly related to the neutron fluence with the result that longer exposure time caused a longer delay tumor growth, as expected. More recent work by this same group[177] showed that boron was selectively delivered to tumors other than melanomas; the KHJJ murine mammary carcinoma in mice and GS-9L gliosarcoma grown in rat brain are representative of such tumors. Boron concentrations as high as 20 μg B per g tumor were attained in the gliosarcomas after oral administration of L-**33**. Other studies of this type are too numerous to mention, but they all support the useful application of L-**33** to amelanoic tumors.

Recently Coderre et al. reported[100] the experimentally determined RBE values of the BSH disulfide dimer BSSB (Scheme 7) and L-**33**, obtained from cell-survival data following thermal neutron irradiation of cells that were enriched in the boron compounds. Gliosarcoma cells (GS-9L) were employed both in vitro and in intracerebral rat tumors. The in vitro RBE values (Section 2.4) ranged from 3.5 to 4.1 for L-**33** and from 1.1 to 1.4 for BSSB. It was pointed out that these BSSB values were physically unrealistic and characteristic of a mechanism for in vivo tumor cell death dependent upon the destruction of vascular endothelial cells through BNC and a resultant loss of vasculature function at the tumor. On the other hand, the higher RBE values observed with L-**33** were consistent with neutron capture by intracellular L-**33**. The destruction of endothelial cells of the vasculature as the principal killing mechanism for BNCT with BSH and BSSB has been noted in Section 7.1.

As pointed out above, the low water solubility of L-**33** hydrochloride at physiological pH has complicated the use of L-**33** in experiments with large animals. This problem has been largely overcome[173] by converting L-**33** to water soluble boronate esters with fructose, diethanolamine, and cyclodextrin derivatives. These species offer the promise of an intravenous injection protocol.

A phase I clinical trial for L-**33**[178] is planned by the New England Medical Center–MIT Program in Neutron Capture Therapy. This clinical trial will join another in progress at the School of Medicine at Kobe University, Japan.

Both DL-2- and DL-3-dihydroxyborylphenylalanine have been synthesized and await thorough evaluation.[179] In addition, the 4-*closo* (**34**) and 4-*nido* (**35**) derivatives of DL-4-carboranylphenylalanine have been prepared[180] and are undergoing biological evaluation. An asymmetric synthesis

of L-**33** has also been developed,[181] which involves the hydrogenation, catalyzed by a chiral rhodium complex, of a substituted α-amino acrylic acid derivative.

7.9.2. *L-Carboranylalanine*

The accelerated rate of synthesis of proteins and amino acid metabolites exhibited by a malignant cell, coupled with the active transport mechanisms available for amino acid accumulation within cells, provides a bioutilization process that may allow boron-containing α-amino acids to enter tumor cells preferentially. The selective uptake of L-**33** by several types of malignant cells appears to follow this cell differentiation mechanism (see Section 7.9.1).

Since one of the most chemically attractive packages for the delivery of boron is the *closo*-1,2-$C_2B_{10}H_{12}$ cage, it is not surprising that the L-phenylalanine surrogate, L-carboranylalanine (**16**) is a highly desired species for biological evaluation. The initial synthesis of **16** was reported[144a] in 1976.

The asymmetric syntheses of the D and L enantiomers have recently become the goal of several research groups, most notably those of Kahl et al.[86a] and Sjöberg et al.[86b] (Schemes 24 and 25, respectively). It was noted by the discov-

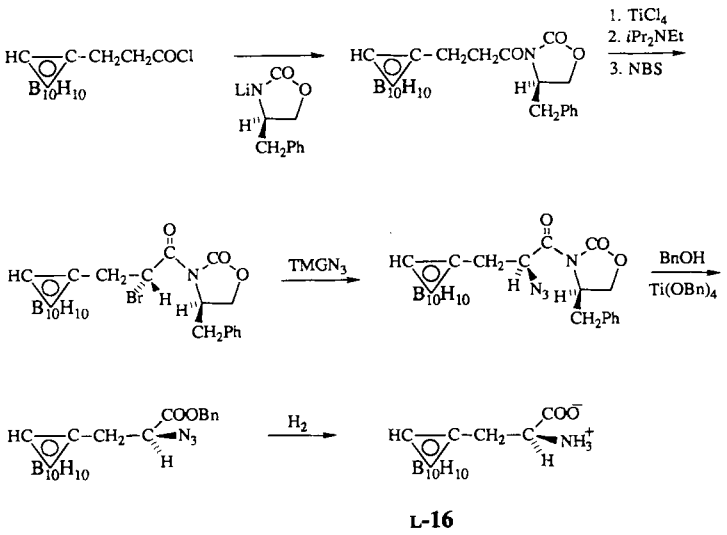

L-16

Scheme 24. The asymmetric synthesis of D- and L-16, devised by Kahl and Radel [86a]. NBS = *N*-bromosuccinimide. $TMGN_3$ = tetramethyl guanidinium azide. The subsequent hydrogenation proceeds catalytically.

erers of **16** that the carborane cage imparted extreme hydrophobicity upon this amino acid,[144a] and Kahl et al.[86a, 128] has pointed out that the steric requirements of the carborane group in **16** is approximately the same as the volume swept out by the rotation of the phenyl group in phenylalanine. Small hydrophilic peptides that incorporate L-carboranylalanine may prove useful to enhance its effective water solubility and bioavailability. Alternatively, its anionic *nido*-

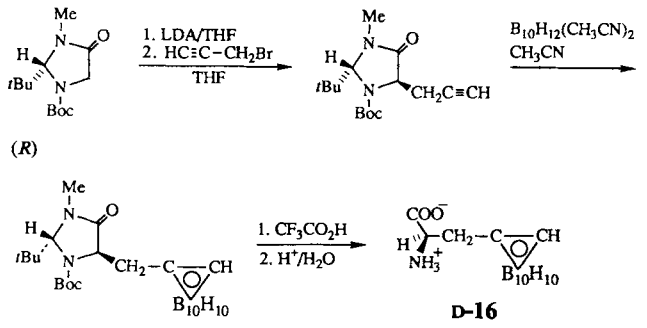

D-16

Scheme 25. An asymmetric synthesis of D- and L-**16**, described by Sjöberg et al. [86b, 128]. LDA = lithium diisopropylamide. The last step takes place on a cation exchange resin.

$C_2B_9H_{11}^-$ derivative will, at the least, be amphiphilic. Nonetheless, the synthesis of **16** makes an important biomolecule readily available for the first time. The results of in vitro and in vivo evaluation of **16** and its derivatives are awaited with great anticipation.

Related to **16** are the amino acids **9**[120, 121] and **10** (Section 7.3.1), which have not been investigated as enantiomerically pure compounds. The asymmetric synthesis of Sjöberg et al.[86b] makes these and related species generally available.

7.9.3. *Ammonium Carboxyborane Analogs of Amino Acids*

Replacement of a neutral carbon atom by an anionic boron atom bearing four valence electrons results in an isoelectronic and isosteric replacement as in the formal relationship of *closo*-$B_{12}H_{12}^{2-}$ and *closo*-1,2-$C_2B_{10}H_{12}$ (see Section 5). This process also provides a pathway for the introduction of boron into simple organic compounds such as α-amino acids and their derivatives. Spielvogel et al.[169, 182] have applied this principle to the BNCT of cerebral tumors by developing a synthesis of **36**, the ammonium carboxyborane analog of glycine. This particular molecule was of importance, because glycine has the lowest rate of transport across the blood–brain barrier of the amino acids, and the ^{14}C-labeled glycine molecule was shown to give a tumor/brain concentration ratio of 10:1 and a tumor/blood concentration ratio of 5:1 twenty-four hours after injection in BALB/c mice carrying brain inplants of Harding–Passey melanoma.[182] Injection of sufficient **36** to provide 40 mg per kg body weight in mice identical to those used in the ^{14}C-labeled glycine experiment gave very disappointing results; rapid total clearance of **36** from the animals and 2 h postinjection tumor, brain, and blood concentrations of 16.2, 7.6, and 8.8 μg B per g tissue, respectively. The blood–brain barrier was apparently more permeable to **36** than to glycine. Additional data obtained by Porschen et al.[183] on adenocarcinoma in C57 mice was consistent with these results. Even more recent data[184] pertaining to small peptide derivatives such as **37** and **38** were equally discouraging from the viewpoint of BNCT. However, it is now well estab-

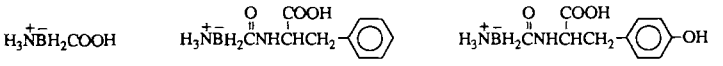

36 **37** **38**

lished[169] that a variety of ammonium carboxyborane derivatives of the type discussed here have great promise as antineoplastic, hypolipidemic, and anti-inflammatory agents and are currently under development.

7.10. Melanoma Differentiation Based Upon Boron-Containing Melanin Precursors and Complexation Agents

The production of the complex pigment, melanin (**39**), by melanosomes present in a preponderance of melanoma types was previously proposed as a tumor cell differentiation process[185] that rationalized the efficacy of L-**33** as a tumor-targetting amino acid.[87] Although this suggestion was not supported by accumulated evidence, and although the true mechanism of boron accretion in tumor with L-**33** is probably related to the accelerated uptake of amino acids such as tyrosine by tumor cells (Section 7.9.1), the actual incorporation of 2-thiouracil (**40**) into the melanin structure during its

in vivo synthesis has been demonstrated.[186–188] This provided an attractive possibility for the selective delivery of boron to the intracellular volume.

The ability of melanin and melanoproteins present in murine melanoma cells to tightly bind phenothiazine derivatives such as the potent tranquilizer chloropromazine[189] (**41**, known under the trade name Thorazine) also suggested a pathway for the selective deposition of boron into melanoma cells.[190] In this case preformed melanin must be available for reaction with the phenothiazine derivative.

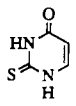

40

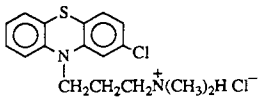

41

7.10.1. 2-Thiouracil Derivatives as Melanoma-Selective Boron Delivery Species

Although it had been determined by Dencker et al.[186,187] that 2-thiouracil (**40**) is selectively incorporated into melanin during its biosynthesis in melanoma cells, Fairchild et al.[188] quantified this process for the first time in 1982 by using ^{14}C-labeled 2-thiouracil ([^{14}C]TU) administered intraperitoneally or intravenously in BALB/c mice bearing Harding–Passey melanoma. The tumor uptake of TU was correlated with melanin content. The tumor uptake of [^{14}C]TU was as high as 9 to 12% of the injected dose per g tumor. Ratios of the concentration in tumor and normal tissue varied from 50:1 in metabolizing organs such as liver and lung, to 80:1 in pigmented whole eye, and 300:1 in muscle and brain. The percentage of uptake of [^{14}C]TU by tumor was virtually unchanged as the administered dose was varied by a factor of 5000 to give as much as 300 μg [^{14}C]TU incorporated per gram of tumor. This is equivalent to 26 μg B per g tumor if only one boron atom were incorporated in each molecule of **40**. These initial results stimulated a major effort to develop new boron-containing delivery agents based upon derivatives of 2-thiouracil and other compounds having at least a loose structural relationship to thiourea. Compounds that have been explored carry boron as a dihydroxyboryl group, an uncharged 1-(*closo*-1,2-$C_2B_{10}H_{11}$) appendage or its anionic 7-(*nido*-7,8-$C_2B_9H_{11}^-$) counterpart, which enhances hydrophilicity. The research groups responsible for the synthesis of this library of derivatives were headed by Gabel.[191,192] and Wilson,[193,194] whose representative contributions are illustrated in Schemes 26 and 27, respectively. In addition to carborane-substituted 2-thiouracil species, Wilson also synthesized the useful carboranylalkylamine building blocks **42** and **43**, which were in turn converted into the corresponding amides[194] **44** and **45** by reaction with 5-carboxy-2-thiouracil. Gabel et al.[192] reported the synthesis of **46** and **47** carborane derivatives of 5-thio-1,2,4-triazole, as well as of **48** and **49**.

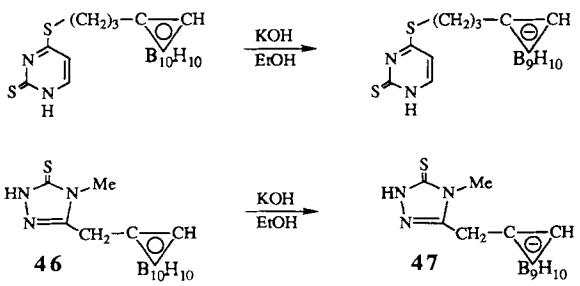

Scheme 26. Thiouracil and thiotriazol derivatives synthesized and evaluated by Gabel et al. [191,192].

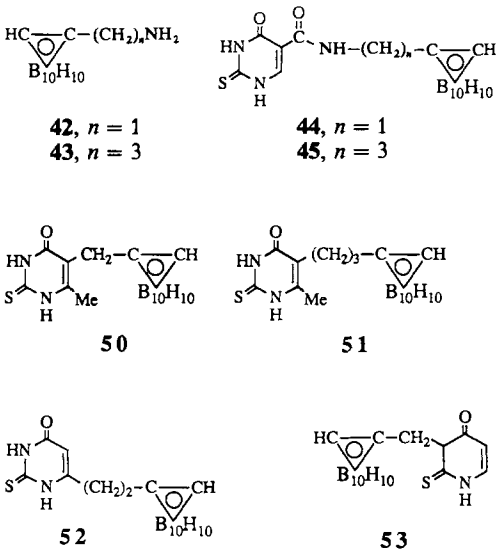

Scheme 27. Carboranylalkylamine and thiouracil derivatives, synthesized and evaluated by Wilson et al. [193,194].

Evaluation of the selective uptake of these candidate species by murine melanoma models has proceeded slowly. Gabel et al.[191,192] report that the dihydroxyboryl derivatives **48a** and **48b** gave boron concentrations in B16 melanomas grown in C57/bl mice (4 h after intraperitoneal administration of 9–16 mg B per kg body weight) of about 30 μg B per g tumor with tumor-to-blood boron concentrations ratios of 4:1 to 7:1. The more hydrophobic 6-propyl

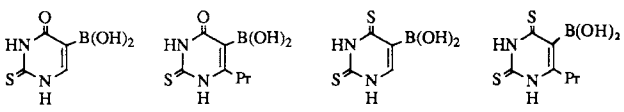

48a **48b** **49a** **49b**

derivative **49b** was taken up to the extent of only 1.7 μg B per g tumor, while **49a** gave intermediate results. The 5-thiotriazole species **46** and **47** gave poor selectivity and accumulated in the liver. The remaining carborane derivatives of Scheme 26 were less effective than the dihydroxyboryl compounds **48** and **49**.

The carborane derivatives **50** through **53** of Wilson et al.[193,194] were quite hydrophobic and too slowly taken up by nude mice bearing Harding–Passey melanoma xenografts to be useful. Incorporation of **51** in the phospholipid bilayer of a liposome (Section 7.7.1) was investigated by

Moore et al.[164] as a means of delivery for this hydrophobic species. High tumor specificity was observed, but no other data were reported.

While the efficacy of boron-containing 2-thiouracil and related compounds remains to be demonstrated and optimized by further molecular design and synthesis work, promising results were indeed obtained, and further work is warrranted. However, the presumed dependence of this delivery mode upon melanogenesis would seem to rule out the ability of these compounds to accumulate in amelanoic melanoma lines and immature premelanoic melanoma metastases having low tyrosinase activity.

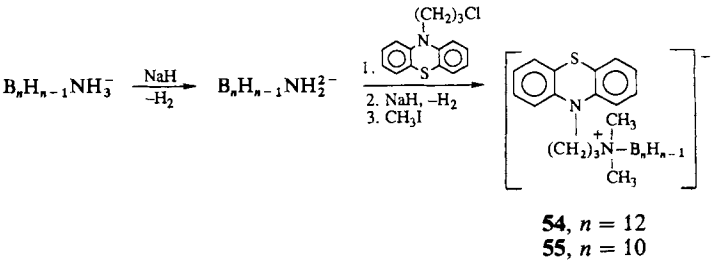

54, $n = 12$
55, $n = 10$

Scheme 28. Phenothiazine derivatives of the polyhedral $B_{10}H_{10}^{2-}$ and $B_{12}H_{12}^{2-}$ ions, synthesized by Nakagawa and Aono [199] and evaluated by Mishima et al. [200].

7.10.2 Phenothiazine Charge-Transfer Complexes with Existing Melanin as a Boron Delivery Mechanism

Investigation of the tranquilizing drug **41** known as chloropromazine in the early 1960s uncovered its remarkable ability to accumulate in the melanin-bearing eye tissues of experimental animals.[189] This apparently selective complexation of **41** and other phenothiazine derivatives was demonstrated with melanin and melanoproteins obtained from many other sources.[189] Melanin and its variations are complex polymeric pigments apparently derived from 5,6-indolequinone and other precursors,[195, 196] some of which contain sulfur (cysteine). It is now accepted that the melanin–phenothiazine complexation reaction is the result of electron-transfer reactions in which melanin serves as the electron acceptor.[197] The chemistry based upon these and other interesting observations is beyond the scope of this article, and the reader is referred to the original literature.

The accumulation of **41** in melanoproteins attracted the interest of Mishima et al.[190] with respect to the possibility of selective transport of boron to melanin-rich melanomas with boron-substituted derivatives of **41**. The biodistribution of ^{35}S-labeled **41** was thoroughly examined by Fairchild et al.[198] in a series of time-course experiments. Both Greene melanoma in Syrian golden hamsters (melanin content about 0.4% by weight of tumor) and Harding–Passey melanoma in BALB/c mice (melanin content about 0.7% by weight of tumor) were employed, since these models closely resembled human melanoma. The drug was administered by intraperitoneal injection. Twenty-four hours postinjection of up to 50 mg **41** per kg body weight, absolute concentrations of **41** in tumor that exceeded 100 μg per g tumor could be obtained; the concomittant tumor-to-liver concentration ratio is about 10:1. The ratios of boron concentration in tumor to that in other tissues such as blood and muscle were greater than 100:1. Computation of hypothetical tissue concentrations of ^{10}B were made with compound **54** as an example (25.4% ^{10}B by weight as sodium salt) and found to be sufficiently high (> 20 μg B per g tumor) for BNCT if this species provided the same performance as **41**.

The results of earlier investigators buttressed by the data of Fairchild et al.[198] stimulated a search for suitable boron-containing derivatives of phenothiazine. Consequently, Nakagawa and Aono[199] reported the syntheses of the polyhedral borane anion derivatives **54** and **55** (Scheme 28). Both **52** and **53** were investigated in BNCT experiments[200] with Greene's melanoma grown in Syrian golden hamsters. Although increased tumor destruction was observed in the presence of these compounds, their cell selectivity significantly differs from that of **41**, and they were not pursued. The compounds **52** and **53** both carried their borane groups as coordination centers on the pendant dimethylaminopropyl group of **41**.[199] Soloway et al.[201] attached 1-(*closo*-1,2-$C_2B_{10}H_{11}^-$) carborane cages to the phenothiazine structure (Scheme 29). The anionic 7-(*nido*-7,8-$C_2B_9H_{11}$) carbor-

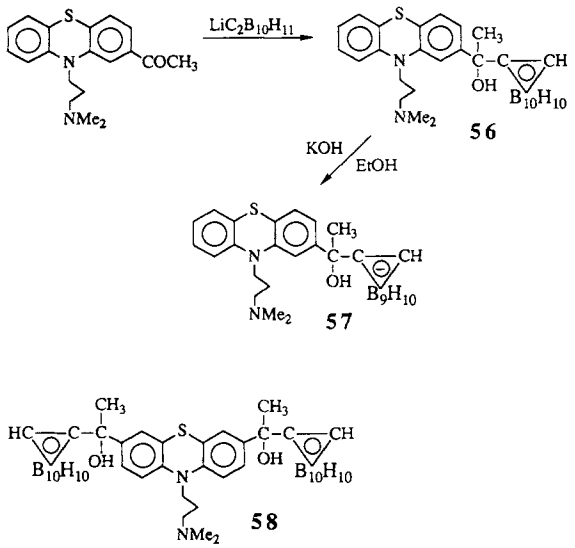

Scheme 29. Phenothiazine derivatives synthesized and evaluated by Soloway et al. [201,202].

ane derivative **57** was obtained by the usual route: removal of a BH^{2+} vertex from **56** with base. The compounds **56** through **58** gave preliminary in vivo evaluation results which suggested that they were too hydrophobic to be of interest, and efforts are underway to synthesize derivatives with improved water solubilities.[202]

The results reviewed above suggest that phenothiazine derivatives may have a place in BNCT if the search for a properly solvated compound is continued. Nonetheless, the fact that **41** and other phenothiazines can be localized only with preformed melanin puts limitations upon the actual therapeutic value of such a compound, even if it were discovered. It is interesting to note that research with phenothiazine derivatives has not been presented at either of the last two international meetings of the International Society for Neutron Capture Therapy convened in 1990 (Sydney) and 1992 (Columbus, Ohio).

7.11. Approaches to the Selective Destruction of the Tumor Cell Nucleus

The spectacular development of the synthetic chemistry of nucleic acids and their derivatives[203] has led to the discovery of new therapeutic agents and useful biological probes based upon modified synthetic nucleosides, mononucleotides, and oligonucleotides. Among these new DNA and RNA precursors are found species that serve as antiviral and anticancer agents either through enzyme inhibition or "antisense" activity, which blocks oncogene expression.[204] Mono- and oligonucleotides have been synthesized which contain altered bases, sugars, and phosphorus-containing linker groups. It is, therefore, not surprising to discover research activities aimed at the modification of nucleotides by the incorporation of boron-containing motifs into all three of these essential structural components. While these boron-containing nucleic acid components are important as such, they also offer new methodologies for the localization of boron in the tumor cell nucleus for purposes of BNCT.

Selectivity for nuclear accretion of boron in tumor cells is provided by the very rapid rate of tumor cell reproduction compared to that of normal cells. An important aspect of this observation is the fact that glioma cells undergo mitosis at a much greater rate than surrounding normal glial cells. Thus, it is possible that boron-containing species useful in BNCT and based upon DNA incorporation might be developed if such an ideal species were capable of Watson–Crick base-pairing, were not susceptible to nuclease activity, and could penetrate cell membranes. Alternatively, if a BNCT reagent were a cytotoxic enzyme inhibitor or "antisense" species, the effective lethality of BNCT would be further enhanced. As stated previously, the nucleus of a malignant cell is the target of highest value, since ^{10}B is at least twice as effective in the cell nucleus as an equal quantity distributed throughout the cytoplasm.

Another approach to the intranuclear accretion of boron is the development of DNA ligand molecules that contain boron.[205, 206] The huge number of available DNA binding sites per tumor cell amplified by the very effective localization of the boron target atoms in the cell nucleus makes this an attractive approach.

The description of a representative variety of boron-containing nucleic acid components is presented in the following section. The mechanisms that provide cellular uptake of these species, where observed, is normally not known nor is their distribution within the cell's interior. Such problems are current research topics of great importance.

7.11.1. *Nucleosides Modified by Base Complexation with Cyanoborane, BH_2CN*

In keeping with their interest in synthesizing α-amino acids in which single carbon atoms are formally replaced by an anionic boron atom having four valence electrons (see Section 7.9.3), Spielvogel et al.[207, 208] have modified the base residues present in representative nucleosides by complexation of specific nitrogen centers with the Lewis acid, BH_2CN. The attachment of BH_2CN to the base residues was accomplished by the displacement of Ph_3P from Ph_3PBH_2CN with a base nitrogen center present in dG, dI, dA, and dC in which the hydroxyl groups are protected followed by deprotection of the nucleoside complex (Scheme 30). The BH_2CN moiety was selectively placed on N^7 of dG and dI, N^1 of dA, and N^3 of dC. The site of coordination in both dG and dI is well

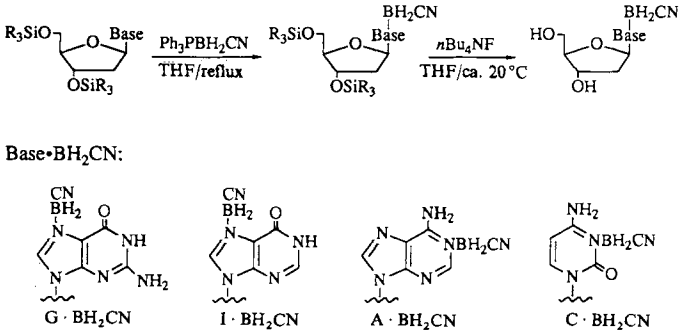

Scheme 30. Nucleoside derivatives synthesized by Spielvogel et al., in which BH_2CN is coordinated to base nitrogen atoms [207,208].

separated from the sites involved in Watson–Crick base-pairing. The dG–N^7-BH_2CN adduct was shown by ^1H NMR experiments to form base pairs with dC as effectively as unmodified dG.[208] Attempts to prepare the BH_2CN complex of dT were unsuccessful. In mice the dC–N^3-BH_2CN complex demonstrates biological activity as an inhibitor of inflammation, while dG–N^7-BH_2CN lowers serum cholesterol.[208] Tumor localization in mice bearing Ehrlich ascites carcinoma was demonstrated with ^{14}C-labeled dC–N^3-BH_2CN and gave a tumor-to-blood concentration ratio of 8.5:1 four hours postinjection.[208] The quantity of boron taken up by tumor was not determined.

7.11.2. *Nucleotide Analogs Containing Boranophosphate Linking Groups*

The formal replacement of the coordinated oxygen atom and its six valence electrons in a nucleotide phosphate linkage by a BH_3 molecule results in the formation of a negatively charged boranophosphate moiety. Such modified nucleotide linkers are isoelectronic with uncharged methylphosphonate linking groups, which have found use in "antisense" constructs.[204] The boranophosphates offer the advantage of a formal negative charge, largely on boron, and greater hydrophobicity than that presented by phosphate. The latter property is thought to be useful in assisting cell-membrane penetration. Modified nucleotides of the boranophosphate type were first prepared by Spielvogel et al.[208, 209] and proposed as boron delivery agents.

Scheme 31 describes the synthesis of typical boranophosphate oligonucleotides and suggests the feasibility of greatly extending the chains of these oligomers by the application of solid phase mediated synthesis methods.

The scope of the biological activity of compounds of the boranophosphate type, including cytotoxicity and enzymatic incorporation into DNA, is presently undergoing evaluation.[210] Superior candidates for BNCT have not yet been identified.

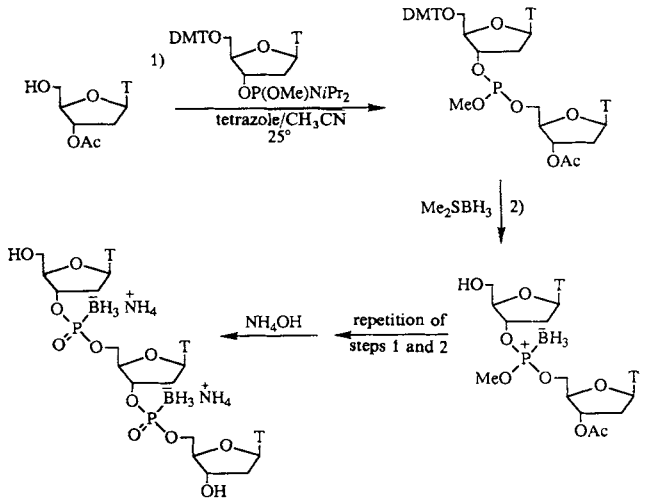

Scheme 31. The synthetic route to nucleotides containing boranophosphate linking groups, which was devised by Spielvogel et al. [208,209].

7.11.3. Boronic Acid Derivatives of Pyrimidine and Purine Nucleosides

The first DNA precursor to be synthesized that contained a carbon–boron bond was 5-dihydroxyboryluracil (**59**, Liao et al.[211] 1964). This was followed by the synthesis of the 5-dihydroxyboryl-2′-deoxyuridine (DBDU, (**60**)) first described by Schinazi and Prusoff[212] in 1978. The syntheses of **59** and **60** were accomplished by lithiation of suitable 5-bromo precursors in which the hydroxyl groups are protected, followed by reaction of the resulting lithium moiety with a trialkyl borate ester.[213] The stereochemical similarity of **60** and natural thymidine (5-methyl-2′-deoxyuridine) suggested this synthesis. The possible modes of incorporation of **60** into the nucleus of tumor cells was envisioned by Schinazi et al.[214] to possibly involve one or more of the following phenomena: 1) **60** is taken up selectively by malignant cells, and trapped within the cell as the 5′-monophosphate. This selectivity for tumor cells could be amplified if **60** were a better substrate for the thymidine kinase present in tumor cells than for the corresponding enzyme found in normal cells. 2) **60** could function as a inhibitor of enzymes involved in pyrimidine nucleoside biosynthesis. 3) **60** might become incorporated in DNA of tumor cells as a substitute for a pyrimidine nucleotide. 4) Any or all of the events listed above could provide ^{10}B-labeled **60** to the nucleus of the tumor cell for selective destruction through neutron capture. In principle, these mechanistic possibilities exist, to varying degrees, in every ^{10}B-labeled nucleoside or nucleotide molecule described here (Section 7.11).

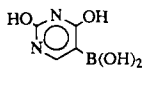

59

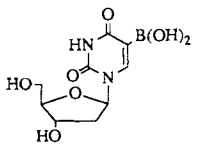

60 DBDU

Evaluation of the biological activity of **60** in vitro proved[214] that it was a good analog of thymidine and inhibited the replication of HSV-1. This inhibition of viral replication was nullified by added thymidine. Preliminary in vitro neutron irradiation experiments with solutions of ^{10}B-enriched **60** containing varying amounts of thymidine and V79 chinese hamster cells (washed) were carried out at the Brookhaven Medical Research Reactor. Pre-equilibration of the subject cells with **60** decreased their survival rate upon exposure to thermal neutrons, and the addition of thymidine to the **60** solution mitigated this effect. These results suggested to the authors that **60** was bound during DNA synthesis, but that it could not effectively compete with thymidine.

Using newly developed synthesis methods Yamamoto has obtained a wide variety of new base and nucleoside derivatives that contain either a 3- or 4-(dihydroxyboryl)-phenyl[215] or an α-hydroxy-4-(dihydroxyboryl)benzyl[216] substituent. Representative syntheses are outlined in Scheme 32. The dihydroxyboryl derivative prepared by these

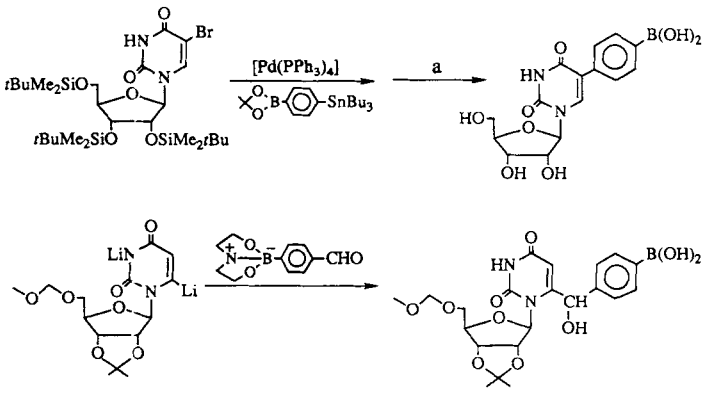

Scheme 32 Examples of two general synthetic routes leading to dihydroxyboryl derivat ves of nucleosides, demonstrated by Yamamoto et al. [215,216]. a: Deprotection.

new procedures are numerous; however, they are most likely susceptible to acid-catalyzed deboronation to form the corresponding phenyl- or α-hydroxybenzyl-substituted nucleoside and boric acid. In addition, the added aryl groups will increase the hydrophobicity of the desired nucleosides with unpredictable results. Selected members of this group of nucleosides are undergoing evaluation with respect to their biological activities including efficacy in BNCT.

7.11.4. Carborane-Substituted Nucleosides

The relatively simple compounds described in the previous section which contain the dihydroxyboryl function are low in boron content and subject to hydrolytic deboronation reactions. As an alternative to these simpler boron compounds, the *closo*-1,2-$C_2B_{10}H_{12}$ carborane has been functionalized to produce carborane-substituted ribose and base components of nucleosides. These species may become trapped in the nucleus of the tumor cell as described in Section 7.11.3. Whereas the boron-rich *closo*-carborane substituent will markedly decrease the hydrophilicity of the substrate to which it is attached, conversion of the *closo*-carborane structure to the corresponding anionic *nido*-carborane structure

may produce an amphiphilic derivative. Because the carborane substituent is comparatively large and has hydrophobic properties, it would not be expected that carborane-substituted nucleotides would actually become incorporated as surrogates in oligomeric DNA or RNA molecules of natural origin. However, intranuclear phosphorylation of a carboranyl-substituted nucleoside may serve to immobilize the resulting monophosphate within the nucleus.

Soloway et al.[217] recently described the first carborane-substituted nucleoside, 2′-*O*-(1,2-carboran-1-ylmethyl)-uridine (**61**), which has been designated CBU-2′ by its discoverers. Both the 3′-*O*- and 5′-*O*-(1,2-carboran-1-ylmethyl)uridine isomers have been described,[218] as well as the anionic *nido*-carborane analog of **61**. More recently, Tjarks et al. have described[219] what may become a general synthesis of nucleosides, which they demonstrated with the synthesis of **61** (Scheme 33). The key precursor in these potential syntheses is 1,3-di-*O*-acetyl-5-*O*-benzoyl-2-*O*-(1′,2′-carboran-1′-ylmethyl)-D-ribofuranose (**62**), which has been shown to afford **61** by reaction with trimethylsilyl-protected uracil in the presence of trimethylsilyl trifluromethanesulfonate followed by alkaline hydrolysis. Only the β-configuration was observed at the 1-position of the ribose moiety. One hopes that this synthesis route will find wide application.

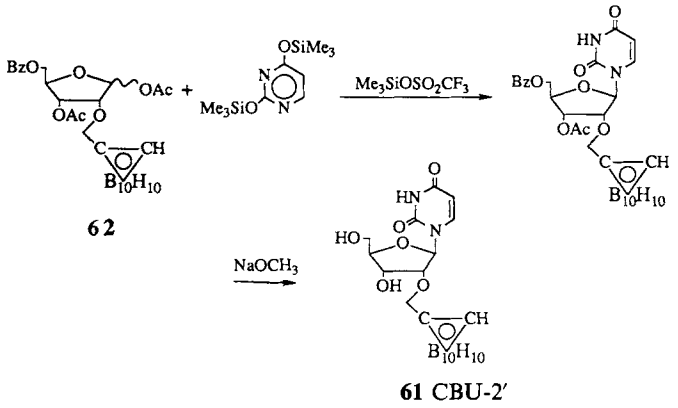

62 **61 CBU-2′**

Scheme 33. An example of the generalized synthesis of carborane derivatives of nucleosides by Tjarks et al. in which **62** is a common precursor [219].

The carborane-substituted nucleoside **61** and its 3′ and 5′ isomers were efficiently taken up by F98 glioma cells in vitro.[218, 220] Morrison et al.[221] have recently shown by SIMS (see Section 2.5.4) that the concentration of **61** in F98 glioma is higher in the cytoplasm than in the cell nucleus by a factor which varies from 1.4 to 2.6. The mechanism of cellular localization of **61** is under investigation.[222]

Yamamoto et al.[223] has recently developed a route to uridine and 2′-deoxyuridine derivatives bearing either a 1,2-carboran-1-yl or 2-hydroxymethyl-1,2-carboran-1-yl substituent in the 5-position of the uracil ring. These syntheses were initiated by using the Pd-catalyzed coupling of 5-iodouridine or 5-iodo-2′-deoxyuridine in which the hydroxyl groups are protected with $HC{\equiv}C\text{-}SiMe_3$ or $HC{\equiv}C\text{-}CH_2OAc$. The resulting 5-alkynyl nucleoside derivatives were converted into the desired products, for example **64**, by the usual reaction with $B_{10}H_{14}$ and a Lewis base. Preliminary findings indicate that 5-carboranyluridine is cytotoxic against P-388 murine leukemia cells in vitro. Schinazi et al.[224] have independently synthesized 5-carboranyl-2′-deoxyuridine (**65**) by a route similar to that reported by Yamamoto et al. Schinazi's group has studied the metabolites produced in CEM cells treated with **65**. A new metabolite was isolated which displays the biochemical properties expected for a 5′-monophosphate of **65**, which is believed to arise by intracellular phosphorylation.[224]

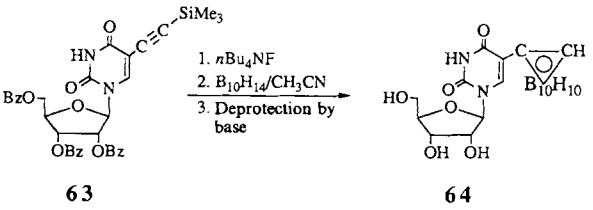

63 **64**

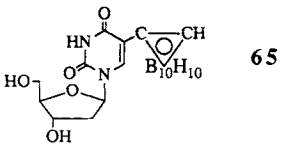

65

A synthesis of racemic 5-carboranyl-2′,3′-dideoxy-3′-thiacytidine (**66**) has been developed by using the Pd-catalyzed alkynylation of 5-iodo-2′,3′-dideoxy-3′-thiacytidine.[224] This and related compounds are undergoing biological evaluation.

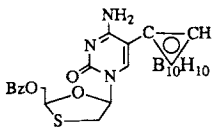

66

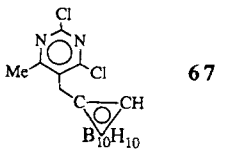

67

Reynolds et al.[225] have described the synthesis of 5-(1,2-carboran-1-ylmethyl)-2,4-dichloro-6-methylpyrimidine (**67**), which may prove to be useful as the synthetic equivalent of substituted pyrimidines.

7.11.5. Intranuclear Localization of Boron with DNA Ligands

The possibility of localizing boron in the DNA of target cells by complexing it with boron-containing ligand molecules has recently been investigated by Whittaker et al.[205] and Corder et al.[206] Dibenzimidazole reagents from Hoechst effectively bind to the minor groove of nuclear DNA, and a variety of reagents based upon this ligand sys-

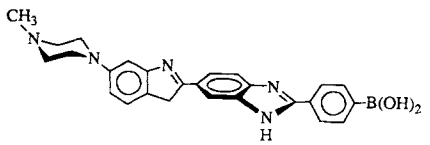

68

tem have been developed. The simple phenylboronic acid derivative **68** has been the subject of preliminary in vitro investigations of cellular boron uptake. Fluorescence microscopy and spectrophotometric analyses of the ligand in isolated nuclei have demonstrated uptake of **68** by a variety of viable cells. Neutron capture experiments demonstrated enhanced cell killing in the presence of 2×10^{-5} M **68**. The observed effect was equivalent to that obtained with a solution of 4×10^{-6} g $^{10}B(OH)_3$ per mL in contact with the cells during irradiation. This result was viewed as quite encouraging, and work is underway with other boron-containing ligands carrying several ^{10}B atoms per ligand.

7.11.6. Selective Delivery of Boron-Containing Species to the Nucleus

Scheme 5 depicts the transport processes involved in bringing a boron-containing agent from blood serum into the nucleus of a tumor cell. Each of the methods outlined in Section 7.11.3 for the intranuclear accretion of boron depends upon the enhanced rate of mitosis of tumor cells, as opposed to normal cells, to provide the required bias for selective tumor cell destruction. In addition, the fact that the walls of malignant cells are penetrated may place structural limitations upon the reagent to be delivered that mitigates its desired function of intranuclear localization. These problems may be circumvented by coupling intranuclear reagents to delivery systems that are known to be biased toward malignant cells. Of the available tumor-selective delivery methods discussed in this review, unilamellar liposomes (Section 7.7.1) are distinguished by their apparent effectiveness in selectively penetrating plasma membranes of tumor cells and by their ability to carry a wide variety of hydrophilic species to the cell's interior. Hydrophilic bases, nucleosides, and nucleotides of all sizes that contain appreciable numbers of boron atoms per molecule are candidates for this mode of delivery. Such research has been initiated in my laboratory.

8. The Needs and Prospects of BNCT

In principle, Locher's original proposal has been demonstrated. BNCT offers great promise for the treatment of cancers not amenable to current management and characterized by high mortality rates such as cerebral glioma and metastatic melanoma. The war on cancer has evolved into trench-warfare, and therapeutic methods that depart from presently accepted therapeutic modalities must be brought to bear if progress is to be resumed. As a therapeutically unique, but superficially complex method, BNCT stands out as just such an opportunity if the research momentum of the present is further increased and applied to the problems that have been identified in this review.

The foremost prerequisite for the adaptation of BNCT as a readily accessible medical tool available for the treatment of patients from the general population requires that pure epithermal neutron beams must be made available from economical sources other than nuclear reactors and placed in urban areas. Such advanced neutron generators could be based upon the spallation of neutrons from a metallic target by accelerated protons (Section 2.3.2). Such devices could possibly be available in prototype form within two to five years.

Also associated with the clinical practice of BNCT is the potential use of real-time NMR imaging techniques (MRI), which employ ^{10}B as the active nucleus, to visualize and quantify ^{10}B-loaded tumor and surrounding tissues (Section 2.5.1). Such a rapid and reliable noninvasive method of obtaining data on ^{10}B targets would be invaluable for determining the required neutron dose, orienting the patient in the epithermal beam, and monitoring changes that occur at the tumor site between the application of fractional doses. Work is now in progress with the more NMR amenable ^{11}B nucleus, which, if successful, will be applied to the development of a more valuable ^{10}B MRI capability.

The outline of biodelivery modes presented in Scheme 6 is based upon data of variable reliability. Consequently, the precise determination of the positioning of ^{10}B target nuclei both on, or in, malignant cells is vital to the intelligent design of new boron-containing compounds. While the subcellular distribution of boron may now be visualized (Section 2.5.4) if the subject cells are derived from an in vitro source, it would be especially useful to have similar data available from cells harvested from in vivo experiments. Data now available from in vitro preparations have been extremely enlightening and prompt further elaboration.

As seems likely, future development of boron-containing compounds will be increasingly directed toward systems designed to enter the tumor-cell nucleus on a cell-selective basis (Section 7.11). In addition to the biosyntheses of DNA or other biochemical processes that take place in the nucleus, the requirement of bringing the molecular tools such as boron-containing DNA precursors, DNA ligands, or antisense species to bear selectively upon malignant cells remains a major challenge. Receptor-mediated species, which may provide a selective means of penetration of the plasma membrane, might be coupled to the nucleus-binding reagent and enzymatically decoupled following cell entry. Cellular selectivity would be provided by the enhanced rate of mitosis and overexpression of receptor sites characteristic of tumor cells. On the other hand, it might prove possible to deliver the nucleus-binding reagent to the cell's cytoplasm through tumor-selective liposomes (Section 7.7.1) followed by migration of the reagent to the nucleus. Regardless of the novelty and elegance of new reagents that specifically interact with nuclear components, the problem of assuring selective binding to tumor cells demands consideration during the conception of the boron-containing agent itself.

The future development of BNCT clearly depends upon the design and synthesis of boron-containing species capable of extensive accretion within tumor cells and the related bioutilization systems that assure their selective delivery to malignant cells. The discoveries of modern microbiology and immunology that are related to practical bioutilization pathways (Section 6) have appeared at such a great rate that the corresponding chemical research effort may have fallen behind. A plea is made here for an extensive expansion of synthesis efforts aimed at the development of new synthesis methodology in the organoborane area and at its interface with bioorganic chemistry. A need exists for boron-contain-

ing molecules and oligomers that may be coupled to biodelivery molecules in a modular fashion. Similarly, modular groups that may be used to overcome the innate hydrophobicity of the *closo*-carborane and the amphiphilic *nido*-anion substituents are needed.

The proper biological evaluation of a candidate boron-containing system is vital to the correlation of chemical structure with biological activity and provides the guidance for further molecular design and synthesis efforts. It may very well be, as shown by recent work with boron-containing nucleosides, that aside from obvious applications in BNCT, some of the new compounds may have biological response profiles that make them desirable for other important applications. The work of Schinazi, Soloway, Spielvogel, and Yamamoto (Sections 7.9.3 and 7.11) provide examples of antiviral, anti-inflammatory, antineoplastic, and hypolipidemic compounds originally developed for BNCT research.

At this time, the concept of BNCT is closer to realization than ever before. New clinical trials with the thioborane anion BSH and dihydroxyborylphenylalanine (BPA, **33**) are beyond the advanced planning stages in Europe and the United States. Trials with melanoma by Mishima and his colleagues continue in Japan, as do the therapeutic procedures of Hatanaka. It must be pointed out, however, that the clinical trials now in progress and those to be initiated in the near future, by necessity, employ boron delivery agents such as BSH (Section 7.1) and BPA (Section 7.9.1). These are not truly high-performance compounds, but they are reasonably well understood and offer reliability. The tumors to be attacked are cerebral gliomas and primary melanoma lesions; the nuclear reactors at Petten and MIT will serve as neutron sources.

Longer range plans for BNCT must proceed irregardless of the upcoming clinical trials, since by the time these trials are completed greatly improved boron delivery agents and new neutron sources could be available, provided increased financial support from both government and industry is forthcoming. It seems certain that the future of BNCT will brighten as more medical practitioners become aware of its virtues. The meeting of knowledge derived from physics, chemistry, biology, and medicine at one point in the multidimensional field of science is a unique circumstance that cries out for exploitation by mankind. Perhaps it was really planned!

I wish to thank my students, postdoctoral associates, and colleagues, both past and present, for their contributions to our group's efforts in BNCT chemistry, and boron cluster chemistry in general. Drs. Debra A. Feakes and Kenneth J. Shelly have made vital contributions to this article by collecting information and critically reviewing the product. I am grateful to Mrs. Diane Gromelski for the preparation of the manuscript, Mr. Albert Calleros for the artwork, and Karin Drechsel for proofreading. I also wish to thank my many friends in the BNCT community for stimulation and the National Institutes of Health (RO1-CA31753 and RO1-CA53870) and the U.S. Department of Energy Idaho National Engineering Laboratory, Office of Energy Research, under DOE Field Office, Idaho, Contract DE-ACO7-761DO1570 for their support of our BNCT research efforts.

Received: March 1, 1993 [A910IE]
German version: *Angew. Chem.* **1993**, *105*, 997

[1] J. Chadwick, *Nature* **1932**, *129*, 312.
[2] J. R. Dunning, G. B. Pegram, G. A. Fink, *Phys. Rev.* **1935**, *47*, 325.
[3] E. Fermi, O. Amaldi, F. D'Agostino, F. Rasetti, E. Segre, *Proc. R. Soc. London A* **1934**, *146*, 483.
[4] J. R. Dunning, G. B. Pegram, G. A. Fink, D. P. Mitchell, *Phys. Rev.* **1935**, *48*, 265.
[5] H. J. Taylor, *Proc. R. Soc. London A* **1935**, *147*, 873.
[6] G. L. Locher, *Am. J. Roentgenol. Radium Ther.* **1936**, *36*, 1.
[7] a) M. Javid, G. L. Brownell, W. H. Sweet, *J. Clin. Invest.* **1952**, *31*, 603; b) W. H. Sweet, *N. Engl. J. Med.* **1951**, *245*, 875; c) W. H. Sweet, M. Javid, *J. Neurosurg.* **1952**, *9*, 200; d) L. E. Farr, W. H. Sweet, J. S. Robertson, C. G. Foster, H. B. Locksley, D. L. Sutherland, M. L. Mendelsohn, E. F. Stickley, *Am. J. Roentgenol. Radium Ther. Nucl. Med.* **1954**, *71*, 279; e) J. T. Godwin, L. E. Farr, W. H. Sweet, J. S. Robertson, *Cancer* **1955**, *8*, 601.
[8] a) *Proc. Third Int. Symp. Neutron Capture Ther. Cancer* (*Strahlenther. Onkol.* **1989**, *165*); b) R. M. Brugger, J. A. Shih in [8a], p. 153; c) R. F. Martin, G. D'Cunha, M. Pardee, B. J. Allen, *Int. J. Radiat. Biol.* **1988**, *54*, 205.
[9] a) *Boron-Neutron Capture Therapy for Tumors* (Ed.: H. Hatanaka), Nishamura, Nigata, Japan, **1986**); b) H. Hatanaka in [9a], p. 5.
[10] R. G. Fairchild, V. P. Bond, *Int. J. Radiat. Oncol. Biol. Phys.* **1985**, *11*, 831.
[11] F. Pfister, G. Hehn, F. El-Husseini in [8a], p. 107.
[12] a) *Abstr. Fifth Int. Symp. Neutron Capture Ther. Cancer* **1992**; b) R. Huiskamp, P. R. Gavin, A. S. Siefert, K. H. I. Phillips in [12a], p. 23.
[13] a) *Proc. Second Int. Symp. Neutron Capture Ther. Cancer* (*Neutron Capture Therapy* (Ed.: H. Hatanaka), Nishamura, Nigata, Japan, **1986**); b) R. M. Brugger, T. J. Less in [13a], p. 110.
[14] R. F. Barth, A. H. Soloway, R. G. Fairchild, *Cancer Res.* **1990**, *50*, 1061.
[15] a) *Proc. Workshop Neutron Capture Ther.* (*Brookhaven Nat. Lab. Rep.* **1986**, BNL 51995; b) R. M. Brugger, T. J. Less, G. G. Passmore in [15a], p. 32.
[16] a) *Proc. Fourth Int. Symp. Neutron Capture Ther. Cancer* (*Progress in Neutron Capture Therapy for Cancer* (Ed.: B. J. Allen, D. E. Moore, B. V. Harrington), Plenum, New York, **1992**); b) V. Benary, R. G. Fairchild, J. Kalef-Ezra, D. Greenberg, Y. Kamen, S. Fiarman, L. Wielopolski in [16a], p. 159.
[17] a) D. W. Nigg, F. J. Wheeler, P. D. Randolf in [16a], p. 145; b) F. J. Wheeler, M. L. Griebenow, D. E. Wessol, D. W. Nigg in [8a], p. 186.
[18] J. C. Yanch, O. K. Harling in [16a], p. 133.
[19] J. C. Yanch, X.-L. Zhou, R. E. Shefer, R. E. Klinkowstein, H. Zhuh in [12a], p. 45.
[20] C.-K. C. Wang, T. E. Blue, R. A. Gahbauer in [8a], p. 75.
[21] a) J. C. Yanch, X.-L. Zhou, R. E. Shefer, R. E. Klinkowstein, G. L. Brownell in [16a], p. 107; b) T. E. Blue, T.-X. B. Que, R. N. Christensen, P. Guo, J. W. Blue in [16a], p. 113; c) R. E. Shefer, R. E. Klinkowstein, J. C. Yanch, G. L. Brownell in [16a], p. 119; d) E. Grusell in [16a], p. 123; e) J. F. Crawford, H. Reiste, H. Conde, K. Elmgren, T. Ronnqvist, E. Grusell, B. Nillsson, O. Pettersson, P. Stromberg, B. Larsson in [16a], p. 129.
[22] R. G. Zamenhof, B. W. Murray, G. L. Brownell, G. R. Wellum, E. I. Tolpin, *Med. Phys.* **1975**, *2*, 47.
[23] R. G. Fairchild in [9a], p. 24.
[24] P. R. Gavin, R. Huiskamp, F. J. Wheeler, M. L. Griebenow in [12a], p. 34.
[25] D. W. Nigg, F. J. Wheeler, P. D. Randolph in [16a], p. 145.
[26] F. J. Wheeler, C. A. Atkinson, P. R. Gavin in [16a], p. 137.
[27] a) R. F. Barth, A. H. Soloway, R. G. Fairchild, *Cancer Res.* **1990**, *50*, 1061; b) *Proc. First Int. Symp. Neutron Capture Ther.* (*Brookhaven Nat. Lab.* **1983**, BNL 51730); c) R. G. Fairchild, V. P. Bond in [27b], p. 1.
[28] The author is indebted to D. W. Nigg and F. J. Wheeler of the Idaho National Engineering Laboratory for these data.
[29] A. Wambersie, L. E. Feinendegen, *Clinical Aspects of Neutron Capture Therapy* (Ed.: R. G. Fairchild, V. P. Bond, A. D. Woodhead), Plenum, New York, **1989**, p. 277.
[30] D. Gabel, S. Foster, R. G. Fairchild, *Radiat. Res.* **1987**, *111*, 14.
[31] M. Ljungberg, S.-E. Strand, *J. Nucl. Med.* **1990**, *31*, 493.
[32] R. J. Paxton, B. G. Beatty, M. F. Hawthorne, A. Varadarajan, L. E. Williams, F. L. Curtis, C. B. Knobler, J. D. Beatty, J. E. Shively, *Proc. Natl. Acad. Sci. USA* **1991**, *88*, 3387.
[33] G. W. Kabalka, M. Davis, P. Bendel, *Magn. Reson. Med.* **1988**, *8*, 231.
[34] T. L. Richards, K. M. Bradshaw, D. M. Freeman, C. H. Stoak, P. R. Gavin in [8a], p. 179.
[35] K. M. Bradshaw, T. L. Richards, S. L. Kraft in [16a], p. 325.
[36] K. M. Bradshaw, M. P. Schweizer, G. H. Glover, J. K. Thomas in [12a], p. 52.
[37] a) S. R. Tamat, D. E. Moore, B. J. Allen, *Anal. Chem.* **1987**, *59*, 2161; b) W. F. Bauer, J. A. Wishard, C. Rae, N. Lassahn in [16a], p. 297.
[38] a) R. F. Barth, A. H. Soloway, D. M. Adams, F. Alam, A. K. M. Anisuzzaman in [16a], p. 305; b) R. F. Barth, D. M. Adams, A. H. Soloway, E. B. Mechetner, F. Alam, A. K. M. Anisuzzaman, *Anal. Chem.* **1991**, *63*, 890.
[39] R. Rogus, O. K. Harling, I. Olmez, S. Wirdzek in [16a], p. 301.
[40] T. Matsumoto, O. Aizawa in [16a], p. 313.

[41] Y. Nakagowa, T. Kobayashi, Y. Ueno, H. Hatanoka, K. Mukai, K. Matsumoto in [16a], p. 283.
[42] M. Abe, K. Amano, K. Kitamura, J. Tateshi, H. Hatanaka, *J. Nucl. Med.* **1986**, *27*, 677.
[43] D. Gabel, H. Holstein, B. Larsson, L. Gille, G. Erikson, D. Sacker, P. Som, R. G. Fairchild, *Cancer Res.* **1987**, *47*, 5451.
[44] J. E. Woollard, Y. Jiang, J. F. Curran, T. E. Blue, R. F. Barth in [16a], p. 317.
[45] B. D. Bennett, X. Zha, I. Gay, G. H. Morrison, *Biol. Cell (1981)* **1992**, *74*, 105.
[46] X. Zha, B. D. Bennett, W. A. Ausserer, G. H. Morrison in [16a], p. 331.
[47] R. D. Leapman, R. L. Ornberg, *Ultramicroscopy* **1988**, *24*, 251.
[48] D. E. Moore, J. R. Stretch, A. L. Dawes, D. J. H. Cockayne, B. J. Allen, G. Constantine in [16a], p. 335.
[49] For the history of BNCT, see: D. N. Slatkin, *Brain* **1991**, *114*, 1609.
[50] See [7b].
[51] See [7c].
[52] A. H. Soloway, personal communication, **1958**.
[53] W. H. Sweet, M. Javid, *Trans. Am. Neurol. Assoc.* **1951**, 60.
[54] See also [7d].
[55] L. E. Farr, W. Haymaker, T. Konikowski, S. W. Lippincott, *Int. J. Neurol.* **1962**, *3*, 564.
[56] J. D. Archarnbeau, *Radiology* **1970**, *94*, 179.
[57] A. H. Soloway, R. L. Wright, J. R. Messer, *J. Pharm. Exp. Ther.* **1961**, *134*, 117.
[58] a) M. F. Hawthorne, A. R. Pitochelli, *J. Am. Chem. Soc.* **1959**, *81*, 5519; b) W. N. Lipscomb, A. R. Pitochelli, M. F. Hawthorne, *ibid.* **1959**, *81*, 5833.
[59] a) A. R. Pitochelli, M. F. Hawthorne, *J. Am. Chem. Soc.* **1960**, *82*, 3228; b) H. C. Miller, N. E. Miller, E. L. Muetterties, *ibid.* **1963**, *85*, 3885.
[60] a) T. L. Heying, J. W. Ager, S. L. Clark, D. J. Mangold, H. L. Goldstein, M. Hillman, R. J. Polak, J. W. Szymanski, *Inorg. Chem.* **1963**, *2*, 1089; b) D. Grafstein, J. Dvorak, *ibid.* **1963**, *2*, 1128.
[61] A. H. Soloway, H. Hatanaka, M. A. Davis, *J. Med. Chem.* **1967**, *10*, 714.
[62] A. K. Asbury, R. G. Ojean, S. L. Nielsen, W. H. Sweet, *J. Neuropathol. Exp. Neurol.* **1972**, *31*, 278.
[63] H. Hatanaka, S. Kamano, K. Amano, S. Hojo, K. Sano, S. Egawa, H. Yasukochi in [9a], p. 349.
[64] H. Hatanaka, Y. Urano in [9a], p. 381.
[65] H. Hatanaka, K. Amano, S. Kamano, K. Sano in [13a], p. 447.
[66] H. Hatanaka, *J. Neurol.* **1975**, *209*, 81.
[67] W. F. Bauer, K. M. Bradshaw, T. L. Richards in [16a], p. 339.
[68] G. R. Wellum, E. I. Tolpin, A. H. Soloway, A. Kaczmarczyk, *Inorg. Chem.* **1977**, *16*, 2120.
[69] E. I. Tolpin, G. R. Wellum, S. A. Berley, *Inorg. Chem.* **1978**, *17*, 2867.
[70] D. Slatkin, P. Micca, A. Forman, D. Gabel, L. Wielopolski, R. Fairchild, *Biochem. Pharmacol.* **1986**, *35*, 1771.
[71] M. F. Hawthorne, R. L. Pilling, *The Preparation of the $B_{10}H_{10}^{2-}$-Ion (Inorg. Synth.* **1967**, *9*, 16).
[72] See [60a, b].
[73] R. N. Grimes, *Carboranes*, Academic Press, New York, **1970**.
[74] E. L. Muetterties, W. H. Knoth, *Polyhedral Boranes*, Dekker, New York, **1968**.
[75] G. B. Dunks, M. F. Hawthorne, *Acc. Chem. Res.* **1973**, *6*, 124.
[76] W. H. Knoth, *J. Am. Chem. Soc.* **1967**, *89*, 1274.
[77] J. H. Morris, S.-A. Khan, F. Mair, G. Peters in [16a], p. 215.
[78] M. F. Hawthorne, *Acc. Chem. Res.* **1968**, *1*, 281.
[79] M. F. Hawthorne, G. B. Dunks, *Science* **1972**, *78*, 462.
[80] R. N. Leyden, B. P. Sullivan, R. T. Baker, M. F. Hawthorne, *J. Am. Chem. Soc.* **1978**, *100*, 3758.
[81] W. N. Lipscomb, *Boron Hydrides*, W. A. Benjamin, New York, **1963**.
[82] K. Wade, *Electron Deficient Compounds*, Appleton-Century-Crofts, New York, **1971**.
[83] *Boron Hydride Chemistry* (Ed.: E. L. Muetterties), Academic Press, New York, **1975**.
[84] *Metal Interactions with Boron Clusters* (Ed.: R. N. Grimes), Plenum, New York, **1982**.
[85] P. Lemmen, B. Werner in [12a], p. 9.
[86] a) P. A. Radel, S. B. Kahl in [12a], p. 5; b) S. Sjöberg, M. F. Hawthorne, P. Lindstrom, J. Malmquist, J. Carlsson, A. Andersson, O. Pettersson in [12a], p. 2.
[87] M. Ichihashi, T. Nakanishi, Y. Mishima, *J. Invest. Dermatol.* **1982**, *78*, 215.
[88] R. F. Schinazzi, W. H. Prusoff, *Tetrahedron Lett.* **1978**, 4981.
[89] B. F. Spielvogel, A. Sood, B. R. Shaw, I. H. Hall, *Pure Appl. Chem.* **1991**, *63*, 415.
[90] K. Shelly, D. A. Feakes, M. F. Hawthorne, P. G. Schmidt, T. A. Krisch, W. F. Bauer, *Proc. Natl. Acad. Sci. USA* **1992**, *89*, 9039.
[91] a) B. H. Laster, S. B. Kahl, E. A. Popenoe, D. A. Pate, R. G. Fairchild, *Cancer Res.* **1991**, *51*, 4588; b) S. B. Kahl, D. W. Pate in [12a], p. 10.
[92] R. M. Straubinger, D. Papahadjopoulis, K. Hong, *Biochemistry* **1990**, *29*, 4929.
[93] R. K. Jain, L. E. Gerlowski, *Crit. Rev. Oncol. Hematol.* **1986**, *5*, 115.
[94] B. A. Allison, E. Waterfield, A. M. Richter, J. T. Ledy, *Photochem. Photobiol.* **1991**, *54*, 709.
[95] W. H. Knoth, J. C. Sauer, D. C. England, W. R. Hertler, E. L. Muetterties, *J. Am. Chem. Soc.* **1964**, *86*, 3973.
[96] W. H. Knoth, *J. Am. Chem. Soc.* **1966**, *88*, 935.
[97] D. Haritz, K. Piscol, D. Gabel in [16a], p. 557.
[98] D. N. Slatkin, D. D. Joel, R. G. Fairchild, P. L. Micca, K. M. Nawrocky, B. H. Laster, J. A. Coderre, C. C. Finkel, C. E. Poletti, W. H. Sweet, *Basic Life Sci.* **1989**, *50*, 179.
[99] R. G. Fairchild, S. B. Kahl, B. H. Laster, J. Kalef-Ezra, E. A. Popenoe, *Cancer Res.* **1990**, *50*, 4860.
[100] J. A. Coderre, M. S. Makar, P. L. Micca, M. M. Nawrocky, D. D. Joel, D. N. Slatkin in [12a], p. 26.
[101] M. Komura, H. Nakai, M. Shiro, *J. Chem. Soc. Dalton Trans.* **1987**, 1953.
[102] W. F. Bale, I. L. Spar, *Adv. Biol. Med. Phys.* **1967**, *5*, 286.
[103] E. I. Tolpin, G. R. Wellum, F. C. Dohan, P. L. Kornblith, R. G. Zamenhof, *Oncology* **1975**, *32*, 223.
[104] R. F. Barth, N. Mafune, F. Alam, D. M. Adams, A. H. Soloway, G. E. Makroglow, O. A. Oredipe, T. E. Blue, Z. Steplewski in [8a], p. 142.
[105] G. Köhler, C. Milstein, *Nature* **1975**, *256*, 495; see also G. Köhler, *Angew. Chem.* **1985**, *97*, 829; *Angew. Chem. Int. Ed. Engl.* **1985**, *24*, 827 (Nobel Lecture).
[106] a) E. Mizusawa, H. L. Dahlman, S. J. Bennett, D. M. Goldenberg, M. F. Hawthorne, *Proc. Natl. Acad. Sci. USA* **1982**, *79*, 3011; b) D. M. Goldenberg, R. M. Sharkey, F. J. Primus, E. Mizusawa, M. F. Hawthorne, *ibid.* **1984**, *81*, 560.
[107] For an example A. R. Horwitz, C. P. Chang, M. Better, K. E. Hellstrom, R. R. Robinson, *Proc. Natl. Acad. Sci. USA* **1988**, *85*, 8678.
[108] For a perspective of immunochemistry till 1968, see D. Pressman, A. L. Grossberg, *The Structural Basis of Antibody Specificity*, W. A. Benjamin, New York, **1968**.
[109] a) A. G. Mallinger, E. L. Jozwiak, J. C. Carter, *Cancer Res.* **1976**, *32*, 1947; b) E. I. Tolpin, H. S. Wong, W. N. Lipscomb, *J. Med. Chem.* **1974**, *17*, 792; c) R. L. Sneath, A. H. Soloway, A. S. Dey, *ibid.* **1974**, *17*, 796; d) P. M. Jacobs, R. L. Sneath, A. H. Soloway, A. S. Dey, *J. Pharm. Sci.* **1976**, *65*, 604; e) R. L. Sneath, J. E. Wright, A. H. Soloway, S. M. O'Keefe, A. S. Dey, W. D. Smolnycki, *J. Med. Chem.* **1976**, *19*, 1290.
[110] M. F. Hawthorne, T. E. Berry, P. A. Wegner, *J. Am. Chem. Soc.* **1965**, *87*, 4746.
[111] M. F. Hawthorne, R. J. Wiersema, *J. Med. Chem.* **1972**, *15*, 449.
[112] a) E. A. Mizusawa, M. R. Thompson, M. F. Hawthorne, *Inorg. Chem.* **1985**, *24*, 1911; b) A. Varadarajan, R. M. Sharkey, D. M. Goldenberg, M. F. Hawthorne, *Bioconjugate Chem.* **1991**, *2*, 102.
[113] J. L. Maurer, F. Berchier, A. J. Serino, C. B. Knobler, M. F. Hawthorne, *J. Org. Chem.* **1990**, *55*, 838 and previous publications in this series.
[114] F. Alam, A. H. Soloway, R. F. Barth, N. Mafune, D. M. Adams, W. H. Knoth, *J. Med. Chem.* **1989**, *32*, 2326.
[115] S. R. Tamat, A. Patwardhan, D. E. Moore, A. Kabral, K. Bradstock, P. Hersey, B. J. Allen in [8a], p. 145.
[116] R. Abraham, R. Müller, D. Gabel in [8a], p. 148.
[117] R. F. Barth, A. H. Soloway, D. M. Adams, F. Alam in [16a], p. 265.
[118] a) *Boron Compounds Suitable for Neutron Capture Therapy for the Treatment of Cancer* (Workshop) (Ed.: A. H. Soloway), Annapolis, MD, USA, **1988**; b) M. F. Hawthorne, A. Varadarajan, J. L. Maurer in [118a].
[119] M. F. Hawthorne, *Pure Appl. Chem.* **1991**, *63*, 327.
[120] A. Varadarajan, M. F. Hawthorne, *Bioconjugate Chem.* **1991**, *2*, 242.
[121] R. J. Paxton, B.-G. Beatty, A. Varadarajan, M. F. Hawthorne, *Bioconjugate Chem.* **1992**, *3*, 243.
[122] M. F. Hawthorne, R. R. Kane, C. S. Lee, C. L. Coe, M. A. St. Rose in [12a], p. 14.
[123] M. F. Hawthorne, R. R. Kane, unpublished results.
[124] C. H. Chang, C. N. Ahlem, B. Wolfert, S. M. Hochschwender, R. Jue, J. M. Frincke, D. J. Carlo, *J. Nucl. Med.* **1986**, *27*, 1041; L. D. Anderson, D. L. Meyer, T. R. Battersby, J. M. Frincke, D. Mackensen, S. Lowe, P. Connolly, *ibid.* **1988**, *29*, 835.
[125] F. J. Primus, M. F. Hawthorne et al., unpublished results, **1991**.
[126] Research in progress: F. J. Primus et al.
[127] D. J. Hnatowich, F. Virzi, M. Ruschowski, *J. Nucl. Med.* **1987**, *28*, 1294.
[128] A. Andersson, J. Andersson, J.-O. Burgman, J. Capola, J. Carlsson, H. Conde, J. Crawford, S. Graffmann, E. Grusell, A. Holmburg, E. Johansson, B. S. Larsson, B. Larsson, T. Liljefors, P. Lindstrom, J. Malmquist, L. Pellettieri, O. Pettersson, J. Ponten, A. Roberti, K. Russel, H. Reist, L. Salford, S. Sjöberg, B. Sternerlöw, P. Strömberg, B. Westermark in [16a], p. 41.
[129] B. D. Albertson, G. Willeke, M. Millan, S. Binney, S. Martsolf, D. L. Loriaux in [12a], p. 22.
[130] J. Capala, R. F. Barth, D. M. Adams, J. Carlsson in [12a], p. 30.
[131] a) S. Sjöberg, J. Malmquist, P. Lindstrom, J. Carlsson, A. Andersson, O. Pettersson in [12a], p. 6; b) J. Malmquist, S. Sjöberg, *Inorg. Chem.* **1992**, *31*, 2534.
[132] H.-C. Chen et al., unpublished results.
[133] M. S. Brown, R. T. Kovanen, J. L. Goldstein, *Science* **1981**, *212*, 628; J. L. Goldstein, R. G. W. Anderson, M. S. Brown, *Nature* **1979**, *279*, 679.
[134] J. L. Goldstein, J. H. S. Holgeson, M. S. Brown, *J. Biol. Chem.* **1979**, *254*, 5403.
[135] See also M. S. Brown, J. L. Goldstein, *Angew. Chem.* **1986**, *98*, 579; *Angew. Chem. Int. Ed. Engl.* **1986**, *25*, 583 (Nobel Lecture).

[136] Y. U. Ho, R. G. Smith, M. S. Brown, J. L. Goldstein, *Blood* **1978**, *52*, 1099.
[137] S. B. Kahl, J. C. Callaway in [8a], p. 137.
[138] S. B. Kahl, *Tetrahedron Lett.* **1990**, *31*, 1517.
[139] a) T. Dougherty, *Photochem. Photobiol.* **1987**, *45*, 879; b) T. F. Delaney, E. Glatstein, *Compr. Ther.* **1989**, *14*, 43.
[140] T. Dougherty, K. R. Weishaupt, C. J. Gomer, *Cancer Res.* **1976**, *36*, 2326.
[141] a) S. B. Kahl in [27b], p. 294; b) S. B. Kahl, D. D. Joel, G. C. Finkel, P. L. Micca, M. M. Nawrocky, J. A. Coderre, D. N. Slatkin, *Basic Life Sci.* **1989**, *50*, 325.
[142] a) M. Miura, D. Gabel, R. G. Fairchild, B. H. Laster, L. S. Warkentien in [8a], p. 131; b) M. Miura, D. Gabel, G. Oenbrink, R. G. Fairchild, *Tetrahedron Lett.* **1990**, *31*, 2247.
[143] S. B. Kahl, M.-S. Koo in [16a], p. 223.
[144] a) R. Schwyzer, K. Q. Do, A. N. Eberle, J. L. Fauchere, *Helv. Chim. Acta* **1981**, *64*, 2078; b) G. Oenbrink, P. Jürgenlimke, D. Gabel, *Photochem. Photobiol.* **1988**, *48*, 51; c) J. Moan, S. Somer, *Cancer Lett. Shannon Irel.* **1983**, *21*, 167.
[145] S. B. Kahl, D. D. Joel, M. M. Nawrocky, P. L. Micca, K. P. Tran, G. C. Finkel, D. N. Slatkin, *Proc. Natl. Acad. Sci. USA* **1990**, *87*, 7265.
[146] M. Miura, P. Micca, D. Gabel in [16a], p. 455.
[147] R. G. Fairchild, S. B. Kahl, B. H. Laster, J. Kalef-Ezra, E. A. Popenoe, *Cancer Res.* **1990**, *50*, 4860.
[148] J. S. Hill, S. B. Kahl, A. H. Kaye, M. F. Gonzales, N. J. Vardaxis, C. I. Johnson, S. S. Stylli, Y. Nakamura in [16a], p. 501.
[149] F. Alam, A. H. Soloway, B. V. Bapat, R. F. Barth, D. M. Adams, *Basic Life Sci.* **1989**, *50*, 107.
[150] R. M. Straubinger, N. G. Lopez, R. J. Debs, K. Hong, D. Papahadjopoulos, *Cancer Res.* **1988**, *48*, 5237.
[151] R. T. Proffitt, L. E. Williams, C. A. Presant, G. W. Tin, J. A. Uliana, R. C. Gamble, J. D. Baldeschwieler, *Science* **1983**, *220*, 502.
[152] R. T. Proffitt, L. E. Williams, C. A. Presant, G. W. Tin, J. A. Uliana, R. C. Gamble, J. D. Baldeschwieler, *J. Nucl. Med.* **1983**, *24*, 45.
[153] a) C. A. Presant, R. T. Proffitt, A. F. Turner, L. E. Williams, D. Windsor, J. L. Werner, P. Kennedy, C. Wiseman, K. Gala, R. J. McKenna, *Cancer* **1988**, *62*, 905; b) C. A. Presant, D. Blayney, R. T. Proffitt, A. F. Turner, L. E. Williams, H. I. Nadel, P. Kennedy, C. Wiseman, K. Gala, R. J. Crossley, S. J. Preiss, G. E. Ksionski, S. L. Presant, *Lancet* **1990**, *335*, 1307.
[154] R. M. Straubinger, K. Hong, D. S. Friend, D. Papahadjopoulos, *Cell Cambridge Mass.* **1983**, *32*, 1069.
[155] K. Shelly, M. F. Hawthorne, P. G. Schmidt in [16a], p. 259.
[156] a) R. L. Pilling, M. F. Hawthorne, E. A. Pier, *J. Am. Chem. Soc.* **1964**, *86*, 3568; b) M. F. Hawthorne, R. L. Pilling, P. M. Garrett, *ibid.* **1965**, *87*, 4740.
[157] B. L. Chamberland, E. L. Muetterties, *Inorg. Chem.* **1964**, *3*, 1450.
[158] M. F. Hawthorne, R. L. Pilling, *J. Am. Chem. Soc.* **1966**, *88*, 3873.
[159] M. F. Hawthorne, R. L. Pilling, P. F. Stokely, *J. Am. Chem. Soc.* **1965**, *87*, 1893.
[160] D. A. Feakes, K. J. Shelly, M. F. Hawthorne, P. G. Schmidt, T. A. Krisch, W. F. Bauer, *Boron USA Workshop III*, Pullmann, WA, USA, **1992**.
[161] D. A. Feakes, K. J. Shelly, M. F. Hawthorne, P. G. Schmidt, C. A. Elstad, G. G. Meadow, W. F. Bauer in [12a], p. 10.
[162] K. J. Shelly, M. F. Hawthorne, C. B. Knobler in [12a], p. 14.
[163] K. J. Shelly, C. B. Knobler, M. F. Hawthorne, *Inorg. Chem.* **1992**, *31*, 2889.
[164] D. E. Moore, A. K. Chandler, S. Corderoy-Buck, J. G. Wilson, B. J. Allen in [16a], p. 451.
[165] H. E. Hadd in [27b], p. 281.
[166] S. B. Kahl in [27b], p. 294.
[167] O. Hechter, I. L. Schwartz in [27b], p. 197.
[168] F. Wellmann, R. Abraham, R. Müller, D. Gabel, *Z. Naturforsch. C* **1991**, *46*, 252.
[169] B. F. Spielvogel, *Mol. Struct. Energ.* **1988**, *5*, 329.
[170] H. R. Snyder, A. J. Reedy, W. J. Lennarj, *J. Am. Chem. Soc.* **1958**, *80*, 835.
[171] Y. Mishima, M. Ichihashi, T. Nakanishi, M. Tsuji, M. Ueda, T. Nakagawa in [27b], p. 355.
[172] a) Y. Mishima, C. Honda, M. Ichihashi, H. Obara, J. Hiratsuka, H. Fukuda, H. Karashima, T. Kobayashi, K. Kanda, K. Yoshino, *Lancet* **1989**, 388; b) Y. Ujeno, K. Akuta, H. Hatanaka, Y. Mishima, Y. Oda, Y. Nakagawa in [16a], p. 593; c) Y. Mishima, M. Ichihashi, C. Honda, M. Shiono, T. Nagogawa, H. Obara, J. Shirkawa, J. Hiratsuka, K. Kanda, T. Kobayashi, T. Nozaki, O. Aizawa, T. Sao, H. Karoshima, K. Yoshino, H. Fukuda in [16a], p. 577.
[173] a) Y. Kinoshita, K. Yoshino, Y. Mori, H. Kakihana, Y. Mishima in [16a], p. 243; b) C. Honda, M. Shiono, N. Wadabayashi, M. Ichihashi, Y. Mishima, T. Kobayashi, K. Kanada, Y. Hori, K. Yoshino in [16a], p. 421.
[174] J. A. Coderre, J. D. Glass, R. G. Fairchild, U. Roy, S. Cohen, I. Fand, *Cancer Res.* **1987**, *47*, 6377.
[175] D. C. Roberts, K. Suda, J. Samanen, D. S. Kemp, *Tetrahedron Lett.* **1980**, *21*, 3435.
[176] J. A. Coderre, J. A. Kalef-Ezra, R. G. Fairchild, P. L. Micca, L. E. Reinstein, J. D. Glass, *Cancer Res.* **1988**, *48*, 6313.
[177] J. A. Coderre, J. D. Glass, R. G. Fairchild, P. L. Micca, I. Fand, D. D. Joel, *Cancer Res.* **1990**, *50*, 138.
[178] R. G. Zamenhof, D. E. Wazer, H. Madoc-Jones, O. K. Harling in [12a], p. 58.
[179] K. Yoshino, T. Maruyama, H. Takahashi, Y. Mori, H. Kakihana, Y. Mishima, M. Ichihashi, C. Honda, M. Shiono in [12a], p. 4.
[180] J. K. Prashar, D. E. Moore, J. G. Wilson, B. J. Allen in [12a], p. 2.
[181] E. G. Samsel, B. M. Simpson in [16a], p. 251.
[182] B. F. Spielvogel, A. T. McPhail, I. H. Hall, R. G. Fairchild, P. L. Micca in [27b], p. 245.
[183] W. Porschen, J. Marx, H. Mühlensiepen, L. E. Feinendegen, F. Dallacker, H. Mückter, W. Müllners, T. Böhmel in [27b], p. 331.
[184] B. F. Spielvogel, A. Good, J. Tomasz, S. Kathikeyan, W. Powell in [12a], p. 6.
[185] Y. Mishima, M. Ichihashi, S. Hatta, C. Honda, K. Yamamura, T. Nakagawa, *Pigm. Cell Res.* **1987**, *2*, 226.
[186] L. Dencker, B. Larsson, K. Olander, S. Ullberg, *Br. J. Cancer* **1982**, *45*, 95.
[187] L. Dencker, B. Larsson, K. Olander, S. Ullberg, M. Yokota, *Pharmacol. Toxicol.* **1981**, *49*, 141.
[188] R. G. Fairchild, S. Packer, D. Greenberg, S. Prantika, A. B. Brill, I. Fand, W. P. McNally, *Cancer Res.* **1982**, *42*, 5126.
[189] A. G. Bolt, I. S. Forrest, *Recent Adv. Biol. Psychiatry* **1968**, *10*, 20.
[190] Y. Mishima, *Pigm. Cell* **1973**, *1*, 215.
[191] W. Tjarks, D. Gabel, *J. Med. Chem.* **1991**, *34*, 315.
[192] H. Ketz, W. Tjarks, D. Gabel, *Tetrahedron Lett.* **1990**, *31*, 4003.
[193] J. G. Wilson, *Pigm. Cell Res.* **1987**, *2*, 297.
[194] J. G. Wilson in [16a], p. 227.
[195] H. S. Mason, D. J. E. Ingram, B. Allen, *Arch. Biochem. Biophys.* **1960**, *86*, 225.
[196] M. S. Blois, A. B. Zahlan, J. E. Maling, *Biophys. J.* **1964**, *4*, 471.
[197] S. Packer, R. G. Fairchild, K. P. Watts, D. Greenberg, S. J. Hannon, *Radiopharmaceuticals: Structure - Activity Relationships* (Ed.: R. P. Spencer), Grune and Stratton, New York, **1981**, Chapter 12, p. 251.
[198] R. G. Fairchild, D. Greenberg, K. P. Watts, S. Packer, H. L. Atkins, P. Som, S. J. Hannon, A. B. Brill, I. Fand, W. P. McNally, *Cancer Res.* **1982**, *42*, 556.
[199] T. Nakagawa, K. Aono, *Chem. Pharm. Bull.* **1976**, *24*, 778.
[200] T. Nakanishi, M. Ichihashi, Y. Mishima, T. Matsuzawa, H. Fukuda, *Int. J. Radiat. Biol.* **1980**, *37*, 573.
[201] F. Alam, A. H. Soloway, R. F. Barth, D. M. Adams in [13a], p. 8.
[202] F. Alam, B. V. Bapot, A. H. Soloway, R. F. Barth, N. Mafune, D. M. Adams in [8a], p. 121.
[203] J. Goodchild, *Bioconjugate Chem.* **1990**, *1*, 165.
[204] *Oligodeoxynucleotides: Antisense Inhibitors of Gene Expression* (Ed.: J. S. Cohen), CRC Press, Boca Raton, FL, USA, **1989**.
[205] A. D. Whittaker, D. P. Kelly, M. Pardee, R. F. Martin in [16a], p. 231.
[206] A. Corder, R. F. Martin, A. Whittaker, D. P. Kelly, H. Meriaty, B. J. Allen in [12a], p. 12.
[207] A. Sood, B. F. Spielvogel, B. R. Shaw, *J. Am. Chem. Soc.* **1989**, *111*, 9234.
[208] a) B. F. Spielvogel, A. Sood, B. R. Shaw, I. H. Hall, *Pure Appl. Chem.* **1991**, *63*, 415; b) B. F. Spielvogel, A. Sood, B. R. Shaw, I. H. Hall, R. G. Fairchild, B. H. Laster, C. Gordon in [16a], p. 211.
[209] a) A. Sood, B. R. Shaw, B. F. Spielvogel, *J. Am. Chem. Soc.* **1990**, *112*, 9000; b) see also J. Tomasz, B. R. Shaw, K. Porter, B. F. Spielvogel, A. Sood, *Angew. Chem.* **1992**, *104*, 1404; *Angew. Chem. Int. Ed. Engl.* **1992**, *31*, 1373.
[210] B. F. Spielvogel, A. Sood, W. Powell, J. Tomasz, K. Porter in [12a], p. 17.
[211] T. K. Liao, E. C. Podrebarac, C. C. Cheng, *J. Am. Chem. Soc.* **1964**, *86*, 1869.
[212] R. F. Schinazi, W. H. Prusoff, *Tetrahedron Lett.* **1978**, 4981.
[213] R. F. Schinazi, W. H. Prusoff, *J. Org. Chem.* **1985**, *50*, 841.
[214] R. F. Schinazi, S. Kusuma, B. H. Laster, E. Popenoe, R. G. Fairchild in [118a].
[215] Y. Yamamoto, T. Seko, H. Nemoto, *J. Org. Chem.* **1989**, *54*, 4734.
[216] a) Y. Yamamoto, T. Seko, F. Rong, H. Nemoto, *Tetrahedron Lett.* **1989**, *30*, 7191; b) Y. Yamamoto, *Pure Appl. Chem.* **1991**, *63*, 423.
[217] A. K. M. Anisuzzaman, F. Alam, A. H. Soloway, *Polyhedron* **1990**, *9*, 891.
[218] W. Tjarks, A. K. M. Anisuzzaman, L. Liang, A. H. Soloway, R. F. Barth, D. J. Perkins, D. M. Adams, *J. Med. Chem.* **1992**, *35*, 1628.
[219] W. Tjarks, A. K. M. Anisuzzaman, A. H. Soloway, *Nucleosides Nucleotides* **1992**, *11*, 1765.
[220] a) L. Liu, R. F. Barth, A. H. Soloway, A. K. M. Anisuzzaman, F. Alam, W. Tjarks, X.-H. Zha, G. H. Morrison, *Proc. Am. Assoc. Cancer Res.* **1991**, *34*, 2418; b) W. Tjarks, A. K. M. Anisuzzaman, A. H. Soloway, L. Liu, R. F. Barth in [12a], p. 11.
[221] See [45].
[222] A. H. Soloway, personal communication, **1992**.
[223] Y. Yamamoto, T. Seko, H. Nakamura, H. Nemoto, H. Hojo, N. Mukai, Y. Hashimoto, *J. Chem. Soc. Chem. Commun.* **1992**, 157.
[224] R. F. Schinazi, N. Goudgaon, J. Soria, D. C. Liotta in [12a], p. 11.
[225] R. C. Reynolds, T. W. Trask, W. D. Sedwick, *J. Org. Chem.* **1991**, *56*, 2391.

Classical and Nonclassical Methyleneboranes

By Armin Berndt*

Dedicated to Professor Heinrich Nöth on the occasion of his 65th birthday

Methyleneboranes are stable compounds when their reactive C=B bonds are shielded by sterically demanding substituents and the electron deficiency at the dicoordinate boron atom is reduced through delocalization of adjacent electron pairs. In the classical amino(methylene)boranes of Nöth and Paetzold, the electron deficiency at the dicoordinate boron atom is relieved through π–π delocalization of a neighboring nitrogen atom's formally nonbonding electron pair, that is, through formation of a classical two-center, two-electron (2c–2e) bond. In *nonclassical* methyleneboranes, which are the focus of this review, the electron-deficient center at the dicoordinate boron atom forms nonclassical three-center, two-electron (3c–2e) bonds with neighboring σ bonds. These methyleneboranes exhibit structural and spectroscopic properties similar to carbenium ions having strong σ–π delocalization (hyperconjugation, bridging) and to transition metal complexes having strong agostic interactions.

1. Introduction

Methyleneboranes (**1**)[1–4] are compounds with a C–B double bond, containing a boron atom which in classical representatives is dicoordinate. They are isoelectronic with vinyl cations (**2**)[5] and are closely related electronically to the carbene complexes of type **3** (M = W, Ta[6, 7]). The properties of compounds **1**–**3** are determined to a large extent by the high electron deficiency at the dicoordinate atoms in **1** and **2** and the metal atoms in **3**.

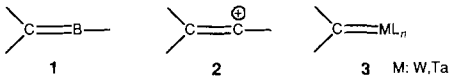

1 **2** **3** M: W,Ta

In classical methyleneboranes, as in the amino-substituted vinyl cations (ketiminium ions) **4**,[8] the electron deficiency at the dicoordinate atom is greatly reduced through π–π delocalization of the formally nonbonding electron pairs on the neighboring atom (Scheme 1). Typical examples are the amino(methylene)boranes **5** of Nöth[2] and Paetzold.[3a–c] The 2-borataallenes **6**[9] and the borataalkynes **7**[10] are considered here as special cases of classical methyleneboranes because of their stabilization through π delocalization of formally nonbonding electron pairs on the carbon atoms adjacent to the dicoordinate boron atom.

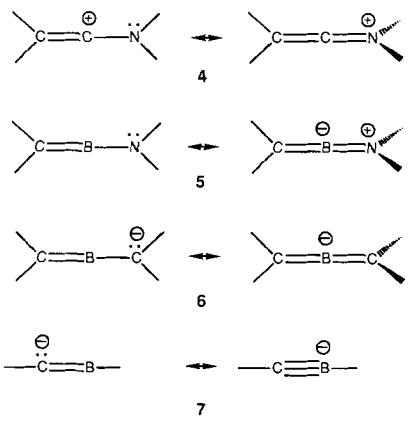

4 **5** **6** **7**

Scheme 1. π–π Delocalization in classical methyleneboranes and related compounds.

In compounds of the type **1** and **2**, and carbocations **8**,[11] where the electron deficiency at the di- or tricoordinate atom is not (or only weakly—see Section 3.2.2) reduced through π–π delocalization, and in **3** and other transition metal complexes of the type **9**,[7, 12] where the metal center has 16 or fewer valence electrons, the electron-deficient centers will form nonclassical 3c–2e bonds with the electrons of the neighboring C–X σ bonds.

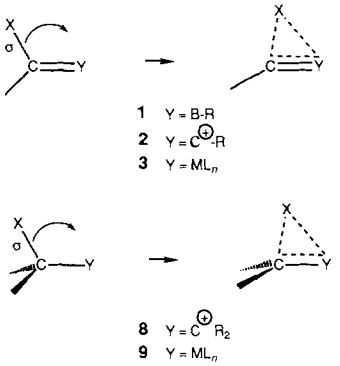

1 Y = B-R
2 Y = C⊕-R
3 Y = ML_n
8 Y = C⊕R_2
9 Y = ML_n

Scheme 2. Nonclassical 3c–2e bonds through interaction of electron-deficient centers with neighboring σ electrons: the α-agostic type.

These interactions are called α agostic effects[7] if the electron-deficient center is a metal, but if it is a positively charged carbon atom, the name C–X hyperconjugation is used. Pronounced effects in carbocations are termed nonclassical bridging. The expression σ–π delocalization[11] is employed as the generic term. Depending upon the extent of the shift of the bonding electrons in the C–X bond towards the electron-deficient center—the X nucleus must follow for electrostatic reasons—a continuum[13] in the degree of 3c–2e bond development can be observed. The following series of formulas show examples of carbocations having no appre-

[*] Prof. Dr. A. Berndt
Department of Chemistry, Universität Marburg
Hans-Meerwein-Strasse, D-35043 Marburg (FRG)
Telefax: Int. code + (6421)28-5547

 © *VCH Verlagsgesellschaft mbH, D-69451 Weinheim, 1993* *0570-0833/93/0707-0985 $ 10.00+.25/0*

ciable hyperconjugation (**8a**[14]), strong C–C hyperconjugation (**8b**,[15] **8e**[16]), unsymmetrical bridging (**8c**,[17] **8f**[18]), and symmetrical bridging (**8d**,[19] **8g**[16]).

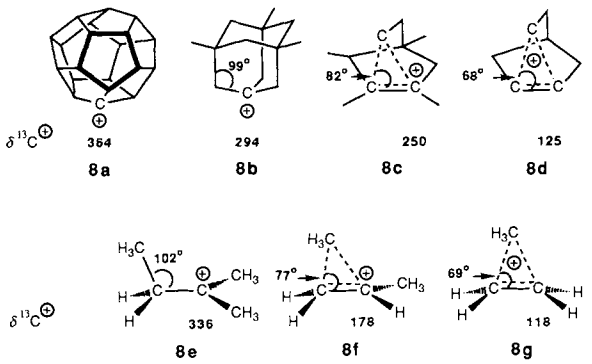

Bond angle distortion and NMR shielding of the electron-deficient center are the most obvious consequences of strong nonclassical interactions.[1d, 1f, 16, 18] The examples demonstrate the influence of geometry, ring strain, and electron deficiency on the extent of C–C hyperconjugation. Very strong C–C hyperconjugation appears with strained σ bonds of three-membered rings.[20, 21]

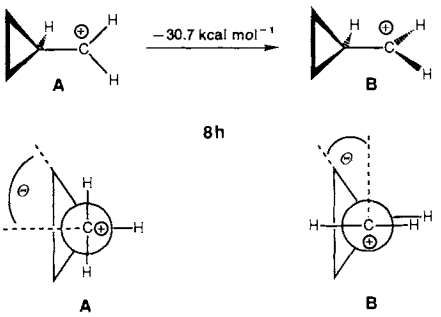

The above example also shows the effect that the dihedral angle θ between the σ and p orbitals has on the strength of the σ–π interactions. The bisected form **8hB** has a small dihedral angle and is 30.7 kcal mol^{-1} [21a] lower in energy than the perpendicular form **8hA** with the large θ.

The salient significance of the X atom's electronegativity is demonstrated by the energy differences between the conformations of the carbocations **8g** and **8i–8k** that *do* (**B**, $\theta = 0°$) and *do not* (**A**, $\theta = 90°$) exhibit C–X hyperconjugation.[22] The calculated stabilization energies for cations exhibiting the "β-Si effect" (that is, type **8i**), have been confirmed impressively by experiment.[23]

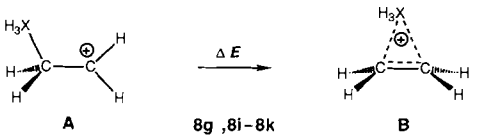

	X	ΔE [kcal mol^{-1}]
8g	C	− 8.3
8i	Si	− 29.1
8j	Ge	− 38.8
8k	Sn	− 47.9

The strength of the nonclassical interactions can be estimated qualitatively with use of the HOMO/LUMO concept.[24] The effect is favored by high electron deficiency (**8g** > **8f** > **8e**, **8d** > **8c**), which induces a low-lying LUMO, and by ring strain (**8h**, **8c** > **8b**), which gives rise to a high-lying HOMO. The overlap between the orbitals of the C–X σ bond and the electron-deficient center will be promoted by a small dihedral angle θ, an electropositive X atom, and a short distance between the σ and p orbitals. Particularly strong effects are therefore to be expected in compounds in which X is an electropositive atom and the C–X bond is part of a three-membered ring bound to the electron-deficient center through a short double bond in an arrangement where $\theta = 0°$ is realized. These conditions are optimally fulfilled in the boriranylideneborane **10u***,[*] whose nonclassical bridged structure **10u** was predicted from ab initio calculations.[25, 26]

The boriranylideneborane **10a** (Sections 2 and 3), with sterically demanding substituents in place of the hydrogen atoms in **10u**, was the first experimentally available methyleneborane.[1a] Bond angle distortions of comparable magnitude to that in **10u** were calculated for the closely related vinyl cation **2a**,[27, 28] and observed in carbene complexes like **3a**.[6, 7] The latter resembles the H-bridged vinyl cation **2u**.[29] Carbocations having electropositive X atoms

[*] The letter "u" will be used for the unsubstituted basic structure of a compound class, and a star "*" will indicate the (nonexistent but more familiar) classical forms of the nonclassical compounds.

Armin Berndt, born in Duisburg in 1936, studied Chemistry at the universities of Marburg and Munich and graduated in 1965 under the supervision of Karl Dimroth with a doctoral thesis on phenoxyl radicals. He completed his habilitation in 1970 with a study on sterically hindered nitro compounds and has been Professor of Organic Chemistry since 1972. At the core of his research interests are syntheses of compounds with sterically demanding substituents and the investigation of the interactions of electron-deficient centers with neighboring σ bonds that are revealed in unusual geometries and spectroscopic properties.

(Si and Sn) at the position β to the electron-deficient center are thermodynamically strongly stabilized by C–Si[22, 23, 30] and C–Sn hyperconjugation[22, 31] (see above) but extremely labile kinetically. NMR spectra of such cations have only recently been recorded,[32] and no crystal structures have been reported to date. Methyleneboranes lacking strong π donors on the dicoordinate boron atom have enabled the investigation by NMR spectroscopy and X-ray diffraction analyses (Section 3) of not only C–Si[1c] and C–Sn hyperconjugation,[1d, e] but also C–B hyperconjugation and the influence of substituents on it,[1i] and have filled a gap in our knowledge of strong σ–π delocalization.

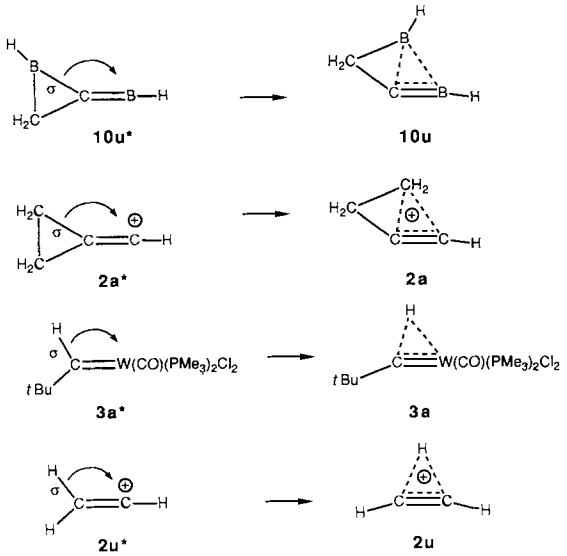

In the extreme form of strong, α-agostic type, nonclassical interactions, the X atom of the C–X σ bond will be transferred to the electron-deficient center. Thus, the borylcarbenes **11**,[33] which are isoelectronic with methyleneboranes and vinyl cations, will be formed from methyleneboranes, and the diborylcarbenes **13** from the (borylmethylene)boranes **12**.

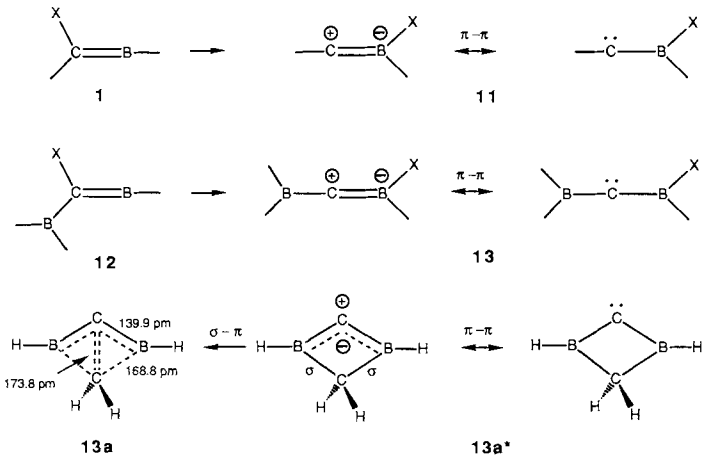

In these carbenes the electron deficiency at the dicoordinate carbon atom will be increased through π–π delocalization of its formally nonbonding electron pair to the boryl substituents. As a result, nonclassical interactions with σ bonds like B–X play a considerable role, as shown by the geometry in **13a**.[25b] Diborylcarbenes of the type **13a** are intermediates in the facile topomerization reactions of **10a–d** (see Section 4.1.2) and, probably, some addition reactions of **10a**.[1k–1o] Additionally, many rearrangement reactions of (borylmethylene)boranes (**12**, Section 2) can be explained, at least formally, by invoking diborylcarbenes (**13**) as intermediates.

The π electrons of the C–B double bond in **12** will be delocalized towards the boryl substituent in a way similar to the nonbonding electron pairs in the carbenes **11** and **13**. Thus, the electron deficiency at the dicoordinate boron atom will be increased in (borylmethylene)boranes, and their nonclassical interactions with neighboring σ electrons will be strengthened (Scheme 3; see 3.3.1.5).

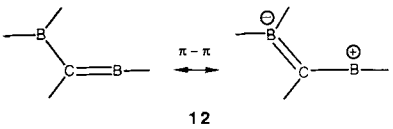

Scheme 3. π–π Delocalization in (borylmethylene)boranes.

In the α-agostic effect and in C–X hyperconjugation, the C–X σ electrons are located in a similar position relative to the electron-deficient center as formally nonbonding electrons in π–π delocalization (compare Scheme 1). Electron-deficient centers can, however, also build nonclassical 3c–2e bonds with other spatially adjacent σ bonds (Scheme 4).

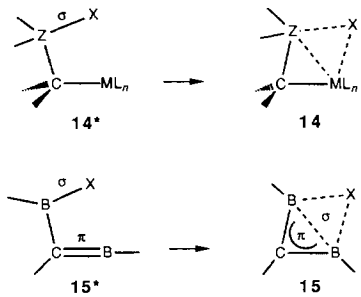

Scheme 4. Nonclassical 3c–2e bonds from interaction of electron-deficient centers with *neighboring* σ electrons: the β-agostic type.

The nonclassical interactions in the transition metal complexes of type **14** have been termed β-agostic effects.[7, 34] Such nonclassical bonds are found in (borylmethylene)-boranes like **15**[1g, 1h, 35] (see Section 3.3.3). The low activation energies of rearrangement reactions involving migration of an X atom from the tri- to the dicoordinate boron atom, which are characteristic of the (borylmethylene)boranes **12** (see Sections 2, 3, and 4), can be explained by stabilized transition states having the structure **15**.

In the extreme case, the weakening of the C–H bond through agostic effects will lead to the formation of a new metal–carbon bond and a transfer of the hydrogen atom to the metal (transition metal)[7] or to a carbanion coordinated to the metal (lithium) (Scheme 5).[36, 37]

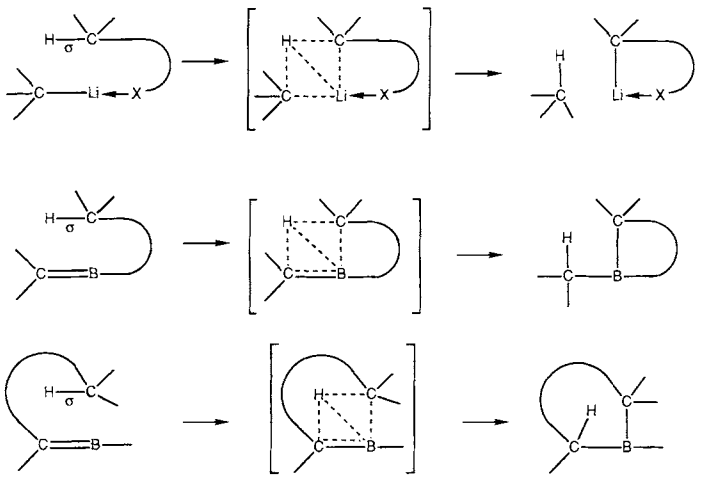

Scheme 5. Extreme cases of agostic interactions with C–H bonds.

Intramolecular C–H bond additions to the C=B double bonds of methyleneboranes (Section 4.2) are reminiscent of such metalation reactions and are therefore described here as γ-, δ-, and ε-agostic effects. The reactivity of methyleneboranes resembles that of vinyl cations ([2 + 2] cycloadditions[1e, 1k, 2h, 38]) and, as Paetzold[3e] has pointed out, also that of methylenesilanes (silaethene $\rangle C{=}Si\langle$)[39]—the tricoordinate silicon atom is related to the dicoordinate boron atom through the diagonal relationship in the periodic system of elements.

2. Syntheses

Like the amino(methylene)boranes **5**, the borataalkynes **7** and the 2-borataallenes **6** are methyleneboranes stabilized by π–π delocalization, but in contrast to **5** they carry a negative charge. Their syntheses will be described here for this reason and also because they can be used as reactants in the synthesis of other methyleneboranes. Clear-cut syntheses without rearrangement reactions will be handled before those involving rearrangements. Exceptions are syntheses of boriranylideneboranes, which are treated before their use in the preparation of methyleneboranes. Syntheses of anionic precursors will also be described prior to their transformation to methyleneboranes.

2.1. Elimination Reactions

Nöth et al.[2b] prepared the first stable amino(methylene)borane **5a** by dehydrohalogenation of the 9-fluorenyl-(2,2,6,6-tetramethylpiperidino)boron halides **16a**.

This procedure is also successful if the di-*tert*-butylamino or the *tert*-butyl(trimethylsilyl)amino derivatives are used instead of the tetramethylpiperidino derivative. With the bis(trimethylsilyl)amino derivative, only the dimer will be obtained.[2c] The intermediacy of fluorenylideneboranes having bulky aryl substituents instead of amino groups on boron can be deduced from their reaction products with the Lewis base tetrahydrofuran[40] or with 3-hexyne ([2 + 2] cycloaddition).[38] Paetzold et al. synthesized not only the amino(methylene)boranes **5d**[3a] and **5e**[3c] but also the methyleneboranes **1a** and **1b**[3d] with methyl and *tert*-butyl groups on the boron atoms by the elimination of fluorotrimethylsilane or trimethyl(methoxy)silane from **17** at temperatures between 470 and 560 °C. Compound **1a** rapidly dimerizes to the corresponding 1,3-diboretane.

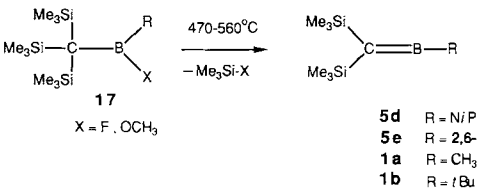

17 X = F, OCH_3

5d R = N*i*Pr$_2$
5e R = 2,6-dimethylpiperidino
1a R = CH_3
1b R = *t*Bu

2.2. Cycloreversion Reactions

The methyleneboranes **5f** and **19** without substituents at the carbon atom of the C–B double bond have been generated by pyrolysis of the bicyclic compounds **18a** and **18b**, isolated in an argon matrix at 10 K, and characterized by IR spectroscopy by Maier et al.[4] As the matrix thawed, the characteristic IR bands disappeared at temperatures as low as 40 K (**19**) and 80 K (**5f**).

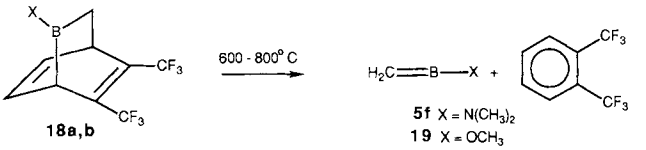

18a,b

5f X = $N(CH_3)_2$
19 X = OCH_3

The methyleneboranes **1c,d** and **1e,f** are obtained by melting the 1,3-diboretanes **20a,b** at 148 and 177 °C, respectively.[1c, 1e] 1,2-Dihydroborete **21a**[1e] yields the methyleneborane **1e** and bis(trimethylsilyl)acetylene on heating at 120 °C (reverse reaction to the formation of **21a**).

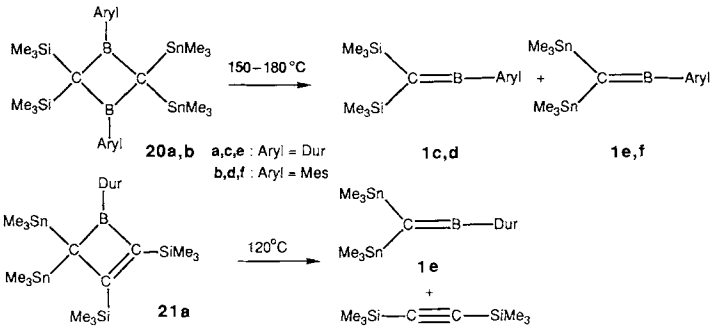

20a,b a,c,e : Aryl = Dur; b,d,f : Aryl = Mes

1c,d **1e,f**

21a

Dur = duryl = 2,3,5,6-tetramethylphenyl; Mes = mesityl = 2,4,6-trimethylphenyl

The [2 + 2] cyclo adduct **22**,[3b] obtained from the reaction of the amino(imino)borane $Me_3Si(tBu)N{-}B{=}NtBu$ with

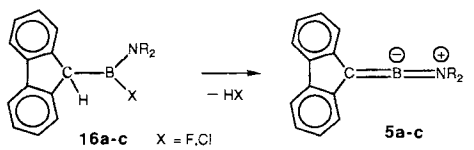

16a-c X = F,Cl

5a-c

NR_2: **a** = 2,2,6,6-tetramethylpiperidino, **b** = $NtBu_2$, **c** = $NtBuSiMe_3$

the alkylidene complex $[(\eta\text{-}C_5H_5)Cl_2Ta{=}CHtBu]$, decomposes at 0 °C into the amino(methylene)borane **5g** and $[(\eta\text{-}C_5H_5)Cl_2Ta{=}Nt\text{-}Bu]$.

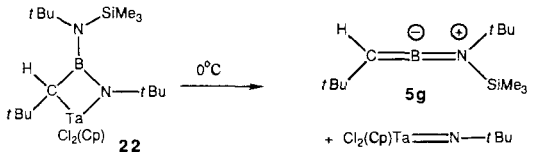

2.3. Boriranylideneboranes (Borandiylboriranes) through Reductive Elimination and Rearrangement

We obtained the methyleneborane **10a** from an attempt to trap an intermediate of the reductive dimerization of **23a**[41] by addition of bis(trimethylsilyl)acetylene. We found that **23a** itself reacted with the alkyne, and the adduct **24a** could be reduced by a sodium/potassium alloy to yield a product with unusual spectroscopic properties. Fortunately, our initial interpretation of the experimental results[42] was subjected to adept and constructive peer review by Budzelaar and van der Kerk, Utrecht, who suggested the constitution **10a*** [1a] with the following comment: "Finally we would venture to remark that all experimental data can also be reconciled with a structure... (**10a***) .... We do not suggest that ...(**10a***)... is a very likely structure; however, neither is [the original suggestion] (see ref. [42])...". Budzelaar and Schleyer[25] and Frenking and Schaefer III[26] have shown by ab initio calculations that the nonclassical structure **10a** is more likely.

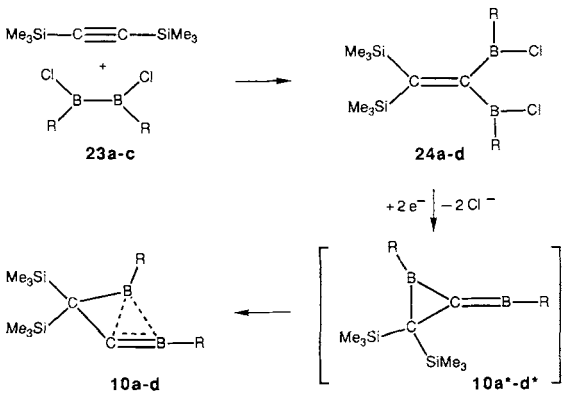

a: R = *t*Bu, **b**: R = Mes
c, d: R = Dur **d**: Me_3Ge instead of Me_3Si

The synthesis of **10a** from **24a**[43] has been optimized by treatment with magnesium under ultrasonication in tetrahydrofuran.[44] In order to verify the calculated, nonclassical structure of the boriranylideneboranes experimentally by X-ray structure analysis, we replaced the *tert*-butyl groups in **23a** and **24a** with mesityl and duryl groups. In contrast to the thermally unstable **23a**, the diboranes(4) **23b** and **23c**[45] do not decompose up to about 90°C and slowly add bis(trimethylsilyl)acetylene in pentane under reflux (3 days to 4 weeks) to form the 1,1-diborylalkenes **24b** and **24c**.[45] Only **24b** reacted with Na/K alloy to form **10b**,[10a] which was, however, obtained as a noncrystalline solid and in only moderate and poorly reproducible yield. Only by employing the highly reactive Bogdanović-magnesium[46] could **10b** and **10c** be synthesized in good yields.[1f] Since the crystals of **10c** were unsuitable for X-ray structure analysis, we finally prepared the diborylalkene **24d** from the reaction of **23c** with bis(trimethylgermyl)acetylene, which gave **10d** upon reduction with Bogdanović-magnesium.[1f] In 1987 we proposed the methylenediborirane **25a** as an intermediate in the transformation of **24a** to **10a**.[47] This suggested a mechanism in which an initial reductive elimination is followed by a rearrangement to form the three-membered ring containing one boron atom.

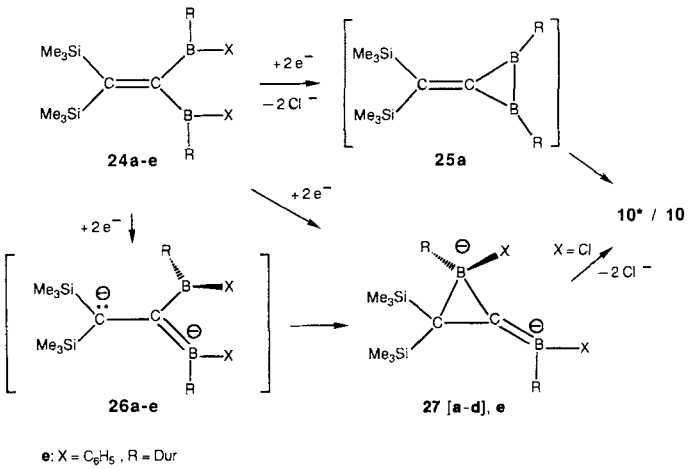

e: X = C_6H_5, R = Dur

Since then we have found that the diborylalkene **24e** can be reduced by lithium in toluene to the dianion **27e**,[48] probably via **26e**. Thus, a boron-containing three-membered ring can also be formed by direct reduction of a 1,1-diborylalkene, which offers an alternative pathway for the transformation of **24** into **10**, via **26** and **27**, in which the elimination reaction *follows* the formation of the boron-containing three-membered ring.

Siebert et al. observed that reduction of the 1,1-diborylalkene **24** bearing diisopropylamino groups in the place of the *tert*-butyl or aryl substituents in **24a–c** led to the formation of 1,3-bis(diisopropylamino)-2,4-bis(trimethylsilyl)-1,3-dihydro-1,3-diborete with migration of a silyl group.[49] Compound **10a** is transformed into the corresponding 1,3-dihydro-1,3-diborete only after heating for several hours at 170 °C.[50]

2.4. Cleavage of B–C Single Bonds in (Borylmethylene)boranes with Retention of the C=B Double Bond

The boriranylideneboranes **10b** and **10c** add sterically hindered phenols[1i] or silanols[51] under cleavage of the Si_2C–B bond of the borirane ring and retention of the C–B double bond to yield the (borylmethylene)boranes **12a–c** in which *one* oxygen atom is bonded to the boron atom of the boryl substituent. These can react with a further equivalent of HOR under cleavage of the B-aryl bond of the boryl

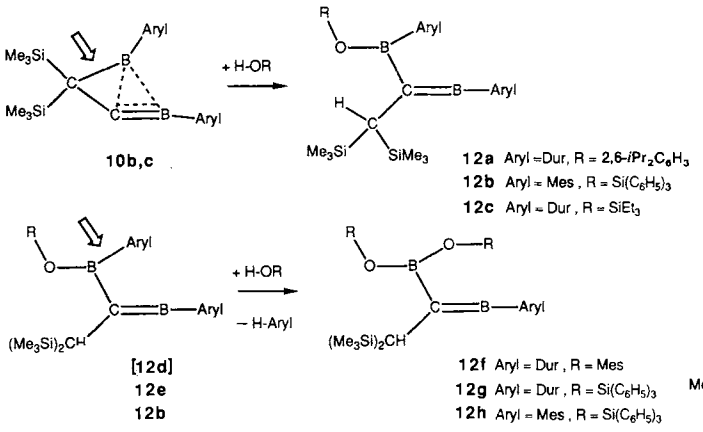

residue and form the (borylmethylene)boranes **12f–h** in which *two* oxygen atoms are bound to the boron atom of the boryl group. When 2,4,6-trimethylphenol is used, the second reaction is so fast that even if just one equivalent of HOR is employed, **12f** is obtained exclusively.[1i]

2.5. Borataalkynes from Reductive Cleavage of the C–C Bond of the Three-Membered Ring of Boriranylideneboranes

The C–C bond of the three-membered ring in the boriranylideneboranes **10b,c** having aryl substituents on the boron atoms is reductively cleaved by lithium in diethyl ether to give the borataalkynes **7a,b**;[10a] however, **7a,b** could be obtained more conveniently by reaction of the **10b,c** precursors **24b,c** with an excess of lithium in diethyl ether.[1b,45]

Protonation of **7a,b** with one equivalent of cyclopentadiene leads to the borylborataalkynes **28a,b**, of which only **28b** was obtained in pure form.[10a]

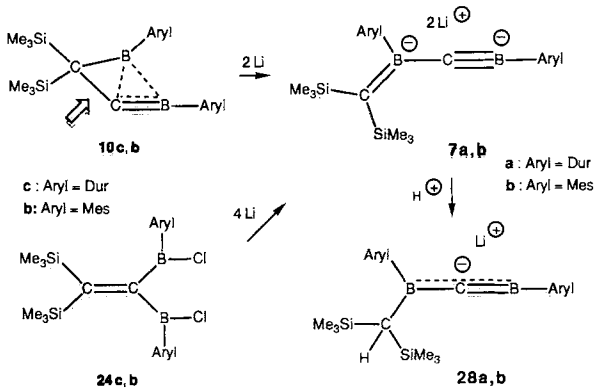

2.6. Reactions of Borataalkynes with Electrophiles

The reaction of the C-borylborataalkyne **28b**[45] with chlorotrimethylstannane yields the [boryl(stannyl)methylene]borane **12i**.[1d]

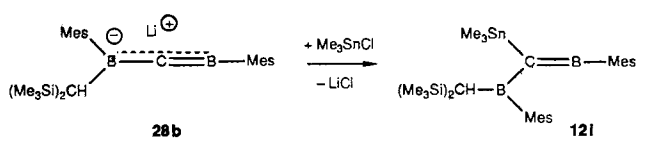

The borataalkynes **7a,b**[10a] react with aryldifluoroboranes to form the (diborylmethylene)boranes (1,3-diboretane-2-ylideneboranes) **29a,b**,[1b] and with 1,1-diaryl-2,2-difluorodiboranes(4) to form the B-boryl(1,3-diboretane-2-ylidene)boranes **30a,b**.[1h]

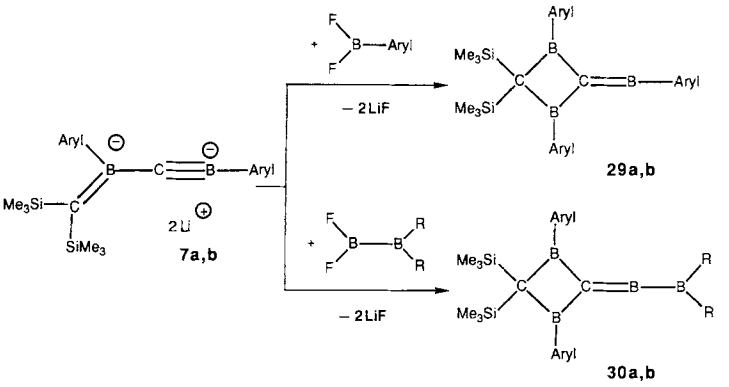

2.7. Rearrangements Involving 1,3 Migrations

From attempts to produce the halo(methylene)boranes **1g,h** by elimination of trimethyl(methoxy)silane (see Section 2.1) from halo(methoxy)[tris(trimethylsilyl)methyl]-boranes, Paetzold et al. obtained the rearrangement products **1i,j**.[3e] The authors conjectured that the anticipated halo(methylene)boranes **1g,h** experienced a double 1,3-shift of the Me and Hal groups, via the intermediate **31**, while still in the hot reaction tube. They could show from the analyses

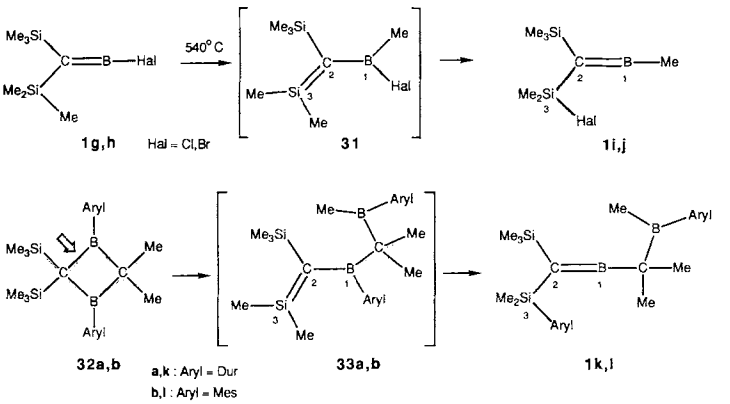

of trapping products that such a double shift is still possible when in place of the halogen a methyl group (in the experiment a CD_3 group) is bound to the boron atom of the methyleneborane (isotopomerization).[3e]

Analogously, the formation of the methyleneboranes **1k,l**[1c] from the thermal isomerization of the 1,3-diboretanes **32a,b** can be explained if one assumes that silaethene intermediates (**33a,b**) are formed. The [boryl(stannyl)-methylene]borane **12i**[1d] transforms below 0°C into the [boryl(stannyl)methylene]borane **12j** in solution,[1d] where **12j** and **12i** coexist in a rapidly established equilibrium. The mutual interconversion takes place by a 1,3-migration of a mesityl group from the tri- to the dicoordinate boron atom, which is a typical reaction for (borylmethylene)boranes (see Sections 3.3.3 and 4.1.1). Upon cooling, the methylene-

borane **12j**, with the bis(trimethylsilyl)methyl group on the dicoordinate boron atom, preferentially crystallizes from a solution of the two isomers in ether.

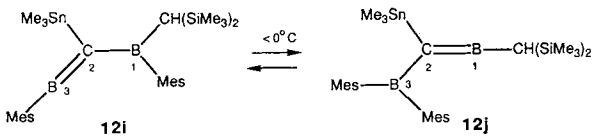

The (borylmethylene)borane **12k**[1i] is generated by thermolysis of **24c** either as a melt at 175°C or by heating under reflux in bis(trimethylsilyl)acetylene at 135°C (this reaction was originally observed when the cooling system failed during the synthesis of **24c**, which is performed in pentane under reflux).

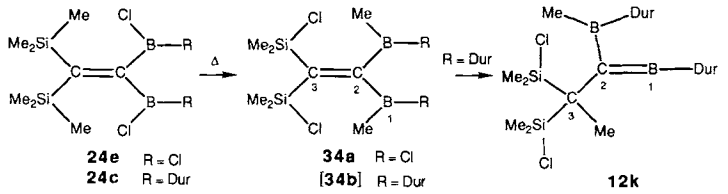

In this reaction, both chlorine atoms migrate from boron to silicon, whereas only one of the methyl groups migrates from silicon to boron, while the other moves to carbon. Analogous to the thermal transformation of **24e** into **34a** described by Siebert et al.,[52] **34b** might be formed as an intermediate, which then gives **12k** by a 1,3 methyl shift from boron to carbon. The remarkable aspect of the **24c** → **12k** isomerization is the thermal formation of a C–B double bond at the expense of a C–C double bond; the compound with the C–B double bond is apparently thermodynamically more stable than the isomer with the C–C double bond (for a discussion of this phenomenon see Section 3.3.1.5).

2.8. Rearrangements Involving 1,2 Migrations

Upon melting at 155°C the (borylmethylene)borane **12b** transforms quantitatively into the (borylmethylene)borane **12l**.[51] In this isomerization the organic substituents on the C–B double bond exchange places (double 1,2 migration); the diborylcarbene **13b** may be an intermediate.

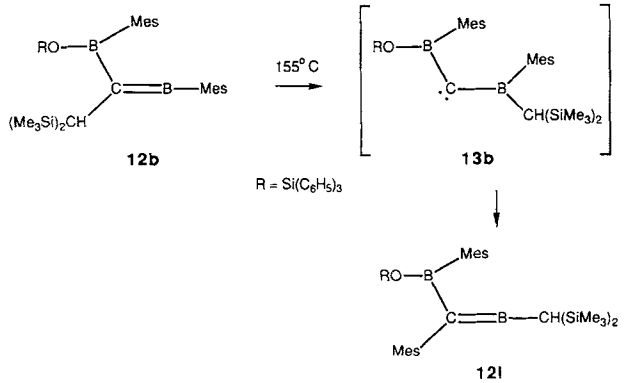

The 1,3-diborataallene **35**, obtained from reaction of the C-borylborataalkyne **28b** with two equivalents of *tert*-butyllithium,[53] can be oxidized by tin(II) chloride to the mesityl-bridged methyleneborane **15a**.[1g] The migration of a mesityl group from the boron to the carbon atom can be most simply explained by employing the diborylcarbene intermediate **13c** and the classical form **15a*** of **15a**.

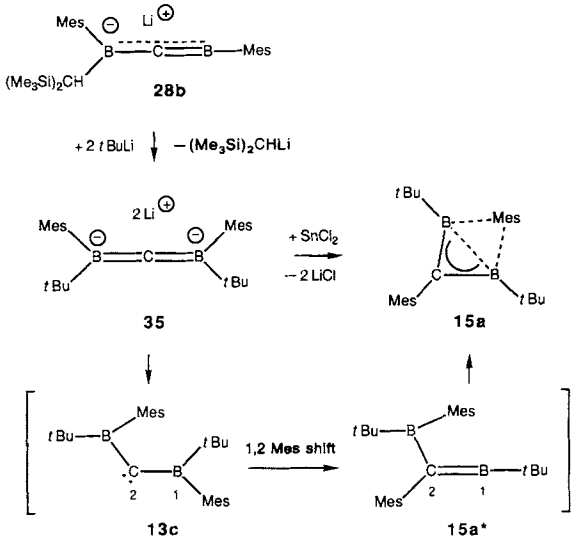

The borylborirane **36a** is quantitatively transformed into the amino(borylmethylene)borane **5h** by heating at 60°C in chloroform or by sublimation at 130°C.[1j] In this reaction, the C–C bond of the three-membered ring is cleaved, a hydrogen atom migrates from the carbon atom bound to two boron atoms to the carbon atom bound to two trimethylsilyl groups, and the *tert*-butyl group migrates from the exocyclic boron atom to the carbon atom bound to the two boron atoms. As intermediate we suggest the diborylcarbene **13d**.

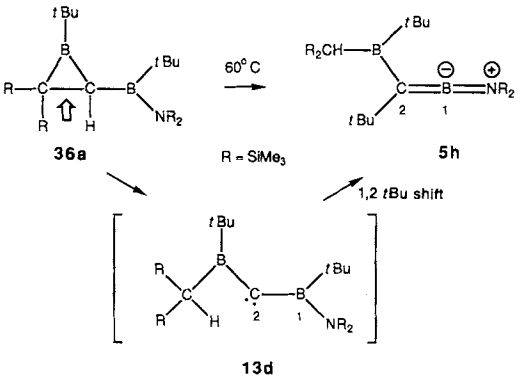

The cyclic methyleneboranes **38a,b**[1h] result from the spontaneous isomerization of the boryl(diborylmethylene)-boranes **30a,b**.[1h] Intermediate steps are likely to contain the diborylcarbene **13e** and the cyclic B-borylmethyleneboranes (dihydrotriboroles) **37**. These react further to form **38***, the classical form of the nonclassical methyleneborane **38a,b**, through a 1,3 migration of an aryl group from the tri- to the dicoordinate boron atom.

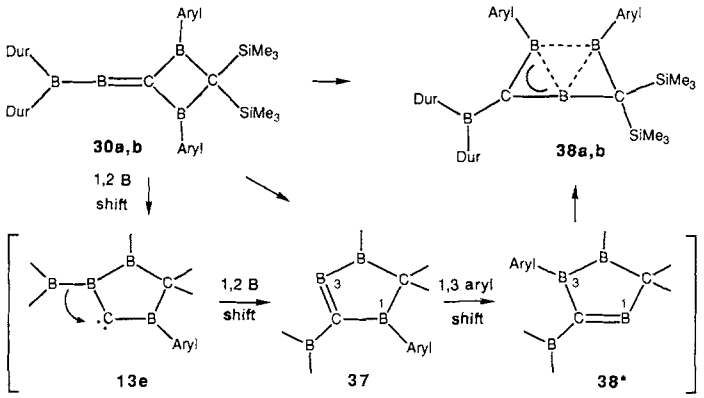

2.9. 2-Borataallenes.

2.9.1. Through Thermal Isomerization of C-Borylboriranides

The borylboriranide **39a**,[9b, 48] prepared from **10c** by reaction with phenyllithium, is transformed in refluxing toluene into a mixture of the 2-borataallene **6a** and the 1,3-diboretanide **42a** from which **6a** can be separated by crystallization. In this reaction, the C—C bond of the three-membered ring is cleaved, and for each product a different duryl group migrates from a boron atom to the carbon atom located between the two boron atoms. The first intermediate in this transformation is likely to be the carbene **40**. A 1,2 migration of the duryl group from the negatively charged boryl substituent to the neighboring coordinatively unsaturated center results in the 2-borataallene **6a**. Migration of the duryl group on the other boron atom would lead to formation of the 1-bora-3-boratabutadiene **41**, whose subsequent electrocyclic ring closure would yield **42a**.

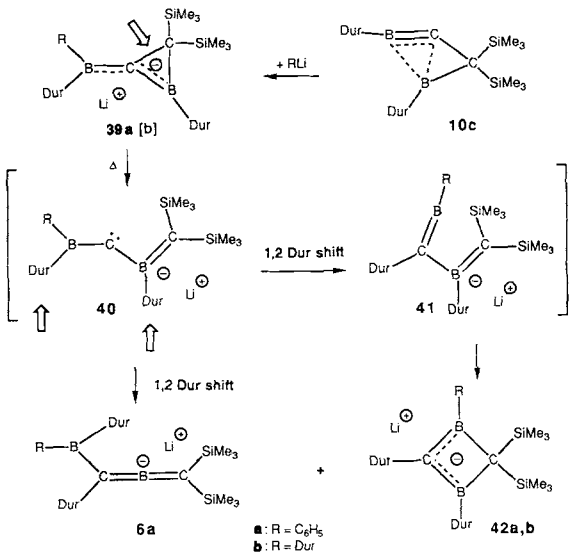

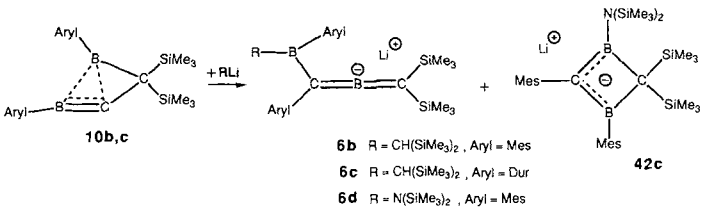

The only products that are formed from the reaction of **10b** or **10c** with $LiCH(SiMe_3)_2$ at room temperature are the corresponding 2-borataallenes **6b**[54] and **6c**,[48] whereas with duryl lithium only **42b** is formed from **10c**.[9b] A mixture of **6d** and **42c** is formed from the reaction of **10b** with $LiN(SiMe_3)_2$ at room temperature.[51]

2.9.2. Through Thermal Isomerization of 2-Boryl-1,3-diboretanides

The 2-boryl-1,3-diboretanides **43a,b** accessible from the reaction of **29a,b** with *tert*-butyllithium are transformed in the melt (200°C) into the 2-borataallenes **6e,f**.[9a, 55] In this reaction, a Si_2C—B bond is cleaved and an aryl group migrates from the tricoordinate ring boron atom to the boron atom which has lost its third coordination partner as a result of the cleavage. We suggest the 1-bora-3-boratabutadiene **44** as an intermediate (compare **41**), whose transformation into **6e,f** requires a 1,3 migration of an aryl group from the tri- to the dicoordinate boron atom, a reaction described repeatedly in this review.

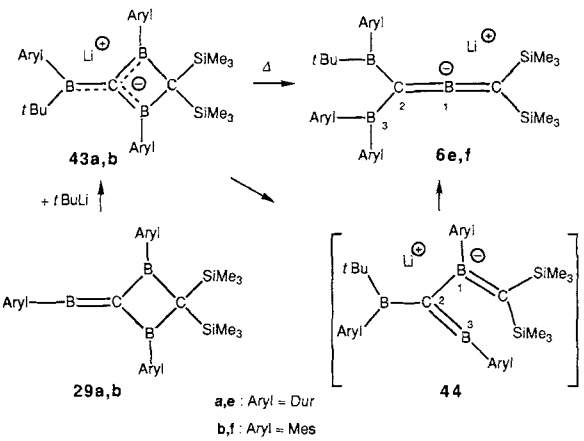

2.9.3. Through Reductive Dimerization of the Methyleneborane 1c

The main product of the reaction of the methyleneborane **1c** with lithium metal in toluene is the 2-borataallene **6g**[9a] (the unsymmetrical dimer of the radical anion of **1c**).

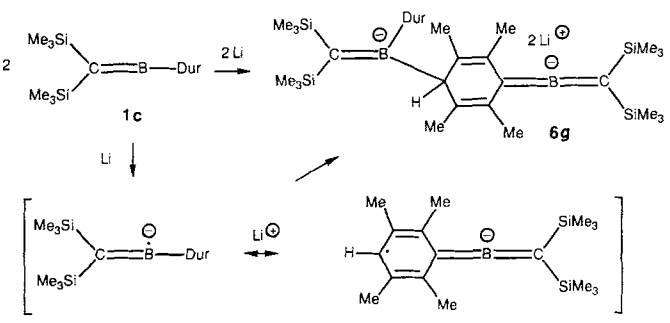

2.10. Reactions of 2-Borataallenes with Electrophiles

The 1-boryl-2-borataallenes **6a–c** react with electrophiles to form the (borylmethylene)boranes **12m–p**.[48, 54, 56] The product **12q**, expected from the protonation of **6d**, is spontaneously transformed into the amino(methylene)borane **5i** through 1,3 migration of a mesityl group.[51]

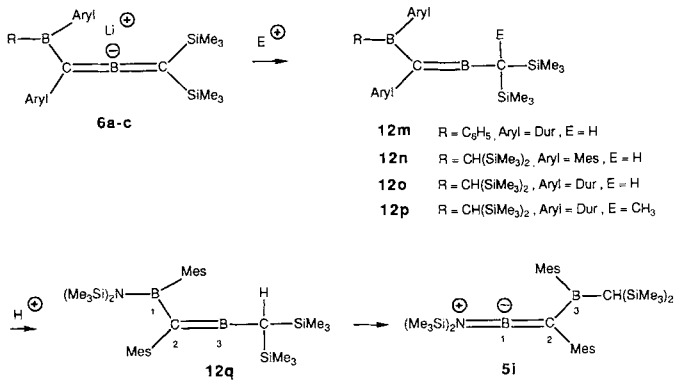

The 1,1-diboryl-2-borataallenes **6e,f** can be protonated with cyclopentadiene to form the (diborylmethylene)boranes **45a,b**.[55–57a] In all cases the electrophiles attack the carbon atom bonded to the two trimethylsilyl groups regioselectively, with the result that only (borylmethylene)boranes and not the isomeric (disilylmethylene)boranes result.

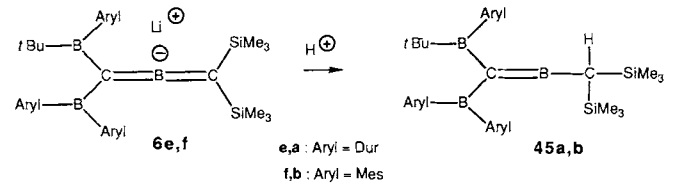

2.11. Protonation of Diboriranides to form H-bridged (Borylmethylene)boranes.

The diboriranides **46a**[44, 35] and **46b**[57b], obtained by reduction of **24a** and **24c** with potassium and Bogdanović-magnesium, respectively, can be protonated with HCl in ether to form the H-bridged (borylmethylene)boranes **15b,c**,[35, 51] as can the intermediate diboriranide **46a**[35] (formed upon monoprotonation of **46a**) and the diboriranide **47c**[51] (formed upon reduction of **12c** with lithium).

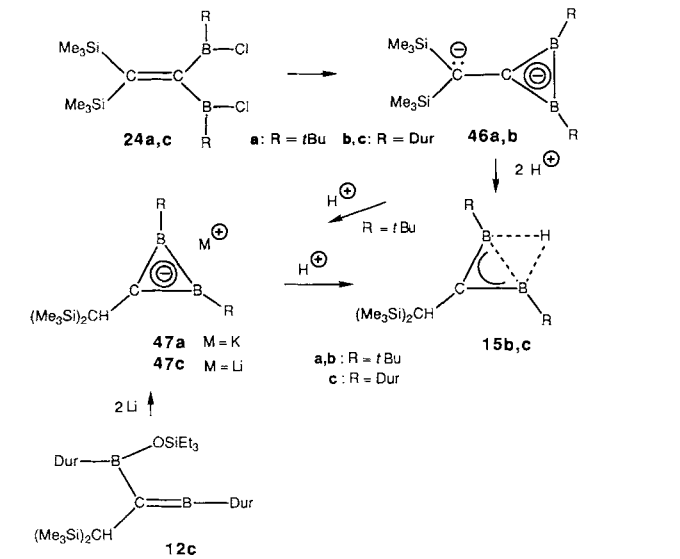

2.12. Elimination of Aryltrimethylstannane and Subsequent Reactions

Upon thermolysis of the 1,3-diboretanes **20a,b**, aryltrimethylstannane and small amounts of the methyleneboranes **49a,b** are formed in addition to the products of the cycloreversion (Section 2.2).[58–60] The primary products of these reactions are likely to be the cyclic methyleneboranes **48a,b (48a*, b*)**. In addition to the dimerization required in going from **48a,b** to **49a,b**, a migration of the trimethylstannyl group from the carbon atom located between the two boron atoms to the carbon atom bonded to the two trimethylsilyl groups must take place.

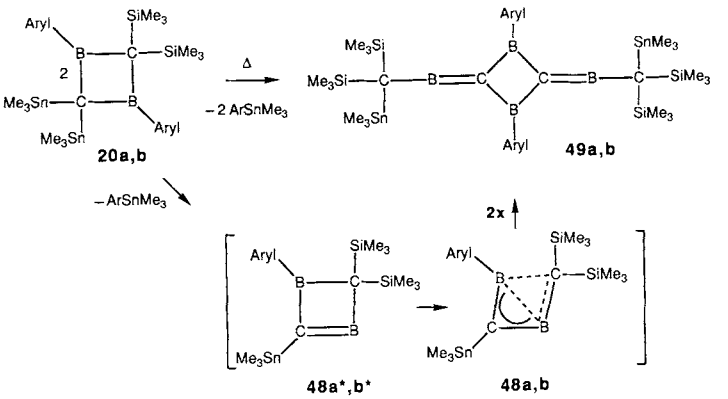

2.13. (Borylmethylene)boranes from Boriranylideneboranes and Alkynes

Boriranylideneborane **10c** reacts with mesityl(trimethylsilyl)acetylene to form the [boryl(silyl)methylene]borane **12r**[51, 61] and with bis(trimethylstannyl)acetylene to form the [boryl(stannyl)methylene]borane **12s**.[51] In these reactions, the three bonds indicated with arrows must be broken, the trimethylsilyl or trimethylstannyl groups of the alkyne must migrate to the carbon atom of the C–B double bond,

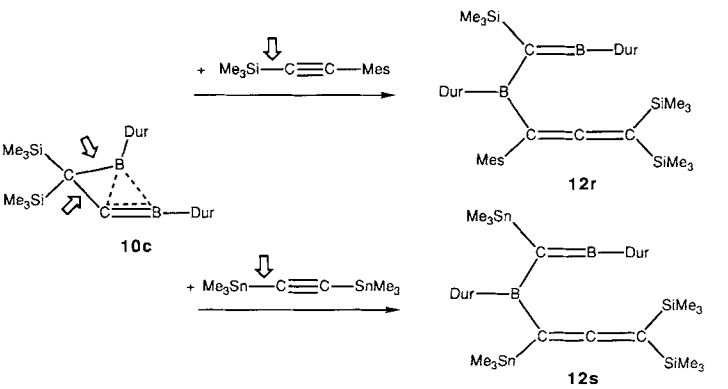

and the $C(SiMe_3)_2$ groups must combine with the alkyne residue to form an allene substructure, which is finally connected to the boryl-B-atom of the resulting methyleneborane.

Thus, stable methyleneboranes are obtained only when the C–B double bond is sterically shielded by large substituents. In addition, electronic stabilization is necessary either through formally nonbonding electron pairs on the atoms directly adjacent to the dicoordinate boron atoms ($=B-\ddot{N}R_2$, $=B-\ddot{C}R_2^{\ominus}-$, or $-^{\ominus}\ddot{C}=B-$) or through electropositive substituents at the position β to the dicoordinate boron atoms. The frequent occurrence of the (borylmethylene)boranes **12** is remarkable (compare Section 3.3).

3. Structures

3.1. Crystal Structure and Spectroscopic Data; Results from Ab Initio Calculations

Selected structural and NMR data of methyleneboranes whose electron deficiency at the dicoordinate boron atom is removed by π–π delocalization are compiled in Tables 1 and 2. Methyleneboranes whose electron deficiency is reduced to some extent through σ–π delocalization are listed in Tables 3 and 4. Table 5 contains the interatomic distances calculated for parent compounds of both types of methyleneboranes with ab initio methods at various levels. The C=B–N(C) bond angles of the methyleneboranes listed in Table 1 deviate from the ideal value for a dicoordinate atom (180°) by a maximum of 4.9°. This is also true for most of the methyleneboranes listed in Table 3. Significant deviations of this angle from 180° are observed when the X–C=B bond angle also deviates significantly from the ideal 120° (for example in **10d**, **15a**, **38a**, and **12j**). In all these cases the chemical shifts observed for the boron atom of the C–B

Table 1. Selected bond angles [°] and bond lengths [pm] of amino(methylene)boranes, 2-borataallenes, and borataalkynes.

Cmpd.	C=B–N(C)	X–C=B Y–C=B	B–C–Li	C=B	B = N(C)	Ref.
5a	177.7(2)	127.6(2) 126.9(2)	–	142.0(3)	134.9(3)	[2c]
5a' [a]	175.1(2)	124.9(2) 128.9(2)	–	142.4(3)	135.3(3)	[2c]
5d	179.6(3)	117.0(2) 117.8(8)	–	139.1(4)	136.3(4)	[3a]
5h	175.8(4)	121.3(3) 111.9(3)	–	140.8(5)	136.7(5)	[62]
6b	175.4(4)	116.9(3) 121.2(3)	87.4(3)	144.7(6)	143.1(6)[b]	[60]
6d	175.9(6)	115.4(5) 116.8(5)	87.3(4)	144.6(7)	141.6(7)[b]	[51]
6e	175.7(8)	115.5(7) 110.9(6)	87.9(6)	145(1)	142(1)[b]	[9a]
28b	176.5(5)	183.5(5)	90.4(4)	133.9(6)	149.2(6)[c]	[10a]
7a	177.2(6)	182.8(6)	88.5(5)	132.3(9)	154.6(9)[d]	[10b]

[a] **5a'** is the symbol for the second independent molecule **5a** in the asymmetric unit. [b] B=C. [c] C≡B. [d] B–C.

Table 2. Selected NMR and IR data for amino(methylene)boranes, 2-borataallenes, and borataalkynes.

Cmpd.	δ^{11}B (C=B)	δ^{11}B (BR_2)	δ^{13}C (C=B)	$C^{11}BN$ ν_{as} [cm^{-1}]	$C^{10}BN$	Ref.
5a	59.2	–	83.2	1717	1780	[2c]
5b	58.9	–	82.9	1720		[2c]
5c	59.8	–	82.3			[2c]
5d	46.3	–	45.2	1710	1766	[3a]
5e	44.8	–	–	1710	1765	[3c]
5f	–	–	–	1780	1829	[4]
5g	60	–	69.1	1705	1758	[3b]
19 [a]	–	–	–	1721 [a]	1765 [a]	[4]
5h	58	70	86.8	1614	1662	[88]
5i	54	63	82.5			[51]
6a	54	65	98.2			[9b]
6b	59	70	97.8			[48]
6d	65	46	90.4			[51]
6e	71	75	108.1			[9a]
28b	41	54	127			[10a]
7a	26	46	110.3			[10b, 45]
7b	26	46	109.6			[10a]

[a] Methoxy(methylene)borane: ν_{as} $C^{11}BO$, $C^{10}BO$.

Table 3. Selected bond angles [°] and bond lengths [pm] of methyleneboranes with aryl or alkyl groups at the dicoordinate boron atom.

Cmpd.	C=B–C	X–C=B	Y–C=B	X–C–Y	C=B	Ref.
12f	175.1(8)	118.3(7)	124.8(6)	116.8(6)	138.4(11)	[1i]
12a	176.6(6)	108.8(5)	131.6(5)	119.5(5)	137.2(9)	[1i]
12k	179.5(7)	98.1(5)	132.2(5)	129.4(5)	140.4(9)	[1i]
45a	173.5(8)	107.2(7)	128.2(7)	124.6(6)	140(1)	[56, 58]
29a	176.7(6)	133.3(5)	148.2(5)	78.3(4)	137.4(8)	[1b]
10d	168.8(6)	78.5(4)	216.8(5)	64.7(5)	135.1	[1f, 57a]
1k	176.6(6)	117.9(5)	120.1(5)	122.0(3)	136.3(9)	[1c]
1b	179.6(4)	118.7(1)	118.7(1)	122.5(2)	136.1(5)	[3d]
12r	169.7(3)	109.1(2)	125.3(3)	124.8(2)	138.6(4)	[51, 61]
12j	173.5(8)	106.0(4)	133.7(6)	120.1(4)	131(1)	[1d]
49a	179.7(3)	141.7(3)	139.1(3)	79.1(3)	137.2(5)	[60]
15a	135.1(5) 138.2(5)	80.7(4)	140.1(4)	139.0(4)	146.2(8) 148.8(8)	[1g, 57a]
38a	170.9(4)	69.3	144.6(3)	145.8(3)	142.5(5)	[1h, 54]

Table 4. Selected NMR data for methyleneboranes with aryl or alkyl groups at the dicoordinate boron atom.

Cmpd.	δ^{11}B (C=B)	δ^{11}B (BR_2)	δ^{13}C (C=B)	Ref.
12p	83	66	98.5	[48]
12l	82	47	84.4	[51]
12f	80	34	67.2	[1i]
12a	79	47	84.1	[1i]
12g	78	31	70.1	[51]
12b	78	45	84.4	[51]
45a	76 [a]	71 [a]	107.1	[56]
12n	72 [b]	72 [b]	97.2	[48]
29a	71	62	115.5	[1b]
12k	62 [c]	62 [c]	104.7	[1i]
15a	42	42	130.3	[1g]
15b	27	27	128	[35]
15c	23	23	140.3	[51]
38a	23	33	140.1	[1h]
10d	20	48	126.0	[1f]
10c	19	51	121.2	[1f]
10a	18	52	115.2	[1a]
1b	70.0	–	49.9	[3d]
1a	69.5	–	52.7	[3d]
1c	63	–	60.9	[1c]
1d	63	–	61.5	[1c]
1e	53	–	46.5 (198 Hz) [d]	[1e]
12j	52	65	77.3 (125 Hz) [d]	[1d]
12s	54	71	75.3 (66 Hz) [d]	[51]

[a] Arbitrary assignments. [b] Averaged value for the rapid exchange. [c] No rapid exchange; values are the same only by coincidence. [d] ^{13}C–Sn coupling constants; the coupling between the two ^{117}Sn and ^{119}Sn isotopes could not be resolved.

Table 5. Calculated interatomic distances [pm] in methyleneboranes, 2-borataallenes, and borataalkynes.

Cmpd.	C=B C≡B	C–B B–B	Method	Ref.
1u	137.7	–	6-31G*	[63]
	138.5		MP2/6-31G*	[64]
	138.8		MP2/6-31 + G*	
	138.4		DZ + P	[26]
	138.3	153.1	6-31G*	[65]
29u **1** [6]	137.3	155.9	6-31G*	[1b]
10u*	136.1	151.1	DZ	[26]
	133.9	152.7	6-31G*	[25a, b]
10u		182.5 (B-B)		
	134.6	153.9		[26]
		182.4 (B-B)	DZ + P	
48u	140.0	149.4	3-21G	[25b]
		174.4		
		151.7		
		174.4 (B-B)		
15u	143.2	173.6 (B-B)	6-31G*	[66a]
	143.8	170.9 (B-B)	MP2/6-31G*	[66c]
5u	134.3	135.7	STO-3G	[2a]
	138.6	137.8 (B-N)	3-21G	[64]
	138.6	136.9 (B-N)	6-31G*	[64]
6u	143.5	143.5	6-31 + G*//	[67]
			6-31 + G*	
7u	132.0		6-31 + G*	[64]
	132.9		MP2/6-31G*	[64]
	134.1		MP2/6-31 + G*	[64]
	131.9		CISD/TZ2P	[68]
28u	133.8	146.7	CISD/TZ2P	[68]

[a] For the meaning of u and u*, see the footnote on page 986. [b] **1** = methylene(vinyl)borane $H_2C=B-C(H)=CH_2$.

double bonds $\delta^{11}B_{C=B}$ differ widely from the maximum values ($\delta^{11}B \approx 80$). Correspondingly large differences for the methyleneboranes in Table 2 appear only for compounds having C–B triple bonds (borataalkynes **7a, b**).

3.2. π–π Delocalization in Methyleneboranes

3.2.1. Strong π–π Interactions of the Dicoordinate Boron Atom with Neighboring Nonbonding Electron Pairs in Classical Methyleneboranes

The short interatomic distances between the dicoordinate boron atom and the nitrogen atom in the amino(methylene)boranes **5** (135.3–136.7 pm) and between the boron and carbon atoms in the 2-borataallenes **6** (141.6–143.1 pm), and the short C–B multiple bonds in **28b** (133.9 pm) and **7a** (132.3 pm) relative to those found from ab initio calculations show that the electron deficiency at the dicoordinate boron atoms in these methyleneboranes is relieved through π–π delocalization of the formally nonbonding electron pairs on the atoms adjacent to the dicoordinate boron atom, that is, through the formation of classical 2c–2e bonds (see Scheme 1). Consistent with this are the NMR shieldings observed at the dicoordinate boron atom of the amino(methylene)boranes ($\delta^{11}B = 44.8-60$), the 2-borataallenes ($\delta^{11}B = 54-71$), and the borataalkynes ($\delta^{11}B = 41$ and 26) compared to those for methyleneboranes without π donors in the neighborhood of the dicoordinate boron atom ($\delta^{11}B = 82-83$; **12l**, **12p**). Characteristic heteroallene IR bands found for the amino(methylene)boranes support the general conclusion that compounds of type **5** are isoelectronic with allenes.

3.2.2. Weak π–π Interactions between the Dicoordinate Boron Atom and Aryl Groups

The electron deficiency at the boron atoms of the methyleneboranes listed in Tables 3 and 4 is reduced only to a small extent through π–π delocalization from the aryl group bound to these boron atoms, as illustrated in Scheme 6. This can be seen from a comparison of **1d**[1c] with

Scheme 6. Weak π–π delocalization in aryl(methylene)boranes.

1b[3d] and **50**.[58] Thus, the boron atom in **1d** is shielded by only $\Delta\delta = 7$ relative to that in **1b**, and the *ortho* and *para* carbon atoms in **1d** are deshielded by only $\Delta\delta = 8.7$ and 7.9 relative to the corresponding atoms in **50**. In contrast, with strong π–π delocalization as found in the vinyl cation **2b**,[32c] the *ortho* and *para* carbon atoms of the aryl substituents are much more strongly deshielded (see values given in the structural formulas). The electron-deficient center in **2b** is more shielded ($\Delta\delta \approx 168$) than the corresponding center in the vinyl cation **2c** ($\delta^{13}C$ from IGLO[69] calculations[32a]). Likewise, the rearrangements **12i** → **12j** (see Section 2.7) and **12b** → **12l** (see Section 2.8) can also be regarded as an indication of the small stabilization through π–π interactions of the type illustrated in Scheme 6. Here, the products in which the bis(trimethylsilyl)methyl groups reside on the dicoordinate boron atom are thermodynamically more stable than the reactants in which aryl groups are in this position.

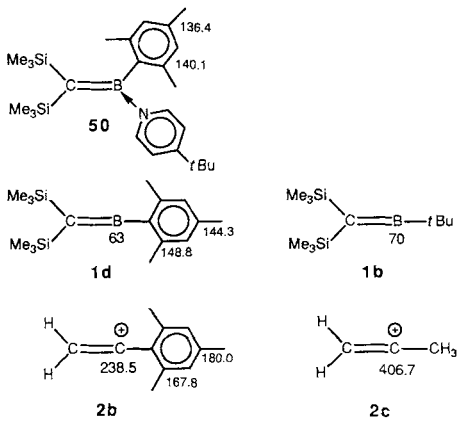

3.3. σ–π Delocalization in Nonclassical Methyleneboranes

The large bond angle distortions of up to 65° at the carbon atom of the C–B double bond, the greater NMR shielding of their boron atoms of up to $\Delta\delta = 65$ (see Section 3.3.1.1), and the decrease in the $^{13}C-^{117/119}Sn$ NMR coupling constants of down to 20% of the normal value (see Section 3.3.1.4), as well as additional smaller effects, can be explained by σ–π delocalization (Scheme 7) of α-agostic type (**A** or **A'**) and β-agostic type (**B**).

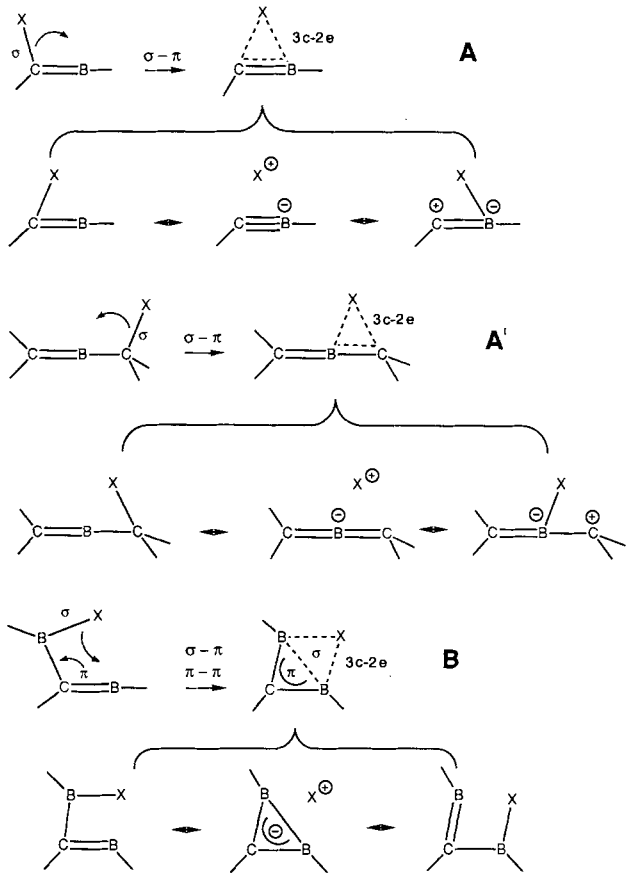

Scheme 7. α-Agostic (type **A**, **A'**) and β-agostic (type **B**) σ–π delocalizations.

The resonance formulas of the 3c–2e bond in **A** and **A'** in which the positive charge is localized on the X atom are identical with those which result from π–π delocalization in the 2-borataallenes **6** and borataalkynes **7** when the counterions are taken into account (Scheme 8). Considered from

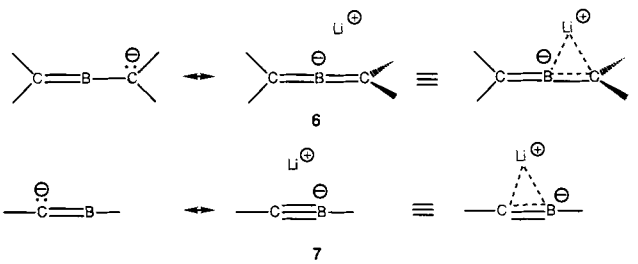

Scheme 8. Borderline cases of classical and nonclassical methyleneboranes; π complexes.

this point of view, π–π delocalization is a borderline case of σ–π delocalization with very electropositive X atoms: the bonding electron pair becomes the formally nonbonding electron pair. One can therefore expect that as the electropositive character of the X atom increases, the properties of methyleneboranes with strong σ–π interactions will approach the properties of systems with π–π delocalization.

Seen from the metal countercations, **6** and **7** are π complexes. Nonclassical carbocations have also been described as π complexes[70] (for example the recently reported bridged β-stannyl- and β-plumbyl-substituted vinyl cations of the types **2d**[71a] and **2e**;[72] see Section 3.3.1.6). Their formation from reactions of alkynes with electrophiles is reminiscent of the "π route" to the nonclassical carbocations. In addition to σ routes,[73] 3c–2e bonds can also form along π routes[74, 75] (the 2-norbornyl and 7-norbornenyl cations **8l** and **8m**, Scheme 9), and only the π route is known for the bishomoborirene **51**.[76, 77] The description "homoaromatic" for **8m** and nonclassical systems of type **51** emphasizes their similarity to 2π-electron aromatic systems having *classical* 3c–2e bonds.

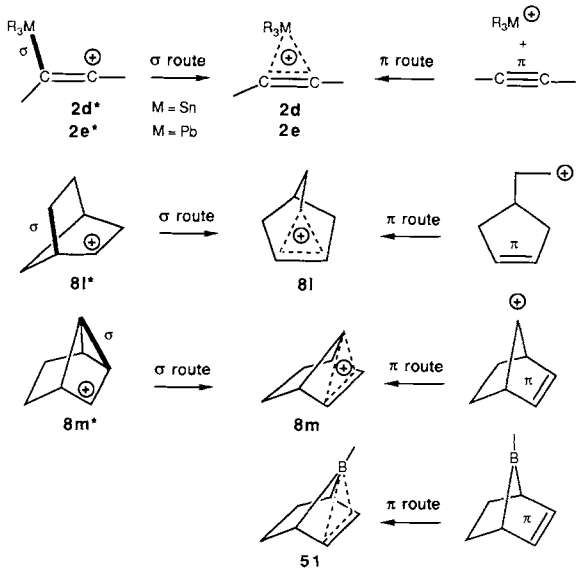

Scheme 9. The σ and π routes to nonclassical 3c–2e bonds.

3.3.1. α-Agostic σ–π Interactions of Type A

3.3.1.1. Nonclassical Bridging, Strong C–B Hyperconjugation and Its Reduction by Electronegative Substituents on the Boryl Groups in (Borylmethylene)boranes

Bond Angle Distortions

It was predicted in 1984 from ab initio calculations that the B–C=B bond angle in **10u** (78.8°[25a] or 78.1°[26]) is compressed by not less than 65° compared to that in the classical **10u*** (146.4°[25b] or 142.7°[26]). The coupled C–C=B angle at the tricoordinate carbon atom is accordingly widened to 217°! The crystal structure of **10d** was obtained in 1990 and revealed B–C=B and C–C=B bond angles of 78.5° and 216.8°,[1f, 57] in impressive agreement with the calculated angles.

The importance of ring strain to the distortion in **10** can be recognized when one compares **10d** to the (borylmethylene)borane **12k**,[1i] in which the boryl substituent is not part of the three-membered ring. Thus, the B–C=B bond angle of 98° in **12k** is approximately 20° larger than the corresponding angle in **10d**. Note that the electron-deficient center is =B–Dur in both cases. On the other hand, the

B–C=B bond angle in **12k** is still more than 20° smaller than the normal bond angle found at a tricoordinate carbon atom and is an indication of the strong C–B hyperconjugation caused by the electropositive nature of the boron atom at the position β to the electron-deficient center. In the (borylmethylene)boranes **12a** and **12f** the β boron atom carries, respectively, one and two substituents in which an electronegative oxygen replaces the carbon substituent in **12k**. These compounds have significantly larger B–C=B bond angles of 109° and 118°; the latter in **12f** is almost the normal size.

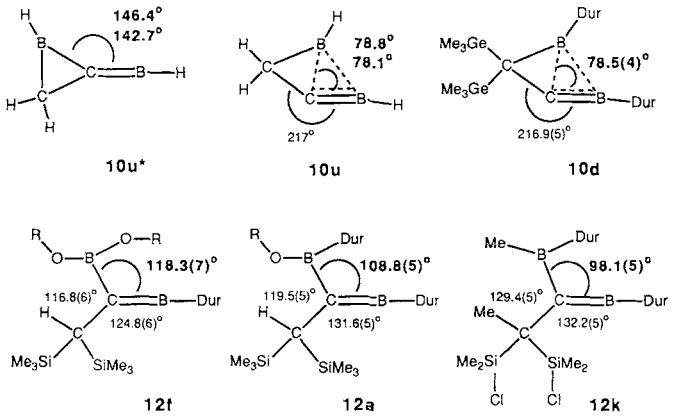

The inverse relationship between the degree of bond angle distortion and the number of electronegative substituents on the β boron atom indicates that the propensity of this boron atom to make the electrons of its bond to the carbon atom of the C–B double bond available for σ–π interactions with the dicoordinate boron atom greatly decreases the higher the number of the electronegative substituents. Thus, as the number of electronegative substituents increases, the electronegativity of the boryl boron atom increases, which leads to weaker σ–π interactions. Carbocations with β-E atoms (E = Si, Ge, Sn) form more slowly when electronegative substituents are introduced at the E atoms. For example, the cation **8n** with a β-$SiMe_3$ group is formed 15600 times faster than **8o**, and the cation **8p** with a β-$SiCl_3$ group is formed about 340 times slower than **8o** despite the presence of a silicon atom in the β position.[78] The rate of formation of carbocations is a generally accepted measure of its stabilization, in this case by C–Si hyperconjugation.

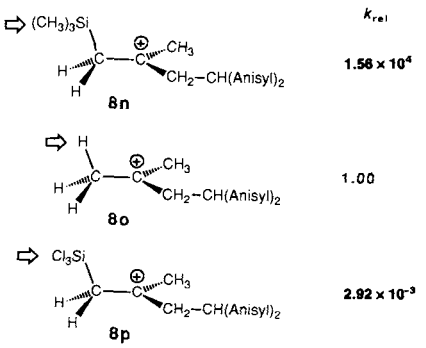

Unfortunately, we have not yet been able to prepare a methyleneborane whose only difference to **12a** is the substitution of an alkyl or an aryl group for the OAr group. The interfering steric requirements of the additional methyl group on the carbon atom carrying the two $SiMe_2Cl$ groups in **12k** primarily result in the widening of the B–C–C (129.4° compared to 119.5° in **12a**) and Me–B–C bond angles (127.5° compared to the 115.0° O–B–C angle) and prevent an even greater widening of the coupled C–C=B angle. C–B hyperconjugation in **12k** may be supported by this steric effect similar to the reinforcement of the β-agostic interactions by steric effects shown recently by Gleiter, Erker et al.[34b]

NMR Shielding of the Electron-Deficient Center

Of all the methyleneboranes with duryl groups at the dicoordinated boron atom, the (borylmethylene)boranes **12** displaying the least distorted B–C=B bond angles (118.3° in **12f**) have the most strongly *deshielded* dicoordinate boron atoms ($\delta^{11}B = 80$) and the nonclassical bridged boriranylideneboranes **10** displaying highly distorted B–C=B bond angles (78.5° in **10d**) have the most strongly *shielded* dicoordinate boron atoms ($\delta^{11}B = 18-20$). This is consistent with the results on carbocations that have strong σ–π interactions, as previously discussed in the Introduction. Bond-angle distortions and NMR shieldings of the electron-deficient centers are general consequences of strong σ–π interactions.[1f, 16, 18]

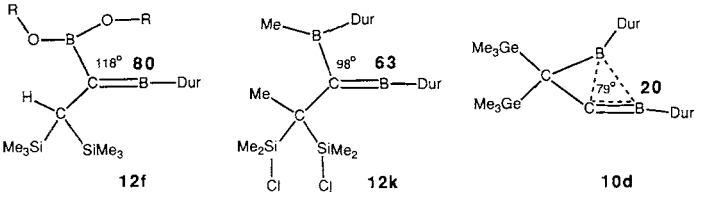

The chemical shift of the dicoordinate boron atom in **12a** ($\delta^{11}B = 79$) can hardly be differentiated from that in **12f**, although significant C–B hyperconjugation is indicated by the approximately 10° smaller B–C=B bond angle in **12a**. Likewise, the dicoordinate boron atom in **12k** is more deshielded ($\delta^{11}B = 63$) than would be expected from the intermediate value of its B–C=B bond angle (118°, 98°, 78.5° for **12f**, **12k**, **10d**). The reason for this deshielding can be seen from the chemical shift of the boron atom of the boryl substituent in **12k** ($\delta^{11}B = 63$) relative to that normally observed for a triorganoborane (e.g., $\delta^{11}B = 85$ in the HCl adduct **52**), which indicates π–π delocalization of the type illustrated in Scheme 3 (see Introduction).

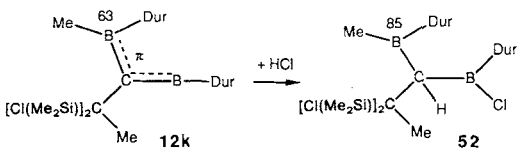

The shielding at the more negative tricoordinate boron atom should correspond to a deshielding at the more positive

dicoordinate boron atom and would explain the discrepancies described above. This π–π delocalization does not play an appreciable role in **12f**, since the electron requirements of the tricoordinate boron atom are already satisfied by the two OR substituents. The deshielding through π–π delocalization in **12a** is compensated for by the shielding through σ–π delocalization, as manifested by the small bond angle. Strong shielding through σ–π delocalization is diminished by the deshielding through significant π–π delocalization in **12k**. Such π–π delocalizations as illustrated in Scheme 3 appear in all (borylmethylene)boranes lacking strong π donors on the boryl boron atom and also in the nonclassical bridged **10**. This has been shown by analysis of the results from calculations[25, 26] and can also be clearly seen in the bond length between the boron atom of the three-membered ring and the carbon atom of the C–B double bond of 154.5 pm (calculated 152.7 and 153.9 pm), which is too short for a 3c–2e C–B bond. B–C bond lengths normally found in 3c–2e bonds are about 170 pm, as, for example, in the nonclassical bridged **53**,[1j] which can be considered as a derivative of **10** "saturated" at the C–B double bond. In the previous description of **10** π–π delocalization was not considered. Taking it into account leads to the more correct form above where the π–π delocalization is represented by the dotted lines.

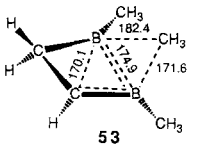

53

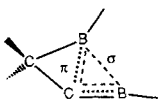

10

3.3.1.2. C–B Hyperconjugation in (Diborylmethylene)boranes

Considerable π–π delocalization in **29a,b**[1b] is indicated by the shielding at the boron atoms of the four-membered ring ($\delta^{11}B = 62$) when compared to that of the boron atoms in the 1,3-diboretanes **20a,b** (see Section 2.2, $\delta^{11}B = 81-82$) and **32a,b** (see Section 2.7, $\delta^{11}B = 76-77$). This, in turn, should lead to a distinct deshielding at the dicoordinate boron atom compared to that found in **12f** ($\delta^{11}B = 80$). The observed chemical shift of $\delta^{11}B = 71$ for the dicoordinate boron atoms in **29a,b** therefore indicates strong C–B hyperconjugation. This interpretation is supported by ab initio calculations (6-31G*) on the unsubstituted **29u** which gave π charges of −0.173 on the ring boron atoms, −0.159 on the carbon atom of the C–B double bond, + 0.504 on the exocyclic boron atom, and a π charge of −0.194 in its "empty" p orbital lying in the B_2CB plane.[1b] π charges of −0.18 and −0.22 on the carbon atom and + 0.18 and + 0.22 on the boron atom have been calculated for in $H_2C{=}B{-}H$.[63b, 26] Thus, the different electronegativities of boron (2.0) and carbon (2.5) alone lead to a considerably lower polarity in the π component of the C–B double bond.

C–B hyperconjugation is also responsible for the longer bond lengths between the tricoordinate carbon atom and the boron atoms of the four-membered ring in **29a** (155.7, 156.6 pm) compared to those in the ether adduct **54** (152.2, 150.7 pm). Adduct **54** exhibits π–π delocalization comparable to that in **29a** but *lacks* σ–π delocalization, since the electron hole on the former dicoordinate boron atom is intermolecularly filled by an electron pair from the diethyl ether. The C=B double bond of 137 pm is about the same length as that calculated for the unsubstituted methyleneborane $H_2C{=}BH$ (138 pm, 6-31G*[63]). The shortening caused by C–B hyperconjugation (additional partial 3c–2e bond) is compensated for by the elongation resulting from π–π delocalization (only partial C–B double bonding). A bond length increase resulting from π–π delocalization *not* compensated for by C–B hyperconjugation can be observed in **38a** (*d*(C=B) 142.5 pm, Section 3.3.3.4).[1h] The short 135.1 pm C=B bond length[1f] in **10d** shows that, in this case, the bond shortening effect through additional 3c–2e bonding is stronger than the bond lengthening effect of π–π delocalization.

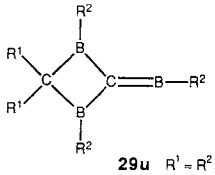

29u $R^1 = R^2 = H$
29a $R^1 = SiMe_3$, $R^2 = Dur$
29b $R^1 = SiMe_3$, $R^2 = Mes$

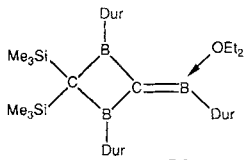

54

3.3.1.3. C–Si Hyperconjugation in (Silylmethylene)boranes

The difference of $\Delta\delta = 17$ between the shielding at the aryl-substituted dicoordinate boron atom in **1c,d** ($\delta^{11}B = 63$) and that in **12f** ($\delta^{11}B = 80$) is a result of strong C–Si hyperconjugation in (disilylmethylene)boranes. Similarly strong shieldings occur in the alkyl-substituted methyleneboranes **1a,b** if one takes into account the shielding ($\Delta\delta \approx 7$) at the dicoordinate boron atom caused by weak π–π delocalization of the π electrons of the aryl substituents in **12f** (see Section 3.2.2).

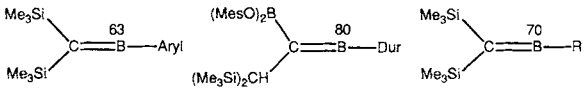

1c Aryl = Dur
1d Aryl = Mes

12f

1a R = CH_3
1b R = *t*Bu

Both theoretical calculations[32a] and experimental measurements[32c] have shown that vinyl cations having β-silyl substituents on the sp^2 carbon atom exhibit increased shielding at the dicoordinate C^+ centers of $\Delta\delta = 158$ (**2f** compared to **2c**) and $\Delta\delta \approx 31$ (**2g** compared to **2b**) as a result of C–Si hyperconjugation.

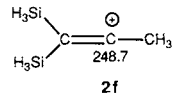

2f

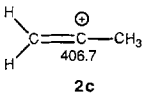

2c

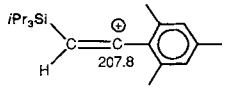

2g

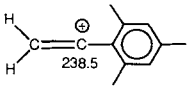

2b

Bond-angle distortion caused by C–Si hyperconjugation effects can be seen in the crystal structure of **12r** (Fig. 1). The Si–C=B bond angle of 109.1(2)° is 9.6° smaller than the corresponding bond angle in **1b** (118.7(1)°[3d]), and the coupled angle B–C=B is widened to 125.3(3)°. The π–π delocalization characteristic for (borylmethylene)boranes, as reflected in the shielding at the tricoordinate boron atom ($\delta^{11}B = 67$), probably contributes to strong C–Si hyperconjugation by increasing the electron deficiency at the dicoordinate boron atom (see also Section 3.3.1.5).

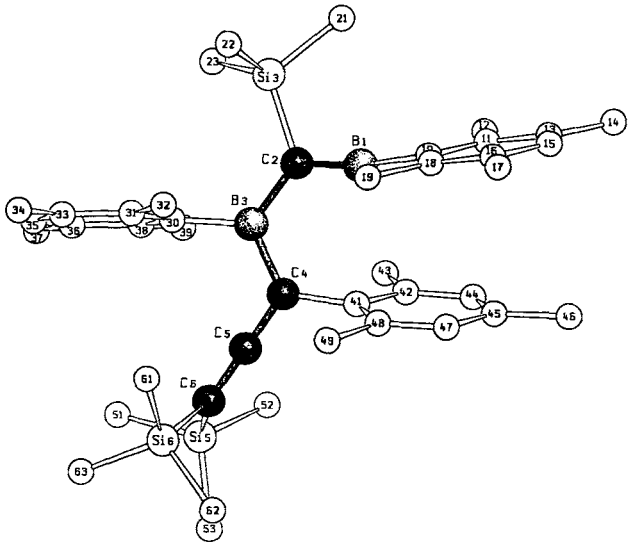

Fig. 1. Schakal representation of the crystal structure of **12r**.

Calculations at the MP2/6-31G* level for the β-silyl-substituted vinyl cation **2h** gave a compressed Si–C=C$^{\oplus}$ bond angle of 92° and a widened H–C=C$^{\oplus}$ angle of 155°.[79]

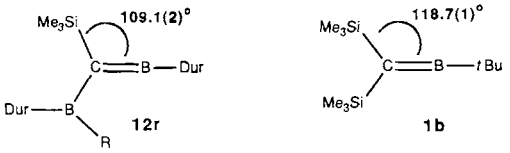

R = 1-mesityl-3,3-bis(trimethylsilyl)allenyl (=All)

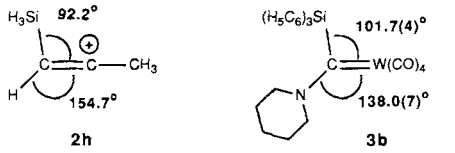

The small Si-C-W angle of 101.7(4)° and the coupled large angle N-C-W of 138.0(7)° in the 16-electron carbene complex **3b** of Schubert et al.[80a] can be plausibly understood as a consequence of an α-C–Si agostic effect.

3.3.1.4. C–Sn Hyperconjugation in (Stannylmethylene)boranes

Strong σ–π interactions in (stannylmethylene)boranes can be recognized from the small Sn–C=B bond angle of 106.0(4)° in **12j**, which approaches the Li–C–B bond angle in the borataalkynes **7a** and **28b** where an electropositive lithium replaces the alkyl tin group in **12j**. Parallel to the bond-angle distortion, strong shielding is observed at the dicoordinate boron atom in **12j** ($\delta^{11}B = 52$), in **1e** ($\delta^{11}B = 53$), and **12s** ($\delta^{11}B = 54$), relative to **12f** and **12l** ($\delta^{11}B = 80$ and 82). Moreover, greatly reduced ^{13}C–$^{117/119}Sn$ coupling constants are found for the carbon atoms

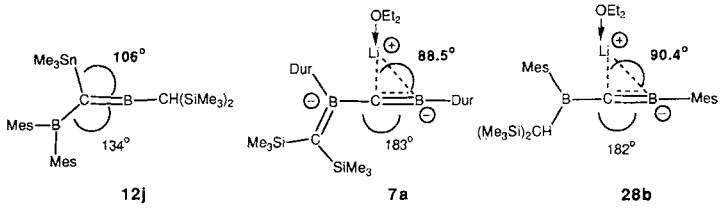

of the C–B double bond. The corresponding coupling constants are of normal magnitude (as in tetra(trimethylstannyl)-allene[80b] or in the allene part of **12s**) in the pyridine adducts **55** and **56**, in which the electron deficiency at the former dicoordinate boron atom is relieved *inter*molecularly. Smaller coupling constants indicate bond weakening, as for example in the C–H bonds of H-bridged carbocations,[81] in this case of the C–$SnMe_3$ bonds, caused by strong C–Sn hyperconjugation. The smaller coupling constant in **12j** relative to that of **1e** can be explained if we consider that the effect in **12j** is concentrated on only *one* C–Sn bond, whereas it is distributed over *two* equivalent σ bonds in **1e**. The even smaller coupling constant in **12s** (66 Hz) may originate from greater electron deficiency and lower steric hindrance at the dicoordinate boron atom in **12s**, which then promote stronger σ–π interactions than in **12j**. The lower stabilization afforded by aryl groups as compared to bis(trimethylsilyl)methyl groups has already been discussed (Section 3.2.2).

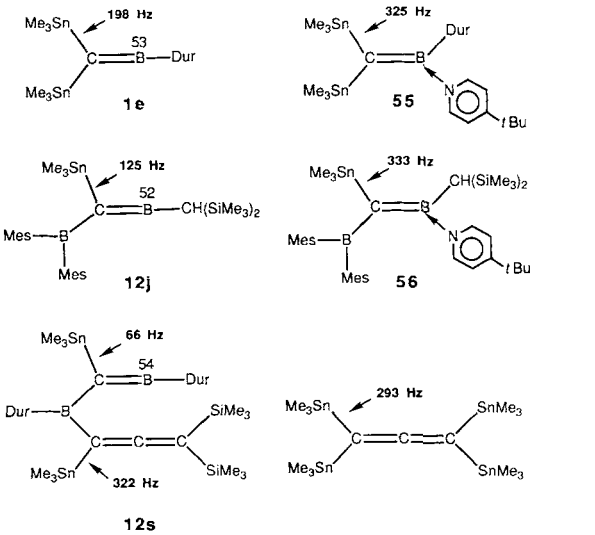

Small ^{13}C–$^{117/119}Sn$ coupling constants comparable to those in **12j** and **12s** have been observed in the compounds **57**[71a] and **58**.[71b] Originally considered as a π complex,[71a] **58** has recently been discussed as a vinyl cation stabilized by

C–Sn hyperconjugation.[71b] The upper portion of the structural formula **58** has been drawn to illustrate its description as a vinyl cation bearing a β-stannyl substituent.

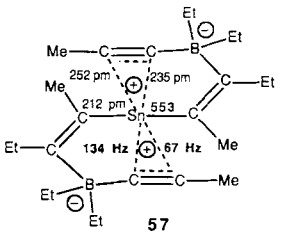

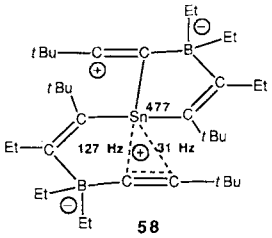

A comparison of the crystal structure data of **57** with that of **8c**[117] (see Introduction) suggests the description "unsymmetrically bridged vinyl cation" for **57**. The similarity between the ^{13}C–$^{117/119}Sn$ coupling constants for **12s** and **57** leads one to expect a strongly distorted Sn–C=B bond angle in **12s**.

3.3.1.5. Strengthening of the σ–π Interactions through π–π Delocalization in (Borylmethylene)boranes

The π–π delocalization in (borylmethylene)boranes illustrated in Scheme 3 increases the electron deficiency at the dicoordinate boron atom and converts it into a better π acceptor (lower lying LUMO) for σ–π interactions. This π–π delocalization will supply additional electron density to the tricoordinate boron atom (Scheme 10) and increase its ability to make the electrons of its σ bond to the carbon atom of the B–C double bond available for σ–π interactions (compare the opposite effect caused by electronegative substituents in **12f** and **12a** in Section 3.3.1.1). Thus, π–π delocalization in the (borylmethylene)boranes leads to stronger σ–π interactions. The abundance of (borylmethylene)boranes **12**, to which over half the reported methyleneboranes belong, and their unexpected thermodynamic stability (see Section 2.7) can be reasonably explained by this synergic stabilization. In (borylmethylene)boranes such as **10**, **12a**, and **12k**, the boron atom of the boryl substituent acts as a π acceptor and its σ bond to the carbon atom of the C–B double bond as a σ donor. In (borylmethylene)boranes that carry a *second* electropositive atom on the carbon atom of the C–B double bond (Sn, Si, B; represented in general by X in Scheme 10), the C–X σ bond can take on the role of the σ donor. Examples in which X = Si or Sn include **12r** (Section 3.3.1.3) and **12j** (Section 3.3.1.4). In (diborylmethylene)boranes, one boryl group can act as the π acceptor, while the =C–B σ bond of the other becomes the σ donor. Such behavior should lead to distinctly different B–C=B bond angles as, in fact, found in the bond angles of 133.3(5) and 148.2(5)° in **29a** (Section 3.3.1.2). One can therefore conjecture that the different B–C=B bond angles observed in **45a** (Section 3.3.2.2, 107.2(7) and 128.2(7)°) are not only a result of the steric hindrance from the *tert*-butyl group on one of the boryl substituent but also, in part, of the above mentioned effect. Attempts to synthesize (diborylmethylene)boranes having identical boryl substituents have not yet been successful.

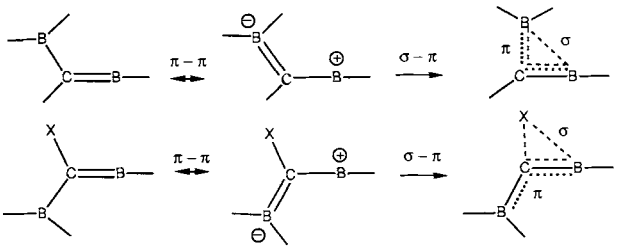

Scheme 10. Synergic strengthening of σ–π delocalization through π–π delocalization.

3.3.1.6. Boryl-, Silyl-, Germyl-, Stannyl-, and Plumbyl-Bridged Vinyl Cations as Reactive Intermediates

The following interpretation of the experimental results in terms of vinyl cations having electropositive bridging atoms at the position β to the electron-deficient center is equivalent to the interpretation by Wrackmeyer et al.[82] in terms of "π complexes of alkynes". The stereoselective formation of the alkenylboranes **60**–**62** with boryl, silyl, or stannyl substituents at the position *cis* to the boryl group, from reactions of the alkynylborates **59** with chlorodiethylborane, chlorotrimethylsilane (Köster[83, 84]), chlorotrimethylstannane (Mortimer[85]) or from reactions of the trimethylsilylalkynylborates **63** with electrophiles E which do *not* react stereoselectively with **59** (Köster[84]) can be explained as follows: In the initially formed vinyl cations **2i***, **2j***, **2k***, and **2l***, one side of the electron-deficient center will be blocked because of strong σ–π interactions (unsymmetrical bridging by BEt_2 in **2i**, $SiMe_3$ in **2j** and **2l**, and $SnMe_3$ in **2k**) with the result that the migrating R^2 fragment can only enter from the opposite side.

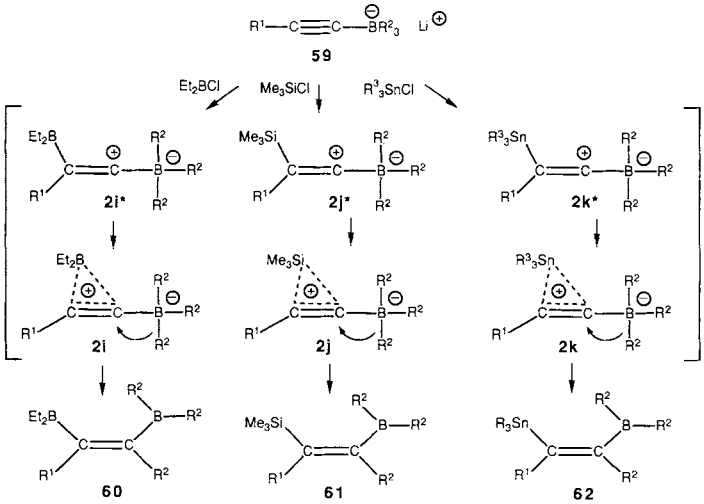

The low stereoselectivity seen in the formation of **65** and **66** from the reaction of **63** with chlorodiethylborane was attributed to the "competition of the trimethylsilyl and the

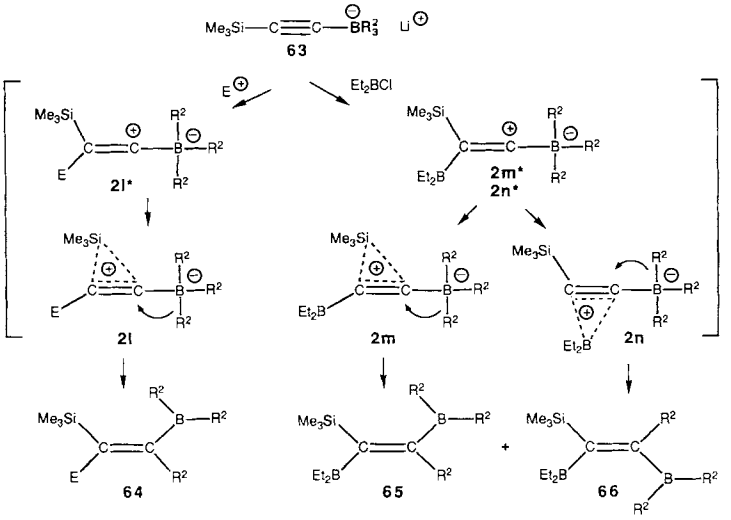

boryl groups",[84] which has to be supplemented by the qualification "in σ–π interactions in the intermediate **2m***,**2n***, which can lead to the bridged vinyl cations **2m** and **2n**". The stereoselectivity found in Wrackmeyer et al.'s syntheses of the alkenylboranes **69** and **70**,[82] with stannyl and plumbyl substituents in the position *cis* to the boryl group from reaction of stannyl- (**67**) or plumbylalkynes (**68**) with trialkylboranes, can be likewise explained with the relevant bridged vinyl cations **2p** and **2r**, these having been formed via **2o*** and **2q*** and their rearrangement products **2p*** and **2r***.

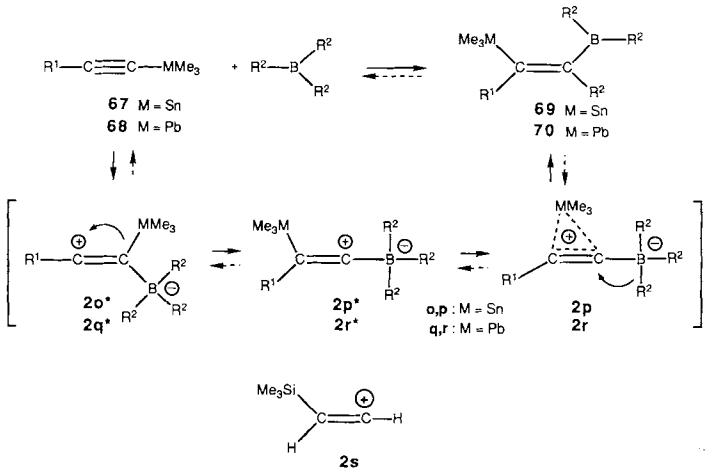

Similarly, the remarkably easy thermal cleavage of the $=C-C(R^2)$ bonds in the vinylboranes **69** and **70**, already at room temperature, to regenerate the trialkylboranes and stannyl- or plumbylalkynes[82] (reverse of the **69** and **70** formation reactions) probably is primarily a result of the considerable thermodynamic stabilization of the vinyl cations **2p** and **2r** through strong C–Sn and C–Pb hyperconjugation. Strong stabilization was recently determined for the β-trimethylsilyl-substituted vinyl cation **2s** by mass spectrometry (43.5 kcal mol^{-1} more stable than $H_2C{=}C^+H$, **2u**).[23c] Large stabilization energies are therefore to be expected for **2p** and **2r** because of the considerably greater stabilization energy of the β-stannyl-substituted ethyl cation **8k** over the β-silyl-substituted ethyl cation **8i** (see Introduction). Wrackmeyer et al. have already emphasized the significance of the weak =C–Sn and =C–Pb bonds and the weakening of the =C–C bond by C–C hyperconjugation with the boryl boron atom.[82]

Closely related to the synthesis of the alkenylboranes **69** and **70** from the reaction of stannyl- or plumbylalkynes with trialkylboranes is the formation of the 1,1-diborylalkenes **24** from reactions of trimethylsilyl- or trimethylgermylalkynes with the diboranes(4) **23** (see Section 2.3). In the first step of these reactions, the vinyl cations **2t*** or **2v*** are probably formed. These then rearrange by 1,2 migration into their respective vinyl cation isomers **2w*** and **2x***. These are small changes when one considers that both types of cations are highly distorted through strong C–Si or C–Ge hyperconjugation (unsymmetrical bridging, see **2t**, **2w** and **2v**, **2x**). The

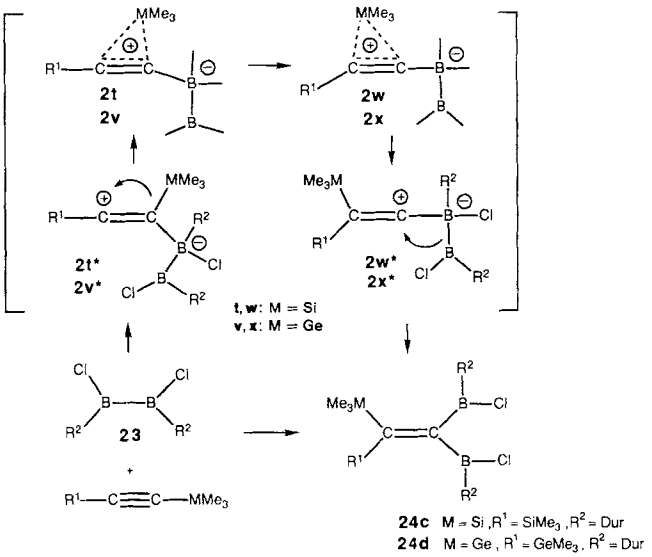

rapid formation of 1,1-diborylalkenes having $GeMe_3$ groups in place of the $SiMe_3$ substituents—the reaction to form **24c** requires four weeks whereas the reaction to form **24d** only three days—is in agreement with the observation that carbocations are more strongly stabilized through C–Ge hyperconjugation (**8j**: 38.8 kcal mol^{-1} [22d]) than through C–Si hyperconjugation(**8i**: 29.1 kcal mol^{-1} [22d]). Stannylalkynes react with **23** with elimination of chlorotrimethylstannane to form borylborirenes.[86]

3.3.2. σ–π Interactions of the α-Agostic Type A'

3.3.2.1. A Methyleneborane with Type A' C–Sn Hyperconjugation

The crystal structure of the methyleneborane **49a**[58–60] is illustrated in Figure 2. Disorder appears in the region of the substituents at the dicoordinate boron atoms. The Sn 5 position has a 57% tin and a 43% silicon occupation; the occupancy of positions Si 6 and Si 7 are likewise 78% silicon and 22% tin.[60] The observed B–C–Sn bond angle of 103.4(2)° therefore reflects only a portion of the distortion due to C–Sn hyperconjugation. This angle approaches that of the

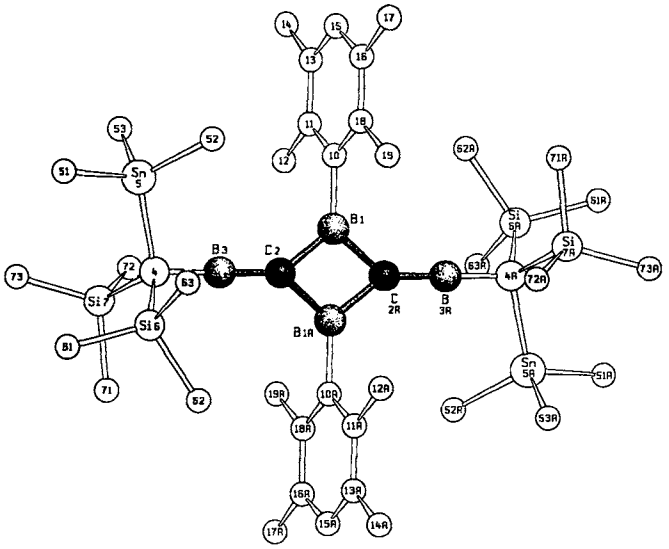

Fig. 2. Schakal representation of the crystal structure of **49a**.

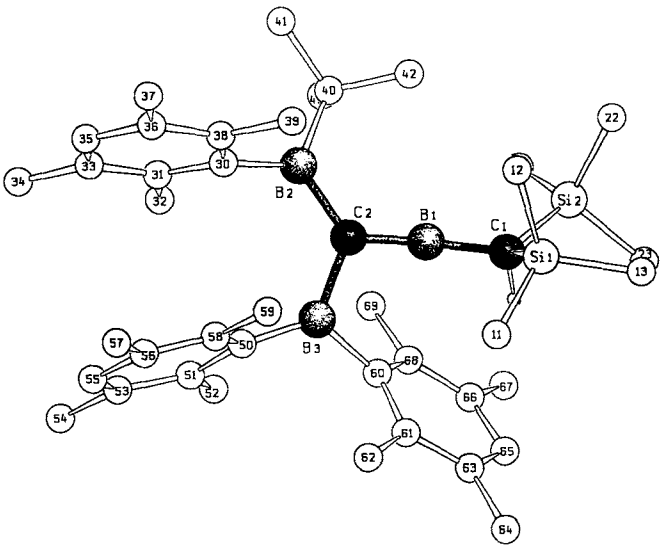

Fig. 3. Schakal representation of the crystal structure of **45a**

B–C–Li bond angle in the borataallene **6e**,[9a] in which an electropositive Li^+ takes up the position of the stannyl substituent in **49a**. The $B-CSi_2$ single bond in **49a** (146.6 pm) is considerably shorter than the corresponding bond in **12j** (155(1) pm) and approaches the length of the $B=CSi_2$ double bond (142(1) pm) observed in the 2-borataallene **6e**.

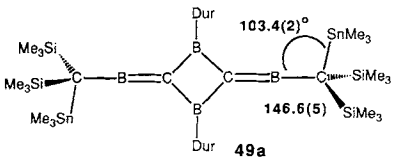

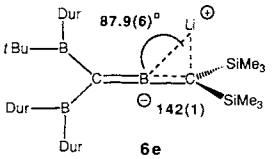

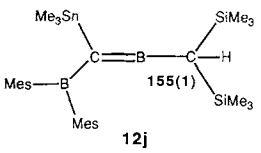

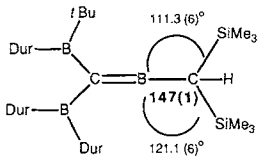

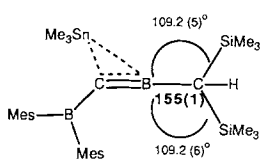

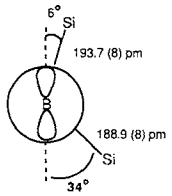

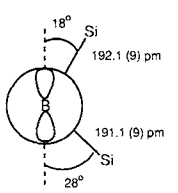

3.3.2.2. Preference for One of Two Equivalent σ Bonds in the Strong σ–π Interaction in a [Bis(trimethylsilyl)methyl]methyleneborane

Figure 3 shows the crystal structure of the methyleneborane **45a**.[56, 57a] Strong **A′** type C–Si hyperconjugation can be recognized in its short $B-CSi_2$ bond (147(1) pm compared to 155(1) pm in **12j**).

While the C–Si distances and the associated torsion angles (see Newman projections) of the two $C-SiMe_3$ bonds in **12j** are only slightly different from each other, in **45a** they differ substantially. The small 6° torsion angle in **45a** is associated with the long C–Si bond of 193.7(8) pm and the small B–C–Si bond angle of 111.3(6)°. The large 34° torsion angle corresponds to the considerably shorter 188.9(8) pm C–Si bond and the larger 121.1(6)° B–C–Si bond angle. These data show that one of the two equivalent $C-SiMe_3$ σ bonds in the bis(trimethylsilyl)methyl group is preferred for σ–π interaction with the electron-deficient dicoordinate boron atom. Preferences for one of two (or three) equivalent σ bonds in the interaction with electron-deficient centers are well-known in carbocations[87] and transition metal complexes exhibiting agostic interactions;[7, 34] typical examples are the vinyl cations **2a** and **2u** (see Introduction).

This effect results in diastereotopic trimethylsilyl groups of the $CH(SiMe_3)_2$ groups of the vinyl cation **2y**, as evident in its ^{13}C NMR spectrum.[32a] The 7.5 kcal mol^{-1} exchange barrier for these groups is a quantitative measure of the magnitude of this preference and is a characteristic consequence of strong nonclassical interactions with concomittant distortion towards 3c–2e bond formation. One-sided preferences are unknown for π–π interactions between an electron-deficient center and two equivalent π donors, for example in the divinylmethyl cation.

3.3.3. σ–π Interactions of the β-Agostic Type B

3.3.3.1. A Mesityl-Bridged (Borylmethylene)borane

The 3c–2e bond in the mesityl-bridged (borylmethylene)-borane **15a** is apparent in the long bond lengths between the boron atoms and the *ipso* carbon atom of the mesityl group (174.8(9) and 176.9(8) pm) and in the short B–B interatomic distance (188.3(9) pm) between the two formally nonbonded boron atoms.[1g] Shielding of the boron atoms through bridging (that is, through an increase in the coordination number) and through symmetrical π–π delocalization—as opposed to the unsymmetrical π–π delocalization shown in Scheme 3 for nonbridged and cyclic methyleneboranes (Sections 3.3.3.3 and 4)—produces a chemical shift ($\delta^{11}B = 42$) that is incompatible with a rapid topomerization equilibrium of the classical methyleneborane **15a*** in solution.[1g]

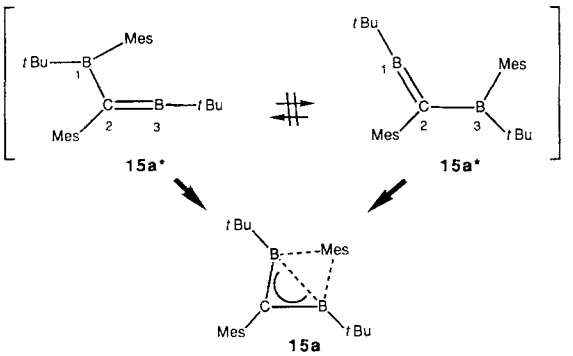

The methyleneborane **12n**,[48] in which bis(trimethylsilyl)methyl groups replace the *tert*-butyl groups in **15a***/**15a**, is not bridged, and its NMR spectra show line broadening typical for a rapid exchange of the mesityl group between the two boron atoms. The transition state of the exchange reaction can be represented by the bridged structure **15d**, and the exchange barrier has been determined from NMR spectroscopy to be 10 kcal mol^{-1}. The energy difference between **15d** (the topomerization transition state of **12n**) and the ground-state bridged form of **15a** must therefore be considerably larger than 10 kcal mol^{-1}. This shows the large effect of the electron-deficient center's $CH(SiMe_3)_2$ substituents on the strength of the 3c–2e bond, which can be explained by a reduction of the electron deficiency at the dicoordinate boron atom through C–Si hyperconjugation (compare Section 3.3.2.2). Additional steric effects cannot be ruled out.

3.3.3.2. H-bridged (Borylmethylene)boranes

The 3c–2e bond in **15b**, which we described in 1985 as a B–H–B bridged 1,3-diboraallyl system,[35] corresponds qualitatively to that found in **15a**.[1g] The B–B interatomic distance of 170.9 pm calculated at the MP2/6-31G* level[66c] for the unsubstituted **15u**[66a, b] is considerably shorter than that in **15a** (188.3(9) pm) and is a clear indication of a stronger 3c–2e bond in **15u**. In order to check the calculated data against a crystal structure we have prepared **15c**[51] but, unfortunately, have not yet obtained a single crystal. The

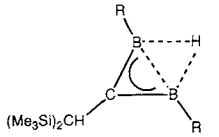

15b R = *t*Bu
15c R = Dur

bridge in **15b**, in contrast to that found in **15a**, can not be opened with either the Lewis base pyridine or *tert*-butyllithium,[35] which is a further indication that the 3c–2e bond in **15b** is stronger than that in **15a**. Additional evidence of the well-developed 3c–2e bonds in **15b,c** is the considerably greater shielding of the boron atoms in **15b** and **15c** ($\delta^{11}B = 27$ and 23) compared to that in **15a** ($\delta^{11}B = 42$), despite their comparable symmetrical π–π delocalization.

3.3.3.3. The Nonclassically Bridged, Cyclic (Borylmethylene)borane 3,4-Dihyro-1,3-diborete

Schleyer showed by ab initio calculations that the cyclic (borylmethylene)borane **48u***/**48u** is the lowest energy system of composition $C_2B_2H_4$, thus suggesting for the first time strong σ–π interactions of the β-agostic type **B** in methyleneboranes.[25b] In addition to unsymmetrical π–π delocalizations of the type observed in open-chain (borylmethylene)-boranes, **48u** exhibits a well-developed 3c–2e bond.

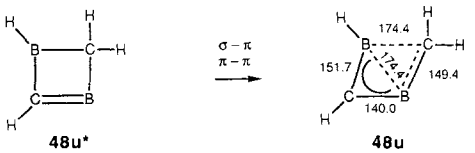

Our attempts to synthesize and isolate compounds of the type **48** have not yet been successful. Compounds **48a,b** may be reactive intermediates in the formation of the methyleneboranes **49** upon thermal elimination of arylstannanes from the 1,3-diboretanes **20a,b** (see Section 2.12).[58–60] We regard the thermodynamic stabilization of **48a,b** through σ–π delocalization to be the reason for the unusually facile 1,2 elimination of arylstannanes from **20a,b**.

3.3.3.4. A Cyclic, Nonclassical (Diborylmethylene)borane Having a Trapezoidal Geometry as a Typical Example of Different Kinds of σ–π Interactions

Except for the boryl substituent, the cyclic methyleneboranes **38**[1h] can be considered as a homologue of **48** hav-

ing an additional B-aryl unit. The 3c–2e bond between three boron atoms with distinctly different B–B bond lengths in **38** replaces a 3c–2e bond between one carbon and two boron atoms in **48**. The formation of this nonclassical bond distorts the hypothetical, classical, five-membered ring **38*** into the trapezoidal form **38**.

As expected, the unsymmetrical π–π delocalization of the π electrons in the C–B double bond leads to a clear lengthening of this bond to 142.5 pm. The short C1–B4 bond (152.0(5) pm) suggests C–B hyperconjugation between the strained C1–B1 and C1–B2 σ bonds and the empty p orbital on the tricoordinate exocyclic boron atom B4. Likewise, this contributes to a lengthening of the C1–B1 bond of the ring. Similar distortions have been calculated for C-borylborirenes[25b] and observed in the C-borylborirene **71**.[86b]

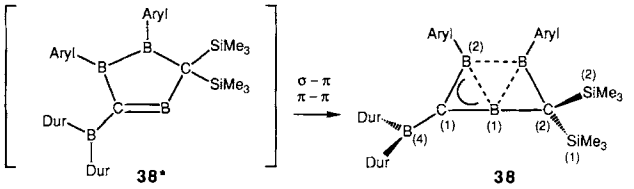

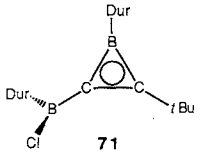

Type **A′** C–Si hyperconjugation, in which σ–π interactions follow the characteristic preference for one of the two equivalent C–$SiMe_3$ σ bonds (compare Section 3.3.2.2), occurs with the boron atom of the C–B double bond whose positive charge is increased through π–π delocalization. The small 102° B1–C2–Si2 bond angle is associated with the long 191 pm C2–Si2 bond length and the small 15° torsion angle between the C2–Si2 bond and the p orbital on the boron. The large 124° B1–C2–Si1 bond angle correlates with the relatively short 188 pm C2–Si bond and the large 34° torsion angle.[1h, 54]

Strong and very strong **A′** and **B** type σ–π interactions (that is, C–B and C–Si hyperconjugation and nonclassical bridging) thus contribute to the structure of **38**. Additionally, the extreme forms of types **A** and **B** are also involved in the 1,2 and 1,3 rearrangements that lead to **38** (see Sections 2.7 and 2.8).

4. Reactions

Numerous reactions typical of methyleneboranes have already been described in the syntheses (Section 2), and, for comparison, the adducts prepared by the addition of Lewis bases were taken into account in Section 3. A description of all the reactions known for methyleneboranes is outside the scope of this review. In the following, intramolecular reactions will be considered for which nonclassical 3c–2e bond formation in the transition state can explain low activation energies. These are α- and β-agostic interactions in rearrangement reactions involving 1,2 and 1,3 migration. C–H bond additions to the C–B double bond will be regarded as extreme forms of γ-, δ-, and ε-agostic interactions as illustrated in Scheme 5 of the Introduction.

4.1. Topomerization Reactions

4.1.1. Topomerization Reactions Involving 1,3 Migrations

Topomerizations through the 1,3 migration of a residue R from the tri- to the dicoordinate boron atom are characteristic reactions of the (borylmethylene)boranes **12** (for **12n**, see Section 3.3.3.1), **12c**,[51] and **72**.[51] They correspond to the topomerization reactions of the (silylmethylene)silanes **73** (Wiberg et al.[39b]) in which methyl groups undergo a 1,3 migration from the tetra- to the tricoordinate silicon atom. The isotopomerization of the Paetzold group's (silylmethylene)borane **1a′** to **1a″** [3e] through a double 1,3 migration, first from the tetracoordinate silicon to the dicoordinate boron and then from the tricoordinate boron to the tricoordinate silicon atom, is to be classified between the topomerization reactions of **72** and **73**.

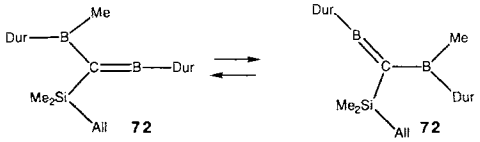

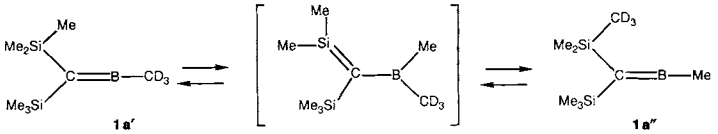

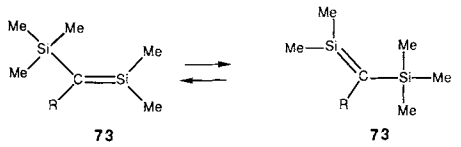

In addition to methyl group migrations (**72**: $\Delta G^{\neq}$ = 12 kcal mol^{-1}), both aryl groups (**12o**,[54] **12n**: $\Delta G^{\neq}$ = 10 kcal mol^{-1}; see Section 3.3.3.1) and $OSiEt_3$ groups (**12c**: $\Delta G^{\neq}$ = 15 kcal mol^{-1} [51]) have been observed to undergo migrations in (borylmethylene)boranes. The relatively low activation energies for these rearrangements in which B–C bonds, or even the B–O bond in **12c**, must be broken can be

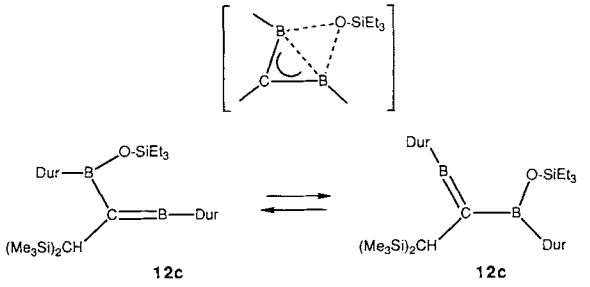

explained quite easily by transition states **15** stabilized through σ–π and π–π delocalizations of the β-agostic type B.

4.1.2. Topomerization Reactions Involving Double 1,2 Migrations

The boron atoms and their bound substituents R in the bridged boriranylideneboranes **10a–d** can be differentiated by NMR spectroscopy only below certain temperatures. Line broadening and coalescence indicate rapid topomerization reactions with exchange barriers of 11.4–12.5 kcal mol^{-1}.[1a, 88, 89]

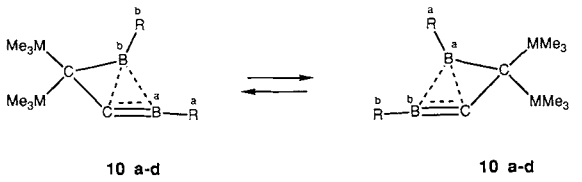

10 a-d **10 a-d**

Schleyer[25b] showed by ab initio calculations on **10e** that this transformation proceeds via the transition state **10f** and the diborylcarbene intermediate **13f/13f***. π–π delocalization as found in other (borylmethylene)boranes (see Scheme 3) can be recognized in **10f** from the short =C–B bond length (146.1 pm). Strong C–C hyperconjugation be-

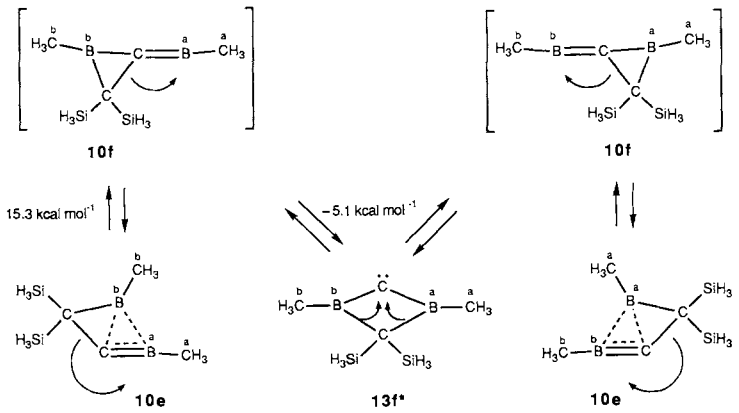

tween the strained C–C σ bond of the three-membered ring and the partially positively charged dicoordinate boron atom (partial charge caused by π–π delocalization) can be seen in the 29° contraction of the C–C=B bond angle to 124° compared to that in **10u***, in the large B–C–B angle of 177.1°, and in the long C–C bond of the three-membered ring (162.3 pm). Complete transfer of this C–C σ bond to the neighboring electron-deficient center provides, through an initial 1,2 migration, the diborylcarbene **13f/13f***, in which the boron atoms and also their bound groups are equivalent. As previously described for **13a** in the Introduction, the severe distortions caused by the σ–π interactions of the Si_2C–B σ bonds with the partially positively charged carbene carbon atom (charge results from π–π delocalization) set up the second 1,2 migration in which the C–B σ bond is transferred to the carbene carbon atom. After this migration, the boron atom B^b that was formerly part of the three-membered ring has now been transformed into the boron atom of the C–B double bond. Redevelopment of the strong σ–π interaction with the C–B σ bond of the three-membered ring, which initially had to be sacrificed, completes the topomerization.

4.2. Intramolecular Addition of C–H Bonds to the C–B Double Bond in Methyleneboranes

4.2.1. Formation of Boron Containing Four-Membered Rings

The methyleneboranes **12g,h** are transformed cleanly into the benzo-1,2-dihydroboretes **74a,b** on melting (166 and 135 °C).[51] Nöth et al. obtained product **76** from the attempt

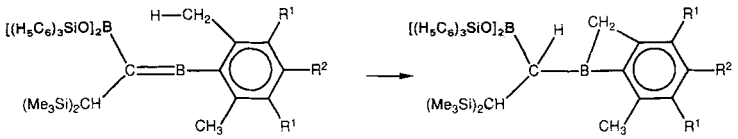

12g $R^1 = CH_3$, $R^2 = H$ **74a** $R^1 = CH_3$, $R^2 = H$
12h $R^1 = H$, $R^2 = CH_3$ **74b** $R^1 = H$, $R^2 = CH_3$

to prepare π complexes by reaction of the amino(methylene)-borane **5a** with either $[\{(H_5C_6)_3P_2Pt(C_2H_4)\}]$ or $[Ni(cod)_2]$ (cod = cyclooctadiene).[2k] The formation of this product can be quite easily explained if one assumes that the metal accepts the lone pair of electrons on the nitrogen to form the methyleneborane **75**, which is no longer stabilized by π–π delocalization and reacts by intramolecular C–H bond addition to the highly reactive C–B double bond, as in the previous example.

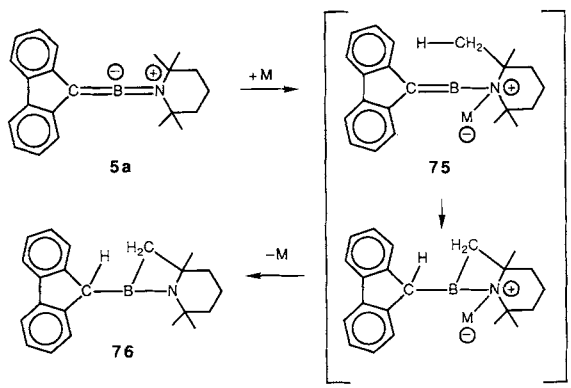

The C–H bond additions to double bonds involving dicoordinate boron atoms described here can be regarded as extreme forms of γ-agostic interactions.[7]

4.2.2. Formation of Boron Containing Five-Membered Rings

From our attempts to synthesize the methyleneborane **79** by reaction of the chloromethyl(methyl)borane **77**,[90] pre-

pared from 2,4,6-tri-*tert*-butylphenyldifluoroborane[90] with lithium tetramethylpiperidide in ether at −65 °C, through α elimination via the borylcarbene **78**, we obtained in good yield (90%) the boraindane **80**[90] in which an ethyl group is bonded to the boron atom. The formation of this compound can be quite easily explained by addition of a C−H bond of an ortho-*tert*-butyl group to the highly reactive C−B double bond in **79**. The direct insertion of the carbene carbon atom

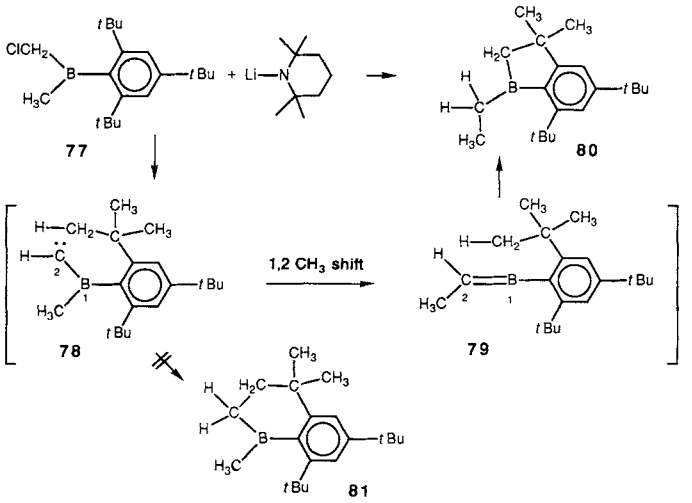

into a C−H bond, which would lead to the six-membered ring **81** in which a methyl group is bonded to the boron atom, occurs only to a minor extent, if at all. From the attempt to synthesize the boraallene **83** or its THF adduct from reaction of the alkynylfluoroborane **82** with *tert*-butyllithium at −120 °C in THF we obtained the vinylboraindane stereoisomers ***E*-84** and ***Z*-84**.[90]

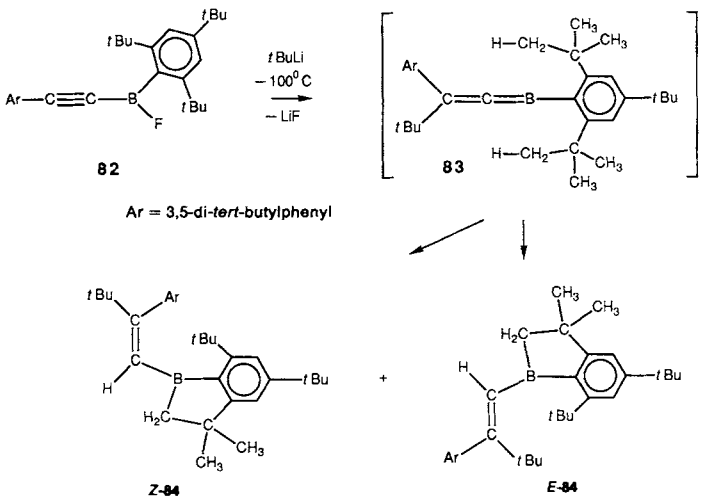

These insertions correspond to those observed for compounds containing the 2,4,6-tri-*tert*-butylphenyl residue bonded to a center of high electron deficiency.[91] For kinetic stabilization of compounds with low-coordinate main group elements *lacking* electron-deficient centers,[93] the "supermesityl" (2,4,6-tri-*tert*-butylphenyl) residue—originally used by Yoshifuji[92] for compounds containing dicoordinate phosphorus—has proven outstanding.

Our attempt to produce **12t** from the reaction of **10a** with 2,4,6-trimethylphenol, analogous to the formation of **12f** under cleavage of the three-membered ring in **10c** (see Section 2.4), yielded the diborolane **85** smoothly.[88] Instead of the expected methyleneborane **12v**, analogous to the formation of **5h** from the borirane **36a** (see Section 2.8), the diborolane **86** formed quantitatively upon melting of the borirane **36b** at 150°C.[94]

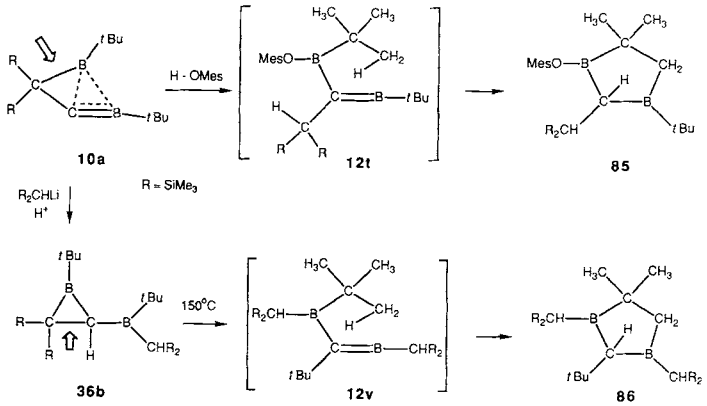

The absence of electronic stabilization and the presence of a favorable geometry for δ-agostic activation of their C−H bonds in the transition states (see Scheme 5) are probably responsible for the low temperatures at which the intramolecular addition reactions occur in the methyleneboranes **79**, **83**, and **12t**. Intermediate **12v** is stabilized by C−Si and C−B hyperconjugation, so C−H bond addition to the C−B double bond probably is caused by the high temperature necessary for the formation of **12v** (compare the reaction conditions for producing **74a,b**).

4.2.3. Formation of Boron Containing Six-Membered Rings

Analogous to the formation reaction of **12r** (see Section 2.13), we attempted to prepare the methyleneborane **12w** from the reaction of **10c** with phenyltrimethylsilylacetylene but instead obtained **87**.[51] Despite the stabiliza-

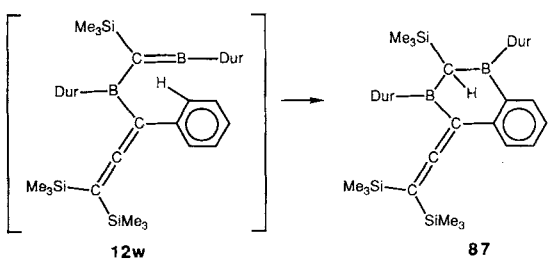

tion of **12w** by C−Si and C−B hyperconjugation, an intramolecular C−H bond addition to the C−B double bond took place already at room temperature, probably as a result of optimal geometry. The formation of **88**[48] from **6b** and

bromine can be explained with the corresponding extreme form of an ε-agostic interaction in intermediate **12x**.

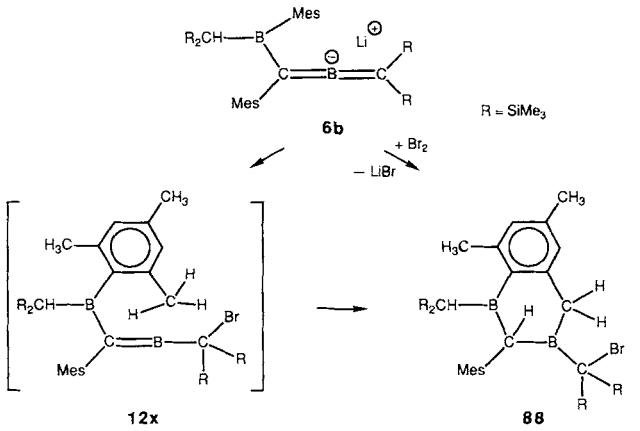

6b **12x** **88**

Closely related to the C–H bond additions to the C–B double bond described here are the high-temperature (560 °C) reactions of (silylmethylene)boranes observed by Paetzold et al.[3e] Here, C–H bonds add intramolecularly to C–Si double bonds formed by the 1,3 migration of a methyl group from a tetracoordinate silicon atom to the dicoordinate boron atom (Scheme 11, compare Section 4.1.1).

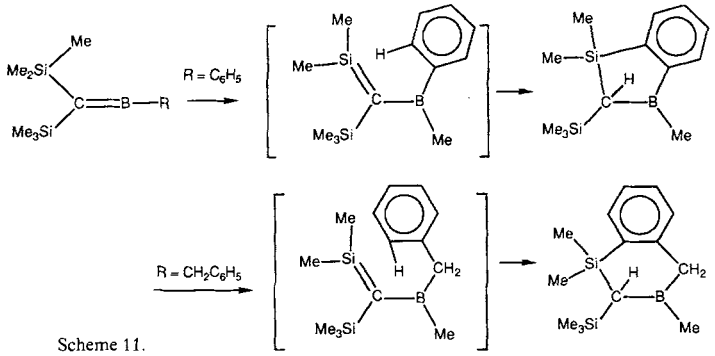

Scheme 11.

5. Summary

Methyleneboranes that are isoelectronic to vinyl cations augment the range of known electron-deficient compounds with members that allow, through spectroscopic and crystal structure analyses, the investigation of σ–π delocalization (hyperconjugation, nonclassical behavior, various degrees of three-center, two-electron bond formation) from σ bonds to electropositive atoms at the position β to an electron-deficient center. σ–π delocalization can be synergically strengthened in methyleneboranes that have tricoordinate boron atoms at the position β to the electron-deficient center by increasing the electron deficiency at the dicoordinate boron atom through concurrent π–π delocalization of the π electrons of its C–B double bond to the boron atom in the boryl substituents. Impressive consequences of strong σ–π delocalization of the α-agostic type include bond angle distortions of up to 65°, reductions in the NMR coupling constants of as much as 80% of their normal values, and NMR shielding at the electron-deficient center of up to $\Delta\delta = 65$. Increasing the electronegativity of the β boron atom with electronegative substituents leads to decreased σ–π delocalization and its associated consequences. Strong σ–π interactions of the β-agostic type are present in mesityl- and H-bridged (borylmethylene)boranes and in a cyclic methyleneborane with trapezoidal geometry. Low activation energies of rearrangement reactions with 1,3 migrations of substituents from tri- to dicoordinate boron atoms—which are characteristic for (borylmethylene)boranes—are explained by transition states stabilized by σ–π interaction of the β-agostic type. The results for methyleneboranes complement the current understanding of σ–π delocalization in an area that is not accessible through carbocations, or only in exceptional cases.

6. Outlook

Our studies on the chemistry of the methyleneboranes have for an essential part been developed not deliberately through planning but serendipitously (to quote G. Wittig[95] "not by intention, but by chance and surprise"). Further pleasant surprises will be welcome. There are several goals that we consider worthwhile, as, for example, the last isoster in the series depicted in Scheme 12, which has only been treated theoretically.[96]

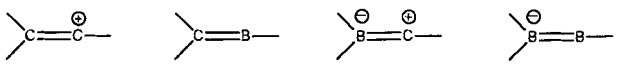

Scheme 12. Isosteres of methyleneboranes.

A simple route to borylcarbenes and diborylcarbenes could open a general access to methyleneboranes and (borylmethylene)boranes. (Halomethylene)boranes would not only be interesting for comparing with β-halogen-substituted vinyl cations[97] but also as starting materials for the synthesis of simple borataalkynes R–C≡B$^{\ominus}$–Ar. These should enable the preparation of a variety of substituted methyleneboranes including the missing β-plumbyl-substituted species and reactants for the synthesis of four-mem-

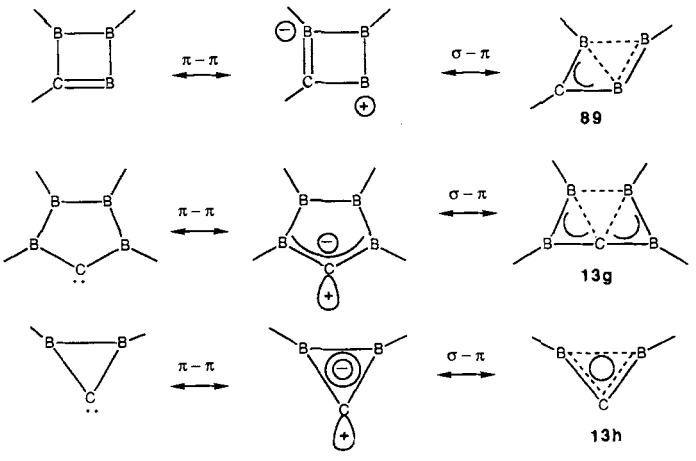

89 **13g** **13h**

H–B≡C≡B–H

90

bered rings containing three boron atoms. With appropriate substituents, the nonclassical cyclic methyleneborane **48**,[25b] the related methyleneborane **89**, and the analogously stabilized diborylcarbene **13g** should be isolable.

The simplest cyclic diborylcarbenes, diboriranylidenes **13h**, which are 2π aromatic systems containing both a classical bond and a nonclassical 3c–2e bond, probably will be detectable only in a matrix. According to calculations by Schleyer et al.,[98] the parent compound (CB_2H_2) exhibits a long B–B bond (194.4 pm) and short C–B bonds (138.0 pm) and is about 1.2 kcal mol^{-1} lower in energy than the recently characterized (in argon matrix) 1,3-diboraallene **90**.[99]

For the results obtained in Marburg and presented in this review I thank the dedicated work of J. Allwohn, C. Balzereit, G. Baum, A. Höfner, R. Hunold, H. Klusik, C. Kybart, K. Kyritsis, U. Lippold, H. Lukasch, S. Mehle, H. Meyer, H. Michel, R.G. Müller, M. Pilz, C. Pues, G. Schmidt-Lukasch, M. Stadler, N. Stamatis, R. Wehrmann, C. Wieczorek, P. Willershausen, and B. Ziegler. I should also like to thank Prof. Dr. W. Massa, Marburg, for the determination of numerous crystal structures and for the instruction and support of to my coworkers, who have themselves performed X-ray structure analyses. Furthrmore I am grateful to Prof. Dr. S. Berger, Marburg, Prof. Dr. P. von R. Schleyer, Erlangen, Prof. Dr. H.-U. Siehl, Tübingen, Prof. Dr. Y. Apeloig, Haifa, and Prof. Dr. B. Wrackmeyer, Bayreuth, for good collaboration, Prof. Dr. B. Bogdanović, Max-Planck-Institute für Kohlenforschung, Mülheim, for information on the preparation of highly reactive magnesium, Prof. Dr. P. Paetzold, Aachen, for valuable suggestions for the organization of this review, and Ms. I. Bublys for her infinite patience during the preparation of the manuscipt. We thank the Deutsche Forschungsgemeinschaft and the Fonds der Chemischen Industrie for financial support.

Received: August 31, 1992
Revised version: March 3, 1993 [A 909 IE]
German version: *Angew. Chem.* **1993**, 105, 1034
Translated by Dr. J. R. Kennedy, Stuttgart

[1] a) H. Klusik, A. Berndt, *Angew. Chem.* **1983**, *95*, 895–896; *Angew. Chem. Int. Ed. Engl.* **1983**, *22*, 877–878; b) R. Hunold, M. Pilz, J. Allwohn, M. Stadler, W. Massa, P. von R. Schleyer, A. Berndt, *ibid.* **1989**, *101*, 759–761 and **1989**, *28*, 781; c) M. Pilz, M. Stadler, R. Hunold, J. Allwohn, W. Massa, A. Berndt, *ibid.* **1989**, *101*, 761–763 and **1989**, *28*, 784; d) J. Allwohn, R. Hunold, R.-G. Müller, W. Massa, A. Berndt, *Z. Naturforsch. B.* **1990**, *45*, 290–298; e) M. Pilz, H. Michel, A. Berndt, *Angew. Chem.* **1990**, *102*, 438–439; *Angew. Chem. Int. Ed. Engl.* **1990**, *29*, 401; f) C. Wieczorek, J. Allwohn, G. Schmidt-Lukasch, R. Hunold, W. Massa, A. Berndt, *ibid.* **1990**, *102*, 435–436 and **1990**, *29*, 398–399; g) M. Pilz, J. Allwohn, W. Massa, A. Berndt, *ibid.* **1990**, *102*, 436–438 and **1990**, *29*, 399; h) A. Höfner, B. Ziegler, R. Hunold, P. Willershausen, W. Massa, A. Berndt, *ibid.* **1991**, *103*, 580–582 and **1991**, *30*, 594; i) P. Willershausen, A. Höfner, J. Allwohn, M. Pilz, W. Massa, A. Berndt, *Z. Naturforsch. B* **1992**, *47*, 983–991; j) P. Willershausen, G. Schmidt-Lukasch, C. Kybart, J. Allwohn, W. Massa, M. L. McKee, P. von R. Schleyer, A. Berndt, *Angew. Chem.* **1992**, *104*, 1417–1420; *Angew. Chem. Int. Ed. Engl.* **1992**, *31*, 1384; k) R. Wehrmann, H. Klusik, A. Berndt, *ibid.* **1984**, *96*, 369–370 and **1984**, *23*, 369; l) R. Wehrmann, H. Klusik, A. Berndt, *ibid.* **1984**, *96*, 810–811 and **1984**, *23*, 826–827; m) H. Meyer, G. Baum, W. Massa, S. Berger, A. Berndt, *ibid.* **1987**, *99*, 559–560 and **1987**, *26*, 546; n) H. Meyer, G. Baum, W. Massa, A. Berndt, *ibid.* **1987**, *99*, 790–791 and **1987**, *26*, 798; o) A. Berndt, H. Meyer, G. Baum, W. Massa, S. Berger, *Pure Appl. Chem.* **1987**, *59*, 1011–1014.

[2] a) H. Nöth, R. Staudigl, H.-U. Wagner, *Inorg. Chem.* **1982**, *21*, 706–716; b) B. Glaser, H. Nöth, *Angew. Chem.* **1985**, *97*, 424–425; *Angew. Chem. Int. Ed. Engl.* **1985**, *24*, 416; c) B. Glaser, E. Hanecker, H. Nöth, H. Wagner, *Chem. Ber.* **1987**, *120*, 659–667; d) H. Nöth, *Proc. 6th Int Meet. Boron Chem. (IMEBORON)* (Eds.: S. Hermanek), World Scientific Singapore, New Jersey, **1987**, p. 438–445; e) H. Nöth, *Nova Acta Leopold.* **1985**, *59*, 277–290; f) B. Glaser, H. Nöth, *Chem. Ber.* **1986**, *119*, 3856–3858; g) B. Glaser, H. Nöth, *ibid.* **1987**, *120*, 345–350; h) B. Glaser, E. P. Mayer, H. Nöth, W. Rattay, V. Wietelmann, *Z. Naturforsch. B* **1988**, *43*, 449–456; i) S. Helm, H. Nöth, *Angew. Chem.* **1988**, *100*, 1378–1384; *Angew. Chem. Int. Ed. Engl.* **1988**, *27*, 1331–1332; j) E. P. Mayer, H. Nöth, *Chem. Ber.* **1990**, *123*, 963–966; k) S. W. Helm, G. Linti, H. Nöth, S. Channareddy, P. Hofmann, *ibid.* **1992**, *125*, 73–86.

[3] a) R. Boese, P. Paetzold, A. Tapper, *Chem. Ber.* **1987**, *120*, 1069–1071; b) I. Manners, P. Paetzold, *J. Chem. Soc. Chem. Commun.* **1988**, 183–185; c) A. Tapper, T. Schmitz, P. Paetzold, *Chem. Ber.* **1989**, *122*, 595–601; d) R. Boese, P. Paetzold, A. Tapper, R. Ziembinski, *ibid.* **1989**, *122*, 1057–1060; e) P. Paetzold, T. Schmitz, A. Tapper, R. Ziembinski, *ibid.* **1990**, *123*, 747–750.

[4] G. Maier, J. Henkelmann, H. P. Reisenauer, *Angew. Chem.* **1985**, *97*, 1061–1062; *Angew. Chem. Int. Ed. Engl.* **1985**, *24*, 1065.

[5] M. Hanack, L. R. Subramanian in *Houben-Weyl Methoden der Organischen Chemie, Vol. E19c* (Eds.: M. Hanack), Thieme, Stuttgart, **1990**, S. 97–250, and references therein.

[6] a) R. R.Schrock, *Acc. Chem. Res.* **1979**, *12*, 98–104; b) A. J. Schultz, R. K. Brown, J. M. Williams, R. R. Schrock, *J. Am. Chem. Soc.* **1981**, *103*, 169–176, and references therein; c) J. H. Wengrovius, R. R. Schrock, M. R. Churchill, H. J. Wasserman, *ibid.* **1982**, *104*, 1739–1740, and references therein

[7] More recent review on agostic interactions: M. Brookhart, M. L. H. Green, L. L. Wong, *Prog. Inorg. Chem.* **1988**, *36*, 1–124.

[8] L. Ghosez, J. Marchand-Brynaert, *Adv. Org. Chem.* **1976**, *9*, 421–532, and references therein.

[9] a) M. Pilz, J. Allwohn, P. Willershausen, W. Massa, A. Berndt, *Angew. Chem.* **1990**, *102*, 1085–1087; *Angew. Chem. Int. Ed. Engl.* **1990**, *29*, 1030; b) P. Willershausen, C. Kybart, W. Massa, M. Bühl, P. von R. Schleyer, A. Berndt, *ibid.* **1992**, *104*, 1278–1280 and **1992**, *31*, 1238.

[10] a) R. Hunold, J. Allwohn, G. Baum, W. Massa, A. Berndt, *Angew. Chem.* **1988**, *100*, 961–963; *Angew. Chem. Int. Ed. Engl.* **1988**, *27*, 961; b) J. Allwohn, M. Pilz, R. Hunold, W. Massa, A. Berndt, *ibid.* **1990**, *102*, 1084–1085 and **1990**, *29*, 1032, and references therein.

[11] a) P. Buzek, P. von R. Schleyer, S. Sieber, *Chem. Unserer Zeit* **1992**, *26*, 116–128, and references therein; b) K. Lammertsma, P. von R. Schleyer, H. Schwarz, *Angew. Chem.* **1989**, *101*, 1313–1335, *Angew. Chem. Int. Ed. Engl.* **1989**, *28*, 1321; c) S. Sieber, P. Buzek, P. von R. Schleyer, W. Koch, J. W. de M. Carneiro, *J. Am. Chem. Soc.* **1993**, *115*, 259–270, and references therein.

[12] H. Jasuda, H. Yamamoto, T. Arai, A. Nakamura, J. Chen, Y. Kai, N. Kasai, *Organometallics* **1991**, *10*, 259–270, and references therein

[13] a) G. Olah, G. J. Liang, *J. Am. Chem. Soc.* **1973**, *95*, 3792–3794; b) D. Lenoir, Y. Apeloig, D. Arad, P. von R. Schleyer, *J. Org. Chem.* **1988**, *53*, 661–675, and references therein; c) D. Lenoir, *Nachr. Chem. Tech. Lab.* **1988**, *36*, 1210–1211, and references therein

[14] G. A. Olah, G. K. S. Prakash, W. D. Fessner, T. Kobayashi, L. A. Paquette, *J. Am. Chem. Soc.* **1988**, *110*, 8599–8605, and references therein.

[15] T. Laube, *Angew. Chem.* **1986**, *98*, 368–369; *Angew. Chem. Int. Ed. Engl.* **1986**, *25*, 349, and references therein.

[16] P. von R. Schleyer, J. W. de M. Carneiro, W. Koch, D. A. Forsyth, *J. Am. Chem. Soc.* **1991**, *113*, 3990–3992, and references therein.

[17] T. Laube, *Angew. Chem.* **1987**, *99*, 580–583; *Angew. Chem. Int. Ed. Engl.* **1987**, *26*, 560, and references therein.

[18] J. W. de M. Carneiro, P. von R. Schleyer, W. Koch, K. Raghavachari, *J. Am. Chem. Soc.* **1990**, *112*, 4064–4066, and references therein

[19] W. Koch, B. Liu, D. J. DeFrees, *J. Am. Chem. Soc.* **1989**, *111*, 1527–1528, and references therein; W. Koch, Technische Universität Berlin, personal communication.

[20] G. A. Olah, V. P. Reddy, G. K. S. Prakasch, *Chem. Rev.* **1992**, *92*, 69–95.

[21] a) M. Saunders, K. E. Laidig, K. W. Wiberg, P. von R. Schleyer, *J. Am. Chem. Soc.* **1988**, *110*, 7652–7659; b) P. C. Myhre, G. G. Webb, C. S. Yannoni, *ibid.* **1990**, *112*, 8992–8994, and references therein.

[22] a) S. G. Wierschke, J. Chandrasekhar, W. L. Jorgensen, *J. Am. Chem. Soc.* **1985**, *107*, 1496–1500; b) M. R. Ibrahim, W. L. Jorgensen, *ibid.* **1989**, *111*, 819–824; c) Y. Apeloig, D. Arad, *ibid.* **1985**, *107*, 5285–5286; d) K. A. Nguyen, M. S. Gordon, G. Wang, J. B. Lambert, *Organometallics* **1991**, *10*, 2798–2803; and references therein; e) C. Dellaire, M. A. Brook, *ibid.* **1990**, *9*, 2873–2874.

[23] a) D. Hajdasz, R. Squires, *J. Chem. Soc. Chem. Commun.* **1988**, 1212–1214; b) G. A. McGibbon, M. A. Brook, J. K. Terlouw, *ibid.* **1992**, 360–362; c) X. Li, J. A. Stone, *J. Am. Chem. Soc.* **1989**, *111*, 5586–5592.

[24] I. Fleming, *Grenzorbitale und Reaktionen organischer Verbindungen*, Verlag Chemie, Weinheim, **1979**, p. 96–97.

[25] a) P. H. M. Budzelaar, P. von R. Schleyer, K. Krogh-Jespersen, *Angew. Chem.* **1984**, *96*, 809–810; *Angew. Chem. Int. Ed. Engl.* **1984**, *23*, 825; b) P. H. M. Budzelaar, K. Krogh-Jespersen, T. Clark, P. von R. Schleyer, *J. Am. Chem. Soc.* **1985**, *107*, 2773–2779.

[26] G. Frenking, H. F. Schaefer III, *Chem. Phys. Lett.* **1984**, *109*, 521–524.

[27] H. Fischer, K. Hummel, M. Hanack, *Tetrahedron Lett.* **1969**, 2169–2172.

[28] Y. Apeloig, J. B. Collins, D. Cremer, T. Bally, E. Haselbach, J. A. Pople, J. Chandrasekhar, P. von R. Schleyer, *J. Org. Chem.* **1980**, *45*, 3496–3501.

[29] K. Raghavachari, R. A. Whiteside, J. A. Pople, P. von R. Schleyer, *J. Am. Chem. Soc.* **1981**, *103*, 5649–5657.
[30] J. B. Lambert, *Tetrahedron* **1990**, *46*, 2677–2689, and references therein
[31] a) T. G. Traylor, W. Hanstein, H. J. Berwin, N. A. Clinton, R. S. Brown, *J. Am. Chem. Soc.* **1971**, *93*, 5715–5725; b) T. G. Traylor, H. J. Berwin, J. Jerkunica, M. L. Hall, *Pure Appl. Chem.* **1972**, *30*, 599–606, and references therein; c) T. G. Traylor, G. S. Koermer, *J. Org. Chem.* **1981**, *46*, 3651–3657, and references therein; d) J. B. Lambert, G.-T. Wang, D. H. Teramura, *ibid.* **1988**, *53*, 5422–5428, and references therein.
[32] a) H.-U. Siehl, F.-P. Kaufmann, Y. Apeloig, V. Braude, D. Danovich, A. Berndt, N. Stamatis, *Angew. Chem.* **1991**, *103*, 1546–1549; *Angew. Chem. Int. Ed. Engl.* **1991**, *30*, 1479; b) G. K. S. Prakash, V. P. Reddy, G. Rasul, J. Casanova, G. A. Olah, *J. Am. Chem. Soc.* **1992**, *114*, 3076–3078; c) H.-U. Siehl, F.-P. Kaufmann, *ibid.* **1992**, *114*, 4937–4939; d) H.-U. Siehl, F. P. Kaufmann, K. Hori, *ibid.* **1992**, *114*, 9343–9349.
[33] a) J. Farràs, S. Olivella, A. Solé, J. Vilarrasa, *J. Comput. Chem.* **1986**, *7*, 428–442; b) P. von R. Schleyer, B. T. Luke, J. A. Pople, *Organometallics* **1987**, *6*, 1997–2000, and references therein.
[34] N. Koga, K. Morakuma, *J. Am. Chem. Soc.* **1988**, *110*, 108–112, and references therein; b) I. Hyla-Kryspin, R. Gleiter, C. Krüger, R. Zwettler, G. Erker, *Organometallics* **1990**, *9*, 517–523; c) T. Ziegler, E. Folga, A. Berces, *J. Am. Chem. Soc.* **1993**, *115*, 636–646, and references therein.
[35] R. Wehrmann, H. Meyer, A. Berndt, *Angew. Chem.* **1985**, *97*, 779–781; *Angew. Chem. Int. Ed. Engl.* **1985**, *24*, 788–790.
[36] N. J. R. van Eikema Hommes, P. von R. Schleyer, *Angew. Chem.* **1992**, *104*, 768–771; *Angew. Chem. Int. Ed. Engl.* **1992**, *31*, and references therein.
[37] J. M. Saá, P. M. Deyá, G. A. Suner, A. Frontera, *J. Am. Chem. Soc.* **1992**, *114*, 9093–9100, and references therein.
[38] C. Pues, G. Baum, W. Massa, A. Berndt, *Z. Naturforsch. B* **1988**, *43*, 275–279.
[39] a) A. C. Brook, K. M. Baines, *Adv. Organomet. Chem.* **1986**, *25*, 1–44; b) N. Wiberg, H. Köpf, *Chem. Ber.* **1987**, *120*, 653–655, and references therein; latest example: c) W. Ziche, N. Auner, P. Kiprof, *J. Am. Chem. Soc.* **1992**, *114*, 4910–4911.
[40] H. Lukasch, G. Schmidt-Lukasch, U. Lippold, A. Berndt, *Angew. Chem.* **1988**, *100*, 959–961; *Angew. Chem. Int. Ed. Engl.* **1988**, *27*, 960.
[41] H. Klusik, A. Berndt, *J. Organomet. Chem.* **1982**, *234*, C17–C19.
[42] *Nachr. Chem. Tech. Lab.* **1983**, *31*, 245.
[43] H. Klusik, C. Pues, A. Berndt, *Z. Naturforsch. B* **1984**, *39*, 1042–1045.
[44] H. Meyer, G. Schmidt-Lukasch, G. Baum, W. Massa, A. Berndt, *Z. Naturforsch. B.* **1988**, *43*, 801–806.
[45] R. Hunold, Dissertation, Universität Marburg, **1988**.
[46] E. Bartmann, B. Bogdanović, N. Janke, S. Liao, K. Schlichte, B. Spliethoff, J. Treber, U. Westeppe, U. Wilczok, *Chem. Ber.* **1990**, *123*, 1517–1528.
[47] A. Berndt, H. Klusik, C. Pues, R. Wehrmann, H. Meyer, U. Lippold, G. Schmidt-Lukasch, R. Hunold, G. Baum, W. Massa in *Proc. 6th Int. Meet. Boron Chem. (IMEBORON)* (Eds.: S. Hermanek), World Scientific Singapore, New Jersey, **1987**, p. 83–103.
[48] P. Willershausen, Dissertation, Universität Marburg, **1992**.
[49] G. Karger, P. Hornbach, A. Krämer, H. Pritzkow, W. Siebert, *Chem. Ber.* **1989**, *122*, 1881–1889, and references therein.
[50] R. Wehrmann, C. Pues, H. Klusik, A. Berndt, *Angew. Chem.* **1984**, *96*, 372–374; *Angew. Chem. Int. Ed. Engl.* **1984**, *23*, 372–374.
[51] N. Stamatis, Dissertation Universität Marburg, **1993**.
[52] W. Siebert, M. Hildenbrand, P. Hornbach, G. Karger, H. Pritzkow, *Z. Naturforsch. B* **1989**, *44*, 1179–1186.
[53] M. Pilz, J. Allwohn, R. Hunold, W. Massa, A. Berndt, *Angew. Chem.* **1988**, *100*, 1421–1422; *Angew. Chem. Int. Ed. Engl.* **1988**, *27*, 1370.
[54] A. Höfner, Dissertation, Universität Marburg, **1991**.
[55] M. Stadler, Diplomarbeit Universität Marburg, **1989**.
[56] P. Willershausen, Diplomarbeit Universität Marburg, **1990**.
[57] a) J. Allwohn, Dissertation Universität Marburg, **1991**; b) C. Balzereit, planned Dissertation, Universität Marburg, **1994**.
[58] M. Pilz, Dissertation Universität Marburg, **1990**.
[59] K. Kyritsis, Diplomarbeit Universität Marburg, **1991**.
[60] C. Kybart, Diplomarbeit Universität Marburg, **1991**.
[61] C. Kybart, planed Dissertation Universität Marburg, **1994**.
[62] J. Allwohn, Diplomarbeit Universität Marburg, **1988**.
[63] a) P. von R. Schleyer, D. Kost, *J. Am. Chem. Soc.* **1988**, *110*, 2105–2109, and references therein; b) B. T. Luke, J. A. Pople, M.-B. Krogh-Jespersen, Y. Apeloig, M. Karni, J. Chandrasekhar, P. von R. Schleyer, *ibid.* **1986**, *108*, 270–284.
[64] P. von R. Schleyer, presented at the *6th Int. Meet. Boron Chem. (IMEBORON)*, Bechyné, CSSR, **1987**.
[65] J. M. Schulman, R. L. Disch, *Organometallics* **1989**, *8*, 733–737.
[66] a) P. von R. Schleyer, footnote 2 in reference [35]; b) K. Krogh-Jespersen, D. Cremer, D. Poppinger, J. A. Pople, P. von R. Schleyer, J. Chandrasekhar, *J. Am. Chem. Soc.* **1979**, *101*, 4843–4851; c) E. D. Jemmis, G. Subramanian, G. N. Srinivas, *ibid.* **1992**, *114*, 7939–7941.
[67] J. C. Sheldon, G. J. Currie, J. H. Bowie, *J. Am. Chem. Soc.* **1988**, *110*, 8266–8267.
[68] I. L. Alberts, H. F. Schaefer III, *Chem. Phys. Lett.* **1990**, *165*, 250–256.
[69] M. Schindler, *J. Am. Chem. Soc.* **1987**, 109, 1020–1033.
[70] M. J. S. Dewar, C. H. Reynolds, *J. Am. Chem. Soc.* **1984**, *106*, 1744–1750.
[71] a) B. Wrackmeyer, H. G. Kehr, R. Boese, *Angew. Chem.* **1991**, *103*, 1374–1376; *Angew. Chem. Int. Ed. Engl.* **1991**, *30*, 1370; b) B. Wrackmeyer, G. Kehr, A. Sebald, J. Kümmerlen, *Chem. Ber.* **1992**, *125*, 1597–1603, and references therein
[72] B. Wrackmeyer, K. Horchler, R. Boese, *Angew. Chem.* **1989**, *101*, 1563–1565; *Angew. Chem. Int. Ed. Engl.* **1989**, *28*, 1500.
[73] J. Lhomme, A. Diaz, S. Winstein, *J. Am. Chem. Soc.* **1969**, *91*, 1548–1549, and references therein.
[74] S. Winstein, P. Carter, *J. Am. Chem. Soc.* **1961**, *83*, 4485–4486.
[75] T. Laube, *J. Am. Chem. Soc.* **1989**, *111*, 9224–9232, and references therein
[76] P. J. Fagan, E. G. Burns, J. C. Calabrese, *J. Am. Chem. Soc.* **1988**, *110*, 2979–2981.
[77] J. M. Schulman, R. L. Disch, P. von R. Schleyer, M. Bühl, M. Bremer, W. Koch, *J. Am. Chem. Soc.* **1992**, *114*, 7897–7901.
[78] G. Hagen, H. Mayr, *J. Am. Chem. Soc.* **1991**, *113*, 4954–4961, and references therein
[79] a) Y. Apeloig, *Theoretical Aspects of Organosilicon Compounds* in *The Chemistry of Organic Silicon Compounds, Vol. 1* (Eds.: S. Patai, Z. Rappoport), Wiley, Chichester, **1989**; b) Y. Apeloig (Technion Israel Institute of Technology, Haifa), personal communication.
[80] a) W. Hepp, U. Schubert, *J. Organomet. Chem.* **1990**, *385*, 221–245; b) E. Liepins, I. Birgele, E. Lukevics, E. T. Bogoradovsky, V. S. Zavgorodny, *J. Organomet. Chem.* **1991**, *402*, 43–54.
[81] R. P. Kirchen, N. Okasawa, K. Ranganayakulu, A. Rauk, T. S. Sorensen, *J. Am. Chem. Soc.* **1981**, *103*, 597–604, and references therein; J. E. McMurry, T. Lectka, C. N. Hodge, *ibid.* **1989**, *111*, 8867–8872, and references therein.
[82] B. Wrackmeyer, K. Horchler, *Organometallics* **1990**, *9*, 1881–1886, and references therein.
[83] L. A. Hagelee, R. Köster, *Synth. React. Inorg. Met.-Org. Chem.* **1977**, *7*, 53–67.
[84] R. Köster, *Pure Appl. Chem.* **1977**, *49*, 765–789, and references therein
[85] J. Hooz, R. Mortimer, *Tetrahedron Lett.* **1976**, 805–808.
[86] a) C. Pues, A. Berndt, *Angew. Chem.* **1984**, *96*, 306–307, *Angew. Chem. Int. Ed. Engl.* **1984**, *23*, 313; b) A. Höfner, B. Ziegler, W. Massa, A. Berndt, *ibid.* **1989**, *101*, 188–190 and **1989**, *28*, 186–187.
[87] M. Saunders, H. A. Jimenez-Vazquez, *Chem. Rev.* **1991**, *91*, 375–397, and references therein.
[88] G. Schmidt-Lukasch, Dissertation, Universität Marburg, **1989**.
[89] C. Wieczorek, Dissertation, Universität Marburg, **1991**.
[90] M. Brock, Dissertation, Universität Marburg, **1990**.
[91] a) M. Groteklaes, P. Paetzold, *Chem. Ber.* **1988**, *121*, 809–810; b) A. Baceiredo, G. Bertrand, P. Mazerolles, J.-P. Majoral, *J. Chem. Soc. Chem. Commun.* **1981**, 1197–1198; c) M. Yoshifuji, I. Shima, K. Ando, N. Inamoto, *Tetrahedron Lett.* **1983**, *24*, 933–936; d) H. H. Karsch, H. U. Reisacher, G. Müller, *Angew. Chem.* **1986**, *98*, 467–468; *Angew. Chem. Int. Ed. Engl.* **1986**, *25*, 454; e) M. Gouygou, C. Tachou, G. Etemad-Moghadam, M. Koenig, *Tetrahedron Lett.* **1989**, *30*, 7411–7614, and references therein; f) A. H. Cowley, F. Gabbai, R. Schluter, D. Atwood, *J. Am. Chem. Soc.* **1992**, *114*, 3142–3144, and references therein; g) L. Lange, B. Meyer, W.-W. du Mont, *J. Organomet. Chem.* **1987**, *329*, C17–C20.
[92] M. Yoshifuji, I. Shima, N. Inamoto, K. Hirotsu, T. Higuchi, *J. Am. Chem. Soc.* **1981**, *103*, 4587–4589; M. Yoshifuji, K. Toyota, N. Inamoto, *J. Chem. Soc. Chem. Commun.* **1984**, 689–690.
[93] a) K. Issleib, H. Schmidt, C. Wirkner, *Z. Anorg. Allg. Chem.* **1982**, *488*, 75–79; b) H. H. Karsch, F. H. Köhler, H.-U. Reisacher, *Tetrahedron Lett.* **1984**, *25*, 3687–3690; c) M. Hesse, U. Klingebiel, *Angew. Chem.* **1986**, *98*, 638–639; *Angew. Chem. Int. Ed. Engl.* **1986**, *25*, 649; d) M. Dräger, J. Escudie, C. Couret, H. Ranalvonjatovo, J. Satge, *Organometallics* **1988**, *7*, 1010–1013; e) G. Märkl, U. Herold, *Tetrahedron Lett.* **1988**, *29*, 2935–2938; f) E. Niecke, M. Nieger, F. Reichert, *Angew. Chem.* **1988**, *100*, 1781–1782; *Angew. Chem. Int. Ed. Engl.* **1988**, *27*, 1715; g) P. Jutzi, A. Becker, C. Leue, H. G. Stammler, B. Neumann, *Organometallics.* **1991**, *10*, 3838–3842; h) W. Luthin, G. Elter, A. Henne, D. Stalke, G. M. Sheldrick, A. Meller, *Z. Anorg. Allg. Chem.* **1992**, *608*, 142–152, and references therein.
[94] C. Balzereit, Diplomarbeit, Universität Marburg, **1992**.
[95] G. Wittig, *Acc. Chem. Res.* **1974**, *7*, 6–14, penultimate sentence.
[96] E. Kaufmann, P. von R. Schleyer, *Inorg. Chem.* **1988**, *27*, 3987–3992.
[97] T. P. Hamilton, H. F. Schaefer III, *J. Am. Chem. Soc.* **1991**, *113*, 7147–7151.
[98] P. von R. Schleyer, Universität Erlangen, personal communication.
[99] P. Hassanzadeh, L. Andrews, *J. Am. Chem. Soc.* **1992**, *114*, 9239–9240.

Syntheses of Polycyclic Natural Products Employing the Intramolecular Double Michael Reaction

New Synthetic Methods (91)

By Masataka Ihara* and Keiichiro Fukumoto*

The one-pot intramolecular double Michael reaction of compounds having two different α,β-unsaturated carbonyl groups to form polycyclic compounds can be carried out by three different methods: in the first the substrate is treated with lithium hexamethyldisilazide, in the second with chlorotrimethylsilane, triethylamine, and zinc chloride at an elevated temperature, and in the third with *tert*-butyldimethylsilyl trifluoromethanesulfonate and triethylamine. The reaction proceeds with complete regioselectivity and high stereoselectivity following a stepwise mechanism. Spiro-fused bicyclo[2.2.2]octane derivatives can be constructed with high stereoselectivity by the intramolecular double Michael reaction by using the first method. Enantiomerically pure atisine and the enantiomer of atisirene were synthesized stereoselectively by application of this methodology. The syntheses of steroids and angular triquinane-type sesquiterpenoids were possible with the second method. Heterocyclic compounds with a bridgehead nitrogen atom were obtained by the reaction of α,β-unsaturated amides following the second and third methods. The asymmetric synthesis of tylophorine with diastereofacial control was achieved by the intramolecular reaction according to the third method. The sulfur-mediated intramolecular double Michael reaction utilizing the third method produced *trans*-hydroindane derivatives. Furthermore, the intramolecular Michael–aldol reaction can be employed in synthesizing polycyclic systems with cyclobutane units by treatment with *tert*-butyldimethylsilyl trifluoromethanesulfonate in the presence of triethylamine. The intermolecular double Michael reaction and related reactions will also be described.

1. Introduction

Since new methods for C–C bond formation with regio- and stereocontrol are needed in synthetic organic chemistry, ring construction is a central theme. If functional group A acts as an electron donor to an electron-accepting group B, which is in the same molecule, and during the reaction the character of the functional groups change to electron-accepting and electron-donating, respectively, formation of a second bond would lead to a polycyclic ring system having a number of stereogenic centers. An example of such a sequence is provided by the intramolecular double Michael reaction shown in Figure 1.

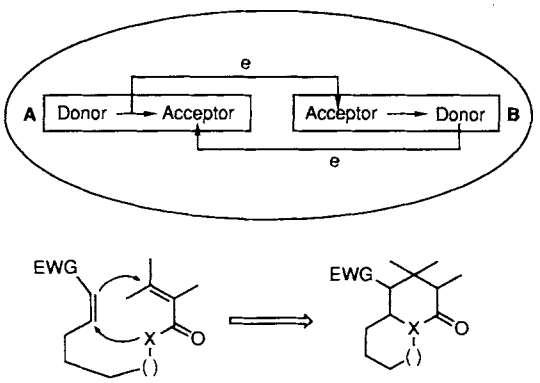

Fig. 1. Schematic representation of the intramolecular double Michael reaction. EWG = electron-withdrawing group; X = electron-donating group. The ellipse represents a molecule with functional groups A and B; the arrows labeled with e indicate intramolecular nucleophilic additions.

[*] Prof. M. Ihara, Prof. K. Fukumoto
Pharmaceutical Institute, Tohoku University
Aobayama, Sendai 980 (Japan)
Telefax: Int. code + (22)263-9205

The Michael reaction of activated methylene groups with α,β-unsaturated esters or ketones is one of the most widely utilized approaches for C–C bond formation.[1] The strategy described consists of two sequential Michael reactions, but the reaction can be also regarded as an anion-assisted or a Lewis acid catalyzed Diels–Alder reaction. Although the determination of the reaction mechanism is difficult, many results support a stepwise mechanism.

The intramolecular double Michael reaction leads to the rapid construction of polycyclic compounds. Hence, it is potentially a powerful weapon for the synthesis of complex natural products.[1b] We would like to show here its usefulness in the field of chemical synthesis. For the purpose of comparison, we will first describe the intermolecular double Michael reaction and several applications.

2. Intermolecular Double Michael Reactions

Double Michael reactions can be carried out under either basic or acidic conditions.[2] In the case of the intermolecular reaction under acidic conditions, it is necessary to convert the first Michael donor into a cross-conjugated silyl enol ether prior to the reaction. In contrast, in the intramolecular variant the sequential conjugate additions directly occur without formation of silyl enol ethers (see Sections 3.1.1–3.1.3, 3.2.4–3.2.7).

2.1. Under Basic Conditions

Cross-conjugated dienolates can be generated from α,β-unsaturated ketones having no hydrogen atom at the γ position by treatment with sodium hydride or potassium *t*-bu-

toxide. The dienolate formed from **1** or **3** underwent double Michael reactions with electron-deficient olefins to give **2**[3] and **4**[4], respectively (Fig. 2).

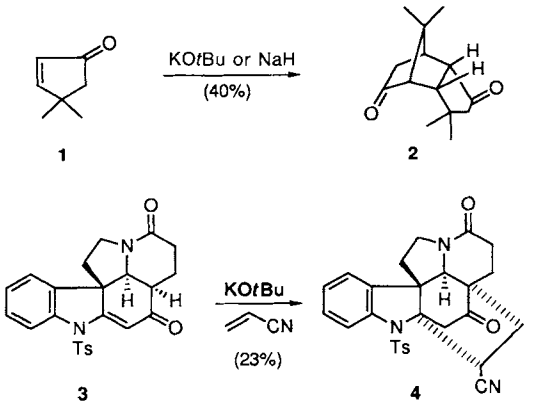

Fig. 2. Intermolecular double Michael reaction of α,β-unsaturated ketones having no γ-hydrogen atoms. Ts = toluenesulfonyl.

The intermolecular double Michael reaction of α,β-unsaturated ketones possessing an γ hydrogen atom was first reported by Lee.[5] Bicyclo[2.2.2]octane derivatives **6** were efficiently synthesized by the reaction of cyclohexenones **5** with methyl acrylate in the presence of lithium diisopropylamide (LDA) (Fig. 3, entries 1 and 2). White and Reusch added several more examples (entries 3–5). They also examined the double Michael reaction of dienolates with methyl vinyl ketone; bicyclic compounds **7** were obtained in good yield when free amine was removed from the reaction mixture (entries 6 and 7).[6] The distinct preference for products **6** and **7** having a *syn* relationship between the two carbonyl groups is noteworthy. These results indicate that the cation is chelated in the transition state by carbonyl groups of the donor and acceptor portions of the moleule.

Hagiwara and Uda also reported the intermolecular double Michael reaction of ethyl α-phenylthio- and α-

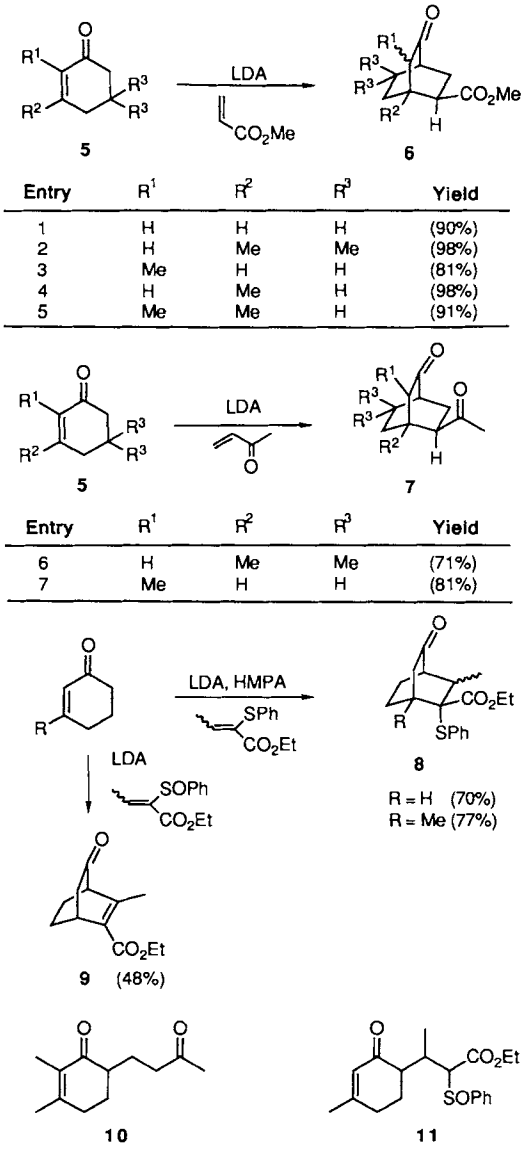

Fig. 3. Synthesis of bicyclo[2.2.2]octane derivatives by intermolecular double Michael reaction. HMPA = hexamethylphosphoric triamide.

Masataka Ihara, born in 1942, was educated at the Pharmaceutical Institute, Tohoku University, and received his Ph.D. degree there in 1970. He has been Associate Professor of Organic Chemistry at the Pharmaceutical Institute, Tohoku University, since 1981. His current interests are the development of new synthetic methods and the syntheses of natural products. He received the Miyata Academic Prize in 1992.

Keiichiro Fukumoto was born in 1934, graduated from the Pharmaceutical Institute, Osaka University, and obtained his Ph.D. degree from Osaka University in 1964. He has been Professor of Organic Chemistry at Pharmaceutical Institute, Tohoku University, since 1981, and his research focuses on the syntheses of natural products. He received the Prize of the Pharmaceutical Society of Japan in 1976.

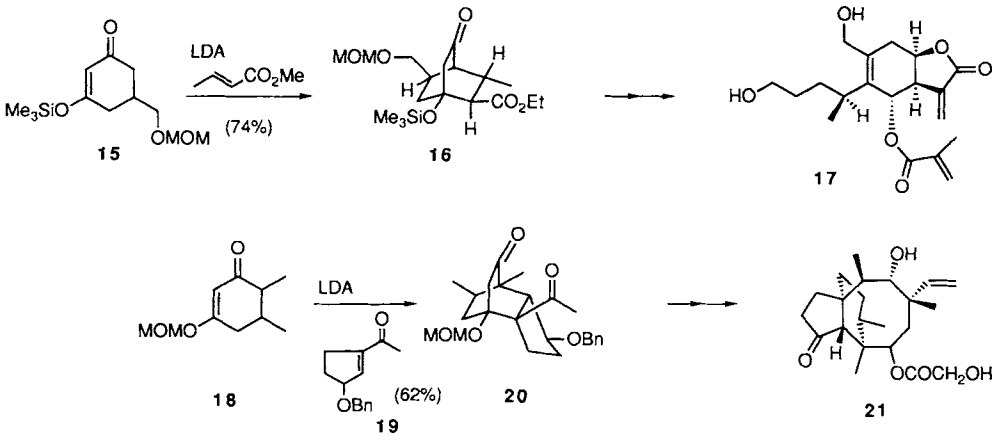

phenylsulfinylcrotonates giving **8** and **9**.[7] In the course of these investigations, several mono Michael adducts such as **10** and **11** were obtained. Failure of the second Michael addition was ascribed to the stability of the enolate anion formed in the first Michael reaction. Formation of adducts **10** and **11** is consistent with a stepwise mechanism. Similar strategies were used for the construction of bridged compounds,[8-14] and mono Michael adducts were detected by several researchers.[8-10]

The stepwise mechanism was clearly supported by the following experiment. Deprotonation of the vinylogous ester **12** with LDA at low temperature was followed by addition of methyl acrylate and in situ silylation to yield the mixed ketene acetal **13** as a rather stable compound. The second Michael addition of **13** proceeded smoothly upon treatment with silica gel to produce **14** (Fig. 4).[15]

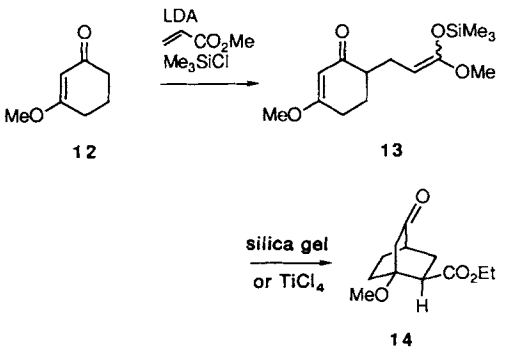

Fig. 4. Intermolecular double Michael reaction via a mixed ketene acetal.

This reaction was applied in the syntheses of many natural products (Fig. 5). Treatment of the dienolate derived from **15** with methyl crotonate gave the bicyclo[2.2.2]octane derivative **16**, which was converted into (±)-eriolanine (**17**).[16,17] Double Michael reaction of **18** with enone **19** provided the tricyclic compound **20**, which was transformed into (±)-pleuromutilin (**21**).[18,19] When the enolate of **22** generated under kinetic control was treated with ethyl sorbate, the synthetic intermediate **23** of (±)-sanadaol (**24**) was produced.[20,21] Double Michael reaction of the enolate of **22** with the (*Z*) ester **25** yielded the bridged product **26** as a single stereoisomer. In contrast, the reaction with the corre-

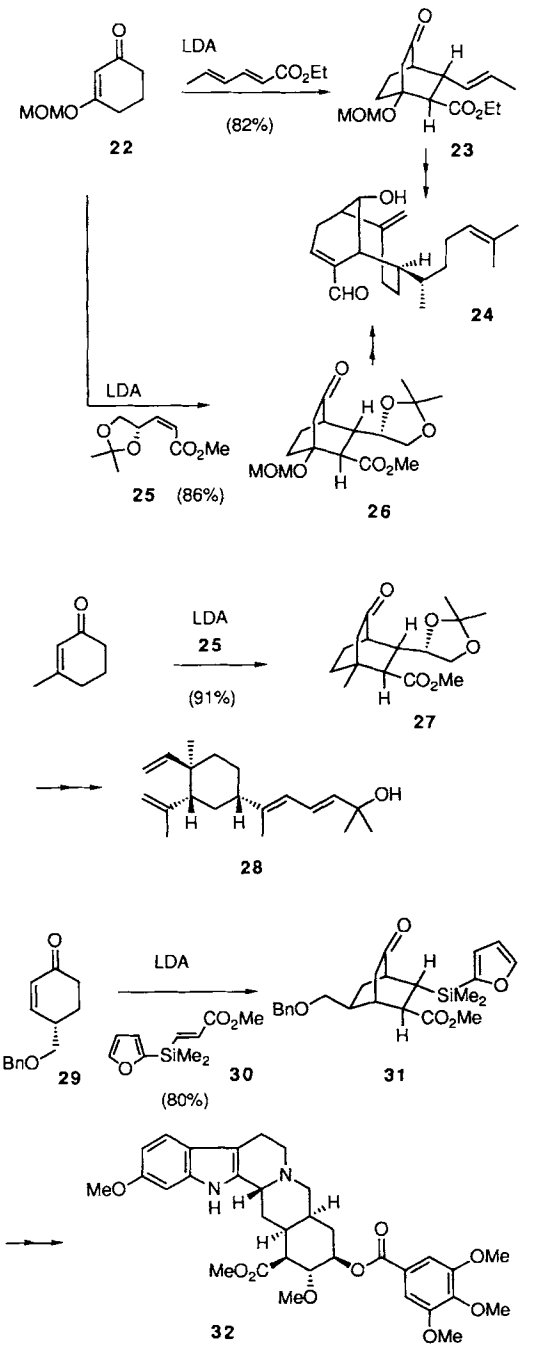

Fig. 5. Natural product syntheses utilizing the intermolecular double Michael reaction. MOM = methoxymethyl.

sponding (*E*) ester provided a mixture of two diastereoisomers. The ratio of the two products was reversed by the addition of HMPA.[22a] Product **26** was converted into (−)-sanadaol (**24**).[22b] The marine diterpene fuscol (**28**)[23] was synthesized via **27**, which was prepared by the double Michael reaction of 3-methyl-2-cyclohexenone with (*Z*) enoate **25**.[24] Stereoselective synthesis of reserpine (**32**)[25] was possible with intermediate **31**, which was obtained by the tandem reaction of **29** with the unsaturated ester **30**.[26]

Construction of bicyclic compounds by base-catalyzed double Michael reaction was devised by Deslongchamps et al.[27] As an example, the *cis*-decalin derivative **35** was prepared stereoselectively by the reaction of **33** with enone **34** in the presence of cesium carbonate (Fig. 6).[27a]

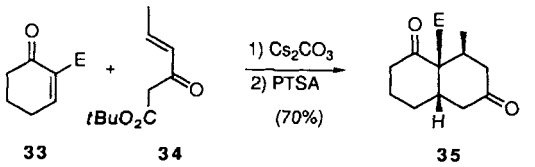

Fig. 6. Synthesis of the *cis*-decalin derivative **35**. E = CO_2Me; PTSA = *para*-toluenesulfonic acid.

2.2. Under Acidic Conditions

The double Michael reaction of cross-conjugated silyl enol ethers with α,β-unsaturated carbonyl compounds in the presence of a Lewis acid could be considered a Lewis acid catalyzed cycloaddition, and it is hard to distinguish between them. Interestingly, the *exo* adduct **38** was selectively formed by the reaction of siloxydiene **36** with enone **37** (Fig. 7).[28] In

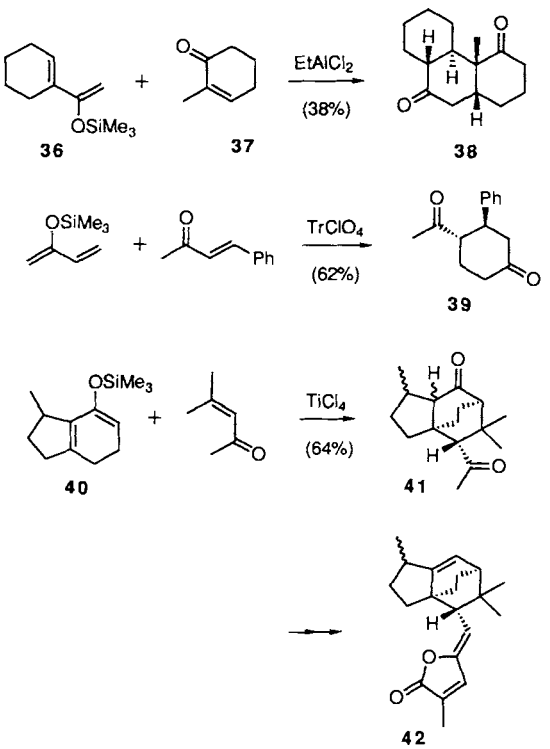

Fig. 7. Lewis acid catalyzed intermolecular double Michael reaction. Tr = trityl.

the presence of a catalytic amount of trityl perchlorate, the double Michael reaction effectively provided the cyclohexanone derivative **39** with selectivity.[29] The reaction of siloxydiene **40** with mesityl oxide in the presence of titanium(IV) chloride afforded a 1:2 mixture of tricyclic compounds **41**, which were transformed into (±)-eremolactone (**42**) (Fig. 7).[30, 31]

3. Intramolecular Double Michael Reactions

3.1. Construction of Polycyclic Ring Systems

3.1.1. Spiro-Fused Bicyclo[2.2.2]octane Derivatives

The bicyclo[2.2.2]octane framework is a partial structure for many natural products. A general method for the stereocontrolled construction of spiro-fused bicyclo[2.2.2]octanes should provide access to a number of interesting compounds. To this end, we studied intramolecular Diels–Alder reactions. But since only poor stereoselection was observed,[32] we were forced to investigate alternative approaches. It was anticipated that compounds having both an enone and an α,β-unsaturated ester group would undergo intramolecular double Michael reactions under either basic or acidic conditions. We also expected that the reaction would be diastereoselective if the ring closure proceeded via a metal-chelate intermediate.

We first examined the intramolecular double Michael reaction of **43** by using several bases (Fig. 8). Treatment with sodium hydride or potassium hydride gave none of the desired tricyclic compounds (entries 1 and 2); however, with LDA and lithium hexamethyldisilazide (LHMDS, $LiN(SiMe_3)_2$), the desired reaction occurred and **46** was produced single isomer (entries 3 and 4). The best results were obtained with LHMDS (entry 4). The stereoselective formation of the desired product **46** can be explained by the intramolecular conjugate addition via intermediate **52** in which the two oxygen atoms are coordinated to a metal cation. This hypothesis is supported by the observed absence of cyclization when NaH or KH was employed and the reduced yield from the reaction carried out in the presence of HMPA (entry 5).[33]

Treatment of the α,β-unsaturated ester **44**, which has hydrogen atoms at the γ position, with LHMDS in THF furnished **47** in poor yield (entry 6). The yield was considerably improved, however, when the reaction was carried out in hexane/ether (entry 7). This observation lends further support for the proposed intramolecular chelation.[34]

The tandem reaction of **45** was also examined with various lithium bases (entries 8–12). Although the racemic product **48** was a single isomer, the yields were dependent on the lithium base and the solvent used. The best results were obtained when **45** was treated with LHMDS in hexane/ether between −78 and 18 °C (2.5 h) and the reaction then quenched with silica gel (entry 10).[35]

The intramolecular tandem reaction of **45** under Lewis acidic conditions was also examined. Among the numerous conditions tested, only two procedures gave the annulation products although with poor stereoselectivity. Heating **45** together with an excess of chlorotrimethylsilane (TMSCl), triethylamine, and zinc chloride in toluene at 180 °C followed by an acidic workup provided **48** and **51** (entry 13).

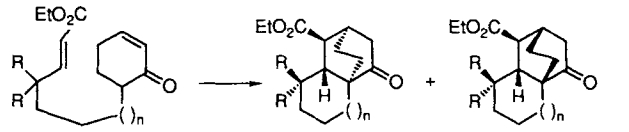

43 R = Me, n = 1 **46** R = Me, n = 1 **49** R = Me, n = 1
44 R = H, n = 1 **47** R = H, n = 1 **50** R = H, n = 1
45 R = Me, n = 0 **48** R = Me, n = 0 **51** R = Me, n = 0

Entry	Substrate	Reaction conditions	Products (yield [%])	
1	**43**	NaH, THF, 66 °C	**46** (0)	**49** (0)
2	**43**	KH, THF, 66 °C	**46** (0)	**49** (0)
3	**43**	LDA, THF, −78 → −20 °C	**46** (45)	**49** (0)
4	**43**	LHMDS, THF, −78 → 18 °C	**46** (60)	**49** (0)
5	**43**	LHMDS, HMPA, THF, −78 → 18 °C	**46** (10)	**49** (0)
6	**44**	LHMDS, THF, −78 → 18 °C	**47** (13)	**50** (0)
7	**44**	LHMDS, hexane/ether, −78 → 18 °C	**47** (50)	**50** (0)
8	**45**	LDA, THF, −78 → −20 °C	**48** (53)	**51** (0)
9	**45**	LHMDS, THF, −78 → 18 °C	**48** (57)	**51** (0)
10	**45**	LHMDS, hexane/ether, −78 → 18 °C	**48** (64)	**51** (0)
11	**45**	LICA, THF, −78 → 18 °C	**48** (26)	**51** (0)
12	**45**	$LiNEt_2$, THF, −78 → 18 °C	**48** (30)	**51** (0)
13	**45**	TMSCl, Et_3N, $ZnCl_2$, 180 °C; H_3O^+	**48** (50)	**51** (13)
14	**45**	TBSOTf, Et_3N, 18 °C; H_3O^+	**48** (21)	**51** (12)

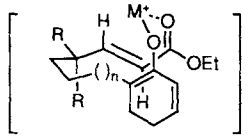

52

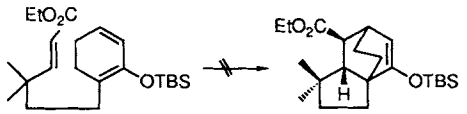

53 **54**

Fig. 8. Construction of spiro-fused bicyclo[2.2.2]octanes. TBS = *tert*-butyldimethylsilyl.

The same products were obtained by the reaction of **45** with *tert*-butyldimethylsilyl trifluoromethanesulfonate (TBSOTf) in the presence of Et_3N at 18 °C for 10 min followed by acidic workup (entry 14).[36] Thus, we found that the tandem reaction could be achieved under three sets of reaction conditions: 1) with LHMDS at a low temperature, 2) with TMSCl, Et_3N, and zinc chloride at elevated temperature, and 3) with TBSOTf in the presence of Et_3N at a low temperature. For the preparation of spiro-fused bicyclo[2.2.2]octane derivatives the first is the method of choice.

The other two methods[37–40] are frequently used in preparing silyl enol ethers. When **45** was treated with TBSOTf in the presence of trimethylamine at a low temperature, the cross-conjugated silyl dienol ether **53** was obtained. Treatment of **53** with TBSOTf and Et_3N at room temperature did not afford the tricyclic product **54**.[35] Thin-layer chromatograms of both reaction mixtures show that **45** gives rise to the cyclic ketones **48** and **51** directly, and these are gradually transformed into the corresponding epimeric silyl enol ethers **54**. This observation speaks against the intramolecuar Diels–Alder reaction of triene **53**.[41]

3.1.2. *Heterocycles with a Bridgehead Nitrogen Atom*

It was assumed that the construction of heterocyclic compounds with a nitrogen atom at the bridgehead position by an intramolecular double Michael reaction would be an efficient method for the synthesis of alkaloids. Treatment of the amide ester **55** under basic conditions with either LDA, LHMDS, potassium *tert*-butoxide, or sodium hydride in the presence of Et_3N led only to the mono Michael product **58** (Fig. 9). Apparently the α,β-unsaturated amide group does

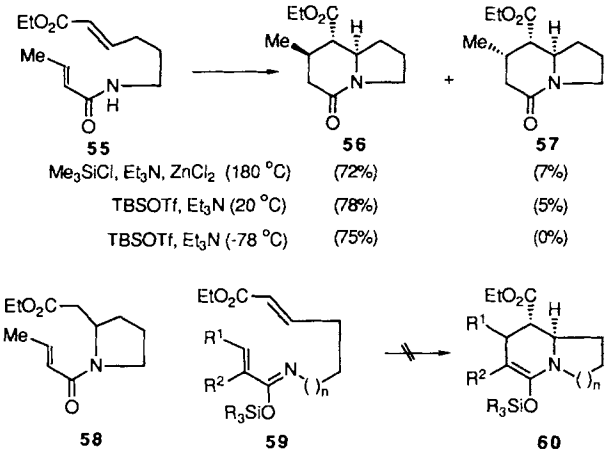

55 **56** **57**

Me_3SiCl, Et_3N, $ZnCl_2$ (180 °C) (72%) (7%)
TBSOTf, Et_3N (20 °C) (78%) (5%)
TBSOTf, Et_3N (−78 °C) (75%) (0%)

58 **59** **60**

Fig. 9. Synthesis of indolizidines.

not function as a Michael acceptor under basic conditions. Various Lewis acids were then examined in order to accomplish the second Michael addition. The desired reaction giving a mixture of **56** and **57** was successfully achieved by treatment of **55** with TMSCl, Et_3N, and $ZnCl_2$ at an elevated temperature and, alternatively, with TBSOTf in the presence of Et_3N at low temperature. When the latter method was applied at −78 °C, **56** was obtained as a single isomer.[42] Formation of 1-azadiene **59** and silyl enol ether **60** was not detected during the reactions.[42] These findings provide further evidence for two sequential conjugate additions in the annulation reactions.

When **61** was subjected to either set of reaction conditions benzo[*a*]quinolizidine **62** was obtained as a single isomer (Fig. 10). Indolo[2,3-*a*]quinolizidine **64** was produced from

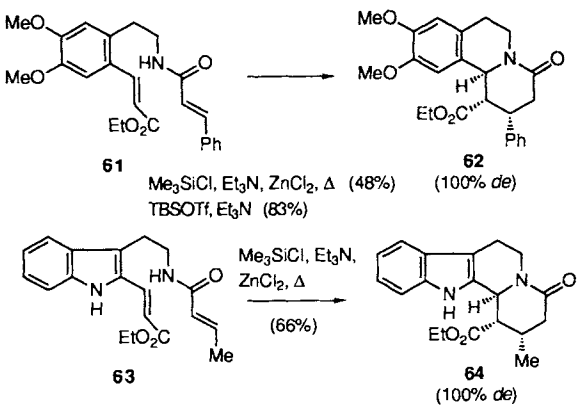

61 **62**

Me_3SiCl, Et_3N, $ZnCl_2$, Δ (48%) (100% *de*)
TBSOTf, Et_3N (83%)

Me_3SiCl, Et_3N, $ZnCl_2$, Δ (66%)

63 **64** (100% *de*)

Fig. 10. Synthesis of benzo[*a*]quinolizidine and indolo[2,3-*a*]quinolizidine.

63 by heating with TMSCl, Et_3N, and $ZnCl_2$. Thus, the intramolecular double Michael reaction allows the efficient assembly of heterocyclic compounds with a bridgehead nitrogen atom under two sets of reaction conditions.[42, 43]

3.1.3. *Hydroindanes*

Since the *trans*-hydroindane framework with a methyl group at the angular position is a partial structure of steroids and various terpenoids, several methods for its construction have been devised.[44] We examined the synthesis of hydroindanes by the intramolecular double Michael reaction. All four geometrical isomers of **65** afforded the same main product, *trans*-fused **66**, upon treatment with TBSOTf in the presence of Et_3N. This procedure provides a useful methodology for the production of polyfunctionalized *trans*-hydroindanes, since **66** can be readily converted into the ketone **67** and the enone **68** (Fig. 11). Because there is no

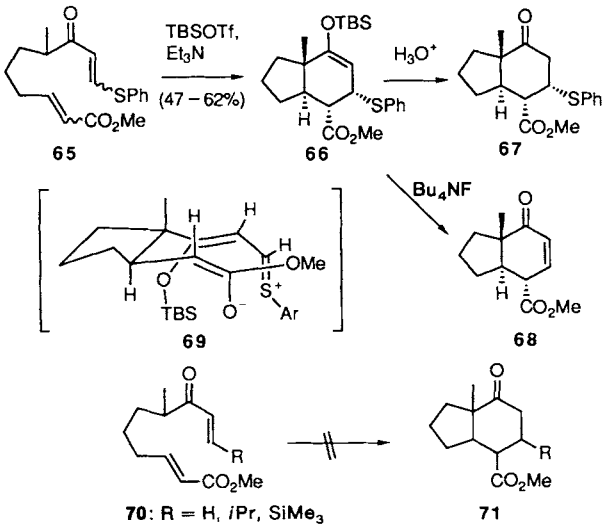

Fig. 11. Sulfur-mediated intramolecular double Michael reaction leading to *trans*-hydroindanes. Ar = aryl.

formation of bicyclic compounds **71** from enone esters **70** in the absence of the sulfenyl group, the sulfur-associated zwitterion **69** was proposed to be the common intermediate.[45] These results reconfirm the stepwise mechanism for the cyclization.

3.2. Syntheses of Natural Products

3.2.1. *Atisirene*

The optically active enone ester **72**, derived from the (+)-Wieland–Miescher ketone,[46] was treated with LHMDS and underwent an intramolecular double Michael reaction to afford the desired tetracyclic compound **74** in excellent yield (Fig. 12). The high stereoselectivity in the formation of **74** arises from the lithium-chelate intermediate **73**, which has no strong nonbonding interactions.[47] Keto ester **74** was converted by deformylation[48] into the synthetic precursor[49] of (+)-atisirene (**75**), the enantiomer of a diterpenoid isolated from *Erythroxylon monogynum*,[50] in order to remove the extra methoxycarbonyl group.[47] It is noteworthy that the corresponding *cis*-substituted substrate **76** produced the cyclized product **77** despite the crowded intermediate.[47a]

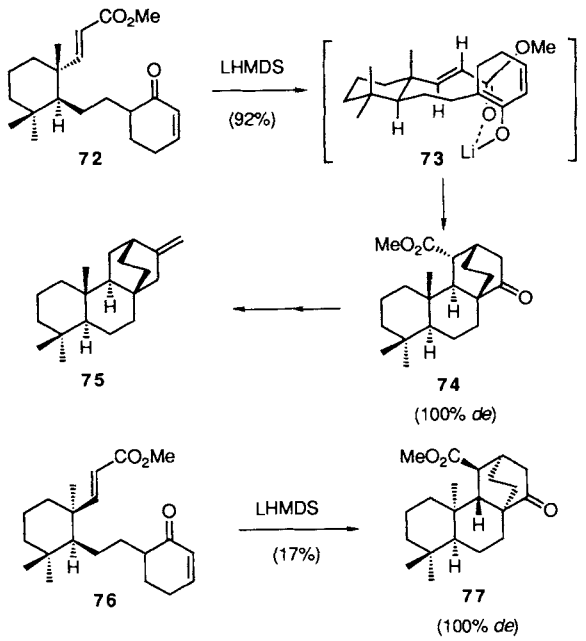

Fig. 12. Synthesis of the enantiomer (**75**) of atisirene.

3.2.2. *Aconitium Alkaloids*

The tricyclic compound **48**, which was mentioned in Section 3.1.1 as the product obtained form the highly stereoselective reaction of **45** with LHMDS, was transformed into the tetracyclic alcohol **78**. After mesylation the synthetic intermediate underwent a Wagner–Meerwein-type rearrangement[51] to give the tetracyclo[7.3.$0^{4,12}0^{5,13}$]tridecane derivative **79** as a single product; **79** corresponds to the CDF part of the *Aconitium* alkaloids **80** (Fig. 13).[35]

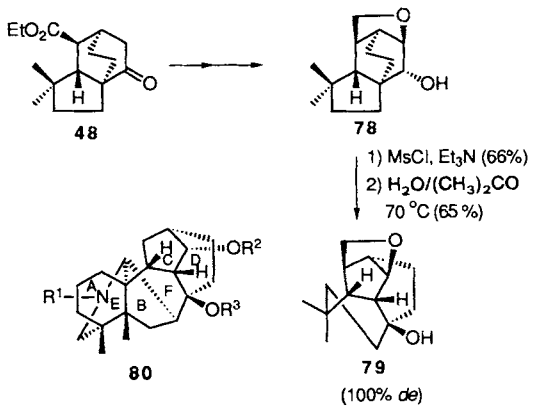

Fig. 13. Synthesis of the CDF part of the *Aconitium* alkaloids.

3.2.3. *Atisine*

Since the determination of the absolute configuration of atisine (**81**), a natural product found in *Aconitium heterophyllum*,[52] the alkaloid has attracted the attention of organic chemists as a target molecule. Three routes[53] were devised leading to Pelletier's synthetic intermediate,[54] but only racemates were obtained. We envisioned the construction of intermediate **82** by the intramolecular double Michael reaction of enone ester **83**.[55] It was further assumed that the substrate for the key step (**83**) could be accessible from the symmetrical azabicyclo[3.3.1]nonane **84** in optically active form (Fig. 14).[56]

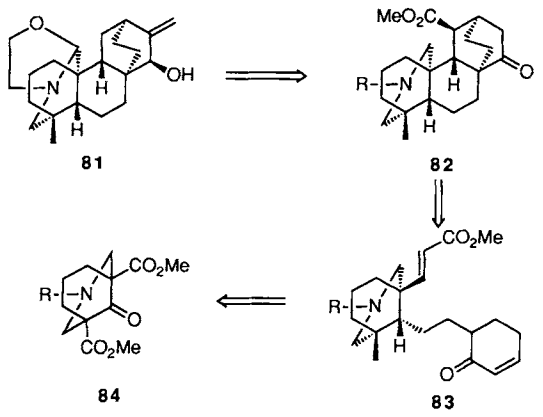

Fig. 14. Retrosynthesis of atisine (**81**).

Azabicyclononane **86**, corresponding to the AE part of atisine (**81**), was prepared quantitatively from diester **85** by a double Mannich reaction[57] (Fig. 15). The *meso* compound **86** is suited for enzyme-catalyzed, enantioselective transformation. After several attempts we were able to pro-

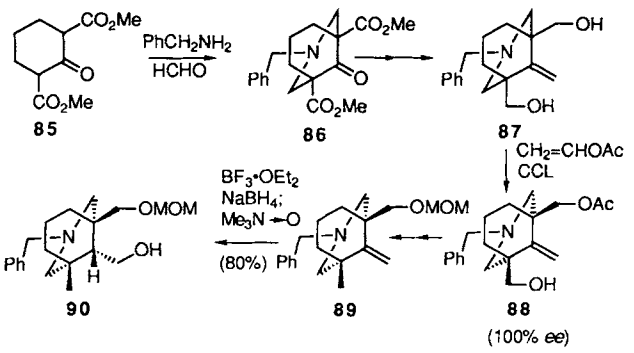

Fig. 15. Preparation of the chiral building block for the synthesis of actonitium alkaloids. CCL = *Candida cylindracea* lipase.

duce optically pure acetate **88** by lipase-catalyzed irreversible transesterification[58] of diol **87**. The absolute configuration was determined by X-ray analysis of the derivative after introduction of the (+)-camphorsulfonyl group with the known absolute configuration.[56] Monoacetate **88** was converted into olefin **89**; the latter could also be prepared from **86** by chemical means by utilizing a chiral auxiliary, however, the enantioselectivity was low.[59]

Stereoselective hydroboration of olefin **89** was not possible with standard borane reagents but was accomplished with sodium borohydride and boron trifluoride etherate, which generate borane in situ. Coordination of boron trifluoride to the amine blocks one side of the double bond, and the desired isomer **90** obtained stereoselectively.

The substrate required for the key step (**91**) was prepared in a straightforward manner from **90** and then subjected to the intramolecular double Michael reaction by treatment with LHMDS (Fig. 16). The highly stereoselective formation of the required pentacyclic compound **93** can be again accounted for by the lithium-chelate intermediate **92**. Removal of the unnecessary methoxycarbonyl group of **93** by Barton's procedure[60] followed by the one-step conversion of the carbamate into the acetamide[61] produced the key synthetic intermediate **94**[54] for atisine (**81**). This enantioselective total synthesis of atisine is the most efficient approach yet reported.[56]

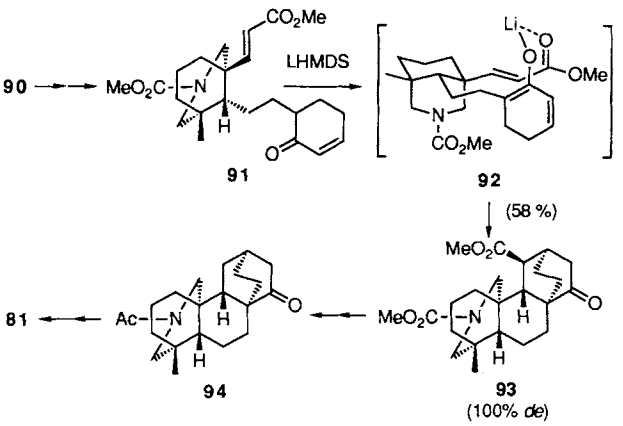

Fig. 16. Total synthesis of atisine (**81**).

The pentacyclic compound **96**, which has an oxygen functionality at the 6-position, was prepared by the intramolecular double Michael reaction of **95** under the same conditions as those above (Fig. 17).[62] It is expected that **96** should be a useful synthetic precursor for other *Aconitium* alkaloids.

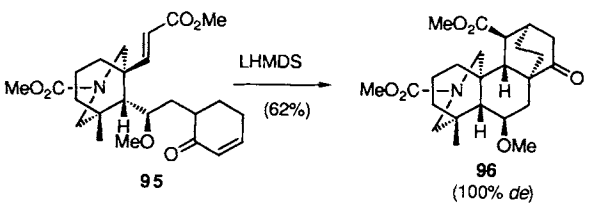

Fig. 17. Synthesis of an atisine derivative having an oxygen functionality at the 6-position.

3.2.4. *Steroids*

Steroids are attractive targets for synthetic work because of their medicinal importance and structural features.[63] We developed syntheses of androgens in which the AB rings are constructed by an intramolecular Diels–Alder reaction[64] and in which the B ring is formed by an intramolecular 1,3-dipolar cycloaddition of a nitrile oxide.[65] As an exten-

sion of this work we applied the intramolecular double Michael reaction to the construction of the AB ring system of estrane.[66] The substrate for the key step (**97**) was synthesized stereoselectively from a chiral indanone derivative.[67] The desired ring closure was achieved only by heating **97** with TMSCl, Et_3N, and $ZnCl_2$, since the vinyl ketone function was too reactive under the other two sets of reaction conditions. Three stereosiomers, **98A**, **98B**, and **99**, were obtained in a 2:1:1 ratio (Fig. 18).[66]

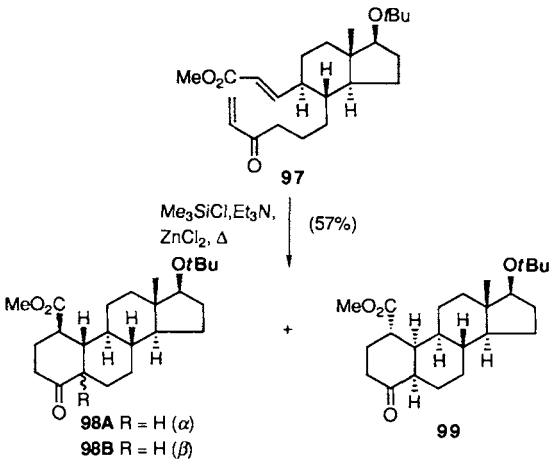

Fig. 18. Synthesis of estranes.

3.2.5. *Angular Triquinanes*

Angular triquinane-type sesquiterpenoids have recently received a great deal of attention from synthetic chemists because of their unique structures.[68] We synthesized the racemate of 3-oxosilphinene, a congener of silphinene, via a tricyclo[7.3.0.$0^{1,5}$]dodecane derivative prepared by an intramolecular Diels–Alder reaction.[69] We envisioned that a structurally related tricyclododecane suitable as a precursor for other triquinanes could be synthesized by the intramolecular double Michael reaction. Vinyl ketone **100** was synthesized in a straightforward manner starting from 5,5-dimethylcyclopent-2-en-1-one. Heating **100** with TMSCl, Et_3N, and $ZnCl_2$ produced two diastereoisomers, **101**, and **102** (Fig. 19). Both the yield and ratio of these products depended on the reaction temperature and solvent. The major product **101** could be transformed into (±)-pentalenic acid (**103**)[70] and (±)-pentalenene (**104**)[71] through ring contraction.[72]

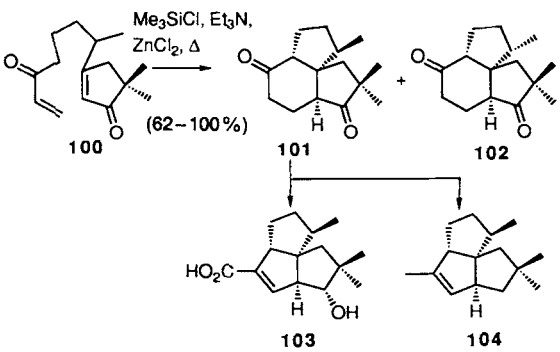

Fig. 19. Synthesis of (±)-pentalenic acid (**103**) and (±)-pentalenene (**104**).

3.2.6. *Epilupinine*

In order to demonstrate the usefulness of the intramolecular double Michael reaction for alkaloid synthesis, we chose epilupinine (**107**)[73] as the first target molecule (Fig. 20). Treatment of the amide ester **105** with TMSCl, Et_3N, and $ZnCl_2$ at an elevated temperature provided quinolizidine **106**. Better yields were possible when the reaction was conducted with TBSOTf *in* the presence of Et_3N at −78 °C. Reduction of **106** gave (±)-epilupinine (**107**).[42]

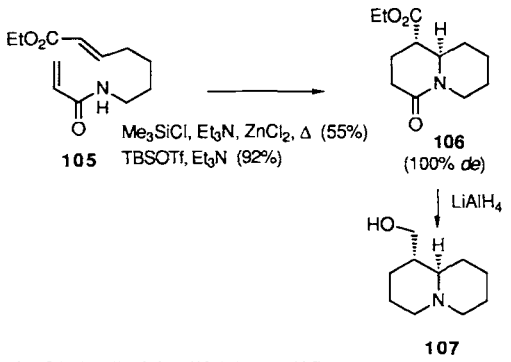

Fig. 20. Synthesis of (±)-epilupinine (**107**) (+ *ent*-**107**).

3.2.7. *Tylophorine*

The absolute configuration of (−)-tylophorine was tentatively assigned as the (*S*) form on the basis of degradation studies.[74] However, synthetic work[75] revealed that the absolute configuration of the natural (−) isomer corresponds to the (*R*) form (**111**). Since synthesis of optically active tylophorine had been carried out with (*S*)-amino acids as chiral precursors,[75] there was no report on the synthesis of the naturally occurring enantiomer. Preliminary experiments for the synthesis of the racemate[76] indicated that the construction of the indolizidine skeleton was possible with the intramolecular double Michael reaction by using TBSOTf in the presence of Et_3N at a low temperature. Therefore, we turned our attention to the asymmetric synthesis of the naturally occurring enantiomer **111**. Based on considerations of the conformation of the transition state, we expected that (−)-phenylmenthol or a secondary alcohol derived from glucose would be a suitable chiral auxiliary for the synthesis of the desired enantiomer. Two chiral amide esters, **108A** and **108B**, were prepared and then subjected to the tandem reaction. It was surprising that only the desired stereoisomers, **109A** and **109B**, respectively, were obtained in excellent yield (Fig. 21). Oxidation of **109A** with thallium(III) trifluoroacetate (TTFA) in the presence of boron trifluoride etherate[77] provided phenanthroindolizidine **110**. (−)-Tylophorine (**111**) was synthesized from both **109A** and **109B** by thermal decarboxylation.[78] These results support the expected transition state **112**, assuming that the conjugated double bond and the ester carbonyl bond of the α,β-unsatu-

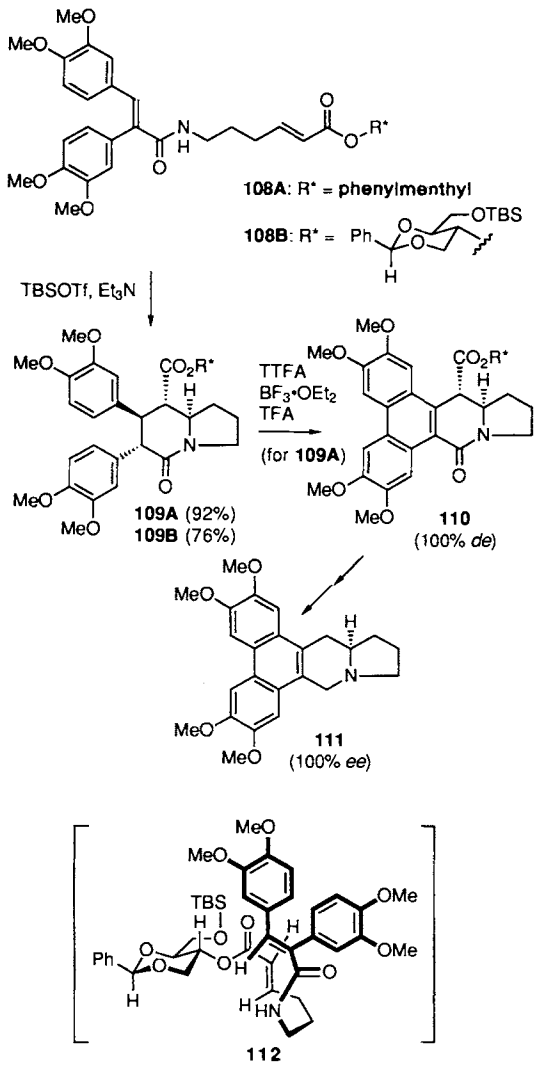

Fig. 21. Asymmetric synthesis of (−)-tylophorine (**111**).

rated ester have an antiplanar disposition and that the alkoxy α-hydrogen atom of the chiral auxiliary and the ester carbonyl oxygen atom have a synplanar arrangement.[44, 79]

4. Extension of Sequential Reactions

Sequential reactions, in which the intermediate in the Michael addition initiates a subsequent reaction, are potentially useful tools for the syntheses of cyclic and polycyclic compounds.

4.1. Other Types of Double Michael Reactions

Disubstituted pyrrolidine and piperidine frameworks were constructed by one-pot tandem Michael reactions, in which a molecule with an electrophilic double bond and a secondary benzylamine bearing an acceptor moiety trap the initially formed enolate.[80] (+)-α-Allokainic acid (**114**)[81] was synthesized by the base-catalyzed reaction of methyl vinyl ketone and the chiral amine **113** (Fig. 22).[80]

Lithium *N*-benzyltrimethylsilylamide (LSA) is an excellent nucleophile which only undergoes 1,4-addition to croton-

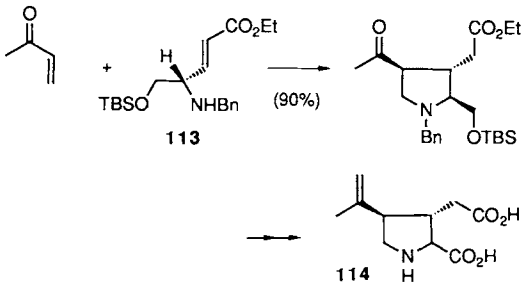

Fig. 22. Synthesis of (+)-α-allokainic acid (**114**).

ate derivatives. The reaction of the symmetrical diester **115** (R = Et) with LSA was followed by treatment with acetic acid to provide a 7:3 mixture of cyclopentane derivatives **116** (Fig. 23).[82] In contrast, treatment of **115** (R = Me) with silyl ketene acetal **117** in the presence of tetrabutylammonium *m*-chlorobenzoate afforded cyclopentane **118** as a single diastereoisomer.[83]

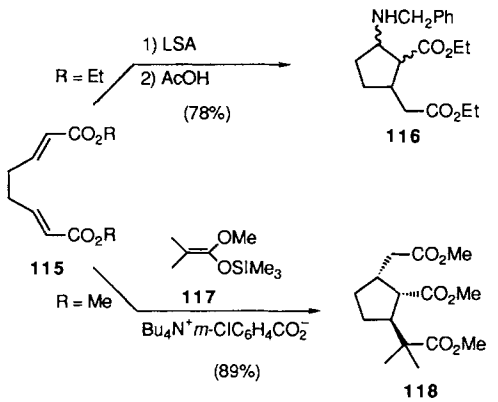

Fig. 23. Synthesis of cyclopentanes by tandem Michael reactions.

4.2. Triple Michael Reactions

Divinyl ketone and the trimethylsilyl enol ether **119** underwent Lewis acid assisted triple Michael reaction to yield tricycle **120**[84] as a single stereoisomer (Fig. 24);[85] **120** is a synthetic intermediate en route to (±)-seychellene (**121**).[86]

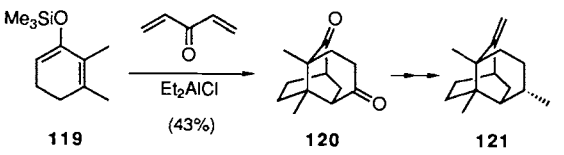

Fig. 24. Synthesis of (±)-seychellene (**121**) by a triple Michael reaction.

4.3. Michael–Michael–Substitution Reactions

If the cross-conjugated dienolate **122** reacts with a Michael acceptor in which the activating group is also a good leaving group, then the double Michael reaction may be followed by intramolecular substitution to generate a polycyclic ring system like **123** with a cyclopropane unit. This transformation was successfully carried out for Michael acceptors with

phosphonium bromide,[87] sulfone,[88] and nitro groups (Fig. 25).[89] For example, the dienolate derived from enone **124** reacted with vinylphosphonium bromide to produce the pentacyclic ketone **125** with high stereoselectivity.[90] A subsequent transformation provided the enantiomer of the diterpene *ent*-trachyloban-19-oic acid (**126**).[91]

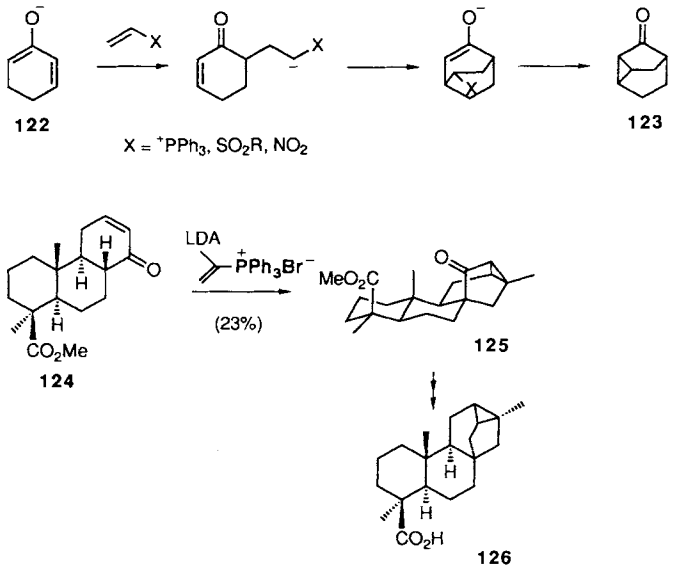

Fig. 25. Synthesis of *ent*-trachyloban-19-oic acid (**126**) by a Michael-Michael-substitution reaction.

Dienolates also undergo smooth Michael–Michael–substitution reactions with acrylic esters bearing a halogen atom at the 2-position.[92] The isolation of the mono Michael adduct as the intermediate supported the stepwise mechanism and ruled out the possibility that the Michael reaction is followed by a carbenoid reaction.[92e] Compound **128**, a precursor of (±)-ishwarane (**129**),[93] was prepared as the major product together with one diastereoisomer in the reaction of enone **127** with methyl α-bromoacrylate (Fig. 26).[92b] Reaction of the dienolate derived from enone **130** with ethyl α-bromocrotonate in the presence of HMPA produced a 4:1 mixture of tricyclic compounds **131** isomeric at the C7 position,[94] which were converted into (±)-helminthosporal (**132**).[95]

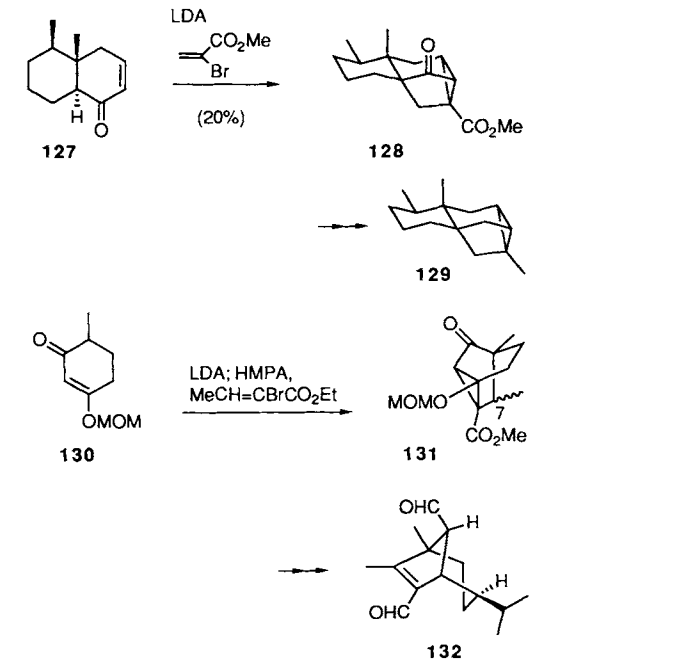

Fig. 26. Synthesis of (±)-ishwarane (**129**) and (±)-helminthosporal (**132**) by Michael-Michael-substitution reactions.

4.4. Michael–Michael–Aldol and Related Reactions

In the reaction shown in Figure 27 the external nucleophile underwent a Michael addition to the β carbon atom of the α-methylene ketone **133** which was then followed by intramolecular Michael addition. The enolate thus produced reacted with the isopropyl ketone part to complete the ring closure. A mixture of a bromohydrin **134** and two diastereoisomeric epoxides **135** was synthesized as a model experiment toward the synthesis of the indole alkaloid aflavinine (Fig. 27).[96]

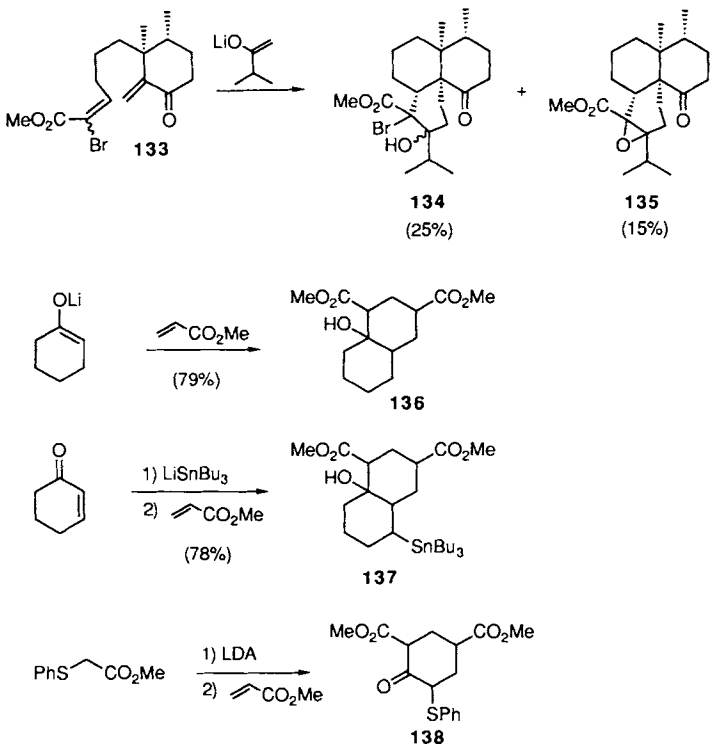

Fig. 27. Three Michael–Michael–aldol reactions (top) and one Michael–Michael–Dieckmann reaction (bottom). Two equivalents of methyl acrylate were used in each case.

Treatment of the lithium enolate from cyclohexanone with two equivalents of methyl acrylate resulted in Michael–Michael–aldol reaction to afford **136**.[97] Furthermore, the lithium enolate prepared by the treatment of 2-cyclohexenone with a trialkylstannyllithium reagent reacted with two equivalents of methyl acrylate to yield **137** (Fig. 27).[98] In contrast, when the lithium enolate of an acyclic or cyclic carboxylate ester was treated with two equivalents of methyl acrylate, a Michael–Michael–Dieckmann reaction afforded

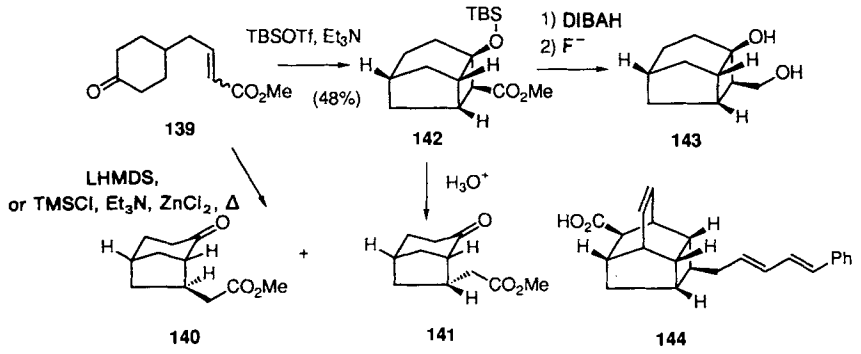

Fig. 28. Synthesis of the partial structure of endiandric acid C (**144**) by intramolecular Michael–aldol reaction.

a cyclohexanone product. In this manner **138** was synthesized in a one-pot procedure (Fig. 27).[99]

4.5. Intramolecular Tandem Michael–Aldol Reactions

A number of polycyclic natural products possessing a cyclobutane unit, for example, endiandric acid C (**144**), trihydroxydecipiadiene (**147**), and italicene (**150**), have been isolated. Although several methods are available for the synthesis of cyclobutane derivatives, [2 + 2] photocycloaddition is the most common.[100] We expected that polycyclic ring systems with cyclobutane units could be constructed by the tandem Michael–aldol reactions of α,β-unsaturated esters having a ketone function at an appropriate position.

When keto ester **139** was treated with LHMDS or TMSCl, Et_3N, and $ZnCl_2$, Michael adduct **140** was obtained as the major product together with diastereoisomer **141** (Fig. 28). In contrast, the reaction of **139** with TBSOTf in the presence of Et_3N resulted in sequential Michael–aldol reactions affording the cyclobutane derivative **142** as a single isomer. The same product **142** was obtained from both the (*E*) and (*Z*) isomers of the unsaturated ester **139**; this observation supports a stepwise mechanism. Acidic treatment of **142** gave the Michael adduct **141** as a single product. The silyl group of **142** was removed after reduction of the ester group leaving the cyclobutane ring intact to afford **143**. Thus, the partial structure of endiandric acid C (**144**)[101] was assembled by the sequential reactions.[102]

Treatment of **145** under the same conditions as above furnished the highly substituted product **146**, whose carbon framework is similar to that of trihydroxydecipiadiene (**147**) (Fig. 29).[103] Compound **149**, which has the framework of italicene (**150**),[104] was quantitatively constructed from **148** by treatment under the same reaction conditions at room temperature for 5 min. These examples demonstrate an effective route to a variety of polycyclic systems with cyclobutane units which is based on modification of the intramolecular double Michael reaction.[102] The intermolecular tandem reaction under the same reaction conditions was not successful.

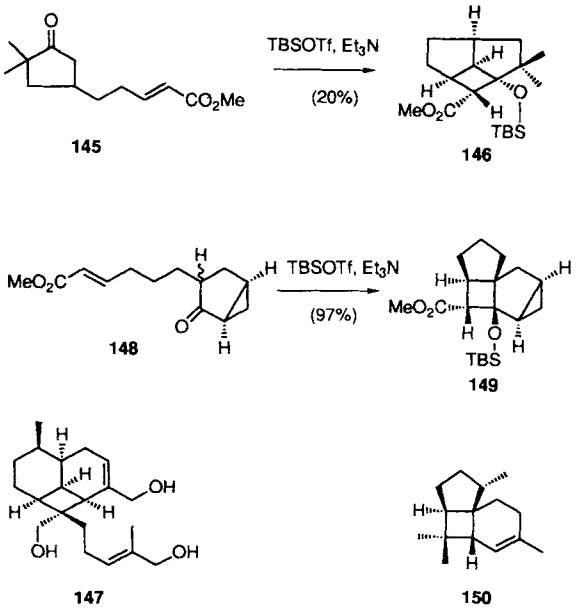

Fig. 29. Synthesis of the frameworks of trihydroxydecipiadiene (**147**) and italicene (**150**).

6. Summary and Outlook

The intramolecular double Michael reaction can be conducted under three sets of fundamentally different conditions—one basic and two acidic. Since a procedure suitable to the substrate can be selected from these, the intramolecular tandem reaction provides a versatile method for the production of polycyclic compounds. Furthermore, this reaction proceeds with complete regioselectivity and high stereoselectivity. Since many bonds are formed in one step, the method is economical. It is expected that this intramolecular sequential reaction will be further utilized as an effective approach to other target molecules.

It is a pleasure to acknowledge the fine efforts of both past and present group members, many of whose names appear in the references related to our work in the area of the intramolecular sequential reactions.

Received: June 6, 1992,
Revised version: August 5, 1992 [A 908 IE]
German version: *Angew. Chem.* **1993**, *105*, 1059

[1] Reviews: a) E. D. Bergmann, D. Ginsburg, R. Pappo, *Org. React.* **1959**, *10*, 179–555; b) D. A. Oare, C. H. Heathcock, *Top. Stereochem.* **1989**, *19*, 227–407; L. F. Tietze, U. Beifuss, *Angew. Chem.* **1993**, *105*, 137–170; *Angew. Chem. Int. Ed. Engl.* **1993**, *32*, 131–163.
[2] M. Ihara, K. Fukumoto, *J. Synth. Org. Chem. Jpn.* **1986**, *44*, 96–108.
[3] A. J. Bellamy, *J. Chem. Soc. (B)* **1969**, 449–455.
[4] T. Ohnuma, T. Oishi, Y. Ban, *J. Chem. Soc. Chem. Commun.* **1973**, 301–302.
[5] R. A. Lee, *Tetrahedron Lett.* **1975**, 3333–3336.
[6] L. B. White, W. Reusch, *Tetrahedron*, **1978**, *24*, 2439–2443.

[7] H. Hagiwara, K. Nakayama, H. Uda, *Bull. Chem. Soc. Jpn.* **1975**, *48*, 3769–3770.
[8] M. L. Quesada, R. H. Schlessinger, W. H. Parsons, *J. Org. Chem.* **1978**, *43*, 3968–3970.
[9] R. A. Holton, A. D. Williams, R. Kennedy, *J. Org. Chem.* **1986**, *51*, 5480–5482.
[10] D. Schinzer, M. Kalesse, *Tetrahedron Lett.* **1991**, *32*, 4691–4694.
[11] W. Weber, D. Spitzner, W. Kraus, *J. Chem. Soc. Chem. Commun.* **1980**, 1212–1213.
[12] A. S. Narula, A. J. Birch, *Tetrahedron Lett.* **1981**, *22*, 591–594.
[13] a) D. Spitzner, *Tetrahedron Lett.* **1978**, 3349–3350; b) *Angew. Chem.* **1982**, *94*, 639; *Angew. Chem. Int. Ed. Engl.* **1982**, *21*, 636–637; c) D. Spitzner, P. Wagner, A. Simon, K. Peters, *Tetrahedron Lett.* **1989**, *30*, 547–550.
[14] H. Nagaoka, K. Ohsawa, T. Takata, Y. Yamada, *Tetrahedron Lett.* **1984**, *25*, 5389–5392.
[15] D. Schinzer, M. Kalesse, J. Kabbara, *Tetrahedron Lett.* **1988**, *29*, 5241–5244.
[16] M. R. Roberts, R. H. Schlessinger, *J. Am. Chem. Soc.* **1981**, *103*, 724–725.
[17] Isolation: S. M. Kupchan, R. L. Baxter, C.-K. Chiang, C. J. Gilmore, R. F. Bryan, *J. Chem. Soc. Chem. Commun.* **1973**, 842–843. Other syntheses: P. A. Grieco, T. Oguri, S. Gilman, *J. Am. Chem. Soc.* **1980**, *102*, 5886–5891.
[18] E. G. Gibbons, *J. Org. Chem.* **1980**, *45*, 1540–1541; *J. Am. Chem. Soc.* **1982**, *104*, 1767–1769.
[19] A. J. Birch, D. W. Cameron, C. W. Holzapfel, R. W. Rickards, *Chem. Ind. (London)* **1963**, 374–375.
[20] H. Nagaoka, K. Kobayashi, T. Matsui, Y. Yamada, *Tetrahedron Lett.* **1987**, *28*, 2021–2024.
[21] Isolation: M. Ishitsuka, T. Kusumi, H. Kakisawa, *Tetrahedron Lett.* **1982**, *23*, 3179–3180.
[22] a) H. Nagaoka, K. Kobayashi, T. Okamura, Y. Yamada, *Tetrahedron Lett.* **1987**, *28*, 6641–6644; b) H. Nagaoka, K. Kobayashi, Y. Yamada, *ibid.* **1988**, *29*, 5945–5946.
[23] Isolation: Y. Gopichand, F. J. Schmitz, *Tetrahedron Lett.* **1978**, 3641–3644.
[24] M. Iwashima, H. Nagaoka, K. Kobayashi, Y. Yamada, *Tetrahedron Lett.* **1992**, *33*, 81–82.
[25] Other syntheses: a) R. B. Woodward, F. E. Bader, H. Bickel, A. J. Frey, R. W. Kierstead, *J. Am. Chem. Soc.* **1956**, *78*, 2023–2025; 2657; b) B. A. Pearlman, *ibid.* **1979**, *101*, 6398–6404; 6404–6408); c) P. A. Wender, J. M. Schaus, A. W. White, *ibid.* **1980**, *102*, 6157–6159; *Heterocycles* **1987**, *25*, 263–270; d) S. F. Martin, H. Rüeger, S. A. Williamson, S. Grzejszczak, *J. Am. Chem. Soc.* **1987**, *109*, 6124–6134.
[26] G. Stork, *Pure Appl. Chem.* **1989**, *61*, 439–442.
[27] a) J.-F. Lavallée, P. Deslongchamps, *Tetrahedron Lett.* **1988**, *29*, 5117–5118; b) R. Ruel, P. Deslongchamps, *ibid.* **1990**, *31*, 3961–3964; c) C. Spino, P. Deslongchamps, *ibid.* **1990**, *31*, 3969–3972.
[28] G. A. Krus, P. Gottshalk, *J. Org. Chem.* **1984**, *49*, 1153–1154.
[29] T. Mukaiyama, Y. Sagawa, S. Kobayashi, *Chem. Lett.* **1986**, 1821–1824.
[30] M. Asaoka, K. Ishibashi, N. Yanagida, H. Takei, *Tetrahedron Lett.* **1983**, *24*, 5127–5130.
[31] A. J. Birch, J. Grimshaw, T. P. Turnbull, *J. Chem. Soc.* **1963**, 2412–2417.
[32] a) T. Kametani, T. Honda, K. Fukumoto, M. Toyota, M. Ihara, *Heterocycles* **1981**, *16*, 1673–1676; b) M. Ihara, M. Toyota, K. Fukumoto, T. Kametani, T. Honda, *J. Chem. Research (S)* **1984**, 252–253.
[33] M. Ihara, M. Toyota, K. Fukumoto, T. Kametani, *Tetrahedron Lett.* **1984**, *25*, 2167–2170.
[34] M. Ihara, M. Toyata, M. Abe, Y. Ishida, K. Fukumoto, T. Kametani, *J. Chem. Soc., Perkin Trans. 1* **1986**, 1543–1549.
[35] M. Ihara, Y. Ishida, M. Abe, M. Toyota, K. Fukumoto, T. Kametani, *Chem. Lett.* **1985**, 1127–1130; *J. Chem. Soc. Perkin Trans. 1* **1988**, 1155–1163.
[36] M. Ihara, Y. Ishida, K. Fukumoto, T. Kametani, *Chem. Pharm. Bull.* **1985**, *33*, 4102–4105.
[37] S. Danishefsky, T. Kitahara, *J. Am. Chem. Soc.* **1974**, *96*, 7807–7808.
[38] H. Emde, D. Domsch, H. Feger, U. Frick, A. Götz, H. H. Hergott, K. Hofmann, W. Kober, K. Krägeloh, T. Oesterle, W. Steppan, W. West, G. Simchen, *Synthesis* **1982**, 1–26.
[39] H. Emde, A. Götz, K. Hofmann, G. Simchen, *Liebigs Ann. Chem.* **1981**, 1643–1657.
[40] L. N. Mander, S. P. Sethi, *Tetrahedron Lett.* **1984**, *25*, 5953–5956.
[41] Diels–Alder reaction using TMSCl-Et_3N-$ZnCl_2$ and TBSOTf-Et_3N: a) R. L. Snowden, *Tetrahedron Lett.* **1981**, *22*, 97–100; *Tetrahedron* **1986**, *42*, 3277–3290; b) H. Lamy-Schelkens, D. Giomi, L. Ghosez, *Tetrahedron Lett.* **1989**, *30*, 5887–5890; 5891–5894; c) S. R. Wilson, M. J. Di Grandi, *J. Org. Chem.* **1991**, *56*, 4766–4772.
[42] a) M. Ihara, T. Kirihara, K. Fukumoto, T. Kametani, *Heterocycles* **1985**, *23*, 1097–1100; b) M. Ihara, T. Kirihara, A. Kawaguchi, M. Tsuruta, K. Fukumoto, T. Kametani, *J. Chem. Soc., Perkin Trans. 1* **1987**, 1719–1726.
[43] M. Ihara, T. Kirihara, A. Kawaguchi, K. Fukumoto, T. Kametani, *Tetrahedron Lett.* **1984**, *25*, 4541–4544.
[44] W. R. Roush, H. R. Gills, A. I. Ko, *J. Am. Chem. Soc.* **1982**, *104*, 2269–2283; G. Stork, C. S. Shiner, J. D. Winkler, *ibid.* **1982**, *104*, 310–312.
[45] M. Ihara, S. Suzuki, N. Taniguchi, K. Fukumoto, C. Kabuto, *J. Chem. Soc., Chem. Commun.* **1991**, 1168–1169; *J. Chem. Soc. Perkin Trans. 1*, **1992**, 2527–2535.
[46] J. Gutzwiller, P. Buckschacker, A. Fürst, *Synthesis* **1977**, 167.
[47] a) M. Ihara, M. Toyota, K. Fukumoto, T. Kametani, *Tetrahedron Lett.* **1984**, *25*, 3235–3238; b) *ibid.* **1985**, *26*, 1537–1540; c) *J. Chem. Soc. Perkin Trans. 1* **1986**, 2151–2161.
[48] K. Ohno, J. Tsuji, *J. Am. Chem. Soc.* **1968**, *90*, 99–107.
[49] L. H. Zalkow, N. N. Girota, *J. Org. Chem.* **1964**, *29*, 1299–1302.
[50] A. H. Kapadi, R. R. Sobti, S. Dev, *Tetrahedron Lett.* **1965**, 2729–2735.
[51] a) J. P. Johnston, K. H. Overton, *J. Chem. Soc. Perkin Trans. 1* **1972**, 1490–1500; b) W. A. Ayer, P. D. Deshpande *Can. J. Chem.* **1973**, *51*, 77–86; c) K. Wiesner, T. Y. R. Tsai, K. Huber, S. E. Bolton, R. Vlahov, *J. Am. Chem. Soc.* **1974**, *96*, 4990–4992.
[52] a) S. W. Pelletier, *Tetrahedron* **1961**, *14*, 76–112; b) K. Wiesner, R. Armstrong, M. F. Bartlett, J. A. Edwards, *Chem. Ind. (London)* **1954**, 132–133.
[53] a) W. Nagata, T. Sugasawa, M. Narisada, T. Wakabayashi, Y. Hatase, *J. Am. Chem. Soc.* **1963**, *85*, 2342–2343; **1967**, *89*, 1483–1499; b) S. Masamune, *ibid.* **1964**, *86*, 291–292; c) R. W. Guthrie, Z. Valenta, K. Wiesner, *Tetrahedron Lett.* **1966**, 4645–4654.
[54] a) S. W. Pelletier, W. A. Jacobs, *J. Am. Chem. Soc.* **1956**, *78*, 4144–4145; b) S. W. Pelletier, P. C. Parthasarathy, *Tetrahedron Lett.* **1963**, 205–208.
[55] M. Ihara, M. Suzuki, K. Fukumoto, T. Kametani, C. Kabuto, *J. Am. Chem. Soc.* **1988**, *110*, 1963–1964.
[56] M. Ihara, M. Suzuki, K. Fukumoto, C. Kabuto, *J. Am. Chem. Soc.* **1990**, *112*, 1164–1171.
[57] F. F. Blicke, F. J. McCarty, *J. Org. Chem.* **1959**, *24*, 1069–1076.
[58] Y.-R. Wang, J. L. Lalonde, M. Momongan, D. E. Bergbreiter, C.-H. Wong, *J. Am. Chem. Soc.* **1988**, *110*, 7200–7205.
[59] M. Ihara, M. Suzuki, K. Fukumoto, *Heterocycles* **1990**, *30*, 381–384.
[60] D. H. R. Barton, D. Crich, W. B. Motherwell, *Tetrahedron* **1985**, *41*, 3901–3924.
[61] M. Ihara, A. Hirabayashi, N. Taniguchi, K. Fukumoto, *Heterocycles* **1992**, *33*, 851–858.
[62] M. Ihara, A. Hirabayashi, N. Taniguchi, K. Fukumoto, *Tetrahedron* **1992**, *48*, 5089–5098.
[63] a) D. Taub in *The Total Synthesis of Natural Products, Vol. 6* (Ed.: J. ApSimon), Wiley, New York, **1984**, pp. 1–89; b) T. Kametani, H. Nemoto, *Tetrahedron* **1981**, *37*, 3–11.
[64] M. Ihara, I. Sudow, K. Fukumoto, T. Kametani, *J. Org. Chem.* **1985**, *50*, 144–145; *J. Chem. Soc. Perkin Trans. 1* **1986**, 117–123.
[65] a) M. Ihara, Y. Tokunaga, K. Fukumoto, *J. Org. Chem.* **1990**, *55*, 4497–4498; b) M. Ihara, Y. Tokunaga, N. Taniguchi, K. Fukumoto, *Tetrahedron* **1991**, *47*, 6635–6648.
[66] M. Ihara, T. Takahashi, N. Shimizu, Y. Ishida, I. Sudow, K. Fukumoto, T. Kametani, *J. Chem. Soc. Chem. Commun.* **1987**, 1467–1468; *J. Chem. Soc. Perkin Trans. 1* **1989**, 529–535.
[67] R. A. Micheli, Z. G. Hajos, N. Cohen, D. R. Parrish, L. A. Portland, W. Sciamanna, M. A. Scott, P. A. Wehrli, *J. Org. Chem.* **1975**, *40*, 675–681.
[68] T. Hudlicky, F. Rulin, T. C. Lovelace, J. W. Reed in *Studies in Natural Products Chemistry, Vol. 3, Stereoselective Synthesis (Part B)* (Ed.: Atta-ur-Rahman), Elsevier, Amsterdam, **1989**, pp. 3–72.
[69] a) M. Ihara, A. Kawaguchi, M. Chihiro, K. Fukumoto, T. Kametani, *J. Chem. Soc. Chem. Commun.* **1986**, 671–672; b) M. Ihara, A. Kawaguchi, H. Ueda, M. Chihiro, K. Fukumoto, T. Kametani, *J. Chem. Soc. Perkin Trans. 1* **1987**, 1331–1337.
[70] Isolation: H. Seto, T. Sasaki, J. Uzawa, S. Takeuchi, H. Yonehara, *Tetrahedron Lett.* **1978**, 4411–4412. Other syntheses: a) K. Sasaki, T. Ohtsuka, M. Misumi, H. Shirahama, T. Matsumoto, *Chem. Lett.* **1981**, 355–358; b) M. T. Crimmins, J. A. DeLoach, *J. Org. Chem.* **1984**, *49*, 2076–2077; *J. Am. Chem. Soc.* **1986**, *108*, 800–806.
[71] Syntheses: a) Y. Ohfune, H. Shirahama, M. Matsumoto, *Tetrahedron Lett.* **1976**, 2869–2872; b) L. A. Paquette, G. D. Annis, *J. Am. Chem. Soc.* **1982**, *104*, 4504–4506; **1983**, *105*, 7358–7363; c) E. Piers, V. Karunaratne, *J. Chem. Soc. Chem. Commun.* **1984**, 959–960; d) G. Pattenden, S. J. Teague, *Tetrahedron Lett.* **1984**, *25*, 3021–3024; e) G. Mehta, K. S. Rao, *J. Chem. Soc. Chem. Commun.* **1985**, 1464–1466; *J. Am. Chem. Soc.* **1986**, *108*, 8015–8021; f) D. H. Hua, *ibid.* **1986**, *108*, 3835–3837; g) T. Imanishi, F. Ninbari, M. Yamashita, C. Iwata; *Chem. Pharm. Bull.* **1986**, *34*, 2268–2271; h) T. Hudlicky, M. G. Natchus, G. Sinai-Zingde, *J. Org. Chem.* **1987**, *52*, 4641–4644.
[72] M. Ihara, M. Katogi, K. Fukumoto, T. Kametani, *J. Chem. Soc. Chem. Commun.* **1987**, 721–722; *J. Chem. Soc. Perkin Trans. 1* **1988**, 2963–2970.
[73] Review: Kh. A. Aslanov, Yu. K. Kushmuradov, A. S. Sadykov in *The Alkaloids, Chemistry and Pharmacology, Vol. 31* (Ed.: A. Brossi), Academic Press, San Diego, **1978**, pp. 117–192. Recent syntheses: a) Y. Nagao, W.-M. Dai, M. Ochiai, S. Tsukagoshi, E. Fujita, *J. Org. Chem.* **1990**, *55*, 1148–1156; b) D. H. Hua, S. W. Miao, A. A. Bravo, D. J. Takemoto, *Synthesis* **1991**, 970–974; c) E. D. Edstrom, *Tetrahedron Lett.* **1991**, *32*, 5709–5712.
[74] T. R. Govindachari, T. G. Rajagopalan, N. Viswanathan, *J. Chem. Soc. Perkin Trans. 1* **1974**, 1161–1165.

[75] a) T. F. Buckley III, H. Rapoport, *J. Org. Chem.* **1983**, *48*, 4222–4232; b) J. E. Nordlander, F. G. Njoroge, *ibid.* **1987**, *52*, 1627–1630.
[76] M. Ihara, M. Tsuruta, K. Fukumoto, T. Kametani, *J. Chem. Soc. Chem. Commun.* **1985**, 1159–1160.
[77] E. C. Taylor, J. G. Andrade, G. J. H. Rall, A. McKillop, *J. Am. Chem. Soc.* **1980**, *102*, 6513–6519.
[78] a) M. Ihara, Y. Takino, K. Fukumoto, T. Kametani, *Tetrahedron Lett.* **1988**, *29*, 4135–4138; b) *Heterocycles* **1989**, *28*, 63–65; c) M. Ihara, Y. Takino, M. Tomotake, K. Fukumoto, *J. Chem. Soc. Perkin Trans 1* **1990**, 2287–2292.
[79] a) W. Oppolzer, C. Robbiani, K. Bätting, *Helv. Chim. Acta* **1980**, *63*, 2015–2018.
[80] a) A. Barco, S. Benetti, A. Casolari, G. P. Pollini, G. Spalluto, *Tetrahedron Lett.* **1990**, *31*, 3039–3042; 4917–4920.
[81] S. Murakami, T. Takemoto, Z. Shimizu, *J. Pharm. Soc. Jpn.* **1953**, *73*, 1026–1028.
[82] T. Uyehara, N. Shida, Y. Yamamoto, *J. Chem. Soc. Chem. Commun.* **1989**, 113–114.
[83] P. G. Klimko, D. A. Singleton, *J. Org. Chem.* **1992**, *57*, 1733–1740.
[84] M. E. Jung, C. A. McCombs, Y. Takeda, Y.-G. Pan, *J. Am. Chem. Soc.* **1981**, *103*, 6677–6685.
[85] H. Hagiwara, A. Okano, H. Uda, *J. Chem. Soc. Chem. Commun.* **1985**, 1047.
[86] Isolation: G. Wolff, G. Ourisson, *Tetrahedron Lett.* **1968**, 3849–3852; *Tetrahedron* **1969**, *25*, 4903–4914.
[87] a) R. M. Cory, D. M. T. Chan, *Tetrahedron Lett.* **1975**, 4441–4444; b) R. M. Cory, M. D. Bailey, D. W. C. Tse, *ibid.* **1990**, *31*, 6839–6842.
[88] R. M. Cory, R. M. Renneboog, *J. Chem. Soc. Chem. Commun.* **1980**, 1981–1982; *J. Org. Chem.* **1984**, *49*, 3898–3904.
[89] a) R. M. Cory, P. C. Anderson, F. R. McLaren, B. R. Yamamoto, *J. Chem. Soc. Chem. Commun.* **1981**, 73–74; b) R. M. Cory, P. C. Anderson, M. D. Bailey, F. R. McLaren, R. M. Renneboog, B. R. Yamamoto, *Can. J. Chem.* **1985**, *63*, 2618–2627.
[90] a) R. M. Cory, Y. M. A. Naguib, M. H. Rasmussen, *J. Chem. Soc. Chem. Commun.* **1979**, 504–506; b) R. M. Cory, D. M. T. Chan, Y. M. A. Naguib, M. H. Rastall, R. M. Renneboog, *J. Org. Chem.* **1980**, *45*, 1852–1863.
[91] J. St. Pyrek, *Tetrahedron* **1970**, *26*, 5029–5032.
[92] a) H. Hagiwara, T. Kodama, H. Kosugi, H. Uda, *J. Chem. Soc. Chem. Commun.* **1976**, 413; b) H. Hagiwara, H. Uda, T. Kodama, *J. Chem. Soc. Perkin Trans. 1* **1980**, 963–977; c) H. Hagiwara, F. Abe, H. Uda, *J. Chem. Soc. Chem. Commun.* **1991**, 1070–1071; d) D. Spitzner, A. Engler, T. Liese, G. Splettstösser, A. de Meijere, *Angew. Chem.* **1982**, *94*, 799–800; *Angew. Chem. Int. Ed. Engl.* **1982**, *21*, 791.
[93] H. Fuhrer, A. K. Ganguly, K. W. Gopinath, T. R. Govindachari, K. Nagarajan, B. R. Pai, P. C. Parthasarathy, *Tetrahedron*, **1970**, *26*, 2371–2390.
[94] H. Nagaoka, A. Baba, Y. Yamada, *Tetrahedron Lett.* **1991**, *32*, 6741–6744.
[95] Isolation: P. de Mayo, E. Y. Spencer, R. W. White, *Can. J. Chem.* **1963**, *41*, 2996–3004. Other syntheses: a) E. J. Corey, S. Nozoe, *J. Am. Chem. Soc.* **1965**, *87*, 5728–5733; b) M. Yanagiya, K. Kaneko, T. Kaji, T. Matsumoto, *Tetrahedron Lett.* **1979**, *20*, 1761–1764; c) Y. Shizuri, K. Suyama, S. Yamamura, *J. Chem. Soc. Chem. Commun.* **1986**, 63–64.
[96] a) S. Danishefsky, S. Chackalamannil, M. Silvestri, J. Springer, *J. Org. Chem.* **1983**, *48*, 3615–3616; b) S. Danishefsky, P. Harrison, M. Silvestri, B. Segmuller, *ibid.* **1984**, *49*, 1321–1322; c) S. Danishefsky, S. Chackalamannil, P. Harrison, M. Silvestri, P. Cole, *J. Am. Chem. Soc.* **1985**, *107*, 2474–2484.
[97] G. H. Posner, S.-B. Lu, E. Asirvatham, E. F. Silversmith, E. M. Shulman, *J. Am. Chem. Soc.* **1986**, *108*, 511–512.
[98] a) G. H. Posner, E. Asirvatham, *Tetrahedron Lett.* **1986**, *27*, 663–666; b) G. H. Posner, K. S. Webb, E. Asirvatham, S.-S. Jew, A. Degl'Innocenti, *J. Am. Chem. Soc.* **1988**, *110*, 4754–4762.
[99] G. H. Posner, E. M. Shulman-Roskes, *J. Org. Chem.* **1989**, *54*, 3514–3515.
[100] H. N. C. Wong, K.-L. Lau, K.-F. Tam in *Small Ring Compounds in Organic Synthesis I* (Ed.: A. de Maijere), Springer, Berlin **1986**, pp. 83–163.
[101] Isolation: J. E. Banfield, D. St. C. Black, S. R. Johns, R. I. Willing, *Aust. J. Chem.* **1982**, *35*, 2247–2256. Syntheses: K. C. Nicolaou, N. A. Petasis, R. E. Zipkin, J. Uenishi, *J. Am. Chem. Soc.* **1982**, *104*, 5555–5557.
[102] M. Ihara, M. Ohnishi, M. Takano, K. Makita, N. Taniguchi, K. Fukumoto, *J. Am. Chem. Soc.* **1992**, *114*, 4408–4410.
[103] Isolation: E. L. Ghisalberti, P. R. Jefferies, P. Sheppard, *Tetrahedron Lett.* **1975**, 1775–1778. Syntheses: a) M. L. Greenlee, *J. Am. Chem. Soc.* **1981**, *103*, 2425–2426; b) W. G. Dauben, G. Shapiro, *J. Org. Chem.* **1984**, *49*, 4252–4258.
[104] Isolation and synthesis: J. Leimner, H. Marschall, N. Meier, P. Weyerstahl, *Chem. Lett.* **1984**, 1769–1772. Other syntheses: T. Honda, K. Ueda, M. Tsubuki, T. Toya, A. Kurozumi, *J. Chem. Soc. Perkin Trans. 1* **1991**, 1749–1754.

Successful X-Ray Structure Analysis of an Alkylidene Carbenoid—A Milestone in Carbenoid Research

By *Adalbert Maercker**

Since the pioneering work of G. Köbrich[1] (1929–1974), whose untimely death unfortunately cut short his work, the interest in carbenoids[2] has not diminished. In contrast to carbenes, the carbenoids show amphiphilic behavior, because a metal atom as well as a leaving group X is bound to a carbon atom. Halogen atoms and -OR or $-NR_2$ groups are possible X groups, but not heteroatoms of higher periods of the periodic system. If the metal is lithium the typical "carbenoid" character, that is, electrophilic properties on the one hand and nucleophilic, "carbanion-oid" properties on the other, is depicted in the two resonance forms of **1**.

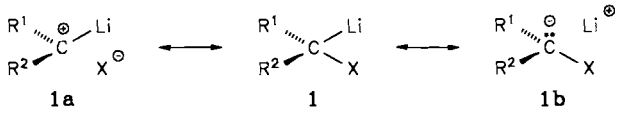

1a **1** **1b**

The lithiocarbenium structure **1a**, and therefore the electrophilic character of the carbenoid, is particularly pronounced only when the lithium atom is σ bound. As soon as an ion pair is present, that is, the ionic character of the C–Li bond is predominant or the negative charge is delocalized, the carbenoid properties disappear or can be observed only with strong nucleophilic partners like alkyllithium compounds. Whether a carbenoid behaves like a carbanion (**1b**) with typical nucleophilic properties depends not only on the substituents R^1 and R^2, but also on the solvent. Thus, the lithiated benzhydryl phenyl ether **3** reacts as a typical Li–OR carbenoid only in diethyl ether, for instance by dimerization to form **5** or by addition of butyllithium to form **2**. In THF, however, the classical carbanion character prevails, and the Wittig rearrangement is observed exclusively, and **4** is formed.[3]

In the dimerization to **6**, the amphiphilic nature of the carbenoid is particularly evident: one particle of **3** reacts as electrophile (**3a**) and one as nucleophile (**3b**).

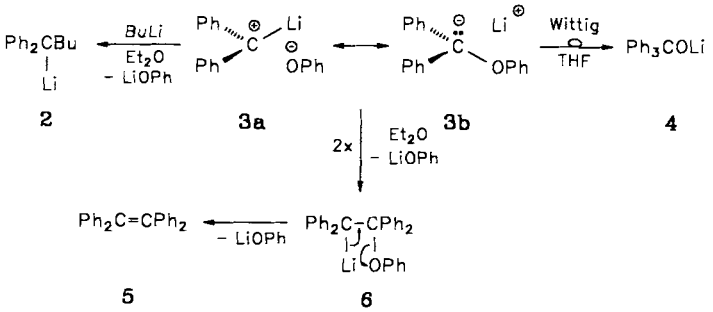

2 **3a** **3b** **4** **5** **6**

The best method of determining whether the electrophilic character of a carbenoid is predominant (that is, it exists mainly as the resonance structure **1a**) is ^{13}C NMR spectroscopy. D. Seebach et al.[4] have studied a variety of typical carbenoids at low temperature and discovered that the carbenoid character (**1a**) can be recognized, amongst other factors, by the strong downfield shift of the ^{13}C NMR shift of the α-carbon atom. The extent of the shift $\Delta\delta$ is distinctly greater than that observed on replacement of a benzylic or vinylic H atom by lithium. Thus, on one hand for the metalated silyl ether analogous to **3** ($OSiMe_3$ instead of OPh),[5] the downfield shift ($\Delta\delta \approx 34.8$) is four units smaller than for the corresponding lithiated hydrocarbon, diphenylmethane ($\Delta\delta = 38.7$), which shows it to be no typical Li–OR carbenoid. On the other hand, this metalated silyl ether displays a distinctly elongated C–O bond, a finding that is likewise considered a criterion for the presence of a carbenoid. The downfield shift of the ^{13}C NMR signal of the α carbon atom should, however, be the more sensitive indicator of the existence of a carbenoid than the C–X distance, especially since according to calculations, the C–O distance for metalated ethers with carbanion character is also distinctly lengthened.[5]

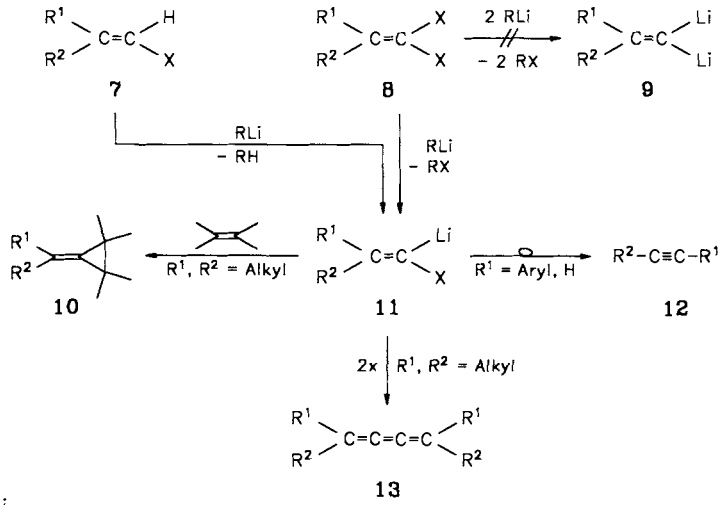

7 **8** **9** **10** **11** **12** **13**

The reactions of the alkylidene carbenoids **11** in which the carbenoid C atom is part of an unsaturated π system are particularly diverse.[6] Because of the stronger C–X bond these carbenoids are more stable than aliphatic carbenoids, and their reactivity is very dependent on the groups R^1 and R^2. Alkylidene carbenoids with aryl groups in a β position can, for instance, no longer be trapped *intermolecularly*, such as by addition of an alkene to alkylidenecyclopropanes like **10** (dimerization to **13** also does not take place), because the intramolecular Fritsch–Buttenberg–Wiechell rearrangement[7] to afford **12** is substantially faster than the addition.

[*] Prof. Dr. A. Maercker
Institut für Organische Chemie der Universität
Adolf-Reichwein Strasse, D-57068 Siegen (FRG)
Telefax: Int. code + (271)7330

The same is valid for the hydride shift of β hydrogen atoms to yield 1-alkynes (**12**, $R^1 = H$).

The alkylidene carbenoids **11** can be prepared either by deprotonation of **7** or by halogen–metal exchange in **8**.[1] Interestingly, the halogen–lithium exchange is accelerated by large groups in a *cis* position,[8] whereas bulky R^1 groups hinder the deprotonation.[1] The report[9] of a double dehalogenation to form the geminal dilithio compound **9** (R^1 = Ph, R^2 = *i*PrO) was disproved.[10]

The first unambiguously characterized Li–Cl carbenoid was 1-chloro-1-lithio-2,2-diphenylethene (**11**, $R^1 = R^2$ = Ph; X = Cl); it was synthesized by G. Köbrich[1] by deprotonation of the appropriate vinyl chloride (**7**). The crystal structure (Fig. 1) of such a carbenoid containing *p*-chlorophenyl instead of phenyl substituents just published by Boche et al.[11] is without doubt a temporary peak in carbenoid research.

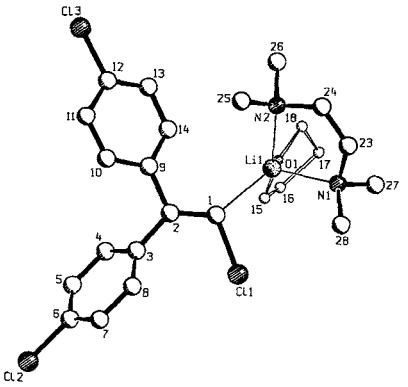

Fig. 1. Crystal structure of 1-chloro-2,2-bis(4-chlorophenyl)-1-lithioethene · TMEDA · 2THF omitting the second THF molecule that occupies a free lattice position and is not bound to Li1.

The pioneer G. Köbrich[1] predicted a rehybridization at the carbenoid carbon atom—he expected the s character of the C–Li bond and the p character of the C–X bond to increase. Exactly that has been shown in this spectacular X-ray structure analysis (at −115 °C!): The Li1-C1-C2 angle is widened from 120 to 137.1°, while the Cl1-C1-C2 angle is only 112.6°. Furthermore, the C1–Cl distance of 185.5 pm is distinctly elongated as anticipated and is about 12 pm longer than the average for C_{sp^2}–Cl bonds. This is consistent with ^{13}C NMR spectra[4] and calculations[12] on Li–halogen carbenoids. In contradiction to the calculations,[12] the lithium atom does *not* bridge the C1–Cl1 bond, presumably because of the solvation of Li1 by tetramethylethylenediamine (TMEDA) and THF.[11] Another feature of the structure is the bond angles at C2. Whereas the aryl group *cis* to Cl1 tilts away from the chlorine atom as expected (C1-C2-C3 129.5°), the *trans* aryl group bends slightly towards C1 (C1-C2-C9 = 116.5°), which seems to set up the Fritsch–Buttenberg–Wiechell rearrangement.[7] The finding that this aryl group is twisted less out of the olefinic plane (39°) than the group *cis* to the Cl atom (57°) is puzzling, as this should affect the overlap of the aromatic π system with the σ* orbital of the rupturing C1–Cl bond unfavorably. The stated cause and effect of the rehydridization at C2[11] could therefore possibly be exchanged—the steric interaction between the large chlorine atom and the aryl group *cis* to it could be the reason for the rehybridization.

In this regard the reactivity of the alkylidene carbenoids towards alkyllithium compounds, which in turn depends strongly on the substituents R^1 and R^2, is interesting. Carbenoids bearing aliphatic substituents react particularly easily,[13] by metal-assisted nucleophilic substitution of the halogen atom (for instance **14** → **15**) accompanied by inversion.[14]

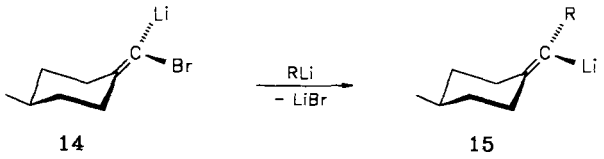

14 **15**

An analogous reaction with alkylidene carbenoids bearing aryl substituents has not yet been observed, even on treatment with *tert*-butyllithium.[10] Instead in this reaction a complex forms that possibly exists in the structure **16** and that in analogy to similar complexes[15] may be considered a Quasi Dianion Complex (QUADAC), especially because with electrophiles it leads to the same products—though in a stepwise mechanism—as the geminal dilithio compound **18**.[10]

1,1-Dilithio-2,2-diphenylethene (**18**) may be prepared from carbenoid **17** in a reaction with lithium-4,4'-di-*tert*-butylbiphenyl (LDBB),[16] a method that has already been used successfully for the synthesis of aliphatic, geminal dilithio compounds.[17] In contrast to the behavior of the QUADAC **16**, **18** rearranges at −70 °C to **21** through an *intra*molecular 1,4-proton shift.[10]

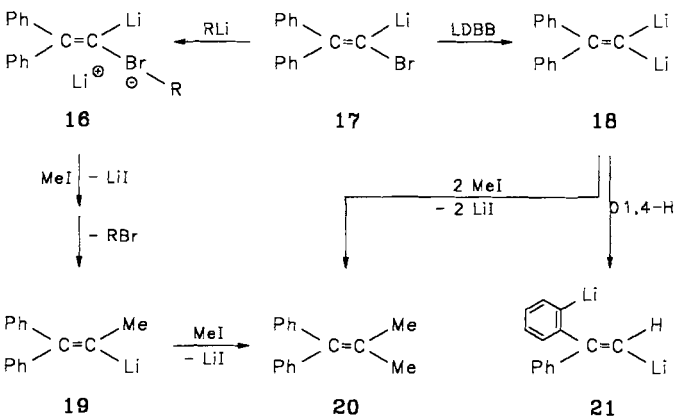

16 **17** **18**

19 **20** **21**

Li–OR carbenoids, and particularly Li–NR_2 carbenoids, have scarcely been studied. The future priority will probably also be the structure and reactivity of these compounds.

German version: *Angew. Chem.* **1993**, *105*, 1072

[1] a) G. Köbrich, *Angew. Chem.* **1967**, *79*, 15–27; *Angew. Chem. Int. Ed. Engl.* **1967**, *6*, 41; b) *ibid.* **1972**, *84*, 557–570 and **1972**, *11*, 473; c) *Bull. Soc. Chim. Fr.* **1969**, 2712–2720.

[2] Other summaries: a) W. Kirmse, *Angew. Chem.* **1965**, *77*, 1–10; *Angew. Chem. Int. Ed. Engl.* **1965**, *4*, 1; b) W. Kirmse, *Carbene Chemistry*, 2nd ed.,

Academic Press, New York, **1971**; *Carbene, Carbenoide und Carbenanaloge*, Verlag Chemie, Weinheim, **1969**; c) H. Siegel, *Top. Curr. Chem.* **1982**, *106*, 55–78.
[3] G. Wittig, E. Stahnecker, *Liebigs Ann. Chem.* **1957**, *605*, 69–93.
[4] a) D. Seebach, H. Siegel, K. Müllen, K. Hiltbrunner, *Angew. Chem.* **1979**, *91*, 844–845; *Angew. Chem. Int. Ed. Engl.* **1979**, *18*, 784; b) H. Siegel, K. Hiltbrunner, D. Seebach, *ibid.* **1979**, *91*, 845-846 and **1979**, *18*, 785; c) D. Seebach, H. Siegel, J. Gabriel, R. Hässig, *Helv. Chim. Acta* **1980**, *63*, 2046–2053; d) D. Seebach, R. Hässig, J. Gabriel, *ibid.* **1983**, *66*, 308–337.
[5] G. Boche, A. Opel, M. Marsch, K. Harms, F. Haller, J. C. W. Lohrenz, C. Thümmler, W. Koch, *Chem. Ber.* **1992**, *125*, 2265–2273.
[6] Reviews: a) P. J. Stang, *Chem. Rev.* **1978**, *78*, 383–405; b) *Acc. Chem. Res.* **1982**, *15*, 348–354.
[7] a) A. A. Bothner-By, *J. Am. Chem. Soc.* **1955**, *77*, 3293–3296; b) D. Y. Curtin, E. W. Flynn, R. F. Nystrom, *ibid.* **1958**, *80*, 4599–4601; c) G. Köbrich, H. Trapp, *Chem. Ber.* **1966**, *99*, 680–688.
[8] a) T. Harada, T. Katsuhira, A. Oku, *J. Org. Chem.* **1992**, *57*, 5805–5807; b) D. Grandjean, P. Pale, *Tetrahedron Lett.* **1993**, *34*, 1155–1158.
[9] J. Barluenga, M. A. Rodriguez, P. J. Campos, G. Asensio, *J. Am. Chem. Soc.* **1988**, *110*, 5567–5568.
[10] a) A. Maercker, B. Bös, *Main Group Met. Chem.* **1991**, *14*, 67–71; b) *6th IUPAC Symp. on Organomet. Chem. directed towards Org. Synth.*, August 25–29, **1991**, Utrecht, The Netherlands, Abstract A 11; c) B. Bös, *Über Bildungstendenzen, Folgereaktionen und Simulationen von 1,1-Dilithio-1-alkenen*, Shaker, Aachen, **1992**; d) A. Maercker in *Lithium Compounds: Principles and Applications* (Eds.: P. von R. Schleyer, A.-M. Sapse), Wiley, New York, in press.
[11] G. Boche, M. Marsch, A. Müller, K. Harms, *Angew. Chem.* **1993**, *105*, 1081; *Angew. Chem. Int. Ed. Engl.* **1993**, *32*, 1032.
[12] a) T. Clark, P. von R. Schleyer, *J. Chem. Soc. Chem. Commun.* **1979**, 883–884; b) *Tetrahedron Lett.* **1979**, 4963–4966; c) *J. Am. Chem. Soc.* **1979**, *101*, 7747–7748, and references therein; d) P. von R. Schleyer, T. Cark, A. J. Kos, G. W. Spitznagel, C. Rohde, D. Arad, K. N. Houk, N. G. Rondan, *ibid.* **1984**, *106*, 6467–6475, and references therein.
[13] H. Günther, A. A. Bothner-By, *Chem. Ber.* **1963**, *96*, 3112–3119.
[14] a) M. Duraisamy, H. M. Walborsky, *J. Am. Chem. Soc.* **1984**, *106*, 5035–5037; b) M. Topolski, M. Duraisamy, J. Rachoń, J. Gawronski, K. Gawronska, V. Goedken, H. M. Walborsky, *J. Org. Chem.* **1993**, *58*, 546–555.
[15] a) P. J. Crowley, M. R. Leach, O. Meth-Cohn, B. J. Wakefield, *Tetrahedron Lett.* **1986**, *27*, 2909–2912; b) W. Zarges, M. Marsch, K. Harms, G. Boche, *Angew. Chem.* **1989**, *101*, 1424–1425; *Angew. Chem. Int. Ed. Engl.* **1989**, *28*, 1392.
[16] P. K. Freeman, L. L. Hutchinson, *Tetrahedron Lett.* **1976**, 1849.
[17] a) N. J. R. van Eikema Hommes, F. Bickelhaupt, G. W. Klumpp, *Recl. Trav. Chim. Pays-Bas*, **1987**, *106*, 514–515; b) *Tetrahedron Lett.* **1988**, *29*, 5237–5240; c) *J. Chem. Soc. Chem. Commun.* **1991**, 438–440; d) C. P. Vlaar, G. W. Klumpp, *Tetrahedron Lett.* **1991**, *32*, 2951–2952.

"Noncoordinating" Anions, II**

By *Konrad Seppelt**

The existence of an anion that has no capacity for coordination in the condensed phase is as impossible as that of a free proton or a naked fluoride ion. However, in the same way that it is possible in the two latter cases to achieve approximate states in which the chemical environment can be neglected, increasingly weaker coordinating anions can also be obtained.[1] This is a worthwhile goal: many compounds with elements with unusual bonding such as R_3Si^+, Fe(porphyrin)$^+$, and many kinds of coordinatively unsaturated metal ions could be prepared. Since cationic alkyl complexes of group 4 metals (Ti, Zr, Hf) function as single-component catalysts for olefin polymerization, these systems are also of great commercial interest.[2]

Each anion in solution competes with the solvent for coordination to the cation. Thus, an anion can, in certain systems, be classed as noncoordinating when it shows a weaker coordination than the solvent. However, the limiting cases of completely nonpolar solvents such as alkanes, perfluorinated alkanes, and even xenon show that we are still a long way from noncoordinating anions in these solvents. Furthermore, as long ago as 1975 complexes of the type $[M(CO)_5Xe]$ (M = Cr, Mo, W) with a dative Xe → M bond were detected.[3]

It is apparent that for a weakly coordinating anion the negative charge—apart from some special cases only singly charged anions are considered—should be distributed over a great number of ligand atoms. In addition, the peripheral atoms should be fluorine or hydrogen atoms, and not oxygen or chlorine atoms, which coordinate more strongly. The solubility of the salts containing weakly coordinating anions in nonpolar solvents is also an important prerequisite.

[*] Prof. Dr. K. Seppelt
Institut für Anorganische und Analytische Chemie der Freien Universität
Fabeckstrasse 34–36, D-14195 Berlin (FRG)
Telefax: Int. code + (30)838-2424

[**] First "highlight" on this topic see ref. [1a]

A further prerequisite is the kinetic stability towards ligand abstraction: the moderately strong coordinating anions such as BF_4^-, PF_6^-, and SbF_6^- are unstable towards electrophilic attack and lose F^-. Finally, the anions should be stable towards oxidative attack. This precludes, for example, the C_{60}^- anion from further consideration, especially when its ability to coordinate to metals through the six-membered ring-six-membered ring double bonds is taken into account.

$B(C_6H_5)_4^-$ and related anions: Tetraarylborates as ligands were only recently the subject of a highlight,[1a] and so we can limit ourselves here to a short addition.

In the series $ClO_4^- > BF_4^- > PF_6^- > B(C_6H_5)_4^-$, the ability to coordinate decreases. The aromatic ring system of the phenyl groups remains as a coordination site of the $B(C_6H_5)_4^-$ ion, and this ring system is mainly coordinated in an η^6 fashion to metal atoms. Coordination through the C–H bonds of the phenyl rings has, however, not yet been observed. The strength of the π interaction of a phenyl ring of $B(C_6H_5)_4^-$ with metals is similar to that of a neutral benzene ligand, if the metal–C bond lengths are regarded as a standard.[4] Since C_6F_6 is a far worse complex ligand than C_6H_6, $B(C_6F_5)_4^-$ or substituted and partially fluorinated tetraphenylborates have also been used. Salts of these anions are particularly soluble,[5] and so far no π-phenyl–metal interaction has been proven. A typical example is $[Zr\text{-}Cp_2^*R]^+[B(C_6F_5)_4]^-$ (R = alkyl, Cp* = η^5-C_5Me_5), which is stable towards aryl group transfer.[6] A recent example that shows the differing coordination abilities of phenyl and pentafluorophenyl groups is the ionic complex **1**.[7] The crystal structure analysis of **1** shows that only the benzyl group

$[Zr(CH_2C_6H_5)_3]^+[B(CH_2C_6H_5)(C_6F_5)_3]^-$ **1**

and not the C_6F_5 group functions as a η^6 ligand. The zirconium atom is bound to two benzyl ligands η^1, one η^2, and

 © VCH Verlagsgesellschaft mbH, D-69451 Weinheim, 1993 0570-0833/93/0707-1025 $ 10.00+.25/0

one η^6. Nevertheless, the preparation of triorgano-substituted silyl cations R_3Si^+ is not achieved with the $[B\{C_6H_3\text{-}3,5\text{-}(CF_3)_2\}_4]^-$ anion, because cations of the type $R_2(CH_3)SiOR'^+_2$ ($R = CH_3$, C_6H_5, C_4H_3S; $R' = C_2H_5$) are formed by addition of the ether solvent.[8] The current state of the debate regarding the existence or nonexistence of silyl cations has recently been summarized.[9] The substitution of the dimeric catecholate anion in $[Cp^*_2SiH]^+[C_6H_4O_2H_3O_2C_6H_4]^-$ by an extremely noncoordinating anion may help to obtain the postulated silyl cation[10] in crystalline form.

$CB_{11}H^-_{12}$: Starting from the BH^-_4 anion, which coordinates in many ways, one can proceed mentally by enlargement of this anion to polyhedral boranes and carboranes, of which the $CB_{11}H^-_{12}$ is weakly coordinating. The most hydridic hydrogen substituent H(12), that is the one opposite the C atom, forms metal$\cdots$H–B bridges,[11] as in $[FeCp(CO)_2]^+[HB_{11}CH_{11}]^-$. The ionic iron porphyrin complex **2**

$[Fe(tpp)]^+[CB_{11}H_{12}]^-$ **2**

(tpp = tetraphenylporphyrin) shows the hitherto weakest interaction between an iron porphyrin cation and any anion, the shortest Fe–N distances, and the smallest shift of the iron atom from the porphyrin plane[12, 13] (Fig. 1). Thus, one is already very close to a square planar surrounded Fe^{3+} ion in $Fe(tpp)^+$.

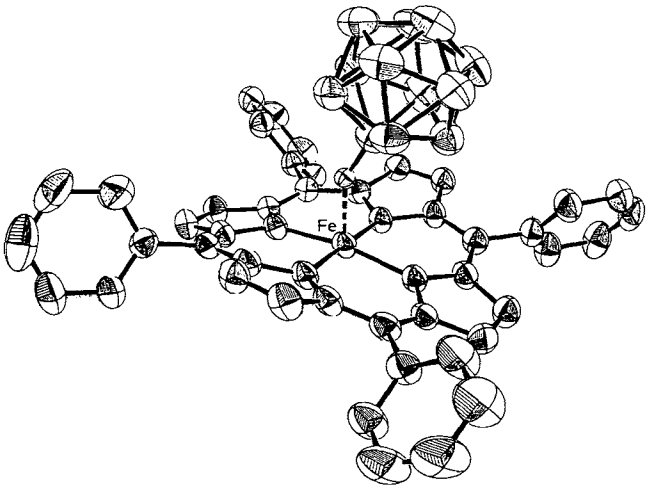

Fig. 1. Crystal structure of **2** [10]. The Fe–H distance is 182(4) pm.

$Nb(OTeF_5)^-_6$ and related anions: If the F^- anion is mentally enlarged to the $OTeF^-_5$ anion, the ability to coordinate is lost to a large degree, whereas the ability to stabilize high oxidation states ($\approx$electronegativity) is retained to a great extent.[14] $OTeF^-_5$ shows a coordinating effect through the oxygen atom. This is the reason why it is inferior to the isoelectronic SbF^-_6 ion and its homologues. Nevertheless, $Ag^+OTeF^-_5$, for example, is very soluble in CH_2Cl_2, in contrast to $Ag^+SbF^-_6$ and $Ag^+BF^-_4$.[15] Since, the $OTeF_5$ group has only one strong donor atom, the metal complexes remain coordinatively unsaturated. $Ag^+OTeF^-_5$ coordinates to, among other weak ligands, CH_2Cl_2 and carbon monoxide![16]

To further enhance these remarkable properties, complex anions of the type $A(OTeF_5)^{m-}_n$ with $m = 1$, 2, and $n = 4$, 6 were constructed. A can be varied in many ways, and the anions are prepared readily by metathesis reactions. $B(OTeF_5)^-_4$ is clearly unstable and readily loses an $OTeF^-_5$ group; however, with its help a dicarbonyl silver complex, the cation of **3**, was prepared for the first time. The spectro-

$[Ag(CO)_2]^+[B(OTeF_5)_4]^-$ **3**

scopic and structural investigation of this complex confirmed the principal weakness of the Ag–CO bond (Fig. 2).

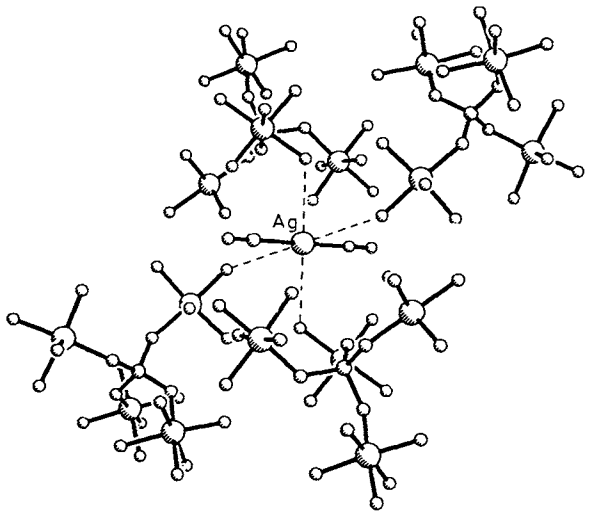

Fig. 2. The coordination sphere of the silver atom in **3** [17]. The Ag$\cdots$F distances to the nearest F atoms of the $OTeF_5$ group are 296(1) and 309(2) pm. Only the weakness of this coordination enables the existence of the carbonyl complexes.

Here, the principle can be explained: the hitherto unknown $[Ag(CO)_2]^+$ cation is formed, despite the weakness of the Ag–CO bond, because the coordination of Ag^+ by the anion is even weaker.[17] $Ti(OTeF_5)^{2-}_6$ and $Nb(OTeF_5)^-_6$ are known,[18, 19] and are particularly weakly coordinating anions.[20] They are extremely stable towards oxidation, towards the loss of a $OTeF^-_5$ group ($^{18}OTeF^-_5$ is not incorporated in $Nb(OTeF_5)^-_6$ in the presence of Ag^+), and like all anions that contain $OTeF^-_5$, these large anions are very stable towards loss of F^-.

$Ag^+_2Ti(OTeF_6)^{2-}_6$ is highly soluble in $C_2Cl_3F_3$ and CH_2Cl_2, and in the latter solvent it is so soluble that the quantitative determination of the solubility is difficult. It crystallizes as $[Ag^+(CH_2Cl_2)_3]_2Ti(OTeF_5)^{2-}_6$ with only two very weak Te–F$\cdots$Ag contacts, each of which is over 300 pm in length.[20] A great deal will probably be heard in the future about compounds with $Ti(OTeF_5)^{2-}_6$ and $Nb(OTeF_5)^-_6$ anions.

Outlook: Many other weakly coordinating anions have been investigated,[1b] for example heteropolyanions such as $PW_{12}O^{3-}_{40}$. So far, however, each of the given systems has its weaknesses. The use of fluorine in the outer sphere of ideally, large spherical anions is sufficient for solvents such as CH_2Cl_2 and chlorofluoro hydrocarbons. In hydrocarbons the weak ability of the fluorine atoms to coordinate will

probably be noticeable, and finally all fluoro compounds are thermodynamically unstable towards Lewis acids such as Fe^{3+}. Thus, the ideal noncoordinating anion should have a spherical hydrocarbon surface and carry the negative charge in the interior; here again a certain oxidation sensitivity will also play a role.

That the preparation of weakly coordinating anions has achieved unexpected significance is exemplified by the fact that the lithium salt of $HC(SO_2CF_3)_3$[21] is used in rechargeable lithium batteries, because it is particularly soluble in ethers and has a high ionic conductivity, and is extremely stable to oxidation.[22] This development could revolutionize present battery technology.

German version: *Angew. Chem.* **1993**, *105*, 1074

[1] a) M. Bochmann, *Angew. Chem.* **1992**, *104*, 1206-1207; *Angew. Chem. Int. Ed. Engl.* **1992**, *31*, 1181-1182. b) Review about weakly coordinating anions: S. H. Strauss, *Chem. Rev.* **1993**, *93*, 927-942.

[2] W. Kaminsky, H. Sinn, *Transition Metals and Organometallics as Catalysts for Olefin Polymerisation*, Springer, New York, **1988**.

[3] R. N. Perutz, J. J. Turner, *J. Am. Chem. Soc.* **1975**, *97*, 4791-4800.

[4] C. J. Krüger, A. L. Du Preez, R. J. Haines, *J. Chem. Soc. Dalton Trans.* **1974**, 1302-1305.

[5] M. Brookhart, S. Sabo-Etienne, *J. Am. Chem. Soc.* **1991**, *113*, 2777-2779.

[6] G. G. Hlatky, *Abstr. 204th Am. Chem. Soc. Nat. Meet.* Washington D.C. **1992**, INOR 387.

[7] C. Pellecchia, A. Grassi, A. Imminzi, *J. Am. Chem. Soc.* **1993**, *115*, 1160-1162.

[8] M. Kira, T. Hino, H. Sakurai, *J. Am. Chem. Soc.* **1992**, *114*, 6697-6700.

[9] P. D. Lickiss, *J. Chem. Soc. Dalton Trans.* **1992**, 1333-1338.

[10] P. Jutzi, E.-A. Bunte, *Angew. Chem.* **1992**, *104*, 1636-1638; *Angew.Chem. Int. Ed. Engl.* **1992**, *31*, 1605-1607. For very recent work on silyl cations with weakly coordinating anions: J. B. Lambert, S. Zhang, *J. Chem. Soc. Chem. Commun.* **1993**, 383-384; Z. Xie, D. J. Liston, T. Jelinek, V. Mitro, R. Bau, C. A. Reed, *ibid.* **1993**, 384-386.

[11] D. J. Liston, Y. J. Lee, W. R. Scheidt, C. A. Reed, *J. Am. Chem. Soc.* **1989**, *111*, 6643-6648.

[12] C. P. Gupta, G. Lang, Y. J. Lee, W. R. Scheidt, K. Shelly, C. A. Reed, *Inorg. Chem.* **1987**, *26*, 3022-3030.

[13] K. Shelly, C. A. Reed, Y. J. Lee, W. R. Scheidt, *J. Am. Chem. Soc.* **1986**, *108*, 3117-3118.

[14] K. Seppelt, *Angew. Chem.* **1982**, *94*, 890-901; *Angew. Chem. Int. Ed. Engl.* **1982**, *21*, 877-888.

[15] M. R. Colsman, T. D. Newbound, L. J. Marshall, M. D. Noirot, M. M. Miller, G. P. Wulfsberg, J. S. Frye, O. P. Anderson, S. H. Strauss, *J. Am. Chem. Soc.* **1990**, *112*, 2349-2362.

[16] P. K. Hurlburt, O. P. Anderson, S. H. Strauss, *J. Am. Chem. Soc.* **1991**, *113*, 6277-6280.

[17] P. K. Hurlburt, J. J. Rack, S. F. Dec, O. P. Anderson, S. H. Strauss, *Inorg. Chem.* **1993**, *32*, 373-374.

[18] K. Schröder, F. Sladky, *Chem. Ber.* **1980**, *113*, 1414-1419.

[19] K. Moock, K. Seppelt, *Z. Anorg. Allg. Chem.* **1988**, *561*, 132-138.

[20] D. M. van Seggen, P. K. Hurlburt, O. P. Anderson, S. H. Strauss, *J. Am. Chem. Soc.* **1992**, *114*, 10995-10997.

[21] L. Turowsky, K. Seppelt, *Inorg. Chem.* **1988**, *27*, 2135-2137.

[22] L. A. Dominey, WO-B 92/02966, USA 91/05262, **1992**; L. A. Dominey, T. J. Blakley, V. R. Koch, *Proc. Intersoc. Energy Convers. Eng. Conf.* **1990**, *25*, 382-384; *Chem. Abstr.* **1991**, *114*, 105617g.

Biologically Active Linear Metabolites of Arachidonic Acid—The First Endogenous Ligand of the Cannabinoid Receptor

By *Wolf D. Lehmann** and *Gerhard Fürstenberger*

The cell membrane is an important site for storage of multiply unsaturated fatty acids. There, these particularly sensitive fatty acids are protected from radical-induced autoxidation by membrane antioxidants such as vitamin E. In addition, membrane fatty acids are esterified and therefore cannot be attacked by cellular enzymes such as lipoxygenases and prostaglandin H synthases, which preferentially accept free fatty acids as substrates. The most abundant multiply unsaturated fatty acids in nonmarine mammals are linoleic acid (9,12-octadecadienoic acid) and arachidonic acid (5,8,11,14-eicosatetraenoic acid) with two and four nonconjugated *cis* double bonds, respectively. As an example, the arachidonyl group is the preferred substituent at the C2 position of glycerol in phosphatidylcholine, an important membrane phospholipid. In unstimulated cells, cytosolic arachidonic acid occurs at a concentration on the order of 0.1 μM, a concentration below the typical K_m values of the main arachidonic acid metabolizing enzymes. Therefore, the release of arachidonic acid from the membrane pool of esterifed fatty acids by activation of phospholipase A_2, C, or D alone or in combination with diacylglycerol lipase or kinase is a key event in the regulation of all metabolic pathways of arachidonic acid. The pathways of archidonic acid release are displayed in the upper half of Figure 1.

[*] Priv.-Doz. Dr. W. D. Lehmann, Dr. G. Fürstenberger
Deutsches Krebsforschungszentrum
Im Neuenheimer Feld 280, D-69120 Heidelberg (FRG)
Telefax: Int. code + (6221)49461

Released free arachidonic acid is either reesterified or effectively metabolized into biologically active metabolites. *Cyclic metabolites* (prostaglandins, prostacyclines, thromboxanes) are generated by attack from a prostaglandin H synthase. The structure and function of these metabolites have been extensively studied since the early 1960s. Interest in the linear metabolic pathway of arachidonic acid was initiated by the discovery of mammalian lipoxygenases and their *linear metabolites* (HETEs, diHETEs, lipoxins, leukotrienes A_4 and B_4) as well as their *linear-branched metabolites* (cysteinyl leukotrienes). Since the early 1970s this area of arachidonic acid metabolism has been extensively investigated.[1] Linear metabolites may also be formed by attack of cytochrome P450 monooxygenase.

So far linear metabolites of arachidonic acid have been predominantly found in cells of the hematopoietic system and of the immune system. Recently, a new linear metabolite of arachidonic acid was isolated from brain and identified as an endogenous ligand of the cannabinoid receptor.[2] We will discuss this work here and describe some new linear metabolites of arachidonic acid with distinct biological activity. These arachidonic acid metabolites and the routes of their formation are given in the lower part of Figure 1.

Chemotaxis by 20-hydroxyleukotriene B_4: Leukotriene B_4 (LTB_4), (5*S*,12*R*)-dihydroxy-(6*Z*,8*E*,10*E*,14*Z*)-eicosatetraenoic acid, is strongly chemotactic for polymorphonuclear leukocytes (neutrophils), the typical defense cells of the immune system. The liver is the main catabolic site for

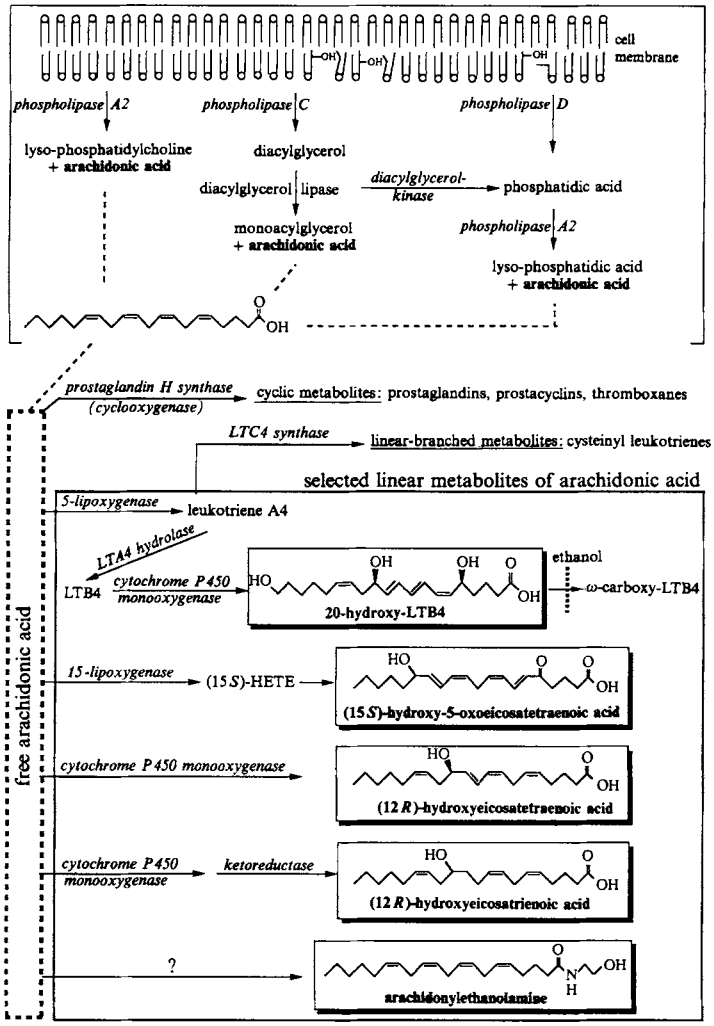

Fig. 1. Formation of free arachidonic acid from the membrane pool of esterified fatty acids and the metabolic pathways leading to the linear arachidonic acid metabolites discussed.

leukotrienes produced systemically, including leukotriene B_4. These are rapidly taken up by liver cells and catabolized by peroxisomal β-oxidation from the ω end. A characteristic feature of fibrotic and cirrhotic liver degeneration is the infiltration of leukocytes, and it is assumed that production of neutrophil-chemotactic metabolites by the liver promotes liver degeneration. One approach to understanding the role of ethanol in this complex pathogenesis is by investigation of the pathways of arachidonic acid metabolism in hepatocytes in vitro with and without the presence of ethanol. By using this approach it was recently shown that ethanol blocks the microsomal β-oxidation of LTB_4 from the ω end at the stage of ω-hydroxy-LTB_4.[3, 4] This intermediate in LTB_4 catabolism is observed only in the presence of ethanol and is an LTB_4 metabolite in which the chemotactic activity is retained. In the absence of ethanol, LTB_4 is rapidly metabolized to ω-carboxy-LTB_4, a chemotactically inactive metabolite. Another biological effect of ethanol that has been observed in the rat is the enhanced synthesis of LTB_4 in the mucus membranes of stomach and colon. Therefore, one factor in the pathogenetic mechanism of acute ethanol-induced hepatitis might be the enhanced systemic production of LTB_4 in combination with the blockage of the peroxisomal inactivation of LTB_4 in the liver.

Chemotaxis by 15-hydroxy-5-oxoeicosatetraenoic acid: A new metabolite with a pronounced chemotactic effect specific for eosinophils was observed following incubation of human peripheral eosinophils with arachidonic acid.[5] This lipid metabolite was identified as 15-hydroxy-5-oxo-6,8,11,13-eicosatetraenoic acid.[6] Moreover, this metabolite could be generated in vitro by incubation of arachidonic acid with soya lipoxygenase (a lipoxygenase with (15*S*)-specificity) in the presence of the heme protein cytochrome c. These investigations showed that in the presence of arachidonic acid, eosinophils can produce a self-specific chemotactic factor.

Chemotaxis and angiogenesis by (12R)-hydroxyeicosatetraenoic acid: By incubating bovine cornea microsomes with arachidonic acid, two new biologically active arachidonic acid metabolites were found.[7] Both metabolites are formed by a cytochrome P450 catalyzed reaction, as was shown by the use of specific inhibitors and by the observation that the formation of these metabolites was NADPH-dependent. The minor metabolite was identified as (12*R*)-hydroxy-(5*Z*,8*Z*,14*Z*)-eicosatrienoic acid [(12*R*)-HETrE].[8] Insight into the mechanism of formation of this metabolite was obtained by using deuterium-labeled arachidonic acid as substrate. Based on these experiments it was proposed that (12*R*)-HETrE is formed via a 12-oxo intermediate which is stereospecifically reduced to the (12*R*)-hydroxy metabolite by a ketoreductase. (12*R*)- and 12(*S*)-HETErE were prepared synthetically and their biological activity was tested separately in vivo in the rabbit eye.[8, 9] Application of 10 ng of the (12*R*) enantiomer caused a strong increase in the protein concentration of the aqueous humor indicating an impairment of the blood–aqueous barrier. Application of the same amount of the (12*S*) enantiomer had no effect. Additional biological effects in the rabbit eye exclusively observed for the physiologic (12*R*) enantiomer and not for the (12*S*) enantiomer were local vasodilation, leukocyte-specific chemotaxis, and angiogenesis (formation of new blood vessels). With a much higher dose of (12*S*)-HETrE, similar in vivo effects could be elicited, but it was suspected that this was actually caused by the contamination of 1–2% (*R*) enantiomer in the applied (12*S*)-HETrE. The effects observed after the application of small amounts of (12*R*)-HETrE are typical for the events observed following injury of the corneal epithelium. Therefore, these investigations support the hypothesis that (12*R*)-HETrE may be a physiologically important mediator of these processes.

Inhibition of an ion transport system by (12R)-hydroxyeicosatetraenoic acid: The main metabolite observed after incubation of corneal microsomes with arachidonic acid was identified as 12-hydroxyeicosatetraenoic acid (12-HETE). In the investigation of the biological effects of this metabolite, a pronounced inhibitory effect on bovine corneal (Na^+/K^+)ATPase was found. This ion transport system is widely distributed in cells and is responsible for maintaining the sodium and potassium concentration gradient across the cell membrane and for the transport of chloride ions out of the cell. These processes are directly connected with the formation of the membrane potential. (Na^+/K^+)ATPase in corneal epithelium probably has additional specialized func-

tions in maintaining transparency. Comparison of the inhibitory potency of the isolated metabolite with pure (12*R*)- and (12*S*)-HETE of synthetic origin showed that only the (12*R*) enantiomer was active. On this basis, the isolated metabolite was identified as (12*R*)-HETE. The inhibitory potency of (12*R*)-HETE towards (Na^+/K^+)ATPase was observed in various other rat and bovine tissues besides corneal epithelium.[10] Thus, (12*R*)-HETE might be a physiological inhibitor of this important ion transport system.

Arachidonylethanolamine as endogenous ligand of the cannabinoid receptor: It is known that fatty acid amides are present in brain tissue. Recently, an amide of arachidonic acid—arachidonylethanolamine—was isolated from porcine brain as the first natural ligand of the cannabinoid receptor.[2] A large number of chromatographically purified fractions obtained from porcine brain were incubated with rat brain synaptosomes, in which the cannabinoid receptor was loaded with a tritium-labeled cannabinol derivative of very high affinity (HU-243, K_D: 45 pM). The ability of the purified brain fractions to replace the specific tritium-labeled ligand at the cannabinoid receptor of the synaptosomes was tested, and it was observed that many lipophilic fractions could liberate the ligand partially by a nonspecific "emulgatory effect". Nevertheless, a compound with a specific affinity towards the cannabinoid receptor was also identified in this way. From 4.5 kg of porcine brain, 600 μg of this compound was isolated and subsequently identified as arachidonylethanolamine by using spectroscopic methods.[2] In addition, the isolated compound was found to be identical to arachidonylethanolamine of synthetic origin. The amino acid sequence of the rat[11] and human[12] cannabinoid receptor is known, and with this study the first endogenous ligand of the cannabinoid receptor could be identified. More than 20 other arachidonic acid metabolites have been tested for specific binding to the cannabinoid receptor, but all have yielded negative results up to now. The cannabinoid receptor plays a key role in the control of important biological functions such as the control of movement, nociception (the perception of pain), and emotional disposition.

The analytical and functional studies on linear arachidonic acid metabolites as described above highlight the important biological role of these fatty acid metabolites in spite of their relatively simple structural characteristics. Among these functions appear to be the regulation of elementary biological processes such as the immune response, the maintainance of membrane potential, and receptor-mediated signal transduction.

German version: *Angew. Chem.* **1993**, *105*, 1076.

[1] B. Samuelsson, *Angew. Chem.* **1983**, *95*, 854; *Angew. Chem. Int. Ed. Engl.* **1983**, *22*, 805; K. C. Nicolaou, J. Y. Ramphal, N. A. Petasis, C. N. Serhan, *ibid.* **1991**, *103*, 1119 and **1991**, *30*, 1100.
[2] D. A. Devane, L.Hanus, A. Breuer, R. G. Pertwee, L. A. Stevenson, G. Griffin, D. Gibson, A. Mandelbaum, A. Etinger, R. Mechoulam, *Science* **1992**, *258*, 1946.
[3] T. Baumert, M. Huber, D. Mayer, D. Keppler, *Eur. J. Biochem.* **1989**, *182*, 223.
[4] M. A. Shirley, C. T. Reidhead, R. C. Murphy, *Biochem. Biophys. Res. Commun.* **1992**, *185*, 604.
[5] E. Morita, J.-M. Schröder, E. Christophers, *J. Immunol.* **1990**, *44*, 1893.
[6] U. Schwenk, E. Morita, R. Engel, J.-M. Schröder, *J. Biol. Chem.* **1992**, *267*, 12482.
[7] M. L. Schwartzman, M. Balazy, J. Masferrer, N. G. Abraham, J. C. McGiff, R. C. Murphy, *Proc. Natl. Acad. Sci. USA* **1987**, *84*, 8125.
[8] R. C. Murphy, J. R. Falck, S. Lumin, P. Yadagiri, J. A. Zirrolli, M. Balazy, J. L. Masferrer, N. G. Abraham, M. L. Schwartzman, *J. Biol. Chem.* **1988**, *263*, 17197.
[9] J. L. Masferrer, J. A. Rimarachin, M. E. Gerritsen, J. R. Falck, P. Yadagiri, M. W. Dunn, M. L. Schwartzman, *Exp. Eye Res.* **1991**, *52*, 417.
[10] J. L. Masferrer, A. P. Rios, M. L. Schwartzman, *Biochem. Pharmacol.* **1990**, *39*, 1971.
[11] L. A. Matsuda, S. J. Lolait, M. J. Brownstein, A. C. Young, T. I. Bonner, *Nature* **1990**, *346*, 561.
[12] C. M. Gerard, C. Mollereau, G. Vassart, M. Parmentier, *Biochem. J.* **1991**, *279*, 129.

 © *VCH Verlagsgesellschaft mbH, D-69451 Weinheim, 1993* *0570-0833/93/0707-1029 $ 10.00+.25/0*

Concerning "An Evaluation of the Peer Review Process at *Angewandte Chemie*"

By *Paul F. Ross**

Research leading to improved practices in peer review in the sciences is badly needed. Daniel's work ("An evaluation of the peer review process at *Angewandte Chemie*"[1]) can contribute to understanding influences on decisions. My work[2] and the demonstration by Peters and Ceci[3] showing that current practices are seriously deficient are a decade old; yet few studies have been stimulated by our work. Daniel's work and *Angewandte Chemie*'s willingness to be examined are welcome.

Daniel's work addresses the validity, reliability, and biases of decisions and follows up on rejected work using a single sample of manuscripts, an approach essential to understanding outcomes of decisions by reviewers and editors. However, as presented, Daniel's work ascribes to scientific value outcomes that are actually caused by circumstances unrelated to scientific content. 1) Daniel's work assumes works published in German only have the same opportunity to be cited as works published in both German and English. That is like expecting the same monthly sales total for a $ 200 fashion item available only in Berlin and an equally fashionable $ 200 item available in both Berlin and New York. 2) Daniel's work assumes that the visibility of the journal in which an item appears has no influence on whether the item is cited. No executive deciding where to publish an advertisement would accept that premise. 3) Daniel's work assumes that the author's reputation, and the reputation of the author's employer, have no effect on the editor's decision to publish and 4) no effect on the citing author's decision to cite. Research shows otherwise (e.g., Peters and Ceci[3]). 5) Daniel's work counts citations for items published in *Angewandte Chemie* over a somewhat longer time period than for items rejected by *Angewandte Chemie* and published elsewhere, exaggerating the observed differences (see Daniel's Figure 1). Daniel's data need to be reexamined, controlling for these and other influences using the statistical method of factor analysis.

For these reasons, I strongly suspect Daniel's conclusion that the 1984 editorial decisions at *Angewandte Chemie* accepted for publication the manuscripts of highest value to scientists from among those it received is an incorrect conclusion.

[*] Dr. Paul F. Ross
Industrial and Organizational Psychologist
The Ross Company
Todd Pond
Lincoln, MA 01773 (USA)

[1] H. D. Daniel, *Angew. Chem.* **1993**, *105*, 247–251; *Angew. Chem. Int. Ed. Engl.* **1993**, *32*, 234–238.
[2] P. F. Ross, unpublished manuscript "The sciences' self-management: Manuscript refereeing, peer review, and goals in Science", **1980**.
[3] D. Peters, S. Ceci, *Behav. and Brain Sci.* **1982**, *5*, 187–195, 246–255.

Reply:

By *Hans-Dieter Daniel**

In his letter to the editor of *Angewandte Chemie* Ross[1] argues that my work[2] on the peer review process fails to control for the language in which the work was published, the visibility of the journal, the author's reputation, and the reputation of the author's employer, and that citations were not counted for equal-length post-publication periods for accepted and rejected-and-published-elsewhere communications.

To start with his last point: the analyses of covariance carried out to test for publication bias and validity of editorial decisions of course took into account the delay period from time of rejection by *Angewandte Chemie* to publication in another journal. The mean citation rates for accepted and rejected-but-published-elsewhere communications were compared, with number of months since publication of the manuscript held constant. It was not necessary to test for bias related to language in which the work was published, since very few of the rejected manuscripts subsequently published elsewhere appeared in German (cf. Table 4 in [2]). Prestige ratings of scientists, departments, and universities are very popular, and are published regularly in the United States. Unfortunately, there has been so far no analogous prestige rankings for most of the 21 different countries from which *Angewandte Chemie* received manuscripts during 1984. Therefore, it is not possible to test for bias related to prestige of author or employer. Moreover, how should one test the provocative thesis that the same paper published in *Angewandte Chemie* and in another journal will be cited more times from *Angewandte Chemie* than from the other journal?

To control for bias variables, Ross proposes a factor analysis with dummy variables. Factor analysis, however, as-

[*] Priv.-Doz. Dr. H.-D. Daniel
Das Rektorat der Universität
Postfach 103462, D-68131 Mannheim (FRG)

sumes interval levels of measurement. A factor analysis with mutually exclusive (i.e., orthogonal) dummy variables [e.g., paper about organometallic chemistry (1) or not (0), paper about physical organic chemistry (1) or not (0), etc.] does not make sense at all. Furthermore, it is unreasonable to expect that factor analysis will produce from a set of data unambiguous, self-evident insights into the validity of referees' recommendations or editor's decision. Factor analysis, in practice, remains highly subjective, as do several other multivariate data analysis techniques.

To provide the reader with more insight into the nature of the data upon which my conclusions on the reliability, fairness, and validity of the peer review process are based, a more detailed version of my study[3] will contain synoptic presentations of four sets of (anonymous) reviewer comments and recommendations, together with the corresponding observations of the editor. The four sets of data are derived from manuscripts differentiated as follows: accepted communications that were later subject to frequent citation, accepted communications that did not lead to citations, rejected communications published elsewhere and then cited relatively frequently, and rejected communications published elsewhere but not subject to citation. These synopses should lead to a clearer picture of the typical reactions of referees and editors.

[1] P. F. Ross, *Angew. Chem.* **1993**, *105*, 1079; *Angew. Chem. Int. Ed. Engl.* **1993**, *32*, Nr. 7.
[2] H.-D. Daniel, *Angew. Chem.* **1993**, *105*, 247–251; *Angew. Chem. Int. Ed. Engl.* **1993**, *32*, 234–238.
[3] H.-D. Daniel in *Guardians of Science*, VCH, Weinheim, **1993**, in press.

Communications may be submitted in English *or* in German. Further details regarding the submission of communications can be found in the "Notice to Authors" reproduced in the January issue of the journal. Copies thereof may be obtained from the editorial office upon request.

1-Chloro-2,2-bis(4-chlorophenyl)-1-lithioethene·TMEDA·2THF: Structure of a Li-Cl Carbenoid**

By *Gernot Boche,* Michael Marsch, Achim Müller,* and *Klaus Harms*

Dedicated to Professor Heinrich Nöth on the occasion of his 65th birthday

Carbenoids are exceptional compounds, because they react not only with electrophiles E–Y, as is usual for "anions", but also with nucleophiles such as RLi, eliminate M–X with the formation of carbenes, and—as in the present case of an aryl-substituted alkylidenecarbenoid—undergo the Fritsch–Buttenberg–Wiechell rearrangement to form alkynes (Scheme 1).[1]

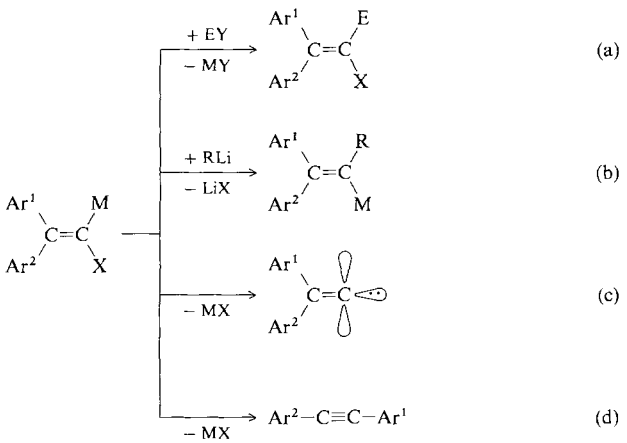

Scheme 1. Reactions of aryl-substituted alkylidene carbenoids: a) reaction with electrophiles EY, b) reaction with nucleophiles RLi, c) α-elimination of MX, d) Fritsch–Buttenberg–Wiechell rearrangement. M = Li, Na, K, MgX; X = F, Cl, Br, I; Y = leaving group; Ar = aryl residue.

What are the structural prerequisites for reactions (b)–(d) in particular? Since carbenoids are thermally labile above about −60 °C, these compounds were previously studied mainly at low temperature by ^{13}C NMR spectroscopy (D. Seebach et al.[2]), or their structure was calculated (P. von R. Schleyer et al.[3]). We crystallized 1-chloro-2,2-bis(4-chlorophenyl)-1-lithioethene (**1**) in the presence of tetrahydrofuran (THF) and tetramethylethylenediamine (TMEDA) at −78 °C as **1**·TMEDA·2THF and determined its crystal structure at −115 °C. It is the first of the lithium halogen carbenoids[4] (Fig. 1).

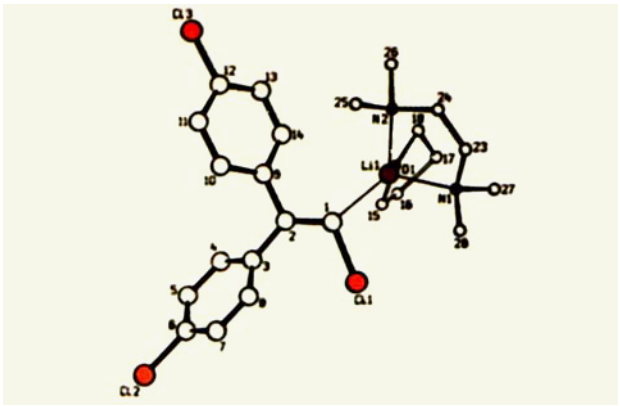

Fig. 1. Crystal structure of **1**·TMEDA·2THF without the second THF molecule, which is situated on a free lattice position and is not bound to the Li1 atom [5]. The carbon atoms are indicated by numbers only. Selected bond lengths [pm] and angles [°]: C1-Cl1 185.5(7), C1-Li1 214.5(14), C1-C2 134.4(10), Li1-O1 196.5(14), Li1-N1 213(2), Li1-N2 215.8(15); Cl1-C1-C2 112.6(5); Li1-C1-C2 137.1(6), Li1-C1-Cl1 108.7(5), C1-C2-C3 129.5(6), C1-C2-C9 116.5(6), C3-C2-C9 114.0(6); Cl1-C1-C2-C3 3(1), Cl1-C1-C2-C9 −175.7(5), C1-C2-C3-C8 57(1), C1-C2-C9-C14 39(1).

At first the distinctly extended C1–Cl1 bond in **1** (12 pm longer than that in the nonlithiated vinyl chlorides) is conspicuous: whereas the mean of 63 vinylic C_{sp^2}–Cl bond lengths lies at 172.9 pm,[9] the C1–Cl1 bond is 185.5(7) pm long. This bond lengthening distinguishes carbenoids from normal acceptor-substituted Li compounds in which the bond of the anionic C atom to the acceptor substituents (e.g., C(O)R, CN, SO_2R, SOR, SR, etc.) is always shortened.[10, 11] However, the elongation is consistent with the conclusions from ^{13}C NMR spectra of LiX carbenoids (X = halogen),[2] calculations on LiX or LiOR carbenoids,[3, 4] and crystal structure data of LiOR carbenoids.[4] The extended C1–Cl1 bond in **1**·TMEDA·2THF[12] is also consistent with the strikingly easy (−90 °C!) nucleophilic substitution of the alkylidenecarbenoid **2** by *tert*-butyllithium that yields **3** (Scheme 2), or after treatment of **3** with CH_3OD the corresponding deuterated compound (H. M. Walborsky et al.).[13]

Also remarkable are the bond angles at C1 and C2 of **1**·TMEDA·2THF. At the carbenoid C1 atom the Cl1-C1-C2 angle of 112.6(5)° is smaller than the 120° angle of a

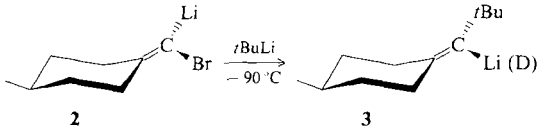

2 **3**

Scheme 2. Stereochemistry of the reaction of the carbenoid **2** with *t*BuLi in Et_2O or THF. If **3** is treated with CH_3OD, the Li atom is exchanged for a deuterium atom (D).

[*] Prof. Dr. G. Boche, M. Marsch, Dipl.-Chem. A. Müller, Dr. K. Harms
Fachbereich Chemie der Universität
Hans-Meerwein-Strasse, D-35032 Marburg (FRG)

[**] This work was supported by the the Deutsche Forschungsgemeinschaft (SFB 260) and the Fonds der Chemischen Industrie.

sp^2-hybridized C atom, while the Li1-C1-C2 angle of 137.1(6)° is much larger. This finding is consistent with an α elimination of LiCl from **1**·TMEDA·2THF to form the corresponding singlet vinylidene,[14] in which the C1-Cl1 bond develops into the empty p orbital and the C1–Li1 bond into the sp orbital filled with two electrons on the carbene C1 atom (see Scheme 1, reaction (c)). The bond angles at C1 also explain the inversion[13] observed for the reaction **2** → **3**: as in **1**·TMEDA·2THF, the side opposite to the leaving group Br^- in the carbenoid **2** should be particularly accessible for the nucleophile *t*BuLi.

For the Fritsch–Buttenberg–Wiechell rearrangement in which it is always the aryl group *trans* to the leaving group X that migrates[15] (see Scheme 1, reaction (d)), the bond angles at the C2 atom are also significant. The chloro-substituted phenyl ring *trans* to the chlorine atom bends slightly towards the C1 atom to which this phenyl ring binds after LiCl elimination (C1–C2–C9 116.5(6)°), while the *cis* Cl-substituted phenyl ring tilts away from the C1 atom (C1–C2–C3 129.5(6)°).

According to calculations the most stable structure of a *nonsolvated* carbenoid is that in which the C–X bond is bridged by the Li atom.[3] This is in accord with formulations that propose easier rupture for the C–X bond when the Li atom assists by "pulling" at X.[1b, 13] As Figure 1 shows, the C1–Cl1 bond in **1**·TMEDA·2THF is, however, not bridged by the Li atom (Cl1–Li1 325.4(9) pm), probably because the Li1 atom is solvated by TMEDA and THF, which agrees with the long-known fact that carbenoids are more stable in THF than in diethyl ether. This stability is attributed to the better solvation of lithium by THF (G. Köbrich[1b]).

Experimental Procedure

1-Chloro-2,2-bis(4-chlorophenyl)ethene (150 mg, 0.53 mmol) was dissolved in a mixture of THF (1.65 mL), diethyl ether (1.1 mL), and *n*-hexane (0.55 mL) to which TMEDA (157 mg, 1.35 mmol) had been added. After cooling to −78 °C, deprotonation with *n*BuLi (0.36 mL, 0.58 mmol) in *n*-hexane ($c = 1.6$ mol L^{-1}) within 30 min with constant shaking formed an orange solution, from which after 10 days at −78 °C colorless crystals suitable for X-ray crystal analysis precipitated. Yield: 113 mg, 39%. The single crystal was mounted on a glass fiber with silicon grease in a stream of cold nitrogen (−90 °C), according to the method of M. Veith and H. Bärninghausen [16b] modified by E. Hahn [16a].

Received: December 22, 1992 [Z 5767 IE]
German version: *Angew. Chem.* **1993**, *105*, 1081

[1] The term carbenoid was coined by G. L. Closs, R. A. Moss, *J. Am. Chem. Soc.* **1964**, *86*, 4042–4053; reviews: a) W. Kirmse, *Angew. Chem.* **1965**, *77*, 1–10; *Angew. Chem. Int. Ed. Engl.* **1965**, *4*, 1; b) G. Köbrich, *ibid.* **1967**, *79*, 15–27 and **1967**, *6*, 41; c) G. Köbrich, *ibid.* **1972**, *84*, 557–596 and **1972**, *11*, 473; d) H. Siegel, *Top. Curr. Chem.* **1982**, *106*, 55–78.

[2] a) H. Siegel, K. Hiltbrunner, D. Seebach, *Angew. Chem.* **1979**, *91*, 845–846; *Angew. Chem. Int. Ed. Engl.* **1979**, *18*, 785; b) D. Seebach, H. Siegel, K. Müllen, K. Hiltbrunner, *ibid.* **1979**, *91*, 844–845 and **1979**, *18*, 784; c) D. Seebach, H. Siegel, J. Gabriel, R. Hässig, *Helv. Chim. Acta* **1980**, *63*, 2046–2053; d) D. Seebach, R. Hässig, J. Gabriel, *ibid.* **1983**, *66*, 308–337.

[3] a) T. Clark, P. von R. Schleyer, *J. Chem. Soc. Chem. Commun.* **1979**, 883–884; b) T. Clark, P. von R. Schleyer, *Tetrahedron Lett.* **1979**, 4963–4966; c) T. Clark, P. von R. Schleyer, *J. Am. Chem. Soc.* **1979**, *101*, 7747–7748, and references therein; d) P. von R. Schleyer, T. Clark, A. J. Kos, G. W. Spitznagel, C. Rohde, D. Arad, K. N. Houk, N. G. Rondan, *ibid.* **1984**, *106*, 6467–6475, and references therein. See also B. Wang, C. Deng, *Chem. Phys. Lett.* **1988**, *147*, 99–104 and B. Wang, C. Deng, L. Xu, T. Tao, *ibid.*, **1989**, *161*, 388–392.

[4] a) As we showed recently, α-oxygen-substituted organolithium compounds ("α-lithiated ethers") are also carbenoids ("LiOR carbenoids"). Accordingly, C–O bond elongation, reaction with nucleophiles RLi, and downfield shifts of the signal of the carbenoid ^{13}C atom are observed: a) G. Boche, A. Opel, M. Marsch, K. Harms, F. Haller, J. C. W. Lohrenz, C. Thümmler, W. Koch, *Chem. Ber.* **1992**, *125*, 2265–2273; b) G. Boche, F. Bosold, J. C. W. Lohrenz, A. Opel. P. Zulauf, in press.

[5] Crystallographic data for **1**·TMEDA·2THF ($C_{28}H_{40}LiN_2O_2Cl_3$, M = 549.9): monoclinic, space group $P2_1/n$, $a = 1273.4(6)$, $b = 1516.0(4)$, $c = 1654.0(6)$ pm, $\beta = 106.67(2)°$, $Z = 4$, $\rho_{calcd} = 1.194$ g cm^{-3}, $\mu(Cu_{K\alpha}) = 3.25$ cm^{-1}. Measurement of the crystal ($1 \times 0.3 \times 0.4$ mm) mounted at 183 K on a Siemens P4 diffractometer ($Mo_{K\alpha}$ radiation, $\lambda = 0.71069$ Å, graphite monochromator, $T = 158$ K); 6791 measured reflections of which 5360 are independent ($R_{int.} = 0.0590$), 2927 with $F > 4\sigma(F)$ were considered observed. Solution with direct methods, and refinement in the Siemens SHELTX-PLUS (VMS) program system, $R = 0.0919$, $wR = 0.0695$ ($w = 1/\sigma^2(F)$), all non-hydrogen atoms anisotropic, H atoms at calculated positions with the isotropic temperature factors of the groups to which they belong. The free THF molecule and the TMEDA ligand are certainly disordered (high temperature factors, unusual bond distances). Disordered models, however, led to a worsening of the R values and standard deviations. All calculations were performed on a Micro-VAX II and a VAX 6000-420 [6–8]. Further details of the crystal structure investigation may be obtained from the Fachinformationszentrum Karlsruhe, Gesellschaft für wissenschaftlich-technische Information mbH, D-76344 Eggenstein-Leopoldshafen (FRG) on quoting the depository number CSD-400037, the names of the authors, and the journal citation.

[6] SHELXTL-PLUS (VMS), Release 4.21, Siemens Analytical Instruments Inc., Madison, **1990**.

[7] A. L. Spek, PLATON 92; Program for Geometrical Analysis of Crystal Structures, Utrecht, **1992**.

[8] E. Keller, SCHAKAL-88B, A FORTRAN Program for the Graphic Representation of Molecular and Crystallographic Models, Freiburg, **1988**.

[9] F. H. Allen, O. Kennard, D. G. Watson, L. Brammer, A. G. Orpen, R. Taylor in *International Tables for Crystallography, Vol. C.* (Eds.: A. J. C. Wilson), Kluwer, Boston, **1992**, p. 696.

[10] D. Seebach, *Angew. Chem.* **1988**, *100*, 1685–1715; *Angew. Chem. Int. Ed. Engl.* **1988**, *27*, 1624.

[11] G. Boche, *Angew. Chem.* **1989**, *101*, 286–306; *Angew. Chem. Int. Ed. Engl.* **1989**, *28*, 277-297.

[12] In an (iodomethyl)zinc compound the C–I bond is not elongated: S. E. Denmark, J. P. Edwards, S. R. Wilson, *J. Am. Chem. Soc.* **1991**, *113*, 723–725.

[13] a) M. Duraisamy, H. M Walborsky, *J. Am. Chem. Soc.* **1984**, *106*, 5035–5037; b) M. Topolski, M. Duraisamy, J. Rachon, J. Gawronski, K. Gawronski, V. Goedken, H. M Walborsky, *J. Org. Chem.* **1993**, *58*, 546–555.

[14] a) P. J. Stang in *Carbene (Carbenoide), Methoden der Org. Chem. (Houben-Weyl), 4th Ed.* **1952–1989**, Band E 19b, Teilband 1, pp. 84–165; b) P. J. Stang, *Acc. Chem. Res.* **1982**, *15*, 348–354, and references therein; c) *Chem. Rev.* **1978**, *78*, 383–405, and references therein.

[15] a) A. A. Bothner-By, *J. Am. Chem. Soc.* **1955**, *77*, 3293–3296; b) D. Y. Curtin, E. W. Flynn, R. F. Nystrom, *ibid.* **1958**, *80*, 4599–4601; c) G. Köbrich, H. Trapp, *Chem. Ber.* **1966**, *99*, 680–688.

[16] a) E. Hahn, Freie Universität Berlin, personal communication; b) M. Veith, H. Bärninghausen, *Acta Crystallogr. Sect. B* **1974**, *30*, 1806–1813.

Formation of Molecular Strands by Hydrogen Bonds at the Gas–Water Interface: Molecular Recognition and Quantitative Hydrolysis of Barbituric Acid Lipids

By *Ramesh Ahuja, Pier-Lorenzo Caruso, Dietmar Möbius,* Wolfgang Paulus, Helmut Ringsdorf,** and *Gerald Wildburg*

Molecular recognition and organization are required for almost all processes at the cell membrane. Besides ionic and dipole–dipole interactions and steric effects, hydrogen bond formation plays a decisive role in molecular recognition and organization. In numerous studies these specific interactions have been examined in model systems, for example, with nucleolipids,[1], diaminotriazine lipids,[2] Kemp's acid,[3]

[*] Prof. Dr. D. Möbius, R. Ahuja, P.-L. Caruso
Max-Planck-Institut für Biophysikalische Chemie
Am Fassberg, W-37077 Göttingen-Nikolausberg (FRG)
Telefax: Int. code + (551)201466
Prof. Dr. H. Ringsdorf, W. Paulus, G. Wildburg
Institut für Organische Chemie der Universität
J.-J.-Becher-Weg 18–22, W-55128 Mainz (FRG)
Telefax: Int. code + (6131)39-3145

guanidinium lipids,[4] and amphiphilic azacrown compounds.[5] We report here on a model system, which in aqueous media forms molecular strands analogous to those described by Lehn et al.[6a] and Whitesides et al.[6b] in organic solvents by the formation of intermolecular hydrogen bonds. This model system undergoes a recognition- and orientation-induced reaction at the gas–water interface based on the formation of complementary hydrogen bonds between the barbituric acid lipids **1** and **2** and substrates like 2,4,6-triaminopyrimidine (TAP), melamine, and urea, as shown in Figure 1.

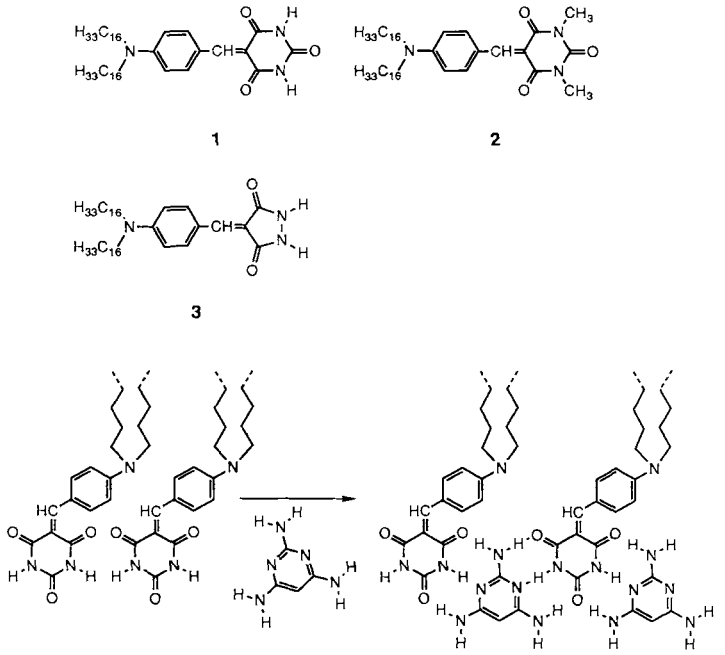

Fig. 1. Receptor lipids **1**–**3** and schematic representation of the formation of the molecular strands of barbituric acid lipid **1** with 2,4,6-triaminopyrimidine (TAP) at the gas–water interface.

The recognition reaction of the substrates and the barbituric acid lipids at the gas–water interface was investigated by measuring the surface pressure–surface area isotherms,[7] by Brewster angle microscopy,[7] and by UV/VIS reflection spectroscopy.[8] The latter method is especially suitable, as the detection of the recognition reaction relies on the disappearence of the aggregation band, which is a measure of the interaction of the lipid chromophore in the monolayer and does not occur in solution. The phase of the monolayer is important in the recognition reaction. The insertion of TAP into the lipid monolayer and formation of the strand structure occurs only when the lipid is in the fluid phase; for lipids **1**–**3** this is above 23 °C. Below this temperature, in the solid phase, the reflection spectra do not change, since TAP does not insert into the monolayer. All monolayer experiments whose results are discussed here were conducted at 25 °C with the same surface area per molecule and at the same pressure.

The reflection spectra of lipid **1** on pure water and 10^{-4} HCl subphases do not change, and the monolayer is stable for 17 h. In contrast, on subphases containing TAP at pH 3 the aggregation band at 430 nm disappears within 4 h (Fig. 2a). The corresponding insertion of TAP in the monolayer is a uniform and defined process, as is indicated by the three isosbestic points at 360, 486, and 544 nm. When the insertion of TAP in the monolayer of lipid **1** is monitored at pH 6.5, then an additional second process is evident—the hydrolytic cleavage of the C=C bond of the chromophore (Fig. 2b). This leads to the formation of the corresponding aldehyde (λ_{max} = 350 nm) and barbituric acid. Two isosbestic points at 298 and 384 nm occur, which again indicates that the reaction proceeds in a uniform and defined fashion. The barbituric acid head of the lipid is cleaved quantitatively after 4 h with formation of the aldehyde. It is quite remarkable that hydrolysis on a 10^{-4} M NaOH subphase (pH 10) is only in the initial stages after 4 h (Fig. 2c). Direct comparison shows that the TAP-catalyzed hydrolysis of the chromophore at pH 6.5 is 14 times faster than the addition of the hydroxide ion to the C=C bond at pH 10.

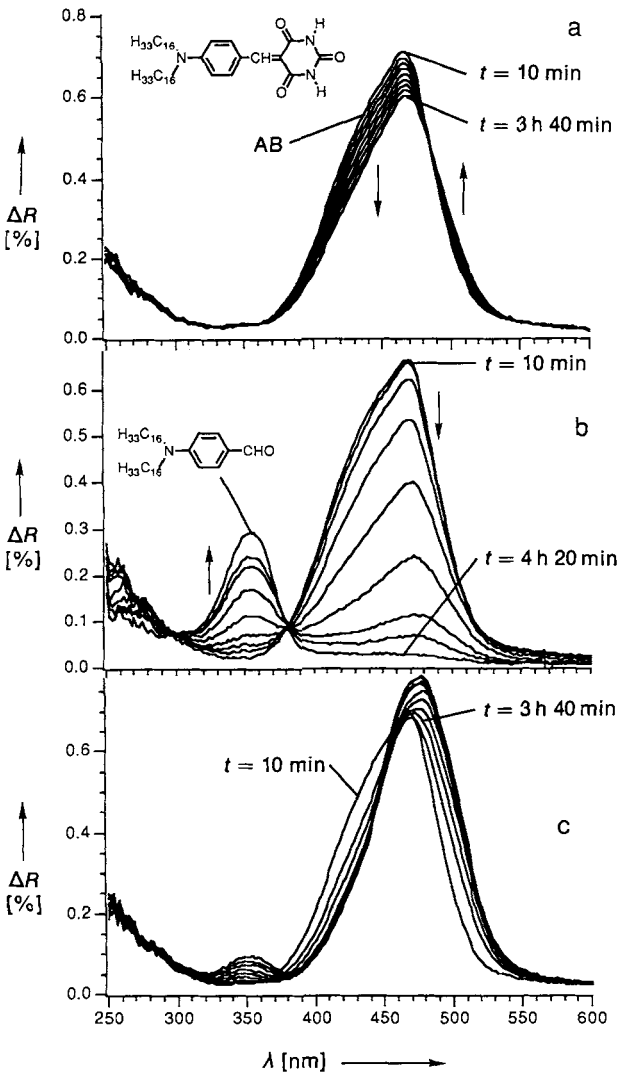

Fig. 2. UV/VIS reflection spectra of barbituric acid lipid **1** at the gas–water interface. R = reflection. a) On a 10^{-4} M TAP subphase at pH 3 containing HCl (disappearance of the aggregate bands (AB) at 430 nm, no hydrolysis); b) on a 10^{-4} M TAP subphase (pH 6.5), fast recognition-induced hydrolysis of barbituric acid lipid **1**; c) on a 10^{-4} M NaOH subphase (pH 10), slow basic hydrolysis of barbituric acid lipid **1**.

The first step of a reaction mechanism that would explain the dramatic increase in the rate of the cleavage of the double bond is shown schematically in Figure 3a and with a space-filling model in Figure 3b. The C—C double bond activated

by the formation of intermolecular hydrogen bonds between the chromophore and TAP is attacked by a water molecule. The high speed of the hydrolysis is not only due to this polarization of the double bond but also to an increase of the nucleophilicity of the water molecule, which is sitting in a hydrophobic pocket as shown schematically in Figure 3b.

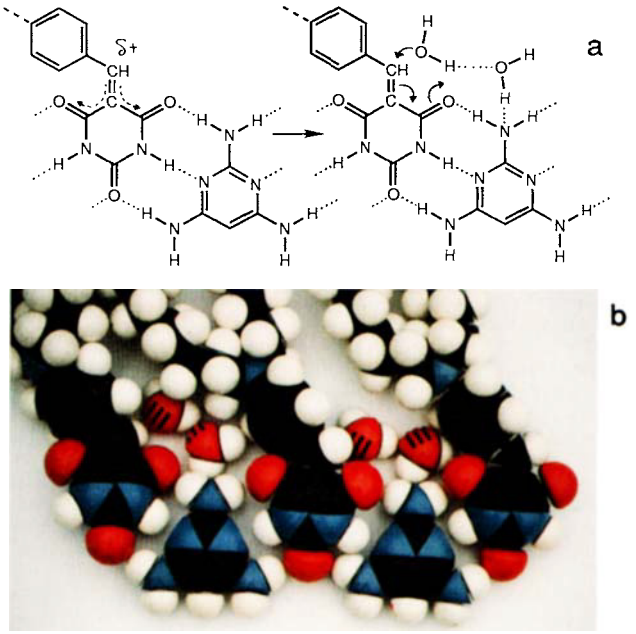

Fig. 3. Addition of water to the activated C=C bond of the chromophore of lipid **1**. a) Polarization of the double bond by hydrogen bonding and nucleophilic addition of water. b) Space-filling model of the molecular strands with water molecules in the hydrophobic environment between the lipids at the gas–water interface.

This proposed mechanism invoking recognition- and orientation-induced C=C cleavage (retro-Knoevenagel reaction) was supported by a series of further experiments. When melamine ($pK_B = 8.9$) was used as a substrate instead of TAP ($pK_B = 7.2$), the insertion was just as rapid (disappearance of the aggregation band), but the hydrolysis reaction was roughly nine times slower. This can be attributed to a weaker activation of the C=C bond, because the hydrogen bonds between the less basic melamine and the carbonyl groups adjacent to the double bond are not as strong. The importance of hydrogen bond formation and the consequent acceleration of the retro-Knoevenagel reaction can be demonstrated by the use of urea as substrate in the subphase.

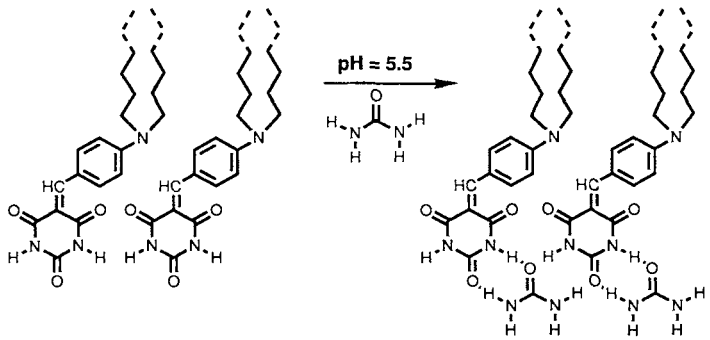

Fig. 4. Schematic representation of the insertion of urea into the monolayer of lipid **1** and formation of a molecular strand.

Figure 4 shows schematically the insertion of urea molecules into the monolayer forming molecular strands. The progress evident in the reflection spectra is analogous to that in Figure 2a, namely, the disappearance of the aggregation band (again three isosbestic points). In this experiment hydrolysis is not observed even at a pH value of 5.5, since the carbonyl groups adjacent to the double bond are not activated by hydrogen bonding.

Cospreading experiments[9] with mixtures of barbituric acid lipids and TAP in different ratios indicate that the insertion and cleavage reaction require the formation of molecular strands at the gas–water interface. The hydrolysis reaction for a 3:1 mixture is depicted at the top of Figure 5.

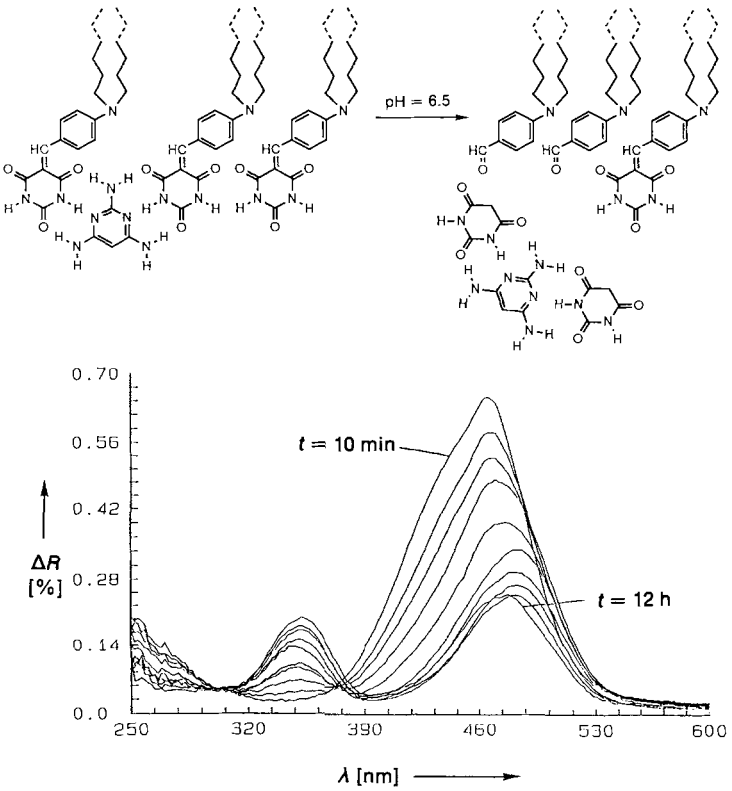

Fig. 5. UV/VIS reflection spectra recorded during the partial hydrolysis of a 3:1 mixture of lipid **1** and TAP, and schematic representation of a 2:1 complex of lipid **1** and TAP; reformation of the aggregation bands after the hydrolysis has ended (see Fig. 2a).

Three points should be noted: the hydrolysis is slower than for the 1:1 mixture (12 h instead of 3 h), the reaction comes to a halt after two-thirds of the lipid molecules are cleaved, and the aggregation band of the barbituric acid lipid reappears. Quantitative cleavage is observed for the 2:1 mixture of lipid **1** and TAP, but the reaction is also slower than for the 1:1 mixture. This implies that each TAP molecule forms hydrogen bonds to two lipid molecules (support for insertion), but only the molecular strand structure (1:1 mixture) leads to a fast reaction; the 2:1 complex (2:1 and 3:1 mixtures) reacts more slowly, since the double bond of the barbituric acid chromophore is activated from one side only. The reappearance of the aggregation band in the experiment with the 3:1 mixture after the reaction had stopped is a further indication that interruption of the lipid aggregates is caused only by the TAP insertion.

The importance of fit in the recognition reaction and the subsequent hydrolysis can be demonstrated by variation of the "receptor" of the barbituric acid (by methylation of the pyrimidine nitrogen atoms; lipid **2**). At pH 3, TAP is inserted into the monolayer of lipid **2** significantly more slowly than into that of lipid **1** (slow disappearance of the aggregation band) due to steric hindrance caused by the space-demanding methyl groups. The rate of the hydrolysis of lipid **2** on a TAP-containing subphase at pH 6.5 is linked to the rate of the insertion (Fig. 6). The aggregation band is observed until the hydrolysis is complete.

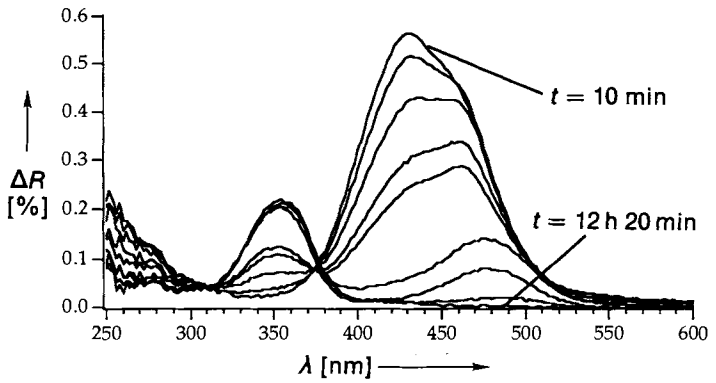

Fig. 6. UV/VIS reflection spectra of lipid **2** on a 10^{-4} M TAP subphase at pH 6.5. Slow insertion (slow disappearance of the aggregation band) followed by hydrolytic cleavage of the C=C bond (see Fig. 2b).

This experiment particularly emphasizes the importance of the organization of lipids at the gas-water interface. Although lipid **2** does not associate with TAP in $CDCl_3$ according to ^{1}H NMR spectra,[9] it does at the gas–water interface even though the solvent is changed from an aprotic to a protic one. The preorientation of the recognition structure by the lipid monolayer ensures that the complex, otherwise weak in solution, is stabilized by this arrangement. In this system the formation of the complex is the rate-determining step.

The importance of molecular recognition is underlined by the investigation of the interaction of the pyrazolidine-3,5-dione lipid **3** with TAP at the gas–water interface. In this case the aggregation band of the chromophore is not interrupted by TAP, because the five- and six-membered ring structures of lipid **3** and TAP do not fit together well enough. The monolayer of lipid **3** is stable on a TAP-containing subphase at pH 3 and pH 6.5 (no changes at all in the UV/VIS reflection spectra).

Preliminary experiments with subphases containing nucleobases indicate a defined interaction, for example, between cytosine and lipid **1**, which is only possible via the enol form of the base. In addition, the reverse systems—water-soluble barbituric acid derivatives and monolayers of amphiphilic triaminopyrimidine and melamine derivatives—are currently under investigation.

Received: March 11, 1993 [Z5918IE]
German version: *Angew. Chem.* **1993**, *105*, 1082

[1] H. Kitano, H. Ringsdorf, *Bull. Chem. Soc. Jpn.* **1985**, *58*, 2826–2828; H. Ringsdorf, B. Schlarb, J. Venzmer, *Angew. Chem.* **1988**, *100*, 143–144; *Angew. Chem. Int. Ed. Engl.* **1988**, *27*, 139–140; M. Ahlers, H. Ringsdorf, H. Rosemeyer, F. Seela, *Colloid Polym. Sci.* **1990**, *268*, 132–142; T. Krauch, S. Y. Zaitsev, V. B. Zubov, *Colloid Surf.* **1991**, *57*, 383–391.
[2] Y. Honda, K. Kurihara, T. Kunitake, *Chem. Lett.* **1991**, 681–684.
[3] V. M. Rotello, E. A. Viani, G. Deslongchamps, B. A. Murray, J. Rebek, Jr., *J. Am. Chem. Soc.* **1993**, *115*, 797–798; Y. Ikeura, K. Kurihara, T. Kunitake, *ibid.* **1991**, *113*, 7342–7350.
[4] D. Y. Sasaki, K. Kurihara, T. Kunitake, *J. Am. Chem. Soc.* **1991**, *113*, 9685–9686.
[5] C. Mertesdorf, T. Plesnivy, H. Ringsdorf, P. A. Suci, *Langmuir* **1992**, *8*, 2531–2537.
[6] a) J.-M. Lehn, M. Mascal, A. Decian, J. Fischer, *J. Chem. Soc. Chem. Commun.* **1990**, 479–481; b) J. A. Zerkowsky, C. T. Seto, D. A. Wierda, G. M. Whitesides, *J. Am. Chem. Soc.* **1990**, *112*, 9025–9026.
[7] The isotherms of lipid **1** show that the lipid has a collapse area of 0.46 nm^2 at a collapse pressure of 20 $mN\,m^{-1}$. The lipid has a liquid–solid coexistence region starting at 23 °C. At lower temperatures only gas- and solid-analogue phases are observed. Fluorescence microscopy shows that the lipids form anisotropic domains in the solid state. The isotherms of the lipid on the water and TAP subphases at pH 3 are almost identical but with slightly differing collapse pressures, which indicates a perfect fit, as shown schematically in Figure 1. The change in the surface potential of the monolayer during the measurements of the isotherms are also the same. The hydrolysis reaction can be followed just as well from the isotherms, since the resulting aldehyde does not form a solid phase at the gas–water interface. Thus the reduction in the collapse area of the barbituric acid lipid reflects the degree of hydrolysis of the monolayer. The same observations are made by Brewster angle micrscopy. Although the insertion does not lead to any noticeable change in the signal, the hydrolysis can be followed very easily.
[8] The UV/VIS reflection spectra were conducted on the monolayer at a subphase temperature of 25 °C and a surface pressure of approximately 5 mN^{-1}. A UV/VIS spectrometer adjusted on the surface of a Fromherz trough by glass fiber optics was used. The spectroscopy of a single monolayer was possible by comparison of the covered and uncovered surface. The experimental setup for the UV/VIS measurements is described in H. Grüniger, D. Möbius, H. Meyer, *J. Chem. Phys.* **1983**, *79*, 3701–3710.
[9] The ratios of the components for the cospreading experiments were determined by weight, and both components were dissolved in $CHCl_3$ as the spreading solvent. ^{1}H NMR spectra had previously established that the 1:1 complex forms in chloroform (quantitative shift of the signals of the amino and imide protons of TAP and barbituric acid by $\Delta\delta = 1.1$ and 2.25, respectively.

Hexakis(benzotriazolato)tetrakis-(2,4-pentanedionato)pentacopper(II): A Model for Corrosion Inhibition**

By *Jane Handley, David Collison, C. David Garner,* Madeleine Helliwell, Robert Docherty, John R. Lawson,* and *Peter A. Tasker**

The coordination chemistry of metal surfaces exposed to atmospheric attack is of considerable economic importance, especially with respect to effective corrosion inhibition. Empirically, specific ligands have been found to inhibit the corrosion of particular metals; benzotriazole (Hbta) is well established as a corrosion inhibitor for copper[1] and copper alloys,[2] performing well when applied in both aerated and deaerated conditions. The characterization of the nature of such ligation presents a significant challenge, not least because the surface to which the corrosion inhibitor is applied is rarely chemically pure or structurally defined. For the copper–benzotriazole interaction, it has been postulated that copper oxide films are prerequisites for successful corrosion inhibition.[2] The formation of polynuclear complexes, in

[*] Prof. C. D. Garner, J. Handley, Dr. D. Collison, Dr. M. Helliwell
Department of Chemistry
University of Manchester
Oxford Road, GB-Manchester M13 9PL (UK)
Telefax: Int. code + (61) 275-4616
Dr. P. A. Tasker, Dr. R. Docherty, Dr. J. R. Lawson
Research Centre, ICI Specialties
Blackley, GB-Manchester M9 3DA (UK)

[**] We acknowledge the financial support of the Science and Engineering Research Council (SERC), the Royal Society and ICI Specialties.

The importance of fit in the recognition reaction and the subsequent hydrolysis can be demonstrated by variation of the "receptor" of the barbituric acid (by methylation of the pyrimidine nitrogen atoms; lipid **2**). At pH 3, TAP is inserted into the monolayer of lipid **2** significantly more slowly than into that of lipid **1** (slow disappearance of the aggregation band) due to steric hindrance caused by the space-demanding methyl groups. The rate of the hydrolysis of lipid **2** on a TAP-containing subphase at pH 6.5 is linked to the rate of the insertion (Fig. 6). The aggregation band is observed until the hydrolysis is complete.

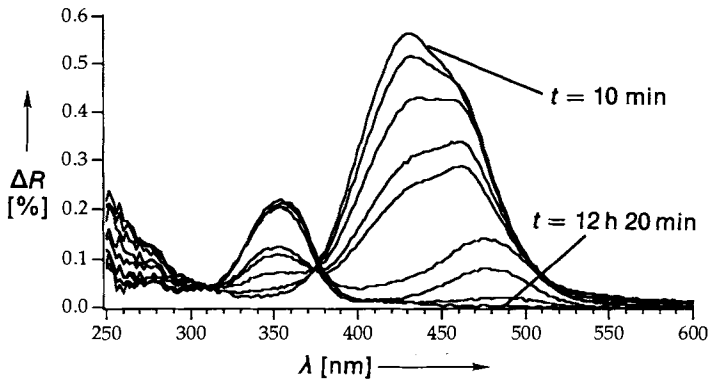

Fig. 6. UV/VIS reflection spectra of lipid **2** on a 10^{-4} M TAP subphase at pH 6.5. Slow insertion (slow disappearance of the aggregation band) followed by hydrolytic cleavage of the C=C bond (see Fig. 2b).

This experiment particularly emphasizes the importance of the organization of lipids at the gas-water interface. Although lipid **2** does not associate with TAP in $CDCl_3$ according to ^{1}H NMR spectra,[9] it does at the gas–water interface even though the solvent is changed from an aprotic to a protic one. The preorientation of the recognition structure by the lipid monolayer ensures that the complex, otherwise weak in solution, is stabilized by this arrangement. In this system the formation of the complex is the rate-determining step.

The importance of molecular recognition is underlined by the investigation of the interaction of the pyrazolidine-3,5-dione lipid **3** with TAP at the gas–water interface. In this case the aggregation band of the chromophore is not interrupted by TAP, because the five- and six-membered ring structures of lipid **3** and TAP do not fit together well enough. The monolayer of lipid **3** is stable on a TAP-containing subphase at pH 3 and pH 6.5 (no changes at all in the UV/VIS reflection spectra).

Preliminary experiments with subphases containing nucleobases indicate a defined interaction, for example, between cytosine and lipid **1**, which is only possible via the enol form of the base. In addition, the reverse systems—water-soluble barbituric acid derivatives and monolayers of amphiphilic triaminopyrimidine and melamine derivatives—are currently under investigation.

Received: March 11, 1993 [Z5918IE]
German version: *Angew. Chem.* **1993**, *105*, 1082

[1] H. Kitano, H. Ringsdorf, *Bull. Chem. Soc. Jpn.* **1985**, *58*, 2826–2828; H. Ringsdorf, B. Schlarb, J. Venzmer, *Angew. Chem.* **1988**, *100*, 143–144; *Angew. Chem. Int. Ed. Engl.* **1988**, *27*, 139–140; M. Ahlers, H. Ringsdorf, H. Rosemeyer, F. Seela, *Colloid Polym. Sci.* **1990**, *268*, 132–142; T. Krauch, S. Y. Zaitsev, V. B. Zubov, *Colloid Surf.* **1991**, *57*, 383–391.
[2] Y. Honda, K. Kurihara, T. Kunitake, *Chem. Lett.* **1991**, 681–684.
[3] V. M. Rotello, E. A. Viani, G. Deslongchamps, B. A. Murray, J. Rebek, Jr., *J. Am. Chem. Soc.* **1993**, *115*, 797–798; Y. Ikeura, K. Kurihara, T. Kunitake, *ibid.* **1991**, *113*, 7342–7350.
[4] D. Y. Sasaki, K. Kurihara, T. Kunitake, *J. Am. Chem. Soc.* **1991**, *113*, 9685–9686.
[5] C. Mertesdorf, T. Plesnivy, H. Ringsdorf, P. A. Suci, *Langmuir* **1992**, *8*, 2531–2537.
[6] a) J.-M. Lehn, M. Mascal, A. Decian, J. Fischer, *J. Chem. Soc. Chem. Commun.* **1990**, 479–481; b) J. A. Zerkowsky, C. T. Seto, D. A. Wierda, G. M. Whitesides, *J. Am. Chem. Soc.* **1990**, *112*, 9025–9026.
[7] The isotherms of lipid **1** show that the lipid has a collapse area of 0.46 nm^2 at a collapse pressure of 20 $mN\,m^{-1}$. The lipid has a liquid–solid coexistence region starting at 23 °C. At lower temperatures only gas- and solid-analogue phases are observed. Fluorescence microscopy shows that the lipids form anisotropic domains in the solid state. The isotherms of the lipid on the water and TAP subphases at pH 3 are almost identical but with slightly differing collapse pressures, which indicates a perfect fit, as shown schematically in Figure 1. The change in the surface potential of the monolayer during the measurements of the isotherms are also the same. The hydrolysis reaction can be followed just as well from the isotherms, since the resulting aldehyde does not form a solid phase at the gas–water interface. Thus the reduction in the collapse area of the barbituric acid lipid reflects the degree of hydrolysis of the monolayer. The same observations are made by Brewster angle micrscopy. Although the insertion does not lead to any noticeable change in the signal, the hydrolysis can be followed very easily.
[8] The UV/VIS reflection spectra were conducted on the monolayer at a subphase temperature of 25 °C and a surface pressure of approximately 5 mN^{-1}. A UV/VIS spectrometer adjusted on the surface of a Fromherz trough by glass fiber optics was used. The spectroscopy of a single monolayer was possible by comparison of the covered and uncovered surface. The experimental setup for the UV/VIS measurements is described in H. Grüniger, D. Möbius, H. Meyer, *J. Chem. Phys.* **1983**, *79*, 3701–3710.
[9] The ratios of the components for the cospreading experiments were determined by weight, and both components were dissolved in $CHCl_3$ as the spreading solvent. ^{1}H NMR spectra had previously established that the 1:1 complex forms in chloroform (quantitative shift of the signals of the amino and imide protons of TAP and barbituric acid by $\Delta\delta = 1.1$ and 2.25, respectively.

Hexakis(benzotriazolato)tetrakis-(2,4-pentanedionato)pentacopper(II): A Model for Corrosion Inhibition**

By *Jane Handley, David Collison, C. David Garner,* Madeleine Helliwell, Robert Docherty, John R. Lawson,* and *Peter A. Tasker**

The coordination chemistry of metal surfaces exposed to atmospheric attack is of considerable economic importance, especially with respect to effective corrosion inhibition. Empirically, specific ligands have been found to inhibit the corrosion of particular metals; benzotriazole (Hbta) is well established as a corrosion inhibitor for copper[1] and copper alloys,[2] performing well when applied in both aerated and deaerated conditions. The characterization of the nature of such ligation presents a significant challenge, not least because the surface to which the corrosion inhibitor is applied is rarely chemically pure or structurally defined. For the copper–benzotriazole interaction, it has been postulated that copper oxide films are prerequisites for successful corrosion inhibition.[2] The formation of polynuclear complexes, in

[*] Prof. C. D. Garner, J. Handley, Dr. D. Collison, Dr. M. Helliwell
Department of Chemistry
University of Manchester
Oxford Road, GB-Manchester M13 9PL (UK)
Telefax: Int. code + (61) 275-4616
Dr. P. A. Tasker, Dr. R. Docherty, Dr. J. R. Lawson
Research Centre, ICI Specialties
Blackley, GB-Manchester M9 3DA (UK)

[**] We acknowledge the financial support of the Science and Engineering Research Council (SERC), the Royal Society and ICI Specialties.

which the Hbta uses its nitrogen atoms to bridge adjacent copper atoms, has been proposed.[3] Alternatively, the formation of a π complex between Hbta and surface copper(I) ions has been suggested.[4] As part of a programme to investigate the possible modes of bonding between copper surfaces and Hbta, a range of copper complexes with this and related ligands have been prepared, including the title compound, **1** (Hacac = 2,4-pentanedione).

$[Cu_5(bta)_6(acac)_4]$ **1**

X-ray structure analysis[5] of prismatic crystals of **1**, obtained from dichloromethane, revealed them to be composed of discrete $[Cu_5(bta)_6(acac)_4]$ molecules (Fig. 1).[6] The pentanuclear copper(II) assembly consists of a distorted tetrahedral arrangement of four copper atoms (Cu2–Cu5) centered on the fifth (Cu1); the cube which envelopes this arrangement is identified in Figure 1. Each of the six bta^- ligands

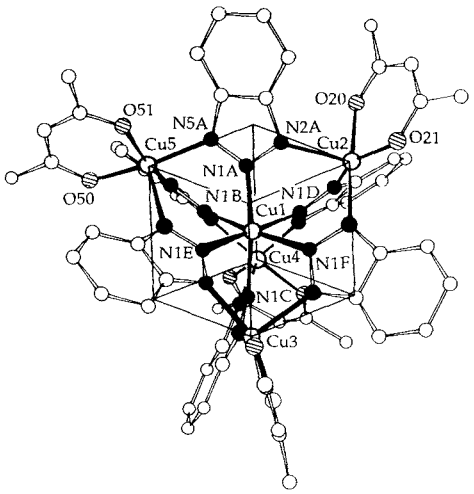

Fig. 1. The molecular structure of **1**; ○ Cu, o C, ● N, ◍ O. Cu1 is the central copper ion. Selected bond lengths [Å]: Cu1-N1A 2.030(9), Cu1-N1B 2.305(8), Cu1-N1C 2.058(9), Cu1-N1D 2.034(9), Cu1-N1E 2.063(9), Cu1-N1F 2.471(9), Cu2-O20 1.931(8), Cu2-O21 1.924(8), Cu2-N2A 2.036(9), Cu2-N2D 2.219(9), Cu2-N2F 1.984(9), Cu3-O30 1.952(7), Cu3-O31 1.929(8), Cu3-N3C 2.182(9), Cu3-N3E 2.026(8), Cu3-N3F 2.011(9), Cu4-O40 1.955(8), Cu4-O41 1.914(7), Cu4-N4B 2.181(9), Cu4-N4C 1.996(8), Cu4-N4D 2.026(9), Cu5-O50 1.920(8), Cu5-O51 1.936(8), Cu5-N5A 2.23(1), Cu5-N5B 1.978(9), Cu5-N5E 2.036(9); selected nonbonding distances [Å]: Cu1-Cu2 3.684(2), Cu1-Cu3 3.715(2), Cu1-Cu4 3.615(2), Cu1-Cu5 3.685(2), Cu2-Cu3 5.740(2), Cu2-Cu4 6.126(2), Cu2-Cu5 6.120(2), Cu3-Cu4 6.063(2), Cu3-Cu5 6.034(2), Cu4-Cu5 5.896(2); selected angles between copper atoms [°]: Cu2-Cu1-Cu3 101.75(5), Cu2-Cu1-Cu4 114.12(6), Cu2-Cu1-Cu5 112.29(6),Cu3-Cu1-Cu5 109.25(5), Cu3-Cu1-Cu4 111.61(5), Cu4-Cu1-Cu5 107.72(5).

spans an edge of the Cu_4 tetrahedron and is ligated to the central copper atom (Cu1) through its central nitrogen atom. Cu1 has a tetragonally distorted (4+2) octahedral coordination geometry. In contrast, each apical copper atom is in an approximately square-based pyramidal $(Cu(N_2O_2)_{eq}(N)_{ax})$ environment, bound to three benzotriazole nitrogen atoms and two oxygen atoms of a bidentate 2,4-pentanedionato group. The structure of **1** corresponds to that proposed by Marshall[7] for a compound he isolated with the same composition.

The arrangement of the $Cu_5(bta)_6$motif in **1** is a repeat of that observed[8] in the mixed-valence cluster **2**,[8] which involves a central Cu^{II} ion, ligated as in **1**, and four apical Cu^{I} ions, each possessing an essentially tetrahedral CuN_3C arrangement. The μ^3-bridging arrangement for bta^- has also been identified[9] in a thallium(I) compound.

$[Cu_5(bta)_6(t\mathrm{BuNC})_4]$ **2**

The mode of bonding of the bta^- ligands to Cu^{II} in **1** and to Cu^{I} and Cu^{II} in **2** could relate directly to the role of Hbta as a corrosion inhibitor of copper metal. Thus, bta^- could anchor to the oxidized metal by binding to two copper atoms in the surface layer and to a copper atom in the layer below. The copper atoms at an oxidized metal surface would be expected to be ligated to O^{2-}, OH^- and/or H_2O and, therefore, the inclusion of O-donor ligands in **1** is consistent with this.

These ideas have been developed further with molecular modeling packages,[11, 12] which have been used to examine the interaction of bta^- with the (110) faces of Cu_2O and CuO. These faces are considered to be the growth faces of these oxides. This is in agreement with classical morphological theory according to Bravais, Friedel, Donnay, and Harker which suggests that "allowing for space group symmetry, the most important growth forms will be those with the greatest interplanar spacings (d_{hkl})".[13, 14] A preliminary study has shown that the best structural match[15] corresponds to the bta^- unit binding to and penetrating the (110) face of Cu_2O, as shown in Figure 2. This arrangement involves the bta^- oriented perpendicular to the (110) face and allows an efficient packing of benzo substituents across the surface. The conclusion is consistent with the ideas of Fang et al.,[17] but contrasts with the idea that the bta^- moiety lies parallel to the surface[4] or is inclined at some intermediate orientation.[18] For CuO the best structural match was also obtained with the (110) face and with bta^- perpendicular to the surface, although the fit was not as good[15] as for the (110) face of Cu_2O. These calculations do not address the binding energies of bta^- to different copper oxide surfaces since an important feature to emerge from the molecular arrangement in **1** is that, even within such a relatively small polynuclear complex, there are significant structural variations which are tolerated within the Cu^{II}_3-bta^- moiety.

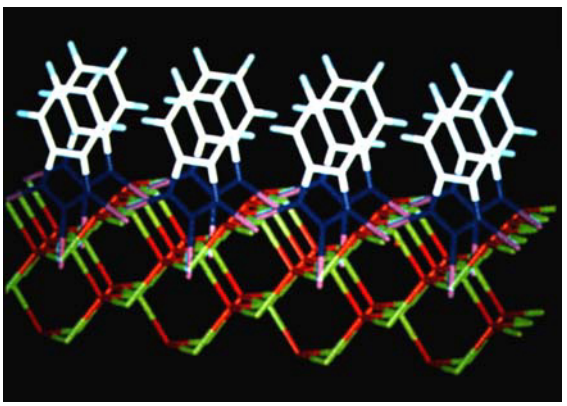

Fig. 2. Molecular modeling representation of binding of benzotriazolate ions to the (110) face of Cu_2O with a goodness of fit [16] of 0.24. The Cu–Cu distances within the unrelaxed triangular units bound by bta^- are 5.667, 3.270, and 3.270 Å; color coding: copper of oxidized surface is green, copper from benzotriazole structure is purple, oxygen is red, nitrogen is dark blue, carbon is white, and hydrogen is pale blue.

1) The inclinations of the bta^- units to the faces of the cube of Figure 1 vary considerably. The angle between a line joining the midpoints of the copper atoms on opposite faces of the cube and the plane of the bta^- penetrating these faces ranges from 1.18 to 27.38°.

2) The torsion angle between the nonadjacent nitrogen atoms of a bta$^-$ ligand and the two copper atoms to which they bind varies between 3.45 and 54.09°.

This versatility suggests that it is possible for benzotriazole to adapt to differences in the binding site geometry presented by various oxidized copper surfaces.

These studies lead to the suggestion that the interaction of benzotriazole with the surface of oxidized copper metal involves a near-normal approach; binding two copper atoms on the surface and one copper atom in the layer below. The flexibility possible with this mode of coordination would allow strong interaction with copper surfaces with varying degrees of oxidation and structure. Such binding of bta$^-$ utilizes its ligating ability to the maximum and would significantly inhibit the corrosion of the metal.

Experimental Procedure

1: A solution of bis(2,4-pentanedionato)copper(II) (3 mmol) in dichloromethane (150 cm^3) was treated with benzotriazole (15 mmol). This resulted in a deep green solution, from which green, prismatic crystals of **1** were isolated after approximately 21 days [5].

Received: January 26, 1993 [Z 5829 IE]
German version: *Angew. Chem.* **1993**, *105*, 1085

[1] I. Dugdale, J. B. Cotton, *Corros. Sci.* **1963**, *3*, 69–74.
[2] D. Chadwick, T. Hashemi, *Corros. Sci.* **1978**, *18*, 39–51.
[3] J. B. Cotton, I. R. Scholes, *Brit. Corros. J.* **1967**, *2*, 1–5.
[4] R. F. Roberts, *J. Elec. Spec. Relat. Phenom.*, **1974**, *4*, 273–291. O. Hollander, G. Dronne, J. Briquet, S. Dunn, M. Fealey, *Proc. 7SEIC Ann. Univ. Ferrara*, **1990**, *9*, 517-533.
[5] Crystal data: $1 \cdot 0.5CH_2Cl_2C_{56.5}H_{53}N_{18}O_8Cu_5Cl$, $M = 1465.34$, monoclinic, space group $P2_1/n$, $a = 16.038(1)$, $b = 22.836(2)$, $c = 17.497(1)$ Å, $\beta = 93.194(6)°$; $V = 6398.0(9)$ Å^3, $Z = 4$; $\rho_{calcd.} = 1.521$ g cm^{-3}; $\lambda(Cu_{K\alpha}) = 1.54178$ Å, $\mu = 27.35$ cm^{-1}, crystal size $0.100 \times 0.170 \times 0.250$ mm, $T = 23$ °C, $F(000) = 2976$, $2\theta_{max} = 119.9°$, $R(R_w) = 0.061$ (0.064), for 4531 unique reflections with $I > 3.00\sigma(I)$. The structure was solved by analyzing the Patterson function, and refined by full-matrix least-squares. The non-hydrogen atoms were refined anisotropically. The hydrogen atoms were included in calculated positions with fixed isotropic thermal parameters. Subsequently, the highest peaks on the difference map were attributed to the presence of dichloromethane, which showed high thermal motion and appeared to be present at an occupancy of a half. Further details of the crystal structure investigation are available on request from the Director of the Cambridge Crystallographic Data Centre, 12 Union Road, GB-Cambridge CB21EZ (UK), on quoting the full journal citation.
[6] Satisfactory elemental analyses (C,H,N,Cu) were obtained; IR (nujol): $\tilde{\nu}$[cm^{-1}] = 1592, 1271, 1214, 1190, 1024, 790, 746; UV/VIS (CH_2Cl_2): λ[nm] (ε[dm^3 mol^{-1} cm^{-1}]) 650 (460); EPR at 25 °C. $g_{iso} = 2.146$, peak-peak linewidth 21.0 mT, no metal hyperfine splitting was observed. Molecular weight (dichloromethane by osmometry) = 1427, positive-ion FAB mass spectrometry shows a group of peaks centered at m/z 1394.6 (molecular ion − CH_3C).
[7] J. H. Marshall, *Inorg. Chem.* **1978**, *17*, 3711–3713.
[8] V. L. Himes, A. D. Mighell, A. R. Siedle, *J. Am. Chem. Soc.* **1981**, *103*, 211–212.
[9] Reedijk et al. [10] have reported the structure of benzotriazolatothallium(I). This compound is constructed from zigzag layers, such that benzotriazolate ions are above and below the layers. All three nitrogen atoms of a given benzotriazolate ion bind to a different Tl^I ion and give a distorted trigonal prismatic geometry at the metal.
[10] J. Reedijk, G. Roelofsen, A. R. Siedle, A. L. Spek, *Inorg. Chem.* **1979**, *18*, 1947–1951.
[11] SYBYL, version 5.3 (1991) Tripos Assoc., 1699 Stanley Road, St. Louis, Missouri, 63144.
[12] CERIUS, version 2.3 (1991) Cambridge, Molecular Design, St. John's Innovation Centre, Cambridge, England.
[13] J. D. H. Donnay, D. Harker, *Am. Miner.* **1937**, *22*, 446–467.
[14] R. Docherty, G. Clydesdale, K. J. Roberts, P. Bennema, *J. Phys. D. App. Phys.* **1991**, *24*, 89–93.
[15] The "goodness of fit" for the model with weighted standard deviations [16] gives a value of 0.24 for the (110) face of Cu_2O, whereas the value was 0.34 for the (110) face of CuO.
[16] S. C. Nyburg, *Acta Crystallogr.* **1974**, *330*, 251–253.
[17] B.-S. Fang, C. G. Olsen, D. W. Lynch, *Surf. Sci.* **1986**, *176*, 476–490.
[18] C. Törnkvist, D. Thierry, J. Bergman, B. Liedberg, C. Leygraf, *J. Electrochem. Soc.* **1989**, *136*, 58–64.

Why is Porphobilinogen the Biological Substrate for the Formation of Porphyrins? Calculations on the Conformation of Acyclic Tetrapyrroles and the Acid-Catalyzed Cyclization of Hydroxymethylpyrroles**

By *Lutz F. Tietze** and *Holger Geissler*

Dedicated to Professor Reinhard W. Hoffmann on the occasion of his 60th birthday

The biological evolution of the plant and animal kingdoms is intimately connected with chemical evolution, that is, with the diversification of those chemical substances required for the development of organisms. In addition to nucleic acids and peptides,[1] the tetrapyrroles—chlorins, porphyrins, and corrins—are important for evolution and absolutely essential for plant and animal life as cofactors in photosynthesis, respiration, and in the formation of methane as well as vitamins; all porphinoid cofactors are formed from uroporphyrinogen III (**6**).

The question raised here is why nature has chosen porphobilinogen (**1**)[2] as the monomer for the biosynthesis of uroporphyrinogen III (**6**) and not the unsubstituted or a monosubstituted 2-aminomethylpyrrole.[3] This cannot have been a problem of the biosynthesis, as a multitude of variously substituted pyrroles occur in nature. On the contrary, one must assume that the substitution pattern found in porphobilinogen (**1**) is critical for the formation of the cyclic tetramer. Franck and Wegner were able to show that even

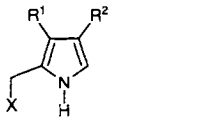

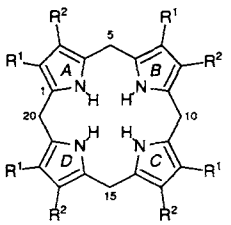

	R^1	R^2	X
1	A	P	NH_2
2	H	H	OH
3	CH_3	CH_3	OH
4	H	CH_3	OH
5	CH_3	H	OH

P = $(CH_2)_2CO_2H$
A = CH_2CO_2H

	R^1	R^2
6	A	P
7	CH_3	CH_3
8	H	CH_3

sterically strained cyclic tetramers could be constructed very easily in vitro by the reaction of 3,4-disubstituted *N*-alkyl-2-aminomethylpyrroles.[4] Thus, the straightforward formation of the cyclic tetramers may be traced back to the conformational fixing of the acyclic tetramers,[5] formed in several steps, in a cyclic conformation as a result of 1,3-allylic strain.[6] To confirm this hypothesis we have investigated the acid-catalyzed cyclization of hydroxymethylpyrroles **2**–**5** and calculated[7] the lowest energy conformation of the substituted and unsubstituted acyclic tetrapyrroles **9** and **10** by using the semiempirical AM1 method.[8]

Since direct determination of the lowest energy conformation for **9** and **10** was not reasonable on account of the size

[*] Prof. Dr. L. F. Tietze, Dr. H. Geissler
Institut für Organische Chemie der Universität
Tammannstrasse 2, D-37077 Göttingen (FRG)
Telefax: Int. code + (551)39-9476

[**] This work was supported by the Deutsche Forschungsgemeinschaft and the Fonds der Chemischen Industrie. We thank Prof. Dr. B. Franck and Prof. Dr. A. Eschenmoser for helpful discussions.

2) The torsion angle between the nonadjacent nitrogen atoms of a bta$^-$ ligand and the two copper atoms to which they bind varies between 3.45 and 54.09°.

This versatility suggests that it is possible for benzotriazole to adapt to differences in the binding site geometry presented by various oxidized copper surfaces.

These studies lead to the suggestion that the interaction of benzotriazole with the surface of oxidized copper metal involves a near-normal approach; binding two copper atoms on the surface and one copper atom in the layer below. The flexibility possible with this mode of coordination would allow strong interaction with copper surfaces with varying degrees of oxidation and structure. Such binding of bta$^-$ utilizes its ligating ability to the maximum and would significantly inhibit the corrosion of the metal.

Experimental Procedure

1: A solution of bis(2,4-pentanedionato)copper(II) (3 mmol) in dichloromethane (150 cm^3) was treated with benzotriazole (15 mmol). This resulted in a deep green solution, from which green, prismatic crystals of **1** were isolated after approximately 21 days [5].

Received: January 26, 1993 [Z 5829 IE]
German version: *Angew. Chem.* **1993**, *105*, 1085

[1] I. Dugdale, J. B. Cotton, *Corros. Sci.* **1963**, *3*, 69–74.
[2] D. Chadwick, T. Hashemi, *Corros. Sci.* **1978**, *18*, 39–51.
[3] J. B. Cotton, I. R. Scholes, *Brit. Corros. J.* **1967**, *2*, 1–5.
[4] R. F. Roberts, *J. Elec. Spec. Relat. Phenom.*, **1974**, *4*, 273–291. O. Hollander, G. Dronne, J. Briquet, S. Dunn, M. Fealey, *Proc. 7SEIC Ann. Univ. Ferrara*, **1990**, *9*, 517-533.
[5] Crystal data: $1 \cdot 0.5CH_2Cl_2C_{56.5}H_{53}N_{18}O_8Cu_5Cl$, $M = 1465.34$, monoclinic, space group $P2_1/n$, $a = 16.038(1)$, $b = 22.836(2)$, $c = 17.497(1)$ Å, $\beta = 93.194(6)°$; $V = 6398.0(9)$ Å^3, $Z = 4$; $\rho_{calcd.} = 1.521$ g cm^{-3}; $\lambda(Cu_{K\alpha}) = 1.54178$ Å, $\mu = 27.35$ cm^{-1}, crystal size $0.100 \times 0.170 \times 0.250$ mm, $T = 23$ °C, $F(000) = 2976$, $2\theta_{max} = 119.9°$, $R(R_w) = 0.061$ (0.064), for 4531 unique reflections with $I > 3.00\sigma(I)$. The structure was solved by analyzing the Patterson function, and refined by full-matrix least-squares. The non-hydrogen atoms were refined anisotropically. The hydrogen atoms were included in calculated positions with fixed isotropic thermal parameters. Subsequently, the highest peaks on the difference map were attributed to the presence of dichloromethane, which showed high thermal motion and appeared to be present at an occupancy of a half. Further details of the crystal structure investigation are available on request from the Director of the Cambridge Crystallographic Data Centre, 12 Union Road, GB-Cambridge CB21EZ (UK), on quoting the full journal citation.
[6] Satisfactory elemental analyses (C,H,N,Cu) were obtained; IR (nujol): $\tilde{\nu}$[cm^{-1}] = 1592, 1271, 1214, 1190, 1024, 790, 746; UV/VIS (CH_2Cl_2): λ[nm] (ε[dm^3 mol^{-1} cm^{-1}]) 650 (460); EPR at 25 °C. $g_{iso} = 2.146$, peak-peak linewidth 21.0 mT, no metal hyperfine splitting was observed. Molecular weight (dichloromethane by osmometry) = 1427, positive-ion FAB mass spectrometry shows a group of peaks centered at m/z 1394.6 (molecular ion − CH_3C).
[7] J. H. Marshall, *Inorg. Chem.* **1978**, *17*, 3711–3713.
[8] V. L. Himes, A. D. Mighell, A. R. Siedle, *J. Am. Chem. Soc.* **1981**, *103*, 211–212.
[9] Reedijk et al. [10] have reported the structure of benzotriazolatothallium(I). This compound is constructed from zigzag layers, such that benzotriazolate ions are above and below the layers. All three nitrogen atoms of a given benzotriazolate ion bind to a different Tl^I ion and give a distorted trigonal prismatic geometry at the metal.
[10] J. Reedijk, G. Roelofsen, A. R. Siedle, A. L. Spek, *Inorg. Chem.* **1979**, *18*, 1947–1951.
[11] SYBYL, version 5.3 (1991) Tripos Assoc., 1699 Stanley Road, St. Louis, Missouri, 63144.
[12] CERIUS, version 2.3 (1991) Cambridge, Molecular Design, St. John's Innovation Centre, Cambridge, England.
[13] J. D. H. Donnay, D. Harker, *Am. Miner.* **1937**, *22*, 446–467.
[14] R. Docherty, G. Clydesdale, K. J. Roberts, P. Bennema, *J. Phys. D. App. Phys.* **1991**, *24*, 89–93.
[15] The "goodness of fit" for the model with weighted standard deviations [16] gives a value of 0.24 for the (110) face of Cu_2O, whereas the value was 0.34 for the (110) face of CuO.
[16] S. C. Nyburg, *Acta Crystallogr.* **1974**, *330*, 251–253.
[17] B.-S. Fang, C. G. Olsen, D. W. Lynch, *Surf. Sci.* **1986**, *176*, 476–490.
[18] C. Törnkvist, D. Thierry, J. Bergman, B. Liedberg, C. Leygraf, *J. Electrochem. Soc.* **1989**, *136*, 58–64.

Why is Porphobilinogen the Biological Substrate for the Formation of Porphyrins? Calculations on the Conformation of Acyclic Tetrapyrroles and the Acid-Catalyzed Cyclization of Hydroxymethylpyrroles**

By *Lutz F. Tietze** and *Holger Geissler*

Dedicated to Professor Reinhard W. Hoffmann on the occasion of his 60th birthday

The biological evolution of the plant and animal kingdoms is intimately connected with chemical evolution, that is, with the diversification of those chemical substances required for the development of organisms. In addition to nucleic acids and peptides,[1] the tetrapyrroles—chlorins, porphyrins, and corrins—are important for evolution and absolutely essential for plant and animal life as cofactors in photosynthesis, respiration, and in the formation of methane as well as vitamins; all porphinoid cofactors are formed from uroporphyrinogen III (**6**).

The question raised here is why nature has chosen porphobilinogen (**1**)[2] as the monomer for the biosynthesis of uroporphyrinogen III (**6**) and not the unsubstituted or a monosubstituted 2-aminomethylpyrrole.[3] This cannot have been a problem of the biosynthesis, as a multitude of variously substituted pyrroles occur in nature. On the contrary, one must assume that the substitution pattern found in porphobilinogen (**1**) is critical for the formation of the cyclic tetramer. Franck and Wegner were able to show that even

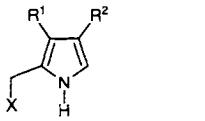

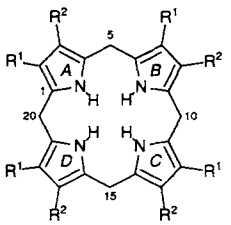

	R^1	R^2	X
1	A	P	NH_2
2	H	H	OH
3	CH_3	CH_3	OH
4	H	CH_3	OH
5	CH_3	H	OH

P = $(CH_2)_2CO_2H$
A = CH_2CO_2H

	R^1	R^2
6	A	P
7	CH_3	CH_3
8	H	CH_3

sterically strained cyclic tetramers could be constructed very easily in vitro by the reaction of 3,4-disubstituted *N*-alkyl-2-aminomethylpyrroles.[4] Thus, the straightforward formation of the cyclic tetramers may be traced back to the conformational fixing of the acyclic tetramers,[5] formed in several steps, in a cyclic conformation as a result of 1,3-allylic strain.[6] To confirm this hypothesis we have investigated the acid-catalyzed cyclization of hydroxymethylpyrroles **2**–**5** and calculated[7] the lowest energy conformation of the substituted and unsubstituted acyclic tetrapyrroles **9** and **10** by using the semiempirical AM1 method.[8]

Since direct determination of the lowest energy conformation for **9** and **10** was not reasonable on account of the size

[*] Prof. Dr. L. F. Tietze, Dr. H. Geissler
Institut für Organische Chemie der Universität
Tammannstrasse 2, D-37077 Göttingen (FRG)
Telefax: Int. code + (551)39-9476

[**] This work was supported by the Deutsche Forschungsgemeinschaft and the Fonds der Chemischen Industrie. We thank Prof. Dr. B. Franck and Prof. Dr. A. Eschenmoser for helpful discussions.

of the molecule, we proceeded in a stepwise fashion. First, the lowest energy conformation of the corresponding dipyrroles was calculated. A third pyrrole moiety was attached to give the tripyrroles, for which a potential energy surface with corresponding energy minima was obtained for the two new C–C bonds as a function of the torsion angle.[9] Further addition of a pyrrole unit gave the acyclic tetrapyrroles **9** and **10** with the conformations **A** and **B**. Once

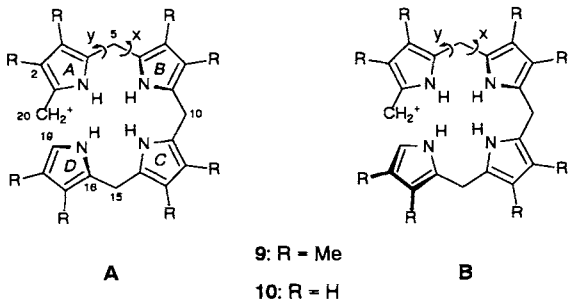

again, the potential energy surfaces *H1* and *H2* for **9** (Fig. 1) and *H3* and *H4* for **10** (Fig. 2) were calculated by variation of the torsion angle[10] of the bonds x and y.

On comparison of the potential energy surfaces *H1* and *H2* with *H3* and *H4* the difference caused by the 1,3-allylic strain becomes immediately apparent. In comparison with *H1* and *H2* the potential energy surfaces *H3* and *H4* are relatively flat, and their minima are considerably less pronounced. In the ground state the cyclic conformation (minima *M1* and *M6*) of the acyclic tetrapyrroles is more favorable than the extended conformation (minima *M5* and *M10*; $\Delta H_f(M1,M5) = 4.53\ kJ\,mol^{-1}$, $\Delta H_f(M6,M10) = 3.34\ kJ\,mol^{-1}$). Although the minimum *M4* corresponds to the energetically lowest point on *H1* and *H2*, on conformational grounds it is only capable of undergoing cyclization via the minimum *M1* (Scheme 1).

Table 1. AM1/RHF energies (H_f) for the minima *M1–M10* for compounds **9** and **10** in $kJ\,mol^{-1}$.

9:	*M1*	*M2*	*M3*	*M4*	*M5*
	1043.0	1049.4	1056.2	1042.1	1047.6
10:	*M6*	*M7*	*M8*	*M9*	*M10*
	1320.9	1327.0	1331.6	1323.9	1324.3

The distance between C20 and C19 in **9** is 395 pm for *M1*; the cyclic tetramer should therefore be formed from this conformation very quickly and easily. The calculations also show that polymerization is anticipated for **10**, as the cyclic conformation is less strongly fixed and the activation energy for the electrophilic substitution is presumably greater than for **9** because of the lower electron density of the pyrrole.

The results of these calculations are in agreement with those of investigations on the acid-catalyzed cyclization of hydroxymethylpyrroles **2**–**5**. Solutions of **2**–**5** in 2-propanol

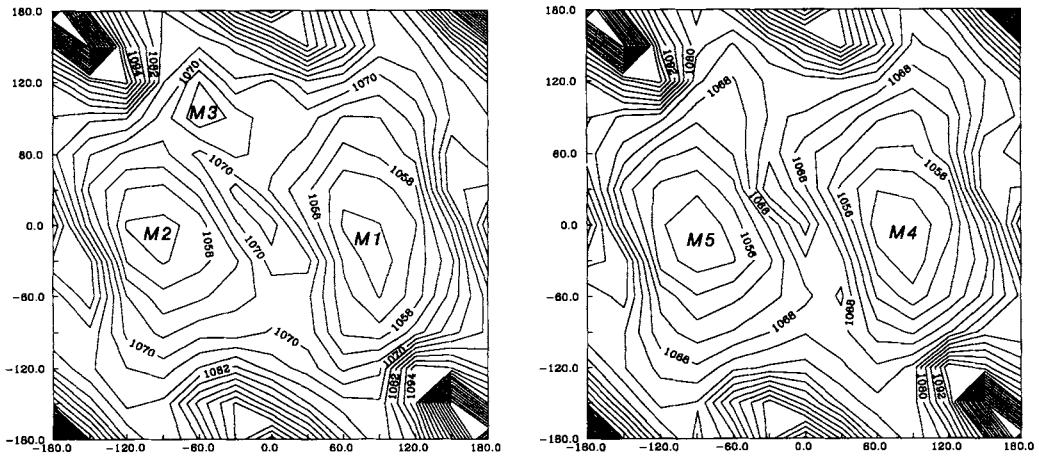

Fig. 1. Left: Potential energy surface *H1* [$kJ\,mol^{-1}$] starting from conformation **A** for **9**; *x* axis: torsion angle C4-C5-C6-N, *y* axis: torsion angle C6-C5-C4-N. Right: Potential energy surface *H2* [$kJ\,mol^{-1}$] starting from conformation **B** for **9**; *x* axis: torsion angle C4-C5-C6-N, *y* axis: torsion angle C6-C5-C4-N[11].

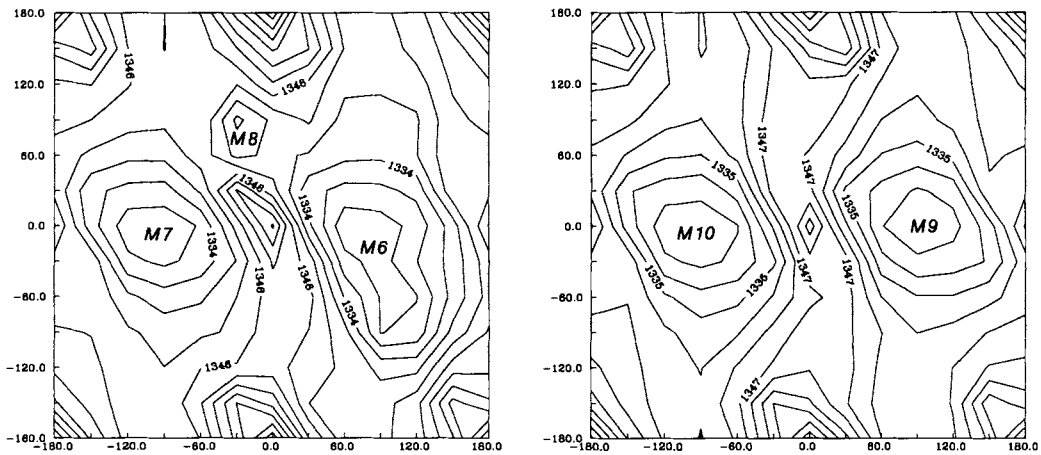

Fig. 2. Left: Potential energy surface *H3* [$kJ\,mol^{-1}$] starting from conformation **A** of **10**; *x* axis: torsion angle C4-C5-C6-N, *y* axis: torsion angle C6-C5-C4-N. Right: Potential energy surface *H4* starting from conformation **B** of **10**; *x* axis: torsion angle C4-C5-C6-N, *y* axis: torsion angle: C6-C5-C4-N[11].

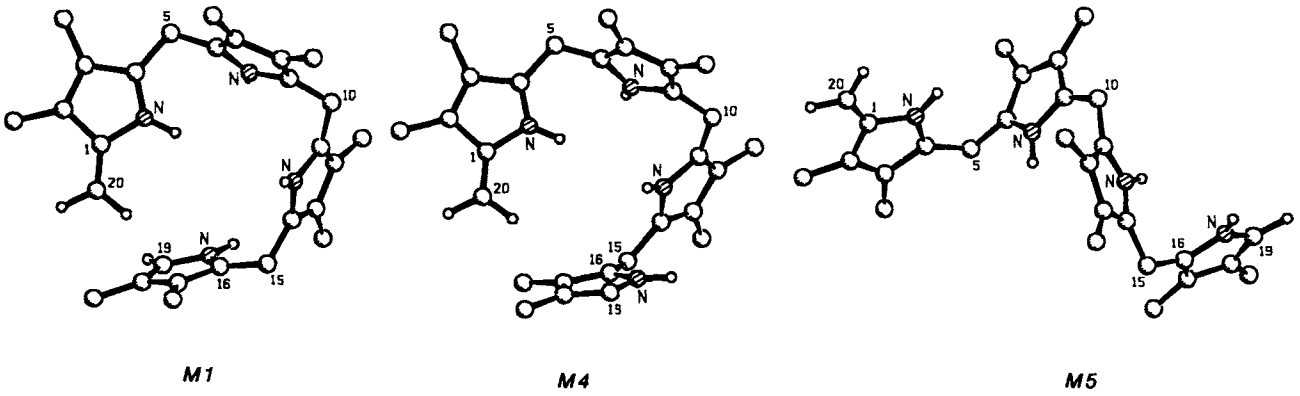

M1 M4 M5

Scheme 1.

were treated with equal amounts of acetic acid under identical reaction conditions (20 °C, 2 h). The yields of the cyclic tetrapyrroles were determined by HPLC with 5,5,10,10,15,15,20,20-octamethylporphyrinogen as internal standard.[12] The reaction of **2** gave no identifiable products; **3** provided an 82% yield of the corresponding cyclic tetrapyrrole **7**.[13] Reaction of **4** and **5** led in each case to a mixture of **8** and the three possible isomeric tetrapyrroles in approximately 20% yield. The calculations and experimental results show unequivocally the importance of substitution at C3 and C4 in the pyrrole ring in the formation of cyclic tetrapyrroles.

Received: February 12, 1993 [Z 58641E]
German version: *Angew. Chem.* **1993**, *105*, 1087

[1] a) M. Eigen, W. Gardiner, P. Schuster, R. Winkler-Oswatitsch, *Sci. Am.* **1981**, *244* (4), 88-92, 96, 99-104, 106-7, 110, 114, 116, 118; b) M. Eigen, W. Gardiner, P. Schuster, R. Winkler-Oswatitsch, *Interdiscip. Sci. Rev.* **1976**, *1*, 19-30.

[2] a) A. I. Scott, *Tetrahedron* **1992**, *48*, 2559-2578; b) N. Crockett, P. R. Alefounder, A. R. Battersby, C. Abell, *ibid.* **1991**, *47*, 6003-6014; c) P. M. Jordan, *Biosynthesis of Tetrapyrroles*, Elsevier, Amsterdam, **1991**; d) A. R. Battersby, F. J. Leeper, *Chem. Rev.* **1990**, *90*, 1261-1274; e) A. I. Scott, *Acc. Chem. Res.* **1990**, 308 317; f) A. R. Battersby, *Pure Appl. Chem.* **1989**, *61*, 337-344; g) F. J. Leeper, *Nat. Prod. Rep.* **1989**, *6*, 171-203; h) F. J. Leeper, *ibid.* **1987**, *4*, 441-469; i) A. Eschenmoser, *Angew. Chem.* **1988**, *100*, 5-40; *Angew. Chem. Int. Ed. Engl.* **1988**, *27*, 5; j) G. Ksander, G. Bold, R. Lattmann, C. Lehmann, T. Früh, Y.-B. Xiang, M. Inomata, H.-P. Buser, J. Schreiber, E. Zass, A. Eschenmoser, *Helv. Chim. Acta* **1987**, *70*, 1115-1172; k) A. R. Battersby, C. J. R. Fookes, K. E. Gustafson-Potter, E. McDonald, G. W. J. Matchham, *J. Chem. Soc. Perkin Trans. 1* **1982**, 2427-2444; l) B. Franck, *Angew. Chem.* **1982**, *94*, 327-337; *Angew. Chem. Int. Ed. Engl.* **1982**, *21*, 343; m) A. I. Scott, *Tetrahedron* **1975**, *31*, 2639-2653.

[3] A similar question has been posed by A. Eschenmoser for the nucleic acids: why does nature use ribose and 2-deoxyribose instead of, for example, glucose and 2-deoxyglucose? a) M. Böhringer, H.-J. Roth, J. Hunziker, M. Göbel, R. Krishnan, A. Giger, B. Schweizer, J. Schreiber, C. Leumann, A. Eschenmoser, *Helv. Chim. Acta* **1992**, *75*, 1414-1477; b) A. Eschenmoser, M. Dobler, *ibid.* **1992**, *47*, 218-259; c) A. Eschenmoser, *Nachr. Chem. Tech. Lab.* **1991**, *39*, 795-807.

[4] B. Franck, C. Wegner, *Angew. Chem.* **1975**, *87*, 419-420; *Angew. Chem. Int. Ed. Engl.* **1975**, *14*, 424. Structure analysis: G. Sawitzki, H. G. von Schnering, *ibid.* **1976**, *88*, 616-617 and **1976**, *15*, 552.

[5] a) J. L. Broeker, R. W. Hoffmann, K. N. Houk, *J. Am. Chem. Soc.* **1991**, *113*, 5006-5017; b) R. W. Hoffmann, *Chem. Rev.* **1989**, *89*, 1841-1860; c) F. Johnson, *ibid.* **1968**, *68*, 375-413.

[6] a) A. R. Battersby, C. J. R. Fookes, G. W. J. Matchham, E. McDonald, R. Hollenstein, *J. Chem. Soc. Perkin Trans. 1* 1983, 3031-3040; b) A. R. Battersby, C. J. R. Fookes, K. E. Gustafson-Potter, E. McDonals, G. W. J. Matchham, *ibid.* **1982**, 2427-2444; c) P. M. Jordan, *J. Am. Chem. Soc.* **1980**, *102*, 6841-6846; d) P. M. Jordan, J. S. Seehra, *FEBS Lett.* **1979**, *104*, 364-366; e) A. R. Battersby, C. J. R. Fookes, G. W. J. Matchham, E. McDonald, *J. Chem. Soc. Chem. Commun.* **1979**, 539-541; f) A. R. Battersby, G. L. Hodgson, E. Hunt, E. McDonald, J. Saunders, *J. Chem. Soc. Perkin Trans. 1* **1976**, 273-282.

[7] The AM1 method was chosen because results of calculations of the geometries of 2-isopropyl-3-methyl-1*H*-pyrrole were in very good agreement with those of ab initio calculations at the 3-21G//MP2/6-31G* level (Gaussian 88 and Gaussian 92).

[8] M. J. S. Dewar, E. G. Zoebisch, E. F. Healy, J. J. P. Stewart, *J. Am. Chem. Soc.* **1985**, *107*, 3902-3909.

[9] All calculations were carried out with the VAMP software package (T. Clark, Universität Erlangen-Nürnberg, unpublished) on an IBM 3090/300e from the Gesellschaft für wissenschaftliche Datenverarbeitung, Göttingen. VAMP is based on AMPAC 1.0 (QCPE no. 506) and MOPAC (QCPE no. 455).

[10] A point was calculated for the potential energy surface every 30°. In this way both torsion angles were fixed and the rest of the structure optimized.

[11] Rotation in a counterclockwise direction carries a positive sign.

[12] To an oxygen-free solution of hydroxymethylpyrroles **2**-**5** (6.00 μmol) in 1 mL of 2-propanol was added 2 μL of acetic acid with stirring at 20 °C under an argon atmosphere and with exclusion of light, and the resulting solution was stirred for another 2 h at 20 °C. After the addition of 4 μL of triethylamine, the solvent was removed by application of high vacuum for 1 h. Subsequently, 1 mL of a solution of 5,5,10,10,15,15,20,20-octamethylporphyrinogen (1 mg) in degassed acetonitrile (10 mL) was added, and quantitative HPLC analysis was conducted on a 5μ-C18 column with CH_3CN/H_2O (76:24, degassed) as solvent.

[13] In the reaction of **3** an acyclic hydroxymethyltetrapyrrole can be formulated as an intermediate corresponding to hydroxymethylbilan, which was demonstrated to be a biosynthetic precursor of uroporphyrinogen III (**6**).

Investigations in the Biosynthesis of the Pigments of Life: Calculations on the Formation of Uroporphyrinogen III from Hydroxymethylbilan and Description of a New Mechanism for the D-Ring Inversion**

By *Lutz F. Tietze** and *Holger Geissler*

Dedicated to Professor Wolfgang Steglich on the occasion of his 60th birthday

The cyclic tetrapyrrole uroporphyrinogen III (**2**) is the biosynthetic precursor for chlorophylls and bacteriochlorophylls, as well as of heme, siroheme, coenzyme F 430, and vitamin B_{12}, which have been described as the pigments of life. Uroporphyrinogen III is formed from porphobilinogen (PBG) by the action of the enzymes hydroxymethylbilan

[*] Prof. Dr. L. F. Tietze, Dr. H. Geissler
Institut für Organische Chemie der Universität
Tammannstrasse 2, D-37077 Göttingen (FRG)
Telefax: Int. code + (551)39-9476

[**] This work was supported by the Deutsche Forschungsgemeinschaft and the Fonds der Chemischen Industrie.

synthase (HMBS) and uroporphyrinogen III synthase (cosynthetase); hydroxymethylbilan (**1**) was shown to be a non-enzyme-bound intermediate.[1] A remarkable step in the biosynthesis of uroporphyrinogen III (**2**) is the inversion of ring D, which takes place only in the presence of cosynthetase.[2] In the absence of this enzyme only uroporphyrinogen I (**3**) is formed, which does not isomerize to give **2** even in the presence of cosynthetase.[3] Countless models (so far unverified), such as the formation of a spiro compound as intermediate,[4] the fragmentation–recombination mechanism,[1,5] [1,5] sigmatropic rearrangements[5b,c] and the intermediate formation of a lactone[6] have been used to explain this phenomenon. We describe here calculations on the formation of uroporphyrinogen III (**2**) from hydroxymethylbilan (**1**) using the model compounds **4** and **5**, and introduce a new mechanism for the inversion of the D ring.

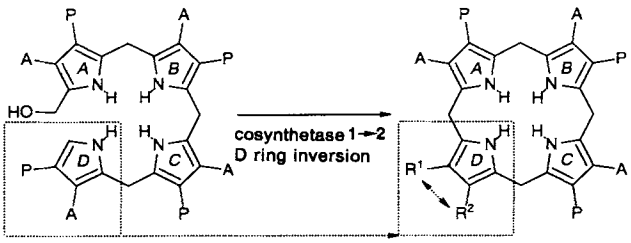

1 A: CH_2CO_2H P: $(CH_2)_2CO_2H$ **2**: R^1=A, R^2=P **3**: R^1=P, R^2=A

In the preceding communication we were able to show, based on calculations, that the cyclic conformations **A** and **B** correspond to energy minima for the acyclic tetrapyrroles **4** and **5**.[7] To investigate the cyclization, we have now determined the transition states[8] and σ complexes involved in the formation of the cyclic tetramer **8** from **4** by attack of C19 at C20 and that of the spiro compound **12** from **4** by attack of C16 at C20 by using the semiempirical method AM1/RHF.[9] We have also conducted similar calculations for the formation of **9** and **13** from the unsubstituted acyclic tetrapyrrole **5**.

Four transition state structures (**TS-4a–d** and **TS-5a–d**) were found for the cyclization of **4** and **5**, respectively. The cyclization of **4** to give the cyclic tetrapyrrole **8** via **6** from the conformation **A** requires the least expenditure of energy (**TS-4a**: $\Delta H_f^{\neq} = 8.36\ kJ\,mol^{-1}$). This corresponds to the formation of uroporphyrinogen I (**3**) from **1** and is in agreement with the acid-catalyzed cyclization of porphobilinogen, which leads first to **3** in a kinetically controlled process; under equilibrating reaction conditions a mixture of uroporphyrinogens I, II, III, and IV in the molar ratio 1:1:4:2 is found.[10] In this context it is worth noting that an activation energy almost twice as great has been calculated for the cyclization of **5** to **9** via **7** (**TS-5a**: $\Delta H_f^{\neq} = 14.7\ kJ\,mol^{-1}$). The lower reactivity of the unsubstituted pyrrole certainly accounts for this figure; the tendency for polymerization[7] becomes understandable when the potential energy surface for the conformation of **5**, which shows only weakly pronounced minima, is considered. Interestingly, the cationic σ complexes **6** and **7**, formed as intermediates in the electrophilic substitution at the pyrrole ring D, and which lead to the tetrapyrroles **8** and **9**, respectively, are considerably more stable than the cationic substrates **4** and **5**; the calculated energy differences ΔH_f amount to $-91.3\ kJ\,mol^{-1}$ for **4** and $-87.3\ kJ\,mol^{-1}$ for **5**. These results could be an indication that a cationic intermediate of type **4** does not arise in the enzymatic cyclization of hydroxymethylbilan and that σ complexes of type **6** have comparatively long lifetimes.

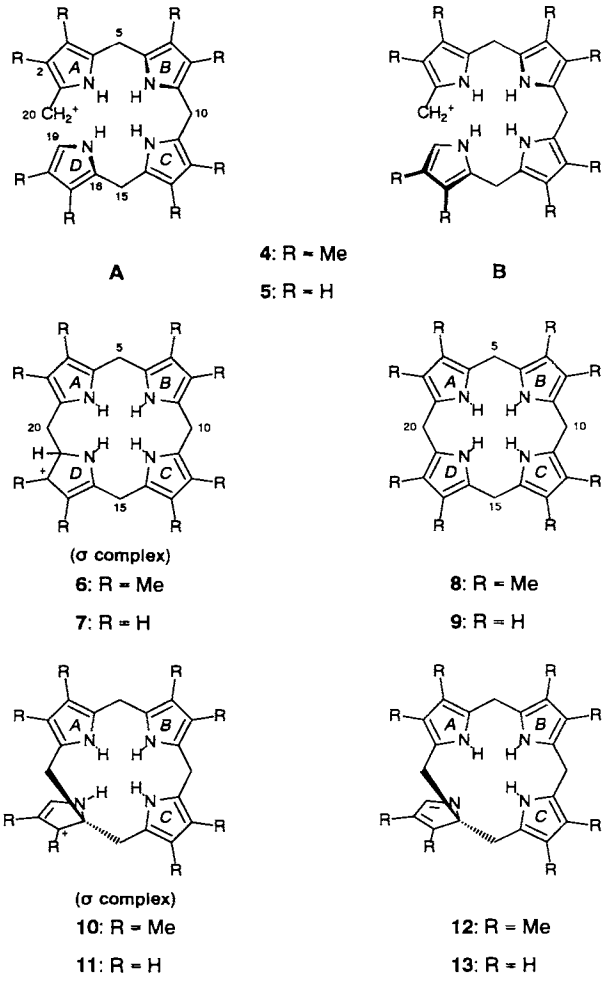

Of considerable importance for the elucidation of the ring inversion in the formation of uroporphyrinogen III (**2**) from **1** is the finding that the calculated activation energies for the formation of the spiro compounds **12** and **13** from **4** and **5** via **10** and **11**, respectively, are considerably higher than the values found for the cyclization to **8** and **9** (see above) (**TS-4b**: $\Delta H_f^{\neq} = 56.0$, **TS-5b**: $\Delta H_f^{\neq} = 54.0\ kJ\,mol^{-1}$). Thus, the difference in energy for the cyclization of **4** to provide the spiro compound **12** relative to that for the cyclization of **4** to **8** amounts to $47.6\ kJ\,mol^{-1}$.

Based on the calculated results, cyclization from conformation **B** can be neglected, as the transition states for both types of cyclization (C19 → C20 and C16 → C20 are higher in energy (**TS-4c**: $\Delta H_f^{\neq} = 35.7$, **TS-5c**: $\Delta H_f^{\neq} = 29.2$, **TS-4d**: $\Delta H_f^{\neq} = 74.5$, **TS-5d**: $\Delta H_f^{\neq} = 72.1\ kJ\,mol^{-1}$).

The calculations show that the direct formation of the spiro compound **12** or of the σ complex **10** from **4** is energetically much less favorable than the formation of **8** or **6** from **4**. Thus, we regard the postulated spirotetrapyrrole model for the formation of uroporphyrinogen III (**2**) from hydroxymethylbilan (**1**) as less likely and therefore suggest the mechanism outlined in Scheme 1 for the formation of **2** from **1**. This mechanism is in agreement with the results of the calculations performed and with the investigations on the biosynthesis of **2** conducted to date.

The first step is the protonation of the hydroxyl group in **1** by an acid moiety in a pocket of the enzyme cosynthetase, followed by formation of the uroporphyrinogen I σ complex

14. The initially formed oxonium ion is attacked from above by the pyrrole ring D to give **14** with a β-directed H atom on C19 (or vice versa). This step is followed by numerous reversible suprafacial [1,5] sigmatropic shifts to provide the spiro σ complex **15** and subsequently the uroporphyrinogen III σ complex **16**, in which the H atom on C19 is now in the α position (or vice versa). Abstraction of this proton by a suitably placed base in the enzymic cleft—presumably the anion of the acid that protonated **1** in the first step—leads to formation of uroporphyrinogen III (**2**) in an irreversible reaction.

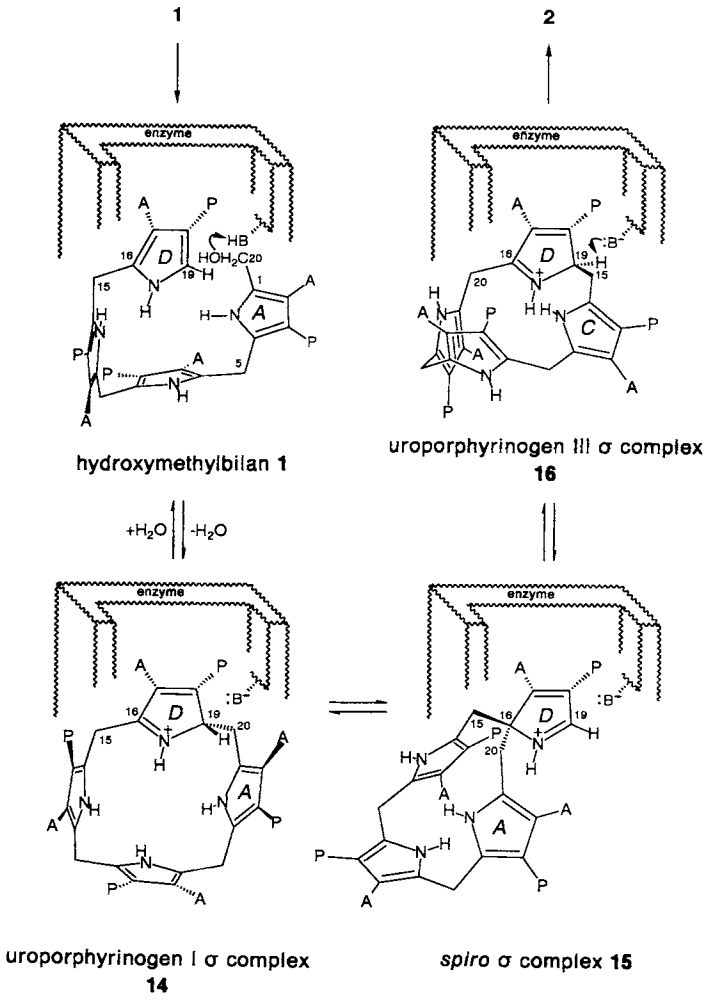

Scheme 1. Postulated biosynthetic route to uroporphyrinogen III (**2**) from hydroxymethylbilan (**1**) (A: CH_2CO_2H, P: $(CH_2)_2CO_2H$).

In summary it can be said that nature had to find a way to improve the unselective synthesis of uroporphyrinogen III in the primordial broth. This was accomplished with the formation of the enzyme cosynthetase, which, as we assume, prohibits the abstraction of a proton of the initially formed uroporphyrinogen I σ complex to give uroporphyrinogen I, whilst the abstraction of a proton from the uroporphyrinogen III σ complex, which is formed in equilibrium, is enhanced giving uroporphyrinogen III. The differentiation of the protons in the σ complexes by the enzyme is possible as they have opposite orientations.

Received: February 12, 1993 [Z 5865 IE]
German version: *Angew. Chem.* **1993**, *105*, 1090

[1] A. R. Battersby, C. J. R. Fookes, K. E. Gustafson-Potter, E. McDonald, G. W. J. Matchham, *J. Chem. Soc. Perkin Trans. 1* **1982**, 2427–2444.
[2] L. Bogorad, *J. Biol. Chem.* **1958**, *233*, 501–509.
[3] L. Bogorad, *J. Biol. Chem.* **1958**, *233*, 510–515.
[4] a) A. R. Battersby, F. J. Leeper, *Chem. Rev.* **1990**, *90*, 1261–1274; b) J. H. Mathewson, A. H. Corwin, *J. Am. Chem. Soc.* **1961**, *83*, 135–137.
[5] a) A. H. Jackson, W. Lertwanawatana, R. K. Pandey, K. R. N. Rao, *J. Chem. Soc. Perkin Trans. 1* **1989**, 374–375; b) A. R. Battersby, M. G. Baker, H. A. Broadbend, C. J. R. Fookes, F. J. Leeper, *ibid.* **1987**, 2027–2028; c) A. R. Battersby, H. A. Broadbend, C. J. R. Fookes, *J. Chem. Soc. Chem. Commun.* **1983**, 1240–1242.
[6] a) A. I. Scott, *Tetrahedron* **1992**, *48*, 2559–2578; b) A. I. Scott, *Acc. Chem. Res.* **1990**, *23*, 308–317.
[7] L. F. Tietze, H. Geissler, *Angew. Chem.* **1993**, *105*, 1087; *Angew. Chem. Int. Ed. Engl.* **1993**, *32*, 1040.
[8] The transition structures were optimized with the NS01A routine (M. J. D. Powell, J. Chandresekar, P. H. M. Budzelaar, T. Clark) of the VAMP software package and characterized with FORCE calculations: J. W. McIver, A. Kormonicki, *J. Am. Chem. Soc.* **1972**, *94*, 2625–2633.
[9] M. J. S. Dewar, E. G. Zoebisch, E. F. Healy, J. J. P. Stewart, *J. Am. Chem. Soc.* **1985**, *107*, 3902–3909.
[10] D. Mauzerall, *J. Am. Chem. Soc.* **1960**, *82*, 2601–2605.

Highly Enantioselective Protonation of Thiol Ester Enolates

By *Charles Fehr,* Isabelle Stempf,* and *José Galindo*

Enantioselective protonation of achiral enolates using an efficient and synthetically useful chiral proton source has long been discussed and has great synthetic potential. Recent progress in this field[1–3] has led to enantioselectivities of up to 91 % *ee*.[2] From both preparative and mechanistic standpoints greater enantiofacial discrimination would be highly desirable. Our efforts have concentrated on the preparation of enantiomerically pure (*R*)- and (*S*)-α-cyclogeranic acid ((*R*)-**1** and (*S*)-**1**)[4] which are pivotal, versatile intermediates in the synthesis of fragences and in medicinal chemistry.[5]

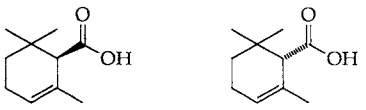

We herein report the large-scale synthesis of thiol esters (*S*)-**4**, (*S*)-**5**, and (*R*)-**4** by an unprecedentedly efficient enantioselective protonation (99 % *ee*) of enolates **4**(Li) and **5**(Li) with readily accessible and easily recoverable (−)- and (+)-*N*-isopropylephedrine ((−)-**7** and (+)-**7**)[11] as the chiral proton source.

The transformations of (*R*)-**4** and (*S*)-**4** into (*R*)-**1** and (*S*)-**1** as well as the perfume components (*R*)- and (*S*)-methyl-α-cyclogeranate ((*R*)-**2** and (*S*)-**2**) and (*S*)-α-damascone ((*S*)-**11**)[11] under nonracemizing conditions (see below) demonstrate the importance of the new enantioselective protonation protocol.[6]

When racemic methyl α-cyclogeranate ((*R*, *S*)-**2**) was deprotonated with *n*BuLi and the resulting enolate **2**(Li)[7] (*Z*/

[*] Dr. C. Fehr, Dr. I. Stempf[+], J. Galindo
Firmenich SA, Research Laboratories
P.O. Box 239, CH-1211 Geneva 8 (Switzerland)
Telefax: Int. code +(22)7803334
[+] Postdoctoral fellow at Firmenich SA (1990–1991).

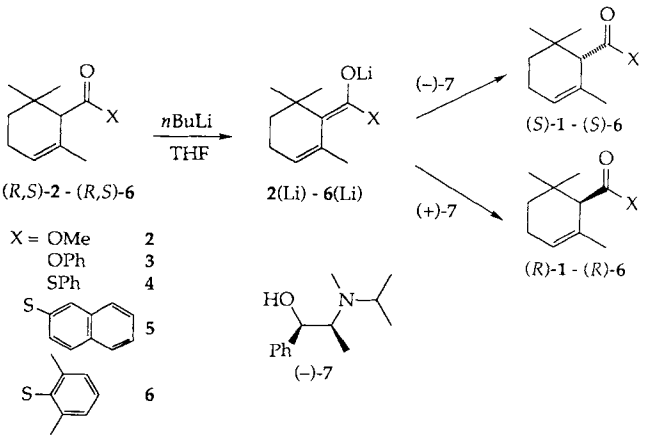

E=19:1)[8] protonated with (−)-7, (*S*)-**2** was obtained with 36% *ee*[9, 10] (Table 1, entry 1). This low enantiofacial discrimination may be due to an insufficient structural differentiation of the enolate substituents on C1 (OLi vs. OMe) for efficient enantiotopic recognition, and an overly rapid protonation of **2**(Li) due to the high pK_a of **2**. Therefore, phenyl ester **3** and the aryl thiol esters **4**,[7] **5**, and **6** were chosen as substrates.

Table 1. Enantioselective protonation of enolates **2**(Li)–**6**(Li).

Entry	Substrate	Reaction conditions (equiv; T [°C] (t[min]))	*ee* [%]	Yield [c] [%]
1	**2**	1) *n*BuLi (2.0; −78 (240)) 2) (−)-**7** (2.6; −100 (60) → −10 (25))	36 (*S*)	–
2	**3**	1) *n*BuLi (3.0; −100 (180)) 2) (−)-**7** (4.0; −100 (60) → −10 (25))	77 (*S*)	–
3	**4**	1) *n*BuLi (1.5; −100 (120))[a], 2) (−)-**7** (2.0; −100 (60) → −10 (25))	**99** (*S*)	87
4	**4**	1) [b], 2) (+)-**7** (2.0; −100 (60) → −10 (25))	**99** (*R*)	87
5	**5**	1) [b], 2) (−)-**7** (2.0; −100 (60) → −10 (25))	**99** (*S*)	82
6	**6**	1) *n*BuLi (1.7; −100 (120)) 2) (−)-**7** (2.3; −100 (60) → −10 (25))	90 (*S*)	–

[a] Use of 1.1 equiv *n*BuLi gave 97% *ee*. [b] As in entry 3. [c] After distillation.

To ensure efficient deprotonation, the starting ester was deprotonated with 1.5–3 equiv *n*BuLi in THF/hexane at −100 °C (liquid N_2/Et_2O).[11] Protonation of **3**(Li) with (−)-**7** at −100 °C (1 h), followed by gradual warming to −10 °C (25 min) afforded (S)-**3** with 77% *ee*[12] (Table 1, entry 2). In line with our expectations, thiol esters **4**–**6** gave even better results (Table 1, entries 3–6): we were very gratified to find an exceptionally high enantioselectivity of more than 200:1[12] for the protonation of both phenyl thiol ester enolate **4**(Li)[13] and 2-naphthyl thiol ester enolate **5**(Li). In addition, when (−)-**7** and (+)-**7** were used, (*S*)-**4** and (*R*)-**4**, respectively, were obtained with 99% *ee* (Table 1, entries 3 and 4). These values are the highest enantioselectivities yet reported for enolate protonations.

The propensity of the thiol ester enolates to form ketenes by elimination of thiolate, and the fact that ketene **8** was detected by GC (≈ 10%) in all cases studied, led us to also consider an alternative mechanism involving elimination/

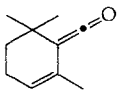

8

enantioselective addition. In order to test this possibility, thiol ester enolate **4**(Li) was treated with lithium 2-naphthyl thiolate prior to protonation with (−)-**7**. The same experiment was then repeated with thiol ester enolate **5**(Li) and lithium phenyl thiolate. In both cases the thiol ester corresponding to the original enolate was isolated with 99% *ee*. The absence of scrambling leads us to the conclusion that a free ketene is not involved. Nevertheless, the addition of lithium phenyl thiolate to **8** in the presence of (−)-**7** was also investigated and showed the same enantiofacial preference as enolate **4**(Li) when treated with (−)-**7**.[14]

A prerequisite for the exceptionally high enantioselectivities obtained in the protonation of aryl thiol ester enolates is the formation of a unique *Z* enolate possessing appropriately differentiated enolate substituents (OLi vs. SAr),[15] coupled with the strong coordination and chelation abilities of ephedrine derivatives.[16] Presumably, protonating agent (−)-**7** or (+)-**7** rapidly forms a 1:1 complex with the enolate leading to a chiral enol/enolate "hybrid" structure,[1a] followed by an irreversible, stereocontrolled C-protonation via an ordered, conformationally rigid transition state.[1a, 3a, 14]

The synthetic value of thiol esters (*R*)-**4** and (*S*)-**4** as versatile chiral building blocks is demonstrated by their ready conversion into (*R*)- and (*S*)-α-cyclogeranic acids ((*R*)-**1** and (*S*)-**1**)[4] (≥ 98% *ee*),[10] methyl esters (*R*)-**2** and (*S*)-**2** (≥ 98% *ee*), (*S*)-α-cyclocitral (**10**)[5a] ($[\alpha]_D^{20} = -743$ (c = 0.05 in $CHCl_3$), 98% *ee*)[10] and (*S*)-α-damascone (**11**)[11] (99% *ee*)[10] (Scheme 1). The saponification (*S*)-

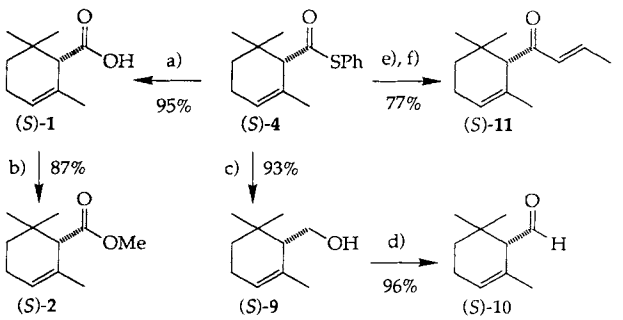

Scheme 1. (*R*)-**4** and (*S*)-**4** as new chiral building blocks (only (*S*) enantiomers are represented). a) H_2O_2 (6.0 equiv), LiOH (3.0 equiv), aq EtOH, 80 °C, 90 min; b) K_2CO_3 (1.2 equiv), MeI (1.2 equiv), acetone, 60 °C, 90 min; c) $LiAlH_4$ (1.0 equiv), Et_2O, 20 °C, 1 h; d) $(COCl)_2$ (1.5 equiv), NEt_3 (5.0 equiv), dimethyl sulfoxide, (2.4 equiv), −70 → 0 °C, 15 min, (Swern oxidation); e) $H_2C{=}CHCH_2MgCl$ (1.70 equiv), LDA (1.05 equiv), THF, 35 °C, 1 h; f) TosOH (cat.), toluene, 20 °C, 15 h.

4 → (*S*)-**1** and the mono-Grignard reaction (*S*)-**4** → (*S*)-**11** merit special comments: the use of LiOOH for the hydrolysis of (*R*)- and (*S*)-**4** without racemization is new.[17, 18] It is not yet clear whether this reaction proceeds via an acyl sulfoxide, followed by O(S) to O(C) rearrangement and hydrolysis of the sulfinyl ester[19] or by normal $B_{AC}2$ (base-catalyzed acyl cleavage via a tetrahedral intermediate) nucleophilic substitution. Conversion of (*S*)-**4** to (*S*)-α-damascone ((*S*)-**11**)[11] with allylmagnesium chloride/LDA proceeds by regioselective deprotonation of the product ketone which favorably competes with nucleophilic attack of a second molecule of the Grignard compound.[20] The fact that no racemization is observed clearly demonstrates that thiol ester (*S*)-**4** is not deprotonated during this process, thus considerably enlarging the scope of possible transformations starting from (*R*)- and (*S*)-**4**.

Experimental Procedure

(*S*)-**4**: A solution of (*R*,*S*)-**4** (40.0 g, 153.8 mmol) in THF (450 mL) was cooled at −100 to −110 °C (Et_2O, liquid N_2) and treated with 1.92 M *n*BuLi in hexane (120.2 mL, 230.8 mmol) (40 min, $T \leq -100$ °C). The solution was stirred between −105 and −100 °C for 2 h. A solution of (−)-**7** (63.7 g, 307.7 mmol) in THF (100 mL) was then added over 50 min at −100 °C. The reaction mixture was cooled to between −102 and −100 °C for 1 h and than allowed to warm up to −10 °C over 25 min. The mixture was poured into vigorously stirred 5% aq. NaOH and extracted with Et_2O. The organic phase was washed successively with H_2O, 5% aq HCl, H_2O, saturated $NaHCO_3$, and saturated NaCl solution, dried over Na_2SO_4, and concentrated. Distillation (110 °C/0.02 Torr) afforded (*S*)-**4** (34.92 g, 87%, ≥ 97% by GC, 99% *ee*[12], $[\alpha]_D^{20} = -421$ ($CHCl_3$, c = 0.04). The combined acidic aqueous phases were basified (10% KOH), extracted (Et_2O), and distilled 90 °C/2 Torr) to afford recovered (−)-**7** (62.4 g, 98%). −(*S*)-**4**: ^{1}H NMR (360 MHz, $CDCl_3$, 25 °C): δ = 0.96 (s, 3 H); 1.05 (s, 3 H); 1.21 (m, 1 H), 1.79 (br. s, 3 H), 1.91 (m, 1 H), 1.98–2.18 (m, 2 H), 2.86 (br. s, 1 H), 5.64 (br. s, 1 H), 7.38 (s, 5 H). IR (neat): $\tilde{\nu}$ = 2970, 1705, 1480, 1440, 980 cm^{-1}. MS (70 eV): *m*/*z*(%): 151 (13), 123 (100), 109 (12), 107 (10), 91 (9), 81 (33).

(*R*)-**4** (≥ 97% pure by GC; 99% *ee*[12], $[\alpha]_D^{20} = +427$ ($CHCl_3$, *c* = 0.06)) was obtained accordingly when (+)-**7** was used.

Reiceived: January 26, 1993 [Z 58321E]
German version: *Angew. Chem.* **1993**, *105* 1091

[1] a) C. Fehr, *Chimia* **1991**, *45*, 253; b) C. Fehr, J. Galindo, *J. Am. Chem. Soc.* **1988**, *110*, 6909.

[2] S. Takeuchi, N. Miyoshi, Y. Ohgo, *Chem. Lett.* **1992**, 551; S. Takeuchi, N. Miyoshi, H. Hirata, H. Hayashida, Y. Ohgo, *Bull. Chem. Soc. Jpn.* **1992**, *65*, 2001; O. Piva, J.-P. Pete, *Tetrahedron Lett.* **1990**, *31*, 5157; D. Potin, K. Williams, J. Rebek, Jr., *Angew. Chem.* **1990**, *102*, 1485; *Angew. Chem. Int. Ed. Engl.* **1990**, *29*, 1420.

[3] a) E. Vedejs, N. Lee, *J. Am. Chem. Soc.* **1991**, *113*, 5483; b) F. Henin, J. Muzart, J.-P. Pete, A.M'Boungou-M'passi, H. Rau, *Angew. Chem.* **1991**, *103*, 460; *Angew. Chem. Int. Ed. Engl.* **1991**, *30*, 416; K. Matsumoto, H. Ohta, *Tetrahedron Lett.* **1991**, *32*, 4729; A. Kumar, R. V. Salunkhe, R. A. Rane, S. Y. Dike, *J. Chem. Soc. Chem. Commun.* **1991**, 485; U. Gerlach, S. Hünig, *Angew. Chem.* **1987**, *99*, 1313; *Angew. Chem. Int. Ed. Engl.* **1987**, *26*, 1283, L. Duhamel, P. Duhamel, S. Fouquai, J. Eddine, O. Peschard, J.-C. Plaquevent, A. Ravard, R. Solliard, J.-Y. Valnot, H. Vincens, *Tetrahedron* **1988**, *44*, 5495 and references therein; c) for enzyme or antibody-catalyzed enantioselective C-protonations of enols (up to 96% *ee*): J.-L. Reymond, K. D. Janda, R. A. Lerner, *J. Am. Chem. Soc.* **1992**, *114*, 2257; K. Matsumoto, S. Tsutsumi, T. Ihori, H. Ohta, *ibid.* **1990**, *112*, 9614; review: H. Waldmann, *Nachr. Chem. Tech. Lab.* **1991**, *39*, 413.

[4] For the resolution of racemic **1**, see: D. J. Bennet, G. R. Ramage, J. L. Simonsen, *J. Chem. Soc.* **1940**, 418; and ref. [5b].

[5] a) T. Matsumoto, S. Usui, *Bull. Chem. Soc. Jpn.* **1979**, *52*, 212; R. Buchecker, R. Egli, H. Regel-Wild, C. Tscharner, C. H. Eugster, G. Uhde, G. Ohloff, *Helv. Chim. Acta* **1973**, *56*, 2548; T. Matsumoto, S. Usui, *Chem. Lett.* **1978**, 105; Y. Masaki, K. Hashimoto, H. Iwai, K. Kaji, *ibid.* **1978**, 1203; b) T. Oritani, K. Yamashita, *Agric. Biol. Chem.* **1987**, *51*, 1271; and ref. [1a].

[6] (*R*)-**2** has a precious flowery, fruity damascone-like fragrance, whereas (*S*)-**2** is characterized by a green, metallic, minty, camphoraceous note, see: C. Fehr, I. Stempf, J. Galindo, Swiss Patent application 13. October 1992.

[7] C. Fehr, J. Galindo, *J. Org. Chem.* **1988**, *53*, 1828.

[8] *E*/*Z* ratios determined by NOE experiments on the corresponding Me_3Si ketene acetals.

[9] Complexation of enolate **2**(Li) with (−)-**7**(Li) or (−)-**7**(MgCl) (metalated (−)-**7**) prior to protonation with (−)-**7** [1b] did not bring any improvement (36% *ee* and < 5% *ee*).

[10] Determined by gas chromatography using permethylated β-cyclodextrin in OV-1701 as chiral stationary phase; column length: 12 m. For use of short columns, see: M. Lindström, *J. High Resolut. Chromatogr.* **1991**, *14*, 765.

[11] Above −80 °, the enolates **3**(Li)–**6**(Li) obtained are converted via ketene **8**[7] to 1-(2,6,6-trimethyl-2-cyclohexenyl)-1-pentanone.

[12] Determined by conversion of **3**–**6** into (2,6,6-trimethyl-2-cyclohexenyl) methyl acetate [1) $LiAlH_4$, Et_2O; 2) AcCl, pyridine, Et_2O] and GC measurements using permethylated β-cyclodextrin in OV-1701 as chiral stationary phase.

[13] Trapping of **4**(Li) with Me_3SiCl gives almost exclusively (*Z*) ketene thiol acetate (*Z*/*E* ≥ 98:2 by GC). After distillation, the *Z*/*E* ratio is 83:17 (GC and NOE experiments).

[14] See C. Fehr, I. Stempf, J. Galindo, *Angew. Chem.* **1993**, *105*, 1093; *Angew. Chem. Int. Ed. Engl.* **1993**, *32*, 1044.

[15] The pK_a of the substrate and the nucleofugal properties of X are also critical. Protonation of the α-cyclothiogeranate enolate with X=*S*n*Bu* showed low enantioselectivity (30% *ee*).

[16] E. M. Arnett, M. A. Nichols, A. T. McPhail, *J. Am. Chem. Soc.* **1990**, *112*, 7059.

[17] Other conditions tested (aq. LiOH, dimethoxyethane (DME), 85 C; aq. NaOH, THF, 65 °C) were inefficient.

[18] Similar conditions have been previously applied in the saponification of esters and amides: E. J. Corey, S. Kim, S. Yoo, K. C. Nicolaou, L. S. Melvin, Jr., D. J. Brunelle, J. R. Falch, E. Tribulski, R. Lett, P. W. Sheldrake, *J. Am. Chem. Soc.* **1978**, *100*, 4620; D. A. Evans, T. C. Britton, J. A. Ellmann, *Tetrahedron Lett.* **1987**, *28*, 6141; W. Oppolzer, J. Blagg, I. Rodriguez, E. Walther, *J. Am. Chem. Soc.* **1990**, *112*, 2767.

[19] K. Schank, A. Frisch, B. Zwanenburg, *J. Org. Chem.* **1983**, *48*, 4580.

[20] C. Fehr, J. Galindo, *Helv. Chim. Acta* **1986**, *69*, 228.

Enantioselective Addition of Aromatic Thiols to a Ketene

By *Charles Fehr*,* *Isabelle Stempf*, and *José Galindo*

In the preceding communication, we reported the enantioselective protonation of *Z* thiol ester enolates **1**(Li) and **2**(Li) with 99% *ee*, using (+)- or (−)-*N*-isopropylephedrine ((+)-**4** or (−)-**4**) as the chiral proton source.[1] A prerequisite for the success of this process is the highly stereoselective formation of a *Z* thiol ester enolate at low temperature, since above −80 °C enolates **1**(Li) and **2**(Li) eliminate lithium thiolate to give ketene **5**.

Both preparative and mechanistic considerations directed our interest to a hitherto unknown reaction, the enantioselective addition of a thiolate to a ketene (e.g. **5** → **1**(Li) → (−)-**1** or (+)-**1**) in the presence of a chiral proton donor.[2, 3] We now describe the successful realization of this procedure (up to 97% *ee*) and its extension to a catalytic version (up to 90% *ee* with 2–5 mol% chiral catalyst).

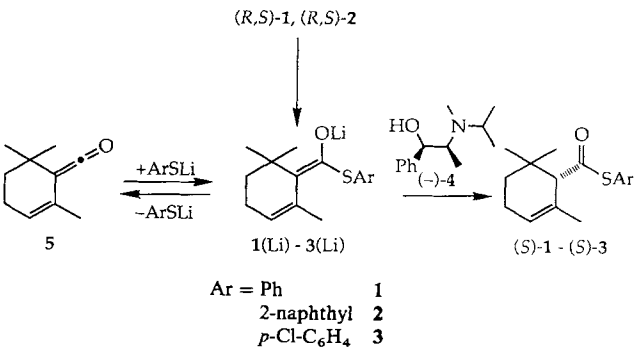

Scheme 1. Enantioselective addition of thiols to **5**. The deprotonation of racemic **1** and **2** is described in ref. [1].

Slow addition (3–4 h) of (−)-**4** to a solution of **5** and lithium thiophenoxide in THF at −55 °C afforded thiol ester (*S*)-**1** in 84% yield and 95% *ee* (Table 1, entry 1). Thiol ester (*S*)-**3** was obtained analogously in 83% yield and 97% *ee* from **5** and lithium *p*-chlorothiophenoxide (Table 1, entry 2). Since under these conditions the equilibrium between **5** and **1**(Li) (or **3**(Li)) lies on the side of **5**, the reaction rate is controlled by the addition of (−)-**4**. This allows rapid and irreversible C-protonation of the incipient enolate. In this

[*] Dr. C. Fehr, Dr. I. Stempf,[+] J. Galindo
Firmenich SA, Research Laboratories
P.O. Box 239, CH-1211 Geneva 8 (Switzerland)
Telefax: Int. code + (22)7803334

[+] Postdoctoral fellow at Firmenich SA (1990–1991).

manner, the concentration of (−)-**4** in the reaction medium is kept low, thus minimizing the risk of proton exchange with the thiolate.[4]

Table 1. Results of the reactions following Scheme 1 (stoichiometric and catalytic).

Entry	Ar	Mol % (−)-**4**	T [°C]	Addition time [h]	Reaction time [h]	*ee* [%] [a]	Yield [%] [c]
1	Ph	100	−55	3	3.5	95 [b]	84
2	*p*-Cl-C_6H_4	100	−55	4	4.5	97	85
3	Ph	5	−27	3	3.5	89	86
4	Ph	2	−27	1	1.5	77	87
5	*p*-Cl-C_6H_4	5	−27	3	3.5	90	81
6	*p*-Cl-C_6H_4	2	−27	3	3.5	57	–

[a] For (*S*)-**1** or (*S*)-**3** the *ee* values and absolute configurations were determined by GC of the corresponding (2,6,6-trimethyl-2-cyclohexenyl)methyl acetate using permethylated β-cyclodextrin in OV-1701 as chiral stationary phase. [b] At −78°: 90% *ee* (72% yield); at −30°; 93% *ee* (83% yield). [c] After distillation.

We next tried to devise a catalytic process, in which the aromatic thiol ArSH serves as both nucleophile and proton source in the presence of a catalytic amount of (−)-**4**(Li). We reasoned that if the rate of introduction of ArSH to a solution of **5** and a catalytic amount of (−)-**4**(Li) in THF is maintained low enough to avoid accumulation of ArSH ([ArSH] ≤ [(−)-**4**(Li)]), and if the added thiol is selectively deprotonated by (−)-**4**(Li) and not by the intermediate thiol ester enolate, a catalytic cycle according to Scheme 2 might be possible. It was envisaged that the mixed reagent ArSLi/(−)-**4** would add in a possibly reversible step to ketene **5**; fast and irreversible C-protonation of enolate complex **6** would then liberate (−)-**4**(Li), which re-enters in the catalytic cycle.

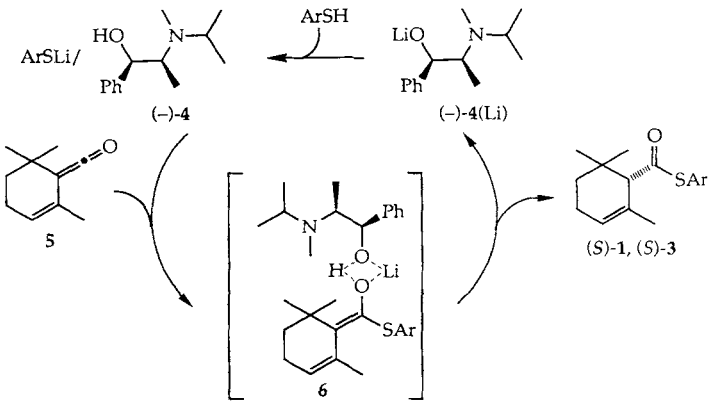

Scheme 2. Catalytic enantioselective addition of aromatic thiols to **5**.

Indeed, this concept proved fruitful. Continuous slow addition of PhSH to a mixture containing 1 mol equiv ketene **5** and 5 mol% (−)-**4**(Li) at −27 °C furnished (−)-**1** (86% yield) with 89% *ee* (Table 1, entry 3). The temperature of −27 °C seems to be optimal: at lower temperature the reaction is too slow, and at 0 °C the enantioselectivity drops markedly (≈ 50% *ee*). This is largely due to the consumption of (−)-**4**(Li) by competing addition to **5** and the accumulation of PhSH. When 2 mol% (−)-**4**(Li) was used, the *ee* value of (−)-**1** decreased to 77% (entry 4). We next applied the catalytic conditions (5 mol% (−)-**4**(Li)) to the addition of *p*-chlorothiophenol (entry 5) and obtained thiol ester (*S*)-**3** with 90% *ee*. The slow addition of the thiols (3 h) turned out to be critical for inducing high enantioselectivities. When *p*-chlorothiophenol was added in 1 h, the *ee* value dropped to 53%. Lowering the amount of (−)-**4**(Li) to 2 mol% proved deleterious (57% *ee*, entry 6) and would presumably require even longer addition times.

Strikingly, the same enantioselectivity trends are observed regardless of whether the esters are generated from **5** or from the racemic esters by deprotonation/protonation.[1,4] Therefore, the mechanism for the chirality-inducing step is likely to be the same in both processes. Taking into consideration the successful catalytic process, in which more than 95% of the protons are supplied by an achiral aromatic thiol, we conclude that a tight transition-state-like complex of type **6** immediately precedes an irreversible stereocontrolled C-protonation.[5–7] Inspection of Table 1 and footnote 4 shows a striking parallel between the *ee* values and the pK_a value of the nucleophile. More acidic thiols such as *p*-chlorothiophenol may be more completely deprotonated to the thiolate;[8] in addition, the lower pK_a of aromatic thiol esters **1**–**3** would allow a slower and more selective protonation.

Experimental Procedure

a) (*S*)-**1** under stoichiometric conditions (1 mol equiv (−)-**4**, Table 1, entry 1): A solution of PhSH (1.47 g, 1.36 mL, 13.33 mmol) in THF (10 mL) containing one crystal of 1,10-phenanthroline was treated without cooling (35–40 °C) with 1.60 M BuLi (8.35 mL, 13.33 mmol) until the colorless solution turned bright violet. The solution was decolorized by addition of one drop of (−)-**4**, diluted with THF (40 mL), cooled to −55 °C, and treated with ketene **5** (2.00 g, 13.33 mmol). Over a period of 3 h, a solution of (−)-**4** (2.76 g, 13.33 mmol) in THF (5 mL) was added with a syringe pump (Bioblock Scientific) (temperature −55 °C). The mixture was stirred for 30 min, poured into vigorously stirred 5% aq NaOH, and extracted with Et_2O. The organic phase was washed successively with H_2O, 5% aq HCl, H_2O, saturated $HaHCO_3$, and saturated NaCl, dried (Na_2SO_4), evaporated, and distilled bulb-to-bulb (oven temperature 130 °C/0.05 Torr) to afford (*S*)-**1** (2.90 g, 84%; 95% *ee*) [1]. The combined acidic aqueous phases were basified (10% aq KOH), extracted (Et_2O), and distilled to afford recovered (−)-**4** (2.70 g, 98%).

b) (*S*)-**1** under catalytic conditions (5 mol% (−)-**4**, Table 1, entry 3): A solution of (−)-**4** (322 mg, 0.67 mmol) in THF (5 mL) containing one crystal of 1,10-phenanthroline was treated with 1.60 M BuLi (0.42 mL, 0.67 mmol) until the colorless solution turned bright violet. Upon addition of the first drop of PhSH (55 mg, 0.05 mL, 0.50 mmol) in THF (0.2 mL) the color faded. The solution was diluted with THF (35 mL), cooled to −27 °C (cryostat at −30 °C) and treated with ketene **5** (2.00 g, 13.33 mmol). Over a period of 3 h, a solution of PhSH (1.35 g, 1.25 mL, 12.30 mmol (total amount 12.80 mmol; 0.96 mol equiv)) in THF (5 mL) was added with a syringe pump (Bioblock Scientific) (temperature −27 °C). Stirring was continued for 30 min. Workup as above afforded (*S*)-**1** (2.98 g, 90% based on PhSH (86% based on **5**); 89% *ee*).

Received: January 26, 1993 [Z 5833 IE]
German version: *Angew. Chem.* **1993**, *105*, 1093

[1] C. Fehr, I. Stempf, J. Galindo, *Angew. Chem.* **1993**, *105*, 1091; *Angew. Chem. Int. Ed. Engl.* **1993**, *32*, 1042.

[2] a) For enantioselective amine-catalyzed additions of alcohols to ketenes, see: H. Pracejus, *Liebigs Ann. Chem.* **1960**, *634*, 9; H. Pracejus, G. Kohl, *ibid.* **1969**, *722*, 1; A. Tille, H. Pracejus, *Chem. Ber.* **1967**, *100*, 196; b) for diastereoselective additions of chiral alcohols to ketenes, see: U. Salz, C. Rüchardt, *Tetrahedron Lett.* **1982**, *23*, 4017; J. Jähme, C. Rüchardt, *Angew. Chem.* **1981**, *93*, 919; *Angew. Chem. Int. Ed. Engl.* **1981**, *20*, 885; R. D. Larsen, E. G. Corley, P. Davis, P. J. Reider, E. J. J. Grabowsky, *J. Am. Chem. Soc.* **1989**, *111*, 7650; c) for reviews on ketene additions, see: T. T. Tidwell, *Acc. Chem. Res.* **1990**, *23*, 273; H. Buschmann, H. D. Scharf, N. Hoffmann, P. Esser, *Angew. Chem.* **1991**, *480*; *Angew. Chem. Int. Ed. Engl.* **1991**, *30*, 477.

[3] For a thio Michael addition/enantioselective protonation, see: A. Kumar, R. V. Salunkhe, R. A. Rane, S. Y. Dike, *J. Chem. Soc. Chem. Commun.* **1991**, 485.

[4] Indeed, when **5** was stirred with an equimolar mixture of lithium thiolate and (−)-**4** in THF at −60 °C for 3 h, (*S*)-**1** or (*S*)-**3** were obtained with diminished enantioselectivities of 81 and 94% *ee*, respectively. Low enantiofacial discriminations (10–40% *ee*) resulted from the reactions of **5** with BnSH or BuSH at −70 °C and with PhOH, MeOH, or (−)-**4** at 20 °C.
[5] For an enantioselective protonation with intramolecular proton return, see: E. Vedejs, N. Lee, *J. Am. Chem. Soc.* **1991**, *113*, 5483.
[6] The postulated mechanism is in line with related nucleophilic additions to ketenes, see refs. [2a, c].
[7] For catalytic enantioselective additions of thiols to cycloalkenones, see: H. Hiemstra, H. Wynberg, *J. Am. Chem. Soc.* **1981**, *103*, 417.
[8] *p*-Chlorothiophenol: $pK_a = 6.96$, thiophenol: $pK_a = 7.76$; see: F. G. Bordwell, H. M. Andersen, *J. Am. Chem. Soc.* **1953**, *75*, 6019. Amine-catalyzed additions of thiols to maleic anhydride also necessitate prior dissociation of the thiol. Indeed, the rate of thiol addition has been found to be proportional to the acid strength of the thiol; *p*-chlorothiophenol reacts faster than *n*BuSH (pK_a 12.4), see: B. Dmuchovsky, B. D. Vineyard, F. B. Zienty, *J. Am. Chem. Soc.* **1964**, *86*, 2874.

Alternating Ferro- and Antiferromagnetic Interactions in a Chainlike Cu^{II} Coordination Polymer**

By *Giovanni De Munno, Miguel Julve,* Francesc Lloret, Juan Faus, Michel Verdaguer*, and *Andrea Caneschi*

One of the best known magneto-structural correlations in systems with magnetic exchange interactions concerns the di-μ-hydroxo-copper(II) complexes $[LCu(OH)_2CuL]^{2+}$.[1] Systematic studies of this family of complexes have established that the singlet–triplet energy gap J is directly proportional to the Cu-OH-Cu bridging angle θ, leading to a singlet ground state for $\theta > 97.5°$ and to a triplet ground state for $\theta < 97.5°$. The value of θ ist strongly influenced by the nature of the terminal ligand L. In this respect we have restricted ourselves to complexes that contain chelating N donor groups as terminal ligands, and for L = diamine[2] antiferromagnetic and for L = 2,2′-bipyridine[2b, 3] ferromagnetic coupling has been observed.

In a recent work, some of us investigated the complex formation between $[Cu(bpym)]^{2+}$ (bpym = 2,2′-bipyrimidine) and OH^- in aqueous solution.[4] The only hydroxo species whose formation was observed in solution is the di-μ-hydroxo $[Cu_2(bpym)_2(OH)_2]^{2+}$ complex. This complex was isolated in the solid state as a perchlorate salt, and displays a relatively strong intramolecular ferromagnetic coupling ($J = 147\ cm^{-1}$), as expected from the θ value (95.0°). Bpym can also act as a bischelating ligand towards transition metal ions,[5] and its ability to transmit antiferromagnetic coupling makes this dinuclear complex a suitable precursor of alternatingly bridged one-dimensional (1D) structures with alternating ferromagnetic (through the hydroxo bridge) and antiferromagnetic (through the bpym bridge) interactions. It should be noted that examples of alternating ferromagnetic/antiferromagnetic exchange in 1D chains are very rare.[6]

Our first attempts along this line led us to prepare the dinuclear precursor **1** and the related Cu^{2+} complex **2**. These

$[Cu_2(bpym)_2(H_2O)_2(OH)_2(NO_3)_2] \cdot 4H_2O$ **1**

$[Cu_2(bpym)(OH)_2(NO_3)_2] \cdot 2H_2O$ **2**

compounds were characterized by elemental analysis, IR spectroscopy, magnetic measurements, and X-ray structural analysis.[7]

The crystal structure of **1** consists of discrete, centrosymmetric di-μ-hydroxocopper(II) dimers with bpym as terminal ligand, weakly coordinated water molecules, and unidentate nitrate anions (bound through an O atom), and molecules of water of crystallization. The coordination geometry around each Cu^{II} ion is approximately octahedral with tetragonal distortion. The two bridging hydroxo groups and the two nitrogen atoms of the bpym ligand form the equatorial plane, and a water molecule and an oxygen atom of a nitrate anion occupy the axial positions (Fig. 1). The Cu–N and

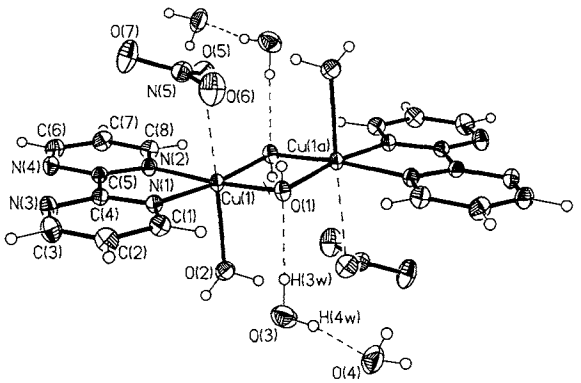

Fig. 1. Molecular structure of **1** (ellipsoids drawn at the 30% probability level). Selected distances [Å] and angles [°] (standard deviations in parentheses): Cu(1)-N(1) 2.014(2), Cu(1)-N(2) 2.018(2), Cu(1)-O(1) 1.944(2), Cu(1)-O(1a) 1.943(2), Cu(1)-O(2) 2.310(2), Cu(1)-O(5) 2.691(2); N(1)-Cu(1)-N(2) 80.7(1), N(1)-Cu(1)-O(1) 96.1(1), N(1)-Cu(1)-O(2) 97.1(1), N(1)-Cu(1)-O(5) 84.3(1), N(1)-Cu(1)-O(1a) 172.5(1), N(2)-Cu(1)-O(1a) 98.0(1), N(2)-Cu(1)-O(2) 91.0(1), N(2)-Cu(1)-O(5) 84.7(1), N(2)-Cu(1)-O(1) 172.7(1), O(1)-Cu(1)-O(1a) 84.3(1), O(1)-Cu(1)-O(2) 95.9(1), O(1)-Cu(1)-O(5) 88.4(1), O(2)-Cu(1)-O(5) 175.3(1), O(2)-Cu(1)-O(1a) 90.3(1) [11].

Cu–O (hydroxo bridge) distances in **1** are very close to those observed in the parent compound $[Cu_2(bpym)_2(H_2O)_4(OH)_2](ClO_4)_2 \cdot 2H_2O$.[4] The main difference between these two compounds is that the axial positions are occupied by two water molecules in the perchlorate species, whereas they are filled by a nitrate group and a water molecule in **1**. The four equatorial atoms are coplanar; no atom deviating from the least-squares plane by more than 0.006(2) Å. The copper atom is displaced by 0.122(1) Å from this plane towards the O(2) atom of the water molecule. Hydrogen bonds link coordinated and uncoordinated water molecules and nitrate anions (some of them are represented by broken lines in Fig. 1). The intramolecular Cu(1)···Cu(1a) separation is 2.881(1) Å; the Cu(1)-O(1)-Cu(1a) bridging angle θ is 95.7(1)°.

The crystal structure of **2** consists of chains of copper(II) ions alternatively bridged by bpym and two hydroxo groups, unidentate nitrate anions (bound through an O atom), and uncoordinated water molecules (Fig. 2). Each copper atom

[*] Prof. M. Julve, Dr. F. Lloret, Prof. J. Faus
Departament de Química Inorgànica
Facultat de Química de la Universitat de València
Dr. Moliner 50, E-46100-Burjassot, València (Spain)
Telefax: Int. code + (6)386-4322-02
Prof. G. De Munno
Università della Calabria, Cosenza (Italy)
Prof. M. Verdaguer
Université Pierre et Marie Curie, Paris (France)
Dr. A. Caneschi
Università degli Studi di Firenze (Italy)

[**] This work was supported by the Spanish DGICYT (Project PB91-0807-C02-01) and the Italian Ministero dell'Università e della Ricerca Scientifica e Tecnologica.

has a distored square pyramidal coordination. Two nitrogen atoms of bpym and two oxygen hydroxo groups form the equatorial plane, whereas an oxygen atom of a nitrate ion occupies the axial position. The Cu(1) and Cu(2) copper atoms are not found in equivalent positions (small differences concerning bond lengths and angles of their surroundings are observed). The maximum deviations from the N(1)N(2)O(1)O(2) and N(3)N(4)O(1)O(2) mean planes are 0.076(5) and 0.006(5) Å, respectively. The copper atoms rise 0.221(1) [Cu(1)] and 0.227(1) Å [Cu(2)] from their mean basal planes in the direction of the nitrate groups. The dihedral angle between the two equatorial mean planes is 6.2(1)°, whereas the dihedral angle formed between Cu(1)O(1)O(2) and Cu(2)O(1)O(2) is 12.2(2)°. Compound **2** grows as a linear chain with the two nitrate ligands in a *cis* arrangement with respect to the (bpym)Cu(OH)$_2$Cu(bpym) plane. Adjacent pairs of nitrate anions are alternatively up and down along the chain. The nitrate-oxygen atoms of one chain point towards the copper atoms of the nearest one (Fig. 2, bottom) [Cu(1)···O(4) and Cu(2)···O(8) distances are 2.9 and 3.1 Å, respectively]. The Cu(1)···Cu(2) separation [2.886(1) Å] and the Cu-μ-OH-Cu angles [θ = 96.2(2) and 96.1(2)° for Cu(1)O(1)Cu(2) and Cu(1)O(2)Cu(2), respectively] are very close to those of **1**. The intrachain metal–metal distances between the metal atoms separated by bpym are 5.451(1) [Cu(1)···Cu(1b)] and 5.574(1) Å [Cu(2)···Cu(2a)], whereas the shortest interchain metal–metal distance is 7.040(1) Å.

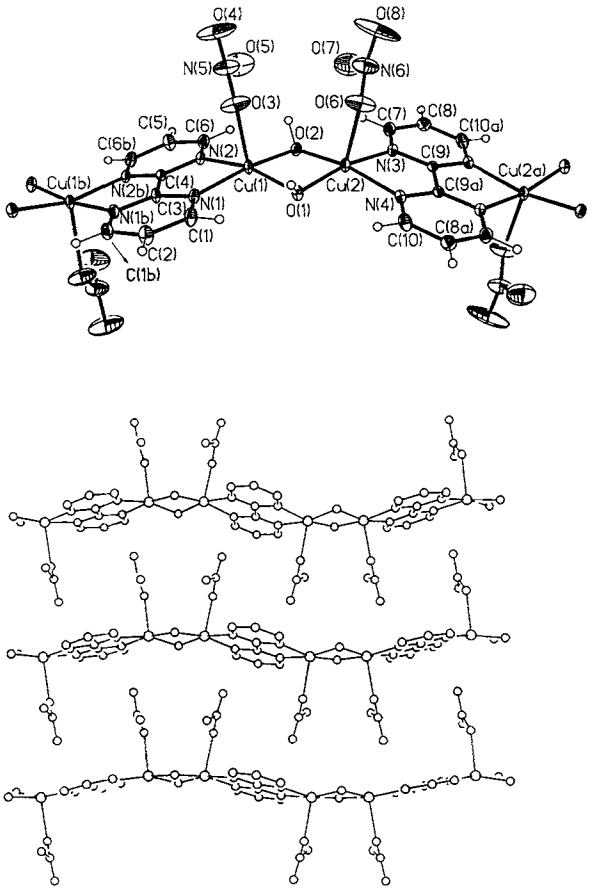

Fig. 2. Crystal structure of **2** (ellipsoids drawn at 30% probability level). Top: View of the alternating chain. Bottom: Arrangement of the chains in the *xz* plane (hydrogen atoms and water molecules have been omitted for clarity). Selected distances [Å] and angles [°] (standard deviations in parentheses): Cu(1)-N(1) 2.054(5), Cu(1)-N(2) 2.035(5), Cu(1)-O(1) 1.921(4), Cu(1)-O(2) 1.923(4), Cu(1)-O(3) 2.298(6), Cu(2)-N(3) 2.036(5), Cu(2)-N(4) 2.055(5), Cu(2)-O(1) 1.931(4), Cu(2)-O(2) 1.930(4), Cu(2)-O(6) 2.320(7); N(1)-Cu(1)-N(2) 81.8(2), N(1)-Cu(1)-O(1) 96.7(2), N(1)-Cu(1)-O(3) 84.1(2), N(1)-Cu(1)-O(2) 171.1(2), N(2)-Cu(1)-O(2) 95.6(2), N(2)-Cu(1)-O(3) 101.0(2), N(2)-Cu(1)-O(1) 163.3(2), O(1)-Cu(1)-O(2) 83.4(2), O(1)-Cu(1)-O(3) 95.4(2), O(2)-Cu(1)-O(3) 104.8(2), N(3)-Cu(2)-N(4) 81.7(2), N(3)-Cu(2)-O(2) 96.0(2), N(3)-Cu(2)-O(6) 96.6(2), N(4)-Cu(2)-O(1) 96.3(2), N(4)-Cu(2)-O(6) 85.2(2), N(4)-Cu(2)-O(2) 166.6(2), O(1)-Cu(2)-O(2) 82.9(2), O(1)-Cu(2)-O(6) 95.9(2), O(1)-Cu(2)-N(3) 167.2(2), O(2)-Cu(2)-O(6) 108.2(2) [12].

The magnetic behavior of **1** is characteristic of compounds with a ferromagnetic interaction with a triplet ground state. The value of $\chi_M T$ (χ_M is the magnetic susceptibility per two Cu^{II} ions) at room temperature is 0.96 cm^3 mol^{-1} K, a value somewhat larger than expected for two uncoupled Cu^{II} ions; $\chi_M T$ increases with decreasing temperature and reaches a plateau at 40 K with $\chi_M T$ = 1.13 cm^3 mol^{-1} K. This value remains constant until 4.2 K. Least-squares fitting through a simple Bleaney–Bowers expression leads to a J value of 114 cm^{-1} and a g value of 2.13.

The $\chi_M T$ value for **2** at room temperature is 0.71 cm^3 mol^{-1} K, a value much smaller than expected for two uncoupled Cu^{II} ions. This value decreases with decreasing temperature and vanishes at temperatures lower than 20 K. The susceptibility curve exhibits a rounded maximum at about 120 K. This compound should exhibit alternating ferromagnetic and antiferromagnetic interactions, since bridging bpym is able to mediate an antiferromagnetic interaction between paramagnetic centers, and the doubly hydroxo bridge with $\theta < 97.5°$, as in **1**, leads to a ferromagnetic coupling. Consequently, the magnetic susceptibility data of **2** were analyzed with a 14-spin ring approximation[13] by using the Hamiltonian $\hat{H} = -J\sum[\hat{S}_{2i}\hat{S}_{2i-1} - \alpha S_{2i}S_{2i+1}]$. This model resulted in an excellent fit to the data (Fig. 3); the best-fit parameters are $J_1 = -140$ cm^{-1}, $J_2 = 105$ cm^{-1}, and

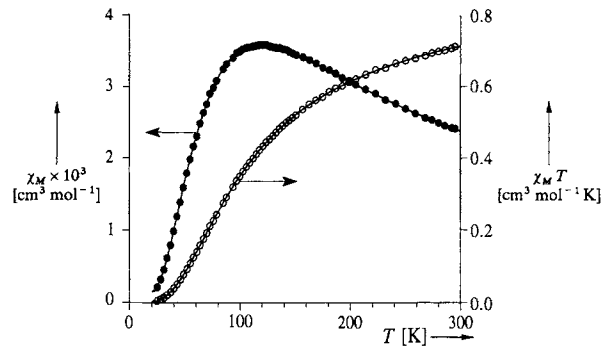

Fig. 3. Plot of $\chi_M T$ (○) and χ_M (●) of **2** versus T. Solid lines correspond to the best theoretical curves.

g = 2.02. The exchange coupling constants of −140 and +105 cm^{-1} are thus accociated with the μ-bpym[14] and di-μ-hydroxo fragments of the alternating chain **2**, respectively. The complex $[Cu_2(bpym)_2(OH)_2]^{2+}$ with its two peripheral potentially bridging ligands appears to be a suitable ferromagnetic building block for the design of new chains with alternating ferro- and antiferromagnetic exchange coupling.

Experimental procedure

1: Blue-green rhombohedral crystals were obtained in good yield by following the previously reported procedure for $[Cu_2(bpym)_2(H_2O)_4(OH)_2](ClO_4)_2 \cdot 2H_2O$ [4].

2: A mixture of **1** and green, chunky single crystals of **2** was obtained by slow evaporation of aqueous solutions containing copper(II) nitrate trihydrate, bpym, and sodium carbonate in a 2:1:1 molar ratio. The yield was low because of the initial precipitation of copper(II) hydroxide. Crystals of **2** were separated manually and studied by X-ray diffraction. The synthesis was repeated until 13 mg of **2** was obtained. This was then used for magnetic measurements. Both **1** and **2** provided correct elemental analysis (C, H, N, Cu).

Received: January 2, 1993 [Z 5792 IE]
German version: *Angew. Chem.* **1993**, *105*, 1122

[1] W. E. Hatfield in *Magneto-Structural Correlations in Exchange Coupled Systems* (Eds.: R. D. Willett, D. Gatteschi, O. Kahn) (*NATO ASI Ser. Ser. C* **1985**, *140*, 555).

[2] a) D. J. Hodgson, *Prog. Inorg. Chem.* **1975**, *19*, 173; b) V. M. Crawford, M. W. Richardson, J. R. Wasson, D. J. Hodgson, W. E. Hatfield, *Inorg. Chem.* **1976**, *15*, 2107, and references therein.

[3] R. J. Majeste, E. A. Meyers, *J. Phys. Chem.* **1970**, *74*, 3497; J. A. Barnes, D. J. Hodgson, W. E. Hatfield, *Inorg. Chem.* **1972**, *11*, 144; M. Toofan, A. Boushehri, M. Ul-Haque, *J. Chem. Soc. Dalton Trans.* **1976**, 217; K. T. McGregor, D. J. Hodgson, W. E. Hatfield, *Inorg. Chem.* **1973**, *12*, 731; I. Castro, J. Faus, M. Julve, M. Verdaguer, A. Monge, E. Gutiérrez-Puebla, *Inorg. Chim. Acta* **1990**, *170*, 251; J. Sletten, A. Sørensen, M. Julve, Y. Journaux, *Inorg. Chem.* **1990**, *29*, 5054; I. Castro, J. Faus, M. Julve, J. A. Real, F. Lloret, C. Bois, *J. Chem. Soc. Dalton Trans.* **1992**, 47.

[4] I. Castro, M. Julve, G. De Munno, G. Bruno, J. A. Real, F. Lloret, J. Faus, *J. Chem. Soc. Dalton Trans.* **1992**, 1739.

[5] a) G. De Munno, G. Bruno, *Acta Crystallogr. Sect. C* **1984**, *40*, 2030; b) G. Brewer, E. Sinn, *Inorg. Chem.* **1985**, *24*, 4580; c) A. Real, J. Zarembowitch, O. Kahn, X. Solans, *ibid.* **1987**, *26*, 2939; d) M. Julve, G. De Munno, G. Bruno, M. Verdaguer, *ibid.* **1988**, *27*, 3160; e) L. W. Morgan, K. V. Goodwin, W. T. Pennington, J. D. Petersen, *ibid.* **1992**, *31*, 1103; f) M. Julve, M. Verdaguer, G. De Munno, J. A. Real, G. Bruno, *ibid.*, **1993**, *32*, 795.

[6] H. J. M. De Groot, L. J. De Jongh, R. D. Willett, J. Reedijk, *J. Appl. Phys.* **1982**, *53*, 8038; C. Benelli, D. Gatteschi, D. W. Carnegie, R. L. Carlin, *J. Am. Chem. Soc.* **1985**, *107*, 2560.

[7] X-ray structure analyses: Siemens R3m/V automatic diffractometer, $Mo_{K\alpha}$, $\lambda = 0.71073$ Å, graphite monochromator, 298 K, Lorentz-polarization and Ψ-scan absorption correction [8]. Data collection, solution and refinement: $\omega - 2\theta$, standard Patterson methods with subsequent Fourier recycling, SHELXTL-PLUS [9]. All non-hydrogen atoms were refined anisotropically. The hydrogen atoms of the water molecules were located on a ΔF map and refined with constraints. The bpym hydrogen atoms were set in calculated positions and refined as riding atoms. They were all refined isotropically. Final geometrical calculations and graphical manipulations were performed with the PARST program [10] and the XP utility of the SHELX-PLUS system, respectively. **1**: $C_{16}H_{26}N_{10}Cu_2O_{14}$ (M_r = 709.5), triclinic, space group $P\bar{1}$, $a = 7.703(1)$, $b = 7.885(1)$, $c = 11.172(2)$ Å, $\alpha = 87.29(1)$, $\beta = 85.85(1)$, $\gamma = 78.17(1)^\circ$, $V = 662.7(2)$ Å^3, $Z = 1$, $\rho_{calcd} = 1.778$ g cm^{-3}, $\mu = 16.9$ cm^{-1}, 2θ range 3–54°, crystal size $0.21 \times 0.19 \times 0.45$ mm^3, $F(000) = 362$; 2901 unique reflections and 2673 assumed as observed with $I > 3\sigma(I)$, 211 parameters, $R(F_o) = 0.030$, $R_w(F_o) = 0.035$ and $S = 1.10$ with $w^{-1} = \sigma^2(F_o) + 0.002000(F_o)^2$. **2**: $C_8H_{12}N_6Cu_2O_{10}$ (M_r = 479.3), monoclinic, space group $C2/c$, $a = 33.619(7)$, $b = 13.040(3)$, $c = 7.040(1)$ Å, $\beta = 101.90(3)^\circ$, $V = 3019.8(10)$ Å^3, $Z = 8$, $\rho_{calcd} = 2.109$ g cm^{-3}, $\mu = 28.9$ cm^{-1}, 2θ-range 2–55°, crystal size $0.27 \times 0.10 \times 0.08$ mm^3, $F(000) = 1920$. 3476 unique reflections and 2032 assumed as observed with $I > 3\sigma(I)$, 255 parameters, $R(F_o) = 0.041$, $R_w(F_o) = 0.047$ and $S = 0.93$ with $w^{-1} = \sigma^2(F_o) + 0.003359(F_o)^2$. Further details of the crystal structure investigations are available on request from the Fachinformationszentrum Karlsruhe, Gesellschaft für wissenschaftlich-technische Information mbH, D-76344 Eggenstein-Leopoldshafen (FRG), on quoting the depository number CSD-57122, the names of the authors, and the journal citation.

[8] A. C. T. North, D. C. Philips, F. S. Mathews, *Acta Crystallogr. Sect. A* **1968**, *24*, 351.

[9] SHELXTL PLUS, Version 3.4, Siemens Analytical X-Ray Instruments Inc., Madison, WI, USA, **1989**.

[10] M. Nardelli, *Comput. Chem.* **1983**, *7*, 95.

[11] Bond lengths and angles in the bpym ligand are in agreement with those reported in the literature. The pyrimidyl rings of bpym are planar, but they form a dihedral angle of 1.4(1)°. The dihedral angle between the equatorial N(1)N(2)O(1)O(1a) and bpym mean planes is 5.5(1)°. The nitrate anion is planar as expected. The N–O bond lengths and the intraanion bond angles average 1.255 Å and 120°, respectively. The nitrate ion contributes to the packing by forming hydrogen bonds involving two of its three oxygen atoms.

[12] Bond lengths and angles of the bridging bpym ligands are close to those of the bpym ligands of **1**. Their pyrimidyl rings are planar. However, only the bpym that bridges the Cu(2) and Cu(2a) atoms is planar, whereas the N(1)C(1)C(2)C(1b)N(1b)C(3) and N(2)C(6)C(5)C(6b)N(2b)C(4) pyrimidyl rings form a dihedral angle of 3.4(2)°. Each water of crystallization is linked through hydrogen bonding to two hydroxo groups of different chains. Only one nitrate-oxygen atom [O(5)] contributes to the network of hydrogen bonds.

[13] J. J. Borrás, Ph. D. Thesis, University of València, **1992**; J. J. Borrás, E. Coronado, J. Curely, J. C. Gianduzzo, R. Georges, *J. Am. Chem. Soc.*, submitted.

[14] The value of J_1 is of the same order of magnitude as previously reported values in bpym-bridged Cu^{II} complexes (see ref. [5d] and references therein), the mechanim of the interaction through bis(bidentate) bridges is now well documented.

Insertion of a Cp Unit into a Metal–Metal Bond: $[Ru_3(CO)_{10}(C_5H_4)]$ and its PPh_3 Derivative**

By *Daniel Heineke* and *Heinrich Vahrenkamp**

Dedicated to Professor Heinrich Nöth on the occasion of his 65th birthday

The field of cyclopentadienylmetal complexes, the oldest and most developed in organotransition metal chemistry, is still fertile and of increasing utility. Recent examples of new compound types[1] and new applications[2] underline this. While only mononuclear cyclopentadienyl complexes have been of practical value, new compositions or structural types are more likely to be found in polynuclear compounds.[3] We demonstrate this here by describing the synthesis and structure of the new Ru_3 clusters **1** with μ_2-η^5:η^1-C_5H_4 units.

Compounds **1a**, **b** were found in the course of our systematic studies of reactions of $[Ru_3(CO)_{12}]$ with phosphorus ylides.[4] These mostly multistep reactions normally lead to organometallic products in which the initially ylidic P–C bond is maintained. An exception to this rule is the reaction between $[Ru_3(CO)_{12}]$ and $Ph_3P{=}C(CH)_4$. Heating the reagents under reflux in cyclohexane for 1 hour results in complete conversion, and after chromatography with hexane over silica gel, yellow **1a** (49%), red $[Ru_3(CO)_{11}PPh_3]$ (8%), and yellow **1b** (29%) are isolated. Thus, the two constituents of the phosphorus ylide are separated and incorporated in one (**1b**) or two (**1a** and $[Ru_3(CO)_{11}PPh_3]$) triruthenium clusters.

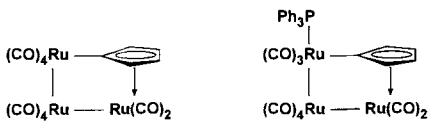

1a **1b**

The compositions of **1a**, **b** were ascertained by mass spectra and NMR data.[5] But only the structure determination of **1b**[6] revealed the new structural type with an open Ru_3 triangle held together by the μ_2-η^5:η^1-C_5H_4 unit (Fig. 1). This C_5H_4 unit is clearly bonded as a metalliocyclopentadienyl (uniform Ru1–C and C–C bond lengths, long Ru2–C1 bond) rather than a cyclopentadienylidene unit (which would bind as a carbene with Ru2 and as an olefin with

[*] Prof. Dr. H. Vahrenkamp, Dr. D. Heineke
Institut für Anorganische und Analytische Chemie der Universität
Albertstrasse 21, D-79104 Freiburg (FRG)
Telefax: Int. code + (761) 203-2900

[**] This work was supported by the Fonds der Chemischen Industrie and by the Volkswagen-Stiftung. We thank Dr. K. Steinbach, Marburg, and Prof. Dr. H. Grützmacher, Freiburg, for mass spectra.

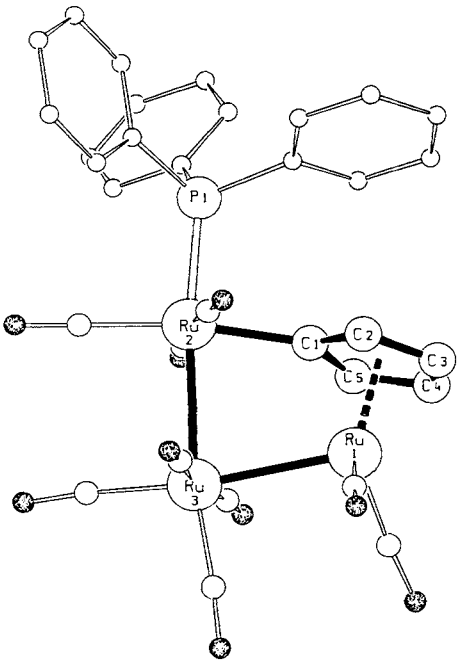

Fig. 1. Molecular structure of **1b**. Selected bond lengths [pm]: Ru2-C1 213.0(5), Ru1-C1 227.1(5), Ru1-C2 222.6(6), Ru1-C3 223.0(6), Ru1-C4 223.4(7), Ru1-C5 222.3(6), C1-C2 143.1(8), C2-C3 142.8(9), C3-C4 138.9(9), C4-C5 143.5(9), C5-C1 143.6(8).

Ru1).[7] Both of these bonding types are known in the chemistry of ruthenium in, for example, **2**[8] and **3**,[9] but this structure in which the cluster geometry is fixed by insertion of a linking Cp unit into a metal–metal bond is, to our knowledge, unprecedented. Compound **4**[10] is, however, an isolobal analogue of **1**, and the mononuclear analogue **5**[11] completes this isoelectronic series of M_3, M_2, and M_1 metallacycles.

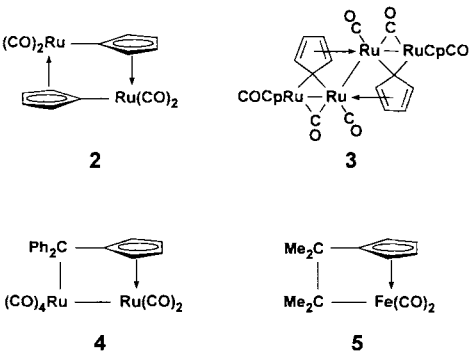

The reaction pathway leading to **1a, b** is as uncommon as their structure. Almost all coordination compounds of $Ph_3P{=}C(CH)_4$ contain this ylide as an intact ligand.[12] Its reactions with $[Os_3(CO)_{10}(MeCN)_2]$, for example, produce closed Os_3 clusters with doubly and triply bridging $Ph_3PC_5H_3$ units.[13] Although the cleavage of phosphorus ylides to generate carbene ligands is not unusual,[12] the separation of the oppositely charged Ph_3P and C_5H_4 fragments and insertion of the cyclopentadienylide fragment into one Ru–Ru bond of $[Ru_3(CO)_{12}]$ are remarkable. Clusters **1a, b** thus extend the long list of product types from reactions of $[Ru_3(CO)_{12}]$ and phosphorus ylides[4, 14] and underline once again the valuable balance of stability and reactivity in triruthenium clusters.

Received: January 15, 1993 [Z 5808 IE]
German version: *Angew. Chem.* **1993**, *105*, 1142

[1] J. L. Kersten, A. L. Rheingold, K. H. Theopold, C. P. Casey, R. A. Wiedenhoefer, C. E. C. A. Hop, *Angew. Chem.* **1992**, *104*, 1364; *Angew. Chem. Int. Ed. Engl.* **1992**, *31*, 1341; see also J. J. Schneider, *ibid.* **1992**, *104*, 1422 and **1992**, *31*, 1392.
[2] See R. F. Jordan, *Adv. Organomet. Chem.* **1991**, *32*, 325–387.
[3] N. J. Coville, K. E. du Plooy, W. Pickl, *Coord. Chem. Rev.* **1992**, *116*, 1–267.
[4] D. S. Bohle, D. Heineke, A. Tiripicchio, M. Tiripicchio Camellini, H. Vahrenkamp, *Angew. Chem.* **1990**, *102*, 938–939; *Angew. Chem. Int. Ed. Engl.* **1990**, *29*, 896–897; D. Heineke, D. S. Bohle, H. Vahrenkamp, *Chem. Ber.* **1993**, *126*, 355–363.
[5] IR (CH_2Cl_2, $\tilde{\nu}$[cm^{-1}]): **1a**: 2115 m, 2065 vs, 2030 vs, 1994 s, 1933 w; **1b**: 2084 vs, 2041 vs, 2004 vs, 1967 sh, 1922 m. ^1H NMR ($CDCl_3$, int. TMS, Cp resonances): **1a**: $\delta = 5.34$ (m, 2H), 4.44 (m, 2H); **1b**: $\delta = 5.05$ (m, 2H), 3.98 (m, 2H). ^{13}C NMR ($CDCl_3$, int. TMS, Cp resonances): **1a**: $\delta = 97.4$ (1C), 90.0 (2C), 85.8 (2C); **1b**: $\delta = 107.5$ (d, $J_{PC} = 8.1$ Hz, 1C), 89.2 (2C), 84.6 (2C). ^{31}P NMR ($CDCl_3$, ext. H_3PO_4): **1b**: $\delta = 29.3$.
[6] Crystal data of **1b**: monoclinic, $P2_1/n$, $a = 11.224(2)$, $b = 16.382(3)$, $c = 17.298(3)$ Å, $\beta = 91.90(3)°$, $Z = 4$ 3441 reflections, $R = 0.031$. Further details of the structure determination may be obtained from the Fachinformationszentrum Karlsruhe, Gesellschaft für wissenschaftlich-technische Information mbH, W-76344 Eggenstein-Leopoldshafen (FRG), upon quotation of the depository number CSD-400041, the authors, and the full journal citation.
[7] For a discussion of these bonding types see W. A. Herrmann, G. Kriechbaum, C. Bauer, E. Guggolz, M. L. Ziegler, *Angew. Chem.* **1981**, *93*, 838–839; *Angew. Chem. Int. Ed. Engl.* **1981**, *20*, 815–816.
[8] K. P. C. Vollhardt, T. W. Weidemann, *J. Am. Chem. Soc.* **1983**, *105*, 1676–1677.
[9] N. D. Feasey, N. J. Forrow, G. Hogarth, S. A. R. Knox, K. A. MacPherson, M. J. Morris, A. G. Orpen, *J. Organomet. Chem.* **1984**, *267*, C41–C44.
[10] S. Töfke, E. T. K. Haupt, U. Behrens, *Chem. Ber.* **1986**, *119*, 96–106.
[11] P. Eilbracht, W. Fassmann, W. Diehl, *Chem. Ber.* **1985**, *118*, 2314–2329.
[12] H. Schmidtbaur, *Angew. Chem.* **1983**, *95*, 980–1000; *Angew. Chem. Int. Ed. Engl.* **1983**, *22*, 907–927.
[13] A. J. Deeming, N. I. Powell, C. Whittaker, *J. Chem. Soc. Dalton Trans.* **1991**, 1875–1880.
[14] D. Heineke, H. Vahrenkamp, *Chem. Ber.* **1993**, *126*, 373–377.

Cs_3AuO, the First Ternary Oxide with Anionic Gold**

By *Claus Feldmann* and *Martin Jansen**

Dedicated to Professor Heinrich Nöth on the occasion of his 65th birthday.

Gold has the highest electron affinity among the metals, 222.73 kJ mol^{-1}, a value comparable to that of iodine (295.30 kJ mol^{-1}).[1] Accordingly, the unusual properties of CsAu, which crystallizes with the CsCl structure type, are attributed to ionic bonding and thus the existence of anionic gold (Au^-).[2] Because of this singular feature,[14] this compound has been intensively studied in recent years. It behaves as a semiconductor with a band gap of approximately 2.6 eV.[3] There is still considerable disagreement whether the cesium auride can be viewed as a purely ionic crystal Cs^+Au^-. Differing ionic contributions to chemical bonding have been discussed, and a value of roughly around 50% is

[*] Prof. Dr. M. Jansen, Dipl.-Chem. C. Feldmann
Institut für Anorganische Chemie der Universität
Gerhard-Domagk-Strasse 1, D-53121 Bonn (FRG)
Telefax: Int. code +(228)735660

[**] This work was supported by the Deutsche Forschungsgemeinschaft and the Fonds der Chemischen Industrie.

the most popular;[2b, 2e, 4] even covalency has been considered.[5] The picture of a pure ionic crystal is weakened by the amazingly high electronic conductivity observed[3b, 6] in comparison to that expected for an ionic model, and by the presence of disorder (Au on Cs positions and vice versa) on the order of 5%.[7, 8] To gain insight into the bonding in CsAu from its chemical behavior, we started conducting solid-state reactions with CsAu to determine whether Au^- ions are transported in solid state through diffusion. We have observed the interdiffusion of Cs_2O and CsAu and established that a new crystalline ternary compound, Cs_3AuO, is formed through transport in the solid. Crystals of higher quality are obtained when CsAu is introduced as the constituting elements in the presence of excess cesium. The rod-shaped ($0.15 \times 0.15 \times 0.38$ mm^3), red-brown, transparent crystals are extremely oxygen and moisture sensitive.

According to the results of X-ray powder diffraction, which were verified by a single-crystal structure determination,[9] Cs_3AuO crystallizes as a hexagonal perovskite with the anti-$CsNiCl_3$ structure type,[10] in which Au and O adopt the crystal-chemical function of Cs and Ni, respectively (Fig. 1). The OCs_6 structural unit is stretched along the threefold axis; the Cs–O distances correspond roughly to those in Cs_2O.[11] Each gold atom is surrounded by 12 cesium atoms in the form of a hexagonal cuboctahedron. The increase in the (averaged) Au–Cs distance (4.08 Å) from that in CsAu (3.69 Å)[2a] is the result of an increase in the coordination number from 8 to 12, and the extent of lengthening corresponds well to that expected. The strong distortion of the polyhedron around Au is striking: the distance between Au and the six Cs neighbors in the a/b level is 3.917(2) Å, and between Au and the 2×3 Cs atoms above and below this layer 4.242(3) Å.

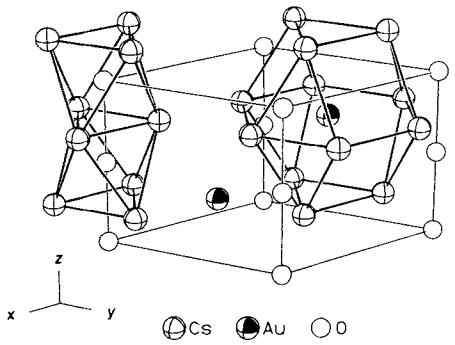

Fig. 1. Unit cell of Cs_3AuO; the polyhedra surrounding Au^- and O^{2-} are emphasized; d(O–Cs) = 2.796(2) Å (6×), d(Au–Cs) = 3.917(2) Å (6×), and 4.242(3) Å (6×).

Every formulation other than the corresponding ionic one, $(Cs^+)_3Au^-O^{2-}$, would require the existence of energetically very high-lying electronic states as well as electron delocalization, which can be excluded due the transparency of the crystals (even in thick layers). Thus, the ionic formulation must correctly describe the fundamental bonding situation. This interpretation is supported by a comparison of the gold L_3-XANES (XANES = X-ray Absorption Near-Edge Structure) spectra of Au_2O_3, $AuCl_3$, AuCN, AuCl, Au, CsAu, and Cs_3AuO (Fig. 2). The area of the prepeak at about 12 keV correlates with the number of unoccupied Au 5d states and is therefore a sensitive indicator for the valence state of gold. One can recognize that the density of free states in the region of the Au valence levels for Cs_3AuO is even lower than that for CsAu. We consider this to be evidence that Au in this compound has an even more distinct anionic character.[12]

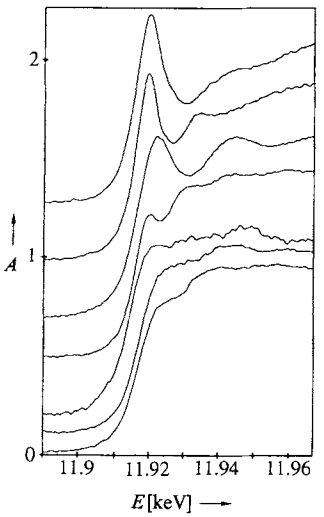

Fig. 2. Au L_3-XANES spectra of Au_2O_3, $AuCl_3$, AuCN, AuCl, Au, CsAu, and Cs_3AuO (from top to bottom).

Experimental Procedure

Cs_3AuO was synthesized by the interdiffusion of equal molar amounts of CsAu (0.601 g, 1.82 mmol) [8] and $CsO_{0.49}$ (0.513 g, 1.82 mmol) [11]. The intimately ground binary components Cs_2O and CsAu were annealled at 300 °C in a gold crucible under argon for 3 weeks. Only small, strongly intergrown crystals of Cs_3AuO were found in the resulting reaction product.

Large, rod-shaped, red-brown, transparent crystals were isolated according to the following method: Equal molar amounts of $CsO_{0.49}$ (0.986 g, 3.50 mmol) and fresh precipitated gold (0.690 g, 3.50 mmol) [13] were heated at 200 °C in a melt of distilled cesium (1.892 g, 14.20 mmol) in a Duran glass tube under argon for eight weeks. The excess cesium was then distilled off under high vacuum (0.01 Pa). To improve the crystal quality, the single-phase residue was annealled for an additional five days at 200 °C in a Duran glass ampule under argon and then cooled slowly (5 K h^{-1}).

Received: February 19, 1993 [Z 5878 IE]
German version: *Angew. Chem.* **1993**, *105*, 1107

[1] H. Hotop, W. C. Lineberger, *J. Phys. Chem. Ref. Data* **1975**, *4*, 539.
[2] a) W. E. Spicer, A. H. Sommer, J. G. White, *Phys. Rev.* **1959**, *115*, 57; b) J. Knecht, R. Fischer, H. Overhof, F. Hensel, *J. Chem. Soc. Chem. Commun.* **1978**, 905; c) R. J. Batchelor, T. Birchall, R. C. Burns, *Inorg. Chem.* **1986**, *25*, 2009.
[3] a) W. E. Spicer, *Phys. Rev.* **1962**, *125*, 1297; b) F. Wooten, G. A. Condas, *Phys. Rev.* **1963**, *131*, 657; c) C. Norris, L. Wallden, *Phys. Status Solidi Sect. A* **1970**, *2*, 381.
[4] J. Robertson, *Phys. Rev. Sect. B* **1983**, *27*, 6322.
[5] G. Steinleitner, W. Freyland, *Phys. Lett. Sect. A* **1975**, *55*, 163.
[6] R. Dupree, D. J. Kirby, W. W. Warren, *Phys. Rev. Sect. B* **1985**, *31*, 5597.
[7] W. Klemm, G. Kienast, J. Verma, *Z. Anorg. Allg. Chem.* **1961**, *310*, 143.
[8] G. A. Tinelli, D. F. Holcomb, *J. Solid State Chem.* **1978**, *25*, 157.
[9] X-ray structural analysis of Cs_3AuO: space group $P6_3/mmc$; $a = 7.830(2)$, $c = 7.059(10)$ Å; $Z = 2$, $\rho_{calcd} = 5.418$ g cm^{-3}; Cs in $6h$ (x = 0.1598(1)), Au in $2d$, O in $2a$; $R = 0.044$; 346 observed reflexions, $F(000) = 504$; Enraf-Nonius CAD-4 diffractometer, ω scan, 2θ range from 3.0° to 34.94°, $Mo_{K\alpha}$ radiation. Further details of the crystal structure investigation may be obtained from the Fachinformationszentrum Karlsruhe, Gesellschaft für wissenschaftlich-technische Information mbH, D-76344 Eggenstein-Leopoldshafen (FRG) on quoting the depository number CSD-57248, the names of the authors, and the journal citation.
[10] G. N. Tishchenko, *Tr. Inst. Kristallogr. Akad. Nauk. SSSR* **1955**, *11*, 93.
[11] A. Helms, W. Klemm, *Z. Anorg. Allg. Chem.* **1939**, *242*, 33.
[12] C. Feldmann, A. Redeker, J. Hormes, M. Jansen, unpublished.
[13] G. Krüss, *Justus Liebigs Ann. Chem.* **1887**, *238*, 43.
[14] Editor's comment: After this communication was submitted, a publication on a Ca_3AuN compound was printed for which Au^- centers were also formulated: J. Jäger, D. Stahl, P. C. Schmidt, R. Kniep, *Angew. Chem.* **1993**, *105*, 738; *Angew. Chem. Int. Ed. Engl.* **1993**, *32*, 709.

Cycloalkano-2*H*-pyrrole as a Stable Intermediate in the Conversion of β-Cycloalkenyl-α-azidoacrylates to Cycloalkano-1*H*-pyrroles**

By *Claus Vogel,* Bernd Schnippenkötter, Peter G. Jones,* and *Peter Bubenitschek*

The thermolysis of substituted vinyl azides in solution has been used to synthesize N-heterocycles such as 2*H*-azirines, 1*H*-pyrroles, indoles, isoquinolines, and benzazepines.[1, 2] In several cases, substituted 2*H*-pyrroles were formed by the thermolysis of 4,4-disubstituted 1-azidobutadienes although with poor yields and as a mixture with the corresponding 1*H*-pyrroles or pyridines.[3] We have found that the thermolysis of β-cycloalkenyl-α-azidoacrylates results in the quantitative formation of substituted cycloalkano-2*H*-pyrroles. In the thermolysis of α-azidocinnamates with *ortho*-alkenyl[2] or -1,3-butadienyl side chains,[4] the vinyl azides or the vinylnitrenes react almost exclusively with these side chains. In our studies of vinyl azides **3**, the vinyl azide unit is not attached to an aryl group but to a cycloalkene bridge in conjugation with a vinyl, phenyl, styryl, or 4-phenylbuta-1,3-dienyl side chain. This structure causes the thermolysis to proceed along a different reaction path.

The conjugated aldehydes **2a–c** were prepared from 2-bromocyclohex-1-ene-1-carbaldehyde (**1**)[5] by the following reaction sequence (Scheme 1): 1. Wittig or Wittig–Horner

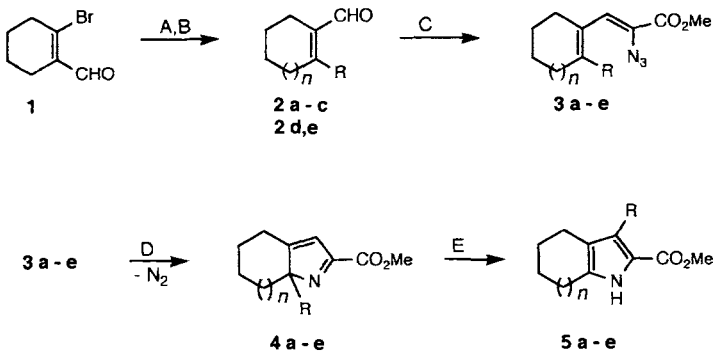

a: R = CH=CH$_2$; *n* = 1; **b**: R = CH=CHPh; *n* = 1;
c: R = CH=CH-CH=CHPh; *n* = 1; **d**: R = Ph; *n* = 1; **e**: R = Ph; *n* = 0

Scheme 1. Synthesis of the substituted 2*H*- and 1*H*-pyrroles **4** and **5**, respectively. Reaction conditions: A: $(EtO)_2P(O)CH_2R^1$/NaH or $Ph_3P{=}CH_2$, THF, room temperature, 70–85%; B: 1.2 equiv *t*BuLi, THF, −78 °C, 2. DMF, −78 °C → room temperature, 80–85%; C: $N_3CH_2CO_2Me$, NaOMe, MeOH, 0 °C → room temperature, 40–60%; D: cyclohexane, xylene, or DMF, 80 °C, 40 min, quantitative; E: for **4a–c**: xylene (or DMF) at reflux, 140 °C, 4 h, 95%; for **4d, e**: tetralin, 200 °C, 2 h, 95%.

reaction (A) for the synthesis of the unsaturated side chain; 2. Br/Li exchange (B) with *tert*-butyllithium following the method of Seebach et al.[6] and subsequent formylation with dimethylformamide (DMF). The functionalized aldehydes **2d, e** were obtained from 1-phenylcyclohexene and 1-phenylcyclopentene, respectively, by Vilsmeier formylation with $POCl_3$/*N*-methylformanilide.[7] The methyl α-azidoacrylates **3a–e** were prepared by the condensation of **2a–e** with methylazidoacetate in the presence of sodium methoxide in methanol (C), according to the method of Knittel to recover methyl α-azidocinnamate.[8] This condensation does not occur if the substituent R in **2** can form a conjugated enolate from the starting aldehyde (e.g. R = methyl).

The thermolysis of vinyl azides **3** in solution at 80 °C (40 min in cyclohexane, xylene, or DMF) proceeded with cleavage of N_2 and gave the substituted cycloalkano-2*H*-pyrroles **4** in quantitative yield. The cyclization products **4a–c** are stable up to 130 °C, **4d, e** even up to 190 °C. Only when the products are heated in refluxing xylene (140 °C, 4 h; **4a–c**) or in tetralin (200 °C, 2 h; **4d, e**) does a slow rearrangement to the substituted 1*H*-pyrroles **5** occur (Scheme 1).

In the thermolysis of vinyl azides, cleavage of nitrogen leads to vinyl nitrenes as the reactive intermediates.[1–3] In the reaction described here, neither the vinyl azide nor the vinyl nitrene reacted with the unsaturated substituent R in **3a–c**, although this was to be expected based on the findings for α-azidocinnamates with unsaturated *ortho* side chains.[2, 4] The products of a 1,7-electrocyclization involving the alkenyl or the phenyl substituents could not be detected. The exclusive formation of the cyclization products **4** can be explained by the quantitative 1,5-electrocyclization of a dienyl nitrene. The cyclization to afford a five-membered ring system apparently proceeds considerably faster than the reaction with the unsaturated side chain. The converse is the case with the corresponding azidocinnamates, whose cyclization would lead to indoles.[1, 2]

The annelated 2*H*-pyrroles **4** rearrange only at high temperatures, presumably by a double 1,5 shift of the substituent R, to give the annelated 1*H*-pyrroles **5**. The first 1,5 shift should lead to the corresponding 3-substituted 3*H*-pyrroles. Then a second 1,5 shift of R and subsequent 1,3 H-migration and aromatization gives **5**. This could well explain the thermal stability of the product **4**.

In the ^1H NMR spectra (400 MHz) of **4a–d**, it is notable that a clearly resolved signal is found for each of the aliphatic ring protons. The structure deduced from the spectroscopic data of the rearranged products **5** was confirmed for **5b** by X-ray crystallography.[9]

Previously, 2*H*-pyrroles were difficult to synthesize. The quantitative synthesis of annelated 2*H*-pyrroles described here provides a good synthetic route to this class of compounds and to isomeric 1*H*-pyrroles.

Experimental Procedure

General thermolysis method: A 0.05 M solution of **3** or **4** was heated (for solvent, temperature, and time, see Scheme 1). After the solvent was distilled off under reduced pressure, the residue was purified by flash chromatography (silica gel, hexane/ethyl acetate 9:1 to 2:1). ^1H NMR data for **4a**: (400 MHz, $CDCl_3$, TMS): δ = 0.94 (dt, *J* = 3.9 Hz, 13.2 Hz, 1H); 1.11 (qt, *J* = 4.4 Hz, 13 Hz, 1H); 1.59 (qt, *J* = 3.5 Hz, 13.4 Hz, 1H); 1.80 (m, 1H); 2.06 (m, 1H); 2.33 (tdd, *J* = 1.7 Hz, 5.7 Hz, 13.1 Hz, 1H; 4-H); 2.68 (m, 1H); 2.84 (m, 1H); 3.92 (s, 3H; OCH_3); 5.00 (d, *J* = 17.5 Hz, 1H; *trans* H of vinyl-CH_2); 5.13 (d, *J* = 10.3 Hz, 1H; *cis* H of vinyl-CH_2); 5.91 (dd, *J* = 17.5 Hz, 10.3 Hz, 1H; vinyl-H); 6.49 (d, *J* = 1.7 Hz, 1H; 3-H).

[*] Dr. C. Vogel, Dipl.-Chem. B. Schnippenkötter, Dipl.-Chem. P. Bubenitschek
Institut für Organische Chemie der Technischen Universität
Hagenring 30, D-38106 Braunschweig
Telefax: Int. code + (531)391-5388
Prof. Dr. P. G. Jones
Institut für Anorganische Chemie der Technischen Universität
Braunschweig

[**] This work was supported by the Deutsche Forschungsgemeinschaft and the Fonds der Chemischen Industrie.

Received: February 5, 1993 [Z 5845 IE]
German version: *Angew. Chem.* **1993**, *105*, 1116

[1] a) A. Hassner in *Azides and Nitrenes* (Ed.: E. F. V. Scriven), Academic Press, Orlando, FL, USA, **1984**, pp. 35–94; b) E. F. V. Scriven, K. Turnbull, *Chem. Rev.* **1988**, *88*, 297.
[2] C. J. Moody in *Studies in Natural Products Chemistry, Vol. 1* (Ed.: A. U. Rahman), Elsevier, Amsterdam, **1988**, pp. 163–185.
[3] a) K. Isomura, M. Okada, H. Taniguchi, *Chem. Lett.* **1972**, 629; b) H. Hemetsberger, I. Spira, W. Schoenfelder, *J. Chem. Res. (S)* **1977**, 247; c) K. Friedrich, G. Boeck, H. Fritz, *Tetrahedron Lett.* **1978**, 3327; d) C. J. Moody, C. W. Rees, J. A. R. Rodrigues, S. C. Tsoi, *J. Chem. Res. (S)* **1985**, 238; e) M. P. Sammes in *The Chemistry of Heterocyclic Compounds, Vol. 48 (1) Pyrroles* (Ed.: R. A. Jones), Wiley, New York, **1990**, pp. 619–620.
[4] a) C. Vogel, P. Delavier, *Tetrahedron Lett.* **1989**, *30*, 1789; b) C. Vogel, P. Delavier, P. G. Jones, D. Döring, *ibid.* **1991**, *32*, 1409.
[5] Z. Arnold, A. Holy, *Collect. Czech. Chem. Commun.* **1961**, *26*, 3059–3073.
[6] H. Neumann, D. Seebach, *Chem. Ber.* **1978**, *111*, 2785.
[7] *Organikum*, 18th ed., Dtsch. Verlag der Wissenschaften, Berlin, **1990**, pp. 327–329.
[8] D. Knittel, *Synthesis* **1985**, 186.
[9] Crystallographic data for methyl 3-β-styryl-4,5,6,7-tetrahydro-1*H*-indol-2-carboxylate **5b**: monoclinic, space group $P2_1/c$, $a = 1069.2(4)$, $b = 1466.1(3)$, $c = 1924.5(6)$ pm, $\beta = 97.35(3)°$, $V = 2.992$ nm^3, $Z = 8$ (two independent molecules). Data collection: colorless prism $0.4 \times 0.3 \times 0.2$ mm, $T = -130$ °C, $Mo_{K\alpha}$ radiation ($\lambda = 71.073$ pm, $2\theta_{max} = 50°$), Stoe-STADI-4 diffractometer, 120489 reflections. Structural refinement: Siemens SHELXTL PLUS software program, *F* anisotropic, H atoms with a riding model, $wR = 0.075$ for 2730 reflections $> 3\sigma(F)$. Further details of the crystal structure investigation may be obtained from the Fachinformationszentrum Karlsruhe, Gesellschaft für wissenschaftliche Information mbH, W-76344 Eggenstein-Leopoldshafen (FRG), on quoting the depository number CSD-57154, the names of the authors, and the journal citation.

Catalytic Hydrogenation with Rhodium Complexes Containing dipamp-pyrphos Hybrid Ligands**

By *Ulrich Nagel** and *Thomas Krink*

The hydrogenation of olefins with rhodium phosphane complexes as catalysts[2] under homogeneous conditions is well established, and chiral complexes and prochiral olefins[3] are known to give rise to mixtures of enantiomers with various compositions. In related work a series of catalysts has been developed for the hydrogenation of dehydroamino acids.[4] Among other empirically determined properties, efficient catalysts should have C_2 symmetry.[5] The development of P- and C-chiral bisphosphane ligands[6] with additional ether groups[7] allows a systematic investigation of the influence of the symmetry on the activity and enantioselectivity of the catalyst.

The introduction of one *ortho* substituent into one of each pair of phenyl groups of diop was described recently.[8] In parallel work we succeeded in synthesizing ligands that can be considered combinations of the two "classic" ligands employed successfully in hydrogenation, dipamp and pyrphos (Fig. 1).[9] In our case the similarity is quite profound, since both dipamp and pyrphos are 1,2-bisphosphanes.

Replacement of one phenyl group on each of the phosphorus atoms in pyrphos with an *ortho*-anisyl group leads to the mixture of diastereomers **1a–c**.[10] The synthesis of these ligands, their purification, and the preparation of the catalysts are described in ref.[1]; in this communication we report on the results in asymmetric hydrogenation.

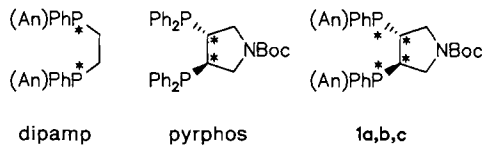

Fig. 1. The structures of dipamp and pyrphos, and their combination to give **1a**, **1b**, **1c**. The stars mark stereogenic centers. An = 2-methoxyphenyl (anisyl), Boc = *tert*-butoxycarbonyl.

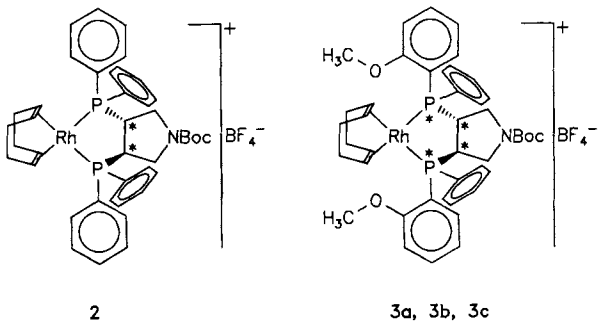

Fig. 2. The structures of catalysts **2**, **3a**, **3b**, and **3c**. The spatial arrangement of the aryl groups in **3a**, **3b**, and **3c** is shown in Figure 3.

Whereas **2** and **3a,b** have C_2 symmetry, **3c** is asymmetric (Fig. 3).[11] By comparing **2** with **3a,b**, it is possible to examine the influence of the additional ether groups while retaining the C_2 symmetry. The consequences of a reduction in symmetry are revealed by a comparison of the activity and enantioselectivity of **3c** with that of **2** and **3a,b**.

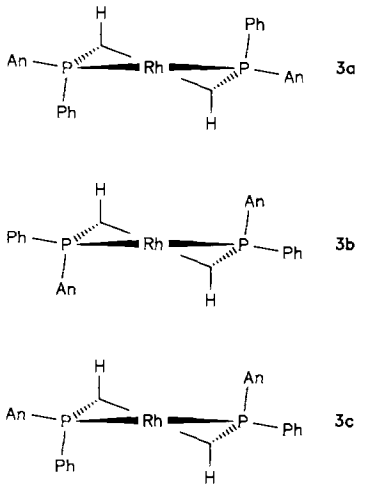

Fig. 3. The spatial arrangement of the aryl groups in **3a**, **3b**, and **3c**. Only the important portions of the molecules are shown (view along the C_2 axis in **3a** and **3b**).

Since both the enantioselectivity and the rate of the catalysis depend on many external parameters, we varied pressure and temperature. The results of these investigations are shown in Figures 4–7 for the hydrogenation of *Z*-α-acetamidocinnamic acid to (*S*)-acetylphenalanine with catalysts **2** and **3a–c**.

The introduction of the additional methoxy groups in catalyst **2** has rate-increasing (**3a** and **3c**) and rate-decreasing

[*] Prof. Dr. U. Nagel, T. Krink
Institut für Anorganische Chemie der Universität
Auf der Morgenstelle 18
D-72076 Tübingen (FRG)
Telefax: Int. code + (7071)292436

[**] Enantioselective Catalysis, Part 10. This research was supported by the Volkswagen-Stiftung and the Fonds der Chemischen Industrie. We thank Priv.-Doz. Dr. B. Koppenhoefer, Tübingen, for valuable suggestions for the analysis of enantiomers and J. M. Briody, Maynooth, for the measurement of some of the enantiomeric excesses. – Part 9: [1].

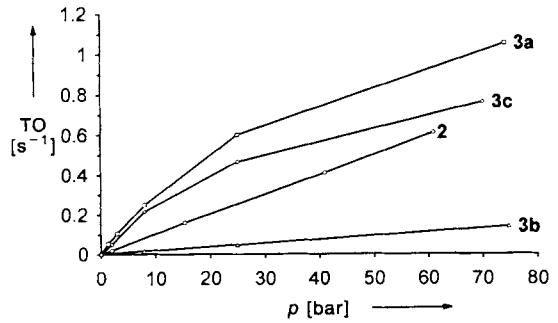

Fig. 4. Reaction rates for the hydrogenation of *Z*-α-acetamidocinnamic acid with catalysts **2**, **3a**, **3b**, and **3c** at 25 °C and at different H_2 pressures. TO = turnover.

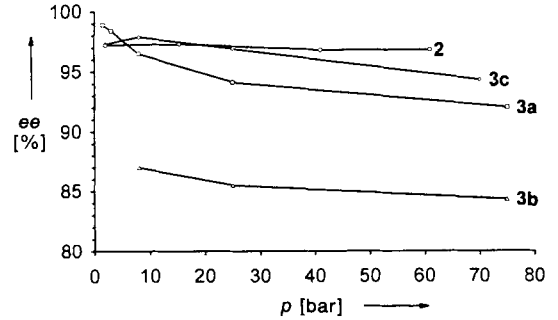

Fig. 5. *ee* Values of the (*S*)-*N*-acetylphenylalanine obtained with catalysts **2**, **3a**, **3b**, and **3c** at different H_2 pressures (reaction conducted at 25.0 °C).

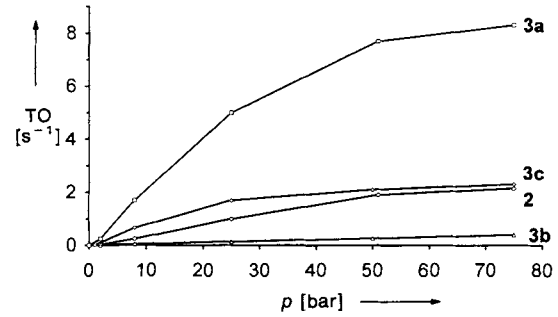

Fig. 6. Reaction rates for the hydrogenation of *Z*-α-acetamidocinnamic acid with catalysts **2**, **3a**, **3b**, and **3c** at 50 °C and at different H_2 pressures.

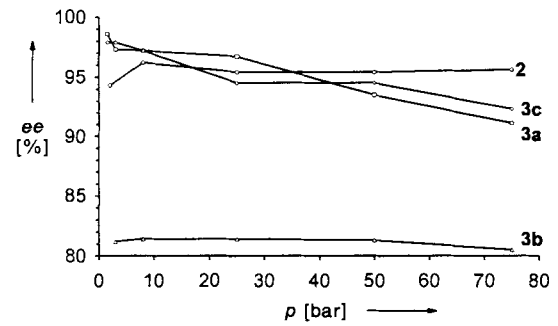

Fig. 7. *ee* Values of the (*S*)-*N*-acetylphenylalanine obtained with catalysts **2**, **3a**, **3b**, and **3c** at different H_2 pressures (reaction conducted at 50.0 °C).

effects (**3b**) because of the effect on ligand symmetry and the resulting relative position to rhodium. The enantiomeric excesses obtained for the hydrogenation of *Z*-α-acetamidocinnamic acid also depend on ligand symmetry. A direct comparison of C_2 symmetry with asymmetry (C_1 symmetry) is possible with compounds **3a**, **3b**, and **3c**, since these are stereoisomers with the same empirical formula. No comparisons of this type have been previously reported. Remarkably, the results from the reaction with asymmetric diastereomer **3c** are almost as good as, and in part even better than, those with **3a**.[12] At least in this case, C_2 symmetry is not essential for high enantiomeric excesses. Whereas the parent compound **2** provides constant enantiomeric excesses over the entire pressure range, the *ee* values obtained with the catalysts **3a**, **3b**, and **3c** decrease to different extents. At pressures over 40 bar **2** is the most selective catalyst; in the low-pressure range **3a** and **3c** are definitely superior to the parent compound **2**. The hybrid ligand in catalyst **3a** (matched pair) combines the partial structures *R*-pyrphos (which gives (*S*)-*N*-acetylphenylalanine in 97% *ee*) and *S*-dipamp (which give the *S* isomer in 95% *ee*) and provides the *S* isomer in up to 99% *ee*. The unsymmetric hybrid ligand in **3c** from *R*-pyrphos and *meso*-dipamp yields the *S* isomer in up to 98% *ee* but is remarkably superior to the matched pair **3a** at higher pressures. In each case the pyrphos structure element dominates the selectivity. In the optimization of a ligand the isoinversion principle[13] helps to only a limited extent. Our measurements show that the selectivities obtained at 25 °C are higher than those at 50 °C; however, the differences are not particularly distinct.

Experimental Procedure

The preparation of the catalysts **2**[6] and **3a–c**[1] were described previously. The hydrogenations were conducted in an autoclave with a stirrer with 5–10 μmol catalyst, 5–10 mmol substrate, and 50 mL methanol. The reaction mixture was initially under argon, which was removed by evacuation, and hydrogen was introduced. The hydrogenation started when stirring started. The H_2 consumption could be determined at any point in the reaction with a resolution of ±0.01 mmol. The hydrogenation reaction has three stages: 1) Saturation phase: when the stirrer is started hydrogen is stirred into the solution (ca. 3 min). 2) Induction phase: in low-pressure hydrogenations (up to 10 bar) the rate of the hydrogenation initially increases only slowly (probably until all of the cyclooctadiene (cod) of the catalyst is hydrogenated). 3) Hydrogenation phase: the rate of the hydrogenation is constant at the selected catalyst/substrate ratio. Workup: The solvent was removed by distillation, and the crude product was dissolved in aqueous NaOH solution and extracted three times with dichloromethane and diethyl ether. The aqueous phase was acidified to pH 3 with 2N HCl. The *N*-acetylphenylalanine formed was extracted with ethyl acetate. Analysis: A solution of *N*-acetylphenylalanine in methanol was converted to the corresponding methyl ester by treatment with HCl/methanol. Baseline separation of the enantiomers was achieved by gas chromatography (GC: Chrompack CP 9000 with a flame-ionization detector; integration: Chrompack integrator with the Mosaic program for data evaluation; capillary column coated with (*S*)-chirasil-Val, standards for calibration prepared from the racemate and a sample of (*S*)-*N*-acetylphenylalanine (99.95% *ee*)).

Received: January 27,
Revised version: March 12, 1993 [Z 5835 IE]
German version: *Angew. Chem.* **1993**, *105*, 1099

[1] U. Nagel, T. Krink, *Chem. Ber.*, **1993**, *126*, 1091–1100.
[2] J. A. Osborn, F. H. Jardine, G. Wilkinson, *J. Chem. Soc. A* **1966**, 1711.
[3] Reviews: K. E. König in *Asymmetric Synthesis, Vol. 5* (Ed.: J. D. Morrison), Academic Press, New York, **1985**, pp. 71–101; H. Brunner in *The Chemistry of the Metal-Carbon Bond, Vol. 5* (Ed.: F. R. Hartley), Wiley, Chichester, **1989**, pp. 109–146; H. Brunner, *Top. Stereochem.* **1988**, *18*, 129–247; I. Ojima, N. Clos, C. Bastos, *Tetrahedron* **1989**, *45*, 6901–6939; R. Noyori, M. Kitamura in *Modern Synthetic Methods, Vol. 5* (Ed.: R. Scheffold), Springer, Berlin, **1989**, pp. 115–198; R. Noyori, *Chem. Soc. Rev.* **1989**, *18*, 187–208.
[4] H. B. Kagan in *Asymmetric Synthesis, Vol. 5*, (Ed.: J. D. Morrison), Academic Press, New York, **1985**, p. 1–39; H. B. Kagan, M. Sasaki in *The Chemistry of Organophosphorus Compounds, Vol. 1* (Ed.: F. R. Hartley), Wiley, Chichester, **1990**, pp. 51–102.
[5] J. K. Whitesell, *Chem. Rev.* **1989**, *89*, 1581–1590; M. J. Burk, *J. Am. Chem. Soc.* **1991**, *113*, 8518–8519 and references therein. For more on C_2-sym-

metric ligands as chiral inductors see also: O. Reiser, *Angew. Chem.* **1992**, *105*, 576; *Angew. Chem. Int. Ed. Engl.* **1992**, *31*, 547.
[6] U. Nagel, B. Rieger, *Chem. Ber.* **1988**, *121*, 1123–1131; U. Nagel, B. Rieger, *Organometallics* **1989**, *8*, 1534–1538; U. Nagel, B. Rieger, A. Bublewitz, *J. Organomet. Chem.* **1989**, *370*, 223–239.
[7] U. Nagel, A. Bublewitz, *Chem. Ber.* **1992**, *125*, 1061–1072; [1].
[8] K. Burgess, M. J. Ohlmeyer, K. H. Whitmire, *Organometallics* **1992**, *11*, 3588–3600. diop = 2,3-*O*-isopropylidene-2,3-dihydroxy-1,4-bis(diphenylphosphino)butane.
[9] B. D. Vineyard, W. S. Knowles, M. J. Sabacky, G. L. Bachman, D. J. Weinkauff, *J. Am. Chem. Soc.* **1977**, *99*, 5946–5952; U. Nagel, E. Kinzel, J. Andrade, G. Prescher, *Chem. Ber.* **1986**, *119*, 3326–3343.
[10] The pyrrolidine nitrogen atom is protected by the Boc group, which can be removed easily.
[11] Rotamers of **2c** exist because of the partial double bond character of the amide bond of the Boc group; they are evident in the $^{31}P\{^1H\}$ NMR spectrum.
[12] Recently the review appeared in this journal "On Quantifying Chirality": A. B. Buda, T. Auf der Heyde, K. Mislow, *Angew. Chem.* **1992**, *104*, 1012–1031; *Angew. Chem. Int. Ed. Engl.* **1992**, *31*, 989–1007. Mislow et al. attempt to give measures of chirality for geometric shapes. A conclusion of their investigations is "that the maximum chirality is associated with minimum symmetry..."
[13] H. Buschmann, H.-D. Scharf, N. Hoffmann, P. Esser, *Angew. Chem.* **1991**, *103*, 480–518; *Angew. Chem. Int. Ed. Engl.* **1991**, *30*, 414. By using the isoinversion principle one can predict that for this type of catalysis a catalyst that has been optimally tailored to the substrates will provide the best *ee* values at 49 °C and 2.3 bar.

Tetrakis(tri-*tert*-butylsilyl)-*tetrahedro*-tetrasilane (tBu$_3$Si)$_4$Si$_4$: The First Molecular Silicon Compound with a Si$_4$ Tetrahedron**

By *Nils Wiberg,* Christian M. M. Finger,* and *Kurt Polborn*

Dedicated to Professor Heinrich Nöth on the occasion of his 65th birthday

In a recently published review on the cluster chemistry of the heavier elements in the fourth main group (Si, Ge, Sn), which is still in its infancy, S. Masamune et al. state in their concluding remarks that the syntheses of tetrasilatetrahedrane **1**, disilyne **2**, and 1,1,1-pentasilapropellane **3** are currently the greatest challenges for silicon chemists.[1] We report here on our achievement of one of these goals—the synthesis of a molecular silicon compound with a Si$_4$ tetrahedron (see note[14] with regard to the question of a disilyne).

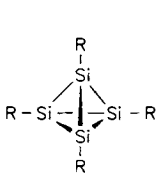

1 (here R = SitBu$_3$)

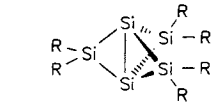

2

3

[*] Prof. Dr. N. Wiberg, Dipl.-Chem. C. M. M. Finger, Dr. K. Polborn
Institut für Anorganische Chemie der Universität
Meiserstrasse 1, D-80333 München (FRG)
Telefax: Int. code + (89)5902-451

[**] Sterically Overloaded Silicon Compounds, Part 6, Silicon Compounds, Part 96. This research was supported by the Deutsche Forschungsgemeinschaft. We thank Dr. J. Evers (Institut für Anorganische Chemie der Universität München) for the measurement and interpretation of various rotating crystal and Weissenberg photographs, and Dr. O. Seligmann (Institut für Pharmazeutische Biologie der Universität München) for recording a FAB mass spectrum. – Part 5 and 95: J. Kovács, G. Baum, G. Fritz, D. Fenske, N. Wiberg, H. Schuster, K. Karaghiosoff, *Z. Anorg. Allg. Chem.* **1993**, *619*, 453.

According to ab initio calculations, the strain energy of (SiH)$_n$ polyhedra increases with the number of three-membered rings in the polyhedron framework (see Scheme 1).[2, 3]

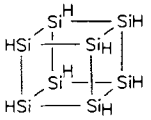

***hexahedro*-octasilane**
(391 kJ mol^{-1}; 239.6 pm)

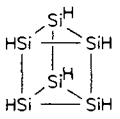

***triprismo*-hexasilane**
(476 kJ mol^{-1}; 237.5 pm)

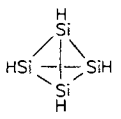

***tetrahedro*-tetrasilane**
(590 kJ mol^{-1}; 231.4 pm)

Scheme 1. (SiH)$_n$ Polyhedra; calculated strain energies and Si-Si distances in parentheses [2, 3].

One expects the difficulty of the syntheses of these fascinating polyhedral compounds[4] to follow the same trend. Indeed, until now only *hexahedro*-octasilane derivatives (Si substituents: SiMe$_2$$tBu, CMe_2$CHMe$_2$, 2,6-Et$_2C_6H_3$) have been synthesized.[5] (For the heavier homologue germanium, a *triprismo*-hexagermane with CH(SiMe$_3$)$_2$ substituents on the germanium atoms has also been generated.[6]) Since compounds with a tetrahedral framework constructed of atoms of one element exist for most of the elements near silicon in the periodic table, boron,[7] aluminum,[8] gallium,[9] carbon,[10] phosphorus (P$_4$), and arsenic (As$_4$), it is especially puzzling that neither a *tetrahedro*-tetrasilane nor a *tetrahedro*-germane have been synthesized previously.

A *tetrahedro*-tetrasilane Si$_4$R$_4$ should be more stable than either a *hexahedro*-octasilane or a *triprismo*-hexasilane if it has sterically demanding R groups (see comment[3]). Thus we chose to synthesize the target tetrahedron molecule **1** with tri-*tert*-butylsilyl groups (R = SitBu$_3$, "supersilyl") (for more on the name supersilyl see comment[8]). Since Si_4^{4-} tetrahedra are anionic components in alkaline and alkaline earth silicides such as NaSi, KSi, and BaSi$_2$, it was reasonable to try to give these "molecular freedom" (e.g. $Si_4^{4-} + 4RX \rightarrow Si_4R_4 + 4X^-$). All attempts at derivatization have failed thus far (one reason for this is the high reducing ability of the silicides; see comment[11, 12]).

Another imaginable approach, the dehalogenation of the previously unknown tBu$_3$Si–SiCl$_3$ with sodium, did not provide access to **1**, although the analogous reaction of the less bulky tBuMe$_2$Si–SiBr$_3$ led to *hexahedro*-octasilane (Si substituents = SiMe$_2$$t$Bu).[5] Treatment of tBu$_3$Si–SiCl$_3$ with sodium in benzene at 80 °C did not give **1**; instead NaCl formation and hydrogen uptake led to a number of products including 1,2-bis(supersilyl)disilane **4**, which can be brominated easily to provide tetrabromobis(supersilyl)disilane **5**, and the very interesting tris(supersilyl)cyclotrisilane **6**.[13]

tBu$_3$Si–SiH$_2$–SiH$_2$–SitBu$_3$
4

tBu$_3$Si–SiBr$_2$–SiBr$_2$–SitBu$_3$
5

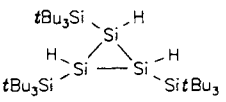

6

At this point we found that **1** (R = SitBu$_3$) can be obtained according to Equation (a) by the reaction of **5** with supersilylsodium tBu$_3$SiNa.[14] Compound **4**, the precursor

$$2\,\mathbf{5} + 4\,t\mathrm{Bu_3SiNa} \longrightarrow \mathbf{1}\ (\mathrm{R} = \mathrm{Si}t\mathrm{Bu_3}) + 4\,t\mathrm{Bu_3SiBr} + 4\,\mathrm{NaBr} \qquad \text{(a)}$$

of **5**, can be synthesized by treating supersilylchlorosilane tBu$_3$Si–SiH$_2$Cl, accessible from SiH$_2$Cl$_2$ and tBu$_3$SiNa, with sodium; the yields here are much better than by the previously mentioned approach.

Compound **1** forms intensely yellow-orange needles, which change color (to deep-red) reversibly upon heating and do not melt below 350 °C. The crystals display high thermo- and photostability and are stable to water and air. Compound **1** cannot be reduced by sodium in benzene in the presence of [18]crown-6 but reacts with oxidants like tetracyanoethylene and Br_2.

X-ray quality crystals of pure **1** have not yet been obtained; however, when a mixture of **1** and hexa-*tert*-butyldisilane tBu$_3$Si–SitBu$_3$ ("superdisilane") was recrystallized from hexadeuteriobenzene,[15] yellow-orange rectangular cubes formed with the composition $2(t\text{Bu}_3\text{Si})_4\text{Si}_4 \cdot (t\text{Bu}_3\text{Si})_2 \cdot \text{C}_6\text{D}_6$ **1a**, whose structure was established by X-ray crystallography.[16] The cubic unit cell (Fig. 1) contains two sets of four molecules of **1** (tetrahedra 1 and 1A), which are located in the eight cube quadrants, as well as four molecules of superdisilane (occupation of the middle of every edge and the center of the cube) and four molecules of hexadeuteriobenzene (occupation of all corners and middles of all the faces of the cube). All the molecules are positioned on threefold symmetry axes. The superdisilane molecules fill the large gaps between the almost sphere-shaped molecules of **1** and thereby apparently stabilize the structure of the crystal.

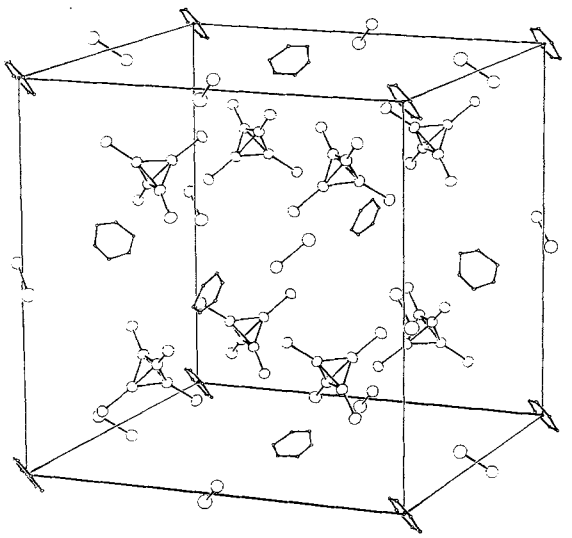

Fig. 1. Cubic unit cell of **1a** (all tBu groups were left out for clarity; the C atoms of C_6D_6 have effective radii; all molecules are found on threefold symmetry axes).

As expected, the units of **1** in crystal **1a** (Fig. 2) are constructed of Si_4 tetrahedra, which have two different Si–Si distances (tetrahedron 1: 233.0 and 231.5 pm; tetrahedron 1A: 232.6 and 234.1 pm) as a consequence of the crystal symmetry. These distances are somewhat longer than those calculated for unsubstituted *tetrahedro*-tetrasilane (231.4 pm; for comparison, in cyclotrisilanes: Si–Si distance in $[(t\text{BuCH}_2)_2\text{Si}]_3$ 239.1 pm, in $(t\text{Bu}_2\text{Si})_3$ 251.1 pm;[18] see also comment[19]). The exocyclic Si–Si separations are somewhat longer than normal Si–Si single bonds as a result of the bulk of the supersilyl groups (tetrahedron 1: 235.5 and 236.5 pm; tetrahedron 1A: 237.1 and 235.6 pm; for comparison[15] the Si–Si distance in Me$_3$Si–SiMe$_3$ 234.0 pm, in tBu$_3$Si–SitBu$_3$ 268.5 pm). The elongated Si–C bonds (range 191.2–197.0 pm) are rationalized in the same way.

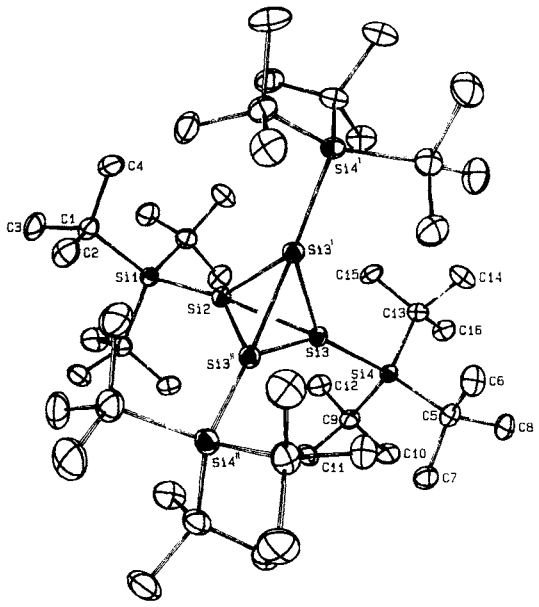

Fig. 2. Structure of **1** in the crystal of **1a** (ORTEP; Si atoms: thermal ellipsoids at the 50% level; C atoms with arbitrary radii for clarity; no H atoms). Selected bond lengths [pm] and angles [°]: Tetrahedron 1: Si1-Si2 235.5(2), Si3-Si4 236.5(2), Si2-Si3 232.0(2), Si3-Si3′ 231.5(2), Si1-C1 194.7(5), Si4-C5 194.0(5), Si4-C9 196.2(5), Si4-C13 191.7(5); Si1-Si2-Si3 144.8(1) (idealized value 144.75), Si2-Si3-Si4 144.9(1), Si4-Si2-Si3′ 59.9 (1) (idealized value 60), Si2-Si1-C1 106.1(1), Si3-Si4-C5 105.8(2), Si3-Si4-C9 106.0(2). Tetrahedron 1A: Si1A-Si2A 237.1(1), Si3A-Si4A 235.6(2), Si2A-Si3A 232.6(2), Si3A-Si3A′ 234.1(2), Si1A-C1A 194.1(5), Si4A-C5A 194.1(5),Si4A-C9A 191.2(5), Si4A-Si13A 197.0(5); Si1A-Si2A-Si3A 144.5(1), Si2A-Si3A-Si4A 144.9(1), Si3A-Si2A-Si3A′ 60.4(1), Si2A-Si1A-C1A 105.8(2), Si3A-Si4A-C5A 107.1(2),Si3A-Si4A-C9A 106.6(2) Si3A-Si4A-C13A 105.8(2).

The superdisilane molecules tBu$_3$Si–SitBu$_3$ in crystals **1a** display almost the same Si–Si distance (268.5 pm) as in crystals containing only superdisilane. As in the pure crystal of superdisilane,[20] in **1a** the two tBu$_3$Si halves are not staggered but twisted out of this symmetric position by 5.2°.

Experimental Procedure

To a solution of **5** (0.428 g, 0.553 mmol) in THF (50 mL) at −20 °C was added dropwise a 0.56 M solution of tBu$_3$SiNa (2.00 mL, 1.12 mmol). The reaction mixture was allowed to warm to room temperature, the THF removed under vacuum, the residue dissolved in pentane (70 mL), the precipitated NaBr filtered off, and the pentane removed by distillation. The crude product was recrystallized a number of times from tBuOMe to provide 0.144 g (0.158 mmol, 57%) pure, yellow-orange **1** (R = SitBu$_3$), m.p. > 350 °C. – ^{1}H NMR (C_6D_6): $\delta = 1.357$; ($CDCl_3$): $\delta = 1.185$; ^{29}Si{^{1}H} NMR (C_6D_6): $\delta = 38.89$ (Si_4), 53.07 (SitBu$_3$); ^{13}C{^{1}H} NMR (C_6D_6): $\delta = 24.68$ (CMe_3), 32.16 (CMe_3); MS (Kratos 80 RFA, Xe (7 kV, 10 W)): m/z (%) 908/909/910/911/912/913/914 (8.5/100/86.3/64.5/31.9/17.6/7.4) [M^+], 710/711/712/713/714 (51.9/47.4/24.5/14.3/7.2) [M^+ − SitBu$_3$]; UV/VIS (isooctane): λ_{max} = 210/235/310/451 nm (extinction 75870/70891/19867/3583). $Si_8C_{48}H_{108}$ (M_r = 908.7): calcd. C 63.33 H 11.97, found C 63.53 H. 12.28.

Received: March 27, 1993 [Z 5949 IE]
German version: *Angew. Chem.* **1993**, *105*, 1140

[1] T. Tsumuraya, S. A. Batcheller, S. Masamune, *Angew. Chem.* **1991**, *103*, 916; *Angew. Chem. Int. Ed. Engl.* **1991**, *30*, 902.
[2] S. Nagase, *Angew. Chem.* **1989**, *101*, 340; *Angew. Chem. Int. Ed. Engl.* **1989**, *28*, 329.
[3] According to calculations *triprismo*-hexasilane is considerably more stable than the isomeric hexasilabenzene; *tetrahedro*-tetrasilane is more stable than tetrasilacyclobutadiene but not as markedly [1]. Bulky R groups help stabilize structure **1**.
[4] M. Weidenbruch, *Angew. Chem.* **1993**, *105*, 574; *Angew. Chem. Int. Ed. Engl.* **1993**, *32*, 545.
[5] H. Matsumoto, K. Higuchi, Y. Hoshino, H. Koike, Y. Naoi, Y. Nagai, *J. Chem. Soc. Chem. Commun.* **1988**, 1083; H. Matsumoto, K. Higuchi, S. Kyushin, M. Goto, *Angew. Chem.* **1992**, *104*, 1410; *Angew. Chem. Int. Ed. Engl.* **1992**, *31*, 1354; A. Sekiguchi, T. Yatabe, H. Kamatani, C. Kabuto, H. Sakurai, *J. Am. Chem. Soc.* **1992**, *114*, 6260.
[6] A. Sekiguhi, C. Kabuto, H. Sakurai, *Angew. Chem.* **1989**, *101*, 97; *Angew. Chem. Int. Ed. Engl.* **1989**, *28*, 55.
[7] T. Mennekes, P. Paetzold, R. Boese, D. Bläser, *Angew. Chem.* **1991**, *103*, 199; *Angew. Chem. Int. Ed. Engl.* **1991**, *30*, 173.
[8] N. Wiberg in *Frontiers of Organosilicon Chemistry* (Eds.: A. R. Bassindale, P. P. Gaspar), R. Soc. Chem. Cambridge, **1991**, p. 263; C. Dohmeier, C. Robl, M. Tacke, H. Schnöckel, *Angew. Chem.* **1991**, *103*, 594; *Angew. Chem. Int. Ed. Engl.* **1991**, *30*, 564.
[9] W. Uhl, W. Hiller, M. Layh, W. Schwarz, *Angew. Chem.* **1992**, *194*, 1378; *Angew. Chem. Int. Ed. Engl.* **1992**, *31*, 1364.
[10] G. Maier, S. Pfriem, U. Schäfer, R. Matusch, *Angew. Chem.* **1978**, *90*, 552; *Angew. Chem. Int. Ed. Engl.* **1978**, *17*, 520. H. Irngartinger, A. Goldmann, R. Jahn, M. Nixdorf, H. Rodewald, G. Maier, K.-D. Malsch, R. Emrich, *ibid.* **1984**, *96*, 967 and **1984**, *23*, 993.
[11] E. Hey-Hawkins, H.-G. von Schnering, *Chem. Ber.* **1991**, *124*, 1167; *Z. Naturforsch. B* **1991**, *46*, 307; *ibid.* **1991**, *46*, 621.
[12] H. Bock, K. Dörr, R. Schlögl, Universität Frankfurt, have attempted to prepare *tetrahedro*-tetrasilane Si_4X_4 by rapid solidification processing of $BaSi_2$ (2000 °C melt under argon on a rotor at 20000 rpm and with additional cooling by *n*-hexane) with halogens; however, only halosilanes like Si_2Cl_6 and SiI_4 could be isolated (lecture at the 25th National Organosilicon Symposium, University of Southern California, Los Angeles, USA, April 3, **1992**, and Diplomarbeit, G. Herrmann, Universität Frankfurt, **1991**).
[13] N. Wiberg, T. Passler, unpublished.
[14] The idea that the conversion of **5** into **1** could proceed by the dimerization of bis(superdisilyl)disilyne $tBu_3Si-Si\equiv Si-SiBu_3$ is quite fascinating: **5** + $tBu_3SiNa \rightarrow (tBu_3Si)BrSi=SiBr(SitBu_3) + tBu_3SiBr + NaBr$; $(tBu_3Si)BrSi=SiBr(SitBu_3) + tBu_3SiNa \rightarrow tBu_3Si-Si\equiv Si-SitBu_3 + tBu_3SiBr + NaBr$.
[15] N. Wiberg, H. Schuster, A. Simon, K. Peters, *Angew. Chem.* **1986**, *98*, 100; *Angew. Chem. Int. Ed. Engl.* **1986**, *25*, 79.
[16] X-ray analysis of **1a**: $2Si_8C_{48}H_{108}\cdot Si_2C_{24}H_{54}\cdot C_6D_6$, $M_r = 2303.15$, cubic, $P2_13$ (no. 198), $a = 2473.3(8)$ pm, $v = 15.1304$ nm^3, $Z = 4$(!), $\rho_{calcd} = 1.011$ Mg m^{-3}, $\mu = 0.185$ mm^{-1}, $T = 296$ K, data collection on a yellow-orange crystal with dimensions of $0.4 \times 0.53 \times 0.53$ mm. 16621 Reflections were collected on an Enraf-Nonius CAD4 diffractometer, of which 6761 were independent and observed, 5940 with ($F > 3\sigma F$). ω-Scan, scan width $0.50° + 0.35\tan\theta$, maximum measurement 180 s per reflection; range: $2° < 2\theta < 46°$. Complete measurement of $\pm h, k, l$ with $|h| \leq l$ and $k < l$; additional reflections without this restriction, i.e. ca. 78% of $\pm h, k, l$ ($R_i = 0.019$), then interruption because of decomposition. Correction for anisotropic disintegration (0.9949, 1.2071). Weissenberg photographs confirm the unit cell found and showed only weak reflections for $0kl$ when $k = 2n + 1$; the reflections h were extinguished when $h = 2n + 1$. The *t*Bu groups of the hexa-*tert*-butyldisilane molecules are more disordered and require geometric constraints; the C atoms of C_6D_6 were also quite disordered; in the final model the D atoms were not included. Solution: SHELX86, block refinement with SHELX76 [17]. Riding hydrogen atoms at geometrical positions, all non-hydrogen atoms refined anisotropically. $R = 0.057$, $R_w = 0.051$, $w = 1/\sigma^2(F_0)$. 433 Parameters. The ratio of reflections to refined parameters is 13.7:1. The absolute configuration was not determined. Further details of the crystal structure investigation may be obtained from the Fachinformationszentrum Karlsruhe, Gesellschaft für wissenschaftlich-technische Information mbH, D-76344 Eggenstein-Leopoldshafen (FRG) on quoting the depository number CSD-57184, the names of the authors, and the journal citation.
[17] G. M. Sheldrick, *SHELX76, Program for the Crystal Structure Determination*. University of Cambridge, **1976**; *SHELX86, Program for the Solution of Crystal Structures*, Göttingen, **1985**.
[18] H. Watanabe, M. Kato, T. Okawa, Y. Nagai, M. Goto, *J. Organomet. Chem.* **1984**, *271*, 225; A. Schäfer, M. Weidenbruch, K. Peters, H. G. von Schnering, *Angew. Chem.* **1984**, *96*, 311; *Angew. Chem. Int. Ed. Engl.* **1984**, *23*, 302.
[19] H. Grützmacher, *Angew. Chem.* **1992**, *104*, 1358; *Angew. Chem. Int. Ed. Engl.* **1992**, *31*, 1329; R. Janoschek, *Chem. Unserer Zeit*, **1988**, *21*, 128.
[20] H. Bock, J. Meuret, K. Ruppert, *Angew. Chem.* **1993**, *105*, 413; *Angew. Chem. Int. Ed. Engl.* **1993**, *32*, 414; *J. Organomet. Chem.* **1993**, 445, 19.

$(C_6F_5NGaMe)_4$ and $(C_6F_5NInMe)_4$: The First Gallium–Nitrogen and Indium–Nitrogen Compounds with Cubane Structures**

By *Thomas Belgardt, Herbert W. Roesky,* Mathias Noltemeyer*, and *Hans-Georg Schmidt*

Dedicated to Professor Hans Bock on the occasion of his 65th birthday

Compounds with heterocubane frameworks have been known for a long time for main group elements.[1] The first aluminum–nitrogen compound with cubane structure $(PhNAlPh)_4$ was prepared in 1962 and structurally characterized ten years later.[2] In the meantime several more compounds of this type have been described.[3] In contrast, there are no indications of analogous gallium–nitrogen and indium–nitrogen compounds. Starting materials for the synthesis of the aluminum–nitrogen compounds with a central cubic Al_4N_4 unit are the aminoalanes $(RNHAlR'_2)_n$, which form cubanes through intermolecular reactions. Power et al. have transferred these reactions to the corresponding aminogallanes and have thus observed that under C–H activation an intramolecular elimination of hydrocarbons takes place.[3b] Corresponding reactions of the aminoindanes are not known. In order to prevent a C–H activation, we have now treated $GaMe_3$ and $InMe_3$ each with pentafluoroaniline (Scheme 1).

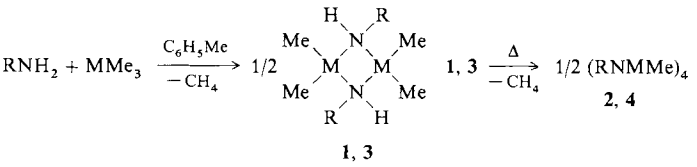

Scheme 1. **1**, **2**: M = Ga; **3**, **4**: M = In. R = C_6F_5.

The aminometallanes **1** and **3** are obtained as intermediates, which precipitate in the form of needlelike crystals in high yield. The compounds **2** and **4**, the first gallium–nitrogen and indium–nitrogen compounds with cubane frameworks, respectively, can be prepared by heating the appropriate aminometallanes without solvent, and subsequent recrystallization of the products from *n*-hexane. Compound **2** belongs to the class of iminogallanes $(RNGaR')_n$, for which to our knowledge only one compound with a complex cage structure is known.[4] Compound **4** is the first structurally characterized iminoindane $(RNInR')_n$.

The crystal structure of **2** is shown in Figure 1.[5] The framework consists of fourfold coordinated Ga and N atoms, which together form a regular cube (angles at Ga and N lie between 85.9(2) and 94.0(2)°). However, the angles here deviate significantly from the 90° angle of a perfect cube, in contrast to $(PhAlNPh)_4$, for which angles of almost 90° are observed. The Ga–N bond lengths lie between 197.2 and 203.9 pm (mean 200.8(4) pm). Thus, they correspond to the atomic distances in aminogallanes, for example those of $(Me_2GaNHPh)_2$.[3b] As expected, the distances are somewhat longer than those for iminoalanes with cubane struc-

[*] Prof. Dr. H. W. Roesky, T. Belgardt, Dr. M. Noltemeyer, H.-G. Schmidt
Institut für Anorganische Chemie der Universität
Tammannstrasse 4, D-37077 Göttingen (FRG)
Telefax: Int. code + (551)39-3373

[**] This work was supported by the Deutsche Forschungsgemeinschaft and the Fonds der Chemischen Industrie.

ture (for $(PhAlNPh)_4$, these lie between 186(2) and 193(1) pm); for comparison we have also prepared the aluminum compound $(C_6F_5NAlMe)_4$ (Al–N bond lengths in the range of 190.5 to 196.7 pm) analogous to **2** and **4** in a similar way.[6] The mean Ga···Ga distance in **2** is 290 pm and the N···N distance 276 pm.

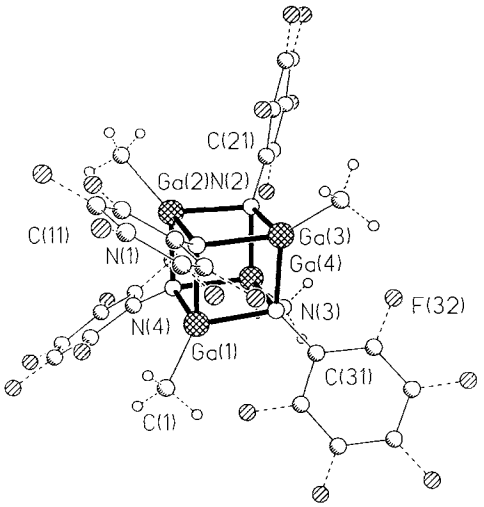

Fig. 1. Crystal structure of **2**. Selected bond lengths [pm] and angles [°]: Ga(1)–N(4) 199.5(4), Ga(2)-N(4) 201.7(4), Ga(1)-C(1) 192.6(6), Ga(4)-C(4) 193.3(5), N(2)-C(21) 142.1(6), N(4)-C(41) 140.1(7); N(3)-Ga(1)-N(4) 88.8(2), Ga(1)-N(1)-N(3) 91.5(2).

The crystal structure of **4** is shown in Figure 2.[7] It is a slightly distorted cube of alternating indium and nitrogen atoms (mean In-N-In angle 95.5(4)°, mean N-In-N angle 84.3(4)°). In this case the angles between the In and N atoms

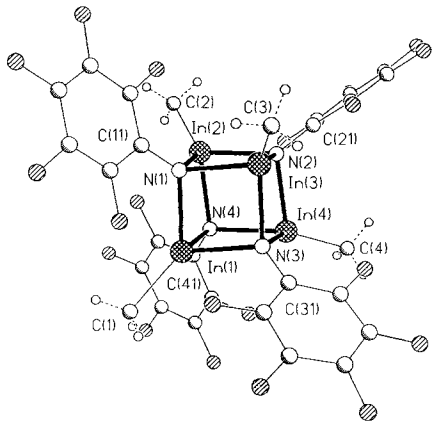

Fig. 2. Crystal structure of **4**. Selected bond lengths [pm] and angles [°]: In(1)-N(3) 220.2(9), In(3)-N(2) 216.7(10), In(4)-N(2) 222.7(10), In(1)-C(1) 211.5(12), In(4)-C(4) 209.9(14); N(1)-In(1)-N(3) 85.4(3), In(1)-N(1)-In(3) 94.9(4).

deviate even more from those of an ideal cube than in compound **2**. Thus, the heavier the participating metal atom is the greater the deviations. This tendency is on the one hand certainly to be attributed to the differences in size of the metals, and also to the fact that the degree of hybridization decreases with increasing atomic mass. In order to be able to make more accurate statements about the bonding, more compounds of this type must be prepared and be compared with **2** and **4**. The In–N distances are between 216.7 and 222.7 pm (mean 220 pm) and are thus significantly longer than those for the homologous aluminum and gallium compounds. The mean In···In distance is 326 pm and the mean N···N distance 296 pm. In the ^1H NMR spectrum of **2**, a septet is observed for the methyl group at gallium, which is attributed to the long-range couplings of the protons with the *ortho*-positioned fluorine atoms of three of the four pentafluorophenyl substituents. For compound **4** these long-range couplings are not observed. In the mass spectra of **2** and **4** the signals of the molecular ions appear with high relative intensities [for **4** 100%]. This indicates that the compounds are also stable in the gas phase.

In conclusion, it is possible to prevent an intramolecular reaction by the use of perfluorinated phenyl substituents and thus transfer the elimination reaction known for aminoalanes to gallium and indium. We will now investigate whether lanthanides behave in a similar fashion.

Experimental Procedure

1: $C_6F_5NH_2$ (4.03 g, 22 mmol) dissolved in freshly distilled toluene (20 mL) was slowly added dropwise to a solution of $GaMe_3$ (1.46M in toluene, 15 mL, 22 mmol) at room temperature and with the exclusion of air and moisture. The reaction mixture was heated for 12 h under reflux. Subsequently the toluene was removed under vacuum and the residual solid was crystallized from *n*-hexane. Yield of **1**: 5.39 g (87%); m.p. 145 °C. ^1H NMR (250.130 MHz, C_6D_6, TMS ext.): $\delta = 2.58$ (s, br, 2H; N-H), −0.22 (s, 12H; Ga-CH_3); ^{19}F NMR (75.39 MHz, C_6D_6, $CFCl_3$ ext.): $\delta = -164.1$ (m, 4F; *o*-F), −165.7 (m, 4F; *m*-F), −174.2 (m, 2F; *p*-F); IR (Nujol): $\tilde{\nu}$[cm^{-1}] = 3327, 3304, 1513, 1351, 1310, 1260, 1241, 1221, 1211, 1134, 1062, 1018, 990, 887, 843, 788, 727, 694, 623, 591, 543. MS (70 eV): *m/z* (%) 563 (5) [M^+], 281 (40) [$M^+/2$], 183 (100) [$C_6F_5NH_2$]. Correct C,H,N analysis.

2: **1** (1.74 g, 3.1 mmol) was heated to 200 °C for 3 h; the methane formed was allowed to escape through a mercury-pressure manometer. Recrystallization of the residue from *n*-hexane led to colorless crystals of **2**. Yield **2**: 1.01 g (61.5%); m.p. 202 °C. 1.01 g (61.5%). ^1H NMR (400.130 MHz, C_6D_6, TMS ext.): $\delta = -0.25$ (sept. 12H; Ga-CH_3); ^{19}F NMR (376.498 MHz, C_6D_6, C_6F_6 ext.): $\delta = 10.82$ (m, 8F; *o*-F), 0.55 (m, 8F; *m*-F), −3.31 (m, 4F; *p*-F); IR (Nujol): $\tilde{\nu}$[cm^{-1}] = 2434, 1512, 1499, 1465, 1452, 1302, 1258, 1218, 1150, 1133, 1020, 1001, 772, 756, 664. MS (70 eV): *m/z* (%) 1064 (59) [M^+], 532 (100) [$M^+/2$]. Correct C,H,N analysis.

3: $C_6F_5NH_2$ (3.66 g, 20 mmol) dissolved in toluene (20 mL) was slowly added dropwise to a solution of $InMe_3$ (3.2 g, 20 mmol) in toluene (20 mL) at room temperature. The reaction mixture was heated under reflux for 12 h. Subsequently the solvent was removed under vacuum and the colorless residue was recrystallized from *n*-hexane. Yield of **3**: 5.1 g (78%); m.p. 159 °C. ^1H NMR (250.130 MHz, C_6D_6, TMS ext.): $\delta = 2.78$ (s, br, 2H; N-H), −0.18 (s, 12H; In-CH_3); ^{19}F NMR (250.320 MHz, C_6D_6, $CFCl_3$ ext.): $\delta = -150.48$ (m, 4F; *o*-F), −161.95 (m, 4F; *m*-F), −164.00 (m, 2F; *p*-F); IR (Nujol): $\tilde{\nu}$[cm^{-1}] = 3288, 1519, 1508, 1450, 1356, 1308, 1260, 1242, 1158, 1133, 1093, 1018, 992, 978, 823, 801, 727, 618, 521. MS (70 eV): *m/z* (%) 654 (4) [M^+], 639 (36) [$M^+ - CH_3$], 327 (25) [$M^+/2$], 145 (100) [$M^+/2 - C_6F_5$]. Correct C,H,N analysis.

4: **3** (2.1 g, 3.21 mmol) was heated to 220 °C for 1 h; the methane formed was allowed to escape and solid **4** was obtained. Crystals suitable for the crystal structure analysis were obtained by the crystallization from *n*-hexane. Yield of **4**: 1.57 g (78.6%); m.p. 225 °C (decomp). ^1H NMR (250.130 MHz, C_6D_6, TMS ext.): $\delta = 0.12$ (s, 12H; In-CH_3); ^{19}F NMR (75.39 MHz, C_6D_6,C_6F_6 ext.): $\delta = 8.50$ (m, 8F; *o*-F), −0.90 (m, 8F; *m*-F), −8.15 (m, 4F; *p*-F); IR (Nujol): $\tilde{\nu}$[cm^{-1}] = 2430, 1646, 1640, 1506, 1437, 1293, 1251, 1140, 1127, 1011, 993, 738, 545. MS (70 eV): *m/z* (%) 1244 (100) [M^+], 622 (20) [$M^+/2$]. Correct C,H,N analysis.

Received: February 4, 1993 [Z 5850IE]
German version: *Angew. Chem.* **1993**, *105*, 1101

[1] M. Veith, *Chem. Rev.* **1990**, *90*, 3–16.
[2] a) T. R. R. McDonald, W. S. McDonald, *Proc. Chem. Soc.* **1962**, 366; b) T. R. R. McDonald, W. S. McDonald, *Acta Crystallogr. Sect B* **1972**, *28*, 1619–1622.
[3] a) G. Del Piero, M. Cesari, G. Dozzi, A. Mazzei, *J. Organomet. Chem.* **1977**, *129*, 281–288; b) K. M. Waggoner, P. P. Power, *J. Am. Chem. Soc.* **1991**, *113*, 3385–3393.

[4] S. Amirkhalili, P. B. Hitchcock, J. D. Smith, *J. Chem. Soc. Dalton Trans.* **1979**, 1206.

[5] Crystal data for **2**: $C_{28}H_{12}F_{20}Ga_4N_4$, triclinic, $P\bar{1}$, $a = 1015.5(2)$, $b = 1045.4(4)$, $c = 1700.7(3)$ pm, $\alpha = 105.34(2)$, $\beta = 90.93(2)$, $\gamma = 98.65(10)°$, $V = 1.7184(6)$ nm^3, $Z = 2$, $\rho_{calcd} = 2.055$ Mg m^{-3}, $\mu(Mo_{K\alpha}) = 3.240$ mm^{-1}, 4494 independent reflections were used for the solution and refinement of the structure. $R1 = 0.0435$, $wR2 = 0.1176$; $wR2 = [\sum w(F_o^2 - F_c^2)^2 / \sum wF_o^4]^{1/2}$, $R1 = \sum(||F_o| - |F_c||/\sum|F_o|)$.

[6] T. Belgardt, H. W. Roesky, H. Gornitzka, D. Stalke, unpublished results. Selected bond lengths of $(C_6F_5NAlMe)_4$ in pm: Al(1)–N(1) 196.4(2), Al(2)–N(3) 196.7(4), Al(3)–N(3) 195.4(4), Al(4)–N(4) 195.0(4).

[7] a) Crystal data for **4**: $C_{28}H_{12}F_{20}In_4N_4$, triclinic, $P\bar{1}$, $a = 995.3(2)$, $b = 1030.0(2)$, $c = 1786.2(4)$ pm, $\alpha = 74.15(3)$, $\beta = 86.27(3)$, $\gamma = 82.91(3)°$, $V = 1.7471(6)$ nm^3, $Z = 2$, $\rho_{calcd} = 2.364$ Mg m^{-3}, $\mu(Mo_{K\alpha}) = 2.743$ mm^{-1}, 4465 independent reflections were used for the solution and refinement of the structure. $R1 = 0.0757$, $wR2 = 0.1992$. $wR2 = [\sum w(F_o^2 - F_c^2)^2 / \sum wF_o^4]^{1/2}$, $R1 = \sum(||F_o| - |F_c||/\sum|F_o|)$. b) Further details of the crystal structure investigations may be obtained from the Fachinformationszentrum Karlsruhe, Gesellschaft für wissenschaftlich-technische Information mbH, D-76344 Eggenstein-Leopoldshafen (FRG), on quoting the depository number CSD-57077, the names of the authors, and the journal citation.

A New Route to Water-Soluble Phosphanes with *para*-Sulfonated Phenyl Substituents. Crystal Structure of $P(C_6H_4\text{-}p\text{-}SO_3K)_3 \cdot KCl \cdot 0.5\,H_2O$**

By *Oliver Herd, Klaus Peter Langhans, Othmar Stelzer,* Norbert Weferling,* and *William S. Sheldrick*

Dedicated to Professor Ulrich Wannagat on the occasion of his 70th birthday

Since the application of water-soluble Rh^I complexes of $P(C_6H_4\text{-}m\text{-}SO_3Na)_3$ (tppts) as catalysts for the industrial hydroformylation of propene in the two-phase system water/organic solvent by the Ruhrchemie/Rhône-Poulenc process, sulfonated triphenylphosphanes have become increasingly important.[1, 2] Because of its extremely good solubility in water the Rh catalyst $[HRh(CO)(tppts)_3]$ can be separated from the hydrophobic products quite simply and reintroduced into the process.

Water-soluble ligands like tppts can be prepared by the direct sulfonation of PPh_3 with fuming sulfuric acid. However, this reaction is not specific, and mixtures of *meta*-sulfonated phenylphosphanes with different degrees of sulfonation are obtained in addition to phosphanoxides and -sulfides. Time-consuming purification procedures are thus necessary for the preparation of uniform and pure products.[3, 4] The modified direct sulfonation of PPh_3 described recently by Larpent, Patin, Thilmont, and Valdor[5] provides the oxide of tppts in good yields, but its conversion into the phosphane requires several low-yielding steps.

We report here that the potassium salt **2** of 4,4′,4″-phosphanetriylbenzenesulfonic acid can be made simply and in high purity by the reaction of potassium *p*-fluorobenzenesulfonate (**1**) with PH_3 in the superbasic medium dimethylsulfoxide (DMSO)/KOH[6] [yield ca. 60%, reaction (b) in Scheme 1)]. Salt **1** was prepared by hydrolyzing *p*-fluorobenzenesulfonyl chloride (**1a**) with aqueous KOH and was used as a mixture with KCl formed in this reaction.[7]

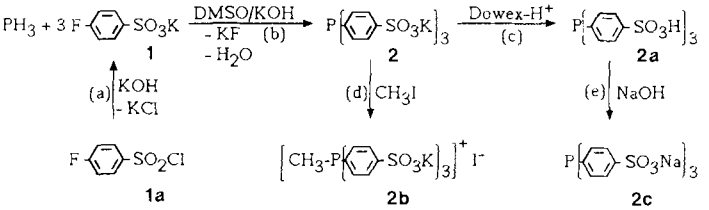

Scheme 1.

Salt **2** is formed according to reaction (b) by stepwise nucleophilic aromatic substitution of the fluorine atom in **1** by the phosphide ions PH_2^-, $[PH(C_6H_4\text{-}p\text{-}SO_3K)]^-$, and $[P(C_6H_4\text{-}p\text{-}SO_3K)_2]^-$, which in the superbasic medium are in equilibrium with PH_3, $PH_2(C_6H_4\text{-}p\text{-}SO_3K)$, $PH(C_6H_4\text{-}p\text{-}SO_3K)_2$.

During the workup of the reaction mixture formed by treatment of PH_3 with a mixture of salt **1** and KCl, product **2** crystallized as a hydrate of a double salt with the composition $\mathbf{2} \cdot KCl \cdot 0.5\,H_2O$. For the preparation of KCl-free **2**, pure **1** was employed in reaction (b); the latter can be obtained by hydrolysis of **1a** with aqueous acetic acid and subsequent neutralization with K_2CO_3 (yield 85%). Salt **2** precipitated as the dihydrate; however, no crystals suitable for X-ray structural analysis could be obtained.

The unit cell of $\mathbf{2} \cdot KCl \cdot 0.5\,H_2O$ (space group $Fd3$)[8] contains 32 formula units, and the anion of **2** has crystallographic C_3 symmetry (Fig. 1). The P–C bonds (1.843(4) Å) are only slightly longer than those in PPh_3 (mean value 1.828(3)[9a] or 1.831(2) Å[9b]). The P-C-P angles in **2** (103.5(2)°) and in PPh_3 (mean value 103.0(8)°[9a] or 102.8(9)°[9b]) are almost identical. The arene substituents are all twisted in the same direction. The angle ω between the plane defined by the three *ipso* C atoms (C(1), C(1a), C(1b)) and the arene ring is 65.7°. The first coordination spheres of the potassium atoms are occupied by eight oxygen and nine chlorine atoms. Compound **2** is the first sulfonated triphenylphosphane whose structure has been determined by X-ray crystallography.

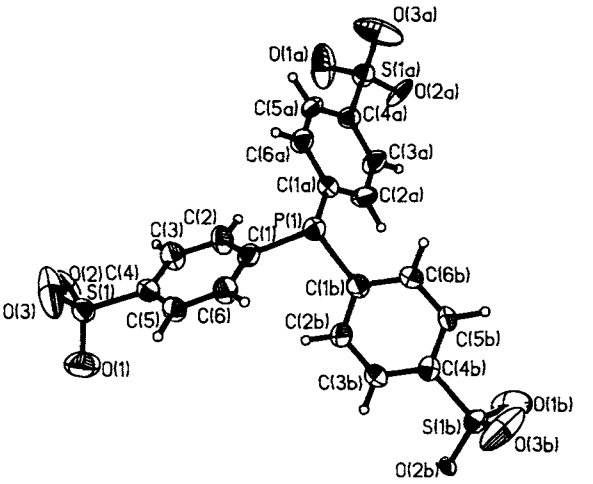

Fig. 1. Structure of the anion $P(C_6H_4\text{-}p\text{-}SO_3^-)_3$ in $\mathbf{2} \cdot KCl \cdot 0.5\,H_2O$. Bond lengths [Å] and angles [°]: P(1)-C(1) 1.843(4), S(1)-O(1) 1.413(4), S(1)-O(2) 1.406(4), S(1)-O(3) 1.440(5); C(1)-P(1)-C(1a, 1b, 1c) 103.5(2), O(1)-S(1)-O(2) 114.1(4), O(1)-S(1)-O(3) 109.5(4), O(2)-S(1)-O(3) 110.5(4).

[*] Prof. Dr. O. Stelzer, O. Herd, K. P. Langhans
Fachbereich 9, Anorganische Chemie der Universität-Gesamthochschule
Gaussstrasse 20, D-42097 Wuppertal (FRG)
Telefax: Int. code + (202)439-2901
Dr. N. Weferling
Hoechst AG, Werk Knapsack
Prof. Dr. W. S. Sheldrick
Lehrstuhl für Analytische Chemie der Ruhr-Universität Bochum

[**] Water-Soluble Phosphanes, Part 1. – This research was supported by the Deutsche Forschungsgemeinschaft and the Fonds der Chemischen Industrie.

The potassium salt **2** was converted into the sulfonic acid **2a** by treatment with the acidic form of an ion-exchange resin (Dowex-H^+) [reaction (c) in Scheme 1]. Salt **2** was quaternized with CH_3I in the two-phase system CH_2Cl_2/water to give the phosphonium salt **2b** [reaction (d) in Scheme 1]. Neutralization of **2a** with NaOH provided the Na salt **2c**.

In analogy to reactions of PH_3, primary and secondary phosphanes such as $PhPH_2$, 2-$PyPH_2$ (2-Py = 2-pyridyl)[10a], Ph_2PH, and 3-Py_2PH[10b] can be arylated with **1** in the superbasic medium to yield the tertiary phosphanes **3**, **4**, **5**, and **6** directly and with a defined degree of sulfonation [reactions (f) and (g) in Scheme 2].[11]

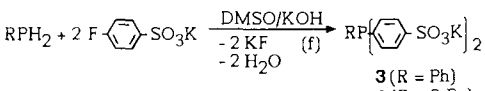

3 (R = Ph)
4 (R = 2-Py)

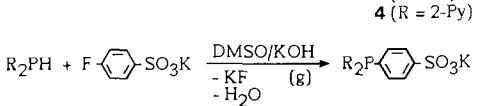

5 (R = Ph)
6 (R = 3-Py)

Scheme 2.

The chemical shifts $\delta^{31}P$ of the phosphanes $Ph_{3-n}P(C_6H_4\text{-}p\text{-}SO_3K)_n$ [**2** ($\delta = -8.9$), **3** (−13.2), **5** (−7.9)] show only a slight dependence on the degree of sulfonation n and the position of the SO_3M group in the arene ring [**2** ($\delta = -8.9$), tppts (−5.3)].[5] The solubility of the anionic phosphanes in water increases with the degree of sulfonation [**2** (0.8) kg L^{-1}), **3** (0.4), **5** (0.1)]. The solubility of **2** and **2c**, 0.8 and 0.9 kg L^{-1}, respectively, is only slightly less than that of the Na salt of tppts (ca. 1.1 kg L^{-1}).

Experimental Procedure

2: *p*-Fluorobenzenesulfonyl chloride (19.5 g, 0.1 mol) was added to 50 mL aqueous 2 N KOH, and the mixture was heated for 2 h at reflux. The solvent was removed at 40 °C (20 mbar), leaving a colorless powder consisting of **1** and KCl. This powder was added during the period of 1 h to a suspension of KOH (26.4 g, 0.4 mol, 85%) in 100 mL DMSO, which was saturated with PH_3. During the addition the PH_3 pressure was held constant at 1.1 bar. Upon addition of 50 mL water and 250 mL ethanol **2** was obtained as a colorless precipitate, which was filtered off and recrystallized twice from water. Correct C,H,P-analysis, 12.4 g (53%) yield. $^{31}P\{^1H\}$ NMR (32.2 MHz, D_2O): $\delta = -8.9$; $^{13}C\{^1H\}$ NMR (62.9 MHz, D_2O): $\delta = 140.1$ (11.0, C1), 135.1 (19.8, C2), 126.7 (7.3, C3), 144.5 (C4); ^1H NMR (250 MHz, D_2O); AA'BB'X spin system (A, A' = H_a, $H_{a'}$; B, B' = H_b, $H_{b'}$; X = ^{31}P): $\delta = 7.28$ [$^3J(PH_a) = 8.0$, $^3J(H_aH_b) = 8.4$, $^4J(H_aH_{a'}) = 1.8$, $^5J(H_aH_{b'}) \approx 0.1$ Hz; H_a], 7.61 [$^4J(PH_b) = 1.3$; $^4J(H_bH_{b'}) = 1.7$ Hz; H_b]. IR (KBr pellet): $\tilde{\nu} = 1205$, 1034 cm^{-1} ($\nu_{as}SO_3$, ν_sSO_3).

Received: January 4, 1993 [Z 5795 IE]
German version: *Angew. Chem.* **1993**, *105*, 1097

[1] E. G. Kuntz, *CHEMTECH*. **1987**, 570; E. Kuntz, (Rhône-Poulenc), FR-B 2314910, **1975**. [*Chem. Abstr.* **1977**, *87*, 101944n].

[2] W. A. Herrmann, J. Kulpe, W. Konkol, H. W. Bach, W. Gick, E. Wiebus, T. Müller, H. Bahrmann (Ruhrchemie AG), DE-B 3822036, **1988** [*Chem. Abstr.* **1990**, *113*, 100262g].

[3] L. Bexten, B. Cornils, D. Kupies (Ruhrchemie AG), DE-A 3431643, **1986** [*Chem. Abstr.* **1986**, *105*, 117009n].

[4] W. A. Herrmann, J. Kulpe, W. Konkol, H. Bahrmann, *J. Organomet. Chem.* **1990**, *389*, 85; W. A. Hermann, J. A. Kulpe, J. Kellner, H. Riepl, H. Bahrmann, W. Konkol, *Angew. Chem.* **1990**, *102*, 408; *Angew. Chem. Int. Ed. Engl.* **1990**, *29*, 391.

[5] C. Larpent, H. Patin, N. Thilmont, J. F. Valdor, *Synth. Comm.* **1991**, *21*, 495.

[6] O. Stelzer, K. P. Langhans, J. Svara, N. Weferling (Hoechst AG), US-A 5003108, **1991**; EP-B 307702, **1989** [*Chem. Abstr.* **1989**, *111*, 97500j]. *Z. Naturforsch. B* **1990**, *45*, 203.

[7] Compound **1a** can be prepared in 90–95% yield by sulfonation of fluorobenzene with chlorosulfonic acid.

[8] X-ray structural analysis of **2**·KCl·0.5H_2O: cubic, $Fd3$, $a = 27.948(5)$ Å, $V = 21830(7)$ Å^3, $Z = 32$, $\rho_{calc} = 1.702$ Mg m^{-3}. The structure was refined to $R = 0.054$, $R_w = 0.051$ for 1332 independent reflections ($Mo_{K\alpha}$, $2\theta \leq 50°$, $F_o^2 > 2\sigma(F_o^2)$, semiempirical absorption correction). Further details of the crystal structure investigation may be obtained from the Fachinformationszentrum Karlsruhe, Gesellschaft für wissenschaftlich-technische Information mbH, D-76344 Eggenstein-Leopoldshafen (FRG) on quoting the depository number CSD-56854, the names of the authors, and the journal citation.

[9] a) J. J. Daly, *J. Chem. Soc.* **1964**, 3799; b) B. J. Dunne, R. B. Morris, A. G. Orpen, *J. Chem. Soc. Dalton Trans.* **1991**, 653.

[10] a) G. U. Spiegel, O. Stelzer, *Chem. Ber.* **1990**, *123*, 989; b) G. U. Spiegel, O. Stelzer, unpublished.

[11] $^{13}C\{^1H\}$ NMR (62.9 MHz,D_2O): **3**: $\delta = 141.0$ (10.9, C1), 134.8 (19.2, C2), 126.5 (7.0, C3), 144.0 (C4), 135.4 (7.6, C5), 135.0 (20.1, C6), 129.9 (7.6, C7) 130.7 (C8); **4**: $\delta = 139.4$ (10.7, C1), 135.3 (19.9, C2), 126.7 (7.4, C3), 144.4 (C4), 161.1 (5.0, C5), 150.8 (12.1, C6), 124.9 (C7), 138.6 (3.0, C8), 129.9 (16.1, C9); **5**: $\delta = 142.0$ (12.0, C1), 134.5 (19.2, C2), 126.9 (6.7, C3), 145.8 (C4), 137.3 (8.8, C5), 134.9 (20.0, C6), 130.0 (7.2, C7), 130.0 (C8); **6**: $\delta = 139.9$ (9.8, C1), 134.6 (19.8, C2), 126.7 (7.2, C3), 144.5 (C4), 132.4 (13.1, C5), 153.7 (27.8, C6), 150.4 (C7), 125.5 (4.2, C8), 143.3 (14.3, C9); values in parentheses "J(PC) ($n = 1-4$); notation for the C atoms: C_6H_4 – SO_3K: C1 (*ipso*), C2 (*o*), C3 (*m*), C4 (*p*); C_6H_5: C5 (*ipso*), C6 (*o*), C7 (*m*), C8 (*p*); 2-Py, 3-Py: C5 (*ipso*), C6 (*o*, 3-Py; *m*, 2-Py), C7 (*p*), C8 (*m*), C9 (*o*).

[{$(Et_2O)_2ClGa$}Ga{$GaCl_2(Et_2O)$}$_3$]: A Molecular Compound with a Tetrahedral Ga_5 unit**

By *Dagmar Loos, Hansgeorg Schnöckel,** and *Dieter Fenske*

In memory of Harald Schäfer

The chemistry of Group IIIA elements in low oxidation states has seen a renaissance during the past years within the realm of solid-state chemistry and, more recently, also in the field of molecular compounds.[1] For solid compounds of the heavier elements, halides with weak metal–metal interactions (such as In_7Cl_9[2]) are known, as well as halides with "true" electron-pair bonding. In_5Br_7,[3] Ga_2I_3,[4] and Ga_2Br_3,[5] in which isolated $M_2X_6^{2-}$ units occur,[6] are among the latter. We are not aware of analogous solvent-free chlorides with Ga–Ga bonds,[7] since Ga_2Cl_4,[9] easily obtainable and known for a long time, must be described as $Ga^+GaCl_4^-$[10] in the crystalline solid[11] and also in the melt.[12]

Ga_2Cl_4 has proven to be an ideal starting compound for the synthesis of lower valent molecular Ga compounds. Interesting Ga^I complexes[14] are formed by adding arenes, whereas stronger donors like dioxane lead to formally divalent gallium compounds with Ga–Ga bonds.[15, 16] [$Ga_2Cl_4(OC_4H_8O)_2$] was the first molecular compound of that kind, with a Ga–Ga distance of 240.6 pm.[17] Starting from this compound, W. Uhl et al. prepared the first solvent-free organometallic compound of Ga with Ga–Ga bonds (254 pm) some years ago: $R_2Ga\text{–}GaR_2$ (R = $CH(SiMe_3)_2$).[18]

Starting from [$Ga_2Br_4(OC_4H_8O)_2$], the same authors recently succeeded in synthesizing the first Ga^I compound stable at room temperature, [Ga_4{$C(SiMe_3)_3$}$_4$],[19] which contains tetrahedral Ga_4 cluster units (d(Ga-Ga) =

[*] Prof. Dr. H. Schnöckel, Dipl.-Chem. D. Loos
Institut für Anorganische Chemie der Universität
Meiserstrasse 1, D-80333 München (FRG)
Telefax: Int. code +(89)5902-451
Prof. Dr. D. Fenske
Institut für Anorganische Chemie der Universität
Engesserstrasse Geb.-Nr. 30–45, D-76128 Karlsruhe (FRG)

[**] This work was supported by the Deutschen Forschungsgemeinschaft and the Fonds der Chemischen Industrie.

268.8 pm). In concurrent studies we showed that Ga^{I} compounds with suitable ligands such as cyclopentadienyl can also be obtained as monomers in solution and in the gas phase (even at approximately $-70\,^{\circ}C$).[20] Crucial to the synthesis of [GaCp] from GaCl and [$MgCp_2$] or [LiCp] was the cryochemical preparation of GaCl.[21] By co-condensing GaCl and a mixture of toluene/diethyl ether (4:1) around $-196\,^{\circ}C$, GaCl, which is metastable at room temperature, was obtained in solution. The structure of this solution species was hitherto unknown. By employing an appropriate crystallization procedure[22] we have now been able to isolate yellow, air- and temperature-sensitive crystals of **1** and have solved the structure by X-ray methods.[23]

$[\{(Et_2O)_2ClGa\}Ga\{GaCl_2(Et_2O)\}_3]$ **1**

Figure 1 shows the result of the X-ray structure analysis. A central atom (Ga1) is tetrahedrally surrounded by another four Ga atoms (Ga2–Ga5). Each of these is likewise coordinated tetrahedrally; two Cl atoms and one ether molecule bind to Ga3, Ga4, and Ga5, while Ga2 is bound to only one Cl atom and two ether molecules. Consequently, the following oxidation states are derived for the Ga atoms: 0 for Ga1, +1 for Ga2, and +2 for Ga3–Ga5. Nevertheless, the Ga–Ga distances vary only little between 241.7(2) and 245.0(2) pm; the longest distance observed is between Ga1 and Ga2. This seems plausible from the individual oxidation states of the respective Ga atoms and their corresponding sizes. In comparison with the distances in the metal, the Ga–Ga bond lengths in **1** also make sense. In Ga metal, a short bond of 244 pm is observed in addition to six longer bonds from 270 to 279 pm.[24] The Ga–Cl bond lengths with distances between 220.8(2) and 222.4(3) pm fall into the expected range, since in $[Ga_2Cl_4(OC_4H_8O)_2]$ the length of the Ga–Cl bond is 217 pm.[17] A shortening of the bond with respect to **1** is plausible, since larger radii of the Ga atoms are expected in **1** due to the lower averaged oxidation number. Therefore, dimeric $GaCl_3$ (containing tetrahedrally coordinated Ga atoms like in **1**) exhibits an unusually short terminal Ga–Cl distance of 206 pm as a consequence of the higher oxidation number for gallium.[25]

The angles measured within the Ga_5 tetrahedron can be explained by repulsive electrostatic interactions. Thus, angles that involve two Ga^{II} ions are wider than the tetrahedral angle. For angles engaging Ga^{I} (e.g. Ga5–Ga1–Ga2) we find smaller values, resulting from less repulsion.[26]

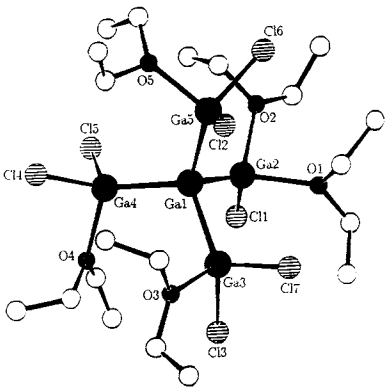

Fig. 1. Crystal structure of **1**. Selected distances [pm] and angles [°] (standard deviations in parentheses): Ga1–Ga2 245.0(2), Ga1–Ga3 242.6(2), Ga1–Ga4 241.7(2), Ga1–Ga5 242.6(2), $d_{max}/d_{min}/\bar{d}$: Ga–Cl 222.4(3)/220.8(3)/221.7, Ga–O 205.8(7)/203.2(7)/205.0; Ga2–Ga1–Ga3 101.27(5), Ga2–Ga1–Ga4 102.45(5), Ga2–Ga1–Ga5 109.01(5), Ga3–Ga1–Ga4 113.05(5), Ga3–Ga1–Ga5 112.44(5), Ga4–Ga1–Ga5 116.81(5).

Compound **1**, in which the Ga atoms are found in different oxidation states, forms in a solution of GaCl, which from the conditions of preparation invariably contains small amounts of $GaCl_3$ (maximum 5%). Formation of **1** therefore must entail disproportionation reactions ($2\,Ga^{I} \rightarrow Ga^{0} + Ga^{II}$), and possibly comproportionation reactions ($Ga^{III} + Ga^{I} \rightarrow 2\,Ga^{II}$) as well. Most likely the mechanism on which such reactions are based is very similar to that of the halogen transfer discussed for analogous reactions of indium compounds.[15]

In this isolation of **1**, an intermediate in the disproportionation of GaCl was successfully trapped and characterized for the first time. Besides their importance for the evaluation of unusual structural relationships, complex **1** and similar compounds may be suitable starting materials for new solid compounds not accessible by the standard high-temperature methods of solid-state chemistry.

Received: January 25, 1993 [Z 5825 IE]
German Version: *Angew. Chem.* **1993**, *105*, 1124

[1] P. Paetzold, *Angew. Chem.* **1991**, *103*, 559–561; *Angew. Chem. Int. Ed. Engl.* **1991**, *30*, 544.
[2] H. P. Beck, *Angew. Chem.* **1991**, *103*, 897–898; *Angew. Chem. Int. Ed. Engl.* **1991**, *30*, 824.
[3] G. Meyer, *Z. Anorg. Allg. Chem.* **1990**, *582*, 128.
[4] G. Gerlach, W. Hönle, A. Simon, *Z. Anorg. Allg. Chem.* **1982**, *486*, 7.
[5] W. Hönle, G. Gerlach, W. Weppner, A. Simon, *J. Solid State Chem.* **1986**, *61*, 171.
[6] The Ga–Ga distance is 243.3 pm [5] in Ga_2Br_3 and 238.8 pm [4] in Ga_2I_3.
[7] Isolated $Ga_2Cl_6^{2-}$ units with a short Ga–Ga distance of 239 pm are found in solid $[\{N(CH_3)_4\}_2(Ga_2Cl_6)]$ [8].
[8] K. L. Brown, D. Hall, *J. Chem. Soc. Dalton Trans.* **1973**, 1843.
[9] W. Klemm, W. Tilk, *Z. Anorg. Allg. Chem.* **1932**, *207*, 175; W. Klemm, F. Dierks, *ibid.* **1934**, *219*, 42.
[10] Ga_2Cl_4 species were, however, detected in the gas phase [13].
[11] G. Garton, H. M. Powell, *J. Inorg. Nucl. Chem.* **1957**, *4*, 84.
[12] J. W. Akitt, N. N. Greenwood, A. Storr, *J. Chem. Soc.* **1965**, 4410.
[13] H. Schäfer, M. Binnewies, *Rev. Chim. Miner.* **1976**, *13*, 24.
[14] H. Schmidbaur, *Angew. Chem.* **1985**, *97*, 893–904; *Angew. Chem. Int. Ed. Engl.* **1985**, *24*, 893.
[15] D. G. Tuck, *Polyhedron* **1990**, *9*, 377.
[16] F. M. Brewer, J. R. Chadwick, G. Garton, *J. Inorg. Nucl. Chem.* **1961**, *23*, 45.
[17] R. W. H. Small, I. J. Worrall, *Acta Crystallogr. Sect. B* **1982**, *38*, 250.
[18] W. Uhl, M. Layh, T. Hildenbrand, *J. Organomet. Chem.* **1989**, *364*, 289.
[19] W. Uhl, W. Hiller, M. Layh, W. Schwarz, *Angew. Chem.* **1992**, *104*, 1378–1380; *Angew. Chem. Int. Ed. Engl.* **1992**, *31*, 1364.
[20] D. Loos, H. Schnöckel, J. Gauss, U. Schneider, *Angew. Chem.* **1992**, *104*, 1376–1378; *Angew. Chem. Int. Ed. Engl.* **1992**, *31*, 1362.
[21] M. Tacke, H. Kreienkamp, L. Plaggenborg, H. Schnöckel, *Z. Anorg. Allg. Chem.* **1991**, *604*, 35.
[22] Pentane was layered onto a solution of GaCl in toluene/diethyl ether (4:1) [21] at $-78\,^{\circ}C$. The resulting reddish brown precipitate was taken up in diethyl ether. Compound **1** crystallized after several days at $-30\,^{\circ}C$. When the solid was warmed to room temperature, disproportionation started at around $0\,^{\circ}C$.
[23] Crystal structure analysis: $C_{20}H_{50}Cl_7Ga_5O_5$, orthorhombic, space group $P2_12_12_1$, $a = 1142.5(5)$, $b = 1212.2(6)$, $c = 2823.9(10)$ pm, $V = 3910.6 \times 10^6$ pm^3, $Z = 4$, $\varrho_{calcd} = 1.55$ g cm^{-3}, Stoe Stadi^{IV} diffractometer, $Mo_{K\alpha}$ radiation, 200 K, ω-scan, 2θ-scan 3–56°, 10405 measured reflections of which 4465 were unique. SHELX76, SHELX86, SCHAKAL programs; 334 parameters refined, C and O isotopic, Ga and Cl anisotropic, $R_1 = 0.048$, $R_w = 0.046$. Maxima/minima of a final difference Fourier synthesis $+0.77/-0.70$ electrons $\times 10^{-6}$ pm^3. Further details of the crystal structure investigation may be obtained from the Fachinformationszentrum Karlsruhe, Gesellschaft für wissenschaftlich-technische Information mbH, D-76344 Eggenstein-Leopoldshafen (FRG), on quoting the depository number CSD-57143, the names of the authors, and the journal citation.
[24] A. J. Bradley, *Z. Kristallogr.* **1935**, *91*, 302.
[25] S. C. Wallwork, I. J. Worrall, *J. Chem. Soc.* **1965**, 1816.
[26] That is why the nonbonding distances between, for example, Ga3 and Ga1 (approximately 377 pm) are also smaller than those between Ga3 and Ga4 (approximately 404 pm).

$CeCl_3$-Mediated Addition of Grignard Reagents to 1,3-Diketones**

By *Giuseppe Bartoli,* Enrico Marcantoni,* and *Marino Petrini*

1,3-Diketones have been always perceived as a practical source of stabilized carbanions owing to the enhanced acidity of the active methylene hydrogen atoms.[1] The alkylation of 1,3-diketones can be carried out with almost complete regio- and stereocontrol of the products.[2] Every attempt at attacking the carbonyl group with organometallic species led to unsatisfactory results, since these nucleophilic reagents are basic enough to promptly deprotonate the active methylene hydrogen atoms. The resulting enolate anion has an extremely stable cyclic structure with pseudoaromatic character and hence it is completely inert towards nucleophilic attack.[3]

We report here that Grignard reagents can be directly added to 1,3-diketones in the presence of dry $CeCl_3$ (Scheme 1). Through the addition of the diketone to a suspension of dry $CeCl_3$ in THF at 0 °C, a 1:1 complex is probably formed.[4] This complex formation enhances the electrophilicity of the carbonyl groups, and the subsequent addition of the organomagnesium reagent at −30 °C proceeds with the attack of the Grignard species at the carbonyl functionality. The usual workup gives β-hydroxy ketones in good yields (Tables 1 and 2).

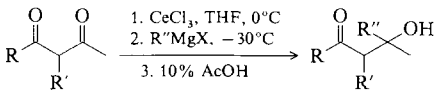

1 a–c **2 a–h**

Scheme 1. Synthesis of β-hydroxyketones **2a–h**. **1a**: R = CH_3, R′ = H; **1b**: R = Ph, R′ = H; **1c**: R + R′ = $-(CH_2)_4-$. R″ = Me, Ph, *n*Pr, H_2C=CH, H_2C=CH–CH_2.

Table 1. Reaction of 1,3-diketones with Grignard reagents in the presence of $CeCl_3$ in THF at −30 °C.

Substrate	R″MgX	Product [10]	Yield [%] [a]
1a	*n*PrMgCl	**2a**	70
1b	*n*PrMgCl	**2b**	75
1c	MeMgCl	**2c**	85
1a	PhMgBr	**2d**	86
1b	PhMgBr	**2e**	73
1b	H_2C=CHMgBr	**2f**	80
1b	H_2C=CHCH_2MgBr	**2g**	88
1c	*n*PrMgCl	**2h**	85

[a] Isolated yields.

The amazing reactivity of the 1,3-diketones was initially attributed to the formation of organocerium intermediates which are known to efficiently add to easily enolizable substrates.[5] However, preformed organocerium reagents[6] are unable to furnish the same products **2**. The starting material is usually recovered in these experiments.[7]

[*] Prof. Dr. G. Bartoli, Dr. E. Marcantoni, Prof. Dr. M. Petrini
Dipartimento di Scienze Chimiche dell'Università
via S.Agostino, 1, I-62032 Camerino (Italy)
Telefax: Int. code +(737) 37345

[**] This work was supported by Ministero dell'Universita' e della Ricerca Scientifica e Tecnologica (MURST) Italy.

Table 2. Selected physical data for **2f–h**.

2f: Oil, ^{1}H NMR (300 MHz, $CDCl_3$, 20 °C): δ = 1.40 (s, 3H, CH_3), 3.10 (d, ^2J(H,H) = 17.1 Hz, 1H, CH_2), 3.38 (d, ^2J(H,H) = 17.1 Hz, 1H, CH_2), 4.44 (s, 1H, OH), 5.05 (dd, ^3J(H,H) = 10.7 Hz, ^2J(H,H) = 1.1 Hz, 1H, =CH_2), 5.27 (dd, ^3J(H,H) = 16.5 Hz, ^2J(H,H) = 1.1 Hz, 1H, =CH_2), 6.00 (dd, ^3J(H,H) = 10.7 Hz, ^3J(H,H) = 16.5 Hz, 1H, CH=), 7.40–7.65 (m, 3H, Ph), 7.90–7.97 (m, 2H, Ph); IR (film): $\tilde{\nu}$[cm^{-1}] = 3490 (OH), 1660 (C=O); MS (70 eV): *m/z* (%) 172 ($M^+ - H_2O$, 8), 160 (51), 105 (100), 77 (50), 71 (14), 51 (17), 43 (18).

2g: Oil, ^{1}H NMR: δ = 1.32 (s, 3H, CH_3), 2.44 (d, ^3J(H,H) = 7.3 Hz, 2H, CH_2 (allyl)), 3.05 (d, ^2J(H,H) = 17.4 Hz, 1H, CH_2), 3.20 (d, ^2J(H,H) = 17.4 Hz, 1H, CH_2), 4.20 (s, 1H, OH), 5.05–5.20 (m, 2H, =CH_2), 5.85–6.00 (m, 1H, CH=), 7.30–7.60 (m, 3H, Ph), 7.90–8.00 (m, 2H, Ph); IR (film): $\tilde{\nu}$[cm^{-1}] = 3440 (OH), 1655 (C=O); MS (70 eV): *m/z* (%) 186 ($M^+ - H_2O$, 0.5), 163 (29), 105 (100), 77 (35), 51 (9), 43 (18), 39 (6).

2h: Oil, ^{1}H NMR: δ = 0.90 (t, ^3J(H,H) = 6.4 Hz, 3H, CH_3), 1.15 (s, 3H, CH_3, diastereomer a), 1.18 (s, 3H, CH_3, diastereomer b), 1.30–2.40 (m, 14H); IR (film): $\tilde{\nu}$[cm^{-1}]: 3490 (OH), 1670 (C=O); MS (70 eV): *m/z* (%) 166 ($M^+ - H_2O$, 84), 151 (100), 137 (35), 123 (31), 109 (50), 95 (35), 81 (37), 67 (57), 55 (30).

We believe that a six-membered ring transition state, favored by the presence of the chelating $CeCl_3$ (Scheme 2), forms in which the Grignard reagent approaches the less hindered carbonyl group. Steric factors should strongly influence the reactivity of the carbonyl groups, since only the less hindered carbonyl group is reactive under our reaction conditions. Furthermore, secondary and tertiary Grignard reagents cannot be introduced even by adopting prolonged reaction times or more elevated temperatures.[8]

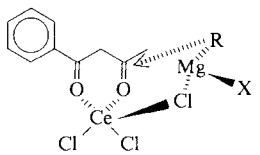

Scheme 2. Proposed transition state for the formation of **2**.

The organomagnesium reagent is added in 0.5 molar excess, and it is worth noting that even when using a larger amount of the reagent no traces of 1,3-dihydroxy compounds, derived from nucleophilic attack at both carbonyl groups, have been found. The present procedure can be used to introduce a large variety of carbon frameworks, including aryl, vinyl, and allyl groups, but it only seems to function with Grignard reagents.[9]

In conclusion, 1,3-ketones in the presence of $CeCl_3$ are extremely reactive towards Grignard reagents. This reaction is considerably chemoselective and allows the straightforward preparation of functionalized β-hydroxy ketones. A study of the synthetic potential of this procedure is currently in progress.

Experimental Procedure

Finely ground $CeCl_3 \cdot 7H_2O$ (0.93 g, 2.5 mmol) was dried by heating at 140 °C/0.1 Torr for 2 h. Dry THF (35 mL) was then added at 0 °C, and the milky suspension was stirred for about 15 h under N_2 at room temperature. The 1,3-diketone (1.66 mmol) was then added at 0 °C, and the mixture was stirred for 1 h at the same temperature. The appropriate Grignard reagent (2.5 mmol) was then added dropwise at −30 °C, and the mixture was stirred at this temperature for a further 30 min. Subsequently 10% acetic acid (45 mL) was poured into the mixture. After extraction with ether (3 × 30 mL), the organic phase was washed with saturated $NaHCO_3$ (10 mL) and saturated NaCl (10 mL), and dried ($MgSO_4$). Flash chromatography (SiO_2, hexane/ethyl acetate 7:3) afforded the pure product.

Received: February 2, 1993 [Z 5846 IE]
German version: *Angew. Chem.* **1993**, *105*, 1115

[1] a) H. O. House, *Modern Synthetic Reactions*, 2nd ed., W. A. Benjamin, Menlo Park, **1972**, p. 492; b) J. March, *Advanced Organic Chemistry*, 4th ed., Wiley, New York, **1992**.

[2] Reviews: a) D. Caine, *Alkylations of Enols and Enolates, in Comprehensive Organic Synthesis, Vol. 3*, (Eds.: B. M. Trost, I. Fleming, G. Pattersen), Pergamon, Oxford, **1991**, p. 54; b) C. M. Thompson, D. L. C. Green, *Tetrahedron* **1991**, *47*, 4223; α,β-unsaturated α-alkoxy ketones: c) G. Stork, R. C. Danheiser, *J. Org. Chem.* **1973**, *38*, 1775; d) G. Stork, R. L. Danheiser, B. Ganem, *J. Am. Chem. Soc.* **1973**, *95*, 3414; α,β-unsaturated β-dialkylamino ketones: e) T. A. Bryson, R. B. Gammill, *Tetrahedron Lett.* **1974**, 3963; f) E. Telshow, W. Reusch, *J. Org. Chem.* **1975**, *40*, 862; β-enamino ketones: g) G. Bartoli, M. Bosco, C. Cimarelli, R. Dalpozzo, G. Palmieri, *J. Chem. Soc., Perkin Trans. 1* **1992**, 2095; h) G. Bartoli, C. Cimarelli, G. Palmieri, G. Rafaiani, *Tetrahedron: Asymmetry* **1992**, *3*, 719.

[3] a) Y. L. Chen, P. S. Mariano, G. M. Little, D. O'Brien, P. L. Huesmann, *J. Org. Chem.* **1981**, *46*, 4643; theoretical calculations (HF/6-31 G/3-21G) have been executed on mono- and dianions of acyclic β-enamino ketones: b) G. Bartoli, M. Bosco, C. Cimarelli, R. Dalpozzo, M. Guerra, G. Palmieri, *J. Chem. Soc. Perkin Trans. 2* **1992**, 649.

[4] Similar chelate intermediates have been invoked to explain the stereoselective reduction of ketones bearing a $P(O)R_2$ functionality in the β position: J. Elliott, S. Warren, *Tetrahedron Lett.* **1986**, *27*, 645.

[5] For comprehensive reviews on this topic see: a) G. A. Molander, *Chem. Rev.* **1992**, *92*, 29; b) H. B. Kagan, J. L. Namy, *Tetrahedron* **1986**, *42*, 6573; for a leading paper on organocerium addition to carbonyl substrates see: c) T. Imamoto, N. Takiyama, K. Nakamura, T. Hatajima, Y. Kamiya, *J. Am. Chem. Soc.* **1989**, *111*, 4392.

[6] These reagents can be efficiently prepared simply by adding the corresponding Grignard reagent to the $CeCl_3$ suspension in THF [5c].

[7] It is known that tris(cyclopentadienyl)ytterbium is able to deprotonate 2,4-pentadione giving a chelate complex: G. Bielang, R. D. Fischer, *Inorg. Chim. Acta* **1979**, *36*, L389.

[8] The low reactivity of secondary and tertiary Grignard reagents may be also ascribed to the increase of basicity observed moving from primary to tertiary organomagnesium reagents.

[9] Organolithium reagents do no react analogously, probably because they are more basic than Grignard reagents.

[10] **2a**: D. P. Curran, *J. Am. Chem. Soc.* **1983**, *102*, 5826; **2b**: C. Najera, M. Yus, D. Seebach, *Helv. Chim. Acta* **1984**, *67*, 289; **2c**: S. Fukuzawa, T. Tsuruta, T. Fujinami, S. Sakai, *J. Chem. Soc., Perkin Trans. 1* **1987**, 1473; **2d**: T. J. Leitereg, D. J. Cram, *J. Am. Chem. Soc.* **1968**, *90*, 4019; **2e**: E. Hasegawa, K. Ishiyama, T. Horaguchi, T. Shimizu, *J. Org. Chem.* **1991**, *56*, 1631.

How N_2 Might Be Activated by the FeMo-Cofactor in Nitrogenase**

By *Haibin Deng* and *Roald Hoffmann**

We finally have a structural model for the nitrogenase FeMo-cofactor, based on 2.7 Å resolution crystal structure of the *Azotobacter vinelandii* MoFe-protein by J. Kim and D. C. Rees.[1] Here we examine the electronic structure of this model, and its possible N_2 binding modes.

The FeMo-cofactor (**1**) contains two clusters of composition 4Fe:3S and 1Mo:3Fe:3S, bridged by three non-protein ligands. The cofactor is linked to the protein through the Fe1 and Mo metal atoms (see **2**). The sulfur atom of the $Cys^{\alpha 275}$ residue coordinates Fe1, whereas the Mo atom is ligated by the imidazole group of the $His^{\alpha 442}$ residue, as well as a homocitrate HC through hydroxyl and carboxyl oxygen atoms.[1] The 4Fe:3S and 1Mo:3Fe:3S clusters may be structurally related to common 4Fe:4S cubane clusters by

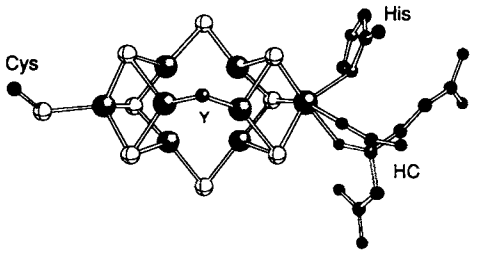

1

removing one of the S atoms of the latter. The six inner iron atoms of the cofactor (Fe2–Fe7 see **2**) form an approximate trigonal prism. The coordination environment around Mo is approximately octahedral and that around Fe1 tetrahedral. Fe2–Fe7 have quite distorted trigonal-planar coordination. Two of the three bridging ligands between the two clusters are sulfide ions S^{2-}, while the third ligand Y is probably a nitrogen or oxygen atom, or a less ordered sulfur.[1]

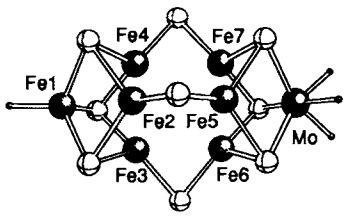

2

We first examine the electronic structure and the bonding in the cofactor model.[2] To simplify the analysis and yet not lose essential chemical information we have replaced the uncertain Y atom with S^{2-}, the ligating atoms from the cysteine, histidine, and homocitrate with the simplest ligands, H^-. Finally we symmetrize the structure to C_{3v} point symmetry.[3] The bond lengths are set at 2.75 (Fe–Fe (all)), 2.85 (Fe–Mo), 2.3 (Fe–S), 2.35 (Mo–S), 1.6 (Fe–H), 1.70 Å (Mo–H). In much previous work we have found it useful to set distances equal and then allow the overlap populations (OPs) to tell us which bonds are stronger. This is why we have equalized the Fe–Fe separations in **2**.

What about the oxidation states of the metal centers in **1**? Mo ENDOR and EXAFS studies indicate that the most likely formal oxidation state for Mo is +4;[4] and Mössbauer investigations show that Mo does not seem to change oxidation state when the MoFe-protein is reduced.[5] We assign the four iron atoms in the 4Fe:3S cluster together a +10 charge, as in the cubane clusters $[Fe_4S_4(SR)_4]^{2-}$.[6] The three iron atoms in the 1Mo:3Fe:3S cluster are given a total +7 charge, to be in line with the spin state of the FeMo-cofactor ($S = 3/2$).[4] Thus the actual molecule calculated, a model of a model, is $[HFe_4S_3(\mu\text{-}S)_3Fe_3S_3MoH_3]^-$ (**2**).

The given charge assignment is by no means unique, or even correct. But we must start somewhere. Thorneley–Lowe kinetic models[7] for dinitrogen reduction indicate that dinitrogen binds to more reduced forms of the cofactor. Thus we will also examine the consequence of adding up to three electrons to the cofactor model **2** (i.e., the reduction of all Fe atoms to Fe^{II}).

An energy level diagram for **2** is shown in Figure 1a. The HOMO is a singly occupied orbital. There is another orbital only 0.03 eV above it; in fact there are nine orbitals within half an eV around the HOMO. Thus the system should be a high-spin one. The electron coupling in the cofactor **1** is

[*] Prof. R. Hoffmann, Dr. H. Deng
Department of Chemistry
Cornell University
Ithaca, NY 14853-1301 (USA)
Telefax: Int. code + (607)255-5707

[**] We are grateful to the National Science Foundation for its support of this work through CHE 8912070. Dr. Douglas Rees was kind enough to transmit to us his refinement of the MoFe-protein structure. We are also grateful to him for discussions of the N_2 binding.

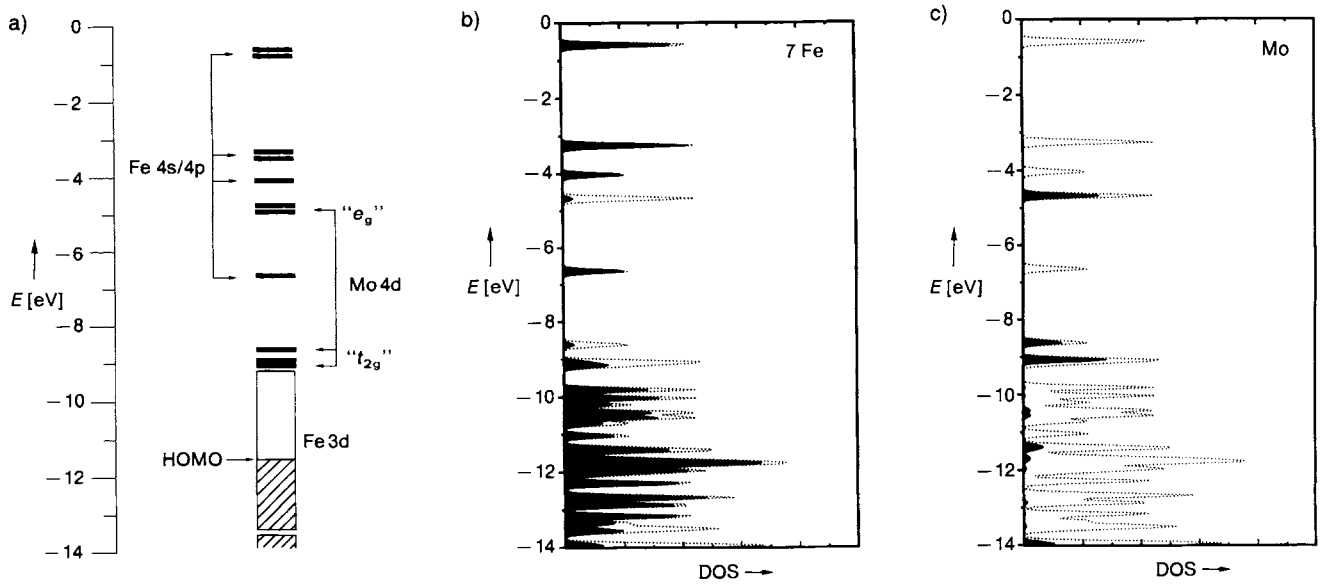

Fig. 1. a) Energy level diagram for **2**. Fe 4s/4p stands for hybrid orbitals, the striped block at the bottom represents ligand-based (S, H) orbitals. b) and c) "Density of states" (DOS) diagrams for **2**; the dotted line is the total DOS of **2**, and the contributions of seven Fe atoms and the Mo atom to the total DOS are shown by the shaded areas in b) and c), respectively.

likely to be complicated, so our results on **2** are not inconsistent with $S = 3/2$ for **1**. We can also show the energy levels in a "density of states" (DOS) fashion,[8] as in Figures 1b and 1c. This is convenient when the contributions of individual atomic orbitals or fragment molecular orbitals are desired. Figures 1b and 1c illustrate such contributions from the Fe and Mo atoms, respectively.

We can analyze these orbitals in some detail. The orbitals below -13.5 eV are mainly ligand-based (S and H) orbitals, which are metal–ligand bonding. A block of 35 levels, mainly Fe 3d orbitals, is concentrated between -13.5 and -9 eV. The bottom of this block is Fe–Fe bonding, while the top part is Fe–Fe antibonding. The HOMO is at about the center of the Fe 3d block. The Mo 4d orbitals are higher in energy than Fe 3d orbitals; the Mo 4d orbitals split into "e_g" and "t_{2g}" sets, typical for an octahedral transition metal complex.[9] The six empty levels (above -7 eV) are composed mainly of combinations of 4s and 4p orbitals on three-coordinate Fe atoms. The resulting hybrids are approximately perpendicular to the local coordination planes of these Fe atoms. One such MO is drawn in Scheme 1. In these orbitals resides the coordinative "unsaturation" of these Fe atoms and their reactivity toward bases. The presence of these acceptor orbitals and the "open" cavity in the trigonal prism formed by Fe2–Fe7 have made people think about occupation of the cavity, even though there is *no* structural evidence for such a species. The model **3** has the geometry in question; when one does a calculation with a main group element in the center, for example, O^{2-} (Fe–O = 2.1 Å), four of the six Fe acceptor orbitals are indeed pushed up. Thus, there is nothing wrong electronically with a central atom in **2**.

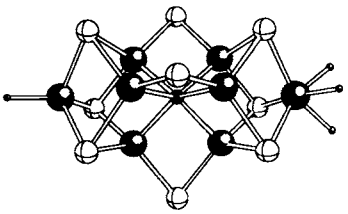

3

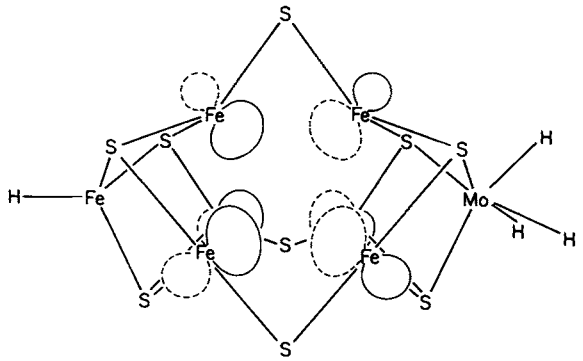

Scheme 1. One of the 4s/4p hybrid orbitals of **2**.

If we now return to the symmetrized cofactor model **2**, the overlap populations (OPs) between three-coordinate Fe atoms (e.g., Fe2–Fe3, Fe2–Fe5, Fe5–Fe6) are substantial (0.14–0.15). This is actually equivalent to something like a single bond. For instance, unbridged $[Fe_2(CO)_8]^{2-}$ at the same Fe–Fe distance has an Fe–Fe OP of 0.21. There definitely is metal–metal bonding everywhere in **2**, and across the trigonal prismatic cavity in particular.[10] This is reflected by the shorter Fe2–Fe5, Fe3–Fe6, and Fe4–Fe7 distances (2.5–2.6 Å) in the structurally refined cofactor model.

We assume that the first step in nitrogen fixation is the binding of N_2 to the FeMo-cofactor.[11] Various models with different N_2 binding sites are shown in Scheme 2. Model **4** has also been suggested by Orme-Johnson.[12] We set all the Fe–N or Mo–N distances at 2.0 Å, and the N–N distance at 1.1 Å, the value in free dinitrogen. We then compared the overlap populations for the N–N bonds and the net charges on the N atoms (Table 1) for various binding modes and for two different redox states of the cofactor (the "reduced" state has three more electrons than the "native" state). As the N–N bond has to be weakened and protonation at N has to occur before the coordinated N_2 can be reduced to NH_3,

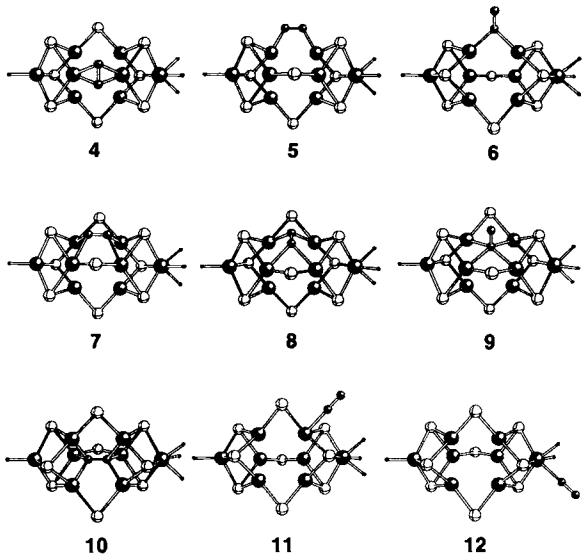

Scheme 2. Theoretically studied complexes from N_2 and **2**.

a small value of N–N OP and a net negative charge on the N atoms should activate an N_2 molecule for reduction.

In models **4**–**6** the Y ligand is replaced by dinitrogen, while in **7**–**9** dinitrogen approaches the cofactor at a face of the Fe_6 trigonal prism. Models **7**–**9** give too close N–S contacts; we would like to reject them for that reason, but hesitate because the cofactor may expand its dimension upon reduction or N_2 binding. In **10**, the simple insertion of N_2 into the Fe_6 trigonal prism gives rise to very short Fe–N distances (ca. 1.8 Å). To obtain an Fe–N separation of 2 Å, a more reasonable value, the Fe_6 trigonal prism has to be expanded until the Fe–Fe distances, originally 2.75 Å, reach 3 Å. Table 1 includes data for both geometries of **10**. Two models involving end-on binding of N_2 are considered in **11** and **12**. One of the ligands on Mo has to be dissociated in order for Mo to bind N_2 in **12**.

Table 1. Overlap populations (OPs) of N–N bonds and net atomic charges on the N atoms for the N_2–FeMo-cofactor models shown in Scheme 2.

	"Native" State		"Reduced" State (three more electrons)	
	OP(N–N)	Charge on N [a]	OP(N–N)	Charge on N [a]
Free N_2	1.73	0		
4	1.47	−0.12	1.47	−0.18
5	1.61	0.11, 0.09	1.60	0.08, 0.06
6	1.58	0.49, −0.37	1.56	0.46, −0.43
7	1.45	0.28, 0.35	1.45	0.26, 0.32
8	1.51	0.20	1.49	0.16
9	1.52	0.58, −0.34	1.52	0.57, −0.39
10 [b]	1.23	0.43, 0.42	1.27	0.41, 0.28
10 [c]	1.35	0.34, 0.33	1.43	0.24, 0.16
11	1.70	0.62, −0.16	1.70	0.62, −0.17
12	1.72	0.45, −0.12	1.71	0.44, −0.14

[a] When two N atoms are not equivalent, the first value is for the "left" (or the bound) nitrogen atom in the structures in Scheme 2. [b] Fe–N = 1.79, Fe–Fe = 2.75 Å (for all edges of the Fe_6 trigonal prism). [c] Fe–N = 2.0, Fe–Fe = 3.03 Å (for all edges of the Fe_6 trigonal prism).

As shown in Table 1, centered **10** gives the smallest OP for the N–N bond; however, the net charges on N are quite positive, which is undesirable for protonation. Model **4** seems to be the best compromise—it has two ingredients important for N_2 reduction: a lowered N–N OP, and negative net charge on N. The reduced OP is primarily a consequence of the occupation of π_g^* orbitals of N_2. The contribution of this fragment MO to all the composite orbitals of **4** is shown in Figure 2. The π_g^* orbital is occupied to the extent of 20%. The models **6** and **9** are also possible binding modes, as the N–N bond is highly polarized and the terminal N atom carries a substantial net negative charge.

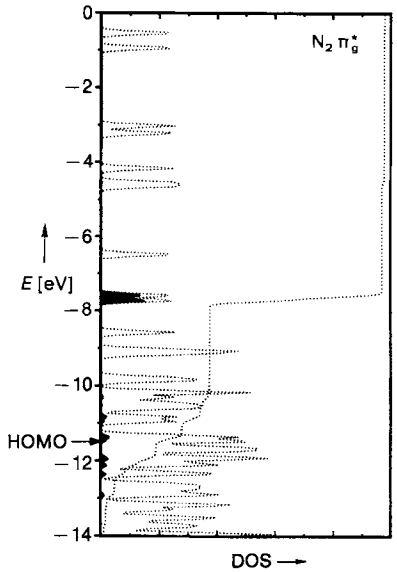

Fig. 2. The contribution of the N_2 π_g^* fragment MO (shaded area) to the total DOS of **4** (dotted line). The integration line indicates the percentage of π_g^* filled, on a scale from 0 to 100%.

The "reduced" state (with three more electrons) gives OPs for the N–N bond and net charges on the N atoms comparable to the "native" state. This is because the three additional electrons enter one or two levels immediately above the HOMO in the Fe 3d block, where there is relatively little N_2 orbital contribution. The net charges on the Fe or Mo atoms that bind N_2 do become more negative.[13]

In conclusion, our initial study finds that metal–metal bonding in the FeMo-cofactor model of nitrogenase is important; the Fe–Fe bonds are especially strong among three-coordinate iron atoms. N_2 coordinated models **4**, and possibly **6** and **9** are, we think, best activated for reduction.

Received: January 29, 1993 [Z 5841IE]
German version: *Angew. Chem.* **1993**, *105*, 1125

[1] J. Kim, D. C. Rees, *Science*, **1992**, *257*, 1677–1682; J. Kim, D. C. Rees, *Nature*, **1992**, *360*, 553–560; see also D. Sellman, *Angew. Chem.* **1993**, *105*, 67; *Angew. Chem. Int. Ed. Engl.* **1993**, *32*, 64. A 2.2 Å resolution refinement has just been published: M. K. Chan, J. Kim, D. C. Rees, *Science* **1993**, *260*, 792–794. There are no major changes in the model.

[2] Our calculations are of extended Hückel type: R. Hoffmann, *J. Chem. Phys.* **1963**, *39*, 1397–1412; R. Hoffmann, W. N. Lipscomb, *ibid.* **1962**, *36*, 2179–2188, 3489–3493. The parameters for Fe, Mo, and S are taken from earlier work: J. Silvestre, R. Hoffmann, *Inorg. Chem.* **1985**, *24*, 4108–4119; R. H. Summerville, R. Hoffmann, *J. Am. Chem. Soc.* **1976**, *98*, 7240–7254. Two other parameter sets were tested – in one the sulfur H_{ii} parameter was raised by 2.3 eV, in the other the Mo 4d H_{ii} parameter was lowered to the energy of the Fe 3d orbitals. The important results on the N–N bond weakening and bound N_2 polarity remain unaffected by these parameter changes.

[3] We also performed calculations on the cofactor model with real ligating atoms and the geometry from the X-ray crystallographic analysis, and obtained similar results.

[4] B. K. Burgess, *Chem. Rev.* **1990**, *90*, 1377–1406.

[5] R. Zimmermann, A. X. Trautwein in *Nitrogen Fixation* (Eds.: A. Müller, W. E. Newton), Plenum, New York, **1983**, pp. 63–81.

[6] S. Harris, *Polyhedron*, **1989**, *8*, 2843–2882.

[7] R. N. F. Thorneley, D. J. Lowe in *Molybdenum Enzymes* (Ed.: T. Spiro), Wiley, New York, **1985**, pp. 221–284.
[8] R. Hoffmann, *Angew. Chem.* **1987**, *99*, 871–906; *Angew. Chem. Int. Ed. Engl.* **1987**, *26*, 846–878; *Solid and Surfaces*, VCH, New York, **1988**; G. F. Holland, D. E. Ellis, W. C. Trogler, *J. Am. Chem. Soc.* **1986**, *108*, 1884–1894.
[9] When the Mo 4d orbitals are put in with an energy of the Fe 3d (see end of ref. [2]), the Mo "t_{2g}" set is filled and the Mo reduced. The results of the N_2 binding are not affected.
[10] In a hypothetical model **3** with a central O atom, all the Fe–Fe (and Fe–Mo) interactions are weak, but definitely bonding (OPs range from 0.04 to 0.09), similar to those in a cubane cluster $[Fe_4S_4(SR)_4]^{2-}$ (OP = 0.07). In addition there is reasonable Fe–O bonding.
[11] One or two protons may also be bound to the MoFe-protein [7]. The protons may not necessarily bind to the cofactor; but if they do they would interact with the donor levels of the cofactor (e.g., the lone pairs of sulfide ions, or the filled Fe 3d orbitals), and should have little effect on the chemical bonding and the N_2-binding properties of the cofactor. We confirmed this by repeating the N_2-Binding studies with two protons bound to two bridging sulfide ions, and to Fe2 and Fe5 along the perpendicular direction of the coordination planes, respectively.
[12] W. H. Orme-Johnson, *Science*, **1992**, *257*, 1639–1640.
[13] We also performed calculations on N_2 binding with the O^{2-}-centered model **3**, but do not present details here. Binding modes **7**–**9** give unreasonably short N–O distances. For **5**, **6**, **11**, **12**, the central O^{2-} has little influence on the OP of the N–N bond. Only for **4** are both the OP for the N–N bond and the net atomic charge on the N atom substantially reduced, to values of 1.39 and −0.32, respectively. This is because the energy levels within half an eV above the HOMO have some contributions from the π^* state of the N_2 fragment, and they are filled when the central O^{2-} raises the energy of the HOMO by 0.4 eV. Of course, **10** is impossible in this case.

Structural Evidence of the Aromaticity of Borepins: A Comparison of 1-Chloroborepin and Tricarbonyl(1-chloroborepin)molybdenum **

By *Arthur J. Ashe, III,* Jeff W. Kampf, Wolfram Klein,* and *Roger Rousseau*

Dedicated to Professor Hans Bock on the occasion of his 65th birthday

Borepins **1** have been intensely investigated since they are the neutral isoelectronic analogues of tropylium **2**.[1–9] However, theoretical work has suggested that the aromaticity of 1 *H*-borepin (**1a**) is more limited than that of **2**.[10] The ready availability of minimally substituted borepins offers the opportunity to obtain experimental data on borepin aromaticity.[8, 9] We report here on the structures of 1-chloroborepin (**1b**) and tricarbonyl(1-chloroborepin)molybdenum (**3b**).[11]

At room temperature **1b** is a moisture- and air-sensitive liquid (m.p. −37 °C). We have determined the X-ray crystal structure of **1b** by using crystals grown from the neat liquid and sealed in capillaries. Selected bond lengths are listed in Table 1, while Figure 1 illustrates the structure, showing a completely planar borepin ring as had been anticipated from theoretical work.[10] The B–C bond length (1.51 Å) is distinctly shorter than those which have been found for nonconjugated B–C bonds (typical range 1.55–1.59 Å),[12] indicating π bonding in the borepin ring. The ring C–C bond lengths range from 1.37 to 1.42 Å; the formal single bonds are somewhat longer than the formal double bonds. However, this range of bond lengths (± 0.058 Å) is considerably smaller than that found for cycloheptatrienes (1.33–1.46 Å)[13] and other cyclic polyenes. Indeed, the range of C–C bond lengths of **1b** is comparable with that of napthalene (1.36–1.42 Å), and is consistent with an aromatic ring.[14]

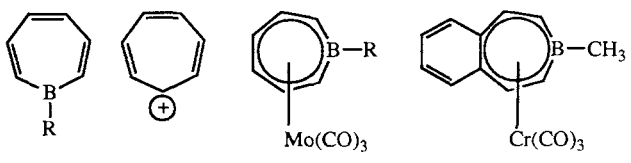

1a, R = H **1b**, R = Cl **2** **3a**, R = H **3b**, R = Cl **3c**, R = C_6H_5 **4**

Table 1. Selected bond lengths [Å] of the borepins **1b** and **3b**.

Bond	**1b** (exp.)	**1b** (6-31G*)	**3b** (exp.)
B1-Cl1	1.802(2)	1.803	1.792(4)
B1-C1	1.514(1)	1.530	1.514(3)
C1-C2	1.369(2)	1.349	1.398(3)
C2-C3	1.424(1)	1.439	1.421(3)
C3-C3a	1.366(1)	1.346	1.413(3)
C-C range	±0.058	±0.093	±0.023
Mo-B1	–	–	2.486(4)
Mo-C1	–	–	2.417(2)
Mo-C2	–	–	2.362(2)
Mo-C3	–	–	2.325(2)

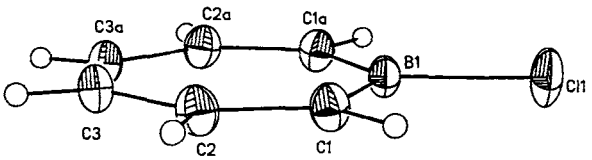

Fig. 1. Crystal structure of **1b** (ORTEP). Bond angles [°]: Cl1-B1-C1 116.76(6), C1-B1-C1a 126.5, B1-C1-C2 127.42(9), C1-C2-C3 128.96(9), C2-C3-C3a 130.4(1).

For purposes of comparison we have performed a Hartree Fock level ab initio MO calculation of **1b** with the 6-31G* basis set.[15] The optimized structural parameters listed in Table 1 do not differ significantly from those reported for **1a** calculated at the same level.[10] While the calculated and experimental structure for **1b** are in reasonable agreement (corresponding bond lengths are ± 0.02 Å), the calculated structure has a larger range of C–C interatomic distances (± 0.093 Å); thus the bond alternation is overestimated.

The reaction of **1b** with tricarbonyltris(pyridine)molybdenum and $BF_3 \cdot OEt_2$ gave the complex **3b**, which serves as a useful precursor for a variety of borepin complexes. The reduction of **3b** with lithium triethylborate afforded 1 *H*-borepin(tricarbonyl)molybdenum (**3a**) as stable crystals. This complex cannot be prepared directly from the very labile free 1 *H*-borepin.

It was of particular interest to obtain a crystal structure of **3b** and to compare it with that of **1b**. Structural data are known for **3c**[9] and **4**[12c] but not for the corresponding free ligands. The structure of **3b** (Fig. 2) consists of a nearly planar chloroborepin ring that is η^7-bound to the $Mo(CO)_3$ unit. The B–Mo distance (Table 1) is slightly longer than the

[*] Prof. Dr. A. J. Ashe, III, Dr. J. W. Kampf, Dr. W. Klein, R. Rousseau
Department of Chemistry, The University of Michigan
Ann Arbor, MI 48109-1055 (USA)
Telefax: Int. code +(313) 747-4865.

[**] This work was supported by the donors of the Petroleum Research Fund, administered by the American Chemical Society. W. K. thanks the Deutsche Forschungsgemeinschaft for a postdoctoral fellowship.

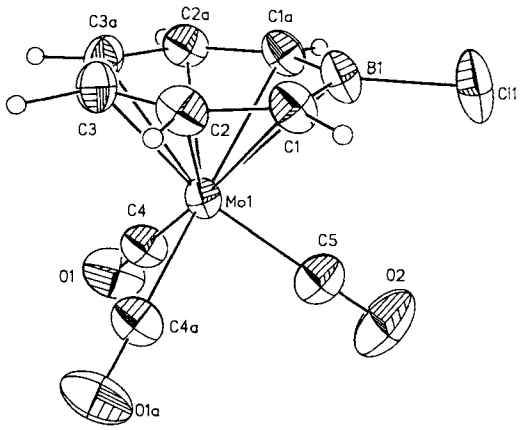

Fig. 2. Crystal structure of **3b** (ORTEP). Ring bond angles: [°]: Cl1-B1-C1 117.3(2), C1-B1-C1a 124.9(3), B1-C1-C2 128.5(2), C1-C2-C3 129.4(2), C2-C3-C3a 129.6(2).

C–Mo distances, and the boron atom is displaced out of the ring plane away from Mo by 0.05 Å. Thus, complexation causes this distortion of the planar free ligand. Similar distortions are found in the structures of **3c** and **4** and indeed in most other complexed boron heterocycles.[16, 17]

In addition, the formal double bonds (C1–C2, C3–C3a) lengthen on complexation, while the formal single bonds (B1–C1, C2–C3) remain unchanged. This suggests that the Mo atom removes electron density primarily from the electron-rich regions of the borepin ring which are *trans* to the CO ligands. The B–Cl unit is thereby eclipsed by one CO ligand. The conformational preferences of similar complexes have been discussed in detail by using an EH-MO model.[18] The effect of complexation is to reduce the C–C bond alternation from ± 0.058 Å in **1b** to ± 0.023 Å in **3b**. Therefore the delocalized π bonding is enhanced in **3b**.

Experimental Procedure

3b: A solution of **1b** (140 mg, 1.1 mmol) in pentane (2 mL) was added to a suspension of $[(C_5H_5N)_3Mo(CO)_3]$ (480 mg, 1.1 mmol) in ether (20 mL) at 25 °C. Then $BF_3 \cdot OEt_2$ (0.84 mL, 6.8 mmol) was added dropwise with stirring over 2 mins. After 3 h the solvent was removed under vacuum, and the residue was extracted with hexane. Crystallization at −20 °C afforded 220 mg (0.7 mmol) of crude crystals. Recrystallization from hexane gave orange cubes, M.p. 132–135 °C. High-resolution EI-MS: calcd. for $C_9H_6{}^{11}B^{35}Cl^{98}MoO_3$: 305.9153; found: 305.9146. IR (hexane): $\tilde{\nu}$ = 2024, 1974, 1947 cm^{-1} (vs, CO); ^1H NMR (360 MHz, C_6D_6): δ = 4.84 (br d, H_β), 4.45 (d, $J_{\alpha\beta}$ = 11.4 Hz, H_α), 4.26 (m, $J_{\beta\gamma}$ = 7.8 Hz, H_γ); ^{11}B NMR (115.5 MHz, C_6D_6): δ = 30.5 (br); ^{13}C NMR (90.6 MHz, C_6D_6): δ = 213.9 (CO), 109.4 (C_β), 95.9 (C_γ), 92.0 (br, C_α).

3a: To a solution of **3b** (40 mg, 0.1 mmol) in toluene (6 mL) at −60 °C was added with stirring 0.32 mL of a 1.0 M solution of $Li[BEt_3H]$ in THF. After the solution had been warmed to 25 °C, the solvent was removed under vacuum. A brown residue remained which was extracted with hexane. Removal of the solvent under vacuum left an orange oil which crystallized at 25 °C. Recrystallization from hexane gave bright orange crystals, M.p. 165 °C (decomp). High-resolution EI-MS: calcd. for $C_9H_7{}^{11}B^{98}MoO_3$: 271.9542; found: 271.9546. IR (hexane): $\tilde{\nu}$ = 2018, 1966, 1943 (vs, CO), 2512 cm^{-1} (w, BH); ^1H NMR (360 MHz, C_6D_6): δ = 5.16 (br d, H_β), 4.62 (dd, $J_{\alpha\beta}$ = 11.4, $^3J_{H\ BH}$ = 6 Hz, H_α), 4.42 (m, $J_{\beta\gamma}$ = 7.8 Hz, H_γ), BH (not observed); ^{11}B NMR (115.5 MHz, C_6D_6): δ = 23.1 (br d, J_{BH} = 94 Hz); ^{13}C NMR (90.6 MHz, C_6D_6): δ = 214.0 (CO), 112.8 (C_β), 97.4 (C_γ) C_α (not observed).

Received: January 27, 1993 [Z 5834 IE]
German version: *Angew. Chem.* **1993**, *105*, 1112

[1] E. E. van Tamelen, G. Brieger, K. G. Untch, *Tetrahedron Lett.* **1960**, *8*, 14.
[2] a) A. J. Leusink, W. Drenth, J. G. Noltes, G. J. M. van der Kerk, *Tetrahedron Lett.* **1967**, 1263; b) G. Axelrad, D. Halpern, *J. Chem. Soc. D.* **1971**, 291; c) A. J. Ashe, III, J. W. Kampf, C. M. Kausch, H. Konishi, M. O. Kristen, J. Kroker, *Organometallics* **1990**, *9*, 2944.
[3] A. T. Jeffries, III, S. Gronowitz, *Chem. Scr.* **1973**, *4*, 183.
[4] a) J. J. Eisch, J. E. Galle, *J. Am. Chem. Soc.* **1975**, *97*, 4436; b) See also: A. Geisberger, dissertation, Universität, Giessen, 1990.
[5] W. Schacht, D. Kaufmann, *Angew. Chem.* **1987**, *99*, 682; *Angew. Chem. Int. Ed. Engl.* **1987**, *26*, 665.
[6] a) A. J. Ashe, III, F. J. Drone, *J. Am. Chem. Soc.* **1987**, *109*, 1879; *ibid.* **1988**, *110*, 6599; b) A. J. Ashe, III, F. J. Drone, C. M. Kausch, J. Kroker, S. M. Al-Taweel, *Pure Appl. Chem.* **1990**, 513.
[7] Y. Sugihara, T. Yagi, I. Murata, A. Imamura, *J. Am. Chem. Soc.* **1992**, *114*, 1479.
[8] Y. Nakadaira, R. Sato, H. Sakurai, *Chem. Lett.* **1987**, 1451.
[9] A. J. Ashe, III, J. W. Kampf, Y. Nakadaira, J. M. Pace, *Angew. Chem.* **1992**, *104*, 1267; *Angew. Chem. Int. Ed. Engl.* **1992**, *31*, 1255.
[10] a) J. M. Schulman, R. L. Disch, M. L. Sabio, *J. Am. Chem. Soc.* **1982**, *104*, 3785; *ibid.* **1984**, *106*, 7696; b) *Tetrahedron Lett.* **1983**, *24*, 1863; c) J. M. Schulman, R. L. Disch, *Organometallics* **1989**, *8*, 733.
[11] **1b**: Monoclinic space group *C2/c* (no. 15) with a = 11.338(6), b = 8.597(5), c = 7.493(4) Å; β = 121.61(4)°; V = 622.1(6) Å^3; Z = 4 (ρ_{calcd} = 1.328 g cm^{-3}); μ ($Mo_{K\alpha}$) = 4.88 cm^{-1}; 1133 unique reflections; 1094 with $F_0 \geq 6.0\sigma(F)$ were used in refinement; R = 0.0365, R_w = 0.0662; GOF = 1.20. **3b**: Orthorhombic space group *Pnma* (no. 62) with a = 8.057(1), b = 10.623(2), c = 12.718(3) Å, Z = 4 (ρ_{calcd} = 1.855 g cm^{-3}); μ ($Mo_{K\alpha}$) = 14.02 cm^{-1}; 1329 unique reflections; 1314 with $F_0 \geq 2\sigma(F)$ were used in refinement; R = 0.0260, R_w = 0.0457; GOF = 2.56. Further details of the crystal structure investigations are available on request from the Director of the Cambridge Crystallographic Data Centre, 12 Union Road, GB-Cambridge CB21EZ (UK), on quoting the full journal citation.
[12] BMe_3 (1.58 Å): L. S. Bartell, B. L. Caroll, *J. Chem. Phys.* **1965**, *42*, 3076.
[13] M. Traetteberg, *J. Am. Chem. Soc.* **1964**, *86*, 4265; S. S. Butcher, *J. Chem. Phys.* **1965**, *42*, 1833; R. E. Davis, A. Tulinsky, *J. Am. Chem. Soc.* **1966**, *88*, 4583.
[14] D. W. J. Cruicksank, R. A. Sparks, *Proc. R. Soc. London, Ser. A* **1960**, *258*, 270.
[15] a) Gaussian 90, Revision I: M. J. Frisch, M. Head-Gordon; G. W. Tucks, J. B. Foresman, H. B. Schlegel, K. Raghavachari, M. Robb, J. S. Binkley, C. Gonzalez, D. J. Fox, R. A. Whiteside, R. Seager, C. F. Melius, J. Baker, R. L. Martin, L. R. Kahn, S. Topiol, J. A. Pople, Gausian Inc. Pittsburgh, PA, USA **1990**; b) 6-31G* basis set: P. C. Hariharar, J. A. Pople, *Theor. Chim. Acta* **1973**, *28*, 213; M. M. Francil, W. J. Pietro, W. J. Hehre, J. S. Brinkley, M. S. Gordon, D. J. DiFries, J. A. Pople, *J. Chem. Phys.* **1982**, *77*, 3654.
[16] For a discussion of complexes of other boron heterocycles see: G. E. Herberich, in *Comprehensive Organometallic Chemistry, Vol. 1* (Eds.: G. Wilkinson, F. G. A. Stone, E. W. Abel), Pergamon, Oxford, **1982**, p. 381.
[17] a) G. E. Herberich, W. Boveleth, B. Hessner, D. P. J. Köffer, M. Negele, R. Saive, *J. Organomet. Chem.* **1986**, *308*, 153; b) W. Siebert, M. Bochmann, J. Edwin, C. Krüger, Y.-H. Tsay, *Z. Naturforsch. B* **1978**, *33*, 1410; c) G. Huttner, W. Gartzke, *Chem. Ber.* **1974**, *107*, 3786; d) G. E. Herberich, B. Hessner, S. Beswetherick, J. A. K. Howard, P. Woodward, *J. Organomet. Chem.* **1980**, *192*, 421; e) G. E. Herberich, B. Hessner, M. Negele, J. A. K. Howard, *ibid.* **1987**, *336*, 29.
[18] a) T. A. Albright, P. Hofmann, R. Hoffmann, *J. Am. Chem. Soc.* **1977**, *99*, 7546; b) T. A. Albright, R. Hoffmann, *Chem. Ber.* **1978**, *111*, 1578; c) T. A. Albright, *Acc. Chem. Res.* **1982**, *15*, 149.

First Structure of a Mixed Organosodium/Lithium Alkoxide Compound: Model for a Superbase**

By *Sjoerd Harder* and *Andrew Streitwieser**

Mixtures of organolithium compounds and alkali metal alkoxides ROM (M = Na, K, Rb, Cs), such as BuLi/KO*t*Bu, are known as "superbases" and widely used in modern organic synthesis.[1] The development and application of these superbase systems have been subjects of chemical research for nearly three decades, yet the molecular structures of such systems are still a matter of controversy. The topic has been reviewed recently.[2] It is generally believed that the high reactivity of RLi/R′OM (M = Na, K, Rb, Cs) mixtures is

[*] Prof. Dr. A. Streitwieser, Dr. S. Harder
Department of Chemistry, University of California
Berkeley, CA 94720 (USA)
Telefax: Int. code +(510)642-8369

[**] S. H. thanks the NWO for a fellowship. This research was supported in part by the National Science Foundation (grant no. CHE87-21134).

caused by metal exchange, forming RM/R'OLi. The interaction of the smaller Li cation with the smaller O anion is favored electrostatically.[3] Organoalkali metal species, however, are commonly aggregated in the solid state and in solution.[4] The superbase mixture may well exist as mixed aggregates of RM and R'OLi monomers (**1**) or may be present as separate aggregates of RM and R'OLi (**2**).

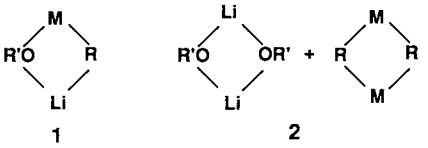

1 **2**

Ab initio calculations on Li/Na dimer systems[5] have shown the importance of Li–O bond formation in the metal-exchange reaction [Eq. (a)]. The number of O–Li bonds is

$$(MeLi)_2 + (NaOH)_2 \longrightarrow (MeNa)_2 + (LiOH)_2 \quad \Delta E = -8.2\ kcal\,mol^{-1} \quad (a)$$

maximized in this reaction. There is, however, only a small energy difference between the separate MeNa and LiOH dimers and a mixed aggregate [Eq. (b)].

$$(MeNa)_2 + (LiOH)_2 \longrightarrow 2(MeNa/LiOH) \quad \Delta E = +1.3\ kcal\,mol^{-1} \quad (b)$$

This result suggests equilibria between **1** and **2** or at least the possible existence of short-lived mixed aggregates.

Because of the extreme reactivity of the superbase metalating reagents, the only report on the molecular structure of these compounds has been an NMR study of the model system cesium triphenylmethane/lithium 3-ethyl-3-heptoxide.[3] The authors could not detect mixed aggregates in this study.

All efforts so far to make crystals of superbase mixtures for X-ray diffraction studies have failed. The mixing of several organolithium compounds with several sodium or potassium alkoxides has resulted in microcrystalline precipitates of the pure organosodium or -potassium compounds.[6] This observation does not rule out the existence of mixed aggregates in solution since the precipitate only represents the least soluble species.

An alternative approach to the study of the structural properties of RM/R'OLi mixtures (M = Na, K, Rb, Cs) is the synthesis, crystallization, and X-ray diffraction analysis of compounds that contain both functionalities (C–M and O–Li) in one molecule. This approach in one sense circumvents the problem but could provide information on bonding and coordination patterns in mixed aggregates. For example, such compounds may form structures in which Li and M are doubly bridging between the anionic centers (**3**), a structure type common for dilithiated species,[4a] or they may form polymeric structures in which distinct C–M and O–Li interactions can be recognized (**4**).

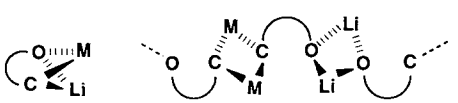

3 **4**

A compound with both functionalities (C–M and O–Li) was obtained by treating sodium 2,4,6-trimethylphenoxide (**5**) with butyllithium in hexane to yield lithium 4,6-dimethyl-2-sodiomethylphenoxide (**6**).[7] Single-crystal X-ray structure analysis[8] of **6** · tmeda (tmeda = tetramethylethylenediamine) reveals a tetrameric aggregate with approximate, noncrystallographic S_4 symmetry (Fig. 1).

5 **6**

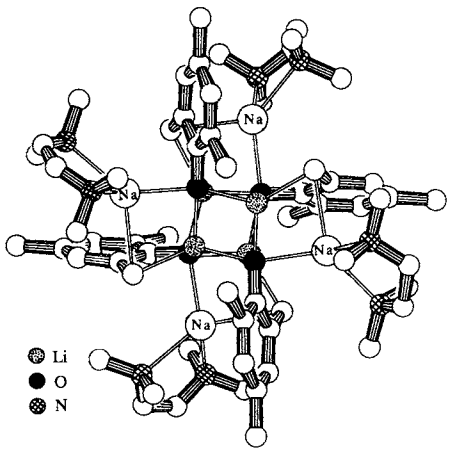

Fig. 1. Crystal structure of **6** · tmeda (hydrogen atoms omitted). The tetrameric aggregate has approximate S_4 symmetry. Average bond lengths [Å] and angles [°]: C-Li 2.17(2), O-Li 1.97(2), C-Na 2.671(9), O-Na 2.410(6), N-Na 2.496(9); Li-O-Li 82.0(7), O-Li-O 97.4(8), N-Na-N 72.6(3).

The core of the structure is a distorted cube made up of O and Li atoms, whose edges are formed by eight O–Li bonds 1.97(2)–2.06(2) Å in length and four significantly shorter O–Li bonds 1.88(2)–1.91(2) Å in length. The four shorter bonds are nearly colinear with the four C_{aryl}–O bonds (C-O-Li angles vary from 165.1(7)° to 171.3(7)°). The Li–O distances are similar to those in a tetrameric Li alkoxide (*O*-lithio-*N*-methylpseudoephedrin, 1.87–1.99 Å)[9] and a tetrameric lithium ester enolate (1.90–2.04 Å).[10]

Each of the Li bridges between the anionic carbon and oxygen centers is part of a puckered five-membered Li-C-C-C-O ring. This type of benzyl–Li interaction is novel for benzyl alkali metal compounds in which the metal atom is usually bonded to an α-benzyl carbon atom and approximately perpendicular to the benzyl plane. The C–Li distances range from 2.14(2) to 2.21(2) Å and are somewhat shorter than those in benzyllithium which range from 2.189(8) to 2.229(8) Å).[11]

The Na atoms are coordinated perpendicular to the plane of the benzyl group with an average distance of 2.671(9) Å to the carbanion center; this is comparable to the average CH_2–Na distance of 2.68 Å in tetrameric benzylsodium · tmeda.[12] Short distances to atoms in the ring system are shown in Figure 2. The Na–O contact (3.75 Å) is quite long, but there is a shorter contact of 2.410(6) Å between the Na atom and another O atom in the LiO cube. This is somewhat longer than the Na–O distances in dimeric sodium 2,4,6-tris(trifluoromethyl)phenoxide, which range from 2.231 to 2.313 Å.[13] The coordination sphere around Na in **6** is completed by chelation to tmeda; the Na–N distances are in the normal range of 2.445(8)–2.528(9) Å. The coordina-

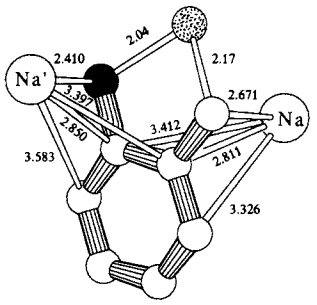

Fig. 2. Metal coordination around each aryl ring in **6** with average distances [Å].

tion sphere of the oxygen atom in this aggregate deviates from the commonly observed trigonal (in ROLi dimers) and tetrahedral (ROLi tetramers/hexamers), and can be described best as tetragonal-pyramidal.

The structure of **6** · tmeda is the first of a "mixed" organosodium/lithium alkoxide aggregate. The structure is dictated by O–Li bonding. The observed cube structure results from the formation of the maximum number of O–Li bonds; Na–O coordination is of minor importance in the coordination sphere of the five-coordinate oxygen atom. The structure of **6** indicates that lithium alkoxides also have a dominating role in superbases in solution and suggests that analogous interactions occur between RM (M = Na, K, Rb, Cs) and R'OLi aggregates. That is, lithium alkoxide dimers or tetramers can be distorted to extend the coordination sphere around the O atom for interaction with the alkali metal (**7**). The resulting reduced coordination of the carban-

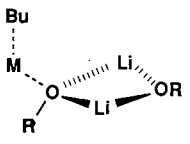

7

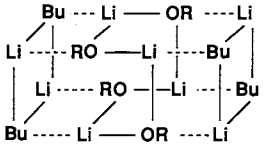

8

ion then effectively increases its basicity; such structural effects thereby contribute to the superbasicity of such mixtures. For comparison, the solid-state structure of (*n*BuLi · LiO*t*Bu)$_4$ may be viewed as a distorted cube made up of a LiO*t*Bu tetramer which is opened on two sides to interact with two BuLi dimers (**8**).[14]

Received: January 26, 1993 [Z 5828 IE]
German version: *Angew. Chem.* **1993**, *105*, 1108

[1] a) L. Lochmann, J. Pospísil, D. Lím, *Tetrahedron Lett.* **1966**, 257; b) M. Schlosser, *J. Organomet. Chem.* **1967**, *8*, 9; c) L. Brandsma, H. D. Verkruijsse, *Preparative Polar Organometallic Chemistry, Vol. 1*, Springer, Berlin, **1987**; d) L. Brandsma, *Preparative Polar Organometallic Chemistry, Vol. 2*, Springer, Berlin, **1990**.

[2] W. Bauer, L. Lochmann, *J. Am. Chem. Soc.* **1992**, *114*, 7482.

[3] This preference for Li–O bonding is shown clearly by replacing anionic and cationic centers in these highly ionic compounds by simple unit negative and positive point charges, and calculating the potential energies. If R is the covalent radius of a nucleus, and $R_M > R_{Li}$ and $R_C > R_O$, then $1/(R_C + R_M) + 1/(R_{Li} + R_O)$ is always larger than $1/(R_C + R_{Li}) + 1/(R_M + R_O)$, no matter what the exact values of R are.

[4] a) W. Setzer, P. von R. Schleyer, *Adv. Organomet. Chem.* **1985**, *24*, 353; b) C. Schade, P. von R. Schleyer, *ibid.* **1988**, *27*, 169; c) W. Bauer, D. Seebach, *Helv. Chim. Acta* **1984**, *67*, 1972.

[5] MP4SDTQ/6-31 + G*//6-31 + G*(+ ZPE) Calculations: S. Harder, T. Kremer, P. von R. Schleyer, *J. Organomet. Chem.*, submitted.

[6] a) L. Lochmann, D. Lim, *J. Organomet. Chem.* **1971**, *28*, 153; b) R. Pi, W. Bauer, P. von R. Schleyer, *ibid.* **1986**, *306*, C1; c) S. Harder, unpublished results.

[7] Compound **6** was synthesized by treating a white suspension of **5** (1.0 g, 6.3 mmol) in 10 mL of hexane with BuLi/hexane (2.0 M, 6.6 mmol) under nitrogen at reflux. The resulting yellow powder (quantitative yield) underwent complete monodeuteration at the benzylic carbon when treated with D_2O.

[8] Crystal structure data of **6** · tmeda, orthorhombic, $a = 19.220(3)$, $b = 18.032(4)$, $c = 39.806(8)$ Å, $V = 13796(5)$ Å^3, space group *Pbca*, formula $\{(C_9H_{10}OLiNa) \cdot (C_6H_{16}N_2)\}_4$, $M = 1121.26$, $Z = 8$, $\rho_{calcd} = 1.080$ g cm^{-3}, $\mu(Mo_{K\alpha}) = 0.8$ cm^{-1}; 9837 unique reflections were measured on a Enraf-Nonius CAD4 diffractometer ($Mo_{K\alpha}$ radiation, graphite monochromator, $T = -95$ °C) and 3704 reflections with $F^2 > 2.5\sigma(F^2)$ were considered observed. Solution by direct methods with SHELXS-86 [15], refinement by minimalization of $\sum w(F_o - F_c)^2$ to $R = 0.077$ and $wR = 0.069$ with $w = 1/\sigma^2(F_o)$, non-hydrogen atoms anisotropic; H atoms were assigned idealized locations and isotropic thermal parameters approximately 1.3 times that of the atoms to which they are attached. Two of the four tmeda molecules show disordering which is common for tmeda and well described in literature [16]. Disorder in the structure of **6** · tmeda was described best with large anisotropic parameters on the disordered atoms. Unfortunately, benzylic hydrogen atoms could not be detected in the difference Fourier map, and the hybridization at the benzylic carbon atom remains unknown. Plots were made with the EUCLID package [17]. Further details of the crystal structure investigation are available from the Director of the Cambridge Crystallographic Data Centre, 12 Union Road, GB-Cambridge CB2 1EZ (UK), on quoting the full journal citation.

[9] E. M. Arnett, M. A. Nichols, A. T. McPhail, *J. Am. Chem. Soc.* **1990**, *112*, 7059.

[10] D. Seebach, R. Amstutz, T. Laube, W. B. Schweizer, J. D. Dunitz, *J. Am. Chem. Soc.* **1985**, *107*, 5403.

[11] a) S. P. Patterman, I. L. Karle, G. D. Stucky, *J. Am. Chem. Soc.* **1970**, *92*, 1150; b) M. A. Beno, H. Hope, M. M. Olmstead, P. P. Power, *Organometallics* **1985**, *4*, 2117; c) W. Zarges, M. Marsch, K. Harms, G. Boche, *Chem. Ber.* **1989**, *122*, 2303.

[12] C. Schade, P. von R. Schleyer, H. Dietrich, W. Mahdi, *J. Am. Chem. Soc.* **1986**, *108*, 2484.

[13] S. Brooker, F. T. Edelmann, T. Kottke, H. W. Roesky, G. M. Sheldrick, D. Stalke, K. H. Whitmire, *J. Chem. Soc. Chem. Commun.* **1991**, 144.

[14] M. Marsch, K. Harms, L. Lochmann, G. Boche, *Angew. Chem.* **1990**, *102*, 334; *Angew. Chem. Int. Ed. Engl.* **1990**, *29*, 308.

[15] G. M. Sheldrick, *SHELXS-86, Program for Crystal Structure Solution*, Göttingen, **1986**.

[16] a) R. Amstutz, T. Laube, W. B. Schweizer, D. Seebach, J. D. Dunitz, *Helv. Chim. Acta* **1984**, *67*, 224; b) S. Harder, Dissertation, University of Utrecht, **1990**, p. 60.

[17] A. L. Spek, The EUCLID package in *Computational Crystallography* (Ed.: D. Sayre), Clarendon Press, Oxford, **1982**, p. 528.

Rapid Carboalumination of Alkynes in the Presence of Water**

By *Peter Wipf** and *Sungtaek Lim*

The carboalumination of alkynes is one of the most versatile routes for the preparation of olefins with defined configurations.[1] Recent applications of this methodology in natural products synthesis include the preparation of segments for lophotoxin,[2] macbecin,[3] and FK-506.[4] Whereas the uncatalyzed carboalumination of nonfunctionalized alkynes is slow even at elevated temperatures, the zirconium-catalyzed variant[5] occurs under mild conditions. Methylalumination of 1-octyne (**1**) in the presence of 1 equiv of [Cp_2ZrCl_2], for example, yields 2-methyl-1-octene (**2**) and 2-nonene (**3**) in a 95:5 ratio after 3 h at 22 °C.[6]

[*] Prof. Dr. P. Wipf, S. Lim
Department of Chemistry, University of Pittsburgh
Pittsburgh, PA 15260 (USA)
Telefax: Int. code + (412) 624-8552

[**] This work was supported by the University of Pittsburgh. We thank Prof. H. Yamamoto for stimulating discussions.

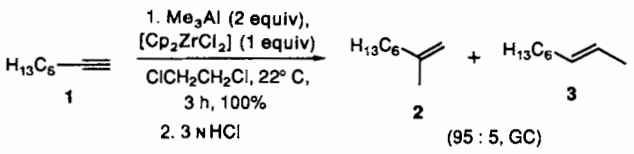

In the course of our studies of transmetalation of alkenylalanes,[7] we discovered that the addition of 1–2 equiv of *water* to the carboalumination reaction mixture led to a considerable increase in the rate of this process. *In fact, even at −70 °C methylalumination of 1-hexyne* (**4**) *was essentially complete in 10 min in the presence of 1.5 equiv of* H_2O*!*

Table 1 summarizes the scope of this novel water effect in carboaluminations.[8] A solution of Me_3Al in hexane or toluene was treated with $[Cp_2ZrCl_2]$ and H_2O, and then alkyne **4**. The vinylalane intermediate formed in 10 min at −23 °C and was trapped with iodine to afford 1-iodo-2-methyl-1-hexene (**7**) and 3-iodo-2-heptene (**8**) (ratio 98:2) in 89% yield after chromatographic purification (entry 1). Trapping with propene oxide (**12**) provided the homoallylic alcohol **13** in 80% yield (entry 3).[9] These results compare very favorably with those from the standard protocols for methylalumination, exemplified in entries 2 and 4, which require reaction times of 4–12 h at room temperature for completion.

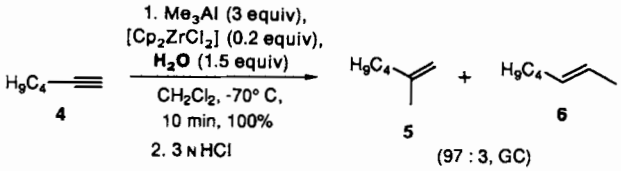

Table 1. Comparison of water-accelerated (methods A and B) and standard (method C) carboalumininations of alkynes.

Entry	Alkyne	Alane	Method	Trapping Agent	Product	Yield [a] [%]	Ref.
1	**4**	Me_3Al	A	I_2	H_9C_4 (I) + H_9C_4 (I) (98: 2, NMR) **7** **8**	89	–
2	Ph (**9**)	Me_3Al	C	I_2	Ph (I) + Ph (I) (98: 2, NMR) **10** **11**	73	[6]
3	**4**	Me_3Al	A	O (**12**)	H_9C_4 (OH) **13**	80 [b]	–
4	**1**	Me_3Al	C	I_2/**12**	$H_{13}C_6$ (OH) **14**	87	[11]
5	**4**	Me_3Al	A	$ClCO_2Et$	H_9C_4 (CO_2Et) **15**	67	–
6	TBDPSO (**16**)	Me_3Al	A	H_2O	TBDPSO **17**	95	–
7	TBDMSO (**18**)	Me_3Al	A [c]	$ClCO_2Et$	TBDMSO (CO_2Et) **19**	52	–
8	TIPSO (**20**)	Me_3Al	A [d]	H_2O	TiPSO **21**	61	–
9	HO (**22**)	Me_3Al	A [e]	I_2	HO (I) **23**	85 [b]	–
10	**22**	Me_3Al	C	I_2	**23**	62 [b]	[5a]
11	**4**	Et_3Al	B	I_2	H_9C_4 (I) + H_9C_4 (I) (73: 27, NMR) **24** **25**	74	–
12	$H_{11}C_5$ (**26**)	Et_3Al	C	H_2O	$H_{11}C_5$ + $H_{11}C_5$ (61: 39, GC) **27** **28**	31	[12]
13	**26**	Et_3Al	$[(TPP)ZrCl_2]$	H_2O	**27** + **28** (88: 12, GC)	52	[12]
14	**4**	Et_3Al	B	**12**	H_9C_4 (OH) **29**	53	–

[a] Yields refer to chromatographically purified products and are based on the alkyne. [b] 8% Regioisomer was present according to the ^1H NMR spectrum. [c] Carboalumination in the presence of 1 equiv of $[Cp_2ZrCl_2]$ for 2 h at $-23 \rightarrow 20$ °C. [d] Carboalumination in the presence of 1 equiv of $[Cp_2ZrCl_2]$ for 18 h at −23 °C. [e] The alcohol was pretreated with 0.33 equiv of Me_3Al; carboalumination for 1 h at $-23 \rightarrow 20$ °C.

The presence of remote functional groups such as silyl ethers[10] or hydroxyl groups does not interfere with the H_2O effect. Thus, methylalumination of **16** was complete after less than 10 min at −23 °C (entry 6). For propargylic and homopropargylic alcohols, however, higher temperatures or longer reaction times were necessary. Methylalumination of **18** followed by trapping with ethyl chloroformate provided ester **19** in 52% yield after 2 h at −23 → 20 °C, and **20** was converted to the silylated methallyl alcohol **21** in 61% yield after 18 h at −23 °C (entries 7 and 8). Treatment of alcohol **22** with 0.33 equiv of Me_3Al, followed by water-accelerated carboalumination at −23 → 20 °C for 1 h and trapping with I_2 led to vinyl iodide **23** in 85% yield (entry 9). In the absence of water, conversion of **22** to the iodide **23** required 12 h reaction time at room temperature for the carboalumination step,[5a] and provided a significantly lower yield of the trapping product (entry 10).

The standard methylalumination with Me_3Al in the presence of $[Cp_2ZrCl_2]$ generally provides quite satisfactory regioselectivities.[5] However, very slow reactions and much inferior regioselectivities are observed in carboaluminations with higher alkylaluminums such as Et_3Al. We therefore investigated the effect of H_2O in the ethylalumination of alkyne **4**. As expected, the turnover number was greatly increased: after 30 min at −23 °C, trapping of the alkenylalane with I_2 provided vinyl iodides **24** and **25** (ratio 73:27) in 74% yield (entry 11). In contrast, hydrolysis of the alkenylalane of **26**, prepared in the absence of H_2O after 24 h reaction time at 20 °C, provided regioisomers **27** and **28** (61:39 ratio) in only 31% yield (entry 12). A more efficient protocol was recently reported by Inoue et al. With Zr^{IV} complexes of tetraphenylporphyrin (TPP) $[(TPP)ZrCl_2]$ in place of $[Cp_2ZrCl_2]$, the turnover of **26** with Et_3Al was slightly improved and led to the ethylalumination products **27** and **28** (ratio 88:12) in 52% yield after 24 h reaction time in benzene (entry 13). Compared to this modified procedure, our water-accelerated ethylalumination provides a lower regioselectivity but still a greatly increased reaction rate and a higher yield. Trapping of the intermediate alane from the low-temperature ethylalumination of 1-hexyne with propene oxide, for example, led to pure homoallylic alcohol **29** in 53% yield after chromatographic separation from the minor regioisomer present in 20% yield (entry 14).

The rate-enhancing effect in Zr-catalyzed carboaluminations seems to be unique to H_2O. We have also used H_2S, alcohols, silanols, diphenylborinic acid (Ph_2BOH), and bis(diisobutylaluminum)oxide, but all of these additives failed to reproduce the effects of water. Zirconocene dichloride is necessary as a cocatalyst, and the rate-enhancing effect is not due to the formation of methylalumoxane ($(AlMeO)_x$, MAO), which is a well-known and highly active cocatalyst for the polymerization of α-olefins.[13, 14] Independently prepared methylalumoxane failed to show any accelerating effects in carboaluminations at low temperatures. Indeed, when the yellowish reaction mixture obtained after addition of $[Cp_2ZrCl_2]$ and H_2O to trialkylalane was warmed from −23 °C to room temperature, which presumably causes the formation of alkylalumoxanes **32**, the resulting medium had greatly reduced catalytic activity for carboalumination. Therefore, we propose that a thermodynamically labile, but catalytically highly active oxo-bridged dimer **31** forms in mixtures of trialkylalane, zirconocene dichloride, and water at temperatures below 0 °C (Scheme 1).

In conclusion, we have demonstrated a novel rate-acceleration by H_2O in the low-temperature carboalumination of alkynes. Alkenylalanes are thus generated within minutes at −23 °C and serve as starting materials for the stereoselective

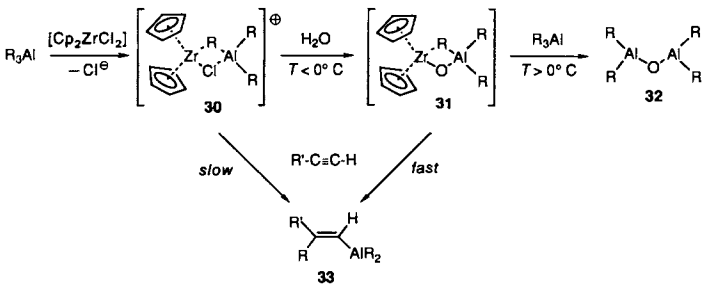

Scheme 1. Proposed mechanism for the formation of a highly active species in the water-accelerated zirconium-catalyzed carboalumination of alkynes.

preparation of functionalized trisubstituted alkenes. This is another example for the unique and yet still basically unexplored effects of water in reactions with organometallic compounds.[15]

Experimental Procedure

Method A: **7**: To a solution of 5 mL (10 mmol) of a 2 M solution of trimethylalane in hexane and 208 mg (0.71 mmol) of $[Cp_2ZrCl_2]$ in 12 mL of CH_2Cl_2 was slowly added 90 μL (5 mmol) of water at −23 °C under vigorous stirring. **Caution: Exothermic reaction!** After 10 min, a solution of 265.8 mg (3.23 mmol) of 1-hexyne in 5 mL of CH_2Cl_2 was added. The reaction mixture was stirred for another 10 min at −23 °C before a solution of 983 mg (3.88 mmol) of iodine in 5 mL of THF was added dropwise. After 10 min, the mixture was allowed to warm to room temperature, and 1 mL of a saturated K_2CO_3 solution was added slowly with vigorous stirring. After 15 min, 2 g of anhydrous $MgSO_4$ was added and the mixture was filtered and extracted with Et_2O. The combined organic layers were concentrated under reduced pressure, and the residue was chromatographed on silica gel (pet. ether) to afford 641.9 mg (89%) of **7** as a colorless oil: ^1H NMR (300 MHz, $CDCl_3$, 22 °C): $\delta = 5.85$ (s, 1H; CH), 2.20 (t, $^3J(H,H) = 7.2$ Hz, 2H; CH_2), 1.82 (s, 3H, CH_3), 1.44–1.37 (m, 2H; CH_2), 1.33–1.22 (m, 2H; CH_2), 0.89 (t, $^3J(H,H) = 7.3$ Hz, 3H; CH_3); ^{13}C NMR (75 MHz, $CDCl_3$, 22 °C): $\delta = 148.4$, 74.4, 39.4, 29.9, 23.8, 22.2, 13.9; IR (neat): $\tilde{\nu} = 2957$, 2930, 2870, 2859, 1617, 1456, 1377, 1267, 1142, 764, 668 cm^{-1}; MS (70 eV): *m/z* 224 (20%) [M^+], 182 (18), 168 (4), 97 (15), 84 (10), 55 (100).

Method B: **24**: To a solution of 3 mL (5.7 mmol) of a 1.9 M solution of triethylalane in toluene and 122 mg (0.42 mmol) of $[Cp_2ZrCl_2]$ in 12 mL of CH_2Cl_2 was slowly added 56 μL (3.1 mmol) of water at −23 °C under vigorous stirring. **Caution: Exothermic reaction!** After 30 min, a solution of 155 mg (1.89 mmol) of 1-hexyne in 3 mL of CH_2Cl_2 was added. After stirring for another 30 min at −23 °C, a solution of 575 mg (2.26 mmol) of iodine in 4 mL of THF was added dropwise. After 10 min the mixture was allowed to warm to room temperature, and 1 mL of a saturated K_2CO_3 solution was added slowly with vigorous stirring. Workup as described for method A afforded 332.3 mg (74%) of a 73:27 mixture of **24** and **25** as a colorless oil. **24**: ^1H NMR: $\delta = 5.80$ (s, 1H; CH), 2.17 (m, 4H; $2CH_2$), 1.44–1.25 (m, 4H; $2CH_2$), 1.00 (t, $^3J(H,H) = 7.6$ Hz, 3H, CH_3), 0.90 (t, $^3J(H,H) = 7.1$ Hz, 3H; CH_3); ^{13}C NMR: $\delta = 153.1$, 73.6, 36.5, 30.5, 30.0, 22.3, 13.9, 11.8; IR (neat): $\nu = 2961$, 2930, 2872, 1462, 1377, 1244, 1142, 762, 668 cm^{-1}; MS (70 eV): *m/z*: 238 (25%) [M^+], 196 (15), 167 (10), 84 (8), 69 (100), 55 (40).

Received: January 20, 1993 [Z 5818 IE]
German version: *Angew. Chem.* **1993**, *105*, 1095

[1] For reviews, see: a) J. F. Normant, A. Alexakis, *Synthesis* **1981**, 841; b) G. Zweifel, J. A. Miller, *Org. React.* **1984**, *32*, 375; c) E. Negishi, *Acc. Chem. Res.* **1987**, *20*, 65; d) E. Negishi, T. Takahashi, *Synthesis* **1988**, 1; e) P. Knochel in *Comprehensive Organic Synthesis, Vol. 4* (Eds.: B. M. Trost, I. Fleming, M. F. Semmelhack), Pergamon, Oxford, **1991**, p. 865.
[2] I. Paterson, M. Gardner, *Tetrahedron* **1989**, *45*, 5283.
[3] R. Baker, J. L. Castro, *J. Chem. Soc. Chem. Commun.* **1989**, 378.
[4] R. E. Ireland, T. K. Highsmith, L. D. Gegnas, J. L. Gleason, *J. Org. Chem.* **1992**, *57*, 5071.
[5] a) C. L. Rand, D. E. Van Horn, M. W. Moore, E. Negishi, *J. Org. Chem.* **1981**, *46*, 4093; b) E. Negishi, *Pure Appl. Chem.* **1981**, *53*, 2333; c) E. Negishi, D. E. Van Horn, T. Yoshida, *J. Am. Chem. Soc.* **1985**, *107*, 6639.
[6] D. E. Van Horn, E. Negishi, *J. Am. Chem. Soc.* **1978**, *100*, 2252.
[7] a) P. Wipf, J. H. Smitrovich, C.-W. Moon, *J. Org. Chem.* **1992**, *57*, 3178; b) P. Wipf, *Synthesis*, **1993**, in press.
[8] Carboaluminations were generally performed at −23 °C in a dry ice/CCl_4 bath. Problems with the rapid freezing of the added H_2O at temperatures below −30 °C were thus avoided. All products were characterized by ^1H NMR, ^{13}C NMR, IR and mass specta.

[9] As the yields of the trapping reactions show, the intermediate vinylalane is not hydrolyzed by any residual water present in the reaction mixture. In a control experiment, 1.5 equiv of D_2O were used in place of H_2O in the accelerated methylalumination of alkyne **18**. After addition of the alkyne at $-23\,^{\circ}C$, the reaction mixture was stirred for 3 h at $0\,^{\circ}C$ before the trapping reagent (I_2) was added. Only 3.4% of the deuterated species **i** besides 66% of the iodide **ii** was detected by ^1H NMR.

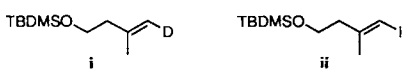

i ii

[10] TBDPS = *tert*-butyldiphenylsilyl, TBDMS = *tert*-butyldimethylsilyl, TIPS = triisopropylsilyl.

[11] M. Kobayashi, L. F. Valente, E. Negishi, *Synthesis* **1980**, 1034. In this procedure, the homoallylic alcohol **14** was prepared by metalation (*n*BuLi) of the intermediate vinyl iodide, followed by treatment with an excess of propene oxide.

[12] K. Shibata, T. Aida, S. Inoue, *Tetrahedron Lett.* **1992**, *33*, 1077.

[13] a) H. Sinn, W. Kaminsky, *Adv. Organomet. Chem.* **1980**, *18*, 99; b) S. Pasynkiewicz, *Polyhedron* **1990**, *9*, 429; c) G. Erker, *Pure Appl. Chem.* **1992**, *64*, 393.

[14] a) D. W. Harney, A. Meisters, T. Mole, *Aust. J. Chem.* **1974**, *27*, 1639; b) A. Storr, K. Jones, A. W. Laubengayer, *J. Am. Chem. Soc.* **1968**, *90*, 3173.

[15] For related effects of water on organometallic reagents, see: a) D. E. Ward, Y. Gai, *Tetrahedron Lett.* **1992**, *33*, 1851; b) M. Miyashita, M. Hoshino, A. Yoshikoshi, *J. Org. Chem.* **1991**, *56*, 6483; c) E. J. Corey, F. J. Hannon, N. W. Boaz, *Tetrahedron* **1989**, *45*, 545.

Stereochemistry of the C–S Bond Cleavage in 1-Phenylethyl Phenyl Sulfide Radical Cation: Evidence for a Unimolecular Pathway**

By *Enrico Baciocchi,* Elisabetta Fasella, Osvaldo Lanzalunga*, and *Mario Mattioli*

Aromatic radical cations are key intermediates in a large number of chemical and biochemical processes.[1] The reactions of these radical cations have therefore attracted continuous attention, particularly the ones involving the cleavage of a σ bond [Eq. (a)].[2] These reactions have a wide scope

$$[Ar-a-b]^{\bullet+} + Nu^- \longrightarrow [Ar-a]^{\bullet} + bNu \qquad (a)$$

and moreover, they exhibit features of theoretical interest, since they represent a new class of nucleophilic displacements in which a free radical is the leaving group. Thus, for these reactions, either a bimolecular, concerted mechanism (S_N2) or a stepwise unimolecular mechanism (S_N1) can be envisaged; interestingly, in the former case, both inversion and retention of configuration are in principle possible, since the radical cation is an open-shell system and either its SOMO or its LUMO may interact with the HOMO of the nucleophile.

Surprisingly, very little information on the mechanisms of these processes is presently available. Unimolecular C–C bond cleavage has been observed for bicumyl[3a] and benzyl acetal radical cations,[3b] whereas clear evidence for a bimolecular mechanism has been provided for ring opening C–C bond cleavage in phenylcyclopropane radical cations[4] as well as for the breaking of the C–Si bond in benzyltrimethylsilane radical cations.[5]

For phenylcyclopropane radical cations, the reaction occurs with complete inversion of configuration, therefore indicating that the LUMO–HOMO interaction is decisive. This has been justified on the basis of theoretical considerations.[6]

Since the nature of the bond to be broken plays a crucial role in the mechanism, we decided to study the C–S bond cleavage in benzyl phenyl sulfide radical cations. We chose the reaction of 1-phenylethyl phenyl sulfide (**1**) promoted by $K_5[Co^{III}W_{12}O_{40}]$, (abbreviated as $[Co^{III}W]$) a "bona fide" outer sphere one-electron oxidant,[7] in $AcOH/H_2O$ (70/30) at $50\,^{\circ}C$. This reaction leads, with an excellent mass balance, to 1-phenylethyl acetate (**2**, X = OAc), 1-phenylethanol (**2**, X = OH), and acetophenone **3**, in a 1.2:2.1:1 molar ratio.

Among the products, diphenyl disulfide and small amounts of styrene are also observed. The oxidation of **1** occurs via the radical cation $\mathbf{1}^{\bullet+}$, which, as shown in Scheme 1, undergoes C–S and C–H bond cleavage, leading to **2** (path b) and **3** (path a), respectively. As expected,[9] when the reaction was carried out in the presence of AcOK (0.25 M), deprotonation becomes more important and acetophenone **3** is the major product: the molar ratio **2**, X = OAc to **2**, X = OH to **3** is 0.65:0.65:1.

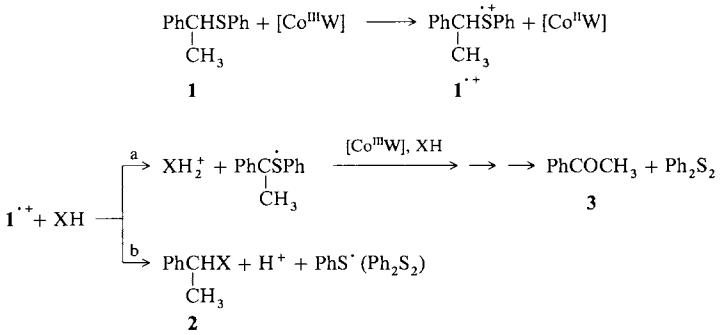

Scheme 1. Possible reaction mechanism for the oxidation of **1** with $[Co^{III}W]$. X = OH, OAc.

When the same reaction was carried out starting from enantiomerically pure (*R*)-(+)-**1**, we observed that the formation of the products **2** took place with racemization, accompanied to some extent (16%) by inversion: The (*S*):(*R*) ratio is 1.4:1 for both products. In the presence of AcOK, the (*S*):(*R*) ratios increase slightly to 1.55:1 (0.25 M AcOK) and 1.8:1 (0.5 M). Again, the (*S*):(*R*) ratio is the same, within the experimental error, for **2**, X = OH and **2**, X = OAc.

These results clearly indicate that the cleavage of the C–S bond in $\mathbf{1}^{\bullet+}$ takes place by two pathways, one leading to racemized **2**, the other to inverted **2**. For the former, there is little doubt that we are dealing with an S_N1 mechanism. This involves the formation of the 1-methylbenzyl carbocation which reacts with the mixed solvent to produce racemic **2** (Scheme 2, path a), or is deprotonated to styrene.

For the pathway with inversion, the situation is less straightforward and two possibilities can be considered. The first is an S_N2 mechanism, occurring with inversion of configuration, as already observed for the C–C bond cleavage in phenylcyclopropane radical cations.[4] The role of this mechanism could become more important in the presence of AcOK, since AcO^- is certainly a much stronger nucleophile than both H_2O and AcOH.

[*] Prof. Dr. E. Baciocchi, Dr. E. Fasella, Dr. O. Lanzalunga, Dr. M. Mattioli
Dipartimento di Chimica, Università "La Sapienza"
P.le A. Moro 5, I-00185 Roma (Italy)
and
Centro CNR di Studio sui Meccanismi di Reazione, Rome
Telefax: Int. code + (396) 490421

[**] This work was supported by the Italian Ministero della Pubblica Istruzione and the European Community, contract n° SC1-CT91-0750 (TSTS).

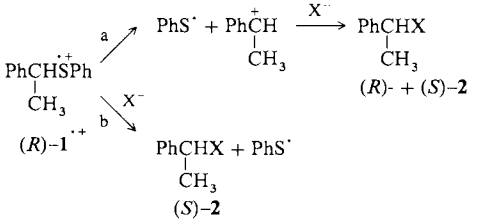

Scheme 2. Competition between unimolecular (path a) and bimolecular mechanisms (path b) for the C–S bond cleavage in $\mathbf{1}^{\bullet+}$.

The second possibility is that the S_N1 mechanism is more complex than indicated in Scheme 2, the unassisted cleavage of the C–S bond first leading to a contact radical–cation pair[10] and then to a solvent-separated radical–cation pair (Scheme 3). Nucleophilic attack on the contact radical–cation pair should lead to the inverted products.

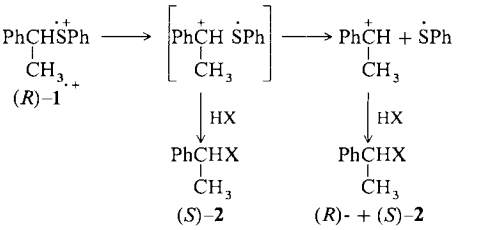

Scheme 3. Possible mechanism for the unimolecular C–S bond cleavage in $\mathbf{1}^{\bullet+}$.

We suggest that the latter hypothesis is the more likely. First, because the effect of AcOK on the (*S*):(*R*) ratio seems too small to be compatible with an S_N1–S_N2 competition. Since some inversion is already present in $AcOH/H_2O$, we would expect a larger effect of AcOK on the (*S*):(*R*) ratio than the one observed. Indeed, this effect is very modest, the percent of inversion changing from 16%, in the absence of AcOK, to 28%, in the presence of AcOK (0.5 M). Such a small increment seems to be more consistent with the mechanism in Scheme 3, where it can be justified by suggesting that, in the presence of AcOK, a larger fraction of the contact radical–cation pairs reacts with the nucleophile before dissociation. Second, a significant contribution of an S_N2 mechanism for the formation of **2** is not in line with the results of preliminary kinetic experiments which indicate that the overall oxidation rate is increased by only 35% in the presence of 0.2 M AcOK. Such an increase is almost exclusively due to the enhanced rate of the deprotonation reaction leading to acetophenone **3**, a process which is certainly base catalyzed.[9] Finally, another argument is the observation that the (*S*):(*R*) ratio is the same for **2**, X = OH and **2**, X = OAc even in the presence of AcOK. This requires that both compounds form in an almost identical ratio in the path leading to inversion and in that leading to racemization. This possibility is very unlikely for the structurally unrelated S_N1 and S_N2 pathways, whereas it is very reasonable if the two reaction channels, as in Scheme 3, involve extremely similar intermediates, namely a solvent-separated and a contact radical–cation pair.

Interestingly, if this hypothesis is correct, the solvolysis of $\mathbf{1}^{\bullet+}$ would closely resemble that of the corresponding closed-shell systems (1-phenylethyl halides) which also exhibit racemization accompanied by some inversion, and have similarly been interpreted on the basis of ion pair formation.[11]

Since the C–S bond dissociation energy in $\mathbf{1}^{\bullet+}$ is about 16 kcal mol^{-1},[12] a value close to that estimated for the C–C bond breaking in the phenylcyclopropane radical cation (ca. 15 kcal mol^{-1}[4]), it is surprising that in $\mathbf{1}^{\bullet+}$ the C–S bond cleavage utilizes an unassisted pathway (unimolecular), whereas the C–C bond cleavage in the phenyl cyclopropane radical cation exclusively occurs by a bimolecular mechanism and is very fast. We suggest that this difference in behavior can be attributed to the fact that small rings, particularly the three-membered ones, exhibit a reactivity in S_N2 ring opening reactions which is many orders of magnitude higher than that expected on the basis of steric strain.[13] However, it should also be considered that phenylcyclopropane radical cations are of π character, whereas $\mathbf{1}^{\bullet+}$ has presumably *n* character.[15]

Experimental Procedure

1: The corresponding ditosylamide was prepared from (*S*)-(1)-phenylethylamine (Aldrich) [14] and this was converted to (*R*)-**1** by reaction with thiophenol in acetone containing potassium carbonate [8]. When treated with H_2O_2 in AcOH, (*R*)-**1** gave the corresponding sulfone, m.p. 120–121 °C (115–116 °C [14]), $[\alpha]_{25}^{D} = 106$ (103 [14]) ($c = 1.5$ g L^{-1}; MeOH). For the oxidation experiments the concentration of **1** was 0.02–0.04 M, and that of [$Co^{III}W$] 0.02–0.08 M. In a typical experiment, 0.23 mmol of substrate was treated with 0.23 mmol of [$Co^{III}W$] in 10 mL of 0.25 M AcOK. After 3 h, 20% of the [$Co^{III}W$] had been consumed, which afforded **3** (0.015 mmol), **2**, X = OH (0.01 mmol), **2**, X = OAc (0.01 mmol), Ph_2S_2 (0.017 mmol), styrene (0.002 mmol), and 0.19 mmol of unreacted **1**. No reaction took place in the absence of [$Co^{III}W$]. In some experiments unreacted (*R*)-**1** was recovered from the reaction mixture and converted into the sulfone which showed no loss of optical activity. Thus, (*R*)-**1** was configurationally stable under the reaction conditions. The products were analyzed by GLC and GC-MS (comparison with authentic specimens) by using two internal standards (anisaldehyde and octadecane). The (*S*)-**2**/(*R*)-**2** ratios were determined by GLC with a Varian Model 3400 flame-ionization gas chromatograph equipped with a chiral capillary column (cyclodex-B, 30 m × 0.25 mm, from J & W Scientific) and He as carrier gas (1.8 atm). Under isothermal conditions (90 °C), the following retention times were obtained for the optically active products **2**: (*R*)-**2**, X = OH: 15.54; (*S*)-**2**, X = OH: 16.16; (*S*)-**2**, X = OAc: 18.91; (*R*)-**2**, X = OAc: 19.57 min. In the experiments in the presence of AcOK, the (*S*):(*R*) ratios showed no change during the course of the reaction, for those in the absence of AcOK, a slight decrease in these ratios was observed at high percent of conversion. This was probably due to some racemization of **2** promoted by the acid which forms during the reaction.

Received: January 8, 1993 [Z 5802 IE]
German version: *Angew. Chem.* **1993**, *105*, 1110

[1] L. Eberson, *Electron Transfer Reactions in Organic Chemistry*, Springer, Berlin, **1987**; R. Sirimanne, Z. Li, D. R. Vanderveer, L. M. Tolbert, *J. Am. Chem. Soc.* **1990**, *112*, 2462, and references therein.

[2] a) E. Baciocchi, *Acta Chem. Scand.* **1990**, *44*, 645; b) *Photoinduced Electron Transfer Part C* (Eds.: A. M. Fox, M. Chanon), Elsevier, Amsterdam, **1988**; c) A. Albini in [2b], Chapter 3; d) X. Ci, D. G. Witten in [2b], Chapter 9.

[3] a) P. Maslak, S. L. Asel, *J. Am. Chem. Soc.* **1988**, *110*, 8260; b) S. Steenken, R. A. McClelland, *ibid.* **1989**, *111*, 4967.

[4] J. P. Dinnocenzo, W. P. Todd, T. R. Simpson, I. R. Gould, *J. Am. Chem. Soc.* **1990**, *112*, 2462.

[5] J. P. Dinnocenzo, S. Farid, J. L. Goodman, I. R. Gould, W. P. Todd, S. L. Mattes, *J. Am. Chem. Soc.* **1989**, *111*, 8973; J. P. Dinnocenzo, S. Farid, J. L. Goodman, I. R. Gould, W. P. Todd, *Mol. Cryst. Liq. Cryst.* **1991**, *194*, 151.

[6] S. S. Shaik, J. P. Dinnocenzo, *J. Org. Chem.* **1990**, *55*, 3434.

[7] a) L. Eberson, *J. Am. Chem. Soc.* **1983**, *105*, 3192; *New. J. Chem.* **1988**, *16*, 151; b) E. Baciocchi, M. Crescenzi, E. Fasella, M. Mattioli, *J. Org. Chem.* **1992**, *57*, 4684. c) The oxidation potential of **1** can be considered the same as that of benzyl phenyl sulfide ($E_p = 1.79$ V vs. NHE) [8] and therefore **1** can certainly undergo an electron transfer process with [$Co^{III}W$] ($E^\circ = 1.0$ vs. NHE) [7a, b] (NHE = normal hydrogen electrode).

[8] E. Baciocchi, D. Intini, A. Piermattei, C. Rol, R. Ruzziconi, *Gazz. Chim. Ital.* **1989**, *119*, 649.

[9] E. Baciocchi, C. Rol, E. Scamosci, G. V. Sebastiani, *J. Org. Chem.* **1991**, *56*, 5498.

[10] S. Saukararam, W. A. Harley, J. K. Kochi, *J. Am. Chem. Soc.* **1987**, *109*, 7824.

[11] F. A. Carey, R. J. Sundberg, *Advanced Organic Chemistry*, Plenum, New York, **1977**, Chapter 5.

[12] a) By a thermochemical cycle, the C–S bond dissociation energy (BDE) in $1^{\bullet+}$ is given by $BDE(1^{\bullet+}) = BDE(1) + I_p(rad) - I_p(1)$, where BDE(1) and $I_p(1)$ are the C–S bond dissociation energy and the ionization potential of 1, respectively, and $I_p(rad)$ is the ionization potential of the 1-phenylethyl radical. BDE(1) was estimated to be about 50 kcal mol^{-1} by subtracting the difference between the C–H BDE values of $PhCH_2$–H (88 kcal mol^{-1}) [12b] and $PhCH(CH_3)$–H (85.4 kcal mol^{-1}) [12c] from the C–S BDE of $PhCH_2$–SPh (52.6 kcal mol^{-1})] [12c]. The latter value is given by the C–S BDE of $PhCH_2$–SH (58.8 kcal mol^{-1}) [12c] minus the difference between the C–S BDE values of CH_3–SH (73.9 kcal mol^{-1}) [12c] and CH_3–SPh (67.7 kcal mol^{-1}) [12c]. $I_p(rad)$ is 6.9 eV [12d] and $I_p(1)$ is taken to be equal to that of benzyl phenyl sulfide (8.36 eV [12e]). The value of BDE($1^{\bullet+}$) obtained in this way refers to the gas phase. However, gas phase bond dissociation energies of radical cations are often similar to those in solution [12f]. b) D. F. McMillen, D. M. Golden, *Annu. Rev. Phys. Chem.* **1982**, *33*, 4390; c) D. Griller, J. A. Martinho Simões, D. D. M. Wayner in *Sulfur-Centered Reactive Intermediates in Chemistry and Biology* (*NATO ASI Ser.* Plenum, New York, **1990**, 43–44); d) S. G. Lias, G. E. Bartmess, J. L. Holmes, R. D. Levin, W. G. Mallard, *J. Phys. Chem. Ref. Data Suppl. n° 1* **1988**, 17; e) Determined by photoelectron spectroscopy; E. Baciocchi, unpublished results. f) D. D. M. Wayner, J. J. Dannenberg, D. Griller, *Chem. Phys. Lett.* **1986**, *131*, 189.

[13] M. L. Di Vona, C. Lillocci, G. Illuminati, *J. Chem. Soc. Chem. Commun.* **1985**, 380; L. Mandolini, *Adv. Phys. Org. Chem.* **1986**, *22*, 1.

[14] P. Müller, M. P. N. Thi, *Helv. Chim. Acta* **1980**, *63*, 2168.

[15] An *n* character has been shown for the structurally similar benzyl phenyl sulfide radical cation [9]. We thank a referee for having called our attention to this point.

Structure and Reactivity of $[HFe(CO)_3(\eta^3\text{-}C_3H_5)]$**

By *Terence M. Barnhart, James De Felippis,* and *Robert J. McMahon**

Transition metal η^3-allyl hydrido complexes were first proposed in 1962 by Pettit et al.[1] and Manuel[2] as key intermediates in the $Fe(CO)_5$-catalyzed isomerization of alkenes. Despite continuing interest in the mechanism of this important process,[3] the extremely high reactivity of first-row η^3-allyl hydrido complexes has precluded direct characterization of catalytically important species in solution.[4] We report here the characterization of a highly reactive iron η^3-allyl hydrido complex, $[HFe(CO)_3(\eta^3\text{-}CH_2CHCH_2)]$ (**2**), by ^1H and ^{13}C NMR spectroscopy in $[D_{14}]$methylcyclohexane at 160 K. This is the first observation of a catalytically significant η^3-allyl hydrido complex in solution, and thus paves the way for further detailed studies concerning the mechanism of alkene isomerization.

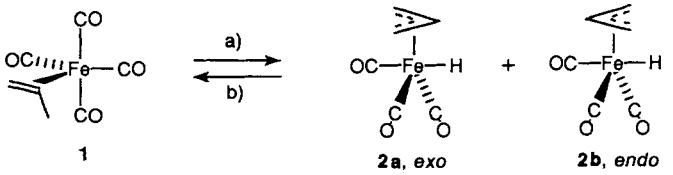

1 **2a**, *exo* **2b**, *endo*

Scheme 1. Reagents and reaction conditions: a) *hν*, −CO, $[D_{14}]$methylcyclohexane, 77 K; b) +CO, $[D_{14}]$methylcyclohexane, $T > 170$ K. Compound **2a** is the major product of the forward reaction.

[*] Prof. R. J. McMahon, T. M. Barnhart, Dr. J. De Felippis
Department of Chemistry
University of Wisconsin
Madison, WI 53706 (USA)
Telefax: Int. code + (608) 262-0381

[**] We gratefully acknowledge financial support from the National Science Foundation, 3M Corp., Rohm and Haas Corp., and DuPont Corp. We thank Prof. C. R. Landis, Prof. C. P. Casey, and Prof. M. Brookhart for helpful discussions.

Photolysis ($\lambda > 280$ nm) of **1** in a $[D_{14}]$methylcyclohexane glass produces **2**,[5] which persists upon warming the glass above its melting point (ca. 140 K). At 160 K, the photolyzed sample displays four new resonances ($\delta = 5.19$, 2.56, 1.80, −12.20, integrated intensities 1:2:2:1) and a fifth, very minor resonance (−12.0) (Fig. 1). We attribute the four major

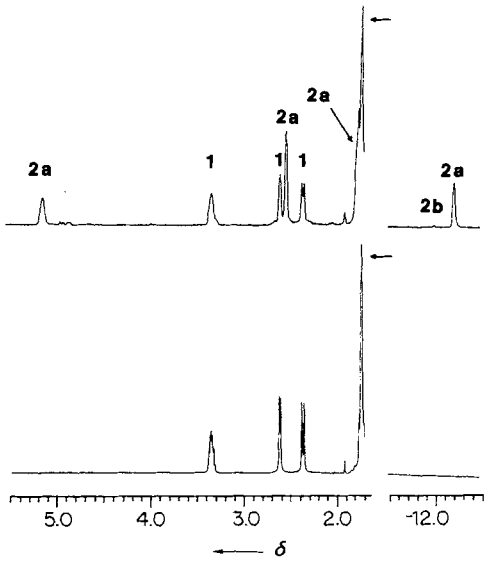

Fig. 1. Bottom: ^1H NMR spectrum **1** in $[D_{14}]$methylcyclohexane at 160 K prior to irradiation. Top: ^1H NMR spectrum of **2a** obtained upon photolysis of **1** ($\lambda > 280$ nm, 1 h). The weak signals near $\delta = 5.0$ are assigned to free propene, and the strong signals marked with arrows are assigned to $[D_{14}]$methylcyclohexane.

resonances to a pseudo-octahedral π-allyl hydrido complex (either **2a** or **2b**), drawing on analogy with π-allyl complexes of iron[6] and with other, less reactive π-allyl hydrides.[4] The high-field resonance ($\delta = -12.2$) is characteristic of a terminal hydrido ligand H_h. The remaining resonances display chemical shifts, coupling constants, and integration consistent with a symmetrical η^3-allyl ligand.[6–8] The signal of the central proton H_c of the allyl ligand ($\delta = 5.19$, m, 1H) exhibits the largest chemical shift, and appears as a broadened multiplet due to coupling with the *syn*-H_s and *anti*-H_a protons. The *syn* protons H_s ($\delta = 2.56$, d, 2H, $J = 5$ Hz) appear

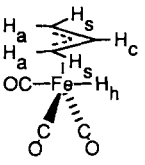

2a, *exo*

upfield of H_c and display the expected small *cis* coupling constant J_{H_c,H_s}. The *anti* protons H_a ($\delta = 1.8$, 2H) appear even further upfield of H_c.[9] The COSY spectrum reveals small coupling constants ($J < 5$ Hz) for the coupling between the hydrido ligand H_h and each of the allyl protons.[4] We could not resolve this coupling in the one-dimensional ^1H NMR spectrum.[7] The observation of two distinct carbonyl resonances in the ^{13}C NMR spectrum of **2** implies that

the CO ligand *trans* to the hydride ($\delta = 212.2$, $^2J_{C,H} = 18$ Hz) and the CO ligands *cis* to the hydride ($\delta = 210.7$, $^2J_{C,H} = 12$ Hz) do not exchange rapidly on the NMR timescale.

Pseudo-octahedral π-allyl halide complexes analogous to **2** exhibit geometric isomerism; the isomers differ in the relative orientation of the allyl ligand with respect to the M–X bond.[6] The isomers interconvert by allyl ligand rotation, but this process is slow on the NMR timescale at 298 K.[6] Thus, the geometric isomers are readily distinguished by ^{1}H NMR spectroscopy. We fully expect to resolve geometric isomers of **2** at 160 K. We tentatively ascribe the additional resonance at $\delta = -12.0$ to the isomer **2b**, although we cannot identify the resonances of the allyl ligand. The integrated ratio of the H_h resonances at $\delta = -12.0$ and -12.2 is $1 : > 20$. We do not know whether this ratio reflects the thermodynamic equilibrium.

We assigned the geometry of the major isomer of **2** on the basis of ^{1}H–^{1}H NOE effects. We used Landis' method to predict the NOE intensities for both *exo* and *endo* isomers.[10] In the *exo* isomer, the NOE intensities for the interactions between H_h and each of the allyl protons are calculated to be roughly comparable. In the *endo* isomer, the NOE intensity for the interaction between H_h and H_a is calculated to be one order of magnitude larger than the NOE intensities for the interactions between H_h and either H_c or H_s. The measured ^{1}H–^{1}H NOESY spectrum shows cross peaks of similar intensity between H_h and each of the allyl protons. The calculations therefore enable us to assign the major product of the photolysis as *exo*-**2a**.[11]

^{1}H and ^{13}C NMR data are inconsistent with various structures involving agostic interactions.[12] An agostic structure such as **3**, in which the methyl group is either static or rotating, would display a 1:1:1 ratio of olefinic resonances in the ^{1}H NMR spectrum. We therefore rule out these structures based on the observation of a 1:2:2 ratio of olefinic resonances. Rapid, reversible 1,3-hydrogen migration in **3**, with accompanying C–C bond rotation, would render all five terminal hydrogen atoms equivalent. This scenario is inconsistent with the observed ^{1}H NMR spectrum. Rapid, reversible 1,3-hydrogen migration in **3**, without accompanying C–C bond rotation, would be consistent with the observed ^{1}H NMR spectrum. In this case, the coupled ^{13}C NMR spectrum should reveal a small $^1J_{C,H}$ coupling of 60–90 Hz.[12] The actual coupled ^{13}C NMR spectrum shows a normal olefinic $^1J_{C,H}$ coupling (170 Hz) and no observable $^2J_{C,H}$ coupling. These observations are inconsistent with a fluxional agostic structure, and consistent with an η^3-allyl hydride structure.

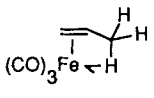

3

The hydrido complex **2** is exceedingly reactive. Warming samples of **2** to temperatures above 170 K results in the back-reaction of **2a** with CO to regenerate the propene complex **1** ($t_{1/2} = 25$ min at 169 K). If CO is removed by freeze-pump-thaw degassing, **2a** persists at temperatures up to 185 K. Above 185 K, **2a** reacts to give an unidentified product. The CO trapping experiment suggests a lower limit on k_{-1} of 6.7×10^{-4} s^{-1} at 169 K. The lack of line broadening in the NMR spectrum at 185 K provides an upper limit on k_{-1} of approximately 10 s^{-1}. These limiting values establish that the Gibbs free energy of activation, $\Delta G^{\neq}$, for hydride migration must be 9–12 kcal mol^{-1}.

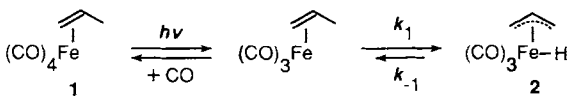

1 **2**

Experimental Procedure

A degassed solution of **1** [13] (ca. 20 mM in [D_{14}]methylcyclohexane) in a sealed 5 mm NMR tube was immersed in liquid nitrogen in a Pyrex dewar, photolyzed ($\lambda > 280$ nm, 1 h, 300 W Xe arc lamp), and transferred to the precooled probe (160 K) of a Bruker AM-500 NMR spectrometer. Data acquisition commenced upon thermal equilibration at 160 K. (Note: it is important to photolyze **1** in a glass; extended photolysis of **1** in solution leads to dimeric products.)

Received: October 24, 1992 [Z 5646 IE]
German version: *Angew. Chem.* **1993**, *105*, 1134

[1] G. F. Emerson, R. Pettit, *J. Am. Chem. Soc.* **1962**, *84*, 4591–4592.
[2] T. A. Manuel, *J. Org. Chem.* **1962**, *27*, 3941–3945.
[3] a) *Comprehensive Organometallic Chemistry* (Eds.: G. Wilkinson, F. G. A. Stone, E. W. Abel), Pergamon, Oxford, **1982**; b) A. J. Deeming in [3a], *Vol. 4*, Chapter 31.3; B. R. James in [3a], *Vol. 8*, Chapter 51.
[4] Several η^3-allyl hydrido complexes of second- and third-row transition metals exhibit sufficiently low reactivity to permit spectroscopic and/or crystallographic characterization. For leading references, see: W. D. McGhee, R. G. Bergman, *J. Am. Chem. Soc.* **1988**, *110*, 4246–4262; J.-M. Zhuang, D. Sutton, *Organometallics* **1991**, *10*, 1516–1527. An early report concerning an η^3-allyl hydrido complex of nickel has never been elaborated: H. Bönnemann, *Angew. Chem.* **1970**, *82*, 699; *Angew. Chem. Int. Ed. Engl.* **1970**, *9*, 736–737.
[5] Y.-M. Wuu, J. G. Bentsen, C. G. Brinkley, M. S. Wrighton, *Inorg. Chem.* **1987**, *26*, 530–540; T. M. Barnhart, R. J. McMahon, *J. Am. Chem. Soc.* **1992**, *114*, 5434–5435.
[6] Gmelin, *Handbuch der Anorganischen Chemie, Fe-Organische Verbindungen, Vol. B5*, pp. 31–67; A. N. Nesmeyanov, Y. A. Ustynyuk, I. I. Kritskaya, G. A. Shchembelov, *J. Organomet. Chem.* **1968**, *14*, 395–403; J. W. Faller, M. A. Adams, *ibid.* **1979**, *170*, 71–80; Y.-M. Wuu, M. S. Wrighton, *Organometallics* **1988**, *7*, 1839–1845; M. Brookhart, J. Yoon, S. K. Noh, *J. Am. Chem. Soc.* **1989**, *111*, 4117–4118.
[7] We attribute our inability to observe small coupling constants to the presence of small amounts of paramagnetic impurities, such as [$Fe(CO)_3(\eta^3$-$CH_2CHCH_2)$].
[8] We exclude the *mer* isomer of **2** as a possible structure, because it would display five nonequivalent allyl protons in the ^{1}H NMR spectrum. We exclude [$Fe(CO)_4(H)(\eta^1$-$CH_2CH{=}CH_2)$] as a possible structure, based on the dissimilarity of the observed ^{1}H NMR spectrum with that of the known [$(\eta^5$-$C_5Me_5)Ir(PMe_3)(H)(\eta^1$-$CH_2CH{=}CH_2)$] [4].
[9] Although this resonance occurs as a shoulder on a large solvent resonance, we can confidently assign it to H_a on the basis of both 1-D and 2-D (COSY and NOESY) spectra. The relative intensity of H_a was determined by integrating the subtracted spectra.
[10] C. Landis, V. S. Allured, *J. Am. Chem. Soc.* **1991**, *113*, 9493–9499. While the sign and magnitude of the NOE intensities depend strongly on the correlation time, the relative intensities do not.
[11] Spectral data for *exo*-**2a**: ^{1}H NMR ([D_{14}]methylcyclohexane, 160 K): $\delta = -12.20$ (brs, 1H), 1.80 (2H), 2.56 (d, 2H, $J = 5$ Hz), 5.19 (m, 1H); ^{13}C NMR ([D_{14}]methylcyclohexane, 160 K): $\delta = 44.2$ (t, J(C,H) = 170 Hz), 87.6 (d, J(C,H) = 163 Hz), 210.7 (d, J(C,H) = 12 Hz), 212.2 (d, J(C,H) = 18 Hz).
[12] M. Brookhart, M. L. H. Green, L.-L. Wong, *Prog. Inorg. Chem.* **1988**, *36*, 1–124.
[13] H. D. Murdoch, E. Weiss, *Helv. Chim. Acta* **1963**, *46*, 1588–1594. ^{1}H NMR ([D_{14}]methylcylohexane, 160 K): $\delta = 3.37$ (m, 1H), 2.63 (d, 1H, $J = 7.3$ Hz), 2.38 (d, 1H, $J = 12.3$ Hz), 1.78 (d, 3H, $J = 4.4$ Hz); ^{13}C NMR ($CDCl_3$, 240 K): $\delta = 24, 41, 57, 212$.

Organometallic Molecular Trees as Multielectron and Multiproton Reservoirs: $CpFe^+$-Induced Nonaallylation of Mesitylene and Phase-Transfer-Catalyzed Synthesis of a Redox-Active Nonairon Complex**

By *Françoise Moulines, Laurent Djakovitch, Roland Boese, Bruno Gloaguen, Werner Thiel, Jean-Luc Fillaut, Marie-Hélène Delville,* and *Didier Astruc**

Dedicated to Professor Hans Bock on the occasion of his 65th birthday

The theory[1] and organic syntheses[2] of multibranched compounds have recently encountered a renewed interest.[3] One especially challenging target is the functionalization of the branches (side chains) with redox systems; in this way molecular electronics devices and multielectron redox catalysis should be accessible.[4] We now present an organometallic strategy for the construction of molecular trees of novel topology. This method uses a one-pot nonafunctionalization of mesitylene and the synthesis of a nonairon complex in which the iron centers are quasi-equivalent reversible Fe^{II}/Fe^{I} redox systems.

Activation of arenes by π complexation to 12-electron transition metal fragments facilitates these nucleophilic reactions.[5-7] Deprotonation of an alkyl side chain followed by electrophilic attack was first shown by Trahanovsky and Card and used with $Cr(CO)_3$,[5a, b, 8] $Mn(CO)_3^+$,[5f, 9] $FeCp^+$ [Cp = (η^5-C_5H_5)][6, 7, 9] and Fe(η^6-arene)$^{2+}$[7c] fragments. We already know that the one-pot reaction of [FeCp(η^6-C_6Me_6)]PF_6 with alkyl, allyl, and benzyl halides in the presence of KOR (R = H, *t*Bu) yields discoid-shaped hexafunctional "tentacled sandwich" complexes.[7b, 9] So far only single[9c, e] and double[9d] branching functionalization of polymethyl arenes (i.e., polymethyl arenes in which each methyl substituent has been converted into a substituent with one or two functionalized branches, respectively) have been disclosed. We now report triple branching functionalization (i.e., each methyl substituent is converted into a substituent with three functionalized branches). The complex **1** (2 g, 5.58 mmol) was treated with KOH (12.54 g, 223 mmol) in allylbromide (20 mL, 223 mmol) for two days at room temperature. After chromatography on alumina the yellow resinous solid **2** (1.59 g, 134 mmol; 60%) with three allyl branches can be isolated [Eq. (a)].

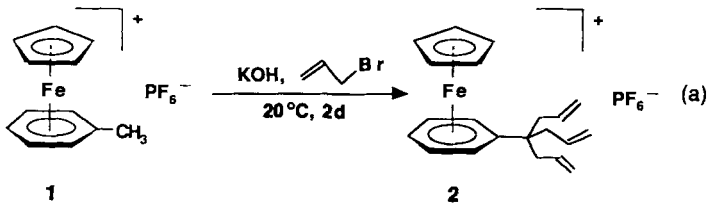

1 **2**

Triple branching functionalization could also be achieved under the same conditions on polymethylarene iron complexes in which the methyl groups have no methyl neighbor (*m*- and *p*-xylene, mesitylene). The reaction of [FeCp(η^6-mesitylene)]PF_6 (**3**) with benzyl bromide does not lead to the replacement of all nine acidic methyl hydrogen atoms because of steric hindrance (maximum: seven or eight branches under forcing conditions). In contrast, we find that with allylbromide and KOH in DME (dimethoxyethane) (Scheme 1), one-pot nonaallylation of **3** proceeds at 20 °C within nine days. The nonaolefin **4**[10b] thus formed was obtained in 68% yield along with the demetalated arene **5** in 30% yield. The cleanest way to demetalate complex **4** is visible-light photolysis in MeCN in the presence of one equivalent of PPh_3[11] (the moderately air-stable complex [FeCp($NCMe)_2(PPh_3)$]PF_6[11b] was filtered off). The compound **5** was recrystallized in pentane (m.p. 35.5 °C, 90% yield). The result of an X-ray structure analysis of **5**[12] is shown in Figure 1. The anisotropic thermal parameters, disorder, and

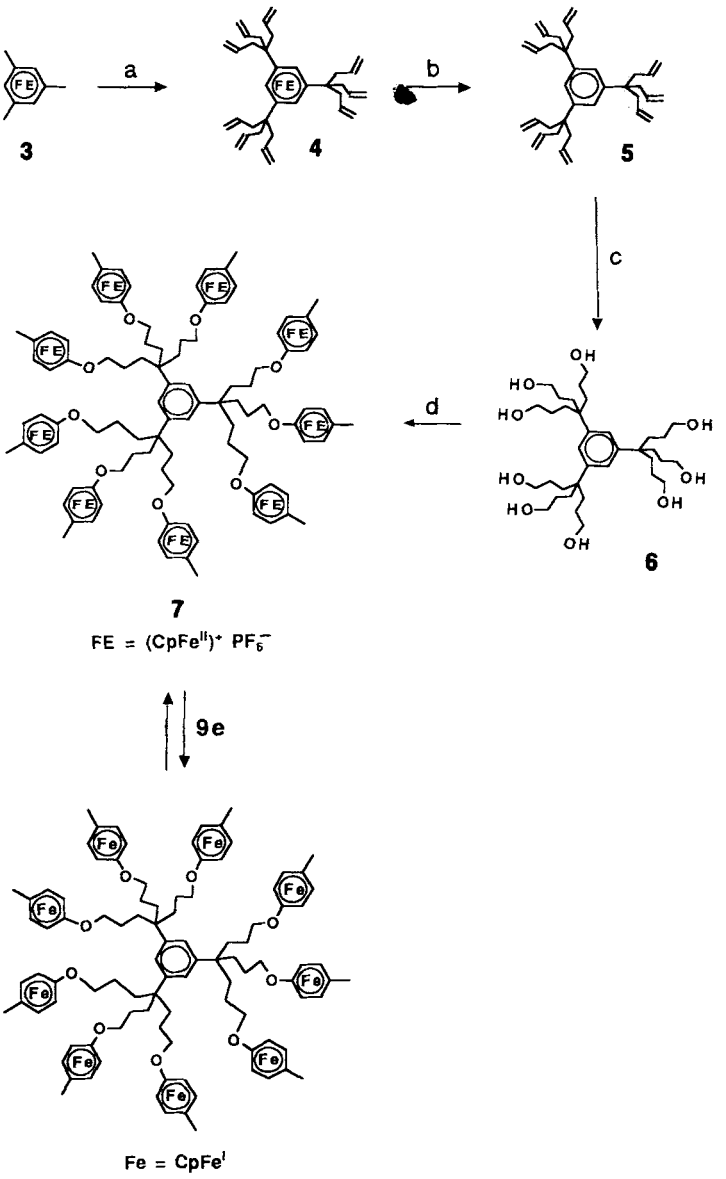

Scheme 1. Synthesis of the nonacation **7**. a) CH_2CHCH_2Br, KOH, DME, 20 °C, 9 days; b) MeCN, PPh_3 (1 equiv), visible light, 7 h, 25 °C; c) Disiamylborane ($Me_2CHCHMe)_2BH$, THF, 20 °C, 1 day, 30% H_2O_2, 3 M NaOH, 50 °C, 1 h; d) [Fe(Cp)(η^6-*p*-MeC_6H_4F)]PF_6, K_2CO_3, $(Bu_4)NBr$, THF/DMSO (80:20), 20 °C, 3 days.

[*] Prof. D. Astruc, Dr. F. Moulines, L. Djakovitch, Dr. B. Gloaguen, Dr. W. Thiel, Dr. J.-L. Fillaut, Dr. M.-H. Delville
Laboratoire de Chimie Organique et Organométallique
URA CNRS N° 35, Université Bordeaux I
351, Cours de la Libération, F-33405 Talence Cédex (France)
Telefax: Int. code (33)5684-6646

Prof. Dr. R. Boese
Institut für Anorganische Chemie der Universität
Universitätsstrasse 3-5, D-45117 Essen (FRG)

[**] This work was partly supported by the Centre National de la Recherche Scientifique (CNRS), the Université Bordeaux I, and the Région Aquitaine. We also thank Rhône-Poulenc (L. D.) and the Alexander von Humboldt Foundation (W. T.) for grants.

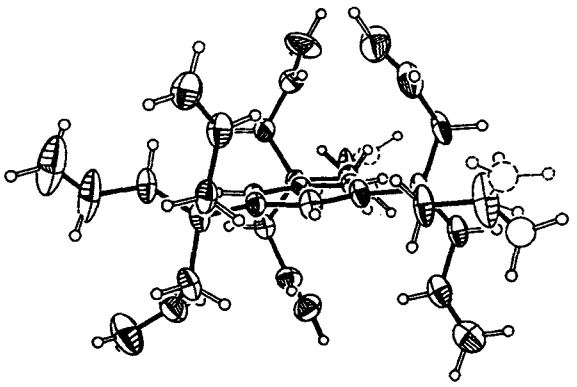

Fig. 1. Crystal structure of **5** (thermal ellipsoids 50% level); view along the plane of the benzene ring. Important distances [Å] (mean values for chemically equivalent bonds) C–C (aromat.) 1.391(3), C(benzene)–C(α) 1.534(3), C(α)–C(β) 1.546(2), C(β)–C(γ) 1.491(2), C(γ)–C(δ) 1.235(17) (this value is strongly affected by thermal movements and disorder).

different orientations of the allyl groups indicate their high flexibility, even in the solid state. The nonaolefin **5**[10c] was regiospecifically hydroborated with disiamylborane, and subsequent alkaline oxidation[9c, 13] gave the very hygroscopic nonaol **6**[10d] (Scheme 1).

The arborol strategy then requires iteration, namely, branching with $[FeCp(arene)]^+$ units in which the arene ligand in the complex fragment bears a methyl group suitable for further starburst reactions such as in Equation (a). Nonaarylmetalation[14] of **6** is activated by the cationic charge of $[FeCp(\eta^6\text{-}p\text{-}MeC_6H_4F)]PF_6$ and also proceeds smoothly at 20 °C with K_2CO_3 and 10% $(Bu_4N)Br$ in THF/DMSO to give the yellow resinous nonairon sandwich **7**.[10e] Phase-transfer catalysis had not yet been used for this type of reaction, but these conditions are indispensable for the sake of the required efficiency. After purification by chromatography on alumina (eluent: CH_2Cl_2/MeCN), the yield of purified **7** was 20% from which satisfactory elemental and spectroscopic analyses were obtained. Note that **7** (like **3**) is fairly soluble in moderately polar solvents in spite of the +9 charge.

The cyclic voltammograms of **7** show a reversible reduction wave[15] (Fig. 2) for Fe^{II} (18e) $\rightleftarrows$ Fe^{I} (19e) at −1.37 V [versus saturated calomel electrode (SCE)] in DMF/0.1 M $(Bu_4N)BF_4$; $\Delta E_p = 100$ mV and remains constant upon variation of scan rates, $I_a/I_c = 0.8$, −30 °C, 0.8 Vs^{-1}, diffusion control [I vs. scan rate was a straight line]. Thus **7** is a reservoir of nine electrons and 27 benzylic protons (the second wave at $E_p = -2.3$ V vs. SCE[15] is irreversible). This aspect of electron transfer (ET) in such large molecules compares with the ET in proteins.[16] Heterogeneous ET from the cathode to the closest redox centers should be faster than to those which are remote. However, the kinetics observed indicates that the rate constants for the ET are so similar that no distinction is made on the electrochemical time scale. From the intensity of the wave in the cyclic voltammogram the number of electrons transferred was calculated to be $n_p = 8 \pm 1$.[17] Using two different equations[18] the diffusion coefficient of **7** was found to be $D_p = 4 \pm 10^{-7}$ $cm^2 s^{-1}$.

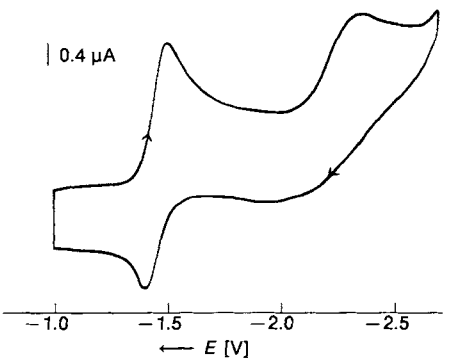

Fig. 2. Cyclic voltammogram of **7** in DMF, 0.1 M $(nBu_4N)BF_4$, Hg electrode, −30 °C, scan rate: 0.4 Vs^{-1} (internal reference: $FeCp_2/FeCp_2^+$).

In conclusion, the one-pot nonafunctionalization of mesitylene reported here has allowed us to design an iterative organometallic strategy for the construction of the molecular tree **7** with quasi-equivalent redox centers, by a very efficient phase-transfer-catalyzed arylmetalation reaction.

Received: February 15, 1993 [Z 5870 IE]
German version: *Angew. Chem.* **1993**, *105*, 1132

[1] For prediction of the cascade limit see: P.-G. de Gennes, H. J. Hervet, *Phys. Lett.* **1983**, *44*, 351.

[2] For pioneering work and most recent highlights see: E. Buhleier, E. Wehner, F. Vögtle, *Synthesis* **1978**, 155; F. Vögtle, E. Weber, *Angew. Chem.* **1979**, *91*, 813; *Angew. Chem. Int. Ed. Engl.* **1979**, *18*, 753; H. Bernhard, M. Burges, W. Jaworek, F. Vögtle, *ibid.* **1992**, *104*, 1609 and **1992**, *31*, 1571.

[3] Arborols, dendrimers: a) G. R. Newkome, C. N. Moorefield, G. R. Baker, A. L. Johnson, R. K. Behera, *Angew. Chem.* **1991**, *103*, 1205; *Angew. Chem. Int. Ed. Engl.* **1991**, *30*, 1176; b) Comprehensive review: D. A. Tomalia, A. M. Taylor, W. A. Goddart III, *ibid.* **1990**, *102*, 119 and **1990**, *29*, 138; c) C. J. Hawker, J. M. Fréchet, *J. Am. Chem. Soc.* **1990**, *112*, 7638; d) H. Uchida, Y. Kabe, K. Yoshino, A. Kawamata, T. Tsumuraya, S. Masamuno, *ibid.* **1990**, *112*, 7077.

[4] a) S. Serroni, G. Denti, S. Campagna, A. Juris, M. Ciano, V. Balzani, *Angew. Chem.* **1992**, *104*, 1540; *Angew. Chem. Int. Ed. Engl.* **1992**, *31*, 1493; b) S. Denti, S. Campagne, M. Serroni, V. Ciano, V. Balzani, *J. Am. Chem. Soc.* **1992**, *114*, 2944.

[5] a) M. F. Semmelhack, *Pure Appl. Chem.* **1981**, *53*, 2379; *J. Organomet. Chem. Libr.* **1976**, *1*, 361; *Ann. N. Y. Acad. Sci.* **1977**, *295*, 36; b) G. Jaouen, *ibid.* **1977**, *295*, 29; c) V. N. Kundig, *Pure Appl. Chem.* **1985**, *57*, 1855; d) V. N. Kalinin, *Russ. Chem. Rev.* **1987**, *56*, 682; e) M. Brookhardt, A. Lukacs, *J. Am. Chem. Soc.* **1984**, *106*, 4161; f) D. M. La Brush, D. Eyman, N. C. Baenzijer, L. M. Mallis, *Organometallics* **1991**, *10*, 1026; g) K. Kirchner, H. Taube, *J. Am. Chem. Soc.* **1991**, *113*, 7039.

[6] a) A. N. Nesmeyanov, N. A. Vol'kenau, I. N. Bolesova, *Dokl. Akad. Nauk. SSSR* **1967**, *175*, 301; b) J. F. Helling, W. A. Hendrickson, *J. Organomet. Chem.* **1976**, *168*, 87; c) C. C. Lee, U. S. Gill, M. Iqbal, C. I. Azogu, R. G. Sutherland, *ibid.* **1982**, *231*, 151.

[7] a) D. Astruc, *Acc. Chem. Res.* **1986**, *19*, 377; b) D. Astruc, *Top. Curr. Chem.* **1991**, *160*, 47; c) D. Astruc in *The Chemistry of the Metal-Carbon Bond, Vol. 4* (Ed.: F. R. Hartley), Wiley, New York, **1987**, pp. 625–731.

[8] a) R. J. Card, W. S. Trahanovsky, *J. Am. Chem. Soc.* **1972**, *94*, 2897; b) J. W. Johnson, P. M. Treichel, *ibid.* **1976**, *98*, 688; *ibid.* **1977**, *99*, 1427; c) C. C. Lee, B. R. Steele, K. J. Demchuk, R. G. Sutherland, *Can. J. Chem.* **1979**, *57*, 946; *J. Organomet. Chem.* **1979**, *181*, 411.

[9] a) D. Astruc, J.-R. Hamon, G. Althoff, E. Román, P. Batail, P. Michaud, J.-P. Mariot, F. Varret, D. Cozak, *J. Am. Chem. Soc.* **1979**, *101*, 5445; b) J.-R. Hamon, J.-Y. Saillard, A. Le Beuze, M. McGlinchey, D. Astruc, *ibid.* **1982**, *104*, 7549; c) F. Moulines, D. Astruc, *Angew. Chem.* **1988**, *100*, 1394; *Angew. Chem. Int. Ed. Engl.* **1988**, *27*, 1347; d) F. Moulines, B. Gloaguen, D. Astruc, *ibid.* **1992**, *104*, 452 and **1992**, *31*, 458; e) J.-L. Fillaut, R. Boese, D. Astruc, *Synlett* **1992**, 55.

[10] a) **2**: ^1H NMR (250 MHz, CD_3COCD_3, TMS) $\delta = 6.4$ (d, aromat. H, 5H); 5.93 (m, allyl-CH, 3H); 5.26 (d, allyl-CH_2, 6H); 5.10 (s, C_5H_5, 5H), 2.65 (d, CH_2, 6H); ^{13}C NMR (62.38 MHz, CD_3COCD_3) $\delta = 134.22$ (allyl-CH), 120.05 (allyl-CH_2), 116 (quart. aromat. C), 88.29, 87.93, 86.17 (aromat. CH); 77.56 (C_5H_5); 44.1 (quart. aliphat. C), 42.91 (CH_2); correct C, H, Fe analysis; b) **4**: ^1H NMR (250 MHz, CD_3COCD_3, TMS) $\delta = 6.30$ (s, complexed aromat. CH, 3H), 5.99–5.89 (m, allyl-CH, 9H), [5.32–5.19 (m, allyl-CH_2, 18H), 5.24 (s, Cp, 5H], 2.75 (d, CH_2, 18H); ^{13}C NMR (62.38 MHz, CD_3COCD_3) $\delta = 134.52$ (allyl-CH), 120.04 (allyl-CH_2), 113.90 (complexed quart. aromat. C), 81.90 (complexed aromat. CH), 77.67 (Cp), 44.55 (quart. aliphat. C), 43.12 (CH_2); correct C, H, Fe analysis; c) **5**: ^1H NMR (250 MHz, CD_3COCD_3) TMS) $\delta = 7.19$ (s, C_6H_3, 3H), 5.53–5.69 (m, $CH{=}CH_2$, 9H), 4.96–5.05 (m, $CH{=}CH_2$, 18H), 2.52 (d, CH_2, 18H); ^{13}C NMR (CD_3COCD_3, 62.38 MHz) $\delta = 42.43$ (CH_2), 44.30 (quart. benzyl-C), 117.79 ($CH{=}CH_2$), 123.5 ($CH{=}CH_2$), 135.58 (aromat. CH), 145.21 (quart. aromat. C); correct C, H analysis; d) **6**: ^1H NMR (D_2O, 250 MHz, TMS) $\delta = 7.22$ (s, C_6H_3, 3H), 3.52 (t, CH_2OH, 18H), 1.75 (m, CH_2-CH_2OH, 18H); 1.34 (m, CH_2-C, 18H); ^{13}C NMR (D_2O, 62.38 MHz) $\delta = 27.47$ (CH_2-CH_2OH), 34.35 (CH_2C), 43.79 (quart. ben-

zyl-C), 63.84 (CH_2OH), 123.59 (aromat. CH), 147.47 (quart. aromat. C); correct C, H, O analysis; e) **7**: ^{1}H NMR (CD_3COCD_3, 250 MHz, TMS) $\delta = 7.51$ (s, C_6H_3, 3H); 6.11 (s, C_6H_4, complexed aromat. H, 36H), 5.01 (s, Cp, 45H), 4.21 (m, CH_2O, 18H); 2.37 (s, CH_3, 27H), 2.09 (m, CH_2-CH_2O, 18H), 1.76 (m, C-CH_2, 18H); ^{13}C NMR (CD_3COCD_3, 62.9 MHz) $\delta = 147.00$ (quart. C of C_6H_3), 134.14 (complexed quart. aromat. C of C-O), 123.43 (aromat CH of C_6H_3), 100.38 (complexed quart. aromat. C of C-CH_3), 87.59 (complexed aromat. CH near O), 77.76 (C_5H_5), 74.57 (complexed aromat. CH near CH_3), 71.21 (complexed CH_2O), 43.84 (quart. aliphat. C), 34.13, 24.39 (CH_2), 19.81 (complexed CH_3); correct C, H, P analysis.

[11] a) T. P. Gill, K. R. Mann, *Inorg. Chem.* **1983**, *22*, 1986; b) D. Catheline, D. Astruc, *J. Organomet. Chem.* **1984**, *272*, 417.

[12] X-Ray structure determination of **5**: A crystal with the approximate dimensions of $0.41 \times 0.36 \times 0.29$ mm^3 was measured on a Nicolet R3m/V diffractometer with $Mo_{K\alpha}$ radiation at 110 K. Cell dimensions, refined from the diffractometer angles of 50 centered reflections, are $a = 8.306(1)$, $b = 17.419(2)$, $c = 21.224(3)$ Å, $\alpha = 90$, $\beta = 97.68(1)$, $\gamma = 90$, $V = 304.32(5)$ Å^3; $Z = 4$, $\varrho_{calcd} = 1.029$ g m^{-3}, $\mu = 0.06$ mm^{-1}, space group $P2_1/c$, data collection of 4059 unique intensities ($2\theta_{max} = 46°$), 3012 observed ($F_o > 4\,\sigma(F)$), extinction correction, structure solution by direct methods and refinement with full-matrix least squares on F (336 parameters) (riding groups for hydrogen atoms; common isotropic U values for each group) and isotropic U values for the disordered atoms C23a, C23b, C35a, and C35b (SOF's 0.5), $R = 0.060$, $R_w = 0.063$, $w^{-1} = \sigma^2(F_o) + 0.0004\,F_o^2$. Further details of the crystal structure investigation are available on request from the Fachinformationszentrum Karlsruhe, Gesellschaft für wissenschaftlich-technische Information mbH in D-76344 Eggenstein-Leopoldshafen, on quoting the following number CSD-57238, the names of the authors and the journal citation.

[13] H. C. Brown, *Organic Syntheses via Boranes*, Wiley, New York, **1975**, p. 52.

[14] For the first arylmetalation of alcohols by $[FeCp(\eta^6\text{-}C_6H_5Cl)]^+$ see [6a]. The authors used refluxing ethanol for several hours. Much milder conditions had to be searched in order to efficiently arylmetalate the nine branches without decomplexation.

[15] a) A. N. Nesmeyanov, L. I. Denisovitch, S. P. Gubin, N. A. Vol'kenau, F. I. Sirotkina, I. N. Bolesova, *J. Organomet. Chem.* **1969**, *20*, 169; b) N. G. Connelly, W. E. Geiger, *Adv. Organomet. Chem.* **1984**, *23*, 1.

[16] *Electron Transfer in Inorganic, Organic and Biological Systems* (Eds.: J.-R. Bolton, V. Mataga, G. McLendon, *Adv. Chem. Ser. 228*, ACS Washington, DC, **1991**.

[17] a) Determination of the number of electrons n_p involved in the redox process is made by using the equation [17b]:

$$n_p = \frac{I_p/c_p}{I_m/c_m}\left(\frac{M_p}{M_m}\right)^{0.275}$$

where I, c, and M are the intensity, the concentration and the molecular weight, respectively; the subcripts p and m refer to **7** and ferrocene respectively; b) J. B. Flanagan, S. Margel, A. J. Bard, F. C. Anson, *J. Am. Chem. Soc.* **1978**, *100*, 4248.

[18] a) F. G. Bordwell, G. D. Cooper, H. Morita, *J. Am. Chem. Soc.* **1957**, *79*, 376; b) T. W. Smith, J. E. Kuder, D. Wychick, *J. Polym. Sci.* **1976**, *14*, 2433.

Novel Alkynylcopper(I) Complexes and Lithium Alkynyl Cuprates**

By *Falk Olbrich, Jürgen Kopf,* and *Erwin Weiss**

Alkynylcopper(I) compounds[1, 2] can exist free of base, stabilized by bases such as neutral amine or phosphane ligands, or as alkynyl cuprates like $[\{Li(OEt_2)(CuPh_2)\}_2]$.[3] Polymeric phenylethynylcopper(I) $[CuC{\equiv}CPh]_n$,[4] stabilized compounds like $[\{CuC{\equiv}CPh(PR_3)\}_4]$, and the adducts with 3,3,6,6-tetramethyl-1-thia-4-cycloheptyne (TMTCH) $[(CuC{\equiv}CtBu)_4(\eta^2\text{-tmtch})_2]$ and $[\{(CuC{\equiv}CPh)(\eta^2\text{-tmtch})\}_2]$[5] that we studied recently have been structurally characterized. No structural data of alkali metal alkynyl cuprates was previously reported.

We report on the unusual stacking structure of the *tert*-butylethynylcopper(I) complex **1** that consists of 24 units, on the tetramer stabilized by triphenylphosphane (**2**), and on the first investigations on the lithium alkynyl cuprates **3** and **4**. X-ray structures illustrate the diverse modes of coordination of the alkynyl ligands.

$[(CuC{\equiv}CtBu)_{24}] \cdot 2C_6H_{14}$ **1**

$[\{CuC{\equiv}CtBu(PPh_3)\}_4] \cdot 2Et_2O$ **2**

$[Li_6(Et_2O)_3Cu_4(C{\equiv}CPh)_{10}]$ **3**

$[Li_6(Et_2O)_3Cu_3(C{\equiv}CPh)_9]$ **4**

The synthesis of the Cu^I complex **1** (18% yield) was adapted from known procedures[6] from copper(I) bromide dimethylsulfide [7] (dms = dimethylsulfide) and $LiC{\equiv}CtBu$ according to Equation (a).

$$[CuBr(dms)]_n + LiC{\equiv}CtBu \xrightarrow[2.\ n\text{-hexane}]{1.\ Et_2O} \underset{\mathbf{1}}{[CuC{\equiv}CtBu]_{24} \cdot 2C_6H_{14}} \quad (a)$$

A crystal structure analysis of **1**[8, 9] revealed a stacking structure unusual for Cu complexes, which consists of an aggregate of 24 $CuC{\equiv}CtBu$ units (Fig. 1). On two sides of a

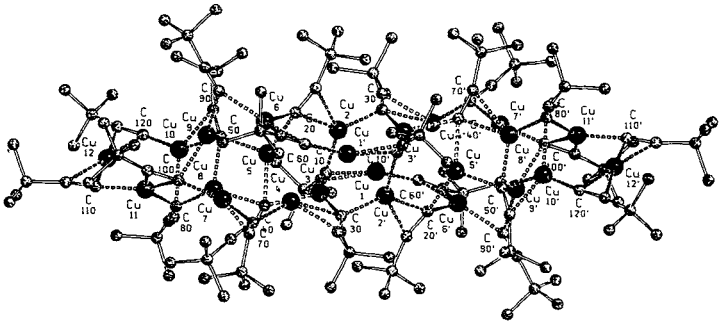

Fig. 1. SCHAKAL representation of the crystal structure of **1**, omitting H atoms and solvent molecules. Important distances [pm]: μ_4–η^2: Cu5–Cu50 215.3(4), Cu8–C50 206.6(4), Cu9–C50 220.5(5), Cu10–C50 209.0(4), Cu10–C51 208.9(4).

distorted central Cu_6 octahedron (Cu1–Cu3 and Cu1′–Cu3′, inversion center in the middle) lie $CuC{\equiv}CtBu$ molecules. The copper atoms Cu12 and Cu12′ situated at the outermost edge of the aggregate are bound in a linear arrangement to two η^2-$C{\equiv}CtBu$ ligands. All other $C{\equiv}CtBu$ ligands are bridging and display a variety of coordination types: μ_2–η^1, μ_2–η^2, μ_3–η^1, and μ_3–η^2. Moreover, a novel mode of coordination, μ_4–η^2, is observed: the alkynyl anion C50–C55 is coordinated through C50 to four different Cu atoms (Cu–C50 distances 207–220 pm), and in addition one of the Cu atoms interacts with the C_β atom of the ligand (C51). The Cu–Cu distances vary widely from 247 to 342 pm. The Cu–C bonds are 190–257 pm long (compare $[CuC{\equiv}CPh]_n$: Cu···Cu 242–247, Cu–C 198–213 pm). Similar stacked structures with different degrees of association were observed for $[Li_{12}(C{\equiv}CtBu)_{12}(thf)_4]$,[10] $[Na_{10}(NMe_2)_{10}(tmeda)_4]$, and $[Na_{12}(NMe)_{12}(tmeda)_4]$ (tmeda = *N*,*N*,*N*′,*N*′-tetramethylethylenediamine).[11]

The known compound **2**[12] was obtained in 4% yield from a new synthesis method according to Equation (b).

$$[CuBr(dms)]_n + LiC{\equiv}CtBu + PPh_3 \xrightarrow{Et_2O} \underset{\mathbf{2}}{[CuC{\equiv}CtBu(PPh_3)]_4 \cdot 2Et_2O} \quad (b)$$

[*] Prof. Dr. E. Weiss, Dr. F. Olbrich, Priv. Doz. Dr. J. Kopf
Institut für Anorganische und Angewandte Chemie der Universität
Martin-Luther-King-Platz 6, D-20146 Hamburg (FRG)

[**] On Metal–Alkyl and Metal–Aryl Complexes, Part 48. This work was supported by the Fonds der Chemischen Industrie. Part 47: S. Corbelin, N. P. Lorenzen, J. Kopf, E. Weiss, *J. Organomet. Chem.* **1991**, *415*, 293.

According to the X-ray crystal structure analysis of **2**,[13] the four Cu atoms form an almost regular tetrahedron (C···Cu 260–265 pm). The μ_3-coordinated C≡C*t*Bu ligands cap the Cu_3 faces (Cu1–C10 215.1(10) pm; Fig. 2). Furthermore each Cu atom binds a PPh_3 ligand (Cu–P 223–224 pm). Similar interatomic distances are observed in the isostructural complexes $[\{CuC{\equiv}CPh(PPh_3)\}_4]$[14] and $[\{CuC{\equiv}CPh(PPh_2py)\}_4]$.[15]

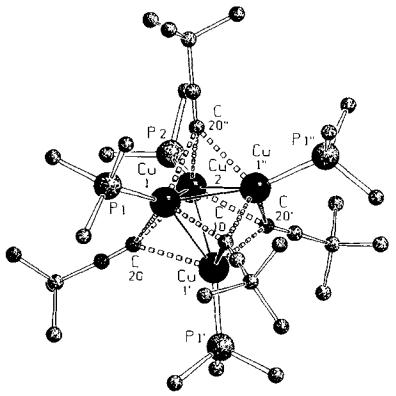

Fig. 2. SCHAKAL representation of the crystal structure of **2**, omitting H atoms and solvent molecules. The phenyl rings are indicated by C atoms.

Organocuprates are known to belong to the most important building blocks of organic synthesis. Apart from the simple organocuprates like R_2CuLi and $[\{Li(OEt_2)(CuPh_2)\}_2]$[3] (Gilman cuprates, low-order (LO) organocuprates), the higher order organocuprates (HO organocuprates) are gaining in importance.[16] Their structures[17] are still subject of a lively and sometimes controversial debate,[18] which includes the point of view, supported by NMR studies, that the HO cuprates do not exist in solution but degrade into LO cuprates that are in equilibrium with one another.[18a]

We have now synthesized the first lithium alkynyl cuprates **3** and **4** according to Equation (c) from $[CuBr(dms)]_n$ and an excess of phenylethynyllithium. The formation of yellow,

$$[CuBr(dms)]_n + LiC{\equiv}CPh \longrightarrow [Li_6(Et_2O)_3Cu_4(C{\equiv}CPh)_{10}]\,\mathbf{3}/[Li_6(Et_2O)_3Cu_3(C{\equiv}CPh)_9]\,\mathbf{4} \quad (c)$$

extremely air- and moisture-sensitive products depend of the reaction conditions.

The solid-state structure of tetracuprate **3** was determined (Fig. 3);[19] it is one of the few structurally characterized organocuprates of higher order[16] and comprises two linked structural units **A** and **B**. Unit **A** is a $[CuC{\equiv}CPh)_4]^{3-}$ anion in which the Cu atom is tetrahedrally surrounded by four C_α atoms of the Cα≡CβPh ligands (C-Cu-C 108–111°,Cu–C 197–202 pm). This structural unit is new for organocopper compounds and resembles the tetraphenyllithate(3−) found in $[\{Na(tmeda)\}_3][LiPh_4]$.[20] The large excess charge at the Cu atom is remarkable and might result in increased nucleophilicity for this unit. The base of the CuC_4 tetrahedron is formed by the C_α atoms C80, C90, and C100, and the apex by C70. Beneath the base lie three solvated Li atoms (Li7–Li9), which are also tetrahedrally coordinated by the oxygen atom of the ether molecule, two C_α atoms of the $C_\alpha{\equiv}C_\beta Ph$ ligand from the structural unit **A** (Li–C 230–236 pm), and another C_α atom from **B**.

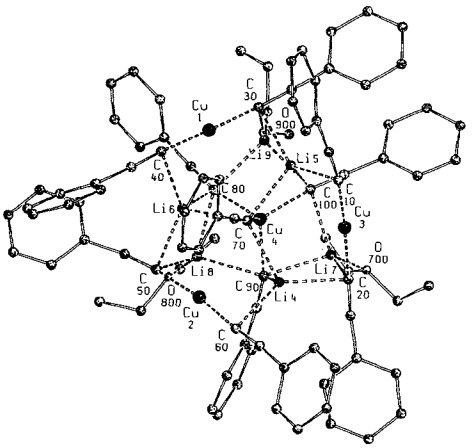

Fig. 3. SCHAKAL representation of the crystal structure of **3**, omitting the H atoms.

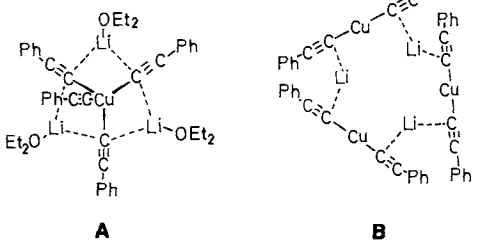

The structural component **B** is set on the threefold axis of the tetrahedral unit **A** like a crown. Unit **B** contains a slightly puckered Cu_3Li_3 six-membered ring (Cu1–Cu3, Li4–Li6; maximum deviation of the atoms from the best plane 13 pm). This plane lies 162 pm above the Cu4 atom. The Cu and Li atoms are bridged by phenylethynyl ligands.

All ten C_α atoms of the phenylethynyl ligands are links between components **A** and **B**. Thus, the Li atoms in the Cu_3Li_3 six-membered ring are also tetrahedrally surrounded by four C atoms. As in $[\{Li(OEt_2)(CuPh_2)\}_2]$,[3] linear cuprate anions $[Cu(C{\equiv}CPh)_2]^-$ are situated within the crown (C-Cu-C 170–173°, Cu–C 183–189 pm.

Experimental Procedure

1: A solution of LiC≡C*t*Bu (0.72 g, 8.2 mmol) in ether (75 mL) was added dropwise at room temperature within 90 min to a suspension of [CuBr(dms)] [7] (0.84 g, 4.1 mmol) in Et_2O (40 mL). The mixture was stirred for 20 h, evaporated almost to dryness (oil pump vacuum), and extracted with *n*-hexane (50 mL) at 50 °C for 2 h. The solution was concentrated to 1/3 of its volume, upon which **1** crystallized at 7 °C as square, yellow plates. Yield 18%; m.p. 104 °C (decomp.); readily soluble in *n*-hexane, Et_2O, and THF. The stoichiometries of **1** determined by X-ray structure analysis and elemental analysis do not agree. Fifteen percent of two *t*BuC≡C ligands are occupied by bromide to yield in the analysis $[Cu_{24}(C{\equiv}C\mathit{t}Bu)_{23.7}Br_{0.3}]\cdot 2C_6H_{14}$.

2: A solution of LiC≡C*t*Bu (0.32 g, 3.6 mmol) in ether (30 mL) was added dropwise at room temperature within 45 min to a suspension of [CuBr(dms)] (0.75 g, 3.7 mmol) in Et_2O (30 mL). After the mixture had been stirred for 30 min, PPh_3 (0.96 g, 3.7 mmol) was added. The mixture was stirred for a further 60 min, the solvent removed under vacuum (oil pump), and the solid extracted at room temperature with *n*-pentane (100 mL) for 15 h. After filtration, yellow crystals of **2** precipitated at 7 °C. Yield: 65 mg (4%); readily soluble in Et_2O and THF, soluble in *n*-hexane. The stoichiometries of **2** determined by X-ray structure analysis and elemental analysis do not agree. Twenty-five percent of three *t*BuC≡C ligands are occupied by bromide to yield in the analysis $[Cu_4(C{\equiv}C\mathit{t}Bu)_{3.25}Br_{0.75}(PPh_3)_4]$.

3: A solution of LiC≡CPh (0.47 g, 4.4 mmol) in ether (60 mL) was added dropwise within 90 min to a suspension of [CuBr(dms)] (0.48 g, 2.3 mmol) in

Et_2O (30 mL). The mixture was stirred for 5 h, filtered, evaporated to dryness, and the residue extracted with benzene (100 mL, 15 h), and filtered again. A small amount of yellow crystals of **3** precipitated from the solution at 7 °C. Decomposition above 206 °C, readily soluble in THF and Et_2O, soluble in benzene, almost insoluble in *n*-hexane.

4: A solution of LiC≡CPh (1.3 g, 12 mmol) in ether (30 mL) was added to a suspension of [CuBr(dms)] (0.56 g, 2.7 mmol) in Et_2O (50 mL) and heated under reflux for 2 h. The solvent was distilled off, the residue extracted with benzene (60 mL) for 24 h under reflux, the resulting solution filtered and evaporated to dryness, and the residue taken up in Et_2O (10 mL) and cooled to −55 °C. The yellow oil that separated was decanted off and dried under reduced pressure; it then appeared finely crystalline and colorless. Decomp. above 80 °C; extremely air-sensitive; readily soluble in THF and Et_2O, soluble in benzene. Correct elemental analysis; ^1H NMR (80 MHz, C_6D_6): δ = 7.69–7.34 (m, 17H; C_6H_5), 7.09–6.87 (m, 30H; C_6H_6), 3.40 (q, 12H; OCH_2), 1.07 (t, 18H; CH_3).

Received: February 5, 1993 [Z 5851 IE]
German version: *Angew. Chem.* **1993**, *105*, 1136

[1] *Gmelin Handbook of Inorganic Chemistry, Cu, Organocupper Compounds, Part 3*, 8th ed., Springer, Berlin, **1986**.
[2] J. G. Noltes, G. van Koten in *Comprehensive Organometallic Chemistry, Vol. 2* (Eds.: G. Wilkinson, F. G. A. Stone, E. W. Abel), Pergamon, New York, **1982**, p. 709 ff., and references therein.
[3] N. P. Lorenzen, E. Weiss, *Angew. Chem.* **1990**, *102*, 322; *Angew. Chem. Int. Ed. Engl.* **1990**, *29*, 300.
[4] a) P. W. R. Corfield, H. M. M. Shearer, *Abstr. Am. Cryst. Assoc. Meeting*, Bozeman, MT, USA, **1964**, 96; b) M. L. H. Green, *Organometallic Compounds Vol. 2: The Transition Elements*, 3rd ed., Methuen, London, **1968**, p. 271.
[5] F. Olbrich, U. Behrens, E. Weiss, unpublished.
[6] a) A. E. Favorskii, L. Morev, *J. Russ. Phys. Chem. Soc.* **1924**, *18*, 2496; b) H. O. House, M. J. Umen, *J. Org. Chem.* **1973**, *38*, 3893; c) E. J. Corey, D. Floyd, B. H. Lipshutz, *ibid.* **1978**, *43*, 3418.
[7] H. O. House, C.-Y. Chu, J. M. Wilkins, M. J. Umen, *J. Org. Chem.* **1975**, *40*, 1460.
[8] Crystal structure analysis of tetracosa[(*tert*-butylethynyl)copper(I)]·2*n*-hexane (**1**): single crystals from *n*-hexane by slow cooling to 7 °C and concentration of the solution. $C_{144}H_{216}Cu_{24}\cdot C_{12}H_{28}$, triclinic, $P\bar{1}$, $Z = 1$, $a = 1419.1(2)$, $b = 1526.3(2)$, $c = 2228.4(5)$ pm, $\alpha = 104.80(2)$, $\beta = 91.03(2)$, $\gamma = 117.32(2)°$, $V = 4094(2) \times 10^6$ pm^3, $\rho_{calcd} = 1.478$ g cm^{-3}, $\mu = 35.1$ cm^{-1} (absorption correction), crystal size $0.20 \times 0.25 \times 0.27$ mm^3, $Cu_{K\alpha}$, Enraf-Nonius CAD4 diffractometer, temperature 173 K, range $2.25° < \theta < 76.5°$, 13295 significant reflections ($|F| > 4\sigma(|F|)$), structure solution with direct methods (SHELXS, G. Sheldrick, Göttingen, **1986**), 869 refined parameters, $R = 0.047$, $R_w = 0.061$ ($[\sigma^2(F) + 0.0002F^2]^{-1}$, all non-hydrogen atoms refined with anisotropic temperature factors. In the asymmetric unit {(CuC≡C*t*Bu)$_{12}$·*n*-hexane} the site of a *tert*-butylethynyl ligand (C90–C95) has 15% bromide occupancy (Br90). The hexane molecule is disordered. Drawing: E. Keller, SCHAKAL 88, Freiburg, **1988**).
[9] Further details of the crystal structure investigation may be obtained from the Fachinformationszentrum Karlsruhe, Gesellschaft für wissenschaftlich-technische Information mbH, D-76344 Eggenstein-Leopoldshafen (FRG) on quoting the depository number CSD-56987, the names of the authors, and the journal citation.
[10] M. Geissler, J. Kopf, B. Schubert, E. Weiss, W. Neugebauer, P. von R. Schleyer, *Angew. Chem.* **1987**, *99*, 569; *Angew. Chem. Int. Ed. Engl.* **1987**, *26*, 587.
[11] N. P. Lorenzen, J. Kopf, F. Olbrich, U. Schümann, E. Weiss, *Angew. Chem.* **1990**, *102*, 1481; *Angew. Chem. Int. Ed. Engl.* **1990**, *29*, 1441.
[12] M. I. Bruce, M. G. Humphrey, J. G. Matisons, S. K. Roy, A. G. Swincer, *Aust. J. Chem.* **1984**, *37*, 1955.
[13] Crystal structure analysis of tetrakis[(μ_3-*tert*-butylethynyl)triphenylphosphanecopper(I)]·2Et_2O (**2**): single crystals from *n*-hexane. $C_{96}H_{96}Cu_4P_4\cdot C_8H_{20}O_2$, rhombohedral, $P\bar{3}$, $Z = 6$, $a = 1531.1(2)$, $c = 6930(1)$ pm, $V = 14069(3) \times 10^6$ pm^3, $\rho_{calcd} = 1.257$ g cm^{-3}, $\mu = 13.8$ cm^{-1}, crystal size $0.43 \times 0.28 \times 0.18$ mm^3, $Mo_{K\alpha}$, CAD4 diffractometer, temperature 293 K, range $2.25° < \theta < 25.0°$, 2377 significant reflections ($|F| < 4\sigma(|F|)$), direct methods, 402 refined parameters, $R = 0.067$, $R_w = 0.067$ ($[\sigma^2(F) + 0.0006F^2]^{-1}$, all non-hydrogen atoms refined with anisotropic temperature factors. The site of a *tert*-butylethynyl ligand (C20–C25) has 25% bromide occupancy (Br2). Both ether molecules are disordered; not all atoms could be localized.
[14] L. Naldini, F. Demartin, M. Manassero, M. Sansoni, G. Rassu, M. A. Zoroddu, *J. Organomet. Chem.* **1985**, *279*, C42.
[15] M. P. Gamasa, J. Gimeno, E. Lastra, X. Solans, *J. Organomet. Chem.* **1988**, *346*, 277.
[16] B. H. Lipshutz, R. S. Wilhelm, J. A. Kozlowski (The Chemistry of Higher Order Organocuprates), *Tetrahedron* **1984**, *40*, 5005.
[17] P. P. Power, (The Structures of Organocuprates and Heteroorganocuprates and Related Species in Solution and in the Solid State), *Progr. Inorg. Chem.* **1991**, *39*, 75.
[18] a) S. H. Bertz, G. Dabbagh, *J. Am. Chem. Soc.* **1988**, *110*, 3668; b) B. H. Lipshutz, S. Sharma, E. L. Ellsworth, *ibid.* **1988**, *110*, 4032.
[19] Crystal structure analysis of tris(diethyl ether)hexalithium deca(phenylethynyl)tetracuprate(I) (**3**): single crystals from benzene. $C_{92}H_{80}Cu_4Li_6O_3$, monoclinic, $P2_1/c$, $Z = 4$, $a = 1763.6(3)$, $b = 1938.3(3)$, $c = 2308.4(3)$ pm, $\beta = 91.34(1)°$, $V = 7889.2(2) \times 10^6$ pm^3, $\rho_{calcd} = 1.288$ g cm^{-3}, $\mu = 15.4$ cm^{-1}, crystal size $0.30 \times 0.20 \times 0.05$ mm^3, $Cu_{K\alpha}$, Enraf-Nonius CAD4 diffractometer, temperature 173 K, range $2.25° < \theta < 60.0°$, 7471 significant reflections ($|F| < 3\sigma(|F|)$), direct methods, 1105 refined parameters, $R = 0.089$, $R_w = 0.090$ ($[\sigma^2(F) + 0.001F^2]^{-1}$, all non-hydrogen atoms refined with anisotropic temperature factors.
[20] U. Schümann, E. Weiss, *Angew. Chem.* **1988**, *100*, 573; *Angew. Chem. Int. Ed. Engl.* **1988**, *27*, 584.

ansa-Metallocenes of Calcium and Strontium: One-Pot Synthesis of Organometallic Complexes of the Heavier Alkaline Earth Metals**

By *Melanie Rieckhoff, Ursula Pieper, Dietmar Stalke,* and *Frank T. Edelmann**

Dedicated to Professor Adolf Knappwost on the occasion of his 80th birthday

Although [Cp_2Ca] (Cp = η^5-C_5H_5) has been known since 1956,[1] the organometallic chemistry of the heavier alkaline earth metals slipped into obscurity for a long time. This field gained new momentum only after the discovery of the high-temperature superconductors of the type $YBa_2Cu_3O_{7-x}$.[2] In particular, the recent pioneering work of Hanusa et al.[3] has shown impressively that the organometallic chemistry of the heavier alkaline earth metals is extremely interesting. However, soluble organometallic compounds of these metals are still very rare; the decamethylmetallocenes [Cp^*_2M] (M = Ca, Sr, Ba; Cp* = η^5-C_5Me_5) and their adducts with Lewis bases are among the most thoroughly studied examples.[4–7] We now report an unusually simple, new route to cyclopentadienylcalcium and -strontium compounds as well as the first X-ray structure determination of an *ansa*-metallocene derivative of calcium.

On addition of 6,6-dimethylfulvene to a suspension of calcium granules (activated by a small amount of $HgCl_2$) in THF, the colorless *ansa*-metallocene complex **1** is formed in 74% yield in a smooth reaction.

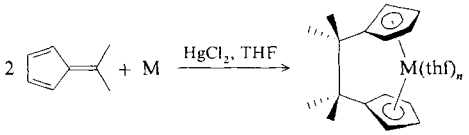

1: M = Ca, $n = 0$
2: M = Sr, $n = 2$

Nonsolvated **1** forms extremely air-sensitive crystals that are readily soluble in toluene and THF. Activated strontium

[*] Priv. Doz. Dr. F. T. Edelmann, Dipl.-Chem. M. Rieckhoff, Dr. U. Pieper, Dr. D. Stalke
Institut für Anorganische Chemie der Universität
Tammannstrasse 4, D-37077 Göttingen (FRG)
Telefax: Int. code + (551)39-3373

[**] This work was supported by the Fonds der Chemischen Industrie and the Deutsche Forschungsgemeinschaft.

powder reacts analogously with 6,6-dimethylfulvene to form the likewise colorless bis(tetrahydrofuran) adduct **2** (38%). Finely divided barium does not react under similar reaction conditions with fulvenes. The colorless complex **3** forms on

$[\{Me_2Et_2C_2(C_5H_4)_2\}Ca]$ **3**

treatment of activated calcium with two equivalents of 6-ethyl-6-methylfulvene. This product, however, crystallizes as a nonseparable mixture of isomers, so the use of unsymmetrically substituted fulvenes does not offer any preparative advantages.

The reductive dimerization of fulvenes was recently reported for the lanthanide elements samarium and ytterbium, too.[8] In fact, this is a good example of the known analogy between the heavier alkaline earth metals and divalent lanthanides.[9] The IR spectrum of **1** is almost superimposable on that of the analogous ytterbium(II) compound $[\{Me_4C_2(C_5H_4)_2\}Yb]$.[8] This phenomenon has already been discussed in detail for the complex pair $[(MeC_5H_4)_2M(dme)]$ (M = Ca, Yb; dme = dimethoxyethane).[10]

The example of the adduct formation of **1** and **3** with 1,4-diazadienes shows that the *ansa*-metallocenes described here can also undergo interesting reactions. Treatment of **1** with *N*,*N*′-di(*tert*-butyl)glyoxaldialdimine in THF/toluene yields an air-sensitive, bright red 1:1 adduct **4**.

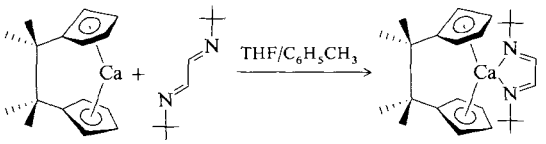

1 **4**

Similarly, **3** reacts with *N*,*N*′-di(*tert*-butyl)glyoxaldialdimine to afford the red, crystalline complex **5**, as a mix-

$[\{Me_2Et_2C_2(C_5H_4)_2\}Ca(tBuN{=}CHCH{=}NtBu)]$ **5**

ture of isomers. Crystallization from toluene/hexane provided single crystals of **4** that were suitable for an X-ray structure analysis.[11] Adduct **4** is monomeric in the solid state (Fig. 1). The reductive dimerization of 6,6-dimethylfulvene leads to the formation of the difunctional cyclopentadienyl ligand $[Me_4C_2(C_5H_4)_2]^{2-}$. The average distance between the

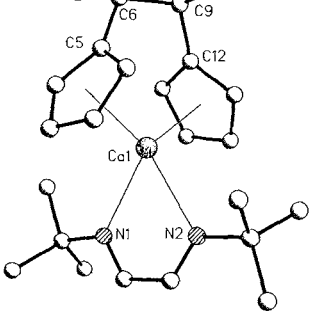

Fig. 1. Structure of **4** in the crystal (one of two crystallographically independent molecules). Selected distances [pm] and angles [°]: Ca1-N1 250.3(6), Ca1-N2 256.4(6), Ca1-X1a 239.6(3), Ca1-X1b 239.1(3), C5-C6 152.9(10), C6-C9 159.1(11), C9-C12 152.8(10); N1-Ca1-N2 68.7(2), (X1a, X1b = centers of Cp rings).

centers of the rings and the calcium atom is 239.4 pm and is thus comparable with the corresponding bond length in the complex $[(MeC_5H_4)_2Ca(dme)]$ (239.9 pm).[10] The diazadiene is coordinated to the central atom in the *cis* form as a chelating ligand. As a result the calcium atom has a distorted pseudo-tetrahedral coordination geometry. The angle between the calcium atom and the center of the rings is 119.0(5)°. However, the N-Ca-N angle of 68.7(2)° is substantially smaller than the tetrahedral angle.

The reductive dimerization of 6,6-dialkylfulvenes by elemental calcium and strontium described here is probably the simplest access to organometallic complexes of these elements. Furthermore, the compounds **1**–**5** are the first *ansa*-metallocene derivatives of the heavier alkaline earth metals.

Experimental Procedure

1: Granulated Ca (2.00 g, 49.9 mmol) was suspended in THF (200 mL) under an inert atmosphere (N_2) and activated by addition of $HgCl_2$ (200 mg; without stirring for 12 h followed by stirring for 1 h). While stirring and cooling (ice/salt mixture) 6,6-dimethylfulvene (5.30 g, 49.9 mmol) [12] was added, and the mixture was allowed to warm slowly to room temperature. After 24 h stirring the excess metal was filtered off, and the colorless filtrate was evaporated to dryness. The residue was dried for 2 h at 100 °C under vacuum and subsequently washed with two 150 mL portions of hexane. Drying under vacuum (2 h, 100 °C) yielded a colorless, very air-sensitive solid (4.66 g, 74%) that decomposed above 163 °C. Correct C,H analysis. IR (Nujol): $\tilde{\nu}$[cm^{-1}] = 3075 s, 1613 m, 1302 m, 1259 m, 1128 m, 1099 m, 1029 vs, 879 m, 848 m, 724 vs, 697 m; ^{1}H NMR (250 MHz, [D$_8$]THF): δ = 6.06–5.97 (m, 4H, C_5H_4), 4.93 (m, 2H, C_5H_4), 4.48–4.42 (m, 2H, C_5H_4), 2.04 (m, 6H, Me), 1.21–1.15 (m, 6H, Me); EI-MS: *m*/*z* (%) 252 (16, M^+), 147 (96, $Me_2CH(C_5H_4)Ca^+$), 107 (53, $Me_2CH(C_5H_4)^+$), 91 (100, $MeC(C_5H_4)^+$).

3: Analogously the reaction of Ca (2.00 g, 49.9 mmol) and 6-ethyl-6-methylfulvene (6.00 g, 49.9 mmol) yields a colorless, very air-sensitive solid (3.61 g, 52%). M.p. 170 °C (decomp.); correct C,H analysis; IR (Nujol): $\tilde{\nu}$[cm^{-1}] = 3074 m, 1610 m, 1260 m, 1096 m, 1029 w, 808 m, 724 vs; EI-MS: *m*/*z* (%) 280 (22, M^+), 161 (100, $MeEtCH(C_5H_4)Ca^+$), 131 (18, $EtCH_2C_2(C_5H_4)^+$), 105 (18, $EtC(C_5H_4)^+$), 93 (26, $MeH_2C(C_5H_4)^+$). The very complex ^{1}H NMR spectrum indicates the presence of a mixture of isomers.

3: Activated strontium powder (1.41 g, 16.0 mmol) and 6,6-dimethylfulvene (1.70 g, 16.0 mmol) were allowed to react for 48 h in THF (50 mL). The suspension was filtered through a thin layer of Celite, the filtrate was evaporated to dryness, and the residue washed with hexane (50 mL). Thorough drying under vacuum afforded a colorless, extremely air-sensitive solid (1.33 g, 38%) that decomposed above 181 °C. Correct C,H analysis. IR (Nujol): $\tilde{\nu}$[cm^{-1}] = 3068 m, 1669 m, 1616 m, 1261 s, 1097 vs, 1039 vs, 800 s, 748 vs, 723 vs; ^{1}H-NMR (250 MHz, C_6D_6/[D$_8$]THF): δ = 5.75 (m, 4H, C_5H_4), 5.14 (m, 2H, C_5H_4), 4.63 (m, 2H, C_5H_4), 3.56–3.44 (m, 4H, THF), 2.15 (m, 6H, Me), 1.70 (m, 6H, Me), 1.52–1.45 (m, 4H, THF); EI-MS: *m*/*z* (%) 429 (14, $M^+ - CH_3$), 91 (100, $MeC(C_5H_4)^+$).

4: A solution of **1** (2.00 g, 7.8 mmol) and $(tBuN)_2C_2H_2$ (1.32 g, 7.8 mmol) [13] was stirred in THF (60 mL) for 2 h at room temperature. After addition of toluene (40 mL), the THF was slowly removed under vacuum at 30 °C. The color changed from yellow to dark red. The solution was filtered, concentrated to about 20 mL, and diluted with hexane (5 mL). Cooling to −25 °C afforded red crystals (2.73 g, 83%). M.p. 157 °C; correct C,H,N analysis; IR (Nujol): $\tilde{\nu}$[cm^{-1}] = 3071 vs, 1650 m, 1613 m, 1601 m, 1590 m, 1385 vs, 1366 vs, 1238 s, 1226 s, 1202 s, 1127 s, 1116 s, 1099 s, 1052 s, 1039 vs, 971 vs, 927 m, 797 vs, 696 s, 466 m; ^{1}H NMR (250 MHz, C_6D_6): δ = 7.11–7.00 (m, 2H, N = CH), 6.31–6.15 (m, 4H, C_5H_4), 5.22–5.07 (m, 2H, C_5H_4), 4.80–4.68 (m, 2H, C_5H_4), 2.19–2.03 (m, 3H, Me), 1.88 (m, 3H, Me), 1.50–1.42 (m, 6H, Me), 1.07 (s, 18H, *t*Bu); EI-MS: *m*/*z* (%) 212 (1, $Me_4C_2(C_5H_4)_2^+$), 197 (3, $Me_3C_2(C_5H_4)_2^+$), 153 (18, $C_4H_9N(CH)_2NC_3H_6^+$), 141 (24, $C_4H_9NH(CH)_2NCH_2CH_3^+$), 112 (23, $C_4H_9N(CH)_2NH^+$), 97 (28, $C_4H_9N(CH)_2^+$), 57 (100, $C_4H_9^+$).

5 is prepared analogously from **3** (2.00 g, 7.0 mmol) and $(tBuN)_2C_2H_2$ (1.20 g, 7.0 mmol) to give 2.35 g of red crystals (75%). M.p. 166 °C; correct C,H,N analysis; IR (Nujol): $\tilde{\nu}$[cm^{-1}] = 3075 s, 1651 m, 1611 m, 1590 m, 1580 m, 1345 m, 1304 m, 1240 m, 1220 m, 1200 m, 1097 m, 1056 s, 1029 s, 972 s, 803 s, 730 s; ^{1}H NMR (250 MHz, C_6D_6): δ = 7.07 (m, 2H, N = CH), 6.30–6.17 (m, 4H, C_5H_4), 5.20–5.08 (m, 2H, C_5H_4), 4.75 (m, 2H, C_5H_4), 1.88 (m, 3H, CH_2CH_3), 1.76 (m, 3H, CH_2CH_3), 1.50–1.41 (m, 6H, Me), 1.40–1.29 (m, 2H, CH_2CH_3), 1.05 (s, 18H, *t*Bu), 0.90–0.81 (m, 2H, CH_2CH_3); EI-MS: *m*/*z* (%) 329 (26, $[Me_2C_2H_3(C_5H_4)]Ca(C_4H_9NCH)_2^+$), 280 (10, $Me_2Et_2C_2(C_5H_4)Ca^+$), 161 (90, $MeEt_2C_2(C_5H_4)^+$), 57 (100, $C_4H_9^+$).

Received: January 9, 1993 [Z 5803 IE]
German version: *Angew. Chem.* **1993**, *105*, 1102

[1] K. Ziegler, H. Froitzheim-Kühlhorn, H. Hafner, *Chem. Ber.* **1956**, *89*, 434–443.
[2] J. G. Bednorz, K. A. Müller, *Angew. Chem.* **1988**, *100*, 757–770; *Angew. Chem. Int. Ed. Engl.* **1988**, *27*, 735–748.
[3] T. P. Hanusa, *Polyhedron* **1990**, *9*, 1345–1362.
[4] M. J. McCormick, R. A. Williams, L. J. Levine, T. P. Hanusa, *Polyhedron* **1988**, *7*, 725–730.
[5] C. J. Burns, R. A. Andersen, *J. Organomet. Chem.* **1987**, *325*, 31–37.
[6] R. A. Williams, T. P. Hanusa, J. C. Huffman, *Organometallics* **1990**, *9*, 1128–1134.
[7] R. A. Andersen, R. R. Blom, C. J. Burns, H. V. Volden, *J. Chem. Soc. Chem. Commun.* **1987**, 768–769.
[8] A. Recknagel, F. T. Edelmann, *Angew. Chem.* **1991**, *103*, 720–721; *Angew. Chem. Int. Ed. Engl.* **1991**, *30*, 693–694.
[9] W. J. Evans, *Polyhedron* **1987**, *6*, 803–835.
[10] A. Hammel, W. Schwarz, J. Weidlein, *J. Organomet. Chem.* **1989**, *378*, 347–361.
[11] Crystallographic data for $[Me_4C_2(C_5H_4)_2]Ca(t\text{BuN=CHCH=N}t\text{Bu})$ **4** (−120 °C): $C_{26}H_{40}CaN_2$, monoclinic, $P2_1/c$, $M = 420.68\ g\,mol^{-1}$, $a = 2077.7(2)$, $b = 1769.3(3)$, $c = 1360.4(3)$ pm, $\beta = 103.91(1)°$, $V = 4.854\ nm^3$, $\rho_{calcd} = 1.15\ g\,cm^{-3}$, $F(000) = 1840$, $Z = 8$, $\mu(Mo_{K\alpha})$, graphite monochromator, $\lambda = 71.073$ pm) $= 0.27\ mm^{-1}$. The data collection was performed on a Siemens-Stoe AED2 diffractometer. Crystal size $0.3 \times 0.3 \times 0.4$ mm; 8834 reflections of which 6422 were independent and 3927 observed with $F > 4\sigma F$; $2\theta_{max} = 45°$; structure determination with direct methods (SHELXS-92 [13]); refinement of 618 parameters with all data and with 1060 restraints according to F^2; *wR2* (all data) = 0.302, *R1* = 0.098, residual electron density 1.15×10^2 and $-0.83 \times 10^2\ e\,nm^{-3}$, respectively. The asymmetric unit contains two crystallographically independent molecules. In one, disorder in a Cp ring and a rotational disorder of a *t*Bu group was resolved and refined by using restraints (SHELXL-92 [14]). Further details of the crystal structure investigation may be obtained from the Fachinformationszentrum Karlsruhe, Gesellschaft für wissenschaftlich-technische Information mbH, W-76344 Eggenstein-Leopoldshafen (FRG) on quoting the depository number CSD-57049, the names of the authors, and the journal citation.
[12] W. Freiesleben, *Angew. Chem.* **1963**, *75*, 576; *Angew. Chem. Int. Ed. Engl.* **1963**, *2*, 396.
[13] G. M. Sheldrick, *Acta Crystallogr. Sect. A* **1990**, *46*, 467.
[14] G. M. Sheldrick, SHELXL-92, Göttingen, **1992**.

A Versatile and Efficient Synthesis of Annulated Cyclopentanes by Stereoselective [3+2] Cycloaddition of Allylsilanes and Cycloalkenyl Methyl Ketones**

By *Hans-Joachim Knölker,* Norbert Foitzik, Helmut Goesmann*, and *Regina Graf*

We recently reported[1, 2] that the "silyl-group-containing by-products" of the Sakurai reaction,[3] originally considered silylmethylcyclobutanes,[4] are in fact silylcyclopentanes. This novel cylcopentane annulation involves a cationic 1,2-silyl shift,[5] which proceeds stereospecifically, thus generating three stereogenic centers. While the cyclization to a silylcyclopentane in the course of the Sakurai reaction was previously unprecedented, the formation of trimethylsilylcyclopentenes has been described for the reaction of trimethylsilylallenes with enones.[6] Following our first communication,[1] more examples of silylcyclopentane formation along with Sakurai reaction products have been reported,[7] and many of the products previously described as silylmethylcyclobutanes have been reassigned as silylcyclopentanes.[8] Related reactions of allylstannanes with α,β-unsaturated acyliron complexes[9] and with aldehydes[10] have also been described. Currently we are investigating metal-mediated processes for the construction of five-membered ring systems.[11] We report here on an elaboration of the silylcyclopentane annulation, a novel [3+2] cycloaddition, which provides a versatile and useful method with broad potential for the synthesis of cyclopentanoid natural products.

In our mechanistic proposal[1] we suggested that a bridged nonclassical pentavalent silicon cation[12] is the crucial intermediate in this novel cycloaddition. A stereospecific cyclization by intramolecular nucleophilic attack of the titanium enolate at the carbon atom of the siliranium ion leads to the product. Thus, the overall process may be regarded as a sila-Wagner–Meerwein rearrangement. The same mechanism has been used to explain more recent examples.[7] We thought that variation of the alkyl substituents at the silicon atom of the allylsilane would allow us to suppress nucleophilic attack at the silicon atom of the pentavalent silicon cation and thus prevent the formation of the Sakurai product.

The allylsilanes that are not commercially available are easily prepared by treatment of allylmagnesium chloride with the appropriate trialkylchlorosilane (Scheme 1).[13] The results of the reactions of cyclohexenyl methyl ketone with a variety of allylsilanes **1** are presented in Table 1. Structural assignments for the bicyclo[4.3.0]nonanes **2** are based on X-ray crystal structure determinations for compound **2d**[8] and the 2,4-dinitrophenylhydrazone derivative of **2a**[1] as well as complete characterization by ^1H and ^{13}C NMR spectroscopy. In every example examined for the cyclopentane annulation onto the six-membered ring (**2a** to **2i**) under op-

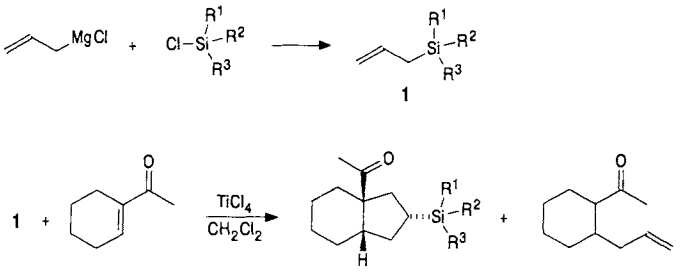

Scheme 1.

Table 1. Optimization of the [3+2] cycloaddition of allylsilanes **1** to cyclohexenyl methyl ketone by variation of the substituents at the silicon atom [a].

	R^1	R^2	R^3	Yield [%] **1**	**2**	**3**
a	Me	Me	Me	-	18	76
b	Me	Me	Ph	89	19	76
c	Me	Ph	Ph	99	26	66
d	Ph	Ph	Ph	99	51	39
e	Me	Me	*t*Bu	-	39	-
f	Me	Me	thexyl	92	53 [b]	trace
g	*t*Bu	Ph	Ph	98	70 [c]	trace
h	*i*Pr	*i*Pr	Ph	59 [d]	68	trace
i	*i*Pr	*i*Pr	*i*Pr	-	86	2

[a] Unless otherwise noted all reactions were carried out according to an optimized standard procedure; after addition of the allylsilane the reaction mixture was stirred for 19 h at −20 °C (see Experimental Procedure). [b] The reaction mixture was stirred for 19 h at −20 °C and for another 24 h at 0 °C. [c] The reaction mixture was stirred for 43 h at 0 °C. [d] Yield based on dichlorodiisopropylsilane to which first 1.2 equiv phenylmagnesium chloride and then 1.2 equiv allylmagnesium chloride were added.

[*] Prof. Dr. H.-J. Knölker, Dipl.-Chem. N. Foitzik, Dipl.-Chem. R. Graf
Institut für Organische Chemie der Universität der Universität
Richard-Willstätter-Allee, D-76131 Karlsruhe (FRG)
Telefax: Int. code +(721)698529
Dr. H. Goesmann
Institut für Anorganische Chemie der Universität Karlsruhe

[**] [3+2] Cycloadditions of Allylsilanes, Part 2. This work was supported by the Deutsche Forschungsgemeinschaft (Gerhard-Hess-Förderpreis) and the Fonds der Chemischen Industrie.—Part 1: [1].

timized reaction conditions (see Experimental Procedure), only the stereoisomer with the silyl group in the position *anti* to the acetyl group could be isolated. The yield of the cycloadduct depends on the steric demand of the alkyl substituents at the silicon atom of the allylsilane moiety. Generally, when bulkier alkyl groups were employed, the cycloadduct was obtained in better yields. This outcome is explained by the inhibition of nucleophilic attack on the silicon at the stage of the intermediate pentavalent silicon cation. A similar observation has been made recently by Mayr et al. in their study on the Lewis acid promoted reaction of diarylmethyl chlorides with allylsilanes.[14]

We next investigated the [3+2] cycloaddition of allylsilanes with cycloalkenyl methyl ketones with different ring sizes (five- to seven-membered rings) by using allyltriphenylsilane **1d** and allyltriisopropylsilane **1i** (Scheme 2, Table 2). Of special interest to us was whether the same mode of stereospecificity would be observed with cyclopentenyl methyl ketone **4a** and cycloheptenyl methyl ketone **4c** as in the cycloaddition of cyclohexenyl methyl ketone **4b**. The

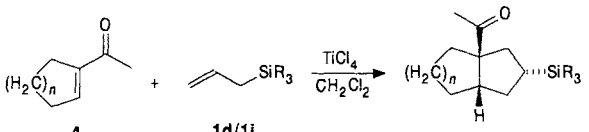

4 **1d/1i** **5/6**

Scheme 2. R = Ph, *i*Pr; $n = 1-3$.

Table 2. [3+2] Cycloadditions of allylsilanes **1d** and **1i** to cycloalkenyl methyl ketones **4**.

Product	R	*n*	Yield [%]
5a	Ph	1	25
5b (= **2d**)	Ph	2	51
5c	Ph	3	34
6a	*i*Pr	1	71 [a]
6b (= **2i**)	*i*Pr	2	86
6c	*i*Pr	3	68

[a] 3:1 Mixture of the *anti*/*syn* stereoisomers (*anti* and *syn* give the position of $SiiPr_3$ group relative to the acetyl group).

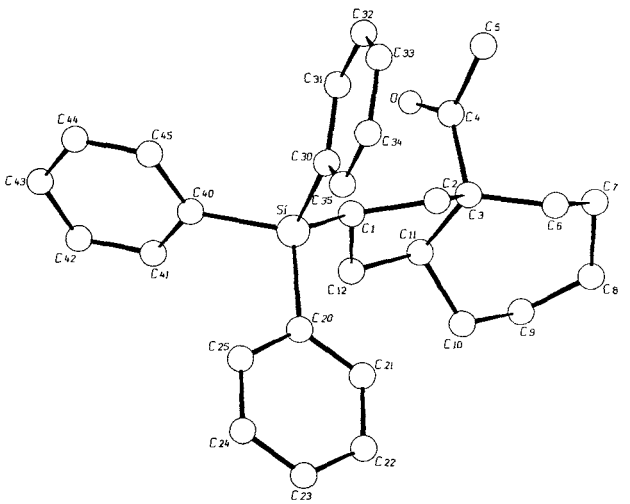

Fig. 1. Molecular structure of **5c** in the crystal. Selected bond lengths [Å]: C1-C2 1.528(5), C2-C3 1.543(5), C3-C11 1.557(5), C11-C12 1.546(4), C1-C12 1.534(6), Si-C1 1.879(4), Si-C20 1.878(3), Si-C30 1.884(4), Si-C40 1.876(3).

cycloaddition of allyltriisopropylsilane **1i** to **4a** gives only a 3:1 selectivity in favor of the product with the bulky triisopropylsilyl group in the *endo* position of the bicyclo[3.3.0]octane ring. Steric effects account for this lack of selectivity. For all other cycloaddition products an *anti* arrangement of the silyl substituent and the angular acetyl group was established. The stereochemical assignments are based on X-ray analyses of the perhydrindane **5b** (= **2d**)[8] and the perhydroazulene derivative **5c** (Fig. 1)[15] and are supported by the ^{13}C NMR data (Table 3).

Table 3. ^{13}C NMR data (δ values) and results of the DEPT experiments (100 MHz, $CDCl_3$) of selected annulated cyclopentanes.

5a: 24.9 (CH_2), 25.2 (CH), 25.9 (CH_3), 33.2 (CH_2), 37.0 (CH_2), 37.7 (CH_2), 39.9 (CH_2), 47.7 (CH), 68.9 (C), 127.9 (CH), 129.4 (CH), 134.5 (C), 135.9 (CH), 211.8 (C=O).

5b (= **2d**): 19.9 (CH), 21.9 (CH_2), 23.3 (CH_2), 25.6 (CH_3), 26.1 (CH_2), 30.4 (CH_2), 32.5 (CH_2), 37.8 (CH_2), 41.0 (CH), 58.5 (C), 127.9 (CH), 129.5 (CH), 134.5 (C), 136.0 (CH), 213.0 (C=O).

5c: 23.1 (CH), 25.1 (CH_3), 26.1 (CH_2), 28.2 (CH_2), 31.0 (CH_2), 33.0 (CH_2), 34.9 (CH_2), 38.1 (CH_2), 42.3 (CH_2), 42.5 (CH), 64.4 (C), 127.8 (CH), 129.5 (CH), 134.5 (C), 135.9 (CH), 213.1 (C=O).

6a (major stereoisomer): 11.4 (CH), 19.2 (CH_3), 25.0 (CH, CH_2), 25.8 (CH_3), 33.2 (CH_2), 37.2 (CH_2), 38.4 (CH_2), 40.6 (CH_2), 47.5 (CH), 68.6 (C), 211.9 (C=O).

6b (= **2i**): 11.2 (CH), 19.2 (CH_3), 20.9 (CH), 22.1 (CH_2), 23.7 (CH_2), 25.6 (CH_3), 26.6 (CH_2), 32.0 (CH_2), 33.6 (CH_2), 39.2 (CH_2), 41.6 (CH), 58.0 (C), 213.1 (C=O).

6c: 11.3 (CH), 19.1 (CH_3), 22.6 (CH), 25.0 (CH_3), 26.2 (CH_2), 28.3 (CH_2), 31.2 (CH_2), 33.5 (CH_2), 35.2 (CH_2), 38.9 (CH_2), 42.1 (CH), 43.2 (CH_2), 64.3 (C), 213.1 (C=O).

7b: 18.0 (CH), 22.5 (CH_3), 22.6 (CH_2), 23.1 (CH_2), 28.0 (CH_2), 30.4 (CH_2), 31.3 (CH_2), 35.8 (CH_2), 44.7 (CH), 91.6 (C), 127.8 (CH), 129.5 (CH), 134.6 (C), 170.7 (C=O).

8b: 18.5 (CH), 23.1 (CH_2), 25.7 (CH_2), 39.3 (CH_2), 127.8 (CH), 129.3 (CH), 134.5 (C), 135.4 (C), 135.9 (CH).

9b: 21.0 (CH), 23.8 (CH_2), 28.1 (CH_2), 32.7 (CH_2), 40.1 (CH), 127.8 (CH), 129.3 (CH), 135.4 (C), 136.2 (CH).

10b: 17.1 (CH), 20.3 (CH_2), 26.5 (CH_2), 35.0 (CH_2), 67.1 (C), 127.9 (CH), 129.5 (CH), 134.6 (C), 135.9 (CH).

11: 19.9 (CH), 23.8 (CH_2), 40.9 (CH_2), 43.4 (CH_2), 128.2 (CH), 129.9 (CH), 132.8 (C), 136.0 (CH), 215.3 (C=O).

The bicyclic products exhibit a useful reactivity for further transformations directed towards the synthesis of cyclopentanoid terpenes. This has been demonstrated for the bicyclo[3.3.0]octane **5a** and the bicyclo[4.3.0]nonane **5b** (= **2d**) (Scheme 3, Table 4).

Table 4. Transformation of the annulated triphenylsilylcyclopentanes **5a** and **5b** (= **2d**) into **7**–**10**.

		Yield [%]			
	n	**7**	**8**	**9**	**10**
a	1	81	87	100	100
b	2	87	97	100	100

The Baeyer–Villiger oxidation to give the acetoxy derivatives **7** is followed by tetrafluoroboric acid promoted elimination of acetic acid to provide the symmetrical bicycloolefins **8** in high yields. In further transformations of the *meso* olefins **8** the triphenylsilyl substituent acts as a stereodirecting group and enforces an approach of the reagent from the opposite face. Thus, hydrogenation with Adam's catalyst affords the saturated bicyclic derivatives **9** stereoselectively. The utility of the bicycloolefins **8** for the synthesis

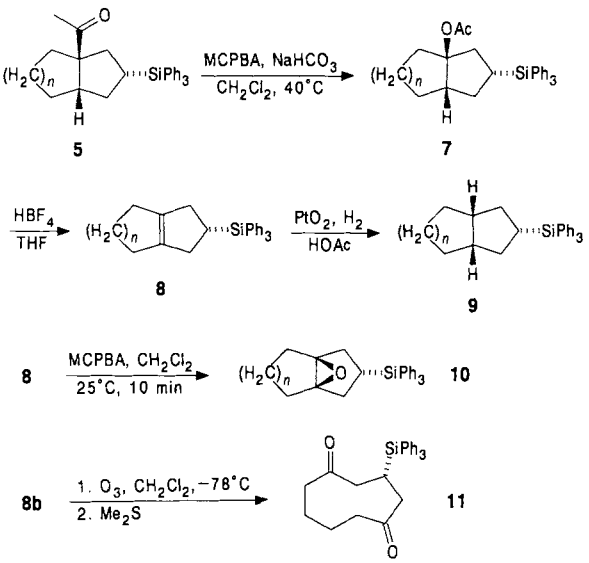

Scheme 3. **a**: $n = 1$, **b**: $n = 2$.

of propellane ring systems has been demonstrated by the stereospecific epoxidations to oxa[3.3.1]propellane **10a** and oxa[4.3.1]propellane **10b**, which proceed quantitatively. Moreover, ozonolysis of bicycloolefin **8b** to afford cyclononadione **11** (46% yield) emphasizes the potential of these intermediates as precursors for compounds with medium-sized rings.

In conclusion we have found a versatile, stereospecific method for the annulation of silylcyclopentanes by cycloaddition of an allylsilane **1** as the synthetic equivalent of the 2-silyl-substituted 1,3-dipole **12**. The stereoselective synthe-

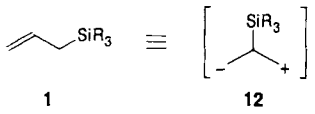

ses and further synthetic transformations of the products emphasize the potential of this method for the synthesis of cyclopentanoid natural products. The oxidative cleavage of the carbon–silicon bond should occur with retention of configuration[16] and is currently under investigation. Preliminary results indicate that asymmetric syntheses of cyclopentanes are feasible by using chiral allylsilanes, and that cyclopentanes with five stereogenic centers can be generated stereospecifically by employing 1,3-disubstituted allylsilanes. The present method thus opens the way for the enantioselective synthesis of highly substituted cyclopentanes.

Experimental Procedure

6b: A solution of **4b** (500 mg, 4.03 mmol) in dry dichloromethane (2 mL) was added to a stirred solution of titanium tetrachloride (840 mg, 4.43 mmol) in dry dichloromethane (5 mL) at −20 °C. The formation of the Lewis acid/enone complex was indicated by the intense yellow color of the resulting suspension. The reaction mixture was cooled to −78 °C, and a solution of allyltriisopropylsilane **1i** (1.2 g, 6.04 mmol) in dry dichloromethane (6 mL) was added. The reaction temperature was raised to −20 °C, during which the color changed to an intense red-violet. The reaction mixture was stirred for 19 h at this temperature then quenched by addition of an aqueous ammonium chloride solution. The organic layer was separated, the aqueous layer was extracted three times with cold dichloromethane, and the combined organic layers were dried over magnesium sulfate. Removal of the solvent and flash chromatography (pentane/ether 20:1) of the residue on silica gel provided bicyclo[4.3.0]nonane **6b** (1.12 g, 86%) as a colorless oil along with the allyl derivative **3** (16 mg, 2%).

Received: March 5, 1993 [Z 5907 IE]
German version: *Angew. Chem.* **1993**, *105*, 1104

[1] H.-J. Knölker, P. G. Jones, J.-B. Pannek, *Synlett* **1990**, 429.
[2] H.-J. Knölker, P. G. Jones, J.-B. Pannek, A. Weinkauf, *Synlett* **1991**, 147; see also H.-J. Knölker, *ibid.* **1992**, 371.
[3] A. Hosomi, H. Sakurai, *J. Am. Chem. Soc.* **1977**, *99*, 1673; T. A. Blumenkopf, C. H. Heathcock, *ibid.* **1983**, *105*, 2354.
[4] a) R. Pardo, J.-P. Zahra, M. Santelli, *Tetrahedron Lett.* **1979**, 4557; b) A. Hosomi, H. Kobayashi, H. Sakurai, *ibid.* **1980**, *21*, 955; c) S. Danishefsky, M. Kahn, *ibid.* **1981**, *22*, 485; d) H. O. House, P. C. Gaa, D. VanDerveer, *J. Org. Chem.* **1983**, *48*, 1661; e) G. Majetich, J. Defauw, C. Ringold, *ibid.* **1988**, *53*, 50; G. Majetich, K. Hull, D. Lowery, C. Ringold, J. Defauw in *Selectivities in Lewis Acid Promoted Reactions* (Ed.: D. Schinzer), Kluwer Academic, Dordrecht, **1989**, p. 169; f) K. Nikisch, H. Laurent, *Tetrahedron Lett.* **1988**, *29*, 1533; g) G. Majetich, J.-S. Song, C. Ringold, G. A. Nemeth, *ibid.* **1990**, *31*, 2239.
[5] A. W. P. Jarvie, A. Holt, J. Thompson, *J. Chem. Soc. B* **1969**, 852; M. A. Cooke, C. Eaborn, D. R. M. Walton, *J. Organomet. Chem.* **1970**, *24*, 301; for more recent reports of cationic 1,2-silyl shifts, see: R. F. Cunico, *J. Org. Chem.* **1990**, *55*, 4474; J. S. Panek, M. Yang, *J. Am. Chem. Soc.* **1991**, *113*, 9868; S. Yamazaki, S. Katoh, S. Yamabe, *J. Org. Chem.* **1992**, *57*, 4.
[6] R. L. Danheiser, D. J. Carini, A. Basak, *J. Am. Chem. Soc.* **1981**, *103*, 1604; R. L. Danheiser, D. J. Carini, D. M. Fink, A. Basak, *Tetrahedron* **1983**, *39*, 935.
[7] K. Ohkata, K. Ishimaru, Y.-G. Lee, K.-Y. Akiba, *Chem. Lett.* **1990**, 1725; S. Imazu, N. Shimizu, Y. Tsuno, *ibid.* **1990**, 1845; Y.-G. Lee, K. Ishimaru, H. Iwasaki, K. Ohkata, K.-Y. Akiba, *J. Org. Chem.* **1991**, *56*, 2058; G. Majetich, J.-S. Song, C. Ringold, G. A. Nemeth, M. G. Newton, *ibid.* **1991**, *56*, 3973; J. Ipaktschi, A. Heydari, *Angew. Chem.* **1992**, *104*, 335; *Angew. Chem. Int. Ed. Engl.* **1992**, *31*, 313; B. B. Snider, Q. Zhang, *J. Org. Chem.* **1991**, *56*, 4908; R. L. Danheiser, B. R. Dixon, R. W. Gleason, *ibid.* **1992**, *57*, 6094.
[8] H.-J. Knölker, N. Foitzik, P. G. Jones, J.-B. Pannek, unpublished results.
[9] J. W. Herndon, C. Wu, *Synlett* **1990**, 411; J. W. Herndon, C. Wu, J. J. Harp, *Organometallics* **1990**, *9*, 3157; J. W. Herndon, C. Wu, J. J. Harp, K. A. Kreutzer, *Synlett* **1991**, 1.
[10] M. Nakatsuka, J. A. Ragan, T. Sammakia, D. B. Smith, D. E. Uehling, S. L. Schreiber, *J. Am. Chem. Soc.* **1990**, *112*, 5583.
[11] H.-J. Knölker, J. Heber, C. H. Mahler, *Synlett* **1992**, 1002.
[12] For more recent discussions on the intermediacy of pentavalent silicon cations (siliranium ions or siloniacyclopropanes; these species have been mistakenly referred to as "siliconium ions") see: T. Drewello, P. C. Burgers, W. Zummack, Y. Apeloig, H. Schwarz, *Organometallics* **1990**, *9*, 1161; J. B. Lambert, *Tetrahedron* **1990**, *46*, 2677; J. B. Lambert, E. C. Chelius, *J. Am. Chem. Soc.* **1990**, *112*, 8120.
[13] T. K. Sarkar, *Synthesis* **1990**, 969, 1101.
[14] G. Hagen, H. Mayr, *J. Am. Chem. Soc.* **1991**, *113*, 4954.
[15] X-ray analysis of **5c**: $C_{30}H_{34}OSi$, triclinic, space group, $P\bar{1}$, $a = 1044.1(5)$, $b = 1195.6(6)$, $c = 1206.9(6)$ pm, $\alpha = 88.27(3)$, $\beta = 65.14(2)$, $\gamma = 69.55(3)°$, $V = 1269 \cdot 10^6$ pm^3, $Z = 2$, $\rho_{calcd} = 1.15$ g cm^{-3}, $\mu = 0.77$ cm^{-1}; $Mo_{K\alpha}$ radiation (graphite monochromator); 2θ range: 3–56°; 5069 independent reflections, 3186 observed ($I > 2\sigma(I)$), $R = 0.053$, $R_w = 0.050$. Further details of the crystal structure investigation may be obtained from the Fachinformationszentrum Karlsruhe, Gesellschaft für wissenschaftlich-technische Information mbH, D-76344 Eggenstein-Leopoldshafen, on quoting the depository number CSD-57205, the names of the authors, and the journal citation.
[16] I. Fleming, R. Henning, H. Plaut, *J. Chem. Soc. Chem. Commun.* **1984**, 29; I. Fleming, *Pure Appl. Chem.* **1990**, *62*, 1879.

Structure and Reactivity of a Highly Twisted Amide**

By *Shinji Yamada**

The preparation and unusual properties of twisted amides have received considerable attention,[1] and a number of such compounds have been synthesized.[2] However, no amides have been reported that have twist angles[2a] about the C(O)–N bonds larger than about 40°. Recently we found

[*] Dr. S. Yamada
Department of Materials Science
Faculty of Science, Kanagawa University
Hiratsuka, Kanagawa 259-12 (Japan)
Telefax: Int. code +(81) 463-58-9684

[**] The author thanks Noriko Kasuga at Kanagawa University for her helpful suggestions about X-ray crystallography.

that 3-pivaloyl-1,3-thiazolidine-2-thione (**1a**), which contains an amide unit, is extremely reactive, and reacts with alcohols to give the corresponding pivalates even at pH $\approx$ 7.[3] These observations prompted us to investigate the relationship between the structure and the reactivities of **1a**. We now report that the C(O)–N bond of **1a** is extremely twisted and that the reactivity is, surprisingly, greater than its analogues **1b–d**.

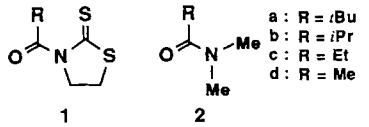

The compounds **1** were synthesized according to the reported method.[4] The rate constants of the reactions of **1a–d** with ethanol[5] at 75 °C were measured at pH $\approx$ 7 to elucidate their reactivities. Although **1a** has the largest substituent group R at the carbon atom of the carbonyl group, the rate constant was 100–1000 greater than those of the other compounds.

Table 1 gives the IR and UV spectral data of **1a–d**, and the ^{13}C NMR chemical shifts of **1** and **2**. The absorption band

Table 1. IR and UV spectroscopic data of **1a–d** and ^{13}C NMR spectroscopic data [a] of **1** and **2**.

	$\tilde{\nu}$(C=O) [cm^{-1}]	λ_{max} [b] [nm]	ε	δ (^{13}C = O)		$\Delta\delta$(^{13}C=O)
1a (**2a**)	1726 [c]	280	8750	187.8	(177.5)	10.3
1b (**2b**)	1701 [d]	309	10870	178.7	(177.0)	1.7
1c (**2c**)	1702 [d]	306	11730	175.6	(173.8)	1.8
1d (**2d**)	1697 [c]	306	11950	171.3	(170.6)	0.7

[a] 400 MHz in $CDCl_3$. [b] In $CHCl_3$. [c] KBr disc. [d] Neat liquid.

of the carbonyl group of **1a** in the IR spectrum appears at 1726 cm^{-1}, those of **1b–d** lie in the range 1697–1702 cm^{-1}. In the UV spectra, the λ value of the longest wavelength band of **1a** is significantly different from those of compounds **1b–d**; however, it is almost identical with that of thiazolidine-2-thione[6] which is the framework structure of the amides. In addition, the absorption coefficient of **1a** is much smaller than those of the compounds **1b–d**. A similar tendency is also seen for the chemical shifts in the ^{13}C NMR spectra. The $\Delta\delta^{13}C$ values listed in Table 1 correspond to the difference in the $\delta(^{13}C)$ value of δ(CO) of the compounds **1** and δ(CO) of the corresponding dimethyl amides. From these results, it is clear that the $\Delta\delta^{13}C$ value of **1a** is higher than those of the other compounds. These results suggest that the C(O)–N bond in the amide **1a** is significantly more twisted than those of the other compounds.

The structural distinction between **1a** and **1b–d** was confirmed by X-ray crystallographic analysis of **1a** and **1d**.[7] The ORTEP representations of **1a** and **1d** are shown in Figure 1, and a projection of the amide groups down the C–N bond of the two thiones is given in Figure 2. As expected, a remarkable difference between **1a** and **1d** exists with respect to their C(O)–N bond. Thus, the twist angle τ[8] of **1d** is 20.1 °, whereas that of **1a** is 74.3 °, which is the highest τ value known to date. Furthermore, the C(O)–N bond length of **1a** is longer than that of **1d** (1.448 Å and 1.413 Å,

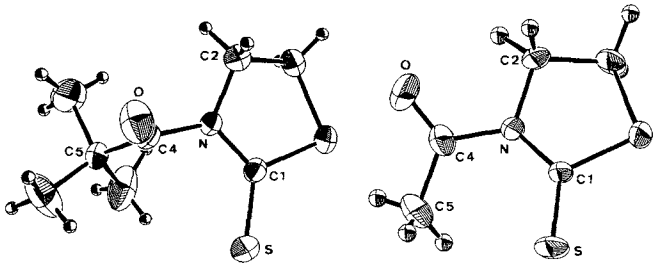

Fig. 1. The molecular structures of **1a** (left) and **1d** (right) (thermal ellipsoids draw at the 35% and 50% probability level, respectively). Selected bond lengths [Å], bond angles [°], and torsion angles [°]: **1a**: O-C4 1.196(4), N-C1 1.351(4), N-C2 1.469(5), N-C4 1.448(4), C4-C5 1.524(5); O-C4-N 117.9(4), O-C4-C5 123.7(4), N-C4-C5 117.8(3), C1-N-C2 114.9(3), C1-N-C4 119.9(3), C2-N-C4 118.8(3); O-C4-N-C1 95.1(4), O-C4-N-C2 −55.4(5), C1-N-C4-C5 −93.2(4), C2-N-C4-C5 116.3(4). **1d**: O-C4 1.21(1), N-C1 1.380(8), N-C2 1.474(8), N-C4 1.413(9), C4-C5 1.50(1); O-C4-N 117.4(6), O-C4-C5 122.6(7), N-C4-C5 119.8(7), C1-N-C2 115.3(5), C1-N-C4 126.9(5), C2-N-C4 116.9(5); O-C4-N-C1 156.1(7), O-C4-N-C2 −12(1), C1-N-C4-C5 −28(1), C2-N-C4-C5 163.7(8).

respectively). As a result, the 1,3-thiazolidine-2-thione ring and the carbonyl group of **1a** are nearly orthogonal, while those of **1d** are nearly planar.

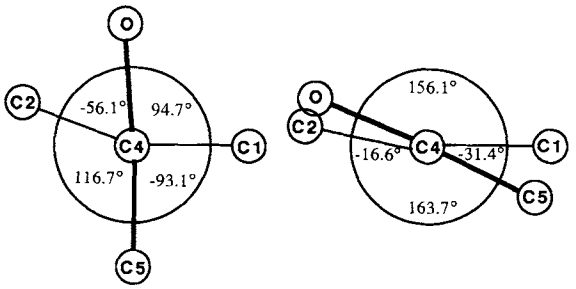

Fig. 2. Projection of the amide groups of **1a** (left) and **1d** (right), down the C–N bond.

From these results, it is apparent that the high reactivity of **1a** is attributed to the significant torsional strain of the C(O)–N bond which seems to arise from the steric repulsion between the bulky *tert*-butyl group and the thione group. Thus, the large rotation about the C(O)–N bond hinders the delocalization of the electrons in the amide unit, and thus causes an increase in the electrophilicity of the carbonyl group and the lengthening of the C(O)–N bond. Consequently, the amide **1a** is the most reactive toward alcohols even at pH $\approx$ 7.

Received: January 16, 1993 [Z 5811 IE]
German version: *Angew. Chem.* **1993**, *105*, 1128

[1] Reviews: a) H. K. Hall, Jr., A. El-Shekeil, *Chem. Rev.* **1983**, *83*, 549; b) A. Greenberg, in *Molecular Structure and Energetics. Vol. 7* (Eds.: J. F. Liebman, A. Greenberg), VCH, New York, **1988**, pp. 139–178.

[2] a) F. K. Winkler, J. D. Dunitz, *J. Mol. Biol.* **1971**, *59*, 169; b) A. H.-J. Wang, I. C. Paul, *J. Chem. Soc. Chem. Commun.* **1972**, 43; c) G. M. Blackburn, J. D. Plackett, *J. Chem. Soc. Perkin Trans. 2* **1972**, 1366; d) M. Tichy, E. Duskova, K. Blaha, *Tetrahedron Lett.* **1974**, 237; e) D. N. J. White, M. H. P. Guy, *J. Chem. Soc. Chem. Commun.* **1975**, 43; f) S. E. Ealick, D. van der Helm, *Acta Crystallogr. Sect. B*, **1975**, *31*, 2676; g) H. K. Hall, Jr., R. G. Shaw, Jr., A. J. Deutschmann, *J. Org. Chem.* **1980**, *45*, 3722; h) V. Somayaji, R. S. Brown, *ibid.* **1986**, *51*, 2676; i) R. M. Williams, B. H. Lee, *J. Am. Chem. Soc.* **1986**, *108*, 6431; j) K. J. Shea, T. G. Lease, J. W. Ziller, *ibid.* **1990**, *112*, 8627; k) Q.-P. Wang, A. J. Bennet, R. S. Brown, B. D. Santarsiero, *ibid.* **1991**, *113*, 5757.

[3] S. Yamada, *Tetrahedron Lett.* **1992**, *33*, 2171.

[4] T. Izawa, T. Mukaiyama, *Bull. Chem. Soc. Jpn.* **1979**, *53*, 555; S. Yamada, *J. Org. Chem.* **1992**, *57*, 1591.

[5] Pseudo-first-order rate constants k [min^{-1}] were determined by using a large excess of ethanol at 75 °C. k (**1a**) $= 1.54 \times 10^{-2}$, k (**1b**) $= 1.06 \times 10^{-4}$, k (**1c**) $= 4.77 \times 10^{-5}$, k (**1d**) $= 1.83 \times 10^{-4}$.

[6] The longest wavelength absorption band of thiazolidine-2-thione appears at 280 nm, and the absorption coefficient is 13200.

[7] Crystal data for **1a** at 296K: $C_8H_{13}NOS_2$, $M = 203.32$, monoclinic, space group $C2/c$, $a = 33.524(3)$, $b = 6.258(2)$, $c = 10.459(3)$ Å, $\beta = 106.71(1)°$, $V = 2101.5(9)$ Å^3, $Z = 4$, $\rho_{calcd} = 0.642$ g cm^{-3}. Anisotropic refinement of all non-hydrogen atoms using 1271 reflections with $I > 3\sigma(I)$, from 1725 unique data collected, gave $R = 0.048$ and $Rw = 0.064$. Crystal data for **1d** at 296K: $C_5H_7NOS_2$, $M = 161.24$, monoclinic, space group $P2_1/n$, $a = 7.3517(8)$, $b = 13.9516(6)$, $c = 7.3806(6)$ Å, $\beta = 104.320(7)°$, $V = 733.5(1)$ Å^3, $Z = 4$, $\rho_{calcd} = 1.406$ g cm^{-3}. Anisotropic refinement of all non-hydrogen atoms using 996 reflections with $I > 3\sigma(I)$, from 1154 unique data collected, gave $R = 0.083$ and $Rw = 0.119$. Further details of the crystal structure investigation are available on request from the Director of the Cambridge Crystallographic Data Centre, 12 Union Road, GB-Cambridge CB2 1EZ(UK), on quoting the full journal citation.

[8] Twist angle τ is defined by F. K. Winkler and J. D. Dunitz (see ref. [2a]) as follows: $\tau = 1/2\,(\omega_1 + \omega_2)$, where ω_1 and ω_2 are torsion angles O-C4-N-C1 and C2-N-C4-C5, respectively. According to their definition, the value of the twist angle τ lies in the range $-180°$ to $180°$. However, the larger the distortion, the nearer the value lies to $90°$ or $-90°$, on the other hand, the smaller the distortion, the nearer the value lies to 0°, 180°, or $-180°$. Therefore, in order to avoid confusion about the magnitude of τ, we represented twist angle as $|\tau|$ (for $0 \leq |\tau| \leq 90°$) or $|180 - |\tau||$ (for $90° \leq |\tau|$).

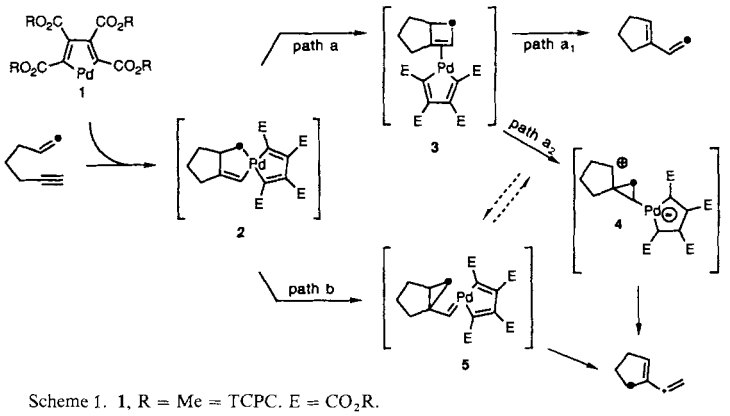

Scheme 1. **1**, R = Me = TCPC. E = CO_2R.

On the Mechanism of the TCPC^{HFB}-Catalyzed Metathesis of 1,6-Enyne: Evidence for Alkylidenepalladium Intermediates**

By *Barry M. Trost** and *A. Stephen K. Hashmi*

Pd^{IV} chemistry is emerging as an exciting new dimension to the organic chemistry of Pd.[1, 2] Pd^{IV} intermediates, for example **2**, are implicated in the metathesis of 1,6- and 1,7-enynes. These reactions are catalyzed by the esters of palladacyclopentadienetetracarboxylic acid (tetrakis(hydroxycarbonyl)palladacyclopentadiene, methyl ester = TCPC) **1**.[3] Labeling studies suggested two paths by which the reaction with terminal acetylenes could proceed, but only one path for the reaction with disubstituted acetylenes (Scheme 1).[4] To account for the labeling patterns, we suggested the intermediacy of the cyclobutene **3** and either cyclopropyl complex **4** or **5** in which we favored **4**. Recent work in which cyclobutenes have now been isolated in good yields validates path a.[5] Studies of the effects of substituents on the metathesis led to a new type of product whose structure strongly implicates the cyclopropylalkylidene complex **5** as a reactive intermediate (in contrast to our earlier preference). This intermediate then undergoes a most unusual further cycloaddition.

Since an ester group on the terminal acetylenic carbon atom promotes the "normal" metathesis,[3] we explored the effect of a nonpolarized sp^2 substituent, a vinyl group (as in **6**). Heating enyne **6** with 5% TCPC^{HFB} (**1**, R = $CH_2C_3F_7$)[3b] and 5% tri-*o*-tolyl phosphite (TOTPO) in the presence of dimethyl acetylenedicarboxylate (DMAD) produced the expected [2+2+2] adduct[3a] from the trapping of the palladacyclopentene (cf. **2**) and a structurally homogenous dimer, which became the exclusive product in the absence of DMAD in 70% yield (Scheme 2). With as little as

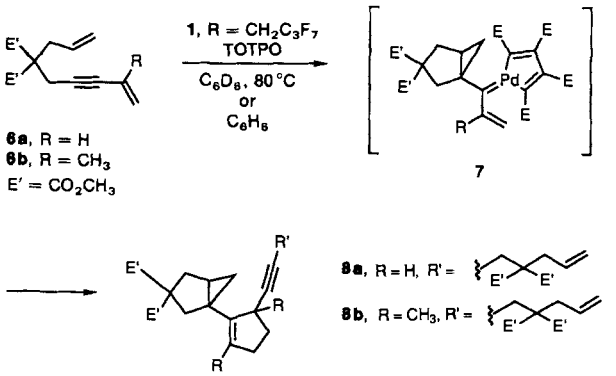

Scheme 2. TOTPO: see text.

0.1 mol% TCPC^{HFB} the yield of dimer was 87%. Since the reactions proceed as well with or without phosphite, in most cases, the phosphite was not added. Extensive ^1H and ^{13}C NMR spectroscopic investigations (see Table 1) (including DEPT, HOM2DJ, COSY, NOESY, and HETCOR), mass spectrometry, and combustion analysis clearly establish **8a**[6] as the structure of the dimer. The methylated starting material **6b** gave a 66% yield of the corresponding dimer **8b**.[6] In both cases, only a single stereoisomer was detected.

We rationalized the formation of the dimer as the trapping of a vinylalkylidene complex **7**[7] with the olefin of the starting enyne, and attempted to intercept this proposed intermediate with strained olefins (e.g. norbornene or norbornadiene), activated olefins (e.g. styrene, methyl acrylate, butoxyethene), and an isolated acetylene (5-decyne) unfortunately without success. In contrast the addition of 2.5 equivalents of 1-nonen-2-yne gave a 65% yield of the cross adduct **10a**[6] in addition to 24% of the homo dimer **8a** (Scheme 3). Strikingly, the addition of as little as one equivalent of methyl (*E*)-2,4-pentadienoate (**11**) led to complete trapping with the formation of the adduct **10b**[6] in 80–86% yield. The adduct from enyne **9** and dienoate **11**, namely **10c**,[6] obtained in 90% yield allows the assignment of all ^1H NMR signals. Examination of all NOEs of nonvicinal hydrogen atoms for **10c** combined with the coupling constants allows assignment of the configuration as depicted in Scheme 3. The formation of such products is best interpreted

[*] Prof. Dr. B. M. Trost, Dr. A. S. K. Hashmi
Department of Chemistry, Stanford University
Stanford, CA 94305-5080 (USA)

[**] We thank the National Science Foundation and the National Institutes of Health, General Medical Sciences, for their generous support of our programs. We are grateful to the Deutsche Forschungsgemeinschaft for fellowship support for A.S.K.H. Mass spectra were generously provided by the University of California-San Francisco Mass Spectrometry Center sponsored by the NIH Division of Research Resources.—TCPC^{HFB} = palladacyclopentadienetetracarboxylic acid (heptafluorobutyl ester).

Table 1. IR and NMR spectroscopic data of **8a, b** and **10a–c**.

8a: IR (neat, NaCl): $\tilde{\nu}$ = 3004, 2955, 2849, 1739, 1733, 1642, 1436, 1325, 1290, 1251, 1218, 1204, 1178, 1097, 1071, 966, 921, 816, 791, 735 cm^{-1}; ^1H NMR (300 MHz, $CDCl_3$): δ = 5.60 (ddt, J = 17.0 Hz, 10.0 Hz, 7.5 Hz, 1 H), 5.48 (m, 1 H), 5.12 (ddm, J = 17.0 Hz, 2.1 Hz, 1 H), 5.09 (ddm, J = 10.0 Hz, 2.1 Hz, 1 H), 3.71 (s, 3 H), 3.70 (s, 3 H), 3.70 (s, 3 H), 3.67 (s, 3 H), 3.13 (br m, 1 H), 2.74 (m, 2 H), 2.71 (m, 1 H), 2.67 (m, 1 H), 2.63 (dd, J = 13.7, 1.4 Hz, 1 H), 2.57 (d, J = 13.7 Hz, 1 H), 2.55 (m, 1 H), 2.49 (dd, J = 13.7 Hz, 4.9 Hz, 1 H), 2.33–2.45 (m, 1 H), 2.21–2.27 (m, 1 H), 2.03–2.18 (m, 1 H), 1.85 (m, 2 H), 0.80 (ddm (W coupling involved), 1 H), 0.36 (dd, J = 5.8 Hz, 4.6 Hz, 1 H); ^{13}C NMR (75 MHz, $CDCl_3$): δ = 173.6, 172.6, 170.7(2), 145.0, 132.2, 125.1, 119.7, 85.9, 75.4, 58.6, 57.2, 52.9, 52.7, 52.5(2), 39.3, 36.5, 36.2, 36.0, 33.2, 30.8, 29.2, 23.5, 23.0, 15.5.

8b: IR (neat, NaCl): $\tilde{\nu}$ = 2955, 2929, 2843, 1737, 1436, 1290, 1250, 1217, 1202, 1177, 1143, 1092, 1071, 925 cm^{-1}; ^1H NMR (400 MHz, $CDCl_3$): δ = 5.62 (ddt, J = 17.0 Hz, 10.0 Hz, 7.5 Hz, 1 H), 5.08–5.15 (m, 2 H), 3.74 (s, 3 H), 3.72 (s, 3 H), 3.71 (s,3 H), 3.69 (s, 3 H), 2.65–2.75 (m, 8 H), 2.41 (dd, J = 13.7 Hz, 1.5 Hz, 1 H), 2.26–2.37 (m, 1 H), 2.09–2.16 (m, 1 H), 1.99–2.07 (m, 1 H), 1.70 (s, 1 H), 1.36–1.42 (m, 1 H), 1.31 (s, 3 H), 0.98 (m, 1 H), 0.27 (dd, J = 5.6 Hz, 4.3 Hz, 1 H); ^{13}C NMR (75 MHz, $CDCl_3$): δ = 173.8, 172.7, 170.8(2), 139.6, 137.6, 132.3, 119.6, 90.7, 74.5, 59.4, 57.3, 52.8, 52.7, 52.4(2), 45.6, 42.2, 41.4, 36.5, 36.2, 35.2, 27.2, 25.9, 23.8, 22.9, 14.7, 12.8.

10a: IR (neat, NaCl): $\tilde{\nu}$ = 2955, 2933, 2858, 1737, 1455, 1435, 1315, 1288, 1249, 1203, 1174, 1114, 1098, 1070 cm^{-1}; 1H NMR (400 MHz, $CDCl_3$): δ = 5.52 (m, 1 H), 3.73 (s, 3 H), 3.70 (s, 3 H), 3.21 (m, 1 H), 2.62–2.78 (m, 4 H), 2.52 (dd, J = 13.7 Hz, 4.9 Hz, 1 H), 2.41 (m, 1 H), 2.21 (m, 2 H), 2.14 (td, J = 7.0 Hz, 2.4 Hz, 2 H), 1.98 (m, 1 H), 1.88 (m, 1 H), 1.47 (m, 2 H), 1.33 (m, 3 H), 0.90 (m, 4 H), 0.38 (dd, J = 5.8 Hz, 4.7 Hz, 1 H); ^{13}C NMR (75 MHz, $CDCl_3$): δ = 173.7, 172.7, 145.2, 125.0, 82.3, 81.5, 58.5, 52.8, 52.7, 39.4, 36.3, 36.1, 33.0, 30.9, 30.8, 29.3, 28.4, 23.5, 22.0, 18.6, 15.3, 13.8.

10b: IR (neat, NaCl): $\tilde{\nu}$ = 3004, 2954, 2849, 1739, 1651, 1435, 1347, 1315, 1249, 1203, 1174, 1152, 1098, 1071, 1045, 1018, 985, 732 cm^{-1}; ^1H NMR (300 MHz, $CDCl_3$): δ = 6.86 (dd, J = 15.6 Hz, 9.2 Hz, 1 H), 5.80 (d, J = 15.6 Hz, 1 H), 5.57 (m, 1 H) 3.74 (s, 3 H), 3.72 (s, 3 H), 3.70 (s, 3 H), 3.23 (br m, 1 H), 2.71 (d, J = 13.5 Hz, 1 H), 2.09–2.57 (m, 6 H), 1.70–1.78 (m, 1 H), 1.47–1.53 (m, 1 H), 0.67–0.72 (m, 1 H), 0.37 (dd, J = 5.7 Hz, 4.4 HZ, 1 H); ^{13}C NMR (75 MHz, $CDCl_3$): δ = 173.4, 172.5, 167.4, 152.3, 146.0, 126.3, 119.9, 58.7, 52.8, 52.7, 51.3, 48.6, 39.3, 35.9, 31.3, 30.6, 29.2, 23.6, 16.0.

10c: IR (neat, NaCl): $\tilde{\nu}$ = 3003, 2954, 2927, 2867, 1733, 1651, 1453, 1435, 1346, 1314, 1249, 1203, 1171, 1130, 1098, 1071, 1041, 994, 854 cm^{-1}; ^1H NMR (400 MHz, $CDCl_3$): δ = 6.86 (dd, J = 15.6 Hz, 9.1 Hz, 1 H), 5.77 (dd, J = 15.6 Hz, 0.9 H, 1 H), 5.46 (dd, J = 1.9 Hz, 1.2 Hz, 1 H), 3.73 (s, 3 H), 3.72 (s, 3 H), 3.70 (s, 3 H), 3.24 (m, 1 H), 2.81 (ddqdd, J = 7.7 Hz, 7.3 Hz, 6.9 Hz, 1.9 Hz, 1.8 Hz, 1 H), 2.71 (d, J = 13.6 Hz, 1 H), 2.58 (d, J = 13.6 Hz, 1 H), 2.56 (dd, J = 13.5 Hz, 1.5 Hz, 1 H), 2.45 (ddm, J = 13.7 Hz, 5.0 Hz, 1 H), 1.92 (ddd, J = 12.8 Hz, 10.1 Hz, 7.3 Hz, 1 H), 1.65 (ddd, J = 12.8 Hz, 8.6 Hz, 7.7 Hz, 1 H), 1.49 (ddd, J = 8.4 Hz, 5.0 Hz, 4.4 Hz, 1 H), 1.00 (d, J = 6.9 Hz, 3H), 0.71 (dddd, J = 8.4 Hz, 5.9 Hz, 1.3 Hz, 1.2 Hz, 1 H), 0.37 (dd, J = 5.9 Hz, 4.4 Hz, 1 Hz); ^{13}C NMR (75 MHz, $CDCl_3$): δ = 173.4, 172.5, 167.4, 152.4, 145.1, 132.3, 119.8, 58.6, 52.9, 52.7, 51.3, 48.4, 40.3, 39.2, 37.8, 35.8, 29.0, 23.8, 20.4, 15.9.

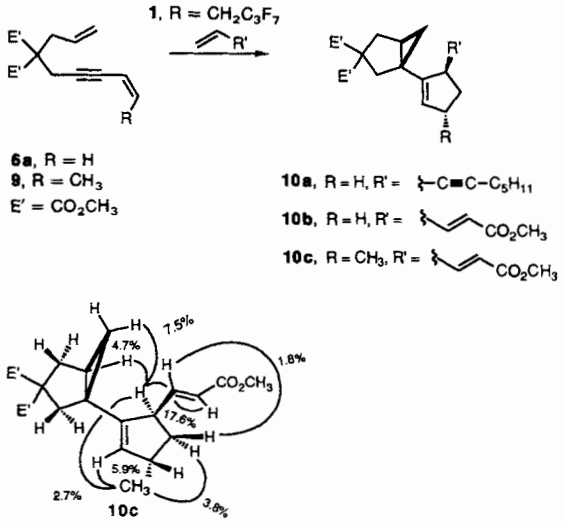

Scheme 3. Synthesis of **10a–c** and NOE effects for **10c** (below).

as arising from intermediates like **7** (Scheme 2). Such an intermediate might be expected to undergo cyclopropanation[8, 9] (Scheme 4, path a) rather than cyclopentannelation via the palladacyclohexene **15** (Scheme 4, path b). However, a vinylcyclopropane–cyclopentene rearrangement of **12** may produce two cyclopentenes **13** and **14**, in which the latter would be anticipated to dominate.[10] On the other hand, a [4+2] cycloaddition of a palladacyclopentadiene followed by reductive elimination nicely accounts for our observations. While such a cycloaddition appears unprecedented,[11] the failure to detect vinylcyclopropanes, the failure to trap **7** with nonconjugated olefins of any kind, and the regioselectivity of the reaction favor path b (Scheme 4). The unusual

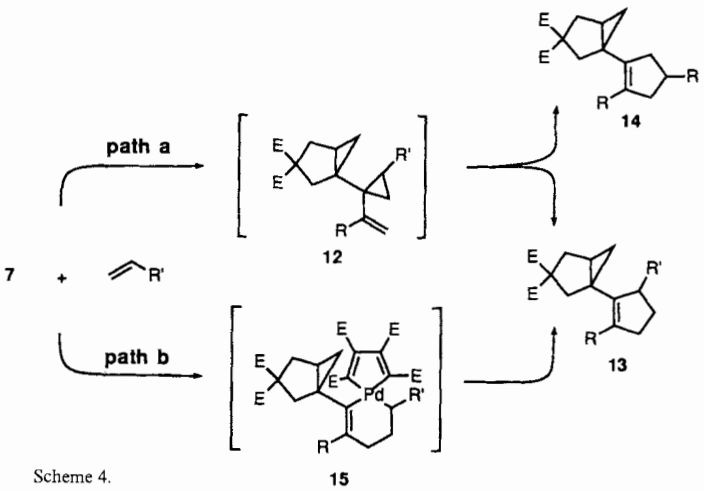

Scheme 4.

structural features required in the trapping agents may be a combination of both electronic and coordinating effects necessary for the metalla-Diels–Alder reaction. Further studies are necessary to understand these requirements. Thus, this transformation involves two novel steps—a metallacyclopentene–metallavinylcyclopropane (cyclopropylalkylidene metal complex[12]) rearrangement and a [4+2] cycloaddition of metalladienes (vinylidene metal complex). These processes appear to be facilitated by Pd^{IV} intermediates, and they support path b of Scheme 1 as the likely major pathway for the metathesis of the terminal acetylenes. The introduction of a vinyl group on the alkylidene carbon atom stabilizes the intermediate and diverts the initial cyclopentene via path b (Scheme 1), whereas an acetylenic ester promotes reductive elimination by path a (Scheme 1). This new process appears to be widely applicable in synthesis.

Received: February 2, 1993 [Z 5847 IE]
German version: *Angew. Chem.* **1993**, *105*, 1130

[1] Reviews: A. J. Canty, *Acc. Chem. Res.* **1992**, *25*, 83; *Platinum Met. Rev.* **1993**, *37*, 2.

[2] For a review of some of our work implicating such species, see B. M. Trost, *Acc. Chem. Res.* **1990**, *23*, 34. See also B. M. Trost, S. Matsubara, J. J. Caringi, *J. Am. Chem. Soc.* **1989**, *111*, 8745; B. M. Trost, C. Chan, G. Rühter, *ibid.* **1987**, *109*, 3486. A reversible slippage of the TCPC unit in **2** to a cyclobutadienylpalladium(II) unit cannot be unambiguously ruled out but appears less likely. Cf.: K. Moseley, P. M. Maitlis, *J. Chem. Soc. Dalton Trans.* **1974**, 169.

[3] a) B. M. Trost, G. J. Tanoury, *J. Am. Chem. Soc.* **1987**, *109*, 4753; b) B. M. Trost, M. K. Trost, *ibid.* **1991**, *113*, 1850; c) *Tetrahedron Lett.* **1991**, *32*, 3647.

[4] B. M. Trost, G. J. Tanoury, *J. Am. Chem. Soc.* **1988**, *110*, 1636.

[5] B. M. Trost, M. Yanai, unpublished results.

[6] This compound has been fully characterized spectrally, and the elemental composition has been established by high-resolution mass spectrometry and/or combustion analysis.
[7] The valence isomer of **7**, a metallacyclobutene, may also be considered as an intermediate, but does not account for the products as straightforwardly as the carbene complex.
[8] For Pd-catalyzed cyclopropanation, see: a) K. Shimamoto, M. Ishida, H. Shinozaki, Y. Ohfune, *J. Org. Chem.* **1991**, *56*, 4167; b) Y. V. Tomilov, A. B. Kostitsyn, E. V. Shulishov, O. M. Nefedov, *Synthesis* **1990**, 246; T. R. Hoye, C. J. Dinsmore, D. S. Johnson, P. F. Korkowski, *J. Org. Chem.* **1990**, *55*, 4518, M. W. Majchrzak, A. Kotelko, J. B. Lambert, *Synthesis* **1983**, 469; M. Suda, *ibid.* **1981**, 714; A. J. Anciaux, A. J. Hubert, A. F. Noels, N. Petiniot, P. Teyssié, *J. Org. Chem.* **1980**, *45*, 695; A. Nakamura, T. Koyama, S. Otsuka, *Bull. Chem. Soc. Jpn.* **1978**, *51*, 593; S. Bien, Y. Segal, *J. Org. Chem.* **1977**, *42*, 1685.
[9] For other metals see: a) M. Buchert, H. U. Reissig, *Chem. Ber.* **1992**, *125*, 2723; b) D. F. Harvey, K. P. Lund, *J. Am. Chem. Soc.* **1991**, *113*, 5066; c) H. Fischer, J. Hofmann, *Chem. Ber.* **1991**, *124*, 981; d) D. F. Harvey, K. P. Lund, *J. Am. Chem. Soc.* **1991**, *113*, 8916; e) J. W. Herndon, S. U. Tumer, *J. Org. Chem.* **1991**, *56*, 286; f) W. D. Wulff, D. C. Yang, C. K. Murray, *J. Am. Chem. Soc.* **1988**, *110*, 2653.
[10] T. Hudlicky, T. M. Kutchan, S. M. Naqvi, *Org. React.* **1985**, *33*, 247; H.-U. Reissig, in *The Chemistry of the Cyclopropyl Group* (Eds.: S. Patai, Z. Rappoport, Wiley, Chichester, **1987**, pp. 375–443; J. Salaün, *ibid.* pp. 809–878.
[11] Vinylalkylidene metal complexes are reported to serve as dienophiles in [4+2] cycloadditions and not as the diene unit. For an excellent leading reference to this type of behavior, see W. D. Wulff, W. E. Bauta, R. W. Kaesler, P. J. Lankford, R. A. Miller, C. K. Murray, D. C. Yang, *J. Am. Chem. Soc.* **1990**, *112*, 3642. While this report deals with Fischer-type carbene complexes, and there are notable effects of the alkoxy group and metal ligands on the behavior of the carbene complex, this type of complex is the only current analogy. Clearly, the contrasting behavior, if any, of less stabilized vinylalkylidene metal complexes is an exciting topic for future endeavors.
[12] For such complexes, see [9e] and J. W. Herndon, G. Chatterjee, P. P. Patel, J. U. Matasi, S. U. Tumer, J. J. Harp, M. D. Reid, *J. Am. Chem. Soc.* **1991**, *113*, 7808; J. W. Herndon, S. U. Tumer, W. F. K. Schnatter, *ibid.* **1988**, *110*, 3334.

Haematopodin, an Unusual Pyrroloquinoline Derivative Isolated from the Fungus *Mycena haematopus*, Agaricales**

By *Carsten Baumann, Martin Bröckelmann, Burkhard Fugmann, Bert Steffan, Wolfgang Steglich,** and *William S. Sheldrick*

Dedicated to Professor Meinhart H. Zenk on the occasion of his 60th birthday

Fruiting bodies of the toadstool *Mycena haematopus* (Pers. ex Fr.) Kummer, contain a red-brown sap which up until now has not been the subject of detailed chemical analysis. We have isolated a pigment from this fungus for which we propose the name haematopodin.

The fruiting bodies were placed in methanol immediately after collection and turned the solvent red-violet. The methanol was removed in vacuum leaving a red-brown, watery residue which was then subjected to chromatography on Sephadex LH-20, eluting with methanol. The haematopodin fraction can be distinguished from the red-violet main fraction as a slower moving rose-colored band. Every time the main fraction was rechromatographed, the haematopodin band reformed, allowing the isolation of the haematopodin in sufficient quantities for further investigations. Final purification by flash chromatography (silica gel, $CHCl_3$/CH_3OH 10/1) yielded pure haematopodin, which crystallized as a monohydrate from dichloromethane/methanol.[1]

The compound is optically active ($[\alpha]_D^{23}$ + 571, c = 0.14 in CH_3OH) and shows absorption maxima in the UV/VIS spectrum (measured in CH_3OH) at 208 (log ε 3.99), 242 (4.27), 344 (4.03), and 514 nm (2.95, broad absorption). The results of high-resolution EI mass spectroscopy indicate an empirical formula of $C_{13}H_{12}N_2O_3$, which was confirmed by the FAB^+ mass spectrum. An intense (M^+ + 2H) peak and the loss of CO from the molecular ion are indicative of the presence of an quinoid structural element.

The aliphatic region of the ^{1}H NMR spectrum (Table 1) shows signals corresponding to the structural elements $OCH_2CH_2CH_2N$ and $CH_2CH(N,O)$, singlets at δ = 5.37 and 7.12 characteristic of arene protons, and a broad NH signal at δ = 12.5. The analysis of the arene and carbonyl signals in the ^{1}H-coupled ^{13}C NMR spectrum (Table 1) indicates the presence of an indole-6,7-quinone chromophore. The fact that the singlet at δ = 180.28 exhibits no H,C coupling indicates that this signal is due to the 6-carbonyl group, whereas the signal due to the 7-carbonyl group at δ = 169.50 (in $CDCl_3$/CD_3OD (1/1)) is split into a doublet by spin–spin coupling with the proton at C-5 (^3J = 5.5 Hz). Selective decoupling experiments in [D_6]DMSO showed the proton at C-5 to have an additional ^3J coupling of 1.5 Hz with the indole-NH. COLOC experiments[2] allow the structural elements to be pieced together showing that haematopodin is identical with the structure 6,6a,9,10-tetrahydro-4*H*,8*H*-[1,3]oxazinol[3,2-*a*]pyrrolo[4,3,2-*de*]quinoline-2,3-dione (**1**).

Table 1. ^{1}H and ^{13}C Data for haematopodin (**1**) (400 and 100.6 MHz, respectively, in [D_6]DMSO, TMS).

^{1}H NMR [a]: δ = 1.53 (m, 9b-H), 1.91 (ddddd, 9α-H), 2.78 (dd, 6β-H), 3.10 (dd, 6α-H), 3.40 (ddd, 10β-H), 3.86 (ddd, 8β-H), 3.95 (m, 10α-H), 3.96 (m, 8α-H), 5.10 (dd, 6α-H), 5.37 (s, 1-H), 7.12 (s, 5-H), 12.5 (br. s, NH).

^{13}C NMR [b]: δ = 24.76 (t, J = 130 Hz, C-9), 26.13 (t, J = 132 Hz, C-6), 46.24 tm, J = 142 Hz, C-10), 67.58 (tm, J = 145, 7 Hz, C-8), 87.88 (dq, J = 161, 7 Hz, C-6a), 94.87 (d, J = 162 Hz, C-1), 114.06 (m, C-5a [c]), 123.11 (m, C-11b [c]), 124.64 (d, J = 8 Hz, C-3a), 124.88 (d, J = 188 Hz, C-5), 151.43 (br. s, C-11a), 169.50 (d [d], J = 5.5 Hz, C-3), 180.28 (s, C-2).

[a] J values [Hz]: $J_{6\alpha,6\beta}$ = 17 Hz, $J_{6\alpha,6a}$ = 6, $J_{6\beta,6a}$ = 3.5, $J_{8\alpha,8\beta}$ = 11.5, $J_{8\alpha,9a}$ = 5, $J_{8\beta,9a}$ = 12, $J_{9\beta,9\beta}$ = 2.5, $J_{9a,9\beta}$ = 13, $J_{9a,10\alpha}$ = 5, $J_{9a,10\beta}$ = 13.2, $J_{9\beta,10\beta}$ = 3.2, $J_{10\alpha,10\beta}$ = 13.5. [b] ^2J and ^3J relationships in 2D COLOC spectrum: C-3: 1-H; C-3a: 5-H; C-5: 6β-H; C-5a: 5-H, 6α-H, 6β-H; C-6a: 6β-H, 8α-H, 8β-H, 10α-H; C-8: 10α-H; C-9: 10α-H, 10β-H; C-11a: 10α-H, 10β-H; C-11b: 1-H, 5-H, 6β-H. [c] Signals could not be assigned unequivocally. [d] In $CDCl_3$/CD_3OD (1/1).

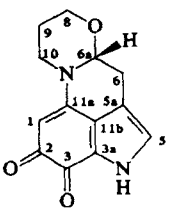

1

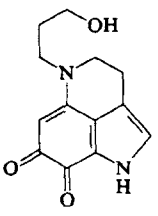

2

[*] Prof. Dr. W. Steglich, Dipl.-Chem. C. Baumann, Dr. M. Bröckelmann, Dr. B. Fugmann, Dr. B. Steffan
Institut für Organische Chemie der Universität
Karlstrasse 23, D-80333 München (FRG)
Telefax: Int. code +(89)5902-483
Prof. Dr. W. S. Sheldrick
Lehrstuhl für Analytische Chemie der Ruhr-Universität Bochum NC 4/72

[**] Pigments of Fungi, Part 62. This work was supported by the Bundesministerium für Wissenschaft und Technologie and by the Fonds der Chemischen Industrie. – Part 61: H. Besl, A. Bresinsky, G. Geigenmüller, R. Herrmann, C. Kilpert, W. Steglich, *Liebigs Ann. Chem.* **1989**, 803.

The structural formula of haematopodin (**1**) was confirmed by X-ray crystallography (Fig. 1).[3] The asymmetric unit (space group $P2_1$) was found to contain two molecules of water in addition to two independent molecules of haematopodin. The molecules of **1** are linked together by N–H···O(water) and O2···H–O(water) hydrogen bonds and in this manner form a 3-D structure. The results of the X-ray crystallographic studies indicate that both molecules of **1** have a 6a-(*R*) configuration.[3]

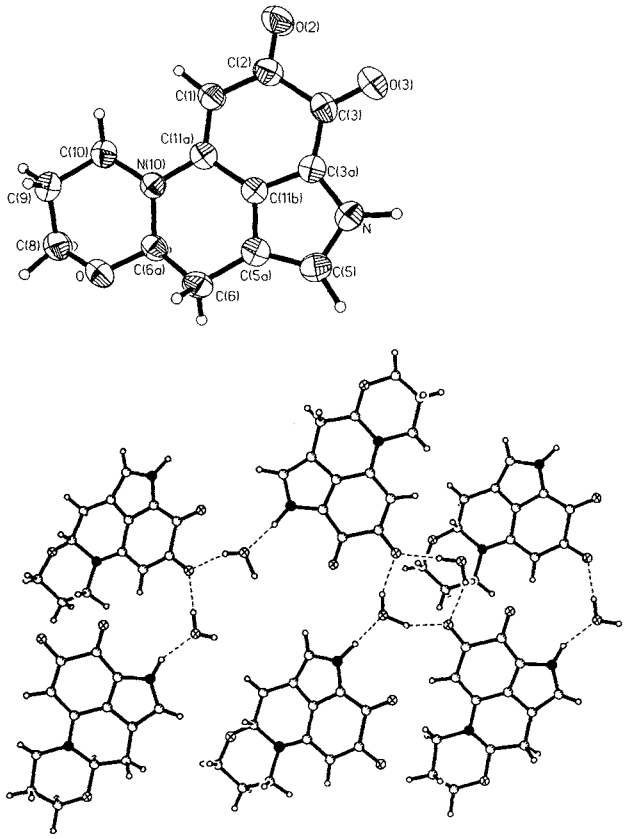

Fig. 1. Top: The structure of the first independent molecule of **1** in the unit cell (projection in accordance with IUPAC guidelines). Bottom: Linkage of the molecules of **1** by hydrogen bonds.

As mentioned in the introduction, haematopodin occurs, when at all, only in trace amounts in fresh fruiting bodies. It is formed by the breakdown of a very sensitive native pigment, which we have not yet been able to isolate in pure form.[4] For example, if a fungal extract is left in methanol in a sealed flask exposed to light for a few weeks, only haematopodin can be detected.

Related 1,3,4,5-tetrahydropyrrolo[4,3,2-*de*]quinoline pigments such as batzellins[5] and damirones[6] have been isolated from sea sponges. It is assumed that for these compounds the key step in the biosynthesis is the intramolecular cyclization of a tryptamine-6,7-quinone. In the case of haematopodin, the open chain compound **2** may be formed first which then undergoes oxidative cyclization to yield the oxazine derivative **1**.

A simple biomimetic synthesis along these lines starting from damirone B (**6**) and compound **2** is possible (Scheme 1, Table 2). The reaction sequence starts from the known compound 6,7-dibenzyloxyindolyl-3-glyoxylic acid chloride (**3**)[7] which in the case of **6** is converted to amide **4** by reaction with methylamine. After reduction to yield amine **5**, the

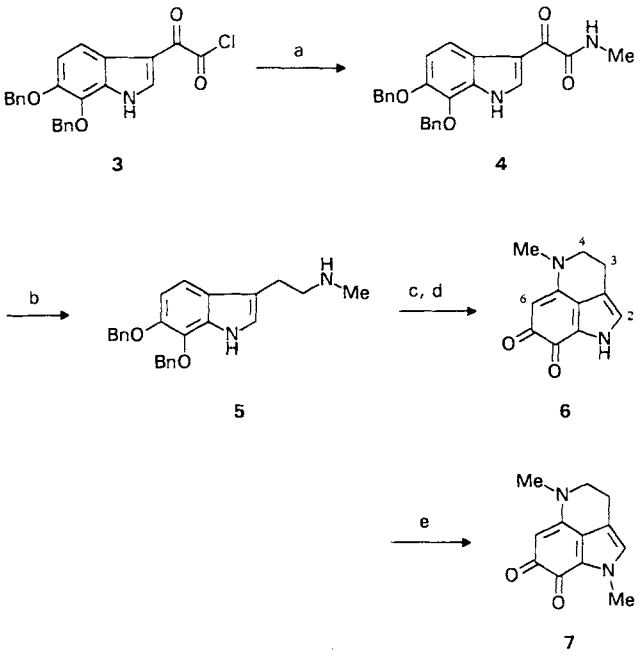

Scheme 1. Synthesis of damirone B (**6**) and damirone A (**7**). Reagents and reaction conditions: a) 1 equiv **3**, 2.0 equiv $MeNH_2 \times HCl$, 4.0 equiv Et_3N, CH_2Cl_2, room temperature (RT), 0.5 h (91%). b) 10 equiv $LiAlH_4$, THF, reflux, 4 h (51%). c) H_2, 10% Pd/$BaSO_4$, MeOH, RT, 1.5 h. d) O_2 from the air, Et_3N, MeOH, RT, 1 h (76%, 2 steps). e) 1.0 equiv **6**, 1 equiv K_2CO_3, 3 equiv CH_3I, EtOH, reflux, 1.5 h (89%).

benzyl protecting groups are removed by hydrogenolysis. The resulting dihydroxyindole derivative is stirred in methanol and triethylamine under air and cyclizes to provide damirone B (**6**). According to spectroscopic data, the synthetic product is identical to the naturally occurring compound.[6] Methylation with methyl iodide and addition of potassium carbonate yielded damirone A (**7**). In an

Table 2. Selected physical and spectroscopic data for compounds **4**–**7** and **2**.

4: Yellow crystals, m.p. 186 °C; ^{1}H NMR (400 MHz, [D$_6$]DMSO): δ = 2.75 (d, J = 4.8 Hz, 3H), 5.18 (s, 2H), 5.21 (s, 2H), 7.17 (d, J = 8.4 Hz, 1H), 7.31–7.52 (m, 10H), 7.87 (d, J = 8.4 Hz, 1H), 8.64 (s, 1H), 8.65 (q, J = 4.8 Hz, amide-NH); EI-MS (70 eV): m/z 414.1582 (15%, M^+), calcd. ($C_{25}H_{22}N_2O_4$) 414.1579.

5-oxalate: M.p. 156 °C; ^{1}H NMR (400 MHz, [D$_6$]DMSO): δ = 2.56 (s, 3H), 2.99 (t, J = 8.0 Hz, 2H), 3.15 (t, J = 8.0 Hz, 2H), 5.13 (s, 2H) 5.15 (s, 2H), 6.93 (d, J = 8.8 Hz, 1H), 7.12 (d, J = 2.5 Hz, 1H), 7.23 (d, J = 8.8 Hz, 1H), 7.32–7.53 (m, 10H), 10.87 (d, J = 2.5 Hz, indole-NH).

6: Dark violet crystals, m.p. 250 °C (decomp); R_f = 0.28 (silica gel, $CHCl_3$/CH_3OH 10/1); ^{1}H NMR (400 MHz, $CDCl_3$/[D$_6$]DMSO): δ = 2.92 (t, J = 6.8 Hz, 2H), 3.14 (s, 3H), 3.67 (t, J = 6.8 Hz, 2H), 4.00 (s, 1H, NH), 5.29 (s, 1H), 6.89 (s, 1H); ^{13}C NMR (100.6 MHz, $CDCl_3$/[D$_6$]DMSO): δ = 20.3, 38.2, 51.7, 92.9, 116.7, 124.3, 125.0, 125.3, 154.0, 170.9, 179.1.

7: Dark violet crystals, m.p. 240 °C (decomp); R_f = 0.38 (silica gel, $CHCl_3$/CH_3OH 15/1); ^{1}H NMR (400 MHz, $CDCL_3$/[D$_6$]DMSO): δ = 2.86 (t, J = 6.8 Hz, 2H), 3.09 (s, 3H), 3.61 (t, J = 6.8 Hz, 2H), 3.91 (s, 3H), 5.27 (s, 1H), 6.67 (s, 1H); ^{13}C NMR (100.6 MHz, $CDCl_3$/[D$_6$]DMSO): δ = 20.3, 36.0, 38.4, 51.9, 93.2, 115.9, 124.8, 125.0, 127.6, 154.5, 171.7, 179.4.

2: Dark violet crystals, m.p. 230 °C (decomp); R_f = 0.31 (silica gel, $CHCl_3$/CH_3OH 5/1); ^{1}H NMR (400 MHz, [D$_6$]DMSO): δ = 1.77 (quint. J = 6.8 Hz, 2H), 2.80 (t, J = 6.8 Hz, 2H), 3.45 (t, J = 6.8 Hz, 2H), 3.49(t, J = 6.8 Hz, 2H), 3.63 (t, J = 6.8 Hz, 2H), 4.63 (s, 1H, OH), 5.20 (s, 1H), 7.08 (s, 1H), 12.36 (s, 1H, indole-NH); ^{13}C NMR (100.6 MHz, [D$_6$]DMSO): δ = 19.7, 29.7, 47.5, 49.4, 58.0, 92.0, 116.4, 123.8, 124.5, 125.0, 152.6, 170.5, 178.4; IR (KBr): $\tilde{\nu}_{max}$ = 3423, 3117, 2934, 2866, 1670, 1608, 1587, 1543, 1432, 1417, 1323, 1241, 1078, 762, 745 cm^{-1}; EI-MS (70 eV): m/z 248 (68%, M^+ + 2H), 247 (44, M^+ + H), 246.1006 (42, M^+), calcd. ($C_{13}H_{14}N_2O_3$) 246.1004, 232 (26), 203 (100), 202 (88), 187(54), 174 (50), 146 (79); UV/VIS: λ_{max} (CH_3OH) = 207, 245, 349, 521 nm.

analogous manner the hypothetical precursor of haematopodin, **2**, was synthesized starting from acid chloride **3** and 3-aminopropanol. However, attempts to oxidatively cyclize this compound to yield **1** by using $Hg(OAc)_2$ or other reagents have not been successful up until now.

These syntheses demonstrate that 6,7-dihydroxytryptamine derivatives are easily converted by oxygen to pyrroloquinolines. Further studies on the chemistry of the *Mycena* pigments and the chemical synthesis of haematopodin are being carried out at the present time.

Received: March 13, 1993 [Z 5921 IE]
German version: *Angew. Chem.* **1993**, *105*, 1120

[1] $\mathbf{1} \times H_2O$: black crystals; $R_f = 0.61$ (silica gel, $CHCl_3/CH_3OH$ 10/1); CD (CH_3OH): $[\theta]_{256} = 0$, $[\theta]_{307} = +2.35 \times 10^3$, $[\theta]_{320} = 0$, $[\theta]_{350} = -6.30 \times 10^3$, $[\theta]_{395} = 0$, $[\theta]_{505} = +5.32 \times 10^3$, $[\theta]_{630} = 0$; IR (KBr): $\tilde{\nu}_{max} = 3440$ (sst), 3120, 3060, 2980, 2950, 2840, 2820 (all m), 1680 (sst), 1640 (w), 1590, 1560, 1520 (br), 1490, 1455 (all sst), 1420 (st), 1400, 1380, 1350 (all w), 1340 (sst), 1300 (m), 1290 (m), 1250 (st), 1180, 1150, 1120 (all m), 1060 (sst), 1090 (st), 1050 (st), 1000, 940, 910 (all w), 900 (m), 870 (m), 800 (w), 680 (w) cm^{-1}; EI-MS: (180 °C, DE): *m/z* 244.0850 (42%, M^+), calcd. ($C_{13}H_{12}N_2O_3$): 244.0848.

[2] H. Kessler, C. Griesinger, Z. Zarbock, H. R. Loosli, *J. Magn. Reson.* **1984**, *57*, 331.

[3] Crystal data for **1**: $C_{13}H_{12}N_2O_3 \times H_2O$, monoclinic, space group $P2_1$, $a = 8.030(2)$, $b = 11.603(4)$, $c = 12.751(2)$ Å, $\beta = 92.79(5)°$, $V = 1186.6(9)$ Å^3, $M = 262.3$, $Z = 4$, $\varrho_{calc} = 1.47$ g cm^{-3}; 4115 observed reflections (including Friedel pairs), Enraf-Nonius CAD4 diffractometer, $Cu_{K\alpha}$ radiation, ω adjustment, $2\theta_{max} = 140°$. After refinement $R = 0.054$ and $R_w = 0.053$. The factor as defined by Rogers was refined to 0.8(6) for the 6a-(*R*) configuration. Further details of the crystal structure investigation may be obtained from the Fachinformationszentrum Karlsruhe, Gesellschaft für wissenschaftlich-technische Information mbH, D-76344 Eggenstein-Leopoldshafen (FRG), on quoting the depository number CSD-57095, the names of the authors, and the journal citation.

[4] The UV/VIS spectrum of the raw extract corresponds in most respects to that of **1**, however, it is markedly bathochromically shifted in the long-wavelength region [λ_{max} (CH_3OH) = 242, 356, 530 nm].

[5] S. Sakemi, H. H. Sun, C. W. Jefford, G. Bernardinelli, *Tetrahedron Lett.* **1989**, *30*, 2517; synthesis of batzellin C: X. L. Tao, S. Nishiyama, S. Yamamura, *Chem. Lett.* **1991**, 1785.

[6] D. B. Stierle, D. J. Faulkner, *J. Nat. Prod.* **1991**, *54*, 1131.

[7] F. G. Lee, D. E. Dickson, J. Suzuki, A. Zirnis, A. A. Manian, *J. Heterocycl. Chem.* **1973**, *10*, 649.

Ylide-Substituted Thioxophosphanes and Dithioxophosphoranes**

By *Georg Jochem, Heinrich Nöth* and *Alfred Schmidpeter**

Chalcogenophosphanes RP=Y (Y = O, S, Se) are extremely reactive, and so far no compound of this type is known that is stable at room temperature.[1b, 2c, 3] Halothioxophosphanes **1** (R = F, Cl, Br) were detected and studied in the gas phase and in argon matrices.[1b] Other thioxophosphanes with R = Me, Et, *n*Bu, Ph, NMe_2, OCH_2CCl_3, OPh, for example, could be generated but were detected only indirectly as adducts and cycloadducts as well as coordinated to metal complexes fragments.[1b] Four (!) independent experiments for the preparation of thioxophosphane **1** with 2,4,6-tri-*tert*-butylphenyl as the substituent R are found in the literature. This substituent was used successfully for the kinetic stabilization of lower coordinated main group elements in many cases before. In the attempted synthesis of **1**, R = 2,4,6-tri-*tert*-butylphenyl, however, only the cyclic trimer **2** and products of disproportionation were found.[2] We have now succeeded in stabilizing thioxophosphanes with an ylide substituent R and isolating them as stable compounds.

1 **2**

Dichloro[organo(triphenylphosphonio)methanidyl]phosphanes **3**, R = Me, Et[4] react smoothly with sodium sulfide in THF to form the ylide-substituted thioxophosphanes **4a, b** which can be isolated as orange-red crystals (Scheme 1). The aryl derivatives **4c, d** are prepared in the same manner but are not stable in solution. Here the reaction does not proceed uniformly. The selenoxophosphanes RP=Se can be prepared analogously from **3** and Na_2Se.[5] Thioxophosphanes **4** were characterized unequivocally by their ^{31}P NMR spectra (Scheme 1), particularly by the low-field signal of the two-coordinate phosphorus. Here the ^{31}P

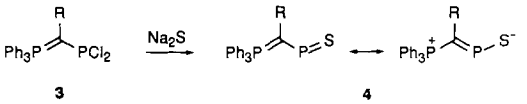

3 **4**

	R	$\delta^{31}PPh_3$	$\delta^{31}PS$	$^2J(P,P)$ in THF
4a	Me	28.9	485.0	116.0 Hz
4b	Et	27.9	488.2	116.0 Hz
4c	Ph	25.0	495.9	107.8 Hz
4d	3-MeC_6H_4	25.3	493.8	107.8 Hz

Scheme 1.

nucleus remains much more strongly shielded, though, than would be expected from extrapolation from $RP=SiR_2$ and $RP=PR$[1f, 6] to RP=S. In keeping with this, the signal of the ylide carbon atom of **4** (**4b**: $\delta^{13}C = 137.2$) is at lower field than those of other ylides, even α-acyl-substituted triphenylphosphonium ylides.[7] Both features point to a considerable contribution of the dipolar resonance formula, in which **4** is depicted as a phosphalkene. The relatively strong P–P coupling indicates that the sulfur atom and the phosphonio group are *trans* to each other[8] as is also found in the crystal structure (see below); the polarity of the solvent (benzene/THF) does not have a discernible influence on the coupling.

Thioxophosphanes **4** prove to be ambident nucleophiles. Compound **4b** reacts with benzyl bromide by S-alkylation forming **5b** (in THF: $\delta^{31}PPh_3 = 25.9$, $\delta^{31}PS = 245.1$, $^2J(P,P) = 173.9$ Hz[9]), but by P-oxidation with sulfur giving **6b**. The latter is also directly accessible from **3** and Na_2S_2 like other dithioxophosphoranes $Ph_3P=Cr-PS_2$ **6**.[10] Oxi-

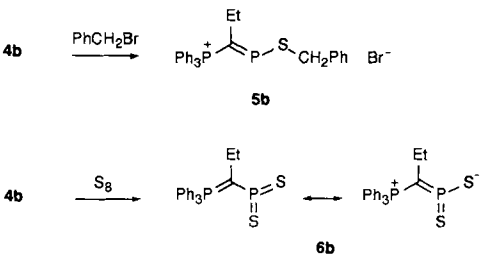

5b

6b

[*] Prof. Dr. A. Schmidpeter, Dipl.-Chem. G. Jochem, Prof. Dr. H. Nöth
Institut für Anorganische Chemie der Universität
Meiserstrasse 1, D-80333 München (FRG)
Telefax: Int. code + (89) 5902-578

[**] This work was supported by the Deutsche Forschungsgemeinschaft and the Fonds der Chemischen Industrie.

dation from **4** to **6** shifts not only the NMR signal of the affected phosphorus atom to higher field ($\Delta\delta^{31}P \approx -250$[10]) but also the NMR signals of the C and P atoms of the ylide substituent ($\Delta\delta^{13}C \approx -50$, $\Delta\delta^{31}P \approx -5$[10]). At the same time $^2J(P,P)$ decreases to less than half its original value.

That the thioxophosphanes **4** are monomeric and nucleophilic at sulfur seems a consequence of their polar nature, as reflected by the second resonance formula; the ^{31}P and ^{13}C NMR shifts are also compatible with this. The contribution of the dipolar resonance formula should be evident in a structure elucidation. The comparison of the structure of **4** to that of a dithioxophosphorane **6** must show, in addition, how the oxidation of the phosphorus affects its bond to the ylide group. Besides the ylide-substituted compounds **6**, three dithioxophosphoranes with bulky aryl substituents are known and their structures have been determined.[1e, 11] In these molecules the aryl and the CPS_2 planes are almost perpendicular to each other. Figure 1 and Table 1 show the results of the structure investigation[12] for single crystals of **4b** and **6c**. In both cases there are discrete molecules with no detectable intermolecular contacts between the S and/or P atoms.

As expected, the ylide carbon atom is surrounded in a planar manner and all sulfur atoms are found in this plane, too. In **4b** the sulfur atom is *trans* to the phophonio group.

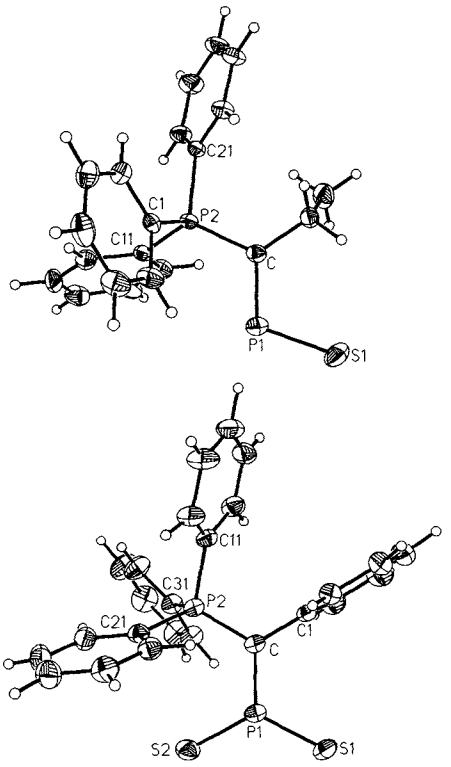

Fig. 1. Crystal structures of **4b** (top) and **6c** (bottom) (thermal ellipsoids at the 25% probability level).

Table 1. Structure parameters [a] of **4b** and **6c**.

Cmpd.	Bond lengths [Å]			Bond angles [°]	
	C-PPh$_3$	C-PS	P-S	C-P-S	S-P-S
4b	1.759(4)	1.704(5)	1.981(2)	109.9(2)	
6c (S1)	1.758(3)	1.689(2)	1.923(1)	117.3(1)	124.3(1)
(S2)			1.929(1)	118.4(1)	

[a] Standard deviations in parentheses.

In **6c** the P–S bonds *cis* and *trans* to the phosphonio groups are of almost equal length. As expected, the C-P-S angle opens on oxidation (**6c** compared to **4b**). Since the planes of the trigonal-planar coordinated C and P atoms in **6c** coincide, the structure of this compound forms a counterpart to the structure of the previously mentioned dithioxophosphoranes, which are stabilized by the steric shielding of the phosphorus.

The Ph_3P–C bond in **4b** and **6c** is longer than the bond in the ylide with an unsubstituted C atom (1.69 Å)[13a] and as long as the bond in α-acyl-substituted ylides (1.70–1.75 Å).[13b] On the other hand, the P–C bond with the two- or three-coordinate phosphorus is far shorter than a single bond (1.84 Å) and corresponds to a relatively long double bond in a phosphaalkene (1.61–1.71 Å).[1c] When **4** is sulfurized to give **6**, the bond is slightly but significantly shortened as is generally observed in the oxidation of a phosphaalkene to a methylenephosphorane.[1d, 14]

The lengths of the P–C bonds of **4b** and **6c** therefore signalize a predominating dipolar resonance formula. This can be seen less clearly in the lengths of the P–S bonds. In **4b** the P–S distance is intermediate to the length of a terminal P=S bond (at the tetrahedral or trigonal-planar surrounded phosphorus, 1.93 Å) and the length of a P–S single bond (2.12 Å; this value relates to a two-coordinate sulfur, however). In **6c**, where the negative charge is distributed between two sulfur atoms, the bond is just as short as the above-mentioned "normal" P=S bond. In other thioxophosphoranes these P–S bonds are also of the same length.[1e, 14]

The calculated angles for ClPS[1b] and for $ClPS_2$[1e] (Cl-P-S: 110° and 117°, respectively, S-P-S: 126°) are identical to those found in **4b** and **6c**. The P=S bond lengths resulting from the MNDO calculations (1.86 and 1.82 Å) are too short, however, as expected. A good comparison is given by the length of the P–S bond in PS_3^-, 1.96 Å, determined by ab initio calculations.[15]

Experimental Procedure

4b: A suspension of **3b** (2.18 g, 5.4 mmol) and Na_2S (0.47 g, 5.4 mmol) in THF (20 mL) was stirred for 15 h at room temperature. After separation of the insoluble products using a reverse frit and concentration of the light-red filtrate to one-third of the original volume, **4b** crystallized. A second fraction was obtained from the concentrated mother liquor to which benzene (5 mL) was added. Yield 1.34 g (68%) orange crystals, m.p. 146–150 °C. Crystals suitable for structural analysis were obtained at room temperature from a saturated solution (1:1 dichloromethane/benzene mixture) after a few mL of pentane was added.

6c: A suspension of **3c** (1.63 g, 3.6 mmol) and Na_2S_2 (0.40 g, 3.6 mmol) in THF (15 mL) was stirred for 15 h at room temperature. After separation of the insoluble products using a reverse frit, concentration of the orange-red filtrate to two-thirds of the original volume, and addition of benzene (8 mL), **6c** · 0.5 C_6H_6 crystallized within 24 h. Yield 1.16 g (66%) yellow crystals, softening >130 °C and decomposing >160 °C.

Received: March 11, 1993 [Z 5912 IE]
German version: *Angew. Chem.* **1993**, *105*, 1117

[1] a) *Multiple Bonds and Low Coordination in Phosphorus Chemistry* (Eds.: M. Regitz, O. J. Scherer), Thieme, Stuttgart **1990**; b) L. D. Quin, J. Szewczyk in [1a], p. 352, and references therein c) R. Appel in [1a], p. 157; d) H. Heydt in [1a], p. 375, and references therein; e) M. Meisel, in [1a], p. 415, and references therein; f) K. Karaghiosoff in [1a], p. 463.

[2] a) B. Cetinkaya, P. B. Hitchcock, M. F. Lappert, A. J. Thorne, H. Goldwhite, *J. Chem. Soc. Chem. Commun.* **1982**, 691–693; b) M. Yoshifuji, K. Toyota, K. Ando, N. Inamoto, *Chem. Lett.* **1984**, 317–318; c) J. Navech, M. Revel, R. Kraemer, S. Mathieu, *Phosphorus Sulfur Relat. Elem.* **1986**, *26*, 83–89; d) E. Lindner, K. Auch, G. A. Weiss, W. Hiller, R. Fawzi, *Chem. Ber.* **1986**, *119*, 3076–3088.

[3] The direct spectroscopic observation of the transient 2,6-di-*tert*-butyl-4-methylphenoxy(oxo)phosphane (a "phosphenite") was reported recently: L. D. Quin, S. Jankowski, A. G. Sommese, P. M. Lahti, *J. Am. Chem. Soc.* **1992**, *114*, 11009–11010.

[4] A. Schmidpeter, G. Jochem, *Tetrahedron Lett.* **1992**, *33*, 471–474.
[5] K. Karaghiosoff, G. Jochem, A. Schmidpeter, unpublished.
[6] S. Lochschmidt, A. Schmidpeter, *Phosphorus Sulfur* **1986**, *29*, 73–109.
[7] a) G. A. Gray, *J. Am. Chem. Soc.* **1973**, *95*, 7736–7742; b) G. Fronza, P. Bravo, C. Ticozzi, *J. Organomet. Chem.* **1978**, *157*, 299–310; c) M. Schlosser, T. Jenny, B. Schaub, *Heteroat. Chem.* **1990**, *1*, 151–156.
[8] If the phosphonio group at the C atom and the substituent at the P atom of a phosphaalkene are fixed *cis* to each other in a ring, then $^2J(P,P) \approx 50$ Hz. E. Fluck, G. Becker, B. Neumüller, R. Knebl, G. Heckmann, H. Riffel, *Z. Naturforsch. B* **1987**, *42*, 1213–1221.
[9] In fact, compound **5b** stays ionic and the bromide ion does not associate with the two-coordinate phosphorus. The same applies to compound **5c**, which is generated from **3c** and Et_2NSiMe_3 and has NEt_2 instead of SCH_2Ph and Cl^- instead of Br^- [4], for which similar ^{31}P NMR data were obtained.
[10] A. Schmidpeter, G. Jochem, K. Karaghiosoff, C. Robl, *Angew. Chem.* **1992**, *104*, 1420–1441; *Angew. Chem. Int. Ed. Engl.* **1992**, *31*, 1350–1352.
[11] a) 2,4,6-Tri-*tert*-butylphenyldithioxophosphorane: R. Appel, F. Knoch, H. Kunze, *Angew. Chem.* **1983**, *95*, 1008–1009; *Angew. Chem. Int. Ed. Engl.* **1983**, *22*, 1004–1005. b) 2,6-Di-*tert*-butyl-4-methylphenyldithioxophosphorane: A. S. Ionkin, V. M. Nekhoroshkov, Y. Y. Efremor, *Izv. Akad. SSSR Ser. Khim.* **1991**, 1654–1656; *Chemical Abstracts* **1991** *115*, 208108s; see also [11c]. c) 2,6-Bis(trifluoromethyl)phenyldithioxophosphorane: G. Grossmann, G. Ohms, H. Beckmann, K. Friedrich, E. Niecke, M. Nieger, R. Serwas, V. von der Gönna, W. W. Schoeller, *Abstr. XIIth Int. Conf. Phosphorus Chem.*, Toulouse, **1992**. Proceedings: *Phosphorus, Sulfur Silicon Relat. Elem.* **1993**, *77*, 248.
[12] X-ray diffraction crystal structure determination: Data were collected at 293 K, Siemens P4/V diffractometer, $Mo_{K\alpha}$ radiation ($\lambda = 0.71073$ Å), graphite monochromator. The structures were solved by direct methods (SHELXTL PLUS, PC version). (Non-hydrogen atoms anisotropic, H atoms in calculated positions and included in the refinement using the riding model $U_{i,H} \approx 1.2\ U_{eq.}$ c). – **4b**: orange-yellow plates, $C_{21}H_{20}P_2S$, $M_r = 366.4$, triclinic, space group $P\bar{1}$; $a = 9.343(4)$, $b = 10.791(5)$, $c = 10.816(5)$ Å, $\alpha = 62.72(1)$, $\beta = 86.55(1)$, $\gamma = 85.95(2)°$, $V = 966(1)$ Å^3, $Z = 2$, $\varrho_{calcd.} = 1.259$ g cm^{-3}, $F(000) = 756$, $\mu = 3.32$ cm^{-1}; ω-scans, $2.0° \leq 2\theta \leq 48°$, 3125 measured reflections, of which 2929 were independent ($R_{int} = 0.0333$), 1904 with $|F| > 3\sigma(F)$. The full-matrix least-squares refinement resulted in $R = 0.0572$ and $R_w = 0.0576$. – **6c** · 0.5 C_6H_6: yellow prisms, $C_{29}H_{23}P_2S_2$, $M_r = 485.5$, triclinic, space group $P\bar{1}$; $a = 9.182(2)$, $b = 11.063(2)$, $c = 13.327(2)$ Å, $\alpha = 89.99(1)$, $\beta = 76.68(1)$, $\gamma = 78.21(1)°$, $V = 1288.0(5)$ Å^3, $Z = 2$, $\varrho_{calcd.} = 1.252$ g cm^{-3}, $F(000) = 506$, $\mu = 3.45$ cm^{-1}; ω-scans, $2.0 \leq 2\theta \leq 50°$, 5398 measured reflections, of which 4486 were independent ($R_{int} = 0.159$), 3671 with $|F| > 3\sigma(F)$. The full-matrix least-squares refinement resulted in $R = 0.0528$ and $R_w = 0.0569$. Further details of the crystal structure investigation may be obtained from the Fachinformationszentrum Karlsruhe, Gesellschaft für wissenschaftlich-technische Information mbH, D-76344 Eggenstein-Leopoldshafen (FRG), on quoting the depository number CSD-57193, the names of the author, and the journal citation.
[13] a) H. Schmidbaur, J. Jeong, A. Schier, W. Graf, D. L. Wilkinson, G. Müller, *New J. Chem.* **1989**, *13*, 341–352; b) M. A. Vincent, H. F. Schaefer III, A. Schier, H. Schmidbaur, *J. Am. Chem. Soc.* **1983**, *105*, 3806–3811, and references therein.
[14] V. D. Romanenko, L. N. Markovskii, A. V. Ruban, *Compounds of Low-Valent Five-Coordinate Phosphorus* (English translation of title), Naukova Dumka, Kiew, **1992**, p. 138.
[15] H. W. Roesky, R. Ahlrichs, S. Brode, *Angew. Chem.* **1986**, *98*, 91–93; *Angew. Chem. Int. Ed. Engl.* **1986**, *25*, 82–83.

Stereoselective Synthesis of C-Glycosides with a Glycosyl Dianion**

By *Valentin Wittman* and *Horst Kessler**

During the past few years the interest in the synthesis of C-glycosides[1] has greatly increased. This is chiefly due to the discovery of C-glycosidic or analogue structures in many natural products,[2] and their potential use as antimetabolites.[3] As with the synthesis of O-glycosides, the traditional approach to C-glycosides is based upon the addition of a suitable C-nucleophile to the electrophilic anomeric center of a 1-activated carbohydrate. The use of glycosyl radicals[1,4] and glycosylidene carbenes[5] has also been described. Direct 1-C-lithiation of sugars generally leads to the elimination of functional groups in the 2-position.[6] Paulsen et al. first reported the C-elongation of open-chain carbohydrates by polarity inversion (umpolung) at the anomeric center via dianions of hydroxy-1,3-dithianes.[7] However, in the case of pyranoses the concept of umpolung has been limited so far to 1-nitrosugars **1**,[8] 2-deoxysugars **2** (X = H,[6a,9] SO_2PH,[10] $^{\oplus}PPh_3$,[11] CO_2R[12]), and glycals **3** (X = H,[9d,13] SOPh,[14] SPh,[15] OBn[15]). Chain elongation of nitrosugars **1** followed by substitution of the nitro group by a hydroxy group leads to higher ketopyranoses with the added residue in the equatorial position. Glycals **3** offer the possibility of subsequent introduction of the missing hydroxy group and therefore access to β-C-glycosides.

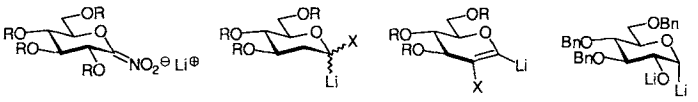

1 **2** **3** **4**

In this communication we present the application of the dilithio compound **4** in the synthesis of C-glucosides. Simple lithiation of the 2-hydroxy group functions both as a means of protection, and efficiently prevents β elimination. Subsequent reaction with electrophiles directly produces 2-hydroxy-substituted C-glucopyranosides, exclusively with α-configuration (see Scheme 1).

Dianions of the general type **5** may be obtained from β-hydroxy organomercury compounds,[16] chlorohydrins,[17] epoxides,[18] carbonyl compounds,[10a,19] or hydroxy-1,3-dithianes,[7] and were used either as carbanions for C–C-coupling reactions (**5** → **6**, El. = electrophile)[7,16–18,19a] or in the synthesis of olefins by Li_2O elimination (**5** → **7**).[19,20]

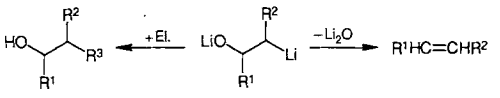

6 **5** **7**

The suitability of **4** for chain elongation reactions at the anomeric center or its tendency to eliminate to give the glucal were not readily predictable. It was reported,[17] for example, that compounds **5** in which lithium is located at a primary carbon (R^2 = H) are stable up to – 60 °C. On the other hand in the case of R^2 = alkyl, they decompose spontaneously even at – 100 °C to the olefin by β elimination. Only compounds **5** with stabilizing substituents like R^2 = Ph or CO_2Et, or cyclic β-lithiocyclohexanolate (R^1,[10] R^2 = $-(CH_2)_4-$) can be converted into the corresponding deuterated alcohols **6** (R^3 = D). Beau and Sinaÿ have postulated[10] the presence of the dilithio derivative **8** and demonstrated that protonation without β elimination is possible.

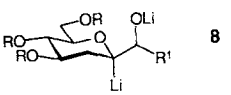

8

[*] Prof. Dr. H. Kessler, Dipl.-Chem. V. Wittmann
Organisch-Chemisches Institut der Technischen Universität München
Lichtenbergstrasse 4, D-85748 Garching (FRG)
Telefax: Int. code +(89)3209-3210

[**] This work was supported by the Fonds der Chemischen Industrie (doctoral fellowship for V. W.) and the Deutsche Forschungsgemeinschaft.

In a first experiment we treated 3,4,6-tri-O-benzyl-α-D-glucopyranosyl chloride **9**[21] in THF at − 78 °C dropwise with 1.1 equivalents of *n*-butyllithium (to generate the alcoholate), and after 15 minutes with 2.2 equivalents of lithium naphthalenide. After a further 15 minutes, quenching with MeOD, work up under acidic conditions, and chromatography on silica gel yielded a mixture of deuterated sugar **10** (66%), the corresponding β-configurated compound (3.1%), and the protonated compound **11** (17%) (Scheme 1). These products suggest that the dilithio compound **4** was formed intermediately during the reaction. The axial configuration of deuterium in **10** is based on the ^{1}H NMR spectrum (250 MHz, $CDCl_3$, $^3J_{H1,H2}$ = 5.3 Hz). The *a*/β ratio of 21 : 1 was determined by deuterium NMR spectroscopy. Obviously no Li_2O elimination leading to 3,4,6-tri-O-benzyl-D-glucal **17** takes place under these conditions.

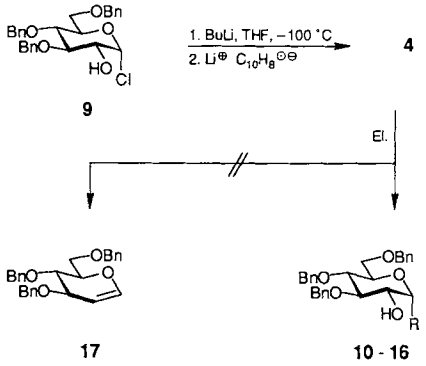

Scheme 1. Synthesis of the α-C-glucosides **10**–**16** (cf. Table 1). Bn = CH_2Ph, El. = electrophile.

Table 1. Results of the C-glucoside synthesis according to Scheme 1.

Electrophile	Product [a]	R	Yield [%] [b]
MeOD	**10**	D	75
MeOH	**11**	H	82
MeCHO	**12a/b**	CH(OH)Me	62
PhCHO	**13a/b**	CH(OH)Ph	70
*i*PrCHO	**14a/b**	CH(OH)*i*Pr	59
HCHO	**15** [23]	CH_2OH	17
MeI [c]	**16**	Me	72

[a] Products were characterized by ^{1}H and ^{13}C NMR spectroscopy (see Table 2) and FAB-MS. [b] Yields of α-anomers after chromatography on silica gel. [c] Addition of 10% CuI.

The best yields were obtained by *quick* addition of the lithium naphthalenide solution. To avoid undue increase of reaction temperature, a precooled lithium naphthalenide solution (−78 °C) is recommended. However, since the solubility of lithium naphthalenide in THF is greatly reduced at this temperature, it is better to work at − 100 °C and add the reagent uncooled. The results presented in Table 1 were obtained by using the latter method.

We next turned our attention to the possibility of using the lithiated sugar **4** in the synthesis of α-C-glucosides. The reaction of **4** with acetaldehyde affords a mixture of diastereomers **12a/b**[22] (ratio 1.4 : 1) in 62% yield. In the same manner benzaldehyde and isobutyraldehyde produced **13a/b** (1 : 1, 70%) and **14a/b** (1 : 1, 59%), respectively. In all cases axial configurated C-glucosides were produced with high stereoselectivity ($\alpha/\beta \geq 20:1$). The use of gaseous formaldehyde gave the desired hydroxymethyl C-glucoside **15** in an unsatisfactory 17% yield; in this case large quantities of polyoxymethylene were formed. However, alkylation of the dianion **4** with MeI proceeded without complications to give α-methyl-C-glucoside **16** in 58% yield. An improved yield of 72% could be obtained by addition of 10% of CuI before addition of the electrophile.

Table 2. Selected ^{1}H and ^{13}C NMR chemical shifts (δ values) and coupling constants *J* [Hz] of **10**–**16** [a,b]. ax = axial, eq = equatorial, n.d. = not determinable.

Compd.	H-1	H-2	H-1′	C-1	C-2	C-1′	$^3J_{H\ 1,H-2}$
10	3.95	3.69		69.1	70.0		5.3
11	3.97 (eq)	3.69		69.5	70.1		5.3 (eq-ax)
	3.18 (ax)						11.1 (ax-ax)
12a	3.50	3.69	4.04	73.6	67.6	67.7	1.6
12b	3.57	3.98	4.10	73.7	68.4	67.0	2.9
13a	3.75	3.34	4.97	73.8	66.1	73.9	1.0
13b	3.93	3.93	5.00	72.4	67.4	74.0	n.d. [c]
14a	3.78	3.75	3.60	69.2	68.9	76.8	<1.0
14b	3.77	3.97	3.77	69.8	68.1	74.3	2.0
15	3.97	3.76	3.76	71.1	68.7	62.2	2.7
			3.87				
16	4.09	3.61	1.23	68.1	70.4	14.2	3.8

[a] NMR spectra in $CDCl_3$ at 300 K, internal standard TMS. ^{1}H: 500 MHz, ^{13}C: 125 MHz. [b] To facilitate comparison, atoms are numbered following that used for the starting sugar **9**.

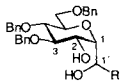

[c] Identical chemical shifts of H1 and H2.

It is remarkable that the formation of tribenzylglucal **17** was not observed under any circumstances. Thus, the dilithio compound **4** proves to be a species which is stable at − 78 °C and reacts with electrophiles with *retention* of configuration at the anomeric center to give a variety of 2-hydroxy-α-C-glucosides. The precursor **9** is crystalline and stable at − 20 °C,[21] and is easily obtained from acetobromoglucose in a four-step synthesis in an overall yield of approximately 55%.

Experimental Procedure

Under argon a 0.15 M solution of **9** in dry THF at − 100 °C was treated with 1.1 equivalents of *n*BuLi (1.6 M in THF), followed by quick addition of 2.2 equivalents of lithium naphthalenide (1 M in THF). After 15 minutes, 1.5 equivalents of aldehyde or MeI were added, and the mixture was stirred for 1 h at − 100 °C and then allowed to warm up to room temperature. A saturated aqueous solution of NH_4Cl was added and the mixture extracted with dichloromethane. After the organic layer had been dried over $MgSO_4$, the product was purified by chromatography on silica gel (eluent: toluene/ethyl acetate or hexane/ethyl acetate).

Received: February 8, 1993 [Z 5856 IE]
German version: *Angew. Chem.* **1993**, *105*, 1138

[1] For an excellent overview see: M. H. D. Postema, *Tetrahedron* **1992**, *48*, 8545–8599 and references cited therein.
[2] a) G. Franz, M. Grün, *Planta Med.* **1983**, *47*, 131–140; b) S. Hanessian, *Total Synthesis of Natural Products: The 'Chiron' Approach*, Pergamon Press, Oxford, **1983**.
[3] a) C. Bertozzi, M. Bednarski, *Carbohydr. Res.* **1992**, *223*, 243–253; b) K. Krohn, H. Heins, K. Wielckens, *J. Med. Chem.* **1992**, *35*, 511–517; c) R. R. Schmidt, H. Dietrich, *Angew. Chem.* **1991**, *103*, 1348–1349; *Angew. Chem. Int. Ed. Engl.* **1991**, *30*, 1328–1329.
[4] a) B. Giese, T. Linker, R. Muhn, *Tetrahedron* **1989**, *45*, 935–940; b) H. Kessler, V. Wittmann, M. Köck, M. Kottenhahn, *Angew. Chem.* **1992**, *104*, 874–877; *Angew. Chem. Int. Ed. Engl.* **1992**, *31*, 902–904.
[5] A. Vasella, C. Witzig, R. Husi, *Helv. Chim. Acta*, **1991**, *74*, 1362–1372.
[6] a) J.-M. Lancelin, L. Morin-Allory, P. Sinaÿ, *J. Chem. Soc. Chem. Commun.* **1984**, 355–356; b) R. R. Schmidt, J. Kast, *Tetrahedron Lett.* **1986**, *27*, 4007–4010.

[7] H. Paulsen, K. Roden, V. Sinnwell, P. Luger, *Liebigs Ann. Chem.* **1981**, 2009–2027.
[8] a) B. Aebischer, J. H. Bieri, R. Prewo, A. Vasella, *Helv. Chim. Acta* **1982**, *65*, 2251–2272; b) K. Mahmood, A. Vasella, B. Bernet, *ibid.* **1991**, *74*, 1555–1583.
[9] a) P. Lesimple, J.-M. Beau, P. Sinaÿ, *J. Chem. Soc. Chem. Commun.* **1985**, 894–895; b) J.-M. Beau, P. Sinaÿ, *Tetrahedron Lett.* **1985**, *26*, 6185–6188; c) P. Lesimple, J.-M. Beau, P. Sinaÿ, *Carbohydr. Res.* **1987**, *171*, 289–300; d) J. Prandi, C. Audin, J.-M. Beau, *Tetrahedron Lett.* **1991**, *32*, 769–772; e) D. K. Hutchinson, P. L. Fuchs, *J. Am. Chem. Soc.* **1987**, *109*, 4930–4939.
[10] a) J.-M. Beau, P. Sinaÿ, *Tetrahedron Lett.* **1985**, *26*, 6189–6192; b) J.-M. Beau, P. Sinaÿ, *ibid.* **1985**, *26*, 6193–6196.
[11] J. B. Ousset, C. Mioskowski, Y.-L. Yang, J. R. Falck, *Tetrahedron Lett.* **1984**, *25*, 5903–5906; Cf. also: S. V. Ley, B. Lygo, *ibid.* **1984**, *25*, 113–116.
[12] a) D. Crich, L. B. L. Lim, *Tetrahedron Lett.* **1990**, *31*, 1897–1900; b) K. Wallimann, A. Vasella, *Helv. Chim. Acta* **1991**, *74*, 1520–1532.
[13] a) K. C. Nicolaou, C.-K. Hwang, M. E. Duggan, *J. Chem. Soc. Chem. Commun.* **1986**, 925–926; b) S. Hanessian, M. Martin, R. C. Desai, *ibid.* **1986**, 926–927; c) P. Lesimple, J.-M. Beau, G. Jaurand, P. Sinaÿ, *Tetrahedron Lett.* **1986**, *27*, 6201–6204; d) K. A. Parker, C. A. Coburn, *J. Am. Chem. Soc.* **1991**, *113*, 8516–8518.
[14] a) R. Preuss, R. R. Schmidt, *Liebigs Ann. Chem.* **1989**, 429–434; b) R. R. Schmidt, R. Preuss, *Tetrahedron Lett.* **1989**, *30*, 3409–3412; c) S. Maier, R. Preuss, R. R. Schmidt, *Liebigs Ann. Chem.* **1990**, 483–489.
[15] R. R. Schmidt, R. Preuss, R. Betz, *Tetrahedron Lett.* **1987**, *28*, 6591–6594.
[16] J. Barluenga, F. J. Fananas, J. Villamana, M. Yus, *J. Org. Chem.* **1982**, *47*, 1560–1564.
[17] a) C. Najera, M. Yus, D. Seebach, *Helv. Chim. Acta* **1984**, *67*, 289–300; b) J. Barluenga, J. Florez, M. Yus, *J. Chem., Soc. Perkin Trans. 1* **1983**, 3019–3026.
[18] a) T. Cohen, I.-H. Jeong, B. Mudryk, M. Bhupathy, M. M. A. Awad, *J. Org. Chem.* **1990**, *55*, 1528–1536; b) E. Bartmann, *Angew. Chem.* **1986**, *98*, 629–631; *Angew. Chem. Int. Ed. Engl.* **1986**, *25*, 653–654.
[19] a) J. Barluenga, J. L. Fernandez-Simon, J. M. Concellon, M. Yus, *J. Chem. Soc., Perkin Trans. 1* **1988**, 3339–3343; b) J. Barluenga, F. Alvarez, J. M. Concellon, M. Yus, *J. Chem. Res. (S)* **1987**, 402–403; (*M*) 3265–3285.
[20] K. N. Gurudutt, B. Ravindranath, *Tetrahedron Lett.* **1980**, *21*, 1173–1174.
[21] H. Yamaguchi, C. Schuerch, *Carbohdr. Res.* **1980**, *81*, 192–195.
[22] Here **a** and **b** refer to the diastereomers produced by addition to both stereoheterotopic faces of the prochiral aldehyde, which are separable by chromatography on silica gel.
[23] G. Stork, H. S. Suh, G. Kim, *J. Am. Chem. Soc.* **1991**, *113*, 7054–7056.

Supramolecular Complexes of Flexible, Extended Cavity Calix[4]arenes—Structural Characterization of a Molecular Venus Flytrap**

By *Jerry L. Atwood,* G. William Orr, Simon G. Bott,* and *Kerry D. Robinson*

The ability of calix[4]arenes to form supramolecular complexes has been responsible for much of the current interest in these macrocycles.[1, 2] While *p*-sulfonatocalix[4]arene has been shown to bind to a range of small molecules and ions,[3–9] there exists a need for calix[4]arenes with larger cavities possessing more binding possibilities. In search of deep-cavity calix[4]arenes, Gutsche and Nam reported[10] in 1988 that calix[4]arene undergoes acetic acid-catalyzed aminomethylation in the presence of formaldehyde and dimethylamine in THF. We have now expanded on this Mannich reaction[11] to synthesize a wide range of aminomethylcalix[4]arenes. One of these, *p*-[4-(2-hydroxyethyl)-piperidinomethyl]calix[4]arene (**1**), possesses a flexible binding capability reminescent of the capture of insects by the Venus flytrap.

In the original synthesis of **1** unidentified resonances appeared in both the ^{1}H and ^{13}C NMR spectra, and efforts to remove the compound causing these signals were unsuccessful. Subsequently, a single-crystal X-ray diffraction study[12] revealed the presence of a guest in the cavity (Fig. 1). This molecule appears to be unreacted, excess 1-(2-hydroxyethyl)piperazine that has been methylated at the position of the secondary nitrogen. Although the hydroxyethyl chain of this molecule is badly disordered (and thus not shown in Fig. 1), the remainder of the atoms are better defined. The ^{1}H and ^{13}C NMR spectra are also consistent with the presence of two different hydroxyethylpiperazine moieites.[13] As Figure 1 reveals, the arms of the calix[4]arene are spread wide to provide a shallow cavity similar to that found in *p*-sulfonatocalix[4]arene.[3–9]

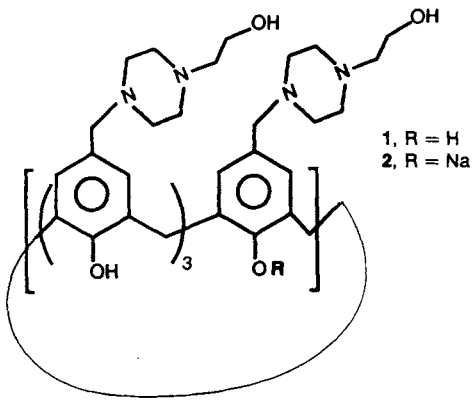

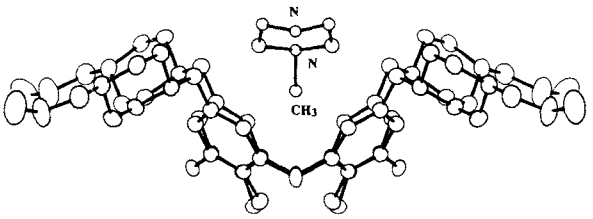

Fig. 1. Structure of *p*-[4-(2-hydroxyethyl)piperazinomethyl]calix[4]arene with the guest $CH_3N(CH_2CH_2)_2NCH_2CH_2OH$. The $-CH_2CH_2OH$ portion of the guest molecule was badly disordered and is not shown.

Preparation of **1** and subsequent neutralization with 10% Na_2CO_3 solution to pH 9 leads to the removal of one of the phenolic protons resulting in the complex **2**. Following crystallization from ethyl acetate, **2** was dried under vacuum for 48 h at 120 °C. The ^{1}H NMR spectrum revealed that even

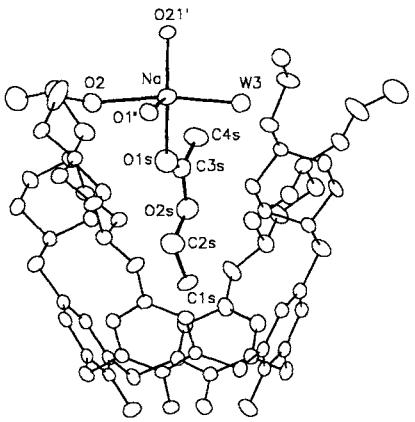

Fig. 2. Structure of Na[*p*-[4-(2-hydroxyethyl)piperazinomethyl]calix[4]-arene] · $CH_3COOCH_2CH_3$.

[*] Prof. Dr. J. L. Atwood, Dr. G. W. Orr, Dr. S. G. Bott, Dr. K. D. Robinson
Department of Chemistry, University of Alabama,
Tuscaloosa, AL 35487 (USA)

[**] This work was supported by the U. S. National Science Foundation.

under these extreme conditions one ethyl acetate molecule was retained. X-ray diffraction quality crystals of this compound afforded the structure[14] shown in Figure 2. In this complex the arms are directed up from the rim of the calix[4]arene to produce a cavity so deep that the ethyl acetate guest molecule is completely enshrouded. The guest is further bound by an electrostatic interaction with the Na^+ ion to the carbonyl oxygen atom. The Na^+ ion further ties the guest to the host by an electrostatic bond to one of the hydroxyl oxygen atoms of the calix[4]arene.[15]

Comparison of Figures 1 and 2 shows that *p*-[4-(2-hydroxyethyl)piperidinomethyl]calix[4]arene under different circumstances can deliver either a shallow or a deep cavity. Ethyl acetate is the largest guest thus far characterized as completely enshrouded by a calix[4]arene.

Experimental Procedure

1: Calix[4]arene (1.00 g, 2.36 mmol), 1-(2-hydroxyethyl)piperazine (1.84 g, 14.2 mmol), and 37% aqueous formaldehyde solution (1.05 mL, 14.2 mmol) were dissolved in 1,2-dimethoxyethane (50 mL). A solution of CF_3COOH (100 mL) in 1,2-dimethoxyethane (20 mL) was added dropwise to the unstirred solution over a period of 1 h. The resulting solution was allowed to stand at room temperature for 1.5 h at which time the solution was pale yellow. The reaction was allowed to continue for a total of 12 h after which time the volatile components were removed under vacuum at 40 °C. The resulting solid was dissolved in MeOH, stirred vigorously for 1 h over solid Na_2CO_3 (0.5 g), and filtered through a fluted filter paper. The filtrate was evaporated to dryness, and crystallization was effected by the addition of hot ethyl acetate to a boiling solution in MeOH, followed by cooling in an ice bath. The solid was collected on a fritted funnel, washed with ice-cold ethyl acetate, and dried under vacuum at 40 °C for 48 h to produce 1.3 g of **1** (50%).

2: Calix[4]arene (1.00 g, 2.36 mmol) and 1-(2-hydroxyethyl)piperazine (1.53 g, 11.8 mmol) were dissolved in THF (25 mL) and glacial acetic acid (2.7 mL). To the resulting colorless solution was added 37% aqueous formaldehyde solution (0.88 mL), and the contents were stirred in a sealed flask at room temperature for 28 h, after which the volatile components were removed under vacuum at 40 °C. The yellow-orange residue was dissolved in distilled water (25 mL) and neutralized to pH 9 with 10% Na_2CO_3 solution. The solution was then subjected to three freeze-pump-thaw cycles at −78 °C to remove traces of CO_2. The solution was then evaporated to dryness, and the residue was dissolved in methanol and filtered. Ethyl acetate was added, followed by cooling in an ice bath to produce the crystalline product. The reaction produced 0.4 g of **2** (17%).

Received: January 30, 1993 [Z 5844 IE]
German version: *Angew. Chem.* **1993**, *105*, 1114

[1] C. D. Gutsche, *Calixarenes*, R. Soc. Chem., Cambridge, **1989**.
[2] *Calixarenes: a Versatile Class of Macrocyclic Compounds* (Eds.: V. Böhmer, J. Vicens), Kluwer, Dordrecht, **1990**.
[3] S. G. Bott, A. W. Coleman, J. L. Atwood, *J. Am. Chem. Soc.* **1988**, *110*, 610.
[4] J. L. Atwood, A. W. Coleman, S. G. Bott, S. D. Morley, C. M. Means, K. D. Robinson, H. Zhang, *Angew. Chem.* **1988**, *100*, 1412; *Angew. Chem. Int. Ed. Engl.* **1988**, *27*, 1361.
[5] S. Shinkai, K. Araki, O. Manabe, *J. Am. Chem. Soc.* **1988**, *110*, 7214.
[6] S. Shinkai, K. Araki, T. Matsuda, N. Nishiyama, H. Ikeda, I. Takasu, M. Iwamoto, *J. Am. Chem. Soc.* **1990**, *112*, 9053.
[7] J. L. Atwood, F. Hamada, K. D. Robinson, G. W. Orr, R. L. Vincent, *Nature* **1991**, *349*, 683.
[8] J. L. Atwood, G. W. Orr, F. Hamada, R. L. Vincent, S. G. Bott, K. D. Robinson, *J. Am. Chem. Soc.* **1991**, *113*, 2760.
[9] J. L. Atwood, G. W. Orr, F. Hamada, S. G. Bott, K. D. Robinson, *Supramol. Chem.* **1992**, *1*, 15.
[10] C. D. Gutsche, K. C. Nam, *J. Am. Chem. Soc.* **1988**, *110*, 6153.
[11] For a review, see M. Tramontini, *Synthesis* **1973**, 703.
[12] The pale yellow crystals of **1** · $[MeN(CH_2CH_2)_2NCH_2CH_2OH] \cdot 7H_2O$ belong to the orthorhombic space group *Pnma* with $a = 11.249(1)$, $b = 33.628(5)$, $c = 19.075(3)$ Å, and $\varrho_{calcd} = 1.17\ g\,cm^{-3}$ for $Z = 4$. Refinement based on 2922 observed reflections led to a final $R = 0.10$. See also [14b].
[13] The CH_2OH and NCH_2 resonances from the calixarene substituent appear as a pair of triplets at $\delta = 3.58$ and 2.44, respectively, corresponding to a total of sixteen protons. The CH_2OH and NCH_2 resonances of the substrate (guest) appear as triplets at $\delta = 3.64$ and 2.52, respectively, corresponding to a total of four protons. The NCH_2CH_2N resonances from the calixarene substituents appear as a very broad multiplet centered at about $\delta = 2.4$. The NCH_2CH_2N resonances of the substrate appear as a pair of broad triplets at $\delta = 2.95$ and 2.58. The ^{13}C resonances of the calixarene substituents appear at $\delta = 64.1$, 61.0, and 54.5 and 54.0 for CH_2OH, NCH_2, and NCH_2CH_2N, respectively. The corresponding substrate resonances appear at $\delta = 62.6$, 59.3, and 55.6 and 55.0, respectively. The CH_3N resonance appears as a singlet at $\delta = 3.35$ (^1H NMR) and $\delta = 42.9$ (^{13}C NMR). The origin of the signal from a CH_3 group was discerned from a DEPT experiment.
[14] a) The compound, Na[4-(2-hydroxyethyl)piperazinomethyl)calix[4]-arene] · $CH_3COOCH_2CH_3 \cdot 3H_2O$, crystallizes in the triclinic space group $P\bar{1}$ with $a = 12.139(1)$, $b = 15.628(2)$, $c = 16.248(1)$ Å, $\alpha = 87.93(1)$, $\beta = 85.76(1)$, $\gamma = 85.75(1)°$, and $\varrho_{calcd} = 1.26\ g\,cm^{-3}$ for $Z = 2$. Refinement based on 4785 observed reflections led to a final $R = 0.065$. b) Further details of the crystal structure investigations are available on request from the Director of the Cambridge Crystallographic Data Centre, 12 Union Road, GB-Cambridge, CB21EZ (UK), on quoting the full journal citation.
[15] The sodium ion which resides at the mouth of the calix[4]arene cavity is found in a roughly trigonal bipyramidal ligand geometry. The bond lengths are Na–O1s = 2.300(7) Å, Na–O2 = 2.414(6) Å, Na–W3 (water oxygen atom) = 2.376(6) Å, Na–O1″ (from a hydroxyethyl group on a neighboring calixarene) = 2.308(6) Å and Na–O21′ (from the phenolic portion of a neighboring calixarene) = 2.397(6) Å.

This section contains book reviews and a list of new books received by the editor. Book reviews are written by invitation from the editor. Suggestions for books to be reviewed and for book reviewers are welcome. Publishers should send brochures or (better) books to the Book Editor, Dr. Gerhard Karger, Redaktion Angewandte Chemie, Postfach 101161, D-69451 Weinheim, Federal Republic of Germany. The editor reserves the right of selecting which books will be reviewed. Uninvited books not chosen for review will not be returned.

Book Reviews

Survey of Industrial Chemistry. 2nd Revised Edition. By *P. J. Chenier*. VCH Publishers, New York, 1992. XV, 527 pp., hardcover \$ 95.00, softcover \$ 45.00.—ISBN 1-56081-082-3/1-56081-622-8

A common complaint in the chemical community is that, even though most chemists work in industry, chemistry is taught as though all graduate chemists would pursue academic careers. Philip Chenier has undertaken to do something about this situation. He has written an advanced undergraduate text that broadly surveys the American chemical industry. The book contains a substantial business perspective in addition to describing how most major industrial chemicals are made and used. The primary intended audience is the chemist who will move into business-orientated employment such as sales or technical service rather than getting an advanced degree. Simultaneously, though, it can provide a useful introduction to industry even for someone anticipating an academic career.

This *Survey of Industrial Chemistry* presents an enormous mass of information. It contains not just a compendium of chemical process technology, but also statistics on the size and scope of the chemical industry, salaries of U. S. chemists, and the sales of the top fifty chemical companies. Chenier has made a significant and largely successful effort to present current data and perspectives on the industry. The information seems to be current through 1990.

The process of packing so much information into a volume affordable by a student has led to a terse writing style. The body of the volume tends to present the facts without the many little anecdotes that might enliven the presentation. Nevertheless it is moderately readable and presents useful perspective not just on how a chemical is made but also on how it is used and what its economic prospects may be. The discussion of manufacturing technology contains many photographs of production facilities and laboratories. The process discussions are clarified with abundant chemical equations and formulas. There are a number of typographical errors in the equations, but they do not usually cause problems for the reader.

The subject matter of the book spans the whole chemical industry, including fields as diverse as pharmaceuticals, plastics, elastomers, mineral products, wood products, and detergents. The greatest attention is given to the fifty largest volume chemicals, but the selection seems repesentative of the industry as a whole. There is a timely and useful section on current environmental and health issues facing the chemical community. Throughout, the author presents a positive but realistic view of the chemical industry.

The survey of individual chemical products, which makes up the greatest part of the book, employs a standard format for each major chemical. For each, there is a discussion of both historic and current manufacturing processes with some perspective on technology trends. For example, the section on acetic acid includes discussion of the obsolescent ethylene-based Wacker process, the oxidation of butane to acetic acid, and the now preferred methanol carbonylation. For each process, the author presents a summary equation, the usual process conditions, and the separation and purification technology. For major processes such as the catalytic carbonylation of methanol there are also sketches of what is known about the reaction mechanism. The process descriptions are followed by summaries of the uses of the compounds together with key physical properties. The book also lists the production volumes and approximate prices for major chemicals.

The *Survey of Industrial Chemistry* is in many respects a mini-encyclopedia of the chemical industry. It meets its goal as a tool for the teacher of a business-orientated chemistry course, but it is also a useful reference source for anyone with a broad interest in the practice of industrial chemistry. The level of detail is not great, but it provides leading references to up-to-date chemical encyclopedias and review articles. After almost forty years in industrial chemistry, I found that I had much to learn from this book. I expect to use it extensively as a general reference source in the near future.

George W. Parshall
DuPont Co.
Wilmington, DE (USA)

Comprehensive Organic Synthesis. Selectivity, Strategy and Efficiency in Modern Organic Chemistry. Volumes 1–9. (Series editor: *B. M. Trost*. Pergamon, Oxford, 1991. CCVI, 10196 pp., hardcover £ 1950.00, \$ 3900.00.—ISBN 0-08-035929-9; **Volume 1: Additions to C–X π-Bonds, Part 1.** Edited by *S. L. Schreiber*. XXI, 989 pp.—ISBN 0-08-040592-4; **Volume 2: Additions to C–X π-Bonds, Part 2**. Edited by *C. H. Heathcock*. XXIII, 1233 pp.—ISBN 0-08-040593-2; **Volume 3: Carbon–Carbon σ-Bond Formation**. Edited by *G. Pattenden*. XXI, 1186 pp.—ISBN 0-08-040594-0; **Volume 4: Additions to and Substitutions at C–C π-Bonds.** Edited by *M. F. Semmelhack*. XXI, 1299 pp.—ISBN 0-08-040595-9; **Volume 5: Combining C–C π-Bonds.** Edited by *L. A. Paquette*. XXV, 1333 pp.—ISBN 0-08-040596-7; **Volume 6: Heteroatom Manipulation**. Edited by *E. Winterfeldt*. XXI, 1194 pp.—ISBN 0-08-040597-5; **Volume 7: Oxidation**. Edited by *S. V. Ley*. XXV, 1012 pp.—ISBN 0-08-040598-3; **Volume 8: Reduction**. Edited by *I. Fleming*. XXV, 1139 pp.—ISBN 0-08-040599-1; **Volume 9: Cumulative Indexes**. XV, 811 pp.—ISBN 0-08-040600-9

Volume 1

Volume 1 of *Comprehensive Organic Synthesis* is essentially concerned with the chemistry of carbanions. This volume is divided into three different sections: "Nonstabilized Car-

 © VCH Verlagsgesellschaft mbH, D-69451 Weinheim, 1993 0570-0833/93/0707-1095 \$ 10.00+.25/0

banion Equivalents," "Heteroatom-stabilized Carbanion Equivalents," and "Transformation of the Carbonyl Group into Nonhydroxylic Groups". These three sections are composed of various chapters authored for the most part by internationally recognized experts.

The first sections contains 13 chapters describing the chemistry of non-stabilized carbanions. A brief introduction to the structure of organometallic compounds is followed by chapters of about 30 pages each, which treat in detail the synthesis and reactions of organometallic compounds of alkali and alkaline earth metals, aluminum, copper, titanium, zirconium, chromium, zinc, cadmium, mercury, and lanthanoids. Special attention is given to the chemo-, regio-, and stereospecificity of the reactions, an essential aspect for any up-to-date compendium of this kind. In the chapter on the chemistry of organocopper compounds the discussion is limited to 1,2 additions of such compounds to carbonyl compounds and their hetero-analogues; 1,4 additions are treated in Volume 4 of the series. The last four chapters of this section describe the Lewis acid mediated reactions of organometallic compounds with carbonyl compounds, epoxides, and acetals, and additions of organometallic compounds to imines and carboxylic acid derivatives. Especially noteworthy here is the description in Chapter 1.10 of studies on asymmetric catalysis, currently a very hot topic.

The second section consists of six chapters dealing with the chemistry of heteroatom-stabilized carbanions. Important topics treated here include the deprotonation of arenes which is mediated by chelating agents, and the deprotonation of compounds in which the CH acidity is increased by –I substituents. As well as carbanions stabilized by nitrogen, boron, sulfur, and silicon, considerable space is devoted to the benzoin reaction and selenium chemistry.

The third section, which consists of about 200 pages divided into only three chapters, deals with the conversion of carbonyl compounds to olefins and epoxides and with ring-enlargement reactions of carbonyl compounds. Although the subject matter of this section does not fit in comfortably with the previous two, some of the methods described are extremely important, for example the olefin-forming reactions just mentioned. The chapter on this topic is 80 pages long, and treats not only the well-known named reactions such as the Wittig, Wittig–Horner, Peterson, Johnson, Tebbe, and Julia reactions, but also modern variants such as modified Tebbe reactions and samarium-induced reactions. The discussion of the advantages and disadvantages of the different reactions is especially useful, enabling the reader to quickly form a view as to which reaction offers the best solution to a specific problem. Under the heading of epoxidation of olefins one is likely to think immediately of the Sharpless epoxidation, but this highly important and elegant method is reserved for Volume 7. The short second chapter describes the preparation of epoxides by addition of heteroatom-stabilized carbanions to carbonyl compounds, which is followed by an intramolecular S_N2 cyclization. The third chapter is concerned mainly with the ring enlargement of cycloalkanones. In addition to the Arndt–Eistert method a number of more modern methods, involving a wide variety of mechanisms, are described.

The bibliographies attached to each of the chapters are a mine of information, citing over 3400 original publications extending up to the beginning of 1990. The detailed subject and author indexes also facilitate quick access to the primary literature. Most, but regrettably not all, chapters include clearly arranged tables from which the reader can obtain a quick overview of the capabilities and range of applicability of the methods described. Also the usefulness of many of the methods is illustrated by numerous examples of natural products syntheses.

Ulrich Groth
Institut für Organische Chemie
der Universität Göttingen (FRG)

Volume 2

Volume 2 consists of four parts as follows: "Uncatalyzed Additions of Nucleophilic Alkenes to C = X" (17 chapters, 526 pp.); "Catalyzed Additions of Nucleophilic Alkenes to C = X" (5 chapters, 134 pp.); "Addition–Elimination Reactions (Acylations)" (7 chapters, 158 pp.); "Additions of Nucleophilic Alkenes to C = NR and C = NR_2^+" (6 chapters, 219 pp.). An 88-page author index and a 61-page subject index are also included.

Nearly all the chapters are very useful reviews of recent developments in the areas covered, written by recognized experts. The topics treated in the first two parts range from "Allyl Organometallics" (W. R. Roush) through "Propargyl and Allenyl Organometallics" (H. Yamamoto) to "Allylsilanes, Allylstannanes and Related Systems" (I. Fleming), "Formation and Addition Reactions of Enol Ethers" (T. H. Chan), "Asymmetric Synthesis with Enol Ethers" (C. Gennari), and "Reactions of Activated Dienes with Aldehydes" (M. D. Bednarski and J. P. Lyssikatos). Between these comes a treatment of the formation and reactions of enolates with a wide variety of counterions. As well as Clayton Heathcock, the undisputed leading expert on the aldol reaction, there are contributions from G. Rosini on the nitroaldol (Henry) reaction, from L. F. Tietze and U. Beifuss on the Knoevenagel reaction, and by T. Rosen on the Perkin reaction. The Darzens condensation is not neglected, nor are metal homoenolates (treated by I. Kuwajima and E. Nakamura). Lastly there are chapters on metalloenamines (S. F. Martin), hydrazone anions (D. E. Bergbreiter and M. Momongan), and the Prins and carbonyl ene reactions (B. B. Snider). One could hardly ask for more from this part of the book. Here the reader will find information on the very latest developments in each of the reactions described.

The contents of the third part come as a slight surprise, but follow quite logically within the subject organization that has been adopted. There are chapters on "Aliphatic Friedel–Crafts Acylations" (S. C. Eyley), "Aromatic Friedel–Crafts Reactions" (H. Heaney), "The Vilsmeier–Haack Reaction" (O. Meth-Cohn and S. P. Stanforth), "Acylation of Esters, Ketones and Nitriles" (W. R. Davies and P. J. Garratt), and "The Eschenmoser Coupling Reaction" (K. Shiosaki).

In some cases it is not obvious why the topic was thought to deserve a separate chapter. For example, it is surprising to find that the Reimer–Tiemann reaction is given a separate chapter of only six pages with 29 references. Other reactions that one would expect to be grouped together in the same part of the book on the grounds of sharing a common mechanism, at least under the arrangement used here, appear elsewhere or are completely absent. For this volume at least the word "comprehensive" in the title should be interpreted as meaning "detailed"; the reader hoping for an exhaustive coverage will be disappointed. A few random checks soon reveal that some chapters have omitted quite important developments, while including others of relatively minor significance. However, this does not detract greatly from the work as a whole, as one can learn about other useful applications from the review articles cited. On the other hand, it is annoying to find that many of the examples mentioned in the text are not backed up by formula schemes that one could take in at a glance; presumably they were left out to save space. This

is a pity, as the chemist can assimilate information so much faster from formula diagrams than from text!

As the series editors point out in the preface, the assignment of subject areas to particular volumes is to some extent arbitrary. The same certainly applies also to the assignment to individual chapters within the volumes. Nevertheless, it can be disconcerting when a long-familiar reaction appears in an unusual context. Examples of this are the Eschenmoser coupling reaction in Chapter 3.7, and to some extent the three sections on different aspects of the Mannich reaction (bimolecular aliphatic, by E. F. Kleinman, bimolecular aromatic, by H. Heaney, and intramolecular, by L. E. Overman and D. J. Ricca) when compared with the chapters on "Reactions of Allyl and Propargyl/Allenyl Organometallic Compounds with Imines and Iminium Ions" (E. F. Kleinman and A. Volkmann) and "Additions to *N*-Acyliminium Ions" (H. Hiemstra and W. N. Speckamp). Several of these chapters are real mines of information for the reader seeking solutions to synthetic problems in heterocyclic chemistry. Here, as elsewhere in this volume, the regio-, stereo-, and enantioselectivity aspects are treated in detail. Also of interest in this context is Chapter 4.6 on "The Passerini and Ugi Reactions" (I. Ugi, S. Lohberger, and R. Karl).

The author index is sensibly planned, giving not only the page number in the present volume but also the number of the reference on the page concerned. In contrast the subject index is totally inadequate: many of the topics are found at best only by chance, as the choice of keywords under which particular topics are entered is rather arbitrary. For example, starting with the keyword "Fenestranes", then moving to the sub-heading "synthesis" (which has no page reference), we eventually find "Dieckmann reaction, p. 829)". But then, under the keyword "Dieckmann reaction", the same page references does not appear. Any number of further examples of this sort could be listed. Under "Dialdehydes" we find just three entries, the first under the sub-heading "Henry reaction", the second under "intramolecular aldol reaction", and the third under "Knoevenagel reaction", with three page numbers altogether. One can hardly believe that only three pages of this hefty volume contain any mention of dialdehydes.

Whoever was responsible for compiling this "Subject Index" may have had a plan in mind, but it is not apparent to the reader. However, perhaps its main purpose is to stimulate thought, which cannot be a bad thing.

Armin de Meijere
Institut für Organische Chemie
der Universität Göttingen (FRG)

Volume 3

The third volume of this series covers the formation of C–C σ-bonds, and is in four parts with a total of 32 chapters. The first part is concerned with alkylations at a carbon atom. Chapter 1.1 by D. Caine is well worth reading, and deals with alkylations of the enol and enolate forms of carbonyl compounds and their nitrogen derivatives. In Chapter 1.2 R. E. Gawley and K. Rein deal with the alkylation of nitrogen-stabilized carbanions, and this is followed by A. Krief's monumental review of the alkylation of sulfur- and selenium-containing carbanions (Ch. 1.3), which could hardly be bettered. Alkylations of carbanions stabilized by other heteroatoms are treated very briefly in Chapter 1.4 by D. R. Cheshire, then in Chapter 1.5 J. M. Klunder and G. H. Posner discuss the corresponding reactions of non-stabilized carbanions. Chapter 1.6 (D. W. Knight) and 1.7 (P. J. Garratt) contain interesting descriptions of alkylations of vinyl and alkynyl anions, respectively. In Chapter 1.8 G. A. Olah, R. Krishnamurti, and G. K. S. Prakash discuss another important type of reaction, Friedel–Crafts alkylations. In Chapter 1.9 J. K. Sutherland shows how polyene cyclizations can be used to synthesize a wide variety of cyclic compounds; however, the title of this chapter is slightly misleading, since the subject matter is not limited solely to rearrangements of polyenes. D. C. Harrowven and the volume editor G. Pattenden conclude this first part with a review of transannular electrophilic cyclizations (Ch. 1.10).

Part 2 is devoted to coupling reactions. The first five chapters are mainly concerned with transition metal catalyzed syntheses. In Chapter 2.1 D. C. Billington describes reactions in which a bond is formed between two sp^3 carbon atoms, then in Chapter 2.2 K. Tamao deals with couplings between sp^2 and sp^3 carbon atoms, and in Chapter 2.3 D. W. Knight describes couplings between two sp^2 carbon atoms. K. Sonogashira completes the picture by reviewing, in Chapters 2.4 and 2.5, couplings between an sp^2 and an sp carbon, and between two sp carbons. Next we come to reductive C–C coupling reactions: Chapter 2.6 (G. M. Robertson) deals with reactions of the pinacol type, and Chapter 2.7 (R. Brettle) with those of the acyloin type. Electrochemical methods are now increasingly important, as is convincingly illustrated in Chapter 2.8 on Kolbe reactions (H. J. Schäfer). In Chapter 2.9 D. A. Whitting concludes this part with a review of the current state of knowledge on the oxidative coupling of phenols and phenol ethers, a topic that continues to attract interest.

Part 3 is devoted to rearrangement reactions, beginning in Chapter 3.1 with an article by J. R. Hanson on the Wagner–Meerwein rearrangement. Next B. Rickborn reports briefly in Chapter 3.2 on the pinacol rearrangement, then in greater detail in Chapter 3.3 on acid-catalyzed rearrangements of epoxides. There follow contributions by D. J. Coveney on the semipinacol rearrangement (Ch. 3.4) and by D. A. Whiting on the dienone–phenol rearrangement (Ch. 3.5). Next come chapters on rearrangements performed under basic conditions: Chapter 3.6, by G. B. Gill, discusses the benzil–benzilic acid rearrangement, then in Chapter 3.7 J. Mann deals with the Favorskii rearrangement and in Chapter 3.8 J. M. Clough with the Ramberg–Bäcklund rearrangement. These are followed by the Wolff rearrangement (G. B. Gill, Ch. 3.9) and an excellent review of ylide rearrangement reactions by I. E. Markó in Chapter 3.10. This part ends with an article by J. A. Marshall (Ch. 3.11) on the Wittig rearrangement. Some of the reactions treated in this part could instead have been assigned to Volume 5 under the heading "sigmatropic processes", and conversely some rearrangements, such as the Fritsch–Buttenberg–Wiechell rearrangement, are not included, but on the whole this is a good representative survey of the present importance of rearrangement reactions in organic synthesis.

Under the rather uninformative title "Other Carbon–Carbon Bond Forming Reactions", Part 4 contains two very interesting articles. The first, by D. J. Thompson (Ch. 4.1), discusses carbonylation and decarbonylation reactions, and the second, by D. F. Taber (Ch. 4.2), is concerned with the formation of C–C bonds by C–H insertion.

The synthetic chemist will find that this volume covers all important aspects of alkylations at carbon atoms, coupling reactions, and rearrangements. Although it has not been possible to describe all the interesting developments in detail, appropriate references to the original literature are given throughout. In nearly all the articles the literature coverage extends up to 1989, and in some cases to 1990. Access to the older literature, where not cited in the original publications, is provided through references to older reviews. Naturally,

one cannot expect a book with this type of format to be completely free of errors, but my impression is that the authors and publisher have taken great care in the preparation of this volume. It is worth pointing out that this is not a comprehensive textbook but a collection of excellent review articles. Its usefulness could have been even further improved by more frequent cross-references to discussions in other chapters. However, the overall verdict is that this book has no rival of its kind, and it can be recommended unreservedly to everyone with an interest in organic synthesis.

Uwe Beifuss
Institut für Organische Chemie
der Universität Göttingen (FRG)

Volume 4

The very generally worded title of Volume 4, "Additions to and Substitutions at C–C π-Bonds", suggests right at the start that here space has had to be provided between the covers of one volume for a whole potpourri of reactions. The contributions by 31 eminent authors are grouped into four lengthy parts, three of which are devoted to the addition and substitution reactions of olefins, allenes, and alkynes, which are so useful to the synthetic chemist. In this otherwise coherent group of topics, Part 2, on nucleophilic substitutions of arenes, seems slightly out of place. This part treats not only classical methods such as the S_NAr reaction, the addition of nucleophiles to arynes, and the $S_{RN}1$ reaction, but also the reactions of nucleophiles with arene–metal complexes, and meets the needs of readers who wish to learn something about the mechanistic fundamentals of such reactions as well as those seeking a solution to a particular synthetic problem.

In the first six chapters of Part 1 the main emphasis is on the formation of C–C bonds by the addition of groups with a nucleophilic carbon atom at electron-deficient double and triple bonds. Not surprisingly, special attention is devoted to the Michael addition which, although quite old, is still an active research topic. The authors cover the whole range of nucleophiles, starting with the classical mesomerically-stabilized carbanions and continuing through lithium compounds and cuprates to boranes and silanes. A recurring theme throughout all the articles is the selectivity of the reactions; there is even a separate chapter devoted to ways of achieving diastereo- and enantioselective reactions. Next come three chapters on electrophilic additions to systems with multiple bonds, although these fit less appropriately under the title of this part ("Polar Additions to Activated Alkenes and Alkynes"). Here, as one would expect, the formation of carbon–heteroatom bonds features prominently.

The excursion into arene chemistry in Part 2, already discussed above, is followed by Part 3 with the rather misleading title "Polar Additions to Alkenes and Alkynes". This is definitely not concerned with "normal" olefins and alkynes; instead the common feature of all five chapters of Part 3 is that the unsaturated system undergoes complexation with fragments of transition metal compounds, making it vulnerable to attack by polar reagents. Three of the chapters describe palladium-induced additions of groups with a nucleophilic carbon atom or heteroatom to alkenes, alkynes, and allylic systems. The noble metal palladium is not essential in every case, as is shown in the two remaining articles. The iron tricarbonyl fragment can form complexes with dienes and polyenes and thereby activate them for attack by electrophiles; alternatively, its cationic pentadienyl complexes can be reacted with nucleophiles to yield a wide variety of substituted dienes.

Part 4 begins with two articles on the addition of free radicals at C–C π-bonds, which are well worth reading. As well as describing how such reactions can be used for synthetic purposes, these chapters equip the reader with much valuable basic knowledge about free radicals and their properties. The next two chapters deal with palladium-catalyzed vinyl substitutions and with the addition of organometallic compounds at carbon–carbon multiple bonds; however, it is a little surprising that they should appear in this part under the overall title "Nonpolar Additions to Alkenes and Alkynes". A further chapter is devoted to hydroformylation, the importance of which is not confined to industrial processes, as it enables one to form a C–C bond with the simultaneous introduction of a carbonyl group, thereby making possible a great variety of further transformations. The closing chapters take one into the broad field of cycloadditions. Two contributions describe the preparation of alkylidene- and keto-carbenes and their addition at carbon–carbon multiple bonds. A third article is concerned with the generation of dihalogen-carbenes, and discusses the impressive synthetic potential of the geminal dihalogen-cyclopropanes obtainable by this route. The volume ends with two articles on inter- and intramolecular 1,3-dipolar cycloadditions.

To summarize, Volume 4 of the series covers many different types of synthetically important reactions of C–C π-bonds in great detail. It is an excellent source of information for the synthetic chemist seeking help. Leaving aside the sometimes rather misleading titles, the presentation of this wealth of information has been carefully thought out, and in combination with a detailed subject index it gives rapid access to the relevant primary literature published up to 1989. Moreover, the needs of newcomers to the field have not been neglected, since most of the articles contain an introductory historical survey with many references to review articles for further reading.

Johannes Belzner
Institut für Organische Chemie
der Universität Göttingen (FRG)

Volume 5

Volume 5 deals with the combining of C–C π-bonds by pericyclic and related reactions. Those discussed include the ene reaction, thermally and photochemically induced [2 + 2]-cycloadditions of alkenes and carbonyl compounds, [3 + 2]- and [4 + 2]-cycloadditions and cycloadditions of higher order, electrocyclic processes, and sigmatropic rearrangements. To complete the volume there are contributions on rearrangements of small rings and reactions involving transition metals.

In the chapter on ene reactions B. B. Snider first describes reactions in which an alkene serves as the enophile (27 pp.), then W. Oppolzer discusses metallo-ene reactions (32 pp.). The carbonyl ene reaction is treated in Volume 2, fortunately indicated by a cross-reference in the introduction to this chapter. Elsewhere, however, such cross-references are rare; on the other hand, this should not be taken as a very serious criticism, since the work as a whole has a good (though not exhaustive) index.

Under [2 + 2]-cycloadditions J. E. Baldwin describes the thermally induced formation of cyclobutane (21 pp.), L. Ghosez and J. Marchand-Brynaert the preparation of four-membered heterocycles (37 pp.), M. T. Crimmins the photochemical cycloaddition of alkenes (27 pp.), J. A. Porco and S. L. Schreiber the Paternò–Büchi reaction (41 pp.), and O. De Lucchi, W. Adam, and M. Demuth di-π-methane photoisomerizations (44 pp.).

[3 + 2]-Cycloadditions are subdivided into those that are thermally induced (31 pp., by R. D. Little) and those cata-

lyzed by transition metals (43 pp., D. M. T. Chan). Almost 300 pages are devoted to the Diels–Alder reaction, underlining yet again the importance of this method, first reported in its general form in 1928. The treatment is divided into separate chapters dealing with the intermolecular Diels–Alder reaction, cycloadditions using heterodienophiles and heterodienes, the intramolecular Diels–Alder reaction, and the retro-Diels–Alder reaction; the authors are W. Oppolzer, S. M. Weinreb, D. L. Boger, W. R. Roush, R. W. Sweger, and A. W. Czarnik.

Coming to the higher-order cycloadditions, A. Hosomi and Y. Tominaga cover the [4 + 3]-cycloadditions (22 pp.), J. H. Rigby the [4 + 4]- and [6 + 4]-cycloadditions (26 pp.), and P. Wender, L. Siggel, and J. M. Nuss the interesting photochemical addition reactions of arenes (28 pp.). After the cycloaddition reactions, electrocyclic processes for the ring-opening of cyclobutenes to give 1,3-dienes (22 pp., by T. Durst and L. Breau) and for the formation of 1,3-cyclohexadienes (51 pp., by W. H. Okamura and A. R. DeLera) are described, as well as the Nazarov reaction, in which divinyl ketones are stereoselectively transformed into cyclopentenones through the influence of acids (33 pp., by S. E. Denmark). Altogether 123 pages are devoted to sigmatropic reactions with their wide variety of synthetic uses: the Cope and oxy-Cope rearrangements (R. K. Hill) and the Claisen rearrangements (P. Wipf). Also in this section, F. E. Ziegler describes the interesting sequential transformations in which two or more sigmatropic processes follow one after another.

The topics covered in the last 300 pages of this volume are: rearrangements of vinylcyclopropanes (T. Hudlicky and J. W. Reed, 71 pp.) and of divinylcyclopropanes (E. Piers, 27 pp.), charge-controlled rearrangements (J. J. Bronson and R. L. Danheiser, 37 pp.), and other transition-metal induced reactions, namely the Pauson–Khand reaction (Co-induced cycloaddition of alkynes with alkenes and CO to yield cyclopentenones, described here by N. E. Schore), the metal–carbene cyclization (W. D. Wulff), the alkene metathesis reaction and the interesting Co-induced [2 + 2 + 2]-cycloadditions of alkynes to arenes (R. H. Grubbs and S. H. Pine), the Zr-induced bicyclization of enynes (E. Negishi), and the metal-catalyzed cycloaddition of small rings (T. Ohta and H. Takaya).

All the articles are written by outstanding experts. A clear arrangement of the subject matter is always indicated at the beginning, and a useful summary is provided in nearly every case. There are, of course, differences in style and in care of presentation between the authors, and some chapters show a higher frequency of errors than others. However, all the articles are of a high quality, and the examples are well chosen in most cases, not only explaining the principles of the synthetic methods but also showing their potency for the synthesis of complex natural products. A small criticism is that some chapters do not devote enough space to the theoretical and mechanistic aspects and to explaining the individual steps in the syntheses. The literature has been carefully and critically reviewed, though it is, of course, unfortunate that two years elapsed between the completion of the articles and the volume's publication.

To summarize, this fifth volume offers a competently prepared, clearly arranged, and critical overview of modern methods for combining C–C π-bonds, and the wealth of interesting and topical examples makes it a rich source of information for scientists and students.

Lutz F. Tietze
Institut für Organische Chemie
der Universität Göttingen (FRG)

Volume 6

The sixth volume is devoted to heteroatom manipulations. In a total of 1194 pages under this main heading the volume covers substitution reactions, acylation type reactions, protecting groups, transformations of functional groups, and elimination reactions. The enormous amount of information is subdivided into individual articles of typically about 30 pages, each with between 100 and 200 literature references. The arrangement is well thought out, but it should be noted that topics have been assigned to chapters and larger sections (and to volumes) not so much on the basis of reaction mechanisms as by certain formal criteria and, so far as possible, classes of compounds. Nevertheless, this meets the needs of the preparative organic chemist very well and makes it easy to find individual topics. The editor, E. Winterfeldt, has in every case recruited expert authors to write the chapters, often those recognized as the leading proponents of their specialist fields.

Part 1 covers methods for synthesizing classes of compounds that are formally derived by substitutions: alcohols and ethers (O. Mitsunobu); glycosides, by all the usual glycosidation methods (R. R. Schmidt); amines and ammonium salts (O. Mitsunobu); nitro and nitroso compounds, hydroxylamines, hydrazines, diazoalkanes, diazoketones, and diazoesters (R. Askani and D. F. Taber); sulfides, thioacetals, sulfoxides, and sulfones (G. Solladié); phosphonium ylides of the alkylidene- and vinylidenephosphorane types, and carbodiphosphoranes (H. J. Bestmann and R. Zimmermann); halides (R. Bohlmann); and nitriles, isonitriles, cyanates, and azides (R. Grashey). Inter- and intramolecular Ritter reactions are also treated (R. Bishop).

Part 2 contains reviews of syntheses of compounds formed by acylation or related reactions: acyl halides, anhydrides, and α-ketonitriles (R. Sustmann); esters, activated esters, and lactones (R. Mulzer); amides, lactams, and imides (G. Benz); thioamides and thiolactams (E. Schaumann); thioesters and thiolactones with –(C=O)S–, –(C=S)O–, and –(C=S)S– groups (J. Voss); selenoesters with –(C=O)Se– and –(C=Se)O– groups, together with selenoamides (A. Ogawa and N. Sonada); iminium salts, orthoesters, and related compounds (W. Kantlehner, 115 pp. with 996 literature references!); and phosphate and phosphite derivatives commonly encountered in nucleotide chemistry (Y. Hayakawa).

Part 3, on protecting groups (70 pp., 409 references), is entirely the work of H. Kunz and H. Waldmann. As well as explaining the general requirements for the blocking of functional groups, the authors discuss specific protecting groups for hydroxy, amino, mercapto, carboxy, and carbonyl groups.

Part 4 discusses methods for the transformation of functional groups, beginning with carbonyl compounds and their derivatives. These chapters describe the conversion of carbonyl compounds into enamines, imines, hydrazones, oximes, and the carbanions derived from these (G. M. Whitesell), methods for synthesizing heterocycles from carbonyl derivatives using nucleophilic, electrophilic, free radical ring-closing, and hetero-Diels–Alder reactions (G. Bringmann, C. L. J. Ewers, and R. Walter), and the conversion of carbonyl derivatives by Beckmann, Neber, and Amadori rearrangements and by Bamford–Stevens and Shapiro reactions (K. Maruoka and H. Yamamoto). A further two chapters are devoted to stereoselective transformations of allylic systems, reactions of the S_N', S_E', and Claisen types being treated by H.-J. Altenbach, while 2,3-sigmatropic rearrangements are treated by R. Brückner. Part 4 also covers the breakdown of carboxylic acid derivatives by means of Hoffmann, Curtius, Schmidt, and Lossen reactions (T. Shiori),

 © VCH Verlagsgesellschaft mbH, D-69451 Weinheim, 1993 0570-0833/93/0707-1099 $ 10.00+.25/0

and transformations based on the Polonovski, Pummerer, and Nef reactions.

Part 5 describes the synthesis of alkenes, allenes, and alkynes by E_1, E_1cB, and E_2 elimination reactions (A. Krebs and J. Swienty-Busch), reductive eliminations, vicinal deoxygenations and vicinal desilylations (P. Kocienski), Cope, sulfoxide, and selenoxide eliminations and related reactions (P. C. Astles, S. V. Mortlock, and E. J. Thomas), and lastly fragmentation reactions of the Grob and Beckmann types (P. Weyerstahl and H. Marschall). The volume is completed by a useful author index (73 pp.) and a rather less useful subject index (49 pp.).

In a multiauthor work of this kind it is inevitable that some reactions are described more than once (for example, transformations of allylic systems also appear in Chapters 1.1–1.3 of Volume 1 and in Chapter 7 of Volume 5). However, this should not be taken as a criticism, as the different viewpoints of the authors result in a more balanced overall picture. On the other hand, a few compound classes that would have fitted very appropriately into Volume 6 are unfortunately omitted or mentioned only briefly. For example, it would certainly not have been out of place in Part 2 to include short chapters on the synthesis of sulfates, sulfonates, sulfonamides, borates, boronates, borinates, and similar compounds, in view of their synthetic importance. Nevertheless, the team of authors and the volume editor have very successfully negotiated the tightrope between too much compression and too much detail, between too much and too little overlapping, and between generality and specificity. It would have been very useful, however, to be able to select information on reactions and on the associated literature with the help of computerized searching. This could be achieved by producing a data bank of reactions in the form of a CD-ROM, which the publishers could offer as a supplement to the set of volumes. CD updates could also be issued at intervals to accommodate the rapid developments occurring in many areas, thus keeping the total work up-to-date for many years to come. Leaving that aside, this is a first-class reference source which no chemical library should be without, and the reasonable price makes it affordable even for some people's private bookshelves.

Günter von Kiedrowski
Institut für Organische Chemie
der Universität Göttingen (FRG)

Volume 7

The seventh volume is devoted entirely to oxidation reactions. The seven parts, each subdivided into several chapters, cover almost every known oxidation method published up to about 1989. Care has been taken to select the methods that are most useful for synthetic purposes, and the many examples enable the reader to quickly review the possibilities and choose the most promising methods for a given problem. The authors of the individual chapters are all recognized experts in their fields, and in many cases the doyen of a particular method has been persuaded to write the contribution; thus one can be confident that the topics are treated expertly.

The division of subject matter between the chapters takes a little getting used to, but in view of the very large number of reactions that can be classified as oxidations it is a quite logical arrangement, enabling one to find a particular topic without difficulty. In this respect the well planned author index turns out to be very useful in cases where one can already associate a name with the reaction in question. Regrettably though, the subject index is much too scanty to give adequate help in finding one's way through the vast amount of information. In the age of computer-aided index compilation the appropriate maxim here should certainly have been: more would mean more!

Part 1 (82 pp.) deals with oxidations of non-activated C–H bonds. The four chapters describe how such oxidations can be performed not only by conventional chemical or biochemical methods but also by nitrene insertion reactions or by suitable intramolecular functionalizations.

Part 2, consisting of about 260 pages divided into eleven chapters, is concerned with oxidations of activated C–H bonds. Here there emerges a clear trend which helps one to quickly decide on the most suitable synthetic approach: methods for oxidations of C–H bonds adjacent to C=C or C=X bonds are contrasted to those for C–H bonds adjacent to sulfur, nitrogen, or oxygen. This part ends with oxidations of vinyl and aryl C–H bonds and the synthesis of quinones.

Part 3 (235 pp.) deals with the oxidation of C=C bonds. Here, as expected, special attention is devoted to asymmetric methods of epoxidation and hydroxylation. The authors have succeeded well in presenting the numerous methods that have been developed, with their respective advantages and disadvantages, in a logical framework. However, the speed of developments in this area is such that the advances made in the last two years, some of which are highly innovative, could not be included in these chapters. As well as a detailed treatment of addition reactions that involve the formation of C–O bonds, we find here methods for functionalizing C=C bonds by the introduction of nitrogen, sulfur, selenium, or halogens using appropriate reagents. Last but not least comes a discussion of the oxidative cleavage of C=C bonds.

In Part 4 (77 pp.) we come to the oxidation of carbon-heteroatom bonds. Methods for oxidizing carbon–metal bonds are treated especially thoroughly, with tin, palladium, and mercury as some of the more important metal atoms. Separate chapters are also devoted to the important topics of oxidations of carbon–boron, carbon–silicon, and carbon–halogen bonds.

Part 5 (63 pp.) is concerned with the oxidation of C–C bonds. Starting from the basis of the Baeyer–Villiger, Beckmann, and Hunsdiecker reactions, and the cleavage of glycols, the various possibilities in this area are described.

Part 6 (53 pp.) provides ample evidence of the interest in the oxidation of heteroatoms. In addition to nitrogen, phosphorus, and sulfur, which have traditionally received most attention as heteroatoms in this context, an appropriate amount of space is devoted to selenium and tellurium in view of their growing importance.

Any readers who have not up to this point found the ideal oxidation reaction for their purpose might usefully take a look at Part 7 (99 pp.), which deals with special methods. As well as electrochemical variants and oxidations using solid-phase reagents, this includes oxidative rearrangements and electron transfer reactions.

While it contains a great wealth of information on oxidation reactions, this book is more than just a survey of the literature. The clearly arranged tables give reliable information about the nature of each reaction, anticipated yields, and relevant review articles. Also it is pleasing to note that in some cases the tables include comments on the general advantages and disadvantages of each method. More information of this sort would certainly have been welcomed, as also would a more user-friendly form of presentation of the various methods: for example, a list identifying compatible and incompatible functionalities for each oxidation method would be very useful.

Despite these minor criticisms, I can recommend chemists to buy this book (and, indeed, the whole work). The defects mentioned above are comparatively trivial when one takes into account the affordable price and the expertly prepared contents.

Oliver Reiser
Institut für Organische Chemie
der Universität Göttingen (FRG)

Volume 8

Volume 8, "Reduction", consists of four parts with the following titles: "Reduction of C=X Bonds" (14 chapters, 356 pp.), "Reduction of X=Y Bonds" (3 chapters, 52 pp.), "Reduction of C=C and C≡C Bonds" (12 chapters, 369 pp.), and "Reduction of C–X to C–H" (8 chapters, 197 pp.). Like the other volumes in the series it also contains an author index (79 pp.) and a subject index (61 pp.).

Part 1 contains the following chapters: "Reduction of C=O to CH(OH) by Metal Hydrides" (N. Greeves, 24 pp., 147 references), "Reduction of C=N to CN(NH) by Metal Hydrides (R. O. Hutchins, 54 pp., 251 references), "Reduction of C=X to CH(XH) by Hydride Delivery from Carbon" (R. M. Kellogg, 28 pp., 131 references), "Reduction of C=X to CH(XH) by Dissolving Metals and Related Methods (J. W. Huffman, 21 pp., 95 references), "Reduction of C=X to CH(XH) Electrolytically" (L. Moëns, 10 pp., 60 references), "Reduction of C=X to CH(XH) by Catalytic Hydrogenation" (K. Harada and T. Munegumi, 20 pp., 203 references), "Reduction of C=X to CH(XH) by Chirally Modified Hydride Reagents" (M. Nishizawa and R. Noyori, 24 pp., 137 references), "Reduction of C=X to CH(XH) Using Enzymes and Microorganisms" (J. B. Jones, 27 pp., 173 references), "Reduction of Acetals, Azaacetals and Thioacetals to Ethers" (J. H. Brewster, 24 pp., 148 references; it is unfortunate, of course, that this chapter went to press before the publication of Nicolaous's imaginative use of the reduction of O,S-acetals as an approach to the synthesis of brevetoxin), "Reduction of Carboxylic Acid Derivatives to Alcohols, Ethers and Amines" (A. G. M. Barrett, 23 pp., 127 references), "Reduction of Carboxylic Acids to Aldehydes by Metal Hydrides" (R. A. W. Johnstone, 23 pp., 158 references), "Reduction of Carboxylic Acids to Aldehydes by Other Methods" (A. P. Davis, 23 pp., 102 references; contrary to what their titles suggest, this and the previous chapter also include reductions of all kinds of carboxylic acid derivatives, but they are much too short to cover these adequately), "Reduction of C=X to CH_2 by Dissolving Metals and Related Methods" (S. Yamamura and S. Nishiyama, 19 pp., 117 references), and "Reduction of C=X to CH_2 by Wolff–Kishner and Other Hydrazone Methods" (R. O. Hutchins, 36 pp., 204 references).

Part 2, covering the reduction of X=Y bonds, consists of three chapters: "Reduction of Nitro and Nitroso Compounds" (G. W. Kabalka and R. S. Varma, 17 pp., 168 references), "Reduction of N=N, N–N, N–O and O–O Bonds" (T. L. Gilchrist, 22 pp., 148 references) and "Reduction of S=O and SO_2 to S, of P=O to P, and of S–X to S–H" (I. W. J. Still, 13 pp., 135 references).

In Part 3 reductions of C=C and C≡C Bonds are covered by the following chapters: "Heterogeneous Catalytic Hydrogenation of C=C and C≡C" (S. Siegel, 26 pp., 85 references), "Homogeneous Catalytic Hydrogenation of C=C and C≡C" (H. Takaya and R. Noyori, 27 pp., 270 references), "Reduction of C=C and C≡C by Noncatalytic Chemical Methods" (D. J. Pasto, 18 pp., 67 references; here the section on reductions of C≡C bonds to olefins by metal hydrides unfortunately does not discuss the questions of *cis* versus *trans* selectivity nor the effects of substituents and reaction media), "Partial Reduction of Aromatic Rings by Dissolving Metals and Other Methods" (by L. N. Mander, the leading expert in this area, 33 pp., 133 references), "Partial Reduction of Enones, Styrenes and Related Systems" (E. Keinan and N. Greenspoon, 54 pp., 486 references), "Partial and Complete Reduction of Pyridines and their Benzo Analogs" (J. G. Keay, 24 pp., 107 references), "Partial and Complete Reduction of Pyrroles, Furans, Thiophenes and their Benzo Analogs" (G. W. Gribble, 31 pp., 188 references), and "Partial and Complete Reduction of Heterocycles Containing more than One Heteroatom" (M. Sainsbury, 32 pp., 123 references). There are four further chapters: "Hydrozirconation of C=C and C≡C and Hydrometalation by Other Metals" (J. A. Labinger, 36 pp., 150 references; but "other metals" here does not include free radical, cuprate-induced, or palladium-catalyzed hydrostannylations), "Hydroboration of C=C and C≡C" (K. Smith and A. Pelter, 29 pp., 199 references), "Hydroalumination of C=C and C≡C" (J. J. Eisch, 29 pp., 171 references), and "Hydrosilylation of C=C and C≡C" (T. Hiyama and T. Kusumoto, 30 pp., 123 references). The inclusion here of these four is surprising, as one thinks of these reactions as additions to carbon–carbon multiple bonds rather than reductions. Moreover, only in a tiny minority of the examples given do the organometallic products undergo a subsequent protonolysis, which might justify their inclusion in this context.

Part 4 treats reductions of C–X to C–H under the following headings: "Reduction of Saturated Alkyl Halides to Alkanes" (T. Imamoto, 17 pp., 129 references), "Reduction of Saturated Alcohols and Amines to Alkanes" (S. W. McCombie, 23 pp., 92 references), "Reduction of Sulfur–Carbon Bonds and Other Heteroatoms Bonded to Tetrahedral Carbon" (P. Caubère and P. Coutrot, 36 pp., 249 references), "Reduction of Epoxides" (S. Murai, T. Murai, and S. Kato, 19 pp., 149 references), "Reduction of Vinyl Halides to Alkenes, and of Aryl Halides and Related Compounds to Arenes" (M. Hudlicky, 28 pp., 121 references), "Reduction of Ketones to Alkenes" (A. R. Chamberlin and D. J. Sall, 32 pp., 177 references), "Hydrogenolysis of Allyl and Benzyl Halides and Related Compounds" (I. D. Entwistle and W. W. Wood, 27 pp., 149 references; the title of this chapter is misleading, since in addition to hydrogenolyses, i.e. bond cleavages by hydrogen, it includes the cleavage of C–X bonds by complex hydrides or by non-noble metals in ammonia, etc., and there are considerably more examples where X is O than where it is a halogen), and lastly "Reduction of α-Substituted Carbonyl Compounds –CX–C(=O)– to Carbonyl Compounds –CH–C(=O)–" (A. J. Fry, 15 pp., 72 references).

This volume, like the rest of the work, contains a wealth of information that no preparative organic chemist can afford to be without. In the examples chosen to illustrate the reactions the opportunity has been taken wherever possible to include interesting stereochemical aspects and/or noteworthy chemoselectivity effects. It has turned out that some reactions are treated in more than one chapter, but this is inevitable in view of the complexity of the subject and the degree of ambiguity in its subdivision. Moreover, to find several treatments of the same topic from different points of view can sometimes be an advantage rather than an annoying repetition. "Sins of omission", where one fails to find topics that should have been included, are far more serious. It is much to the credit of the team of editors (and others) that there is little to complain about in this respect. However, one topic that has been entirely overlooked is reductions of

glycols and their derivatives (halogen hydrins and the ethers or esters derived from them, *vic*-dihalides) to olefins, and also ring-opening reactions of cyclopropanes would perhaps have been of interest to some readers. The aromatic radical anions such as lithium naphthalide, lithium 4,4′-di-*tert*-butylbiphenylide, and lithium-1-(dimethylamino)naphthalenide (LDMAN), which have been used increasingly in recent years as reducing agents, also seem to have been overlooked. It is also regrettable, though understandable in view of the work involved, that the editor has not been able to persuade anyone to compile a table listing the reactivities and selectivities of different reducing agents. There can hardly be a single user of the book who would not welcome a table showing which transformations can be performed in the presence of which other functionalities without the latter being attacked.

In a work as substantial as this, in which the arrangement of the subject matter can never be ideal in *all* respects, it is essential to provide a well planned subject index which covers the contents as fully as possible and offers the reader a high probability of finding the required answer. Unfortunately the 61-page index is a total failure by these criteria. On the one hand the reader finds reducing agents listed with indications of the substrates that they are capable of reducing, and conversely he can look up a given substrate to locate information on its reactions with different reducing agents. However, the information given by the index is neither well organized nor complete. Suppose, for example, that we want to know how lactones can be reduced: under "Lactones" we find two page references, one with the (self-evident) sub-heading "reduction" and the other with the sub-heading "metal hydrides". But then under "Aldonolactones", if it occurs to us to look up this keyword, we find two different page references corresponding to "electrochemical reduction" and "formation of aldoses", respectively. Finally, under "γ-Butyrolactone" we find yet another (different) page reference with the sub-heading "hydrogenation".

Another type of question that the synthetic chemist may want to ask is "How can I obtain my target molecule via a reduction?" Here it is very unlikely that the subject index could yield an answer. An example will illustrate this: if one wishes to know how allyl alcohols can be obtained reductively, and to compare the possibilities of preparing these by reduction of the corresponding malonic ester, enone, propargyl alcohol, vinyl epoxide, or α,β-epoxyalcohol, the subject index does not yield a single page reference that could help. Even when we look under "Alcohols" for reductive methods of preparation we find only six references (under "via carboxylic acids", "via enantiomeric (!) reduction of carbonyl compounds", "via epoxide reduction", "via hydrogen transfer", "via metal hydride reduction", and "via reduction of hydroperoxides"). Examples of this kind could be continued at will; thus, for reductive routes to alkanes the index lists only three possibilities: "via alcohols and amines", "via alkyl halide reduction", and "via enzyme reduction of alkenes"; no references whatever are given to whole chapters that relate to this problem, nor to the heterogeneously or homogeneously catalyzed hydrogenation of carbon–carbon multiple bonds, nor to the Wolff–Kishner reduction! These inadequacies prompt one to ask whether chemists were really involved in the preparation of the subject index, and to doubt whether one should recommend buying this otherwise really excellent work (!!) until the publishers have replaced the present "Cumulative Indexes" volume by a revised version.

Reinhard Brückner
Institut für Organische Chemie
der Universität Göttingen (FRG)

A Semiempirical Life. (Series: Profiles, Pathways, and Dreams. Series editor: *J. I. Seeman.*) By *M. J. S. Dewar.* American Chemical Society, Washington, DC, 1992. XXIII, 215 pp., hardcover $ 24.95—ISBN 0-8412-1771-8

The title of this lively and informative scientific and personal autobiography derives from Professor Dewar's parametric ("semiempirical") method of determining reaction mechanisms based on an all-valence-electron SCF (self-consistent field) MO (molecular orbital) treatment, in contrast to the "ab initio" SCF approach—an approximation to the Hartree–Fock (HF) SCF MO method involving the linear combination of atomic orbitals (LCAO), introduced independently by C. C. Roothaan and G. G. Hall. Unlike many theoreticians, Dewar recalls that his interest in theory was "purely practical" from the beginning; his own experimental results had made him extremely skeptical of the reaction mechanisms that are "stated so confidently in organic texts." He maintains that reaction mechanisms cannot be observed directly because reactions take place too rapidly and because of the restrictions imposed by the uncertainty principle.

Although Dewar's prediction that most ab initio methods would fail to produce reliable results was confirmed, and although—or because—his treatments based on PNDDO, the various versions of MINDO, and later MNDO and AM1, required a thousand times less computing time than ab initio treatments, "every effort was made to suppress publication of [his] papers and papers by others reporting calculations that used [his] procedures, using every dirty trick in the book."

However, one of Dewar's traits is persistence: "Nothing ever works the first time in organic chemistry, but almost everything does eventually if you try hard enough" (p. 52). Undeterred by criticism, he went on to apply his theoretical-experimental approach to π-complexes, nonclassical carbocations, biomimetic cyclizations, pericyclic reactions (e.g., Diels–Alder reactions and the Cope, Claisen, and benzidine rearrangements), nucleophilic substitutions, enzyme reactions, elimination reactions, singlet oxygen, a refutation of frontier orbital theory, and dozens of other reactions. Dewar has made all his programs freely available rather than commercializing them, and he claims that "My group alone has studied more reactions than all the ab initioists put together with far more chemical effect and at a tiny fraction of the cost" (p. 167).

"Chemistry is, or should be, fun" Dewar proclaims (p. 184). His pursuit of this goal has led him in one direction after another in a long, distinguished multifaceted career that has not prevented him from also pursuing such hobbies as classical music, bridge, chess, running, ice skating, and rock climbing. He has even made original contributions to astronomy and geology.

In this book Michael James Steuart Dewar describes his life from his birth on September 24, 1918 in Ahmednagar, India, where his father, Francis, was a member of the Indian Civil Service, to his current activity as Research Professor of Chemistry at the University of Florida at Gainesville, where he is attempting to develop an effective theoretical treatment for transition metals, a major goal of his for the past decade and a half. In the course of his engrossing tale he discusses his education at a boarding school in England and at Winchester College, one of the leading English public (private) schools (1931–1936), where he taught himself science in general and chemistry in particular by reading books. ("If my thoughts about chemistry have often been unorthodox, this is probably the reason," p. 14). He then attended Balliol College, Oxford University (1936–1945). Here he supported

himself by means of two scholarships, was influenced by R. P. (Ronnie) Bell and Sir Robert Robinson, and received his B. A. (1940), D. Phil. (1942), and M. A. (1943). In addition to discussing his research on alkaloids (yohimbine) and his wartime work on explosives, sulfa drugs, antimalarials, and penicillin (the last two as a postdoctoral fellow with Sir Robert Robinson at Oxford's Dyson Perrins Laboratory), he relates "the most important event of my life," his meeting with "someone who was more than my equal," Mary Williamson, whom he wed on June 3, 1944, three days before D-Day. Because Mary was a historian, scholar, and author rather than a scientist, their relationship has been a mutually beneficial one ("we tend to look at things from different viewpoints"). Their almost half-century marriage has been a very close and happy one, resulting in two sons, Robert and Steuart, both of whom now work with computers.

From 1945 to 1951 Dewar was a "physical chemist" at the new laboratory set up by Courtaulds, Ltd. (the rayon and acetate fibers manufacturer) at Maidenhead near London, where he carried out basic research on polymerization and other problems, while teaching himself physical chemistry and writing his first book, *The Electronic Theory of Organic Chemistry* (1949), "the first general account of organic chemistry in terms of MO theory." Although a move from an industrial position to an academic position is unusual (another exception to the rule was Carl Djerassi's move from Syntex to Wayne State University, related in *Steroids Made It Possible*, an earlier volume in the *Profiles* series), in 1951 Dewar was offered the position of Professor of Chemistry and Department Head at Queen Mary College, University of London, the youngest person (age 33) to be appointed to a chair in London except for one or two mathematicians. At QMC, where Mary belatedly obtained her Ph.D., Dewar carried out research on resonance theory, bond localization, molecular orbital (PMO) theory, structures of phosphonitrile chlorides, condensation of steam on metal surfaces, liquid crystals, and NMR, ESR, and NQR spectroscopy.

In 1959 Dewar was appointed to the late Morris S. Kharasch's chair at the University of Chicago, the first full professor to defect in the "brain drain". Here he continued his work on borazaromatic compounds and "one-off" projects--relatively short-term projects designed to answer a specific question and providing ideal training for graduate students. He also began his current theoretical program described at the beginning of this review, which he developed fully during his tenure as Robert A. Welch Professor of Chemistry at the University of Texas at Austin (1963–1990). In the course of his account he discusses with praise or sometimes with scorn the contributions of others, and the book reads like a "Who's Who" of organic chemistry. He champions the contributions of chemists such as Christopher Longuet-Higgins and M. G. Evans, whose work he thinks has not been sufficiently appreciated.

This picture of Dewar that emerges from these pages is one of a complex, brilliant, no-nonsense scientist and devoted husband and father. Insight into his character is best conveyed in his own words. Being scrupulously realistic in evaluating his own abilities and shortcomings and those of others, he expresses himself with a refreshing frankness and matter-of-fact candor that sometimes appears brash or controversial: "Because I have ... never been a respecter of persons, let alone of 'experts', my contributions have ... not always been expressed too tactfully" (p. 183). Being secure and comfortable with who he is, he can make statements that might be considered boastful if uttered by others: "My arrival in Texas put the place on the academic map" (p. 112). "I probably know more about [the mechanism of pericyclic reactions] than any other chemist who is still active" (p. 139). At other times his characteristic forthrightness results in statements that might be misconstrued as false modesty: "I have come up with a number of similar contributions that have given me an undeserved reputation for original thinking. I am not, in fact, original in the proper sense of the term. I am, however, good at solving problems..." (pp. 39–40). "I am hopeless at administration. I am good at seeing what has to be done but hopeless at getting it done. A good administrator operates by manipulating people. I have never been any good at this" (p. 67). "I have always been very bad at publicizing the things I have done" (p. 91). Unlike too many of us, he benefits from his experiences. In his concluding chapter, titled "Debts Owed, Lessons Learned," he decries the growing trend for conformity and the tendency for chemists to take their work too seriously, and he criticizes the policies of the National Science Foundation and the *Journal of the American Chemical Society*. Although he voices his opinions strongly, he is not opinionated: "I have always been ready, as the record shows, to abandon *any* chemical belief in the face of valid arguments or new evidence" (p. 184).

We warmly recommend this eminently readable and very human autobiography of Professor Dewar, graced by 46 photographs from his family albums, to organic chemists, undergraduate and graduate chemistry students, historians of chemistry, and anyone interested in the development of chemistry, the conduct of research, and the personal and professional lives of scientists.

George B. Kauffman, Laurie M. Kauffman
California State University
Fresno, CA (USA)

The Inositol Phosphates. Chemical Synthesis and Biological Significance. By *D. C. Billington*. VCH Verlagsgesellschaft, Weinheim/VCH Publishers, New York, 1993. XIV, 153 pp., hardcover DM 126.00—ISBN 3-527-28152-5/0-89573-977-1

It is now almost a decade since Michael Berridge and his collaborators reported in *Nature*: ".... micromolar concentrations of Ins(1,4,5)P_3 (1D-*myo*-inositol 1,4,5-trisphosphate) release Ca^{2+} from a non-mitochondrial intracellular store in pancreatic acinar cells. Our results strongly suggest that this is the same store that is released by acetylcholine." Thus, some 30 years after the beginnings of this field with the observation by Lowell Hokin of agonist-stimulated phospholipid turnover (the so-called "phospholipid effect") and 8 years after the correlation made by Michell in 1975 with agonist-stimulated intracellular Ca^{2+} release, the final missing molecular link was found in 1983 in the form of a second messenger, the polyphosphorylated cyclitol Ins(1,4,5)P_3.

Since 1983 progress in this new area of signal transduction has been nothing short of breathtaking. Indeed, Lowell Hokin recently remarked: "The phosphoinositide field is currently the number one field in biochemistry in the number of citations (excluding molecular biology)." Small wonder, then, that most workers in the field, be they chemists or biologists, find it almost impossible to keep fully abreast of events. Thus one tends to rely upon the all-too-frequent biological reviews to escape the need to digest the voluminous primary literature. Such reviews, however, rarely address chemical matters in any depth, if at all, and it is therefore a pleasure to see at last this new book, where the author has clearly made an effort to focus upon a very particular need, that of the biological and medicinal chemist.

With the opening of this new chapter in cellular signalling it was soon clear that there was a prime need for synthetic chemical involvement, and there has been a very significant revival of interest in the chemistry of inositols since the mid-1980s, beginning with the first synthesis of Ins(1,4,5)P_3 in 1986. While progress here has also been relatively rapid, and necessarily highly competitive, the chemistry of the new inositol phosphates is still a small enough field to be concisely reviewed. Until now, however, there have only been two comprehensive major chemical reviews in this area, and one, indeed, by the author of this present book. While "The Inositol Phosphates" clearly represents a useful addition to this literature, I admit to being more than a little apprehensive about how much further this book could go in relation to these existing reviews.

The chemical synthesis of inositol polyphosphates presented a number of problems, namely: the regiospecific protection of inositol in order to afford suitable intermediates for phosphorylation; the optical resolution of such intermediates; the polyphosphorylation of intermediates possessing vicinal diol functionalities, where it is essential to avoid the facile formation of 5-membered cyclic phosphates; deblocking of fully protected polyphosphates, without concomitant migration of phosphate groups; and finally, purification of the final water-soluble polyphosphate. Essentially, these problems have all been overcome and it is now, at least in principle, possible to synthesize any inositol polyphosphate. This message is well conveyed by the book. Much effort, however, is still being expended in the development of novel routes to optically active inositol phosphates and improvement upon the established methods developed to combat the above problems. All this information, and more, with clear summaries of a large number of synthetic strategies, is provided excellently in this book. Although clearly aimed at chemists, it would perhaps also be useful to biologists who want a concise survey of chemical progress and, as many do, a basic grounding in the more structural, and particularly stereochemical, aspects of this field. In view of this, the biological background here, while adequate for a chemical audience, forms only a minor part of the book and the author, wisely, does not attempt to become embroiled in any of the many controversies currently raging in this expansive field.

After equipping the reader in the earlier chapters with enough background biology to understand the rationale behind the synthetic work, the author launches into Chapter 3 which discusses in depth the basic problems of inositol polyphosphate synthesis, namely the protection, phosphorylation, deprotection, and resolution steps mentioned above. A systematic treatment of mono-, bis-, tris-, and tetrakisphosphates then follows, with detailed accounts of various approaches, covering most of the chemical literature up to 1991. A most welcome Chapter 8 describes some of the efforts expended in the synthesis of inositol phosphate analogues, now a major theme in organic chemistry, with the prospect of developing enzyme inhibitors, receptor antagonists, and perhaps even therapeutic agents of the future.

The final chapter provides an insight into some of the more recent synthetic activity, including some 1992 publications. Nevertheless, I regretted that the book as a whole could not be more up-to-date, presumably due to the production time-scale. As always in such a field, review articles and books run the risk of rapidly becoming out of date, and sadly this has been all too true for biological articles and books on the polyphosphoinositide pathway. However, since the volume of chemical work is clearly smaller than that in biology, and the synthetic chemistry reported here is well established and not the subject of anywhere near as much controversy, this may be less important in this case. I felt that the book ended rather abruptly, and I would have liked to see space given to a concise summary of chemical progress to date and, more especially, to speculation, philosophical and otherwise, on future chemical directions in this research area.

Despite these shortcomings, I can recommend "The Inositol Phosphates" to anyone who requires a comprehensive summary of some seven years of chemical research in this rapidly expanding field. It will provide an invaluable compendium for anyone contemplating synthetic work in this area. This book deserves a place upon the bookshelf of any active inositol phosphate or carbohydrate chemist, and it will hopefully give encouragement and heart to those chemists who have been too afraid of the fast-moving nature of this field to join in the game.

B. V. L. Potter
Department of Medicinal Chemistry
School of Pharmacy & Pharmacology
University of Bath (UK)

Fundamentals of Crystallography. (Series: IUC Texts on Crystallography, Vol. 2.) Edited by *C. Giacovazzo*. International Union of Crystallography, Oxford University Press, Oxford, 1992. XI, 654 pp., paperback £ 27.50.—ISBN 0-19-855578-4

Although chemical crystallography has undergone rapid developments and become more widely used during the last few decades, one could hardly claim that this has been accompanied by a corresponding surge in the publication of up-to-date monographs and textbooks on the subject. As in most cases, exceptions prove the rule; in particular the International Union of Crystallography has recently published a number of excellent books that go some way towards remedying this. The volume reviewed here also belongs to this category; under the editorship of C. Giacovazzo it deals with important aspects of modern crystallography, mainly chemical. All the authors are eminent representatives of the Italian school of crystallography, as also is the editor who has contributed three of the chapters.

What detailed aspects are covered? Appropriately one should first mention the three chapters by C. Giacovazzo: "Symmetry in Crystals", "Crystallographic Computing", and "The Diffraction of X-Rays by Crystals". These are followed by "Experimental Methods in X-Ray Crystallography" (H. L. Monaco), "Solution and Refinement of Crystal Structures" (D. Viterbo), "Ionic Crystals" (F. Scordari), "Molecules and Molecular Crystals" (G. Gilli), and "Protein Crystallography" (G. Zanotti). The book ends with a treatment of "Physical Properties of Crystals" by M. Catti. The last four chapters introduce aspects of crystal structure science that go far beyond merely describing the tools used for structure determination, and especially here one notes with approval that the authors have avoided following well-trodden paths in their presentation of the material. The book also excels by the exemplary way in which this has been done, and by the unusually clear layout, which is in the style of the textbooks by Atkins (lots of attractive illustrations and diagrams!). Furthermore, each chapter includes an account of the latest developments, while always taking care to put these into a practical context, which is a highly commendable approach. Thus the book makes very worthwhile reading, even for those with long experience in using the methods, especially as there are plentiful references to recent relevant

literature (about 850 citations!). A few minor criticisms follow. Chapter 2 on "Crystallographic Computing" seems a little out of place, and it would probably have been better to treat this subject in conjunction with "Solution and Refinement of Crystal Structures". The treatment of molecular crystals could definitely have been improved by omitting the discussion of bonding theory, which is in any case very elementary, and instead devoting more space to molecular mechanics. Lastly, the index could have been made rather more comprehensive.

To summarize, this book can certainly be recommended, and the remarkably low price is a further reason for approval. However, one might ask: is it only for the specialist? Happily it is not. It is exactly because it treats the more chemical and physical aspects of crystals and crystal structures that it should also be read by those who are interested only in the results of crystal structure determinations. If at the same time these readers take a glance at the sections on techniques, so much the better. However, all readers must be prepared to recognize that the authors make few concessions to those who would prefer a non-mathematical treatment.

Gerhard Müller
Fakultät für Chemie
der Universität Konstanz (FRG)

Chemistry of the Solid-Water Interface. Processes at the Mineral-Water and Particle-Water Interface in Natural Systems. By *W. Stumm*. Wiley, Chichester, 1992. X, 428 pp., paperback £ 32.50.—ISBN 0-471-57672-7

The distribution and reactions of substances present in water are crucially affected by processes at the solid–water interfaces, and consequently the understanding of interfacial reactions has become one of the most important tasks for modern chemistry and neighboring disciplines. Where the interest is combined with ecological aspects, this task offers a particularly attractive field for those involved in water research. Werner Stumm, one of the leading pioneers of systematic water research, has made an important contribution towards the solution of this problem.

By approaching the subject from a physicochemical standpoint and making use of the latest knowledge, the author has written a textbook that is of value not only to water chemists but also to geochemists, chemical engineers, and others with an interest in aquatic systems. What are the main aspects covered? The introduction at once identifies adsorption, surface complexation, and colloids as topics for detailed consideration. This is followed by necessary digressions into the coordination chemistry of oxide surfaces with both inner sphere and outer sphere complexes and into surface charges, including an impressive image of a lead sulfide surface obtained by scanning tunneling microscopy (STM), which is also reproduced on the book's dust-cover.

The substances dealt with in the chapter on adsorption include synthetic surface-active agents from detergents, soil-derived substances, and various others that cannot be precisely identified but are of hydrological importance. Modern approaches to this topic emphasize the importance of kinetics and reversibility. The role of surface-controlled solvation processes in weathering is discussed in relation to precipitation studies, and the behavior of minute particles is considered from the standpoints of nucleation and solubility. On the important topic of the stability of colloidal systems the author discusses the particle–particle interactions in considerable detail. In contrast, the chapter on the reactivity and solubility of carbonates is relatively brief, giving the impression that readers are expected to be already familiar with this classical topic. Under redox processes the vanadates find a place as comparative outsiders alongside the iron and manganese compounds usually considered in this context.

The book ends with two chapters written by Stumm's coworkers: one on heterogeneous photochemistry (B. Sulberger) and another on trace levels of elements in surface waters (L. Sigg). Both articles begin with the theoretical fundamentals and lead up to examples illustrating the practical importance of the results. Not surprisingly, iron again emerges here as the main performer!

The literature references given for each of the eleven chapters are a good representative selection. The many schemes and diagrams are a useful aid to understanding the otherwise not readily digestible text. The didactic value of the book lies in its successful progression from simple considerations through more complex ideas to the applications. The textbook character is reinforced by the appendixes attached to the individual chapters, which include amplification of particular points, examples from practical situations, and exercise problems. It is unfortunate that this excellent approach has only been consistently followed in the early chapters. Also students would have greatly appreciated being given solutions, which they could use when appropriate, to the often quite difficult exercise problems. However, even without such help they will benefit greatly from working through this well written and sturdily produced book. It will quickly find a place on the desks of those who teach water science and others working in the field of heterogeneous aquatic systems.

Fritz H. Frimmel
Lehrstuhl für Wasserchemie
der Universität Karlsruhe (FRG)

Metals in Biological Systems. By *M. J. Kendrick, M. T. May, M. J. Plishka* and *K. D. Robinson*. Ellis Horwood, New York, 1992. 183 pp., hardcover $ 68.00.—ISBN 0-13-577727-5

There has been a need for an updated text at this level to cover short (5–10 lecture) undergraduate courses in the fast-moving field of metals in biological systems, so this publication will be of interest to students and teachers of the subject. The subject is now a required component of most chemistry courses, and is taught to students of biochemistry and medicinal chemistry. The book aims to provide both introductory and background material to the subject for over a dozen metal ions, together with details of physical techniques required for their study. The authors faced the considerable problem of what to leave out in such a book. Their selection of topics is pertinent and timely, but may not suit all potential readers. The book appears to aim at the market already covered by the more detailed book of M. N. Hughes (1972, 1981) or that by R. W. Hay (1983). Despite the advantage of its more recent publication date, the book under review is unlikely to replace these established texts, although it could be used to supplement either.

Certain aspects of this book make it unsuitable as an undergraduate text; indeed only sections of it could be recommended, and then only if accompanied by errata slips. The coverage of the topics is very uneven, betraying the four different hands involving in the writing, and a lack of cohesive overview of the camera-ready copy. The introduction illustrates the uneven approach, comprising a brief 1–2-page sum-

mary of the relevant elements via the Periodic Table, followed by three pages on the entatic state. Introductory coverage of proteins and amino acids perversely takes two pages in the middle of the 45-page chapter on physical techniques. Extensive biochemical background is assumed elsewhere.

Of the other 16 chapters, most are 4–6-page essays on a single element; the depth and coverage of these varies idiosyncratically, with the focus generally on metal ions as enzyme activators. The chapter on iron (25 pages) covers much of the expected ground and provides 8 references (the most recent 1982), but omits from the Fe–S protein section any mention of the Fe_3S_3 clusters, while the vanadium chapter (8 pages, 17 references mostly to recent primary sources) is generous for the present state of knowledge. The treatment of calcium, magnesium, and sodium in short separate chapters is very perfunctory—for calcium, only calmodulin-dependent processes are mentioned, with nothing on the mechanism of skeletal muscle control, one of the best-known allosteric processes in biology; nor is there any mention of the major role of calcium in bones and teeth. The sodium coverage has almost a page on non-biological ligands, and potassium does not merit a chapter on its own. Ion channels are not mentioned. Likewise, an effect of tungstate on steroid receptor complexes is quoted, but the short zinc chapter makes no mention of the much better understood zinc fingers. On the other hand, cobalt, manganese, molybdenum, and nickel are covered at about the right introductory level, as also are inorganic drugs.

Many whose native tongue is not English will read such texts; it is especially incumbent on authors to ensure clarity of text and accuracy in science and grammar, so that beginners will not be confused. The authors of this text did not succeed. Amongst the obvious slips, labels on legends did not match those on the figures or sometimes the text; a Nobelist's name is given two spellings on opposite pages, 66 and 67 (both wrong!); the crystal structure resolution for calmodulin is quoted on page 46 as 3.0 Å (long outdated) while on page 59 it is stated that no structure has been obtained! The number of grammatical and other trivial slips is high for such a short text, and the whole book clearly lacked an overall editorial survey. Any future edition will no doubt put right these faults. In the meantime, publishers should note that there is still a market for an updated text at this level.

Joyce C. Lockhart
Department of Chemistry
University of Newcastle upon Tyne (UK)

Theoretical Aspects of Physical Organic Chemistry. The S_N2 Mechanism. By *S. S. Shaik, H. B. Schlegel,* and *S. Wolfe.* Wiley, New York, 1992. XV, 285 pp., hardcover $ 47.50.—ISBN 0-471-84041-6.

The Nobel award to R. A. Marcus for his efforts to relate thermodynamic and kinetic properties in order to describe the "simplest" chemical reaction, the transfer of a single electron, has certainly renewed interest in methods for the theoretical description of chemical reactions. In this book the authors set out to analyze S_N2 reactions by means of a semi-quantitative model on the basis of quantum-mechanical valence-bond considerations with configuration interaction. Their model also includes elements of the Marcus theory. According to the authors, "the model leads not only to linear free-energy relationships, the Marcus equation, and the Leffler–Hammond postulate, but also accounts for the role of frontier MO's, orbital symmetry, and so forth". Therefore, the book as a whole is also intended to serve as a general introduction to physical organic chemistry. The reader is first given a short introduction to the history of this discipline, starting with Menschutkin; nearly half the citations are to the authors' own publications. In the first chapter (36 pp.) the reader is made familiar with some fundamental concepts of physical organic chemistry. The Brønsted relationship, the significance of its exponent α, the Bell–Evans–Polanyi principle, and the Leffler–Hammond postulate are lucidly presented. A brief introduction to the Marcus theory is also given. However, other books or articles, such as those by L. Eberson, would do better service to beginners. The properties of energy hypersurfaces are described in Chapter 2 (47 pp.), mainly from a quantum-chemical point of view. The reader is confronted with numerical methods for the determination of stationary points on these hypersurfaces, even though these are not needed for the following discussions. In the next chapter (41 pp.), the basics of MO- and VB-models are presented in a mathematical fashion, taking the hydrogen atom and its radical anion and cation as examples. The authors' state correlation model is introduced in connection with the exchange reaction between H_2 and H. The thermodynamic parameters of an S_N2 reaction, such as the ionization potentials and electron affinities of the reactants, are defined in Chapter 4 (27 pp.), and methods for determining them are discussed. Parameters of importance for the model are deduced from them. In Chapter 5 (62 pp.) the thermodynamic and kinetic parameters are interrelated for the analysis of identity S_N2 reactions in the gas phase and in solution. Activation barriers and geometries of transition states are calculated by ab initio methods in combination with the authors' model, and are compared with experimental data. The final chapter (49 pp.) treats non-identity reactions. Author and subject indexes conclude the book.

The authors' aim is to make the virtues of their model known to a wider audience (their previous work is described in the preface as "seminal"). Justification for such an intention should be provided by the model's predictive power. For a publication designed as a textbook it is reasonable to expect authors to adopt a more critical approach to their own results than in original papers. Despite the authors' claim on page IX that "All of these predictions [of the model] were consistent with experimental data ...", a literature search yields at least one exception. On the basis of elements of the model presented in this book it was concluded that the direct reaction of nucleophiles with radical cations should be a "forbidden" process (A. Pross, *J. Am. Chem. Soc.* **1986**, *108*, 3537). This prediction proved to be incorrect, as shown experimentally (N. M. M. Nibbering, H. Schwarz et al., *ibid.* **1987**, *109*, 4810; see also H. I. Kettämaa et al., *Chem. Rev.* **1992**, *92*, 1649). At least a little hint ought to have been given to the reader, as the book covers the literature up to 1988 (in some instances up to 1990).

This book certainly cannot serve as an introduction to physical organic chemistry. Firstly, it covers only one part of this discipline, though an important one. Secondly, many aspects are treated so briefly that the novice is likely to misunderstand them, for example the Marcus theory and the ab initio MO methods. Topics that are not necessary to understand the model or its consequences are given much space, especially the lucid but essentially superfluous chapter on the numerical analysis of hypersurfaces. The authors' predilection for abbreviations tends to make the reader feel uncomfortable. Most often, they are explained only once (sometimes never, as in the cases of the RRKM theory or the "CEPA" approximation), but are used throughout the book.

A little help is provided by the brief subject index; otherwise the reader has to consult the original literature.

Nobody expects a book free of errors, and one can disregard misprints such as the resonance arrow for the Menschutkin reaction on page 1. More annoying is the use of different letters to describe the same property, for example, $\mathcal{A}$ on pages 136–7, but a three pages later. On account of the profusion of newly introduced symbols, this is very disturbing.

Whether the considerable time spent in understanding the mathematics and terminology of this model pays off for the "common" chemist, in order to describe experimental data semi-quantitatively with a better theoretical basis, may be left to his or her own discretion. The specialist familiar with the authors' original publications will probably not discover much new material. Most of the diagrams in this book have also been taken from the primary literature, sometimes in severely reduced form which makes them difficult to decipher.

To conclude: this book was meant to serve many, but turns out to be superficial in many aspects. Apart from the discussion about the quantitative validity of the model, the form of the book means that it will probably be useful to few other than specialists.

J. Jens Wolff
Organisch-Chemisches Institut
der Universität Heidelberg (FRG)

Synthetic Fluorine Chemistry. Edited by *G. A. Olah, R. D. Chambers* and *G. K. Surya Prakash.* Wiley, New York, 1992. XVII, 402 pp., hardcover £ 75.00.—ISBN 0-471-54370-5

The properties of fluorine, both as an element and in its compounds, differ so markedly from those of the other halogens that fluorine chemistry has developed as a distinct subject with its own special methods. Now, 106 years after elemental fluorine was first obtained, this branch of chemistry has become so extensive that to review it all is scarcely possible, even for an expert in the field. Accordingly, the aim of this book is not to present a systematic survey; instead it consists of 17 chapters in which leading scientists from universities and industry give comprehensive reviews of selected areas of inorganic and, more especially, organic fluorine chemistry. The book is based on papers presented at a symposium on Synthetic Fluorine Chemistry, which was organized by the Loker Hydrocarbon Research Institute of the University of Southern California in February 1990.

In Chapter 1 Schrobilgen describes the preparation and Lewis acid behavior of noble gas fluoride cations. Christe, Wilson, and Schack (Ch. 2) describe methods for replacing fluorine by oxygen in fluorides and oxyfluorides. Aubke, Cader, and Mistry (Ch. 3) present a comprehensive review of transition metal derivatives of strong protonic acids and superacids. Seppelt (Ch. 4) describes the preparation and properties of compounds containing carbon–sulfur multiple bonds stabilized by fluorine. Lagow, Bierschenk, Juhlke, and Kawa (Ch. 5) report on direct fluorination methods for the synthesis of perfluoropolyethers and on possible areas of application for these compounds. Adcock (Ch. 6) describes aerosol direct fluorination, claimed to be a universal method for perfluorinations. Rozen (Ch. 7) describes electrophilic fluorinations of organic compounds using fluorine or other fluorinating agents. Olah and Li (Ch. 8) demonstrate that onium-polyhydrogenfluorides have a wide range of applications as fluorinating agents. Burton (Ch. 9) describes the use of organometallic compounds containing perfluoroalkyl groups for the synthesis of organofluoro compounds. Prakash (Ch. 10) reports on nucleophilic perfluoroalkylations using perfluorotrialkylsilanes. Farnham (Ch. 11) describes the use of organosilicon reagents in synthetic organofluorine chemistry. Shteingarts (Ch. 12) discusses electrophilic *ipso* reactions of polyfluoroarenes from the standpoint of synthetic applications. Takenaka and Lemal (Ch. 13) discuss the perfluorobenzeneoxide–perfluorooxepin system. Krespan and Dixon (Ch. 14) describe the chemistry of perhalogenated dioxans and dioxens. Welch, Yamakazi, and Gimi (Ch. 15) report on the Claisen rearrangement of fluoroacetamide acetal as a method for asymmetric syntheses of compounds of biological interest. Chambers (Ch. 16) describes the preparation of some unusual fluorinated alkenes and dienes by reactions involving fluoride ions. Lastly Baum (Ch. 17) describes syntheses of fluorinated monomers for condensation polymerization.

The book covers quite a broad range of topics and gives a very good overview of the present state of experimental fluorine chemistry. It includes about a thousand references which afford a convenient way into the relevant literature. There is a nine-page subject index which greatly facilitates using the book as a reference source. The fact that it originates from a symposium is readily apparent from the widely differing styles of the chapters, some giving detailed treatments of only a few compounds while others treat many in a brief manner. However, this variety makes the book agreeable to read for someone who, like this reviewer, works through it from start to finish—for example, the reader who is just beginning work in fluorine chemistry.

Stephan Rüdiger
Projektgruppe Fluorchemie
Berlin (FRG)

Adsorption of Molecules at Metal Electrodes. (Series: Frontiers of Electrochemistry.) Edited by *J. Lipkowski* and *P. N. Ross.* VCH Publishers, New York/VCH Verlagsgesellschaft, Weinheim, 1992. XI, 414 pp., hardcover DM 246.00, $ 145.00.—ISBN 0-89573-786-8, 0-89573-789-2 (set)/3-527-28008-1, 3-527-28007-3 (set)

An electrochemical double layer is formed at almost every type of phase boundary. The driving forces causing this are differences in the chemical potentials of the charge carriers that are common to both phases, even though they may be present in very different concentrations. The resulting electrical potential difference cannot be measured directly. Adsorbed molecules have a secondary effect on the electrochemical double layer. Where dipolar molecules are involved there is not only a chemical interaction with the surface but also a strong electrostatic field effect.

The volume reviewed here contains eight articles dealing with the adsorption of molecules at metal electrodes. However, the topics covered are much more specialized than the title leads one to expect. Of the metals considered, mercury and platinum are by far the predominant ones. Where the use of surface enhanced Raman spectroscopy (SERS) is described, silver and gold also feature, since these metals are specific for the technique. The two most important utility metals, iron and aluminum, are discussed only very briefly in the article by Plieth et al. The other phase is an electrolyte solution which contains not only the organic molecules but also ions such as HSO_4^- or CN^- that can be adsorbed. The methods used to study adsorption include the classical tech-

niques of ellipsometry and optical reflection spectroscopy, and also more modern methods such as infrared reflection absorption spectroscopy (IRRAS), SERS, and Raman second harmonic spectroscopy. It has thus become possible to obtain detailed information about the structure of the double layer, the nature of the adsorption, and the dynamics of phase transformations in monolayers. For example, benzonitrile molecules can be adsorbed in four different configurations relative to the electron lone pair of the nitrile group: planar, bent so that the triple bond of the nitrile group has a strong interaction with the surface through the formation of either two or four bonds, or "perpendicular". In the first two articles, by Guidelle and by Buess-Herman, the emphasis is on theoretical considerations and the use of molecular models, whereas the remaining chapters report detailed experimental results obtained by the various surface analytical techniques.

For the specialist this volume is undoubtedly a useful source of detailed information on the theory and methodology of such studies, and it covers the literature up to the end of the 1980s. Electrochemists can learn much from these impressive results. However, the practitioner who wishes to know, for example, how an acrylonitrile molecule lies on the surface of a cadmium cathode (as in the Monsanto process for the electrosynthesis of adiponitrile), or how typical corrosion inhibitors are adsorbed on iron, will find no information here. Also it is regrettable that none of the authors has taken the trouble to write a summary and evaluation of the methods, but that is usually the case. The book will find its way into libraries, but the high price is likely to deter individual scientists from buying it.

Fritz Beck
Fachgebiet Elektrochemie
der Universität-Gesamthochschule Duisburg (FRG)

Tandem Organic Reactions. By *Tse-Lok Ho*. Wiley, Chichester, 1992. X, 502 pp., hardcover \$ 79.95.—ISBN 0-471-57022-2

Tandem reactions, also called cascade, domino, sequential, or one-pot reactions, are strictly speaking old hat. Perhaps one of the best-known tactical combinations is the Robinson tropinone synthesis, discovered more than 75 years ago, which makes four new σ bonds from three components in biomimetic fashion, and also the Robinson annulation, which has proved so valuable in steroid synthesis.

Tse-Lok Ho, previously with the NutraSweet company in Chicago and now at the National Taiwan University, a well-known author and prolific writer, whose earlier books include *Hard and Soft Acids in Organic Chemistry* (Academic Press, 1977), *Carbon–Carbon Bond Formation in Terpene Synthesis* (VCH, 1988) and *Polarity Control for Synthesis* (Wiley, 1991), has now produced a timely monograph on tandem reactions, selecting examples right up to 1992.

After a short preface and an introduction (Chapter 1), tandem reactions are classified, as far as this is possible and practical, by the *last step* of the sequence. The following 14 chapters deal with a wealth of practical examples, which have been put together by the author thanks to his wide knowledge of the literature and excellent memory, and also from his previous books. All methods for making carbon–carbon bonds are represented, including ionic, pericyclic, free radical, and transition metal mediated transformations. The headings of the 14 chapters are as follows: 2. Aldol Condensation; 3. Michael Reactions; 4. Tandem Vicinal Difunctionalization of Alkenes and Alkynes; 5. Dieckmann and Claisen Cyclizations; 6. Mannich Reactions; 7. Diels–Alder Reactions; 8. Other Cycloadditions; 9. Retro-Diels–Alder and Cheletropic Reactions; 10. Electrocyclic Reactions; 11. Ene, Retro-Ene, and Some Other Thermal Reactions; 12. Sigmatropic Reactions; 13. Rearrangements and Fragmentations; 14. Free Radical Reactions; 15. Miscellaneous Tandem Reactions.

However, the headings can only be a rough guide and cannot give the full flavor of the diverse chemistry that is described. For example, Chapter 4 contains examples of the Pauson–Khand and the Dötz reaction as well as biosynthetically patterned cationic polyene cyclizations. Chapter 8 includes the Vollhardt [2 + 2 + 2] and also higher cycloadditions. Structurally simpler examples and also complex natural products chemistry are well represented.

The structural formulas are well produced and capture the essence of a procedure, with a concise commentary. Thus the book complements and contrasts with other recent texts which focus mainly on the tools of the trade, i.e. *methods* for manipulating functional groups and the growing number of *reagents* for organic synthesis. As far as I could see the book contains no more than a few minor misprints and some inevitable misspellings of authors' names.

Whither tandem reactions? As a strategem or even as a principle of organic chemistry and synthesis, tandem reactions will undoubtedly continue to flourish. Elegance, aesthetic appeal, atom economy and functional group economy, convergence and also stereocontrol often blend to provide optimum access to complex molecular structures. In future it will be important to somehow measure the quality of a tandem reaction, since the number of steps is not necessarily an absolute criterion, for example if the flexibility and applicability are too narrow, or when it becomes too difficult to find the "reaction window" which may not be wide enough.[1] In this case, it may still be possible that two or three "inelegant" but well worked out steps are superior to the elegant but difficult tandem procedure.[2] Of course, the time factor, so important for industry for obtaining material for initial biological tests, may also be in favor of the linear and more conventional step-by-step approach.

In summary, Tse-Lok Ho's text is a welcome source book, also for graduate seminars, and it is a must for a young organic chemist setting out on his or her career. By exposing gaps in our current knowledge the book, together with other recent articles,[3–8] will stimulate discussion and new experimental work. Thus, it will help to evaluate the current state of the art and synthetic efficiency.[9]

H. Martin R. Hoffmann
Department of Organic Chemistry
University of Hannover (FRG)

[1] For example, the important modification of using acetonedicarboxylic *acid* instead of acetonedicarboxylic *ester* in the tropinone synthesis was introduced by Schöpf almost 20 years after Robinson's first paper. See obituary of Clemens Schöpf by J. Thesing, *Chem. Ber.* **1979**, *112*, I–XIX.

[2] The converse also applies. For example, the tandem bicyclization of β-keto allyl alcohols to 6,8-dioxabicyclo[3.2.1]octanes involves an unfavorable hetero-Diels–Alder reaction in the first step, which is potentially reversible.

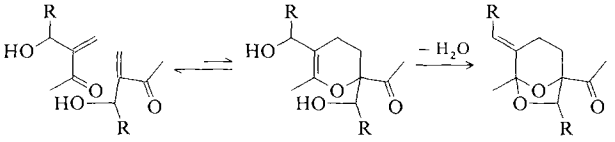

However, thanks to the hydroxy groups, the reaction is driven by the irreversible final cyclization (see Scheme). See also N. Daude, U. Eggert, H. M. R. Hoffmann, *J. Chem. Soc. Chem. Commun.* **1988**, 206; H. M. R.

Hoffmann, U. Vogt, *Synlett* **1990**, 581; A. Weichert, H. M. R. Hoffmann, *J. Org. Chem.* **1991**, *56*, 4098.
[3] L. F. Tietze, U. Beifuss, *Angew. Chem.* **1993**, *105*, 137.
[4] H. Waldmann, *Nachr. Chem. Tech. Lab.* **1992**, *40*, 1133.
[5] H. M. R. Hoffmann, *Angew. Chem.* **1992**, *104*, 1361.
[6] F. E. Ziegler, *Chem. Rev.* **1988**, *88*, 1423.
[7] G. H. Posner, *Chem. Rev.* **1986**, *86*, 831.
[8] B. M. Trost, *Science* **1991**, *254*, 1471.
[9] Cf. S. H. Bertz, *J. Am. Chem. Soc.* **1982**, *104*, 5801.

Spectroscopy of Polymers. By *J. L. Koenig*. American Chemical Society, Washington DC, 1992. XVI, 328 pp., paperback $ 49.95.—ISBN 0-8412-1924-9

To characterize the structures of synthetic polymers one needs to determine various properties that are specific to polymers, such as the molar mass, tacticity, configuration and conformation, copolymerization statistics, etc. To these must be added the organization and dynamic behavior of the molecular chains in the solid state, or in the different forms of liquid crystalline polymers. Spectroscopic methods are becoming increasingly important as ways of investigating these properties. During the last decade there have been especially rapid developments in the areas of vibrational spectroscopy (Fourier transform infrared (FTIR) and Raman spectroscopy) and NMR spectroscopy, and these advances are described in the book by J. L. Koenig reviewed here. However, the title is somewhat misleading, since in addition to these two areas there are many other spectroscopic methods that are successfully applied to polymer studies. The book is based on the author's many years of experience in research and teaching in the two fields described, and it replaces his earlier book on the same subject. It is intended for graduate students and polymer scientists who are not experts in these areas of spectroscopy. Its purpose is to enable them to choose the most suitable methods to solve specific polymer problems, and to equip them with enough basic knowledge to make intelligent use of more advanced monographs and of the original literature.

This approach is an extremely useful one for practical laboratory work, and Koenig fulfills the task outstandingly well. In addition to clearly explaining the standard methods used, for example, to determine the microstructure of polymers in solution, he describes more recent developments such as attenuated total reflection (ATR) Raman spectroscopy and FT-Raman spectroscopy. Even some techniques that are complicated to explain, such as two-dimensional (2D) FTIR spectroscopy, are treated in a concise and understandable way. In the case of NMR spectroscopy a considerable amount of space is devoted to structural characterization, and especially to the dynamics of polymers in the solid state. The discussion makes it clear that the current state of the art in the NMR spectroscopy of solid polymers allows not only the determination of chemical structure using the CP–MAS (cross-polarization magic angle spinning) technique but also the measurement of various relaxation parameters. Last but not least, Koenig devotes a chapter to NMR imaging techniques and shows the potential of these methods for the characterization of elastomers and for studying diffusion processes, mainly using examples from his own work.

For each of the techniques covered Koenig begins with the basic physical principles, deliberately keeping the number of mathematical formulas to a minimum. This is followed by a discussion of the experimental details that are important in practice, then the applications of the method are illustrated by numerous examples from different areas of polymer research. The advantages and disadvantages of each method are clearly set out; here the author is not afraid to state his personal views which sometimes conflict with those expressed in the literature.

The book makes easy reading, thanks to the many useful illustrations and the excellently written text, and can be recommended for all graduate students and polymer scientists. It should find a place in the library of every laboratory concerned with the physics or chemistry of macromolecules, which expressly includes industrial laboratories.

Hans Wolfgang Spiess
Max-Planck-Institut für Polymerforschung
Mainz (FRG)

New Books
see next page

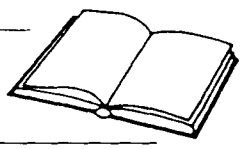

New Books

Flow Injection Separation and Preconcentration. By **Z. Fang.** VCH, Weinheim/New York, **1993**. 259 pp., hardcover, DM 148.–/$ 100.—ISBN 3-527-28308-0/1-56081-147-1

Handbuch der Naturfarbstoffe. By **H. Schweppe.** Ecomed, Landsberg, **1993**. 800 pp., hardcover, DM 298.—ISBN 3-609-65130-X

GLP – Handbuch für Praktiker. By **Hembeck, Christ, Harston.** GIT Verlag, Darmstadt, **1992.** 282 pp., DM 89.—ISBN 3-928865-03-X

Solutions Manual to accompany The Elements of Physical Chemistry. By **D. Goss.** Oxford Science Publications, Oxford, **1993.** 164 pp., paperback, $ 9.95.—ISBN 0-19-855784-1

The Analysis of Natural Waters. (Volumes I and II as a set). By. **T.R. Crompton.** Oxford Science Publishers, Oxford, **1993.** Vol. I: 232 pp., Vol. II: 232 pp., hardback, $ 75.—ISBN 0-19-855752-3

NEW IN PAPERBACK. **The Biological Chemistry of the Elements.** The Inorganic Chemistry of Life. By **J.J.R. Fraústo da Silva, R.J.P. Williams.** Oxford Science Publishers, Oxford, **1993.** 582 pp., paperback, $ 25.—ISBN 0-19-855802-3

Advances in Polymer Science, 106. Polymer Characteristics. By **A. Grosberg, S. Nechaev et al.** Springer-Verlag, Berlin, **1993**. 195 pp., hardcover, DM 158.—ISBN 3-540-56140-4

Fish. Ecotoxicology and Ecophysiology. Edited by **T. Braunbeck, W. Hanke, H. Segner**. VCH Verlagsgesellschaft mbH, Weinheim/New York, **1993**. 418 pp., hardcover, $ 125.—/DM 184.—ISBN 3-527-30010-4/1-56081-704-6

Horizonte der Biologie. Edited by **P. Sitte**. VCH Verlagsgesellschaft mbH, Weinheim, **1993**. 160 pp., hardcover, DM 48.—ISBN 3-527-30018-X

X-Ray-Diffraction at Elevated Temperatures. A Method for in situ Process Analysis. By **D.D.L. Chung, P.W. DeHaven, H. Arnold, D. Ghosh**. VCH Verlagsgesellschaft mbH, Weinheim/New York, **1993**. 268 pp., hardcover, $ 95.—/DM 158.—ISBN 3-527-27842-7/0-89573-745-0

Reviews in Computational Chemistry, Vol 4.. Edited by **K.B. Lipkowitz, D.B. Boyd**. VCH Verlagsgesellschaft mbH, Weinheim/New York, **1993**. 280 pp., hardcover, $ 79.—/DM 138.—ISBN 3-527-89620-1/1-56081-620-1

Phthalocyanines. Properties and Applications. Edited by **C.C. Leznoff, A.B.P. Lever**. VCH Verlagsgesellschaft mbH, Weinheim/New York, **1993**. 303 pp., hardcover, $ 125.—/DM 198.—ISBN 3-527-89638-4/1-56081-638-4

X-Ray Optics and Microanalysis 1992. Edited by **P.B. Kenway, P.J. Duke, G.W. Lorimer, T. Mulvey, I.W. Drummond, G. Love, A.G. Michette, M. Stedman**. IOP Publishing Ltd., Bristol, **1993**. 652 pp., hardcover, £ 99.—ISBN 0-7503-0255-0

Photodissociation Dynamics. (Cambridge Monographs on Atomic, Molecular and Chemical Physics, Vol. 1). By **R. Schinke.** Cambridge University Press, Cambridge, **1993**. 417 pp., hardcover, £ 50.—ISBN 0-521-38368-4

Polymer Surfaces and Interfaces II. Edited by **W.J. Feast, H. S. Munro, R.W. Richards**. Wiley Publishers, Chichester, Great Britain, **1993.** 297 pp., hardcover, £ 49.50.—ISBN 0-471-93456-9

Ceramics and Earths/Keramik und Erden. Dictionary/Wörterbuch. By **B. Pfannkuche, J. Baur**. VCH, Weinheim/New York, **1993.** 555 pp., hardcover, DM 168.–/$ 110.—ISBN 3-527-28409-5/1-56081-207-9

Modernes Online-Retrieval. By **S. von Keitz, W. von Keitz, H. Gerlach.** VCH, Weinheim, **1993.** 341 pp., hardcover, DM 98.—ISBN 3-527-28398-6

Coordination Chemistry of Aluminium. Edited by **G. H. Robinson.** VCH, Weinheim/New York, **1993**. 234 pp., hardcover, DM 189.–/$ 115.—ISBN 3-527-28149-5/1-56081-059-9

Organic Synthesis. (Collective, Vol. 8.). A Revised Edition of Annual Volumes 65-69. Edited by **J.P. Freeman et al.** Wiley Publishers, Chichester, Great Britain, **1993.** 696 pp., hardcover, £ 49.50.—ISBN 0-471-58565-3

Handbuch der Technischen Polymerchemie. By **A. Echte.** VCH, Weinheim, **1993**. 721 pp., hardcover, DM 276.– ISBN 3-527-28564-4

Quantitative Calculations in Pharmaceutical Practice and Research. (Analytical Techniques in Clinical Chemistry and Laboratory Medicine). Edited by **T.P. Hadjiioannou, G.D. Christian, M.A. Koupparis, P.E. Macheras.** VCH Weinheim/New York, **1993**. 461 pp., hardcover, DM 198.—/$ 120.—ISBN 3-527-89654-6/0-89573-282-3

Compounds with Germanium-Oxygen Bonds. Edited by **F. Glockling et al.** Springer, Heidelberg, **1993.** 546 pp., hardcover, DM 3.150.—ISBN 3-540-93660-2

Optical Spectra of Ce and Pr. Edited by **K. Gürs et al.** Springer, Heidelberg, **1993.** 275 pp., hardcover, DM 1.598.—ISBN 3-540-93663-7

Alloys of Thorium with Metals of Main Groups I to IV. Edited by **H. U. Borgstedt, H. Wedemeyer.** Springer, Heidelberg, **1992.** 189 pp., hardcover, DM 1.150.—ISBN 3-540-93656-4

Metallurgy of Iron 4th (Vol. 11a, Vol 11b). Springer, Heidelberg, **1992.** 809 pp., hardcover, DM 4.500.—ISBN 3-540-93654-8

Medicinal Implications in Cytochrome P-450 Catalyzed Biotransformation. (Frontiers in Biotransformation, Vol. 8). Edited by **K. Ruckpaul, H. Rein.** Akademie Verlag, Berlin, **1993.** 210 pp., hardcover, DM 228.—ISBN 3-05-501366-2

Ferroelectric Ceramics. Tutorial reviews of materials, theory, processing and applications. By **N. Setter, E.L. Colla.** Birkhäuser, Basel, **1992.** 329 pp., hardcover, sFr. 98.—/DM 118.—ISBN 3-7643-2838-X

Hepatocyte Growth Factor - Scatter Factor (HGF-SF) and the C-Met-Receptor. By **I.D. Goldberg, E.M. Rosen.** Birkhäuser, Basel, **1993**. 396 pp., hardcover, sFr. 178.—/DM 198.—ISBN 3-7643-2777-4

DNA Methylation. By **J.-P. Jost, H.P. Saluz.** Birkhäuser, Basel, **1993.** 572 pp., hardcover, sFr. 178.—/DM 198.—ISBN 3-7643-2778-2

Comparative Molecular Neurobiology. By **Y. Pichon.** Birkhäuser, Basel, **1993.** 434 pp., hardcover, sFr. 178.—/DM 198.—ISBN 3-7643-2785-5

Physical Properties of III-V Semiconductor Compounds. By **S. Adachi.** Wiley, West Sussex, **1992.** 318 pp., hardcover, £ 55.—ISBN 0-471-57329-9

Basic One- and Two-Dimensional NMR Spectroscopy. By **H. Friebolin.** VCH, Weinheim/New York, **1993.** 368 pp., paperback, DM 58.—ISBN 3-527-29059-1/1-56081-796-8

Ecotoxicology Monitoring. By **M. Richardson.** VCH, Weinheim/New York, **1993.** 384 pp., hardcover, DM 192.—/$ 125.—ISBN 3-527-28560-1/1-56081-736-4

Eine Branche lernt Umweltschutz. Motive und Verhaltensmuster der deutschen chemischen Industrie. By **S. Longolius.** Rainer Bohn Verlag, Berlin, **1993.** 181 pp., paperback, DM 29.80.—ISBN 3-89404-346-6

Registered names, trademarks, etc. used in this journal, even when not marked as such, are not to be considered unprotected by law.

© VCH Verlagsgesellschaft mbH, D-69451 Weinheim, 1992. – Printed in the Federal Republic of Germany by Konrad Triltsch Druck- und Verlagsanstalt Würzburg.

All rights reserved (including those of translation into foreign languages). No part of this issue may be reproduced in any form — by photoprint, microfilm, or any other means — nor transmitted or translated into a machine language without written permission from the publishers. Only single copies of contributions, or parts thereof, may be made for personal use. This journal was carefully produced in all its parts. Nevertheless, authors, editors, and publisher do not warrant the information contained therein to be free of errors. Readers are advised to keep in mind that statements, data, illustrations, procedural details, or other items may inadvertently be inaccurate.

Valid for users in the USA: The appearance of the code at the bottom of the first page of an article (serial) indicates the copyright owner's consent that copies of the article may be made for personal or internal use, or for the personal or internal use of specific clients. This consent is given on the condition, however, that the copier pay stated per-copy fee through the Copyright Clearance Center, Inc. (CCC), for copying beyond that permitted by Sections 107 or 108 of the U.S. Copyright Law. This consent does not extend to other kinds of copying, such as copying, for general distribution, for advertising or promotional purposes, for creating new collective works, or for resale. For copying from back volumes of this journal see 'Permissions to Photo-Copy: Publisher's Fee List' of the CCC.

Editorial office: Postfach 10 11 61, D-69451 Weinheim, Federal Republic of Germany, Telephone (06201) 606 315, Telex 465 516 vchwh d, Telefax (06201) 606 328, E-Mail Z16@DHDURZ2 in Earn Bitnet.

Editor: *Peter Gölitz*

Associate editors: *N. A. Compton, R. H. Schmidt-Radde, K. J. Schneider.* **Book editor:** *G. Karger.* **Editorial assistant:** *E. Schweikart*

Publishers: VCH Verlagsgesellschaft mbH. (Managing Directors: *Hans Dirk Köhler, Dr. Karlheinz Köpfer*), Pappelallee 3, D-69451 Weinheim, Federal Republic of Germany.

Advertising office (Advertising Manager: *N. Schippel*): Postfach 10 11 61, D-69451 Weinheim, Federal Republic of Germany, Telephone (0 62 01) 606 312, Telefax (0 62 01) 606 328.

ANGEWANDTE CHEMIE
International Edition in English
Volume 32 · Number 8
August 1993
Pages 1111–1222

Electron Transfer Reactions in Chemistry: Theory and Experiment (Nobel Lecture)**

By Rudolph A. Marcus*

Since the late 1940s, the field of electron transfer processes has grown enormously, both in chemistry and biology. The development of the field, experimentally and theoretically, as well as its relation to the study of other kinds of chemical reactions, presents to us an intriguing history, one in which many threads have been brought together. In this lecture, some history, recent trends, and my own involvement in this research are described.

1. Electron Transfer Experiments since the Late 1940s[***]

The early experiments in the electron transfer field were on "isotopic exchange reactions" (self-exchange reactions) and, later, "cross reactions." These experiments reflected two principal influences. One of these was the availability after the Second World War of many radioactive isotopes, which permitted the study of a large number of isotopic exchange electron transfer reactions in aqueous solution such as depicted in Equations (1) and (2), where the asterisk denotes a radioactive isotope.

$$Fe^{2+} + {}^*Fe^{3+} \rightleftharpoons Fe^{3+} + {}^*Fe^{2+} \quad (1)$$

$$Ce^{3+} + {}^*Ce^{4+} \rightleftharpoons Ce^{4+} + {}^*Ce^{3+} \quad (2)$$

There is a two-fold simplicity in typical self-exchange electron transfer reactions (so-called because other methods beside isotopic exchange were later used to study some of them): 1) the reaction products are identical with the reactants, thus eliminating one factor that usually influences the rate of a chemical reaction in a major way, namely the relative thermodynamic stability of the reactants and products; and 2) no chemical bonds are broken or formed in simple electron transfer reactions. Indeed, these self-exchange reactions represent, for these combined reasons, the simplest class of reaction in chemistry. Observations stemming directly from this simplicity were to have major consequences, not only for the electron transfer field, but also, to a lesser extent, for the study of other kinds of chemical reactions as well (see Shaik et al.[2]).

A second factor in the growth of the electron transfer field was the introduction of new instrumentation, which permitted the study of the rates of rapid chemical reactions. Electron transfers are frequently rather fast compared with many reactions that undergo, instead, breaking of chemical bonds and forming of new ones. Accordingly, the study of a large body of fast electron transfer reactions became accessible with the introduction of this instrumentation. One example was the stopped-flow apparatus, pioneered for inorganic electron transfer reactions by N. Sutin. It permitted the study of bimolecular reactions in solution in the millisecond time scale (a fast time scale at the time). Such studies led to the investigation of what has been termed electron transfer

[*] Prof. Dr. R. A. Marcus
Noyes Laboratory of Chemical Physics
California Institute of Technology
MS 127-72
Pasadena, CA 91125 (USA)
Telefax: Int. code + (91)818-792-8485

[**] Copyright © The Nobel Foundation 1993. – We thank the Nobel Foundation, Stockholm, for permission to print this lecture.

[***] This article has not been consistently annotated. The relevant articles in the reference section have been arranged as follows: In [1] some of my important articles, largely from the 1956–1965 period, are listed. Some general references which review the overall literature are listed in [2], and several additional references for Table 1 and for the Figures in [3]. Classic texts on unimolecular reactions are given in [4].

cross reactions, that is, electron transfer reactions between two different redox systems, as in Equation (3), which sup-

$$Fe^{2+} + Ce^{4+} \rightleftharpoons Fe^{3+} + Ce^{3+} \quad (3)$$

plemented the earlier studies of the self-exchange electron transfer reactions. A comparative study of these two types of reaction, self-exchange and cross-reactions, stimulated by theory, was also later to have major consequences for the field and, indeed, for other areas.

Again, in the field of electrochemistry, the new post-war instrumentation in chemical laboratories led to methods that permitted the study of fast electron transfer reactions at metal electrodes. Prior to the late 1940s, only relatively slow electrochemical reactions, such as the discharge of an H_3O^+ ion at an electrode to form H_2, had been investigated extensively. They involved the breaking of chemical bonds and the forming of new ones.

Numerous electron transfer studies have now also been made in other areas. Some are depicted in Figure 1. Some of

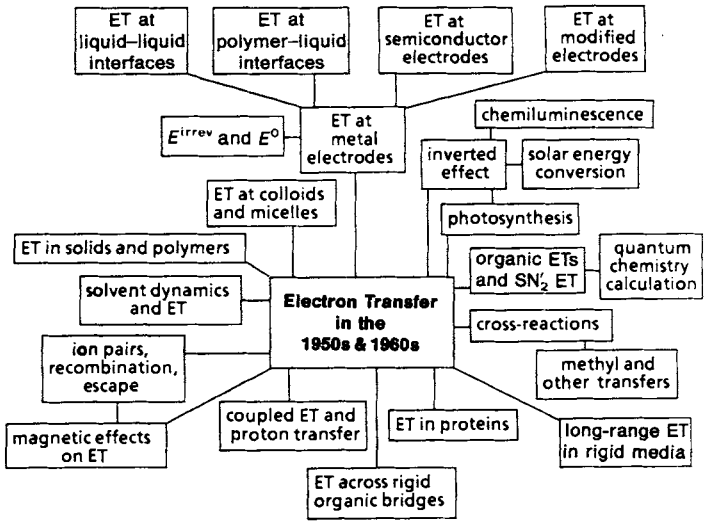

Fig. 1. Examples of topics in the electron transfer (ET) field (Marcus and Siddarth [2]).

these investigations were made possible by newer technology, in particular that of lasers, and now include studies in the picosecond and subpicosecond time regimes. Just recently, the non-laser technique of nanometer-sized electrodes has been introduced to study electrochemical processes that are still faster than those hitherto investigated. Still other recent investigations, important for testing aspects of the electron transfer theory at electrodes, involve the new use of an intervening, ordered, adsorbed monolayer of long-chain organic compounds on the electrode to facilitate the study of several effects such as varying the metal–solution potential difference on the electrochemical electron transfer rate.

In some studies of electron transfer reactions in solution, there has also been a skillful blending of these measurements of chemical reaction rates with organic or inorganic synthetic methods, as well as with site-directed mutagenesis, to obtain more hitherto unavailable information. The use of chemically modified proteins to study the distance dependence of electron transfer, notably by Gray and co-workers, has opened a whole new field of activity.

The interaction of theory and experiment in these many electron transfer fields has been particularly extensive and exciting, and each has stimulated the other. This lecture addresses the underlying theory and this interaction.

2. Early Experience

My own involvement in the electron transfer field began in a rather circuitous way. My background was in experimental measurements of reaction rates as a chemistry graduate student at McGill University (1943–1946) and as a post-doctoral associate at the National Research Council of Canada (NRC, 1946–1949). A subsequent post-doctoral study at the University of North Carolina (1949–1951) on the theory of reaction rates resulted in what is now known as RRKM theory (Rice, Ramsperger, Kassel, Marcus).

This field of unimolecular reactions reflects another long and extensive interaction between theory and experiment. RRKM theory enjoys widespread use and is now usually referred to in the literature only by its acronym (or by the texts written about it[4]), instead of by citation of the original articles.

After the theoretical post-doctoral period, I joined the faculty of the Polytechnic Institute of Brooklyn in 1951 and wondered what theoretical research to do next after writing the RRKM papers (1951–1952). I remember vividly how a friend of mine and a colleague at Brooklyn Poly, Frank Collins, came down to my office every day with a new idea on the liquid-state transport theory that he was developing, while I had none for my theoretical research. Perhaps this gap of not doing anything immediately in the theoretical field was, in retrospect, fortunate: In not continuing with the study of the theory of unimolecular reactions, for which there were too few legitimate experimental data at the time to make the subject one of continued interest, I was open for investigating quite different problems in other areas. I did, however, begin a program of experimental studies in gas phase reactions prompted by my earlier studies at NRC and by the RRKM work.

I also recall how a student in my statistical mechanics class in this period (Abe Kotliar) asked me about a particular problem in polyelectrolytes. It led to my writing two papers on the subject (1954–1955), one of which required a considerable expansion in my background in electrostatics to analyze different methods for calculating the free energy of these systems: in polyelectrolyte molecules, the ionic charges along the organic or inorganic molecular backbone interact with each other and with the solvent. In the process I read the relevant parts of the texts that were readily available on electrostatics (Caltech's Mason and Weaver's book was later to be particularly helpful!) When shortly thereafter I encountered some papers on electron transfer, a field entirely new to me, I was reasonably well prepared for treating the problems that lay ahead.

3. Developing an Electron Transfer Theory

3.1. Introduction

My first contact with electron transfer reactions came in 1955 as a result of chancing upon a 1952 symposium issue on the subject in the Journal of Physical Chemistry. An article by Bill Libby caught my eye—a use of the Franck–Condon principle to explain some experimental results, namely, why some isotopic exchange reactions that involve electron transfer between pairs of small cations in aqueous solution, such as reaction (1), are relatively slow, whereas electron transfers involving larger ions, such as $[Fe(CN)_6]^{3-}/[Fe(CN)_6]^{4-}$ and MnO_4^-/MnO_4^{2-}, are relatively fast.

Libby explained this observation in terms of the Franck–Condon principle, as discussed in Section 4.1. The principle was used extensively in the field of spectroscopy for interpreting spectra for the excitation of the molecular electronic–vibrational quantum states. An application of that principle to chemical reaction rates was novel and caught my attention. In that paper Libby gave a "back-of-the-envelope" calculation of the resulting energy barrier for solvation that slowed the reaction. However, I felt instinctively that even though the idea—that somehow the Franck–Condon principle was involved—seemed strikingly right, the calculation itself was incorrect. The next month of study of the problem was, for me, an especially busy one. To place the topic in some perspective I first digress and describe the type of theory that was used for other types of chemical reaction rates at the time and continues to be useful today.

3.2. Reaction Rate Theory

Chemical reactions are often described in terms of the motion of the atoms of the reactants on a potential energy surface. This potential energy surface is really the electron energy of the entire system, plotted against the positions of all the atoms. A very common example is the transfer of an atom or a group B from molecule AB to form BC [Eq. (4)].

$$AB + C \longrightarrow A + BC \qquad (4)$$

An example of reaction (4) is the transfer of a hydrogen atom, such as in IH + Br → I + HBr, or the transfer of a CH_3 group from one aromatic sulfonate to another. To aid in visualizing the motion of the atoms in this reaction, the potential energy function for reaction (4) is frequently plotted as constant energy contours in a space whose axes are chosen to be two important relative coordinates such as a scaled AB bond length and a scaled distance from the center of mass of AB to C, as in Figure 2.

A point representing the reactants of this reacting system begins its trajectory in the lower right region of the figure in a valley in this plot of contours. When the system has enough energy, appropriately distributed between the various motions, it can cross the "mountain pass" (saddle-point region) separating the initial valley from the products' valley in the upper left of Figure 2, and so form the reaction products. The line xy in Figure 2, analogous to the continental divide in the Rocky Mountains in the United States separates systems that could spontaneously flow into the reactants' valley from those that could flow into the products' one. In chemists' terminology this line represents the transition state of the reaction.

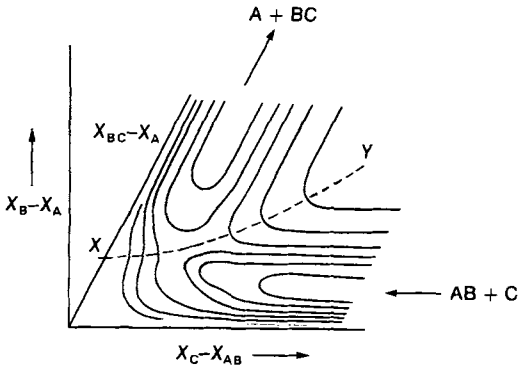

Fig. 2. Potential energy contours for reaction (4) in the collinear case. X_A = coordinates of A, etc.

In transition state theory, a quasi-equilibrium between the transition state and the reactant is frequently postulated, and the reaction rate is then calculated with equilibrium statistical mechanics. A fundamental dynamical basis, which replaces this apparently ad hoc but common assumption of transition state theory and which is perhaps not as well known in the chemical literature as it deserves to be, was given in 1938 by the physicist and one-time chemical engineer, Eugene Wigner. He used a classical mechanical description of the reacting system in the many-dimensional space (of coordinates and momenta). Wigner pointed out that the quasi-equilibrium would follow as a dynamical consequence, if each trajectory of a moving point representing the reacting system in this many-dimensional space did not recross the transition state (and if the distribution of the reactants in the reactants' region were a Boltzmann one). In recent times, the examination of this recrossing has been a common problem in classical mechanical trajectory studies of chemical reactions. Usually, recrossings are relatively minor, except in nonadiabatic reactions, where they are readily treated (see Section 4.1).

In practice, transition state theory is generalized to include as many coordinates as are needed to describe the reacting system. Further, when the system can tunnel quantum mechanically through the potential energy barrier (the pass) separating the two valleys, as for example frequently happens at low energies in H-transfer reactions, the method of treating the passage across the transition state region needs, and has received, refinement. (The principal problem encountered here has been the lack of "dynamical separability" of the various motions in the transition state region.)

4. Electron Transfer Theory: Formulation

4.1. Fundamental Considerations

In contrast to the above picture, we have already noted that in simple electron transfer reactions no chemical bonds are broken or formed, and so a somewhat different picture of the reaction is needed.

In his symposium paper in 1952, Libby noted that when an electron is transferred from one reacting ion or molecule to another, the two new molecules or ions formed are in the wrong environment of the solvent molecules, since the nuclei do not have time to move during the rapid electron jump: in reaction (1) an Fe^{2+} ion would be formed in some configuration of the many nearby dipolar solvent molecules that was appropriate to the original Fe^{3+} ion. Analogous remarks apply to the newly formed Fe^{3+} ion in the reaction. On the other hand, in reactions of complex ions, such as those in the $[Fe(CN)_6]^{-3}/[Fe(CN)_6]^{-4}$ and MnO_4^-/MnO_4^{2-} self-exchange reactions, the two reactants are larger, and so the change of electric field in the vicinity of each ion, upon electron transfer, would be smaller. The original solvent environment would therefore be less foreign to the newly formed charges, and so the energy barrier to reaction would be less. In this way Libby explained the faster self-exchange electron transfer rate for these complex ions. Further confirmation was noted in the ensuing discussion in the symposium: the self-exchange $[Co(NH_3)_6]^{3+}/[Co(NH_3)_6]^{2+}$ reaction is very slow, and it was pointed out that there was a large difference in the equilibrium Co–N bond lengths in the Co^{III} and Co^{II} ions. Again, each ion would be formed in a very foreign configuration of the vibrational coordinates, even though the ions are complex ions.

After studying Libby's paper and the symposium discussion, I realized that what troubled me in this picture for reactions occurring in the dark was that energy was not conserved: the ions would be formed in the wrong high-energy environment, but the only way such a non-energy-conserving event could happen would be by the absorption of light (a vertical transition), and not in the dark. Libby had perceptively introduced the Franck–Condon principle to chemical reactions, but something was missing.

In the present discussion, as well as in Libby's treatment, it was supposed that the electronic interaction of the reactants that causes the electron transfer is relatively weak. That view is still the one that seems appropriate today for most of these reactions. In this case of weak-electronic interaction, the question becomes: how does the reacting systm behave in the dark so that it satisfies both the Franck–Condon principle and energy conservation? I realized that fluctuations had to occur in the various nuclear coordinates, such as in the orientation coordinates of the individual solvent molecules and indeed in any other coordinates whose most probable distribution for the products differs from that of the reactants. With such fluctuations, values of the coordinates could be reached which satisfy both the Franck–Condon and energy conservation conditions and so permit the electron transfer to occur in the dark.

An example of an initial and final configuration of the solvent molecules for reaction (1) is depicted in Figure 3. Fluctuations from the original equilibrium ensemble of configurations were ultimately needed, prior to the electron transfer, and were followed by a relaxation to the equilibrium ensemble for the products after electron transfer.

The theory then proceeded as follows. The potential energy U_r of the entire system, reactants plus solvent, is a function of the many hundreds of relevant coordinates of the system, coordinates which include, among others, the position and orientation of the individual solvent molecules (and

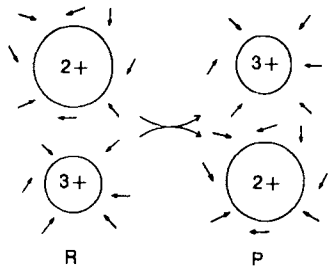

Fig. 3. Typical arrangement of solvent molecules surrounding reactants and products in reaction (1). The longer M–OH_2 bond length in the cation is indicated schematically by the larger ionic radius (Sutin, [2]).

hence of their dipole moments, for example), and the vibrational coordinates of the reactants, particularly those in any inner coordination shell of the reacting ions. (For example, the inner coordination shell of an ion such as Fe^{2+} or Fe^{3+} in water is known from EXAFS (*e*xtended *X*-ray *a*bsorption *f*ine *s*tructure) experiments to contain six water molecules.) No longer were there just the two or so important coordinates that were dominant in reaction (4).

Similarly, after the electron transfer, the reacting molecules have the ionic charges appropriate to the reaction products, and so the relevant potential energy function U_p is that for the products plus solvent. These two potential energy surfaces will intersect if the electronic coupling which leads to electron transfer is neglected. For a system with N coordinates this intersection occurs on an $(N-1)$ dimensional surface, which then constitutes in our approximation the transition state of the reaction. The neglected electronic coupling causes a well-known splitting of the two surfaces in the vicinity of their intersection. A schematic profile of the two potential energy surfaces in the N-dimensional space is given in Figure 4. (The splitting is not shown.)

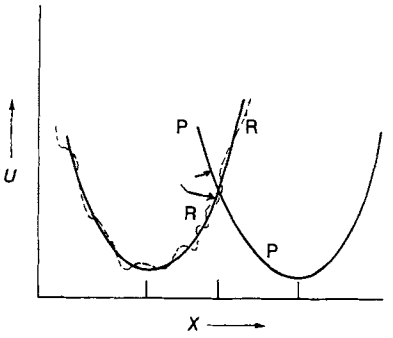

Fig. 4. Profile of potential energy surfaces for reactants plus environment (R) and for products plus environment (P). Solid curve: schematic. Dashed curve: schematic but slightly more realistic. The typical splitting at the intersection of the potential energy curves U_r and U_p is not shown (Marcus and Siddarth [2]). X = nuclear coordinates.

Due to the effect of the previously neglected electronic coupling and the coupling between the electronic motion and the nuclear motion near the intersection surface S, an electron transfer can occur at S. In classical terms, the transfer at S occurs at fixed positions and momenta of the atoms; the Franck–Condon principle is satisfied. Since U_r equals U_p at S, energy is also conserved. The details of the electron trans-

fer depend on the extent of electronic coupling and how rapidly the point representing the system in this N-dimensional space crosses S. (It has been treated, for example, by using as an approximation the well-known one-dimensional Landau–Zener expression for the transition probability at the near-intersection of two potential energy curves.)

When the splitting caused by the electronic coupling between electron donor and acceptor is large enough at the intersection, a system crossing S from the lower surface on the reactants' side continues onto the lower surface on the products' side; an electron transfer in the dark has then occurred. When the coupling is, instead, very weak, ("nonadiabatic reactions") the probability of successfully reaching the lower surface on the products' side is small and can be calculated by using quantum mechanical perturbation theory—for example, by using Fermi's "Golden Rule," an improvement over the 1-dimensional Landau–Zener treatment.

Thus, there is some difference and some similarity with a more conventional type of reaction such as reaction (4), whose potential energy contour plots were depicted in Figure 2. In both cases, fluctuations of coordinates are needed to reach the transition state, but since so many coordinates can now play a significant role in the electron transfer reaction because of the major and relatively abrupt change in charge distribution on passing through the transition state region, a rather different approach from the conventional one was needed to formulate the details of the theory.

4.2. Electron Transfer Theory: Treatment

In the initial paper (1956) I formulated the picture of the mechanism of electron transfer described in the previous section and, to make the calculation of the reaction rate tractable, treated the solvent as a dielectric continuum. Because of the orientation and vibrations of the solvent molecules, the position-dependent dielectric polarization $P_u(r)$ of the solvent in the transition state was not the one in equilibrium with the reactants' or the products' ionic charges. It represented instead, some macroscopic fluctuation from them. The electronic polarization of the solvent molecules, on the other hand, can rapidly respond to any such fluctuations and therefore is that dictated by the reactants' charges and by the instantaneous $P_u(r)$.

With these ideas as a basis, what was then needed was a method of calculating the electrostatic free energy G of this system and its still unknown polarization function $P_u(r)$. I obtained this free energy G by finding a reversible path for reaching this state of the system. Upon then minimizing G, subject to the constraint imposed by the Franck–Condon principle (reflected in the electron transfer occurring at the intersection of the two potential energy surfaces), I was able to find the unknown $P_u(r)$ and, hence, to find G for the transition state. That G was then introduced into transition state theory, and the reaction rate calculated.

During this research I also read and was influenced by a lovely paper by Platzmann and Franck (1952) on the optical absorption spectra of halide ions in water and later by work of physicists such as Pekar and Fröhlich (1954) on the closely related topic of polaron theory. As best as I can recall now, my first expressions for G during this months of intense activity seemed rather clumsy, but then with some rearrangement a simple expression emerged that had the right "feel" to it and that I could also derive by a somewhat independent argument. The expression also reduced reassuringly to the usual one, when the constraint of arbitrary $P_u(r)$ was removed. Obtaining the result for the mechanism and rate of electron transfer was indeed one of the most thrilling moments of my scientific life.

The expression for the rate constant k of the reaction is given by Equation (5), where ΔG^* is represented by Equation (6).

$$k = A\exp\left(\frac{-\Delta G^*}{k_B T}\right) \tag{5}$$

$$\Delta G^* = \frac{\lambda}{4}\left(1 + \frac{\Delta G^0}{\lambda}\right)^2 \tag{6}$$

The term A in Equation (5) depends on the nature of the electron transfer reaction (e.g., bimolecular or intramolecular), ΔG^0 is the standard free energy of reaction (and equals zero for a self-exchange reaction), and λ is a "reorganization term" composed of solvational (λ_o) and vibrational (λ_i) components [Eq. (7)].

$$\lambda = \lambda_o + \lambda_i \tag{7}$$

In a two-sphere model of the reactants, λ_o was expressed in terms of the two ionic radii a_1 and a_2 (which encompass the radii of any inner coordination shell), the center-to-center separation distance R of the reactants, the optical (D_{op}) and static (D_s) dielectric constants of the solvent, and the charge transferred (Δe) from one reactant to the other [Eq. (8)].

$$\lambda_o = (\Delta e)^2\left(\frac{1}{2a_1} + \frac{1}{2a_2} - \frac{1}{R}\right)\left(\frac{1}{D_{op}} - \frac{1}{D_s}\right) \tag{8}$$

For a bimolecular reaction, work terms, principally electrostatic, are involved in bringing the reactants together and in separating the reaction products, but are omitted from Equation (6) for notational brevity. The expression for the vibrational term λ_i is given by (9), where Q_j^r and Q_j^p are equi-

$$\lambda_i = \tfrac{1}{2}\sum_j k_j (Q_j^r - Q_j^p)^2 \tag{9}$$

librium values for the jth normal mode coordinate Q, and k_j is a reduced force constant $2k_j^r k_j^p/(k_j^r + k_j^p)$ associated with it. The superscripts r and p refer to reactants and products. (I introduced a "symmetrization" approximation for the vibrational part of the potential energy surface to obtain this simple form of (6)–(9), and tested it numerically.)

In 1957 I published the results of a calculation of the λ_i arising from a stretching vibration in the innermost coordination shell of each reactant, (the equation used for λ_i was given in the 1960 paper). An early paper on the purely vibrational contribution calculated by using chemical bond length coordinates and neglecting bond–bond correlation had already been published for self-exchange reactions by George and Griffiths in 1956.

I also extended the theory to treat electron transfers at electrodes, and distributed it as an Office of Naval Research

Report in 1957. The equations were published later in a journal paper in 1959. I had little prior knowledge of the subject, and my work on electrochemical electron transfers was facilitated considerably by reading a beautiful and logically written survey article of Roger Parsons on the equilibrium electrostatic properties of electrified metal–solution interfaces.

In the 1957 and 1965 work I showed that the electrochemical rate constant is given by (5)–(9), but A now is a value appropriate to the different "geometry" of the encounter of the participants in the reaction. The term $1/(2a_2)$ in Equation (8) is now absent because only one reaction ion is present, and R denotes twice the distance from the center of the reactant's charge to the electrode (it equals the ion–image distance). A term $e\eta$ replaces ΔG^0 in Equation (6), where e is the charge transferred between the ion and the electrode, and η is the activation overpotential, namely, potential difference between metal and solution relative to the value it would have if the rate constants for the forward and reverse reactions were equal. These rate constants are equal when the minima of the two free energy curves in Figure 5 have the same value for G.

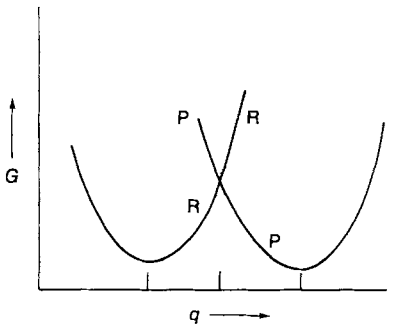

Fig. 5. Plot of the free energy of reactants plus environment vs. the reaction coordinate q (R) and of the free energy of products plus environment vs. reaction coordinate q (P). The three vertical lines on the abscissa denote, from left to right, the value for the reactants, the transition state, and the products (Marcus and Siddarth [2]).

When $|e\eta| < \lambda$, most electrons go into or out of quantum states in the metal that are near the Fermi level. However, because of the continuum of states in the metal, the inverted effect described below was now predicted to be absent for this process; that is, the electrochemical counterpart of Eq. (6) is applicable only in the region $|e\eta| < \lambda$: In the case of an intrinsically highly exothermic electron transfer reaction at an electrode, the electron can remove the immediate "exothermicity" by (if entering) going into a high, unoccupied quantum state of the metal, or (if leaving) departing from a low, occupied quantum state, each far removed from the Fermi level. (The inverted region effect should, however, occur for the electron transfer when the electrode is a narrow-band semiconductor.)

After these initial electron transfer studies, which were based on a dielectric continuum approximation for the solvent outside the first coordination shell of each reactant, I introduced a purely molecular treatment of the reacting system. The solvent was treated by statistical mechanics as a collection of dipoles in the 1960 paper, and later in 1965 a general charge distribution was used for the solvent molecules and the reactants. At the same time I found a way in this 1960 paper of introducing rigorously a global reaction coordinate in this many-dimensional (N) coordinate space of the reacting system. The globally defined coordinate so introduced was equivalent to using $U_p - U_r$, the potential energy difference between the products plus solvent (U_p) and the reactants plus solvent (U_r) (see A. Warshel, 1987). This coordinate is thus defined everywhere in this N-dimensional space.

The free energy G_r of a system containing the solvent and the reactants, and that of the corresponding system for the products, G_p, could now be defined along this globally defined reaction coordinate. (By contrast, in reactions such as that depicted by Figure 2, it is customary, instead, to define a reaction coordinate locally in the vicinity of a path leading from the valley of the reactants through the saddle point region and into the valley of the products.)

The potential energies U_r and U_p in the many-dimensional coordinate space are simple functions of the vibrational coordinates, but complicated functions of the hundreds of relevant solvent coordinates: there are many local minima corresponding to locally stable arrangements of the solvent molecules. However, I introduced a "linear response approximation," in which any hypothetical change in charge of the reactants produces a proportional change in the dielectric polarization of the solvent. (Recently I utilized a central limit theorem to understand this approximation better than is possible with simple perturbation theory and plan to submit the results for publication shortly.) With this linear approximation the free energies G_r and G_p became simple quadratic functions of the reaction coordinate.

Such an approach had major consequences. It depicted the reaction in terms of parabolic free energy plots in simple and readily visualized terms, as in Figure 5. With these plots the trends predicted from the equations were readily understood. It was also important to use the free energy curves, instead of oversimplified potential energy profiles, because of the large entropy changes which occur in many electron transfer cross-reactions, caused by changes in strong solvent interactions between ions and polar solvent. (The free energy plot is legitimately a one-coordinate plot, whereas the potential energy plot is at most a profile of the complicated U_r and U_p functions in N-dimensional space.)

With the new statistical mechanical treatment of 1960 and 1965 one could also see how certain relations between rate constants initially derivable from the dielectric continuum-based equations in the 1956 paper could also be valid more generally. The relations were based, in part, on Equations (5) and (6) and (initially via (8) and (9)) on the approximate relation (10), where λ_{12} is the reoganization term for

$$\lambda_{12} \cong \tfrac{1}{2}(\lambda_{11} + \lambda_{22}) \tag{10}$$

the cross-reaction, and λ_{11} and λ_{22} are those of the self-exchange reactions.

5. Predictions Based on the Theory

In the 1960 paper I had listed a number of theoretical predictions resulting from these equations, in part to stimu-

late discussion with experimentalists in the field at a Faraday Society meeting on oxidation–reduction reactions, where this paper was to be presented. At the time I certainly did not anticipate the subsequent involvement of the many experimentalists in testing them. Among the predictions was one that became one of the most widely tested aspects of the theory, namely, the cross-relation. This expression, which follows from Equations (5), (6), and (10), relates the rate constant k_{12} of a cross-reaction to the two self-exchange rate constants, k_{11} and k_{22}, and to the equilibrium constant K_{12} of the reaction [Eq. (11)], where f_{12} is a known function of k_{11}, k_{22} and K_{12} and is usually close to unity.

$$k_{12} \cong (k_{11} k_{22} K_{12} f_{12})^{1/2} \tag{11}$$

Another prediction in the 1960 paper concerned what I termed there the inverted region: In a series of related reactions, similar in λ but differing in ΔG^0, a plot of the activation free energy ΔG^* vs. ΔG^0 is seen from Equation (6) first to decrease as ΔG^0 is varied from zero to some negative value, to be zero at $\Delta G^0 = -\lambda$, and then to increase when ΔG^0 is made still more negative. The initial decrease of ΔG^* with increasingly negative ΔG^0 is the expected trend in chemical reactions and is similar to the usual trend in "Brønsted plots" of acid- or base-catalyzed reations and in "Tafel plots" of electrochemical reactions. I termed that region of ΔG^0 the "normal" region. However, the prediction for the region where $-\Delta G^0 > \lambda$, the inverted region, was the unexpected behavior, or at least unexpected until the present theory was introduced.

This inverted region is also easily visualized from Figures 6 and 7: Successively making ΔG^0 more negative by lowering the products' G curve vertically relative to the reactant curve, decreases the free energy barrier ΔG^* (given by the intersection of the reactants' and products' curves); that barrier is seen in Figure 6 to vanish at some ΔG^0 and then to increase again.

Other predictions dealt with the relation between the electrochemical and the corresponding self-exchange electron transfer rates, the numerical estimate of the reaction rate constant k, and, in the case of nonspecific solvent effects, the dependence of the reaction rate on solvent dielectric properties.

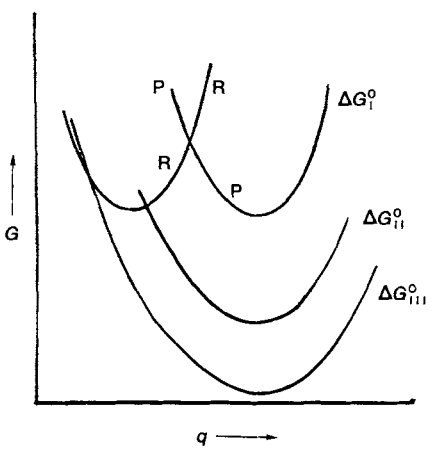

Fig. 6. Plot of the free energy G versus the reaction coordinate q for reactants (R) and products (P), for three different values of ΔG^0; the cases I to III refer to Figure 7 (Marcus and Siddarth [2]).

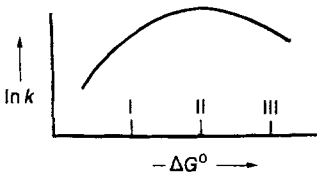

Fig. 7. Plot of $\ln k_r$ vs. $-\Delta G^0$. Points I and III are in the normal and inverted regions, respectively, while point II at which $\ln k_r$ is a maximum occurs at $-\Delta G^0 = \lambda$ (Marcus and Siddarth, [2]).

The testing of some of the predictions was delayed by an extended sabbatical in 1960–1961, which I spent auditing courses and attending seminars at the nearby Courant Mathematical Institute.

6. Comparison of Experiment and Theory

Around 1962 during one of my visits to Brookhaven National Laboratory, I showed Norman Sutin the 1960 predictions. Norman had either measured on his stopped-flow apparatus or otherwise knew rate constants and equilibrium constants that permitted the cross-relation [Eq. (11)] to be tested. He had about six such sets of data available. I remember vividly the growing sense of excitement we both felt as, one by one, the observed rate constants k_{12} more or less agreed with the predictions of the relation. I later collected the results of this and of various other tests of the 1960 predictions and published them in 1963. Perhaps by showing that the previously published expressions were not mere abstract formulae, but rather had concrete applications, this 1963 paper and many tests by Sutin and others appear to have stimulated numerous subsequent tests of the cross-rela-

Table 1. Comparison of calculated and experimental k_{12} values (Bennett [3]).

Reaction [a]	k_{12} [$M^{-1}s^{-1}$] observed	calculated
$[IrCl_6]^{2-} + [W(CN)_8]^{4-}$	6.1×10^7	6.1×10^7
$[IrCl_6]^{2-} + [Fe(CN)_6]^{4-}$	3.8×10^5	7×10^5
$[IrCl_6]^{2-} + [Mo(CN)_8]^{4-}$	1.9×10^6	9×10^5
$[Mo(CN)_8]^{3-} + [W(CN)_8]^{4-}$	5.0×10^6	4.8×10^6
$[Mo(CN)_8]^{3-} + [Fe(CN)_6]^{4-}$	3.0×10^4	2.9×10^4
$[Fe(CN)_6]^{3-} + [W(CN)_8]^{4-}$	4.3×10^4	6.3×10^4
$Ce^{IV} + [W(CN)_8]^{4-}$	$>10^8$	4×10^8
$Ce^{IV} + [Fe(CN)_6]^{4-}$	1.9×10^6	8×10^6
$Ce^{IV} + [Mo(CN)_6]^{4-}$	1.4×10^7	1.3×10^7
L-$[Co\{(-)pdta\}]^{2-} + [Fe(bpy)_3]^{3+}$	8.1×10^4	$\geq 10^5$
L-$[Fe\{(-)pdta\}]^{2-} + [Co(edta)]^-$	1.3	1.3
L-$[Fe\{(-)pdta\}]^{2-} + [Co(ox)_3]^{3-}$	2.2×10^2	1.0×10^3
$[Cr(edta)]^{2-} + [Fe(edta)]^-$	$\geq 10^6$	10^9
$[Cr(edta)]^{2-} + [Co(edta)]^-$	ca. 3×10^5	4×10^7
$[Fe(edta)]^{2-} + [Mn(Cydta)]^-$	ca. 4×10^5	6×10^6
$[Co(edta)]^{2-} + [Mn(Cydta)]^-$	0.9	2.1
$[Fe(pdta)]^{2-} + [Co(Cydta)]^-$	1.2	1.8
$[Co(terpy)_2]^{2+} + [Co(bpy)_3]^{3+}$	6.4	3.2
$[Co(terpy)_2]^{2+} + [Co(phen)_3]^{3+}$	2.8×10^2	1.1×10^2
$[Co(terpy)_2]^{2+} + [Co(bpy)(H_2O)_4]^{3+}$	6.8×10^2	6.4×10^4
$[Co(terpy)_2]^{2+} + [Co(phen)(H_2O)_4]^{3+}$	1.4×10^3	6.4×10^4
$[Co(terpy)_2]^{2+} + [Co(H_2O)_6]^{3+}$	7.4×10^4	2×10^{10}
$[Fe(phen)_3]^{2+} + MnO_4^-$	6×10^3	4×10^3
$[Fe(CN)_6]^{4-} + MnO_4^-$	1.3×10^4	5×10^3
$[V(H_2O)_6]^{2+} + [Ru(NH_3)_6]^{3+}$	1.5×10^3	4.2×10^3
$[Ru(en)_3]^{2+} + [Fe(H_2O)_6]^{3+}$	8.4×10^4	4.2×10^5
$[Ru(NH_3)_6]^{2+} + [Fe(H_2O)_6]^{3+}$	3.4×10^5	7.5×10^6
$[Fe(H_2O)_6]^{2+} + [Mn(H_2O)_6]^{3+}$	1.5×10^4	3×10^4

[a] pdta = propylenediaminetetraacetate, bpy = bipyridine, edta = ethylenediaminetetraacetate, Cydta = *trans*-1,2-diaminocyclohexane-*N*,*N*,*N*',*N*'-tetraacetate, terpy = terpyridine, phen = phenanthroline, en = ethylenediamine.

tion and of the other predictions. A few examples of the cross-relation test are given in Table 1.

The encouraging success of the experimental tests given in the 1963 paper suggested that the theory itself was more general than the approximations (for example, treating solvent as dipoles or employing unchanged force constants) used in 1960 and stimulated me to give a more general formulation (1965). The latter paper also contains a unified treatment of electron transfer reactions in solution and at metal electrodes, and served, thereby, to generalize my earlier (1957) treatment of the electrochemical electron transfer reactions.

The best experimental evidence for the inverted region was provided in 1984 by Miller, Calcaterra, and Closs, almost 25 years after it was predicted. This successful experimental test, which was later obtained for other electron transfer reactions in other laboratories, is reproduced in Figure 8. Possible reasons for not observing it in the earlier tests are severalfold and have been discussed elsewhere.

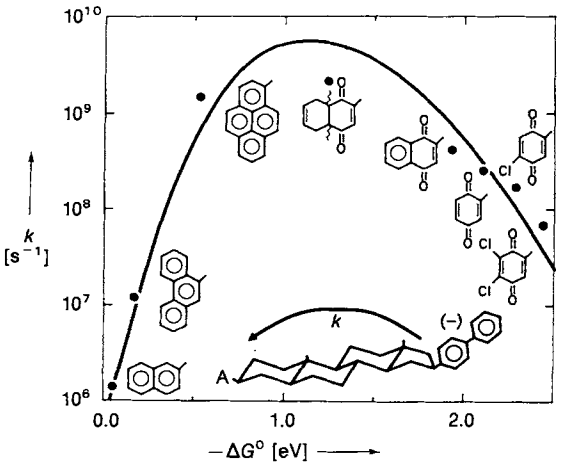

Fig. 8. Inverted region in the chemical electron transfer from a biphenyl group to an acceptor A. Dihydronaphthoquinone marks the changeover from normal (left) to inverse behavior (right). The solid curve was calculated for $\lambda_0 = 0.75$ and $\lambda_i = 0.45$ eV. The frequency of the high-frequency vibrations ω was 1500 cm^{-1} (Miller et al. [3]).

Previously, indirect evidence for the inverted region had been obtained by observing that electron transfer reactions with a very negative ΔG^0 may result in chemiluminescence: when the intersection of the G_r and G_p curves in such cases results in a high free energy of activation ΔG^* because of the effect of the inverted region, there may be an electron transfer to a more easily accessible G_p curve in which one of the products is electronically excited and which intersects the G_r curve in the normal region at a low ΔG^* (Fig. 9). Indeed, experimentally in some reactions 100% formation of an electronically excited state of a reaction product has been observed by Bard and co-workers, and results in chemiluminescence.

Another consequence of Equations (5) and (6) is the linear dependence of $k_B T \ln k$ on $-\Delta G^0$ with a slope of 1/2 when $|\Delta G^0/\lambda|$ is small. The behavior at electrodes is similar, but ΔG^0 is replaced by $e\eta$, that is, the product of the charge transferred and the activation overpotential. Extensive verification of both these results has been obtained. More recently, the curvature of plots of $\ln k$ vs. $e\eta$, expected from these equations, has been demonstrated in several experiments. The very recent use of ordered organic molecular monolayers on electrodes, either to slow down the electron transfer rate or to bind a redox-active agent to the electrode, but in either case to avoid or minimize diffusion control of the fast electron transfer processes, has considerably facilitated this study of the curvature in the $\ln k$ vs. $e\eta$ plot.

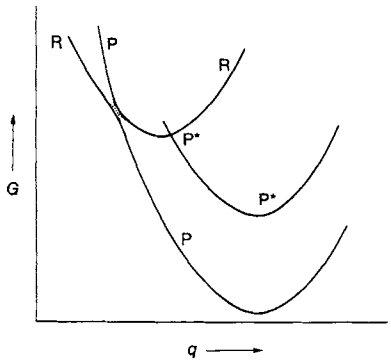

Fig. 9. The favored formation of an electronically excited state of the products (Marcus and Siddarth [2]), which prevents the observation of the inverse region.

Comparison of experiment and theory has also included the testing of absolute reaction rates of self-exchange reactions and the effect on the rate of varying the solvent (an effect sometimes complicated by ion pairing in the low dielectric constant media involved). The related problem of charge transfer spectra, as portrayed in (12) has also been examined. Here, the frequency of the spectral absorption maximum ν_{max} is given by Equation (13).

$$DA + h\nu \longrightarrow D^+A^- \tag{12}$$

$$h\nu_{max} = \lambda + \Delta G^0 \tag{13}$$

Comparisons with Equation (13) in which λ is expressed as in Equation (8) have included examples with effects of separation distance and solvent dielectric constant.

Comparisons have also been made of the self-exchange reaction rates in solution with the rates of the corresponding electron transfer reactions at electrodes. An example of the latter is the plot given in Figure 10, where the self-exchange

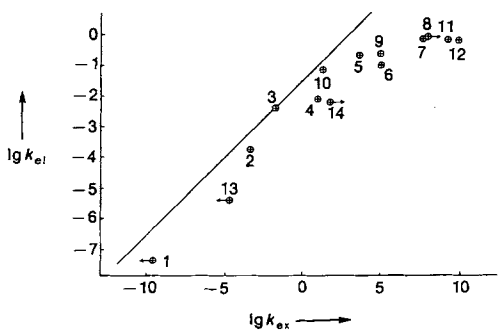

Fig. 10. Comparison of self-exchange electron transfer rates k_{ex} in solution, covering 20 orders of magnitude with rates of corresponding electron transfers at metal electrodes (k_{el}). The line with slope 1/2 shows the behavior predicted by theory (Cannon [2]).

rates are seen to vary by some twenty orders of magnitude. The discrepancy at high rate constants k is currently the subject of some reinvestigation of the fast electrode reaction rates, using the new nanotechnology. Most recently, a new type of interfacial electron transfer rate has also been measured: electron transfer at liquid–liquid interfaces. In treating the latter, I extended the cross relation to this two-phase system. It is clear that much is to be learned from this new area of investigation. (The study of the transfer of ions across such an interface, on the other hand, goes back to the time of Nernst and of Planck around the turn of the century.)

7. Other Applications and Extensions of the Theory

As noted in Figure 1, one aspect of the electron transfer field has been its continued and, indeed, ever-expanding growth in so many directions. One of these is in the biological field, where there are now detailed experimental and theoretical studies in photosynthetic and other protein systems. The three-dimensional structure of a photosynthetic reaction center, the first membrane protein to be so characterized, was obtained by Deisenhofer, Michel, and Huber, who received the Nobel Prize in Chemistry in 1988 for this work. A bacterial photosynthetic system is depicted in Figure 11; the protein framework holding fast the constituents in this reaction center is not shown.

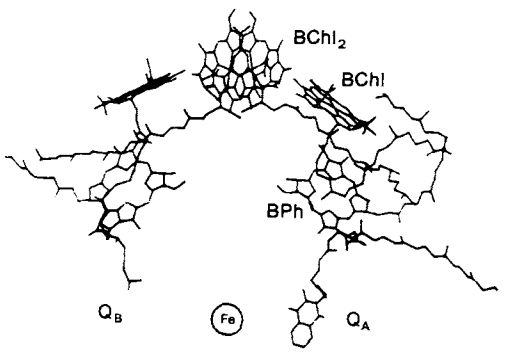

Fig. 11. The redox-active species involved in the initial charge separation in a bacterial photosynthetic center (Deisenhofer et al. and Yeates et al. [3]). The labels added conform to the present text; they include a missing Q_B.

In the photosynthetic system there is a transfer of electronic excitation from "antenna" chlorophylls (not shown in Figure 11) to a special pair $BChl_2$. The latter then transfers an electron to a pheophytin BPh within a very short time (≈ 3 ps), from it to a quinone Q_A in 200 ps, and thence to the other quinone Q_B. (Other chemical reactions then occur with these separated charges at each site of the membrane, bridged by this photosynthetic reaction center.)

To avoid wasting the excitation energy of the $BChl_2^*$ unduly, it is necessary that $-\Delta G^0$ of this first electron transfer to BPh be small. (It is only about 0.25 eV out of an overall excitation energy of $BChl_2^*$ of 1.38 eV.) In order that this electron transfer also be successful in competing with two wasteful processes, the fluorescence and the radiationless transition of $BChl_2^*$, it is also necessary that ΔG^* for that first electron transfer step be small and hence, by Equation (6), that λ be small. The reactants are large, and the immediate protein environment is largely nonpolar, so leading to a small λ [see Eq. (8)]. Nature appears, indeed, to have constucted a system with this desirable property.

Furthermore, to prevent another form of energy wastage, it is also important that an unwanted back electron transfer reaction from the BPh^- to the $BChl_2^+$ not compete successfully with a second forward electron transfer step from BPh^- to Q_A. That is, it is necessary that the back transfer, a "hole–electron recombination" step, be slow, even though it is a very highly exothermic process (about 1.1 eV). It has been suggested that the small λ (about 0.25 eV) and the resulting inverted region effect play a significant role in providing this essential condition for the effectiveness of the photosynthetic reaction center.

There is now a widespread interest in synthesizing systems that can mimic the behavior of nature's photosynthetic systems, and so offer other routes for harnessing solar energy. The current understanding of how nature works has served to provide some guidelines. In this context, as well as in that of electron transfer in other proteins, there are also relevant experiments in long-range electron transfer. Originally the studies were of electron tansfer in rigid glasses, performed by Miller and co-workers. More recently the studies have involved a donor and receptor held together by constructed rigid molecular bridges. The effect of varying the bridge length has been studies in the various systems. A theoretical estimate of the dependence of electron transfers on distance in a photosynthetic system was first made by Hopfield, who used a square barrier as model and an estimate of the barrier height based on molecular considerations.

Recently, in their studies of long-range electron transfer in chemically modified proteins, Gray and co-workers have studied systematically the distance or site dependence of the electronic factor by attaching an appropriate electron donor or acceptor to a desired site. For each such site the reactant was chosen so that $-\Delta G^0 \approx \lambda$, that is, the rate constant k is at the maximum of the $\ln k$ vs. $-\Delta G^0$ curve (see Eqs. (5)–(6)). The value of k then no longer depends on ΔG^*. Since ΔG^* is distance-dependent [see Eq. (8)], it is particularly desirable to make $\Delta G^* \approx 0$, so that the relative k values at the various sites now reflect only the electronic factor. Dutton and co-workers have treated data similarly for a number of reactions by using, where possible, the k at the maximum of each $\ln k$ vs. ΔG^0 curve. Of particular interest in such studies is whether there is a simple exponential decrease of the electronic factor on the separation distance between donor and acceptor, or whether there are deviations from this monotonic behavior, due to local structural factors.

In a different development, the mechanism of various organic reactions has been explored by several investigators, notably by Eberson,[2] in the light of current electron transfer theory, and also by Shaik and Pross in their analysis of a possible electron transfer mechanism vs. a conventional mechanism.

Theoretical calculations of the donor–acceptor electronic interactions, initially by McConnell and by Larsson, and later by others, my group among them, have been used to treat long-range electron transfer. The methods have recently been adapted to large protein systems. In our studies with

Siddarth we used an "artificial intelligence" searching technique to limit the number of amino acids used in the latter type of study.

Another area of much current activity in the field of electron transfer is that of solvent dynamics, which follows the pioneering treatment for general reactions by Kramers (1940). Important later developments for electron transfer were made by many contributors. Solvent dynamics affects the electron transfer reaction rate when the solvent is sufficiently sluggish. As we showed recently with Sumi and Nadler, the solvent dynamics effect can also be modified significantly when there are vibrational (λ_i) contributions to λ.

Computational studies, such as the insightful one of David Chandler and co-workers on the Fe^{2+}/Fe^{3+} self-exchange reaction, have also been employed recently. Using computer simulations they obtained a verification of the parabolic G curves, even for surprisingly strong fluctuations in G. They also extended their studies to dynamic and quantum mechanical effects of nuclear motion. Studies of the quantum mechanical effects of the nuclear motion on electron transfer reactions were initiated in 1959 by Levich and Dogonadze, who assumed a harmonic oscillator model for the polar solvent medium and employed perturbation theory. Their method was related to that used for other problems by Huang and Rhys (1951) and Kubo and Toyozawa (1954).

Important subsequent developments by various authors on these quantum effects include the first discussion of quantum effects for the vibrations of the reactants by Sutin in 1962 and the important work of Jortner and co-workers in 1974–1975, who combined a Levich and Dogonadze type approach to treat the high frequency vibrations of the reactants with the classical expression that I described earlier for the polar medium. These quantum effects have implications for the temperature dependence of k, among other effects. Proceeding in a different (classical) direction Savéant recently showed how to extend Equation (6) to reactions involving the rupture of a chemical bond by electron transfer, which he had previously studied experimentally: $M(e) + RX \rightarrow M + R + X^-$, where R is an alkyl group, X a halide, and M a metal electrode.

A particularly important early development was that by Taube in the 1950s, who received the Nobel Prize for his work in 1983. Taube introduced the idea of different mechanisms for electron transfer, the outer sphere and inner sphere electron transfers, which he had investigated experimentally. His experimental work on charge transfer spectra of strongly interacting systems ("Creutz–Taube" ion, 1959, 1973) and of weakly interacting ones has been similarly influential. Also notable has been Hush's theoretical work on charge transfer spectra, both of intensities and absorption maxima (1967), which supplemented his earlier theoretical study of electron transfer rates (1961).

There has been a spin-off of the original electron transfer theory to other types of chemical reactions as well. In particular, the ΔG^* vs ΔG^0 relation and the cross-relation have been extended to these other reactions, such as the transfer of atoms, protons, or methyl groups. (Even an analog of Equations (6) and (10) for binding energies instead of energy barriers has been introduced to relate the stability of isolated proton-bound dimers AHB^+ to those of AHA^+ and BHB^+!)

Since the transfer of these nuclei involves strong electronic interactions, it is not well represented by intersecting parabolic free energy curves, and a different theoretical approach was needed. For this purpose I adapted in 1968, a "bond-energy–bond-order" model of H. Johnston in order to treat the problem for a reaction of type (4). The resulting simple expression for ΔG^* is similar to Equation (6) when $|\Delta G^0/\lambda|$ is not large ($<\frac{1}{2}$), but differs from it in not having any inverted region. It has the same λ property as that given by Equation (10) and has resulted in a cross-relation analogous to Equation (11). The cross-relation has been tested experimentally for the transfer of methyl groups by E. Lewis, and the ΔG^* vs ΔG^0 relation has been used or tested for other transfers by the groups of Albery and Kreevoy, among others.

It is naturally gratifying to see one's theories used. A recent article, which showed the considerable growth in the use of papers such as the 1956 and 1964 articles,[5] points up the impressive and continued vitality of the field itself. The remarks above on many areas of electron transfer and on the spin-off of such work on the study of other types of reactions represent a necessarily brief picture of these broad-based investigations.

I would like to acknowledge my many fellow researchers in the electron transfer field, notably Norman Sutin, with whom I have discussed so many of these matters for the past thirty or more years. I also thank my students and post-doctorals, whose presence was a constant source of stimulation to me, both in the electron transfer field and in the other fields of research which we have explored. In its earliest stage and for much of this period, my research was supported by the Office of Naval Research and also later by the National Science Foundation. The support of both agencies continues to this day, and I am very pleased to acknowledge its value and timeliness here.

In my Nobel lecture, I concluded on a personal note with a slide of my great-uncle, Henrik Steen (né Markus), who came to Sweden in 1892. He received his doctorate in theology from the Univeristy of Uppsala in 1915, and was an educator and a prolific writer of pedagogic books. As I noted in the biographical sketch in Les Prix Nobel, he was one of my childhood idols. During my trip to Sweden to receive the Nobel prize, visiting with my Swedish relatives – some thirty or so of his descendants – has been an especially heartwarming experience for me and for my family. In a sense I feel that I owed him a debt, and that it is most fitting to acknowledge that debt here.

Received: March 10, 1993 [A 914 IE]
German version: *Angew. Chem.* **1993**, *105*, 1161

[1] R. A. Marcus, *J. Chem. Phys.* **1956**, *24*, 966, 979; *ibid.* **1957**, *26*, 867, 872; *Trans. N.Y. Acad. Sci.* **1957**, *19*, 423; *ONR Tech. Rep. 12*, Project NR 051-331, **1957**, reproduced in *Spec. Top. Electrochem.* **1977**, 181; *Can. J. Chem.* **1959**, *37*, 155; *Discuss. Faraday Soc.* **1960**, *29*, 21; *J. Phys. Chem.* **1963**, *67*, 853, 2889; *J. Chem. Phys.* **1963**, *38*, 1858; *ibid.* **1963**, *39*, 1734; *Annu. Rev. Phys. Chem.* **1964**, *15*, 155; *J. Chem. Phys.* **1965**, *43*, 679, 1261; *ibid.* **1965**, *43*, 2654, correction *ibid.* **1970**, *52*, 2803; *J. Phys. Chem.* **1968**, *72*, 891.

[2] R. A. Marcus, N. Sutin, *Biochim. Biophys. Acta* **1985**, *811*, 265; assorted articles in *Adv. Chem. Ser.* **1991**, *228*; M. D. Newton, N. Sutin, *Annu. Rev. Phys. Chem.* **1984**, *35*, 437; N. Sutin, *Prog. Inorg. Chem.* **1983**, *30*, 441; M. D. Newton, *Chem. Rev.* **1991**, *91*, 767; R. D. Cannon, *Electron Transfer*

Reactions, Butterworths, London, **1980**; L. Eberson, *Electron Transfer Reactions in Organic Chemistry*, Springer, New York, **1987**; *Photoinduced Electron Transfer Vol. 1–4* (Eds.: M. A. Fox, M. Chanon), Elsevier, New York, **1988**; J. F. Endicott, D. H. Macartney in *Mechanisms of Inorganic and Organometallic Reactions, Vol. 7* (Ed.: M. V. Twigg), Plenum, New York, **1991**, Chapters 1, 2, and earlier volumes. R. A. Marcus, P. Siddarth in *Photoprocesses in Transition Metal Complexes, Biosystems and Other Molecules: Experiment and Theory* (Ed.: E. Kochanski), Kluwer, Norwall, MA, USA, **1992**, p. 49; S. S. Shaik, H. B. Schlegel, S. Wolfe, *Theoretical Aspects of Physical Organic Chemistry*, J. Wiley, New York, **1992**; N. Sutin, *Pure Appl. Chem.* **1988**, *60*, 1817; assorted articles in *Chem. Rev.* **1992**, *92*, (3); *J. Phys. Chem.* **1986**, *90*, R. A. Marcus Commemorative Issue).

[3] L. E. Bennett, *Prog. Inorg. Chem.* **1973**, *18*, 1; J. R. Miller, L. T. Calcaterra, G. L. Closs, *J. Am. Chem. Soc.* **1984**, *106*, 3047; J. Deisenhofer, O. Epp, K. Miki, R. Huber, H. Michel, *J. Mol. Biol.* **1984**, *180*, 385; R. Huber, *Angew. Chem.* **1989**, *101*, 849; *Angew. Chem. Int. Ed. Engl.* **1989**, *28*, 848; J. Deisenhofer, H. Michel, *ibid.* **1989**, *101*, 872 or **1989**, *28*, 829; T. G. Yeates, H. Komiya, D. C. Rees, J. P. Allen, G. Feher, *Proc. Natl. Acad. Sci.* **1987**, *84*, 6438.

[4] P. J. Robinson, H. A. Holbrook, *Unimolecular Reactions*, J. Wiley, New York, **1972**; W. Forst, *Theory of Unimolecular Reactions*, Academic Press, New York, **1973**; see also the very recent publication by R. G. Gilbert, S. C. Smith, *Theory of Unimolecular and Recombination Reactions*, Blackwell, Oxford, **1990**.

[5] *Science Watch* **1992**, *3* (9), p. 8.

Protein Phosphorylation and Cellular Regulation I (Nobel Lecture)**

By Edwin G. Krebs*

Introduction

This presentation and the one to be given immediately thereafter [***] will be concerned with the reversible phosphorylation of proteins and the role of this process in biological regulation. In addition to discussing our own early contributions to this field, Ed Fischer and I will describe some of the developments that have occurred subsequently. These developments have led to the realization that protein phosphorylation constitutes a major mechanism by which cellular processes are controlled. My own remarks will review the historical background that provided the setting in which our joint work was carried out in the 1950s and early 1960s. Then I'll turn to a discussion of this work itself, to be followed by comments to the cyclic AMP dependent protein kinase. Finally I will talk about the intracellular transmission of hormone and growth factor signals through protein kinase cascades.

Background

By 1940, which is the year in which I entered medical school at Washington University in St. Louis, it was well established that the breakdown of glycogen in skeletal muscle and other types of cells occurs by the process of phosphorolysis, catalyzed by the enzyme phosphorylase (reviewed in ref.[1]). Carl Cori was Professor and Chairman of the Department of Pharmacology at Washington University when I started my training there, but he was soon to take over the Department of Biological Chemistry. I gradually came to know him, at first distantly, the way medical students usually know their professors, but later on somewhat better after I had become a teaching assistant in biochemistry. In this latter role I also became acquainted with Arda Green, who, together with Carl and Gerty Cori, was purifying rabbit muscle phosphorylase. It was not long until I began to hear about the unusual properties of this remarkable enzyme, which they had found existed in skeletal muscle in two different forms that they designated as phosphorylase *a* and phosphorylase *b*.[2, 3] The *a* form was purified and obtained as a crystalline enzyme. Kinetically, it was shown that phosphorylase *b* requires high concentrations of 5'-AMP for activity, whereas phosphorylase *a* is active in the absence of this nucleotide. Since the concentration of 5'-AMP required for the activity of phosphorylase *b* was considerably higher than that found in muscle, this form was considered to be physiologically inactive. Phosphorylase *a* was thought of as the physiologically active species. Evidence was obtained that the two forms are interconvertible within the cell, and it was postulated by the Coris that interconversion of the forms of phosphorylase constitutes a physiologically significant regulatory mechanism. Resting muscle was reported to contain phosphorylase predominantly in the *a* form, whereas electrically stimulated muscle contained the *b* form.[4] As will be discussed later (see below) the reverse is actually true. Regardless of this latter point, however, the finding that an enzyme might shuttle back and forth between two forms within the cell was a remarkable advance, which set the stage for important later developments.

The Coris were unaware of the chemical nature of the interconversion reactions of phosphorylase, but they did discover an enzyme that would convert phosphorylase *a* to phosphorylase *b* in vitro. This enzyme was called the "PR enzyme" based on the assumption that it acted by removing a prosthetic group from phosphorylase *a*, which was thought of as a holoenzyme form;[2] phosphorylase *b*, lacking the putative group, was considered to be the apoenzyme form. Based on the fact that phosphorylase *b* could be activated by 5'-AMP, this nucleotide bound to the enzyme was thought of as the likely candidate for the prosthetic group of phosphorylase *a*. However, all attempts to identify 5'-AMP as a product formed when phosphorylase *a* was converted to phosphorylase *b* by the PR enzyme were unsuccessful.[2, 3] Because trypsin treatment of phosphorylase *a* led to the formation of a phosphorylase *b*-like form, in other words an enzyme that could be activated by 5'-AMP,[3] it was believed that the PR enzyme might be a protease. No enzyme that could convert phosphorylase *b* to *a* in vitro in the presene of 5'-AMP, or under any other condition that these workers tried, could be demonstrated. This did not seem unreasonable, however, if it were supposed that such a conversion might require peptide bond biosynthesis, because at that time the likelihood that such a reaction could be shown to occur in vitro was considered unlikely. These early concepts with respect to the interconversion reactions of phosphorylase are illustrated in Figure 1.

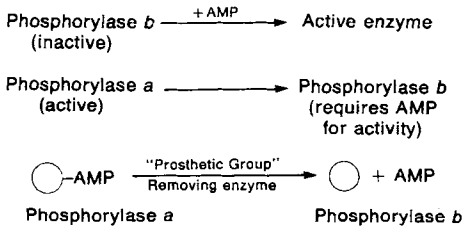

Fig. 1. Early concepts of the interconversion reactions of muscle phosphorylase. Inactive phosphorylase *b* becomes an active enzyme in the presence of 5'-AMP. Phosphorylase *a*, the physiologically active form of the enzyme, is inactivated by the prosthetic group removing (PR) enzyme. It was thought likely that 5'-AMP would be product of this reaction, but this could not be demonstrated.

[*] Prof. E. G. Krebs
Departments of Pharmacology and Biochemistry
School of Medicine, SL-15
University of Washington
Seattle, WA 98195 (USA)
Telefax: Int. code + (206)543-0858

[**] Copyright © The Nobel Foundation 1993. – We thank the Nobel Foundation, Stockholm, for permission to print this lecture.

[***] See the article immediately following: E. H. Fischer, *Angew. Chem.* **1993**, *105*, 1173–1180; *Angew. Chem. Int. Ed. Engl.* **1993**, *32*, 1130–1137.

Although as a medical student I heard about the research on phosphorylase, particularly as a result of my friendship with Arda Green, my first "hands-on" experience with this enzyme came after World War II had ended, when I started postdoctoral work in the Coris' laboratory. (My residency training in internal medicine had been interrupted by the war, and although at that time I expected to return to clinical medicine in due course, I had decided to work in a basic science department for a year or two before resuming hospital-based training.) The problem that was given to me by the Coris involved solubility measurements on phosphorylase, and I also studied the effect of protamine and polylysine on the two forms of the enzyme. It was of interest that in the presence of these polyanionic substances, inosinic acid and 5'-AMP were both very effective as activators of phosphorylase *b*. All of these studies on the effects of nucleotides on phosphorylase were carried out before the revelations of Jacob and Monod concerning allosterism and protein conformation and at that time were viewed simply as unexplained phenomenology. Indeed for several years Carl Cori advised against my publishing these findings unless I could explain them. Eventually, after Neil Madsen found that protamine could physically bind to phosphorylase, which was at least a step in the direction of how it might affect the activity of the enzyme, Cori let me send in my paper.

Although, as I have pointed out, knowledge with respect to the properties of phosphorylase as an enzyme increased significantly during the 1940s, it was often difficult to explain their physiological importance. This can be understood if one considered what was known about glycogen metabolism at that time. The epochal work of Leloir on the mechanism of glycogen synthesis was still to come, that is, the role of uridinediphosphate (UDG) in polysaccharide synthesis and the existence of the enzyme glycogen synthase were completely unknown. Hence, it was believed that phosphorylase is involved in glycogen synthesis as well as in glycogenolysis (Fig. 2). It was assumed that the direction of the phosphorylase reaction would be determined by the concentrations of the components of the reaction, particularly by the concentration of inorganic phosphate (P_i). This situation obviously made it difficult to interpret findings relating to the interconversion reactions of phosphorylase *a* and *b*. Nonetheless, in the late 1940s and the early 1950s a clear story was beginning to emerge with respect to the action of the glycogenolytic hormones, glucagon and epinephrine, and their effects on interconversion of the forms phosphorylase as studied in liver cells. Earl Sutherland, working initially in the Coris' laboratory and later independently at Western Reserve University, found that epinephrine and glucagon caused the rapid conversion of liver phosphorylase *a* to phosphorylase *b*,[5] and it was also shown that epinephrine caused the same change in the muscle diaphragm.[6] Inasmuch as epinephrine and glucagon were known to be glycogenolytic hormones, Sutherland's findings clearly supported the concept that the activation of phosphorylase is associated with glycogen degradation. Why then, should electrical stimulation and muscle contraction, which were also known to result in glycogenolysis, be associated with the conversion of phosphorylase *a* to the inactive form, phosphorylase *b*?[4]

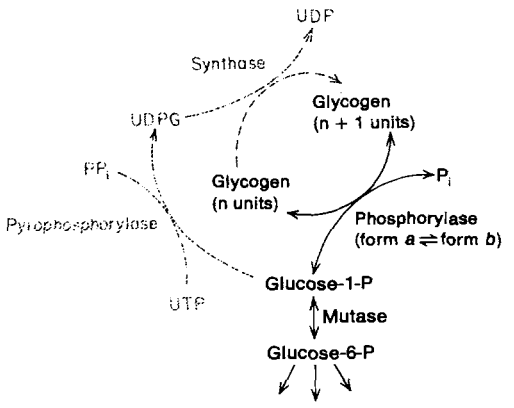

Fig. 2. Glycogen metabolism as depicted circa 1945. The stippled portion of the metabolic scheme was unknown. It was assumed that glycogen synthesis and degradation were catalyzed by phosphorylase and that the direction of the reaction was determined by the concentration of reaction components. Within the cell, phosphorylase was believed to shuttle back and forth between forms *a* and *b*, but the chemical nature of the interconversion reaction was unknown. Conversion of phosphorylase *a* to *b* had been demonstrated in vitro.

Conversion of Rabbit Skeletal Muscle Phosphorylase *b* to Phosphorylase *a* In Vitro

In Fall 1953, Ed Fischer joined the Department of Biochemistry at the University of Washington, where I was already a faculty member. As a graduate student in Geneva, Ed had worked on potato phosphorylase, and we thus shared a common interest in this particular enzyme. We discussed some of the puzzling features of phosphorylase and were particularly intrigued by the still-unsolved nature of the 5'-AMP effect, that is, how 5'-AMP activates phosphorylase *b* but is seemingly unnecessary for phosphorylase *a*. It seemed worthwhile purely as a secondary undertaking for each of us, since we both had problems that we considered as our major areas of concentration, to pool our efforts to see whether or not we could obtain information on this point. The initial experiment that we undertook together was simply to prepare pure crystalline phosphorylase *a* by the Coris' procedure.[7] However, our initial attempts to do this were woefully unsuccessful. The enzyme would not crystallize, a step that was essential in order to obtain pure protein. More puzzling was the fact that the partially pure enzyme, which we did obtain, was always in the *b* form rather than the *a* form. Insofar as we could determine we had followed the Coris' procedure exactly except that we had clarified the original muscle extract by centrifugation rather than by filtration through paper. Although this seemed like a trivial change, we nonetheless included the filtration step in our next preparation. To our surpise, this time we obtained phosphorylase *a*, which crystallized readily as it was supposed to do. Two conclusions could be drawn that would explain these results. First, "resting" rabbit muscle extracts must contain phosphorylase predominantly in the *b* form rather than the *a* form as had been postulated by the Coris,[4, 8] and second, filtration of muscle extracts through paper must trigger conversion of phosphorylase *b* to *a* in vitro.[9] Subsequently, we found that thorough washing of the filter paper before use eliminated conversion of *b* to *a*, implying that some component in the paper must have been extracted to account for the effect. It was also found that this conversion failed to occur if the muscle extract were aged prior to filtra-

tion. The critical component from the filter paper that was required in the *b*-to-*a* step was shown to be calcium ions, and the essential component in the extract that was lost on aging was found to be ATP.

Armed with the knowledge that there is an ATP requirement for conversion of phosphorylase *b* to phosphorylase *a*, we thought it likely that we were dealing with a phosphotransferase reaction in which the terminal phosphoryl group of ATP is being transferred either to the protein itself or possibly to a nonprotein component bound to the enzyme. It soon became apparent data a "converting enzyme", which could be separated that phosphorylase *b*, was required in the reaction.[10] After it had been determined that ADP as well as phosphorylase *a* were products of the reaction,[11] we spoke of this enzyme as phosphorylase *b* kinase, or simply phosphorylase kinase, rather than converting enzyme.[11] The nature of the Ca^{2+} requirement for the *b*-to-*a* reaction was not apparent immediately, but eventually it was determined by one of our graduate students, William L. Meyer, that the effect of this metal ion was twofold. On the one hand, Ca^{2+} was needed for the activation of a kinase activating factor (KAF), but in addition it was also required for the activity of phosphorylase kinase itself.[12] KAF was later shown to be a Ca^{2+}-dependent protease by another student, R. Bruce Huston.[13] (The current name for this protease is calpain.) We determined the stoichiometry of the conversion of phosphorylase *b* into phosphorylase *a*[11] and also obtained the amino acid sequence surrounding the phosphorylated serine in phosphorylase *a*.[14] It was demonstrated that inorganic phosphate is released in the muscle phosphorylase *a*-to-*b* reaction catalyzed by the PR enzyme, which could now be termed phosphorylase phosphatase. Thus, by the late 1950s, it was possible to write specific equations for the interconversion reactions of muscle phosphorylase (Scheme 1).

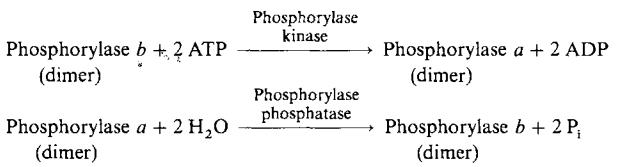

Scheme 1.

During the same period that our work on the muscle phosphorylase system was being carried out, very similar studies relating to liver phosphorylase were being conducted independently in the laboratory of Earl Sutherland at Western Reserve University. Sutherland's major co-workers in this effort were Walter D. Wosilait and Theodore W. Rall. In an early study[15] these investigators obtained evidence that inorganic phosphate was released when partially purified active liver phosphorylase was incubated with what they referred to as inactivating enzyme, and they also determined that phosphate was incorporated into phosphorylase when liver slices were incubated in the presence of ^{32}P-phosphate. Later they showed that both of the interconversion reactions of liver phosphorylase could be demonstrated in cell-free systems.[16, 17] A monumental "ancillary finding" that grew out of the work on liver phosphorylase by the Sutherland laboratory was, of course, the discovery of cyclic AMP, the first identified "second messenger" of hormone action.[18]

It is of interest to consider whether there had been any indications that the phosphorylation and dephosphorylation of proteins might be of regulatory significance prior to elucidation of the muscle and liver phosphorylase systems. The existence of phosphoproteins had, of course, been known for many years before 1950. Phosphoproteins were classified as "conjugated proteins" and for the most part consisted of proteins of nutritional significance associated with the feeding of the young, for example, casein in milk and several phosphoproteins found in egg yolk. Interestingly, it was also appreciated that pepsinogen contained one mole of firmly bound phosphate per mole of enzyme, but the significance of this was not (and still is not) known. It was also known that nonspecific phosphatases could catalyze the release of phosphate from phosphoproteins. In an important study that was carried out at about the same time as the work on phosphorylase was underway, Burnett and Kennedy described an enzyme that catalyzed the phosphorylation of casein.[19] These workers were aware of the high rate of turnover of phosphate in proteins and were the first to describe a protein kinase. In general, however, the realization that protein phosphorylation–dephosphorylation is a dynamic process affecting enzymes and that it is important in the control of metabolism and other cellular processes had not been foreseen.

Protein Phosphorylation and the Transmission of Extracellular Signals

As we have seen, an interest in the mechanisms of action of epinephrine and glucagon had an important part in work on the interconversion reactions of phosphorylase,[5, 6] which in turn led to the discovery of the dynamic phosphorylation and dephosphorylation of proteins. Going back even further, however, it can be noted that the original studies of the Coris, which led to the finding of phosphorylase itself, grew out of the longstanding interest of these investigators in the role of epinephrine in the regulation of glycogen metabolism.[20] That an interest in hormone action would contribute importantly to the development of the field of protein phosphorylation–dephosphorylation was no accident, since we now know that one of the major functions of protein phosphorylation as a regulatory process is in the transmission of signals that impinge on cells. This is true not only with respect to the transduction of hormone and growth factor signals but for other types of stimuli as well. For example, as mentioned earlier, electrical stimulation of muscle leads to changes in protein phosphorylation within the cell. It is probably more than coincidental that the extent of protein phosphorylation is much greater in eukaryotic cells than it is in prokaryotes, particularly in eukaryotic cells of higher animals that are subject to complex forms of external regulation.

It was apparent very early on that the relative amounts of phosphorylase *a* and *b* that are present within the cell at any particularly time depend on the relative rates of the phosphorylase kinase and phosphatase reactions, and it was anticipated that one or both of these enzymes must be subject

to regulation. Furthermore, two factors capable of influencing the balance between the two forms of phosphorylase had been found. As noted, these were calcium ions, identified as the metal ion that caused phosphorylase *a* formation in muscle extracts,[9] and cyclic AMP, which promoted phosphorylase *a* formation in liver cells and homogenates (reviewed in ref.[21]). We subsequently showed that cyclic AMP would also cause phosphorylase *a* formation in muscle extracts.[22] In the muscle system it was determined that the effects of Ca^{2+} and cyclic AMP in stimulating phosphorylase activation in vitro were a result of phosphorylase kinase activation rather than phosphorylase phosphatase inhibition.[11]

The Coupling of Muscle Contraction to Glycogenolysis

The finding that the major form of phosphorylase present in resting muscle is phosphorylase *b*[8] rather than phosphorylase *a*,[4, 7] together with the realization that phosphorylase *b* can be converted to phosphorylase *a* if Ca^{2+} is introduced into muscle extracts containing ATP,[9] made it possible to arrive at a rational position with respect to the effect of electrical stimulation on phosphorylase. In 1956[23] Cori was able to demonstrate that muscle contraction causes conversion of phosphorylase *b* to *a*, rather than the other way around; this was in keeping with the known effect of contraction on glycogen breakdown. The effect of Ca^{2+} on the activation of phosphorylase kinase now fit well into a scheme (Fig. 3), whereby this metal ion, acting as a messen-

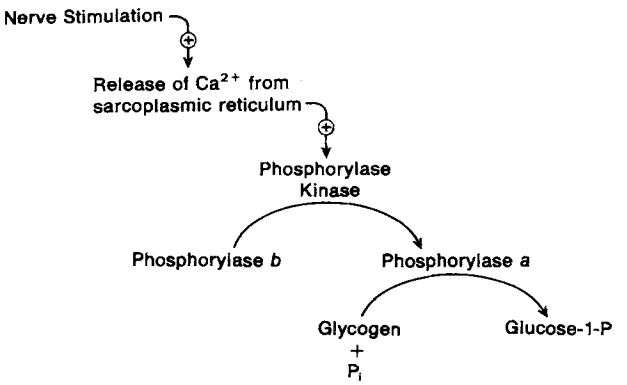

Fig. 3. The role of calcium ions in regulating glycogenolysis (ca. 1962).

ger substance associated with muscle contraction, could be responsible for the coupling of glycogenolysis (an energy-yielding process) to contraction (an energy-utilizing process). Of the two different mechanisms by which Ca^{2+} could regulate phosphorylase kinase, through limited proteolysis involving KAF or as a result of the requirement of phosphorylase kinase for Ca^{2+} per se,[12] only the latter was considered to be physiologically significant. The work of Ozawa et al.,[24] who quantified the effect of Ca^{2+} on the phosphorylase kinase reaction, was critical with respect to our understanding of this process. Many years later the actual mechanism by which Ca^{2+} stimulates phosphorylase kinase became apparent when it was found that calmodulin is a subunit of phosphorylase kinase.[25]

The Mechanism of Action of Cyclic AMP and the Cyclic AMP Dependent Protein Kinase

The mechanism by which cyclic AMP causes an increase in phosphorylase kinase activity turned out to be more complex than that of Ca^{2+}. Whereas Ca^{2+} is an essential activating component in the phosphorylase *b*-to-*a* reaction itself, cyclic AMP causes activation of phosphorylase kinase by promoting its phosphorylation. The first clue that phosphorylation might be involved in the activation of the kinase came with the finding that ATP is required in order to observe the activation reaction and the cyclic AMP effect in rabbit skeletal muscle extracts.[22] A key co-worker who carried out the initial experiment that revealed this requirement was a graduate student, Donald A. Graves. Activation of muscle phosphorylase kinase was characterized by marked enhancement of its activity as measured at pH 7 or below, and only moderate increases in activity were seen when the *b*-to-*a* reaction was carried out at higher pH values. The ratio of activity at pH 6.8 to activity at pH 8.2 was found to serve as a useful index of the state of phosphorylase kinase activation.[26] Significantly, once phosphorylase kinase had been activated by preincubation with ATP, the presence of cyclic AMP was no longer essential—as might be anticipated if the kinase were being modified covalently in an activation process stimulated by cyclic AMP.[22]

Phosphorylase kinase was purified extensively and obtained as a nearly homogeneous high molecular weight protein ($M_r = 1.2 \times 10^6$), which still retained the ability to be activated by preincubation with MgATP in a reaction that was strongly stimulated by cyclic AMP. Although there were indications that a second protein kinase might be involved in the activation process,[27] the kinetics of the reaction were complex and the work of DeLange et al.[28] suggested instead that an autocatalytic reaction was occurring. However, the existence of a separate "cyclic AMP dependent phosphorylase kinase kinase", which accompanied phosphorylase kinase kinase during its purification, was eventually established by Donal A. Walsh and John P. Perkins, postdoctoral fellows in my laboratory.[29] They succeeded in concentrating the new kinase about 200-fold from rabbit muscle extract and separated it completely from phosphorylase kinase. The kinase was referred to as the "cyclic AMP dependent protein kinase" rather than phosphorylase kinase kinase, because it was found[29] to have a broader specificity than would have been implied by use of the more restrictive name. In retrospect, the cyclic AMP dependent protein kinase probably represents the same activity reported by Huijing and Larner[30] to be involved in cyclic AMP stimulated glycogen synthase phosphorylation. The finding of a cyclic AMP dependent protein kinase separable from phosphorylase kinase made it possible to construct a complete cascade mechanism showing the effect of epinephrine on glycogenolysis (Fig. 4). This was the first example of a protein kinase cascade in which one protein kinase is phosphorylated and activated by another. Despite the potential usefulness of a cascade device (amplification of the signal, provision of branch points, etc.) very few other examples have been reported. Recently, however, a complicated multistep protein kinase cascade related to the action of numerous growth factors has been detected; this will be discussed at the end of this lecture.

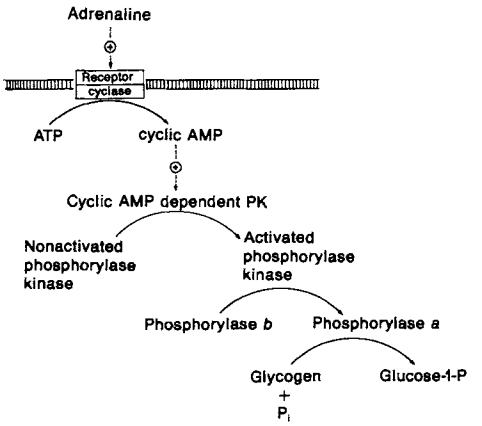

Fig. 4. The regulation of glycogenolysis by epinephrine (adrenaline).

The cyclic AMP dependent protein kinase has served as a prototype for studies on protein kinases in general. This kinase is made up of regulatory (R) and catalytic (C) subunits and has the general structure R_2C_2. In the next lecture Ed Fischer will speak about the mechanism by which cyclic AMP regulates the activity of the kinase. The catalytic subunit of this enzyme was the first protein kinase for which the complete amino acid sequence was determined,[31] and it was also the first protein kinase to have had its X-ray crystallographic structure elucidated.[32] The cyclic AMP dependent protein kinase also played a very significant part in our understanding of protein kinase specificity, which has become increasingly important as the number of known kinases has skyrocketed. Although it will not be possible to do more than touch on this latter topic here, it can be noted that the cyclic AMP dependent protein kinase was the first kinase for which a "consensus" phosphorylation site sequence was clearly recognized.[33-37] This sequence, Arg-Arg-X-Ser-X, is found in many, but not all, substrates for the cyclic AMP dependent protein kinase. In connection with the specificity studies that were carried out within my own laboratory, I would like to call particular attention to the work of David B. Bylund and Bruce E. Kemp.

A Protein Serine/Threonine Kinase Cascade Activated in Response to Insulin and Related Growth Factors

One of the enduring problems in endocrinology has been the question of the mechanism of action of insulin. Indeed, investigators have been interested in this area for decades, and over the years information on this subject has gradually accumulated through the application of whatever tools became available. At first, experiments were carried out with animals, later with perfused organs, eventually with isolated tissues such as the muscle diaphragm, and finally with cells in culture. Until comparatively recently it had not been possible, however, to demonstrate a meaningful insulin response in homogenates or other types of cell-free systems. Approximately ten years ago, however, it was found that the EGF receptor (EGF = epidermal growth factor) is a protein tyrosine kinase, and shortly after that it was determined that this is also true for the insulin receptor.[38,39] Now it is known that eight or nine different growth factor receptors are protein tyrosine kinases. These findings ushered in a new era of research with respect to insulin and related hormones and growth factors. However, although most workers in the field felt that it would now be a simple matter to identify meaningful substrates for these receptor/kinases and to elucidate the complete intracellular signal transduction pathway involved, this did not occur. Several tyrosine-phosphorylated proteins were found in cells treated with insulin or the other growth factors, but none of these proteins could at first be readily connected with the known cellular actions of the growth factors involved. Nonetheless, it was clearly demonstrated that the protein tyrosine kinase activity of these receptors is essentially for their action, and there was little if any doubt that initiation of their signals must involve ligand-stimulated tyrosine phosphorylation.

An investigator who is interested in determining the steps of a signal transduction pathway can either work "downstream" from a receptor in order to identify components of the pathway, or he can work "upstream" toward the receptor starting with a well-established cellular effect of the growth fact in question. A number of laboratories, including my own, which are interested in signaling from the insulin or related receptors, have used the latter strategy in their approach. The particular cellular effect that these groups have chosen as their starting point has been the activation of protein serine and threonine kinases, which results from the simulation of tyrosine kinases. It has long been known that the stimulation of protein tyrosine kinases in cells results in changes in serine/threonine phosphorylation as well as in changes in tyrosine phosphorylation, but the mechanism involved in the coupling of the two types of protein phosphorylation has been unknown.[40]

One of the cellular proteins that is readily phosphorylated on serine residues in response to the stimulation of receptors having protein tyrosine kinase activity is ribosomal protein S6, although the role of this phosphorylation insofar as the regulation of protein synthesis is not clear. This phenomenon had been discovered a number of years before, prior to the involvement of my own laboratory in the problem, and a good start had already been made in identifying components involved in regulating S6 phosphorylation. For example, it had been shown that in adipocytes or Swiss 3T3 cells stimulated by insulin an S6 kinase becomes activated,[41,42] and there was good evidence that the activation was due to covalent modification, in other words, phosphorylation. It was determined that the protein serine/threonine phosphatases would inactivate the activated proteins.[43,44] Maller and co-workers had shown that an S6 kinase (S6 kinase II), purified to homogeneity from *Xenopus laevis* eggs, could also be inactivated by protein phosphatases.[45] Importantly, this latter S6 kinase could be reactivated by a different protein serine/threonine kinase, microtubule-associated protein 2 kinase (MAP kinase), which was known to be stimulated by insulin treatment of 3T3 L1 cells.[46] These results strongly suggested the existence of a protein serine/threonine kinase cascade in which one growth-factor-activated protein kinase phosphorylated and activated a second protein kinase. Gregory et al.[47] confirmed these findings using a phosphatase-treated S6 kinase from rabbit liver and MAP kinase from insulin-stimulated rat 1 HIR_c B cells. Then in our laboratory we showed that an EGF or insulin-

stimulated MAP kinase from Swiss 3T3 cells could phosphorylate and activate an S6 kinase obtained from this same cell type.[48] MAP kinase, in its active form, appeared to have been activated as a result of serine/threonine phosphorylation, since it could be inactivated by protein phosphatase 2A. This suggested the existence of even a third protein serine/threonine kinase in this growth factor stimulated process.

A finding of major significance from Sturgill's laboratory was the fact that MAP kinase in its active form contains phosphotyrosine as well as phosphothreonine, and that in addition to being inactivated by protein phosphatase 2A, it can also be inactivated by CD45, a protein tyrosine phosphatase.[49] These investigators went on to show that phosphorylation of MAP kinase on tyrosine and threonine is essential for its activity, and it seemed likely that two different types of protein kinase, a protein serine/threonine kinase and a protein tyrosine kinase, would be involved as upstream components in its activation. There was no evidence, however, that a receptor-type protein tyrosine kinase could serve as either one of these kinases. It was thus of great interest to search for an enzyme or enzymes, MAP kinase kinases, that would catalyze MAP kinase phosphorylation and activation.

In our laboratory Natalie Ahn et al.[50] discovered two separable protein factors from Swiss 3T3 cells that catalyzed the activation of an inactive form of MAP kinase in vitro. Each of these factors required the presence of MgATP in order to bring about activation of MAP kinase, and it did not matter whether the latter had first been inactivated by a protein serine/threonine phosphatase or by a protein tyrosine phosphatase. This made it appear probable that the factors were "dual specificity" kinases capable of phosphorylating proteins or serine and threonine residues as well as tyrosine residues. The existence of such kinases had, in fact, been found in yeast. At first we hesitated to call the activating factors "MAP kinase kinases", because in work carried out by Rony Seger et al.[51] we had determined that MAP kinase can undergo a slow but distinct autophosphorylation reaction, in other words, that it can catalyze its own phosphorylation, and that in this reaction threonine and tyrosine residues are phosphorylated. Moreover, autophosphorylation resulted in activation of the kinase. This result made it appear possible that a MAP kinase kinase as such might be unnecessary and that the next "upstream" component could be a protein activator that simulated autophosphorylation. Eventually it was shown, however, that the MAP kinase activators were, in fact, protein kinases capable of phosphorylating a mutant form of MAP kinase that lacked enzymic activity.[52, 53] Moreover, amino acid sequence data obtained in our laboratory and elsewhere, showed that the activators contain protein kinase sequence motifs. Later, similar "activators", MAP kinase kinases, were found in PC12 cells stimulated by nerve growth factors or bradykinin.[54, 55] Gomez and Cohen showed that activated MAP kinase kinase could be inactivated by a protein serine/threonine phosphatase but was not affected by protein tyrosine phosphatases.[54] This latter result indicated that an additional "upstream" protein serine/threonine kinase, in other words a MAP kinase kinase kinase, was probably a component of the pathway. The present status of the MAP kinase cascade, without the putative MAP kinase kinase kinase, is shown in Figure 5.

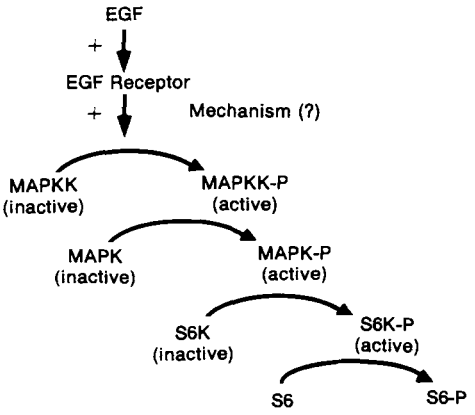

Fig. 5. The MAP kinase cascade. EGF = epidermal growth factor, MAP = microtubule-associated protein, K = kinase, SG = ribosomal protein S6.

Intense effort on the part of many different laboratories is currently centered on the question of the identity of MAP kinase kinase kinase and the mechanism by which such an enzyme might be regulated. It was reported by Kyriakis et al. that Raf-1 activates MAP kinase kinase and thus might itself be a candidate for the kinase kinase kinase.[56] This result was confirmed by Dent et al.[57] Other studies have implicated the possibility that cdc2 might be an "upstream" component of the MAP kinase cascade but not an immediate kinase kinase kinase itself.[58] Finally, there is considerable evidence that p21 ras is a component acting at some site between the receptor and the components of the cascade as currently identified.[59-62] A somewhat neglected area of study with respect to the MAP kinase cascade relates to the question of its precise function and the reasons for the existence of such a complicated scheme. It is probable that numerous substrates may exist for each of the protein kinases in the cascade, and in this connection it is noteworthy that a number of transcription factors appear to be targeted by MAP kinase and by the S6 kinase. The different kinases may also have specific metabolic enzyme targets that have not as yet been identified. Finally, some of the kinases may branch off and regulate still other kinases.[63]

Conclusion

In this talk I have reviewed the early work on the interconversion reactions of the two forms of glycogen phosphorylase and phosphorylase kinase. A third enzyme that played an important part in early work on protein phosphorylation–dephosphorylation was glycogen synthase. Much of the original research on that enzyme was carried out by Joseph Larner and his associates during the early 1960s. These investigators found that, in contrast to the effect of phosphorylation on phosphorylase and phosphorylase kinase, phosphorylation caused a decrease in the activity of the synthase. Because of the "field" of protein phosphorylation during the first ten years was dominated by those interested in glycogen metabolism, some even expressed the idea that perhaps regulation of enzymes by phosphorylation–dephos-

phorylation might be restricted to this area. However, the finding of a multifunctional cyclic AMP dependent protein kinase, which was almost immediately shown by Kuo and Greengard[64] to be very widespread in nature, served to change this concept. Another important finding that dispelled the idea that protein phosphorylation was very limited in scope was the report that pyruvate dehydrogenase is regulated by phosphorylation.[65] As can be noted in Figure 6, the number of enzymes reported to undergo regulation as a result of being phosphorylated started growing precipitously in 1970. If reports on protein phosphorylation involving nonenzymic proteins were included, the growth curve in Figure 6 would be even steeper. In the next talk Ed Fischer will

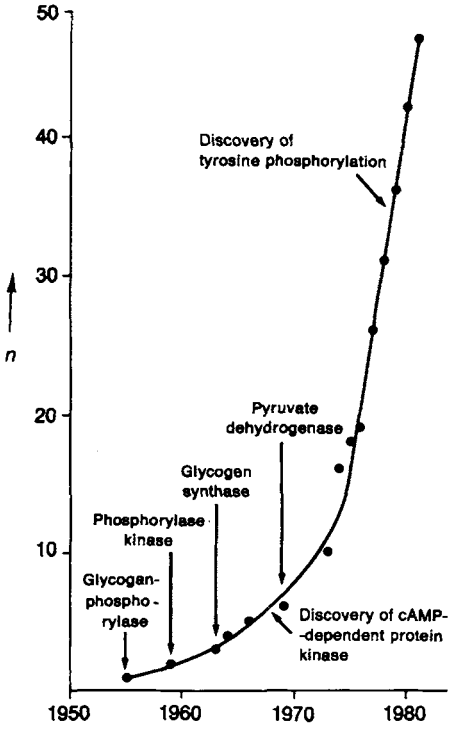

Fig. 6. Growth in an awareness of protein phosphorylation as a mechanism for regulating enzymes. The total number n of enzymes reported to undergo phosphorylation-dephosphorylation is plotted against years.

trace some of the developments that have contributed to this explosion. I anticipate that he may also "correct" some of the errors that I may have made in my historical account of our work together.

I would like to dedicate this lecture to my parents, who had the education of their children as a major goal in their lives, and to my wife, Deedy, who has always been extremely supportive of my work. In addition, I recognize the very important contributions made by numerous talented students and postdoctoral fellows, some of whom are not mentioned here, who for the most part carried out the actual experiments reported here, and in addition helped to provide direction for many of the studies that are reported.

Received: February 12, 1993 [A 912 IE]
German version: *Angew. Chem.* **1993**, *105*, 1173

[1] C. Cori, *Cold Spring Harbor Symp. Quant. Biol.* **1939**, *7*, 260–268.
[2] G. T. Cori, A. A. Green, *J. Biol. Chem.* **1945**, *158*, 321–332.
[3] G. T. Cori, C. F. Cori, *J. Biol. Chem.* **1943**, *151*, 31–38.
[4] G. T. Cori, *J. Biol. Chem.* **1945**, *158*, 333–339.
[5] E. W. Sutherland, C. F. Cori, *J. Biol. Chem.* **1951**, *188*, 531–543.
[6] E. W. Sutherland, *Recent Prog. Horm. Res.* **1950**, 441–463.
[7] A. A. Green, G. T. Cori, *J. Biol. Chem.* **1943**, *151*, 21–29.
[8] E. G. Krebs, E. H. Fischer, *J. Biol. Chem.* **1955**, *216*, 113–120.
[9] E. H. Fischer, E. G. Krebs, *J. Biol. Chem.* **1955**, *216*, 121–132.
[10] E. G. Krebs, E. H. Fischer, *Biochim. Biophys. Acta* **1956**, *20*, 150–157.
[11] E. G. Krebs, A. B. Kent, E. H. Fischer, *J. Biol. Chem.* **1958**, *231*, 78–83.
[12] W. L. Meyer, E. H. Fischer, E. G. Krebs, *Biochemistry*, **1964**, *3*, 1033–1039.
[13] R. B. Huston, E. G. Krebs, *Biochemistry* **1968**, *7*, 2116–2122.
[14] E. H. Fischer, D. J. Graves, E. R. S. Crittenden, E. G. Krebs, *J. Biol. Chem.* **1959**, *234*, 1698–1704.
[15] E. W. Sutherland, W. D. Wosilait, *Nature* **1955**, *175*, 169.
[16] T. W. Rall, E. W. Sutherland, W. D. Wosilait, *J. Biol. Chem.* **1956**, *218*, 483.
[17] W. D. Wosilait, *J. Biol. Chem.* **1958**, *233*, 597.
[18] E. W. Sutherland, T. W. Rall, *J. Biol. Chem.* **1958**, *233*, 1077–1091.
[19] G. Burnett, E. P. Kennedy, *J. Biol. Chem.* **1954**, *211*, 969–988.
[20] C. F. Cori, G. T. Cori, *J. Biol. Chem.* **1928**, *79*, 309–355.
[21] E. W. Sutherland, *The Harvey Lectures, Series 57*, Academic Press, New York, **1962**, pp. 17–33.
[22] E. G. Krebs, D. J. Graves, E. H. Fischer, *J. Biol. Chem.* **1959**, *234*, 2867–2873.
[23] C. F. Cori, *Enzymes: Units of Biological Structure and Function* (Ed.: O. H. Gaebler), Academic Press, New York, **1956**, p. 573.
[24] E. Ozawa, K. Hosoi, S. Ebashi, *J. Biochem.* **1967**, *61*, 531–533.
[25] R. J. A. Grand, S.Shenolikar, P. Cohen, *Eur. J. Biochem.* **1981**, *113*, 359–367.
[26] J. B. Posner, R. Stern, E. G. Krebs, *J. Biol. Chem.* **1965**, *240*, 982–985.
[27] E. G. Krebs, R. J. DeLange, R. G. Kemp, W. D. Riley, *Pharmacol. Rev.* **1966**, *18*, 163–171.
[28] R. J. DeLange, R. G. Kemp, W. D. Riley, R. A. Cooper, E. G. Krebs, *J. Biol. Chem.* **1968**, *243*, 2200–2208.
[29] D. A. Walsh, J. P. Perkins, E. G. Krebs, *J. Biol. Chem.* **1968**, *243*, 3763–3765.
[30] F. Huijing, J. Larner, *Biochem. Biophys. Res. Commun.* **1966**, *23*, 259–263.
[31] S. Shoji, D. C. Parmelee, R. D. Wade, S. Kumar, L. H. Ericsson, K. A. Walsh, H. Neurath, G. L. Long, J. G. DeMaille, E. H. Fischer, K. Titani, *Proc. Natl. Acad. Sci. USA*, **1981**, *78*, 848–851.
[32] D. R. Knighton, J. Zheng, L. F. T. Eyck, V. A. Ashford, N.-H. Xuong, S. S. Taylor, J. M. Sowadski, *Science*, **1991**, *253*, 407–414.
[33] B. E. Kemp, D. B. Bylund, T. S. Huang, E. G. Krebs, *Proc. Natl. Acad. Sci. USA*, **1975**, *72*, 3448–3452.
[34] E. Humble, L. Berglund, V. Titanji, O. Ljunstrom, B. Edlund, O. Zetterquist, L. Engstrom, *Biochem. Biophys. Res. Commun.* **1975**, *66*, 614–621.
[35] P. Daile, P. R. Carnegie, J. D. Young, *Nature* **1975**, *257*, 416–418.
[36] O. Zetterquist, U. Ragnarsson, E. Humble, L. Berglund, L. Engstrom, *Biochem. Biophys. Res. Commun.* **1976**, *70*, 696–703.
[37] B. E. Kemp, D. J. Graves, E. Benjamini, E. G. Krebs, *J. Biol. Chem.* **1977**, *252*, 4888-4894.
[38] S. Cohen, G. Carpenter, L. E. King, Jr., *J. Biol. Chem.* **1980**, *255*, 4835–4842.
[39] M. Kasuga, Y. Zick, D. L. Blithe, F. A. Karlsson, H. U. Häring, C. R. Kahn, *J. Biol. Chem.* **1982**, *257*, 9891–9894.
[40] R. M. Denton, *Adv. Cyclic Nucleotide Protein Phosphorylation Res.* **1986**, 293–341.
[41] M. H. Cobb, O. M. Rosen, *J. Biol. Chem.* **1982**, *258*, 12472–12481.
[42] I. Novak-Hofer, G. Thomas, *J. Biol. Chem.* **1984**, *259*, 5995–6000.
[43] L. M Ballou, P. Jenö, G. Thomas, *J. Biol. Chem.* **1988**, *263*, 1188–1194.
[44] L. M. Ballou, M. Siegmann, G. Thomas, *Proc. Natl. Acad. Sci. USA* **1988**, *85*, 7154–7158.
[45] J. L. Andres, J. L. Maller, *J. Biol. Chem.* **1989**, *264*, 151–156.
[46] T. W. Sturgill, L. B. Ray, E. Erickson, J. L. Maller, *Nature* **1988**, *334*, 715–718.
[47] J. S. Gregory, T. G. Boulton, B.-C. Sang, M. H. Cobb, *J. Biol. Chem.* **1989**, *264*, 18397–18401.
[48] N. G. Ahn, E. G. Krebs, *J. Biol. Chem.* **1990**, *265*, 11495–11501.
[49] N. G. Anderson, J. L. Maller, N. K. Tonks, T. W. Sturgill, *Nature* **1990**, *343*, 651–653.
[50] N. G. Ahn, R. Seger, R. L. Bratlien, C. D. Diltz, N. K. Tonks, E. G. Krebs, *J. Biol. Chem.* **1991**, *226*, 4220–4227.
[51] R. Seger, N. G. Ahn, T. G. Boulton, G. D. Yancopoulos, N. Panayotatos, E. Radziejewska, L. Ericsson, R. L. Bratlien, M. H. Cobb, E. G. Krebs, *Proc. Natl. Acad. Sci. USA* **1991**, *88*, 6142–6146.
[52] J. Posada, J. A. Cooper, *Science* **1992**, *255*, 212–215.
[53] R. Seger, N. G. Ahn, J. Posada, E. S. Munar, A. M. Jensen, J. A. Cooper, M. H. Cobb, E. G. Krebs, *J. Biol. Chem.* **1992**, *267*, 14373–14381.
[54] N. Gomez, P. Cohen, *Nature* **1991**, *351*, 69–72.
[55] N. G. Ahn, D. J. Robbins, J. W. Haycock, R. Seger, M. H. Cobb, E. G. Krebs, *J. Neurochem.* **1992**, *59*, 147–156.

[56] J. M. Kyriakis, H. App, X. Zhang, P. Banerjee, D. L. Brautigan, U. R. Rapp, J. Avruch, *Nature* **1992**, *358*, 417–421.
[57] P. Dent, W. Haser, T. A. J. Haystead, L. A. Vincent, T. M. Roberts, T. W. Sturgill, *Science* **1992**, *257*, 1404–1406.
[58] S. Matsuda, H. Kosako, K. Takenaka, K. Moriyama, H. Sakai, T. Akiyama, Y. Gotoh, E. Nishida, *EMBO J.* **1992**, *11*, 973–982.
[59] S. M. Thomas, M. DeMarco, G. D'Arcangelo, S. Halegoua, J. S. Brugge, *Cell* **1992**, *68*, 1031–1040.
[60] K. W. Wood, C. Sarnecki, T. M. Roberts, J. Blenis, *Cell* **1992**, *68*, 1041–1050.
[61] A. M. M. deVries-Smits, B. M. T. Burgering, S. J. Leevers, C. J. Marshall, J. L. Bos, *Nature* **1992**, *357*, 602–604.
[62] D. J. Robbins, M. Cheng, E. Zhen, C. A. Vanderbilt, L. A. Feig, M. H. Cobb, *Proc. Natl. Acad. Sci. USA* **1992**, *89*, 6924–6928.
[63] D. Stokoe, D. G. Campbell, S. Nakielny, H. Hidaka, S. J. Leevers, C. Marshall, P. Cohen, *EMBO J* **1992**, *11*, 3985–3994.
[64] J. F. Kuo, P. Greengard, *J. Biol. Chem.* **1969**, *244*, 3417–3419.
[65] T. C. Linn, F. H. Pettit, F. Hucho, L. J. Reed, *Proc. Natl. Acad. Sci. USA* **1969**, *64*, 227–234.

Protein Phosphorylation and Cellular Regulation II (Nobel Lecture)**

By Edmond H. Fischer*

Introduction

In the preceeding contribution,[***] Ed Krebs retraced the early history of glycogen phosphorylase and its regulation by reversible phosphorylation. In retrospect, we were extraordinarily lucky in more ways than one to have selected this particular enzyme to work on. First, it is extremely abundant in skeletal muscle so that material was never limiting. In fact, when 20 years later, we undertook its total amino acid sequence with Ko Titani and Ken Walsh,[1] we used no less than 10 grams of the crystalline enzyme to complete the analysis. Second, the phosphorylation reaction was unambiguous, converting a totally inactive enzyme into a fully active species. Third, the phosphorylation ran to completion, introducing 1 mole of phosphate per mole of enzyme subunit. Fourth, only one site became phosphorylated; and fifth, this site occurred within a loose N-terminal arm of the molecule that could be easily cleaved by limited proteolysis, leaving behind the bulk of the enzyme intact. This made it easy to separate the phosphopeptide and determine its structure,[2] though it took a long time, since in the mid fifties sequences had to be carried out by paper chromatography. We could show that a single seryl residue had been phosphorylated (Fig. 1). Incidentally, it took another five years to

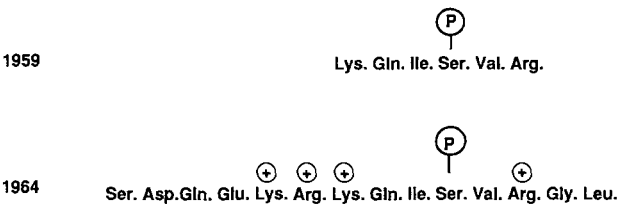

Fig. 1. Sequence of the site phosphorylated during the phosphorylase *b* to *a* reaction.

extend this sequence by nine residues.[3] The longer structure showed the presence of several positive charges, mainly upstream, and forming those recognition motifs whose significance became apparent only later.[4, 5]

The phosphorylation reaction was so straightforward and simple that there was no doubt in our minds that it would represent the prototype for such kinds of interconversions. As it turned out, it was really the exception. Six years went by before Joe Larner et al. identified the next enzyme to be regulated by phosphorylation–dephosphorylation, namely, glycogen synthase.[6] He found that this enzyme was inactivated rather than activated by phosphorylation,[7] which made sense: closing off the backward reaction when the forward one is turned on guarantees that there would be no recycling of the system that would inevitably result in a useless expenditure of energy. Joe Larner rapidly found, however, that far more than one phosphate was introduced during the interconversion;[8] about six per mole of synthase. At that time, the idea that a single phosphorylation event was all that was needed to alter the state of activity of an enzyme was so ingrained that I remember that we thought: "How can this be possible? It would imply that glycogen synthase is made up of six identical subunits, each of approximately 15000 molecular weight." And Joe Larner himself thought along these lines.[8, 9] Of course, we know today from his work as well as that of Phil Cohen,[10] Peter Roach,[11] and others, that the enzyme is phosphorylated on no less than seven sites by seven different protein kinases, all totally unknown at that time (Fig. 2). Furthermore, some of these

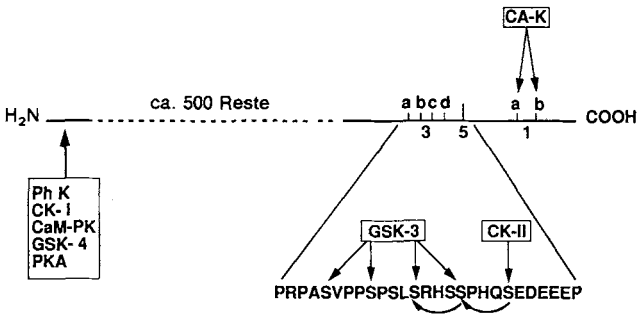

Fig. 2. Major phosphorylation sites in glycogen synthase. PhK, phosphorylase kinase; CK, casein kinase; CaM-PK, multifunctional calcium/calmodulin-dependent kinase; GSK, glycogen synthase kinase; PKA or CA-K, cAMP-dependent protein kinase (from ref. [11]).

phosphorylation events follow a most complicated program of successive reactions that have to proceed in a strictly prescribed order. The enzyme is inhibited by phosphorylation by glycogen synthase kinase 3 (GSK-3) but not until a first phosphate is introduced by casein kinase 2 (CK-2). This then allows phosphorylation of the next residue, then the next and the next after that until all sites are finally occupied.[12] Imagine the incredible difficulties we would have encountered had we decided to study this enzyme rather than phosphorylase.

We did not know at that time whether the phosphorylation reaction was a unique occurrence, a rare event restricted to the control of these two enzymes, or perhaps to carbohydrate metabolism. It was well known, for example, that during glycogenolysis, inorganic phosphate was picked up from the medium and used for the production of many sugar phosphate intermediates. Could nitrogen metabolism be reg-

[*] Prof. E. H. Fischer
Department of Biochemistry, SJ-70
University of Washington
Seattle, WA 98195 (USA)
Telefax: Int. code + (206) 685-1792

[**] Copyright © The Nobel Foundation 1993. – We thank the Nobel foundation, Stockholm, for permission to print this lecture.

[***] See preceeding article: E. Krebs, *Angew. Chem.* **1993**, *105*, 1173; *Angew. Chem. Int. Ed. Engl.* **1993**, *32*, 1122.

ulated by another type of covalent modification, for instance, amidation/deamidation, or lipid metabolism by acetylation/deacetylation? Or had we discovered a more general type of reaction that would apply widely to many different systems. Once again, as luck would have it, reversible protein phosphorylation turned out to be one of the most widespread mechanisms by which cellular processes can be regulated.[13, 14]

Allosteric and Covalent Regulation

Here, a question should be raised. Ed Krebs already mentioned that phosphorylase could also be activated by AMP. Why are two mechanisms required to control the activity of an enzyme when, in both cases, they lead to an active conformation (Fig. 3)? According to the allosteric model proposed

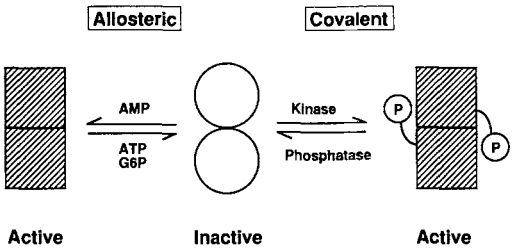

Fig. 3. Allosteric and covalent regulation of phosphorylase.

by Jacques Monod in the early 1960s, the enzyme responds to effectors that are generated during the normal maintenance of the cell and reflect its overall internal condition: is it proliferating or quiescent, actively metabolizing or not, what is its energy balance like, that is, its ratio of AMP to ATP, etc. According to the rule that enzymes are subjected to end-product or feed-back inhibition, phosphorylase would be expected to be inhibited by glucose-6-phosphate (G6P) that accumulates during its reaction, and by ATP, the ultimate end product of carbohydrate metabolism. By the same token, it would be activated by AMP as indeed it is. But then, many enzymes of carbohydrate metabolism would be similarly affected by the same effectors; in proceeding down the metabolic path, all these "doors" would become open at the same time. By contrast, the kinase reaction is highly specific: it allows the activation of phosphorylase only without affecting the activity of any other enzyme. Furthermore, and this is perhaps one of the major lessons we have learned over the last 30 years, covalent regulation responds mainly to extracellular signals (Fig. 4). These external signals come in the form of hormones, or neurotransmitters, growth factors, and other stimuli such as drugs, light, odorants, and perhaps touch in plants. Each signal will act on its own membrane receptor and either cause the release of second messengers (cAMP, cGMP, Ca^{2+}, diacylglycerol (DAG), inositol triphosphate (IP3), etc.) in reactions regulated by G-proteins, or induce the intrinsic tyrosine kinase activity of the receptors themselves. These second messengers or internal signals will act on kinases or phosphatases, then on target enzymes to finally elicit a physiological response. One finds here all the elements of a cascade system such as those described by Ed Krebs: enzymes acting on enzymes, resulting in the enormous amplification of an external signal. In addition, it allows the coordinated regulation of different physiological events through the pleiotropic action of some of the enzymes involved.

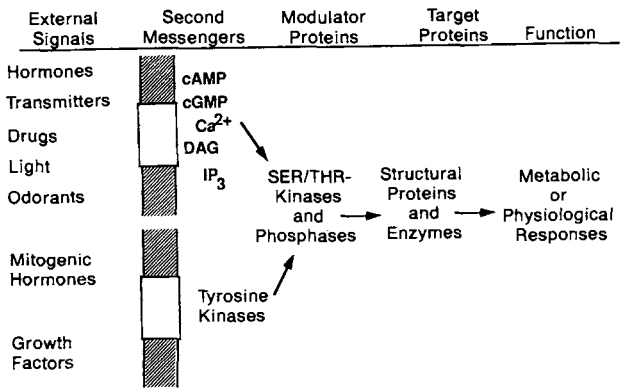

Fig. 4. Control of cellular processes by protein phosphorylation. Cascade systems triggered by extracellular stimuli.

The Protein Kinases

Today, one knows several hundred protein kinases that can be classified according to their mode of regulation or substrate specificity[15] (Table 1). Among the large family of

Table 1. Classification of protein kinases (PKs).

I.	Second messenger-dependent Ser/Thr PKs
A.	cyclic nucleotides: cAMP, cGMP PKs
B.	Ca^{2+}/calmodulin (CaM)-dependent kinase: phosphorylase kinase, MLCK, CaM kinase II
C.	diacylglycerol (DAG)/Ca^{2+}: PKC
II.	Second messenger-independent Ser/Thr PKs
A.	heme-, ds RNA-, (INF)-dependent eIF2 PKs
B.	CK-I, CK-II, GSK-3, S6 kinases
III.	Dual specificity (Ser/Thr and Tyr) PKs MAPK, MAPKK Wee1
IV.	Protein tyrosine kinases (PTKs)
A.	cellular or viral (oncogenic) PTKs
B.	receptor-linked PTKs

Ser/Thr kinases, some are dependent on the second messengers mentioned above, others on specific components of the system that they are called upon to regulate. Such is the case of the heme-regulated kinase that blocks the initiation of globin synthesis when heme or iron comes to be missing, or the double-stranded RNA-dependent kinase that is induced by interferon in cells under viral attack. There are also the so-called "independent kinases" such as the casein kinases for which no precise mode of control has been elucidated as yet.

Next come the mixed-function kinases that can phosphorylate their substrates on both tyrosine or serine/threonine, or that can be regulated by tyrosine and serine/threonine phosphorylation. This is the case for the enzymes that Ed Krebs has recently described:[16] microtubule-associated

protein (MAP) kinase, the MAP kinase kinase, perhaps Raf, or the cell cycle kinases such as $p34^{cdc2}$.[17] They stand guard at crucial crossroads of signal transduction. They form the link between a signaling system that originates at the membrane level and relies on tyrosine phosphorylation, and the more widespread serine/threonine phosphorylation reactions that occur downstream. Their dual control and specificity would ensure that no accidental initiation of important cellular events occurs at inappropriate times, just as one would need two keys to get access to a safety deposit box.

Finally, there is the large class of tyrosine kinases that will be discussed later. Not listed are the less common histidine kinases such as those involved in bacterial chemotaxis[18] and the double-headed kinase/phosphatase that regulates bacterial isocitrate dehydrogenase.[19]

Regulation of Protein Kinases

All these enzymes have homologous catalytic domains but vary greatly in the structure of their regulatory segments. They have consensus sequences, such as the motifs that are involved in the binding of ATP, by which they can be identified by searching the database.[20, 21] Most are regulated by segments that block their activity, often by virtue of the fact that they contain pseudo-substrate motifs that interact with, and shield, their catalytic sites. These autoinhibitory domains can exist on separate subunits as in the cAMP-dependent protein kinase (cAMP PK) first characterized by Ed Krebs, Don Walsh et al.,[22] or within the same peptide chain, as in the cGMP PK, where the two segments have become fused in the course of evolution. Initially, for the cAMP PK, the reaction seemed simple enough: the enzyme exists as an inactive complex between catalytic and regulatory subunits; cAMP induces a change in conformation in the regulatory subunits, resulting in the dissociation of the enzyme and the liberation of active catalytic subunits. It soon became apparent, however, that the inactive complex had a more substantial purpose, namely, to prevent the translocation of the free catalytic subunits to other compartments of the cell, particularly the nucleus.[23] But we know today that the regulation of this enzyme is even more sophisticated: the regulatory subunits themselves contain structural determinants that allow them to recognize and bind with high affinity to anchoring proteins distributed at specific locations within the cell.[24–27] More than two dozen of these have been identified; they are particularly abundant in the brain and the thyroid. Conceivably, some of these could colocalize with particular cAMP-generating receptors. This would confer a certain degree of selectivity to the hormonal response, by targeting the kinase toward a given set of substrates[27] (Fig. 5).

Enzyme translocation may also play an important role in the regulation of protein kinase C first described by Nishizuka et al.[28, 29] Depending on which subspecies of PKC is involved, the enzyme contains up to three regulatory domains responsible for the binding of Ca^{2+}, diacylglycerol, and phospholipids. Binding of these allosteric effectors can promote the translocation of the enzyme to the plasma membrane where it could bind to specific anchoring proteins.[30]

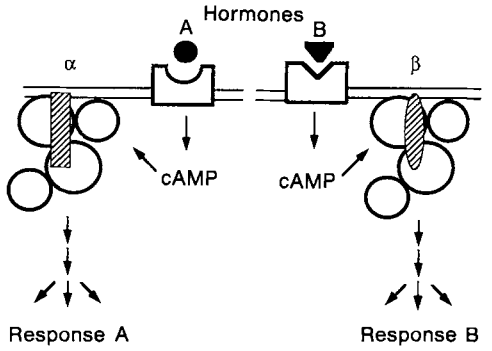

Fig. 5. Hypothetical selectivity in hormonal response by juxtaposition of cAMP-dependent protein kinase anchoring proteins with specific adenylate cyclase receptors.

Once again, this could determine which particular signal pathway would become affected.

Enzyme translocation might also be one of the functions of the cyclins, those regulatory subunits that are transiently expressed during various phases of the cell cycle. They associate strongly with the cell cycle-dependent kinases and operate particularly at the G1/S and G2/M transitions.[31–33] In *S. cerevisiae*, for instance, between four and five dozen cyclins have been identified.[34] While their multiciplicity would provide the cell with the redundancy it needs to protect itself from accidental failures, it would seem unlikely that their sole purpose would be to modulate the activity of the kinases. Some of these complexes must become operative at other set points along the cell cycle. More importantly, perhaps, they could be essential to target the enzymes toward those elements that become operative during the profound cytoskeletal reorganizations that accompany cell division.

Targeting of Serine/Threonine Phosphatases

Targeting subunits are particularly crucial for serine/threonine phosphatases because these enzymes are not geared to recognize specific sequences, or structural determinants within their substrates. Furthermore, unlike the kinases, they consist of just a few types of enzymes that have broad and overlapping specificities.[35–37] Thus they have to depend on regulatory subunits or binding proteins to direct them toward particular compartments of the cell where they will encounter particular substrates. That is the case, for instance, of the type 1 phosphatase whose catalytic subunit can bind to a glycogen-recognizing subunit, a myosin-recognizing subunit, or an inhibitory molecule called Inhibitor 2. In each of these forms, the enzyme recognizes a particular set of substrates. Formation or dissociation of these complexes is under hormonal control.[38–41] This is the theme that I propose to develop in the second part of this lecture, which is devoted to the role of regulatory/localization domains in the function of tyrosine phosphatases.

Protein Tyrosine Phosphorylation

Three remarkable discoveries, 15 years ago, generated considerable excitement in the field of cellular regulation by

protein phosphorylation. First, the finding by the groups of Ray Erickson[42,43] and Varmus and Bishop[44] that the product of the src gene responsible for the oncogenicity of Rous sarcoma virus was a protein kinase they designated as $pp60^{src}$. Second, the unexpected report by Tony Hunter and Bart Sefton that this kinase, unlike all previously known enzymes, phosphorylated its protein substrates exclusively on tyrosyl residues.[45] Third, the nontransforming homologue of v-src,[46-50] that is the cellular c-src, was identified. c-src encodes a product ($pp60^{c\text{-}src}$), which differs from its oncogenic viral counterpart by having, among other discrete mutations, a short extension at the C terminus. This extension carries a phosphotyrosyl residue that keeps the activity of the enzyme under control. Today we know of more than a dozen tyrosine kinases of cellular or viral origin, and their number continues to grow.[15,50]

Finally came the seminal discovery from the laboratory of Stanley Cohen[51,52] that the receptor for epidermal growth factor was itself a tyrosine kinase whose activity was induced by binding of the ligand. Since then, many families of receptors with tyrosine kinase activities have been identified.[53] They all have an external, ligand-binding domain, some with cystein-rich regions, a single transmembrane segment, and a cytoplasmic tyrosine kinase (PTK) domain (Fig. 6).

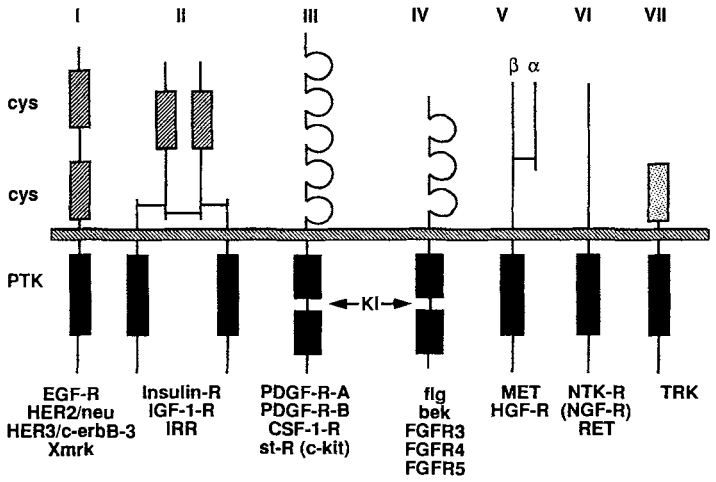

Fig. 6. Growth factor tyrosine kinase receptors.

Just as mutation of the intracellular tyrosine kinases can lead to cell transformation, mutation of the growth factor receptors can lead to oncogenic products. The first to be identified was the retroviral oncogene v-erb B[54,55] generated by a truncation of the external domain of the EGF receptor, its cellular progenitor. Many others have since been cloned and characterized; they usually result from truncation of the molecule at one end or the other or both, fusion with certain viral elements, and other kinds of mutations.

With accumulating evidence implicating tyrosine phosphorylation in cell proliferation and transformation, it is hardly surprising that many groups would become interested in the enzymes that would catalyze the reverse reaction, namely, the protein tyrosine phosphatases.

Protein Tyrosine Phosphatases

First evidence for phosphotyrosine dephosphorylation was obtained by Graham Carpenter and Stanley Cohen[51,56] by using A431 cell membranes overexpressing the EGF receptor, and allowing these to undergo autophosphorylation, and then monitoring their rate of dephosphorylation. Similar observations were made by Bart Sefton and Tony Hunter by using cells transformed with a temperature sensitive mutant of Rous sarcoma virus.[57] Then followed a flurry of studies by a number of groups, including our own six years ago.[58-60] The work was originated with Nick Tonks, a superb Post Doctoral Fellow and second generation Seattleite, since he had just obtained his PhD with Phil Cohen at Dundee, who himself had been in our laboratory some 20 odd years before. When we started, we also assumed that if transformation could be brought about by overexpression of the tyrosine kinases, or mutations that would render them constitutively active, then overexpression of the phosphatases might block or reverse these reactions. This assumption was too simplistic.

Within a couple of years, a tyrosine phosphatase was isolated in homogeneous form from human placenta.[61,62] The enzyme was totally specific for phosphotyrosyl residues and extremely active. It had a specific activity about one order of magnitude higher than most viral tyrosine kinases and up to three orders of magnitude higher than certain receptor tyrosine kinases. This high activity suggested that it had to be tightly regulated to allow for those mitogenic signals that are necessary for normal cell development.

The Leukocyte Common Antigen, CD45: A Tyrosine Phosphatase

The surprise came when the amino acid sequence of the enzyme was determined by Ken Walsh and Harry Charbonneau because it showed no homology with any of the other protein phosphatases.[63] However, a search of the data base indicated that the enzyme was structurally related to an abundant and already well-known surface antigen, the leukocyte common antigen also designated as CD45[64] (Fig. 7). The leukocyte common antigen represents a broad

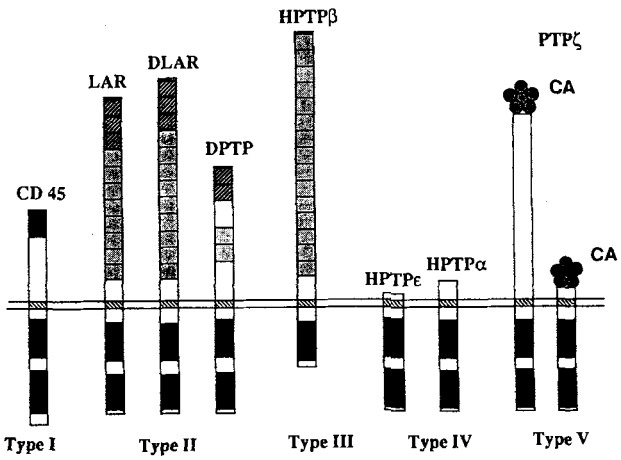

Fig. 7. Tyrosine phosphatase receptors.

family of membrane-spanning molecules found in all hematopoietic cells except mature erythrocytes.[65] Their intracellular moiety is highly conserved and contains two homologous domains of approximately 30 kDa each. It is those two domains that are structurally related to the placenta phosphatase. CD45 has been implicated in the regulation of lymphocyte function, including cytotoxicity, proliferation, and differentiation and in modulating interleukin-2 (IL2) receptor expression.

Here, I must open a parenthesis with biblical overtone. Had we obtained the sequence of the placenta phosphatase before that of CD45 was determined, nobody would have paid much attention—and we neither—because it would just have been the sequence of another enzyme. And it is those working on CD45—Ian Trowbridge, Allen Williams, Matt Thomas, etc.—who, once they got their sequence and searched for it through the data base, would have made the surprising observation that their receptor was, in fact, a tyrosine phosphatase. What this means is that in this business, it really pays to be last, precisely as recorded in the Gospel which states that "The last shall be first and the first last".

Since then, a great variety of receptor forms have been identified.[58-60] All but one display the same double catalytic domains in their cytoplasmic portion, but considerable diversity in their external segments (Fig. 7). Some have structural characteristics of cell adhesion molecules such as the leukocyte common antigen-related (LARs) first cloned by Saito and Schlossman. They are related to the Neural Cell Adhesion Molecules (N-CAMs) and fasciclin II, suggesting that they might be involved in homophilic cell–cell interactions and perhaps modulate morphogenesis and tissue development. Others contain fibronectin type III repeats and might be involved in cell–cell or cell–matrix signaling. Some have very short external domains. Perhaps the most intriguing receptors are the ones recently cloned independently by Schlessinger et al.[66] and Saito et al.[67] At the end of an external segment, one finds a large globular domain almost identical to carbonic anhydrase (CA) except that it contains only one of the three histidines involved in the binding of Zn^{2+}. Except for CD45, no ligand has been found for any of these structures.

The Intracellular Tyrosine Phosphatases in Cell Cycle Progression and Transformation

Likewise, the low molecular weight, intracellular protein tyrosine phosphatases (PTPs) display a great diversity of structures, either preceding or following a highly conserved catalytic core. These are undoubtedly involved in the regulation and localization of the enzymes (Fig. 8). Some PTPs have segments homologous to cytoskeletal proteins such as band 4.1, ezrin, and talin; others contain two src-homology 2 (SH2) domains which might allow them to interact with phosphotyrosyl residues at sites of autophosphorylation of growth factor receptors. Tyrosine phosphatases are also found as the gene products (YOPs) of virulence plasmids from bacteria of the genus *Yersinia* (such as *Y. pestis* responsible for the bubonic plague).

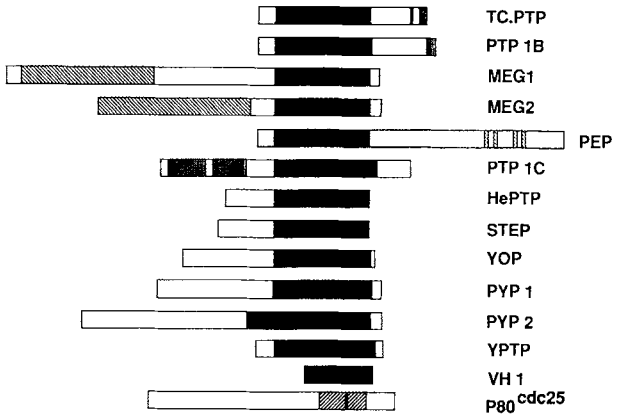

Fig. 8. Intracellular tyrosine phosphatases, aligned on the basis of their conserved, catalytic domains.

I would like to discuss now the role that these regulatory domains might play in enzyme localization and function, focussing on the human T-cell enzyme (Tc-PTP) cloned by Debbie Cool[68] (Fig. 9). The regulatory domain is entirely

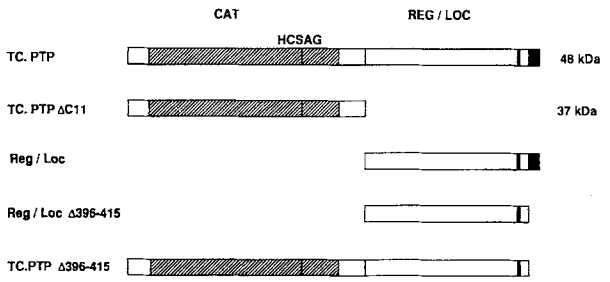

Fig. 9. Schematic representation of the human T-cell tyrosine phosphatase (TC-PTP) and some of its mutated forms. Illustrated are the full-length, wild-type 48 kDa enzyme, the 37 kDa truncated form containing only the catalytic domain; the 11 kDa regulatory/localization domain; and two mutant forms in which the hydrophobic 19-residue segment at the C terminus (dark band) has been deleted.

hydrophilic until one reaches the last 19 residues that are very hydrophobic, reminiscent of a transmembrane domain. There is also a short stretch of five basic residues that could serve as a nuclear localization signal.[68]

The 11 kDa segment of the enzyme, as well as other segments of putative physiological importance, was mutated. As a first step, a premature stop codon was introduced after the catalytic domain to delete the entire C-terminal tail. When this is done, the truncated enzyme becomes soluble, whereas the wild-type protein is particulate,[69, 70] localizing with the endoplasmic reticulum (ER). Expression of the C-terminal tail as a fusion protein with β-galactosidase shows that the soluble β-galactosidase now becomes attached to the ER. Finally, if one deletes just the C-terminal hydrophobic stretch, the enzyme localizes in the nucleus (J. A. Lorenzen, unpublished results).

Because of lack of time, I will only discuss the differences one observes in cell cycle progression and transformation when one expresses the wild-type enzyme versus its truncated form obtained by introducing a premature stop codon after the catalytic domain. In BHK cells, in which the wild-type enzyme is overexpressed, there is no obvious change in cell

morphology. By contrast, 60–70% of the cells expressing the truncated form become multinucleated[71] due to a failure in cytokinesis.

Multinucleation is not unusual; it can occur by cell fusion, with certain drugs or with antibodies against myosin ATPase since cytokinesis is an actomyosin-dependent process.[72, 73] But in all these instances, when nuclear division goes on, it goes on synchronously. What is unusual in these BHK cells is that nuclear division is more often than not asynchronous (Fig. 10): that is, one nucleus will divide while the other will not. Therefore, one will see cells with nuclei at all phases of cell cycle. At this time, we do not know which signals between the nuclei have been disrupted.

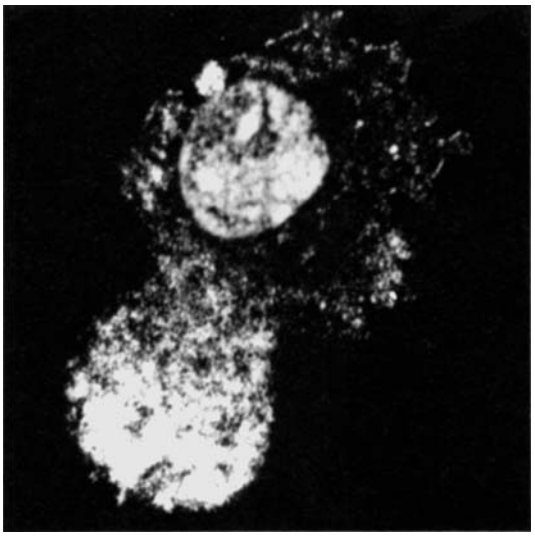

Fig. 10. BHK cells overexpressing the truncated 37 kDa form of the T-cell tyrosine phosphatase showing asynchronous nuclear division. The cell has rounded up around the lower nucleus ready to undergo mitosis. The nucleus on top is in an interphase configuration [7, 71].

Differences in cell behavior brought about by expression of the wild-type verses truncated T-cell enzyme can also be seen in cell transformation, by using the same highly tumorigenic BHK cell line. Transformation is the change a cell undergoes when it becomes malignant and no longer abides by the constraints under which a normal cell must operate. A normal cell does not grow on soft agar as it needs a solid support to which it can adhere, whereas a transformed cell will. As expected, the transformed BHK cell line grows readily on soft agar but it grows just as well, if not better, when transfected with the wild-type enzyme. By contrast, overexpression of the truncated form nearly abolishes growth under these conditions, as if transformation had been suppressed (D. Cool, unpublished results).

A similar enhancement in tumorigenicity by overexpression of the full-length phosphatase is observed when these cells are injected into athymic nude mice. The tumors produced are highly vascularized, as compared to tumors formed from control BHK cells. On the other hand, tumor formation is greatly reduced if not suppressed with BHK cells containing the truncated form. In several animals, no tumor was detected.

Since the nature of the transforming agent in these BHK cells was not defined, these studies were repeated in embryonic Rat-2 cells transformed with the well-characterized viral oncogene v-fms;[74] v-fms was first isolated from a feline sarcoma virus and belongs to the platelet-derived growth factor (PDGF) family of tyrosine kinase receptors.[75] Its nontransforming progenitor, the cellular protooncogene c-fms, encodes the receptor for CSF-1, the macrophage colony-stimulating factor. Binding of CSF-1 triggers signaling events that lead to the transcription of CSF-1 genes necessary for mononuclear phagocyte growth, differentiation and survival.[76]

Control Rat-2 cells display typical, nontransformed, cobblestone morphology—as opposed to the spindle-shape v-fms transformed cells.[74] Cells overexpressing the full-length enzyme have the same stringy transformed appearance, whereas clones containing the truncated form have the Rat-2, nontransformed cobblestone phenotype (Fig. 11). The

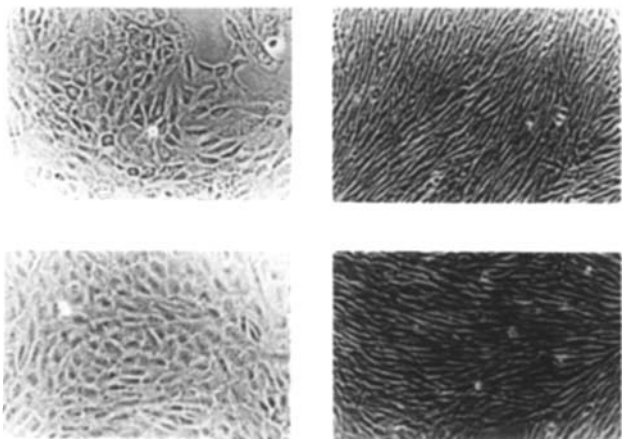

Fig. 11. Morphology of nontransformed Rat-2 cells (upper left) or cells transformed with v-fms (upper right). The v-fms-transformed cell lines were cotransfected with full-length T-cell tyrosine phosphatase (lower right) or its 37 kDa truncated form (lower left). The data indicate that while the full-length enzyme has not altered the transformed (spindle-shape) morphology, cells containing the truncated enzymes display a nontransformed phenotype.

transformed cells will grow on soft agar, the others will not. To achieve a high level of expression of the tyrosine phosphatase, the enzyme was packaged in retroviruses with which the cells were infected. None of the cells containing the truncated enzyme grew very well on soft agar. That these cells had reverted to a nontransformed state was further demonstrated by the appearance of their cytoskeleton (Fig. 12). Transformed cells exhibit a disruption of actin microfilaments and a loss of focal adhesions; that is, the structures through which normal cells adhere to their substratum. The actin fibers are restored in cells expressing the truncated enzyme and many more focal adhesions can be seen (D. Cool, unpublished results).

Finally, the same differences were observed in the ability of these two types of cells to form tumors when injected into nude mice. All cells containing the v-fms oncogenes produced large tumors, similar to those coexpressing the wild-type phosphatase. As observed in BHK cells, tumor formation was prevented in most cells transfected with the truncated enzyme.

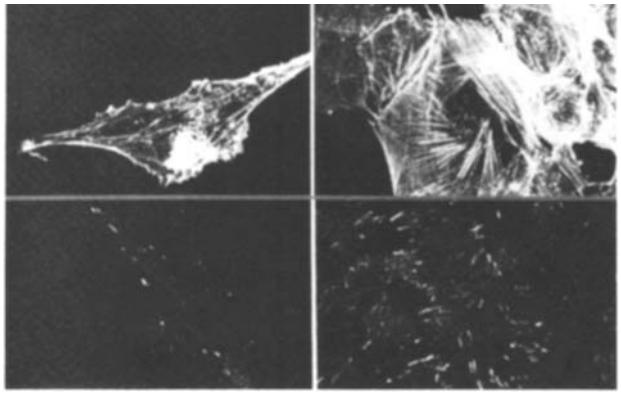

Fig. 12. Cytoskeleton morphology of v-fms transformed Rat-2 cells before (left) and after detransformation by coexpression of the truncated (37 kDa) form of the T-cell enzyme. Upper frames: actin stained with rhodamine-conjugated phalloidin; lower frames: stained with anti-vinculin antibodies to mark the focal adhesions (bright spots).

Concluding Remarks

The above results, plus others I did not have the time to develop, indicate that phosphatases cannot be viewed simply as providing an "off" switch in an "on/off" kinase/phosphatase system. In certain cases, and depending on the form of the enzyme involved, tyrosine phosphatases can clearly act synergistically with the kinases to bring about a particular physiological response. An obvious way by which they could do that would be by activating the src family kinases which are repressed by phosphorylation at the C terminus (Fig. 13). Furthermore, the factors that would determine

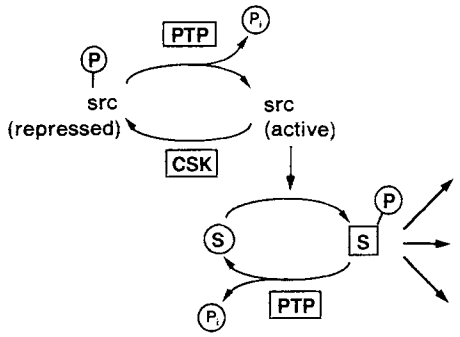

Fig. 13. Possible dual role of protein tyrosine phosphatases (PTP) in signal transduction. Upper reaction, activation of src family tyrosine kinases by dephosphorylation of the C-terminal phosphotyrosyl residue. Lower reaction, dephosphorylation of other tyrosine phosphorylated substrates to return the system to its original state. CSK is the cellular src kinase that represses enzymatic activity by tyrosine phosphorylation at the C terminus.

whether a phosphatase would enhance or oppose a kinase reaction would seem to depend less on its state of activity than on its subcellular localization. An analogous situation is found with $pp60^{v-src}$. Removal of the myristoyl group required for its binding to the plasma membrane does not affect its enzymatic properties but prevents its transforming abilities.[77] Association with the membrane is, therefore, essential for its oncogenicity. The above data indicate that if one wanted to control transformation through the phosphatases, one should try to manipulate the segments involved in their localization—or whatever anchoring proteins to which they may bind—rather than their catalytic domains. There are, of course, many questions that need to be answered. To mention a few:

a) What controls the activity of phosphatases under normal conditions? It may be easier to achieve high level expression of these enzymes in transformed lines in which the signal pathways are turned on, rather than in normal cells; as if a balance existed between kinases and phosphatases.

b) Do the differences between wild-type and truncated enzymes depend solely on their localization or is enzyme specificity also implicated?

c) Would the same effects be observed with any oncogene, including those that are not tyrosine kinases (such as ras, raf, mos, etc.)?

d) Which are the steps in the signaling pathway that are specifically affected by the enzymes? And finally:

e) If oncogenicity can result from an overexpression of tyrosine kinases, could oncogenicity also result from an underexpression of certain phosphatases?

All the processes Ed Krebs and I have described here have had something in common; they followed a similar pattern at the molecular level. Under the influence of an external stimulus, the state of phosphorylation of a protein or enzyme has been altered. This, in turn, has triggered a given cellular response. The finding that certain oncogenic agents may operate along the same principles may provide some clues as to the very mechanism of cell transformation. And who knows, perhaps with a little luck, a deeper understanding of these signaling pathways may suggest new avenues by which oncogenicity can be brought under control.

My scientific career has been profoundly marked by two long-standing collaborations, first with the late Eric A. Stein on α-amylases, then with Edwin G. Krebs, with whom I share this Award, on the protein phosphorylation problem. In addition to being the most valuable of colleagues, they have been two of my closest friends. I also owe a debt of gratitude to all those who joined the laboratory over the years, contributing their skills, original ideas, and maximum effort before moving on to pursue their own personal academic or research careers. The list would be too long were I to name them all; suffice to recall a few in chronological order: T. Yamamoto, M. Appleman, J. Hedrick, S. Shaltiel, S. Hurd, P. Cohen, L. Heilmeyer, B. Boeker, D. Gratecos, D. Malencik, C. Heizmann, H. Blum, M. Fosset, K. Lerch, J. Demaille, D. Brautigan, E. Villa-Moruzzi, L. Ballou, S. McNall, and N. Tonks. They have been superb collaborators; without them and all those I haven't been able to mention by name, including all my present collaborators, nothing that has happened could have happened.

I also owe a debt of gratitude to my wife Beverley for keeping her cool in the midst of recurring crises, whenever I had to prepare last-minute lectures or rush to the airport. Finally, a mountain of thanks goes to my secretary, Carmen Westwater for, time after time, wading through countless drafts of manuscripts, and retrieving lost letters, articles, or plane tickets. But those around me exaggerate when they call my office the "Bermuda Triangle".

My indebtedness goes to the National Institute of Diabetes and Digestive and Kidney Disease, NIH, for supporting my work from day one, and the Muscular Dystrophy Association for their unfailing help.

Received: February 12, 1993 [A 913 IE]
German version: *Angew. Chem.* **1993**, *105*, 1181

[1] K. Titani, A. Koide, J. Hermann, L. H. Ericsson, S. Kumar, R. D. Wade, K. A. Walsh, H. Neurath, E. H. Fischer, *Proc. Natl. Acad. Sci. USA* **1977**, *74*, 4762–4766.
[2] E. H. Fischer, D. J. Graves, E. R. Snyder Crittenden, E. G. Krebs, *J. Biol. Chem.* **1959**, *234*, 1698–1704.
[3] C. Nolan, W. B. Novoa, E. G. Krebs, E. H. Fischer, *Biochemistry* **1964**, *3*, 542–551.
[4] B. E. Kemp, D. J. Graves, E. Benjamini, E. G. Krebs, *J. Biol. Chem.* **1977**, *252*, 4888–4894.
[5] R. B. Pearson, B. E. Kemp, *Methods Enzymol.* **1991**, *200*, 62–81.
[6] M. Rosell-Perez, C. Villar-Palasi, J. Larner, *Biochemistry* **1962**, *1*, 763–768.
[7] D. L. Friedman, J. Larner, *Biochemistry* **1963**, *2*, 669–675.
[8] J. Larner, C. Villar-Palasi, *Curr. Top. Cell. Regul.* **1971**, *3*, 195–236.
[9] C. H. Smith, N. E. Brown, J. Larner, *Biochim. Biophys. Acta* **1971**, *3*, 81–88.
[10] P. Cohen, *The Enzymes* **1986**, *17A*, 461–497.
[11] P. J. Roach in *Enzymes* (Eds.: P. D. Boyer, E. G. Krebs), Academic Press, Orlando, **1986**, p. 499–539.
[12] P. J. Roach, *FASEB J.* **1990**, *4*, 2961–2968.
[13] E. G. Krebs, *The Enzymes* **1986**, *17*, 3–18.
[14] A. M. Edelman, D. K. Blumenthal, E. G. Krebs, *Annu. Rev. Biochem.* **1987**, *56*, 567–613.
[15] T. Hunter, *Methods Enzymol.* **1991**, *200*, 3–37.
[16] R. Seger, N. G. Ahn, J. Posada, E. S. Munar, A. M. Jensen, J. A. Cooper, M. H. Cobb, E. G. Krebs, *J. Biol. Chem.* **1992**, *267*, 14373–14379.
[17] J. Pines, T. Hunter, *New Biol.* **1990**, *2*, 389–401.
[18] R. B. Bourret, K. A. Borkovich, M. I. Simon, *Annu. Rev. Biochem.* **1991**, *60*, 401–441.
[19] D. C. LaPorte, P. E. Thorness, D. E. Koshland, Jr. *J. Biol. Chem.* **1985**, *260*, 10563–10568.
[20] S. K. Hanks, A. M. Quinn, T. Hunter, *Science* **1988**, *241*, 42–52.
[21] S. K. Hanks, A. M. Quinn, *Methods Enzymol.* **1991**, *200*, 38–62.
[22] D. A. Walsh, J. P. Perkins, E. G. Krebs, *J. Biol. Chem.* **1968**, *243*, 3763–3765.
[23] M. Castagna, W. K. Palmer, D. A. Walsh, *Eur. J. Biochem.* **1975**, *55*, 193–199.
[24] M. Leiser, C. S. Rubin, J. Erlichman, *J. Biol. Chem.* **1986**, *261*, 1904–1908.
[25] C. B. Bergman, N. Bhattacharyya, C. S. Rubin, *J. Biol. Chem.* **1989**, *264*, 4648–4656.
[26] D. W. Carr, Z. E. Hausken, E. D. C. Fraser, R. E. Stofko-Hahn, J. D. Scott, *J. Biol. Chem.* **1992**, *267*, 13376–13382.
[27] J. D. Scott, D. W. Carr, *News Physiol. Sci.* **1992**, *7*, 143–148.
[28] Y. Takai, A. Kishimoto, Y. Iwasa, Y. Kawahara, T. Mori, Y. Nishizuka, *J. Biol. Chem.* **1979**, *254*, 3692–3695.
[29] Y. Nishizuka, *Science* **1992**, *258*, 607–614.
[30] D. Mochly-Rosen, H. Khaner, J. Lopez, B. L. Smith, *J. Biol. Chem.* **1991**, *266*, 14866–14868.
[31] M. Lee, P. Nurse, *Trends Genet.* **1988**, *4*, 287–290.
[32] P. Nurse, *Nature* **1990**, *344*, 503–508.
[33] C. Norbury, P. Nurse, *Annu. Rev. Biochem.* **1992**, *61*, 441–470.
[34] C. Norbury, P. Nurse, *Curr. Biol.* **1992**, *1*, 23–27.
[35] P. Cohen, *Annu. Rev. Biochem.* **1989**, *58*, 453–508.
[36] P. Cohen, P. T. W. Cohen, *J. Biol. Chem.* **1989**, *264*, 21435–21438.
[37] S. Shenolikar, A. Nairn, *Adv. Second Messenger Phosphoprotein Res.* **1990**, 1–121.
[38] P. Stralfors, A. Hiraga, P. Cohen, *Eur. J. Biochem.* **1985**, *149*, 295–303.
[39] M. J. Hubbard, P. Cohen, *Eur. J. Biochem.* **1989**, *180*, 457–465.
[40] A. A. Chisholm, P. Cohen, *Biochim. Biophys. Acta* **1988**, *971*, 163–169.
[41] A. A. DePaoli Roach, *Adv. Protein Phosphatases* **1989**, *5*, 479–500.
[42] J. S. Brugge, R. L. Erikson, *Nature* **1977**, *269*, 346–347.
[43] M. S. Collett, R. L. Erikson, *Proc. Natl. Acad. Sci. USA* **1978**, *75*, 2021–2024.
[44] A. D. Levinson, H. Oppermann, L. Levintow, H. E. Varmus, J. M. Bishop, *Cell* **1978**, *15*, 561–572.
[45] T. Hunter, B. M. Sefton, *Proc. Natl. Acad. Sci. USA* **1980**, *77*, 1311–1315.
[46] M. S. Collett, J. S. Brugge, R. L. Erikson, *Cell* **1978**, *15*, 1363.
[47] H. Oppermann, A. R. Levinson, H. E. Varmus, L. Levintow, J. M. Bishop, *Proc. Natl. Acad. Sci. USA* **1979**, *76*, 1804–1808.
[48] L. R. Rohrschneider, R. N. Eisenman, C. R. Leitch, *Proc. Natl. Acad. Sci. USA* **1979**, *76*, 4479–4483.
[49] A. P. Czernilofsky, A. D. Levinson, H. E. Varmus, J. M. Bishop, E. Tischer, H. M. Goodman, *Nature* **1980**, *287*, 198–203.
[50] *Oncogenes and the Molecular Origins of Cancer* (Ed.: R. A. Weinberg) Cold Spring Harbor Laboratory Press, Cold Spring Harbor, NY, USA, **1989**.
[51] H. Ushiro, S. Cohen, *J. Biol. Chem.* **1980**, *255*, 8363–8365.
[52] G. Carpenter, *Annu. Rev. Biochem.* **1987**, *56*, 881–914.
[53] Y. Yarden, A. Ullrich, *Annu. Rev. Biochem.* **1988**, *57*, 443–478.
[54] J. Downward, Y. Yarden, E. Mayes, G. Scrace, N. Totty, P. Stockwell, A. Ullrich, J. Schlessinger, M. D. Waterfield, *Nature* **1984**, *307*, 521–527.
[55] L. Ullrich, L. Coussens, J. S. Hayflick, T. J. Dull, A. Gray, A. W. Tam, J. Lee, Y. Yarden, T. A. Libermann, J. Schlessinger, J. Downward, E. L. V. Mayes, N. Whittle, M. D. Waterfield, P. H. Seeburg, *Nature* **1984**, *309*, 418–425.
[56] G. Carpenter, L. King, S. Cohen, *J. Biol. Chem.* **1979**, *254*, 4884–4891.
[57] B. M. Sefton, T. Hunter, K. Beemon, W. Eckhart, *Cell* **1980**, *20*, 807–816.
[58] E. H. Fischer, H. Charbonneau, N. K. Tonks, *Science* **1991**, *253*, 401–406.
[59] H. Saito, M. Streuli, *Cell Growth Differ.* **1991**, *2*, 59–65.
[60] H. Charbonneau, N. K. Tonks, *Annu. Rev. Cell. Biol.* **1992**, *8*, 463–493.
[61] N. K. Tonks, C. D. Diltz, E. H. Fischer, *J. Biol. Chem.* **1988**, *263*, 6731–6737.
[62] N. K. Tonks, C. D. Diltz, E. H. Fischer, *J. Biol. Chem.* **1988**, *263*, 6722–6730.
[63] H. Charbonneau, N. K. Tonks, S. Kumar, C. D. Diltz, M. Harrylock, D. E. Cool, E. G. Krebs, E. H. Fischer, K. A. Walsh, *Proc. Natl. Acad. Sci. USA* **1989**, *86*, 5252–5256.
[64] H. Charbonneau, N. K. Tonks, K. A. Walsh, E. H. Fischer, *Proc. Natl. Acad. Sci. USA* **1988**, *85*, 7182–7186.
[65] M. L. Thomas, *Annu. Rev. Immunol.* **1989**, *7*, 339–369.
[66] G. Barnea, O. Silvennoinen, B. Shaanan, A. M. Honegger, P. D. Canoll, P. D'Eustachio, B. Morse, J. B. Levy, S. LaForgia, K. Huebner, J. M. Musacchio, J. Sap, J. Schlessinger, *Mol. Cell. Biol.* **1992**, *13*, 1497–1506.
[67] N. X. Krueger, H. Saito, *Proc. Natl. Acad. Sci. USA* **1992**, *89*, 7417–7421.
[68] D. E. Cool, N. K. Tonks, H. Charbonneau, K. A. Walsh, E. H. Fischer, E. G. Krebs, *Proc. Natl. Acad. Sci. USA* **1989**, *86*, 5257–5261.
[69] D. E. Cool, N. K. Tonks, H. Charbonneau, E. H. Fischer, E. G. Krebs, *Proc. Natl. Acad. Sci. USA* **1990**, *87*, 7280–7284.
[70] N. F. Zander, J. A. Lorenzen, D. E. Cool, N. K. Tonks, G. Daum, E. G. Krebs, E. H. Fischer, *Biochemistry* **1991**, *30*, 6964–6970.
[71] D. E. Cool, P. R. Andreassen, N. K. Tonks, E. G. Krebs, E. H. Fischer, R. L. Margolis, *Proc. Natl. Acad. Sci. USA* **1992**, *89*, 5422–5426.
[72] K. Fujiwara, T. D. Pollard, *J. Cell Biol.* **1976**, *71*, 848–875.
[73] N. Sato, S. Yonemura, T. Obinata, S. Tsukita, *J. Cell. Biol.* **1991**, *113*, 321–330.
[74] N. F. Zander, D. E. Cool, C. D. Diltz, L. R. Rohrschneider, E. G. Krebs, E. H. Fischer, *Oncogene*, **1993**, *8*, 1175–1182.
[75] S. K. McDonough, S. Larsen, R. S. Brodey, N. D. Stock, W. D. Hardy, Jr., *Cancer Res.* **1971**, *31*, 953–956.
[76] C. J. Sherr, *Biochim. Biopyhs. Acta* **1988**, *948*, 225–243.
[77] M. L. Kamps, J. E. Buss, B. M. Sefton, *Proc. Natl. Acad. Sci. USA* **1985**, *82*, 4625–4628.

The Chemistry of the Fullerenes: An Overview

By *Andreas Hirsch**

Chemists' fascination with the fullerenes, the new soluble forms of carbon, is not founded merely on the geometric beauty of the molecules. Following the development of the synthesis of these spherical, cavity-containing molecules in preparative amounts,[1] these compounds and their chemically modified derivatives have been found to possess novel, remarkable properties. The soccerball-shaped buckminsterfullerene C_{60} has been at the forefront of these investigations. One notable feature of this molecule is its ready and reversible uptake of up to six electrons.[2] This high electron affinity was exploited in the first chemical modifications of C_{60}. For example, superconductors like K_3C_{60}[3] and ferromagnets like $[TDAE]C_{60}$ (TDAE = tetrakis(dimethylamino)ethylene)[4] were prepared by charge transfer with electropositive metals and organic donor molecules, respectively. Atoms may be deposited in the cavity within the cage. Helium was introduced to C_{60},[5a] and other noble gases[5b,c] and metal atoms[6] were included in fullerenes during their preparation.

Exohedral modifications of fullerenes in three dimensions by addition reactions and the development of preparative fullerene chemistry are particularly attractive to chemists. Materials with promising properties can be expected from these experiments. In principle the structure of the fullerenes provides access to a multitude of reaction products and positional isomers. Of course this can also make the purification and characterization of individual isomerically pure compounds more difficult. The following questions concerning the derivatization of fullerenes have been asked from the start: What kind of reactivity do the fullerenes have? Do they behave like a three-dimensional "superbenzene"? What are the structures of exohedral fullerene derivatives and how stable are they? In the meantime an entire series of successful reactions with C_{60} and also with C_{70} have been conducted, leading to well-defined fullerene derivatives (Scheme 1). Distinct regularities are already evident, which suggest a summary of the reactivity of the fullerenes. In order to avoid the problem of multiple derivatives that are difficult to separate, mainly monoadducts were prepared at first.

The first characterizable monoadduct $[C_{60}(OsO_4)(4\text{-}tert\text{-}butylpyridine)_2]$ was reported by Hawkins et al.[7] Its X-ray crystal structure confirmed the soccerball shape of C_{60}.[7b] The O-Os-O unit was shown to add regioselectively exclusively at a double bond common to two annelated six-membered rings (6-6 bond) in the fullerene framework. This structural analysis also provided the important finding that the 6-6 bonds (double bonds) are shorter than the bonds common to both a five- and a six-membered ring (5-6 bonds), which have single-bond character. According to this, C_{60} can be described topologically by annelated cyclohexatriene and [5]radialene units, as was also confirmed by the crystal structure analyses[8] and calculations[9] of underivatized C_{60}. The olefin character was also underlined in the reactions with coordinatively unsaturated transition metal complexes ML_n (M = Pt, Ir, etc.) conducted by Fagan et al. and Balch et al.[10] The formation of monoadducts always occurs at a 6-6 double bond (Scheme 1).

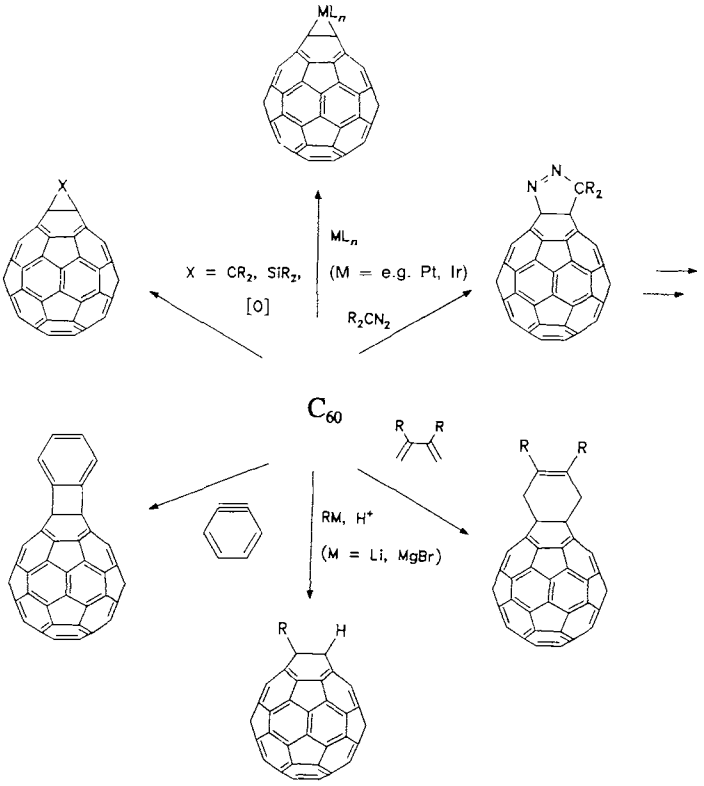

Scheme 1. Syntheses of exohedral fullerene derivatives. For clarity only the front sides of the fullerenes are shown.

The first investigations of the reactivity of C_{60} to organic reagents[11] proved that it is distinctly electrophilic and dieno/dipolarophilic. In a series of experiments[12] Wudl et al. and Diederich et al. showed that stoichiometrically controlled reactions with diazoalkanes and diazoacetates provide σ- or π-homoaromatic fullerenes with methano bridges. In several cases it was demonstrated that the primary step in these reactions is a [3 + 2] cycloaddition to form a dihydropyrazole.[12e] The thermally stable final products in these reactions are the opened, π-homoaromatic compounds **1** bridged at a 5-6 ring juncture, the corresponding opened compounds **2** bridged at a 6-6 ring juncture, or the closed, σ-homoaromatic fullerenes **3** bridged at the 6-6 ring juncture. In some cases several valence isomers are formed simultaneously, which are then converted into the most stable derivative by heating.[12e] The precise spectroscopic investigation of the fullerenes with methano bridges ("fulleroids")

[*] Dr. A. Hirsch
Institut für Organische Chemie der Universität
Auf der Morgenstelle 18, D-72074 Tübingen (FRG)
Telefax: Int. code + (7071)5244

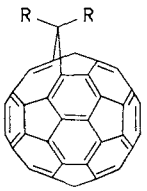

1

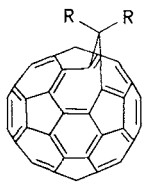

2

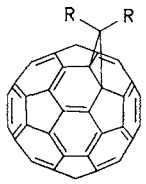

3

shows an impressive analogy to the annulenes with methano bridges. Reactions with suitable diazoalkanes allowed the synthesis of bridged fullerenes and polymers with fullerene units in the side chains.[12f] The opened azafulleroids **4** were obtained from C_{60} and organic azides by [3 + 2] cycloadditions and subsequent loss of nitrogen.[13]

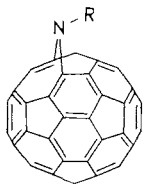

4

Defined, stable Diels–Alder adducts of C_{60} (Scheme 1) can be obtained from reactions with suitable dienes[14] and with isobenzofuran.[15] They are formed with high regioselectivity by addition to a 6-6 double bond exclusively, as was proved by ^{13}C NMR spectroscopy[14] and X-ray structure analysis.[14b]

The nucleophilic additions of Grignard and organolithium compounds and the subsequent protonation to form 1-organo-1,9-dihydrofullerenes-60[16, 17] reveal much about the reactivity of C_{60} (Scheme 1). Even in these two-step processes isomerically pure compounds are obtained. For good yields of the monoadduct, the reactions with reactive carbanionic nucleophiles must be carefully regulated. The nucleophile is added in portions and the reactions are monitored by high-performance liquid chromatography (titration).[16a, b] The fact that the stable final products isolated are exclusively the 1,9 derivatives clearly demonstrates that the negative charge in the anionic intermediates RC_{60}^- (C_s symmetry) is localized primarily on C9. Correspondingly, in these compounds the proton bound to the fullerene framework is very acidic. A pH value of 5.7 was determined for $C_{60}HtBu$.[16c] More recently the parent compound of the 1,9-dihydrofullerenes-60, $C_{60}H_2$, has been synthesized.[18] This simplest hydrocarbon derivative of C_{60} was obtained by addition of BH_3 and hydrolysis of the initial hydroboration product $C_{60}H(BH_2)$ with acetic acid. When deuterolysis was the last step, ^1H NMR spectroscopy proved that the 1,9 isomer was formed regioselectively.

The reaction of C_{60} with benzyne[19] does not provide a [4 + 2] cycloadduct but formally a [2 + 2] adduct (Scheme 1). The hypothetical [4 + 2] adduct would require formation of a 5-6 double bond, which is energetically unfavorable for the fullerene system.[20]

Carbenes,[21] silanediyls,[22], and oxygen[23] react with the double bonds of C_{60} (Scheme 1), and the monoadducts obtained were characterized completely. In all of these cases the products are closed fullerenes bridged at a 6-6 bond. An especially impressive example is the addition of glycosylidene carbenes to give fullerene sugar derivatives.[21]

Defined diaminofullerenes **5** have also been obtained by the reaction of C_{60} with secondary diamines such as *N,N'*-dimethylethylenediamine.[24] Noteworthy here is that dehydrogenated C_{60} derivatives are produced. The products are monoadducts that have lost the hydrogen atoms introduced with the diamine units.

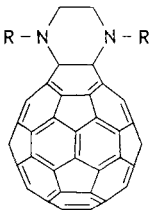

5

A variety of substituents can be bound covalently to the fullerene framework with the addition reactions discussed briefly here. This preparative organic fullerene chemistry allows the synthesis of derivatives in which the properties of the fullerenes are combined with those of other classes of compounds. High regioselectivities and in most cases satisfactory to good yields are obtained.

Extensive investigations of the reaction of radicals with C_{60} and C_{70} were conducted in situ by ESR spectroscopy.[25] A series of alkyl radicals was generated either thermally or photochemically, and the ready formation of multiple addition products $C_{60}R_n$ was observed. The reaction was also directed to give monoalkyl radical adducts. The analysis of the spectra of $RC_{60}^{\cdot}$ (C_s symmetry) showed that the unpaired electron is predominently localized directly adjacent to the R-substituted C atom at position 9, as is also the case in the anions RC_{60}^-. The monoalkyl radical adducts are in equilibrium with their diamagnetic dimers $R-C_{60}-C_{60}-R$.

Multiple additions to fullerenes readily lead to reaction mixtures that are difficult to separate because of polyfunctionality. Several examples for defined multiple adducts are now known.[26] In the organometallic derivatives $[C_{60}\{M(PEt_3)_2\}_6]$ (M = Ni, Pd, Pt) the C_{60} framework is coordinated in an octahedral fashion by six η^2-$(Et_3P)_2M$ units,[26a, b] leading to the uncommon, approximately ideal T_h point group (ethyl groups neglected). The reaction of C_{60} with an excess of $[Ir(CO)Cl(PMe_2Ph)_2]$ provides two conformational isomers of $[C_{60}\{Ir(CO)Cl(PMe_2Ph)_2\}_2]$.[26c] In both isomers the iridium atoms are bound to 6-6 double bonds of the fullerene framework exactly across from each other; in other words, the second addition takes place on the opposite hemisphere. Bisosmylation of C_{60} affords five positional isomers of $[C_{60}\{OsO_4(py)\}_2]$,[26e] which were all separated. Here, too, the second attack takes place on the opposing hemisphere for electronic and steric reasons.

Whereas fluorination[27] and chlorination[28] of C_{60} led to uncharacterizable mixtures of products, the bromides $C_{60}Br_6$, $C_{60}Br_8$, and $C_{60}Br_{24}$ were crystallized and characterized.[29] The previously discussed examples mainly concerned 1,2-additions to 6-6 bonds. In contrast, bromination is preferentially a 1,4-addition for steric reasons. The regular

arrangement of the 24 bromine atoms in T_h-$C_{60}Br_{24}$ arises from two 1,4-additions at each pair of annelated six-membered rings such that the bromine substituents closest to each other are at 1,3-positions.[29b] Subsequent additions of Br_2 are unfavorable, since the bromine atoms would be bound to directly adjacent C atoms. The 1,4-addition mode is attributed to the large spatial requirement of bromine atoms. The fullerene framework must thus accept the energetically unfavorable formation of a 5-6 double bond.[20] The ratio of 1,2- to 1,4-additions (Fig. 1) depends in general on the interplay of the spatial requirement of the bound ligands and the destabilization associated with the 5-6 double bond. The bromides $C_{60}Br_6$ and $C_{60}Br_8$ are relatively unstable[29a] ($C_{60}Br_{24}$ is somewhat more stable) and lose Br_2 to regenerate C_{60}.

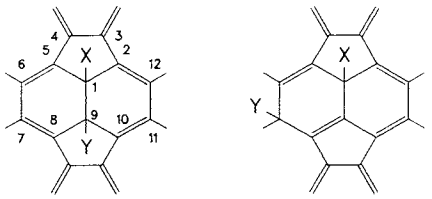

Fig. 1. 1,2-Addition product (A) and 1,4-addition product (B) of fullerene-60 with systematic numbering of the carbon atoms.

Other successful reactions of C_{60} include hydroaminations with primary and secondary amines,[11] addition of triethylphosphite,[11] addition of hydroxide,[30] reaction with lithium and subsequent methylation,[31] hydrogenation,[32] reaction with Lewis acids,[33] and reaction with NO_2^+.[34] The reaction products have not yet been separated or completely characterized in any of these cases. The addition reactions are frequently reversible.

The reaction of fullerene-60 with polymers having NH_2 groups in their side chains is an elegant method for the synthesis of polymer-bound C_{60}.[35] Some of these polymers are soluble, fulfilling an important prerequisite for further manipulations of these materials.

While all positions in C_{60} are identical, five sets of C atoms are found in C_{70}. It can be anticipated that the different bonds display different reactivities.[36] In both the reaction of C_{70} with $[Ir(CO)Cl(PPh_3)_2]$ to give $[(\eta^2\text{-}C_{70})Ir(CO)Cl(PPh_3)_2]$ (**6**)[37] and in hydroalkylations of C_{70},[16b] attack occurs at the a-b bonds at the poles. In the formation of the bisadduct from C_{70} and $[Ir(CO)Cl(PPh_3)_2]$, the second addition takes place at the a'-b' bond in the opposite hemisphere.[26b]

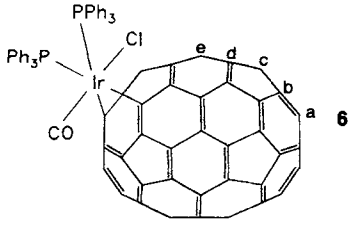

6

Based on the results obtained up until now, the chemistry of the fullerenes[38] can be summarized as follows:

- C_{60} reacts as an electron-poor olefin with fairly localized double bonds.
- Additions occur preferentially at a 6-6 double bond.
- Fullerenes with methano bridges may have either σ- or π-homoaromatic structures.
- 1,4-Additions take place with sterically demanding ligands; the introduction of the energetically unfavorable 5-6 double bond must be taken into account.
- In general the second addition occurs in the opposite hemisphere.
- Additions to C_{70} take place selectively at the most reactive double bonds at the poles.

German version: *Angew. Chem.* **1993**, *105*, 1189

[1] W. Krätschmer, L. D. Lamb, K. Fostiropoulos, D. R. Huffman, *Nature* **1990**, *347*, 354.

[2] Q. Xie, E. Perez-Cordero, L. Echegoyen, *J. Am. Chem. Soc.* **1992**, *114*, 3978.

[3] R. C. Haddon, *Acc. Chem. Res.* **1992**, *25*, 127.

[4] P.-M. Allemand, K. C. Khemani, A. Koch, F. Wudl, K. Holczer, S. Donovan, G. Grüner, J. D. Thompson, *Science* **1991**, *253*, 301.

[5] a) T. Weiske, D. K. Böhme, J. Hrusak, W. Krätschmer, H. Schwarz, *Angew. Chem.* **1991**, *103*, 898; *Angew. Chem. Int. Ed. Engl.* **1991**, *30*, 884; b) K. A. Caldwell, D. E. Giblin, C. S. Hsu, D. Cox, M. L. Gross, *J. Am. Chem. Soc.* **1991**, *113*, 8519; c) M. Saunders, H. A. Jimenez-Vazquez, R. J. Cross, R. J. Poreda, *Science* **1993**, *259*, 1428–1430.

[6] A) R. D. Johnson, M. S. de Vries, J. Salem, D. S. Bethune, C. S. Yannoni, *Nature* **1992**, *355*, 293; b) E. G. Gillan, C. Yeretzian, K. S. Min, M. M. Alvarez, R. L. Whetten, R. B. Kaner, *J. Phys. Chem.* **1992**, *96*, 6869.

[7] a) J. M. Hawkins, T. A. Lewis, S. D. Loren, A. Meyer, J. R. Heath, Y. Shibato, R. J. Saykally, *J. Org. Chem.* **1990**, *55*, 6250; b) J. M. Hawkins, A. Meyer, T. Lewis, S. Loren, F. J. Hollander, *Science* **1991**, *252*, 312; c) J. M. Hawkins, S. Loren, A. Meyer, R. Nunlist, *J. Am. Chem. Soc.* **1991**, *113*, 7770.

[8] a) W. I. F. David, R. M. Ibberson, J. C. Matthewman, K. Prassides, T. J. S. Dennis, J. P. Hare, H. W. Kroto, R. Taylor, D. R. Walton, *Nature* **1991**, *353*, 147; b) K. Hedberg, L. Hedberg, D. S. Bethune, C. A. Brown, H. C. Dorn, R. D. Johnson, M. de Vries, *Science* **1991**, *254*, 410; c) S. Liu, Y.-J. Kappers, J. A. Ibers, *ibid.* **1991**, *254*, 408.

[9] a) R. Sachidanandam, A. B. Harris, *Phys. Rev. Lett.* **1991**, *67*, 1447; b) M. Haeser, J. Almhöf, G. E. Scuseria, *Chem. Phys. Lett.* **1991**, *181*, 497.

[10] a) P. J. Fagan, J. C. Calabrese, B. Malone, *Science* **1991**, *252*, 1160; b) *Acc. Chem. Res.* **1992**, *25*, 134; c) A. L. Balch, V. J. Catalano, J. W. Lee, *Inorg. Chem.* **1991**, *30*, 3980; d) A. L. Balch, V. J. Catalano, J. W. Lee, M. M. Olmstead, *J. Am. Chem. Soc.* **1992**, *114*, 5455.

[11] F. Wudl in *Fullerenes: Synthesis, Properties, and Chemistry of Large Carbon Clusters* (*ACS Symp. Ser.* **1992**, *481*), pp. 161–176.

[12] a) T. Suzuki, Q. Li, K. C. Khemani, F. Wudl, Ö. Almarsson, *Science* **1991**, *254*, 1186; b) T. Suzuki, Q. Li, K. C. Khemani, F. Wudl, *J. Am. Chem. Soc.* **1992**, *114*, 7300; c) *ibid.* **1992**, *114*, 7301; d) F. Wudl, *Acc. Chem. Res.* **1992**, *25*, 157; e) L. Isaacs, A. Wehrsig, F. Diederich, *Helv. Chim. Acta* **1993**, in press; f) S. Shi, K. C. Khemani, Q. Li, F. Wudl, *J. Am. Chem. Soc.* **1992**, *114*, 10656.

[13] M. Prato, Q. Li, F. Wudl, V. Lucchini, *J. Am. Chem. Soc.* **1993**, *115*, 1148.

[14] a) P. Belik, A. Gügel, J. Spikermann, K. Müllen, *Angew. Chem.* **1993**, *105*, 95; *Angew. Chem. Int. Ed. Engl.* **1993**, *32*, 78; b) Y. Rubin, S. Khan, D. I. Freedberg, C. Yeretzian, *J. Am. Chem. Soc.* **1993**, *115*, 344; c) S. I. Khan, A. M. Oliver, M. N. Paddon-Row, Y. Rubin, *J. Am. Chem. Soc.* **1993**, *115*, 4919.

[15] M. Prato, T. Suzuki, H. Foroudian, Q. Li, K. Khemani, F. Wudl, J. Leonetti, R. D. Little, T. White, B. Rickborn, S. Yamago, E. Nakamura, *J. Am. Chem. Soc.*, in press.

[16] a) A. Hirsch, A. Soi, H. R. Karfunkel, *Angew. Chem.* **1992**, *104*, 808; *Angew. Chem. Int. Ed. Engl.* **1992**, *31*, 766; b) A. Hirsch, T. Grösser, A. Skiebe, A. Soi, *Chem. Ber.* **1993**, *126*, 1061; c) P. J. Fagan, P. J. Krusic, D. H. Evans, S. A. Lerke, E. Johnston, *J. Am. Chem. Soc.* **1992**, *114*, 9697.

[17] Numbering of the fullerene C atoms according to P. R. Birkett, P. B. Hitchcock, H. W. Kroto, R. Taylor, *Nature* **1992**, *357*, 479.

[18] C. C. Henderson, P. A. Cahill, *Science* **1993**, *259*, 1885–1887.

[19] S. H. Hoke II, J. Molstad, D. Dilettato, M. J. Jay, D. Carlson, B. Kahr, R. G. Cooks, *J. Org. Chem.* **1992**, *57*, 5069.

[20] a) D. A. Dixon, N. Matsuzawa, T. Fukunaga, F. N. Tebbe, *J. Phys. Chem.* **1992**, *96*, 6107; b) N. Matsuzawa, D. A. Dixon, T. Fukunaga, *ibid.* **1992**, *96*, 7594; c) N. Matsuzawa, T. Funkunaga, D. A. Dixon, *ibid.* **1992**, *96*, 10747.

[21] A. Vasella, P. Uhlmann, C. A. A. Waldraff, F. Diederich, C. Thilgen, *Angew. Chem.* **1992**, *104*, 1383; *Angew. Chem. Int. Ed. Engl.* **1992**, *31*, 1388.
[22] T. Akasaka, W. Ando, K. Kobayashi, S. Nagase, *J. Am. Chem. Soc.* **1993**, *115*, 1605.
[23] a) K. M. Creegan, J. L. Robbins, W. K. Robbins, J. M. Millar, R. D. Sherwood, P. J. Tindall, D. M. Cox, J. M. McCauley, Jr., D. R. Jones, R. Gallagher, A. B. Smith III, *J. Am. Chem. Soc.* **1992**, *114*, 1103; b) Y. Elemes, S. K. Silverman, C. Sheu, M. Kao, C. S. Foote, M. M. Alvarez, R. L. Whetten, *Angew. Chem.* **1992**, *104*, 364; *Angew. Chem. Int. Ed. Engl.* **1992**, *31*, 351.
[24] K.-D. Kampe, N. Egger, M. Vogel, *Angew. Chem.* **1993**, *105*, 1203; *Angew. Chem. Int. Ed. Engl.* **1993**, *32*, 1174.
[25] a) P. J. Krusic, E. Wasserman, P. N. Keizer, J. R. Morton, K. F. Preston, *Science* **1991**, *254*, 1183; b) J. R. Morton, K. F. Preston, P. J. Krusic, S. A. Hill, E. Wasserman, *J. Phys. Chem.* **1992**, *96*, 3576; c) *J. Am. Chem. Soc.* **1992**, *114*, 5454; d) P. N. Keizer, J. R. Morton, K. F. Preston, *J. Chem. Soc. Chem. Commun.* **1992**, 1259; e) P. J. Krusic, D. C. Roe, E. Johnston, J. R. Morton, K. F. Preston, *J. Phys. Chem.* **1993**, *97*, 1736.
[26] a) P. J. Fagan, J. C. Calabrese, B. Malone, *J. Am. Chem. Soc.* **1991**, *113*, 9408; b) *Acc. Chem. Res.* **1992**, *25*, 134; c) A. L. Balch, J. W. Lee, B. C. Noll, M. M. Olmstead, *J. Am. Chem. Soc.* **1992**, *114*, 10984; d) A. L. Balch, J. W. Lee, M. M. Olmstead, *Angew. Chem.* **1992**, *104*, 1400; *Angew. Chem. Int. Ed. Engl.* **1992**, *31*, 1356; e) J. M. Hawkins, A. Meyer, T. A. Lewis, U. Bunz, R. Nunlist, G. E. Ball, T. W. Ebbesen, K. Tanigaki, *J. Am. Chem. Soc.* **1992**, *114*, 7954.
[27] a) J. H. Holloway, E. G. Hope, R. Taylor, G. J. Langley, A. G. Avent, T. J. Dennis, J. P. Hare, H. W. Kroto, D. R. M. Walton, *J. Chem. Soc. Chem. Commun.* **1991**, 966; b) H. Selig, C. Lifshitz, T. Peres, J. E. Fisher, A. R. McGhie, J. W. Romanov, J. P. McCauley, Jr., A. B. Smith III, *J. Am. Chem. Soc.* **1991**, *113*, 5475.
[28] G. A. Olah, I. Bucsi, C. Lambert, R. Anizfeld, N. J. Trivedi, D. K. Sensharma, G. K. S. Prakash, *J. Am. Chem. Soc.* **1991**, *133*, 9358.
[29] a) F. N. Tebbe, R. L. Harlow, D. B. Chase, D. L. Thorn, G. C. Campbell, J. C. Calabrese, N. Herron, R. J. Young, E. Wasserman, *Science* **1992**, *256*, 822; b) P. R. Birkett, P. B. Hitchcock, H. W. Kroto, R. Taylor, D. R. M. Walton, *Nature* **1992**, *357*, 479.
[30] A. Naim, P. B. Shevlin, *Tetrahedron Lett.* **1992**, *33*, 7097.
[31] J. W. Bausch, G. K. S. Prakash, G. A. Olah, D. S. Tse, D. C. Lorents, Y. K. Bae, R. Malhorta, *J. Am. Chem. Soc.* **1991**, *113*, 3205.
[32] a) R. E. Haufler, J. Conceicao, L. P. F. Chibante, Y. Chai, N. E. Byrne, S. Flanagan, M. M. Haley, S. C. O'Brian, C. Pan, Z. Xiao, W. E. Billups, M. A. Ciufolini, R. H. Hauge, J. L. Margrave, L. J. Wilson, R. F. Curl, R. E. Smalley, *J. Phys. Chem.* **1990**, *94*, 8634; b) C. Rüchardt, M. Gerst, J. Ebenhoch, H.-D. Beckhaus, E. E. B. Campbell, R. Tellgmann, H. Schwarz, T. Weiske, S. Pitter, *Angew. Chem.* **1993**, *105*, 609; *Angew. Chem. Int. Ed. Engl.* **1993**, *32*, 584.
[33] G. A. Olah, I. Bucsi, C. Lambert, R. Anizfeld, N. J. Trivedi, D. K. Sensharma, G. K. S. Prakash, *J. Am. Chem. Soc.* **1991**, *113*, 9387.
[34] L. Y. Chiang, R. B. Upasani, J. W. Swirczewski, *J. Am. Chem. Soc.* **1992**, *114*, 10154.
[35] a) A. O. Patil, G. W. Schriver, B. Carstensen, R. D. Lundberg, *Polym. Bull.* **1993**, *30*, 187–190; b) K. E. Geckeler, A. Hirsch, *J. Am. Chem. Soc.* **1993**, *115*, 3850–3851.
[36] H. R. Karfunkel, A. Hirsch, *Angew. Chem.* **1992**, *104*, 1529; *Angew. Chem. Int. Ed. Engl.* **1992**, *31*, 1468.
[37] A. L. Balch, V. J. Catalano, J. W. Lee, M. M. Olmstead, S. R. Parkin, *J. Am. Chem. Soc.* **1991**, *113*, 8953.
[38] For a very recent review see also R. Taylor, D. R. M. Walton, *Nature* **1993**, *363*, 685.

Prediction of the Secondary Structure of Proteins from the Amino Acid Sequence with Artificial Neural Networks

By *Gisbert Schneider* and *Paul Wrede**

How does an amino acid sequence fold into its native three-dimensional structure (that is, the correct arrangement for the biological function of the protein)? A comprehensive answer to this question cannot be given yet. Too many factors influence the folding in vivo and in vitro. One potential approach to the solution is to consider the spatial structure of a protein molecule as a hierarchically constructed system (amino acid sequence → secondary structure → structure domains → tertiary structure and, where applicable, quaternary structure[1]), in order to understand the elementary steps of the folding process in this modular concept. An important first step is the prediction of secondary structures from the amino acid sequences.

A method frequently applied is the procedure of P. Chou and G. Fasman, which is based on a statistical analysis of known secondary structures.[2] The propensity of each amino acid to form part of a helix, a folded sheet, or a loop, calculated in this way, can then be used in the prediction of these structures for new sequences. The prediction is achieved through a concept that views the formation of a secondary structure as a local event that is limited to a short section of the amino acid sequence (a "window"). To predict the secondary structure at individual amino acids the window moves across the sequence. This has the particular advantage that the secondary structure at a certain sequence position is seen in the context of adjacent amino acids, and interactions between the amino acid residues within the sequence in question can be taken into account. Several concepts for the prediction of secondary structure have been developed that are based mainly on the moving window principle. A consistent approach stems from the interdisciplinary field of molecular biocomputing: sequence analysis with artificial neural networks.

Neural networks are ideally suited for parallel sequence processing and are increasingly applied for the study of biological macromolecules. The aim is the classification of nucleic acid and amino acid sequences on one hand and the prediction of the spatial structures and their functions on the other. For classification, mainly self-organizing Kohonen networks[3] and multilayer perceptrons[4] are used, which achieve a high precision and accuracy in classification, for example, of amino acid sequences according to their biological function.[5] However, we are still far away from an exact prediction of the tertiary and quaternary structure from amino acid sequences with these systems.[6–8] If such a prediction were possible, new routes for rational protein design through an intermediate synthesis of amino acid sequences entirely based on theoretical considerations and models would be opened. The reliable prediction of secondary structures is an important initial step. Other applications of other types of artificial neural nets in chemistry, for instance for

[*] Priv.-Doz. Dr. P. Wrede, Dipl.-Biochem. G. Schneider
Freie Universität Berlin
FB Physik, AG Biophysik
Arnimallee 14, D-14195 Berlin (FRG)
Telefax: Int. code + (30)838-5186

the processing of spectroscopic data of for the control of chemical processes, were described comprehensively by J. Gasteiger and J. Zupan.[9]

The development of artificial neural nets for the prediction of secondary structures from amino acid sequences was first attempted in 1988 by Qian and Sejnowski and in 1989 by Holley and Karplus.[4, 6, 10] The accuracy of their predictions was 63–64% (α, β, or random structures). This accuracy is also achieved by statistical methods. Now for the first time Burkhard Rost, Reinhard Schneider, and Chris Sander of the European Molecular Biology Laboratory (EMBL) in Heidelberg have reached an accuracy of over 70%[11, 12] in the prediction of secondary structures with neural networks. Also in the context of the Human Genome Project—the sequencing of the human genome—and the successfully completed sequencing of the chromosome III of the yeast *S. cerevisiae*,[13] the development of both existing and new methods for predictive and analytic methods is necessary for a systematic processing of the vast amounts of data. Apart from the potential application for the design of proteins, the EMBL group's distinctly improved prediction of secondary structures with artificial neural nets simply from the knowledge of the amino acid sequences reveals a promising approach for the biocomputing field for the study of the enormous amount of information in sequence data banks.

An artificial neural net for the analysis of the sequence of proteins is a computer program that recognizes patterns and correlations in sequence data. The success of the process depends among other factors upon the ability of the system to separate relevant from irrelevant information by parallel processing.[4, 9] Along the lines of the moving window concept, each new position within the sequence section is examined by the artificial neural net in relation to every other position of the sequence window. An example with a window span of five positions is shown in Figure 1.

The networks used by Rost et al. belong to the type most frequently used for sequence analysis in the class of feedforward nets (Fig. 1). The flow of information is in one direction: from the input to the output layer of the network. This

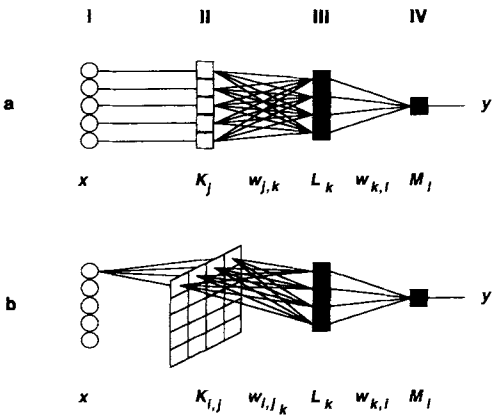

Fig. 1. Model of a general architecture for a three-layered artificial neural network for the analysis of amino acid sequences. The flow of information is in one direction only, from the sequence x (I) to the output unit (IV), which yields the value y, for example, a secondary structural type ("feedforward"). The net's units of the hidden layer (III) enable the calculation of any desired transformation function between an amino acid sequence (I) and the output unit (IV) of the network. An amino acid j is described a) by a binary or a physicochemical parameter K_j (II) or b) by a series of physicochemical properties $K_{i,j}$ (here $i = 1-4$)

is achieved by linking every unit of one layer only with units of the next layer. A significant advantage of this network architecture lies in the ability to approximate any input–output transformation.[14] This means that transformations between amino acid sequences (network input) and their structure or function (network output) can also be calculated. The transformation function $T(x)$ of a sequence pattern x that can be determined by a three-layered net (Fig. 1 a) is given by the number of the net's units (K_j,L_k,M_l) and the connections of the net with assigned weights $w_{j,k}$, $w_{k,l}$ [Eq. (a)]. $S(\mathrm{net_{in}})$ is the "transfer function" of a net unit, given in Equation (b).

$$T(x) = S(\sum_{l} w_{k,l} S(\sum_{j,k} w_{j,k} \xi_j)) \qquad \text{(a)}$$

$$S(\mathrm{net_{in}}) = \frac{1}{1 + e^{-(\tau\, \mathrm{net_{in}} + \sigma)}} \qquad \text{(b)}$$

As a rule a nonlinear sigmoidal function (Fermi function) is chosen; τ determines the steepness of the curve, σ its point of inflection.[9] In Equation (a), ε_j is the representation chosen for the amino acid j, for example, as a twenty-bit binary number (distributed coding, Fig. 1 b) or a set of physicochemical parameters (Fig. 1 b). An advantage of binary coding is that each amino acid can be precisely defined in a technical and complete manner, which is not self-evident for a description of the constitution by physicochemical properties. Nevertheless, relationships and similarities between amino acids can be expressed through their properties, which is particularly advantageous for the study of sequences that have little or no sequence homology in the formal description. The use of a nonlinear transfer function $S(x)$ allows the units also to represent nonlinear relationships between input and output that are often difficult to calculate[9] with statistical procedures, including those of Chou and Fasman.[2]

Therefore, when a description of relationships between sequence and structure or function has been achieved with an artificial neural network, similar structures or functions in new sequences can be predicted exactly. A penetrating, but easily understandable description of the way artificial networks function and their architecture is offered, for instance, by the book of J. Hertz, A. Krogh, and R. G. Palmer.[15]

How does an artificial neural network "learn" the right transformation between sequence and structure or function? To set up the desired transformation function, such as for the prediction of secondary structures, known exemplary sequences must be presented to the network. Such a training set contains sequences with known, experimentally confirmed secondary structures. The parameters of the transformation function of the network, in particular the connection weights, are then changed iteratively by learning and optimization algorithms until the secondary structures of the amino acid sequences predicted by the neural network correspond to the experimentally known data as well as possible. The back-propagation algorithm,[16] a gradient process for multilayer network models, and evolutionary algorithms[17, 18] have proved outstanding as optimization procedures. The evolutionary algorithm is based on a local stochastic search.

Whether a trained network is indeed suitable for general predictions of, for example, secondary structures is determined by giving it one or more test sets. A test set contains

sequences with known structures, like the training set, which were, however, not used in the training phase. A test set is thus a collection of data independent of the training set with which the artificial network's ability to generalize can be tested. This ability, apart from the fundamental question whether the prediction can be performed by the chosen method at all, is also determined by several, mostly empirical parameters, for example by the network architecture, the learning algorithm, the size and number of the net layers, and the suitability of the data representation. A new approach to computer-assisted optimization of these parameters has already been proposed ("structure evolution");[19] however, its applicability in the development of artificial neural networks for sequence analysis remains to be demonstrated.

A suitable representation of the sequence data that enables the general characteristic for the prediction to be found is crucial for the success of the method. On one hand, attention must be given to the representation of the amino acids; on the other hand the selection of the sequences and their grouping into one or more training sets is important.[10, 20, 21] In particular, the latter is apparently extremely important, as Rost and Sander pointed out. They established a series of training sets, each of which contained a number of homologous sequences—in other words, a "protein family". The artificial neural network thus had access in the learning phase to additional information on the evolutionary relationships between the sequences of a protein family and its secondary structures. This procedure was the decisive step that distinctly improved the accuracy of the prediction of secondary structure. The authors recommended it for the development of other predictive systems as well. So besides a suitable method for extraction of the salient characteristics (artificial neural networks), a suitable representation of the data is extremely important for success in the development of predictive systems!

Since the method for secondary structure prediction will be made available to a wide range of users through Electronic Mail at EMBL, the generalizability of the system ("PHD" method i.e., *P*rofile network from *Heid*elberg) can be subjected to a severe test. In addition, detailed instructions can be requested through the "Help" command to the address *PredictProtein@EMBL-Heidelberg.de*.[11, 12]

A criticism of secondary structure prediction itself is its limited implications, even when it is completely correct! The tertiary structure of a protein is the essential factor for the function of proteins, and their prediction lies far in the future. Nevertheless, the application of artificial neural networks point to a promising means to this end, not least because of their simplicity and universal applicability.

German version: *Angew. Chem.* **1993**, *105*, 1192

[1] C. Branden, J. Tooze, *Introduction to Protein Structure*, Garland Publishing, New York, **1991**.
[2] P. Y. Chou, G. D. Fasman, *Biochemistry* **1974**, *13*, 211–222, 222–245.
[3] T. Kohonen, *Self-Organization and Associative Memory*, Springer, Berlin, **1989**.
[4] J. D. Hirst, M. J. E. Sternberg, *Biochemistry* **1992**, *31*, 7211–7218.
[5] C. Wu, G. Whitson, J. McLarty, A. Ermongkonchai, T. C. Chang, *Protein Sci.* **1992**, *1*, 667–677.
[6] L. H. Holley, M. Karplus, *Proc. Natl. Acad. Sci. USA* **1989**, *86*, 152–156.
[7] H. Bohr, J. Bohr, S. Brunak, R. M. J. Cotterill, B. Lautrup, L. Norskov, O. H. Olsen, S. B. Petersen, *FEBS Lett.* **1988**, *241*, 223–228.
[8] H. Bohr, J. Bohr, S. Brunak, R. M. J. Cotterill, H. Fredholm, B. Lautrup, S. B. Petersen, *FEBS Lett.* **1990**, *261*, 43–46.
[9] J. Gasteiger, J. Zupan, *Angew. Chem.* **1993**, *105*, 510–536; *Angew. Chem. Int. Ed. Engl.* **1993**, *32*, 503–527.
[10] N. Quian, T. J. Sejnowski, *J. Mol. Biol.* **1988**, *202*, 865–884.
[11] B. Rost, C. Sander, *Nature* **1992**, *360*, 540.
[12] B. Rost, R. Schneider, C. Sander, *Trends Biochem. Sci.* **1993**, *18*, 120–123.
[13] S. G. Oliver et al., *Nature* **1992**, *357*, 38–46.
[14] K. Hornik, M. Stinchcombe, H. White, *Neural Networks* **1989**, *2*, 359–366.
[15] J. Hertz, A. Krogh, R. G. Palmer, *Introduction to the Theory of Neural Computation*, Addison-Wesley, Redwood City, CA, USA, **1991**.
[16] D. E. Rumelhart, G. E. Hinton, R. J. Williams, *Nature* **1986**, *323*, 533–536.
[17] I. Rechenberg, *Evolutionsstrategie – Optimierung technischer Systeme nach Prinzipien der biologischen Evolution*, Frommann-Holzboog, Stuttgart, **1973**.
[18] D. E. Goldberg, *Genetic Algorithms in Search, Optimization and Machine Learning*, Addison-Wesley, Reading, MA, USA, **1989**.
[19] R. Lohmann, *Structure Evolution* in *Dynamic, Genetic and Chaotic Programming* (Eds.: B. Suocek & The IRIS Group), Wiley, New York, **1992**, pp. 395–411.
[20] G. Schneider, P. Wrede, *Endocytobiosis Cell Res.* **1992**, *9*, 1–12.
[21] G. Schneider, P. Wrede, *J. Mol. Evol.* **1993**, *36*, 586–595.

Metal-Mediated Oxyfunctionalization of Organic Substrates by Organometallic Intermediates—More Recent Developments and Perspectives

By *Jörg Sundermeyer**

The complex-catalyzed oxyfunctionalization of organic substrates is of fundamental importance, for example in chemical processes of Nature, in the synthesis of fine chemicals, and in the production of commodity chemicals.[1] Regardless of the results achieved in this interdisciplinary area of research, there is still a great lack of experimental evidence that could help to settle very controversial debate[2] about the mechanism of the metal-mediated C–O bond formation. The catalytically active complexes are usually differentiated on the basis of their mechanisms.[1e] Thus, there is a group of metal complexes that catalyzes the homolytic cleavage of the O–O bond of peroxides and triplet oxygen, a second group that induces its heterolytic cleavage, and a third that has at its disposal polarizable and transferable oxo functions such as $M-O^{\delta-}$, M=O, and $M\equiv O^{\delta+}$. The first group includes low- and high-spin complexes of Fe, Co, Ni, Mn, Cu, and other biologically relevant metals, which, for example, control the radical chain initiations as well as the propagation and inhibition of autoxidation reactions. In contrast, d^0 complexes of the second category (e.g. those of Ti, V, Mo, W, and Re) are diamagnetic and strong Lewis acids. These compounds activate H_2O_2 or alkyl hydroperoxides by formation of reactive d-block metal peracids [M–OOH], peroxides [$M(\eta^2\text{-}O_2)$], or peracid esters [M–OOR], that is, they polarize the O–O bond for nucleophilic attack of the substrate at the peroxidic oxygen atom. In contrast, electron-rich transition metals (Rh, Ir, Pd, Pt) cause an inverse polarization, which makes an electrophilic attack at the peroxy function more favorable. The group of reactive oxo complexes includes, for example, $[MnO_4]^-$, RuO_4, and OsO_4, well-established for hydroxylations.

Not so long ago the suggestion that organometallic intermediates might participate in polar oxygen-transfer reactions would have been refuted and considered as unrealistic. The knowledge accumulated over the last few years about oxo and peroxo complexes functionalized with organometallic groups demonstratrates that, in particular, the relatively nonpolar M–C bonds in complexes of molybdenum(VI), tungsten(VI), and rhenium(VII) can be stable under catalytic conditions (protic medium, hydroperoxides, O_2), and that they are sometimes essential for the activity and lifetime of a catalyst. In this respect the results of Herrmann et al. should be considered a breakthrough.[3] They have succeeded in bridging the gap between the Mimoun reagents of the type **1** (L = HMPA, DMF, etc.)[4] well established for epoxidations, and the classic Milas reagent $OsO_4/H_2O_2/t$BuOH[5] for the catalytic *syn* hydroxylation of olefins. The isolation and complete characterization of the catalytically active species **2**, R = CH_3,[3b] in the catalyst system $[ReO_3R]/H_2O_2/t$BuOH is worthy of note and stimulates comment.

Compounds **1** and **2** have the same pentagonal-bipyramidal molecular structure;[3b,4c] however, the equatorial [d^0-Mo-L] building block in **1** is replaced by the isoelectronic [d^0-Re-R] fragment in **2**. The symmetry and relative arrangement of all frontier orbitals[1b] are similar in the two compounds. This relationship between **1** and **2** is reflected in the similar reactivity of the two compounds, particularly in the *anti* hydroxylation of alkenes by means of the opening of epoxides formed as intermediates, and in the Baeyer–Villiger oxidation of ketones. However, it is already apparent that the Herrmann reagent excels as a result of higher reactivity (oxyfunctionalization of certain alkynes, similar as OsO_4[5d]) and high catalytic activity, whereas the readily prepared Mimoun reagent has proved successful primarily for stoichiometric reactions.[2a,4]

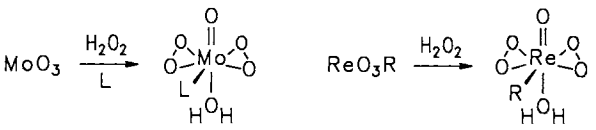

Why has it taken so long for the quality of oxo complexes of rhenium for catalytic oxygen-transfer reactions to be recognized and proven? As strange as it may sound, the key to success with **2** lies in its organometallic functionality. More polar Re–X groups (X = OR, NR_2, Cl, etc.) are generally more rapidly protolyzed to give catalytically inactive compounds than the relatively nonpolar Re–R unit in **2**, which is stable under catalytic conditions (weakly acidic, protic medium). From the Brønsted acidities of $[ReO(O_2)_2(CH_3)(H_2O)]$ (pK_s = 3.8) and $[ReO_3(CH_3)(H_2O)]$ (pK_s = 7.5) it can be concluded indirectly that the σ,π donor ability of an oxo ligand O^{2-} is significantly higher than that of a peroxo ligand O_2^{2-}, and that consequently the catalytically active species **2** is more Lewis acidic than its catalytically inactive monoperoxo precursor $[ReO_2(O_2)(CH_3)(H_2O)]$. Thus, not a low coordination number, but the π acidity of the d^0 metal center appears to be decisive for the catalytic activity of a peroxo complex. A molecular catalyst design based on adjustable ligand parameters from compounds of the type $[ReO(O_2)_2(R)(L)]$ has therefore moved within reach. We can eagerly await the catalytic efficiency of polymer-bound alkylrhenium peroxides.

Other organometallic compounds have also proven their value as precursors for catalysts in the activation of hydroperoxides. For example, Trost and Bergman have reported[6] that the molybdenum complex **3** catalyzes the epoxidation of olefins by alkyl hydroperoxides ROOH. In sharp contrast to **2**, **3** is not capable of activating H_2O_2, conversely **2** cannot activate alkyl hydroperoxides. The catalytically active species in the ROOH/**3**/olefin system has not been characterized unambiguously as yet; the authors report, however, that the surprisingly catalytic, inactive peroxo complex **4** forms from **3** and ROOH or H_2O_2 in a *deactivating* side reaction. Complexes with a $[(\eta^5\text{-}C_5Me_5)Mo(\eta^2\text{-}OOR)]$

[*] Dr. J. Sundermeyer
Institut für Anorganische Chemie der Universität
Am Hubland, D-97074 Würzburg (FRG)
Telefax: Int. code + (931)888-4605

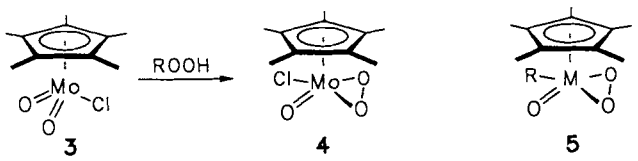

building block could be considered as a plausible organometallic intermediate for the oxygen-transfer step.

The stability of M–C bonds in the presence of hydroperoxides could also be confirmed for the structurally related alkyl complexes **5** (M = Mo, W; R = CH_3, CH_2SiMe_3).[7] An intramolecular [1,2] shift of the alkyl groups to one of the peroxidic oxygen atoms (similar to that which occurs in the tantalocene complexes, for example **6**, investigated in detail by Bercaw et al.[8a]) does not appear to be a preferred reaction pathway in analogous complexes of Mo, W, and Re. However, Bercaw et al. were able to show that the rearrangement of **6** into the alkoxy complex **7** does not take place either spontaneously or according to a first-order rate law, but is initiated by the attack of an electrophile (e.g. H^+) at the peroxo group.[8b]

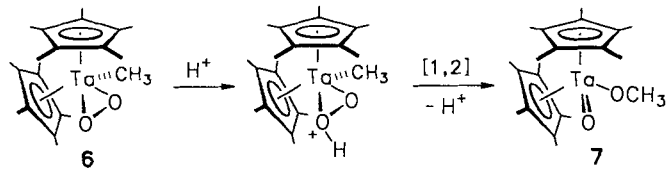

In spite of intensive efforts the knowledge accumulated to date about polar oxygen-transfer reactions on peroxo, hydroperoxo, and alkylperoxo complexes is not yet sufficient to decide whether to agree with the direct attack of the olefin at the positively polarized oxygen center[9] ("butterfly mechanism" without an organometallic intermediate, step A in Scheme 1) discussed by Chong and Sharpless, or with the

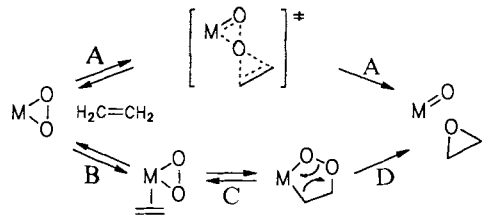

Scheme 1. Mechanistic alternatives for polar oxygen-transfer reactions of peroxo complexes.

mechanism postulated by Mimoun based on an olefin coordination, followed by a 1,3-dipolar cycloinsertion with the formation of a metalladioxacyclopentane and its cycloreversion (steps B–D in Scheme 1).[2a] The question of whether the metal center adopts only the activating role of a π-acidic substituent, analogous to that of a −I,−M substituent in percarboxylic acids or persulfonic acids, or whether in an equilibrium on account of unoccupied metal acceptor orbitals it forms weak π interactions[10] with the olefin to be oxidized, remains unanswered for the moment.

How easily well-established mechanistic ideas about the metal-mediated oxyfunctionalization of organic substrates can begin to falter is also illustrated by a very recent kinetic study by Göbel and Sharpless on the influence of the reaction temperature on the enantioselectivity of the asymmetric *syn* hydroxylation of olefins with chirally modified alkaloid–OsO_4 complexes.[11a] The Eyring plots for several olefin/alkaloid combinations provide clear indications of a multistep mechanism with at least two diastereoselective steps. Thus, a concerted mechanism (step A in Scheme 2) in the form of a 1,3-dipolar cycloaddition of the OsO_4 to the olefin can be ruled out, a fact which can be considered as evidence for but not proof of the two diastereomeric metallaoxetanes discussed as intermediates by Sharpless (step B in Scheme 2)[11b] and their diastereoselective [1,2] rearrangement into the glycolate complexes **8** (step C in Scheme 2). As for the

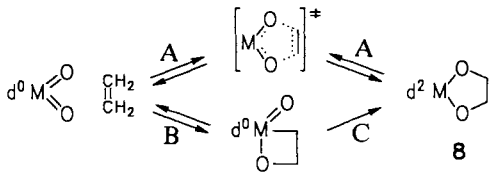

Scheme 2. Mechanistic alternatives for *syn* hydroxylations of olefins with OsO_4 complexes.

examples mentioned in Scheme 1, it is also shown here that the characterization of intermediate products on the reaction coordinate, even in matrix studies, is the safest way to remove doubts concerning the participation of organometallic intermediates.

The formation of the irida(III)oxetane **10** may serve as a model reaction for the metal-mediated transfer of oxygen to a coordinated olefin; the formation is explained by autoxidation of the iridium(I) cyclooctadiene complex **9** via the plausible dinuclear oxoiridium(III) intermediate.[12]

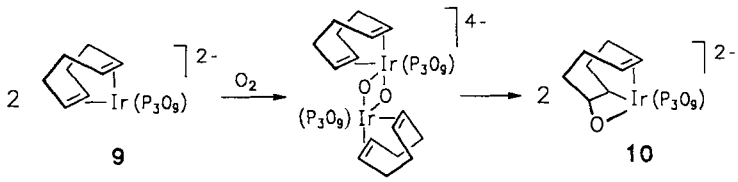

Closely related with steps B and C in Scheme 2 is also the [2 + 2] cycloaddition of ethylene to the neopentylidene function of [Re(C*t*Bu)(CH*t*Bu)(O*t*Bu)$_2$], followed by [1,2] rearrangement of the d^0-rhenacyclobutane intermediate into a d^2-rhenacyclopentene, recently described by Schrock et al.[13]

Many unanswered questions remain as a challenge to the researchers in this field, for example, the indisputable proof for a [2 + 2] cycloaddition of an olefin to an M=O group, proof of possible π interactions of olefins with the d^0 metal center of oxo and peroxo complexes and the existence of d^0-peroxymetallacycles (Scheme 1), and unequivocal evidence for a [1,2] shift of a metal-bound organic group R to a geminal oxo function (step C in Scheme 2) with reduction of the metal center.

German version: *Angew. Chem.* **1993**, *105*, 1195

[1] See also the Highlight from C. Bolm, *Angew. Chem.* **1991**, *103*, 414–415; *Angew. Chem. Int. Ed. Engl.* **1991**, *30*, 403–404; Reviews: a) R. H. Holm, *Chem. Rev.* **1987**, *87*, 1401–1449, b) K. A. Jørgensen, *ibid.* **1989**, *89*, 431–458; c) B. Meunier, *ibid.* **1992**, *92*, 1411–1456; d) H. Mimoun in *Comprehensive Coordination Chemistry, Vol. 6*, (Eds.: G. Wilkinson, R. D. Gillard, J. A. McCleverty), Pergamon, Oxford, **1987**, p. 317–410; e) R. A. Sheldon, J. K. Kochi; *Metal-Catalyzed Oxidation of Organic Compounds*, Plenum, New York, **1981**.

[2] a) H. Mimoun, *Angew. Chem.* **1982**, *94*, 750–766; *Angew. Chem. Int. Ed. Engl.* **1982**, *21*, 734–750; b) K. A. Jørgensen, B. Schiøtt, *Chem. Rev.* **1990**, *90*, 1483–1506.

[3] a) W. A. Herrmann, R. W. Fischer, D. W. Marz, *Angew. Chem.* **1991**, *103*, 1706–1709; *Angew. Chem. Int. Ed. Engl.* **1991**, *30*, 1638–1641; b) W. A. Herrmann, R. W. Fischer, W. Scherer, M. U. Rauch, *ibid.* **1993**, *105*, 1209–1212 and **1993**, *32*, 1157–1160.

[4] a) H. Mimoun, I. Seree de Roch, L. Sajus, *Bull. Soc. Chim.* **1969**, 1481–1492; b) *Tetrahedron* **1970**, *26*, 37–50; c) P. J.-M. Le Carpentier, R. Schlupp, R. Weiss, *Acta Crystallogr. Sect. B* **1972**, *28*, 1278–1288; d) Ref. [1e], p. 93f.

[5] N. A. Milas, S. Sussman, *J. Am. Chem. Soc.* **1936**, *58*, 1302–1304; *ibid.* **1937**, *59*, 2345–2347; b) N. A. Milas, S. Sussman, H. S. Mason, *ibid.* **1939**, *61*, 1844–1847; c) R. Criegee, *Angew. Chem.* **1937**, *50*, 153–155; *ibid.* **1938**, *51*, 519–520; d) Review: M. Schröder, *Chem. Rev.* **1980**, *80*, 187–213.

[6] M. K. Trost, R. G. Bergman, *Organometallics* **1991**, *10*, 1172–1178.

[7] a) P. Legzdins, E. C. Phillips, S. J. Rettig, L. Sánchez, J. Trotter, V. C. Yee, *Organometallics* **1988**, *7*, 1877–1878; b) P. Legzdins, E. C. Phillips, L. Sánchez, *ibid.* **1989**, *8*, 940–949; c) J. W. Faller, Y. Ma, *ibid.* **1988**, *7*, 559–561; d) *Organomet. Chem.* **1989**, *368*, 45–56; e) G. Parkin, J. E. Bercaw, *Polyhedron* **1988**, *7*, 2053–2082.

[8] a) A. van Asselt, M. S. Trimmer, L. M. Henling, J. E. Bercaw, *J. Am. Chem. Soc.* **1988**, *110*, 8254-8255; b) Protonation results in an additional increase of the polarity of the O–O bond.

[9] A. O. Chong, K. B. Sharpless, *J. Org. Chem.* **1977**, *42*, 1587-1590; for η^2-alkyl peroxides both reaction pathways can also be formulated.

[10] $p_\pi \rightarrow d_\pi$ Charge transfer interactions between ligand and metal center in d^0 electron configuration, without participation of metal $d\pi \rightarrow p\pi$ backbonding; spectroscopic indications: W. A. Nugent, *J. Org. Chem.* **1980**, *45*, 4533–4534.

[11] a) T. Göbel, K. B. Sharpless, *Angew. Chem.* **1993**, *105*, no. 9; *Angew. Chem. Int. Ed. Engl.* **1993**, *32*, no. 9; b) K. B. Sharpless, A. Y. Teranishi, J.-E. Bäckvall, *J. Am. Chem. Soc.* **1977**, *99*, 3120–3128.

[12] V. W. Day, W. G. Klemperer, S. P. Lockledge, D. J. Maine, *J. Am. Chem. Soc.* **1990**, *112*, 2031–2033.

[13] G. A. Vaughan, R. Toreki, R. R. Schrock, W. M. Davis, *J. Am. Chem. Soc.* **1993**, *115*, 2980–2981.

Communications may be submitted in English *or* in German. Further details regarding the submission of communications can be found in the "Notice to Authors" reproduced in the January issue of the journal. Copies thereof may be obtained from the editorial office upon request.

Separation of the Enantiomers of 2,2′-Dihydroxy-1,1′-binaphthyl and 10,10′-Dihydroxy-9,9′-biphenanthryl by Complexation with *N*-Alkylcinchonidinium Halides**

By *Koichi Tanaka, Toru Okada*, and *Fumio Toda**

The enantiomers of 2,2′-dihydroxy-1,1′-binaphthyl **1** are important C_2 symmetrical, chiral compounds, whose use is not only limited to asymmetric syntheses.[1] They are also used for the separation of racemates by the formation of inclusion complexes[2] and as chiral shift reagents.[3] The enantiomers of 10,10′-dihydroxy-9,9′-biphenanthryl **3** are also important chiral host compounds.[4]

Several methods for the separation of the enantiomers of **1**[5, 6] and **3**[6] have been reported. One of the most effective of these methods is the formation of inclusion complexes with optically active (*R,R*)-(+)-2,3-dimethoxy-*N,N,N′,N′*-tetramethylsuccinamide (**4**) and (*R,R*)-(+)-*N,N,N′,N′*-tetramethyl-2,2-dimethyl-1,3-dioxolane-*trans*-4,5-dicarboxamide (**5**), respectively.[6] One disadvantage of this method, however, is that the amide host compounds (**4** and **5**)[7] are not commerically available, and must be synthesized from tartaric acid prior to the resolution experiment.

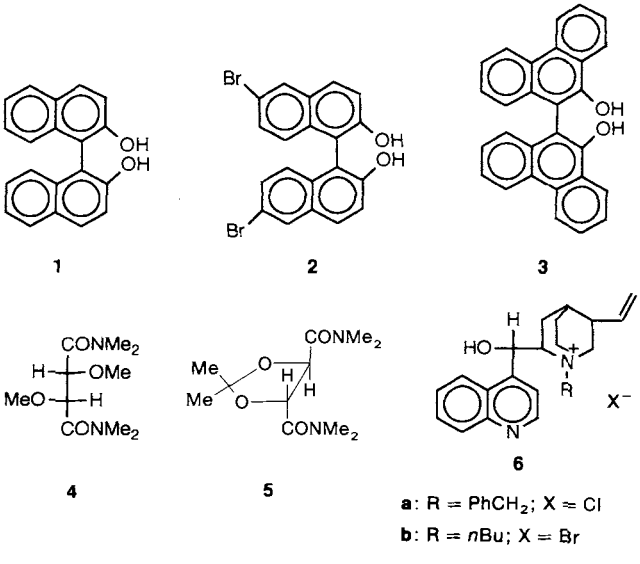

1 **2** **3**

4 **5**

6

a: R = $PhCH_2$; X = Cl

b: R = *n*Bu; X = Br

Recently we have found that commercially available *N*-alkylcinchonidinium halides (**6**) are very effective for the resolution of **1**, the 6,6′-dibromo derivative **2**, and the biphenanthryldiol **3** by the formation of inclusion complexes. For example, when a solution of *N*-benzylcinchonidinium chloride (**6a**)[8] (0.74 g, 1.76 mmol) and *rac*-**1** (1 g, 3.5 mmol) in MeOH (20 mL) was kept at room temperature for 6 h, a 1:1 inclusion complex of **6a** and (+)-**1** was obtained, which precipitated as colorless prisms (0.89 g, 72% yield, m.p. 240–244 °C). The 1:1 complex was decomposed with dilute HCl. Subsequent extraction with AcOEt, followed by evaporation of the solvent gave (+)-**1** (95% *ee*; 0.35 g, 70% yield, $[\alpha]_D = +31.5$ ($c = 1.0$, THF)). Recrystallization of the crude product from MeOH gave (+)-**1** (100% *ee*; 0.3 g, 60% yield, $[\alpha]_D = +33.2$ ($c = 1.0$, THF)). The filtrate left after separation of the complex of **6a** and (+)-**1** was treated with dilute HCl to give (−)-**1** (42% *ee*; 0.62 g, 124% yield, $[\alpha]_D = -13.9$ ($c = 1.0$, THF)). This method is also effective for the separation of the enantiomers of **2**. In this case when a solution of **6a** (0.95 g, 2.26 mmol) and *rac*-**2**[9] (2 g, 4.5 mmol) in MeOH (2 mL)/AcOEt (10 mL) was kept at room temperature for 6 h, a 1:1 inclusion complex of **6a** and (−)-**2** was obtained, which precipitated in the form of colorless prisms (1.7 g, 89% yield, m.p. 229–232 °C). Decomposition of the complex with dilute HCl gave (−)-**2** (99% *ee*; 0.82 g, 82% yield, $[\alpha]_D = -51.0$ ($c = 0.9$, THF)). From the filtrate left after the separation of the inclusion complex, (+)-**2** (79% *ee*; 1.1 g, 110% yield, $[\alpha]_D = +40.7$ ($c = 1.0$, THF)) was isolated by treatment with dilute HCl. The enantiomeric purities of **1** and **2** were determined by HPLC by using a column containing an optically active solid phase, Chiralpak AS,[10] and hexane/EtOH (95:5) as an eluent.

Interestingly, however, **6a** was not suitable for the separation of the enantiomers of **3**, because **6a** does not form an inclusion complex with **3**. In contrast this separation was achieved by the use of *N*-butylcinchonidinium bromide (**6b**).[11] For example, when a solution of **6b** (0.14 g, 0.33 mmol) and *rac*-**3** (0.25 g, 0.65 mmol) in MeCN (10 mL) was kept at room temperature for 24 h, a 1:1 inclusion complex of **6b** and (+)-**3** was obtained, which precipitated as colorless prisms (0.22 g, 83% yield, m.p. 168–169 °C). Decomposition of the complex with dilute HCl gave (+)-**3** (100% *ee*; 0.1 g, 80% yield, $[\alpha]_D = +58$ ($c = 1.0$, $CHCl_3$)). From the filtrate left after the separation of the inclusion complex, (−)-**3** (58% *ee*; 0.15 g, 80% yield, $[\alpha]_D = -35$ ($c = 1.5$, $CHCl_3$)) was isolated by treatment with dilute HCl. The enantiomeric purity of **3** was determined by HPLC by using a column containing an optically active solid phase, Chiralcel OC,[10] and hexane/*i*PrOH (90:10) as an eluent. The cinchonidinium salt **6b**, however, does not form inclusion complexes with **1** or **2**. It is interesting that the inclusion behavior of the cinchonidinium derivatives **6** varies dramatically depending on the alkyl substituent at the bridgehead N atom of these compounds. This might be due to a kind of molecular recognition in the inclusion crystal.

Previously we have shown that **1** forms crystalline inclusion complexes with the alkali metal hydroxides LiOH, NaOH, KOH, and CsOH, and that these hydroxides can be isolated from aqueous solution by using the complex formation with **1**.[12] The presence of strong hydrogen bonds between the OH groups of **1** and the HO^- ions of the alkali

[*] Prof. F. Toda, Associate Prof. K. Tanaka, T. Okada
Department of Applied Chemistry, Faculty of Engineering
Ehime University, Matsuyama, Ehime 790 (Japan)
Telefax: Int. code + (899) 230672

[**] This work was supported by the Japanese Ministry of Education, Science, and Culture (Grant-in-Aid for Scientific Research (B), no. 04453102).

metal hydroxide in these complexes has been observed by the measurement of the IR spectra. Hydrogen bonds are also formed between the OH groups of **1**, **2**, and **3** and the halogen counterions of **6**. This was clarified by X-ray structure analyses of the corresponding inclusion complexes.[13] The X-ray crystal structures of these complexes will be reported in detail in the future.

Noteworthy is the very efficient chiral recognition in the formation of inclusion complexes of **6** with C_2 symmetrical chiral biaryldiol derivatives such as **1**, **2**, or **3**. They are particularly useful for the separation of the enantiomers of biaryldiols. It is also interesting that the behavior of the cinchonidine derivatives **6** is completely different from that of cinchonidine itself; the latter does not form inclusion complexes with **1**, **2**, or **3**.[14] These findings may be applicable to other combinations of salts of alkaloids or simple chiral alkylamines with biaryldiol derivatives.

Received: March 12, 1993 [Z 5913 IE]
German version: *Angew. Chem.* **1993**, *105*, 1266

[1] R. Noyori, I. Tomino, Y. Tanimoto, M. Nishizawa, *J. Am. Chem. Soc.* **1984**, *106*, 6709; D. Seebach, A. K. Beck, S. Roggo, A. Wonnacott, *Chem. Ber.* **1985**, *118*, 3673; B. M. Trost, D. J. Murphy, *Organometallics* **1985**, *4*, 1143; J.-T. Wang, X. Fan, X. Feng, Y.-M. Qian, *Synthesis* **1989**, 291.
[2] F. Toda, K. Mori, Z. Stein, I. Goldberg, *Tetrahedron Lett.* **1989**, *30*, 1841; K. Mori, F. Toda, *Bull. Chem. Soc. Jpn.* **1990**, *63*, 2127; F. Toda, K. Mori, *J. Chem. Soc. Chem. Commun.* **1986**, 1059; F. Toda, K. Mori, *ibid.* **1986**, 1357; F. Toda, K. Mori, Z. Stein, I. Goldberg, *J. Org. Chem.* **1988**, *53*, 308.
[3] F. Toda, K. Mori, J. Okada, *Chem. Lett.* **1988**, 131.
[4] F. Toda, K. Tanaka, *Tetrahedron Lett.* **1988**, *29*, 1807; F. Toda, K. Tanaka, *J. Org. Chem.* **1991**, *56*, 7332; G.-H. Lee, Y. Wang, K.Tanaka, F. Toda, *Chem. Lett.* **1988**, 781.
[5] J. Brussee, J. L. G. Groenedijk, J. M. te Koppele, A. C. A. Jansen, *Tetrahedron* **1985**, *41*, 3313; S. Miyano, K. Kawahara, Y. Inoue, H. Hashimoto, *Chem. Lett.* **1987**, 355; M. Kawashima, A. Hirayama, *ibid.* **1990**, 2299.
[6] F. Toda, K.Tanaka, *J. Org. Chem.* **1988**, *53*, 3607; F. Toda, K. Tanaka, L. R. Nassimbeni, M. Niven, *Chem. Lett.* **1988**, 1371.
[7] D. Seebach, H.-O. Kalinowskyi, B. Bastani, G. Crass, H. Daum, H. Dörr, N. P. DuPreez, V. Ehrig, W. Langer, C. Nüssler, H.-A. Oei, M. Schmidt, *Helv. Chim. Acta* **1977**, *60*, 301.
[8] S. Colonna, A. Re, H. Wynberg, *J. Chem. Soc. Perkin Trans. 1* **1981**, 547.
[9] M. Vondenhof, J. Mattay, *Tetrahedron Lett.* **1990**, *31*, 985.
[10] Chiralpak AS and Chiralcel OC are available from Daicel Chemical Industries, Ltd., Himeji (Japan).
[11] S. Julia, A. Ginebreda, J. Guixer, J. Masana, A. Tomas, S. Colonna, *J. Chem. Soc. Perkin Trans. 1* **1981**, 574.
[12] F. Toda, K. Tanaka, M. C. Wong, T. C. W. Mak, *Chem. Lett.* **1987**, 2069.
[13] F. Toda, K. Tanaka, I. Goldberg, unpublished results.
[14] However, quinine itself forms an inclusion complex with the 7,7'-bis(benzyloxy) derivative of **1**: P. P. Castro, T. M. Georgiadis, F. Diederich, *J. Org. Chem.* **1989**, *54*, 5835.

Porphyrins with Aromatic 26π-Electron Systems**

By *Thomas Wessel, Burchard Franck,* Manfred Möller,* Ute Rodewald,* and *Mechthild Läge*

In memory of Franz Sondheimer

With the synthesis of the aromatic [18]annulene **1a**, the hexavinylogous benzene, Sondheimer[1] achieved a major breakthrough: he provided valuable experimental evidence in support of the wide-reaching validity of the $(4n + 2)$ rule for aromatic π-electron systems.[2] Moreover, in agreement with HMO calculations,[3] it has been determined that also [22]annulene **1b** shows aromaticity at low temperatures, whereas resonance stabilization in [26]annulene **1c** is no longer[4] sufficient to stabilize the molecule in a planar conformation with aromatic properties.

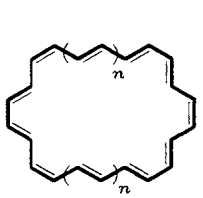

1a: $n = 0$ (18π)
1b: $n = 1$ (22π)
1c: $n = 2$ (26π)

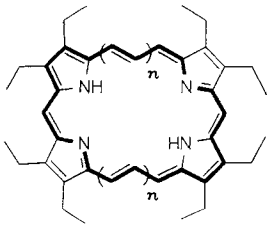

2a: $n = 0$ (18π)
2b: $n = 1$ (22π)
2c: $n = 2$ (26π)

We report here on the synthesis of [26]porphyrin **2c**, its crystal structure, its diatropicity, and initial investigations on electrophilic substitution. Thus it has been demonstrated that this cyclic, conjugated system with 26 π electrons is aromatic. Furthermore, the phenyl- and alkyl-substituted [26]porphyrins **8a** and **8b**, respectively, and a [26]azaporphyrin **9** were synthesized.

We recently described the synthesis of stable, aromatic [22]porphyrins, for example, **2b** with 22 π-electron perimeters;[5, 6] like the parent porphyrin **2a**, **2b** is a bisazaannulene. The pyrrole units situated at the corners stabilize the planar conformation without impairing the annulenoid conjugation, by the formation of individual π-electron sextets. Octaethyl[18]porphyrin **2a** prepared by Hans Fischer et al.[7] developed into the most frequently used porphyrin. In a similar way the bis- and tetravinylogues **2a** and **2c**, respectively, may find manifold applications.

Our synthesis of [26]porphyrin **3**[11] had helped to clarify whether the $(4n + 2)$ rule no longer applies to [26]annulene **1c** in general or only to annulene-type conjugated cyclic systems. Like compound **4**,[12] described almost at the same time by LeGoff et al., significant diamagnetic ring current effects in the ^{1}H NMR spectrum demonstrated that this system is aromatic. Furthermore, diatropic 26 π-electron systems have been described in which the annulene perimeter is planar, stabilized by six pyrrole units,[13, 14] or by allene and ethyne groups (dehydroannulenes).[15] In one case, a crystal structure analysis was carried out for a corrinoid hexapyrrole.[14]

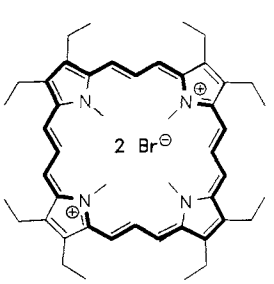

3

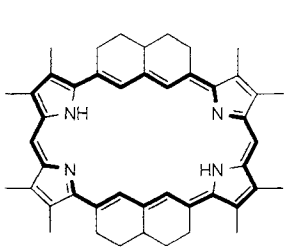

4

[*] Prof. Dr. B. Franck, Dr. T. Wessel
Organisch-chemisches Institut der Universität
Orléansring 23, D-48149 Münster (FRG)
Telefax: Int. code + (251)839-772
Dr. M. Möller, Dipl.-Ing. U. Rodewald, M. Läge
Anorganisch-chemisches Institut der Universität Münster (FRG)

[**] Novel porphyrinoids, Part 12. This work was supported by the Deutsche Forschungsgemeinschaft, the Fonds der Chemischen Industrie, and BASF AG (Ludwigshafen). Part 11: [5].

Analogous to the synthesis of the 22π compound **2b**,[6] for the octaethyl[26]porphyrin **2c**, a buildup by the "biladiene synthesis path" was considered, because it allows the simultaneous preparation of *meso*-substituted derivatives and a 14-aza[26]porphyrin (Scheme 1). However, it seemed doubtful whether the required, still unknown open-chain tetrapyrrole **7** with two heptavinylogous amidine systems was sufficiently stable. The condensation of **7** required that this compound although being a dication in acidic condensation medium can adopt the "hairpin" conformation.

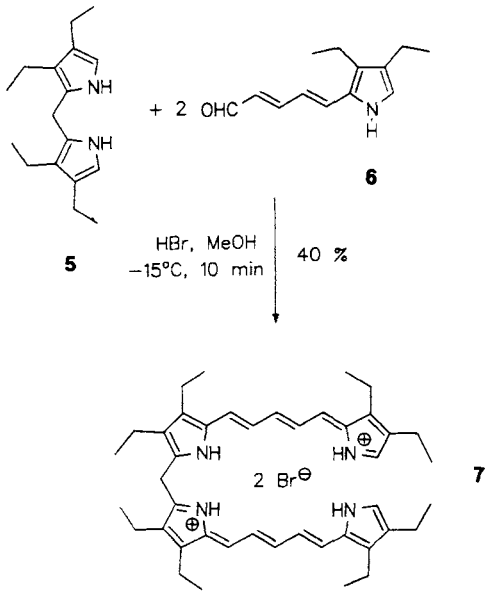

Scheme 1. Synthesis of tetravinylogous biladiene **7**.

After intensive examination of alternative routes for the construction of **7**, its synthesis was achieved by condensation of dipyrrylmethane **5**[16] with the bisvinylogous pyrrole aldehyde **6**[17] in 40% yield. The bisvinylogous Vilsmeier formylation[17] of 3,4-diethylpyrrole with dimethylaminopentadienal proved to be suitable for the synthesis of **6**. Acid-catalyzed condensation of the open-chain tetrapyrrole **7** with formaldehyde/HBr and in situ dehydrogenation of the hydroporphyrinoid intermediate with DDQ (2,3-dichloro-5,6-dicyano-1,4-benzoquinone) gave the [26]porphyrin **2c** (red-violet in solution) in 43% yield (Scheme 2). Analogously, cyclization of **7** with benzaldehyde or propionaldehyde gave the 14-phenyl derivative **8a** and the 14-ethyl derivative **8b**, respectively. By reaction with ammonia and subsequent dehydrogenation, **7** could be converted into the 14-aza[26]porphyrin **9**. The spectroscopic data for these compounds are summarized in Table 1.

Experience has shown[6] that, because of its ethyl side chains, **2c** provides good preconditions for obtaining suitable single crystals for crystal structure analysis (Fig. 1). Crystallization from dichloromethane/trifluoroacetic acid (TFA) (20:1) gave the bistrifluoroacetate of **2c** as green, metallic, shiny cubic crystals. Measurements on this system, which had to be carried out at 170 K in order to fix the conformation of the [26]porphyrin dication, produced an unusual result. For example, the unit cell contains two different conformers of $\mathbf{2c}^{2+}$ in a ratio of 2:1. Two molecules occur—as regards the arrangement of their ethyl groups towards the ring plane—in an all-*trans* conformation with pseudo-C_2 symmetry. In this conformation, the ethyl side

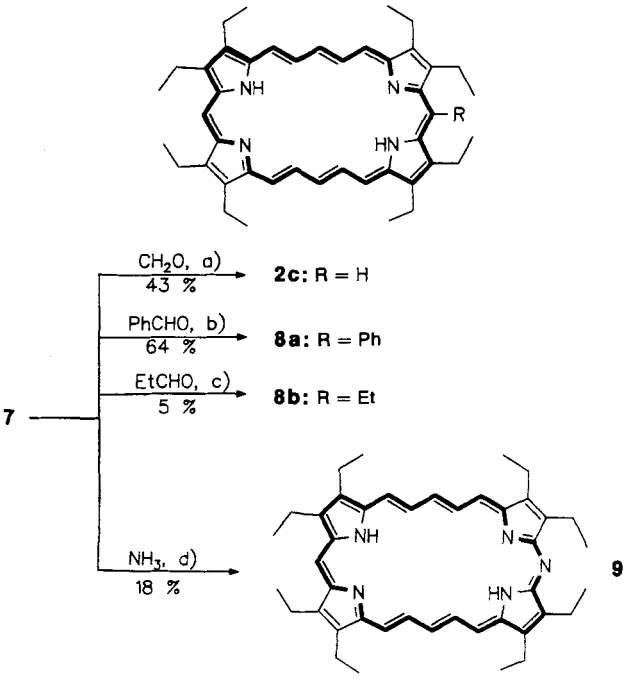

Scheme 2. Synthesis of octaethyl[26]porphyrin **2c**, its 14-phenyl and 14-ethyl derivatives **8a** and **8b**, respectively, and its 14-aza derivative **9**. Reaction conditions: a) aqueous CH_2O, MeOH, HBr, 20 min reflux, then DDQ/CH_2Cl_2, 20 °C, 1.5 h; b) PhCHO, MeOH, HBr, 20 °C, 48 h (without DDQ); c) EtCHO, MeOH, HBr, 20 °C, 48 h (without DDQ); d) NH_3, MeOH, 10 min at 20 °C, then DDQ 1 h at 20 °C.

Table 1. Analytical data of **2c**, **8a**, **8b**, **9**, and **7** (without ^{1}H NMR signals of CH_2CH_3 groups; the new compounds have been completely characterized by elemental analyses and spectra).

2c: ^{1}H NMR (300 MHz, [D$_6$]DMSO/[D$_1$]TFA, TMS): $\delta = -9.79$ (t, $J = 13.8$ Hz, 4H, CHC*H*CHC*H*CH), −5.77 (br. s, NH), 12.26 (s, 2H, monomethine bridges CH), 13.51 (d, $J = 13.8$ Hz, 4H, C*H*CHCHCHC*H*), 14.35 (t, $J = 7.4$ Hz, 2H, CHCHC*H*CHCH); IR (KBr): $\tilde{\nu}$[cm^{-1}] = 2980, 2920, 2910 (CH), 1590 (conj. C = C); UV/VIS (CH_2Cl_2): λ_{max} [nm] (lgε) = 507 (5.44), 528 (5.23), 553 (4.93), 663 (4.39); UV/VIS (CH_2Cl_2 + 1% TFA): λ_{max} [nm] (lgε) = 512 (5.84), 694 (4.61); high-resolution MS: $C_{44}H_{54}N_4$: calcd. 638.4348, found 638.4362; correct C,H,N analysis.

8a: ^{1}H NMR (300 MHz, [D$_6$]*DMSO*/[D$_1$]*TFA, TMS*): $\delta = -7.95$ (m, 4H, CHC*H*CHC*H*CH), −4.27 (br. s, NH), −3.03 (br. s, NH), 8.17 (m, 3H, *m*- and *p*-Ph-H), 8.89 (d, $J = 7.1$ Hz, 2H, *o*-Ph-H), 11.39 (s, 1H, monomethine bridges CH), 12.68, 12.73 (2d, $J = 15.2$ Hz, each 2H, C*H*CHCHCHC*H*), 13.60 (t, $J = 12.9$ Hz, 2H, CHCHC*H*CHCH); IR (KBr): $\tilde{\nu}$[cm^{-1}] = 3020 (= CH), 2960, 2920, 2870 (CH), 1600 (conj. C = C), 760, 700 (monosubst. arene); UV/VIS (CH_2Cl_2): λ_{max} [nm] (lgε) = 512 (5.56), 544 (5.02), 673 (4.44); UV/VIS (CH_2Cl_2 + 1% TFA): λ_{max} [nm] (lgε) = 525 (5.69), 7.11 (4.52); high-resolution MS: $C_{50}H_{58}N_4$: calcd. 714.4661, found 714.4678; correct C,H,N analysis.

8b: ^{1}H NMR (300 MHz, [D$_6$]*DMSO*/[D$_1$]*TFA, TMS*): $\delta = -7.42$ (t, J = 13.4 Hz, 4H, CHC*H*CHC*H*CH), −3.92 (br. s, NH), −2.97 (br. s, NH), 11.08 (s, 1H, monomethine bridges CH), 12.39, 12.43 (2d, $J = 13.0$ Hz, each 2H, C*H*CHCHCHC*H*), 13.28 (t, $J = 12.8$ Hz, 2H, CHCHC*H*CHCH); IR (KBr): $\tilde{\nu}$[cm^{-1}] = 3015 (= CH), 2975, 2916, 2890 (CH); UV/VIS (CH_2Cl_2): λ_{max} [nm] (lgε) = 512 (5.59), 546 (5.20), 673 (4.53); UV/VIS (CH_2Cl_2 + 1% TFA): λ_{max} [nm] (lgε) = 520 (5.81), 545 (5.35), 710 (4.56); high-resolution MS $C_{46}H_{58}N_4$: calcd. 666.4661, found 666.4645.

9: ^{1}H NMR (300 MHz, [D$_1$]TFA, TMS): $\delta = -4.47$ (m, 4H, CHC*H*CHC*H*CH), 11.26 (s, 1H, monomethine bridges CH), 11.77, 12.03 (2d, $J = 12.5$ Hz, 4H C*H*CHCHCHC*H*), 12.53 (t, $J = 12.7$ Hz, 2H, CHCHC*H*CHCH); IR (KBr): $\tilde{\nu}$[cm^{-1}] = 3410 (NH), 2960, 2920, 2860 (CH); UV/VIS (CH_2Cl_2): λ_{max} [nm] (lgε) = 490 (5.23), 649 (4.45), 697 (4.18); UV/VIS (CH_2Cl_2 + 1% TFA): λ_{max} [nm] (lgε) = 503 (5.56), 681 (4.51), 735 (4.44); high-resolution MS $C_{43}H_{53}N_5$: calcd. 639.4300, found 639.4295; correct C,H,N analysis.

7: ^{1}H NMR (300 MHz, [D$_6$]DMSO, TMS): $\delta = 5.56$, 5.61 (2 br. s, 2H, bridges CH_2), 6.75–7.27 (m, 12H, C*H* = C*H*-C*H* = C*H*-C*H* and pyrrole-α-H), 11.06, 11.18 (2 br. s, each 2H, NH); IR (KBr): $\tilde{\nu}$[cm^{-1}] = 2980, 2910, 2860 (CH), 1570 (conj. C = C); UV/VIS (CH_2Cl_2): λ_{max} [nm] (lgε) = 785 (4.34), 621 (5.54), 410 (4.24), FD-MS (CH_2Cl_2, 8 kV, 8–15 mA): *m/z* 629 (M^+ − 2Br − H, 100%), 628 (M^+ − 2HBr, 78%); $C_{43}H_{58}Br_2N_4$; correct C,H,N,Br analysis.

chains of both dipyrrylmethane units are bent away from one another (Fig. 1a). The third molecule is in the *cis-trans* conformation and is centrosymmetric. The ring systems of the all-*trans* and the *cis-trans* conformations are almost planar with, comparably,[14] very small maximum deviations from the mean plane (19.8 and 18.0 pm, respectively). The bond lengths in the conjugated perimeter (Fig. 1b), that is in

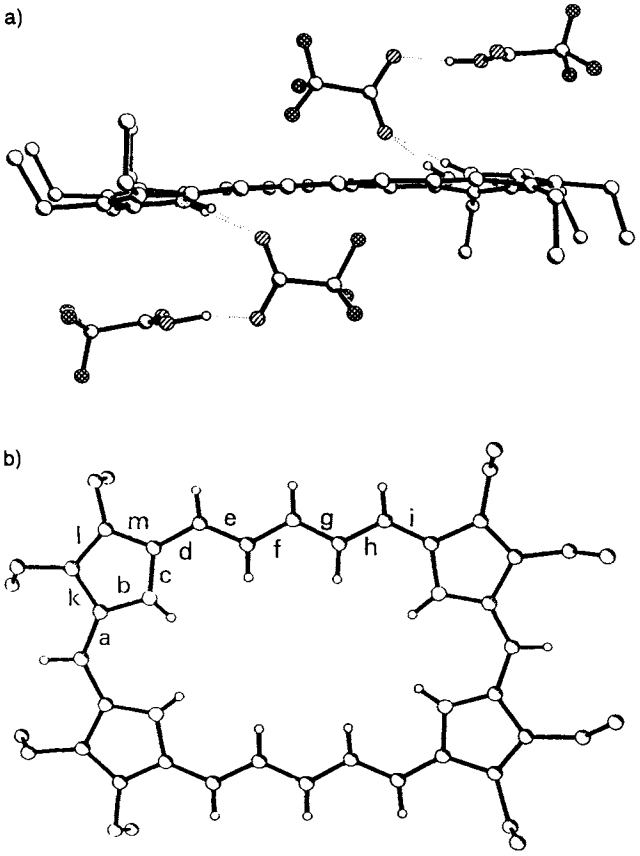

Fig. 1. Crystal structure of $\mathbf{2c}^{2+}$ bistrifluoroacetate. a) Side view of the all-*trans* conformation; b) View perpendicular to the arene plane of the all-*trans* conformation. Some characteristic distances [pm]: a = 139.1, b = 137.1, c = 137.3, d = 139.6, e = 138.1, f = 138.8, g = 139.2, h = 138.1, i = 139.1, k = 143.9, l = 137.5, m = 142.9.

the C_1 and C_5 bridges and in the pyrrole units, are approximately equal (137.1–139.6 pm), and are in good agreement with those of $\mathbf{2a}^{2+}$.[19] Therefore, the [26]porphyrin **2c** fulfills the structural criteria of an aromatic system, that is it is planar and the bond lengths are approximately equal.

As expected, the ^{1}H NMR spectrum of **2c** as arene, shows significant diatropic ring current effects (Table 2, Scheme 3). The maximum difference between the δ values of the inner and outer protons $\Delta\delta = 24.1$ is approximately equal to the corresponding values for the [26]porphyrins **3** (25.31) and **4** (25.95). The diatropicity of the *meso*-substituted derivatives decreases from **8a** via **8b** to the aza derivative **9**, and lies in the range of that of [22]porphyrin **2b**.

The UV/VIS absorption spectra of the bisprotonated forms of the new [26]porphyrins, measured in CH_2Cl_2/TFA (Tables 1 and 2), are very similar. Compared with **2b**, they exhibit a bathochromic shift of 40–60 nm in the range of their most intensive Soret bands.

With the 14-phenyl[26]porphyrin **8a**, which is somewhat more stable than **2c**, electrophilic deuteration was carried out in D_2SO_4 (Scheme 3). NMR spectroscopic and mass

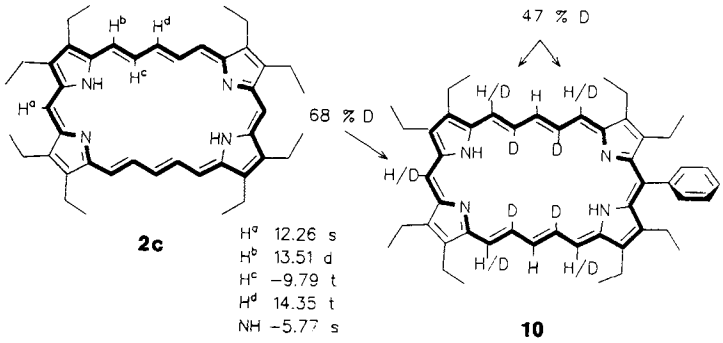

Scheme 3. ^{1}H NMR data of octaethyl[26]porphyrin **2c** and electrophilic deuteration of 14-phenyloctaethyl[26]porphyrin **9**.

Table 2. Maximum shift differences $\Delta\delta$ between the inner and outer protons in the ^{1}H NMR spectra of the new octaethyl[26]porphyrins(5.1.5.1) [20] (**2c**, **8a**, **8b**, **2b** in [D_6]DMSO/[D_1]TFA, **9** in [D_1]TFA); and their most intense (Soret bands) and longest wave UV/VIS bands in CH_2Cl_2/TFA.

Compound [20]	$\Delta\delta$	λ_{max} [nm] (lgε)
[26]porphyrin(5.1.5.1) **2c**	24.1	512 (5.84) 694 (4.61)
14-phenyl[26]porphyrin(5.1.5.1) **8a**	21.6	525 (5.69) 711 (4.52)
14-ethyl[26]porphyrin(5.1.5.1) **8b**	20.7	520 (5.81) 710 (4.56)
14-aza[26]porphyrin(5.1.5.1) **9**	18.9	503 (4.51) 735 (4.44)
[22]porphyrin(3.1.3.1) **2b**	22.3	460 (6.05) 691 (3.90)

spectrometric studies of the deuteration product **10** revealed that all of the inner bridge protons, and some of the outer bridge protons had been exchanged at a degree of deuteration of approximately 70% (determined by mass spectrometry). This result agrees with the aromaticity of **8a**. Noteworthy is especially the difference to the deuteration of [22]porphyrin **2b**, in which only the outer protons are replaced.[6] An explanation for this phenomenon, which will be reported later in connection with further deuterations of vinylogous porphyrins, is based on the size of the porphyrinoid rings, and the inductive effect of the phenyl substituents.[21]

Received: February 23, 1993 [Z 5884 IE]
German version: *Angew. Chem.* **1993**, *105*, 1201

[1] F. Sondheimer, *Acc. Chem. Res.* **1972**, *5*, 81–91.
[2] D. Lloyd, *The Chemistry of Conjugated Cyclic Compounds*, Wiley, New York, **1989**.
[3] M. J. S. Dewar, G. J. Gleicher, *J. Am. Chem. Soc.* **1965**, *87*, 685–692.
[4] R. M. McQuilkin, B. W. Metcalf, F. Sondheimer, *Chem. Commun.* **1971**, 338–339.
[5] S. Beckmann, T. Wessel, B. Franck, W. Hönle, H. Bormann, H. G. von Schnering, *Angew. Chem.* **1990**, *102*, 1439–1441; *Angew. Chem. Int. Ed. Engl.* **1990**, *29*, 1395–1397.
[6] H. König, C. Eickmeier, M. Möller, U. Rodewald, B. Franck, *Angew. Chem.* **1990**, *102*, 1437–1439; *Angew. Chem. Int. Ed. Engl.* **1990**, *29*, 1393–1394.
[7] H. Fischer, R. Bäumler, *Liebigs Ann. Chem.* **1929**, *468*, 58–98.
[8] This applies particularly to the use of porphyrins as photosensitizers for photodynamic tumor therapy (PDT)[9] and the deactivation of viruses in transfusion blood (PDV)[10]. Owing to the longer wave VIS absorption of vinylogous porphyrins, light can be employed which is not absorbed by hemoglobin. Moreover, they do not form complexes with iron or other transition metals by which they would be deactivated in organisms as photosensitizers.
[9] T. J. Dougherty, *Adv. Photochem.* **1992**, *17*, 275–311; *Photochem. Photobiol.* **1987**, *45*, 879–889.
[10] J. T. Matthews, J. T. Newman, F. Sogandares-Bernal, M. M. Judy, H. Skiles, J. R. E. Leveson, A. J. Marengo-Rowe, T. C. Chan, *Transfusion (Philadelphia)* **1988**, *28*, 81–83.
[11] M. Gosmann, B. Franck, *Angew. Chem.* **1986**, *98*, 1107–1108; *Angew. Chem. Int. Ed. Engl.* **1986**, *25*, 1100–1101.

[12] E. LeGoff, O. G. Weaver, *J. Org. Chem.* **1987**, *52*, 711–712.
[13] H. Rexhausen, A. Gossauer, *J. Chem. Soc. Chem. Commun.* **1983**, 275; A. Gossauer, *Chimia* **1983**, *37*, 341–342.
[14] J. L. Sessler, T. Morishima, V. Lynch, *Angew. Chem.* **1991**, *103*, 1018–1020; *Angew. Chem. Int. Ed. Engl.* **1991**, *30*, 977–980.
[15] M. Nakagawa, *Pure Appl. Chem.* **1975**, *44*, 885–924.
[16] A. W. Johnson, I. T. Kay, *J. Chem. Soc.* **1965**, 1620–1629; H. Ogoshi, H. Sugimoto, T. Nishiguchi, T. Watanabe, Y. Matsuda, Z. Yoshida, *Chem. Lett.* **1978**, 29–32.
[17] G. Knübel, B. Franck, *Angew. Chem.* **1988**, *100*, 1203–1204, 1211; *Angew. Chem. Int. Ed. Engl.* **1988**, *27*, 1170–1172.
[18] X-ray structural analysis **2c**: Measurements were carried out at 170 K on a dark green, metallic, shiny cubic crystals (0.25 × 0.45 × 0.88 mm) with a Siemens R3m/V.0 diffractometer ($Mo_{K\alpha}$ radiation) 14907 reflections. Crystal data: space group $P1$ $a = 1117.3(2)$, $b = 1851.7(3)$, $c = 20.027(3)$ pm, $\alpha = 89.87(1)$, $\beta = 75.80(1)$, $\gamma = 83.28(1)^{\circ}$, $Z = 2$. $R = 0.0697$ (1020 variables, 8505 F_0-values), $R_w = 0.0663$. Further details of the crystal structure investigation may be obtained from Fachinformationszentrum Karlsruhe, Gesellschaft für wissenschaftlich-technische Information mbH, D-76344 Eggenstein-Leopoldshafen (FRG), on quoting the depository number CSD-57264, the names of the authors, and the journal citation.
[19] E. Cetinkaya, A. W. Johnson, M. F. Lappert, G. M. Maclaughlin, K. W. Muir, *J. Chem Soc. Dalton Trans.* **1974**, 1236–1243.
[20] For the nomenclature of vinylogous porphyrins, based on our suggestion [11], the number of C atoms in the *meso* bridges are in brackets after the name of the porphyrin. In the case of vinylogous porphyrins with different bridge lengths, the number of C atoms in the *meso* bridges, starting with the α-pyrrole unit (upper left) and moving clockwise, is given. Thus, the ring system **2c** has the name "[26]porphyrin(5.1.5.1)".
[21] C. Eickmeier, dissertation, Universität Münster, **1993**.

Synthesis of 4-Deoxyaklanonic acid and Its Microbial Conversion into Anthracyclinones**

By *Karsten Krohn,* Ernst Roemer, Michael Top,* and *Christina Wagner**

Dedicated to Professor Eckehard Volker Dehmlow on the occasion of his 60th birthday

Very little is known about the intermediates in the biosynthesis of polyketides on the way from the hypothetical enyzme-bound open-chain polyketo precursor to the cyclized final products.[1] A notable exception to this is aklanonic acid **1**, a partially cyclized anthracycline precursor which is produced by mutants of *Streptomyces galilaeus* and *Streptomyces peucetius*.[2] It was isolated as a block mutant product and is considered to be the most important intermediate in anthracycline biosynthesis.[3] The incorporation of isotopically labeled alkanonic acid **1** into a variety of anthracyclines has demonstrated that aklanonic acid is really an intermediate and not merely a shunt product.[4]

The discovery of aklanonic acid **1** led us to attempt the enantioselective cyclization of achiral ketoester precursors—

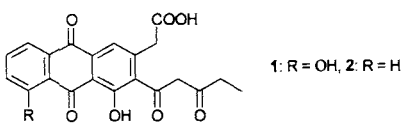

1: R = OH, **2**: R = H

as yet an unsolved problem in the synthesis of anthracylines—using a microbial conversion. We report here the synthesis and the biotransformation of the unnatural 4-deoxyaklanonic acid **2** to anthracyclinones of the aklavinone type.

The synthesis of **2** starts from the well-known homophthalate monoester **3**,[5] which is treated with an excess of the dilithium salt of *tert*-butylacetoacetate dianion (Scheme 1).

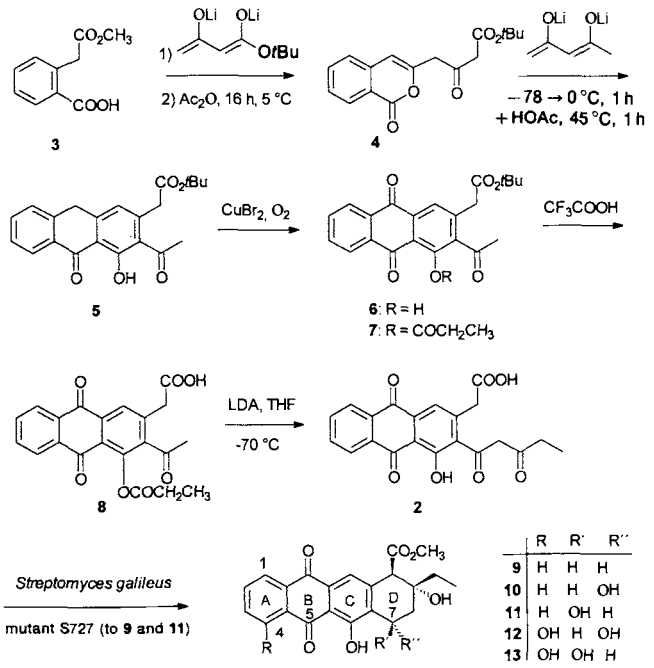

Scheme 1. LDA = lithium diisopropylamide.

The open-chain acid formed initially is cyclized without isolation with acetic anhydride to isocoumarin **4**[6] (57%). Treatment with a threefold excess of the dilithium salt of the acetylacetone dianion according to the procedure of Yamaguchi et al.[7] led to the formation of anthrone **5** (72%), which is oxidized by oxygen in the air in the presence of copper bromide to the anthraquinone **6** (87%). The transformation of the not very reactive phenol into the corresponding propionate **7** (82%) was achieved by using propionyl chloride in the presence of 5% 4-dimethylaminopyridine. To prevent a premature base-catalyzed cyclization during the final chain elongation step by a Venkataraman rearrangement,[8] the *tert*-butylester **7** was first saponified with trifluoroacetic acid to yield the acid **8** (98%). The intramolecular rearrangement of the acyl groups was achieved by reaction at −40 °C with LDA in THF. In addition to 70% of the chain elongation product 4-deoxyaklanonic acid **2** (C-acylation), about 30% of the saponification product **6** was isolated; **6** was probably formed by an O-acylation and can be reused in the reaction. The synthesis of aklanonic acid **1** was achieved in an analogous manner.[9]

The synthetic product **2** was then given to mutants of *Streptomyces* to see if they could use this unnatural precursor as substrate and convert it into enantiomerically pure 4-deoxyanthracyclinones not found so far in nature.

The mutant strain used (S727) was obtained by treating *Streptomyces galilaeus* (cinerubin producer) with the potent mutagen *N*-methyl-*N'*-nitro-*N'*-nitrosoguanidine (MNNG) (2 mg mL^{-1} at pH 9.0). The mutant strain S727 does not enrich anthracyclines or anthracyclinones and was first used to convert aklanonic acid **1** into cinerubin.[10] The wild type is known for it's abililty to produce aklavinone **12** and aklavinone-II **13**.[11]

[*] Prof. Dr. K. Krohn, Dr. E. Roemer, M. Top
Fachbereich Chemie und Chemietechnik der
Universität-Gesamthochschule
Postfach 1621, D-33098 Paderborn (FRG)
Telefax: Int. code + (5251)60-3245
Dr. C. Wagner
Hans-Knöll-Institut für Naturstoff-Forschung e.V.
Beutenbergstrasse-11, D-07745 Jena (FRG)

[**] This work was supported by the Bundesministerium für Forschung und Technologie.

A total of 34 mg of 4-deoxyaklanonic acid **2** was added to the cultures of the strain S727 in the feeding experiments (11 flasks each with 80 mL of culture medium). After an incubation period of 24 h, the pH of the cultures was adjusted to 8.5, and the metabolites were extracted with chloroform/methanol (9:1, v/v). Thin-layer chromatography revealed three red to violet minor products and two yellow major products. The polar compound (3 mg) exhibits the typical behavior of anthracyclinones hydroxylated twice in ring A (dehydration to yield fluorescent naphthacenediones). However, the results of NMR studies indicate that it is not identical with synthetic 4-deoxyaklavinone **10**,[12] and that in fact the compound in question is the C-7 epimeric 4-deoxyaklavinone-II **11**.[11, 12] The nonpolar major product, (17 mg, $[\alpha]_D^{20} = 31$ ($c = 0.2$ in methanol); m.p. 174.5 °C), was identified as 4,7-dideoxyaklavinone **9** by comparison with racemic synthetic compounds.[12] The enantiomeric purity was checked by using HPLC with a chiral column (Chiradex, Merck; gradient: T_0: 50%: 0.1% triethylamine buffered with HOAc to pH 4.4/50% methanol; t_{15}: 100% methanol). The racemic 4,7-dideoxyaklavinone[12] showed, as expected, two peaks; the product **9** from the microbial transformation corresponded to the enantiomer with a lower retention time. Although no values are available (e.g. optical rotation values) which could be used for a direct comparision for the determination of the absolute configuration, we assume that **9** has the natural (9*R*,10*R*) configuration, since the wild type of the mutant used also produces aklavinones with this absolute configuration.

Thus, we have demonstrated for the first time that relatively simple achiral unnatural precursors can be converted in a multistep biotransformation with high yield (56%) into optically active anthracyclinones. 4-Demethoxy analogues of daunorubicin compounds have already been clinically used and have proved to be more effective against tumors in vitro than the natural compounds.[13] With this new "hybrid" synthetic technique, in which chemical synthesis is combined with a multistep biotransformation, it will be possible to use other mutants to produce glycosidic anthracyclinones.[14] Furthermore, the synthesis of the biosynthetic intermediates **1** and **2** is designed to enable isotopic labeling and thus allow the biosynthesis to be investigated in more detail.

Received: March 13, 1993 [Z 5920IE]
German version: *Angew. Chem.* **1993**, *105*, 1220

[1] a) R. B. Herbert, *The Biosynthesis of Secondary Metabolites*, Chapman and Hall, London, **1989**, pp. 31–62; b) D. O'Hagan, *The Polyketide Metabolites*, Horwood, New York, **1991**.
[2] K. Eckardt, D. Tresselt, G. Schumann, W. Ihn, C. Wagner, *J. Antibiot.* **1985**, *38*, 1034–1039.
[3] C. Wagner, K. Eckhardt, W. Ihn, G. Schumann, C. Stengel, W. F. Fleck, D. Tresselt, *J. Basic Microbiol.* **1991**, *31*, 223–240.
[4] K. Eckardt, G. Schumann, U. Gräfe, W. Ihn, C. Wagner, W. F. Fleck, H. Thrum, *J. Antibiot.* **1985**, *38*, 1096–1097.
[5] L. F. Fieser, M. Fryt, *J. Am. Chem. Soc.* **1940**, *62*, 3489–3494.
[6] T. M. Harris, C. H. Harris, T. A. Oster, L. E. Brown Jr., J. Y.-C. Lee, *J. Am. Chem. Soc.* **1988**, *110*, 6180–6186.
[7] M. Yamaguchi, K. Hasebe, H. Higashi, M. Uchida, A. Irie, T. Minami, *J. Org. Chem.* **1990**, *55*, 1611–1623.
[8] U. S. Cheema, K. C. Gulati, K. Venkataraman, *J. Chem. Soc.* **1932**, 925–933.
[9] E. Roemer, dissertation, Universität Braunschweig, **1992**.
[10] G. Schumann, C. Stengel, K. Eckardt, W. Ihn, *J. Basic Microbiol.* **1986**, *26*, 249–255.
[11] D. Tresselt, K. Eckardt, J. Tax, *Tetrahedron* **1975**, *31*, 613–617.
[12] K. Krohn, M. Klimars, H. J. Köhle, E. Ebeling, *Tetrahedron* **1984**, *40*, 3677–3694.
[13] F. Arcamone in *Doxorubicin*, Academic Press, New York **1981**, p. 259–279.
[14] C. Wagner, unpublished results.

Competing $M{=}C_{carbonyl}$ and $M{=}C_{carbene}$ Bonds: Cycloaddition to the Metal–$C_{carbonyl}$ Bond in η^2-Thiocarbene Complexes**

By *Fritz R. Kreissl,** *Wolfgang Schütt, Josef Ostermeier,* and *Eberhardt Herdtweck*

Dedicated to Professor Ernst Otto Fischer on the occasion of his 75th birthday

Cycloadditions to metal–carbon multiple bonds are attaining increasing significance in metathesis[1–5] as well as in preparative organic and organometallic chemistry. In complexes in which the carbon atoms of the M=C units belong exclusively to carbonyl[6–10] or isonitrile ligands,[7, 11, 12] 1,3-dipoles preferably attack the M=C bond; thus, among other products, five-membered metallaheterocycles are formed. However, if additional carbene,[5, 13, 14] vinylidene,[15, 16] or carbyne ligands[17, 18] are present, the attack of the 1,3-dipole takes place at the M–C multiple bond of these groups.

Starting from $[Cp(CO)LM{\equiv}CR]$[19, 20] (M = Mo, W; R = Me, Ph, *p*-tolyl, NEt_2; L = CO, PR_3), 3*H*-1,2,3,4-triazametallol complexes[18, 21] can be prepared through a [2 + 3] cycloaddition with azido esters. In comparable cationic η^2-thiocarbene complexes $[Cp(CO)LM{=}C(R)SMe]^+$[22, 23] (M = Mo, W; R = Me, Ph, *p*-tolyl; L = CO), which include the complexes **1a** (M = W, R = Ph) and **1b** (M = W, R = *p*-tolyl) reported here, the attack of the dipole occurs at the $M{=}C_{carbene}$ bond and not at the $M{=}C_{carbonyl}$ bond; thus, thiatriazametallabicyclo[3.1.0]hexenes[24] are formed.

However, the attempt to bridge the metal–carbene bond with thio- or selenourea, which are significantly weaker dipoles failed! Furthermore, the $M{=}C_{carbonyl}$ bond, which is in competition with the $M{=}C_{carbene}$ bond, is more reactive; to our knowledge the first example of such reactivity. In the reaction of **1** with $X{=}C(NH_2)_2$ (X = S, Se) (Scheme 1), which occurs rapidly, the M=CO bond is bridged with the formation of a 1-thia/selena-3-aza-5-tungstacyclopenten-4-one. Together with the thiatungstacyclopropane system, the

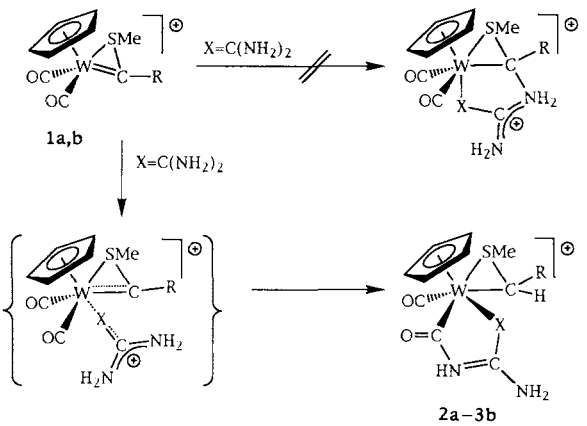

Scheme 1. **1a–3a**: R = Ph; **1b–3b**: R = *p*-tolyl; **2**: X = S; **3**: X = Se.

[*] Prof. Dr. F. R. Kreissl, Dipl.-Chem. W. Schütt, Dipl.-Chem. J. Ostermeier, Dr. E. Herdtweck
Anorganisch-chemisches Institut der Technischen Universität München
Lichtenbergstrasse 4, D-85747 Garching (FRG)
Telefax: Int. code + (89)3209-3473

[**] This work was supported by the Deutsche Forschungsgemeinschaft and the Fonds der Chemischen Industrie.

spirocycles **2** and **3** are obtained which precipitate in the form of yellow to red crystals.

The cycloaddition of thio- or selenourea leads to the appearance of two additional broad signals for the NH protons and one sharp singlet for the newly formed CH group in the ^{1}H NMR spectrum. In the $^{13}C\{^1H\}$ NMR spectrum, the protonation of the carbene carbon atom results in a drastic high-field shift ($\Delta\delta \approx 180$) of the corresponding signal. The molecular ion peaks of the spirocycles **2a,b**, and **3b** can be observed in the positive ion FAB mass spectra.

Compound **2a** crystallizes from acetonitrile/diethyl ether in the form of rhombohedral crystals. The single-crystal X-ray structure analysis[25] of **2a** shows a spirocyclic system with the central tungsten atom as the bridgehead between a heteroatom-substituted three-membered ring and a nearly planar metallaheterocycle (Fig. 1). The metal–sulfur bonds

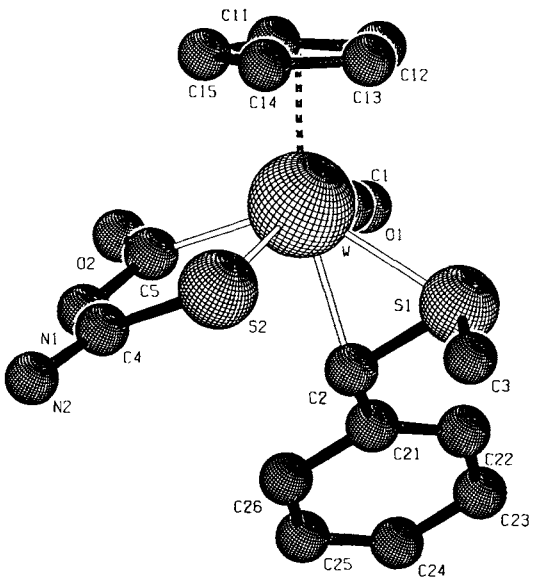

Fig. 1. Crystal structure of **2a**. Selected bond lengths [pm] and angles [°]: W-S1 244.2(1), W-S2 250.2(1), W-C1 201.1(5), W-C2 224.9(4), W-C5 218.8(4), C2-S1 178.6(4), S2-C4 171.5(4), C4-N1 134.4(5), C4-N2 131.2(4), N1-C5 139.8(4), C5-O2 121.8(5), C1-O1 114.8(5); S1-W-C1 85.8(04), S1-W-C2 44.5(1), S2-W-C5 79.3(1), C1-W-C2 76.3(2), W-S1-C2 62.0(1), W-C2-S1 73.5(2), W-C5-N1 117.0(3), C5-N1-C4 124.3(3), N1-C4-S2 119.7(3), N1-C4-N2 120.1(3), N2-C4-S2 120.2(3), C4-S2-W 99.6(1).

in both rings are between 244 and 250 pm long and, in comparison to those in $[Cp(CO)_2\overline{W=C(Ph)SMe}]^+$[22] (242.9 pm) and $[Cp(CO)_2(CF_3COO)\overline{W-CH(Me)SMe}]^+$[26] (247.5 pm), are considered to be single bonds. The protonation of the carbene carbon atom in the W-S-C three-membered ring leads to a lengthening of the W–C distance (224.9 pm). This distance now corresponds to those found for W–C single bonds (cf. $[Cp(CO)_3W(Ph)]$[27] ($d(W-C_{ipso}) = 232$ pm) and $[Cp(CO)_2(CF_3COO)W-CH(Me)SMe]^+$[26] ($d(W-C) = 224.8$ pm). The conversion of the terminal into a bridging carbonyl function is shown in the significant lengthening of the $W-C_{CO}$ bond; its length now lies between those found for double and single bonds.

For the formation of **2** and **3**, the nucleophilic attack of the chalcogen (S, Se) in $X=C(NH_2)_2$ at the tungsten center is considered to be the initial step. Thus, the resulting increase in the positive charge at the $C(NH_2)_2$ group should increase the acidity of the amine protons to such an extent that the protonation of the nucleophilic carbene carbon atom[13, 15] in **1** is made possible. The final linkage of the $C_{CO}-N$ bond between the carbonyl carbon atom and the imine nitrogen atom leads formally to the 1-thia-3-aza-5-metallacyclopenten-4-one. A protonation of the nucleophlic carbene carbon atom as initial step, as in the reaction of $[Cp(CO)_2\overline{W=C(R)SMe}]^+[BF_4]$ with CF_3COOH,[26] seems unlikely due to urea's lack of acidity. Furthermore, urea acts as a nitrogen base towards the comparable methyl-substituted cationic η^2-thiocarbene complex $[Cp(CO)_2\overline{W=C(Me)SMe}]^+$, and like triethylamine deprotonates the C methyl group with the formation of the thiovinyl complex $[Cp(CO)_2\overline{W-C(=CH_2)SMe}]$.[28]

Experimental Procedure

2a: **1a** (0.30 g, 0.57 mmol) in acetonitrile (10 mL) was treated with a solution of thiourea (0.04 g, 0.53 mmol) in acetonitrile (5 mL) at room temperature. During the reaction, the initially red solution slowly lightened in color. After 4 h the solvent was removed under high vacuum, the orange-yellow residue was washed several times with small amounts of dichloromethane, and subsequently recrystallized from acetonitrile/diethyl ether at −35 °C. Red crystals. Yield: 70%; m.p. 139.4 °C (decomp). IR (CH_3CN): $\tilde{\nu}$[cm^{-1}] = 2015 vs, 1634 m; MS (FAB): *m/z*: 517 $[M]^+$; ^{1}H-NMR (270.27 MHz, CD_3NO_2): δ = 9.71 (br, NH), 7.60 (br, NH_2), 7.24 (m, 5H, C_6H_5), 5.74 (s, 5H, C_5H_5), 4.87 (s, 1H, CH), 2.62 (s, 3H, SCH_3); $^{13}C\{^1H\}$ NMR (67.94 MHz, CD_3NO_2, 20 °C): δ = 209.3 (CO), 209.4 (W-CO-N), 184.6 (N-C-S), 142.4, 129.7, 128.3, 127.4 (C_6H_5), 92.9 (C_5H_5), 74.6 (W-C), 21.6 (SCH_3).

2b: Analogous to the preparation of **2a**, **1b** (0.27 g, 0.50 mmol) was treated with thiourea (0.035 g, 0.46 mmol) in acetonitrile (5 mL) and worked up. Pale yellow powder. Yield: 75%. IR (CH_3CN): $\tilde{\nu}$[cm^{-1}] = 2015, vs, 1635 m; MS (FAB): *m/z*: 531 $[M]^+$; ^{1}H NMR (270.27 MHz, CD_3NO_2): δ = 9.66 (br, NH), 7.56 (br, NH_2), 7.15 (m, 4H, C_6H_4), 5.73 (s, 5H, C_5H_5), 4.84 (s, 1H, CH), 2.61 (s, 3H, SCH_3), 2.38 (s, 3H, CH_3); $^{13}C\{^1H\}$ NMR (67.94 MHz, CD_3NO_2, 20 °C): δ = 209.4 (CO), 209.3 (W-CO-N), 184.7 (N-C-S), 139.4, 138.5, 130.2, 127.3 (C_6H_4), 92.8 (C_5H_5), 74.8 (W-C), 21.5 (SCH_3), 20.9 (CH_3).

3a: **1a** (0.37 g, 0.70 mmol) in dichloromethane (10 mL) was treated (in small portions) with selenourea (0.08 g, 0.65 mmol) in acetonitrile (10 mL) at −30 °C. After 6 h the mixture was worked up as for **2a**. Pale yellow powder. Yield: 60%. IR (CH_3CN): $\tilde{\nu}$[cm^{-1}] = 2014 vs, 1634 m; MS (FAB): *m/z*: 441 $[M]^+$; ^{1}H NMR (270.27 MHz, CD_3COCD_3): δ = 9.36 (br, NH), 8.57 (br, NH_2), 7.24 (m, 5H, C_6H_5), 5.85 (s, 5H, C_5H_5), 3.75 (s, 1H, CH), 2.71 (s, 3H, SCH_3); $^{13}C\{^1H\}$ NMR (67.94 MHz, CD_3COCD_3, −50 °C, $^1J(^{183}W,^{13}C)$ in parentheses): δ = 209.3 (CO, 140.5 Hz), 210.6 (W-CO-N, 125.1 Hz), 184.7 (N-C-Se, 106.0 Hz), 142.4, 129.7, 128.3, 127.3 (C_6H_4), 92.9 (C_5H_5), 74.6 (W-C), 21.5 (SCH_3)

3b: Analogous to the preparation of **3a**, **1b** (0.54 g, 1.00 mmol) in dichloromethane (10 mL) was treated (in small portions) with selenourea (0.11 g, 0.89 mmol) in acetonitrile (10 mL) at −30 °C. Analogous workup gave **3b** as a pale yellow powder. Yield: 69%. IR (CH_3CN): $\tilde{\nu}$[cm^{-1}] = 2013 vs, 1634 m; MS (FAB): *m/z*: 578 $[M]^+$; ^{1}H NMR (270.27 MHz, CD_3COCD_3): δ = 9.30 (br, NH), 8.60 (br, NH_2), 7.05 (m, 4H, C_6H_4), 5.84 (s, 5H, C_5H_5), 3.75 (s, 1H, CH), 2.69 (s, 3H, SCH_3), 2.33 (s, 3H, CH_3); $^{13}C\{^1H\}$ NMR (67.94 MHz, CD_3COCD_3, −50 °C): δ = 209.4 (CO), 210.3 (W-CO-N), 178.6 (N-C-Se), 139.3, 136.4, 129.3, 126.3 (C_6H_4), 91.4 (C_5H_5), 70.5 (W-C), 21.8 (SCH_3), 20.6 (CH_3).

Received: April 5, 1993 [Z 5980 IE]
German version: *Angew. Chem.* **1993**, *105*, 1233

[1] R. R. Schrock, *J. Organomet. Chem.* **1986**, *300*, 249–262.
[2] R. Toreki, G. A. Vaughan, R. R. Schrock, W. M. Davies, *J. Am. Chem. Soc.* **1993**, *115*, 127–137.
[3] J.-L. Couturier, M. Leconte, J.-M. Basset in *Transition Metal Carbyne Complexes* (Ed.: F. R. Kreissl), Kluwer, Dordrecht, **1993**, pp. 39–50.
[4] C. B. Gorman, E. J. Ginsburg, R. H. Grubbs, *J. Am. Chem. Soc.* **1993**, *115*, 1397–1409.
[5] K. Weiss, R. Goller, M. Denzner, K. Lössel, J. Ködel in *Transition Metal Carbyne Complexes* (Ed.: F. R. Kreissl), Kluwer, Dordrecht, **1993**, pp. 55–66.
[6] J. P. Collman, M. Kubota, F. D. Vastine, J. Y. Sun, J. W. Kang, *J. Am. Chem. Soc.* **1968**, *90*, 5430–5437.
[7] W. Beck, *J. Organomet. Chem.* **1990**, *383*, 143–160.
[8] W. P. Fehlhammer, G. Christian, A. Mayr, *J. Organomet. Chem.* **1980**, *199*, 87–98.
[9] H. Werner, J. Wolf, U. Schubert, *Chem. Ber.* **1983**, *116*, 2848–2854.
[10] W. A. Herrmann, A. Stiffl, M. L. Ziegler, K. Weidenhammer, *Chem. Ber.* **1979**, *112*, 1731–1742.
[11] H. Werner, B. Heiser, H. Otto, *Chem. Ber.* **1985**, *118*, 3931–3938.
[12] H. Werner, B. Strecker, *J. Organomet. Chem.* **1991**, *413*, 379–397.

[13] K. H. Dötz in *Transition Metal Carbene Complexes* (Eds.: K. H. Dötz, H. Fischer, P. Hofmann, F. R. Kreissl, U. Schubert, K. Weiss), Verlag Chemie, Weinheim **1983**, pp. 191–226.
[14] J. Wolf, R. Zolk, U. Schubert, H. Werner, *J. Organomet. Chem.* **1988**, *340*, 161–178.
[15] A. Höhn, H. Werner, *Chem. Ber.* **1988**, *121*, 881–886.
[16] H. Werner, U. Brekau, M. Dziallas, *J. Organomet. Chem.* **1991**, *406*, 237–260.
[17] K. Weiss in *Carbyne Complexes* (Eds.: H. Fischer, P. Hofmann, F. R. Kreissl, R. R. Schrock, U. Schubert, K. Weiss), VCH Verlagsgesellschaft, Weinheim **1988**, pp. 205–228.
[18] C. M. Stegmair, W. Ullrich, W. Schütt, P. Kiprof, F. R. Kreissl, *Chem. Ber.* **1992**, *125*, 1571–1573.
[19] E. O. Fischer, T. L. Lindner, G. Huttner, P. Friedrich, F. R. Kreissl, J. O. Besenhard, *Chem. Ber.* **1977**, *110*, 3397–3404.
[20] H. Fischer, P. Hofmann, F. R. Kreissl, R. R. Schrock, U. Schubert, K. Weiss, *Carbyne Complexes*, VCH Verlagsgesellschaft, Weinheim, **1988**.
[21] C. M. Stegmair, W. Schütt, W. Ullrich, P. Kiprof, J. Ostermeier, F. R. Kreissl, *J. Organomet. Chem.* **1993**, *447*, 251–259.
[22] N. Ullrich, C. M. Stegmair, H. Keller, E. Herdtweck, F. R. Kreissl, *Z. Naturforsch. B* **1990**, *45*, 921–925.
[23] W. Schütt, N. Ullrich, F. R. Kreissl, *J. Organomet. Chem.* **1991**, *408*, C5–C8.
[24] C. M. Stegmair, J. Ostermeier, W. Schütt, F. R. Kreissl, unpublished results.
[25] Crystal structure data for complex **2a**: $C_{16}H_{17}BF_4N_2O_2S_2W \cdot 0.25Et_2O \cdot 0.125CH_3CN$, $M_r = 604.1$ (without solvent), rhombohedral, $R\bar{3}$, $a = b = 3052.2(2)$, $c = 1402.1(1)$ pm, $\gamma = 120°$, $V = 11312(2) \times 10^6$ pm^3, $Z = 18$, -80 ± 3 °C, $\rho_{calcd} = 1.596$ (without solvent) g cm^{-3}, 6308 measured reflections (without R centering), of which 3683 were unique and 3467 observed with $I > 1.0\sigma(I)$ (ω scan, $1.0° < \theta < 25.0°$, $(0.75 + 0.25 \cdot \tan\theta)°$ ±25%, $\pm h, +k, +l$, $Mo_{K\alpha}$, $\lambda = 71.073$ pm, Enraf-Nonius CAD4). $R = 0.035$, $R_w = 0.035$, goodness of fit = 3.237, $\Delta\rho_{fin}$ (max./min) + 0.61/−0.59 eÅ^{-3}. There are large cavities, each of about 1000 Å^3 around the lattice positions (0,0,0), (1/3,2/3,2/3), and (2/3,1/3,1/3). In total, about 25% of the lattice is empty! Even with a complete occupation of the ether positions, about 260 Å^3 of unoccupied lattice positions still remain, almost 10% of the cell volume. Small quantities of solvent incorporated in the cavities are not observed by X-ray crystallography. The cations interact with the anions through weak hydrogen bonds. Further details of the crystal structure investigation may be obtained from the Fachinformationszentrum Karlsruhe, Gesellschaft für wissenschaftlich-technische Information mbH, D-76344 Eggenstein-Leopoldshafen (FRG) on quoting the depository number CSD-57414, the names of the authors, and the journal citation.
[26] F. R. Kreissl, F. X. Müller, D. L. Wilkinson, G. Müller, *Chem. Ber.* **1989**, *122*, 289–290.
[27] V. A. Semion, Y. T. Struchkov, *Zh. Strukt. Khim.* **1968**, *9*, 1046–1047.
[28] F. R. Kreissl, N. Ullrich, *Chem. Ber.* **1989**, *122*, 1487–1488.

On the BO Bond Length in Oxadiboriranes**

By *Michael Bühl, Henry Frederick Schaefer III,** *Paul von Ragué Schleyer,** and *Roland Boese**

High-level ab initio calculations, an important source of accurate structural data,[1] can help decide among competing structural models obtained from experimental refinements.[2] Recently the first oxadiborirane (**1d**)[3] was synthesized and characterized by X-ray structure analysis. The accuracy was reduced due to disorder, but the refinement favored (model A) gave extremely long BO bond lengths (1.545(5) and 1.510(6) Å). These disagreed with the much shorter BO distances (1.409[4] and 1.403 Å[3]) which were calculated for the parent compound **1a**, both at the modest (HF/3-21G)[4] and at the higher (MP2/6-31G*)[3] level. We now report the results of a variety of quantum mechanical calculations which reveal that a second refinement (model B), although more disordered, provides a better description of the molecular geometry than the previously published crystal structure.

Conventional refinement of the X-ray diffraction data for **1d** (model A) resulted in an essentially linear CBBC arrangement; in accord with crystallographic centrosymmetry, the oxygen atoms were found with 50% probability on each side of the B–B bond.[3] The BBC angles of 178 and 182° exaggerated the trend towards linearity predicted computationally for the parent compound **1a**.[3,4] More importantly, the

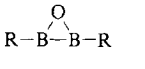

1a, R = H **1c**, R = $C(SiH_3)_3$
1b, R = CH_3 **1d**, R = $C(SiMe_3)_3$

BO bond lengths of this model (A) did not agree with the ab initio calculated distances. An alternative, preliminary refinement with split positions, allowing for disorder of the boron atoms as well as the oxygen atom (model B), afforded BO separations of around 1.38 Å which are in much better agreement with the theoretical results. The R value of this model B, however, was not significantly better than that of model A. Since the theoretical geometries of the parent system **1a** might be different from those of the highly substituted compound **1d**, it was decided to publish the results for model A, the conventional refinement.[3]

We now have investigated the substituted derivatives **1b** and **1c** at the SCF/DZP level, as well as the parent oxadiborirane **1a** at higher levels of theory including large basis sets and more sophisticated treatments of electron correlation.[5,6] As apparent from the results in Table 1, there is no change in the theoretical conclusion. The computational evidence requires that **1a** does not possess a BO bond longer than about 1.39 Å. The CCSD(T)/TZ2Pf value (1.388 Å) should be reliable. The geometry changes upon methyl (**1b**)

Table 1. Geometries of oxadiboriranes **1a**–**1d**.

Cmpd.	R	Level	B-O [Å]	B-B [Å]	B-H [Å]	B-B-H [°]
1a	H	SCF/3-21G [4]	1.409	1.594	1.169	173.4
		SCF/6-21G*	1.368	1.567	1.178	174.8
		SCF/DZP	1.373	1.576	1.176	174.2
		SCF/TZP	1.362	1.568	1.177	174.9
		SCF/TZ2Pf	1.361	1.567	1.177	174.8
		MP2/6-31G* [3]	1.403	1.562	1.183	175.2
		CISD/DZP	1.391	1.575	1.175	174.6
		CCSD(T)/DZP	1.405	1.538	1.179	175.0
		CISD/TZP	1.378	1.562	1.174	175.0
		CCSD(T)/TZP	1.393	1.568	1.179	175.3
		CCSD(T)/TZ2Pf	1.388	1.566	1.180	175.4

Cmpd.	R	Level	B-O	B-B	B-C	B-B-C
1a	H	SCF/DZP	1.373	1.576	-	174.2
1b	CH_3	SCF/DZP	1.378	1.584	1.561	173.8
1c	$C(SiH_3)_3$	SCF/DZP	1.378	1.587	1.549	172.8
1d	$C(SiMe_3)_3$	exp. model A [3]	1.545(5)	1.601(7)	1.544(4)	177.7(3)
			1.510(6)			182.3(3)
		exp. model B	1.365(7)	1.599(9)	1.510(7)	172.2(5)
			1.347(7)		1.607(7)	171.9(5)

[*] Prof. Dr. H. F. Schaefer III, Dr. M. Bühl
Center for Computational Quantum Chemistry
University of Georgia
Athens, GA 30602 (USA)
Telefax: Int. code + (706)542-0406
Prof. Dr. P. von R. Schleyer
Institut für Organische Chemie der Universität Erlangen-Nürnberg
Henkestrasse 42, D-91054 Erlangen (FRG)
Telefax: Int. code + (9131)859-132
Priv. Doz. Dr. R. Boese
Institut für Anorganische Chemie der Universität-Gesamthochschule
Universitätsstrasse 5–7, D-45117 Essen (FRG)
Telefax: Int. code + (201)183-2535

[**] This work was supported by the Deutsche Forschungsgemeinschaft, the Fonds der Chemischen Industrie, and the U.S. National Science Foundation.

and trisilylmethyl (**1c**) substitution are less than 0.01 Å for the BO separations (SCF/DZP level, lower part in Table 1). The structural differences between **1c** and **1d** should be even smaller.

Energy considerations also argue against model A: a partially optimized structure **1a′**, based on the published X-ray structure (i.e. **1a** with a fixed three-membered BBO ring but with freely optimized (B)–H positions), was 12.4 kcal mol^{-1} less stable (CISD/DZP level) than the fully optimized geometry (**1a**, C_{2v}).[7] Finally, the averaged IGLO ^{11}B NMR chemical shift[8] calculated by using this hypothetical structure (**1a′**), $\delta = 81.1$, does not agree with the value observed experimentally for **1d** ($\delta = 65.7$).[3] In contrast, the computed structures for **1a** give very good agreement: $\delta = 67.0$ (II′//MP2/6-31G*) and 66.3 (II′//CISD/DZP).[9]

Prompted by these apparent deficiencies of model A, the second, split model B was refined further.[10] The final molecular structure (Fig. 1) can be viewed as a superposition

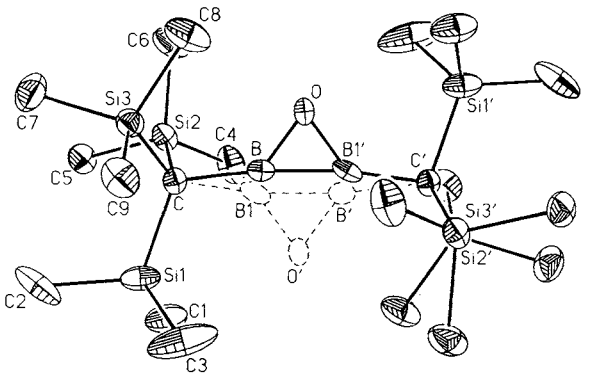

Fig. 1. Molecular structure of **1d** in the solid state (model B). The ellipsoids correspond to 50% probability of electron occupation, hatched and unhatched atoms are equivalent by crystallographic centrosymmetry, the disordered oxygen and boron atoms are drawn with dashed outlines, and the hydrogen atoms are omitted for clarity. Selected distances [Å] and angles [°] (standard deviation in parentheses): B-B1′ 1.599(9), B-O 1.347(7), B1′-O 1.365(7), B-C 1.607(7), B1′-C′ 1.510(7), O-B-B1′ 54.4(3), B-O-B1′ 72.3(4), C-B-B1′ 172.2(5), C′-B1′-B 171.9(5).

of two independent molecules disordered about the crystallographic inversion center. The "averaging" of the B and B1 as well as B1′ and B′ positions, leads to the apparently elongated BO separations of model A. The BO distances deduced from model B (1.347(7) and 1.365(7) Å) are now in much better agreement with the results of the ab initio calculations (1.378 Å for **1c**, Table 1). In contrast to model A, these BO bond lengths are also within the usual range observed for trigonal-coordinated boron (1.28–1.43 Å, mean value 1.365 Å),[11] and are close to the BO separations in Me_2B-O-BMe_2 (1.359(4) Å[12]), an acyclic reference compound.

Likewise, the BBC bond angles from model B (172.2(5) and 171.9(5)°) are in better accord with the ab initio values for **1c** (172.8°, Table 1) than those of model A (177.7(3)° and 182.3(3)°[3, 13]). Finally, the computed energy of **1a″**, employing the BBO ring dimensions derived from model B, is only 1.5 kcal mol^{-1} higher than that of the fully optimized structure of **1a** (CISD/DZP level).

In summary, the refinement employing model B results in much better agreement of theory and experiment and represents the molecular geometry of **1d** more reliably than that derived from model A.[3] However, correlations between the refined parameters (ADPs) increase the error margins of the experimental data beyond the commonly used 3 σ criterion. In addition, the large vibrational motion of the oxygen atom perpendicular to the BBO ring plane is expected to shorten the observed BO distance artificially. Also, the $SiMe_3$ positions should be affected by the disorder of the BBO ring. Some evidence for this can be detected by investigation of the ADPs of the respective atoms, but it was not possible to resolve them in split positions. Based on the ab initio data in Table 1, we recommend 1.39 Å as reference value for the equilibrium BO bond length in oxadiboriranes. While crystallographic criteria (i.e. *R* values) could not decide between the two alternative structural models A and B for **1d**, our theoretical results (geometries, energies, and NMR chemical shifts) unambiguously demonstrate that model B (Fig. 1) affords the more realistic experimental geometrical parameters.

This again demonstrates a general admonition: when their results do not agree with high level ab initio computations, experimentalists are encouraged to consider other possible interpretations of their data if this leads to better accord between theory and experiment.

Received: February 9, 1993 [Z 5857 IE]
German version: *Angew. Chem.* **1993**, *105*, 1265

[1] See for example A. Domenico, I. Hargittai, *Accurate Molecular Structures*, Oxford University Press, Oxford, **1992**.
[2] Experimental and theoretical borane and carborane geometries have been assessed by means of computed energies and chemical shifts: M. Bühl, P. von R. Schleyer, *J. Am. Chem. Soc.* **1992**, *114*, 477.
[3] P. Paetzold, L. Geret-Baumgarten, R. Boese, *Angew. Chem.* **1992**, *104*, 1071; *Angew. Chem. Int. Ed. Engl.* **1992**, *31*, 1040; see also "highlight": H. Grützmacher, *ibid.* **1992**, *104*, 1358 and **1992**, *31*, 1329.
[4] C. Liang, L. C. Allen, *J. Am. Chem. Soc.* **1991**, *113*, 1878.
[5] Geometries have been fully optimized in C_{2v} symmetry for **1a** and in C_2 symmetry for **1b** and **1c**, at the SCF/CISD [6a], and CCSD(T) levels [6b], employing the following contracted Huzinaga/Dunning basis sets [6c]: DZP (9s5p1d/4s2p1d) for B ($\alpha_d = 0.7$), C ($\alpha_d = 0.75$), and O ($\alpha_d = 0.85$), (11s7p1d/6s4p1d) for Si ($\alpha_d = 0.5$), (4s1p/2s1p) for H ($\alpha_p = 0.75$); TZP (10s6p1d/5s/3p1d) for B and O, (5s1p/3s1p) for H; TZ2Pf (10s6p2d1f/5s2d1f) for B ($\alpha_d = 1.4$, 0.35, $\alpha_f = 0.5$) and O ($\alpha_d = 1.7$, 0.425, $\alpha_f = 1.4$), TZP for H.
[6] a) P. Saxe, D. J. Fox, H. F. Schaefer III, N. C. Handy, *J. Chem. Phys.* **1982**, *77*, 5584; J. E. Rice, R. D. Amos, N. C. Handy, T. J. Lee, H. F. Schaefer III, *ibid* **1986**, *85*, 963; b) A. C. Scheiner, G. E. Scuseria, J. E. Rice, H. F. Schaefer III, *ibid.* **1987**, *87*, 5461; G. E. Scuseria, C. L. Janssen, H. F. Schaefer III, *ibid.* **1988**, *89*, 7382; c) S. Huzinaga, *ibid.* **1965**, *42*, 1293; T. H. Dunning, Jr., *ibid.* **1970**, *53*, 2823; *ibid.* 1971, *55*, 716.
[7] **1c** was optimized by employing the Turbomole program: a) M. Häser, R. Ahlrichs, *J. Comput. Chem.* **1989**, *10*, 104. b) R. Ahlrichs, M. Bär, M. Häser, H. Horn, C. Kölmel, *Chem. Phys. Lett.* **1989**, *162*, 165.
[8] Chemical shifts have been evaluated by using the IGLO (Individual Gauge for Localized Orbitals) method (W. Kutzelnigg, *Isr. J. Chem.* **1980**, *19*, 193; M. Schindler, W. Kutzelnigg, *J. Chem. Phys.* **1982**, *76*, 1919), employing the following contracted Huzinaga basis set (S. Huzinaga, *Approximate Atomic Wave Functions*, University of Alberta, Edmonton, **1971**): II′ (9s5p1d, 5s4p1d) for B ($\alpha_d = 0.5$) and O ($\alpha_d = 1.0$); (3s,2s) for H. See also reference [7] and W. Kutzelnigg, M. Schindler, U. Fleischer, in *NMR, Basic Princ. Prog.* **1990**, 165.
[9] Similar values were obtained with P. Pulay's GIAO program by employing a TZP basis set; H. Sulzbach, P. von R. Schleyer, unpublished results.
[10] Crystal structure of **1d**: Cell data identical to those reported in reference [3]; refinement with disordered boron and carbon atoms with SOF = 0.5; 2098 independent reflections, 1799 of which observed with $F_o \geq 4\sigma(F)$; anisotropic temperature factors for non-hydrogen atoms; 172 parameters refined; $R = 0.0420$, $R_w = 0.0451$. (Model A: 163 parameters, $R = 0.0424$, $R_w = 0.0520$) Further details of the crystal structure investigation may be obtained from the Fachinformationszentrum Karlsruhe, Gesellschaft für wissenschaftlich-technische Information mbH, D-76344 Eggenstein-Leopoldshafen (FRG) on quoting the depository number the names of the authors CSD-400 204 and the journal citation.
[11] A. F. Wells, *Structural Inorganic Chemistry, 5th ed.*, Clarendon Press, Oxford, **1984**.
[12] G. Gundersen, H. Vahrenkamp, *J. Mol. Struct.* **1976**, *33*, 97.
[13] ELF calculations (ELF = electron localization function) (A. Savin, A. D. Becke, J. Flad, R. Nesper, H. Preuss, H. G. von Schnering, *Angew. Chem.* **1991**, *30*, 421; *Angew. Chem. Int. Ed. Eng.*, **1991**, 409) indicate that the BB bond in **1a** is bent outward, but the BO bonds are strongly polarized toward oxygen and can hardly be regarded as having bent character. We thank M. Kaupp, Stuttgart, for this analysis.

A Highly Electrophilic Unsaturated Ditungsten Dication**

By *M. Angeles Alvarez, M. Esther García, Victor Riera,* Miguel A. Ruiz, Claudette Bois*, and *Yves Jeannin*

Organometallic transition metal dimers with formal metal–metal bond order of two or higher are attractive species, since they usually react with a great variety of molecules under mild conditions. Members of this class of compounds include, for example, $[M_2(CO)_4L_2]$ $(M{\equiv}M)$ (M = Cr, Mo, W),[1a,b] or $[M_2(CO)_2L_2]$ $(M{=}M)$ (M = Co, Rh, Ir),[1b] (L = η^5-C_5H_5 (Cp), or related ligands); the electrophilicity of these complexes is perhaps their most chracteristic property. A positive charge in a molecule with a metal–metal multiple bond should therefore greatly enhance its electrophilicity. Such organometallic cations are, however, very scarce, and are generally synthesized through redox reactions,[2] and their chemistry has been little explored. Further interest in such transition-metal-based Lewis acids, arises from their potential use as homogeneous catalysts in a number of organic reactions.[3] We report here the preparation of the novel unsaturated cationic ditungsten complex $[W_2(\mu\text{-CO})_2(CO)_2(\mu\text{-dppm})Cp_2]^{2+}$ $(W{=}W)$ (dppm = $Ph_2PCH_2PPh_2$) as PF_6^- salt **2**, and about the remarkable electrophilicity of this complex; its reactions are summarized in Scheme 1.

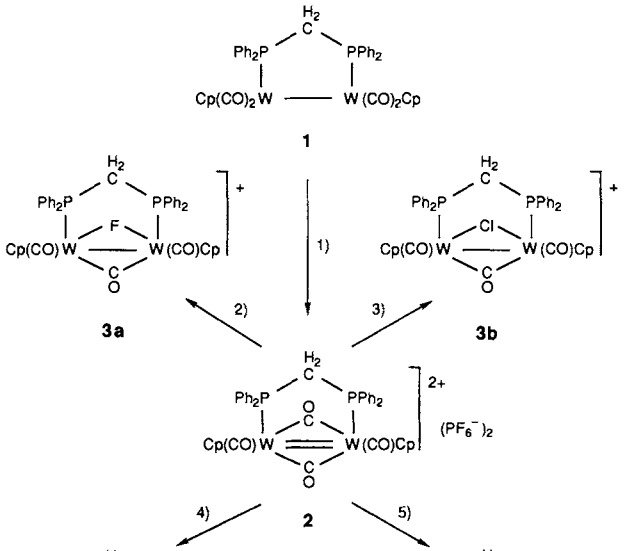

Scheme 1. 1) 2[$FeCp_2$]PF_6, −10 °C, CH_2Cl_2, 5 min. 2) 25 °C, CH_2Cl_2, 10 min. 3) [$AsPh_4$]Cl, CH_2Cl_2, −30 °C, 10 min. 4) BH_3 · THF, CH_2Cl_2, −30 °C, 10 min. 5) MeOH, −30 °C, CH_2Cl_2, 5 min. The counterion for the cationic complexes **3a**, **3b**, **4** and **6** is PF_6^-.

[*] Prof. Dr. V. Riera, Lda. M. A. Alvarez, Dr. M. E. García, Dr. M. A. Ruiz
Departamento de Química Organometálica
Universidad de Oviedo, E-33071 Oviedo (Spain)
Telefax: Int. code + (8)5103446
Dr. C. Bois, Prof. Dr. Y. Jeannin
Laboratoire de Chimie des Metaux de Transition, Université Pierre et Marie Curie, Paris (France)

[**] This work was supported by the Dirección General de Investigación Cientifica y Tecnica (D.G.Y.C.I.T.) (PB91-0678) of Spain.

The Reaction of **1** with two equivalents of $[FeCp_2]PF_6$ in dichloromethane at −10 °C gave almost quantitatively compound **2** as a violet microcrystalline precipitate.[4] The salt **2** is stable as a solid below −10 °C, but reacts rapidly in solu-

$[W_2(CO)_4(\mu\text{-dppm})Cp_2]$ **1**

$[W_2(\mu\text{-CO})_2(CO)_2(\mu\text{-dppm})Cp_2](PF_6)_2$ **2**

tion even below that temperature (for example, in acetone at −40 °C),[5] to give the green-brown fluorobridged tricarbonyl complex **3a** (as PF_6^- salt).[6] In this reaction a fluoride

$[W_2(\mu\text{-F})(\mu\text{-CO})(CO)_2(\mu\text{-dppm})Cp_2](PF_6)$ **3a**-PF_6

ion is transferred from the anion to the cation, and a CO ligand is liberated. Although fluoride abstraction from PF_6^- by mononuclear transition metal complexes has been observed in several instances,[7] there appears to be only one reported example involving a dinuclear system.[8] On the other hand, compound **3a**-PF_6 is, to our knowledge, the first organometallic complex in which a fluoro ligand bridges a metal–metal bond.[9] So far, we have not succeeded in growing suitable crystals of **3a**-PF_6, but have characterized its chloro analogue **3b**-PF_6 by X-ray crystallography (Fig. 1).[10]

$[W_2(\mu\text{-Cl})(\mu\text{-CO})(CO)_2(\mu\text{-dppm})Cp_2](PF_6)$ **3b**-PF_6

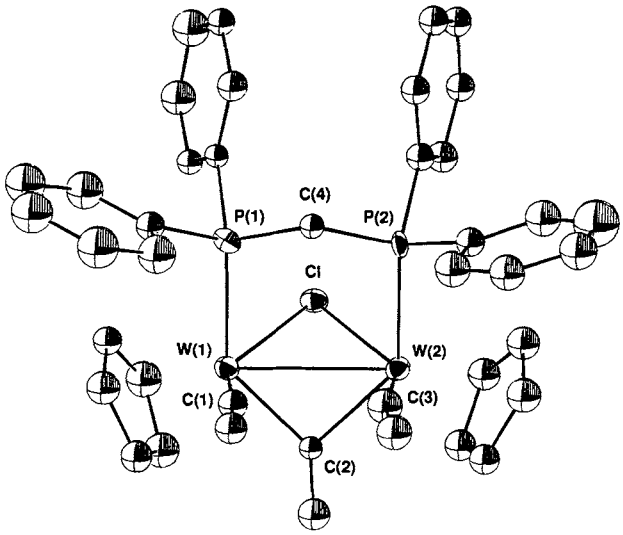

Fig. 1. Molecular structure of the cationic complex **3b** (ORTEP, thermal vibrational ellipsoids with 30% probability). Selected bond lengths [Å] and angles [°]: W(1)-W(2) 3.040(3), W(1)-Cl 2.494(8), W(2)-Cl 2.457(9), W(1)-C(1) 1.96(3), W(1)-C(2) 2.11(3), W(2)-C(2) 2.13(3), W(2)-C(3) 1.87(3); W(1)-Cl(1)-W(2) 75.8(2), W(1)-C(2)-W(2) 91.7(9), W(1)-C(2)-O(2) 136.8(30), P(1)-W(1)-C(1) 84.5(10), P(1)-W(1)-C(2) 134.0(9), Cl-W(1)-C(1) 134.8(11), Cl-W(1)-C(2) 76.5(8).

The latter is formed almost instantaneously through the reaction of **2** with [$AsPh_4$]Cl in dichloromethane at −30 °C. Spectroscopic data for these halogeno complexes indicate that they are isostructural,[6,11] and are in agreement with the geometry found in the crystal for **3b**-PF_6.[10] A metal–metal single bond is formulated for these compounds on the basis of the 18-electron rule, and this is consistent with the intermetallic separation in **3b** (3.040(3) Å). This lies in the range found for related cations with metal–metal single bonds (for example, 3.001(2) Å in $[Mo_2(\mu\text{-I})(\mu\text{-CH}_2PPh_2)$-

$(\mu\text{-PPh}_2)(CO)_2Cp_2]^{+}$[12] or 3.008(2) Å in $[Mo_2(\mu\text{-S}t\text{Bu})_2(CO)_4Cp]^{2+}$[13]).

Further evidence of the high electrophilicity of **2** is the unusual hydride abstraction forced upon $BH_3 \cdot THF$. This occurs quickly in dichloromethane at $-30\,^{\circ}C$ and gives the novel unsaturated hydrido complex **4**-PF_6 in very high yield

$[W_2(\mu\text{-H})(CO)_2(\mu\text{-dppm})Cp_2](PF_6)$ $(W{\equiv}W)$ **4**-PF_6

through spontaneous liberation of two CO ligands (Scheme 1). Compound **4**-PF_6 displays a resonance signal shifted to unusually low field for bridging hydrido ligands at $\delta = -2.6$,[14] which remains unchanged down to $-90\,^{\circ}C$. This deshielding may be an effect of the metal–metal multiple bonding.[15] As expected, this unsaturated hydrido complex reacts readily with CO to yield the saturated species **5**

$[W_2(\mu\text{-H})(CO)_4(\mu\text{-dppm})Cp_2](PF_6)$ **5**-PF_6

(counterion PF_6^-, two isomers),[16] similar to the dimolybdenum complex previously prepared by us,[3] and its hydrido ligands show resonances in the usual region in the ^1H NMR spectrum (δ = ca. -20).[17]

Other simple compounds interact with **2** at low temperatures. For example, **2** reacts instantaneously with MeOH at $-30\,^{\circ}C$ to give the methoxy-bridged species **6**,[18] which is

$[W_2(\mu\text{-OMe})(\mu\text{-CO})(CO)_2(\mu\text{-dppm})Cp_2](PF_6)$ **6**-PF_6

isostructural with compounds **3a** and **3b**. More complex reactions occur with compounds with P–H or C–H bonds, such as PPh_2H, MeC(O)H, or HC≡CPh, and these are currently under investigation.

Received: January 2, 1993
Revised version: March 25, 1993 [Z 5791 IE]
German version: *Angew. Chem.* **1993**, *105*, 1232

[1] a) M. D. Curtis, *Polyhedron* **1987**, *6*, 759–782; b) M. J. Winter, *Adv. Organomet. Chem.* **1989**, *29*, 101–162, and references therein.

[2] a) N. G. Connelly, *Chem. Soc. Rev.* **1989**, *18*, 153–185, and references therein; b) N. G. Connelly, W. E. Geiger, *Adv. Organomet. Chem.* **1985**, *24*, 87–130.

[3] T. K. Hollis, N. P. Robinson, B. Bosnich, *Organometallics* **1992**, *11*, 2745–2748.

[4] Complex **1** was prepared as described for its molybdenum analogue. V. Riera, M. A. Ruis, F. Villafañe, *Organometallics* **1992**, *11*, 2854–2863. IR (toluene): $\tilde{\nu}$ [cm^{-1}] = 1911 m, 1875 vs, 1837 m, 1815 m (νCO).

[5] The solid-state IR spectrum of **2** (nujol) showed no indication of PF_6^- coordination to the cation. $\tilde{\nu}$[cm^{-1}] = 2024 vs, 1980 w, 1864 s, 1814 vs (νCO).

[6] Chemical shifts were referenced against internal standards TMS (^1H, ^{13}C) and $CFCl_3$ (^{19}F), or external standard 85% aqueous H_3PO_4 (^{31}P); signs of J(P,W) are only relative. Data recorded at room temperature. Selected spectroscopic data for **3a**: IR (CH_2Cl_2): $\tilde{\nu}$[cm^{-1}] = 1969 vs, 1907 w, 1681 m (νCO). $^{31}P\{^1H\}$ NMR (121.50 MHz, [D$_6$]acetone: δ = 55.1 (d, ^2J(P,F) = 29 Hz, ^1J(P,W) = 257 Hz, ^2J(P,W) = − 59 Hz); $^{13}C\{^1H\}$ NMR (75.47 MHz, CD_2Cl_2): δ = 304.1 (br, μ-CO), 232.9 (s, 2 × W-CO); $^{19}F\{^1H\}$ NMR (188.31 MHz, [D$_6$]acetone: δ = − 523.8 (t, ^2J(F,P) = 29 Hz).

[7] N. M. Doherty, N. W. Hoffman, *Chem. Rev.* **1991**, *91*, 553–573.

[8] R. Mathieu, R. Poilblanc, P. Lemoine, M. Gross, *J. Organomet. Chem.* **1979**, *165*, 243–252.

[9] In $[Mn_3(\mu_2\text{-F})(\mu_3\text{-OEt})_2(CO)_9]$, the fluoro ligand bridges two metal atoms separated by only 2.829(7) Å. E. W. Abel, I. D. H. Towle, T. S. Cameron, R. E. Cordes, *J. Chem. Soc. Dalton Trans.* **1979**, 1943–1949. However, the presence of a metal–metal bond in this trimetallic species with 52 valence electrons is doubtful.

[10] Crystal data for **3b** · CH_2Cl_2: orthorhombic, space group *Pcab*; a = 18.001(5), b = 19.719(15), c = 24.178(9) Å, V = 8582(12) Å^3, Z = 8, ϱ_{calcd} = 1.91 g cm^{-3}. Crystal size 0.65 × 0.50 × 0.30 mm. 4534 reflections in the range $1^{\circ} < 2\theta < 25^{\circ}$ ($\mu(Mo_{K\alpha})$ = 60.4 cm^{-1}) were collected at 18 °C on a Phillips PW1100 diffractometer, of which 1721 with $I_o \geq 3\sigma(I)$ were used for the refinement of the structure. Structure solved by direct methods and subsequent Fourier maps. An absorption correction was applied. Refinements were carried out by least-squares methods in four cycles (202 parameters). Only W, Cl, and P atoms were refined with anisotropic thermal parameters, Ph and Cp ligands as rigid groups; hydrogen atoms were not located. R = 0.051 (Rw = 0.057). Further details of the crystal structure investigation are available on request from the Director of the Cambridge Crystallographic Data Centre, 12 Union Road, GB-Cambridge CB2 1EZ (UK), on quoting the full journal citation.

[11] Selected spectroscopic data for **3b**: IR (CH_2Cl_2): $\tilde{\nu}$[cm^{-1}] = 1973 vs, 1911 w, 1678 m (νCO). $^{31}P\{^1H\}$ NMR (121.50 MHz, CD_2Cl_2): δ = 31.1 (s, ^1J(P,W) = 214 Hz, ^2J(P,W) = − 17 Hz); $^{13}C\{^1H\}$ NMR (75.47 MHz, CD_2Cl_2): δ = 294.5 (s, μ-CO), 229.0 (s, 2 × W-CO).

[12] V. Riera, M. A. Ruiz, F. Villafañe, C. Bois, Y. Jeannin, *J. Organomet. Chem.* **1989**, *375*, C23–C26.

[13] J. Courtot-Coupez, M. Gueguen, J. E. Guerchais, J. Talarmin, F. Y. Pétillon, R. Mercier, *J. Organomet. Chem.* **1986**, *312*, 81–95.

[14] Selected spectroscopic data for **4**: IR [D$_6$]acetone: $\tilde{\nu}$[cm^{-1}] = 1917 m, 1801 vs (νCO). ^1H NMR (200.13 MHz, CD_2Cl_2): δ = − 2.60 (t, ^2J(H,P) = 8 Hz, ^1J(H,W) = 102 Hz, 1H, μ-H).

[15] The large magnetic anisotropy of M–M multiple bonds and its deshielding effect on proton nuclei lying alongside them is well stablished. See, for example, F. A. Cotton, R. A. Walton, *Multiple Bonds Between Metal Aoms*, Wiley, New York, **1982**, p. 221.

[16] Selected spectroscopic data for **5**: IR (CH_2Cl_2): $\tilde{\nu}$[cm^{-1}] = 1981 vs, 1958 s, 1896 sh, m, 1881 s (νCO). ^1H NMR (400.13 MHz, CD_2Cl_2): δ = − 20.79 (td, ^2J(H,P) = 27 Hz, ^4J(H,H) = 5 Hz, ^1J(H,W) = 102 Hz, 1H, μ-H, major (*syn*) isomer) [4]).

[17] D. S. Moore, S. D. Robinson, *Chem. Soc. Rev.* **1983**, *12*, 415–452.

[18] Selected spectroscopic data for **6**: IR (CH_2Cl_2): $\tilde{\nu}$[cm^{-1}] = 1963 vs, 1896 w, 1674 m (νCO). ^1H NMR (200.13 MHz, CD_2Cl_2): δ = 4.00 (s, 3H, μ-OMe).

Methyltrioxorhenium(VII) as Catalyst for Epoxidations: Structure of the Active Species and Mechanism of Catalysis**

By *Wolfgang A. Herrmann,* Richard W. Fischer, Wolfgang Scherer,* and *Monika U. Rauch*

Dedicated to Professor Hans Bock on the occasion of his 65th birthday

Oxides of transition metals in high oxidation states are common reagents and catalysts for olefin oxidation.[1] Despite many attempts no oxidation catalyst able to be "tuned" with substituents was found. This possibility is now in sight with the class of compounds $[RReO_3]$: the parent compound (R = CH_3) as well as derivatives (for example, R = $CH_2CH_2CH_2N(C_2H_5)_2$, cyclopropyl (c-C_3H_5)) efficiently catalyze the epoxidation of olefins with hydrogen peroxide under mild conditions, and direct the subsequent chemistry of the epoxides.[2]

We have now elucidated the active species of the catalytic system $[CH_3ReO_3]/H_2O_2$ and describe here the first isolated peroxo–metal complex with a metal–alkyl group that is stable to hydrolysis and to peroxide.

On treatment of methyltrioxorhenium (MTO, **1**) in water (or organic solvents) with an excess of hydrogen peroxide, a yellow solution (λ_{max} = 364 nm, $\varepsilon_\lambda(H_2O)$ = 610 L mol^{-1} cm^{-1}, ε_λ(THF) = 700 L mol^{-1} cm^{-1}) is obtained according to Scheme 1. This solution is stable for

[*] Prof. Dr. W. A. Herrmann, R. W. Fischer, W. Scherer, M. U. Rauch
Anorganisch-chemisches Institut der Technischen Universität München
Lichtenbergstrasse 4, D-85747 Garching (FRG)
Telefax: Int. code + (89)3209-3473

[**] Multiple Bonds between Main Group Elements and Transition Metals, Part 122. This work was supported by the Fonds der Chemischen Industrie. Part 121: W. A. Herrmann, P. Kiprof, F. E. Kühn, W. Scherer, M. Kleine, M. Elison, K. Rypdal, H. V. Volden, S. Gundersen, A. Haaland, *Bull. Soc. Chim. Fr.* **1992**, *129*, 655–662.

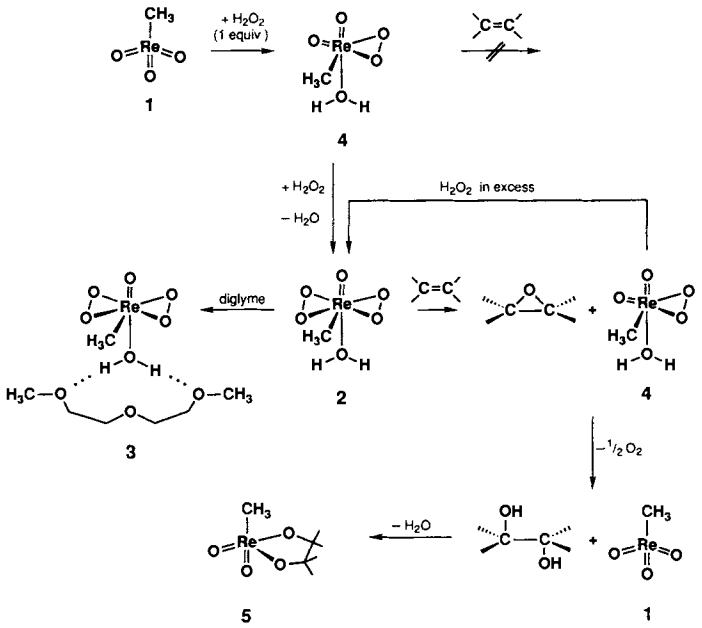

Scheme 1.

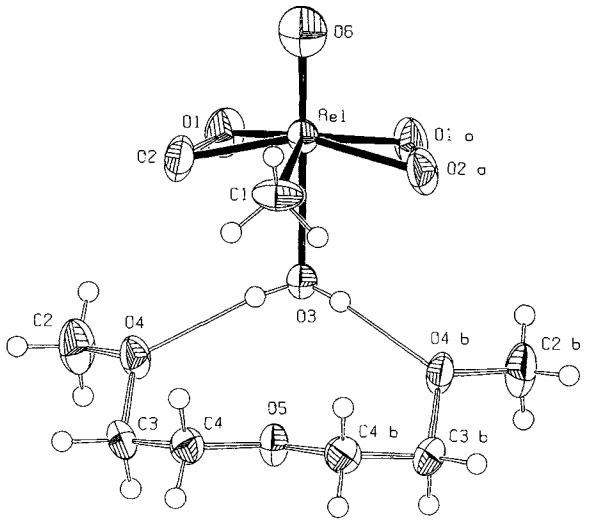

Fig. 1. Crystal structure (PLATON) of the diglyme adduct **3**. Selected distances [pm] and angles[°]: Re-C1 213.2(6), Re-O1 191.8(3), Re-O2 190.4(3), Re-O3 225.3(4), Re-O6 166.8(6), O1-O2 147.4(4), O3···O4 276.3(3), O3-H1 76(5), *H1*···O4 201(5); C1,Re,O3 80.4(2), C1,Re,O6 95.6(2), O3,Re,O6 175.9(2), O1,Re,O2 45.4(1), O3,H1,O4 168.7(7), M,Re,O3 77.8, M,Re,O6 103.4, M,Re,C1 105.4, M,Re,M 136.5 (M: center of the O1–O2 bond). The atoms labeled with a and b are generated by symmetry (reflection across the mirror plane $y = 1/4$ on which the atoms Re, C1, O3, O6, and O5 lie).

weeks at 0 °C and for days at room temperature. The compound **2** of composition $[CH_5O_6Re]$ can be extracted from it with diethyl ether, isolated as a solid (m.p. 55 °C, decomp. 65°C),[3] and sublimed under high vacuum at 25 °C; nevertheless heat stress should be carefully avoided (*danger of explosion*). In water **2** is a medium-strength Brønsted acid ($pK_s = 3.8$; cf. $[CH_3ReO_3]/H_2O$: $pK_s = 7.5$). The acidity of the coordinated water molecule is, however, not restricted to aqueous media: the (auto)protolysis has been detected by spectroscopy in dichloromethane and THF as well.[3]

Compound **2** is the first authentic organorhenium peroxo complex. It is particularly surprising that a metal-bound CH_3 group ($\delta(^1H) = 2.60$, $\delta(^{13}C) = 31$ in D_2O, 25 °C) can exist beside a peroxo ligand and coordinated water. Dissolved in THF, **2** exchanges its oxo group (Re=O) rapidly with $H_2{}^{17}O$, but *not* its peroxo oxygen atoms.[4] On addition of a little diglyme (diethyleneglycol dimethyl ether) to *n*-pentane/diethyl ether solutions, **2** affords thermally stable, orange-yellow single crystals of the 1:1 diglyme adduct **3** (yield > 95%). Like **2** this is very soluble in dichloromethane or ethereal solutions as well as in water. It melts at 40 °C without decomposition. Consistent with elemental analyses and IR and NMR spectra,[3, 5] and confirmed by single-crystal X-ray structure analysis (− 80 °C),[6] **3** displays two η^2-coordinated peroxo ligands besides the CH_3 ligand, as well as a coordinated water molecule, an oxo group, and one molecule of the triether diglyme per formula unit (Fig. 1). The aqua ligand holds the solvating ether molecule in the molecular arrangement by hydrogen bonds. The coordination of water is required by the type of constitution of the present complex: when **2** is crystallized from dichloromethane *without* diglyme, it also contains H_2O, apparently as a result of the very large Lewis acidity of peroxo-coordinated Re^{VII} (cf. pK_s!) In the crystal **2** is not solvated by diethyl ether. An entropic effect of the "half" crown ether diglyme appears to determine the constitution and exert a stabilizing influence. The strong water–rhenium bond in **2** and **3** explains why the H_2O ligand does not exchange with $H_2{}^{17}O$ (^{17}O NMR).

If each O_2 group is considered a coordinative unit, the molecular structure of the peroxo complex **3** can be described as a trigonal bipyramid; otherwise it is a pentagonal bipyramid. The *trans* ligands O6 and H_2O (O3) occupy the apical, and the methyl and both peroxo groups the equatorial positions. Diglyme is bound by linear hydrogen bonding between O3 and O4 to the peroxo complex. The interatomic distances in the peroxo groups correspond to published values (144.5(2)–144.9(2) pm).[7, 8] A similar geometry is displayed by adducts of bases of alkylrhenium oxides $[RReO_3 \cdot L]$ (L = quinuclidine; R = CH_3),[9] when both the η^2-O_2 ligands are (formally) replaced by two oxo ligands. The ligand L is, however, *trans* to the methyl group. As the existence of **3** shows, these complexes are certainly not sterically congested. Both the *cis* arrangement of the CH_3 and H_2O ligands and the stable H_2O coordination suggest that the prospect of generating configuratively stable, chiral peroxorhenium complexes with C,O- and C,N-chelating ligands is good.

The Re^{VII} peroxo complex **2**, which, surprisingly, could be isolated in the solid state, is the active species in the olefin epoxidation catalyzed by $[CH_3ReO_3]$ (**1**): λ_{max} and ε_λ of the UV/VIS spectra of **2** generated in situ (tenfold excess of H_2O_2 simulates catalytic conditions) and of isolated, analytically pure **2** (in each case in ether as solvent) are identical, as are the IR and NMR spectra (solvents CH_2Cl_2 and D_2O, respectively). In the ^{17}O spectrum of **2** in diethyl ether, two broad signals at $\delta = 422$ and 363 can be assigned to the peroxo groups ($\Delta_{1/2} = 1250$ Hz); the relatively small difference in chemical shift ($\Delta\delta = 59$) indicates that a rigid, η^2-coordination is also present in solution at −20 °C. From ^1H NMR studies it can be concluded that *two* equivalents of H_2O_2 are required for the formation of the active species;[2a] thus olefins like 2,3-dimethylbut-2-ene can be titrated or transformed very rapidly in solution even at temperatures as low as −25 °C with *isolated* **2** according to Scheme 1 in stoichiometric amounts (n(**2**):n(olefin) = 1:1) and form epoxides as primary products. In contrast, the monoperoxo complex **4** does not react with olefins to an extent worth mentioning. Only at 25 °C does the generated epoxide undergo slow ring opening to form the 1,2-diol as a result of water present in **2**. In the process the catalyst MTO (**1**) is released

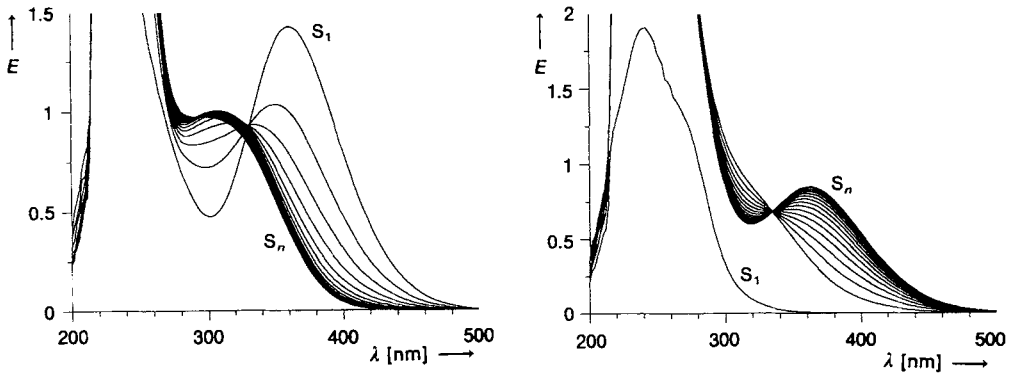

Fig. 2. Left: Change in the UV/VIS spectra during the course of the reaction of 2,3-dimethylbut-2-ene with isolated **2** in the absence of H_2O_2 in THF. $c(\mathbf{2}) = 2 \times 10^{-3}$ mol L^{-1}, c(olefin) $= 4 \times 10^{-3}$ mol L^{-1}, $T = 10\,^{\circ}C$, $t =$ 30 min. Right: Changes in the UV/VIS spectra during the course of the reaction of regenerated **1** with H_2O_2 to form **2**. $c(\mathbf{1}) = 1.1 \times 10^{-3}$ mol L^{-1}, $T = 20\,^{\circ}C$, $t =$ 60 min.

and forms the isolable condensation product **5** in a subsequent reaction (75% yield).[10] The reaction can be followed and quantified by gas chromatography.

Consistent with the results from gas chromatography, the regeneration of MTO (**1**) on the oxidation of 2,3-dimethylbut-2-ene from **2** is confirmed by UV/VIS spectroscopy. This regeneration is, however, not direct, but occurs via intermediate **4**, detectable in UV/VIS and NMR spectroscopy ($\lambda_{max} = 310$ nm, $\varepsilon_\lambda \approx 600$ L mol^{-1} cm^{-1}, $\delta(CH_3) = 3.2$, in [D$_8$]THF; isosbestic points are observed in the UV/VIS spectra of Fig. 2, left). Compound **4** is formed rapidly from **2** in the presence of olefins ($k_1 = 0.2\ s^{-1}$ at 10 °C) and finally transformed into **1** (Fig. 2, left). The decomposition **4** → **1** is accelerated only slightly by olefins (in contrast to the reaction **2** → **4**: in comparison to **2**, the monoperoxo complex **4** oxidizes olefins very slowly and inefficiently (^{1}H NMR) and can thus be considered inactive as regards epoxidation catalysis.[11] Alternatively, **4** can be generated directly from **1** (for example, in THF) and *one* equivalent of H_2O_2 according to an NMR/UV/VIS study. Consequently, **1** forms 1:1 and 1:2 adducts with aqueous H_2O_2. These adducts form concentration-dependent equilibria at low concentrations ($n(\mathbf{1})/n(H_2O_2) \leq 3$) according to NMR data.[2e] Regenerated **1** rapidly gives **2** with an excess of H_2O_2 (Fig. 2, right; here without detectable intermediate steps, $k_2 = 1.7 \times 10^{-3}\ s^{-1}$ at 20 °C).

In the absence of olefins, **2** decomposes much more slowly to **4**: $k_3(10\,^{\circ}C) = 3.5 \times 10^{-4}\ s^{-1}$, $k_3(40\,^{\circ}C) = 4.0 \times 10^{-3}\ s^{-1}$ (cf. Fig. 3, left). Under the catalytic conditions (excess of H_2O_2) **2** is, however, very stable. It can be assumed that in the catalytic cycle no free MTO (**1**) is generated, because **4** reacts much more rapidly with H_2O_2 to form **2** ($k_4(20\,^{\circ}C) = 5.0 \times 10^{-3}\ s^{-1}$) than it decomposes to form **1**. The reaction **1** → **4** with H_2O_2 is similarly slow (see Scheme 1 and Fig. 3, right).

The oxidizing power of **2** can also be seen in the immediate evolution of chlorine, bromine, and iodine on mixing **2** with solid or dissolved KCl, KBr, or KI. These reagents are also oxidized by **4**, which is additional proof of the presence of a peroxo group.

If the η^2-coordinated peroxo groups were not essential for the olefin epoxidation, organic hydroperoxides would also be active in oxidations with MTO (**1**). This does not occur.[2] Organic peroxides like *tert*-butylhydroperoxide, di-*tert*-butylperoxide, and organic peracids do not react with MTO. Since the existence—exemplified by compounds **2** and **3**—of bis(peroxo) Re^{VII} complexes like **2** is now proven, we give no significance to the hydroperoxo tautomer **2'** [Eq. (a)]. The ^{17}O NMR spectra (position and form of signals[12]) and the IR spectra in solution speak against the hydroperoxo form that is considered for many peroxo–metal species.

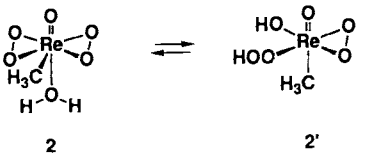

2 **2'** (a)

Our present results explain why MTO (**1**) is by far the most active rhenium epoxidation catalyst. In contrast to all other rhenium oxides, the molecularly defined, very reactive catalyst **2** is formed *quantitatively* with H_2O_2 and is not only stable to peroxide, light, acid, and water, but also to temperature in the presence of an excess of H_2O_2. The low metal coordination of MTO (**1**) and the H_2O_2-resistant Re–CH_3 group are the two crucial prerequisites for all these properties. All in all, the peroxide formation has a stabilizing function for alkyltrioxorhenium(VII) complexes: thermolabile

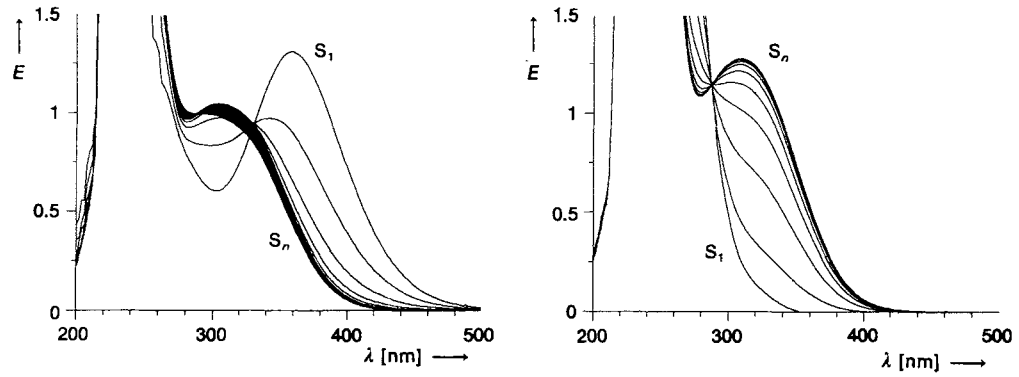

Fig. 3 Left: Changes in the UV/VIS spectra during the decomposition of **2** to form **1** via the intermediate **4**. $c(\mathbf{2}) = 2 \times 10^{-3}$ mol L^{-1}, $T = 40\,^{\circ}C$, $t = 48$ min. Right: Changes in the UV/VIS spectra during the course of the formation of **4** from **1** and H_2O_2. $c(\mathbf{1}) = c(H_2O_2) = 2 \times 10^{-3}$ mol L^{-1}, $T =$ 20 °C, $t = 8$ h.

 © VCH Verlagsgesellschaft mbH, D-69451 Weinheim, 1993 0570-0833/93/0808-1159 $ 10.00+.25/0

cyclopropyltrioxorhenium yields a catalyst with H_2O_2 that is stable at elevated temperatures and even more active in epoxidation than the MTO derivative **2**.

Experimental Procedure

2: MTO (1.00 g, 4 mmol) was dissolved in distilled water (20 mL) at 25 °C. The solution was cooled to 0 °C, and perhydrol p.A. (5 mL of 30% H_2O_2) was added dropwise. After 10 min the yellow-orange solution was extracted with diethyl ether (50 mL). The ether extract was washed with water (3 × 20 mL) and dried twice with Na_2SO_4, and finally over 4 Å molecular sieves. (These operations should be performed as rapidly as possible to avoid decomposition.) The organic phase was quickly evaporated to dryness at 0 °C under high vacuum. The yellow residue was washed with *n*-pentane at 0 °C and finally dissolved in dichloromethane (if necessary with addition of a little diethyl ether). Analytically pure product was obtained on crystallization at −30 °C. Yield 960 mg (80%). Single crystals of **3** were obtained after addition of a small amount of diglyme to solutions of **2** in a mixture of diethyl ether and *n*-pentane (1:25) and slow cooling to −30 °C in screw-top vials that were not tightly closed.

Received: March 8, 1993 [Z5908IE]
German version: *Angew. Chem.* **1993**, *105*, 1209

[1] Surveys: a) R. A. Sheldon, J. K. Kochi, *Metal-Catalyzed Oxidation of Organic Compounds*, Academic Press, New York, **1981**; b) *Organic Syntheses by Oxidation with Metal Compounds* (Eds.: W. J. Mijs, C. R. H. I. de Jonge), Plenum, New York, **1986**; c) R. A. Sheldon in *Aspects of Homogeneous Catalysis, Vol. 4*, (Ed.: R. Ugo), Reidel, Dordrecht, **1981**, p. 3 ff.; d) H. A. *Jørgensen, Chem. Rev.* **1989**, *89*, 431–458.

[2] a) W. A. Herrmann, R. W. Fischer, D. W. Marz, *Angew. Chem.* **1991**, *103*, 1706–1709; *Angew. Chem. Int. Ed. Engl.* **1991**, *30*, 1638–1641; b) W. A. Herrmann, D. W. Marz, W. Wagner, J. Kuchler, G. Weichselbaumer, R. W. Fischer (Hoechst AG), DE-B 3.902.357, **1989/1990**; c) R. W. Fischer, *GIT Fachz. Lab.* **1992**, *10*, 997–1002; d) W. A. Herrmann, R. W. Fischer, M. U. Rauch, W. Scherer, *J. Mol. Catal.* **1993**, in press.

[3] **2**: Yellow, hygroscopic crystals; m.p. 55 °C, decomp. 65 °C. IR (CH_2Cl_2 or Nujol(*), {$[CH_3ReO(O_2)_2 \cdot D_2O]$, ca. 90%}: $\tilde{\nu}$(ReO) [cm^{-1}] = 1020 (vs) [2 × 1020 (vw)]; ν(Re-O_2)* = 330 {328} (w); δ(Re-OH) = 1121 {800} (w); ν(O_2) = 877; ν(Re-CH_3) = 571 {572} (s); CH_3 rocking mode: 814 (w); ν(H_2O) = 3616, 3536 {2634} (vs); δ(H_2O) = 1599 {1180} (s); {δ(HDO) = 1430 (w)}; δ(H_3O^+) = 1752 {1282} (w); $\nu_{deg}(CH_3)$ = 3058 {3055} (s); $\nu_{sym}(CH_3)$ = 2968 {2987} (s); $\delta_{asym}(CH_3)$ = 1399 {1403} (m); $\delta_{sym}(CH_3)$ = 1213 {1217}. ^{1}H NMR (400 MHz, D_2O, 20 °C, {[D_8]THF, −20 °C}): δ = 2.6 (CH_3, s) {2.71 (CH_3, s), 9.4 (H_2O-coord., br)}; $^{13}C\{^1H\}$ NMR (100.5 MHz, D_2O, 20 °C): δ = 31. ^{13}C NMR (100.5 MHz, [D_8]THF, −10 °C): δ = 30.53 (q, $^2J(^{13}C, ^1H)$ = 135 Hz); ^{17}O NMR (54.21 MHz, −20 °C, Et_2O): δ = 762 (ReO), 422 and 363 (η^2-O_2, signal width 1250 Hz), −26 (H_2O). UV/VIS (Et_2O, 20 °C): λ_{max} = 364 nm, ε_λ = 700 $Lmol^{-1}cm^{-1}$. MS (EI, 70 eV, ^{187}Re, correct isotope pattern): *m/z*: 282 [M − H_2O], 250 [CH_3ReO_3], 220 [$HReO_2$, *M* − H_2O − H_2CO, base peak]; (CI, isobutane, ^{187}Re, correct isotope pattern): *m/z*: 299 [M + 1 − H_2], 281 [M + 1 − H_2 − H_2O, base peak]. Correct elemental analysis (C,H,O,Re).

[4] A little decomposition occurs during the NMR experiment.

[5] Yellow-orange, slightly hygroscopic crystals. M.p. 40 °C. ^{1}H NMR (400 MHz, [D_8]THF, 20 °C): δ = 2.66 (Re-CH_3, s, 3H), 3.27 (CH_3, s, 6H), 3.43 (CH_2, t, 4H), 3.52 (CH_2, t, 4H), 3.39 (H_2O/CH_3OH; from decomposition, br). MS (EI, 70 eV, ^{187}Re, correct isotope pattern): *m/z*: 266 [$CH_3Re(O_2)O_2$], 250 [CH_3ReO_3], 89 [$C_4H_9O_2$], 59 [C_3H_7O, base peak], M^+ not observed. Correct elemental analysis (C,H,O,Re).

[6] **3**: $C_7H_{19}O_9Re$; *a* = 1246.4(2), *b* = 1496.4(3), *c* = 714.9(1) pm, *V* = 1333 × 10^6 pm^3, measurement at −80 °C, ρ_{calcd} = 2.16 gcm^{-3}, μ = 92.7 cm^{-1}, *Z* = 4, orthorhombic, *Pnma* (no. 62), Enraf-Nonius CAD4, λ = 71.07 pm ($Mo_{K\alpha}$, graphite monochromator), ω scan; of 3002 measured reflections (+*h*, +*k*, ±*l*), 1211 were independent, and 1104 with $I > 3\sigma(I)$ were used for the refinement; structure solution with Patterson methods and difference Fourier syntheses, empirical absorption correction on the basis of psi scan data, transmission coefficients 0.608–0.999, 125 refined parameters, all H atoms found and refined freely with isotropic auslenkung parameters. $R = \sum(||F_o| - |F_c||)/\sum|F_o| = 0.019$, $R_w = [\sum w(|F_o| - |F_c|)^2/\sum w|F_o|^2]^{1/2} = 0.021$, residual electron density +1.75, −0.99 $\Delta e_o/Å^3$. Further details of the crystal structure investigation may be obtained from the Fachinformationszentrum Karlsruhe, Gesellschaft für wissenschaftlich-technische Information mbH, D-76344 Eggenstein-Leopoldshafen (FRG) on quoting the depository number CSD-57189, the names of the authors, and the journal citation.

[7] W. A. Herrmann, W. R. Thiel, J. G. Kuchler, J. Behm, E. Herdtweck, *Chem. Ber.* **1990**, *123*, 1963–1970.

[8] a) P. Legzdins, E. C. Philips, S. J. Rettig, L. Sánchez, J. Trotter, V. C. Yee, *Organometallics* **1988**, *7*, 1877–1878. b) H. Mimoun in *The Chemistry of Functional Groups, Peroxides* (Ed.: S. Patai), Wiley, New York, **1983**, Chap. 15; c) M. J. Nolte, E. Singleton, M. Laing, *J. Am. Chem. Soc.* **1975**, *97*, 6396–6400, and references therein; d) G. Henrici-Olivé, S. Olivé, *Angew. Chem.* **1974**, *86*, 1–12; *Angew. Chem. Int. Ed. Engl.* **1974**, *13*, 29–38.

[9] W. A. Herrmann, C. C. Romaõ, R. W. Fischer, P. Kiprof, C. de Mèric de Bellefon, *Angew. Chem.* **1991**, *103*, 183–185; *Angew. Chem. Int. Ed. Engl.* **1991**, *31*, 185–186.

[10] W. A. Herrmann, P. Watzlowik, P. Kiprof, *Chem. Ber.* **1991**, *124*, 1101–1106.

[11] k_1 was calculated on the basis of pseudo-first-order kinetics (olefin in excess) for the reaction **2** + olefin → **4** (c(olefin) = 2 × 10^{-1} $molL^{-1}$, c(**2**) = 2 × 10^{-3} $molL^{-1}$); k_2 (c(**1**) = 1.1 × 10^{-3} $molL^{-1}$, $c(H_2O_2)$ = 1 × 10^{-1} $molL^{-1}$), and k_4 (c(**4**) = 1.6 × 10^{-3} $molL^{-1}$, $c(H_2O_2)$ = 2.9 × 10^{-1} $molL^{-1}$) were determined analogously. The reaction **2** → **4** (k_3) is first order. *E* = extinction; S_1 = initial spectrum, S_n = final spectrum.

[12] a) M. Postel, C. Brevard, H. Arzoumanian, J. G. Riess, *J. Am. Chem. Soc.* **1983**, *105*, 4922–4926; b) I. P. Gerothanassis, M. Momenteau, *ibid.* **1987**, *109*, 6944–6947; c) B. 1. P. Gerothanassis, M. Momenteau, B. Loock, *ibid.* **1989**, *111*, 7006–7012, d) S. Berger, S. Braun, H.-O. Kalinowski, *NMR-Spektroskopie von Nichtmetallen, Band 1* (Grundlagen, ^{17}O-, ^{33}S- und ^{129}Xe NMR-Spektroskopie), Thieme, Stuttgart, **1992**, p. 107 ff., and references therein.

Golcondane: A Novel, Caged, Nonacyclic $C_{20}H_{24}$-Hydrocarbon of D_{2d} Symmetry**

By *Goverdhan Mehta** and *S. Hari Krishna Reddy*

The conception and creation of space-enclosing polycyclic hydrocarbons (polyhedranes) of novel shape and symmetry is an area of contemporary interest that elegantly blends aesthetics with synthetic challenge.[1] In recent years, the assembly of C_{20}-polyhedranes in particular received a great deal of attention from organic chemists and culminated in many notable achievements. These include the syntheses of $C_{20}H_{20}$-dodecahedrane by Paquette et al.[2a] and Prinzbach et al.,[2b] $C_{20}H_{20}$-pagodane by Prinzbach et al.,[2c] and $C_{20}H_{24}$-propella[3$_4$]prismane by Gleiter et al.[2d] to mention a few.

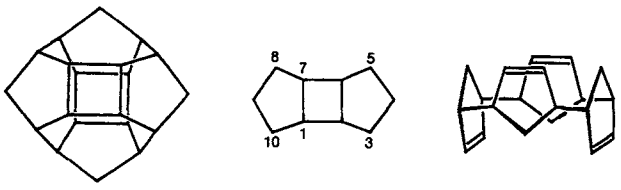

1 **2** **3**

Through this communication, we add a new member to this esoteric C_{20}-family and describe a short synthesis of a nonacyclic $C_{20}H_{24}$-hydrocarbon **1** ("golcondane")[3] of D_{2d} symmetry. Interestingly, the polycyclic ring system of **1** could be regarded either as a dimer of *cis,syn,cis*-tricyclo[5.3.0.0^{2,6}]decane (**2**) with an orthogonal union of the two units through C_3, C_5, C_8, and C_{10} or as a subsequent product of a head-to-tail, cyclic 1,4 tetramer of 1,3-cyclopen-

[*] Prof. G. Mehta, S. H. K. Reddy
School of Chemistry, University of Hyderabad
Hyderabad 500134 (India)
Telefax: Int. code + (842)253145
and
Jawaharlal Nehru Center for Advanced Scientific Research
Indian Institute of Science Campus
Bangalore 560012 (India)

[**] We thank the Indian National Science Academy (award of Ramanujan Research Professorship to GM) and the Council for Scientific and Industrial Research (CSIR; award of a Research Fellowship to SHKR). We thank Dr. D. S. K. Reddy and Dr. M. S. Reddy for their interest.

tadiene (**3**), in which the diametrically opposite pairs of double bonds have undergone [2 + 2] ring closure.

Reaction between *syn*-bisnorborneno-1,4-benzoquinone (**4**)[4] and cyclobutadiene (liberated from its iron tricarbonyl complex with ceric ammonium nitrate) furnished two [4 + 2] *endo* adducts **5**[5, 6] and **6**[5, 6] in a 55:45 ratio and 70% yield. On irradiation with a Hanovia 450 W Hg lamp through a pyrex filter, **5** and **6** underwent smooth intramolecular $[\pi_s^2 + \pi_s^2]$ ring closure to give nonacyclic, annulated bishomocubane diones **7**[5, 7] (61%) and **8**[5] (35%), respectively. The bishomocubanone moiety in **7** was opened through the reductive scission of cyclobutyl bonds conjugating the 1,4-dicarbonyl functionality.[8] Thus, reaction of **7** with Zn in acetic acid under ultrasonication furnished **9**[5] and **10**[5] (16:1, 85%). The octacyclic dione **9** in which one bond has been cleaved could be transformed to heptacycle **10**[5] on further exposure to Zn in ethanol in 30–40% yield. Alternatively, **10** could be accessed directly from **7** in a single-pot reaction with Zn in ethanol, albeit in somewhat lower yield (about 25%). The reductive opening of the cage in **7** rendered the two double bonds proximal, and irradiation of **10** from a 450 W Hanovia lamp led to the desired intramolecular [2 + 2] cycloaddition, and the nonacyclic dione **11**[5] (40%) was readily realized. Its structure was secured through X-ray crystal structure determination.[9] Deoxygenation of **11** presented considerable difficulties, but eventually a modified Wolff–Kishner reduction could be carried out to furnish the $C_{20}H_{24}$-hydrocarbon, golcondane (**1**, 10–20%),[5] which as expected exhibited a 3-line ^{13}C NMR spectrum (δ = 45.63, 41.04, 39.21), while **11** showed a 6-line ^{13}C NMR spectrum. The energy-minimized structure of **1** determined with MMX force-field calculations (Scheme 1, strain energy = 132.4 kcal mol^{-1}, ΔH_f° = 74.9 kcal mol^{-1}) exhibited structural parameters closely resembling those for its precursor dione **11** obtained by X-ray studies.

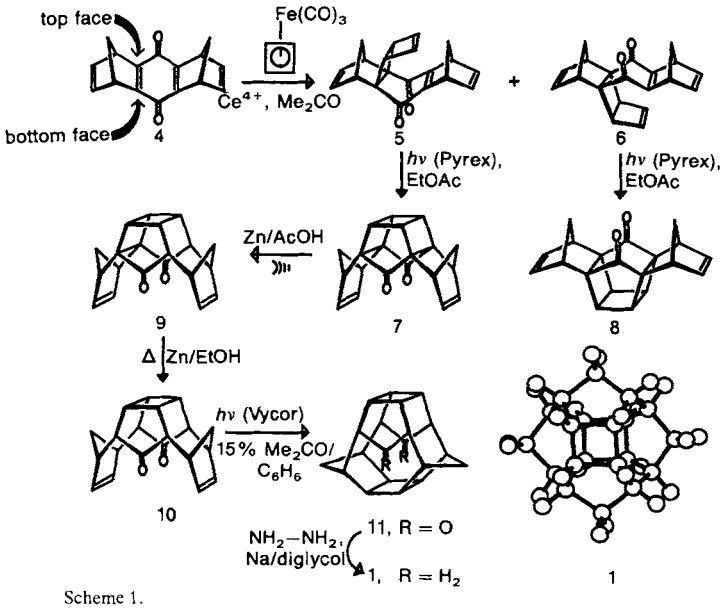

Scheme 1.

The nonacyclic, annulated bishomocubanedione **8** on zinc/acetic acid reduction also furnished the corresponding heptacyclic dione **12** (50%) through reductive scission of two C–C bonds. Several attempts at thermal [2 + 2] cycloreversion in **12** to furnish the novel head-to-head 1,4-cyclic tetramer **13** of 1,3-cyclopentadiene have not borne fruit so far (Scheme 2). Nonetheless, **10** and **12** are potential precursors for **3** and **13**, respectively, besides many other novel polycycles. These possibilities are currently being explored.

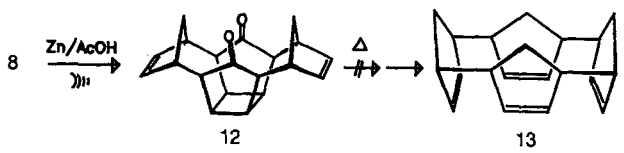

Scheme 2.

Received: January 26, 1993 [Z 5830 IE]
German version: *Angew. Chem.* **1993**, 105, 1230

[1] a) *Cage Hydrocarbons* (Ed.: G. Olah), Wiley, New York, **1990**; b) *Carbocyclic Cage Compounds. Chemistry and Applications* (Eds.: E. Osawa, O. Yonemitsu), VCH Publishers, New York, **1992**; c) N. Anand, T. S. Bindra, S. Ranganathan, *Art in Organic Synthesis*, 2nd ed., Wiley, New York, **1988**.

[2] a) Review: L. A. Paquette, *Chem. Rev.* **1989**, *89*, 1051; b) review: W. D. Fessner, H. Prinzbach in *Organic Synthesis, Modern Trends* (Ed.: O. Chizov), Blackwell, Oxford, **1987**, p. 23; c) W. D. Fessner, G. Sedelmeier, P. R. Spurr, G. Rihs, H. Prinzbach, *J. Am. Chem. Soc.* **1987**, *109*, 4626; d) R. Gleiter, M. Karcher, *Angew. Chem.* **1988**, *100*, 851; *Angew. Chem. Int. Ed. Engl.* **1988**, *27*, 840.

[3] In honor of the 400th anniversary of the founding of the city of Hyderabad, in Southern India, we have named **1** as golcondane, derived from Golconda, the old name of Hyderabad; see the *New Oxford Encyclopedic Dictionary*, Bay Books, Oxford University Press, Oxford, **1983**, p. 720. IUPAC nomenclature for **1**: Nonacyclo[10.7.1.$0^{2,6}$.$0^{4,17}$.$0^{5,8}$.$0^{7,11}$.$0^{9,15}$.$0^{13,19}$.$0^{14,18}$]icosane.

[4] a) G. Mehta, S. Padma, S. R. Karra, K. R. Gopidas, D. R. Cyr, P. K. Das, M. V. George, *J. Org. Chem.* **1989**, *54*, 1342; b) G. Mehta, S. H. K. Reddy, *Tetrahedron Lett.* **1991**, *32*, 4989.

[5] All new compounds were characterized on the basis of ^1H and ^{13}C NMR spectra and analytical data (MS and/or elemental analysis). ^{13}C NMR data in $CDCl_3$ for some key compounds: **1**: ^{13}C NMR (50 MHz): δ = 45.63, 41.04, 39.21; **5**: ^{13}C NMR (25.0 MHz): δ = 197.71, 170.60, 142.83, 140.18, 136.95, 73.88, 62.76, 49.29, 49.00, 48.47, 42.41; **6**: ^{13}C NMR (25.0 MHz): δ = 197.66, 171.00, 143.18, 138.06, 136.24, 72.65, 62.41, 50.59, 49.82, 48.65, 48.29; **7**: ^{13}C NMR (25.0 MHz): δ = 213.07, 134.95, 65.71, 45.06, 43.53, 38.35; **8**: ^{13}C NMR (25 MHz): δ = 214.60, 136.58, 66.88, 49.82, 41.76, 37.41; **10**: ^{13}C NMR (25.0 MHz): δ = 222.95, 134.41, 58.06, 41.88, 41.76, 35.17; **11**: ^{13}C NMR (25.0 MHz): δ = 219.48, 54.06, 42.35, 41.94, 38.00, 36.41.

[6] The stereochemistry of **5** and **6** follows from the analyses of ^1H NMR data and chemical transformations. Further confirmation was obtained through the X-ray crystal structure determination of an interesting photoproduct derived from **5**; see, G. Mehta, S. H. K. Reddy, V. Pattabhi, *J. Chem. Soc. Chem. Commun.* **1992**, 991.

[7] Besides **7**, minor photoproduct(s) resulting from β cleavage were also encountered during the photoirradiation.

[8] E. Wenkert, J. E. Yoder, *J. Org. Chem.* **1970**, *35*, 2986; G. Mehta, K. S. Rao, *ibid.* **1985**, *50*, 5537.

[9] The X-ray crystal structure of **11** was kindly determined by Prof. V. Pattabhi, Department of Biophysics, Madras University, Madras, and will be published elsewhere.

Decamercuration of Ruthenocene**

By *Charles H. Winter*,* *Young-Hee Han*, *Robert L. Ostrander*, and *Arnold L. Rheingold*

The mercuration of transition metal cyclopentadienyl complexes has been largely limited to ferrocene and its

[*] Prof. Dr. C. H. Winter, Y.-H. Han
Department of Chemistry, Wayne State University
Detroit, MI 48202 (USA)
Telefax: Int. + (313) 577-1377
Dr. R. L. Ostrander, Prof. Dr. A. L. Rheingold
Department of Chemistry, University of Delaware
Newark, DE 19716 (USA)

[**] This work was supported by the Air Force Office of Scientific Research (F49620-93-1-0072 to C.H.W.).

derivatives, due to the electron-rich character and high stability of the bis(cyclopentadienyl)iron(II) framework.[1] An early study by Fischer et al. on the mercuration of ruthenocene reported impure mono- and dimercurated complexes,[2a] while Nesmeyanov et al. demonstrated that ruthenocene could be monomercurated in low yield.[2b] Subsequent investigations have revealed that the reaction of ruthenocene with Hg^{II} salts often affords adducts with Ru–Hg bonds, rather than electrophilic substitution products.[3] We recently reported that pentamethylruthenocene is preferentially pentamercurated at the unsubstituted cyclopentadienyl ligand with mercuric acetate.[4] However, extension of mercuration reactions to other transition metal cyclopentadienyl complexes remains speculative due to the electron-poor nature of many complexes relative to ferrocene and pentamethylruthenocene. Herein we report that ruthenocene can be decamercurated in nearly quantitative yield and that the permercurated ruthenocene can be directly halogenated to efficiently afford decahaloruthenocenes. Permercuration of the electron-deficient ruthenocene suggests that a wide variety of permercurated cyclopentadienyl complexes may be accessible. Subsequent derivatization should then provide entry to a variety of new pentahalogenated cyclopentadienyl ligands.

Treatment of ruthenocene with mercuric acetate (10 equiv) in refluxing dichloroethane for 18 h afforded deca(acetoxymercurio)ruthenocene (**1**) in 88% yield as an off-white solid which precipitated from the reaction medium (Scheme 1). Complex **1** was rigorously insoluble in all common solvents, which prevented its analysis by NMR spectroscopy. The complex was, however, characterized by microanalysis and IR spectroscopy. In particular, the IR spectrum of **1** revealed strong absorption bands characteristic of the HgO_2CCH_3 functionality at 1570, 1403, 1382, 1337, and 643 cm^{-1}. By comparison, mercuric acetate showed strong absorption bands at 1555, 1400, 1330, and 653 cm^{-1}.

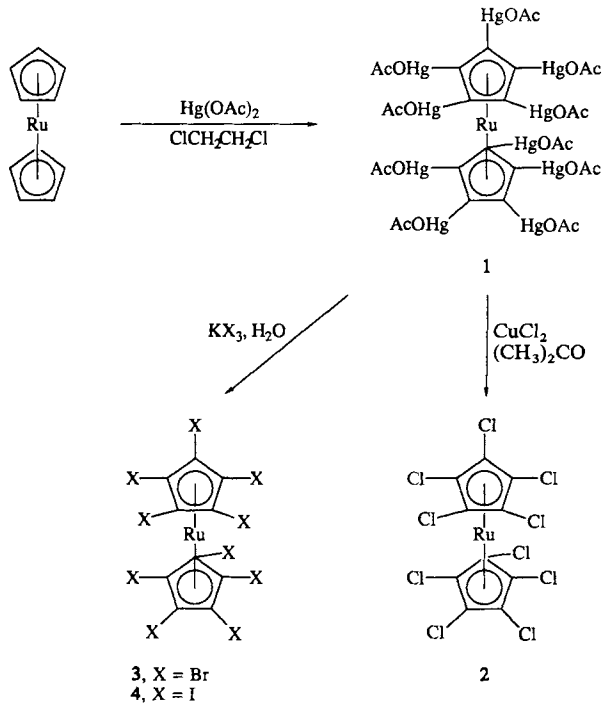

Scheme 1. Synthesis and reactions of **1**. The complexes **1** and **2** were prepared under reflux.

The fully mercurated nature of **1** was confirmed by its reaction with halogenating agents. Treatment of **1** with $CuCl_2$ (50 equiv) in refluxing acetone for 12 h afforded decachlororuthenocene (**2**) in 73% yield as a white crystalline solid after workup (Scheme 1). ^1H NMR spectra of the crude product **2** showed no signals that could be attributed to partially chlorinated ruthenocenes. Reaction of **1** with KBr_3 and KI_3 (prepared from KX and X_2 in water where X = Br or I) afforded decabromoruthenocene (**3**, 47%) and decaiodoruthenocene (**4**, 39%) as white and yellow-ochre solids, respectively.

In order to gain insight into the bonding involved in the decahalometallocenes, the X-ray crystal structure of **3** was determined.[5, 6] Figure 1 shows a perspective view of **3**, in

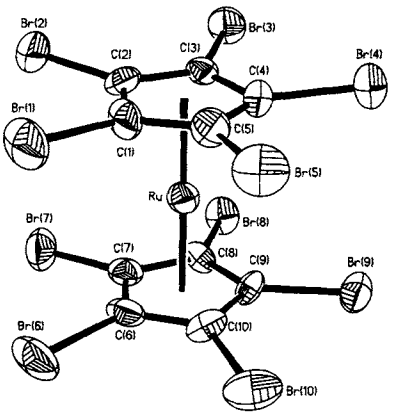

Fig. 1. An ORTEP view of **3** with 35% probability ellipsoids. Selected bond lengths [Å] and angles [°]: Ru-C(1) 2.153(23), Ru-C(2) 2.193(18), Ru-C(3) 2.167(16), Ru-C(4) 2.161(20), Ru-C(5) 2.176(24), Ru-C(6) 2.163(18), Ru-C(7) 2.168(20), Ru-C(8) 2.175(20), Ru-C(9) 2.169(19), Ru-C(10) 2.172(19), Ru-Cp(1) 1.80(2), Ru-Cp(2) 1.81(2); Cp(1)-Ru-Cp(2) 179.4(8).

which two eclipsed η^5-C_5Br_5 ligands are η^5-bonded to the ruthenium atom. The mean Ru–C bond lengths are 2.17 Å and the mean C–C and C–Br bond lengths 1.42 and 1.87 Å, respectively. The ruthenium–cyclopentadienyl centroid distances are 1.80(2) and 1.81(2) Å, with a (C_5Br_5)-Ru-$(C_5Br_5)'$ angle of 179.4(8)°. The ring-to-ring distance is 3.61 Å; thus the distance between the eclipsed interannular bromine substituents is shorter than the sum of their covalent radii (3.84 Å).[7] The bromine substituents are bent slightly out of the plane of the cyclopentadienyl ligands (range 1.7–6.4°, mean 4.2°), away from the ruthenium atom. Despite such close Br–Br contacts, the molecule retains an eclipsed conformation. The structure of **3** is very similar to that previously reported for **2**.[6b, 8] The halogen substituents are eclipsed in both **2** and **3**, and the interannular distances (**3**, 3.61 Å; **2**, 3.598 Å) and average Ru–C distances (**3**, 2.17 Å; **2**, 2.17 Å) are nearly identical. Moreover, the halogen atoms in **2** and **3** show small displacements out of the plane of the C_5 ring away from the ruthenium atom. Unlike **3**, the position of the halogen atoms in **2** could not be attributed to interannular interactions, since the Cl–Cl distances were larger than the sum of their van der Waals radii.

Decamercuration of the relatively electron-poor ruthenocene ($E^0 = 1.03$ V,[9] compared to ferrocene ($E_{1/2} = 0.31$ V[6c]) and pentamethylruthenocene ($E_{1/2} = 0.54$ V[6c])) suggests that a wide variety of other transition metal cyclopentadienyl complexes should undergo pentamercuration. In analogy with **1**, ferrocene can be decamercurated with mercuric acetate in refluxing dichloroethane to afford deca(acetoxymercurio)ferrocene, which can be halogenated

to afford decahaloferrocenes.[10] Chlorination, bromination, and iodination of **1** provides the complexes **2**–**4** in 39–73% yields. Complex **2** was previously prepared in 14% yield by repetitive lithiation/chlorination of ruthenocene.[11] The present synthesis of **2** from **1** is clearly superior.

In summary, pentamercurated cyclopentadienyl ligands should not be viewed as exotic species, but rather as potentially accessible and useful synthetic intermediates.

Experimental Procedure

1: A 250 mL round-bottomed flask was charged with Cp_2Ru (0.231 g, 1.00 mmol), $Hg(OAc)_2$ (3.187 g, 10.0 mmol), and dichloroethane (100 mL). The mixture was refluxed for 18 h, during which time an off-white solid precipitated. The precipitate was collected on a medium glass frit and was washed with hexane (40 mL). Vacuum drying afforded **1** as an off-white powder (2.492 g, 88%). M.p. 200–220 °C (decomposition range, with evolution of elemental mercury); IR (KBr): $\tilde{\nu}$[cm^{-1}] = 1570 (vs, C=O); correct C,H analysis.

2: A 250 mL round-bottomed flask was charged with **1** (1.00 g, 0.355 mmol), $CuCl_2$ (3.03 g, 17.8 mmol), and acetone (80 mL). The resultant mixture was refluxed for 12 h. The volatiles were removed under reduced pressure to give a dark oily solid. The solid was extracted with hexane (100 mL). The hexane extract was applied to a 3 cm column of silica gel on a coarse frit and was eluted with hexane (100 mL) to afford a colorless solution. Removal of the volatile components under reduced pressure, followed by vacuum drying afforded **2** as a white powder (0.149 g, 73%). M.p. > 300 °C (sublimes) [11]; $^{13}C\{^1H\}$ NMR ($CDCl_3$): δ = 91.46 (s, C_5Cl_5); IR (KBr): $\tilde{\nu}$[cm^{-1}] = 1386 (m), 1351 (s), 1310 (m), 1095 (w), 928 (w), 811 (w), 703 (s), 564 (w), 409 (s); MS (20 eV): *m/z* 576 (M^+, 100%), the isotope distribution pattern of the parent mass envelope was identical with the calculated pattern.

3: A 100 mL round-bottom flask was charged with KBr (0.484 g, 4.07 mmol), bromine (0.208 mL, 4.07 mmol), and water (50 mL). The resultant mixture was stirred at ambient temperature for 0.5 h, and then **1** (1.146 g, 0.407 mmol) was added. The mixture was stirred at ambient temperature for 3 h, during which time a white precipitate formed. The crude product was collected on a medium-porosity glass frit and washed with methanol (20 mL). The precipitate was then extracted with dichloromethane (100 mL) to afford a colorless solution. This solution was applied to a 3 cm pad of silica gel on a coarse glass frit. Elution with dichloromethane (50 mL) afforded a colorless solution. Removal of the volatile components under reduced pressure afforded **3** as an analytically pure white powder (0.194 g, 47%). M.p. (sealed tube) > 300 °C; $^{13}C\{^1H\}$ NMR ($CDCl_3$): δ = 84.51 (s, C_5Br_5); IR (KBr): $\tilde{\nu}$[cm^{-1}] = 1379 (m), 1302 (s), 1274 (w), 589 (s); MS (20 eV): *m/z* 1020 (M^+, 100%), the isotope distribution pattern of the parent mass envelope was identical with the calculated pattern; correct C,H analysis.

4: A 100 mL round-bottom flask was charged with KI (0.830 g, 5.00 mmol), iodine (1.269 g, 5.00 mmol), water (50 mL), and a stir bar. The resultant mixture was stirred at ambient temperature for 1 h and then **1** (1.409 g, 0.50 mmol) was added. The mixture was stirred at ambient temperature for 5 h, during which time an orange-colored precipitate formed. The crude product was collected on a medium-porosity glass frit and was washed with aqueous potassium iodide (0.1 M, 100 mL), water (20 mL), water (20 mL), and methanol (100 mL) to remove mercury impurities. The residue was placed in a paper thimble and was extracted with acetone in a Soxhlet extractor for 24 h to remove additional mercury impurities. Vacuum drying in a drying pistol for 24 h afforded **4** as a yellow-ochre powder (0.292 g, 39%). M.p. 240–260 °C (decomposition range); $^{13}C\{^1H\}$ NMR ([D$_6$]DMSO): δ = 69.94 (s, C_5I_5); IR (KBr): $\tilde{\nu}$[cm^{-1}] = 1246 (m), 506 (m); MS (20 eV): *m/z* 1110 ([M − 3I]$^+$, 3%), the isotope distribution pattern of the [M − 3I]$^+$ mass envelope was identical with the calculated pattern; correct C,H analysis.

Received: March 4, 1993 [Z 5903 IE]
German version: *Angew. Chem.* **1993**, *105*, 1247

[1] For leading references, see: C. W. Fung, R. M. G. Roberts, *Tetrahedron* **1980**, 3289; B. Floris, G. Illuminati, *Coord. Chem. Rev.* **1975**, *16*, 107; W. Kitching, *Organomet. Chem. Rev.* **1968**, *3*, 35; L. G. Makarova in *Organometallic Reactions, Vol. 1* (Eds.: E. I. Becker, M. Tsutsui), Wiley-Interscience, New York, **1970**, p. 119; V. I. Popov, M. Lieb, A. Haas, *Ukr. Khim. Zh.* **1990**, *56*, 1115. See also: G. Amiet, K. Nicholas, R. Pettit, *J. Chem. Soc. Chem. Commun.* **1970**, 161; A. N. Nesmeyanov, K. N. Anisimov, Z. P. Valuava, *Izv. Akad. Nauk. SSSR Otdel. Khim. Nauk.* **1962**, 1683; M. D. Rausch, R. A. Genetti, *J. Org. Chem.* **1970**, *35*, 3888.

[2] a) M. D. Rausch, E. O. Fischer, H. Grubert, *J. Am. Chem. Soc.* **1960**, *82*, 76; b) A. N. Nesmeyanov, A. A. Lubovich, S. P. Gubin, *Izv. Akad. Nauk. SSSR Ser. Khim.* **1972**, 1823.

[3] W. H. Morrison, D. H. Hendrickson, *Inorg. Chem.* **1972**, *11*, 2912; A. I. Gusev, Y. T.Struchkov, *Zh. Strukt. Khim.* **1972**,*6*, 1121; L. I. Denisovich, N. V. Zakurin, A. A. Bezrukova, S. P. Gubin, *J. Organomet. Chem.* **1974**, *81*, 207.

[4] C. H. Winter, Y.-H. Han, M. J. Heeg, *Organometallics* **1992**, *11*, 3169. For the decamercuration of ferrocene, see: V. I. Boev, A. V. Dombrovskii, *Zh. Obshch. Khim.* **1977**, *47*, 727; *Izv. Vyssh. Uchebn. Zaved. Khim. Khim. Tekhnol.* **1977**, *20*, 1789.

[5] $C_{10}Br_{10}Ru$ (**3**): M = 1020.3, triclinic, P$\bar{1}$, a = 7.600(2), b = 8.915(3), c = 14.617(5) Å, α = 89.50(3), β = 84.88(2), γ = 78.14(2)°, V = 965.3(5) Å^3, Z = 2, ϱ_{calcd} = 3.510 g cm^{-3}, $\mu(Mo_{K\alpha})$ = 214.97 cm^{-1}, T = 295 K, 3398 independent reflections with $4° \le 2\theta \le 50°$ were collected (Siemens P4), of which 1624 reflections with F_o greater than $5\sigma(F_o)$ were used in refinement. R = 0.0525, R_w = 0.060, GOF = 1.19. The centrosymmetric space group was chosen on the initial basis of E values and was retained on the basis of the refinement statistics. A semiempirical absorption correction based on 216 data (ψ-scans of 6 reflections at 10° increments) was applied, T(max)/T(min) = 4.82. There were no unusual bond lengths or angles. All atoms were refined anisotropically. Further details of the crystal structure investigation may be obtained from the Fachinformationszentrum Karlsruhe, Gesellschaft für wissenschaftlich-technische Information mbH, D-76344 Eggenstein-Leopoldshafen (FRG), on quoting the depository number CSD-57327, the names of the authors, and the journal citation.

[6] For crystal structure determinations of complexes containing pentachlorocyclopentadienyl and pentabromocyclopentadienyl ligands, see: a) V. W. Day, K. J. Reimer, A. Shaver, *J. Chem. Soc. Chem. Commun.* **1975**, 403; b) G. M. Brown, F. L. Hedberg, H. Rosenberg, *ibid.* **1972**, 5; c) P. G. Gassman, C. H. Winter, *J. Am. Chem. Soc.* **1988**, *100*, 6130; d) W. Priebsch, M. Hoch, D. Rehder, *Chem. Ber.* **1988**, *121*, 1971. See also: O. J. Curnow, R. P. Hughes, *J. Am. Chem. Soc.* **1992**, *114*, 5895.

[7] A. Bondi, *J. Phys. Chem.* **1964**, *68*, 441.

[8] For selected structure determinations of ruthenocenes, see: P. Seiler, J. D. Dunitz, *Acta Crystallogr. Sect. B* **1980**, *36*, 2946; D. C. Liles, A. Shaver, E. Singleton, M. B. Wiege, *J. Organomet. Chem.* **1985**, *288*, C33; J. Trotter, *Acta Crystallogr.* **1963**, *16*, 571; G. Small, J. Trotter, *Can. J. Chem.* **1964**, *42*, 1746; H. Schmid, M. L. Ziegler, *Chem. Ber.* **1976**, *109*, 125; E. O. Fischer, F. J. Gammel, J. O. Besenhard, A. Frank, D. Neugebauer, *J. Organomet. Chem.* **1980**, *191*, 261.

[9] M. G. Hill, W. M. Lamanna, K. R. Mann, *Inorg. Chem.* **1991**, *30*, 4690.

[10] Y. H. Han, C. H. Winter, unpublished results.

[11] F. L. Hedberg, H. Rosenberg, *J. Am. Chem. Soc.* **1973**, *95*, 870.

Synthesis and Structure of a Diphospha[4]radialene**

By *Kozo Toyota, Katsuya Tashiro*, and *Masaaki Yoshifuji**

Sterically protected phosphorus-containing multiple-bonded compounds are currently of interest. Our studies have centered on compounds that contain cumulative double bonds or conjugated π-electron systems with phosphorus atom(s) in low coordination states,[1,2] as well as diphosphenes[3] and phosphaethenes.[4] Recently Appel et al.,[5] Märkl et al.,[6] and ourselves[7–9] have reported the preparation and isolation of diphosphinidenecyclobutenes **1a**–**c**, which utilizes 2,4,6-tri-*tert*-butylphenyl (Ar) as a protecting group. We now report the synthesis and structure of a diphosphinidenecyclobutene with an extended π-electron system, namely a diphospha[4]radialene (1,2-dimethylene-3,4-diphosphinidenecyclobutane) **5**.

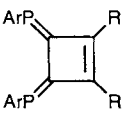

1a: R = $SiMe_3$
1b: R = Ph
1c: R = H

Ar = 2,4,6-tBu$_3$C$_6$H$_2$

[*] Prof. Dr. M. Yoshifuji, Dr. K. Toyota, K. Tashiro
Department of Chemistry, Faculty of Science
Tohoku University, Aoba, Sendai 980 (Japan)
Telefax: Int. code + (22)224-2029

[**] This work was supported in part by the Japanese Ministry of Education, Science and Culture (Grants-in-Aid for Scientific Research), and Funds from the Asahi Glass Foundation. We thank Tosoh Akzo Co., Ltd. and Shin-Etsu Chemical Co., Ltd. for chemicals.

The alkynyl-substituted phosphane **2** was prepared by the reaction of 3-phenyl-1-propynylmagnesium bromide with ArPHCl (spectroscopic data of **2** and the other new compounds are given in Table 1). By using the method employed for the preparation of **1a**, compound **2** was then converted into **3** (Scheme 1).[7] Subsequent bromination of **3** with 2 equivalents of *N*-bromosuccinimide (NBS) gave **4** as an intermediate, which was then allowed to react with butyllithium at −78 °C to give the first diphospha[4]radialene **5** as an orange solid.

Table 1. Selected spectroscopic data of **2**, **3**, and **5** [a].

2: Pale yellow needles (acetonitrile), m.p. 64–65 °C. ^{31}P NMR (81 MHz, $CDCl_3$, 25 °C, 85% H_3PO_4 ext.): $\delta = -100.9$ (d, $^1J(P,H) = 246.9$ Hz); ^1H NMR (200 MHz, $CDCl_3$, 25 °C, TMS): $\delta = 1.41$ (s, 9H; *p*-*t*Bu), 1.72 (s, 18H; *o*-*t*Bu), 3.67 (d, $^4J(P,H) = 4.6$ Hz, 2H; CH_2), 5.88 (d, $^1J(P,H) = 247.0$ Hz, 1H; PH), 7.28 (bs, 5H; Ph), 7.55 (d, $^4J(P,H) = 2.0$ Hz, 2H; *m*-Ar); $^{13}C\{^1H\}$ NMR (50 MHz, $CDCl_3$, 25 °C, TMS): $\delta = 26.6$ (d, $^3J(P,C) = 1.4$ Hz, CH_2), 31.4 (s, *p*-CMe_3), 33.8 (d, $^4J(P,C) = 6.8$ Hz, *o*-CMe_3), 35.2 (s, *p*-CMe_3), 38.6 (d, $^3J(P,C) = 0.7$ Hz, *o*-CMe_3), 80.0 (d, $^1J(P,C) = 19.4$ Hz, PC≡C), 101.7 (s, PC≡*C*), 122.8 (d, $^3J(P,C) = 4.4$ Hz, *m*-Ar), 126.4 (s, Ph) 126.5 (d, $^1J(P,C) = 25.7$ Hz, *ipso*-Ar), 127.9 (s, Ph), 128.4 (s, Ph), 136.5 (d, $^4J(P,C) = 1.5$ Hz, *ipso*-Ph), 150.6 (s, *p*-Ar), 155.5 (d, $^2J(P,C) = 10.0$ Hz, *o*-Ar). IR (KBr): $\tilde{\nu}$[cm^{-1}] = 2403, 2183, 1595, 1495, 1454, 1363, 729, 696. UV/VIS (hexane): λ_{max} (lg ε) = 235 (sh 4.11), 284 nm (3.25). MS (EI, 70 eV): *m*/*z* (%): 392 (19) [M^+], 391 (34) [$M^+ - 1$], 277 (18) [$ArP^+ + 1$], 57 (100) [$t Bu^+$]; HRMS (EI, 70 eV): found: *m*/*z* 392.2633; calcd for $C_{27}H_{37}P$: M = 392.2631.

3: Pale yellow powder, m.p. 190.5–191.5 °C. $^{31}P\{^1H\}$ NMR ($CDCl_3$): $\delta = 154.0$; ^1H NMR ($CDCl_3$): $\delta = 1.23$ (s, 18H; *p*-*t*Bu), 1.53 (s, 36H; *o*-*t*Bu), 2.00 (s, 4H; CH_2), 6.31 (d, $^3J(H,H) = 7.6$ Hz, 4H; *o*-Ph), 6.92 (dd, $^3J(H,H) = 7.6$ Hz, $^3J(H,H) = 7.6$ Hz, 4H; *m*-Ph), 6.95 (t, $^3J(H,H) = 7.6$ Hz, 2H; *p*-Ph), 7.30 (s, 4H; Ar); $^{13}C\{^1H\}$ NMR (150 MHz, $CDCl_3$): $\delta = 31.3$ (s, *p*-CMe_3), 32.2 (s, CH_2), 33.1 (s, *o*-CMe_3), 34.9 (s, *p*-CMe_3), 38.1 (s, *o*-CMe_3), 121.1 (s, *m*-Ar), 125.4 (s, *p*-Ph) 127.6 (s, *m*-Ph), 128.2 (s, *o*-Ph), 134.9 (ABX, *ipso*-Ar), 137.4 (s, *ipso*-Ph), 149.9 (s, *p*-Ar), 155.4 (s, *o*-Ar), 160.7 (ABX, P = C-*C*), 180.6 (d, $^1J(P,C) = 25.1$ Hz, P = *C*-C). IR (KBr): $\tilde{\nu}$[cm^{-1}] = 1589, 1477, 1392, 1362, 1240, 876, 756, 729, 696. UV/VIS (hexane): λ_{max} (lg ε) = 244 (4.50), 298 (4.58), 340 nm (4.03). MS (70 eV): *m*/*z* (%): 782 (27) [M^+], 537 (26) [$M^+ - Ar$], 275 (26) [$ArP^+ - 1$], 57 (100) [$t Bu^+$]; HRMS (70 eV): found: *m*/*z* 782.5109; calcd for $C_{54}H_{72}P_2$: M = 782.5106.

5: Orange prisms (toluene/CH_2Cl_2), m.p. 223–224.5 °C. $^{31}P\{^1H\}$ NMR ($CDCl_3$): $\delta = 190.7$; ^1H NMR ($CDCl_3$): $\delta = 1.41$ (s, 18H; *p*-*t*Bu), 1.59 (s, 36H; *o*-*t*Bu), 4.50 (s, 2H; C*H*Ph), 6.17 (d, $^3J(H,H) = 7.3$ Hz, 4H; *o*-Ph), 6.52 (dd, $^3J(H,H) = 7.4$ Hz, $^3J(H,H) = 7.3$ Hz, 4H; *m*-Ph), 6.70 (t, $^3J(H,H) = 7.4$ Hz, 2H; *p*-Ph), 7.51 (s, 4H; Ar); $^{13}C\{^1H\}$ NMR (150 MHz, $CDCl_3$): $\delta = 31.6$ (s, *p*-CMe_3), 32.5 (s, *o*-CMe_e), 35.1 (s, *p*-CMe_3), 38.2 (s, *o*-CMe_3), 122.2 (s, *m*-Ar), 123.7 (dd, $^3J(P,C) = 5.4$ Hz, $^4J(P,C) = 5.4$ Hz, *C*HPh), 126.3 (s, *m*-Ph), 126.6 (s, *p*-Ph), 128.2 (s, *o*-Ph), 135.0 (ABX, *ipso*-Ar), 136.8 (s, *ipso*-Ph), 143.0 (s, P = C-*C*), 150.5 (s, *p*-Ar), 154.5 (s, *o*-Ar), 182.5 (dd, $^1J(P,C) = 15.0$ Hz, $^2J(P,C) = 10.5$ Hz, P = *C*-C). IR (KBr): $\tilde{\nu}$[cm^{-1}] = 1591, 1477, 1394, 1363, 877, 758, 742, 696. UV/VIS (CH_2Cl_2): λ_{max} (lg ε) = 243 (4.52), 327 (4.67), 425 (3.87), 502 nm (sh, 3.72). MS (70 eV): *m*/*z* (%): 780 (50) [M^+], 535 (18) [$M^+ - Ar$], 390 (8) [$M^+/2$], 57 (100) [$t Bu^+$]; HRMS (70 eV): found: *m*/*z* 780.4952; calcd for $C_{54}H_{70}P_2$: M = 780.4949.

[a] NMR spectra: Bruker AC200P or Bruker AM600.

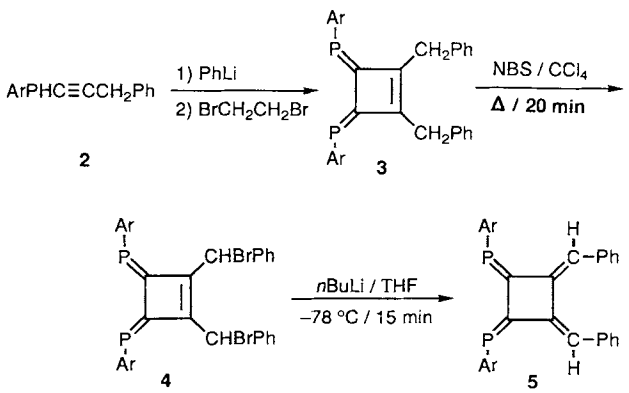

Scheme 1. Δ: heating under reflux.

The structure of (*E*,*E*,*E*,*E*)-1,2-dibenzylidene-3,4-bis-[(2,4,6-tri-*tert*-butylphenyl)phosphinidene]cyclobutane (**5**) was unambiguously confirmed by X-ray crystallography (Fig. 1).[10] The arrangement of the two phenyl groups in the benzylidene moieties is more crowded than that of the two bulky Ar groups, which point away from each other.

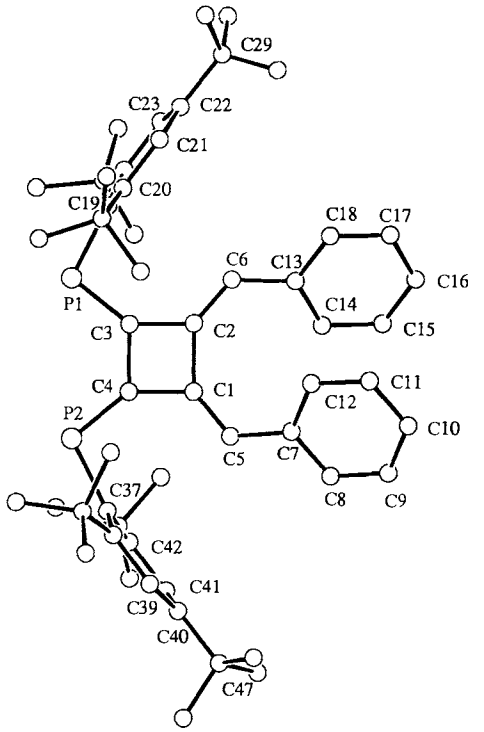

Fig. 1. Molecular structure of **5** (ORTEP). Important bond lengths [Å] and angles [°]: C1-C2 1.521(7), C2-C3 1.481(6), C3-C4 1.499(6), C4-C1 1.507(7), P1-C3 1.683(5), P2-C4 1.669(5), P1-C19 1.851(5), P2-C37 1.849(5), C1-C5 1.345(7), C2-C6 1.332(6), C5-C7 1.472(7), C6-C13 1.463(7); C3-P1-C19 101.2(2), C4-P2-C37 102.1(2), C1-C2-C3 89.6(4), C2-C3-C4 91.2(4), C3-C4-C1 89.4(4), C4-C1-C2 89.4(4), P1-C3-C2 141.1(4), P1-C3-C4 127.7(4), P2-C4-C3 129.4(4), P2-C4-C1 140.9(4), C1-C2-C6 139.1(5), C3-C2-C6 130.8(5), C2-C1-C5 139.5(5), C4-C1-C5 130.7(5), C1-C5-C7 127.9(5), C2-C6-C13 130.2(5), C5-C7-C8 119.4(6), C6-C13-C14 121.1(6), P1-C19-C20 119.6(4), P2-C37-C38 119.5(4).

The atoms C1, C2, C3, and C4 are coplanar within 0.03 Å, and the atoms P1 and P2 only deviate from this plane by 0.15 and −0.01 Å, respectively. Furthermore, the atoms C5 and C6 lie almost in the plane (C1–C4) (deviations 0.22 and −0.23 Å, respectively); thus this radialene framework is almost planar. The two phenyl groups (C7–C12) and (C13–C18) form angles of 34.1 and 38.3°, respectively, with the (C1–C4) plane. The two Ar protecting groups are tilted by 78.2 and 91.9° from the plane (C1–C4), while their benzene rings are slightly deformed into boat forms; commonly observed for compounds with Ar–P units.[11] The "bow" atoms (C19 and C37) of these boat-shaped benzene rings are located 6.1° and 9.3° above the bottoms (C20, C21, C23, C24) and (C38, C39, C41, C42), respectively, while the "stern" atoms, (C22 and C40) are 4.2° and 4.2°, respectively, above the bottoms. In contrast to the octaphenyl[4]-radialene **6** reported by Iyoda et al.,[12] the overall shape of this diphospha[4]radialene **5** is highly symmetric.

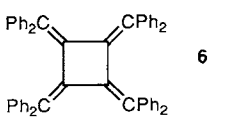

6

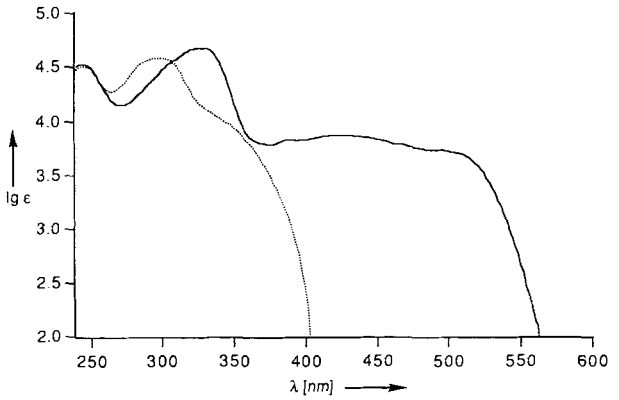

Fig. 2. UV/VIS spectra of **5** (solid line) and **3** (dotted line).

Figure 2 shows the UV/VIS spectra of the radialene **5** and the diphosphinidenecyclobutene **3**, indicating that the absorption spectrum of **5** shows a red shift compared to that of **3**. The absorption peaks due to $\pi-\pi^*$ transition for both **3** and **5** appeared at 243–244 nm with almost equal intensities, in contrast the absorption band at 298 nm due to the conjugated double bonds associated with phosphorus atom(s) for **3** is shifted by about 30 nm to a longer wavelength at 327 nm with a slightly increased intensity for **5**. Moreover, a featureless band above 400 nm appeared in the spectrum of **5**, indicating a very extended conjugated π-electron system. Similar bands also occur in the carbon analogues of **5**,[12, 13] suggesting that the diphospha[4]radialene **5** contains a new π-electron system,[14] which in terms of its electro-, photo-, and coordination chemistry is of interest.

Experimental Procedure

2: Under argon at room temperature, 3-phenyl-1-propyne (0.92 g, 7.9 mmol) in THF (5 mL) was added to one equivalent of ethylmagnesium bromide in THF (12 mL), and stirred for 3 h. To this solution was added 2,4,6-tri-*tert*-butylphenyl(chloro)phosphane (ArPHCl) (7.2 mmol)[15] in THF (10 mL) at 0 °C, and the mixture was stirred for 20 min. After workup (including chromatography on silica gel) and recrystallization from acetonitrile, **2** (1.3 g, 3.3 mmol) was obtained in 46% yield (based on the starting material $ArPH_2$ (2.0 g, 7.2 mmol) used for the preparation of ArPHCl).

3: Under argon and in the dark, **2** (1.3 g, 3.3 mmol) in THF (15 mL) was allowed to react with one equivalent of phenyllithium (1.05 M, cyclohexane/ether solution) at −78 °C, and then stirred for 30 min at room temperature. The solution was cooled to −78 °C and 1,2-dibromoethane (0.28 mL, 3.2 mmol) was added, the mixture was then gradually allowed to warm up to room temperature and stirred for 1 h. The chromatographic workup on silica gel gave **3** (0.31 g, 0.40 mmol) in 24% yield.

5: The cyclobutene **3** (52.8 mg, 0.0674 mmol) in CCl_4 (2.5 mL) was brominated with NBS (24.7 mg, 0.139 mmol) under reflux for 25 min. After the succinimide had been filtered off, the filtrate was concentrated to give a yellow solid. This solid contained about 60% [16] bromobenzylcyclobutene **4** (a 1:1 mixture of *dl* and *meso* form $\delta(^{31}P) = 175.8$ and 175.7). The dibromide **4** thus obtained was dissolved in THF (5 mL) and was allowed to react with butyllithium (0.135 mmol, 1.63 M, hexane) for 15 min at −78 °C and 30 min at room temperature in THF to give an orange solution. The solution was concentrated, and the resulting solid was washed with acetonitrile. Chromatographic workup (silica gel, hexane) gave 11.1 mg of **5** as an orange solid in 21% yield (based on **3**). Similar results were obtained when zinc powder (4 equiv) was used to eliminate the bromine (in diglyme at 50 °C for 13 h) (**5**, 21% yield).

Received: March 27, 1993 [Z 5948 IE]
German version: *Angew. Chem.* **1993**, *105*, 1256

[1] M. Yoshifuji, K. Toyota, K. Shibayama, N. Inamoto, *Tetrahedron Lett.* **1984**, *25*, 1809; M. Yoshifuji, H. Yoshimura, K. Toyota, *Chem. Lett.* **1990**, 827.

[2] M. Yoshifuji, K. Toyota, N. Inamoto, *J. Chem. Soc. Chem. Commun.* **1984**, 689; M. Yoshifuji, S. Sasaki, N. Inamoto, *ibid.* **1989**, 1732; H. H. Karsch, F. H. Köhler, H.-U. Reisacher, *Tetrahedron Lett.* **1984**, *25*, 3687; R. Appel, P. Fölling, B. Josten, M. Siray, V. Winkhaus, F. Knoch, *Angew. Chem.* **1984**, *96*, 621; *Angew. Chem. Int. Ed. Engl.* **1984**, *23*, 619.

[3] M. Yoshifuji, I.Shima, N. Inamoto, K. Hirotsu, T. Higuchi, *J. Am. Chem. Soc.* **1981**, *103*, 4587; *ibid.* **1982**, *104*, 6167.

[4] M. Yoshifuji, K. Toyota, I. Matsuda, T. Niitsu, N. Inamoto, K. Hirotsu, T. Higuchi, *Tetrahedron* **1988**, *44*, 1363.

[5] R. Appel, V. Winkhaus, F. Knoch, *Chem. Ber.* **1987**, *120*, 243.

[6] G. Märkl, P. Kreitmeier, H. Nöth, K. Polborn, *Angew. Chem.* **1990**, *102*, 958; *Angew. Chem. Int. Ed. Engl.* **1990**, *29*, 927.

[7] M. Yoshifuji, K. Toyota, M. Murayama, H. Yoshimura, A. Okamoto, K. Hirotsu, S. Nagase, *Chem. Lett.* **1990**, 2195.

[8] K. Toyota, K. Tashiro, M. Yoshifuji, *Chem. Lett.* **1991**, 2079.

[9] K. Toyota, K. Tashiro, M. Yoshifuji, S. Nagase, *Bull. Chem. Soc. Jpn.* **1992**, *65*, 2297.

[10] Crystal data of **5**: recrystallized from a mixture of toluene and dichloromethane. $C_{54}H_{70}P_2$, $M_r = 781.09$. Monoclinic, space group $P2_1/c$, $a = 15.03(1)$, $b = 15.405(5)$, $c = 21.288(3)$ Å; $\beta = 93.93(3)°$; $V = 4918(3)$ Å^3, $Z = 4$, $\varrho_{calcd} = 1.055$ g cm^{-3}, $\mu = 1.16$ cm^{-1}; 9383 reflections with $2\theta \leq 50.0°$ were recorded on a four-circle diffractometer ($Mo_{K\alpha}$ radiation, graphite monochromator). Of these, 4047 with $I > 3\sigma(I)$ were judged as observed. The structure was solved with MULTAN88 [17]. The non-hydrogen atoms were refined anisotropically. Hydrogen atoms were included, but their positions were not refined. $R = 0.069$, $R_w = 0.045$. Further details of the crystal structure investigation are available on request from the Director of the Cambridge Crystallographic Data Centre, 12 Union Road, GB-Cambridge CB2 1EZ, (UK), on quoting the full journal citation.

[11] M. Yoshifuji, N. Inamoto, K. Hirotsu, T. Higuchi, *J. Chem. Soc. Chem. Commun.* **1985**, 1109.

[12] M. Iyoda, H. Otani, M. Oda, Y. Kai, Y. Baba, N. Kasai, *J. Am. Chem. Soc.* **1986**, *108*, 5371.

[13] F. Toda, K. Kumada, N. Ishiguro, K. Akagi, *Bull. Chem Soc. Jpn.* **1970**, *43*, 3535; K. Tanaka, F. Toda, *Tetrahedron Lett.* **1980**, *21*, 2713.

[14] H. Hopf, G. Maas, *Angew. Chem.* **1992**, *104*, 953; *Angew. Chem. Int. Ed. Engl.* **1992**, *31*, 931.

[15] M. Yoshifuji, S. Sasaki, N. Inamoto, *Tetrahedron Lett.* **1989**, *30*, 839.

[16] In addition the yellow solid contained 1,6-bis(2,4,6-tri-*tert*-butylphenyl)-3,4-bis(α-bromobenzyl)-1,6-diphospha-1,2,4,5-hexatetraene (about 40%) which was also a 1:1 mixture of the *dl* and *meso* forms ($\delta(^{31}P) = 49.7$ and 47.9). Attempted purification has not yet been successful because of the instability of **4**. Therefore the subsequent reaction was carried out without purification.

[17] T. Debaerdemaeker, G. Germain, P. Main, L. S. Refaat, C. Tate, M. M. Woolfson, *Computer Programs for the Automatic Solution of Crystal Structures from X-Ray Diffraction Data*, University of York, **1988**.

Molecular Self-Organization of Amphotropic Cyanobiphenyl Mesogens**

By *Detlev Joachimi, Carsten Tschierske,* Henning Müller, Joachim Heinz Wendorff, Ludolf Schneider,* and *Ralf Kleppinger*

Hydrogen bonds are directed interactions whose energies lie between those of covalent bonds and nonspecific, intermolecular interactions. Intermolecular hydrogen bonds are, therefore, very important in the formation of macrostructures in biological systems. Molecular self-organization through hydrogen bonds also plays an important role in materials science. This is expressed, amongst other properties, in the formation of liquid crystalline phases which represent a state of matter characterized by order and mobility at the molecular level. The amphiphilic carbohydrate deriva-

[*] Dr. habil. C. Tschierske, Dr. D. Joachimi, H. Müller
Institut für Organische Chemie der Universität Halle-Wittenberg
Weinbergweg 16, PSF 8, D-06120 Halle (FRG)
Telefax: Int. code + (345) 649065
Prof. Dr. J. H. Wendorff, L. Schneider, R. Kleppinger
Institut für Physikalische Chemie der Universität Marburg (FRG)

[**] This work was supported by the Deutsche Forschungsgemeinschaft and the Fonds der Chemischen Industrie. We thank Merck for the donation of chemicals. The names of the compounds in this publication do not conform to IUPAC nomenclature since cyanobiphenyl is an accepted term in the field of liquid crystals (Editorial note).

tives and polyhydroxyl amphiphiles which form lamellar or columnar macrostructures are an important class of compounds whose mesogenicity depends on the ability to form hydrogen bonds.[1] Amphiphilic *n*-alkane-1,2-diols, for example **1**, may be regarded as the simplest compounds of this type.[2] In certain temperature ranges these compounds show lamellar mesophases in which the molecules are arranged in layers, and the hydroxyl groups are linked through a dynamic network of cooperative hydrogen bonds. The liquid crystalline phases of these compounds can be modified and stabilized by the inclusion of rigid calamitic structural elements (Fig. 1).[3,4] Comparison of compounds **3** and **4** shows that

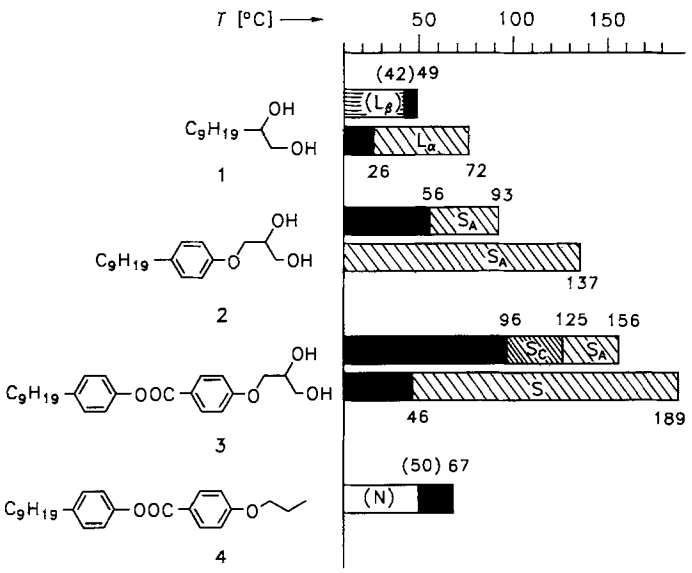

Fig. 1. The influence of calamitic structural elements of different lengths on the liquid crystalline properties of amphiphilic diols, and the comparison of the amphiphilic diol **3** [4] with a nonamphiphilic mesogen **4** [5]. The lower bars for compounds **1**, **2**, and **3** represent the lyotropic mesophase behavior of samples saturated with water. For an explanation of the abbreviations see Table 1 [a].

the introduction of a 1,2-diol unit to the end of an *n*-alkyl side chain of the nonamphiphilic phenyl benzoate **4** causes the change from a nematic mesophase to a smectic phase.

4'-Alkoxy-4-cyanobiphenyls are also known to be calamitic liquid crystals.[5] We have attempted to combine the two types of mesogenic molecular structures—the amphiphilic diols and the calamitic cyanobiphenyl mesogens—and have examined how this affects the ability for molecular self-organization.

The phase transition temperatures of the 4'-[ω,(ω − 1)-dihydroxyalkoxy]-4-cyanobiphenyls **5** which we have synthesized are collected in Table 1, and compared with the analogous 4'-alkoxy-4-cyanobiphenyls **6**. It can be seen that the stability of liquid crystalline phases is raised considerably by the introduction of the 1,2-diol unit. But in spite of the diol group no induction of a smectic phase is observed. On the contrary, while compound **6c** shows a smectic A phase stable up to 67 °C, the 1,2-diol derivative **5d** can be supercooled to 55 °C without any sign of a phase transition. The appearance of a smectic A phase is first observed with compound **5e**. Its stability increases with further chain extension (**5f**) and finally completely displaces the nematic phase. X-ray scattering measurements on the nematic phase of **5c** shows two diffuse halos. The halo observed in the wide angle range at $2\theta = 20°$ corresponds to a mean distance of

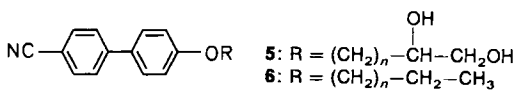

Table 1. Comparison of the phase transitions [a] and associated temperatures T [°C] of 4'-[ω,(ω −1)-dihydroxy]-4-cyanobiphenyls **5** [b] and 4'-alkoxy-4-cyanobiphenyls **6** [5].

n	Compd.	Phase, *T*	Compd.	Phase, *T*
1	**5a**	cr116 N* 129is [c]		
2	**5b**	cr115 N 133is	**6a**	cr78 (N77.5) is
		cr86 S_A 166is [d, e]		
4	**5c**	cr97 N 125is	**6b**	cr57 N75.5is
		cr57 S_A 133is [d, f]		
6	**5d**	cr82 N 119is	**6c**	cr54 S_A 67N80is
		cr S_A 128is [d, e]		
8	**5e**	cr98 S_A 110N 110.5is	**6d**	cr59.5 S_A 87.5is
		cr S_A 122is [d, e]		
9	**5f**	cr111 S_A 127is		

[a] Determined on a hot table by using a polarization microsope; abbreviations: cr = crystalline; N = nematic mesophase; N* = cholesteric mesophase; S_A = smectic A phase; S_c = smectic C phase; is = isotropic liquid; L_α, L_β = lamellar mesophases; the values in parentheses characterize monotropic (metastable) mesophases. [b] Correct C,H analyses, ^{1}H NMR and ^{13}C NMR spectra available. [c] (*S*) enantiomer, see [6]. [d] Phase transition temperatures of the water-saturated samples. [e] Determined by observations of contact preparations in sealed glass capillaries with a polarization microscope. [f] From DSC measurements.

0.44 nm, and is assigned to the closely associated alkyl chains. In the narrow angle region there is a broad halo which is typical for a nematic phase. The average distance is about 1.5 nm, which indicates that no stable dimers, such as those known to occur with mesogenic carboxylic acids, are found in the nematic phase. Thus no influence of hydrogen bonding on the structural parameters can be demonstrated. Here the hydrogen bonds function exclusively as stabilizers of the mesophase. In Figure 2 sections of the IR spectra of compound **5c** and 1,2-propanediol are compared. The absorption maximum for both compounds shifts to higher wave numbers with rising temperature. This is a result of the breaking of intermolecular hydrogen bonds between the diol groups with rising temperature. In comparison with 1,2-

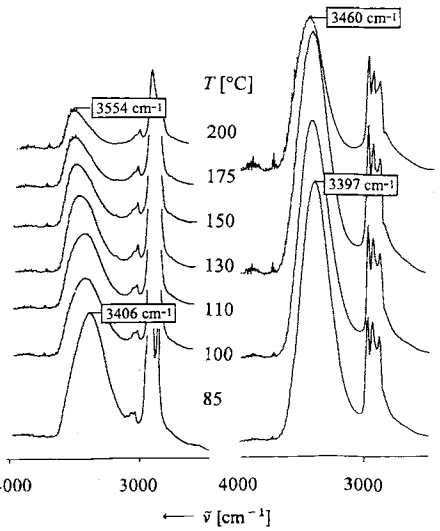

Fig. 2. Sections of the temperature-dependent IR spectra of compound **5c** (left) and 1,2-propanediol (right) in the range 2500–4000 cm^{-1}; measured with a BIORAD-FTS-40 spectrophotometer, in a heated thermal cell SPECAC P/N 21.500.

propanediol, the temperature dependence of the mesogenic diol **5c** is much more evident, and an especially large shift is observed in the region of the phase transition. This verifies that, already, in the nematic phase, some of the hydroxyl groups are not intermolecularly associated during the average time of the measurement. The formation of the nematic mesophase can, therefore, be explained by disorder in the layer structure. The cyano group could be responsible for this, since these can form hydrogen bonds with hydroxy groups.[7] This clearly gives rise to disorder in the smectic layer structure, and a nematic phase is thus favored. But when the length of the alkylene spacers between the diol head group and the cyanobiphenyl unit is further extended the effect of the separation of the hydrophobic and hydrophilic parts of the molecule becomes evident and leads to the formation of smectic layer structures. Similar results were also obtained by Griffin et al. in the investigation of 4′-(ω-hydroxyalkoxy)-4-cyanobiphenyls (for example **7** in Fig. 3).[8]

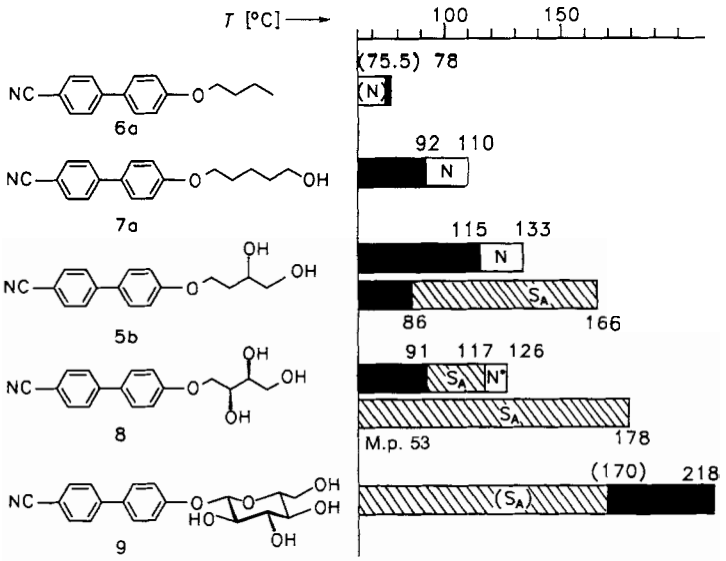

Fig. 3. The influence of the number of hydroxyl groups on the thermotropic mesophase behavior of 4-cyanobiphenyl mesogens **5**–**7** [8], **8** [10], and **9** [11]. The lower bars for compounds **5** and **8** represent the lyotropic mesophase behavior of the water saturated samples. For an explanation of the abbreviations see Table 1 [a].

With respect to mesophase stability, these compounds, since they only have one hydroxyl group available for intermolecular association, lie between the nonamphiphilic compounds **6** and the 1,2-diol derivatives **5**. Smectic mesophases could not be detected even for long-chain compounds of this class of substances.

Since the 4′-(ω,ω-1-dihydroxyalkoxy)-4-cyanobiphenyls **5** are amphiphilic compounds, their mesogenic properties should be influenced by the addition of water. The phase transition temperatures of samples of compounds **5b**–**e**, saturated with water, are compared with those of the anhydrous substances in Table 1. It is clear that the addition of water leads not only to a considerable stabilization of the mesophase, but also to the induction of a smectic layer structure.[9] We interpret this as meaning that the water molecules can be incorporated into the network of hydrogen bonds of the diol head group, strengthening the interactions between the groups and thus hindering the parallel movement of single molecules.

Increasing the number of hydrogen bonds should be possible not only by the inclusion of water molecules but, in general, by increasing the number of available hydroxyl groups in the vicinity of the head group. A comparison of **5b** with compounds **8**[10] and **9**[11] in Figure 3 clearly hows that covalent hydroxyl groups can also cause the induction of smectic mesophases. Thus, by influencing hydrogen bonds, it is possible to control specifically the molecular arrangement of amphiphilic molecules.

Received: February 23, 1993 [Z 5887 IE]
German version: *Angew. Chem.* **1993**, *105*, 1205

[1] G. A. Jeffrey, L. M. Wingert, *Liq. Cryst.* **1992**, *12*, 179–202, and references therein; K. Praefcke, B. Kohne, A. Eckert, J. Hempel, *Z. Naturforsch. B* **1990**, *45*, 1084, and references therein; G. Lattermann, G. Staufer, G. Brezesinski, *Liq. Cryst.* **1991**, *10*, 169.

[2] C. Tschierske, G. Brezesinski, F. Kuschel, H. Zaschke, *Mol. Cryst. Liq. Cryst. Lett. Sect.* **1989**, *6*, 139.

[3] C. Tschierske, F. Hentrich, D. Joachimi, O. Agert, H. Zaschke, *Liq. Cryst.* **1991**, *9*, 571–582.

[4] C. Tschierske, A. Lunow, D. Joachimi, F. Hentrich, D. Girdziunaite, H. Zaschke, A. Mädicke, G. Brezesinski, F. Kuschel, *Liq. Cryst.* **1991**, *9*, 821–829.

[5] D. Demus, H. Demus, H. Zaschke, *Flüssige Kristalle in Tabellen*, 1st ed. VEB Deutscher Verlag für Grundstoffindustrie, Leipzig, **1974**, p. 64; D. Demus, H. Zaschke, *Flüssige Kristalle in Tabellen II*, 1st ed. VEB Deutscher Verlag für Grundstoffindustrie, Leipzig, **1984**, p. 278.

[6] Compounds **5a**–**6f** were obtained by the etherification of 4′-hydroxy-4-cyanobiphenyl with the corresponding 1,2-*O*-isopropylidene-1,2-dihydroxyalkan-ω-ols, by using the method of O. Mitsunobu, *Synthesis* **1981**, 1, and subsequent acid-catalyzed cleavage of the isopropylidene protective group. For the synthesis of **5a** (*S*)-1,2-*O*-isopropylidene glycerol was used. All other compounds of type **5** are racemic mixtures.

[7] A. Allerhand, P. von R. Schleyer, *J. Am. Chem. Soc.* **1963**, *85*, 866.

[8] A. C. Griffin, S. R. Vaidya, *Mol. Cryst. Liq. Cryst.* **1989**, *173*, 85–88.

[9] The water uptake of these compounds is limited. To determine the water miscibility of the diols, mixtures of **5c** with increasing amounts of water were investigated by differential scanning calorimetry (DSC). With a molar ratio of diol to water of 1:3, the appearance of an ice peak, which is attributed to the crystallization of the "nonbound" water, could already be seen. At higher temperatures the water uptake should, however, be considerably higher.

[10] Compound **8** was obtained by the Mitsunobu etherification of 4′-hydroxy-4-cyanobiphenyl with 1,2-*O*-isopropylidene-3-(*O*-tetrahydropyran-2-yl)-L-threitol (L. De Gaudenzi, S. Apparao, R. R. Schmidt, *Tetrahedron* **1990**, *46*, 277–290), followed by removal of the protective group.

[11] The synthesis of compound **9** was achieved by treating acetobromoglucose with the sodium salt of 4′-hydroxy-4-cyanobiphenyl according to the method of J. Conchie, G. A. Levvy in *Methods in Carbohydrate Chemistry, Vol. 20* (Eds.: R. L. Whistler, M. L. Wolfrom), Academic Press, New York, **1963**, pp. 335–337.

The "Phosphonioyl(phosphoranediyl)carbene" $[(i\mathrm{Pr}_2\mathrm{N})_2\mathrm{P(H)CP}(\mathrm{N}i\mathrm{Pr}_2)_2]^+$ as a Source of New 1,3-Diphosphaallene Ylides: The First Carbodiphosphoranes with P–H Bonds**

By *Michèle Soleilhavoup, Antoine Baceiredo,* and *Guy Bertrand**

Several types of diphosphaallenes possessing either ylidic and/or genuine phosphorus–carbon double bonds (**A**,[1] **B**,[2] and **C**[3]) are known, and we recently the synthesis of the titel compound **1** which can be formally regarded as **D**.[4]

[*] Dr. G. Bertrand, M. Soleilhavoup, Dr. A. Baceiredo
Laboratoire de Chimie de Coordination du CNRS
205, route de Narbonne, F-31077 Toulouse Cédex (France)
Telefax: Int. code + (61) 553 003

[**] This work was supported by the Centre National de la Recherche Scientifique. We thank Prof. R. Ahlrichs, Karlsruhe, for the preliminary communication of calculations and Dr. R. Reed for helpful discussions.

On the other hand, ylides with P–H bonds (**E**) are rare, and most of them are in equilibrium with the alkylphosphane form **F** (Scheme 1).[5] Here, we report the synthesis and rearrangement of the first carbodiphosphoranes (diphosphoranediylmethanes) with P–H bonds, as well as the deprotonation of the phosphonioyl(phosphoranediyl)carbene **1**, which leads formally to a transient new type of diphosphaallene $\overset{+}{P}=C=\overset{-}{P}$.

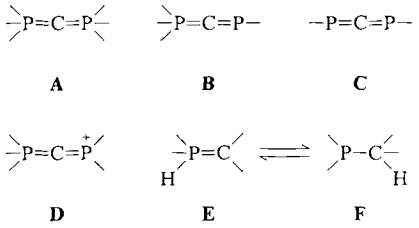

A **B** **C**

D **E** **F**

Scheme 1.

Surprisingly, compound **1** is stable with respect to the possible migration of the hydrogen atom to the central carbon atom, although calculations on the hydrogen analogue (H in place of *i*Pr) predict **2** to be more stable than **1** by 54 and 70 kJ mol^{-1} at the SCF and MP2 levels, respectively[6] (Scheme 2).

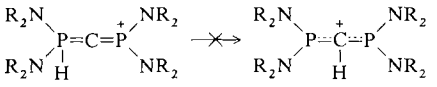

1 **2**

Scheme 2. Counterion $CF_3SO_3^-$ (Tf), R = *i*Pr.

This observation prompted us to treat compound **1** with a nucleophile in the hope of obtaining a carbodiphosphorane with a P–H bond. Indeed, the reaction of **1**-Tf with sodium tetrafluoroborate led to the desired carbodiphosphorane **3**. The ^{31}P NMR spectrum of **3** shows a doublet ($^1J_{PF}$ = 951.8 Hz) of doublets ($^2J_{PP}$ = 32.9 Hz) of doublets ($^3J_{PH}$ = 4.0 Hz) of quintets ($^3J_{PH}$ = 17.8 Hz) centered at δ = + 59.5, and a doublet ($^1J_{PH}$ = 524.2 Hz) of doublets ($^2J_{PP}$ = 32.9 Hz) of doublets ($^3J_{PF}$ = 15.3 Hz) of quintets ($^3J_{PH}$ = 16.1 Hz) centered at δ = 9.2, demonstrating that the carbodiphosphorane structure possesses a P–H and a P–F bond; this was further confirmed by a doublet of doublets of doublets at δ = 18.9 ($^1J_{PC}$ = 143.8 and 195.0 Hz, $^2J_{FC}$ = 24.8 Hz) in the ^{13}C NMR spectrum. Carbodiphosphorane **3** is thermally quite stable as a solid (m.p. 116 °C); in solution, **3** slowly rearranges into the isomeric phosphorus ylide **4** after one week at room temperature. It should be noted that **3**, the first carbodiphosphorane with a P–H bond, can be directly obtained by addition of tetrafluoroboric acid to diphosphinodiazomethane **5** (Scheme 3).

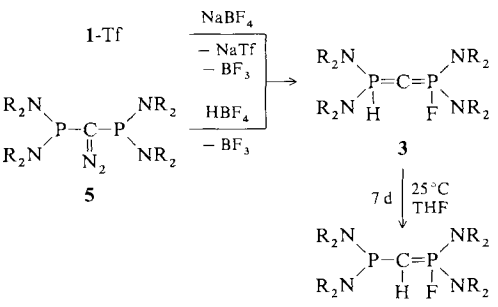

5 **3** **4**

Scheme 3. R = *i*Pr.

It was thus tempting to try to synthesize a carbodiphosphorane featuring two P–H bonds. Reaction of **1** with *tert*-butyllithium[7] gave the desired compound **6** which was characterized in solution. The $^{31}P\{^1H\}$ spectrum showed a singlet at δ = – 8.0, but the definitive proof of the structure was given by the ^{31}P NMR ^1H coupled spectrum which was an AA'XX'$M_4M'_4$ system with $^1J_{PH}$ = 465, $^3J_{PH}$ = 1, $^2J_{PP}$ = 158, $^4J_{HH}$ = 0, and $^3J_{PH(CH)}$ = 15 Hz; the calculated and experimental spectra are shown in Figure 1. The carbodiphosphorane **6** rearranged in solution at room temperature in the course of about 16 h to give the phosphorus ylide with a P–H bond (**7**). This compound was also not stable and was completely transformed overnight into the diphosphinomethane **8** (Scheme 4).

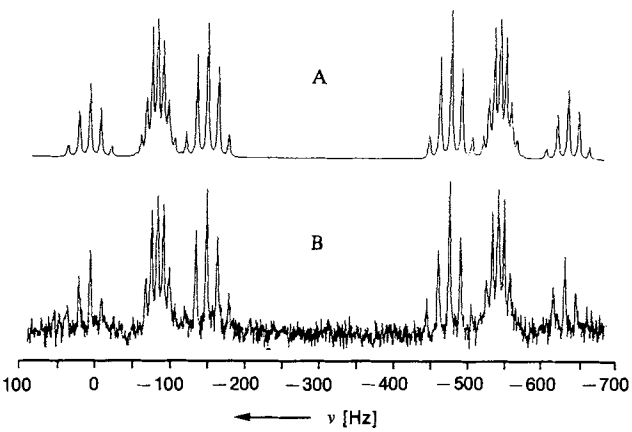

Fig. 1. Calculated (A) and experimental (B) ^{31}P NMR spectra (32.438 MHz) of **6**. Standard: 85% H_3PO_4.

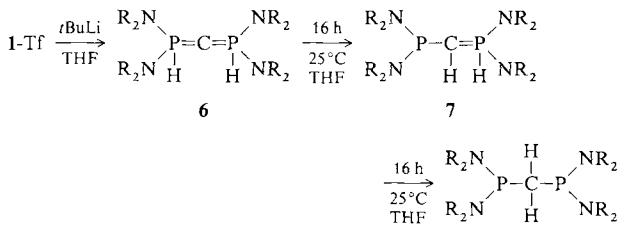

6 **7** **8**

Scheme 4. R = *i*Pr.

The addition of fluoride in the reaction of **1** with boron tetrafluoroborate demonstrated the strong Lewis acid character of the three-coordinate phosphorus center of **1**, while the reaction with *tert*-butyllithium showed that **1** can be easily reduced. It is also possible to abstract the proton from **1**. A clean reaction occurred when **1** was treated with potassium *tert*-butoxide leading to the phosphaalkene **10**, resulting from 1,2-shift of a diisopropylamino group from phosphorus to carbon. Note that the intermediate in this reaction can be formally regarded as a diphosphaallene **9a** or a diphosphinocarbene **9b**; indeed, we have already shown that the phosphaalkene **10** can be obtained by photolysis of the corresponding diazo compound **5**[8] (Scheme 5).

It is of interest to compare these experimental results with theoretical predictions for model compounds carrying amino

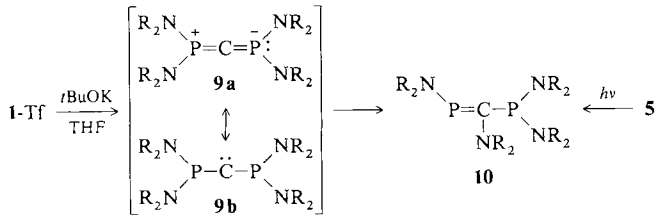

Scheme 5. R = *i*Pr.

in place of diisopropylamino substituents.[6] Compound **3** is a local minimum on the potential energy surface, but appeared to be 110 and 116 kJ mol^{-1} above **4**, at the SCF and MP2 level, respectively. In the same way, **6** is 120 kJ mol^{-1} above **7**, which is 140 kJ mol^{-1} higher than **8**. The surprising stabilities of **3**, **6**, and **7** are probably due to the presence of bulky substituents, since the tetracoordinate P–H ylide form better accommodates the steric hindrance than does the tricoordinate CH form. Lastly, the isomerization of **9** → **10** is not surprising since phosphaalkene **10** was found to be 220 kJ mol^{-1} lower in energy than **9**.

This work demonstrates the great potential of **1** as a building block for the synthesis of new metastable species, predicted by theory to be thermodynamically high in energy.

Experimental Procedure

3: To a solution of **1** (1 mmol) in dichloromethane (5 mL) was added the equimolar amount of $NaBF_4$ at room temperature. After the solution had been stirred for 2 h, the solvent was removed under vacuum, and the residue was washed several times with Et_2O. This afforded **3** as white powder (70%; m.p. 116 °C.) ^{31}P NMR: δ = 59.5 (dddq, J(P,P) = 32.9 Hz, J(P,F) = 951.8 Hz, J(P,H) = 4.0 and 17.3 Hz), 9.2 (dddq, J(P,P) = 32.9 Hz, J(P,F) = 15.3 Hz, J(P,H) = 524.2 and 16.1 Hz); ^{13}C NMR: δ = 17.9 (ddd, J(P,C) = 143.8 and 195.0 Hz, J(F,C) = 24.8 Hz, =C=), 22.7 (s, CH_3), 22.9 (d, J(P,C) = 2.6 Hz, CH_3), 46.4 (d, J(P,C) = 4.4 Hz, CHNP), 48.1 (dd, J(P,C) = 5.7 Hz, J(F,C) = 2.5 Hz, CHNPF); ^{1}H NMR: δ = 1.25 (d, J(H,H) = 6.8 Hz, 48 H, CH_3), 3.70 (m, J(H,H) = 6.8 Hz, 8 H, CHNP), 7.20 (dt-like, J(P,H) = 524.2 Hz, J(P,H) = J(F,H) = 4.0 Hz, 1 H, HP=C=P).

4: A solution of **3** (1 mmol) in THF (5 mL) was stirred at room temperature for one week. After evaporation of the solvent, **4** was obtained as a viscous oil (90%); ^{31}P NMR: δ = 71.2 (dddq, J(P,P) = 81.1 Hz, J(P,F) = 1015.4 Hz, J(P,H) = 17.3 and 16.8 Hz), 39.3 (broad d, J(P,P) = 81.1 Hz); ^{13}C NMR: δ = 22.7 and 23.2 (s, CH_3), 23.8 and 23.9 (d, J(P,C) = 7.1 and 6.8 Hz, CH_3), 28.1 (ddd, J(P,C) = 99.6 and 44.5 Hz, J(F,C) = 15.3 Hz, = CH), 47.6 (d, J(P,C) = 12.1 Hz, CHNP), 49.0 (t-like, J(P,C) and J(F,C) < 2 Hz, CHNPF); ^{1}H NMR: δ = 1.11 and 1.21 (d, J(H,H) = 6.6 Hz, 24 H, CH_3), 1.35 and 1.42 (d, J(H,H) = 6.9 Hz, 24 H, CH_3), 2.75 (ddd, J(P,H) = 16.8 and 5.4 Hz, J(F,H) = 10.9 Hz, 1 H, = CH), 3.4 (dsept, J(P,H) = 12.8 Hz, J(H,H) = 6.6 Hz, 4 H, CHNP), 3.9 (dsept, J(P,H) = 17.3 Hz, J(H,H) = 6.9 Hz, 4 H, CHNP).

6: To a solution of **1** (1 mmol) in [D_8]THF (5 mL) was added the equimolar amount of *t*BuLi at −78 °C. Compound **6** was characterized in solution by ^{31}P NMR without any further purification (Fig. 1).

7: After 16 hours at room temperature **6** in [D_8]THF solution rearranged to give **7** in near quantitative yield, according to NMR spectroscopy. ^{31}P NMR: δ = 49.5 (br d, J(P,P) = 174.7 Hz), 13.1 (br dd, J(P,P) = 174.7 Hz, J(P,H) = 486.3 Hz).

8: After 16 hours at room temperature **7** in [D_8]THF solution rearranged to give **8**. The solvent was removed under vacuum, and compound **8** was crystallized at −20 °C from a toluene/pentane solution as colorless crystals (85%); m.p. 167–168 °C; MS: m/z 477 (M + H$^+$); ^{31}P NMR: δ = 44.0; ^{13}C NMR: δ = 24.2 and 24.6 (s, CH_3), 24.1 and 24.5 (d, J(P,C) = 3.3 and 10.7 Hz, CH_3), 30.3 (t, J(P,C) = 21.9 Hz, CH_2), 46.3 (t-like, J(P,C) = 5.0 Hz, NCH); ^{1}H NMR: δ = 1.15 and 1.17 (d, J(H,H) = 6.6 Hz, 48 H, CH_3), 2.1 (t, J(P,H) = 5.0 Hz, 2 H, CH_2), 3.40 (dsept, J(P,H) = 7 Hz, J(H,H) = 6.6 Hz, 8 H, CHN).

10: To a solution of **1** (1 mmol) in THF (5 mL) was added at −78 °C the equimolar amount of *t*BuOK. After the solution had been warmed up to room temperature, the solvent was removed under vacuum, and the residue was extracted with pentane (10 mL). Evaporation of the solvent afforded **10** as a viscous oil (45%) [8].

Received: January 22, 1993 [Z 5822 IE]
German version: *Angew. Chem.* **1993**, *105*, 1245

[1] For reviews, see H. J. Bestmann, R. Zimmermann, *Fortschr. Chem. Forsch.* **1971**, *20*, 1; C. N. Matthews, G. H. Birum, *Acc. Chem. Res.* **1969**, *2*, 373; H. J. Bestmann, R. Zimmermann, *Methoden Org. Chem. (Houben-Weyl), 4th ed. 1952–, Vol.* E1, **1982**, p. 616; H. J. Bestmann, R. Zimmermann in *Comprehensive Organic Synthesis, Vol. 6* (Ed. B. M. Trost, I. Fleming, E. Winterfeldt), Pergamon, Oxford, **1991**, p. 171.
[2] R. Appel, V. Barth, H. Kunze, B. Laubach, V. Paulen, F. Knoll, *ACS Symp. Ser.* **1981**, *171*, 395.
[3] For a review, see R. Appel in *Multiple Bonds and Low Coordination in Phosphorus Chemistry* (Eds. M. Regitz, O. J. Scherer) Thieme, Stuttgart, **1990**, p. 181.
[4] M. Soleilhavoup, A. Baceiredo, O. Treutler, R. Ahlrichs, M. Nieger, G. Bertrand, *J. Am. Chem. Soc.* **1992**, *114*, 10959.
[5] For a review, see O. I. Kolodyazhnyi, V. P. Kukhar, *Russ. Chem. Rev.* **1983**, *52*, 1096.
[6] R. Ahlrichs, O. Treutler, Universität Karlsruhe, personal communication.
[7] E. J. Corey, S. M. Albonico, U. Koelliker, T. K. Schaaf, R. K. Varma, *J. Am. Chem. Soc.* **1971**, *93*, 1491.
[8] A. Baceiredo, A. Igau, G. Bertrand, M. J. Menu, Y. Dartiguenave, J. J. Bonnet, *J. Am. Chem. Soc.* **1986**, *108*, 7868; M. J. Menu, M. Dartiguenave, Y. Dartiguenave, J. J. Bonnet, G. Bertrand, A. Baceiredo, *J. Organomet. Chem.* **1989**, *372*, 201.

Complexation of Methane and Chlorofluorocarbons by Cryptophane-A in Organic Solution**

By *Laurent Garel, Jean-Pierre Dutasta*, and *André Collet**

The design of hosts capable of binding neutral substrates is of great interest in supramolecular chemistry, and, in this context, the capture of the smallest aliphatic hydrocarbons and fluorocarbons still remains a challenging problem.[1] We report here the complexation of methane and of some small chlorofluorocarbons (CFCs) by a synthetic receptor of the cryptophane family.[2] The methane complex is amazingly stable, and the study of its properties sheds light on some important factors that may govern the formation of supramolecular assemblies made of neutral partners.

We have shown that cryptophane-E (**1**) is an excellent receptor for neutral tetrahedral substrates such as isobutane, even in an organic solvent in which hydrophobic forces are absent.[3] This host proved unsuitable for the complexation of methane, presumably because this substrate is too small (V_{vdW} = 28.4 Å^3).[4] This result led us to use cryptophane-A (**2**),[5] the cavity of which is about 8% smaller in volume than that of **1**.[6] Prior to this work, little had been reported about the complexing properties of **2**.[2]

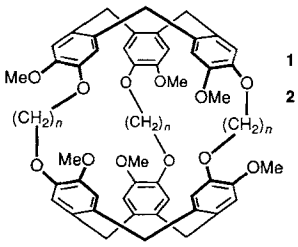

1 n = 3 (cryptophane-E)
2 n = 2 (cryptophane-A)

When methane was bubbled for 30 s at room temperature through a solution of **2** in $(CDCl_2)_2$,[7] the ^{1}H NMR spectrum showed a broad singlet at δ_{obs} = − 3.05, indicating that

[*] Prof. Dr. A. Collet, Dipl.-Chem. L. Garel, Dr. J.-P. Dutasta
Ecole normale supérieure de Lyon
Stéréochimie et Interactions moléculaires, UMR CNRS no 117
F-69 364 Lyon Cedex 07 (France)
Telefax: Int. code + (72)728483

[**] We are grateful to the Centre National de la Recherche Scientifique (CNRS) for a grant (to L. G.).

CH_4 was reversibly bound, and that a fast exchange occurred between the free (signal at δ_f) and complexed (δ_c) molecules (Fig. 1a). On increasing the amount of CH_4 stepwise up to 1.35 times that of **2**, (Fig. 1b to g), δ_{obs} moved downfield (from $\delta = -3.05$ up to $\delta \approx -2$), as a result of the decrease of the host/guest ratio; a plot of $\delta_f - \delta_{obs}$ as a function of this ratio showed that only *one* methane molecule is present in the host cavity. When a solution containing (0.9 equivalents of methane was cooled to 199 K, the guest signal split into two singlets at $\delta_f = +0.14$ and $\delta_c = -4.36$, corresponding to the free and complexed molecules (Fig. 1h).

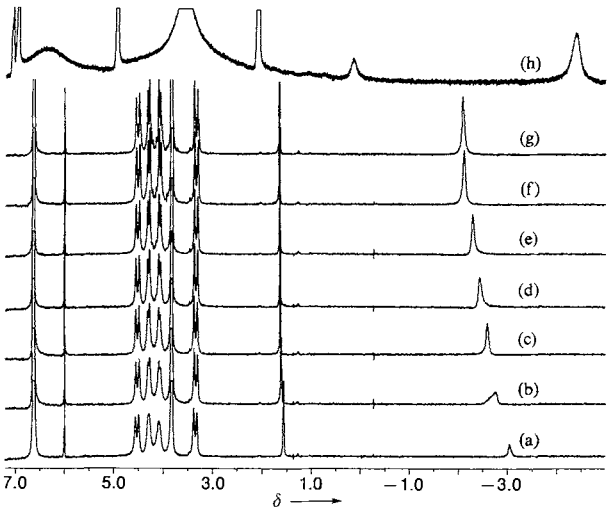

Fig. 1. 200 MHz ^{1}H NMR spectra of host **2** (2.5×10^{-2} M) in $(CDCl_2)_2$ at 298 K, in the presence of increasing concentrations of methane (from 0.33 equivalents in (a) to 1.35 equivalents in (g); (h) spectrum recorded at 199 K in the presence of 0.9 equivalents of methane (ca. 40% of [D_8]toluene was added to prevent freezing).

Treatment of the NMR data[8] provided the binding constant for the complexation of CH_4 to **2** in $(CDCl_2)_2$ at 298[9] and 199 K ($K_a = 130 \pm 20$ M^{-1} and 520 ± 160 M^{-1}, respectively). The enthalpy of binding ΔH_a^0 is therefore negative (around -1.6 kcal mol^{-1}), and the entropy ΔS_a^0 weakly positive ($+4$ cal mol^{-1} K^{-1}). The methane complex of **2** is thus about as stable as the isobutane complex of **1**.[3] Lineshape analysis[10] of the guest NMR signals between 199 and 298 K furnished the half life of the complex $t_{1/2}$ of 6×10^{-6} s at 298 K and 9×10^{-3} s at 199 K; the corresponding dissociation barriers are $\Delta G_d^{\#} = 10.5$ and 9.8 kcal mol^{-1}, respectively.

To our knowledge, the only reported studies on the complexation of small fluorinated hydrocarbons have dealt with the enantioselective recognition of the anesthetic halothane by α-cyclodextrin,[11] and of CHFClBr by cryptophane-C.[12] We investigated the interaction of CHF_2Cl and CF_2Cl_2 with **2** in $(CDCl_2)_2$, and found that both were complexed, albeit less strongly than CH_4. For CHF_2Cl, K_a was (roughly) 0.3 M^{-1} at 298 K and 12 ± 3 M^{-1} at 253 K;[13] owing to the lack of precision, the measurements at 298 K do not provide reliable ΔH_a^0 and ΔS_a^0 values. For CF_2Cl_2, K_a was 13 ± 4 M^{-1} at 298 K.

Relevant data on the properties of these complexes are given in Table 1. In Figure 2, the free energy of binding ($-\Delta G_a^0$) for all the complexes of **2** known to date is plotted as a function of the guest size, together with a similar plot for

Table 1. ^{1}H and ^{19}F NMR chemical shifts ($\Delta\delta = \delta_f - \delta_c$), binding constants ($K_a$), free energies of association (ΔG_a^0), and energy barrier for dissociation ($\Delta G_d^{\#}$) for some complexes of **2** with various guests in 1,1,2,2-[D_2]tetrachloroethane.

Guest	V_{vdW} [Å^3]	$\Delta\delta$	K_a [M^{-1}] (298 K)	ΔG_a^0 [kcal mol^{-1}] (298 K)	ΔH^0 [kcal mol^{-1}]	ΔS^0 [cal mol^{-1} K^{-1}]	$\Delta G_d^{\#}$ (T [K]) [kcal mol^{-1}]
CH_4	28.4	4.50	130	−2.9	−1.6	+4	10.5 (298)
CHF_2Cl	50.6	4.59 (^{1}H) 1.80 (^{19}F)	0.3	+0.7			
CF_2Cl_2	65.2	4.85 (^{19}F)	13	−1.5			14.1 (283)
CH_2Cl_2	55.6	4.33	475	−3.7	−3.3	+1	13.1 (265)
CH_2Br_2	64.8	4.28	320	−3.4	−1.3	−7	12.8 (258)
$CHCl_3$	72.2	4.33	230	−3.2	−8.2	−16	14.7 (298)

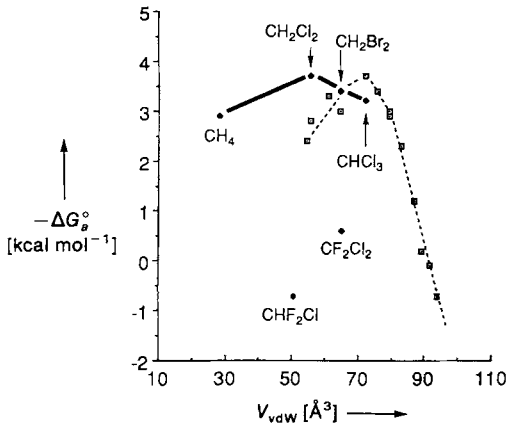

Fig. 2. The solid line represents the free energy of formation $-\Delta G_a^0$ at 298 K for a series of complexes of **2** as a function of the size (V_{vdW}) of the guest molecules; the dotted line shows a similar set of data for host **1** (taken from ref. [3]).

cryptophane-E **1**.[3] For the non-fluorinated substrates, host **2** appears to be less selective than **1**, and its size preference is around 55 Å^3 (dichloromethane), instead of 72 Å^3 (chloroform) for **1**. The amazing stability of the methane complex is both enthalpic and entropic in origin (see Table 1), and this feature may result from favorable host–guest interactions and disfavorable solvent–guest interactions. The observation that cryptophane-E **1** does not bind methane in $(CDCl_2)_2$ suggests that the host–guest interactions are dominant in the stabilization of the methane complex of **2**; this view is supported by the results of MMX force field calculations. A stereoview of the energy-minimized structure of the supermolecule (or host–guest complex) is shown in Figure 3. The methane molecule lies close to the

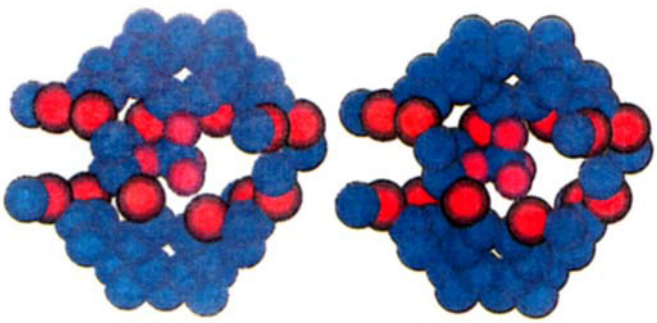

Fig. 3. Stereoview of the energy-minimized structure of the [CH_4/**2**] supermolecule (MMX force field calculation). For clarity, the van der Waals radii of the atoms shown have been reduced by 0.65 Å.

center of the cavity, and the mean distance between the guest and the arene carbon atoms of the host is 4.5 Å; about 20% larger than the sum of the van der Waals radii. This separation is almost exactly that required to reach the *maximum of attractive forces* in a van der Waals interaction potential.[14]

It is obvious from Figure 2 that the relatively large stability difference between the CH_4 complex and the CFC complexes of **2** is not related to size parameters. We cannot yet give a good interpretation for this observation. The CFCs are much more soluble in $(CDCl_2)_2$ than methane, which may indicate the existence of favorable solvent–guest interactions, and may disfavor their inclusion in the cavity of **2**.

At the microscopic level, the fact that methane and related small molecules can be so easily captured by a cryptophane to form stable supermolecules raises some questions about the *state of matter* in the interior of the host cavity. For one molecule of chloroform in host **2**, which has a spherical cavity of 81.5 Å^3, the occupancy factor[15] ϱ is 0.886, which would correspond to a *very closely packed crystal*. In this case, the magnitudes of ΔH_a^0 (-8.2 kcal mol^{-1}) and of ΔS_a^0 (-16 cal mol^{-1} K^{-1}) are actually quite comparable with the heat and entropy of crystallization of organic compounds, and the description of this complex as an ordered *pseudocrystal*, in which host and guest are at contact distance, may seem relevant. For one molecule of methane in the same cavity, the occupancy factor is 0.348; by comparison, the magnitude of ϱ is 0.77×10^{-3} in the gas state (1 atm and 298 K), 0.173 at the critical point (45.6 atm and 190.6 K), and 0.67 in the solid at 0 K. It follows that the best description of the interior of the complex would be a *supercritical fluid*, in which the methane molecule behaves like a small sphere colliding with the walls of the cavity of **2** for a few μs (at 298 K) before escaping. It is amazing to consider that, translated to the macroscopic level, one molecule of methane in the cavity of **2** is equivalent to one mole of methane reduced to a volume of 49 mL and exerting a pressure of 610 atm at 298 K![16]

Even though our knowledge of the guest behavior in the interior of such supermolecules is still very imprecise, we suggest that a description of these species in terms of equivalent macroscopic states of matter is soundly based, and may provide an interesting clue to understanding their properties. Such information may also be of great interest for the design and synthesis of new host systems.

Received: March 2, 1993 [Z 5901 IE]
German version: *Angew. Chem.* **1993**, *105*, 1249

[1] For review on the complexation of neutral species by synthetic hosts. See: R. M. Izatt, J. S. Bradshaw, K. Pawlak, R. L. Bruening, B. J. Tarbet, *Chem. Rev.* **1992**, *92*, 1261–1354, and references therein.
[2] A. Collet, *Tetrahedron* **1987**, *43*, 5725–5759.
[3] J. Canceill, M. Cesario, A. Collet, J. Guilhem, L. Lacombe, B. Lozach, C. Pascard, *Angew. Chem.* **1989**, *101*, 1249–1251; *Angew. Chem. Int. Ed. Engl.* **1989**, *28*, 1246–1248.
[4] Molecular sizes are expressed here as van der Waals volumes (V_{vdw}), calculated according to A. Bondi, *J. Phys. Chem.* **1964**, *68*, 441-451.
[5] J. Gabard, A. Collet, *J. Chem. Soc. Chem. Commun.* **1981**, 1137–1139; J. Canceill, A. Collet, *ibid.* **1988**, 582–584.
[6] The cavity volume in **1** and **2** was estimated with the molecular modeling software PCMODEL. For both cryptophanes, the cavity is almost spherical in shape, with a mean diameter D of 9.07 Å for **1** and 8.92 Å for **2**. The corresponding van der Waals diameters D_{vdw} (obtained by substracting from D twice the van der Waals radius of an arene carbon atom (1.77 Å)) were 5.53 Å for **1** and 5.38 Å for **2**, and the van der Waals volumes of the cavities were 88.5 and 81.5 Å^3, respectively. These volumes are in agreement with those of the largest neutral molecules that could be complexed in the cavity of these hosts: *tert*-butyl chloride (91 Å^3) for **1**, chloroform (72 Å^3) for **2**. These volumes do not apply to charged guests such as $(Me_3NR)^+$ ions; see A. Collet, J.-P. Dutasta, B. Lozach, *Bull. Soc. Chim. Belg.* **1990**, *99*, 617–633.
[7] This solvent (110 Å^3) is too big for the cavity of **2**.
[8] See for example R. Macomber, *J. Chem. Educ.* **1992**, *69*, 375–378.
[9] There is no significant difference between the values of K_a in pure $(CDCl_2)_2$ and in the mixture of $(CDCl_2)_2$ and [D$_8$]toluene (1.6:1, v:v) used for the low-temperature experiments.
[10] M. L. Martin, G. J. Martin, J.-J. Delpuech, *Practical NMR Spectroscopy*, Heyden, Chichester, England, **1980**, p. 291.
[11] J. Knabe, N. S. Agarwal, *Dtsch. Apoth. Ztg.* **1973**, *113*, 1449–1453.
[12] J. Canceill, L. Lacombe, A. Collet, *J. Am. Chem. Soc.* **1985**, *107*, 6993–6996.
[13] The ^{1}H and ^{19}F NMR spectra gave the same values of K_a.
[14] The attraction between two neutral atoms is maximum at a separation 1.24 times larger than the sum of the van der Waals radii; see J. Israelachvili, *Intermolecular and Surface Forces*, 2nd ed., Academic Press, London, **1992**. This feature sheds light on earlier remarks that, in such host–guest complexes, the size of the best guest is about 20% smaller than that suggested by CPK models: see [3], and F. Diederich, *Angew. Chem.* **1988**, *100*, 372; *Angew. Chem. Int. Ed. Engl.* **1988**, *27*, 362–386.
[15] The occupancy factor (sometimes called packing coefficient) is defined as $\varrho = V_{vdw}(\text{guest})/V_{vdw}(\text{cavity})$.
[16] This pressure was calculated by using the principle of corresponding states, for an occupancy factor of 0.348. For details, see, for example, P. W. Atkins, *Physical Chemistry*, 4th ed., Oxford University Press, Oxford **1990**, pp. 4–26.

[*tert*-Butylcyanide · Lithium Bis(trimethylsilyl)-amide]$_2$, a Model of the Intermediate RCN · MR′ Complex Formed in Reactions of Cyanides RCN with Organometallic Compounds R′M**

By *Gernot Boche*,* *Ira Langlotz*, *Michael Marsch*, *Klaus Harms*, and *Gernot Frenking*

Dedicated to Professor H. M. Walborsky on the occasion of his 70th birthday

Cyanides RCN (R = alkyl, aryl, heteroaryl, etc.) can react with organometallic compounds R′M (R′ = alkyl, aryl, NR_2, etc.; M = Li, Na, K, etc.) by deprotonation or addition.[1] As in the case of the reactions of carbonyl compounds with organometallic compounds,[2] the initial formation of a complex RCN · MR′ is possible. Wakefield et al.[3] consider the RCN · MR′ complex **3** to be a necessary intermediate in reactions of benzyl cyanide (**1**) with *two* molar equivalents of the base R′M (lithium bis(trimethylsilyl)amide, lithium diisopropylamide, or *n*-butyllithium) followed either by dialkylation (on treatment with ≥ 2 molar equivalents of R″-Hal) or dideuteration (with ≥ 2 molar equivalents of D_2O) to give **5** (Scheme 1).[4]

Evidence for the quasi-dianion complex (QUADAC) **2** from the NMR spectrum indicated that a *sequential* deprotonation/alkylation (deuteration) process should be involved rather than the proposed reaction via the "dianion" **6**: QUADAC **2** is selectively alkylated (deuterated) to give the RCN · MR′ complex **3**, which in turn is converted by an *intra*molecular proton shift (R″Hal or D_2O (!) compete with the complexed cyanide RCN for the base R′M!) to the dimeric mono "anion" **4**; a further alkylation of the latter then gives **5**. We have been able to demonstrate the existence of QUADAC **2**[5] and the dimeric "anion" **4**[6] by means of X-ray crystal structure determinations. We now present

[*] Prof. Dr. G. Boche, I. Langlotz, M. Marsch, Dr. K. Harms, Prof. Dr. G. Frenking
Fachbereich Chemie der Universität
D-35032 Marburg (FRG)
Telefax: Int. code + (6421)285547

[**] This work was supported by the Deutsche Forschungsgemeinschaft (SFB 260) and the Fonds der Chemischen Industrie.

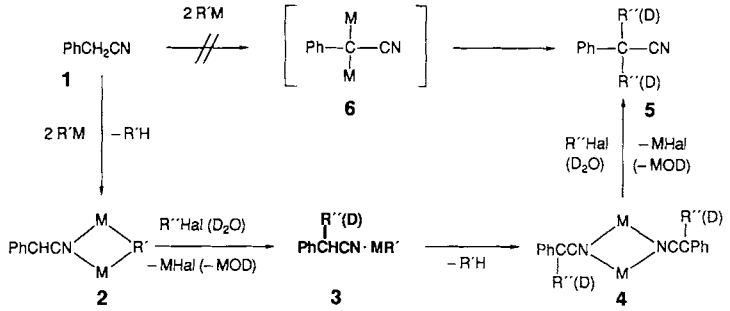

Scheme 1. Sequential reactions with the RCN·MR′ complex **3** as intermediate in the dialkylation (dideuteration) of **1** to give **5**.

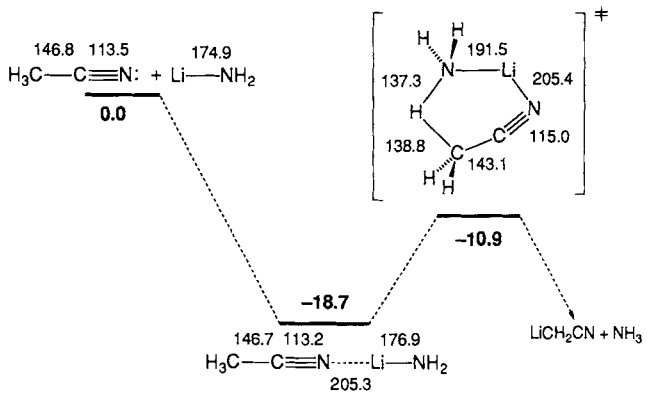

Scheme 2. Results of MP2/6-31 + G*//HF/6-31G* calculations of H_3CCN (C_{3v}), $LiNH_2$ (C_{2v}), the complex $H_3CCN \cdot LiNH_2$ (C_s), and the transition state for the deprotonation of H_3CCN in the $H_3CCN \cdot LiNH_2$ complex (C_s); E_{rel} [kcal mol^{-1}] and bond lengths [pm] are given. Bond and torsional angles [°] in the transition state: C-C-N 165.9, C-N-Li 92,6, N-Li-N 114.2, Li-N-H 92.5, N-H-C 161.2, H-C-C 93.8; H-N-Li-N ±113.4, H-C-C-N ±117.0.

proof of the existence of the "missing link", an RCN·MR′ complex of the type **3**: Figure 1 shows the structure of [*tert*-butylcyanide·lithium bis(trimethylsilyl)amide]$_2$ (**7**).[7–10]

[*t*BuCN·LiN(SiMe$_3$)$_2$]$_2$ **7**

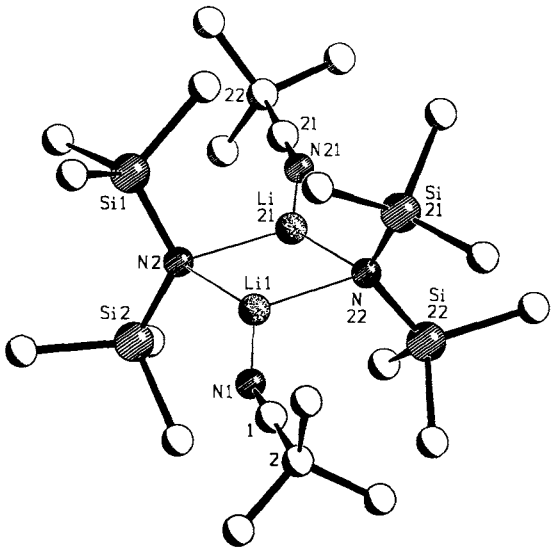

Fig. 1. Crystal structure of **7**. Selected distances [pm] and angles [°]: C1-N1 113.6(5), C21-N21 114.2(6), C1-C2 147.1(6), C21-C22 145.1(7), Li1-N2 203.0(7), Li1-N22 203.7(7), Li21-N2 203.4(7), Li21-N22 201.7(7), Li1-N1 204.6(7), Li21-N21 205.1(8); N1-C1-C2 179.5(4), N21-C21-C22 179.7(5), C1-N1-Li1 159.8(4), C21-N21-Li21 163.1(4). The carbon atoms are denoted only by a number.

As is often the case for lithium amides,[14] **7** exists in the form of a Li-bridged dimer; the third coordination sites of Li1 and Li2 are occupied by *t*BuCN. The structure of **7** is thus similar to those of the complexes of lithium bis(trimethylsilyl)amide with the esters *tert*-butylisobutyrate and *tert*-butylpivalate recently characterized by Williard, Liu, and Lochmann;[2e] the analogous dietherates containing Et_2O and THF have been known for some time.[15]

Ab initio calculations[16] at the MP2/6-31 + G*//HF/6-31G* level confirm both the stability of RCH·MR′ complexes such as **3** and **7** and the energetically favorable *intra*molecular proton shift which must occur in the case of **3** (Scheme 2).[18]

Thus the complex $H_3CCN \cdot LiNH_2$ is 18.7 kcal mol^{-1} more stable than its components H_3CCN and $LiNH_2$. Only 7.8 kcal mol^{-1} is required to reach the transition state for the proton shift in the complex $H_3CCN \cdot LiNH_2$. The initial complexation of RCN and MR′ to give RCN·MR′ thus also favors the subsequent reaction of the latter. It is therefore apparent that complexes of the type RCN·MR′ are probably of general importance in the reactions of cyanides RCN with organometallic compounds R′M.

Experimental Procedure

Preparation of single crystals of **7**: *n*-Butyllithium (0.63 mL, 1.6 M in hexane, 1.00 mmol) was added to a solution of hexamethyldisilazane (161 mg, 1.00 mmol) in diethyl ether (0.5 mL) at 0 °C. After 30 min the solvent mixture was removed under vacuum (oil pump) and the remaining lithium bis(trimethylsilyl)amide dissolved in 0.6 mL diethyl ether. The solution was cooled to −78 °C and treated with *tert*-butylcyanide (83 mg, 1.00 mmol). Single crystals of **7** were obtained after 3 d at −26 °C. Yield: 53 mg (21%).

Received: February 25, 1993 [Z 5891 IE]
German version: *Angew. Chem.* **1993**, *105*, 1207

[1] a) D. J. Cram, *Fundamentals of Carbanion Chemistry*, Academic Press, New York, **1965**; b) B. J. Wakefield, *The Chemistry of Organolithium Compounds*, Pergamon Press, Oxford, **1974**; c) E. Buncel, *Carbanions: Mechanistic and Isotopic Aspects*, Elsevier, Amsterdam, **1975**; d) J. C. Stowell, *Carbanions in Organic Synthesis*, Wiley, New York, **1979**.

[2] Reviews: a) D. Seebach, *Angew. Chem.* **1988**, *100*, 1685–1715; *Angew. Chem. Int. Ed. Engl.* **1988**, *27*, 1624; crystal structures: b) P. G. Williard, J. M. Salvino, *Tetrahedron Lett.* **1985**, *26*, 3931–3934; c) R. Amstutz, J. D. Dunitz, T. Laube, W. B. Schweizer, D. Seebach, *Chem. Ber.* **1986**, *119*, 434–443; d) P. G. Williard, G. B. Carpenter, *J. Am. Chem. Soc.* **1986**, *108*, 462–468; e) P. G. Williard, Q.-Y. Liu, L. Lochmann, *ibid.* **1992**, *114*, 348–350; calculations: f) E. Kaufmann, P. von R. Schleyer, K. N. Houk, Y.-D. Wu, *ibid.* **1985**, *107*, 5560–5562; g) M. L. McKee, *ibid.* **1987**, *109*, 559–565; h) S. M. Bachrach, A. Streitwieser, Jr., *ibid.* **1986**, *108*, 3946–3951.

[3] P. J. Crowley, M. R. Leach, O. Meth-Cohn, B. J. Wakefield, *Tetrahedron Lett.* **1986**, *25*, 2909–2912.

[4] The degree of aggregation of a complex of the type RCN·MR′ was initially less important for us than its actual existence. The same is true for compounds **2**, **3**, and **4** as formulated by Wakefield (Scheme 2). It is also clear that $H_3CCN \cdot LiNH_2$, for which calculations of the complex stability and the *intra*molecular proton abstraction were carried out, is only a model.

[5] α-Lithiophenylacetonitrile·lithium diisopropylamide·2 tetramethylethylenediamine: W. Zarges, M. Marsch, K. Harms, G. Boche, *Angew. Chem.* **1989**, *101*, 1424-1425; *Angew. Chem. Int. Ed. Engl.* **1989**, *28*, 1393.

[6] [(α-Cyanobenzyllithium·tetramethylethylenediamine)$_2$·benzene]: G. Boche, M. Marsch, K. Harms, *Angew. Chem.* **1986**, *98*, 373-374; *Angew. Chem. Int. Ed. Engl.* **1986**, *25*, 373.

[7] *Intra*molecular acid–base reactions are also found for complexes between enolates and amines; for the crystal structure of the lithium (*Z*)-enolate of *N*,*N*-dimethylpropionamide, which exists as a dimer and crystallizes with two molecules of *N*,*N*,*N*′-trimethylethylenediamine see T. Laube, J. D. Dunitz, D. Seebach, *Helv. Chim. Acta* **1985**, *68*, 1373-1393 and ref. [2a].

[8] Other organolithium "acid–base" complexes: a) R. A. Wanat, D. B. Collum, G. Van Duyne, J. Clardy, R. T. DePue, *J. Am. Chem. Soc.* **1986**, *108*, 3415–3422; b) S. Buchholz, K. Harms, M. Marsch, W. Massa, G. Boche, *Angew. Chem.* **1989**, *101*, 57–58; *Angew. Chem. Int. Ed. Engl.* **1989**, *28*, 72–73; see also S. Buchholz, K. Harms, W. Massa, G. Boche, *ibid.* **1989**, *101*, 58–59 and *28*, 73–75.

[9] RCN complexes with Lewis acids: a) B. Swanson, D. F. Shriver, J. A. Ibers, *Inorg. Chem.* **1969**, *8*, 2182–2189; b) T. N. Majid, M. C. P. Yeh, P. Knochel, *Tetrahedron Lett.* **1989**, *30*, 5069–5072.

[10] Crystal structure data for **7**: $C_{22}H_{54}Li_2N_4Si_4$, triclinic, $Z = 2$, space group $P\bar{1}$, $a = 9.229(3)$, $b = 13.091(2)$, $c = 14.967(4)$ Å, $\alpha = 94.37(2)$, $\beta = 100.10(2)$, $\gamma = 100.94(2)^\circ$. 4653 Reflections were measured using an Enraf-Nonius diffractometer ($Cu_{K\alpha}$ radiation, graphite monochromator, T = 193 K), 4321 of these were independent and 4037 with $F_o > 4\sigma(F_o)$ were considered as observed. Solution using direct methods (SHELXTL PLUS), refined (SHELXTL PLUS) to $R = 0.0629$, $Rw = 0.0763$. Non-hydrogen atoms anisotropic, H atoms at calculated positions and refined in groups with common temperature factors; 292 parameters. All calculations were carried out on a Microvax II and a VAX 6000-420[11-13]. Further details of the crystal structure investigation may be obtained from the Fachinformationszentrum Karlsruhe, Gesellschaft für wissenschaftlich-technische Information mbH, D-76344 Eggenstein-Leopoldshafen (FRG) on quoting the depository number CSD-400062, the names of the authors, and the journal citation.

[11] SHELXTL-PLUS (VMS), Release 4.2, Siemens Analytical Instruments, Madison, **1991**.

[12] A. L. Spek, *PLATON 88*, Program for Geometrical Analysis of Crystal Structures, Utrecht, **1988**.

[13] E. Keller, *SCHAKAL-88B*, A FORTRAN Program for the Graphic Representation of Molecular and Crystallographic Models, Freiburg, **1988**.

[14] Review on Li amide structures: a) R. E. Mulvey, *Chem. Soc. Rev.* **1991**, *20*, 67–209; b) K. Gregory, P. von R. Schleyer, R. Snaith, *Adv. Inorg. Chem.* **1991**, *37*, 47–142.

[15] a) M. F. Lappert, M. J. Slade, A. Snigh, J. L. Atwood, R. D. Rogers, R. Shakir, *J. Am. Chem. Soc.* **1983**, *105*, 302–304; b) L. M. Engelhardt, A. S. May, C. L. Raston, A. H. White, *J. Chem. Soc. Dalton Trans.* **1983**, 1671–1673; c) L. M. Engelhardt, B. S. Jolly, P. C. Junk, C. L. Raston, B. W. Skelton, A. H. White, *Aust. J. Chem.* **1986**, *39*, 1337–1345.

[16] The calculations were carried out with complete geometry optimization and subsequent calculation of the vibrational frequencies at the HF/6-31G* level. The transition state is characterized by an imaginary frequency, while the minima show only real frequencies. The reaction energies were obtained by taking the correlation energy into account with the help of second-order Møller–Plesset perturbation calculations [17] at the MP2/6-31 + G* level. The zero-point vibration energy was scaled with a factor of 0.9 and is contained in the calculated energies. The program package Gaussian 90 was used: M. J. Frisch, M. Head-Gordon, G. W. Trucks, J. B. Foreman, H. B. Schlegel, K. Raghavachari, M. A. Robb, J. S. Binkley, C. Gonzalez, D. J. DeFrees, D. J. Fox, R. A. Whiteside, R. Seeger, C. F. Melius, J. Baker, R. Martin, L. R. Kahn, J. J. P. Stewart, S. Topiol, J. A. Pople, Gaussian 90, Gaussian Inc., Pittsburgh, **1990**.

[17] a) C. Møller, M. S. Plesset, *Phys. Rev.* **1934**, *46*, 618; b) J. S. Binkley, J. A. Pople, *Int. J. Quantum Chem.* **1975**, *9*, 229.

[18] The *intra*molecular proton shift in complex **3**, in other words the deprotonation of the cyanide PhCH(R″;D)CN ($pK_a \approx 22$) by the strong base MR′ (MR′ = lithium bis(trimethylsilyl)amide, lithium diisopropylamide, or *n*BuLi) *in the presence of D_2O, which is orders of magnitude more acidic than the cyanide*, is a further lucid example of the importance of the proximity effect in intramolecular (organic) and enzymatic reactions, see for example T. C. Bruice, S. J. Benkovic, *Bioorganic Mechanisms, Vol. 1*, W. A. Benjamin Inc., New York, **1966**, 119–211; D. E. Koshland Jr., *J. Theor. Biol.* **1962**, *2*, 75–86; S. Scheiner, W. N. Lipscomb, D. A. Kleier, *J. Am. Chem. Soc.* **1976**, *98*, 4770–4777; D. Detar, N. P. Luthra, *J. Am. Chem. Soc.* **1980**, *102*, 4505–4512; I. M. Page, W. P. Jencks, *Proc. Natl. Acad. Sci. USA* **1971**, *68*, 1678–1683; K. N. Houk, J. A. Tucker, A. E. Dorigo, *Acc. Chem. Res.* **1990**, *23*, 107–113; F. M. Menger, *ibid.* **1993**, *26*, 206–212, and references cited in these publications.

Domino Reactions of 4-Ene-1,2,3-triol Derivatives

By *Johann Mulzer*,* *Stefan Greifenberg*, *Jürgen Buschmann*, and *Peter Luger*

Domino reactions via carbocationic intermediates are of considerable importance in synthesis and biosynthesis.[1] We report a sequence consisting of at least eight individual steps which is terminated by dimerization to give bis(furanoside) derivatives.

The enetriol derivatives **1a–c**,[2] readily available from (*R*)-2,3-isopropylideneglyceraldehyde in two steps, were treated with trimethylsilyl iodide to give the diastereomerically pure bicyclic products **2a–c** in acceptable yields (Scheme 1). With other Lewis acids such as aluminum

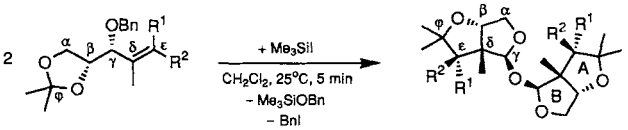

Scheme 1. **a**, $R^1 = H$, $R^2 = Me$; **b**, $R^1 = R^2 = H$; **c**, $R^1 = Et$, $R^2 = H$. Yields based on **1**; 50% is considered to be the maximum possible yield: **2a**, 24%; **2b**, 37%; **2c**, 18%.

trichloride, tin tetrachloride, trimethylsilyl trifluoromethanesulfonate, trimethylsilyl cyanide, and trimethylsilyl chloride, unidentifiable mixtures were obtained or the starting material was recovered. As expected, the ^1H and ^{13}C NMR spectra of **2a–c** show only half of the signals because of the C_2 symmetry of the molecules (Table 1). The dimeric structures can be deduced from the high-resolution mass spectra. The relative configuration was confirmed by X-ray structure analysis (Fig. 1)[3] for **2a** and by NOE difference spectra for **2b** and **2c**. The absolute configuration follows from the fact that the stereogenic center at C_β is unchanged throughout the reaction.

Table 1. Selected spectroscopic data for compounds **2a–c**.

2a: Colorless crystals; $[\alpha]_D^{20} = -124.2$ ($c = 0.95$ in $CHCl_3$); ^1H NMR ($CDCl_3$, 270 MHz): $\delta = 0.86$ (d, $J = 7.5$ Hz, 3H), 1.05 (s, 3H), 1.08 (s, 3H), 1.24 (s, 3H), 1.69 (q, $J = 7.5$ Hz, 1H), 3.72 (d, $J = 10$ Hz, 1H), 3.80 (dd, $J_1 = 10$ Hz, $J_2 = 3.2$ Hz, 1H), 4.04 (d, $J = 3.2$ Hz, 1H), 4.41 (s, 1H); ^{13}C NMR ($CDCl_3$, 68 MHz): $\delta = 10.14$, 15.07, 21.61, 28.29, 51.32, 57.63, 72.21, 84.84, 87.52, 104.82; IR (KBr pellet): $\tilde{\nu} = 2972$ s, 2935 m, 2898 m, 2974 w, 1465 m, 1389 m, 1379 w, 1369 m, 1258 w, 1227 m, 1177 m, 1141 m, 1104 m, 1069 s, 980 vs, 932 m, 902 m, 860 m, 763 w, 612 w, 519 w cm^{-1}; MS (EI, 80 eV, 60 °C): *m/z* (%): 339 (0.8), 199 (3.6), 185 (7.6), 169 (100), 43 (49.8).

2b: Colorless oil: $[\alpha]_D^{20} = -110.3$ ($c = 1.06$ in $CHCl_3$); ^1H NMR ($CDCl_3$, 250 MHz): $\delta = 1.19$ (s, 6H), 1.25 (s, 3H), 1.72 (d, $J = 12.5$ Hz, 1H), 1.80 (d, $J = 12.5$ Hz, 1H), 3.69 (d, $J = 9.7$ Hz, 1H), 3.79 (dd, $J_1 = 9.7$ Hz, $J_2 = 3.7$ Hz, 1H), 4.12 (d, $J = 3.7$ Hz, 1H), 4.59 (s, 1H); ^{13}C NMR ($CDCl_3$, 63 MHz): $\delta = 20.23$, 27.86, 29.35, 52.51, 54.64, 71.66, 83.02, 89.04, 111.32; IR (KBr pellet): $\tilde{\nu} = 2973$ s, 2932 s, 2899 m, 2831 w, 1458 m, 1382 m, 1367 m, 1263 w, 1188 m, 1101 vs, 1074 m, 1055 s, 1010 s, 979 m, 923 m, 868 w cm^{-1}; MS (EI, 80 eV, 60 °C): *m/z* (%): 171 (12.0), 155 (19.2), 126 (85.4), 111 (54.4), 59 (33.8), 43 (100).

2c: Colorless oil; $[\alpha]_D^{20} = -95.3$ ($c = 1.15$ in $CHCl_3$); ^1H NMR ($CDCl_3$, 270 MHz): $\delta = 1.01$ (t, $J = 7.5$ Hz, 3H), 1.20 (s, 3H), 1.21 (s, 3H), 1.28 (s, 3H), 1.50 (m_c, 2H), 1.76 (dd, $J_1 = 15$ Hz, $J_2 = 7.5$ Hz, 1H), 3.79 (d, $J = 10$ Hz, 1H), 3.91 (dd, $J_1 = 10$ Hz, $J_2 = 3.5$ Hz, 1H), 4.14 (d, $J = 3.5$ Hz, 1H), 4.92 (s, 1H); ^{13}C NMR ($CDCl_3$, 68 MHz): $\delta = 13.40$, 20.21, 21.06, 23.44, 31.64, 55.61, 60.65, 71.56, 84.46, 88.78, 106.83; IR (KBr pellet): $\tilde{\nu} = 2968$ s, 2933 s, 2878 s, 2830 w, 1462 m, 1385 m, 1365 m, 1199 m, 1151 m, 1104 vs, 1057 vs, 1006 s, 974 m, 943 m, 914 m, 876 w, 756 w, 628 w cm^{-1}; MS (EI, 80 eV, 80 °C). *m/z* (%): 199 (64.5), 183 (57.3), 154 (70.9), 139 (42.8), 125 (70.7), 111 (61.6), 96 (91.5), 69 (70.6), 53 (61.4), 43 (100).

Scheme 2 shows a plausible pathway for the conversion of **1** into **2**. Although none of the postulated intermediates (**3–9**) can be isolated or trapped, the course of the reaction is clear from the connectivity and the relative configuration of the products. The acetonide ring in **1** is cleaved by silyl iodide to give the oxonium ion **3**, which is converted into **4** by a

[*] Prof. Dr. J. Mulzer, Dipl.-Chem. S. Greifenberg
Institut für Organische Chemie der Freien Universität
Takusstrasse 3, D-14195 Berlin (FRG)
Telefax: Int. code + (30)838-5163
Dr. J. Buschmann, Prof. Dr. P. Luger
Institut für Kristallographie der Freien Universität Berlin (FRG)

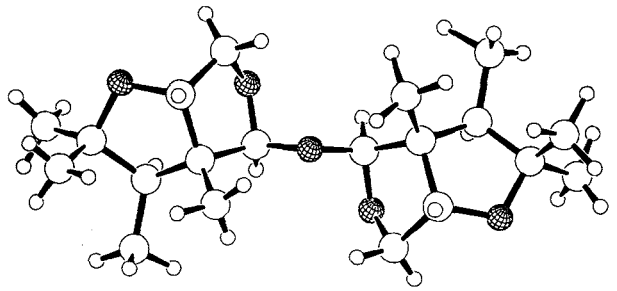

Fig. 1. Crystal structure of **2a** [3,4].

Prins cyclization. Subsequent pinacol rearrangement provides **5**.[5] Desilylation and cyclization affords the tetrahydrofuran **6**, whose labile glycosidic bond is cleaved by trimethylsilyl iodide to give the cyclic oxonium ion **8**. Unreacted glycoside **6** adds to **8** to form dimer **9**, which eliminates benzyl iodide giving **2a**. The overall yield is roughly 50%, which indicates an average yield of 91% for each step.

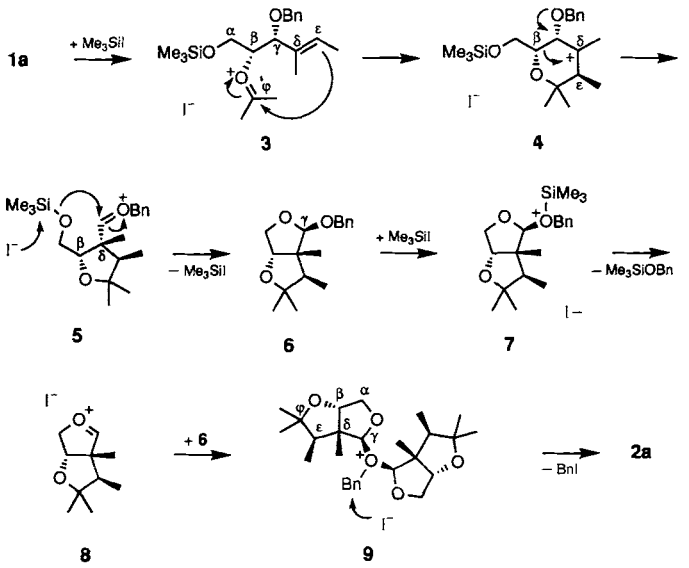

Scheme 2. Mechanism for the formation of **2a**.

In this sequence the stereogenic center at C_β controls the configurations at C_α, C_δ, and C_ε. Conformations **3** and **10** are the possible transition states for the Prins cyclization (Scheme 3). Conformation **3** is clearly preferred, since the side chain at C_β is equatorial. This explains the formation of **4**. The pinacol rearrangement proceeds suprafacially, and thus only **5** is formed from **4**. Starting from **10**, an analogous sequence would generate **12**, which cannot form a second ring due to the *trans* arrangement of the necessary appendages.[6] Finally, the stereogenic center at C_γ is formed by attack of **6** at the less hindered, convex face[7] of the bicyclo[3.3.0]octane structure **8**. According to our proposed mechanism, the geometry of the double bond in **1** reappears in the A ring in **2**. The rearrangements of **1a–2a** (*E* olefin) and **1c–2c** (*Z* olefin) do confirm this.

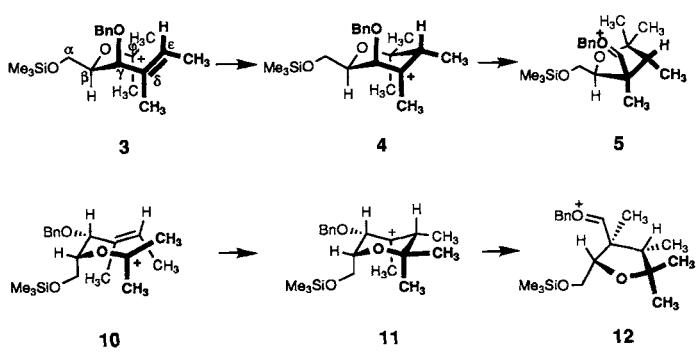

Scheme 3. Intermediates in the formation of the glycoside.

Within the limits of HPLC detection (±5%) the rearrangements are stereoselective. Their preparative value lies in the synthesis of complex bis(furanosides) from simple precursors. At present we are investigating the formation of cross-coupled bis(furanosides) from mixtures of unlike enetriols **1**.

Experimental Procedure

1a (1.00 g, 3.6 mmol) in CH_2Cl_2 (2 mL) was stirred at 0 °C with Me_3SiI (0.57 mL, 4.0 mmol, 1.1 mol equiv). After 5 min the reaction was quenched with MeOH, and stirred for approximately 15 h over solid $Na_2S_2O_3$. The mixture was concentrated under vacuum and diluted with ether. The organic phase was washed several times with water and dried over Na_2SO_4, and the solvent was removed under vaccum. Preparative column chromatography (silica gel, hexane/ethyl acetate 5:1) gave **2a** (310 mg, 24%) as colorless crystals, m.p. 134 °C.

Received: March 30, 1993 [Z 5963 IE]
German version: *Angew. Chem.* **1993**, *105*, 1214

[1] Review: L. F. Tietze, U. Beifuss, *Angew. Chem.* **1993**, *105*, 137; *Angew. Chem. Int. Ed. Engl.* **1993**, *32*, 131, and references therein [8]–[29].
[2] G. Funk, *Dissertation*, Freie Universität Berlin, **1992**.
[3] **2a**: Space group $P2_12_12_1$; $a = 6.7772(6)$, $b = 13.8324(6)$, $c = 21.889(1)$ Å; $Z = 4$; $\varrho_{calcd} = 1.1475\ g\,cm^{-3}$; $Cu_{K\alpha}$ radiation; $0 \le h \le 7$, $0 \le k \le 16$, $0 \le l \le 25$; 1993 reflections, 1741 of which were independent with $F_o > 3\sigma(F_o)$ for the structural solution (direct methods [8]) and least squares refinement with XTAL program package [9]: $R = 0.037$, $R_w = 0.028$. Further details of the crystal structure investigation may be obtained from the Fachinformationszentrum Karlsruhe, Gesellschaft für wissenschaftlich-technische Information mbH, D-76344 Eggenstein-Leopoldshafen FRG, on quoting the depository number CSD-57249, the names of the authors, and the journal citation.
[4] E. Keller, SCHAKAL88, graphics program for crystallography and molecular modeling, Universität Freiburg, **1988**.
[5] M. H. Hopkins, L. E. Overman, *J. Am. Chem. Soc.* **1987**, *109*, 4748; G. C. Hirst, P. N. Howard, L. E. Overman, *ibid.* **1989**, *111*, 1514.
[6] As the yield of **2** is not quantitative, the route via **10** → **11** → **12** cannot be completely disregarded. Nevertheless, it can be assumed that **12** would be stable under the reaction conditions and isolable after hydrolytic workup.
[7] This is one of the basic principles of quinane chemistry, see for example: L. A. Paquette, *Top. Curr. Chem.* **1979**, *79*, 41; J. Mulzer, H. J. Altenbach, M. Braun, K. Krohn, H. U. Reissig, *Organic Synthesis Highlights*, VCH, Weinheim, **1991**, p. 323.
[8] G. M. Sheldrick, *Acta Crystallogr. Sect. A* **1990**, *A46*, 467.
[9] S. R. Hall, J. M. Stewart, *XTAL 2.2 Users Manual*, University of Western Australia, Nedlands, WA, Australia, and University of Maryland, College Park, MO, USA, **1987**.

Diamino and Tetraamino Derivatives of Buckminsterfullerene C_{60}

By *Klaus-Dieter Kampe,* Norbert Egger*, and *Martin Vogel*

The addition of amines was one of the first reactions of buckminsterfullerene C_{60} (**1**) to be investigated.[1] A large excess of the amine was invariably employed, leading to a

[*] Dr. K.-D. Kampe
Hoechst AG, Hauptlaboratorium
Postfach 800320, D-65926 Frankfurt am Main (FRG)
Telefax: Int. + (69)3036 65-66
Dr. N. Egger, Dr. M. Vogel
Analytisches Laboratorium der Hoechst AG (FRG)

complex mixture of addition products,[1] which could not be separated. We report here on a simple method for the synthesis of defined products from the addition of secondary diamines to C_{60} (Scheme 1).

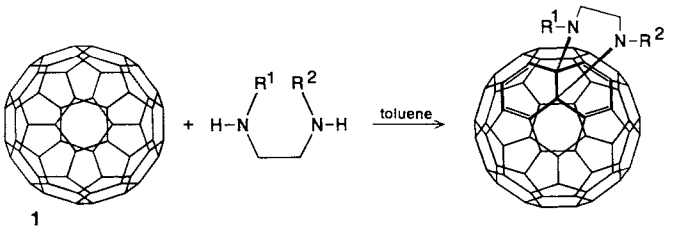

	R^1	R^2
2	CH_3	CH_3
3	$(CH_2)_2$	
4	$(CH_2)_3$	

	R^1	R^2
5	CH_3	CH_3
6	$(CH_2)_2$	
7	$(CH_2)_3$	

Scheme 1. Synthesis of the fullerene bases **5**, **6**, and **7**.

If a diamine such as *N,N'*-dimethylethylenediamine (**2**), piperazine (**3**), or homopiperazine (**4**) is allowed to react with C_{60} (**1**) in toluene between 0 and 100 °C and both reactants are present in low concentrations,[2] the predominant products formed are the mono- and bisadducts.[3] Contrary to expectations, an exact 1:1 ratio of reactants is not necessary in order to obtain high proportions of the monoadduct. Even in the presence of up to a 14-fold molar excess of the diamines **2**, **3**, or **4**, relatively high proportions of the corresponding monoaddition products are obtained when the reaction is stopped at 50–80% conversion of C_{60} (**1**). The bias towards formation of the monoadduct is also influenced by the structure of the diamine and is most pronounced in the case of piperazine (**3**) and least pronounced in the case of *N,N'*-dimethylethylenediamine (**2**).

The mono- and bisaddition products[3] formed in the reaction of **2**, **3**, or **4** with C_{60} (**1**) as well as unreacted **1** can be separated by conventional column chromatography on silica gel. In the case of the piperazine–C_{60} adducts, six regioisomeric bisaddition products can be separated on SiO_2 in addition to recovered **1** and the principal product, the monoadduct. Separation of the regioisomeric bisaddition products in the case of the reactions with the diamines **2** and **4** requires more effort; further chromatography is necessary after removal of unreacted **1** and the monoadduct.[4] The mono- and bisadducts isolated by the above procedure were found to be pure according to thin-layer chromatography (TLC). The homogeneous composition of the samples was further confirmed by high-performance liquid chromatography (HPLC) on two different stationary phases (RP 18 and SiO_2).

Adducts containing more than two diamine units per **1** are also formed in yields of around 15–50% with respect to reacted **1** when up to a 14-fold molar excess of the diamine is employed. These adducts are not isolated by the procedure described above.

The mono- and bisadducts crystallize as deep brown-black solids, in part as well-formed needles. They are soluble in CS_2, but are otherwise only sparingly soluble in solvents over a range of polarities. The presence of the mono- and bisadducts was established from the elemental analyses and mass spectra. Mass spectrometric and NMR spectroscopic analyses show that these derivatives are not adducts arising from nucleophilic addition, that is to say with two hydrogen atoms attached to C_{60} for every diamine unit. They are actually the corresponding "dehydrated" C_{60} derivatives. The expected signals characteristic of hydrogen atoms bonded to

Table 1. Selected physical data for the monoadducts **5**, **6**, and **7** (all compounds gave correct C,H,N analyses) [a].

5: $C_{64}H_{10}N_2$; M = 806.80; MS (FAB): m/z 807 (MH^+), 806 (M^-); IR [b] (strong bands): ν = 2940, 2880, 2840, 2795, 1465, 1445, 1430, 1050, 730 cm^{-1}; ^1H NMR (360 MHz, $CS_2/CDCl_3$): δ = 3.49 (s, 6H; CH_3), 3.96 (s, 4H; CH_2)

6: $C_{64}H_8N_2$, M = 804.78; MS (FAB): m/z 805 (MH^+), 804 (M^-); IR [b] (strong bands): ν = 2970, 2940, 2870, 1455, 1430, 1300, 1245, 1040, 1015, 850 cm^{-1}

7: $C_{65}H_{10}N_2$; M = 818.81; MS (FAB): m/z 819 (MH^+); IR [b] (strong bands): ν = 2950, 2910, 2860, 1460, 1450, 1430, 1180, 1110, 1035, 1010 cm^{-1}; ^1H NMR (360 MHz, $CS_2/CDCl_3$): δ = 4.63 (m, 2H; CH_2), 4.49 (q, 2H; CH_2), 3.94 (m, 2H, CH_2) 3.82 (q, 2H; CH_2), 2.63 (m, 1H; CH_2) 2.47 (m, 1H, CH_2)

[a] As a result of fragmentation, a signal at m/z 720 (molecular peak of **1**) also appears in every mass spectrum (matrix: 3-nitrobenzyl alcohol). M^+ or M^-: Mass spectra in which cations or anions, respectively, are observed after ionization. [b] IR spectra were recorded on crushed crystal aggregates on KBr with a Bruker IR microscope coupled to a Bruker IFS 88 spectrometer.

C_{60} are absent both in the ^1H and ^{13}C NMR spectra. Both hydrogen atoms introduced with each diamine unit have thus been eliminated. The mass spectra of the monoadducts **5**, **6**, and **7** (Table 1) provide further support for the dehydrogenated structure. Only 15 signals appear in the C_{60} region of the ^{13}C NMR spectrum of **6** (Fig. 1). This is an

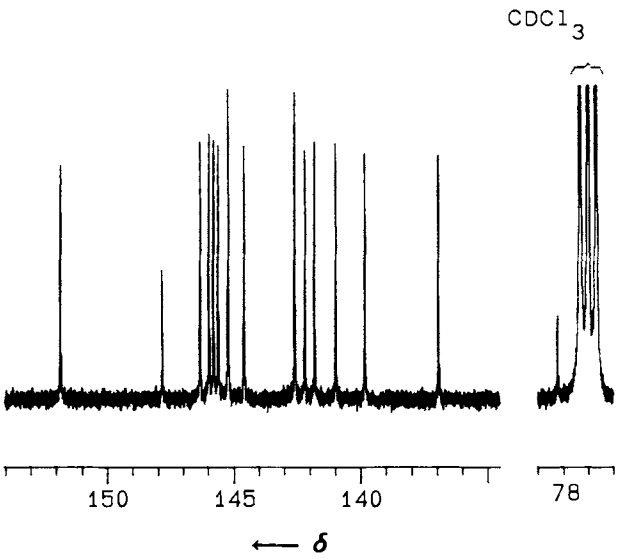

Fig. 1. ^{13}C NMR spectrum (90.5 MHz, $CS_2/CDCl_3$) of **6** in the C_{60} region.

indication of a highly symmetrical structure. The ^1H NMR spectra of **5**, **6** (Fig. 2), and **7** also point to a highly symmetrical structure. The simple pattern of signals in the ^1H and ^{13}C NMR spectra clearly show that **5**, **6**, and **7** have a symmetrical dehydrogenated structure (see Scheme 1) in which both nitrogen atoms of the diamine are bonded to neighboring C_{60} atoms of a 6-6 bond. This is yet another example of the strong preference shown by C_{60} (**1**) towards reaction at what is probably the energetically most favored position,[5] the 6-6 bond. The bonding of a diamine across a 5-6 bond, which would result from the formal addition of the diamine to two neighboring 6-6 bonds that form part of the [5]radialene structure of a pyracylene unit, can be rejected.

The purified regioisomeric bisadducts formed in the reactions of **2**, **3**, and **4** with **1** have analogous structures to those of the monoadducts. The mass spectra once again provide unambiguous support for the dehydrogenated structure. Six regioisomeric bisadducts from the reaction of **1** with **3** were separated cleanly by chromatography. They show striking differences in polarity as seen from the large variations in the

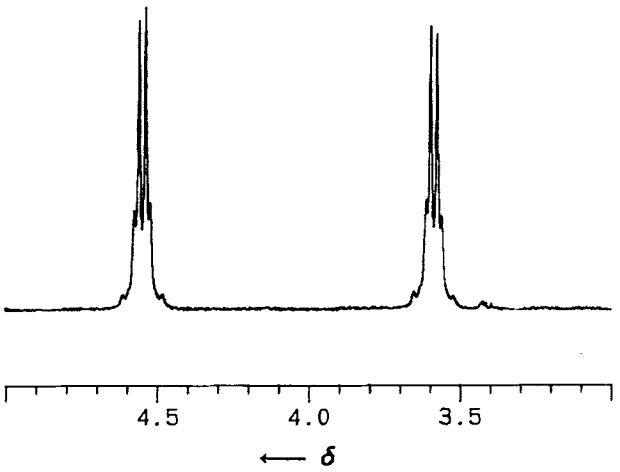

Fig. 2. ^{1}H NMR spectrum (360 MHz, $CS_2/CSCl_3$) of **6**.

TLC R_f values. The R_f values for the six bisadducts measured on Kieselgel 60 (coating thickness 0.25 mm; eluent CH_2Cl_2/C_2H_5OH 10/1) vary between 0.46 and 0.10, whereas the R_f value for the monoadduct **6** is 0.56 ($\pm$0.02). The IR spectra of the six bisadducts differ in the fine structure of the bands. No N–H bands were observed (typically around 3300 cm^{-1}).

Mono- and bisadducts were obtained in overall yields of 50–85% calculated on the basis of reacted **1** (45–70% based on total quantity of **1** used); compound **6**, for example, was isolated in yields of up to 53% with respect to the total quantity of **1** used in the reaction.

This reaction provides selective access to diamino and tetraamino derivatives of C_{60} **1** for the first time.

Experimental Procedure

6: A solution of 1110 mg of **1** (C_{60}/C_{70} 98/2) (1.5 mmol **1**) in 600 mL of toluene was treated with a solution of 1035 mg of **3** (12 mmol) in 183 mL of toluene under a nitrogen atmosphere. The resulting mixture was stirred for five days at 50 °C. After filtration, the solution was loaded onto a silica gel/CH_2Cl_2 column (40 × 3.6 cm), and 192 mg of **1** was eluted with 1200 mL of CH_2Cl_2. A CH_2Cl_2/CH_3OH (100/0.8) mixture was then used as eluent. After 2.5 L of compound-free eluate was collected, 560 mg of a brown-black compound was eluted from the column with a further 1.5 L. After treatment with ether, suction filtration, and drying, 507 mg of pure, crystalline **6** was isolated (42% with respect to total amount of **1** used; 49.5% with respect to reacted **1**). The column was further eluted with CH_2Cl_2/CH_3OH (100/2 and 100/4). After 1 L of compound-free eluate, 4 L (100/4) containing 110 mg of a mixture of five bisadducts were collected. These bisadducts were in turn be separated on a silica gel column (80 × 3.0 cm) using an analogous procedure to that described above. Further elution with 1.5 L (100/6) gave, after addition of ether to the crystalline residue, suction filtration, and drying, 90 mg of the most polar bisadduct according to TLC (SiO_2) (HPLC >92% pure); $C_{68}H_{16}N_4$ (M = 888.91); elemental analysis; calculated: C 91.88, H 1.81, N 6.30%, found: C 90.2, H 1.7, N 6.0%.

Received: March 20, 1993 [Z 5939 IE]
German version: *Angew. Chem.* **1993**, *105*, 1203

[1] a) F. Wudl, A. Hirsch, K. C. Khemani, T. Suzuki, P.-M. Allemand, A. Koch, H. Eckert, G. Srdanov, H. Webb in *Fullerenes* (Eds.: G. S. Hammond, V. J. Kuck) (*ACS Symp. Ser.* **1992**, *481*, 161–175); b) A. Hirsch, Q. Li, F. Wudl, *Angew. Chem.* **1991**, *103*, 1339–1341; *Angew. Chem. Int. Ed. Engl.* **1991**, *30*, 1309–1310; c) R. Seshadri, A. Govindaraj, R. Nagarajan, T. Pradeep, C. N. R. Rao, *Tetrahedron Lett.* **1992**, *33*, 2069–2070.

[2] The total concentration of both reactants was between 8 and 55 mmol L^{-1}; the concentration of **1** was between 2.3–3.3 mmol L^{-1}.

[3] For the sake of simplicity the term "adduct" is used even though, as shown below, these compounds are not adducts in the strict sense of the word.

[4] Separation of **1**, the monoadduct, and the bisadducts en bloc is generally successful when a total of 1.7–2.2 g is chromatographed on a silica gel column of 80–100 cm in length (particle size 0.063–0.20 mm; d 2.5–3.0 cm).

[5] A. Hirsch, A. Soi, H. R. Karfunkel, *Angew. Chem.* **1992**, *104*, 808–810; *Angew. Chem. Int. Ed. Engl.* **1992**, *31*, 766–768.

A Catalytic Enantioselective Michael Addition of a Simple Malonate to Prochiral α,β-Unsaturated Ketones and Aldehydes**

By *Masahiko Yamaguchi,** *Tai Shiraishi*, and *Masahiro Hirama*

Distinct progress has been made in the catalytic asymmetric Michael addition of prochiral enolates to acceptors for example, enantioselective addition of indane-1-one-2-carboxylate to methyl vinyl ketone.[1] These reactions rely on the differentiation of donor enantiofaces by chiral catalysts. In contrast, very little success has been achieved in the enantioselective Michael addition of an enolate to prochiral acceptors, despite the high potential of this reaction to produce various chiral carbon centers.[2] The conventional methods appear to be highly substrate specific, and enantiomeric excesses attained have generally not been high. We disclose herein the first catalytic asymmetric Michael addition of a simple malonate ion to prochiral enones and enals, which employs the readily available rubidium salt of L-proline (**2**).[3] The optical yields are substantial for this type of reaction, and the method can be applied to a range of acceptors to give adducts of predictable absolute configurations.

The Michael addition of dimethyl malonate in methanol catalyzed by the lithium salt of L-proline gave racemates.[4] However, appreciable asymmetric inductions were observed when the reactions were carried out in chloroform. Furthermore, the rubidium salt **2**[5] was found to possess remarkably high catalytic activity compared with the lithium salt, and higher optical yields were attained with diisopropyl ester **1**[6] (Scheme 1). Enantioselectivities up to 77% *ee* were

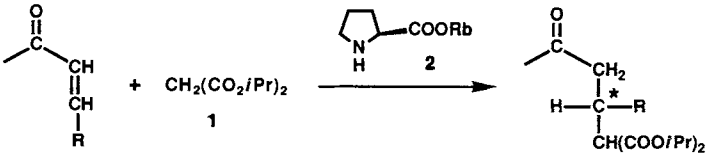

Scheme 1. The asymmetric Michael addition of diisopropyl malonate **1** to prochiral acceptors catalyzed by the rubidium salt of L-proline (**2**).

attained with 5 mol% of catalyst **2** (or 20 mol% with the less reactive substrates) (Table 1). Applicability to various Michael acceptors such as aliphatic and aromatic cyclic enones, cyclic enones, and enals should also be noted.

The catalyst **2** used contains water molecules as shown by elemental analysis.[7] The reaction rate was considerably lower in the presence of molecular sieves (4 Å), and a small amount of water was found to promote the reaction. Yields of adducts were very low with 5 or 10 mol% of the rubidium salts of *N*-methyl-L-proline and *N*-benzyl-L-proline, L-prolinol, L-proline, pyrrolidine, or triethylamine. Thus, both the secondary amine moiety and the metal carboxylate moiety of **2** are essential for the high catalytic activities. Since the activities and basicities of these amines are not correlated, **2** not only functions as a base but also involves some substrate activation.

[*] Prof. Dr. M. Yamaguchi, T. Shiraishi, Prof. Dr. M. Hirama
Department of Chemistry, Faculty of Science
Tohoku University
Aoba, Sendai 980 (Japan)
Telefax: Int. code + (22)263-9207

[**] This work was supported by a Grant-in-Aid for Scientific Research on Priority Areas (no. 01649515) from the Ministry of Education, Science, and Culture, Japan.

Table 1. A catalytic asymmetric Michael addition of **1** to enals and enones.

Entry	Enones or enals	*t* [h]	Yields [%] [a]	*ee* [%] [b]	$[\alpha]_D$ [c]	Config.
1	(*E*)-$CH_3CH{=}CHCOCH_3$	21	71	76	+12.7°	*S* [d]
2	(*E*)-$CH_3CH{=}CHCO(n\text{-}C_3H_7)$	46	73 [e]	74	+11.2°	*S* [f]
3	(*E*)-$(n\text{-}C_5H_{11})CH{=}CHCOCH_3$	7d	62	77	+8.0°	
4	(*E*)-$PhCH{=}CHCOCH_3$	9d	79 [e]	53	+10.8°	*S* [d]
5	2-cycloheptenone	59	91	59	+22.4°	*R* [d]
6	2-cyclohexenone	46	87	49	+2.3°	*R* [d, g]
7	(*E*)-$(n\text{-}C_3H_7)CH{=}CHCHO$	17	58	41	+4.6°	
8	(*E*)-$CH_3CH{=}CHCHO$	3	63	35	+5.6°	*S* [f]

[a] Isolated yields are shown. All the adducts gave satisfactory ^1H NMR, ^{13}C NMR, and IR spectra, as well as elemental analyses. [b] Enantiomeric excesses were determined by ^1H NMR spectroscopy (400 or 600 MHz) on ketals synthesized from the adducts and (2*R*,3*R*)-2,3-butanediol. [c] Obtained in $CHCl_3$ at 22–26 °C, $c = 1.01 - 1.04$. [d] The adducts were converted into known methyl esters by decarboxylation and esterification for the determination of the absolute configurations. Entry 1: D. Enders, K. Papadopoulos, *Tetrahedron Lett.* **1983**, *24*, 4967; Entry 4: K. Tomioka, K. Yasuda, K. Koga, *ibid.* **1986**, *27*, 4611. Entry 5: Compared with the compound described in footnote [g]. Entry 6: G. H. Posner, M. Weitzberg, T. G. Hamill, E. Asirvatham, H. Cun-Heng, J. Clardy, *Tetrahedron* **1986**, *42*, 2919. [e] 20 mol% of **2** was employed. [f] The product of the entry 8 was treated with MeLi or PrMgBr (THF, −78 °C) and oxidized (pyridinium dichromate or Swern oxidation) to give the products of the entries 1 and 2, respectively. The three compounds possessed the same absolute configuration. [g] Methyl(*R*)-(+)-3-oxocyclohexaneacetate, synthesized from the adduct by decarboxylation and esterification, was treated with diazomethane for ring enlargement: T. J. Boer, H. J. Backer, *Org. Synth. Collect. Vol.* **1963**, *4*, 225. Separation of the regioisomers gave methyl (*R*)-(+)-3-oxocycloheptaneacetate, $[\alpha]_D^{24} = +21.4$ ($c = 1.27$, $CHCl_3$).

The malonate **1** attacked cyclic (*Z*)-enones preferentially from the *Re* face (entry 5 and 6 of Table 1), and acyclic (*E*)-enones from the *Si* face (entries 1, 2, 4, and 8).[8] In other words, the nucleophile attacks from the same side of the enone plane irrespective of its stereochemistry (Fig. 1). The preference was also observed in reactions of a nitroalkane.[9]

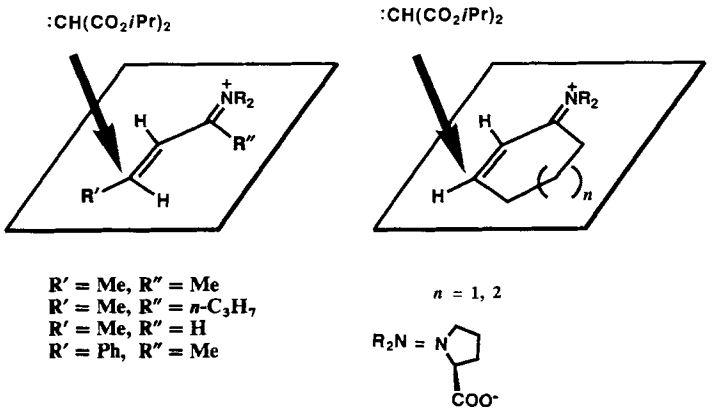

Fig. 1. The attack of the malonate ion on a postulated intermediate in the asymmetric addition.

These asymmetric inductions take place through enantioface differentiation of acceptors rather than recognition of differences in two β substituents. They therefore are relatively inert to structure variations of acceptors and donors, which may be the origin of the wide applicability of the present asymmetric process. Although related phenomena have been known in the diastereoselective Michael addition reactions to chiral unsaturated amides,[10] we are not aware of the concept in catalytic reactions. We presume that the unfavorable substrate specificity of the conventional reactions[2] may at least be partially due to the use of methods to recognize β substituents, which can be quite sensitive to the structure of acceptors and donors.

Reversible iminium salt formation in nonprotic solvents is one explanation for the above asymmetric inductions. Independent experiments demonstrated a high reactivity of an unsaturated iminium salt towards malonate addition. When an iminium salt, prepared from (*E*)-4-phenyl-3-buten-2-one and pyrrolidine,[11] was treated with dimethyl malonate in the presence of a catalytic amount of triethylamine at 25 °C, the starting material was consumed in several hours giving the 1,4 adduct after an aqueous workup. No 1,2 adduct was detected. Essentially no reaction took place with the enone itself under these conditions.

Experimental Procedure

Under an argon atmosphere, a mixture of **1** (1.30 mL, 6.72 mmol), 2-cycloheptenone (0.50 mL, 4.48 mmol), and catalyst **2** (46 mg, 0.22 mmol) in chloroform (5 mL) was stirred for 59 h at 25 °C. The reaction was quenched by adding 2 N HCl. Diisopropyl (+)-(3-oxocycloheptyl)malonate (1.21 g, 91%) was obtained by the usual workup.

Received: March 15, 1993 [Z 5930 IE]
German version: *Angew. Chem.* **1993**, *105*, 1243

[1] For recent examples, see: G. Desimoni, P. Quadrelli, P. P. Righetti, *Tetrahedron* **1990**, *46*, 2927; H. Brunner, H. Zintl, *Monatsh. Chem.* **1991**, *122*, 841; E. W. Dehmlow, V. Knufinke, *Liebigs Ann. Chem.* **1992**, 283; H. Sawamura, H. Hamashima, Y. Ito, *J. Am. Chem. Soc.* **1992**, *114*, 8295.

[2] Acceptable enantiomeric excesses have been attained mostly with chalcone and related compounds. See the following and references cited therein: A. Sera, K. Takagi, H. Katayama, H. Yamada, K. Matsumoto, *J. Org. Chem.* **1988**, *53*, 1157; N. Iwasawa, T. Yura, T. Mukaiyama, *Tetrahedron* **1989**, *45*, 1197; A. Loupy, J. Sansoulet, A. Zaparucha, C. Merienne, *Tetrahedron Lett.* **1989**, *30*, 333; C. Botteghi, S. Paganelli, A. Schionato, C. Boga, A. Fava, *J. Mol. Cat.* **1991**, *66*, 7. Exceptions: In the following references, reactions of a single Michael acceptor are described in which moderate enantiomeric excesses were achieved and applicability to other acceptors was not shown. M. Takasu, H. Wakabayashi, K. Furuta, H. Yamamoto, *Tetrahedron Lett.* **1988**, *29*, 6943; Y. Hayashi, K. Otaka, N. Saito, K. Narasaka, *Bull. Chem. Soc. Jpn.* **1991**, *64*, 2122.

[3] Use of proline in asymmetric intramolecular aldol reactions: U. Eder, G. Sauer, R. Wiechert, *Angew. Chem.* **1971**, *83*, 492; *Angew. Chem. Int. Ed. Engl.* **1971**, *10*, 496; Z. G. Hajos, D. R. Parrish, *J. Org. Chem.* **1974**, *39*, 1615. Use of proline in asymmetric Michael additions: R. B. Woodward, E. Logusch, K. P. Nambiar, K. Sakan, D. E. Ward, B.-W. Au-Yeung, P. Balaram, L. J. Browne, P. J. Card, C. H. Chen, R. B. Chênevert, A. Fliri, K. Frobel, H.-J. Gais, D. G. Garratt, K. Hayakawa, W. Heggie, D. P. Hesson, D. Hoppe, I. Hoppe, J. A. Hyatt, D. Ikeda, P. A. Jacobi, K. S. Kim, Y. Kobuke, K. Kojima, K. Krowicki, V. J. Lee, T. Leutert, S. Malchenko, J. Martens, R. S. Matthews, B. S. Ong, J. B. Press, T. V. Rajan Babu, G. Rousseau, H. M. Sauter, M. Suzuki, K. Tatsuta, L. M. Tolbert, E. A. Truesdale, I. Uchida, Y. Ueda, T. Uyehara, A. T. Vasella, W. C. Vladuchick, P. A. Wade, R. M. Williams, H. N.-C. Wong, *J. Am. Chem. Soc.* **1981**, *103*, 3210; A. P. Kozikowski, B. B. Mugrage, *J. Org. Chem.* **1989**, *54*, 2274. The corresponding alkali metal salts, however, have not been used in asymmetric synthesis.

[4] M. Yamaguchi, N. Yokota, T. Minami, *J. Chem. Soc. Chem. Commun.* **1991**, 1088.

[5] To obtain reasonable yields of the optically active Michael adducts in chloroform, 100 mol% of the lithium salt was required. Use of 10 mol% of the sodium or potassium salt of L-proline gave adducts in high yields but in low enantiomeric excesses.

[6] Reaction of dimethyl malonate in the presence of 10 mol% of **2** for 15 h gave the (*R*)-adduct in 88% yield and 40% *ee* Di-*tert*-butyl ester gave the (*R*)-adduct in 39% yield and 65% *ee* after 63 h.
[7] The catalyst **2** was conventiently prepared from the reaction of one equivalent of L-proline and rubidium hydroxide monohydrate (Kanto Chemical Co.) in methanol at 25 °C for 1–3 h. After evaporating the solvent, **2** was dried at 25 °C in vacuo. M.p. 269–271 °C (decomp); $[\alpha]_D^{23} = -61.2$ ($c = 0.99$, MeOH). Correct elemental analysis (C,H,N) for $C_5H_8NO_2Rb \cdot 1/2\,H_2O$.
[8] Although **1** attacked from the *Re* face of (*E*)-4-phenyl-3-buten-2-one (entry 4), this is simply a matter of the nomenclature. The sense of the asymmetric induction is the same as with other acyclic Michael acceptors (Fig. 1).
[9] Reaction of 2-nitropropane with 2-cyclohexenone and (*E*)-3-penten-2-one in the presence of **2** (5 mol%) for 24 h gave the adducts of the same asymmetric induction mode in 58% *ee* (61% yield) and 69% *ee* (48% yield), respectively. Details will be reported elsewhere.
[10] W. Oppolzer, H. J. Löher, *Helv. Chim. Acta* **1981**, *64*, 2808; W. Oppolzer, G. Poli, *Tetrahedron Lett.* **1986**, *27*, 4717.
[11] The iminium salt was prepared from the enone and pyrrolidine perchlorate in methanol at 25 °C in the presence of a catalytic amount of triethylamine: N. J. Leonard, J. V. Paukstelis, *J. Org. Chem.* **1963**, *28*, 3021.

A Novel Mixed-Valence Tetranuclear V^{II}/V^{III} Complex Isolated from 3,5-Di-*tert*-Butylcatechol/Vanadium(II)/Sodium Methoxide System for Dinitrogen Reduction

By *Nataly P. Luneva,* Svetlana A. Mironova, Alexander E. Shilov, Mikhail Yu. Antipin,* and *Yuri T. Struchkov*

Development of the coordination chemistry of bivalent vanadium, particularly for nonorganometallic complexes, lagged well behind that of most other first-row transition elements.[1] There has, however, been a steady growth of interest in the synthesis, structural characterization, and reactivity of bivalent vanadium complexes because of their ability to reduce a variety of substrates.[2] The complexes of vanadium(II) with catechol are of particular interest because they can reduce molecular dinitrogen under ambient conditions.[2b]

We report here the crystal structure of a novel mixed-valence tetranuclear V^{II}/V^{III} complex isolated from a solution of VCl_2, 3,5-di-*tert*-butylcatechol (dbcat), and $NaOCH_3$. The complexes of V^{II} with dbcat formed in methanol in the presence of sodium methoxide are powerful reducing agents: they evolve H_2 from the solvent [Eq. (a)] and reduce dinitrogen [Eq. (b)]. Figure 1a shows that H_2 evolution occurs at a

$$2\,V^{II} + 2CH_3OH \longrightarrow 2\,V^{III} + H_2 + 2CH_3O^- \quad (a)$$

$$6\,V^{II} + N_2 + 6CH_3OH \longrightarrow 6\,V^{III} + 2NH_3 + 6CH_3O^- \quad (b)$$

considerable rate for 3–4 h, and the total H_2 yield[3] is about 50%. The complete oxidation of V^{II} to V^{III} [Eq. (a)] requires 8–10 days. The reduction by V^{II} of N_2 [Eq. (b)] competes with that of methanol [Eq. (a)], and the NH_3 yield[3] gives a measure of the activity of the V^{II} complexes to reduce N_2. The increase in $NaOCH_3$ concentration results in the enhancement of the NH_3 yield up to the apparently limiting value of 40–45% at $[NaOCH_3] \geq 0.8$ M. Figure 1b shows that the reduction of N_2 to NH_3 proceeds for 2–3 hours, and

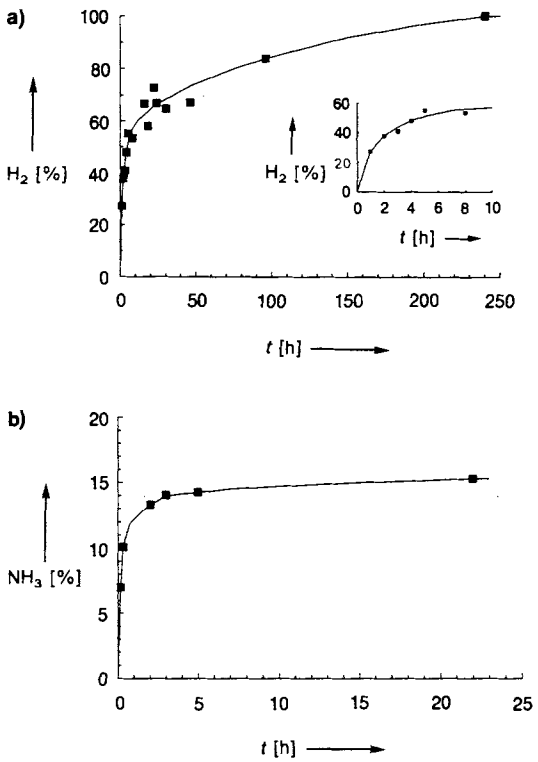

Fig. 1. The variation with time of the dihydrogen evolution (a) and ammonia formation (b). Initial conditions: VCl_2 3.5×10^{-4} mol, dbcat 1.88×10^{-3} mol, $NaOCH_3$ 1.5×10^{-3} mol, $V = 7.5$ mL, N_2 pressure 75 atm.

further reduction is practically brought to a stop. Chemical analysis shows that during the first 2–3 hours approximately 50% of the initial V^{II} oxidizes to V^{III}, and 15–18% of NH_3 [Eq. (b)] and 35–38% of H_2 [Eq. (a)] is formed. The retardation of the V^{II} oxidation rate may be explained by the formation of the relatively stable mixed-valence V^{II}/V^{III} complex, which is not able to reduce N_2 and demonstrates poor activity in the dihydrogen evolution from methanol.

The mixed-valence V^{II}/V^{III} complex with the composition of **1** is crystallized in the form of yellow-brown rhombuses.

$$[Na_2V_4(OMe)_2\{O_2C_6H_2(tBu)_2\}_4\{OC_6H_2(OH)(tBu)_2\}_2(MeOH)_8] \quad \mathbf{1}$$

The structure of **1** was elucidated by X-ray analysis (Fig. 2)[4] In **1** two V^{II} ions and two V^{III} ions are present on the base of chemical analysis, but from the X-ray data the V atoms are undistinguishable. Each vanadium center exhibits a distorted octahedral coordination involving the oxygen atoms. V1 is coordinated to two O atoms (O(8) and O(9)) of the methanol molecules, two μ_3-bridging atoms (O(7) and O(7a)) of the methoxy ligands, and another two bridging O atoms (O(1) and O(6)) from different dbcat molecules. V2 is coordinated to the μ_3-bridging O(7a) atom of the methoxy ligand, the μ_2-bridging O(1a) atom of a dbcat molecule, and four O atoms (O(3), O(4), O(5), and O(6) of two chelating dbcat molecules. The V–O distances range from 1.954(5) to 2.158(5) Å and correspond to the expected values. Sodium atoms are located in the centers of distorted tetrahedrons formed by oxygen atoms. Each sodium atom is coordinated by two O atoms (O(10) and O(11)) of the methanol molecules and by two O atoms (O(3) and O(5)) of different dbcat molecules. Na and V atoms are linked by the μ_2-bridging O(3) and O(5) atoms.

The architecture of the central part of **1** is similar to that found earlier for the Mg–Mo–alkoxide complexes.[5] It is

[*] Dr. N. P. Luneva, S. A. Mironova, Prof. A. E. Shilov
Institute of Chemical Physics
Russian Academy of Sciences, Chernogolovka, 142432 (Russia)
Prof. M. Yu. Antipin, Prof. Yu. T. Struchkov
Institute of Organoelement Compounds
Russian Academy of Sciences, Moscow (Russia)

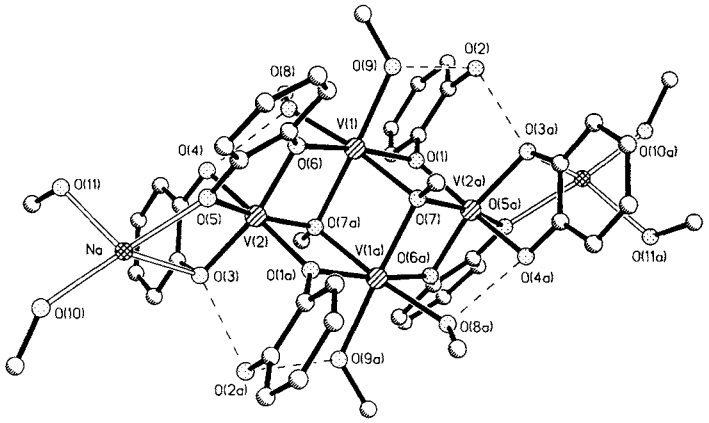

Fig. 2. Crystal structure of the complex **1** (*tert*-butyl groups and H atoms omitted). Important distances [Å]: V(1)–O(1) 2.110(5), V(1)–O(6) 2.118(5), V(1)–O(7) 2.122(4), V(1)–O(7a) 2.149(5), V(1)–O(8) 2.158(5), V(1)–O(9) 2.142(5), V(2)–O(1a) 1.970(5), V(2)–O(3) 2.010(5), V(2)–O(4) 2.036(4), V(2)–O(5) 1.980(5), V(2)–O(6) 1.954(5), V(2)–O(7a) 2.060(5), V(1)···V(2) 3.059(2), V(1)···V(1a) 3.193(2), V(1)···V(2a) 3.241(2), Na–O(10) 2.285(7), Na–O(11) 2.292(6), Na–O(3) 2.246(6), Na–O(5) 2.296(6), Na···V (2) 3.250(4), O(2)···H···O(3a) 2.796(5), O(9)···H···O(2) 2.815(5), O(8)···H···O(4) 2.644(5). The index a indicates the centrosymmetrical coordinate transformation.

probably stabilized by the intramolecular hydrogen bonds, whose geometrical parameters correspond to hydrogen bonds of the medium strength. The OH groups of the coordinated methanol molecules and "free" OH groups of dbcat ligands are the proton donors in these hydrogen bonds.

The formation of relatively stable **1** is a characteristic feature of the V^{II} system with dbcat. In the V^{II} systems with another catechols,[6] a mixed valence V^{II}/V^{III} complex is not formed, and all initial V^{II} is oxidized to the mononuclear V^{III} complex containing three ligands. An X-ray analysis of this type of complex, e.g. $K_3[V^{III}(cat)_3]$, showed that six O atoms of three catechol (cat) molecules are arranged octahedrally around the metal center.[7] In the case of dbcat, the coordination of the third ligand is hindered sterically, and it is possible that structure of the isolated V^{II} complex is not substantially different from that of the initial V^{II} complex that reduces molecular nitrogen.

Experimental Procedure

N_2 reduction and H_2 evolution kinetics have been performed as previously described [2d]. VCl_2 was synthesized by dissolving vanadium metal in hydrogen chloride under argon. The mixed valence V^{II}/V^{III} complex **1** was crystallized from the solution containing VCl_2 (3×10^{-4} mol), dbcat (1.5×10^{-3} mol), and $NaOCH_3$ (4×10^{-3} mol) in 10 mL of methanol. Thirty to forty hours are required for the formation of proper crystals from the initial reaction mixture (yield about 10–15% of total vanadium). The crystals dissolve easily in methanol. The concentration of V^{II} in the solution has been determined by titration with $(NH_4)_2Fe(SO_4)_2$ in sulfuric acid in the presence of safranine T. The total V concentration has been determined by atomic absorption analysis.

Received: December 23, 1992,
Revised version: April 19, 1993 [Z 5769 IE]
German version: *Angew. Chem.* **1993**, *105*, 1240

[1] a) A. Butler, C. J. Carrano, *Coord. Chem. Rev.* **1991**, *109*, 61–105; b) L. V. Boas in *Comprehensive Coordination Chemistry, Vol. 3* (Eds.: G. Wilkinson, R. D. Gillard, J. A. McCleverty), Pergamon, Oxford, **1987**, pp. 462–473.

[2] a) A. E. Shilov, N. T. Denisov, O. N. Efimov, V. F. Shuvalov, N. I. Shuvalova, A. K. Shilova, *Nature (London)* **1971**, *231*, 460–462; b) L. A. Nikonova, S. A. Isaeva, N. I. Pershikova, A. E. Shilov, *J. Mol. Catal.* **1975/76**, *1*, 367–374; c) S. A. Isaeva, L. A. Nikonova, A. E. Shilov, *Nouv. J. Chim.* **1981**, *5*, 21–25; d) N. P. Luneva, A. P. Moravsky, A. E. Shilov, *ibid.* **1982**, *6*, 245–251; R. A. Henderson, G. J. Leigh, C. J. Pickett, *Adv. Inorg. Chem. Radiochem.* **1983**, *27*, 197; e) J. Y. Becker, B. Rosin, *J. Electroanal. Chem.* **1988**, *250*, 385–397; e) C. Woitha, D. Rehder, *Angew. Chem.* **1990**, *102*, 1495–1497, *Angew. Chem. Int. Ed. Engl.* **1990**, *29*, 1438–1440; f) G. J. Leigh, R. Prieto-Alcón, J. R. Sanders, *J. Chem. Soc. Chem. Commun.* **1991**, 921–922; g) C. Woitha, D. Rehder, W. Priebsch, H. Gailus, *ibid.* **1992**, 364–365.

[3] According to Equations (a) and (b) the hydrogen and ammonia yields are $(2\,a_{H_2}/a_V)\times100\%$, $(3\,a_{NH_3}/a_V)\times100\%$, where a_{H2} is the amount of H_2 evolved, a_{NH_3} the amount of NH_3 formed, and a_V the amount of V^{II} consumed, all in moles.

[4] **1**: $C_{94}H_{160}O_{22}V_4Na_2$, $M=1892.1$, monoclinic, space group $P2_1/n$, $a=16.748(3)$, $b=16.459(3)$, $c=21.764(3)$ Å, $\beta=109.53(2)^\circ$, $V=5654.2(3.5)$ Å^3, $\varrho_{calc}=1.12\,g\,cm^{-3}$, $Z=2$, $T=140$ K. Siemens P3/PC diffractometer, $Mo_{K\alpha}$ radiation, graphite monochromator, $\theta/2\theta$-scan, $2\theta\le46^\circ$ were used. At $T=140$ K 6740 independent reflections were measured; 3111 observed reflections with $I\ge2\sigma(I)$ were used in the calculations: direct methods; Na, V, O anisotropic; C and H atoms of the OH groups isotropic; least-squares refinement (H atoms of the Me groups and phenyl rings included in the calculated positions as fixed contributors with constant temperature factors $U_{iso}=0.08$ Å^2); 369 refined parameters, $R=0.064$, $R_w=0.053$, GOF = 1.92. All calculations were performed by the PC/AT computer using SHELXTL PLUS programs. Further details of the crystal structure investigation are available on request from the Director of the Cambridge Crystallographic Data Centre, 12 Union Road, GB-Cambridge CB21EZ (UK), on quoting the full journal citation.

[5] M. Yu. Antipin, L. P. Didenko, L. M. Kachapina, A. K. Shilova, A. E. Shilov, Yu. T. Struchkov, *J. Chem. Soc. Chem. Commun.* **1989**, 1467–1468.

[6] S. A. Isaeva, L. A. Nikonova, *Izv. Akad. Nauk SSSR Ser. Khim.* **1977**, 1968–1971.

[7] S. R. Cooper, Yu. B. Koh, K. N. Raymond, *J. Am. Chem. Soc.* **1982**, *104*, 5092–5102.

The First Neutral Adamantanoid Iron(III)–chelate Complex: Spontaneous Formation, Structure, and Electrochemistry**

By *Rolf W. Saalfrank,* Bernd Hörner, Dietmar Stalke,* and *Josef Salbeck*

One of the most interesting new aspects of synthetic chemistry is endohedral chemistry, that is, the chemistry inside cages.[2] Consequently it is necessary to be able easily to build up intramolecular cavities with variable diameters.

On treatment of dimethyl malonate with methylmagnesium iodide or methyllithium/metal(II) chloride and oxalyl chloride at −78 °C in tetrahydrofuran and subsequent workup with aqueous ammonium chloride, we obtained, by spontaneous self-assembly,[1, 3, 4] the tetranuclear chelate complexes **1a** (M^{2+} = Mg, Mn, Co, Ni, Zn).[1, 5]

The doubly bidentate bridging ligand L^1 is formally obtained by the template coupling of two dimethyl malonate monoanions with oxalyl chloride to form tetramethyl 2,3-dihydroxy-1,3-butadiene-1,1,4,4-tetracarboxylate followed by subsequent spontaneous double deprotonation.

[*] Prof. Dr. R. W. Saalfrank, Dipl.-Chem. B. Hörner
Institut für Organische Chemie der Universität Erlangen-Nürnberg
Henkestrasse 42, D-91054 Erlangen (FRG)
Telefax: Int. code + (9131)85-6864
Dr. D. Stalke [+]
Institut für Anorganische Chemie der Universität Göttingen (FRG)
Priv.-Doz. Dr. J. Salbeck [++]
Institut für Organische Chemie der Universität Regensburg (FRG)

[+] Single-crystal X-ray structure analysis.

[++] Electrochemistry.

[**] "Adamantanoid" Chelate Complexes, Part 3. This work was supported by the Deutsche Forschungsgemeinschaft and the Fonds der Chemischen Industrie. B. H. thanks the Freistaat Bayern for a post-graduate fellowship; J. S. thanks Prof. Dr. J. Daub, University of Regensburg, for supporting his research. We are grateful to Priv.-Doz. Dr. H. U. Hummel, University of Erlangen-Nürnberg, for advice and Prof. Dr. R. Glaser, Ben-Gurion University of the Negev, Beersheva, Israel for stimulating discussions. We thank Prof. Dr. F. Vögtle and Dr. S. Schuth, University of Bonn, for recording the FAB-MS spectrum, Prof. Dr. A. X. Trautwein, Dr. E. Bill and C. Butzlaff (Dipl.-Phys.), Medizinische Universität zu Lübeck, for the recording of a Mössbauer spectrum, as well as magnetic measurements.—Part 2: [1].

We were convinced that the size of the cavity of the tetrametallate(4−) ions **1a** could be tailored with suitable spacers. In place of the anions **1a**, it should also be possible to obtain *neutral* tetranuclear metal–chelate complexes by using M^{3+}, instead of M^{2+}, ions.

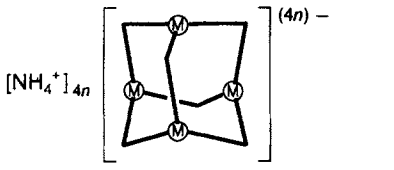

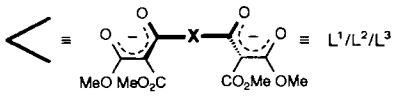

1a: Ⓜ ≡ M^{2+}, $n = 1$, L^1:X = —

1b: Ⓜ ≡ Fe^{3+}, $n = 0$, L^1:X = —

1c: Ⓜ ≡ Fe^{3+}, $n = 0$, L^2:X =

1d: Ⓜ ≡ Fe^{3+}, $n = 0$, L^3:X =

Consequently we doubly deprotonated tetramethyl 2,2'-terephthaloyldimalonate[6] with sodium hydride at 20 °C. We then treated the resulting dianion L^2 with an iron(III) chloride solution and obtained ruby-red crystals upon workup. According to elemental analysis and FAB-MS data (FAB = Fast Atom Bombardment) the compound, of composition $Fe_4L_6^2$, is the tetranuclear iron(III) chelate complex **1c** (for details see [8]).

The ^1H and ^{13}C NMR spectra of $Fe_4L_6^2$ (**1c**) do not unambiguously establish the structure of this compound. Thus an X-ray crystallographic structure analysis of this complex was carried out.[9] According to this analysis, **1c** crystallizes as a neutral, adamantanoid, tetranuclear iron(III) chelate complex (Fig. 1)—the first of its kind.[12] The nucleus of the complex forms an almost ideal tetrahedron, with an Fe(III) ion in each of the corners. The six edges of the tetrahedron are each formed by the doubly bidentate, doubly negatively charged, bridging ligands L^2 (distances between facing phenyl centers approximately 10 Å). Six oxygen atoms surround each of the four Fe^{III} ions in an octahedral arrangement (Fig. 2).[13]

Two enantiomeric pairs [(*Δ*)-, (*Λ*)-*fac*, and (*Δ*)-, (*Λ*)-*mer*] are principally possible for octahedral complexes of the type MA_3B_3 [with bidentate ligands $M(AB)_3$].[14] The $Fe_4L_6^2$ complex has an exact S_4 symmetry in the crystal and is thus achiral (*meso* form). This means that the ligands L^2 around the four iron centers in **1c** are arranged facially and that two of the four iron centers have the same configuration [(*Δ*, *Δ*)-/(*Λ*, *Λ*)-*fac*]. This is in contrast to the chiral, racemic, *T*-symmetrical complexes **1a**, in which all four metal centers (M^{2+} = Mg, Mn, Co, Ni, Zn) are identically coordinated [(*Δ*, *Δ*, *Δ*, *Δ*)-*fac* or (*Λ*, *Λ*, *Λ*, *Λ*)-*fac*].[1, 5]

The cyclic voltammogram under aprotic conditions[15] shows the reduction of the $Fe_4L_6^2$ complex **1c** as a quasi-reversible signal pair centered at −550 mV (Fig. 3, left). The peak potential difference ΔE_p at a scan rate of 250 mVs^{-1} is 170 mV; the reduction peak is slightly broadened ($E_p - E_{p/2}$ = 135 mV), but shows no further splitting.[16] In thin-layer voltammetry, at a layer thickness of 15 μm and a scan rate of 10 mVs^{-1}, the reduction is also seen as a quasi-reversible signal pair with a peak potential difference of 60 mV. The half-peak widths are also broader ($\Delta E_{p/2}$ = 220 mV for the reduction, 170 mV for the reoxidation), but the signals show no further structure. Thin-layer coulometry shows that four electrons are transferred under every signal, whereas a multi-

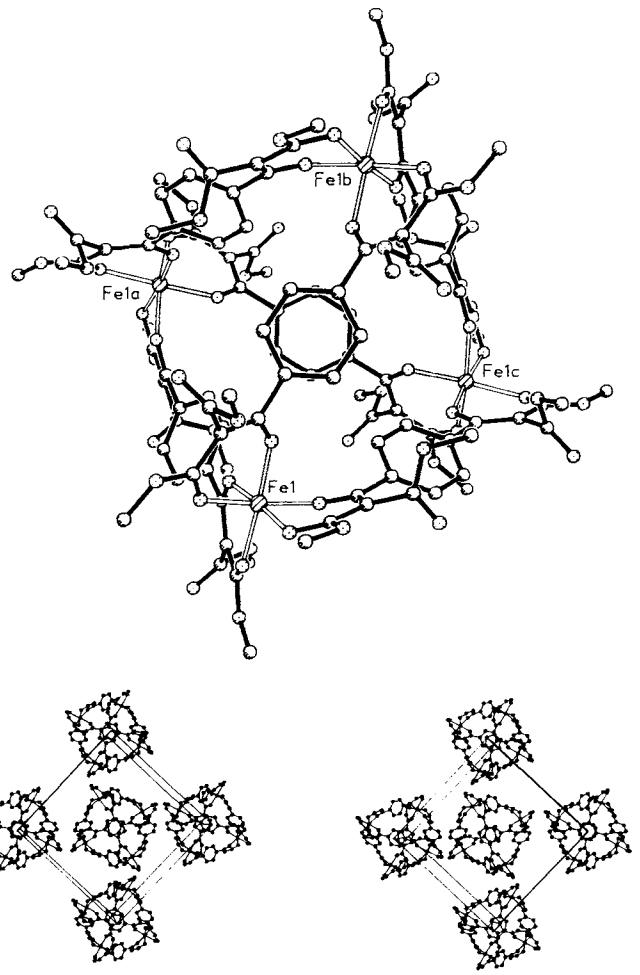

Fig. 1. Top: Crystal structure of **1c** (view along the crystallographic S_4 axis; H atoms omitted; C atoms white; O atoms dotted). Bottom: Stereoview of the crystal packing of **1c** (view along the crystallographic S_4 axis; for reasons of clarity the methoxy and methoxycarbonyl groups as well as the solvents of crystallization $C_4H_{10}O$, C_3H_6O, and H_2O have been omitted).

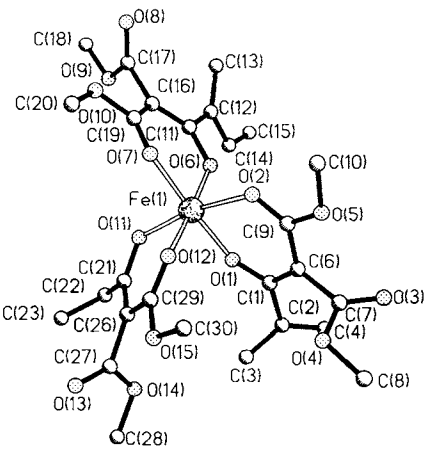

Fig. 2. Coordination sphere of a Fe^{3+} ion in **1c**. Selected distances [Å] and angles [°]: Fe(1)-O(1) 1.946(4), Fe(1)-O(2) 2.039(4), Fe(1)-O(6) 1.926(4), Fe(1)-O(7) 2.016(4), Fe(1)-O(11) 1.950(4), Fe(1)-O(12) 2.043(4), Fe(1)···Fe(1a) 10.028, Fe(1)···Fe(1b) 10.375; O(1)-Fe(1)-O(2) 85.66(15), O(6)-Fe(1)-O(7) 85.7(2), O(11)-Fe(1)-O(12) 85.0(2).

sweep experiment shows the complete chemical reversibility of the redox process. This reversibility is confirmed by spectroelectrochemical as well as voltabsorptometric measurements. Following the reduction spectroelectrochemically gives continually changing absorption signals, but no recognizable intermediates for a partially reduced complex are observed. It is conspicuous that the longest wave absorption signal of **1c** at 450 nm does not completely disappear, but only reduces in intensity to a quarter of its extinction. Also, no further absorptions at long wavelengths for mixed-valent species occur (Fig. 3, right). In the UV region the spectral changes are analogous. Thus no, or only very weak, electronic interactions ("metalloautism") exist between the iron centers in **1c**. The redox process is therefore formally a one-potential four-electron transfer.[17, 20]

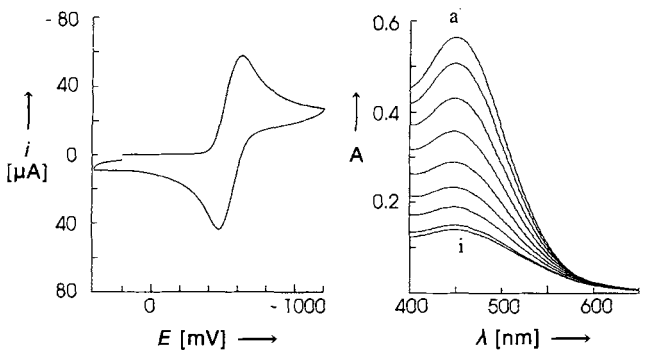

Fig. 3. Left: Cyclic voltammogram of **1c** in a 0.1 M solution of tetraethylammonium tetrafluoroborate in acetonitrile, $c = 10^{-3}$ M, scan speed 250 mVs^{-1}. Potentials vs. ferrocene/ferrocenium (Fc/Fc^+). Right: Spectroelectrogram of **1c** in solution of 0.1 M tetrabutylammonium hexafluorophosphate in acetonitrile. Potentials (a–i): −300, −400, −500, −550, −600, −700, −750, −800 (vs. Fc/Fc^+).

Furthermore Mössbauer and magnetic measurements are in agreement with the results of the electrochemical studies on **1c**. The Mössbauer spectrum shows a signal broadened by relaxation with an isomeric shift δ at 293 K of 0.6 mm s^{-1}. Magnetic measurements (SQUID-susceptometer, temperature range 10–300 K) give a temperature-independent value of 11.55 μ_B for the effective magnetic moment μ_{eff}.[24] This result agrees well with the calculated value of the magnetic moment ($\mu_{calc} = 11.83\ \mu_B$) for four magnetically isolated high-spin iron(III) centers that show no interactive phenomena in the investigated temperature range.[25]

We shall report elsewhere on the simple iron(III) chelate complex **1b** and the iron(III) chelate complex **1d** with biphenyl as spacer.

Received: March 13, 1993 [Z 5922 IE]
German version: *Angew. Chem.* **1993**, *105*, 1223

[1] R. W. Saalfrank, A. Stark, M. Bremer, H.-U. Hummel, *Angew. Chem.* **1990**, *102*, 292–294; *Angew. Chem. Int. Ed. Engl.* **1990**, *29*, 311–314.

[2] T. Weiske, T. Wong, W. Krätschmer, J. K. Terlouw, H. Schwarz, *Angew. Chem.* **1992**, *104*, 242–244; *Angew. Chem. Int. Ed. Engl.* **1992**, *31*, 183–185; H. Hopf, *ibid.* **1991**, *103*, 1137–1139 and **1991**, *30*, 1117–1118; C. Seel, F. Vögtle, *ibid.* **1992**, *104*, 542–563 and **1992**, *31*, 528–549.

[3] P. Baxter, J.-M. Lehn, A. DeCian, J. Fischer, *Angew. Chem.* **1993**, *105*, 92–95; *Angew. Chem. Int. Ed. Engl.* **1993**, *32*, 69–72; J.-M. Lehn in *Perspectives in Coordination Chemistry* (Eds.: A. F. Williams, C. Floriani, A. E. Merbach), VCH, Weinheim, **1992**, pp. 447–462.

[4] Reviews: J.-M. Lehn, *Angew. Chem.* **1988**, *100*, 91–116; *Angew. Chem. Int. Ed. Engl.* **1988**, *27*, 89–112, *ibid.* **1990**, *102*, 1347–1362 and **1990**, *29*, 1304–1319.

[5] R. W. Saalfrank, A. Stark, K. Peters, H. G. von Schnering, *Angew. Chem.* **1988**, *100*, 878–880; *Angew. Chem. Int. Ed. Engl.* **1988**, *27*, 851–853.

[6] Synthesis based on ref. [7] starting with dimethyl malonate, triethylamine, anhydrous magnesium(II) chloride and terephthaloyl chloride in acetonitrile at −10 °C (16 h) and workup with 15 percent hydrochloric acid.

[7] M. W. Rathke, M. A. Nowak, *Synth. Commun.* **1985**, *15*, 1039–1049; M. W. Rathke, M. A. Nowak, *J. Org. Chem.* **1985**, *50*, 2624–2626; M. W. Rathke, P. J. Cowan, *ibid.* **1985**, *50*, 2622–2624.

[8] **1c** (preparation): To sodium hydride (0.2 g, 8 mmol) in THF (10 mL) was added tetramethyl 2,2′-terephthaloyl dimalonate [6] in dry THF (40 mL) (under nitrogen) at 20 °C, and the mixture stirred for 1 h. Then a solution of iron(III) chloride (0.3 g, 2 mmol) in THF (40 mL) was added dropwise over 15 min, and the mixture was stirred for 16 h, filtered in air through a fluted filter, and concentrated to 15 mL. Acetone (50 mL) was added. After 3 d ruby-red microcrystals could be isolated from the solution. Yield: 0.73 g (57%). Decomp. above 150 °C. IR (KBr): $\tilde{\nu} = 1720\ cm^{-1}$ (C = O). FAB-MS (3-nitrobenzyl alcohol matrix): *m/z* 2578 $[Fe_4L_6^2 + H^+]$, 2185 $[Fe_4L_5^2 + H^+]$, 1793 $[Fe_4L_4^2 + H^+]$. Correct C, H, N analyses.

[9] Crystal data for **1c**: $C_{108}H_{96}O_{60}Fe_4 \cdot C_4H_{10}O \cdot C_3H_6O \cdot H_2O$, $M_r = 777.49$, tetrahedral, space group $P\bar{4}n2$, $a = b = 21.631(1)$, $c = 17.371(3)$ Å, $V = 8127.9(15)$ Å^3, $Z = 8$, $\varrho_{calcd.} = 1.271$ Mg m^{-3}, $F(000) = 3240$, $\lambda = 0.71073$ Å, $T = 180$ K, $\mu(Mo_{K\alpha}) = 0.439$ mm^{-1}. The data were collected on a Stoe–Siemens AED diffractometer. Intensity determinations were performed on a shock-cooled crystal (dimensions 1.2 × 1.0 × 0.8 mm) in an oil drop according to the $2\theta/\omega$ method in the region $8° < 2\theta < 45°$. Of the 7537 collected reflections, 5328 were unique and were absorption-corrected according to a semiempirical method; highest minima and maxima: 1.0 and −0.46 eÅ^{-3}, respectively; $R1 = 0.068$ and $wR2 = 0.179$ (all data), the absolute structure was refined by using the Flack parameters (H. D. Flack, *Acta Crystallogr. Sect. A* **1983**, *39*, 876) to 0.01(3). The structure was solved by direct methods (SHELXS-90) [10] and refined according to the least-squares method (SHELXL 92) [11]. All hydrogen atom positions were located in a difference Fourier map and refined by using a riding model. The *U* values for chemically equivalent hydrogen atoms were refined together in groups. Further details concerning the X-ray structure analysis can be obtained from the Director of the Cambridge Crystallographic Data Centre, 12 Union Road, GB-Cambridge CB2 1EZ (UK), on quoting the full journal citation.

[10] G. M. Sheldrick, *Acta Crystallogr. Sect. A* **1990**, *46*, 467–473.

[11] G. M. Sheldrick, *SHELXL-92*, University of Göttingen, **1992**.

[12] Tetranuclear iron(III) complexes: S. R. Boone, G. H. Purser, H.-R. Chang, M. D. Lowery, D. N. Hendrickson, C. G. Pierpont, *J. Am. Chem. Soc.* **1989**, *111*, 2292–2299; J. K. McCusker, J. B. Vincent, E. A. Schmitt, M. L. Mino, K. Shin, D. K. Coggin, P. M. Hagen, J. C. Huffman, G. Christou, D. N. Hendrickson, *ibid.* **1989**, *113*, 3012–3021; K. S. Hagen, A. D. Watson, R. H. Holm, *ibid.* **1983**, *105*, 3905–3913; M. A. Whitener, J. K. Bashkin, K. S. Hagen, J.-J. Girerd, E. Gamp, N. Edelstein, R. H. Holm, *ibid.* **1986**, *108*, 5607–5620; J. L. Sessler, J. D. Hugdahl, V. Lynch, B. Davis, *Inorg. Chem.* **1991**, *30*, 334–336; Q. Chen, J. B. Lynch, P. Gomez-Romero, A. Ben-Hussein, G. B. Jameson, C. J. O'Conor, L. Que, Jr., *ibid.* **1988**, *27*, 2673–2681.

[13] In regard to the topology of the four-centered chelate complex **1c** (bridgeheads: Fe^{3+} ions), compare also the conditions in spherical tricycles (bridgeheads: N atoms): Ref. [4]. F. P. Schmidtchen, *Angew. Chem.* **1977**, *89*, 751–752; *Angew. Chem. Int. Ed. Engl.* **1977**, *16*, 720–721; J.-M. Lehn, *Pure Appl. Chem.* **1977**, *49*, 857–870; E. Graf, J.-M. Lehn, *J. Am. Chem. Soc.* **1975**, *97*, 5022–5024; E. Weber, F. Vögtle, *Kontakte (Darmstadt)* **1981**, (1), 24–36; E. Weber: *Phase Transfer Catalysts, Properties and Applications* (Merck-Schuchardt publication, **1987**, pp. 32–76; F. P. Schmidtchen, *Nachr. Chem. Tech Lab.* **1988**, *36*, 8–1.

[14] M. Becke-Goehring, H. Hoffmann, *Komplexchemie*, Springer, Berlin **1970**, p. 26ff; see also *Nomenclature of Inorganic Chemistry* (Ed.: G. J. Leigh), Blackwell, Oxford, **1991**, p. 179ff. (in octahedral complexes of type $MA^1B^1A^2B^2A^3B^3$, five enantiomeric pairs occur: J. Leong, K. N. Raymond, *J. Am. Chem. Soc.* **1975**, *97*, 293–296). See also the descriptions OC-6-22 (for facial) and OC-6-21 (for meridonal) recommended by IUPAC.

[15] Amel System 5000 with IR compensation. Undivided cell with Pt-disc electrodes. Potentials vs. Fc/Fc^+. For experimental details on electrochemistry, spectroelectrochemistry and voltabsorptometry, see J. Salbeck, *J. Electroanal. Chem.* **1992**, *340*, 169–195.

[16] The peak potential difference ΔE_p of 170 mV, and also the peak width $E_p - E_{p/2}$ of 135 mV, stay essentially constant with variation of the scan speed in the region 50–250 mV^{-1}. In the region 50–250 mV the ratio of peak current i_p and the square root of the scan rate are constant. The use of tetrabutylammonium hexafluorophosphate as conducting salt leads to considerably larger values: $\Delta E_p = 300$ mV, $E_p - E_{p/2} = 299$ mV at 250 mVs^{-1}.

[17] A random number of noninteracting identical redox centers in a molecule should show a current potential behavior with the same characteristics as a reversible one-electron transfer (e.g. $\Delta E_p = 58$ mV). This is only valid, however, when the redox centers show *Nernstian behavior* [18]. In the case of a partial diffusion control, signal broadening occurs. Signal forms comparable to ours result from the simulation of cyclic voltammograms for a

formal two-electron transfer under similar conditions for the rate constants of the charge transfers [19].
[18] J. B. Flanagan, S. Margel, A. J. Bard, F. C. Anson, *J. Am. Chem. Soc.* **1978**, *100*, 4248–4253.
[19] K. Hinkelmann, J. Heinze, *Ber. Bunsenges. Phys. Chem.* **1987**, *91*, 243–249.
[20] See refs. [21–23] for details concerning multielectron transfer processes.
[21] D. E. Fenton, R. R. Schroeder, R. L. Lintvedt, *J. Am. Chem. Soc.* **1978**, *100*, 1931–1932; D. E. Fenton, R. L. Lintvedt, *ibid.* **1978**, *100*, 6367–6375; D. T. Pierce, W. E. Geiger, *ibid.* **1989**, *111*, 7636–7638; B. Tulyathan, W. E. Geiger, *ibid.* **1985**, *107*, 5960–5967; J. Salbeck, J. Schöberl, J. Daub, *Z. Phys. Chem.* **1991**, *171*, 191–212.
[22] E. Kimura, S. Joko, T. Koike, M. Kodama, *J. Am. Chem. Soc.* **1987**, *109*, 5528–5529.
[23] W. F. Sokol, D. H. Evans, K. Niki, T. Yagi, *J. Electroanal. Chem.* **1980**, *108*, 107–115; K. Fan, H. Akutsu, K. Niki, N. Higuchi, Y. Kyogoku, *ibid.* **1990**, *278*, 295–306.
[24] The diamagnetic corrections were determined by using Pascal constants: E. A. Budreaux, L. N. Mulay, *Theory and Applications of Molecular Paramagnetism*, J. Wiley, New York, **1976**; A. Weiss, H. Witte, *Magnetochemie*, VCH, Weinheim, **1973**.
[25] F. E. Mabbs, D. J. Machin, *Magnetism and Transition Metal Complexes*, Chapman and Hall, London, **1973**; A. Bencini, D. Gatteschi, *EPR of Exchange Coupled Systems*, Springer, Berlin, **1990**.

Dilithiation of Two Diphenyl Ethers Each Containing Two $NHCH_2CH_2Y$ (Y = OMe, NMe_2) Side Arms in *ortho* Positions: Assembly of "Adamantanoid" $Li_4O_2N_4$ Cores**

By *Ian Cragg-Hine, Matthew G. Davidson,* Oldrich Kocian, Francis S. Mair, Ehmke Pohl, Paul R. Raithby, Ronald Snaith, Neil Spencer*, and *J. Fraser Stoddart**

Lithium amides are important synthetic organic reagents, and consequently much work has been done in order to elucidate their structures both in solution and in the solid state.[1, 2] Until recently however, the structures of only simple monolithiated complexes of secondary amines were known. To our knowledge only two dilithiated amide complexes exist. Recently we published the results of dilithiating naphthylamine, providing the first example of a dilithiated primary amine; it is a Li_{20} species held together by $(NaphN)^{2-}$ anions (Naph = naphtyl) and ether ligands.[3] We have also obtained the structure of a dilithiated diamine $(PhLiNCH_2CH_2NLiPh) \cdot 3\,HMPA$[4] (HMPA = hexamethylphosphoric triamide), containing the commonly observed[2] Li_2N_2 core. Such a core also featured in the first lithiated diazacrown.[5] We now report on the dilithiation of two diamines, 2,2′-bis(2-methoxyethylamino)diphenyl ether (**1**) and 2,2′-bis(*N*,*N*-dimethylethylenediamino)diphenyl ether (**2**), which give the lithium amides **3** and **4**, respectively.

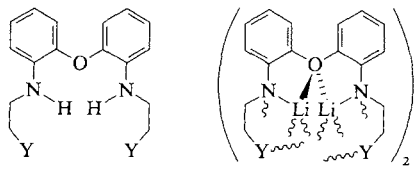

1, Y = OMe
2, Y = NMe_2

3, Y = OMe
4, Y = NMe_2

The possibility of intramolecular coordination, coupled with the increased flexibility of **1** and **2** over the cyclic crown ethers suggested that the use of an additional Lewis base donor such as $(C_2H_5)_2O$ or HMPA would be unnecessary. Indeed, dilithiation of the diamines **1** and **2** and the subsequent crystallization of products **3** and **4** from toluene solution was achieved in the absence of a Lewis base donor.

The X-ray crystal structure analyses[6] of diamines **3** and **4** exhibit an adamantanoid metal-containing core, a structural motif that is unprecedented in the chemistry of Group I metal complexes (Fig. 1 and 2).[7, 8]

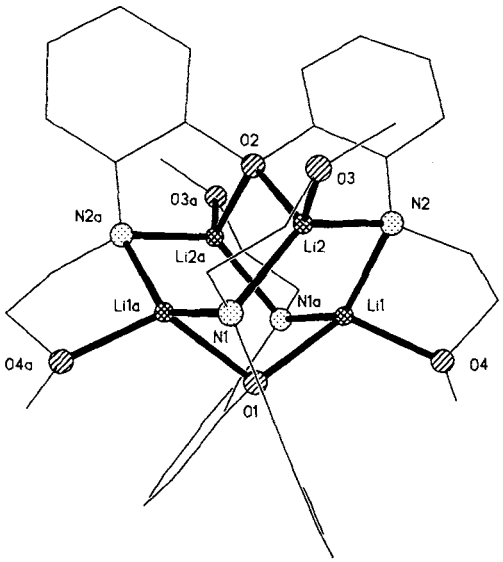

Fig. 1. Molecular structure of **3** (for clarity, the carbon framework is not shown in detail and hydrogen atoms have been omitted).

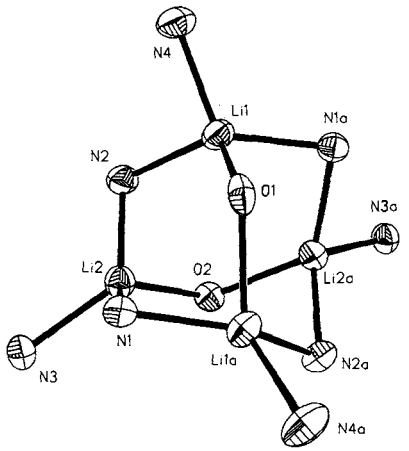

Fig. 2. Adamantanoid $Li_4O_2N_8$ central core of **4** (thermal ellipsoids at the 50% probability level).

[*] M. G. Davidson, I. Cragg-Hine, Dr. F. S. Mair, Dr. P. R. Raithby, Dr. R. Snaith
University Chemical Laboratory
Lensfield Road, Cambridge CB2 1EW (UK)
Telefax: Int. code + (223)336-362
Prof. J. F. Stoddart, Dr. O. Kocian, Dr. N. Spencer
School of Chemistry, University of Birmingham
Edgbaston, Birmingham B15 2TT (UK)
E. Pohl
Institut für Anorganische Chemie, University of Göttingen (FRG)

[**] This work was supported by the U. K. Science and Engineering Research Council (O. K., R. S., and J. F. S.) and The Associated Octel Company Ltd. (CASE Studentships for M. G. D. and I. C.-H.). F. S. M. thanks Queens' College, Cambridge, and The Associated Octel Company and M. G. D. thanks St. John's College, Cambridge, for research fellowships. We would like to thank Prof. Dr. G. M. Sheldrick and Dr. D. Stalke (University of Göttingen) for the use of X-ray facilities for the determination of the structure of **3**.

Formation of an Li_2N_2 ring within a monomeric dilithiated diamine (perhaps with additional coordination between the Li ions and the O and Y centers) was not observed. Molecular models show that such an arrangement would be highly strained. Considering structure 3 (Fig. 1) and firstly just one monomeric unit within it reveals that N1a–H has been deprotonated by Li1 and N1–H by Li1a. These two lithium centers are then both coordinated by the diaryl ether linkage (Li1–O1 and Li1a–O1). This is the first observation of this bonding mode for Ar–O–Ar (Ar = aryl) with lithium.[2, 9] The OMe groups of the side arms cannot satisfactorily act as intramolecular Lewis base donors so it is at this stage that the complex dimerizes spontaneously. The monomeric units containing (as yet) two two-coordinate lithium ions and two noncoordinating side arms slot together almost orthogonally, and each deprotonated amide N atom forms an intermolecular μ_2-bridge (Li1–N2, Li1a–N2a, Li2–N1, and Li2a–N1a), thus forming the adamantanoid core. Such an arrangement now allows the side arms of each monomer to coordinate to the lithium ions and complete their coordination spheres. In **4**, precisely the same intra- and intermonomer coordinations operate, save that the side arms are now Me_2 groups (Fig. 2). In retrospect, for both **3** and **4**, such an arrangement, although unpredicted, appears (as shown by space-filling molecular models) to be ideal. The two monomer units have been clamped together by the tendency of the lithium atoms to attain their favored fourfold coordination without inducing steric strain on the organic framework.

The conceptual view of this dimerization as self-recognition of two monomers is lent credence by considering the bond lengths within the cores of the solid-state structures (Fig. 3). The bonds within one monomeric unit are highlighted in boldface. In **3** the averaged[10] amide N–Li bonds within a monomeric unit are shorter (196 pm) than the amide N–Li bonds between monomers (203 pm). The Li–O linkages between Li atoms of one monomer and the OMe groups of the other are considerably shorter (192 pm) than the intramonomer one involving the O atom of the Ar–O–Ar unit (207 pm). This is significant as it is these intermolecular Li–OMe interactions that clamp the two monomers together. Furthermore, of all the interactions with Li of electronegative centers only these Li–Y ones are terminal; all others involve *bridging* of two Li atoms. In **4** where $Y = NMe_2$, however, these side-arm interactions are no longer the shortest bonds (Fig. 3).

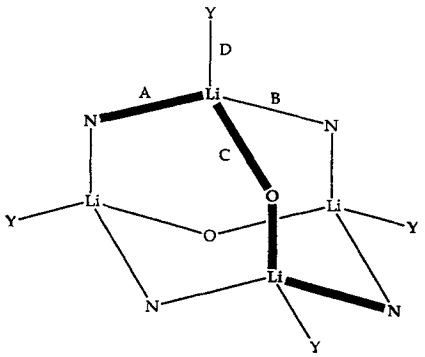

	A	B	C	D
3 [Y=OMe]	196	203	207	192
4 [Y=NMe_2]	199	206	212	211

Fig. 3. The core of complexes **3** and **4** showing average intramolecular (A and C) and intermolecular (B and D) bond lengths in pm [10]. Bonds and atoms of one monomeric unit are in boldface.

This subtle difference in the binding between monomeric units in **3** and **4** is reflected in the solution studies. The room-temperature ^1H NMR of **3** in C_6D_6 shows an ABCD coupling pattern for the pair of methylene groups on the side arm of the ligand that is consistent with the persistence of the solid-state structure in solution. Cryoscopy in benzene also indicates that the dimer remains intact in solution [$n = 1.97 \pm 0.06$ for a 0.025 M solution (concentration expressed in terms of monomer)]. In **4**, the room-temperature solution behavior indicates a less rigid structure, consistent with the looser solid-state binding.

Further differences in behavior are to be expected with variation of metal size, metal valency, and identity of bridging and terminal functionalities. Such variations are being investigated.

Experimental Procedure

For **1**, bis(2-aminophenyl) ether, readily available from reduction of bis(2-nitrophenyl) ether [11] with hydrazine hydrate in the presence of 10% Pd on carbon, was converted into a bis(methoxyacetamide) by reaction with methoxyacetyl chloride. This amide was then reduced with $LiAlH_4$ in boiling THF to give the diamine **1** as a yellow oil, which crystallized on standing. Yield 90%, m.p. 42–43 °C. Satisfactory C,H, and N analyses. ^1H NMR (300 MHz, $CDCl_3$, 293 K, TMS): $\delta = 3.34$ (s, 6H, OCH_3), 3.34 (t, 4H, $J = 5.5$ Hz, CH_2), 3.59 (t, 4H, $J = 5.5$ Hz, CH_2), 4.58 (bs, 2H, NH), 6.56–6.64 (m, 2H, ArH), 6.71–6.78 (m, 4H, ArH), 6.96–7.07 (m, 2H, ArH). ^{13}C NMR (75 MHz, $CDCl_3$): $\delta = 144.06, 139.90, 124.21, 117.68, 116.92, 111.38, 71.11, 58.79, 43.38$. MS(CI): m/z 317 ($M + H^+$, 100%), 259(43), 201(14), 186(12), 166(13), 152(32), 132(18), 120(26), 110(35) 94(50), 76(47), 59(18), 44(28).

For **2**, bis(2-aminophenyl) ether was converted into a bis(chloroacetamide) by reaction with chloroacetyl chloride. This was then treated with 40% aqueous $(CH_3)_2NH$ to form the corresponding bis(N,N-dimethylacetamide). Reduction of this, again with $LiAlH_4$, gave the diamine **2** as a yellow oil. Yield 89%. Satisfactory C,H, and N analyses. ^1H NMR (300 MHz, $CDCl_3$, 293 K, TMS): $\delta = 2.20$ (s, 12 H, CH_3), 2.53 (t, 4H, $J = 6$ Hz, CH_2), 3.21 (q, 4H, $J = 5.5$ Hz, CH_2), 4.70 (t, 2H, $J = 5$ Hz, NH), 6.59 (dt, 2H, $J = 8$ Hz, $J = 1.5$ Hz, ArH), 6.73 (dt, 4 H, $J = 8$ Hz, $J = 1.5$ Hz, ArH), 6.99 (dt, 2H $J = 8$ Hz, $J = 1.5$ Hz, ArH). ^{13}C NMR (75 MHz, $CDCl_3$) $\delta = 143.94, 140.12, 124.14, 117.53, 116.52, 111.28, 58.18, 45.31, 41.37$. MS(CI): m/z 343 ($M + H^+$, 100%) 298(5), 272(20), 181(10), 165(10), 110(16), 94(18), 72(50), 58(84), 46(25).

3: *n*-Buthyllithium (4.0 mmol, 2.5 mL of a 1.6 M hexane solution) was added to a chilled solution (0 °C) of **1** (0.632 g, 2.0 mmol) in dry toluene (8 mL) under nitrogen. The product, a white precipitate, was warmed into solution (60 °C). A crop of colorless crystals was deposited after standing at room temperature overnight (0.322 g, 49%); m.p. > 300 °C, satisfactory C, H, and N analyses. ^1H NMR (250 MHz, C_6D_6, 293 K, TMS): $\delta = 2.77$ (s, 3H, OMe) 2.80, 2.92, 3.28, 3.45 (D,C,B and A, respectively, of an ABCD system; see above for labels; 4×1 H, $^2J_{AB} = 7$ Hz, $^3J_{AC} = 17$ Hz, $^3J_{AD} = 16$ Hz, $^3J_{BC} = 28$ Hz, $^3J_{BD} = 7$ Hz, $^2J_{CD} = 7$ Hz), 6.45 (t of d, 1 H, aryl H *meta* to amide), 6.67 (dd, 1 H, aryl H *ortho* to amide), 7.10–7.2 (m, 2H, other arene-H). Assignments were by a combination of coalesence behavior, selective decoupling, and COSY experiments and were confirmed by a NMR simulation program.

4: As for **3**, **2** (0.684 g, 2.0 mmol) was lithiated (4.0 mmol, 2.5 mL of 1.6 M *n*-butyllithium in hexane) to produce crystals of **4** (0.361 g, 51%); m.p. 230–233 °C, satisfactory C,H, and N analyses. ^1H NMR (250 MHz, C_6D_6, 293 K, TMS): $\delta = 1.70$ (s, 6H, Me_2N), 2.24, 2.89 (br.s, 2×2H, CH_2CH_2), 6.23 (t of d, 1H, aryl *meta* to amide), 6.48 (dd, 1H, aryl *ortho* to amide), 6.95 (t of d, 1H, aryl *meta* to ether), 7.14 (dd, 1H, aryl *ortho* to ether).

Received: March 13, 1993 [Z 5923 IE]
German version: *Angew. Chem.* **1993**, *105*, 1254

[1] K. Gregory, P. von R. Schleyer, R. Snaith, *Adv. Inorg. Chem.* **1991**, *37*, 47–142.
[2] R. E. Mulvey, *Chem. Soc. Rev.* **1991**, *20*, 167–209.
[3] D. R. Armstrong, D. Barr, W. Clegg, S. R. Drake, R. J. Singer, R. Snaith, D. Stalke, D. S. Wright, *Angew. Chem.* **1991**, *104*, 1702–1704; *Angew. Chem. Int. Ed. Engl.* **1991**, *30*, 1707–1709.
[4] D. R. Armstrong, D. Barr, A. T. Brooker, W. Clegg, K. Gregory, S. M. Hodgson, R. Snaith, D. S. Wright, *Angew. Chem.* **1990**, *102*, 443–445; *Angew. Chem. Int. Ed. Engl.* **1990**, *29*, 410–411.

[5] D. Barr, D. J. Berrisford, L. Méndez, A. M. Z. Slawin, R. Snaith, J. F. Stoddart, D. J. Williams, D. S. Wright, *Angew. Chem.* **1991**, *103*, 97–100; *Angew. Chem. Int. Ed. Engl.* **1991**, *30*, 82–84.

[6] X-ray crystal data for **3**: $C_{36}H_{44}N_4O_6Li_4$, $M_r = 656.51$, monoclinic, space group $P2_1/c$, $a = 18.899(5)$, $b = 10.386(5)$, $c = 18.995(5)$ Å, $\beta = 107.06(2)°$, $V = 3564(2)$ Å^3, $Z = 4$, $\varrho_{calcd} = 1.223$ Mg m^{-3}, $F(000) = 1392$, $\lambda(Mo_{K\alpha}) = 0.71073$ Å, $\mu(Mo_{K\alpha}) = 0.081$ mm^{-1}, $T = 153.0(20)$K. Data were collected on a Stoe-Siemens diffractometer in the range $8° \leq 2\theta \leq 50°$ (6793 reflections collected, 4926 independent reflections). The structure was solved by direct methods [12] and refinement, based on F^2, was by full-matrix least-squares techniques [13] (all non-hydrogen atoms were refined anisotropically and hydrogen atoms were included in calculated positions) to $R_1 = 0.0428$, $wR_2 = 0.1022$ for 4040 unique reflections [$F > 4\sigma(F)$]. – X-ray crystal data for **4**: $C_{20}H_{28}N_4OLi_2$, $M_r = 354.34$, monoclinic, space group $C2/c$, $a = 20.289(4)$, $b = 10.790(2)$, $c = 19.426(4)$ Å, $\beta = 108.51(3)°$, $V = 4032.7(14)$ Å^3, $Z = 8$, $\varrho_{calcd} = 1.167$ Mg m^{-3}, $F(000) = 1520$, $\lambda(Mo_{K\alpha}) = 0.71073$ Å, $\mu(Mo_{K\alpha}) = 0.072$ mm^{-1}, $T = 153.0(20)$K. Data were collected on a Stoe four-circle diffractometer in the range $5° \leq 2\theta \leq 45°$ (5276 reflections collected, 2638 independent reflections). The structure was solved and refined as above to $R_1 = 0.0413$, $wR_2 = 0.1207$ for 2139 unique reflections [$F > 4\sigma(F)$]. Further details of the crystal structures are available on request from the Director of the Cambridge Crystallographic Data Centre, 12 Union Road, GB-Cambridge CB2 1EZ (UK), by quoting the full journal citation.

[7] A structurally very different magnesium chelate complex has been reported in which four metals and six dianionic ligand units together form an "adamantanoid" anion: R. W. Saalfrank, A. Stark, K. Peters, H. G. von Schnering, *Angew. Chem.* **1988**, *100*, 878–880; *Angew. Chem. Int. Ed. Engl.* **1988**, *27*, 851–853. Similar anionic species have also been observed for transition metal species: R. W. Saalfrank, A. Stark, M. Bremer, H.-U. Hummel, *ibid.* **1990**, *102*, 292–295 and **1990**, *29*, 311–313. Recently a crystal structure of a neutral Fe^{III} adamantanoid complex has been obtained: R. W. Saalfrank, personal communication.

[8] In a very recent publication a trilithiated triamine is described as having an adamantanoid structure, but this involves the organic framework and not assembly of a metal core: L. H. Gade, N. Mahr, *J. Chem. Soc. Dalton Trans.* **1993**, 489–494.

[9] W. Setzer, P. von R. Schleyer, *Adv. Organomet. Chem.* **1985**, *24*, 353–451.

[10] In **3** the dimer is the crystallographic asymmetric unit; all bond lengths within it are therefore independent and each quoted bond length is an average of four values. In **4** the asymmetric unit is only half the dimeric molecule and so each quoted bond length is an average of only two values.

[11] J. F. K. Wilshire, *Aust. J. Chem.* **1988**, *41*, 995–1001.

[12] G. M. Sheldrick, *Acta Crystallogr. Sect. A* **1990**, *46*, 467.

[13] G. M. Sheldrick, SHELXL-92, program for crystal structure refinement, University of Göttingen.

Polymeric Hemiporphyrazines, a New Class of Rodlike Macromolecules Suitable for the Langmuir–Blodgett Technique

By *Andreas Ferencz, Roland Ries*, and *Gerhard Wegner**

Macromolecules composed of stacks of macrocyclic repeat units have received considerable attention as building blocks of supramolecular architectures.[1–7] Such rodlike macromolecules are frequently insoluble as a consequence of inherent chain-stiffness. Attachment of flexible, short side chains to the perimeter of the macrocyclic subunits makes these macromolecules soluble in ordinary organic solvents, thus allowing their processing. Macromolecules of this type are called "hairy rods". They can be spread at the air–water interface of a Langmuir trough, if the overall geometry of the macromolecules and the structure of the side chains are suitably chosen. The side-chain segments may be considered as bound solvent that helps in the formation of the monomolecular layers on the Langmuir trough, which are subsequently transferred layer by layer to planar substrates by the Langmuir–Blodgett (LB) technique. The rheological features linked to the transfer process lead to a preferential alignment of the macromolecules with their long axes in the direction of transfer. The main-chain orientation thus produced is fixed during the course of the transfer. Therefore, a highly ordered and anisotropic layered structure is achieved in which all macromolecules are aligned parallel with their director axes in the plane of the substrate pointing in the dipping direction.

This correlation of geometry and chemical structure of the macromolecules with ordering phenomena, and thus the possibility to create novel supramolecular architectures, was first exemplified with alkoxy-substituted phthalocyaninato-poly(siloxane)s **1a**.[8] It has since been extended to a variety of chemically quite different, but topologically related systems.[9, 10] Among these are helical poly(peptide)s, for example, poly(alkyl L-glutamate)s, cellulose ethers, poly(silane)s with sterically demanding substituents, and poly(2,5-dialkoxy-2,4-phenylene)s. The prominent feature common to all of these types of molecules is the cladding of the stiff backbone with flexible side chains that results in ideal or nearly ideal cylindrical symmetry. The consequence of this topological structure is the densest hexagonal packing of the molecules in the layered structure yet observed experimentally by X-ray techniques in many cases. However, polarization of the side-chain segments ("hairs") at the air–water interface of the Langmuir trough gives rise initially to double layers in the course of the transfer, which relax into the dense hexagonal packing after a short annealing of the samples.

These results triggered the question whether other fundamental geometries of molecularly defined objects exist that could produce supramolecular architectures with different packing symmetries. Stimulated by the very interesting optical and electrical properties of the systems obtained from stacked macromolecules (the phthalocyaninatopoly(siloxane) **1a** (PcPS) being a good example), hemiporphyrazinatopoly(germanoxane) (hpPG, **1b**) was selected as a target (Fig. 1). Macromolecules of this type should be shaped like a square box and therefore exhibit a completely different packing in the solid state, which is enhanced by the substitution pattern of the alkoxy side chains.

The synthesis of **1b** starts from 2,6-diaminopyridine, which is treated with dialkoxy-substituted isoindoline to give the hemiporphyrazine hpH_2.[11] The latter reacts with germanium tetrachloride in quinoline to give the hemiporphyrazinato-dichlorogermane, the monomer of the subsequent polycondensation.[12–14] This is achieved in di-2-methoxyethyl ether with the addition of stoichiometric amounts of tetra(acetonitrilo)copper(I) trifluoromethanesulfonate in analogy to the preparation of PcPS. In the case of dimethoxydioctyloxy-hemiporphyrazinatopoly(germanoxane) ($hpPGC_1C_8$), the polymer precipitates as a brownish solid when the reaction medium is cooled from 140 °C to room temperature. The polymer is completely soluble in chloroform or THF. The degree of polymerization P_n, determined by HPLC, shows a broad distribution; the fraction of highest molecular mass has a degree of polymerization of 12. Solutions of the polymer in chloroform show broad absorption bands in the UV/VIS spectra, the exact spectral location and extinction depending on P_n. The unfractionated polymer **1b** ($hpPGC_1C_8$, R_1 = methyl, R_2 = *n*-octyl) exhibits these bands at $\lambda \approx 280$, 340, and 390 nm. The polymer is actually a copolymer composed of two monomer units that are positional isomers. The monomers were not separated into the isomers, because previous investigations on the spreading and ordering behavior of "hairy-rod" systems had shown that the creation of supramolecular architectures by the LB

[*] Prof. Dr. G. Wegner, A. Ferencz, R. Ries
MPI für Polymerforschung
Ackermannweg 10, D-55021 Mainz (FRG)
Telefax: Int. code + (6131) 379-330m

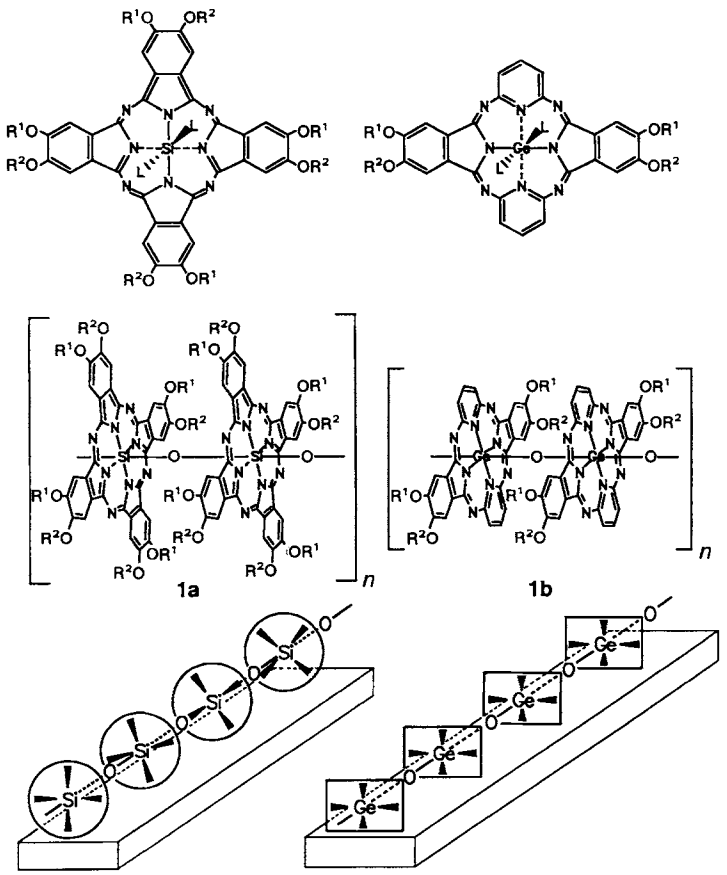

Fig. 1. Structure of surface-active derivatives of phthalocyaninatopoly(siloxane)s (**1a**) and hemiporphyrazinatopoly(germanoxane)s (**1b**) for comparison. Top: monomers, L = Cl; middle: section of the polymer chain; bottom: position of the macromolecules relative to the substrate plane in the Langmuir–Blodgett layers. $R^1 = OCH_3$; $R^2 = OC_8H_{17}$ (in reality, mixtures of the positional isomers are used).

technique is substantially enhanced if ordering phenomena in the side-chain region of the macromolecules are suppressed by introducing positionally isomeric repeat units.

The unfractionated polymer hpPGC$_1$C$_8$ (that is a mixture of homologues with approximately normal distribution of chain lengths) can be spread at the surface of a Langmuir trough from a dilute solution in chloroform. A monomolecular film is thus obtained, the force–area diagram of which is very similar to those reported for PcPS (20 °C, pure water subphase). The films collapse at a surface pressure $\pi > 30\ mN\,m^{-1}$; the area per monomer unit is calculated to be 1.00 nm^2. Transfer to hydrophobic substrates is straightforward and is carried out at $\pi = 20\ mN\,m^{-1}$ (20 °C) and a transfer speed of about $1\ cm\,min^{-1}$. The transfer ratio is unity and remains constant even after more then 100 layers have been transferred to the same substrate. A dependence of the spreading and transfer properties on the degree of polymerization has not been found in our investigations.

The measurements that serve to characterize the structure of the layered assemblies have been performed on samples of 20–30 monolayers each. The UV/VIS spectra demonstrate dichroic behavior of the samples if recorded with polarized light. The absorption is always larger for light polarized normal to the dipping direction. The films are birefringent—as expected—with $n_{\parallel}$ (parallel to the dipping direction) $< n_{\perp}$ (normal to dipping direction). The dichroism is particularly strong in the IR region of the spectrum. The dichroic ratio of certain vibrational bands in the region of 860–710 cm^{-1} reaches a value $D = A_{\parallel}/A_{\perp} = 7$ even for fresh samples.[15] The reverse behavior is seen for the bands associated with ring vibrations around 1600 cm^{-1}. However, in the region of the valence bands of the side-chain segments at 2800–3000 cm^{-1}, no dichroism is observed. Consequently, the bond directions and groups associated with the side chains must be isotropically distributed as in a liquid. Grazing-incidence-reflection (GIR) spectroscopy allows further characterization of the IR-active groups with regard to their orientation normal to the substrate plane.[16]

In this mode all bands that have an associated dipole transition moment containing a component in the direction of the polymer backbone are very small, and the bands of the alkoxy side chains have the identical intensity distribution as in the transmission spectra, but substantial changes become obvious in the intensity pattern of the ring vibrations. This points toward a double orientation of the macromolecules within the substrate plane with regard to their main axes and leads to the speculation that consecutive macrocycles are threaded onto the Ge-O-Ge-O main chain in an eclipsed fashion. Further evidence comes from the X-ray powder diagram of the freeze-dried samples. It shows three peaks, the corresponding Bragg distances of which are $d = 2.80$, 1.32, and 0.35 nm. These values correspond to the width and height of the constitutional units and the periodicity of the repeat (0.35 nm) predicted by molecular models. The product of molecular width (2.80 nm) and periodicity (0.35 nm) gives the value of the base area (0.98 nm^2), in excellent agreement with the value of 1.00 nm^2 determined from the force–area isotherms.

An important question is the following: how are the molecules arranged within the LB layers relative to the substrate plane—flat, edge-on, like tiles on a roof, or disordered? X-ray investigations at grazing incidence of the beam serve to answer the question. The corresponding diagram obtained from a multilayer sample (30 monolayers) on a silicon substrate is shown in Figure 2. A series of Kiessig

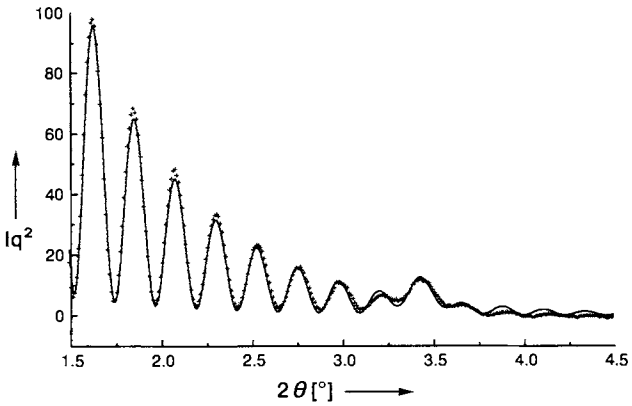

Fig. 2. X-ray diffractogram (at grazing incidence) of 30 monolayers of hpPGC$_1$C$_8$ (**1b**) deposited onto a silicon wafer. The coordinates are diffracted intensity $I\cdot$ (momentum transfer $q = 2\sin\theta/\lambda)^2$ and glancing angle θ; (+) measured data, (−) data calculated according to [19].

fringes is seen, which indicates an excellent quality of the film (homogeneity, lack of surface defects). The surface roughness is ±50 pm. The total thickness of the film is readily calculated from the angular distance between consecutive minima; a value of $D = 38.85$ nm is obtained. The periodicity of the layers is calculated as $d = 2.59$ nm from the position of the weak Bragg peak. These data demonstrate

the presence of double layers (since $(30/2) \times 2.59\ \text{nm} = 38.85\ \text{nm}$) and that the molecules lie flat within the layers ($2.59\ \text{nm}/2 \approx 1.30\ \text{nm}$).

Further proof of these findings comes from the results of electron diffraction on 20-monolayer films that were transferred directly to a carbon film-coated microscopic grid. The diffraction pattern found at normal incidence of the electron beam shows a crescent-shaped reflection on the meridian ($d = 0.35$ nm) and a strong reflection on the equator at $d = 2.87$ nm. A reflection corresponding to a d value of 1.30 nm is not observed. This corroborates the model in which the molecules are pictured as extended, rectangular boxes lying flat within the layers. The lateral interaction between the molecules contained in the individual layers occurs through the alkoxy side chains, which serve as a "glue". This type of packing of the macromolecules is sketched schematically in Figure 3.

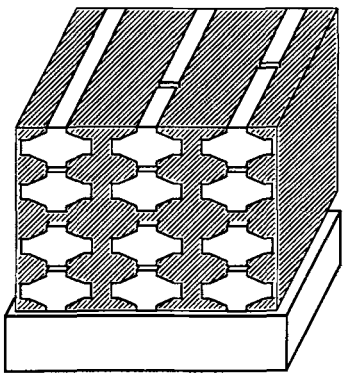

Fig. 3. Sketch of the supramolecular architecture of LB multilayers obtained from hpPGC$_1$C$_8$ (**1b**); the volume filled by the side-chain moieties (C$_1$ and C$_8$) is hatched.

The discrepancy in the Bragg values of the lateral reflections in X-ray and electron diffraction is—most probably—caused by small variations in the packing density, which depend to some extent on preparation and annealing conditions. The effect has been known quite well from previous investigations on PcPS.[9]

The quality of the mutual correlation of the layers can be deduced from the changes in intensity of the 2.87 nm reflection when the sample is rotated around the direction of the long axes of the macromolecules. The correlation length amounts to approximately 4 layers; that is, consecutive layers are in register.

A few experiments in combination with PcPS serve to indicate the usefulness of hpPG: it is not only possible to prepare alternating double layers of high quality, but one can also co-spread PcPS and hpPG (c(PcPS): c(hpPG) = 1:2); the force area diagram of this mixture shows only one step (collapse pressure at 30 mNm^{-1}), the area required of PcPS and hpPG is additive, and the transfer ratio ($\pi \approx 20$ mNm^{-1}, 20 °C, 1 cm min^{-1}) amounts to unity. The LB film obtained shows Kiessig fringes at grazing incidence diffraction, although the reduced intensity indicates a certain roughness of the film, which may be induced by the differences in thickness of the constituent macromolecules. The polymer hpPG seems to lie predominantly flat in these films, since the intensity pattern in the GIR spectra remains identical to the pure substance.

Experimental Procedure

Solvents were obtained from Fluka or Aldrich and were used as received except where stated otherwise. Dialkoxydiiminoisoindoline and tetra- (acetonitrilo)copper(I) trifluoromethanesulfonate were synthesized as described in references [8, 17, 18].

Dimethoxydioctyloxy-hemiporphyrazine, hpH$_2$ C$_1$, C$_8$: Freeze-dried 5-methoxy-6-octyloxy-1,3-diiminoiso-indoline (9.56 g, 31.5 mmol) and 2,6-diaminopyridine (3.44 g, 31.5 mmol) were dissolved in 80 g chloronaphthalene. The mixture was repeatedly degassed and stirred under nitrogen for 40 hours at 170 °C. To stop the reaction the mixture was cooled to about 50 °C and poured into 200 mL of *n*-hexane. The fine red or green-brown precipitate was washed with *n*-hexane and acetone. Repeated recrystallization from toluene gave the red product with a yield of approximately 15% (freeze-dried from benzene). IR(KBr): $\tilde{\nu}$[cm^{-1}] = 3445 m, 3070 vw, 2990 vw, 2920 m sh, 2870 m sh, 2850 m, 1660 s sh, 1655 s, 1605 w, 1585 m, 1545 m, 1495 s, 1465 m, 1455 m sh, 1435 w, 1350 s br, 1270 m, 1225 s, 1215 s sh, 1150 w, 1140 w, 1035 m, 860 w, 815 m, 760 w, 730 w, 710 w, 550 w br, 500 w br; ^{1}H NMR (CDCl$_3$, 300 MHz): δ = 10.21 (s, 2H, N-H), 7.68 (t, 2H, pyr-H), 7.38 (d, 4H, ind-H), 6.96 (d, 4H, pyr-H), 4.14 (t, 4H, CH$_2$), 3.99 (d, 6H, OCH$_3$), 1.90 (q, 4H, CH$_2$), 1.52–1.10 (m, 20H, CH$_2$), 0.87 (t, 6H, CH$_3$); UV/VIS: λ_{max} [nm] = 266, 306, 344 sh, 358, 376 sh.

Dimethoxydioctyloxy-hemiporphyrazinatogermanium dichloride, GehpCl$_2$ C$_1$,C$_8$: Freeze-dried hpH$_2$ (C$_1$,C$_8$) (1.8 g, 2.38 mmol) and freshly distilled quinoline (7 mL) were mixed under nitrogen and degassed. After addition of GeCl$_4$ (0.51 mL, 4.47 mmol) by syringe through a septum, the mixture was heated as fast as possible with an oil bath preheated to 170 °C. After about 8 minutes when the color changed to green-blue, the reaction was stopped by pouring the reaction mixture into 150 mL of methanol. The greenish-blue precipitate was rinsed with methanol and acetone, dissolved in chloroform (red-violet solution), and after evaporation of the solvent, freeze-dried from benzene (yield approximately 75%). For further purification column-filtration through neutral Al$_2$O$_3$ with chloroform/methanol (99:1) as eluent is possible. IR(KBr): $\tilde{\nu}$[cm^{-1}] = 3430 m br, 2950 m sh, 2920 m, 2870 m sh, 2850 m, 1670 m, 1620 s, 1580 s, 1550 m, 1495 m, 1470 m, 1455 w sh, 1445 w, 1360 s, 1290 w, 1245 s, 1215 w, 1155 w br, 1055 m, 820 w, 770 vw, 725 w; ^{1}H NMR (CDCl$_3$:CD$_3$OD = 20:1, 300 MHz): δ = 7.44 (t, 2H, pyr-H), 7.15 (d, 4H, ind-H), 6.80 (d, 4H, pyr-H), 4.05 (t, 4H, CH$_2$), 3.89 (s, 6H, OCH$_3$), 1.84 (q, 4H, CH$_2$), 1.50–1.10 (m, 20H, CH$_2$), 0.87 (t, 6H, CH$_3$); UV/VIS: λ_{max} [nm] = 271, 353, 385, 407, 532 sh, 562, 622 sh.

Dimethoxydioctyloxy-hemiporphyrazinatopoly(germanoxane), hpPGC$_1$C$_8$: Freeze-dried GehpCl$_2$(C$_1$,C$_8$) (100 mg, 0.11 mmol) and tetra(acetonitrilo)-copper(I)trifluoromethanesulfonate (102 mg, 0.27 mmol) were combined in freshly distilled, dry di-2-methoxyethyl ether and degassed. The mixture was heated under nitrogen for 1–2 h to 140 °C. After cooling to room temperature it was poured into 50 mL of methanol. The deep brown precipitate was washed with methanol, dissolved in chloroform, and filtered through a Teflon membrane filter (pore-size 5 μm). Evaporating the solvent and freeze-drying from benzene gave the product in a yield of nearly 100%. HPLC (RP18 column, 12.8 cm length, 5 μm diameter, in methanol–THF gradient (0 to 100%)) results in sharply resolved peaks for trimers (first peak) to dodecamers (last peak). IR(KBr): $\tilde{\nu}$[cm^{-1}] = 2950 m sh, 2920 m, 2870 m sh, 2850 m, 1660 w, 1625 s, 1580 s, 1545 m, 1495 s, 1470 w sh, 1450 w, 1360 s, 1300 w, 1245 s, 1215 m, 1150 w br, 1070 s, 1030 w, 860 m br, 810 m, 770 vw, 715 m, 635 w; ^{1}H NMR (CDCl$_3$, 300 MHz): δ = 7.0–5.7 (m, br, ≈ 10H), 3.65 (s br, ≈ 10H), 1.78 (s br, ≈ 8H), 1.32 (m, ≈ 20H), 0.88 (s br, ≈ 6H); UV/VIS: λ_{max} [nm] = 276, 343, 387, 414 sh.

For the electron diffraction experiment, carbon films with a thickness of about 6 to 10 nm were applied to Ni electron-microscopy grids. These grids could be fastened to a Teflon-coated magnetic rod and used directly in the LB technique. The preparation of the other LB substrates and the characterization of the LB films used methods described elsewhere [9, 10].

Received: March 5, 1993 [Z 5905 IE]
German version: *Angew. Chem.* **1993**, *105*, 1251

[1] J. Simon, J.-J. André, A. Skoulios, *New J. Chem.* **1984**, *10*, 295.
[2] M. Hanack, G. Pawlowski, *Naturwissenschaften* **1982**, *69*, 266.
[3] M. Hanack, A. Datz, R. Fay, K. Fischer, U. Keppeler, J. Koch, J. Metz, M. Mezger, O. Schneider, H.-J. Schulze in *Handbook of Conducting Polymers* (Ed.: T. A. Skotheim), Dekker, New York, **1986**, p. 133.
[4] T. Shimidzu, T. Iyoda, *Chem. Lett.* **1981**, 853.
[5] J. F. van der Pol, M. P. de Haas, J. M. Warman, W. Drenth, *Mol. Cryst. Liq. Cryst.* **1990**, *183*, 411.
[6] C. W. Dirk, E. A. Mintz, A. F. Schoch, Jr., T. J. Marks, *J. Macromol. Sci. Chem. A* **1981**, *16*, 275.
[7] D. Adam, F. Closs, T. Frey, D. Funhoff, D. Haarer, H. Ringsdorf, P. Schuhmacher, K. Siemensmeyer, *Phys. Rev. Lett.* **1993**, *70*, 457.
[8] E. Orthmann, G. Wegner, *Angew. Chem.* **1986**, *98*, 1114; *Angew. Chem. Int. Ed. Engl.* **1986**, *25*, 1105.
[9] G. Wegner, *Thin Solid Films* **1990**, *216*, 105, and references therein.

[10] G. Wegner, *Ber. Bunsen-Ges. Phys. Chem.* **1991**, *95*, 1326, and references therein.
[11] J. A. Elvidge, R. P. Linstead, *J. Chem Soc.* **1952**, 5008.
[12] J. N. Eposito, L. E. Sutton, M. E. Kenney, *Inorg. Chem.* **1967**, *6*, 1116.
[13] G. Meyer, D. Wöhrle, *Makromol. Chem.* **1974**, *175*, 714.
[14] C. W. Dirk, T. J. Marks, *Inorg. Chem.* **1984**, *23*, 4325.
[15] T. Sauer, T. Arndt, D. N. Batchelder, A. A. Kalachev, G. Wegner, *Thin Solid Films* **1990**, *187*, 357.
[16] D. L. Allara, J. D. Swalen, *J. Phys. Chem.* **1982**, *86*, 2700.
[17] W. Caseri, T. Sauer, G. Wegner, *Makromol. Chem. Rapid Commun.* **1988**, *9*, 651.
[18] T. Sauer, G. Wegner, *Mol. Cryst. Liq. Cryst.* **1988**, *162*, 97.
[19] M. Schaub, K. Mathauer, S. Schwiegk, P.-A. Albouy, G. Wenz, G. Wegner, *Thin Solid Films* **1992**, *210/211*, 397.

Tetrakis(trialkylsilylethynyl)butatriene and 1,1,4,4-Tetrakis(trialkylsilylethynyl)-1,3-butadiene: Novel Cross-Conjugated Chromophores**

By *Jan-Dirk van Loon, Paul Seiler,* and *François Diederich**

Dedicated to Professor Jack D. Dunitz on the occasion of his 70th birthday

Following the preparation of tetraethynylethene (**1a**)[1] and differentially protected derivatives,[2] we became interested in the preparation of tetraethynylcumulenes, which are new chromophores of substantial theoretical and practical interest.[3] Allene **2** is a possible precursor to a three-dimensional all-carbon network,[4] and butatriene **3** could be transformed by carbene or carbenoid addition[5] into the

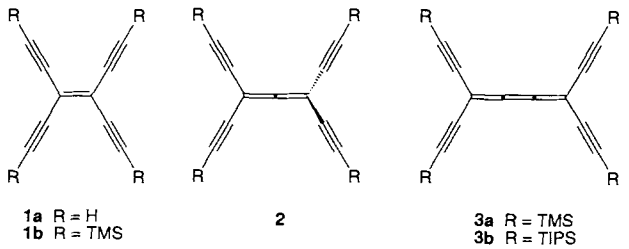

[3]radialene **4** or by photochemical, thermal,[6] or metal-catalyzed[7] dimerization into the [4]radialene **5**, possible precursors to other two-dimensional all-carbon networks (Scheme 1).[4, 5]

When the TMS-protected dibromoolefin **6a** was treated with one equivalent of *n*BuLi in Et_2O at $T < -100\,^{\circ}C$ and subsequently with one equivalent of $CuI \cdot PBu_3$ at $T < -85\,^{\circ}C$,[8] the tetraethynylbutatriene **3a** was obtained in 55% yield as a brown solid with a metallic luster.[9] Similarly, the TIPS-protected olefin **6b** afforded the cumulene **3b** as a yellow solid in 42% yield. The TMS-protected compound **3a** decomposes in the solid state, even at $-20\,^{\circ}C$, but is stable in dilute hexane solutions. On the contrary, the TIPS derivative **3b** can be kept as a stable solid at room temperature and decomposes only above 150 °C. The two butatrienes **3a** and **3b** show similar spectral properties. In

[*] Prof. F. Diederich, Dr. J.-D. van Loon, P. Seiler
Laboratorium für Organische Chemie
ETH-Zentrum
Universitätstrasse 16, CH-8092 Zürich (Switzerland)
Telefax: Int. code +(1)261-3524

[**] J.-D. v. L. thanks the Dutch National Science Foundation (NWO) for a postdoctoral fellowship.

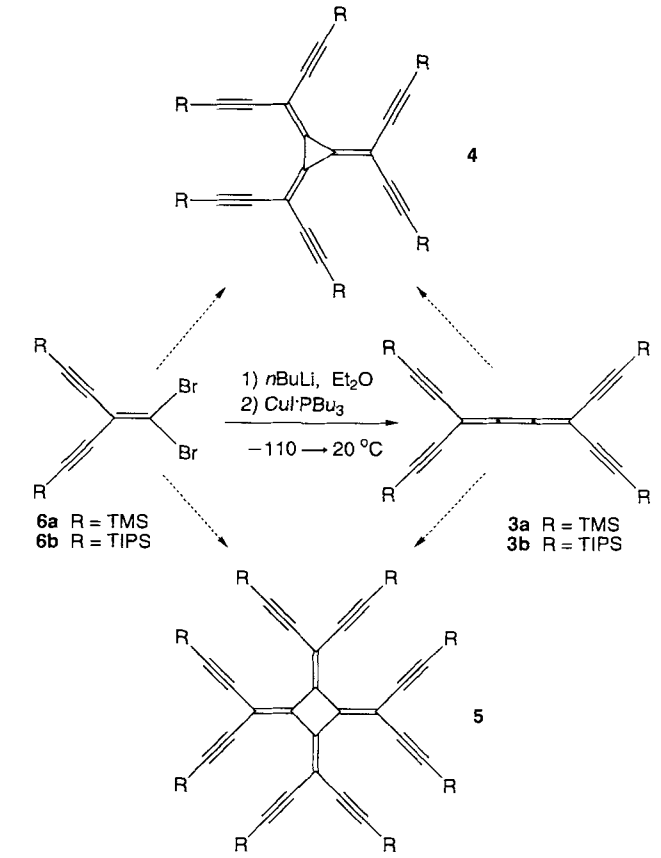

Scheme 1. Synthesis of the tetraethynylbutatrienes **3a/b** and possible routes to the perethynylated radialenes **4** and **5**. *TMS* = trimethylsilyl; *TIPS* = triisopropylsilyl.

the ^{13}C NMR spectrum of **3b** in $CDCl_3$, four signal for quaternary carbon atoms are observed and the signal for the two central carbon atoms of the butatriene moiety appears as a characteristic peak at $\delta = 150.6$. The IR spectrum shows a weak C≡C stretch at 2144 cm^{-1} and a weak C=C stretch at 1628 cm^{-1}. The electronic absorption spectrum of **3b** in hexane reflects the greater extension of the chromophore, compared to **1b** (Fig. 1).[1] The longest wavelength band in the spectrum of **3b** at 424 nm shows a remarkably high mo-

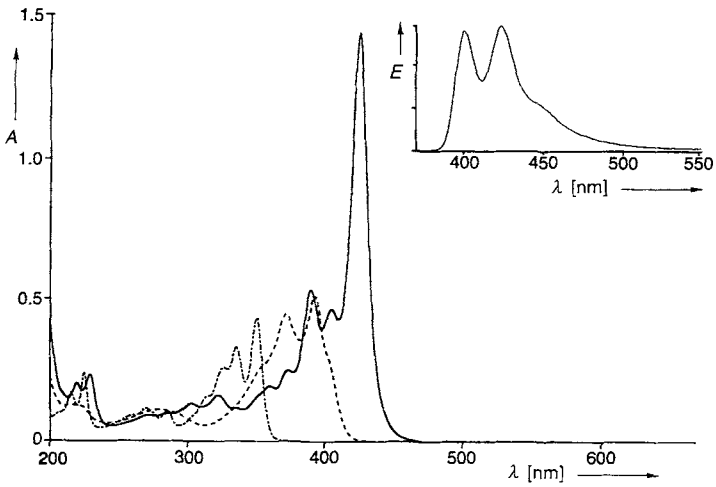

Fig. 1. Electronic absorption spectra of **1b** (·····), **3b** (—), and **7a** (-----) recorded in hexane. $T = 298$ K, $d = 1$ cm, $c = 1.053 \times 10^{-5}$ M for all compounds. Insert: Fluorescence spectrum of **7a**, $\lambda_{exc} = 350$ nm.

 © *VCH Verlagsgesellschaft mbH, D-69451 Weinheim, 1993* *0570-0833/93/0808-1187 $ 10.00+.25/0*

[10] G. Wegner, *Ber. Bunsen-Ges. Phys. Chem.* **1991**, *95*, 1326, and references therein.
[11] J. A. Elvidge, R. P. Linstead, *J. Chem Soc.* **1952**, 5008.
[12] J. N. Eposito, L. E. Sutton, M. E. Kenney, *Inorg. Chem.* **1967**, *6*, 1116.
[13] G. Meyer, D. Wöhrle, *Makromol. Chem.* **1974**, *175*, 714.
[14] C. W. Dirk, T. J. Marks, *Inorg. Chem.* **1984**, *23*, 4325.
[15] T. Sauer, T. Arndt, D. N. Batchelder, A. A. Kalachev, G. Wegner, *Thin Solid Films* **1990**, *187*, 357.
[16] D. L. Allara, J. D. Swalen, *J. Phys. Chem.* **1982**, *86*, 2700.
[17] W. Caseri, T. Sauer, G. Wegner, *Makromol. Chem. Rapid Commun.* **1988**, *9*, 651.
[18] T. Sauer, G. Wegner, *Mol. Cryst. Liq. Cryst.* **1988**, *162*, 97.
[19] M. Schaub, K. Mathauer, S. Schwiegk, P.-A. Albouy, G. Wenz, G. Wegner, *Thin Solid Films* **1992**, *210/211*, 397.

Tetrakis(trialkylsilylethynyl)butatriene and 1,1,4,4-Tetrakis(trialkylsilylethynyl)-1,3-butadiene: Novel Cross-Conjugated Chromophores**

By *Jan-Dirk van Loon, Paul Seiler,* and *François Diederich**

Dedicated to Professor Jack D. Dunitz on the occasion of his 70th birthday

Following the preparation of tetraethynylethene (**1a**)[1] and differentially protected derivatives,[2] we became interested in the preparation of tetraethynylcumulenes, which are new chromophores of substantial theoretical and practical interest.[3] Allene **2** is a possible precursor to a three-dimensional all-carbon network,[4] and butatriene **3** could be transformed by carbene or carbenoid addition[5] into the

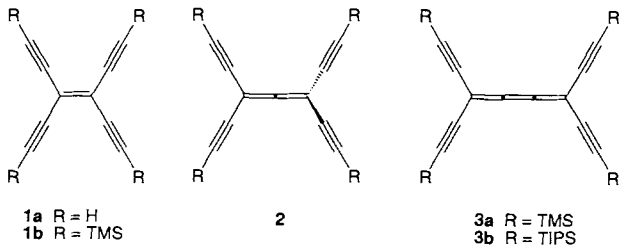

[3]radialene **4** or by photochemical, thermal,[6] or metal-catalyzed[7] dimerization into the [4]radialene **5**, possible precursors to other two-dimensional all-carbon networks (Scheme 1).[4, 5]

When the TMS-protected dibromoolefin **6a** was treated with one equivalent of *n*BuLi in Et_2O at $T < -100\,^{\circ}C$ and subsequently with one equivalent of $CuI \cdot PBu_3$ at $T < -85\,^{\circ}C$,[8] the tetraethynylbutatriene **3a** was obtained in 55% yield as a brown solid with a metallic luster.[9] Similarly, the TIPS-protected olefin **6b** afforded the cumulene **3b** as a yellow solid in 42% yield. The TMS-protected compound **3a** decomposes in the solid state, even at $-20\,^{\circ}C$, but is stable in dilute hexane solutions. On the contrary, the TIPS derivative **3b** can be kept as a stable solid at room temperature and decomposes only above 150 °C. The two butatrienes **3a** and **3b** show similar spectral properties. In

[*] Prof. F. Diederich, Dr. J.-D. van Loon, P. Seiler
Laboratorium für Organische Chemie
ETH-Zentrum
Universitätstrasse 16, CH-8092 Zürich (Switzerland)
Telefax: Int. code +(1)261-3524

[**] J.-D. v. L. thanks the Dutch National Science Foundation (NWO) for a postdoctoral fellowship.

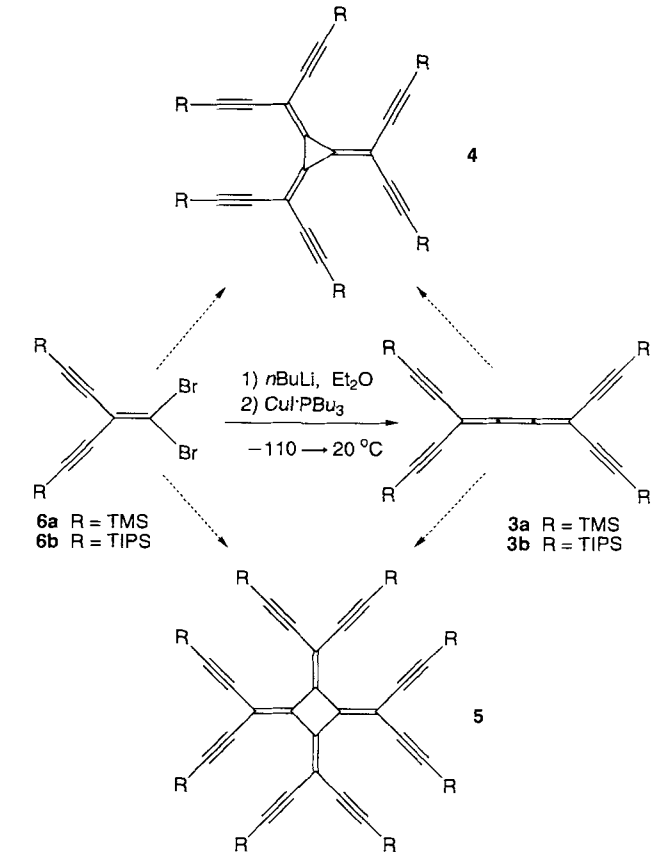

Scheme 1. Synthesis of the tetraethynylbutatrienes **3a/b** and possible routes to the perethynylated radialenes **4** and **5**. *TMS* = trimethylsilyl; *TIPS* = triisopropylsilyl.

the ^{13}C NMR spectrum of **3b** in $CDCl_3$, four signal for quaternary carbon atoms are observed and the signal for the two central carbon atoms of the butatriene moiety appears as a characteristic peak at $\delta = 150.6$. The IR spectrum shows a weak C≡C stretch at 2144 cm^{-1} and a weak C=C stretch at 1628 cm^{-1}. The electronic absorption spectrum of **3b** in hexane reflects the greater extension of the chromophore, compared to **1b** (Fig. 1).[1] The longest wavelength band in the spectrum of **3b** at 424 nm shows a remarkably high mo-

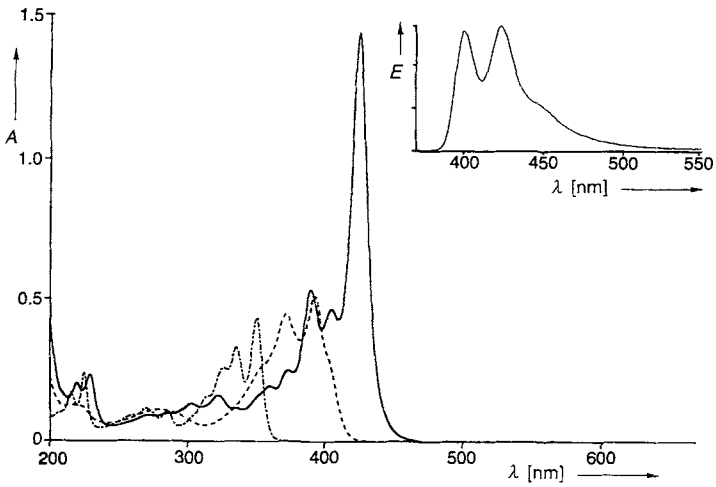

Fig. 1. Electronic absorption spectra of **1b** (·····), **3b** (—), and **7a** (-----) recorded in hexane. $T = 298$ K, $d = 1$ cm, $c = 1.053 \times 10^{-5}$ M for all compounds. Insert: Fluorescence spectrum of **7a**, $\lambda_{exc} = 350$ nm.

 © *VCH Verlagsgesellschaft mbH, D-69451 Weinheim, 1993* *0570-0833/93/0808-1187 $ 10.00+.25/0*

lar extinction coefficient ($\varepsilon = 138000$) and appears bathochromically shifted by 74 nm relative to the longest wavelength band in the spectrum of **1b**.

Unambiguous structural proof for the cross-conjugated butatriene structure of **3a** was obtained by low-temperature X-ray analysis of crystals grown from acetone (Fig. 2).[10]

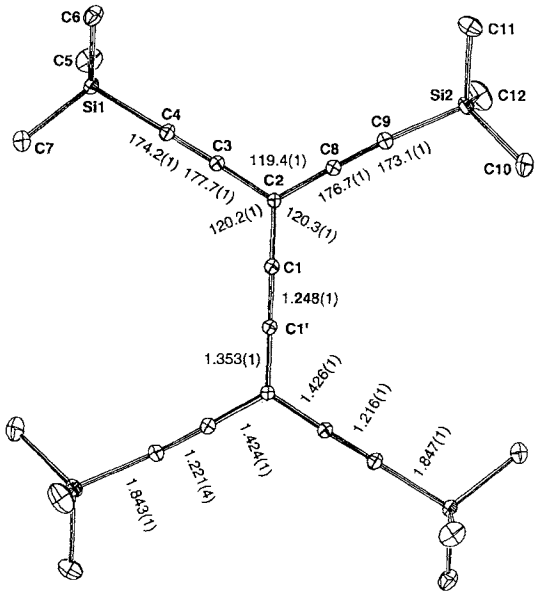

Fig. 2. X-ray crystal structure of **3a**. Vibrational ellipsoids are shown at the 50% probability level.

The chromophore in **3a** is nearly planar: the maximum deviation from the least-squares plane through the tetraethynyl[3]cumulene framework is 0.09 Å. Bond lengths and angles are within the range expected from previous X-ray data for tetraethynylethene[1,2] and butatriene derivatives.[11] All attempts to deprotect **3a** or **3b** without decomposition or polymerization have so far been unsuccessful.

In an attempt to prepare the [4]radialene **5**, we followed a procedure of West et al., who had dimerized "diquinoethylene, a cross-conjugated butatriene, to form a [4]radialene in the presence of triphenylphosphane, which presumably initiates the reaction by nuleophilic attack on the central cumulenic double bond.[7] When the tetraalkynylcumulene **3b** was treated for 12 h at 20 °C with an excess of PPh_3 in hexane, benzene, or CH_2Cl_2 solutions, no evidence for formation of the [4]radialene **5** was obtained but, instead, the 1,3-butadiene **7a** was isolated as a yellow oil in 78% yield.[9] In the ^1H NMR spectrum of **7a**, the olefinic protons appear at $\delta = 7.24$. The UV/VIS spectrum of **7a** (Fig. 1) is less structured than the spectrum of **1b** or **3b**, which is indicative of a less rigid chromophore, and the longest wavelength band of **7a** at $\lambda_{max} = 392$ nm appears at a position between the corresponding bands in **1b** and **3b**. In contrast to **1b** and **3b**, the cross-conjugated 1,3-butadiene **7a** is highly fluorescent, and the emission maxima are observed at $\lambda_{em} = 400$, 423, and 447 nm (Fig. 1, insert).

The specific and very mild reduction[12] of cumulene **3b**, initiated by attack of triphenylphosphane at the central double bond, yields a zwitterion, which is protonated at the vinylic carbanion center by traces of moisture.[13a] The resulting hydroxide ion subsequently reacts with the vinylic phosphonium ion by elimination of triphenylphosphane oxide and a second protonation to form **7a**. This mechanism is

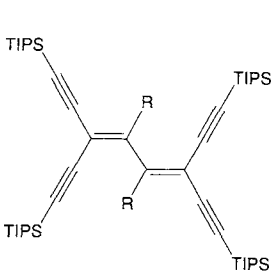

7a R = H
7b R = D

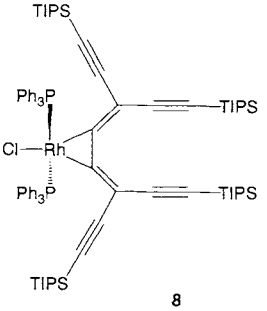

8

supported by the observation that reduction of **3b** in the presence of D_2O affords exclusively the dideuterated butadiene **7b**. Previously, the reduction of double bonds with phosphanes had only been described for activated olefins HRC=CRH (R = CO_2Me, COPh),[13a] and for 7,7,8,8-tetracyanoquinomethane (TCNQ) and tetracyanoethylene (TCNE).[13b] We propose that facile reduction of **3b** occurs, since a) the two diethynylmethylene fragments with their sp carbon atoms exert an activating, electron-withdrawing effect on the central double bond, therefore facilitating the attack of PPh_3, and b) these fragments help to stabilize the resulting zwitterion through delocalization of the anionic charge.[14] Accordingly, 1,4-bis(pentamethylene)-1,2,3-butatriene[6] is not sufficiently activated to be reduced with PPh_3.

Rhodium(I) is known to form stable η^2 complexes with both butatrienes[15] and alkynes,[16] and we were interested to determine whether regioselective complexation occurs with **3b**, which features both types of π systems. When **3b** was treated at 20 °C with one equivalent of $[Rh(PPh_3)_3Cl]$ in CH_2Cl_2, complex **8** (m.p. 202–203 °C) was obtained in 57% yield as an orange-yellow solid.[9] In this conversion, butadiene **7a** was consistently isolated as a by-product in 40% yield, presumably due to the reaction of **3b** with the one equivalent of PPh_3 that is liberated during the formation of **8**. The ^1H NMR spectrum of **8** in $CDCl_3$ shows a complex pattern for protons of the TIPS group, presumably due to hindered rotation of these groups as a result of steric hindrance in the complex. The ^{13}C NMR spectrum shows two sets of acetylenic carbons at $\delta = 108.4$ and 104.3 (Si–*C*≡C) and at 93.6 and 92.7 (Si–C≡*C*), which is indicative of the symmetrical structure resulting from complexation at the central cumulenic bond. The two metallacyclic carbon atoms exhibit a multiplet at $\delta = 146.7$ due to coupling to both rhodium as well as phosphorous.

Unambiguous proof for the selective complexation at the central double bond of the butatriene unit in **8** was provided by the low-temperature X-ray analysis on crystals grown from acetone solution.[10] The compound crystallizes in the space group $P\bar{1}$, and the asymmetric unit contains two independent molecules of which molecule 1 is shown in Figure 3. The Rh–C bond lengths of 2.00 ± 0.01 Å are within the range of those previously found in cumulene–rhodium complexes.[15] The C–C bond in the metallacycle (1.35 Å) is considerably longer than the C=C bond in **3b** (1.25 Å), which reflects the lower bond order due to the coordination with the rhodium. The two PPh_3 ligands are axially coordinated; the analysis of the C(phenyl)–P coupling constants in the ^{13}C NMR spectrum also provides support for *trans* coordination of the phosphanes in the solution complex.

The geometry of the central framework of the complex, consisting of the tetraethynylcumulene carbon atoms, the rhodium, and the chlorine atoms, is roughly planar (within 0.34 Å) in both molecules 1 (Fig. 3B) and 2. However, the

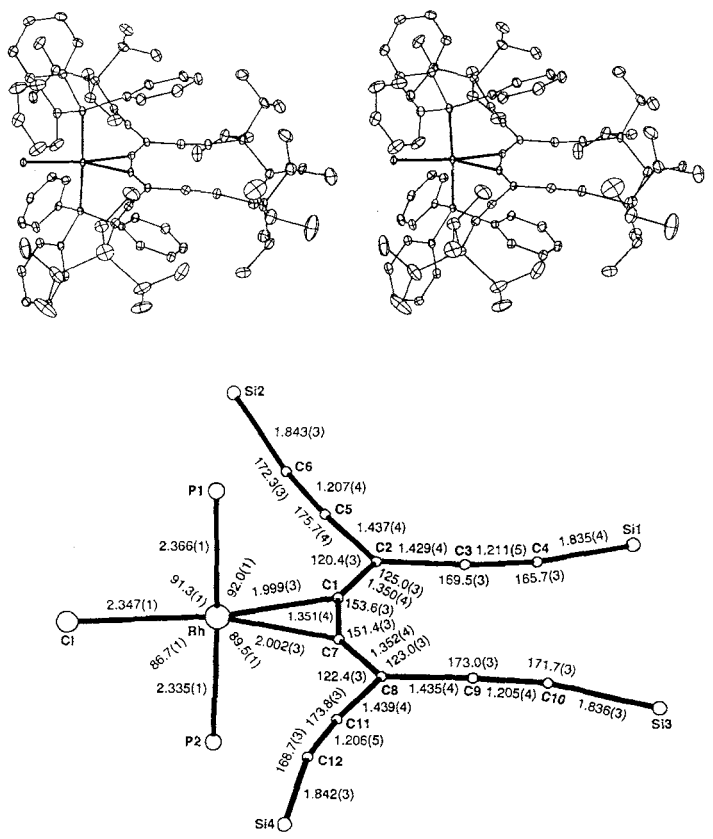

Fig. 3. X-ray crystal structure of **8**. Vibrational ellipsoids are shown at the 30% probability level.

complexation to rhodium and the presence of the two bulky phosphane ligands lead to marked angle distortions in the cross-conjugated π system of **8**. In molecule 1 (Fig. 3B), the exocyclic CCC angles at the metallacycle are 153.6(3)° and 151.4(3)°. These angles would force the two TIPS groups Si1 and Si3 into very close contact if the corresponding two C–C≡C–Si fragments were perfectly linear. To avoid severe violation of van der Waals space, bond angles at sp carbon atoms in these fragments adopt values between 165.7° and 173.0°, and, as a result, the distance between the two TIPS groups increases. The two other ethynyl fragments are also distorted by the steric hindrance between the TIPS groups Si2 and Si4 and the bulky triphenylphosphane ligands. To minimize steric repulsion, bond angles at sp carbon atoms in these two fragments vary between 168.7° and 175.7°. Similar distortions are also observed for molecule 2 in the unit cell of **8**.

Following the preparation of the first tetraethynylcumulene derivatives, we are now directing our efforts towards the synthesis of perethynylradialenes.

Experimental Procedure

3b: To a solution of the dibromoolefin **6b** (1.0 g, 1.83 mmol) in dry Et_2O (15 mL) at −110 °C was added dropwise 1.14 mL of a solution of *n*BuLi (1.83 mmol, 1.6 M) in hexane. The mixture was stirred for 1 h at −100 °C, after which a solution of CuI · PBu_3 (1.83 mmol) in Et_2O (15 mL) was added. The resulting red solution was stirred for 1 h at −85 °C, then allowed to warm to 20 °C within 5 h. The reaction mixture was filtered over SiO_2 and, after evaporation of the solvent, purified by chromatography (SiO_2, hexane) to afford 300 mg of **3b** (42% yield) as a yellow solid; m.p. (MeOH) >150 °C (decomp.); IR (KBr) $\tilde{\nu}$ = 2943, 2865 (C–H), 2144 (C≡C), 1628 (C=C), 1224 (C–Si) cm^{-1}; ^1H NMR ($CDCl_3$) δ = 1.09 (s, 84H); ^{13}C NMR ($CDCl_3$) δ = 150.6 (s, =C=), 104.2 (s, C≡C–Si), 100.1 (s, C≡C–Si), 87.7 (s, C–C≡C), 18.5 (q, CH_3), 11.3 (d, CH); UV/VIS (hexane): λ_{max} = 424 (ε = 138000), 404 (44600), 390 (51200), 373 (23800), 360 (18500), 322 (15400), 303 (12600), 230 (22300), 220 nm (19400); EI-MS *m/z* 773 (M^+, 100% relative intensity). Correct elemental analysis for C, H.

Received: March 5, 1993 [Z 5906 IE]
German version: *Angew. Chem.* **1993**, *105*, 1235

[1] Y. Rubin, C. B. Knobler, F. Diederich, *Angew. Chem.* **1991**, *103*, 708–710; *Angew. Chem. Int. Ed. Engl.* **1991**, *30*, 698–700.

[2] a) A. M. Boldi, J. Anthony, C. B. Knobler, F. Diederich, *Angew. Chem.* **1992**, *104*, 1270–1273; *Angew. Chem. Int. Ed. Engl.* **1992**, *31*, 1240–1242; b) J. Anthony, C. B. Knobler, F. Diederich, *ibid.* **1993**, *105*, 437–440; *ibid.* **1993**, *32*, 406–409; c) H. Hopf, M. Kreutzer, P. G. Jones, *Chem. Ber.* **1991**, *124*, 1471–1475, and references therein.

[3] Monoalkynylbutatrienes: a) P. J. Stang, M. Ladika, *J. Am. Chem. Soc.* **1981**, *103*, 6437–6443; b) F. Bohlmann, C. Zdero, *Chem. Ber.* **1971**, *104*, 1329–1331.

[4] F. Diederich, Y. Rubin, *Angew. Chem.* **1992**, *104*, 1123–1146; *Angew. Chem. Int. Ed. Engl.* **1992**, *31*, 1101–1123.

[5] H. Hopf, G. Maas, *Angew. Chem.* **1992**, *104*, 953–977; *Angew. Chem. Int. Ed. Engl.* **1992**, *31*, 931–955.

[6] M. Iyoda, S. Tanaka, H. Otani, M. Nose, M. Oda, *J. Am. Chem. Soc.* **1988**, *110*, 8494–8500.

[7] L. Hagelee, R. West, J. Calabrese, J. Norman, *J. Am. Chem. Soc.* **1979**, *101*, 4888–4892.

[8] M. Iyoda, H. Otani, M. Oda, Y. Kai, Y. Baba, N. Kasai, *J. Am. Chem. Soc.* **1986**, *108*, 5371–5372.

[9] All new compounds have been fully characterized by ^1H NMR, ^{13}C NMR, IR, and UV spectroscopy, mass spectrometry, and elemental analysis.

[10] Single crystals of **3a** ($C_{24}H_{36}Si_4$, M_r = 436.89) were grown at 235 K from acetone and mounted, without warming, on a CAD4 diffractometer equipped with a graphite monochromator ($Mo_{K\alpha}$ radiation) and a cooling device. X-ray crystal data at 85 K: monoclinic space group $P2_1/c$ (no. 14), ϱ_{calcd} = 1.024 g cm^{-3}, Z = 2; a = 10.870 (2), b = 10.121(2), c = 15.241(2) Å, β = 122.30(2)°, V = 1417.3 Å^3. The molecule has a crystallographic center of symmetry. The structure was solved by direct methods (SHELXS86) and refined by full-matrix least-squares (SHELXL92) with an exponentially modified weight factor with r = 4 Å^2 (J. D. Dunitz, P. Seiler, *Acta Crystallogr. Sect. B* **1973**, *29*, 589–595). $R(F)$ = 0.027, $wR(F^2)$ = 0.105 for 146 variables and 4552 reflection intensities with $I_o > 3\sigma(I_o)$ and $H = 2\sin\theta/\lambda < 1.62$ Å^{-1} (C and Si atoms anisotropic, H atoms isotropic with a riding model). Single crystals of **8** ($C_{84}H_{114}P_2Si_4RhCl$, M_r = 1436.5) were first obtained at 293 K from acetone and mounted on the diffractometer described above. Cooling of the crystals from 293 to 85 K produced twinned intergrowths with a large mosaic spread. To circumvent this problem, crystals were grown at ≈ 235 K, then mounted on the diffractometer without warming and cooled slowly to 85 K during 24 h. X-ray crystal data at 85 K: triclinic space group $P\bar{1}$ (no. 2), ϱ_{calcd} = 1.13 g cm^{-3}, Z = 4; a = 13.738(3), b = 23.426(4), c = 27.769(6) Å, α = 108.48(2), β = 92.78(2), γ = 95.32(2)°, V = 8411(3) Å^3. The asymmetric unit contains two independent molecules and probably one or two highly disordered acetone molecules. The structure was solved by the Patterson method (SHELXTL PLUS) and refined by full-matrix least-squares, with an exponentially modified weight factor r = 5 Å^2. $R(F)$ = 0.034 for 1657 variables and 19909 reflection intensities with $I_o > 3\sigma(I_o)$ and $H = 2\sin\theta/\lambda < 1.2$ Å^{-1} (all non-H atoms anisotropic, H atoms isotropic and fixed). All TIPS groups show relatively large thermal motion, even at 85 K, and some exhibit orientational disorder as well (especially in molecule 2). Further details of the crystal structure investigations are available on request from the Director of the Cambridge Crystallographic Data Centre, 12 Union Road, GB-Cambridge CB2 1EZ (UK), on quoting the full journal citation.

[11] a) Z. Berkovitch-Yellin; L. Leiserowitz; *Acta Crystallogr. Sect. B* **1977**, *33*, 3657–3669. b) Y. Morimoto, Y. Higuchi, K. Wakamatsu, K. Oshima, K. Utimoto, N. Yasuoka, *Bull. Chem. Soc. Jpn.* **1989**, *62*, 639–641.

[12] Regioselective reductions of butatrienes: a) S. Kishigami, K. Tanaka, F. Toda, *Chem. Lett.* **1990**, 1877–1880; b) R. Kuhn, H. Fischer, *Chem. Ber.* **1960**, *93*, 2285–2289; c) *ibid.* **1961**, *94*, 3060–3071.

[13] a) M. G. Burnett, T. Oswald, B. J. Walker, *J. Chem. Soc. Chem. Commun.* **1977**, 155–156; b) M. P. Naan, R. L. Powell, C. D. Hall, *J. Chem. Soc. (B)* **1974**, 1683–1691.

[14] The production of 1,5-diene-3-yne as a by-product in the [Ni(PPh_3)$_4$]-catalyzed dimerization of tetraphenyl[5]cumulene can also be explained by a PPh_3-mediated reduction; M. Iyoda, Y. Kuwatani, M. Oda, *J. Am. Chem. Soc.* **1989**, *111*, 3761–3762.

[15] a) P. J. Stang, M. R. White, G. Maas, *Organometallics* **1983**, *2*, 720–725; b) R. O. Angus, Jr., M. N. Janakiraman, R. A. Jacobson, R. P. Johnson, *ibid.* **1987**, *6*, 1909–1912.

[16] D. Schneider, H. Werner, *Angew. Chem.* **1991**, *103*, 710–712; *Angew. Chem. Int. Ed. Engl.* **1991**, *30*, 700–702.

The Absolute Configuration of Michellamine B, a "Dimeric", Anti-HIV-Active Naphthylisoquinoline Alkaloid**

By *Gerhard Bringmann,* Rainer Zagst, Manuela Schäffer, Yali F. Hallock, John H. Cardellina II,* and *Michael R. Boyd*

Dedicated to Professor Wolfgang Steglich on the occasion of his 60th birthday

The michellamines constitute an intriguing novel class of naturally occurring "dimeric" naphthylisoquinoline alkaloids, isolated from a West African *Ancistrocladus* species.[1] Of these, especially michellamine B is distinguished by a high anticytopathic activity aginst HIV-1 and HIV-2.[1] Also, from a chemical point of view these naturally occurring quateraryls are remarkable in many regards: Besides the unprecedented "dimeric" naphthylisoquinoline structure, even the molecular "halves" are unique with respect to their high polarity resulting from the presence of three phenolic OH groups. Furthermore, they are based on an unusual 5,8′-coupling type,[2] which is otherwise realized only in the "monomeric" naphthylisoquinoline alkaloid ancistrobrevine B (**2**).[3,4] The constitution of michellamine B was established by extensive ^1H and ^{13}C NMR experiments.[1] The relative configuration at the two stereocenters C1 and C3 was proved to be *trans* for both isoquinoline parts. While constitutionally identical, the molecular halves were shown to be diastereomorphous to each other, for example by the nonequivalence in ^{13}C NMR, which exhibits 46 signals for michellamine B. As simultaneously established for ancistrobrevine B (**2**),[3,4] the configurations at the biaryl axes relative to the stereocenters in michellamine B were elucidated by specific NOE interactions of the protons at C1′ and C7′ with the corresponding diastereotopic protons at C4.[1] According to these studies, the two molecular halves have different relative configurations at their centers relative to their axes. By contrast, no information has so far been obtained concerning the *absolute* configuration of michellamine B, which was arbitrarily assigned as **1a**, that is, (1*S*, 3*S*)-configurated,[1] consistent with most other *Ancistrocladus* alkaloids,[5] such as **2**. In this paper, we describe the elucidation of the absolute configuration of michellamine B as **1b**, by application of an oxidative degradation procedure recently developed for "ordinary", that is, "monomeric", naphthylisoquinoline alkaloids.[6]

Based on the above-mentioned NMR findings, michellamine B could indeed be represented either by **1a**, with (*S*)-configuration at *all* the stereocenters and different absolute configurations at the axes, or by its enantiomer **1b**. Yet, the diastereomorphous relationship of the two molecular moieties might also arise from a heterochiral character of the stereocenters (i.e., 1*R*, 3*R*, 1‴*S*, 3‴*S*), with the axes having identical configurations (i.e., 5*M*, 5‴*M* or 5*P*, 5‴*P*, respectively). These two additional stereoisomers would also fit in with the above-mentioned experimental results and did not seem too improbable, since West African *Ancistrocladus* plants do produce pairs of related alkaloids that are stereochemically identical at the axes, but different, for example, at C3.[7–9]

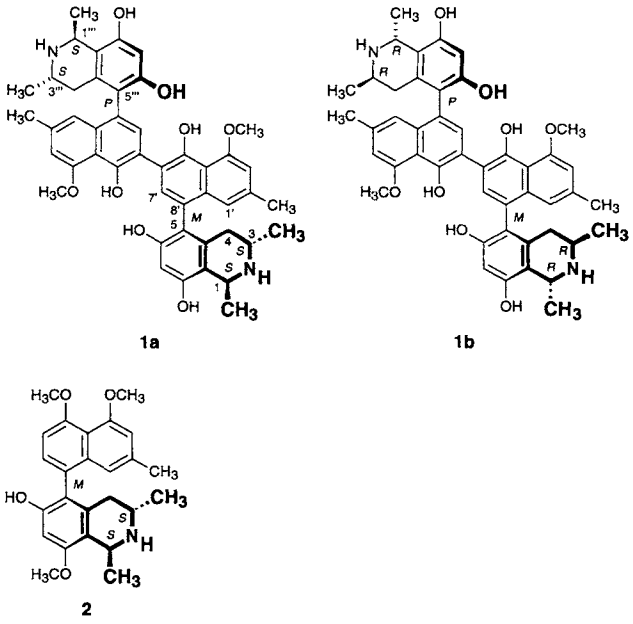

For this reason, the absolute configuration at C1 and C3 of both halves of michellamine B would be best analyzed by a ruthenium-mediated transformation into the amino acids alanine and 3-aminobutyric acid, simple chiral compounds that are easy to analyze stereochemically. The oxidative degradation of michellamine B (9.3 mg) was performed as developed for "monomeric" naphthylisoquinolines,[6] by treatment of the alkaloid with $NaIO_4$ (99 mg) and catalytic amounts of $RuCl_3$ (0.1 mg) in $MeCN/CCl_4$/aqueous phosphate buffer at room temperature (Scheme 1). The resulting amino acids were converted into their methyl esters with MeOH/HCl and derivatized with (*S*)-α-methoxy-α-trifluoromethylphenylacetic acid via its acid chloride ("*R*-MTPA-Cl"), to give the Mosher-type derivatives. Analysis by gas chromatography (fused silica capillary column, 30 m × 0.33 mm inner diameter, coated with DB1) revealed two peaks, which could unambiguously be assigned as (*R*)-3-aminobutyric acid (**3**, t_R=21.2 min) and D-alanine (**4**, t_R=15.6 min) by coinjection with racemic as well as enantiomerically pure standard samples.

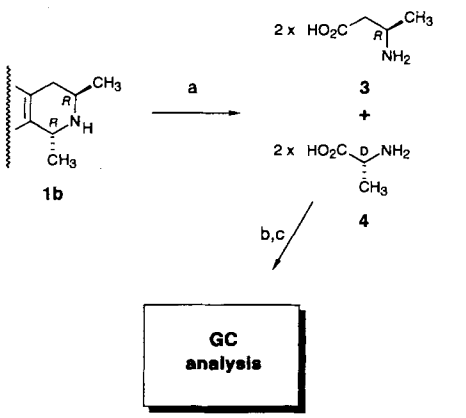

Scheme 1. Oxidative degradation of michellamine B (**1**). Reaction conditions: a) $RuCl_3$, $NaIO_4$, 1 h; b) MeOH, HCl, 5 h; c) MTPA-Cl, NEt_3, 1 h.

For a further confirmation, the configurationally known[10,11] naphthylisoquinoline alkaloids ancistro-

[*] Prof. Dr. G. Bringmann, Dipl.-Chem. R. Zagst, M. Schäffer
Institut für Organische Chemie der Universität
Am Hubland, D-97074 Würzburg (FRG)
Telefax: Int. code + (931)888-4606
Dr. Y. F. Hallock, Dr. J. H. Cardellina II, Prof. Dr. M. R. Boyd
Laboratory of Drug Discovery Research and Development
National Cancer Institute
Building 1052, Room 121, Frederick, MD 21702-1201 (USA)

[**] Acetogenic Isoquinoline Alkaloids, Part 51. This work was supported by the Fonds der Chemischen Industrie. – Part 50: G. Bringmann, R. Weirich, H. Reuscher, J. R. Jansen, L. Kinzinger, T. Ortmann, *Liebigs Ann. Chem.* **1993**, in press.

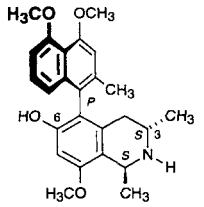

5

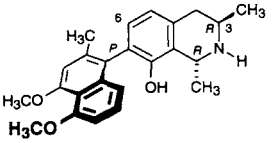

6

cladine (**5**, 1*S*, 3*S*) and dioncophylline A (**6**, 1*R*, 3*R*) were also subjected to the same degradation conditions, thus serving as additional standards. The exclusive formation of the amino acids (*R*)-**3** and D-**4** in a practically enantiomerically pure form (> 95:5) clearly shows that both tetrahydroisoquinoline parts are stereochemically identical. This excludes the above-mentioned stereoisomers with identical configurations at the axes, but enantiomorphous tetrahydroisoquinoline parts. Furthermore, the identification of both amino acids in their (*R*)-configurated forms clearly rules out stereoisomer **1a**, thus unambiguously demonstrating michellamine B to be represented by the stereostructure **1b**, that is, a (1*R*, 3*R*, 5*M*, 1‴*R*, 3‴*R*, 5‴*P*) configuration. Of course, this result again and independently confirms the relative *trans* configurations in both heterocyclic systems.

The work described in this paper represents the first complete elucidation of the full stereostructure of a "dimeric" naphthylisoquinoline alkaloid. Michellamine b (**1b**) is a constitutionally symmetrical, but heterochiral coupling product of two atropodiastereomeric biaryl alkaloids. These two naphthylisoquinoline "halves" formally do not constitute typical Ancistrocladaceae-type alkaloids (that is, with (*S*)-configuration at C3 and an oxygen function at C6, as realized, for example, in **2** and **5**), nor typical Dioncophyllaceae-type alkaloids, that is, with (3*R*)-configuration and no oxygen at C6, like in **6**), but rather one of the "mixed" Ancistrocladaceae/Dioncophyllaceae-type hybrids,[7, 12] since they combine the two properties by having (3*R*)-configuration *and* an oxygen function at C6.

Received: March 20, 1993 [Z 5941 IE]
German version: *Angew. Chem.* **1993**, *105*, 1242

[1] K. P. Manfredi, J. W. Blunt, J. H. Cardellina II, J. B. McMahon, L. L. Pannell, G. M. Cragg, M. R. Boyd, *J. Med. Chem.* **1991**, *34*, 3402–3405.
[2] For an easier comparison of naphthylisoquinoline alkaloids of different coupling types, the naphthalene part is, as introduced [13] and applied [1,3,4] earlier, numbered such that (contrary to the IUPAC rules) it is always attributed a 2-methyl-4,5-dioxy substitution pattern, independent of the site of the axis.
[3] G. Bringmann, R. Zagst, L. Aké Assi, *Planta Med.* **1991**, *57* (*Suppl. 2*), 96–97.
[4] G. Bringmann, R. Zagst, H. Reuscher, L. Aké Assi, *Phytochemistry* **1992**, *31*, 4011–4014.
[5] G. Bringmann in *The Alkaloids*, Vol. 29 (Ed.: A. Brossi), Academic Press, New York, **1986**, pp. 141–184.
[6] G. Bringmann, T. Geuder, M. Rübenacker, R. Zagst, *Phytochemistry* **1991**, *30*, 2067–2070.
[7] G. Bringmann, F. Pokorny, M. Stäblein, L. Aké Assi, *Planta Med.* **1991**, *57* (*Suppl. 2*), 97.
[8] G. Bringmann, F. Pokorny, M. Stäblein, M. Schäffer, L. Aké Assi, *Phytochemistry* **1993**, in press.
[9] G. Bringmann, R. Weirich, D. Lisch, L. Aké Assi, *Planta Med.* **1992**, *58* (*Suppl. 1*), 703–704.
[10] T. R. Govindachari, K. Nagarajan, P. C. Parthasarathy, T. G. Rajagopalan, H. K. Desai, G. Kartha, S. Lai Chen, K. Nakanishi, *J. Chem. Soc. Perkin Trans. 1* **1974**, 1413–1417.
[11] G. Bringmann, J. R. Jansen, H. Reuscher, M. Rübenacker, K. Peters, H. G. von Schnering, *Tetrahedron Lett.* **1990**, *31*, 643–646.
[12] G. Bringmann, R. Zagst, D. Lisch, L. Aké Assi, *Planta Med.* **1992**, *58* (*Suppl. 1*), 702–703.
[13] G. Bringmann, M. Rübenacker, T. Geuder, L. Aké Assi, *Phytochemistry* **1991**, *30*, 3845–3847.

Novel Synthesis of Tetrasubstituted β-Lactones: The Use of Indium in the Electrochemically Supported Reformatsky Reaction**

By *Hans Schick,** *Ralf Ludwig, Karl-Heinz Schwarz, Katharina Kleiner,* and *Annamarie Kunath*

Dedicated to Professor Hans Gross on the occasion of his 65th birthday

The discovery of biologically active natural products with a β-lactone structure, for example, lipstatin,[2] esterastin,[3] lupeolactone,[4] valilactone,[5] obafluorin,[6] and oxazolomycin,[7] has attracted more interest in efficient syntheses for β-lactones. An up-to-date summary of the synthetic methods available today for this class of substances may be found in the literature.[8, 9] We chanced across a surprisingly simple synthesis of tetrasubstitued β-lactones during studies on the electrochemical generation of the Reformatsky reagent from ethyl 2-bromo-2-methylpropanoate (**2**) by using indium as the sacrificial anode.[10]

In previous investigations heat evolution in a Reformatsky reaction, which is often difficult to control, could be regulated conveniently if the Reformatsky reagent is not generated by the reaction of the α-bromoalkanoate with zinc powder, but by using a zinc anode in an electrolysis cell. With this method succinic anhydride was converted by reaction with alkyl 2-bromoalkanoates in good yields into 2-substituted 1-alkyl 5-hydrogen 3-oxohexanedioates.[11] The use of other metals as sacrificial anode showed that indium gave even better yields than zinc.[1] This prompted us to study the electrochemical transformation of 2-bromoalkanoates with ketones at an indium anode as well.

On electrolysis of **2** and cyclohexanone (**1a**) at an indium anode with a cell voltage of 30 V, the crystalline β-lactone **3a** was obtained in 80% yield instead of the expected liquid β-hydroxy ester **4a** (Scheme 1). The structure of **3a** could be

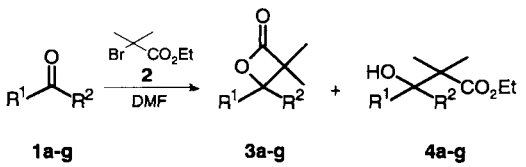

1a-g **3a-g** **4a-g**

Scheme 1. Addition of the bromo ester **2** to the carbonyl compounds **1a–g** in the electrochemically supported Reformatsky reaction at an indium anode. For **a–g**, see Table 1.

deduced unambiguously from the characteristic IR band at 1810 cm^{-1}, the elemental analysis, and the agreement of the ^1H and ^{13}C NMR signals, as well as of the melting point with published data.[8] Under the same conditions the ketones **1b–f** afforded the β-lactones **3b–f** in yields of about 60%. A high-pressure liquid chromatographic (HPLC) study of the crude products obtained by flash chromatography allowed the detection of the expected β-hydroxy esters **4** in small amounts as minor product. The yields and the ratios of β-lactones **3** to β-hydroxyalkanoates **4** are collated in Table 1.

[*] Prof. Dr. H. Schick, Dipl.-Chem. R. Ludwig, Dr. K.-H. Schwarz, Chem.-Ing. K. Kleiner, Dr. A. Kunath
Zentrum für Selektive Organische Synthese
Rudower Chaussee 5, D-12489 Berlin (FRG)
Telefax: Int. code + (30)6392-4103

[**] Reactions of Electrochemically Generated Organometallic Compounds, Part 3. This work was supported by the Deutsche Forschungsgemeinschaft and the Fonds der Chemischen Industrie. Part 2: [1].

Table 1. Reaction of the carbonyl compounds **1a–g** with **2** to form the β-lactones **3a–g** and the ethyl β-hydroxycarboxylates **4a–g**.

1, 3, 4	R^1	R^2	Yield (3 and 4) [%] [a]	IR (3) $\tilde{\nu}_{CO}$ [cm^{-1}]	3:4 [b]
a	$(CH_2)_5$		84	1810	95:5
b	$(CH_2)_2CMe(CH_2)_2$		66	1800	91:9 [c]
c	Et	Et	61	1815	>99:1
d	*n*Pr	*n*Pr	57	1810	>99:1
e	*n*Bu	*n*Bu	61 [d]	1810	>99:1
f	Ph	Ph	61	1820	>99:1
g	Ph	H	93	-	<1:100

[a] The yields refer to the fractions containing **3** and **4** obtained by flash chromatography. [b] The ratio of **3**:**4** was determined by HPLC of the crude product obtained from flash chromatography. [c] According to HPLC the two isomers of **3b** are formed in a ratio of 4:1. [d] The yield is based on **1e** that reacts. The conversion was not complete.

Although the Reformatsky reaction has often been employed—also with other metals like magnesium,[12] cadmium,[13] nickel,[14] cerium,[15] manganese,[16] and also indium[17–19]—as a standard method for the synthesis of β-hydroxyalkanoates, the formation of β-lactones has apparently not been observed before. At any rate, no reference to such a possibility appears in surveys either on the Reformatsky reaction[20] or on β-lactones.[8, 9]

To explain the course of the reaction, it can be assumed that organoindium compounds of type **5**[21] or indium enolates of type **6**[22] are formed in the electrochemical reaction of indium and the bromo ester **2** (Scheme 2). These react as

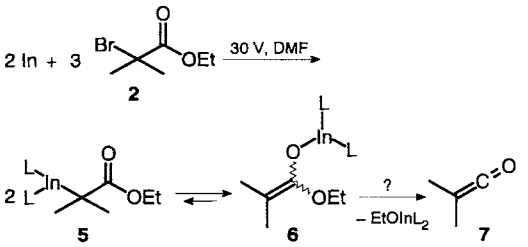

Scheme 2. Formation of possible intermediates in the electrolysis of bromo ester **2** at an indium anode (L = Br, Me_2CCO_2Et, or $Me_2C{=}C(O)OEt$).

nucleophiles, for instance with the carbonyl group of **1a** to form the adduct **8** (Scheme 3). This seems to afford preferentially the β-lactone **3a** by elimination of an indium alcoholate from the ortho ester derivative **9**. The hydroxy ester **4a** formed as minor product arises in the hydrolytic workup if **8** first rearranges to the indium alcoholate **10**. This is in any event the generally accepted course of the Reformatsky reaction with zinc.[20] That the β-lactone **3a** in the described reaction is formed before the hydrolytic workup can be seen from the typical signals of **3a**—in particular at $\delta = 85.1$ and 176.1—in the ^{13}C NMR spectra of the unhydrolyzed reaction solution.

Although the Lewis acid catalyzed addition of ketenes to aldehydes and ketones is a general possibility for the synthesis of β-lactones,[8, 9] this reaction can apparently be disregarded for the formation of the β-lactones **3** observed here. If the ketene **7** could be formed from the ester enolate **6** by elimination of an indium alcoholate (see Scheme 2), it should then add more readily to aldehydes than to ketones.[23] This was, however, not observed: benzaldehyde, in contrast to benzophenone, afforded exclusively the β-hydroxy ester **4g** (Table 1).

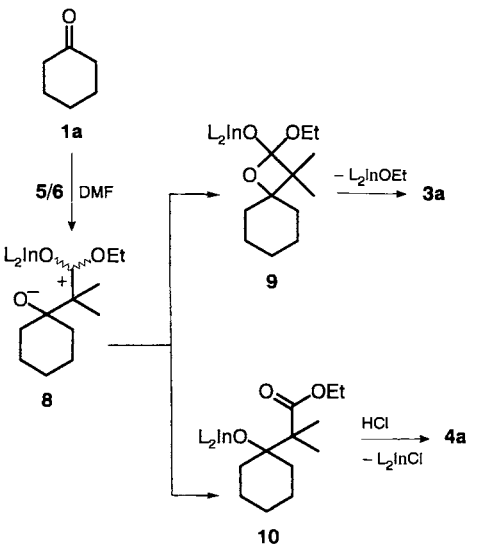

Scheme 3. Interpretation of the formation of the β-lactone **3a** and the hydroxy ester **4a** from the ketone **1a**.

According to the results available at present, tetrasubstituted β-lactones can be prepared in good yields from ketones and ethyl 2-bromo-2-methylpropanoate (**2**) in an electrochemically supported Reformatsky reaction with indium as sacrificial anode. The preparative possibilities and limitations of this special application of the Reformatsky reaction for the synthesis of β-lactones containing four different substituents and the suitability of other metals are under investigation.

Experimental Procedure

3a: In a thermostatable, one-compartment electrolysis cell provided with an indium rod as anode and a nickel gauze as cathode, **1a** (0.491 g, 5 mmol) and **2** (2.926 g, 15 mmol) were electrolyzed under argon in *N*,*N*-dimethylformamide (DMF)/tetrahydrofuran (1/1, 10 mL) in the presence of tetrabutylammonium bromide (0.322 g, 0.1 mmol) at 50 °C at a cell voltage of 30 V. When no more **1a** could be detected by thin-layer chromatography, the mixture was stirred without current for a further 2 h. Ice (25 g) and HCl (5%, 25 mL) were added, and the mixture was extracted with EtOAc (5 × 20 mL). The combined extracts were washed with water (3 × 10 mL), dried with Na_2SO_4, and evaporated to dryness under reduced pressure. The residue was purified by flash chromatography on silica gel 60 (230–400 mesh, E. Merck) with hexane/EtOAc (10/1) and recrystallized from hexane; yield 0.672 g (80%), m.p. 108–110 °C (published value [8]: 109–111 °C).

Received: March 29, 1993 [Z 5955 IE]
German version: *Angew. Chem.* **1993**, *105*, 1218

[1] K.-H. Schwarz, K. Kleiner, R. Ludwig, H. Schick, *Chem. Ber.* **1993**, *126*, 1247–1249.
[2] E. K. Weibel, P. Hadvary, E. Hochuli, E. Kupfer, H. Lengsfeld, *J. Antibiot.* **1987**, *40*, 1081–1085.
[3] S. Kondo, K. Uotani, M. Miyamoto, T. Hazato, H. Naganawa, T. Aoyagi, H. Umezawa, *J. Antibiot.* **1978**, *31*, 797–800.
[4] H. Kikuchi, A. Tensho, I. Shimizu, H. Shiokawa, A. Kuno, S. Yamada, T. Fujiwara, K. Tomita, *Chem. Lett.* **1983**, 603–606.
[5] M. Kitahara, M. Asano, H. Naganawa, K. Maeda, M. Hamada, T. Aoyagi, H. Umezawa, Y. Iitaka, H. Nakamura, *J. Antibiot.* **1987**, *40*, 1647–1649.
[6] A. A. Tymiak, C. A. Culver, M. F. Malley, J. Z. Gougoutas, *J. Org. Chem.* **1985**, *50*, 5491–5495.
[7] T. Mori, K. Takahashi, M. Kashiwabara, D. Uemura, C. Katayama, S. Iwadare, Y. Shizuri, R. Mitomo, F. Nakano, A. Matasuzaki, *Tetrahedron Lett.* **1985**, *26*, 1073–1076.
[8] R. L. Danheiser, J. S. Nowick, *J. Org. Chem.* **1991**, *56*, 1176–1185, and references therein.
[9] J. Mulzer in *Comprehensive Organic Synthesis, Vol. 6* (Eds.: B. M. Trost, I. Fleming), Pergamon, Oxford, **1991**, pp. 342–350.

[10] Review on use of sacrificial anodes in preparative electrochemistry: J. Chaussard, J.-C. Folest, J.-Y. Nedelec, J. Perichon, S. Sibille, M. Troupel, *Synthesis* **1990**, 369–381.
[11] K.-H. Schwarz, K. Kleiner, R. Ludwig, H. Schick, *J. Org. Chem.* **1992**, *57*, 4013–4015.
[12] T. Moriwake, *J. Org. Chem.* **1966**, *31*, 983–985.
[13] E. Burkhardt, R. D. Rieke, *J. Org. Chem.* **1985**, *50*, 416–417.
[14] S. N. Inaba, R. D. Rieke, *Tetrahedron Lett.* **1985**, *26*, 155–156.
[15] T. Imamoto, T. Kusumoto, Y. Tawarayama, Y. Sugiura, T. Mita, Y. Hatanaka, M. Yokoyama, *J. Org. Chem.* **1984**, *49*, 3904–3912.
[16] G. Cahiez, P.-Y. Chavant, *Tetrahedron Lett.* **1989**, *30*, 7373–7376.
[17] L.-C. Chao, R. D. Rieke, *J. Org. Chem.* **1975**, *40*, 2253–2255.
[18] S. Araki, H. Ito, Y. Butsugan, *Synth. Commun.* **1988**, *18*, 453–458.
[19] P. S. Johar, S. Araki, Y. Butsugan, *J. Chem. Soc. Perkin Trans.* **1992**, 711–713.
[20] A. Fürstner, *Synthesis* **1989**, 571–590, and references therein
[21] Organoindium compounds of a similar structure are discussed in [18].
[22] For the Reformatsky reagent formed from zinc and **2**, the structure of an analogous zinc ester enolate seems plausible (W. R. Vaughan, S. C. Bernstein, M. E. Lorber, *J. Org. Chem.* **1965**, *30*, 1790–1795). The manner in which these enolates aggregate was left open.
[23] D. Borrmann, R. Wegler, *Chem. Ber.* **1969**, *102*, 64–70.

Transformation of the First Zirconocene Alkyne Complex without an Additional Phosphane Ligand into a Dinuclear σ-Alkenyl Complex by Hydrogen Transfer from η^5-C_5H_5 to the Alkyne Ligand**

By *Uwe Rosenthal,* Andreas Ohff, Manfred Michalik, Helmar Görls, Vladimir V. Burlakov,* and *Vladimir B. Shur*

Dedicated to Dr. habil. Erhard Kurras on the occasion of his 65th birthday

Metallocene alkyne complexes with Group 4 metals without additional ligands $[Cp_2M(RC{\equiv}CR')]$ are highly reactive and can be prepared and characterized only in rare cases. We synthesized the first complexes of this type with M = Ti, **1a**,[1] **1b**,[2, 3] and **1c**,[4] according to Equation (a). Complex **1b** is the only one of this type that was characterized by X-ray crystal structure analysis. In addition, a thermally unstable complex with R = R′ = Me was described.[5]

$$[Cp_2TiCl_2] + Mg + RC{\equiv}CR' \xrightarrow[-MgCl_2]{20\,^\circ C,\ THF} Cp_2Ti(C(R)=C(R'))\quad (a)$$

1a: R = R′ = Ph
b: R = Ph, R′ = $SiMe_3$
c: R = R′ = $SiMe_3$

Analogous zirconium complexes $[Cp_2Zr(RC{\equiv}CR')]$ are unknown, however, since in the reactions analogous to (a) they react further with the alkyne to form substituted zirconacyclopentadienes $[Cp_2Zr{-}C(R')=C(R){-}C(R)=C(R')]$, for example for R = R′ = Ph[6] and R = Ph, R′ = $SiMe_3$.[7] Nevertheless, a series of zirconocene alkyne complexes $[Cp_2Zr(PR_3)(RC{\equiv}CR')]$ has been synthesized with stabilizing phosphane ligands.[8–12] When bis(trimethylsilyl)acetylene was used, the first zirconocene alkyne complex without an additional phosphane ligand, **2**, was obtained; we report here on its synthesis, structure, and properties.

Complex **2** was prepared from the reaction of zirconocene dichloride with equimolar amounts of magnesium and

$[Cp_2Zr(thf)(Me_3SiC{\equiv}CSiMe_3)]$ **2**

bis(trimethylsilyl)acetylene in THF at room temperature [Eq.(b)]; the complex contains a weakly bound THF molecule.

$$[Cp_2ZrCl_2] + Mg + Me_3SiC{\equiv}CSiMe_3 \xrightarrow[-MgCl_2]{20\,^\circ C,\ THF} Cp_2Zr(thf)(C(SiMe_3)=C(SiMe_3))\quad (b)$$

2

Complex **2** crystallizes in orange, monoclinic prisms, which become colorless above about 100 °C and melt at 139–141 °C with decomposition. The compound is very air and moisture sensitive.

Although the acetylene carbon atoms in **2** should not be equivalent, in ^{13}C NMR spectra between + 30 and −30 °C they give rise to only one singlet at $\delta = 212.9$[13] ($[Cp_2Zr(PMe_3)(Me_3SiC{\equiv}CSiMe_3)]$ has signals at $\delta = 177.3$ and 205.1[12]). Accordingly, the carbon and hydrogen atoms of the Me_3Si groups in **2** also give rise to one singlet each in the ^{13}C and ^1H NMR spectra, respectively. This apparent equivalence of the two halves of the alkyne in solution can be explained by a fast exchange of free and coordinated THF molecules. Measurements in noncoordinating solvents such as [D_6]benzene are not possible because cleavage of THF is immediately followed by a spontaneous reaction (see [Eq.(c)]).

The IR spectrum of **2** ($\nu(C{\equiv}C) = 1581\ cm^{-1}$) indicates a complex with zirconacyclopropene structure. In the X-ray structure analysis[14] of **2** (Fig. 1) the zirconium center has a

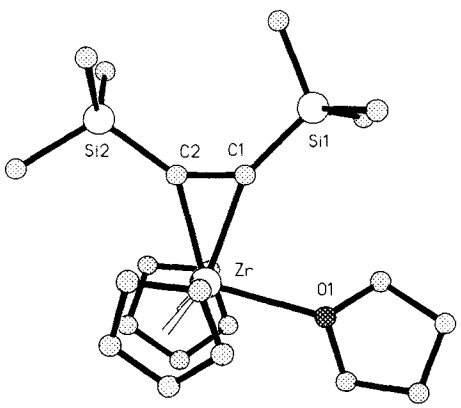

Fig. 1. Crystal structure of **2**. Selected distances [Å] and angles [°]: C1-C2 1.302(9), Zr-C1 2.260(7), Zr-C2 2.204(7), Zr-O1 2.390(5); C1-C2-Si2 143.5(6), C2-C1-Si1 134.4(6), C1-Zr-C2 33.9(2), O1-Zr-C1 86.8(2), O1-Zr-C2 120.7(2), Cp1-Zr-Cp1A 130.5(3).

[*] Dr. habil. U. Rosenthal, Dipl.-Chem. A. Ohff
Max-Planck-Gesellschaft, Arbeitsgruppe "Komplexkatalyse"
an der Universität Rostock
Buchbinderstrasse 5-6, D-18055 Rostock (FRG)
Telefax: Int. code + (381)4669324
Dr. habil. M. Michalik
Institut für Organische Katalyseforschung an der Universität Rostock e.V.
Dr. H. Görls
Max-Planck-Gesellschaft, Arbeitsgruppe "CO_2-Chemie"
an der Universität Jena
Dr. V. V. Burlakov, Prof. V. B. Shur
Institute of Organoelement Compounds of the
Russian Academy of Sciences, Moscow (Russia)

[**] This research was supported by the Max-Planck-Gesellschaft and the Fonds der Chemischen Industrie. We thank Prof. Dr. G. Oehme, Institut für Organische Katalyseforschung an der Universität Rostock e.V., for his support.

tetrahedral coordination sphere composed of Cp ligands, alkyne, and tetrahydrofuran. The molecule has *m* symmetry; the mirror planes pass through the central atom, the alkyne carbon atoms, the Si atoms, and the O atoms as well as both β-C atoms of the THF ligand. Thus, in the solid the halves of the alkyne are not equivalent.

The distance between the two alkyne carbon atoms in the complex (1.302(9) Å) is close to that of a C–C double bond (in $[Cp_2^*Ti(Me_3SiC{\equiv}CSiMe_3)]$ 1.309(4) Å ($Cp^* = \eta^5$-C_5Me_5),[3] $[Cp_2Zr(PMe_3)(HC{\equiv}CnBu)]$ 1.286(5) Å[8]). The relatively long Zr–O separation of 2.390(5) Å in **2** (in $Cp'_2Zr\{(Z)$-$C(CH_3){=}C(CH_3)(nPr)\}(thf)](BPh_4)$ 2.289(6) Å ($Cp' = C_5H_4Me$),[15] in $[Cp_2Zr(CH_3)(thf)]$-(BPh_4) 2.122(14) Å,[16] in $[Cp_2Zr(thf)(Me_3SiN{=}CHPh)]$ 2.376(9) Å[17]) is further proof of the loose Zr–THF interaction deduced from spectroscopic data which is the cause for the reaction shown in Equation (c).

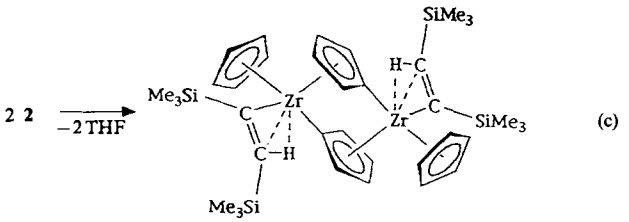

(c)

3

When complex **2** is dissolved in pentane or benzene, or heated under vacuum (oil pump), the THF ligand is lost completely; the shift of a hydrogen atom from the η^5-C_5H_5 ligand to the alkyne then results in formation of the dinuclear σ-alkenyl complex **3** [Eq.(c)].

Complex **3** crystallizes in colorless prisms which melt at 142–143 °C with decomposition and are very air and moisture sensitive. The structure of the compound was determined by NMR spectroscopy[18] and X-ray structure analysis [19] (Fig. 2). In this dinuclear complex the zirconium

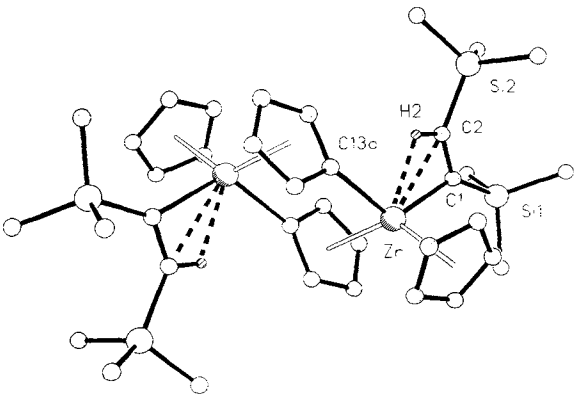

Fig. 2. Crystal structure of **3**. Selected distances [Å] and angles [°]: C1-C2 1.318(5), Zr-C1 2.244(3), Zr-C2 2.566(3), Zr-H2 2.14(1), C2-H2 1.10(3), Zr-C13 2.349(3), C13a-H2 2.41(1); C1-C2-Si2 135.3(3), C2-C1-Si1 133.3(3), C1-Zr-C2 30.9(1), Zr-H2-C2 99.5(8), Cp1-Zr-Cp2 132.3(1).

atoms are linked by two bridging $\eta^1{:}\eta^5$-cyclopentadienyl ligands. The agostic interaction between the alkenyl C–H bonds and the zirconium centers is an interesting structural feature in this complex.

Bridging C_5H_4 ligands are not unusual (see for example $[\{Cp[\mu$-$(\eta^1{:}\eta^5$-$C_5H_4)]Ti(PMe_3)\}_2]$[20]). The distances and angles in the Zr–C=C–H portion of **3** correspond for the most part to those of zirconocene alkenyl halides (see for example $[Cp_2Zr(Cl)\{C(SiMe_3){=}CHPh\}]$[21]).

The agostic interaction CH → Zr in **3** is also evident from the small coupling constants $^1J(C_\beta$-H) of 96 and 97 Hz, the large difference in the ^{13}C NMR chemical shifts between the signals of the C_α and C_β carbon atoms ($\Delta\delta = 130$), and the downfield shifts of the C_β–H signals in the ^1H NMR spectra, $\delta = 7.28$ and 7.52.[21] The distance between the hydrogen atom involved in the agostic bond and the zirconium atom is 2.14(1) Å.

Two sets of signals appear in the ^1H and ^{13}C NMR spectra of **3** in THF or benzene; even the spectra of the isomerically pure sample characterized by X-ray crystallography show these sets of signals in the ratio 1:2.5, which indicates the formation of two isomers not previously characterized. In addition, **3** converts slowly into **2** in THF. Complexes **2** and **3** display the typical reactivity of zirconocene alkyne complexes, for example, in reactions with acetone, water, and CO_2.[22] The results of these studies will be reported in due course.

The differences in the synthesis and reactivity of the titanocene and zirconocene alkyne complexes can be traced back to the difference in the atomic radii of the central atoms. Thus in the case of the larger atom, zirconium, coordination of THF to give **2** and the subsequent elimination of THF providing **3** are possible.

Experimental Procedure

All experiments were conducted under anaerobic and anhydrous conditions.

2: A mixture of $[Cp_2ZrCl_2]$ (2.10 g, 7.2 mmol), finely cut magnesium (0.18 g, 7.4 mmol), and bis(trimethylsilyl)acetylene (1.62 mL, 1.23 g, 7.2 mmol) in THF (25 mL) was stirred at 20 °C for 3 h and then concentrated under vacuum until crystals started to form. Pentane (15 mL) was added and the reaction mixture filtered through a G3 frit. The solid was washed with THF/pentane (1/3, 15 mL) and then extracted with this solvent mixture (50–60 mL). The extract was concentrated to dryness under vacuum, leaving the orange complex **2** (2.5 g, 75%) (correct elemental analysis).

3: a) Complex **2** (0.988 g) was dissolved in benzene (20 mL), the solution filtered, and concentrated under vacuum to a volume of approximately 5 mL. Colorless crystals formed after one day. The remaining solution was decanted off and the crystals washed with benzene/pentane (1/1) and then dried under vacuum (oil pump) to give **3** (0.573 g, 69%) (correct elemental analysis).

b) Complex **2** (0.1 g) was heated at 100 °C for 10 min under vacuum (oil pump); a colorless powder formed which is identical to product **3** obtained from method a).

Received: April 15, 1993 [Z6009IE]
German version: *Angew. Chem.* **1993**, *105*, 1228

[1] V. B. Shur, V. V. Burlakov, M. E. Vol'pin, *J. Organomet. Chem.* **1988**, *347*, 77.
[2] V. V. Burlakov, U. Rosenthal, R. Beckhaus, A. V. Polyakov, Yu. T. Struchkov, G. Oehme, V. B. Shur, M. E. Vol'pin, *Metalloorg. Khim.* **1990**, *3*, 476 [English translation: *Organomet. Chem. USSR* **1990**, *3*, 237].
[3] U. Rosenthal, H. Görls, V. V. Burlakov, V. B. Shur, M. E. Vol'pin, *J. Organomet. Chem.* **1992**, *426*, C53–C57.
[4] V. V. Burlakov, U. Rosenthal, P. V. Petrovski, V. B. Shur, M. E. Vol'pin, *Metalloorg. Khim.* **1988**, *1*, 953 [English translation: *Organomet. Chem. USSR* **1988**, *1*, 526].
[5] H. G. Alt, G. S. Herrmann, *J. Organomet. Chem.* **1990**, *390*, 159.
[6] J. L. Atwood, W. E. Hunter, H. Alt, M. D. Rausch, *J. Am. Chem. Soc.* **1976**, *98*, 2454; W. E. Hunter, J. L. Atwood, G. Fachinetti, C. Floriani, *J. Organomet. Chem.* **1981**, *204*, 67; E. Negishi, F. E. Cederbaum, T. Takahashi, *Tetrahedron Lett.* **1986**, *27*, 2829.
[7] G. Erker, R. Zwettler, C. Krüger, I. Hyla-Kryspin, R. Gleiter, *Organometallics* **1990**, *9*, 524; G. Erker, R. Zwettler, *J. Organomet. Chem.* **1991**, *409*, 179.
[8] S. L. Buchwald, B. T. Watson, J. C. Huffmann, *J. Am. Chem. Soc.* **1987**, *109*, 2544; S. L. Buchwald, R. B. Nielsen, *Chem. Rev.* **1988**, *88*, 1047.
[9] T. Takahashi, D. R. Swanson, E. Negishi, *Chem. Lett.* **1987**, 623.

[10] H. G. Alt, H. E. Engelhardt, M. D. Rausch, L. B. Kool, *J. Organomet. Chem.* **1987**, *329*, 61.
[11] P. Binger, P. Müller, R. Benn, A. Rufinska, B. Gabor, C. Krüger, P. Betz, *Chem. Ber.* **1989**, *122*, 1035.
[12] F. Langhauser, Dissertation, Universtität Kaiserslautern, **1991**.
[13] **2**: IR (Nujol): 1581 cm^{-1} (ν(C≡C)); ^1H NMR ([D_8]THF, Bruker ARX 300, TMS, 30 °C): δ = 0.10 (s, $SiMe_3$), 5.55 (s, Cp); $^{13}C\{^1H\}$ NMR ([D_8]THF, TMS, 30 °C): δ = 2.3 (s, $SiMe_3$), 107.0 (s, Cp); 212.9 (s, C≡C).
[14] Crystal data for **2**: $C_{22}H_{36}OSi_2Zr$, M_r = 463.9 g mol^{-1}, *Pnma*, *a* = 20.091(2), *b* = 11.955(2), *c* = 10.256(3) Å, *V* = 2459(1) $Å^3$, *Z* = 4, ρ_{calc} = 1.25 g cm^{-3}, λ = 0.71069 Å, μ = 5.4 cm^{-1}, 4769 measured reflections, 4436 independent reflections, of which 2031 were observed ($I > 2\sigma(I)$), 142 refined parameters, *R* = 0.065, *Rw* = 0.065, ($w = 1/\sigma^2(F_0)$), residual electron density 0.94 e $Å^{-3}$. Further details of the crystal structure investigation may be obtained from the Fachinformationszentrum Karlsruhe, Gesellschaft für wissenschaftlich-technische Information mbH, D-76344 Eggenstein-Leopoldshafen (FRG) on quoting the depository number CSD-57254, the names of the authors, and the journal citation.
[15] R. F. Jordan, R. E. LaPointe, P. K. Bradley, N. Baenziger, *Organometallics* **1989**, *8*, 2892.
[16] R. F. Jordan, C. S. Bajgur, R. Willett, B. Scott, *J. Am. Chem. Soc.* **1986**, *108*, 7410.
[17] S. L. Buchwald, B. T. Watson, M. W. Wannamaker, J. C. Dewan, *J. Am. Chem. Soc.* **1989**, *111*, 4486.
[18] **3**: ^1H NMR (C_6D_6), Bruker ARX 300, *cyclo*-C_6H_{12}, δ = 1.42, 30 °C): two isomers A and B (2.45:1), A: δ = 7.52 (s, =CH); 5.62 (s, Cp), 4.50, 5.14, 6.29, 6.42 (m, C_5H_4), 0.13 (s, $SiMe_3$), 0.41 (s, $SiMe_3$); B: δ = 7.28 (s, =CH), 5.53 (s, Cp), 4.48, 5.36, 6.24, 6.53 (m, C_5H_4), 0.29 (s, $SiMe_3$), 0.44 (s, $SiMe_3$); $^{13}C\{^1H\}$ NMR (C_6D_6, δ = 127.96; 30 °C) A: δ = 230.2 (s, $CSiMe_3$), 101.7 (s, $CHSiMe_3$), 106.9 (s, Cp), 110.5, 111.7, 118.2, 121.9 (s, CH), 135.0 (s, C_qCp), B: δ = 230.3 (s, $CSiMe_3$), 100.4 (s, $CHSiMe_3$), 106.9 (s, Cp), 111.5, 112.8, 116.6, 121.6 (s, CH), 135.2 (s, C_qCp).
[19] Crystal data for **3**: $C_{36}H_{56}Si_4Zr_2$, M_r = 783.6 g mol^{-1}, $P2_1/c$, *a* = 11.305(3), *b* = 10.863(3), *c* = 16.174(3) Å, β = 97.69(2), *V* = 1968(1) $Å^3$, *Z* = 2, ρ_{calc} = 1.32 g cm^{-3}, λ = 0.71069 Å, μ = 6.6 cm^{-1}, 4892 measured reflections, 4487 independent reflections, of which 3193 were observed ($I > 2\sigma(I)$), 194 refined parameters, residual electron density 0.68 e $Å^{-3}$. The H atoms were first localized by using difference Fourier synthesis. In the refinement all H atoms except H2 were placed in idealized positions (*d*(C–H) = 0.95 Å) and treated with a common isotropic temperature factor B_{iso} = 8.0 $Å^2$. The position of H2, which was obtained by difference Fourier synthesis, is essential to the interpretation of the structure. Both this position and the temperature factor were refined, then the temperature factor alone was refined. Comparison of the distances and angles for the atoms interacting with H2 (Zr, C2, and C13A) shows the structures obtained by the two refinement procedures do not differ significantly. Thus the position of H2 seems realistic. The final *R* value converged at 0.039 (R_w = 0.043)[14].
[20] L. B. Kool, M. D. Rausch, H. G. Alt, M. Herberhold, U. Thewalt, B. Honold, *J. Organomet. Chem.* **1986**, *27*, 310.
[21] I. Hyla-Kryspin, R. Gleiter, C. Krüger, R. Zwettler, G. Erker, *Organometallics* **1990**, *9*, 517.
[22] U. Rosenthal, A. Ohff, M. Michalik, H. Görls, V. V. Burlakov, V. B. Shur, unpublished.

Host–Guest Complexes between Calix[4]arenes Derived from Resorcinol and Alkylammonium Ions**

By *Tino Lippmann, Horst Wilde, Maren Pink, Andrea Schäfer, Manfred Hesse,* and *Gerhard Mann**

Interest in water-soluble calix[4]arenes as models for synthetic enzymes and receptors has increased during the last few years.[1–6] The tetraanion of all-*cis*-tetramethylcalix[4]-arene **1** derived from resorcinol, which exists in aqueous alkaline solution, serves as the anionic host molecule in complexes with alkylammonium ions; the energy of formation of such complexes ΔG°_{298} is between 1.3 and 6.4 kcal mol^{-1} ($K = 10–10^4$).[7–9] We have now obtained crystals of a complex of **1** for the first time. The structure of these complexes

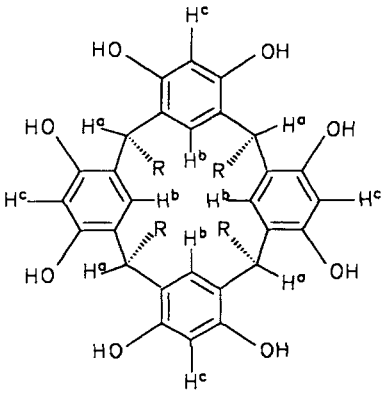

1: R = CH_3
2: R = *n*-C_9H_{19}

is of particular interest because tetraphenols with a crown conformation (C_{4v} symmetry) have hitherto been known only for calix[4]arenes[10] derived from phenol, not resorcinol. Disregarding bridged resorcinol tetramers,[11,12] crystal structure analyses of phenolic calixarenes show the complexation of solvents, for example, acetonitrile[13] and methyl ethyl ketone;[14] in these complexes the hosts exist in the C_{2v}-symmetric boat conformation.

Octol **1** was dissolved with alkylammonium sulfates **3**–**11** in neutral or slightly acidic solution (ethanol/water 2:1) by warming. The complexes that crystallized were examined by using elemental analysis and ^1H NMR spectroscopy.

$(Et_3HN)_2SO_4$ **3**	$(nPr_2H_2N)_2SO_4$ **4**
$(nBu_2H_2N)_2SO_4$ **5**	$(MeH_3N)_2SO_4$ **6**
$(Me_2H_2N)_2SO_4$ **7**	$(Me_3HN)_2SO_4$ **8**
$(Et_2H_2N)_2SO_4$ **9**	$[(tBuCH_2)H_3N]_2SO_4$ **10**
$[(c\text{-}C_6H_{11})H_3N]_2SO_4$ **11**	

Distinct 1:1 complexes with sharp melting points were obtained with the ammonium sulfates **3**–**5**; crystalline complexes with undefined stoichiometric composition formed with **6**–**9**.

The ^1H NMR spectra (400 MHz) of the complexes **1**·**3** (m.p. 248–250 °C), **1**·**4** (m.p. 242–243 °C), and **1**·**5** (m.p. 227–231 °C) (all recrystallized from ethanol) with the same absolute concentrations show a slight shift of the signals caused by complex formation compared with those of the pure host compound: $\Delta\delta = 0.02–0.07$. The signals of the aromatic protons H^c bonded to the upper rim and those of the H^b protons are shifted to low field, the H^a protons are shifted to high field.[15] Integration of the ^1H NMR signals and the elemental analyses support a 1:1 ratio between the host compound **1** and the bis(alkylammonium sulfates).

The marked complexation of the alkylammonium ions by the calixarene crowns is made clearer by the mass spectra obtained with electrospray ionization (ESI).[16,17] The most intense peak in the ESI spectrum of complex **1**·**3** is assigned to the species complexed to one triethylammonium ion (*m/z*

[*] Prof. Dr. G. Mann, Dipl.-Chem. T. Lippmann, Prof. Dr. H. Wilde, Dipl.-Chem. M. Pink
Fachbereich Chemie der Universität
Talstrasse 35, D-04103 Leipzig (FRG)
Dr. A. Schäfer, Prof. Dr. M. Hesse
Organisch-chemisches Institut der Universität Zürich (Switzerland)

[**] This work was supported by the Deutsche Forschungsgemeinschaft, the Fonds der Chemischen Industrie, and the Schweizerischen Nationalfonds zur Förderung der wissenschaftlichen Forschung.

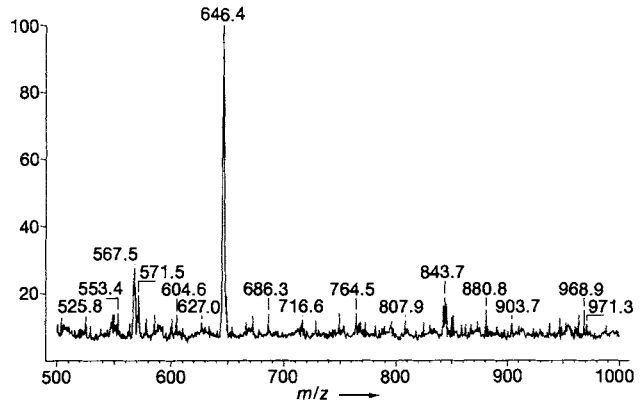

Fig. 1. ESI mass spectrum of the 1:1 complex **1**·**3**.

646 = 544 + 102) (Fig. 1). Although intense peaks can be detected for an excess of ammonium ions, only a weak signal is observed for the uncomplexed host molecule **1** (M = 544). Stable complexes in the gas phase, in other words free from solvophobic interactions, have hitherto been described only for a few host–guest compounds.[18–20]

The proposed host–guest composition is supported by variation of the substituents. Complex **1**·**5** with the nBu$_2$H$_2$N$^+$ ion as guest shows the expected base peak at m/z 674 = 544 + 130, complex **2**·**3** correspondingly at m/z 1095 = 993 + 102. As expected, ammonium ions with branched alkyl groups, for example **10** and **11**, do not form complexes with the hosts **1** and **2**.

Complex **1**·**3**, which we examined after recrystallization from ethanol at low temperature,[21] is the first crystalline host–guest compound in which the all-*cis*-tetramethylcalix[4]arene derived from resorcinol exists in approximately conical form with C_{4v} symmetry (Fig. 2).

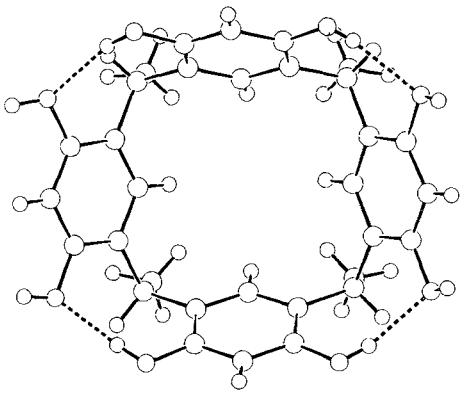

Fig. 2. Molecular geometry of the host compound **1** in the crystal (crown conformation).

The eight torsional angles of **1** reflect the conformation of the macrocycle.[22] Comparison of the torsional angles of the boat form of the host–guest compound **1**·MeC(O)Et with those of **1**·**3**·4EtOH (appropriate elemental analysis and ^{1}H NMR spectrum) makes the difference in conformation quite clear.[23] As shown in Figure 3, the crystalline compound **1**·**3** has a layer structure, composed of alternating hydrophilic and hydrophobic layers.

The hydrophobic layers are formed from pairs of calixarene molecules, which are facing each other in the region of the methyl groups (lower rim). The hydrophilic layer is formed from triethylammonium ions, sulfate ions, the hydroxyl groups of the calixarene, and also from the solvent (ethanol).

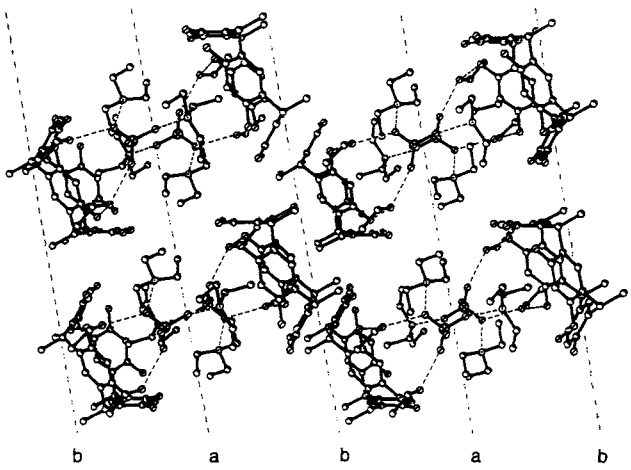

Fig. 3. Structure of **1**·**3**·4EtOH (SHELXTL-PLUS, viewing direction (010)) showing the paired arrangement of the calixarene crowns with intercalated hydrophilic compounds (triethylammonium ions, sulfate ions, ethanol molecules); hydrophilic/hydrophobic layers are formed in the crystal. Hydrophilic layer = a, hydrophobic layer = b.

Received: March 15, 1993 [Z 5927/5928 IE]
German version: *Angew. Chem.* **1993**, *105*, 1258

[1] C. D. Gutsche in *Monographs in Supramolecular Chemistry, Vol. 1* (Ed.: J. F. Stoddart), The Royal Society of Chemistry, Cambridge, **1989**.
[2] J. Vicens, V. Böhmer in *Calixarenes: A Versatile Class of Macrocyclic Compounds* (Eds.: J. Vicens, V. Böhmer), Kluwer, Dordrecht, **1991**.
[3] V. Böhmer, M. A. McKervey, *Chem. Unserer Zeit* **1991**, *4*, 195.
[4] R. M. Izatt, J. S. Bradshaw, K. Pawlak, R. L. Bruening, B. J. Tarbet, *Chem. Rev.* **1992**, *92*, 1261.
[5] K. Kurihara, K. Ohto, Y. Tanaka, Y. Aoyama, T. Kunitake, *J. Am. Chem. Soc.* **1991**, *113*, 444.
[6] Y. Kikuchi, K. Kobayashi, Y. Aoyama, *J. Am. Chem. Soc.* **1992**, *114*, 1351.
[7] H. J. Schneider, D. Güttes, U. Schneider, *Angew. Chem.* **1986**, *98*, 635; *Angew. Chem. Int. Ed. Engl.* **1986**, *25*, 647.
[8] H. J. Schneider, D. Güttes, U. Schneider, *J. Am. Chem. Soc.* **1988**, *110*, 6442.
[9] H. J. Schneider, R. Kramer, S. Simova, U. Schneider, *J. Am. Chem. Soc.* **1988**, *110*, 6449.
[10] G. D. Andreetti, R. Ungaro, A. Pochini, *J. Chem. Soc. Chem. Commun.* **1979**, 1005.
[11] J. R. Moran, S. Karbach, D. J. Cram, *J. Am. Chem. Soc.* **1982**, *104*, 5826.
[12] D. J. Cram, K. D. Stewart, I. Goldberg, K. N. Trueblood, *J. Am. Chem. Soc.* **1985**, *107*, 2574.
[13] L. M. Tunstad, J. A. Tucker, E. Dalcanale, J. Weiser, J. A. Bryant, J. C. Sherman, R. C. Helgeson, C. B. Knobler, D. J. Cram, *J. Am. Chem. Soc.* **1989**, *54*, 1305.
[14] G. Mann, L. Hennig, F. Weinelt, K. Müller, R. Meusinger, G. Zahn, T. Lippmann, *Supramol. Chem.*, submitted.
[15] ^{1}H NMR (400 MHz, [D$_6$]DMSO): **1**: δ = 4.56 (q, H^a), 6.25 (s, H^b), 6.90 (s, H^c); **1**·**3**: δ = 4.54 (q, H^a), 6.27 (s, H^b), 6.96 (s, H^c); **1**·**4**: δ = 4.54 (q, H^a), 6.26 (s, H^b), 6.97 (s, H^c); **1**·**5**: δ = 4.54 (q, H^a), 6.28 (s, H^b), 6.97 (s, H^c).
[16] J. B. Fenn, M. Mann, C. K. Meng, S. F. Wong, C. M. Whitehouse, *Mass Spectrom. Rev.* **1990**, *9*, 1.
[17] R. D. Smith, J. A. Loo, C. G. Edmonds, C. J. Barinaga, H. R. Udseth, *Anal. Chem.* **1990**, *62*, 882.
[18] K. Laali, R. P. Lattimer, *J. Org. Chem.* **1989**, *54*, 496.
[19] M. Vincenti, E. Dalcanale, P. Soncini, G. Guglielmetti, *J. Am. Chem. Soc.* **1990**, *112*, 445.
[20] H. Zhang, I.-H. Chu, S. Leming, D. V. Dearden, *J. Am. Chem. Soc.* **1991**, *113*, 7415.
[21] a) Preparation and structure data for (**1**·**3**·4EtOH): The crystal used for measurements, 0.5 × 0.4 × 0.7 mm, moistened with mother liquor, was prepared under Ar in a Mark tube $C_{52}H_{88}N_2O_{16}S$, triclinic, space group $P\bar{1}$, a = 10.809(2), b = 16.177(3), c = 16.374(4) Å, α = 90.42(2), β = 100.19(2), γ = 90.12(2)°, Z = 2, ρ_{calc} = 1.214 g cm^{-3}. The measurements were made

on a Stoe-STADI4 diffractometer ($Mo_{K\alpha}$, $\lambda = 0.71069$ Å; graphite monochromator; $T = 273$ K). From 13681 reflections, 12332 were independent ($3° < 2\theta < 54°$), from which 6386 with $F > 3\sigma(F)$ were regarded as observed. Solution was by direct methods, all non-hydrogen atoms were refined anisotropically to $R = 0.0621$, $R_w = 0.0544$ ($w = 1/\sigma^2$)[21b]. Further details of the crystal structure investigation may be obtained from the Fachinformationszentrum Karlsruhe, Gesellschaft für wissenschaftlich-technische Information GmbH, D-76344 Eggenstein-Leopoldshafen (FRG) on quoting the depository number CSD-400153, the names of the authors, and the journal citation. b) G. M. Sheldrick, SHELX86, SHELX76 Program for crystal structure determination, University of Cambridge, **1986**.

[22] F. Ugozzoli, G. D. Andreetti, *J. Inclusion Phenom. Mol. Recognit. Chem.* **1992**, *13*, 337.

[23] Torsional angles w [°] von **1** · MeC(O)Et: +107, −77, +77, −107, +106, −78, +78, −106, $\Delta w = 30$; of **1** · **3** · 4EtOH: +100, −86, +89, −98, +98, −86, +89, −100, $\Delta w = 14$.

Selective Dehydrogenation of Aldonic and Aldaric Acid with an *R*-Configurated α-Carbon Atom to 2-Oxocarboxylic Acids, and Reduction of the Oxo Group of *N*-Acetylneuraminic Acid with *Proteus mirabilis***

By *Carsten Schinschel* and *Helmut Simon**

Dedicated to Professor Lothar Jaenicke on the occasion of his 70th birthday

Regio- and stereoselective reactions of carbohydrates and their derivatives that proceed without the use of protecting groups are of considerable interest. The key reaction in the synthesis of L-ascorbic acid is, for example, the microbial dehydrogenation of D-sorbitol to L-sorbose by *Acetobacter suboxidans*. We have found that suitably cultivated cells of *Proteus mirabilis* can selectively and quantitatively dehydrogenate an *R*-configurated C- atom in α-position to the carboxylate group of aldonic or aldaric acids to an oxo group.

The sequence of reactions shown in Scheme 1 yielded pent-2-ulosones and hex-2-ulosones from aldonic acids of the pentose and hexose series, respectively. We carried out the reactions on a preparative scale (10 mmol) with resting cells of *P. mirabilis* in 100–200 mM solution without buffer. Even in 500 mM solution D-gulonate was dehydrogenated almost quantitatively. The stable and inexpensive artificial electron acceptor AQDS ($E_0' = -184$ mV) proved useful here.

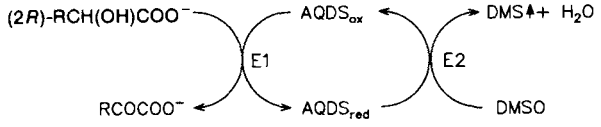

Scheme 1. Enzymatic dehydration of (2*R*)-aldonic and -aldaric acids. E1 = HVOR [(2*R*)-hydroxycarboxylate-viologen oxidoreductase]; AQDS = anthraquinone 2,6-disulfonate, E2 = dimethyl sulfoxide reductase; DMSO = dimethyl sulfoxide; DMS = dimethyl sulfide. (2*S*)-RCH(OH)COO⁻ is not converted and has no inhibitory effect. The R groups can be inferred from Table 1.

The enzyme HVOR(E1) that we found in *P. mirabilis* and *P. vulgaris*[1] dehydrogenates (2*R*)-hydroxycarboxylates and transfers the electrons to AQDS (1 mM). This reagent then donates them to DMSO reductase (E2), which is also present in the cells, and finally reduces DMSO to DMS. Because of its volatility and its low solubility in water, DMS is lost from the system, which is maintained at 38 °C, but can be condensed and reoxidized. By using AQDS concentrations of approximately 200 mM, it is also possible to carry out the reaction with HVOR alone, although the isolation of the oxo acid is more complex by this method. The acids were obtained as their sodium or potassium salts.

A summary of the results is given in Table 1. In all but one case, the microbial reactions proceeded almost quantitatively. Reactions with phosphorylated or glycosylated aldonates also proceeded smoothly, as was demonstrated by the dehydrogenations of 6-phospho-D-gluconate and 4-*O*-(β-D)-galactopyranosido)-D-gluconate (lactobionate). Although the two aldaric acids (Table 1) reacted more slowly than the aldonic acids, the products were obtained in good yield.

Table 1. Isolated pent- and hex-2-ulosonates and 2-oxoaldarates characterized by ^{13}C NMR spectroscopy.

Products	Conversion [%] [a]	Yield of isolated product [%]	δ (^{13}C) of C-2 [b]	PN [c] after 50%/final conversion
Pent- and Hex-2-ulosonates				
L-*erythro*-	≥98	65	102.99/107.02	1040/280
D-*erythro*-	≥99	71	103.01/107.15	1320/690
D-*threo*-	≥99	78	103.76 [d]	1400/270
D-*xylo*-	≥97	95	99.47 [e]	1600/740
D-*lyxo*-	≥99	98	99.67/102.40	4000/650
L-*arabino*-	≥98	88	99.87/102.31	1580/210
D-*arabino*-	≥96	85	99.89/102.33	3100/760
6-phospho-D-*arabino*-	≥99	98	102.35/107.06	1560/250
4-*O*-(β-D-galactopyranosido)-D-*arabino*-	≥99	70	99.82/105.42	1040/480
2-Oxoaldarates				
2-oxo-D-gluc-	≥99	91	103.17/107.49	310/270
2-oxogalact-	79	70	103.71/107.31	280/140

[a] According to HPLC [TEAP = Si 100, 5 μm, 4.6 × 250 mm (Serva Heidelberg), 10% acetonitrile, 20 mM KH_2PO_4/H_3PO_4, pH 3.0–3.2, 1 mL min^{-1}]. [b] 360 MHz, D_2O, pH 7, 25 °C, 3-trimethylsilylpropanesulfonate. The values refer to the ^{13}C NMR signals of C-2 in the α and β form. [c] PN = mmol product per kg biocatalyst and hour [4]. [d] D-*threo*-Pent-2-ulosonate appears to exist in solution at pH 7 not only as a hemiacetal but also to a considerable extent as a lactone. The chemical shift of the α-CO group of the lactone at δ = 85.90 indicates that it may be hydrated. [e] According to the NMR spectrum only one hemiacetal form is found. The product was converted into D-ascorbic acid.

The productivity numbers (PN) vary by up to a factor of four. However, yields are generally very high, even for the more slowly reacting aldonic acids. The PN ratios for 50% conversion and complete conversion also vary. Since the K_m values we determined for various aldonic acids are less than 1 mM, the variation in the PN ratios may be due to differences in the k_{cat} values or to product inhibition. No overoxidation was observed. The products were also isolated in analytically pure form in passable to very good yields (Table 1).

None of the starting materials revealed a peak in the ^{13}C NMR spectrum near $\delta = 100$ (in D_2O), but this signal was present in all the products, and is characteristic of the carbonyl group arising from the dehydrogenation, which is

[*] Prof. Dr. H. Simon, Dr. C. Schinschel
Lehrstuhl für Organische Chemie und Biochemie
der Technischen Universität München
Lichtenbergstrasse 4, D-85747 Garching (FRG)
Telefax: Int. code + (89)3209-3345

[**] This research was supported by the Deutsche Forschungsgemeinschaft (Sonderforschungsbereich 145), BASF AG, and the Fonds der Chemischen Industrie. We thank Dr. H. White for assistance with all cultivation, N. Schmuderer for technical assistance, and Prof. Dr. C. Wandrey, Jülich, for several grams of *N*-acetylneuraminic acid.

present as a hemiacetal.[2] L-Gluconic acid does not fulfill the steric requirements for the reaction with HVOR, and was indeed not transformed.

D-*xylo*-Hex-2-ulosonate, the dehydrogenation product of D-gulonate, was converted to D-ascorbic acid. Its ^{13}C NMR spectrum is identical to that of authentic L-ascorbic acid.

The dehydrogenations described were also carried out with purified HVOR.

The reaction sequence shown in Scheme 1 is also suitable for selective dehydrogenation of the (*R*) enantiomer of racemates.[3] Reductions of 2-oxocarboxylic acids in the carbohydrate series are also effectively possible. Thus, the α-carbonyl group of *N*-acetylneuraminic acid was reduced quantitatively to the hydroxyl group by *P. mirabilis* when formate was used as the reducing agent. The ^{13}C NMR signal at $\delta = 97.99$ disappeared, and a new signal emerged at $\delta = 71.52$. We assume that the resulting product has an (*R*)-configurated α-position, as we have proved in several dozen other cases.[4, 5]

We have recently reported the reduction of numerous other multifunctional 2-oxocarboxylic acids to (2*R*)-hydroxycarboxylic acids and their chemical transformation to a variety of compounds with three chiral centers.[5] From structurally very diverse 2-oxocarboxylic acids it is therefore possible to obtain enantiomerically pure (2*R*)-hydroxycarboxylic acids, from (2*R*)-hydroxycarboxylic acids one may produce 2-oxocarboxylic acids, and from *rac*-2-hydroxycarboxylic acids both the pure (*S*) enantiomers and the 2-oxocarboxylic acids are accessible.

The dehydrogenations shown in Scheme 1 were in principle carried out using the methods previously developed for the preparative synthesis of pyruvate from (*R*)-lactate in up to 650 mM solutions.

Several years ago, the preparation of 2-oxoaldonic acids by catalytic oxidation of aldonic acids was described.[7] The yields in this case reveal a pronounced time optimum, and in most cases, the product contained five or six by-products.

In the transformations described here, specially cultivated *P. mirabilis* cells were used which have $>20\ U\,mg^{-1}$ of HVOR in the crude extract with respect to pyruvate reduction, and approximately $8\ U\,mg^{-1}$ for (*R*) lactate dehydrogenation (1 U produces 1 μmol product per minute).[8] These are exceptionally high values for redox enzymes in crude extracts. The activities are significantly less for the carbohydrate derivatives we studied, but for the transformations described they are nonetheless very useful indeed. In assessing these results, one must take into account that baker's yeast typically reduces keto compounds with productivity numbers of 5–50. Dehydrogenations (i.e. oxidations) with yeast are virtually unknown.

The enzyme present in *P. mirabilis* and *P. vulgaris*, HVOR, reveals by far the broadest substrate range of any 2-hydroxycarboxylate oxidoreductase yet studied. This is true not only for the enzyme substrates, but also for the artificial electron carriers. We have found up to twenty suitable electron carriers, which vary in their standard redox potential by more than 650 mV and therefore allow both quantitative reductions and dehydrogenations (i.e. oxidations).[8] The enzyme is nonetheless completely stereospecific. Till now, this substrate range has not even been nearly matched by any pyridine nucleotide-dependent 2-oxoacid reductase,[9] even after extensive protein engineering.[9, 10] For pyridine nucleotide-dependent redox enzymes, cofactor regeneration is generally more complicated, and quantitative dehydrogenations on a preparative scale are difficult to carry out for thermodynamic reasons. In addition, severe product inhibition often occurs.

Experimental Procedure

Commercially unavailable aldonic acids were synthesized by oxidation of the corresponding aldoses [11].

Preparation of the reaction solution and the dehydrogenation itself were carried out under a nitrogen atmosphere, and the pH of the buffer-free solution was held constant during the reaction with the help of a pH-stat and 2 N sodium hydroxide. The reaction solution consisted of 200 mM substrate as its sodium or potassium salt, 300 mM DMSO, 1 mM AQDS, 5 mM ethylenediaminetetraacetic acetate, and 0.001 mM tetracycline in 50 mL water, and contained 0.8 g (dry weight) of *P. mirabilis* cells. A slow stream of nitrogen was passed through the gently stirred mixture at 38 °C, and the course of the reaction was monitored by high-performance liquid chromatography (HPLC). At the end of the reaction, the pH of the mixture was brought to 3.5 with perchloric acid, the protein precipitate was removed by centrifugation, and the supernatant was treated with active charcoal and filtered. The free acid was isolated by chromatography on a 10 × 210 mm AG-50-W-XB (200–400 mesh) column in the H^+ form (Bio-rad, Munich). The pale yellow solution was then brought to pH 8.0 with sodium or potassium hydroxide and lyophilized. The residue was taken up in 200 mL methanol containing almost 2% water and stirred for one hour. The sparingly soluble sodium or potassium salts were filtered off and washed with methanol and acetone.

D-ascorbic acid was synthesized from D-*xylo*-hex-2-ulosonate as previously described [12].

The reduction of *N*-acetylneuraminic acid to 5-acetylamido-3,5-dideoxy-D-*erythro*-L-manno-nonanoic acid was carried out at 38 °C with *P. mirabilis* instead of *P. vulgaris* as previously reported [5]. The reaction solution consisted of 100 mM substrate as its sodium salt, 100 mM formate, and 1 mM benzylviologen in 40 mL water, and contained 0.2 g (dry weight) of *P. mirabilis* cells. The pH was held constant at 7.0 with 1 N formic acid. Yield 98%.

Received: April 2, 1993 [Z 5969 IE]
German version: *Angew. Chem.* **1993**, *105*, 1221

[1] I. Thanos, J. Bader, H. Günther, S. Neumann, F. Krauss, H. Simon, *Meth. Enzymol.* **1987**, *136*, 302–317; S. Neumann, H. Simon, *FEBS Lett.* **1984**, *167*, 29–32.
[2] E. Breitmaier, G. Haas, W. Voelter, *Atlas of Carbon-13 NMR Data*, Heyden, London, **1979**; J. Wu, A. S. Serianni, *Carbohydr. Res.* **1991**, *210*, 51–70.
[3] We converted *rac*-glycerate, for example, virtually quantitatively into a 1:1 mixture of 3-hydroxypyruvate and (*S*)-glycerate. The analogous reaction with *rac*-(3*E*)-2-hydroxy-4-phenylbutenoate could also be performed, and from the resulting 1:1 mixture of (3*E*)-2-oxo-4-phenylbutenoate and (2*S*,3*E*)-2-hydroxy-4-phenylbutenoate both components could be isolated in pure form (unpublished results).
[4] H. Simon, J. Bader, H. Günther, S. Neumann, J. Thanos, *Angew. Chem.* **1985**, *97*, 541–555; *Angew. Chem. Int. Ed. Engl.* **1985**, *24*, 539–553.
[5] a) A. Schummer, H. Yu, H. Simon, *Tetrahedron* **1991**, *47*, 9019–9034; b) D. Bonnaffé, H. Simon, *ibid.* **1992**, *48*, 9695–9706.
[6] C. Schinschel, H. Simon, *J. Biotechnol.*, in press.
[7] P. C. C. Smits, EP-A 0151498, **1985** (Cl. C 07 H 7/027).
[8] C. Schinschel, H. Simon, *Appl. Microbiol. Biotechnol.* **1993**, *38*, 531–536.
[9] H. K. W. Kallwass, *Enzyme Microb. Technol.* **1992**, *14*, 28–35.
[10] H. K. W. Kallwass, J. K. Hogan, E. L. A. Macfariane, V. Martichonok, W. Parris, C. M. Kay, M. Gold, J. B. Jones, *J. Am. Chem. Soc.* **1992**, *114*, 10704–10710.
[11] S. Moore, K. P. Link, *J. Biol. Chem.* **1940**, *133*, 293–311.
[12] K. Gätzi, T. Reichstein, *Helv. Chim. Acta* **1938**, *21*, 456–463.

A Self-Replicating System from *Three* Starting Materials**

By *Thomas Achilles* and *Günter von Kiedrowski**

Nucleic acid systems capable of self-replicating in the absence of enzymes probably played a key role in the origin of life on earth.[1] The first example for nonenzymatic self-replication was found in the condensation of the complementary trideoxynucleotides $^{Me}CCGp$[2] and $^{HO}CGGp$,[2] which

[*] Prof. Dr. G. von Kiedrowski, Dipl.-Chem. T. Achilles
Institut für Organische Chemie und Biochemie der Universität
Albertstrasse 21, D-79104 Freiburg (FRG)
Telefax: Int. code + (761)203-2815

[**] This work was supported by the Deutsche Forschungsgemeinschaft and the Fonds der Chemischen Industrie.

yields the self-complementary hexadeoxynucleotide template ^{Me}CCGCGGṗ in the presence of 1-(3-dimethylaminopropyl)-3-ethylcarbodiimide (EDC).[3] The product was formed by two reaction pathways, one of which was autocatalytic and described by a rate equation with a reaction order of 1/2 with respect to the template concentration (square root law).[3,4] Substituting the 5′-OH group of ^{HO}CGGṗ with an amino group resulted in a drastic increase of the reaction rates particularly for the autocatalytic reaction path for which the expected parabolic increase of template concentration could be observed.[5]

Meanwhile, a series of self-replicating systems have been reported in which the templates are always formed from two constituents.[6] Other approaches to self-replication of artificial systems have also been developed.[7] However, it was pointed out that in the previous systems selection processes cannot occur and that to study information transfer phenomena, complex systems with three or more starting materials are required.[1a]

Here, we report on self-replication experiments with three starting materials: 5′-methylthiomethyl(MTM)-trideoxynucleotide-3′-phosphate (**A**), 5′-aminodimer-3′-phosphate (**B**), and 5′-amino-2′,5′-dideoxyguanosine-3′-(*o*-chlorophenyl)-phosphate (**C**). These compounds and other model compounds were synthesized by the phosphotriester method in solution.[8] In the presence of EDC and 1-methylimidazole (MeIm), the 3′-phosphate groups of reactants **A** and **B** react with the 5′-amino groups of reactants **B** and **C** to form 3′-5′-phosphoamidate bonds (Fig. 1).[2] The reactions were carried out at 20 °C on a nanomole scale in 1 μL capillaries[9] and were monitored by HPLC on a RPC-18 column.[10] The phosphoamidate products **AB**, **AC**, and **BC** were identified from conversions of pairs of the appropriate reactants. In the reaction of all three of the reactants, the product **ABC** was also detected. **ABC** is formed both from **AB** + **C** and from **A** + **BC**, which causes the concentrations of the intermediates **AB** and **BC** pass through maxima (Fig. 2, left). As neither **AB** nor **BC** is present initially, the rate of formation of **ABC** at the start is zero. The tetramer **AC** is always formed

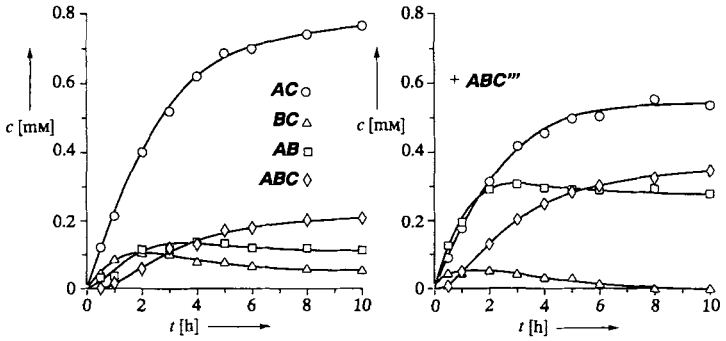

Fig. 2. Left: concentrations as a function of time of the trimer **BC**, the tetramer **AC**, the pentamer **AB**, and the hexamer **ABC** formed from the condensation of **A**, **B**, and **C** in the presence of EDC and 1-methylimidazole [9], as determined by HPLC [10]. Right: the same condensation in the presence of 1 mM of the hexamer template **ABC'''**.

as the major product in this reaction (Fig. 2, left). Most likely, the tetramer **BB** is a further major product which, however, could not be separated from its precursor **B** on RPC-18 columns under a variety of conditions.[11,12]

In order to estimate the amount of **BB** synthesized, the reaction between 5′-azidodimer-3′-phosphate ^{N3}CGp (**B″**) and 5′-aminodimer-3′-(2-phenylthioethyl)phosphate ^{H2N}CGp^{PTE} (**B′**) in the presence of EDC and 1-methylimidazole was examined (model reaction 3, see below). The tetramer **BB′** could be separated from its precursors by HPLC.[12] The conversion reached 30% after four hours;[9] under the same reaction conditions for **B**, the conversion rate of a 2 mM solution should be doubled, as there are two equivalent synthetic pathways leading to **BB**. Analogous model reactions, each with a 5′-protected 3′-phosphate reactant and a 3′-protected 5′-amino reactant were also carried out for the other individual reaction steps [reactions (1) to (7)].[2,9]

$$^{MTM}CCGp\ (\mathbf{A}) + {}^{H2N}CGp^{PTE}\ (\mathbf{B'}) \longrightarrow {}^{MTM}CCGpnCGp^{PTE}\ (\mathbf{AB'}) \quad (1)$$

$$^{MTM}CCGp\ (\mathbf{A}) + {}^{H2N}G\dot{p}\ (\mathbf{C}) \longrightarrow {}^{MTM}CCGpnG\dot{p}\ (\mathbf{AC}) \quad (2)$$

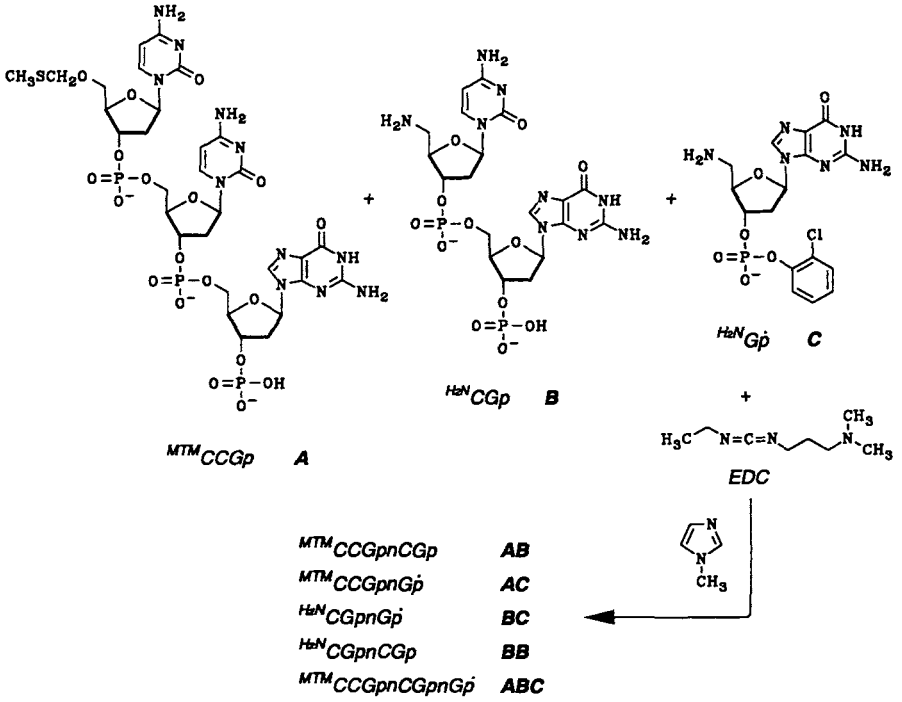

Fig. 1. Overall reaction of the self-replicating system from **A**, **B**, and **C**.

^{N3}CGp (**B''**) + ^{H2N}CGp^{PTE} (**B'**) ⟶ ^{N3}CGpnCGp^{PTE} (**BB'**) (3)

^{N3}CGp (**B''**) + ^{H2N}Gṗ (**C**) ⟶ ^{N3}CGpnGṗ (**BC'**) (4)

^{N3}CGp (**B''**) + ^{H2N}Cṗ (**X**) ⟶ ^{N3}CGpnCṗ (**BX**) (5)

^{HO}CCGCGp (**AB''**) + ^{H2N}Gṗ (**C**) ⟶ ^{HO}CCGCGpnGṗ (**ABC'**) (6)

^{MTM}CCGp (**A**) + ^{H2N}CGGṗ (**BC''**) ⟶ ^{MTM}CCGpnCGGṗ (**ABC''**) (7)

In order to detect possible catalytic, cross-catalytic, or autocatalytic effects (couplings) caused by the products, the condensation reaction between **A**, **B**, and **C**, as well as the above model reactions were followed in the presence of the oligodeoxynucleotides ^{HO}CCGG (**AC'**),[13] ^{HO}CCGCG (**AB'''**),[13] and ^{Me}CCGCGGṗ (**ABC'''**).[2, 3] These oligonucleotides have the same base sequences as the products **AC**, **AB**, and **ABC**, but differ in respect of their backbone and the terminal groups. Investigations into the template-dependent synthesis of ^{MTM}CCGpnCGGṗ from ^{MTM}CCGp and ^{H2N}CGGṗ showed that ^{Me}CCGCGGṗ (**ABC'''**), which has a central 3′-5′-phosphodiester bond, displays the same template properties within the limits of measurement as ^{HO}CCGpnCGGṗ, which has a central 3′-5′-phosphoamidate bond.[5] From this, we assume that **AC'**, **AB''**, and **ABC'''** also have at least similar template properties to **AC**, **AB**, and **ABC**, respectively. In the case of template effects of the products, the observed rates always obey the square root law,[3, 4] that is, the reaction order is 1/2 with respect to the template. To determine the apparent rate constants of the template-dependent and -independent reaction pathways (k_a and k_b, respectively) the initial stage of each experimental concentration–time profile was analyzed by means of the computer program SimFit[6g] on the basis of the reaction model portrayed in reactions (8) and (9). **P** and **N** represent the

P + **N** → **PN** (k_b) (8)

P + **N** + 1/2 **T** → **PN** + 1/2 **T** (k_a) (9)

3′-phosphate and 5′-amino components respectively, **PN** the reaction product, and **T** the template. Provided that **PN** and **T** have the same sequence, the initial concentration of **PN** was taken to be the template concentration, and the sum of the concentrations (**PN** + **T**) was then evaluated. The results of these model studies are summarized in Figure 3 in a semiquantitative fashion.

The template-independent synthesis of the products **PN** can proceed from single-stranded reactants as well as double-stranded complexes between the reactants. Complexes of the type **P** · **N**, **P** · **P**, and **N** · **N** are conceivable. Investigations into the synthesis of hexameric 3′-5′-phosphoamidates from trimeric reactants have shown that a complementary trimer pair—as, for example, in model reaction 7—always react faster than a noncomplementary trimer pair, both in the template-dependent (autocatalytic) and in the template-independent reaction pathways.[14] The enhancement of the template-independent synthetic pathway was explained by the stabilization of the transition state through stacking interactions when two **P** · **N** complexes come together.[14] Thermodynamic data for the formation of complexes of oligonucleotides show that complexes with less than three consecutive CG base pairs are unstable under the reaction conditions and can only exist in very small concentrations.[15] The reactions (4) and (5) should thus represent G-G and G-C couplings in single-stranded reactions: $k_{GG} = 1.8 \times 10^{-2}\ M^{-1}s^{-1}$, $k_{GC} = 0.9 \times 10^{-2}\ M^{-1}s^{-1}$. The model reactions (6) and (7) proceed much faster than (4) and (5), respectively. For these model reactions it must be assumed that double-stranded complexes of the type **P** · **P** and **P** · **N**, containing four and three CG base pairs, respectively, participate in the reaction: $k_b(6) \approx 5 \times k_{GG}$, $k_b(7) \approx 4 \times k_{GC}$. In the case of reaction (6), the assumption of a high population of **P** · **P** complexes is supported by the fact that this reaction is first order with respect to **AB''**, and in addition, that no measurable acceleration by **ABC'''** and **AB'''** can be detected. The synthesis of **ABC'** should proceed within a termolecular complex, in which the pentamer **AB''** functions on the one hand as a reaction partner of **C** and on the other as a template (Fig. 3, dashed line). It should be noted, however, that this template-catalysis by a reactant is not an autocatalytic or a cross-catalytic feedback.

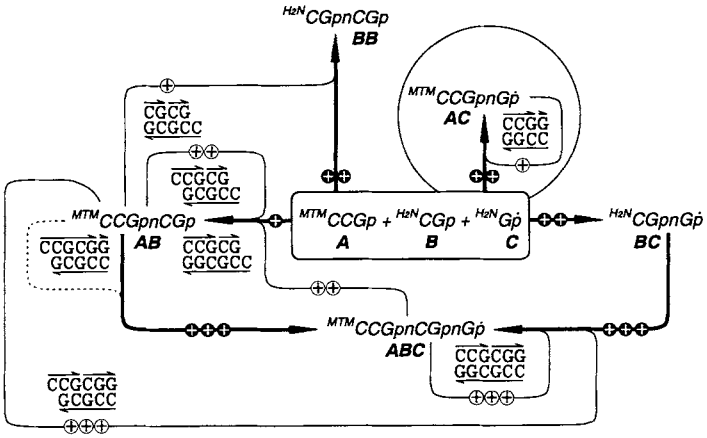

Fig. 3. Reaction scheme of the condensations between **A**, **B**, and **C**. The synthetic pathways to the products are depicted with boldface arrows. The apparent rate constants of the template-independent syntheses are classified as follows (symbols on dark background): ⊕ $k_b < 10^{-2}\ M^{-1}s^{-1}$, ⊕⊕ $10^{-2}\ M^{-1}s^{-1} \le k_b \le 3 \times 10^{-2}\ M^{-1}s^{-1}$, ⊕⊕⊕ $k_b > 3 \times 10^{-2}\ M^{-1}s^{-1}$. The thin lines represent template effects that originate from the templates and lead to the synthetic pathways. The coupling strength (efficiency) of these template effects—as ascertained by using the model templates **AC'**, **AB'''**, and **ABC'''**—are depicted by the quotient $\varepsilon = k_a/k_b$ and are classified as follows (symbols on light background): ⊕ $\varepsilon \le 20\ M^{-1/2}$, ⊕⊕ $20\ M^{-1/2} < \varepsilon < 150\ M^{-1/2}$, ⊕⊕⊕ $\varepsilon \ge 150\ M^{-1/2}$. In the immediate vicinity of the symbols are the relevant termolecular complexes. The arrows above and below the symbols for bases represent the 5′ → 3′ direction. No couplings exist at all between the main product (circled) and the rest of the products. EDC acts as activator.

The whole reaction process of the condensation of **A**, **B**, and **C** can be understood as a catalytic network with a total of six (feedback) couplings (Fig. 3). However, only those couplings with sufficient efficiency (categories ⊕⊕ and ⊕⊕⊕) exert a notable influence. The latter couplings only affect the synthesis of the hexameric template **ABC** and that of its pentameric precursor **AB**, but not the synthesis of the tetrameric main product **AC**. Furthermore, a situation exists where **AB** and **ABC** compete with **AC** to incorporate the common reactants **A** and **C**. If two (noncoupled) self-replicating molecules compete for one or more reactants, the addition of one autocatalyst ought to augment its own synthesis, while the synthesis of the competitor is suppressed. In fact, a comparison of the left and right parts of Figure 2 shows that the formation of the tetramer **AC** decreases in the presence of the hexameric model template **ABC'''**, whereas the autocatalysts **AB** and **ABC** are clearly formed more quickly. Broadly speaking, this finding can be regarded as a first, though very concealed, example of information transfer and selection. A true ("Darwinian") selection process will only be realized in a system in which the autocatalytic growth of the template concentration is exponential rather than parabolic.[1e, 4a, 16]

Received: April 8, 1993 [Z 5988]
German version: *Angew. Chem.* **1993**, *105*, 1225

[1] Recent reviews: a) L. E. Orgel, *Nature* **1992**, *358*, 203–209; b) A. Eschenmoser, E. Loewenthal, *Chem. Soc. Rev.* **1992**, 1–16; c) S. Hoffmann, *Angew. Chem.* **1992**, *104*, 1032–1035; *Angew. Chem. Int. Ed. Engl.* **1992**, *31*, 1013–1016; d) M. Famulok, J. S. Nowick, J. Rebek, *Acta Chem. Scand.* **1992**, *46*, 315–324; e) G. von Kiedrowski, J. Helbing, B. Wlotzka, S. Jordan, M. Matzen, T. Achilles, D. Sievers, A. Terfort, B. C. Kahrs, *Nachr. Chem. Tech. Lab.* **1992**, *40*, 578–588.

[2] Sequence notations principally concern oligodeoxynucleotide derivatives; the prefix d for deoxy is omitted here. Abbreviations: ^{Me} = 5′-*O*-methyl, ^{MTM} = 5′-*O*-methylthiomethyl, ^{N3} = 5′-azido-5′-deoxy, ^{H2N} = 5′-amino-5′-deoxy, ^{HO} = 5′-hydroxy, p = 3′-phosphate, ṗ = 3′-(2-chlorophenyl)-phosphate, p^{PTE} = 3′-(2-phenylthioethyl)phosphate, pn = 3′-5′-phosphoamidate (the sequences, when not otherwise specified, are always in the 5′ → 3′ direction); HPLC = high-performance liquid chromatography, RPC = reversed-phase column.

[3] G. von Kiedrowski, *Angew. Chem.* **1986**, *98*, 932–934; *Angew. Chem. Int. Ed. Engl.* **1986**, *25*, 932–935.

[4] a) For the theory of the square root law and parabolic growth see: G. von Kiedrowski, *Bioorg. Chem. Front.* **1993**, *3*, 113–146. b) Interestingly, parabolic growth is also described in connection with the propagation of computer viruses: J. O. Kephart, S. R. White *Proc 1991 IEEE Computer Soc. Symp. Res. Securacy and Privacy*, IEEE Computer Society, Washington, **1991**, 343–359.

[5] G. von Kiedrowski, B. Wlotzka, J. Helbing, M. Matzen, S. Jordan, *Angew. Chem.* **1991**, *103*, 456–459, 1066; *Angew. Chem. Int. Ed. Engl.* **1991**, *30*, 423–426, 892.

[6] Further self-replicating systems with self-complementary templates from two starting materials: a) W. S. Zielinski, L. E. Orgel, *Nature* **1987**, *327*, 346–347; b) G. von Kiedrowski, B. Wlotzka, J. Helbing, *Angew. Chem.* **1989**, *101*, 1259–1261; *Angew. Chem. Int. Ed. Engl.* **1989**, *28*, 1235–1237; c) T. Tjivikua, P. Ballester, J. Rebek, Jr., *J. Am. Chem. Soc.* **1990**, *112*, 1249–1250; d) J. S. Nowick, Q. Feng, T. Tjivikua, P. Ballester, J. Rebek, Jr., *ibid.* **1991**, *113*, 8831–8839; e) J.-I. Hong, Q. Feng, V. Rotello, J. Rebek, *Science* **1992**, *255*, 848–850; f) Q. Feng, T. K. Park, J. Rebek, *ibid.* **1992**, *256*, 1179–1180; g) A. Terfort, G. von Kiedrowski, *Angew. Chem.* **1992**, *104*, 626–628; *Angew. Chem. Int. Ed. Engl.* **1992**, *31*, 654–656. Related examples: h) W. S. Zielinski, L. E. Orgel, *J. Mol. Evol.* **1989**, *29*, 281–283; i) K. E. Ng, L. E. Orgel, *ibid.* **1989**, *29*, 101–107; j) J. T. Goodwin, D. G. Lynn, *J. Am. Chem. Soc.* **1992**, *114*, 9197–9198; k) F. Persico, J. D. Wuest, *J. Org. Chem.* **1993**, *58*, 95.

[7] Other systems: Self-replicating micelles: a) P. A. Bachmann, P. Walde, P. L. Luisi, J. Lang, *J. Am. Chem. Soc.* **1990**, *112*, 8200–8201; b) P. A. Bachmann, P. L. Luisi, J. Lang, *Nature* **1992**, *357*, 57–59. En route to self-replicating ribozymes: c) J. A. Doudna, J. W. Szostak, *ibid.* **1989**, *339*, 519; d) J. A. Doudna, J. Couture, J. W. Szostak, *Science* **1991**, *251*, 1605–1610. e) For self-replicating algorithms, see articles in *Artificial Life. The Proceedings of an Interdisciplinary Workshop on the Synthesis and Simulation of Living Systems Held September, 1987 in Los Alamos, New Mexico* (Ed.: C. G. Langton), Addison-Wesley, Redwood City, USA, **1989**; f) J. A. Reggia, S. L. Armentrout, H.-H. Chou, Y. Peng, *Science* **1993**, *259*, 1282–1287.

[8] a) J. Helbing, Dissertation, Göttingen, **1990**; b) T. Achilles, G. von Kiedrowski, unpublished; c) synthesis method employed: V. A. Efimov, O. G. Chakhmakhcheva, Y. A. Ovchinnikov, *Nuclic Acids Res.* **1985**, *13*, 3651–3670.

[9] The following standard conditions were chosen for all described reactions: T = 20 °C; 0.2 M EDC; 0.1 M MeIm/pH 7.2; reactant concentrations: 2 mM.

[10] Nucleosil C18, 4 × 250 mm; A: 0.1 M sodium hydrogen carbonate, B: acetonitrile/water 30:70 (v/v); flow rate 1 mL min^{-1}; gradient (B): 18%–28% in 5 min, 28%–42% in 2 min, 42%–50% in 4 min, 50%–75% in 2.5 min, and 0.5 min 75%; detection at λ = 254 nm.

[11] As trace products in the conversion of (**A** + **B** + **C**), all possible oligomerization products of the type $\mathbf{B}_n$, $\mathbf{AB}_n$, $\mathbf{B}_n\mathbf{C}$, and $\mathbf{AB}_n\mathbf{C}$ are assumed ($n > 1$), because each amino reactant ($\mathbf{B}_n$, $\mathbf{B}_n\mathbf{C}$) can in principle be condensed with each 3′-terminal phosphate reactant ($\mathbf{AB}_n$, $\mathbf{B}_n$) to give the corresponding 3′,5′-phosphoamidate. However, with the exception of **ABC**, higher condensation products could not be reliably identified in the HPLC profile.

[12] The elution behavior of the nucleotide reactants on C18 is determined mainly by the terminal groups. Compounds with polar termini, for example **B** and **BB**, elute immediately and hence cannot be separated.

[13] **AC′**, **AB″** and **AB‴** were prepared by solid-phase synthesis (phosphoamidite method). The formation of phosphodiesters between 3′-phosphates and the terminal hydroxy groups of these templates is negligible under the reaction conditions; the templates can be regarded as inert.

[14] B. Wlotzka, Dissertation, Göttingen, **1992**.

[15] a) S. M. Freier, A. Sinclair, T. Neilson, D. H. Turner, *J. Mol. Biol.* **1985**, *185*, 645–648; b) K. H. Breslauer, R. Frank, H. Blöcker, L. A. Marky, *Proc. Natl. Acad. Sci. USA* **1986**, *83*, 3746–3749.

[16] E. Szathmáry, I. Gladkih, *J. Theor. Biol.* **1989**, *138*, 55–58.

Metallomesogens with a Cholesteric Mesophase**

By *Maria J. Baena, Julio Buey, Pablo Espinet,* Heinz-S. Kitzerow*, and *Gerd Heppke*

Metallomesogens, liquid crystals containing coordinated metal atoms, have seen a rapid development in the last few years.[1] In a very short period metallomesogens displaying almost every mesophase previously found in organic mesogens—calamitic (nematic and smectic phases), discotic, polymeric, and amphiphilic phases—have been reported. Rather surprisingly, chiral metallomesogens are scarce; only one material displaying a chiral smectic C mesophase (and hence ferroelectric) had been reported[2] until very recently, when two paramagnetic chiral smectic C metallomesogens were described.[3] There is no representative of the chiral nematic (cholesteric, Ch) mesophase. We report here the first metallomesogens displaying cholesteric behavior, which have been obtained within the now-large family of metallomesogens derived from *ortho*-palladated imines and azines.[2, 4]

p-$C_6H_{13}O$–C_6H_4–CH=N–C_6H_4–OC_6H_{13}-p **1**

Imine **1** reacts with $Pd(OAc)_2$ in acetic acid (50 °C, overnight) to give complex **2a** (X = OAc) which shows no mesogenic behavior (crystalline/217 °C/isotropic) (Scheme 1).[5] Treatment of **2a** in CH_2Cl_2 with HCl (Pd/HCl = 1/1) affords **2b** (X = Cl) (crystalline/176 °C/S_A/247 °C/isotropic) which, on treatment with (*R*)-$KO_2CCHClMe$ in CH_2Cl_2/acetone (1/1), yields complex **3** (crystalline/152 °C/S_A/186 °C/isotropic/203 °C/S_A'/224 °C/isotropic). All the complexes gave satisfactory C,H,N-analyses. The mesogenic behavior of the planar complex **2b** and the nonmesogenic behavior of the folded compound **2a** are to be expected from our previous results,[2, 4] but the meso-

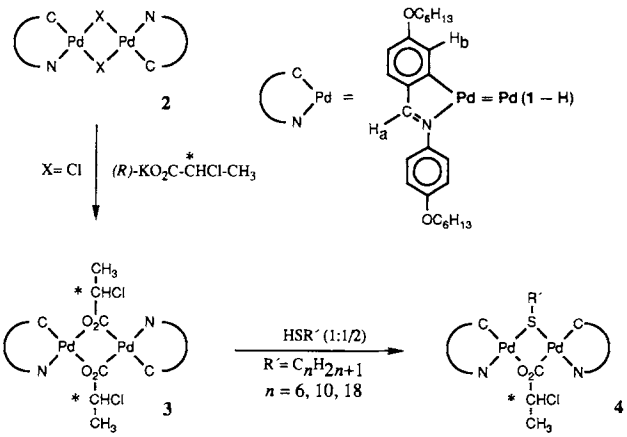

Scheme 1. **2a**: X = OAc; **2b**: X = Cl.

[*] Prof. Dr. P. Espinet, Dr. M. J. Baena, J. Buey
Departamento de Química Inorgánica
Facultad de Ciencias
Universidad de Valladolid, E-47005 Valladolid (Spain)
Telefax: Int. code + (83)423-013

Dr. H.-S. Kitzerow, Prof. Dr. G. Heppke,
Technische Universität Berlin -ER 11-
Strasse des 17. Juni 135, D-10623 Berlin (FRG)

[**] This work was supported by the Comisión Interministerial de Ciencia y Tecnología (Project MAT90-0325), the Consejería de Cultura de la Junta de Castilla y León, Iberdrola, (stipend for M. J. B.), and the Deutsche Forschungsgemeinschaft (SFB 335).

genic behavior of the folded complex **3** is unexpected and remarkable. We had expected that the 2-chloropropionato ligand, which is bulkier than the acetato ligand, would disturb the molecular packing and hinder mesogenic behavior more; however, the dipole moment introduced with the C–Cl bond apparently increases the strength of the intermolecular interactions enough to compensate for the unfavorable steric effect, and **3** is indeed mesomorphic. The compound is also remarkable for its double-melting behavior.[6]

Treatment of **3** with mercaptans HSC_nH_{2n+1} (Pd/HSR = 2/1) produces the mixed-bridge compounds **4** (**4a**: $n = 6$; **4b**: $n = 10$; **4c**: $n = 18$). The complexes gave satisfactory C,H,N-analyses; molecular weight determinations in $CHCl_3$ and ^1H NMR spectra are also consistent with a bridged dinuclear compound. We discuss only the data obtained for **4a**; the results for **4b** and **4c** are similar. The easily observable signals for H_a ($\delta = 7.83$, s) and H_b ($\delta = 7.49$ d, $J = 2.34$ Hz) indicate a unique *cis* arrangement of the two imine moieties in the complex.[7] In contrast, the chloro- and carboxylato-bridged complexes **2** and **3**, respectively, have *trans* structures. To the best of our knowledge bridged dimers with *ortho*-palladated ligands either have *trans* structures (and hence have no net dipole moment) or are mixtures of *trans* and *cis* isomers, in which the latter is typically the very minor component. The carboxylato/thiolato bridges of the compounds described here seem to force a *cis* arrangement. This is particularly interesting in view of possible applications of these compounds as frequency doublers in nonlinear optics, where a net dipole moment is required.[8]

All three compounds **4a–4c** show a cholesteric mesophase in a certain range of temperatures (**4a**: crystalline/140 °C/cholesteric/157 °C/isotropic; **4b**: crystalline/109.5 °C/S_A/115.2 °C/cholesteric/137.6 °C/isotropic; **4c**: crystalline/92 °C/S_A/128.3 °C/cholesteric/131.7 °C/isotropic). In order to characterize their chirality in mesophase conditions,[9] we measured the pitch of the cholesteric phase induced by **4a** and **4c** in mixtures of the respective chiral metallomesogen and RO-TN 404 (a commercial, wide-range nematic solvent from Hoffmann-La Roche, containing cyano-substituted biphenyls and pyrimidine derivatives), by applying the Grandjean–Cano method.[10]

The cholesteric mixtures show a temperature dependence of the pitch p which is characterized by a divergence of p and an inversion of the helical screw sense with changing temperature (Fig. 1). At low temperatures we found a right-handed cholesteric helix ($p > 0$), at high temperatures a left-handed one ($p < 0$). Similar inversions of the helical pitch have been previously reported in organic systems.[11–14] The induced chirality can be described by the helical twisting power $k = p^{-1}c^{-1}$, which is independent on the concentration c of the chiral compound for most substances. From the temperature dependence of this quantity (Fig. 2) the inversion temperatures $T_i = 89.8$ °C for compound **4a** and $T_i = 100.4$ °C (extrapolated) for compound **4c** are obtained.

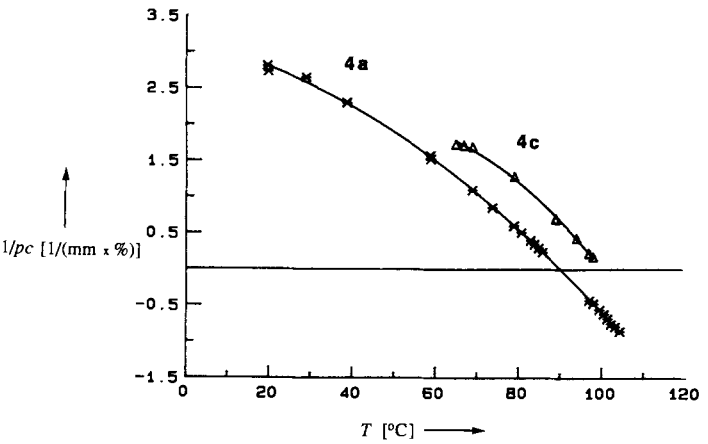

Fig. 2. Temperature dependence of the helical twisting power for **4a** and **4c** (p = cholesteric helical pitch, c = concentration of the chiral compound in wt%).

The relationship between the unusual temperature dependence of the pitch of the cholesteric helix and the chemical structure of the new mesogens calls to mind earlier investigations on mesogenic esters of (*S*)-1,2-propanediol and (*R,R*)-2,3-butanediol which also show a helix inversion.[12] Like compounds **4a–4c**, the structure of these esters is characterized by two large mesogenic groups that are connected to each other. It was proposed that the inversion effect is due to the presence of two conformers, which induce cholesteric structures with opposing helical screw senses, and which are in temperature-dependent thermodynamic equilibrium. The observations presented here seem to confirm that molecules containing two mesogenic wings tend to favor helix inversion. However, it should be noted that twist inversion has also been observed in compounds exhibiting a different type of structure.[13, 14]

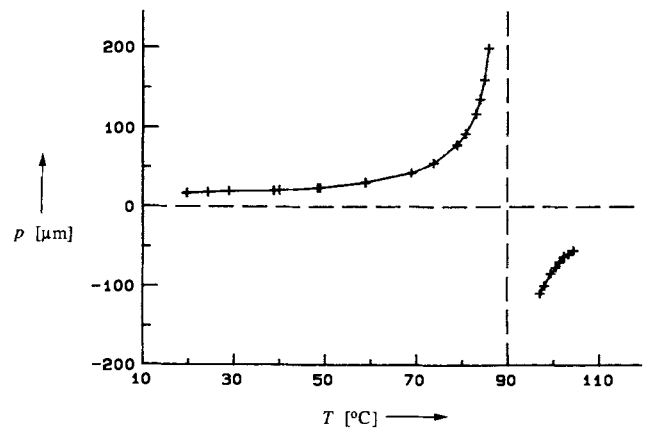

Fig. 1. Temperature dependence of the cholesteric pitch p for a mixture of 21.2 wt% of **4a** and 78.8 wt% of the commmercial nematic solvent RO-TN 404.

Received: November 27, 1992,
Revised version: February 11, 1993 [Z 5707 IE]
German version: *Angew. Chem.* **1993**, *105*, 1238

[1] Reviews: A. M. Giroud-Godquin, P. M. Maitlis, *Angew. Chem.* **1991**, *103*, 370; *Angew. Chem. Int. Ed. Engl.* **1991**, *30*, 375; P. Espinet, M. A. Esteruelas, L. A. Oro, J. L. Serrano, E. Sola, *Coord. Chem. Rev.* **1992**, *117*, 215; *Inorganic Materials* (Eds.: D. Bruce, D. O'Hare), Wiley, New York, **1992**.
[2] P. Espinet, J. Etxebarría, M. Marcos, J. Pérez, A. Remón, J. L. Serrano, *Angew. Chem.* **1989**, *101*, 1076; *Angew. Chem. Int. Ed. Engl.* **1989**, *28*, 1065.
[3] M. Marcos, J. L. Serrano, T. Sierra, M. J. Giménez, *Angew. Chem.* **1992**, *104*, 1523; *Angew. Chem. Int. Ed. Engl.* **1992**, *31*, 1471.
[4] J. Barberá, P. Espinet, E. Lalinde, M. Marcos, J. L. Serrano, *Liq. Cryst.* **1987**, *2*, 833; P. Espinet, E. Lalinde, M. Marcos, J. Pérez, J. L. Serrano, *Organometallics* **1990**, *9*, 555; P. Espinet, J. Pérez, M. Marcos, M. B. Ros, J. L. Serrano, J. Barberá, A. M. Levelut, *ibid.* **1990**, *9*, 2028; M. B. Ros, N. Ruiz, J. L. Serrano, P. Espinet, *Liq. Cryst.* **1991**, *9*, 77; M. J. Baena, P. Espinet, M. B. Ros, J. L. Serrano, *Angew. Chem.* **1991**, *103*, 716; *Angew. Chem. Int. Ed. Engl.* **1991**, *30*, 711.
[5] The phases observed were characterized with a polarizing microscope; the abbreviation S_A that appears later in the text refers to a smectic A phase characterized by an untilted, liquid-crystalline layer structure.

[6] Other examples of compounds with double-melting behavior: K. Ohta, M. Yokohama, S. Kusabayashi, H. Mikawa, *J. Chem. Soc. Chem. Commun.* **1980**, 392; K. Ohta, H. Muroki, K. I. Hatada, I. Yamamoto, K. Matsuzaki, *Mol. Cryst. Liq. Cryst.* **1985**, *130*, 249; K. Ohta, H. Muroki, K. I. Hatada, A. Takagi, H. Ema, I. Yamamoto, K. Matsuzaki, *ibid.* **1986**, *140*, 163; K. Ohta, H. Ema, H. Muroki, I. Yamamoto, K. Matsuzaki, *ibid.* **1987**, *147*, 61.

[7] The nonequivalence of the two halves of the dimer caused by the chiral center becomes apparent only at $-20\,^{\circ}C$ in the ^1H NMR spectrum: at this temperature the two nonequivalent H_a atoms give rise to two very close but distinct singlets.

[8] Modified complexes of type **4** have been measured, and frequency doubling was observed: J. Zyss, I. Ledoux, J. Martín, J. Buey, P. Espinet, unpublished.

[9] $[\alpha]_D^{20}$ of the complexes ($c = 1$, CH_2Cl_2): **4a**, -8.8; **4b**, -8.0; **4c**, -7.7.

[10] R. Cano, *Bull. Soc. Fr. Mineral. Cristallogr.* **1967**, *90*, 333. Cholesteric mixtures containing about 20 wt% of the chiral additive were placed between a flat glass slide and a spherical lens. Both surfaces were rubbed to provide a uniform planar anchoring. The disclination rings in the sample, which correspond to steps of $p/2$, were observed using a polarizing microscope. The pitch p was calculated from the diameters of these rings.

[11] H. Finkelmann, H. Stegemeyer, *Z. Naturforsch. A* **1973**, *28*, 799.

[12] G. Heppke, D. Lötzsch, F. Oestreicher, *Z. Naturforsch. A* **1987**, *42*, 279.

[13] L. Komitov, S. T. Lagerwall, B. Stebler, G. Anderson, K. Flatiscler, *Ferroelectrics* **1991**, *114*, 167.

[14] A. J. Slaney, I. Nishiyama, P. Styring, J. W. Goodby, *J. Mater. Chem.* **1992**, *2*, 805.

Improved Properties of Ferroelectric Liquid Crystals from Palladium β-Diketone Complexes**

By *María Jesús Baena, Pablo Espinet,* María Blanca Ros, José Luis Serrano,** and *Amaya Ezcurra*

Ferroelectric liquid crystals (FLCs)[1] are one of the main interests in research on liquid crystals. Although many organic mesogens are known for FLCs, there are few examples of analogous metal complexes[2, 3] and most of them have high transition temperatures that affect their thermal stability. The first FLC metallomesogen reported,[2] a dimeric *ortho*-palladated azine complex (a mixture of isomers), displayed some undesirable drawbacks: high transition temperatures (K 102 °C SmC* 119 °C SmA 149 °C I) leading to thermal instability in the mesophases and a very long switching time (nearly one second). We then discovered that altering the highly symmetrical molecular shape of these dimers results in lower melting points.[4] Whereas dimeric compounds $[\{(C\text{-}N)PdCl\}_2]$ (C-N = *ortho*-palladated imine with long alkyl chains) form SmA and SmC phases at high temperatures,[5] monomeric complexes [(C-N)Pd(acac)] form N and SmA phases at noticeably lower temperatures. Thus the monomeric complexes may be taken repeatedly to the isotropic state without signs of decomposition.[4]

Taking these two observations into account, we aimed to synthesize ferroelectric metallomesogens with low transition temperatures, which would allow potential applications as both liquid crystals and in nonlinear optics.[6] Our first approach was the introduction of chirality in the alkyl chains of the above-mentioned acac complexes,[4] but this did not lead to the desired SmC* phases. However, analogues **3a** ($n = 10$) and **3b** ($n = 14$) with modified β-diketonate ligands formed a ferroelectric SmC* liquid crystalline phase at lower temperatures, showed thermal stability under working conditions, and displayed switching times a *thousand times shorter* than that of the first ferroelectric metallomesogen described.[2]

The synthesis of compounds **3** from **1** (Scheme 1) proceeded via the dinuclear complexes **2**. The reaction of **2a, b**[5] with thallium(I) β-diketonate[7] in CH_2Cl_2 provided the mononuclear complexes **3a** and **3b**, respectively. Both complexes gave correct elemental analyses, and ^1H NMR and IR spectra in full agreement with the structure proposed.

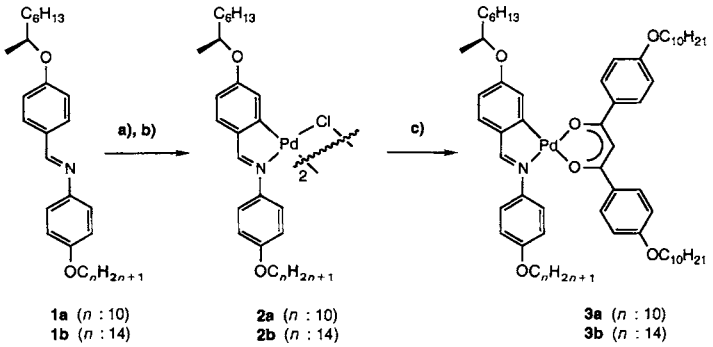

Scheme 1. a) $Pd_3(AcO)_6$/AcOH; b) HCl/MeOH; c) Tl [*p*-$H_{21}C_{10}OC_6H_4CO)_2$-CH]/CH_2Cl_2.

The thermotropic behavior of the β-diketonate derivatives was studied by optical microscopy and differential scanning calorimetry (DSC) at 10 K min^{-1} (Table 1). Smectic A and chiral smectic C phases were assigned on the basis of their optical textures and confirmed by X-ray diffraction studies. The chiral smectic C phase showed a characteristic focal-conic texture, and no dechiralization lines were observed. The ferroelectric properties of these two β-diketonate complexes—spontaneous polarizations (P_s), switching times (τ_E), viscosities (γ_c), and tilt angles (θ)—are summarized in Table 1.[8] Figure 1 shows the dependence of P_s and θ of the ferroelectric palladium complexes on temperature.

These metallomesogens have moderate P_s values with maxima at 29 and 22 nC cm^{-2} for **3a** and **3b** respectively, and maximum optical tilt angles very close to the optimum tilt angle in FLCs of 22.5°. It is noteworthy that the tilt angles could not be calculated from the X-ray diffraction measurements, as no significant differences between the layer thickness at the SmA and SmC* phases were detected.[10]

The switching times of the new ferroelectric palladium complexes **3a, b** are on the order of milliseconds. Although this is noticeably slower than the switching times of typical organic FLCs (microseconds), these new complexes switch three orders of magnitude faster than the first palladium

[*] Dr. P. Espinet, M. J. Baena
Química Inorgánica, Facultad de Ciencias
Universidad de Valladolid
E-47005 Valladolid (Spain)
Telefax: Int. code + (83)423-013
Dr. J. L. Serrano, Dr. M. B. Ros
Química Orgánica, Facultad de Ciencias-I.C.M.A.
Universidad de Zaragoza-C.S.I.C.
E-50009 Zaragoza (Spain)
Telefax: Int. code + (76)56 7920
Dr. A. Ezcurra
Física Aplicada II, Facultad de Ciencias
Universidad del País Vasco, Aptdo. 644
E-48080 Bilbao (Spain)

[**] This work was financed by the Comisión Interministerial de Ciencia y Tecnología (Projects MAT90-0325, MAT90-0813, and MAT91-0962CO2-01) and the Consejería de Cultura de la Junta de Castilla y León. M. J. B. thanks Iberduero for a fellowship. We thank Dr. J. Barberá for the X-ray measurements and M. M. Zurbano for supplying the β-diketone. – Abbreviations: C = crystalline, SmC* = chiral smectic C phase, SmA = smectic A phase, I = isotropic, N = nematic, FLC = ferroelectric liquid crystal.

Table 1. Phase transition data and ferroelectric properties of complexes **3**.

Complex	Transition [a]	T [°C] (ΔH [kJ mol^{-1}])	P_s (max) [nC cm^{-2}]	τ_E [b] [μs V μm^{-1}]	[Pa s]	θ [b] [°]	$P_s/\sin\theta$ [b] [nC cm^{-2}]
(*S*)-**3a**	K-SmA	114.4	−29	984	0.120	21.3	−59
	SmA-I	118.4 (29.67) [c]					
	I-SmA	118.2 (−4.66)					
	SmA-SmC* [d]	110.8 (−0.27)					
	SmC*-K	88.7 (−17.53)					
(*S*)-**3b**	K-I	110.9 (26.84)	−22	1596	0.185	21.5	−55
	I-SmA	110.3 (−4.55)					
	SmA-SmC* [d]	99.2 (−0.16)					
	SmC*-K	85.1 (−17.63)					

[a] See footnote[**]. [b] Data measured at $T_c - T = 10$ °C (T_c: SmA–SmC* transition temperature determined by DSC). [c] Combined enthalpies. [d] Monotropic transition.

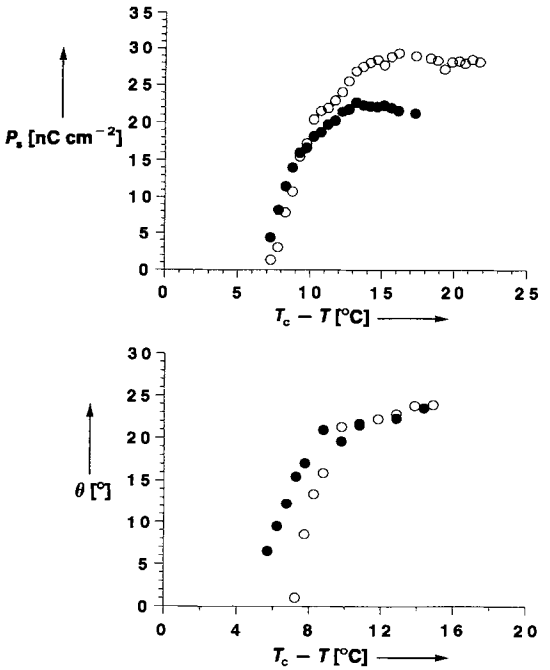

Fig. 1. Temperature dependence of the spontaneous polarization P_s and tilt angle θ of complexes **3a** (○) and **3b** (●). T_c is the temperature of the SmA–SmC* transition determined by DSC.

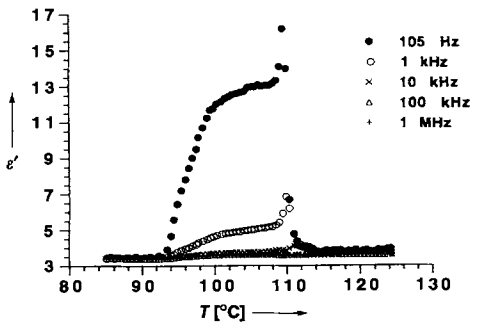

Fig. 2. Temperature dependence of the dielectric permitivity ε′ of compound **3a** at different frequencies.

Table 2. Ferroelectric properties of the binary mixtures of the chiral imines **2** [a].

Cmpd.	T [°C] [b]	P_s [nC cm^{-2}]	P_s (ext) [nC cm^{-2}]	$\theta(T)$ [°C]	P_s (ext)/sinθ (T)
(*S*)-**1a**	57.0	−5.5 [c]	−33	25.4	77
(*S*)-**1b**	58.7	−3.5 [c]	−24	21.8	64

[a] 15% binary mixture of **1** [14]. [b] $T = T_c - 10$ °C (T_c = SmA–SmC* transition temperature determined by optical microscopy). [c] Maximum value.

complex described,[2] and are even faster than polymeric FLCs[11] and in the range of FLCs from dimeric organic compounds.[12]

The dielectric behavior of **3a, b** was also studied at different frequencies (Fig. 2) by using a method described elsewhere.[9a, 13] The SmC* phase is characterized, as usual, by an additional contribution to ε', which is mainly due to the helical structure. This additional contribution decreases and finally disappears when the frequency increases, as the responsible mechanism relaxes.

It is worth noting that none of the Schiff bases used as ligands are liquid crystals (**1a**, C-I 60.3 °C and **1b**, C-I 44.3 °C). The ferroelectric behavior of these chiral organic compounds was evaluated in 15% binary mixtures[14] in which the SmC* phase was induced. As can be seen in Table 2, the $P_s/\sin\theta$ values extrapolated to 100% **1a** and **1b** are 77 and 64 nC cm^{-2}, respectively, at temperatures 10 K below the SmA–SmC* transition of the corresponding binary mixture.

If we compare the $P_s/\sin\theta$ values of compounds **1** and **3** (data independent of T), it seems that the P_s values of the chiral organic ligands slightly decrease on complexation. However, since complexation leads to dramatic structural changes, which undoubtedly modify the arrangement of the molecular dipoles at the SmC* mesophase, this may be a misleading effect and further studies will be needed before any conclusions about the effect of the metal atom can be reached.

Experimental Procedure

3a, b: To a stirred solution of the corresponding dimeric complex **2** (0.05 mmol) in 20 mL of CH_2Cl_2 was added a stoichiometric amount of thallium β-diketonate. A white precipitate of TlCl immediately formed. After stirring at room temperature for 1 h, the precipitate was filtered off and the solution was filtered through a 20-cm silicagel column using CH_2Cl_2 as an eluent. The resulting solution was concentrated to dryness, and the residue was triturated in a mixture of acetone/ethanol (1/3) to obtain a yellow solid, which was filtered and washed with ethanol. Complexes **3a** and **3b** gave correct elemental analyses. Representative spectroscopic data of the palladium complexes: **3a** IR (Nujol), $\tilde{\nu}$[cm^{-1}] = 1608(C=N), 1591 (C=O), 1544 (C=C), 1254 (C-O), 1023 (C-O); ^{1}H NMR (300 MHz, $CDCl_3$): δ = 0.83–0.95 (m, 12H, CH_3), 1.24–1.60 (m, 50H, CH_2), 1.39 (d, 3H, J(H,H) = 6.0 Hz, CH_3), 1.72–1.90 (m, 8H, CH_2), 3.9–4.0 (m, 6H, CH_2), 4.59 (m, 1H, CH), 6.60 (dd, 1H, J(H,H) = 8.24 Hz, J(H,H) = 2.40 Hz, CH), 6.61 (s, 1H, CH), 6.79 (d, 2H, J(H,H) = 8.97 Hz, CH), 6.90 (d, 2H, J(H,H) = 8.97 Hz, CH), 6.93 (d, 2H, J(H,H) = 8.97 Hz, CH), 7.29 (d, 1H, CH), 7.31 (d, 2H, J(H,H) = 8.79 Hz, CH), 7.42 (d, 2H, J(H,H) = 8.79 Hz, CH), 7.71 (d, 2H, J(H,H) = 8.79 Hz, CH), 7.97 (d, 2H, J(H,H) = 8.97 Hz, CH), 7.99 (s, 1H, CH).

Received: February 9, 1993 [Z 5858 IE]
German version: *Angew. Chem.* **1993**, *105*, 1260

[1] For an introduction to FLCs see: S. T. Lagerwall, B. Otterholm, K. Skarp, *Mol. Cryst. Liq. Cryst.* **1987**, *152*, 503; L. A. Beresnev, L. M. Blinov, M. A. Osipov, S. A. Pikin, *ibid.* **1988**, *158A*, 3; D. M. Walba, *Adv. Synth. React. Solids* **1991**, *1*, 173; L. A. Beresnev, S. A. Pikin, W. Hasse, *Condens. Matter News* **1992**, *1*, 13.

[2] P. Espinet, J. Etxebarría, M. Marcos, J. Pérez, A. Remón, J. L. Serrano, *Angew. Chem.* **1989**, *101*, 1076; *Angew. Chem. Int. Ed. Engl.* **1989**, *28*, 1065. Review on metallomesogens: A. M. Giroud-Godquin, P. M. Maitlis, *Angew. Chem.* **1991**, 103, 370–398; *Angew. Chem. Int. Ed. Engl.* **1991**, *30*, 375.

[3] M. Marcos, J. L. Serrano, T. Sierra, M. J. Giménez, *Angew. Chem.* **1992**, *104*, 1523; *Angew. Chem. Int. Ed. Engl.* **1992**, *31*, 1471.

[4] M. J. Baena, P. Espinet, M. B. Ros, J. L. Serrano, *Angew. Chem.* **1991**, *103*, 716; *Angew. Chem. Int. Ed. Engl.* **1991**, *30*, 711.

[5] J. Barberá, P. Espinet, E. Lalinde, M. Marcos, J. L. Serrano, *Liq. Cryst.* **1987**, *2*, 833.

[6] D. Walba, M. B. Ros, N. A. Clark, R. Shao, M. G. Robinson, J.-Y. Liu, K. Johnson, D. Doroski, *J. Am. Chem. Soc.* **1991**, *113*, 5471, and references therein.

[7] J. Barberá, C. Cativiela, J. L. Serrano, M. M. Zurbano, *Adv. Mater.* **1991**, *3*, 602.

[8] P_s, τ_E and γ were measured simultaneously using the triangular-wave method [9] with cells of 10 μm thickness and polyimide-coated indium tin oxide electrodes. For these measurements fields of 50 Hz and peak-to-peak voltages of 30–40 V were used. The optical evaluations were performed using the same cell and sample and applying electrical fields of 30 V.

[9] a) K. Miyasato, S. Abe, H. Takezoe, A. Fukuda, E. Kuze, *Jpn. J. Appl. Phys.* **1983**, *22*, 661; b) M. R. De la Fuente, A. Ezkurra, M. A. Pérez-Jubindo, J. Zubía, *Liq. Cryst.* **1990**, *7*, 51.

[10] R. Bartolino, J. Doucet, G. Durand, *Ann. Phys.* **1978**, *3*, 389; R. Halfon, E. N. Keller, E. Nachatiel, D. Davidov, C. Escher, *Ferroelectrics* **1991**, *114*, 354.

[11] M. Dumon, H. T. Nguyen, M. Mauzac, C. Destrade, M. F. Achard, H. Gasparoux, *Macromolecules* **1990**, *23*, 355; H. Poths, A. Schonfeld, R. Zentel, F. Kremer, K. Siemensmeyer, *Adv. Mater.* **1992**, *4*, 351.

[12] M. Marcos, A. Omenat, J. L. Serrano, T. Sierra, A. Ezcurra, *Adv. Mater.* **1992**, *4*, 285.

[13] M. A. Pérez-Jubindo, A. Ezcurra, M. R. de la Fuente, C. Santamaría, J. Etxebarría, J. L. Serrano, M. Marcos, *Ferroelectrics* **1988**, *81*, 405.

[14] Achiral host: 4-hexyloxyphenyl-4′-decyloxybenzoate, K 62.5 °C/SmC 78.2 °C/SmA 84.5 °C/N 90.5 °C/I.

1,3-Bis(triphenylphosphoranylidene)allene and Tribenzyl(4-methyldiphenylphosphoniobutadiynyl)borate, Stabilized C_3 and C_4: Confirmation of a Hypothesis

By *Hans Jürgen Bestmann,* Dariusch Hadawi, Harald Behl, Matthias Bremer,* and *Frank Hampel*

Different hypotheses have been put forth for the formation of fullerenes. According to one proposal, for example, small carbon units arise from C_1 and grow into long chains, which in turn then form rings.[1, 2] The fragmentation of fullerenes apparently proceeds by the continuous cleavage of C_2 units.[3] C_3 is found in interstellar space.[4] The chemical reactivity of short-lived C_1, C_2, C_3, and C_4 is being investigated in particular by Skell et al.[5] The question of whether these small, highly reactive species can be stabilized can be answered as follows:[6] In hexaphenylcarbodiphosphorane **1**, a compound known for many years, a C_1 unit is stabilized by two triphenylphosphane donor molecules.[7] In complex **2**, which has a betaine structure, stabilized C_2 was prepared by attaching a donor molecule (tertiary phosphane) to one C atom and an acceptor molecule (borane) to the other C atom.[6] We postulated[6] that C_3 should also be stabilized by two donor molecules in **3** and C_4 with a donor molecule and an acceptor molecule at either end of the C_4 chain as in **4**. We report here on our verification of this postulate.

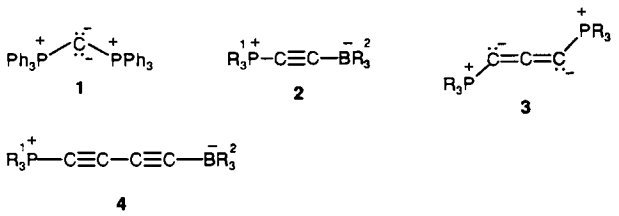

1 **2** **3**

4

A compound of type **4** could be prepared quite easily, since its synthesis follows that of **2**. Treatment of diacetylene **5**[8] with ethylmagnesium bromide (**6**) provided the Grignard compound **7**, which was allowed to react with chlorodiphenylphosphane (**8**) to give the light-sensitive butadiynyldiphenylphosphane (**9**).[9, 10] The reaction of **9** with butyllithium (**10**) in THF provided the corresponding Li compound **11**,[11] which was converted into the borate complex **13** by treatment with tribenzylborane (**12**).[12] The reaction of **13** with methyl iodide led to the desired product, tribenzyl(4-methyldiphenylphosphoniobutadiynyl)borate (**15**).[13] The crystals that formed from the reaction mixture were recrystallized from dimethylformamide. They are colorless, light sensitive, and can be stored in a refrigerator only for a limited time. The spectroscopic data of **15** are listed in the references.[13] Two C≡C stretching bands are found in the IR spectrum. In the ^{13}C spectra the values of the coupling constants $J(P,C)$ decrease as expected from C_α to C_β (C_α: $^1J(P,C) = 193.8$ Hz, C_β: $^2J(P,C) = 38.1$ Hz); C_γ does not couple with the P atom. The signal for C_δ cannot be recognized due to the effects of the quadrupole moment of the neighboring B atom, similar to the case for compounds of type **2**.[6] The positions of the ^{31}P NMR and ^{11}B NMR signals indicate that both atoms are tetracoordinate, as in **2**.

Recrystallization of **15** from dimethylformamide provided crystals suitable for an X-ray structure determination; the resulting structure is shown in Figure 1.[14a] The solvent dimethylformamide is included in the crystal lattice. The diacetylene character of the betaine compound is apparent. The distances between C1 and C2, and C3 and C4 (120.5(6) and 121.1(7) pm, respectively) correspond to those of triple bonds. The C2–C3 separation, 136.1(6) pm, is in accord with that of a single bond between two sp-hybridized C atoms.[15] The P1–C4 distance is 171.7(5) pm and that between B1 and C1 159.5(7) pm. These bond lengths are almost identical to the analogous data for compound **2** with $R^1 = C_6H_5$, CH_3, $R^2 = C_6H_5$. The structure of **15**, like that of **2**, is also not linear but slightly bent.

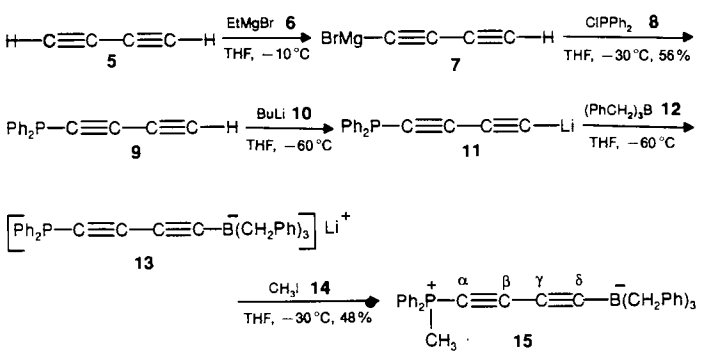

[*] Prof. Dr. H. J. Bestmann, Dipl.-Chem. D. Hadawi, Dr. H. Behl, Dr. M. Bremer, Dipl.-Chem. F. Hampel
Institut für Organische Chemie der Universität Erlangen-Nürnberg
Henkestrasse 42, D-91054 Erlangen (FRG)
Telefax: Int. code + (9131)856864

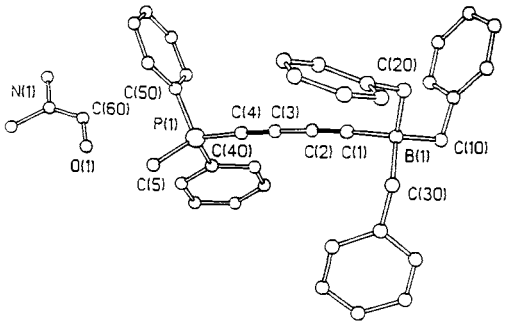

Fig. 1. Crystal structure of **15**. Selected bond angles [°]: B1-C1-C2 176.7(5), C1-C2-C3 177.0(5), C2-C3-C4 179.2(5), P1-C4-C3 175.7(5).

The synthesis of a compound of type **3** was more difficult. The final successful synthesis is outlined here. 1,3-Dibromoacetone was converted into bisphosphonium ylide **16**[16] and then treated with trifluoromethanesulfonic anhydride (**17**) in benzene. Besides allene-1,3-diylbisphosphonium trifluoromethanesulfonate (**19**), compound **25**[17] and bisphosphonium salt **22** formed. The compounds were separated by fractional crystallization from dichloromethane/ether. We assume that **16** and **17**,in analogy to reactions of other acyl ylides, react to give primarily *O*-trifluromethylsulfonated phosphonium triflate **18**[18] which is not isolable but is converted into **19** by an E1-cb-type reaction. We explain the simultaneous formation of **22** and **25** as follows: allenediylbisphosphonium salt **19** reacts with unreacted bisylide **16** by ylide transfer[19] to yield **22** and the "half ylide" **21**, which attacks the middle, strongly electrophilic C atom of the cumulene unit of **19**. The resulting intermediate **24** is converted into **25** by a proton shift. Consistent with this proposed mechanism, **25** is formed when **19** is treated with one mole equivalent of a base such as sodium (bistrimethylsilyl)amide (**26**).[20] Under optimized conditions the formation of **22** and **25** can be suppressed in the reaction of **16** with **17**.

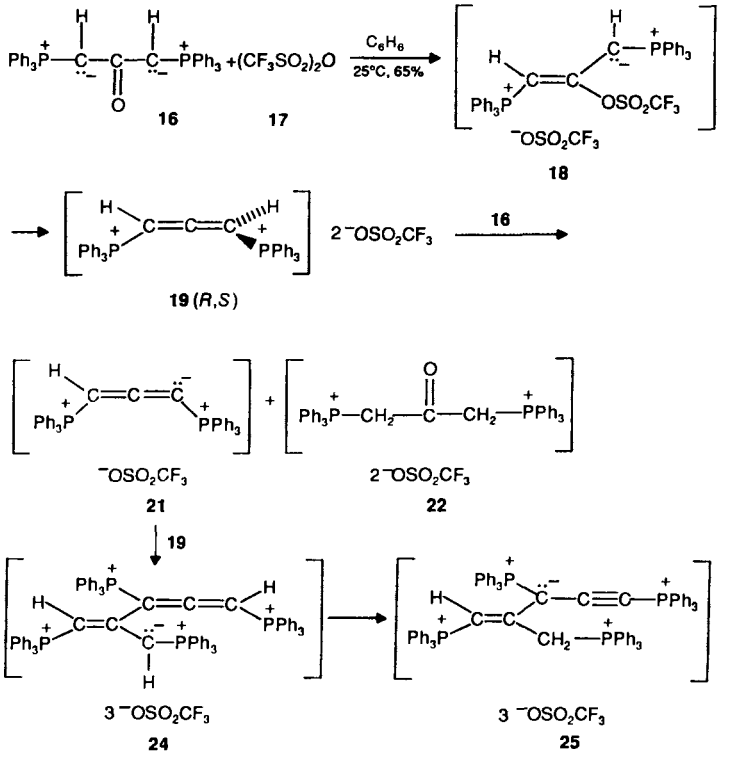

The strong electrophilicity of the middle C atom in **19** is also evident from the quantitative reaction of **19** upon dissolution in pyridine. Compound **23** is obtained both in solution and after evaporation of the solvent as an oily compound; this bis(phosphonio)propenide cation[21] shows typical NMR signals.[22]

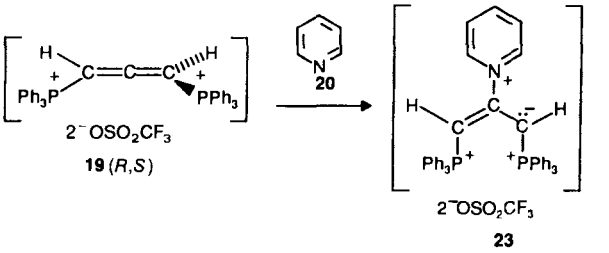

Both **19**[23] and **25** were characterized by X-ray crystallography. The structure of **19** does not have any special features. The result of the structure analysis of **25** is shown in Figure 2.[14b] In this molecule overburdened with phenyl groups, the geometry about the triple bond is not linear (C1-C2-C3-P2; for angles and distances see Fig. 2), as is also the case in **15**.

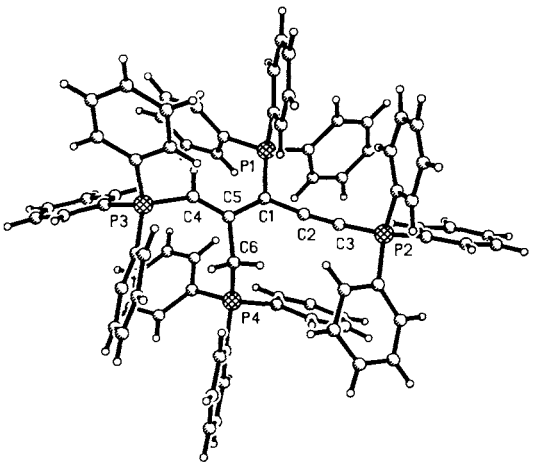

Fig. 2. Crystal structure of **25**. Selected bond lengths [pm] and angles [°]: C2-C3 120.7(23), C4-C5 134.3(21), C5-C6 155.7(19); C1-C2-C3 173.3(15), C2-C3-P2 156.5(14).

Treatment of allenediylbisphosphonium salt **19** with two mole equivalents of sodium (bistrimethylsilyl)amide (**26**)[20] led to **27**, the first compound of type **3**.[24] In the IR spectrum of this orange-red amorphous powder the absorption at 2060 cm^{-1} provides evidence of a cumulene system. In the ^{31}P NMR spectrum a signal is observed at $\delta = -10.4$, which is shifted to much higher field relative to that of **19** ($\delta = +19.9$); we observed a similar upfield shift previously in the conversion of vinylphosphonium salts into phosphacumulene ylides.[25] Only the signals of the aromatic H atoms are seen in the ^1H NMR spectrum of **27**. In the ^{13}C NMR spectrum the triplet at $\delta = 159.2$ ($^2J(P,C) = 30$ Hz) is assigned to the middle atom of the allene unit. The equivalent quasi-anionic C atoms give rise to a doublet of doublets at $\delta = 36.8$ ($^1J(P,C) = 122.1$ Hz, $^3J(P,C) = 15.3$ Hz).

The reaction of **27** with alkyl iodides provides further support for the proposed structure. The reaction with methyl

iodide yields (1,3-dimethylallene-1,3-diyl)bisphosphonium diiodide **29a**; with benzyl iodide the corresponding bis(benzyl) derivative **29b** is obtained.[26] Characteristic allene bands are found in the IR spectrum. In the ^{13}C NMR spectra of **29a** and **29b** no coupling is evident between the two P atoms and the middle C atom of the allene unit; in **27**, on the other hand, the corresponding C atom gives rise to a triplet. One explanation is that the $^2J(P,C)$ coupling constant in allenediyl(bisphosphonium) salts happens to be zero.[27]

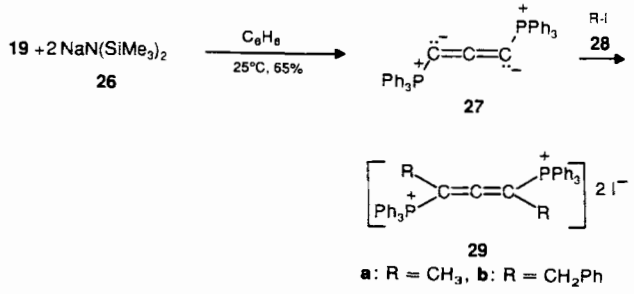

The synthesis of **15** and **27** provides experimental confirmation for the simple theoretical approach for stabilizing "naked" C_1 to C_4 previously proposed. We assume that in general C_n units, when n is odd, can be stabilized by two donor molecules (e.g. phosphanes) at either end of the C_n unit; when n is even, C_n can be stabilized analogously by one donor molecule and one acceptor molecule.

Received: February 19, 1993 [Z 5879 IE]
German version: *Angew. Chem.* **1993**, *105*, 1198

[1] F. Diederich, R. L. Whetten, *Acc. Chem. Res.* **1992**, *25*, 119–126.
[2] For the mechanism of fullerene formation see, for example, A. L. Zhang, S. C. O'Brien, S. R. Heath, Y. Liu, R. D. Curl, H. W. Kroto, R. F. Smally, *J. Phys. Chem.* **1986**, *90*, 525–528; J. M. Hawkins, *Acc. Chem. Res.* **1992**, *25*, 150–156; S. R. Heath, *Fullerene-Synthesis, Properties and Chemistry of Large Carbon Clusters*, (*ACS Symp. Ser.* **1992**, *481*, 1–21), as well as [3].
[3] R. E. Smalley, *Acc. Chem. Res.* **1992**, *25*, 98.
[4] J. P. Hare, H. W. Kroto, *Acc. Chem. Res.* **1992**, *25*, 106.
[5] P. S. Skell, J. J. Havel, M. J. McGlinchey, *Acc. Chem. Res.* **1973**, *6*, 97.
[6] H. J. Bestmann, H. Behl, M. Bremer, *Angew. Chem.* **1989**, *101*, 1303; *Angew. Chem. Int. Ed. Engl.* **1989**, *28*, 1219.
[7] Summaries: C. N. Matthews, G. H. Birum, *Acc. Chem. Res.* **1969**, *2*, 373; H. Schmidbaur, *Nachr. Chem. Tech. Lab.* **1979**, *27*, 620.
[8] L. Brandsma, *Preparative Acetylenic Chemistry*, 2nd edition, Elsevier, Amsterdam, **1988**, p. 180.
[9] C. Charrier, W. Chodkiewicz, P. Cadiot, *Bull. Soc. Chim. Fr.* **1966**, 1002.
[10] **9**: IR(KBr): $\tilde{\nu}$[cm^{-1}] = 3300, 2150, 2035; ^{31}P NMR (161.7 MHz, Et_2O/$CDCl_3$ ext., 25 °C, H_3PO_4 ext.): $\delta = -30.75$.
[11] **11**: ^{31}P NMR (161.7 MHz, THF/$CDCl_3$, 25 °C, H_3PO_4 ext.): $\delta = -28.68$.
[12] **13**: ^{31}P NMR (161.7 MHz, THF/$CDCl_3$, 25 °C, H_3PO_4 ext.): $\delta = -28.70$; ^{11}B NMR (128.2 MHz, THF/$CDCl_3$ ext., 25 °C): $\delta = -16.08$.
[13] **15**: M.p. 159 °C; IR(KBr): $\tilde{\nu}$[cm^{-1}] = 3060, 3040, 3010, 2890, 2810, 2130 (C≡C), 2055 (C≡C), 1585, 1480, 1430, 1260, 1205, 1110, 890, 800, 735, 690, 625; ^1H NMR (400 MHz, [D$_7$]DMF, 27 °C, TMS): δ = 8.07 (q, 4H, *o*-H(PPh)), 7.91 (m, 2H, *p*-H(PPh)), 7.82 (m, 4H, *m*-H(PPh)), 7.07 (m, 12H, *o*-, *m*-H(BPh)), 6.89 (m, 3H, *p*-H(BPh)), 3.09 (d, $^2J(P,H)$ = 13.3 Hz, 3H, P-CH_3), 1.67 (br. 6H, B-CH_2); ^{13}C NMR (100.4 MHz, [D$_7$]DMF, 27 C, TMS): δ = 135.43 (d, $^4J(P,C)$ = 3 Hz, 2C, *p*-C(PPh)), 132.64 (d, $^2J(P,C)$ = 12.2 Hz, 4C, *o*-C(PPh)), 130.77 (d, $^3J(P,C)$ = 13.9 Hz, 4C, *m* C(PPh)), 122.24 (d, $^1J(P,C)$ = 99.2 Hz, 2C, *i*-C(PPh)), 150.51 (s, BPh), 129.24 (s, BPh), 127.42 (s, BPh), 122.43 (s, BPh), 103.93 (d, $^2J(P,C)$ = 38.1 Hz, 1C, P–C≡*C*–), 78.76 (s, 1C, –*C*≡C–B), 48.78 (d, $^1J(P,C)$ = 193.8 Hz, 1C, P–*C*≡C–), 36.0 (br., B-CH_2), 11.39 (d, $^1J(P,C)$ = 62.5 Hz, 1C, P-CH_3); ^{31}P NMR (161.7 MHz, [D$_7$]DMF, 27 °C, H_3PO_4 ext.): δ = 4.6 (s); ^{11}B NMR (128.2 MHz, [D$_7$]DMF, 27 °C): $\delta = -15.98$.
[14] a) **15**: Crystals with orthorhombic symmetry, space group $P2_12_12_1$, a = 1005.7(4), b = 1222.0(7), c = 2849.0(2) pm, $V = 3501 \times 10^6$ pm^3, ρ_{calcd} = 1.149 g cm^{-3}; 4757 measured reflections; 4650 reflections unique, of which 3451 with $F > 4\sigma(F)$ were observed; R = 0.064, R_w = 0.078, 410 refined parameters. b) **25**: Yellow crystals, triclinic, space group $P\bar{1}$; a = 1353.7(5), b = 1507.2(10), c = 1857.4(5) pm, ρ_{calcd} = 1.393 g cm^{-3}; 16107 measured reflections; 16068 reflections unique, of which 3284 with $F > 6\sigma(F)$ were observed; R = 0.0761, R_w = 0.081, 917 refined parameters. Further details of the crystal structure investigation may be obtained from the Fachinformationszentrum Karlsruhe, Gesellschaft für wissenschaftlich-technische Information mbH, D-76344 Eggenstein-Leopoldshafen (FRG) on quoting the depository number CSD-56980, the names of the authors, and the journal citation.
[15] F. H. Allen, O. Kennard, D. G. Watson, L. Brammer, A. G. Orpen, R. Taylor, *J. Chem. Soc. Perkin Trans. 2* **1987**, 1.
[16] H. J. Bestmann, W. Schlosser, *Synthesis* **1979**, *201*.
[17] **19**: Colorless flakes; m.p. 208–210 °C; IR(KBr): $\tilde{\nu}$[cm^{-1}] = 1960 (C=C=C); ^1H NMR (400 MHz, CD_2Cl_2; 26 °C): δ = 8.1 (dd, $^2J(P,H)$ = 7.5 Hz, $^4J(P,H)$ = 2.9 Hz, C=C=C–H), 7.4–7.9 (m, 30H, PPh); ^{13}C NMR (100.4 MHz, CD_2Cl_2, 26 °C): δ = 217.2 (s, 1C, C=*C*=C), 136.4 (s, 6C, *p*-C(Ph)), 134.1 (t, virtual $J(P,C)$ = 5.3 Hz, A part of an AXX′ systems, 12C, *o*-C(Ph)), 131.0 (t, virtual $J(P,C)$ = 6.8 Hz, A part of an AXX′ system, 12C, *m*-C(PH)), 121.1 (q, $^1J(F,C)$ = 321.1 Hz, 2C, CF_3SO_3), 116.4 (d, $^1J(P,C)$ = 93.0 Hz, 6C, *i*-C(Ph)), 81.1 (dd, $^1J(P,C)$ = 93.1 Hz, $^3J(P,C)$ = 9.2 Hz, 2C, P–*C*=C=*C*–P); ^{31}P NMR (161.7 MHz, CD_2Cl_2, 27 °C, H_3PO_4 ext.): δ = 19.9 (s, 2P, PPh). – **25**: M.p. 286–288 °C; IR(KBr): $\tilde{\nu}$[cm^{-1}] = 2080 (C≡C); ^1H NMR (400 MHz, $CDCl_3$, 25 °C, TMS): δ = 6.9–7.9 (m, 60H, Ph), 4.5 (d, $^2J(P,H)$ = 15.6 Hz, 1H), 4.65 (d, $^2J(P,H)$ = 4 Hz, 1H), 5.66 (d, $^2J(P,H)$ = 11.6 Hz, 1H); ^{31}P NMR (161.7 MHz, $CDCl_3$, 25 °C, H_3PO_4): δ = 21.6 (dd, $^4J(P,P)$ = 7.6 Hz, $^4J(P,P)$ = 2.3 Hz, 1P, CH_2-P), 16.1 (dd, $^4J(P,P)$ = 4.6 Hz, $^4J(P,P)$ = 2.3 Hz, 1P, CH-P), 12.2 (d, $^4J(P,P)$ = 4.6 Hz, 1P, C-P), 3.1 (d, $^4J(P,P)$ = 7.6 Hz, 1P, C-C≡C-P); ^{13}C NMR (100.4 MHz, $CDCl_3$, 26 °C): δ = 195.4 (s, 1C), 154.8 (s, 1C), 135.7 (s, C(Ph)), 134.8 (s, C(Ph)), 134.3 (d, $J(P,C)$ = 10.7 Hz, C(Ph)), 134.1 (d, $J(P,C)$ = 9.1 Hz, C(Ph)), 133.7 (d, $J(P,C)$ = 10.7 Hz, C(Ph)), 133.5 (d, $J(P,C)$ = 10.7 Hz, C(Ph)), 133.0 (d, $J(P,C)$ = 12.3 Hz, C(Ph)), 130.9 (d, $J(P,C)$ = 12.2 Hz, C(Ph)), 130.7 (s, C(Ph)), 130.6 (s, C(Ph)), 130.4 (d, $J(P,C)$ = 13.8 Hz, C(Ph)), 130.1 (d, $J(P,C)$ = 12.2 Hz, C(Ph)), 130.0, (d, $J(P,C)$ = 13.8 Hz, C(Ph)), 128.8 (q, $^1J(F,C)$ = 321 Hz, 3C, CF_3SO_3), 119.52 (d, $^1J(P,C)$ = 99.2 Hz, *i*-C(Ph)), 119.49 (d, $^1J(P,C)$ = 91.6 Hz, *i*-C(Ph)), 119.2 (d, $^1J(P,C)$ = 90.1 Hz, *i*-C(Ph)), 116.6 (d, $^1J(P,C)$ = 87.0 Hz, *i*-C(Ph)), 86.6 (dd, $^1J(P,C)$ = 101.5 Hz, $^3J(P,C)$ = 6.9 Hz, 1C, P=*C*–C≡C–), 73.9 (dd, $^1J(P,C)$ = 195.3 Hz, $^3J(P,C)$ = 7.6 Hz, 1C, C≡*C*–P), 39.2 (dd, $^1J(P,C)$ = 61.8 Hz, $^3J(P,C)$ = 6.8 Hz, 1C, CH_2), 30.7 (dd, $^1J(P,C)$ = 55.7 Hz, $^3J(P,C)$ = 6.8 Hz, 1C, CH).
[18] H. J. Bestmann, K. Kumar, W. Schaper, *Angew. Chem.* **1983**, *95*, 154; *Angew. Chem. Int. Ed. Engl.* **1983**, *22*, 167; H. J. Bestmann, A. Pohlschmidt, K. Kumar, *Tetrahedron Lett.* **1992**, *33*, 5955.
[19] H. J. Bestmann, *Chem. Ber.* **1962**, *95*, 58; H. J. Bestmann, *Angew. Chem.* **1965**, *77*, 609; *Angew. Chem. Int. Ed. Engl.* **1965**, *4*, 583.
[20] For the preparation of ylides from the reaction of the appropriate phosphonium salts with **26**, see H. J. Bestmann, W. Stransky, O. Vostrowsky, *Chem. Ber.* **1976**, *109*, 1694.
[21] H. Schmidbaur, C. Paschalidis, O. Steigelmann, G. Müller, *Angew. Chem.* **1989**, *101*, 1739; *Angew. Chem. Int. Ed. Engl.* **1989**, *28*, 1700; H. J. Bestmann, L. Kisielowski, *Tetrahedron Lett.* **1990**, *31*, 3301.
[22] **23**: IR (NaCl): no allene bands between 1900 and 2000 cm^{-1}; ^1H NMR (400 MHz, [D$_5$]pyridine, 26 °C): δ = 7.4–8.2 (m, 35H, H(Ph, py), 4.9 (dd, $^2J(P,H)$ = 13 Hz, $^4J(P,H)$ = 6.9 Hz, 1H), 3.9 (d, $^2J(P,H)$ = 5.2 Hz, 1H); ^{13}C NMR (100.4 MHz, [D$_5$]pyridine, 26 °C): δ = 162.9 (d, $^2J(P,C)$ = 13.7 Hz, 1C, C-*C*-C), 121.0–134.7 (m, 41C, C (Ph, py)), 56.0 (d, $^1J(P,C)$ = 120.6 Hz, 1C, *C*-C-C), 63.7 (dd, $^1J(P,C)$ = 108.5 Hz, $^3J(P,C)$ = 12.1 Hz, 1C, C-C-*C*); ^{31}P NMR (161.7 MHz, [D$_5$]pyridine, 26 °C): δ = 10.9 (s, 1P), 12.3 (s, 1P).
[23] A. Bram, H. Burzlaff, D. Hadawi, H. J. Bestmann, *Acta Crystallogr. Sect. C* **1992**, *48*, 1904.
[24] **27**: M.p. 73 °C (charring); IR(NaCl): $\tilde{\nu}$[cm^{-1}] = 2060 (C=C=C); ^{31}P NMR (161.7 MHz, C_6D_6, 26 °C): $\delta = -10.4$ (s, 2P, PPh); ^{13}C NMR (100.4 MHz, C_6D_6, 26 °C): δ = 159.2 (t, $^2J(P,C)$ = 30 Hz, 1C, P=C=*C*=C=P), 133.6 (d, $^1J(C,P)$ = 94.6 Hz, 6C, *i*-C(Ph)), 132.8 (t, virtual $J(C,P)$ = 4.6 Hz, A part of an AXX′ system, 12C, *o*-C(Ph)), 130.5 (s, 6C, *p*-C(Ph)), 128.3 (t, virtual $J(C,P)$ = 6.1 Hz, A part of an AXX′ systems, 12C, *m*-C(Ph)), 36.8 (dd, $^1J(P,C)$ = 122.1 Hz, $^3J(P,C)$ = 15.3 Hz, 2C, =C=*C*=PPh); ^1H NMR (400 MHz, C_6D_6, 26 °C): δ = 6.9–7.9 (m, 30H, Ph).
[25] H. J. Bestmann, K. Roth, *Tetrahedron Lett.* **1981**, *22*, 1681; the phosphonium salts corresponding to the phosphacumulene ylides described there show a band in the ^{31}P NMR spectrum around δ = +11; H. J. Bestmann, R. Engler, H. Hartung, K. Roth, *Chem. Ber.* **1979**, *112*, 28; K. R. Roth, *Dissertation*, Universität Erlangen-Nürnberg, **1981**, 475.
[26] **29a**: Beige needles, m.p. 259 °C; IR(KBr): $\tilde{\nu}$[cm^{-1}] = 1940 (C=C=C); ^1H NMR (400 MHz, CD_2Cl_2, 29 °C): δ = 7.4–8.0 (m, 30H, Ph), 2.4 (dd, $^3J(P,H)$ = 12.82 Hz, $^5J(P,H)$ = 6.72 Hz, 6H, CH_3); ^{13}C NMR (100.4 MHz, CD_2Cl_2, 29 °C): δ = 215.7 (s, 1C, C=*C*=C), 136.5 (s, 6C,

p-C(Ph)), 134.5 (t, virtual J(C,P) = 5.4 Hz, A part of an AXX′ system, 12C, *o*-C(Ph)), 131.4 (t, virtual J(C,P) = 6.8 Hz, A part of an AXX′ system, 12C, *m*-C(Ph)), 115.4 (d, ^1J(P,C) = 91.5 Hz, 6C, *i*-C(Ph)), 91.9 (dd, ^1J(P,C) = 86.95 Hz, ^3J(P,C) = 7.65 Hz, 2C, C=*C*-P), 17.8 (s, 2C, CH_3); ^{31}P NMR (161.7 MHz, CD_2Cl_2, 30 °C, H_3PO_4 ext.): δ = 24.9 (s, 2P, PPh). **29b**: M.p. 220 °C; IR(KBr): $\tilde{\nu}$[cm^{-1}] = 1920 (C=C=C); ^{1}H NMR (400 MHz, CD_2Cl_2; 29 °C): δ = 6.9–8.0 (m, 40H, Ph), 4.09 (m, 2H, CH_2), 3.67 (m, 2H, CH_2); ^{13}C NMR (100.4 MHz, CD_2Cl_2, 29 °C): δ = 217.0 (s, 1C, C=*C*=C), 136.9 (s, 6C, *p*-C(PPh)), 134.8 (t, virtual J(C,P) = 5.4 Hz, A part of an AXX′ system, 12C, *o*-C(PPh)), 131.5 (t, virtual J(C,P) = 6.1 Hz, A part of an AXX′ systems, 12C, *m*-C(PPh)), 130.5 (s, 4C, CH_2-*Ph*), 129.7 (s, 4C, CH_2-*Ph*), 129.1 (s, 2C, CH_2-*Ph*), 128.9 (s, 2C, CH_2-*Ph*), 115.2 (d, ^1J(P,C) = 90.0 Hz, 6C, *i*-C(PPh)), 101.0 (d, ^1J(P,C) = 85.8 Hz, 2C, C=*C*-PPh), 36.9 (s, 2C, CH_2); ^{31}P NMR (161.7 MHz, CD_2Cl_2, 25 °C, H_3PO_4 ext.): δ = 24.4 (s, 2P, PPh).

[27] It is known that the $^2J(^{13}C,^{31}P)$ coupling constants for phosphonium salts may be either positive or negative: G. Mavel, *Annu. Rep. NMR Spectrosc.* **1973**, *5*, 1.

$[\{(Me_3Si)_2N\}_2Sm\{\mu\text{-}(\eta^8\text{:}\eta^8\text{-}C_8H_8)\}\text{-}Sm\{N(SiMe_3)_2\}_2]$: An Inverse Organolanthanoid Sandwich Complex**

By *Herbert Schumann,* Jörn Winterfeld, Lothar Esser,* and *Gabriele Kociok-Köhn*

Dedicated to Professor Hans Bock on the occasion of his 65th birthday

The planar π-electron system of aromatic hydrocarbons is not only capable of forming bonds to metals on one of its faces leading to half-sandwich or sandwich complexes such as $[(\eta^6\text{-}C_6H_6)Cr(CO)_3]$ or ferrocene, respectively, but can also bind metals on both of its faces (inverse sandwich); this was first observed in triple-decker sandwich complexes discovered by Werner and Salzer in 1972.[1] Later Schmidbaur et al.[2] found that "Menshutkin complexes"[4] which are formed between benzene and either arsenic, antimony, and bismuth, and which have been known since 1882[3] also belong to the type of inverse-sandwich complexes. Also the 10 π-electron system of the cyclooctatetraene dianion can bind a metal atom to each of the two faces of the arene, giving rise to symmetric complexes such as [K(diglyme)-$\{\mu\text{-}(\eta^8\text{:}\eta^8\text{-}C_8H_4Me_4)\}$K(diglyme)][5] and [K(diglyme)-$\{\mu\text{-}(\eta^8\text{:}\eta^8\text{-}C_8H_8)\}Ce(\eta^8\text{-}C_8H_8)$] (diglyme = diethyleneglycol dimethyl ether)[6] as well as to unsymmetric complexes such as $[(\eta^8\text{-}C_8H_8)Nd(thf)_2\{\mu\text{-}(\eta^2\text{:}\eta^8\text{-}C_8H_8)\}Nd(\eta^8\text{-}C_8H_8)]$[7] and $[Li(thf)_2\{(\mu\text{-}(\eta^2\text{:}\eta^8\text{-}C_8H_8)\}Sm\{CH(SiMe_3)_2\}_2]$.[8]

We have now found in the form of (cyclooctatetraene)bis{di[bis(trimethylsilyl)amido]samarium(III)} **3**, a simple inverse sandwich complex of a 4f element: (cyclooctatetraene)lanthanoid chloride (lanthanoid = Y, Gd, Er, and Lu) react as expected with sodium bis(trimethylsilyl)amide to form the half-sandwich complexes **1a–d**. In contrast to that, (cyclooctatetraene)samarium chloride reacts under the same conditions to give the inverse-sandwich complex **3** and sodium bis(cyclooctatetraene)samarate(III) **2** (Scheme 1).

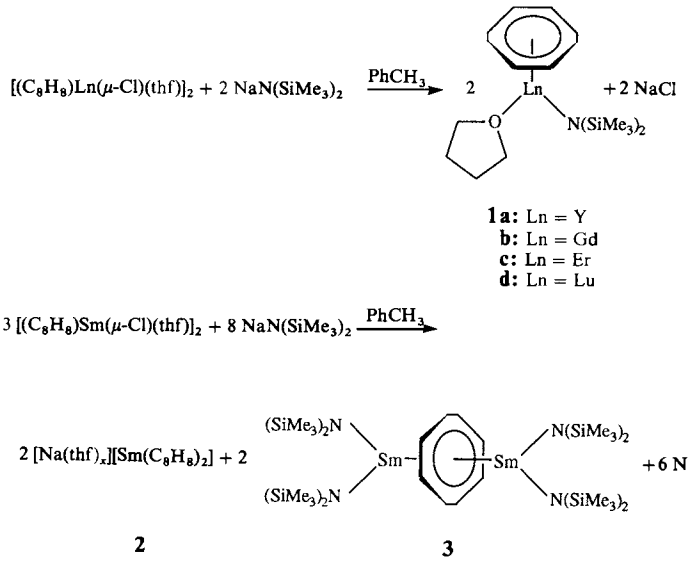

Scheme 1.

The extremely air- and moisture-sensitive compounds **1a–d** can be obtained in a crystalline form in yields of 42–58%. The presence of THF in **1a–d** can clearly be shown by elemental analyses, as well as by NMR spectroscopy (^{1}H, ^{13}C) of the diamagnetic compounds **1a** and **1d**. We obtained well-shaped single crystals of the lutetium complex **1d** by slow cooling of a saturated cyclopentane solution. The X-ray crystal structure analysis[9] revealed three symmetrically independent molecules per asymmetric unit. The solid-state structure of **1** is shown in Figure 1. Assuming that the centroid of the η^8-bound cyclooctatetraene unit is the center of this ligand, we can consider the lutetium atom to be pseudo-trigonal planar coordinated. The mean Lu–C distances

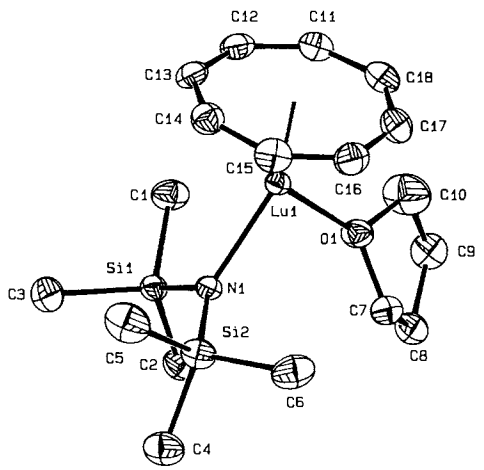

Fig. 1. Structure of **1d** (one molecule of the asymmetric unit [9], without hydrogen atoms). Selected bond lengths [pm] and angles [°] with standard deviations: Lu1-N1 219.7(3), Lu1-O1 231.1(2), Lu1-$(C_8H_8)_z$-(molecule 1) 172.9, Lu...C1 317.0(4); N1-Lu1-O1 86.4(1), $(C_8H_8)_z$(molecule 1)-Lu1-N1 147.0, $(C_8H_8)_2$ (molecule 1)-Lu1-O1 126.0, Lu1-N1-Si1 113.1(2), Lu1-N1-Si2 123.5(2), N1-Si1-C1 108.5(2), N1-Si1-C2 114.2(2), N1-Si1-C3 113.9(2), N1-Si2-C4 113.3(2), N1-Si2-C5 111.7(2), N1-Si2-C6 110.4(2).

[*] Prof. Dr. H. Schumann, Dr. J. Winterfeld, Dr. L. Esser, Dr. G. Kociok-Köhn
Institut für Anorganische und Analytische Chemie
der Technischen Universität
Strasse des 17. Juni 135 D-10623 Berlin (FRG)
Telefax: Int. code + (30)3142-2168

[**] Organometallic Compounds of the Lanthanoids, Part 79. This work was supported by the Fonds der Chemischen Industrie (doctoral grant for J. W.), the Deutsche Forschungsgemeinschaft, and the Bundesministerium für Bildung und Wissenschaft in the framework of the research area "Synthese und Strukturaufklärung niedermolekularer Verbindungen". Part 78: H. Schumann, M. Glanz, H. Hemling, F. H. Görlitz, *J. Organomet. Chem.* in press.

(251.2(5) pm for molecule 1, 250.0(5) pm for molecule 2, and 251.2(5) pm for molecule 3) are in good agreement with the corresponding bond length in $[(\eta^8\text{-}C_8H_8)Lu(o\text{-}C_6H_4CH_2NMe_2)(thf)]$ (255(1) pm),[10] when the different coordination numbers are taken into consideration. The mean value of the Lu–N bond (219.3(3) pm) is similar to the Y–N bond length in $[(\eta^5\text{-}C_5Me_5)_2Y\{N(SiMe_3)_2\}]$ (227.4(5) and 225.3(5) pm),[11] provided that the smaller ionic radius of lutetium has been taken into consideration. Noteworthy is the asymmetric conformation of the amido ligand. Thus, in molecule 1 the Lu-N1-Si1 angle (113.1(2)°) is 10.4(4)° smaller than the Lu1-N1-Si2 angle. The same is true for the N1-Si1-C1 angle (108.5(2)°), which is smaller than the N1-Si1-C2 (114.2(2)°) and N1-Si1-C3 (113.9(2)°) bond angles. Analogous distortions also occur in molecules 2 and 3. It is, however, unclear whether these distortions are due to γ-agostic bonds between the methyl groups of the amido ligand and the Lewis acidic lanthanoid center, or only a result of packing effects, since the shortest Lu–C(methyl) distance in molecule 1 is 317.0(4) pm (322.0(4) pm in molecule 2 and 318.0(4) pm in molecule 3), and this is very large in comparison with Lu–C-σ bonds such as in $[\{Me_2Si(\eta^5\text{-}C_5Me_4)\}(\eta^5\text{-}C_5H_4)Lu\{CH(SiMe_3)_2\}]$ (d(Lu–C$_\alpha$) = 236.5(7) pm)[12] or in $[(\eta^5\text{-}C_5H_5)_2Lu(CH_2SiMe_3)(thf)]$ (d(Lu–C$_\alpha$) = 237.6(17) pm).[13]

The compounds **2** and **3** are also very highly air and moisture sensitive. Compound **3** is thermally extremely stable (decomp 196 °C). In the ^{1}H NMR spectra of **2** and **3**, the influence of the paramagnetism of the Sm^{3+} ion on the protons of its ligands is evident. Thus, the C_8H_8 ring of **3** (in [D$_8$]toluene) has a chemical shift of $\delta = 9.29$, and the $SiMe_3$ groups a chemical shift of $\delta = -2.32$, whereas in the ^{1}H NMR spectrum of **2** (in [D$_8$]THF) the signal of the C_8H_8 ring occurs at $\delta = 13.3$ ($\nu_{1/2}$ = 50 Hz). Compounds **2** and **3** can be separated easily from each other as a result of their differing solubilities in various solvents. Whereas the sandwich complex **2** is only highly soluble in polar solvents such as THF, the trimethylsilyl groups in **3** provide for good solubility in nonpolar solvents such as *n*-hexane or cyclopentane. Suitable single crystals of **3** for an X-ray crystal structure analysis[14] were obtained by cooling a saturated *n*-hexane solution. In the crystal, **3** is a centrosymmetric molecule with an inverse sandwich structure (Fig. 2). Like the Lu^{3+} ion in **1d**, the Sm^{3+} ions in **3** have a pseudo-trigonal planar coordination sphere consisting of one η^8 interaction with the bridging cyclooctatetraene unit and two σ bonds to the amido ligands. The Sm–cyclooctatetraene vectors are almost perpendicular (88.9°) to the plane of the cyclooctatetraene ligand. The amido ligands are eclipsed; the N1-Sm-Sm'-N2' torsion angle is 4.45(8)° (Fig. 3). Owing to the competition of

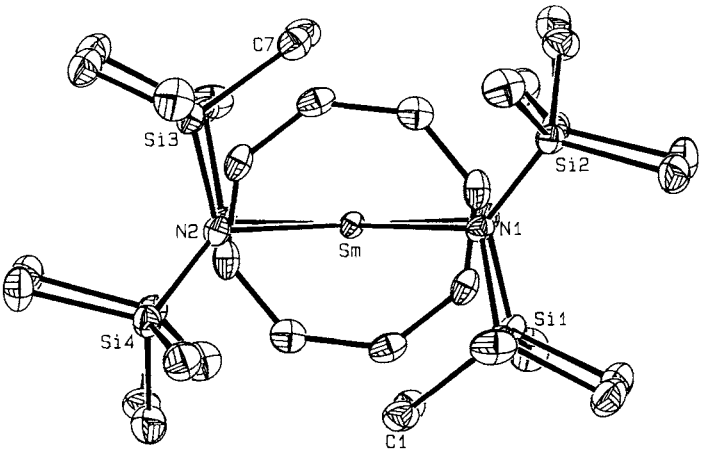

Fig. 3. View of **3** along the Sm–Sm axis.

two Sm^{3+} ions for ten π electrons of the bridging eight-membered ring, the mean Sm–C distance is 14.3 pm greater than the corresponding distance in $[Li(thf)_2\{\mu\text{-}(\eta^2\text{:}\eta^8\text{-}C_8H_8)\}Sm\{CH(SiMe_3)_2\}_2]$ (d(Sm–C) = 268.8(5) pm).[8] The mean Sm–N bond length (228.0(2) pm), however, correlates with the corresponding distances in the homoleptic amido lanthanoid complexes $[Eu\{N(SiMe_3)_2\}_3]$ (d(Eu–N) = 225.9(9) pm)[15] and $[Nd\{N(SiMe_3)_2\}_3]$ (d(Nd–N) = 229(9) pm).[16] Remarkably, in the solid-state structure of **3**, one methyl carbon atom (C1 and C7) of each amido ligand is found very close to the lanthanoid center. The Sm···C1 distance is 310.5(2) pm and the Sm···C7 distance 297.0(2) pm. These distances are thus significantly shorter than the sum of the van der Waals radii of a methyl group and of a samarium(III) ion, but somewhat longer than the Sm–C(methyl) bonds in $[(\eta^5\text{-}C_5Me_5)_2Sm\{\mu\text{-}Me)AlMe_2\}_2(\mu\text{-}Me)\}_2Sm(\eta^5\text{-}C_5Me_5)_2]$ (d(Sm–C(Me)) = 274.3(16) and 275.0(16) pm)[17] or in $[(\eta^5\text{-}C_5Me_5)_2SmMe(thf)]$ (d(Sm–C(Me)) = 248.4(14) pm).[17] Due to the close contact of the two methyl groups to the Lewis acidic lanthanoid center, the Sm-N1-Si1 (110.5(1)°) and the Sm-N2-Si3 angles (106.8(1)°) are smaller than the Sm-N1-Si2 (130.2(1)°) and the Sm-N2-Si4 angles (133.0(1)°). The same is true for the N1-Si1-C1 and N2-Si3-C7 bond angles (107.8(1) and 107.1(1)°, respectively), which are about 5–8° smaller than the usual N1-Si1-C and N2-Si3-C angles. Finally, Scheme 2 summarizes complexes that also display the type of γ-agostic interaction, which has been described for **3**.

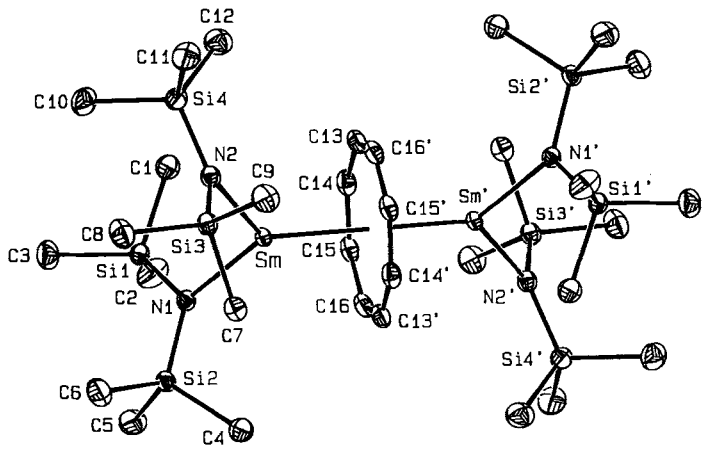

Fig. 2. Structure of **3** (without hydrogen atoms). Selected bond lengths [pm] and angles [°] with standard deviations: Sm-N1 227.5(2), Sm-N2 228.6(2), Sm-(C_8H_8)$_z$ 215.4, Sm···C1 310.6(3), Sm···C7 297.0(3); N1-Sm-N2 109.44(7), (C_8H_8)$_z$-Sm-N1 126.72(5), (C_8H_8)$_z$-Sm-N2 123.71(5), Sm-N1-Si1 110.5(1), Sm-N1-Si2 130.2(1), N1-Si1-C1 107.8(1), N1-Si1-C2 115.2(1), N1-Si1-C3 113.0(1), N2-Si2-C4 111.3(1), N2-Si2-C5 114.3(1), N2-Si2-C6 111.7(1), Sm-N2-Si3 106.8(1), Sm-N2-Si4 133.0(1), N2-Si3-C7 107.1(1), N2-Si3-C8 114.9(1), N2-Si3-C9 114.8(1), N2-Si4-C10 111.3(1), N2-Si4-C11 113.0(1), N2-Si4-C12 113.2(1).

$[(\eta^8\text{-}C_8H_8)Th\{N(SiMe_3)_2\}_2]$[18]
$[(\eta^5\text{-}C_5Me_5)Ce\{N(SiMe_3)_2\}_2]$[19]
$[(\eta^5\text{-}C_5Me_5)_2Y\{N(SiMe_3)_2\}]$[11]
$[Sm\{N(SiMe_3)_2\}_2(thf)_2]$[20]
$[Yb\{N(SiMe_3)_2\}_2(dmpe)]$[21]

Scheme 2. dmpe = 1,2-bis(dimethylphosphino)ethane

Experimental Procedure

All operations were carried out under an argon atmosphere in dry, oxygen-free solvents.

General procedure: To a suspension of $[(\eta^8\text{-}C_8H_8)Ln(\mu\text{-}Cl)(thf)]_2$ [22, 23] (Ln = Y, Gd, Er, Lu, Sm) in toluene (50 mL) at −60 °C was added $NaN(SiMe_3)_2$, the mixture was continually stirred and allowed to warm up to room temperature over 12 h. After the solvent had been removed under vacuum, the residue was treated with *n*-hexane (70 mL), stirred, allowed to settle, and the solution was decanted off. When the extract was cooled to −25 °C, **1a**–**d** and **3** were obtained in a crystalline form.

1a: $[(\eta^8\text{-}C_8H_8)Y(\mu\text{-}Cl)(thf)]_2$ (0.88 g, 1.46 mmol), $NaN(SiMe_3)_2$ (0.54 g, 2.94 mmol); yield 0.58 g (47 %) colorless crystals; m.p. 119 °C (decomp); correct C, H, N analysis; ^{1}H NMR (270 MHz, C_6D_6, 25 °C, TMS): δ = 6.59 (s, 4H, C_8H_8), 3.12 (m, 2H, THF), 0.94 (m, 2H, THF), 0.06 (s, 9H, $SiMe_3$); ^{13}C NMR (67.9 MHz, C_6D_6, 25 °C, TMS): δ = 94.9 (d, $^1J(^{13}C,^{89}Y)$ = 2.5 Hz, C_8H_8), 71.2 (THF), 25.0 (THF), 3.9 ($SiMe_3$); MS (70 eV): *m/z* (%): 353 (19) $[M^+-THF]$, 338 (41) $[M^+-THF-Me]$, 193 (26) $[(C_8H_8)Y^+]$, 146 (100) $[Si_2Me_6^+]$.

1b: $[(\eta^8\text{-}C_8H_8)Gd(\mu\text{-}Cl)(thf)]_2$ (0.66 g, 0.89 mmol), $NaN(SiMe_3)_2$ (0.33 g, 1.80 mmol); yield 0.45 g (51 %) colorless crystals; m.p. 112 °C (decomp); correct C, H, N analysis; MS (70 eV, ^{158}Gd): *m/z* (%): 422 (3) $[M^+-THF]$, 407 (9) $[M^+-THF-Me]$, 262 (9) $[(C_8H_8)Gd^+]$, 146 (100) $[Si_2Me_6^+]$.

1c: $[(\eta^8\text{-}C_8H_8)Er(\mu\text{-}Cl)(thf)]_2$ (0.54 g, 0.71 mmol), $NaN(SiMe_3)_2$ (0.26 g, 1.42 mmol); yield 0.30 g (42 %) pink crystals; m.p. 116 °C (decomp); correct C, H, N analysis; MS (70 eV, ^{166}Er): *m/z* (%): 430 (1) $[M^+-THF]$, 415 (5) $[M^+-THF-Me]$, 270 (2) $[(C_8H_8)Er^+]$, 146 (100) $[Si_2Me_6^+]$.

1d: $[(\eta^8\text{-}C_8H_8)Lu(\mu\text{-}Cl)(thf)]_2$ (0.64 g, 0.83 mmol), $NaN(SiMe_3)_2$ (0.30 g, 1.64 mmol); yield 0.49 g (58 %) colorless crystals; m.p. 143 °C (decomp); correct C, H, N analysis; ^{1}H NMR (270 MHz, C_6D_6, 25 °C, TMS): δ = 6.55 (s, 4H, C_8H_8), 3.08 (m, 2H, THF), 0.91 (m, 2H, THF), 0.07 (s, 9H, $SiMe_3$); ^{13}C NMR (67.9 MHz, C_6D_6, 25 °C, TMS): δ = 94.0 (C_8H_8), 71.8 (THF), 25.0 (THF), 4.2 ($SiMe_3$); MS (70 eV): *m/z* (%): 439 (13) $[M^+-THF]$, 424 (36) $[M^+-THF-Me]$, 279 (14) $[(C_8H_8)Lu^+]$, 146 (100) $[Si_2Me_6^+]$.

3: $[(\eta^8\text{-}C_8H_8)Sm(\mu\text{-}Cl)(thf)]_2$ (0.71 g, 0.98 mmol), $NaN(SiMe_3)_2$ (0.48 g, 2.62 mmol); yield 0.22 g (32 %) orange crystals; m.p. 196 °C (decomp); correct C, H, N analysis; ^{1}H NMR (270 MHz, [D$_8$]toluene, 25 °C, TMS): δ = 9.29 (s, 2H, C_8H_8), −2.32 (s, 9H, $SiMe_3$); ^{13}C NMR (67.9 MHz, [D$_8$]toluene, 25 °C, TMS): δ = 82.6 (C_8H_8), 1.9 ($SiMe_3$).

Received: February 27, 1993 [Z 5896 IE]
German version: *Angew. Chem.* **1993**, *105*, 1212

[1] H. Werner, A. Salzer, *Synth. Inorg. Met. Org. Chem.* **1972**, *2*, 239.
[2] A. Schier, J. M. Wallis, G. Müller, H. Schmidbaur, *Angew. Chem.* **1986**, *98*, 742; *Angew. Chem. Int. Ed. Engl.* **1986**, *25*, 757.
[3] W. Smith, G. W. Davis, *J. Chem. Soc. Trans.* **1882**, *41*, 411.
[4] B. N. Menshutkin, *Zh. Russ. Fiz. Khim. Ova. Chast. Khim.* **1911**, *43*, 1298, 1786.
[5] S. Z. Goldberg, K. N. Raymond, C. A. Harmon, D. H. Templeton, *J. Am. Chem. Soc.* **1974**, *96*, 1348.
[6] K. O. Hodgson, K. N. Raymond, *Inorg. Chem.* **1972**, *11*, 3030.
[7] a) S. R. Ely, T. E. Hopkins, C. W. DeKock, *J. Am. Chem. Soc.* **1976**, *98*, 1624; b) C. W. DeKock, S. R. Ely, T. E. Hopkins, M. A. Brault, *Inorg. Chem.* **1978**, *17*, 625.
[8] H. Schumann, J. Winterfeld, F. H. Görlitz, J. Pickardt, *J. Chem. Soc. Chem. Commun.* **1993**, 623.
[9] Crystal data for **1d**: $C_{18}H_{34}LuNOSi_2$, M_r = 511.61, colorless, parallelepiped-shaped crystals ($0.24 \times 0.15 \times 0.42$ mm^3), monoclinic space group $P2_1/c$ (no. 14), a = 2392.8(6), b = 2115.0(2), c = 1320.4(4) pm, β = 104.68(3)°, $V = 6464(3) \times 10^{-30}$ m^3 determined from 96 reflections with 24° < 2θ < 27.4°, Z = 12, ρ_{calcd} = 1.58 g cm^{-3}, λ = 71.069 pm, $\mu(Mo_{K\alpha})$ = 47.0 cm^{-1}. Absorption correction by ψ scan. 10448 independent reflections in the range 1° ≤ 2θ ≤ 50° with ω-2θ scan were measured at a crystal temperature of −155 °C on an Enraf-Nonius diffractometer. The structure was solved with Patterson (SHELXS-86) and difference Fourier methods (SHELX-76). The full-matrix least-squares refinement of 622 parameters derived from 9346 reflections with $F_o > 4\sigma(F_o)$ converged at R = 0.022 and R_w = 0.029 ($w = 1/\sigma^2(F_o) + 0.0003F_o^2$). The three symmetrically independent molecules in an asymmetric unit have no close contacts. By superimposing any pair of molecules such that the Lu, O, and N atoms coincide, we find that the C_8H_8 ring atoms also coincide. This result contrasts with that observed for the THF molecules and the amido ligands, which exhibit considerable angular dispersion about the Lu–O and Lu–N bonds, respectively. Thus, three clearly different conformers are present in the asymmetric unit [14].
[10] A. L. Wayda, R. D. Rogers, *Organometallics* **1985**, *4*, 1440.
[11] K. H. den Haan, J. L. de Boer, J. H. Teuben, A. L. Spek, B. Kojic-Prodic, G. R. Hays, R. Huis, *Organometallics* **1986**, *5*, 1726.
[12] D. Stern, M. Sabat, T. J. Marks, *J. Am. Chem. Soc.* **1990**, *112*, 9558.
[13] H. Schumann, W. Genthe, N. Bruncks, *Angew. Chem.* **1981**, *93*, 126; *Angew. Chem. Int. Ed. Engl.* **1981**, *20*, 120.
[14] Crystal data for **3**: $C_{32}H_{80}N_4Si_8Sm_2$, M_r = 1046.41, orange, parallelepiped crystals ($0.42 \times 0.24 \times 0.06$ mm^3), triclinic space group $P\bar{1}$ (no. 2), a = 869.8(2), b = 1070.0(3), c = 1400.6(4) pm, α = 97.86(2), β = 101.97(2), γ = 100.24(2)°, $V = 1234.3(6) \times 10^{-30}$ m^3, Z = 1, ρ_{calcd} = 1.41 g cm^{-3}, λ = 71.069 pm, $\mu(Mo_{K\alpha})$ = 25.8 cm^{-1}. The crystal on the Enraf-Nonius diffractometer was cooled to −155 °C. Absorption correction by ψ scan. There were 4289 reflections measured in the range 1 ≤ 2θ ≤ 49° with ω-2θ scan, of which 3956 reflections with $F_o \geq 4\sigma(F_o)$ were used in the solution (Patterson/Difference Fourier methods) and refinement of the structure. All hydrogen atoms were freely refined. The full-matrix least-squares refinement of 368 parameters converged at R = 0.018 and R_w = 0.025 ($w = 1/\sigma^2(F_o) + 0.0005F_o^2$). Further details of the crystal structure investigations may be obtained from the Fachinformationszentrum Karlsruhe, Gesellschaft für wissenschaftlich-technische Information mbH, D-76344 Eggenstein-Leopoldshafen (FRG) on quoting the depository number CSD-57255, the names of the authors, and the journal citation.
[15] J. S. Ghotra, M. B. Hursthouse, A. J. Welch, *J. Chem. Soc. Chem. Commun.* **1973**, 669.
[16] R. A. Andersen, D. H. Templeton, A. Zalkin, *Inorg. Chem.* **1978**, *17*, 2317.
[17] W. J. Evans, L. R. Chamberlain, T. A. Ulibarri, J. W. Ziller, *J. Am. Chem. Soc.* **1988**, *110*, 6423.
[18] T. M. Gilbert, R. R. Ryan, A. P. Sattelberger, *Organometallics* **1988**, *7*, 2514.
[19] H. J. Heeres, A. Meetsma, J. H. Teuben, R. D. Rogers, *Organometallics* **1989**, *8*, 2637.
[20] W. J. Evans, D. K. Drummond, H. Zhang, J. L. Atwood, *Inorg. Chem.* **1988**, *27*, 575.
[21] T. D. Tilley, R. A. Andersen, A. Zalkin, *J. Am. Chem. Soc.* **1982**, *104*, 3725.
[22] K. O. Hodgson, F. Mares, D. F. Starks, A. Sreitwieser, *J. Am. Chem. Soc.* **1973**, *95*, 8650.
[23] A. L. Wayda, *Organometallics* **1983**, *2*, 565.

Investigation of the Surface Structure of the Zeolites FAU and EMT by High-Resolution Transmission Electron Microscopy**

By *Viveka Alfredsson,* Tetsu Ohsuna, Osamu Terasaki,* and *Jan-Olov Bovin*

Synthetic zeolites, produced in tons per year, are important products in the chemical industry. Although synthetic zeolites are primarily used in detergents, synthetic faujasites (FAU) are most widely employed as catalysts and as adsorbents of water or organic compounds. Naturally occurring zeolites are used in wastewater treatment. The cubic zeolite FAU has, aside from its recently discovered hexagonal polymorph EMT, the most open zeolite framework known (although there exist aluminium phosphates with less dense structures). The structure of FAU consists of sodalite cages (truncated octahedra) joined with double six-rings.[1] The sodalite cages are related by inversion in all four directions.

[*] V. Alfredsson, J.-O. Bovin
National Center for HREM, Inorganic Chemistry 2
Lund University
P.O. Box 124, S-221 00 Lund (Sweden)
Telefax: Int. code +(46)104012
T. Ohsuna
Department of Material Science, Iwaki Meisei University
Iwaki (Japan)
O. Terasaki
Department of Physics, Tohoku University
Aramaki Aoba, Sendai 980 (Japan)

[**] This work was supported by the Swedish Natural Science Research Council and the Swedish Research Council for Engineering Sciences (V. A. and J.-O. B.). We thank M. W. Andersson, Manchester, and S. W. Carr, Unilever Research, for providing the EMT specimen and A. Carlsson, Lund, for help with the computer graphics. T. O. thanks Prof. D. Watanabe, Iwaki, for encouragement; O. T. thanks Prof. S. Andersson, Lund, for encouragement. We also thank the National Center for Electron Microscopy, Lawrence Berkeley Laboratory, and the U.S. Department of Energy for providing the NCEMSS and IFTOOL software programs. A. Fogden, Lund, is acknowledged for linguistic comments on the text.

So-called supercages with a diameter of 13 Å are thus created within the framework. Along the [110] directions, channels are formed by interconnection of the super cages. The space group of FAU is $Fd\bar{3}m$, and its lattice parameter is 24.7 Å.[2] In the closely related structure of EMT (space group $P6_3/mmc$, $a = 17.3$ Å, $c = 28.8$ Å),[2] the double six-rings possess mirror symmetry along the c axis. Two different types of large cages are thus formed—one larger than the cubic supercage and one smaller with an elliptical shape. Until recently the hexagonal polytype was merely a hypothetical structure known as Breck's structure six (BSS),[1, 3] but it can now be synthesized with crown ethers serving as crystallization templates.[4] Intergrowths of the two polymorphs have been confirmed: the recurrent twinning of FAU results in a local formation of EMT,[5] and in the synthesis of both structures crown ethers direct the crystallization towards EMT or FAU.[6] Slabs of the faujasite structure (Fig. 1) are then connected either by inversion (FAU) or by mirror reflections (EMT).

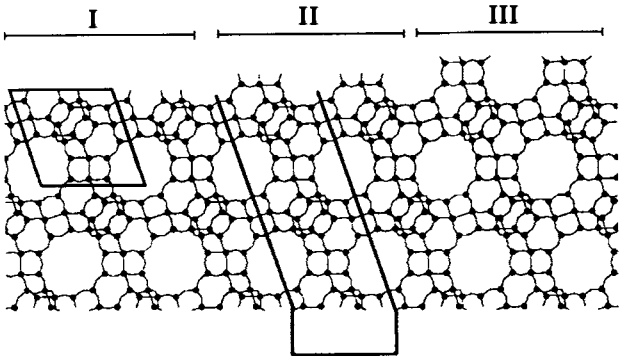

Fig. 1. Projection of the FAU structure along [110]. The Si atoms are drawn as black spots and the Si-O-Si bonds as bent lines. A FAU slab is defined as the part of the structure between the two heavy diagonal lines. In the hexagonal EMT structure the slabs are related by mirror symmetry. The upper edge of the structure displays the atom arrangements of the three structure models used in the computer image simulations. The rhombus marks the possible surface growth unit at the steps of the surface.

High-resolution transmission electron microscopy (HRTEM) gives a direct image of crystal structures, their defects, and local variations. It is an indispensable method for the elucidation of intergrowths. HRTEM investigations of zeolites have previoulsy been limited to the Si-richer forms. Usually the zeolite structures disintegrate rapidly in the electron beam, and it has been suggested that the amount of water retained by the framework, in turn depending on the number of aluminum atoms, is a critical factor.[7] Hence, the hydrophobic ultrastable zeolite Y (USY) and silicalite are normally better suited to HRTEM investigations. The NaY zeolites (FAU) (Si/Al = 2.8) investigated here, which are in the original form, were sufficiently stable for the atomic structure images of clean surfaces to be recorded for the first time. We attribute this stability to the high crystallinity of the samples. The crystals investigated contained practically no defects, apart from the twin planes in FAU, which are equivalent to intergrowths of narrow slabs of the hexagonal structure (EMT). The surfaces were also clear and sharp without contamination. The possibility of observing untreated zeolites is, of course, a great advantage, as the samples do not have to be altered in any way prior to the HRTEM studies and can thus be imaged exactly in their original form.

The crystals of the zeolite samples were dispersed in water or acetone and then collected on perforated carbon films. Since the crystals were not crushed, the HRTEM images show the form of the surfaces as they appear after synthesis or after the hydrothermal treatment (USY). The Si/Al ratios were 2.8 for the FAU samples and 3.1 for the EMT samples. The electron micrographs were recorded with a JEM-4000EX microscope operated at 400 keV. This microscope has a spherical aberration constant of 1.0 mm and a resolution limit of 1.6 Å. A television camera (Gatan 622) with an image intensifier was employed to permit focusing at very low beam intensities. The crystal structure of FAU determined from X-ray diffraction was taken as a basis for creation of the different models of the {111} surfaces with the IFTOOL programs (R. Kilaas, Berkeley, personal communication). The image simulations were performed with the NCEMSS programs.[8] The optical parameters of the microscope were used in the calculations.

The form of the FAU crystals investigated in this work is determined almost exclusively by {111} faces. Other kinds of faces sometimes appear at the intersection of the {111} faces, but these are poorly defined. The crystals are often wedge-shaped, becoming thinner at the position where four {111} faces intersect. This intersection, corresponding to the corner of an octahedron, is rounded off in all cases. The particles are crystalline to the very edge. It has been observed that the shape of the zeolite crystals can be altered when they become amorphous during irradiation,[9] but this was not the case here.

There are clear resemblances between the experimental images and the model of the crystal and surface structure shown in Figure 1. When a FAU crystal is viewed along the [110] direction, one set of channels is parallel to the electron beam. Between the large channels, recognizable as large white spots in the micrographs (Fig. 2), three smaller white

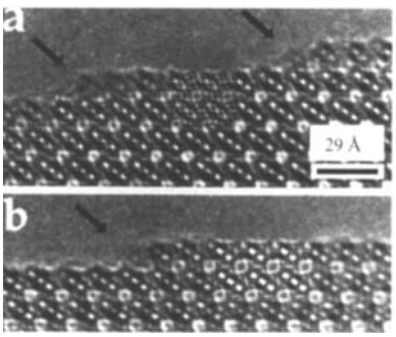

Fig. 2. HRTEM surface profile images of a {111} surface on a FAU (NaY) crystal recorded with the electron beam parallel to [110]. a) Image of the surface showing two surface steps, each 14.3 Å high, close to the octahedral top of the crystal. A simulated image for the surface model I (see Fig. 1) calculated for a focus of −900 Å and a crystal thickness of 50 Å is inserted. b) A surface step situated on the same {111} surface. A computer-simulated image of model I calculated for a focus of −700 Å and a crystal thickness of 50 Å is inserted.

spots are visible, which correspond to smaller channels in the framework (see Fig. 1). The middle spot is a projection of three Si-O four-rings, while the other two correspond to six-rings of Si-O. The dark spots at the centers of the large channels are artefacts due to insufficient transfer by the objective lens for reflections with small scattering vectors.[10, 11]

The {111} surfaces of the FAU crystals observed in this investigation are always terminated identically. Since the

surface terminates in the middle of the large channels, the edge seen in the image resembles the edge of a postage stamp. The most likely surface structure was determined by comparison of HRTEM images with computer simulations for three types of surface models (see Fig. 1). All of the models have the same number of "dangling" bonds, each ending with an oxygen atom. The hydrogen atom in the terminal OH group[1] was ignored in the image calculations since it is a very weak scatterer of electrons. The three surface models were chosen to terminate in the following ways:

1) with an incomplete sodalite cage (model I),
2) with a complete sodalite cage (model II),
3) with a complete double six-ring (model III).

The computer-simulated HRTEM images were calculated for crystal thicknesses of 50 Å and 200 Å with an objective lens focus series ranging from 0 to −900 Å (underfocus conditions) in steps of 100 Å. The simulated images displaying the closest match to the experimental ones are inserted in Figures 2 and 3.

The electron micrographs in Figures 2a and b show two different areas of the same {111} surface of a FAU crystal. Since the crystal is wedge-shaped and its support angle is unknown, the focus conditions are not identical. The variation in the crystal thickness has very little influence when the thickness does not exceed 200 Å. For this crystal surface model I gives the best fit, although distinguishing between model II with the completed sodalite cage and model I is somewhat difficult. The third model is easily rejected, since the surface in this model typically possesses two types of depressions: one is formed by the half-sphere of the supercage, has only the "closed" SiO_4 bonds on its surface, and has a diameter of 13 Å—the perfect size to accommodate a small 55-atom metal cluster; the second depression created by half of a sodalite cage, is significantly smaller (6.2 Å), and has an entrance surrounded by six dangling Si-O-H groups.

The crystal imaged in Figure 3a reveals an intergrowth of the hexagonal zeolite EMT and FAU, its cubic counterpart.

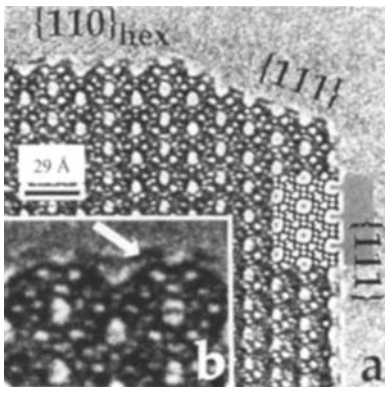

Fig. 3. a) Surface profile image of an EMT crystal along [110] showing the intergrowth with FAU (right). A simulated image for model III calculated for a crystal thickness of 200 Å and a focus of −700 Å is inserted. b) The enlargement of the $\{110\}_{hex}$ surface shows clearly (arrow) the contrast from the double Si-O six-rings, similar to that on the {111} surface.

The right side of the crystal is FAU. As was the case for FAU in Figure 2, the surfaces of the crystal are clear and without contamination. Crystals of EMT are plate shaped; as the specimen here is imaged end-on, the projection distance is great (several hundred Å). The inserted image was calculated for a crystal thickness of 200 Å. The {111} surface of the FAU part of the crystal (Fig. 3a, on the right) displays a structure image closely related to that of model III (see Fig. 1). This is apparent on comparison of the simulated image of focus −700 Å with the experimental one. Models III and I posess the common feature of completed double six-rings. The image of the $\{110\}_{hex}$ surface (the horizontal crystal surface in Fig. 3b) exhibits a similar termination of the surface structure. Since the EMT structure arises from chemical twinning[12] of unit-cell-width slabs of the FAU structure (marked in the model in Fig. 1) with mirror reflection as the twin operation, the EMT $\{110\}_{hex}$ surface would be expected to consist of unit-cell-width $\{111\}_{cubic}$ surface planes of the FAU structure. This is the appearance of the $\{110\}_{hex}$ surface in the image displayed in Figure 3b with a surface termination made up of double six-membered Si-O rings.

The {111} surface structures are different, as shown in Figures 2 and 3a. Although the latter possesses the large depression made out of the supercage, the sodalite cage is now closed. In this case the supercage is more complete, and the overall surface is more "rugged". The different surface structures can be traced back to the manner of preparation of the two samples. The EMT sample was synthesized with crown ethers as templates,[4] whereas the FAU crystal was prepared by the conventional hydrothermal method. The rugged {111} surface structures of the EMT crystal can be explained by the fact that the crown ether is probably adsorbed on the surface during the crystal growth and gives rise to more complete cages when incorporated in the crystal.

In several cases we found steps on the {111} surface of FAU crystals (see Figs. 2a and b). These steps are positioned at the ends of the crystal growth planes, suggesting that the crystal growth took place along the {111} surface one layer at the time. This implies that the growth rate is high along the {111} surface and relatively low perpendicular to it. The {111} planes will thus dominate the shape of the crystal, conferring upon it an octahedral habit, which is confirmed by the HRTEM images. The height of the surface steps is identical to the distance of unit cell repeat in this direction (14.3 Å). In the three steps shown in Figure 2, the detailed image contrasts differ in structure, permitting some conclusions to be drawn. The step at the left in Figure 2a is situated near the top of the octahedral crystal and has an appearance distinct from that of the other two steps. It comprises two unfinished rows of the unit marked as a rhombus in Figure 1, which contains the three small channels (the three white spots in the HRTEM image). This image is obtained from the projection of the top triangular {111} surface of the crystal. The step at the right in Figure 2a displays only one unfinished unit with the small channels but is of almost the same contrast as the adjacent one. This indicates that the row is nearly as long as the whole surface. The contrast of the third step (Fig. 2b) is weaker than the former one, implying that this row of units is shorter in projection. Similar surface steps caused by incomplete {001} planes have been observed by HRTEM for EMT.[13]

USY, the ultrastable form of FAU, is obtained after several post-synthesis treatments. The standard means of accomplishing a siliceous form of zeolite Y is hydrothermal treatment. First, Na^+ is exchanged for NH_4^+, whereupon the zeolite is heated in steam. This process is repeated several times in order to remove the aluminum as completely as possible, after which the zeolite is leached in acid to extract the intrachannel aluminum species. This treatment creates "mesopores", believed to be large cavities in the framework.

The HRTEM images of USY crystals differ from those of NaY (see Fig. 2), although the average crystal structure images appear similar and the crystal habit is also preserved. For USY zeolites we never observed clean crystal edges such as those in NaY. The crystals of USY are always completely enclosed by a thin amorphous layer (see Fig. 4). We are certain that these layers are not caused by irradiation, since they are present even when the bulk of the crystal is undamaged. We have also found USY crystals to be more stable under the electron beam than the zeolite forms containing aluminum. Under the amorphous layer, surface steps (see arrow in Fig. 4) similar to those observed in FAU (see Fig. 2) can be discerned. This may be taken as an indication that the structure as a whole is not changed in any significant way during the dealumination process and that the amorphous constituents originally come from inside the particle (possibly from the mesopore areas) and not from the surface. Alternatively, it may be postulated that the crystal disintegrates during dealumination, starting with the outer surface layers, progressing one layer at the time. In this case the step will actually be the antithesis of a growth mechanism.

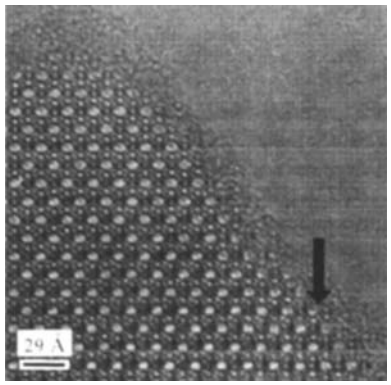

Fig. 4. HRTEM image of the top part of an octahedrally shaped USY crystal (dealuminated FAU zeolite), recorded with the electron beam parallel to [110]. The {111} surface, and most likely the whole crystal, is covered with a thin amorphous layer approximately 25 Å thick. The arrow points to what might have been a step on the {111} surface before the dealumination process.

Received: January 23, 1993 [Z 5824 IE]
German version: *Angew. Chem.* **1993**, *105*, 1262

[1] D. W. Breck, *Zeolite Molecular Sieves*, Wiley, New York, **1974**.
[2] W. M. Meier, D. H. Olson, *Atlas of Zeolite Structure Types*, 3rd ed., Structure Commission of the International Zeolite Association, Butterworths-Heinemann, Stoneham, **1992**.
[3] P. B. Moore, J. V. Smith, *Mineral. Mag.* **1964**, *34*, 1008–1014.
[4] F. Delprato, L. Delmotte, J. L. Guth, L. Huve, *Zeolites* **1990**, *10*, 546–552.
[5] M. Audier, J. M. Thomas, J. Klinowski, D. A. Jefferson, L. A. Bursill, *J. Phys. Chem.* **1982**, *86*, 581–584.
[6] M. W. Anderson, K. S. Pachis, F. Prebin, S. W. Carr, O. Terasaki, T. Ohsuna, V. Alfredsson, *J. Chem. Soc. Chem. Commun.* **1991**, 1660–1664.
[7] L. A. Bursill, J. M. Thomas, K. J. Rao, *Nature* **1981**, *289*, 157–158.
[8] R. Kilaas, *Proc. Annu. Meet. Electron Microsc. Soc. Am.* **1987**, *45*, 66–67.
[9] M. M. J. Treacy, J. M. Newsam, *Ultramicroscopy* **1987**, *23*, 411–420.
[10] V. Alfredsson, O. Terasaki, J.-O. Bovin, *J. Solid State Chem.*, in press.
[11] R. Csencsits, R. Gronsky, *Ultramicroscopy*, **1987**, *23*, 421–432.
[12] S. Andersson, B. G. Hyde, *J. Solid State Chem.* **1974**, *9*, 92–101.
[13] O. Terasaki, T. Ohsuna, V. Alfredsson, J.-O. Bovin, D. Watanabe, S. W. Carr, M. W. Andersson, *Chem. Mater.*, **1993**, *5*, 452–458.

C–H-Activation by Reaction of (Butadiene)zirconocenes and -hafnocenes with 9-BBN**

By *Gerhard Erker*,* *Ralf Noe*, *Doris Wingbermühle*, and *Jeffrey L. Petersen*

Activation and designed functionalization of organic substrates in organometallic compounds through the simultaneous influence of two metallic centers on a ligand is a matter of current discussion. Experimental realization of this basically attractive concept, however, could only be accomplished in a few cases.[1] Generally, a combination of transition elements, for the most part even of two like d-block elements, were employed. Had there been more attempts to combine the effects of a transition metal and an electropositive main group element, there would probably have been more examples of dimetallic activation of organic compounds to date. With just that combination we achieved stoichiometric C-H activation of 1,3-butadiene under fairly mild reaction conditions.

We treated (η^4-butadiene)bis(η^5-methylcyclopentadienyl)-zirconium (**2a**)[2] with a molar equivalent of 9-borabicyclo[3.3.1]nonane (9-BBN, **1**; in the following the abbreviation 9-BBN is used for the borane as well as the boryl substituent). The addition is complete in toluene at room temperature within 5 h, and compound **4a** can be isolated in 86% yield (Scheme 1). The product **4a** has a metallacyclic framework with an endocyclic (π-allyl)zirconocene unit. The assignment of the structure follows from the characteristic

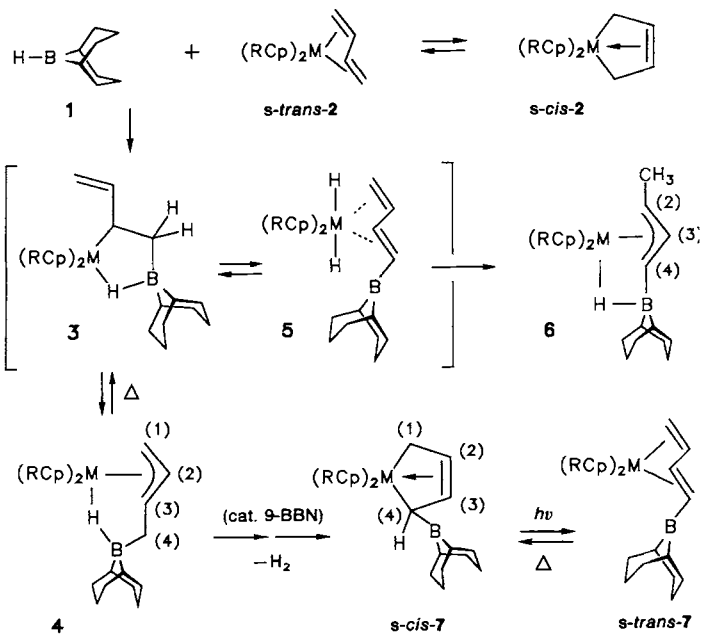

Scheme 1. M = Zr, R = CH_3 (**a**), R = H (**b**); M = Hf, R = H (**c**).

[*] Prof. Dr. G. Erker, Dipl.-Chem. R. Noe, D. Wingbermühle
Organisch-chemisches Institut der Universität
Corrensstrasse 40, D-48149 Münster (FRG)
Telefax: Int. code + (251)83-9772
Prof. Dr. J. L. Petersen
Department of Chemistry, West Virginia University
Morgantown, WV 26506 (USA)

[**] This work was supported by the Volkswagen-Stiftung, the Fonds der Chemischen Industrie, the NATO, and the Alfried-Krupp-von-Bohlen-und-Halbach-Stiftung.

spectroscopic properties (Table 1) and a comparison with typical data of many analogous addition compounds of (butadiene)metallocenes.[3]

Table 1. Characterization and spectroscopic data of the new organometallic compounds.

4a: 320 mg (86%) isolated, m.p. 114 °C (DSC); correct C,H analysis. – ^{1}H NMR ([D$_6$]benzene, 200 MHz): δ = 5.60, 5.33, 5.22, 5.17, 5.14, 5.09, 4.93, 4.87 (m, each 1 H, C$_5H_4$CH$_3$), 4.55 (m, 1 H, 3-H), 3.81 (m, 1 H, 2-H), 2.60 (m, 1 H, 1-H *syn*), 2.40–1.90 (m, 12 H, CH$_2$, 9-BBN), 1.60, 1.54 (2s, each 3 H, CH$_3$), 1.82 (dd, 1 H, 4-H), 1.43 (m, 1 H, 1-H *anti*), 1.33 (m, 1 H, 4-H'), 0.65 (br m, 2 H, CH, 9-BBN), -4.35 (br s, 1 H, Zr-*H*-B), coupling constants [Hz]: ^2J = 11.3 (1-H *syn*, 1-H *anti*), 5.2 (4-H, 4-H'), ^3J = 15.9 (2-H, 3-H), 3.3 (1-H *syn*, 2-H), 11.4 (1-H *anti*, 2-H), 8.2 (3-H, 4-H), 13.3 (3-H, 4-H'); ^{13}C NMR ([D$_6$]benzene, 75 MHz): δ = 117.9, 117.2 (*ipso*-C, MeCp), 112.2, 109.1, 107.0, 105.4, 104.8 (doubled intensity), 102.1, 101.9 (CH, MeCp), 113.7 (^1J(C,H) = 149 Hz, C-3), 97.8 (140 Hz, C-2), 48.0 (153 and 144 Hz, C-1), 25.0 (C-4), 33.4, 33.0 (CH$_2$, 9-BBN), 28.4 (br, CH, 9-BBN), 14.8 (127 Hz, CH$_3$); ^{11}B NMR ([D$_6$]benzene, 64 MHz): δ = –19.5. IR (KBr): $\tilde{\nu}$ = 1594 cm^{-1} (br, m-H)

6a: 270 mg (98%) isolated. – ^{1}H NMR ([D$_6$]benzene, 200 MHz): δ = 5.16–4.94 (m, 5 H), 4.90 (m, 1 H), 4.68 (m, 1 H), 4.52 (m, 1 H, C$_5H_4$CH$_3$), 4.32 (m, 1 H, 3-H), 2.60–2.00 (m, 14 H, 4-H, 2-H and CH$_2$, 9-BBN), 1.83 and 1.66 (s, each 3 H, C$_5H_4CH_3$), 1.74 (d, 3 H, allyl-CH$_3$), 0.86 and 0.45 (br m, each 1 H, CH, 9-BBN), –4.44 (br s, 1 H, Zr-H-B); ^{13}C NMR ([D$_6$]benzene, 50 MHz): δ = 116.0, 111.8 (*ipso*-C, MeCp), 110.3, 107.7, 107.1, 104.5, 102.8, 102.0, 101.6, 98.4 (CH, MeCp), 128.3, 80.3 (^1J(C,H) = 145 Hz), 89 (br, ^1J(C,H) ≈ 125 Hz, C-2, C-3, C-4), 38.5, 38.4, 35.4, 34.0, 26.4, 26.0 (CH$_2$, 9-BBN; CH, 9-BBN not observed). 19.1 (125 Hz, allyl-CH$_3$); 15.1 and 14.8 (127 Hz, C$_5$H$_4$-CH$_3$); ^{11}B NMR ([D$_6$]benzene, 64 MHz): δ = 4.6. IR (KBr): $\tilde{\nu}$ = 1610 cm^{-1} (br, m-H)

4b: 1.7 g (86%) isolated, m.p. 130 °C; correct C,H analysis. – ^{1}H NMR ([D$_6$]benzene, 200 MHz): δ = 5.30 and 5.13 (s, each 5 H, Cp), 4.48 (m, 1 H, 3-H), 3.81 (m, 1 H, 2-H), 2.56 (m, 1 H, 1-H *syn*), 2.40–1.75 (m, 12 H, CH$_2$, 9-BBN), 2.01 (dd, 1 H, 4-H), 1.40 (m, 1 H, 1-H *anti*), 1.29 (dd, 1 H, 4-H'), 0.64 (br m, 2 H, CH, 9-BBN), -4.47 (br. s, 1 H, Zr-H-B); coupling constants [Hz]: ^2J = 11.5 (1-H *syn*, 1-H *anti*), 5.1 (4-H, 4-H'), ^3J = 16.3 (2-H, 3-H), 4.1 (1-H *syn*, 2-H), 12.0 (1-H *anti*, 2-H), 8.0 (3-H, 4-H), 13.3 (3-H, 4-H'); ^{13}C NMR ([D$_6$]benzene, 75 MHz): δ = 105.9 and 104.5 (Cp), 112.4 (^1J(C,H) = 148 Hz, C-2), 95.7 (142 Hz, C-3), 44.8 (153 and 146 Hz, C-1), 33.3, 32.8 (CH$_2$, 9-BBN), 28.3, 26.2 (CH, 9-BBN), 24.9 (C-4); ^{11}B NMR ([D$_6$]benzene, 64 MHz): δ = –19.5. IR (KBr): $\tilde{\nu}$ = 3116, 1441, 1016, 808 cm^{-1} (Cp), 1617 (br, m-H)

6b: 330 mg (87%) isolated (9:1 mixture of **6b** and s-*cis*-**7b**), m.p. 178 °C (DSC). – ^{1}H NMR ([D$_6$]benzene, 200 MHz): δ = 5.00 and 4.98 (s, each 5 H, Cp), 4.23 (m, 1 H, 3-H), 2.66 (m, 1 H, 2-H), 2.55–2.00 (br m, 13 H, CH$_2$, 9-BBN, and 4-H), 1.73 (d, 3 H, allyl-CH$_3$), 0.76 and 0.36 (br m, each 1 H, C*H*, 9-BBN), –4.69 (br s, 1 H, m-H), coupling constants [Hz]: ^3J = 17.6 (4-H, 3-H), 14.8 (3-H, 2-H), 6.0 (2-H, CH$_3$), ^4J = 1.2 (4-H, 2-H); ^{13}C NMR ([D$_6$]benzene, 75 MHz): δ = 102.6 and 102.4 (Cp), 127.3 (^1J(C,H) = 146 Hz, C-2), 88 (br, ^1J(C,H) ≈ 125 Hz, C-4), 79.1 (145 Hz, C-3), 38.5 (double intensity), 35.3, 34.1, 26.5, 26.0 (CH$_2$, 9-BBN), 28.8 and 24.2 (*C*H, 9-BBN), 19.6 (125 Hz, CH$_3$); ^{11}B NMR ([D$_6$]benzene, 64 MHz): δ = 4.1. IR (KBr): $\tilde{\nu}$ = 3113, 1438, 1017, 803 cm^{-1} (Cp)

s-*cis*-**7b**: ^{1}H NMR ([D$_6$]benzene, 50 MHz, 300 K): δ = 5.47 and 4.92 (s, each 5 H, Cp), 5.30 and 4.9 (m, each 1 H, 3-H, 2-H), 3.31 (dt, 1 H, 1-H), 2.2–1.4 (br m, 14 H, CH$_2$, CH, 9-BBN), 0.29 (d, 1 H, 4-H), –0.30 (m, 1 H, 1-H'); ^{13}C NMR ([D$_6$]benzene, 50 MHz): δ = 118.1 and 116.8 (C-2 and C-3), 104.8 and 101.3 (Cp), 77.2 (br, C-4), 51.7 (C-1), 36.8, 36.3, 32.1, 31.9, 26.4, 21.8 (*C*H$_2$, 9-BBN), 30.2, 24.6 (CH, 9-BBN); ^{11}B NMR ([D$_6$]benzene, 64 MHz): δ = 60.3

s-*cis*-**7c**: 310 mg (46%) isolated, m.p. 195 °C, correct C,H analysis. – ^{1}H NMR ([D$_6$]benzene, 200 MHz): δ = 5.45 and 4.94 (s, each 5 H, Cp), 5.40 (m, each 1 H, 3-H), 5.05 (m, 1 H, 2-H), 3.09 (dt, 1 H, 1-H), 2.2–1.4 (br m, 14 H, 9-BBN), 0.33 (d, 1 H, 4-H), –0.52 (dt, 1 H, 1-H'); ^{13}C NMR ([D$_6$]benzene, 50 MHz): δ = 118.8 (^1J(C,H) = 157 Hz) and 117.7 (157 Hz, C-2 and C-3), 104.5 and 100.8 (Cp), 72 (br, C-4), 46.6 (^1J(C,H) = 152 and 133 Hz, ^2J(C,H) = 9 Hz, C-1), 36.7, 36.1, 31.9, 31.7, 26.6, 21.5 (CH$_2$, 9-BBN), 30.0, 24.5 (CH, 9-BBN); ^{11}B NMR ([D$_6$]benzene, 64 MHz): δ = 62. IR (KBr): $\tilde{\nu}$ = 3111, 1440, 1014, 804 cm^{-1} (Cp)

s-*trans*-**7c**: ^{1}H NMR ([D$_8$]toluene, 200 MHz, 300 K): δ = 4.87 and 4.79 (s, each 5 H, Cp), 3.45–3.33 (m, 2 H, 2-H, 3-H), 3.02 (m, 1 H, 1-H *syn*) 2.2–1.8 (br m, 14 H, 9-BBN), 1.52 and 1.25 (m, each 1 H, 1-H *anti*, 4-H); ^{13}C NMR ([D$_8$]toluene, 50 MHz, 235 K): δ = 99.8 and 99.6 (C-2, C-3), 99.4 and 99.0 (Cp), 76.5 (^1J(C,H) = 127 Hz, C-4), 57.8 (^1J(C,H) = 154 and 147 Hz, C-1), 38.1, 38.0, 32.5, 29.5, 26.6, 22.0 (*C*H$_2$, 9-BBN), 30.9, 26.3 (*C*H, 9-BBN).

Thermolysis of **4a** (approximately 2 wt% in toluene, 100 °C, 40 min) yields nearly quantitatively **6a**, isomeric to **4a**, as a rearrangement product. It still contains a μ-H bridge spanning Zr and B. Typical spectroscopic data indicate that a crotyl ligand carrying a 9-BBN substituent at C4 (for numbering see Scheme 1) is now η^3-coordinated to the zirconium atom. X-ray structure analysis (Fig. 1[4]) shows **6a** to possess

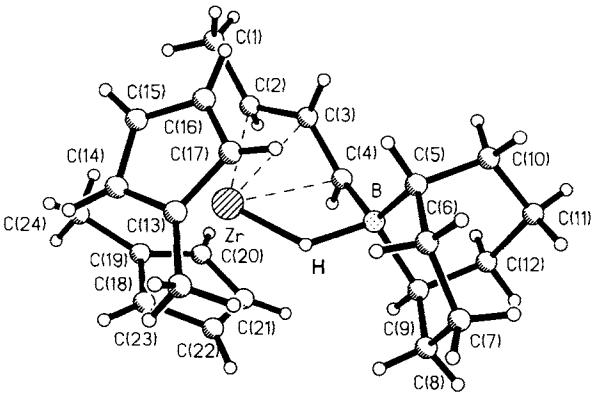

Fig. 1. Molecular structure of **6a** in the crystal. Selected bond lengths [Å] and angles [°]: Zr-C(2) 2.564(8), Zr-C(3) 2.449(8), Zr-C(4) 2.425(6), Zr-H 1.85(6), B-H 1.40(5), B-C(5) 1.604(11), B-C(9) 1.611(12), B-C(4) 1.556(12), C(3)-C(4) 1.393(12), C(2)-C(3) 1.402(13), C(1)-C(2) 1.492(13); center of Cp(1)-Zr-center of Cp(2) 128.0, Zr-H-B 119.1(40), H-B-C(4) 94.2(28), C(5)-B-C(9) 107.5(7), C(1)-C(2)-C(3) 124.9(8), C(2)-C(3)-C(4) 122.9(8), C(3)-C(4)-B 127.7(6).

a metallacyclic skeleton with a 1,3-disubstituted (π-allyl)zironocene unit. The two substituents (CH$_3$ at C2 and R$_2$B of 9-BBN at C4) have a *syn* arrangement with respect to the π-allyl unit.

This thermally induced isomerization, after addition of the boryl substituent, involves transfer of a hydrogen atom from one end of the initial butadiene ligand to the other. We think that this C-H activation first requires the formation of a (σ-allyl)metallocene **3** from **4**.[5] β-Hydride elimination in the five-membered metallacycle[6] then leads to an equilibrated mixture of isomers of [η^2-1-(9-BBN)butadiene]dihydridozirconocene (**5**) from which the observed product **6** can be formed by intramolecular hydrozirconation.

A [1-(9-BBN)butadiene]zirconocene unit is preformed in the hypothetical intermediate **5** of this reaction sequence. By successive addition and elimination of hydrido ligands, it should be possible to generate an isomer of **5** with hydrido ligands in a *cis* arrangement. The *cis* isomer can then form a stable [η^4-1-(9-BBN)butadiene]metallocene by eliminating molecular hydrogen. This was actually accomplished: addition of 9-BBN to [η^4-butadiene]zirconocene (**2b**) at room temperature yields the metallacyclic compound **4b**. Subsequent thermolysis (100 °C, 1 h) leads to a 9:1 mixture of the zirconium complex **6b** containing a boryl-substituted crotyl ligand and the [s-*cis*-η^4-1-(9-BBN)butadiene]zirconocene (s-*cis*-**7b**). At 100 °C, product **7** formed by H$_2$-elimination competes with the rearrangement product **6**. A high yield of [η^4-1-(9-BBN)butadiene]zirconocene can be obtained by direct transformation of **4b** at an elevated temperature (approximately 100 °C) with more 9-BBN (approximately 10 mole percent) as a catalyst. Mechanistic details of the dialkylborane-induced formation of **7** are presently underway.

Starting from the easily available (s-*cis*-η^4-butadiene)-hafnocene[2], we have developed a simple direct route to [η^4-1-(9-BBN)butadiene]hafnocene. An equimolar mixture of (butadiene)hafnocene and 9-BBN in toluene was stirred for 1 h at 50 °C and heated for another 3 h at 100 °C. The solvent was distilled off, and the residue extracted with boiling *n*-heptane. From the extract, [s-*cis*-η^4-1-(9-BBN)-

butadiene]hafnocene (s-*cis*-**7c**) precipitated as orange crystals in approximately 50% yield.[7] Photolysis of s-*cis*-**7c** (10% solution in toluene) quantitatively yields the s-*trans*-**7c** isomer, which in turn isomerizes to the more stable s-*cis*-**7c** above 0°C [s-*trans*-**7c** → s-*cis*-**7c**: $\Delta G^{\neq}$ (300 K) = 22.6 ± 0.5 kcal mol^{-1}].[8]

Our experiments show that C–H bonds in simple organic substrates can be easily activated by using a combination of a main group element and a transition metal. Since many complexes with combinations of moieties containing d-block metals and main group elements are now easily accessible,[9] we shall devote attention to these "heterodimetallic" compounds as stoichiometric reagents or catalysts for the activation of organic substrates.

Received: March 23, 1993 [Z 5952 IE]
German version: *Angew. Chem.* **1993**, *105*, 1216

[1] See for example: F. Antwi-Nsiah, M. Cowie, *Organometallics* **1992**, *11*, 3157; Y. Ishii, Y. Ishino, T. Aoki, M. Hidai, *J. Am. Chem. Soc.* **1992**, *114*, 5429; V. Dufand, J. Thivolle-Cazat, J. M. Basset, R. Mathieu, J. Jand, J. Waissermann, *Organometallics* **1991**, *10*, 4005; J. Schwank, *Stud. Surf. Sci. Catal.* **1991**, *64*, 225; *Chem. Abstr.* **1991**, *115*, 240877c; M. Ichikawa, *Polyhedron* **1988**, *7*, 2351; A. Fukuoka, M. Ichikawa, J. A. Hriljac, D. F. Shriver, *Inorg. Chem.* **1987**, *26*, 3643; S. Sato, B. Chaudret, D. Gervais, R. Poilblanc, *Nouv. J. Chim.* **1981**, *5*, 597; C. P. Horwitz, D. F. Shriver, *Adv. Organomet. Chem.* **1984**, *23*, 219; E. L. Muetterties, J. Stein, *Chem. Rev.* **1979**, *79*, 479; E. L. Muetterties, T. N. Rhodin, E. Band, C. F. Brucker, W. R. Pretzer, *ibid.* **1979**, *79*, 91, and references therein, cf.: J. Hine, *Acc. Chem. Res.* **1978**, *11*, 1.

[2] G. Erker, J. Wicher, K. Engel, F. Rosenfeldt, W. Dietrich, C. Krüger, *J. Am. Chem. Soc.* **1980**, *102*, 6344; H. Yasuda, Y. Kajihara, K. Mashima, K. Nagasuna, K. Lee, A. Nakamura, *Organometallics* **1982**, *1*, 388; G. Erker, K. Engel, C. Sarter in *"Organometallic Synthesis" Vol. 3* (Eds.: R. B. King, J. J. Eisch), Elsevier, Amsterdam, **1986**, p. 32.

[3] G. Erker, K. Engel, U. Dorf, J. L. Atwood, W. E. Hunter, *Angew. Chem.* **1982**, *94*, 915; *Angew. Chem. Int. Ed. Engl.* **1982**, *21*, 914; G. Erker, U. Dorf, R. Benn, R.-D. Reinhardt, J. L. Petersen, *J. Am. Chem. Soc.* **1984**, *106*, 7649; G. Erker, T. Mühlenbernd, R. Benn, A. Rufinska, *Organometallics* **1986**, *5*, 402; G. Erker, R. Lecht, R. Schlund, K. Angermund, C. Krüger, *Angew. Chem.* **1987**, *99*, 708; *Angew. Chem. Int. Ed. Engl.* **1987**, *26*, 666; G. Erker, R. Lecht, J. L. Petersen, H. Bönnemann, *Organometallics* **1987**, *6*, 1962; G. Erker, R. Lecht, Y.-H. Tsay, C. Krüger, *Chem. Ber.* **1987**, *120*, 1763. Review: G. Erker, *Angew. Chem.* **1989**, *101*, 411; *Angew. Chem. Int. Ed. Engl.* **1989**, *28*, 397.

[4] Crystal structure analysis of **6a**: Crystal size 0.10 × 0.26 × 0.54 mm, monoclinic, space group $P2_1$, a = 10.665(5), b = 7.819(1), c = 13.429(4) Å, β = 109.87(3)°, V = 1053.2(4) Å^3, Z = 2, ρ_{calcd} = 1.342 g cm^{-3}, F(000) = 448, $\mu(Mo_{K\alpha})$ = 5.27 cm^{-1}, Siemens-P4-diffractometer, T = 295 K, graphite-monochromated $Mo_{K\alpha}$ (λ = 0.71073 Å), 2θ-scan 2–50.0°, 2642 measured reflections of which 2278 were unique and 1868 observed at $F > 4.0\,\sigma(F)$. 237 independent parameters refined, Siemens SHELXTL PLUS program, direct methods, R = 0.0393, R_w = 0.0415. Further details of the crystal structure investigation may be obtained from the Fachinformationszentrum Karlsruhe, Gesellschaft für wissenschaftlich-technische Information mbH, D-76344 Eggenstein-Leopoldshafen, on quoting the depository number CSD-57168, the names of the authors, and the journal citation.

[5] G. Erker, K. Engel, J. L. Atwood, W. E. Hunter, *Angew. Chem.* **1983**, *95*, 506, *Angew. Chem. Int. Ed. Engl.* **1983**, *22*, 494. See also: E. G. Hoffmann, R. Kallweit, G. Schroth, K. Seevogel, W. Stempfle, G. Wilke, *J. Organomet. Chem.* **1975**, *97*, 183; G. Erker, K. Berg, K. Angermund, C. Krüger, *Organometallics* **1987**, *6*, 2620, and references therein.

[6] U. Dorf, K. Engel, G. Erker, *Angew. Chem.* **1982**, *94*, 916, *Angew. Chem. Int. Ed. Engl.* **1982**, *21*, 914; J. S. McDermott, J. F. White, G. M. Whitesides, *J. Am. Chem. Soc.* **1976**, *98*, 6521, 6529; T. M. Miller, G. M. Whitesides, *Organometallics* **1986**, *5*, 1473.

[7] For conventional syntheses of 1-(9-BBN)-substituted 1,3-butadiene and other boryl-substituted olefins see: R. Köster, A. Bussmann, G. Schroth, *Liebigs Ann. Chem.* **1975**, 2130; G. M. Clark, K. G. Hancock, G. Zweifel, *J. Am. Chem. Soc.* **1971**, *93*, 1308; G. Zweifel, G. M. Clark, N. L. Polston, *ibid.* **1971**, *93*, 3395; R. Köster, *Pure Appl. Chem.* **1977**, *49*, 765; D. A. Singleton, J. P. Martinez, G. M. Ndip, *J. Org. Chem.* **1992**, *57*, 5768; T. E. Cole, R. Quintanilla, *ibid.* **1992**, *57*, 5768; T. E. Cole, R. Quintanilla, *ibid.* **1992**, *57*, 7366; R. H. Wallace, K. K. Zong, *Tetrahedron Lett.* **1992**, *33*, 6941; I. Rivera, J. C. Colberg, J. A. Soderquist, *ibid.* **1992**, *33*, 6919; N. Noiret, Y. Youssofi, B. Carboni, M. Vaultier, *J. Chem. Soc. Chem. Commun.* **1992**, 1105; H. C. Brown, U. R. Khire, U. S. Racherla, *Tetrahedron Lett.* **1993**, *34*, 15; R. Köster, G. Seidel, K. Wagner, B. Wrackmeyer, *Chem. Ber.* **1993**, *126*, 305. R. Köster, G. Seidel, K. Wagner, B. Wrackmeyer. *ibid.* **1993**, *126*, 319, and references therein. Review: R. Köster in *"Organobor-Verbindungen I"* (*Methoden Org. Chem. (Houben-Weyl) 4th Ed. 1952–*), Band 13/3a, **1982**, p. 206ff.

[8] G. Erker, J. Wicher, K. Engel, C. Krüger, *Chem. Ber.* **1982**, *115*, 3300; G. Erker, K. Engel, C. Krüger, A.-P. Chiang, *ibid.* **1982**, *115*, 3311; U. Dorf, K. Engel, G. Erker, *Organometallics* **1983**, *2*, 462; G. Erker, C. Krüger, G. Müller, *Adv. Organomet. Chem.* **1985**, *24*, 1; G. Erker, T. Mühlenbernd, A. Rufinska, R. Benn, *Chem. Ber.* **1987**, *120*, 507.

[9] G. Erker, R. Zwettler, C. Krüger, R. Noe, S. Werner, *J. Am. Chem. Soc.* **1990**, *112*, 9620; G. Erker, M. Albrecht, C. Krüger, S. Werner, *Organometallics* **1991**, *10*, 3791; M. Albrecht, G. Erker, M. Nolte, C. Krüger, *J. Organomet. Chem.* **1992**, *427*, C21; G. Erker, *Comments Inorg. Chem.* **1992**, *13*, 111; G. Erker, M. Albrecht, S. Werner, M. Nolte, C. Krüger, *Chem. Ber.* **1992**, *125*, 1953; G. Erker, M. Albrecht, C. Krüger, S. Werner, P. Binger, F. Langhauser, *Organometallics* **1992**, *11*, 3517; G. Erker, M. Albrecht, C. Krüger, S. Werner, *J. Am. Chem. Soc.* **1992**, *114*, 8531; G. Erker, R. Noe, C. Krüger, S. Werner, *Organometallics* **1992**, *11*, 4174.

BOOKS

This section contains book reviews and a list of new books received by the editor. Book reviews are written by invitation from the editor. Suggestions for books to be reviewed and for book reviewers are welcome. Publishers should send brochures or (better) books to the Book Editor, Dr. Gerhard Karger, Redaktion Angewandte Chemie, Postfach 101161, D-69451 Weinheim, Federal Republic of Germany. The editor reserves the right of selecting which books will be reviewed. Uninvited books not chosen for review will not be returned.

Book Reviews

The Chemistry of Organophosphorus Compounds. Vol. 2: Phosphine Oxides, Sulphides, Selenides and Tellurides. (Series: The Chemistry of Functional Groups. Series editor: *S. Patai.*) Edited by *F. R. Hartley*. Wiley, Chichester, 1992. XVI, 647 pp., hardcover £ 160.00.—ISBN 0-471-93056-3

The comments of this reviewer (*Angew. Chem.* **1992**, *104*, 109; *Angew. Chem. Int. Ed. Engl.* **1991**, *30*, 1046) on the first volume of the four-volume series "The Chemistry of Organophosphorus Compounds", which appeared in 1990, are also applicable to this second volume. No major handbook on

organophosphorus chemistry has been published for a long time, and this new series is therefore very welcome. Many developments have occurred in this field during the last twenty years, and it is important that they should be covered in a work of this kind.

The area covered by Volume 2, namely phosphine oxides, sulfides, selenides, and tellurides, is certainly one of the most important parts of organophosphorus chemistry. However, some related compound classes are not covered in this volume, for example the important class of phosphine imides of the type XYZP(=NR), where X, Y, and Z are hydrocarbon groups, which can be regarded as formally related to phosphine oxides. In reviewing this volume it would have been helpful to be given a detailed plan for the complete series. Such an overall plan should at least be provided with Volumes 3 and 4 that are still to be published.

Returning to the present volume, there is no doubt that it offers an up-to-date and (almost) complete description of a very important area of organophosphorus chemistry, which is treated in detail in more than 600 pages. The editor has aimed at emphasizing important recent developments rather than attempting an encyclopedic coverage. The subjects covered by the eight chapters are: structure and bonding in tertiary phosphine chalcogenides (D. G. Gilheaney); structure and stereochemistry of secondary and tertiary phosphine chalcogenides (M. J. Gallagher); electrochemistry of organophosphorus(v) compounds (K. V. S. Santhanam—here the subject matter is by no means limited to phosphine chalcogenides); photochemistry of phosphine chalcogenides (M. Dankowski); spectroscopy of phosphine chalcogenides (G. Davidson); methods for preparing phosphine chalcogenides (A. K. Bhattacharya and N. K. Roy); chemical properties and reactions of phosphine chalcogenides (R. S. Edmundson); coordination chemistry of phosphine chalcogenides, and analytical and catalytic applications (T. S. Lobana).

The volume gives a comprehensive and up-to-date survey of the field of phosphine chalcogenides. Numerous references to the original literature are included, extending to very recent work. Each chapter begins with an introduction giving the background to the topic, and continues up to the most recent developments. As well as giving an overall picture, the chapters indicate where more detailed information can be found.

The chapter on the spectroscopy of phosphine chalcogenides is especially welcome, and covers UV/visible, vibrational, and NMR spectroscopy. It would have been desirable to have a chapter like this in Volume 1, especially with regard to NMR studies, and one hopes that Volumes 3 and 4 will also include these aspects.

The sequence of the chapters does not seem entirely appropriate; in particular, Chapters 6 and 7 (on preparative methods, chemical properties, and reactions) should, in my view, have been placed at the beginning of the book. The term "phosphine chalcogenides" is not interpreted in the same way by all the authors: in some chapters it is taken to mean only tertiary phosphine chalcogenides, whereas in others it includes both secondary and tertiary phosphine chalcogenides. There is also a lack of uniformity in the formula diagrams, with the phosphorus–chalcogen double bonds shown too long in some cases, giving an unattractive appearance. Inconsistencies are also evident in the literature coverage. For example, there is some confusion with regard to citing the Russian literature, which is especially important in organophosphorus chemistry: sometimes only the English translation is cited, whereas in other (rarer) cases only the Russian original is cited; it would have been better always to give both. Where citations in unusual or obscure journals are given, they are not always accompanied by the *Chemical Abstracts* reference. Unfortunately some authors' names have become garbled; sometimes the same name appears several times with different spellings, and so on. Moreover, it seems that the authors essentially interpret phosphine chalcogenides as compounds with only one phosphorus atom; I found no obvious mention of related compounds with two or more phosphine chalcogenide centers (for example, linked together through heteroatoms). Some other related compound types also appear to be absent. Thus, in cases where one needs to make an exhaustive search it is necessary to consult other sources. The volume includes a detailed author index and a (less comprehensive) subject index, both of which are useful.

Now that two of the four volumes have appeared, it can be said that the overall impression is still favorable, and the remaining two volumes are awaited with interest.

Reinhard Schmutzler
Institut für Anorganische und Analytische Chemie
der Technischen Universität Braunschweig (FRG)

Enantioselective Synthesis. Natural Products from Chiral Terpenes. By *Tse-Lok Ho*. Wiley, Chichester, 1992. XII, 324 pp., hardcover £ 56.00.—ISBN 0-471-54819-7.

The development of methods for the synthesis of enantiomers (rather than racemates) is a very important area of research. A new book on this subject will therefore interest many, but expectations will be high. This book deals with an important sub-domain, namely natural product synthesis starting from simple, chiral natural building blocks having high enantiopurity—the chiral pool, in the present case terpenes. The essential point is, of course, that the chirality and the enantiopurity of the building block are transferred, wherever feasible, into the synthetic target compound.

In the preface it is stated that "... there is an apparent lack of a comprehensive summary of terpene-based syntheses" and one sentence later that "... consequently it seems worthwhile to collate and discuss the important contributions in this area". Now it is clearly impossible to treat this huge area in this single, relatively thin volume. A selection must have been made, but it is up to the reader to find out what the selection is. This is the only really serious criticism I have. Nowhere does the author define the actual scope of the book.

The author has restricted himself mainly to multi-step syntheses, which are described and discussed, but with very little background information, and to starting materials that are almost exclusively monoterpenes (citronellene, citronellol, linalool, oxidized derivatives; limonene; menthone, piperitone, perilla aldehyde and related compounds; pulegone; carvone; carenes and thujone; pinenes; camphor and congeners; other terpenes).

The chapter on the camphors, for example, contains about 50 references, whereas the review article on the same subject by Money—which is cited—contains 240 primary references, many of which contain multiple citations. The difference is due to the fact that the latter review covers not only the types of syntheses dealt with in the book, but also all the classical chemistry that has made the multiple functionalizations of the camphors possible. This chemistry is only mentioned in passing in the book, and without real help as to how to get access to it ("... a thorough knowledge of its (camphor's) chemistry is most critical [Money, 1985]").

It is more difficult to judge how comprehensive the coverage of the syntheses is. We again selected the camphors and

made a computer on-line search in *Chemical Abstracts*; almost everything we found there was dealt with in the book. But I also compared with one of our lists of publications that are important for the perfumery industry, and only a fraction of that material was covered. The coverage is thus not comprehensive, but in my opinion a good representative selection has been made.

The book contains a total of about 450 references, almost exclusively from the primary literature. There are also a few theses, abstracts of ACS meetings, private communications, and two books, namely Simonsen's *The Terpenes* and the author's *Polarity Control*. The reader is referred to Simonsen's multivolume text as a source of basic terpene chemistry. It is still an important text, but it appeared in the fifties. If one cites this, then one should at least also give a selection from the many more recent handbooks, such as Erman's *Chemistry of the Monoterpenes; an Encyclopedic Handbook* (1985). Books that have similar or related objectives, such as the indispensable five-volume standard text *Asymmetric Synthesis* by Morrison and Scott (1983–1985), Hanessian's *Total Synthesis of Natural Products: The 'Chiron' Approach* (1983), and Corey and Cheng's *The Logic of Chemical Synthesis* (1989), are not mentioned. Corey's "logic-centered methodology" is instead covered by the 1969 article by Corey and Wipke in *Science*. To the best of my knowledge, the word carbogen ("During the last fifty years complex carbogen synthesis has extended its frontier to near the conceivable limit.") comes from the book by Corey and Cheng. A related word is chirogen (neologism?, "camphor is an excellent chirogen...") but the sense that it has here does not fit an earlier definition by Eschenmoser (chirogenic, *Helv. Chim. Acta* **1990**, *73*, 1373). Both terms are used without explanation or reference. A few review articles such as the one by Money are there but are not recognizable as such in the text. The limits of the literature coverage are not indicated. Most of the references are from the eighties. There is one from 1958 and five from 1991, none before or after.

I return to the contents, which are of course mirrored by the references that I discussed. I estimate that about 350 syntheses (!) are summarized in the accepted format, by means of schemes composed of formulas, arrows, letters, and footnotes. The formulas are well-drawn but usually not identified (no numbers or letters). When they are, and this is mainly done for the final products, they are identified by a name. The schemes are likewise not identified but appear in the text where they are discussed. The text consists of concise—sometimes perhaps too concise—analyses of the synthetic strategies ("Space is devoted therefore mostly to strategic considerations and unusual observations"), in a rather personal style, but that is a minor matter of taste. The whole, schemes and text, is well-integrated, and one does get a good overview. Here the author has done a very good job.

But also with regard to indexes and to some really essential data, limited and sometimes arbitrary and inconsistent choices have been made. Also the citations in the text (e.g., Money, T. (1985)) and the format of the references in the bibliography at the end of the book (Money, T. (1985) *Nat. Prod. Rep.* **2**: 253.) are inconvenient and different from standard practice in the chemical literature. There is a four-page index of the synthetic targets covered [from achillin via cornorsterone, (+)-7,8-epoxy-2-basmen-6-one, estrone, *ar*-himachalene, nootkatone, sex pheromone (banded cucumber beetle, California red scale, corn rootworm, stink bug, yellow scale) to zonarene], but neither an index of starting materials nor an author index. However, the starting materials can be found via the list of contents at the beginning of the book. The 15-page bibliography at the end of the book is of little use when one is searching for a senior author, as the references are listed alphabetically by the first-named author and, moreover, one cannot refer back to the text (no page number is given). With a few exceptions, authors and research groups are only identified by these first-author citations.

The "optical purities" of the starting materials are not always defined, and when they are then only qualitatively ("not of high optical purity"). It would be better to refer to the enantiopurities since these are relevant and the term enantiomerically pure is used in parallel to optical purity. $[\alpha]_D$-values are also not given routinely, and when they are given this is done without specifying the solvent and temperature (e.g., "(*R*)-pulegone, $[\alpha]_D$ +23°, has found frequent service in synthesis due to its optical purity..."). The chiralities of the starting materials and the products are not defined uniformly [(−)-camphor, (*R*)-(+)-pulegone, β-elemenone, *ent*-occidentalol]. There are almost no references dealing with enantiopurities, $[\alpha]_D$-values, and chiralities. Prices are sometimes indicated qualitatively ("The cost of (−)-carvone is much less than that of the (+)-isomer." "(*R*)-(+)-Limonene, $[\alpha]_D$ +126.8°, is probably the most abundant and cheapest enantiomerically pure cyclic olefin available from natural sources.")

Last but not least, the title is misleading. A step in a synthetic sequence that leads more or less preferentially to one enantiomer is enantioselective, for example the enantioselective hydrogenation of a prochiral substrate (according to Eschenmoser, a chirogenic step), and one can extend that meaning to the entire sequence. The book deals with something else and this is indicated in the subtitle, but racemates are also chiral.

Valentin Rautenstrauch
Firmenich SA
Geneva (Switzerland)

McGraw-Hill Encyclopedia of Science and Technology. 7th Edition. Edited by *S. P. Parker*. McGraw-Hill, New York, 1992. 20 volumes; 13450 pp., hardcover $ 1900.00.—ISBN 0-07-909206-3

Since 1960, when the first edition of the *McGraw-Hill Encyclopedia of Science and Technology* first appeared, it has served the science information needs of students, scholars, and the general public by offering up-to-date, authoritative, and comprehensive coverage of all disciplines in science and engineering. The new 7th edition, which continues to fulfill this purpose, represents the culmination of five years of substantial revision and updating to reflect the numerous scientific and technological developments that have occurred since the 6th edition (1987). The material on entire disciplines, including chemistry, medicine, physics, electronics, computers, telecommunications, and the earth sciences, has been extensively revamped. Three thousand distinguished scientists and engineers from around the world (including 21 Nobel laureates), more than 200 of whom are new to this edition, participated in this work of accurate, lucid, objective, thorough, and rigorous scholarship.

Prepared with the assistance of a 15-member international advisory board and 75 distinguished consulting editors, the encyclopedia contains 7500 signed, alphabetically arranged, and cross-referenced articles (230 entirely new, 700 rewritten by new authors, and 800 extensively revised), covering 81 major subject areas from acoustics to virology. Among the new articles are those on adhesive bonding, anxiety states, atom clusters, bioelectronics, chaos, climate modeling, compact disk, laser cooling, foot disorders, fiber-optic

imaging, fuzzy sets and systems, superstring theory, oxygen toxicity, magnetic levitation, psychosomatic disorders, Kepler's laws, sonochemistry, flexible manufacturing systems, and quasicrystals. Each article begins with a clear definition of the subject, establishing the conceptual foundation for the following discussion that moves progressively from elementary to advanced concepts. The articles consistently discuss both theoretical and practical aspects, thus providing valuable insights into real-world connections between the two.

Lavishly illustrated, the set contains more than 13000 drawings, maps, charts, diagrams, and photographs (1960 of which are new to this edition); 15 of the 81 pages of striking full-color photographs are new. The volumes are exceptionally well-designed with an outstanding visual layout (wide margins, easy-to-read type, and bold headings). Numbered figures, equations, and reactions are referenced throughout the text, 50000 cross-references allow quick access to related articles, and up-to-date bibliographies (some with references as late as 1990) facilitate further research. Numerical data are given throughout in both U.S. customary and international (SI) units.

Volume 20 contains a list of contributors (79 two-column pages), a 13-page discussion of scientific notation with conversion tables, and six new comprehensive study guides based on standard curriculum outlines in physics, chemistry, biology, geosciences, health, and engineering. It also includes a subject index (28 four-column pages) listing alphabetically all 7500 article titles under the 81 major subject headings, making subject-related browsing easy, and an analytical index (more than 160000 entries in 478 four-column pages, referred to by library educators as the "perfect index") permitting quick access to specific terms. The encyclopedia can be updated annually by the *McGraw-Hill Yearbook of Science and Technology*, which is cross-referenced to the parent set and features the same extensive illustrations and bibliographies.

I was disappointed by the lack of entries for two of the most active recent research areas in my own field of chemistry, namely buckminsterfullerenes and cold fusion, but considering the broad interdisciplinary scope of the encyclopedia it was inevitable that some topics would be omitted. Thus the series remains the preeminent, essential reference source for accurate information in any area of science or technology. Its cost will probably limit its purchase to libraries and laboratories, and therefore students, teachers, scholars, and laypersons may wish to buy the one-volume *McGraw-Hill Concise Encyclopedia of Science and Technology*, 2nd edition, abridged from the Encyclopedia's 6th edition (lxxvi + 2222 pp., $ 110, 1989; for review see George B. Kauffman, *Today's Chemist* Dec. **1989**, *2(6)*, 16).

George B. Kauffman
California State University
Fresno, CA (USA)

Electron and Proton Transfer in Chemistry and Biology. (Series: Studies in Physical and Theoretical Chemistry, Vol. 78.) Edited by *A. Müller, H. Ratajczak, W. Junge*, and *E. Diemann*. Elsevier, Amsterdam, 1992. XVI, 394 pp., hardcover HFl 355.00/$ 203.00.—ISBN 0-444-88862-4

In 1992 the Nobel Prize for Chemistry was awarded to Rudolph A. Marcus in recognition of his work on the theory of electron transfer, and thus the publication of this book on electron transfer processes is timely (although it was, of course, planned before the announcement of the Nobel Committee's decision). This volume of nearly 400 pages reports on the proceedings of an international conference held on 19–21 September 1990 at the Center for Interdisciplinary Research of the University of Bielefeld.

The wide range of topics includes contributions from physical, inorganic, organic, and organometallic chemistry, as well as from biochemistry, microbiology, biophysics, and theoretical physics. There is a correspondingly broad spread in the disciplines, origins, and objectives of the authors, and likewise in those of the potential readers. Accordingly, the editors have faced a demanding task in choosing the contributions and in arranging and linking them together.

The description of systems in which *electron transfer* occurs begins with simple metal ions and complexes (R. D. Cannon, B. Jezowska-Trzebiatowska et al., A. Vogler et al., W. Kaim, H. So et al.), then goes on to systems of increasing complexity, such as membrane systems (M. Grätzel), proteins (C. C. Moser et al., W. Haase et al., D. J. Lowe), and eventually whole microorganisms (A. Kröger et al.). Next comes a group of articles on biological systems in which there is a coupled transfer of *electrons and protons* (G. von Jagow et al., T. A. Link, E. Takahashi et al., E. K. Pistorius, W. Junge et al.). Continuing then to studies of *proton transfer*, the topics move from biological processes (M. Gutman et al., C. Sandorfy) back again to "purely chemical" reactions (H. Ratajczak, G. Zundel, H.-H. Limbach, D. Borgis, E. Kryachko).

The basic reaction mechanisms are discussed, including a very brief introduction to the "Marcus–Hush paradigm", and articles which focus on thermal or photochemically induced inter- or intramolecular electron transfer, and the problem of mixed valency in metal-oxygen clusters. The elementary processes involved can be studied in detail for model systems by spectroscopic methods, magnetic measurements, or neutron diffraction. Models for both natural and artificial photosynthetic systems have been investigated. Remarkably high efficiencies for the conversion of solar to electrical energy have been obtained with an "artificial leaf". The Marcus equations for the rate of electron transfer are used to analyze the redox reactions in bacterial photosynthesis centers, leading to conclusions about the spatial arrangement of the redox centers in the protein. Another aspect of biochemical electron transfer that is examined is the magnetic interaction between the metal centers. In the context of nitrogen fixation and analogous reactions, the occurrence of successive or concerted multielectron transfer is discussed (in the latter case the formation of highly reactive free radical intermediates is avoided). This is followed by a discussion of the enzyme-controlled flux of electrons in the bacterial system *Wolinella succinogenes*.

Redox reactions are closely related to the uptake or release of protons. This aspect is discussed for biological reaction pathways, taking as examples quinol oxidation, quinone reduction, water oxidation, and the formation of adenosine triphosphate (ATP) in respiration and photosynthesis. The diffusion of protons within apomyoglobin and their reaction with the Schiff base chromophore in rhodopsin is then discussed. The volume ends with a discussion of hydrogen bonding and its effects on proton transport in liquid phases (amine/hydrogen halide and amine/phenol complexes in aprotic solvents), solid phases, and organic glasses, first for small-molecule model systems then from a theoretical standpoint.

The book ranges over all aspects of the subject, from theoretical studies (e.g., Kryachko's description of the soliton model of proton transfer) to practical applications (Grätzel's article on solar energy conversion), and thus it undoubtedly

lives up to the title and the claims made in the preface. It would certainly have been possible to produce a book with a different balance of emphasis. For example, there are scarcely any references to electrochemical reactions, despite the fact that in many cases these are good model systems for coupled and biologically relevant electron and proton transfer processes. However, any choice of topics for such a book is inevitably subjective, and reflects the interests of the conference participants and organizers. A more serious criticism in my view is that insufficient attention has been given to linking together the individual contributions. The preface emphasizes the interdisciplinary approach ("...biology has become the ground where the various disciplines of science ... are meeting again"; "students of the life sciences will always rely on ... investigations of simpler and cleaner systems that are the object of pure physics and chemistry"), and that is exactly why it would have been desirable to have sections in the text to link and interrelate the disciplines, so as to overcome the barriers that exist, often even in the terminology. Also only a few of the articles are in the nature of reviews, and some report results on the authors' special research topics. Consequently the book is not very suitable as an introduction to the field, but is rather in the nature of a snapshot of current research activity.

On careful reading of some individual articles one is struck by the large number of errors, leading one to ask whether the manuscripts were checked before typesetting. For example, pages 95–109 contain 22 cases of incomplete sentences, incorrect symbols, errors of sign in equations (!), and spelling errors. To cite only the most glaring example found, what is one supposed to make of "dimethyltetraaza (ref. 14) annulene" (p. 338)? Presumably what is meant is dimethyltetraaza[14]annulene (although strictly speaking it refers to the dibenzo derivative of this compound). One might reasonably expect that, for a book costing over $ 200, errors of this kind would not occur so frequently as is found here. The same applies to the lack of consistency in book and journal citations. In some of the articles the style is too much like a transcript of a lecture. Occasionally the English would have benefited from a little polishing by the editors, as there are whole sentences whose meaning can only be deciphered with difficulty.

For readers who are engaged in research in the fields described and want to look beyond the confines of their own specialism, this book should be worth buying, provided that they are prepared to overlook the minor shortcomings of presentation mentioned above. They will discover from it some surprising parallels between chemistry and biology in the area of electron and proton transfer.

Bernd Speiser
Institut für Organische Chemie
der Universität Tübingen (FRG)

Organic Photochemistry. A Comprehensive Treatment. (Physical Chemistry Series.) By *W. Horspool* and *D. Armesto*. Ellis Horwood/Prentice Hall, New York, 1992. XVI, 521 pp., hardcover $ 90.00.—ISBN 0-13-639477-9

As editor of the book *Synthetic Organic Photochemistry* (1984) and as the author of the annual reviews of the photochemistry of carbonyl compounds in the Royal Chemical Society's *Specialist Periodical Reports on Photochemistry*, W. Horspool is certainly widely recognized as a leading expert on light-induced reactions of organic molecules. It was therefore almost a foregone conclusion that a new book on organic photochemistry should have him as one of its authors.

The book consists of seven chapters as follows: a brief general introduction to molecules in electronically excited states; the photochemical behavior of hydrocarbons; photochemical reactions of molecules containing oxygen, sulfur, nitrogen, and halogens; and lastly a survey of the main experimental requirements for carrying out photochemical reactions. The authors have undoubtedly succeeded in putting together a very comprehensive summary of the armory of light-induced reactions of organic molecules that can be used for synthetic purposes. The book can therefore be recommended for all readers seeking a good general overview of this subject. As seems to be generally unavoidable, there are a few printing errors, such as the repetition of a whole sentence (p. 234) or of a literature citation (p. 345), and also quite a number of errors in authors' names in the references. German-speaking readers will notice that the literature survey in the introduction fails to mention the photochemistry volume (IV 5a, b) of "Houben-Weyl".

Although the publishers describe the book as a "timely review" it is, unfortunately, not really so in the sense of being up-to-date. Except for the chapter on organonitrogen compounds, which has been partly updated by including the authors' most recent work on aza-di-π-methane rearrangements (with five literature references for 1990 onwards), the most recent publications are not adequately covered. It is certainly possible to cover the latest work in books of this kind, as J. Kopecky has clearly demonstrated in his book *Organic Photochemistry* (VCH, 1992). Leaving aside the fact that these two books treat the subject differently, and the significant difference in price between the two, this matter of up-to-dateness is by itself a sufficient reason for me to recommend that students wishing to learn about this field should preferably buy Kopecky's book.

Paul Margaretha
Institut für Organische Chemie
der Universität Hamburg (FRG)

Organic Synthesis in Japan. Past, Present, and Future. In Commemoration of the 50th Anniversary of the Society of Synthetic Organic Chemistry, Japan. Edited by *R. Noyori*. Tokyo Kagaku Dozin, Tokyo, 1992. XI, 565 pp., hardcover ¥ 14000.—ISBN 4-8079-0369-1

The Society of Synthetic Organic Chemistry in Japan was founded in 1942. At that time chemists in Europe could already look back on more than fifty years of achievement in this field, both in the laboratory and on an industrial scale, and also on some impressive successes in natural products chemistry, especially in structure determination. The aim of the newly formed society was to foster close collaboration between universities and industry, and to stimulate and encourage research in organic synthesis. As R. Noyori points out in the preface, chemists in Japan have a different scientific and cultural background from their counterparts in other countries, which influences motivation, the approach to solving problems, and the way that research projects are carried out in practice. These special circumstances and Japan's geographical position have contributed to the fact that initially the development of chemistry there was not so rapid as that occurring in Europe and the USA during the same period. Even today, although the successes of Japanese chemical research compare well with those in other leading industrial countries, certain characteristics that we generally associate with the "Japanese mentality" are discernible. To mark the fiftieth anniversary of its formation the Japanese

 © *VCH Verlagsgesellschaft mbH, D-69451 Weinheim, 1993* *0570-0833/93/0808-1219 $ 10.00+.25/0*

Society of Synthetic Organic Chemistry has now undertaken a sort of stocktaking review, with contributions by 60 authors drawn from academia and industry. These mainly very personal contributions highlight some important developments that have taken place in Japan in synthetic organic chemistry, and describe the most outstanding research results achieved in recent times.

The first part of the book is devoted to the history of the development of synthetic chemistry in Japan, with descriptions of some milestones in the areas of the synthesis of natural products and biologically active substances (Y. Ban, M. Matsui, M. Yamaguchi), organic synthesis in the pharmaceutical industry (K. Morita), industrial synthesis (Y. Ito), and syntheses of molecular energy storage media, organic conductors, and ferromagnetic materials (Z. Yoshida). In a more general article H. Nozaki discusses the changes that have occurred over the years in the areas on which synthetic organic chemistry has concentrated.

In the second part 53 authors (of whom 36 are from universities and 17 from industry) describe their best research results. The majority of the literature citations belong to the last ten years. The contributions extend over a wide range of synthetic organic chemistry, but an emphasis on certain topics is clearly evident. These include the synthesis and modification of complex natural products (e.g., 1-oxacephems, taxanditerpenoids, 1,3-polyols, macrolides, glycoconjugates, pyrethroid insecticides), metal-assisted selective transformations (especially those using palladium or the ruthenium(II)-BINAP reagent, and new Lewis acid catalyzed reactions), syntheses based on organoboranes and organosilanes, and stereochemically controlled reactions. On the other hand, some classes of interesting compounds other than natural products that have been synthesized in Japan are perhaps somewhat under-represented here. Rather predictably, modern developments in the chemistry of organoheteroelement compounds are treated only in the context of aids to organic synthesis (see above), not from the standpoint of the synthesis of the compounds themselves. Looking at the list of authors one can, of course, point to a few notable omissions, but it is certainly not possible to achieve completeness in a collection of this kind.

With regard to the future of Japanese organic chemistry as mentioned in the title, most of the comments are to be found in the first part of the book, but some of the authors in the second part also make projections. In academic research some important future trends are: a) studies aimed at a better understanding of organometallic reactions, especially with regard to (stereo)selective reactions, and closer links between inorganic chemistry and synthetic organic chemistry; b) chemical synthesis in combination with methods based on fermentation and enzyme-catalyzed reactions; c) the synthesis of molecules with useful photochemical, electrical, or magnetic properties. For industry, Y. Ito predicts that future objectives will include: a) technologies for protecting the global environment and conserving natural resources—such projects will require cooperation between industry and universities; b) a strengthening of speculative basic research, with a willingness on the part of management to take risks; c) international collaboration in the development of new chemical technologies; d) a close integration of chemistry, biotechnology, electronics, and physics at the molecular level. Many of these future perspectives could apply equally in Germany, as also could the urgent appeal to policy-makers to increase investment in education and basic research.

The book has a consistent layout and very attractive presentation, which is greatly helped by the clear and excellently reproduced formula diagrams. The title page of each contribution carries a photograph of the author with a biographical note on his scientific work. Although the book does not cover the whole field exhaustively, it is certainly an important and valuable source of information on the present state of synthetic organic chemistry in Japan.

Gerhard Maas
Fachbereich Chemie
der Universität Kaiserslautern (FRG)

Orbital Symmetry and Reaction Mechanism. The OCAMS View. By *E. A. Halevi.* Springer, Berlin/New York, 1992. XXII, 310 pp., hardcover DM 68.00.—ISBN 3-540-50164-9/0-387-50164-9

When, in 1992, someone writes a book about the relationship between orbital symmetry and reaction mechanism, it can be assumed that it is not so much an account of the latest results as a review and appraisal of a line of development that extends back at least to 1965. It was then that Woodward and Hoffmann, with their principle of the conservation of orbital symmetry, initiated a revolution in chemistry that is almost without equal. This book leaves no doubt that the stimulus generated by that simple idea could not have come about without the existence at that time of a receptive intellectual climate, characterized by a lack of the fundamental knowledge needed to understand reaction mechanisms. The author does not assume that the reader will be satisfied with a superficial argument; instead he adopts a rigorous approach that is a continuous theme throughout the book. He starts by noting that it would be very convenient if one could make predictions about a reaction mechanism on the basis of symmetry. The second stage is to determine whether or not the system goes beyond the range of validity of the molecular orbital (MO) theory; in other words, one has to distinguish between MO, configurational, and state correlation. The third stage is concerned with the rigorous description of the transition structure in energetic terms, from which one can decide whether a symmetry argument is to be accepted or rejected.

The author takes considerable care to prepare the ground by explaining aspects of symmetry that are needed later. The uninitiated reader is gently "led by the hand" through the necessary stages, and the reader with previous knowledge will probably not start with any special advantage. The unconventional approach in which symmetry and symmetry reduction are treated simultaneously is certainly very convincing, but the combining of this with the illustration of the behavior of atomic p-orbitals in a magnetic field relates only to an imaginary experiment and not to the actual situation. Because of the electron spin the 2p state undergoes not a threefold but a fourfold splitting. The treatment of the Zeeman effect without including the electron spin is a dubious approach, and should at least have been preceded by an explanatory note. Considering that fundamental aspects of d-orbitals are discussed in some detail, it would have been appropriate to explain that there is an infinite number of legitimate ways of choosing a set of five d-orbitals. In fact the discussion is always confined to the one set that can easily be generated from the complex functions for spherical symmetry, and which is easy to handle in the case of octahedral symmetry, where the axes can be chosen in accordance with the ligands. Thus even the equivalence of the functional forms is abandoned. On the whole this first third of the book covers all the most important preparative material for what is to follow. This includes molecular orbitals and normal

 © VCH Verlagsgesellschaft mbH, D-69451 Weinheim, 1993 0570-0833/93/0808-1220 $ 10.00+.25/0

vibrations, as well as orbital correlation diagrams for diatomic molecules. The two fundamental rules, namely the non-crossing rule and the Walsh rules, are only briefly mentioned, and the reader is apparently expected to understand these already.

The next 100 pages are devoted to classical thermal reactions. These are analyzed from the OCAMS (orbital correspondence analysis in maximum symmetry) standpoint that the author has himself developed. Compared with the Woodward–Hoffmann rules this has the advantage of providing a rigorous formalism that leads directly to the thermally favored reaction mechanism, avoiding the need to consider all conceivable mechanisms in turn (and perhaps to overlook the one that is of most interest). The information that OCAMS gives about a mechanism is of a relative nature, and is conceptually related, in a broad sense, to the Walsh rules. It therefore undoubtedly comes nearer to the truth than topological considerations. About 40 topical examples are described in detail and clearly illustrated.

It is only in the final third of the book that the electron spin is introduced. Spin-forbidden processes are incorporated into the OCAMS approach, and examples that involve intersystem crossing are described. About a dozen carefully chosen examples of reactions involving electronically excited states are described. At the time when the Woodward–Hoffmann rules were being applied to photochemical reactions without sufficient care, inappropriate mechanisms were assumed in many cases. Only four examples from inorganic chemistry are described, and from these one can conclude that the orbital symmetry approach is best reserved for carbon compounds, since there is always doubt as to whether the condition of kinetic stability is satisfied for inorganic compounds, so that no reliance can be placed on results from symmetry considerations. The appendix contains character tables and group correlation tables that are a valuable aid in studying the examples.

The text is excellent in both its intellectual content and style, and the book provides ample evidence of the author's rich fund of experience.

Rudolf Janoschek
Institut für Theoretische Chemie
der Universität Graz (Austria)

Science as Writing. By *D. Locke*. Yale University Press, New Haven, 1992. X, 237 pp., hardcover \$ 30.00/£ 18.50.—ISBN 0-300-05452-1

The author of this book, David Locke, started as a chemist. His mentor was S. William Pelletier, with whom he synthesised atisine, an alkaloid. The work was published in the *Journal of the American Chemical Society* in 1959. At present, David Locke teaches English at the University of Florida. He is thus able to describe science as an insider. When he refers to style in science, the example he brings forward (who else?) is that of Robert B. Woodward. This issue of scientific style is one that elicits considerable current interest. A whole periodical, *Science in Context*, is devoted to the question of style in science, not only on the part of an individual, but within a field of science or a national tradition. This book is well-researched and jargon-free. It puts to rest our cherished notion of science as methodically built from the objective gathering of facts. It has other uses also. It will help to devise an efficient rhetoric for one's scientific discourse. It should help to restore to science a measure of personal style, as opposed to the fastidiously repetitive hyperspecialization that masquerades in its stead.

Locke brings to bear on his precious little book an in-depth understanding of the scientific process. The third chapter contrasts expressionless, humorless writing, as seemingly required in publications, both with shop talk in the laboratory, and with the emotional involvement in their work by eminent scientists such as Charles Darwin. This empathy for one's brainchild is beautifully exemplified by Barbara McClintock's animation of the genome; it is for her a living entity. Locke deals next with the rhetoric of science, of which *The Origin of Species* is a prime example. He shows convincingly that the lack of impact of Mendel's discovery, even though the contemporaries knew of it, stems from a revolutionary finding having been presented in the language of normal, run-of-the-mill science. He uses Einstein's introduction of relativity theory to demonstrate the importance of story-telling to conveying a novel world-view. In a chapter with the felicitous title "The Art of Artless Prose", the author focuses on the irony that permeates great texts, such as Galileo's *Dialogues* or *The Double Helix*. He draws attention also to the virtue of understatement, as a device to prepare for the hard-hitting punch line (such as that, one may add, in Woodward and Hoffmann's *The Conservation of Orbital Symmetry*: "Exceptions? There are none.") The book throbs with vital insights. In Chapter 5, on "The Putative Purity of Science", Locke comments perceptively on the existence of a scientific oligarchy, in between decision-makers and the scientific community: "ultimately, it determines what is scientifically thinkable, until the unorthodox idea thrusts its way into the arena, with the force of scientific genius, skillful rhetoric, and iron determination behind it."

The main virtues of Locke's book are his intimate familiarity with living science; the smooth readability buoyed by a constantly pleasing style and by recourse to major texts, known by everyone, for its examples; the constant criticism of the myth of science as an objective and neutral process. These qualities are sometimes drawbacks. One might argue that to focus on scientific revolutions and masterpieces is too selective. Normal science is also to be considered advantageously as writing. One might also argue, on a different tack, that scientific advances can be uncoupled from ideological hangups: Jacques Loeb (p. 154ff.) is remembered for the study of tropisms, more than for his obsession with getting rid of free will.

Deconstruction has been a slogan during the post-modern, post-structuralist period from which we are emerging. This debunking movement has helped to jettison the myth of science as the progressive buildup of the laws of nature from objective facts. Its own mythological view of science nevertheless borders on the ridiculous and, to this writer, is unacceptable. It rests on microsociological studies of laboratory life. They find that science is akin to a power play: its conclusions would be, according to this critical analysis, merely a negotiated settlement between the human participants. Locke's essay is far above such ultrasimplifications. He uses various complementary approaches so as to provide a realistic, multidimensional view of science. His metaphor of science as writing is much more productive, and he pushes it to all its implications without ever forcing the evidence to conform to his model.

Pierre Laszlo
Laboratoire de Chimie
École Polytechnique, Palaiseau (France)

New Books

see next page

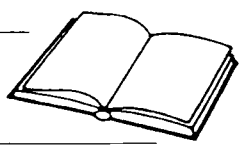

New Books

Complexity. Life at the edge of chaos. By **R. Lewin.** Maxwell Macmillan International, Oxford, **1993.** 208 pp., hardcover, £ 17.95.—ISBN 0-02-570485-0

Structure of Electrified Interfaces. Edited by **J. Lipkowski, P.N. Ross.** VCH, Weinheim/New York, **1993.** 406 pp., hardcover, DM 196.—/$ 125.—ISBN 3-527-28787-6/0-89573-787-6

Grundkurs Chemie. By **A. Arni.** VCH, Weinheim, **1993.** 354 pp., paperback, DM 48.—ISBN 3-527-29008-7

HPLC Detection. Newer Methods. Edited by **G. Patonay.** VCH, Weinheim/New York, **1993.** 236 pp., hardcover, DM 158.—/$ 95.—ISBN 3-527-28219-X/0-89573-327-7

Electrode Kinetics for Chemists, Chemical Engineers, and Materials Scientists. By **E. Gileadi.** VCH, Weinheim/New York, **1993.** 597 pp., hardcover, DM 189.—/$ 115.—ISBN 3-527-89561-2/1-56081-561-2

Plants as Biomonitors. Indicators for Heavy Metals in the Terrestrial Environment. Edited by **B. Markert.** VCH, Weinheim/New York, **1993.** 644 pp., hardcover, DM 298.—/$ 200.—ISBN 3-527-30001-5/1-56081-272-9

Data Analysis for the Chemical Sciences. A Guide to Statistical Techniques. By **R.C. Graham.** VCH, Weinheim/New York, **1993.** 536 pp., hardcover, DM 78.—/$ 49.50.—ISBN 3-527-28114-2/1-56081-048-3

Scanning Tunneling Microscopy and Spectroscopy. Theory, Techniques, and Applications. Edited by **D.A. Bonnell.** VCH, Weinheim/New York, **1993.** 436 pp., hardcover, DM 196.—/$ 125.—ISBN 3-527-27920-2/0-89573-786-X

Capillary Electrophoresis of Small Molecules and Ions. By **P. Jandik, G. Bonn.** VCH, Weinheim/New York, **1993.** 298 pp., hardcover, DM 108.—/$ 65.—ISBN 3-527-89533-7/1-56081-533-7

Electrochemical and Electrocatalytic Reactions of Carbon Dioxide. Edited by **B.P. Sullivan, K. Krist, H.E. Guard.** Elsevier, Amsterdam, **1993.** 298 pp., hardcover, Dfl. 340.—ISBN 0-444-88316-9

Applied Chaos Theory. A Paradigma for Complexity. By **A.B. Çambel.** Academic Press, London, **1993.** 246 pp., hardcover, £ 33.—ISBN 0-12-155940-8

Principles of Biochemistry. 2. Auflage. By **A. Lehninger, D.L. Nelson, M.M. Cox.** Worth Publishers, New York, **1993.** 1013 pp., hardcover, $ 56.95.—ISBN 0-87901-500-4

Soil Chemistry and its Applications.(Cambridge Environmental Chemistry Series 5). By **M. Cresser, K. Killham, T. Edwards.** Cambridge University Press, Cambridge, **1993.** 192 pp., paperback, £ 35.—ISBN 0-521-32269-3

Atomic and Molecular Properties. (Methods in Computational Chemistry, Vol. 5). Edited by **S. Wilson.** Plenum Press, New York, **1993.** 349 pp., hardcover, $ 79.50.—ISBN 0-306-44263-9

Characterization of Ceramics. (Materials Characterization Series). Edited by **R.E. Loehmann.** Butterworth-Heinemann, Oxford, **1993.** 295 pp., hardcover, £ 47.50.—ISBN 0-7506-9253-7

An Introduction to Metal Matrix Composites. (Cambridge Solid State Science Series). Edited by **T.W. Clyne, P.J. Whiters.** Cambridge University Press, Cambridge, **1993.** 509 pp., hardcover, £ 55.—ISBN 0-521-41808-9

Anorganikum. By **L. Kolditz.** Hüthig, Heidelberg, **1993.** 1125 pp., hardcover, DM 98.—ISBN 3-335-00341-1

Relaxation and Thermodynamics in Polymers. Glas Transition. By **E.-J. Donth.** Akademie Verlag, Berlin, **1993.** 350 pp., hardcover, DM 148.—ISBN 3-05-501392-1

New Frontiers in Catalysis. Proc. 10th Int. Congr. Catalysis, 1992. Edited by **L. Guczi, F. Solymosi, P. Teteny.** Elsevier, Amsterdam, **1993.** 2878 pp., hardcover, Dfl. 895.—ISBN 0-444-89621-X

Half a Century of Free Radical Chemistry. By **D.H.R. Barton, S.I. Parekh.** Cambridge University Press, Cambridge, **1993.** 164 pp., paperback/hardback, £ 12.95/30.—ISBN 0-531-44580-9/0-531-44005-X

Silica Gel and Bonded Phases. Their Production, Properties and Use in LC. (Separation Science Series). Edited by **R. P. W. Scott.** Wiley, West Sussex, Great Britain, **1993.** 261 pp., hardcover, £ 35.—ISBN 0-471-93985-4

Metal Extraction by Bacterial Oxidation of Minerals. (Ellis Horwood Series in Inorganic Chemistry). By **J. Barrett, M. N. Hughes, G. I. Karavaiko, P. A. Spencer.** Ellis Horwood, London, **1993.** 191 pp., hardcover, £ 64.60.—ISBN 0-13-577735-6

Biopolymers I. (Advances in Polymer Sciences, Vol. 107). Edited by **N. A. Peppas, R. S. Langer.** Springer, Heidelberg, **1993.** 272 pp., hardcover, DM 218.—ISBN 3-540-56148-X

Electro-Osmosis. (Ellis Horwood Series in Physical Chemistry). By **K. P. Tikhomolova.** Ellis Horwood, London, **1993.** 219 pp., hardcover, £ 99.—ISBN 0-13-249806-5

Pest Control with Enhanced Environmental Safety. (ACS Symposium Series, Vol. 524). Edited by **S. O. Duke, J. J. Menn, J. R. Plimmer.** American Chemical Society, Washington, **1993.** 357 pp., hardcover, $ 84.95.—ISBN 0-8412-2638-5

Chromatography of Polymers. Characterization by SEC and FFF. (ACS Symposium Series, Vol. 521). Edited by **T. Provder.** American Chemical Society, Washington, **1993.** 337 pp., hardcover, $ 94.95.—ISBN 0-8412-2625-3

Polymeric Delivery Systems. Properties and Applications. (ACS Symposium Series, Vol. 520). Edited by **M. A. El-Nokaly, D. M. Piatt, B. A. Charpentier.** American Chemical Society, Washington, **1993.** 411 pp., hardcover, $ 99.95.—ISBN 0-8412-2624-5

Nuclear Magnetic Shielding and Molecular Structure. (Nato Advanced Science Institutes Series). Edited by **J. A. Tossell.** Kluwer, Dordrecht, **1993.** 600 pp., hardcover, Dfl 330.—ISBN 0-7923-2119-7

Physical Methods in Chemistry. By **V. A. Afanasiev, G. E. Zaikov.** Nova Science, Commack, USA, **1993.** 182 pp., hardcover, $ 79.—ISBN 1-56072-063-8

Biomembranes. Physical Aspects. Edited by **M. Shinitzky.** VCH, Weinheim/New York, **1993.** 378 pp., hardcover, DM 198.—/$.135.—ISBN 3-527-30021-X/1-56081-771-2

Industrial Organic Chemistry. Second, Revised and Extended Edition. By **K. Weissermel, H.-J. Arpe.** VCH, Weinheim/New York, **1993.** 457 pp., hardcover, DM 128.—/$.80.—ISBN 3-527-26995-9/0-89573-861-9

Registered names, trademarks, etc. used in this journal, even when not marked as such, are not to be considered unprotected by law.

© VCH Verlagsgesellschaft mbH, D-69451 Weinheim, 1992. – Printed in the Federal Republic of Germany by Konrad Triltsch Druck- und Verlagsanstalt Würzburg.

All rights reserved (including those of translation into foreign languages). No part of this issue may be reproduced in any form — by photoprint, microfilm, or any other means — nor transmitted or translated into a machine language without written permission from the publishers. Only single copies of contributions, or parts thereof, may be made for personal use. This journal was carefully produced in all its parts. Nevertheless, authors, editors, and publisher do not warrant the information contained therein to be free of errors. Readers are advised to keep in mind that statements, data, illustrations, procedural details, or other items may inadvertently be inaccurate.

Valid for users in the USA: The appearance of the code at the bottom of the first page of an article (serial) indicates the copyright owner's consent that copies of the article may be made for personal or internal use, or for the personal or internal use of specific clients. This consent is given on the condition, however, that the copier pay stated per-copy fee through the Copyright Clearance Center, Inc. (CCC), for copying beyond that permitted by Sections 107 or 108 of the U.S. Copyright Law. This consent does not extend to other kinds of copying, such as copying, for general distribution, for advertising or promotional purposes, for creating new collective works, or for resale. For copying from back volumes of this journal see 'Permissions to Photo-Copy: Publisher's Fee List' of the CCC.

Editorial office: Postfach 10 11 61, D-69451 Weinheim, Federal Republic of Germany, Telephone (06201) 606 315, Telex 465 516 vchwh d, Telefax (06201) 606 328, E-Mail Z16@DHDURZ2 in Earn Bitnet.

Editor: *Peter Gölitz*

Associate editors: *N. A. Compton, R. H. Schmidt-Radde, K. J. Schneider.* **Book editor:** *G. Karger.* **Editorial assistants:** *J. Göhrig, E. Schweikart*

Publishers: VCH Verlagsgesellschaft mbH. (Managing Directors: *Hans Dirk Köhler, Dr. Karlheinz Köpfer*), Pappelallee 3, D-69451 Weinheim, Federal Republic of Germany.

Advertising office (Advertising Manager: *N. Schippel*): Postfach 10 11 61, D-69451 Weinheim, Federal Republic of Germany, Telephone (0 62 01) 606 312, Telefax (0 62 01) 606 328.

ANGEWANDTE CHEMIE
International Edition in English
Volume 32 · Number 9
September 1993
Pages 1223–1376

How Nature Synthesizes Vitamin B_{12}—A Survey of the Last Four Billion Years

By A. Ian Scott*

This review contains an account of recent experimental results in the continuing saga of vitamin B_{12} biosynthesis (largely from the author's laboratory) as well as a personal view of future directions of research in natural product biosynthesis. The emphasis is on the powerful combination of molecular biology in the search for, and the expression of, the genes encoding the biosynthetic enzymes and state-of-the-art spectroscopic techniques, in order to "view" the biochemical events as they take place in the NMR tube. As a logical development of these approaches, the feasibility of one-flask, multienzyme synthesis of natural products is addressed.[**] Implicit throughout is the profound change in the "tools of the trade" of the bioorganic chemist, thanks to the harnessing and exploitation of cloning techniques and the resultant availability of enzymes which can make carbon–carbon bonds. It is also our desire to alert organic chemists, who may wish to take advantage of these technical developments, to the fact that they will be rewarded by a new world of natural catalysts capable of high yielding, synthetic chemistry often with a surprising, but welcome, lack of substrate specificity. Finally we hope to convey our enthusiasm for the methods now at the disposal of present and future generations of chemists for studying Nature's synthetic routes to complex natural products.

1. Introduction: The Early Experiments

"It is a tangled skein and I am looking for a loose end."
"The Creeping Man"[***]

The complex mechanisms underlying the biosynthesis of the tetrapyrrolic cofactors (Fig. 1) which mediate such diverse processes as respiration (heme), photosynthesis (chlorophyll), methanogenesis (coenzyme F430), six-electron sulfite and nitrite reduction (siroheme), and vitamin function (B_{12} and its coenzyme—the corrinoids) have intrigued biochemists since the 1940s when Shemin et al.[1] and Neuberger et al.[2] began their classic studies of heme biosynthesis. Indeed, by ingesting [^{15}N]glycine, Shemin showed that his own heme nitrogen atoms were labeled by this amino acid.[1] From these and other pioneering studies using [^{14}C] labeling and chemical degradation,[3] it was revealed by painstaking experiments that in mammals, glycine and succinyl CoA combined to form 5-aminolevulinic acid (ALA), the universal building block for both porphyrins and vitamin B_{12}. Our own work in this field began 25 years ago when, by whole cell feeding of ^{13}C-enriched precursors to *Propionibacterium shermanii*, it was established by NMR spectroscopy that the pathway to B_{12}, beginning with ALA, continues via porphobilinogen (PBG) to the unsymmetrical

[*] Prof. A. I. Scott
Department of Chemistry, Texas A&M University
College Station, TX 77843-3255 (USA)
Telefax: Int. code + (409) 845-5992

[**] Based on a lecture given at the 27th Euchem Conference on Stereochemistry, 26th April to 4th May, 1992, Bürgenstock, Switzerland. A more explicit account of this new field has been given in "Genetically Engineered Synthesis of Complex Natural Products" (A. I. Scott *Tetrahedron*, **1992**, *48*, 2559).

[***] The quotations that appear in the text are all taken from the works of Sir Arthur Conan Doyle (1859–1930) and are spoken by Sherlock Holmes.

 © *VCH Verlagsgesellschaft mbH, D-69451 Weinheim, 1993* *0570-0833/93/0909-1223 $ 10.00+.25/0*

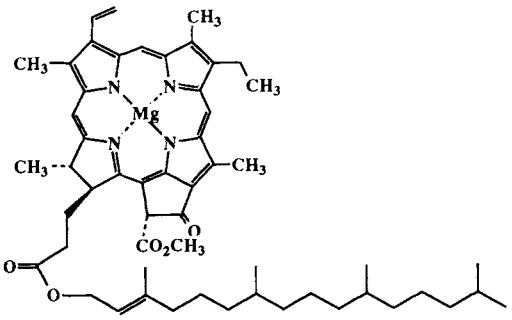

chlorophyll-a

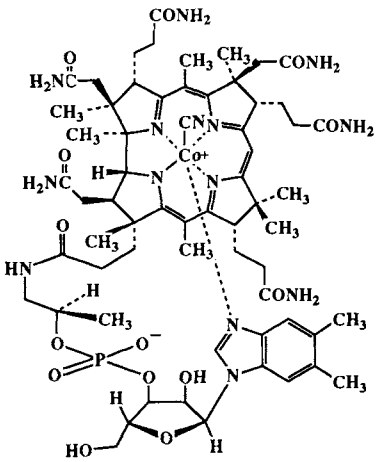

vitamin B_{12}: cyanocobalamin

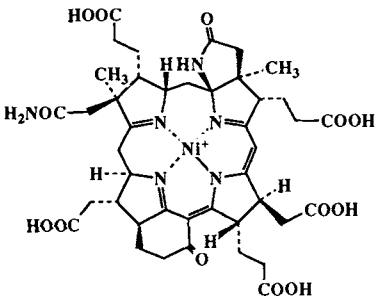

coenzyme F 430

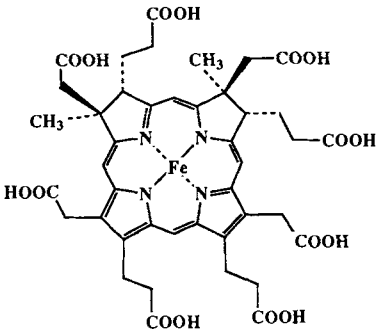

siroheme

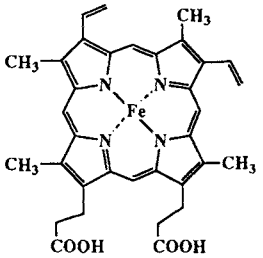

heme

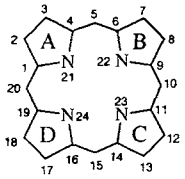

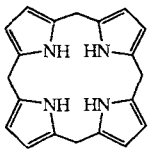

porphyrinogen

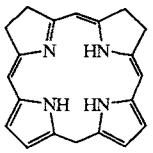

dipyrrocorphin

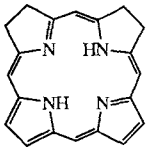

isobacteriochlorin

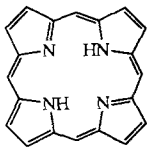

porphyrin

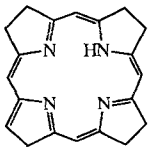

corphin

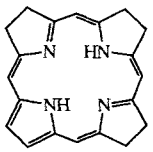

pyrrocorphin

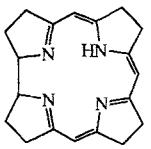

corrin

Fig. 1. Top: The cofactors derived from uroporphyrinogen (uro'gen)III. Bottom: The chromophores of the macrocyclic tetrapyrroles.

A. Ian Scott was born in Glasgow, Scotland in 1928 and received B.Sc., Ph.D., and D.Sc. degrees from Glasgow University. Following postdoctoral studies with M. S. Newman (Ohio State University) and Sir Derek Barton (Birkbeck College and Glasgow), and a lectureship at Glasgow University (1957–62), he occupied chairs of organic chemistry at U.B.C., Vancouver, Sussex, and Yale, before moving to Texas A & M University in 1977 where he is now Davidson Professor of Science and Director of the Center for Biological NMR. His research insterests are concentrated at the interfaces of organic chemistry, NMR spectroscopy and genetic engineering of natural product biosynthesis. The combination of these techniques have led his investigations into the use of stable isotopes, enzymology, and gene expression to study the mechanisms and synthetic power of the enzymes which mediate the biosynthesis of alkaloids, antibiotics, vitamins, and steroids. His work has been recognized by numerous awards, the most recent being the A. C. Cope Scholar Award of the American Chemical Society. He is a Fellow of the Royal Societies of London and Edinburgh and the European Academy of Arts and Science, a Member of the Scientific Academy of Siena, and a Founding Member of the Yale Sherlock Holmes Society.

uroporphyrinogen (uro'gen), (a route shared with all the cofactors in Fig. 1) before entering the chiral world of corrins, whose stereochemical complexity is largely a result of C methylation of the pyrrolic rings by *S*-adenosylmethionine (SAM).[4] The next 10 years witnessed the isolation (with L. Siegel and G. Müller) of two partially methylated intermediates (factors II and III) on the way to corrins, by using cell-free systems of *P. shermanii* and *Clostridium tetanomorphum*.[4] It is now clear that these oxidized pigments or "factors", are carried through the biosynthetic machinery at the level of hexahydroporphyrin, and although the stable isobacteriochlorin structures of factors II and III were conveniently elucidated by ^{13}C NMR spectroscopy on submilligram amounts,[4] the true substrates for the biosynthetic methyltransferases are now known to be their reduced (and much more labile) forms, the precorrins 1–3 (Fig. 2).[5a]

1.1. Dating of the B_{12} Pathway and Some Medical Implications

There is no apparent, formal change in oxidation level throughout the pathway from ALA to the corrinoid structure of B_{12}. This fact, taken together with the phylogeny of the B_{12}-producing organisms[6] and Eschenmoser's remarkable prebiotic simulation of uro'gen III synthesis from glutamine dinitrile[7] suggests that the prerequisite not only of the type III porphyrinogen, but of a prebiotic corrin template, bearing protons at the positions associated with biological C methylation, was quite feasible. The primitive anaerobes (methanogenic bacteria) which make B_{12} (but not heme) can be dated to about 3.79×10^9 years,[8] whereas the modulation of oxygen by the respiratory (heme) pigments and oxygenic photosynthesis (chlorophyll) was not required

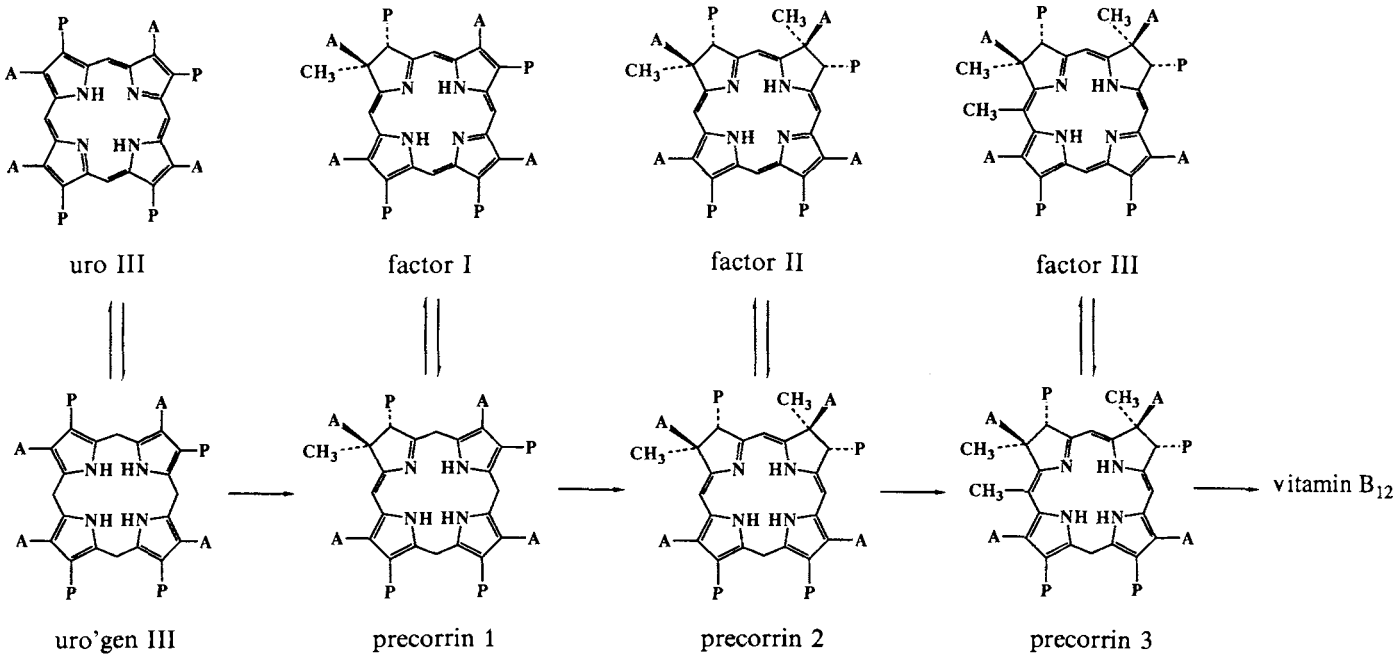

Fig. 2. The precorrins 1–3 and the corresponding oxidized "factors" I–III.

Our discussion will concentrate on what is now known about the biosynthetic enzymes which produce corrin from ALA; a process which involves as many as 20 steps along a pathway rich in mechanistic complexity. We have omitted any discussion of the events which transform the simplest corrin, cobyrinic acid, to cyanocobalamin (vitamin B_{12}), by amidation and addition of the "nucleotide loop" whose aminoisopropyl alcohol, phosphate, ribose, and dimethyl benzimidazole moieties are furnished from threonine, guanosine triphosphate, ribose, and riboflavin, respectively. The physiologically active coenzyme B_{12} bears a 5-deoxyadenosyl group in place of the cyanide function in cyanocobalamin. Due to the facile exchange of the sixth (axial) ligand it appears that the cyanide group was first introduced as an artifact of the original isolation of B_{12} due to the presence of CN^-/ions in the animal charcoal used in the purification process.[5b]

until sufficient O_2 entered the earth's atmosphere about 1.7 billion years ago.[6, 8] Thus, the ancient organisms had learned to synthesize corrins from type III uro'gen or to produce methane from coenzyme F430 long before the oxidized pigments (hemes, cytochromes) were required.[6] Although endowed with a much more complex stereochemical motif than planar heme, the cobalt–corrin complex was surely the earliest organometallic cofactor, along with nickel-containing coenzyme F430, whose biosynthetic pathway shares precorrin 2 as a common precursor. Whereas primitive methanogenesis mediated by F430 can be understood, the function of the early corrins is not so easy to deduce. One possibility would be methyl transfer from methyl cobalamin leading to cobalamin-dependent methionine synthesis[9] or the carboxylation of methyl cobalamin to form acetate.[10] Whatever may have been the biological function of corrins in archaebacteria, their subsequent evolution and recruitment

to a functional coenzyme has now provided modern organisms (and man) with a spectacular series of 1,2-shifts mediated by coenzyme B_{12}—to say nothing of ribonucleotide reductase. All of these reactions depend on homolytic fission of the unique cobalt–carbon bond embedded in a water-soluble structure—the hallmark of the B_{12} coenzyme rearrangements.[11] As discussed later, this evolutionary hierarchy is of considerable interest with regard to the ubiquitous presence of type III uroporphyrinogen-derived pigments right down to present-day man who requires the four genes, *hem*A-D, necessary for synthesis of uro'gen III, to produce heme for his hemoglobin. As an historical aside, the disease of acute intermittent porphyria caused by the deficiency of the *hem*C gene (which encodes porphobilinogen (PGB) deaminase, the polymerizing enzyme of tetrapyrrole biosynthesis) lay at the heart of the "Royal Madness" in the House of Hanover,[12] whose most celebrated victim was George III. It has recently been suggested[13] that this congenital deficiency (and hence deranged behavior) was also linked with the tragic life of Vincent van Gogh.

2. The Enzymes of Tetrapyrrole Assembly Encoded by *hem*A-D

"When a fact appears to be opposed to a long chain of deductions
it invariably proves to be capable of bearing some other interpretation."
"A Study in Scarlet"

2.1. ALA Synthesis: Two Routes to a Simple Molecule

The structure of the C_5 building block, ALA, in fact conceals a duality of genetic origin. Thus, the action of ALA synthase, discovered by Shemin, involves the decarboxylative condensation of glycine and succinyl CoA mediated by pyridoxal phosphate (Fig. 3a). A more primitive route features the reduction of glutamyl-tRNA to glutamate semialdehyde (GSA) (Fig. 3b) by a dehydrogenase encoded by the *hem*A gene of *Escherichia coli*. This is followed by a remarkable intramolecular transposition of the amine and carbonyl functionalities of GSA to ALA under the control of *hem*L. This "C_5 pathway" was first discovered in plants[14] (which do not make B_{12}), but has now been found to operate[14] in many B_{12}-producing organisms such as *Salmonella* and *Clostridium thermoaceticum*.[15] The classical Shemin sequence,[1,3] however, is probably restricted to photosynthetic bacteria, yeast and mammals.

Regardless of the origin of the ALA, the next step involves the dehydrative self condensation of ALA to PBG. This reaction is catalyzed by the enzyme ALA dehydratase, which is encoded by *hem*B. Overexpression of dehydratase[16,17] (to 40 mg/L^{-1} in engineered *E. coli* cells), and immobilization on sepharose has provided us with a convenient synthesis of PBG in ^{13}C-labeled forms, suitable for the many studies involving ^{13}C enrichment of the later, more complex intermediates and has furnished the first enzyme in the repertoire of catalysts for multienzyme synthesis, using the readily available ALA as substrate.

2.2. Porphobilinogen Deaminase: An Enzyme with Many Surprises in Store!

The next enzyme, PBG deaminase, encoded by *hem*C, catalyzes the tetramerization of PBG **1** to preuro'gen (hydroxymethylbilane, HMB) **2**,[18,19] which is cyclized with rearrangement to the unsymmetrical uro'gen III **3** by uro'gen III synthase[19–21] (Fig. 4). In the absence of the uro'gen III synthase, HMB **2** dehydrates spontaneously to uro'gen I **4**, which, although strictly not a natural product, turns out to be a substrate for some of the methyltransferases of the vitamin B_{12} pathway.

We have constructed a plasmid pBG101, containing the *E. coli hem*C gene[22,23] encoding deaminase. *Escherichia coli* (TB1) transformed with this plasmid produces deaminase at levels greater than 200 times those of the wild strain[23] (30–40 mg L^{-1}). This allows access to substantial quantities of pure enzyme for detailed study of the catalytic mechanism and for the preparation of the later intermediates.

Deaminase is an unusually helpful enzyme since a covalent bond is formed between each incoming substrate molecule and enzyme,[24–30] thus allowing isolation of covalent complexes containing up to 3 PBG units (E-S_1–E-S_3). With adequate deaminase in hand it was found that a novel cofactor is covalently attached to one of the four cysteine residues of the enzyme (Cys 242) in the form of a substrate-derived dipyrromethane. The free α-position of which becomes the site of attachment of the four PBG-molecules during the catalytic cycle (Figs. 5 and 6).

Thus, a mutant strain of *E. coli* (*hem*A-requiring ALA for growth) in the presence of [5-^{13}C]ALA **6** afforded highly

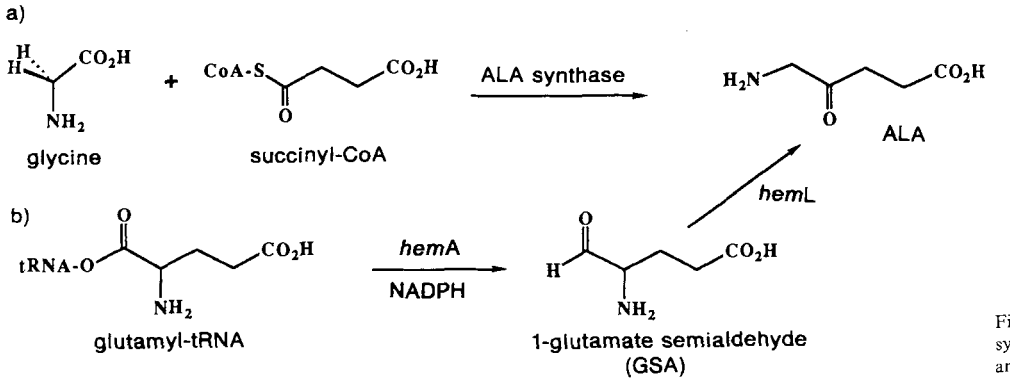

Fig. 3. The two mechanisms of ALA synthesis: a) the "Shemin" pathway and b) the "C_5" pathway.

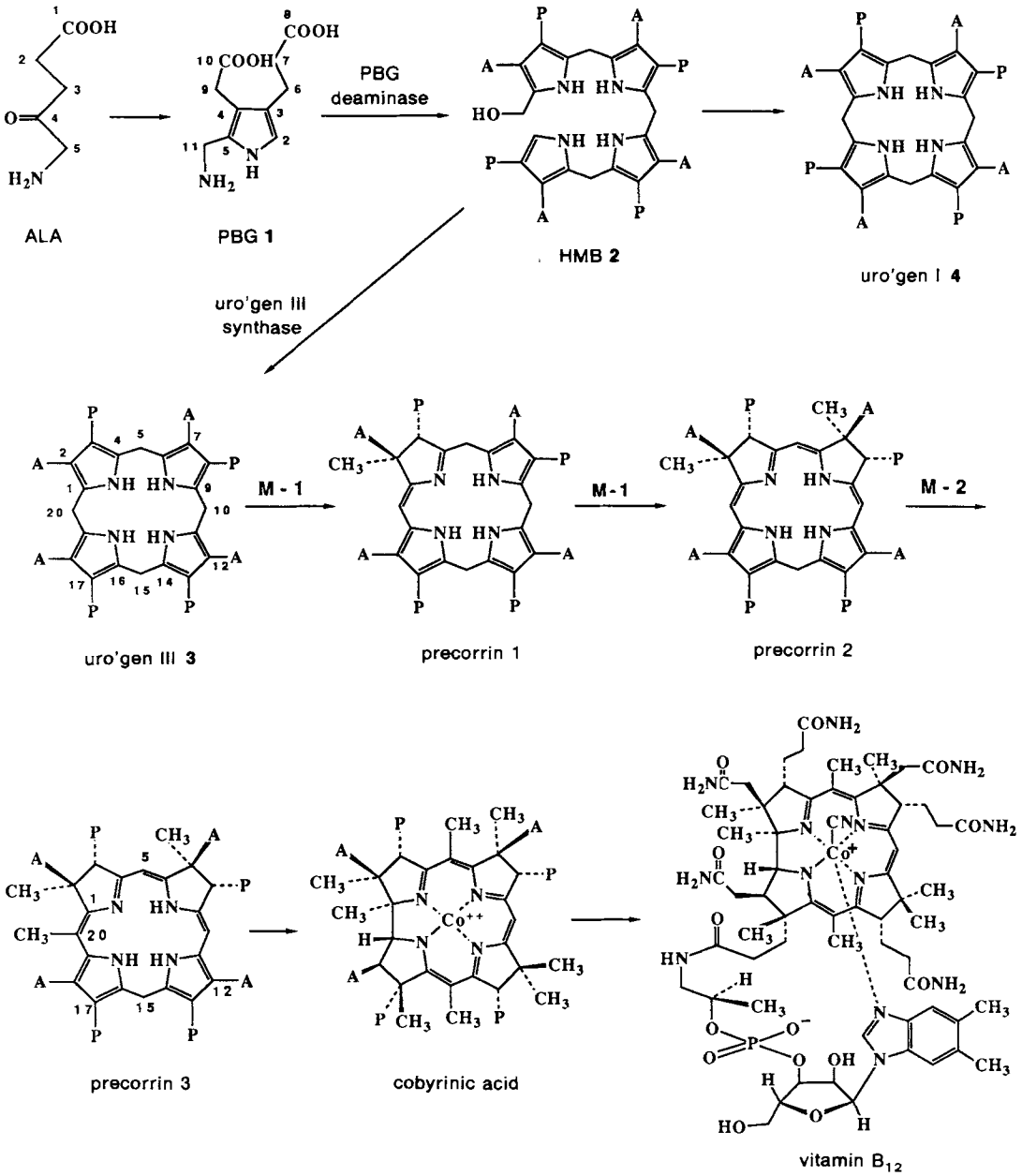

Fig. 4. The "early" precursors of vitamin B_{12}. From ALA to precorrin 3. A = CH_2COOH, P = CH_2CH_2COOH.

^{13}C-enriched enzyme for NMR studies. At pH 8, the signals for the enriched carbon atoms of the dipyrromethane cofactor were clearly recognized at $\delta = 24.0$ (py-CH_2-py), 26.7 (py-CH_2-X), 118.3 (α-free pyrrole), and 129.7 (α-substituted pyrrole) (Fig. 5A). The signals are sharpened at pH 12 (Fig. 5B), and the CH_2X resonance is shifted to $\delta = 29.7$ in the unfolded enzyme. Comparison with synthetic models reveals that a shift of $\delta = 26.7$ is in the range expected for an α-thiomethyl pyrrole (py-CH_2-SR). Confirmation of the dipyrromethane (rather than oligopyrromethane) came from the ^{13}C INADEQUATE spectrum taken at pH 12 which reveals the expected coupling only between the py-CH_2-py group ($\delta = 24.7$) and the adjacent substituted pyrrole carbon atom ($\delta = 128.5$) (Fig. 5C). When the enriched deaminase was studied by ^1H-detected heteronuclear filtered spectroscopy (Fig. 5D), only five protons (from a total of nearly two thousand!) attached to ^{13}C-enriched nuclei were observed in accord with structure **5** (Fig. 5 top). A specimen of deaminase was then covalently inhibited with the suicide inhibitor [2,11-$^{13}C_2$]2-bromo PBG **8** (Fig. 6) to give a spectrum consistent only with structure **9**, recently confirmed by electrospray mass spectrometry ($M_r = 34\,559$).[30b] The site of covalent attachment of substrate (and inhibitor) is therefore the free α-pyrrole carbon atom of the dipyrromethane cofactor in the native enzyme, leading to the structural and mechanistic proposal for deaminase portrayed in Figure 6.

It was then found that two moles of PBG are incorporated autocatalytically into the apoenzyme (isolated by overexpression in a *hem*B-strain of *E. coli* which does not make PBG)[28] and that the first (kinetic) encounter of PBG deaminase with substrate involves attachment of PBG (with loss of NH_3) to the α-free pyrrole position of the dipyrromethane to form the E-S_1 complex **7** (Fig. 6).[29, 30a] The process is repeated to produce the unstable "tetra PBG" (E-S_4) adduct

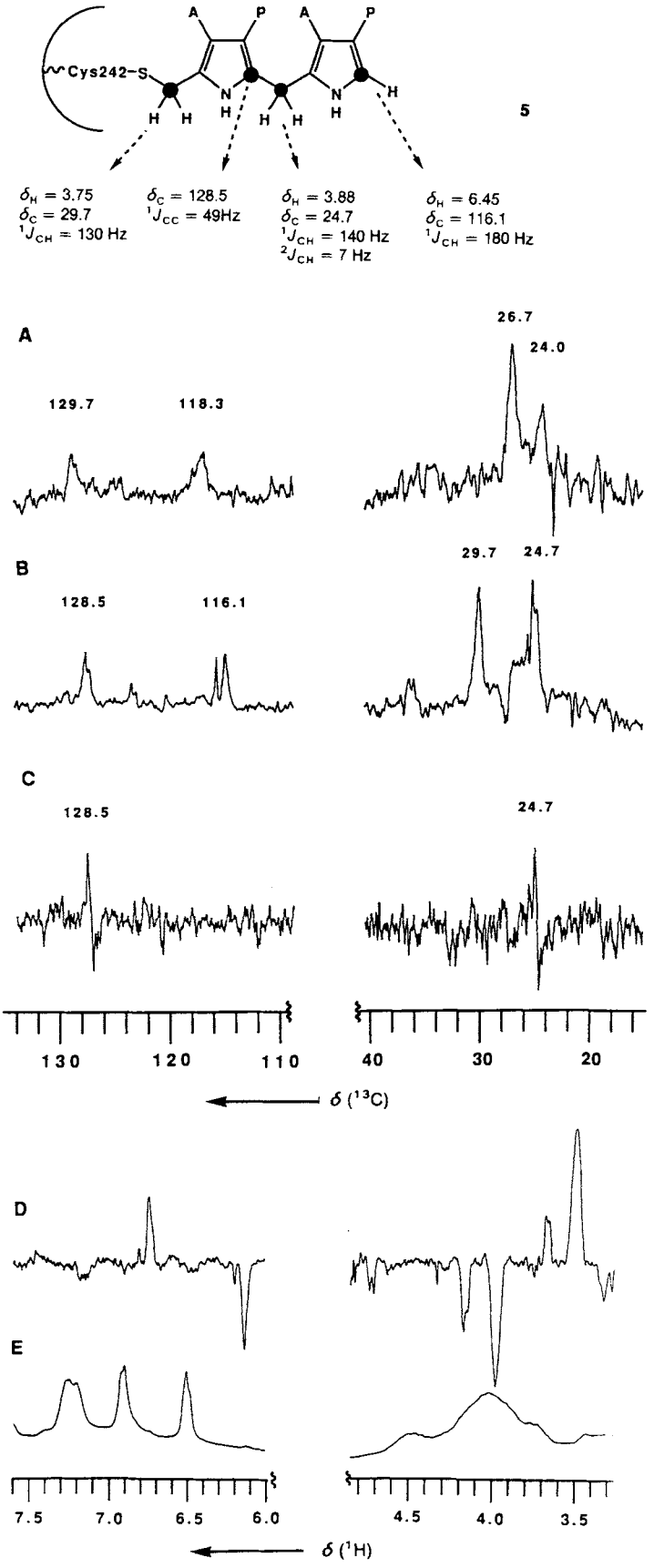

Fig. 5. High-field NMR spectra of PBG deaminase from *E. coli* (ca. 1 mM) specifically ^{13}C-enriched in the dipyrromethane cofactor by [5-^{13}C]ALA (**6**). A) 125 MHz ^{13}C NMR difference spectrum between separate deaminase samples (pH 8) grown in the presence or absence of [5-^{13}C]ALA **6**, which shows the four signals of the ALA-derived ^{13}C-enriched carbon atoms. B) Difference spectrum of the same samples as in (A), recorded at pH 12. Upon alkaline denaturation, the resonance signal assigned to the thiomethyl carbon atom shifts downfield to δ = 29.7; in closer agreement to a model cysteine thiomethylpyrrole conjugate. C) ^{13}C INADEQUATE NMR spectrum (pH 12) of [5-^{13}C]ALA-derived deaminase which demonstrates the coupling of adjacent carbon atoms, confirming the head-to-tail dipyrromethane structure. D) Isotope-edited 300 MHz ^{1}H NMR spectrum (pH 12) of biosynthetically enriched deaminase (2 mM), showing the three pairs of signals originating from only those protons directly bound to the ^{13}C carbon atoms derived from [5-^{13}C]ALA **6**. The observed antiphase splittings are due to the one-bond ^{1}H-^{13}C coupling. E) Normal ^{1}H NMR spectrum of the same sample, illustrating the degree of selection afforded by the pulse sequence for spectrum D. Above the spectra is shown the structure of the dipyrromethane cofactor **5**; the ^{1}H and ^{13}C NMR chemical shifts and coupling constants obtained at pH 12 are given.

10, which was recently detected (M_r = 35107) by electrospray MS.[30b] Site-specific cleavage of the hexapyrrole chain (at ⟶ ; see Fig. 6) releases the azafulvene (**11**) which becomes the substrate of uro'gen III synthase after stereospecific hydration[19] to HMB **2**. The bilane **2** is stable at pH 12, but is cyclized chemically to uro'gen **4** at pH $\leq$8 (Fig. 4). Independent, complementary work in 1987/1988 from two other laboratories[31, 32] reached identical conclusions regarding the catalytic site. The ^{13}C labeling defines the number of PBG units (two) attached in a head-to-tail motif to the native enzyme at pH 8, and reveals the identity of the nucleophilic group (Cys-SH) which anchors the dipyrromethane (and hence the growing oligopyrrolic chain) to the enzyme. Site-specific mutagenesis[23] and chemical cleavage[31, 32] were employed to determine that Cys 242 is the point of attachment of the cofactor.

The use of the α-carbon atom of a dipyrromethane as the nucleophilic group responsible for oligomerization of four moles of PBG (with loss of NH_3 at each successive encounter with an α-free pyrrole) is not only remarkable for the exquisite specificity and control involved, but is, as far as we know, a process unique in the annals of enzymology in that the substrate is actually used not only once, but twice in the genesis of the active site cofactor! Even more remarkable is the fact that the apoenzyme is automatically transformed to the active holoenzyme by addition of two PBG units without the intervention of another enzyme.

2.3. Uro'gen III Synthase: The Molecular Acrobatics of the "Ring D Inversion"

We now turn briefly to the enzyme for the rearrangement, uro'gen III synthase. The early ideas of Bogorad et al.[33] involving the aminomethylbilane (AMB) **12** as a putative substrate, were helpful in finally tracking down the elusive species which, after synthesis by PBG deaminase, becomes the substrate for uro'gen III synthase. This was shown to be HMB **2**, and at this stage (1978) the lack of activity of AMB (**12**) as substrate relegated the latter bilane to an interesting artefact produced quantitatively by addition of ammonia to deaminase incubations (Fig. 6). However, with the acquisition of substantial quantities of pure uro'gen III synthase obtained by cloning the genes *hem*C and *hem*D together[34] and overexpression in *E. coli*, now at a level several hundred times greater than that described elsewhere,[35a] the substrate specificity of the synthase (formerly called cosynthetase) has been reinvestigated. Ever since its conception by Mathewson and Corwin in 1961,[33b] the spiro compound **13** (Fig. 6) has been a favorite construct with organic chemists, since both

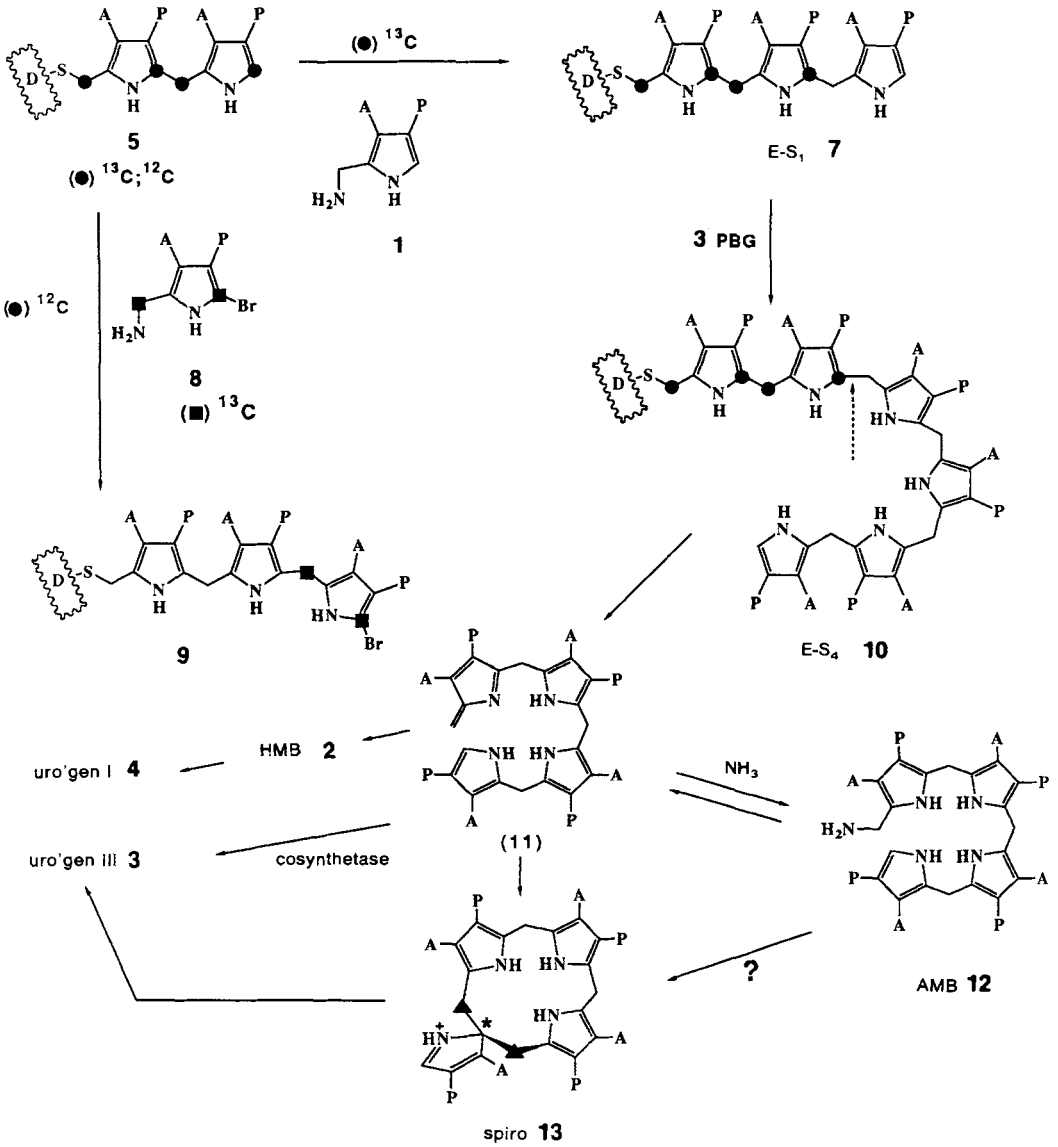

Fig. 6. The remarkable dipyrromethane cofactor of PBG deaminase, covalently attached to Cys242 of the enzyme and its role in tetrapyrrole assembly, showing the "spiro" mechanism (**13**) for the action of uro'gen III synthase (cosynthetase).

its genesis through α-pyrrolic reactivity and its fragmentation—recombination rationalize the remarkable intramolecular formation of uro'gen III from the linear bilane preuro'gen (HMB) **2** through inversion of ring D. A careful search for the spiro compound (**13**) was conducted at subzero temperatures in a cryosolvent (−24 °C; ethylene glycol/buffer) by using various ^{13}C isotopomers of HMB as substrate.[34] Although the synthase reaction could be slowed down (20 h rather than 20 s), no signals corresponding to the quaternary carbon atom (labeled with an asterisk in **13**; $\delta \approx 80$) or to the α-pyrrolic methylene groups (labeled with a black triangle; $\delta = 35-40$) could be observed. It was also found that totally synthetic AMB **12** (thus free of deaminase which can catalyze interconversion of AMB into HMB) also served as a slow but productive substrate for uro'gen III synthase at high concentrations (1 mmol in both enzyme and substrate). Regardless of which version of the bilane system (HMB, AMB) is involved, the fact that no intervening species free of enzyme was observed strongly suggests that the intermediate is enzyme-bound and therefore difficult to detect. Indirect evidence for the "spiro" mechanism was adduced when it was found that one of the enantiomers of the corresponding synthetic ring D-lactam served as an inhibitor of uro'gen III synthase.[36a] We recently proposed an alternative to the "spiro intermediate" **13** hypothesis, which is still consistent with the known facts.[34] and is based on a concept of self assembly with the formation of a lactone (see Fig. 7). It was suggsted that generation of the azafulvene (**11**) is followed not by carbon–carbon bond formation (to give **13**, but by closure of the macrocycle to the macrolide. The regiospecificity of this step is reflected by the failure[21] of synthetic bilanes lacking the acetic acid side chain at position 17 in ring D to undergo enzyme-catalyzed rearrangement to the type III system, together with the observation that a "switched" bilane carrying a propionate at position 17 (and an acetate at position 18) does indeed give a certain amount of (rearranged) uro'gen I (but also uro'gen III) enzymatically.[21, 36b] This indicates that lactone formation could also be achieved (but less efficiently) by a propionate group at position 17. The subsequent chemistry is

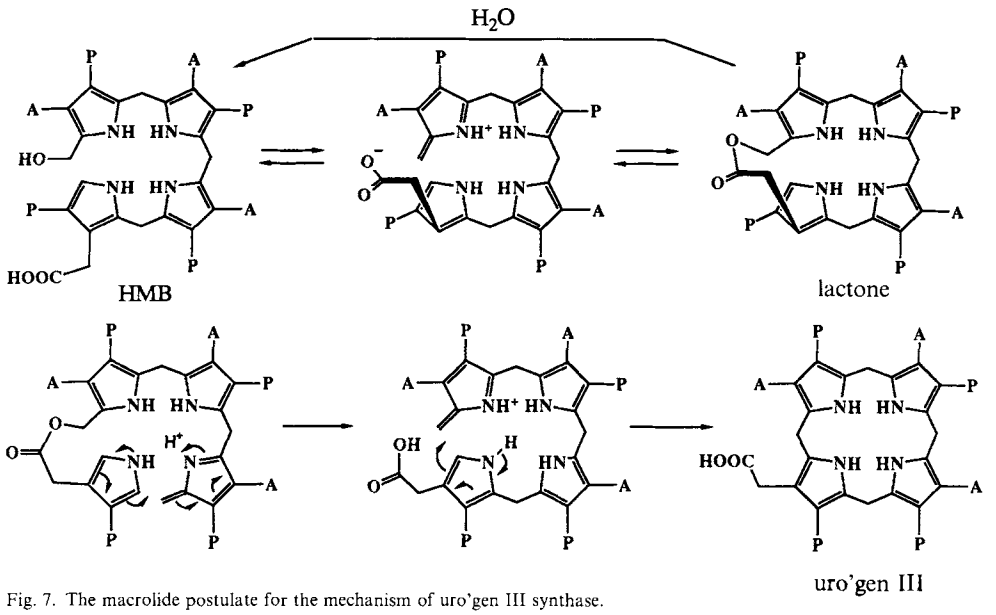

Fig. 7. The macrolide postulate for the mechanism of uro'gen III synthase.

quite similar to the fragmentation–recombination postulated for the spiro system except that a "twisted macrolide" becomes the pivotal intermediate species and the sequence proceeds as shown in Figure 7. Although this novel hypothesis is rather difficult to test experimentally, specific chemical traps for a lactonic intermediate, combined with the use of ^{18}O labeling are being employed to confirm or refute the possible role of a macrolide mechanism for uro'gen III synthase, whose cryptic mechanism has posed a biochemical puzzle for over three decades.

3. The Search for the Missing Intermediates: Genetic Engineering to the Rescue

"It is an old maxim of mine that when you have excluded the impossible, whatever remains, however improbable, must be the truth."
"The Beryl Coronet"

3.1. The First Methyltransferases: Their Specifities, and the Synthesis of Precorrins 1 and 2

The first of the methylases catalyzes the sequential formation of factors I and II (Fig. 2) and has been named *S*-adenosylmethionine uro'gen III methyltransferase (SUMT). SUMT was first partially purified from *P. shermanii* by G. Müller[37] and has been overexpressed in *Pseudomonas denitrificans*.[38] In *E. coli* it was found that the *Cys*G gene encodes uro'gen III methylase (M-1) as part of the synthetic pathway to siroheme, the cofactor for sulfite reductase, and overproduction (30 mg L^{-1}) was achieved by the appropriate genetic engineering.[39a] Although, SUMT and M-1 appear to perform the same task, it has been found that their substrate specificities differ.[39b,c] Thus, it has been possible to study in detail the reaction catalyzed by M-1 directly by NMR spectroscopy and to provide rigorous proof that the structure of precorrin 2 is that of the dipyrrocorphin tautomer of dihydro-factor II (dihydrosirohydrochlorin). Uro'gen III (enriched from [5-^{13}C]ALA **6** at the positions labeled with a black square in Fig. 8) was prepared by mixing dehydratase, deaminase, and uro'gen III synthase and then incubating them with M-1 and [$^{13}CH_3$]SAM. The resultant ^{13}C NMR spectrum of precorrin 2 revealed only one sp^3-enriched carbon atom assigned to C-15, thereby locating the reduced center. By using a different set of ^{13}C labels (● from [3-^{13}C]ALA) and [$^{13}CH_3$]SAM, the sp^2 carbon atoms at C-12 and C-18 were located as well as the sp^3 centers coupled to the pendant ^{13}C-enriched methyl groups at (*) C-2 and C-7. This result confirms an earlier NMR analysis[40a] of precorrin 2 isolated by careful anaerobic purification of the methyl ester, and shows that no further tautomerism takes place during the latter procedure. The two sets of experiments mutually reinforce the postulate that precorrins 1, 2, and 3 all exist as hexahydroporphinoids, and recent labeling experiments[40b] have provided good evidence that precorrin 1 is discharged from the methylating enzyme (SUMT) as the species with the structure shown in Figure 4.

However, prolonged incubation (2 h) of uro'gen III with M-1 provided a surprising result: the UV and NMR spectra changed dramatically from those of precorrin 2 (a dipyrrocorphin) to the chromophore of a pyrrocorphin, hitherto known only as a synthetic tautomer of hexahydroporphyrin.[41a] At first sight, this event seemed to signal a further tautomerism of a dipyrrocorphin to a pyrrocorphin catalyzed by the enzyme, but when [$^{13}CH_3$]SAM was added to the incubation, it was found that a third methyl group signal appeared in the region $\delta = 19-21$ of the NMR spectrum. When uro'gen III was provided with appropriate ^{13}C labels (● in Fig. 8), three pairs of doublets appeared in the sp^3 region ($\delta = 50-55$) of the pyrrocorphin product. The necessary ^{13}C pulse-labeling experiments[41c] together with appropriate FAB-MS data finally led to the structural proposal (Fig. 8)[41b,42] for the novel trimethylpyrrocorphin produced by "overmethylation" of the normal substrate, uro'gen III, in presence of high concentration of enzyme. Thus, M-1 has been recruited to insert a methyl group in the

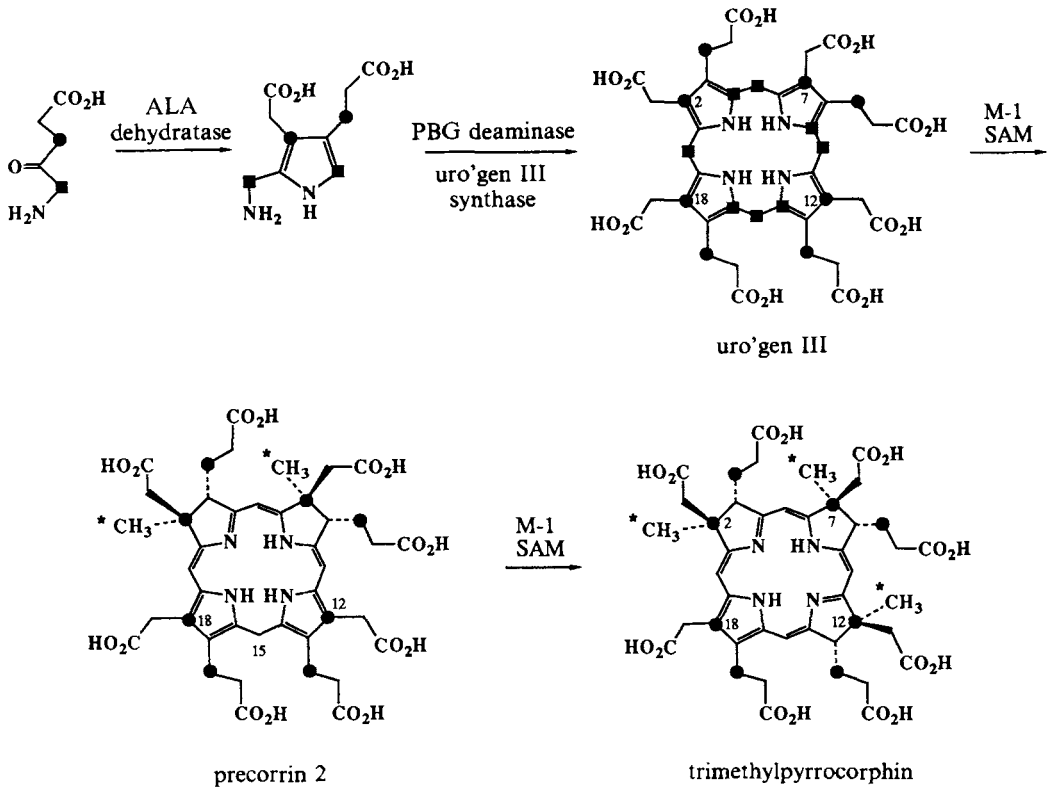

Fig. 8. Synthesis of procorrin 2, C methylation of uro'gen III by the enzyme uro'gen III methylase (M-1) and "overmethylation" of the product in a clockwise direction. The ^{13}C-enriched centers used to assign the carbon centers and C–C coupling were inserted from [3-^{13}C](●)-[5-^{13}C](■) ALA and [$^{13}CH_3$]SAM (*).

C ring and to synthesize the long sought "natural" chromophore. This chromophore corresponds to that of the postulated precorrin **4**, although in this case the regiospecificity is altered from ring D to ring C. The lack of specificity of M-1 was further exploited to synthesize a range of "unnatural" isobacteriochlorins and pyrrocorphins based on isomers of uro'gen III. Thus, uro'gen I produces the methylated products corresponding to precorrin 2 and the type I pyrrocorphin (Fig. 9). These compounds are reminiscent of a series of tetramethyl type I corphinoids, factors S1–S4, isolated from *P. shermanii*[43,44] which occur as their zinc complexes as discussed in Section 3.2. The totally synthetic isomers, uro'gens II and IV, in which the acetate (A) and propionate (P) side chains are positioned in the orders AP, PA, AP, PA and AP, AP, PA, PA, respectively, can also serve as substrates for M-1, remarkably producing the corresponding 2,7-dimethylisobacteriochlorins in both cases.[42b] When uro'gen I was incubated with SUMT,[45] isolation of factor II of the type I (sirohydrochlorin I) family revealed a lack of specificity for this methyltransferase also, although in the latter studies no pyrrocorphins were observed. This may reflect a control mechanism in the *P. denitrificans* enzyme (SUMT) which does not "overmethylate" precorrin 2, as is found for the M-1 from *E. coli*, whose physiological function is to manufacture sirohydrochlorin (factor II)[39b] for sulfite reductase, which itself is necessary for cysteine synthesis.[4] The fact that *E. coli* does not synthesize B_{12} could reflect an evolutionary process in which the C-methylation machinery has been retained, but is only required to insert the C-2 and C-7 methyl groups.

The sites of C methylation in both the type I and III series are also reminiscent of the biomimetic C methylation of the

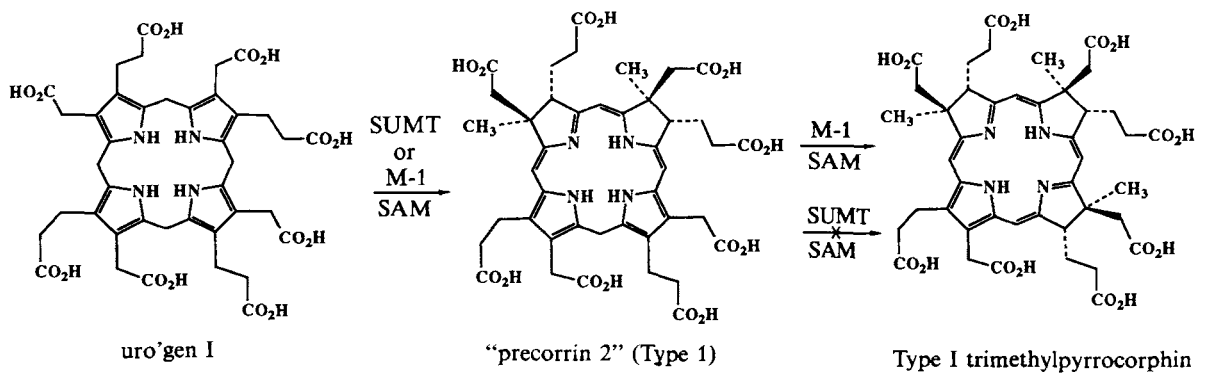

Fig. 9. Overmethylation of uro'gen I by M-1 (but not by SUMT!).

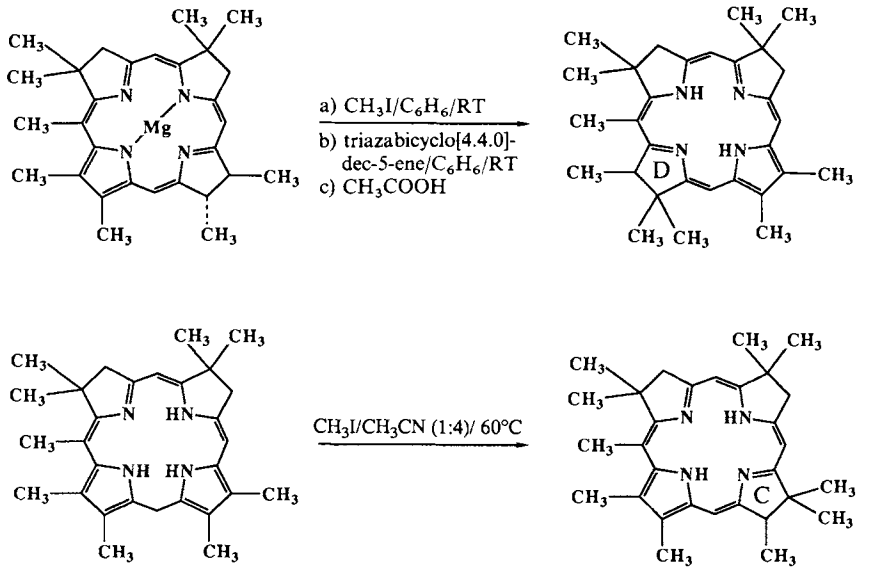

Fig. 10. "Metallic" control of regiospecificity in Eschenmoser's biomimetic C methylation of pyrrocorphins. Note that in the presence of Mg^{2+}, methylation occurs in ring D rather than ring C. RT = room temperature.

hexahydroporphyrins discovered by Eschenmoser et al.,[46] and the regiospecificity is in accord with the principles adumbrated[47] for the stabilizing effect of a vinylogous ketimine system (Fig. 10). Thus, the chemical dipyrrocorphin to pyrrocorphin conversion not only leads to the favored ketimine system of the pyrrocorphin but in the presence of a methyl group at C-20 becomes controllable through the presence of coordinating metal. The fascinating result of these in vitro models is that ring D (C-17) methylation can be achieved in the presence of magnesium, which corresponds to the methylation sequence found in Nature. The above experiments made us more optimistic that the methylases of the B_{12} pathway, which synthesize both natural and unnatural pyrrocorphins and corphins, could now be harnessed to prepare several of the missing intermediates of the biosynthetic pathway. Also of note is that the instability of these substances towards oxygen rationalizes our previous inability to isolate any new intermediates under aerobic conditions (> 5 ppm O_2), other than factors I–III formed by oxidation of the corresponding precorrins 1–3 (Fig. 2).

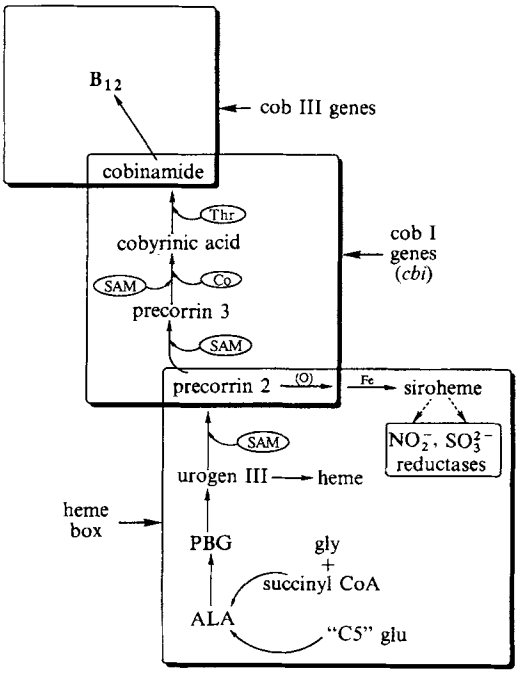

Fig. 11. The heme (*E. coli*) and Cob (*Salmonella*) gene boxes of B_{12} biosynthesis.

3.2. On the Road to Corrins: A Change of Horses from *E. coli* to *Salmonella*

Our search for the biosynthetic enzymes leading to precorrin 2 has so far relied on the "heme gene box" (Fig. 11) in *E. coli*. This is responsible for the synthesis of precorrin 2, a precursor of sirohydrochlorin[39b] (factor II), which, by insertion of iron, forms siroheme, a cofactor for the six-electron *E. coli* sulfite reductase.[4] Fortunately, the heme and corrin pathways intersect in *E. coli* and *Salmonella typhimurium*. Although *E. coli* does not make B_{12}, the discovery by J. Roth et al.[48a] that anaerobic fermentation of *S. typhimurium* produces vitamin B_{12}, has opened the way to enhance our knowledge of vitamin B_{12} synthesis by using the vast array of genetic and cloning techniques available with this organism. Three loci at minutes 13, 34, and 41 have been identified by mutation and complementation studies.[48] The main gene cluster at 41 minutes contains the machinery (Cob I) necessary for the synthesis of cobinamide from precorrin 2 (Fig. 11), a process involving six C methylations (at C-1, C-5, C-12, C-15, C-17, and C-20), decarboxylation (of the acetate residue at C-12), ring contraction, loss of acetic acid (from C-20 and its attached methyl), amidation, and cobalt insertion under control of the *cbi* genes. Thus, the CobI region responsible for cobinamide synthesis contains all of the *cbi* genes encoding these biosynthetic functions. Through the generosity of Professor Roth we were able to use his 10 kb sequence data to clone and overexpress the gene products, corresponding to the 12 open reading frames (ORFs) necessary to synthesize cobyrinic acid from precorrin 2 (Fig. 12).

Ten of the *cbi* genes found in the *cob* operon of *S. typhimurium* were subcloned for expression from the four different plasmids (Fig. 12). All of these genes except *cbi*D were

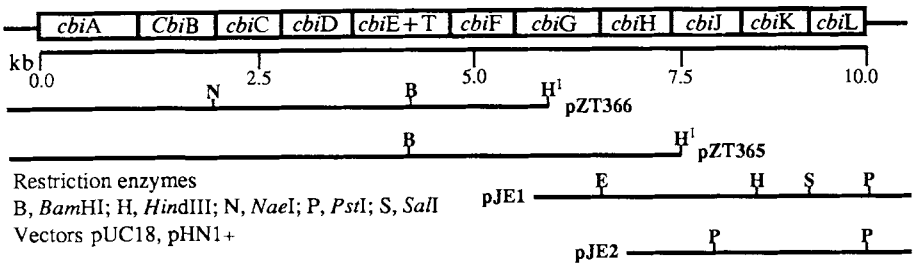

Genes	Plasmid	Construction
*cbi*C & D	pCAR345	pZT366 (N-B) into pHN1+
*cbi*E	pCAR340	ecpcr[3] product into pHN1+
*cbi*T & F	pCAR276	pZT366 (B-H) into pUC18
*cbi*T,F,G,[4]H	pCAR293	pZT365 (B-H) into pUC18
*cbi*H &J[4]	pCAR309	pJE1 (E-H) into pUC18
*cbi*K & L	pCAR292	pJE1 (P-P) into pUC18
*cbi*K	pCAR311	pJE2 (S-P) into pUC18
*cob*F[2]	pCAR332	ecpcr[3] product into pHN1+
*cob*I[2]	pCAR333	ecpcr[3] product into pHN1+

[1] *Hin*dIII site in pBR329 cloning vector
[2] *P.-denitrificans* gene
[3] Expression cassette polymerase chain reaction
[4] Form insoluble inclusion bodies

Fig. 12. Subcloning of the *cbi* genes from *S. typhimurium* for expression. The *cbi* genes in plasmid pBR 329 (pZT365, pZT366, pJE1, and pJE2) were a generous gift from Dr. J. Roth, University of Utah. The superscripts (1–4) relate to the footnotes at the bottom of the figure.

expressed in *E. coli* as determined by SDS-PAGE polyacrylamide gel electrophoresis), and seven of the gene products were purified from the soluble fraction of cell lysates of the appropriate strain. Two further gene products, those of *cbi*G and *cbi*J were found in the insoluble fraction. The amino terminal sequence of each of the purified proteins was determined and used to confirm the location of the open reading frames predicted from the nucleotide sequence.[48c] The gene products of *cbi*E, *cbi*F, *cbi*H, and *cbi*L were shown to be SAM-binding proteins, and based on their homology with other methyltransferases,[49a, b] are considered to be the most likely candidates for methyltransferase activity. The *P. denitrificans cob*L gene product has recently been reported[49c] to have two functions, methylation (of C-5 and C-15) and decarboxylation of the ring C acetate. SDS-PAGE and NH_2-terminal sequence analysis revealed that two separate gene products in *S. typhimurium* (*cbi*E and *cbi*T) correspond to the *cob*L gene product with *cbi*E homologous to the methyltransferase region and *cbi*T homologous with the decarboxylase region, that is in *Salmonella* the 5,15-methylase and decarboxylation activities are separated.

From its homology with the gene product of *cob*I in *P. denitrificans* (31% identity, 71% conservation), the *cbi*L gene product was predicted to be the *S. typhimurium* precorrin 2 methyltransferase (M-2), and using this expressed protein, or more efficiently the *cob*I enzyme, the multienzyme one-flask synthesis of precorrin 3 from the building block ALA was accomplished (Fig. 13).This was achieved both in the NMR tube and preparatively (on the multimilligram scale), by adding the five overexpressed enzymes to the substrate ALA in the presence of SAM.[50] The structure of precorrin 3, a dipyrrocorphin with the constitution shown (Fig. 13), revealed subtle differences compared with the precorrin 2 in the ^{13}C NMR spectrum, which reflected the influence of the new methyl group at C-20 on the conjugated system. This resulted in a preponderance of the tautomer whose electronic array is prepared for the next C-methylation step, and is directly observed by ^{13}C enrichment by NMR spectroscopy.

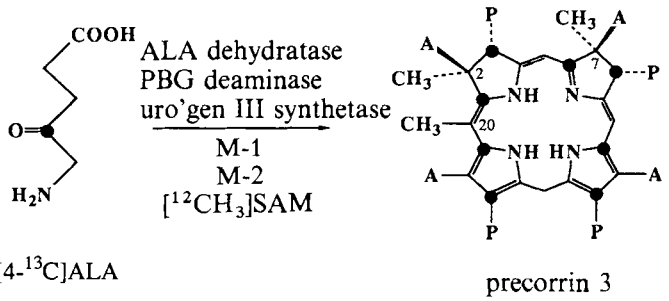

Fig. 13. Multienzyme synthesis of precorrin 3. M-2 is precorrin 2 methyltransferase.

As a guide to the anticipated order of insertion of the remaining methyl groups on the periphery of this last intermediate, precorrin 3, we recall the earlier pulse-labeling experiments. In these experiments the substrates uro'gen III and precorrins 2 and 3 (as factors II and III respectively) were incubated with SAM for several hours with a cell-free extract capable of synthesizing cobyrinic acid followed by a pulse of [$^{13}CH_3$]-labeled SAM. By examining the different intensities of the [$^{13}CH_3$]methyl resonances in the resultant cobester, the sequence of methyl group insertion was found (in three independent studies)[51a–c] to correspond to C methylation at C-17, followed by that at C-12 (now known to occur first at C-11, see below) then at C-1, C-5, and C-15. This differentiation between C-5 and C-15 was found in *P. shermanii*,[51a] while the reverse order for the C-5 and C-15 insertions was deduced by using *Clostridium tetanomorphum* extracts.[51b] In the third study (*P. denitrificans*)[51c] no distinction could be made between the C-5 and the C-15 methylation. However, the welcome agreement that C-17 is the first site of alkylation on the precorrin 3 template and is followed by C methylation at C-11 then C-1 imposes certain restrictions on the type of structure expected for the missing intermediates precorrins 4, 5, and 6, corresponding to methyl insertion at C-17, C-11, and C-1, respectively. Inspection of the stereochemistry of the methyl group ab C-17 in vitamin B_{12} reveals that, of the five methyl groups on quarternary

carbon centers in the vitamin, only that at C-17 is β oriented. This configuration was rationalized as long ago as 1976[4] when we suggested that methylation actually occurred at C-19 followed by ring opening and reclosure (by an allowed 16π-electron process) to give the β-oriented C_{19}-methyl group. Subsequently two [1,5]sigmatropic shifts led to the β-oriented methyl group at C-17. In other words, just like the situation now revealed at C-11 in which the attached methyl group migrates later to C-12, the final resting place of the fourth methylation (at C-17) might be preceded by a similar event, in which case precorrin 4 might correspond to either C-19 or C-18 β-methylated structures shown in Figure 14.

In order to begin the task of unveiling the remaining precorrin intermediates, precorrin 3 was incubated in turn with each of the putative, overexpressed methyltransferases from *cbi*E, H, F, and L in the presence of SAM. A surprising result was obtained. The only C methylation observed was that catalyzed by the gene product of ORF-7 (*cbi*F) and turned out to be methylation at C-11! The new compound, identified as the kinetic product by direct NMR observation (Fig. 15), is a modified corphin bearing a fourth methyl group at C-11. Since biochemical conversion of this corphin to cobyrinic acid has not yet been demonstrated, we have named the new compound 4x,[52] and its structural variant recalls one of the four possible structures proposed for factor S3.[43, 44] The spectroscopic data for the latter metabolite

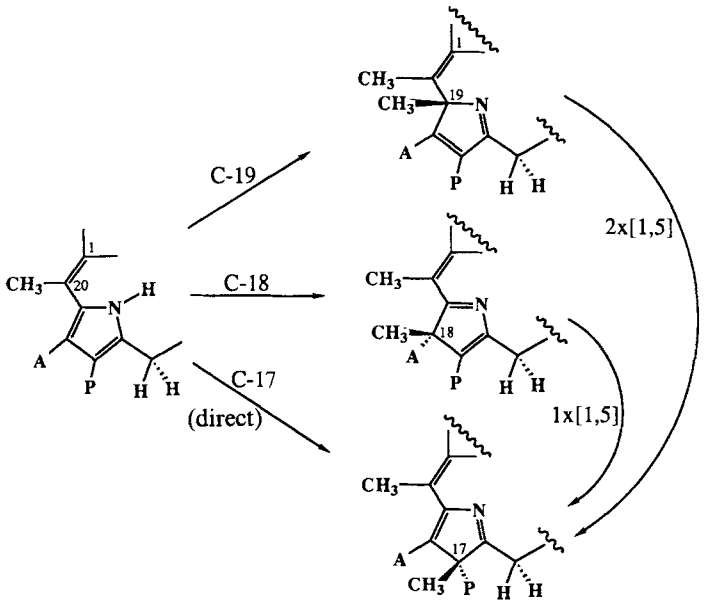

Fig. 14. Possible sites of C methylation in ring D of precorrin 3 and subsequent [1,5] sigmatropic shifts which rationalize the methyl group insertion finally observed at C-17 in corrins.

isolated from *P. shermanii*[43, 44] could not distinguish between methylation at C-1 or C-11, but it is now clear that the correct isomer is the one in which (α)-methylation at C-11

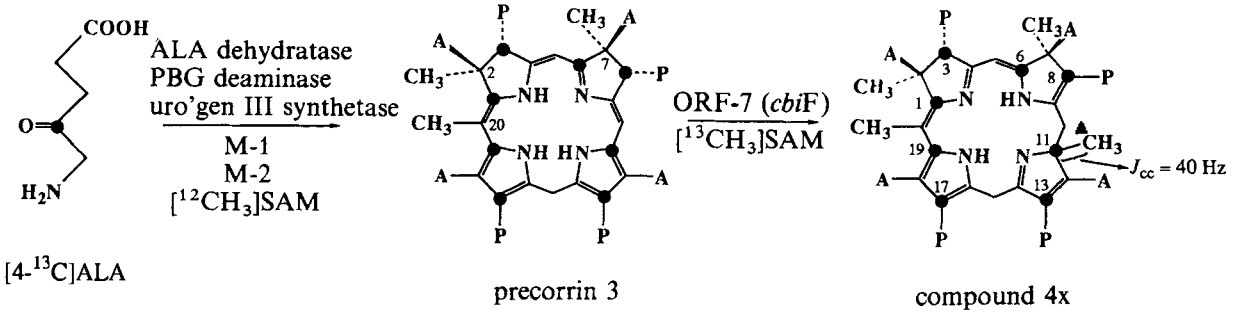

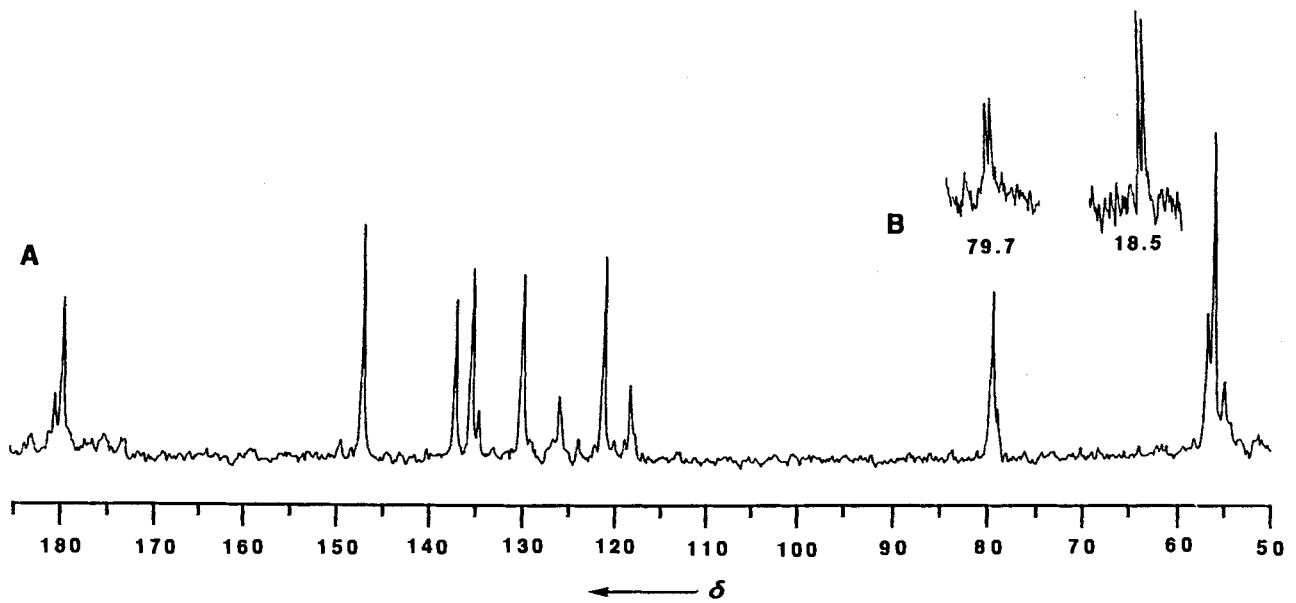

Fig. 15. Multienzyme synthesis of compound 4x with the gene product from *cbi*F and SAM. The ^{13}C NMR spectrum of 4x (A) reveals three sp^2 resonances at $\delta = 134.8$, 136.5, and 120.7 (C-8, C-13, and C-17, respectively), but only one signal at $\delta = 55.5$ for one sp^2 propionate terminus (C-3), and one at $\delta = 79.7$, typical of an sp^3 carbon atom (C-11) adjacent to a nitrogen atom. The inset B shows the coupling (J(C,C) = 40 Hz) of the new signal for $^{13}CH_3$ ($\delta = 18.5$) to the signal for C-11 at $\delta = 79.7$.

(≡C-16) has taken place on the uro'gen I template. The new structural proposal for factor S3 was nicely confirmed by a second multienzyme synthesis, this time using [4-^{13}C]ALA as substrate in a one-flask reaction mixture, containing dehydratase, deaminase (→ uro'gen I) *cys*G,[*] *cbi*F, and SAM (Fig. 16a). In the absence of the last of these enzymes (*cbi*F) the product 2,7,12-trimethylpyrrocorphin (Fig. 9) accumulates, but when the fourth enzyme (*cbi*F) was added, a new signal appeared at $\delta = 79$ heralding the insertion of a fourth (α-) methyl group on the C-16 position (Fig. 16a). The resultant zinc complex (in the form of its octamethyl ester) was identical in every respect with factor S3 isolated earlier from *P. shermanii*.[52b] It only remains to define the absolute configuration of the new chiral center at C-16 and to test for the putative [1,5]sigmatropic shift to transform factor S3 into factor S1 (Fig. 16b). These new findings[52] suggest a lack of substrate specificity in C methylation by the methyltransferases and provide a welcome confirmation of the function of *cbi*F as a methyltransferase which attacks the α position of pyrrole rings of pyrrocorphins, whether type III or type I. Furthermore, these results open the door to synthetic chemistry based on C methylation at electron-rich centers.

The discovery that factor S3 could be synthesized from uro'gen I, M-1, and *cbi*F,[52b] has profound implications for the methylation sequence and stereochemistry of corrin biosynthesis, since stereospecific methyl transfer has been effected on an "unnatural" substrate. In the light of these recent findings we now return to a discussion of the modulation of the regio- and stereochemistry of the post-precorrin 3 methylases by coordination with divalent metals.

[*] This abbreviation is used for both the gene and the gene product.

3.3. The Role of Metals in Corrin Biosynthesis

Since coordinating metal ions, for example Zn^{2+}, Co^{3+}, are present in the substrate for both type I and type III te-

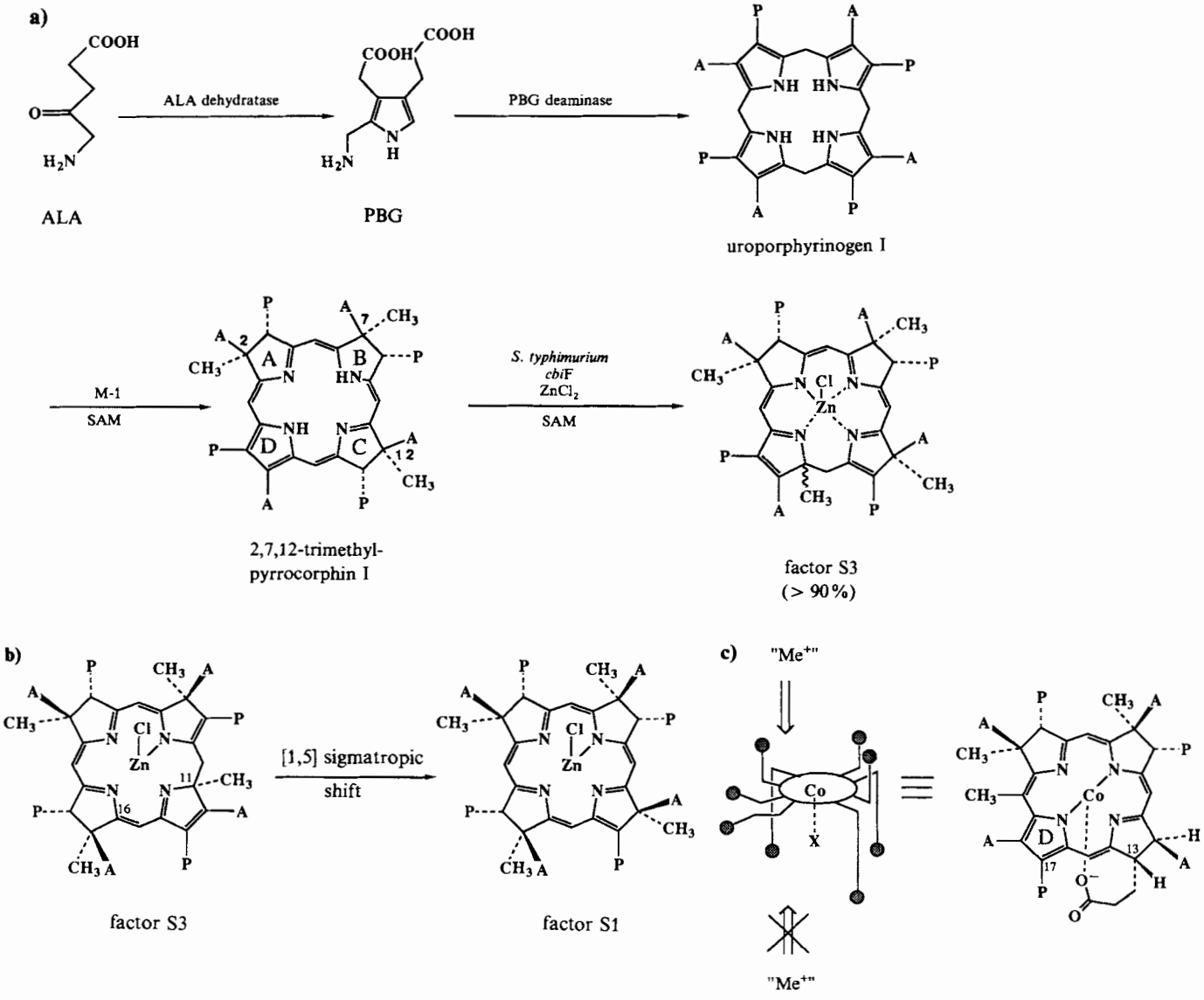

Fig. 16. a) Multienzyme synthesis of factor S3. b) A rationalization of a (chemical?) connection between factors S3 and S1. Note that the symmetry of the type I template allows clockwise rotation of the structure shown for factor S3 through 90° to change the apparent order of the C-methylation steps. c) Possible role of the three propionate side chains in the ring D pyrrocorphin tautomer of cobalt precorrin 3 to direct the incoming methyl group from SAM to the (upper) β face at the fourth (southwest) propionate terminus.

tramethylation, we can now speculate that the regio- and stereospecific C methylation of metalated precorrin 3 is controlled both by the inductive effect of the methyl group at C-20 and by the coordinating metal. Thus, cobalt precorrin 3 can be prepared for C-17 methylation by tautomerization to the ring D pyrrrocorphinate (Fig. 16c) which has the thermodynamically favorable all-*trans* configuration of the side chains (beginning with ring A). This process requires an α-orientated ring C propionate at C-13 whose interaction with the coordinating sphere of the metal together with the propionate side chains at C-3 and C-8 provide steric shielding on the α face of the macrocycle, allowing the fourth methylation (at C-17) to occur exclusively on the β face. This argument also holds for possible β methylation at C-18 (or even C-19) as discussed above.

On the other hand, in the recently described *P. denitrificans* mutant,[49, 53, 54] which harbors the eight genes necessary for the synthesis of the metal-free precorrin 6x[53, 54] (and hence hydrogenobyrinic acid), the absence of cobalt suggests that zinc or magnesium can be substituted for cobalt in order to achieve the same regio- and stereospecificity of C methylation and ring contraction as found in the cobalt series. Since the presence of a coordinating metal obviously exercises strict regiocontrol on this type of process, our metal-free substrates must now be reinvestigated in the form of their complexes with cobalt and zinc in order to determine the effect of the metal on the specificity of C methylation in corrin biosynthesis. The special role of cobalt is discussed in Section 4.

3.4. Comparison of *Salmonella* and *P. denitrificans* Genes for Corrin Synthesis

We are now in a position to compare the homologies and functions of the cloned genes of *Salmonella* and *Pseudomonas* (Fig. 17). Amino acid sequence comparisons of the gene products predicted from the nucleotide sequence of the *P. denitrificans* and *S. typhimurium* genes revealed homology between: *cob*H and *cbi*C; *cob*I and *cbi*L; *cob*J and *cbi*H; *cob*K and *cbi*J; *cob*L and *cbi*E + T; and the *cob*M and *cbi*F gene products. No homologues were found for the *cob*F, *cob*G, *cbi*D, and *cbi*G gene products (Fig. 17).

The *P. denitrificans* enzymes responsible for reduction of precorrin 6x to 6y (*cob*K), the bismethylation and decarboxylation of 6y to 8x (*cob*L), and the rearrangement of the latter to hydrogenobyrinic acid (*cob*H) have recently been described (Fig. 18).[49, 55, 56a] The remaining genes (*cob*F, G, J, M) most likely encode enzymes responsible for the synthesis of precorrin 6x from precorrin 3, a process which must involve several labile intermediates derived from SAM-dependent C methylations at C-1, C11, C-17, and ring contraction/deacylation (from C-20 and its attached methyl). None of these intermediates has been isolated from lysates of the recombinant *P. denitrificans* strain; they are presumably destroyed by the procedures used for the isolation of precorrin 6x (oxidation/esterification).

We have still to find C-17 and C-1 methylases, the ring contractase/deacylase and cobalt insertase enzymes. The structure recently suggested for precorrin 8x formed by C-5, C-15 methylation and decarboxylation in ring C, and the

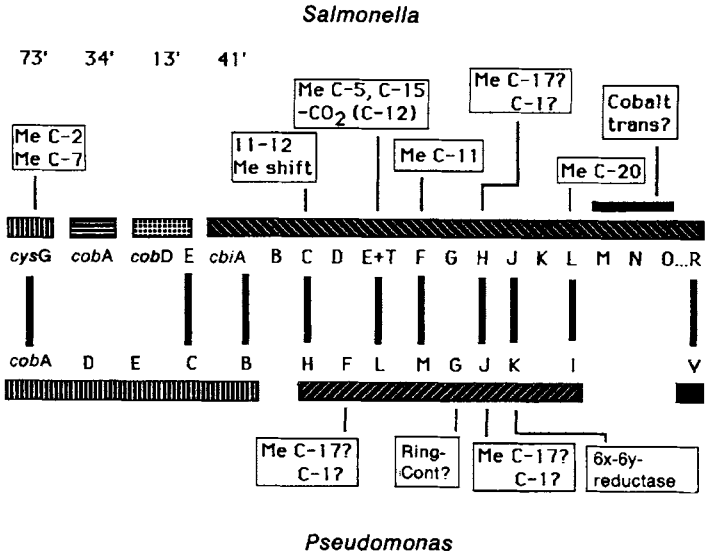

Fig. 17. The location and functions of some of the known genes for B_{12} biosynthesis in *Salmonella typhimurium* [49, 50] and *Pseudomonas denitrificans* [50, 53–56]. In *S. typhimurium* the genes map at 13', (*cob*D, *cob*E: addition of aminopropanol), 34' (*cob*A; adenosylation), 41' (*cbi*A-R; cobinamide biosynthesis), and 73' (*cys*G; uro'gen III methyltransferase). Homologies between the *S. typhimurium* and *P. dentrificans* gene products are shown. See the text for a discussion of their functions.

gene (*cob*H) encoding the mutase for the subsequent C-11 → C-12 transposition (Fig. 18) are important clues[55, 56, 56c] for the mechanism of corrin biosynthesis. It must be borne in mind, however, that none of these species bear cobalt, and that the final product in the eight gene system overexpressed in *P. denitrificans* is hydrogenobyrinic acid (cobalt-free cobyrinic acid). The absence of cobalt in the *P. denitrificans* metabolites precorrin 6x to 8x suggests that the gene for cobalt insertion resides elsewhere than the eight gene cluster used for overexpression,[56b] and that in this organism, amidation of cobyrinic acid takes place before cobalt insertion, remembering that complete cobalt-free corrinoids (including the nucleotide loop) have been found in photosynthetic bacteria. Thus, *Rhodopseudomonas spheroides* and *Chromatium vinosium* produce cobalt-free corrinoids,[57] as does the *P. denitrificans* strain that has been genetically altered by introduction of a plasmid bearing eight genes for corrin synthesis.[53] On the other hand, hydrogenobyrinic acid is not a precursor of cobyrinic acid in *P. shermanii*,[58] and even in the genetically altered *P. denitrificans* strain, cobalt can be inserted into the product, hydrogenobyrinic acid, only by chemical means. Since metallic cofactors seem important in the anaerobic B_{12} producers, it can be suggested that, in aerobes, divalent metal ions such as Mg^{2+} and Zn^{2+} can act as surrogates for cobalt and, on extraction (≡decomplexing), the metal-free corrinoid or precorrinoid is isolated. The reverse situation is found in *P. shermanii* (and presumably in *S. typhimurium*), since once cobalt is inserted into precorrins 2 and 3 (see Section 4), it cannot escape at a later stage from the strong coordinating ligands of the ring-contracted intermediates corresponding to precorrin 6x etc. for it is well known that cobalt cannot easily[59] be removed chemically from cobyrinic acid, cobalamins, and B_{12} without destroying, or at least cutting open, the macrocyclic ligand. Whether the presence (or absence) of cobalt in the precorri-

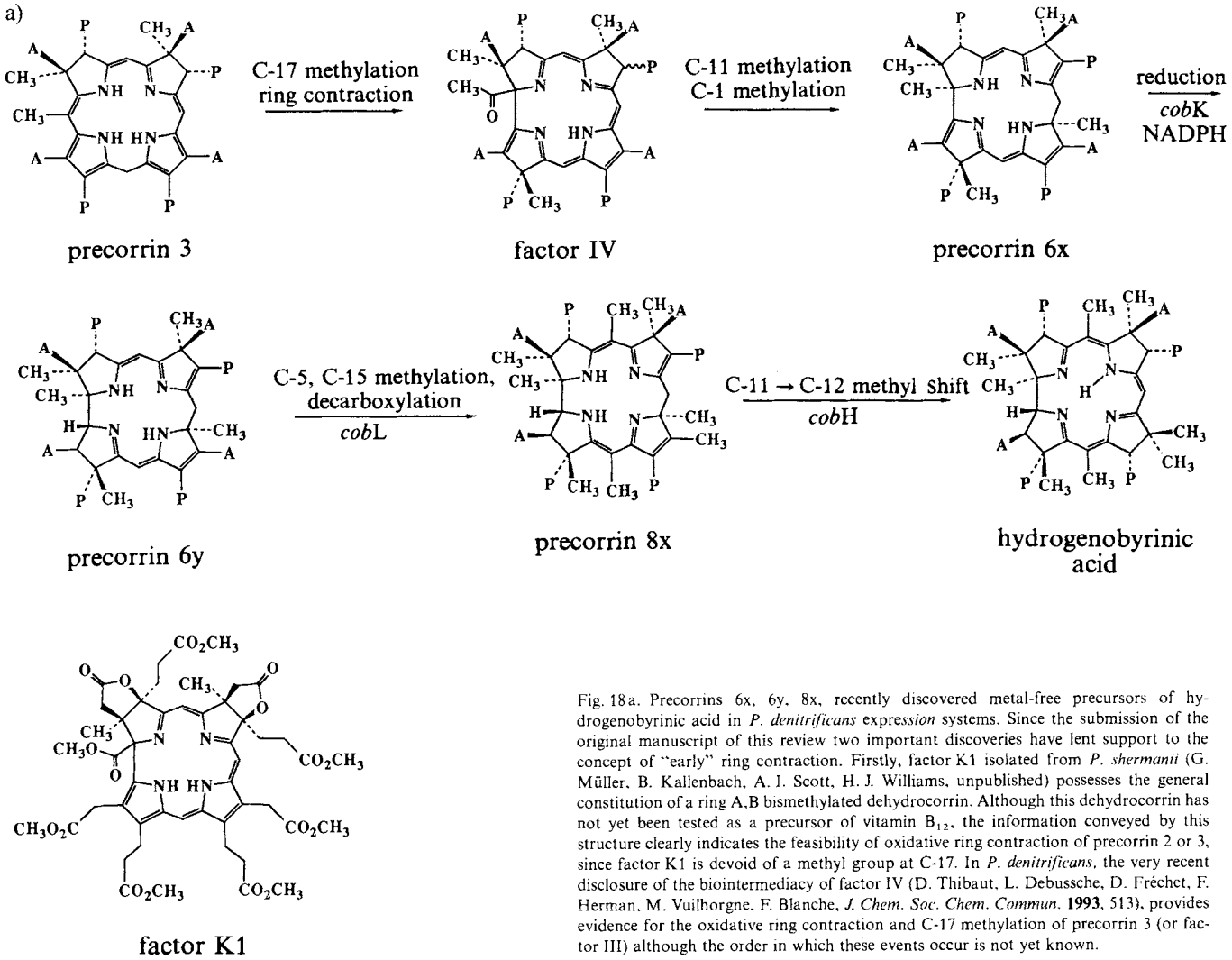

Fig. 18a. Precorrins 6x, 6y, 8x, recently discovered metal-free precursors of hydrogenobyrinic acid in *P. denitrificans* expression systems. Since the submission of the original manuscript of this review two important discoveries have lent support to the concept of "early" ring contraction. Firstly, factor K1 isolated from *P. shermanii* (G. Müller, B. Kallenbach, A. I. Scott, H. J. Williams, unpublished) possesses the general constitution of a ring A,B bismethylated dehydrocorrin. Although this dehydrocorrin has not yet been tested as a precursor of vitamin B_{12}, the information conveyed by this structure clearly indicates the feasibility of oxidative ring contraction of precorrin 2 or 3, since factor K1 is devoid of a methyl group at C-17. In *P. denitrificans*, the very recent disclosure of the biointermediacy of factor IV (D. Thibaut, L. Debussche, D. Fréchet, F. Herman, M. Vuilhorgne, F. Blanche, *J. Chem. Soc. Chem. Commun.* **1993**, 513), provides evidence for the oxidative ring contraction and C-17 methylation of precorrin 3 (or factor III) although the order in which these events occur is not yet known.

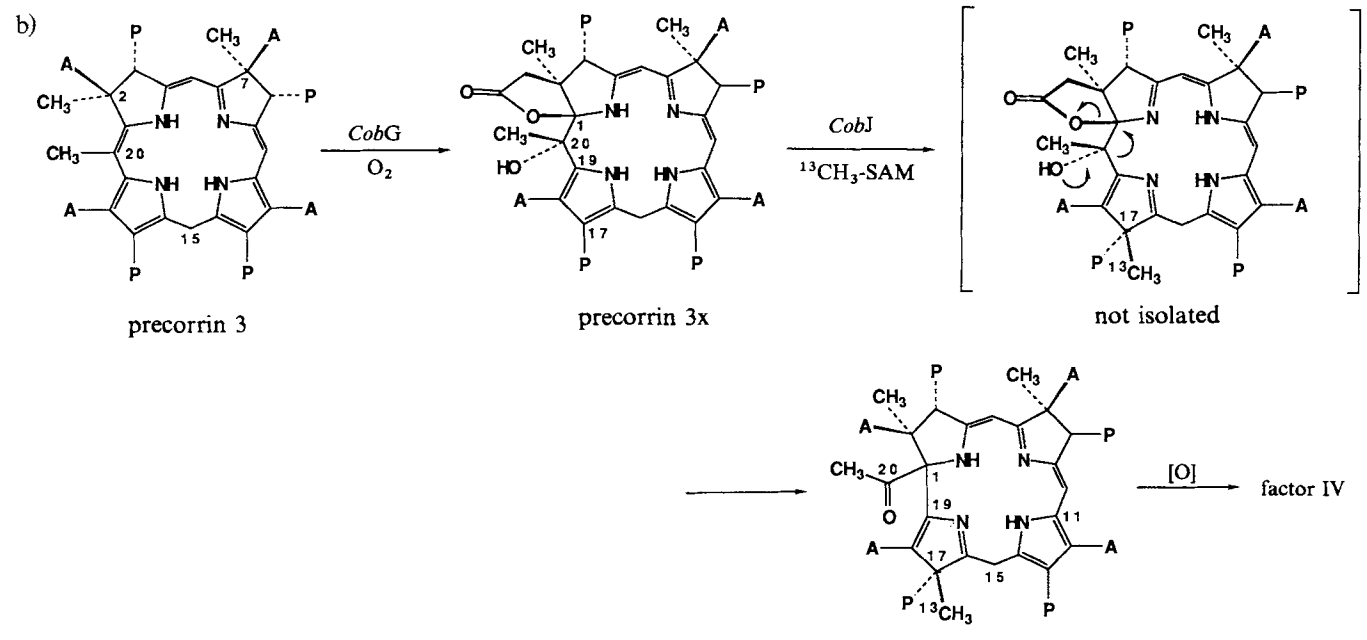

Fig. 18b. Note added in proof (July 15, 1993): Experimental evidence for the sequence between precorrin 3 and factor IV involving a new intermediate, precorrin 3x, with the *P. denitrificans* genes *cob*G and J has been obtained recently. An oxidative step (*cob*G) is followed by pinacol-type ring contraction and methylation at C-17 (*cob*J) to give precorrin 4, which on oxidation gives a product identical with factor IV (A. I. Scott, C. A. Roessner, N. J. Stolowich, J. B. Spencer, C. Min, *FEBS Lett.*, **1993**, in press).

noid intermediates radically alters the sequence of biosynthetic events such as C methylation, ring contraction, oxidation level, and amidation remains to be determined by exchange of the two classes of substrate, metalated and metal-free, between the biosynthetic enzymes of the aerobic and anaerobic B_{12}-producing bacteria.

Although it would seem inconceivable to organic chemists (and evolutionary theorists) that two distinct pathways should run parallel to such a complex target as B_{12} (or even cobyrinic acid), the circumstantial evidence now suggests that the enzymes of the aerobic and anaerobic pathways make and handle subtly different substrates—one set cobalt-free, the other coordinated with cobalt.

4. Cobalt Insertion: Experiments with *P. shermanii*

"When you follow two separate chains of thought, Watson, you will find some point of intersection which should approximate the truth."
"The Disappearance of Lady Frances Carfax"

In collaboration with G. Müller[60] we have shown that in *P. shermanii* extracts, cobalt is inserted into precorrins 2 and 3, and that the resultant metal complexes serve as substrates for cobyrinic acid synthesis in this organism (Fig. 19).

When we compared the synthetic capabilities of cell-free extracts from *P. shermanii* grown (A) in the absence and (B) in the presence of Co^{2+}, the oxidized cobalt complex of precorrin 2 (cobalt factor II) could be isolated only after incubation of extract (A) with ALA, SAM, and Co^{2+}, while the cobalt complex of factor III was isolated directly from extract (B). Extracts (A) and (B) were then partially purified (gel filtration) to remove endogenous small molecules. While the purified system **A** synthesizes cobyrinic acid only with the added substrates SAM/Co^{2+}/ALA or SAM/Co^{2+}/factor III, purified system **B** is capable of corrin synthesis in the presence of SAM but in the absence of Co^{2+} or any other substrate.

Direct confirmation of the role of cobalt precorrin 3 as a true substrate came from the incorporation of doubly labeled ($C^3H_3/^{14}C$) cobalt factor III with retention of two-thirds of the original $^3H/^{14}C$ ratio, as required for the loss of the C^3H_3 group and C-20 as acetic acid. Competition experiments clearly demonstrate intact bioconversion without interchange of coordinated metal, of cobalt factors II and III to cobyrinic acid, although in the absence of ethylenediaminetetraacetic acid (EDTA) some exchange of cobalt between the complexes can be detected. By careful experimentation it was possible to demonstrate the cell-free conversion of ^{14}C-labeled cobalt factor II in the presence of [C^3H_3]SAM to cobalt factor III, which exhibits a $^3H/^{14}C$ ratio of 1.15, and to cobyrinic acid with the $^3H/^{14}C$ ratio (5.65) expected for the five introduced methyl groups. Finally it could be shown that cobalt insertion in *P. shermanii* is an enzymatic process, when cobalt factor III was isolated after incubation of factor III with a *P. shermanii* homogenate.[60b] Thus, there is no longer any doubt that in *P. shermanii* (and presumably in *Salmonella*) cobalt is inserted much earlier in the pathway than in *P. denitrificans*.

5. Ring Contraction: Temporal Resolution of a Unique Isotope Exchange at a Carbonyl Group on the Way to B_{12}

"It is quite a three-pipe problem."
"The Red Headed League"

The structure of precorrin 6x dictates that, in *P. denitrificans*, ring contraction takes place between precorrins 3 and

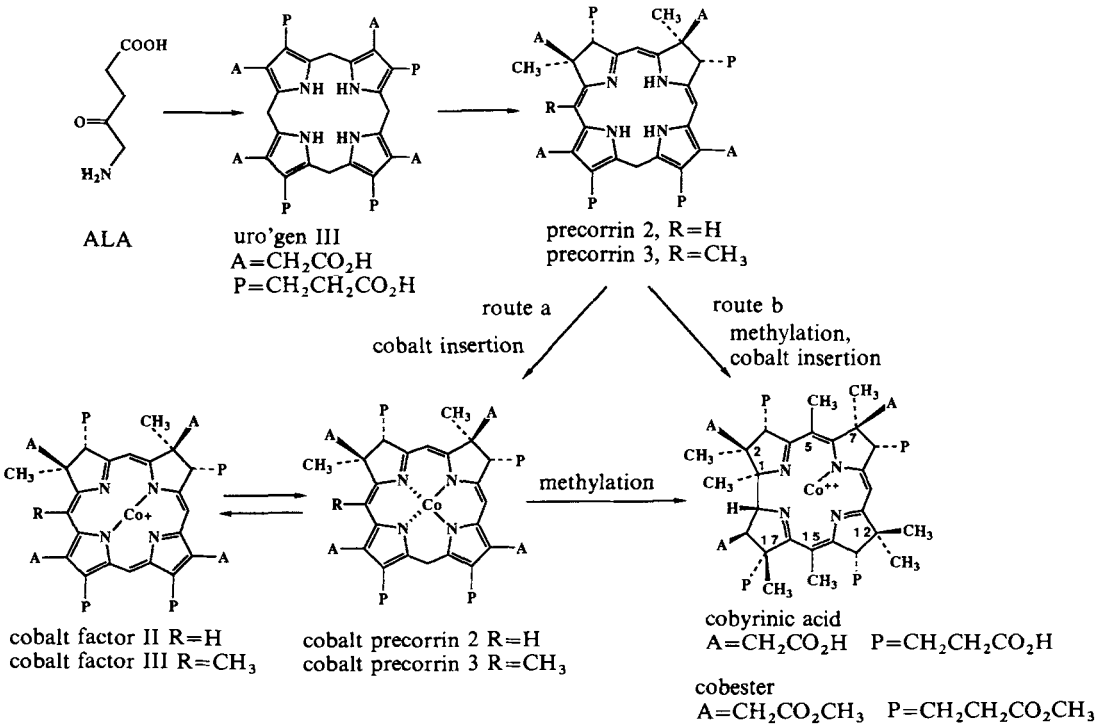

Fig. 19. Temporal resolution of cobalt insertion (into precorrins 2 and 3; route a) in *P. shermanii*.

6x, that is before the last two methylations (C-5 and C-15) and decarboxylation (C-12 acetate). No evidence is yet available for the intermediacy of species corresponding to precorrins 4a, 5a, and 6a; the structures of which are shown in Figure 20. However, in *P. shermanii* it has been possible to

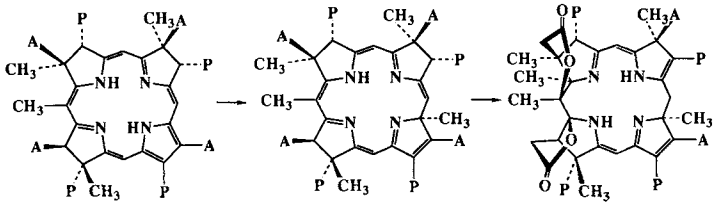

Fig. 20. Proposed structures of the missing intermediates, precorrins 4a, 5a, and 6a. Since several tautomeric and even isomeric(!) structures are possible for the undiscovered tetra- and pentamethyl intermediates, we have used the term 4a and 5a to denote this uncertainty. The same is true for the hexamethyl series where only 6x has been characterized. Thus, C-1 methylation in ring A may have been preceeded by C-20 alkylation and 1,2-migration as part of the ring contraction process. Although C-11 methyltransferase activity has been shown (Fig. 15), none of the research groups involved in B_{12} biosynthesis has yet identified the gene product responsible for C-17 methylation, corresponding to the putative structure for precorrin 4a but see Figure 18. The logical possibility, therefore, remains that ring contraction precedes methylation at C-17 (and hence C-11). In other words, the ring-contractase may use precorrin 3 (or even factor III!) as a substrate. This would constitute some violation of our cherished preconceptions about the timing of the extrusion of acetic acid from C-20, and its attached methyl group, and yet another major surprise in the convoluted saga of Nature's synthetic strategy for corrin synthesis. Experimental proof must now be sought for such a hypothesis by using the gene libraries from *S. typhimurium* and *P. denitrificans*. See also legend for Figure 18.

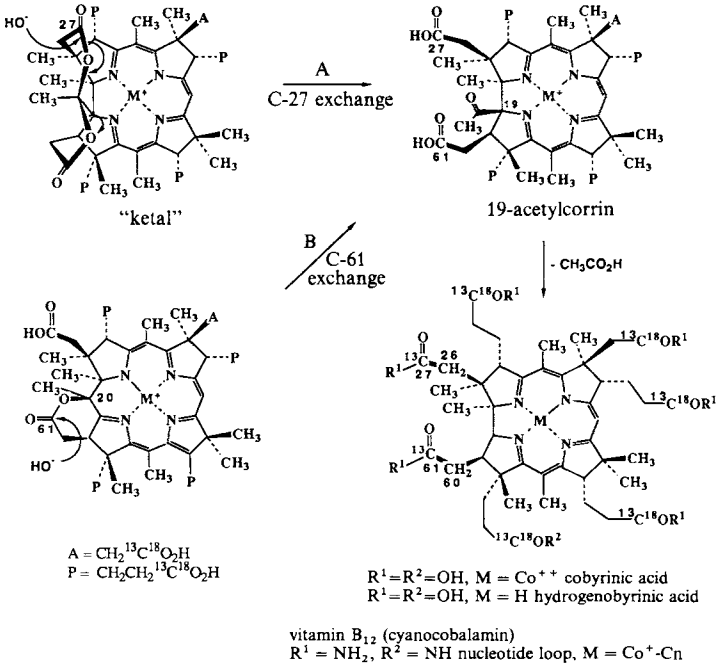

Fig. 21. Proposed mechanisms for $^{18}O/^{16}O$ exchange during ring contraction. The proposals are given in their original form although it is now known that ring contraction can take place on a cobalt-free structure with six or less methyl groups and that in aerobic organisms the acetyl group is at C-1 rather than C-19 (see Fig. 18).

show by NMR experiments that a unique carbonyl group at C-27 (the ring A carboxyamide group of B_{12}) is involved in the mechanism of ring contraction following C methylation at C-17, C-11, and C-1.

It was found[61] by ^{18}O labeling that during B_{12} biosynthesis almost complete $^{18}O/^{16}O$ exchange of the carbonyl oxygen atom of one of the three acetamido groups takes place. This result has profound bearing on the proposed mechanism of corrin biosynthesis. Thus, in one hypothesis,[62] δ-lactone formation between the acetate group (C-27) of ring A and C-20 has been proposed to rationalize the ring contraction of the porphyrinoid to the corrinoid template (mechanism A; Fig. 21), leading to incorporation of solvent label by hydrolysis. A second hypothesis[63] involves the sole intervention of the ring D acetate carbonyl group (C-61) in δ-lactone formation to C-20, followed by a subsequent hydrolysis step in which exchange of ^{18}O label ($\geq 50\%$) exclusively at C-61 would be observed (mechanism B; Fig. 21). The unambiguous assignment of the ^{13}C NMR signals for these two acetate carbonyl C atoms now become crucial, since the analysis for $^{18}O/^{16}O$ exchange is based on the isotopic shifts of ^{18}O on the $^{13}C{=}O$ resonances. Unfortunately, in the NMR spectra of cobalamins[64-66] the two carbonyls in question (C-27 and C-61) usually differ by less than $\Delta\delta = 0.3$ in chemical shift, and in several instances are superimposable.[65,66] The problem was solved by enhancing the resolution of the 2D experiment by specific ^{13}C enrichment. Cyanocobalamin was biosynthetically enriched at all seven carbonyl carbon atoms from [1-^{13}C]ALA, using cells of *P. shermanii*. The resulting high-resolution (<4 Hz/pt in F_1) HMBC spectrum clearly resolves all seven carbonyl carbon atoms. More importantly, C-27 and C-61, separated by only $\Delta\delta = 0.2$ in the one-dimensional spectrum, can be assigned unambiguously by correlation to their adjacent protons, H-26 ($\delta = 2.35$) and H-60 ($\delta = 2.70$) (Figs. 22A, B). The chemical shifts of these protons have been previously assigned.[65] This establishes that the correct assignment for C-27 ($\delta = 178.40$) had indeed been chosen in the earlier work, that is the acetate group of ring A, rather than that of ring D, uniquely participates at least once (and possibly more than once) in reactions whose mechanisms require almost complete exchange of ^{16}O from the medium with the ^{18}O-labeled carbonyl group at C-27.[67]

The next question concerns the timing of the loss of ^{18}O, that is before or after the formation of uro'gen III, the first tetrapyrrolic macrocycle of the B_{12} pathway. This question can, in principle, be answered by observation of the ^{18}O induced chemical shift changes in the ^{13}C NMR spectrum of a sample of urogen III derived from [1-^{13}C,1-$^{18}O_2$]5-aminolevulinic acid (ALA). Although distinction can be made between the two sets of ^{13}C signals comprised of four acetate and four propionate carbonyl groups of urogen III, specific assignments for the individual acetate and propionate carbonyl groups cannot be made for reasons of symmetry. Accordingly, a method for removing this impasse was devised in order to provide unequivocal assignment for the acetate carbonyl groups of rings A and D, and information about possible ^{18}O exchange beyond urogen III, that is, after the insertion of the first two methyl groups in the biosynthetic intermediate precorrin 2 at C-2 and C-7. As discussed in

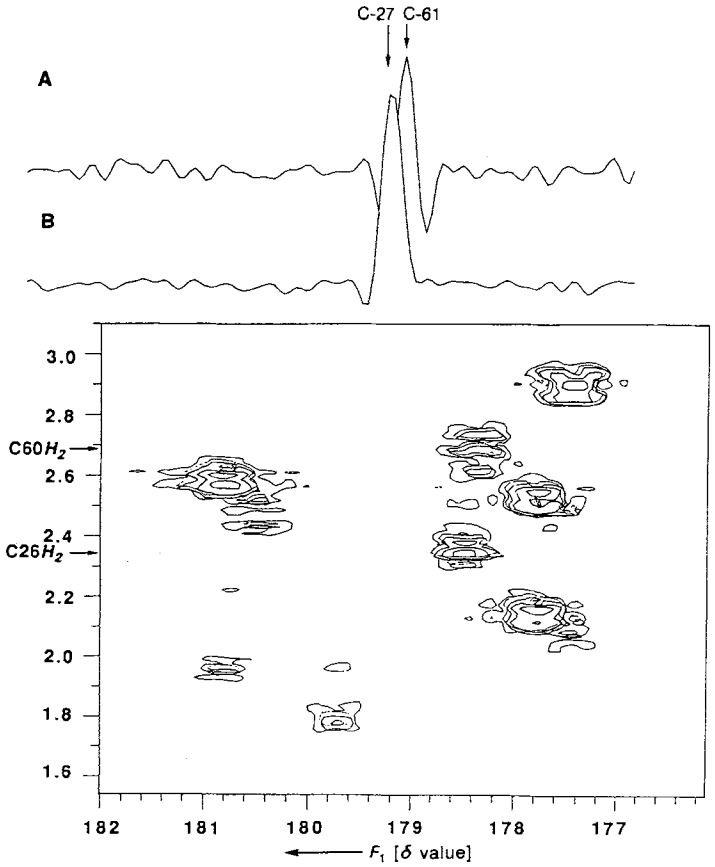

Fig. 22. 2D HMBC NMR spectrum (300 MHz, ^1H; 75 MHz, ^{13}C) of cyanocobalamin isolated from *P. shermanii* grown on [1-^{13}C]ALA. Spectra **A** and **B** represent slices through $\delta = 2.70$ and $\delta = 2.35$, respectively, confirming the two bond correlation between C-61 ($\delta = 178.28$) and H-60 in **A**, and C-27 ($\delta = 178.40$) and H-26 in **B**. See Figure 21 for numbering system.

Section 3.1, uro'gen III can be efficiently C methylated in the presence of SAM by M-1 to give the trimethylpyrrocorphin in which all four acetate carbonyl groups are cleanly resolved in the ^{13}C NMR spectrum. When the trimethylpyrrocorphin (Fig. 8) was prepared from [1-^{13}C,1-$^{18}O_2$]ALA with the required set of enzymes in $H_2{}^{16}O$, analysis of the ^{18}O perturbed ^{13}C chemical shifts for the acetate and propionate carbonyl groups of the product revealed that no exchange of ^{18}O by solvent ^{16}O had taken place. Thus, the major exchange of the oxygen atom of the ring A acetate carbonyl group of cyanocobalamin with water from the medium must occur in an intermediate after precorrin 2. The result[67] is important not only in defining the timing of the exchange, but in providing a protocol for analyzing the fate of ^{18}O in the carbonyl groups of urogen III. One of these carbonyl groups might be induced to undergo trapping of ^{16}O under conditions of high pH. This would be a test for possible lactonic intermediates during uro'gen III formation as discussed above.

Returning to the mechanism of corrin biosynthesis, it is now clear that the ring A acetate (C-27) serves at least once in a scaffolding role before and/or during the ring contraction step, and is released by hydrolysis at C-27. The ring D acetate, which may still be involved in ketal formation of the 19-acetyl system (Fig. 21), however, neither suffers direct hydrolysis nor participates in the hydrolytic step envisaged in a previous hypothesis.[63]

6. Evolution of the Porphyrin–Corrin Pathway: Why Type III?

"In solving a problem of this sort, the grand thing is to be able to reason backwards."
"A Study in Scarlet"

There seems no doubt that dual or parallel pathways exist for corrin synthesis in the primitive anaerobes when compared with the (anaerobic) photosynthetic and aerobic microorganisms (Fig. 23). The "preregistration"[47] of a prebiotic corrin template may well have diverted the subsequent biochemical machinery to a type III rather than a type I world, since the genes for uro'gen III synthesis were required for the subsequent ring-contraction step which requires juxtaposition of the two adjacent acetate side chains[47] in ring A and D of uro'gen III. Thus, when heme, chlorophyll, and the cytochrome pigments became necessary cofactors for oxygen transport, photosynthesis, and O_2 activation, respectively, the natural choice was uro'gen III, since this template was already in place as a necessary component of corrin synthesis under genetic control. These intriguing questions will be difficult to answer directly, but even within the context of "modern" B_{12} biosynthesis the duality of pathways (with or without O_2) suggest a vestige of evolutionary preference which now appears to be lateral rather than vertical.

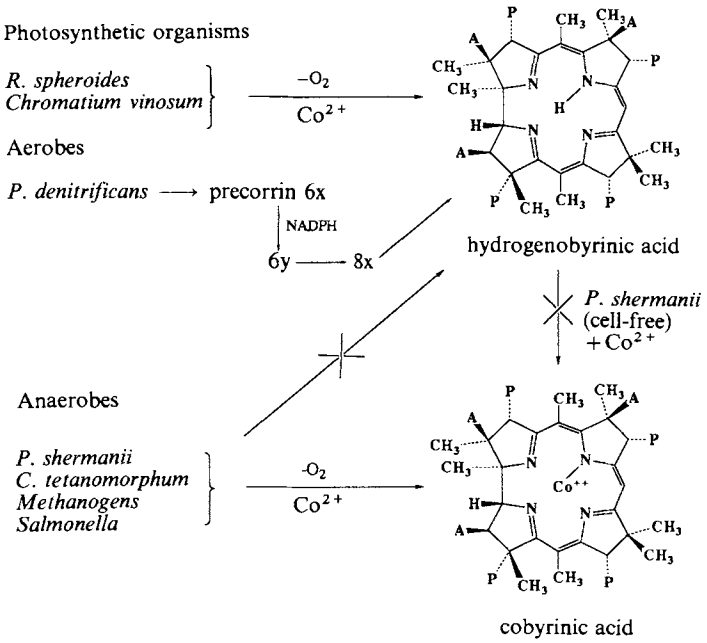

Fig. 23. Parallel, oxidative and metal-free routes to corrins in bacteria.

7. Epilogue

"It is a capital mistake to theorize before you have all the evidence."
"A Study in Scarlet"

This account of vitamin B_{12} biosynthesis has shown how, over the last 25 years, both our earlier ideas and the tech-

niques available for the experimental resolution of the problems of the B_{12} biosynthetic mechanisms, including the isolation of post-uro'gen III intermediates, have been tempered by the fire of experience. By use of modern gene technology and NMR spectroscopy it has at last been possible to break through the previously impenetrable shroud of mystery surrounding Nature's chosen route to vitamin B_{12}. Even with these superb tools, given to us from physics and biology, several steps of the pathway remain cryptic, and it may take yet another technical advance to solve the remaining fascinating problems of enzymatic methylations at carbon atoms C-1 and C-17, the "black box" of ring contraction/deacetylation, and finally cobalt insertion. However, it does appear that at last the beginning of the end is in sight. The many surprises encountered along the way have deepened our respect for the elegant and finely tuned processes used to forge the enigmatic porphyrinoid–corrinoid connection. The adage "to travel hopefully is better than to arrive" can truly be applied to our journey along the road to corrins, and in many ways we will be exhilarated, yet saddened, when the last mysteries of vitamin B_{12} enzymology are solved.

Our expedition along the road to B_{12}, frequently uphill, was shared and made possible by my previous graduate students, postdoctorals, and technical assistants, all of whom contributed great skill and energy to this convoluted, yet rewarding search. In chronological order beginning in 1967 they were: Dr. D. White (Upjohn), Dr. C. A. Townsend (John Hopkins), Dr. K. Okada (Nagoya), Dr. M. Kajiwara (Tokyo), Dr. R. J. Cushley (Victoria, B.C.), Dr. E. Lee (Seoul), Dr. B. Yagen (Jerusalem), Dr. N. Georgopapadakou (Roche), Dr. K. S. Ho (Massachusetts), Dr. S. Klioze (Hoechst), Dr. G. H. Temme (Dow), Dr. I. M. Armitage (Yale), Dr. S.-L. Lee (Corning), Dr. T. Takahashi (Japan), P. Demou (Yale), Dr. D. Petrocine (New York), Dr. K. Kang (Korea), Dr. H. Klein (Cologne), Dr. A. Gossauer (Fribourg), Dr. A. J. Irwin (Ontario), Dr. S. K. Chung (Korea), (The late) Dr. K. Obata (Japan), Dr. P. J. Whitman (New Jersey), Dr. G. Burton (Buenos Aires), Dr. H. Nordlov (Stockholm), Dr. P. Fagerness (Upjohn), Dr. S. Hosozawa (Otsuka Co.), Dr. H. Matsumoto (Daiichi Co.), Dr. J. B. Hansen (Kopenhagen), Dr. K. Shishido (Japan), Dr. J. N. S. Evans (Pullman, Washingon), Dr. N. E. Mackenzie (Tucson), Dr. R. L. Baxter (Edinburgh), Dr. A. Boyd (Edingburgh), Dr. R. C. Davies (Edinburgh), Dr. I. Ichinose (Japan), Dr. T. Oh-hama (Japan), Dr. S. K. Grant (Merck), Dr. P. Karuso (Australia), Dr. T. Hoshino (Japan), Dr. K. Clemens (Scripps Institut), Dr. A. R. Jacobson (Cambridge, Mass.), Dr. P. Yon-Hin (Houston), and Dr. D. Becker (Israel).

A special word of thanks is due to my senior collaborators: Professors G. Müller (Stuttgart), P. M. Jordan (London) and J. Roth (Utah). I am indebted to the present group of highly motivated, young colleagues whose recent discoveries form the main theme of this account: Drs. P. J. Santander, R. Danso-Danquah, M. D. Gonzalez, M. J. Warren, K. Iida, C. Pichon, T. Xue, P. Nayar, J. B. Spencer, Ms. B. P. Atshaves, Ms. K. Campbell, Ms. S. Estrada, and Messrs. N. Anousis, C. Min, S. Ozaki, and J. Park. Their research efforts in the areas of molecular biology, enzymology, and NMR spectroscopy were guided at all times by Drs. Charles Roessner, Neal Stolowich, and Howard Williams whilst Mr. Y. Gao provided untiring help with NMR instrumentation.

We thank the National Institues of Health (NIH), the National Science Foundation (NSF), the Robert A. Welch Foundation, the Science and Engineering Research Council (SERC) (UK), and NATO for generous financial support.

Received: September 21, 1992
Revised: April 29, 1993 [A 916 IE]
German version: *Angew. Chem.* **1993**, *105*, 1281

[1] D. Shemin, D. Rittenberg, *J. Biol. Chem.* **1945**, *159*, 567.
[2] H. M. Muir, A. Neuberger, *Biochem. J.* **1950**, *47*, 97.
[3] P. M. Jordan, *New Compr. Biochem.* **1991**, *19*, 1.
[4] Review: A. I. Scott, *Acc. Chem. Res.* **1978**, *11*, 29. Factor II turned out to be identical with sirohydrochlorin, the metal-free cofactor of *E. coli* sulfite reductase which requires siroheme, the iron complex of factor II, as part of its biochemical machinery to synthesize cysteine in a six-electron reductive process. It is remarkable that sulfite reductase employs a B_{12} intermediate in this way. (A. I. Scott, A. J. Irwin, L. M. Siegel, J. N. Shoolery, *J. Am. Chem. Soc.* **1978**, *100*, 316).
[5] a) F. J. Leeper, *Nat. Prod. Rep.* **1985**, *2*, 561; *ibid.* **1987**, *4*, 441; *ibid.* **1989**, *6*, 171; b) H. A. Barker, H. Weissbach, R. D. Smyth, *Proc. Natl. Acad. Sci. USA* **1958**, *44*, 1093.
[6] N. H. Georgopapadokou, A. I. Scott, *J. Theor. Biol.* **1977**, *69*, 381.
[7] G. Ksander, G. Bold, R. Lattmann, C. Lehmann, T. Früh, Y.-B. Yiang, K. Inomata, H.-P. Buser, J. Schreiber, E. Zass, A. Eschenmoser, *Helv. Chim. Acta* **1987**, *70*, 1115.
[8] M. Eigen, B. F. Lindemann, M. Tietze, R. Winkler-Oswatitsch, A. Dress, A. von Haeseler, *Science* **1989**, *244*, 673; S. F. Mason, *Chemical Evolution: Origins of the Elements, Molecules, and Living Systems*, Oxford University Press, Oxford, **1991**; *Earth's Earliest Biosphere* (Ed.: W. Schopf), Princeton University Press, Princeton, NJ, USA, **1983**. The time-honored British billion (10^{12}) has recently been usurped by the "New World" billion (10^9) as used in this article. British readers therefore should make the mental adjustment and note that the journal *Nature*, a bastion of correct English usage, will henceforth adopt this convention (1 billion = 10^9) as discussed therein (*Nature*, **1992**, *358*, 2).
[9] R. T. Taylor in *B_{12}, Vol. 2*, (Ed.: D. Dolphin), Wiley, New York, **1982**, Chapter 12.
[10] L. J. Ljungdahl, H. G. Wood in *B_{12}, Vol. 2*, (Ed.: D. Dolphin), Wiley, New York, **1982**, Chapter 7.
[11] Almost the entire second volume of *B_{12}* [(Ed.: D. Dolphin) Wiley, New York, **1982**] is devoted to the fascinating rearrangements catalyzed by coenzyme B_{12}. It is quite remarkable that although organisms such as *Salmonella typhimurium* do not appear to require B_{12} for their well-being, the genes for B_{12} synthesis have been retained, albeit silently. Thus, *S. typhimurium*, normally cultivated aerobically, only makes the vitamin when grown anaerobically (R. M. Jeter, B. M. Olivera, J. R. Roth, *J. Bacteriol.* **1984**, *170*, 2078). The question then arises as to what "anaerobic" function can be ascribed to B_{12} in these and related organisms such as the methanogenic bacteria.
[12] I. Macalpine, R. Hunter, *George III and the Mad Business*, Random House, New York, **1969**.
[13] *New York Times*, December 21, **1991**.
[14] Review: S. I. Beale, *New Compr. Biochem.* **1991**, *19*, 155.
[15] T. Oh-hama, N. J. Stolowich, A. I. Scott, *Int. J. Biochem.* **1991**, *23*, 1417.
[16] C. A. Roessner, unpublished results.
[17] See ref. [3], p. 19.
[18] G. Burton, P. E. Fagerness, S. Hosazawa, P. M. Jordan, A. I. Scott, *J. Chem. Soc. Chem. Commun.* **1979**, 202.
[19] A. R. Battersby, C. J. R. Fookes, K. E. Gustafson-Potter, G. W. J. Matcham, E. McDonald, *J. Chem. Soc. Chem. Commun.* **1979**, 1115.
[20] P. M. Jordan, G. Burton, H. Nordlov, M. M. Schneider, L. M. Pryde, A. I. Scott, *J. Chem. Soc. Chem. Commun.* **1979**, 204.
[21] Reviews: F. J. Leeper, *Nat. Prod. Rep.* **1985**, *2*, 19, 561; *ibid.* **1987**, *4*, 441; *ibid.* **1989**, *6*, 171.
[22] A. I. Scott, *J. Heterocycl. Chem.* **1987**, *14*, p. 75.
[23] A. I. Scott, C. A. Roessner, N. J. Stolowich, P. Karuso, H. J. Williams, S. K. Grant, M. D. Gonzalez, T. Hoshino, *Biochemistry* **1988**, *27*, 7984.
[24] P. M. Anderson, R. J. Desnick, *J. Biol. Chem.* **1980**, *255*, 1993.
[25] A. Berry, P. M. Jordan, J. S. Seehra, *FEBS Lett.* **1981**, *129*, 220.
[26] A. R. Battersby, C. J. R. Fookes, G. Hart, G. W. J. Matcham, P. S. J. Pandey, *J. Chem. Soc. Perkin Trans. 1* **1983**, 3041.
[27] P. M. Jordan, A. Berry, *Biochem. J.* **1981**, *195*, 177.
[28] A. I. Scott, C. A. Roessner, K. R. Clemens, N. J. Stolowich, P. J. Santander, M. D. Gonzalez, *FEBS Lett.* **1988**, *242*, 319.
[29] A. I. Scott, N. J. Stolowich, H. J. Williams, M. D. Gonzalez, C. A. Roessner, S. K. Grant, C. Pichon, *J. Am. Chem. Soc.* **1988**, *110*, 5898.
[30] a) P. M. Jordan, M. J. Warren, H. J. Williams, N. J. Stolowich, C. A. Roessner, S. K. Grant, A. I. Scott, *FEBS Lett.* **1988**, *235*, 189. b) R. T. Aplin, J. E. Baldwin, C. Pichon, C. A. Roessner, A. I. Scott, C. J. Schofield, N. J. Stolowich, M. J. Warren, *Bioorg. Med. Chem. Lett.* **1991**, *1*, 503.
[31] a) M. J. Warren, P. M. Jordan, *FEBS Lett.* **1987**, *225*, 87; b) M. J. Warren, P. M. Jordan, *Biochemistry* **1989**, *27*, 9020.

[32] a) G. J. Hart, A. D. Miller, F. J. Leeper, A. R. Battersby, *J. Chem. Soc. Chem. Commun.* **1987**, 1762; b) A. D. Miller, G. J. Hart, L. C. Packman, A. R. Battersby, *Biochem. J.* **1988**, *254*, 915; c) C. J. Hart, A. D. Miller, A. R. Battersby, *ibid.* **1988**, *252*, 909; d) U. Beifuss, G. J. Hart, A. D. Miller, A. R. Battersby, *Tetrahedron Lett.* **1988**, *29*, 2591.

[33] a) R. Radmer, L. Bogorad, *Biochemistry* **1972**, *11*, 904; b) J. H. Mathewson, A. H. Corwin, *J. Am. Chem. Soc.* **1961**, *83*, 135.

[34] A. I. Scott, C. A. Roessner, P. Karuso, N. J. Stolowich, B. P. Atshaves, unpublished results; A. I. Scott, *Pure Appl. Chem.* **1990**, *62*, 1269.

[35] a) A. F. Alwan, B. I. A. Mgbeje, P. M. Jordan, *Biochem. J.* **1989**, *264*, 397; b) N. Crockett, P. R. Alefounder, A. R. Battersby, C. Abell, *Tetrahedron* **1991**, *47*, 6003.

[36] a) W. M. Stork, M. G. Baker, P. R. Raithby, F. J. Leeper, A. R. Battersby, *J. Chem. Soc. Chem. Commun.* **1985**, 1294; b) A. R. Battersby, J. R. Fookes, G. W. J. Matcham, E. McDonald, R. Hollenstein, *J. Chem. Soc. Perkin Trans.1* **1983**, 3031.

[37] G. Müller in *Vitamin B_{12}* (Eds.: B. Zagalak, W. Friedrich), de Gruyter, New York, **1979**, p. 279. He described a methylase from *P. shermanii* capable of using Uro'gen I as substrate. The product was not characterized.

[38] B. Cameron, K. Briggs, S. Pridmore, G. Brefort, J. Crouzet, *J. Bacteriol.* **1989**, *171*, 547; F. Blanche, D. Debussche, D. Thibaut, J. Crouzet, B. Cameron, *ibid.* **1989**, *171*, 4222.

[39] a) M. J. Warren, C. A. Roessner, P. J. Santander, A. I. Scott, *Biochem. J.* **1990**, *265*, 725. b) Recent investigation [39c] of the *cysG* gene product, M-1, has revealed that the enzyme is, in fact, bifunctional and in the presence of NAD behaves both as a methyltransferase and as a specific dehydrogenase responsible for the synthesis of sirohydrochlorin (factor II) (required for siroheme production) from precorrin 2. Only in the absence of NAD does M-1 show catalytic activity in overmethylating precorrin 2. c) J. B. Spencer, C. A. Roessner, N. J. Stolowich, A. I. Scott, unpublished results.

[40] a) A. R. Battersby, K. Frobel, F. Hammerschmidt, C. Jones, *J. Chem. Soc. Chem. Commun.* **1982**, 455; b) R. D. Brunt, F. J. Leeper, I. Grgurina, A. R. Battersby, *ibid.* **1989**, 428.

[41] a) R. Schwesinger, R. Waditschatka, J. Rigby, R. Nordmann, W. B. Schweizer, E. Zass, A. Eschenmoser, *Helv. Chim. Acta* **1982**, *65*, 600; R. Waditschatka, Dissertation, no. 7707, *Die Porphyrinogen ⇄ Pyrrocorphin-Tautomerisierung*, ETH Zürich, **1985**; b) M. J. Warren, N. J. Stolowich, P. J. Santander, C. A. Roessner, B. A. Sowa, A. I. Scott, *FEBS Lett.* **1990**, *261*, 76. c) That the structure of the trimethylpyrrocorphin (Fig. 8) conforms to a "clockwise" direction of C methylation could be shown by a pulsed isotopic dilution experiment in which heavy ^{13}C enrichment at C-2 and C-7, medium enrichment at C-12, and very slight enrichment at C-18 in the substrate, uro'gen III was achieved by conversion of differentially ^{13}C-enriched E-S complexes of deaminase to HMB (Fig. 4), thence to uro'gen III with cosynthase. The ^{13}C NMR spectrum of the C-methylated product of this specimen of uro'gen III, the trimethylpyrrocorphin (Fig. 8), showed strong (sp^3) signals for C-2, C-7, a medium (sp^3) signal for C-12, and almost no signal in the sp^2 region corresponding to C-18, showing that the third methylation had occurred at C-12. On the other hand, due to the inherent symmetry of the type I template, the corresponding trimethylpyrrocorphin (Fig. 9) does not betray its methylation sequence, since the third methyl group could have been introduced formally at C-12 or C-17, as can be seen by rotating the structure through 90°. We will assume for the subsequent argument that the methylations are in conformity with the type III system (Fig. 8), that is they are always performed in a *clockwise* direction.

[42] a) A. I. Scott, M. J. Warren, C. A. Roessner, N. J. Stolowich, P. J. Santander, *J. Chem. Soc. Chem. Commun.* **1990**, 593; b) M. J. Warren, M. D. Gonzalez, H. J. Williams, N. J. Stolowich, A. I. Scott, *J. Am. Chem. Soc.* **1990**, *112*, 5343.

[43] G. Müller, J. Schmiedl, E. Schneider, R. Sedlmeier, G. Worner, A. I. Scott, H. J. Williams, P. J. Santander, N. J. Stolowich, P. E. Fagerness, N. E. Mackenzie, *J. Am. Chem. Soc.* **1986**, *108*, 7875.

[44] G. Müller, J. Schmiedl, L. Savidis, G. Wirth, A. I. Scott, P. J. Santander, H. J. Williams, N. J. Stolowich, H.-P. Kriemler, *J. Am. Chem. Soc.* **1987**, *109*, 6902.

[45] A. I. Scott, H. J. Williams, N. J. Stolowich, P. Karuso, M. D. Gonzalez, F. Blanche, D. Thibaut, G. Müller, G. Wörner, *J. Chem. Soc. Chem. Commun.* **1989**, 522.

[46] C. Leumann, K. Hilpert, J. Schreiber, A. Eschenmoser, *J. Chem. Soc. Chem. Commun.* **1983**, 1404.

[47] Review: A. Eschenmoser, *Angew. Chem.* **1988**, *100*, 5; *Angew. Chem. Int. Ed. Engl.* **1988**, *27*, 5.

[48] a) R. M. Jeter, J. R. Roth, *J. Bacteriol.* **1987**, *169*, 3189; b) J. R. Roth, C. Crabau, T. G. Doak in *Chemical Aspects of Enzyme Biotechnology; Fundamentals*. (Eds.: T. O. Baldwin, F. M. Raushel, A. I. Scott), Plenum, New York, **1990**, p. 317; c) J. R. Roth, personal communication.

[49] a) D. Thibaut, M. Corder, J. Crouzet, L. Debussche, B. Cameron, F. Blanche, *J. Bacteriol.* **1990**, *172*, 6245, and references therein; b) J. Crouzet, F. Blanche, B. Cameron, D. Thibaut, L. Debusche in *Chemical Aspects of Enzyme Biotechnology; Fundamentals* (Eds.: T. O. Baldwin, F. M. Raushel, A. I. Scott), Plenum, New York, **1990**, p. 299; c) F. Blanche, A. Famechon, D. Thibaut, L. Debussche, B. Cameron, J. Crouzet, *J. Bacteriol.* **1992**, *174*, 1050.

[50] M. J. Warren, C. A. Roessner, S.-I. Ozaki, N. J. Stolowich, P. J. Santander, A. I. Scott, *Biochemistry* **1992**, *31*, 603.

[51] a) A. I. Scott, *Acc. Chem. Res.* **1990**, *23*, 308, and references therein; b) H. C. Uzar, A. R. Battersby, T. A. Carpenter, F. J. Leeper, *J. Chem. Soc. Perkin Trans. 1* **1987**, 1689; c) F. Blanche, D. Thibaut, D. Frechet, M. Vuilhorgne, J. Crouzet, B. Cameron, G. Müller, K. Hlineny, U. Traub-Eberhard, M. Zboron, *Angew. Chem.* **1990**, *102*, 947; *Angew. Chem. Int. Ed. Engl.* **1990**, *29*, 884.

[52] a) C. A. Roessner, M. J. Warren, P. J. Santander, B. P. Atshaves, S.-I. Ozaki, N. J. Stolowich, K. Iida, A. I. Scott, *FEBS Lett.* **1992**, *301*, 73; b) S.-I. Ozaki, C. A. Roessner, N. J. Stolowich, G. Müller, unpublished results. We have recently found (J. B. Spencer, A. I. Scott, unpublished results) that the *cysG* gene product (M-1) turns out to have at least three functions in addition to C methylation of uro'gen III to precorrin 2. Thus, in the presence of M-1 and NAD, precorrin 2 is dehydrogenated to factor II (sirohydrochlorin; Fig. 2) which, on addition of Fe^{2+} (again in the presence of M-1) is catalytically metalated to siroheme (Fig. 1). It has also been found with uro'gen I as substrate, that *cysG* not only inserts three C-methyl groups (at C-2, C-7, and C-12) (Fig. 9), but also catalyzes the insertion of Zn^{2+} in the resultant trimethylpyrrocorphin, and surprisingly, uses this metal substrate for inserting a fourth methyl group at C-17, leading to the multienzyme synthesis of factor S1. Contrary to our previous ideas, this has a separate biosynthesis and is not derived by a 1,2-shift of the C-11 methyl group of factor S3 (Fig. 14). Also in recent work (with J. B. Spencer, C. A. Roessner, and N. J. Stolowich) it has been demonstrated that *cysG* not only serves as an iron and zinc chelatase, but will also introduce Co^{2+} into factor II. Thus, *cysG* is the first methyltransferase and may also be the cobaltochelatase of the anaerobic B_{12} pathway, a proposal which has received welcome confirmation by the demonstration (B. S. Goldman and J. R. Roth, *J. Bacteriol.*, **1993**, *175*, 1457–1466) that 66 *cysG* mutants of *Salmonella typhimurium* are unable to synthesize either siroheme or vitamin B_{12}. To summarize, *cysG* ($M_r \approx 50000$) appears to be the ancestral methyltransferase/dehydrogenase of anaerobic B_{12}-producing bacteria, and the subsequent specialized methyltransferases (such as SUMT, $M_r \approx 26000$) have lost this multifunctionality which also includes metal insertion (Fe^{2+}, Co^{2+}, Zn^{2+}, Ni^{2+}) and the capacity to "overmethylate" the (di)pyrrocorphinate template at positions C-12 and C-17. The metal and NAD binding sites are associated with the N-terminus residues 1–200, as evidenced by mutagenesis and truncation studies (M. J. Warren, personal communication). The *cysG* gene product should therefore be renamed siroheme synthase.

[53] D. Thibaut, L. Debussche, F. Blanche, *Proc. Natl. Acad. Sci. USA* **1990**, *87*, 8795.

[54] D. Thibaut, F. Blanche, L. Debussche, F. J. Leeper, A. R. Battersby, *Proc. Natl. Acad. Sci. USA* **1990**, *87*, 8800.

[55] F. Blanche, D. Thibaut, A. Famechon, L. Debussche, B. Cameron, J. Crouzet, *J. Bacteriol.* **1992**, *174*, 1036.

[56] a) D. Thibaut, M. Couder, A. Famechon, L. Debussche, B. Cameron, J. Crouzet, F. Blanche, *J. Bacteriol.* **1992**, *174*, 1043. b) The gene for cobalt insertion has recently been found in *P. denitrificans* and encodes cobaltochelatase whose substrate is the *a,c diamide* of hydrogenobyrinic acid. L. Debussche, M. Couder, D. Thibaut, B. Cameron, J. Crouzet, F. Blanche, *Abstr. 18th IUPAC Symp. Chem. Nat. Prod.*, Strasbourg, **1992**, 473. c) D. Thibaut, F. Kiuchi, L. Debussche, F. Blanche, M. Kodera, F. J. Leeper, A. R. Battersby, *J. Chem. Soc. Chem. Commun.* **1992**, 982.

[57] V. B. Koppenhagen in *B_{12}, Vol. 2*, (Ed.: D. Dolphin), Wiley, New York, **1982**, p. 105.

[58] T. E. Podschun, G. Müller, *Angew. Chem.* **1985**, *97*, 63; *Angew. Chem. Int. Ed. Engl.* **1985**, *24*, 46.

[59] For removal of cobalt in a model corrin see: N. J. Lewis, A. Pfaltz, A. Eschenmoser, *Angew. Chem.* **1983**, *95*, 743; *Angew. Chem. Int. Ed. Engl.* **1983**, *22*, 735.

[60] a) G. Müller, F. Zipfel, K. Hlineny, E. Savvidis, R. Hertle, U. Traub-Eberhard, A. I. Scott, H. J. Williams, N. J. Stolowich, P. J. Santander, M. J. Warren, F. Blanche, D. Thibaut, *J. Am. Chem. Soc.* **1991**, *113*, 9893; b) P. J. Santander, unpublished results.

[61] K. Kurumaya, T. Okazaki, M. Kajiwara, *Chem. Pharm. Bull.* **1989**, *37*, 1151.

[62] The mechanism suggested for the ring-contraction step is a stereoelectronically dictated dyotropic 1,2-migration of antiperiplanar groups within the dilactonic ensemble (ref. [47]). Precorrins 4a, 5a, and 6a are hypothetical structures predicted by the sequence of C methylation deduced indirectly from pulse-labeled ^{13}C NMR experiments, and are based on chemical models (ref. [47]). The connection between the postulated 6a and precorrin 6x, the known metal-free intermediate from *P. denitrificans*, involves ring contraction and loss of acetic acid in a process which raises the oxidation level (in precorrin 6x) by one double bond equivalent (Fig. 18). It has yet to be proved if the same mechanism is operational in *P. shermanii* since a) cobalt is already in place before ring contraction and b) there appears to be no requirement for NADPH (6x → 6y). This again suggests dual pathways for aerobic and anaerobic B_{12}-producing organisms, the latter requiring no change in the oxidation level from ALA to cobyrinic acid.

[63] H. C. Uzar, A. R. Battersby, *J. Chem. Soc. Chem. Commun.* **1985**, 585; F. J. Leeper, *Nat. Prod. Rep.* **1985**, *2*, 561. In the two mechanisms proposed in references [47, 63] it has been assumed that all five C methylations and decarboxylation in ring C have taken place before ring contraction. The actual sequence may be modulated by the presence or absence of cobalt in the substrates. Thus, in aerobic, genetically engineered *P. denitrificans* the isolable intermediate precorrin 6x has already undergone ring contraction and deacylation, but still has to receive C-5 and C-15 methyl groups, to undergo a C-11 to C-12 methyl shift with decarboxylation, and NADPH-mediated reduction to form hydrogenobyrinic acid which is not metalated enzymatically in this system (Fig. 18). However, in *P. shermanii* the substrates for subsequent C methylations (and ring contraction) are the cobalt complexes of the precorrins (Fig. 19). For clarity the mechanistic proposals for ring contraction are given in their original form.

[64] G. T. Bratt, H. P. C. Hogenkamp, *Biochemistry* **1984**, *23*, 5653.

[65] M. F. Summers, L. G. Marzilli, A. Bax, *J. Am. Chem. Soc.* **1986**, *108*, 4285.

[66] T. G. Pagano, P. G. Yohannes, B. P. Hay, J. R. Scott, R. G. Finke, L. G. Marzilli, *J. Am. Chem. Soc.* **1989**, *111*, 1484; T. G. Pagano, L. G. Marzilli, *Biochemistry* **1989**, *28*, 7213.

[67] A. I. Scott, N. J. Stolowich, B. P. Atshaves, P. Karuso, M. J. Warren, H. J. Williams, M. Kajiwara, K. Kurumaya, T. Okazaki, *J. Am. Chem. Soc.* **1991**, *113*, 9891.

Peptidomimetics for Receptor Ligands—Discovery, Development, and Medical Perspectives

By Athanassios Giannis* and Thomas Kolter

Peptides, as neurotransmitters, neuromodulators, and hormones, influence a multitude of physiological processes by signal transduction mediated through receptors. In addition, during the last 20 years their role in the appearance or maintenance of various diseases could be unequivocally proven. Agents that can imitate or block the biological functions of bioactive peptides (agonists or antagonists, respectively) can be considered as aids for the investigation of peptidergic systems and also as therapeutic agents. The suitability of bioactive peptides as therapeutic agents was examined after preliminary pharmacological experiments. It was thereby shown that based on their pharmacological properties, for example degradation by peptidases or poor bioavailability, they could be employed as drugs in only a few cases. To solve this problem peptidomimetics, compounds that act as substitutes for peptides in their interaction with receptors, have been synthesized. In comparison with native peptides they show higher metabolic stability, better bioavailability, and longer duration of action. Peptidomimetics with antagonistic properties were also developed within the range of these investigations. As a result, new types of treatment and therapy for a series of diseases are possible. Although peptidomimetics have been developed largely by empirical methods (e.g. modification of native peptides, optimization of lead structures), methods for rational design based on investigations into the structure of peptide–peptide receptor complexes and studies of conformation energies, among others, are gradually being established.

1. Introduction

A multitude of biologically active peptides have been discovered and characterized during the last 30 years.[1–3] Many of these have been found in both neuronal and in nonneuronal tissues. Representative examples include somatostatin, substance P, cholecystokinin, endorphin, enkephalin, angiotensin II, and endothelin. After binding to their membrane-bound receptors, these neurotransmitters, neuromodulators, and hormones influence cell–cell communication and control a series of vital functions such as metabolism, immune defense, digestion, respiration, sensitivity to pain, reproduction, behavior, and electrolyte levels. Thus, they are of enormous medical interest. The number of native and modified peptides used as drugs is constantly increasing, and this trend should continue during the next few years.[4]

As a result of major advances in organic chemistry and in molecular biology[5] most bioactive peptides have been prepared in larger quantities and made available for pharmacological and clinical experiments. Thus, in the last few years new methods have been established for the treatment and therapy of a series of diseases, and hopes have also been raised for the therapy of other illnesses in which peptides have been implicated. However, the use of peptides as drugs is limited by the following factors: a) their low metabolic stability towards proteolysis in the gastrointestinal tract and in serum; b) their poor absorption after oral ingestion, in particular due to their relatively high molecular mass or the lack of specific transport systems or both; c) their rapid excretion through liver and kidneys; and d) their undesired effects caused by interaction of the conformationally flexible peptides with various receptors (Fig. 1). In addition, a bioactive peptide can cause effects in several types of cells and

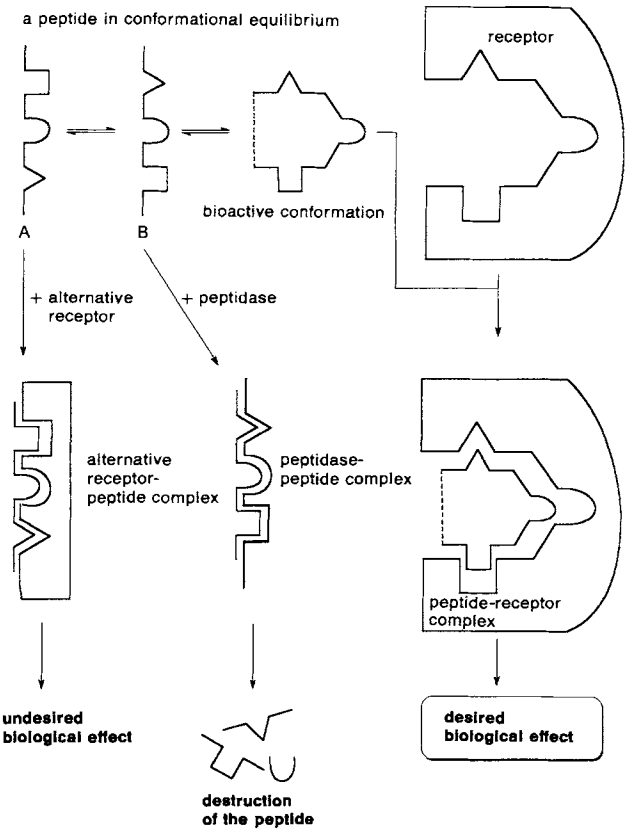

Fig. 1. In solution peptides exist in a variety of conformations that are in dynamic equilibrium with each other. If a conformational restriction (broken line) is introduced to the bioactive conformation of the peptide, forms A and B cannot arise. Thus, the interaction with alternative receptors and peptidases is suppressed or does not occur. In this fashion a desired biological effect can be obtained (modified after ref.[6]).

[*] Priv.-Doz. Dr. A. Giannis, Dr. T. Kolter
Institut für Organische Chemie und Biochemie der Universität
Gerhard-Domagk-Strasse 1, D-53121 Bonn (FRG)
Telefax: Int. code + (228)73-5683

organ systems, since peptide receptors and/or isoreceptors can be widely distributed in an organism.

From the pharmacological and medical viewpoint it is frequently desirable to not only imitate the effect of the peptide at the receptor level (agonism) but also to block the receptor when required (antagonism). The same pharmacological considerations mentioned above hold for peptidal antagonists, but, in addition, their development in the absence of lead structures is more difficult. Even today it is not unequivocally clear which factors are decisive for the agonistic effect and which for the antagonistic.[12]

In recent years intensive efforts have been made to develop peptidomimetics[6-14] that display more favorable pharmacological properties than their prototypes. A *peptidomimetic* is a compound that, as the ligand of a receptor, can imitate or block the biological effect of a peptide at the receptor level.[8, 15] As the ligand of an enzyme it can serve as substrate or as inhibitor. Ligands as enzyme inhibitors will be considered here only in special cases. We will restrict our discussion to peptidomimetics for receptor ligands including not only ligands of peptidal nature but also nonpeptide ligands.

2. Discovery and Development of Peptidomimetics

The following requirements exist for the pharmacological properties of a peptidomimetic: a) metabolic stability, b) good bioavailability, c) high receptor affinity and receptor selectivity, and d) minimal side effects. A major problem in the development of such agents is the discovery of a lead structure that can then be optimized, for example by the use of molecular modeling programs. Information concerning the three-dimensional structure of the peptide–receptor complex, the subsequent signal transduction, and the coordination and interaction with other signal transduction systems and integration in the organism, as well as knowledge of the biosynthesis, transport, release, and inactivation of the peptide are also extremely helpful.

Regardless of their mode of action (as neurotransmitters, neuromodulators, hormones), biologically active peptides show some common characteristics:[16] they are synthesized in the ribosomes as higher molecular forms (prepro forms). The pro forms are formed by cleavage of an N-terminal signal peptide by peptidases. During the subsequent vesicular transport to the Golgi apparatus they are processed further to their active forms and finally transported to the intracellular storage pools. They are released from the latter after stimulation (exocytosis). Inactivation of these peptides results mainly from the action of proteolytic enzymes (endo- and exopeptidases).

Although considerable progress has been made in the characterization of the receptors and in research into the mechanism of signal transduction, difficulties are encountered in structural investigation of the peptide–receptor complex. The application of newer NMR methods here is quite promising.[17b]

The native peptide itself, the pharmacological properties of which should be optimized, generally serves as lead structure for the development of peptidomimetics. With few exceptions peptides of small to medium size ($< 30-50$ amino acid units) exist unordered in dilute aqueous solution in a multitude of conformations in dynamic equilibrium (see Fig. 1). If a receptor ligand has the biologically active conformation per se, in other words the receptor-bound conformation, then an increased affinity toward the receptor is expected, since the decrease in entropy on binding is less than that on the binding of a flexible ligand. In solution and in the absence of the receptor, the biologically active conformation can be poorly populated and is frequently quite different from the conformation obtained by, for example, X-ray structure analysis in the solid state.[17]

A generally applicable and successful method so far for the development of peptidomimetics involves formation of conformationally restricted analogues that imitate the receptor-bound conformation of the endogenous ligands as closely as possible.[6, 14, 18, 19] Investigations of these analogues show them to have increased resistance toward proteases,

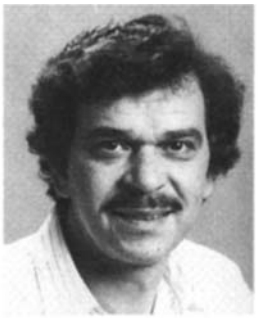

Athanassios Giannis was born in 1954 in Drama, Greece. He studied chemistry from 1972 to 1980 and medicine from 1978 to 1988 at the University of Bonn. After completing his diploma thesis with Prof. Reetz, he worked on his doctoral thesis with Prof. Sandhoff on the synthesis of glycosides. He received his "habilitation" in chemistry and biochemistry in 1992 for his research on the synthesis of chiral building blocks from D-glucosamine hydrochloride and of inhibitors of the glycosphingolipid metabolism. His research interests include amino sugars, amino aldehydes, and amino alcohols, as well as biochemical aspects of glycoconjugates, peptide aldehydes, and peptidomimetics.

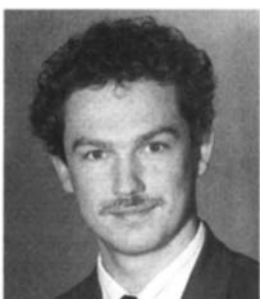

Thomas Kolter was born in 1963 in Bonn and studied chemistry there from 1984 to 1989. The subject of his diploma thesis with Prof. Sandhoff was the synthesis of inhibitors of the sphingolipid metabolism. He received his Ph.D. at the beginning of 1993 for his research on chiral amino aldehydes and the synthesis of peptidomimetics with A. Giannis. Currently, he is working on the total synthesis of modified gangliosides under the auspices of the "Sonderforschungsbereich" for research on glycoconjugates and contact structures of the cell surface.

that is, an increase in the metabolic stability, as well as increased selectivity and thereby fewer side effects.[6] The fact that frequently only a small number of four to eight amino acid side chains of the peptide are responsible for the recognition of the ligand by the receptor turns out to be favorable for this approach.[9, 17a] In such cases the rest of the molecular framework serves to fix the pharmacophores in a specific spatial arrangement. In addition, in the part of the peptide not directly involved in the interaction between the ligand and the receptor, additional binding affinity to various receptor types (an "address") or to an interface (the plasma membrane) can be localized. The half-life of the ligand can also be controlled by the existence of cleavage sites for proteases in this region of the molecule. Simplification of the structure of the ligand by removal or modification of this part of the molecule leads to a simultaneous increase in the protease resistance by the removal of cleavage sites. The resistance toward amino- and carboxypeptidases can be increased independently by acylation of the N-terminal group and by amidation of the C-terminus.

An important step in the development of conformationally restricted peptide ligands is the identification of the amino acid side chains necessary for receptor recognition. For this reason shorter analogues are also synthesized to identify the minimal sequence required for biological activity. The significance of parameters such as stereochemistry, charge, and hydrophilicity can be examined by systematic changes in the individual amino acids. Compounds with rigid conformations are then produced, and the most active structures selected by studying the conformation–activity relationships. This more-or-less empirical procedure is time-consuming and costly. New techniques that permit the controlled synthesis of a great variety of peptides (peptide libraries) and allow the careful examination of receptor binding are promising.[5, 20, 21] The hope of discovering new lead structures in this way and optimizing these with respect to their pharmacological properties appears to be justified.

The poor bioavailability of peptide-based drugs can hinder or even prevent their therapeutic use. A generally applicable concept for overcoming these difficulties is not yet available. Despite the advances in this area[22] "it is ironic that, with the exception of angiotensin converting enzyme (ACE) inhibitors and cholecystokinin antagonists (CCK), medicinal chemists have been unable to harness the profound pharmacologic effects of peptides by the discovery of bioavailable analogues."[8] If one also takes into account that the application of peptide-based drugs can cause immunological reactions,[23] the development of low molecular mass nonpeptide ligands appears to be urgently necessary.

The design of *nonpeptide ligands* is still in its infancy: the discovery of lead structures in large-scale screening is essential. Collections of substances (compound libraries) and single compounds, mostly natural products, are examined for their biological activity. These compounds are frequently conformationally restricted analogues of peptides that show the required characteristics for recognition by receptors. The structure is then optimized with regard to receptor affinity, selectivity, and other pharmacological properties. The fungal metabolite asperlicin can be mentioned here as an example of a lead structure discovered by large-scale screening and optimized in research aimed at the development of cholecystokinin antagonists (see Section 4.5).

The opioid alkaloids are classic examples of nonpeptide ligands that were later discovered to be mimetics of endogenous peptides. Morphine (**1**) imitates the effect of, for example, β-endorphin (**2**) (an endogenous opioid composed of 31 amino acids), at one of the recognition sites on the receptor common to both compounds. This example demonstrates unequivocally that it is possible, in principle, to use a small compound as a substitute for a relatively large peptide. In addition to morphine there is a whole series of other known drugs whose peptidomimetic character has already been demonstrated (see Sections 4 and 5).

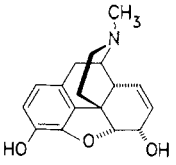

1

Tyr–Gly–Gly–Phe–Met–Thr–Ser–Glu–Lys–Ser–
Gln–Thr–Pro–Leu–Val–Thr–Phe–Lys–Asn–Ala–
Ile–Ile–Lys–Asn–Ala–Tyr–Lys–Lys–Gly–Glu

2

In the following sections established methods available for the design of peptidomimetics will be discussed. Selected examples of peptidomimetics (both peptide- and nonpeptide-based), including their possible use in therapy, are the topic of Section 4. Biological and biochemical aspects of the endogenous peptides will also be treated there.

3. Strategies for the Synthesis of Peptidomimetics

3.1. Modification of Amino Acids

Several possibilities exist for the synthesis of conformationally restricted and/or metabolically stable peptidomimetics at the amino acid level. The systematic exchange of individual amino acids by α-C-alkylated-, α-N-alkylated-, and D-amino acids is well established. In addition, α,β-unsaturated, cyclic, and β-amino acids, as well as amino acids with sterically demanding side chains may also be employed.

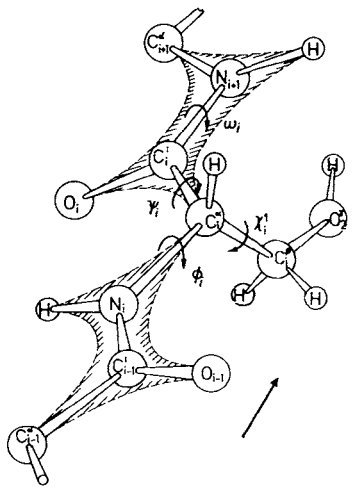

Fig. 2. Definition of the dihedral angles Φ,Ψ,χ, and ω of a peptide[24b].

Since the effect of such substitution on the conformational parameters Φ, Ψ, χ, and ω (for definitions see ref.[24] and Fig. 2) and also on the biological activity of the resulting peptides has been summarized in other reviews,[7a, 10] we will only refer here to examples of structures and syntheses of individual compounds.

The structures of some analogues of the amino acid phenylalanine (Phe) are shown in Scheme 1. The number of possible conformations can be limited by the introduction of sterically demanding groups (**3** and **4**) or rigid bridging units. Compounds **3** and **5** are components of potent ligands of the angiotensin II receptor with agonistic or anatagonistic activity.[25] A simple preparative approach to indanaminocarboxylic acid **5** and other related compounds was achieved by alkylation of the benzylidene derivative of glycine ethyl ester with suitable electrophiles.[26] Gonadotropin-releasing hormone (GnRH) antagonists, which contain 2-naphthylalanine **4** in addition to other nonnatural amino acids, show high affinity for the receptor by negligible release of histamine (compound **125**). A new enantioselective synthesis of (*S*)-**4** and other α-amino acids of general utility was recently described by Corey et al.[27] Compound **4** and other Phe analogues can also be obtained in optically pure form by alkylation of chiral imidazolidinones.[28]

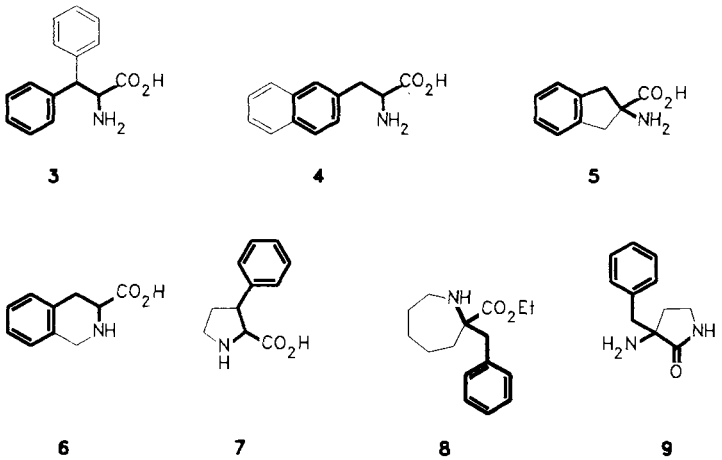

Scheme 1. Sterically demanding and conformationally fixed analogues of phenylalanine; the structure of the amino acid is highlighted.

The tetrahydroisoquinolinecarboxylic acid **6** (Tic) is a phenylalanine analogue in which the dihedral angle χ can only encompass a very small range. The preferred conformation and thus the topology of the side chain depends on whether Tic is N-terminal ($\chi = +60°$ for D-Tic) or N-acylated ($\chi = -60°$ for D-Tic) in the peptide.[29] D-Tic is a component of various opioid antagonists with high selectivity for the μ receptor.[30] Tic, together with other Phe analogues, has been incorporated into a cyclic opioid peptide analogue and the corresponding effects on conformation and receptor selectivity examined.[31]

An asymmetric synthesis based on the imidazolidinone method of Seebach et al.[32] provides access to the four stereoisomeric α,β-dimethyl derivatives of Phe and Tic.[33] Proline derivative **7**, substituted in the 3-position, was synthesized in racemic form and the *trans* derivative obtained enantiomerically pure after cleavage of the racemate.[34] The corresponding 3-propyl derivative was incorporated as a norleucine analogue in a C-terminal tetrapeptide of cholecystokinin (CCK), which shows higher affinity for the central CCK receptor than Boc-CCK itself.[35] Lactam **8** is also a Phe analogue,[36] lactam **9** a C-terminal phenylalanine amide analogue.[37]

The 4-methyl-substituted proline derivative **10** and compound **11** are conformationally restricted leucine[38] and tryptophan analogues,[39] respectively. (The structure of the amino acids is highlighted; the stereochemistry of **10** and **11** is not shown.) A new entry to C-alkylated peptides has been described by Seebach et al.:[40] the alkylation of polydeprotonated *N*-Boc-protected oligopeptides was achieved regio- and stereoselectively on glycine and sarcosine residues without racemization.

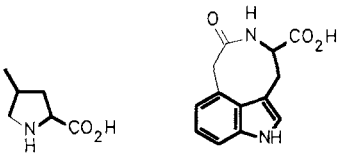

3.2. Dipeptide Analogues

Bridging between two neighboring amino acids in a peptide leads to a dipeptide mimetic, the conformative flexibility of which is limited in comparison with that of regular dipeptides. Some possibilities for forming such bridges are shown by the structural modifications of peptide **12**: incorporation of lactams (→ **13**–**15**) and piperazinones (→ **16**, **17**). γ-Lactams and δ-lactams[41] of type **13** have been designed to some extent as "turn mimetics"; in several cases the incorporation of such structures into peptides leads to biologically active compounds. Syntheses that permit the incorporation of side chains have also been described. The structural variation in compounds of type **13** can be extended further by

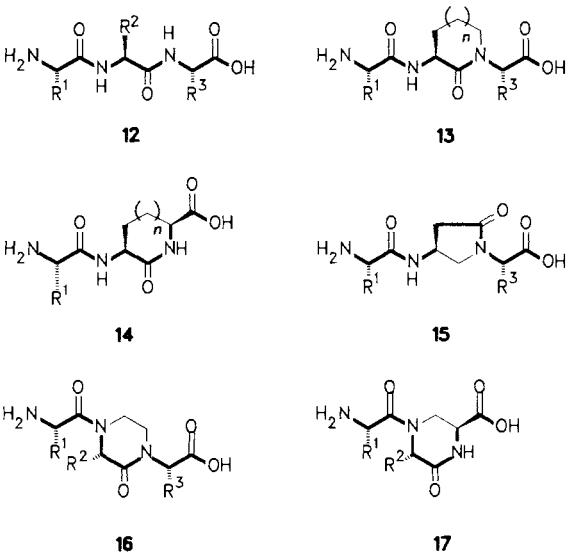

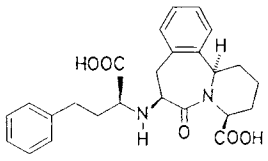

18

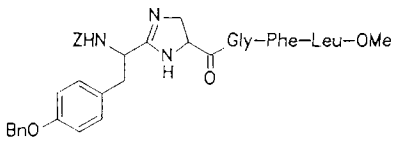

19

reduction or increase in the size of the lactam ring, by incorporation of heteroatoms,[42] or by annelation to aromatic rings. Compounds such as **18**,[43] currently the most potent inhibitor of the angiotensin-converting enzyme (ACE) known, belong to this category. Lactams of type **14** ($n = 1$)[44] and compounds **29** and **30** are also dipeptide mimetics. In **29** and **30** two neighboring methylene groups in the eight- and seven-membered rings, respectively, have been formally replaced by sulfur or with benzoannelated methine groups. The lactam derivative **15** was designed following the observation[45] that a corresponding aspartimide, which appeared as an artefact in peptide synthesis, led to an octapeptide derivative of the human growth hormone (hGH) with biological activity.[46] The incorporation of a lactam of type **15**, synthesized as the racemate, led to a biologically active hGH analogue.

Various substituted 2-oxopiperazines, for example **16** and **17**, are components of leu-enkephalin analogues.[47] A piperazinone of type **16** is a component in the structure of compound **91**, a selective antagonist of the neurokinin (NK)2 receptor. A synthesis of suitably substituted 2-oxopiperazines as precursors to compounds of type **17** is shown in Scheme 2.[48] The configuration of the chiral center is adjusted by choice of starting material or by the reaction conditions. Further syntheses of chiral piperazinones are summarized in the references.[49]

Another possible approach to bridging two neighboring amino acids by bridging the peptide strand in the direction of the original amide oxygen atom is illustrated by imidazoline **19**.[50]

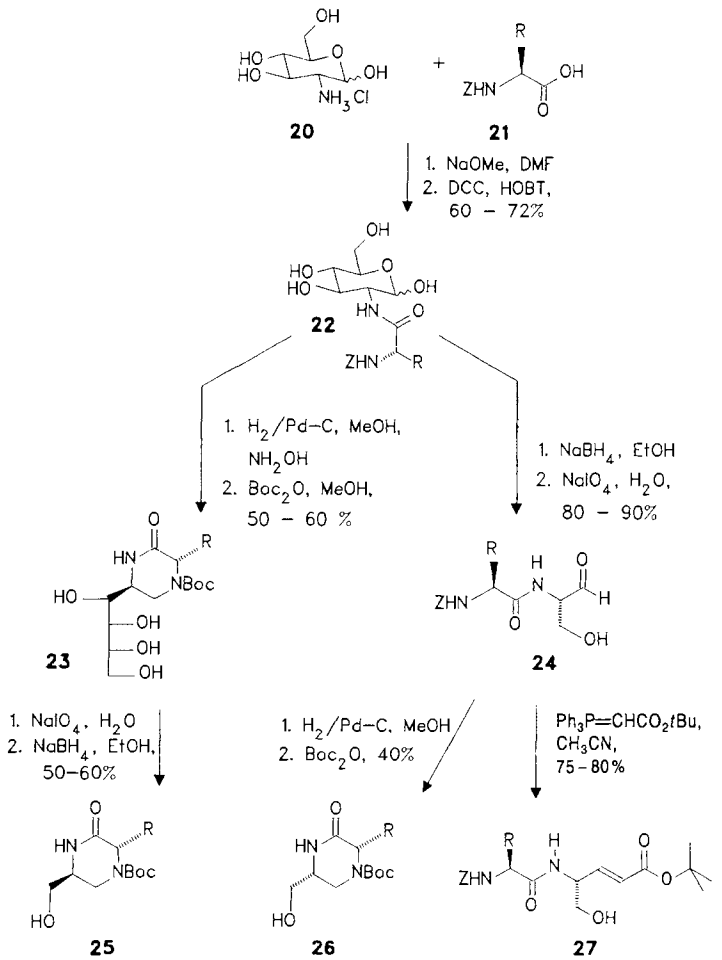

Scheme 2. Synthesis of chiral 2-oxopiperazines of type **17**. The stereochemistry of products **25** and **26** is adjusted by choice of starting material and reaction conditions. Compound **27** is a dipeptide analogue with C-terminal vinylogous amino acids; R = benzyl, isopropyl, methyl. DMF = dimethyl formamide, DCC = dicyclohexylcarbodiimide, HOBT = hydroxybenzotriazole, BOC = *tert*-butoxycarbonyl, Z = benzyloxycarbonyl.

3.2.1. Analogues of Dipeptides with cis Configuration at the Amide Bond

The partial double bond character of the amide C–N bond leads to *E*/*Z* isomers. In peptides generally only the more stable (by about 8 kJ mol^{-1}) *trans* configuration is found. An exception is given by peptidyl-proline and peptidyl-*N*-alkyl amino acid groups, in which the *cis* configuration can also be appreciably populated.[51] Amide bonds with *cis* configurations not involving imino acids have been found, for example, in cyclic peptides[52] and in a linear peptide in the conformation induced by binding to a model membrane.[53] β Turns can also contain *cis*-configurated amide bonds.[54] In order to simulate the "*cis*-amide bonds" that could occur in the biologically active conformation of a peptide, the corresponding dipeptide analogues were synthesized. Compounds **28**,[55] **29**,[56] **30**,[57] and **31**[58] are examples; incorporation of **31** into a cyclic hexapeptide analogue of somatostatin led to a compound with biological activity. Whether the concept of *cis*-amide mimetics will prove itself in practice remains to be seen.

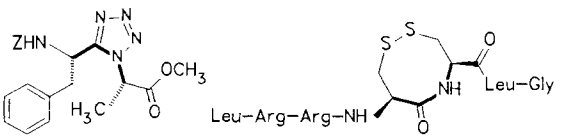

28

29

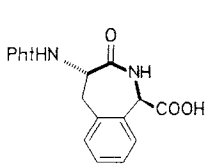

30

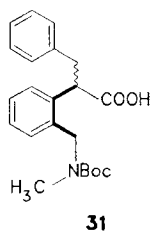

31

3.3. Modification of the Peptide Backbone

Modification of the peptide backbone leads primarily to an increase in the biological half-life in comparison with that

of parent compounds, and only secondarily, if at all, to restrictions in conformation.

3.3.1. Isosteric Replacement of the Amide Bond

Replacement of an amide bond by a suitable mimetic[59] was particularly important for the development of enzyme inhibitors. In the area of receptor ligands this concept has hitherto been less successful. Examples of ligands that are still biologically active after exchange of an amide group for an isosteric group include the [Tyr^1-(*E*)-CH=CH-Gly^2]-leu-enkephalin analogue[60] and the [Phe^8-(*E*)-CF=CH-Gly^9]-substance P analogue.[61] A route to the discovery of antagonists could lie in the exchange of the amide group for (CH_2NH), which led to the development of a gastrin[62] and bombesin antagonist.[63] Compounds containing the isosteric CH_2NH group are quite different, especially in their electronic properties, from those containing the amide group; the isosteric compounds may be obtained by reduction of the latter with $LiBH_4/(CH_3)_3SiCl$.[64, 67] Another preparative possibility is the reductive amination of suitably protected α-aminoaldehydes with amino acid derivatives,[65] during which racemization of the aldehyde can occur. An example of the racemization-free synthesis of such a derivative is shown in Scheme 3.[66] In a recent publication[67]

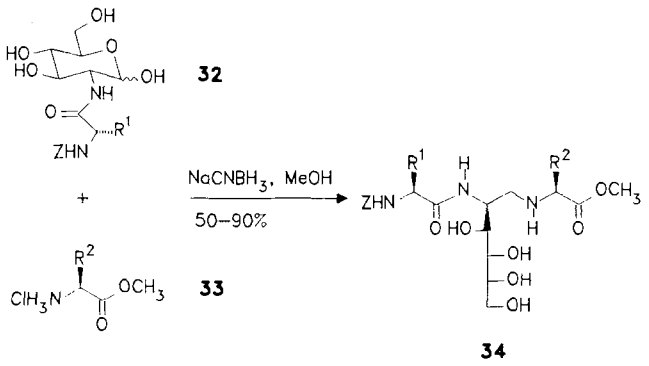

Scheme 3. Racemization-free synthesis of an isosteric aminomethylene peptide derivative; R^1 = benzyl, *para*-hydroxybenzyl, R = methyl.

amide surrogates were incorporated into a CCK-B receptor ligand and the influence of the various structures systematically analyzed and quantified. An accurate imitation of the amide bond with regards to lipophilicity, geometry, and hydrogen bond donor or acceptor properties could not be correlated with the measured receptor affinity. Apparently, parameters other than those investigated, possibly also conformational effects, are responsible, and a convincing imitation of the amide bond in the ground state has not yet been achieved.

3.3.2. Retro-Inverso Isomers

A further approach for changing the peptide backbone is the use of retro-inverso modifications.[68] In this method the L-amino acids of a peptide are exchanged for D-amino acids, and simultaneously the direction of the peptide is reversed. The topology of the side chains, with the exception of proline groups, is largely maintained, and such structures are no longer substrates for proteases. The retro-inverso modification itself does not contain any conformational restrictions when compared with the native peptide. One problem is that for noncyclic peptides the end groups and, thereby, their charges are not complementary to those of the native peptide and must either be substituted by the introduction of "false" ends or the retro-inverso structure must be incorporated into a larger peptide. Examples are shown in Schemes 4[71] and 5.[69] A more recent example of the synthesis of such a compound is given in the literature.[70] The small number of retro-inverso derivatives[71] that actually show activity comparable to that of the original compounds indicates that the peptide backbone is also important for recognition by the

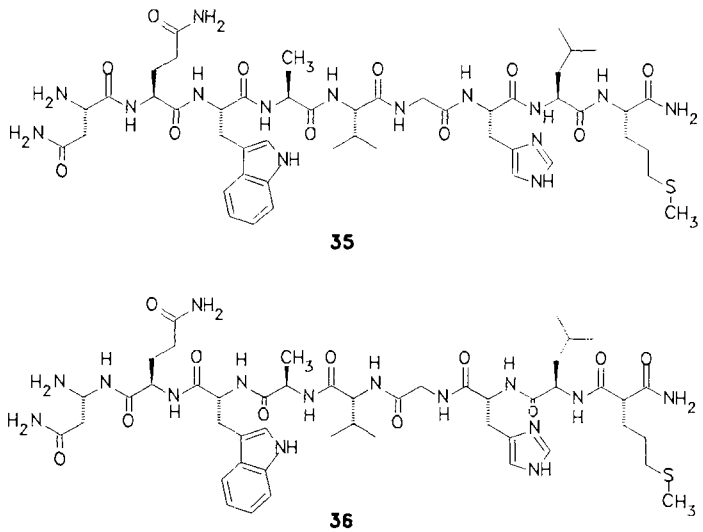

Scheme 4. The C-terminal nonapeptide **35**, which has the full agonist activity of bombesin (see **102**), and the retro-inverso isomer **36** with modified end groups, which does not bind to the receptor.

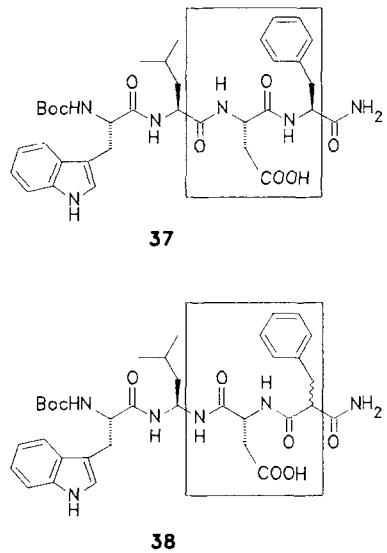

Scheme 5. The C-terminal *N*-Boc nonapeptide of gastrin **37** and the partially retro-inverso isomer **38**, which is an antagonist of the gastrin receptor.

receptor or that there are indeed differences in the topology[72] of both compound classes.

3.3.3. *Further Modifications of the Peptide Backbone*

In a recently published study[73] it was shown that peptides containing vinylogous amino acids **39** in place of "normal" amino acids are rich in secondary structure elements. Peptides such as **40**, for example, are conceptually related to

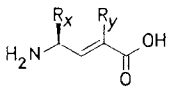

39

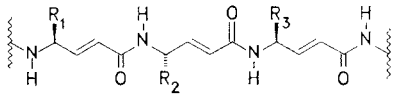

40

hexose-DNA and could lead to the development of substances similar to peptides with modified backbones. A new entry to vinylogous peptides of type **27** via the chemically and configurationally stable dipeptide aldehyde **24** is shown in Scheme 2.[48b]

3.4. Global Restrictions of Conformation

Global[10] restrictions in the conformation of a peptide are possible by limiting the flexibility of the peptide strand through cyclization. For this purpose, amino acid side chains that are not involved in receptor recognition are connected together or to the peptide backbone. Three representative examples are compounds **41**–**43**: partial structures of each peptide are made into rings by linking two penicillamine residues with a disulfide bridge, by formation of an amide bond between a lysine and an aspartate group, or by connecting two lysine groups with a succinate unit.

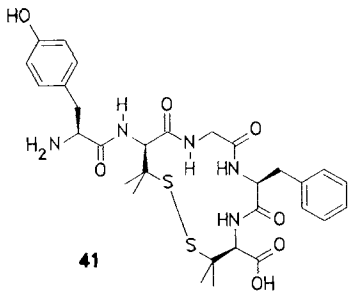

41

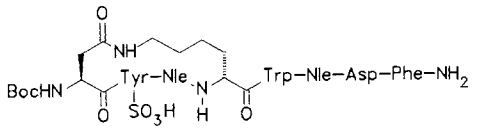

42

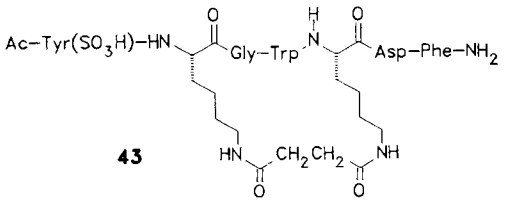

43

Compound **41** is a cyclic enkephalin analogue with selectivity for the δ opiate receptor;[74] BC 197 (**42**)[75] and JMV 30 (**43**)[76] (IC_{50}[*] = 1.3 nM, 10000 times more selective to the cholecystokinin A receptor) are agonists to the cholecystokinin B receptor, found largely in the brain.

3.5. Imitation of Secondary Structures: β Turns

A crucial disadvantage of the methods referred to so far is that the resulting conformation cannot be predicted. As a result biophysical investigations are necessary to obtain conformation–activity relationships for each and every derivative prepared. For this reason it is desirable to have methods available that induce a specific target conformation. Numerous experiments in the design and synthesis of secondary structure mimetics have been conducted. A secondary structure mimetic is a building block that forces a defined secondary structure after its incorporation into a peptide. The requirements of such a conformation mimetic are the following: the desired conformation should be mimicked as exactly as possible, and the synthesis should permit the introduction of the desired side chains. In addition, practical aspects such as stability under the conditions used for synthesis of the peptide and removal of protecting groups must be considered.

A β turn is a segment composed of four amino acids (*i* to *i* + 3) that occurs when a peptide strand changes its direction. If, on the other hand, the segment is composed of three amino acids, one speaks of a γ turn. β Turns are classified according to their conformation. The criteria employed include the torsion angles at the amino acids *i* + 1 and *i* + 2. These angles are compared to those observed in proteins and peptides with secondary structure[7b] (for a definition of the torsion angles see Fig. 2). In linear peptides (and proteins) turns arise mainly due to the tendency to form intramolecular hydrogen bonds.[17a] The β turn is a structural motif common to many biologically active, cyclic peptides and has been postulated in many cases for the biologically active form of linear peptides.[7b] For this reason it is the most frequently imitated secondary structure. It can be assumed that the side chains are important for the recognition by the receptor. γ Turns are also found in peptides, albeit to a lesser extent, and are imitated by appropriate mimetics.[77]

A selection of compounds designed and synthesized as β turn mimetics is shown in Scheme 6.[11] The majority of these compounds have been shown to be inactive after incorporation in model peptides. Compound **59** (Scheme 7)[91] imitates a β turn in the sequence Tyr-Ser-Gly-Ser-Thr (**58**), a component of the hypervariable region of a monoclonal antibody against the reovirus type 3 receptor.[92] Compound **59** is the first example of a low molecular mass immunoglobulin mimetic developed on the basis of an X-ray structure analysis of the antigen–antibody complex. Cyclopeptide **59** is resistant toward proteases and imitates the binding and functional properties of the native antibody. The synthesis of **59**

[*] IC_{50} is the concentration of an antagonist that reduces the maximum action of an agonist by 50%.

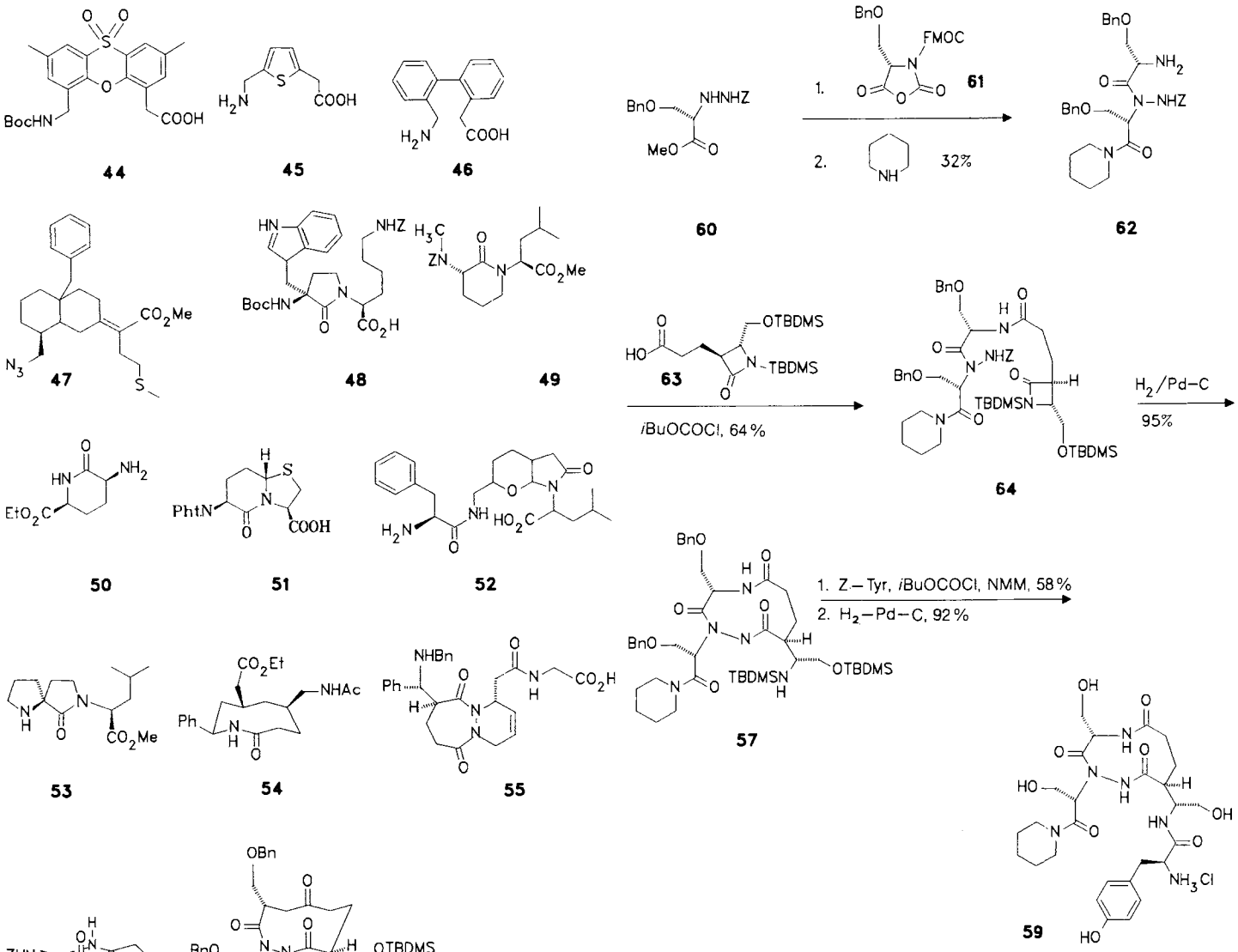

Scheme 6. Representative β turn mimetics. **44**[78], **45**[79], **46**[80], **47**[81], **48**[82], **49**[83], **50**[84], **51**[85], **52**[86], **53**[87], **54**[88], **55**[89], **56**[90], and **57** (see Scheme 7). Z = benzyloxycarbonyl, Pht = phthaloyl, TBDMS = *tert*-butyldimethylsilyl.

Scheme 8. Overview of the synthesis of **59**. FMOC = 9-fluorenylmethoxycarbonyl, NMM = *N*-methylmorpholine.

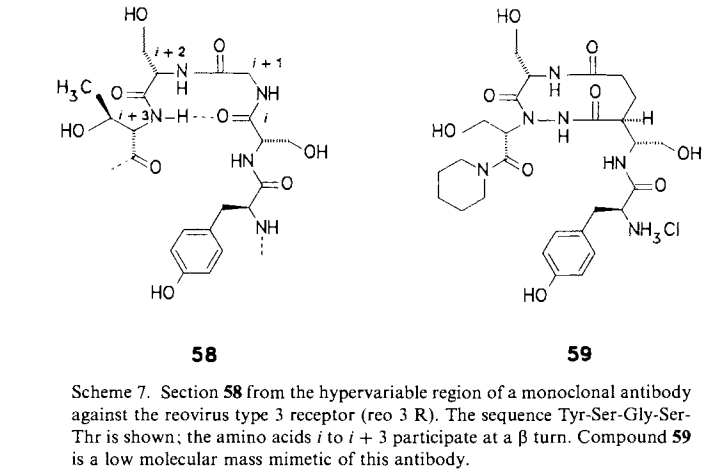

Scheme 7. Section **58** from the hypervariable region of a monoclonal antibody against the reovirus type 3 receptor (reo 3 R). The sequence Tyr-Ser-Gly-Ser-Thr is shown; the amino acids *i* to *i* + 3 participate at a β turn. Compound **59** is a low molecular mass mimetic of this antibody.

is shown in Scheme 8. Three other biologically active derivatives of β turn mimetics are **65**–**67**. Compound **65** is a GnRH derivative and agonist, in which the amino acids glycine and

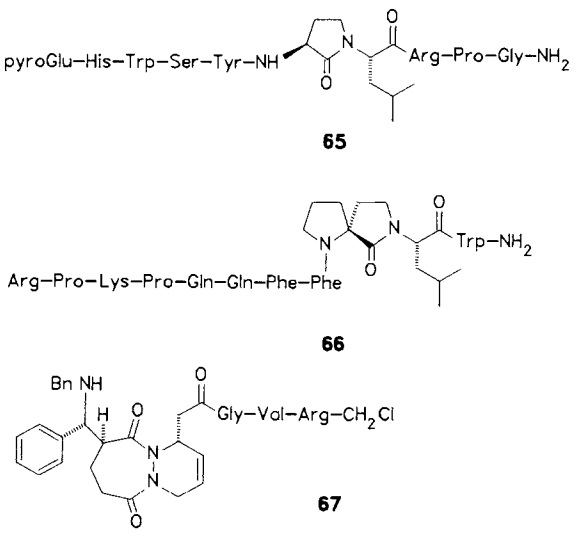

leucine in the positions $i+1$ and $i+2$ of a postulated β turn have been replaced by a γ-lactam. In vivo **65** is 2.4 times more effective than GnRH and in vitro 8.9 times more effective.[93] Compound **66** contains spirolactam **53** in place of Gly^9 and Leu^{10} in [Trp^{11}]-substance P. It is one of the most potent peptide-based antagonists of the neurokinin 1 receptor.[94] Compound **67** imitates the thrombin-bound structure of the fibrin peptide A and is an inhibitor of this protease. An overview of the synthesis of **67** is given in Scheme 9.

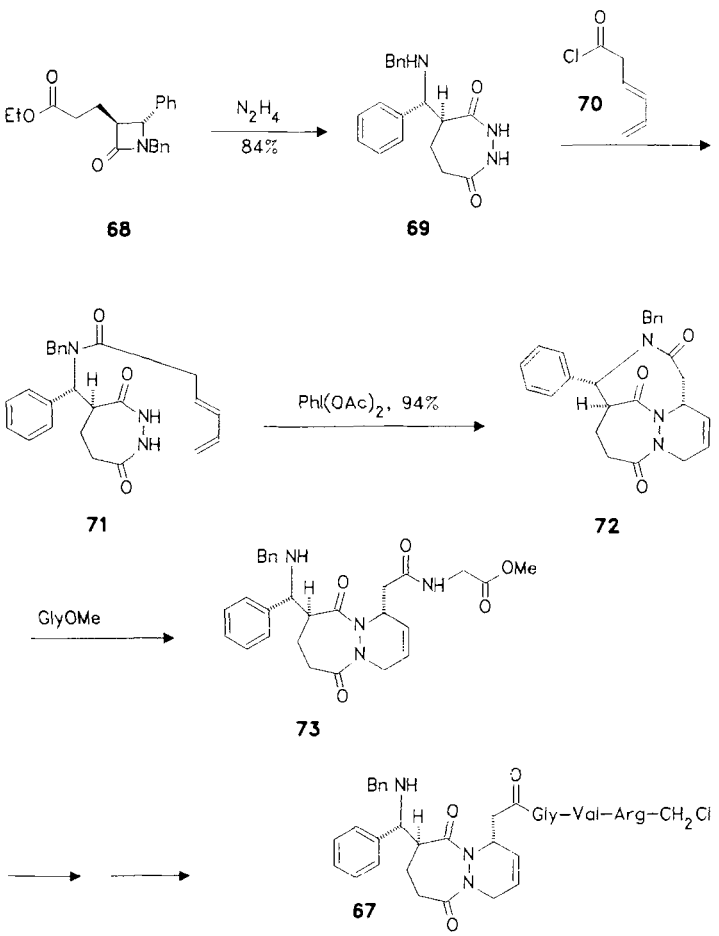

Scheme 9. Synthesis of **67**.

4. Examples of Peptidomimetics

4.1. Opioids (Endorphins, Enkephalins, Dynorphins)

Morphine—the main constituent of opium—has been used and misused for its pain-killing and euphoria-generating effect for over two and a half thousand years. Countless morphine derivatives have been synthesized and examined in the search for morphine's mechanism of action and with the aim of developing a nonaddictive analgesic. With the help of these compounds it was possible to discover various opioid receptors in animal organisms. The demonstration of such receptors[95] suggested the existence of the corresponding endogenous ligands: the characterization of enkephalin in the mid-1970s[96] was followed by the discovery of endorphin[97] and dynorphin.[98] These endogenous opioids are biosynthesized by posttranscriptional processing[99] of the corresponding higher molecular mass precursors pro-opiomelanocortin, proenkephalin A, and proenkephalin B, both in neurons and also in nonneuronal cells, for example in cells of the adrenal medulla and in leucocytes.[100] Surprisingly, the presence of morphine and codeine in the brain of various animals was recently demonstrated.[101] To answer the question whether they are of exogenous origin or—as speculated at the beginning of this century[102]—of endogenous origin, cell culture experiments were conducted which showed that liver cells from mice possess the enzymes necessary for the decisive step of conversion of exogenously administered reticulin to salutaridine (with morphinan framework)![103] Adrenal and brain cells, on the other hand, are not able to convert reticulin into salutaridine. Thus, the question of the existence of a complete biosynthetic route for morphine in animal organisms remains unanswered.

From the pharmacological viewpoint endogenous opioids are very similar to morphine:[104] they also have analgesic properties, lead to physical addiction and depression of respiration, depress the cough reflex, stimulate the release of vasopressin, and inhibit gastric fluid secretion and the motor activity of the intestine. In addition, they appear to act as tumor suppressants and as inhibitors of cell division.[105] The effects of opioids are transmitted by receptor-induced modulation of the intracellular levels of c-AMP and Ca^{2+}, apparently involving various G proteins.[106]

Opium alkaloids were later shown to be mimetics of the endogenous opioids. Independent experiments on the interaction of opiate receptors with the corresponding agonists and antagonists demonstrated that there are at least three distinct types of opiate receptors with differing specificity, anatomic location (in both central and peripheral nervous systems; both pre- and postsynaptic in neurons), and physiological importance. These three types are designated μ, κ, and δ. The δ opioid receptor was recently cloned for the first time, expressed in COS cells, and characterized pharmacologically.[106c] It is assumed that dynorphin (**74**) and enkephalin (**75**) are the endogenous ligands for the κ and δ receptors, respectively, whilst a protein with selectivity for the μ receptor has not yet been found (Scheme 10).[107] Comparison of the amino acid sequence of the endogenous peptide ligands shows that their N-terminals have the common grouping Tyr-Gly-Gly-Phe, regardless of the receptor specificity. This sequence is apparently essential for molecular recognition by the opiate receptor, is the same for all receptor types, and, after a concept[108] developed for adrenocorticotropic hormone (ACTH), is designated as "message". A different, neighboring sequence for the given receptor types, designated as "address", is responsible for the selectivity. According to a modified[109] interpretation of this model, which also can be extended to nonpeptide ligands of opiate receptors, the message is located in the Tyr^1 residue and separated by two glycine groups that function as spacers from the address sequence, which begins with Phe. On the basis of this model it was possible to develop ligands of type **77** from the μ-selective opioid antagonist oxymorphone (**76a**) by attaching the appropriate "address" sequence. Ligands **77** bind selectively to the δ and κ receptors. Naltrindole (**78**) was synthesized analogously as the first nonpeptide anatagonist with selectivity for the δ opioid receptor.[109]

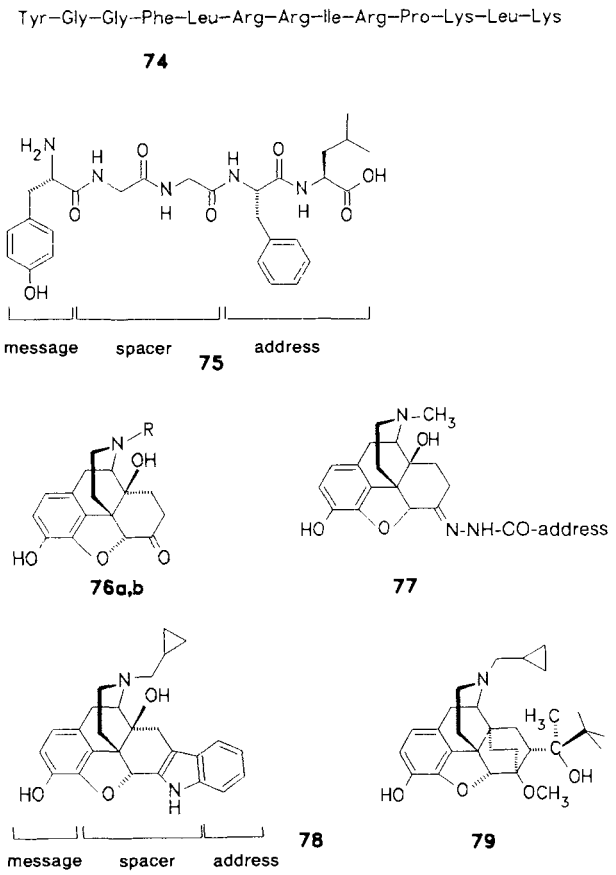

Scheme 10. Dynorphin (**74**), Leu-enkephalin (**75**), oxymorphone (**76a**, R = methyl), naloxone (**76b**, R = allyl), a universal opioid antagonist **77**, and synthetic opioid derivatives **78**, **79**. Hybrid structures **77** containing a morphine framework (message) and peptide (address) are selective ligands of the δ receptor (address = Phe-Leu-OH) and the κ receptor (address = Phe-Leu-Arg-Arg-Ile-OMe). Naltrindole (**78**) is the first nonpeptide ligand for the δ receptor. Buprenorphin (**79**) is an opioid with low potential dependency. Other ligands with selectivity for the opioid receptor types include compounds **80**–**83**, morphine (**1**, μ agonist), amd DPDP 50 (**41**, δ agonist).

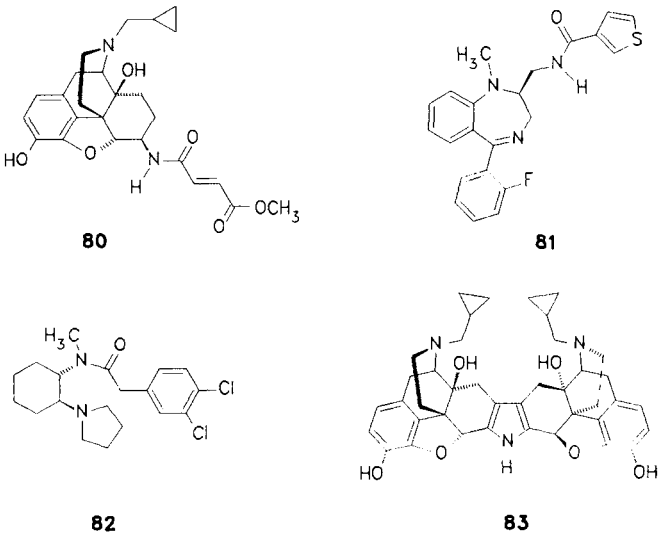

The pyrrole ring of the indole residue serves as a rigid spacer, fixing the phenylene group in the conformation required for it to serve as a component of the δ address. Finally, a comparison of the structure of oxymorphone (**76a**) with that of naloxone (**76b**) appears to be interesting: replacement of the *N*-methyl group of **76a** with an *N*-allyl group leads to the universal opioid antagonist naloxone (**76b**)! Other ligands for the various opioid receptors are the selective and irreversible μ antagonist β-funaltrexamine (**80**),[110a] as well as the κ-selective agonists tifluadom (**81**) and U-50488 (**82**).[110b] The C_2-symmetric compound norbinaltorphimine (NorBNI, **83**)[111] is a highly potent opioid antagonist with good selectivity for the κ receptor.

A wealth of other peptide- and nonpeptide-based ligands of opioid receptors have been synthesized and investigated pharmacologically.[109, 112, 113] "While our knowledge of the opioid receptor system has increased tremendously, this new information has not yet led to the development of a major new therapeutic agent."[113] In particular it has not yet been possible, despite initial hopes, to develop an opiate with strong analgesic potency that is not addictive and does not suppress respiration (a frequent cause of death following morphine overdose). Nevertheless, some practical successes and interesting new developments in the area have been achieved:

a) Buprenorphine (**79**) is a partial agonist of the μ receptor. After sublingual application approximately 50% is absorbed (for comparison, only 5% of the morphine applied orally passes into the blood stream). After successful absorption buprenorphine binds slowly to the receptor and dissociates from it equally slowly. It is precisely this property that leads to the unusually low potential for addiction of this agent. After treatment has stopped only mild withdrawal symptoms are observed. This pharmacological profile, together with the absence of respiratory suppressant and psychotomimetic effects, has contributed to the clinical success of buprenorphine.[114]

b) Based on the knowledge that 1) nerve endings of peripheral sensory neurons possess opioid receptors and that 2) the leucocytes that migrate to inflamed tissues may help alleviate pain by virtue of their opioids,[115] a new approach for producing analgesia was recently reported. In arthroscopic knee operations morphine is applied intra-articularly (in the knee joint). It has been shown that the postoperative analgesia is both stronger and longer lasting than that obtained by intravenous application of morphine. The well-known side effects of morphine do not appear with this type of application.[116] These results suggest that central opioid receptors are not the exclusive target of systemically administered morphine (Fig. 3) and confirm the necessity for the development of potent, orally active opioid analgesics that cannot pass the blood–brain barrier, thus precluding the serious side effects triggered by their action in the central nervous system.[117]

c) An exciting and interesting possibility for the pharmacotherapy of pain is offered by the benzodiazepine derivative tifluadom (**81**), a κ receptor agonist. Although clinical studies are still not available, animal experiments show that **81** is an effective opioid analgesic without undesired effects such as respiratory depression or addictive potential.[118]

Considering the importance of substance P (Fig. 3) and cholecystokinin for the perception of pain and the fact that potent substance P and cholecystokinin antagonists (see Sections 4.2 and 4.5) are now available, the future of pain therapy can be viewed with optimism.

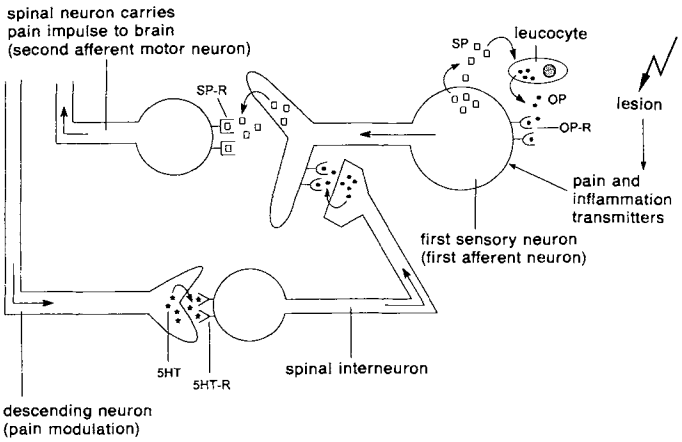

Fig. 3. Components of the pain transmission system (OP = opioid, OP-R = opioid receptor, 5HT = serotonin (5-hydroxytryptamine), 5HT-R = serotonin receptor, SP = substance P, SP-R = substance P receptor). Specific interneurons of the spinal cord use opioids as neurotransmitters. The interneurons act directly on the centrally directed ends of the primary sensory neurons (first afferent neuron) and suppress the conduction of pain impulses from the periphery to the spinal cord by release of opioids. Substance P is an important neurotransmitter in the pain-transmitting synapses. The pain impulse is carried to the brain by the second afferent neuron. The neuron descending from the brain modulates the activity of the spinal interneuron and in this process uses serotonin, among others, as a neurotransmitter. The activation of the peripheral nerve endings of sensory neurons, for example, during inflammation, also leads to the release of substance P in the area of the lesion. The result is that leucocytes migrate to this area. Endogenous opioids released from the leucocytes bind to the peripheral opioid receptors of the first afferent neurons, leading to a reduction in intensity of the pain impulses (modified after ref.[258] and taking refs. [115,259] into account).

4.2. Tachykinins (Substance P, Neurokinins A and B)

Tachykinins are peptides with a length of ten or eleven amino acids that act as neurotransmitters or neuromodulators in various parts of the central and peripheral nervous systems.[119] These peptides possess a common C-terminal sequence Phe-X-Gly-Leu-Met-NH_2. The best known and most investigated tachykinin, substance P (**84**), was discovered by von Euler and Gaddum in 1931.[120] In 1971 the amino acid sequence of substance P was determined,[121] and it was synthesized using solid-phase synthesis.[122] Peptides with structural similarities to tachykinins have also been isolated from lower organisms.

The biosynthesis of tachykinins takes place by way of two preproproteins; substance P (**84**) and neurokinin A (**85**) are released from one of these by posttranscriptional processing and neurokinin B (**86**) from the other. The receptors for substance P and for neurokinins A and B are designated NK 1–3. The supposed endogenous ligands are, corresponding to the different relative receptor affinities, substance P for NK 1, neurokinin A for NK 2, and neurokinin B for NK 3. NK 2 is found predominantly in the peripheral nervous system and NK 3 in the central nervous system, whereas NK 1 exists in both the central and peripheral nervous systems. The receptors from various mammals were sequenced and expressed.[123] They belong to the G protein-coupled receptor superfamily with seven α-helical transmembrane segments as the common structural feature. The transmembrane segments V–VII are responsible for the recognition of the common tachykinin sequence (message sequence), whereas the segments I–IV and the N-terminal (extracellular) part of the receptors bind to the variable part of the tachykinin (address sequence).[124] The individual receptors are quite homologous; after they bind their endogenous ligands they act by intracellular release of 1,4,5-inositoltrisphosphate, diacylglycerol, and cyclo-AMP (c-AMP) as second messengers.

The physiological significance of tachykinins is still poorly understood, not least because of the absence of selective antagonists. The effects of substance P have been examined the most. It triggers contraction of the smooth muscles of the respiratory, the gastrointestinal, and the urogenital tract, has diuretic and natriuretic properties, and in addition is a potent stimulator for the secretion of saliva, pancreatic juice,

Arg–Pro–Lys–Pro–Gln–Gln–Phe–Phe–Gly–Leu–Met–NH_2 **84**

His–Lys–Thr–Asp–Ser–Phe–Val–Gly–Leu–Met–NH_2 **85**

Asp–Met–His–Asp–Phe–Phe–Val–Gly–Leu–Met–NH_2 **86**

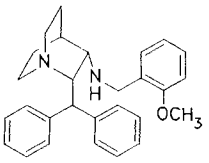

87

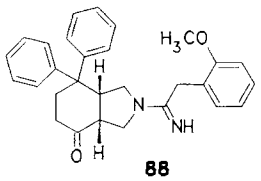

88

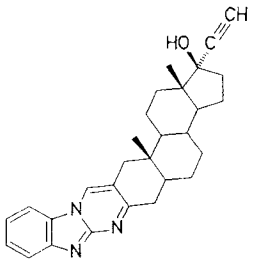

89

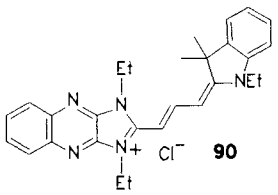

90

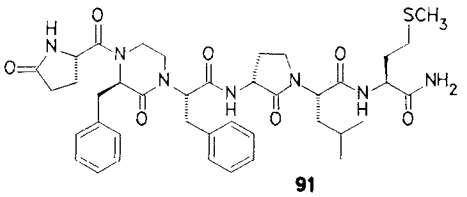

91

cyclo (Gln–Trp–Phe–Gly–Leu–Met) **92**

Boc–Arg–Ala–D–Trp–Phe–D–Pro–$NleNH_2$ **93**

PhCO–Ala–Ala–D–Trp–Phe–D–Pro–Pro–$NleNH_2$ **94**

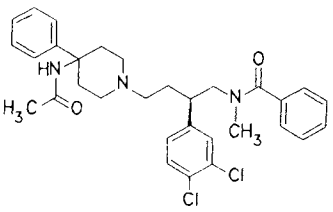

95

and bile. Substance P acts in the periphery, causing the symptoms characteristic of inflammation, including dilation of blood vessels (vasodilation) and the extravasation of plasma from the blood vessels. It induces the release of interleukin-1, interleukin-6, and tumor necrosis factor-a from human monocytes.[125] On the other hand, some cytokines appear to increase the rate of biosynthesis of substance P.[126] This mutual influence of substance P and cytokines could be significant in rheumatoid arthritis.[127] There is also evidence for the participation of substance P in pathophysiological events of inflammatory intestinal diseases (Crohn's disease, colitis ulcerosa):[128] in general the specific sensory neurons of the dorsal root ganglions seem to use substance P as a transmitter substance at pain-conveying synapses. The same neurons, on the other hand, can regulate or maintain an inflammatory process (for example, rheumatoid arthritis) by release of substance P into the area of an inflammation innervated by them (see Fig. 3). Neurokinin A has effects similar to those of substance P, whereas neurokinin B operates as a pain reliever by the release of ligands of the opiate receptor. Substance P and neurokinin A facilitate the dopaminergic excitation pathway. Thus, an agonist could be useful in the therapy of Parkinson's disease, which is characterized by a loss of dopaminergic neurons in the substantia nigra. Finally, substance P acts neurotrophically and is able to arrest the neurotoxic effects of the β-amyloid protein regarded as causing the pathogenesis of Alzheimer's disease.[129]

In the development of antagonists it became apparent that residues 7–11 of substance P contain the minimal sequence required for biological activity. Exchange of Phe^7 or Gly^9 by D-Trp or other aromatic D-amino acids leads to an antagonistic effect of the resulting peptides.[119a] The compounds developed on this basis initially showed an affinity for the receptors several orders of magnitude lower than that of the endogenous ligands and allowed only an incomplete characterization of the receptors, because of overlapping specificity.

The first potent, competitive nonpeptide antagonist for the NK 1 receptor is CP-96345 (**87**),[130] which emerged from a screening process. Only the (2*S*,3*S*) enantiomer of **87** is effective; it shows no agonistic activity and has an affinity for the NK 1 receptor comparable to that of its endogenous ligand, substance P. Other potent nonpeptide antagonists for the NK 1 receptor are RP 67580 (**88**)[131] and the steroid derivative **89**.[132] Compound **90**[133] is also a nonpeptide NK 1 antagonist, although it is not suitable for further tests because of its lower affinity and high toxicity.

More recent examples of NK 2 selective antagonists based on peptides include **91**,[134] the cyclic hexapeptide **92**,[135] and the hexa- and heptapeptides **93** and **94**.[136] Recently, SR 48968 (**95**) was described as a potent, selective NK 2 antagonist.[137] Presently the most potent NK 3 antagonists are a (4–10) fragment of neurokinin A, in which Val^7 and Gly^8 have been replaced by Trp and β-alanine, respectively, and a (4–10) fragment of neurokinin B that contains MePhe instead of Val^7 and β-alanine in place of Gly^8.[138]

Tachykinin antagonists promise useful properties, in particular inhibition of inflammation and relief of pain. In addition, it is also conceivable that they could be used in asthma therapy and in the treatment of some autocrine tumors.

4.3. Somatostatin (Somatotropin-Release Inhibiting Factor, SRIF)

Somatostatin (**96**),[139–141] a cyclic tetradecapeptide, is formed in the hypothalmus and inhibits the release of growth hormone (GH) by the pituitary gland. In other parts of the brain somatostatin acts as a neurotransmitter and as a neuromodulator; participation of somatostatin in the peripheral nervous system in the perception of pain has been proposed. Outside the nervous system it has been found in the secretory cells of the intestine and pancreas, and in the salivary glands. It serves in these organs as an autocrine and paracrine regulator. Somatostatin formed in the δ cells of the pancreas inhibits the release of insulin and glucagon by the β and α cells of the pancreas, respectively. In the digestive tract motility is inhibited by somatostatin and the blood supply restricted. The secretion of gastric acid and gastrin is also reduced. Another effect is the reduction in secretion of pancreatic enzymes and the absorption of carbohydrates, triglycerides, and water.

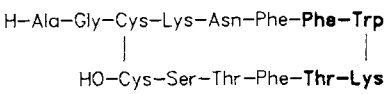

96

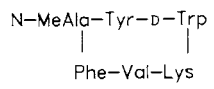

97

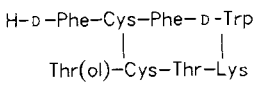

98

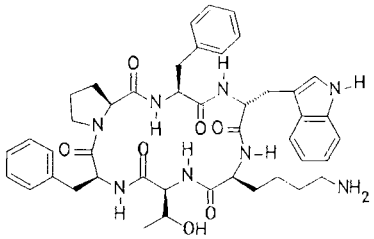

99

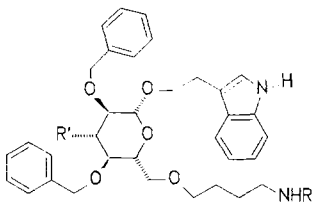

100a : R=R'=H
100b : R=CH_3CO, R'=OCH_2Ph

Somatostatin is synthesized as a preproprotein with a molecular mass of approximately 8 kDa. Through alternative posttranscriptional processing it is transformed into the mature hormone and to SRIF-28, which is also active. Receptors for somatostatin have been isolated from various tissues and biochemically characterized.[139] The somatostatin receptor from the brains of rats has recently been cloned and expressed in COS-1 cells.[142] This receptor belongs to the family of receptors coupled to G proteins with seven transmembrane regions. The binding of somatostatin to its receptor causes a G protein-mediated inhibition of adenylate cyclase activity and reduces the permeability of the plasma membrane to calcium ions.[139]

The main therapeutic use of somatostatin is in the treatment of acute gastrointestinal diseases such as gastric ulcers and particularly in the treatment of life-threatening bleeding in the gastrointestinal tract. It is also used in the treatment of pancreatitis and after surgery on the pancreas. Somatostatin has not been successful, however, in the treatment of diabetes mellitus. In patients with type I diabetes (juvenile form, absolute shortage of insulin), a temporary reduction in the blood glucose level has been observed after infusion of somatostatin. The condition of patients with type II diabetes (adult diabetes, relative shortage of insulin) deteriorates after application of somatostatin because of inhibition of the remaining insulin secretion.

Numerous peptide-based somatostatin agonists have been synthesized and pharmacologically tested, especially by Veber and co-workers. A critical discussion of this topic has been published recently.[143] Seglitide (MK 678, **97**)[144] is more active than somatostatin by one to two orders of magnitude, but clinical trials with the compound were terminated because of side effects (steatorrhea = malfunction of the absorption of fats). Another somatostatin agonist, octreotide (SMS 201-995, **98**)[145] is used in the therapy of acromegalia (enlargement of the ends of body parts and inner organs because of increased release of growth hormone by the pituitary gland).[146] The treatment of carcinoid tumors[147] and intestinal scleroderma, which is otherwise difficult to treat,[148] with octreotide appears promising. Octreotide labeled with ^{123}I has also been used successfully as a diagnostic agent for the detection of various tumors that have somatostatin receptors.[149]

Compounds **97**, **98**, and **99**[150] simulate a β turn between the Phe^7 and Thr^{10} residues of somatostatin, a structural characteristic that was postulated after extensive studies of structure–activity relationships. In agreement with the theory that a D-amino acid in the $i+1$ position stabilizes a β turn,[151] Trp^8 is replaced by D-Trp in these compounds.

Compound **100a** was described as the first nonpeptide somatostatin mimetic.[152] 3-Deoxy-β-D-glucose serves as a scaffold for the attachment of the first three side chains of the postulated β turn: Phe^7, Trp^8, and Lys^9. The compound binds to a somatostatin receptor of the pituitary gland with an IC_{50} value of 1.3 μM. A compound that contains a 1,2,3,5-tetrasubstituted D-xylofuranose unit in place of the central deoxyglucose shows comparable activity.[153]

In more recent investigations with **100a** and the structurally related derivative **100b** the following interesting aspects were reported: at low concentration **100a** behaves as a somatostatin agonist, whereas at higher concentration it shows antagonistic properties; thus it is the first somatostatin antagonist ever reported. Furthermore, **100a** behaves as an antagonist of the β_2-andrenergic receptor (IC_{50} = 3 μM), which is also coupled to G protein. Surprisingly, **100a** displays a much higher affinity toward the substance P receptor (agonistic effect, IC_{50} = 0.18 μM), whereas derivative **100b** is a potent antagonist (IC_{50} = 60 nM) for the substance P receptor!

4.4. Gastrin-Releasing Peptide (GRP, Bombesin-27)

Gastrin-releasing peptide (GRP, **101**), a peptide composed of 27 amino acids, is closely related to bombesin (**102**), a

Ala–Pro–Val–Ser–Val–Gly–Gly–Gly–Thr–Val–Leu–Ala–Lys–Met–Tyr–Pro–Arg–Gly–Asn–His–Trp–Ala–Val–Gly–His–Leu–Met–NH_2

101

pyroGlu–Gln–Arg–Leu–Gly–Asn–Gln–Trp–Ala–Val–Gly–His–Leu–Met–NH_2

102

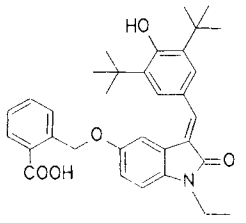

103

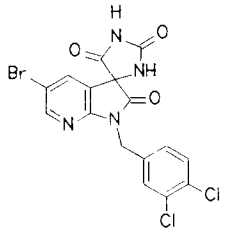

104

tetradecapeptide isolated from amphibians. It has been found in the central and peripheral nervous systems, as well as in the gastrointestinal tract and in neuroendocrine cells of the lungs. It effects the contraction of the smooth muscles of the gastrointestinal tract and the uterus, and stimulates the release of gastrin, glucagon, pancreatic amylase, cholecystokinin, and somatostatin.[154]

The GRP receptor from Swiss 3T3 cells was recently cloned, sequenced, and expressed in xenopus oozytes.[155] It is a G protein-coupled receptor that surprisingly also stimulates a tyrosine kinase.[156] The substrate of this kinase is the focal adhesion kinase p125 ($p125^{FAK}$), which is activated by phosphorylation and as a result has an effect on cell growth and cell adhesion.[156b, 156c]

The interest in GRP antagonists results from the fact that GRP acts as a potent autocrine/endocrine growth factor in small-cell lung cancer (SCLC).[157] Various GRP antagonists are capable of inhibiting the GRP-induced growth of these bronchial carcinomas in vitro.[158] [Leu^{14}-ψ-CH_2NH-Leu^{13}]bombesin[159] and the nonapeptide pyroGlu-Gln-Trp-Ala-Val-Gly-His-Phe-ψ-[CH_2S]Leu-NH_2 with a dissociation constant K_d of 3 nM[160] are among the most potent GRP antagonists presently known. Interestingly, the nonapeptide pyroGlu-Gln-Trp-Ala-Val-Gly-His-Phe-Leu-NH_2 is a potent GRP agonist (K_d = 0.2 nM)! This example also proves the value of the CH_2S group (another isosteric group for the amide bond) in the development of peptide antagonists.

The synthesis and properties of two nonpeptide antagonists of GRP have been described recently.[161] Compounds **103** and **104** are antagonists of the binding of GRP to the corresponding receptors in the rat brain (IC_{50} = 1.5 μM). However, the same compounds are, up to a concentration of 30 μM, inactive toward the human SLCL cell line N592. Unlike the endogenous ligands these mimetics are apparently capable of discriminating between species-specific receptor types.

4.5. Cholecystokinin and Gastrin

The peptide hormone cholecystokinin[162, 163] (CCK) exists in numerous biologically active forms (CCK-58, CCK-

39, CCK-33, CCK-8 **105**, CCK-4 = tetragastrin) with a common C-terminus. It exists in the nervous system both centrally (CCK-8 is the most common neuropeptide in the brain) and peripherally. It was originally demonstrated to be one of the hormones responsible for regulating the function of the digestive tract. Structurally it is related to the intestinal hormone gastrin (**106**); the two compounds have a common C-terminal pentapeptide. Similarities also exist with the decapeptide caerulein isolated from frogs.

Asp–Tyr(SO_3H)–Met–Gly–Trp–Met–Asp–Phe–NH_2 **105**

pyroGlu–Gly–Pro–Trp–Leu–Glu–Glu–Glu–Glu–Ala–Tyr(SO_3)–Gly–Tyr–Gly–Trp–Met–Asp–Phe–NH_2 **106**

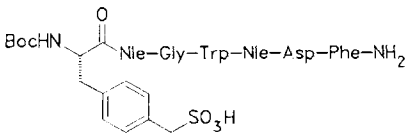

107

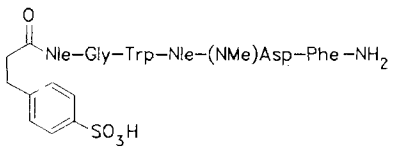

108

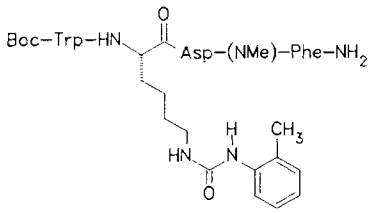

109

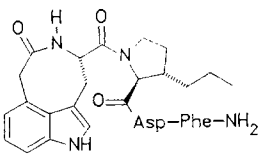

110

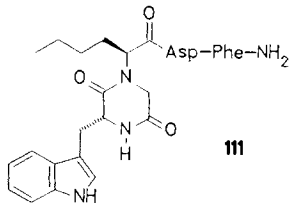

111

In the digestive tract cholecystokinin stimulates the contraction of the gall bladder and simultaneous relaxation of the sphincter of oddi, increases the release of insulin, increases the secretion of enzymes from the pancreas, and inhibits the secretion of gastrin and the emptying of the stomach.

In the central nervous system cholecystokinin acts as a neuromodulator/neurotransmitter, has an anxiety-generating (anxiogenic) and appetite-suppressing effect, whilst at the spinal level it antagonizes the effect of opiates and thereby acts as an antianalgesic.[164]

Two receptor subtypes could be characterized: the predominantly peripheral CCK-A receptor and the largely central CCK-B receptor. At the molecular level the binding of an agonist with the CCK-A receptor in acinus cells of the pancreas causes the G protein-mediated release of inositol 1,4,5-trisphosphate and calcium ions, activation of the protein kinase C, and the opening of calcium-dependent chloride channels. The CCK-A receptor from the rat pancreas has been cloned, sequenced, and expressed in foreign cells (xenopus oocytes).[165] The sequence shows similarities to other representatives of the G protein-coupled receptor family. The CCK-B receptor, a protein with a molecular mass of 74 kDa,[166] is closely related or possibly identical to the peripheral gastrin receptor and effects a G protein-mediated phosphatidylinositol-4,5-bisphosphate hydrolysis after stimulation through an agonist.[167] The canine CCK-B (gastrin) receptor has been cloned, sequenced, and expressed in COS-7 cells.[168] It also shows similarities to representatives of the family of G protein-coupled receptors.

Numerous CCK-A receptor agonists based on peptides have been developed. In contrast to the endogenous peptides these show much higher metabolic stability. An example of such a compound is the CCK-7 analogue **107**: replacement of the sulfuric acid ester function (acid labile and essential for biological function) by a methyl sulfonyl group and of methionine by norleucine increases the stability. This analogue shows higher receptor affinity ($K_i = 1$ nM) and complete agonistic affinity (amylase secretion by the pancreas and contraction of the ileum).[169] Exchange of the sulfuric acid group by an acetate or tetrazolyl group is tolerated by the receptor.[170] Other peptidal CCK-A selective agonists are A-71378 (**108**, $IC_{50} = 0.42$ nM, 700 times more selective for the CCK-A receptor)[171] and A-71623 (**109**, $IC_{50} = 4$ nM, >1000 times more selective).[172]

Several peptide-based CCK-B receptor agonists have also been developed. Examples include the two cyclic compounds **42** and **43** mentioned in Section 3.4, and the conformationally rigid derivatives A-63387 (**110**) and **111**. Compound **110** ($IC_{50} = 0.7$ nM, 9000-fold selectivity for the CCK-B receptor)[173] contains the tryptophan analogue **11**, referred to in Section 3.1, whereas compound **111**[174] contains a dioxopiperazine as a dipeptide analogue.

While the area of indications for the CCK agonists appears to be limited, the therapeutic potential of CCK antagonists lies in the treatment of diseases of the digestive tract (gastritis, pancreatitis, endocrinic tumors such as insulinomes and gastrinomes), neuropsychiatric disorders (anxiety, panic, cognitive dysfunction, schizophrenia), and pain.

Potent nonpeptide antagonists of the CCK receptors have been developed by optimization of lead structures. Proglumide (**112**), which has been used for a long time in therapy of pancreatitis, served as the lead structure in the development of, for example, the CCK-A antagonist **113**.[175] Benzotript (**114**) and **112** served as the models in the development of the CCK-A antagonist **115**[176] ($IC_{50} = 21$ nM). The discovery of the fungal metabolite asperlicin (**116**)[177] as a CCK-A antagonist ($IC_{50} = 1$ μM) represents a milestone in this area and permitted the development of the selective, orally active CCK-A antagonist MK-329 (**117**)[178] (previously L-364718, $IC_{50} = 0.08$ nM), as well as the CCK-B antagonist L-365260 (**118**)[179] ($IC_{50} = 2$ nM). The

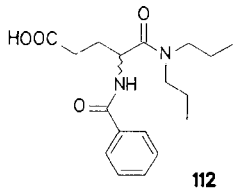

112

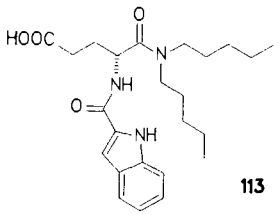

113

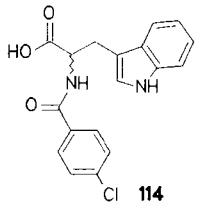

114

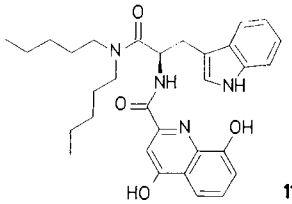

115

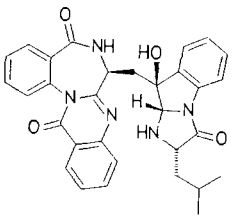

116

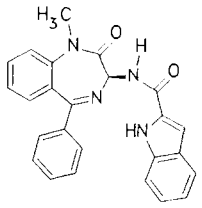

117

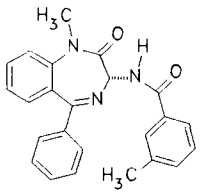

118

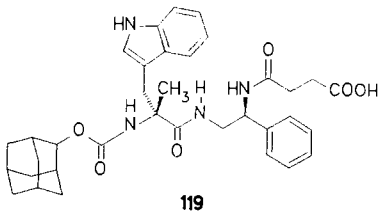

119

similarity of asperlicin with the clinically well-established benzodiazepines was the main driving force for the synthesis of the compounds MK-329 and L-365260. In this context it is worth mentioning that some benzodiazepines such as diazepam act as weak CCK-A antagonists. The benzodiazepine derivative tifluadom (**81**) developed initially as a κ-opioid receptor *agonist* later also turned out to be a CCK-A *antagonist*![180]

The observation that the minimal sequence of the C-terminal tetrapeptide of CCK (Trp-Met-Asp-Phe-NH_2) is necessary for the biological activity at central CCK receptors led to the synthesis of the dipeptide derivative Boc-Trp-Phe-NH_2 as a weaker CCK-B agonist.[181] The modification of this structure, supported by investigations of conformational energy[182] of the tetrapeptide Trp-Met-Asp-Phe-NH_2, culminated in the synthesis of the orally active dipeptoid CI-988 (previously PD-134308) **119**, which showed itself to be a selective CCK-A antagonist ($IC_{50} = 1.7$ nM with 1000 times greater selectivity for the CCK-B receptor).[183] The compound CI-988 is the first example of a rationally developed nonpeptide ligand for a neuropeptide receptor.

Compounds CI-988 (**119**) and L-365260 (**118**) have shown very interesting pharmacological effects in animal experiments. They have strong anxiolytic properties, but at the same time show no sedatory effects. The generation of dependence has not been observed.[184] Regarding these properties they are far superior to the benzodiazepines. Nevertheless, an appetite-increasing effect seen in animal experiments should be taken into consideration before clinical application of these new CCK-B antagonists.[185] Neither CI-988 nor L-365260 alone have analgesic properties; however, they can increase the analgesic effect of morphine and the duration of this effect.[186] These results suggest that CCK is the physiological opioid antagonist.[187]

4.6. Gonadotropin-Releasing Hormone (GnRH, LH-RH)

The gonadotropin-releasing hormone GnRH[188] (**120**) is synthesized in the hypothalmus and then secreted. In the anterior lobes of the pituitary gland it acts to release gonadotropins, in other words, luteinizing hormone (LH) and follicle-stimulating hormone (FSH). After GnRH binds to its membrane-bound receptor, LH and FSH are released. Then a G protein-mediated activation of phospholipase C together with an increase in the intracellular concentration of free Ca^{2+}[189] occurs, and activation of calmodulin follows as a direct consequence. Recent investigations[189] also confirm the participation of leukotrienes as second messengers in the GnRH-induced release of gonadotropins by cells of the pituitary gland.

The gonadotropins are heterodimeric glycoproteins with common α and different β subunits. They function as nonspecific superordinate sex hormones: FSH stimulates maturation of follicles and estrogen biosynthesis in females, and the generation of spermatozoa in males; in females LH causes ovulation and formation of corpus luteum and estrogen;

pyroGlu–His–Trp–Ser–Tyr–Gly–Leu–Arg–Pro–Gly–NH_2 **120**

[D–Leu^6, Pro^{9}NHEt]–GnRH **121**

[D–Ser(*t*Bu)^6, Pro^{9}NHEt]–GnRH **122**

[D–His(Bn)^6, Pro^{9}NHEt]–GnRH **123**

[D–3–(2–naphthylalanine)^6]–GnRH **124**

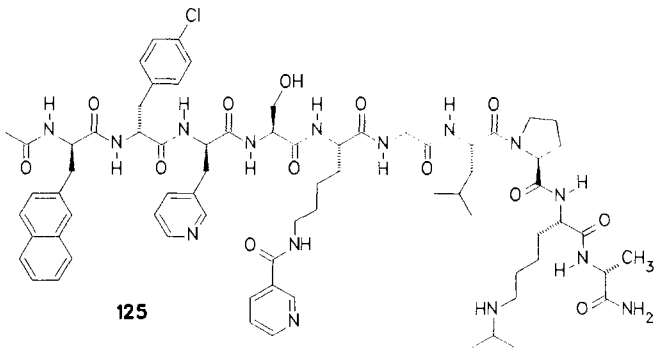

125

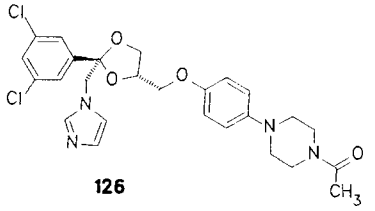

126

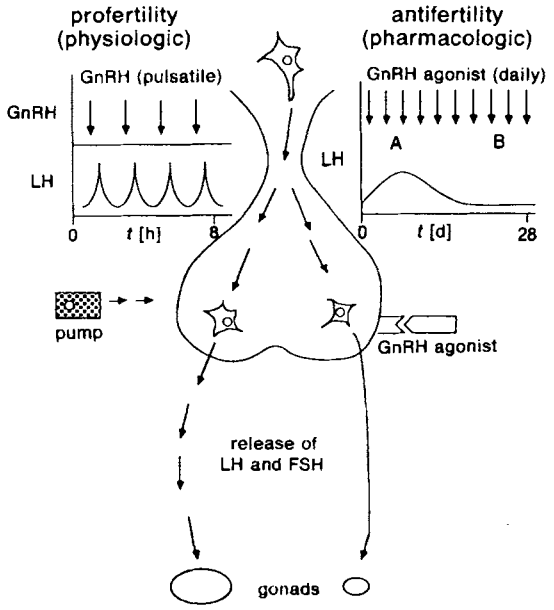

Fig. 4. Mechanism of action of gonadotropin-releasing hormone (GnRH) and GnRH agonists with long-lasting effects. The treatment of fertility problems requires the pulsatile application of natural GnRH (physiological type of application, left). This type of application imitates the physiological secretion of GnRH by the hypothalmus. For suppression of the pituitary gland gonadal axis, long-lasting GnRH agonists are administered in depot form or taken once daily (pharmacological application, right). After an agonistic initial phase A, which can last several days to weeks, a long-lasting inhibition of the gonadotropin secretion results that is practically complete and selective (antagonistic phase B). By terminating administration of the GnRH agonist the inhibition can be reversed[188].

in males the release of testosterone and biosynthesis of androgens is triggered.

Under physiological conditions GnRH is released in a pulsatile fashion (Fig. 4).[188] Continuous application of GnRH (or a GnRH agonist) causes an initial increase in gonadotropin release by the pituitary gland, followed by reduction and finally cessation of gonadotropin release. The exact molecular mechanism responsible for this phenomenon has not yet been unequivocally clarified, but there is some evidence suggesting that it involves a loss of GnRH receptors in the pituitary gland (down-regulation of the receptors) or their decoupling from the intracellular effector system in the pituitary gland or both. Thus, the action of GnRH can be both imitated and antagonized by the choice of the method of application!

Suppression of the release of the gonadotropins is possible directly by application of GnRH antagonists. It is advantageous hereby that the initial phase of increased secretion of LH, FSH, and sexual hormones is not observed. GnRH and its analogues are used primarily in the following areas:[191]

a) In the treatment of fertility disorders, for example in patients with a deficiency of GnRH. The use of an external pump, through which native GnRH is administered in pulses, is necessary for the reasons previously given.

b) For the selective and reversible suppression of the pituitary gland gonadal axis. The continuous application of GnRH is necessary here. Alternatively, long-lasting GnRH agonists or antagonists can be used. Examples of diseases that can be treated in this fashion include endometriosis, polycystic ovarian disease, and prostate carcinomas. GnRH agonists have been used hitherto for this purpose because, overall, they show fewer side effects in comparison with the first-generation antagonists. For the antagonists tested to date, the side effects are generally caused by the release of histamine.

A multitude of peptide-based GnRH analogues has been synthesized so far. The exchange of Gly^6 by D-amino acids and substitution in the 10-position leads to agonists that are much more potent in comparison with GnRH itself and that to some extent have found clinical application. Among these are leuprolide (**121**), buserelin (**122**), and histrelin (**123**), which are 15, 20, and 210 times more active than native GnRH, respectively. Another potent GnRH agonist is the azapeptide [D-Ser(tBu)^6,azaGly^{10}]-GnRH (goserelin).[192] The improved effect of these compounds can be traced back both to the blocking of catabolism at positions 6 and 10 and to the better receptor binding and increased hydrophobicity, which leads to depot formation in the body and increased half-life.

There are indications that the receptor-bound conformation of GnRH shows a Tyr^5-Gly^6-Leu^7-Arg^8-β-II′ turn.[193] Incorporation of a β turn mimetic in this position leads to peptide **65**. Although this compound shows an in vivo effect only 2.4 times greater than that of GnRH,[194] it provides an indication for the existence of a β turn in the biologically active GnRH conformation. This observation also initiated the application of lactams as turn mimetics.

GnRH agonists such as buserelin[195] and leuprolide[196] find application in the treatment of metastasic prostate cancer, the growth of which is dependent on sex hormones. Thus the simultaneous application of antiandrogens is necessary in order to forestall an androgen-induced initial intensification of the symptoms.

The GnRH agonist nafarelin (**124**) has recently been used successfully in the therapy of the gynecological disease endometriosis (an increased estrogen level seems to be responsible for the pathogenesis of this disease), treatment of which is otherwise difficult.[197] In comparison with the steroid derivative danazol used hitherto for this purpose, nafarelin possesses fewer side effects and is apparently tolerated very well by patients.[198] In this context is it also important to comment that many endocrinologists believe that GnRH analogues are the most important advance since the discovery and application of synthetic estrogens and progestagens in the treatment of gynecological diseases.[198]

Typically GnRH antagonists are modified at positions 1 and 10 for protection from exopeptidases, and a D-amino acid is incorporated at position 2. An example for an antagonist with negligible histamine release is antide (**125**).[199]

The accidental observation[200] that high oral doses of the antimycotic drug ketoconazole (**126**) cause a reduction of the serum testosterone level and subsequent remission in prostate cancer led to the discovery that ketoconazole is a weakly competitive antagonist of the GnRH receptor.[201] Its affinity lies in the micromolar range. Thus, a nonpeptide lead structure is available for the first time, the receptor affinity of which can still be improved.

4.7. Angiotensin II (A II)

The renin–angiotensin system plays an important role in the regulation of blood pressure. The enormous interest in

this system has come about because of the high incidence of cardiovascular diseases, for example hypertension and heart failure.

The biosynthesis of angiotensin II starts from angiotensinogen, a protein with a mass of about 60 kDa, which is largely synthesized in the liver and then passes into the blood. In the kidneys it is cleaved by the aspartyl protease renin into the decapeptide angiotensin I, which in turn is converted by the angiotensin-converting enzyme (ACE), a carboxypeptidase found primarily in the lungs, into the biologically active angiotensin II (**127**). Its inactivation results from C-terminal cleavage of a further amino acid and leads to angiotensin III. The brain is also capable of synthesizing angiotensin II. This octapeptide was the most potent substance known for increasing the blood pressure until the discovery of endothelin-1. It affects the blood pressure directly by constriction of the blood vessels and indirectly by release of aldosterone through the cortex of the adrenal gland.

In addition to its action on the blood pressure, angiotensin II transmits numerous other effects,[202] for example release of catecholamines from the adrenal medulla and stimulation of glycogenolysis in the liver. In the kidneys it stimulates the synthesis of prostaglandins and the resorption of sodium ions, and inhibits the release of renin and, thereby, its own biosynthesis. Angiotensin effects contraction of the uterus and stimulates ovulation, and in the brain it stimulates the secretion of vasopressin and adrenocorticotropic hormone (ACTH) by the pituitary gland and also functions as a neuromodulator.

Asp–Arg–Val–Tyr–Ile–His–Pro–Phe **127**

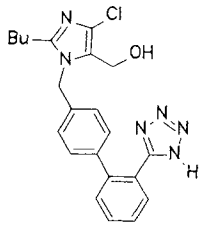

128

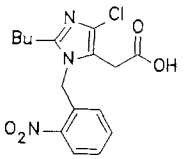

129

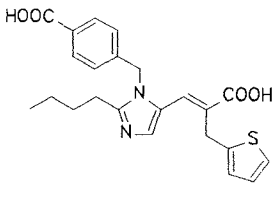

130

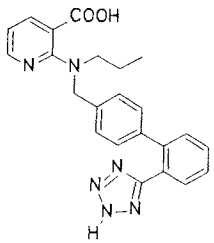

131

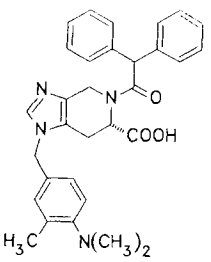

132

Based on the variable selectivity of synthetic ligands, two receptor subtypes, AT-1 and AT-2, could be differentiated.[203] Recently, with the help of an oligonucleotide primer derived from AT-1, an additional receptor subtype, AT-3, from the adrenal cortex of the rat, was cloned, sequenced, and expressed in COS cells and in xenopus oocytes.[204]

All known physiological effects of angiotensin II have hitherto been attributed to the AT-1 receptor, which has been demonstrated in several tissue types (adrenal cortex, liver, kidney, brain, and smooth muscles of blood vessels, bronchi, and the digestive tract), and whose c-DNA has been cloned from various species (cow,[205] rat,[206] humans[207]) and expressed in COS cells. A G protein-mediated action through various second-messenger systems, including the inhibition of adenylate cyclase activity, increase in the intracellular calcium concentration by mobilization of intracellular reserves or by opening of calcium channels, and hydrolysis of phosphatidylinositol-4,5-bisphosphate could be demonstrated. In comparison with AT-1, the receptor subtype AT-2 is found predominantly in the adrenal cortex and in the uterus. Unlike AT-1, AT-2 is not deactivated by reaction with disulfide-reducing agents and is apparently not coupled to a G protein. Its biological function is unknown.

There are indications that angiotensin II plays a role in embryonic development. A growth-factor-like effect of angiotensin II is possibly mediated by the AT-2 receptor.[208] A development-dependent differential expression of the two receptors AT-1 and AT-2 has been observed in the aorta[209] and the brain[210] of the rat.

In principle there are numerous possibilities for the pharmacological influence of the renin–angiotensin system, for example, by application of renin inhibitors, ACE inhibitors, or of antagonists of the A II receptor. ACE inhibitors have proven to be useful in the treatment of hypertension. In addition to the development of effective, orally active renin inhibitors, dramatic activity has taken place most recently in the development of angiotensin II analogues. While A II agonists are of interest for biochemical and pharmacological investigations (e.g. characterization and localization of the various A II receptors), the A II antagonists are of high therapeutic potential. One of the newer peptide-based ligands of the A II receptor is [Sar^1,(2′,3′,4′,5′,6′,-Br_5)Phe^8]-A II, a strong noncompetitive antagonist with a long-lasting effect in vivo.[211] Derivatives of [Sar^1]-A II, in which Phe^8 is replaced by β,β'-diphenylalanine (**3**), are potent agonists of the A II receptor, whereas [Sar^1]-A II analogues with 2-naphthylalanine (**4**) and 2-amino-2-indanecarboxylic acid (**5**) in place of Phe^8 are antagonists. Global restriction of the conformational flexibility of A II led to the agonist [$HCy^{3,5}$]-A II as well as the agonist [Sar^1,$HCy^{3,5}$,Ile^8]-A II, both with higher affinity for the receptor (HCy = homocysteine).[212] Peptide antagonists with selectivity for the AT-2 receptor include [*p*-aminophenylalanine^6]-A II[213] and nicotinic acid-Tyr-(*N*-Z-Arg)-Lys-His-Pro-IleOH.[214]

The first potent, orally active nonpeptide antagonist of the AT-1 receptor and prototype of a series of further compounds of similar structure[202] is DuP 753 (MK-954, **128**)[215] (IC_{50} = 19 nM). Compound **128** was developed by superpositioning the lead structure of S-8308 (**129**), a weak

but specific antagonist of the AT-1 receptor,[216] with the structure of angiotensin II, assisted by the use of molecular modeling. In clinical trials the blood pressure of volunteers could be reduced as a function of the concentration used. This discovery spurred intensive research in this area which culminated in the design of more potent and selective antagonists of the AT-1 receptor such as SK & F 108566 (**130**, $IC_{50} = 1$ nM)[217] and A-81988 (**131**, $K_i = 0.76$ nM; K_i for AT-2 > 10000 nM).[218] Selective antagonists of the AT-2 receptor were also discovered: PD-123319 (**132**), a nonpeptide antagonist of the AT-2 receptor ($IC_{50} = 34$ nM)[219] is representative here of other compounds with similar structures.

Investigations with **128** and other nonpeptide ligands suggest that angiotensin III is taken up into the cell and then inhibits cGMP-phosphodiesterase, resulting in opposite effects (relaxation of smooth muscle) to those of angiotensin II.[220] Since controlled clinical studies with nonpeptide A II antagonists are not yet available, the suitability of such agents for the treatment of cardiovascular diseases cannot be judged at this time.

4.8. Endothelins

Endothelin-1 (**133**),[221] a peptide consisting of 21 amino acids which has a marked blood vessel contracting action (10 times stronger than angiotensin II), was first isolated in 1988 from cultivated endothelial cells.[222] Later, two other related peptides were found, endothelin-2 (**134**) and endothelin-3 (**135**).[223] They are related to the sarafotoxins (snake toxins) in terms of structure and also from the pharmacological viewpoint. The endothelins belong to a series of substances that can be secreted from endothelial cells (cells of the inner walls of blood vessels) and which transmit a regulatory effect of the endothelial cells on the vascular tonus and thereby on the blood pressure (Fig. 5).[221] In addition to the endothelins[224] other substances belong to this class, including prostacyclins and the endothelium-derived relaxing factor (EDRF-NO), recently identified as nitrogen monoxide. The endothelins cause a long-lasting contraction of arteries and veins, minimize the excretion of sodium ions by the kidneys, and mediate a series of other biological effects, for example contraction of smooth bronchial, intestinal, and uterine muscles.[221] In the central nervous system the endothelins appear to be involved in the regulation of GnRH secretion.[225]

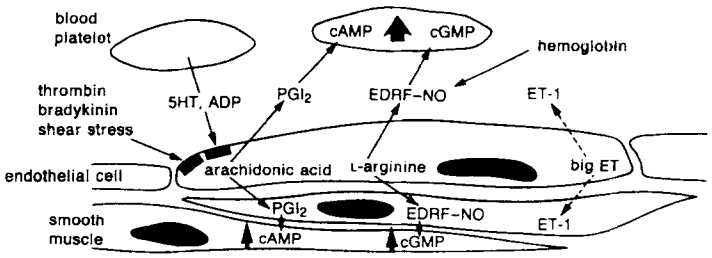

Fig. 5. Production of prostacyclin (PGI2), endothelial-derived relaxing factor nitrogen monoxide (EDRF-NO) and endothelin-1 (ET-1) in cells of the interior walls of blood vessels (endothelial cells). The blood platelets (thrombocytes) release serotonin (5HT) and adenosine diphosphate (ADP) through the influence of thrombin and bradykinin, or from the application of shear stress. The stimulation of the cell receptors by serotonin or adenosine diphosphate leads to the release of vessel-active mediators. Prostacyclin, formed from arachidonic acid, relaxes the smooth muscles of the blood vessels and inhibits the aggregation of blood platelets by increasing the concentration of *cyclo*-adenosine monophosphate (cAMP). EDRF-NO, formed from L-arginine, has the same effect but by increasing the *cyclo*-guanosine monophosphate (cGMP) level. Prostacyclin and EDRF-NO thereby function synergistically in inhibiting blood platelet aggregation by the simultaneous increase of the cAMP and cGMP concentration. Hemoglobin inactivates EDRF-NO. Endothelin-1 is generated in the endothelial cells by proteolysis of big endothelin (big ET). After exocytosis it binds to the membrane receptors of the smooth muscle cells and causes a contraction of the blood vessel muscles[224].

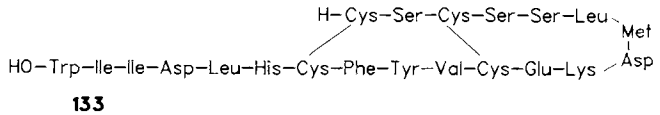

133

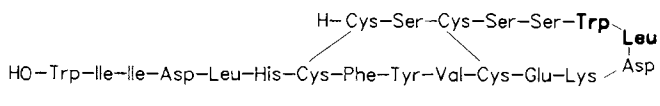

134

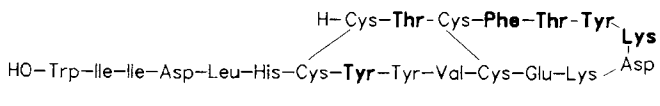

135

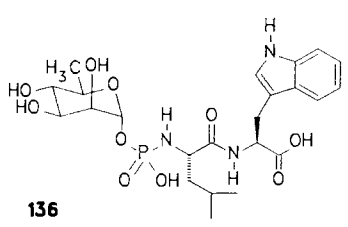

136

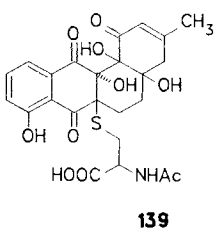

139

cyclo(-D-Glu-Ala-allo-D-Ile-Leu-D-Trp-) **137**

cyclo(-D-Trp-D-Asp-Pro-D-Val-Leu-) **138**

The biosynthesis of the most investigated member, endothelin-1, occurs by way of a preproendothelin (203 amino acids) and a proendothelin (39 amino acids). This peptide, also known as "big endothelin", is cleaved by the endothelin-converting enzyme, which can be inhibited by the metalloprotease inhibitor phosphoramidon (**136**).[226] So far two endothelin (ET) receptor types have been isolated: ET_A with selectivity for endothelin-1 and ET_B without selectivity for the isopeptides. They have subsequently been sequenced, cloned, and expressed.[227] The receptors display seven transmembrane regions. They are coupled by G proteins to the phosphatidylinositol-4,5-bisphosphate second-messenger system and effect the mobilization of calcium ions from intracellular stores. Interestingly, after endothelin is bound to its receptor (Swiss 3T3 cells), a tyrosine kinase is also stimulated.[156a] Endothelins and their receptors occur in peripheral tissues and also in various regions of the brain.[228]

A linear endothelin-1, in which all four cystein residues are replaced by alanine, acts as a selective agonist for the ET_B receptor.[229] If the outer of the two disulfide bridges in endothelin-1 is exchanged for an amide bond between di-

aminopropionic acid and aspartic acid in position 15 (the position of the outer cysteine residue), a specific, potent antagonist for the ET_A receptor is obtained.[230] The authors discuss a direct participation of the outer disulfide bridge in the recognition of endothelin-1 by its receptor, possibly by a disulfide exchange between ligand and receptor.[231]

Screening revealed another selective ET_A antagonist,[232] the cyclopeptide **137**. Structure–activity analysis based on this compound led to **138**, which has improved affinity and selectivity for the ET_A receptor.[233] Apparently this compound acts as a noncompetitive antagonist.[234] IRL-1038 [Cys^{11}-Cys^{15}]-endothelin-1(11-21) was recently described as a selective antagonist for the ET_B receptor,[235] and the anthraquinone derivative **139** was described as the first nonpeptide antagonist of the ET receptor.[236]

Apart from pharmacological and pathophysiological aspects, the main therapeutic potential of ET_A-selective antagonists lies in the treatment of elevated blood pressure. Other possible applications for ET_A antagonists include the treatment of arteriosclerosis, vasospasms in brain and heart, asthma, and malfunction of the kidneys. No concrete hypothesis concerning the potential of the ET_B receptor antagonists can be made at present, especially as the physiological significance of the ET_B receptor is still not clear. An opposite action to that of the ET_A receptor (relaxation of the vessel muscles and thereby a reduction in blood pressure) is being discussed.[237]

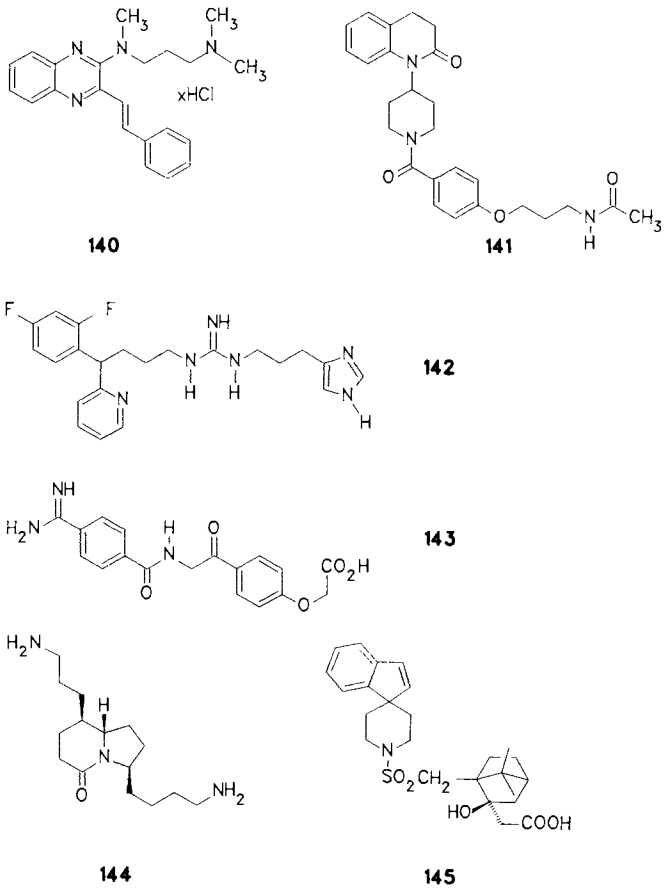

4.9. Miscellaneous

A series of other long-known agents have been shown recently to be mimetics of endogenous peptide ligands. In addition to the examples discussed above the following can be mentioned:

a) The antibiotic erythromycin has been shown to be an agonist of the polypeptide motilin, which is responsible for the coordination of the contraction of the gastrointesinal tract.[238] This observation led to the successful application of erythromycin for the treatment of the delayed emptying of the stomach caused by diabetes, thereby extending its indication area.[239]

b) Drugs based on sulfonylurea, long used for treatment of diabetes mellitus type II, are mimetics of the endosulfines, the endogenous peptide ligands of the sulfonylurea receptor.[240]

c) The endogenous ligands of the benzodiazepine receptor—an integral component of the $GABA_A$ receptor (GABA = γ-aminobutyric acid)[241]—are peptide based.[242]

Other nonpeptide ligands for peptide receptors include the glucagon receptor antagonist CP-99711 (**140**),[243] the vasopressin V1 receptor antagonist OPC-21268 (**141**),[244] the neuropeptide Y antagonist He-90481 (**142**),[245] and the glycoprotein (GP) IIb-IIIa antagonist (**143**) (highly potent inhibitor of thrombocyte aggregation),[246] the antagonist **144**[247] of the immune-stimulating tetrapeptide tuftsin (Thr-Lys-Pro-Arg), and the first nonpeptide oxytocin antagonist **145**.[248]

The steroid derivative **146**[249] was recently synthesized as an analogue of a postulated typeI β turn **147** of the glycoprotein GpIIb-IIIa-bound sequence Arg-Gly-Asp (RGD) of fibrinogen. Compound **146** binds to the GpIIb-IIIa receptor and shows an IC_{50} value of 100 μM when fibrinogen is used as ligand. In comparison the peptide *cyclo*(Arg-Gly-Asp-Phe-D-Val) (**148**, IC_{50} = 2 μM) is much more potent.[250] The RGD conformation relevant for the binding of the glycoprotein GpIIb-IIIa is apparently imitated better by **148**. According to NMR spectroscopic investigations, the Arg residue of this cyclopeptide in the position $i + 2$ takes up a βII′ turn, whereas the Asp residue in the central position adopts a γ turn.[251]

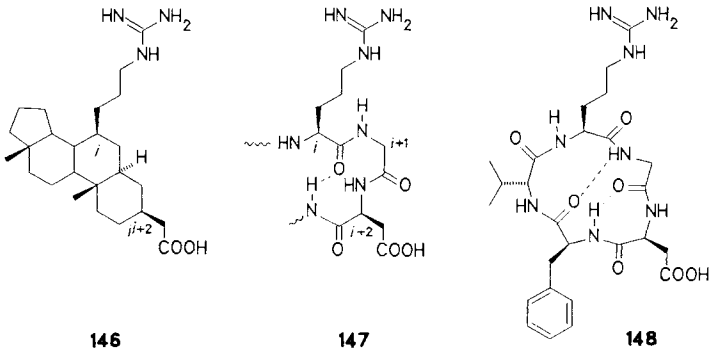

5. Summary and Outlook

Despite the disadvantages referred to at the beginning of this article, the development of peptide-based receptor lig-

ands will certainly remain of interest in the future.[252] The successes in this area cannot be denied. The marked trend of the last few years is the design of effective, orally active nonpeptide ligands for peptide receptors. Of significance in this regard is the fact that it is possible, in principle, to imitate or to block the function of a relatively large peptide at the receptor level with low molecular mass compounds. The opioid alkaloids are excellent examples here. The peptidomimetic character of other drugs such as ketoconazole, erythromycin, the sulfonylureas, and benzodiazepines have only recently been discovered.

Most of the peptide receptors known to date are coupled with proteins that bind guanine nucleotides (G proteins).[253] If one then contemplates the structures of the previously mentioned nonpeptide ligands, it is noticeable that they frequently contain hydrophobic and in particular aromatic structure elements. This suggests the existence of lipophilic domains at the ligand binding site of these receptors. Aromatic groups on the ligand appear generally to play a central role in recognition and in subsequent receptor activation. The elimination of such groups often leads to an inversion of the action at the receptor.[254] This is shown quite impressively, for example, by a comparison of structures **100a** (substance P agonist) and **100b** (substance P antagonist).

A major problem in the design of ligands for peptide receptors with favorable pharmacalogical properties was and remains the discovery of a lead structure. That this can also take place rationally is shown unequivocally by the example of **119**: The correct spatial positioning of the pharmacophores of a peptidal CCK agonist provided a "peptoid" with high affinity and antagonistic properties to a CCK receptor. In this case an endogenous peptide served as a lead compound. The importance of the appropriate spatial arrangement was also demonstrated in studies of immunoglobulin mimetic **59**, the development of which was based on the X-ray crystallographic analysis of an antigen–antibody complex. This compound, as well as the somatostatin agonist octreotide (**98**), the GnRH agonist **65**, and the thrombin inhibitor **67**, demonstrates unequivocally the value of the concept of conformative restriction and the application of secondary structure mimetics in the development of ligands that imitate the conformation of a peptide bound to a receptor. NMR spectroscopy has been shown to be increasingly useful in the investigation of bioactive peptide conformations. Of great importance here is the fact that receptor proteins are becoming available in larger quantities with the help of molecular biology—for example, by expression in foreign cells. In this way the production of isotopically labeled receptor proteins is also possible. The importance of NMR spectroscopy in studies of peptide–receptor complexes[17b] under physiological conditions was demonstrated recently for the example of cyclosporin A and its interaction with the protein cyclophilin.[17c, d] A general method for the application of such knowledge to conformational design[255] is, nevertheless, not yet available. In conformational design the aim is often the conception of suitable scaffolds that carry the functional groups required for binding to the receptor in a suitable spatial arrangement. Structure–activity investigations have shown that only a relatively small peptide sequence of four to eight amino acids is responsible for the biological activity, and that the amide backbone is not involved in occupation of the receptor and its activation.[12, 254] In addition, conformation–activity investigations show that these sequences of folded and compact bioactive conformations are generally 10×15 Å in size. These are the same dimensions of a benzodiazepine like **117** (MK-329) or a cyclic hexapeptide such as **99**.[9]

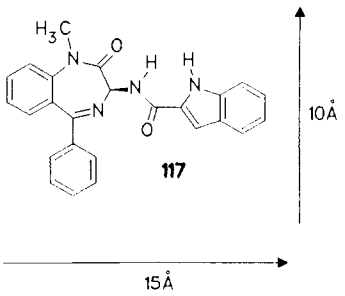

117

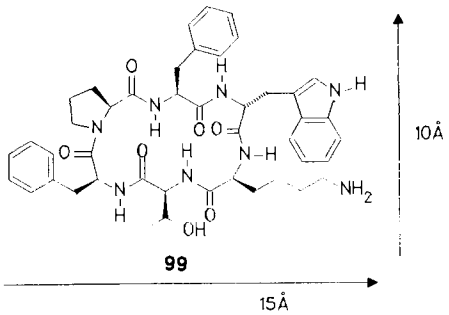

99

The benzodiazepine skeleton has proven to be versatile and leads not only to neuropeptide mimetics like tifluadom (**81**), MK-329 (**117**), and L-365260 (**118**) but also to HIV protease inhibitors (HIV = human immunodeficiency virus).[256] Thus, it would appear that benzodiazepines[257] and related structures will provide years of research for both chemists and physicians.

The biochemical and pharmacological properties of the compounds **100a** and **100b** finally suggest the potential of the carbohydrate skeleton in the design of nonpeptide ligands. Carbohydrates offer advantages of structural diversity and the facile derivatization with a multitude of functional groups.[260]

We thank the Deutsche Forschungsgemeinschaft for financial support. Thomas Kolter thanks the state of North Rhine-Westphalia for a stipend.

Received: November 5, 1992
Revised version: January 30, 1993 [A915 IE]
German version: *Angew. Chem.* **1993**, *105*, 1303
Translated by Dr. M. D. Ravenscroft, Bischwiller (France)

[1] G. Schmidt, *Top. Curr. Chem.* **1986**, *136*, 109.
[2] D. T. Krieger, *Science* **1983**, *222*, 975.
[3] J. H. Schwarz in *Principles of Neural Science* (Eds.: E. R. Kandel, J. H. Schwarz, T. M. Jessel), Elsevier, **1991**, p. 213.
[4] a) *A Textbook of Drug Design and Development* (Eds.: P. Krogsgaard-Larsen, H. Bundgaard), Harwood Academic Publishers, Chur, **1991**; b) M. Williams, A. M. Nadzan in [4a], p. 1.
[5] G. Jung, A. G. Beck-Sickinger, *Angew. Chem.* **1992**, *104*, 375; *Angew. Chem. Int. Ed. Engl.* **1992**, *31*, 367.

[6] D. F. Veber, R. M. Freidinger, *Trends Neurosci.* **1985**, 392.
[7] a) W. F. De Grado, *Adv. Protein Chem.* **1988**, *39*, 51; b) G. D. Rose, L. M. Gierasch, J. A. Smith, *ibid.* **1985**, *37*, 1.
[8] B. A. Morgan, J. A. Gainor, *Annu. Rep. Med. Chem.* **1989**, *24*, 243.
[9] R. M. Freidinger, *Trends Pharmacol. Sci.* **1989**, 270.
[10] V. J. Hruby, F. Al-Obeidi, W. Kazmierski, *Biochem. J.* **1990**, *268*, 249.
[11] G. Hölzemann, *Kontakte (Darmstadt)* **1991**, 3, 55.
[12] R. Hirschmann, *Angew. Chem.* **1991**, *103*, 1305; *Angew. Chem. Int. Ed. Engl.* **1991**, *30*, 1278.
[13] E. C. Griffith in [4a], p. 486.
[14] J. Rizo, L. M. Gierasch, *Annu. Rev. Biochem.* **1992**, *61*, 387.
[15] In order to take this meaning into account Veber has suggested the term *peptidlimeticum* (from peptide ligand mimetic): D. F. Veber in *Peptides: Chemistry and Biology, Proceedings of the Twelfth American Peptide Symposium*, Escom, **1992**, p. 3.
[16] a) M. J. Brownstein in *Basic Neurochemistry* (Eds.: G. J. Siegel, B. W. Agranoff, R. W. Albers, P. B. Molinoff), Elsevier, Amsterdam, **1989**, p. 287; b) J. van Nispen, R. Pinder, *Annu. Rep. Med. Chem.* **1986**, *21*, 51.
[17] a) H. Kessler, *Angew. Chem.* **1982**, *94*, 509; *Angew. Chem. Int. Ed. Engl.* **1982**, *21*, 512; for NMR investigations of receptor–ligand complexes: b) S. W. Fesik, *J. Med. Chem.* **1991**, *34*, 2937; c) K. Wüthrich, B. von Freiberg, C. Weber, G. Wider, R. Traber, H. Widmer, W. Braun, *Science* **1991**, *254*, 953; d) W. L. Jorgensen, *ibid.* **1991**, *254*, 954.
[18] S. K. Burt, J. Greer, *Annu. Rep. Med. Chem.* **1988**, *23*, 285.
[19] *Conformationally Directed Drug Design – Peptides and Nucleic Acids as Templates or Targets, ACS Symp. Ser.* **1984**, *251*.
[20] Reviews: a) [5]; b) M. Mutter, *Nachr. Chem. Tech. Lab.* **1992**, *40*, 172; c) W. J. Dower, S. P. A. Fodor, *Annu. Rep. Med. Chem.* **1991**, *26*, 271; d) H.-E. Radunz, *GIT Fachz. Lab.* **1992**, *9*, 869.
[21] a) K. S. Lam, S. E. Salmon, E. M. Hersh, V. J. Hruby, W. M. Kazmierski, R. J. Knapp, *Nature* **1991**, *354*, 82; b) R. A. Houghten, C. Pinilla, S. E. Blondelle, J. R. Appel, C. T. Dooley, J. H. Cuervo, *ibid.* **1991**, *354*, 84; c) R. J. Simon, R. S. Kania, R. N. Zuckermann, V. D. Huebner, D. A. Jewell, S. Banville, S. Ng, L. Wang, S. Rosenberg, C. K. Marlowe, D. C. Spellmeyer, R. Tan, A. D. Frankel, D. V. Santi, F. E. Cohen, P. A. Bartlett, *Proc. Natl. Acad. Sci. USA* **1992**, *89*, 9367.
[22] H. Bundgaard in [4a], p. 113.
[23] E. T. Kaiser, F. J. Kézdy, *Science* **1984**, *223*, 249.
[24] a) IUPAC-IUB Commission on Biochemical Nomenclature, *Biochemistry* **1970**, *9*, 3471; b) Fig. 3: G. E. Schulz, R. H. Schirmer, *Principles of Protein Structure* (Ed.: C. R. Cantor), Springer, New York, **1979**, p. 19.
[25] K.-H. Hsieh, T. R. LaHann, R. C. Speth, *J. Med. Chem.* **1989**, *32*, 898.
[26] a) S. Kotha, A. Kuki, *Tetrahedron Lett.* **1992**, *33*, 1565; b) S. Kotha, D. Anglos, A. Kuki, *ibid.* **1992**, *33*, 1569.
[27] a) E. J. Corey, J. O. Link, *J. Am. Chem. Soc.* **1992**, *114*, 1906; b) E. J. Corey, J. O. Link, Y. Shao, *Tetrahedron Lett.* **1992**, *33*, 3435.
[28] D. Seebach, E. Dziadulewicz, L. Behrendt, S. Cantoreggi, R. Fizzi, *Liebigs Ann. Chem.* **1989**, 1215.
[29] W. M. Kazmierski, H. I. Yamamura, V. J. Hruby, *J. Am. Chem. Soc.* **1991**, *113*, 2275.
[30] a) W. Kazmierski, V. J. Hruby, *Tetrahedron* **1988**, *44*, 697; b) W. Kazmierski, W. S. Wire, G. K. Lui, R. J. Knapp, J. E. Shook, T. F. Burks, H. I. Yamamuran, V. J. Hruby, *J. Med. Chem.* **1988**, *31*, 2170; c) P. W. Schiller, T. M. D. Nguyen, G. Weltrowska, B. C. Wilkes, B. J. Marsden, C. Lemieux, N. N. Chung, *Proc. Natl. Acad. Sci. USA* **1992**, *89*, 11871.
[31] P. W. Schiller, G. Weltrowska, T. M. D. Nguyen, C. Lemieux, N. N. Chung, B. J. Marsden, B. C. Wilkes, *J. Med. Chem.* **1991**, *34*, 3125.
[32] a) R. Naef, D. Seebach, *Helv. Chim. Acta* **1985**, *68*, 135; b) D. Seebach, J. D. Aebi, R. Naef, T. Weber, *ibid.* **1985**, *68*, 144; c) R. Fitzi, D. Seebach, *Tetrahedron* **1988**, *44*, 5277.
[33] W. M. Kazmierski, V. J. Hruby, *Tetrahedron Lett.* **1991**, *32*, 5769.
[34] J. Y. L. Chung, J. T. Wasicak, W. A. Arnold, C. S. May, A. M. Nadzan, M. W. Holladay, *J. Org. Chem.* **1990**, *55*, 270.
[35] M. W. Holladay, C. W. Lin, C. S. May, D. S. Garvey, D. G. Witte, T. R. Miller, C. A. W. Wolfram, A. M. Nadzan, *J. Med. Chem.* **1991**, *34*, 455.
[36] G. I. Georg, X. Guan, J. Kant, *Bioorg. Med. Chem. Lett.* **1991**, *1*, 125.
[37] M. W. Holladay, A. M. Nadzan, *J. Org. Chem.* **1991**, *56*, 3900.
[38] Asymmetric synthesis of 4-alkyl-substituted proline derivatives: a) A. M. P. Koskinen, H. Rapoport, *J. Org. Chem.* **1989**, *54*, 1859, and references therein; b) F. Soucy, D. Wernic, P. Beaulieu, *J. Chem. Soc. Perkin Trans. 1* **1991**, 2885, and references therein.
[39] J. Y. L. Chung, J. T. Wasicak, A. M. Nadzan, *J. Chem. Soc. Chem. Commun.* **1992**, 1039.
[40] D. Seebach, H. Bossler, H. Grondler, S-i. Shoda, *Helv. Chim. Acta* **1991**, *74*, 197.
[41] Examples: a) R. M. Freidinger, D. F. Veber, D. S. Perlow, J. R. Brooks, R. Saperstein, *Science* **1980**, *210*, 656; b) R. M. Freidinger, D. S. Perlow, D. F. Veber, *J. Org. Chem.* **1982**, *47*, 104; c) Z. Procházka, M. Lebl, T. Barth, J. Hlaváček, A. Trka, M. Budešinsky, K. Jošt, *Collect. Czech. Chem. Commun.* **1984**, *49*, 64; d) R. M. Freidinger, *J. Org. Chem.* **1985**, *50*, 3631; e) T. M. Zydowsky, J. F. Dellaria, Jr., H. N. Nellans, *ibid.* **1988**, *53*, 5607; f) S. Thaisrivongs, D. T. Pals, S. R. Turner, L. T. Kroll, *J. Med. Chem.* **1988**, *31*, 1369; g) J. D. Aebi, D. Guillaume, B. E. Dunlap, D. H. Rich, *ibid.* **1988**, *31*, 1805; h) J. P. Wolf, H. Rapoport, *J. Org. Chem.* **1989**, *54*, 3164; i) G. Valle, M. Crisma, C. Toniolo, K.-L. Yu, R. L. Johnson, *J. Chem. Soc. Perkin Trans. 2* **1989**, 83; k) D. S. Garvey, P. D. May, A. M. Nadzan, *J. Org. Chem.* **1990**, *55*, 936.
[42] H. Yanagisawa, S. Ishihara, A. Ando, T. Kanazaki, S. Miyamoto, H. Koike, Y. Iijima, K. Oizumi, Y. Matsushita, T. Hata, *J. Med. Chem.* **1987**, *30*, 1984, and references therein.
[43] G. A. Flynn, E. L. Giroux, R. C. Dage, *J. Am. Chem. Soc.* **1987**, *109*, 7914.
[44] a) D. S. Kemp, E. T. Sun, *Tetrahedron Lett.* **1982**, *23*, 3759; b) D. S. Kemp, P. E. McNamara, *ibid.* **1982**, *23*, 3761; c) *J. Org. Chem.* **1984**, *49*, 2286; d) *ibid.* **1985**, *50*, 5834.
[45] N. J. Ede, I. D. Rae, M. T. W. Hearn, *Tetrahedron Lett.* **1990**, *31*, 6071.
[46] V. M. Robson, I. D. Rae, F. Ng, *Biol. Chem. Hoppe-Seyler* **1990**, *371*, 423.
[47] J. DiMaio, B. Belleau, *J. Chem. Soc. Perkin Trans. 1* **1989**, 1687, and references therein.
[48] a) Piperazinones: A. Giannis, T. Kolter, A. Klein, *Chemiedozententagung Heidelberg – Programmübersicht und Kurzreferate* **1992**, Abstract B 33; b) vinylogous dipeptides: T. Kolter, A. Klein, A. Giannis, *Angew. Chem.* **1992**, *104*, 1394; *Angew. Chem. Int. Ed. Engl.* **1992**, *31*, 1391; c) T. Kolter, Dissertation, Universität Bonn, **1992**.
[49] a) [47]; b) T. Yamashita, J. Maruo, A. Fujimoto, K. Shibata, Y. Kojima, A. Ohsuka, *Macromol. Chem.* **1990**, *191*, 1261; c) A. Bravo, I. Gómez-Monterrey, R. González-Muñiz, M. T. García-López, *J. Chem. Soc. Perkin Trans. 1* **1991**, 3117; d) T. P. Curran, S. M. Abelleira, R. J. Messier, G. F. Musso in *Peptides (Chemistry and Biology, Proc. 12th Am. Peptide Symp.* June 16–21, Cambridge, MA, USA), Escom, Leiden, **1992**, p. 573; e) S. Jain, K. Sujatha, K. V. Rama Krishna, R. Roy, J. Singh, N. Anand, *Tetrahedron* **1992**, *48*, 4985.
[50] R. C. F. Jones, G. J. Ward, *Tetrahedron Lett.* **1988**, *29*, 3853.
[51] a) H. Kessler, *Angew. Chem.* **1970**, *82*, 237; *Angew. Chem. Int. Ed. Engl.* **1970**, *9*, 219; b) W. E. Stewart, T. H. Siddall, *Chem. Rev.* **1970**, *70*, 517.
[52] a) D. F. Mierke, T. Yamazaki, O. E. Said-Nejad, E. R. Felder, M. Goodman, *J. Am. Chem. Soc.* **1989**, *111*, 6847; b) H. Kessler, U. Anders, M. Schudok, *ibid.* **1990**, *112*, 5908.
[53] E. Bairaktari, D. F. Mierke, S. Mammi, E. Peggion, *J. Am. Chem. Soc.* **1990**, *112*, 5383.
[54] P. K. C. Paul, P. A. Burney, M. M. Campell, D. J. Osguthorpe, *Bioorg. Med. Chem. Lett.* **1992**, *2*, 141, and references therein.
[55] a) K.-L. Yu, R. L. Johnson, *J. Org. Chem.* **1987**, *52*, 2051; b) J. Zabrocki, G. D. Smith, J. B. Dunbar, Jr., H. Iijima, G. R. Marshall, *J. Am. Chem. Soc.* **1988**, *110*, 5875.
[56] D. K. Suumaran, M. Prorok, D. S. Lawrence, *J. Am. Chem. Soc.* **1991**, *113*, 706.
[57] G. A. Flynn, T. P. Burkholder, E. W. Huber, P. Bey, *Bioorg. Med. Chem. Lett.* **1991**, *1*, 309.
[58] M. Elseviers, L. Van Der Auwera, H. Pepermans, D. Tourwé, G. Van Binst, *Bioorg. Biochem. Res. Commun.* **1988**, *154*, 515.
[59] Review: A. F. Spatola, *Chem. Biochem. Amino Acids Pept. Proteins* **1983**, *7*, 267.
[60] M. M. Hann, P. G. Sammes, P. D. Kennewell, J. B. Taylor, *J. Chem. Soc. Perkin Trans. 1* **1982**, 307.
[61] T. Allmendinger, E. Fehler, E. Hungerbühler, *Tetrahedron Lett.* **1990**, *31*, 7301.
[62] J. Martinez, J. P. Bali, M. Rodriguez, B. Castro, R. Magous, J. Laur, M. F. Ligon, *J. Med. Chem.* **1985**, *28*, 1874.
[63] D. H. Coy, P. Heinz-Erian, N.-Y. Jiang, Y. Sasaki, J. Taylor, J.-P. Moreau, W. T. Wolfrey, J. D. Gardner, R. T. Jensen, *J. Biol. Chem.* **1988**, *263*, 5056.
[64] A. Giannis, K. Sandhoff, *Angew. Chem.* **1989**, *101*, 220; *Angew. Chem. Int. Ed. Engl.* **1989**, *28*, 218.
[65] See [49d].
[66] a) C. Dahl, Diplomarbeit, Universität Bonn, **1993**; b) see [48c].
[67] C. I. Fincham, M. Higginbottom, D. R. Hill, D. C. Horwell, J. C. O'Toole, G. S. Ratcliffe, D. C. Rees, E. Roberts, *J. Med. Chem.* **1992**, *35*, 1472.
[68] M. Goodman, M. Chorev, *Acc. Chem. Res.* **1979**, *12*, 1.
[69] M. Rodriguez, P. Dubreuil, J.-P. Bali, J. Martinez, *J. Med. Chem.* **1987**, *30*, 758.
[70] H. Dürr, M. Goodman, G. Jung, *Angew. Chem.* **1992**, *104*, 773; *Angew. Chem. Int. Ed. Engl.* **1992**, *31*, 785.
[71] M. Cushman, J. Jurayj, J. D. Moyer, *J. Org. Chem.* **1990**, *55*, 316, and references therein.
[72] R. M. Freidinger, D. F. Veber, *J. Am. Chem. Soc.* **1979**, *101*, 6129.
[73] M. Hagihara, N. J. Anthony, T. J. Stout, J. Clardy, S. L. Schreiber, *J. Am. Chem. Soc.* **1992**, *114*, 6568.
[74] H. I. Mosberg, R. Hurst, V. J. Hruby, K. Gee, H. I. Yamamura, J. J. Galligan, T. F. Burks, *Proc. Natl. Acad. Sci. USA* **1983**, *80*, 5871.
[75] a) B. Charpentier, D. Pelaprat, C. Durieux, A. Dor, M. Reibaud, J. C. Blanchard, B. P. Roques, *Proc. Natl. Acad. Sci. USA* **1988**, *85*, 1986; b) B. Charpentier, A. Dor, P. Roy, H. England, H. Pham, C. Durieux, B. P. Roques, *J. Med. Chem.* **1989**, *32*, 1184.
[76] M. Rodriguez, M. Amblard, M. C. Galas, M. F. Lignon, A. Aumelas, J. Martinez, *Int. J. Pept. Protein Res.* **1990**, *35*, 441.
[77] M. Sato, Y. H. Lee, H. Nakanishi, M. E. Johnson, R. A. Chrusciel, M. Kahn, *Biochem. Biophys. Res. Commun.* **1992**, *187*, 999.

[78] M. Feigel, *Liebigs Ann. Chem.* **1989**, 459.
[79] M. Feigel, G. Lugert, C. Heichert, *Liebigs Ann. Chem.* **1987**, 367.
[80] V. Brandmeier, M. Feigel, *Tetrahedron* **1989**, *45*, 1365.
[81] P. C. Belanger, C. Dufresne, J. Scheigetz, R. N. Young, J. P. Springer, G. I. Dimitrienko, *Can. J. Chem.* **1982**, *60*, 1019.
[82] R. M. Freidinger, *J. Org. Chem.* **1985**, *50*, 3631.
[83] J. D. Aebi, D. Guillaume, B. E. Dunlap, D. H. Rich, *J. Med. Chem.* **1988**, *31*, 1805.
[84] D. S. Kemp, E. T. Sun, *Tetrahedron Lett.* **1982**, *23*, 3759.
[85] U. Nagai, K. Sato, *Tetrahedron Lett.* **1985**, *26*, 647.
[86] J. L. Krstenansky, R. L. Baranowski, B. L. Currie, *Biochem. Biophys. Res. Commun.* **1982**, *109*, 1368.
[87] M. Hinds, N. G. J. Richards, J. A. Robinson, *J. Chem. Soc. Chem. Commun.* **1988**, 1447.
[88] M. Kahn, B. Chen, *Tetrahedron Lett.* **1987**, *28*, 1623.
[89] H. Nakanishi, R. A. Chrusciel, R. Shen, S. Bertenshaw, M. E. Johnson, T. J. Rydel, A. Tulinsky, M. Kahn, *Proc. Natl. Acad. Sci. USA* **1992**, *89*, 1705.
[90] D. S. Kemp, W. E. Stites, *Tetrahedron Lett.* **1988**, *29*, 5057.
[91] H. U. Saragovi, D. Fitzpatrick, A. Raktabutr, H. Nakanishi, M. Kahn, M. I. Greene, *Science* **1991**, *253*, 792.
[92] W. V. Williams, T. Kieber-Emmons, J. VonFeldt, M. I. Greene, D. B. Weiner, *J. Biol. Chem.* **1991**, *266*, 5182.
[93] See [41a].
[94] a) P. Ward, G. B. Ewan, C. C. Jordan, S. J. Ireland, R. M. Hagan, J. R. Brown, *J. Med. Chem.* **1990**, *33*, 1848. b) For studies on the recognition of a spirolactam by antibodies and for an α-alkylproline as turn mimetic: M. G. Hinds, J. H. Welsh, D. M. Brennand, J. Fisher, M. J. Glennie, N. G. J. Richards, D. L. Turner, J. A. Robinson, *ibid.* **1991**, *34*, 1777.
[95] C. B. Pert, S. H. Snyder, *Science* **1973**, *179*, 1011.
[96] J. Hughes, T. W. Smith, H. W. Kosterlitz, L. A. Fothergill, B. A. Morgan, H. R. Morris, *Nature* **1975**, *258*, 577.
[97] S. Nakanishi, A. Inoue, T. Kita, M. Nakamura, A. C. J. Chang, S. N. Cohen, S. Numa, *Nature* **1979**, *278*, 423.
[98] S. Tachibama, K. Araki, S. Ohya, S. Yoshida, *Nature* **1982**, *295*, 339.
[99] D. R. Lynch, S. H. Snyder, *Annu. Rev. Biochem.* **1986**, *55*, 773.
[100] a) G. Zurawski, M. Benedik, B. J. Kamb, J. S. Abrams, S. M. Zurawski, F. D. Lee, *Science* **1986**, *232*, 772; b) E. M. Smith, A. C. Morrill, W. J. Meyer III, J. E. Blalock, *Nature* **1986**, *321*, 881.
[101] C. J. Weitz, L. I. Lowney, K. F. Faull, G. Feistner, A. Goldstein, *Proc. Natl. Acad. Sci. USA* **1987**, *83*, 9784.
[102] M. Mavroyannis, *CR Soc. Biol.* **1903**, *55*, 1092.
[103] C. J. Weitz, K. F. Faull, A. Goldstein, *Nature* **1987**, *330*, 674.
[104] E. J. Simon, J. M. Hiller in *Basic Neurochemistry* (Eds.: G. J. Siegel, B. W. Agranoff, R. W. Albers, P. B. Molinoff), Elsevier, Amsterdam, **1989**, p. 271.
[105] a) R. Maneckjee, J. D. Minna, *Proc. Natl. Acad. Sci. USA* **1992**, *89*, 1169; b) *ibid.* **1990**, *87*, 3294; c) I. S. Zagon, P. J. McLaughlin, *Science* **1983**, *221*, 671.
[106] a) M. Wollemann, *J. Neurochem.* **1990**, *54*, 1095; b) A. R. Ginzler, H. Xu, *Proc. Natl. Acad. Sci. USA* **1991**, *88*, 4741; c) B. L. Kiefer, K. Befort, C. Gaveriaux, C. G. Hirth, *ibid.* **1992**, *89*, 12048.
[107] P. S. Portoghese, *J. Med. Chem.* **1991**, *34*, 1757; see also ref. [99].
[108] R. Schwyzer, *Ann. NY Acad. Sci.* **1977**, *297*, 3.
[109] a) P. S. Portoghese, M. S. Sultana, A. E. Takemori, *J. Med. Chem.* **1990**, *33*, 1714; b) P. S. Portoghese, *ibid.* **1991**, *34*, 1757; c) *ibid.* **1992**, *35*, 1927.
[110] a) P. S. Portoghese, D. L. Larson, L. M. Sayre, D. S. Fries, A. E. Takemori, *J. Med. Chem.* **1980**, *23*, 233; b) J. Szmuszkovicz, P. F. Von Voigtlander, *ibid.* **1982**, *25*, 1125.
[111] P. S. Portoghese, A. W. Lipkowski, A. E. Takemori, *J. Med. Chem.* **1987**, *30*, 238.
[112] S. M. Evans, G. R. Lenz, R. A. Lessor, *Annu. Rep. Med. Chem.* **1990**, *25*, 11, and references therein.
[113] D. M. Zimmerman, J. D. Leander, *J. Med. Chem.* **1990**, *33*, 895.
[114] J. W. Lewis in *Medicinal Chemistry – The Role of Organic Chemistry in Drug Research* (Eds.: S. M. Roberts, B. J. Price), Academic Press, London, **1985**, p. 119.
[115] C. Stein, A. H. S. Hassan, R. Przewlocki, C. Gramsch, K. Peter, A. Herz, *Proc. Natl. Acad. Sci. USA* **1990**, *87*, 5935.
[116] C. Stein, K. Comisel, E. Haimeri, A. Yassouridis, K. Lehrberger, A. Herz, K. Peter, *N. Engl. J. Med.* **1990**, *325*, 1123.
[117] A. I. Basbaum, J. D. Levine, *N. Engl. J. Med.* **1990**, *325*, 1168.
[118] D. Römer, H. H. Büscher, R. C. Hill, R. Maurer, T. J. Petcher, H. Zeugner, W. Benson, E. Finner, W. Milkowski, P. W. Thies, *Nature* **1982**, *298*, 759.
[119] a) M. E. Logan, R. Goswami, B. E. Tomczuk, B. R. Venepalli, *Annu. Rep. Med. Chem.* **1991**, *26*, 43; b) J. E. Maggio, *Annu. Rev. Neurosci.* **1988**, *11*, 13.
[120] U. S. von Euler, J. H. Gaddum, *J. Physiol.* **1931**, *72*, 74.
[121] M. M. Chang, S. E. Leeman, H. D. Niall, *Nature* **1971**, *232*, 86.
[122] G. W. Tregear, H. D. Niall, J. T. Potts, S. E. Leeman, M. M. Chang, *Nature* **1971**, *232*, 87.
[123] a) Y. Masu, K. Nakayama, H. Tamaki, Y. Harada, M. Kuno, S. Nakanishi, *Nature* **1987**, *329*, 836; b) Y. Yokota, Y. Sasay, K. Tanaka, T. Fujiwara, K. Tsuchida, R. Shigemoto, A. Kahizuka, H. Ohkubo, S. Nakanishi, *J. Biol. Chem.* **1989**, *264*, 17649; c) R. Shigemoto, Y. Yokota, K. Tsuchida, S. Nakanish, *ibid.* **1990**, *265*, 623; d) A. D. Hershey, J. E. Krause, *Science* **1990**, *247*, 958; e) A. Graham, B. Hopkins, S. J. Powell, P. Danks, I. Briggs, *Biochem. Biophys. Res. Commun.* **1991**, *177*, 8; f) Y. Takeda, K. B. Chou, J. Takeda, B. S. Sachais, J. E. Krause, *ibid.* **1991**, *179*, 1232; g) B. Hopkins, S. J. Powell, P. Danks, I. Briggs, A. Graham, *ibid.* **1991**, *180*, 1110.
[124] Y. Yokota, C. Akazawa, H. Ohkubo, S. Nakanishi, *EMBO J.* **1992**, *11*, 3586.
[125] M. Lotz, J. H. Vaughan, D. A. Carson, *Science* **1988**, *241*, 1218.
[126] M. Freidin, J. A. Kessler, *Proc. Natl. Acad. Sci. USA* **1991**, *88*, 3200.
[127] a) M. Lotz, D. A. Carson, J. H. Vaughan, *Science* **1987**, *235*, 893; b) E. D. Harris, Jr., *N. Engl. J. Med.* **1990**, *322*, 1277.
[128] C. R. Mantyh, T. S. Gates, R. P. Zimmerman, M. L. Welton, E. P. Passaro, Jr., S. R. Vigna, J. E. Maggio, L. Kruger, P. W. Mantyh, *Proc. Natl. Acad. Sci. USA* **1988**, *85*, 3235.
[129] a) N. W. Kowall, M. F. Beal, J. Busciglio, L. K. Duffy, B. A. Yankner, *Proc. Natl. Acad. Sci. USA* **1991**, *88*, 7247; b) M. Robertson, *Nature* **1992**, *356*, 103.
[130] a) R. M. Snider, J. W. Constantine, J. A. Lowe III, K. P. Longo, W. S. Lebel, H. A. Woody, S. E. Drozda, M. C. Desai, F. J. Vinick, R. W. Spencer, H.-J. Hess, *Science* **1991**, *251*, 435; b) S. McLean, A. H. Ganong, T. F. Seeger, D. K. Bryce, K. G. Pratt, L. S. Reynolds, C. J. Siok, J. A. Lowe III, J. Heym, *ibid.* **1991**, *251*, 437.
[131] a) C. Garret, A. Carruette, V. Fardin, S. Moussaoui, J.-F. Peyronel, J.-C. Blanchard, P. M. Laduron, *Proc. Natl. Acad. Sci. USA* **1991**, *88*, 10208; b) J.-F. Peyronel, A. Truchon, C. Mountonnier, C. Garret, *Bioorg. Med. Chem. Lett.* **1992**, *2*, 37.
[132] B. R. Venepalli, L. D. Aimone, K. C. Appel, M. R. Bell, J. A. Dority, R. Goswami, P. L. Hall, V. Kumar, K. B. Lawrence, M. E. Logan, P. M. Scensny, J. A. Seelye, B. E. Tomczuk, J. M. Yanni, *J. Med. Chem.* **1992**, *35*, 374.
[133] K. C. Appell, B. E. Babb, R. Goswami, P. L. Hall, K. B. Lawrence, M. E. Logan, R. Przyklek-Elling, B. E. Tomczuk, B. R. Venepalli, J. M. Yanni, *J. Med. Chem.* **1991**, *34*, 1751.
[134] C. T. Dourish, M. L. Clark, D. Hawley, B. J. Williams, S. D. Iversen, *Regul. Pept.* **1988**, *22*, 58.
[135] A. T. McKnight, J. J. Maguire, B. J. Williams, A. C. Forster, R. Tridgett, L. L. Iversen, *Regul. Pept.* **1988**, *22*, 127.
[136] A. B. McElroy, S. P. Clegg, M. J. Deal, G. B. Ewan, R. M. Hagan, S. J. Ireland, C. C. Jordan, B. Porter, B. C. Ross, P. Ward, A. R. Whittinton, *J. Med. Chem.* **1992**, *35*, 2582.
[137] C. Advenier, N. Rouissi, Q. T. Nguyen, X. Emonds-Alt, J.-C. Breliere, G. Neliat, E. Naline, D. Regoli, *Biochem. Biophys. Res. Commun.* **1992**, *184*, 1418.
[138] G. Drapeau, N. Rouissi, F. Nantel, N.-E. Rhaleb, C. Tousignant, R. D. Reguli, *Regul. Pept.* **1990**, *31*, 125.
[139] S. Rens-Domiano, T. Reisine, *J. Neurochem.* **1992**, *58*, 1987.
[140] S. Reichlin, *N. Engl. J. Med.* **1983**, *309*, 1495.
[141] S. Reichlin, *N. Engl. J. Med.* **1983**, *309*, 1556.
[142] F.-W. Kluxen, C. Bruns, H. Lübert, *Proc. Natl. Acad. Sci. USA* **1992**, *89*, 4618.
[143] See [15].
[144] D. Veber, R. Saperstein, R. Nutt, R. Freidinger, S. Brady, P. Curley, D. Perlow, W. Palveda, C. Colton, A. Zacchei, D. Tocco, D. Hoff, R. Vandlen, J. Gerich, L. Hall, L. Mandarino, E. Cordes, P. Anderson, R. Hirschmann, *Life Sci.* **1984**, *34*, 1371.
[145] W. Bauer, U. Briner, W. Doepfner, R. Haller, R. Huguenin, P. Marbach, T. J. Petcher, J. Pless, *Life Sci.* **1982**, *31*, 1133.
[146] S. W. J. Lamberts, P. Uitterlinden, L. Verschoor, K. J. van Dongen, E. del Pozo, *N. Engl. J. Med.* **1985**, *313*, 1576.
[147] L. K. Kvols, C. G. Moertel, M. J. O'Connell, A. J. Schutt, J. Rubin, R. G. Hahn, *N. Engl. J. Med.* **1986**, *315*, 702.
[148] H. C. Soudah, W. L. Hasler, C. Owyang, *N. Engl. J. Med.* **1991**, *325*, 1508.
[149] S. W. J. Lamberts, W. H. Bakker, J.-C. Reubi, E. P. Krenning, *N. Engl. J. Med.* **1990**, *323*, 1246.
[150] D. F. Veber, R. M. Freidinger, D. S. Perlow, W. J. Paleveda, Jr., F. W. Holly, R. G. Strachan, R. F. Nutt, B. H. Arrison, C. Homnick, W. C. Randall, M. S. Glitzer, R. Saperstein, R. Hirschmann, *Nature* **1981**, *292*, 55.
[151] R. Chamdrasekaren, A. V. Lakshminarayanau, U. V. Pandya, G. N. Ramachandran, *Biochim. Biophys. Acta* **1973**, *303*, 14.
[152] a) K. C. Nicolaou, J. M. Salvino, K. Raynor, S. Pietranico, T. Reisine, R. M. Freidinger, R. Hirschmann, *Pept. Chem. Struct. Biol. Proc. Am. Pept. Symp. 11th* **1990**, 881; b) R. Hirschmann, K. C. Nicolaou, S. Pietranico, J. Salvino, E. M. Leahy, P. A. Sprengler, G. Furst, A. B. Smith III, C. D. Strader, M. A. Cascieri, M. R: Candelore, C. Donaldson, W. Vale, L. Maechler, *J. Am. Chem. Soc.* **1992**, *114*, 9217.
[153] C. Papageorgiou, R. Haltiner, C. Bruns, T. J. Petcher, *Bioorg. Med. Chem. Lett.* **1992**, *2*, 135.

[154] Y. Tache, M. Brown, *Trends Neurosci.* **1982**, *5*, 431; E. Spindel, *ibid.* **1986**, *9*, 130.
[155] J. F. Battley, J. M. Way, M. H. Corjay, H. Shapira, K. Kusano, R. Hapkins, J. M. Wu, T. Slattery, E. Mann, R. I. Feldman, *Proc. Natl. Acad. Sci. USA* **1991**, *88*, 395.
[156] a) I. Zachary, J. Gil, W. Lehmann, J. Sinnet-Smith, E. Rozengurt, *Proc. Natl. Acad. Sci. USA* **1991**, *88*, 4577; b) I. Zachary, J. Sinnet-Smith, E. Rozengurt, *J. Biol. Chem.* **1992**, *267*, 19031; c) Review: I. Zachary, E. Rozengurt, *Cell* **1992**, *71*, 891.
[157] F. Cuttita, D. N. Carney, J. Milshine, T. W. Moody, J. Fedorko, A. Fischler, J. D. Minna, *Nature* **1985**, *316*, 823.
[158] E. R. Larson, P. H. Fischer, *Annu. Rep. Med. Chem.* **1989**, *24*, 121.
[159] a) D. H. Coy, P. Heinz-Erian, N.-Y. Jiang, Y. Sasaki, J. Taylor, J.-P. Moreau, W. T. Wolfrey, J. D. Gardner, R. T. Jensen, *J. Biol. Chem.* **1988**, *263*, 5056; b) M. A. Shipp, G. E. Tarr, C.-Y. Chen, S. N. Switzer, L. B. Hersh, H. Stein, M. E. Sunday, E. L. Reinhez, *Proc. Natl. Acad. Sci. USA* **1991**, *88*, 10662.
[160] J. A. Malikayil, L. V. Edwards, L. R. McLean, *Biochemistry* **1992**, *31*, 7043.
[161] J. J. Valentine, S. Nakanishi, D. L. Hageman, R. M. Schneider, R. W. Spencer, F. J. Vinick, *Bioorg. Med. Chem. Lett.* **1992**, *2*, 333.
[162] A. M. Nadzan, J. F. Kerwin, Jr., *Annu. Rep. Med. Chem.* **1991**, *26*, 191.
[163] H. F. Bradford, *Chemical Neurobiology* Freeman, New York, **1986**, p. 265.
[164] P. L. Faris, B. R. Komisaruk, L. R. Watkins, D. J. Mayer, *Science* **1983**, *219*, 310.
[165] S. A. Wank, R. Harkins, R. T. Jensen, H. Shapira, A. De Weerth, T. Slattery, *Proc. Natl. Acad. Sci. USA* **1992**, *89*, 3125.
[166] G. S. Baldwin, R. Chandler, D. B. Scanlon, J. Weinstock, *J. Biol. Chem.* **1986**, *261*, 12252.
[167] a) S. Muallem, G. Sachs, *Biochim. Biophys. Acta* **1984**, *805*, 181; b) C. S. Chew, M. R. Brown, *ibid.* **1986**, *888*, 116; c) S. Roche, J. P. Bali, R. Magous, *ibid.* **1990**, *1055*, 287.
[168] A. S. Kopin, Y.-M. Lee, E. W. McBride, L. J. Miller, M. Lu, H. Y. Lin, J. F. Kolakowski, Jr., M. Beinborn, *Proc. Natl. Acad. Sci. USA* **1992**, *89*, 3605.
[169] I. Marseigne, P. Roy, A. Dor, C. Durieux, D. Pelaprat, M. Reibaud, J. C. Blanchard, B. P. Roques, *J. Med. Chem.* **1989**, *32*, 445.
[170] J. W. Tilley, W. Danho, K. Lovey, R. Wagner, J. Swistok, R. Makofske, J. Michalewsky, J. Triscan, D. Nelson, S. Weatherford, *J. Med. Chem.* **1991**, *34*, 1125.
[171] C. W. Lin, M. W. Holladay, D. G. Witte, T. R. Miller, C. A. W. Wolfram, B. R. Bianchi, M. J. Bennett, A. M. Nadzan, *Am. J. Physiol.* **1990**, *258*, G648.
[172] K. Shiosaki, C. W. Lin, H. Kopecka, R. Craig, F. L. Wagenaar, B. Bianchi, T. Miller, D. Witte, A. M. Nadzan in *Peptides 1990* (Eds.: E. Giralt, D. Andreu), Escom, Leiden, **1991**, p. 710.
[173] J. Y. L. Chung, M. D. Tufano, P. D. May, K. Shiosaki, A. M. Nadzan, D. S. Garvey, Y. K. Shue, M. Brodie, M. W. Holladay, *Eur. Pat. Appl.* **1991**, *405*, 506.
[174] a) *Peptides, Chemistry and Biology* (Ed.: J. Rivier), Escom, Leiden, **1990**; b) K. Shiosaki, R. Craig, C. W. Lin, R. W. Barrett, T. Miller, D. Witte, C. A. W. Wolfram, A. Nadzan in [174a], p. 978.
[175] R. M. Freidinger, W. L. Whitter, N. P. Gould, M. K. Holloway, R. S. L. Chang, V. J. Lotti, *J. Med. Chem.* **1990**, *33*, 591.
[176] J. R. Kerwin, Jr., F. Wagenaar, H. Kopecka, C. W. Lin, T. Miller, D. Witte, A. M. Nadzan in [174a], p. 149.
[177] R. S. L. Chang, V. J. Lotti, R. L. Monaghan, J. Birnbaum, E. O. Stapley, M. A. Goetz, G. Albers-Schonberg, A. A. Pachett, J. M. Liesch, O. D. Hensens, J. P. Springer, *Science* **1985**, *230*, 177.
[178] B. E. Evans, M. G. Bock, K. E. Rittle, R. M. Dipardo, W. L. Whitter, D. F. Veber, P. S. Anderson, R. M. Freidinger, *Proc. Natl. Acad. Sci. USA* **1986**, *83*, 4918.
[179] M. G. Bock, R. M. Dipardo, B. E. Evans, K. E. Rittle, W. L. Whitter, D. F. Veber, P. S. Anderson, R. M. Freidinger, *J. Med. Chem.* **1989**, *32*, 13.
[180] a) [116]; b) M. G. Bock, R. M. DiPardo, B. E. Evans, K. E. Rittle, W. L. Whitter, D. F. Veber, R. M. Freidinger, R. S. L. Chang, T. B. Chen, V. J. Lotti, *J. Med. Chem.* **1990**, *33*, 450.
[181] D. C. Horwell, A. Beeby, C. R. Clarc, J. Hughes, *J. Med. Chem.* **1987**, *30*, 729.
[182] M. R. Pincus, R. P. Carty, J. Chen, J. Lubowsky, M. Avitable, D. Shah, H. A. Scheraga, R. B. Murphy, *Proc. Natl. Acad. Sci. USA* **1987**, *84*, 4821.
[183] D. C. Horwell, J. Hughes, J. C. Hunter, M. C. Pritchard, R. S. Richardson, E. Roberts, G. N. Woodruff, *J. Med. Chem.* **1991**, *34*, 404.
[184] J. Hughes, P. Boden, B. Costall, A. Domeney, E. Kelly, D. C. Horwell, J. C. Hunter, R. D. Pinnock, G. N. Woodruff, *Proc. Natl. Acad. Sci. USA* **1990**, *87*, 6728.
[185] C. T. Dourish, W. Rycroft, S. D. Iversen, *Science* **1989**, *245*, 1509.
[186] Z. Wiesenfeld-Hallin, X.-J. Xu, J. Hughes, D. C. Horwell, T. Höckelt, *Proc. Natl. Acad. Sci. USA* **1990**, *87* 7105.
[187] E. P. Wiertelak, S. F. Maier, L. R. Watkins, *Science* **1992**, *256*, 830.
[188] P. M. Conn, W. F. Crowley, Jr., *N. Engl. J. Med.* **1991**, *324*, 93.
[189] A. Tse, B. Hille, *Science* **1992**, *255*, 462.
[190] L. Kiesel, A. F. Przylipiak, A. J. R. Habenicht, M. S. Przylipiak, B. Runnenbaum, *Proc. Natl. Acad. Sci. USA* **1991**, *88*, 8801.
[191] J. J. Nestor, Jr., B. H. Vickery, *Annu. Rep. Med. Chem.* **1988**, *23*, 211.
[192] For the synthesis and biological properties of azapeptides: J. Gante, *Synthesis* **1989**, 405.
[193] F. A. Momany, *J. Am. Chem. Soc.* **1976**, *98*, 2990.
[194] R. M. Freidinger, D. F. Veber, D. S. Perlow, J. R. Brooks, R. Saperstein, *Science* **1980**, *210*, 656.
[195] J.-M. Kuhn, T. Billebaud, H. Navratil, A. Moulognuet, J. Fiet, P. Grise, J.-F. Jouis, P. Costa, J.-M. Husson, R. Dahan, C. Bertagna, R. Edelstein, *N. Engl. J. Med.* **1989**, *321*, 413.
[196] E. D. Crawford, M. A. Eisenberger, D. G. McLeod, J. T. Spaulding, R. Benson, F. A. Dorr, B. A. Blumenstein, M. A. Davies, P. J. Goodman, *N. Engl. J. Med.* **1989**, *321*, 419.
[197] M. R. Henzl, S. L. Corson, K. Moghissi, V. C. Buttram, C. Berquist, J. Jacobson, *N. Engl. J. Med.* **1988**, *318*, 485.
[198] R. L. Barbieri, *N. Engl. J. Med.* **1988**, *318*, 512.
[199] a) A. Ljungqvist, D.-M. Feng, P.-F. L. Tang, M. Kubota, T. Okamoto, Y. Zhang, C. Y. Bowers, W. A. Hook, K. Folkers, *Biochem. Biophys. Res. Commun.* **1987**, *148*, 849; b) improvements on this basis: A. Ljungqvist, D.-M. Reng, C. Bowers, W. A. Hook, K. Folkers, *Tetrahedron* **1990**, *46*, 3297.
[200] S. Bhasin, S. Sikka, T. Fielder, U. Sod-Moriah, H. B. Levine, T. S. Swerdloff, J. Rajfer, *J. Endocrinol.* **1986**, *118*, 1229.
[201] D. Biswanath, J. J. Plattner, E. N. Bush, H.-S. Jae, G. Diaz, E. S. Johnson, T. J. Perun, *J. Med. Chem.* **1989**, *32*, 2038.
[202] W. J. Greenlee, P. K. S. Siegl, *Annu. Rep. Med. Chem.* **1991**, *26*, 63.
[203] A. T. Chiu, W. F. Herblin, D. E. McCall, R. J. Ardecky, D. J. Carini, J. V. Duncia, L. J. Pease, P. C. Wong, R. R. Wexler, A. L. Johnson, P. B. M. W. M. Timmermans, *Biochem. Biophys. Res. Commun.* **1989**, *165*, 196.
[204] K. Sandberg, H. Ji, A. J. L. Clark, H. Shapira, K. J. Catt, *J. Biol. Chem.* **1992**, *267*, 9455.
[205] K. Sasaki, Y. Yamano, S. Bardhan, N. Iwai, J. J. Murray, M. Hasegawa, Y. Matsuda, T. Inagami, *Nature* **1991**, *351*, 230.
[206] T. J. Murphy, R. W. Alexander, K. K. Griendling, M. S. Runge, K. E. Bernstein, *Nature* **1991**, *351*, 233.
[207] D. J. Bergsma, C. Ellis, C. Kumar, P. Nuthulaganti, H. Kersten, N. Eishourbagy, E. Griffin, J. M. Stadel, N. Alyar, *Biochem. Biophys. Res. Commun.* **1992**, *183*, 989.
[208] P. Feuillan, M. A. Millan, G. Aguilera, *FASEB J.* **1991**, *5*, A872.
[209] M. Viswanathan, K. Tsutsumi, F. M. A. Correa, J. M. Saavedra, *Biochme. Biophys. Res. Commun.* **1991**, *179*, 1361.
[210] M. A. Millan, D. M. Jacobowitz, G. Aguilera, K. J. Catt, *Proc. Natl. Acad. Sci. USA* **1991**, *88*, 11440.
[211] M. Holk, R. Bossé, W. Fischli, H. Gerold, E. Escher, *Biochem. Biophys. Res. Commun.* **1989**, *160*, 1350.
[212] K. L. Spear, M. S. Brown, E. J. Reinhard, E. G. McMahon, G. M. Olins, M. A. Palomo, D. R. Patton, *J. Med. Chem.* **1990**, *33*, 1935.
[213] R. C. Speth, K. H. Kim, *Biochem. Biophys. Res. Commun.* **1990**, *169*, 997.
[214] S. Whitebread, M. Mele, B. Kamber, M. de Gasparo, *Biochem. Biophys. Res. Commun.* **1989**, *163*, 284.
[215] D. J. Carini, J. V. Duncia, P. E. Aldrich, A. T. Chiu, A. L. Johnson, M. E. Pierce, W. A. Price, J. B. Santella III, G. J. Wells, R. R. Wexler, P. C. Wong, S. Yoo, P. B. M. W. M. Timmermans, *J. Med. Chem.* **1991**, *34*, 2525.
[216] Y. Furukawa, S. Kishimoto, K. Nishikawa, US-A 4340598, **1982**.
[217] J. Weinstock, R. M. Keenan, J. Samanen, J. Hempel, J. A. Finkelstein, R. G. Franz, D. E. Gaitanopoulos, G. R. Girard, J. G. Gleason, D. T. Hill, T. M. Morgan, C. E. Peishoff, N. Aiyar, D. P. Brooks, T. A. Fredrickson, E. H. Ohlstein, R. R. Ruffolo, Jr., E. J. Stack, A. C. Sulpizio, E. F. Weidley, R. M. Edwards, *J. Med. Chem.* **1991**, *34*, 1514.
[218] B. De, M. Winn, T. M. Zydowsky, D. J. Kerkman, J. F. DeBernardis, J. Lee, S. Buckner, R. Warner, M. Brune, A. Hancock, T. Opgenorth, K. Marsh, *J. Med. Chem.* **1992**, *35*, 3714.
[219] C. J. Blankley, J. C. Hodges, S. R. Klutchko, R. J. Himmelsbach, A. Chucholowski, C. J. Conolly, S. J. Neergaard, M. S. Van Nieuwenhze, A. Sebastian, J. Quin III, A. D. Essenburg, D. M. Cohen, *J. Med. Chem.* **1991**, *34*, 3248.
[220] R. K. Sharma, J. R. Smith, G. J. Moore, *Biochem. Biophys. Res. Commun.* **1991**, *179*, 85.
[221] A. M. Doherty, *Annu. Rep. Med. Chem.* **1991**, *26*, 83.
[222] M. Yanagisawa, H. Kurihara, S. Kumura, Y. Tomobe, M. Kobayashi, Y. Mitsui, Y. Yazaki, K. Goto, T. Masaki, *Nature* **1988**, *332*, 411.
[223] a) A. Inoue, M. Yanagisawa, S. Kimura, Y. Kasuya, T. Miyauchi, K. Goto, T. Masaki, *Proc. Natl. Acad. Sci. USA* **1989**, *86*, 2863; b) H. Matsumoto, N. Suzuki, H. Onda, M. Fujino, *Biochem. Biophys. Res. Commun.* **1989**, *164*, 74.
[224] Review: J. R. Vane, E. E. Änggård, R. M. Botting, *N. Engl. J. Med.* **1990**, *323*, 27.
[225] L. Z. Krsmanovic, S. S. Stjlkovic, T. Balla, S. Al-Damluji, R. I. Weiner, K. J. Catt, *Proc. Natl. Acad. Sci. USA* **1991**, *88*, 11124.

[226] E. G. McMahon, M. A. Palomo, W. M. Moore, J. F. McDonald, M. K. Stern, *Proc. Natl. Acad. Sci. USA* **1991**, *88*, 703.
[227] a) H. Arai, S. Hori, I. Aramori, H. Ohkubo, S. Nahanishi, *Nature* **1990**, *348*, 730; b) T. Sakurai, M. Yanagisawa, Y. Takuwa, H. Miyazaki, S. Kimura, K. Goto, T. Masaki, *Nature* **1990**, *348*, 732.
[228] S. S. Stojilkovic, F. Merelli, T. Iida, L. Z. Krsmanovic, K. J. Catt, *Science* **1990**, *248*, 1663.
[229] T. Saeki, M. Ihara, T. Fukuroda, M. Yamagawa, M. Yano, *Biochem. Biophys. Res. Commun.* **1991**, *179*, 286.
[230] M. J. Spinella, A. B. Malik, J. Everitt, T. T. Andersen, *Proc. Natl. Acad. Sci. USA* **1991**, *88*, 7743.
[231] a) D. B. Morrison, M. L. Swanson, L. J. Swanson, L. J. Sweet, J. E. Pessin, *J. Biol. Chem.* **1988**, *263*, 8706; b) P. A. Wilden, J. L. Treadway, B. D. Morrison, J. E. Pessin, *Biochemistry* **1989**, *28*, 9734.
[232] M. Ihara, T. Fukuroda, T. Saeki, M. Nishikibe, K. Kojiri, H. Suda, M. Yano, *Biochem. Biophys. Res. Commun.* **1991**, *178*, 132.
[233] K. Ishikawa, T. Fukami, T. Nagase, K. Fujita, T. Hayama, K. Niijyama, T. Mase. M. Ihara, M. Yano, *J. Med. Chem.* **1992**, *35*, 2139.
[234] C. R. Hiley, D. J. Cowley, J. T. Pelton, A. C. Hargreaves, *Biochem. Biophys. Res. Commun.* **1992**, *184*, 504.
[235] Y. Urade, Y. Fujitani, K. Oda, T. Watakabe, I. Umemura, M. Takai, T. Okada, K. Sakata, H. Karaki, *FEBS Lett.* **1982**, *311*, 12.
[236] N. Oochata, M. Nishikawa, S. Kiyoto, S. Takase, K. Hemmi, H. Murai, M. Okuhara, *Eur. Pat. Appl.*, EP-A 405421.
[237] R. Takayanagi, K. Kitazumi, C. Tadasaki, K. Ohnaka, S. Aimoto, K. Tasaka, M. Ohashi, H. Nawata, *FEBS Lett.* **1991**, *282*, 103.
[238] Y. Kondo, K. Torii, S. Omura, Z. Ito, *Biochem. Biophys. Res. Commun.* **1988**, *150*, 877.
[239] J. Janssens, T. J. Peters, G. Vantrappen, J. Tack, J. L. Urban, M. De Roo, E. Muls. R. Bouillon, *N. Engl. J. Med.* **1990**, *322*, 1028.
[240] A. Virsolvy-Vergine, H. Leray, S. Kuroki, B. Lupo, M. Dufour, D. Bataille, *Proc. Natl. Acad. Sci. USA* **1992**, *89*, 6629.
[241] D. H. Hinzen, L. Pieri, *Nachr. Chem. Tech. Lab.* **1992**, *40*, 811.
[242] a) H. Alho, E. Costa, P. Ferrero, M. Fujimoto, D. Cosenza-Murphy, A. Guidotti, *Science* **1985**, *229*, 179; b) H. Marquardt, G. J. Todaro, M. Shoyad, *J. Biol. Chem.* **1986**, *261*, 9727.
[243] J. L. Collins, P. J. Collins, S. W. Goldstein, W. S. Faraci, *Bioorg. Med. Chem. Lett.* **1992**, *2*, 915.
[244] Y. Yamamura, H. Ogawa, T. Chihara, K. Kondo, T. Onogawa, S. Nakamura, T. Mori, M. Tominaga, Y. Yabuuchi, *Science* **1991**, *252*, 572.
[245] H. J. Motulsky, M. C. Michel, International Society of Hypertension, Montreal, Abstract P5.15, 1990, cited in A. M. Doherty, *Annu. Rep. Med. Chem.* **1991**, *26*, 88.
[246] L. Alig, A. Edenhofer, M. Müller, A. Trzeciak, T. Weller, US-A 5039805.
[247] M. Kahn, B. Devens, *Tetrahedron Lett.* **1986**, *27*, 4841. The observation that the tripeptide Lys-Pro-Arg antagonizes the effects of tuftsins led to the synthesis of **144**.
[248] B. E. Evans, J. L. Leighton, K. E. Rittle, K. F. Gilbert, G. F. Lundell, N. P. Gould, D. W. Hobbs, R. M. DiPardo, D. F. Veber, D. J. Pettibone, B. V. Clineschmidt, P. S. Anderson, R. M. Freidinger, *J. Med. Chem.* **1992**, *35*, 3919.
[249] R. Hirschmann, P. A. Sprengler, T. Kawasaki, J. W. Leahy, W. C. Shakespeare, A. B. Smith III, *J. Am. Chem. Soc.* **1992**, *114*, 9699.
[250] M. Aumailley, M. Gurrath, G. Müller, J. Calvete, R. Timpl, H. Kessler, *FEBS Lett.* **1991**, *291*, 50.
[251] G. Müller, M. Gurrath, H. Kessler, R. Timpl, *Angew. Chem.* **1992**, *104*, 341; *Angew. Chem. Int. Ed. Engl.* **1992**, *31*, 326.
[252] a) [4]; b) [13].
[253] A. D. Strosberg, *Eur. J. Biochem.* **1991**, *196*, 1.
[254] G. R. Marshall, *Curr. Opin. Struct. Biol.* **1992**, *2*, 904.
[255] R. W. Hoffmann, *Angew. Chem.* **1992**, *104*, 1147; *Angew. Chem. Int. Ed. Engl.* **1992**, *31*, 1124.
[256] a) R. Pauwels, K. Andries, J. Desmyter, D. Schols, M. Kukla, H. Breslin, A. Raeymaeckers, J. Van Gelder, R. Woestenborghs, J. Heykants, K. Schellekens, M. A. C. Janssen, E. De Clercq, P. Janssen, *Nature* **1990**, *343*, 470; b) V. J. Merluzzi, K. D. Hargrave, M. Labadia, K. Grozinger, M. Skoog, J. C. Wu, C.-K. Shih, K. Eckner, S. Hattox, J. Adams, A. S. Rosenthal, R. Faanes, R. J. Eckner, R. A. Koup, J. L. Sullivan, *Science* **1990**, *250*, 1411; c) G. V. De Luca, M. J. Otto, *Bioorg. Med. Chem. Lett.* **1992**, *2*, 1639.
[257] Benzodiazepines such as *N*-desmethyldiazepam were surprisingly found in the brains of people who had not been treated with benzodiazepines. Moreover, *N*-desmethyldiazepam could be detected in material obtained from human autopsies over 52 years ago, long before the first benzodiazepine was synthesized. The biosynthetic route has still not been clarified. a) L. Sangameswaran, H. M. Fales, P. Friedrich, A. L. De Blas, *Proc. Natl. Acad. Sci. USA* **1986**, *83*, 9236; b) J. D. Rothstein, W. Garland, G. Puia, A. Guidotti, R. Weber, E. Costa, *J. Neurochem.* **1992**, *58*, 2102; c) Review: F. A. Stephenson, *Trends Neurosci.* **1987**, *10*, 185.
[258] L. L. Iversen, *Sci. Am.* **1979**, *241*, 134.
[259] T. M. Jessel, D. D. Kelly in *Principles of Neural Science* (Eds.: E. R. Kandel, J. H. Schwarz, T. M. Jessel), Elsevier, New York, **1991**, p. 385.
[260] Note added in proof: We would like to point out *Tetrahedron* **1993**, *43*, No. 17 (Peptide Secondary Structure Mimetics) and *Bioorg. Med. Chem. Lett.* **1993**, *3*, No. 5 (Approaches to Non-peptide Ligands for Peptide Receptor Sites).

Ultramicroelectrodes in Electrochemistry

By Jürgen Heinze*

Dedicated to Professor Herbert Zimmermann on the occasion of his 65th birthday

In the 1950s and 1960s fundamental developments in electrochemical methods included voltammetry and low signal techniques. A generation later, the discovery of the unusual properties of ultramicroelectrodes has opened new possibilities of analyzing electrode processes. The changes in mass transport conditions bring about extremely high current densities at ultramicroelectrodes, whereas the currents themselves become very small. This little-noticed phenomenon allows for many electroanalytical applications that are not possible with conventional electrodes, especially experiments in solutions with very low electrolyte concentrations, in nonpolar solvents, in solids, and even in gases. In addition, two factors—changes in the experimental time scale at low scan rates because of the size of the electrode, and insignificant *iR* effects at very high scan rates—make it possible to study very fast homogeneous and heterogeneous electrode processes.

1. Introduction

Electrodes are systems of coupled electrically conducting phases, which are usually in electrochemical equilibrium. An exchange of charges takes place across the interfaces between the phases. The reaction at the phase interface is known as an electrode reaction, and the exchange of charged particles across the phase interface is a charge transfer reaction. As a rule, one phase conducts electrons and at least one phase ions (metal or semiconductor electrode). In principle, an electrode can also consist of two ion-conducting phases.

In textbooks, some such definition will introduce the electrode as the crucial instrument of electrochemistry. Accordingly, almost all our knowledge in this field concerns electrodes directly or indirectly. In basic research, electrode kinetics[1] and electrochemical thermodynamics provide comprehensive theories that are continually being extended to explain the properties of electrodes and the processes at or through them. Hence, it comes as a surprise to learn that in the past electrochemists paid little attention to the influence that size and geometry of the electrode surface have on electrochemical processes, apart from the direct proportionality between size and the measured signal.[2]

The development of polarography[3] made the relatively small spherical Hg drop electrode widely known as early as 1922. Initially, however, no one appears to have obtained theoretical or experimental findings that indicated a direct relationship between the size of the drop and its electrochemical properties. In 1937 MacGillavry and Rideal[4] set up a current–time equation for the stationary, spherical electrode for the first time, which predicted that the course of the diffusion-controlled current over time depended on the size of the radius. Two years later, Laitinen and Kolthoff were unable to verify this relationship experimentally.[5a] In 1941 the same authors reported the results of voltammetric experiments using thin wire electrodes.[5b] They interpreted the stationary currents they observed as a consequence of natural convection, and did not relate them to surface size or geometry of the electrode. Only in the mid 1960s, when current–time measurements at small stationary disk electrodes excluded the influence of convection, was it accepted that the results did not agree with the theory of planar diffusion. These phenomena were interpreted as edge effects due to surface size, for the most part the result of quasi-spherical diffusion processes.[6] At about this time, almost twenty-five years after it had been theoretically predicted, experiments confirmed for the first time that the current response in chronoamperometric experiments with spherical electrodes becomes time-independent and stationary. The time lapse before the stationary value is attained depends on the electrode radius.[7] Although the subject attracted some interest in the following years,[8–7] only at the end of the 1970s did Fleischmann and co-workers at the University of Southampton[18] establish beyond question that diminishing electrode surface size has not only quantitative effects, but also—and always—unusual qualitative effects.[19, 20] For instance, chronoamperometric measurements at electrodes with μm dimensions (≤ 20 μm) showed that, in contradiction of Cottrell's theory,[21] even with planar electrodes a time-independent stationary state is reached very rapidly. Other conspicuous phenomena included high current densities in spite of small measuring currents, the possibility of measuring transients at considerably shorter time scales as well as a drastic decrease in the ohmic drop caused by the resistance of the solution. In 1981 Wightman provided a first comprehensive survey of the special properties and perspectives of microvoltammetric electrodes.[22]

These discoveries have encouraged numerous research groups to study the properties and applications of ultramicroelectrodes in theory and practice.

The concept of ultramicroelectrodes (UME) is now a widely accepted term in the literature. However, unlike in the field of electrophysiology, in electrochemistry it is not necessary for all dimensions of probes to be extremely small. In principle, only one, the characteristic dimension that is given by the geometry of the electrode, must be very small. For instance, a very narrow, but long band electrode makes a suitable ultramicroelectrode.

In their enthusiasm, electrochemists should not forget that microelectrodes with diameters of 25 μm have long been

[*] Prof. Dr. J. Heinze
Institut für Physikalische Chemie der Universität
Albertstrasse 21, D-79104 Freiburg (FRG)
Telefax: Int. code + (761)203-2815

used in medical and biological research.[23] They were initially developed to determine the oxygen content of living tissue and tissue liquids.[24, 25] Accordingly, the electrodes had to be as small as possible. The users either did not notice the unconventional properties of these electrodes, or did not think anything of it.

Electrochemists are interested in ultramicroelectrodes mainly because their application in accordance with the general principles of practice used in voltammetry and chronoamperometry opens totally new possibilities for studying electrode reactions. The results of dynamic measurements in solvents with low electrolyte concentrations or in poorly conducting media,[26] or in the solid state,[27] or even in the gas phase[28] have been particularly spectacular. This will ensure that in future electrochemical data will be obtained under similar experimental conditions as, for example, in spectroscopy.

Moreover, using microelectrodes expands the time scale for measurements by several orders of magnitude, which makes it much easier to study rapid homogeneous or heterogeneous reactions with microelectrodes than with, for example, rotating electrodes. Over and above this, the combination of exceptionally high current densities and low measuring currents promises new applications in the fields of analysis, sensors, and scanning electrochemical microscopy.[29] At the same time, the small dimensions of the electrodes guarantee that the experiment will not alter or destroy the object measured, a very important aspect in, for instance, biophysical examinations.

A growing number of communications, progress reports,[30] and books[31] indicates that the above-mentioned set of examples is by no means complete. As ultramicroelectrodes become commercially available, this technique will soon find new friends outside specialized electrochemical laboratories. It is hoped that this survey will encourage this development.

2. Electrochemistry at Ultramicroelectrodes

2.1. Mass Transport

In principle, experiments using ultramicroelectrodes are similar to those using conventional electrodes. A stationary electrode immersed in an unstirred electrolytic solution is given either a constant potential or one that changes linearly over time. Provided there is an electroactive substance, that is, one that can undergo oxidation or reduction, in the electrolytic solution, a heterogeneous charge transfer will occur at the metal/liquid interface, during which, in the case of reduction, for example, electrons will be transferred from the electrode to the electroactive substance.[1, 32] At the same time, the concentrations at the electrode surface start to change, which sets off diffusive mass transport to and from the electrode.

Depending on the size of the electrode and the volume of electrolytic solution used, one can distinguish between three limiting cases of diffusion. The simplest case is an electrode in a thin-layer cell with a very low ratio of cell volume to electrode surface. Under these conditions, mass transport within the cell is negligible, and no diffusion gradient develops.[33] By reducing the ratio between the electrode surface and the electrolyte volume, one approximates the normal situation of a voltammetric experiment with semi-infinite planar diffusion.[34] With the transition to extremely small electrode surfaces, the conditions change yet again, and the diffusion process becomes dependent on the size and geometry of the electrode[2, 30, 31] (Fig. 1).

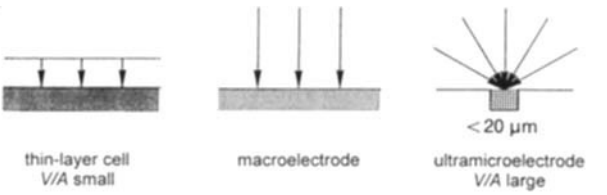

Fig. 1. Limiting cases of diffusive mass transport in electrochemical cells. Left: Thin-layer cell; the available transport paths are short, and no diffusion gradient develops. The ratio between electrolyte volume (V) and electrode area (A) is very low. Center: Macroelectrode (for example, disk with diameter ≥ 0.01 m); mass transport perpendicular to electrode is in form of a semi-infinite planar diffusion. In mathematical terms, the process corresponds to mass transport in a one-dimensional diffusion field [Eq. (1)]. Right: Ultramicroelectrode; the diffusion process depends on the shape of the electrode. A spatial diffusion field develops (hemispheric in the case of a disk electrode) [Eqs. (2–6)]. The V/A ratio is extremely high.

As one might expect, the voltammetric current–voltage curves of these three cases differ markedly. In the case of a thin electroactive layer, the cathodic and anodic waves appear as perfect mirror images. Normal electrodes produce the characteristic cyclic voltammograms,[34] and extremely

Jürgen Heinze was born in Dresden in 1939. He studied chemistry in Cologne and Munich from 1960 to 1966. After obtaining his Diploma, he completed a PhD under Herbert Zimmermann in Freiburg in 1971 on the synthesis and physical properties of azole systems. In 1980 he habilitated in Physical Chemistry with studies on microelectrodes and was appointed professor in 1987. Since 1991 he has been a member of the newly founded Freiburger Materialforschungszentrum. He is chairman of the Baden-Württemberg priority research program, "Electroactive Materials for Sensor Technology". His main research subjects are mechanistic investigations of electron-transfer-induced processes and their coupled chemical reactions, and the development of new and improved methods of electrode kinetics (cyclic voltammetry), in particular, those involving microelectrodes. Further interests include electroactive materials, such as conductive polymers, and the development of electrochemical sensors.

small electrodes (ultramicroelectrodes) yield steady-state current–voltage curves, which resemble the classic polarograms as well as the current–voltage curves of rotating electrodes (Fig. 2).

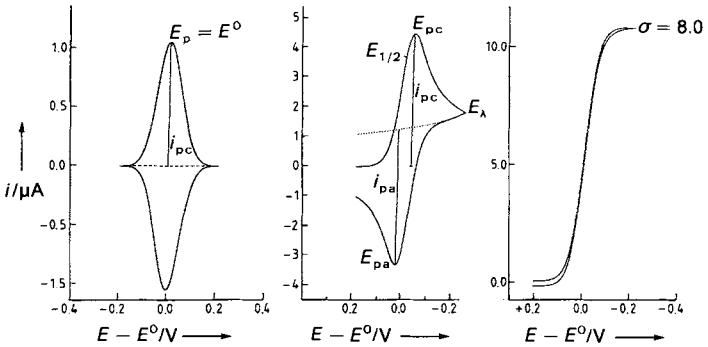

Fig. 2. Voltammetric current–voltage curves. Left: for the thin-layer cell; center: for semi-infinite planar diffusion ($\sigma = 0$) to a macroelectrode; right: for semi-infinite hemispheric diffusion to a microdisk electrode ($\sigma = 8.0$). E_λ = switching potential, $E_{\frac{1}{2}}$ = half-wave potential, E_p = peak potential, E_{pa} = anodic peak potential, E_{pc} = cathodic peak potential, i_{pa} = anodic peak current, i_{pc} = cathodic peak current. The V/A ratio increases from left to right.

The phenomena at ultramicroelectrodes are caused by time-dependent changes in mass transport, in which one-dimensional diffusion fields transform into spatial fields. In the case of planar electrodes, besides the usual axial diffusion, an additional, radial diffusive component becomes effective parallel to the electrode surface. In the case of curved electrode surfaces, spherical or cylindrical diffusion fields form over time at rates that depend on electrode size.

In mathematical terms, the diffusion is described by Fick's Laws, which vary for spatial fields [Eqs. (1–5)] according to the electrode geometry.[35]

$$\frac{\partial c}{\partial t} = D\frac{\partial^2 c}{\partial x^2} \quad \text{(planar diffusion)} \tag{1}$$

$$\frac{\partial c}{\partial t} = D\left(\frac{\partial^2 c}{\partial r^2} + \frac{1}{r}\frac{\partial c}{\partial r}\right) \quad \text{(cylindrical electrode)} \tag{2}$$

$$\frac{\partial c}{\partial t} = D\left(\frac{\partial^2 c}{\partial r^2} + \frac{2}{r}\frac{\partial c}{\partial r}\right) \quad \text{(spherical electrode)} \tag{3}$$

$$\frac{\partial c}{\partial t} = D\left(\frac{\partial^2 c}{\partial r^2} + \frac{1}{r}\frac{\partial c}{\partial r} + \frac{\partial^2 c}{\partial z^2}\right) \quad \text{(disk)} \tag{4}$$

$$\frac{\partial c}{\partial t} = D\left(\frac{\partial^2 c}{\partial x^2} + \frac{\partial^2 c}{\partial z^2}\right) \quad \text{(band)} \tag{5}$$

The introduction of further boundary conditions determines whether the diffusion will be finite (thin-layer cell) or semi-infinite and whether the electrode reaction will proceed galvanostatically (constant current), potentiostatically (constant potential), or potentiodynamically (variable potential). When ultramicroelectrodes are used, measurements are generally potentiostatic (chronoamperometry) or potentiodynamic (cyclic voltammetry).

The planar disk is the most popular electrode in experiments (Fig. 3). It is constructed relatively easily by encasing a metal wire or a carbon fiber in glass or embedding it in

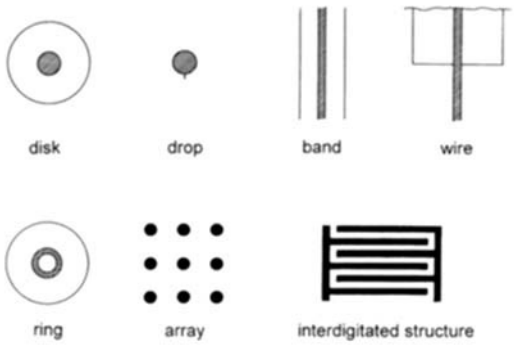

Fig. 3. Typical configurations of ultramicroelectrodes.

plastic; the flat surface of the end of the insulated wire serves as the active electrode surface.[6, 36–38] Recently, greater use has been made of band[39–42] and ring electrodes,[43, 44] whose surface areas can be enlarged by altering the length of the band or the circumference of the ring without losing the specific properties of ultramicroelectrodes. The same objective can be achieved with electrode arrays,[45–47] that is, several electrodes arranged, for example, in the form of an interdigitated structure. However, with arrays the diffusion conditions change depending on the arrangement of the electrodes. This means that, during very long experiments, the diffusion field eventually returns to a planar form.[48, 49] From a theoretical point of view, spherical (Hg drop)[49] and cylindrical (wire) electrodes[17, 41, 51] are particularly interesting, as they allow for one-dimensional solutions to the diffusion problem.[2, 4, 35]

2.2. Chronoamperometry

Notwithstanding different diffusion equations, when the surface area is reduced, qualitatively similar changes take place in the current response of all electrodes, irrespective of shape. This is because at electrodes generally the particle flux per surface unit increases as the distance from the electrode surface decreases. A study of chronoamperometric experiments reveals the details of this phenomenon.

In the simplest case of a chronoamperometric (potential step) experiment, a working electrode is given a potential sufficient to completely reduce or oxidize at the electrode surface a dissolved electroactive substance of concentration c^*. The corresponding initial and boundary conditions are compiled in Equations (6)–(8).

$$c(x,0) = c^* \qquad (t = 0) \tag{6}$$

$$\lim_{x \to \infty} c(x,t) = c^* \quad (t > 0) \tag{7}$$

$$c(0,t) = 0 \tag{8}$$

Experiment and theory show that under these conditions a diffusion-controlled, faradaic current i flows over the electrode. Its value (in A, proportional to j, the flux in $\mathrm{mol\,s^{-1}\,m^{-2}}$) is directly proportional to the concentration gradient at the electrode surface [Eq. (9), where F is the faradaic constant, D the diffusion coefficient, and A the area

$$\frac{i}{nFA} = j(0,t) = -D\left[\frac{\partial c}{\partial x}\right]_{x=0} \quad (9)$$

of the electrode]. This gradient causes the formation of a diffusion layer in front of the electrode, which gradually spreads into the solution (Fig. 4, top). For a purely planar

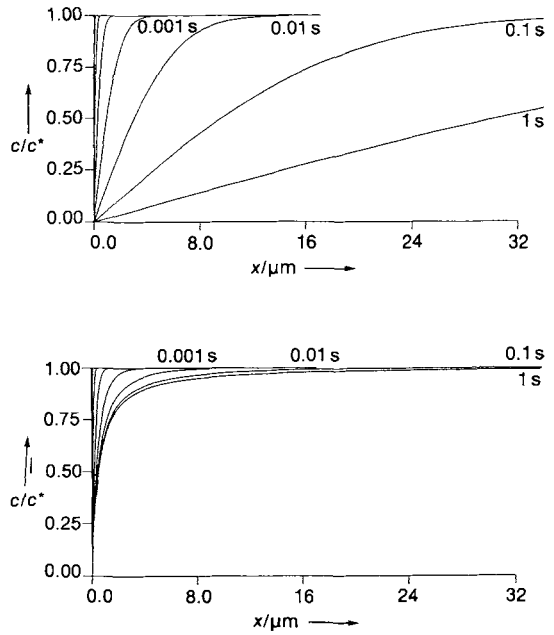

Fig. 4. Concentration profiles of diffusion layers (diffusion coefficient $D = 1 \times 10^{-9}\ m^2 s^{-1}$) in a chronoamperometric experiment for different times t after application of a potential step (concentration of the electroactive species at electrode surface is zero). Top: semi-infinite planar diffusion; bottom: spherical diffusion for a spherical microelectrode with $r_0 = 0.5$ μm. c/c^* = normed concentration, x = distance from electrode.

diffusion, the time-dependent current obeys the Cottrell equation [Eq. (10)],[21] which predicts that the current in

$$\frac{it^{1/2}}{nFAD^{1/2}c^*} = \frac{1}{\pi^{1/2}} \quad (10)$$

the chronoamperometric experiment is inversely proportional to $t^{\frac{1}{2}}$.

The conditions for planar diffusion are properly fulfilled only if the electrode surface is very large. In the case of a disk electrode, edge effects become increasingly noticeable as surface area decreases: in addition to the mass transport perpendicular to the electrode, mass transport also develops parallel to the electrode. The size of the edge effects depends on duration of the measurement and electrode radius. Figure 5 shows computed concentration profiles at disk electrodes with different radii recorded after 1 s of measuring.

From this it is clear that as the electrode radius decreases, semi-infinite planar diffusion gradually transforms into semi-infinite hemispherical diffusion. Longer experiment duration produces the same phenomenon. Due to the time-dependent change in the diffusion profile, the solid angle occupied by the diffusion layer in front of the electrode increases, and hence, grows considerably relative to the electrode surface. As a consequence, many more electroactive particles per unit time and area reach the electrode than in

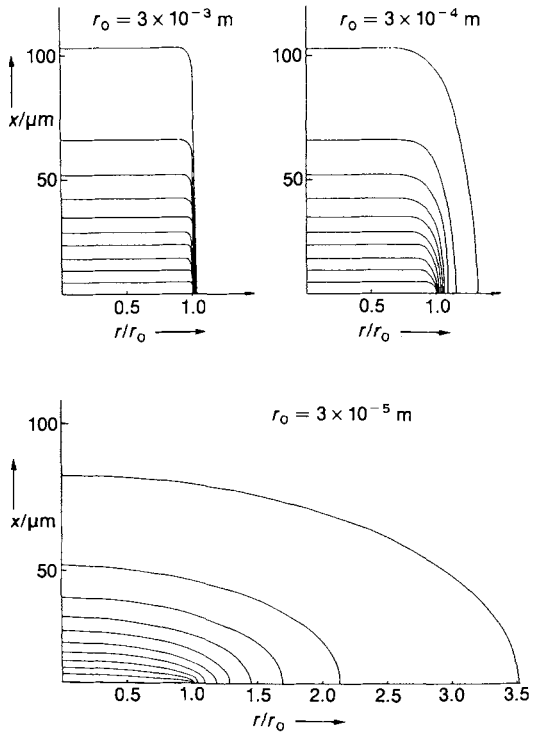

Fig. 5. Normalized calculated concentration profiles c/c^* calculated for disk electrodes with different radii ($r_0 = 3 \times 10^{-3}$, 3×10^{-4}, 3×10^{-5} m; $D = 1 \times 10^{-9}\ m^2 s^{-1}$) 1 s after start of a chronoamperometric experiment; concentration of the electroactive species at the electrode is zero because of a high potential pulse. Concentration curves are separated by 0.1 of a concentration unit. x = distance perpendicular to the electrode.

the case of pure planar diffusion. On the other hand, the growing volume within the prescribed solid angle means that the particle flux in and out of the volume eventually becomes stationary (Fig. 4b) and the diffusion layer stops growing. The mass transport rate in the stationary case is given by the mass transport coefficient m (in $m s^{-1}$). Its value in a (hemi)spherical field is indirectly proportional to the electrode radius r_0 [Eq. (11)]. Consequently, for extremely small electrodes the diffusion rate can be extraordinarily high.

$$m = Dr_0^{-1} \quad (11)$$

Hence, the calculation of the current–time curve produces a modified Cottrell equation [Eq. (12)]. For the disk elec-

$$\frac{it^{1/2}}{nFAD^{1/2}c^*} = \frac{1}{\pi^{1/2}}\left(1 + b\left(\frac{Dt}{r_0^2}\right)^{1/2}\right) \quad (12)$$

trode,[6, 13, 52] $\pi^{\frac{1}{2}} \leq b \leq 4\pi^{-\frac{1}{2}}$. The value of the prefactor b changes in the transition from the planar to the hemispherical diffusion field. Approximate formulas for this intermediate case may be found in the literature.[53, 54] By analogy, Equation (13) is valid for the spherical electrode.[2, 4] As long

$$\frac{it^{1/2}}{nFAD^{1/2}c^*} = \frac{1}{\pi^{1/2}}\left(1 + \pi^{1/2}\left(\frac{Dt}{r_0^2}\right)^{1/2}\right) \quad (13)$$

as planar diffusion dominates and the measuring time is short, the second term on the right-hand side of Equations (12) and (13) can be neglected, which results in the

limiting case of Equation (10). By contrast, if the measuring time is very long, the first term on the right-hand side becomes negligible, and the result is a stationary current. The smaller the electrode surface, the shorter the time lapse before the stationary state is established. The parameter (14)

$$\eta = \left(\frac{Dt}{r_0^2}\right)^{1/2} \tag{14}$$

characterizes the extent of the nonplanar diffusion. For values of η greater than 6, the current becomes stationary; for smaller values, one approximates the limiting case of planar diffusion. Oldham's comprehensive theoretical studies[55-57] have shown that one can set up an identity for the stationary limiting currents i_{Gr} (in A) for the spherical, hemispherical, and disk electrodes by introducing a surface diameter d [Eq. (15)]. For the sphere, $d = 2\pi r_0$, for the hemi-

$$i_{Gr} = 2nFc^*Dd \tag{15}$$

sphere $d = \pi r_0$, and for the disk electrode $d = 2r_0$. The attainable stationary limiting currents for the different electrode forms are listed in Table 1.[41,56-59] In contrast to

Table 1. Limiting currents for ultramicroelectrodes.

Sphere
$i_{Gr} = 4\pi r_0 nFDc^*$

Hemisphere
$i_{Gr} = 2\pi r_0 nFDc^*$

Disk:
$i_{Gr} = 4r_0 nFDc^*$
is identical with the sphere when $= (\pi/2)r_0$ (hemisphere)

Cylinder (approximate)
$i = 2nFADc^* \dfrac{1}{\ln[4(Dt)/r_0^2]}$
where A = cylinder surface area ($2\pi r_0 l$) or
hemicylinder surface area ($\pi r_0 l$), l = length of the cylinder

Band electrode (approximate)
$i = 2\pi nFDc^* l \dfrac{1}{\ln[4(Dt)/r_0^2]}$
l = length of the band

Ring
$\dfrac{\lim_{t\to\infty} i(t)}{nFDc^*} = \dfrac{\pi^2(a+b)}{\ln[16(b+a)/(b-a)]}$
where $a - b \ll a$ and
b = inner radius of the ring, a = outer radius of the ring

macroelectrodes, with microelectrodes current and electrode surface are not proportional for diffusion-controlled processes; instead current is proportional to the characteristic electrode diameter or radius. Thus, with microelectrodes under diffusion control, the current density is larger the smaller their diameter, whereas with macroelectrodes it is usually independent of surface area.

The time lapse before a stationary state is reached depends both on the size of the electrode and on the diffusion coefficient of the electroactive system. Calculations of Oldham et al.[57] show that for an average diffusion coefficient of $10^{-9}\,m^2s^{-1}$, a 10 μm disk electrode takes approximately 1.3 s and a 1 μm electrode 0.01 s to reach a stationary state, with a deviation $\varepsilon = 5\%$. (According to Equation (12), stationary states can, in theory, also form at macroelectrodes. This would take about 360 h in the case of a 1 cm disk electrode, so that in any event convection influences would dominate.) As it is obvious that several parameters determine the specific properties of such electrodes—the influence exerted by iR will be discussed in Section 2.5—it is very difficult to define an "ultramicroelectrode" in terms of a precise limit for its characteristic dimension. It has become practice to use the term UME for disk electrodes with a diameter smaller than or equal to 20 μm. The term nanode is used for electrodes with a diameter of less than 1 μm.

As expected, the influence of electrode shape is greatest for spherical diffusion fields. The comparison with planar diffusion (Fig. 6) shows that already after 1 s, despite a small

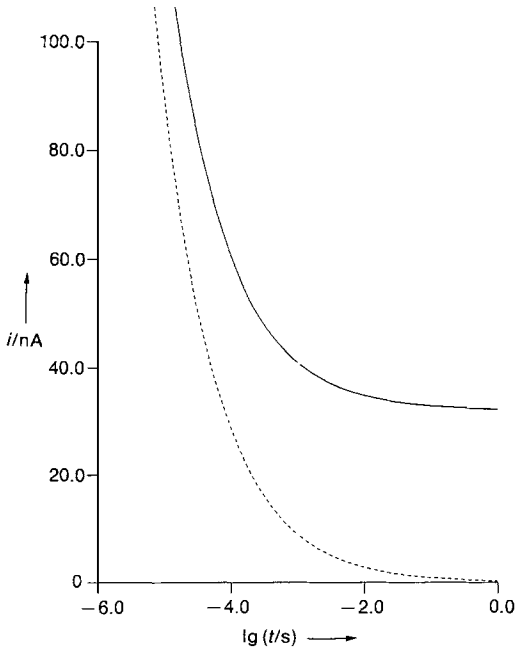

Fig. 6. Simulated current–time curve in chronoamperometry (Cottrell experiment) ($D = 1 \times 10^{-9}\,m^2s^{-1}$, $c^* = 5.4 \times 10^{-2}$ M, $c(0,t) = 0$) for planar (——) and spherical (- - - -) diffusion ($r_0 = 0.5$ μm).

absolute current, the current density at a spherical microelectrode with a diameter of 1 μm is nearly 100 times greater than that at a normal electrode [Eq. (16)].

$$\frac{i_{spher}}{i_{plan}} = 1 + \left(\pi \frac{Dt}{r_0^2}\right)^{1/2} \tag{16}$$

The calculations for cylindrical, band, and ring electrodes prove that these attain only a quasi-stationary state, as the equations for their currents contain time-dependent terms. On the other hand, the current response can be considerably increased by altering band length or ring circumference without changing the diffusion field. This opens interesting perspectives for analytical applications.

2.3. Voltammetry

Whereas in chronoamperometry the potential at the electrode is constant after a single step from the initial to the

final value, in voltammetry the potential changes linearly over time. Starting from an initial potential E_i, a linear potential sweep (potential ramp) is applied to the electrode. After reaching a switching potential E_λ, the sweep is reversed and the potential returns linearly to its initial value,[32, 34] which explains the term *cyclic* voltammetry. The experimental time scale is determined by the potential scan rate (also known as the sweep rate) $v = \Delta E/\Delta t$. This popular electrochemical method was presented in a previous issue of *Angewandte Chemie*.[34]

Ultramicroelectrodes in cyclic voltammetry produce, in principle, the same phenomena as in chronoamperometry. The transition to the stationary state is achieved by reducing the scan rate—and the smaller the characteristic radius of the electrode, the faster the transition. Initially the cyclic voltammograms at "high" v values are wave-shaped; as v declines they become sigmoid polarograms (Fig. 7). As such, they are

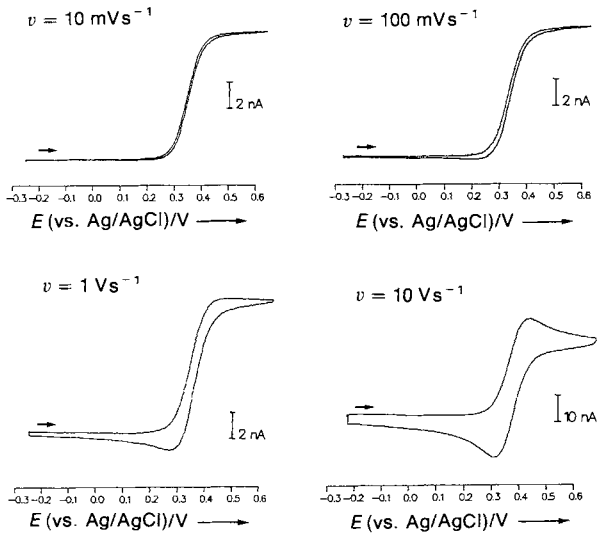

Fig. 7. Experimental cyclic voltammograms of the oxidation of ferrocene ($c = 3.2$ nM) in CH_2Cl_2/0.1 M [TBA]PF_6 (TBA = tetra-*n*-butylammonium) at different scan rates. Measurements taken with a Pt microdisk electrode ($r_0 = 6$ μm).

comparable with the steady-state voltammograms at rotating disk electrodes. This resemblance is due to the formation of stationary (Nernst) diffusion layers, which in the case of rotating electrodes are caused by rapid convectional mass transport, and in the case of microelectrodes are a result of the particular shape of the diffusion field and the high diffusive mass transport rate.

In the stationary state, the currents are time-independent, and the scan rate no longer affects the shape and size of the voltammetric wave. The conditions for the formation of a steady-state differ according to the geometry of the electrodes used. Whereas the diffusion-limited current or the current density corresponds to the values obtained for the stationary state in chronoamperometry (Table 1), theoretical modeling of the entire current–voltage curve has to be done numerically.[60, 61] The only exception is the case of the simple reversible redox process during spherical diffusion to a spherical electrode. For this, Reinmuth[62] has developed a correction formula that can be used to calculate the dimensionless current function $\pi^{\frac{1}{2}}\chi^s(at)$ (which corresponds to a normalized current—s stands for spherical) from the known current function $\pi^{\frac{1}{2}}\chi^p(at)$ (p stands for planar) for planar diffusion [Eq. (17), where σ is the sphericity (17b) and Φ the spherical correction factor (17c)]. The factor a is the normal-

$$\pi^{1/2}\chi^s(at) = \pi^{1/2}\chi^p(at) + \sigma\Phi(at) \tag{17a}$$

$$\sigma = \sqrt{\frac{D}{ar_0^2}} \tag{17b}$$

$$\Phi = \frac{1 - e^{-at}}{1 + e^{\eta - \eta^0}} \tag{17c}$$

ized scan rate in cyclic voltammetry (defined as $a = vnF(RT)^{-1}$) and $\eta^{(0)} = E^{(0)}nF(RT)^{-1}$ is a normalized potential. The sphericity σ characterizes the extent of the spherical diffusion. For $\sigma = 0$, the limiting case of normal planar diffusion ($r \to \infty$) characterized by the typical transient voltammogram is observed, whereas from $\sigma > 1$ the stationary state ensues (Fig. 8). The transition to the stationary

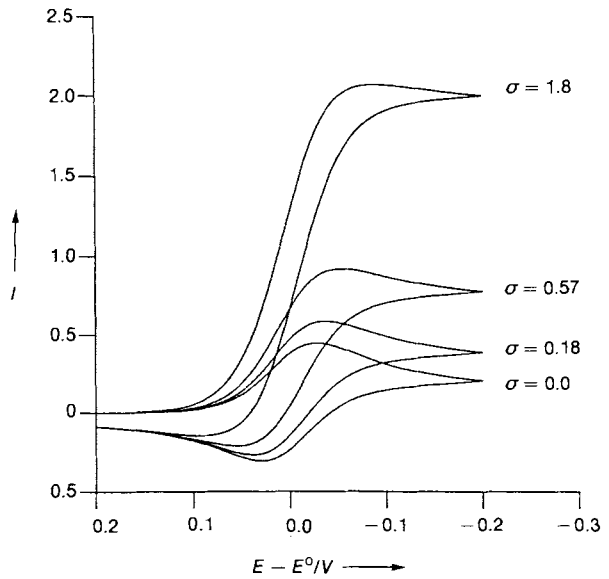

Fig. 8. Simulated cyclic voltammetric diagrams for spherical electrodes with different sphericities. The ordinate gives the current function $\pi^{\frac{1}{2}}\chi(at)$ (= normalized current i) [8].

state takes place at somewhat higher σ values for other electrode geometries.

Larger σ values, usually a consequence of smaller electrode radii, imply higher transport coefficients m (Eq. 11) and therefore higher current densities. A comparison with rotating electrodes (RDE) reveals that the transport coefficient of a spherical electrode with a diameter of 10 μm corresponds to a speed of 10000 rpm. Whereas this is the maximum speed for rotating electrodes, the dimensions of ultramicroelectrodes can be considerably smaller.

One property that distinguishes ultramicroelectrodes from stationary electrodes of conventional size is the increase in the transport rate of the electroactive particles as the electrode radius decreases. The high transport rates mean that with very small electrodes this process can take place as fast or even faster than heterogeneous charge transfer; that is,

instead of being diffusion-controlled, the process becomes kinetically controlled. Unlike the diffusion-controlled case, which is in thermodynamic (Nernst) equilibrium at the electrode, the corresponding stationary current–voltage curves shift and change their shapes depending on the rate of electron transfer (Fig. 9). Thus, ultramicroelectrodes are very

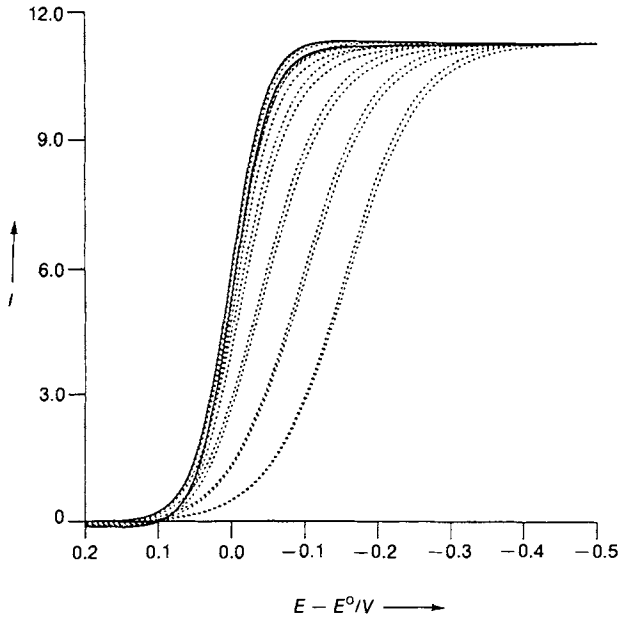

Fig. 9. Steady-state cyclic voltammograms with an ultramicrodisk electrode ($\sigma = 11.1$, ($D = 1 \times 10^{-10} m^2 s^{-1}$, $r = 0.5$ μm, (hemi)spherical diffusion field). k_s^0: (——) > 1, (----) 0.011, 0.0035, 0.0011, 0.00035, 0.00011, 0.000035, 0.000011 ms^{-1}. For $k_s^0 > 1\ ms^{-1}$ and a mass transport coefficient of $m = 0.002\ ms^{-1}$, the electrode process is diffusion-controlled (Nernst case). For $k_s^0 \leq 0.002\ ms^{-1}$, the reaction is kinetically controlled, and the steady-state voltammograms shift with simultaneous minor changes in shape along the potential axis. With the help of theory [63], k_s^0 can be determined from the curves' potential shift.

elegant instruments for determining kinetic parameters of rapid electron transfer reactions. As theoretical considerations show,[63] rapid transfer processes with heterogeneous rate constants of the order of $10^{-2}\ ms^{-1}$ can be analyzed by disk electrodes with a diameter of between 5 μm and 0.05 μm. For slower processes, electrodes with significantly larger diameters are adequate. By applying a suitable set of ultramicroelectrodes of different sizes to obtain steady-state voltammograms, one can determine the kinetic parameters of the heterogeneous charge transfer (the transfer coefficient α and the transfer rate k_s^0) as well as the thermodynamic standard redox potential.[63, 64]

There is also another reason why ultramicroelectrodes can accurately determine standard redox potentials. As a result of the high transport rates, the homogeneous chemical processes associated with the heterogeneous charge transfer in the experimental time scale—the latter expressed by the σ value [Eq. (17b)] or the mass transport coefficient m [Eq. (11)]—take place only partially or not at all (Fig. 10). Because the diffusion rates rise with decreasing electrode radius while the rates of homogeneous chemical processes do not change, the effect of diffusion rates on the shape and position of the voltammetric current–voltage curves decreases continuously. Provided that the heterogeneous

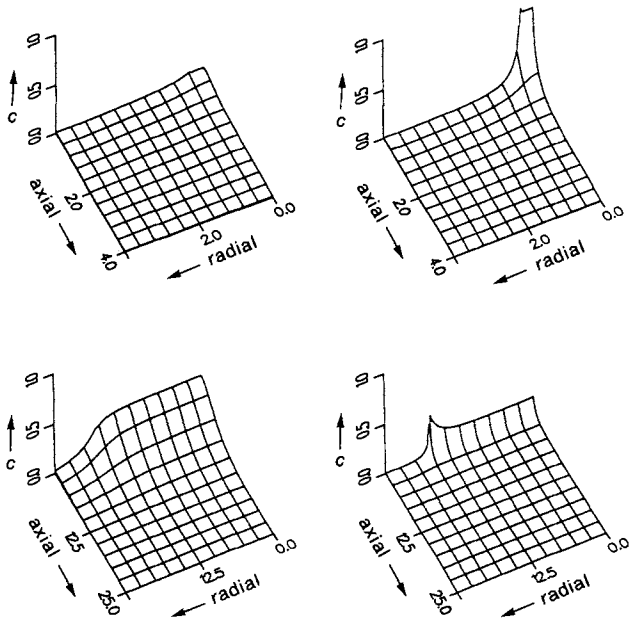

Fig. 10. Two-dimensional concentration profiles for an electron transfer reaction ($R \rightarrow R^-$), to which an irreversible dimerization is coupled ($2R^- \rightarrow R_2^{2-}$, EC_{2irr}, $k_f c/a = 20.0$). Top: microdisk electrode, $\sigma = 5.0$, for the dimer (left) and the anion (right); bottom: macrodisk electrode, $\sigma = 0.1$, for the dimer (left) and the anion (right). The formation of the dimer close to the macroelectrode is very clear; in the case of the microelectrode, the concentration profile of the first anion formed predominates.

charge transfer is very fast, appropriately small electrodes enable the direct determination of the formal redox potential of an electrode reaction by measurement of the half-wave potential $E_{\frac{1}{2}}$.[64] As shall be seen in Section 3.1.1, the relationship between diffusion rate, on one hand, and the reaction rate of the associated chemical reactions, on the other, can be applied to quantitative analysis of the kinetics of such chemical processes.

2.4. The Influence of the Capacitive Current

As with all dynamic electrochemical experiments, chronoamperometry and cyclic voltammetry have to take account of the faradaic current as well as the capacitive current i_c that flows along the electrode when the electrical double layer is charged. The simplest way of simulating the capacitive current is by applying an electrical equivalent circuit, with a resistance that corresponds to the resistance of the solution R_u and a capacitance in series that corresponds to the double layer capacitance C_d. For a single potential step ΔE, i_c (in A) is given by Equation (18), which shows that

$$i_c = \frac{\Delta E}{R_u} \exp\left(-\frac{t}{R_u C_d}\right) \tag{18}$$

the capacitive charging current falls exponentially over time. The smaller the corresponding time constant for charging the double layer (contained in the term RC), the faster the process. According to the expression (19), the drop-off time

$$R_u C_d \sim r_0 \tag{19}$$

for the charging current for ultramicroelectrodes becomes extremely short; they, therefore, hold great potential for measurements in very small time domains.

Because of continual potential sweep, the capacitive current in cyclic voltammetry has two components, one transient, the other steady-state [Eq. (20)]. As the latter predominates at medium and low scan rates, as a rule (20) simplifies to (21).

$$i_c = \left[\left(\frac{E_a}{R_u} - vC_d\right)\exp\left(-\frac{t}{R_uC_d}\right)\right] + vC_d \tag{20}$$

$$i_c = vC_d \tag{21}$$

The capacitive current component i_c disturbs studies on electrochemically induced electron transfer reactions (the faradaic processes), because voltammetric measurements always give the sum of both currents. The capacitive current increases linearly with the scan rate v, whereas the faradaic current i_f changes at $v^{\frac{1}{2}}$. Moreover, when the concentrations of the active redox system are low ($< 10^{-5}$ M), i_f and i_c cannot be adequately separated. Although there is some capacitive effect when ultramicroelectrodes are used in the stationary state, the current ratio i_f/i_c improves drastically as the faradaic component of the current density increases with r_0^{-1}, whereas the capacitive component is independent of the radius. The relationship (22) holds either exactly or approximately for most geometric shapes.

$$\frac{i_F}{i_c} \approx \frac{1}{r_0C_dv} \tag{22}$$

The smaller the characteristic dimension of the electrode and the lower the scan rate, the better the current ratio i_f/i_c in the stationary state of a voltammetric measurement.

2.5. The Ohmic *iR* Drop

As a consequence of the ohmic resistance in an electrolyte, in every electrochemical experiment involving current flow, any prescribed (time-dependent) potential $E_a(t)$ (in V) will be incorrect because of an ohmic potential drop [Eq. (23)]. The

$$E_{eff}(t) = E_a(t) - iR_u \tag{23}$$

lower the conductivity of the electrolyte system and the larger the total current, the larger this effect will be. This influence is particularly conspicuous when the faradaic current is accompanied by a strong capacitive component, as observed, for instance, at high scan rates in cyclic voltammetry (Fig. 11). Moreover, as the combination of R and C_d acts as a low pass filter on the current response (its properties are given by the time constant RC_d), sudden changes in current are more or less strongly distorted.[64b, 65] Because of all these effects, current and potential are mutually dependent in voltammetric analysis, and instead of the set potential scan rate v, an effective rate v' is operative [Eq. (24), Fig. 12].

$$E_{eff}(t) = E_{start} - v't + R_u(C_dv' + i_f) \tag{24}$$

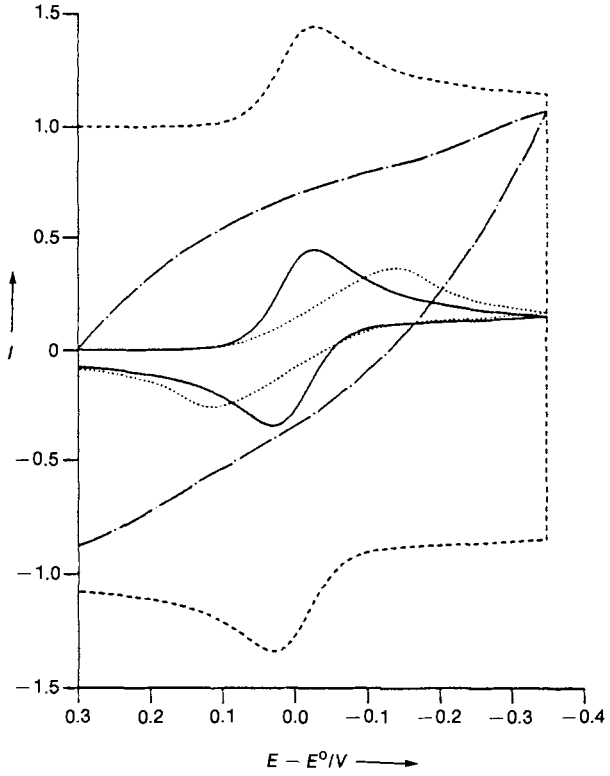

Fig. 11. Simulated cyclic voltammogram for a reversible charge transfer with planar diffusion (——). Presence of a normalized capacitance [65] $\gamma = 1$ (– – –), of a normalized uncompensated solution resistance $\rho = 10$ (· · · ·), and of a combination of these properties (—·—·—) [80b].

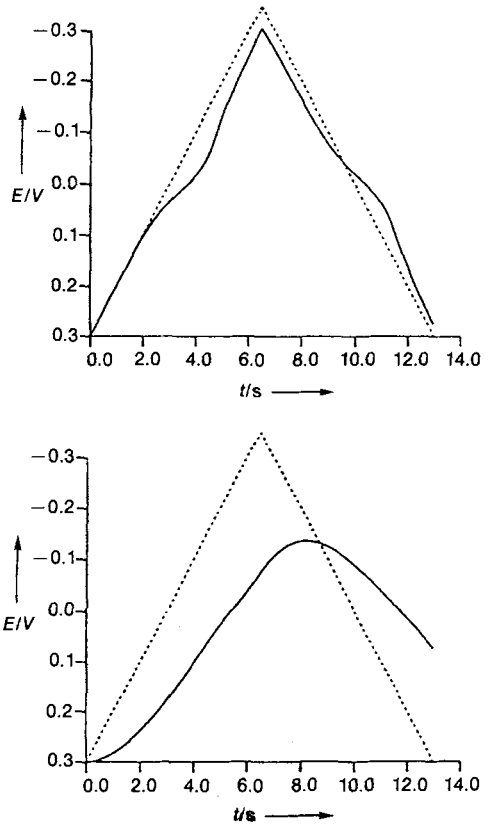

Fig. 12. Potential–time curves for the cyclic voltammograms in Figure 11; measured (effective) potential (——), applied potential (· · · ·). Top: only resistance $\rho = 10$; bottom: resistance $\rho = 10$ and capacitance $\gamma = 1$ [65].

Hence, even in electrolytic solutions with high conductivity, the maximum scan rate for ordinary electrodes with a radius greater than 1 mm is approximately 400 Vs^{-1}.[2, 32] In solutions with low conductivity, this value falls drastically. For example, in benzene the current–voltage curves measured at scan rates of less than 0.1 Vs^{-1} are so distorted that they cannot be interpreted, even though the time constant is negligible, and the only effect is the ohmic potential drop.

In the past one attempted to reduce the iR drop by improving equipment, usually by including a potentiostat in combination with a three-electrode configuration.[32, 66] Through the potentiostat, a reference electrode with high impedance provided a correction signal large enough to compensate for most of the loss of potential at the working electrode. The remaining uncompensated solution resistance was further reduced by electronic feedback,[67] which resulted in possible scan rates of greater than 1000 Vs^{-1} for systems with high conductivity electrolytes and conventional electrodes.

Using ultramicroelectrodes reduces the iR drop so much that it is possible to interpret the results of measurements taken even in extremely diminished electrolytic solutions. Several limiting cases must be distinguished, depending on the experimental conditions. Theoretical[68] and experimental[69] studies show that in the stationary state with a diffusion-controlled limiting current, the ohmic potential drop is no longer dependent on the size and geometry of the microelectrode, but solely on the properties of the electrolyte [Eq. (25), $\varkappa$ = conductivity of the electrolyte system].

$$iR = nFc^{*}D\varkappa^{-1} \tag{25}$$

The iR drop in the case of a low conductivity electrolyte ($\varkappa = 10^{-2}\,Sm^{-1}$, $D = 10^{-9}\,m^2s^{-1}$, $c^{*} = 0.1\,mol\,m^{-3} = 10^{-4}$ M, concentration of an electroactive system) is, according to Equation (25), then 1 mV.

The situation becomes more complicated when the level of the conducting electrolyte in the solution is reduced, for then, in addition to the diffusive mass transport, migration effects can also play a role.[70] As Oldham's calculations and experiments show,[36, 71] the quantitative ratio of conducting electrolyte to electroactive substance can fall to 1:1 without any significant distortion of the current–voltage curve in the stationary state. One reason for this is that the charge transfer at the solution/metal interface raises the ionic density immediately in front of the electrode, which improves the local conductivity $\varkappa$.

The relationship (26) is valid for purely planar diffusion, as exists in the case of high scan rates. Accordingly, as electrode size decreases, so does the ohmic potential drop. As, according to Equation (19), the time constant of the cell decreases parallel to iR, the smaller the radius of the ultramicroelectrode, the more suitable it is for measurements at high scan rates.

$$iR \sim r_0 \tag{26}$$

3. Applications of Ultramicroelectrodes

3.1. Reaction Mechanisms

3.1.1. *Voltammetry under Steady-State Conditions*

As shown in Section 2.3, the magnitude of the diffusion-limited current depends not only on the simple charge transfer, but on whether chemical reactions also take place, possibly coupled with further charge transfer steps. If one uses "large" UMEs ($r_0 < 100\,\mu m$) for the analysis of a three-step reaction[34] comprising one charge transfer followed by a chemical step and subsequently a second charge transfer (ECE reaction), the diffusion-limited current as a rule corresponds to the transfer of two electrons. With smaller microelectrodes, the rate of the chemical step decreases relative to that of the diffusive mass transport (Fig. 10). As a result, the time scale used in steady-state voltammetry is too short for the overall reaction, and therefore n_{app}, the number of electrons measured by the limiting current, gradually declines to 1. This change in the current as a function of the electrode radius can be used to determine the rate constant and the activation parameters of chemical steps in reactions of this nature.[64, 72, 73]

The stationary limiting current's dependence on electrode size can also be used to determine the rate constants of the chemical step in the catalytic EC′ mechanism,[73–77] in which the starting species is regenerated in a chemical step after the heterogeneous charge transfer, and of the reactions preceding the charge transfer. By contrast, in pure EC mechanisms —only a chemical step after the charge transfer—the limiting current is independent of the rate of the next step. Information on the kinetics can only be obtained from the shifts of steady-state voltammograms as a function of the electrode radius.[73]

The use of microelectrodes in steady-state voltammetry to determine rate constants of homogeneous processes has been described several times.[64, 72, 74–79] This method has the advantage that by measuring the diffusion-limited currents with a set of microelectrodes of varying size, the rate constant of a chemical step can quickly be determined. However, this assumes that the precise relationship between the characteristic electrode radius and the kinetics is known, which was as yet only partly the case.

Apart from the catalytic EC′ mechanism,[75–78] the classical ECE mechanism has also been studied in detail. A typical example is the dimerization of triphenylamine (TPA)[80, 81] after its radical cation formation. Under the given experimental conditions ($E_1^0 > E_2^0, E_3^0$), the product tetraphenylbenzidine (TPB) is oxidized to its dication. Overall, a two-electron transfer has apparently taken place [Eq. (27)].

$$2\,TPA \xrightarrow{E_1^0} TPB^{2+} + 2e^{-} + 2H^{+} \tag{27}$$

Figure 13 shows the change in the number of electrons n_{app} at an 8 μm disk electrode as a function of the concentration of TPA. Because the dimerization is a second-order reaction, the rate of the coupling step, and thus the number of electrons transferred, decreases as the concentration of TPA diminishes. A comparison between the experimental data and computer simulations[80] gave a rate constant of

$2.2 \times 10^3\ M^{-1} s^{-1}$, which is in very close agreement with values in the literature.[81] There was some difficulty in interpreting the finding that, in high concentrations of TPA, measurements at microdisk electrodes give rate constants greater than $10^4\ M^{-1} s^{-1}$ on account of the significantly higher n_{app} values (Fig. 13).[72] However, the results did not support the

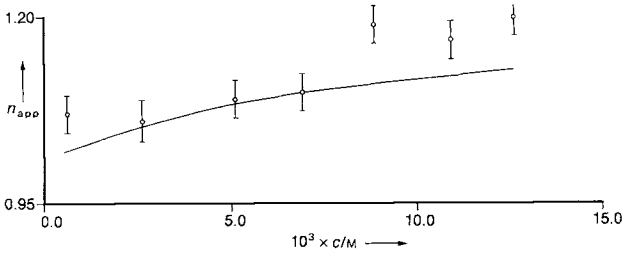

Fig. 13. Numbers of electrons transferred (n_{app}) for the oxidation of triphenylamine for different concentrations in CH_2Cl_2/0.1 M [TBA]PF_6. Experimental points (o) and simulated curve (——). Diffusion-controlled limiting currents measured at a Pt microdisk electrode with diameter 8 μm.

initial assumption that the changes in current density at a microdisk electrode, obtained using a spherical diffusion model with uniform current density over the entire electrode surface, would be false.[72] Rather, it turns out that TPA electropolymerizes to a conducting polymer at a microelectrode[64] (Fig. 14).

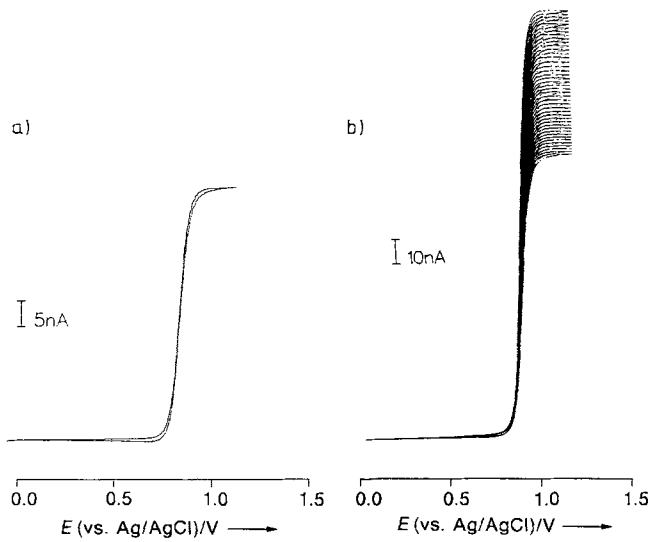

Fig. 14. Experimental steady-state voltammograms for the oxidation of triphenylamine. a) $c = 2.3 \times 10^{-3}$ M, b) $c = 1.2 \times 10^{-2}$ M in CH_2Cl_2/0.1 M [TBA]PF_6, measured at an 8 μm microdisk electrode. The rise in the current in b) is due to electropolymerization effects.

The mechanisms of a whole series of processes used in industrial electrosynthesis have been analyzed.[82] The chief advantage of microelectrodes is the absence of *iR* distortion in the current–voltage curves, even in extremely high concentrations of the reactants, which, of course, enables kinetic and thermodynamic data to be accurately evaluated. For instance, steady-state measurements revealed the experimental conditions under which hydrodimerization of acrylonitrile to adiponitrile (Monsanto process) dominates over the simple reduction of acrylonitrile to propionitrile.[83] Other examples include the catalytic mechanism to methoxylize furane by indirect anodic oxidation in the presence of bromide and methanol[84] and the reductive hydrodimerization of formaldehyde to ethyleneglycol.[85]

Finally, reports on microelectrodes with modified surfaces include studies on electrocatalytic effects of simple redox systems[86] as well as charging processes at conducting polymers or their formation mechanisms.[87, 88] Microelectrodes can also be used in the analysis of slow homogeneous chemical reactions of redoxactive compounds in a reactor to determine the rate constants of the chemical step directly from the time-dependent changes in the diffusion limited currents.[89]

As pointed out above, as the mass transport coefficients *m* increase (that is, as the electrode radius decreases), the diffusion rate may exceed the rate of the associated heterogeneous charge transfer. This makes it possible to determine the rate constants directly from the shift and change in slope in steady-state voltammograms relative to the reversible case.[63] Steady improvements in the construction of ultramicroelectrodes have reduced their characteristic dimensions.[30a, 36, 58a, 90, 91] There have already been reports of microelectrodes with radii of 1–100 nm.[92–94] Hence, theoretically, it should be possible to determine standard rate constants k_s^0 smaller than 1 ms^{-1}. Recent results published by Penner et al.[94] appear to confirm this. Using nanodes ($r_0 = 1-2$ nm), they measured a series of outer-sphere redox couples, for example, $[Ru(NH_3)_6]^{2+/3+}$ (H_2O, 0.5 M KCl) and ferrocene ($Fc^{0/+}$)(CH_3CN, 0.3 M [nBu$_4$N]ClO_4), and obtained k_s^0 values of 0.79 ± 0.44 ms^{-1} and 2.2 ± 1.2 ms^{-1}. Somewhat earlier studies by Bond et al.[95] on ferrocene with 0.3 and 0.5 μm Pt electrodes also produced an unusually high k_s^0 value of 0.064 ms^{-1}. Such high standard rate constants could not be measured in the past. These new results compare surprisingly well with the values predicted by the electron transfer theory of Marcus.[96] Hitherto, standard rate constants of charge transfers obtained with conventional electrodes had produced much lower values, which had raised doubts about the reliability of the theoretical predictions. Apparently, the high transport rates hinder the formation of passivating films, which would otherwise retard the charge transfers in proportion to their thickness and electrode coverage. On the other hand, Penner's results have drawn a lot of criticism. Baranski[97] has shown that relatively large electrodes that are in contact with the electrolyte (through a hollow lagoon left by imperfect fusing and subsequently filled with solution) produce current–voltage curves that are almost identical to those obtained with nanodes. In these circumstances, the theoretical predictions for nanodes are certainly no longer valid; thus the postulated high rate constants have not been unequivocally substantiated.

3.1.2. *Voltammetry with High Scan Rates*

On gradually raising the scan rate when the steady state of an ultramicroelectrode has already been established, one observes the transfer to the semi-infinite planar diffusion as a change from a sigmoid voltammogram to the classic cyclic voltammogram with potential-separated anodic and cathod-

ic waves. These so-called edge effects first drew electrochemists' attention to the peculiar properties of microelectrodes.[6, 13, 19, 55, 98, 99] When microelectrodes with radii between 25 and 500 μm are used, the influence of these edge effects is noticeable at upper scan rates of 5 and 0.05 Vs^{-1}, respectively. Thus, the quantitative data on the kinetics of the heterogeneous charge transfer in these time domains must take into consideration the influence of these edge effects on the peak separation and the shape of the voltammogram.[19, 100–102] On the other hand, in this time scale the iR drop and the capacitance C_d will have little effect on the voltammetric signal. Therefore, using a single microelectrode and varying the scan rate can provide very reliable data on the rate constants of the heterogeneous charge transfer, as described by Nicholson and Shain.[8, 103]

The qualitative jump that makes ultramicroelectrodes so interesting takes effect at scan rates above, say, 500 Vs^{-1}. From about this level the growing iR drop as well as the increasing influence of the RC time constant normally render data obtained with conventional electrodes impossible to interpret. For rates greater than 500 Vs^{-1}, however, conditions for planar diffusion are more or less fulfilled, even for nanodes with radii as small as 1 μm ($\sigma \leq 0.2$). Thus, as v increases, the faradaic current i_f increases proportional to $v^{\frac{1}{2}}$ and the capacitive charging current i_c proportional to v. However, due to the reduction in the radius and the corresponding lower current values, both the RC term [Eq. (19)] and the iR drop [Eq. (24)] decline, and as a result UMEs can be used in a fast-scan range up to 10^5–10^6 Vs^{-1}. "Classical" cyclic voltammetry reaches its limits at scan rates of a few megavolts per second, because the diffusion layer and the electrical double layer then assume almost the same size and can no longer be separated, as theory requires.[104]

In principle, the fast-scan technique provides much the same kind of information as conventional cyclic voltammetry,[34] with one important distinction: the time scale for measurements extends to below 1 μs (for example, at 10^6 Vs^{-1} $\tau = 25$ ns where $\tau = RT/vF$). Thus, it has become possible to measure the redox potentials of highly reactive intermediates[106–108] and rate constants for the rapid heterogeneous charge transfer,[38, 106, 109] as well as to analyze complex mechanisms including chemical steps.[64, 110, 111] Quantitative evaluations of the diffusion-controlled steps of second-order reactions are now also reality. Nor is there any difficulty in investigating and evaluating simple EC reactions.[112]

The group of McCreery were the first to obtain small time constants using ultramicroelectrodes.[113] They were able to prove through chronoamperometry and spectroelectrochemical techniques that within 150 ns concentration profiles of electroactive particles build up in the diffusion-layer region of microelectrodes. With time-dependent absorption measurements of chronoamperometrically produced radical cations of chlorpromazine (CPZ) in the presence of equimolar quantities of dopamine, they obtained values of 6.2×10^7 $M^{-1}s^{-1}$ for the rate constant of the homogeneous $CPZ^{\cdot+}$ cation reduction by dopamine at pH 6.8.

Since then, many voltammetric investigations have been carried out on electron transfer systems with coupled chemical reactions, such as addition,[106, 114] isomerization,[115] dimerization,[116] and homolytic cleavage,[112, 117] to name some examples.

In some cases, the fast-scan technique has made it possible to obtain direct evidence of the existence of reactive intermediates as well as new, unequivocal findings on reaction mechanisms. For instance, in the very rapid homolytic cleavage of halide ions from radical anions of aryl halides, it was not always clear whether the bond-breaking step occurred concurrently with the charge transfer as an inner sphere reaction,[118] or whether the cleavage took place after the formation of the radical anion, that is, in a two-step reaction. Measurements by Saveant et al.[117] of the reduction of 9-bromoanthracene confirm that at scan rates above 100 000 Vs^{-1} the formation of the radial anion is reversible. This proves the intermediacy of a highly reactive anion; the rate constant for the subsequent cleavage of the bromide ion is $k_f = 5.9 \times 10^6$ s^{-1}.

For a long time it was disputed whether the cation in the dimerization of radical cations of aromatic amines and heterocyclic compounds first coupled with its neutral species (RS dimerization) or immediately underwent radical cation coupling (RR coupling). Several independent studies support the assumption of RR coupling reactions in most cases.[116] The electropolymerization of heterocycles such as pyrrole and thiophene also involve dimerization steps. Again, Saveant et al. have demonstrated the existence of highly reactive cations of pyrrole and some derivatives within the voltammetric time scale[119] and determined the associated redox potentials. Pyrrole dimerization ($c = 4$ mM) becomes partially reversible at scan rates greater than 18 000 Vs^{-1}, which corresponds to an average cation lifetime of 30 μs. The oxidation of 3,3′-dimethoxy-2,2′-bithiophene[120] demonstrates the complexity of the reaction path involving coupling steps in a growing polymer chain. Fast-scan experiments show that the cations formed at the electrode with a rate constant of 10^{+5} initially couple to form a tetramer, which, in turn, after the loss of two protons, also transforms into a dication (Fig. 15). At scan rates greater than or equal to 5000 Vs^{-1} ($c = 1$ mM) the reaction at the electrode is chemically reversible. Further measurements at high concentrations and slow scan rates confirm that the dications comproportionate in solution with unchanged starting monomer, thereby autocatalytically initiating a new coupling step.

The fast-scan technique has proved particularly successful in investigating the kinetics of fast heterogeneous charge transfer reactions.[106, 109, 121–127] Even C_{60}, only recently accessible in large quantities, has already been measured.[114, 127] Provided that the iR influence is reduced to a negligible minimum, the method of Nicholson and Shain[8, 103] can be used without any complications to obtain rate constants from the separation of the peak potentials of the anodic and cathodic waves ($\Delta E_p = E_{pa} - E_{pc}$) (Fig. 16). To determine values between 0.01 and 0.1 ms^{-1}, scan rates must lie between 1000 and 50 000 Vs^{-1}. Independently of one another, several groups have established that anthracene, a particularly well-studied compound with a low reorganization energy during charging, has a k_s^0 value of about 0.035 ms^{-1}.[38, 109, 120, 121, 128] Similarly high values were obtained for the ferrocene/ferrocinium redox couple. It

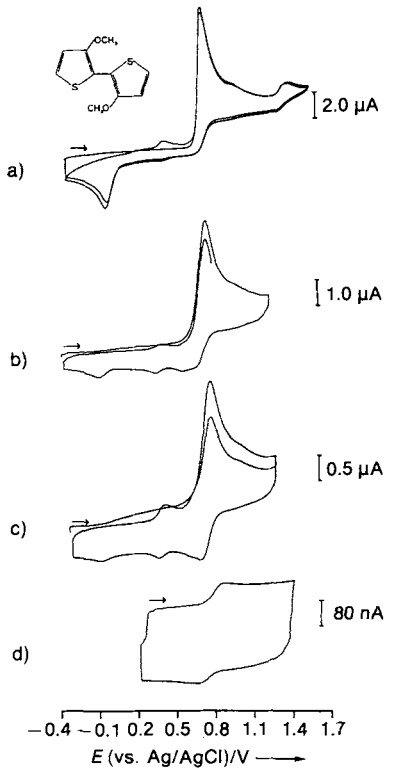

Fig. 15. Experimental cyclic voltammograms for the oxidation of 3,3'-dimethoxy-2,2'-bithiophene in acetonitrile/0.1 M [TBA]PF_6: a) $c = 2 \times 10^{-3}$ M, $v = 100\ mVs^{-1}$, $r_0 = 500\ \mu m$; in the reverse sweep the reduction of the cleaved protons is visible at 0.0 V; b) $c = 3 \times 10^{-3}$ M, $v = 20\ Vs^{-1}$, $r_0 = 100\ \mu m$; in the reverse sweep the reduction signals of the di- and monocations of the tetramer are also visible; c) $c = 3 \times 10^{-3}$ M, $v = 100\ Vs^{-1}$, $r_0 = 100\ \mu m$; d) $c = 3 \times 10^{-3}$ M, $v = 5000\ Vs^{-1}$, $r_0 = 2.5\ \mu m$.

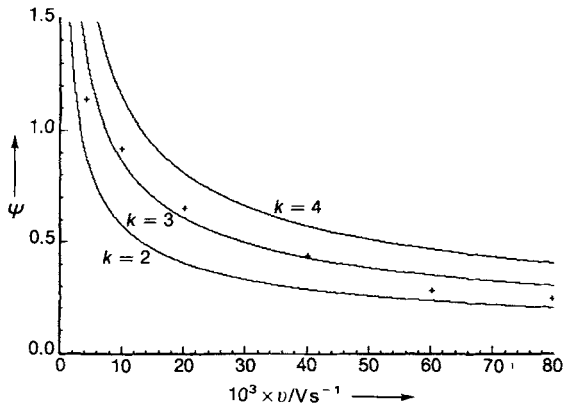

Fig. 16. Experimental and calculated data of the dimensionless ψ parameter as a function of the scan rate [34, 103]. Fast-scan experiments of the reduction of anthracene provided the experimental ψ values from ΔE_p values at different scan rates according to the equation $\psi = f(\Delta E_p)$. The calculation of the ψ values assumes that $k_s^0 = 0.02$, 0.03, or 0.04 ms^{-1}, and $D = 1 \times 10^{-9}\ m^2s^{-1}$.

is noticeable that this technique provides much higher rate constants than conventional techniques. This supports the assumption that, as in the steady-state experiments, no passivation occurs at the electrode surface.

At present, the fast scan rather than the steady state technique is preferred for studying reaction mechanisms and measuring kinetic parameters of homogeneous and heterogeneous electrochemical processes. Its crucial advantage is that all methods of evaluation used in classical cyclic voltammetry, including simulation, can be applied. Thus, all the usual mechanisms can be analyzed, and scan rates up to $10^5\ Vs^{-1}$ are accessible even with relatively large electrodes with radii of up to 2.5 μm (Fig. 17). This requires that, apart

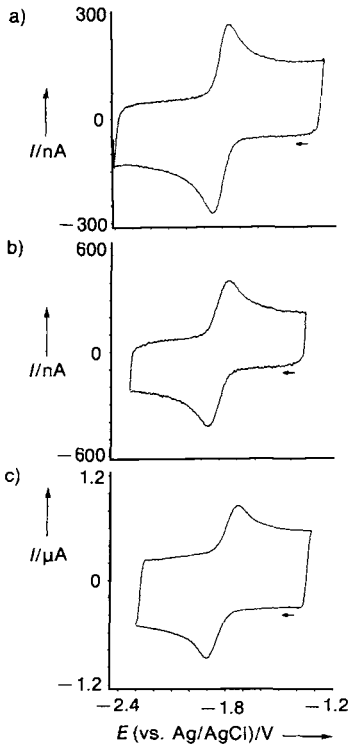

Fig. 17. Fast-scan voltammetry of the reduction of anthracene ($c = 5 \times 10^{-3}$ M) in acetonitrile/0.5 M [TBA]PF_6 at different scan rates. Gold ultramicroelectrode with $r_0 = 2.5\ \mu m$: a) $v = 20\,000\ Vs^{-1}$; b) $v = 40\,000\ Vs^{-1}$; c) $v = 120\,000\ Vs^{-1}$.

from experimental effects due to electrode size and electrolyte resistance, all instrumental influences which might distort the current–voltage curve must be kept as small as possible. Critical features are the construction of the potentiostat, including the current transducer, and the construction of the microelectrode. In respect of the potentiostat and the current transducer, it is very important that amplifiers have an extremely rapid time response and, hence, large band widths are used.[112a, 122, 125] Stray capacitances in the microelectrodes and the cables can cause heavy distortion of the current–voltage curve. For this reason, electrodes with radii of less than 5 μm have to be shielded,[129, 130] and connected to the current transducer and the potentiostat by very short leads. The appropriate *iR* compensation can produce further improvements.[121, 131]

If very high scan rates of 10^5 to greater than $10^6\ Vs^{-1}$ are used, cell resistance and the time constant will always distort the current–voltage curve. In poorly conducting electrolytes these effects are already apparent at much lower scan rates. It is then better to use simulation to evaluate the data, by inserting the capacitances and resistance values in the Butler–Volmer equation in accordance with Equation 24[60b] (Fig. 18), or by obtaining the real scan rates from the experimental voltammogram and applying them directly in the simulation.[124] Wightman et al.[132] have proposed a method that, given a suitable apparatus, will measure the

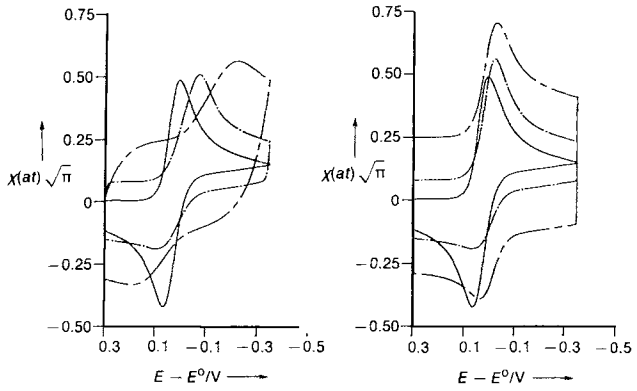

Fig. 18. Simulated cyclic voltammograms for an EC_{2rev} mechanism. Left: with uncompensated resistance $R_u = 41\ \Omega$ and double-layer capacitance $C_d = 1.56\ \mu F$. Right: after correction for the iR drop. Simulation data: $E^0 = 0.0$ V, $D = 1 \times 10^{-9}\ m^2 s^{-1}$, $K_{eq} = 10$, $k_f \times c = 0.1\ s^{-1}$, $k_s^0 = 0.04\ ms^{-1}$; scan rates: (——) $0.1\ Vs^{-1}$, (— · —) $100\ Vs^{-1}$, (— · · —) $1000\ Vs^{-1}$.

background voltammogram without the electroactive system, and then subtract this background current after adding the electroactive sample. However, this technique is only possible if the iR influence is small enough to be neglected.

3.2. Electrochemistry in Poorly Conducting Electrolytic Media

In conventional electrochemical experiments the basic electrolytic solution and the polar solvent ensure high conductivity. Hence, there are no iR problems and consequently no migration effects even at low or medium scan rates. This changes drastically when nonpolar solvents are used, or the concentration of electrolyte is very low, or measurements have to be taken in the solid state or the gas phase. In all these cases the iR drop is very large and cannot be controlled by the usual methods.

As indicated in Section 2.4, the use of UMEs reduces the iR effects, permitting interpretation of voltammetric or amperometric signals even under extremely unfavorable conditions. For example, Bond et al.[36, 133–135] measured the same diffusion-limited currents with 50 μm disk electrodes for the oxidation of ferrocene in electrolyte-free acetonitrile and in electrolytic solution. Moreover, the shape of the steady-state current–voltage curve obtained with electrodes with diameters of less than 1 μm resembles the ideal case of reversible charge transfer very closely. Other authors report similar findings.[136–139] The experimental results agree with Oldham's theoretical predictions[71] that even minute quantities of conducting "impurities" are enough for a sufficiently high conductivity in the immediate vicinity of the electrode. Voltammetric measurements of the oxidation of ferrocene in virtually electrolyte-free acetonitrile with microband electrodes[133] show that the influence of the iR drop depends not on the amplitude of the current response, but mainly on the special flux conditions in the vicinity of the electrode.[68] Despite relatively large currents, the voltammograms show only minor distortions. Some effects have still not been explained. The purpose of measuring in electrolytes with diminished or no conductivity is to obtain electrochemical data under the same conditions as used in spectroscopy or analytical chemistry. Usually, electrolytes have high ionic strengths, imparting significantly different thermodynamic and kinetic properties from those in ideal solutions without added electrolytes. This implies, for example, that in the transition from high to low ionic strengths, ion-pair equilibria, redox potentials, and rate constants of ionic reactions change. Apart from the activity of the involved reactants, the electric properties of the double layer at the electrode also change when the electrolyte concentration is reduced, which renders it difficult to draw unequivocal conclusions from the such experiments. Hence, researchers concentrate on systematically investigating the influence of the concentration of the ground electrolyte on migration and double-layer effects, comparing experimental findings with theoretical predictions, and, finally, determining the limits of electrolytic variations in nonpolar solvents.[70, 71, 134–142] The unexplained phenomena include the frequent appearance of typical cyclic voltammograms in non-electrolytic solutions, despite established steady-state conditions. Presumably the cause lies in changes in solubility after recharging the redox system.

UMEs enable the expansion of the utilizable potential range of aprotic solvents. This is confirmed by measurements in electrolyte-free acetonitrile and SO_2. It could be shown that alkanes are oxidized in acetonitrile[142] at potentials above + 3.5 V, and alkali metal ions were successfully oxidized in liquid SO_2 at potentials[143] of + 5.0 V.

Nonpolar solvents used to be taboo in electrochemical measurements. However, with ultramicroelectrodes the extremely high iR drop falls to tolerable values, and, by choosing suitable electrolytes such as tetrahexylammonium perchlorate ([THA]ClO_4) or $NaBPh_4$–crown ether complexes, amperometric or potentiodynamic experiments in solvents such as benzene, toluene, or even hexane provide interpretable results.[26, 36, 106, 144, 145] The precondition for the success of such experiments is that the electrolytes are soluble enough, and that they dissociate to some degree to provide an acceptable level of conductivity in the solution. Up to now, the chemistry of redox reactions in hydrocarbons could only be analyzed with spectroscopic methods; now, for the first time, it will be possible to use electrochemical measurements for quantitative studies. The growing interest in electrochemical investigations in aromatic hydrocarbons, alkenes, and alkanes is largely due to the fact that ionic reactions take place at quite different rates in weakly polar solutions and in polar media. Measurements that cover as wide a range of polarity as possible provide precise insights into the relationships between solvation and chemical reactivity, including the kinetics of electron transfer. For example, voltammetric studies[64] on the kinetics of the dimerization of radical anions of 9-cyanoanthracene show that the corresponding rate constants increase by almost four orders of magnitude from 1.4×10^3 to $9.0 \times 10^6\ s^{-1} M^{-1}$ between benzene ($\varepsilon = 2.27$) and the extremely polar *N*-methylformamide ($\varepsilon = 190$) (Fig. 19). Experiments of this nature show that particles with the same charge can form a covalent bond at high rates despite coulombic repulsion.

The use of nonpolar solvents also has interesting analytical applications. There is a discussion, for instance, on the use of supercritical CO_2 as a mobile phase in capillary chromatography.[146] Voltammetric measurements in this medi-

um are reproducible only after small quantities of water have been added; the use of ion-conducting membranes improves the results.[147]

Steady-state voltammetry is another challenging field for ultramicroelectrode techniques. However, to ensure that the *iR*-drop component always remains sufficiently small for the use of nanodes, conductivity values may not fall below $10^{-6}\,S\,cm^{-1}$. For this reason, inorganic[148] and organic[149] steady-state electrolytes as well as frozen electrolytic solutions[27, 150] (cryoelectrochemistry) are the most popular areas of research. Because under solid-state conditions, diffusion coefficients lie between 10^{-11} and $10^{-16}\,m^2\,s^{-1}$ ($\sigma \leq 0.3$), that is, orders of magnitude smaller than in solution, instead of steady-state curves, voltammetric measurements at UMEs often reveal a range of conditions from a transition between the steady state and planar diffusion up to classical cyclic voltammetric situation. An additional complication is the appearance, especially at very low temperatures, of voltammetric curves typical of surface processes without diffusive mass transport. Although many details are still unclear, one plausible explanation assumes that liquid microphases survive in solution well below freezing point,[150, 151] adhering to the electrode surface in thin layers.

One field of electrochemistry with spectacular promise is UME applications in the gas phase. Pons and Fleischmann have published several reports on such experiments.[28, 152, 153] It is important that a very narrow insulating field separate the working and the auxiliary electrodes, for example, in a ring–disk arrangement or two half-disks. The conductivity across the insulating gap takes place either by means of a conducting membrane or in the presence of moisture in the form of proton transport.[152a] Microelectrode detectors, affixed for this purpose at the outlet of a gas chromatograph, were able to determine the individual components of a hydrocarbon mixture as well as a heat conducting detector (Fig. 20).

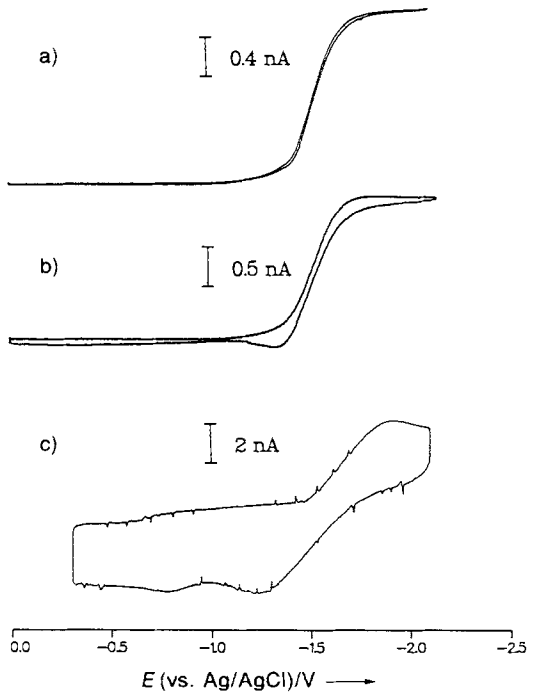

Fig. 19. Cyclic voltammograms for the reduction of 9-cyanoanthracene ($c = 1 \times 10^{-3}$ M) in benzene/0.5 M $[TBA]ClO_4$ at different scan rates: a) 100 $mV\,s^{-1}$, b) 1 $V\,s^{-1}$, c) 100 $V\,s^{-1}$.

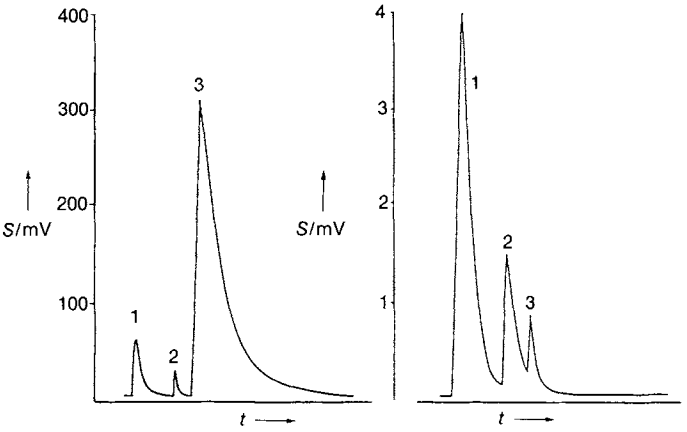

Fig. 20. Response of detectors in gas chromatography for an injection volume of 1 μL of a sample containing 30% toluol (1), 30% *ortho*-xylol (2), and 40% cyclohexanone (3). Injection port 190 °C, column 90 °C, outlet port 120 °C. Left: palladium microelectrode (potential + 3.0 V); right: thermal-conductivity detector. S = signal strength [152b].

3.3. Exploiting the Smallness of Microelectrodes

As already mentioned in the introduction, UMEs have a cardinal advantage because of their size, which makes it possible to conduct electrochemical measurements in minute volumes and observe discrete spatial events in microscopically small areas. Hence, it is not surprising that microelectrodes were first used for measurements in living systems. A report on electrochemical studies on the partial pressure of oxygen in tissue was published as early as 1938.[23] Baumgärtl and Lübbers' invention of the microcoaxial needle electrode, which, including the reference electrode, was only 0.3 to 0.5 μm at the tip, enabled routine measurements of oxygen gradients in cell tissue as well as at the gas/liquid interface or in pores of polymers.[154] Another important aspect of in vivo voltammetry is tracing neurotransmitters (catecholamines) or their metabolites (ascorbic acid) in the brain or in nerve cells. Building on pioneering work of Adams et al.,[155] improvements in the manufacture of microelectrodes[156–158] as well as technical progress[159, 160] have made it possible to take measurements both in living tissue and in unicellular organisms or single cells.[161] Surface-modified electrodes are becoming increasingly popular as they provide greater selectivity and sensitivity.

The patch-clamp technique,[162] for which Neher and Sakmann recently received the Nobel Prize,[163] also uses "microelectrodes". Whereas the above-mentioned microvoltammetric electrodes can cause and measure redox processes in a cell, the patch-clamp technique employs micropipettes, which measure electric currents that appear when the stimulated cell causes ions to move through channels in the cell membrane. Efforts are now being made to combine the two methods.[164]

A lot of work has been done on the electrocrystallization of metals, metal oxides, and organic salts. But quantitative

descriptions of growth processes in progress were extremely difficult because, statistically, nuclei form at several points on an electrode surface, and the measured current transients would integrate all these events. Naturally, the number of nucleation processes on the minute surface of ultramicroelectrodes is considerably smaller than on macroelectrodes. Therefore, under favorable circumstances it should be possible to detect the individual steps in the formation of a single nucleus and to analyze the kinetics of its growth process[20, 165, 166] (Fig. 21). Measurements obtained with

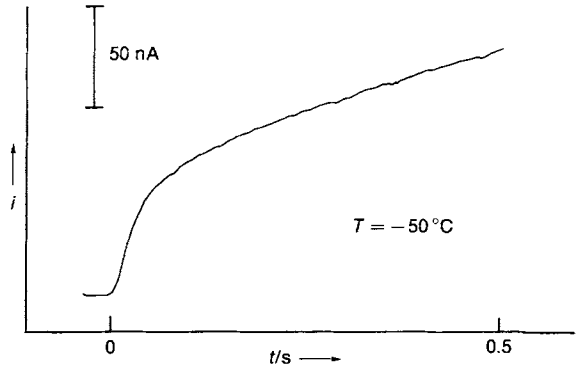

Fig. 21. Potentiostatic current–time transient for the growth of a crystal nucleus of a fluoranthene radical cation salt ($c = 2 \times 10^{-2}$ M) in acetonitrile/0.1 M [TBA]PF_6, measured at an 8 μm Pt disk electrode with a potential of +1.4 V vs. Ag/AgCl.

an ensemble of microelectrodes should provide unequivocal information on the rates of nucleus formation. The relatively large distances between the individual microelectrodes prevents the individual crystal nuclei from colliding with one another as they grow, which would unleash an undesirable dispersion of growth.[166] In recent articles, Oldham et al.[167] discuss the different mechanism of electrochemical mercury precipitation on carbon or metal microelectrodes from a thermodynamic point of view, and show that the type of precipitation process is conditioned by the surface energy at the electrode/electrolyte interface and the relative sizes of all the components involved.

The small size of UMEs is also useful for studying corrosion phenomena. They can be employed as probes to scan corrosive processes in closely defined spaces,[168] on the one hand, and serve as experimental models for local corrosive processes,[169] on the other. The small time constants are another advantage: rapid events can be recorded without complications, and interference from background currents during corrosive processes are kept to a minimum.[170]

A fascinating new development in UME techniques is based on the fact that the faradaic current, which, in the presence of an electroactive substance under diffusion-controlled conditions flows over the "tip" of the ultramicroelectrode, depends on whether the diffusion field of the microelectrode is disturbed by external influences. One consequence is that in the immediate vicinity of an insulating surface the current flowing over the UME is smaller than the undisturbed limiting current (Fig. 22). The extent of the change in current is determined exactly by the distance between the microelectrode and the nonconducting surface. Moreover, the smaller the electrode, the stronger the effect.

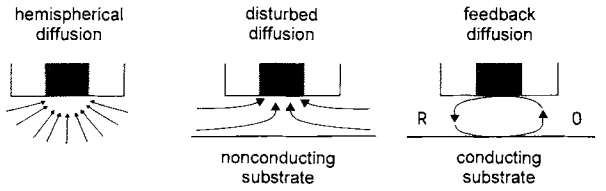

Fig. 22. Typical shapes of diffusion fields in scanning electrochemical microscopy. Left: undisturbed hemispherical diffusion field far from the substrate; diffusion-limited current i_l according to Equation (15). Center: disturbed diffusion field close to a nonconducting surface, $i < i_l$. Right: electroactive starting system regenerated (feedback effect) at a conducting substrate, $i > i_l$ [172b].

Thus, a piezoelectric scanner that moves the tip of the microelectrode parallel to the surface of a structured substrate can monitor the tip current as a function of its position. This setup generates an image of the surface topography of the sample (Fig 23). The recording technique resembles scanning

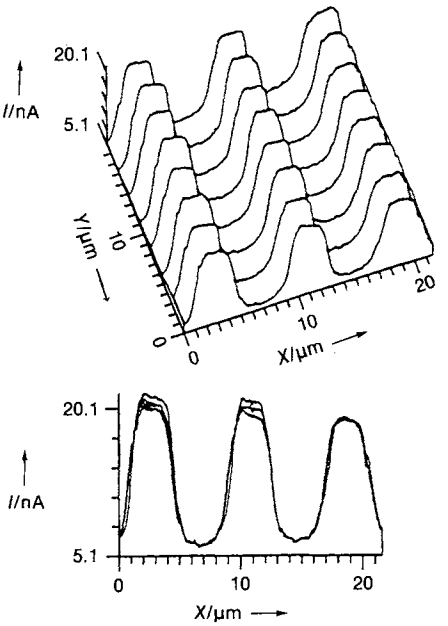

Fig. 23. SECM image of a Pt interdigitated structure on a SiO_2 substrate. Probe: Pt disk electrode embedded in a 0.3 μm poly(methyl methacrylate) layer, disk diameter ~0.5 μm, $E_s = -0.77$ V vs. SCE (saturated calomel electrode); aqueous solution with 40 mM methyl viologen and 2 M KCl. Top: three-dimensional view. Bottom: side view [174b].

tunneling microscopy (STM)[171] as far as the movement of the electrode across the substrate surface under investigation is concerned, but the principles of measurement differ. Whereas in STM a tunnel current flows between the tip of the electrode and the substrate, the current flow in the case described here is based on redox processes that take place at the tip of the electrode or at the substrate surface (see below). Their extent is controlled by the kinetics of the charge transfer at the phase interfaces as well as by the diffusive mass transport. For this reason, this method is known as scanning electrochemical microscopy (SECM). It is a fairly recent development, largely a product of Bard's group.[29, 172] Its resolution is not as high as that of STM, but should, with further improvement, approach the 50 nm limit. In a variant of this technique, the substrate surface itself is conductive,

and thus can be given a different potential than the microelectrode. This allows, for example, a substance R produced by reduction ($O + e \rightarrow R$) at the electrode tip to be reoxidized at the substrate, a feedback which increases the diffusion current at the microelectrode (Fig. 22). This technique has advantages: the insulating shield of the electrode causes less interference than in the direct mode, and the stronger current improves depth resolution.[173] Both methods have been used to study surfaces of interdigitated arrays[174,175] (Fig. 23), polymers,[175,176] and biological samples.[177] Apart from topographical information, the SECM technique provides data on heterogeneities of the charge transfer at different points on a substrate surface.[178,179] This enables one to detect space-dependent changes in the chemical properties of surfaces, including, for instance, biocatalytic activities.[180] Furthermore, varying the perpendicular distance between the microelectrode and the substrate will provide information on diffusion profiles and kinetic parameters of homogeneous reactions.[181] This is achieved by generating different potentials at the substrate electrode and the microelectrode with a bipotentiostat, analogous to the ring–disk electrode.[182] Thus, the particles generated at the substrate can be detected with spatial and temporal resolution at the microelectrode (generator-collector mode[182]). Instead of using the microelectrode as detector, Anson[183] used the substrate electrode. This not only provides greater sensitivity to current and a better current-to-noise ratio; it also allows the two electrodes to be placed farther apart.

Interesting technical applications of SECM in the field of microsystem technologies include electroplating and etching.[184] Using the direct mode, one can generate, for example, thin metal strips in an ionic conducting polymer film, for instance Nafion containing gold, silver, or palladium ions, by polarizing the microelectrode tip to a negative potential and the substrate tip attached to the back of the polymer film to a positive potential. In the feedback mode, a mediator is oxidized or reduced at the microelectrode, which, after oxidative etching or reductive metal deposition at the substrate, is then transported back to the microelectrode, where it undergoes a new redox reaction.[185]

Reports on the SECM principle indicate an enormous range of possibilities for surface analysis, microgalvanization, and microetching. Present efforts to increase the resolution and sensitivity of the technique focus on reducing the size of the microelectrode tip[174b] and improving procedures.[186]

The aforementioned generator–collector principle can also be applied to stationary electrodes by polarizing a series of band electrodes in very close proximity (μm range) at different potentials. Reactive intermediates generated at one electrode, or which emerge in a subsequent chemical step, are detected at the collector electrode.[187] Measuring the current density (collector efficiency) as a function of the distance between the band electrodes and evaluating the findings with the aid of digital simulation provides kinetic and mechanistic information on the system under investigation. Studies of this nature have been carried out on recombination and electrochemical luminescence (ECL) of radical ion pairs, and on the catalytic oxidation of ascorbic acid and aminopyrine by $K_3[Fe(CN)_6]$.[39,188] Not only pairs of band electrodes, but also triple band electrodes[189] and interdigitated array electrodes[190] are now also being used for such work.

3.4. Ultramicroelectrodes in Chemical Analysis

Although analytical problems in the widest sense constitute an important aspect of this article, so far not much has been said about the use of UMEs in analytical chemistry, apart from electrochemical measurements of concentrations in the gas phase.

In principle, all the unconventional properties of ultramicroelectrodes can be exploited with advantage in chemical analysis. High mass transport rates and reduced capacitive effects produce both a marked improvement in the faradaic/capacitive current ratio [i_f/i_c; see Eq. (22)] and a better signal-to-noise ratio, which raises overall system sensitivity.[39,191] Digital and analog filters hold promise of further improvements.[192] The low values of the *RC* time constants lead to a fast drop in the capacitive charging current. As a result, traditional voltammetric pulse methods[32] used in chemical analysis, such as (differential) pulse voltammetry, staircase voltammetry, and square-wave voltammetry, should prove particularly suitable for UME measurements. This has been largely confirmed in experiments, some of which introduce new technical improvements.[133,138c,193–195] By using square-wave voltammetry in conjunction with a hydrodynamic modulation achieved by vibrating a microcylinder, the detection limit for ferrocene in acetonitrile could be lowered to 3×10^{-8} M.[196]

UMEs also have great potential in the stripping methods used in trace-element analysis. Because of the high mass transport coefficients, the solution does not have to be stirred during accumulation, and accumulation proceeds far faster. As the substance being analyzed was concentrated in a very small volume (the microelectrode), it is stripped completely during the anodic scan. This provides very sharp, easily interpretable peaks.[50,197–199]

If the characteristic dimensions of the microelectrodes are less than 10 μm, the high mass transport coefficients will keep the convection and hydrodynamic influences on a microelectrode's current response so small that they can be ignored. This phenomenon can be exploited to great advantage for electrochemical detection in flow systems, for example, in flow injection analysis or high performance liquid chromatography (HPLC).[200–202]

Because the *iR* drop has little influence on the current response, additional electrolytes are unnecessary, and the solution requires minimal conditioning. Furthermore, investigations can be carried out directly in samples, for example in fruit[203] (Fig. 24). Recently, band,[49] cylinder,[204] and array electrodes[133,203,205] have been used for these measurements instead of microdisk electrodes. They make it possible to measure relatively large currents in the lower μA range with the typical advantages of ultramicroelectrodes, which considerably reduces time and effort compared with other analytical techniques. The advantage of array electrodes is that they are easy and cheap to reproduce with modern lithographic techniques (see Section 4), and thus can be discarded after use.[206] Array electrodes also find in-

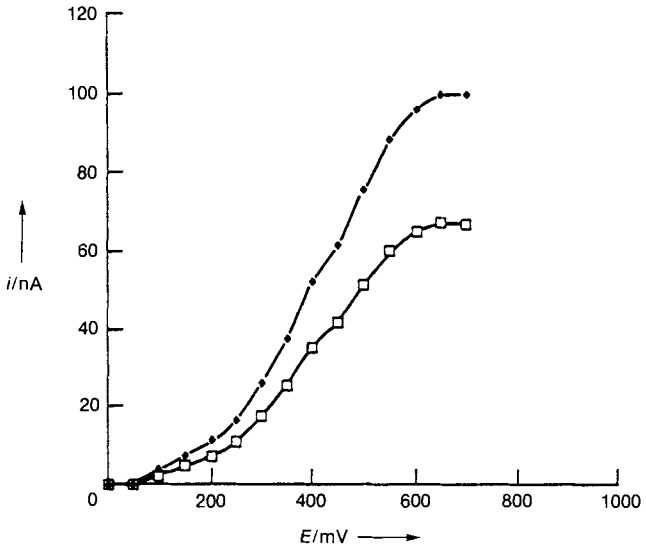

Fig. 24. Steady-state measurements of the oxidation of ascorbic acid in a Granny Smith apple with a gold microband electrode. $v = 20\ mVs^{-1}$: • at the surface, □: in the apple [203].

creasing application in the manufacture of electrochemical chemo- and biosensors, because their combination of small dimensions and relatively large sensitive area reduces response times and the signal-to-noise ratio.[207]

4. Construction of Ultramicroelectrodes

By now it should be clear that the main variables in the use of ultramicroelectrodes are geometry and size. The choice depends on the field of application. In recent years, therefore, many techniques have been developed to produce ultramicroelectrodes in varying geometries, sizes, and materials.

The most important type of electrode is still the disk electrode, which is usually made of platinum, palladium, gold, or carbon and, apart from the disk surface, fused into glass or embedded in plastic to isolate it completely from the electrolytic environment.[6b, 36–38, 63a, 90–94, 125, 132] It is essential that the electrode is reusable. This means that the electrode surface must be easy to clean; details can be found in the literature.[30a, 158] The details of techniques for manufacturing disk electrodes with diameters smaller than 0.6 μm have also been published. Because the electrode material becomes increasingly sensitive to temperature as the diameter decreases, "pullers" are used in the fusion process.[163] This step has been borrowed from the patch-clamp technique, which has long used pullers in the manufacture of extremely thin glass capillaries. They make it possible to set the exact temperatures needed to gradually soften the glass. The perfect seal obtained at the interface between glass and electrode material, a precondition for quantitative investigations with ultramicroelectrodes (Fig. 25), corroborates the quality of these fusion processes. Another problem with electrodes with diameters below 10 μm is the stray capacitances caused by additional capacitance between the electrode wire, the insulating environment, and the electrolytic solution.[129, 208, 209] It can lead to a drastic decline in the faradaic/capacitive current ratio (Figs. 26a and 27a). Recently, shielded electrodes have brought a noticeable improvement in this respect: the electrode capacitance is

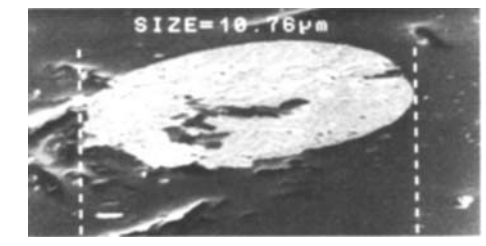

Fig. 25. Electron micrograph of a platinum disk electrode with a diameter of 10 μm embedded in soft glass.

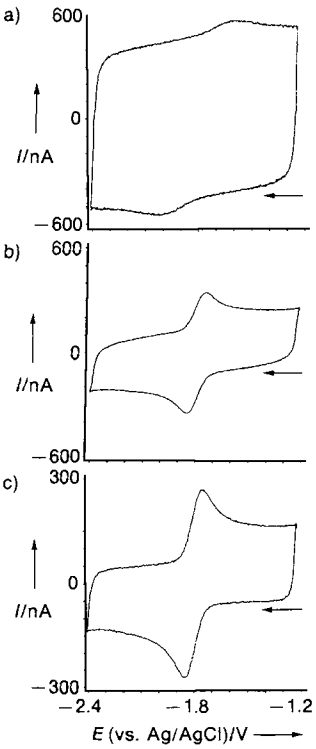

Fig. 26. Fast-scan voltammetry of the reduction of anthracene (5×10^{-3} M) in CH_3CN/0.5 M [TBA]PF_6; $v = 20000\ Vs^{-1}$; measured with a gold ultramicroelectrode with $r_0 = 2.5$ μm; a) without shield, b) shield incorporated but not activated, c) shield incorporated and activated.

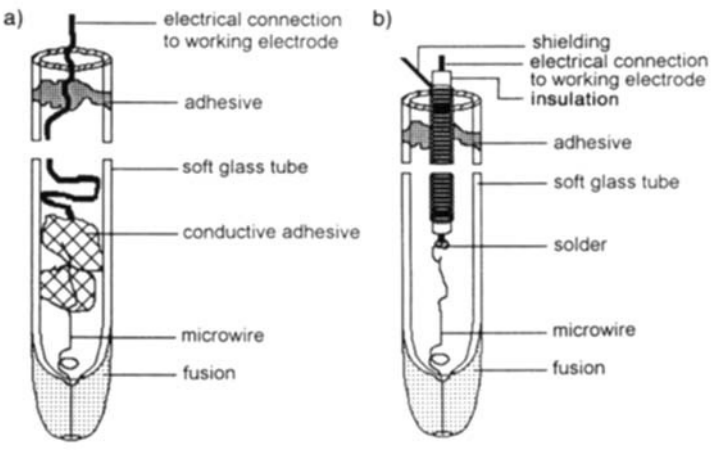

Fig. 27. Schematic setup of microdisk electrodes. a) Conventional electrode without shield. b) Electrode with electric shield.

significantly reduced by incorporating an additional, grounded metal shield or a coaxial cable in the glass fusion[129, 130b, 210] (Figs. 26b,c and 27b).

Whereas a metal wire fused into the glass is virtually indispensable in disk-electrode experiments in aprotic solutions, there is no problem in using carbon fibers as electrode material for studies in aqueous media, especially on biological objects.[30a, 211–215] The carbon fiber tips with characteristic diameters of up to 400 nm are produced by, for example, electrochemical etching or burning in a flame and isolated from the medium by electropolymerization of polyoxyphenylene.[212, 215, 216] The thin polymer layer adheres well and ensures that only the narrow tip retains its conductivity (Figs. 28 and 29). A common problem associated with carbon fiber electrodes is very slow electron transfer, which calls for appropriate activation of the tip.

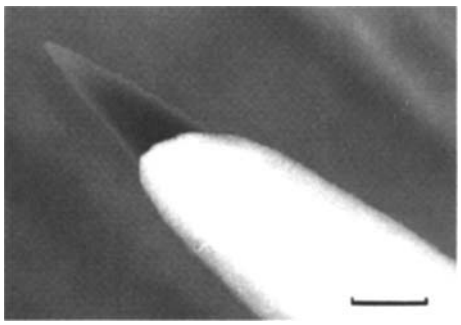

Fig. 28. Electron micrograph of a carbon-fiber tip (pitch fiber P100, Union Carbide), stuck into silicon rubber and then copper-plated. This was an experiment to test the possibility of leaving just a few μm free at the tip of the fiber on the principle of regioselective insulation. To heighten the contrast, Cu was chosen instead of insulating polyoxyphenylene [215]. The bar represents 3 μm.

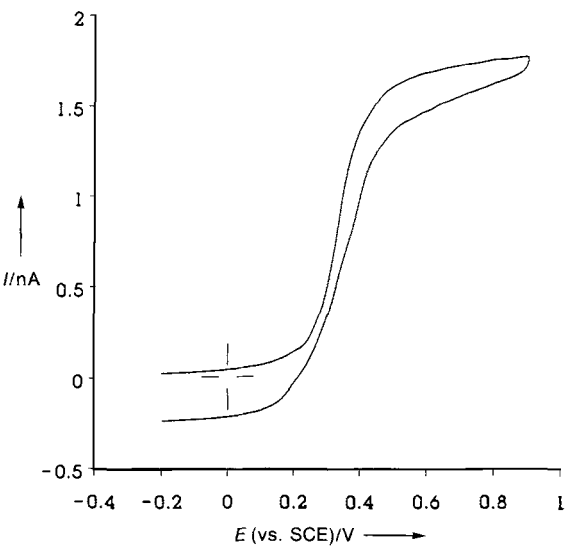

Fig. 29. Steady-state voltammogram of the oxidation of $K_4[Fe(CN)_6]$ ($c = 2$ mM) in H_2O/0.1 M KCl, $v = 1\ Vs^{-1}$, measured with a carbon-fiber tip [215].

Apart from the microdisk, microcylinder,[41, 51] microring,[43, 44] and microband electrodes[39–42] are also used. Band electrodes, employed as single-band electrodes, as double or triple band arrangements, or as arrays, have become increasingly popular in recent years. One reason is that, despite their narrowness, microband electrodes have a relatively large surface, and, therefore, give a favorable signal-to-noise ratio. Band electrodes serve as chromatographic detectors in analytical chemistry, are used to study reaction mechanisms and diffusion processes, and act as devices in microelectronics. There are different ways of manufacturing these electrodes.[217] The classical method is to fuse very thin strips of metal foil between sheets of glass or to embed them in a synthetic material with the aid of epoxy resins or films of Teflon. A far more elegant method, applicable into the lower nm range, consists of evaporation or sputtering of metals onto insulating substrates, which are then covered with a second insulating layer.[38–40, 218–220] Promising developments are microlithographic techniques, which have long been used in the electronic and semiconductor industries.[133, 187, 188, 217, 221–223] The most popular variants in electrode manufacturing are photolithographic techniques, which produce structures as narrow as 0.5 μm.[217]

5. Conclusions

Though the unconventional properties of ultramicroelectrodes were recognized only at the beginning of the 1980s, the exponential growth in literature on the subject testifies to their success. Numerous applications have stimulated the development of new methods and opened up previously inaccessible fields of research to electrochemistry. Present research goals include voltammetric measurements of the thermodynamics and analytical chemistry of poorly conducting electrolytic media from the solid state, through nonelectrolytic solutions, to the gas phase, as well as of the mechanisms and kinetics of very fast electrochemical reactions. With in vivo voltammetry, metabolic processes can be observed in cell tissue without causing any damage, and in the field of applied electrochemistry new strategies for sensor development[207] and corrosion research[224] are emerging. Moreover, with the new SECM technique an electrochemical method is available, which, for the first time, makes it possible to derive images of surface structures by measuring faradaic currents, as well as to microgalvanize and etch surfaces.

The persistent trend to smaller electrodes and simpler manufacturing techniques, assisted by efficient microsystem technologies and advances in laser research,[225] will considerably expand the scope of applications. The many aspects of an electrochemistry in a "natural" environment will surely encourage more intense interdisciplinary cooperation with other fields in chemistry, biology, and the material sciences. The priority status of the fast-scan technique and probably the SECM technique, too, should ensure that they reach a degree of perfection in the near future, which will turn them into routine methods using commercial equipment. The application of the techniques of microelectroplating will soon be used to build elements for microelectronics and micromechanics that will be able to compete with the products of photolithographic techniques. After an extraordinarily successful start, microelectrochemistry has a very promising future.

I am indebted to my excellent co-workers for their commitment and their considerable contributions in the form of ideas and experiments, which have gained for my research group its reputation in the field of ultramicroelectrodes. Their names will be found in the references. Dr. Michael Störzbach's conception of simulation models and his construction and application of UMEs were pioneering developments in this field. To him go my special thanks. I am grateful to the Deutsche Forschungsgemeinschaft, the Volkswagen Foundation, and the Fonds der Chemischen Industrie for the generous support they have given our work. Mr. Danny O'Hare, Imperial College, London, and Dr. Christian Amatore, Ecole Normale Supérieure, Paris, provided many suggestions in numerous discussions, for which I thank them both. Some aspects of the work mentioned in the text were only possible through the cooperation of other groups, in particular the Max-Planck-Institut für Systemphysiologie in Dortmund and the research group of Professor Besenhard, University of Münster. Finally, I wish to thank Dipl.-Chem. Peter Tschuncky, whose work on the fast-scan technique has set new standards for quality in microelectrodes.

Received: February 3, 1993 [A 917IE]
German version: *Angew. Chem.* **1993**, *105*, 1337
Translated by John Richardson, Freiburg

[1] K. J. Vetter, *Elektrochemische Kinetik*, Springer, Berlin, **1961**.
[2] P. Delahay, *New Instrumental Methods in Electrochemistry*, Interscience, New York, **1954**.
[3] a) J. Heyrovsky, *Chem. Listy* **1992**, *16*, 256; b) J. Heyrovsky, *Recl. Trav. Chim. Pays-Bas* **1925**, *44*, 488.
[4] D. MacGillavry, E. K. Rideal, *Recl. Trav. Chim. Pays-Bas* **1937**, *56*, 1013.
[5] a) H. A. Laitinen, I. M. Kolthoff, *J. Am. Chem. Soc.* **1939**, *61*, 3344; b) H. A. Laitinen, I. M. Kolthoff, *J. Phys. Chem.* **1941**, *45*, 1061.
[6] a) A. J. Bard, *Anal. Chem.* **1962**, *33*, 11; b) P. J. Lingane, *Anal. Chem.* **1964**, *36*, 1723; c) Z. G. Soos, P. J. Lingane, *J. Phys. Chem.* **1964**, *68*, 3821.
[7] a) I. Shain, K. J. Martin, *J. Phys. Chem.* **1961**, *65*, 254; b) I. Shain, K. J. Martin, J. W. Ross, *ibid.* **1961**, *65*, 259.
[8] R. S. Nicholson, I. Shain, *Anal. Chem.* **1964**, *36*, 706.
[9] D. I. Dornfield, D. H. Evans, *J. Electroanal. Chem.* **1968**, *20*, 341.
[10] Y. Saito, *Rev. Polarogr.* **1968**, *15*, 177.
[11] W. Grunewald, *Pfluegers Arch.* **1970**, *320*, 24.
[12] C. R Ito, S. Asokura, K. Nobe, *J. Electrochem. Soc.* **1972**, *119*, 698.
[13] J. B. Flanagan, L. Marcoux, *J. Phys. Chem.* **1973**, *77*, 1051.
[14] R. N. Adams, *Anal. Chem.* **1976**, *48*, 1126A.
[15] R. Lines, V. D. Parker, *Acta Chem. Scand. Ser. B* **1977**, *31*, 369.
[16] B. Speiser, A. Rieker, *Electrochim. Acta* **1978**, *23*, 983.
[17] J.-L. Ponchon, R. Cespuglio, F. Gonon, M. Jouvet, J.-F. Pujol, *Anal. Chem.* **1979**, *51*, 1483.
[18] P. N. Swan, Dissertation, University of Southampton, **1980**.
[19] J. Heinze, *Ber. Bunsenges. Phys. Chem.* **1980**, *84*, 785; *ibid.* **1981**, *85*, 1096.
[20] a) B. R. Scharifker, G. J. Hills, *J. Electroanal. Chem.* **1981**, *130*, 81; b) G. Hills, A. K. Pour, B. Sharifker, *Electrochim Acta* **1983**, *28*, 891.
[21] F. G. Cottrell, *Z. Phys. Chem. Stoechiom. Verwandschaftsl.* **1902**, *42*, 385.
[22] R. M. Wightman, *Anal. Chem.* **1981**, *53*, 1125A.
[23] a) L. R. Blinks, R. K. Skow, *Proc. Natl. Acad. Sci. USA* **1938**, *24*, 420. b) P. W. Davies, F. Brink, *Rev. Sci. Instrum.* **1942**, *13*, 524.
[24] Y. H. Lee, G. T. Tao, *Adv. Biochem. Eng.* **1979**, *13*, 36.
[25] H. Baumgärtl, D. W. Lübbers in *Polarographic Oxygen Sensors* (Eds.: E. Gnaiger, H. Forstner), Springer, Berlin, **1983**, p. 37.
[26] A. M. Bond, T. F. Man, *Electrochim. Acta.* **1987**, *32*, 863.
[27] A. M. Bond, M. Fleischmann, J. Robinson, *J. Electroanal. Chem.* **1984**, *180*, 257.
[28] J. Ghorogchian, F. Sarfarazi, T. Dibble, J. Cassidy, J.-J. Smith, A. Russell, G. Dunmore, M. Fleischmann, S. Pons, *Anal. Chem.* **1986**, *58*, 2278.
[29] A. J. Bard, F.-R. F. Fan, J. Kwak, O. Lev, *Anal. Chem.* **1989**, *61*, 132.
[30] a) R. M. Wightman, D. O. Wipf in *Electroanalytical Chemistry, Vol. 15* (Ed.: A. J. Bard), Marcel Dekker, New York, **1989**, p. 267; b) A. M. Bond, K. B. Oldham, C. G. Zoski, *Anal. Chim. Acta.* **1989**, *216*, 177; c) J. Robinson in *Comprehensive Kinetics, Vol. 29* (Ed.: C. H. Bamford, R. G. Compton), Elsevier, Amsterdam, **1989**, p. 149; d) J. Heinze, *Angew. Chem.* **1991**, *103*, 175; *Angew. Chem. Int. Ed. Engl.* **1991**, *30*, 170; e) R. M. Penner, N. S. Lewis, *Chem. Ind.* **1991**, 788; f) B. R. Scharifker in *Microelectrode Techniques in Electrochemistry Mod. Aspects of Electrochem.)* **1992**, *22*.
[31] a) M. Fleischmann, S. Pons, D. R. Rolison in *Ultramicroelectrodes* (Ed.: P. P. Schmidt), Datatech Systems. Inc. Morganton, **1987**; b) *Microelectrodes: Theory and Application* (Ed.: M. I. Montenegro, M. A. Queiros, J. L. Daschbach) (*NATO ASI Ser. Ser. E* **1991**, *197*).
[32] A. J. Bard, L. R. Faulkner, *Electrochemical Methods, Fundamentals and Applications*, Wiley, New York, **1980**.
[33] A. T. Hubbard, F. C. Anson, *Electroanal. Chem.* **1970**, *4*, 129.
[34] J. Heinze, *Angew. Chem.* **1984**, *96*, 823; *Angew. Chem. Int. Ed. Engl.* **1984**, *23*, 831.
[35] J. Crank, *The Mathematics of Diffusion*, Clarendon, Oxford, **1976**.
[36] A. M. Bond, M. Fleischmann, J. Robinson, *J. Electroanal. Chem.* **1984**, *168*, 299.
[37] M. A. Dayton, J. C. Brown, K. J. Stutts, R. M. Wightman, *Anal. Chem.* **1980**, *52*, 946.
[38] J. O. Howell, R. M. Wightman, *Anal. Chem.* **1984**, *56*, 524.
[39] K. R. Wehmeyer, M. R. Deakin, R. M. Wightman, *Anal. Chem.* **1985**, *57*, 1913.
[40] T. V. Shea, A. J. Bard, *Anal. Chem.* **1987**, *59*, 2101.
[41] P. M. Kovach, W. L. Caudill, D. G. Peters, R. M. Wightman, *J. Electroanal. Chem.* **1985**, *185*, 285.
[42] J. S. Symanski, S. Bruckenstein, *J. Electrochem. Soc.* **1984**, *131*, 110C.
[43] D. R. MacFarlane, D. K. Y. Wong, *J. Electroanal. Chem.* **1985**, *185*, 197.
[44] M. Fleischmann, S. Bandyopadhyay, S. Pons, *J. Phys. Chem.* **1985**, *89*, 5537.
[45] T. Gueshi, K. Tokuda, H. Matsuda, *J. Electroanal. Chem.* **1978**, *89*, 247; *ibid.* **1979**, *101*, 29; *ibid.* **1979**, *102*, 41.
[46] F. Belal, J. L. Anderson, *Analyst* **1985**, *110*, 1493.
[47] M. Ciszkowska, Z. Stojek, *J. Electroanal. Chem.* **1985**, *191*, 101.
[48] H. Reller, E. Kirowa-Eisner, E. Gileadi, *J. Electroanal. Chem.* **1982**, *138*, 65; *ibid.* **1984**, *161*, 247.
[49] D. Shoup, A. Szabo, *J. Electroanal. Chem.* **1984**, *160*, 19.
[50] K. R. Wehmeyer, R. M. Wightman, *Anal. Chem.* **1985**, *57*, 1989.
[51] P. M. Kovach, M. R. Deakin, R. M. Wightman, *J. Phys. Chem.* **1986**, *90*, 4612.
[52] J. Heinze, *J. Electroanal. Chem.* **1981**, *124*, 73.
[53] a) K. Aoki, J. Osteryoung, *J. Electroanal. Chem.* **1981**, *122*, 19; b) K. Aoki, J. Osteryoung, *ibid.* **1984**, *160*, 335.
[54] D. Shoup, A. Szabo, *J. Electroanal. Chem.* **1982**, *140*, 237.
[55] K. B. Oldham, *J. Electroanal. Chem.* **1981**, *122*, 1.
[56] K. B. Oldham, C. G. Zoski, *J. Electroanal. Chem.* **1988**, *256*, 11.
[57] C. G. Zoski, A. M. Bond, E. T. Allinson, K. B. Oldham, *Anal. Chem.* **1990**, *62*, 37.
[58] a) M. Fleischmann, S. Pons, *J. Electroanal. Chem.* **1987**, *222*, 107; b) A. Szabo, *J. Phys. Chem.* **1987**, *91*, 3108.
[59] a) S. Coen, D. K. Cope, D. E. Tallman, *J. Electroanal. Chem.* **1986**, *215*, 29; b) K. Aoki, K. Tokuda, H. Matsuda, *ibid.* **1987**, *225*, 19.
[60] a) J. Heinze, M. Störzbach, *Ber. Bunsenges. Phys. Chem.* **1986**, *90*, 1043; b) M. Störzbach, J. Heinze, *J. Electroanal. Chem.* **1993**, *346*, 1.
[61] a) C. A. Amatore, M. R. Deakin, R. M. Wightman, *J. Electroanal. Chem.* **1986**, *206*, 23; b) M. R. Deakin, R. M. Wightman, C. A. Amatore, *ibid.* **1986**, *215*, 49; c) C. A. Amatore, B. Fosset, M. R. Deakin, R. M. Wightman, *ibid.* **1987**, *225*, 33; d) C. Michael, R. M. Wightman, C. A. Amatore, *ibid.* **1989**, *267*, 33.
[62] W. H. Reinmuth, *J. Am. Chem. Soc.* **1957**, *79*, 6358.
[63] a) K. B. Oldham, C. G. Zoski, A. M. Bond, D. Sweigart, *J. Electroanal. Chem.* **1988**, *248*, 467; b) K. B. Oldham, J. C. Myland, C. G. Zoski, A. M. Bond, *ibid.* **1989**, *270*, 79; c) Z. Galus, J. Golas, J. Osteryoung, *J. Phys. Chem.* **1988**, *92*, 1103.
[64] a) J. Heinze, in [31b], 283); b) M. Störzbach, Disseration, Freiburg, **1991**.
[65] J. C. Imbeaux, J. M. Saveant, *J. Electroanal. Chem.* **1970**, *28*, 325.
[66] J. A. Frauenhofer, C. H. Bank, *Potentostats and its Applications*, Butterworth, London, **1972**.
[67] a) D. Britz, *J. Electroanal. Chem.* **1978**, *88*, 309; b) D. Garreau, J.-M. Saveant, *ibid.* **1974**, *50*, 1.
[68] a) K. B. Oldham, *J. Electroanal. Chem.* **1987**, *237*, 303; b) S. Bruckenstein, *Anal. Chem.* **1987**, *59*, 2098.
[69] A. M. Bond, D. Luscombe, K. B. Oldham, C. G. Zoski, *J. Electroanal. Chem.* **1988**, *249*, 1.
[70] a) K. B. Oldham, C. G. Zoski in *Comprehensive Kinetics, Vol. 26* (Eds.: G. H. Bamford, R. G. Compton), Elsevier, Amsterdam, **1986**, p. 79; b) C. A. Amatore, M. R. Deakin, R. M. Wightman, *J. Electroanal. Chem.* **1987**, *220*, 49.
[71] a) K. B. Oldham in ref. [30b], p. 83; b) K. B. Oldham, *J. Electroanal. Chem.* **1988**, *250*, 1.
[72] M. Fleischmann, F. Lasserre, J. Robinson, *J. Electroanal. Chem.* **1984**, *177*, *115*.
[73] K. B. Oldham, *J. Electroanal. Chem.* **1991**, *313*, 3.
[74] M. Fleischmann, F. Lasserre, J. Robinson, D. Swan, *J. Electroanal. Chem.* **1984**, *177*, 97.
[75] a) A. Denault, M. Fleischmann, D. Pletcher, O. R. Tutty, *J. Electroanal. Chem.* **1990**, *280*, 243; b) A. Denault, M. Fleischmann, D. Pletcher, *J. Electroanal. Chem.* **1990**, *280*, 255; c) A. Denault, D. Pletcher, *ibid.* **1991**, *305*, 131; C. G. Philips, *ibid.* **1990**, *296*, 255.
[76] M. A. Dayton, A. S. Ewing, R. M. Wightman, *Anal. Chem.* **1980**, *52*, 2392.

[77] a) M. Dong, G. Che, *J. Electroanal. Chem.* **1991**, *309*, 103; b) C. L. Miaw, J. F. Rusling, A. Owlia, *Anal. Chem.* **1990**, *62*, 268.
[78] C. G. Zoski, D. A. Sweigart, N. J. Stone, P. H. Reiger, E. Mocellin, T. F. Mann, D. R. Mann, D. K. Gosser, M. M. Doeff, A. M. Bond, *J. Am. Chem. Soc.* **1988**, *110*, 2109.
[79] A. M. Bond, G. Jaouen, T. F. Mann, E. Mocellin, S. Top, *Organometallics* **1989**, *8*, 2382.
[80] a) J. Heinze, M. Störzbach in ref. [31 b], p. 99; b) M. Störzbach, Dissertation, Freiburg, **1991**.
[81] a) L. S. Marcoux, R. N. Adams, S. W. Feldberg, *J. Phys. Chem.* **1969**, *73*, 2611; b) K. Debrodt, K. Heussler, *Z. Phys. Chem. (Munich)* **1981**, *125*, 35.
[82] M. I. Montenegro in ref. [31 b], p. 429.
[83] M. I. Montenegro, D. Pletcher, *J. Electroanal. Chem.* **1988**, *248*, 229.
[84] M. J. Medeiros, M. I. Montenegro, D. Pletcher, *J. Electroanal. Chem.* **1990**, *290*, 155.
[85] M. I. Montenegro, D. Pletcher, E. A. Liolios, D. J. Mazur, C. Zawodzinski, *J. Appl. Electrochem.* **1990**, *20*, 54.
[86] a) S. Dong, G. Che, *J. Electroanal. Chem.* **1991**, *315*, 191; b) G. Che, S. Dong, *Electrochim. Acta* **1992**, *37*, 2695, 2701.
[87] M. Kalaji, L. Nyholm, L. M. Peter, *J. Electroanal. Chem.* **1992**, *325*, 269.
[88] R. John, G. G. Wallace, *J. Electroanal. Chem.* **1991**, *306*, 157.
[89] a) S. U. Pedersen, K. Daasbjerg, *Acta Chem. Scand.* **1989**, *43*, 301; b) K. Daasbjerg, S. U. Pedersen, H. Lund, *ibid.* **1989**, *43*, 875.
[90] C. D. Baer, N. J. Stome, D. A. Sweigart, *Anal. Chem.* **1988**, *60*, 188.
[91] J. D. Norton, H. S. White, S. W. Feldberg, *J. Phys. Chem.* **1990**, *94*, 6772.
[92] K. Itaya, T. Abe, I. Uchida, *J. Electrochem. Soc.* **1987**, *134*, 1191.
[93] B. D. Pendley, H. D. Abruna, *Anal. Chem.* **1990**, *62*, 782.
[94] a) R. M. Penner, M. J. Herben, N. S. Lewis, *Anal. Chem.* **1989**, *61*, 1630; b) R. M. Penner, M. J. Herben, T. L. Longin, N. S. Lewis, *Science*, **1990**, *250*, 1118.
[95] A. M. Bond, T. I. Henderson, D. R. Mann, T. F. Mann, W. Thormann, C. G. Zoski, *Anal. Chem.* **1988**, *60*, 1678.
[96] R. A. Marcus, *J. Phys. Chem.* **1963**, *67*, 853. Nobel-Vortrag: R. A. Marcus, *Angew. Chem.* **1993**, *105*, 1161; *Angew. Chem. Int. Ed. Engl.* **1993**, *32*, 1111.
[97] A. S. Baranski, *J. Electroanal. Chem.* **1991**, *307*, 287.
[98] J. C. Myland, K. B. Oldham, *J. Electroanal. Chem.* **1983**, *147*, 295.
[99] B. Speiser, S. Pons, *Can. J. Chem.* **1982**, *60*, 1352.
[100] I. Lavagnini, P. Pastore, F. Magno, *Can. J. Chem.* **1992**, *333*, 1.
[101] A Neudeck, J. Dittrich, *J. Electroanal. Chem.* **1991**, *313*, 37.
[102] L. K. Safford, M. J. Weaver, *J. Electroanal. Chem.* **1991**, *312*, 69.
[103] R. S. Nicholson, *Anal. Chem.* **1965**, *37*, 1351.
[104] C. A. Amatore, C. Lefrou, *J. Electroanal. Chem.* **1990**, *296*, 335.
[105] R. M. Wightman, D. O. Wipf, *Acc. Chem. Res.* **1990**, *23*, 64.
[106] J. W. Howell, R. M. Wightman, *J. Phys. Chem.* **1984**, *88*, 3915.
[107] J. O. Howell, J. Goncalves, C. Amatore, L. Klasinc, J. Kochi, R. M. Wightman, *J. Am. Chem. Soc.* **1984**, *106*, 3968.
[108] P. Hapiot, J. Pinson, C. Francesch, F. Mhamdi, C. Rolando, S. Schneider, *J. Electroanal. Chem.* **1992**, *328*, 327.
[109] M. I. Montenegro, D. Pletcher, *J. Electroanal. Chem.* **1986**, *200*, 371.
[110] C. P. Andrieux, P. Hapiot, J.-M. Saveant, *Chem. Rev.* **1990**, *90*, 723.
[111] W. J. Bowyer, D. H. Evans, *J. Org. Chem.* **1988**, *53*, 5234.
[112] a) D. O. Wipf, R. M. Wightman, *Anal. Chem.* **1988**, *60*, 2460; b) D. O. Wipf, R. M. Wightman, *J. Phys. Chem.* **1989**, *93*, 4286.
[113] a) R. S. Robinson, R. L. McCreery, *Anal. Chem.* **1981**, *53*, 997; b) R. S. Robinson, C. W. McCurdy, R. L. McCreery, *ibid.* **1982**, *54*, 2356; c) R. S. Robinson, R. L. McCreery, *J. Electroanal. Chem.* **1985**, *182*, 61.
[114] K. Meerholz, P. Tschuncky, J. Heinze, *J. Electroanal. Chem.* **1993**, *347*, 425.
[115] a) A. Fitch, D. H. Evans, *J. Electroanal. Chem.* **1986**, *202*, 83; b) W.-J. Boyer, D. H. Evans, *ibid.* **1988**, *240*, 227.
[116] a) D. Larumbe, I. Gallando, C. P. Andrieux, *J. Electroanal. Chem.* **1991**, *304*, 241; b) H. Yang, D. O. Wipf, A. J. Bard, *ibid.* **1992**, *331*, 913; c) C. A. Amatore, A. Jutan, F. Pflüger, *ibid.* **1987**, *218*, 361.
[117] C. P. Andrieux, P. Hapiot, J.-M. Saveant, *J. Phys. Chem.* **1988**, *92*, 5987; *ibid.* **1988**, *92*, 5992.
[118] H. Taube, H. Myers, *J. Am. Chem. Soc.* **1954**, *76*, 2103.
[119] C. P. Andrieux, P. Audebert, P. Hapiot, J.-M. Saveant, *J. Am. Chem. Soc.* **1990**, *112*, 2439.
[120] a) P. Tschuncky, J. Heinze, *Synth. Met.* **1993**, *55*, 1603; b) P. Tschuncky, Diplomarbeit, Freiburg, **1991**; P. Tschuncky, J. Heinze, unpublished results.
[121] C. A. Amatore, C. Lefrou, F. Pflüger, *J. Electroanal. Chem.* **1989**, *270*, 43.
[122] a) C. P. Andrieux, D. Garreau, P. Hapiot, J. Pinson, J.-M. Saveant, *J. Electroanal. Chem.* **1988**, *243*, 321; b) C. P. Andrieux, D. Garreau, P. Hapiot, J.-M. Saveant, *ibid.* **1988**, *248*, 447; c) D. Garreau, P. Hapiot, J.-M. Saveant, *ibid.* **1989**, *272*, 1; d) D. Garreau, P. Hapiot, J.-M. Saveant, *ibid.* **1990**, *289*, 73.
[123] G. M. Brisard, M. Manzini, A. Lasia, *J. Electroanal. Chem.* **1992**, *326*, 317.
[124] W. J. Bowyer, E. E. Engelman, D. H. Evans, *J. Electroanal. Chem.* **1989**, *262*, 67.
[125] D. W. Wipf, E. W. Kristensen, M. R. Deakin, R. M. Wightman, *Anal. Chem.* **1988**, *60*, 306.
[126] L. K. Safford, M. J. Weaver, *J. Electroanal. Chem.* **1992**, *331*, 857.
[127] N. Oyama, S. Kikuyama, T. Tatsuma, *J. Electroanal. Chem.* **1993**, *344*, 367.
[128] A. S. Baranski, K. Winkler, W. R. Fawcett, *J. Electroanal. Chem.* **1991**, *313*, 367.
[129] D. O. Wipf, A. C. Michael, R. M. Wightman, *J. Electroanal. Chem.* **1989**, *269*, 15.
[130] a) K. Nuzaki, M. Oyama, H. Hatano, S. Okazaki, *J. Electroanal. Chem.* **1989**, *270*, 191; b) S. Nomura, K. Nozaki, S. Okazaki, *Anal. Chem.* **1991**, *63*, 2665.
[131] C. A. Amatore, C. Lefrou, *J. Electroanal. Chem.* **1992**, *324*, 33.
[132] J. O. Howell, W. G. Kuhr, R. E. Ensman, R. M. Wightman, *J. Electroanal. Chem.* **1986**, *209*, 77.
[133] a) W. Thormann, P. van den Bosch, A. M. Bond, *Anal. Chem.* **1985**, *57*, 2764; b) A. M. Bond, T. L. E. Henderson, W. Thormann, *J. Phys. Chem.* **1986**, *90*, 2911.
[134] A. M. Bond, P. A. Lay, *J. Electroanal. Chem.* **1986**, *199*, 285.
[135] a) J. B. Cooper, A. M. Bond, *J. Electroanal. Chem.* **1991**, *315*, 143; b) J. B. Cooper, A. M. Bond, K. B. Oldham, *ibid.* **1992**, *331*, 877.
[136] J. D. Norton, H. S. White, *J. Electroanal. Chem.* **1992**, *325*, 341.
[137] a) C. A. Amatore, B. Fosset, J. Bartelt, M. R. Deakin, R. M. Wightman, *J. Electroanal. Chem.* **1988**, *256*, 255; b) S. M. Drew, R. M. Wightman, C. A. Amatore, *ibid.* **1991**, *317*, 117.
[138] a) M. Ciszkowska, Z. Stojek, *J. Electroanal. Chem.* **1986**, *213*, 189; b) Z. Stojek, J. Osteryoung, *Anal. Chem.* **1988**, *60*, 131; c) M. Ciszkowska, Z. Stojek, J. Osteryoung, *ibid.* **1990**, *62*, 349.
[139] C. Lea, F. C. Anson, *J. Electroanal. Chem.* **1992**, *323*, 381.
[140] A. M. Bond, M. Fleischmann, J. Robinson, *J. Electroanal. Chem.* **1984**, *172*, 11.
[141] a) J. D. Norton, W. E. Benson, H. S. White, B. D. Pendley, H. D. Abruna, *Anal. Chem.* **1991**, *63*, 1909; b) B. D. Pendley, H. D. Abruna, J. D. Norton, W. E. Benson, H. S. White, *ibid.* **1991**, *63*, 2766.
[142] J. Cassidy, S. B. Khoo, S. Pons, M. Fleischmann, *J. Phys. Chem.* **1985**, *89*, 3933.
[143] C. Jehoulet, A. J. Bard, *Angew. Chem.* **1991**, *103*, 882; *Angew. Chem. Int. Ed. Engl.* **1991**, *30*, 836.
[144] a) L. Geng, A. G. Ewing, J. C. Jernigan, R. W. Murray, *Anal. Chem.* **1986**, *58*, 85; b) L. Geng, R. W. Murray, *Inorg. Chem.* **1986**, *25*, 311.
[145] S. Nakabayashi, A. Fujishima, K. Honda, *J. Electroanal. Chem.* **1980**, *111*, 391; *ibid.* **1983**, *149*, 149.
[146] M. V. Novotny, S. R. Springston, P. A. Peaden, J. C. Fjeldsted, M. L. Lee, *Anal. Chem.* **1981**, *53*, 407A.
[147] a) M. E. Philips, M. R. Deakin, M. V. Novotny, R. M. Wightman, *J. Phys. Chem.* **1987**, *91*, 3934; b) D. Niehaus, M. Philips, A. Michael, R. M. Wightman, *ibid.* **1989**, *93*, 6232; c) A. C. Michael, R. M. Wightman, *Anal. Chem.* **1989**, *61*, 2193; *ibid.* **1989**, *61*, 2770.
[148] W. Gorski, J. A. Cox, *J. Electroanal. Chem.* **1992**, *323*, 163.
[149] a) R. A. Reed, L. Geng, R. W. Murray, *J. Electroanal. Chem.* **1986**, *208*, 185; b) L. Geng, R. A. Reed, R. W. Murray, *J. Phys. Chem.* **1987**, *91*, 2914; c) L. Geng, R. A. Reed, M.-H. King, T. T. Wooster, B. N. Oliver, J. Egekeze, R. T. Kennedy, J. W. Jorgenson, J. F. Parcher, R. W. Murray, *J. Am. Chem. Soc.* **1989**, *111*, 1614; d) R. A. Reed, T. T. Wooster, R. W. Murray, D. R. Yaniv, J. S. Tonge, D. F. Shriver, *J. Electrochem. Soc.* **1989**, *136*, 2565; e) H. Nishihara, F. Dalton, W. Murray, *Anal. Chem.* **1991**, *63*, 2955; f) T. T. Wooster, M. L. Longmine, H. Zhang, M. Watanabe, R. W. Murray, *ibid.* **1992**, *64*, 1132.
[150] a) A. M. Bond, M. Svestka, *J. Electroanal. Chem.* **1991**, *301*, 139; b) A. M. Bond, V. B. Pfund, *ibid.* **1992**, *325*, 281.
[151] D. K. Gosser, Q. Huang, *J. Electroanal. Chem.* **1989**, *267*, 333.
[152] a) R. Brina, S. Pons, M. Fleischmann, *J. Electroanal. Chem.* **1988**, *244*, 81; b) R. Brina, S. Pons, *ibid.* **1989**, *264*, 121.
[153] J. Ghoroghchian, S. Pons, M. Fleischmann, *J. Electroanal. Chem.* **1991**, *317*, 101.
[154] a) H. Baumgärtl, D. W. Lübbers in *Oxygen Supply* (Eds.: M. Kessler, D. F. Bruley, L. C. Clark, D. W. Lübbers, I. A. Silver, J. Strauss), Urban und Schwarzenberg, München, **1973**, p. 130–136; b) H. Baumgärtl in *Clinical Oxygen Measurement* (Eds.: A. M. Ehrly, J. Hauss, R. Huch), Springer, Heidelberg, **1987**, p. 17–42; c) H. Baumgärtl, U. Heinrich, D. W. Lübbers, *Pfluegers Arch.* **1989**, *414*, 228; d) J. Beunink, H. Baumgärtl, W. Zimelka, H.-J. Rehm, *Experientia* **1989**, *45*, 1041.
[155] a) R. N. Adams, *Anal. Chem.* **1976**, *48*, 1126A; b) R. M. Wightman, E. Strope, P. M. Plotsky, R. N. Adams, *Nature* **1976**, *262*, 145.
[156] a) R. Kelly, R. M. Wightman, *Anal. Chim. Acta* **1986**, *187*, 79; E. W. Kristensen, W. G. Kuhr, R. M. Wightman, *Anal. Chem.* **1987**, *59*, 1751; J. E. Baur, E. W. Kristensen, L. J. May, D. J. Wiedemann, R. M. Wightman, *ibid.* **1988**, *60*, 1268.
[157] B. Poulain, G. Baux, L. Tauc, D. Henzel, *Anal. Chem.* **1986**, *58*, 2091.
[158] P. A. Broderick, *Electroanalysis* **1990**, *2*, 241.
[159] a) M. Armstrong-James, K. Fox, Z. I. Kruk, J. Millar, *J. Neurosci. Methods* **1981**, *4*, 385; b) W. G. Kuhr, R. M. Wightman, *Brain Res.* **1986**, *381*, 168; c) D. J. Wiedemann, K. T. Kawagoe, R. T. Kennedy, E. Ciolkowski, R. M. Wightman, *Anal. Chem.* **1991**, *63*, 2965.

[160] a) T. K. Chen, Y. Y. Lau, D. K. Y. Wong, A. G. Ewing, *Anal. Chem.* **1992**, *64*, 1264; b) F. Bailey, T. Malinski, F. Kiechle, *ibid.* **1991**, *63*, 395.

[161] a) R. M. Wightman, L. J. May, A. C. Michael, *Anal. Chem.* **1988**, *60*, 769A; b) R. M. Wightman, R. T. Kennedy, D. J. Wiedemann, K. T. Kawagoe, J. B. Zimmerman, D. J. Leszczyszyn in ref. [30b], p. 453M; c) K. T. Kawagoe, J. A. Jankowski, R. M. Wightman, *Anal. Chem.* **1991**, *63*, 1589.

[162] W. P. Hamil, A. Marty, E. Neher, B. Sakmann, F. J. Sigworth, *Pfluegers Arch.* **1981**, *391*, 85.

[163] a) E. Neher, *Angew. Chem.* **1992**, *104*, 837; *Angew. Chem. Int. Ed. Engl.* **1992**, *31*, 824; b) B. Sakmann, *ibid.* **1992**, *104*, 844 or **1992**, *31*, 830.

[164] L. von Rüden, H. Chow, E. Neher, *Tagungsband DECHEMA* Symp. Mikroelektrochemie, Friedrichroda, **1992**.

[165] a) K. Bade, V. Tsakova, J. W. Schulze, *Electrochim. Acta* **1992**, *37*, 2255; b) M. Fleischmann, S. Pons, J. Daschbach in ref. [31b], p. 393.

[166] a) R. L. Deutscher, S. Fletcher, *J. Electroanal. Chem.* **1988**, *239*, 17; *ibid.* **1990**, *270*, 1; b) S. Fletcher in ref. [31b], p. 341.

[167] a) C. L. Colyer, D. Luscombe, K. B. Oldham, *J. Electroanal. Chem.* **1990**, *283*, 379; b) C. L. Colyer, K. B. Oldham, S. Fletcher, *ibid.* **1990**, *290*, 33.

[168] H. S. Isaacs, *J. Electrochem. Soc.* **1988**, *135*, 2180.

[169] a) R. C. Newman, *Corros. Sci.* **1985**, *25*, 341; b) R. T. Atanasoski, H. S. White, W. H. Smyrl, *J. Electrochem. Soc.* **1986**, *133*, 2435; K. Wikiel, J. Osteryoung, *ibid.* **1988**, *135*, 1915.

[170] a) D. E. Williams, C. Westcott, M. Fleischmann, *J. Electroanal. Chem.* **1985**, *132*, 1796; *ibid.* **1985**, *132*, 1804; b) D. E. Williams, in ref. [31b], p. 445.

[171] a) G. Binning, H. Rohrer, *Angew. Chem.* **1987**, *99*, 622; *Angew. Chem. Int. Ed. Engl.* **1987**, *26*, 606; b) J. Frommer, *ibid.* **1992**, *104*, 1325 or **1992**, *32*, 1298.

[172] a) A. J. Bard, F.-R. R. Fan, J. Kwak, O. Lev, *Anal. Chem.* **1989**, *61*, 132; b) A. J. Bard, G. Denuault, C. Lee, D. Mandler, D. O. Wipf, *Acc. Chem. Res.* **1990**, *23*, 357; c) A. J. Bard, F.-R. F. Fan, D. T. Pierce, P. R. Unwin, D. O. Wipf, F. Zhou, *Science* **1991**, *254*, 68.

[173] J. Kwak, A. J. Bard, *Anal. Chem.* **1989**, *61*, 1221.

[174] a) J. Kwak, A. J. Bard, *Anal. Chem.* **1989**, *61*, 1794; b) C. Lee, C. J. Miller, A. J. Bard, *ibid.* **1991**, *63*, 78.

[175] C. Lee, A. J. Bard, *Anal. Chem.* **1990**, *62*, 1906.

[176] J. Kwak, C. Lee, A. J. Bard, *J. Electrochem. Soc.* **1990**, *137*, 1481.

[177] C. Lee, J. Kwak, A. J. Bard, *Proc. Natl. Acad. Sci. USA* **1990**, *87*, 1740.

[178] D. O. Wipf, A. J. Bard, *J. Electrochem. Soc.* **1991**, *138*, 469.

[179] R. C. Engstrom, B. Small, L. Kattan, *Anal. Chem.* **1992**, *64*, 241.

[180] J. Wang, L.-H. Wu, R. Li, *J. Electroanal. Chem.* **1989**, *272*, 285.

[181] a) R. C. Engstrom, M. Weber, D. J. Wunder, R. Burgess, S. Winquist, *Anal. Chem.* **1986**, *58*, 844; b) R. C. Engstrom, T. Meaney, R. Tople, R. M. Wightman, *ibid.* **1987**, *59*, 2005; R. C. Engstrom, R. M. Wightman, E. W. Kristensen, *ibid.* **1988**, *60*, 652.

[182] W. J. Albery, M. L. Hitchman, *Ring-Disc-Electrodes*, Clarendon, Oxford, **1971**.

[183] C. Lee, J. Kwak, F. C. Anson, *Anal. Chem.* **1991**, *63*, 1501.

[184] a) D. H. Craston, C. W. Lin, A. J. Bard, *J. Electrochem. Soc.* **1988**, *135*, 785; b) O. E. Hüsser, D. H. Craston, A. J. Bard, *J. Vac. Sci. Technol. B* **1988**, *6*, 1873; c) O. E. Hüsser, D. H. Craston, A. J. Bard, *J. Electrochem. Soc.* **1989**, *136*, 3222; d) T.-M. Wuu, F.-R. F. Fan, A. J. Bard, *ibid.* **1989**, *136*, 885.

[185] a) D. Mandler, A. J. Bard, *J. Electrochem. Soc.* **1989**, *136*, 3143; b) *ibid.* **1990**, *137*, 1079; c) *ibid.* **1990**, *137*, 2468.

[186] a) C. Lee, D. O. Wipf, A. J. Bard, K. Bartels, A. C. Bovik, *J. Electrochem. Soc.* **1991**, *63*, 2442; b) D. O. Wipf, A. J. Bard, *ibid.* **1992**, *64*, 1362.

[187] A. J. Bard, J. A. Crayston, G. P. Kittlesen, T. V. Shea, M. S. Wrighton, *Anal. Chem.* **1986**, *58*, 231.

[188] C. E. Chidsey, B. J. Feldman, C. Lundgren, R. W. Murray, *Anal. Chem.* **1986**, *58*, 601.

[189] a) J. E. Bartelt, M. R. Deakin, C. Amatore, R. M. Wightman, *Anal. Chem.* **1988**, *60*, 2167; b) B. Fosset, C. Amatore, J. Bartelt, R. M. Wightman, *ibid.* **1991**, *63*, 1403.

[190] O. Niwa, M. Morita, H. Tabei, *Anal. Chem.* **1990**, *62*, 447.

[191] W. F. Berry, S. G. Weber, *J. Electroanal. Chem.* **1986**, *208*, 77.

[192] D. J. Wiedemann, K. T. Kawagoe, R. T. Kennedy, E. L. Ciolkowski, R. M. Wightman, *Anal. Chem.* **1991**, *63*, 2965.

[193] a) D. P. Whelan, J. J. O'Dea, J. Osteryoung, *J. Electroanal. Chem.* **1986**, *202*, 23; b) J. J. O'Dea, M. Wojciechowski, J. Osteryoung, *Anal. Chem.* **1985**, *57*, 954; c) K. Aoki, K. Tokuda, H. Matsuda, J. Osteryoung, *J. Electroanal. Chem.* **1986**, *207*, 25; d) L. Sinru, J. Osteryoung, J. J. O'Dea, R. Osteryoung, *Anal. Chem.* **1988**, *60*, 1135; e) M. J. Nuwer, J. Osteryoung, *ibid.* **1989**, *61*, 1954; f) C. Wechter, J. Osteryoung, *ibid.* **1989**, *61*, 2092; g) J. Osteryoung, M. M. Murphy, in ref. [30b], p. 123; h) J. Osteryoung in ref. [31b], p. 139.

[194] A. G. Ewing, M. A. Dayton, R. M. Wightman, *Anal. Chem.* **1981**, *53*, 1842.

[195] a) F. G. Gonon, C. M. Fombarlet, M. J. Buda, J. F. Pujol, *Anal. Chem.* **1981**, *53*, 1386; b) F. G. Gonon, F. Navarre, M. J. Buda, *ibid.* **1984**, *56*, 573.

[196] a) S. A. Schuette, R. L. McCreery, *J. Electroanal. Chem.* **1985**, *191*, 329; b) S. A. Schuette, R. L. McCreery, *Anal. Chem.* **1986**, *58*, 1778.

[197] a) A. S. Baranski, H. Quon, *Anal. Chem.* **1986**, *58*, 407; b) A. S. Baranski, *ibid.* **1987**, *59*, 662.

[198] C. Wechter, J. Osteryoung, *Anal. Chem.* **1989**, *61*, 2092.

[199] J. F. Coetzee, M. J. Ecoff, *Anal. Chem.* **1991**, *63*, 957.

[200] a) D. C. Johnson, S. G. Weber, A. M. Bond, R. M. Wightman, R. E. Shoup, I. S. Krull, *Anal. Chim. Acta* **1986**, *180*, 187; J. W. Bixler, A. M. Bond, *Anal. Chem.* **1986**, *58*, 2859; c) L. A. Knecht, E. J. Guthrie, J. W. Jorgenson, *ibid.* **1984**, *56*, 479; d) J. W. Bixler, M. Fifield, J. C. Poler, A. M. Bond, W. Thormann, *Electroanalysis* **1989**, *1*, 23; e) J. L. Anderson, K. K. Whiten, J. D. Brewster, T. Y. Ou, W. K. Nonidez, *Anal. Chem.* **1985**, *57*, 1366; f) M. Takahashi, M. Morita, O. Niwa, H. Tabei, *J. Electroanal. Chem.* **1992**, *335*, 253.

[201] J. M. Zadeii, R. Mitchell, T. Kuwana, *Electroanalysis* **1990**, *2*, 209.

[202] A. Aoki, T. Matsue, I. Uchida, *Anal. Chem.* **1992**, *64*, 44.

[203] D. H. Craston, C. P. Jones, D. E. Williams, *Talanta* **1991**, *38*, 17.

[204] a) S. T. Singleton, J. O'Dea, J. Osteryoung, *Anal. Chem.* **1989**, *61*, 1211; b) M. M. Murphy, J. O'Dea, J. Osteryoung, *ibid.* **1991**, *63*, 2743.

[205] N. Sleszynski, J. Osteryoung, M. Carter, *Anal. Chem.* **1984**, *56*, 130.

[206] D. E. Williams, in ref. [31b], p. 415.

[207] K. Camman, U. Lemke, A. Rohen, J. Sander, H. Wilken, B. Winter, *Angew. Chem.* **1991**, *103*, 519; *Angew. Chem. Int. Ed. Engl.* **1991**, *30*, 516.

[208] T. Zeuthen, *Med. Biol. Eng.* **1978**, *16*, 489.

[209] S. Fletcher in ref. [31b], p. 243.

[210] P. Tschuncky, J. Heinze, *Anal. Chem.*, submitted.

[211] A. Meulemans, B. Poulain, G. Baux, L. Tauc, D. Hanzel, *Anal. Chem.* **1986**, *58*, 2088.

[212] a) K. Potje-Kamloth, J. Janata, M. Josowicz, *Ber. Bunsenges. Phys. Chem.* **1989**, *93*, 1480; b) K. Potje-Kamloth, J. Janata, M. Josowicz, *Sens. Actuators* **1989**, *18*, 415; c) K. T. Kawagoe, J. A. Jankowski, R. M. Wightman, *Anal. Chem.* **1991**, *63*, 1589.

[213] F. Bailey, T. Malinski, F. Kiechle, *Anal. Chem.* **1991**, *63*, 395.

[214] a) T. G. Strein, A. G. Ewing, *Anal. Chem.* **1991**, *63*, 194; b) T. G. Strein, A. G. Ewing, *ibid.* **1992**, *64*, 1368; c) Y. Y. Lau, T. Abe, A. G. Ewing, *ibid.* **1992**, *64*, 1702.

[215] a) J. O. Besenhard, A. Schulte, K. Schur, P. D. Jannakoudakis, in ref. [30b], p. 189; b) A. Schulte, J. Besenhard, P. D. Jannakoudakis, J. Heinze, P. Tschuncky, *Tagungsband DECHEMA* Symp. *Mikroelektrochemie*, Friedrichroda, **1992**.

[216] G. Mengoli, P. Bianco, S. Dalio, M. T. Munari, *J. Electrochem. Soc.* **1981**, *128*, 2276.

[217] R. L. McCarley, M. G. Sullivan, S. Ching, Y. Zhang, R. W. Murray, in ref. [30b], p. 205.

[218] A. M. Bond, T. L. E. Henderson, W. Thormann, *J. Phys. Chem.* **1986**, *90*, 2911.

[219] a) R. S. Morris, D. J. Franmta, H. S. White, *J. Phys. Chem.* **1987**, *91*, 3559; b) J. B. Seibold, E. R. Scott, H. S. White, *J. Electroanal. Chem.* **1989**, *264*, 281.

[220] K. Aoki, K. R. Tokuda, *J. Electrochem. Chem.* **1987**, *237*, 163.

[221] L. F. Thompson, C. G. Wilson, *Introduction to Microlithography* (Ed.: M. J. Bowden), American Chemical Society, Washington, D.C., **1983**.

[222] a) G. P. Kittlesen, H. S. White, M. S. Wrighton, *J. Am. Chem. Soc.* **1984**, *106*, 7289; b) G. P. Kittlesen, H. S. White, M. S. Wrighton, *ibid.* **1985**, *107*, 7373; c) E. W. Paul, A. J. Ricco, M. S. Wrighton, *J. Phys. Chem.* **1985**, *89*, 1441; d) E. T. Turner Jones, O. M. Chyan, M. S. Wrighton, *J. Am. Chem. Soc.* **1987**, *109*, 5526.

[223] M. Samuelsson, M. Armgarth, C. Nylander, *Anal. Chem.* **1991**, *63*, 931.

[224] J. W. Schultze, *Nachr. Chem. Tech. Lab.* **1993**, *42*, 205.

[225] a) J. W. Schultze, J. Thietke, *Electrochim. Acta* **1989**, *34*, 1769; b) J. W. Schultze, K. Bade, O. Kartens, A. Michaelis, *Ber. Bunsenges. Phys. Chem.* **1991**, *95*, 1350.

Carboranes, Anti-Crowns, and Big Wheels

By *Russell N. Grimes**

Carboranes – polyhedral boranes containing carbon in the framework—have been around for over 30 years, and their intrinsic stability, versatility, structural variety, and electronic properties have been put to use in a number of diverse areas,[1] for example in the synthesis of extraordinarily heat-stable polymers, in boron neutron capture therapy (BNCT), as ligands in metallacarborane catalysts, as complexing agents for extraction of metal ions, as precursors to ceramics, conducting polymers, and nonlinear optical materials, as anticancer agents, and as carriers for radioactive metals in radioimmunodetection and radioimmunotherapy.

Although polyhedral carboranes having as few as five and as many as twelve vertices (fourteen if metal atoms are included) are known,[2] most research and applications have centered on the exceptionally stable seven- and twelve-vertex cage systems. Largely for reasons of accessibility, the twelve-vertex $C_2B_{10}H_{12}$ icosahedral carboranes have been most widely studied. The three known isomers, in which the carbon atoms occupy *ortho* (1,2), *meta* (1,7), or *para* (1,12) vertices, are white solids that rank among the most stable molecular compounds known. These clusters can be viewed as "superaromatic" systems in which 26 electrons fill the 13 bonding molecular orbitals on the polyhedral framework; moreover, the cage volume approximates that displaced by a benzene molecule rotating on one of its twofold axes. The very high intrinsic stability of the $C_2B_{10}H_{12}$ isomers, together with the acidic character of the hydrogen atoms bound to the cage carbon atoms (which allows facile introduction of functional groups at carbon), is the basis of extensive development of icosahedral carborane chemistry over three decades and its application to practical problems.[1, 2]

The remarkable versatility of carboranes presents an almost limitless range of possible roles in designed synthesis, a fact that is drawing increasing attention in organic and inorganic chemistry, materials science, engineering, and biologically related areas. A particularly elegant recent example is the design and construction of novel carborane-based macrocycles, in which both the electron-withdrawing character of the carborane cage and the close geometric relationship of icosahedral $C_2B_{10}H_{12}$ to planar C_6H_6 are exploited. In a series of papers,[3] Hawthorne et al. report the synthesis of "mercuracarborands" which incorporate three or more $C_2B_{10}H_{10}$ cages linked by an equal number of mercury atoms. The reaction of 1,2-dilithio-*ortho*-carborane $Li_2C_2B_{10}H_{10}$ with $HgCl_2$ afforded the tetramer shown in Figure 1a, which binds to a Cl^- ion, resulting in a nearly square-planar geometry for this ion (Fig. 1c), an unprecedented coordination mode for halide ions.[3a]

Since the uncomplexed THF adduct of the host macrocycle has been shown by X-ray crystallography to have S_4 symmetry with the centers of the icosahedra well outside the plane of the four mercury atoms,[3b] it has been proposed that the chloride ion functions as a template, creating the square-planar conformation. The carborane macrocycle is a Lewis acid and coordinates nucleophiles; it is therefore an "anti-crown",[4] that is, a charge-reversed analogue of the well-known family of nucleophilic hosts such as [12]crown-4 (Fig. 1b) that have figured prominently in molecular recognition studies.[5]

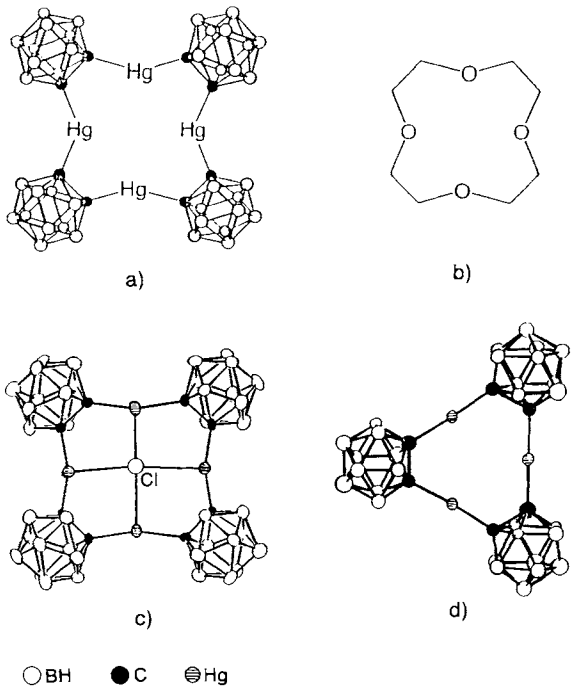

Fig. 1. a) Structure of the host tetramer $(1,2\text{-}C_2B_{10}H_{10}Hg)_4$ in its planar conformation [3a]. b) Structure of [12]crown-4. c) Structure of the tetramer with a bound chloride ion [3a]. d) Structure of the host trimer $(1,2\text{-}C_2B_{10}H_{10}Hg)_3$ (bound CH_3CN molecules not shown) [3f].

Treatment of the 1,2-dilithiocarborane with HgI_2 generated the dianionic species $[(1,2\text{-}C_2B_{10}H_{10})_4Hg_4I_2]^{2-}$ in which two iodide ions bind to the four mercury atoms;[3c] the corresponding reaction of the 1,2-dilithio-3-phenylcarborane gave a cyclic tetramer with only one I^- ion bound in the sterically encumbered cavity.[3d] Surprisingly, of the four possible stereoisomers, the only one formed was that having two phenyl rings directed "up" and two "down" with respect to the cavity. Addition of Ag^+ ions to the mercuracarborand complexes was found to remove the halide ion(s) and afford the free host molecule.[3a, c]

A related example of complexation by the mercuracarborand tetramer involves two polyhedral $B_{10}H_{10}^{2-}$ guest dianions that are bound to the four Hg atoms through three-center, two-electron B–H–Hg bonds.[3e] The reaction of dilithiocarborane with mercuric acetate[3f] yielded yet another macrocycle, this time a trimer (Fig. 1d) which coordi-

[*] Prof. Dr. R. N. Grimes
Department of Chemistry
University of Virginia
Charlottesville, VA 22901 (USA)
Telefax: Int. code + (804)924-3710

nates acetonitrile in a most unusual manner: the solid-state structure features two cocrystallized adducts having three and five CH_3CN-bound molecules, respectively. This anti-crown is analogous to trimeric *ortho*-phenylene mercury, but its mean Hg–Hg distance of more than 3.7 Å implies a larger central cavity than the latter compound.[3f] On treatment of $Hg_3(C_2B_{10}H_{10})_3$ with LiCl, an anionic chloride complex was formed in which the Cl^- ion is proposed to reside at the center of the Hg_3 triangle. The binding ability of these mercuracarborands toward Lewis bases implies that nitrogen-containing bases of biological relevance—adenine, guanine, and the like—may be similarly bound.[3f]

In a different synthetic tour de force that combined chemistry with art, Wade et al.[6] prepared the macrocycle shown in Figure 2. In this case the starting reagent was the dicopper

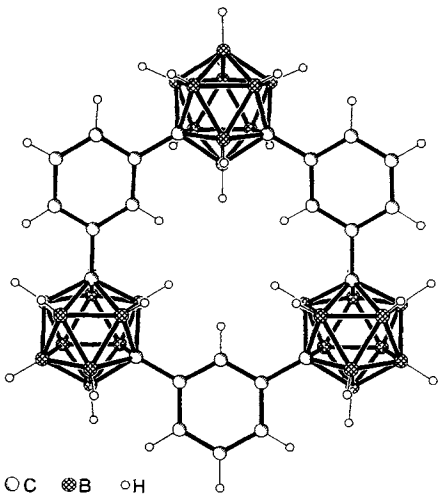

Fig. 2. Structure of $(1,7\text{-}C_2B_{10}H_{10}\text{-}1',3'\text{-}C_6H_4)_3$ [6].

meta-carborane, $1,7\text{-}Cu_2C_2B_{10}H_{10}$, which reacted with *meta*-diiodobenzene to give the desired trimeric product in low yield. As revealed by X-ray crystallography, the carborane cages are tilted away by 17° from the plane defined by their carbon atoms, while the benzene rings are tilted in the opposite direction by the same amount; consequently, the molecule has a dish-shaped structure whose central cavity is defined by three inward-directed carborane hydrogen atoms (mean separation 3.16 Å) and three phenylene hydrogen atoms that lie almost in the same plane; three other carborane hydrogen atoms are much further apart (ca. 4.47 Å). Boron atoms on the inside of the macrocycle could be removed and replaced with metals,[6] which opens truly intriguing possibilities for catalysis and other applications wherein the three metal centers act in concert.

Macrocycles incorporating the $1,2\text{-}C_2B_{10}H_{10}$ cage and linked by trimethylene or 1,3-xylyl groups have been prepared in Hawthorne's laboratory, and these include both trimers and tetramers.[7] The X-ray crystallographically determined structure of a xylyl-linked tetramer that features a remarkable 28-membered ring is shown in Figure 3.

While the geometries of the 1,2- and $1,7\text{-}C_2B_{10}$ cages are made to order for the synthesis of macrocycles through substitution at the carbon atoms, the 1,12-carborane (*para*-isomer) has carbon atoms at opposite ends of the polyhedron and is ideally suited for the assembly of rigid linear rods

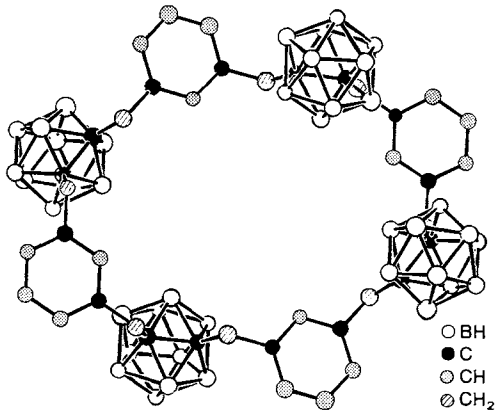

Fig. 3. Structure of $(1,2\text{-}C_2B_{10}H_{10}\text{-}1',3'\text{-}CH_2C_6H_4CH_2)_4$ [7].

through direct C–C connections, as has been demonstrated by two research groups.[8] As all these examples illustrate, the special stereochemistry of the icosahedral carboranes can be used to advantage in very innovative and creative ways. Molecular engineering employing nonicosahedral carborane or organoborane clusters is also under active investigation, as in the multidecker sandwich systems that incorporate seven-vertex MC_2B_3M' or MC_3B_2M' pentagonal bipyramidal cages.[9]

The beauty of the chemistry highlighted in this article lies in its essential simplicity, in that preorganized cyclic host molecules are generated in one or two steps from readily available reagents—an advantage not afforded by crown ethers and cryptands. These synthetic advances vividly exemplify the rapidly evolving art of "designer chemistry" in which inorganic and organometallic assemblies of specified architectures are obtained in directed reactions from available building-block molecules. It seems clear that carboranes and other boron clusters are destined to play a significant role in this field. Philosophically and historically, designed synthesis is derived from organic chemistry; but for inorganic chemists, given the entire periodic table of elements to play with, the scope of possibility seems far larger and the ultimate achievements hardly imaginable at present.

German version: *Angew. Chem.* **1993**, *105*, 1350

[1] J. Plesek, *Chem. Rev.* **1992**, *92*, 269, and references therein.

[2] a) V. I. Bregadze, *Chem. Rev.* **1992**, *92*, 209; b) B. Stibr, *ibid.* **1992**, *92*, 225; c) R. N. Grimes, *Carboranes*, Academic Press, New York, **1970**.

[3] a) X. Yang, C. B. Knobler, M. F. Hawthorne, *Angew. Chem.* **1991**, *103*, 1519; *Angew. Chem. Int. Ed. Engl.* **1991**, *30*, 1507; b) X. Yang, S. E. Johnson, S. I. Khan, M. F. Hawthorne, *ibid.* **1992**, *104*, 886 and **1992**, *31*, 893; c) X. Yang, C. B. Knobler, M. F. Hawthorne, *J. Am. Chem. Soc.* **1992**, *114*, 380; d) Z. Zheng, X. Yang, C. B. Knobler, M. F. Hawthorne, *ibid.* **1993**, *115*, 5320; e) X. Yang, C. B. Knobler, M. F. Hawthorne, *ibid.* **1993**, *115*, 4904; f) X. Yang, Z. Zheng, C. B. Knobler, M. F. Hawthorne, *ibid.* **1993**, *115*, 193.

[4] For a summary of published reports on anion complexation by multidentate Lewis acid hosts, see ref. [3f].

[5] a) D. J. Cram, *Science* **1983**, *219*, 1177; b) F. Vögtle, E. Weber, *Host-Guest Complex Chemistry/Macrocycles*, (Eds.: F. Vögtle, E. Weber), Springer, Berlin, **1985**; c) L. F. Lindoy, *The Chemistry of Macrocyclic Ligands*, Cambridge University Press, Cambridge, **1989**.

[6] W. Clegg, W. R. Gill, J. A. H. MacBride, K. Wade, *Angew. Chem.* **1993**, *105*, 1402; *Angew. Chem. Int. Ed. Engl.* **1993**, *32*, 1328.

[7] I. T. Chizhevsky, S. E. Johnson, C. B. Knobler, F. A. Gomez, M. F. Hawthorne, *J. Am. Chem. Soc.*, **1993**, *115*, 6981.

[8] a) X. Yang, W. Jiang, C. B. Knobler, M. F. Hawthorne, *J. Am. Chem. Soc.* **1992**, *114*, 9719; b) J. Müller, K. Base, T. F. Magnera, J. Michl, *ibid.* **1992**, *114*, 9721.

[9] a) R. N. Grimes, *Chem. Rev.* **1992**, *92*, 251; b) W. Siebert, *Pure Appl. Chem.* **1987**, *59*, 947; c) X. Meng, M. Sabat, R. N. Grimes, *J. Am. Chem. Soc.* **1993**, *115*, 6143.

New Developments in the Chemistry of Catalytic Antibodies

By *Christian Leumann**

Since the first reports of chemical reactions catalyzed by antibodies were published in 1986,[1-2] research in this field, which borders chemistry and biology, has been rapidly established and has led to many interesting results. Within the first five years, antibodies have been elicited for the catalysis of about 40 reactions.[3] The range of transformations catalyzed by antibodies includes carbonate, ester, and amide hydrolysis reactions as well as the corresponding reverse reactions, Claisen rearrangements, light-induced cycloaddition and reversion reactions, redox processes, β-eliminations, *cis–trans* isomerizations, metal chelating reactions, and Diels–Alder reactions. The art of generating such catalysts lies in the design of the hapten which must be chemically stable while at the same time mimicking the structure and electronic properties of the transition state of the reaction in question. To produce such antibodies the immune system is challenged with the appropriate haptens conjugated to carrier proteins. The resulting antibodies bind preferentially to the transition state of the target reaction and thus accelerate the reaction. Such catalysts rival natural enzymes in terms of catalytic efficiency and substrate selectivity. The state of current knowledge has already been reviewed in a number of articles.[3-5] Current research in the field of catalytic antibodies is being carried out on a wide front, including research devoted to practical applications of this technology. In the following, several examples from the more recent literature will be used to illustrate the direction in which current research is headed.[11]

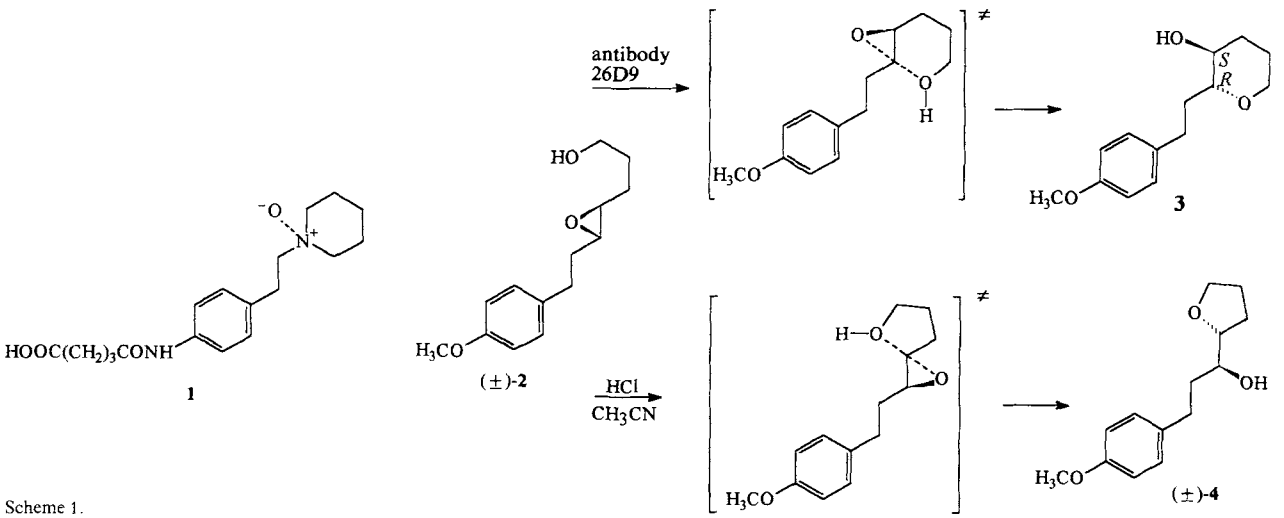

Scheme 1.

For example, the stereochemical course of an intramolecular substitution reaction can be controlled by antibodies (Scheme 1).[6] An antibody raised against hapten **1** catalyzes the intramolecular substitution reaction of the hydroxyepoxide **2** to give the tetrahydropyran derivative **3**, whereas acid catalysis in the absence of the antibody exclusively leads to the formation of the tetrahydrofuran derivative **4**. Furthermore, the antibody is substrate specific, transforming only one enantiomer of **2** into (enantiomerically pure) **3**. The structure of the hapten **1** is responsible for the observed stereochemical course of the antibody-catalyzed reaction, since this structure closely resembles the transition state on the way to the tetrahydropyran derivative **3**. This is a remarkable approach since in this case a reaction is not only accelerated but also forced in a direction that does *not* correspond to the inherent reactivity of the free substrate. Whereas the structural requirements for the transition state of an S_N2 reaction can be fulfilled in the acid-catalyzed reaction leading to **4**, the formation of **3** in the antibody-catalyzed reaction appears to be a mechanistic paradox that, however, is partly resolved by the fact that the substitution center (part of a three-membered ring) can be regarded structurally as a special case.

The antibody-catalyzed reduction of a diketone (Scheme 2) serves as a further example of regioselectivity not accessible by previous synthetic routes.[7] The antibody (37B.39.3) raised against the hapten **5**—again an *N*-oxide is used to mimic the transition state—catalyzes not only the enantioselective reduction of the *para*-nitrobenzylketones **6–8** by $NaBH_4$ to yield the corresponding alcohols **9–11** (86–96% *ee* (*S*) configuration in **9**), but also controls the reduction of the diketone **12**, such that of the three possible reaction products **13–15**, **13** is formed selectively in 95% yield (57% conversion) with 96% *ee*. While in the antibody-catalyzed reduction of **12** the keto group next to the nitrobenzyl residue reacts about 75 times faster than the keto group next to the methoxybenzyl residue, in the absence of the antibody practically no kinetic preference for one of the two reacting groups is observed. Remarkably, the antibody will tolerate a range of residues R in the ketones **6–8** but can discriminate strongly between methoxybenzyl and nitrobenzyl groups; this is a further indication of the relative insensitivity of the

[*] Prof. Dr. C. Leumann
Institut für Organische Chemie der Universität
Freiestrasse 3, CH-3012 Bern (Switzerland)
Telefax: Int. code + (31)658057

 © VCH Verlagsgesellschaft mbH, D-69451 Weinheim, 1993 0570-0833/93/0909-1291 $ 10.00+.25/0

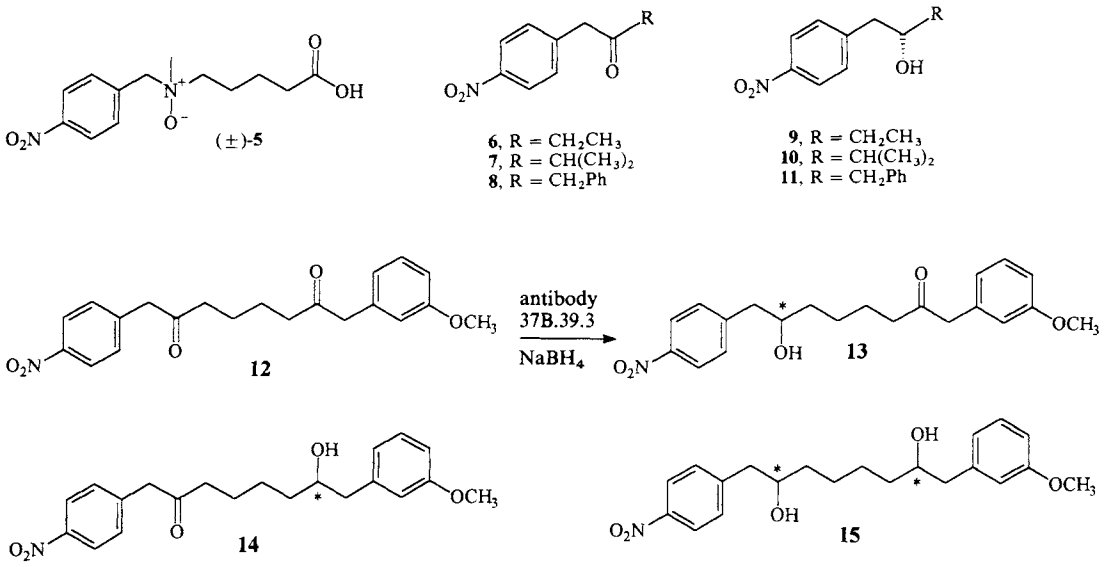

Scheme 2.

antibody to structural variations in the substrate near the conjugation site of the hapten–protein conjugate.

In the early research the main emphasis was placed on expanding the range of reactions catalyzed by antibodies and on mechanistic studies. More recent research now focuses on practical applications, in which catalytic antibodies play a central role. An example is the development of an antibody that catalyzes the hydrolysis of cocaine to (−)-ecgonine (Scheme 3).[8] This work was inspired by the wish to develop

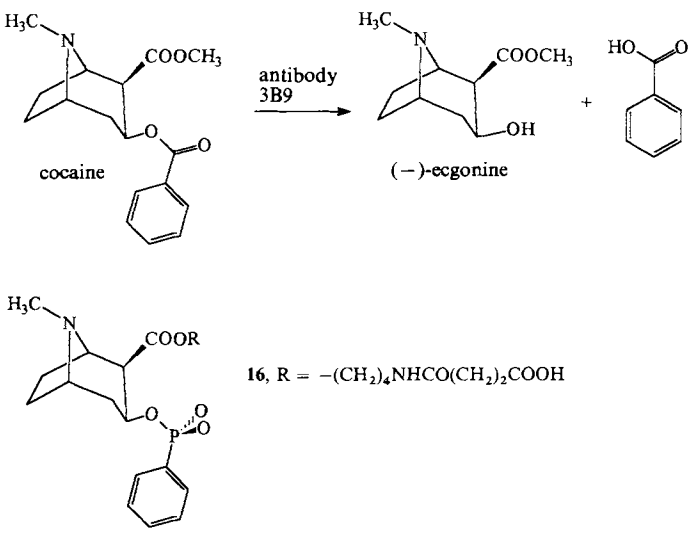

Scheme 3.

a new cure for drug addiction. A number of factors, such as peak concentration, positive concentration gradients, and changes in the level of cocaine in the blood serum, reinforces self-administration of the drug. This led to the idea of developing a drug that could degrade cocaine in the blood before it is transported to the central nervous system. Thus, this antibody, which catalyzes the hydrolysis of cocaine to give the inactive substance ecgonine, could serve this purpose. The production of the antibodies against phosphonate **16** can already be considered as an application of an existing procedure for the development of antibodies with esterase properties. Indeed the resulting antibody exhibits a catalytic activity similar to that of the main enzyme responsible for the breakdown of cocaine in the blood, namely butyrylcholinesterase. However, to be effective an antibody would have to exhibit yet higher activity. Nevertheless, this work points the way to future applications in drug development.

Recently significant advances have also been made in the preparation of antibodies. A difficult problem here is the time-consuming and expensive immunization process in addition to the unavoidable use of test animals for the induction and production of antibodies. By using the tools and techniques of molecular biology, it is now possible to produce and screen entire antibody libraries for binding to a given hapten in vitro. A step in this direction is the "reorientation" of an anti-tetanus-toxoid antibody into an antibody that binds fluorescein.[9] This was achieved by replacing the part of the gene coding for one of the hypervariable regions of the heavy chain of the original antibody with a synthetically prepared mixture of oligodeoxynucleotides of the same length. The resulting large number of antibodies was then expressed on the surface of phages. After the selection of the phages on the basis of their ability to bind to fluorescein followed by amplification and isolation steps, the molecular nature of the individual redefined antibodies was determined. Some of the resulting antibodies exhibited a binding affinity to fluorescein comparable with those obtained by direct immunization of mice with derivatives thereof.

Whether practical applications of catalytic antibodies as drugs or diagnostic tools will find widespread use in the future not only depends on further improvements of their catalytic activities, but also on the successful elaboration of methods that avoid the immunization procedure and thus the use of test animals.[10] The first promising steps in this direction have already been taken.

German version: *Angew. Chem.* **1993**, *105*, 1352

[1] S. J. Pollack, J. W. Jacobs, P. G. Schultz, *Science* **1986**, *234*, 1570–1573.
[2] A. Tramontano, K. D. Janda, R. A. Lerner, *Science* **1986**, *234*, 1566–1570.
[3] R. A. Lerner, S. J. Benkovic, P. G. Schultz, *Science* **1991**, *252*, 659–667.
[4] P. G. Schultz, *Angew. Chem.* **1989**, *101*, 1336–1348; *Angew. Chem. Int. Ed. Engl.* **1989**, *28*, 1283.
[5] P. G. Schultz, *Acc. Chem. Res.* **1989**, *22*, 287–294; *ibid.* **1993**, *26*, in press.
[6] K. D. Janda, C. G. Shevlin, R. A. Lerner, *Science* **1993**, *259*, 490–493.
[7] L. C. Hsieh, S. Yonkovich, L. Kochersperger, P. G. Schultz, *Science* **1993**, *260*, 337–339.
[8] D. W. Landry, K. Zhao, G. X.-Q. Yang, M. Glickman, T. M. Georgiadis, *Science* **1993**, *259*, 1899–1901.
[9] C. F. Barbas III, J. D. Bain, D. M. Hoekstra, R. A. Lerner, *Proc. Natl. Acad. Sci. USA* **1992**, *89*, 4457–4461.
[10] R. A. Lerner, A. S. Kang, J. D. Bain, D. R. Burton, C. F. Barbas III, *Science* **1992**, *258*, 1313–1314.
[11] After the completion of this manuscript the following communications appeared: S. C. Sinha, E. Keinan, J.-L. Reymond, *J. Am. Chem. Soc.* **1993**, *115*, 4893–4894; W. S. Wade, J. A. Ashley, G. K. Jahangiri, G. McElhaney, K. D. Janda, R. A. Lerner, *ibid.* **1993**, *115*, 4906–4907; H. Miyashita, Y. Karaki, M. Kikuchi, I. Fujii, *Proc. Natl. Acad. Sci. USA* **1993**, *90*, 5337–5340.

[Cp*Ru(acac)] Is Not a Coordinatively Unsaturated, Stable 16-Valence-Electron Complex**

By *Michael E. Smith, Frederick J. Hollander,* and *Richard A. Andersen**

A recent publication in this journal reported that the X-ray crystal structure of [Cp*Ru(acac)] (Cp* = η^5-C_5Me_5) shows it to be a coordinatively unsaturated, sixteen-electron complex in which the angle defined by the intersection of the Me_5C_5-centroid-Ru line with the plane defined by Ru-O-O substantially deviates from 180°.[1] Kölle et al. state that [Cp*Ru(acac)] "exhibits two independent molecules in the asymmetric unit and does not show the intermolecular metal–acac interactions often observed for acac complexes (shortest intermolecular distance, Ru···C(13), >5 Å)." The authors quote preliminary extended-Hückel calculations that trace the stability of the bent geometry to a large HOMO–LUMO gap.

In recent X-ray crystallographic studies of monomeric [Cp*Co(acac)] and [Cp*Ni(acac)] we observed no deviation from linear geometry.[2] This observation led us to question the results of the X-ray crystallographic study of [Cp*Ru(acac)]. The atomic position data were retrieved from the Cambridge Structural Database.[3] A packing diagram produced by ORTEP[4] showed that the X-ray data for [Cp*Ru(acac)] had been incorrectly interpreted. Figure 1 shows the contents of the unit cell. There are indeed two independent molecules in the asymmetric unit, but they are linked through an inversion center to form dimers, and each ruthenium atom is bonded to the γ-carbon atom of the symmetry-related acetylacetonate group. The Ru1···C13 and Ru2···C28 distances are 2.418 and 2.417 Å, respectively. The geometry of the dimers is essentially identical to that reported for the isoelectronic dication in $[Cp^*_2Rh_2(acac)_2](BF_4)_2$.[5] There the Rh···C contact distance of 2.287(6) Å is 0.13 Å shorter than that found in the neutral ruthenium compound, probably due to the cationic nature of the rhodium center.

The reinterpretation of the published X-ray crystallographic data shows that the bent geometry of [Cp*Ru(acac)] is due to the interaction of the Ru atom with the γ-carbon atom of the acac group in a neighboring [Cp*Ru(acac)] molecule. The ruthenium center thus avoids coordinative unsaturation.

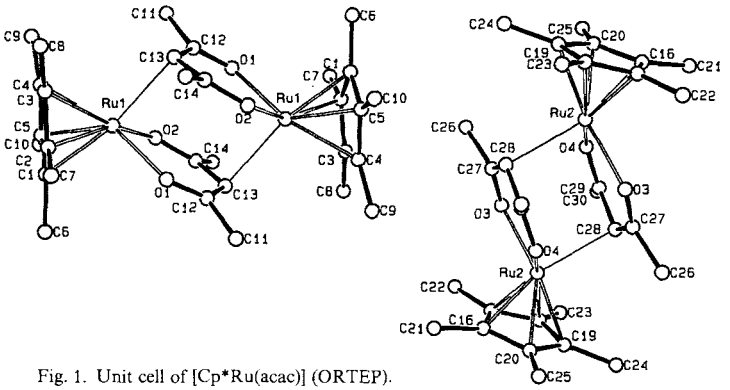

Fig. 1. Unit cell of [Cp*Ru(acac)] (ORTEP).

Received: April 23, 1993
German version: *Angew. Chem.* **1993**, *105*, 1355

[1] U. Kölle, J. Kossakowski, G. Raabe, *Angew. Chem.* **1990**, *120*, 839; *Angew. Chem. Int. Ed. Engl.* **1990**, *29*, 773.
[2] M. E. Smith, unpublished.
[3] Address: Cambridge Crystallographic Data Centre, 12 Union Road, GB-Cambridge CB21EZ.
[4] C. K. Johnson, ORTEP, Report ORNL-3794, Oak Ridge National Laboratory, Oak Ridge, TN, USA, **1965**.
[5] W. Rigby, H. B. Lee, P. M. Bailey, J. A. McCleverty, P. M. Maitlis, *J. Chem. Soc. Dalton Trans.* **1979**, 387.

Reply*

In our interpretation of the solid-state structure of [Cp*Ru(acac)] we apparently made a mistake: the intermolecular distance Ru···C13 was not determined correctly. In the meantime we have obtained numerous results from derivatives of the same complex type that indicate their coordinatively unsaturated nature in solution, for example, inversion at the metal (observed by NMR spectroscopy). We will report on these findings shortly.

[*] Prof. R. A. Andersen, M. E. Smith, Dr. F. J. Hollander
Department of Chemistry
University of California, Berkeley, CA 94720 (USA)
Telefax: Int. code + (510) 642-8369

[**] This research was supported by the National Science Foundation (fellowship for M. E. S.). – Hacac = acetylacetone.

[*] Prof. Dr. U. Kölle
Institut für Anorganische Chemie der Technischen Hochschule
Templergraben 55, D-52062 Aachen (FRG)
Telefax: Int. + (241) 87-1984
Dr. G. Raabe
Institut für Organische Chemie der Technischen Hochschule Aachen

Communications may be submitted in English *or* in German. Further details regarding the submission of communications can be found in the "Notice to Authors" reproduced in the January issue of the journal. Copies thereof may be obtained from the editorial office upon request.

Photoswitchable Catenanes**

By *Fritz Vögtle,** *Walter Manfred Müller, Ute Müller, Martin Bauer,* and *Kari Rissanen*

Catenanes are not longer freaks of the laboratory since they became preparatively accessible through the use of template effects.[1-3] The strategy developed by Stoddart[4, 5] in which the formation of a donor–acceptor complex is used to preorient the building blocks participating in ring formation was applied by us to synthesize catenanes with *unsymmetrical* paraquat rings (Scheme 1).[6] This enables the use of almost any bis(bromomethyl)arene for linking the second ring. Other variations are described in the following communication by Stoddart et al.[7]

In the simplest case, two dibromides with different substitution patterns form the closely interlocked catenane **1**, which contains a *meta*-phenylene building block. More interesting examples employ photochemically or electrochemically active building blocks[8] to close the gap. We report here on the catenanes **2** and **3**, in which a photoactive switching function is integrated into one of the two large rings.

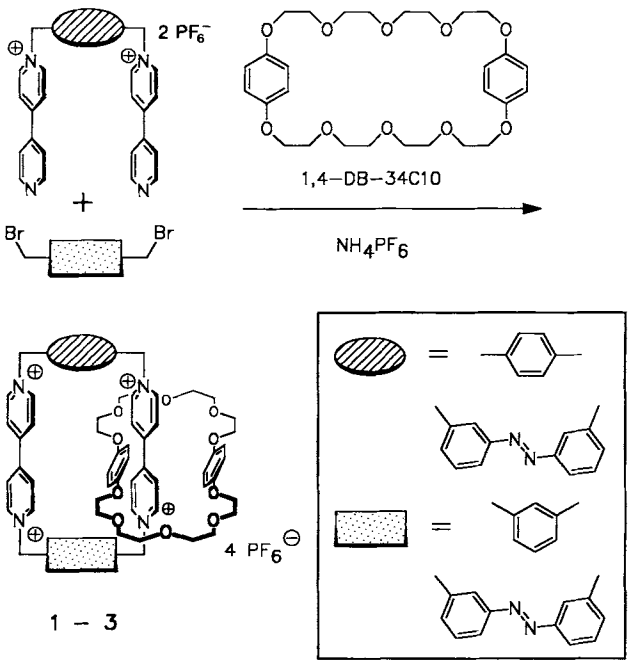

Scheme 1. Synthesis of the catenanes **1–3** containing two different spacers in each case (schematic).

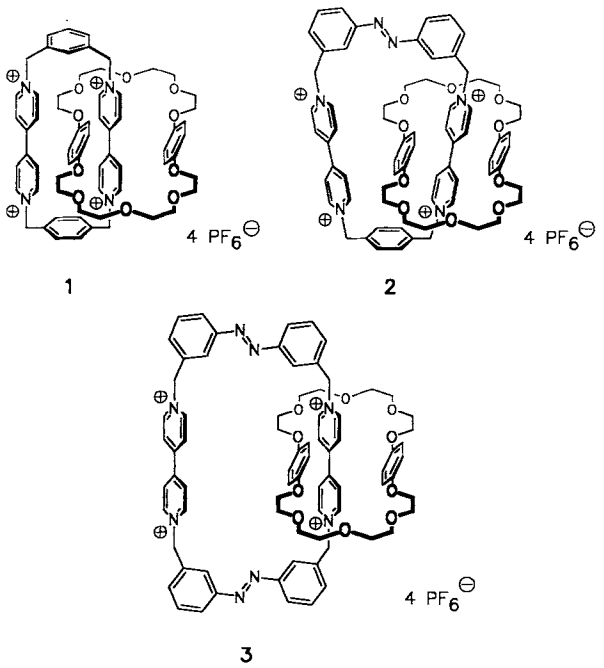

The azobenzene unit in **2** and **3**, and in the new azo compounds **4–6** prepared for comparison, can be converted from the (*E*) configuration formed in their synthesis into the (*Z*) configuration by irradiation at 310 nm and revert to the (*E*) configuration on irradiation with blue light (440 nm).

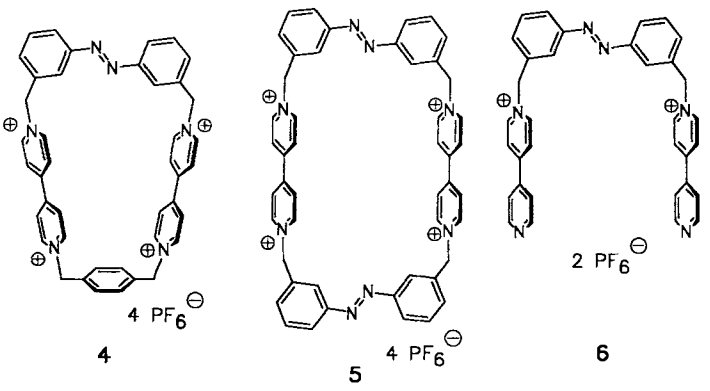

Whereas photochemical switching leads to two photostationary equilibria (PSE) characterized by different (*E*)/(*Z*) populations, the starting state (that of the pure (*E*) isomer) can be attained by prolonged heating in solution (thermal reisomerization) (Scheme 2).[9]

[*] Prof. Dr. F. Vögtle, W. M. Müller, U. Müller, Dr. M. Bauer
Institut für Organische Chemie und Biochemie der Universität
Gerhard-Domagk-Strasse 1, D-53121 Bonn (FRG)
Telefax: Int. code + (228)73-5662

Doz. Dr. K. Rissanen
Department of Chemistry
University of Jyväskylä
PL 35, SF-40351 Jyväskylä (Finland)

[**] This work was supported by the Bundesministerium für Forschung und Technologie, Project 0329120 A.

Thus, a mixture of the (*E*) and (*Z*) isomers is obtained from the catenane **2**, and a mixture of the (*E*,*E*), (*E*,*Z*), and (*Z*,*Z*) isomers from **3**. The switching can be monitored by ^{1}H NMR spectroscopy. Remarkably, in **2** not only the proton signals of the azobenzene unit itself are affected by the change in configuration at the N=N bond; it also influences the signals of the bipyridine unit of the same large ring and of the paraphenylene ring fourteen bonds away (!), as well as those of the second catenane ring, that is, of the hydroquinone component and, to some extent, the ethano groups.

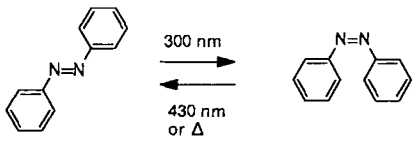

Scheme 2. (*E*)/(*Z*) isomerization for the example of azobenzene.

The rate of the thermal (*Z*) → (*E*) reisomerization of the azobenzene unit depends both on the size of the macrocycle containing it and on whether the cavity is occupied, which in catenanes must be the case. The half-life of (*Z*)-**2** in acetonitrile at room temperature is about 20.5 h, while the reisomerization to (*E*,*E*)-**3** from the (*Z*,*Z*)-configurated and mixed configurated isomers proceeds with a half-life of 12 days. The "quat rings" **4** and **5** that contain no guest reisomerize more slowly than the corresponding catenanes (Table 1). The

Table 1. Rate constants k and half-lives $\tau_{1/2}$ for the reisomerization of catenanes **2** and **3**, as well as (for comparison) the corresponding empty macrocycles **4** and **5** and the open chain precursor **6** in [D_3]acetonitrile at 20 °C.

	2	**3** [a]	**4**	**5** [b]	**6**
k[s^{-1}]	9.4×10^{-6}	–	9.7×10^{-7}	5.6×10^{-7}	4.8×10^{-7}
$\tau_{1/2}$	20.5 h	12 d	8.3 d	14 d	17 d

[a] This value for $\tau_{1/2}$ refers to the backformation of (*E*,*E*)-**3** from the (*Z*) isomer mixture in the PSE. Signal overlap prevents the accurate determination of the isomerization rate of the (*Z*,*Z*) isomer. [b] These values refer to the reisomerization of (*Z*,*Z*)-**5**; for the reaction of both (*Z*) isomers to form (*E*,*E*)-**5** from the PSE the half-life is about 24 days.

crown ether apparently forces the bipyridine units that restrict it apart, particularly those in the (*Z*) configuration, thus mechanically assisting the isomerization. The comparison of catenane **2** with the macrocycle **4** clearly demonstrates this auxiliary effect: in catenane **2** the cavity is particularly crowded and consequently the mechanical forces are especially strong. The open-chain starting material **6**, in which the (*Z*) form is not favored by bridging, reisomerizes much more slowly than the catenanes or the narrow macrocycle **4**.

The results of the X-ray analysis of **1** and **2**[10, 11] suggest that the crown part of the catenanes cannot rotate freely around the bipyridine component. In **2** the enclosed hydroquinone unit does not lie in the center of the paraquat ring: the shortest distance is 3.41 Å to the inner bipyridine unit; the distance to the outer unit is 3.56 Å. The larger azobenzene spacer enables a more pronounced twisting of the outer bipyridine unit (30.8°); the torsional angle of the inner unit is only 12.1°.

In both the ^{13}C and ^{1}H NMR spectra the inner and outer part of the polyether ring of **1** give rise to different signals. The broadening of the proton signals for **2** can be observed at room temperature, but the exchange takes place too rapidly on the ^{13}C NMR time scale for a broadening to be visible in this spectrum. Finally, the bis(bipyridine) ring of **3** has been so stretched by the two azogroups that also in its ^{1}H NMR spectrum only a single averaged signal appears for the aromatic protons of the crown ether.

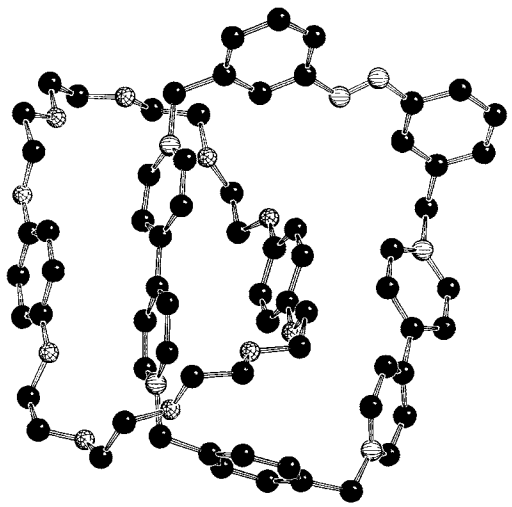

Fig. 1. X-ray crystal structure of **2**.

In the context of host/guest chemistry, the catenanes are on the one hand ideal model compounds in which the interactions between the molecule's two components are maximized. The properties observed for them—here, for example, the (*Z*) → (*E*) isomerization behavior—can, at least, be considered as a measure of the stability of a complex. On the other hand the empty monocycles **4** and **5** offer the possibility of manipulating the strength of bonding of electron-rich arene molecules by light.[12] An alternative to the incorporation of potential photoswitches will be presented in the following communication.[7]

Experimental Procedure

Preparation of the catenane **3** and the macrocycle **5**: The azo compound **6** (0.81 g, 1.0 mmol) and the crown ether 1,4-DB-34C10 (1.07 g, 2.0 mmol) were dissolved in dry acetonitrile (40 mL), treated with a solution of 3,3'-bis(bromomethyl)azobenzene (0.37 g, 1.0 mmol) in acetonitrile (40 mL), and stirred for one week at room temperature. Filtrate and precipitate were purified separately on silica gel (solvent system: methanol/5% aqueous NH_4Cl solution/nitromethane 7:2:1) by medium pressure liquid chromatography (MPLC). After anion exchange with NH_4PF_6, **3** is obtained from the filtrate in 12% yield (R_f = 0.19), and **5** from the precipitate in 4.1% yield (R_f = 0.10).

6: 3,3'-bis(bromomethyl)azobenzene (3.68 g, 10.0 mmol) and dry 4,4'-bipyridine (6.25 g, 40.0 mmol) were heated in acetonitrile (150 mL) for 12 h under reflux. The precipitate was purified on silica gel (solvent system: methanol/5% aqueous NH_4Cl solution 7:2) by MPLC (R_f = 0.34). A double exchange with NH_4PF_6 solution afforded hexafluorophosphate **6** in 53% yield.

Received: March 20, 1993 [Z 5940IE]
German version: *Angew. Chem.* **1993**, *105*, 1356

[1] Reviews: G. Schill, *Catenanes, Rotaxanes, and Knots*, Academic Press, New York, **1971**; C. O. Dietrich-Buchecker, J.-P. Sauvage, *Chem. Rev.* **1987**, *87*, 795–810.
[2] D. Philp, J. F. Stoddart, *Synlett* **1991**, 445–458.
[3] C. A. Hunter, *J. Am. Chem. Soc.* **1992**, *114*, 5303–5311; F. Vögtle, S. Meier, R. Hoss, *Angew. Chem.* **1992**, *104*, 1628–1631; *Angew. Chem. Int. Ed. Engl.* **1992**, *31*, 1619.

[4] P. R. Ashton, T. T. Goodnow, A. E. Kaifer, M. V. Reddington, A. M. Z. Slawin, N. Spencer, J. F. Stoddart, C. Vicent, D. J. Williams, *Angew. Chem.* **1989**, *101*, 1404–1408; *Angew. Chem. Int. Ed. Engl.* **1989**, *28*, 1396–1400; P. R. Ashton, C. L. Brown, E. J. T. Chrystal, T. T. Goodnow, A. E. Kaifer, K. P. Parry, A. M. Z. Slawin, N. Spencer, J. F. Stoddart, D. J. Williams *ibid.* **1991**, *103*, 1055–1058 and **1991**, *30*, 1039.

[5] P. L. Anelli, P. R. Ashton, R. Ballardini, V. Balzani, M. Delgado, M. T. Gandolfi, T. T. Goodnow, A. E. Kaifer, D. Philp, M. Pietraszkiewicz, L. Prodi, M. V. Reddington, A. M. Z. Slawin, N. Spencer, J. F. Stoddart, C. Vicent, D. J. Williams, *J. Am. Chem. Soc.* **1992**, *114*, 193–218.

[6] See also F. Vögtle, H. Förster, *Chem. Ztg.* **1973**, *97*, 386–387; F. Vögtle, D. Brombach, *Chem. Ber.* **108**, *1975*, 1682–1693; W. Geuder, S. Hünig, A. Suchy, *Tetrahedron* **1986**, *42*, 1665–1677; M. Bühner, W. Geuder, W.-K. Gries, S. Hünig, M. Koch, T. Poll, *Angew. Chem.* **1988**, *100*, 1611–1614; *Angew. Chem. Int. Ed. Engl.* **1988**, *27*, 1553.

[7] D. B. Amabilino, P. R. Ashton, M. S. Tolley, J. F. Stoddart, D. J. Williams, *Angew. Chem.* **1993**, *105*, 1358–1362; *Angew. Chem. Int. Ed. Engl.* **1993**, *32*, 1297–1301.

[8] G. W. Gokel, *Crown Ethers and Cryptands*, The Royal Society of Chemistry, London, **1991**, Chapter 5.5.

[9] F. Vögtle, *Supramolecular Chemistry*, Wiley, Chichester, **1993**, Chapter 7; H.-W. Losensky, H. Spelthann, A. Ehlen, F. Vögtle, J. Bargon, *Angew. Chem.* **1988**, *100*, 1225–1226; *Angew. Chem. Int. Ed. Engl.* **1988**, *27*, 1189; M. Bauer, F. Vögtle, *Chem. Ber.* **1992**, *125*, 1675–1686; H.-B. Mekelburger, K. Rissanen, F. Vögtle, *ibid.* **1993**, *126*, 1161–1169.

[10] Crystals of **1** and **2** were obtained by vapor diffusion of diisopropyl ether into a solution of the catenane in acetonitrile. Details of the crystal structure analysis are available on request from the Director of the Cambridge Crystallographic Data Centre, 12 Union Road, GB-Cambridge CB2 1EZ, on quoting the full journal citation.

[11] The preliminary refinement (*R* value 0.15) in the X-ray analysis of **1**, which crystallizes in the monoclinic space group *C*2/*c* (no. 15), confirms the catenane structure and shows substantial disorder of the solvent, acetonitrile. Crystal data: $a = 4980.9(8)$, $b = 1401.5(2)$, $c = 2904.4(3)$ pm, $\beta = 119.74(1)^\circ$, $V = 17604(5) \times 10^6$ pm^3, $Z = 8$.

[12] For the idea of (electrochemical) "reversed" switching of the "guest molecule" in a rotaxane, see P. R. Ashton, R. A. Bissell, N. Spencer, J. F. Stoddart, M. S. Tolley, *Synlett* **1992**, 923–926 and earlier papers.

Isomeric Self-Assembling [2]Catenanes**

By *David B. Amabilino, Peter R. Ashton, Malcolm S. Tolley, J. Fraser Stoddart,** and *David J. Williams*

In 1989 we reported the efficient, template-directed[1] self-assembly[2] of the tetracationic cyclophane cyclobis(paraquat-*p*-phenylene)[3] with bis(*p*-phenylene)[34]crown-10 (BPP34C10) to form[4] the [2]catenane $\mathbf{1}\cdot 4PF_6$ in 70% yield. The noncovalent bonding—the π–π stacking interactions and [C-H···O] hydrogen bonding that combine to enhance the efficiency of the macrocyclization[5] of the tetracationic cyclophane—'lives on' both in the solution and solid-state structures of $\mathbf{1}\cdot 4PF_6$. A subsequent objective was to explore the self-assembly of molecular structures isomeric with **1** for the controlled creation of nanometer-scale, ordered supramolecular architectures.[6] To achieve this goal, we had to understand the effects of constitutional changes upon the efficiency of the self-assembly process. Here we describe the syntheses of two constitutional isomers of

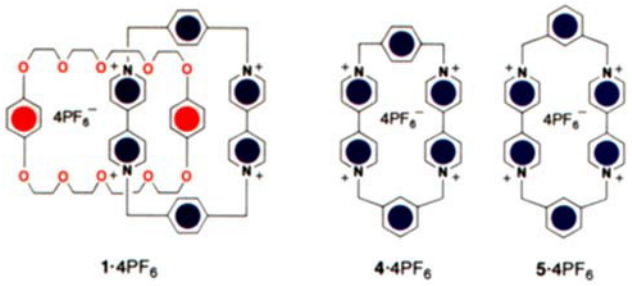

$\mathbf{1}\cdot 4PF_6$, $\mathbf{2}\cdot 4PF_6$ and $\mathbf{3}\cdot 4PF_6$, in which the incorporated tetracationic cyclophanes are different, and compare the efficiency of the self-assembly process leading to the isomeric [2]catenanes with the binding properties of the free tetracationic macrocycles $\mathbf{4}\cdot 4PF_6$ and $\mathbf{5}\cdot 4PF_6$.[7] We also discuss the X-ray crystal structures of $\mathbf{2}\cdot 4PF_6$ and $\mathbf{3}\cdot 4PF_6$, and their dynamic ^{1}H NMR spectroscopic behavior in solution.

The [2]catenane $\mathbf{2}\cdot 4PF_6$ was prepared by two different routes according to Scheme 1. Although the catenations were performed under identical conditions, when **6** was added to $\mathbf{7}\cdot 2PF_6$ in dimethylformamide (DMF) in the presence of an excess of BPP34C10, $\mathbf{2}\cdot 4PF_6$ was obtained in 18% yield after counterion exchange, whereas when the self-

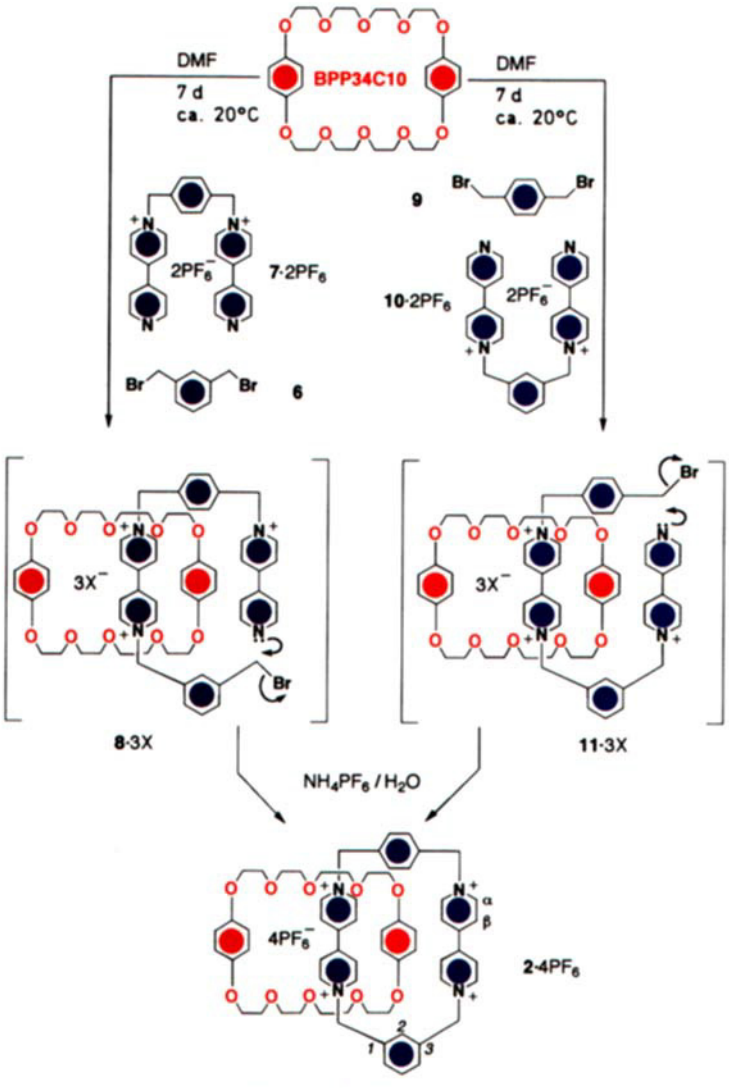

Scheme 1. Synthesis of the [2]catenane $\mathbf{2}\cdot 4PF_6$ by self-assembly by two routes.

[*] Prof. J. F. Stoddart, Dr. D. B. Amabilino, P. R. Ashton, M. S. Tolley
School of Chemistry, The University of Birmingham
Edgbaston, Birmingham B152TT (UK)
Telefax: Int. code + (21)414-3531
Dr. D. J. Williams
Chemical Crystallography Laboratory
Department of Chemistry, Imperial College
London SW72AY (UK)

[**] This research was supported by the Science and Engineering Research Council in the United Kingdom, and first presented at the XIIth Royal Society of Chemistry UK Macrocycle Group Meeting at the University of Oxford (January 1993).

assembly was performed using **9** and **10**·2PF_6, the yield of the catenane isolated was 40%. Clearly, the intermediate tricationic complex **11** undergoes ring closure to give **2** much more readily than does **8**. The positive-ion FAB mass spectrum[8] of **2**·4PF_6 is similar to that[4, 5] of its isomer **1**·4PF_6, displaying peaks at *m/z* 1636 for the parent ion and at *m/z* 1491, 1346, and 1201 for loss of one, two, and three PF_6^- ions, respectively.

The catenane structure of **2** was confirmed by X-ray crystallography. The crystal structure[9, 10] of **2**·4PF_6 reveals (Fig. 1) a geometry similar to that[4, 5] of **1**·4PF_6 in the solid state. One hydroquinone ring in the crown ether component

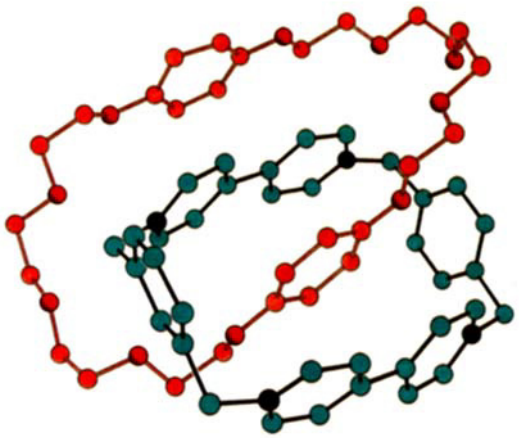

Fig. 1. The structure of **2** in the crystal; the donor and acceptor macrocycles are shaded light red and light blue, respectively. O atoms are dark red and N atoms are dark blue.

is located within the cavity of the tetracationic cyclophane such that it is sandwiched between the two π-electron deficient bipyridinum units, forming an angle of approximately 45° between its OC_6H_4O axis and the equatorial plane[11] of the cyclophane. Whereas in **1**·4PF_6 the methylene groups of the "inside" $CH_2-OC_6H_4O-CH_2$ unit are *anti* and those of the "alongside" unit are *syn*, in **2**·4PF_6 both units adopt *anti* geometries. As in **1**·4PF_6, one of the protons of the "inside" hydroquinone ring in **2**·4PF_6 is directed into the center of the *p*-xylyl spacer of the cyclophane (H···ring centroid distance, 2.75 Å; in **1**·4PF_6, 2.85 Å), whilst the hydroquinone proton directed towards the opposite end of the cyclophane makes an orthogonal approach to the carbon atom at the 2-position of the *m*-xylyl unit (H···C distance, 2.79 Å).[12] On going from **1**·4PF_6 to **2**·4PF_6, the maximum separation between the bipyridinium units is reduced[13] from 7.0 to 6.9 Å, and the distance between the xylyl spacers decreases from 10.3 to 10.0 Å. The bowing of the bipyridinium units is the same in both isomers; the angles subtended by the pairs of $N-CH_2$ bonds are approximately 26° in each case. The small diminution in the length of the tetracationic cyclophane component in **2**·4PF_6, which results in the reduced H–xylyl distance mentioned previously is supported by a low-temperature ^{1}H NMR spectroscopic study (vide infra) of **2**·4PF_6 in solution. Both **1**·4PF_6 and **2**·4PF_6 (Fig. 2) form polar stacks[14] in the solid state, comprising alternating π-electron rich and π-electron deficient aromatic moieties.

The tetracationic cyclophane component of **2**·4PF_6 was obtained as free **4**·4PF_6 from a template-directed reaction of **9** with **10**·2PF_6 in 7% yield, using a method identical to that described[5] for the preparation of cyclobis(paraquat-*p*-phenylene). When a solution of **4**·4PF_6 in CD_3COCD_3 is

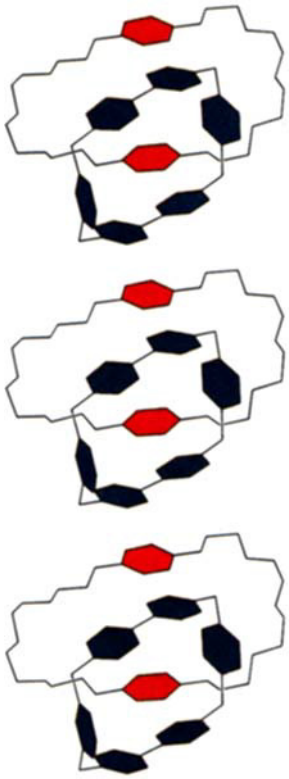

Fig. 2. Part of a polar stack of the [2]catenane **2** in the crystal illustrating the alternating sequence of π-electron-deficient and π-electron-rich aromatic moieties.

mixed with an excess of the template, 1,4-bis[(2-hydroxyethoxy)-ethoxy]benzene (BHEEB), an intensely orange-colored solution develops immediately, indicating charge transfer between the π-electron-rich and π-electron-deficient aromatic rings and therefore inclusion[15] of the template within the cavity of the cyclophane.[16] In a similar experiment, when **5**·4PF_6[7] and BHEEB are combined in CD_3COCD_3, a colorless solution results which gives rise to an ^{1}H NMR spectrum that can be superimposed upon the spectra of the components, indicating that *no* complex is

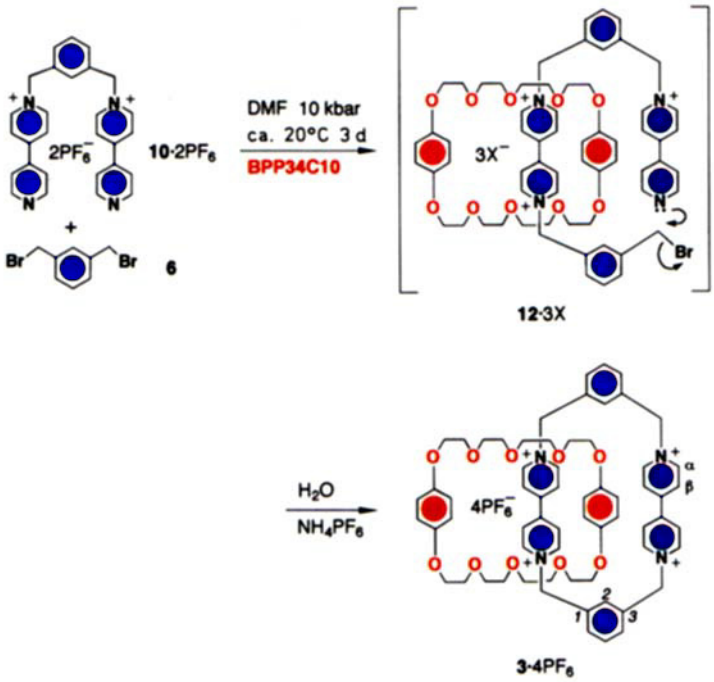

Scheme 2. Synthesis of the [2]catenene **3**·4PF_6 by self-assembly at ultrahigh pressure.

ployed[23] along with the chemical shift difference between the signals at ambient temperature ($\Delta\nu = 206$ Hz) to obtain a $\Delta G_c^{\ddagger}$ value of 16.3 kcal mol^{-1} for the site exchange.

At +25 °C, the ^{1}H NMR spectrum (CD_3CN, 90 MHz) of $\mathbf{3}\cdot 4PF_6$ is remarkably simple, since the cyclophane component exhibits averaged D_{2h} symmetry. However, the equilibration between the "inside" and "alongside" hydroquinone rings of the BPP34C10 component is slow, as evidenced by a sharp singlet at $\delta = 6.55$ for the protons on the latter ring, which broadens when the temperature is raised. The exchange method of analysis[25] of the temperature dependence of this signal gave a $\Delta G^{\ddagger}$ value of 17.6 kcal mol^{-1}. Cooling down a CD_3COCD_3 solution of $\mathbf{3}\cdot 4PF_6$ increases the complexity of its ^{1}H NMR spectrum. At −70 °C, four signals are observed for the α-CH bipyridinium protons, whilst the "inside" hydroquinone protons appear as two doublets centered on $\delta = 3.19$ and 5.63. This observation suggests that, as with $\mathbf{2}\cdot 4PF_6$, at low temperature, the degenerate structural changes of $\mathbf{3}\cdot 4PF_6$ are slow on the ^{1}H NMR timescale, and that the gross structure in solution is similar to that observed in the solid state. Coalescence of the resonances arising from the included hydroquinone ring at −1 °C indicates that the approximate barrier[23] to the rocking process[24] in $\mathbf{3}\cdot 4PF_6$ is $\Delta G_c^{\ddagger} = 11.7$ kcal mol^{-1} based on a $\Delta\nu$ value of 976 Hz.

The results presented here provide us with three important conclusions: 1) The self-assembly of isomeric [2]catenanes of the type described in this communication is extremely sensitive to constitutional changes in the tetracationic cyclophane component; the most favored[26] is cyclobis(paraquat-*p*-phenylene). 2) Changing the constitution[27] of the π-electron-deficient cyclophane influences dramatically the dynamic behavior of the isomeric [2]catenanes. 3) The solid-state structures of the [2]catenanes in and beyond their molecules is isomer dependent. It follows that it should be possible to control prescribed functions of these molecules by the most subtle of structural changes—isomerism!

Experimental Procedure

$\mathbf{2}\cdot 4PF_6$: 1,4-Bis(bromomethyl)benzene (**9**) (31 mg, 0.12 mmol), $\mathbf{10}\cdot 2PF_6$ (80 mg, 0.11 mmol), and BPP34C10 (201 mg, 0.38 mmol) were dissolved in dry DMF (5 mL), and the solution was stirred at room temperature for one week. $\mathbf{2}\cdot 4PF_6$ was isolated according to a previously described workup procedure [5] as a red solid (74 mg, 40%), m.p. > 250 °C. Single crystals suitable for X-ray crystallography were grown by vapor diffusion of iPr$_2$O into a solution of $\mathbf{2}\cdot 4PF_6$ in MeCN.

$\mathbf{3}\cdot 4PF_6$: 1,3-Bis(bromomethyl)benzene (**6**) (48 mg, 0.18 mmol), $\mathbf{10}\cdot 2PF_6$ (128 mg, 0.18 mmol), and BPP34C10 (267 mg, 0.50 mmol) were dissolved in dry DMF (5 mL) in a high-pressure reaction vessel which was pressurized to 10 kbar for 3 d at 20 °C. Following the purification procedure described above for $\mathbf{2}\cdot 4PF_6$, $\mathbf{3}\cdot 4PF_6$ was isolated as a red solid (82 mg, 28%), m.p. > 250 °C. Single crystals suitable for X-ray crystallography were grown by vapor diffusion of iPr$_2$O into a solution of $\mathbf{3}\cdot 4PF_6$ in MeCN.

$\mathbf{4}\cdot 4PF_6$: 1,4-Bis(bromomethyl)benzene (**9**) (0.42 g, 1.59 mmol), $\mathbf{10}\cdot 2PF_6$ (1.12 g, 1.59 mmol) and BHEEB (1.00 g, 3.49 mmol) were dissolved in dry DMF (30 mL), and the reaction mixture was stirred at room temperature for four weeks. $\mathbf{4}\cdot 4PF_6$ was isolated according to a previously described workup procedure [5], as a white solid (122 mg, 7%), m.p. > 250 °C, *m/z* (positive-ion FAB-MS [8]) 955 $(M - PF_6)^+$, 810 $(M - 2PF_6)^+$, 665 $(M - 3PF_6)^+$; ^{1}H NMR (300 MHz, CD_3COCD_3) $\delta = 6.18$ and 6.19 (overlapping s, 8H, NCH_2), 7.70 (t, 1H, 5-position of *m*-xylyl spacer), 7.82 (s, 4H, arom. protons of the *p*-xylyl spacer), 7.89 (s, 1H, 2-position of *m*-xylyl spacer), 7.95 (d, 2H, 4- and 6-positions of *m*-xylyl spacer), 8.40 (d, 4H, β-CH bipyridinium protons), 8.45 (d, 4H, β-CH bipyridinium protons), 9.30–9.39 (overlapping d, 8H, α-CH bipyridinium protons).

Received: April 28, 1993 [Z 6044 IE]
German version: *Angew. Chem.* **1993**, *105*, 1358

[1] For more information about the recent developments in the template-directed synthesis of interlocked structures refer to C. Dietrich-Buchecker, J.-P. Sauvage, *Bull. Soc. Chim. Fr.* **1992**, *129*, 113; D. H. Busch, *J. Inclusion Phenom. Mol. Recognit. Chem.* **1992**, *12*, 389; J.-C. Chambron, C. Dietrich-Buchecker, J.-P. Sauvage, *Top. Curr. Chem.* **1993**, *165*, 131; D. M. Walba, Q. Y. Zheng, K. Schilling, *J. Am. Chem. Soc.* **1992**, *114*, 6259. For a discussion about the self-assembly of synthetic helicates using metal-ion templates see J.-M. Lehn, A. Rigault, *Angew. Chem.* **1988**, *100*, 1121; *Angew. Chem. Int. Ed. Engl.* **1988**, *27*, 1095; E. C. Constable, *Tetrahedron*, **1992**, *48*, 10013; and more recently: K. T. Potts, K. A. Gheysen Raiford, M. Keshavarz-K, *J. Am. Chem. Soc.* **1993**, *115*, 2793.

[2] For a general review on self-assembly, see J. S. Lindsey, *New J. Chem.* **1991**, *15*, 153, and for systems of the type discussed here refer to D. Philp, J. F. Stoddart, *Synlett* **1991**, 445. The self-assembly of [2]catenanes by means of a hydrogen-bonding motif has been described recently: C. A. Hunter, *J. Am. Chem. Soc.* **1992**, *114*, 5303; F. Vögtle, S. Meier, R. Hoss, *Angew. Chem.* **1992**, *104*, 1628; *Angew. Chem. Int. Ed. Engl.* **1992**, *31*, 1619. The self-assembly of catenated cyclodextrins has been described by D. Armspach, P. R. Ashton, C. P. Moore, N. Spencer, J. F. Stoddart, T. J. Wear, D. J. Williams, *Angew. Chem.* **1993**, *105*, 944; *Angew. Chem. Int. Ed. Engl.* **1993**, *32*, 854.

[3] B. Odell, M. V. Reddington, A. M. Z. Slawin, N. Spencer, J. F. Stoddart, D. J. Williams, *Angew. Chem.* **1988**, *100*, 1605; *Angew. Chem. Int. Ed. Engl.* **1988**, *27*, 1547.

[4] P. R. Ashton, T. T. Goodnow, A. E. Kaifer, M. V. Reddington, A. M. Z. Slawin, N. Spencer, J. F. Stoddart, C. Vicent, D. J. Williams, *Angew. Chem.* **1989**, *101*, 1404; *Angew. Chem. Int. Ed. Engl.* **1989**, *28*, 1396.

[5] P. L. Anelli, P. R. Ashton, R. Ballardini, V. Balzani, M. Delgado, M. T. Gandolfi, T. T. Goodnow, A. E. Kaifer, D. Philp, M. Pietraszkiewicz, L. Prodi, M. V. Reddington, A. M. Z. Slawin, N. Spencer, J. F. Stoddart, C. Vicent, D. J. Williams, *J. Am. Chem. Soc.* **1992**, *114*, 193.

[6] J.-M. Lehn, *Angew. Chem.* **1988**, *100*, 91; *Angew. Chem. Int. Ed. Engl.* **1988**, *27*, 89; J.-M. Lehn, *ibid.* **1990**, *102*, 1347 and **1990**, *29*, 1304.

[7] W. Geuder, S. Hünig, A. Suchy, *Angew. Chem.* **1983**, *95*, 501; *Angew. Chem. Int. Ed. Engl.* **1983**, *22*, 489; *Tetrahedron* **1986**, *42*, 1665; M. Buhner, W. Geuder, W.-K. Gries, S. Hünig, M. Koch, T. Poll, *Angew. Chem.* **1988**, *100*, 1611; *Angew. Chem. Int. Ed. Engl.* **1988**, *27*, 1555.

[8] The FAB mass spectra were measured on a Kratos MS80RF mass spectrometer (accelerating voltage 3 kV; resolution 1500) coupled to a DS90 data system. The atom gun was an adapted saddle field source (Ion Tech Limited) operated at 7 keV and a tube current of approximately 2 mA. Krypton was used to provide a primary beam of atoms. The samples $\mathbf{2}\cdot 4PF_6$, $\mathbf{3}\cdot 4PF_6$, and $\mathbf{4}\cdot 4PF_6$ were dissolved in 3-nitrobenzyl alcohol that had previously been coated onto a stainless steel probe tip. Spectra were recorded in the positive-ion mode at a scan speed of 30 s per decade.

[9] Crystal data for $\mathbf{2}\cdot 4PF_6\cdot 5MeCN$: monoclinic, $a = 49.47(7)$, $b = 13.945(16)$, $c = 28.88(3)$ Å, $\beta = 119.16(2)°$, $V = 17400$ Å^3, space group $C2/c$, $Z = 8$, $\rho_{calcd} = 1.40$ g cm^{-3}, $\mu(Cu_{K\alpha}) = 18$ cm^{-1}, 4543 independent observed reflections with $[|F_o| > 4\sigma(|F_o|), 2\theta \leq 110°]$ refined to a current $R = 0.139$, $R_w = 0.137$.

[10] Siemens-P3/PC diffractometer, ω scans, $Cu_{K\alpha}$ radiation (graphite monochromator). The structure was solved by direct methods and refined anisotropically. Further details of the crystal structure can be obtained from the Cambridge Crystallographic Data Centre, 12 Union Road, GB-Cambridge CB2 1EZ (UK), on quoting the full journal citation.

[11] The equatorial plane of the cyclophane is defined as the mean plane of the four methylene carbon atoms.

[12] In the solid-state structure of $\mathbf{2}\cdot 4PF_6$, there are additional weak stabilizing C–H···O interactions between, for example, the α-CH proton of the included bipyridinium unit nearest to the *m*-xylyl spacer and the central oxygen atom of the BPP34C10 component (H···O = 2.52 Å, C–H···O angle = 153°) and between the diametrically opposite central oxygen atom of the crown ether and one of the aromatic protons in the *p*-xylyl spacer (H···O = 2.57 Å, C–H···O angle = 159°).

[13] In $\mathbf{2}\cdot 4PF_6$, there is an accompanying reduction to 6.95 Å in the interplanar separation between the "inside" and "alongside" hydroquinone rings (in $\mathbf{1}\cdot 4PF_6$ this separation is 6.95 Å).

[14] Each stack contains only one of the enantiomeric forms of the [2]catenane.

[15] P. R. Ashton, B. Odell, M. V. Reddington, A. M. Z. Slawin, J. F. Stoddart, D. J. Williams, *Angew. Chem.* **1988**, *100*, 1608; *Angew. Chem. Int. Ed. Engl.* **1988**, *27*, 1550.

[16] In the ^{1}H NMR spectrum of the complex, the resonances for protons in both the template and $\mathbf{4}\cdot 4PF_6$ are shifted significantly from those observed in the spectra of free BHEEB and free cyclophane.

[17] P. R. Ashton, D. Philp, M. V. Reddington, A. M. Z. Slawin, J. F. Stoddart, N. Spencer, D. J. Williams, *J. Chem. Soc. Chem. Commun.* **1991**, 1680.

[18] Crystal data for $\mathbf{3}\cdot 4PF_6\cdot 4MeCN$: triclinic, $a = 12.669(5)$, $b = 15.553(4)$, $c = 21.801(9)$ Å, $\alpha = 84.50(2)$, $\beta = 119.16(2)$, $\gamma = 78.21(2)°$, $V = 4154$ Å^3, space group $P\bar{1}$, $Z = 2$, $\rho_{calcd} = 1.45$ g cm^{-3}, $\mu(Cu_{K\alpha}) = 19$ cm^{-1}, 7173 independent observed reflections with $[|F_o| > 3\sigma(|F_o|), 2\theta \leq 116°]$ refined to a current $R = 0.100$, $R_w = 0.097$.

[19] As in $\mathbf{2}\cdot 4PF_6$, there are additional intramolecular stabilizing interactions in the solid-state structure of $\mathbf{3}\cdot 4PF_6$. There are, for example, short H···O contacts between the central oxygen atom of the BPP34C10 component and one of the methylene protons of the tetracationic cyclophane component (H···O = 2.35 Å, C–H···O angle = 157°) and between the diametrically opposite central ether oxygen atom and one of the α-CH

protons on the included bipyridinium unit (H···O = 2.58 Å, C-H···O angle = 147°).
[20] P. R. Ashton, C. L. Brown, E. J. T. Chrystal, T. T. Goodnow, A. E. Kaifer, K. P. Parry, A. M. Z. Slawin, N. Spencer, J. F. Stoddart, D. J. Williams, *Angew. Chem.* **1991**, *103*, 1055; *Angew. Chem. Int. Ed. Engl.* **1991**, *30*, 1032.
[21] ^{1}H NMR data for **2**·4PF$_6$ (400 MHz, CD_3COCD_3, 25 °C): δ = 3.40 (m, 4H, CH_2O), 3.63 (m, 6H, CH_2O and "inside" hydroquinone ring protons nearest to the π-faces of the xylyl spacers), 3.77 (m, 4H, CH_2O), 3.82 (m, 4H, CH_2O), 3.83–4.03 (m, 16H, remaining CH_2O protons), 4.42 (br. s, 2H, "inside" hydroquinone protons directed away from the cavity of the cyclophane), 6.03 (s, 4H, CH_2N), 6.10 (s, 4H, CH_2N), 6.27 (s, 4H, "alongside" hydroquinone ring protons), 7.87 (t, 1H, 5-position of *m*-xylyl spacer), 7.98 (s, 1H, 2-position of *m*-xylyl spacer), 8.05 (s, 4H, *p*-xylyl spacer arom. protons), 8.12–8.20 (overlapping d, 6H, 4- and 6-positions of *m*-xylyl spacer and β-CH bipyridinium protons), 8.25 (d, 4H, β-CH bipyridinium protons), 9.15 (d, 4H, α-CH bipyridinium protons), 9.27 (d, 4H, α-CH bipyridinium protons). ^{1}H NMR data for **3**·4PF$_6$ (400 MHz, CD_3COCD_3, 45 °C): δ = 3.42 (m, 4H, CH_2O), 3.66 (m, 4H, CH_2O), 3.80 (m, 12H, CH_2O), 3.88 (m, 4H, CH_2O), 3.98 (m, 4H, CH_2O), 4.09 (m, 4H, CH_2O), 4.41 (br. s, 4H, "inside" hydroquinone ring protons), 6.13 (s, 8H, NCH_2), 6.31 (s, 4H, "alongside" hydroquinone ring protons), 7.87 (t, 2H, 5-position of *m*-xylyl spacer), 8.04 (s, 2H, 2-position of *m*-xylyl spacer), 8.17 (d, 4H, 4- and 6-positions of *m*-xylyl spacer), 8.23 (d, 8H, β-CH bipyridinium protons), 9.13 (d, 8H, α-CH bipyridinium protons).
[22] The value of $\Delta G_c^{\neq}$ was obtained from the observed coalescence (T_c = −28 °C) of the "inside" hydroquinol resonances (δ = 3.17 and 5.53 at −60 °C, $\Delta\nu$ = 944 Hz) nearest to the *m*-xylyl spacer (see [23] for calculation).
[23] Values of k_c were obtained (I. O. Sutherland, *Annu. Rep. NMR Spectrosc.* **1971**, *4*, 71) by using the approximate expression $k_c = \pi(\Delta\nu)/\sqrt{2}$, and the Eyring equation was then used to calculate $\Delta G_c^{\neq}$ values at T_c.
[24] A process whereby the tetracationic cyclophane passes through the BPP34C10 component is also evident in the variable temperature ^{1}H NMR spectroscopic study, but estimation of the barrier to circumrotation was not possible owing to the complexity of the spectra at low temperature.
[25] The exchange method involves obtaining values of k (J. Sandström, *Dynamic NMR Spectroscopy*, Academic Press, London, **1982**, Chapter 6) from the approximate expression $k = \pi(\Delta\nu)$, where $\Delta\nu$ is the difference between the line width at a given temperature and the line width in the absence of exchange. The Eyring equation is then used to obtain values of $\Delta G^{\neq}$.
[26] Constitutional control of catenane formation can be exploited to advantage in the highly selective self-assembly of a chiral bis([2]catenane). See P. R. Ashton, A. S. Reder, N. Spencer, J. F. Stoddart, *J. Am. Chem. Soc.* **1993**, *115*, 5286.
[27] After the research described in this communication had been completed, we became aware that F. Vögtle, W. M. Müller, U. Müller, M. Bauer, and K. Rissanen (*Angew. Chem.* **1993**, *105*, 1356; *Angew. Chem. Int. Ed. Engl.* **1993**, *32*, 1295) had also prepared and obtained a crystal structure of **2**·4PF$_6$.

A Photochemically Driven Molecular Machine**

By *Roberto Ballardini,* Vincenzo Balzani,* Maria Teresa Gandolfi, Luca Prodi, Margherita Venturi, Douglas Philp, Howard G. Ricketts,* and *J. Fraser Stoddart**

In everyday life, we make extensive use of macroscopic devices called machines, which are assemblies of components designed for specific functions. The concept of a machine can be extended to the molecular level.[1–9] Whereas the machines of the macroscopic world are designed and constructed by mechanical engineers, molecular machines, which have dimensions on the nanometer scale, are constructed by "molecular engineers", that is, chemists. Molecular machines, like macroscopic machines, need energy to operate. For several reasons, the most convenient form of energy to make molecular machines work is light. In this paper, we describe some preliminary studies aimed at the construction of simple, light-driven mechanical molecular machines that could play a role in storing and processing information at the molecular level.[10]

Amongst the numerous new types of compounds recently constructed by chemists are the rotaxanes (**1**),[11] which are composed of a macrocyclic ring threaded by a linear component resembling a dumbbell, with bulky groups at either end. When one or both of the bulky end-groups are absent, the ring can unthread. This supramolecular species is called a pseudorotaxane (**2**).[12] In the last few years a variety of rotaxanes and pseudorotaxanes have been obtained by exploiting self-assembly processes based on π-electron donor–acceptor interactions.[6–8, 11c, 13, 14]

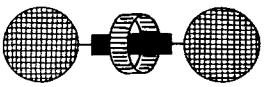

When the molecular thread **3**, which has a 1,5-dioxynaphthalene electron-donating group, is added to a solution of the electron-accepting cyclophane **4**, it threads itself spontaneously through the center of the tetracationic cyclophane producing the 1:1 complex or pseudorotaxane **5** as indicated by the ^{1}H NMR spectra.[14] The threading process can also

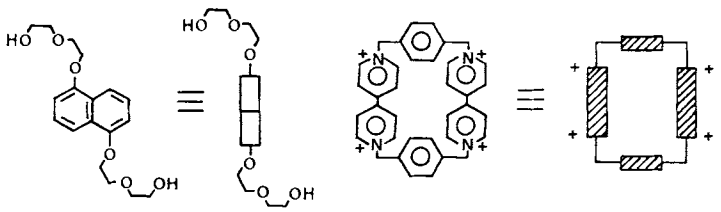

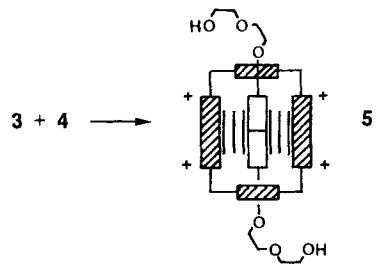

be followed by absorption and emission spectra. The interaction between the π-electron donor and the π-electron acceptor causes the formation of a charge-transfer band in the visible region (λ_{max} = 520 nm, $\varepsilon_{max} \approx 700\ M^{-1}cm^{-1}$) and the disappearance of the intense luminescence of **3** (λ_{max} = 345 mm, τ = 7.5 ns).[15] The threading process takes place in a variety of solvents,[14] reaching an equilibrium more or less displaced towards the formation of the pseudorotaxane **5**. The solvent chosen for the present investigation was water, wherein, starting with a 6.0×10^{-5} M solution of **3** and **4** (as

[*] Dr. R. Ballardini
Istituto FRAE-CNR
via De Castagnoli 1, I-40126 Bologna (Italy)
Prof. V. Balzani, Prof. M. T. Gandolfi, Dr. L. Prodi, Prof. M. Venturi
Dipartimento di Chimica "G. Ciamician" dell'Università
Via Selmi 2, I-40126 Bologna (Italy)
Prof. J. F. Stoddart, Dr. D. Philp, H. G. Ricketts
School of Chemistry, The University of Birmingham
Edgbaston, Birmingham B15 2TT (UK)

[**] This work was supported by the Consiglio Nazionale delle Ricerche (Progetto Finalizzato Chimica Fine II) and the Italian Ministero dell'Università e della Ricerca Scientifica e Tecnologica, and by SERC and Glaxo Group Research in the UK. We thank Anna Godi for some preliminary experiments.

its tetrachloride), 80% of the species formed at room temperature is the pseudorotaxane.[16]

Since the superstructure of the pseudorotaxane is based on the donor–acceptor interaction between its two components, reduction of the electron acceptor or oxidation of the electron donor is expected[7] to destabilize the supramolecular array and cause unthreading.[17] We have now devised a simple photochemical method to govern the unthreading process in this system.

It is well known[19] that the first excited state of 9-anthracenecarboxylic acid (hereafter abbreviated as **P**) is a long-lived (250 μs) and powerful reductant ($E_{red}(P^+/{}^*P) = -0.88$ V, vs. SCE). Therefore, one might expect that irradiation of a deoxygenated solution containing **P** (5.0×10^{-6} M) and **5** (4.8×10^{-5} M) should cause the reduction of the electron acceptor component **4** of the pseudorotaxane ($E_{red} = -0.32$ V) and, as a consequence, promote the unthreading process (Fig. 1). However, the departure of the

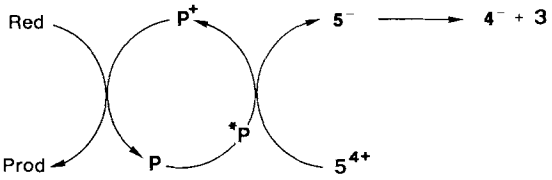

Fig. 1. Schematic representation of the light-induced unthreading process. The photosensitizer **P** is 9-anthracenecarboxylic acid and the "sacrificial" reductant Red is triethanolamine. For more details, see text. Prod = product of the oxidation of triethanolamine.

thread from the ring is slow because the process requires extensive nuclear motions. Therefore, it cannot compete with the fast back electron-transfer from the reduced **5** to the oxidized species P^+.[19] However, when a "sacrificial" reductant (like triethanolamine, 0.01 M) is also present in the solution, the oxidized species P^+, produced by the excited-state electron-transfer reaction, can be rapidly scavenged (Fig. 1). The result is that the back electron-transfer reaction is prevented and the pseudorotaxane remains reduced, as evident from the appearance of the characteristic bands of reduced paraquat-type units in the absorption spectrum of the solution (Fig. 2). Under such conditions, the charge-transfer interaction between the thread and the ring is permanently reduced, and the unthreading process takes place,

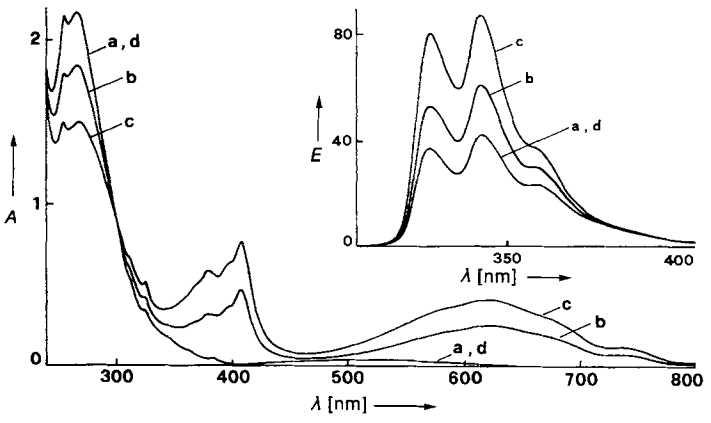

Fig. 2. Changes in the absorption (A) and luminescence spectrum (E [a.u.], of the pseudorotaxane **5** on irradiation. Curve a: starting solution; curves b and c: solutions irradiated for 4 and 15 min, respectively; curve d: solution c after oxidation with O_2.

as proven by the appearance of the fluorescence of free **3** (Fig. 2, inset).[20] Under the experimental conditions[15] 35% of the pseudorotaxane species was unthreaded after 25 minutes of irradiation. The unthreading reaction can also be performed by using $[Ru(bpy)_3]^{2+}$ (bpy = 2,2′-bipyridine) as a photosensitizer, but the reaction is not as efficient, mainly because of shorter excited-state lifetime of the complex.[21]

If oxygen is allowed to enter the irradiated solution, the reduced cyclophane is promptly reoxidized and **3** again threads through it, as shown by the decrease in the intensity of the fluorescence band and the reappearance of the initial absorption spectrum (Fig. 2). In principle, the rethreading process could also be photoinduced if a suitable "sacrificial" oxidant was added to the solution.

The strategy described above could be extended to more interesting systems in which the photosensitizer is incorporated as a stopper in the molecular structure of a rotaxane. A particularly appealing system based on the molecular shuttles[6, 8, 13] already described is shown in Fig. 3. In such

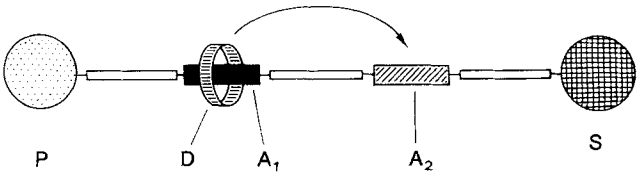

Fig. 3. Proposed structure for a light-driven molecular shuttle.

a system, an electron donor ring **D** is threaded by a dumbbell component composed of two electron acceptor "stations" $\mathbf{A}_1$ and $\mathbf{A}_2$, a bulky photosensitizer **P**, an inert stopper **S**, and suitable connectors. If $\mathbf{A}_1$ is a better electron acceptor than $\mathbf{A}_2$, the ring will reside on it preferentially. Light excitation of the photosensitizer **P** in the presence of a "sacrificial" electron donor could then be used to reduce $\mathbf{A}_1$, which would cause the displacement of the ring to $\mathbf{A}_2$. This movement would amount to the use of light to operate a molecular abacus.

Received: April 26, 1993 [Z 6036 IE]
German version: *Angew. Chem.* **1993**, *105*, 1362

[1] V. Balzani, L. Moggi, F. Scandola in *Supramolecular Photochemistry* (Ed.: V. Balzani), Reidel, Dordrecht, **1987**, p. 1.
[2] a) J.-M. Lehn, *Angew. Chem.* **1988**, *100*, 91; *Angew. Chem. Int. Ed. Engl.* **1988**, *27*, 89; b) *ibid.* **1990**, *102*, 1347 and **1990**, *29*, 1304.
[3] *Molecular Electronic Devices* (Eds.: F. L. Carter, R. E. Siatkowsky, H. Woltjien), North Holland, Amsterdam, **1988**; P. Ball, L. Garwin, *Nature* **1992**, *355*, 761.
[4] V. Balzani, F. Scandola, *Supramolecular Photochemistry*, Horwood, Chichester, **1991**, Chap. 12.
[5] H. Kuhn in *Molecular Electronics* (Ed.: P. I. Lazaraev), Kluwer, Dordrecht, **1991**, p. 175.
[6] P. L. Anelli, N. Spencer, J. F. Stoddart, *J. Am. Chem. Soc.* **1991**, *113*, 5131.
[7] P. L. Anelli, P. R. Ashton, R. Ballardini, V. Balzani, M. Delgado, M. T. Gandolfi, T. T. Goodnow, A. E. Kaifer, D. Philp, M. Pietraszkiewicz, L. Prodi, M. V. Reddington, A. M. Z. Slawin, N. Spencer, J. F. Stoddart, C. Vicent, D. J. Williams, *J. Am. Chem. Soc.* **1992**, *114*, 193.
[8] P. R. Ashton, R. A. Bissell, N. Spencer, J. F. Stoddart, M. S. Tolley, *Synlett* **1992**, 923.
[9] K. E. Drexler, *Nanosystems: Molecular Machinery, Manufacturing, and Computation*, Wiley, New York, **1992**.
[10] D. Bradley, *Science* **1993**, *259*, 890.
[11] a) G. Schill, *Catenanes, Rotaxanes, and Knots*, Academic Press, New York, **1971**; b) C. O. Dietrich-Buchecker, J.-P. Sauvage, *Chem. Rev.* **1987**, *87*, 795; c) J. F. Stoddart in *Frontiers in Supramolecular Organic Chemistry and Photochemistry* (Eds.: J. Schneider, H. Dürr), VCH, Weinheim, **1991**, p. 251.
[12] D. Philp, J. F. Stoddart, *Synlett* **1991**, 445.
[13] P.R. Ashton, D. Philp, N. Spencer, J. F. Stoddart, *J. Chem. Soc. Chem. Commun.* **1992**, 1124.

[14] a) P. R. Ashton, R. Ballardini, V. Balzani, M. Blower, M. Ciano, M. T. Gandolfi, L. Prodi, C. H. McLean, D. Philp, N. Spencer, J. F. Stoddart, M. S. Tolley, *New J. Chem.*, in press; b) P. L. Anelli, P. R. Ashton, N. Spencer, A. M. Z. Slawin, J. F. Stoddart, D. J. Williams, *Angew. Chem.* **1991**, *103*, 1052; *Angew. Chem. Int. Ed. Engl.* **1991**, *30*, 1306.

[15] The experiments were carried out at room temperature in deaerated, aqueous 0.1 M MeCOONa solution. Absorption and luminescence spectra were recorded with Perkin-Elmer λ6 and LS50 instruments. Luminescence lifetimes were measured with an Edinburgh 199 single-photon counting instrument. Light excitation was performed with a Hanau Q 400 medium-pressure Hg lamp, equipped with a 365 nm filter. The incident light intensity on the 3 mL reaction cell was 2×10^{-6} N$h\nu$ min^{-1}. The fraction of the incident light absorbed by the photosensitizer was 13%.

[16] The amount of pseudorotaxane present under the conditions used for the photochemical experiments was determined from the quenching of the intensity of the luminescence of **3** and the intensity of the charge-transfer absorption band. The ^{1}H NMR spectrum (300 MHz) of the complex composed of **3** and **4** (0.013 M of each) in D_2O at room temperature shows significant changes in the chemical shifts of the aromatic protons of **3**. The largest change ($\Delta\delta = -4.52$) is for the H4 and H8 protons on the naphthalene ring. This large $\Delta\delta$ value, along with the strong charge-transfer interaction between the two components, is compelling evidence for the formation of complex **5**, whose structure in aqueous solution is best described as pseudorotaxane-like: a) P. Ashton, D. Philp, N. Spencer, J. F. Stoddart, *J. Chem. Soc. Chem. Commun.* **1991**, 1677; b) P. R. Ashton, C. L. Brown, E. J. T. Chrystal, T. T. Goodnow, A. E. Kaifer, K. P. Parry, A. M. Z. Slawin, N. Spencer, J. F. Stoddart, D. J. Williams, *Angew. Chem.* **1991**, *103*, 1055; *Angew. Chem. Int. Ed. Engl.* **1991**, *30*, 1039; c) P. R. Ashton, D. Philp, N. Spencer, J. F. Stoddart, unpublished results.

[17] In principle, the donor–acceptor interaction can be destroyed by direct excitation of the supramolecular species in its charge-transfer band. However, the back electron-transfer reaction is, as expected [4], much faster than the unthreading process [18]. Such a "direct-excitation approach", therefore, does not seem to be very promising.

[18] P. L. Anelli, A. C. Benniston, A. Harriman, J. F. Stoddart, *J. Chem. Soc. Chem. Commun.*, submitted.

[19] O. Johansen, A. W. H. Mau, W. H. F. Sasse, *Chem. Phys. Lett.* **1983**, *94*, 107.

[20] If the unthreading process does not take place, the luminescence of the bound **3** would be quenched by the reduced cyclophane in **5** by energy transfer.

[21] V. Balzani, F. Barigelletti, L. De Cola, *Top. Curr. Chem.* **1990**, *158*, 31.

A New Copper Selenide Cluster with PPh_3 Ligands: $[Cu_{146}Se_{73}(PPh_3)_{30}]$**

By *Harald Krautscheid, Dieter Fenske,* Gerhard Baum,* and *Marcus Semmelmann*

Dedicated to Professor Hans Bock on the occasion of his 65th birthday

Complexes of transition metal halides with cyclopentadienyl, carbonyl, and above all tertiary phosphane ligands react with silylated elements of the fifth and sixth main groups to give trimethylsilyl halide and metal-rich cluster compounds.[1] In these reactions, the structure of the clusters formed is influenced by the steric demand of the phosphane ligand. For example, copper–chalcogenide clusters of differing sizes are obtained from the reaction of CuCl with PEt_3, $PiPr_3$, $PtBu_3$, or PEt_2Ph, and $E(SiMe_3)_2$ (E = Se, Te) (Scheme 1).[2]

In analogous reactions of $[CuCl(PPh_3)]_4$, $[Cu_2Cl_2(PPh_3)_3]$, or $[CuCl(PPh_3)_3]$ with $Se(SiMe_3)_2$, we found that in organic solvents either dark brown powders or black crystals were formed, which were unsuitable for X-ray crystal structure analysis.[2] However, we have now succeeded in obtaining suitable single crystals from the reaction of CuCl with PPh_3 and $Se(SiMe_3)_2$ in THF.[3] In this reaction, the reaction rate decreases with an increasing ratio of PPh_3 to CuCl. Whereas attempts at recrystallization have so far not been successful, the reaction rate and therewith also the rate of crystallization was slowed by the high phosphane concentration, so that the crystal quality improved. According to the results of the crystal stucture analysis, the product has the composition $[Cu_{146}Se_{73}(PPh_3)_{30}]$ (**2**).

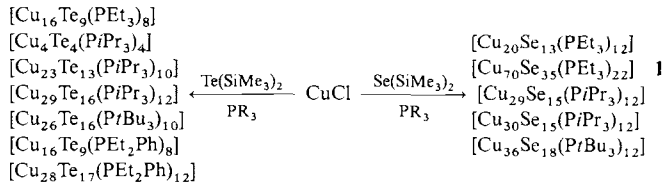

Scheme 1.

$$146\ CuCl + 73\ Se(SiMe_3)_2 + 30\ PPh_3 \xrightarrow{THF} [Cu_{146}Se_{73}(PPh_3)_{30}] + 146\ Me_3SiCl$$

2

No structural information could be derived from NMR spectroscopic investigations of **2** in solution because of the low solubility of the cluster and the rapid exchange of the phosphane ligands. Only bands of weak intensity for the coordinated PPh_3 ligands are found in the IR spectrum of **2**.

Based on the systematic absences the solution and the refinement of the structure was carried out in the space groups $P\bar{3}1c$ and $P6_3/mmc$.[4] Whereas the $Cu_{146}Se_{73}$ cluster core and the P atoms of the PPh_3 ligands comply with the space group symmetry of $P6_3/mmc$, only some of the C atoms could be located and these were disordered. In contrast, the difference Fourier syntheses in $P\bar{3}1c$ yielded all the C atoms; for which a phenyl group of one PPh_3 ligand is disordered. This disorder and the large thermal ellipsoids of Cu 17, Cu 18, and Cu 25 indicate that the trigonal or hexagonal symmetry, respectively, is possibly not real. It could be a consequence of triple twinning during the growth of the crystal, and in reality a lower symmetry may exist.[5]

Compound **2** crystallizes with two formula units per unit cell and has a threefold and three twofold axes. Compound **2** (Fig. 1, top) is constructed according to the same structural principle as $[Cu_{70}Se_{35}(PEt_3)_{22}]$ **1**. As Figure 1 (bottom left) shows, the PPh_3 ligands, which are bound to 30 peripheral copper atoms (Cu 1, Cu 6, Cu 11, Cu 12, Cu 23; Cu–P 218.4–224.4 pm, mean 222.2 pm), shield the $Cu_{146}Se_{73}$ cluster core almost perfectly. In **1** and **2**, the Se atoms are organized into three planar layers with 10, 15, and 10 atoms in **1**, and 21, 31, and 21 atoms in **2** (ABA stacking). The maximum deviations from the ideal planes in **2** are 5.4 pm for the middle layer and 15.5 pm for the outer layers. As shown in Figure 1, bottom right, these layers are constructed according to the principle of a two-dimensional closest packing and have an interlayer distance of 362 pm. Only Se 1 does not follow this order. The Se–Se distances within these layers range from 371.5 to 467.7 pm (mean 412 pm), and between the layers from 418.1 to 453.4 pm (mean 436 pm).

In β-Cu_2Se, a layer structure of the Se atoms is also found, which, however, in contrast to **1** and **2** form a cubic closest packing. Here, the nonbonding Se–Se distance is 414.4 pm, and the distance between the Se layers is 338.3 pm.[6]

[*] Prof. Dr. D. Fenske, Dr. H. Krautscheid, G. Baum, M. Semmelmann
Institut für Anorganische Chemie der Universität
Engesserstrasse, Geb. Nr. 30.45, D-76128 Karlsruhe (FRG)
Telefax: Int. code + (721)661921

[**] This work was supported by the Deutsche Forschungsgemeinschaft (SFB 195) and the Fonds der Chemischen Industrie.

The holes generated by the Se packing are filled with Cu atoms (blue), as shown in Figure 2. Of the 146 Cu atoms 120 are found between the Se layers, 12 Cu atoms (Cu 7, Cu 14, and Cu 24) in the middle Se layer, and 14 Cu atoms (Cu 6, Cu 23, and Cu 26) outside the Se layers. If all the Cu–Se distances in the cluster less than 282 pm are considered as bonds, 12 μ_4-(Se 1, Se 13; Cu–Se 236.1–248.2 pm), 6 μ_5-(Se 8; Cu–Se 237.7–268.3 pm), 25 μ_6- (Se 7, Se 9–Se 12; Cu–Se 237.3–267.8 pm), 21 μ_7-(Se 2, Se 3, Se 5, Se 14; Cu–Se 233.8–277.4 pm), and 9 μ_8-Se bridges (Se 4, Se 6; Cu–Se

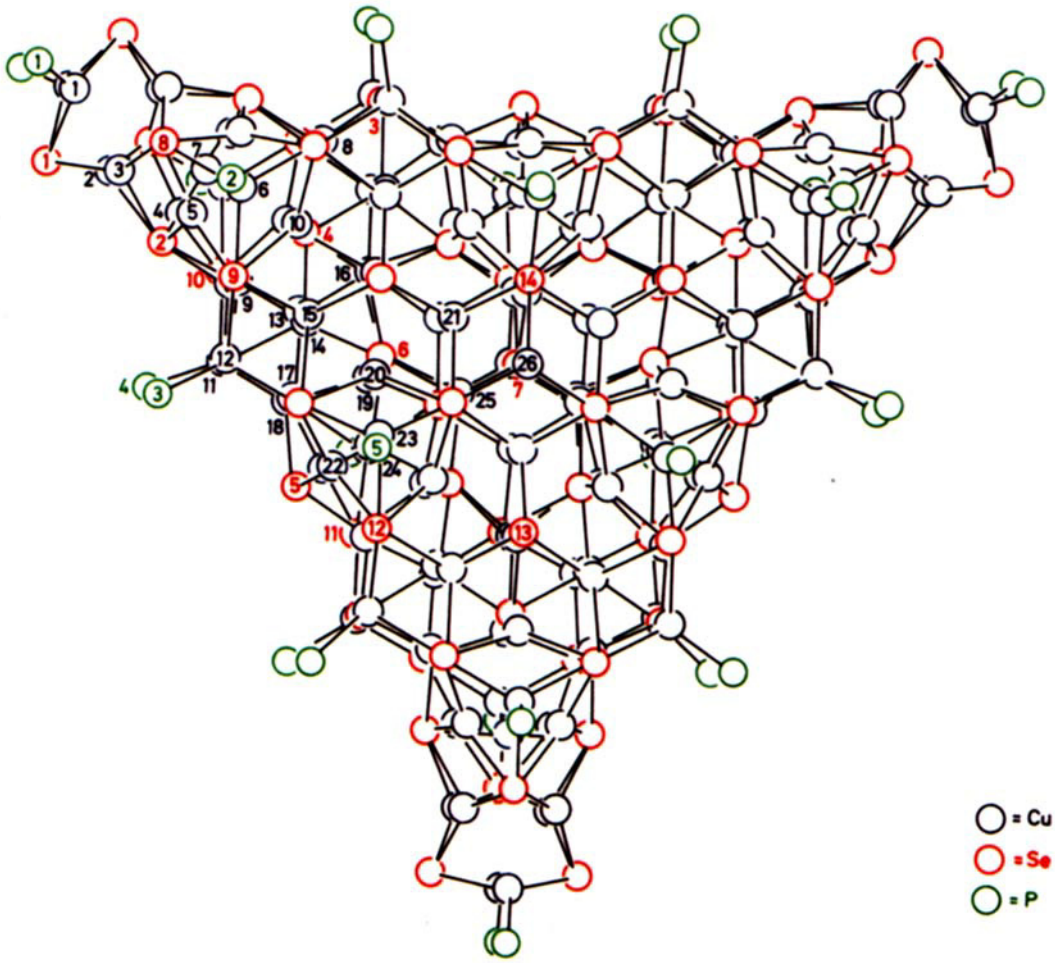

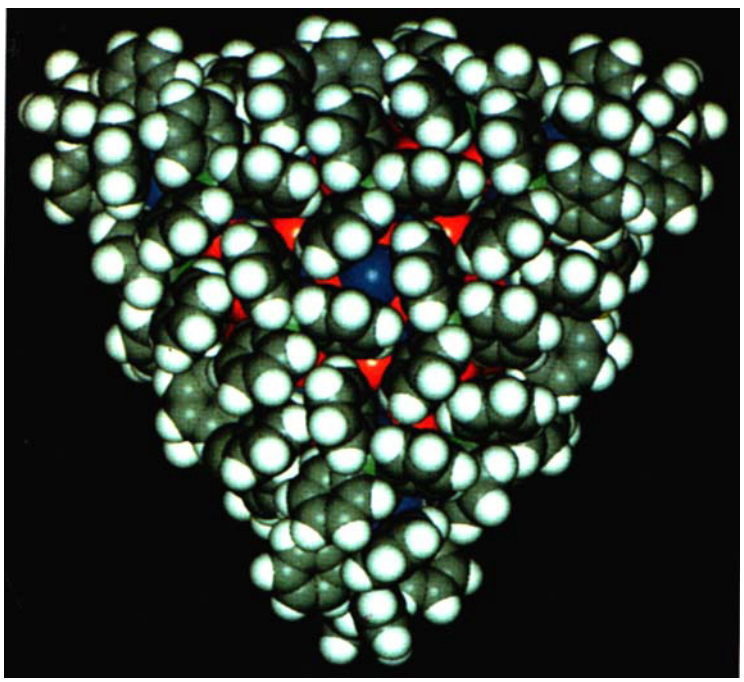

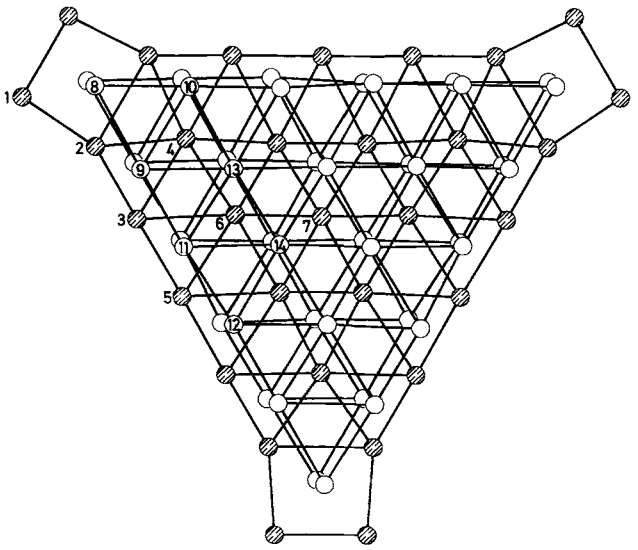

Fig. 1. Top: Crystal structure of **2** (without phenyl groups; Cu: blue, Se: red, P: green) viewed approximately down the threefold axis. For a better overview only one set of symmetrically independent atoms was labeled with atom numbers in the corresponding color. Cu–Cu bonds are not shown, but Cu–Se distances up to 282 pm are drawn. Bottom left: space-filling model of **2** in the same orientation (with phenyl groups); bottom right: stacking of the Se layers in **2**.

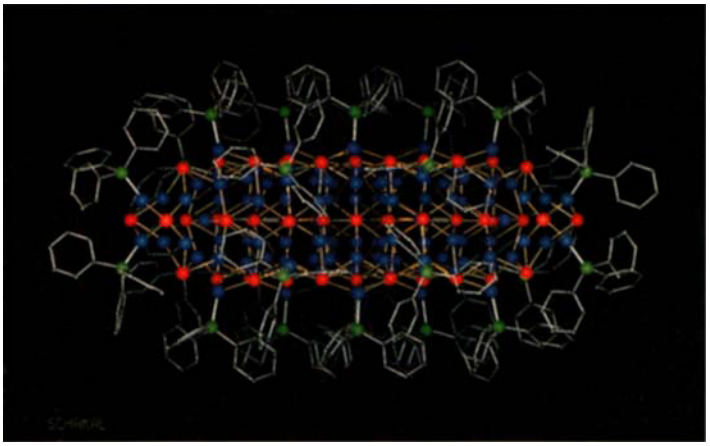

Fig. 2. Structure of **2** viewed along the Se layers (Cu: blue, Se: red, P: green). Cu–Se distances up to 282 pm are drawn.

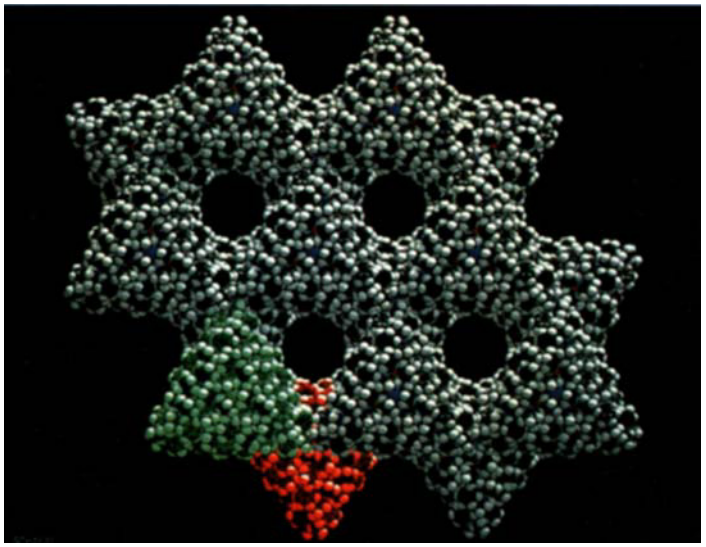

238.7–281.1 pm) are found. The mean Cu–Se distance is 251.2 pm.

The Cu atoms predominantly fill sites with threefold Se coordination. Only Cu14 and Cu24 lie in the middle of nearly equilateral Se_3 triangles, whereas the other Cu atoms are found outside the Se planes. Eighteen Cu atoms (Cu9, Cu16, Cu25) are bound nearly tetrahedrally to four Se atoms, and 24 Cu atoms (Cu6, Cu11, Cu12, Cu23) are coordinated to three Se atoms and one phosphane ligand, also in an almost tetrahedral manner. Cu1 is coordinated by one PPh_3 and two Se atoms. Cu7, which is bound to only two Se ligands, has the lowest coordination number.

In cubic β-Cu_2Se, half of the Cu atoms fill tetrahedral holes, the other half are distributed on octahedral sites and those sites which lie between the middle of the Se_3 faces and the unoccupied tetrahedral holes. For example, the Cu atoms in $Cs_2Cu_5Se_4$ are found mainly in tetrahedral holes, they are, however, shifted toward the middle of a tetrahedral face, so that here also the tendency for the coordination number 3 is apparent.[6]

The Cu–Se distances in β-Cu_2Se for the Cu atoms in octahedral holes are 293.0 pm, for Cu atoms in tetrahedral holes 253.7 pm, and for Cu atoms in a distorted trigonal environment 243.2 pm. Thus, it is clear that **2** does not exactly represent a section from the β-Cu_2Se structure; however, the coordination and separations between the Se layers show similarities.

Compound **2** forms molecules with approximately trigonal prismatic shape with an edge length of about 40 Å and a thickness of about 20 Å. The copper selenide cluster core has a maximum width of 26.7 Å and a thickness of 8.7 Å. The shortest distance between two cluster cores is found between the Se1 atoms of two molecules of one layer (Fig. 3), and is only 11.2 Å. Since Cu_2Se behaves like a semimetal, the question arises of whether the cluster unit surrounded by the insulating PPh_3 envelope already possesses physical properties similar to those of Cu_2Se. According to initial impedance spectroscopic investigations on single crystals of **2**, the electric conductivity is frequency and temperature dependent.[7] Comparable measurements on powder samples of **1** give an electric conductivity of $10^{-2}\,\Omega^{-1}\,cm^{-1}$, whereas $[Cu_{36}Se_{18}(PtBu_3)_{12}]$ is an insulator.[8] The direct current conductivity of crystalline **2** at room temperature is $\sigma' = 1.5 \times 10^{-2}\,\Omega^{-1}\,cm^{-1}$;[7] it is, however, significantly less than the value found for Cu_2Se.

As a result of the packing, channellike cavities with a diameter of about 16 Å form in the crystal along the c axis (Fig. 3). In organic solvents, the channels are probably filled with solvent molecules, which, however, can be removed under mild conditions, without destroying the crystal lattice. In the crystal structure analysis of **2**, 42 THF molecules per formula unit were located in the immediate vicinity of the PPh_3 ligands.

Received: March 19, 1993 [Z 5937 IE]
German version: *Angew. Chem.* **1993**, *105*, 1364

[1] D. Fenske, J. Ohmer, J. Hachgenei, K. Merzweiler, *Angew. Chem.* **1988**, *100*, 1300; *Angew. Chem. Int. Ed. Engl.* **1988**, *27*, 1277.

[2] D. Fenske, H. Krautscheid, S. Balter, *Angew. Chem.* **1990**, *102*, 799; *Angew. Chem. Int. Ed. Engl.* **1990**, *29*, 796; D. Fenske, H. Krautscheid, *ibid.* **1990**, *102*, 1513 and **1990**, *29*, 1453; D. Fenske, J.-C. Steck, *ibid.* **1993**, *105*, 254 and **1993**, *32*, 238.

[3] Preparation of **2**: To a suspension of CuCl (0.50 g, 5.0 mmol) in THF (100 mL) was added PPh_3 (6.6 g, 25 mmol). After dissolution of the CuCl, the mixture was treated with $Se(SiMe_3)_2$ (0.6 mL, 2.5 mmol) at room temperature; the reaction mixture turned yellow and within a few minutes this had changed to dark brown. After two to five days, **2** formed as black, hexagonal columns (with sharp ends) of up to 4 mm in length. Yield: about 50%. Correct elemental analyses for C, H, Cu, P, Se.

[4] X-ray structure analysis: STOE-IPDS, $Mo_{K\alpha}$, data collection and refinement: lattice constants (210 K): $a = b = 37.984(10)$, $c = 39.723(7)$ pm, $V = 49630 \times 10^6$ pm^3; space group $P\bar{3}1c$ (no. 163), $Z = 2$, $\mu(Mo_{K\alpha}) = 56.7$ cm^{-1}, $2\theta_{max} = 48°$; 120661 reflections, 24894 of which are independent reflections, 10939 with $I > 4\sigma(I)$, 707 parameters (Se, Cu, P anisotropic; phenyl rings refined as rigid groups), $R = 0.089$. One phenyl group at P1 is disordered. Seven solvent molecules (THF) per asymmetric unit could be located. - A second modification of **2** crystallizes in the space group $R\bar{3}c$ (no. 167) with $a = b = 48.430$, $c = 70.962$ pm, $V = 144140 \times 10^6$ pm^3, when the preparation is carried out from copper acetate instead of copper chloride. Further details of the crystal structure investigations may be obtained from the Fachinformationszentrum Karlsruhe, Gesellschaft für wissenschaftlich-technische Information mbH, D-76344 Eggenstein-Leopoldshafen (FRG) on quoting the depository number CSD-57250, the names of the authors, and the journal citation.

[5] H. Bärnighausen, personal communication.

[6] R. McLaren Murray, R. D. Heyding, *Can. J. Chem.* **1975**, *53*, 878; A. L. N. Stevels, F. Jellinek, *Recl. Trav. Chim. Pays-Bas* **1971**, *90*, 273; P. Rahlfs, *Z. Phys. Chem. Abt. B* **1936**, *31*, 157; W. Borchert, *Z. Kristallogr.* **1945**, *106*, 5; L. De Montreuil, *Econ. Geol.* **1975**, *70*, 384; W. Bronger, H. Schils, *J. Less-Common Met.* **1982**, *83*, 279.

[7] A. Enderle, Diplomarbeit, Universität Karlsruhe, **1993**.

[8] A. C. Kolbert, H. J. M. de Groot, D. van der Putten, H. B. Brom, L. J. de Jongh, G. Schmid, H. Krautscheid, D. Fenske, *Z. Phys. D* **1993**, in press.

[9] *SCHAKAL 92, a computer program for the graphic representation of molecular and crystallographic models*, E. Keller, Universität Freiburg, **1992/1993**.

Polynitrile- and Polyamine-Functional Poly(trimethylene imine) Dendrimers**

By *Christof Wörner* and *Rolf Mülhaupt**

Dedicated to Professor K. Takemoto

Symmetrical cascade polymers, often referred to as dendrimers or starburst polymers, can be prepared by divergent or convergent synthetic methods.[1] In the divergent synthesis the generation are prepared by sequential construction of stepwise branched polymers starting from a polyfunctional core and multiplying the functionalities in each branching step.[2-9] The ideal starburst-type growth is restricted to a certain limiting generation,[10,11] and when the density of the functional groups reaches a limit, steric hindrance accounts for incomplete branching reaction and consequently increased content of structural defects. Furthermore, for the divergent syntheses large excesses of the reagents must be used. In contrast, in the convergent synthetic strategy large dendritic precursors are prepared which are subsequently coupled.[12,13] Our research is aimed at the development of high yield divergent syntheses which do not require large excess of reagents and purification.

Vögtle et al.[2] had first proposed a conceptual approach involving a branching reaction sequence through cyanoethylation of amines with acrylonitrile followed by chemical reduction to double the amine end group functionality and stepwise branching the dendritic polyamines, thus forming poly(trimethylene imines). As a consequence of rather low

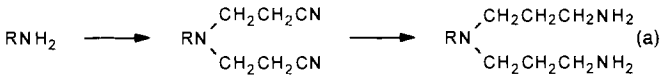

yields obtained in the reduction step, this reaction sequence was restricted to low molecular weight polyamine-functional oligo(trimethylene imines). The nitriles are quantitatively hydrogenated in the presence of Raney-nickel at room temperature and 8 bar hydrogen pressure, when small amounts of sodium hydroxide is added to the ethanol solvent.[14] Under such reaction conditions, the only partially ethanol-soluble polynitrile-functional poly(trimethylene imine) is suspended and hydrogenated to form ethanol-soluble polyamine-functional poly(trimethylene imines). This hydrogenation slurry process eliminates side reactions between amines and nitriles. Also it was found that in the presence of methanol the cyanoethylation occurs without formation of monosubstituted side products. In acetic acid[2] colored reaction products are formed that contain small quantities of monocyanoethylated amines, which lead to the structural defects in the dendrimers.

Since acrylonitrile, methanol, and cyanoethylated methanol are readily removed under vacuum, this synthetic route does not require special purification processes.

Starting from ammonia as initiator core, it was possible to build five generations of polynitrile- (X = CN) and polyamine-functional ($X = CH_2NH_2$, Scheme 1) cascade

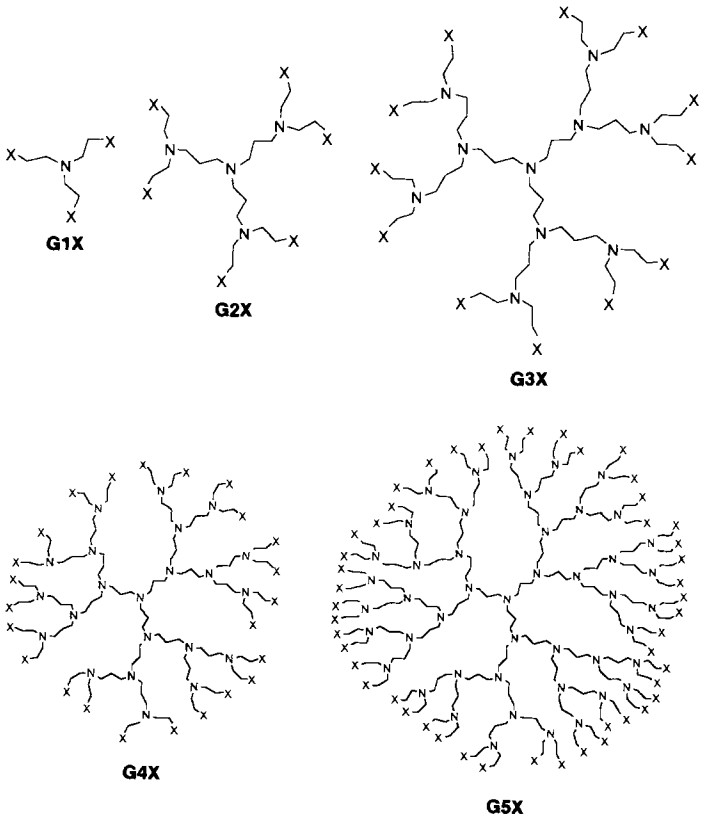

Scheme 1. Starburst poly(trimethylene imine) generations G*n*X ($n = 1-5$) with X = N for nitrile (CN) and X = A for amino (CH_2NH_2) end groups.

molecules by repeating the cyanoethylation/catalytic hydrogenation reaction sequence (Table 1). Although according to growth statistics, the fifth generation is not considered to be the theoretical limitation for ideal growth, G5N could not be completely hydrogenated. Most likely, the steric hindrance of 48 nitrile groups located at the surface is sufficient to reduce the catalytic activity of the Raney-nickel. In fact, the reaction time required for quantitative hydrogenation increases substantially with increasing number of generations: G1N is hydrogenated in seven hours, G4N in four days.

Table 1. Polynitrile- and polyamine-functional poly(trimethylene imines). G*n*X represents the generations from $n = 1-5$ with X = N for nitrile- and X = A for amine end groups.

G*n*X	End groups [mol mol^{-1}]	Yield [%]	$\bar{M}_n$ theor. [g mol^{-1}]	$\bar{M}_n$ [a] [g mol^{-1}]	$\bar{M}_n$ [b] [g mol^{-1}]	$\bar{M}_w/\bar{M}_n$ [b]
G1N	3	77	176	–	180	1.02
G1A	3	67	188	–	185	1.05
G2N	6	96	506	494	480	1.02
G2A	6	86	530	–	530	1.07
G3N	12	94	1167	1060	1200	1.02
G3A	12	79	1216	–	1250	1.08
G4N	24	96	2489	2470	2570	1.04
G4A	24	69	2586	–	2480	1.08
G5N	48	93	5133	4880	4810	1.07

[a] Determined by vapor pressure osmometry (VPO). [b] Determined by gel permeation chromatography (GPC).

For applications of such poly(trimethylene imines) cascade molecules it is important to identify structural defects which may account for changes in the supramolecular archi-

[*] Prof. Dr. R. Mülhaupt, C. Wörner
Institut für Makromolekulare Chemie
Hermann-Staudinger-Haus
Stefan-Meier-Strasse 31, D-79104 Freiburg (FRG)
Telefax: Int. code +(761)276-453

[**] This work was supported by the Deutsche Forschungsgemeinschaft. During preparation of this manuscript the authors became aware of similar results from E. M. M. de Brabander-van den Berg, E. W. Meijer, *Angew. Chem.* **1993**, *105*, 1370-1372; *Angew. Chem. Int. Ed. Engl.* **1993**, *32*, 1308-1311

tecture. The structures proposed for the individual generations in Scheme 1 have been confirmed with elemental analysis, end group titration, ^{1}H NMR, ^{13}C NMR, and IR spectroscopy, mass spectrometry, vapor pressure osmometry (VPO) and gel permeation chromatography (GPC). In addition to the molecular weights, the content of primary NH_2 end groups, and secondary NRH structural defects were determined. By potentiometric end group titration, it was possible to distinguish between primary and tertiary amine content only in the first generation G1A.[15] The ^{1}H NMR spectra of polynitrile-functional G4N (Fig. 1) and in polyamine-functional G4A (Fig. 2) show no secondary NHR structural defects, since the signals of the methylene group adjacent to the secondary amino group at $\delta = 2{,}7$ (between a and c in Fig. 1) and $\delta = 2{,}5$ (between b and d in Fig. 2) are observed in the expected region. According to the

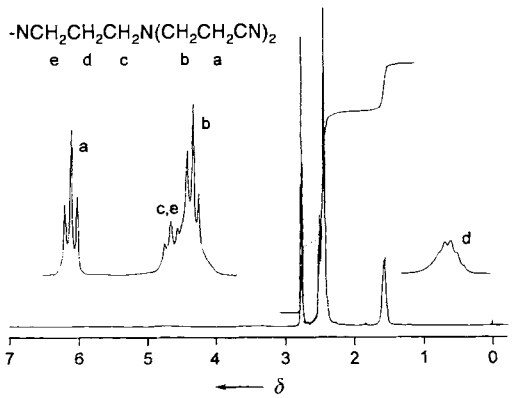

Fig. 1. ^{1}H NMR spectrum (400 MHz, CD_2Cl_2) of G4N.

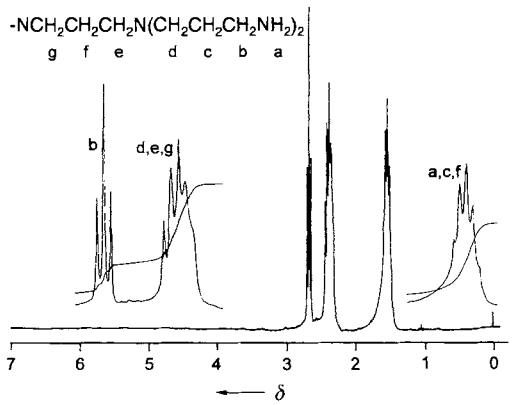

Fig. 2. ^{1}H NMR spectrum (250 MHz, $CDCl_3$) of G4A.

signal intensity ratio, highly symmetrical cascade polymers are formed. Also the signals of the CH_2 groups bound to the end groups have been assigned (triplet a in Fig. 1 at $\delta = 2{,}83$ triplet b in Fig. 2 at 2.67). The ^{13}C NMR spectra of the generations 1–4 confirm the high purities of the dendrimers. In the cyanoethylation of G4N small quantities of monocyanoethylated secondary NHR end groups are observed since steric hindrance increases drastically in the fifth reaction sequence. The ^{13}C NMR spectrum of the generation G5N (Fig. 3) reveals the signals of the methylene groups adjacent to the secondary amine (signals n and l at $\delta = 47.9$ and 45.5 respectively) and to the tertiary amine (signals d and c at $\delta = 51.6$ and 49.8 respectively). In a rough estimate based upon the signal intensities, the proportion of dendrimers with structural defects is less than 2 mol%. This means that on the surface of G5N, on average only 47 of the 48 possible nitrile groups per mol of dendrimer is achieved. This NMR study confirms that the cyanoethylation/hydrogenation reaction sequence provides excellent control of the molecular structure of these highly symmetrical cascade molecules.

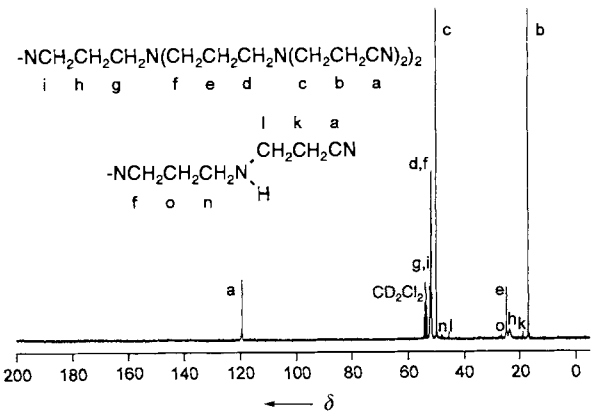

Fig. 3. ^{13}C NMR spectrum (100 MHz, CD_2Cl_2) of G5N. Spectrum confirms structural defects in the cascade molecule through monosubstitution (secondary amino end groups).

For the determination of the molecular weights, end group titration confirms the expected values for G1A and mass spectrometry for the generations G1(N, A) and G2(N, A). As apparent from Table 1, vapor pressure osmometry gives good agreement with the theoretical molecular weights over the entire range. Since in each generation size and hydrodynamic volume of the cascade molecules change substantially, gel permeation chromatography (GPC) has proven to be the best method for the characterization of the polyamine- and polynitrile-functional poly(trimethylene imines). In order to overcome adsorption problems of the highly surface-functional cascade molecules, which cause a broadening of the GPC chromatographs, electrolytes must be added to the eluent used in GPC chromatography. The characterization of the dendrimers was achieved by using an aqueous 0.05 M K_2HPO_4 buffer solution and a methanol/water (70:30) solvent mixture at pH = 11 and 60 °C. In Figure 4 the GPC chromatographs of the polyamine- and polynitrile-functional generations are shown.

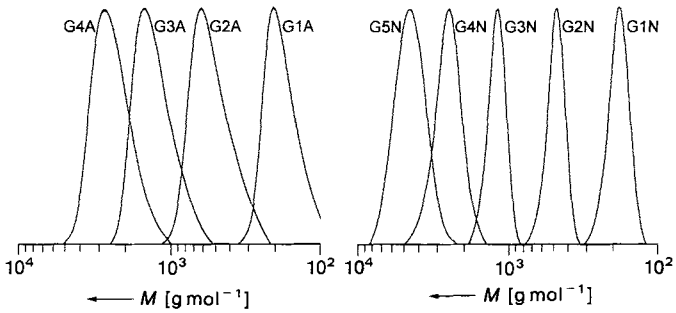

Fig. 4. Molecular weight distributions of the polyamine- and polynitrile-functional dendrimers (determined with GPC).

Using the values from vapor pressure osmometry for calibration, the polydispersities and number as well as weight average molecular weights have been determined. All generations exhibit monodisperse molecular weight distributions with polydispersities $\bar{M}_w/\bar{M}_n$ increasing with increasing number of the generation from 1.02 to 1.08. On the basis of the

GPC analyses, coupling reactions can be excluded. Interestingly, the solution behavior of poly(ethylene oxide), a typical random-coil polymer, is quite different from that of the two types of highly functional poly(trimethylene imine) cascade molecules prepared by us. As apparent from Figure 5, the polyamine-functional cascade molecules require higher elution volumes, which increase with increasing number of generations. In agreement with earlier observations,[1, 16] it ap-

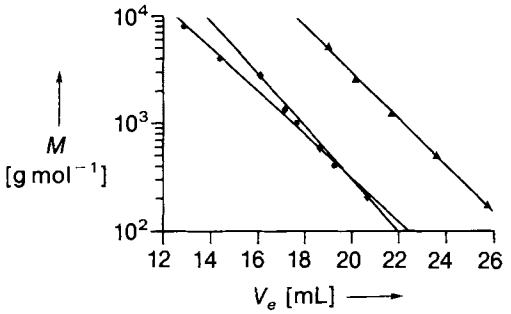

Fig. 5. Correlation of molecular weight M and elution volume V_e in GPC analyses of poly(ethylene oxide) (●), polynitrile- (▲) and polyamine-functional poly(trimethylene imines) (◆).

pears likely that cascade molecules when compared with conventional random-coil polymers exhibit higher densities, which increase with increasing molecular weight. The very high elution volumes found for the polynitrile-functional cascade molecules may result from adsorption phenomena, which do not interfer with the GPC analysis of the molecular weight distributions. In all three polymers there exists a linear correlation between molecular weight, determined by vapor pressure osmometry, and elution volume.

In conclusion, the divergent synthesis involving cyanoethylation and catalytic hydrogenation efficiently doubles the amino groups. With this reaction sequence poly(trimethylene imine) cascade molecules can be prepared in high yields and purity without requiring extensive purifications and excess reagent.

Experimental Procedure

Typical syntheses for the higher generations G4N, G4A, and G5N; the yields are summarized in Table 1.

G4N: To a cold solution of G3A (2.56 g, 2.10 mmol) in methanol (20 mL) were added acrylonitrile (20.0 mL, 305 mmol) (distilled over CaH_2 and stabilized with 0.05 wt% hydroquinonemonomethyl ether) within 90 minutes at 5–10 °C. After stirring 1 h at 10 °C and 4 days at 60 °C, the quantitative bis(cyanoethylation) was obtained. For separation of the stabilizer, the reaction mixture was passed through a neutral Al_2O_3 column and eluted with methanol/ethyl acetate (7:3), and the methanol content was increased slowly to 100%. The solvent was evaporated in vacuo to obtain 5.02 g (96%) of the highly viscous G4N. Correct elemental analysis for $C_{135}H_{222}N_{46}$ (2489.55 g mol^{-1}); ^{1}H NMR (400 MHz, CD_2Cl_2): δ = 1.62 (q, J = 7 Hz, 42 H; $CH_2CH_2CH_2$), 2.56 (m, 132 H; CH_2N), 2.83 (t, J = 7 Hz, 48 H; CH_2CN); ^{13}C NMR (100 MHz, CD_2Cl_2): δ = 17.3 (CH_2CN), 23.9, 25.1 ($CH_2CH_2CH_2$), 49.9 (CH_2CH_2CN), 51.7, 51.9, 52.2, 52.4 (CH_2N), 119.5 (CN); IR (neat): $\tilde{\nu}$[cm^{-1}] = 2920, 2800, 2220, 1450, 1410, 1350, 1250, 1160, 1120, 1050.

G4A: The hydrogenation was carried out in a 2 L stainless steel autoclave (Büchi AG, Uster/Switzerland). To 100 mL of a 1.4 M solution of NaOH in EtOH/H_2O (95:5), G4N (4.20 g, 1.69 mmol) was added. Under nitrogen the mixture was treated with Raney-nickel (2.5 g) (slurry in water, Aldrich), and the mixture was hydrogenated at 1000 rpm at 8 bar H_2 pressure for 4 days at 25 °C. The catalyst was filtered and washed with EtOH/H_2O (95/5). After diluting the filtrate with H_2O (100 mL), EtOH was evaporated and the residue extracted several times with CH_2Cl_2. Thereby, the NaOH concentration in the aqueous phase was increased in every extraction step. The organic layers were dried with Na_2SO_4 and the solvent evaporated in vacuo to give 3.01 g (69%) G4A. Correct elemental analysis for $C_{135}H_{318}N_{46}$ (2586.31 g mol^{-1}); ^{1}H NMR (250 MHz, $CDCl_3$): δ = 1.54 (m, 138 H; $CH_2CH_2CH_2$, NH_2), 2.36 (m, 84 H; CH_2N), 2.42 (t, J = 7 Hz, 48 H; $CH_2CH_2CH_2NH_2$), 2.67 (t, J = 7 Hz, 48 H; CH_2NH_2); ^{13}C NMR (100 MHz, $CDCl_3$): δ = 24.6 ($NCH_2CH_2CH_2N$), 30.9 ($CH_2CH_2NH_2$), 40.7 (CH_2NH_2), 51.9, 52.3, 52.4, 52.6 (CH_2N); IR (neat): $\tilde{\nu}$[cm^{-1}] = 3300, 3260, 2910, 2780, 1570, 1450, 1360, 1170, 1070, 960–770.

G5N: The procedure was equivalent to that reported for the synthesis of G4N. From G4A (600 mg, 0.232 mmol) was obtained 1.11 g (93%) of the highly viscous substance G5N. Correct elemental analysis for $C_{279}H_{462}N_{94}$ (5133.35 g mol^{-1}): ^{1}H NMR (400 MHz, CD_2Cl_2): δ = 1.62 (m, 90 H; $CH_2CH_2CH_2$), 2.52 (m, 276 H; CH_2N), 2.82 (t, J = 7 Hz, 96 H; CH_2CN); ^{13}C NMR (100 MHz, CD_2Cl_2): δ = 17.2 (CH_2CN), 23.8, 25.1 ($CH_2CH_2CH_2$), 49.8 (CH_2CH_2CN), 51.6, 51.8, 52.1, 52.3 (CH_2N), 119.5 (CN); IR (neat): $\tilde{\nu}$[cm^{-1}] = 2920, 2790, 2220, 1450, 1410, 1350, 1230, 1160, 1120, 1060.

The ^{1}H NMR and ^{13}C NMR spectra were measured with a Bruker AC 400 spectrometer with tetramethylsilane as internal standard; CD_2Cl_2 was used for the nitrile-functional and $CDCl_3$ for the amine-functional generations. End group titration was performed in a solution of H_2O/Et_2O (1:1) with 0.1 N HCl with a Mettler DC 25 titrator. Vapor pressure osmometry was carried out with a Perkin-Elmer Molecular Weight Apparatus Type 115 at 30 °C with $CHCl_3$ as solvent. The GPC analysis was performed on a Shimadzu LC-4A at 60 °C with a 0.05 M K_2HPO_4 buffer MeOH/H_2O (70:30) at pH = 11 (HEMA 40 and HEMA 100 column (MZ Analysentechnik), flow rate 0.5 mL min^{-1}, UV detector 228 nm, RI detector, calibrated with the values obtained from vapour pressure osmometry).

Received: April 1, 1993 [Z 5968 IE]
German version: *Angew. Chem.* **1993**, *105*, 1367

[1] D. A. Tomalia, A. M. Naylor, W. A. Goddard III, *Angew. Chem.* **1990**, *102*, 119–157; *Angew. Chem. Int. Ed. Engl.* **1990**, *29*, 138–175.
[2] E. Buhleier, W. Wehner, F. Vögtle, *Synthesis* **1978**, 155–158.
[3] H.-B. Mekelburger, W. Jaworek, F. Vögtle, *Angew. Chem.* **1992**, *104*, 1609–1614; *Angew. Chem. Int. Ed. Engl.* **1992**, *31*, 1571–1576.
[4] R. G. Denkewalter, J. F. Kolc, W. J. Lukasavage, US-A 4410688, **1983** (*Chem. Abstr.* **1984**, *100*, 103907p).
[5] A. M. Naylor, W. A. Goddard III, G. E. Kiefer, D. A. Tomalia, *J. Am. Chem. Soc.* **1989**, *111*, 2339–2341.
[6] D. A. Tomalia, H. Baker, J. Dewald, M. Hall, G. Kallos, S. Martin, J. Roeck, J. Ryder, P. Smith, *Polym. J.* **1985**, *17*, 117–132.
[7] D. A. Tomalia, H. Baker, J. Dewald, M. Hall, G. Kallos, S. Martin, J. Roeck, J. Ryder, P. Smith, *Macromolecules* **1986**, *19*, 2466–2468.
[8] G. R. Newkome, G. R. Baker, S. Arai, M. J. Saunders, P. S. Russo, K. J. Theriot, C. N. Moorefield, L. E. Rogers, J. E. Miller, T. R. Lieux, M. E. Murray, B. Phillips, L. Pascal, *J. Am. Chem. Soc.* **1990**, *112*, 8458–8465.
[9] X. Lin, G. R. Newkome, *Macromolecules* **1991**, *24*, 1443–1444.
[10] P. G. de Gennes, H. Hervert, *Phys. Lett.* **1983**, *44*, 351–360.
[11] R. L. Lescanec, M. Muthukumar, *Macromolecules* **1990**, *23*, 2280–2288.
[12] C. J. Hawker, J. M. J. Fréchet, *J. Am. Chem. Soc.* **1990**, *112*, 7638–7647.
[13] K. L. Wooley, C. J. Hawker, J. M. J. Fréchet, *J. Am. Chem. Soc.* **1991**, *113*, 4252–4261.
[14] R. J. Bergeron, J. R. Garlich, *Synthesis* **1984**, 782–784.
[15] O. C. Dermer, G. E. Ham, *Ethyleneimine and other azaridines*, Academic Press, New York, **1969**, p. 334.
[16] S. M. Aharoni, C. R. Crosby, E. K. Walsh, *Macromolecules* **1982**, *15*, 1093–1098.

Poly(propylene imine) Dendrimers: Large-Scale Synthesis by Hetereogeneously Catalyzed Hydrogenations**

By *Ellen M. M. de Brabander-van den Berg** and *E. W. Meijer*

Dendritic macromolecules are hyperbranched polymers that emanate from a central core, have a defined number of generations and functional end groups, and are synthesized in a stepwise way by a repetitive reaction sequence.[1] The syntheses described so far are either convergent, this is discrete

[*] Dr. E. M. M. de Brabander-van den Berg, Prof. Dr. E. W. Meijer [+]
DSM Research
P.O. Box 18, NL-6160 MD Geleen (The Netherlands)
[+] Present address:
Laboratory of Organic Chemistry, Eindhoven University of Technology
P.O. Box 513, NL-5600 MB Eindhoven (The Netherlands)
Telefax: Int. code + (31)40-451036

[**] We thank many colleagues at DSM Research, especially A. Nijenhuis, J. Keulen, M. Muré, B. Bosman, F. Vanderbooren, R. Reintjens, and S. van der Wal for their valuable input.

organic compounds are synthesized, or divergent, that is the construction of dendrimers can be regarded as a step polymerization with polydispersities of almost 1.[2-4] Detailed studies show that only a limited number of reaction schemes can be used for the synthesis of these dendrimers;[1,5-7] all known methods to date do not deliver pure dendrimers in large quantities, which is due to the use of sophisticated building blocks and/or (large excesses of) expensive reagents and/or complicated purifications.[6] In this paper we present a very convenient reaction sequence for the large-scale production of pure poly(propylene imine) dendrimers.

The reaction sequence presented here (Scheme 1) is based on the first approaches to dendrimeric structures by Vögtle et al. in which the low yields in the reduction hampered the synthesis of higher generations.[8] Our sequence is a repeti-

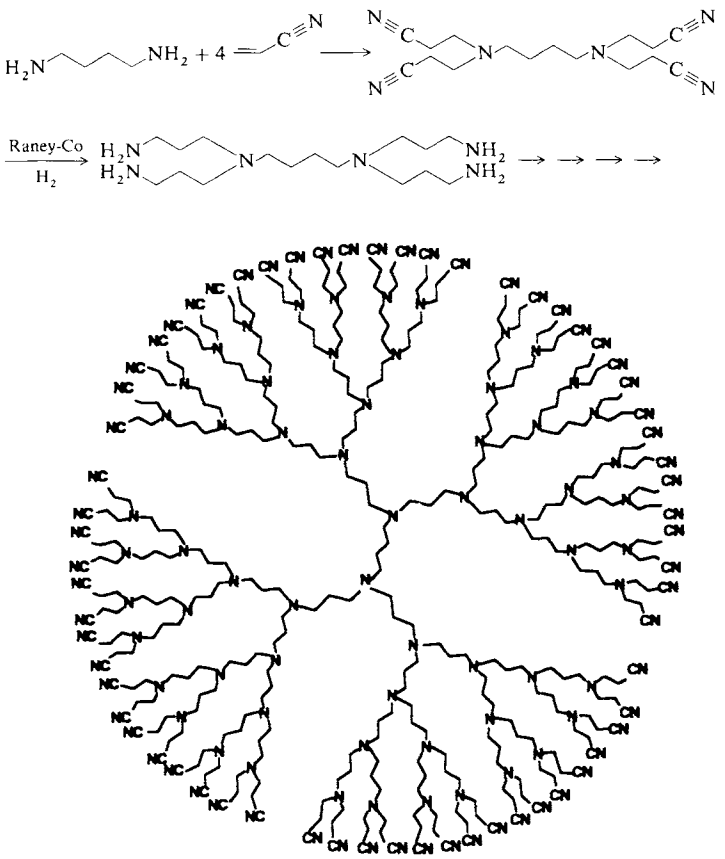

Scheme 1. Synthetic scheme for poly(propylene imine) dendrimers with diaminobutane as core.

tion of a double Michael addition of acrylonitrile to primary amines, followed by the heterogeneously catalyzed hydrogenation of the nitriles, resulting in a doubling of the number of primary amines. In this sequence 1,4-diaminobutane has been used as the dendrimer core; but a variety of molecules with primary or secondary amine groups can also be used. We have optimized conditions for both reaction steps in the sequence so that this occurs almost quantitatively and with optimal selectivity.[9]

All Michael reactions were performed similarly; 2.5–4 equivalents of acrylonitrile per primary amine are used at a concentration of 0.1 M in water; the first equivalent of acrylonitrile is added at room temperature and the second equivalent at 80 °C. The reaction time for complete conversion increases with every generation: 1 h for generation 0.5 (DAB-*dendr*-$(CN)_4$), 3 h for generation 4.5 (DAB-*dendr*-$(CN)_{64}$).[10] The excess of acrylonitrile is distilled off as a water azeotrope, leaving a clear two-phase system, from which the pure dendrimers with nitrile end groups can be isolated by pouring off the water layer. If necessary the water-soluble side products for example $HOCH_2CH_2CN$ (the Michael addition adduct of H_2O to acrylonitrile) or incompletely cyanoethylated products can be separated by washing the residue with water.

The hydrogenations of the cyanoethylated structures with H_2 (30–70 bar) and Raney/Cobalt as catalyst are also performed preferably in water. The reaction time required for complete hydrogenation increases at higher generations, but even at the higher generations this heterogeneous hydrogenation is quantitative and selective. Dendrimers with NH_2 end groups are isolated by evaporating the water from the filtered reaction mixture. The process window for a quantitative hydrogenation is small and side reactions easily occur. Three major side reactions which lead to dendrimers with structural defects have been observed, and the corresponding side products have been characterized: a) the occurrence of the retro-Michael addition during the hydrogenation, yielding secondary amines,[11] b) incomplete cyanoethylation in the Michael addition, resulting in dendrimers missing one ethyl cyanide side chain, and c) the formation of cyclic diamines and NH_3 by intramolecular addition of amines to the intermediate imines during the hydrogenation reactions. Under the optimized conditions these side products are not detectable and poly(propylene imine) dendrimers can be synthesized up to generation 4.5 with 64 terminal nitrile groups, a molecular weight of 6912 g mol^{-1} and in quantities of several grams up to several kilograms. Apart from the first generation (0.5) which is a white crystalline solid, all other generations are colourless oils, which are readily soluble: the DAB-*dendr*-$(NH_2)_x$ in H_2O and methanol, the DAB-*dendr*-$(CN)_x$ in common organic solvents.

All products were characterized by ^1H, ^{13}C NMR and IR spectroscopy, mass spectrometry, HPLC, gel permeation chromatography (GPC), differential scanning calorimetry (DSC), thermogravimetric analysis (TGA), and intrinsic viscosity. All data are consistent with the proposed dendrimer structures. NMR spectroscopy appears to be a very suitable technique to detect and assign structural failures in the outermost dendrimer generation. In the ^1H NMR spectra of the dendrimers with CN end groups the shape and intensity of the most downfield triplet of the NCH_2CH_2CN group at $\delta = 2.85$ is characteristic for defects in the outer generation, whilst the growth of the dendrimers is clearly indicated by the ratio of the integrals of the signal at $\delta = 1.40$ ($NCH_2CH_2CH_2CH_2N$ protons of the dendrimer core) to the integral of the signal at $\delta = 1.58$ ($NCH_2CH_2CH_2N$ branch protons). Incompletely cyanoethylated dendrimers are most readily concluded from additional signals in the ^{13}C NMR spectra at $\delta = 45.1$ ($NHCH_2CH_2CN$) and 18.7 ($NHCH_2CH_2CN$) as well as the products of retro-Michael additions of dendrimers with NH_2 end groups with signals at $\delta = 47.7$, 46.7, 39.1, 32.0, and 25.6.

Dendrimers with CN end groups can be separated and analyzed with HPLC. In Figure 1 a typical chromatogram of DAB-*dendr*-$(CN)_8$ from a kg-scale run is shown. From mass spectrometric experiments it has been concluded that the small peak corresponds with the fully cyanoethylated product of DAB-*dendr*-$(NH_2)_3$. If equal absorption coefficients are assumed for both compounds, the average selectivity per conversion in the first three steps is 99.8%.

Figure 2 shows a typical gel permeation chromatogram of various dendrimers with NH_2 end groups taken from a large-scale synthesis. The absence of detectable impurities is evi-

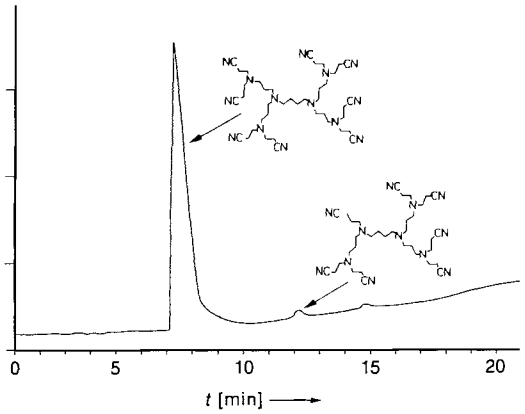

Fig. 1. Typical HPLC chromatograph of DAB-*dendr*-$(CN)_8$.

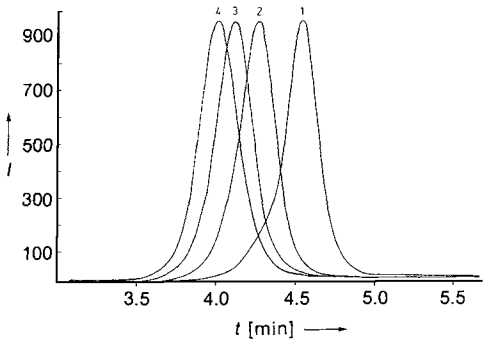

Fig. 2. Typical GPC trace of DAB-*dendr*-$(NH_2)_4$ (1), DAB-*dendr*-$(NH_2)_8$ (2), DAB-*dendr*-$(NH_2)_{16}$ (3), and DAB-*dendr*-$(NH_2)_{32}$ (4).

dent from the chromatograms. Furthermore, the characteristic relation between the molecular weight M_n and the intrinsic viscosity η is presented in Figure 3. As reported for two other classes of dendrimers, the intrinsic viscosity of the poly(propylene imine) dendrimers with CN end groups decreases with increasing molecular weight at a certain generation;[11, 12] in this case after the fourth generation.

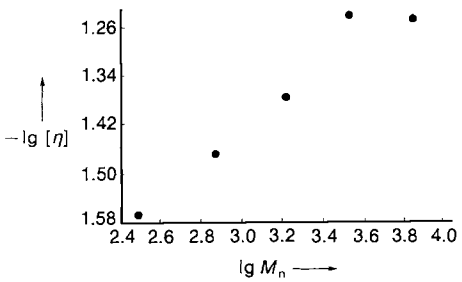

Fig. 3. Plot of $-\lg\eta$ vs. $\lg M_n$ of the various poly(propylene imine) dendrimers with CN end groups.

Thermal analysis of the dendrimers synthesized shows a number of interesting features. The glass transition temperature Tg has been recorded with DSC (Fig. 4); in both series of dendrimers with NH_2 and CN end groups the Tg's observed are low and an increase in Tg is observed by increasing molecular weight. In all cases the CN dendrimers possess the highest Tg, which is expected on basis of the dipole–dipole interaction of the CN groups. The thermal stability of the dendrimers with NH_2 end groups is unexpectably high and again increases with increasing molecular weight as determined by TGA (For DAB-*dendr*-$(NH_2)_4$, DAB-*dendr*-$(NH_2)_8$, DAB-*dendr*-$(NH_2)_{16}$, DAB-*dendr*-$(NH_2)_{32}$, TGA_{max} are 330, 378, 424, and 470 °C, respectively. For the DAB-*dendr*-$(NH_2)_8$ less than 1.0% weight loss is observed at $T = 310$ °C and scan speed 20 °C min^{-1}.) Dendrimers with CN end groups are less stable, although also in this case the stability increases at higher generations. With TGA-MS, a thermally induced retro-Michael addition is observed for DAB-*dendr*-$(CN)_{64}$, followed by a degradation similar to DAB-*dendr*-$(NH_2)_{32}$. A molecular interpretation of the latter is not possible with the data available.

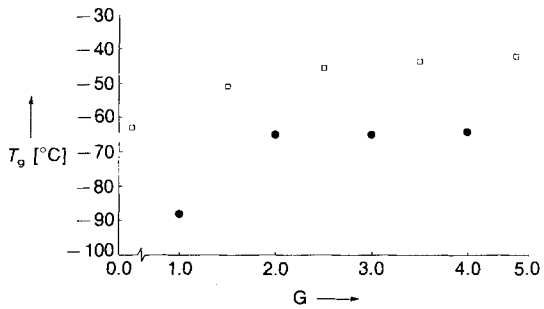

Fig. 4. Plot of the glass transition temperatures (T_g) of the poly(propylene imine) dendrimers with nitrile (□) and amino groups (●). G = generation.

As a consequence of the extensive purifications and low yields in the first approaches,[8] it was assumed until recently that this acrylonitrile–hydrogenation sequence is not suitable for dendrimer synthesis. However, by the correct choice of reagents and reaction conditions we have shown that this reaction sequence is very efficient. The main advantages of our synthetic procedures are 1) the simple reaction and isolation procedures which can readily be scaled up; 2) the use of one solvent for all reaction steps, so that the intermediates must not be isolated; 3) the use of readily available reagents which do not have to be protected; 4) the high yields and selectivities obtained; 5) a simple purification method which can easily be applied to large-scale quantities; 6) the versitility of the reaction sequence which allows for the introduction of a variety of end and core groups.

The dendrimers with NH_2 end groups offer remarkable thermal and good hydrolytic stability, and have a low T_g. The drop in intrinsic viscosity after the fourth generation indicates that a spherical shape with a sterically hindered shell is formed at the fifth generation. The low T_g indicates that the dendrimers possess a large degree of conformational freedom, despite their hyperbranching and well-defined chemical and geometrical structure. Research into the synthesis of higher generations and the functionalization of the dendrimers is in progress.

Experimental Procedure

DAB-*dendr*-$(CN)_4$: Acrylonitrile (8.35 mol, 443 g) was added to a solution of diaminobutane (1.67 mol, 147 g) in 1.176 kg water. The exothermic reaction caused the temperature to rise to 38 °C. After this exothermic effect the reaction mixture was heated at 80 °C for 1 h to complete the addition. Then the excess of acrylonitrile was removed as a water azeotrope by vacuum distillation (16 mbar, bottom temperature 40 °C). Phase separation of the reaction mixture afforded 499 g (99%) HPLC-pure DAB-*dendr*-$(CN)_4$, which was recrystallized from methanol.

^{13}C NMR (50 MHz, $CDCl_3$): $\delta = 119$ (CN), 53.1 ($NCH_2CH_2CH_2CH_2N$), 49.4 (NCH_2CH_2-CN, 24.9 ($NCH_2CH_2CH_2CH_2N$), 16.9 (CH_2CN); ^1H NMR (200 MHz, $CDCl_3$): $\delta = 2.85$ (t, 8H, NCH_2CH_2CN), 2.55 (m, 4H, $NCH_2CH_2CH_2CH_2N$), 2.48 (t, 8H, CH_2CN), 1.55 (m, 4H, $NCH_2CH_2CH_2CH_2N$); IR (KBr): $\tilde{\nu} = 2245\ cm^{-1}$ (CN).

DAB-*dendr*-$(NH_2)_4$: To a hydrogenation vessel, filled with Raney Cobalt catalyst (Cr promoted, Grace 2724, pretreated with hydroxide, 900 g) and water (22.5 L) was added DAB-*dendr*-$(CN)_4$ (450 g) dissolved in methanol. Subsequently the mixture was hydrogenated at 40 atm hydrogen pressure at 70 °C for 1 h. The cooled reaction mixture was then filtered and the solvents were evaporated at reduced pressure. The residue contained 450 g (95%) NMR spectroscopically pure DAB-*dendr*-$(NH_2)_4$ as a colorless oil.

^{13}C NMR (50 MHz, D_2O): $\delta = 53.4$ ($NCH_2CH_2CH_2CH_2N$), 51.1 ($NCH_2CH_2CH_2NH_2$), 39.5 (CH_2NH_2), 28.8 ($CH_2CH_2NH_2$), 23.9 ($NCH_2CH_2CH_2CH_2N$); ^1H NMR (200 MHz, $CDCl_3$): $\delta = 2.70$ (t, 8H, CH_2NH_2), 2.44 (t, 8H, $NCH_2CH_2CH_2NH_2$), 2.40 (m, 4H, $NCH_2CH_2CH_2CH_2N$), 1.58 (quin, 8H, $CH_2CH_2NH_2$), 1.42 (m, 12H, $NCH_2CH_2CH_2CH_2N$, NH_2); IR (film): $\tilde{\nu} = 3284$, 3355 cm^{-1} (NH_2).

Received: April 28, 1993 [Z 6041 IE]
German version: *Angew. Chem.* **1993**, *105*, 1370

[1] D. A. Tomalia, A. M. Naylor, W. A. Goddard III, *Angew. Chem.* **1990**, *102*, 119; *Angew. Chem. Int. Ed. Engl.* **1990**, *29*, 138–175.
[2] D. A. Tomalia, H. Baker, J. Dewald, M. Hall, G. Kallos, S. Martin, J. Roeck, J. Ryder, P. Smith, *Polym. J. Tokyo* **1985**, *17*, 117–132.
[3] C. J. Hawker, J. M. J. Fréchet, *J. Am. Chem. Soc.* **1990**, *112*, 7638.
[4] G. R. Newkome, X. Lin, *Macromolecules* **1991**, *24*, 1443; G. R. Newkome, A. Nayak, R. K. Behera, C. N. Moorefield, G. R. Baker, *J. Org. Chem.* **1992**, *57*, 358.
[5] C. J. Hawker, J. M. J. Fréchet, *Polymer* **1992**, *33*, 1507.
[6] H.-B. Mekelburger, W. Jaworek, F. Vögtle, *Angew. Chem.* **1992**, *104*, 1609; *Angew. Chem. Int. Ed. Engl.* **1992**, *31*, 1571.
[7] T. M. Miller, E. W. Kwock, T. X. Neenan, *Macromolecules* **1992**, *25*, 3143; A. W. van der Made, P. W. N. M. van Leeuwen, *J. Chem. Soc. Chem. Commun.* **1992**, 1400; A. Morikawa, M. Kakimoto, Y. Imai, *Macromolecules* **1991**, *24*, 3469.
[8] E. Buhleier, W. Wehner, F. Vögtle, *Synthesis* **1978**, 155–158.
[9] Independently C. Wörner and R. Mülhaupt (*Angew. Chem.* **1993**, *105*, 1367–1370; *Angew. Chem. Int. Ed. Engl.* **1993**, *32*, 1306–1308) have disclosed a similar reaction scheme.
[10] DAB-*dendr*-$(CN)_x$ means a dendrimer with DAB (DiAminoButane) as core and x nitrile end groups; DAB-*dendr*-$(NH_2)_x$ one with x primary amine end groups. A proposal for the systematic naming of dendrimers is given by G. R. Newkome, G. R. Baker, J. K. Young, J. G. Traynham, *J. Polym. Sci. Part A* **1993**, *31*, 641–651.
[11] Retro-Michael addition during the hydrogenations is strongly base-catalyzed by dendrimers with NH_2 end groups.
[12] T. H. Mourey, S. R. Turner, M. Rubinstein, J. M. J. Tréchet, C. J. Hawker, K. L. Wooley, *Macromolecules* **1992**, *26*, 2401.

Intramolecular Base Stabilization of Silicenium Ions: A New Route to Siliconium Ions

By *Claude Chuit, Robert J. P. Corriu,* Ahmad Mehdi,* and *Catherine Reyé*

The possible existence of trisubstituted silylium "silicenium" ions (R_3Si^+) has intrigued chemists for a long time.[1, 2] Nevertheless claims to have generated such species in solution[3] have been disputed,[4] and the question whether triorganylsilyl perchlorates undergo ionization in solvents has been reviewed by Eaborn[5] and Lickiss.[6] Recently silyl cations have been prepared in nonnucleophilic solvents with weakly coordinating anions.[7–8] However, the structural analysis of one of these derivatives showed a strong interaction between anion and cation.[8]

Some silyl cations that can be prepared are stabilized by the π-pentamethylcyclopentadienyl ligand,[9] intermolecular coordination,[8, 10–13] or intramolecular coordination.[14–15] However, these examples do not constitute a general route to cationic silicon species with a functional group at silicon that enables reactivity studies.

Some years ago, we showed that pentacoordinate neutral and anionic silicon species have unusual, often unexpected reactivity.[16] That led us to prepare cations containing pentacoordinate silicon centers (siliconium ions) in order to study their reactivity.

Since intramolecular coordination of the amino group stabilizes silanethione,[17] silaphosphene,[18] silanimine,[18] and transition metal silanediyl complexes very efficiently,[18, 19] we decided to extend this intramolecular stabilization to the silylium ions. We report here a novel and general route to functional and nonfunctional siliconium ions using the potentially bischelating ligand **A**.[20]

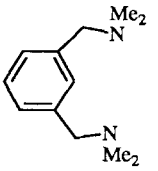

A

The reaction of the silane **1** with half an equivalent of iodine in ether at room temperature results in the formation of a precipitate and loss of half an equivalent of H_2 in a redox reaction. The precipitate was identified as the ionic species **2a** (Scheme 1).

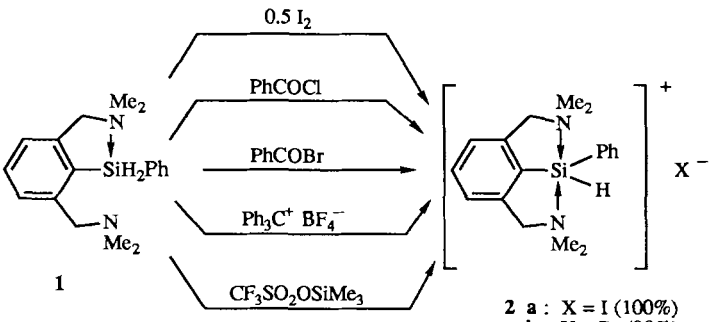

Scheme 1.

The ^1H NMR spectrum of **2a** shows a singlet at $\delta = 5.3$, shifted to low field with respect to the resonance signal of the SiH_2 protons of **1** and assigned to the SiH proton. The signal of the methylene protons in **2a** has an AB pattern. The two NMe_2 groups are magnetically equivalent as a result of the coordination of both nitrogen atoms to the silicon center and give rise to two singlets of equal intensity. In the coupled ^1H ^{29}Si NMR spectrum of **2a**, a doublet is observed at $\delta = -29.7$ ($^1J_{Si,H} = 280$ Hz), whereas the ^{29}Si resonance of the pentacoordinate silane **1**[21] appears as a triplet at $\delta = -51.5$ ($^1J_{Si,H} = 200$ Hz). Interestingly, the ^{29}Si NMR spectrum of **2a** in the solid state shows a sharp signal with the same chemical shift ($\delta = -28.8$) as in solution, which indicates that **2a** remains ionic even in the solid state.

The IR spectrum of **2a** in $CHCl_3$ shows a Si–H stretch at $\tilde{\nu} = 2202$ cm^{-1}, substantially higher than for **1** (2111 cm^{-1}). Moreover this frequency is very close to that observed by Jutzi et al.[9] for the silyl cation $[(\pi\text{-}Me_5C_5)_2SiH]^+$.

[*] Prof. Dr. R. J. P. Corriu, Dr. C. Chuit, A. Mehdi, Dr. C. Reyé
Université de Montpellier II
Sciences et Techniques du Languedoc, URA 1097
Place Eugène Bataillon, case 007, F-34095 Montpellier Cédex 5 (France)
Telefax: Int. code + (67)1438-88

The positive-ion FAB mass spectrum (FAB = fast atom bombardement) of **2a** shows an ion at *m/z* 297 corresponding to the mass of the siliconium ion.

The same cation can also be generated by treating **1** with one equivalent of various electrophiles such as *N*-chlorosuccinimide, PhCOX (X = Cl, Br; reduced to PhCHO[22]), $AgBF_4$, $Ph_3C^+BF_4^-$, or $CF_3SO_3SiMe_3$ (Scheme 1). Species **2b**–**2e** have all the same IR spectra, ^1H and ^{29}Si NMR spectra, and the same positive-ion FAB mass spectra as **2a**. These salts are air- and moisture-sensitive but they are stable in solution under argon, as well as in the solid state.

As a confirmation of the ionic nature of the salts **2** we carried out conductivity titrations: aliquots of reagents in CH_2Cl_2 (PhCOCl, PhCOBr, I_2, $CF_3SO_3SiMe_3$) were added to a solution of the silane **1** in CH_2Cl_2; the conductivity was measured after each addition. Figure 1 depicts a plot of conductivity as a function of the added reagent. The conductivity increases until one molar equivalent of reagent has been added, and thereafter it is constant.

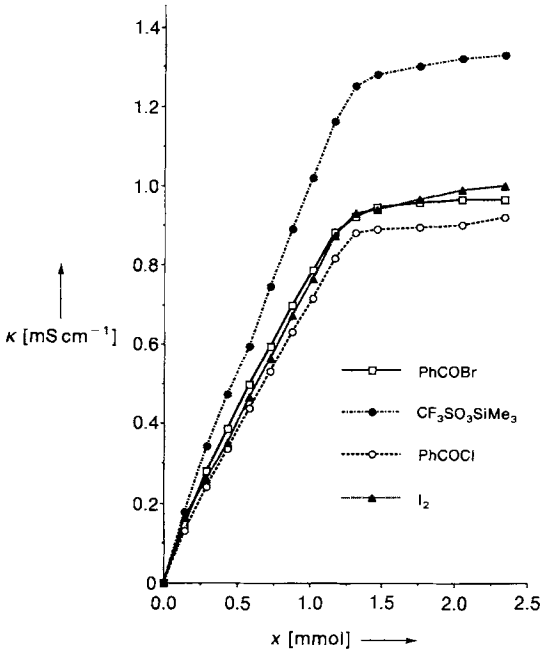

Fig. 1. The conductivity (κ) as a function of the amount of electrophilic reagent added (x) to a solution of 0.146 moles of silane **1** in CH_2Cl_2.

In contrast, the chlorosilane **4** resulting from the reaction of *N*-chlorosuccinimide with the silane **3** [Eq. (a), NClS = *N*-chlorosuccinimide] shows no conductance in dichloromethane, as expected for a covalent chlorosilane.[23,24]

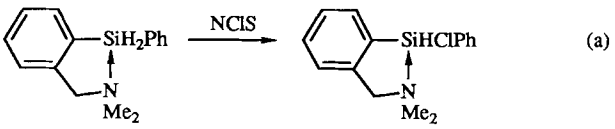

(a)

The preparation of siliconium ions by reaction of a electrophile on a silane bearing the ligand **A** and at least one hydrogen atom is quite general. As indicated in Equations (b) and (c), difunctional and nonfunctional siliconium ions have also been obtained with a good yield by this process.

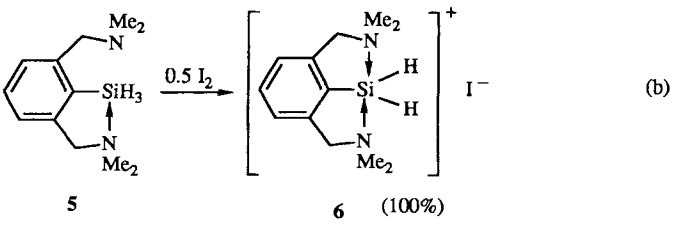

(b)

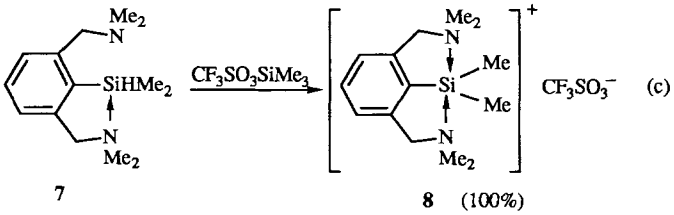

(c)

The reaction of the lithium derivative **9**[25] and dichlorophenylsilane or trichlorosilane also affords the corresponding siliconium ions (Scheme 2).

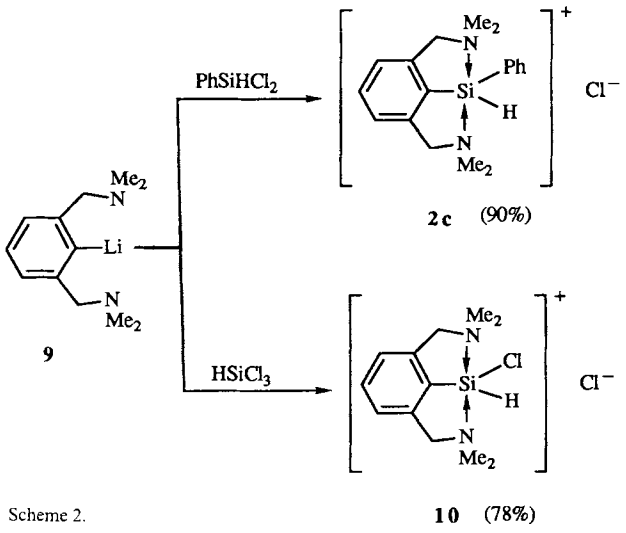

Scheme 2.

The formation of these siliconium ions should result either from the abstraction of a hydride ion (when $Ph_3C^+BF_4^-$ or $CF_3SO_3SiMe_3$ is the reagent) or from the substitution of an hydrogen atom by a halogen atom that is displaced by the nucleophilic coordination of the second NMe_2 group at silicon.

It is interesting to note that the dichlorosilane **11**, the X-ray structure of which has been determined,[19] is covalent.

11

This indicates the importance of the geometry of the ligand **A** in the formation of siliconium ions.

Experimental procedure

1: A solution of **9** [25] (22 mmol) in Et_2O (40 mL) was added slowly over 15 min at 0 °C to a solution of phenylsilane (2.4 g, 22 mmol) in Et_2O (40 mL). The mixture was stirred at room temperature for 2 h and then hydrolyzed at 0 °C with 0.4 mL of H_2O. After filtration on celite, distillation gave 5.4 g (83%) of **1** as a colorless oil. B.p. 115–117 °C/0.02 Torr; ^{1}H NMR (250 MHz, $CDCl_3$, TMS): $\delta = 2.0$ (s, 12H, CH_3), 3.51 (s, 4H, CH_2), 4.82 (s, 2H, SiH_2); ^{29}Si NMR (200 MHz, $CDCl_3$, TMS): $\delta = -51.5$ (t, ^1J(SiH), 200 Hz); IR (CCl_4): $\tilde{\nu}$[cm^{-1}] = 2111 (SiH_2). Correct elemental analyses (C,H,N,Si).

2a: A solution of iodine (0.43 g, 1.67 mmol) in ether (10 mL) was added dropwise to a solution of silane **1** (1 g, 3.35 mmol) in Et_2O (10 mL) at room temperature under argon. The resulting mixture was stirred until evolution of H_2 had ceased. It became progressively colorless as a precipitate appeared. The mixture was then filtered, and the residue washed twice with ether to give 1.4 g (100% yield) of a white microcrystalline powder. M.p. 135 °C (decomp); ^{1}H NMR (250 MHz, CD_2Cl_2, TMS): $\delta = 2.2$ (s, 6H, CH_3), 2.85 (s, 6H, CH_3), 4.0 (d, ^2J(H,H) = 16 Hz, 2H, CH_2), 4.25 (d, ^2J(H,H) = 16 Hz, 2H, CH_2), 5.3 (s, 1H, SiH); ^{13}C NMR (200 MHz, $CDCl_3$, TMS): $\delta = 63.1$ (CH_2N), 47.1, 47.6 ($N(CH_3)_2$), 123.2, 124.2, 127.3, 128.8, 131.2, 134.0, 143.0; ^{29}Si NMR (200 MHz, $CDCl_3$, TMS): $\delta = -29.7$ (d, ^1J(Si,H) = 280 Hz); IR (KBr): $\tilde{\nu}$[cm^{-1}] = 2202.

2c: A solution of **9** [25] (7.38 mmol) in Et_2O (50 mL) was added slowly to a solution of dichlorophenylsilane (1.1 mL, 7.38 mmol) in Et_2O (50 mL). The mixture was stirred at room temperature for 2 h. After filtration, the solid obtained was dissolved in CH_2Cl_2 to precipitate LiCl which was removed by filtration. After concentration, Et_2O was added to precipitate crude **2c** as a white solid (1.9 g, 90%) whose characteristics are the same as those of **2a**.

6: A solution of I_2 (0.4 g, 1.56 mmol) in Et_2O (15 mL) was added dropwise at −5 °C to a solution of silane **5** (b.p. = 45–50 °C/0.1 Torr) (0.7 g, 3.15 mmol) in Et_2O (15 mL). The mixture was stirred at room temperature for 4 h, filtered, and the solid obtained washed twice with Et_2O to give 1.1 g (100%) of crude **6**. M.p. 145 °C (decomp); ^{1}H NMR (80 MHz, $CDCl_3$, TMS): $\delta = 2.9$ (s, 12H, CH_3), 4.4 (s, 4H, CH_2), 4.9 (s, 2H, SiH_2); ^{29}Si NMR (250 MHz, $CDCl_3$, TMS): $\delta = -46.4$ (t, ^1J(Si,H) = 265 Hz); IR (KBr): $\tilde{\nu}$[cm^{-1}] = 2191 and 2209.

8: $CF_3SO_3SiMe_3$ (0.57 mL, 2.95 mmol) was added dropwise at 0 °C to a solution of 7 (b.p. = 120 °C/0.2 Torr) (0.7 g, 2.8 mmol) in Et_2O (15 mL). After stirring (30 min), the solvent was removed, and the solid obtained washed twice with Et_2O to give 1.1 g (100%) of crude **8**. M.p. = 118–121 °C; ^{1}H NMR (250 MHz, $CDCl_3$, TMS): $\delta = 0.4$ (s, 6H, $Si(CH_3)_3$), 2.4 (s, 12H, $N(CH_3)_2$), 3.8 (s, 4H, CH_2); ^{19}F NMR (80 MHz, $CDCl_3$, C_6F_6), $\delta = 85$ (s); ^{29}Si NMR (250 MHz, $CDCl_3$, TMS): $\delta = -4.1$ (s); positive-ion FAB-MS: m/z 249 (M^+, 100%).

10: A solution of **9** [25] (11.1 mmol) in Et_2O (30 mL) were added slowly to a solution of $HSiCl_3$ (1.2 g, 11.1 mmol) in Et_2O (30 mL). After 1 h at room temperature, the solvent was removed under vacuum, and CH_2Cl_2 (50 mL) was added. After filtration and evaporation of the solvent the oil obtained was solidified by addition of Et_2O. After washing twice with Et_2O, 2.5 g (78%) of crude **10** was obtained as a light yellow-green solid. M.p. 140 °C (decomp); ^{1}H NMR (250 MHz, $CDCl_3$, TMS): $\delta = 2.9$ (s, 12H, CH_3), 4.4 (s, 4H, CH_2), 5.2 (s, 1H, SiH); ^{29}Si-NMR (250 MHz, $CDCl_3$, TMS): $\delta = -40.3$ (d, ^1J(Si,H) = 334 Hz). IR (KBr): $\tilde{\nu}$[cm^{-1}] = 2204.

Received: April 11, 1993 [Z 5977 IE]
German version: *Angew. Chem.* **1993**, *105*, 1372

[1] R. J. P. Corriu, M. Henner, *J. Organomet. Chem.* **1974**, *74*, 1, and references therein.
[2] J. B. Lambert, W. J. Schulz, Jr., in *The Chemistry of Organic Silicon Compounds* (Eds.: S. Patai, Z. Rappoport), Wiley, Chichester, **1989**, S. 1007, and references therein.
[3] a) J. B. Lambert, W. J. Schulz, Jr., J. A. A. McConnell, W. Schilf, *J. Am. Chem. Soc.* **1988**, *110*, 2201; J. B. Lambert, W. Schilf, *ibid.* **1988**, *110*, 6364; b) J. B. Lambert, L. Kania, W. Schilf, J. A. A. McConnell, *Organometallics* **1991**, *10*, 2578.
[4] G. K. S. Prakash, S. Keyaniyan, R. Aniszfeld, L. Heiliger, G. A. Olah, R. C. Stevens, H. K. Choi, R. Bau, *J. Am. Chem. Soc.* **1987**, *109*, 5123; G. A. Olah, L. Heiliger, X.-Y. Li, G. K. S. Prakash, *ibid.* **1990**, *112*, 5991.
[5] C. Eaborn, *J. Organomet. Chem.* **1991**, *405*, 173.
[6] P. D. Lickiss, *J. Chem. Soc. Dalton Trans.* **1992**, 1333, and references therein.
[7] J. B. Lambert, S. Zhang, *J. Chem. Soc. Chem. Commun.* **1993**, 383.
[8] Z. Xie, D. J. Liston, T. Jelinek, V. Mitro, R. Bau, C. A. Reed, *J. Chem. Soc. Chem. Commun.* **1993**, 384.
[9] P. Jutzi, E. A. Bunte, *Angew. Chem.* **1992**, *104*, 1636; *Angew. Chem. Int. Ed. Engl.* **1992**, *31*, 1605.
[10] J. Y. Corey, R. West, *J. Am. Chem. Soc.* **1963**, *85*, 4034.
[11] H. J. Campbell-Ferguson, E. A. V. Ebsworth, *J. Chem. Soc. A* **1967**, 705.
[12] A. R. Bassindale, T. Stout, *J. Chem. Soc. Chem. Commun.* **1984**, 1387.
[13] M. Kira, T. Hino, H. Sakurai, *J. Am. Chem. Soc.* **1992**, *114*, 6697.
[14] E. L. Muetterties, H. Roesky, C. M. Wright, *J. Am. Chem. Soc.* **1966**, *88*, 4856.
[15] G. Schott, K. Golz, *Z. Anorg. Allg. Chem.* **1971**, *383*, 314; *ibid.* **1973**, *399*, 7.
[16] R. J. P. Corriu, J. C. Young in *The Chemistry of Organic Silicon Compounds* (Eds.: S. Patai, Z. Rappoport), Wiley, Chichester **1989**, S. 1241; R. J. P. Corriu, *J. Organomet. Chem.*, **1990**, *400*, 81; C. Chuit, R. J. P. Corriu, C. Reyé, J. C. Young, *Chem. Rev.* **1993**, *93*, 1371.
[17] P. Arya, J. Boyer, F. Carré, R. Corriu, G. Lanneau, J. Lappasset, M. Perrot, C. Priou, *Angew. Chem.* **1989**, *101*, 1069; *Angew. Chem. Int. Ed. Engl.* **1989**, *28*, 1016.
[18] R. Corriu, G. Lanneau, C. Priou, *Angew. Chem.* **1991**, *103*, 1153; *Angew. Chem. Int. Ed. Engl.* **1991**, *30*, 1130.
[19] R. Probst, C. Leis, S. Gamper, E. Herdtweck, C. Zybill, N. Auner, *Angew. Chem.* **1991**, *103*, 1155; *Angew. Chem. Int. Ed. Engl.* **1991**, *30*, 1132.
[20] G. van Koten, J. T. B. H. Jastrzebski, J. G. Noltes, A. L. Spek, J. C. Schoone, *J. Organomet. Chem.* **1978**, *148*, 233.
[21] J. Boyer, C. Brelière, F. Carré, R. J. P. Corriu, A. Kpoton, M. Poirier, G. Royo, J. C. Young, *J. Chem. Soc. Dalton Trans.* **1989**, 43.
[22] R. Corriu, G. Lanneau, M. Perrot, *Tetrahedron Lett.* **1988**, *29*, 1271.
[23] A suspension of *N*-chlorosuccinimide (0.56 g, 4.15 mmol) in CCl_4 (15 mL) was added slowly at 0 °C to a solution of the silane **3** (b.p. 104–110 °C/0.06 Torr) (1 g, 4.15 mmol) in CCl_4 (15 mL). The mixture was then stirred for 5 h at room temperature. After the succinimide had been filtered off and the solvent removed, **4** was obtained in 85% yield; ^{1}H NMR (80 MHz, $CDCl_3$, TMS): $\delta = 1.85$ (s, 6H, CH_3), 3.4 (q, ^2J(H,H) = 6 Hz, 2H, CH_2), 5.5 (s, 1H, SiH); ^{29}Si NMR (250 MHz, $CDCl_3$, TMS): $\delta = -53.6$ (d, ^1J(Si,H) = 279 Hz).
[24] R. J. P. Corriu, A. Kpoton, M. Poirier, G. Royo, A. de Saxcé, J. C. Young, *J. Organomet. Chem.* **1990**, *395*, 1.
[25] J. T. B. H. Jastrzebski, G. van Koten, M. Konijn, C. H. Stam, *J. Am. Chem. Soc.* **1982**, *104*, 5490.

Photochemical 1,2 Shift of the Phosphane Ligands in the Silanediyl Complex $[(2\text{-}Ph_2PCH_2C_6H_4)_2Si{=}Cr(CO)_5]$**

By *Hermann Handwerker, Martin Paul, Janet Blümel,* and *Christian Zybill**

Dedicated to Professor Robert West on the occasion of his 65th birthday

The successive 1,2 shifts of two intramolecular donor groups from an atom A to an atom B in a molecule can be considered as a tandem reaction;[1] in the case discussed here A=Si and B=M=Cr.

Tandem reactions of this kind permit the abstraction of weakly bonded donor groups from silicon atoms in silanediyl complexes, by migration to the metal (Scheme 1).

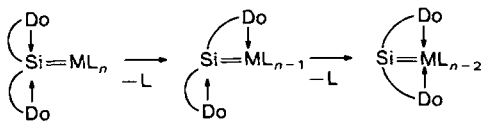

Scheme 1.

Thus, the 1,2 shift of phosphane or amine donor groups opens up a thermodynamically favored route to silanediyl complexes containing a three-coordinate silicon atom.[2]

[*] Dr. C. Zybill, Dr. H. Handwerker, Dipl.-Chem. M. Paul, Dr. J. Blümel
Anorganisch-chemisches Institut der Technischen Universität München
Lichtenbergstrasse 4, D-85747 Garching (FRG)
Telefax: Int. code + (89)3209-3125

[**] We thank Professor H. Schmidbaur for generous support, as well as J. Riede for creating a crystallographic data base.

The key silanediyl complex **1** is prepared by the reaction of the corresponding dichlorosilane with $Na_2[Cr(CO)_5]$;[3] complex **1** is remarkable in many ways:

The single-crystal X-ray analysis of **1** (Fig. 1) shows a Cr–Si double bond length of 2.414(1) Å.[4] The P1–Si distance (2.380(1) Å) is longer than that of the covalent P–Si bond in H_3SiPH_2 (2.25 Å), and the P2–Si distance of 3.725(1) Å is considered as nonbonding.[5] The phosphorus atom P2 of the diphenylphosphino unit is orientated towards the silicon atom in the crystal; this configuration also corresponds to the sterically most favored arrangement of the phenyl substituents. The sum of the bond angles of the three substituents covalently bonded to the silicon atom is 352.1°.[6]

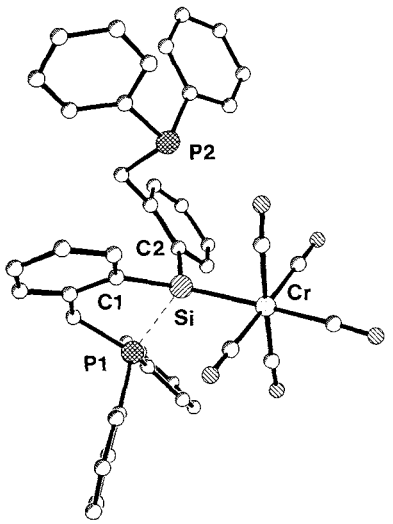

Fig. 1. Crystal structure of **1**. Selected distances [Å] and angles [°]: Cr–Si 2.414(1), P1–Si 2.380(1), P2–Si 3.725(1); C1-Si-Cr 121.8(1), C2-Si-Cr 121.0(1), C2-Si-C1 109.3(1).

A solid-state ^{31}P CP-MAS NMR spectrum (CP = cross polarization, MAS = magic angle spinning) of **1** as a powder shows two distinct signals for the two phosphane ligands at $\delta = -5.3$ and 19.6 (Fig. 2).

A dynamic "flip-flop" coordination of each phosphorus atom to the silicon is observed in solution.[7] The C_2-symmetrical transition state of this rapid exchange process can be detected by NMR spectroscopy (^{31}P NMR: $\delta = 1.78$ (s); ^{29}Si NMR: $\delta = -73.2$ (t, $^1J(^{31}P^{29}Si) = 17.5$ Hz); ^1H NMR: $\delta = 3.20, 3.47$ (ABX system, CH_2). In the ^{13}C NMR spectrum two sets of signals are found for the diphenylphosphino units. The C_6H_5 rings are diastereotopic due to the rigid tetrahedral geometry at the P atom. Therefore, in contrast to complexes with N donor groups such as **4**, the flip-flop coordination in **1** occurs without simultaneous inversion at the P atom. A related example with similar molecular dynamics is the stannanediyl complex $[(2\text{-}Ph_2PCH_2C_6H_4)_2Sn{=}W(CO)_5]$ reported by Abicht and Issleib.[3, 8] An asymmetric coordination of both phosphane or amine ligands to the silicon atom in the silanediyl complexes **1** and **4** in the ground state can be proven by the consistent results of the crystal structure analyses and variable temperature NMR studies. The two energetically degenerate ground states are interconverted via a C_2-symmetric transition state, with the retention of configuration at the silicon atom. The C_2-symmetric transition state is "seen" NMR spectroscopically in solution at 22 °C; the determination of the activation barrier for this exchange process has been described.[5a, c]

$[(2\text{-}Me_2NCH_2C_6H_4)Si{=}Cr(CO)_5]$ **4**

The photolysis of **1** results in the direct formation of **3** in a tandem reaction (Scheme 2). In the reaction of **4** with (2-dimethylaminomethyl)phenyl ligands, the intermediate **5** of one 1,2 amine shift was isolated and characterized by a single-crystal X-ray analysis.[5a] The product **6** of the tandem

$[(2\text{-}Me_2NCH_2C_6H_4)(2\text{-}Me_2\overline{NCH_2C_6H_4)Si{=}Cr(CO)_4}]$ **5**

$[(2\text{-}Me_2NCH_2C_6H_4)(2\text{-}Me_2\overline{NCH_2\text{-}C_6H_4)Si{=}Cr(CO)_3}]$ **6**

reaction **4** → **5** → **6** is thermally labile, but can be detected by trapping reactions with MeOH or HCl.[9a]

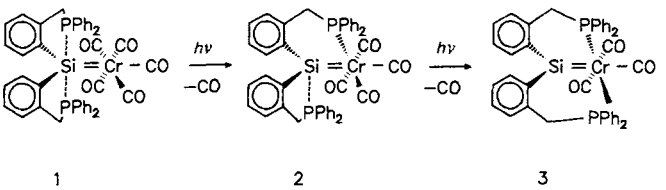

Scheme 2.

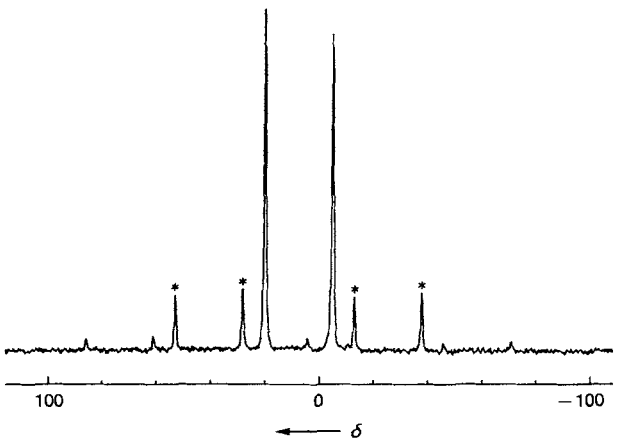

Fig. 2. Solid-state ^{31}P CP-MAS NMR (121.5 MHz) spectrum of **1**, spin frequency 4 kHz, ext. standard $\delta[(NH_4)H_2PO_4] = 0$, contact pulse = 1 ms, 90° pulse = 4 μs. Asterisks denote spinning bands.

The rearrangement **1** → **2** → **3** (Scheme 2) proceeds more quickly by an order of magnitude, however, **2** can be observed by IR spectroscopy (2021, 1901, 1875 cm^{-1}). Finally, the (phosphino)silanediylchromium complex **3** is obtained as an extremely air-sensitive, deep red powder, and is spectroscopically fully characterized. (^{29}Si NMR: $\delta = 159.7$, see also Experimental Procedure).[10] According to this the two phosphane ligands in **3** are arranged in a *trans* and the CO ligands in a meridional configuration. The silicon atom in **3** is three-coordinate. Photochemical 1,2 shifts of the donor ligands from silicon to the metal thus allow general access to complexes with low-coordinate silicon.

Experimental Procedure

1: A solution of bis(2-diphenylphosphinomethyl)phenyldichlorosilane (3.57 g, 5.5 mol) in THF (50 mL) was added slowly to a solution of $Na_2[Cr(CO)_5]$ (1.37

g, 5.8 mmol) in THF (150 mL) at −40 °C. The mixture was stirred for a further 5 h at room temperature after which the precipitated NaCl was filtered off. Compound **1** was isolated as a pale yellow powder in 34% yield. The compound was recrystallized from THF/pentane.

^{1}H NMR (400 MHz, CD_2Cl_2, 25 °C, TMS): δ = 3.20 (dd), 3.47 (d, ABX system, ^2J(HH) = 14.0, ^2J(H^{31}P) = 8.5 Hz, 4H, CH_2), 6.75 (t, ^3J(HH) = 7.3, 2H), 6.86 (d, ^3J(HH) = 7.3, 2H), 6.97 (t, ^3J(HH) = 7.9, 2H), 7.20–7.28 (br, 12H), 7.30–7.38 (br, 6H), 7.43 (t, ^3J(HH) = 7.0, 2H), 7.64 (d, ^3J(HH) = 7.9, 2H, C_6H_5P); ^{13}C NMR (CD_2Cl_2, 25 °C): δ = 33.9 (tdd, ^1J(H^{13}C) = 126, ^1J(H^{13}C) = 9.2, ^1J(H^{13}C) = 3.9, P-CH_2), 128.9 (dd, ^1J(H^{13}C) = 160, ^3J(H^{31}P^{13}C) = 8.7), 130.4 (dd, ^1J(H^{13}C) = 160, ^2J(H^{13}C) = 8.3, *m*-C_6H_5), 130.5 (d, ^1J(H^{13}C) = 155), 130.8 (d, ^1J(H^{13}C) = 156, *p*-C_6H_5), 133.3 (dd, ^1J(H^{13}C) = 161, ^2J(H^{31}P^{13}C) = 13.5, 133.6 (dd, ^1J(H^{13}C) = 161, ^2J(H^{31}P^{13}C) = 14.3, *o*-C_6H_5), 126.5 (d, ^1J(H^{13}C) = 158), 129.3 (d, ^1J(H^{13}C) = 160, *i*-C_6H_5), 130.8 (d, ^1J(H^{13}C) = 160), 131.8 (dm, ^1J(H^{13}C) = 156), 138.3 (dm, ^1J(H^{13}C) = 157, 139.4 (dm, ^1J(H^{13}C) = 159), 140.9 (m), 141.2 (m), 222.3 (s, CO_{ax}), 226.1 (t, ^3J(H^{31}P^{13}C) = 1.8, CO_{eq}); ^{31}P{^{1}H} NMR (CD_2Cl_2): 1.78 (s); ^{29}Si NMR (CD_2Cl_2, 25 °C, TMS): 73.2 (t, ^1J(H^{29}Si) = 17.5. IR (CH_2Cl_2), $\tilde{\nu}$[cm^{-1}] = 2038 (s), 1981 (w), 1912 (ss, br). Correct elemental analysis (C, H, P). M.p. 156 °C.

3: **1** (0.26 g, 0.3 mmol) was suspended in methylcyclohexane (100 mL) in a quartz Schlenk tube at −30 °C and photolyzed at 254 nm (Hg low-pressure lamp) for 30 h. The color of the suspension changed from pale yellow to dark red. After removal of the solvent, **3** was obtained (171 mg) as a red powder in 80% yield.

^{1}H NMR (400 MHz, CD_2CL_2, 25 °C, TMS): δ = 2.3 (s, 2H, CH_2), 7.6–7.1 (m, 14H, C_6H_5); ^{13}C{^{1}H} NMR (C_7D_8, 25 °C, TMS): δ = 36.2 (d, ^1J(H^{31}P^{13}C) = 8.7, CH_2), 129.3 (d, ^3J(H^{31}P^{13}C) = 8.5), 132.5 (s), 134.1 (d, ^2J(H^{31}P^{13}C) = 12.1), 142.1 (d, ^1J(H^{31}P^{13}C) = 5.1, C_6H_5), 220.1 (t, ^2J(H^{31}P^{13}C) = 5.2, CO), 227.1 (t, ^2J(H^{31}P^{13}C) = 9.2, CO); ^{31}P NMR (CD_2Cl_2 49.2 (s); ^{29}Si NMR (CD_2Cl_2: 159.7 (t, ^2J(H^{31}P^{29}Si) = 12 Hz). IR (methylcyclohexane): $\tilde{\nu}$[cm^{-1}] = 2038 (s), 1988 (s) (νCO). MS (70 eV): *m/z* 714 (M^+ for $C_{41}H_{32}CrO_3P_2Si$ with correct isotope distribution, 5%), 686 (M^+ − CO, 1.5%), 658 (M^+ − 2 CO, 0.9%), 630 (M^+ − 3 CO, 0.8%). M.p. 148 °C. Correct elemental analysis (C, H, P).

Received: April 19, 1993 [Z 6021 IE]
German version: *Angew. Chem.* **1993**, *105*, 1375

[1] L. F. Tietze, U. Beifuss, *Angew. Chem.* **1993**, *105*, 137; *Angew. Chem. Int. Ed. Engl.* **1993**, *32*, 131.

[2] a) C. Zybill, *Top. Curr. Chem.* **1992**, *160*, 1; b) C. Zybill, *Nachr. Chem. Tech. Lab.* **1989**, *37*, 248; c) C. Zybill, H. Handwerker, H. B. Friederich, *Adv. Organomet. Chem.* **1993**, in press; d) C. Zybill, C. Leis, H. Handwerker, *Chem. Rev.* **1993**, *93*, in press; e) C. Zybill, H. Handwerker, *GIT Fachzeitschrift*, **1993**, *7*, 594; f) T. D. Tilley in *The Silicon Heteroatom* (Eds.: S. Patai, Z. Rappoport), Wiley, New York, **1991**, p. 309.

[3] The synthesis of lithiated phosphane precursors was first described by Issleib et al.: H. P. Abicht, K. Issleib, *Z. Anorg. Allg. Chem.* **1976**, *422*, 237.

[4] **1**: Crystallographic data: $C_{43}H_{32}CrO_5P_2Si$ (0.4 × 0.45 × 0.4 mm) M_r = 770.76, triclinic $P\bar{1}$ (no. 2), a = 11.795(1), b = 12.225(1), c = 15.051(1) Å, V = 1890.0 Å^3, Z = 2, ρ_{calcd} = 1.35 g cm^{-3}, μ(Mo$_{K\alpha}$) = 4.52 cm^{-1}, F(000) = 800 e. Measurement parameters: Enraf-Nonius CAD4-Turbo, T = 23 °C, 5928 measured reflections (13, ±13, ±17 *hkl*), of which three reflections were discarded and 4623 unique reflections with $F_o > 3\sigma(F_o)$ were used for the refinement. Decomposition (56 h, −1.8%), no decomposition, extinction, or absorption corrections were carried out. Structure solution: direct methods (SHELX86), 597 parameters, Refinement: full matrix least squares ($R = [\Sigma||F_o| - |F_c||]/\Sigma|F_o|$, $R_w = [\Sigma(|F_o| - |F_c|)^2]/[\Sigma wF_o^2]^{1/2}$, $w = l/[\sigma^2(F_o) - kF_o^2]$, k = 0.00, l = 2.5090, R = 0.038, R_w = 0.027, all heavy atoms were refined with anisotropic and all hydrogen atoms with isotropic displacement parameters; residual electron density + 0.22/−0.20 eÅ^3. Further details of the crystal structure investigation may be obtained from the Fachinformationszentrum Karlsruhe, Gesellschaft für wissenschaftlich-technische Information mbH, D-76344 Eggenstein-Leopoldshafen (FRG) on quoting the depository number CSD-57430, the names of the authors, and the journal citation.

[5] a) H. Handwerker, C. Leis, R. Probst, P. Bissinger, A. Grohmann, P. Kiprof, E. Herdtweck, J. Blümmel, N. Auner, C. Zybill, *Organometallics*, **1993**, *12*, 2162. b) C. Leis, D. L. Wilkinson, H. Handwerker, C. Zybill, G. Müller, *ibid.* **1992**, *11*, 514; c) R. Probst, C. Leis, S. Gamper, E. Herdtweck, N. Auner, C. Zybill, *Angew. Chem.* **1991**, *103*, 1155; *Angew. Chem. Int. Ed. Engl.* **1991**, *30*, 1132; d) C. Leis, C. Zybill, J. Lachmann, G. Müller, *Polyhedron*, **1991**, *10*, 1163.

[6] Similar pyramidalization effects at the silicon atom are known in the structures of several disilaethenes: R. West, *Angew. Chem.* **1987**, *99*, 1231; *Angew. Chem. Int. Ed. Engl.* **1987**, *26*, 1201.

[7] a) F. Carré, C. Cerveau, C. Chuit, R. J. P. Corriu, C. Reye, *Angew. Chem.* **1989**, *101*, 474; *Angew. Chem. Int. Ed. Engl.* **1989**, *28*, 489; b) R. J. P. Corriu, *Pure Appl. Chem.* **1988**, *60*, 99; c) E. Colomer, R. J. P. Corriu, M. Lheureux, *Chem. Rev.* **1990**, 265; d) J. T. B. H. Jastrzebski, P. A. van der Schaaf, J. Boersma, G. van Koten, D. J. A. de Ridder, D. Heijdenreijk, *Organometallics* **1992**, *11*, 1521.

[8] H. P. Abicht, K. Jurkschat, A. Tzschach, K. Peters, E. M. Peters, H. G. von Schnering, *J. Organomet. Chem.* **1987**, *326*, 357.

[9] a) H. Handwerker, dissertation, TU München *1993*; b) H. Handwerker, M. Paul, C. Zybill, *J. Organomet. Chem.* **1993**, in press.

[10] A single-crystal X-ray analysis of **3** has failed to date because of twinning of the crystals.

Metal-Initiated Coupling of C_2 Units to Enynes and Butatrienes: Two Different Routes for the Dimerization of 1-Alkynes**

By *Martin Schäfer, Norbert Mahr, Justin Wolf,* and *Helmut Werner**

Dedicated to Professor Reinhard W. Hoffmann on the occasion of his 60th birthday

It has recently been shown that the dimerization of 1-alkynes to enynes with electron-rich transition-metal compounds as catalysts can occur either by alkynyl–vinyl or alkynyl–vinylidene coupling.[1] The enyne is liberated, sometimes stereoselectively, from the enynyl metal complexes formed as intermediates, on treatment with an additional molecule of the 1-alkyne RC≡CH. Furthermore, Wakatsuki et al. observed[2] that the dimerization of *t*BuC≡CH with $[RuH_2(CO)(PPh_3)_3]$ as catalyst does not lead to the enyne *t*BuC≡CCH=CH*t*Bu but, surprisingly, to the isomeric butatriene (*Z*)-*t*BuCH=C=C=CH*t*Bu. The authors postulated that in this case an enynyl complex is also formed as intermediate which is in equilibrium with the σ-butatrienyl metal species that affords the butatriene. Using alkynyl(vinylidene)rhodium compounds as starting materials, we have now succeeded in preparing not only enyne but also enynyl metal complexes which react with acids HX to give, predominantly either enynes or butatrienes, depending on the strength of HX.

The key to success is the η^3-benzylrhodium(I) compound **2**. It is formed in the same way as the derivative **3**[3] on treatment of **1** with the appropriate Grignard reagent; the yield in both cases is about 80%. In solution, **2** and **3** show fluxional behavior. At low temperatures, a suprafacial rearrangement takes place,[4, 5] which is shown by the equivalence of the benzylic protons and of the ring protons in *ortho* and *meta* position; at higher temperatures a σ-to-π conversion[6] occurs in addition to the suprafacial rearrangement, which is confirmed by the equivalence of the phosphane ligands. During this process, the coordinatively unsaturated intermediate $[Rh(\eta^1\text{-}CH_2C_6H_4R)(PiPr_3)_2]$ is generated. Its formation explains why compound **2**, in contrast to the related allyl complex $[Rh(\eta^3\text{-}C_3H_5)(PiPr_3)_2]$,[7] smoothly reacts with PhC≡CH and *t*BuC≡CH to give **4** and **5**, respectively. The addition of NEt_3 to the reaction mixture facilitates the formation of the alkynyl(vinylidene) species. If the reaction of **2** is carried out with phenylacetylene in pentane at −40 °C, the alkyne(alkynyl)rhodium(I) intermediate **6** can be isolat-

[*] Prof. Dr. H. Werner, Dipl.-Chem. M. Schäfer, Dipl.-Chem. N. Mahr, Dr. J. Wolf
Institut für Anorganische Chemie der Universität
Am Hubland, D-97074 Würzburg (FRG)
Telefax: Int. code + (931)888-4605

[**] This work was supported by the Fonds der Chemischen Industrie and by Degussa AG. We thank Dr. O. Nürnberg for his assistance with the X-ray crystal structure analysis.

ed. In solution, there is an equilibrium between **6** and **7**, the ratio of which is 60:40 at −40 °C in [D_8]toluene. Compound **7** rearranges quantitatively in benzene at room temperature in 3 hours to yield **4**. The alkynyl(vinylidene) complexes **4** and **5**, isolated as blue-green crystalline solids, slowly decompose in solution; they thus behave differently to the remarkably stable chloro(vinylidene) compounds *trans*-[RhCl(=C=CHR)($PiPr_3$)$_2$] (R = Ph,[8] *t*Bu[9]), which cannot be used for the preparation of **4** and **5**.

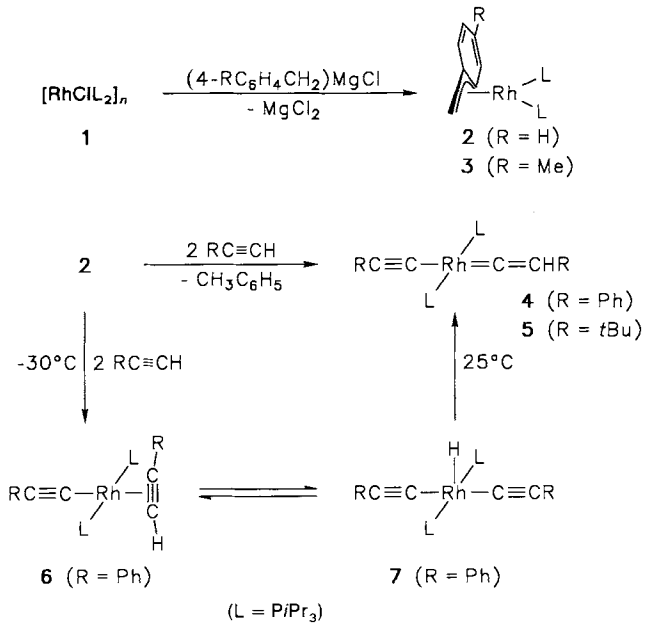

Surprisingly, the reaction of **4** with a solution of HCl in benzene at room temperature does not cause the elimination of phenylacetylene but gives the enyne complex **8** in about 50% yield. If **4** is treated in ether at −40 °C with gaseous HCl, instead of **8** the alkynyl(vinyl) compound **9** is formed quantitatively. Presumably, in the initial step an oxidative addition of HCl to the metal center takes place, followed by the migration of the hydride ligand to the α-carbon atom of the vinylidene unit.[10] The reaction of **4** with HCl to give **9** is both regio- and stereoselective. The exclusive formation of the (*Z*) isomer is probably due to the kinetically preferred transfer of the hydride from the side opposite to the phenyl group. The rearrangement of **9** to **8** occurs quantitatively in benzene at room temperature and is equally selective; only the compound containing the enyne in the (*Z*) configuration is formed. On treatment of **8** with CO (C_6H_6, 25 °C), a ligand exchange occurs spontaneously to give (*Z*)-PhC≡CCH=CHPh and the carbonyl complex **10**.[11]

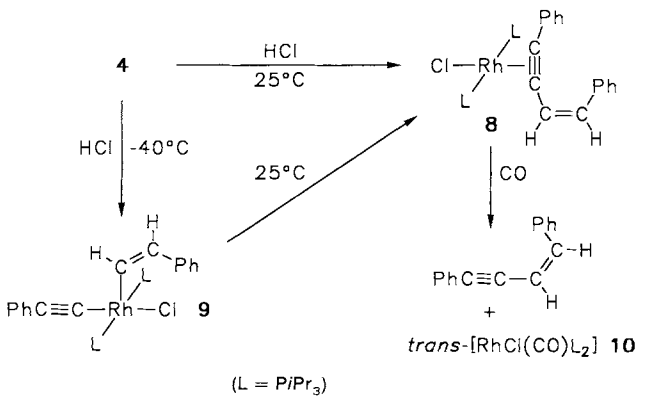

Coupling of the C_2 units of **4** (and also of **5**) occurs in a different way if the sequence of the addition of HX and CO is reversed. Both **4** and **5** react with CO in pentane at −40 °C to give exclusively the (*Z*) isomers of the enynyl metal complexes **13** and **14** in about 80% yield (Scheme 1). We assume

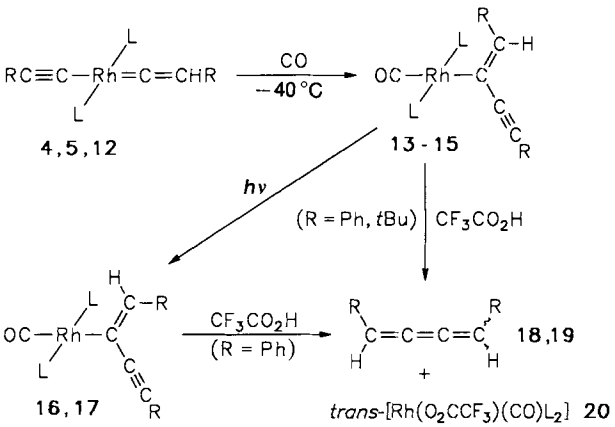

Scheme 1. **4**, **13**, **16**, **18**: R = Ph; **5**, **14**, **17**, **19**: R = *t*Bu; **12**, **15**: R = CO_2Me. L = $PiPr_3$.

that initially CO adds to the rhodium atom, thus generating a five-coordinate intermediate, which after migration of the alkynyl ligand to the α-carbon of the vinylidene unit transforms into the isolated product. The importance of steric factors probably explains why the attack of the alkynyl residue occurs only at that side of the molecule which is opposite to the group R (Ph or *t*Bu). Photolysis of a solution of **13** or **14** in benzene leads to an isomerization, which affords the thermodynamically preferred (*E*) isomers **16** and **17**. The stepwise conversion of **4** to **13** and finally to **16** (or **5** to **14** and finally **17**) is noteworthy insofar as Wakatsuki et al.[2] reported the exclusive formation of the (*E*) isomer of the enynyl ruthenium complex [RuCl(η^1-(*E*)-C(=CH*t*Bu)-C≡C*t*Bu)(CO)(PPh_3)$_2$] in the reaction of [$RuCl_2$-(=C=CH*t*Bu)(PPh_3)$_2$] with LiC≡C*t*Bu and CO.

The stereochemistry of the primary products formed in the reaction with CO by coupling of the C_2 units is confirmed by

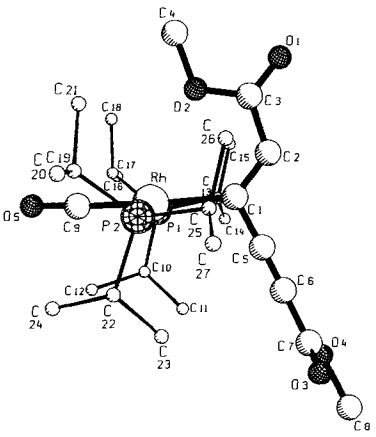

Fig. 1. Crystal structure of **15**. Selected bond distances [Å] and angles [°]: Rh-C1 2.099(4), Rh-C9 1.833(4), Rh-P1 2.347(1), Rh-P2 2.345(1), C1-C2 1.352(5), C2-C3 1.459(5), C1-C5 1.421(5), C5-C6 1.198(5), C6-C7 1.430(6), C9-O5 1.147(5); C1-Rh-C9 177.5(1), P1-Rh-P2 168.18(3), Rh-C9-O5 177.7(3), Rh-C1-C2 130.3(3), Rh-C1-C5 113.9(3), C1-C2-C3 126.8(4), C2-C1-C5 115.8(3), C1-C5-C6 177.4(5), C5-C6-C7 175.9(5).

the X-ray crystal structure analysis of **15**. In contrast to **4** and **5**, compound **12**, which is needed as a precursor to prepare **15**, cannot be obtained directly from **2** and $HC{\equiv}CCO_2Me$ but is accessible on treatment of $[Rh(\eta^2\text{-}O_2CCH_3)(PiPr_3)_2]$ (**11**)[7] with two equivalents of the alkyne in presence of Na_2CO_3. The conversion of **12** to **15** occurs under similar conditions (pentane, $-40\,^{\circ}C$) as described for **13** and **14**. The square-planar coordination of the metal center and the *trans* arrangement of the phosphane ligands in **15** is shown in Figure 1. The enynyl unit is perpendicular to the plane of the molecule; the dihedral angle between the planes [C2, C1, C5] and [P1, Rh, P2] is $91.13 \pm 0.48^{\circ}$. The bond lengths Rh–C5 (2.973(4) Å), Rh–C6 (> 3.5 Å), together with the bond angle C5-C6-C7 (175.9(5)°) and the distance Rh–O2 (3.028(3) Å), speak against an additional interaction between the C≡C bond or the cisoid ester group with the metal atom.

The cleavage of the enynyl–rhodium bond in **13**, **14**, and **16** by CF_3CO_2H in acetone or benzene gives, besides small amounts of the corresponding enyne, the butatrienes **18** and **19** in 90–95% yield. The carboxylato complex **20** is also formed (Scheme 1). Whereas compound **13** is inert toward acetic acid, the reaction of **14** with CH_3CO_2H leads to a 40:60 mixture of (*E*)-*t*BuC≡CCH=CH*t*Bu and **19**, and that of **16** gives (*Z*)-PhC≡CCH=CHPh. Both the product distribution and the isomer ratio of the (*E*/*Z*)-butatrienes (see Table 1) indicate that, with a strong proton donor such as CF_3CO_2H, the attack of the acid does not occur at the Lewis basic metal center but directly at the triple bond of the enynyl ligand. We assume that a cationic butatriene rhodium complex is formed as an intermediate,[18] from which the cumulene is displaced by the carboxylate anion. The molecular structure of **15** reveals that the proton probably attacks the C≡C bond from the side opposite to the metal, which would explain why the (*Z*)-enynyl complexes **13** and **14** predominantly afford the (*Z*) isomer, and the (*E*)-enynyl rhodium compound **16** the (*E*) isomer of the substituted butatriene.

Table 1. Product distribution and (*E*/*Z*)-isomer ratio after elimination of the C_4 unit from **13**, **14**, and **16** with HX [13].

Complex	HX/*T* [°C], *t*	Solvent	Butatriene Yield [%] (*E*/*Z*)	Enyne Yield [%] (*E*/*Z*)
13	CF_3CO_2H/40, 30 min	C_6H_6	90 (20/80)	10 (100/0)
13	CF_3CO_2H/25, 30 min	$(CH_3)_2CO$	95 (45/55)	5 (0/100)
14	CH_3CO_2H/40, 2 h	C_6H_6	40 (80/20)	60 (100/0)
14	CF_3CO_2H/25, 2 h	$(CH_3)_2CO$	> 95 (30/70)	< 5 (100/0)
16	CH_3CO_2H/25, 10 min	C_6H_6	0	100 (0/100)
16	CF_3CO_2H/25, 10 min	$(CH_3)_2CO$	95 (90/10)	5 (0/100)

In conclusion, the results described in this paper prove that the rhodium-mediated coupling of two alkyne molecules can lead to the formation of either enynes or butatrienes, provided that the reaction proceeds via an alkynyl(vinylidene) complex as a common intermediate. By changing the sequence of the reaction steps it is possible to convert this intermediate into an enyne or enynyl rhodium compound from which the dimers are liberated (spectroscopic data of the complexes are listed in Table 2). We are now investigating whether, besides the alkynyl–vinylidene coupling described here, analogous metal-initiated alkynyl–allenylidene and vinyl–vinylidene couplings can be achieved, and whether two reaction pathways are feasible also in these cases.

Table 2. Selected spectroscopic data of **8** and **13**–**17** (omitting ^1H and ^{13}C NMR data for the phosphane ligands and phenyl groups).

8: IR (KBr): $\tilde{\nu}$[cm^{-1}] = 1850 (C≡C), 1585 (C=C); ^1H NMR (90 MHz, C_6D_6): δ = 6.75 [dd, *J*(HH) = 12.4, *J*(RhH) = 1.5 Hz, *CH*=CHPh], 6.45 [d, *J*(HH) = 12.4 Hz, CH=*CH*Ph]; ^{13}C NMR (100.6 MHz, C_6D_6): δ = 133.69 (s, =*C*HPh), 119.52 [d, *J*(RhC) = 1.9 Hz, *C*H=CHPh], 91.68 [dt, *J*(RhC) = 17.1, *J*(PC) = 3.0 Hz, C≡*C*Ph], 78.50 [d, *J*(RhC) = 12.8 Hz, *C*≡CPh]; ^{31}P NMR (36.2 MHz, [D$_8$]toluene): δ = 31.99 [d, *J*(RhP) = 118.7 Hz].

13: IR (hexane): $\tilde{\nu}$[cm^{-1}] = 2155 (C≡C), 1945 (CO); ^1H NMR (90 MHz, C_6D_6): δ = 8.02 [dt, *J*(RhH) = 2.4, *J*(PH) = 2.3 Hz, =*CH*Ph]; ^{13}C NMR (100.6 MHz, C_6D_6): δ = 195.83 [dt, *J*(RhC) = 55.8, *J*(PC) = 15.5 Hz, Rh-CO], 159.67 [dt, *J*(RhC) = 28.4, *J*(PC) = 14.2 Hz, Rh-C], 146.40 [t, *J*(PC) = 4.3 Hz, =*C*HPh], 102.57 [t, *J*(PC) = 1.9 Hz, *C*≡CPh], 97.46 (s, C≡*C*Ph); ^{31}P NMR (36.2 MHz, C_6D_6): δ = 43.09 [d, *J*(RhP) = 139.2 Hz].

14: IR (KBr): $\tilde{\nu}$[cm^{-1}] = 2160 (C≡C), 1930 (CO); ^1H NMR (400 MHz, C_6D_6): δ = 6.81 [dt, *J*(RhH) = 2.3, *J*(PH) = 2.2 Hz, =*CH*t*Bu*], 1.29, 1.28 (each s, $C(CH_3)_3$); ^{13}C NMR (50.3 MHz, C_6D_6): δ = 196.24 [dt, *J*(RhC) = 55.6, *J*(PC) = 16.5 Hz, Rh-CO], 155.17 [t, *J*(PC) = 4.5 Hz, =*CH*t*Bu*], 143.22 [dt, *J*(RhC) = 27.4, *J*(PC) = 13.7 Hz, Rh-C], 100.61 (s, C≡*C*t*Bu*), 90.17 [dt, *J*(RhC) = 1.3, *J*(PC) = 1.8 Hz, *C*≡C*t*Bu], 34.30 [dt, *J*(RhC) = 0.9, *J*(PC) = 1.3 Hz, =CH*C*(CH$_3$)$_3$], 31.95 [s, ≡CC(*C*H$_3$)$_3$], 31.21 [t, *J*(PC) = 1.8 Hz, =CHC(*C*H$_3$)$_3$], 28.84 (s, ≡C*C*(CH$_3$)$_3$); ^{31}P NMR (162.0 MHz, C_6D_6): δ = 40.75 [d, *J*(RhP) = 143.7 Hz].

15: IR (hexane): $\tilde{\nu}$[cm^{-1}] = 2155 (C≡C), 1955 (CO); ^1H NMR (200 MHz, C_6D_6): δ = 7.21 [dt, *J*(RhH) = 2.6, *J*(PH) = 2.7 Hz, =*CH*CO$_2$CH$_3$], 3.51, 3.34 (each s, CO$_2$CH$_3$); ^{13}C NMR (50.3 MHz, C_6D_6): δ = 196.28 [dt, *J*(RhC) = 57.8, *J*(PC) = 15.6 Hz, Rh-CO], 186.60 [dt, *J*(RhC) = 27.8, *J*(PC) = 13.9 Hz, Rh-C], 169.74 [dt, *J*(RhC) = 1.9, *J*(PC) = 1.4 Hz, =CH*C*O$_2$CH$_3$], 155.59 (s, C≡C*C*O$_2$CH$_3$), 135.11 [dt, *J*(RhC) = 1.9, *J*(PC) = 3.9 Hz, =*C*HCO$_2$CH$_3$], 100.61 (s, C≡*C*CO$_2$CH$_3$), 96.60 [t, *J*(PC) = 1.6 Hz, *C*≡CCO$_2$CH$_3$], 51.46, 50.69 (each s, CO$_2$*C*H$_3$); ^{31}P NMR (162.0 MHz, C_6D_6): δ = 44.10 [d, *J*(RhP) = 136.3 Hz].

16: IR (hexane): $\tilde{\nu}$[cm^{-1}] = 2120 (C≡C), 1945 (CO); ^1H NMR (200 MHz, C_6D_6): δ = 6.91 [dt, *J*(RhH) = 1.8, *J*(PH) = 1.8 Hz, =*CH*Ph]; ^{13}C NMR (100.6 MHz, C_6D_6): δ = 196.46 [dt, *J*(RhC) = 57.2, *J*(PC) = 14.8 Hz, Rh-CO], 152.09 [dt, *J*(RhC) = 26.9, *J*(PC) = 14.3 Hz, Rh-C], 144.44 [t, *J*(PH) = 5.0 Hz, =*C*HPh], 106.04, 97.99 (each s, C≡C); ^{31}P NMR (162.0 MHz, C_6D_6): δ = 45.09 [d, *J*(RhP) = 140.7 Hz].

17: IR (KBr): $\tilde{\nu}$[cm^{-1}] = 2175 (C≡C), 1930 (CO); ^1H NMR (400 MHz, C_6D_6): δ = 5.44 [dt, *J*(RhH) = 1.9, *J*(PH) = 1.9 Hz, =*CH*t*Bu*], 1.36 (s, =CHC(*CH*$_3$)$_3$) 1.28 (s, C≡CC(*CH*$_3$)$_3$); ^{13}C NMR (100.6 MHz, C_6D_6): δ = 196.36 [dt, *J*(RhC) = 56.4, *J*(PC) = 15.1 Hz, Rh-CO], 150.65 [t, *J*(PC) = 5.0 Hz, = *CH*t*Bu*], 145.89 [dt, *J*(RhC) = 26.2, *J*(PC) = 13.9 Hz, Rh-C], 112.28 (s, C≡*C*t*Bu*), 85.62 [dt, *J*(RhC) = 1.0, *J*(PC) = 1.9 Hz, C≡*C*t*Bu*], 36.13 [dt, *J*(RhC) = 1.1 Hz, *J*(PC) = 1.0 Hz, =CH*C*(CH$_3$)$_3$], 31.37 (s, C≡CC(*C*H$_3$)$_3$), 30.72 [t, *J*(PC) = 1.2 Hz, =CHC(*C*H$_3$)$_3$], 29.20 (s, ≡CC(*C*H$_3$)$_3$); ^{31}P NMR (162.0 MHz, C_6D_6): δ = 44.45 [d, *J*(RhP) = 145.9 Hz].

Received: April 27, 1993 [Z 6038 IE]
German version: *Angew. Chem.* **1993**, *105*, 1377

[1] a) A. Dobson, D. S. Moore, S. D. Robinson, M. B. Hursthouse, L. New, *Polyhedron* **1985**, *4*, 1119–1130; b) L. Dahlenburg, K.-M. Frosin, S. Kerstan, D. Werner, *J. Organomet. Chem.* **1991**, *407*, 115–124; c) A. M. Echavarren, J. Lopez, A. Santos, J. Montoya, *ibid.* **1991**, *414*, 393–400; d) C. Bianchini, M. Peruzzini, F. Zanobi, P. Frediani, A. Albinati, *J. Am. Chem. Soc.* **1991**, *113*, 5453–5454; e) I. P. Kovalev, K. V. Yevdakow, Y. A. Strelenko, M. G. Vinogradow, G. I. Nikishin, *J. Organomet. Chem.* **1990**, *386*, 139–146; f) J. Ohshita, K. Furumori, A. Matsuguchi, M. Ishikawa, *J. Org. Chem.* **1990**, *55*, 3277–3280; g) B. M. Trost, C. Chan, G. Ruhter, *J. Am. Chem. Soc.* **1987**, *109*, 3486–3487.

[2] Y. Wakatsuki, H. Yamazaki, H. Kumegawa, T. Satoh, J. Y. Satoh, *J. Am. Chem. Soc.* **1991**, *113*, 9604–9610.

[3] X-ray structure analysis: O. Nürnberg, Dissertation, Universität Würzburg, **1993**.

[4] a) $\Delta G^{\ddagger}_{208}$ = 40.2 for **2**, $\Delta G^{\ddagger}_{203}$ = 39.4 kJ mol^{-1} for **3**; for calculations see [5]; b) similar example: M. D. Fryzuk, D. H. McConville, S. J. Rettig, *J. Organomet. Chem.* **1993**, *445*, 245–256.

[5] H. Günther, *NMR-Spektroskopie*, 3rd ed., Thieme, Stuttgart, **1992**, pp. 306–313.

[6] a) $\Delta G^{\ddagger}_{313}$ = 59.3 for **2**, $\Delta G^{\ddagger}_{313}$ = 58.9 kJ mol^{-1} for **3**; for calculations see [5]; b) similar example: L. E. Crascall, J. L. Spencer, *J. Chem. Soc. Dalton Trans.* **1992**, 3445–3452.

[7] M. Schäfer, J. Wolf, H. Werner, *J. Chem. Soc. Chem. Commun.* **1991**, 1341–1343.
[8] H. Werner, F. J. Garcia Alonso, H. Otto, J. Wolf, *Z. Naturforsch. B* **1988**, *43*, 722–726.
[9] H. Werner, U. Brekau, *Z. Naturforsch. B* **1989**, *44*, 1438–1446.
[10] For related reactions at an iridium metal center see: a) A. Höhn, H. Werner, *Angew. Chem.* **1986**, *98*, 745–746; *Angew. Chem. Int. Ed. Engl.* **1986**, *25*, 737–738; b) *J. Organomet. Chem.* **1990**, *382*, 255–272; c) M. D. Fryzuk, N. T. McManus, S. J. Rettig, G. S. White, *Angew. Chem.* **1990**, *102*, 67–68; *Angew. Chem. Int. Ed. Engl.* **1990**, *29*, 73–75; d) M. D. Fryzuk, L. Huang, N. T. McManus, P. Paglia, S. J. Rettig, G. S. White, *Organometallics* **1992**, *11*, 2979–2990.
[11] C. Busetto, A. D'Alfonso, F. Maspero, G. Perego, A. Zazzetta, *J. Chem. Soc. Dalton Trans.* **1977**, 1828–1834.
[12] Crystals from methanol (−30 °C); crystal size 0.25 × 0.2 × 0.15 mm; monoclinic, space group $P2_1/c$ (Nr. 14), $Z = 4$, $a = 12.713(4)$, $b = 12.954(2)$, $c = 20.235(6)$ Å, $\beta = 106.95(1)°$, $V = 3187$ Å^3; $\varrho_{calcd} = 1.289$ g cm^{-3}; $T = 293$ K; max. $2\theta = 46°$ [$Mo_{K\alpha}$ radiation, $\lambda = 0.70930$ Å, graphite monochromator, zircon-filter (factor 15.41)]; 4599 independent reflections, 3205 observed [$F_0 > 3\sigma(F_0)$], Lp- and empirical absorption corrections (Ψ-scan method, min. transmission 96.89%); direct methods (SHELXS-86), refinement with full-matrix least-squares, 359 parameters (Enraf-Nonius-SDP); $R = 0.025$, $R_w = 0.027$; reflex/parameter-ratio 8.89; residual electron density +0.23/−0.24 eÅ^{-3}. Further details of the X-ray structure analysis are available on request from the Fachinformationszentrum Karlsruhe, Gesellschaft für wissenschaftlich-technische Information mbH, D-76344 Eggenstein-Leopoldshafen (FRG), on quoting the depository number CSD-57299, the names of the authors, and the journal citation.
[13] The trienes and enynes were characterized spectroscopically (^{1}H, ^{13}C NMR) by comparison with published data: (*E*)-**18** [14]; (*Z*)-**18** [14]; (*E*)-**19** [14, 15]; (*Z*)-**19** [14–16]; (*E*)-PhC≡CCH = CHPh [1b]; (*Z*)-PhC≡CCH=CHPh [1c]; (*E*)-*t*BuC≡CCH=CH*t*Bu [17].
[14] M. Tigchelaar, H. Kleijn, C. J. Elsevier, J. Meijer, P. Vermeer, *Tetrahedron Lett.* **1981**, 2237–2238.
[15] a) H. Westmijze, I. Nap, J. Meijer, H. Kleijn, P. Vermeer, *Recl. Trav. Chim. Pays-Bas* **1983**, *102*, 154–157; b) H. Kleijn, M. Tigchelaar, R. J. Bullee, C. J. Elsevier, J. Meijer, P. Vermeer, *J. Organomet. Chem.* **1982**, *240*, 329–333.
[16] Y. Wakatsuki, M. Satoh, H. Yamazaki, *Chem. Lett.* **1989**, 1585–1588.
[17] W. T. Boese, A. S. Goldman, *Organometallics* **1991**, *10*, 782–786.
[18] Recently, a related neutral compound was isolated: T. Rappert, O. Nürnberg, H. Werner, *Organometallics* **1993**, *12*, 1359–1364.

The First Trigonal-Bipyramidal Cluster with an Interstitial C_2 Unit: $[Rb\{Pr_5(C_2)\}Cl_{10}]$**

By *Gerd Meyer** and *Stefan Uhrlandt*

The structures of the metal-rich rare earth halides are built predominantly of octahedral M_6 or tetrahedral M_4 clusters, stabilized, almost without exception, by interstitial atoms Z (that is, also by M–Z bonds). Examples are $[(Zr_6Be)Cl_{12}]$,[1] $[(Gd_2N)Cl_3]$,[2] and $[Na_2(Pr_4O_2)Cl_9]$.[3] These compounds are formed at high temperature by symproportionation ($MX_3 + M$, X = halogen) in the presence of the element Z, sometimes with addition of alkali metal chlorides as a flux. An alternative route is the metallothermic reduction of trihalides with alkali metals A ($MX_3 + A + Z$),[4] which leads to ternary halides like $[\{Er_{10}(C_2)_2\}Br_{18}]$,[5] and also, more often, to quaternary halides such as $[Cs\{Er_{10}(C_2)_2\}I_{18}]$[6] or $[Cs_2\{Pr_6(C_2)\}I_{12}]$.[7] Surprisingly, with **1** we have now obtained an isolated trigonal-bipyramidal cluster stabilized by a C_2 unit as the first such example in the chemistry of the metal-rich rare earth halides.

$[Rb\{Pr_5(C_2)\}Cl_{10}]$ **1**

In the crystal structure of **1**,[8] each of the nine edges of the trigonal bipyramid of five Pr atoms and an interstitial C_2 unit is bridged by a chlorine atom. According to the nomenclature of Schäfer and Schnering,[9] these chlorine atoms must be labeled Cl^i atoms. In addition to the nine Cl^i atoms, twelve chlorine atoms (Cl^a) complete the coordination sphere. Of these twelve, two sets of three are located at the apexes of the bipyramid, and three sets of two around the Pr atoms of the pyramidal base (Fig. 1). The complete unit is thus described as $[\{Pr_5(C_2)Cl^i_9\}Cl^a_{12}]$.

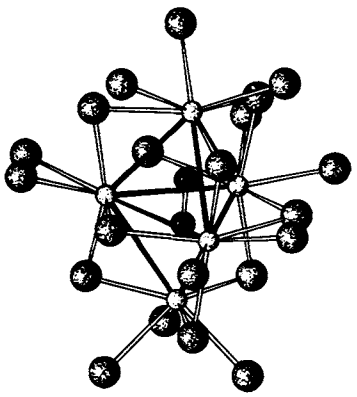

Fig. 1. The $[\{Pr_5(C_2)\}Cl_{21}]$ unit in the solid-state structure of **1**. All of the 21 Cl atoms are shared by adjacent bipyramids to yield the empirical formula $[\{Pr_5(C_2)\}Cl_{10}]$. Every edge of the trigonal Pr_5 bipyramid is bridged by one Cl^i atom. In addition, three terminal Cl^a atoms are coordinated to each of the apexes and two such atoms to each of the three Pr atoms forming the base. Solid circles are C atoms, lightly shaded circles Pr atoms, and darkly shaded circles Cl atoms.

An arrangement of 21 chlorine atoms around a trigonal bipyramid seems to be sterically demanding at first, especially since octahedral M_6 clusters like those in $[Cs_2\{Pr_6(C_2)\}I_{12}]$ are surrounded by not more than 18 halogen atoms. Yet a comparison of the $[\{M_5(C_2)\}X_{21}]$ unit in **1** with the (even smaller) tetrahedral $[\{M_4O\}X_{18}]$ unit in $[(Eu_4O)Cl_6]$[10] reveals that an arrangement of 21 chlorine atoms around an M_5 cluster is indeed possible.

In contrast to the established connections of octahedral and bioctahedral clusters, in **1** all chlorine atoms participate in the intercluster connections. We even find chlorine atoms which connect three clusters through unprecedented Cl^{a-a-a} bridges (Fig. 2). One trigonal bipyramid is connected to twelve others, of which six are in the same plane and three each above and below the central bipyramid. Connection along [001] to the out-of-plane bipyramids above and below is effected by Cl^{i-a} bridges in such a way that a chlorine atom belongs to the inner coordination sphere of one cluster and to the outer sphere of the next cluster and vice versa. Accordingly, connectivity along [001] must be described as $[\{Pr_5(C_2)Cl^{i-a}_{6/2}\}Cl^{a-i}_{6/2}]$. In-plane connectivity between the six bipyramids around a central bipyramid is achieved by Cl^{i-a} bridges of the three edge-bridging chlorine atoms positioned around the base, and three Cl^{a-i} bridges as well as three Cl^{a-a-a} bridges of the six terminal chlorine atoms. This leads to $[\{Pr_5(C_2)Cl^{i-a}_{3/2}\}Cl^{a-i}_{3/2}Cl^{a-a-a}_{3/3}]$ as a description for this plane. Figure 2 shows the connectivity within the hexagonal plane. Combination of these two motifs leads to $[\{Pr_5(C_2)Cl^{i-a}_{9/2}\}Cl^{a-i}_{9/2}Cl^{a-a-a}_{3/3}]$ as a full description of **1**. Along [001] the cluster layers are stacked with the ABAB

[*] Prof. Dr. G. Meyer, Dipl.-Chem. S. Uhrlandt
Institut für Anorganische Chemie der Universität
Callinstraße 9, D-30167 Hannover
Telefax: Int. + (511)762-3006

[**] This work was supported by the Deutsche Foschungsgemeinschaft and the Fonds der Chemischen Industrie.

sequence as in a hexagonal closest packing. Eight rubidium atoms are located on the edges of the unit cell. Of these eight, four each are in the same plane as the apexes of the bipyramid; they thus form a layer together with the Pr atoms. The coordination around Rb is a distorted tricapped trigonal prism of [6 + 3] chlorine atoms [$\bar{d}$(Rb-Cl) = 337.2 pm].

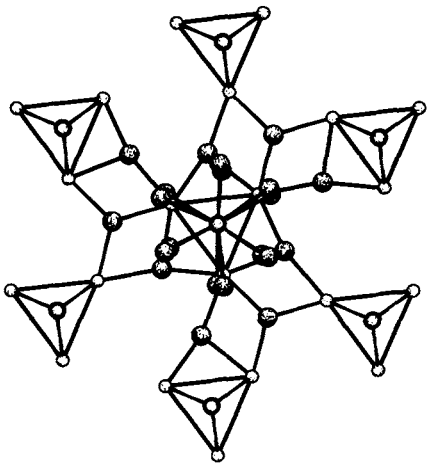

Fig. 2. Connection of a central bipyramid in **1** with six others in the hexagonal plane. Three pyramids are connected to the central one through Cl^{i-a} bridges and three through Cl^{a-a-a} bridges.

The trigonal bipyramids of five Pr atoms and an interstitial C_2 unit are not elongated as is observed when C_2 units are incorporated into M_6 octahedra, but rather contracted: the Pr–Pr distances are 404.4 pm in the base and 382.4 pm from the base to the apex. The distance from the carbon atoms of the C_2 units to the apexes is 228.5 pm. Within the carbon pair the C–C distance of 148.8 pm is somewhat longer than C–C distances observed inside octahedral clusters (143–148 pm).[11, 12] In fact, MO calculations show that the cluster electrons are localized in carbon levels, so that formally a C_2^{6-} unit results. For $[\{Gd_{10}(C_2)_2\}Cl_{18}]$,[13] similar calculations give an analogous result.

Compound **1** is to date the only known example in the chemistry of solid state clusters of transition metals (including the lanthanides and the actinides) featuring a trigonal-bipyramidal M_5 unit with an incorporated C_2 unit. All other known and isolated Pr clusters, namely, $[Cs_2\{Pr_6(C_2)\}I_{12}]$ and $[Cs_4\{Pr_6(C_2)\}I_{13}]$,[14] contain octahedral M_6 units. Main group elements do form trigonal bipyramidal clusters such as Sn_5^{2-} or Bi_5^{3+}, which must be counted among the Zintl-type polyions.[15] In transition metal chemistry $[\{(C_4H_9)N\}Mo_5Cl_{13}]$[16] has been reported as well as $(NH_4)_6[Ta_5(NH)_4Cl_{17}]$,[17] which was described only recently. These two compounds contain M_5 clusters in the form of tetragonal pyramids; in the Ta cluster, four NH^{2-} ions bridge the Ta atoms of the pyramidal base. The successful synthesis of **1** now adds the trigonal bipyramid, stabilized by M–Z bonds, as a third polyhedron to the tetrahedrons and octahedrons in the chemistry of metal-rich rare earth halides.

Experimental Procedure

1 was obtained by treating 32 mg Rb with 555 mg $PrCl_3$, 211 mg Pr, and 18 mg C. The starting materials were weighed inside an argon-filled glove box into a niobium container, which in turn was jacketed in a quartz glass ampoule and sealed under vacuum. The mixture was melted at 950 °C (4 h) and subsequently kept in the furnace at 800 °C for 50 days. Carmine red crystals of **1** were obtained in an approximately 95% yield. The remaining 5% consisted of some unchanged $PrCl_3$ and yellow needles, which were identified as $[Pr_2NCl_3]$ [18]. **1** reacts violently with water (gas is evolved) and is sensitive to air.

Received: April 23, 1993 [Z 6028 IE]
German Version: *Angew. Chem.* **1993**, *105*, 1379

[1] R. P. Ziebarth, J. D. Corbett, *J. Solid State Chem.* **1989**, *80*, 56.
[2] A. Simon, U. Schwanitz-Schüller, *Z. Naturforsch. B* **1985**, *40*, 705.
[3] H. Mattfeld, G. Meyer, *Z. Anorg. Allg. Chem.*, in press.
[4] G. Meyer, T. Schleid, *Inorg. Chem.* **1987**, *26*, 217; G. Meyer, *Chem. Rev.* **1988**, *88*, 93.
[5] H. M. Artelt, S. Uhrlandt, G. Meyer, unpublished.
[6] H. M. Artelt, G. Meyer, *J. Chem. Soc. Chem. Commun.* **1992**, 1320.
[7] H. M. Artelt, G. Meyer, *Z. Anorg. Allg. Chem.* **1993**, *619*, 1.
[8] Crystal structure analysis of $[Rb\{Pr_5(C_2)\}Cl_{10}]$: hexagonal, space group $P6_3/m$ (No. 176), a = 8.4499(7), c = 14.976(4) Å, V = 926 Å^3, Z = 2, 7438 measured reflections of which 1188 were unique and 1137 observed at $F_o^2 > 3\sigma(F_o^2)$; anisotropic refinement except for the carbon atoms which were fixed at U_{11} = 300 pm^2; R = 0.083, R_w = 0.052; Siemens-Stoe AED-2 four-circle diffractometer ($Mo_{K\alpha}$ radiation; μ = 162 cm^{-1}, 2θ_{max} = 71°). Structure solution with SHELX 76 and SHELXS 86, empirical absorption correction. Further details of the crystal structure investigation may be obtained from the Fachinformationszentrum Karlsruhe, Gesellschaft für wissenschaftlich-technische Information mbH, D-76344 Eggenstein-Leopoldshafen, on quoting the depository number CSD-400114, the names of the authors, and the journal citation.
[9] H. Schäfer, H. G. Schnering, *Angew. Chem.* **1964**, *76*, 833.
[10] T. Schleid, G. Meyer, *Z. Anorg. Allg. Chem.* **1987**, *554*, 118.
[11] A. Simon, *J. Solid State Chem.* **1985**, *57*, 2.
[12] H. M. Artelt, G. Meyer, unpublished.
[13] A. Simon, *Mater. Chem. Phys.* **1991**, *29*, 143.
[14] H. M. Artelt, T. Schleid, G. Meyer, unpublished.
[15] J. D. Corbett, *Chem. Rev.* **1985**, *85*, 383.
[16] K. Jödden, H. G. von Schnering, *Angew. Chem.* **1975**, *87*, 594; *Angew. Chem. Int. Ed. Engl.* **1975**, *14*, 570.
[17] M. Simon, G. Meyer, *J. Chem. Soc. Chem. Commun.* **1993**, 460.
[18] $[Pr_2NCl_3]$ crystallizes in the orthorhombic system, space group *Ibam* (No. 72), a = 13.531(1), b = 6.8512(7), c = 6.107(1) Å, R = 0.051, R_w = 0.039.

Giant Organometallic Networks Derived from Ferrocenepolysulfides**

By *Collin P. Galloway* and *Thomas B. Rauchfuss**

We recently reported a new type of organometallic polymer based on disulfido-linked metallocenes, prepared according to Equation (1).[1]

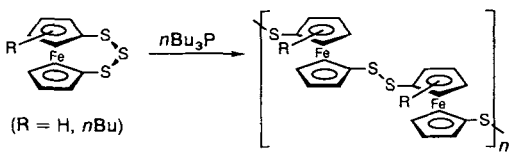

(1)

We now describe routes to related three-dimensional networks; this has involved the preparation of stereochemically novel crosslinking agents and their conversion to very high molecular weight organometallic aggregates. Conceptually related to this work are two other network materials, poly-

[*] Prof. Dr. T. B. Rauchfuss, C. P. Galloway
School of Chemical Sciences and the Materials Research Laboratory
University of Illinois
505 S. Mathews Street,
Urbana, IL 61801 (USA)
Telefax: Int. code + (217)333-2685

[**] This work was supported by the U.S. Department of Energy (DE-FG02-91ER45439). We thank David Compton for experimental assistance.

silynes, prepared by dehalogenation of trichlorosilanes,[2] and (bipyridine)ruthenium arborols.[3]

Crosslinking groups for polymeric metallocenes with disulfido bridges could in principle be prepared from the higher order ferrocenepolysulfides $[Fe(C_5H_{5-x})_2(S_3)_x]$ $(x > 1)$.[4] The hexasulfide $(x = 2)$ is available by tetralithiation of 1,1'-ferrocenedithiol followed by sulfurization with S_8; a process also described by Long et al.[5] This methodology involves deprotonation of the thiol groups followed by *ortho* metalation on each of the rings, as observed in the metalation of thiophenols.[6] An extractive workup of the reaction mixture gives **1** in about 20% yield. The spectro-

$[Fe(C_5H_3)_2(S_3)_2]$ **1**

scopic properties for **1** agree with the published values. Additionally, solutions of **1** in CH_2Cl_2 reversibly oxidize at 1.02 V (vs. Ag/AgCl). Under the same conditions the $E_{1/2}$ values for $[Fe(C_5H_5)_2]$ and $[Fe(C_5H_4)_2S_3]$ are 540 and 857 mV, respectively.[7]

Solutions of **1** react readily with the desulfurization agent nBu$_3$P [Eq. (2)] to deposit a bright orange solid with an Fe:S ratio of about 1:4. Evaluation of the molecular weight distri-

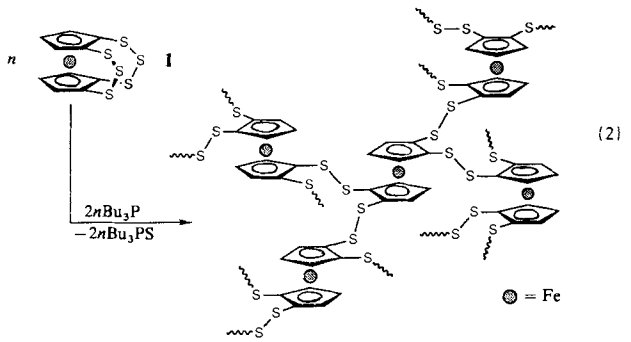

(2)

bution of this material was precluded by its complete insolubility in organic solvents. Cross polarization magic angle spinning (CP/MAS) ^{13}C NMR spectroscopy showed two signals, one at $\delta = 80$ for the CH centers and another at $\delta = 91$ for the CS centers. These chemical shifts are similar to those for the related one-dimensional polymer $[Fe(C_5H_4S)_2]_n$.[1]

In order to prepare soluble ferrocene networks we first synthesized alkyl-substituted analogues of **1**. This was accomplished in a completely regiospecific manner starting from $[Fe(t\text{BuC}_5H_3SH)(C_5H_4SH)]$.[8] Ring lithiation of this species is cleanly directed adjacent to the thiolates and away from the *tert*-butyl group to give, after sulfurization, **2**.

$[Fe(t\text{BuC}_5H_2)(C_5H_3)(S_3)_2]$ **2**

^{1}H NMR measurements (Fig. 1) confirm that this synthesis is regioselective: one observes a single CH_3 resonance signal as well as a singlet and an A_2B coupling pattern for the protons of the trisubstituted and disubstituted cyclopentadienyl rings, respectively, consistent with the conformer of C_s symmetry.[4] In the course of this analysis we discovered that **2** undergoes conformational isomerism in solution. The intensity of the signals assigned to the conformer of C_s symmetry diminish over a period of several minutes; concurrent with this is the appearance of a second CH_3 resonance signal and a new pattern for the ring protons (ABC spin system for the disubstituted ring). These new signals are assigned to the conformer of C_1 symmetry. Separate experiments confirmed that this same dynamic process applies to **1**, provided that the NMR solutions are very freshly prepared. These results reconcile the observation[5] that two isomers of **1** are present in solution, while only one conformer is seen in the crystal lattice.[9] Recrystallization of equilibrated samples of **1** and **2** affords only single conformers, although flash evaporation gives a mixture of the two. The rate constants k_1 and k_{-1} for the isomerization (19 °C) of **1** in C_6D_6 are 6.5×10^{-4} and $7.0 \times 10^{-4}\ s^{-1}$, with $K_{eq} = 0.93$. The rate constant for the inversion of individual S_3 bridges in the C_{2v} isomer is $0.5k_1$ since there are two equivalent trisulfides.[10]

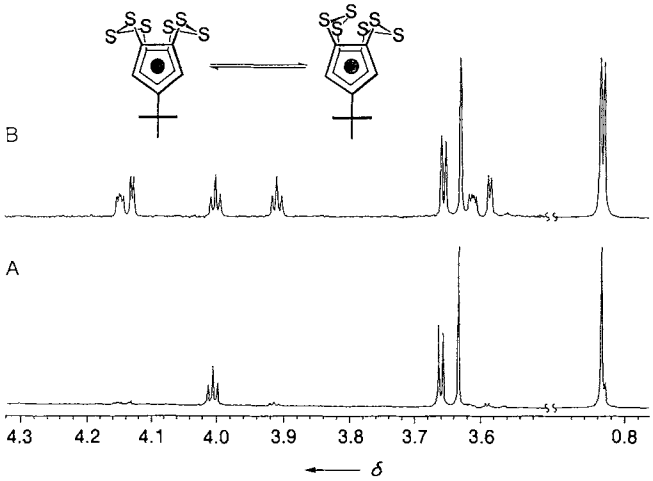

Fig. 1. ^{1}H NMR spectrum of **2** (400 MHz, C_6D_6). Spectrum A was recorded within 5 min of dissolution of the compound, spectrum B was recorded 24 h later and represents the equilibrated sample.

Desulfurization of **2** gave orange polymeric species whose molecular weight distributions proved sensitive to the reaction conditions. Treatment of **2** with two equivalents nBu$_3$P gave primarily materials with MW < 50000. This effect is attributed to the degradation of the network of S–S bonds by the phosphane. Particularly exciting results were obtained when **2** was desulfurized with only 1.5 equivalents nBu$_3$P. The clean conversion of the phosphane to SPBu$_3$ was confirmed by ^{31}P NMR spectroscopy. As indicated by gel permeation chromatographic (GPC) analysis, the initial product has a wide molecular weight distribution to $> 10^6$ Da (Fig. 2). The lighter fractions may correspond to linear polymers with relatively few crosslinks, as seen in the polymerization of the trisulfide $[Fe(t\text{BuC}_5H_3)(C_5H_4)(S_3)]$.[8] Over a period of several minutes, network formation leads to very high molecular weight species.[11] The two trisulfido groups in the monomers clearly participate in the formation of these large organometallic networks, since polymerization of $[Fe(t\text{BuC}_5H_3)(C_5H_4)(S_3)]$ affords mainly a polymer of low molecular weight $M_n < 6000$.[7]

The yellow network polymer $[Fe(t\text{BuC}_5H_2)(C_5H_3)(S_{3-x})_2]_n$ $(x = 0,1)$ was purified by preparative-scale GPC on crosslinked polystyrene; this allowed easy removal of the low molecular weight fractions. Based on analysis of the GPC traces, the purified polymer has $M_n \approx 8.5 \times 10^5$ and $M_w \approx 3.0 \times 10^6$. The observed molecular weights are exceptional for organometallic polymers and can be attributed to the networking capability of the two trisulfido groups in **2**.[12]

To summarize, a three-dimensional network of S–S linkages has been employed in the formation of particularly high molecular weight organometallic superstructures. These findings, together with the widespread occurrence of S–S

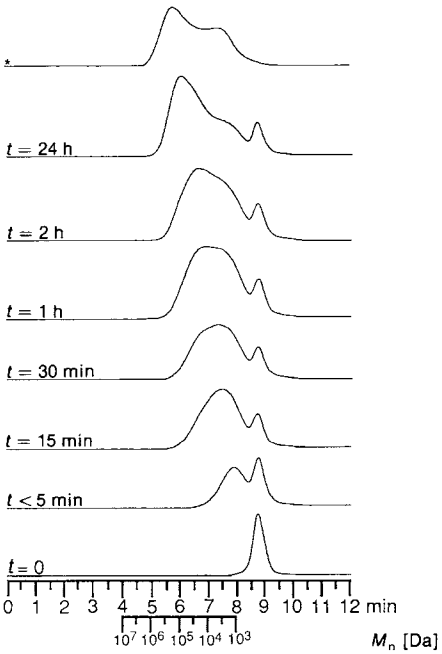

Fig. 2. GPC traces for the reaction mixture of **2** and 1.5 equivalents nBu$_3$P in THF. The top trace (*) is the reaction mixture after purification on Biobeads SX-1 (1 wt% divinylbenzene crosslinked polystyrene). The data for the average molecular weights, M_n, correspond to polystyrene standards which cover the range between 10^3 and 3×10^7 Da.

crosslinks in proteins and minerals, suggest that this structural motif could be more widely applied in synthetic polymers.

Experimental Procedure

All reactions were conducted under a dinitrogen atmosphere.

Polymerization of **1**: A solution of **1** (0.080 g, 0.02 mmol) in dry THF (20 mL) was treated with nBu$_3$P (106 μL, 0.04 mmol). A bright orange precipitate appeared immediately. After 4 h, the solid was collected and washed with THF. Yield: 65 mg (100%). Correct elemental analysis (C, H, Fe, S) for $[Fe(C_5H_3S_2)_2]_n$. IR (KBr): $\tilde{\nu}$ = 3085 (m), 2951 (m), 2921 (m), 2858 (m), 825 (s), 515 (s), 430 (s) cm^{-1}. ^{13}C CP/MAS NMR (75.5 MHz): δ = 80 (CH), 91 (CS).

Synthesis of **2**: [Fe(tBuC$_5$H$_3$SH)(C$_5$H$_4$SH)] was prepared from the trisulfide by LiAlH$_4$ reduction followed by acidification according to the literature method [13]. A solution of [Fe(tBuC$_5$H$_3$SH)(C$_5$H$_4$SH)] (2.62 g, 8.55 mmol) in hexane (50 mL) was added to a stirred solution of 1.6 M nBuLi (21.9 mL, 35 mmol) and TMEDA (5.29 mL). After 16 h at 60 °C, excess elemental sulfur (3.6 g, 112 mmol) was added and the slurry heated under reflux for 6 h. The reaction mixture was filtered and the residue was extracted with hexane (1.5 L). The hexane fractions were washed with 10% NaOH (100 mL) and dried over Na$_2$SO$_4$. Fractional crystallization from THF gave 0.500 g of **2** (12%). ^{1}H NMR (400 MHz, C$_6$D$_6$): C_s conformer δ = 0.84 (s, 9H), 3.69 (s, 2H), 3.71 (d, 2H), 4.06 (t, 1H); C_1 conformer δ = 0.83 (s, 9H), 3.64 (d, 1H), 3.67 (dd, 1H), 3.97 (t, 1H), 4.18 (d, 1H), 4.21 (dd, 1H); ^{13}C NMR (75.5 MHz, C$_6$D$_6$): both conformers (18 of 20 possible signals observed): δ = 108.7, 106.4, 101.6, 99.8, 90.3, 89.4, 80.6, 77.6, 76.1, 73.8, 72.5, 70.5, 69.3, 67.3, 31.2, 31.1. Correct elemental analysis (C, H, Fe, S) for [Fe(tBuC$_5$H$_2$)(C$_5$H$_3$)(S$_3$)$_2$]. EI-MS: (m/z): 430 (M^+). $E_{1/2}$ = 975 mV.

Polymerization of **2**: A solution of **2** (0.025 g, 0.058 mmol) in purified THF (5 mL) was treated with nBu$_3$P (21.6 μL, 0.087 mmol). An immediate color change from yellow to red occurred and the progress of the polymerization was monitored by GPC on a TSK-Gel polystyrene column (Tosoh Corp.) (λ_{det} = 300 nm, 1.5 mL min^{-1} of THF), calibrated with 13 polystyrene standards over the range 10^3 to 3×10^7 Da.

Received: March 3, 1993 [Z 5902 IE]
German version: *Angew. Chem.* **1993**, *105*, 1407

[1] P. F. Brandt, T. B. Rauchfuss, *J. Am. Chem. Soc.* **1992**, *114*, 1926.
[2] P. A. Bianconi, F. C. Schilling, T. W. Weidman, *Macromolecules* **1989**, *22*, 1697.
[3] S. Serroni, G. Denti, S. Campagna, A. Juris, M. Ciano, V. Balzani, *Angew. Chem.* **1992**, *104*, 1540; *Angew. Chem. Int. Ed. Engl.* **1992**, *31*, 1493.
[4] A.Davison, J. C. Smart, *J. Organomet. Chem.* **1979**, *174*, 321.
[5] N. J. Long, S. J. Sharkey, M. B. Hursthouse, M. A. Mazid, *J. Chem. Soc. Dalton Trans.* **1993**, 23.
[6] D. M. Giolando, T. B. Rauchfuss, A. L. Rheingold, *Inorg. Chem.* **1987**, *26*, 1636; G. D. Figuly, C. K. Loop, J. C. Martin, *J. Am. Chem. Soc.* **1989**, *111*, 654; E. Block, V. Eswarakrishnan, M. Gernon, G. Ofori-Okai, C. Saha, K. Tang, J. Zubieta, *ibid.* **1989**, *111*, 658; K. Smith, C. M. Linday, G. J. Pritchard, *ibid.* **1989**, *111*, 664.
[7] Correct C,H,S analysis for [Fe(C$_5$H$_3$)$_2$(S$_3$)$_2$]. Cyclic voltammetry data were measured at 60 mV sec^{-1} and potentials were referenced to Ag/AgCl. Solutions were 1 mM in the ferrocene and 0.1 M in NBu$_4$PF$_6$.
[8] D. L. Compton, T. B. Rauchfuss, *A. C. S. Polym. Prepr.* **1993**, *34*, 351.
[9] In the case of **1**, the A$_2$B and ABC coupling patterns for the two isomers were verified by two-dimensional NMR measurements (^{1}H–^{1}H COSY).
[10] For **2**, $k_1 = 4.5 \times 10^{-4}$ s^{-1}; $K_{eq} = 0.92$ (19 °C). For representative examples of slow conformational equilibria in cyclic polysulfides: (Me$_2$C)$_2$S$_4$: C. H. Bushweller, *J. Am. Chem. Soc.* **1969**, *91*, 6019; [Cp$_2$TiS$_5$]: H. Köpf, B. Block, M. Schmidt, *Chem. Ber.* **1968**, *101*, 272; [(C$_5$H$_4$)$_2$FeE$_3$] (E = S, Se, Te): E. W. Abel, K. G. Orrell, A. G. Osborne, V. Sik, W. Guoxiong, *J. Organomet. Chem.* **1991**, *411*, 239; RP(S)S$_n$: J. Hahn, A. Borkowsky, T. Nataniel, *Phosphorus, Sulfur, Silicon Relat. Elem.* **1989**, *41*, 57.
[11] The extinction coefficients (per Fe) of the polymer and monomer were found to be virtually identical at the detection wavelength of 300 nm.
[12] Recent work on organotransition metal polymers: M. Herberhold, H.-D. Brendel, O. Nuyken, T. Pühlmann, J. *Organomet. Chem.* **1991**, *413*, 65; S. C. Tenhaeff, D. R. Tyler, *Organometallics* **1991**, *10*, 473; H. B. Fyfe, M. Mlekuz, D. Zargarian, N. J. Taylor, T. B. Marder, *J. Chem. Soc. Chem. Commun.* **1991**, 188; A. E. Dray, R. Rachel, W. O. Saxton, J. Lewis, M. S. Khan, A. M. Donald, R. H. Friend, *Macromolecules* **1992**, *25*, 3473; D. A. Foiucher, B.-Z. Tang, I. Manners, *J. Am. Chem. Soc.* **1992**, *114*, 6246; see also a review: J. E. Mark, H. R. Allcock, R. West, *Inorganic Polymers*, Prentice Hall, New York, **1992**.
[13] J. J. Bishop, A. Davison, M. L. Katcher, D. W. Lichtenberg, R. E. Merrill, J. C. Smart, *J. Organomet. Chem.* **1971**, *27*, 241.

Molecular Recognition within a Rigid Host: Structural Changes Induced in μ-Carboxylato Dimetal(II) Complexes by Replacing Steric Repulsions with Hydrogen Bonds**

By *Karl S. Hagen,** *Rene Lachicotte, Alex Kitaygorodskiy,* and *Abdelaziz Elbouadili*

Dedicated to Professor Richard H. Holm on the occasion of his 60th birthday

The diverse reactivity of dioxygen with the diiron(II) nonheme proteins,[1] hemerythrin (Hr, reversible binding), ribonucleotide reductase (R2, generation of tyrosine radical),[2] and methane monooxygenase (MMO, hydroxylation of CH_4 to CH_3OH), is presumably due to the identity of the coordinated ligands and varied stereochemistry induced by the tertiary protein structure, which is an α barrel constructed from a four-helix bundle for Hr and R2. The two Fe^{II} centers in Hr are bridged by two RCO_2^- and a OH^- group and terminally ligated by five histidine residues, whereas those in R2 are bridged by only two RCO_2^- groups and terminally ligated by two histidine residues and two additional RCO_2^- groups. The ligand sphere of the reactive center in MMO is less well characterized, but the iron centers are thought to be in an oxygen-rich environment. The structure of apo-R2[2d] reveals a group of four carboxylato ligands,

[*] Prof. K. S. Hagen, R. Lachicotte, Dr. A. Kitaygorodskiy, Dr. A. Elbouadili
Department of Chemistry, Emory University
1515 Pierce Drive, Atlanta, GA 30322 (USA)
Telefax: Int. code + (404) 727-6586

[**] This research was supported in part by the University Research Committee of Emory University and the National Institutes of Health (GM 46506).

two of which have O···O separations of 290 pm, and two histidine residues. Our initial structural models of the reduced proteins have the general formula $[M_2(OH_2)(O_2CR)_4(tmen)_2]$ **1** (M = Fe^{II}, R = CH_3, Ph,[3] CF_3 (=1-Fe), CMe_3; M = Co^{II}, R = CF_3 (= **1**-Co); tmen = *N,N,N′,N′*-tetramethyl-1,2-diaminoethane) and involve two Fe^{II} centers that interact with four carboxylato ligands. As these complexes

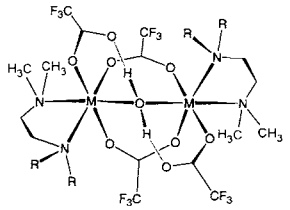

1-Fe R = CH_3; M = Fe^{II}
1-Co R = CH_3; M = Co^{II}
4 R = H; M = Co^{II}

lack the asymmetry of the protein, we have sought ligands that provide multiple, stereochemically constrained functional groups that more closely mimic the constraints of the protein sites. The series of rigid molecules having molecular clefts such as **2a**, developed by Rebek and coworkers,[5] appear to have a favorable structural configuration to serve as hosts for model complexes of metalloproteins, and in particular non-heme proteins in which the diiron(II) centers are coordinated by carboxylato ligands. In order to provide a system with potentially greater flexibility than the previously reported ligand (**2a**), alter the symmetry, and introduce ^{19}F labels for NMR spectroscopic studies, we have prepared the new dicarboxylic acids **2b** and **2c**. Ligand-exchange reac-

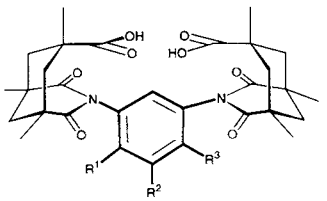

2a $R^1 = R^3 = CH_3$; $R^2 = H$
2b $R^1 = CH_3$; $R^2 = R^3 = H$
2c $R^2 = CF_3$; $R^1 = R^3 = H$

tions have been carried out between **2a**–**c** and **1**-Fe/**1**-Co to form aqua-bridged dinuclear complexes of type **3**; the analogous reaction with the dmen (*N,N*-dimethyl-1,2-diaminoethane) dicobalt complex **4** afforded a complex of type **5**.

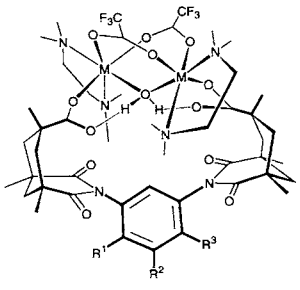

3-Co M = Co^{II}
3-Fe M = Fe^{II}

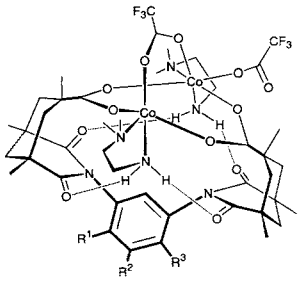

5

The optimal method for monitoring ligand-exchange reactions is not UV-VIS but rather ^{19}F NMR spectroscopy, since the paramagnetism of Co^{II} and Fe^{II} ions affords large isotropic shifts of the resonance of the bound trifluoroacetato ligands and dicarboxylic acid **2c** (Fig. 1). The Co^{II} complexes were chosen because of the higher resolution of their spectra relative to those of Fe^{II} complexes, which results from larger dipolar contributions to the isotropic shifts of the former due to the larger magnetic anisotropy of high-spin Co^{II} relative to high-spin Fe^{II} ions.[6]

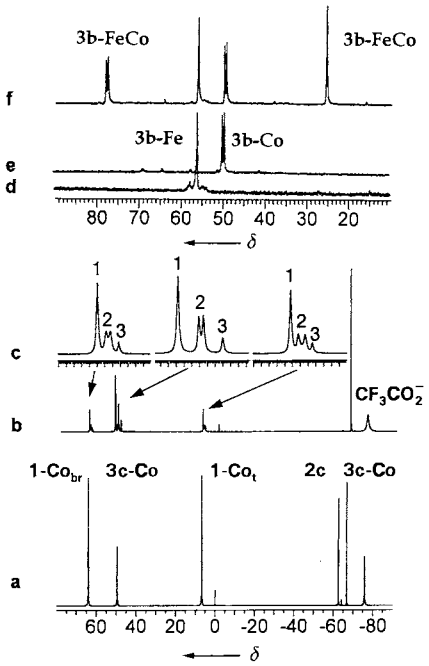

Fig. 1. 470 MHz ^{19}F NMR spectra (for abbreviations see ref. [4], values given are δ values) of a) **1**-Co (F_b 64, F_t 7.5; standard $CFCl_3$ in $CDCl_3$, 24 °C) with excess **2c** (−62.8) affords **3c**-Co (F_b 49.5, −66.8); free $CF_3CO_2^-$ (−76.0) ($1\text{-}Co_{br}$, and $1\text{-}Co_t$ mark the signals corresponding to the bridging and terminal trifluoroacetato ligands in 1-Co); b) isotopomeric mixture with excess **1**-Co; c) expanded spectrum of isotopomeric mixture: (1) D_2O as bridging ligand (1-Co F_{bD} 65.5, F_{tD} 8.1, **3c**-Co 52.4), (2) DOH as bridging ligand (1-Co $F_{b'HD}$ 64.9, $F_{b''HD}$ 64.7, $F_{t'HD}$ 7.6, $F_{t''HD}$ 7.2, **3c**-Co 51.1, 50.8), and (3) H_2O as bridging ligand (**1**-Co F_{bH} 64.1, F_{tH} 6.7, **3c**-Co 49.5); d) **3b** Fe (56); e) **3b**-Co (49.9, 49.4); f) **3b**-FeCo ($F_{b'}$ 78.0, 77.6, $F_{b''}$ 25.5).

Four experiments prove that a quantitative ligand-exchange reaction occurs and that the product has the same stereochemistry as the starting complexes **1**-Fe and **1**-Co. 1) When **1**-Fe (or **1**-Co) is treated with dicarboxylic acid **2c**, no reaction occurs until base is added, whereupon the ^{19}F NMR signals arising from the two $CF_3CO_2^-$ groups of **1**-Fe (or **1**-Co) are lost and replaced by signals of equal intensity corresponding to the diamagnetic, free $CF_3CO_2^-$ ion and paramagnetic, coordinated $CF_3CO_2^-$ ion in **3c**-Fe (or **3c**-Co, Fig. 1a). When a 1:1 mol ratio of **1**-Co and **2c** is employed with an excess of base, the ^{19}F NMR signal for the diamagnetic dicarboxylic acid **2c** at $\delta = -62.6$ is lost, and a new signal corresponding to **3c**-Co is observed at $\delta = -66.8$, indicating that the reaction is quantitative. 2) The presence of two $CF_3CO_2^-$ groups in the product is demonstrated in the reaction of **2b** and **1**-Co affording **3b**-Co, where the lack of any symmetry (C_1 point group) is reflected in two closely spaced, isotropically shifted $CF_3CO_2^-$ resonances (Fig. 1e) which are not resolved in **3b**-Fe (Fig. 1d). 3) The dinuclear nature of the complex is demonstrated by mixing solutions of **3b**-Fe with **3b**-Co which, within time of mixing, affords

the mixed-metal complex, **3b**-FeCo through facile metal exchange.[7] The spectrum of this reaction mixture (Fig. 1f) shows a statistical distribution of the resonances of **3b**-Fe and **3b**-Co as well as two new signals of **3b**-FeCo. 4) The presence of a bridging aqua ligand can be verified by using a mixture of H/D isotopomers.[8] Four ^{19}F NMR resonances of the three isotopomers (H_2O, D_2O (one signal each for C_2 point group) and HOD (two signals for each $CF_3CO_2^-$ ligand in C_1 point group)) are observed in the spectra of **1**-Co and **3c**-Co (Fig. 1b, c).

The ^{19}F NMR chemical shifts of **3**-Co and **3**-Fe suggest that it is the terminal rather than the bridging carboxylato ligands of **1**-Co and **1**-Fe that are replaced by the dicarboxylic acid. This is confirmed by crystal structures of **3a**-Co (Fig. 2) and **3a**-Fe.[9] The $[Co_2(H_2O)(O_2CCF_3)_2(tmen)_2]^{2+}$ fragment of **1**-Co has docked with the molecular cleft of **2a** through coordinate bonds between the dicarboxylic acid and the Co centers and two hydrogen bonds to the bridging aqua ligand. The positions of the C and H atoms in **1**-Co[9, 10]

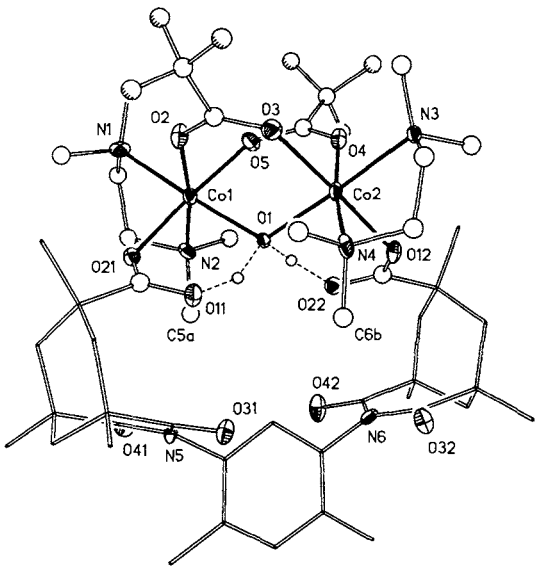

Fig. 2. Crystal structure of **3a**-Co showing 30% probability thermal ellipsoids for Co, N, and O atoms, and open and shaded circles of arbitrary size for C and F, respectively. The host (**2a**) is shown as a stick figure apart from its heteroatoms. Selected interatomic distances [pm] and angles [°] for **3a**-Co: Co1 ··· Co2 370.1; O atoms in hydrogen bonds: O1 ··· O11 249.3, O1 ··· O22 253.4; steric interactions: C5a ··· O41 331, C5a ··· O42 382, C6b ··· O31 341, C6b ··· O32 341; bonds: Co1-O1 211.5(5), Co2-O1 211.7(4), Co1-O2 210.6(5), Co1-O5 210.7(6), Co2-O3 210.0(6), Co2-O4 211.4(6), Co1-O21 208.7(5), Co2-O12 206.2(5), Co1-N1 217.7(7), Co1-N2 219.8(7), Co2-N3 217.7(6), Co2-N4 220.8(7); Co1-O1-Co2 122.0(2).

differ only slightly from those of the corresponding atoms of **3a**-Co. The distance between the convergent carboxylate groups of the dicarboxylic acid has increased considerably upon binding the complex, as compared to that between the carboxylate pair in **2b**, which have a strong hydrogen bond.[11] The carboxylate carbon atoms are 581 pm apart in **3a**-Co compared to 385 pm in **2b**. The O ··· O contacts in **3a**-Co are shorter than in **1**-Co (by 11 and 5 pm) indicating that the hydrogen bonds between the dicarboxylic acid and the bridging aqua ligand are stronger than between the aqua ligand and unrestrained terminal carboxylato ligands in **1**-Co.

The dicarboxylic acid ligand and the dimetal unit are both U-shaped with hydrophobic exteriors and hydrophilic interiors. The two units fit together tightly, and only steric interactions between the methyl groups on the amines and the diimide oxygens of **2a** prevent the closer interaction in which the carboxylate groups of the dicarboxylic acid would become bridging. In the reaction of **4** (a complex analogous to **1**-Co in which the offending methyl groups have been removed) with **2a**, these repulsive steric interactions are replaced by attractive hydrogen bonds, and **5a** forms (Fig. 3).

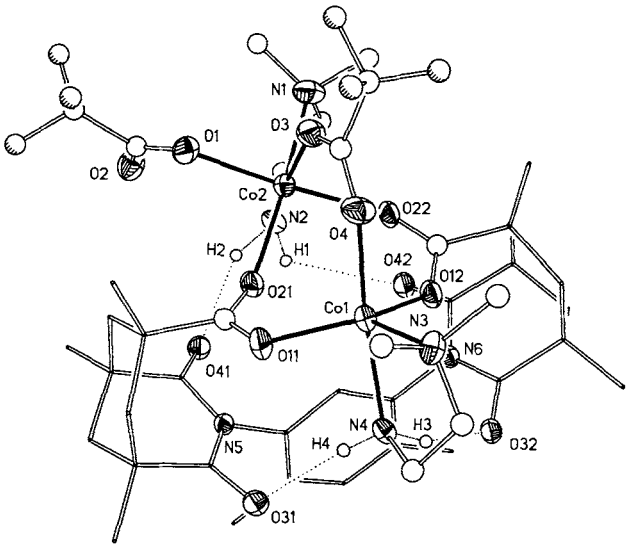

Fig. 3. Crystal structure of one of the two independent dimers of **5a** showing 30% probability thermal ellipsoids for Co, N, and O atoms, and open and shaded circles of arbitrary size for C and F, respectively. The host (**2a**) is shown as a stick figure apart from its heteroatoms. Selected interatomic distances [pm] for **5**: Co1 ··· Co2 389.5; N atoms in hydrogen bonds: N2 ··· O41 307, N2 ··· O42 332, N4 ··· O31 304, N4 ··· O32 311; bonds: Co1-O4 208.2(6), Co1-O11 198.5(6), Co1-O12 195.3(6), Co2-O1 201.7(6), Co2-O3 208.0(6), Co2-O21 214.9(6), Co2-O22 215.6(5), Co1-N3 212.3(7), Co1-N4 218.2(6), Co2-N1 225.4(8), Co2-N2 209.6(6).

The better fit and new hydrogen bonds have pulled the metal ions a further 140 pm into the cleft, and the carboxylate groups of the dicarboxylic acid now bridge the two metal centers. The bridging aqua ligand is lost and replaced by one bridging trifluoroacetato ligand affording a tris(μ-carboxylato) complex.[12] One of the metal centers is terminally coordinated only by dmen and therefore adopts trigonal-bipyramidal five-coordinate geometry. The other metal center is six coordinate with one dmen and one terminal trifluoroacetato ligand. The ^{19}F NMR spectrum of **5** shows two broad resonances at $\delta = 42$ and -4 consistent with the solid-state structure (bridging and terminal trifluoroacetato ligands).

By taking advantage of molecular recognition (weak noncovalent interactions between guest and host in the second coordination sphere of the metal ions) we have been able to alter the geometry of the metal complexes. In doing so we have formed an asymmetric complex with two different types of carboxylato ligands and a six-coordinate as well as a five-coordinate metal center, which is less coordinatively saturated. The asymmetry is relevant to di-iron(II) centers in proteins, which require open coordination sites for reaction with dioxygen. This ligand system allows for diverse terminal ligands with which to tune the stereochemistry and the reactivity of analogous diiron(II) model complexes.

Experimental Procedure

The preparations of dicarboxylic acids **2b** and **2c** were analogous to that of **2a** [5a, 13]. Compounds **3a**-Co, **3a**-Fe, and **3c**-Co were isolated in high yield by cooling acetonitrile solutions of one equivalent each of **1**-Co or **1**-Fe and **2a** or **2c**, respectively, in the presence of an excess of Et_3N under a dry, dinitrogen atmosphere. Compounds **4** and **5** were prepared analogously to **1**-Co and **3a**-Co, respectively, by using dmen instead of tmen.

Received: December 23, 1992
Revised version: May 27, 1993 [Z 5779 IE]
German version: *Angew. Chem.* **1993**, *105*, 1404

[1] Recent reviews: a) S. J. Lippard, *Angew. Chem.* **1988**, *100*, 353–371; *Angew. Chem. Int. Ed. Engl.* **1988**, *27*, 344–361; b) J. B. Vincent, G. L. Olivier-Lilley, B. A. Averill, *Chem. Rev.* **1990**, *90*, 1447–1467; c) L. Que, Jr., A. True, *Prog. Inorg. Chem.* **1990**, *38*, 97–200; d) E. I. Solomon, Y. Zhang, *Acc. Chem. Res.* **1992**, *25*, 343–352; d) R. G. Wilkins, *Chem. Soc. Reviews* **1992**, 171–178.

[2] a) B.-M. Sjöberg, A. Gräslund, *Adv. Inorg. Biochem.* **1983**, *5*, 87–110; b) P. Nordlund, B.-M. Sjöberg, H. Eklund, *Nature* **1990**, *345*, 593–598; c) R2 with Mn^{II} instead of Fe^{II}: M. Atta, P. Nordlund, A. Åberg, H. Eklund, M. Fontecave, *J. Biol. Chem.* **1992**, *267*, 20682–20688; d) Structure of apo-R2: A. Åberg, P. Nordlund, H. Eklund, *Nature* **1990**, *361*, 276–278.

[3] K. S. Hagen, R. Lachicotte, *J. Am. Chem. Soc.* **1992**, *114*, 8741–8742.

[4] Abbreviations: F_b: bridging $CF_3CO_2^-$; F_t: terminal $CF_3CO_2^-$; $F_{b'}$ and $F_{b''}$: nonequivalent bridging $CF_3CO_2^-$; F_{bD}, F_{tD}: $CF_3CO_2^-$ with bridging D_2O; $F_{b'HD}$, $F_{b''HD}$, $F_{t'HD}$, $F_{t''HD}$: nonequivalent $CF_3CO_2^-$ with bridging HOD; F_{bH}, F_{tH}: bridging and terminal $CF_3CO_2^-$ with bridging H_2O.

[5] a) J. Rebek, Jr., L. Marshall, R. Wolak, K. Parris, M. Killoran, B. Askew, D. Nemeth, N. Islam, *J. Am. Chem. Soc.* **1985**, *107*, 7476–7481; b) J. Rebek, Jr., B. Askew, M. Killoran, D. Nemeth, F.-T. Lin, *ibid.* **1987**, *109*, 2426–2431; c) J. Rebek, Jr., *Science* **1987**, *235*, 1478–1484; d) J. Rebek, Jr., *Angew. Chem.* **1990**, *102*, 261; *Angew. Chem. Int. Ed., Engl.* **1990**, *29*, 245.

[6] a) *NMR of Paramagnetic Molecules* (Eds.: G. N. LaMar, W. D. Horrocks, Jr., R. H. Holm), Academic Press, New York, **1973**, b) I. Bertini, C. Luchinat, *NMR of Paramagnetic Molecules in Biological Systems*, Benjamin/Cummings, Menlo Park, CA, USA, **1986**.

[7] Mixed Ni-Co dimers have been characterized by UV/VIS and EPR spectroscopy and by X-ray crystallography: U. Turpeinen, R. Hämäläinen, J. Reedijk, *Polyhedron* **1987**, *7*, 1603–1610.

[8] R. Lachicotte, A. Kitaygorodskiy, K. S. Hagen, unpublished.

[9] Crystal data: **3a**-Co · MeCN: monoclinic space group $C2/c$; a = 35.245(7), b = 15.116(3), c = 23.408(5) Å, β = 101.07(3)°, V = 12239(4) Å^3, ϱ_{calcd} = 1.318 g cm^{-3}, Z = 8. For **3a**-Co and **3a**-Fe reflections were collected at 173 K with $Mo_{K\alpha}$ radiation (λ = 0.71073 Å), $2\theta_{max}$ = 45° on a single-crystal X-ray diffractometer. The structures were solved by Patterson interpretation and expansion (SHELXS-86) and difference Fourier methods and refined by full-matrix least-squares (SHELXTL). 5483 Reflections were used in refinement, $R(wR)$ = 0.0740 (0.1009). – **3a**-Fe · MeCN is isostructural to **3a**-Co: monoclinic space group $C2/c$; a = 35.475(17), b = 15.139(7), c = 23.360(12), β = 101.03(3)°, V = 12311(12) Å^3, ϱ_{calcd} = 1.303 g cm^{-3}, Z = 8. 5343 Reflections were used in refinement, $R(wR)$ = 0.0675–0.0956. – **1**-Co: monoclinic space group $P2_1/n$, a = 15.377(4), b = 13.729(3), c = 16.921(5) Å, β = 113.98(2)°, V = 3264(2) Å^3, ϱ_{calcd} = 1.670 g cm^{-3}, Z = 4. 4398 Reflections were used in refinement $2\theta_{max}$ = 50°, $R(wR)$ = 0.0562–0.0756). – **5**: monoclinic space group $P2_1/c$, a = 20.807(4), b = 12.872(3), c = 40.099(8), β = 93.73(2)°, V = 10717(4) Å^3, ϱ_{calcd} = 1.407 g cm^{-3}, Z = 8. 8230 Reflections used in refinement, $R(wR)$ = 0.0615 (0.0724). Further details of the crystal structure investigations of **1**-Co, **3a**-Co, and **5** are available on request from the Director of the Cambridge Crystallographic Data Centre, 12 Union Road, GB-Cambridge CB2 1EZ (UK), on quoting the full journal citation.

[10] For the isostructural Ni complex, see: M. Ahlgrén, U. Turpeinen, *Acta Crystallogr. Sect. B* **1982**, *32*, 276–279.

[11] Structure of **2b**: R. Lacicotte, A. Elbouadili, A. Kitaygorodskiy, K. S. Hagen, unpublished.

[12] $[Mn_2(\mu\text{-}O_2CCH_3)_3(Me_3tacn)_2](BPh_4)$ (Me_3tacn = *N*,*N*′,*N*″-trimethyl-1,4,7-triazacyclononane) is the only other example of a dimer bridged by three carboxylato ligands. K. Wieghardt, U. Bossek, B. Nuber, J. Weiss, J. Bonvoisin, M. Corbella, S. E. Vitols, J. J. Girerd, *J. Am. Chem. Soc.* **1988**, *110*, 7398–7411.

[13] Correct C,H,N-analyses for **2b** · H_2O, **2c** · H_2O, **3a**-Co · MeCN, **4**, and **5a** · MeCN. – **2b**: MS (LSI-MS): m/z 573 $[M^+Li]^+$, 579 $[M - H^+2Li]^+$, 585 $[M - 2H^+3Li]^+$. IR (Nujol): $\tilde{\nu}$ = 1738, 1706, 1690 (sh) cm^{-1}. Mp > 300 °C. – **2c**: MS (LSI-MS) m/z: 627 $[M^+Li]^+$, 633 $[M - H + 2Li]^+$, 639 $[M \cdot 2H + 3Li]^+$. IR (Nujol): $\tilde{\nu}$ = 1738, 1706, 1690 (sh) cm^{-1}. MP > 300 °C. **3a**-Co · MeCN: IR (Nujol): $\tilde{\nu}$ = 1731, 1714, 1690 cm^{-1}.

A Novel 1,6-Methano[10]annulene Derivative with Bisnorcaradiene Structure—Syntheses with Transition Metal Complexes**

By *Richard Neidlein** and *Ulrich Kux*

Dedicated to Professor Werner Schroth on the occasion of his 65th birthday

Almost 30 years ago, E. Vogel and H. D. Roth[1] prepared 1,6-methano[10]annulene **1**, a 10π electron Hückel arene, some derivatives of which have a bisnorcaradiene structure (**2**). Ab initio calculations[2] have shown that **1** is lower in energy than its valence tautomer **2** by only approximately 4.5 kcal mol^{-1},[2a] a value virtually identical to the difference in energy between cycloheptatriene and norcaradiene.[3] The equilibrium shown above can be shifted in the direction of the valence tautomer **2** in several ways:

1 **2**

1) Substitution of the methylene bridge carbon atom C-11 with electron-withdrawing substituents as in, for example, 1,6-methano[10]annulene-11,11-dicarbonitrile.[4]
2) Complexation with organometallic complex fragments, for example with cyclopentadienylcobalt.[5]
3) Bridging the 2- and 10-positions with an etheno or ethano bridge as in 2,10-etheno-1,6-methano[10]annulene.[6]

In order to explore the little-studied reactivity of 1,6-methano[10]annulene derivatives with organometallic reagents, we treated 2,10-bis(phenylethynyl)-1,6-methano-[10]annulene **3**[7] and the corresponding 1,8-bis(phenylethynyl)naphthalene **4**[8] with 2,6-dimethylphenyl isocyanide (**5**) in the presence of transition metal complexes. The reaction of **3** produced **7**, which confirms that a *peri*-2,10-ethano bridge shifts the equilibrium between **1** and **2** towards **2**.

The reaction of **3** with π-cyclopentadienylbis(triphenylphosphine)cobalt[9] in benzene at room temperature produced a brownish-red compound, which is presumably

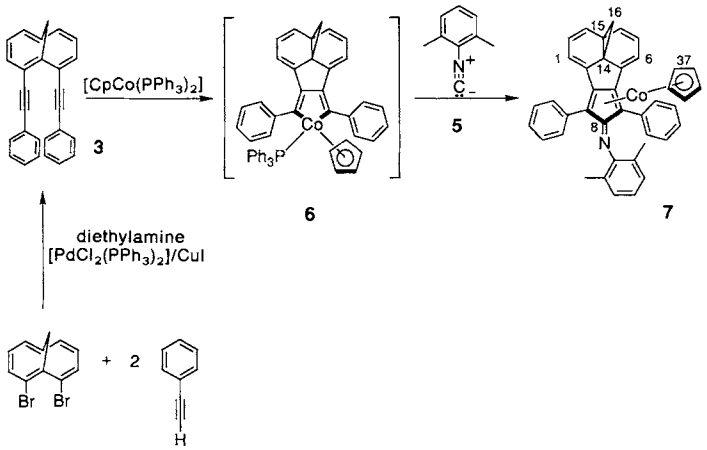

[*] Prof. Dr. R. Neidlein, Dr. U. Kux
Pharmazeutisch-chemisches Institut der Universität
Im Neuenheimer Feld 364, D-69120 Heidelberg (FRG)
Telefax: Int. code + (6221) 56-3430

[**] We thank Dr. W. Kramer for obtaining the NMR spectra.

cobaltocycle **6**, and was not further characterized. After addition of isocyanide **5**, the reaction mixture was heated to reflux. The reaction mixture was cooled and *n*-hexane was added to precipitate a dark solid. Recrystallization from CH_2Cl_2 gave shiny black crystals of **7** in 66% yield over both steps.

The NMR spectra show that **7** is present exclusively as the bisnorcaradiene valence tautomer (Table 1). In the ^1H NMR spectrum the signals of H-1 to H-6 are shifted to higher field relative to those of **1**; selective decoupling experiments allowed the exact assignments of these protons. Additionally,

Table 1. Selected physical data for **7** and **10** (RT = room temperature).

7: M.p. 175–176 °C (CH_2Cl_2); ^1H NMR (250.13 MHz, $CDCl_3$, RT): $\delta = 1.22$ (s, 2H; H-16), 1.62 (s, 3H; CH_3), 2.52 (s, 3H; CH_3), 4.86 (s, 5H; H-37), 6.03 (m, 2H), 6.26 (m, 1H), 6.37 (m, 3H), 6.48 (m, 2H), 6.75 (m, 1H), 7.16 (br. s, 6H; Ph), 7.70–8.08 (br. s, 4H; Ph); ^{13}C NMR (62.89 MHz, $CDCl_3$, RT): $\delta = 18.8$ (q; CH_3), 19.2 (q; CH_3), 22.0 (t, $^1J_{C,H} = 166.0$ Hz; C-16), 45.5 (s; C-14 or C-15), 56.4 (s; C-14 or C-15), 83.0 (d; C-37), 88.6 (s), 114.5 (d), 120.5 (d), 121.1 (d), 126.4 (s), 126.7 (d), 126.74 (d), 126.9 (d), 127.1 (d), 127.3 (s), 127.9 (d), 129.9 (d), 135.3 (s), 138.0 (s), 146.5 (s), 148.9 (s), 173.2 (s; C-8); IR (KBr): $\tilde{\nu} = 1568\ cm^{-1}$ (C=N).

10: M.p. 227–228 °C; ^1H NMR (250.13 MHz, $CDCl_3$, −60 °C): $\delta = 2.15$ (s, 6H; CH_3), 6.66 (m, 3H; H-24/25/26), 7.12 (m, 5H), 7.46 (m, 2H), 7.59 (m, 4H), 7.79 (m, 2H), 8.00 (m, 3H); ^{13}C NMR (62.89 MHz, $CDCl_3$, −60 °C): $\delta = 19.1$ (q; CH_3), 119.7 (d), 120.0 (d), 121.8 (s), 123.3 (d), 124.8 (s), 126.5 (d), 126.6 (d), 126.8 (d), 127.0 (d), 127.6 (d), 127.9 (d), 128.1 (d), 128.4 (d), 129.9 (d), 131.2 (s), 131.4 (s), 132.8 (s), 132.9 (s), 144.0 (s), 147.7 (s), 147.8 (s), 153.1 (s), 171.2 (s; C-8); IR (KBr): $\tilde{\nu} = 1629\ cm^{-1}$ (C=N).

it was determined which of the three 1,3-diene systems is complexed to the cyclopentadienylcobalt unit. The fact that eight protons of the 1,6-methano[10]annulene segment of **7** give rise to only four signals suggests the complexation of the iminocyclopentadiene unit. According to ^1H-^1H nuclear Overhauser effect (NOE) experiments, the cyclopentadienylcobalt unit and the protons of the 1,6-methano[10]annulene bridge are on the same side of **7**. Final proof for the bisnorcaradiene structure of **7** was obtained from the ^{13}C NMR spectrum: the bridgehead carbon atoms C-14 and C-15 give rise to singlets at $\delta = 45.5$ and 56.4, respectively, the methylene bridge atom C-11 shows a triplet at $\delta = 22$ (multiplicities were determined in a gated decoupling experiment). The ^{13}C-^1H coupling constant of 166 Hz is within the range characteristic for cyclopropyl carbon atoms (160–170 Hz).

Not only is **7** one of the few known complexes of 1,6-methano[10]annulene,[5] it is also the first 1,6-methano[10]annulene derivative in which a transition metal complex achieves a regioselective C–C connection between "parallel"[10] triple bonds at the *peri*-2,10-positions. Compounds such as **7** bridge the gap to the fullerenes C_{60} and C_{70}, which upon cyclopropanation produce compounds with 1,6-methano[10]annulene subunits and *peri*-2,10-annulations just as in **7**.

Surprisingly, the reaction of **3** with isocyanide **5** in the presence of an equivalent of bis(1,5-cyclooctadienyl)nickel at 120 °C in toluene gave the expected reaction product **8** in only low yield; the nearly exclusive product was iminocyclopentadiene **10**, which had previously been prepared by two independent routes.[7, 12] The formation of **8** could be proved by mass spectroscopy from the presence of the molecular ion and the virtual identity of the mass spectra of **8** and **10**. Insufficient material was at hand to allow a rigorous characterization.

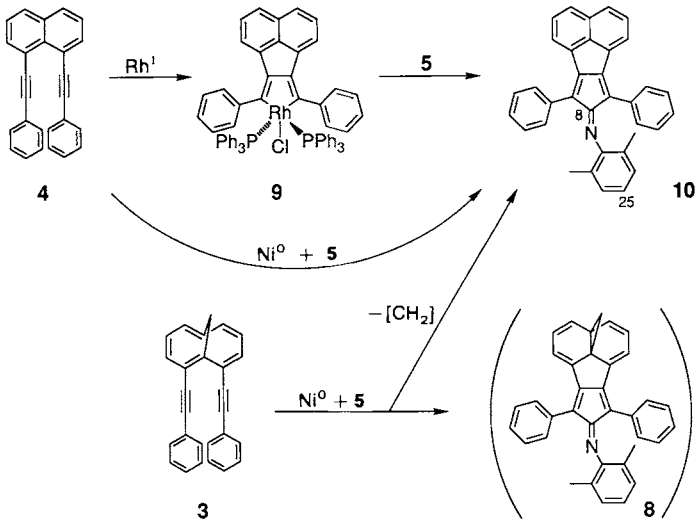

The transformation of **3** into **10** is very unusual, as 1,6-methano[10]annulene derivatives, with the exception of 11,11-dihalo derivatives,[13] undergo upon heating a carbene decomposition through the energetically favored "Berson–Willcott rearrangement", in which one of the bridge or cyclopropyl C–C bonds is broken. In this case the gain of the naphthalene resonance energy is apparently sufficient to allow for the loss of the methylene group. Energy-optimized molecular models of **8** and **10** might offer an explanation (Fig. 1). Not surprisingly, the naphthalene framework in **10**

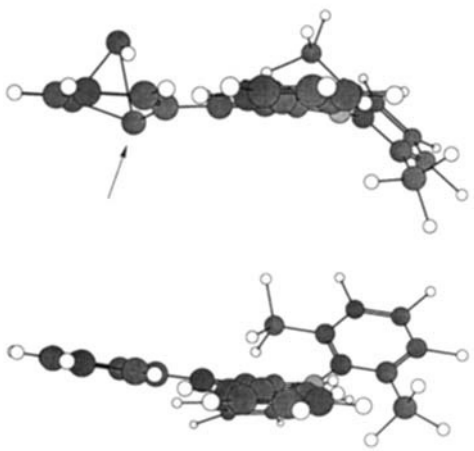

Fig. 1. Energy-minimized molecular models of **8** (above) and **10** (below) obtained using the program Chem3D, version 2.0, Cambridge Scientific Computing.

is planar, but in **8** the bridgehead carbon atom of the 1,6-methano[10]annulene leaning towards the annulated ring is clearly displaced from the plane of the molecule (arrow). This seems to suggest a distortion of the molecule which might facilitate the cleavage of the methylene bridge. The role of the nickel complex in the reaction is not yet known.

Received: April 17, 1993 [Z 6017 IE]
German version: *Angew. Chem.* **1993**, *105*, 1381

[1] E. Vogel, H. D. Roth, *Angew. Chem.* **1964**, *76*, 145; *Angew. Chem. Int. Ed. Engl.* **1964**, *3*, 228.

[2] a) D. Cremer, B. Dick, *Angew. Chem.* **1982**, *94*, 877; *Angew. Chem. Int. Ed. Engl.* **1982**, *21*, 865; b) L. Farnell, L. Radom, *J. Am. Chem. Soc.* **1982**, *104*, 7650; c) R. C. Haddon, K. Raghavachari, *ibid.* **1985**, *107*, 289.

[3] M. B. Rubin, *J. Am. Chem. Soc.* **1981**, *103*, 7791; H. Frauenrath, M. Kapon, M. B. Rubin, *Isr. J. Chem.* **1989**, *29*, 307.
[4] E. Vogel, T. Scholl, J. Lex, G. Hohlneicher, *Angew. Chem.* **1982**, *94*, 878; *Angew. Chem. Int. Ed. Engl.* **1982**, *21*, 869.
[5] P. Mues, R. Benn, C. Krüger, Y.-H. Tsay, E. Vogel, G. Wilke, *Angew. Chem.* **1982**, *94*, 879; *Angew. Chem. Int. Ed. Engl.* **1982**, *21*, 868.
[6] R. Arnz, J. Walkimar de M. Carneiro, W. Klug, H. Schmickler, E. Vogel, R. Breuckmann, F.-G. Klärner, *Angew. Chem.* **1991**, *103*, 702; *Angew. Chem. Int. Ed. Engl.* **1991**, *30*, 683.
[7] U. Kux, Dissertation, Universität Heidelberg, **1993**.
[8] a) B. Bossenbroek, H. Shechter, *J. Am. Chem. Soc.* **1967**, *89*, 7111; b) J. Ipaktschi, H. A. Staab, *Tetrahedron Lett.* **1967**, *45*, 4403; c) A. E. Jungk, Dissertation, Universität Heidelberg, **1970**.
[9] H. Yamazaki, Y. Wakatsuki, *J. Organomet. Chem.* **1977**, *139*, 157.
[10] Parallel is not meant in the strictly mathematical sense: an X-ray structure [8c] of **4** shows a clear deviation from a precise parallel arrangement of the triple bonds. For steric reasons an even larger mutual repulsion of the triple bonds is to expected for **3**, since the vicinal *peri* positions in 1,6-methano[10]annulene are, as a result of the slightly folded structure, closer than in the planar naphthalene[13].
[11] T. Suzuki, Q. Li, K. C. Khemani, F. Wudl, *J. Am. Chem. Soc.* **1992**, *114*, 7300; L. Isaacs, A. Wehrsig, F. Diederich, *Helv. Chim. Acta* **1993**, *76*, 1231.
[12] Compound **9** was prepared according to E. Müller, *Synthesis* **1974**, 761.
[13] E. Vogel, *Pure Appl. Chem.* **1969**, *20*, 237.
[14] J. A. Berson, M. R. Willcott III, *J. Am. Chem. Soc.* **1965**, *87*, 2752.

Selective Pd^0-Mediated C–C Bond Constructions on the Imidazole Ring of L-Histidine: A Practical Approach to the Synthesis of Diphthamide and Related Histidine Analogues**

By *David A. Evans** and *Thorsten Bach*

Dedicated to Professor Reinhard W. Hoffmann on the occasion of his 60th birthday

The unique amino acid diphthamide **1**, the target of diphtheria toxin-catalyzed ADP-ribosylation in elongation factor 2 (EF-2) has raised much scientific interest, in particular concerning its role in protein biosynthesis.[1] In our efforts to devise a practical synthesis of diphthamide,[2] we were attracted to the prospect of utilizing L-histidine as one of the principal building blocks for this amino acid (Scheme 1). In particular, the idea of introducing the methionine-derived, C_4 side chain late, and possibly fully functionalized, in the synthesis led us to consider mild Pd-catalyzed coupling reactions[3] for the decisive C–C bond formation. The weakness in this synthetic strategy was associated with the fact that there are few suitable literature procedures available for the regioselective functionalization of histidine at the C2 position of the imidazole nucleus. Of the various reactions reported,[4] only the reactions with diazonium salts proceed with high selectivity at C2.[5] On the other hand, histidine can be converted selectively into 4-iodo[6] or 2,4-diiodo derivatives[7] depending upon the iodine/substrate ratio. Accordingly, with the potential availability of diiodohistidine derivatives such as **3**,[8] we entertained the prospect of carrying out C2 selective Pd^0-catalyzed reactions with substituted alkynes and other organometallic reagents. In spite of the discouraging literature precedent,[9] we thought that selective cross coupling might be achieved at the more sterically accessible, electronically deficient C2 position of the imidazole nucleus.

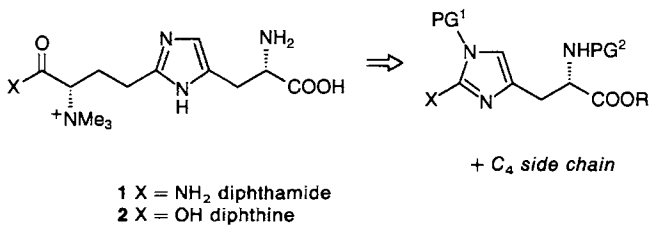

1 X = NH_2 diphthamide
2 X = OH diphthine

Scheme 1. PG^1, PG^2 = protecting group.

Surprisingly, phenylacetylene, in the presence of Pd^0, functioned as a reducing agent to afford, by a selective H–I exchange (ca. 3/1) at the C4 atom, the monoiodide **4**, which was readily obtained in isomerically pure form by flash chromatography (Scheme 2). In addition to **4**, 1,4-diphenylbutadiyne was isolated as the major by-product of the reaction. If the same reaction is carried out in the presence of phosphane ligands, the Heck coupling[10] product **5** is obtained in 52% yield in high enantiomeric purity [>95% *ee* as determined by NMR analysis of the derivatives with (+)- and (−)-α-methoxy-α-(trifluoromethyl)phenylacetyl chloride]. This pivotal reaction thus solves the dual problem of the dehalogenation at the C4 atom and the bond construction at the C2 atom in a single operation. Although a concise mechanism cannot be established at the present time, it seems likely that the proximity of a comparably acidic NH-proton facilitates an intramolecular proton transfer to a Pd–C intermediate, initially formed by oxidative addition. Indeed, simple 5-alkyl-substituted diiodoimidazoles underwent sluggish, poorly selective dehalogenations under identical conditions.

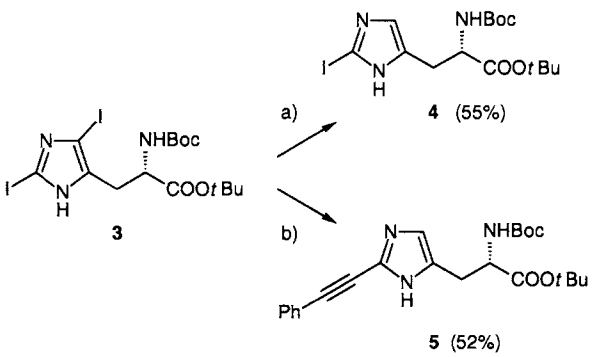

Scheme 2. Deiodination and coupling reactions of compound **3**. Reagents and conditions: a) 3 equiv PhCCH, 0.05 equiv $[Pd(dba)_2]$ (dba = dibenzylidenacetone), 0.07 equiv CuI in NEt_3; 65 °C; 5 h. b) 3 equiv PhCCH, 0.1 equiv $[PdCl_2(PPh_3)_2]$, 0.05 equiv CuI in NEt_3; 65 °C; 12 h.

The extension of the C2 coupling process with representative alkynes was then investigated. *N*-Protection of **4** (Boc_2O, NEt_3 in CH_2Cl_2; 97%) yielded the monoiodohistidine derivative **6** which proved to be a versatile substrate for Pd-catalyzed coupling reactions (Table 1).

With **6** in hand we turned our attention towards reactions that might lead to the incorporation of functionalized car-

[*] Prof. Dr. D. A. Evans, Dr. T. Bach
Department of Chemistry, Harvard University
Cambridge, MA 02138 (USA)

[**] This work was supported by the National Institutes of Health (NIH). The NIH BRS Shared Instrument Grant Program 1-S10-RR04870 and NSF grant CHE88-14019 are acknowledged for providing NMR facilities. T. B. wishes to thank the Deutsche Akademische Austauschdienst for a NATO fellowship.

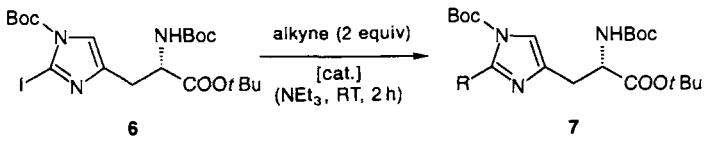

Table 1. Pd-catalyzed coupling of alkynes with **6**.

Alkyne	Catalyst	Equiv	Yield [%]	Product
Bu—≡—H	$[PdCl_2(PPh_3)_2]$/CuI	0.05/0.1	91	**7a**
Ph—≡—H	$[PdCl_2(PPh_3)_2]$/CuI	0.05/0.1	98	**7b**
*t*Bu—≡—H	$[PdCl_2(PPh_3)_2]$/CuI	0.05/0.1	96	**7c**
Me_3Si—≡—H	$[PdCl_2(PPh_3)_2]$/CuI	0.05/0.1	83	**7d**
HO—≡—H	$[PdCl_2(PPh_3)_2]$/CuI	0.05/0.1	94	**7e**
Ph—≡—$SnBu_3$	$[PdCl_2(PPh_3)_2]$	0.1	97 [a]	**7b**

[a] Conditions: THF, reflux, 4 h.

bon chains at C2. In this regard, the reaction of alkylzinc compounds with iodoarenes has been shown to tolerate a high degree of functionalization.[11] We therefore sought to employ a homoserine-based 4-iodobutanoic acid ester as a C_4 precursor. These esters were quantitatively metalated by using an activated Zn/Cu couple.[12] Addition of the resulting alkylzinc iodide in *N,N*-dimethylacetamide (DMA) to a solution of **6** in DMA under the influence of Pd catalysis afforded the desired products in excellent yields (Table 2).

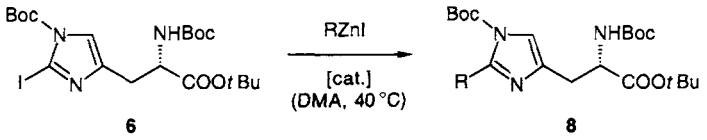

Table 2. Pd-catalyzed coupling of functionalized alkylzinc iodides with **6**.

RZnI	Equiv	Catalyst	Equiv	Yield [%]	Product
EtO(C=O)—ZnI	2	$[PdCl_2(PPh_3)_2]$	0.1	84	**8a**
BnO(C=O)—ZnI, NHBoc	4	$[PdCl_2(PPh_3)_2]$	0.1	65	**8b**
BnO(C=O)—ZnI, NHTrt	3	$[PdCl_2(PPh_3)_2]$	0.1	79	**8c**

The required amino acid esters were prepared stepwise from L-homoserine by standard methods.[13] The coupling reaction proceeded smoothly without detectable epimerization, which was demonstrated by comparison of **8c** with its diastereomer, obtained from *rac*-homoserine. The practicability of this route was finally illustrated in the completion of a total synthesis of diphthine **2**, the most important degradation product of diphthamide[14] (Scheme 3). The trityl group (Trt) in **8c** was selectively cleaved by titration with 0.1 N HCl in 90% aqueous trifluoroethanol (TFE) without loss of the Boc-protecting groups.[15] Subsequent reductive elimination, quaternization, and deprotection led to (*S,S*)-diphthine **2**. Other analogues and diphthamide itself should be equally well accessible by combining this coupling sequence with previously described methods.[2]

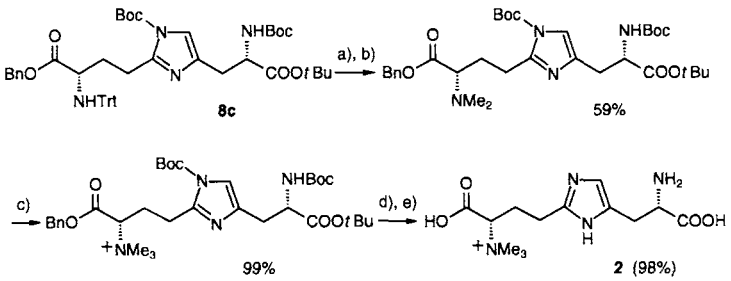

Scheme 3. Completion of the total synthesis of (*S,S*)-diphthine **2**. Reagents and conditions: a) 0.1 N HCl in TFE (aq, 90%), pH > 4; room temperature (RT). b) CH_2O, NaOAc in $HOAc/H_2O$/MeOH; $NaCNBH_3$; RT. c) 25 equiv MeI in MeOH; RT; 2 d. d) H_2 (500 psi), Pd/C (100% w/w) in $HOAc/H_2O$/MeOH (1/1/3); RT; 14 h. e) 2 N HCl (aq); RT; 14 h.

In conclusion, the preceding study establishes the first reliable methodology for the selective carbofunctionalization of the imidazole moiety at the C2 atom in L-histidine. An extension of the Pd-catalyzed transformations to related, simpler imidazole derivatives appears possible.

Received: April 16, 1993 [Z 6011 IE]
German version: *Angew. Chem.* **1993**, *105*, 1414

[1] B. G. van Ness, J. B. Howard, J. W. Bodley, *J. Biol. Chem.* **1978**, *253*, 8687–8690; *ibid.* **1980**, *255*, 10710–10716; *ibid.* **1980**, *255*, 10717–10720; J. W. Bodley, J.-Y. Chen, *ibid.* **1988**, *262*, 11692–11696.
[2] D. A. Evans, K. M. Lundy, *J. Am. Chem. Soc.* **1992**, *114*, 1495–1496.
[3] For a comprehensive review on Pd-catalyzed C–C bond-formation reactions of heterocycles, see: V. N. Kalinin, *Russ. Chem. Rev.* **1991**, *60*, 173–191.
[4] a) Radical substitution: H. Kimoto, S. Fujii, L. A. Cohen, *J. Org. Chem.* **1984**, *49*, 1060–1064; b) fluorination: K. L. Kirk, W. Nagai, L. A. Cohen, *J. Am. Chem. Soc.* **1973**, *95*, 8389–8392; c) sulfenylation: S. Ito, *J. Org. Chem.* **1985**, *50*, 3636–3638.
[5] W. Nagai, K. L. Kirk, L. A. Cohen, *J. Org. Chem.* **1971**, *38*, 1971–1974.
[6] M. Miyashita, Y. Seyama, K. Kaji, S. Yamashita, *Chem. Pharm. Bull.* **1983**, *31*, 386–393.
[7] K. Brunings, *J. Am. Chem. Soc.* **1947**, *69*, 205–208.
[8] Prepared from 2,4-diiodohistidine [6] in two steps: a) Boc_2O, $KHCO_3$ in H_2O/*t*BuOH, room temperature; 48 h (97%); b) $(tBuO)_2CH(NMe_2)$ in benzene; 80 °C; 30 min (74%).
[9] K. Edo, H. Yamanaka, T. Sakamoto, *Heterocycles* **1978**, *9*, 271–274.
[10] K. Sonogashira, Y. Tohda, N. Hagihara, *Tetrahedron Lett.* **1975**, 4467–4470.
[11] a) R. F. W. Jackson, N. Wishart, A. Wood, K. James, M. J. Wythes, *J. Org. Chem.* **1992**, *57*, 3397–3404, and references cited therein. b) For related cuprate reagents, see R. F. W. Jackson, N. Wishart, M. J. Wythes, *Synlett* **1993**, 219–220.
[12] Reviews on activation methods: a) E. Erdik, *Tetrahedron* **1987**, *43*, 2203–2212; b) A. Fürstner, *Synthesis* **1988**, 571–590.
[13] a) J. E. Baldwin, M. North, A. Flynn, *Tetrahedron* **1988**, *44*, 637–642; b) C. Coutsogeorgopoulos, L. Zervas, *J. Am. Chem. Soc.* **1961**, *83*, 1885–1888.
[14] Diphthamide has not yet been isolated in pure form and diphthine is the most closely related material for comparison.
[15] B. Riniker, B. Kamber, P. Sieber, *Helv. Chim. Acta* **1961**, *58*, 1086–1094.

$(1,7\text{-}C_2B_{10}H_{10}\text{-}1',3'\text{-}C_6H_4)_3$, a Cyclic Trimer from *meta*-Carboranediyl and *meta*-Phenylene Units: A New Category of Macrocycle**

By *William Clegg, Wendy R. Gill, J. A. Hugh MacBride,* and *Kenneth Wade**

Icosahedral carboranes $R'R''C_2B_{10}H_{10}$ with suitably functionalized aryl groups R on one or both of their carbon atoms are of considerable potential value in various respects; in boron neutron capture therapy (BNCT),[1] in polymers for high-temperature applications,[2] as precursors for boron carbide-type ceramics,[3] and in connection with their nonlinear optical (NLO) properties.[4] Here, we describe a new type of arylcarborane, the cyclic trimer **1**, that not only extends dramatically the range of systems available for applications of the above types, but also provides the first example of a new category of cyclophane[5] capable of conversion into multifunctional ligands related to calix-arenes,[6] macrocycles, and spherands.[7]

Compound **1** was first isolated in 5% yield from the reaction between $1,7\text{-}Cu_2C_2B_{10}H_{10}$, the dicopper(I) derivative of *meta*-carborane, and *meta*-diiodobenzene in 1,2-dimethoxyethane (DME) in the presence of pyridine [Eq. (a)] (a reaction type we have developed for arylation of *ortho*- and *meta*-carboranes[8]).

$$3\ 1,7\text{-}Cu_2C_2B_{10}H_{10} + 3\ 1,3\text{-}C_6H_4I_2 \longrightarrow 6\,CuI + \underset{\mathbf{1}}{(1,7\text{-}C_2B_{10}H_{10}\text{-}1',3'\text{-}C_6H_4)_3} \quad (a)$$

Compound **1** crystallized as well-formed prisms from benzene. Its cyclic trimeric molecular structure (Fig. 1), which has near threefold symmetry, and in which the skeletal B–B, B–C, and C–C bond lengths and angles are normal for icosahedral carboranes and benzene rings, was established by an X-ray crystallographic study.[9] Although the ^1H, ^{13}C, and ^{11}B NMR spectra of **1** in solution (see below) are consistent with the D_{3h} symmetry expected if all three benzene rings were coplanar (and the carborane icosahedra were bisected by that plane), in the crystal the molecules adopt a dished conformation in which the icosahedra are tilted back by an average of 17° from the plane defined by their carbon atoms. The benzene rings tilt forward by an average of 17° from the same plane. These distortions bring the hydrogen atoms connected to boron atoms of type B3 (the most inward-pointing boron atoms) much closer together (mean interatomic H–H distance 3.16 Å) than those attached to atoms B2 (the other set of inward-pointing boron atoms: mean interatomic H–H distance 4.47 Å). The hydrogen atoms on the inward pointing ring carbon atoms C2′ define a nearly equilateral triangle of mean edge length 3.70 Å. The center of the molecule is thus surrounded by a truncated trigonal pyramid of B-attached hydrogen atoms, the basal triangle of which has edge length 4.47 Å, while the upper triangle has an edge length of 3.16 Å. The C-attached hydrogen atoms occupy sites close to the plane of the upper triangle of B-attached hydrogen atoms. The hydrogen atom positions thus differ markedly from the tricapped trigonal prismatic array that would obtain in the D_{3h} structure that is indicated by solution NMR studies.

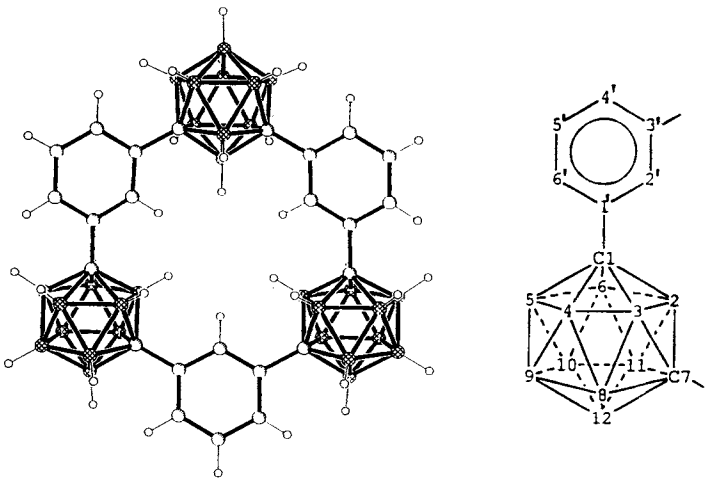

Fig. 1. Left: Molecular structure of crystalline **1**. Selected mean bond lengths [Å]: C1-C1′ and C7-C3′ 1.510, C-C (phenylene) 1.388, C1/7-B2/3 1.709, C-B (carborane) 1.730, B-B 1.774, B-H 1.10, C-H 1.00. Right: Numbering scheme for **1**.

The ^1H NMR spectrum of **1** in $CDCl_3$ solution shows the resonance signal attributable to the inward-pointing C-attached protons (H2′) at remarkably low field ($\delta = 8.14$) compared with normal values ($\delta = 7.21$ for H5′, $\delta = 7.34$ for H4′,6′) for the external protons on these benzene rings. The downfield shift of the internal protons is evidently associated with the macrocyclic structure, since the corresponding protons of the model fragment **2** (prepared from $1,7\text{-}Cu_2C_2B_{10}H_{10}$ and $1,3\text{-}C_6H_4I_2$ in 2:1 molar proportion) resonate at $\delta = 7.48$. In the ^{13}C NMR spectra, three of the four types of phenylene carbon atoms in **1** and **2** resonate at similar fields, but C2′ resonates at higher field for **1** ($\delta = 125.0$) than **2** ($\delta = 127.7$). Preliminary $^1H\{^{11}B\}$NMR spectroscopic studies on **1** and **2** show an unusually low field signal for **1** compared with **2** that appears attributable to the three pairs of internal protons (H2 and H3), since it is coupled to the highest field ^{11}B resonance signal, usually (B2 and B3).[10] Comparison of the ^{11}B NMR spectra of **1** with those of **2** and other diaryl-*meta*-carboranes[10] shows an upfield shift of the lowest field resonance signal, probably that of the boron atoms (B5 and B12) antipodal to the carbon atoms. The UV spectra of **1** and **2** are similar, revealing no cyclic conjugative effect.

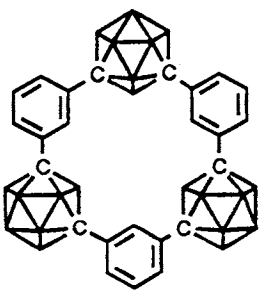

1

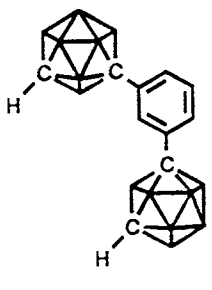

2

Standard deboronation/metalation reactions[11] of **1**, accessible also from the dicopper derivative of **2** and $1,7\text{-}(3'\text{-}IC_6H_4)_2C_2B_{10}H_{10}$, should allow it to be used as a frame

[*] Prof. K. Wade, Dr. W. R. Gill, Dr. J. A. H. MacBride
Chemistry Department, Durham University
South Road, GB-Durham DH1 3LE (UK)
Telefax: Int. code +(91)374-3745
Prof. W. Clegg
Chemistry Department, Newcastle University (UK)

[**] This work was supported by the Science and Engineering Research Council (SERC).

on which to build di- and trinuclear arrays of metal atoms in the icosahedral sites originally occupied by B2-H2 or B3-H3 units in **1**, for example, structure **3**. Suitably derivatized, **1** could be incorporated in polymers or used for BNCT. Heterocyclic variations on **1**, such as result from reactions between 1,7-$Cu_2C_2B_{10}H_{10}$ and 2,6-dibromopyridine,[12] add a further dimension to the ligand potential of cluster compounds of this type.

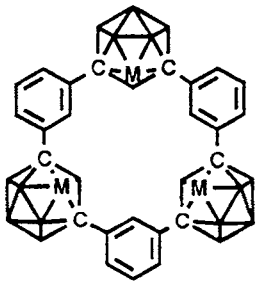

3

Experimental Procedure

1: *meta*-carborane (1,7-$C_2B_{10}H_{12}$: 2.89 g, 20 mmol) in DME (80 cm^3) was treated successively with *n*BuLi (42 mmol in 26 cm^3 hexane), Cu^ICl (4.65 g, 47 mmol), pyridine (12 cm^3), and 1,3-diiodobenzene (6.64 g, 20 mmol), and heated under reflux for 86 h. The product was precipitated by pouring the solution into dilute HCl (4 M, 300 cm^3), washed, dried, dissolved in toluene, and chromatographed on silica. The first fraction eluted by cyclohexane and recrystallized from benzene was identified as **1**, m.p. 375–378 °C. Correct C,H analysis. MS: *m/z* 625–661 (M^+, correct isotope pattern for $C_{24}H_{42}B_{30}$). IR (KBr): $\tilde{\nu}_{max}$ [cm^{-1}] = 3080w, 3040w (ArCH), 2642vs, 2596vs (BH), 1609s, 1588s, 1491s (arene skeleton), 1432s, 1327m, 1185m, 1108s, 1098s, 1018m, 1004m, 912m, 884m, 844s, 812s, 778m, 738s (carborane skeleton), 688s (*m*-C_6H_4), 610m, 442m. ^{13}C NMR ($CDCl_3$, 125.8 MHz): δ = 76.3 (carborane C); 125.0 (C2'), 128.9 (C4',6'), 129.2 (C5'), 135.2 (C3'); ^1H NMR ($CDCl_3$, 250 MHz): δ = 1.8–4.2 (m, 10H, BH), 7.21 (t, J = 7.6 Hz, 1H, H5'); 7.34 (dd, J = 7.6, 1.8 Hz, 2H, H4',6'), 8.14 (t, J = 1.8 Hz, 1H, H3'); ^1H {^{11}B} NMR ($CDCl_3$, 250 MHz): δ = 2.37 (s, 2H), 2.54 (s, 4H, H4,6,8,11) 2.87 (s, 2H), 3.59 (s, 2H), 7.21 (m, 1H, H5'); 7.34 (m, 2H, H4',6'), 8.14 (s, 1H, H3'); ^{11}B NMR ($CDCl_3$, 160.5 MHz): δ = 7.0 (br s), −9.6, −10.3 (br d), −13.7 (br s). UV/VIS (THF): λ_{max} [nm] (lg ε) = 261 (3.93), 267 (4.04); 273.5 (3.99).

2: **2** was prepared similarly, but using a 2:1 molar ratio of *meta*-carborane: diiodobenzene. The crude product was extracted with boiling butanol and recrystallized from ethanol. M.p. 240–244 °C. Correct C,H, analysis. MS: *m/z* 344–366 (M^+, correct isotope pattern for $C_{10}H_{26}B_{20}$). IR (KBr): $\tilde{\nu}_{max}$ [cm^{-1}] = 3065 (carborane CH); 2600 (BH), 1608, 1592s, 1488 (arene skeleton), 1090, 1008, 996, 909, 832, 812, 684 (*m*-C_6H_4), 728 (carborane skeleton). ^{13}C NMR ($CDCl_3$, 125.8 MHz): δ = 55.1 (C7); 77.5 (C1); 127.7 (C2'); 128.0 (C4',6'); 128.4 (C5'); 135.2 (C1',3'); ^1H NMR ($CDCl_3$, 250 MHz): δ = 3.07 (carborane CH); 7.14 (t, J = 7.9 Hz, 1H, H5'); 7.35 (d, J = 7.9 Hz, 2H, H4',6'); 7.48 (s, 1H, H2') ^1H {^{11}B} NMR ($CDCl_3$): δ = 2.18, 2.25, 2.44, 2.59 (BH) and carborane CH and aryl CH signals as before. ^{11}B NMR ($CDCl_3$, 160.5 MHz, relative intensities in parentheses): δ = −4.15 (1), −8.63 (1), −10.49 (4), −13.41 (2), −15.27 (2). UV/VIS (THF): λ_{max} [nm] (lg ε) = 274 (3.27).

Received: April 16, 1993 [Z 6010 IE]
German version: *Angew. Chem.* **1993**, *105*, 1402

[1] J. Plesek, *Chem. Rev.* **1992**, *92*, 269; M. F. Hawthorne, *Pure Appl. Chem.* **1991**, *63*, 327.
[2] H. M. Colquhoun, J. A. Daniels, I. R. Stephenson, K. Wade, *Polym. Commun.* **1991**, *32*, 272; D. A. Brown, H. M. Colquhoun, J. A. Daniels, J. A. H. MacBride, I. R. Stephenson, K. Wade, *J. Mater. Chem.* **1992**, *2*, 793.
[3] L. G. Sneddon, M. G. L. Mirabelli, A. T. Lynch, P. J. Fazen, K. Su, J. S. Beck, *Pure Appl. Chem.* **1991**, *63*, 407.
[4] D. M. Murphy, D. M. P. Mingos, J. M. Forward, *J. Mater. Chem.* **1993**, *3*, 67; D. M. Murphy, D. M. P. Mingos, J. L. Hagitt, H. R. Powell, S. A. Westcott, T. B. Marder, N. J. Taylor, D. R. Kanis, *ibid.* **1993**, *3*, 139.
[5] F. Diederich, *Cyclophanes* Royal Soc. Chem., Cambridge, **1991**.
[6] C. D. Gutsche, *Calixerenes* Royal Soc. Chem., Cambridge, **1989**.
[7] G. Gokel, *Crown Ethers and Cryptands* Royal Soc. Chem., Cambridge, **1991**.
[8] R. Coult, M. A. Fox, W. R. Gill, P. L. Herbertson, J. A. H. MacBride, K. Wade, *J. Organomet. Chem.* **1993**, in press.
[9] **1**: M_r = 654.88, monoclinic, $P2_1/n$, a = 12.147(4), b = 14.596(7), c = 21.263(7) Å, β = 91.73(4)°, V = 3768(3) Å^3, Z = 4, ϱ_{calcd} = 1.154 g cm^{-3}, $F(000)$ = 1344, $Cu_{K\alpha}$ radiation, λ = 1.54184 Å, μ = 0.36 mm^{-1}. The structure was determined by direct methods and refined on F^2 for all 6260 independent reflections measured at 170 K with a Stoe-Siemens diffractometer ($2\theta_{max}$ = 130°), with anisotropic atomic displacement parameters and with freely refined isotropic H atoms: $wR2 = [\Sigma w(F_o^2 - F_c^2)^2 / \Sigma w(F_o^2)^2]^{1/2}$ = 0.1927, conventional R [on F values for 4789 reflections with $F_o^2 > 2\sigma(F_o^2)$] = 0.0565, goodness of fit on F^2 = 1.051 for 656 parameters. Programs: SHELXS-86 and SHELXL-93, G. M. Sheldrick, University of Göttingen. Further details of the crystal structure investigation can be obtained from the Director of the Cambridge Crystallographic Data Centre, 12 Union Road, Cambridge, CB2 1EZ (UK), on quoting the full journal citation.
[10] M. A. Fox, Ph.D. Thesis, University of Durham, **1991**.
[11] R. N. Grimes, *Metal Interactions with Boron Clusters*, Plenum, New York, **1982**.
[12] J. A. H. MacBride, K. Wade, unpublished results.

Temperature Effects in Asymmetric Dihydroxylation: Evidence for a Stepwise Mechanism**

By *Thomas Göbel* and *K. Barry Sharpless**

More than fifty years have passed since Rudolf Criegee's pioneering work on the oxidation of olefins with osmium tetroxide. It is extraordinary that he already envisioned all the essential features of the reaction in these early papers.[1] The concerted mechanism implied by Criegee (Scheme 1) is still the accepted "textbook mechanism" for the reaction of OsO_4 or MnO_4^- with olefins. The remarkable ligand-accel-

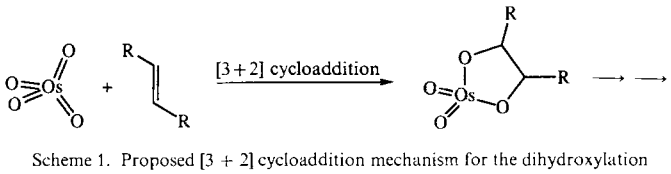

Scheme 1. Proposed [3 + 2] cycloaddition mechanism for the dihydroxylation of alkenes [1]. The heterocycle dimerizes or adds an additional ligand.

eration phenomenon in the osmylation, also discovered by Criegee, enabled us to develop an asymmetric version of this process.[2] These asymmetric *cis* dihydroxylations of olefins have been the subject of intensive research in recent years.[3] Nevertheless, the reaction mechanism is still not understood, a fact which severely hampers the development of a useful model for predicting the transfer of chirality during these reactions. Two mechanisms have been postulated, a concerted [3 + 2],[4] and a stepwise [2 + 2] process.[5] In this latter mechanism, the olefin first coordinates to the osmium center and this intermediate undergoes a fast and reversible rearrangement to the oxaosmetane intermediates **1**. Bond migration then leads to the five-membered cyclic complex **3** (Scheme 2). The coordination of an amine ligand leads to the osmium(VIII) complex **2** which is more likely than **1** to undergo rearrangement to the glycolate **3**, thus explaining the ligand-acceleration effect.[6]

[*] Prof. Dr. K. B. Sharpless, Dr. T. Göbel
Department of Chemistry, The Scripps Research Institute
10666 N. Torrey Pines Road, La Jolla, CA 92307 (USA)
Telefax: Int. code + (619) 554-6406

[**] This work was supported by the National Institutes of Health and the National Science Foundation. T. G. thanks the Deutsche Forschungsgemeinschaft for providing a fellowship.

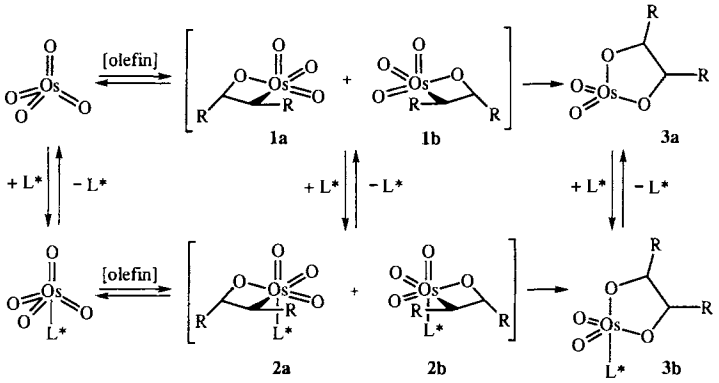

Scheme 2. Proposed [2 + 2] mechanism for the dihydroxylation of alkenes [5]. L* symbolizes the chiral alkaloid ligands.

In this communication we report the influence of reaction temperature on the enantioselectivity of the asymmetric dihydroxylation. The results show that the reaction proceeds via at least two different pairs of diastereomeric transition states, and are therefore inconsistent with a concerted mechanism.

The dihydroxylation of olefins **4**–**6** were performed by using stoichiometric amounts of OsO_4 in presence of an excess[7] of hydroquinidine derivatives **7**–**10** as chiral ligands in toluene,[8] and the temperature was varied over a range of about 100 °C. The enantiomeric excesses of the products were determined by GLC or HPLC analysis of either the diols or the corresponding α-methoxy-α-trifluoromethylphenylacetic acid esters (MTPA esters).

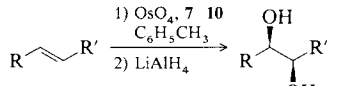

4: R = R′ = C_4H_9
5: R = C_6H_5; R′ = H
6: R = C_8H_{17}; R′ = H

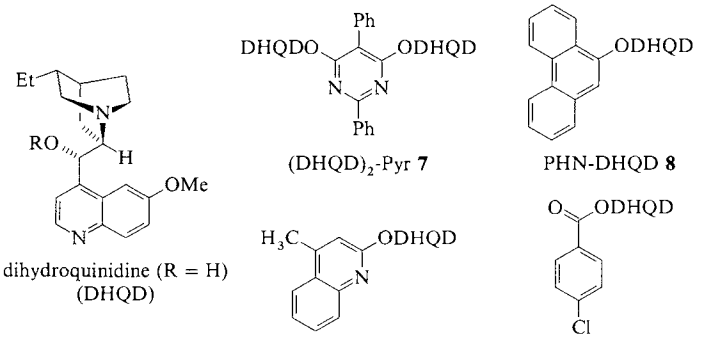

Scheme 3.

The temperature dependence of the *ee* values was analyzed according to the modified Eyring formalism:[9] $\ln P = -(\Delta\Delta H^{\ddagger}/RT) + (\Delta\Delta S^{\ddagger}/R)$ where $P = k(\text{major diol})/k'(\text{minor diol})$ and k and k' are the overall rate constants. The results are summarized in Figures 1 and 2.

Each olefin/catalyst combination[10] shows two linear regions in the Eyring plot with a characteristic inversion point. The temperature at the inversion point is the so-called "inversion temperature" of each system. Inversion points have already been observed in a wide range of stereoselective catalytic systems, including the transition metal-catalyzed asymmetric hydrogenations,[11] and can be explained by a

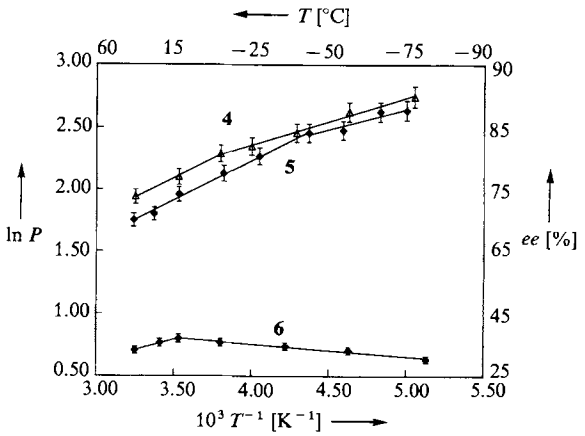

Fig. 1. Eyring plots for the enantiomeric excesses of the dihydroxylation of olefins **4**–**6** with **9** as ligand. The error bars represent confidence levels of ±95% and were determined by standard statistical analysis.

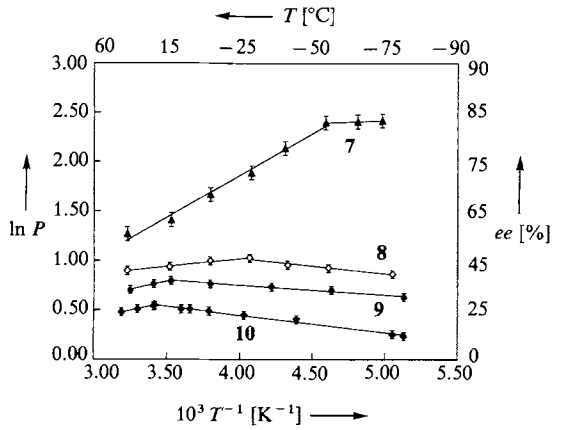

Fig. 2. Eyring plots for the enantiomeric excesses of the dihydroxylation of 1-decene (**6**) with the chiral alkaloid ligands **7**–**10**. The error bars represent confidence levels of ±95% and were determined by standard statistical analysis.

reaction pathway with at least two enantioselective steps that are weighted differentially according to temperature. Our results are therefore consistent with a stepwise process like the [2 + 2] mechanism[12] (Scheme 2) with one selectivity level being the reversible formation of the two diastereomeric oxaosmetanes **2** and the second level the rearrangement to the glycolate **3**. Depending on temperature, either the one or the other reaction is rate and therefore selectivity determining. The two lines observed in the Eyring plot reflect the different $\Delta\Delta H^{\ddagger}$ and $\Delta\Delta S^{\ddagger}$ values for the two steps. On the other hand, a concerted mechanism like the [3 + 2] cycloaddition should show no inversion point because the stereoselectivity would only depend on the difference of the free energy of activation for the two diastereomeric transition states.[13]

Experimental Procedure

In a typical experiment **9** [14] (23 mg, 0.1 mmol) was dissolved in toluene (1.75 mL) and OsO_4 (0.25 mL of a 0.2 M solution in toluene, 0.05 mmol) was added. The reaction mixture was cooled to the desired temperature (T: ±0.5 °C) and 1-decene (**6**) (28.0 mg, 0.2 mmol) was added. After the color had changed from orange to dark green the reaction was quenched with $LiAlH_4$ (1 mL of a 1.0 M solution in THF). After the mixture had been stirred at room temperature for 30 min, ethyl acetate (10 mL) was added, followed, after an additional 10 min, by 1 N HCl (5 mL). The mixture was first passed through Celite, and then the organic layer was separated and dried over $MgSO_4$. Chro-

matography over a short silica gel column yielded 1,2-decanediol which was then converted to the MTPA diester. The *ee* value was determined by HPLC (Pirkle 1 A, 0.5% *i*PrOH in hexane, 1.5 mL min^{-1}).

Received: April 13, 1993 [Z 5999 IE]
German version: *Angew. Chem.* **1993**, *105*, 1417

[1] a) R. Criegee, *Justus Liebigs Ann. Chem.* **1936**, *522*, 75; b) R. Criegee, *Angew. Chem.* **1937**, *50*, 153; c) R. Criegee, *Angew. Chem.* **1938**, *51*, 519; d) R. Criegee, B. Marchand, H. Wannowias, *Justus Liebig Ann. Chem.* **1942**, *550*, 99.
[2] S. G. Hentges, K. B. Sharpless, *J. Am. Chem. Soc.* **1980**, *102*, 5974.
[3] a) K. B. Sharpless, W. Amberg, Y. L. Bennani, G. A. Crispino, J. Hartung, K.-S. Jeong, H.-L. Kwong, K. Morikawa, Z.-M. Wang, D. Xu, X. L. Zhang, *J. Org. Chem.* **1992**, *57*, 2768; b) R. A. Johnson, K. B. Sharpless, in *Catalytic Asymmetric Synthesis* (Ed.: I. Ojima), VCH, Weinheim, scheduled for summer **1993**; c) B. B. Lohray, *Tetrahedron: Asymmetry* **1992**, *3*, 1317.
[4] The mechanism favoured by Criegee and originally proposed by Böseken: J. Böseken, *Rec. Trav. Chim.* **1922**, *41*, 199.
[5] K. B. Sharpless, A. Y. Teranishi, J.-E. Bäckvall, *J. Am. Chem. Soc.* **1977**, *99*, 3120; b) K. A. Jorgensen, B. Schiott, *Chem. Rev.* **1990**, *90*, 1483.
[6] H. C. Kolb, H.-L. Kwong, K. B. Sharpless, unpublished results.
[7] Depending on the temperature a 2 ($T < -10$ °C) to 20 ($T > 10$ °C) fold excess of the ligand was employed to suppress reaction of the olefin with uncomplexed OsO_4; see: E. N. Jacobsen, I. Marko, M. B. France, J. S. Svendsen, K. B. Sharpless, *J. Am. Chem. Soc.* **1989**, *111*, 737.
[8] For the preparation and the structure of the ligands **7**–**10** see: a) K. B. Sharpless, W. Amberg, M. Beller, H. Chen, J. Hartung, Y. Kawanami, D. Lübben, E. Manoury, Y. Ogino, T. Shibata, T. Ukita, *J. Org. Chem.* **1991**, *56*, 4587; b) K. B. Sharpless, G. A. Crispino, K.-S. Jeong, H. C. Kolb, Z.-M. Wang, D. Xu, *J. Org. Chem.*, submitted.
[9] a) H. Eyring, *J. Phys. Chem.* **1935**, *3*, 107; b) S. Glasstone, K. J. Laidler, H. Eyring, *The Theory of Rate Processes*; McGraw-Hill: New York, **1941**.
[10] Similar studies with the systems **9**/3,3-dimethyl-1-butene and **9**/2-methyl-2-heptene in the same temperature range showed no inversion points.
[11] For a review see: H. Buschmann, H.-D. Scharf, N. Hoffmann, P. Esser, *Angew. Chem.* **1991**, *103*, 480; *Angew. Chem. Int. Ed. Engl.* **1991**, *30*, 477.
[12] Of course, the results presented herein do not favor any particular stepwise mechanism. The reaction scheme involving oxaosmetane intermediates receives prominence only because no other stepwise process has been suggested to date.
[13] For two recent examples providing further evidence for a stepwise mechanism in related redox processes see: a) G. A. Vaughan, R. Toreki, R. R. Schrock, W. M. Davis, *J. Am. Chem. Soc.* **1993**, *115*, 2980; b) K. P. Gable, Oregon State University, private communication.
[14] Ligands **8**–**10** are commercially available from Aldrich.

Aminocyclodextrins as Selective Hosts with Several Binding Sites for Nucleotides**

By *Alexey V. Eliseev* and *Hans-Jörg Schneider**

The selective recognition of nucleotides by synthetic host compounds[1–5] is of great importance for the understanding of biological processes as well as for future uses of supramolecular chemistry in analytical chemistry and biological or medicinal fields. The known host–guest complexes are based primarily on ionic bonding between the phosphate units of the nucleotides and positive charges on the host compounds. The host compounds may be modified by the introduction of additional functional groups which can result in some degree of selectivity with regard to the nucleobases, based on the formation of hydrogen bonds with nucleobases in lipophilic solvents.[1–6] Here we report on systems that exhibit additional selectivity by discrimination between 3′- and 5′-phosphate groups, as well as for the first time between the presence or absence of hydroxyl groups in the 2′ position of the riboses (2′-oxy and 2′-deoxy sugar phosphates).

In contrast to the unsubstituted parent compounds,[7] cyclodextrins (CD) with amino groups at the 6 position can form ionic bonds with nucleotides in which the strength of bonding can be regulated by the number of ammonio substituents (Scheme 1). The energies of complexation for such

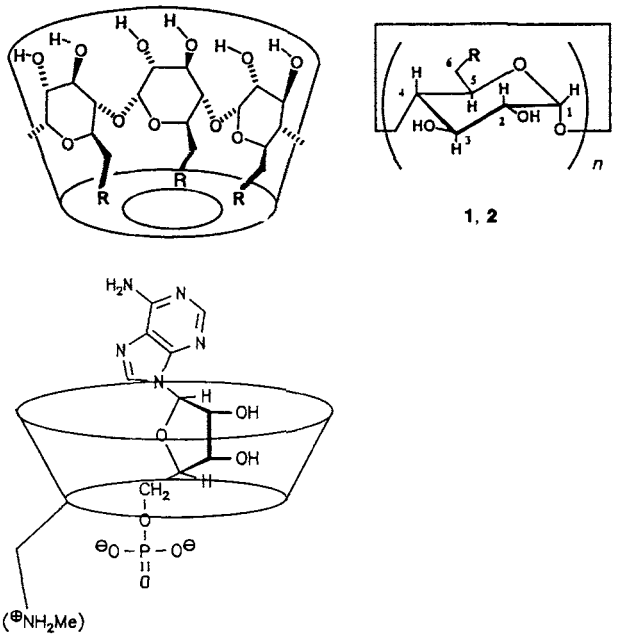

Scheme 1. Top: Schematic representation of the aminodeoxy-β-cyclodextrins ($n = 7$) **1** (= CD-N7 with seven residues R = $^+NH_2Me$) and **2** (= CD-N2 with two R residues at position 6 of the glucose units A and D). Bottom: Postulated structure of the complex.

aminocyclodextrins[8] in water, found for example, for the binding of catecholates, in principle, agree with the general increment of about 5 kJ mol^{-1} per salt bridge found by analysis of over 60 ion pairs.[9] The binding constants K[10] (mostly determined potentiometrically) that we have measured with ATP^{4-} can reach more than 10^6 M^{-1}; they decrease as expected with decreasing number of charges on the nucleotide or on the cyclodextrin (Scheme 2). While the heptakis(6-methylamino-6-deoxy)-β-cyclodextrin CD-N7 **1** discriminates more strongly between ATP and AMP than the only doubly charged β-cyclodextrin CD-N2 **2** (with two methylamino groups at the 6 position of the glucose units A and D), the opposite is true for the discrimination with respect to the isomeric 3′- and 5′-phosphates.

Furthermore, the diamino derivative CD-N2 **2** can also recognize the presence or absence of 2′-hydroxyl groups, and this not only in nucleotides, but also in sugar phosphates for which, despite their large hydrophilicity, binding constants of still over 10^4 M^{-1} were observed (Scheme 3). The affinities increase as expected with CD-N7 **1**, however, here again at the expense of selectivity.

Finally, supramolecular complex formation proved useful in the discrimination of nucleobases (Scheme 4); as is the case with most of the host compounds investigated to date[1–7] adenine derivatives are preferred. In total, there-

[*] Prof. Dr. H.-J. Schneider, Dr. A. V. Eliseev
Fachrichtung Organische Chemie der Universität
D-66041 Saarbrücken (FRG)
Telefax: Int. code + (681)302-4105

[**] Supramolecular Chemistry, Part 37. This work was supported by the Deutsche Forschungsgemeinschaft and the Fonds der Chemischen Industrie. A. E. Eliseev thanks the Alexander-von-Humboldt-Stiftung for a fellowship. Part 36: H.-J. Schneider, F. Werner, T. Blatter, *J. Phys. Org. Chem.* in press.

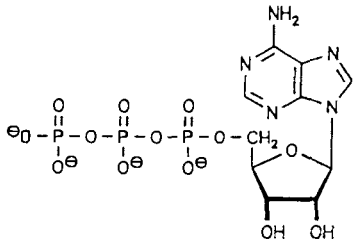

ATP

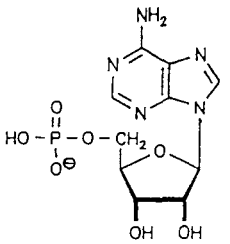

AMP

	ATP	AMP
1 (CD-N7): $10^{-3} \times K =$	3240	126 M^{-1}
2 (CD-N2): $10^{-3} \times K =$	98	14 M^{-1}

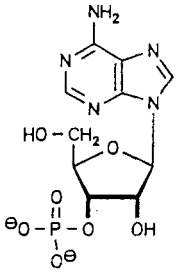

3′-AMP

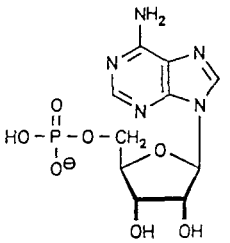

5′-AMP

	3′-AMP	5′-AMP
1 (CD-N7): $K_{rel} =$	1	1.37
2 (CD-N2): $K_{rel} =$	1	9.34

Scheme 2. Discrimination between the type and position of the phosphate groups (absolute complex constants K, measured in water at 25 °C).

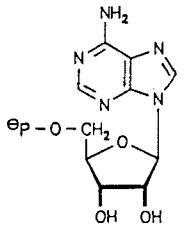

5′-AMP

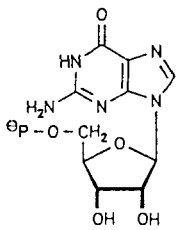

5′-GMP

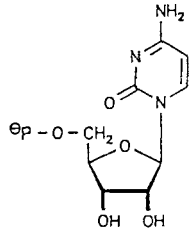

5′-CMP

	5′-AMP	5′-GMP	5′-CMP
1 (CD-N7): $K_{rel} =$	1	0.32	0.16
2 (CD-N2): $K_{rel} =$	1	0.44	0.059

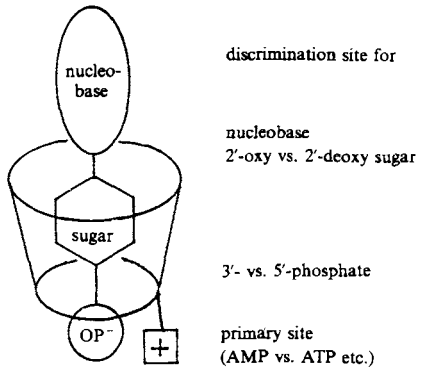

Scheme 4. Top: Discrimination between the nucleobases. Bottom: Schematic representation of the binding sites.

fore, the systems investigated exhibit four selection possibilities which, moreover, can work in parallel and which can function in water, the biologically dominant matrix.

The inclusion geometries postulated in Schemes 1 and 4 are in agreement with molecular mechanics simulations as well as, in some cases, with preliminary NOE measurements and NMR shifts due to complex formation.[11] For instance, in the case of complexes with **1** saturation of the CD protons (H-3) located inside the CD cavity leads, for example with AMP, to Overhauser effects on the ribose protons of up to 6%. In contrast, all other intermolecular effects are less than 0.3%. In addition, only the protons (H-3 and H-5) on the inside of the CD show upfield shifts of up to $\Delta\delta = -0.16$ (calculated for 100% complexation), while all other protons have values of less than $\Delta\delta = 0.01$. To the best of our knowledge these results demonstrate for the first time the inclusion of sugars *inside* the lipophilic CD cavity.[12]

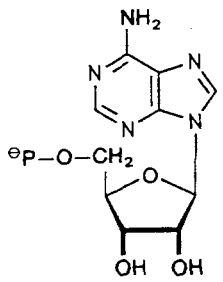

5′-AMP

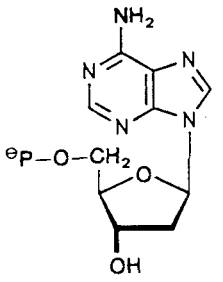

2′-deoxy-5′-AMP

	5′-AMP	2′-deoxy-5′-AMP
1 (CD-N7): $K_{rel} =$	1	0.94
2 (CD-N2): $K_{rel} =$	1	0.034

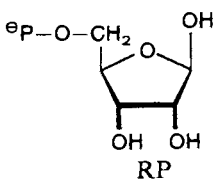

RP

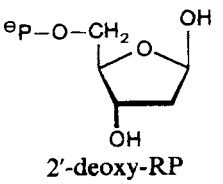

2′-deoxy-RP

	RP	2′-deoxy-RP
1 (CD-N7): $10^{-3} \times K =$	850	815 M^{-1}
2 (CD-N2): $10^{-3} \times K =$	11.2	2.4 M^{-1}

Scheme 3. Discrimination between 2′-oxy and 2′-deoxy nucleotides.

Received: April 2, 1993 [Z 5972 IE]
German version: *Angew. Chem.* **1993**, *105*, 1423

[1] J. M. Lehn, *Angew. Chem.* **1990** *102*, 1347; *Angew. Chem. Int. Ed. Engl.* **1990** *29*, 1304.
[2] E. Kimura, *Top. Curr. Chem.* **1985**, *128*, 131, 141.
[3] M. P. Mertes, K. Bowman Mertes, *Acc. Chem. Res.* **1990**, *23*, 413.
[4] a) A. D. Hamilton, N. Pant, A. V. Muehldorf, *Pure Appl. Chem.* **1988**, *60*, 533; b) *Bioorg. Chem. Front* **1991**, *2*, 115.
[5] Nucleobase bonding in chloroform etc.: J. Rebek, Jr., *Angew. Chem.* **1990**, *102*, 261; *Angew. Chem. Int. Ed. Engl.* **1990**, *29*, 245.
[6] Recent work on host compounds for nucleotides: a) T. K. Park, J. Schroeder, J. Rebek, Jr., *J. Am. Chem. Soc.* **1991**, *113*, 5125; b) V. Kral, J. L. Sessler, H. Furuta, *ibid.* **1992**, *114*, 8704; c) H.-J. Schneider, T. Blatter, B. Palm, U. Pfingstag, V. Rüdiger, I. Theis, *ibid.* **1992**, *114*, 7704; d) T. J. Murray, S. C. Zimmermann, *ibid.* **1992**, *114*, 4010; e) T. Motomura, Y. Aoyama, *J. Org. Chem.* **1991**, *56*, 7224; f) Z. Yang, H. B. Lin, C. M. Lee, H. M. Chang, H. N. C. Wong, *ibid.* **1991**, *57*, 7248; g) D. Y. Sasaki, K. Kurihara, F. Kunitake, *J. Am. Chem. Soc.* **1992**, *114*, 10994. h) A. Galán, E. Pueyo, A. Salmerón, J. de Mendoza, *Tetrahedron Lett.* **1991**, 1827; i) G. Deslongchamps, A. Galán, J. de Mendoza, J. Rebek, Jr., *Angew. Chem.* **1992**, *104*, 58; *Angew. Chem. Int. Ed. Engl.* **1992**, *104*, 61; j) T. Li, S. J. Krasne, B. Persson, H. R. Kaback, F. Diederich, *J. Org. Chem.* **1993**, *58*, 380.

[7] Earlier work on complexation of nucleotides and nucleosides with cyclodextrins: a) T.-X. Xiang, B. D. Anderson, *Int. J. Pharm.* **1990**, *59*, 35; *ibid* **1990**, *59*, 45; b) M. Komiyama, S. Sawata, Y. Takeshige, *J. Am. Chem. Soc.* **1992**, *114*, 1070, and references therein.
[8] A. K. Yatsimirski, A. V. Eliseev, *J. Chem. Soc. Perkin Trans. 2* **1991**, 1769.
[9] H.-J. Schneider, T. Schiestel, P. Zimmermann, *J. Am. Chem. Soc.* **1992**, *114*, 7698.
[10] Some of the binding constant K determinations carried out in water at 25 °C were checked against NMR measurements (in D_2O). The agreements and deviations obtained indicated that the errors in determining K were mostly less than 10%. The CD and nucleotide solutions, generally about 10^{-3} M, were adjusted with HCl (in the presence of 0.1 M NaCl), to the initial pH necessary for the potentiometric determination. Further details and measurements will be published later [11].
[11] A. V. Eliseev, H.-J. Schneider, unpublished results.
[12] Compare with Y. Aoyama, Y. Nagai, J. Otsuke, K. Kobayashi, H. Toi, *Angew. Chem.* **1992**, *104*, 785; *Angew. Chem. Int. Ed. Engl.* **1992**, *31*, 745.

Porphyrin-Like [22]Annulenoquinones**

By *Gottfried Märkl** and *Ulrich Striebl*

Dedicated to Professor Heinrich Nöth on the occasion of his 65th birthday

The porphyrin homologues [22]porphyrin(2.2.2.2),[1] [26]porphyrin(3.3.3.3),[2] and [34]porphyrin(5.5.5.5)[3] are as fascinating as macrocyclic "super"-heteroarenes as the dicationic porphyrinoids,[4] derived from furan, thiophene, and selenophene. The simplest porphyrin analogue, porphycene **1** ([18]porphyrin(2.0.2.0), X = −NH−, =N−) was first described in 1986 by Vogel et al.[5] The next highest porphyrin analogue, the [20]porphyrin(1.2.1.2) **2** (X = −NH−, $=\overset{\oplus}{N}-$) and the corresponding porphyrinoids **2** (X = −O−, $=\overset{\oplus}{O}-$, −S−, $=\overset{\oplus}{S}-$) as well as the corresponding dihydro derivatives **3**, which can be regarded as bridged [22]annulenes, are not yet known. The next highest analogue to **2**, the

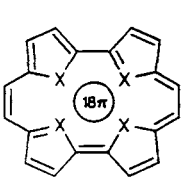

1

X = −NH−, =N−
X = −O−, $=\overset{\oplus}{O}-$
X = −S−, $=\overset{\oplus}{S}-$

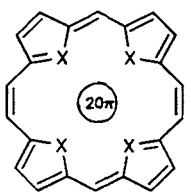

2

X = −NH−, =N−
X = −O−, $=\overset{\oplus}{O}-$
X = −S−, $=\overset{\oplus}{S}-$

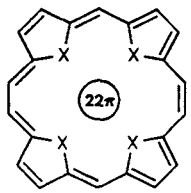

3

X = NR, O, S

[22]porphyrin(1.3.1.3), was first prepared in 1990 as the octaethyl derivative by Franck et al.[6] We report here on the diketones **4**, which can be regarded as [22]annulenoquinones, derived from the tetraoxa- and dioxadithia-bridged annulenes **3**, X = O, S.

Hitherto, of the annulenoquinones of general structure **5** only a few, very special compounds are known as quinoid systems: for example, the cyclooctadecatetraenetetrayne-1,6-dione **5a** ($m = 6$, $n = 2$, four triple bonds) and the cyclooctadecatetraenetetrayne-1,10-dione **5b** ($m = n = 4$, four triple bonds) of Sondheimer et al.[7, 8], together with the di-*tert*-butylbisdehydro[14]annulenedione **5c** ($m = n = 3$, two triple bonds) and the di-*tert*-butylbisdehydro[18]annulenedione **5d** ($m = n = 4$, two triple bonds) of Nakagawa et al.[9] Fuhrhop et al.[10] have proposed the description "paraporphoquinone" for an α,γ-dioxoporphomethene, although this nomenclature does not prove the quinoid character of this system.

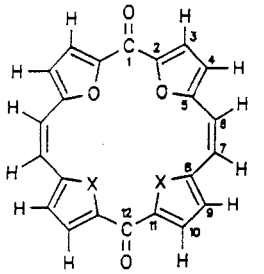

4a, X = O
4b, X = S

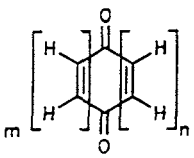

5

The [22]annulenoquinone **4** was obtained by double Wittig cyclization of the dialdehyde **6** with the bis-ylide from **7** in accordance with the Ruggli–Ziegler dilution principle. Preparation of the ketodialdehydes **6a,b**[11b] was achieved according to the method of Cresp et al.[11a] by metalation of the 1,3-dioxolanes from 5-bromofuran-2-carbaldehyde[12] or 5-bromothiophene-2-carbaldehyde[13], respectively, and subsequent reaction with *N*,*N*-diethyl-ethylcarbamate. The bisphosphonium salt **7** was accessible, as described,[11a] from the 5,5′-bis(chloromethyl) derivative of 2,2′-difurylketone.[14] The Wittig reaction of the bis-ylide obtained from **7** was carried out in such a fashion that a freshly prepared solution of lithium methanolate in methanol was added dropwise at 90 °C (reaction time 3 d) to a dilute solution of **6** and **7** in anhydrous dimethylformamide (DMF). In this manner it is probable that only the mono-ylide of **7** is formed initially, which then reacts with the dialdehyde **6**, present in excess, to give the open-chain olefin. The reaction mixture was worked up by hydrolysis, followed by extraction with ether. After removal of the solvent and treatment with a little CH_2Cl_2, the [22]annulene-1,12-dione **4a**[15] precipitated out as a red, fine crystalline powder. To isolate the unsymmetrical [22]annulene-1,12-dione **4b**,[15] which crystallizes as yellow needles, repeated chromatography on silica gel 60 with diethyl ether/petroleum ether (1:1) was necessary.

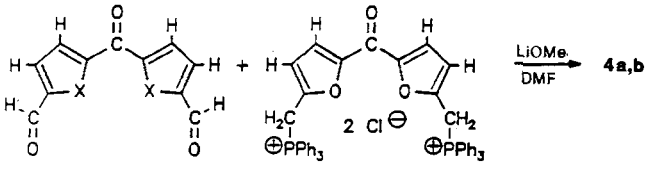

6a, X = O
6b, X = S

7

4a,b

X-Ray crystal structure analysis[16] of **4b** (Fig. 1) shows that the molecule is not planar and that a furan ring is twisted out of the "molecular" plane. The bond lengths in **4b**

[*] Prof. Dr. G. Märkl, Dipl.-Chem. U. Striebl
Institut für Organische Chemie der Universität
Universitätsstrasse 31, D-93040 Regensburg (FRG)
Telefax: Int. code + (941)943-4505

[**] We thank Prof. Dr. H. Nöth, Munich, for the X-ray crystal structure analysis of **4b**, Prof. Dr. D. Troll for the cyclovoltammetry studies, and Priv.-Doz. Dr. J. Salbeck and M. Porsch for the spectroelectrochemical investigations.

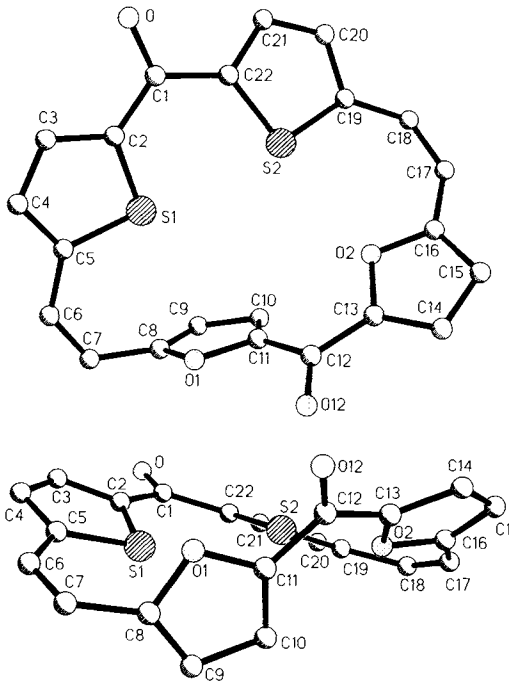

Fig. 1. Structure of **4b** in the crystal. Above: plane view, Below: side view. Selected bond lengths [Å] and angles [°] (standard deviations in parentheses): O-C1 1.227(6), C12-O12 1.217(6), C18-C19 1.464(9), C18-C17 1.318(11), C17-C16 1.411(8), C6-C5 1.456(8), C6-C7 1.312(8), C7-C8 1.467(7), C20-C19 1.383(9), C20-C21 1.357(10), C21-C22 1.387(8); C16-C17-C18 133.2(6), C17-C18-C19 134.5(5), C2-C1-C22 123.6(4), C11-C12-C13 118.0(4), C19-S2-C22 93.4(3), C13-O2-C16 107.0(3), O2-C16-C17 119.9(5); interplanar angle between two thiophene rings is 24.1°, between two furan rings is 134.7°, between furan ring (O1) and thiophene ring (S1) is 73.8°; distance S1 from plane of furan ring (O1) 3.05 Å; torsion angles: C16-C12-C18-C19 4.6°; C5-C6-C7-C8 5.8°; C10-C11-C12-C13 31.5°.

correspond to those in *p*-benzoquinone (C=O: 1.218 Å; C(=O)–CH: 1.467 Å; C=C: 1.312 Å).

The annulenodiones **4a** and **4b** dissolve in $CHCl_3$ and in concentrated H_2SO_4 to give yellow and green solutions, respectively. The UV/VIS spectra of the $CHCl_3$ solutions (Fig. 2, Table 1) are comparable with those of 1,4-benzoquinones:[17] $\lambda = 240-300$ ($\pi \rightarrow \pi^*$), 420–460 nm ($n \rightarrow \pi^*$). The spectra of **4b** show a marked bathochromic shift and simultaneously a dramatic increase in the molar extinction coefficients on changing the solvent from $CHCl_3$ to concentrated H_2SO_4. Protonation of **4** is expected to give the dicat-

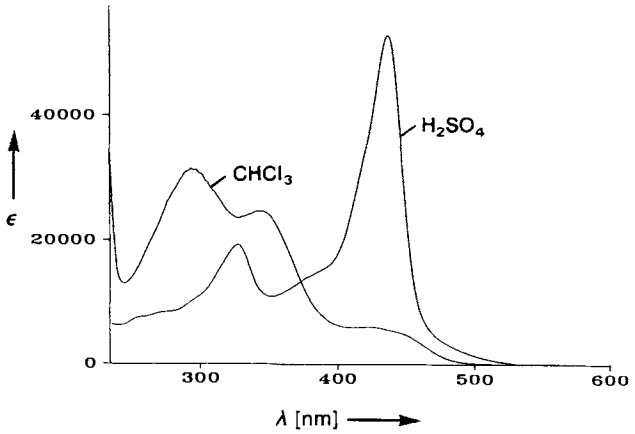

Fig. 2. UV/VIS spectra of **4b** in $CHCl_3$ and in concentrated H_2SO_4.

ions **8**, which can be described both as annulenoid and as a porphyrinoid antiaromatic 20π-electron system.

The ^1H NMR spectra of **4a**, **b** (Table 1) indicate a dynamic structure in solution in which conformational exchange results in a symmetric, planar molecular structure on the NMR timescale. In contrast to the expectation that the ring protons in the diprotonated species **8a**, **b**, as an antiaromatic, paratropic 20π system, experience a high-field shift in the ^1H NMR spectrum compared with those of **4**, quite significant low-field shifts can be observed to some extent (for **4b**

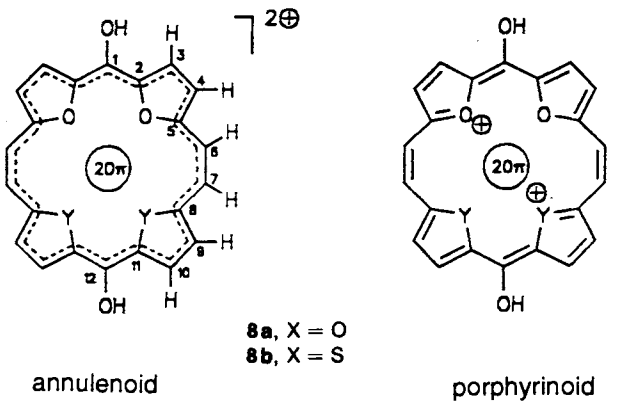

Table 1. UV/VIS and ^1H NMR data for **4a**, **4b**. Coupling constants $^3J(H,H)$ in Hz.

UV/VIS	λ_{max} [nm] (ε)					
4a ($CHCl_3$)	326 (38.200), 408 (sh, 9.300), 452 (sh 3.000)					
4a (conc. H_2SO_4)	344 (12.400), 363 (28.700), 414 (54.000), 490 (sh, 6.200)					
4b ($CHCl_3$)	297 (31.360), 343 (25.100), 423 (6.300)					
4b (conc. H_2SO_4)	328 (31.600), 438 (79.400)					
^1H NMR	3-H	4-H	6-H	7-H	9-H	10-H
4a ($CDCl_3$, 250 MHz)						
δ, $^3J(H,H)$	7.30(d), 3.60	6.50(d)	6.40(s)			
4a (CF_3COOD, 250 MHZ)						
δ	7.60(d)	7.40(d)	6.50(s)			
4b ($CDCl_3$, 80 MHz)						
δ, $^3J(H,H)$	7.83(d), 4.2	7.13(d)	6.95(AB), 12.1	6.45(AB)	6.60(d), 3.5	7.36(d)
4b (conc. H_2SO_4, CF_3COOH, green solution)						
δ, $^3J(H,H)$	8.89(d), 4.1	8.13(d)	7.93(AB), 12.4	7.46(AB)	7.67(d), 4.6	8.52(d)
4b (CF_3COOD/CF_3COOH, red solution)						
δ, $^3J(H,H)$	8.04(d), 4.2	7.32(d)	7.15(AB), 12.0	6.65(AB)	6.84(d), 4.2	7.72(d)

in H_2SO_4: $\Delta\delta = 0.98-1.16$). A plausible interpretation of this finding could be that the low-field shifts resulting from the double positive charge carry more weight than that of the possible high-field shift caused by the paratropic system. Accordingly, the low-field shifts observed by Ogawa et al.[18] in the ^{1}H NMR spectrum on the protonation of a [15]annulenone with CF_3COOH could not be correlated unequivocally with the formation of an aromatic, diatropic [14]annulene.

Electrochemical investigations of **4a, b** in CH_3CN and in DMF show two discrete, reversible one-electron transitions, first to give the radical anions (semiquinones) **9** and then to give the dianions **10** (Fig. 3). The reduction potentials E_1 and

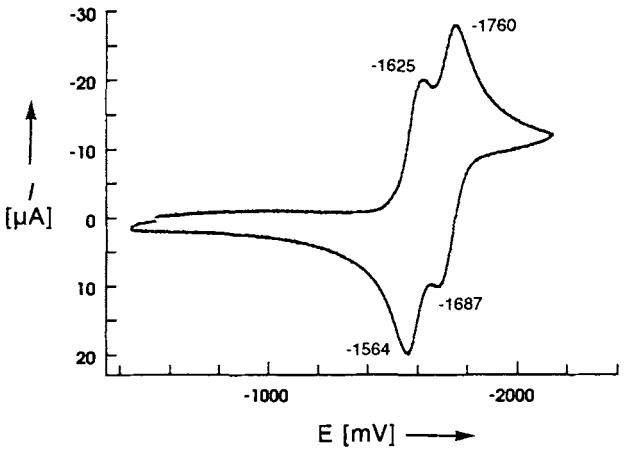

Fig. 3. Cyclic voltammogram for **4b** (acetonitrile, electrolyte tetrabutylammonium hexafluorophosphate; working electrode: Pt; reference electrode: Ag/AgCl; 250 mVs^{-1}, potentials given versus ferrocene as reference, calibrant: ferrocene versus Ag/AgCl: **4a**, 518 mV; **4b** 546 mV).

E_2 of **4a, b**, together with those of *p*-benzoquinone, 1,4-naphthoquinone, and of **5a** and **5c**, are given in Table 2. In agreement with the considerations of Breslow et al.[8] the $(E_1 + E_2)$ values reflect the energy change from the dione to the dianion and thereby further to the aromatically stabilized "hydroquinones". The required flattening of **4** in the transi-

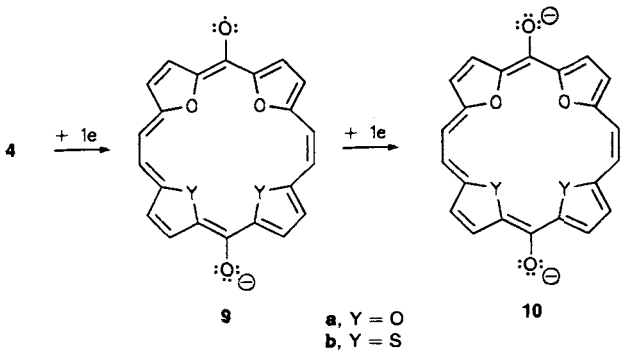

tion from the dione to the semiquinone **9** and to the aromatic "hydroquinone" dianions **10** is probably also partly responsible for the relatively high $(E_1 + E_2)$ values of **4a** and **4b**.

Table 2. Electrochemical reduction potentials.

Compound	E_1	E_2	$E_1 + E_2$	$E_1 - E_2$
p-benzoquinone	−0.42	−1.18	−1.60	0.76
1,4-naphthoquinone	−0.59	−1.30	−1.89	0.71
5a	−0.70	−1.04	−1.74	0.34
5c	−0.72	−0.92	−1.64	0.20
4a	−1.58	−1.72	−3.31	0.13
4b	−1.66	−1.77	−3.43	0.11

The results of spectroelectrochemical experiments, as well as reactivity studies, which substantiate the quinoidal properties of the annulenoquinones **4**, will be reported elsewhere.

Received: April 2, 1993 [Z 5971 IE]
German version: *Angew. Chem.* **1993**, *105*, 1387

[1] E. Vogel, N. Jux, E. Rodriguez-Val, J. Lex, H. Schmickler, *Angew. Chem.* **1990**, *102*, 1431; *Angew. Chem. Int. Ed. Engl.* **1990**, *29*, 1387; N. Jux, P. Koch, H. Schmickler, J. Lex, E. Vogel, *ibid.* **1990**, *102*, 1429 and **1990**, *29*, 1385.

[2] M. Gosmann, B. Franck, *Angew. Chem.* **1986**, *98*, 1107; *Angew. Chem. Int. Ed. Engl.* **1986**, *25*, 1100.

[3] G. Knübel, B. Franck, *Angew. Chem.* **1988**, *100*, 1203; *Angew. Chem. Int. Ed. Engl.* **1988**, *27*, 1170.

[4] E. Vogel, *Pure Appl. Chem.* **1990**, *62*, 557.

[5] E. Vogel, M. Köcher, H. Schmickler, J. Lex, *Angew. Chem.* **1986**, *98*, 262; *Angew. Chem. Int. Ed. Engl.* **1986**, *25*, 257.

[6] H. König, C. Eickmeier, M. Möller, U. Rodewald, B. Franck, *Angew. Chem.* **1990**, *102*, 1437; *Angew. Chem. Int. Ed. Engl.* **1990**, *29*, 1393.

[7] N. Darby, K. Yamamoto, F. Sondheimer, *J. Am. Chem. Soc.* **1974**, *96*, 248.

[8] R. Breslow, D. Murayama, R. Drury, F. Sondheimer, *ibid.* **1974**, *96*, 249.

[9] Y. Onishi, M. Iyoda, M. Nakagawa, *Tetrahedron Lett.* **1981**, *37*, 3641; M. Iyoda, Y. Onishi, M. Nakagawa, *ibid.* **1981**, *37*, 3645.

[10] J.-H. Fuhrhop, S. Besecke, J. Subramanian, C. Mengersen, D. Riesner, *J. Am. Chem. Soc.* **1975**, *97*, 7141.

[11] a) T. M. Cresp, M. V. Sargent, *J. Chem. Soc. Perkin Trans. 1*, **1973**, 2961; b) **6a**, yield 51%; m.p. 189–191 °C (CH_2Cl_2/petroleum ether); IR (KBr): $\tilde{\nu}$(C=O, aldehyde) = 1665 cm^{-1}; $\tilde{\nu}$(C=O, ketone) = 1625 cm^{-1}; UV ($CHCl_3$): λ_{max} = 294 (13600), 325 nm (25100); ^{1}H NMR: δ = 9.90 (s, 2H, CHO); **6b**: yield 67%; M.p. 202–203 °C (acetone); IR (KBr): $\tilde{\nu}$(C=O) = 1660 cm^{-1}; UV ($CHCl_3$): λ_{max} = 260 (9000), 327 nm (24500); ^{1}H NMR: δ = 9.92 (s, 2H, CHO); **7**, yield 90%; m.p. ca. 210 °C (decomp).

[12] H. Gilman, G. F. Wright, *J. Am. Chem. Soc.* **1930**, *52*, 1170; **8a**: yield 90%; b.p. 135 °C/15 Torr.

[13] S. Gronowitz, A. Biezais, B. Mathiasson, *Ark. Kemi* **1964**, *21*, 265; **8b**: yield 98%, b.p. 138–141 °C/15 Torr.

[14] U. Michael, A.-B. Hörnfeldt, *Tetrahedron Lett.* **1970**, *11*, 2013.

[15] **4a**: M.p. >300 °C (decomp), yield 10%; MS (70 eV), *m/z* (%): 372 (100) [M^+], 344 (2) [M^+ − CO], 316 (3) [M^+ − 2CO], 186 (5) [$M/2^+$]; IR (KBr): $\tilde{\nu}$ = 3140, 3100, 3050 cm^{-1} (m, CH arom.), 1620 cm^{-1} (s, C=O); **4b**: M.p. 275–276 °C, yellow needles, yield 19%; MS (70 eV), *m/z* (%): 404 (100) [M^+], 376 (22) [M^+ − CO], 348 (9) [M^+ − 2CO], 202 (12) [$M/2^+$]; ^{13}C NMR ($CDCl_3$): δ = 177.2 (C-1), 172.0 (C-12), 146.5 (C-2), 134.2, 132.8 (C-3, C-4), 142.4 (C-5), 129.2 (C-6), 120.8 (C-7), 152.3 (C-8), 116.8, 114.6 (C-9, C-10), 154.6 (C-11); IR (KBr): $\tilde{\nu}$ = 3120, 3080 cm^{-1} (m, C-H arom.), 1610, 1585 cm^{-1} (s, C=O).

[16] **4b**: $C_{22}H_{12}O_4S_2$, M_r = 404.4, yellow needles; orthorhombic, a = 5.998(2), b = 10.909(4), c = 27.733(9) Å, V = 1817(1) Å^3, Z = 4, ρ_{calcd} = 1.480 Mgm^{-3}, $F(000)$ = 832. Data collection: Siemens P4, $Mo_{K\alpha}$ radiation, single crystal: 0.14 × 0.40 × 0.6 mm^3, 2θ = 2–50° in h, k, $\pm l$, variable rate of measurement: 3.3–60° per minute, ω scans, 4309 reflections, of which 3174 were independent and 2517 observed ($F > 3\sigma(F)$). Structure solution: SHELXTL PLUS PC. Direct methods, $w^{-1} = \sigma^2F + 0.0004F^2$, 253 parameters, H: fixed U_i, non-hydrogen atoms treated as anisotropic, R = 0.0512, R_w = 0.0564; all data: R = 0.0664, GOF 1.37, difference peaks: 0.52/−0.37 e Å^{-3}. Further details of the crystal structure investigation may be obtained from the Fachinformationszentrum Karlsruhe, Gesellschaft für wissenschaftlich-technische Information GmbH, D-76344 Eggenstein-Leopoldshafen (FRG) on quoting the depository number CSD-57152, the names of the authors, and the journal citation.

[17] S. Berger, P. Hertl, A. Riecker in *The Chemistry of Quinoid Compounds, Part 1* (Ed.: S. Patai), Wiley, Chichester, England **1974**, p. 231.

[18] H. Ogawa, N. Shimojo, M. Yoshida, *Tetrahedron Lett.* **1971**, *12*, 2013; see also G. P. Cotterrell, G. H. Mitchell, F. Sondheimer, G. M. Pilling, *J. Am. Chem. Soc.* **1971**, *93*, 259.

Posttranslational Backbone Modifications in the Ribosomal Biosynthesis of the Glycine-Rich Antibiotic Microcin B17**

By *Anja Bayer, Stefan Freund, Graeme Nicholson,* and *Günther Jung**

Dedicated to Professor Murray Goodman on the occasion of his 65th birthday

The antibiotic microcin B17 (McB17) belongs to a group of polypeptides called microcins,[1] which were discovered by Asensio et al. in 1976.[2] In contrast to the commonly known peptide antibiotics synthesized by multienzyme complexes, microcins are produced by ribosomal synthesis and posttranslational modification of precursor proteins by nonsporulating microorganisms such as Enterobacteriae. McB17 inhibits DNA replication with an impressive bactericidal activity against gram-negative bacteria: only one molecule is sufficient to kill a bacterial cell.[1] The mode of action resembles that of quinolines and a variety of antitumor drugs currently used in chemotherapy. McB17 binds to a DNA-bound gyrase, and induces thereby double-strand cleavage, because the normal gyrase activity (DNA untwisting and rejoining of the cleaved DNA) is suppressed.[3]

In previous attempts,[4] the nature of the posttranslational modifications present in McB17 could not be determined. Here, we elucidate the structure of McB17 by using various analytical techniques, including multidimensional NMR spectroscopy of ^{15}N-labeled McB17.

McB17 is produced by several strains of *Escherichia coli*.[5] The genetic determinants for the McB17 production are located in a cluster on the plasmid. The gene mcbA codes for the inactive 69 amino acid precursor molecule of McB17[6] (Fig. 1). McB17 exhibits rather unusual features: Of the 43 amino acid residues in the DNA-derived sequence of McB17, 26 are glycine residues. The mature polypeptide is very thermostable and resistant to extreme pH conditions; its poor solubility in aqueous buffers and most organic solvents is also remarkable. These properties severely hampered the isolation, purification, and enzymatic cleavage, for example by lysostaphin.

The structure of the highly purified McB17[7] was elucidated by UV-spectroscopy, mass-spectrometry, amino acid analysis, protein sequencing, GC-MS, and in particular multidimensional NMR.

The molecular mass of McB17 was determined by on-line HPLC–electrospray mass spectrometry.[8] Due to its low solubility McB17 had to be dissolved in 50% aqueous formic acid. From the triply and doubly positively charged quasi-molecular ions, a molecular mass of 3092 Da was determined. This experimental mass differs from the one calculated on the basis of the DNA sequence (Fig. 1) by 160 Da. The 48 amu higher mass of the ^{15}N-labeled McB17 proved the complete uptake of ^{15}N from a medium containing $(^{15}NH_4)_2SO_4$ as sole nitrogen source.

McB17 was hydrolyzed in the gas phase at 160 °C in 6 N HCl in a fully automated amino acid analyzer, and after derivatization with phenyl thioisocyanate and separation as phenyl thiocarbamoyl derivatives on a microbore PP-HPLC, all amino acids predicted from the DNA-sequence were found except for the following: Although four Cys and six Ser residues are predicted, none of the Cys and only two Ser residues were detected. The number of Gly residues varied from 13 to 21 out of 26. These results point clearly to a modification of four Ser, four Cys, and some of the Gly residues. The reduction of McB17 with $NaBH_4$ should yield free thiol groups in the case of disulfide bridges, but the reaction of Ellman's reagent was negative.

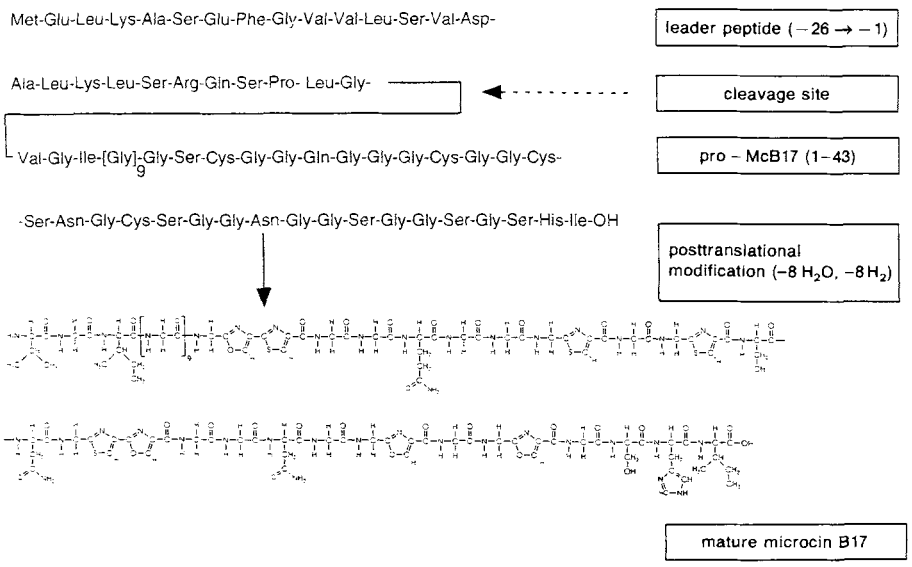

Fig. 1. Primary sequence of the precursor protein of Microcin B17 and its posttranslational modification to the mature McB17 containing 2-aminomethylthiazol-4-carboxylic acid (Atc), 2-aminomethyloxazol-4-carboxylic acid (Aoc), 2-(2-aminomethylthiazolyl)oxazol-4-carboxylic acid (Atoc) and 2-(2-aminomethyloxazolyl)thiazol-4-carboxylic acid (Aotc) as heteroaromatic residues.

Chiral-phase GC-MS investigations[9] with a derivatized total hydrolyzate of McB17 detected all amino acids expected from the results of the amino acid analysis as *N*-trifluoroacetylamino acid *n*-propyl esters by their molecular mass and rentention time. Again cysteine was not detected and only two of the six Ser residues were found. One additional compound was eluted with a very long retention time. It was identified as 2-aminomethylthiazole-4-carboxylic acid (Atc) by its characteristic MS fragmentation pattern. A possible

[*] Prof. Dr. G. Jung, Dipl.-Biol. A. Bayer, Dr. S. Freund, G. Nicholson
Institut für Organische Chemie der Universität
Auf der Morgenstelle 18, D-72076 Tübingen (FRG)
Telefax: Int. code + (7071)29-6925

[**] We acknowledge financial support from the Deutsche Forschungsgemeinschaft (SFB 323, project C2-Jung). We are grateful to Prof. Dr. V. Braun for providing laboratory equipment and to Prof. Dr. K. Hantke for the microcinogenic strain. We acknowledge Dr. M. Spraul, Bruker Karlsruhe for providing the 750 MHz NOESY spectrum of McB17.

mechanism for such a ring formation must involve attack of the thiol group of cysteine on the peptide carbonyl of the preceding N-terminal Gly residue with elimination of water and H_2 (Fig. 1).

The UV spectrum of McB17 indicated two absorption maxima at 210 nm and 270–280 nm, although the DNA-derived amino acid sequence of McB17 contains no aromatic amino acid residues. The UV absorptions were indicative of the presence of further heteroaromatic ring systems in addition to the Atc residues ($\lambda_{max} = 225$ nm).

The sequencing of McB17 with automated Edman degradation stopped after the first 12 N-terminal amino acid residues: VGIGGGGGGGGG (Fig. 1). Thus we concluded that the next amino acid residues Gly^{13} and Ser^{14} are modified in the mature peptide antibiotic.

The standard approach to define the primary sequence of peptides by 2D-NMR experiments is to use scalar-coupled experiments such as double quantum-filtered correlation spectroscopy (DQF-COSY) and total correlation spectroscopy (TOCSY) for the assignment of spin systems of residues and to connect them to adjacent residues by nuclear Overhauser effects (NOEs).[10] However, judging from the DNA-derived precursor sequence (Fig. 1), such an approach has to fail in the case of microcin B17 because up to 26 out of the 43 residues of microcin B17 are glycine units and therefore lack characteristic side-chain signals.

Furthermore, several heteroaromatic components such as Atc were expected from a deuterium exchange experiment where seven or eight singlet signals remained in the aromatic region after exchange of all labile amide signals. The preparation of uniformly ^{15}N-labeled McB17 and the extensive use of inverse-detected heteronuclear experiments with ^{13}C at natural abundance and ^{15}N labeling (100%) allowed us to record a set of two-dimensional NMR spectra that enabled us to unravel the peculiarities of McB17.

The amino acid and GC-MS analysis of the ^{15}N-labeled derivative showed that modifications in the primary structure of the precursor peptide should be found for at least five glycine, all four cysteine, and four out of the six serine residues. Obviously the three Gly-Cys sites in McB17 are modified to thiazole derivatives as shown by GC-MS; however, the analogue 2-aminomethyloxazole-4-carboxylic acid (Aoc) that would result from a similarly modified Gly-Ser could not be found in the acid hydrolyzates. As a working hypothesis, we explained the mass difference of -160 Da between pro-McB17 and McB17 as a modification of eight sites ($-H_2O$, $-H_2$) to thiazole and oxazole rings as shown in Figure 1. In the following, we summarize our 2D NMR data that enabled us to define and to localize these modification sites.

A homonuclear TOCSY experiment yielded the spin systems of all amino acid residues already found in the amino acid analysis; however, one of the two suggested unmodified Ser spin systems could be assigned only in the $^{15}N-^1H$ TOCSY spectrum (Fig. 2). Most of the signals of the Gly residues were located completely overlapped within the region of $\delta = 3.8-4.0$ in the ^1H spectra. This situation did not change in a $^{13}C-^1H$ HSQC (HSQC = heteronuclear single quantum coherence) experiment, which allowed the assignment of all carbon atoms of the standard residues mentioned above. In these two experiments several additional peaks became apparent, which had to be attributed to modified residues. A NOESY spectrum yielded sequential NOEs within the terminal positions 1–4, and 40–43 and for residues adjacent to the two Asn and one Gln residue. The NOE assignments proved that one of the unmodified serine residues was in position 41. The lack of sequential NOEs from Gly^{40} to residue 39 indicated a modification site at the position of Ser^{39}. The absence of long-range contacts in this NOESY experiment (750 MHz) points to an extended structure for McB17 and renders cross linking highly unlikely. The assignment of the N-terminus was hampered by the $(Gly)_9$ segment (Fig. 1), most of the proton and carbon signals of which overlap.

The $^{13}C-^1H$ HSQC experiment revealed eight signals with characteristic heteroaromatic carbon chemical shifts. Thus it was expected, that these CH fragments are part of modification sites that have to involve not only the four Cys but also Ser residues. In a $^{13}C-^1H$ HMQC experiment optimized for long-range couplings, four of these heteroaromatic singlet signals exhibited long-range contacts to signals in the range of $\delta = 140$, four others to signals in the region of $\delta = 160$. These signals can be attributed to C4 (at $\delta = 140$) and C2 (at $\delta = 160$) in oxazole or thiazole ring systems. Signals for the expected aminomethyl backbone fragments were found as three isolated doublets as well as three overlapping signals in the 1D experiment, with characteristic ^{13}C chemical shifts of $\delta = 40$ and $\delta = 44$. Long-range $^{13}C-^1H$ contacts to signals at $\delta = 160$ proved the connection of these aminomethyl fragments to C2 carbon atoms of adjacent heterocyclic backbone fragments. The precursor sequence (Fig. 1) shows that the modification of adjacent Ser and Cys residues should not only lead to isolated monocyclic units but also to linked cyclic systems. If all the possible modification sites are count-

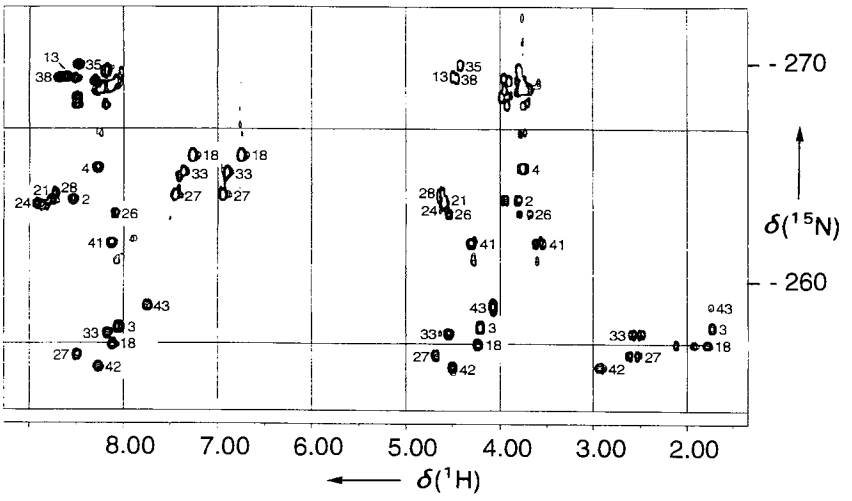

Fig. 2. $^{15}N-^1H$ HSQC–TOCSY spectrum of McB17 in [D_6]DMSO. The numbering of the residues in the mature McB17 is according to the unmodified residues in the prepeptide (Fig. 1). Gly residues are not assigned because of signal overlap. The region shown contains the signals of NH, CH_α and $CH_{\beta,\gamma}$ protons connected to the amide ^{15}N of the same spin system. The NH_2 signals of Asn and Gln appear in the spectrum at $\delta = 7.5-6.5$. The internal [D_5]DMSO (^1H, $\delta = 2.50$) signal as well as external $MeNO_2$ (^{15}N, $\delta = 0$) were used as references.

ed, six aminomethyl fragments from glycine would be expected. This is in agreement with the six partly overlapping NH–CH_2 fragments found. Thus we proved so far, that not only Gly–Cys but also Gly–Ser must be modified to aminomethyl heterocyclic backbone residues.

A direct detection of the ^{15}N signals in these heterocyclic ring systems is hampered by the low sensitivity of this nucleus. If thiazole and oxazole residues are indeed present, an inverse-detected ^{15}N–^{1}H long-range HMBC spectrum (HMBC = heteronuclear multiple bond coherence) should be able to connect the thiazole/oxazole ^{15}N through $^{3}J_{N,H}$ coupling with the C5 proton and with the methylene protons of the aminomethyl fragment in the case of isolated monocyclic residues or the aminomethylated fragment of linked cyclic systems, respectively. Figure 3 shows two regions of the long-range HMBC spectrum with signals at chemical shift positions of $\delta = -80$ and $\delta = -120$. The ^{15}N chemical shifts of these signals are characteristic for oxazoles and thiazoles.[11, 12] In both regions, four signals indicating long-range coupling between C5–H and ^{15}N were found. This finding proves that four Ser and four Cys residues are modified to oxazoles and thiazoles. In both regions, three ^{15}N signals exhibit additional long-range contacts to aminomethyl protons, which confirmed the modification of six Gly residues to aminomethyl fragments. The remaining ^{15}N signals which are not connected to aminomethyl fragments have to be part of linked ring systems, Atoc and Aotc, stemming from modified Gly-Cys-Ser and Gly-Ser-Cys segments. Thus the Aotc modification in position 13–15 can be unambiguously assigned, whereas there are two possibilities for the Atoc site. Sequential NOEs from Asn^{27} to Ser^{26} in a ^{15}N HMQC–NOESY spectrum unambiguously proved the location of Atoc at positions 28 to 30. As a further confirmation, the total synthesis of McB17 is in progress.

In summary, McB17 contains eight backbone modification sites involving three Gly-Cys, three Gly-Ser, one Gly-Ser-Cys, and one Gly-Cys-Ser segment of the precursor protein. Apart from the completely overlapping $(Gly)_9$ segment, all the standard residues as well as the modification sites could be assigned on the basis of the primary sequence of the prepeptide. A complete sequential assignment is hampered by the lack of NOEs as well as long-range contacts between the modification sites and the residues following them. The independent proof for the directly connected heteroaromatic, five-membered ring structures (Fig. 1) could only be a specific ^{13}C-labeling of Gly and/or Ser residues, which is underway.

Until now, the lantibiotics had been the only known class of ribosomally synthesized polypeptides with posttranslational modifications to unusual *side chains* such as α,β-didehydroamino acids and several cyclic sulfides.[13, 14] Here, however, for the first time posttranslational *backbone* modifications of a protein include the formation of heteroaromatic five-membered rings.

Experimental Procedure

Isolation of Microcin B17: The McB17 overproducing strain was cultivated under optimized conditions. The antibiotic remains associated to the cell envelope and is not secreted into the culture medium; we therefore harvested the bacterial cells by centrifugation. For the extraction of McB17 the cell suspension was heated in buffer containing acetic acid and EDTA (pH 4.0) at 100 °C for 10 min. After centrifugation the McB17-containing supernatant was evaporated to dryness, and the residue was dissolved in formic acid (50%). After gel chromatography to accumulate McB17 and to separate it from the low molecular mass components in the cell extract, reversed-phase HPLC on RP18 of the pooled, antibiotically active fractions yielded the antibiotic McB17 with a purity of 95%. ^{15}N-labeled McB17 was obtained from a cell culture containing $(^{15}NH_4)_2SO_4$ as the only nitrogen source in the medium.

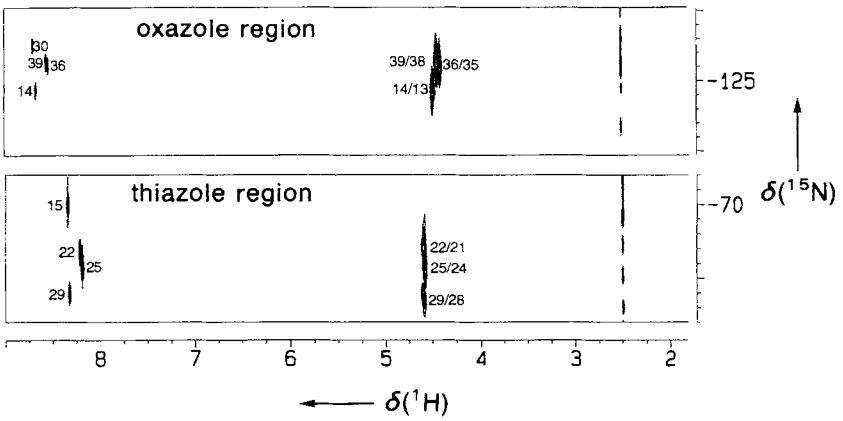

Fig. 3. ^{15}N–^{1}H HMBC spectrum of McB17 in [D_6]DMSO. The regions shown contain long-range contacts between ^{15}N (F1) and the C5 protons (F2) of the heterocyclic modification sites as well as between ^{15}N and the aminomethyl fragments. The internal [D_6]DMSO (^{1}H, $\delta = 2.50$) signal as well as external $MeNO_2$ (^{15}N, $\delta = 0$) were used as references.

NMR: 2D NMR experiments were carried out at 400 and 750 MHz on Bruker AMX spectrometers equipped with "inverse" triple resonance probes and X32 computers. All 2D experiments were recorded in the pure-phase absorption mode by using the time-proportional phase-incrementation method. NOESY experiments with mixing times of 250 ms and clean-TOCSY spectra with a MLEV17 mixing sequence of 50 ms between 2.5 ms trim pulses were recorded at 305 K. ^{13}C–^{1}H HSQC spectra and an HMQC spectrum optimized for long-range couplings ($J = 7$ Hz) were acquired with a sample at natural abundance. ^{15}N–^{1}H HSQC, HSQC-TOCSY, HMQC-NOESY, and HMQC spectra were recorded with a uniformly ^{15}N-labeled sample. Typically, 512–700 increments of 2K data points were collected with a digital resolution of 4–5 Hz in the acquisition (F2) dimension, which was set to 4800 Hz (400 MHz) and 10500 Hz (750 MHz). The ^{13}C–^{1}H HSQC and HMQC spectra were recorded with a sweep width of $\delta = 180$ in the F1 dimension. For the ^{15}N–^{1}H HSQC, HSQC-TOCSY, and HMQC-NOESY spectra, a sweep width of $\delta = 25$ was sufficient in the F1 dimension. The ^{15}N–^{1}H HMBC spectrum was recorded with a F1 sweep width of $\delta = 360$. Data processing consisted of filling up a 2K × 2K data matrix with zeros, apodization with a squared sine bell weighting function, and in the case of the NOESY experiment, linear prediction of up to 700 points in the F1 dimension.

Received: April 1, 1993 [Z 5967 IE]
German version: *Angew. Chem.* **1993**, *105*, 1410

[1] F. Baquero, F. Moreno, *FEMS Microbiol. Lett.* **1984**, *23*, 117–124.
[2] C. Asensio, J. C. Perez-Diaz, M. C. Martinez, F. Baquero, *Biochem. Biophys. Res. Commun.* **1976**, 7–14.
[3] J. L. Vizan, C. Hernandez-Chico, I. del Castillo, F. Moreno, *EMBO J.* **1991**, *10*, 467–476.
[4] P. Yorgey, J. Lee, R. Kolter in *Bactericins, Microcins and Lantibiotics* (Eds.: R. James, C. Ladzunski, F. Pattus), Springer, New York, **1992**, pp. 19–31.

[5] J. Davagnino, M. Herrero, D. Furlong, F. Moreno, R. Kolter, *Proteins* **1986**, *1*, 230–238.
[6] M. Herrero, F. Moreno, *J. Gen. Microbiol.* **1986**, *132*, 393–402.
[7] A. Bayer, S. Stevanovic, S. Freund, J. Metzger, G. Jung in *Peptides 1992* (Eds.: C. Schneider, A. Eberle), Escom, Leiden, **1993**, pp. 117–118.
[8] J. Metzger, W. Beck, G. Jung, *Angew. Chem.* **1992**, *104*, 235–237; *Angew. Chem. Int. Ed. Engl.* **1992**, *31*, 226–228.
[9] H. Frank, G. J. Nicholson, E. Bayer, *J. Chromatogr.* **1978**, *146*, 197–206.
[10] K. Wüthrich, *NMR of Proteins and Nucleic Acids*, Wiley, New York, **1986**.
[11] S. Berger, *NMR-Spektroskopie von Nichtmetallen*, Band 2, Thieme, Stuttgart, **1992**.
[12] a) U. Schmidt, R. Utz, *Angew. Chem.* **1984**, *96*, 723–724; *Angew. Chem. Int. Ed. Engl.* **1984**, *23*, 725–726; b) M. A. J. Akkermann, Dissertation, University of Nijmegen, **1992**; c) H. G. Floss, J. M. Beale, *Angew. Chem.* **1989**, *101*, 147–179; *Angew. Chem. Int. Ed. Engl.*, **1989**, *28*, 146–178.
[13] G. Jung, *Angew. Chem.* **1991**, *103*, 1067–1084; *Angew. Chem. Int. Ed. Engl.* **1991**, *30*, 1051–1068.
[14] *Nisin and Novel Lantibiotics* (Eds.: G. Jung, H.-G. Sahl), Escom, Leiden, **1991**.

Substituent Effects on the Zero-Field Splitting Parameters of Localized Triplet 1,3-Cyclopentanediyl Biradicals**

By *Waldemar Adam,* Lothar Fröhlich, Werner M. Nau, Hans-Gert Korth,* and *Reiner Sustmann**

EPR spectra of many localized triplet biradicals[1] are readily obtained in solvent matrix at 4–77 K.[2] These spectra afford the zero-field splitting parameters which may provide valuable information on the electronic structure of the biradicals.[3] In particular, the D parameter is an effective probe for the average distance r between the unpaired spins.[4] According to the dipole approximation,[5] D varies as $1/r^3$; consequently, for r of the order of 3.5 Å and with an experimental accuracy of 0.5 mT, a change by 0.01 Å in the r value should be accessible. Unfortunately, little is presently known about substituent effects on the D parameter in localized triplet biradicals[6] except that phenyl and vinyl substitution at the radical termini decrease D in conformity with π delocalization.[7]

To fill this gap, it was desirable to study electronic substituent effects on the D parameter, namely the influence of *para* substitution in bisbenzylic triplet 1,3-cyclopentanediyl biradicals like **1**. Of particular interest was to assess whether spin delocalization by *para* substituents would show up in the D parameter and whether the observed substituent effects would coincide with observations made for the spin delocalization in substituted monobenzylic radicals. As model system, we chose a series of *para*-substituted biradicals **2**, which are readily obtained by irradiation (400–320 nm) of the corresponding azo compounds **3**. Such triplet biradicals should be sufficiently persistent in a matrix at 77 K.[8] The azo precursors **3** were, in turn, obtained by cycloaddition of cyclopentadiene and substituted 4,4-dimethyl-3,5-diphenylisopyrazoles according to a multistep synthesis published for the parent compound.[9]

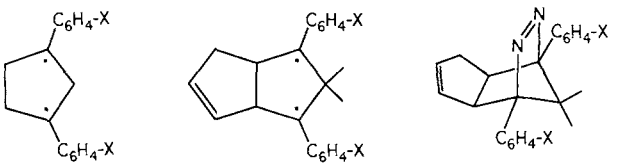

2a: X = *p*-H
2b: X = *p*-Me
2c: X = *p*-MeO
2d: X = *p*-F
2e: X = *p*-Cl
2f: X = *p*-Br
2g: X = *p*-NO_2

3

As our EPR results reveal (Table 1), symmetric *para*-phenyl substitution decreases the zero-field splitting parameter D in the order F > MeO > H ≈ Me > Br > Cl ≫ NO_2. For ease of argumentation we have defined a ΔD parameter, which gives the relative D with respect to the parent compound **2a** (Table 1); thus, negative ΔD values correspond to a larger D for the substituted derivatives. The structural similarity and the common *para* substitution suggest that steric interactions with the matrix are not responsible for the observed trends in the D parameter and even a small ΔD should be significant for assessing variations of the electronic structure through substituent effects in the biradical.

Table 1. Zero-field splitting parameters [a] of substituted biradicals **2** and radical substituent constants [b].

Compd.	X	$\lvert D/hc\rvert$ [cm^{-1}]	$10^2\,\Delta D$ [c] [cm^{-1}]	$\sigma^{\bullet}$	$\sigma^{\bullet}_{\alpha}$
2a	H	0.0504	0.00	0.00	0.000
2b	Me	0.0502	0.02	−0.02	0.015
2c	MeO	0.0509	−0.05	−0.12	0.018
2d	F	0.0521	−0.17	−0.25	−0.011
2e	Cl	0.0495	0.09	0.08	0.011
2f	Br	0.0499 [d]	0.05 [d]	0.17	–
2g	NO_2	0.0414	0.90	0.27	–

[a] In MTHF matrix at 77 K; $\lvert E/hc\rvert < 0.001\ cm^{-1}$; accuracy for $\lvert D/hc\rvert \geq 0.0002\ cm^{-1}$. [b] Values for $\sigma^{\bullet}$ and $\sigma^{\bullet}_{\alpha}$ taken from ref. [11]. [c] ΔD values are relative to **2a**. [d] The correction for the contribution of spin-orbit coupling from ref. [6] gives $D^{*} = 0.0493\ cm^{-1}$ and $10^2\,\Delta D^{*} = 0.11\ cm^{-1}$ (see text).

Spin-orbit coupling contributions to the zero-field splitting of localized biradicals are generally assumed to be negligibly small[4, 6, 10] as long as heavy atoms like bromine are absent. Hence, the D parameter should reflect the average separation (r) of the spins and the ΔD parameter its variation with substituents. The negative ΔD values for *para*-fluorine and *para*-methoxy substituents indicate an increase of spin density towards the radical sites in the biradicals **2**. The *para*-methyl group leaves the D value essentially unchanged within the experimental accuracy, whereas bromine, chlorine, and nitro substituents (**2e–g**) give rise to positive ΔD values, which suggest delocalization of spin density away from the benzylic radical termini.

Since Dougherty has proposed that the spin densities in the radical sites of a biradical are similar to those in isolated monoradicals and that there are no special delocalizing effects,[4] we have compared our ΔD values for the biradicals **2** with known data for the α spin densities of benzylic monoradicals. Five σ scales have been suggested to estimate the α spin densities or, inherently related, the chemical reactivities of substituted benzylic radicals.[11] Negative σ values indicate a larger α spin density or a higher reactivity of the benzylic position in radical reactions. Fisher's $\sigma^{\bullet}$ and Arnold's $\sigma^{\bullet}_{\alpha}$ parameters are given in Table 1 for comparison.

[*] Prof. Dr. W. Adam, L. Fröhlich, W. M. Nau, M.Sc.
Institut für Organische Chemie der Universität
Am Hubland, D-97074 Würzburg (FRG)
Telefax: Int. code + (931)888-4606
Prof. Dr. R. Sustmann, Dr. H.-G. Korth
Institut für Organische Chemie der Universität-Gesamthochschule
Universitätsstrasse 5, D-45141 Essen (FRG)

[**] The authors gratefully acknowledge the financial support by the Deutsche Forschungsgemeinschaft. W. M. N. thanks the Fonds der Chemischen Industrie for a Kekulé doctoral fellowship.

They are derived from bromination rates of substituted *meta* tolylcarbonitriles and from EPR hyperfine splitting constants of *meta*- and *para*-substituted benzyl radicals.[11]

Evidently the $\sigma^{\bullet}$ values are in better agreement with the measured ΔD values. For **2a** and **2b** ΔD and $\sigma^{\bullet}$ are quite similar, whereas for **2c** and **2d** both parameters suggest an enhanced α spin density (relative to **2a**). The latter result is at variance with Arnold's $\sigma_{\alpha}^{\bullet}$ scale which indicates a decrease in spin density for the *para*-methoxy substituent.[11] The exceptional behavior of the *para*-methoxybenzyl radical is not only suggested by the $\sigma^{\bullet}$ values, but also implied by earlier theoretical arguments[12] and further substantiated by recent reaction rates of oxygenation.[13] The larger D value for **2f** versus **2e** is attributed to a small, but significant spin-orbit coupling effect of the bromine substituents.[14] It was shown for the related series of substituted biradicals **1**[6] that two *para*-bromine atoms give rise to an increase of D by $0.0006\ cm^{-1}$. With this spin-orbit correction, a smaller D value for **2f** results ($D^* = 0.0493\ cm^{-1}$, $10^2\ \Delta D^* = 0.11\ cm^{-1}$), in accordance with Fisher's $\sigma^{\bullet}$ scale.

The better correlation of the ΔD parameters with Fisher's kinetic $\sigma^{\bullet}$ values rather than with Arnold's $\sigma_{\alpha}^{\bullet}$ values is surprising if one recalls the fact that the D and $\sigma_{\alpha}^{\bullet}$ values are obtained from EPR spectra. However, it is noteworthy that the D parameter reflects the spin densities at all positions of the spin-bearing benzylic moiety ("average spin separation"), whereas the $\sigma_{\alpha}^{\bullet}$ parameter is regarded as a measure for the spin density in the α position only. One may argue that the D parameter is a better measure for the overall electronic nature of the benzyl radical, which is a crucial feature for chemical reactivity.

The effect of *para*-nitro substitution in **2g** is substantial. Indeed, the ΔD value for *para* nitrophenyl is larger than the relative variation of D on going from phenyl to vinyl.[7] The corresponding calculated r values[5] are 3.71 ± 0.04 Å for **2a**–**2f** and 3.97 Å for **2g**.[14] These data indicate a significant change in the chemical environment for the unpaired electrons. The propensity of the nitro group (compare $\sigma^{\bullet}$) to accept electrons cannot alone account for the drastic decrease in the D parameter. In addition, the center of gravity of the spin is more displaced in the direction of the *para*-nitro substituent, since the oxygen atoms of the nitro group can accommodate spin density as well. For the other substituents, spin density is only transferred to the atom directly attached to the phenyl ring.

Whereas the examination of additional substituents and the reproduction of experimental findings by more refined[14] MO calculations remain synthetic and theoretical challenges, the set of available data already indicates novel effects, which deserve more detailed attention.[6] Even though we cannot offer an explanation for the variations of the D parameter with substituents at this point, it appears useful that the D parameters of biradicals provide the opportunity to assess electronic effects on the reactivity of simple radicals. Since such effects are typically small and quite difficult to study,[15–17] the D parameters of the substituted triplet biradicals **2** may indeed be an appealing alternative to the kinetic measurements.[11]

Received: March 30, 1993 [Z5962 IE]
German version: *Angew. Chem.* **1993**, *105*, 1383

[1] In "localized" biradicals the radical sites are not connected through a π-electron system; note that the radical sites themselves may be delocalized, for example by phenyl groups.

[2] D. A. Dougherty in *Kinetics and Spectroscopy of Carbenes and Biradicals* (Ed.: M. S. Platz), Plenum Press, New York, **1990**, p. 117.
[3] M. S. Platz in *CRC Handbook of Organic Photochemistry, Vol. 2* (Ed.: J. C. Scaiano), CRC Press, Boca Raton, FL, USA, **1989**, p. 3.
[4] D. A. Dougherty, *Acc. Chem. Res.* **1991**, *24*, 88.
[5] S. S. Eaton, K. M. More, B. M. Sawant, G. R. Eaton, *J. Am. Chem. Soc.* **1983**, *105*, 6560.
[6] Prof. D. A. Dougherty has made available to us unpublished results of similar work on triplet biradicals **1** (X = Me, MeO, Br, $PhSO_2$); see E. G. Stewart, Ph.D. Thesis, California Institute of Technology, **1992**. The conclusions drawn in this thesis are in good agreement with our results. We thank Prof. Dougherty for providing us with this valuable data.
[7] R. Jain, M. B. Sponsler, F. D. Coms, D. A. Dougherty, *J. Am. Chem. Soc.* **1988**, *110*, 1356; F. D. Coms, D. A. Dougherty, *Tetrahedron Lett.* **1988**, *29*, 3753.
[8] W. Adam, G. Reinhard, H. Platsch, J. Wirz, *J. Am. Chem. Soc.* **1990**, *112*, 4570.
[9] K. Beck, S. Hünig, *Chem. Ber.* **1987**, *120*, 47.
[10] M. Rule, A. R. Matlin, D. E. Seeger, E. F. Hilinski, D. A. Dougherty, J. A. Berson, *Tetrahedron* **1982**, *38*, 787.
[11] $\sigma^{\bullet}$: T. H. Fisher, A. W. Meierhoefer, *J. Org. Chem.* **1978**, *43*, 224; $\sigma_{\alpha}^{\bullet}$: D. R. Arnold in *Substituent Effects in Radical Chemistry* (Ed.: H. G. Viehe, Z. Janousek, R. Merényi), Reidel, Dordrecht, **1986**, p. 171; $\sigma_{j}^{\bullet}$: H. Ağirbaç, R. A. Jackson, *J. Chem. Soc. Perkin Trans. 2* **1983**, 739. $\sigma_{\zeta}^{\bullet}$: X. Creary, M. E. Mehrsheikh-Mohammadi, S. McDonald, *J. Org. Chem.* **1987**, *52*, 3254. $\sigma_{\uparrow}^{\bullet}$: X. K. Jiang, X. Y. Li, C. X. Zhao, G. Z. Ji, *Rev. Chem. Intermed.* **1986**, *7*, 195.
[12] J. W. Timberlake, M. L. Hodges, *Tetrahedron Lett.* **1970**, *48*, 4147.
[13] K. Tokumura, T. Ozaki, H. Nosaka, Y. Saigusa, M. Itoh, *J. Am. Chem. Soc.* **1991**, *113*, 4974.
[14] The r values obtained from the $1/r^3$ formula are considerably smaller than expected from MO calculations (AM1). This discrepancy is due to the approximations in the $1/r^3$ formula, which strictly applies for localized radical sites.
[15] R. Sustmann, H.-G. Korth, *Adv. Phys. Org. Chem.* **1990**, *26*, 131.
[16] T. H. Fisher, S. M. Dershem, M. L. Prewitt, *J. Org. Chem.* **1990**, *55*, 1040.
[17] *Substituent Effects in Radical Chemistry* (Ed.: H. G. Viehe, Z. Janousek, R. Merényi), Reidel, Dordrecht, **1986**.

Dicyanopolyynes: Formation of New Rod-Shaped Molecules in a Carbon Plasma**

By *Thomas Grösser* and *Andreas Hirsch**

Fullerenes can be obtained in preparative amounts by the vaporization of graphite in a helium atmosphere.[1] The replacement of carbon atoms by heteroatoms in the spherical structure of these fascinating molecules presents a great synthetic challenge. Calculations carried out by us to determine the heat of formation of azafullerenes[2] revealed cyanogen $(CN)_2$ to be a very promising molecule for the insertion of nitrogen atoms into the fullerene framework due to its thermodynamic properties and reactivity in a plasma.[3] This gave us reason to investigate experimentally the interaction of carbon vapor with $(CN)_2$. To this end, we vaporized graphite under Krätschmer–Huffman conditions in the presence of $(CN)_2$. Under the chosen conditions, a homologous series of dicyanopolyynes was obtained as the main product.

The reaction was carried out in a simple fullerene reactor[4] modified specifically for the present purpose (Fig. 1). The lemon-yellow colored toluene extract of the reaction products consisted of several components but did not include any of the usual fullerenes (HPLC). The major portion contained five components, which were eluted together as the first fraction on a silica gel column (toluene/hexane, 80:20). The following products have been synthesized for the

[*] Dr. A. Hirsch, Dipl.-Chem. T. Grösser
Institut für Organische Chemie der Universität
Auf der Morgenstelle 18, D-72076 Tübingen (FRG)
Telefax: Int. code + (7071)29-5244

[**] This work was supported by the Deutsche Forschungsgemeinschaft.

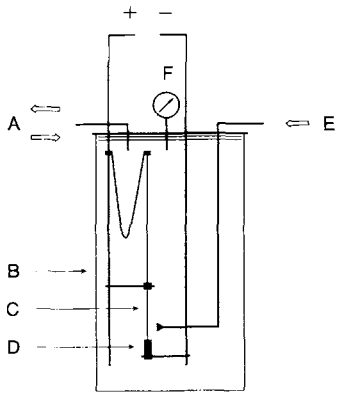

Fig. 1. Schematic diagram of the reactor used for the vaporization of graphite in the presence of $(CN)_2$ or Cl_2. Helium supply and connection to vacuum system (A), pyrex bell jar (B), graphite rod (3 mm) (C), graphite block (10 mm) (D), gas inlet tube for $(CN)_2$ or Cl_2 (E), manometer (F).

first time: $D_{\infty h}$-symmetrical dicyanopolyynes C_8N_2 **1**, $C_{10}N_2$ **2**, $C_{12}N_2$ **3**, $C_{14}N_2$ **4**, and $C_{16}N_2$ **5**.[5] The subsequent fractions have not yet been identified. The polyyne fraction consisted of up to approximately 55% **1** and 35% **2**; the higher homologues **3**–**5** formed less than 10% of the total (HPLC).

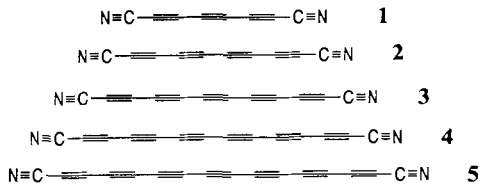

Compound **1** was obtained with a purity of 98.8% (GC) by sublimation from the remaining dicyanopolyynes, allowing complete characterization.[6] The compound forms colorless crystals, which are very soluble in toluene and chloroform but only sparingly in hexane. In the solid state, compound **1** decomposes gradually at room temperature and turns black. However, in the absence of light and moisture, dilute solutions of **1** may be stored at −18 °C without change. Compound **1** is very electrophilic; its cyclic voltammogram shows an irreversible reduction at −0.56 V (vs. Ag/AgCl) accompanied by the deposition of a black conducting film on the electrode.

Investigations by mass spectrometry have shown that the formation of the polyynes $H\text{-}(C{\equiv}C)_n\text{-}H$ occurs to a considerable extent during laser vaporization of graphite in the presence of H_2,[7] and that small amounts of dicyanopolyynes form in the presence of N_2.[7a] This is explained[7a] by the addition of H or N atoms to the ends of C_n chain species, which are considered as early intermediate products in the formation of fullerenes.[8] In addition to polyynes, monocyclic compounds and polycyclic aromatic hydrocarbons have also been detected as capture products.[7] Similar products as well as fullerenes have also been found in acetylene–oxygen flames.[9] The preferential formation of chain or cyclic products depends largely on the reaction conditions such as partial pressure of H_2,[7a] where the capture reaction takes place, and the C:O ratio.[9] The temperatures prevailing in the hot reaction zone during graphite vaporization by the Krätschmer–Huffman process are sufficiently high (6000 °C) for the formation of radicals such as CN or NCN from cyanogen to be expected.[10] If the dicyanopolyynes isolated here are to be viewed as terminal capture products arising from intermediate chains formed from carbon atoms,[11] then two alternative mechanisms of formation must be considered. One possibility is that the dicyanopolyynes could originate from subsequent reactions of other, initially formed intermediates. On the other hand, it is known that low concentrations of dicyanopolyynes up to C_8N_2 are formed in cyanogen–oxygen flames.[10] It is unlikely that the dicyanopolyynes isolated here are formed exclusively from the reactant cyanogen for the following reasons: 1) The observed intensity ratio of the mass lines corresponding to the compounds C_2N_2, C_4N_2, C_6N_2, and C_8N_2 produced in cyanogen–oxygen flames is 1000:100:9.5:0.5.[10] Our total yield of dicyanopolyynes **1**–**5**[12] is at least 50% relative to the cyanogen used and thus lies at least three orders of magnitude higher. 2) The formation of fullerenes is drastically reduced even at low cyanogen concentrations and is completely suppressed with gas mixtures having compositions below a set $(CN)_2$:He ratio of 4:6. 3) No further increase in the yield of **1**–**5** was observed when the $(CN)_2$ partial pressure was increased or when the reaction was conducted under flow conditions. The maximum yield amounts to 5% of the vaporized graphite and corresponds approximately to that obtained for fullerenes (8%) when a pure He atmosphere was used.

In order to show beyond doubt that reaction products can be formed from the C plasma and other gases, the same experiments were carried out with Cl_2. The toluene extract of the products still contained a small amount of fullerenes (<5%), but the main components that could be isolated by preparative HPLC and completely characterized were hexachlorobenzene (**6**) (60%) and perchloroacenaphthylene (**7**) (9%).[13] In addition, further perchlorinated compounds were present (in total 17%), which absorbed at longer wavelengths in the UV/VIS spectrum (up to 480 nm), and whose masses[14] matched those of perchlorinated polycondensed arenes such as decachlorocoroannulene (**8**). The carbon

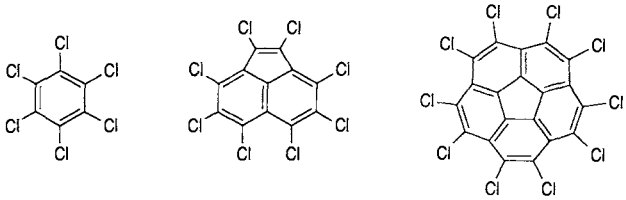

6 **7** **8**

frameworks of these compounds are sections of the C_{60} structure, in which the occurence of five-membered rings necessary for the formation of fullerene is particularly noteworthy. In the cyanogen experiments no cyclic compounds were formed, whereas in the chlorine capture reaction no rod-shaped reaction products could be detected. This indicates that the interactions with the C plasma are different.

The extension of the Krätschmer–Huffman process to incorporate the use of suitable foreign gases allows access to new and interesting classes of compounds. The dicyanopolyynes synthesized here for the first time are rod-shaped molecules with the highest possible number of π electrons. Linear polyynes can be produced by traditional methods but only in multistep syntheses[15] and are considered interesting precursors of carbyne and other hypothetical carbon modifications.[16] Analogous polyynes such as HC_nN ($n = 1, 3, 5, 7$)

have been detected by Kroto et al. as molecules in interstellar space.[17] The formation of cyclic perchlorinated compounds such as **6**–**8** provides new and valuable clues to the formation of fullerenes. The isolation and characterization of capture products within the C plasma, such as the hitherto unknown **8** and components seen preferentially at low $(CN)_2$ concentrations, are the subject of further investigations.

Experimental Procedure

The fullerene reactor used was modified for the admission of $(CN)_2$ or Cl_2 by the addition of a gas inlet tube with a flat nozzle (Fig. 1). After it was synthesized [18], cyanogen was condensed in an autoclave, the outlet of which (needle valve) was connected to the gas inlet tube of the reactor. The following operating conditions were used: a voltage of 30 V DC, a current of 40 A, and a reactor pressure of 140 mbar He. After ignition of the electric arc, $(CN)_2$ or Cl_2 was fed into the reactor. The supply was quantitatively regulated so that the pressure in the reaction vessel remained constant. The cool surfaces of the reactor interior became coated with a yellow film in addition to soot. After completion of the reaction, the crude product was extracted with toluene. In each case the yield corresponded to 6–7% of the vaporized graphite.

Received: March 30, 1993
Revised version: June 4, 1993 [Z 5961 IE]
German version: *Angew. Chem.* **1993**, *105*, 1390

[1] W. Krätschmer, L. Lamb, K. Fostiropoulos, D. R. Huffman, *Nature* **1990**, *347*, 354.
[2] H. R. Karfunkel, T. Dressler, A. Hirsch, *J. Comput. Aided. Mol. Des.* **1992**, *6*, 521.
[3] H. W. Roesky, H. Hofmann, *Chem. Ztg.* **1984**, *108*, 231.
[4] A. Koch, K. C. Khemani, F. Wudl, *J. Org. Chem.* **1991**, *56*, 4543.
[5] MS (FD): *m/z* 124 (C_8N_2 (**1**)), 148 ($C_{10}N_2$ (**2**)), 172 ($C_{12}N_2$ (**3**)), 196 ($C_{14}N_2$ (**4**)), 220 ($C_{16}N_2$ (**5**)); UV/VIS (*n*-hexane): λ_{max}[nm] = 215, 225, 236, 248 (sh), 261, 284, 306, 322, 327, 338, 344, 363, 371, 399, 408; FT-IR (KBr): ν[cm^{-1}] = 2245 (sh, CN), 2237 (C≡N), 2187 (C≡C), 2120 (C≡C); ^{13}C NMR (62.9 MHz, $CDCl_3$, 25 °C, TMS): δ = 104.28, 104.10, 66.21, 65.64, 64.56, 63.27, 61.92, 51.99, 51.19 (quart. C atoms, spin-echo, coupled spectrum).
[6] Spectroscopic data for C_8N_2 **1**: UV/VIS (*n*-hexane): λ_{max} [nm] = 206 (sh), 215, 225, 236, 248 (sh), 261; FT-IR (NaCl): ν[cm^{-1}] = 2247 (C≡N), 2187 (C≡C), 2120 (C≡C); MS (FD) *m/z* 124 ($M^{\oplus}$, 100%); ^{13}C NMR (62.9 MHz, $CDCl_3$, 25 °C, TMS): δ = 104.10, 65.64, 63.27, 51.99.
[7] a) J. R. Heath, Q. Zhang, S. C. O'Brien, R. F. Curl, H. W. Kroto, R. E. Smalley, *J. Am. Chem. Soc.* **1987**, *109*, 359; b) A. A. Rohlfing, *J. Chem. Phys.* **1990**, *93*, 7851; c) M. Broyer, A. Goeres, M. Pellarin, E. Sedlmayer, J. L. Vialle, L. Wöste, *Chem. Phys. Lett.* **1992**, *198*, 128.
[8] a) A. Goeres, E. Sedlmayr, *Chem. Phys. Lett.* **1991**, *184*, 310; b) J. R. Chelikowsky, *Phys. Rev. Lett.* **1991**, *67*, 2970; c) C. Z. Wang, C. H. Xu, C. T. Chan, K. M. Ho, *J. Phys. Chem.* **1992**, *96*, 3563; d) J. R. Chelikowsky, *Phys. Rev. B.* **1992**, *45*, 12062; e) R. Kerner, K. A. Penson, K. H. Bennemann, *Europhys. Lett.* **1992**, *19*(5), 363.
[9] P. Gerhardt, K. H. Homann, *J. Phys. Chem.* **1990**, *94*, 5381.
[10] R. A. Albers, K. H. Homann, *Z. Phys. Chem. (Munich)* **1968**, *58*, 220.
[11] a) C. S. Yannoni, P. P. Bernier, D. S. Bethune, G. Meijer, J. R. Salem, *J. Am. Chem. Soc.* **1991**, *113*, 3190; b) J. M. Hawkins, A. Meyer, S. Loren, R. Nunlist, *J. Am. Chem. Soc.* **1991**, *113*, 9394; c) T. W. Ebbesen, J. Tabuchi, K. Tanigaki, *Chem. Phys. Lett.* **1992**, *191*, 336.
[12] The exact determination of the yield is difficult, since the dicyanopolyynes are transformed into a black voluminous soot within a split-second by the effect of pressure or upon heating. The yields given should be interpreted as a lower limit. It has also been shown that polyynes decompose into primary soot even in the solid state.
[13] W. Mack, *Tetrahedron Lett.* **1966**, *25*, 2875.
[14] The peaks in the mass spectra (FD, EI) of the fraction containing the higher capture products are attributed to $C_{14}Cl_8$, $C_{16}Cl_{10}$, $C_{20}Cl_{10}$ and show the isotopic pattern corresponding to the degree of chlorination.
[15] a) R. Eastmond, T. R. Johnson, D. R. M. Walton, *Tetrahedron* **1972**, *28*, 4601; b) R. Eastmond, D. R. M. Walton, *ibid.* **1972**, *28*, 4591; c) T. R. Johnson, D. R. M. Walton, *ibid.* **1972**, *28*, 5221.
[16] F. Diederich, Y. Rubin, *Angew. Chem.* **1992**, *104*, 1123; *Angew. Chem. Int. Ed. Engl.* **1992**, *31*, 1101.
[17] J. P. Hare, H. W. Kroto, *Acc. Chem. Res.* **1992**, *25*, 106.
[18] D. J. Park, A. G. Stern, R. L. Willer, *Synth. Commun.* **1990**, *20*, 2901.

Continuous Catalytic Synthesis of *N*-Acetyllactosamine**

By *Guido F. Herrmann, Udo Kragl,* and *Christian Wandrey**

Oligosaccharides are attracting much interest in immunological and pharmacological research because of their significance as fundamental structures of glycoproteins and glycolipids.[1] As well as the chemical syntheses of O-glycosides, syntheses employing enzymes have been established for a decade.[2] Access to large quantities of target compounds by means of both methods has been very limited.[3] The use of enzymes, in homogeneous solution, for reactions in an enzyme membrane reactor has proved to be a valuable tool in organic synthesis.[4] The enzyme-catalyzed synthesis of *N*-acetylneuraminic acid in an enzyme membrane reactor showed that large quantities of this compound could be produced in this way.[5]

We report here the enzyme-catalyzed continuous synthesis of *N*-acetyllactosamine (**3**, LacNAc) in an enzyme membrane reactor. Like *N*-acetylneuraminic acid, **3** is a structural component of many biologically active oligosaccharides.[1] Alongside the chemical syntheses of **3**[6] and as a part of higher oligosaccharides,[7] several authors used a galactosyltransferase (E.C. 2.4.1.38)[8] for the synthesis of **3**. The hitherto limited availability of this enzyme, its high price,[9] and its instability hampered its use. An alternative biocatalyst is a β-galactosidase (E.C. 3.2.1.23),[10] in particular the use of the β-galactosidase from *Bacillus circulans* resulted in high regioisomeric purity of the synthesized **3**.[10a]

Figure 1 shows the reaction scheme of the continuous synthesis described here. Starting with lactose **1**, transgalactosylation results in the transfer of the galactose moiety of **1** to *N*-acetylglucosamine **2** to afford **3** (Fig. 1a).

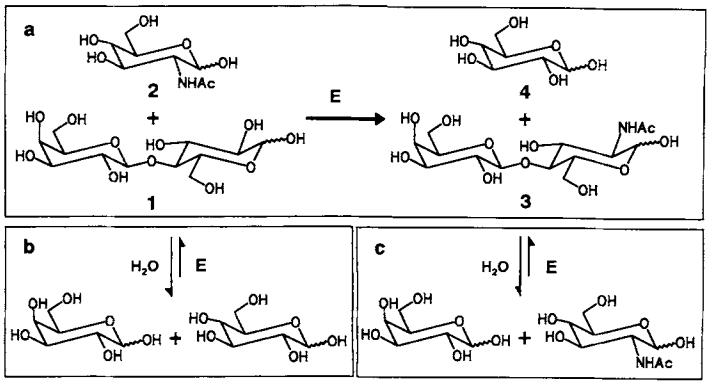

Fig. 1. Enzyme-catalyzed synthesis of *N*-acetyllactosamine **3**; the enzyme E is β-galactosidase a) Transgalactosylation, b) hydrolysis of **1** (side reaction), c) hydrolysis of the product (secondary hydrolysis).

The galactosyl donor **1** is hydrolyzed to galactose and glucose in a side reaction (Fig. 1 b). The desired product **3** is also a substrate for the β-galactosidase and is hydrolyzed

[*] Prof. Dr. C. Wandrey, G. F. Herrmann, Dr. U. Kragl
Forschungszentrum Jülich, Institut für Biotechnologie
D-52425 Jülich (FRG)
Telefax: Int. code +(2461)61-3870

[**] We would like to thank the company Daiwa Kasei K. K., Osaka (Japan) for supplying β-galactosidase.

again in a subsequent reaction by the enzyme (secondary hydrolysis, Fig. 1c).

Experiments to investigate the stability of the enzyme showed that the β-galactosidase is a very stable enzyme,[11] and because of its low price and availability, it is a useful enzyme for synthesis.[12] The ratio of transgalactosylation to hydrolysis of **1**, that is, the selectivity[13] of the enzymatic reaction, could be optimized for the continuous process by changing the concentration ratio of **1** and **2**.

By selecting a suitable residence time τ for the reaction mixture in the reactor, the secondary hydrolysis of compound **3** could be minimized. Figure 2 shows the concentration-time curve for this continuous enzyme-catalyzed synthesis of **3** in an enzyme membrane reactor over 100 hours.

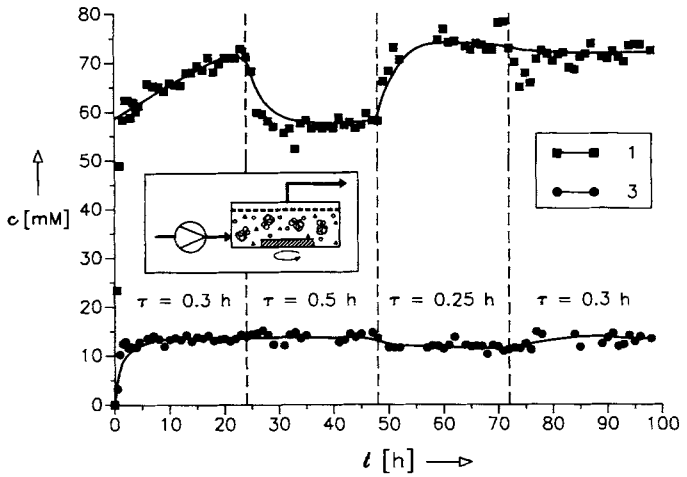

Fig. 2. Concentration-time curve for the continuous synthesis of *N*-acetyllactosamine **3** in an enzyme membrane reactor; starting concentrations: 120 mM lactose **1**, 300 mM *N*-acetylglucosamine **2**, 100 mM KH_2PO_4, 2 mM $MgCl_2 \cdot 6H_2O$, 5 mM dithiothreitol; pH 6.8; 25 °C; 3 mg mL^{-1} β-galactosidase; residence time: $\tau = 0.25$ h to $\tau = 0.5$ h.

During the course of the reaction there was no noticeable deactivation of the enzyme. The residence time was varied between $\tau = 0.25$ h and $\tau = 0.5$ h. With increasing residence time the concentration and therefore also the yield of **3** increased slightly.[14] The conversion of **1** increased from 0.37 to 0.51. The selectivity decreased with increasing conversion from 0.26 ($\tau = 0.25$ h) to 0.22 ($\tau = 0.5$ h). The space-time yield was 442 g L^{-1} d^{-1} at a residence time of $\tau = 0.25$ h and decreased to 261 g L^{-1} d^{-1} at a residence time of $\tau = 0.5$ h. After 100 h, 11.3 g of **3** was produced. The space-time yield was increased by a factor of 130 relative to the synthesis of **3** by using galactosyltransferase by Wong et al.[8a] Since reactions in a membrane reactor can be scaled up linearly,[4, 15] this method opens up an economic and a simple way of producing large amounts of **3**.[16] The process described here is the first continuous synthesis of a disaccharide that employs homogeneous catalysis. As a result of the broad spectrum of substrates for β-galactosidase from *B. ciruculans*,[17] the synthesis of derivatives of **3** with this advantageous technique is also possible.

Experimental Procedure

The enzyme membrane reactor (volume 10 mL; Bioengineering, Wald, Switzerland) fitted with an ultrafiltration membrane (YM-3, Amicon, Witten) preceded by a sterile filter (0.2 μm, Sartorius, Göttingen) was sterilized in an autoclave for 0.3 h at 120 °C (the experimental procedure corresponds to that described in [4] and [5]). Subsequently, bovine serum albumin (10 mg) and β-galactosidase (30 mg, 150 units) from *Bacillus circulans* (Daiwa Kasei K. K., Osaka, Japan) were fed into the reactor using buffer solution (100 mM KH_2PO_4, 2 mM $MgCl_2 \cdot 6H_2O$, 5 mM dithiothreitol, pH 6.8). A sterile solution (2.6 L) of the substrates (120 mM lactose **1**, 300 mM *N*-acetylglucosamine **2** in buffer solution) was then pumped through the reactor with residence times between $\tau = 0.25$ h and 0.5 h. Samples were taken regularly from the reactor outlet and analyzed by chromatography (HPLC: column ET 250/8/4 Nucleosil 5 NH_2 (Macherey-Nagel, Düren), 250 mm × 4 mm; eluent 75/25 (v/v) acetonitrile/water; flow-rate 1 mL min^{-1}; RI detection; capacity factors k': *N*-acetylglucosamine 0.84, galactose 1.26, **3** 2.09, lactose 3.09). To isolate the product **3**, the solution (containing 11.3 g of **3**) was concentrated to 0.68 L. The product was characterized by chromatography of a small portion of the solution (0.02 L) on 2/1 (w/w) activated charcoal (Darco, 20-40 mesh)/celite AFA (38 cm × 3.5 cm, eluent: H_2O with 0%-10% (v/v) ethanol, 0.5 bar). The fractions of **3** were collected and lyophilized. Yield 0.19 g. Analysis by gas chromatography (column: OV1 (Machery-Nagel, Düren); 25 m × 0.25 mm; He; temperature 275 °C, silylation according to [18] showed 4.7% *N*-acetylallolactosamine (Galβ(1,6)GlcNAc) as a by-product. Capacity factors k': **3** 5.00/5.35, allo-**3** 3.65/4.24. Correct elemental analysis.

$[\alpha]_{20.5\,°C}^{D} = 25.38$ ($c = 0.1$ in H_2O). The ^{1}H NMR spectrum (500 MHz, D_2O, internal standard [D$_4$]DSS (DSS = 3-trimethylsilyl-1-propanesulfonic acid), $\delta = 2.04$ (3 H, s, NHAc, GlcNAc), 4.47 (1 H, d, $J_{1,2} = 7.5$ Hz, HI, Gal), 5.2 (1 H, s, H1, GlcNAc)) and the 50 MHz ^{13}C NMR spectrum for **3** are consistent with published values [8a, 10d].

Received: April 14, 1993 [Z 5946 IE]
German version: *Angew. Chem.* **1993**, *105*, 1399

[1] a) L. A. Lasky, *Science* **1992**, *258*, 964-969; b) A. Kobata, *Eur. J. Biochem.* **1992**, *209*, 483-501; c) T. Feizi, *Nature* **1985**, *314*, 53-57.
[2] a) Y. Ichikawa, G. C. Look, C.-H. Wong, *Anal. Biochem.* **1992**, *202*, 215-238, and references therein; b) H. Waldmann, *Nachr. Chem. Tech. Lab.* **1992**, *40*, 828-834, and references therein.
[3] S. Bormann, *Chem. Eng. News* **1992**, *70* (49), 25-28.
[4] a) U. Kragl, D. Vasic-Racki, C. Wandrey, *Chem. Ing. Tech.* **1992**, *64* (6), 499-509, and references therein; b) G. Herrmann, A. Schwarz, C. Wandrey, M.-R. Kula, G. Knaup, K. H. Drauz, H. Berndt, *Biotechnol. Appl. Biochem.* **1991**, *13*, 346-353.
[5] U. Kragl, D. Gygax, O. Ghisalba, C. Wandrey, *Angew. Chem.* **1991**, *103*, 854-855; *Angew. Chem. Int. Ed. Engl.* **1991**, *30*, 827-828.
[6] a) R. Kuhn, W. Kirschenloher, *Liebigs Ann. Chem.* **1956**, *600*, 135-143; b) E. Lattová, L. Petrus, *Carbohydr. Res.* **1992**, *235*, 289-293.
[7] a) A. Kameyama, H. Ishida, M. Kiso, A. Hasegawa, *Carbohydr. Res.* **1991**, 209, c1-c4; b) K. C. Nicolaou, C. W. Hummel, Y. Iwabuchi, *J. Am. Chem. Soc.* **1992**, *114*, 3126-3128; c) A. Toepfer, R. R. Schmidt, *Tetrahedron Lett.* **1992**, *33*, 5161-5164; d) Y. Matsuzaki, Y. Ito, Y. Nakahara, T. Ogawa, *ibid.* **1993**, *34*, 1061-1064.
[8] a) C.-H. Wong, S. L. Haynie, G. M. Whitesides, *J. Org. Chem.* **1982**, *47*, 5416-5418; b) H. Yuasa, O. Hindsgaul, M. M. Palcic, *J. Am. Chem. Soc.* **1992**, *114*, 5891-5892; c) J. Thiem, T. Wiemann, *Angew. Chem.* **1990**, *102*, 78-80; *Angew. Chem. Int. Ed. Engl.* **1990**, *29*, 827-828.
[9] 25 units of the galactosyltransferase from bovine milk is available for $ 637 (Sigma Chemie).
[10] a) K. Sakai, R. Katsumi, H. Ohi, T. Usui, Y. Ishido, *J. Carbohydr. Chem.* **1992**, *11*, 553-565; b) L. Hedbys, E. Johansson, K. Mosbach, P.-O. Larsson, A. Gunnarsson, S. Svensson, H. Lönn, *Glycoconjugate J.* **1989**, *6*, 161-168; c) F. Zilliken, P. N. Smith, C. S. Rose, P. György, *J. Biol. Chem.* **1955**, *217*, 79-82; d) K. Ajisaka, H. Fujimoto, H. Nishida, *Carbohydr. Res.* **1988**, *180*, 35-42; e) K. G. I. Nilsson, *Trends Biotechnol.* **1988**, *6*, 256-264, and references cited therein.
[11] Half-life of the enzyme: $t_{1/2} = 262$ h at pH 7 and 22 °C (McIlvaine buffer, 5 mM dithiothreitol, 2 mM $MgCl_2 \cdot 6H_2O$).
[12] β-galactosidase from *B. circulans* is available for $ 350 per kg (5×10^6 units) (Daiwa Kasei, Osaka Japan).
[13] Selectivity is defined as the quotient of product concentration (LacNAc **3**) and concentration of converted substrate (lactose **1**).
[14] At $\tau = 0.5$ h the concentration of **3** is 5.4 g L^{-1} (13.85 mmol L^{-1}). This corresponds to a yield of 11.5%. Concentration of allo-LacNAc is 0.25 g L^{-1}.
[15] A 0.2 L enzyme membrane reactor was used to produce 3.5 kg *N*-acetylneuraminic acid (unpublished results).
[16] 1 g β-galactosidase from *B. circulans* affords 376 g of **3** by the technique described here.
[17] G. F. Herrmann, Y. Ichikawa, C. Wandrey, F. C. A. Gaeta, J. C. Paulson, C.-H. Wong, *Tetrahedron Lett.* **1993**, *34*, 3091-3094.
[18] C. C. Sweeley, R. Bentley, W. W. Wels, *J. Am. Chem. Soc.* **1963**, 85, 2497-2507.

Carbenes in Constrained Systems I: 1,3 C–H Insertion Reaction of Adamantylidene within the β-Cyclodextrin Cavity**

By *Udo H. Brinker,* Rüdiger Buchkremer, Margaret Kolodziejczyk, René Kupfer, Murray Rosenberg, Mark D. Poliks, Mario Orlando*, and *Michael L. Gross*

Dedicated to Professor Emanuel Vogel on the occasion of his 65th birthday

The chemistry of reactive intermediates (guests) within the confined spaces of another species (host) presents interesting opportunities for the discovery of new reactions.[1] The reactive behavior of carbenes in constrained systems is expected to be very different from that of free carbenes in solution or in the gas phase. The "tight fit" between the structures of hosts and the guest carbenes should alter both inter- and intramolecular reactions. Furthermore, suitable cavity sizes will restrict the mobility of the entrapped carbenes, which are then anticipated to react more selectively.

Carbene chemistry in different media has been studied extensively over the past decades.[2] Nearly nothing, however, is known about carbenes generated in constrained systems. Although α- and β-cyclodextrin (CD) have been the only molecules employed as hosts,[3] the intermediacy of carbenes or the corresponding carbenoids has not been firmly established.[3]

The relatively stable[4] diazirine **1** derived from adamantane[5] was chosen as the guest-carbene precursor and β-CD as the molecular reaction vessel (see Scheme 1). Compound **1** was prepared according to the literature,[6] purified by column chromatography (silica gel) under the exclusion of light, and shown to be pure by ^{1}H NMR spectroscopy. The β-CD complex of **1** (**1** · β-CD) was synthesized (ratio of host: guest ca. 3:1) and characterized. To avoid the replacement of entrapped guest molecules in the β-CD cavity by solvent molecules, solid-state NMR spectroscopy was used for the characterization. Cross polarization/magic angle spinning (CP/MAS) ^{13}C NMR spectra provide convincing evidence that an inclusion complex was formed.[7] This is further supported by powder X-ray diffraction spectra of **1**, β-CD, **1** · β-CD, and a physical mixture of **1** and β-CD. Under the conditions of fast atom bombardment (FAB) mass spectrometry, however, the loosely bound complex does not survive, and only the $(M - H)^-$ peak of β-CD is observed.[8]

In addition, molecular modeling was used to gain information about the fit and possible position of **1** within the CD cavity.[9] According to calculations carried out by using the SYBYL force field with default parameters, **1** is nearly completely submerged into the β-CD cavity with the diazirine function at the wider rim of the truncated cone.

Photolysis (Hanovia 400 W) of the solid inclusion complex of **1** · β-CD (Scheme 1) yielded the intramolecular carbene insertion product, 2,4-didehydroadamantane, as **3** · β-CD, and 2-adamantanone azine · β-CD[10] in a ratio of about 35:65.[11] Both products were identified by comparison of the NMR spectra with those of β-CD complexes of 2-adamantanone azine and 2,4-didehydroadamantane, synthesized by independent routes. When a physical mixture of β-CD and **1** was photolyzed, only about 1% of 2,4-didehydroadamantane **3** was formed! Furthermore, photolysis of **1** in the solid state leads to no detectable **3**.

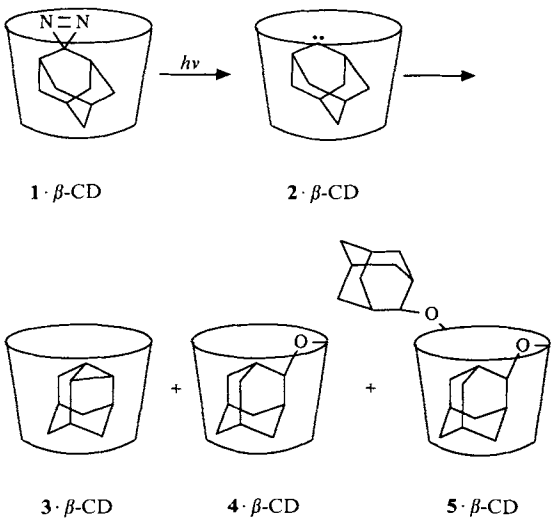

1 · β-CD **2** · β-CD **3** · β-CD **4** · β-CD **5** · β-CD

Scheme 1. All guest molecules might be positioned differently within and outside the β-CD cavity. Insertion reactions of the carbene might have taken place into the secondary or primary hydroxyl groups at the wider and narrower rims, respectively, of the β-CD molecules.

Our results contrast strongly with the product distribution of the photolysis of **1** in hydrocarbon solvents, in which the carbene insertion product is not[12] (or only in traces) formed (0.2% in heptane[13]). In the photolysis in solution the formation of azine (76–85%) and adamantanone clearly dominates.[12]

Why is **3** · β-CD, the 1,3 C-H insertion product of **2** · β-CD, formed in yields as high as approximately 30% in the solid state, whereas yields of 0.2% or less are obtained by the photolysis in solution? β-CD complexation has dramatically altered the reactivity of adamantylidene; the intramolecular 1,3 C-H insertion reaction is now more likely by a factor of 150.

In the clean CP/MAS ^{13}C NMR spectrum of the product mixture, all signals of 2,4-didehydroadamantane and most of those of the azine can be assigned directly. No clear indication of the formation of products resulting from insertion of adamantylidene into the O–H bonds of β-CD, however, could be found. According to FAB and tandem mass spectrometry, however, adamantylidene inserts into one of the 21 O–H bonds of β-CD[14] to make a covalently bound host-guest complex with an $(M - H)^-$ ion of m/z 1267. Proof was obtained by treating a sample with D_2O to exchange the number of active hydrogen atoms left,[14] and by collisionally activating the m/z 1267 ion; no loss of 2,4-didehydroadamantane could be detected. A low abundance ion of m/z 1401.5 was also observed in the FAB mass spectra; it is probably due to a β-CD with *two* $C_{10}H_{14}$ moieties attached. This is confirmed by the fact that only 19 hydrogen atoms

[*] Prof. U. H. Brinker, Dr. R. Buchkremer, M. Kolodziejczyk, Dipl.-Chem. R. Kupfer, M. Rosenberg
Department of Chemistry
State University of New York at Binghamton
Binghamton, NY 13902-6000 (USA)
Telefax: Int. code + (607)777-4478
Dr. M. D. Poliks
IBM Corporation
1701 North Street, Endicott, NY 13760 (USA)
Dr. M. Orlando, Prof. M. L. Gross
Department of Chemistry, University of Nebraska
Lincoln, NE 68588-0304 (USA)

[**] Carbene Rearrangements, Part 41. We thank the American Maize-Products Company, Hammond, Indiana, for providing the cyclodextrins used in this study. Part 40: L. Xu, G. Lin, F. Tao, U. H. Brinker, *Acta Chem. Scand.*, **1992**, *46*, 650.

can be exchanged with D_2O. Thus, two insertions of two adamantylidenes into two different O–H bonds of β-CD have taken place. The absolute amount of OH insertion products **4** · β-CD and **5** · β-CD detected by FAB mass spectrometry (Scheme 1) is not yet known. Since these compounds could not be found by CP/MAS ^{13}C NMR spectroscopy, they must have been formed each in less than 5% yield.

Adamantylidene is believed to be a ground-state singlet carbene, and the generation of the triplet state fails even in the presence of photosensitizers.[15] The question of whether adamantylidene entrapped in β-CD is also a singlet cannot be answered at this time. Laser flash photolysis studies may solve this problem, as well as answer questions concerned with the detailed differences in the reactive behavior of a "free" adamantanylidene and a (partially) entrapped one.

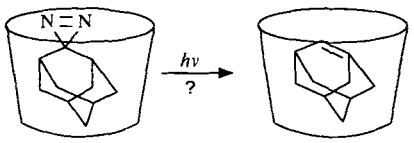

1 · β-CD **6** · β-CD

If the carbene **2** · β-CD cannot easily encounter another reaction partner, it could rearrange to the highly strained adamantene **6**, which is known to dimerize[16] immediately, although it has been shown to exist in a matrix at low temperature.[17] This reaction, however, does not appear to take place if adamantylidene **2** is entrapped in β-CD.[18]

In conclusion, our results strongly suggest that we have established the first intra- and intermolecular carbene insertions within any constrained molecular reaction vessel.

Experimental Procedure

1 · β-CD: A solution of **1** (0.49 g, 3 mmol) in diethyl ether (12 mL) was added to a solution of β-CD hydrate (3.4 g, 3 mmol) in water (150 mL). After the mixture had been stirred for one day, the precipitate was filtered off, washed several times with water and ether, and then dried in the desiccator. Yield: 2.9 g (2.4 mmol, 81%).

Received: March 17, 1993
Revised: April 30, 1993 [Z 5933 IE]
German version: *Angew. Chem.* **1993**, *105*, 1427

[1] *Photochemistry in Organized and Constrained Media* (Ed.: V. Ramamurthy), VCH, Weinheim, **1991**.
[2] a) W. Kirmse, *Carbene Chemistry*, Academic Press, New York, **1971**; b) *Carbenes, vols. 1–3* (Eds.: M. Jones, Jr., R. A. Moss), Wiley, New York, **1973**, **1975**, **1978**; c) W. M. Jones, U. H. Brinker in *Pericyclic Reactions* (Eds.: A. P. Marchand, R. E. Lehr), Academic Press, New York, **1977**; d) *Methoden Org. Chem. (Houben-Weyl) 4th ed. 1952–*, vol. E19, **1989**.
[3] a) M. Komiyama, H. Hirai, *Bull. Chem. Soc. Jpn.* **1981**, *54*, 2053; b) *J. Am. Chem. Soc.* **1983**, *105*, 2018; c) C. J. Abelt, J. M. Pleier, *J. Org. Chem.* **1988**, *53*, 2159.
[4] Since **1** sublimes easily, it should be kept in the freezer.
[5] a) E. Schmitz, *Dreiringe mit zwei Heteroatomen*, Springer, Berlin, **1967**; b) *Chemistry of Diazirines, vols. I, II* (Ed.: M. T. H. Liu), CRC Press, Boca Raton, FL, USA, **1987**.
[6] S. D. Isaev, A. G. Yurchenko, F. N. Stepanov, G. G. Kolyada, S. S. Novikov, N. F. Karpenko, *Zh. Org. Khim.* **1973**, *9*, 724.
[7] In **1** · β-CD the signals at $\delta = 27$–28 and 37 appear as doublets; when resolution enhancements were applied they became two distinct signals. For a physical mixture, these signals remained singlets. Cross polarization dynamics, as measured by the contact time and the proton rotating-frame relaxation time $T_{1\rho}(H)$, differed between **1** · β-CD and the physical mixture, indicating a single proton-spin reservoir for the complex and two distinct proton-spin reservoirs which are separated in space for the physical mixture (see J. R. Garbow, B. J. Gaede, *J. Agric. Food Chem.* **1992**, *40*, 156).
[8] FAB mass spectra were obtained by bombarding the samples in a glycerol or triethanolamine matrix with approximately 33 keV beam of Cs^+ ions, and the desorbed ions were analyzed with the first stage of a VG analytical ZAB-T four-sector mass spectrometer. Exact mass measurements were within <3.8 ppm of theoretical values. Collisional activation of the *m/z* 1267.4 ion and mass analysis of products with the second stage produces evidence for rupture of the CD ring but not for loss of $C_{10}H_{14}$. The mass spectrometer was briefly described by M. L. Gross *Methods Enzymol.* **1990**, *193*, 131.
[9] The calculations were performed with the SYBYL 6.0 version from Tripos Associates, Inc., on an 4D/35 IRIS workstation from Silicon Graphics.Inc. The "dock molecules" program was used to obtain the total energy of the complex with consideration of different possible conformations of **1** within β-CD.
[10] For the azine formation at least three mechanisms have to be discussed, two of them require the intermediacy of a carbene (see ref. [5b] *vol. I*, p. 111).
[11] In addition, variable amounts of adamantanone were formed.
[12] S. D. Isaev, V. P. Sherstyuk, O. F. Kozlov, V. Skripkin, I. Yanku, *Teor. Eksp. Khim.* **1991**, *27*, 211.
[13] R. Kupfer, planned Ph.D. dissertation, State University of New York at Binghamton.
[14] This sample which contained "empty" and "filled" β-CD molecules (ratio: ca. 2:1, determined by NMR spectroscopy) was treated with D_2O in order to exchange the number of active hydrogen atoms. The $(M - H)^-$ ion of β-CD shifts from *m/z* 1133.4 to 1153.4, indicating that all 21 active hydrogen atoms of β-CD had been replaced with deuterium atoms, and that an $(M - D)^-$ ion had been desorbed. The exchange was not complete; there were still some isomers with 20, 19, 18, and 17 deuterium atoms, but it was the most exchange that could be accomplished. For **4** · β-CD, 20 active hydrogen atoms could be exchanged as indicated by a shift from *m/z* 1267.4 for $(M - H)^-$ to *m/z* 1286.5 for $(M - D)^-$. One active hydrogen atom was lost owing to carbene insertion into an O–H bond.
[15] S. Morgan, J. E. Jackson, M. S. Platz, *J. Am. Chem. Soc.* **1991**, *113*, 2782.
[16] a) D. J. Martella, M. Jones, Jr., P. von R. Schleyer, W. F. Maier, *J. Am. Chem. Soc.* **1979**, *101*, 7634; b) D. Lenoir, J. Firl, *Liebigs Ann. Chem.* **1974**, 1467.
[17] J. Michl, G. J. Radziszewski, J. W. Downing, K. B. Wiberg, F. H. Walker, R. D. Miller, P. Kovačić, M. Jawdosiuk, V. Bonačić-Koutecký, *Pure Appl. Chem.* **1983**, *55*, 315.
[18] This could also mean that adamantene **6** is not formed from the carbene **2** but from the diazirine **1** or the rearranged linear diazo precursor (see J. E. Jackson, M. S. Platz in *Advances in Carbene Chemistry, vol. 1* (Ed.: U. H. Brinker), JAI, Greenwich, CT, in press.

Conjugated, Liquid Crystalline Polymers**

By *Luping Yu,** *Zhenan Bao*, and *Rubing Cai*

Liquid crystalline (LC) polymers are of great interest in fundamental science and the development of advanced materials.[1] Three main types of LC polymers have been extensively studied: 1) side-chain LC polymers, 2) main-chain LC polymers with flexible spacers, and 3) rigid main-chain LC polymers. The study of type 3 LC polymers stemmed from the discovery that poly(*p*-phenyleneterephthalamide) forms an LC solution from which high-modulus fibers may be spun.[2, 3] These polymers are particularly important because of their exceptional strength and high-temperature properties induced by the LC ordering. However, since these materials are not very soluble, fabrication is extremely difficult. To overcome these problems, in recent years there has been considerable efforts to prepare LC polymers with a rigid

[*] Prof. L. Yu, Z. N. Bao
Department of Chemistry, The University of Chicago
5735 S. Ellis Avenue, Chicago, IL 60637 (USA)
Telefax: Int. code + (312) 702-0805
Dr. R. Cai
The Sherwin-Williams Co, Chicago IL

[**] This work was supported by the Office of Naval Research (grants N00014-93-1-0092), the Camille & Henry Dreyfus Foundation (New Faculty Award), and The Petroleum Research Fund, administered by the American Chemical Society.

main chain and flexible side chains, for example, polyamides and polyesters with alkyl side chains.[4]

In the past decades, conjugated polymers have attracted much attention due to their electrical properties, for example conductivity, and optical properties;[5-7] however, structural studies of these materials have been limited.[8] Their potential as liquid crystalline materials has not yet been explored largely because traditional conjugated polymers are intractable and infusible.[5-7] Nevertheless, conjugated polymers obviously have a stiff chain which could act as the mesogenic unit and lead to properties known for type 3 LC polymers. In these compounds electrical, optical, and liquid crystalline properties are interrelated. For example, the conductivity and the third-order nonlinear optical (NLO) susceptibility strongly depend upon the orientation of conjugated polymer chains.[6] After a conjugated polymer is aligned by mechanical stretching, the conductivity parallel to the stretching directions is much greater than in the perpendicular direction, and the anisotropy of physical properties is enhanced.

These considerations have led to the synthesis of soluble and fusible conjugated polymers.[6] Recently, we found that the Stille reaction is very versatile for the synthesis of conjugated polymers.[9] We prepared poly(1,4-phenylene-2,5-thiophene) with different alkyl side chains utilizing this reaction (Scheme 1). Our latest studies show that these polymers form

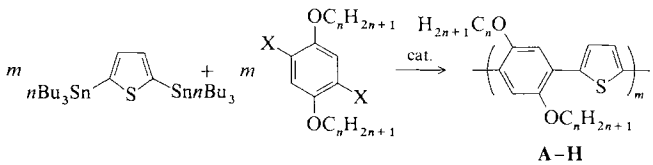

A–H

Scheme 1. Synthesis of poly(1,4-phenylene-2,5-thiophene) **A**–**H**. **A**: $n = 4$, **B**: $n = 5$, **C**: $n = 6$, **D**: $n = 7$, **E**: $n = 8$, **F**: $n = 9$, **G**: $n = 12$, **H**: $n = 16$. [Pd(P-Ph$_3$)$_2$Cl$_2$] was used as catalyst when X = I, [Pd(PPh$_3$)$_4$]/LiCl when X = CF$_3$SO$_3$.

nematic phases when they are heated above their melting points, proving that conjugated polymers may also be liquid crystals. This paper reports our results on the LC properties of polymers **A**–**H**; the syntheses and physical properties are described in detail elsewhere.[9, 10] The spectroscopic studies (NMR, FT-IR, UV/VIS) and elemental analyses support the structures we proposed.

Thermogravimetric analyses (TGA) show that all of these polymers remain stable up to 400 °C under nitrogen. Thermograms obtained from differential scanning calorimetry (DSC; DuPont 90 calorimeter) were recorded at heating rates of 10 °C min^{-1} under a nitrogen flow. Polymers **A**, **B**, and **C** show glass transition temperatures (second-order transition) at 100, 90, and 75 °C, respectively. All of these thermograms display at least two transitions as the temperature is increased from 50 to 300 °C (Fig. 1), corresponding to the melting of the side chains (T_{m1}) and the backbones (T_{m2}). Two more transitions above the sharp melting transition for polymer **A** can also be noted. The higher temperature transition corresponds to the transition (T_c) from the liquid crystalline to the isotropic phase and was confirmed by the optical microscopy. The other transition cannot be assigned, although the difference between the phases in these two temperature regions is apparent in the X-ray diffractogram (Fig. 2). Similar behavior observed in aromatic polyesters[11]

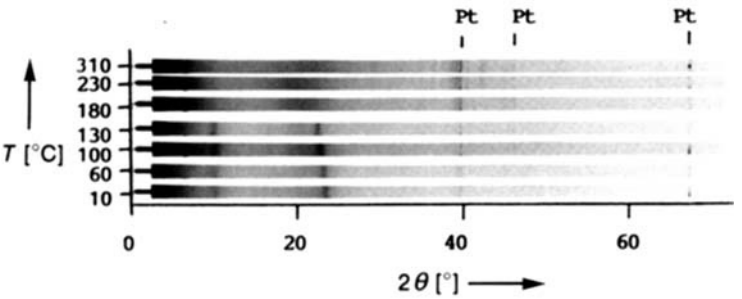

Fig. 2. Results of a temperature-dependent X-ray diffraction experiment with synchronized radiation. Each experiment lasted 8 h. The Pt line was used for calibration, the X-ray source was Ni-filtered $Cu_{K\alpha}$ radiation.

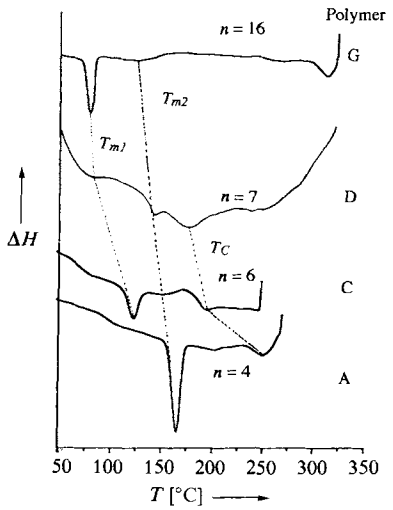

Fig. 1. DSC thermograms of polymers **A**, **C**, **D**, and **G**; heating rate 10 °C min^{-1}, nitrogen atmosphere. The polymers were annealed before the DSC scan: polymer **A**, 145 °C for 12 h; polymer **C**, 100 °C for 12 h; polymer **D**, 115 °C for 16 h; polymer **G**, 65 °C for 12 h.

has been ascribed to the smectic-to-nematic phase transition. However, polymer **A** did not show any typical smectic patterns under the optical microscope.

Since we could not detect the nematic-to-isotropic phase transition of other polymers having alkyl side chains with more than eight carbon atoms by DSC measurements, polarizing microscopy was performed (Nikon HFX-IIA microscope equipped with a Linkam (TMS-90) hot stage). All of the polymers exhibit a birefringent fluid melt above their melting temperatures and a characteristic shear opalescence, indicating a nematic phase. Figure 3 shows the textures of the mesophases of polymers **A** and **E**. Typical schlieren textures can be seen, further demonstrating the presence of a nematic phase. Both DSC studies and observations from polarizing optical microscopy indicate that the melting and the clearing transition temperatures are affected by the lengths of the side chains. In Figure 4 the transition temperatures of polymers **A**–**H** are plotted against the number of carbon atoms n in the alkyl side chain. As n increases, the melting (T_m) and clearing temperatures (T_c) of the polymers decrease steadily. Depending upon the length of the side chain, the liquid crystal range is between 56 and 20 °C.

The X-ray diffraction studies indicate that the polymers precipitated as crystalline materials. The X-ray diffraction results for polymer **A** with a synchronized diffractometer are shown in Figure 2. Two strong diffraction maxima at 2θ values of 10 and 23.5° can be noted. As temperature was increased, the spacings at 8.51 and 3.79 Å increased due to

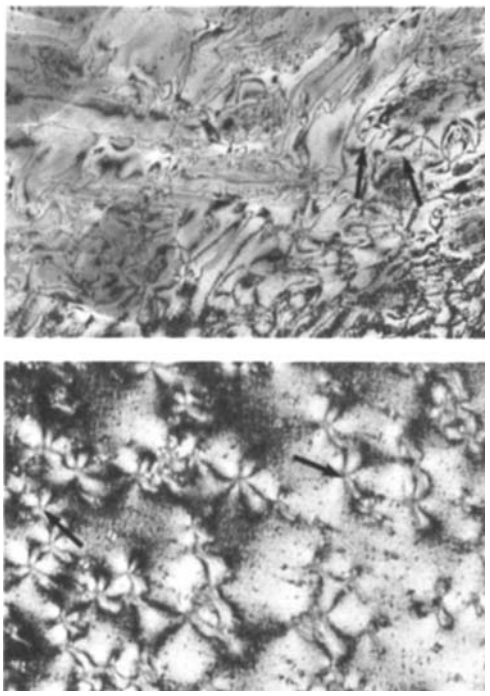

Fig. 3. The textures of the mesophases of polymers **A** (top) and **E** (bottom) under crossed polarizers at 220 °C and 159 °C, respectively, (× 100). The arrows indicate the recognizable singularities $S = \pm 1/2$.

thermal expansion. As the temperature increased above the melting temperature, these two diffraction peaks became very diffuse (barely visible), which is typical for a nematic phase.

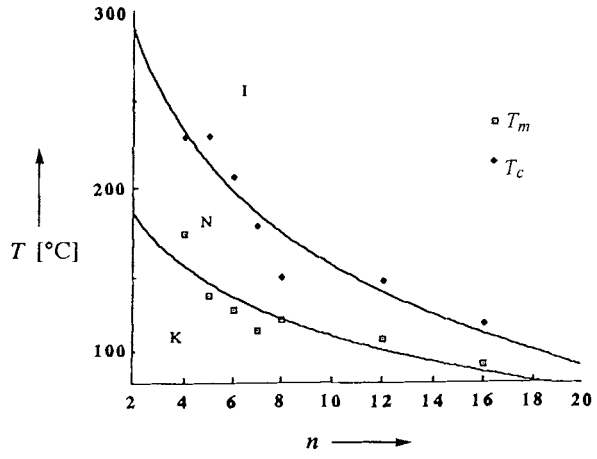

Fig. 4. Transition temperatures of polymers with different alkyl side chains.

From these results, we can see that polymers **A**–**H** have promising LC properties. Ballauff has pointed out that the side chains behave more or less like bound solvent molecules, rendering the polymer soluble and fusible.[12] This model of bound solvent molecules accounts for the change in the transition temperature as a function of the length of the side chain.

We have shown clear evidence of a nematic LC phase for the new conjugated polymers **A**–**H**, which were prepared by the Stille coupling reaction. Certain properties of the polymers such as transition temperatures, solubility, and fusibility of polymers can be controlled by the length of the side chains. We also can easily change the structure of the conjugated main chain. For example, the 2,5-linkage of thiophene results in a main chain with a bent structure, and the chain packing should thus be different from that of polymers with linear structures such as 2,5-phenylene and 1,4-naphthalene. (Although polyphenylene has been synthesized before, to our knowledge no liquid crystal property study was reported.) Our findings should serve as a basis for further investigations of LC behavior in conjugated polymers.

Received: March 15, 1993 [Z 5926 IE]
German version: *Angew. Chem.* **1993**, *105*, 1392

[1] *Liquid Crystalline Polymers, ACS Symp. Ser.* **1990**, *435*.
[2] P. W. Morgan, *Macromolecules* **1977**, *10*, 1381.
[3] S. L. Kwolek, P. W. Morgan, J. R. Schaefer, L. W. Gulrich, *Macromolecules* **1977**, *10*, 1390.
[4] M. Ballauff, *Angew. Chem.* **1989**, *101*, 261; *Angew. Chem. Int. Ed. Engl.* **1989**, *28*, 253, and references therein.
[5] *Handbook of conducting polymers, Vol. 1, 2* (Ed.: T. A. Skotheim), Dekker, New York, **1986**.
[6] *Electroresponsive Molecular and Polymeric Systems, Vol. 2* (Ed.: T. A. Skotheim), Dekker, New York, **1991**.
[7] *Conjugated Conducting Polymers* (*Springer Ser. Solid State Sci.* **1992**, 102).
[8] T. J. Pross, M. J. Winokur, J. Moulton, P. Slith, A. J. Heeger, *Macromolecules* **1992**, *25*, 4364.
[9] Z. N. Bao, W. K. Chan, L. P. Yu, *Chem. Mater.* **1993**, *5*, 2.
[10] Z. N. Bao, L. P. Yu, *Macromolecules*, submitted.
[11] M. Ballauff, G. F. Schmidt, *Mol. Cryst. Liq. Cryst.* **1987**, *147*, 163.
[12] M. Ballauff, *Macromolecules* **1986**, *19*, 1366.

Structure and Electrochemical Behavior of the Paramagnetic Anion $[Ir_{14}(CO)_{27}]^-$, Possessing a Trigonal Bipyramidal Arrangement of Metal Atoms**

By *Roberto Della Pergola, Luigi Garlaschelli,* Mario Manassero, Norberto Masciocchi,** and *Piero Zanello**

The number of well-defined and structurally characterized, high-nuclearity clusters is increasing, but slowly. Knowledge in this field is somehow hampered by experimental difficulties: most compounds are obtained in very small amounts with reactions of low reproducibility, and the characterization is simply restricted to the crystal structure. In other cases in which a large number of physico-chemical measurements are available, high nuclearity clusters have been shown to possess unusual properties which deserve more detailed investigation.[1]

Within the latter group, $[Ir_{12}(CO)_{26}]^{2-}$[2] and $[Ir_{12}(CO)_{24}]^{2-}$[3] were obtained by oxidation of $[Ir_6(CO)_{15}]^{2-}$ with $[Cu(NCCH_3)_4]^+$, through the intermediacy of the

[*] Prof. L. Garlaschelli, Dr. R. Della Pergola
Dipartimento di Chimica Inorganica e Metallorganica
via G. Venezian 21, I-20133 Milano (Italy)
Dr. N. Masciocchi, Prof. M. Manassero
Istituto di Chimica Strutturistica Inorganica
via G. Venezian 21, I-20133 Milano (Italy)
Prof. P. Zanello
Dipartimento di Chimica dell' Università
Pian dei Mantellini 44, I-53100 Siena (Italy)

[**] We acknowledge the financial support of the Ministero dell'Università e della Ricerca Scientifica et Tecnologica (MURST) and of Consiglio Italiano delle Ricerche (CNR). ESR spectra were recorded by Prof. Franca Morazzoni, to whom we are indebted.

$[Ir_6(CO)_{15}\{CuNCCH_3\}]^-$ adduct;[4] the dodecanuclear clusters represented the maximum nuclearity achieved for iridium, until we were able to synthesize the new monoanion $[Ir_{14}(CO)_{27}]^-$ ($\mathbf{1}^-$) by oxidation of $[Ir_6(CO)_{15}]^{2-}$ with ferrocenium ions. This type of reaction was previously exploited for the synthesis of substituted hexanuclear iridium clusters.[5] In the absence of any coordinating ligands, the major product is the red isomer of $[Ir_6(CO)_{16}]$,[6] but other clusters are also produced. Of these, $[Ir_{14}(CO)_{27}]^-$ can be recovered as $[N(PPh_3)_2]^+$ salt. Single crystal X-ray diffraction analysis[7] showed that $[Ir_{14}(CO)_{27}]^-$ possesses an approximate D_{3h} symmetry and contains a metal core polyhedron of ν_2-trigonal bipyramidal shape,[8] showing an ABCBA stacking sequence of metal atoms down the pseudo-threefold axis (Fig. 1). This arrangement of 14 metal atoms has never been observed before, although it can be recognized as a part of the framework of $[Os_{17}(CO)_{36}]^{2-}$;[9] other truncated ν_2-trigonal bipyramids are also known, for example, $[Ir_{12}(CO)_{24}]^{2-}$[3] and $[H_xNi_{12}(CO)_{21}]^{x-4}$ ($x = 0, 1, 2$).[10]

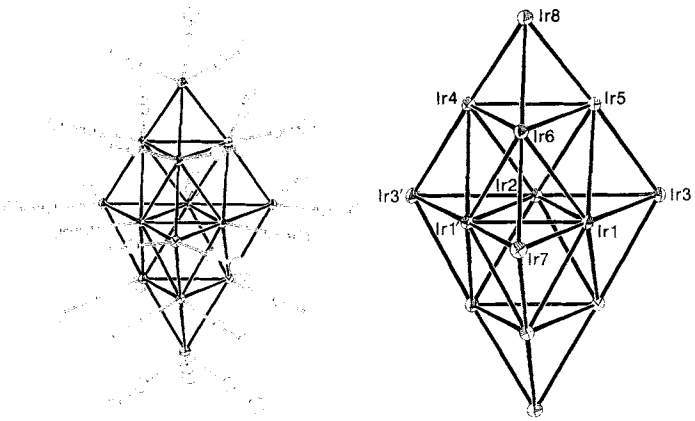

Fig. 1. Left: ORTEP drawing of the $[Ir_{14}(CO)_{27}]^-$ ion. Thermal ellipsoids are drawn at the 30% probability level. Right: Schematic drawing of the Ir_{14} metal core. Primed atoms are generated by rotation about the (crystallographic) twofold axis passing through the Ir(2) and Ir(7) atoms. Ir–Ir distances [Å]: 1–1′ 2.643(2), 1–2 2.646(2), 1–3 2.692(1), 1–4′ 2.760(1), 1–5 2.750(1), 1–6 2.767(1), 1–7 2.700(2), 2–3 2.702(1), 2–4 2.740(1), 2–5 2.770(1), 3–4′ 2.735(1), 3–5 2.724(1), 4–5 2.763(1), 4–6 2.767(1), 4–8 2.674(1), 5–6 2.758(1), 5–8 2.676(1), 6–7 2.742(1), 6–8 2.681(1).

The metal framework of $[Ir_{14}(CO)_{27}]^-$ is only slightly distorted: the 33 Ir–Ir distances (average value 2.720 Å, range 2.643–2.770 Å) can be grouped into four homogeneous subsets: 1) only the equatorial [Ir1, Ir2, Ir3 and Ir7] atoms (average 2.680 Å), 2) only the upper layer [Ir4, Ir5, Ir6] atoms, (average 2.763 Å), 3) the apical Ir8 atom (average 2.677 Å), and 4) interlayer connections (average 2.751 Å).

All the carbonyl ligands in $\mathbf{1}^-$ are terminally bound, three on each apical, two on each equatorial vertex, and one on each Ir atom in the center of the edges of the equatorial plane: this disposition matches the requirement of densest coverage of metallic surface, as observed in the ν_2-tetrahedral osmium clusters $[Os_{10}C(CO)_{24}]^{2-}$[11] and in $[Os_{17}(CO)_{36}]^{2-}$. Average distances and angles for the carbonyl ligands are 1.83 Å (range 1.73–1.92 Å) for Ir–C and 1.17 Å (range 1.10–1.22 Å) for C–O; Ir-C-O angles range from 173(3) to 180°.

Cluster $\mathbf{1}^-$ possesses 181 cluster valence electrons (CVE), corresponding to 91 occupied molecular orbitals. This number conforms to the $6N + 7$ rule suggested by Ciani and Sironi[12] and is in fairly good agreement with predictions of Teo et al.,[8] but can not be rationalized in terms of the Polyhedral Skeletal Approach,[13] probably because it is rather awkward to describe the regular ν_2 polyhedron as being derived by condensation of two octahedra, three trigonal bipyramids, and two tetrahedra. The agreement of the number of electrons with attributable to the bipyramidal core of $[Os_{17}(CO)_{36}]^{2-}$ is even lower (176 CVEs).

The odd number of electrons, which was confirmed by ESR measurements, suggests that electrons could be added or removed. As a matter of fact, Figure 2 shows that, in dichloromethane solution, the monoanion undergoes an oxidation as well as a reduction process. Both redox changes

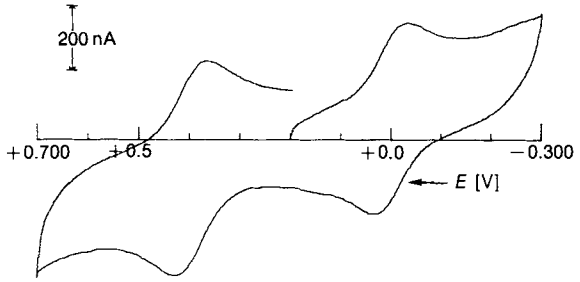

Fig. 2. Cyclic voltammetric response exhibited by a solution of $[N(PPh_3)_2][Ir_{14}(CO)_{27}]$ (1×10^{-4} mol dm^{-3}) and $[NBu_4][ClO_4]$ (0.2 mol dm^{-3}) in CH_2Cl_2. Platinum working electrode. Scan rate 0.05 Vs^{-1}. Ag/AgCl reference electrode.

look like chemically and electrochemically reversible one-electron transfers ($E^{o\prime}_{1/1^-} = +0.39$ V; $\Delta E_p(0.05\,\mathrm{Vs}^{-1}) = 65$ mV; $E^{o\prime}_{1/1^{2-}} = 0.00$ V; $\Delta E_p(0.05\,\mathrm{Vs}^{-1}) = 64$ mV). The slight increase of the peak-to-peak separation of each process from 60 mV at 0.02 Vs^{-1} to 90 mV at 1.00 Vs^{-1} in the high-resistive dichlorometane solution clearly supports the electrochemical reversibility of the redox changes. This implies that the original cluster framework does not undergo significant structural reorganizations upon the actual electron addition or removal.[14]

Experimental Procedure

$[N(PPh_3)_2]_2[Ir_6(CO)_{15}]$ (0.19 g, 0.07 mmol) was dissolved in THF (20 mL) and cooled to 0 °C under a light stream of nitrogen. Solid $[(C_5H_5)_2Fe]PF_6$ (0.05 g, 0.15 mmol) was added, and the reaction mixture stirred for two hours. The brownish-black solution was evaporated to dryness in vacuum, ferrocene was extracted with hexane (2 × 15 mL), and the residue was dissolved in CH_2Cl_2 and filtered. The filtrate was layered with cyclohexane and, after slow diffusion, produced a large number of white colorless needles of $[(N(PPh_3)_2]PF_6$ together with a few black crystals. This residue was washed with 2-propanol, toluene, and CH_3CN, leaving only black crystals of the highly insoluble product. Approximate yield: 10 mg; $\tilde{\nu}_{CO}$ (CH_2Cl_2 solution): 2082s, 2068w, 2042vs, 2014m, 1994w cm^{-1}; g (polycrystalline sample at 120 K): 2.37.

In this preliminary report, the electrochemical behavior of $[N(PPh_3)_2]$ **1** was studied only by cyclic voltammetry, because a very small amount of it (2.3 mg) remained after characterization. The number of electrons involved in the electron transfer processes was roughly evaluated by comparison with the response of an equimolar amount of $[NEt_4][Fe_5N(CO)_{14}]$[15]. The electrochemical apparatus was a BAS 100A Electrochemical Analyzer connected to a MF-1065 microcell equipped with an Ag/AgCl reference electrode and a button and a spiral platinum electrode as working and auxiliary electrodes, respectively. Under these experimental conditions, the one electron oxidation of ferrocene occurs at $E^{o\prime} = +0.47$ V vs. Ag/AgCl.

Received: February 15, 1993 [Z 5871 IE]
German version: *Angew. Chem.* **1993**, *105*, 1415

[1] G. Longoni, A. Ceriotti, M. Marchionna, G. Piro in *Surface Organometallic Chemistry: Molecular Approaches to Surface Catalysis (NATO ASI Ser. Ser. C, 231*, **1988**, 157–172; L. J. de Jongh, H. B. Brom, G. Longoni, J. M. van Ruitenbeek, G. Schmid, H. H. A. Smit, M. P. J. Staveren, R. C. Thiel, *New J. Chem.* **1990**, *14*, 559–560, and references therein.

[2] R. Della Pergola, F. Demartin, L. Garlaschelli, M. Manassero, S. Martinengo, M. Sansoni, *Inorg. Chem.* **1987**, *26*, 3487–3491.
[3] R. Della Pergola, F. Demartin, L. Garlaschelli, M. Manassero, S. Martinengo, N. Masciocchi, P. Zanello, *Inorg. Chem.*, **1993**, in press.
[4] R. Della Pergola, L. Garlaschelli, F. Demartin, M. Manassero, N. Masciocchi, *J. Organomet. Chem.* **1992**, *436*, 241–253.
[5] A. Cinquantini, P. Zanello, R. Della Pergola, L. Garlaschelli, S. Martinengo, *J. Organomet. Chem.* **1991**, *412*, 215–224; A. Ceriotti, R. Della Pergola, F. Demartin, L. Garlaschelli, M. Manassero, N. Masciocchi, *Organometallics* **1992**, *11*, 756–760.
[6] L. Garlaschelli, S. Martinengo, P. L. Bellon, F. Demartin, M. Manassero, M. Y. Chiang, C. Y. Wei, R. Bau, *J. Am. Chem. Soc.* **1984**, *105*, 6664–6667.
[7] Crystal data for $[N(PPh_3)_2][Ir_{14}(CO)_{27}]$: $C_{63}H_{30}Ir_{14}NO_{27}P_2$, monoclinic, $C2/c$, $a = 16.541(4)$, $b = 34.599(6)$, $c = 14.640(12)$ Å, $\beta = 91.62(4)°$, $M = 3985.6\ g\,mol^{-1}$, $V = 8375(10)$ Å^3, $Z = 4$, $\varrho_{calcd} = 3.161\ g\,cm^{-3}$; $F(000) = 6956$, $Mo_{K\alpha}$ radiation, $\lambda = 0.71069$ Å, $\mu(Mo_{K\alpha}) = 221\ cm^{-1}$. Of a total of 7359 reflections (corrected for absorption and crystal decay), 3945 were observed [$I > 3\sigma(I)$] in the $6 < 2\theta < 50$ range. $R = 0.037$, $Rw = 0.036$. The structure was solved by a combination of direct methods and difference Fourier techniques and refined by full-matrix least-squares methods. All iridium and phosphorous atoms were refined anisotropically, while the carbonyl ligands were isotropically refined at a later stage. Two half-occupancy cations have also been refined (their phenyl rings, treated as rigid bodies, occupy the same cavities between the large anions). Crystal packing drawings clearly demonstrate that their van der Waals surfaces closely match those of their centrosymmetric (disordered) images. Refinements of the structure in the non-centrosymmetric $C2$ or Cc groups did not lead to an ordered model. Further details of the crystal structure investigation are available on request from the Director of the Cambridge Crystallographic Data Centre, 12 Union Road, GB-Cambridge CB2 1EZ (UK), on quoting the full journal citation.
[8] B. K. Teo, N. J. A. Sloane, *Inorg. Chem.* **1985**, *24*, 4545–4558.
[9] E. Charalambous, L. H. Gade, B. F. G. Johnson, J. Lewis, M. McPartlin, H. R. Powell, *J. Chem. Soc. Chem. Commun.* **1990**, 688–690.
[10] R. W. Broack, L. F. Dahl, G. Longoni, P. Chini, *Adv. Chem. Ser.* **1978**, *167*, 93.
[11] P. F. Jackson, B. F. G. Johnson, J. Lewis, M. McPartlin, W. J. H. Nelson, *J. Chem. Soc. Dalton Trans.* **1982**, 2099–2107.
[12] G. Ciani, A. Sironi, *J. Organomet. Chem.* **1980**, *197*, 233–248.
[13] D. M. P. Mingos, *Acc. Chem. Res.* **1984**, *17*, 311.
[14] P. Zanello in *Molecular Electrochemistry of Inorganic, Bioinorganic and Organometallic Compounds (NATO ASI Ser. Ser. C* **1993**, *385*, 229–245.
[15] R. Hourihane, T. R. Spalding, G. Ferguson, T. Deeney, P. Zanello, *J. Chem. Soc. Dalton Trans.* **1993**, 43–46.

Sequential Analysis of Oligosaccharide Structures in a Few Minutes**

By *Harald Schröder* and *Ernst Haslinger**

Polysaccharides and compounds containing oligosaccharide partial structures are widespread in nature and are often highly biologically active. In order to determine the structure, not only must the monosaccharide residues be known but also their anomeric configuration, their sequence, and the positions of the glycoside linkages. NMR spectroscopy is proving to be the best method of determining both of the latter structural characteristics.[1–3] In past years, the application of 3D NMR techniques to structural investigations of oligosaccharides has gained in importance.[4–6] All the desired structural parameters, for instance, can be obtained by a 3D TOCSY-ROESY experiment.[7] However, the low digital resolution, low sensitivity, and hence the high time requirement are the greatest obstacles for routine application of 3D NMR techniques.

If the first pulse in a 3D TOCSY-ROESY experiment is replaced by a selective Gaussian pulse,[8] which only excites a particular proton, then the signals are obtained in the form of a 2D spectrum. We have carried out selective TOCSY-ROESY experiments on verbascosaponin (**1**). The spectra obtained are shown in Figures 1 and 2. Each spectrum makes it possible to determine the sugar residues adjacent to a given monosaccharide and the glycoside linkage positions. The critical advantage of this measuring technique is its high sensitivity and hence the exceptional gain in time.

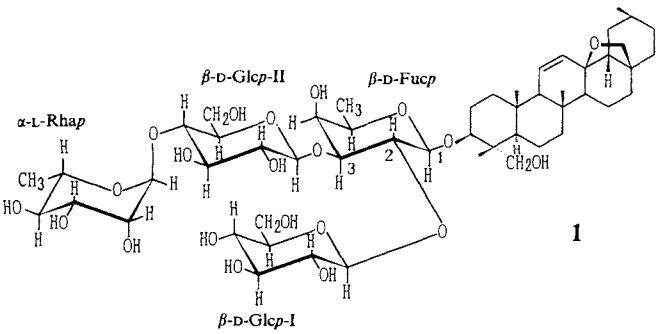

The principle can be briefly explained: A nonoverlapping proton resonance signal of a monosaccharide unit (usually the anomeric H atom) is selectively excited by a Gaussian pulse. The magnetization thus generated is transferred to other protons in the same sugar residue by a subsequent TOCSY step. After this preparation, the ROESY experiment is carried out, and the magnetization is transferred through space by dipolar coupling to any proton in the neighboring sugar building blocks that is connected at the

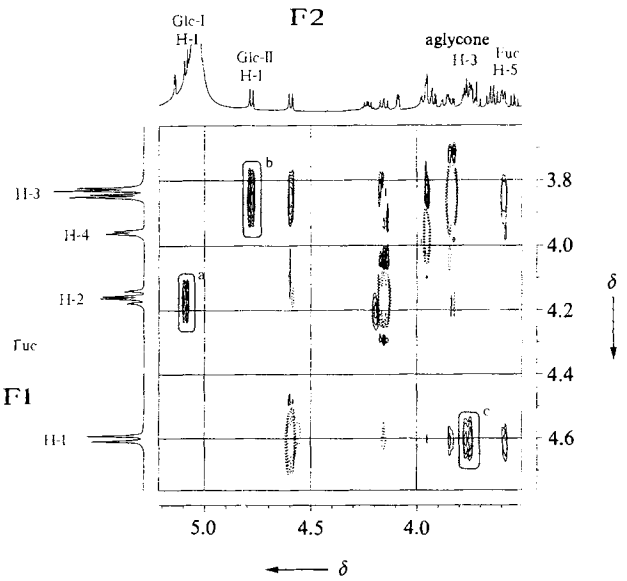

Fig. 1. 2D TOCSY-ROESY spectrum, selective excitation of the H1 atom of the fucose unit. The anomeric proton of the fucose building block is selectively excited and the magnetization transferred to the H2, H3, and H4 protons of this building block. After this preparation, the ROESY experiment is carried out. The fucose peaks in F1 give rise to diagonal peaks to the same proton (shown negative, dotted), weak COSY-like peaks (appearing antiphase), and ROESY cross-peaks (positive, solid line) within the sugar building block and to protons at the glycoside linkages of the neighboring sugar units which can be seen in the spectrum. Three interglycosidal peaks (circled, a: Fuc-H2/Glc-I-H1, b: Fuc-H3/Glc-II-H1, c: Fuc-H1/aglycone-H3) verify the partial sequence Glc-II-(1 → 3)-[Glc-I-(1 → 2)-]Fuc-(1 → 3)-aglycone. Furthermore, ROE correlations can be seen within the fucose unit: H1/H3, H1/H5, and H3/H5. A selective TOCSY of the fucose unit is shown in the F1 dimension, and a ^{1}H NMR spectrum of **1** is shown in the F2 dimension as a reference spectrum. 512 W data points, 40 experiments, TOCSY mixing time 70 ms, experiment time 4 min.

[*] Prof. Dr. E. Haslinger, Dipl.-Chem. H. Schröder
Abteilung für Organische Chemie I der Universität
Albert-Einstein-Allee 11, D-89069 Ulm (FRG)
Telefax: Int. code +(731) 502-2803

[**] This work was supported by the Fonds der Chemischen Industrie.

glycoside linkage position. This leads to interglycosidic correlation between protons at the glycoside linkage.

We illustrate the application of selective 3D TOCSY-ROESY measurements using verbascosaponin (**1**) as the example. Two experiments were sufficient for the complete sequencing of **1**. Figure 1 shows the spectrum obtained when the anomeric proton of the fucose unit is selectively excited. There are three interglycosidic correlation signals, a, b, and c. Signal a verifies the linkage between the C1 atom of the glucose-I unit and the C2 atom of the fucose building block. The glucose-II unit is connected at position C3 of fucose (signal b); fucose is thus the starting point for branching of the sugar chain. Magnetization transfer from the anomeric H atom to H3 of the aglycone at the site of the third glycosidic linkage accounts for signal c. The information still to be determined concerning the structure of the sugar chain can be obtained from Figure 2. Here the anomeric proton of the glucose-II unit was selectively excited and the magnetization distributed among all other protons of this sugar. Correlation signal a verifies that the rhamnose building block is connected at position 4 of the glucose-II unit. Signal b again correlates H3 proton of fucose to the anomeric proton of the glucose-II unit.

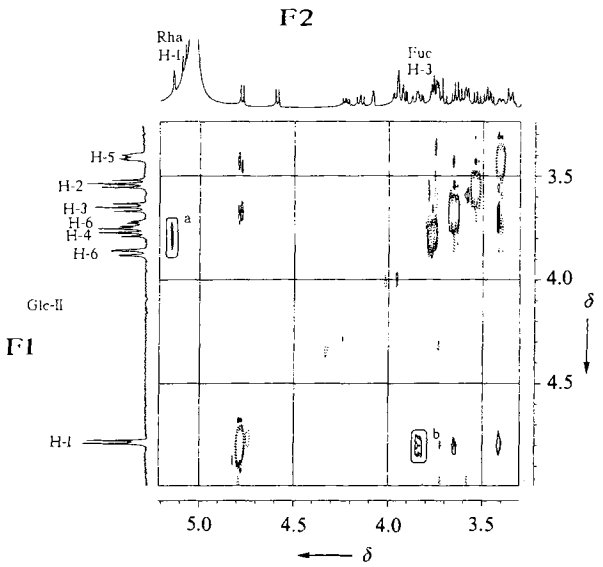

Fig. 2. 2D TOCSY-ROESY spectrum, selective excitation of the H1 atom of the glucose-II unit. The anomeric proton of the glucose-II unit is selectively excited, the magnetization transferred to all other protons in the glucose building block and the ROESY experiment then carried out. Two interglycosidal ROE cross-peaks (circled a: Glc-II-4/Rha-1, b: Glc-II-1/Fuc-3) verify the partial sequence Rha-(1 → 4)-Fuc. Therefore, the sequence and the positions of the glycoside linkages of **1** are completely determined by this experiment and that in Figure 1. The following intraglycosidal ROE peaks of the glucose-II unit can be seen: H1/H3, H1/H5, and H3/H5. A selective TOCSY of the glucose-II unit is shown in the F1 dimension, and the ^{1}H NMR spectrum of **1** in the F2 dimension serves as a reference spectrum. 512 W data points, 40 experiments, TOCSY mixing time 70 ms, experiment time 4 min.

The application of a TOCSY-ROESY pulse sequence instead of a TOCSY-NOESY experiment[9] is necessary for medium-sized molecules such as verbascosaponin since nuclear Overhauser effects (NOE) are small or nonexistent.[10] A requirement for sequencing the sugar chain is the previous assignment of the proton signals, for example by a COSY spectrum. The selective TOCSY-ROESY experiment makes unambiguous sequencing possible even with severely overlapping signals. Of course, if signals due to the selectively excited sugar unit are superimposed on one another, even this method can fail. The measurement technique described exclusively combines the advantages of selective excitation (frequency selectivity, low time and computer memory requirement) with those of 3D spectroscopy (dispersion in an additional frequency dimension and hence generation of partial spectra). We succeeded in a complete sequence analysis of **1** within 10 minutes by measuring the two spectra in Figures 1 and 2. Structural determination of oligosaccharides is simplified considerably by this method.

Experimental Procedure

The NMR spectra were recorded on a Bruker AMX-500 spectrometer (^{1}H NMR frequency: 500.13 MHz) and processed with an Aspect X32 computer using the UXNMR program. Sample tubes 5 mm in diameter, solvent: 0.2 mL [D_4]methanol/[D_5]pyridine (3:2), sample concentration: 3×10^{-5} mol, temperature: 310 K. The CD_3OD peak was used as an internal reference (^{1}H NMR: $\delta = 3.3$).

Pulse sequence for the selective 3D TOCSY-ROESY experiment: 90° soft pulse – d1 – [MLEV-17] – t_1 – [spin-lock] FID (t_2); 90° soft pulse length P1: 70 ms (64 dB, truncation level 1%), TOCSY mixing time: 70 ms (60 MLEV-17 cycles, each with two trim pulses lasting 2.5 ms, ROESY spin-lock CW pulse: 250 ms, d1 = 1/J – P1/2, ^3J(H1, H2) = 7.8 Hz (fucose and glucose), acquisition time + relaxation delay: 300 ms, 8 scans, 512 W data points, 40 increments (t_1), measurement time 4 min. A Gaussian pulse is very selective and offers advantages over Dante and semi-Gaussian pulses. A selective excitation pulse of 70 ms was chosen to achieve the required selectivity. The subsequent TOCSY transfer requires in-phase magnetization. As the delay required for this (d1 = 1/J – P1/2 = 95 ms) results in a loss in sensitivity due to relaxation, the delay chosen was as short as possible (5 μs). The loss in sensitivity due to the antiphase magnetization component was accepted. This offers the additional advantage that d1 does not have to be adjusted for different coupling constants.

Received: April 16, 1993 [Z 6014 IE]
German version: *Angew. Chem.* **1993**, *105*, 1431

[1] J. Dabrowski in *Two-dimensional NMR Spectroscopy* (Eds.: W. R. Croasmun, R. M. K. Carlson), VCH, Weinheim, **1987**, pp. 366–370.
[2] L. Poppe, J. Dabrowski, *Biochem. Biophys. Res. Commun.* **1989**, *159*, 618–623.
[3] E. Haslinger, S. Korhammer, M. Schubert-Zsilavecz, *Liebigs Ann. Chem.* **1990**, 713–714.
[4] C. Griesinger, O. W. Sørensen, R. R. Ernst, *J. Magn. Reson.* **1987**, *73*, 574–579.
[5] G. W. Vuister, P. de Waard, R. Boelens, J. F. G. Vliegenthart, R. Kaptein, *J. Am. Chem. Soc.* **1989**, *111*, 772–774.
[6] L. Poppe, H. van Halbeek, *J. Magn. Reson.* **1992**, *96*, 185–190.
[7] H. Schröder, E. Haslinger, *Liebigs Ann. Chem.* **1993**, in press.
[8] H. Kessler, S. Mronga, G. Gemmecker, *Magn. Reson. Chem.* **1991**, *29*, 527–557.
[9] V. Sklenar, J. Feigon, *J. Am. Chem. Soc.* **1990**, *112*, 5644–5645.
[10] A. Bax, D. G. Davis, *J. Magn. Reson.* **1985**, *63*, 207–213.

$Ba_9N[N_3][TaN_4]_2$: A Nitridotantalate(v) with Nitride and Azide Ions**

By *Peter Höhn, Rüdiger Kniep,** and *Joachim Maier**

A simple method of preparing nitrodometalates is by reaction of binary or ternary metal melts (Li-EA-TE systems; where EA is a group 2 element, and TE an element of groups 4–11 of the periodic system) with elemental nitrogen.[1, 2] The compounds prepared by this method contain

[*] Prof. Dr. R. Kniep,[+] Prof. Dr. J. Maier, Dr. P. Höhn
Max-Planck-Institut für Festkörperforschung
Heisenbergstrasse 1, D-70569 Stuttgart (FRG)
Telefax: Int. code + (711)6891-722
[+] Permanent address:
Eduard-Zintl-Institut der Technischen Hochschule
Hochschulstrasse 10, D-64289 Darmstadt (FRG)
Telefax: Int. code + (6151)16-4073

[**] This work was funded by the Deutsche Forschungsgemeinschaft and the Fonds der Chemischen Industrie.

nitrogen reduced to nitride, which participates in the "covalent" arrangement of complex anions (as in $Li_4[FeN_2]$[3] and $Sr_2Li[Fe_2N_3]$[4]) or is found as "isolated" nitride species surrounded by cations of an electropositive metal (as in Ca_3AuN[5]). In the course of our investigations in nitridotantalates,[2] we have now succeeded in preparing $Ba_9N[N_3][TaN_4]_2$, a compound containing the complex anions $[Ta^VN_4]^{7-}$, "isolated" nitride ions, and simultaneously also azide ions N_3^-, from the elements. The only way to prepare this metastable phase was by quenching the high-temperature system in direct contact with excess tantalum. This, together with the results of the crystal structure analysis, provide evidence that elemental nitrogen is reduced to the nitride stage via the azide under the given conditions.

$Ba_9N[N_3][TaN_4]_2$ was prepared by heating barium (Ventron, 99.5%; peeled under argon) and tantalum (Ventron, 99.9%; powder) in 10:1 molar ratio in a tantalum crucible (Plansee, 99.95%) under a stream of nitrogen (Messer Griesheim, 99.999%, 5 L h^{-1}) at a rate of 100 K h^{-1} to 1223 K, maintaining this temperature for 12 h, and finally quenching to room temperature. The reaction tube (quartz glass) containing the tantalum crucible was disconnected from the nitrogen supply, sealed, withdrawn from the oven (1223 K), and dipped into a water bath at room temperature. After temperature equilibrium was attained, black shining orthorhombic prisms of $Ba_9N[N_3][TaN_4]_2$, which appear red and translucent in thin layers, grew on the upper rim of the tantalum crucible. The reaction product at the bottom of the crucible consisted primarily of $Ba_2[TaN_3]$.[6]

In the crystal structure of $Ba_9N[N_3][TaN_4]_2$ the anionic part (Fig. 1) consists of isolated $[Ta^VN_4]^{7-}$ tetrahedra (forming a double layer parallel to (001)), "isolated" nitride ions (roughly at the boundaries of the double-layers), and azide ions (between the double layers). The bond lengths and bond

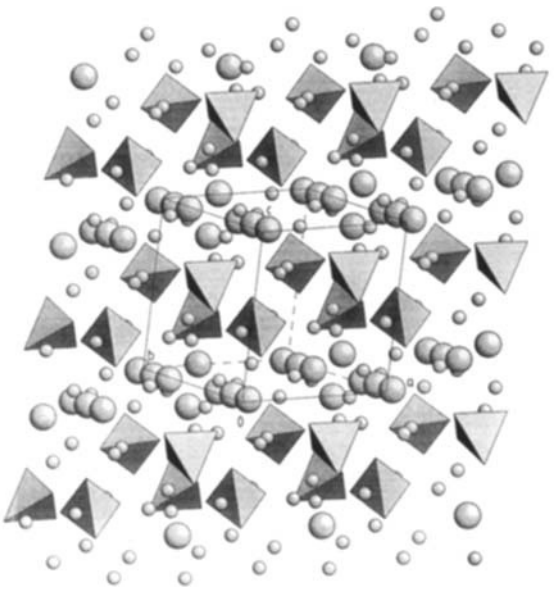

Fig. 1. Section of the crystal structure of $Ba_9N[N_3][TaN_4]_2$. Tetrahedra: $[TaN_4]^{7-}$, large spheres: nitrogen (N_3^- or N^{3-}), small spheres: Ba^{2+}.

angles within the isolated TaN_4 tetrahedra (194(2)–199(2) pm and 104.49(1)–114.30(1)°, respectively) are of the same order of magnitude as those in $Li_7[TaN_4]$[8] (195.5(2) and 196.7(3) pm, 109.0(1) and 110.0(1)°, respectively). The azide group is only slightly bent ($N_{terminal}$-$N_{bridging}$-$N_{terminal}$: 176.21(2)°; compare also the angle at the central N atom of the azide group in iodine azide, as described recently:[9] 171(7) and 174(6)°). The lengths of the $N_{terminal}-N_{bridging}$ bonds are 121(2) and 126(2) pm; the crystal structure of the binary azide $Ba[N_3]_2$[10] also contains unsymmetrical azide ions (two independent ions with bond lengths of 119.6/114.3 pm and 118.2/120.3 pm). The azide ions in the crystal structure of $Ba_9N[N_3][TaN_4]_2$[7] are surrounded by eight barium ions; the $Ba-N_{(azide)}$ distances (283 to 320 pm) lie in the range of the sum of the effective ionic radii (282 to 308 pm),[11] so that this ternary compound can be regarded as an ionic azide.[12] The N–N bonds in the ternary azide (mean value: 124(2) pm) are rather long compared with those in $Ba[N_3]_2$[10] (mean value: 118.1 pm) and in the alkali metal compounds $M[N_3]$ (M = K, Rb, Cs; mean value: 117(1) pm);[13] this corresponds with the high coordination number (CN) of the azide ions (CN = 8, in contrast to CN = 4–5 in $Ba[N_3]_2$) and the higher charge on the surrounding cations compared with the alkali metal compounds, which also contain eight-coordinate azide ions. Figure 2 illustrates the coordination of azide ions by barium ions.

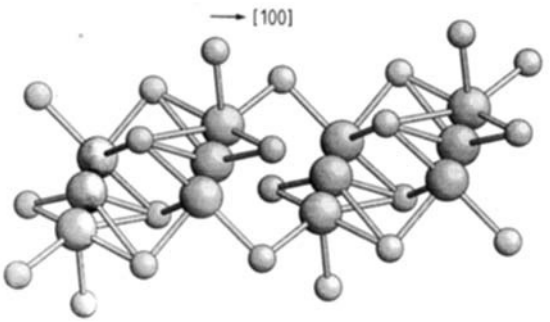

Fig. 2. Coordination of the azide ions (large spheres) by barium ions (small spheres) in $Ba_9N[N_3][TaN_4]_2$ and linkages forming ribbons along the [100] direction.

The specific arrangement of the cations and anions leads to ribbons along the [100] direction. The terminal N atoms of the azide groups are surrounded by five (291(2)–320(2) pm) or four (283(2)–312(2) pm) barium ions, whereas the central N atom has only three neighboring Ba ions (294(2)–306(2) pm). This result is in complete agreement with MO calculations for azide ions,[12, 14] according to which the central N atom has a formal charge of +0.6, while the terminal N atoms have a formal charge of −0.8, which implies that the latter should have a stronger interaction with the neighboring cations.

The isolated nitride ions are surrounded by barium ions (distorted octahedral coordination; 264(2)–295(1) pm); the mean distance of 280(2) pm is similar to that found recently for the octahedral coordination of N^{3-} by Ba^{2+} ions (273.4 pm) in the subnitride Ba_3NaN.[15]

The formation of an azide at a reaction temperature of 1223 K is rather unlikely and has never been observed before. It can thus be assumed that $Ba_9N[N_3][TaN_4]_2$ is formed only at lower temperatures during the rapid temperature equilibration between 1223 K and room temperature. The preparation is certainly reproducible, although the yield is limited to only a few small crystals. Thus it has not yet been possible to extend these studies (for example, by vibrational spectroscopy measurements).

Received: April 5, 1993 [Z 5981 IE]
German version: *Angew. Chem.* **1993**, *105*, 1409

[1] A. Gudat, *Ternäre und quaternäre Nitride und Nitridometallate in Systemen Lithium-Erdalkalimetall-Übergangsmetall-Stickstoff*, Dissertation, Universität Düsseldorf, **1990**.
[2] P. Höhn, *Ternäre und quaternäre Nitridometallate: Verbindungen in den Systemen Lithium-Erdalkalimetall-Übergangsmetall-Stickstoff*, Dissertation, Technische Hochschule Darmstadt, **1993**.
[3] A. Gudat, R. Kniep, A. Rabenau, *Angew. Chem.* **1991**, *103*, 217–218; *Angew. Chem. Int. Ed. Engl.* **1991**, *30*, 199–200.
[4] S. Haag, P. Höhn, R. Kniep, W. Milius, *Angew. Chem.* **1991**, *103*, 874–875; *Angew. Chem. Int. Ed. Engl.* **1991**, *30*, 831–832.
[5] J. Jäger, D. Stahl, P. C. Schmidt, R. Kniep, *Angew. Chem.* **1993**, *105*, 738–739; *Angew. Chem. Int. Ed. Engl.* **1993**, *32*, 709–710.
[6] F. K.-H. Helmlinger, P. Höhn, R. Kniep, *Z. Naturforsch. B*, **1993**, *48*, 1015–1018.
[7] Structural analysis of $Ba_9N[N_3]TaN_4]_2$: space group $P\bar{1}$; $a = 801.2(2)$, $b = 964.7(3)$, $c = 11265.5(2)$ pm, $\alpha = 75.86(2)$, $\beta = 85.78(1)$, $\gamma = 87.55(2)$; $Z = 2$, $\varrho_{calcd} = 6.20\ g\,cm^{-3}$; 3430 independent observed reflections ($I \geq 3\sigma(I)$); STOE Stadi-4 diffractometer, 2θ from 3° to 60°; $Mo_{K\alpha}$ radiation; $R(R_w) = 0.059\ (0.036)$. Further details of the crystal structure investigation may be obtained from the Fachinformationszentrum Karlsruhe, Gesellschaft für wissenschaftlich-technische Information mbH, D-76344 Eggenstein-Leopoldshafen (FRG), on quoting the depository number CSD-57257, the names of the authors, and the journal citation.
[8] C. Wachsmann, H. Jacobs, *J. Alloys Comp.* **1992**, *190*, 113–116.
[9] P. Buzek, T. M. Klapötke, P. von Ragué Schleyer, I. C. Tornieporth-Oetting, P. S. White, *Angew. Chem.* **1993**, *105*, 289–290; *Angew. Chem. Int. Ed. Engl.* **1993**, *32*, 275–276.
[10] E. M. Walitzi, H. Krischner, *Z. Kristallogr.* **1970**, *132*, 19–26.
[11] W. H. Bauer, *Cryst. Rev.* **1987**, *1*, 59–83.
[12] U. Müller, *Struct. Bonding (Berlin)* **1972**, *14*, 141–172.
[13] U. Müller, *Z. Anorg. Allg. Chem.* **1972**, *392*, 159–166.
[14] J. F. Wyatt, I. H. Hillier, V. R. Saunders, J. A. Connor, *J. Chem. Phys.* **1971**, *54*, 5311–5315.
[15] P. E. Rauch, A. Simon, *Angew. Chem.* **1992**, *104*, 1505–1506; *Angew. Chem. Int. Ed. Engl.* **1992**, *31*, 1519–1520.

Bi[1,3-bis(dicyanomethylene)indan-2-ylidene]—An Ethylene Derivative with Extremely Pronounced Twisting of the C=C Bond**

By *Albert Beck, Rudolf Gompper,* Kurt Polborn,* and *H.-U. Wagner*

Dedicated to Professor Heinrich Nöth on the occasion of his 65th birthday

The activation energies of the (*Z*)/(*E*) isomerization of ethylene derivatives, which is usually quite large (for example, $E_a = 64.9\ kcal\,mol^{-1}$ for ethylene[1]), can be reduced by a stabilization of the transition state or by a destabilization of the ground state occasioned by mutual steric hinderance of bulky substituents (see ref.[2]) or by ring strain (Bredt, cf. ref.[3]). The steric congestion at the C=C bond can be relieved by *syn* or *anti* pyramidalization of the olefinic C atoms or a twisting about the bond axis between them. The energy content of the molecule increases with decreasing overlap of the p_z orbitals (see Table 1), and the HOMO–LUMO gap diminishes (see ref.[4] for the $\pi-\pi^*$ absorption energy as a function of strain).

A twisting of 90° in ethylene derivatives of the type $A_2C{=}CA_2$ (A = acceptor) or $Do_2C{=}CDo_2$ (Do = donor) leads to diradicals that are expected to have a singlet ground state.[5, 6] These twisted systems represent the transition state

[*] Prof. Dr. R. Gompper, Dipl.-Chem. A. Beck, Dr. K. Polborn, Dr. H.-U. Wagner
Institut für Organische Chemie der Universität
Karlstrasse 23, D-80333 München (FRG)
Telefax: Int. code + (89)5902-420

[**] This work was supported by the Deutsche Forschungsgemeinschaft and the Fonds der Chemischen Industrie.

Table 1. Heats of formation H_f and HOMO/LUMO energies for different geometries of ethylene (MNDO). θ = twist angle.

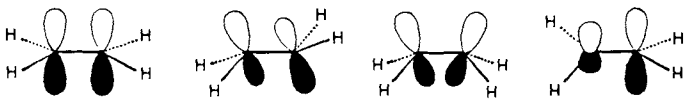

	planar	*anti*-pyramidalized	*syn*-pyramidalized	twist
θ [°]	0	30	30	30
H_f [kcal mol^{-1}]	15.4	28.5	32.4	44.2
E (LUMO) [eV]	1.3	1.0	0.9	0.4
E (HOMO) [eV]	−10.2	−10.2	−10.0	−8.9
ΔE	11.5	11.2	10.9	9.3

of the *cis*/*trans* isomerization of alkenes. A similar twisting of ethylenes of the type $A_2C{=}CDo_2$ affords 1,2-dipoles (cf. ref.[7]). Twisted olefinic structures play an important role in photochemistry, because the reversion of the excited state to the ground state might occur from the 90° twisted state.[8]

The molecular structures of some sterically hindered ethylene derivatives in the solid state are known: The C atoms of the central double bond of the thermochromic bianthron,[9] bixanthylidene,[10] and heptafulvalene[11] are *anti* pyramidalized. Five-membered ring systems like perhalogenated fulvalenes[12] and 9,9′-bifluorenylidene[13] are twisted about the central double bond.

Tetra-*tert*-butylethylene, for which a torsional angle of 44° has been determined by force field calculations,[14] would be the most strongly strained acyclic olefin. Till now, however, it could not be synthesized.[15] Hitherto, the largest twist angles found in sterically hindered tetrakis(trialkylsilyl)-substituted alkenes were 48.7[16] and 49.6°.[17]

The data in Table 1 show that the twisting of a (symmetrically substituted) C=C bond causes a bathochromic shift of the longest wavelength absorption maximum (see also refs.[4,18]). However, only scant data can be found in the literature on such an effect. *N*,*N*′-Dialkylindigo derivatives with increasingly bulky alkyl groups, for instance, absorb at substantially longer wavelengths than the parent compound.[19] Moreover, quantum mechanical calculations on fulvalene predict that the bathochromism caused by twisting is accompanied by a decrease in the band intensity.[20]

The availability of semiconductor lasers with emission wavelengths between 780 and 840 nm has created a need for dyes that absorb in the near infrared (NIR). The synthesis of twisted ethylene derivatives could make a contribution to this topical research field.[21] A prerequisite is the presence of subchromophores that absorb at long wavelengths; twisting could then shift the absorption into the NIR. Such compounds have the additional advantage that information on the bonding can be obtained not only from the crystal structure analysis, but also from electronic spectra on the structure in solution.

We chose 1,3-bis(dicyanomethylene)indane (**1**)[22] as starting material, because it is sterically demanding and affords deeply colored merocyanines with donor-substituted benzaldehydes or *p*-nitrosodialkylanilines.[23] Their structures are, however, unknown. Indane **1** reacts with the dibromo derivative **2** in the presence of Hünig base (the blue color of the anion of **1** appears temporarily) to form the sparingly soluble, yellow "dimer" **3**, which is extremely susceptible to nucleophiles. The maximum of the longest wavelength absorption band of **3** at 405 nm suggests that the C atoms at the

double bond are planar or weakly pyramidalized. The relevant band in the structure-related bi(indanedionylidene) lies at 348 nm.[24]

A suspension of **3** in dry acetonitrile at room temperature converts slowly into the shiny black compound **4**; this process is complete after about six months. A qualitative electronic spectrum of the dark red mother liquor of the sparingly soluble, readily decomposable product was recorded. The longest wavelength absorption maximum (λ = 510 nm) has undergone a bathochromic shift of 105 nm relative to that of **3**.

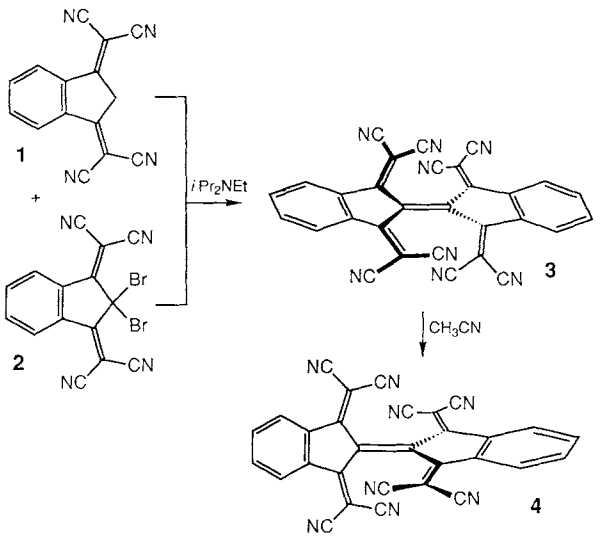

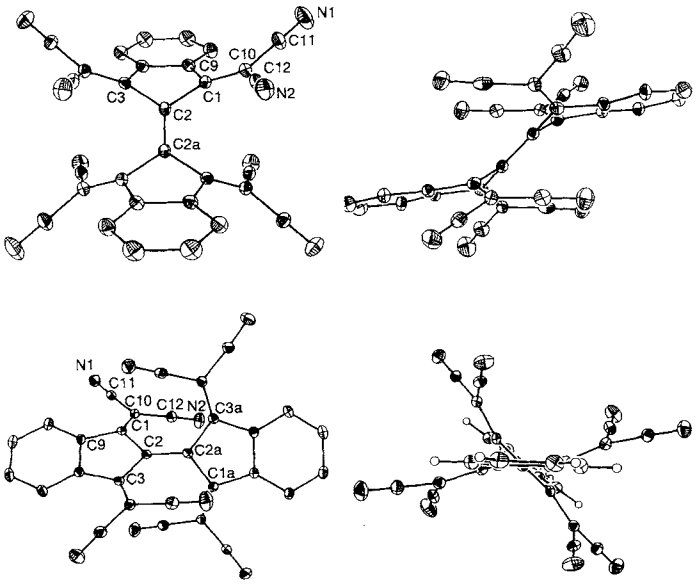

Fig. 1. Crystal structures of **3** (top) and **4** (bottom) (ORTEP). Left: View onto the central double bond. Right: side view (**3**) and view along the central double bond (**4**). Selected bond lengths [pm] and pyramidalization angles [°] for **3**: C1-C2 148.7(2), C1-C9 147.2(2), C1-C10 134.9(3), C2-C2a 134.1(3), C10-C11 143.9(3), C10-C12 143.6(3), C11-N1 113.4(3), C12-N2 113.9(3); C2-C2a: C1-C2-C3 8.0, C1-C10: C2-C1-C9 9.5, C1-C10: C11-C10-C12 5.8. **4**: Selected bond lengths [pm] and pyramidalization angles [°]: C1-C2 146.8(2), C1-C9 146.7(3), C1-C10 136.2(3), C2-C2a 140.2(3), C10-C11 143.7(3), C10-C12 143.8(3), C11-N1 113.6(3), C12-N2113.9(3); C1-C2-C2a-C3a 49.9, C3-C2-C2a-C1a 49.9; C1-C10: C2-C1-C9 9.7, C1-C10: C11-C10-C12 3.7.

The isomers **3** and **4** have different physical properties and are not interconvertible by heating the solid. Crystal structure analyses[26] show that **3** is a planar, only weakly pyramidalized ethylene derivative (Fig. 1, top), whereas **4** is a severely twisted system (Fig. 1, bottom).

The C atoms of the central double bond of **3** are weakly *anti* pyramidalized; the pyramidalization angle (definition in ref.[25]) of C2 and C2a is 8°. The C=C bond length of 134.1(3) pm is within experimental error in accord with the standard value of 133.0(9) pm.[27] The steric hinderance between the Y-shaped dicyanomethylene groups leads to a butterflylike arrangement of these groups. Each pair forms an angle of 47.2 or 47.8° with the C=C bonding plane, which is accompanied by an unusual folding of the five-membered ring of 32.0°, counteracting a strong pyramidalization of the atoms C1 and C3 of the dicyanomethylene groups. The dicyanomethylene groups are *syn* pyramidalized and twisted by 4.4 and 3.7° (definition in ref.[28]). The pyramidalization angles of the endocyclic C atoms C1 and C3 are 9.5 and 9.1°, respectively, whereas those of the exocyclic C atoms C10 and C13 are 5.8 and 6.9°, respectively. The C=C bond length in the dicyanomethylene groups (134.8 and 134.9 pm) agree with literature values.[29]

In **4** the central C=C bond is severely twisted (twist angle of 49.9°). The result is a pronounced lengthening of this double bond to 140.2 pm (134.1 in **3**). This value corresponds to 50% double-bond character. The C=C bond in the tetrasilylethylenes synthesized by Sakurai et al. are slightly shorter (136.9 pm (48.7°)[16], 137.0 pm (49.6°)[17]) and twisted to the same extent.

The remaining bond lengths of **3** are very similar to the corresponding bond lengths of **4**. The torsion in **4** causes the planarization of the indane framework to be lost. To relieve the steric congestion at the central double bond in **4**, too, the dicyanomethylene groups are *syn* pyramidalized (C1 9.7°, C3 13.9°, C10 3.7°, C13 5.1°) and slightly twisted (7.8°).

Indane **4** is probably the most twisted, symmetrically substituted ethylene derivative that has been synthesized to date. Though Sakurai et al.[16] reported a twisting of 50.2°, the twist angle is defined[28] as the average of both twist angles (50.2, 47.1°) and is thus actually 48.7° for the *anti*-pyramidalized alkene studied by them. Ballester et al.[30] give a twist angle of 67° for perchlorobifluorenylidene; the crystal structure analysis has, however, not yet been published. The structural data in a further paper on this work[31a] is very inaccurate, and this twist angle cannot be considered confirmed.

The synthesis of **3** and **4** affords for the first time an alkene[31b] in two conformations that differ by a partial rotation about the C=C bond, which allows a quantative description of the bonding changes during torsion in the crystal and in solution.

The electronic spectra of **3** and **4** calculated with an MNDO-CI program[32] from the X-ray structural data placed the longest wavelength $\pi-\pi^*$ transitions at 353 nm (oscillator strength f = 0.368) for **3** and 566 nm (f = 0.087) for **4**. The calculated excitation energies agree satisfactorily with the experimental λ_{max} values of **3** (405 nm) and **4** (510 nm).

The finding that the twisting about the central double bond in **4** relative to the almost planar structure **3** leads to a bathochromic shift of the longest wavelength absorption maximum of approximately 105 nm is the first direct experimental evidence for the thermo- and photochromism of some ethylene derivatives.[33] Torsion has already been postulated as cause of the color change on heating or irradiation; this was hitherto supported only indirectly by quantum mechanical calculations and NMR experiments.[34]

Experimental Procedure

3: Compounds **1** (0.48 g, 2 mmol) and **2** (0.88 g, 2 mmol) were suspended in dry dichloromethane (15 mL). After addition of ethyldiisopropylamine (0.70 mL, 4 mmol), the light yellow suspension immediately turned deep blue; after 15 min yellow microcrystals began to precipitate. The mixture was stirred for three days at room temperature before the crystals were filtered off by suction, washed with dichloromethane till the washings were colorless, and finally washed again with hot glacial acetic acid and with ether. Yield: 0.17 g (85%). Correct elemental analysis. Yellow prisms, m.p. > 350 °C (from CH_3CN); IR (Nujol): $\tilde{\nu}$ = 2253 (m, C≡N), 2235 (s, C≡N), 2230 (m, C≡N), 1603 (s, C=C), 1575 (s, C=C) cm^{-1}; UV/VIS(CH_2Cl_2): λ_{max} (lg ε) = 278 (42700), 293 (43100), 405 nm (8900); MS (325 °C): *m/z* = 480 (100, M^+), 4541(15, M^+−CN),453 (11%, M^+−HCN). A cubic crystal, suitable for crystal structure analysis, was obtained by recrystallization from dry acetone at 4 °C.

4: A suspension of the recrystallized compound **3** in dry acetonitrile was allowed to stand for about six months under nitrogen at room temperature. The solution slowly became very dark red, and black crystals grew at the expense of the yellow ones. Correct elemental analysis. Shiny black crystals, m.p. 280–282 °C (decomp.); IR (Nujol): $\tilde{\nu}$ = 2228(s, C≡N), 2220(m, C≡N), 2211(m, C≡N), 1584(m, C=C), 1556(s, C=C), 1510(s, C=C), 1502(s, C=C); UV/VIS(CH_3CN): λ_{max} (lg ε) = 242, 293(sh), 329, 510 nm; MS (155 °C): *m/z* = 482 (100, M^+ + 2H), 480(34, M^+), 454(13%, M^+−CN), 418(40), 390(10%).

Received: April 10, 1993 [Z 5991 IE]
German version: *Angew. Chem.* **1993**, *105*, 1424

[1] W. von E. Doering, W. R. Roth, F. Bauer, R. Breuckmann, T. Ebbrecht, M. Herbold, R. Schmidt, H. W. Lennartz, D. Lenoir, R. Boese, *Chem. Ber.* **1989**, *122*, 1263.
[2] W. Luef, R. Keese, *Top. Stereochem.* **1991**, *20*, 231–318.
[3] G. Köbrich, *Angew. Chem.* **1973**, *85*, 494; *Angew. Chem. Int. Ed. Engl.* **1973**, *12*, 464; D. Lenoir, *Nachr. Chem. Tech. Lab.* **1979**, *27*, 762.
[4] T. T. Tidwell, *Tetrahedron* **1978**, *34*, 1855; A. Krebs, B. Kaletta, R. M. Frank, *ibid.* **1986**, *42*, 1693.
[5] J. Michl, V. Bonačić-Koutecký, *Tetrahedron* **1988**, *44*, 7559; see also V. Bonačić-Koutecký, J. Koutecký, J. Michl, *Angew. Chem.* **1987**, *99*, 216; *Angew. Chem. Int. Ed. Engl.* **1987**, *26*, 170.
[6] O. Takahashi, O. Kikuchi, *Tetrahedron* **1990**, *46*, 3803.
[7] J. Sandström, *Top. Stereochem.* **1983**, *14*, 83.
[8] a) L. Salem, C. Rowland, *Angew. Chem.* **1972**, *84*, 86; *Angew. Chem. Int. Ed. Engl.* **1972**, *11*, 92; b) B. R. Brooks, H. F. Schäfer, *J. Am. Chem. Soc.* **1979**, *101*, 307; c) R. J. Buenker, V. Bonačić-Koutecký, L. Pigliani, *J. Chem. Phys.* **1980**, *73*, 1836.
[9] E. Harnik, G. M. J. Schmidt, *J. Chem. Soc.* **1954**, 3295.
[10] J. F. D. Mills, S. C. Nyburg, *J. Chem. Soc.* **1963**, 308, 927.
[11] R. Thomas, P. Coppens, *Acta Crystallogr. Sect B* **1972**, *28*, 1800.
[12] H. L. Ammon, G. L. Wheeler, *Tetrahedron* **1973**, *29*, 2695; L. Fallon, H. L. Ammon, R. West, V. N. M. Rao, *Acta Crystallogr. Sect B* **1974**, *30*, 2407.
[13] J.-S. Lee, S. C. Nyburg, *Acta Crystallogr. Sect C* **1985**, *41*, 560.
[14] A. Krebs, W. Rüger, W.-U. Nickel, M. Wilke, U. Burkert, *Chem Ber.* **1984**, *117*, 310.
[15] J. Dannheim, W. Grahn, H. Hopf, C. Parrodi, *Chem Ber.* **1987**, *120*, 871.
[16] H. Sakurai, K. Ebata, C. Kabuto, Y. Nakadaira, *Chem. Lett.* **1987**, 301.
[17] H. Sakurai, H. Tobita, Y. Nakadaira, C. Kabuto, *J. Am. Chem. Soc.* **1982**, *104*, 4288.
[18] E. Heilbronner, H. Bock, *Das HMO-Modell und seine Anwendung, Grundlagen und Handhabung*, 2nd ed., Verlag Chemie, Weinheim, **1978**, p. 315.
[19] G. Miehe, P. Susse, V. Kupcik, E. Egert, M. Nieger, G. Kunz, R. Gerke, B. Knieriem, M. Niemeyer, W. Lüttke, *Angew. Chem.* **1991**, *103*, 1008; *Angew. Chem. Int. Ed. Engl.* **1991**, *30*, 964.
[20] A. Y. Meyer, H. Yinnon, *Tetrahedron* **1972**, *28*, 3915.
[21] J. Fabian, R. Zahradnik, *Angew. Chem.* **1989**, *101*, 693; *Angew. Chem. Int. Ed. Engl.* **1989**, *28*, 677.
[22] E. Y. Gudriniece, P. V. Pastors, A. F. Ievins, *Dokl. Akad. Nauk SSSR* **1972**, *204*, 874; *Dokl. Chem. (Engl. Transl.)* **1972**, *204*, 471.
[23] K. A. Bello, L. Cheng, J. Griffiths, *J. Chem. Soc. Perkin Trans. 2*, **1987**, 815.
[24] F. Campagna, A. Carotti, G. Casini, M. Ferappi, *Gazz. Chim. Ital.* **1983**, *113*, 507.
[25] W. V. Volland, E. R. Davidson, W. T. Borden, *J. Am. Chem. Soc.* **1979**, *101*, 533.
[26] Crystal structure analysis of **3**: Enraf-Nonius CAD4 diffractometer, $\mu(Mo_{K\alpha})$ = 0.769 cm^{-1}, single crystal 0.13 × 0.4 × 0.4 mm^3, *T* = 294 K. Crystal data: M_r = 562.56, ρ_{calcd} = 1.294 $g\,cm^{-3}$, monoclinic, space group $P2_1/c$ (no. 14), *a* = 1053.6(3), *b* = 956.7(2), *c* = 1439.9(4) pm, β = 96.01(2)°, *V* = 1.4433 nm^3, *Z* = 2. ω data collection: 2θ = 4–46°, maximum measuring time 150 s, scan width 0.90° + 0.35 tan θ. Of 2248 measured reflections (±*h*, + *k*, + *l*), 2101 were symmetry-independent and 1762 of those were considered observed [$I > 2\sigma(I)$]. Refined parameters: 199. Structure solution with SHELXS 86, refinement SHELXTL-Plus. Non-hydrogen atoms anisotropic, hydrogen atoms isotropic according to a riding model in calculated positions. *R* = 0.0384, R_w = 0.0363; largest residual electron density + 0.17 and −0.19 10^{-6} e pm^{-3}. The unit cell contains two molecules of acetonitrile.—Crystal structure analysis of **4**: Enraf-Nonius CAD4 diffractometer, $\mu(Mo_{K\alpha})$ = 0.834 cm^{-1}, single crystal 0.13 × 0.27 × 0.27 mm^3, *T* = 294 K. Crystal data: M_r = 480.45, ρ_{calcd} = 1.409 $g\,cm^{-3}$, rhombic, space group *Pbcn* (no. 60), *a* = 1761.4(4), *b* = 731.5(2), *c* = 1757.6(5) pm, *V* = 2.2646 nm^3, *Z* = 4. ω data collection: 2θ = 4–46°, scan width 0.90° + 0.35 tan θ. Of 1842 measured reflections (+ *h*, + *k*, + *l*), 1440 were symmetry-independent and 1250 of those were considered observed [$I > 2\sigma(I)$]. Refined parameters: 172. Structure solution with MULTAN, refinement SHELXTL-Plus. Non-hydrogen atoms anisotropic, hydrogen atoms isotropic according to a riding model in calculated positions. *R* = 0.0307, R_w = 0.0261; largest residual electron density + 0.13 and −0.15 10^{-6} e pm^{-3}. Further details of the crystal structure investigation may be obtained from the Fachinformationszentrum Karlsruhe, Gesellschaft für wissenschaftlich-technische Information mbH, D-76344 Eggenstein-Leopoldshafen (FRG) on quoting the depository number CSD-57256, the names of the authors, and the journal citation.
[27] F. H. Allen, O. Kennard, D. G. Watson, L. Brammer, A. Guy Orpen, R. Taylor, *J. Chem. Soc. Perkin Trans. 2* **1987**, 1.
[28] O. Ermer, *Angew. Chem.* **1974**, *86*, 672; *Angew. Chem. Int. Ed. Engl.* **1974**, *13*, 604.
[29] B. Rosenau, C. Krieger, H. A. Staab, *Tetrahedron Lett.* **1985**, *26*, 2081; K. Maruyama, H. Imahori, K. Nakagawa, N. Tanaka, *Bull. Chem. Soc. Jpn.* **1989**, *62*, 1626.
[30] M. Ballester, J. Castaner, J. Riera, G. de la Fuente, M. Camps, *J. Org. Chem.* **1985**, *50*, 2287.
[31] a) F. H. Herbstein, *Acta Crystallogr. Sect. B* **1991**, *47*, 288. b) Note added in proof (July 14, 1993): The donor–acceptor substituted 2(thioxanthen-9-ylidene)indane-1,3-dione crystallizes in a folded and in a folded-twist conformation (twist angle 11.1°); UV/VIS spectra measured for solutions prepared from either conformer are the same (J. J. Stezowsky, P. U. Biedermann, T. Hildenbrand, J. A. Dorsch, C. J. Eckhardt, I. Agranat, *J. Chem. Soc. Chem. Commun.* **1993**, 213).
[32] J. Fabian, Universität Dresden, private communication, (MNDO-CI with configuration interaction of 148 singly and doubly excited states, program SCAMP 4.30 (based on AMPAC 1.0 and MOPAC 4.0)).
[33] G. Kortüm, *Ber. Bunsenges. Phys. Chem.* **1974**, *78*, 391; E. Fischer, *Chem. Unserer Zeit* **1975**, *9*, 85.
[34] R. Korenstein, K. A. Muszkat, S. Sharafy-Ozeri, *J. Am. Chem. Soc.* **1973**, *95*, 6177.

Rapid Construction of Large-size Phenylacetylene Dendrimers up to 12.5 Nanometers in Molecular Diameter**

By *Zhifu Xu* and *Jeffrey S. Moore**

The preparation and characterization of dendrimers or cascade molecules[1] are currently of widespread interest. With dendritic macromolecules, high molecular weight and a high level of structural control are possible with tremendous synthetic efficiency, because the methods of preparation rely on repetitive, nonlinear growth schemes.[2] To date, the nonlinear mathematical relationship that forms the basis of dendrimer growth has been simple geometric progression. The corresponding molecular structures quickly fill space in three dimensions, resulting in compact, globular shapes. In fact, the increase in volume per generation, based on added the properties of these macromolecules.

[*] Prof. J. S. Moore,[+] Dr. Z. Xu
The Willard H. Dow Laboratories
Department of Chemistry
The University of Michigan
Ann Arbor, MI 48109-1055 (USA)
Telefax: Int. code + (313)747-4865
[+] New address:
Department of Chemistry
University of Illinois at Urbana-Champaign
505 South Mathews Avenue, Urbana, IL 61801 (USA)

[**] Stiff Dendritic Macromolecules, Part 3. Acknowledgment is made to the National Science Foundation (NSF) for support (grant DMR-9212054) and the NSF Young Investigator Program. J. S. M. also thanks the 3M company for support through their awards program for untenured faculty. Part 2: See reference [6].

molar mass, changes at a rate that is faster than the space available given the monomer's geometric constraints.[3] We envisioned that other patterns of nonlinear repetitive growth, when translated into synthetic chemistry, would lead to molecules with molecular architectures completely different than the highly compact globular shapes of traditional dendrimers. Here we describe one strategy that leads to greatly expanded structures, enabling large-size macromolecules to be realized after only a few repetitive cycles.[4] The idea for this new strategy was proposed two years ago,[5] but poor solubility in the original dendrimers prevented growth beyond a monodendron with 17 monomer units. The solubility of phenylacetylene dendrimers is greatly enhanced by using di-*tert*-butylphenyl peripheral groups,[6] and here we use this finding to demonstrate the full utility of this new convergent synthetic method.

The new strategy combines a linear increase in monomer size per generation with the conventional convergent[1] dendrimer growth method.[7] Scheme 1 illustrates this method for dendrimers constructed from phenylacetylene monomers. In this scheme, benzene rings are represented by filled circles (•) and C≡C linkages between rings by solid lines. The angle defined by the benzene ring connectivity (*meta* or *para*) is represented in the scheme as 120° or 180° at each vertex, respectively. The advantage of constructing dendrimers from rigid building blocks such as phenylacetylene units is that the resulting macromolecules have overall dimensions that are almost invariant of conformation; thus, the interpretation of molecular size data does not depend strongly on experimental conditions nor does it require assumptions about the macromolecule's conformational state. The concept of macromolecules that are "dimension-persistent" or "shape-persistent" is important for developing molecular scaffoldings that control functional group placement on the size scale of 1–10 nm.

As shown in Scheme 1, the method requires a series of monomers (**M-1**, **M-3**, **M-5**) as well as cores (**C-1**, **C-4**, **C-7**, **C-10**) that gradually increase in size. For both monomers and cores, enlargement is accomplished by catenation of *para*-linked phenylacetylene structural units. Cores **C-1**, **C-4**, **C-7**, **C-10** span radii of 2.8, 9.7, 16.6, and 23.4 Å, respectively, as determined by molecular models. Core **C-10** is only sparsely soluble in organic solvents, but it has proven to be adequately soluble for subsequent transformations. These enlarged units are easily synthesized by using the repetitive protection/deprotection chemistry that we have described for linear phenylacetylene oligomers [Eqs. (a) and (b), dba = dibenzylideneacetone].[8]

For example, **M-3** is prepared by coupling **M-1** with two equivalents of *para*-protected phenylacetylene **1** followed by transformation of the triazene to the iodo functionality. Similarly, **C-4** is synthesized by coupling **C-1** and three equiva-

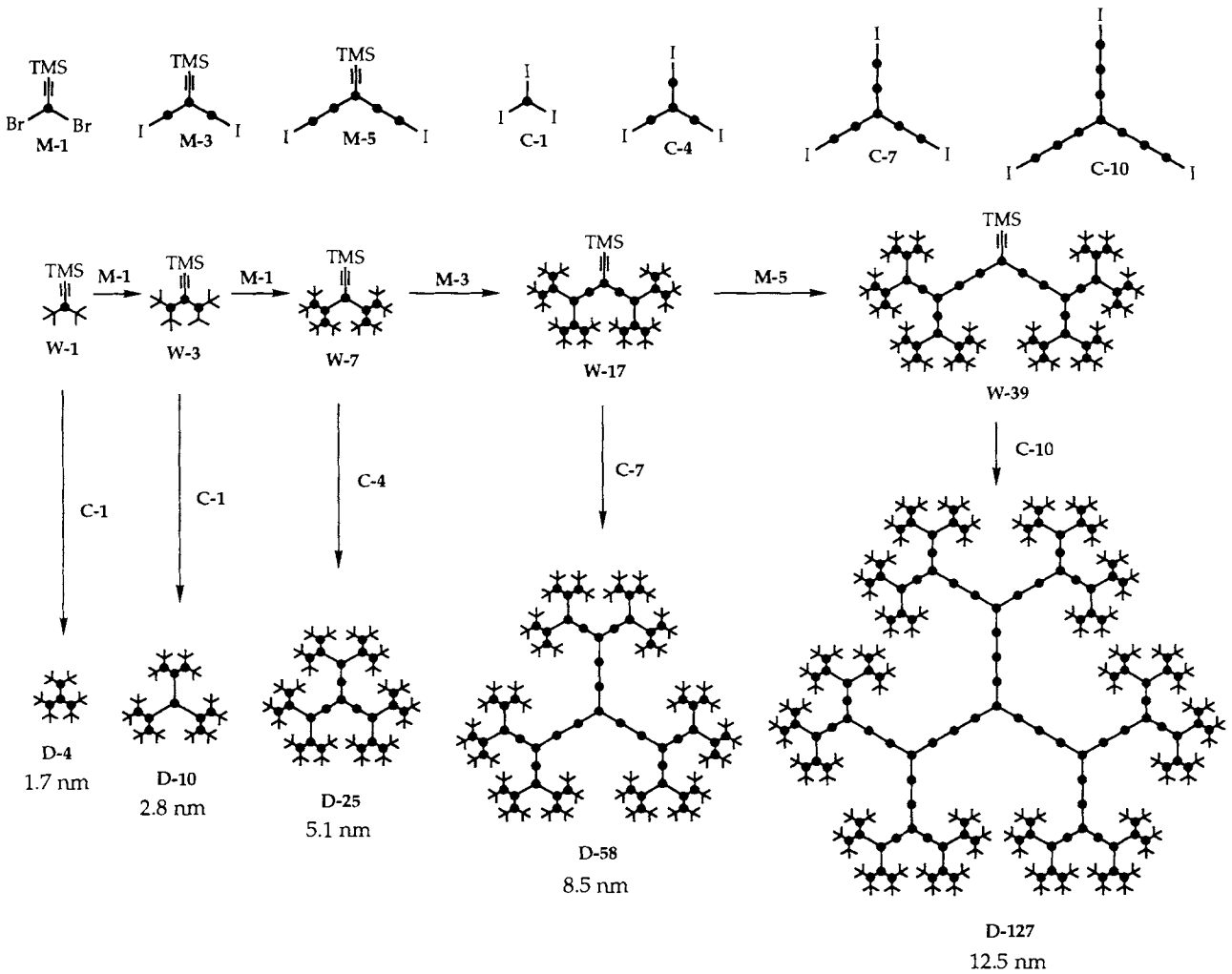

Scheme 1. Method for the preparation of phenylacetylene dendrimers that combines a linear increase in monomer/core size per generation with the convergent dendrimer growth process. Structural elements: ⅄: 1,3,5-connected benzene ring, —•—: 1,4-connected phenylene unit, ⋋⋌: 1,3-di-*tert*-butylphenyl unit, —: C≡C unit. TMS = trimethylsilyl.

 © *VCH Verlagsgesellschaft mbH, D-69451 Weinheim, 1993* *0570-0833/93/0909-1355 $ 10.00+.25/0*

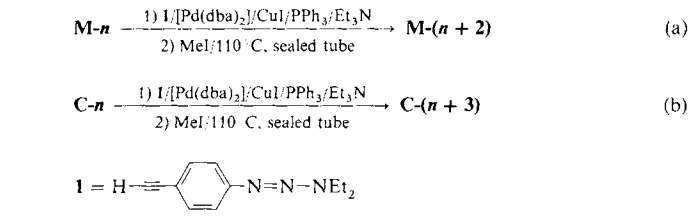

lents of **1**, and subsequently converted to the iodide. These enlarged monomers are integrated with the convergent method of dendrimer growth as shown in Scheme 1 to prepare a series of monodendrons (**W-3**, **W-7**, **W-17**, and **W-39**) containing 3 to 39 monomeric units. This is accomplished by repetitive trimethylsilyl deprotection and then palladium-catalyzed coupling with the appropriate size monomer. All of these monodendrons have been fully characterized by ^{1}H and ^{13}C NMR spectroscopy, elemental analysis, size-exclusion chromatography (SEC), and thin-layer chromatography (TLC). ^{1}H NMR spectra acquired under carefully chosen conditions (temperature, solvent) give adequate chemical shift dispersion for **W-39** for complete assignment of all the resonance signals. Finally, the new tridendrons are obtained by coupling the deprotected monodendrons with the indicated core. The process ultimately leads to the 127-mer tridendron, **D-127**, whose overall diameter as measured from molecular models spans 125 Å. This size would be nearly impossible to achieve simply by following the traditional convergent route alone.

Structure and purity (>95%) for **D-4**, **D-10**, **D-25** has been confirmed by the characterization methods described previously. Characterization of the higher members of the series has been more challenging. By using two-dimensional H,H-COSY and *J*-resolved experiments, the signals in the ^{1}H NMR spectrum of **D-58** have been completely assigned. For spectra recorded in [D_6]benzene resonances from protons on all the *para*-linked phenyl rings are fully resolved from the resonances from protons on the 1,3,5-connected aromatic rings. The former are located further upfield and exhibit the characteristic AA'BB' pattern. The two-dimensional *J*-resolved ^{1}H NMR spectrum of the aromatic region of **D-58** shows four AB_2 (nearly AX_2) spin systems at low field corresponding to four triplet–doublet pairs and a singlet corresponding to the A_3 spin system of the core. The two-dimensional H,H-COSY-45 ^{1}H NMR spectrum also confirms the expected *J*-coupling correlations, and integration is consistent with the expected composition within ±5%. In the case of **D-127**, complete characterization has been even more difficult. Elemental analysis data of the isolated product is consistent with the chemical structure of **D-127** ($C_{1398}H_{1278}$: calcd: C, 92.87; H, 7.13; found: C, 92.84; H, 7.19). SEC data are consistent with its high purity (M_n = 31 000 and M_w/M_n = 1.04 relative to polystyrene). While NMR spectral data are consistent with the expected structure, complete assignment for this molecule has not been possible. The triconnected rings in the inner two tiers as well as all of the *para*-connected rings are strongly second order and severely overlapped. Attempts at increasing dispersion through variation of temperature, solvent, and the addition of silver-lanthanide shift reagents[9] have not proven successful. Moreover, dendrimer **D-127** shows a very strong tendency to tail on both normal and reverse phases, thus deteriorating the resolution of analytical chromatography. Because of these problems, we have not been able to unambiguously prove the structure or purity of **D-127**.

Molecular models and SEC data show that all the tridendrons made by the present method have greatly expanded molecular dimensions compared with the dendrimers prepared from the standard convergent method. Hydrodynamic radii of **D-58** and **D-127** relative to polystyrene were measured by SEC to be 40 and 59 Å, respectively.[10] Thus, the advantage of Scheme 1 for dendrimer preparations is that large sizes are achieved after only a few cycles through the repetitive process. To illustrate how rapidly the size of the molecule increases by this new method, the *third* generation tridendron **D-58** containing 58 aromatic units elutes with a polystyrene equivalent hydrodynamic radius that is almost 1.5 times larger than that of the *fourth* generation compact tridendron prepared[6] by the traditional convergent growth scheme (containing 94 aromatic units). The polystyrene equivalent hydrodynamic radius of the 94-mer was determined to be 29 Å. The rapid growth in size observed for these dendrimers is efficiently expressed because of the stiff nature of the phenylacetylene monomeric unit.

It is evident that by coupling the nonlinear character of dendrimer syntheses to a linear increase in monomer size as a function of generation, growth in terms of size is dramatically accelerated. This method also results in significant changes in molecular architecture, leading to much more expanded structures. We believe that there are other nonlinear repetitive growth schemes, each perhaps leading to unique and interesting macromolecular architectures. These structural variations may have important consequences on the properties of these macromolecules.

Experimental Procedure

General procedure for tridendron (**D-4**, **D-10**, **D-25**, **D-58**, **D-127**) synthesis: A single-neck flask with a side arm was charged with **W-*x*** (3.3 equiv), **C-*y*** (1.0 equiv), [Pd(dba)$_2$] (0.02 equiv), triphenylphosphane (0.1 equiv), copper(I) iodide (0.02 equiv), and dry triethylamine. The concentrations of the reaction varied from 0.3 to 0.01 M depending on the molecular weight of the reactants. The flask was then evacuated and back-filled with nitrogen three times, capped, and stirred at 40 °C. The disappearance of terminal acetylene was checked by TLC. After completion, the reaction mixture was diluted with dichloromethane, washed with water (3 ×) and saturated aqueous sodium chloride, dried over anhydrous sodium sulfate, and filtered. Following concentration, the product was purified by careful flash chromatography, eluting with a mixture of petroleum ether and dichloromethane.

D-4: Yield 77%, m.p. 229–231 °C. ^{1}H NMR (360 MHz, [D_6]benzene, 295 K): δ = 7.81 (s, 3H), 7.663 (d, ^4J(H,H) = 1.8 Hz, 6H), 7.518 (t, ^4J(H,H) = 1.8 Hz, 3H), 1.25 (s, 54H); ^{13}C NMR (360 MHz, $CDCl_3$): δ = 150.94, 133.87, 125.97, 124.26, 123.06, 121.91, 91.61, 86.80, 34.83, 31.35. Correct C,H analysis ($C_{54}H_{66}$).

D-10: Yield 73%. ^{1}H NMR (360 MHz, [D_6]benzene, 295K): δ = 7.845 (t, ^4J(H,H) = 1.4 Hz, 3H), 7.812 (d, ^4J(H,H) = 1.4 Hz, 6H), 7.698 (d, ^4J(H,H) = 1.8 Hz, 12H), 7.665 (s, 3H), 7.53 (t, ^4J(H,H) = 1.8 Hz, 6H), 1.25 (s, 108H); ^{13}C NMR (360 MHz, $CDCl_3$): δ = 151.00, 134.52, 134.47, 133.98, 126.02, 124.45, 123.90, 123.42, 123.17, 121.81, 91.88, 89.38, 88.59, 86.62, 34.85, 31.35. Correct C,H analysis ($C_{126}H_{138}$).

D-25: Yield 87%. ^{1}H NMR (360 MHz, [D_6]benzene, 295K): δ = 7.85 (t, ^4J(H,H) = 1.5 Hz, 6H), 7.802 (d, ^4J(H,H) = 1.5 Hz, 12H), 7.75 (s, 3H), 7.711 (d, ^4J(H,H) = 1.5 Hz, 6H), 7.702 (d, ^4J(H,H) = 1.8 Hz, 24H), 7.672 (t, ^4J(H,H) = 1.5 Hz, 3H), 7.53 (t, ^4J(H,H) = 1.8 Hz, 12H), 7.39–7.45 (m, 12H, protons on the *para*-linked phenyl rings), 1.25 (s, 216H); ^{13}C NMR (360 MHz, $CDCl_3$): δ = 150.94, 134.46, 134.35, 133.90, 131.71, 125.97, 124.44, 123.98, 123.91, 123.83, 123.40, 123.12, 123.00, 122.95, 121.81, 91.91, 90.43, 90.37, 89.81, 89.74, 89.36, 88.62, 86.62, 34.81, 31.33. Correct C,H analysis ($C_{294}H_{294}$).

D-58: Yield 88%. ^{1}H NMR (360 MHz, [D_6]benzene, 295K): δ = 7.853 (t, ^4J(H,H) = 1.6 Hz, 12H), 7.806 (d, ^4J(H,H) = 1.6 Hz, 24H), 7.75 (t, ^4J(H,H) = 1.5, 3H), 7.733 (d, ^4J(H,H) = 1.5, 6H), 7.72 (s, 3H), 7.71–7.70 (m, 60H), 7.675 (t, ^4J(H,H) = 1.5 Hz, 6H), 7.53 (t, ^4J(H,H) = 1.8 Hz, 24H), 7.37–7.45 (m, 48H, protons on the *para*-linked phenyl rings), 1.25 (s, 432H); ^{13}C NMR (360 MHz, $CDCl_3$): δ = 150.98, 134.50, 134.38, 133.93, 131.76, 131.73, 131.66, 125.99, 124.44, 123.97, 123.88, 123.39, 123.16, 121.79, 91.87, 90.35, 89.74, 89.37, 88.57, 86.60, 34.85, 31.34. Correct C,H analysis ($C_{654}H_{618}$).

D-127: Yield 61%. ^{1}H NMR (360 MHz, [D_6]benzene, 336K): δ = 7.82 (t, ^4J(H,H) = 1.6 Hz, 24H), 7.775 (d, ^4J(H,H) = 1.6 Hz, 48H), 7.708–7.765 (m, 30H), 7.70 (d, ^4J(H,H) = 1.6 Hz, 24H), 7.676 (t, ^4J(H,H) = 1.6 Hz, 12H), 7.649 (d, ^4J(H,H) = 1.8 Hz, 96H), 7.519 (t, ^4J(H,H) = 1.8 Hz, 48H), 7.367–7.455 (m, 132H, protons on the *para*-linked phenyl rings), 1.26 (s, 864H); ^{13}C NMR (360 MHz, $CDCl_3$): δ = 150.97, 134.49, 134.37, 133.92, 131.74, 131.72, 131.65,

125.98, 124.42, 123.95, 123.86, 123.38, 123.15, 123.01, 121.76, 91.87, 90.35, 89.75, 89.36, 88.58, 86.60, 34.85, 31.33. Correct C,H analysis ($C_{1398}H_{1278}$).

Received: April 17, 1993 [Z 6018 IE]
German version: *Angew. Chem.* **1993**, *105*, 1394

[1] H.-B. Mekelburger, W. Jaworek, F. Vögtle, *Angew. Chem.* **1992**, *104*, 1609–1614; *Angew. Chem. Int. Ed. Engl.* **1992**, *31*, 1571–1576.
[2] J. S. Moore, *Polym. News* **1993**, *18*, 5–10.
[3] P. G. de Gennes, H. Hervet, *J. Phys. Lett.* **1983**, *44*, L351.
[4] The recursive mathematical relationship that describes the growth of these dendrimers in terms of the total number of benzene rings, T_n, as a function of generation, n, is given by $T_0 = 4$, $T_1 = 10$, $T_{n-1} = 3T_n - 2T_{n-1} + 3$.
[5] J. S. Moore, Z. Xu, *Macromolecules* **1991**, *24*, 5893–5894.
[6] Z. Xu, J. S. Moore, *Angew. Chem.* **1993**, *105*, 261–263; *Angew. Chem. Int. Ed. Engl.* **1993**, *32*, 246–248.
[7] We refer to this method as the SYNDROME method (*SYN*thesis of *D*endrimers by *R*epetition *O*f *M*onomer *E*nlargement).
[8] J. S. Moore, E. D. Weinstein, Z. Wu, *Tetrahedron Lett.* **1991**, *32*, 2465–2467; J. Zhang, J. S. Moore, Z. Xu, R. A. Aquirre, *J. Am. Chem. Soc.* **1992**, *114*, 2273–2274.
[9] T. J. Wenzel, *NMR Shift Reagents*, CRC Press, Boca Raton, FL, USA, **1987**; K. A. Kime, R. E. Sievers, *Aldrichimica Acta* **1977**, *10*, 54; T. J. Wenzel, R. E. Sievers, *Anal. Chem.* **1981**, *53*, 393.
[10] W. W. Yau, J. J. Kirkland, D. D. Bly, *Modern Size-Exclusion Liquid Chromatography*, Wiley, New York, **1979**, p. 35 and pp. 43–46.

Zirconium Phosphite (3,3′,5,5′-Tetramethylbiphenyl)diphosphonate, a Microporous, Layered, Inorganic–Organic Polymer**

By *Giulio Alberti,** *Umberto Costantino, Fabio Marmottini, Riccardo Vivani,* and *Piergiorgio Zappelli*

The chemistry of layered materials was greatly extended after the observation that organophosphonates with four-coordinate metal ions can be obtained in crystalline form with a layered structure similar to that of α-zirconium phosphate.[1] An appreciable number of pure and mixed metal(IV) phosphonates have already been prepared and characterized in various laboratories, and some of these may have practical applications as catalysts, hosts in intercalation compounds, and protonic conductors.[2–5] Only some years after the preparation of the first layered α-zirconium organophosphonate, metal(IV) diphosphonates $M^{IV}(O_3P\text{–}R\text{–}PO_3)$ were obtained by a similar procedure.[6] In these compounds, adjacent inorganic α-type layers are joined covalently by the organic R groups. Since materials with specific interlayer porosity can be prepared by simply changing the length of the organic R group, metal(IV) diphosphonates were termed MELS (Molecularly Engineered Layered Structures) to emphasize their practical potential.[7]

The structure of a typical "pillared" compound in which the organic group joining the α layers is an aromatic ring is shown schematically in Figure 1a. It is evident from this figure that the R groups are very crowded owing to the small distance (5.3 Å) between adjacent attachments in the α layer, and that the free space in the interlayer region is insufficient, regardless of the length of the organic R group. It was initially believed[8] that crystalline compounds would result if a number of pillars were replaced with small $O_3P\text{–}R'$ groups (R′ = H, OH, CH_3) (Fig. 1b). Unfortunately, only compounds with a low degree of crystallinity and low surface area, mainly because of intercrystalline mesoporosity, were obtained with the usual preparation methods.[9] A new synthetic strategy led to the realization of the first zirconium diphosphonate with covalently attached, interlamellar pillars with a high degree of crystallinity and interlayer porosity. To understand this approach, one should consider the O_3P groups on one side of the α layer to be arranged at alternate vertices of a hexagonal array structure separated by 5.3 Å and with a free area of 24 Å^2 around each O_3P group.[10] If the maximum van der Waals cross section of the pillar groups R is less than 24 Å^2, all the binding sites of the inorganic framework can be occupied, and a regular distribution of the pillars is expected. On the other hand, if the cross section of the pillars is greater than 24 Å^2, adjacent positions cannot be occupied by the large pillars, and pure zirconium diphosphonates cannot be obtained. The formation of mixed phosphonate phases containing large and small interlayer groups R and R′, respectively, is nevertheless possible if the sum of the cross section radii ($r_R + r_{R'}$) of two adjacent groups is ≤5.3 Å.

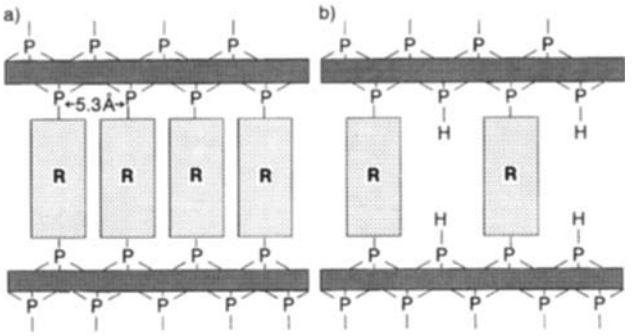

Fig. 1. a) Schematic model of a pillared zirconium phenyl diphosphonate. The size of the pillars, R = benzenediyl, is described by their van der Waals radii. b) Here some of the pillars have been substituted with small O_3PH groups.

The distribution of the large and small groups should be similar to that illustrated schematically in Figure 2. Note that the correspondenting composition is $Zr(O_3P\text{–}H)_{1.33}(O_3P\text{–}R\text{–}PO_3)_{0.33}$. Six small phosphite groups surround each large diphosphonate pillar. If the cross section of the

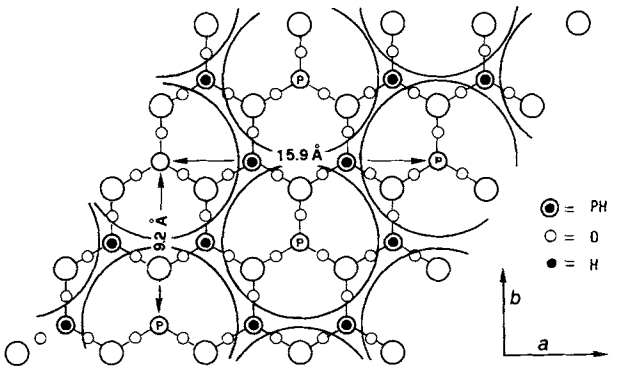

Fig. 2. Idealized arrangement of small phosphite groups and large diphosphonate pillars on one side of the α layers; the idealized structure corresponds to the composition $Zr(O_3PH)_{1.33}(O_3P\text{–}R\text{–}PO_3)_{0.33}$.

[*] Prof. Dr. G. Alberti, Prof. Dr. U. Costantino, Dr. F. Marmottini, Dr. R. Vivani
Dipartimento di Chimica, Università di Perugia
Via Elce di Sotto 8, I-06123 Perugia (Italy)
Dr. P. Zappelli
Enitricerche Spa
Via Ramarini 32, I-00016 Monterotondo (Italy)

[**] This work was supported by Enitricerche Spa, Milan, Italy.

large pillars is uniform, little or no interlayer porosity is expected (Fig. 3a). However, if the cross section is not uniform, and in particular if the cross section of the pillar in the middle is smaller than at the ends, interlayer porosity results (Fig. 3b). This type of pillar could be prepared with the R

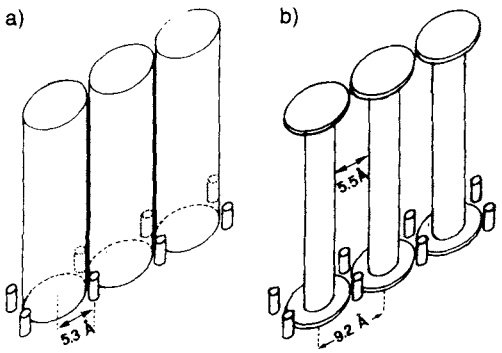

Fig. 3. a) Schematic representation of the structure described in Figure 2 (small phosphite groups and large diphosphonate groups with uniform cross section). View along the *a* axis. Note that no appreciable interlayer porosity is created. b) Here the large diphosphonate groups are broader at the ends than in the middle. Interlayer porosity is created.

groups shown in Scheme 1. Thus we synthesized diphosphonic acid **1**, and the corresponding pillared zirconium phosphite diphosphonate **2**.

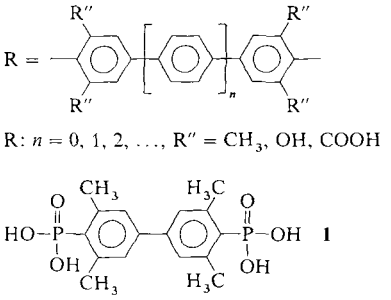

Scheme 1.

The chemical and NMR spectroscopic analyses gave a P:Zr molar ratio of 2:1 and a phosphite:diphosphonate molar ratio of 3:1, which implies that the composition of this compound is $Zr(HPO_3)_{1.2}(O_3P–R–PO_3)_{0.4}$ ($R = Me_2H_2C_6–C_6H_2Me_2$). The X-ray diffraction powder pattern of **2** is typical of a fairly crystalline, α-layered, pillared compound.[11]

The high phosphite content and the good degree of crystallinity are in agreement with the model in Figure 2; furthermore, the predicted microporosity was experimentally confirmed. The specific surface area, calculated by the BET analysis, was 375 $m^2 g^{-1}$. The micropore distribution curve obtained by the T-plot analysis, has a sharp maximum for a pore size of about 5 Å (Fig. 4). This result was also confirmed by ^{129}Xe NMR spectroscopy.[12]

A computer-generated structural model for the ideal composition $Zr(HPO_3)_{1.33}(O_3P–R–PO_3)_{0.33}$ is shown in Figure 5. In this model it was assumed that the diphosphonate groups are perpendicular to the α layers and that all the arene rings have the same orientation. Although these assumptions might be too strict, it can be noted that both the interlayer spacing (14.5 Å) and the free average intercolumnar distance

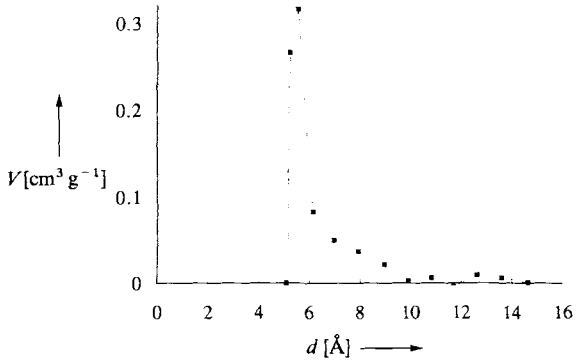

Fig. 4. Micropore-size distribution of $Zr(HPO_3)_{1.2}(O_3P–R–PO_3)_{0.4}$; R = 3,3',5,5'-tetramethylbiphenyl. *d* = pore size.

deduced from the model (5 Å) are in good agreement with the position of the first reflection in the X-ray diffraction pattern (14 Å) and with the pore size determined experimentally. The structure of this pillared compound in which the pillars have broadened bases, is reminiscent of the architecture of a Greek temple.

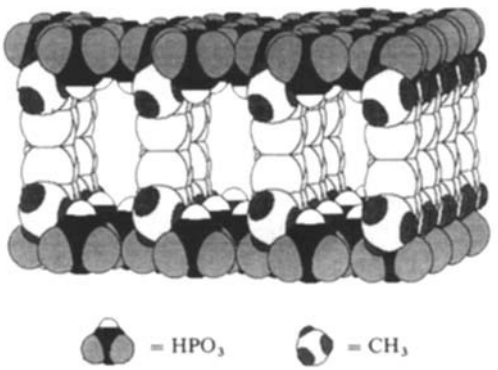

Fig. 5. Computer-generated structural model of the pillared compound with the idealized composition $Zr(HPO_3)_{1.33}(O_3P–R–PO_3)_{0.33}$; R = 3,3',5,5'-tetramethylbiphenyl. Zirconium atoms are omitted for clarity.

This type of microporous inorganic–organic polymer with tailor-made cavities of uniform size, possibly containing catalytic sites, opens the way for their application as molecular sieves and "shape-selective" catalysts.

Experimental Procedure

1: To a solution of *tert*-butyl nitrite (32 g, 312 mmol) in bromoform (75 mL) was added a solution of 3,3',5,5'-tetramethylbenzidine (25 g, 104 mmol) in bromoform (175 mL). The mixture was stirred for 2 h at 65 °C. After workup and column chromatography (silica gel, petroleum ether), the intermediate 4,4'-dibromo(3,3',5,5'-tetramethyl)biphenyl was recovered (16.5 g, 43% yield). This was then subjected to a photocatalyzed phosphonation reaction by irradiating a solution in triethyl phosphite with a high-pressure mercury vapor UV lamp. After workup and column chromatography (silica gel, ethyl acetate/petroleum ether (7:3)), the next intermediate, tetraethyl-[(3,3',5,5'-tetramethyl)biphenyl]-4,4'-bisphosphonate was collected (11.2 g, 51.7% yield). This second intermediate was hydrolyzed by heating for 4 h at 80 °C with HBr in acetic acid to afford **1** (94% yield). ^1H NMR (400 MHz, [D$_6$]DMSO, 25 °C): $\delta = 2.65$ (s, 12H, CH_3), 7.40 (4H, Ar); ^{31}P NMR (400 MHz, [D$_6$]DMSO, 25 °C): $\delta = 17.02$, relative to H_3PO_4, external.

2: Preparation according to the method of thermal decomposition of fluorozirconium complexes [13]. Diphosphonic acid **1** (1.036 g, 2.8 mmol) and H_3PO_3 (4.14 g, 50.5 mmol) were dissolved in DMSO (28 mL) and water (6 mL) in a plastic vessel, then treated with a solution of $ZrOCl_2 \cdot 8H_2O$ (0.602 g, 1.9 mmol) in conc. HF (1.6 mL) and water (4.4 mL). The closed vessel was placed in a thermostated bath at 70 °C, and the temperature was increased at the rate of 5 °C per hour. When the solution began to show a slight turbidity (at

about 80 °C), the temperature was reduced by 5 °C and then slowly increased at the rate of 2 °C per day up to 95 °C. The solid product was filtered, washed with DMSO and then acetone, dried under air, and stored under P_4O_{10}. Correct elemental analysis. ^{31}P NMR (200 MHz, DMSO/D_2O (2:1), 50 mg of **2** dissolved in 1 mL of 2 M HF, 25 °C): $\delta = 19.6$ (br. m, PCH(Ar)), 6.9 (d, $^1J(P,H) = 665.3$ Hz, PH), the shifts are relative to 85% D_3PO_4 in D_2O, external.

Received: April 5, 1993 [Z 5979 IE]
German version: *Angew. Chem.* **1993**, *105*, 1396

[1] G. Alberti, U. Costantino, S. Allulli, N. Tomassini, *J. Inorg. Nucl. Chem.* **1978**, *40*, 1113.
[2] M. B. Dines, P. D. Di Giacomo, *Inorg. Chem.* **1981**, *20*, 92.
[3] G. Alberti, U. Costantino, J. Kornyei, M. L. Luciani, *React. Polym.* **1985**, *5*, 1.
[4] G. Alberti, U. Costantino in *Inclusion Compounds 5* (Eds.: J. L. Atwood, J. E. D. Davis, D. D. MacNicol), Oxford University Press, **1991**, Chap. 5, and references therein.
[5] D. A. Burwell, M. E. Thompson in *Supramolecular Architecture* (*ACS Symp. Ser.* **1992**, *499*, 166); A. Clearfield, C. Y. Ortiz-Avila, *ibid.* **1992**, *499*, 178.
[6] M. B. Dines, P. D. Di Giacomo, K. P. Gallahan, P. C. Griffith, R. H. Lane, R. E. Cooksey in *Chemically Modified Surface in Catalysis and Electrocatalysis* (*ACS Symp. Ser.* **1982**, *192*, 223).
[7] J. Alper, *Chem. Ind.* **1986**, 335.
[8] M. B. Dines, R. E. Cooksey, P. C. Griffith, R. H. Lane, *Inorg. Chem.* **1983**, *22*, 1003.
[9] G. Alberti, U. Costantino, R. Vivani, P. Zappelli, *Mater. Res. Soc. Symp. Proc.* **1991**, *233*, 101.
[10] J. M. Troup, A. Clearfield, *Inorg. Chem.* **1977**, *16*, 3311.
[11] The X-ray diffractogram was indexed as describing a monoclinic cell with $a = 15.286$, $b = 9.365$, $c = 28.478$ Å, $\beta = 94.99°$; structure analysis conduced using the program TREOR (*J. Appl. Crystallogr.* **1985**, *18*, 367).
[12] J. A. Ripmeester, C. I. Ratcliffe, J. S. Tse, *J. Chem. Soc. Faraday Trans. 1* **1988**, *84*, 3731. The chemical shift in the ^{129}Xe NMR spectrum extrapolated to pressure zero ($d_s = 119$ pm) is close to the value found for ZSM5-type zeolite ($d_s = 114$ ppm).
[13] G. Alberti, U. Costantino, R. Giulietti, *J. Inorg. Nucl. Chem.* **1980**, *42*, 1062.

increase in charge separation between the phosphorus and carbon atoms of the double bond of about 0.2–0.3 e per silyl group, which acts as a π acceptor.[6] Replacement of the hydrogen atoms at the phosphorus center with methyl groups increases this difference still further. The polarizing effect of the silyl group can be utilized in a simple and productive synthesis of novel, four-membered phosphorus–carbon heterocycles.[7]

Thus, halogenated ylides **5** react almost quantitatively with $AlCl_3$ to give the previously unknown dihydrophosphetium salts **6** (Scheme 1).[8] The formation of **6** may be

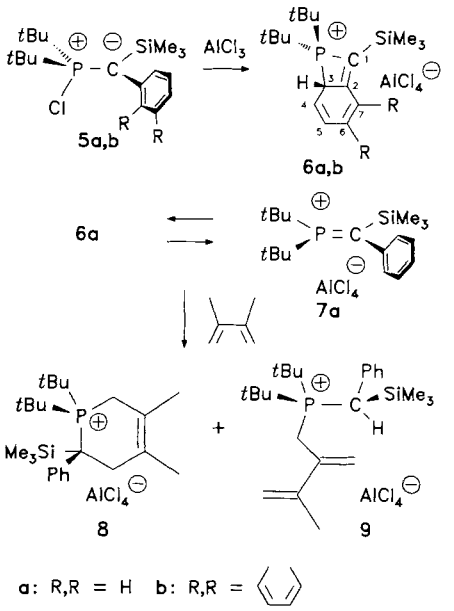

Scheme 1.

explained in terms of an *intra*molecular electrocyclic ring closure of intermediate methylenephosphonium ions **7** (**7a**: aryl = phenyl, **7b**: aryl = naphthyl). A change in coordination geometry at the electrophilic phosphorus center from trigonal-planar in **7** to tetrahedral in **6** is energetically favorable, and compensates for the loss of conjugation energy of the aryl ring as well as the ring strain caused by the formation of the four-membered ring. The ring closure that leads to **6a** is reversible, and the methylenephosphonium ion **7a**, which is present at equilibrium in low concentration, reacts with 2,3-dimethylbutadiene (DMB) to give the [2 + 4] cycloadduct **8** and ene reaction product **9** [ratio **8**:**9** ca. 2:1; ^{31}P NMR: $\delta = 45.3$ (**8**), $\delta = 53.6$ (**9**); c.f. ref.[3]]. We could not, however, detect **7a** spectroscopically.

Whereas solutions of **6a** decompose within 24 h to products of indeterminate composition (not, however, **10a**), **6b** is stable, and likewise does not react with DMB. This cyclization reaction of methylenephosphonium ions described here

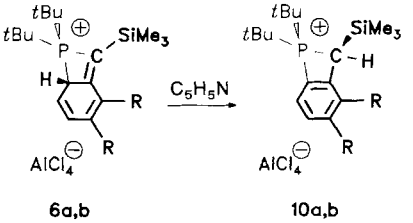

Benzoannulated Phosphorus–Carbon Four-Membered Rings**

By *Udo Heim, Hans Pritzkow, Ulrich Fleischer,* and *Hansjörg Grützmacher**

Dedicated to Professor Hans Bock on the occasion of his 65th birthday

The polarizing effect of silyl substituents[1] on multiply bonded systems is highly pronounced, and well defined experimentally.[2] We have previously investigated the influence of a trimethylsilyl group on the double bond of methylenephosphonium salts.[3] Population analyses for the molecules $H_2P{=}CH_2^+$ (**1**) [q(P): +0.7, q(C): −0.2], $H_2P{=}C(SiH_3)_2^+$ (**2**) [q(P): +0.7, q(C): −0.7],[4] $Me_2P{=}CH_2^+$ (**3**) [q(P): +1.0, q(C): −0.2], and $Me_2P{=}CH(SiH_3)^+$ (**4**) [q(P): +1.0, q(C): −0.5][5] show an

[*] Prof. Dr. H. Grützmacher
Institut für Anorganische und Analytische Chemie der Universität
Albertstrasse 21, D-79104 Freiburg (FRG)
Telefax: Int. code + (761)203-2815
Dipl.-Chem. U. Heim, Dr. H. Pritzkow
Anorganisch-chemisches Institut der Universität Heidelberg (FRG)
Dr. U. Fleischer
Fakultät für Chemie, Lehrstuhl für Theoretische Chemie
an der Universität Bochum (FRG)

[**] This work was supported by the Deutsche Forschungsgemeinschaft (SFB 247) and the Fonds der Chemischen Industrie. We thank the referees for their stimulating comments.

can be compared with the Bischler–Napieralski cyclization of iminium ions $R_2N{=}CR'^{+}_2$, in which the C terminus acts as the electrophilic center.[9] An *inter*molecular phosphorylation of arenes (toluene, anisole) with methylenephosphonium ions has not been achieved to date.

Upon addition of a tertiary amine base (preferably pyridine), both **6a** and **6b** undergo irreversible and quantitative rearrangement to the stable, isomeric phosphetanes **10a** and **10b**.[10] Whereas **6b** is unreactive towards acids (e.g. $HBF_4 \cdot OEt_2$), **6a** gives rise mainly to $tBu_2PClCHPh(SiMe_3)^+X^-$ (X = BF_4, Cl) **11**, small amounts of **10a**, and a further uncharacterized product (^{31}P NMR: $\delta = 158.3$).

The molecular structures of the heterocycles **6b** and **10b** (Fig. 1) were determined by single-crystal X-ray diffraction analyses.[11] Within the planar four-membered rings of **6b**

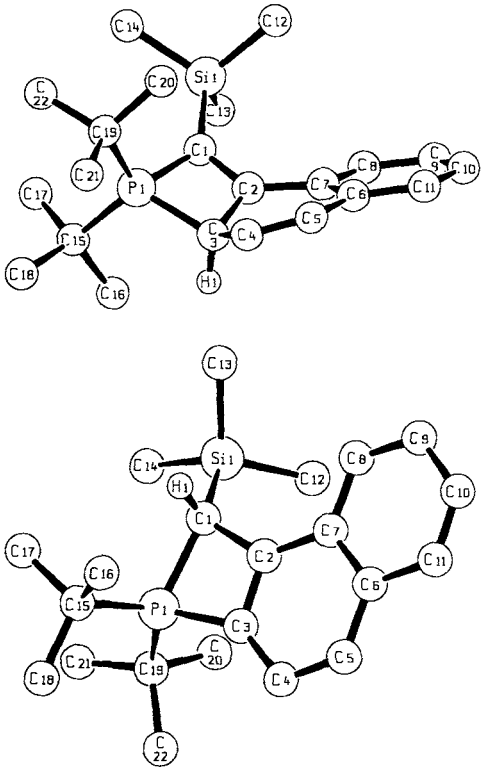

Fig. 1. Top: Crystal structure of cation **6b**: Selected distances [Å] and angles [°]: P1-C1 1.798(3), C1-C2 1.366(4), C2-C3 1.514(4), C3-P1 1.856(3), C3-C4 1.495(5), C4-C5 1.317(5), C5-C6 1.458(5), C6-C7 1.408(4), C7-C8 1.385(4), C8-C9 1.384(5), C9-C10 1.372(5), C10-C11 1.370(5), C11-C6 1.398(4), C2-C7 1.463(4); C3-P1-C1 79.1(1), P1-C1-C2 89.7(2), C1-C2-C3 107.7(2), C2-C3-P1 83.2(1), C2-C3-C4 111.7(3), C4-C3-P1 128.0(2), P1-C1-Si1 137.3(1), Si1-C1-C2 132.2(2), C1-C2-C7 132.9(2), C7-C2-C3 118.6(2). Bottom: Crystal structure of cation **10b**: Selected distances [Å] and angles [°]: P1-C1 1.859(3), C1-C2 1.549(5), C2-C3 1.360(5), C3-P1 1.781(3), C3-C4 1.420(5), C4-C5 1.350(6), C5-C6 1.409(6), C6-C7 1.438(5), C7-C8 1.402(6), C8-C9 1.360(6), C9-C10 1.401(8), C10-C11 1.328(8), C11-C6 1.421(6), C2-C7 1.424(4); C3-P1-C1 78.7(1), P1-C1-C2 83.8(2), C1-C2-C3 105.0(3), C2-C3-P1 92.5(2), C2-C3-C4 123.7(3), C4-C3-P1 143.8(3), P1-C1-Si1 129.8(2), Si1-C1-C2 123.7(2),C1-C2-C7 133.7(3), C7-C2-C3 121.2(3).

and **10b**, the bond angle at the phosphorus center is the smallest, and is almost identical for both heterocycles (79.1° **6b**, 78.7° **10b**). The P–C bonds in the four-membered ring are conistent with normal P–C(sp^3) and P–C(sp^2) distances. In the course of the de- and reprotonation, the change in coordination number of carbon atoms C1 and C3 gives rise to the predicted differences in the molecular geometry: the C1–C2 double bond in **6b** [1.366(4) Å] is lengthened to 1.549(5) Å in **10b**, corresponding to a single bond, whereas the C2–C3 distance in **6b** [1.514(4) Å] is shortened to 1.360(5) Å in **10b**. In accordance with this, a reciprocal shortening/lengthening is observed in the P1–C1 [**6b**: 1.798(3) Å; **10b**: 1.859(3) Å] and P1–C3 [**6b**: 1.856(3) Å; **10b**: 1.781(3) Å] distances. Consideration of the C–C distances in **6b** (Fig. 1 top) indicates that the bonding system in **6** is accurately represented by the valence-bond formula illustrated in Scheme 1. The C–C bond lengths in **10b** differ only slightly from those in naphthalene,[12] and only the C6–C7 distance (1.429(4) Å) is longer than that of the parent hydrocarbon (1.393 Å). Analogous with **6a** and **10a** are 3-methylene-1,4-cyclohexadiene **12** (*ortho*-isotoluene) and toluene **13**, where the latter is 24 ± 1.8 kcal mol^{-1} more stable than its isomer **12**.[13] Benzoannulation reduces the energy difference between conjugated polyenes and arenes [cf. $\Delta(\Delta H_f) = 15.8 \pm 1.8$ kcal mol^{-1}] for 1-methylene-1,4-dihydronaphthalene **14** and 1-methylnaphthalene **15**), and this explains the high stability of **6b**. Compared with **12** and **14**, compounds **6a**, **b** are remarkably resistant towards acid-catalyzed rearrangement to cyclic, conjugated electron systems. This is attributed to the π electron withdrawing effect of the Me_3Si group and to a greater degree the π electron withdrawing effect of the phosphonio group.[14] Rearrangement is thus prevented by the reduced basicity of the C1=C2 bond in the position α to the heterosubstituents in addition to the positive charge of the cation (Coulomb barrier).

With a strong base such as sodium bis(trimethylsilyl)amide, the cyclic phosphonium salt **10a** is deprotonated smoothly, to give, as expected, the neutral λ^5-phosphete **16**.[7b, 15] This ring

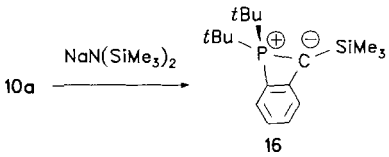

system has not, to our knowledge, been reported to date, and is prepared here for the first time with classical methods.[16]

Experimental Procedure

All manipulations were carried out in dry, oxygen-free solvents.

6a, b: 3 mmol of the phosphorus ylide **5a** (1.03 g) or **5b** (1.25 g) was dissolved in CH_2Cl_2 (10 mL) and added dropwise at -78 °C to a suspension of powdered $AlCl_3$ (0.53 g, 4 mmol). The reaction mixture was stirred for 10 min at -78 °C, and then filtered rapidly below -30 °C. After removal of all volatiles at 0.01 Torr, the product was obtained spectroscopically pure as a pale yellow powder, which was recrystallized from CH_2Cl_2 by layering with *n*-hexane. Yield 80–85%.

10a, b: A solution of **6a, b** in CH_2Cl_2 was treated with an equimolar quantity of pyridine. After removal of all volatiles from the clear reaction mixture at 0.01 Torr, the colorless solid residue was recrystallized as described above from a little CH_2Cl_2/*n*-hexane. Yield >90%.

16: A solution of $NaN(SiMe_3)_2$ (0.38 g) in toluene (10 mL) was added dropwise at 0 °C with a syringe to a solution of **10a** (1.0 g, 2.1 mmol) in toluene (20 mL). After stirring at 0 °C for 30 min, the bright orange reaction mixture was filtered, concentrated under reduced pressure (0.01 Torr), treated with *n*-hexane until **16** began to precipitate, and left for 24 h at -30 °C. Yield 64%. Loss of yield arose through slow decomposition of **16** in the reaction solution, which we attribute to the reaction of $NaAlCl_4$ with $HN(SiMe_3)_2$. Warming of the reaction mixture or a longer reaction time should therefore be avoided.

Received: March 27, 1993 [Z 5953 IE]
German version: *Angew. Chem.* **1993**, *105*, 1400

[1] a) H. Bock, *Angew. Chem.* **1989**, *101*, 1659; *Angew. Chem. Int. Ed. Engl.* **1989**, *28*, 1627; b) Y. Apeloig in *The Chemistry of Organic Silicon Compounds* (Eds.: S. Patai, Z. Rappoport), Wiley, Chichester, **1989**, p. 57.

[2] For example: Investigations into methylenephosphanes $RP{=}CR_2$ and iminophosphanes RP=NR: a) W. W. Schoeller, J. Niemann, R. Thiele, W. Haug, *Chem. Ber.* **1990**, *124*, 417, and references therein; b) E. Niecke, D. Gudat, *Angew. Chem.* **1991**, *103*, 251; *Angew. Chem. Int. Ed. Engl.* **1991**, *30*, 217, and references therein.

[3] a) H. Grützmacher, H. Pritzkow, *Angew. Chem.* **1991**, *103*, 721; *Angew. Chem. Int. Ed. Engl.* **1991**, *30*, 709; b) H. Grützmacher, H. Pritzkow, *ibid.* **1992**, *104*, 92; **1992**, *31*, 99; c) U. Heim, H. Pritzkow, H. Schönberg, H. Grützmacher, *J. Chem. Soc. Chem. Commun.* **1993**, 673.

[4] M. Ehrig, H. Horn, C. Kölmel, R. Ahlrichs, *J. Am. Chem. Soc.* **1991**, *113*, 3701.

[5] U. Fleischer, unpublished results.

[6] H. Bock, J. Meuret, K. Ruppert, *Angew. Chem.* **1993**, *105*, 413; *Angew. Chem. Int. Ed. Engl.* **1993**, *32*, 414, and references therein.

[7] Phosphetanes: a) O. Stelzer, *Chem. Ber.* **1992**, *125*, 1987; b) E. Fluck, B. Neumüller in *Rings Clusters, and Polymers of Main Group and Transition Metals* (Ed.: H. W. Roesky), Elsevier, Amsterdam, **1989**, p. 201.

[8] **5a**: M.p. 82–83 °C; ^{31}P NMR: $\delta = 98.3$; ^{13}C NMR: $\delta = 45.6$ [^1J(P,C) = 67 Hz, PCSi]; ^1H NMR: $\delta = 0.34$ (s, H_3CSi), 1.32 [d, ^3J(P,H) = 16.1 Hz, CH_3], 6.91–7.63 [aromat. CH], ^{29}Si NMR: $\delta = -0.9$ [d, ^2J(P,Si) = 6.2 Hz]. **5b, b'** (two rotamers, interconvertible through a 90° rotation about the bond to the ylidic carbon atom, and distinguishable only through their ^1H NMR spectra. Other data refer to the mixture.): M.p. 106–107 °C; ^{31}P NMR: $\delta = 101.9$; ^{13}C NMR: $\delta = 47.8$ [^1J(P,C) = 61 Hz, PCSi]; ^1H NMR: $\delta = -0.05$ (s, H_3CSi), 1.26 [d, ^3J(P,H) = 16.3 Hz, CH_3], 1.52 [d, ^3J(P,H) = 16.0 Hz, CH_3], 7.33–8.46 [aromat. CH]; ^{29}Si NMR: $\delta = -3.7$ [d, ^2J(P,Si) 4.3 Hz]. – **5b'**: ^1H NMR: $\delta = -0.04$ (s, H_3CSi), 1.27 [d, ^3J(P,H) = 16.3 Hz, CH_3], 1.53 [d, ^3J(P,H) = 16.0 Hz, CH_3], 7.33–8.46 [aromat. CH]. – **6a**: M.p. 102–103 °C; ^{31}P NMR: $\delta = 82.3$; ^{13}C NMR (numbering as in Scheme 1): $\delta = 43.8$ [d, ^1J(P,C) = 44 Hz, C3], 132.6 [d, ^1J(P,C) = 26 Hz, C1], 172.9 [d, ^2J(P,C) = 29 Hz, C2]; ^1H NMR: $\delta = 0.33$ (s, H_3CSi), 1.47 [d, ^3J(P,H) = 16.9 Hz, CH_3], 1.52 [d, ^3J(P,H) = 16.6 Hz, CH_3], 4.34 [d, ^2J(P,H) = 26.6 Hz, CH], 6.44–6.64 [aromat. CH], ^{29}Si NMR: $\delta = -9.4$ [d, ^2J(P,Si) = 5.8 Hz]. – **6b**: m.p. 135–136 °C; ^{31}P NMR: $\delta = 81.7$; ^{13}C NMR (numbering as in Scheme 1): $\delta = 42.4$ [d, ^1J(P,C) = 46 Hz, C3], 131.4 [d, ^1J(P,C) = 11 Hz, C1], 172.7 [d, ^2J(P,C) = 26 Hz, C2]; ^1H NMR: $\delta = 0.39$ (s, H_3CSi), 1.55 [d, ^3J(P,H) = 16.7 Hz, CH_3], 1.60 [d, ^3J(P,H) = 16.5 Hz, CH_3], 4.43 [d, ^2J(P,H) = 20.8 Hz, CH], 6.30–7.59 [aromat. CH], ^{29}Si NMR: $\delta = -10.6$ [d, ^2J(P,Si) = 5.8 Hz].

[9] G. Fodor, S. Nagubandi, *Tetrahedron* **1980**, *36*, 1279.

[10] **13a**: M.p. 122 °C; ^{31}P NMR: $\delta = 89.5$; ^{13}C NMR: $\delta = 34.1$ [d, ^1J(P,C) = 32.5 Hz, PCSi]; ^1H NMR: $\delta = 0.42$ (s, H_3CSi), 1.49 [d, ^3J(P,H) = 16.6 Hz, CH_3], 1.68 [d, ^3J(P,H) = 17.1 Hz, CH_3], 3.71 [d, ^2J(P,H) = 16.1 Hz, CH], 7.20–7.90 [aromat. CH]. – **13b**: M.p. 142 °C; ^{31}P NMR: $\delta = 84.5$; ^{13}C NMR: $\delta = 35.4$ [d, ^1J(P,C) = 30.8 Hz, PCSi]; ^1H NMR: $\delta = 0.54$ (s, H_3CSi), 1.55 [d, ^3J(P,H) = 11.6 Hz, CH_3], 1.73 [d, ^3J(P,H) = 12.5 Hz, CH_3], 4.04 [d, ^2J(P,H) = 16.1 Hz, CH], 7.47–8.19 [aromat. CH].

[11] **6b**: $P2_1/c$, $a = 13.981(7)$, $b = 12.632(6)$, $c = 17.302(9)$ Å, $\beta = 113.48(4)°$, $V = 2803$ Å^3, $Z = 4$, 3646 observed reflections [$I > 2\sigma(I)$], $R = 0.051$ (320 parameters); **10b**: *Pcab*, $a = 15.437(8)$, $b = 17.987(9)$, $c = 20.256(10)$ Å, $V = 5624$ Å^3, $Z = 8.3042$ observed reflections [$I > 2\sigma(I)$], $R = 0.052$ (320 parameters). Intensity measurement: Four-circle diffractometer ($Mo_{K\alpha}$ radiation, ω-scan); Refinement: Non-hydrogen atoms anisotropic, hydrogen atoms of the methyl groups as part of a rigid group with common isotropic thermal parameters, all other H atoms in found positions isotropically refined. Further details of the crystal structure investigations may be obtained from the Fachinformationszentrum Karlsruhe, Gesellschaft für wissenschaftlich-technische Information mbH, D-76344 Eggenstein-Leopoldshafen (FRG) on quoting the depository number CSD-57361, the names of the authors, and the journal citation.

[12] J. M. Robertson, *Organic Crystals and Molecules*, Cornell Univ Press, New York, **1953**, Chapter 8.

[13] J. E. Bartmess, S. S. Griffith, *J. Am. Chem. Soc.* **1990**, *112*, 2931.

[14] W. Kaim, U. Lechner-Knoblauch, P. Hänel, H. Bock, *J. Org. Chem.* **1983**, *48*, 4206; H. Bock, U. Lechner-Knoblauch, H. Hänel, *Chem. Ber.* **1986**, *119*, 3759.

[15] **16**: ^{31}P NMR: $\delta = 78.3$; ^1H NMR: $\delta = 0.19$ (s, H_3CSi), 1.47 [d, ^3J(P,H) = 14.0 Hz, CH_3], 5.8–7.1 [m, aromat. CH].

[16] H. J. Bestmann, R. Zimmermann in *Methoden der Organischen Chemie, Vol. E1* (Ed.: Houben-Weyl-Müller), Thieme, Stuttgart, **1982**, p. 616.

How Strong and How Hindered Can Uncharged Phosphazene Bases Be?**

By *Reinhard Schwesinger,* Christian Hasenfratz, Helmut Schlemper, Leonhard Walz, Eva-Maria Peters, Karl Peters,* and *Hans Georg von Schnering*

In 1987 we reported on the extraordinarily basic, uncharged polyaminophosphazenes **1**–**4a**[1] exhibiting $^{MeCN}pK_{BH^+}$ values[2] of up to 42.6. These compounds, readily available from **5a**,[3] **6a**,[4] and Me_2NH, are of increasing interest as bulky auxiliary bases for sensitive reactions in the basicity range of classical organometallic compounds.[5]

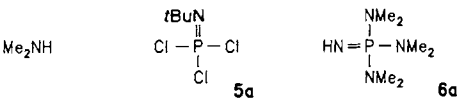

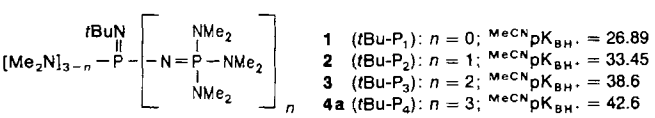

With the exception of proton sponges, uncharged bases are kinetically highly active even towards weak acids, and the naked anions thus generated are often extremely reactive. In reactions of such substrates with electrophiles, a low equilibrium concentration of the anion often suffices as long as the base is inert to the electrophile. Thus both an increase in basicity and steric bulk of the phosphazene bases should extend their range of applications.

An apparent approach for increasing the basicity of the phosphazene bases is homologation of their chains; the extension of the P_4 system in **4** ("*t*Bu-P_4")[5n] by one PN_3 unit proved to be the best strategy. For this synthetic concept P_2 building blocks[6] **10** must be generally accessible (Scheme 1). Coupling of the P_1 units **6a** and **7a** afford **8a**;[7] the further reactions leading to **10a** correspond to those previously employed to convert hexamethylphosphoric triamide (HMPA) into **6a**; however, the chlorination of **8** requires a somewhat higher temperature than the analogous reaction with HMPA.[9] After compound **5a** is coupled with **10a** and then with **6a** (in this order), the counterion is exchanged to provide **11a**·HBF_4. In analogy to **4a**, this salt is treated with KNH_2 in liquid NH_3 to liberate **11a**. Like all higher phosphazene bases **11a** (*t*Bu-P_5), a stable solid, is extremely hygroscopic, lipophilic, and approximately[10] 3 pK units more basic than **4a**.

[*] Priv.-Doz. Dr. R. Schwesinger, Dipl.-Chem. C. Hasenfratz
Chemisches Laboratorium der Universität
Institut für Organische Chemie und Biochemie
Albertstrasse 21, D-79104 Freiburg (FRG)
Telefax: Int. code + (761)203-2815

Dr. H. Schlemper
Fluka AG, CH-9470 Buchs SG (Switzerland)

Dr. L. Walz
Daimler Benz AG, Forschungszentrum, D-89081 Ulm (FRG)

E.-M. Peters, Dr. K. Peters, Prof. Dr. H. G. von Schnering
Max-Planck-Institut für Festkörperforschung, D-70569 Stuttgart (FRG)

[**] This research was supported by the Deutsche Forschungsgemeinschaft, the Fonds der Chemischen Industrie, and the Wissenschaftliche Gesellschaft Freiburg.

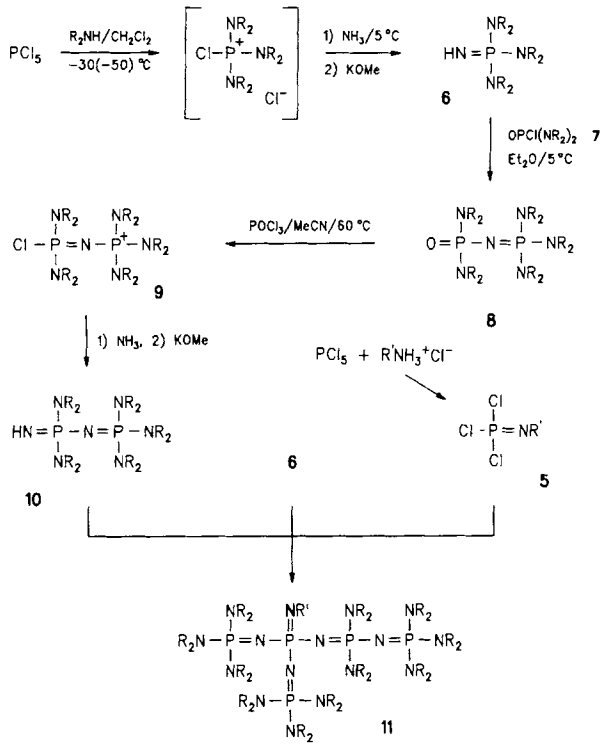

Scheme 1. **5a**: R′ = *t*Bu; **5b**: R′ = CMe_2*t*Bu; **5c**: R′ = CMe_2CH_2*t*Bu; **6a**–**10a**: R = Me; **6b**–**10b**: $R_2 = -(CH_2)_4-$; **11a**: R = Me, R′ = *t*Bu; **11b**: $R_2 = -(CH_2)_4-$, R′ = *t*Bu; **11c**: R = Me, R′ = CMe_2*t*Bu.

The easily prepared P_7 system **12** shows the limits of this homologation concept, which is surprising in a number of ways. Cation **12**·H^+ is extremely acid sensitive; traces of acetic acid in acetate solvents, for example, lead to rapid decomposition. Phosphazene **12** is not more basic than **11a**[10] and has not yet been isolated in pure form presumably on account of its oxygen sensitivity.

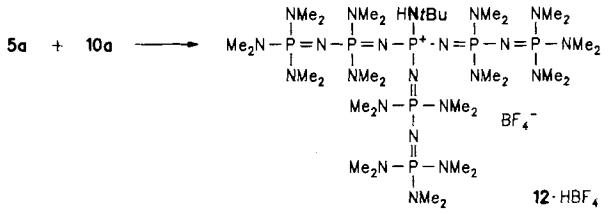

When all Me_2N groups of **1** are exchanged for pyrrolidine groups,[11] the basicity increases by 1.4 pK units, which is an even greater increase than when pairs of amino groups are incorporated into six-membered rings.[5a] The efficiency of this strategy with phosphazene bases was confirmed with the readily available P_4 system **4b**, the basicity of which lies between that of **4a** and that of **11a**.[10]

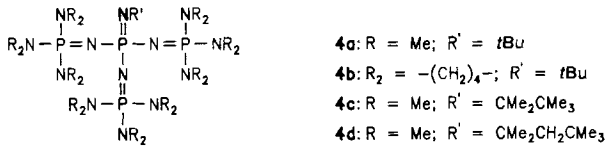

4a: R = Me; R′ = *t*Bu
4b: $R_2 = -(CH_2)_4-$; R′ = *t*Bu
4c: R = Me; R′ = CMe_2CMe_3
4d: R = Me; R′ = $CMe_2CH_2CMe_3$

Both strategies for increasing basicity can be effectively combined: **6b** is coupled with **7b**[12] to provide **8b**,[13] which leads to the stable base **11b**, the strongest uncharged base to date with a $^{MeCN}pK_{BH^{\oplus}}$ value of approximately 47[10] (corresponding to a $^{DMSO}pK_{BH^{\oplus}}$ value of 34–35). The thermodynamic deprotonation behavior of **11b** in THF with hydrocarbon indicators like triphenylmethane is comparable to that of lithium diethylamide; however, **11b** is kinetically much more active than the latter and less nucleophilic than lithium diisopropylamide relative to the kinetic activity.

The synthesis of the *t*Oct-P_4 base **4d**[5n] via **5b**, which is analogous to the preparation of **4a**, is a step in the direction towards even less nucleophilic bases. Amine units suitable for the synthesis of bases with even greater steric bulk were not commericially available. 1,1,2,2-Tetramethylpropylamine (*tert*-heptylamine)[14] was chosen because of its ready accessibility and, judging from molecular modeling studies, the efficient shielding effect of the alkyl group with the respect to the molecular weight.

The enormous steric bulk of the *t*Hept-P_4 base **4c**, synthesized via **5c** in high yields, is apparent from comparison of the relative rates of methylation (with MeI) of the bases in the series **4a**-**4d**-**4c** (Table 1). This high steric hindrance offers the opportunity of effectively controlling alkylations of CH acids by means of the deprotonation step; **4c** and **4d** are markedly more selective than **4a**.[5b,k]

An X-ray structure analysis of the HPF_6 salt of the *t*Hept-P_5 base **11c**, which is prepared analogously to **11a**, **b**, was conducted (Fig. 1).[16] Despite formal symmetry the cation is unsymmetric; the phosphazene chain is fairly stretched, the P-N-P angles lie between 138 and 158°, and the Me_2N

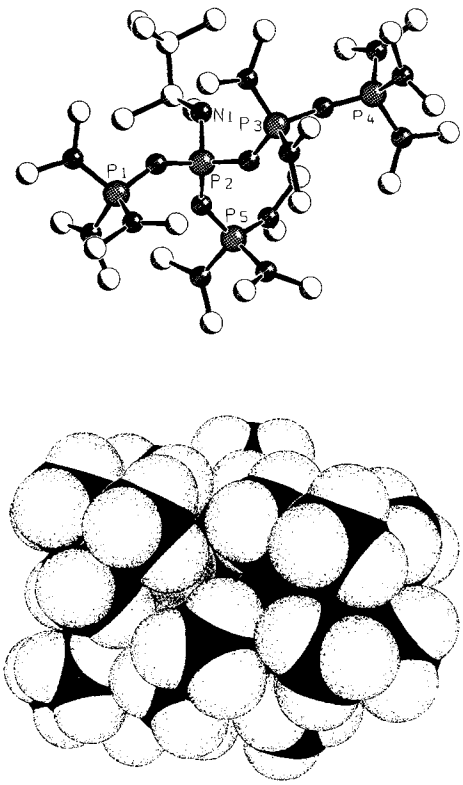

Fig. 1. Crystal structure of the cation in **11c**·HPF_6. Top: Schakal[17] representation without H atoms; bottom: space-filling model, positions of the H atoms from molecular modeling (perspective projection without the NH proton, N1 gray).

Table 1. Melting points, calculated or estimated $^{MeCN}pK_{BH^{\oplus}}$ values[10], and relative rates of methylation of **4a–d** and **11a–c**.

Compd.	M.p. [°C]	$^{MeCN}pK_{BH^{\oplus}}$ [2]	k_{Mel} (rel.)
4a [1]	208 (decomp)	42.6	1
4d	165–167 (decomp)	42.6	0.22
4c	202 (decomp)	42.6	0.001
4b	280 (decomp)	ca. 44	
11a	97	45–46	
11c	96	45–46	
11b	214 (decomp)	ca. 47	

groups are roughly trigonal planar (average sum of angles 355°). The space-filling model shows the unusually strong steric shielding of the basic N1 atom, which is almost completely hidden by the methyl groups of the side chains. Molecular modeling studies suggest that the conformations of such phosphazenium ions are determined primarily by steric interactions and that in solution several conformations of similar energy most likely exist.

Table 2. Physical and spectroscopic data[15] as well as yields of the new compounds.

4b · HBF_4 (88%): M.p. 208 °C (decomp); ^1H NMR (250 MHz, $CDCl_3$, 30 °C, TMS): $\delta = 1.26$ [s, 9H, $C(CH_3)_3$], 1.77 (m, 36H, NCH_2CH_2), 2.17 (br. d, $^2J_{P,H} = 7$ Hz, 1H, NH), 3.11 (m, 36H, NCH_2CH_2)

4b (95%): ^1H NMR (250 MHz, [D_6]benzene, 30 °C, TMS): $\delta = 1.71$ (m, 36H, NCH_2CH_2), 1.80 [s, 9H, $C(CH_3)_3$], 3.35 (m, 36H, NCH_2CH_2)

4c · HBF_4 (88%): M.p. 229 °C; ^1H NMR (250 MHz, $CDCl_3$, 30 °C, TMS): $\delta = 0.90$ [s, 9H, $C(CH_3)_3$], 1.32 [s, 6H, $C(CH_3)_2$], 2.21 (d, $^2J_{P,H} = 6$ Hz, 1H, NH), 2.64 [d, $^3J_{P,H} = 10$ Hz, 54H, NCH_3]

4c (94%): ^1H NMR (250 MHz, [D_6]benzene, 30 °C, TMS): $\delta = 0.91$ [s, 9H, $C(CH_3)_3$], 1.30 [s, 6H, $C(CH_3)_2$], 2.54 [d, $^3J_{P,H} = 10$ Hz, 54H, NCH_3]

4d · HBF_4 (73%): M.p. 205 °C; ^1H NMR (250 MHz, $CDCl_3$, 30 °C, TMS): $\delta = 1.00$ [s, 9H, $C(CH_3)_3$], 1.39 [s, 6H, $C(CH_3)_2$], 1.57 (br. s, 2H, CH_2), 2.38 (d, $^2J_{P,H} = 6$ Hz, 1H, NH), 2.66 [d, $^3J_{P,H} = 10$ Hz, 54H, NCH_3]

4d (95%): ^1H NMR (250 MHz, [D_6]benzene, 30 °C, TMS): $\delta = 1.07$ [s, 9H, $C(CH_3)_3$], 1.44 [s, 6H, $C(CH_3)_2$], 1.66 (br. s, 2H, CH_2), 2.60 [d, $^3J_{P,H} = 10$ Hz, 54H, NCH_3]

11a · HBF_4 (78%): M.p. 153 °C; ^1H NMR (250 MHz, $CDCl_3$, 30 °C, TMS): $\delta = 1.26$ [s, 9H, $C(CH_3)_3$], 2.56 (d, $^3J_{P,H} = 10$ Hz, 12H, NCH_3), 2.65 [d, $^3J_{P,H} = 10$ Hz, 36H, NCH_3), 2.66 (d, $^3J_{P,H} = 10$ Hz, 18H, NCH_3); ^{13}C NMR (100 MHz, $CDCl_3$, 30 °C, TMS): $\delta = 31.72$ [d, $^3J_{P,C} = 5$ Hz, $C(CH_3)_3$], 37.14 [d, $^2J_{P,C} = 5$ Hz, NCH_3], 37.19 [d, $^2J_{P,C} = 5$ Hz, NCH_3], 37.34 (d, $^2J_{P,C} = 5$ Hz, NCH_3], 50.09 (s, CMe_3)

11a (96%): ^1H NMR (250 MHz, [D_6]benzene, 30 °C, TMS): $\delta = 1.93$ [s, 9H, $C(CH_3)_3$], 2.57 (d, $^3J_{P,H} = 10.5$ Hz, 18H, NCH_3), 2.85 [d, $^3J_{P,H} = 10.5$ Hz, 36H, NCH_3], 3.08 (d, $^3J_{P,H} = 10.5$ Hz, 12H, NCH_3)

11b · HBF_4 (71%): M.p. 144 °C (decomp); ^1H NMR (250 MHz, $CDCl_3$, 30 °C, TMS): $\delta = 1.24$ [s, 9H, $C(CH_3)_3$], 1.59 (br. s, 1H, NH), 1.72 (m_c, 8H, NCH_2CH_2), 1.78 (m_c, 24H, NCH_2CH_2), 1.84 (m_c, 12H, NCH_2CH_2), 3.04(m_c, 8H, NCH_2CH_2), 3.14 (m_c, 24H, NCH_2CH_2), 3.18 (m_c, 12H, NCH_2CH_2)

11b (94%): ^1H NMR (250 MHz, [D_6]benzene, 30 °C, TMS): $\delta = 1.66$ (m_c, 12H, NCH_2CH_2), 1.78 (m_c, 24H, NCH_2CH_2), 1.80 [s, 9H, $C(CH_3)_3$], 1.88 (m_c, 8H, NCH_2CH_2), 3.20 (m_c, 12H, NCH_2CH_2), 3.48 (m_c, 24H, NCH_2CH_2), 3.56 (m_c, 8H, NCH_2CH_2)

11c · HBF_4 (46%): M.p. 112 °C; ^1H NMR (250 MHz, $CDCl_3$, 30 °C, TMS): $\delta = 0.90$ [s, 9H, $C(CH_3)_3$], 1.32 [s, 6H, $C(CH_3)_2$], 2.56 (d, $^3J_{P,H} = 11$ Hz, 12H, NCH_3), 2.61 (d, $^3J_{P,H} = 10$ Hz, 18H, NCH_3), 2.61 [d, $^3J_{P,H} = 10$ Hz, 36H, NCH_3]

11c (94%): ^1H NMR (250 MHz, [D_6]benzene, 30 °C, TMS): $\delta = 1.51$ [s, 9H, $C(CH_3)_3$], 1.79 [s, 6H, $C(CH_3)_2$], 2.43 (d, $^3J_{P,H} = 10$ Hz, 18H, NCH_3), 2.73 [d, $^3J_{P,H} = 10$ Hz, 36H, NCH_3], 2.88 (d, $^3J_{P,H} = 10$ Hz, 12H, NCH_3)

12 · HBF_4 (86%): M.p. 261 °C (decomp); ^1H NMR (250 MHz, $CDCl_3$, 30 °C, TMS): $\delta = 1.25$ [s, 9H, $C(CH_3)_3$], 2.60 (d, $^3J_{P,H} = 10.5$ Hz, 36H, NCH_3), 2.63 (d, $^3J_{P,H} = 10.5$ Hz, 54H, NCH_3); ^{13}C NMR (100 MHz, $CDCl_3$, 30 °C, TMS): $\delta = 31.67$ [d, $^2J_{P,C} = 5.0$ Hz, $C(CH_3)_3$], 37.23 (d, $^2J_{P,C} = 4.85$ Hz, $P[N(CH_3)_2]_3$), 37.85 (d, $^2J_{P,C} = 4.3$ Hz, $P[N(CH_3)_2]_2$), 49.71 (d, $^2J_{P,C} = 3.0$ Hz, CMe_3)

We suspect that the phosphazene bases described here (for physical and spectroscopic data see Table 2) may define the limits of the base strength of stable, uncharged nitrogen bases and may approach the limits of steric bulk within this extreme range of basicities. We are currently examining whether this new class of auxiliary bases can lift the restrictions of base-catalyzed reactions and thus open completely new possibilities.

Received: April 16, 1993 [Z 6013 IE]
German version: *Angew. Chem.* **1993**, *105*, 1420

[1] R. Schwesinger, H. Schlemper, *Angew. Chem.* **1987**, *99*, 1212; *Angew. Chem. Int. Ed. Engl.* **1987**, *26*, 1167.
[2] Absolute scale relative to 1,4-diaminobutane = 20.12 (J. F. Coetzee, *Prog. Phys. Org. Chem.* **1967**, *4*, 45).
[3] C. Glidewell, *Angew. Chem.* **1975**, *87*, 875; *Angew. Chem. Int. Ed. Engl.* **1975**, *14*, 826.
[4] Compound **6a** has been prepared by another approach with low efficiency: G. N. Koidan, A. P. Marchenko, A. A. Kudryartsev, A. M. Pinchuk, *Zh. Obshch. Khim.* **1982**, *52*, 2001.
[5] a) R. Schwesinger, *Chimia* **1985**, *39*, 269; b) *Nachr. Chem. Tech. Lab.* **1990**, *38*, 1214; c) F. P. Montforts, U. M. Schwartz, *Angew. Chem.* **1985**, *97*, 767; *Angew. Chem. Int. Ed. Engl.* **1985**, *24*, 775; d) J. Schubert, R. Schwesinger, L. Knothe, H. Prinzbach, *Liebigs Ann. Chem.* **1986**, 2009; e) T. Netscher, R. Schwesinger, B. Trupp, H. Prinzbach, *Tetrahedron Lett.* **1987**, *28*, 2115; f) R. Kühlmeyer, B. Seitz, T. Weller, H. Fritz, R. Schwesinger, H. Prinzbach, *Chem. Ber.* **1989**, *122*, 1729; g) B. S. Sproat, B. Beijer, A. Iribarren, *Nucleic Acid Res.* **1990**, *18*, 41; h) M. Fletschinger, B. Zipperer, H. Fritz, H. Prinzbach, *Tetrahedron Lett.* **1987**, *28*, 2517; i) H.-J. Gais, J. Vollhardt, C. Krüger, *Angew. Chem.* **1988**, *100*, 1108; *Angew. Chem. Int. Ed. Engl.* **1988**, *27*, 1092; j) M. Falk-Heppner, M. Keller, H. Prinzbach, *ibid.* **1989**, *101*, 1281 and **1989**, *28*, 1253; k) T. Pietzonka, D. Seebach, *Chem. Ber.* **1991**, *124*, 1837; l) *Angew. Chem.* **1992**, *104*, 1543; *Angew. Chem. Int. Ed. Engl.* **1992**, *31*, 1481; m) *ibid.* **1993**, *105*, 741 and **1993**, *32*, 716; n) several of the bases, **1** (*t*Bu-P_1), **4a** (*t*Bu-P_4), and **4d** (*t*Oct-P_4), are available from Fluka Chemie AG.
[6] N-silylated **10a** and N-unsubstituted diphosphazenes with larger alkyl groups of this type are known: O. Schlak, W. Stadelmann, O. Stelzer, R. Schmutzler, *Z. Anorg. Allg. Chem.* **1976**, *419*, 275; A. P. Marchenko, G. N. Koidan, A. M. Pinchuk, *Zh. Obshch. Khim.* **1983**, *53*, 670.
[7] Compound **8a** was already prepared by a different approach[8], but we found the subsequent purification difficult.
[8] H. R. Allcock, N. M. Tollefson, R. A. Arcus, R. R. Whittle, *J. Am. Chem. Soc.* **1985**, *107*, 5166.
[9] B. Castro, J.-R. Dormoy, B. Dourtoglou, G. Evin, C. Selve, J.-C. Ziegler, *Synthesis* **1976**, 751; J.-R. Dormoy, B. Castro, *Tetrahedron Lett.* **1979**, *20*, 3321; H. Nöth, H. J. Vetter, *Chem. Ber.* **1965**, *98*, 1981; S. Poignant, J. R. Gauvreau, G. J. Martin, *Can. J. Chem.* **1980**, *58*, 946.
[10] These are estimated by qualitative experiments with indicators; A. Streitweiser et al. plan to conduct titrations of P_4 and P_5 bases.
[11] R. Schwesinger, J. Willaredt, unpublished results.
[12] S. R. Wilson, M. F. Price, *Synth. Commun.* **1982**, *12*, 657.
[13] Compound **8b** was already prepared by a lower yielding route: Z. Kiliç, N. Gündüz, E. Kiliç, H. Nazir, *Synth. React. Inorg. Met. Org. Chem.* **1989**, *19*, 453.
[14] Z. J. Vejdelek, V. Trcka, M. Vanecek, B. Kakác, J. Holubek, *Collect. Czech. Chem. Commun.* **1970**, *35*, 2810.
[15] Correct C,H,N analysis and IR data were obtained for all of the BF_4 salts; because of their extreme hygroscopicity the free bases could be characterized only by NMR spectroscopy.
[16] Structural data of **11c**, $[C_{29}H_{82}N_{16}P_5]PF_6$, $M = 954.93$; crystal dimensions [mm] $0.2 \times 0.2 \times 0.4$, $a = 2507.1(7)$, $b = 2303.8(6)$, $c = 1813.3(8)$ pm, $\beta = 101.25(3)°$; $\rho_{calcd} = 1.235\ g\,cm^{-3}$; linear absorption coefficient = $0.26\ mm^{-1}$ ($Mo_{K\alpha}$); monoclinic, space group $C2/c$, $Z = 8$; number of measured reflections between $\theta = 1.75$ and 25.0°: 7710 ($2\theta/\theta$), number of independent reflections: 6727, number of observed reflections with $F > 3\sigma(F)$: 3040; $R = 0.139$, $R_w = 0.076$, number of refined parameters: 521. Difference Fourier synthesis: greatest residual density = $0.63\ e\,Å^{-3}$, greatest residual disorder = $-0.61\ e\,Å^{-3}$; empirical absorption correction; no extinction correction. Further details of the crystal structure investigation may be obtained from the Fachinformationszentrum Karlsruhe, Gesellschaft für wissenschaftlich-technische Information mbH, D-76344 Eggenstein-Leopoldshafen (FRG) on quoting the depository number CSD-57300, the names of the authors, and the journal citation.
[17] E. Keller, *Chem. Unserer Zeit* **1986**, *20*, 178.

The Dynamic Jahn–Teller Effect in the Benzene Cation: Rotationally Resolved ZEKE Photoelectron Spectra of the $\nu_6(e_{2g})$ Mode**

By *Reiner Lindner, Hiroshi Sekiya,* and *Klaus Müller-Dethlefs**

Consideration of vibronic interactions is fundamental for understanding the dynamics of molecules and the mechanisms of chemical reactions such as chemical activation and catalysis.[1] One of the most important effects of vibronic interactions on degenerate electronic states of nonlinear molecules is the Jahn–Teller effect,[2] best described as the instability of a molecule with respect to distortions from its most symmetric configuration. The decline in the adiabatic potential energy surface along the Jahn–Teller active coordinate can cause a reduction of the activation energy and may thus favor the course of chemical reactions that proceed in the direction of this coordinate.[3] The classical textbook example of the Jahn–Teller effect is given by the benzene cation, the properties of which have been thoroughly examined theoretically and experimentally.[3] Until just recently, however, it was not possible to examine the benzene cation by spectroscopy with sufficient resolution for a meaningful description of its structure and symmetry. By means of rotationally resolved ZEKE spectroscopy (ZEKE = *z*ero *k*inetic *e*nergy) of the vibrational ground state $D_0\,^2E_{1g}$ of the benzene cation in the gas phase it was shown that this state is planar and has D_{6h} symmetry.[4] The high symmetry of the free ion is certainly not self-evident, since a reduction in symmetry to D_{2h} is expected as a result of the Jahn–Teller (JT) effect associated with its electronic degeneracy;[3a] this reduced symmetry was also observed by ESR in matrix studies.[5]

It is interesting to see the effect of excitation of a Jahn–Teller active vibrational mode on the structure of the ion and how vibronic interactions affect the vibrational structure of the ion's ground state. According to theory, excitation of a degenerate vibration in a degenerate electronic state should lift the degeneracy, and splitting into vibronic states of different energies is expected.[6] Because of vibronic coupling, the electronic wave function depends on the vibrational coordinate. The Jahn–Teller effect is thus one of the most significant examples of the breakdown of the Born–Oppenheimer approximation, which has as its basic tenet the separability of the motion of electrons and nuclei.

In the case of linear vibronic coupling, a good quantum number for the characterization of the vibronic wave function for a doubly degenerate electronic state is simply the sum $j = l \pm \lambda$ of the vibrational angular momentum $l = \pm v$ and half of the electronic angular momentum $\lambda = 1/2\Lambda$ ($\Lambda = \pm 1$), and not the individual angular momenta alone.[6, 7] For the benzene cation this implies that excitation of one quantum of the degenerate $\nu_6(e_{2g})$ vibrational mode (6^1) results in a splitting into two states with different vibronic angular momenta $j = \pm 1/2$ and $j = \pm 3/2$. The state with angular momentum $j = \pm 3/2$ should split further into two states with $j = +3/2$ and $j = -3/2$ due to quadratic JT coupling.[6, 7] This differing behavior of the two components with $j = \pm 1/2$ and $j = \pm 3/2$ can also be explained by group theory. The direct product of the irreducible representations of the electronic state E_{1g} and the ν_6 vibrational mode e_{2g} generates one doubly degenerate state with the symmetry species E_{1g} and two states with the symmetry species B ($\Gamma_e \otimes \Gamma_v = E_{1g} \oplus B_{1g} \oplus B_{2g}$). Higher order couplings can only split the state $\Gamma_{ev} = B_{1g} \oplus B_{2g}$ ($j = \pm 3/2$); the state $\Gamma_{ev} = E_{1g}$ ($j = \pm 1/2$) remains degenerate. An unambiguous assignment of the individual, split vibronic states and an exact determination of their energies is necessary for a precise determination of the strengths of the vibronic coupling. Rotationally resolved ZEKE spectroscopy is the method for the unequivocal assignment of the symmetry species of the vibronic states and thus the vibrational modes of the benzene cation, thereby providing very reliable values for the vibronic coupling strengths.

The rotational state of an oblate symmetric rotor is characterized by two quantum numbers. For the ground state (S_0) and the intermediate state (S_1) of the neutral benzene molecule, these are the quantum number J of the total angular momentum and the quantum number K for its projection along the molecule-fixed principal axes. For the benzene cation with the electronic spin $S = 1/2$, the rotational states are characterized (with the assumption of only a weak spin–orbit interaction) by the quantum number N^+, which describes the total angular momentum without electronic spin, and the projection quantum number K^+. In degenerate vibronic states the rotational states split by Coriolis interactions must be differentiated by an additional quantum number l.[8]

The determination of the rotational structure of the benzene cation and the assignment of the rotational transitions observed in the ZEKE spectra allow the determination of the vibronic symmetry species of the corresponding vibrational state. We employed a method that was already successfully applied to ammonia[9, 10] and to the vibrationless ground state of the benzene cation.[4] Starting with the known symmetry of the intermediate state, in which only one rovibronic state is populated, the possible final states are determined based on group theoretical considerations. The conservation of symmetry of the nuclear spin wave function and the rules for electronic symmetry selection and the coupling of angular momenta greatly restrict the possible transitions; depending on the vibronic symmetry of the final state, only a few rotational progressions can be observed.[4, 9, 10, 11]

For the benzene cation the $\nu_6(e_{2g})$ mode is the Jahn–Teller active mode with the lowest frequency.[3] Photoelectron spectra of benzene[12] indicate a splitting of the $j = 3/2$ and $j = 1/2$ components of the 6^1 band by roughly 300 cm^{-1}. Measurements with a variant of the ZEKE method, in which the ion remaining after the pulsed field ionization is detected (*m*ass *a*nalyzed *t*hreshold *i*onization, MATI[13, 14]), show vibrational structure in the region up to 800 cm^{-1} above the first ionization potential. In this vibrational structure the splitting of the two components with $j = 3/2$ and $j = 1/2$ and to some extent the separation of the components $j = +3/2$ and $j = -3/2$ can be seen.[15] However, rotational resolution, which would ensure the unambiguous assignment of the bands, was not achieved in these measurements. This is especially necessary for the $j = \pm 1/2$ band, as it lies close to high-intensity combination modes of other vibrations.

Figure 1 shows the completely rotationally resolved ZEKE spectrum in the region of the 6^1 ($j = \pm 1/2$) band of the benzene cation. The first laser is tuned to the $S_1\,6^1 \leftarrow S_0\,^rR_0(0)$ transition, and thus a single rovibronic level

[*] Dr. K. Müller-Dethlefs, Dipl.-Phys. R. Lindner, Dr. H. Sekiya[+]
Institut für Physikalische und Theoretische Chemie
der Technischen Universität München
Lichtenbergstrasse 4, D-85747 Garching (FRG)
Telefax: Int. code + (89)3209-2727

[+] Permanent address:
Institute of Advanced Material Study
Kyushu University, Fukuoka (Japan)

[**] This research was supported by the EC (contract no. SC1-CT90-0462-(MD)). H. S. thanks the Alexander-von-Humboldt-Stiftung for a one-year research fellowship (1991–1992).

($J' = 1, K' = 1, +l$) in the intermediate state is populated.[16] The second laser is scanned over the range $\nu_2 = 36598-36638\ cm^{-1}$, and the ZEKE signal is recorded versus ν_2. Figure 1 shows two vibrational bands in this region with almost the same intensity and both with resolved rotational structure. Without rotational resolution it is not possible to decide with certainty which of the two states should be assigned to the $6^1(j = \pm 1/2)E_{1g}$ band. Starting from the rotational transitions characteristic for a given vibronic symmetry, two rotational progressions with $K^+ = 1$ and $K^+ = 5$ can be assigned to the state higher in energy (right in Fig. 1).

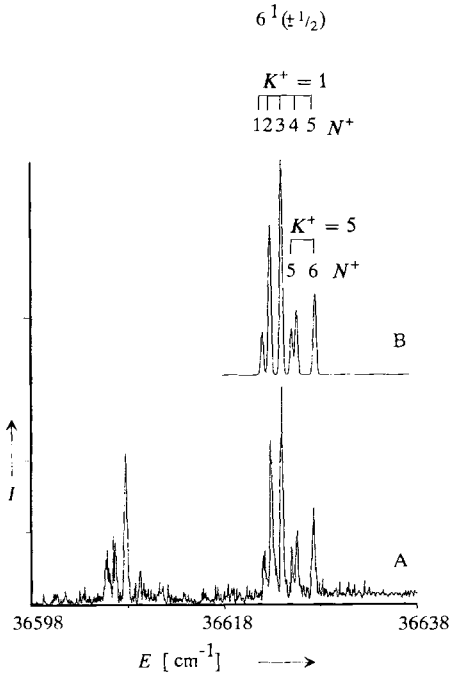

Fig. 1. Measured (A) and simulated (B) ZEKE spectra of the $6^1(j = \pm 1/2)$ band of the electronic ground state of the benzene cation via the intermediate state $S_1 6^1(J' = 1, K' = 1, +l)$. Gaussian bands with a width of 0.4 cm^{-1} (FWHM) were assumed for the simulation. The intensities are taken from the measured spectrum. *I*: ZEKE signal, *E*: energy of the ionizing laser.

The rotational structure indicates that E_{1g} is the vibronic symmetry species of this band, which can thus be unambiguously assigned to the $6^1(j = \pm 1/2)E_{1g}$ state. This assignment is supported by comparison with the spectrum of the vibrationless ground state,[4] which also has E_{1g} symmetry. The two spectra are very similar with the exception of the Coriolis splittings resulting from Coriolis coupling constants (ζ) of different sizes and signs. In contrast, the rotational structure of the lower energy state (left in Fig. 1) is not compatible with an E_{1g} symmetry species. This probably corresponds to a component of the combination mode $16^16^1(j = \pm 3/2)$.[17]

The second component of the split ν_6 band, the state with vibronic angular momentum $j = \pm 3/2$, is split due to the quadratic, dynamic Jahn–Teller effect into two states with B_{1g} and B_{2g} symmetry.[6, 7] Since both vibronic states have the same symmetry species *B* and their rotational constants should have close to the same values, very similar rotational structures are expected for the two states. Figure 2 shows the ZEKE spectrum via the same intermediate state $S_1 6^1(J' = 1, K' = 1, +l)$, in which the second laser is scanned over the range $\nu_2 = 36288-36328\ cm^{-1}$. Two clearly separated vibronic states with almost identical rotational structures can be seen, which can both be assigned to a progression with $K^+ = 3$. This leads to the vibronic symmetry species B_{1g} and B_{2g}, in agreement with the symmetry selection rules for ZEKE spectroscopy; these components must be assigned to the states $6^1(j = -3/2)$ and $6^1(j = +3/2)$. It cannot be determined yet which state has the vibronic symmetry species B_{1g} and which B_{2g}. The separations of each set of two transitions with the same quantum numbers N^+ and K^+ agree to within $\pm 0.1\ cm^{-1}$. The mean splitting between the states with $j = -3/2$ and $j = +3/2$ is 20 cm^{-1}.

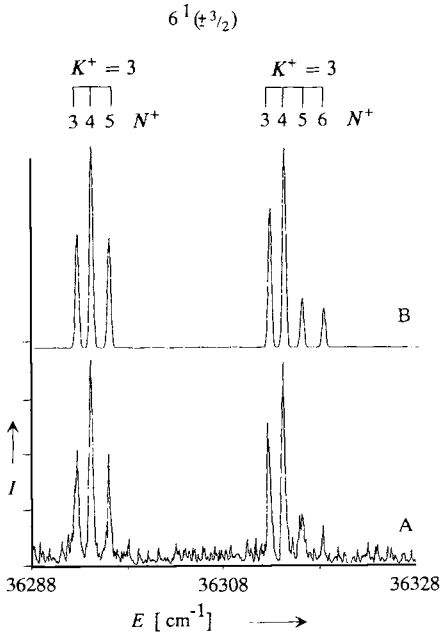

Fig. 2. Measured (A) and simulated (B) ZEKE spectra of the $6^1(j = \pm 3/2)$ band of the electronic ground state of the benzene cation via the intermediate state $S_1 6^1(J' = 1, K' = 1, +l)$. Gaussian bands with a width of 0.4 cm^{-1} (FWHM) were assumed for the simulation. The intensities are taken from the measured spectrum. *I*: ZEKE signal, *E*: energy of the ionizing laser.

With twelve rovibronic levels of the (neutral) $S_1 6^1$ state as intermediate resonance, we were able to assign 50–55 lines in the ZEKE spectrum of the individual bands. A preliminary least-squares approximation of the rotational constants based on these lines gave the values listed in Table 1. Neither the margins of error for the constants nor the standard deviation of 0.1 to 0.2 cm^{-1} are as good as expected based on the quality of the spectra and the low standard deviation (0.04 cm^{-1}) obtained for the vibrationless ground state.[4] The large difference in the rotational constant C for the two almost degenerate vibronic states of the $6^1(j = \pm 3/2)$ band, which are split due to quadratic Jahn–Teller coupling, is not plausible, and the resulting significant rotational defects of +7 and −5 amu Å^2 disagree with the planar structure of the benzene cation recently proven.[4] Apparently the simple model of the symmetric rotor, which was applied successfully for the vibrationless ground state of the cation, does not correctly describe the rotational energy of the molecule with linear and quadratic, dynamic Jahn–Teller coupling. A theory that correctly specifies the position of the rotational states in these cases must still be worked out for the benzene cation. Between the two almost degenerate components of the $6^1(j = \pm 3/2)$ state there may exist an off-diagonal Coriolis coupling such as that observed between the components of a degenerate electronic state[18] or a degenerate vibration[19] split by asymmetric isotopic substitution. Even with

the accuracy given for the rotational constants listed in Table 1, a marked expansion of the benzene ring is apparent; however, the details must still be clarified.

Table 1. Spectroscopic constants of the benzene cation for the vibrational states $6^1(j = +3/2)$, $6^1(j = -3/2)$, and $6^1(j = \pm 1/2)$ of the electronic ground state $D_0\,^2E_{1g}$.

	$6^1(j=-3/2)$	$6^1(j=+3/2)$	$6^1(j=\pm 1/2)$
Band origin [cm^{-1}]	345.4	365.4	676.4
B [cm^{-1}]	0.1867 ± 0.0008	0.1868 ± 0.0008	0.184 ± 0.002
C [cm^{-1}]	0.0895 ± 0.0004	0.0966 ± 0.0004	0.094 ± 0.001
ζ_{eff}	–	–	−0.19 ± 0.03

The differences in band origin energy between the $6^1(j = \pm 1/2)$ bands and the $6^1(j = -3/2)$ and $6^1(j = +3/2)$ bands is 331 and 311 cm^{-1}, respectively. This corresponds to roughly half of the vibrational energy of the ν_6 mode. Thus the benzene cation is a good example for intermediate coupling, in which the vibrational frequency of the Jahn–Teller active mode and the accompanying coupling strengths have almost the same values.[3b] With the precise values given here for the energies of the components of the ν_6 band affected by vibronic interaction, the results of quantum chemical ab initio calculations can be examined very closely. Comparison with values published recently shows how well these latest dynamic Jahn–Teller calculations can take into account several active modes.[20] The difference between the caluculated value for the $6^1(j = \pm 1/2)$ band of 694 cm^{-1} and the measured value of 676.4 cm^{-1} is only 3 percent.

The determination of the symmetry of a vibronic state by rotationally resolved ZEKE spectroscopy, which is demonstrated here for the ν_6 mode, would allow the elucidation of the vibrational structure of the benzene cation, which is predicted to be very irregular due to multiple-mode Jahn–Teller coupling. This would be a significant contribution to the understanding of the Jahn–Teller effect and vibronic interactions. High-resolution experimental analysis of the cation of the benzene molecule, the prototypical aromatic molecule which is frequently the subject of theoretical studies, was not possible previously.[21]

Experimental Procedure

The principles behind ZEKE spectrosopy and the exact experimental setup were described in ref. [4]. Benzene coexpanded with argon as carrier gas (p_0 = 4 bar) was ionized in a skimmed, pulsed, supersonic beam by two-photon two-color ionization (1 + 1′ REMPI). The laser system consists of a Nd:YAG laser (Continuum NY-82/20) that pumps two (frequency-doubled) dye lasers (Lumonics HD-500). The first laser populates a specific rovibronic state in the first excited electronic state $S_1\,6^1$ of the molecule. The second laser promotes the molecules to extremely long-lived Rydberg states (with very high principal quantum numbers $n > 150$) converging to rovibronic states of the cation. After a delay time of about 3 μs a pulsed electric extraction field was applied, and the resulting field-ionized electrons were detected, resolved in time[4,22,23].

Received: March 12, 1993 [Z 5914 IE]
German version: *Angew. Chem.* **1993**, *105*, 1384

[1] I. B. Bersuker, *The Jahn-Teller Effect and Vibronic Interactions in Modern Chemistry*, Plenum Press, New York, **1984**.
[2] H. A. Jahn, E. Teller, *Proc. R. Soc. London A* **1937**, *161*, 220–235.
[3] Numerous publications address the Jahn–Teller effect in the benzene cation. See, e.g. a) K. Raghavachari, R. C. Haddon, T. A. Miller, V. E. Bondybey, *J. Chem. Phys.* **1983**, *79*, 1387–1395; b) J. Eiding, R. Schneider, W. Domcke, H. Köppel, W. von Niessen, *Chem. Phys. Lett.* **1992**, *177*, 345, and references therein.
[4] R. Lindner, H. Sekiya, B. Beyl, K. Müller-Dethlefs, *Angew. Chem.* **1993**, *105*, 631–634; *Angew. Chem. Int. Ed. Engl.* **1993**, *32*, 603–606.
[5] M. Iwasaki, K. Toriyama, K. Nunome, *J. Chem. Soc. Chem. Commun.* **1983**, 320–322.
[6] a) H. C. Longuet-Higgins, U. Öpik, M. H. L. Pryce, F. R. S. Sack, R. A. Sack, *Proc. R. Soc. London A* **1958**, *244*, 1–16; b) T. A. Miller, V. E. Bondybey, *Molecular Ions: Spectroscopy, Structure and Chemistry*, North-Holland, Amsterdam, **1983**, and references therein
[7] R. L. Whetten, K. S.Haber, E. R. Grant, *J. Chem. Phys.* **1986**, *84*, 1270–1284.
[8] G. Herzberg, *Molecular Spectra and Molecular Structure, Vol. 3*, Van Nostrand, Princeton, USA, **1966**.
[9] W. Habenicht, G. Reiser, K. Müller-Dethlefs, *J. Chem. Phys.* **1991**, *95*, 4809–4820.
[10] K. Müller-Dethlefs, *J. Chem. Phys.* **1991**, *95*, 4821–4839.
[11] H. Rudolph, V. McKoy, S. N. Dixit, *J. Chem. Phys.* **1989**, *90*, 2570–2574.
[12] S. R. Long, J. T. Meek, J. P. Reilly, *J. Chem. Phys.* **1983**, *79*, 3206–3219.
[13] L. Zhu, P. Johnson, *J. Chem. Phys.* **1991**, *94*, 5769–5771.
[14] C. Jouvet, C. Dedonder-Lardeux, S. Martrenchard-Barra, D. Solgadi, *Chem. Phys. Lett.* **1992**, *198*, 419–423.
[15] H. Krause, H. J. Neusser, *J. Chem. Phys.* **1992**, *97*, 5923–5926.
[16] E. Riedle, T. Knittel, Th. Weber, H. J. Neusser, *J. Chem. Phys.* **1989**, *91*, 4555–4563.
[17] R. Lindner, H. Sekiya, K. Müller-Dethlefs, unpublished results.
[18] L. Yu, D. W. Cullin, J. M. Williamson, T. A. Miller, *J. Chem. Phys.* **1993**, *98*, 2682–2698.
[19] E. Riedle, A. Beil, D. Luckhaus, M. Quack, *Mol. Phys.* **1993**, in press.
[20] J. Eiding, W. Domcke, *Chem. Phys.* **1992**, *163*, 133–147.
[21] K. Müller-Dethlefs, *Nachr. Chem. Tech. Lab.* **1993**, *41*, 200–202.
[22] a) K. Müller-Dethlefs, M. Sander, E. W. Schlag, *Z. Naturforsch. A* **1984**, *39*, 1089–1091; b) G. Reiser, W. Habenicht, K. Müller-Dethlefs, E. W. Schlag, *Chem. Phys. Lett.* **1988**, *152*, 119–123.
[23] K. Müller-Dethlefs, E. W. Schlag, *Annu. Rev. Phys. Chem.* **1991**, *42*, 109–136.

Crystal Structure of [(α-Cyanoisopropylsodium · Tetramethylenediamine)$_4$]: How Coordination Expansion from Li to Na Centers can Increase the Aggregation State of an α-Nitrile "Carbanion"**

By *James Barker, Nicholas D. R. Barnett, Donald Barr, William Clegg, Robert E. Mulvey,** and *Paul A. O'Neil*

"Carbanions" generated by alkali metalation of organic nitriles possessing α-hydrogen atoms have long been important synthetic intermediates in organic chemistry. Though studies of such species abound, the first crystal structure determination appeared only in 1986.[1] This structure analysis of [(α-cyanobenzyllithium · tmeda)$_2$ · benzene] (TMEDA = *N,N,N′,N′*-tetramethylethylenediamine) **1** highlighted obstacles which have severely hindered the development of this aspect of α-nitrile carbanion chemistry, for as well as being air- and moisture-sensitive, the crystals decompose in the X-ray beam (this accounts for the unavoidably high *R* value of 0.115). The crystal structure of **1** emphasized the strong

[{Li(tmeda)CH(CN)C$_6$H$_5$}$_2$] · C$_6$H$_6$ **1**

[{Na(tmeda)CH(CN)Me$_2$}$_4$] **2**

[*] Dr. R. E. Mulvey, N. D. R. Barnett
Department of Pure and Applied Chemistry
University of Strathclyde
GB-Glasgow, G1 1XL (UK)
Telefax: Int. code + (41)552-5664
Dr. J. Barker, Dr. D. Barr
The Associated Octel Company Limited
GB-Ellesmere Port, L65 4HF (UK)
Prof. W. Clegg, P. A. O'Neil
Department of Chemistry
University of Newcastle
GB-Newcastle upon Tyne, NE1 7RU (UK)

[**] This work was supported by the Associated Octel Company Limited and by the UK Science and Engineering Research Council.

influence exerted by the metal cation (Li^+, in this example) on the molecular arrangement adopted, particularly with regard to the degree of aggregation and solvation, since it revealed that **1** was a dimer with a four-membered $(NLi)_2$ ring, in which each Li atom is bound to a bidentate tmeda ligand. MO calculations on model compounds also recognized the important structural role of the metal cation.[2] In this communication, we report the synthesis and crystal structure (refined to a final R value of 0.061) of [(α-cyanoisopropylsodium · tmeda)$_4$] **2**, a sodium complex closely related to the lithium complex **1**. Interestingly, although oligomerization is generally accepted to be more important with organolithium compounds[3] due to electrostatic considerations, here we find that the sodium complex **2** exhibits the higher (tetrameric) aggregation state.

Formally, isopropylcyanide $Me_2C(H)C{\equiv}N$ converts to α-cyanoisopropylsodium $Me_2C(Na)C{\equiv}N$ in the preparation of **2**. However, in reality, the crystal structure of **2** (Fig. 1)[4] shows that C–Na bonding does not occur, instead the Na^+ ions preferentially bind to the more electronegative N^- centers of the CN groups with concomitant formation of stable, near-linear $C{=}C{=}N$ units (mean bond angle, 178.53°; mean bond lengths, 1.360 and 1.187 Å, respectively;[5] the "anionic" C atoms are surrounded essentially trigonal planar). Furthermore, these contact ion pairs exist in a discrete tetrameric arrangement, with an $(NNa)_4$ pseudocubane core reminiscent of that in the ketimide–ketimine complex [(tBu$_2$C=NNa)$_4$·(HN=CtBu$_2$)$_2$][6] described as a stack[7] of two $(NNa)_2$ rings (one complexed and one uncomplexed). A similar description could be applied to the structure of **2** though there is no clear pattern to the N_{anion}–Na bond lengths (range, 2.424–2.489 Å) to permit identification of the stacking direction.[8]

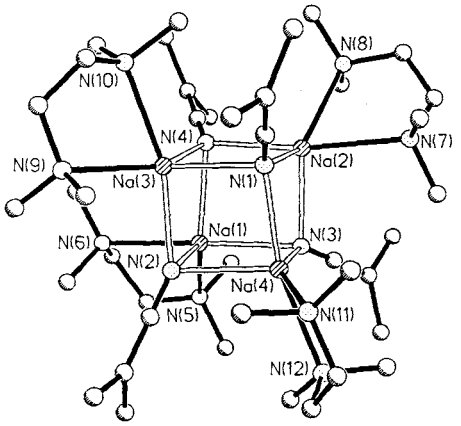

Fig. 1. Crystal structure of **2** (excluding hydrogen atoms). Principal distances [Å] and angles [°]: Na1-N2 2.424(6), Na1-N3 2.470(6), Na1-N4 2.489(6), Na1-N5 2.498(6), Na1-N6 2.567(6), Na2-N1 2.467(6), Na2-N3 2.477(6), Na2-N4 2.457(6), Na2-N7 2.528(6), Na2-N8 2.542(7), Na3-N2 2.435(6), Na3-N4 2.460(7), Na3-N1 2.474(5), Na3-N10 2.499(6), Na3-N9 2.541(6), Na4-N3 2.464(6), Na4-N1 2.467(6), Na4-N2 2.473(6), Na4-N12 2.529(6), Na4-N11 2.572(6); N2-Na1-N3 90.3(2), N2-Na1-N4 97.5(2), N3-Na1-N4 86.9(2), N2-Na1-N5 128.7(2), N3-Na1-N5 101.1(2), N4-Na1-N5 132.6(2), N2-Na1-N6 97.0(2), N3-Na1-N6 171.9(2), N4-Na1-N6 95.5(2), N5-Na1-N6 71.6(2), N1-Na2-N4 93.9(2), N3-Na2-N4 87.4(2), N1-Na2-N3 96.5(2), N4-Na2-N7 169.1(2), N1-Na2-N7 94.8(2), N3-Na2-N7 98.1(2), N4-Na2-N8 97.5(2), N1-Na2-N8 133.4(2), N3-Na2-N8 128.9(2), N7-Na2-N8 71.7(2), N2-Na3-N4 98.0(2), N2-Na3-N1 87.8(2), N1-Na3-N4 93.7(2), N2-Na3-N10 164.7(2), N4-Na3-N10 91.2(2), N1-Na3-N10 103.9(2), N2-Na3-N9 94.2(2), N4-Na3-N9 145.7(2), N1-Na3-N9 118.8(2), N10-Na3-N9 71.6(2), N1-Na4-N3 96.9(2), N2-Na4-N3 89.3(2), N1-Na4-N2 87.2(2), N3-Na4-N12 93.0(2), N1-Na4-N12 160.6(2), N2-Na4-N12 109.7(2), N3-Na4-N11 153.2(2), N1-Na4-N11 94.0(2), N2-Na4-N11 115.7(2), N12-Na4-N11 70.5(2).

Figure 1 shows one of three stacking possibilities; the other two being perpendicular to the N1-Na4-N2-Na3 and N1-Na2-N3-Na4 faces. Irrespective of the direction, this vertical association of dimeric rings raises the coordination number of their constituent Na^+ ions from two to three, making them five-coordinate in total, when the bidentate tmeda ligands are taken into account. Since Li^+ ions are significantly smaller than Na^+ ions, their coordination sphere is also appreciably smaller, that is they can bind fewer ligands. Thus, the $(NLi)_2$ ring in the related complex **1** remains discrete, and its Li^+ ions are coordinatively saturated in a fourfold environment. The scale of the steric "expansion" from Li to Na can be gauged by a comparison of mean N_{tmeda}–metal bond lengths (2.05 Å in **1**;[1] 2.534 Å in **2**; difference 0.484 Å). As a consequence of the distorted cubic morphology of **2**, the five-coordinate Na^+ ions and the four-coordinate N^- ions are greatly distorted from the respective trigonal bipyramidal and tetrahedral geometries often associated with these coordination numbers, as reflected by the bond angles (mean internal-cube angles at Na, 92.12°; at N, 87.28°: range of external-cube angles at Na, 70.5–171.9°; at N, 110.7–146.5°).

A comparison of the structures of **2** and the related sodium "carbanions" $NaC(CN)_3$ (**3**)[9] and [Na{N(nBu)$_4$}·{HC(CN)$_2$}$_2$ · THF] (**4**),[10] shows that there is a definite correlation between the N_{anion}–Na bond lengths and the coordination numbers of the Na atoms. Thus, in general the bond lengths increase sequentially (2.364–2.396 (**4**), 2.424–2.489 (**2**), 2.373–2.613 Å (**3**)) as the coordination number increases from four (in **4**) to five (in **2**) and to six (in **3**).

An IR spectrum of **2** (in Nujol) revealed a strong [ν_{as}(C=C=N)] band at 2030 cm^{-1}. Donor-free α-cyanobenzylsodium PhCH(Na)C≡N, which may have a different aggregation state, was reported to have a similar absorption band at the slightly higher value of 2080 cm^{-1}.[11]

Thus, we conclude that the structures of α-nitrile "carbanions" can differ, depending on whether they are produced by lithiation or by sodiation, since they are in reality contact ion pair aggregates, and as structure is intimately linked to reactivity this should be borne in mind when generating such intermediates for synthetic purposes.

Experimental Procedure

2: Under anaerobic and anhydrous conditions, isopropylcyanide (10 mmol) was added to a Schlenk vessel which contained a chilled, stirred hexane suspension of nBuNa (10 mmol). A yellowish precipitate formed almost immediately. Introduction of TMEDA (10 mmol) followed by mild heating redissolved the solid, and a homogeneous orange solution was formed. Refrigeration at −30 °C afforded a large crop of yellow crystalline **2**. Yield, 45%. Satisfactory C,H,Na analyses. The yellow crystals decomposed on contact with moisture or oxygen. Single crystals suitable for X-ray crystallography were sealed under argon in Lindemann capillary tubes prior to data collection.

Received: March 16, 1993 [Z 5931 IE]
German version: Angew. Chem. **1993**, *105*, 1419

[1] See G. Boche, M. Marsch, K. Harms, *Angew. Chem.* **1986**, *98*, 373–374; *Angew. Chem. Int. Ed. Engl.* **1986**, *25*, 373–374, and references therein.

[2] J. Kaneti, P. von R. Schleyer, T. Clark, A. J. Kos, G. W. Spitznagel, J. G. Andrade, J. B. Moffat, *J. Am. Chem. Soc.* **1986**, *108*, 1481–1492.

[3] C. Schade, P. von R. Schleyer, *Adv. Organomet. Chem.* **1987**, *27*, 169–278. A review of the crystal structures of organometallic compounds of higher alkali metals. The introductory section (pp. 169–186) provides an excellent account of the general principles involved, drawing comparisons with organolithium structures.

[4] **2**: M_r = 829.2, monoclinic, $P2_1/c$, a = 20.204(11), b = 11.885(5), c = 22.663(12) Å, β = 92.72(3)°, V = 5435.8 Å^3, Z = 4, ϱ_{calcd} = 1.013 g cm^{-3}, $F(000)$ = 1824, $Mo_{K\alpha}$ radiation, λ = 0.71073 Å, μ = 0.09 mm^{-1}. The structure was determined by direct methods and refined on F^2 using all 7082 independent reflections measured at 180 K with a Stoe-Siemens diffractometer ($2\theta_{max}$ = 45°), with anisotropic atomic displacement parame-

ters, with isotropic H atoms in calculated positions and some restraints on the disordered ligand at N4: $wR_2 = [\Sigma\{w(F_o^2 - F_c^2)^2\}/\Sigma\{w(F_o^2)^2\}]^{1/2} = 0.2031$, conventional R[on F values for 2949 reflections with $I > 2\sigma(I)$] = 0.0610, S(on F^2) = 1.03 for 550 parameters. Further details of the crystal structure investigation can be obtained from the Director of the Cambridge Crystallographic Data Centre, 12 Union Road, GB-Cambridge CB2 1EZ (UK), on quoting the full journal citation.

[5] Respective dimensions of the corresponding triatomic unit in 1: 178.4°, 1.38 and 1.15 Å, see ref. [1].

[6] W. Clegg, M. MacGregor, R. E. Mulvey, P. A. O'Neil, *Angew. Chem.* **1992**, *104*, 74–76; *Angew. Chem. Int. Ed. Engl.* **1992**, *31*, 93–95.

[7] For an explanation of the term "ring stacking", and its relevance to a wide assortment of lithium compounds, see R. E. Mulvey, *Chem. Soc. Rev.* **1991**, *20*, 167–209. See also K. Gregory, P. von Schleyer, R. Snaith, *Adv. Inorg. Chem.* **1991**, *37*, 47–142.

[8] D. Barr, R. Snaith, W. Clegg, R. E. Mulvey, K. Wade, *J. Chem. Soc. Dalton Trans.* **1987**, 2141–2147. This paper describes how to deduce the stacking direction in the related imidolithium cubane, $[(Ph_2C{=}NLi \cdot NC_5H_5)_4]$.

[9] P. Anderson, B. Klewe, E. Thom, *Acta Chem. Scand.* **1967**, *21*, 1530–1542.

[10] W. Hiller, S. Frey, J. Strähle, G. Boche, W. Zarges, K. Harms, M. Marsch, R. Wollert, K. Dehnicke, *Chem. Ber.* **1992**, *125*, 87–92.

[11] C. Krüger, *J. Organomet. Chem.* **1967**, *9*, 125–134.

Copper-Catalyzed 1,4-Additions of Trialkylaluminum Compounds to Enones

By *Jürgen Westermann** and *Klaus Nickisch*

The 1,4-addition of organometallic compounds to enones is an important reaction in organic chemistry, which frequently provides the desired products only with low-order or high-order cuprates.[1, 2] In the reactions of enones with organomagnesium halides and organolithium compounds in the presence of catalytic amounts of copper salts according to the method of Kharasch, 1,2-addition is often a side reaction resulting from the undesired attack at the carbonyl group.

Our goal was to conduct the 1,4-addition of an alkyl group to enones and cross-conjugated dienones catalytically. Previously it was not possible to introduce aliphatic groups to, for example, the cross-conjugated system **1** to give **2**. The latter, a steroid with a methyl substituent in position 1 and an important pharmaceutical intermediate, was previously prepared from **1** only with stoichiometric amounts of Me_2CuLi[3] or under catalytic conditions only from an unconjugated dienone (Scheme 1).[3c]

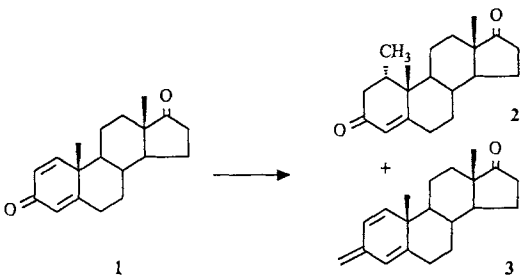

Scheme 1. 1,4-Additions to steroid **1** with methylcopper and methylmagnesium compounds (reaction conditions, yield of **2** [%], yield of **3**[%]): 1.8 equiv Me_2CuLi, 0 °C, 75, 15–20; 1.1 equiv MeMgBr/10 mol% CuX, < 5, > 80; $Me_2CuLi + Me_3SiCl$, −78 to 0 °C, < 10, > 80; MeMgBr + Me_3SiCl/10 mol% CuX, < 5, > 90.

[*] Dr. J. Westermann, Dr. K. Nickisch
Schering AG Berlin
Müllerstrasse 178, D-13342 Berlin (FRG)
Telefax: Int. code + (30)4691-8008

When Me_3SiCl or $BF_3 \cdot Et_2O$ was added to the reaction of **1** with equimolar amounts of low-order or high-order cuprates, or to the highly reactive organometallic compounds MeMgX or MeLi under Cu catalysis,[1, 4] then mainly the carbonyl group was attacked, leading to product **3** after hydrolysis. Thus, for achieving catalytic 1,4-addition the organometallic compounds should not react readily with carbonyl groups so that the competing 1,2-addition is suppressed. For this reason we examined trialkylaluminum compounds in more detail.

The reactions of the trialkylaluminum compounds with carbonyl groups by 1,2-addition depend on the reaction conditions,[5] but in our studies they were less reactive than expected.[6] A number of 1,4-additions of organoaluminum compounds are known: Kabalka et al. reported on a 1,4-addition of triisopropylaluminum initiated by air,[7] dialkylaluminum chlorides react with α,β-unsaturated carbonyl compounds in part without a catalyst,[8] and copper-catalyzed reactions of trialkylaluminum with acid chlorides are important routes to ketones.[9] Nickel-catalyzed 1,4-additions of Me_3Al[10a] were not selective with **1** (in our studies the yield of **2** was only 35%; see entry 18 in Table 1). Another metal-catalyzed reaction, the 1,4-addition of Me_3Al to isophorone with $[Cu(acac)_2]$ (acac = acetylacetonate), was also reported.[10b] However, Mole et al. could not reconfirm this result,[10c] and we also failed to observe this type of reaction when $[Cu(acac)_2]$ was employed as a catalyst. 1,4-Additions of the more reactive alkenyl- and alkynylaluminum compound to enones proceed smoothly,[11, 12] but until now alkyl groups from aluminum compounds could not be transferred to α,β-unsaturated ketones under Cu catalysis.

In our search for suitable catalysts we found that the 1,4-addition of Me_3Al to enones is catalyzed by CuBr. Here the transfer of the methyl group of Me_3Al to the transition metal atom and subsequently to the enone is apparently faster than the competing attack at the carbonyl group. This process could follow the path outlined in Scheme 2.

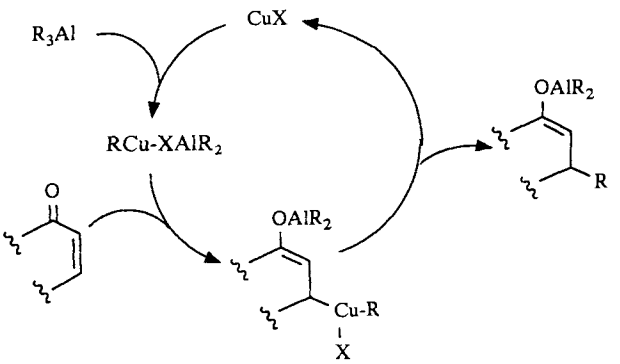

Scheme 2. CuX-catalyzed addition of R_3Al to enones. X = halogen.

Employing this method we converted dienone **1** into **2** under catalytic conditions (method A); addition of Me_3SiCl increased the reaction rate (method B). Apparently the Lewis acid promotes the reaction of trialkylaluminum with 3-keto-$\Delta^{1,4}$ steroids like **1** and suppresses competing reactions of the aluminum enolate formed as an intermediate, resulting in improved yields. In the addition of a methyl group to **1**, a high regioselectivity of >98:2 (position 1 vs. position 5) was achieved; with Me_2CuLi this selectivity was 93:7 and with $Me_3Al/[Ni(acac)_2]$ 62:38. The reaction of **1** with Et_3Al in the presence of Me_3SiCl proceeded smoothly

and furnished **4** in 87% yield. Besides steroidal enones, other cyclic and open-chain enones were tested (Scheme 3).

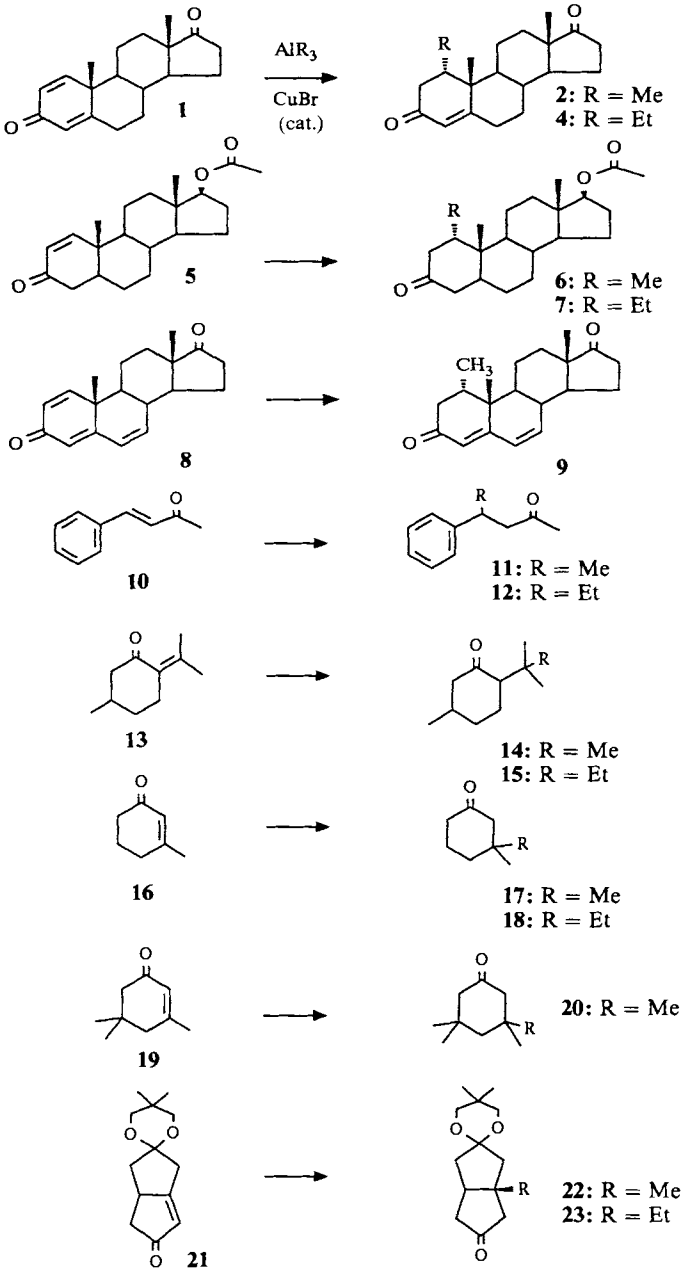

Scheme 3. 1,4-Additions to enones.

17β-acetoxyandrost-1-en-3-one (**5**) reacted with Me_3Al and CuBr (1 mol%) at room temperature in ethyl acetate giving **6** in 90% yield (method A). The acetoxy group was not attacked. The reactions may be conducted in either ether solvents (THF, dioxane) or ethyl acetate (for reaction conditions see Table 1).

The products obtained (Table 1) demonstrate that the copper-catalyzed 1,4-addition of alkylaluminum compounds to enones is a useful reaction, in which ethyl groups can also be transferred, in contrast to the reactions with Ni catalysis.[10] Besides CuBr, $CuBr_2$ and CuCN are suitable catalysts; CuCl, CuI,CuI·2LiCl, CuCN·2LiCl,[13] MeCu, and thienylcopper are not as effective. The amount of catalyst used in the experiments described (1–5 mol%) can be reduced further, but the reaction does not occur without catalyst.[6, 8] The high regioselectivity and good chemoselectivity of this method is notable. The catalytic aspect of this reaction and the use of ethyl acetate, a solvent with minimal environmental impact, are important in view of industrial applications.

Table 1. CuBr-catalyzed 1,4-additions of R_3Al to enones. RT = room temperature, EA = ethyl acetate.

Entry	Enone	R	Prod.	Method [a]	CuBr [mmol]	Conditions	Yield [b]
1	**1**	Me	**2**	A	5	dioxane, 3 h 35 °C	70
2	**1**	Me	**2**	B	2	THF, 2 h, RT	89
3	**1**	Et	**4**	A	5	EA, 2 h, RT	83
4	**1**	Et	**4**	B	5	THF, 1 h, RT	87
5	**5**	Me	**6**	A	1	EA, 0.5 h, RT	90
6	**5**	Et	**7**	A	5	EA, 1 h, RT	92
7	**8**	Me	**9**	A	5	THF, 1 h, RT	89
8	**10**	Me	**11**	B	5	THF, 0.5 h, 0 °C	94
9	**10**	Et	**12**	B	5	THF, 0.5 h, RT	93
10	**13**	Me	**14**	B	5	THF, 0.5 h, RT	91
11	**13**	Et	**15**	B	5	THF, 1 h, RT	76
12	**16**	Me	**17**	B	2	THF, 1 h, 0 °C	97
13	**16**	Et	**18**	B	2	THF, 1 h, 0 °C	91
14	**19**	Me	**20**	A	5	EA, 1 h, RT	80
15	**19**	Me	**20**	B	5	THF, 1 h, RT	93
16	**21**	Me	**22**	A	5	EA, 1 h, RT	64
17	**21**	Et	**23**	A	5	EA, 1 h, 0 °C	87
18	**1**	Me	**2**	-	-	$[Ni(acac)_2]$, Et_2O	35

[a] Method A: 1.1 equiv R_3Al, 1 equiv enone, 1–5 mol% CuBr (no Me_3SiCl). Method B: 1.1 equiv R_3Al, 1 equiv enone, 1–5 mol% CuBr, 1.2 equiv Me_3SiCl. [b] The purity of products **2**, **4**, and **6** (determined by gas chromatography) is >99%, that of the other products >97%. The ^1H NMR data of the products are in accord with the structures shown.

Experimental Procedure

Preparation of **2** according to method B: Enone **1** (8.52 g, 30 mmol) and CuBr (86 mg, 0.6 mmol) were dissolved in THF (70 mL) under nitrogen, and a solution of 10% Me_3Al in toluene (28.4 mL, 33 mmol) was added. Me_3SiCl (3.92 g, 36 mmol) was added dropwise to the solution, which was then stirred for 2 h at 25 °C. The reaction mixture was hydrolyzed with water (3 mL) and the solid filtered off and washed. The crude product was purified by chromatography on silica gel (eluent: ethyl acetate/hexane) to give **2** (8 g, 89% yield). M.p. 154 °C; $[\alpha]_D^{20} = -205.6$ ($c = 1$ in $CHCl_3$); ^1H NMR (300 MHz, $CDCl_3$, 25 °C, TMS) $\delta = 0.95$ (s, 3H; 19-CH_3), 0.97 (d, 3H, $^2J = 7$ Hz; 1α-CH_3), 1.35 (s, 3H; 18-CH_3), 1–2.75 (m, 17H), 5.73 (s, 1H, H-4).

Preparation of **6** according to method A: Enone **5** (3.3 g, 10 mmol) and CuBr (14 mg, 0.1 mmol) were dissolved in ethyl acetate (15 mL) under nitrogen, and a solution of 10% Me_3Al in toluene (9.5 mL, 11 mmol) was added. The solution was stirred for 0.5 h at room temperature, the reaction mixture hydrolyzed with water (1 mL), and the solid filtered off and washed. The solution was concentrated to dryness to give more crude product, which then totaled 3.45 g. Recrystallization from acetone at −10 °C gave **6** (3.1 g, 90% yield). M.p. 154 °C; $[\alpha]_D^{20} = -205.6$ ($c = 1$ in $CHCl_3$); ^1H NMR (300 MHz, $CDCl_3$, 25 °C, TMS) $\delta = 0.95$ (s, 3H; 19-CH_3), 0.97 (d, 3H, $^2J = 7$ Hz; 1α-CH_3), 1.35 (s, 3H; 18-CH_3), 1–2.75 (m, 17H), 5.73 (s, 1H, H-4).

Received: April 24, 1993 [Z 6031 IE]
German version: *Angew. Chem.* **1993**, *105*, 1429

[1] Review: a) G. H. Posner, *An Introduction to Synthesis Using Organocopper Reagents*, Wiley, New York, **1980**; b) Y. Yamamoto, *Angew. Chem.* **1986**, *98*, 945–957; *Angew. Chem. Int. Ed. Engl.* **1986**, *25*, 947–959; c) E. Nakamura, *Synlett* **1991**, 539–547; d) B. H. Lipshutz, *ibid.* **1990**, 119–128; e) B. H. Lipshutz, *Synthesis* **1987**, 325–341; g) G. H. Posner, *Org. React.* **1972**, *19*, 1–113.

[2] P. Perlmutter, *Conjugate Addition Reactions in Organic Synthesis*, Pergamon, Oxford, **1992**.

[3] a) H. Laurent, R. Wiechert in *Organic Reactions in Steroid Chemistry*, *Vol. 2* (Eds.: J. Fried, J. A. Edwards), Van Nostrand Reinhold, New

York, **1972**, pp. 53–126; b) R. Philippson, E. Kaspar (Schering AG), DE-A 2046640, **1972**; c) Addition to an 3-keto-$\Delta^{1,5}$ steroid: M. Tanabe, D. F. Crowe, *Can. J. Chem.* **1967**, *45*, 475–479; R. Wiechert, U. Kerb (Schering AG), DE-A 1223837, **1966**.

[4] Acceleration of the reaction of organocuprates by polar additives and Lewis acids such as Me_3SiCl: a) C. R. Johnson, T. J. Marren, *Tetrahedron Lett.* **1987**, *28*, 27–30; b) E. Nakamura, S. Matsuzawa, Y. Horiguchi, I. Kuwajima, *ibid.* **1986**, *27*, 4029–4032; c) C. Chuit, J. P. Foulon, J. F. Normant, *Tetrahedron* **1980**, *36*, 2305–2310; *ibid.* **1981**, *37*, 1385–1389; d) E. J. Corey, N. W. Boaz, *Tetrahedron Lett.* **1985**, *26*, 6015–1618; *ibid.* **1985**, *26*, 1619–1622; e) A. Alexakis, J. Berlan, Y. Besace, *ibid.* **1986**, *27*, 1047–1050.

[5] Reviews on organoaluminum compounds: a) K. Maruoka, H. Yamamoto, *Tetrahedron* **1988**, *44*, 5001–5032; b) T. Mole, E. A. Jeffery, *Organoaluminium Compounds*, Elsevier, Amsterdam, **1972**.

[6] Without catalyst the reaction of **1** with Me_3Al in THF gave less than 1% of the 1,2-addition product (THF, 5 h, 22 °C); the reaction providing **2** was not observed in the presence of oxygen.

[7] G. W. Kabalka, R. F. Daley, *J. Am. Chem. Soc.* **1973**, *95*, 4428–4429.

[8] a) H. Kunz, K. Rück, *Angew. Chem.* **1991**, *103*, 712–715; *Angew. Chem. Int. Ed. Engl.* **1991**, *30*, 694–696; b) K. Rück, H. Kunz, *Synlett* **1992**, 343–344; c) H. Kunz, K. J. Pees, *J. Chem. Soc. Perkin Trans. 1* **1989**, 1168–1169.

[9] a) K. T. Takai, K. Oshima, H. Nozaki, *Bull. Chem. Soc. Jpn.* **1981**, *54*, 1281–1282; b) F. Sato, H. Kodama, Y. Tomuro, M. Sato, *Chem. Lett.* **1979**, 623–626.

[10] a) E. A. Jeffry, A. Meisters, T. Mole, *J. Organomet. Chem.* **1974**, *74*, 365–371; b) E. C. Ashby, G. Heinsohn, *J. Org. Chem.* **1974**, *39*, 3297–3299; c) L. Bagnell, E. A. Jeffry, A. Meisters, T. Mole, *Aust. J. Chem.* **1975**, *28*, 801–815.

[11] a) P. Wipf, H. Smitrovich, C.-W. Moon, *J. Org. Chem.* **1992**, *57*, 3178–3186; b) B. H. Lipshutz, S. H. Dimock, *ibid.* **1991**, *56*, 5761–5763; c) G. Zeifel, J. A. Miller, *Org. React.* **1984**, *32*, 375–513.

[12] a) J. Schwartz, D. B. Carr, R. T. Hansen, F. M. Dayrit, *J. Org. Chem.* **1980**, *45*, 3053–5061; b) R. T. Hansen, D. B. Carr, J. Schwartz, *J. Am. Chem. Soc.* **1978**, *100*, 2244–2245.

[13] a) CuCN · 2LiCl: P. Knochel, M. P. C. Yeh, S. C. Berk, J. Talbert, *J. Org. Chem.* **1988**, *53*, 2390–2392; b) CuI · 2LiCl: M. Arai, E. Nakamura, B. H. Lipshutz, *ibid.* **1991**, *56*, 5489–5491.

BOOKS

This section contains book reviews and a list of new books received by the editor. Book reviews are written by invitation from the editor. Suggestions for books to be reviewed and for book reviewers are welcome. Publishers should send brochures or (better) books to the Book Editor, Dr. Gerhard Karger, Redaktion Angewandte Chemie, Postfach 101161, D-69451 Weinheim, Federal Republic of Germany. The editor reserves the right of selecting which books will be reviewed. Uninvited books not chosen for review will not be returned.

Book Reviews

UV-VIS Atlas of Organic Compounds. Part 1: Spectra A1/1-C9/13. Part 2: Spectra D1/1-M19. 2nd Edition. Edited by *H.-H. Perkampus*. VCH Verlagsgesellschaft, Weinheim/VCH Publishers, New York, 1992. Part 1: VIII, pp. 1–336, Part 2: VII, pp. 336–1525, hardcover DM 750.00.—ISBN 3-527-28510-5/1-56081-268-0

To bring out a second edition of a specialist book in unaltered form twenty years after its predecessor is a remarkably brave step, and is only possible for a standard work with an undisputed international reputation, such as the "UV-VIS Atlas". This differs from other spectral collections in having the organic compounds arranged according to typical chromophores, for which 1167 representative spectra are given, with a quality of presentation unrivalled by anything else in the available literature. In addition to the displayed spectra there are 170 tables listing extinction coefficients and positions of absorption maxima for 740 further substances, which are related to the basic chromophores with variations of structure or solvent. Short review articles on the main chromophore groups are included, and these are still relevant and topical today.

The chromophores are arranged in groups as follows: groups A1 to A15: compounds containing multiply bonded carbon atoms; B1 to B21: compounds containing C=O and C=S groups; C1 to C9: compounds containing multiply bonded nitrogen atoms; D1 to D11: monocyclic aromatics; E1 to E7: polycyclic aromatics; F1 to F4: aromatic compounds containing non-benzenoid rings; G1 to G12: mononuclear heterocyclic compounds; H1 to H22: polynuclear heterocyclic compounds; I: saturated organic compounds; J1 to J10: selected compounds of biochemical and clinical interest; K1 to K3: inorganic systems. The atlas is completed by collections of spectra of UV-VIS spectrophotometric standards (Group L) and of 19 solvents (Group M).

Thus the scientific world has access here to a wealth of comparative information on UV-VIS spectra of organic compounds, which is indispensable for a wide variety of applications in fields such as analytical chemistry (titrimetry, chromatography), laser physics (laser dyes, materials for nonlinear optics), photochemistry, clinical chemistry, molecular biology (immunoassay, photodynamic effects), and ecology (reference materials for pollution studies).

The appearance of the new edition is an appropriate occasion to emphasize the great service that was performed by the original editors. At that time the Institut für Spektrochemie und angewandte Spektroskopie in Dortmund and the Photoelectric Spectrometry Group in London together succeeded in recruiting as contributors over 200 scientists from about 80 scientific institutions and 20 industrial laboratories throughout the world. These include many names of international renown.

Obviously a reprinting of such a work without change has meant that none of the developments of the past 25 years are reflected in it. Consequently many highly interesting chromophores such as the fullerenes, the cyclophanes, the many different laser dyes, the cyclopentadienyl dyes, reference materials for fluorescence spectroscopy, many new organic solvents, and a host of others are all absent. The publishers and the institutions responsible for the scientific development program need to remedy this situation as soon as possible by issuing a supplementary volume.

The "revision" that has been carried out for the second edition deserves criticism; in fact, in the form presented here it would have been better to leave things alone. The usefulness of such an atlas stands or falls according to how well the information is organized. In this case there are only two indexes that one can use: the molecular formula index and the alphabetical index of compound names based on the Chemical Abstracts nomenclature system. However, as the latter places the substituents (which are often unimportant in relation to light absorption) at the beginning of the name, it is of no help in searching for classes of compounds with similar chromophores. The search is made even more difficult by the occasional use of trivial names instead of the systematic ones. One therefore wonders why the index of core structural units, which corresponded most closely to the layout of the atlas, has now been dropped. In the first edition one could find all the acridine derivatives, all the ethylene derivatives, all the aniline derivatives, etc. under their corresponding keyword headings. Now in contrast, for example, the 26 substituted anilines must be extracted from four different tables, and the spectra of aniline derivatives from 15 widely scattered entries in the index—a hopeless task, especially as the systematic classification means that the spectra of the substituted anilines are distributed over Groups C6, D6, D8, D9, and D10, some of which are very large!

Another fault is that the spectral data tables no longer appear immediately after the spectra of the basic chromophores. Thus, for example, considerable effort is needed to discover that Table H22/T6 on page 1396 belongs to spectrum 36 of Group H22 on page 1055. Furthermore, in the second edition the compounds listed in the tables have been deleted from the formula and alphabetical indexes, with the result that they are lost to the majority of users.

Also the decimal classification given with the spectra is useless without a corresponding index. Such an index would at least have made it possible to search for compounds according to their basic chromophores, conjugation, heteroatoms, ring sizes, substituents, etc.

The lack of additional useful indexes is even more regrettable when one considers that 31 pages of the atlas have been used for an index of *R*-values, which aims to describe by a single quantity the degree of unsaturation of a molecule and hence the position of its light absorption. If one takes this index as a guide one finds, for example, that the aliphatic compound cubane, with $R = 5.0$, has the same degree of unsaturation as tetralin or decapentaene, and is even more unsaturated than the bisdimethylamino-nonamethinium cation ($R = 4.5$, listed in the index only under *N*-(9-dimethylaminonona-2,4,6,8-tetraenylidene)dimethylammonium perchlorate!); this despite the facts that cubane absorbs at about 200 nm, tetralin at 275 nm, decapentaene above 300 nm, and the nonamethine dye at as high as 625 nm. It remains a mystery why the *R*-index, unlike the other two indexes, includes compounds listed in the tables, whereas over 700 compounds have been left out of both the spectra collection and the tables. Thus, the user who wishes to have access to the whole of this wealth of information must systematically comb through the spectra and tables of Groups A to K. The publishers would be well advised to include better indexes along with the supplementary volume suggested above.

Although some printing errors in the first edition have been corrected in the revision, the frequency of errors has, on the whole, increased significantly. Some which affect the meaning are: the omission of the words "absorption intensity" after "log ε_λ specific for the..." (p. 1), benzene ring anellation has become "annealing" (p. 3), the association of ε_{max} with the dipole moment rather than with the transition dipole moment (p. 3), "future" instead of "feature" (p. 11), "p-electrons" instead of π-electrons (pp. 12, 19), "$\varepsilon \geq 5$" instead of $\log \varepsilon \geq 5$ (p. 39), "$n \rightarrow \pi$" instead of $n \rightarrow \pi^*$ excitation (p. 40), "E1/44; E1/45" instead of E1/T3 (p. 44), and "methylene bridges" instead of methine bridges (p. 56). It is also unfortunate that in the revision six literature citations in Pestemer's review article have been wrongly numbered. Lastly, in the introduction to UV-VIS spectroscopy, the only contribution that is described as having been rewritten, one would have expected to find a more representative and up-to-date collection of literature citations. The standard work on UV-VIS spectroscopy should at least have included a reference to G. Kortüm's book "Kolorimetrie, Photometrie und Spektrometrie" (Springer, Berlin, 1992).

Despite the shortcomings mentioned above, no science library should be without the atlas. It is a valuable working resource for all laboratories concerned in any way with UV-VIS spectroscopy, and can be thoroughly recommended.

Siegfried Dähne
Bundesanstalt für Materialforschung und -prüfung
Berlin (FRG)

Michael Faraday and the Royal Institution: The Genius of Man and Place. By *J. M. Thomas*. Adam Hilger, Bristol, 1991. XII, 234 pp., paperback £12.50.—ISBN 0-7503-0145-7

Few subjects appealed so strongly to Victorian biographers as did Michael Faraday, the bookbinder's apprentice unschooled beyond the age of 12, who through native talent, determination, hard work, kindness, eloquence, pluck, and simple virtue became a dominant figure in British intellectual society and one of the leading physicists and chemists of all time. Within three years of his death in 1867 three biographies appeared; the first, by his colleague and successor John Tyndall, went through five editions. Childless himself, Faraday delighted in children. Introducing them, and the general public, to the wonders and promise of experimental science was a calling that he felt as strongly as that of fundamental research. So it is fitting that a series of biographies over more than a century, and the enduring presence of *The Chemical History of a Candle* and others of Faraday's timeless writings, have inspired successive generations of the young to consider devoting their lives to science.

The present biography, published during the bicentennial of Faraday's birth, aims for accessibility to "all layfolk interested in, but not well informed about, modern science and especially young people in the arts and in all branches of the sciences." Because of the author's unique perspective and authority, and his skills as a writer and analyst of human endeavors, it will also appeal to professional scientists.

Professor Thomas writes as a special admirer of Faraday. For five years he has worked in Faraday's laboratory, lectured in his theater, lived in his home, and kept vibrant the scientific and educational tradition that he labored half a century to establish. This affinity with his subject not only gives the author access to rare materials, it also sharpens his insight into the symbiosis between Faraday and the Royal Institution of Great Britain.

Five of the book's eight chapters are devoted mostly to Faraday. The longest concerns his scientific contributions; others describe his youth, his skill and productivity as a writer, and his personal character. Every reader can profit by observing the nonpareil of experimental scientists, the discoverer of benzene and of electromagnetic induction, whose scientific rigor was not a whit diminished by his ignorance of

mathematics. Extracts from Faraday's writings are particularly effective at illuminating his personality. One example comes from his letter to Tyndall after an acrimonious scientific meeting in 1855: "I found....as a general rule, it was better to be a little dull of apprehension where phrases seemed to imply pique, and quick in perception when, on the contrary they seemed to imply kindly feeling."

The remaining three chapters focus on the Royal Institution, the unique legacy that is "part university, part museum, part research centre, part classroom, part library, part club, part exhibition and broadcasting center amongst other things." Readers who have known it primarily as the address of such luminaries as Davy, Huxley, Rayleigh, and most of the outstanding X-ray crystallographers of our century will learn a great deal about the people and traditions behind this remarkable institution. Impressive extracts and lists demonstrate the scope of its famous Friday Evening Discourses and Christmas Lectures through the years and are accompanied by capsule biographies of many lecturers and members.

Faraday did much to establish the model for the clear, precise, elegant lectures that characterize the Royal Institution. The contents and writing of this book give evidence that the tradition continues healthily towards its third century.

J. Michael McBride
Department of Chemistry
Yale University, New Haven (USA)

Artificial Life II. A Proceedings Volume in the Santa Fe Institute Studies on the Sciences of Complexity. Edited by *C. G. Langton, C. Taylor, J. D. Farmer,* and *S. Rasmussen.* Addison-Wesley, Redwood City, 1992. XXI, 854 pp., hardcover $ 57.95, paperback $ 41.25.—ISBN 0-201-52570-4

This volume describes part of the proceedings of a conference that brought together individuals interested in modeling living systems. The title of the book was sufficiently provocative to attract this reviewer's attention, especially as it was apparently a sequel to an earlier book, *Artificial Life,* which was interesting to read. Unfortunately, *Artificial Life II* is a disappointment by comparison with its predecessor, and will interest only the very mathematical specialist. *Artificial Life II* contains a collection of articles discussing various attempts to model, in a largely mathematical way, certain processes and properties characteristic of living systems. As with mathematical models generally, the relationship between life and the model described in this volume is often superficial. In *Artificial Life*, the novelty of the ideas and the obvious enthusiasm created by the assembling of individuals from various backgrounds compensated for this shortcoming. Neither the novelty nor the enthusiasm has been convincingly retained in the sequel. Most of the ideas in *Artificial Life II* are extensions of those in the earlier volume, and often rather simple extensions. Most disappointing was the absence of the experimental work on modeling chemical processes found in living systems that has emerged since the first volume was prepared. Several groups of experimental scientists, including von Kiedrowski in Germany, Luisi in Zurich, and Szostak, Orgel, Rebek, and their coworkers in the United States, have constructed in the laboratory experimental systems that serve as models for several of the key behavioral patterns of living systems. Although again these models are still in a very simple form, their availability makes purely mathematical models less exciting, especially as there was little in *Artificial Life II* to suggest that the contributors were aware of this work, and little that might guide experimentalists in their efforts. It would seem that contact between the mathematical modelers and the experimental chemists would be productive on both sides, offering the experimentalists some new insights and relieving the modeler of the vapidity that comes from computations disconnected from reality. One hopes that this will be recognized when the time comes to prepare the conference that yields *Artificial Life III.*

Steven Benner
Laboratorium für Organische Chemie
Eidgenössische Technische Hochschule
Zürich (Switzerland)

Capillary Electrophoresis. Principles, Practice and Applications. (Journal of Chromatography Library, Vol. 52.) By *S. F. Y. Li.* Elsevier, Amsterdam, 1992. XXVI, 582 pp., hardcover HFl 395.00, $ 225.50.—ISBN 0-444-89433-0

Capillary Electrophoresis (CE) is a new instrumental method of analysis which is undergoing very rapid development. This is matched by the rate of appearance of new monographs on the subject. This book by S. F. Y. Li differs from most in being an attempt by a single author to cover the whole field. Surprisingly, the author has not previously published much in the area of CE. The declared aim of the book is to give an easily understandable survey of CE, but it turns out to be more a collection of illustrated abstracts of individual publications. There are 1089 literature citations, so taking into account the fact that some of these are repeated in different chapters, this figure is consistent with the approximately 800–900 publications on CE that have appeared up to the beginning of 1992. This indicates that the literature on the subject has been fully covered.

The eight chapters vary in quality and length. Chapter 1 ("Introduction") gives a good survey of the historical development, followed by an explanation of the theoretical principles of CE and a comparison of this new separation method with conventional methods. Chapter 2 is concerned with sample introduction techniques, which are all described in great detail but not evaluated. Little is said about the problems that can arise with individual methods. However, the discussion of the problems of overcharging and excessive concentration (sample stacking) is highly topical. Chapter 3, the longest with over 100 pages, deals with all the types of detectors that have been described in the literature. However, it is doubtful whether it was appropriate to include detailed electronic circuit diagrams here. It would certainly have been better to reduce this to a critical summary, although it might have involved more work. The ability of the author to do this is shown by the table at the end of this chapter listing the most important detector properties.

The arrangement of subject matter in the rest of the chapters seems a little arbitrary. The chapter on "Column Technology" describes the preparation of both coated and gel-packed capillaries, whereas the principles of electrophoresis in gel-packed capillaries are treated just in the final section of this chapter. The chapter on "Electrolyte Systems" discusses capillary zone electrophoresis and micellar electrochromatography, whereas the other techniques (isoelectric focussing, isotachophoresis, and methods for coupling to a mass spectrometer) are treated in the chapter on "Special Systems and Methods". The chapter on "Applications" summarizes the uses of electrophoretic separation methods in a wide variety of fields. Here the space devoted to applications involving different classes of substances (peptides and proteins: 36 pp., nucleotides: 19 pp., pharmaceuticals: 18 pp., etc.) is in keeping with the relative importance of CE

in these areas. There is a table giving a quick survey of the types of substances that have been separated, with references to the original publications. The final chapter includes a late list of publications that appeared while the book was in preparation, extending the coverage to about the end of March 1992.

To summarize, the book offers a detailed and apparently complete survey of the literature on capillary electrophoresis. The information content is greater than that in the usual *Annual Reviews of Analytical Chemistry*. On the other hand, the published work is reviewed in an uncritical way. Consequently, one finds quite contradictory results cited in short succession, and some material is repeated in the individual chapters, thus increasing the length unnecessarily. However, these criticisms should not detract from the author's achievement in having produced a book of this kind that is so up-to-date (reflecting the state of knowledge at the beginning of 1992). It should be regarded as a handbook and reference source on CE rather than a textbook. It will be extremely useful to everyone who wishes to have rapid access to the literature on the subject.

Heinz Engelhardt
Angewandte Physikalische Chemie
Universität des Saarlandes
Saarbrücken (FRG)

Electrochemistry in Colloids and Dispersions. Edited by *R. A. Mackay* and *J. Texter*. VCH Publishers, New York/VCH Verlagsgesellschaft, Weinheim, 1992. XV, 546 pp., hardcover DM 210.00.—ISBN 1-56081-573-6/3-527-89573-6

This book contains 36 contributions by 83 authors. Some of the contributions are written in the style of review articles, while others report original research. They are based on papers presented at the Symposium on Electrochemistry in Microheterogeneous Fluids, which was held in August 1991 in New York under the auspices of the Division of Colloid and Surface Chemistry of the American Chemical Society. The aim of the symposium was to review the current state of knowledge in this rapidly developing interdisciplinary field, which lies between electrochemistry and the physical chemistry of colloidal systems. Studies on biophysical systems were deliberately excluded.

The book consists of five sections as follows: 1. Electroanalytical Methods and Applications (6 articles); 2. Transport Phenomena in Micellar Systems, Suspensions of Liposomes, and Microemulsions (9 articles); 3. Polymers and Latices (5 articles); 4. Electrosyntheses and Electrocatalytic Reactions (4 articles); 5. Colloidal Metals and Semiconductors (12 articles). Readers with interests in electrochemistry and in the physical chemistry of colloidal systems will probably not find much here that is new, except for the articles in the section on colloidal metals and semiconductors which together present a good picture of current development trends in this area. For those wishing to learn about the electrochemistry of colloidal systems the introductory chapter by one of the editors (J. Texter) will be of particular interest. In about 20 pages (with 252 literature references) Texter gives a comprehensive overview of the background to the individual contributions that follow, with examples taken from important results obtained by leading workers in this field.

Although the editors acknowledge the "cheerful and professional assistance" of a number of people at the research laboratories of the Eastman Kodak Company in enabling them to submit the articles to the publishers in camera-ready form, the book is by no means cheap. What, then, makes it particularly useful? Owing to the rising costs of scientific journals and the fact that departmental libraries have had their budgets frozen for several years, they have been forced to cut out more and more titles. The disturbingly impoverished state of such libraries is readily apparent to everyone using them. As a result scientists in Germany find that access to original publications is increasingly laborious and time-consuming. Copies of articles that seem to be especially important can be obtained from central libraries, but the cost is then charged to the research group's basic operating budget, which is usually small. In view of this situation it could be worthwhile to buy this volume, provided that the interested reader can persuade the library committee to do so despite the high price.

Dietrich Woermann
Institut für Physikalische Chemie
der Universität Köln (FRG)

Proton Conductors. Solids, Membranes and Gels—Materials and Devices. (Series: Chemistry of Solid State Materials, Vol. 2, series editors: *A. R. West* and *H. Baxter*.) Edited by *P. Colomban*. Cambridge University Press, Cambridge, 1992. XXXII, 581 pp., hardcover £ 75.00.—ISBN 0-521-38317-X

The second volume of the series "Chemistry of Solid State Materials" is concerned with an aspect of the chemistry of hydrogen that is relatively unfamiliar to the chemist, namely protons in "solids with pathological symptoms". To qualify as a *solid electrolyte* a material must have disorder, which can be induced thermally or chemically. In solids the ions become mobile enough for conduction to occur only at high temperatures. Chemical modifications can be achieved in a multistage synthesis so as to introduce specific structural defects which confer the high temperature conductivity needed for applications in high performance batteries or fuel cells. In Chapter 3 of this book the special characteristics of solid ionic conductors, with the emphasis on proton conductors, are skillfully and concisely presented by the editor, P. Colomban, and A. Novak. From this it already becomes clear that, because of the complicated nature of most proton conductors, they do not yet offer the basis for a reliable technology or a large commercial market. Nevertheless, the authors report many novel and exciting results of fundamental research on hydrogen-containing materials, which are seldom adequately covered in conventional textbooks and data complications. One moves on eagerly to the chapters that treat particular groups of materials with special types of defect structures, the effects that these have on proton conduction, and especially the technology of applying them.

The chapter on "Hydrogen Bond and Protonic Species" (100 pp.) describes the fundamentals of chemical bonding and proton structure in the compounds formed by hydrogen with the strongly electronegative elements oxygen, fluorine, and nitrogen. The special position of proton conductors compared with other types of solid ionic conductors is emphasized here. This chapter also includes a contribution on hydrogen in metals, by I. Svare. The discussions of adsorption and desorption, diffusion, tunneling, and the structure of metal hydrides go beyond the area defined by the book's title: here one is not mainly concerned with the proton H^+ but with the valence states H^- and H^0. Nevertheless, the article serves a useful purpose in completing the picture of the behavior of hydrogen in its compounds, and especially the dynamics of the bonding, and at the same time defining a boundary to the subject!

Chapter 2 (225 pp.) is concerned with "Materials: Preparation, Structures and Properties". Here the reader is introduced to many different types of materials, and the temperature-dependent conducting properties of several well-known families of proton conductors such as Nafion and β″-alumina are described. In the contribution by Dickens and Chippendale we get to grips with the problems of the nonstoichiometric oxides of the transition metals W, Mo, V, Cr, and U. The analysis of the constitution of these materials has only been possible through a combination of methods, some of which are fairly unusual in chemistry: vibrational spectroscopy, magic-angle-spinning (MAS) NMR spectroscopy, and incoherent inelastic neutron scattering. To develop quantitative relationships that describe how the hydrogen in these compounds influences the constitution and properties calls for lateral thinking and an imaginative approach to analytical results, analogous to dealing with macromolecular materials in biochemistry, for example. Next some specific groups of proton conductors are discussed: perovskites, hydroxides of the alkaline earth metals, the oxyacids of phosphorus, arsenic, sulfur, selenium, and chlorine, and graphite intercalation compounds. However, it is not obvious why it was thought necessary to treat the next three groups of materials, the β- and β″-polyaluminates, the zeolites, and the Nasicon phases, in a separate sub-chapter entitled "Inorganic Ion Exchangers". The same also applies to the following sub-chapter on "Layer Hydrates"; this includes some very special groups of proton conductors (e.g., γ-$Zr(HPO_4)_2$), which are not hydrates at all but hydroxo salts or hydrogen phosphates of the tetravalent metals Ti, Zr, and Ce, and, moreover, do not necessarily have layer structures.

Chapter 3 (115 pages) is entitled "Proton Dynamics and Charge Transport", and deals with the special methods used for characterizing proton conductors. The eight articles describe the use of vibrational spectroscopy, NMR spectroscopy, various methods for measuring dielectric constants, impedance spectroscopy, and neutron scattering. Emphasis is placed on the discussion of typical results for some specific materials, thereby providing readers who intend to use these methods with the theoretical background needed to interpret spectra or other data.

Chapter 4, "Proton Diffusion Mechanisms", consists of three short articles by Slade, Colomban, Novak, and Kreuer which discuss specific proton conduction mechanisms. These discussions link up with some fundamental aspects of bonding and thermodynamics in proton conductors (e.g., the dynamics of the proton in hydrogen bonding, as treated in Chapter 1). However, it is difficult to see why the fundamental article by I. A. Ryzhkin on "Ice" was not included here instead of in Chapter 2.

In Chapter 5, "Devices", we learn something about the latest state of the art in applications to secondary energy storage and to primary energy generation using fuel cells. Also in the fields of gas sensors, electrochromic devices, field effect transistors, and super-capacitors there are articles reporting on recent developments, results with pilot systems, and prospects for new types of thin film elements.

The editor, P. Colomban, has made a good choice of topics and authors. In putting together the specialized contributions of 38 authors in five main chapters with altogether 575 pages he has, remarkably, managed to avoid over-stretching the material or losing the reader's attention by offering too heterogeneous a presentation. Chemists, physicists, and engineers will all find the book informative. The detailed introduction, comprehensive subject index, and table of symbols all afford clear and easy access to the material. References are given throughout to original papers as well as reviews, a mark of quality in a specialist book such as this with an international team of authors.

Jürgen Felsche
Fakultät für Chemie
der Universität Konstanz (FRG)

Metallothioneins. Synthesis, Structure and Properties of Metallothioneins, Phytochelatins and Metal–Thiolate Complexes. Edited by *M. J. Stillman, C. F. Shaw III*, and *K. T. Suzuki*. VCH Verlagsgesellschaft, Weinheim/VCH Publishers, New York, 1992. IX, 443 pp., hardcover DM 218.00.—ISBN 3-527-28011-1/0-89573-785-X

Seven years after the publication of the two-volume work "Metalloproteins", edited by P. Harrison, the same publishing house has now brought out a volume devoted expressly to metallothioneins. The editors' aim is to present a collection of review articles by recognized experts so as to cover the rapid developments that have occurred in this field. The book consists of 16 chapters. After a succinct introduction in Chapter 1 to the metallothioneins and related polypeptides (cadystins and phytochelatins), the following topics are treated: preparation, isolation, and identification (Ch. 2), X-ray structure determination (Ch. 3), studies using circular dichroism (CD), magnetic circular dichroism (MCD), and emission spectroscopy (Chs. 4 and 5), kinetic studies of cluster formation, metal exchange reactions, and ligand substitution (Ch. 7), phytochelatins and cadystins: synthesis and biosynthesis, and studies of their role in Cd^{2+} and S^{2-} metabolism (Chs. 9–12), and model complexes: metal–thiolate complexes and NMR studies of complexes with adamantane-like structures (Chs. 13 and 14). Other topics covered include aurothioneins (Ch. 6), analysis for mercury (Ch. 8), models of Cu^{II} proteins (Ch. 15), and metallodrugs (Ch. 16).

The book gives comprehensive accounts of the present state of knowledge in each of the areas treated. The treatment of "Optical Spectroscopy of Metallothioneins" in Chapter 4 is especially interesting. So many results are presented here that one is confused at first, but the author goes on to provide the interested reader with a clear picture of the dynamics of cluster formation and the wide variety of metallothionein structures produced in this way. The picture is completed by the article on "Kinetic Reactivity of Metallothioneins" in Chapter 7. On the basis of the results on metal exchange reactions and ligand substitution the author has succeeded in reaching a better understanding of the hitherto obscure function of thioneins in an organism. Four further chapters deal with phytochelatins and cadystins. Since these peptides have only been studied for about ten years, some questions remain unanswered, for example concerning the relationship between sulfide metabolism and production of phytochelatin. Also no clear picture of the structures of these cadmium- and zinc-containing peptides has yet emerged, since there have as yet been no single crystal X-ray studies. Chapter 11 on "Metal:sulfide Quantum Crystallites in Yeast" gives a suggested structure for the metal centers in these sulfide-containing cadmium-binding proteins, based on powder X-ray diffraction patterns. The article on "Metal–Thiolate Compounds" (Ch. 13) reviews the latest findings on coordination principles in synthetic metal–thiolate and metal sulfide–thiolate complexes. Readers seeking a quick and straightforward summary of the latest developments in this area will much appreciate the clearly set out table which lists all the new complexes synthesized in the last six years. This chapter and Chapter 14 on "Adamantane-

Like Cages" together serve to bridge the gap between inorganic chemistry and biochemistry.

One of the book's weaknesses is undoubtedly that the potential of NMR spectroscopy only emerges in Chapter 14, and no mention is made of the great importance of ^{113}Cd–^{1}H NMR spectroscopy in elucidating the three-dimensional structures of metallothioneins. In recent years NMR spectroscopy has become such a powerful method in this area that even the interpretation of X-ray crystallographic data has had to rely on NMR results. The neglect of NMR spectroscopy is probably due to the fact that the book has developed out of papers presented at the symposium on "The Chemistry of Heavy Metals in Physiologically Important Roles" (Hawaii, 1989).

Altogether, this book is of interest to those involved in all aspects of metallothionein research, as it is clearly presented and contains nearly 1000 literature references which afford easy access to the original publications. It should therefore be available in every departmental library.

Hans-Oscar Stephan
Fachbereich Anorganische und Festkörperchemie
der Universität Duisburg (FRG)

Inorganic Polymeric Glassses. (Series: Studies in Inorganic Chemistry, Vol. 15.) By *R. C. Popp*. Elsevier, Amsterdam, 1992. XIV, 322 pp., hardcover HFl 365.00.—ISBN 0-444-89500-0

This book contains a useful survey of experimental results on glass-forming phosphate systems, explaining clearly how these relate to applications. Special attention is devoted to the suitability of these materials for immobilizing and sealing in radioactive wastes in the nuclear energy industry.

The introductory chapter deals with the fundamentals of glass formation, the important properties that can be controlled by adjusting the process variables, and the main technological methods used in glass manufacture, including a brief survey of aspects such as sol–gel technology and fiber optics processes. However, the emphasis on phosphate glasses as inorganic polymeric glasses, thereby making a distinction between these and glasses made from other glass-forming systems, seems rather arbitrary, and can hardly be justified on structural grounds.

The main part of the book is concerned with efforts to produce glasses with the highest possible chemical stability, and with the analytical and diagnostic methods used to evaluate them. Much space is devoted to the resistance to hydrolysis and acids, and the effects of impurities (especially contamination from the crucible wall during melting) on the properties, including the recrystallization and segregation behavior, illustrated throughout by electron micrographs. However, in the course of this the author makes some statements that are unsupported by experimental evidence and do not take into account other results reported in the literature. Thus, he denies the existence of a specific mechanism for internal diffusion in glasses of this type, whereas it is known, for example, that $Na^{\oplus}$ ions have a higher mobility in $NaPO_3$ glasses than they do at comparable concentrations in silicate or borate glasses. As the book describes, glass-forming phosphate systems are used not only for encapsulating radioactive wastes but also in luminescent glasses, and the range of uses is being further extended to medical applications based on their proven biocompatibility; for example, glasses of this type or suitable glass ceramics can be used as bone cements or in dental prosthetics.

Each chapter ends with a bibliography listing important original papers and, most usefully, review articles. This is a monograph on a specialized field, in which a notable feature is the thorough survey of knowledge on the inorganic structural chemistry of condensed phosphates.

The excellent layout makes the text quick and easy to assimilate. The book will certainly be welcomed and used by specialists in the field of phosphate-containing materials. It has been produced using a computer text-processing program, and this becomes apparent especially in the diagrams, which do not always have the necessary captions. In view of this, the rather high price seems surprising.

Adalbert Feltz
Institut für Anorganische Chemie
der Universität Jena (FRG)

New Books
see next page

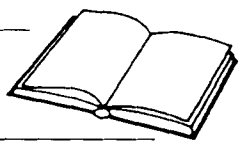

 © *VCH Verlagsgesellschaft mbH, D-69451 Weinheim, 1993* *0570-0833/93/0909-1375 $ 10.00+.25/0*

New Books

Complexity. Life at the edge of chaos. By **R. Lewin.** Maxwell Macmillan International, Oxford. **1993.** 208 pp., hardcover, £ 17.95.—ISBN 0-02-570485-0

Structure of Electrified Interfaces. Edited by **J. Lipkowski, P.N. Ross.** VCH, Weinheim/New York, **1993.** 406 pp., hardcover, DM 196.—/$ 125.—ISBN 3-527-28787-6/0-89573-787-6

Grundkurs Chemie. By **A. Arni.** VCH, Weinheim, **1993.** 354 pp., paperback, DM 48.—ISBN 3-527-29008-7

HPLC Detection. Newer Methods. Edited by **G. Patonay.** VCH, Weinheim/New York, **1993.** 236 pp., hardcover, DM 158.—/$ 95.—ISBN 3-527-28219-X/0-89573-327-7

Electrode Kinetics for Chemists, Chemical Engineers, and Materials Scientists. By **E. Gileadi.** VCH, Weinheim/New York, **1993.** 597 pp., hardcover, DM 189.—/$ 115.—ISBN 3-527-89561-2/1-56081-561-2

Plants as Biomonitors. Indicators for Heavy Metals in the Terrestrial Environment. Edited by **B. Markert.** VCH, Weinheim/New York, **1993.** 644 pp., hardcover, DM 298.—/$ 200.—ISBN 3-527-30001-5/1-56081-272-9

Data Analysis for the Chemical Sciences. A Guide to Statistical Techniques. By **R.C. Graham.** VCH, Weinheim/New York, **1993.** 536 pp., hardcover, DM 78.—/$ 49.50.—ISBN 3-527-28114-2/1-56081-048-3

Scanning Tunneling Microscopy and Spectroscopy. Theory, Techniques, and Applications. Edited by **D.A. Bonnell.** VCH, Weinheim/New York, **1993.** 436 pp., hardcover, DM 196.—/$ 125.—ISBN 3-527-27920-2/0-89573-786-X

Capillary Electrophoresis of Small Molecules and Ions. By **P. Jandik, G. Bonn.** VCH, Weinheim/New York, **1993.** 298 pp., hardcover, DM 108.—/$ 65.—ISBN 3-527-89533-7/1-56081-533-7

Electrochemical and Electrocatalytic Reactions of Carbon Dioxide. Edited by **B.P. Sullivan, K. Krist, H.E. Guard.** Elsevier, Amsterdam, **1993.** 298 pp., hardcover, Dfl. 340.—ISBN 0-444-88316-9

Applied Chaos Theory. A Paradigma for Complexity. By **A.B. Çambel.** Academic Press, London, **1993.** 246 pp., hardcover, £ 33.—ISBN 0-12-155940-8

***Principles* of Biochemistry.** 2. Auflage. By **A. Lehninger, D.L. Nelson, M.M. Cox.** Worth Publishers, New York, **1993.** 1013 pp., hardcover, $ 56.95.—ISBN 0-87901-500-4

Soil Chemistry and its Applications.(Cambridge Environmental Chemistry Series 5). By **M. Cresser, K. Killham, T. Edwards.** Cambridge University Press, Cambridge, **1993.** 192 pp., paperback, £ 35.—ISBN 0-521-32269-3

Atomic and Molecular Properties. (Methods in Computational Chemistry, Vol. 5). Edited by **S. Wilson.** Plenum Press, New York, **1993.** 349 pp., hardcover, $ 79.50.—ISBN 0-306-44263-9

Characterization of Ceramics. (Materials Characterization Series). Edited by **R.E. Loehmann.** Butterworth-Heinemann, Oxford, **1993.** 295 pp., hardcover, £ 47.50.—ISBN 0-7506-9253-7

An Introduction to Metal Matrix Composites. (Cambridge Solid State Science Series). Edited by **T.W. Clyne, P.J. Whiters.** Cambridge University Press, Cambridge, **1993.** 509 pp., hardcover, £ 55.—ISBN 0-521-41808-9

Anorganikum. By **L. Kolditz.** Hüthig, Heidelberg, **1993.** 1125 pp., hardcover, DM 98.—ISBN 3-335-00341-1

Relaxation and Thermodynamics in Polymers. Glas Transition. By **E.-J. Donth.** Akademie Verlag, Berlin, **1993.** 350 pp., hardcover, DM 148.—ISBN 3-05-501392-1

New Frontiers in Catalysis. Proc. 10th Int. Congr. Catalysis, 1992. Edited by **L. Guczi, F. Solymosi, P. Teteny.** Elsevier, Amsterdam, **1993.** 2878 pp., hardcover, Dfl. 895.—ISBN 0-444-89621-X

Half a Century of Free Radical Chemistry. By **D.H.R. Barton, S.I. Parekh.** Cambridge University Press, Cambridge, **1993.** 164 pp., paperback/hardback, £ 12.95/30.—ISBN 0-531-44580-9/0-531-44005-X

Silica Gel and Bonded Phases. Their Production, Properties and Use in LC. (Separation Science Series). Edited by **R. P. W. Scott.** Wiley, West Sussex, Great Britain, **1993.** 261 pp., hardcover, £ 35.—ISBN 0-471-93985-4

Metal Extraction by Bacterial Oxidation of Minerals. (Ellis Horwood Series in Inorganic Chemistry). By **J. Barrett, M. N. Hughes, G. I. Karavaiko, P. A. Spencer.** Ellis Horwood, London, **1993.** 191 pp., hardcover, £ 64.60.—ISBN 0-13-577735-6

Biopolymers 1. (Advances in Polymer Sciences, Vol. 107). Edited by **N. A. Peppas, R. S. Langer.** Springer, Heidelberg, **1993.** 272 pp., hardcover, DM 218.—ISBN 3-540-56148-X

Electro-Osmosis. (Ellis Horwood Series in Physical Chemistry). By **K. P. Tikhomolova.** Ellis Horwood, London, **1993.** 219 pp., hardcover, £ 99.—ISBN 0-13-249806-5

Pest Control with Enhanced Environmental Safety. (ACS Symposium Series, Vol. 524). Edited by **S. O. Duke, J. J. Menn, J. R. Plimmer.** American Chemical Society, Washington, **1993.** 357 pp., hardcover, $ 84.95.—ISBN 0-8412-2638-5

Chromatography of Polymers. Characterization by SEC and FFF. (ACS Symposium Series, Vol. 521). Edited by **T. Provder.** American Chemical Society, Washington, **1993.** 337 pp., hardcover, $ 94.95.—ISBN 0-8412-2625-3

Polymeric Delivery Systems. Properties and Applications. (ACS Symposium Series, Vol. 520). Edited by **M. A. El-Nokaly, D. M. Piatt, B. A. Charpentier.** American Chemical Society, Washington, **1993.** 411 pp., hardcover, $ 99.95.—ISBN 0-8412-2624-5

Nuclear Magnetic Shielding and Molecular Structure. (Nato Advanced Science Institutes Series). Edited by **J. A. Tossell.** Kluwer, Dordrecht, **1993.** 600 pp., hardcover, Dfl 330.—ISBN 0-7923-2119-7

Physical Methods in Chemistry. By **V. A. Afanasiev, G. E. Zaikov.** Nova Science, Commack, USA, **1993.** 182 pp., hardcover, $ 79.—ISBN 1-56072-063-8

Biomembranes. Physical Aspects. Edited by **M. Shinitzky.** VCH, Weinheim/New York, **1993.** 378 pp., hardcover, DM 198.—/$.135.—ISBN 3-527-30021-X/1-56081-771-2

Industrial Organic Chemistry. Second, Revised and Extended Edition. By **K. Weissermel, H.-J. Arpe.** VCH, Weinheim/New York, **1993.** 457 pp., hardcover, DM 128.—/$.80.—ISBN 3-527-26995-9/0-89573-861-9

Registered names, trademarks, etc. used in this journal, even when not marked as such, are not to be considered unprotected by law.

© VCH Verlagsgesellschaft mbH, D-69451 Weinheim, 1993. – Printed in the Federal Republic of Germany by Konrad Triltsch Druck- und Verlagsanstalt Würzburg.

All rights reserved (including those of translation into foreign languages). No part of this issue may be reproduced in any form – by photoprint, microfilm, or any other means – nor transmitted or translated into a machine language without written permission from the publishers. Only single copies of contributions, or parts thereof, may be made for personal use. This journal was carefully produced in all its parts. Nevertheless, authors, editors, and publisher do not warrant the information contained therein to be free of errors. Readers are advised to keep in mind that statements, data, illustrations, procedural details, or other items may inadvertently be inaccurate.

Valid for users in the USA: The appearance of the code at the bottom of the first page of an article (serial) indicates the copyright owner's consent that copies of the article may be made for personal or internal use, or for the personal or internal use of specific clients. This consent is given on the condition, however, that the copier pay stated per-copy fee through the Copyright Clearance Center, Inc. (CCC), for copying beyond that permitted by Sections 107 or 108 of the U.S. Copyright Law. This consent does not extend to other kinds of copying, such as copying, for general distribution, for advertising or promotional purposes, for creating new collective works, or for resale. For copying from back volumes of this journal see 'Permissions to Photo-Copy: Publisher's Fee List' of the CCC.

Editorial office: Postfach 10 11 61, D-69451 Weinheim, Federal Republic of Germany, Telephone (06201) 606 315, Telex 465 516 vchwh d, Telefax (06201) 606 328, E-Mail Z16@DHDURZ2 in Earn Bitnet.

Editor: *Peter Göltz*

Associate editors: *N. A. Compton, R. H. Schmidt-Radde, K. J. Schneider.* **Book editor:** *G. Karger.* **Editorial assistants:** *J. Göhrig, E. Schweikart*

Publishers: VCH Verlagsgesellschaft mbH. (Managing Directors: *Hans Dirk Köhler, Dr. Karlheinz Köpfer*). Pappelallee 3, D-69451 Weinheim, Federal Repuhlic of Germany.

Advertising office (Advertising Manager: *N. Schippel*): Postfach 10 11 61, D-69451 Weinheim, Federal Republic of Germany, Telephone (0 62 01) 606 312, Telefax (0 62 01) 606 328.

ANGEWANDTE CHEMIE
International Edition in English
Volume 32 · Number 10
October 1993
Pages 1377–1500

The Battle of Calicheamicin γ_1^I

By K. C. Nicolaou*

*In memory of Franz Sondheimer***

The first total synthesis of calicheamicin γ_1^I was achieved approximately a year ago. In this article, the author presents a personal account of the events, in chronological order, that led to this success story in total synthesis.

Introduction

Chaliche, a word of Greek origin (χαλιξ≡chaliche) means "pebble made of lime stone". No one could have ever imagined that this little pebble would hide for millions of years the secrets of calicheamicin γ_1^I (**1**) (Fig. 1).[1] A microorganism attached to the pebble produces this antitumor antibiotic that has created so much excitement in scientific circles and continues to fascinate those who get to know it. Among the many groups who had the good fortune to work with this unique molecule was ours, and below we unfold the story of our battle for the total synthesis of calicheamicin γ_1^I. The drive for the conquest of this highly prized natural product generated excitement and drama rarely seen before in synthesis and, as such, it is worthwhile to record some of its details.

We begin with some rather esoteric, but fundamental, observations from the 1970s which were destined to become one of the most celebrated reactions of the 1980s and beyond. In 1972, Robert Bergman, then at the California Institute of Technology (CalTech), reported the thermal cycloaromatization of conjugated *cis*-enediynes to 1,4-benzenoid diradicals, a reaction he ingeniously designed and thoroughly studied (Fig. 2).[2] Neither he, nor anyone else could have dreamed that this fundamental process, which had also been observed by Sondheimer et al.[3] and Masamune et al.[4] and is known today as the Bergman reaction (Fig. 2), could have been used by Nature for eons in chemical warfare amongst microorganisms. For at the heart of the

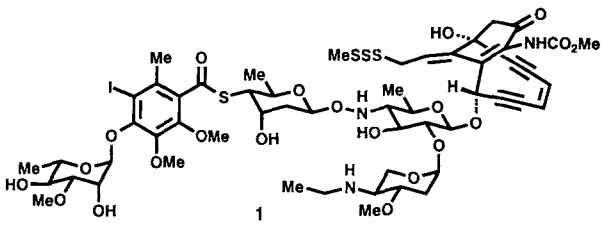

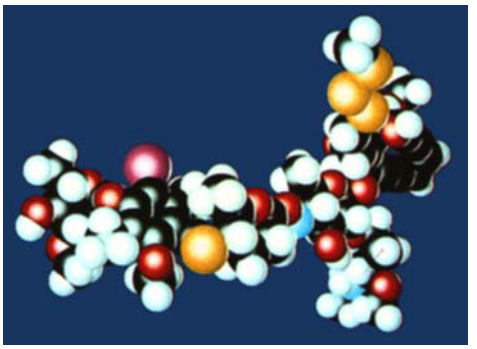

Fig. 1. Structural formula (top) and computer-generated space-filling model (bottom) of calicheamicin γ_1^I **1**.

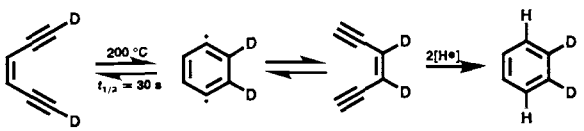

Fig. 2. The Bergman cycloaromatization.

[*] Prof. Dr. K. C. Nicolaou
Department of Chemistry, The Scripps Research Institute
10666 N. Torrey Pines Road, La Jolla, CA 92037 (USA)
and
Department of Chemistry, University of California, San Diego
9500 Gilman Drive, La Jolla, CA 92093 (USA)
Telefax: Int. code + (619)554-6738

[**] Professor Franz Sondheimer was one of the most influential acetylene chemists of the 20th century and from whom the author learned his first acetylene chemistry while studying at University College, London, as a doctoral student jointly with him and P. J. Garratt.

 © VCH Verlagsgesellschaft mbH, D-69451 Weinheim, 1993 0570-0833/93/1010-1377 $ 10.00+.25/0

mechanism of action of calicheamicin γ_1^I as a powerful antibiotic lies this very reaction (Fig. 3).

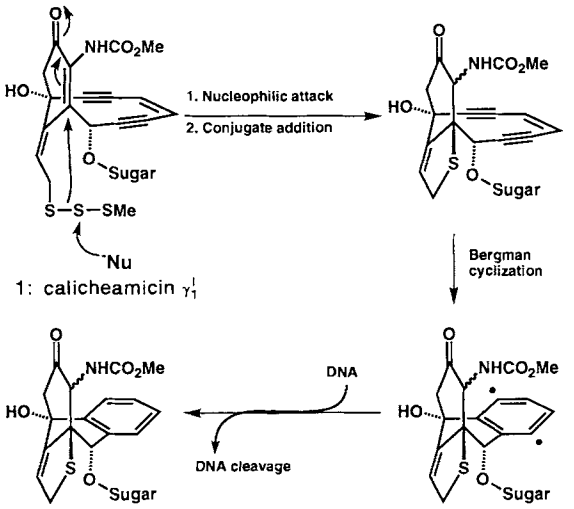

Fig. 3. Proposed mechanism of action of calicheamicin γ_1^I 1.

In July 1986, I was attending the Natural Products Gordon Conference in New Hampton, New Hampshire, where I had the good fortune of making the acquaintance of Robert Babine of Lederle Laboratories. He tantalizingly brought to my attention a new natural product that the Lederle group was working on with an "amazing structure and phenomenal biological activity" as he put it. Without revealing the structure of the molecule, Robert assured me that the structure would intrigue me, and that he would see to it that I heard about it before publication!

In September 1986, a phone call from Robert Babine brought me to Pearl River, New Jersey, the next day where the Lederle group, which included May Lee and George Ellestad, were waiting. After the obligatory signature to assure confidentiality, I was allowed to take my first glance at the structure of LL-E33288 γ_1^I –the code number for that "amazing natural product" (Fig. 4). Indeed, I was amazed!

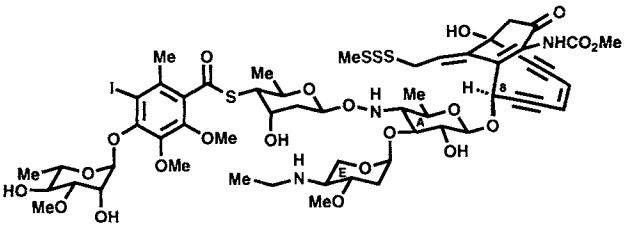

Fig. 4. September 1986: First look at the structure of LL-E33288 γ_1^I (calicheamicin γ_1^I) on a visit to Lederle Laboratories. The early structure turned out to be partly incorrect (configuration at C-8 of the aglycon and point of attachment of ring E to ring A) and was later rectified. R. Babine, M. D. Lee, G. Ellestad, personal communication.

Speechless, I proceeded to scan the structure with my eyes and mind with mixed feelings best described as alternating among disbelief, excitement, admiration, and hope! Finally, I chose to utter in disbelief, but with a secret hope of optimism, "The structure must be wrong. I cannot believe that those acetylenes could allow such a strained ring system to exist. And what about that trisulfide? Are you sure about that NH–O bond?" By the end of the day, however, the Lederle group had convinced me of the "correctness" of their structure and I drove home to Philadelphia that evening, quite excited, contemplating what this molecular structure was holding for us in terms of chemical synthesis, molecular design, biology, and medicine.

The Daring Proposal

The next morning I held a meeting in my office at the University of Pennsylvania with two of my best students, Nicos A. Petasis and Guido Zuccarello, to whom I entrusted the secret of the structure of LL-E33288 γ_1^I; together we began planning a strategy for the total synthesis and the solution of the associated chemical problems. The project was code named "Molecular Robotics" and no one was to leak the structure until we received permission from the Lederle group. By February 1987 a synthetic strategy was ready, and a proposal was submitted to the National Institutes of Health (NIH). By the summer of 1987 the structure of LL-E33288 γ_1^I, now renamed calicheamicin γ_1^I, was in the public domain (Fig. 5). At about the same time we learned from

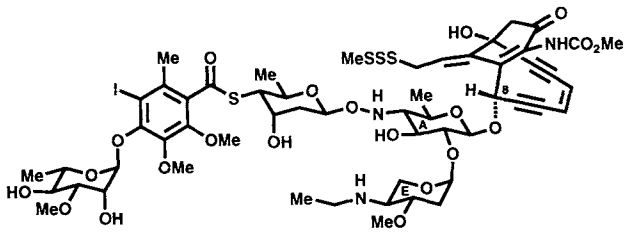

Fig. 5. February 1987: The Lederle group reports the structure of calicheamicin γ_1^I. The configuration at C-8 on the aglycon is now correct. M. D. Lee, T. S. Dunne, M. M. Siegel, C. C. Chang, G. O. Morton, D. B. Borders, *J. Am. Chem. Soc.* **1987**, *109*, 3464; M. D. Lee, T. S. Dunne, C. C. Chang, G. A. Ellestad, M. M. Siegel, G. O. Morton, W. J. McGahren, D. B. Borders, *ibid.* **1987**, *109*, 3466.

NIH that our grant had been recommended for approval with a score of 3.15 (out of 5, 1: best, 5: worst) or 87.2 percentile level (ranked worse than 87.2% of the proposals reviewed in that round!). This was obviously disappointing to us, to say the least, and remains to this day by far the worst score this group ever received from NIH! The study section at NIH was right, however: besides, the many questionable steps in our proposed synthesis (indeed, how could one not have questionable steps in a strategy towards such a diabolical and, at the time, questionable molecular structure!), we had directed our approach toward the incorrect structure! As it turned out, the structure revealed to us by the Lederle group in September 1986 had the wrong stereochemistry at C-8, and the wrong attachment site for the aminosugar (Figs. 4 and 6)!

Much to their credit, the study section enthusiastically endorsed our second attempt to secure funding from NIH in the next round. This time our strategy was directed at the correct structure, although it was, in essence, very similar to the one originally proposed. A brief consideration of our plans included in that fatal first proposal, particularly in the

context of the chemistry subsequently developed in the field, may be constructive and amusing.

In Figure 6 the retrosynthetic analysis of the target structure (incorrect) indicates how we intended to utilize the Schmidt trichloroacetimidate method for the coupling of the carbohydrate and aglycon fragments. Interestingly, this turned out to be the way we and the Danishefsky group – our major competitors (see below)—successfully carried out this step.

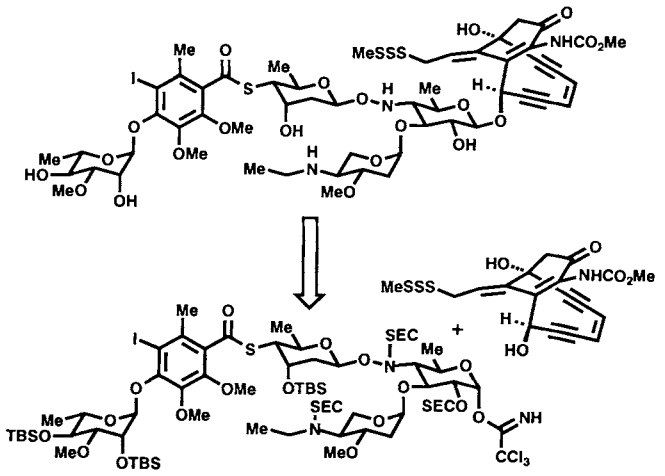

Fig. 6. Early 1987: Retrosynthetic analysis of LL-E33288 γ_1^I (incorrect isomer) according to the orginal proposal. Abbreviations and acronymns, for example for protecting groups, are not explained in this article; for details the reader should consult the orginal literature or for example the enediyne review article from Nicolaou et al. in November 1991 in *Angewandte Chemie* [1 b].

In Figure 7 a retrosynthetic analysis of the aglycon fragment is shown, depicting the original five alternative approaches to this unusual skeleton. Again, it is interesting to

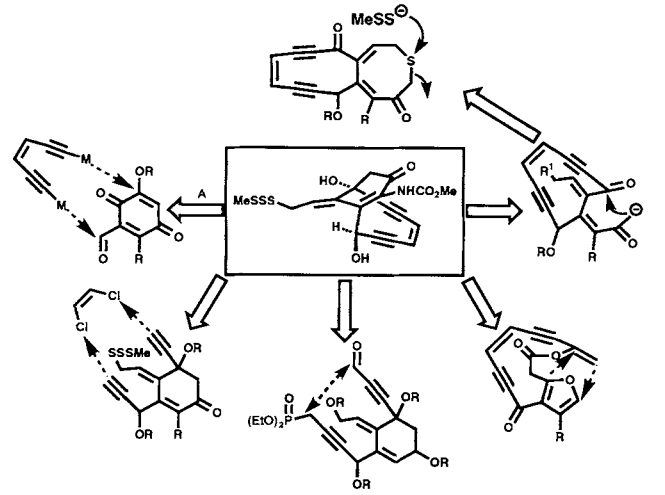

Fig. 7. Early 1987: Retrosynthesis of the aglycon of calicheamicin γ_1^I in the original proposal; a wide range of approaches was considered.

observe that one of them (approach A) contained the essence of the intramolecular acetylide–aldehyde condensation as the key step in forming the 10-membered enediyne ring, a concept that proved crucial in building calicheamicinone and related systems and was used by ourselves and by several research groups including those of Danishefsky and Kende

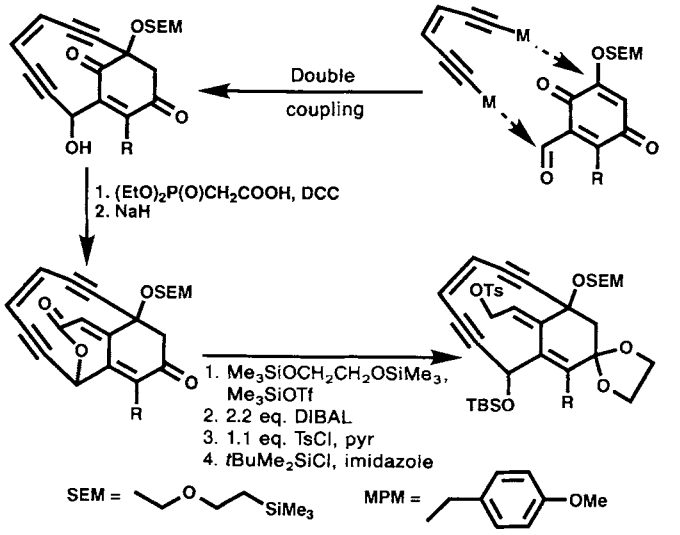

Fig. 8. Early 1987: Proposed synthesis of the aglycon of calicheamicin γ_1^I based on an acetylide–aldehyde condensation in the original proposal.

(see below). Figure 8 gives a more detailed version of this original plan and illustrates our projected elaborations towards more advanced intermediates. Some of the other strategies shown in Figure 7, however, remain curiosities to this day.

In Figure 9 our original ideas pertaining to the construction of the oligosaccharide fragment are summarized. Al-

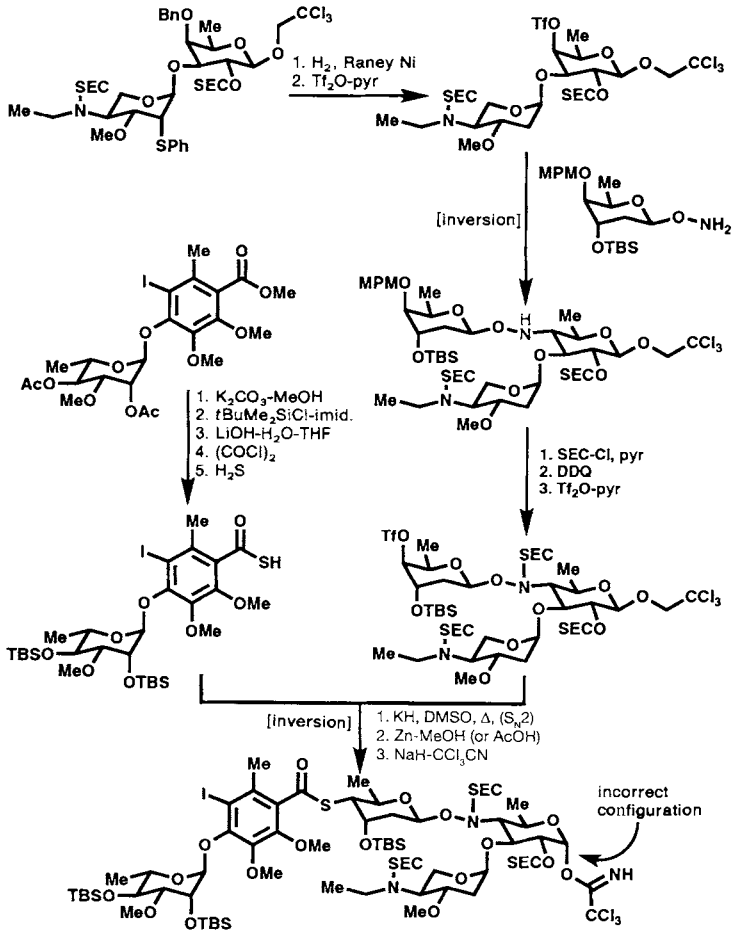

Fig. 9. Early 1987: Proposed synthesis of the oligosaccharide of calicheamicin γ_1^I in the original proposal.

though neither of the two proposed coupling reactions were used in our synthesis, the feasibility of the nucleophilic displacement of a trifluoromethanesulfonate (triflate) by a nitrogen nucleophile as a means of constructing the NH–O bond was demonstrated independently by the Kahne and Danishefsky groups in their pioneering studies on calicheamicin γ_1^I. As it turned out, we opted for an oxime forming reaction followed by reduction as a strategy for the construction of this unusual bond of calicheamicin (see below).

The Competition

The emergence of calicheamicin γ_1^I as a challenging synthetic target provided a rare opportunity for creativity in organic synthesis and molecular design. Although such endeavors should not ideally be subject to time constraints and the pressures of competition, these elements of human nature always surface, particularly when the projects are attractive and the stakes are high. Such was the case of calicheamicin γ_1^I. It is almost certain that most who entered the arena, including ourselves, had, at the outset, strong misgivings whether the total synthesis of such a complex and constrained molecule could be achieved! All of us, however, were quite convinced that interesting scientific results should emerge from such an undertaking. For the interest of the reader, and in order to extend credit to those groups who contributed so importantly to the feat of the calicheamicin total synthesis, the main landmark events along the way to this molecule are highlighted.

The first "bombshell" was dropped by Schreiber and Kiessling who submitted a paper in August 1987 to the *Journal of the American Chemical Society* (JACS) claiming the synthesis of the first calicheamicinone model system by a breathtaking intramolecular Diels–Alder reaction (Fig. 10).

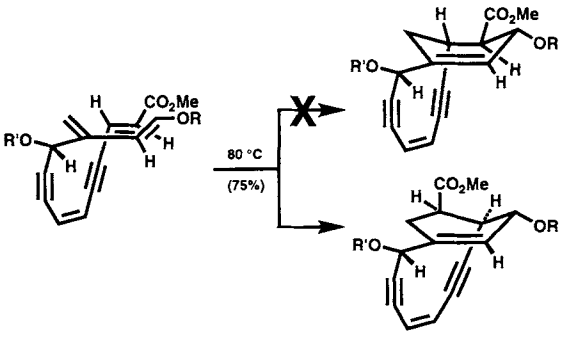

Fig. 10. August 1987: Schreiber et al. drop the first "bombshell" claiming the first synthesis of a calicheamicinone model (S. L. Schreiber, L. L. Kiessling, *J. Am. Chem. Soc.* **1988**, *110*, 631); this was later (1988) proven to be the wrong isomer and shortly thereafter (1989) was converted to the correct isomer by a clever pinacol rearrangement (see Fig. 11).

However, a little later (1988) it was determined that the major product of this reaction had the "incorrect" regiochemistry, prompting Schreiber to withdraw his claim but also to devise an ingenious solution to the isomer problem based on a clever pinacol rearrangement (1989) (Fig. 11) which had previously been reported by Tsuchihashi et al.[5]

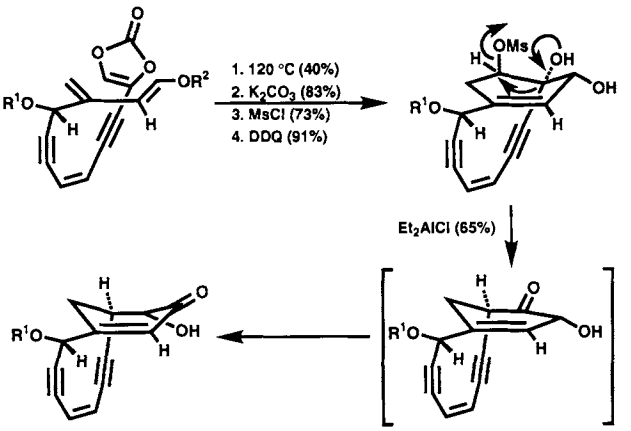

Fig. 11. May 1989: Schreiber et al. convert a Diels–Alder adduct by the pinacol rearrangement to deliver a calicheamicinone model system with the correct regiochemistry. F. J. Schoenen, J. A. Porco, Jr., S. L. Schreiber, *Tetrahedron Lett.* **1989**, *30*, 3765.

In February 1988, a paper was submitted by our group to JACS describing the synthesis and properties of the 10-membered ring parent hydrocarbon which represented the enediyne moiety of calicheamicin (Fig. 12). In May, later that year, we reported the first demonstration of DNA cleavage by a synthetic 10-membered ring enediyne system through a Bergman cyclization in the same journal. Much more work in this field was to follow from ourselves and other research groups around the world.

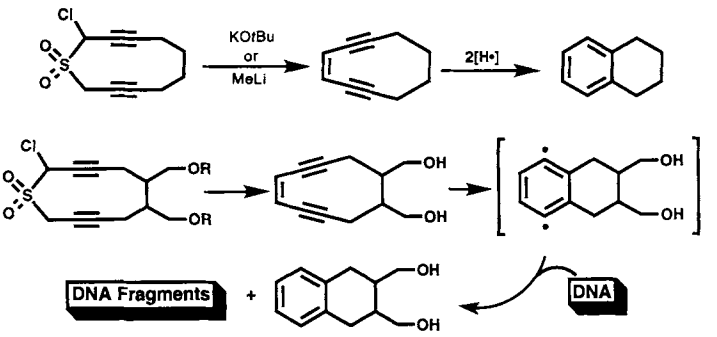

Fig. 12. February 1988: The Nicolaou group synthesizes the parent 10-membered ring enediyne unit such as in calicheamicinone (K. C. Nicolaou, G. Zuccarello, Y. Ogawa, E. J. Schweiger, T. Kumazawa, *J. Am. Chem. Soc.* **1988**, *110*, 4866) and provides the first demonstration of its ability to cleave DNA (K. C. Nicolaou, Y. Ogawa, G. Zuccarello, H. Kataoka, *ibid.* **1988**, *110*, 7247).

In March 1988, our group also reported, in a submission to *Angewandte Chemie*, the first synthesis of the aromatic ring (ring C) of calicheamicin γ_1^I and the observation of the rare phenomenon of spontaneous resolution of two enantiomeric forms of this "seemingly achiral" molecule upon crystallization (cf. Pasteur and tartaric acid) (Fig. 13).

In June 1988, Magnus and his group established the elegant cobalt route to calicheamicinone model systems (Fig. 14). This entry allowed Magnus et al. to carry out a series of mechanistic studies in the field and to penetrate further into more sophisticated models of the calicheamicinone system. The same method was also demonstrated later by Tomioka et al. [6] who reported a similar synthesis of a related enediyne system.

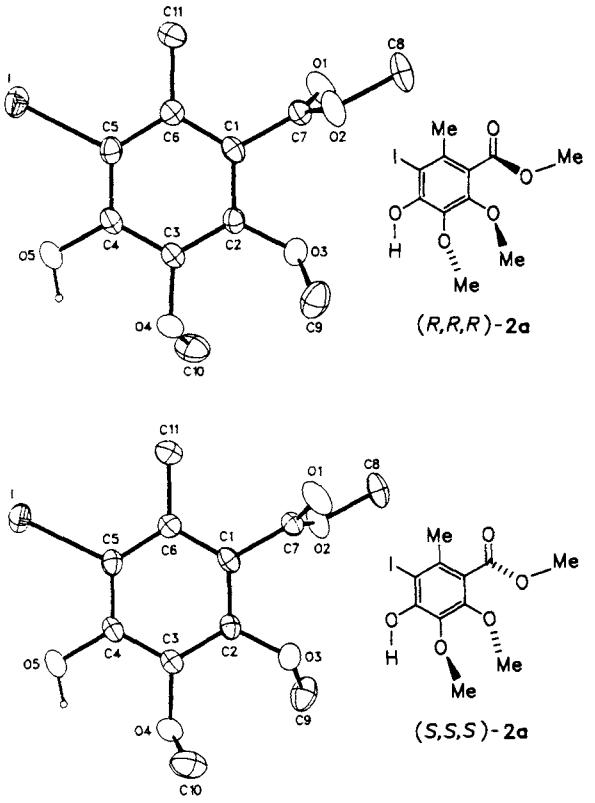

Fig. 13. March 1988: The Nicolaou camp reports the first synthesis of the aromatic ring of calicheamicin and observes spontaneous resolution of the enantiomers upon crystallization. K. C. Nicolaou, T. Ebata, N. A. Stylianides, R. D. Groneberg, P. J. Carrol, *Angew. Chem.* **1988**, *100*, 1138; *Angew. Chem. Int. Ed. Engl.* **1988**, *27*, 1097.

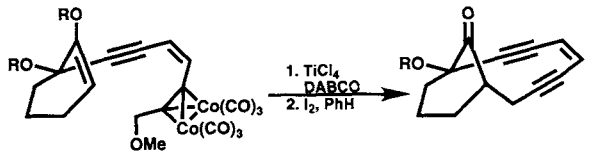

Fig. 14. June 1988: The Magnus group establishes the cobalt route to calicheamicinone model systems. P. Magnus, R. T. Lewis, J. C. Huffman, *J. Am. Chem. Soc.* **1988**, *110*, 6921.

June 1988 was also the month in which both Danishefsky et al. and Kende et al. reported their landmark demonstrations of the intramolecular acetylide–aldehyde condensation approach to the calicheamicinone core. Danishefsky's sophisticated system was reported in JACS (Fig. 15) and Kende's work appeared in *Tetrahedron Letters* (Fig. 16). The Danishefsky group extensively utilized this entry to produce

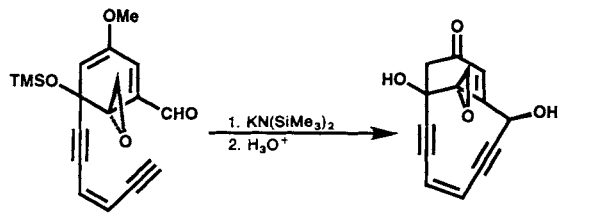

Fig. 15. June 1988: The Danishefsky group establishes the first entry into calicheamicinone skeleton. S. J. Danishefsky, N. B. Mantlo, D. S. Yamashita, G. Schulte, *J. Am. Chem. Soc.* **1988**, *110*, 6890.

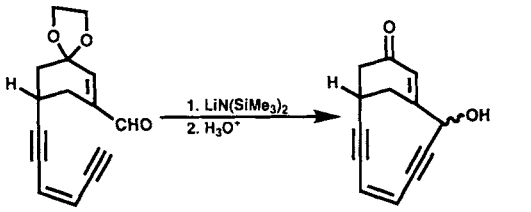

Fig. 16. The Kende group demonstrates the acetylide–aldehyde condensation approach to a model calicheamicinone system. A. S. Kende, C. A. Smith *Tetrahedron Lett.* **1988**, *29*, 4217.

a series of more advanced calicheamicinone systems and eventually to arrive at calicheamicinone itself (see below).

In January 1989, the Magnus group achieved the first introduction of the trisulfide moiety onto a calicheamicinone model system from a thiol by using the Harpp–Boustany method with *N*-(methyldithio)phthalimide (Fig. 17).

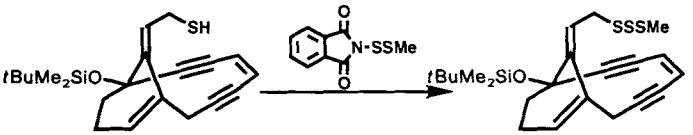

Fig. 17. January 1989: The Magnus group installs the trisulfide moiety (90% yield 1.3:1 mixture of tri- and disulfide) on a calicheamicinone model system for the first time. P. Magnus, R. T. Lewis, F. Bennett, *J. Chem. Soc. Chem. Commun.* **1989**, 916.

In December 1989, we—the Nicolaou group—reported the synthesis of an ABC model system for the carbohydrate fragment of calicheamicin γ_1^I by using a [3,3] sigmatropic rearrangement to install the sulfur group in ring B shown in Figure 18, and the oxime-based technology to construct the N–O bond (Fig. 18). This method was later adopted by the

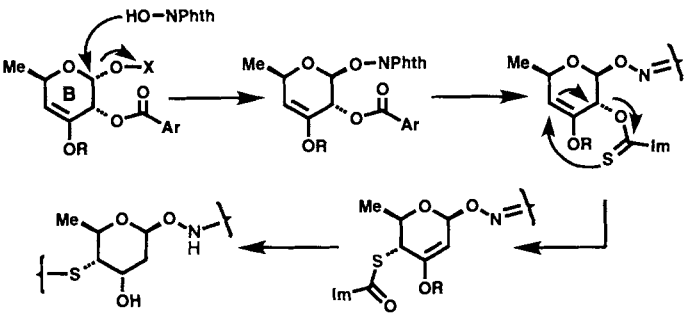

Fig. 18. December 1989: The Nicolaou group report the synthesis of an ABC model system of the oligosaccharide, in which a [3,3] sigmatropic rearrangement is used to install the sulfur group and the oxime method is used to construct the N–O bond. K. C. Nicolaou, R. D. Groneberg, *J. Am. Chem. Soc.* **1990**, *112*, 4085.

same group in the synthesis of the complete oligosaccharide segment (see below). As often is the case in total synthesis, this successful strategy was not the first we attempted. Extensive experimentation and considerable fine-tuning had to be done prior to final success. One such abortive attempt to set up the ring B functionality is shown in Figure 19 in which the [3,3] sigmatropic rearrangement was to be followed by in-

tramolecular delivery of the requisite oxygen atom. The latter operation was not to be realized, however, which forced us to redesign our strategy (see Fig. 18).

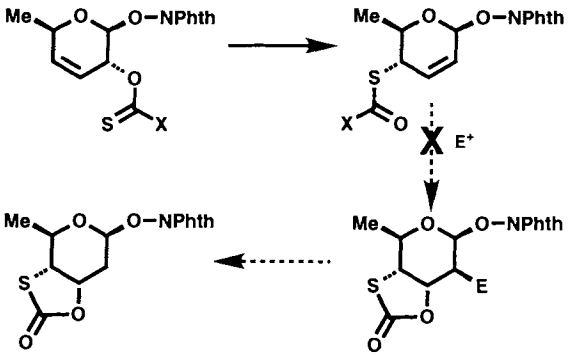

Fig. 19. A proposed electrophilically induced ring closure fails, forcing modifications of the scheme to include the requisite C-3 oxygen in the rearrangement substrate (see Fig. 18). X = NHPh, $OCH_2C_6H_4OMe$, imidazolyl.

In January 1990, the Danishefsky group moved ahead with the report of the first synthesis of racemic calicheamicinone (Fig. 20). This brilliant work was a significant breakthrough in that it provided an entry to the aglycon fragment of calicheamicin for coupling with the oligosaccharide segment which was still, however, elusive to any of the groups involved.

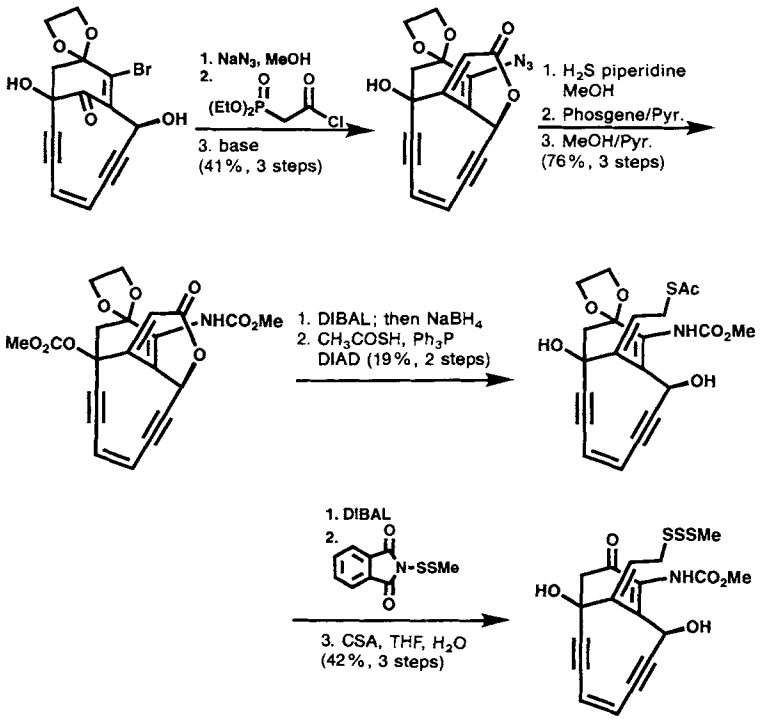

Fig. 20. January 1990: The Danishefsky group reports the first total synthesis of racemic calicheamicinone and thus moves ahead. M. Paz Cabal, R. S. Coleman, S. J. Danishefsky, *J. Am. Chem. Soc.* **1990**, *112*, 3253.

The first total synthesis of the carbohydrate fragment of calicheamicin γ_1^I was reported in July 1990 by our group (Fig. 21). Headed by Robert D. Groneberg, the group working on this fragment was able to overcome the many difficulties encountered and deliver the saccharide fragment in multigram quantities. The team, however, was still anxiously searching for a calicheamicinone route and serious concern about this problem was building in La Jolla.

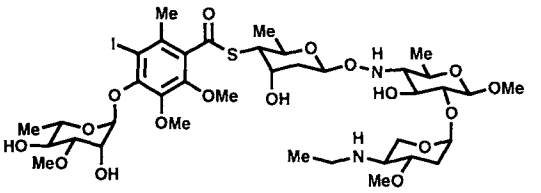

Fig. 21. July 1990: The Nicolaou group reports the first total synthesis of the pentacyclic oligosaccharide by using the sigmatropic rearrangement–oxime method. K. C. Nicolaou, R. D. Groneberg, T. Miyazaki, N. A. Stylianides, T. J. Schulze, W. Stahl *J. Am. Chem. Soc.* **1990**, *122*, 8193.

In December 1990, our group reported the first demonstration of the trichloroacetimidate-based methodology for the construction of the crucial glycoside bond which links the carbohydrate and aglycon fragments of calicheamicin. In this study we coupled the AE oligosaccharide segment with a dynemicin enediyne model system (Fig. 22). This originally

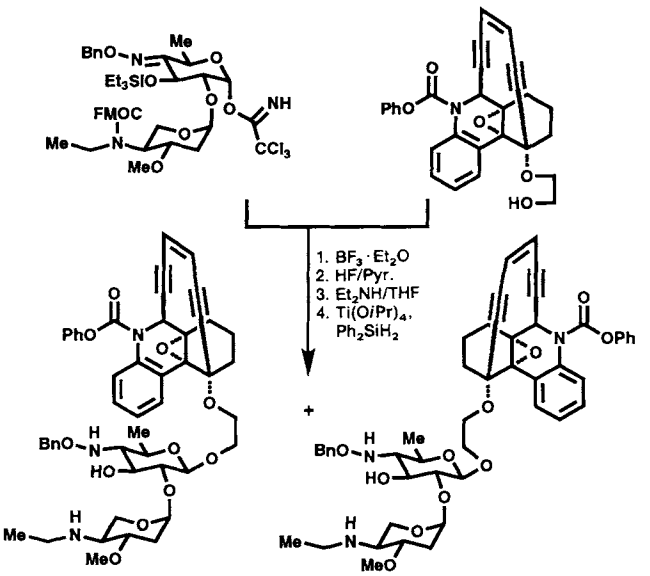

Fig. 22. December 1990: The Nicolaou camp demonstrates for the first time the viability of Schmidt's trichloroacetimidate method in the coupling of the oligosaccharide and aglycon fragments by using model systems. K. C. Nicolaou, E. P. Schreiner, W. Stahl, *Angew. Chem.* **1991**, *103*, 566; *Angew. Chem. Int. Ed. Engl.* **1991**, *30*, 585.

proposed method (see Fig. 6) was later successfully used by both ourselves and the Danishefsky groups to construct more advanced calicheamicin–dynemicin hybrid compounds and potential calicheamicin precursors (see below). Eventually, the same technology played a crucial role in the successful total synthesis of calicheamicin γ_1^I.

December 1990 was also the time of submission of the first demonstration of the triflate nucleophilic displacement approach to construct the N–O bond of calicheamicin by the Kahne group (Fig. 23). This work also included the synthesis of the oligosaccharide ABE ring system.

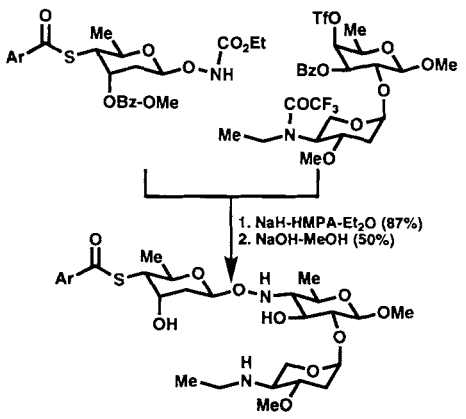

Fig. 23. December 1990: The Kahne group reports the synthesis of an ABE oligosaccharide in which the N–O bond is constructed by nucleophilic substitution of a triflate. D. Yang, S.-H. Kim, D. Kahne, *J. Am. Chem. Soc.* **1991**, *113*, 4715.

In March 1991, the Danishefsky group reported the application of the triflate displacement method for the construction of an oligosaccharide ABE model system (Fig. 24). This compound was actually one of the oligosaccharide fragments of the related esperamicin A_1.

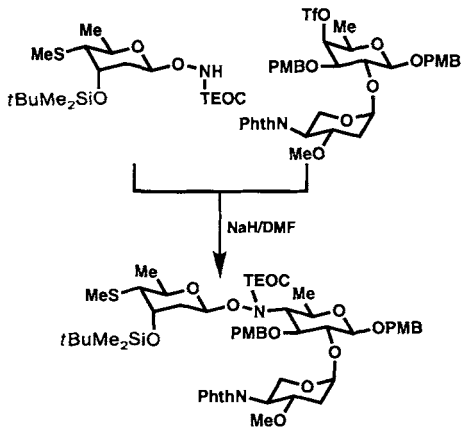

Fig. 24. March 1991: The Danishefsky group reports the synthesis of an ABE oligosaccharide model compound in which the N–O bond is also constructed by triflate displacement. R. L. Halcomb, M. D. Wittman, S. H. Olson, S. J. Danishefsky, J. Golik, H. Wong, D. Vyas, *J. Am. Chem. Soc.* **1991**, *113*, 5080.

As the autumn of 1991 was approaching our group had still not found a synthesis for calicheamicinone and there was still no sign that Danishefsky had successfully obtained the pentasaccharide fragment. We, however, had the pentasaccharide, whereas they had the aglycon. The thought of combining forces in the final drive towards calicheamicin had already crossed our minds but both Danishefsky and I politely rejected the idea. The battle was now reaching a climax as these and other groups were racing to secure the missing fragments and to establish base camps along the way.

In October 1991, our group reported the coupling of the intact pentasaccharide fragment of calicheamicin γ_1^I with dynemicin model systems by using the trichloroacetimidate technology (Fig. 25). This maneuver produced a series of calicheamicin–dynemicin hybrid compounds but also revealed, at the same time, our weakness in admitting that we still did not have the aglycon at hand! Concurrently, the Danishefsky group reported the coupling of advanced intermediates of the oligosaccharide and aglycon fragments by utilizing similar methodology (Fig. 26). It looked, for the moment, that final success in the Danishefsky camp was imminent! Despite these setbacks, we continued to surge forward, suspecting that many obstacles would still lie ahead before anyone could reach the final objective.

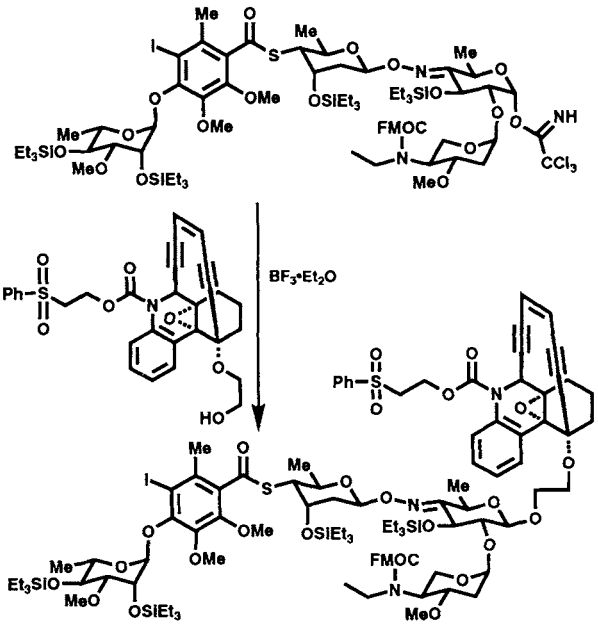

Fig. 25. October 1991: The Nicolaou group reports the total synthesis of the calicheamicin–dynemicin hybrid structure by coupling a fully functionalized pentacyclic oligosaccharide with dynemicin model compounds by using the trichloroacetimidate method. K. C. Nicolaou, E. P. Schreiner, Y. Iwabuchi, T. Suzuki, *Angew. Chem.* **1992**, *104*, 317; *Angew. Chem. Int. Ed. Engl.* **1992**, *31*, 340.

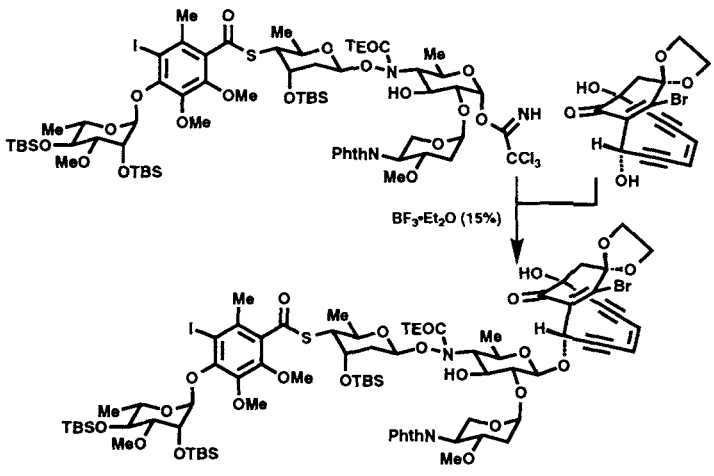

Fig. 26. October 1991: The Danishefsky group reports the coupling of a pentacyclic oligosaccharide with an aglycon precursor by using the trichloroacetimidate method. R. L. Halcomb, S. H. Boyer, S. J. Danishefsky, *Angew. Chem.* **1992**, *104*, 314; *Angew. Chem. Int. Ed. Engl.* **1992**, *31*, 338.

By the end of 1991, postdoctoral fellow Adrian L. Smith and his team were rewarded with success, and in December

of that year, we submitted a paper that described the first total synthesis of enantiomerically pure calicheamicinone; the key step in this synthesis proved to be a nitrile–oxide cycloaddition (Fig. 27). As was the case in the synthesis of

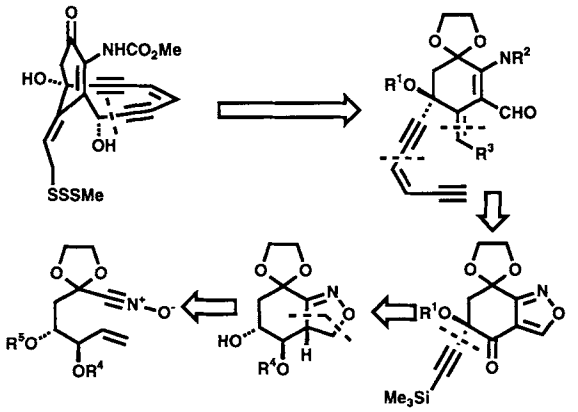

Fig. 27. December 1991: The Nicolaou group reports the first total synthesis of enantiomerically pure calicheamicinone by using the nitrile–oxide cycloaddition strategy. The long sought synthesis revives the race. A. L. Smith, C.-K. Hwang, E. Pitsinos, G. R. Scarlato, K. C. Nicolaou, *J. Am. Chem. Soc.* **1992**, *114*, 3134.

the oligosaccharide fragment, and for that matter most complex natural products, in the synthesis of the aglycon many hurdles had to be crossed. The following two paradigms exemplify the kinds of problems one often encounters in total synthesis and their role in precipitating unusual solutions. The first example involved the necessity for the protection of the amine function and the realization that most protecting groups would engage the aldehyde oxygen atom, rather than the nitrogen atom. To combat this unusual reactivity we used phthaloyl chloride, a bifunctional reagent, which reacted with both the oxygen and the nitrogen of the vinylogous amide to form a novel 9-membered ring heterocycle. This heterocycle was easily induced to rearrange to an acceptable derivative for further elaboration (Fig. 28). The next operation, the crucial ring closure to afford the 10-membered ring enediyne, was clouded with the wrong configuration at the newly generated hydroxyl center! A beauti-

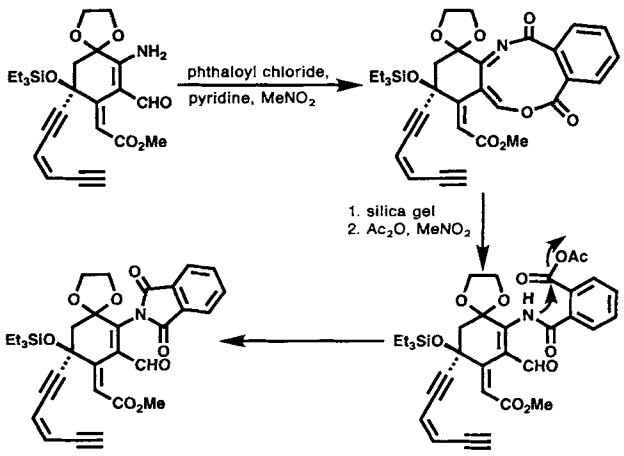

Fig. 28. The protection of the amino group of a vinylogous amide gives problems which are overcome by using a novel reaction sequence.

ful solution was, however, devised, based on the inspection of molecular models, which involved an intramolecular S_N2 type reaction with inversion of configuration (Fig. 29), thus fully correcting the course and allowing for eventual success. In the meantime, the Danishefsky camp had reported a resolution of a precursor to calicheamicinone, giving them, in principle, the capability of producing enantiomerically pure material.

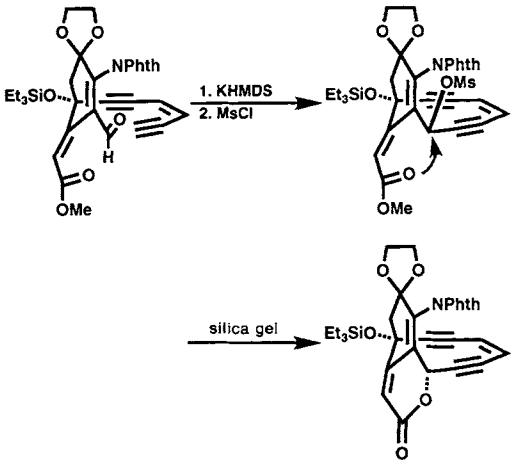

Fig. 29. The acetylide–aldehyde coupling leads to the 10-membered enediyne ring system, but with the wrong configuration! An intramolecular reaction sequence corrects the errant center and brings us back on course.

The race to the finish was now in its final lap! By this time it became evident that we were among the front-runners and that we had a good shot at completing the synthesis. As we later learned, our strong conviction that the final goal was achievable perhaps gave us the edge over a number of the other groups. However, the complexity and sensitivity of the intermediates involved, as well as the logistics of personnel continuity and of bringing starting materials to the "front" were posing enormous problems to us and persumably to the other groups involved. Even though the relationship of the participating groups was extremely cordial and friendly throughout the competition, exchange of information regarding the frontiers was scant. No group had any idea where the others were, although the fear of losing the race must have been playing on the minds of all of the members of the competing teams. We, of course, had tremendous regard and respect for the other camps and were prepared for the "worst" as we pushed for the final goal! Luck perhaps was to play the final role...

The Final Success

Finally, early in September 1992, success in our laboratories was knocking on the door. The final finish, however, was not without its scary moments! A particularly fearful moment came when, on attempting to persilylate an advanced intermediate in preparation for a pending major operation, TLC analysis indicated a heterogeneous streak, suggesting a disastrous decomposition at that step. A short time later, however, a suggestion to treat the mixture with acetic acid in dichloromethane containing silica gel resulted in the joyful

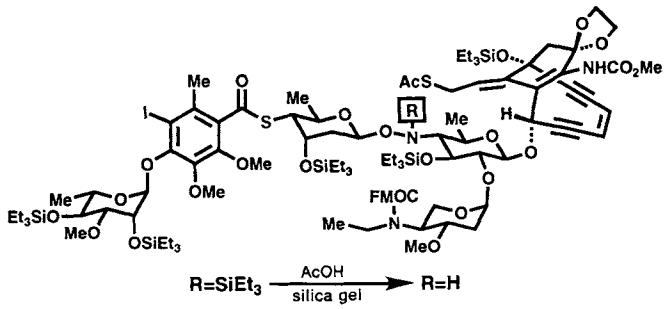

Fig. 30. A fearful moment! TLC analysis reveals a streak which soon clears up to a single spot.

observation of a clean, one-spot thin-layer chromatogram! What transpired is explained in Figure 30: Apparently, the silylation had not only taken place at all the hydroxyl groups but also at the NH–O function, giving rise to a labile intermediate which was smoothly and continuously decomposing on silica gel as the sample was moving up the plate!

The first indication that the job was complete came on Tuesday, September 16, 1992 when graduate student Conrad Hummel, the front man on the project for the last six months, obtained the first TLC picture on the final step (Fig. 31). The product matched an authentic sample! Subse-

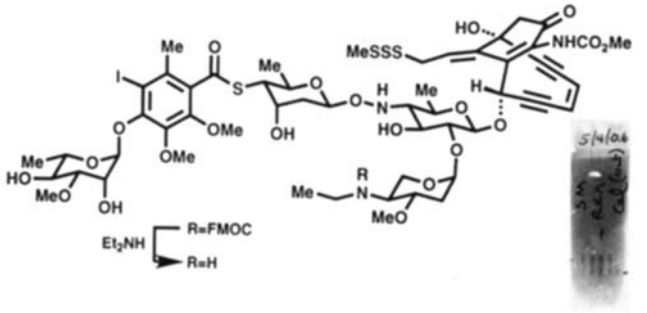

Fig. 31. September 1992: The Nicolaou group completes the first total synthesis of calicheamicin γ_1^I! The first indication of success, a TLC picture! K. C. Nicolaou, C. W. Hummel, M. Nakada, E. N. Pitsinos, A. L. Smith, K. Shibayama, H. Saimoto, *J. Am. Chem. Soc.* **1992**, *114*, 10082.

quent purification and spectroscopic measurements confirmed the identity of synthetic material with authentic calicheamicin γ_1^I! The mission was complete! Calicheamicin had been synthesized in the laboratory. Champagne was in order! (Fig. 32) On September 29, 1992, the communication announcing the total synthesis of calicheamicin γ_1^I was submitted to the JACS. In December 1992, exactly the month which we had suggested in our original NIH proposal for the completion of the synthesis, the publication appeared[7] and as well as a report in *Chemical & Engineering News*.[8] And so it was done! With this chapter closed, several new chapters opened...

Conclusion

This story was written in the hope of being interesting reading, educational, and revealing of the usually hidden side of such endeavors as the one covered here. The excite-

Fig. 32. A toast was in order. Together with the correspondence author of this review Dr. K. C. Nicolaou (seated in the center) are other members of the research group (standing from left to right: Dr. Katsuhiro Shibayama, Conrad Hummel, Dr. Masahisa Nakada, Emmanuel Pitsinos, Dr. Hiroyuki Saimoto; bottom left: Dr. Adrian Smith).

ment of my students and postdoctoral fellows who worked on this project in the period between 1987 and 1992, and the gratification I felt as their leader was too much not to share with others. Thus, this article was written in the hope that the reader will enjoy the behind the scenes emotions, setbacks, and triumphs of total synthesis.

This story could have not been written without the dedication, enthusiasm, and persistence of the talented group of students and postdoctoral fellows who participated on this project (alphabetically): K.-U. Baldenius, T. Ebata, R. D. Groneberg, C. W. Hummel, C.-K. Hwang, Y. Iwabuchi, T. Miyazaki, Y. Mizuno, M. Nakada, N. A. Petasis, E. N. Pitsinos, H. Saimoto, G. R. Scarlato, E. P. Schreiner, T. J. Schulze, K. Shibayama, A. D. Smith, W. Stahl, N. A. Stylianides, T. Suzuki, and G. Zuccarello. To these, and the rest of the members of my past and present group, I am indebted for their invaluable contributions to the research for which this group is credited. I am also indebted to Robert Babine, May Lee, George Ellestad, and Don Borders of the Lederle group for bringing my attention to this challenging molecule, calicheamicin, and for staying with me until the end! This work was carried out at the University of Pennsylvania (1987–1989), The Scripps Research Institute (1989–1992), and the University of California, San Diego (1989–1992). Financial support from the National Institutes of Health, Lederle Laboratories (USA), Merck Sharp and Dohme (USA), Schering Plough, Pfizer, and Rhone-Poulenc Rorer is gratefully acknowledged.

Received: May 12, 1993 [A 920 1E]
German version: *Angew. Chem.* **1993**, *105*, 1462

[1] a) M. D. Lee, G. A. Ellestad, D. B. Borders, *Acc. Chem. Res.* **1991**, *24*, 235; b) K. C. Nicolaou, W.-M. Dai, *Angew. Chem.*, **1991**, *103*, 1453–1481; *Angew. Chem. Int. Ed. Engl.* **1991**, *30*, 1387–1416.
[2] R. G. Bergman, *Acc. Chem. Res.* **1973**, *6*, 25.
[3] H. N. C. Wong, F. Sondheimer, *Tetrahedron Lett.* **1980**, *21*, 217.
[4] N. Darby, C. U. Kim, J. A. Salaun, K. W. Sheldon, S. Takada, S. Masamune, *Chem. Commun.* **1971**, 1516.
[5] K. Suzuki, E. Katayama, G. Tsuchihashi, *Tetrahedron Lett.* **1983**, *24*, 4497; K. Suzuki, T. Ohkuma, M. Miyazawa, G. Tsuchihashi, *ibid.* **1986**, *27*, 373.
[6] K. Tomioka, H. Fujita, K. Koga, *Tetrahedron Lett.* **1989**, *30*, 851.
[7] Communication: K. C. Nicolaou, C. W. Hummel, E. N. Pitsinos, M. Nakada, A. L. Smith, K. Shibayama, H. Saimoto, *J. Am. Chem. Soc.* **1992**, *114*, 10082; full papers: K. C. Nicolaou et al., *ibid.* **1993**, *115*, 7593–7635.
[8] S. Borman, *Chem. Eng. News* **1992**, *70* (49), 29.

Organoelement Compounds with Al–Al, Ga–Ga, and In–In Bonds

By Werner Uhl*

Dedicated to my daughter Anna Katharina

In the attempt to synthesize compounds with aluminum in a low oxidation state and an Al–Al bond, by the reduction of alkylaluminum halides with alkali metals, analogous to a Wurtz coupling, in general the deposition of elemental aluminum and the formation of the corresponding trialkylaluminum compounds is observed. Thus, tetrasubstituted dialuminum compounds $R_2Al-AlR_2$, apart from a few poorly characterized examples, were for a long time considered part of an unverified class of substances. Only with the sterically very highly shielded tetrakis[bis(trimethylsilyl)methyl]dialuminum did we achieve the synthesis of the first completely characterized organoelement compound with unlimited stability, which shows aluminum in the oxidation state + II and has an Al–Al bond. In the meantime, corresponding compounds for the elements gallium and indium have been obtained. With the simple access to tetrasubstituted dimetal compounds, a fascinating new research area has opened for preparative chemistry, in which the particular interest will naturally lie in the reactive properties of the metal–metal bond.

1. Introduction

Organoelement compounds with an element–element single bond and central atoms from the third main group were for a long time only known for the lightest element boron. The preparation of diborane(4) compounds, which are stabilized through the interaction between the empty p orbital on the boron atom and a lone pair of electrons in the α position at nitrogen, oxygen, or halogen atoms, was achieved a long time ago,[1, 2] whereas diboranes(4) substituted exclusively with alkyl groups were obtained concurrently in the research groups of Nöth[3] and Berndt[4] only in 1980. Their synthesis, transferred in the meantime to numerous compounds,[5] is achieved by the reaction of alkyllithium compounds with tetra(methoxy)diborane(4), which already contains a B–B bond (Scheme 1). They are very stable towards disproportionation because of the steric shielding by the bulky substituents.

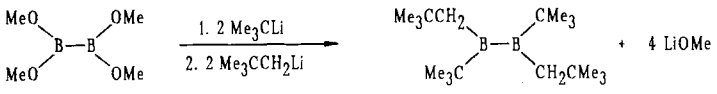

Scheme 1. Synthetic route to tetraalkylsubstituted diboranes(4) [3,4].

The corresponding compounds for aluminum and the higher homologues could at this time not be proven unambiguously. Element–element bonds, however, have been known for a long time in typical inorganic compounds, such as Ga_2Br_3,[6] In_5Br_7,[7] InS,[8] In_4Se_3,[9] and others,[10] as well as recently in the field of aluminum chemistry in Al_7Te_{10}[11] or Al_3Te_3I.[12] By treatment of the mixed-valent subhalides $Ga[GaX_4]$ (X = halogen) with Lewis bases such as dioxane, the corresponding adducts of the divalent elements can be synthesized very readily.[13, 14] Attempts to synthesize organoelement compounds, in which the metal atom has a low oxidation state, starting from such subhalides by the reaction with alkyllithium compounds, however, remained unsuccessful for a long time.[15, 16] Theoretical investigations on Al_2H_4 show that the mixed-valent form $Al^+AlH_4^-$ is preferred over that with divalent Al atoms. Moreover, the conformation is favored for the compound with an Al–Al bond, in which the substituents are arranged staggered.[17] The present review concentrates exclusively on the synthesis of stable organoelement compounds of the elements Al, Ga, and In in unusual oxidation states and with metal–metal bonds.

2. Synthesis and Physical Properties of Tetrasubstituted Dialuminum, Digallium, and Diindium Compounds

2.1. $[(Me_3Si)_2HC]_2Al-Al[CH(SiMe_3)_2]_2$

After numerous unsuccessful attempts the synthesis of a tetraalkyldialuminum compound (**1**) was achieved with the bis(trimethylsilyl)methyl substituent[18] by the reduction of the appropriate aluminum chloride with elemental potassium.[19] The compound **1** isolated in 60% yield shows a surprisingly high thermal stability and melts not before 220 °C with very little decomposition. Two reasons are chiefly responsible for this: first the high steric shielding by the bulky substituents kinetically prevents a disproportionation, and second, electronic effects caused by the $CH(SiMe_3)_2$ group, known to be a very effective electron donor.[20] The UV/VIS

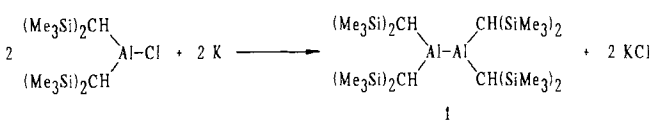

1

[*] Prof. Dr. W. Uhl
Fachbereich Chemie der Universität
Postfach 2503, D-26111 Oldenburg (FRG)
Telefax: Int. code + (441)798-3329

spectra and the crystal structure still to be discussed indicate an electron transfer from the orbitals of the substituent into suitable atomic orbitals on the metal. Remarkably, in the ^{1}H NMR spectra of **1**, as well as in the other dimetal compounds (**10** and **11**) still to be described, a strong downfield shift of the signal for the methine protons of about $\Delta\delta = 0.7$ in comparison to the corresponding resonance signals of trialkylaluminum compounds without an Al–Al bond is observed.

The Al–Al bond in **1** (266.0(1) pm) is longer than those in the tellurides Al_7Te_{10}[11] and Al_3Te_3I[12] by 6 and 11 pm, respectively. On the basis of the unit cell shown in Figure 1, it is clear that the central Al_2C_4 unit in **1** is almost ideally planar, and the torsion angles about the metal–metal bond deviate from the values of 0° and 180° expected for a planar unit by only 8°. From a molecular model the preference of

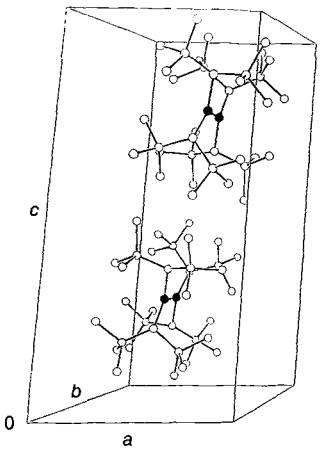

Fig. 1. Representation of a unit cell of **1**. The size of the atoms was chosen arbitrarily; aluminum atoms black; hydrogen atoms are not shown [19].

the planar Al_2C_4 conformation cannot be explained on steric grounds; however, the previously mentioned hyperconjugative interactions may be responsible for this. The C_α–Si bonds are arranged so that they adopt an optimal position for an electron transfer into the unoccupied p orbitals at the metal center and that the torsion angles between the σ and the p orbitals never become larger than the ideal value of 30°.[20] This, assumes an electronic system delocalized over the Al–Al bond.

The by-product **2** is obtained in very low and very variable yield by treatment of the precipitate formed in the synthesis of **1** with toluene. This by-product is a KCl adduct of the dialkylaluminum chloride, and forms readily and almost quantitatively in the reaction of the two components.[21] According to the results of the cryoscopic molar mass determination in benzene, **2** is monomeric and undissociated in solution, whereas in the solid state, through the formation of K_2Cl_2 heterocycles, it exists as a one-dimensional infinite coordination polymer. Remarkably, a very short contact is

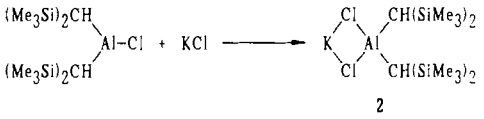

2

observed between one of the C–H bonds of a methyl group and the potassium atom, which is insufficiently coordinated by four chlorine atoms.

2.2. Other Tetraalkyldialuminum Compounds

As has long been known for methyl, ethyl, or *n*-propyl compounds,[22] sterically less shielded dialkylaluminum halides react with potassium under deposition of elemental aluminum and the formation of the corresponding trialkyl compounds. We varied the substituents systematically (Scheme 2). For example, we used *sec*-butyl, (trimethylsilyl)methyl, neopentyl, and aromatic mesityl groups; however, no products were detected with aluminum in an unusual oxidation state, and the reaction course described above, corresponding to a disproportionation of intermediate tetraalkyldialuminum compounds, occurs. KCl was then added quantitatively to the aluminum chlorides so that only half of the starting material is converted under the chosen conditions at room temperature over 24 hours in hexane.

Scheme 2. Reaction of sterically less demanding dialkylaluminum chlorides. R = Me [22], Et [22], Pt [22], *sec*-butyl, H_2CCMe_3, H_2CSiMe_3, $C_6H_2Me_3$.

Remarkably, following the careful workup of the reaction of di(neopentyl)aluminum chloride with potassium, a dark red, highly viscous residue was obtained which cannot be recrystallized from any of the common solvents, and which

Werner Uhl was born in 1953 in Lich (Hessen, FRG), studied chemistry between 1972 and 1977 at the Universität Karlsruhe, and received his doctorate there in 1980 after two years at the Universität Marburg under the supervision of G. Becker with work on alkylidenephosphanes with P=C double bonds. Thereafter he undertook two years of industrial experience in the research and development department at the NUKEM company (Hanau, FRG), before he followed G. Becker to the Universität Stuttgart in 1983. In 1989 he completed his habilitation in inorganic chemistry and in 1992 became a professor of inorganic chemistry at the Universität Oldenburg. His main research interests are sterically highly shielded organoelement molecules with the heavier elements of the third main group.

in addition to signals of low intensity in the NMR spectra reveals mainly the presence of a single product. On the basis of a hydrolysis experiment and a molar mass determination Schram et al.[23] assumed the occurrence of a tetrameric aluminum(I) compound, similar to $Al_4Cp^*_4$ ($Cp^* = C_5Me_5$)[24] which was characterized by crystal structure analysis, and which will be discussed later.

Di(*tert*-butyl)aluminum halides (Cl, Br) form with potassium in hexane a highly reactive, paramagnetic gray-green powder, which has so far not been fully characterized. If this product is dissolved in benzene or ether, spontaneous decomposition takes place and the powder turns black. From this black product, small quantities of the anion $(Me_3C)_3AlH^-$ can be isolated, and readily characterized by NMR and IR spectroscopy.[25]

For a systematic investigation of the chemical properties of compounds with an Al–Al bond, we were interested in the syntheses of further derivatives. In the literature reports are found on stable compounds, which are substituted by isobutyl groups.[26–28] We repeated these reactions; however, in no case did we obtain the described molecules. Tri(isobutyl)aluminum is supposed to yield the hexa(isobutyl)dialuminate **3** with potassium,[26] instead, in agreement with the results previously obtained for other substituents,[29] the tetra(isobutyl)aluminate **4** was formed, whose NMR spectroscopic parameters are consistent with the published values. Its crystal structure[30] shows layers of

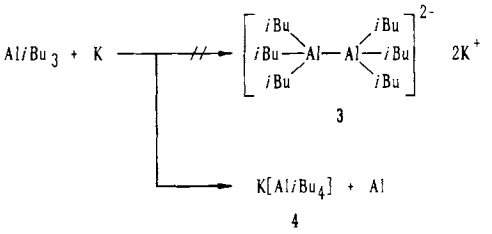

aluminate ions which are bridged by potassium ions; the alkali metal ion becomes six-coordinate, bonded to four α-C atoms and two C–H bonds of methyl groups. This coordination of C–H bonds is similar to the agostic interaction[31] and is also detected in the IR spectrum because of the unusual position of one C–H valence stretch (2600 cm^{-1}).[30]

The second dialuminum compound described in the literature is **5**, which had supposedly been prepared analogously to **1**. In the reaction of di(isobutyl)aluminum chloride with potassium, a dark brown, highly viscous liquid is formed,[27] whose spectra have unfortunately remained mainly unpublished, so that the direct comparison of the compounds obtained is impossible. The main product of the reaction cannot be recrystallized from any of the common solvents, and

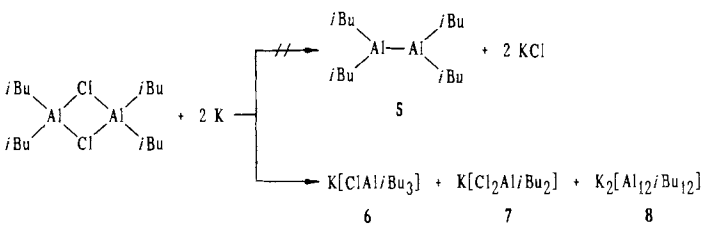

decomposes on distillation with the formation of tri(isobutyl)aluminum. By a comparison of the NMR spectra obtained by us it was concluded that only an adduct from KCl and iBu_3Al (**6**) is present. Compound **6**, synthesized in a highly pure form by the stoichiometric reaction of the constituents, exhibits the same properties as those of the product obtained from the reduction with potassium and can be neither recrystallized nor distilled. With triphenylphosphane both products form $PPh_3 \cdot AliBu_3$ in over 80% yield with the displacement of the chloride ions, and with [18]crown-6, the crystalline ether adduct K([18]crown-6)[ClAliBu$_3$] is obtained almost quantitatively (Scheme 3).[25]

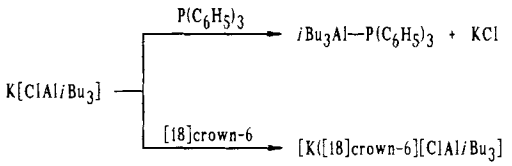

Scheme 3.

On treatment with toluene two compounds can be extracted from the residue of the reaction of di(isobutyl)aluminum chloride with potassium, and these compounds can be separated from each other by recrystallization: the KCl adduct **7**, as well as $K_2[Al_{12}iBu_{12}]$ **8** in low, but reproducible yield. Compound **8** forms as dark red crystals; the result of the crystal structure determination is shown in Figure 2.[32] Ac-

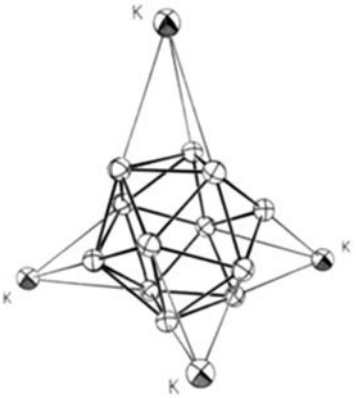

Fig. 2. Drawing of the Al_{12} icosahedron in $K_2[Al_{12}iBu_{12}]$ **8** (thermal ellipsoids drawn at 30% probability level). For clarity, only the Al and K atoms are drawn [32].

cording to this the Al_{12} dianion has an almost undistorted icosahedral framework which corresponds with the boron $B_{12}H_{12}^{2-}$ dianion both in terms of its structure and the number of electrons. The Al–Al distances in the cluster (268.5 pm) are only slightly longer than that in the tetraalkyldialuminum compound **1** with an isolated Al–Al bond (266.0 pm). The icosahedron is surrounded by a tetrahedron comprising four potassium ions, each bridging two icosahedra through contacts to six α-carbon atoms of *i*Bu groups (Fig. 3) The interaction exists, however, between the potassium ions and the C–H bonds of the *i*Bu substituents. The potassium atom is thus coordinated by six C atoms and has an almost undistorted octahedral environment. In this way a

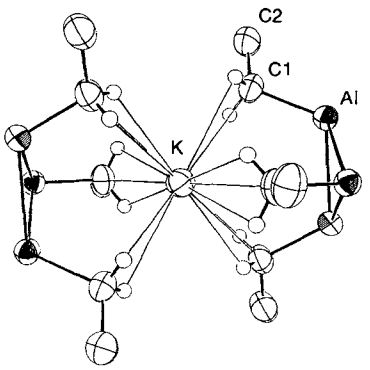

Fig. 3. Coordination of the K atoms in **8** (thermal ellipsoids drawn at 30% probability level). For clarity, the methyl groups of the *i*Bu substituents are omitted and only the α-hydrogen atoms which interact with the K atom are drawn [32].

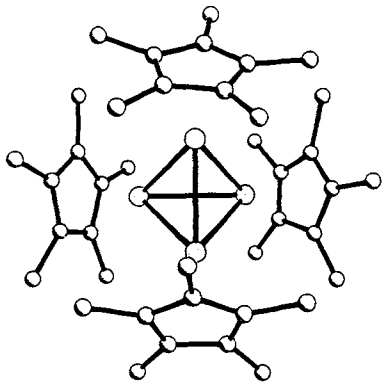

Fig. 4. Crystal structure of $Al_4Cp_4^*$ **9** (atoms with arbitrary radius; no hydrogen atoms) [24].

three-dimensional structure is obtained that is reminiscent of the structure of cuprite, as a result of the linear coordination of the K^+ ion by two icosahedra and of the tetrahedrally surrounded $[Al_{12}iBu_{12}]^{2-}$ anion. In the crystal structure of **8** very highly disordered toluene molecules are inserted into the cavities present. These solvent molecules can be removed by thorough evacuation, the crystals, however, become more unstable and disintegrate to a microcrystalline powder on the slightest touch.

Compound **8** is very unstable in solution, whereas it is very stable as a solid. Even in air, it is almost two hours before a decomposition reaction is observed. Cyclic voltammetric investigations[25] reveal a reversible one-electron oxidation, followed by a second, irreversible loss of an electron. Also in this respect the dodecaaluminate **8** is similar to the corresponding boron compounds.[33]

A further organoaluminum cluster (**9**) was obtained by Schnöckel et al.[24] by the reaction of pentamethylcyclopentadienylmagnesium with AlCl (Scheme 4). AlCl was pre-

$$2\,Al + 2\,HCl \xrightarrow{1200K} 2\,AlCl + H_2$$

$$2\,(C_5Me_5)_2Mg + 4\,AlCl\cdot O(C_2H_5)_2 \xrightarrow{-O(C_2H_5)_2} \underset{\mathbf{9}}{Al_4(C_5Me_5)_4} + 2\,MgCl_2$$

Scheme 4.

pared in a high-temperature synthesis from elemental aluminum and HCl, and in solution has a half life[34] long enough so that reactions can be carried out. For the yellow crystals of **9** a crystal structure was determined which shows a tetrahedral Al_4 framework and an η^5-coordinated cyclopentadienyl group at each Al atom (Fig. 4). The Al–Al distance (mean 276.9 pm) is as expected significantly longer than that of the isolated Al–Al bond in **1**, and also than those in the $[Al_{12}iBu_{12}]^{2-}$ dianion (**8**).

2.3. Tetrasubstituted Digallium and Diindium Compounds

For the synthesis of the digallium compound **10** and the diindium compound **11** we did not use the reduction of the dialkyl element halides as for the preparation of **1**, since these are not accessible by simple reactions. Instead, we used halides that already contained the element–element bond. Thus, the reaction of $Ga_2Br_4\cdot 2$ dioxane[13] with four equivalents of bis(trimethylsilyl)methyllithium[18] leads to the tetraalkyldigallium **10** in over 70% yield.[35] Compound **10**

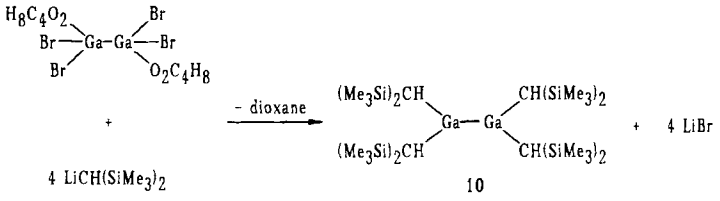

crystallizes isotypical to the corresponding aluminum compound and forms large dark yellow crystals. The Ga–Ga bond in **10** (254.1(1) pm) is, however, in comparison with the Al–Al bond in **1**, significantly shorter by 12 pm, which again shows the special role of gallium in the third main group. This exceptional role is due to the insertion of electrons into the d orbitals of the preceding 3d elements in the periodic table and the associated contraction of the atomic radius. The Raman spectrum of **10** shows a weak band at 268 cm^{-1} that is probably assigned to the vibration of the Ga–Ga bond and which only lies at slightly higher wavenumbers than the corresponding values of Ga^{II} chlorides.[36]

The UV/VIS spectra for the three compounds **10**, **1**, and $Al[CH(SiMe_3)_2]_3$[37] are given in Figure 5. In all three spectra two absorptions at the same wavelengths of 245 and 275 (shoulder) nm are observed, which we ascribe to transitions from the orbitals of the substituent, known to be a good electron donor,[20] into the empty orbitals of the metal atoms. Only in the two spectra of the dimetal compounds does an additional absorption occur at 370 nm, and is thus evidently characteristic for the metal–metal bond. For the digallium compound **10** the base of this band extends into the visible region and is thus responsible for the yellow color of **10**: the absorption band of the dialuminum compound **1** is, in contrast, narrower, which, therefore, explains the pale yellow color of **1** only recognizable in thick layers.

The preparation of the compound **11** with an In–In bond is achieved in a way similar to the synthesis of **10**. LiCH-

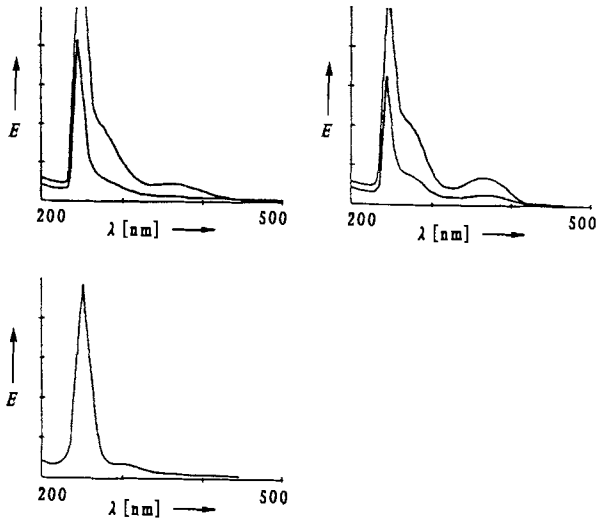

Fig. 5. UV/VIS spectra of the dimetal compounds **10** (with Ga–Ga bond; top left), **1** (with Al–Al bond; top right), and of the tris[bis(trimethylsilyl)methyl]aluminum (without a metal–metal bond, bottom) between 200 and 500 nm [35].

$(SiMe_3)_2$ is allowed to react with $In_2Br_4 \cdot 2\,tmeda$ (tmeda = *N,N,N',N'*-tetramethylethylenediamine), whose simple synthesis is achieved in a one-pot reaction from In metal, $InBr_3$, and TMEDA.[38] Compound **11** forms orange-red crystals and crystallizes no longer isotypically to the two homologous compounds **1** and **10**; instead, a stacking variant of the nearly planar molecules occurs which are packed to give layers.[38] The In–In bond is 282.8(1) pm long . This

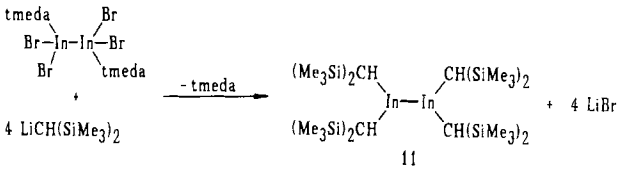

value lies—as does the Ga–Ga bond length—in the upper region of the bond lengths of typical inorganic compounds of each bivalent element. Whereas **1** and **10** are remarkably thermally stable, the indium compound **11** decomposes under metal deposition at 100 °C or with exposure to light, even at room temperature.

The UV/VIS absorption bands of In compounds are given in Table 1, and these again show the absorption characteristic for the metal–metal bond at 380 nm. In addition the dimetal compounds have very high extinction coefficients, which are 10 times higher than those in the coordinatively unsaturated trialkylindium compound without a metal–metal bond. In contrast, in the compound with a coordinatively saturated central atom only very small extinction coefficients are obtained, which are perhaps due to decomposition products of the dialkylindium dibromide which is not particularly stable in solution. Thus, the tetrasubstituted dimetal compounds, in addition to an absorption at about 370 nm, are also characterized by high extinction values in the region of the electron transfers from the substituent to the metal atom, which may occur due to an electronic system delocalized through the metal–metal bond.

Table 1. UV/VIS spectroscopic investigations of bis(trimethylsilyl)-methylindium compounds.

	11	$In[CH(SiMe_3)_2]_3$	$(tmeda)LiBr_2In[CH(SiMe_3)_2]_2$
λ (ε)	240 nm (24000)	240 nm (1900)	250 nm (60)
	270 nm (9500)	270 nm (1300)	270 nm (50
	380 nm (800)		

Recently in a way analogous to that for the preparation of **10**, Power et al.[39] obtained the tetraaryldigallium **12**, which unlike **10** does not have a planar central C_2GaGaC_2 unit in the solid state, but the substituents are staggered to avoid steric interactions (torsion angle about the Ga–Ga bond 43.8°). Compounds with a Ga–Ga (**13**) or an In–In bond

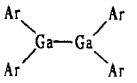

12: Ar = 2,4,6-$C_6H_2iPr_3$

and nitrogen substituents were obtained by Veith et al. from the reduction of the corresponding halides with Na/naphthalene.[40] The indium compound analogous to **13** was investigated by X-ray crystallography; this structure shows a significantly shorter In–In distance (276.8(1) pm) than that in the tetraalkyldiindium **11**. Similar to the corresponding C

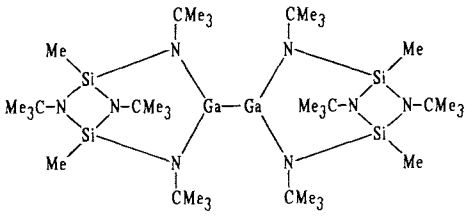

13

atoms in **11**, the four nitrogen atoms bound directly to the indium atoms lie almost ideally in a plane with the two metal atoms; however, an additional nitrogen atom of the substituent is coordinated to each In atom with only a slightly longer contact (15 pm), so that the coordination number at the metal atom increases to four. A compound with an In–In bond that has not been investigated by X-ray crystallography is evidently also formed on treatment of metallic indium with tetrachloro-*o*-benzoquinone in the presence of phenanthroline.[41] Recently Cowley et al. reported a tetraaryldiindium compound, which is formed from indium monochloride and 2,4,6-tris(trifluoromethyl)phenyllithium (Scheme 5). The In–In bond (274.4(2) pm) is significantly shorter than that in **11**, and the substituents are staggered; however, the coordination number at the indium atom is increased through an interaction with the fluorine atoms of

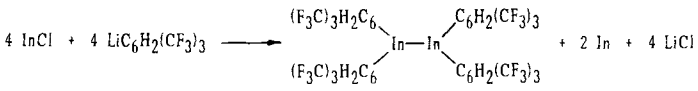

Scheme 5.

the trifluoromethyl groups.[42] Theoretical studies on the In–In interactions have also been discussed.[43]

If the attempt is made to transfer the synthesis of **10** from $Ga_2Br_4 \cdot 2$dioxane and four equivalents of an alkyllithium compound to less sterically demanding substituents such as the (trimethylsilyl)methyl or neopentyl group, disproportionation resulting in the deposition of elemental gallium is always observed. Depending on the solvent different products are obtained; in *n*-pentane/diethyl ether the formation of the corresponding trialkylgallium compounds **14** and **15** is observed, whereas in pure pentane exclusively the tetraalkyl compounds **16** and **17** are formed, which crystallize with differing dioxane content. The crystal structure was determined for **16**, and this showed a formula unit dimerized through the formation of a dioxane bridge.[44]

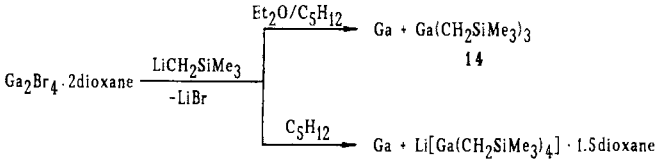

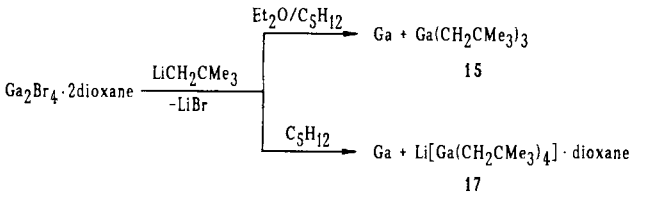

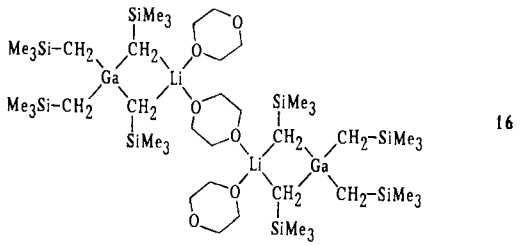

16

2.4. Reactions of Digallium and Diindium Bromides with Solvent-Free $LiC(SiMe_3)_3$

Since the reactions of $Ga_2Br_4 \cdot 2$dioxane with sterically less demanding alkyllithium compounds did not produce the desired dimetal compounds, we attempted to carry out this synthesis with the very bulky tris(trimethylsilyl)methyllithium. This lithium compound is readily accessible in the form of its THF adduct;[45] however, the reaction with the gallium(II) halide ether adduct led, with cleveage of ether, only to tris(trimethylsilyl)methane $HC(SiMe_3)_3$. The necessary solvent-free lithium compound **18** was not known; it was obtained from *n*-butyllithium and tris(trimethylsilyl)methylmercury bromide[46] by applying a method described by Bickelhaupt et al. for the synthesis of 1,3-dilithiopropanes.[47] Compound **18** is monomeric in benzene, but

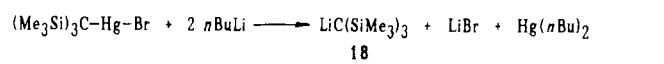

dimeric in the solid state due to the formation of Li–C bridges. However, an unexpected pathway is observed in the reaction with $Ga_2Br_4 \cdot 2$dioxane: evidently for steric reasons four of the bulky substituents cannot be arranged around the Ga–Ga unit, and thus a compound is formed with at least one halogen atom bound to the gallium atom; however, this compound is not stable, and disproportionates, because one halogen atom possibly migrates through a bridging position to the second gallium atom. The disproportionation, however, does not lead to the deposition of elemental metal, as is the case for smaller substituents, but stops at an alkylgallium(I) compound **19**, which can be isolated in the form of dark red crystals.[48] Compound **19** is remarkably thermally

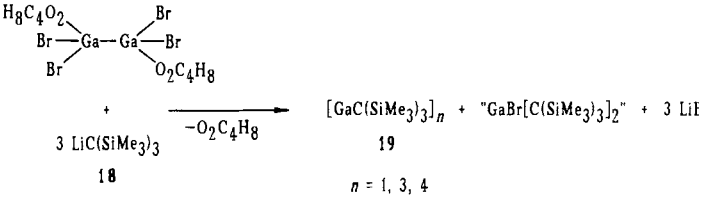

stable; it remains completely unaltered over several months in air. Depending on the method of characterization one of several degrees of oligomerization is determined: in the mass spectrum only the monomer with a relative intensity of 100% is detected. The cryoscopic molar mass determination in benzene in the usual concentration range (0.023 mol L^{-1}) indicates approximately a trimer, whereas with increasing dilution the dissociation increases, and at a concentration of 0.0014 mol L^{-1} finally only the monomer is present. In the solid state (Fig. 6), **19** has an almost undistorted tetrahedral Ga_4 framework, in which the Ga–Ga distance (mean 268.8 pm) is as expected very much longer (ca. 15 pm) than in the digallium compound **10** with an isolated Ga–Ga bond. An absorption band at 435 nm characteristic for the

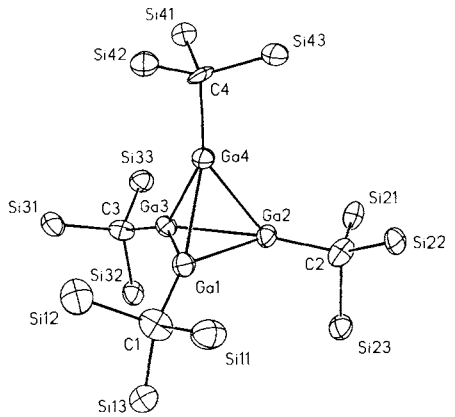

Fig. 6. Crystal structure of **19** (thermal ellipsoids drawn at 40% probability level). For a better overview, the methyl groups are not drawn [48].

Ga_4 framework is observed in the UV/VIS spectrum, which, in comparison to those bands for compounds with an isolated metal–metal bond, shows a slight bathochromic shift, and with increasing dilution of the spectroscopically investi-

gated solution of **10**, and corresponding increasing dissociation, there is a significant loss in the intensity of this band.

In the meantime the preparation of the indium cluster analogous to **19** has been achieved by the reaction of $In_2Br_4 \cdot 2$ tmeda with **18**. This cluster is also obtained in the form of dark red crystals, and in the mass spectrum only the peak for the monomer is detected. However, the color as well as the dimensions of the unit cell are in agreement with the existence of an In_4 cluster.[49]

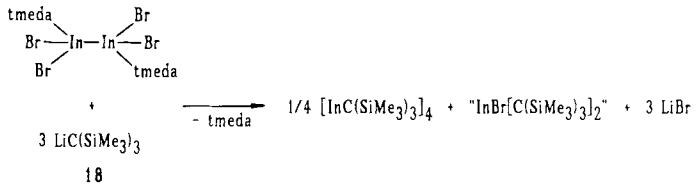

Similar to AlCl, GaCl can also be prepared by a high-temperature synthesis from gallium and HCl and subsequent rapid cooling to liquid nitrogen temperature.[50] In toluene and diethyl ether GaCl is thermally stable enough to allow reproducible reactions. With cyclopentadienylmagnesium or -lithium Schnöckel et al.[51] obtained colorless, crystalline cyclopentadienylgallium(I) **20**, which is extremely volatile; thus it cannot be isolated by removal of the solvent under vacuum. Compound **20** was characterized by its mass spec-

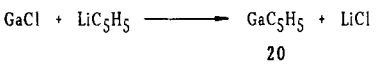

trum, in which, as for **19**, only the molecular ion of the monomer was detected, and by its ^{71}Ga NMR spectrum which showed the shift ($\delta = -714$) characteristic for Ga^I compounds. Calculations support the existence of monomeric molecules with an η^5-coordinated cyclopentadienyl group in solution, whereas in the solid, in contrast to the yellow $Al_4Cp^*_4$ **9** or the red $Ga_4[C(SiMe_3)_3]_4$ **19** (with $n = 4$), one-dimensional infinite polymers might occur similar to those in cyclopentadienylindium[52] or -thallium.[53] For InC_5Me_5 a different geometry was observed with an octahedral arrangement of the metal atoms; the very long contact distance of 395 pm precludes a strong In–In interaction.[54] With the sterically more demanding $[C_5(CH_2C_6H_5)_5]$ substituent pseudodimers are obtained, which also have a very long In–In distance (363.1 pm).[55] Similarly, no cluster structure was observed in the tris(trifluoromethyl)phenoxyindium(I) compound reported by Roesky et al.[56]

3. Chemical Properties of the Dimetal Compounds

After the successful synthesis of compounds with Al–Al, Ga–Ga, and In–In bonds, studies into the chemical properties of these compounds should now be the main focus of attention. Numerous reactions may be possible: addition of Lewis bases to the unsaturated, three-coordinate metal atoms, further reduction with the transfer of electrons into the unoccupied p orbitals, insertion reactions both into the metal–metal bond and the metal–carbon bond, substitution reactions, and in the particular case of the bis(trimethylsilyl)methyl compounds deprotonation reactions at the C–H acidic substituent by the reactions with strong bases. Most of these reactions are considered in the following.

3.1. UV Irradiation of $[(Me_3Si)_2HC]_2Al–Al[CH(SiMe_3)_2]_2$

We began our studies into the reactivity of the dialuminum compound **1** with the irradiation, in order to establish whether the Al–Al bond can be homolytically cleaved. Initially we carried out these experiments in an ESR spectrometer, to allow the detection of possible intermediate paramagnetic species. The result based on the ESR spectra is illustrated in Figure 7:[57] the top spectrum was recorded approximately three minutes after the start of the irradiation; it shows the resonance signals of two radicals, of which that of one radical stands out only a little from the background and forms a sextet of doublets, whose three inner signals are covered by the main signal. With increasing irradiation times this sextet can no longer be detected, and only the second signal of 11 equidistant lines is observed, which is scaled up in Figure 7 (bottom). This radical is very stable; it can still be detected several hours after the end of the irradiation.

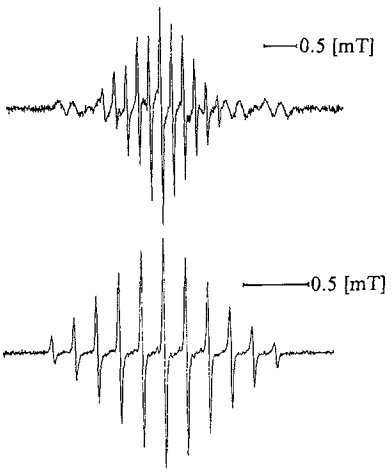

Fig. 7. The ESR spectra obtained on irradiation of a sample of **1** in *n*-pentane with UV light. The top spectrum was recorded after three minutes, the bottom spectrum after 30 minutes [57]. Sextet of doublets: $a_{Al} = 0.612$ mT; $a_H = 0.216$ mT; undecet: $a_{Al} = 0.172$ mT.

Evidently, **1** decomposes under UV irradiation by two different pathways: 1) The Al–Al bond is cleaved homolytically with the formation of two symmetrical fragments; these fragments are responsible for the sextet with low intensity ($I_{Al} = 5/2$, $a_{Al} = 0.612$ mT, Scheme 6). The further splitting to give a doublet may be due to the coupling to a hydrogen atom ($a_H = 0.216$ mT). 2) The intense signal shows 11 lines ($a_{Al} = 0.172$ mT); here the electron interacts with the two aluminum atoms, and the Al–Al bond has remained intact. The formation of this radical can be understood by the homolysis of an Al–C bond; however, the

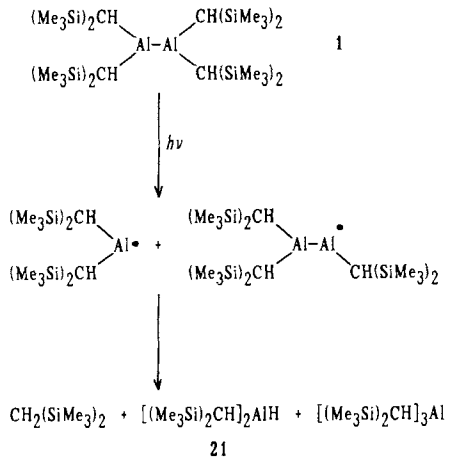

Scheme 6. Decomposition of **1** on irradiation with UV light. Reaction equation is not stoichiometric.

bis(trimethylsilyl)methyl radical formed in addition to the dialuminum radical could not be detected by ESR spectroscopy. The high stability of the aluminum radical may be due to the fact that one of the three remaining alkyl groups adopts the bridging position between the two Al atoms. In agreement with the proposed mechanism products exist which were obtained from preparative irradiation reactions in pentane: bis(trimethylsilyl)methane from the bis(trimethylsilyl)methyl radical, bis[bis(trimethylsilyl)methyl]-aluminum **21** with Al–H bond from the monoaluminum radical as well as $Al[CH(SiMe_3)_2]_3$.[37] The subsequent product of the dialuminum radical has so far not been isolated. Additional decomposition reactions do not occur, and in particular, no elemental aluminum is deposited. Compound **21** so far only accessible in this way is in equilibrium with its dimeric form in the cryoscopic molar mass determination in benzene. With increasing dilution of the sample this equilibrium shifts to the side of the monomer. Generally, dialkylaluminum hydrides exist as trimers in benzene with Al–H–Al bridges.[58]

3.2. Reactions of $[(Me_3Si)_2HC]_2Al–Al[CH(SiMe_3)_2]_2$ with Alkali Metals

The two unoccupied p orbitals of the Al–Al unit in **1** suggest that **1** can be reduced to give compounds with aluminum in the oxidation state + I. In nonpolar solvents no reaction is observed with alkali metals, whereas in DME (DME = 1,2-dimethoxyethane) with potassium or sodium,

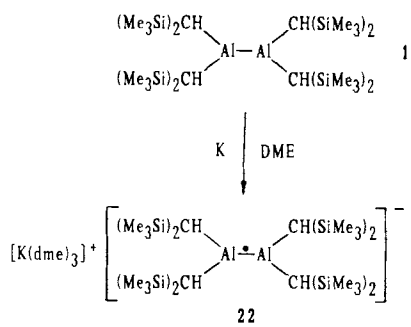

dark blue solutions are obtained in the course of 16 hours at room temperature, from which deep blue crystals of the paramagnetic compound **22** were isolated after distillation of the solvent and recrystallization from DME/*n*-pentane. These crystals are amorphous and thus their constitution could not be elucidated by an X-ray structure determination. The existence of the radical monoanion **22** containing an Al–Al bond is, however, clearly evident from the elemental analysis with a K:Al ratio of 1:2 as well as from the ESR spectra. These spectra show 11 equidistant lines (Fig. 8), which, as a result of an insufficient averaging of anisotropic contributions, increase in width with increasing distance from the center and show additional couplings to ^{29}Si nuclei.

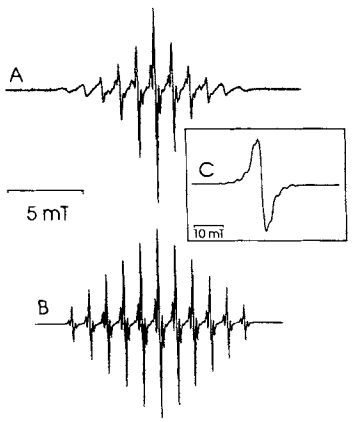

Fig. 8. A) ESR spectrum of **22**·$Li(tmeda)_2^+$ at 295 K in diethyl ether with strong anisotropic line broadening. B) Computer simulation with $a(^{27}Al)$ = 1.11 mT (2 Al atoms), $a(^{29}Si)$ = 0.435 mT (8 Si atoms). C) ESR spectrum at 110 K in glassy rigid diethyl ether [59].

The anisotropic components of the hyperfine splitting determined from the sprectra of the radicals immobilized in the solid ether matrix, the closeness of the g value ($g = 2.0025$) to that of the free electron, and the small isotropic hyperfine splitting $a(^{27}Al) = 1.17$ mT confirm the existence of a radical with an Al–Al π bond.[59] Pörschke et al. obtained a corresponding radical anion from **1** with $[Li(tmeda)_2]^+$ as counterion in a similar way, whose crystal structure has been determined.[60] The shortening of the Al–Al distance by 13 pm in comparison to the starting material **1**, as well as the ideal planar arrangement of the central C_2AlAlC_2 unit reveal likewise the existence of a π bond in **22**. Similar compounds are known for boron,[61] and in the meantime Power et al. have also synthesized gallium analogues (Scheme 7).[39]

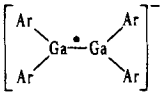

Scheme 7. Ar = 2,4,6-$C_6H_2iPr_3$.

Whereas the compound **22** purified by recrystallization can be stored even in solution at room temperature and in daylight for weeks without change, it decomposes when attempts are made to transfer a second electron by treatment with excess potassium in DME. As the NMR spectra show, three new compounds are formed, which cannot be separat-

ed from one another by recrystallization, not even after the addition of crown ether, or by distillation. As a result of its characteristic NMR spectrum, the structure of one of the products (**23**) was determined and verified by desired synthesis and a crystal structure determination; the corresponding lithium compound forms as the only product in the reaction of excess lithium with **1** in DME.[62]

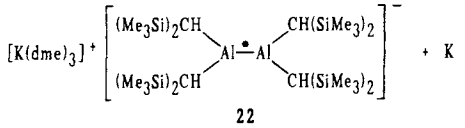

22

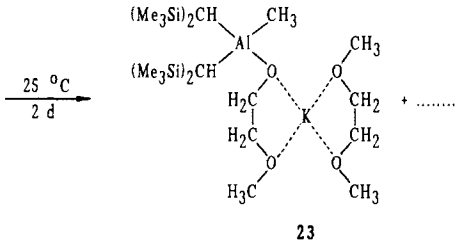

23

We propose the following pathway for the formation of **23** from **1**: initially the aluminum compound **1** is reduced with the transfer of only one electron and the formation of the radical anion **22** isolable with potassium or sodium. The desired second reduction step to an Al^I compound, however, evidently does not give a stable compound under the chosen reaction conditions in DME. Thus, the alkoxyaluminate **23** is isolated, which can be described as the product of the insertion of a molecular fragmemt with Al in the oxidation state + I into a H_3C-O bond of a DME molecule.

3.3. Reactions of $[(Me_3Si)_2HC]_2Al-Al[CH(SiMe_3)_2]_2$ with Alkyllithium Compounds

We set out to investigate the reactions of **1** with alkyllithium compounds for two reasons: first deprotonation reactions at the C–H acidic substituents should be possible. Thus, the previously mentioned sterically highly shielded $Al[CH(SiMe_3)_2]_3$ reacts with *tert*-butyllithium under deprotonation of a methyl group in the periphery of the molecule; the resulting carbanion is subsequently stabilized through an interaction with the coordinatively unsaturated aluminum atom, leading to the formation of a four-membered heterocycle.[37] Second, in certain cases, the reaction with alkyllithium compounds leads to the cleavage of element–element bonds with the formation of lithium–element compounds that are valuable as synthetic building blocks.[63]

With *tert*-butyllithium and **1** in the presence of the chelating ligand TMEDA none of the expected reactions is observed. Instead a β-elimination from the lithium compound occurs, and the formed hydride ion is bound to one of the aluminum atoms of the Al–Al bond (**24**), which in this reaction is retained. The length of the metal–metal bond in **24** (266.7(3) pm) remains unchanged within the range of standard deviations in comparison to the starting material **1**.[64] Remarkably, the hydride ion does not bridge the two coordinatively unsaturated metal atoms; thus, in **24** a saturated, four-coordinate Al atom is in close proximity to an unsaturated, three-coordinate Al atom.

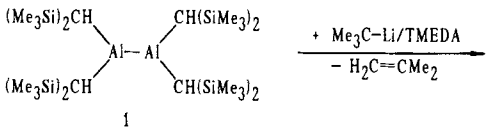

1

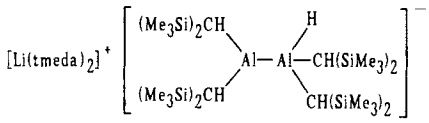

24

A similar adduct (**25**) with a methyl group bound to an aluminum atom is formed in the reaction of **1** with methyllithium.[64] Here, a significant lengthening of the Al–Al bond by 9 pm to 275.2(3) pm is observed, which is in agreement with the facile decomposition of **25** in solution with the deposition of elemental aluminum. The addition of the nucleophile in a terminal position is initially surprising, since dimers exist like $Me_2Al(\mu\text{-}H)_2AlMe_2$ (gas phase)[65] and $Me_2Al(\mu\text{-}Me)_2AlMe_2$[66] with the corresponding bridging ligands, which compensate the formal lack of electrons at the two metal atoms. With Al–Al distances of 262 and 261 pm, respectively, the structural parameters of the central molecular unit in these dimers do not deviate significantly from those observed in **24** and **25**. Apparently, also through the

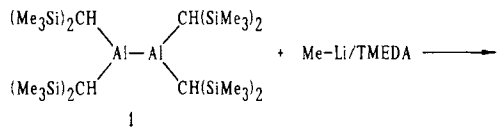

1

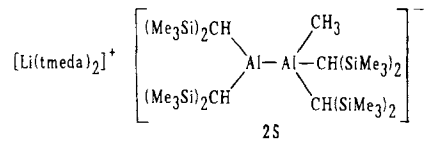

25

hyperconjugation, which can be established at the three-coordinate metal centers on the basis of molecular conformation shown in Figure 9 and the UV/VIS spectroscopic results similar as in **1**, the Lewis acidity of the bivalent aluminum atoms is reduced to such an extent that the formation of a two-center bond to the newly added substituent is more favorable than the occupation of a bridging position with the loss of the hyperconjugative interaction to both metal atoms.

To avoid the formation of an adduct we therefore used sterically more demanding (trimethylsilyl)methyl- and neopentyllithium, which are not subject to β-elimination, with **1** and obtained a completely different reaction course. In this an electron transfer from the lithium compounds to **1** is observed with the formation of the radical anion **22** with a different cation ($Li(tmeda)_2^+$) which precipitates in the

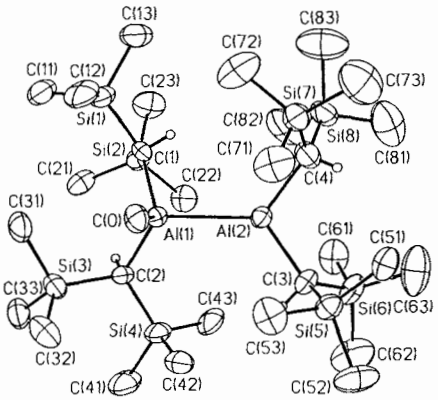

Fig. 9. Anionic part of the structure in methyldialuminate **25** (thermal ellipsoids drawn at 40% probability level). For a better overview, the hydrogen atoms of the methyl groups are not drawn, the remaining hydrogen atoms are drawn with arbitrary radius [64].

form of dark blue crystals.[59] The g value and the coupling constants in the ESR spectrum correspond to the parameters observed for **22**·K(dme)$_3^+$.

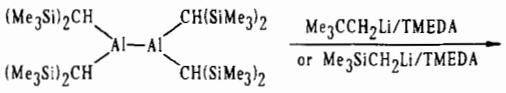

1

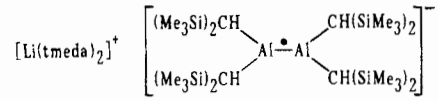

22

On careful observation it can be seen that the dark blue precipitate from the reaction of neopentyllithium with **1** contains small quantities of a yellow product, which can be extracted by treatment with nonpolar solvents. Crystals of probably two compounds can be obtained from this extract, of which, however, only one was completely characterized. As the crystal structure determination shows, the originally intended deprotonation of **1** to give **26** occurs as a side reaction. The proton is removed from a methyl group of a $SiMe_3$ group, and the resulting carbanion is stabilized by the interaction with one of the coordinatively unsaturated aluminum atoms; thus, the five-membered Al_2C_2Si heterocycle **26** is formed. The Al–Al bond is only slightly shorter (264.1(2) pm) than that in the starting material.[67]

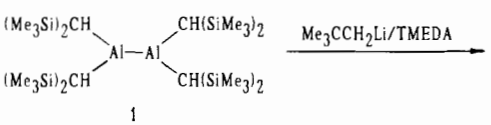

1

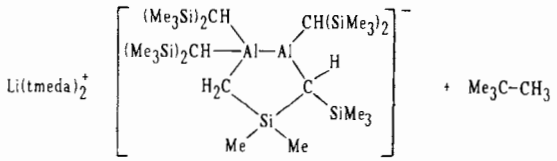

26

The reaction of **1** with lithium alcoholates does not occur as clearly as that with alkyllithium compounds. The cleavage of the Al–Al bond with the formation of the alkoxyaluminates **27** and **28** is always observed in addition to mostly inseparable product mixtures.[67]

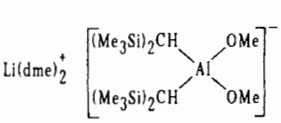

27

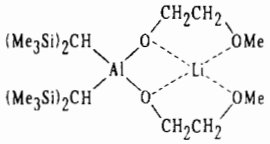

28

3.4. Reaction of $[(Me_3Si)_2HC]_2Al–Al[CH(SiMe_3)_2]_2$ with Carbon Disulfide

We have carried out preliminary experiments on the insertion of small molecules into compound **1** with carbon disulfide. Remarkably, irrespective of the solvent and of the reaction time, no reaction took place when stoichiometric quantities of both compounds were combined. A reaction is only observed when **1** is dissolved directly in a large excess of CS_2, and even then it takes 24 hours before the starting material **1** can no longer be detected. Thus, two compounds are formed (**29** and **30**), which can be separated from each other by repeated recrystallizations.[68] In the colorless main

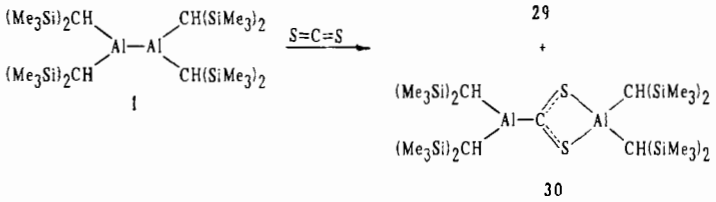

1 **29** **30**

product **29**, an S atom is inserted into the Al–Al bond. This results in a molecule with a short Al–S distance and a very large Al-S-Al angle (117°). But, from the spectroscopic and crystal structure data no additional interaction can be derived between a lone pair of electrons at the sulfur atom and the empty p orbital on the aluminum atom. The large angle can be ascribed to a steric repulsion of the bulky substituents or to an electrostatic repulsion between the two positively charged Al atoms. For the same reasons we observe a corresponding increase in the angle for a compound in which the sulfur bridge is replaced by a CH_2 group.[69]

In the second product (**30**) isolated in 15% yield, a CS_2 molecule was inserted into the Al–Al bond, which binds to one of the Al atoms with the C atom and surrounds the second Al atom in a chelate-like fashion with the two S atoms. In the solid state, as in the starting material **1**, the four α-C atoms of the bis(trimethylsilyl)methyl groups lie in a plane with the two Al atoms, and the CS_2 fragment is almost perpendicular to this plane. Compound **30** can be compared with dithiocarbamates, in which the three-coordinate Al atom is replaced by a N atom. Whereas a strong interaction between the lone pair of electrons on the nitrogen atom and

the delocalized π-electron system of the CS_2 unit is observed in such compounds, in **30** as a result of the described conformation of the molecule and of a very long Al–C distance of 205 pm, an inverse electron transfer to the metal atom can certainly be precluded. Also here a different arrangement of the substituents exists in the two halves of the molecule; whereas at the four-coordinate aluminum atom the two substituents are almost perpendicular, they adopt a parallel arrangement at the coordinatively unsaturated aluminum atom. Thus, the α-C–H bonds at the three-coordinate Al atom lie in a plane with both Al atoms, and all C–Si bonds to the two methine carbon atoms, as described several times in previous sections, are in a favorable position for the electron transfer into the unoccupied p orbital at the aluminum atom.

3.5. A Monomeric Gallium Telluride

The chemistry of the tetrasubstituted digallium and diindium compounds has been studied very little to date; the formation of a radical anion of a tetraaryldigallium compound was described in Section 3.2.[39] A remarkable reaction of the compound **10** is achieved with the sterically highly shielded bis[tris(trimethylsilyl)silyl]ditellane. In toluene at 100 °C in the course of four days complete metathesis is achieved with the formation of the gallium telluride **31**, which is monomeric both in solution and in the solid state.[70] The synthesis of

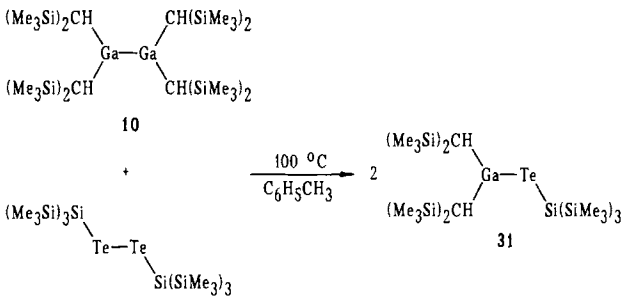

31 is also achieved by the reaction of the corresponding lithium telluride with bis[bis(trimethylsilyl)methyl]gallium bromide **32**, which is only accessible by disproportionation in the reaction of $Ga_2Br_4 \cdot 2$ dioxane with three equivalents of the alkyllithium compound.[70]

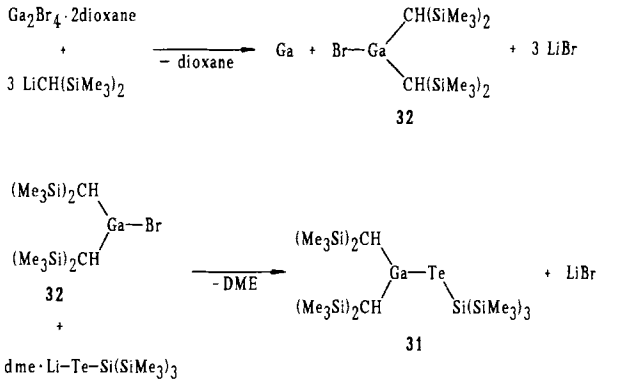

Compound **31** is the only monomeric organoelement gallium telluride reported to date which shows a range of remarkable properties. The molecular framework consisting of the atoms Ga, Te, Si1, Si2, C1, and C2 (Fig. 10) is planar; it lies on a crystallographic mirror plane. The Ga–Te distance is significantly shorter (253.5(1) pm) than the mean value of the Ga–Te distances in typical inorganic compounds and that calculated from the covalent radii of 262 pm. A hindered rotation about the Ga–Te bond with an estimated rotation barrier of 50 kJ mol^{-1} as well as an unusual chemical shift for the central methine protons is observed in the NMR spectra. The observations described may possibly be explained by an additional π interaction between the lone pair of electrons on the tellurium atom and the empty p orbital on the gallium atom.

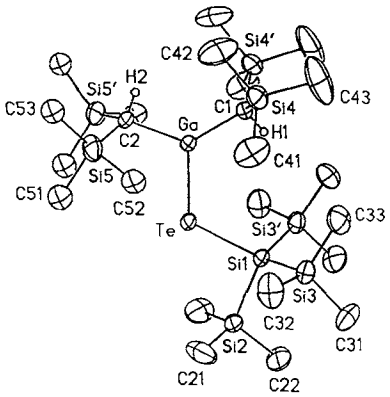

Fig. 10. Molecular structure of the gallium telluride **31** (thermal ellipsoids drawn at 40% probability level). Only the hydrogen atoms of the two CH groups were drawn with arbitrary radius; they denote the position of the $(Me_3Si)_2CH$ groups [70].

4. Outlook

The described synthesis and the preliminary studies into the reactivity of the tetrasubstituted dimetal (M–M) compounds of the heavier elements of the third main group (Al, Ga, and In) have opened the way to a fascinating and interesting new field of research in organoelement chemistry, which in the meantime has attracted many more research groups. The preparative potential of this class of compounds has by no means been completely exhausted, and the reducing properties of the metal–metal bonds in particular offer a field of activity, little studied to date. Moreover, the addition of a second Lewis base, which would lead to compounds analogous to the disilanes, or the ligand exchange with the retention of the element–element bond as well as the introduction of heteroatom substituents with coordinating oxygen or nitrogen atoms at the metal atoms is now at the forefront of current investigations.

I would like to thank the Deutsche Forschungsgemeinschaft and the Fonds der Chemischen Industrie for the financial support of this work. My thanks also go to Prof. Dr. G. Becker and Prof. Dr. W. Kaim (Universität Stuttgart) as well as Prof. Dr. W. Hiller (München) for their generous cooperation.

Received: April 10, 1993 [A 921 IE]
German version: *Angew. Chem.* **1993**, *105*, 1449

[1] H. Nöth, W. Meister, *Chem. Ber.* **1961**, *94*, 509; R. J. Brotherton, A. L. McCloskey, L. L. Petterson, H. Steinberg, *J. Am. Chem. Soc.* **1960**, *82*, 6242; R. J. Brotherton, A. L. McCloskey, J. L. Boone, H. M. Manasevit, *ibid.* **1960**, *82*, 6245; H. Nöth, H. Pommerening, *Angew. Chem.* **1980**, *92*, 481; *Angew. Chem. Int. Ed. Engl.* **1980**, *19*, 482.

[2] A. G. Massey, *Adv. Inorg. Chem. Radiochem.* **1983**, *26*, 1.

[3] W. Biffar, H. Nöth, H. Pommerening, *Angew. Chem.* **1980**, *92*, 63; *Angew. Chem. Int. Ed. Engl.* **1980**, *19*, 56; H. Nöth, H. Pommerening, *Chem. Ber.* **1981**, *114*, 3044.

[4] K. Schlüter, A. Berndt, *Angew. Chem.* **1980**, *92*, 64; *Angew. Chem. Int. Ed. Engl.* **1980**, *19*, 57.

[5] A. Moezzi, M. M. Olmstead, R. A. Bartlett, P. P. Power, *Organometallics* **1992**, *11*, 2383.

[6] W. Hönle, G. Gerlach, W. Weppner, A. Simon, *J. Solid State Chem.* **1986**, *61*, 171.

[7] T. Staffel, G. Meyer, *Z. Anorg. Allg. Chem.* **1988**, *563*, 27; R. E. Marsch, G. Meyer, *ibid.* **1990**, *582*, 128.

[8] K. Schubert, E. Dörre, E. Günzel, *Naturwissenschaften* **1954**, *41*, 448; W. J. Duffin, J. H. C. Hogg, *Acta Crystallogr.* **1966**, *20*, 566.

[9] J. H. C. Hogg, H. H. Sutherland, D. J. Williams, *Acta Crystallogr. Sect. B* **1973**, *29*, 1590.

[10] A. Kuhn, R. Chevalier, A. Rimsky, *Acta Crystallogr. Sect. B* **1975**, *31*, 2841; F. Jellinek, H. Hahn, *Z. Naturforsch. B* **1961**, *16*, 713; A. Kuhn, A. Chevy, R. Chevalier, *Acta Crystallogr. Sect. B* **1976**, *32*, 983; W. Frank, W. Hönle, A. Simon, *Z. Naturforsch. B* **1990**, *45*, 1; W. Hönle, A. Simon, *ibid.* **1986**, *41*, 1391; G. Gerlach, W. Hönle, A. Simon, *Z. Anorg. Allg. Chem.* **1982**, *486*, 7; J. Weis, H. Schäfer, *Z. Naturforsch. B* **1976**, *31*, 1341; G. Wagner, R. Hoppe, *J. Less Common Met.* **1986**, *116*, 129; H. Mattausch, A. Simon, E.-M. Peters, *Inorg. Chem.* **1986**, *25*, 3428; J. H. C. Hogg, W. J. Duffin, *Acta Crystallogr.* **1967**, *23*, 111; J. H. C. Hogg, *Acta Crystallogr. Sect. B* **1971**, *27*, 1630; A. Likforman, D. Carre, J. Etienne, B. Bachet, *ibid.* **1975**, *31*, 1252; T. Staffel, G. Meyer, *Z. Anorg. Allg. Chem.* **1987**, *552*, 113; H. Bärnighausen, *Z. Kristallogr.* **1989**, *186*, 16.

[11] R. Nesper, J. Curda, *Z. Naturforsch. B* **1987**, *42*, 557.

[12] S. Paashaus, R. Kniep, *Z. Naturforsch. B* **1990**, *45*, 667; *Angew. Chem.* **1986**, *98*, 725; *Angew. Chem. Int. Ed. Engl.* **1986**, *25*, 752.

[13] J. C. Beamish, A. Boardman, I. J. Worrall, *Polyhedron* **1991**, *10*, 95; R. W. H. Small, I. J. Worrall, *Acta Crystallogr. Sect. B* **1982**, *38*, 250; *ibid.* **1982**, *38*, 86; M. Khan, C. Oldham, M. J. Taylor, D. G. Tuck, *Inorg. Nucl. Chem. Lett.* **1980**, *16*, 469; J. C. Beamish, R. W. H. Small, I. J. Worrall, *Inorg. Chem.* **1979**, *18*, 220; H. J. Cumming, D. Hall, C. E. Wright, *Cryst. Struct. Commun.* **1974**, *3*, 107; K. L. Brown, D. Hall, *J. Chem. Soc. Dalton Trans.* **1973**, 1843; C. A. Evans, K. H. Tan, S. P. Tapper, M. J. Taylor, *ibid.* **1973**, 988.

[14] M. A. Khan, C. Peppe, D. G. Tuck, *Can. J. Chem.* **1984**, *62*, 601; I. Sinclair, I. J. Worrall, *ibid.* **1982**, *60*, 695; M. J. Taylor, D. G. Tuck, L. Victoriano, *ibid.* **1982**, *60*, 690.

[15] D. G. Tuck in *Comprehensive Organometallic Chemistry, Vol. 1* (Eds.: G. Wilkinson, F. G. A. Stone, E. W. Abel), Pergamon, Oxford, **1982**, p. 684.

[16] A. J. Carty, M. J. S. Gynane, M. F. Lappert, S. J. Miles, A. Singh, N. J. Taylor, *Inorg. Chem.* **1980**, *19*, 3637.

[17] K. Lammertsma, O. F. Güner, R. M. Drewes, A. E. Reed, P. von R. Schleyer, *Inorg. Chem.* **1989**, *28*, 313; Al_2H_2: Z. Palagyi, R. S. Grev, H. F. Schaefer III, *J. Am. Chem. Soc.* **1993**, *115*, 1936.

[18] P. J. Davidson, D. H. Harris, M. F. Lappert, *J. Chem. Soc. Dalton Trans.* **1976**, 2268.

[19] W. Uhl, *Z. Naturforsch. B* **1988**, *43*, 1113.

[20] H. Bock, W. Kaim, *J. Am. Chem. Soc.* **1980**, *102*, 4429; *Acc. Chem. Res.* **1982**, *15*, 9.

[21] W. Uhl, *Z. Naturforsch. B* **1990**, *45*, 1349.

[22] A. V. Grosse, J. M. Mavity, *J. Org. Chem.*, **1940**, *5*, 106; radical anions formed in the presence of pyridine: R. Köster, G. Benedikt, H. W. Schrötter, *Angew. Chem.* **1964**, *76*, 649; *Angew. Chem. Int. Ed. Engl.* **1964**, *3*, 514; H. Lehmkuhl, G. Fuchs, R. Köster, *Tetrahedron Lett.* **1965**, 2511.

[23] E. P. Schram, N. Sudha, *Inorg. Chim. Acta* **1991**, 183, 213.

[24] C. Dohmeier, C. Robl, M. Tacke, H. Schnöckel, *Angew. Chem.* **1991**, *103*, 594; *Angew. Chem. Int. Ed. Engl.* **1991**, *30*, 564; theoretical investigations on the Al_4 cluster: U. Schneider, R. Ahlrichs, H. Horn, A. Schäfer, *ibid.* **1992**, *104*, 327 and **1992**, *31*, 353..

[25] W. Uhl, J. Wagner, unpublished results.

[26] H. Hoberg, S. Krause, *Angew. Chem.* **1978**, *90*, 1013; *Angew. Chem. Int. Ed. Engl.* **1978**, *17*, 949.

[27] H. Hoberg, S. Krause, *Angew.Chem.* **1976**, *88*, 760; *Angew. Chem. Int. Ed. Engl.* **1976**, *15*, 694.

[28] Some further questionable examples for compounds with an Al–Al bond, which are very poorly characterized, are given in the following publications: E. P. Schram, *Inorg. Chem.* **1966**, *5*, 1291; E. P. Schram, R. E. Hall, J. D. Glore, *J. Am. Chem. Soc.* **1969**, *91*, 6643; see also: H. Nöth, *Prog. Boron Chem.* **1970**, *3*, 211; V. V. Gavrilenko, L. A. Chekulaeva, L. I. Zakharkin, *Zh. Obshch. Khim.* **1983**, 53, 481; *J. Gen. Chem. USSR* **1983**, *53*, 423; see also: E. P. Schram, *Inorg. Chim. Acta* **1987**, *134*, 117.

[29] L. I. Zakharkin, V. V. Gavrilenko, *Zh. Obshch. Khim.* **1962**, *32*, 689; *J. Gen. Chem. USSR* **1962**, *32*, 688; F. Hein, E. Petzchner, K. Wagler, F. A. Segitz, *Z. Anorg. Allg. Chem.* **1924**, *141*, 161; G. Tatzel, H. Schrem, J. Weidlein, *Spectrochim. Acta Part A* **1978**, *34*, 549.

[30] W. Uhl, J. Wagner, *J. Organomet. Chem.* **1992**, *427*, 151.

[31] R. H. Crabtree, D. G. Hamilton, *Adv. Organomet. Chem.* **1988**, *28*, 299.

[32] W. Hiller, K.-W. Klinkhammer, W. Uhl, J. Wagner, *Angew. Chem.* **1991**, *103*, 182; *Angew. Chem. Int. Ed. Engl.* **1991**, *30*, 179.

[33] J. Morris, D. Gysling, D. Reed, *Chem. Rev.* **1985**, *85*, 51; R. L. Middaugh, F. Farha, *J. Am. Chem. Soc.* **1966**, *88*, 4147; R. J. Wiersema, R. L. Middaugh, *ibid.* **1967**, *89*, 5078; A. P. Schmitt, R. L. Middaugh, *Inorg. Chem.* **1974**, *13*, 163; R. J. Wiersema, R. L. Middaugh, *ibid.* **1969**, *8*, 2074.

[34] M. Tacke, H. Schnöckel, *Inorg. Chem.* **1989**, *28*, 2895.

[35] W. Uhl, M. Layh, T. Hildenbrand, *J. Organomet. Chem.* **1989**, *364*, 289.

[36] J. C. Beamish, A. Boardman, R. W. H. Small, I. J. Worrall, *Polyhedron* **1985**, *4*, 983; C. A. Evans, M. J. Taylor, *J. Chem. Soc. D* **1969**, 1201; see also [13].

[37] W. Uhl, *Z. Anorg. Allg. Chem.* **1989**, *579*, 75.

[38] W. Uhl, M. Layh, W. Hiller, *J. Organomet. Chem.* **1989**, *368*, 139.

[39] X. He, R. A. Bartlett, M. M. Olmstead, K. Ruhlandt-Senge, B. E. Sturgeon, P. P. Power, *Angew. Chem.* **1993**, *105*, 761; *Angew. Chem. Int. Ed. Engl.* **1993**, *32*, 717.

[40] M. Veith, F. Goffing, S. Becker, V. Huch, *J. Organomet. Chem.* **1991**, *406*, 105; M. Veith, J. Pöhlmann, *Z. Naturforsch. B* **1988**, *43*, 505.

[41] T. A. Annan, D. G. Tuck, *Can. J. Chem.* **1989**, *67*, 1807; T. A. Annan, R. K. Chadha, P. Doan, D. H. McConville, B. R. McCarvey, A. Ozarowski, D. G. Tuck, *Inorg. Chem.* **1990**, *29*, 3936.

[42] R. D. Schluter, A. H. Cowley, D. A. Atwood, R. A. Jones, M. R. Bond, C. J. Carrano, *J. Am. Chem. Soc.* **1993**, *115*, 2070.

[43] C. Janiak, R. Hoffmann, *J. Am. Chem. Soc.* **1990**, *112*, 5924.

[44] W. Uhl, K.-W. Klinkhammer, M. Layh, W. Massa, *Chem. Ber.* **1991**, *124*, 279.

[45] A. H. Cowley, N. C. Norman, M. Pakulski, G. Becker, M. Layh, E. Kirchner, M. Schmidt, *Inorg. Synth.* **1990**, *27*, 235.

[46] W. Hiller, M. Layh, W. Uhl, *Angew. Chem.* **1991**, *103*, 339; *Angew. Chem. Int. Ed. Engl.* **1991**, *30*, 324.

[47] J. W. F. L. Seetz, G. Schat, O. S. Akkerman, F. Bickelhaupt, *J. Am. Chem. Soc.* **1982**, *104*, 6848.

[48] W. Uhl, W. Hiller, M. Layh, W. Schwarz, *Angew. Chem.* **1992**, *104*, 1378; *Angew. Chem. Int. Ed. Engl.* **1992**, *31*, 1364.

[49] W. Uhl, M. Layh, U. Schütz, unpublished results.

[50] M. Tacke, H. Kreienkamp, L. Plaggenborg, H. Schnöckel, *Z. Anorg. Allg. Chem.* **1991**, *604*, 35.

[51] D. Loos, H. Schnöckel, J. Gauss, U. Schneider, *Angew. Chem.* **1992**, *104*, 1376; *Angew. Chem. Int. Ed. Engl.* **1992**, *31*, 1362.

[52] O. T. Beachley, Jr., J. C. Pazik, T. E. Glassman, M. R. Churchill, J. C. Fettinger, R. Blom, *Organometallics* **1988**, *7*, 1051; O. T. Beachley, Jr., J. F. Lees, T. E. Glassman, M. R. Churchill, L. A. Buttrey, *ibid.* **1990**, *9*, 2488; O. T. Beachley, Jr., J. F. Lees, R. D. Rogers, *J. Organomet. Chem.* **1991**, *418*, 165.

[53] E. Frasson, F. Menegus, C. Panattoni, *Nature* **1963**, *199*, 1087; H. Schumann, H. Kucht, A. Dietrich, L. Esser, *Chem. Ber.* **1990**, *123*, 1811; S. Harvey, C. L. Raston, B. W. Skelton, A. H. White, M. F. Lappert, G. Srivastava, *J. Organomet. Chem.* **1987**, *328*, C1.

[54] O. T. Beachley, Jr., M. R. Churchill, J. C. Fettinger, J. C. Pazik, L. Victoriano, *J. Am. Chem. Soc.* **1986**, *108*, 4666.

[55] H. Schumann, C. Janiak, F. Görlitz, J. Loebel, A. Dietrich, *J. Organomet. Chem.* **1989**, *363*, 243.

[56] M. Scholz, M. Noltemeyer, H. W. Roesky, *Angew. Chem.* **1989**, *101*, 1419; *Angew. Chem. Int. Ed. Engl.* **1989**, *28*, 1383.

[57] W. Uhl, A. Vester, W. Kaim, V. Kasack, unpublished results.

[58] J. J. Eisch in *Comprehensive Organometallic Chemistry, Vol. 1* (Eds.: G. Wilkinson, F. G. A. Stone, E. W. Abel), Pergamon, Oxford, **1982**, p. 583.

[59] W. Uhl, A. Vester, W. Kaim, J. Poppe, *J. Organomet. Chem.*, **1993**, *454*, 9.

[60] C. Pluta, K.-R. Pörschke, C. Krüger, K. Hildenbrand, *Angew. Chem.* **1993**, *105*, 451; *Angew. Chem. Int. Ed. Engl.* **1993**, *32*, 388.

[61] H. Klusik, A. Berndt, *Angew. Chem.* **1981**, *93*, 903; *Angew. Chem. Int. Ed. Engl.* **1981**, *20*, 870; *J. Organomet. Chem.* **1982**, *232*, C21.

[62] W. Uhl, A. Vester, D. Fenske, G. Baum, *J. Organomet. Chem.*, in press.

[63] E. Fluck, R. Riedel, H. D. Hausen, G. Heckmann, *Z. Anorg. Allg. Chem.* **1987**, *551*, 85; G. Fritz, K. Stoll, *ibid.* **1986**, *539*, 65; G. Fritz, T. Vaahs, J. Härer, *ibid.* **1987**, *552*, 11; K. Issleib, F. Krech, *J. Organomet. Chem.* **1968**, *13*, 283; W. C. Still, *J. Org. Chem.* **1976**, *41*, 3063; G. Becker, H.-M. Hartmann, A. Münch, H. Riffel, *Z. Anorg. Allg. Chem.* **1985**, *530*, 29; G. Gutekunst, A. G. Brook, *J. Organomet. Chem.* **1982**, *225*, 1; H. Gilman, J. M. Holmes, C. L. Smith, *Chem. Ind. (London)* **1965**, 848.

[64] W. Uhl, A. Vester, *Chem. Ber.* **1993**, *126*, 941.

[65] A. Almenningen, G. A. Anderson, F. R. Forgaard, A. Haaland, *Acta Chem. Scand.* **1972**, *26*, 2315.

[66] R. G. Vranka, E. L. Amma, *J. Am. Chem. Soc.* **1967**, *89*, 3121; J. C. Huffman, W. E. Streib, *J. Chem. Soc. Chem. Commun.* **1971**, 911.

[67] W. Uhl, U. Schütz, A. Vester, unpublished results.

[68] W. Uhl, A. Vester, W. Hiller, *J. Organomet. Chem.* **1993**, *443*, 9.

[69] M. Layh, W. Uhl, *Polyhedron* **1990**, *9*, 277.

[70] W. Uhl, M. Layh, G. Becker, K. W. Klinkhammer, T. Hildenbrand, *Chem. Ber.* **1992**, *125*, 1547.

Bacteria and the Biodegradation of Chemicals Achieved Naturally, by Combination, or by Construction

By Gerhard Gottschalk* and Hans-Joachim Knackmuss

The natural potential of bacteria for the biological degradation of synthetic compounds is greater than is commonly supposed and extends to many heteroarenes and even some chloroarenes. An increase in the number of substituents on the aromatic ring or a certain substitution pattern is what confers xenobiotic character to a compound. In addition, when enzymes with low substrate specificity encounter foreign compounds with random variations, products with very strong xenobiotic character often result. In this case, changing the conditions or introducing a cooperation between several different types of bacteria can be used to degrade these compounds. Finally, mineralization, the complete breakdown of organic substances into carbon dioxide and inorganic salts, of xenobiotics previously regarded as persistent can be achieved by taking advantage of natural or induced gene transfer to construct hybrid degradative pathways. After an introduction to the world of bacteria and their place in nature, we will describe their natural potential for biodegradation with reference to aliphatic and aromatic hydrocarbons. The discussion will then turn to the types of the substituents that confer xenobiotic properties to compounds and how these compounds are degraded despite their xenobiotic character.

1. The Two Faces of Bacteria

Bacteria do not generally have a very good reputation. Most people think only of the pathogens, the cause of the plague, cholera, typhus, tuberculosis, and sexually transmitted diseases. This is of course understandable, since in the Middle Ages, for example, far more people died from the plague than in wars. The worst plague epidemic of all time occurred between 1347 and 1352.[1, 2] Starting in the Black Sea area, the plague was carried by sea travelers and traders to neighboring countries and spread from Italy to central Europe and then back to the East, leaving a death count of 30–40 million. Cholera has also been one of the great banes of mankind; the last large cholera epidemic in Germany occurred in 1892 in Hamburg. Robert Koch personally led the struggle against it. Indeed, the danger from the pathogen *Vibrio cholerae* is not over yet, as the more recent news from South America indicates. New pathogens make themselves known every so often, as in the case of the causitive agent of "Legionnaires' disease" first described in 1976 which appeared during a veterans' convention in Philadelphia. As it was later shown, the veterans were infected with a new kind of bacterium spread by the air-conditioning system while they slept. Many became ill with lung inflammations and 31 died. The bacterium was named *Legionella pneumophila* following this incident.[3]

That is, however, only one aspect of bacteria; they also play a useful and vital role in recycling elements essential for life (carbon, nitrogen, and sulfur) on our planet. With the help of sunlight, green plants and phototropic bacteria convert carbon dioxide into biomass and thus provide the basis for all other organisms. Some of this biomass is respired as CO_2 by the phototropic organisms themselves and some by animals in the food chain. Large amounts of plant and animal material die and then decay, a process which to a large extent is carried out by bacteria. Organic material accumulates everywhere on the Earth—in the soil and in sediments of bodies of water and in the sewage and rubbish dumps of our civilization. In all these places microorganisms are at work mineralizing this organic material and thereby returning CO_2 to the atmosphere.[4]

A summary of the terrestrial and marine carbon cycles is shown in Figure 1. Every year roughly 200 gigatons of carbon in the form of biomass is oxidized and released into the atmosphere as CO_2; an estimated 70% of this results from the activities of fungi and bacteria.[5] Fungi mineralize wood and other cellulose-containing material; bacteria are crucial in the breakdown of organic material for three main reasons:

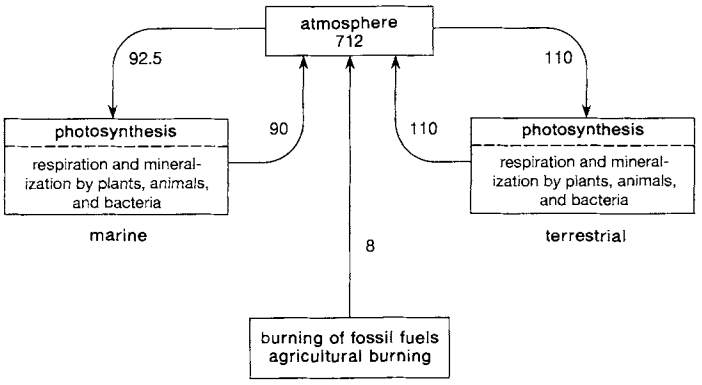

Fig. 1. The carbon cycle on the continents and in the oceans including carbon release into the atmosphere by combustion processes. Values in gigatons (10^9 t) of carbon.

[*] Prof. Dr. G. Gottschalk
Institut für Mikrobiologie der Universität
Grisebachstrasse 8, D-37077 Göttingen (FRG)
Telefax: Int. code + (551)3937-93
Prof. Dr. H.-J. Knackmuss
Institut für Mikrobiologie der Universität
Allmandring 31, D-70569 Stuttgart (FRG)
Telefax: Int. code + (711)685-5725

1) The substrate spectrum of bacteria corresponds to the variety of naturally occurring compounds. This is apparent from the observation that no organic compounds of natural origin are accumulated on the Earth's surface or in its waters. The tremendous degradative potential of bacteria includes hydrocarbons, a large number of aromatic compounds, and even chlorine-containing compounds; thus a link to the degradation of pollutants exists already.

2) Bacteria are able to survive under a wide range of conditions. The limits for bacterial growth and survival are delineated in Table 1. Certain archaebacteria often called extremophiles are found in places where life under the prevailing conditions (temperature, pH, pressure, ionic strength) is hard to imagine.

3) Bacteria possess an enormously high metabolic activity due in part to their small size and consequent large surface-to-volume ratio. A cross section of a bacterial cell is shown schematically in Figure 2. It is evident that energy produc-

Table 1. The limits of bacterial growth.

Condition	Limits	Examples
temperature	90–110 °C	*Pyrodictium occultum* *Methanopyrus kandleri*
	15–0 °C	*Photobacterium phosphoreum*
pH	3–1.5	*Acidianus brierleyi*
	9–11	*Bacillus alcalophilus*
salinity	up to 5.2 M NaCl	*Halobacterium halobium*
O_2 concentration	0%	fermentation organisms like methanogenic bacteria and clostridia
	about 1%	microaerophilic bacteria like *Thiomicrospira denitrificans*
	20%	common bacteria found in soil and water

[a] Examples taken from refs.[6,7].

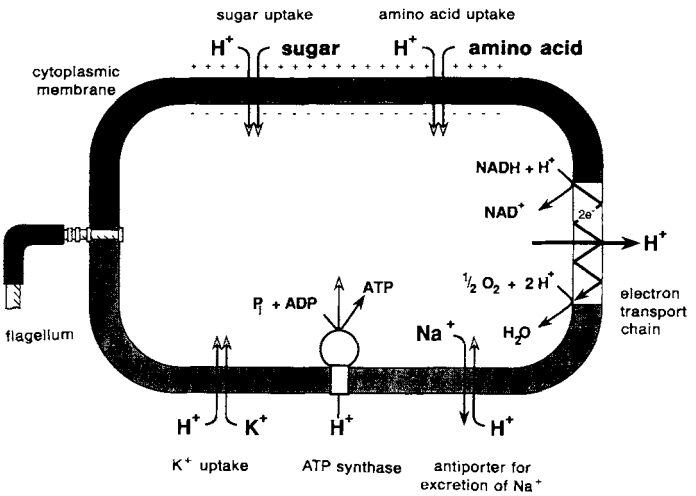

Fig. 2. Schematic diagram of a bacterial cell showing the many activities that take place in the cytoplasmic membrane. The outer cell wall and the intermediate metabolism that occurs in the cytoplasmic membrane are not shown.

Gerhard Gottschalk was born in 1935 in Schwedt/Oder and studied chemistry at the Humboldt University in Berlin from 1953 to 1959. After receiving his diploma, he moved to Göttingen in 1960, where he completed his Ph.D. dissertation in 1963 for his work with H. G. Schlegel on the biosynthesis of poly-β-hydroxybutyric acid. Following two years of postdoctoral research with H. A. Barker at the Department of Biochemistry at UC Berkeley, he completed his habilitation in microbiology at the University of Göttingen. He received a faculty appointment at the University of Münster in 1969 and took up his present position in 1970 at the University of Göttingen. He has been a guest professor at UC Davis and UC Berkeley and is a member of the Akademie der Wissenschaften zu Göttingen. In 1992 he recieved the Philip-Morris-Forschungspreis "Herausforderung Zukunft" together with A. Steinbüchel and H. G. Schlegel. His major research interests are the metabolism of anaerobic bacteria, in particular methane-producing bacteria, the enzymology and genetic organization of microbial metabolic processes, and biodegradation. He is the author of the textbook "Bacterial Metabolism".

Hans-Joachim Knackmuss, born in 1936 in Halle/Saale, studied chemistry in Heidelberg from 1957 to 1962. He obtained his diploma and Ph.D. (1963–1964) for research he conducted with Richard Kuhn at the Max-Planck-Institut in Heidelberg on natural product synthesis directed toward the structural determination of bacterial indigoidine. After one year of postdoctoral research with M. P. Starr at the Department of Bacteriology at UC Davis, he completed his habilitation at the University of the Saarland in Saarbrücken in 1970. He then switched research areas and joined the scientific staff at the Institut für Mikrobiologie der Gesellschaft für Strahlen- und Umweltforschung mbH München in Göttingen. In 1979 he was appointed professor at the Universität-Gesamthochschule Wuppertal. He took up his present position as a director of the Institut für Microbiologie at the University of Stuttgart in 1986. His main research interests are the development of microbial systems for the targeted biotransformation of synthetic compounds and for the removal of xenobiotics from the environment. His work on the physiology and enzymology of the microbial degradation of xenobiotics and the experimental evolution of new catabolic activities in microorganisms form the basis for biological waste management techniques, which are being developed in cooperation with a group at the Fraunhofer Institut für Grenzflächen and Bioverfahrenstechnik in Stuttgart.

tion and transport of material in and out of the cell occur in the cytoplasmic membrane enclosing the cell. The greater the surface area of this membrane in comparison to the volume of the cytoplasm, the more substrate and therefore the more energy in the form of ATP can be made available for the synthetic machinery in the cytoplasm. For example, the respiration rate of the nitrogen-fixing *Azotobacter vinelandii* is 2000 times greater than that of cells in liver tissue. The rate of growth and reproduction of bacterial cells is also much faster. Under optimum conditions an *Escherichia coli* cell, for example, can divide every 20 minutes, and this is not even the record. Other bacteria need only 11 minutes for one generation. The impact of such rapid cell division is shown in the following (somewhat imaginary) example.

If we ask how much bacterial mass would be produced from a single *E. coli* cell in 48 hours, assuming that cell division takes place every 20 minutes, we come up with a rather incredible answer. In this time 144 cell divisions would take place, and $N = 1 \times 2^{144} = 10^{43}$ cells would result. Since a single *E. coli* cell weighs 10^{-12} grams, 10^{43} cells would weigh 10^{25} tons (for comparison, the Earth weighs 6×10^{21} tons). Thus the weight of the bacteria produced in only two days would be 1000 times the mass of the Earth. This calculation shows that the growth of *E. coli* and other bacteria must be controlled by limiting utilizable substrates or by allowing the products of degradation to accumulate. Nevertheless, it is obvious that under the right conditions utilizable compounds are quickly broken down by bacteria.

2. Everything Depends on an Energized Cytoplasmic Membrane

A bacterium is not a passive biocatalyst, not a closed net full of enzymes that swims in an aqueous milieu allowing everything to enter and then somehow transforming these substances and releasing the products to the outside. Bacteria are in fact compartments well shielded from their surroundings. The differences in the concentrations of substances inside and outside of the cell are enormous. For example, the K^+ concentration in a bacterial cell is around 250 mM, (outside the cell the concentration of K^+ is often 20 mM or less); the Na^+ concentration is only a few mM even in bacteria in sea water, where the concentration of Na^+ is 600 mM. It is the cytoplasmic membrane, a phospholipid bilayer containing proteins,[8] that shields the cell from the outside world. This membrane does not just form a shell around the inside of the cell; the membrane is also "energized" as a result of the proton gradient across it. Consequently, the cell's interior is more alkaline than the exterior, and the inside is negatively and the outside positively charged. These combined parameters are called the protomotive force (Fig. 2).

This energized state of the cytoplasmic membrane is crucial for the survival of a bacterial cell, allowing the selective uptake and release of compounds such as neutral or charged organic compounds and inorganic ions. The gradient also makes possible the synthesis of adenosine triphosphate (ATP). Substrates are taken up by bacteria and partially oxidized through respiration, leading to the production and maintenance of the proton gradient and protomotive force just mentioned.[9] Lack of substrate leads to the death of the bacteria, as they are not able to maintain the energized state of the membrane. However, substrates themselves can be a problem: lipophilic substrates can destroy the energized state of the membrane and thus prevent ATP synthesis. Such uncoupling agents include compounds like 2,4-dinitrophenol, tetrachlorosalicylanilide, and also weak organic acids, which can pass through the phospholipid bilayer in undissociated form[10] and dissociate inside the cell, thus destroying the pH gradient between the interior and exterior (Fig. 3).

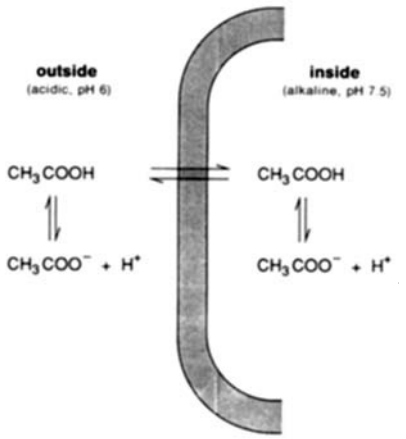

Fig. 3. The uncoupling effect of weak organic acids. The concentrations of the undissociated acid inside and outside equalize, and the difference in pH is minimized by dissociation inside.

For this reason organic acids like acetic acid or lactic acid are good food preservatives. Solvents like toluene and butanol function differently: they make "holes" in the membrane and prevent the maintenance of ion gradients. It is therefore even more remarkable that Horikoshi et al. were able to isolate strains of *Pseudomonas putida* and *P. aeruginosa* that grow on agar under a 2-mm-thick layer of toluene, *p*-xylene, cyclohexane, or *n*-heptanol.[11] Although exceptions, these strains are very interesting, and attention should be directed to understanding their fundamental tolerance mechanisms.

From the discussion so far it is clear that the lack of substrate as well as certain lipophilic substrates can cause problems for bacteria. Lipophilic compounds in particular are a potential danger, which bacteria are generally able to circumvent by metabolizing the compounds at a rate faster than the rate at which they diffuse into the neighborhood of the cell. An aqueous milieu, low concentrations of such compounds, and possible enzymatic transformations are requirements for the breakdown of many compounds, natural as well as synthetic.

3. The Degradation of Natural Compounds Is Fascinating in Itself

A few examples should serve to document the range of reactions used by microorganisms for the breakdown of substances. This catabolism extends beyond glycolysis and related reactions. Oxygen is generally directly involved in the breakdown of aliphatic and aromatic compounds. Aliphatic

hydrocarbons like **1** are converted into primary alcohols such as **2** by means of monooxygenase reactions [Eq.(a)].[8]

$$C_{15}H_{31}\text{-}CH_3 + O_2 + NADH + H^+ \longrightarrow C_{15}H_{31}\text{-}CH_2OH + H_2O + NAD^+ \quad (a)$$

It is characteristic of this reaction that in addition to the hydrocarbon, a coenzyme in the cell such as nicotinamide adenine dinucleotide (NADH) is also oxidized. The resulting primary alcohol can then be converted via the aldehyde into the corresponding carboxylic acid, which can then be activated by esterification with coenzyme A and then broken down further by the β-oxidation pathway.

The degradation of aromatic compounds proceeds by the following scheme: First compounds with hydroxyl groups next to each other are formed by "dioxygenase reactions". In the simplest case, the degradation of benzene, the cyclohexadienediol derivative **5** is formed, which is then dehydrogenated in a separate NAD^+-dependent reaction to give catechol (**6**) [Eq.(b)]. Dioxygenases that act on aromatic ring systems

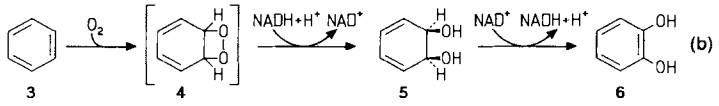

are multicomponent systems (Fig. 4). A reductase component, a flavoprotein, accepts an electron from NADH and passes this on via ferredoxin to the oxygenase itself, which contains iron–sulfur centers (Fe-S), specifically Fe^{2+}, in its reaction center.[12] A few of these dioxygenases are listed in

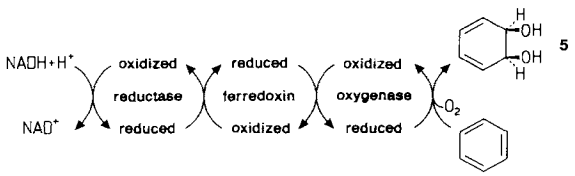

Fig. 4. Benzene dioxygenase, a three-component system.

Table 2. Benzoate and *ortho*-phthalate dioxygenases are two-component systems in which electrons are transferred directly from the reductase to the oxygenase via the Fe-S centers. Catechol (**6**) and protocatechuate are cleaved with O_2 between the hydroxyl groups (*ortho* cleavage) or at a position directly next to one of the hydroxyl groups (*meta* cleavage), leading to the formation of *cis,cis*-muconic acid and hydroxymuconic acid semialdehyde, respectively, or corresponding derivatives (Scheme 1). The ability to cleave

Table 2. Multicomponent systems for the hydroxylation of arenes (dioxygenases).

Dioxygenase	Reductase			Ferredoxin	Oxygenase		
	M [a]	flavin	Fe-S center	*M*	*M*	Fe-S center	Fe^{2+}
benzene 1,2-	60	FAD	–	12	168	+	+
toluene 2,3-	46	FAD	–	15	151	+	–
naphthalene 1,2-	36	FAD	2Fe-2S	14	158	+	–
benzoate 1,2-	38	FAD	2Fe-2S	–	201	+	+
o-phthalate 1,2-	34	FMN	2Fe-2S	–	217	+	–

[a] Molecular mass in kilodalton. Data taken from refs. [12,15].

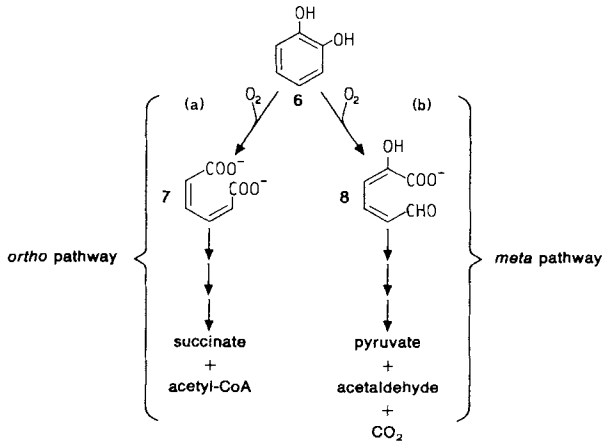

Scheme 1. Cleavage of catechol (**6**) by a 1,2-dioxygenase (a) and a 2,3-dioxygenase (b).

an aromatic ring system is amazingly widely distributed among bacteria. The genes required may lie on the bacterial chromosome (as is often the case with *ortho* cleavage), or on a plasmid (primarily for *meta* cleavage). Plasmids are small, circular, double-stranded DNA molecules, which though similar to the bacterial chromosome are much smaller (around 1% the mass of the bacterial chromosome). Plasmids often carry genes whose gene products confer resistance to specific antibiotics.

Heteroarenes, found frequently in nature in nucleic acids and some amino acids, vitamins, and alkaloids, are also biodegradable.[13] The microbial attack on unsubstituted heterocycles often begins with the introduction of a hydroxyl group next to the heteroatom. In this case the hydroxyl oxygen atom does not come from oxygen but rather from water; the enzymes responsible contain a molybdenum cofactor and in most cases flavins as well (Table 3).

Table 3. Molybdenum-containing enzymes that hydroxylate heterocycles using water.

Enzyme	Other prosthetic groups	Product
xanthine DH [a]	FAD, Fe-S	uric acid
nicotine DH	FAD, Fe-S	6-hydroxynicotine
isonicotinic acid DH	FAD	6-hydroxyisonicotinic acid
picolinic acid DH	FAD	6-hydroxypicolinic acid
quinoline DH	FAD	2-hydroxyquinolinic acid
furan-2-carboxyl-CoA DH		5-hydroxyfuran-2-carboxyl-CoA

[a] DH = dehydrogenase.

The molybdenum cofactor that occurs in bacteria is a molybdopterin guanine or cytosine dinucleotide (Fig. 5).[14]

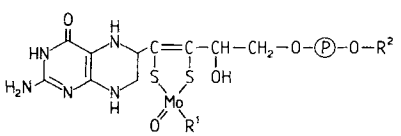

Fig. 5. Molybdenum cofactors. R^1 = O: nitrate reductase, sulfite oxidase; R^1 = S: most known molybdenum enzymes; R^1 = Se: a few molybdenum enzymes of anaerobic bacteria; R^2 = cytosine or guanosine monophosphate. Ⓟ = phosphodiester group.

How the cofactor is involved in the hydroxylation is shown in the postulated mechanism for the xanthine dehydrogenase reaction (Fig. 6).[15]

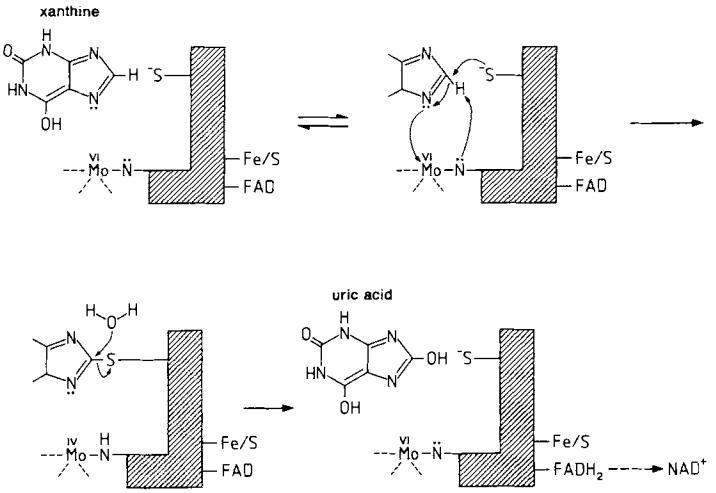

Fig. 6. A possible mechanism for the xanthine dehydrogenase reaction[15]. The shaded area represents the active center of the enzyme (S^- groups and the redox-active components).

It is reasonable that these enzymes require flavine adenine nucleotide (FAD) in addition and contain Fe-S centers. In the course of the hydroxylation Mo^{VI} is reduced to Mo^{IV}; in the reoxidation mediated by the Fe-S centers and FAD the electrons are finally transferred to NAD^+.

4. No Suitable Degradation Mechanisms Exist for a Number of Synthetic Compounds

Some of the synthetic compounds released deliberately or accidentally into the environment are xenobiotic in nature. Substituents like chlorine, bromine, and sulfonic acid and nitro groups occur relatively rarely in natural compounds; fluoro- and fluoroalkyl-substituted arenes and those with phenylazo groups are unknown. Besides the nature of the substituents, their number and position also confer xenobiotic character to synthetic compounds. For example, although methyl substituents occur widely in natural compounds, they can hinder the biodegradation of synthetic compounds. A methyl group vicinal to a substituent already present hinders the primary attack by oxygenases on aromatic structures and also hinders the degradation of aliphatic compounds by β-oxidation.

Since microorganisms have not been exposed to such xenobiotic structures during the course of evolution, corresponding degradation mechanisms have not been developed. The lack of specific enzymes for the degradation of xenobiotics in natural microbial communities is *one* of the reasons for the persistence of these compounds.

The enzymes produced by bacteria for the degradation of naturally occurring compounds do not have absolute specificity. Accordingly, xenobiotics undergo "gratuitous" changes in structure, which is referred to as cometabolism.[16] These reactions generally do not lead to the mineralization of xenobiotics, that is to say a complete breakdown into CO_2, H_2O, and inorganic nitrogen compounds etc. does not take place. Instead, complex product mixtures are produced which are subject to further biological and chemical reactions (see Section 6). The rate of such cometabolic reactions is generally slow for a number of reasons. Firstly, they do not generate any energy for the microorganism involved, and thus the active biomass does not increase. Secondly, the oxidative catabolism supporting the oxygenases actually requires energy (e.g. NADH). The only way to increase the rate of these reactions by external influences is by adding growth substances. Therefore cometabolism is referred to as unproductive, or when energy is lost and cell damage occurs it is even referred to as a counterproductive catabolism. Cometabolically active organisms therefore require a cosubstrate to provide energy and to induce the production of the cometabolically active enzymes.

5. Process Conditions and Cosubstrates Can Be Decisive

Despite the problems mentioned, many observations confirm the role of cometabolic transformations as the key reactions for the biodegradation of xenobiotics. A good illustration is provided by nitrobenzene, which can only be broken down with great difficulty by aerobic bacteria. In contrast, the ability to mediate the gratuitous reduction of nitrobenzene to yield aniline, in other words, the cometabolic reduction by nonspecific enzymes designed for other substrates, is generally present in anaerobic populations of bacteria. The reduction to aniline occurs rapidly in the presence of electron donors like glucose or alcohols, and the resulting aniline can be easily and completely broken down in a subsequent aerobic degradation step.[16a]

The nonspecific gratuitous reduction of xenobiotics can be applied to other electrophilic compounds. The potential of such reductions in making compounds that are difficult to tackle by oxidation accessable for complete biodegradation by aerobic microorganisms has remained largely untapped. It is possible, for example, to use gratuitous reduction to cleave azo compounds yielding aromatic amines, which can then be subjected to electrophilic attack by oxygenases (see Section 7). In the case of highly chlorinated compounds like tetrachloroethene or polychlorinated biphenyls (PCBs) some of the chlorine substituents can be reductively eliminated,[17, 18] which considerably reduces the persistence of such compounds to oxidative biodegradation by bacteria.

Whereas tetrachloroethene is only slowly attacked by oxygenases, the rate of reaction increases markedly in the following series trichloroethene (**12**), dichloroethene, and vinyl chloride.[19] Here, monooxygenases whose natural function is the oxidation of naturally occurring substances like methane, alkylarenes,[20] or alkenes[21] are particularly effective. Bacterial strains that degrade isoprene have proved to be especially effective.[22] In this case, a monooxygenase transforms isoprene (**9**) to 3,4-epoxy-3-methyl-1-butene (isoprene oxide, **10**) (Scheme 2), which in turn is hydrolyzed to diol **11** by a glutathione (GSH)-dependent enzyme. In contrast to methylotrophic bacteria, isoprene-degrading bacteria can tolerate high levels of trichloroethene (**12**). The methane monooxygenases from methylotrophic bacteria are

irreversibly inactivated by the reactive epoxide **13** produced by the cooxidation of **12**.[23] In contrast, in the same reaction with isoprene-degrading bacteria three equivalents of chloride are eliminated without any loss of activity. The advantage of isoprene (**9**) over methane as cosubstrate is that the latter, which is structurally related to **12**, stimulates the growth of those bacteria able to eliminate three equivalents of chloride by means of a epoxide hydrolase, thus protecting themselves against suicide inactivation. The release of three

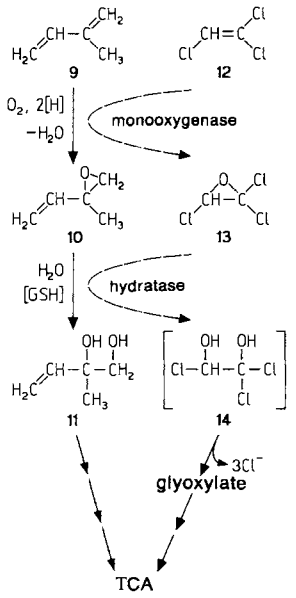

Scheme 2. Initial reactions of the degradation of isoprene and the cometabolism of trichloroethene (dotted arrows) by *Rhodococcus erythropolis* JE77. TCA = tricarboxylic acid cycle.

equivalents of chloride from **12** is also observed in its transformation by bacteria isolated with isopropylbenzene (cumene) as energy substrate.[20] In this case, it is apparent that a nonspecific isopropylbenzene-2,3-dioxygenase is responsible for the direct formation of **14**.

6. Bacteria Help Each Other in the Degradation of Xenobiotics

With more complex xenobiotics, structural alterations are possible by cooxidation reactions; however, complete degradation (i.e. mineralization) cannot be expected. The wide range of degradative activities of a typical mixed population of bacteria lead to products with at least as much variety. The aromatic 1,2-diols referred to in Section 3 are formed from aromatic compounds. These diols are not degraded further but undergo autoxidation and polymerization, which negatively influences the COD (chemical oxygen demand) elimination of biological wastewater treatment plants.

An improvement in the degree of biodegradation of a xenobiotic substance can be expected when the degradative activities present in a mixed microbial community complement each other, and the participation of several organisms finally leads to the mineralization of the substance concerned.

Such syntrophic interactions within mixed cultures actually occur and can lead to a complete mineralization of complex xenobiotic compounds. The aerobic degradation of 6-aminonaphthalene-2-sulfonate (**15**) illustrates this principle (Scheme 3).[24] The ability to partially degrade substituted naphthalenes to the corresponding salicylates is ubiquitous. The regioselective dioxygenation in the 1,2-position is of vital importance for the selection of baceteria that degrade naphthalene sulfonates (see also ref.[40]). This makes the

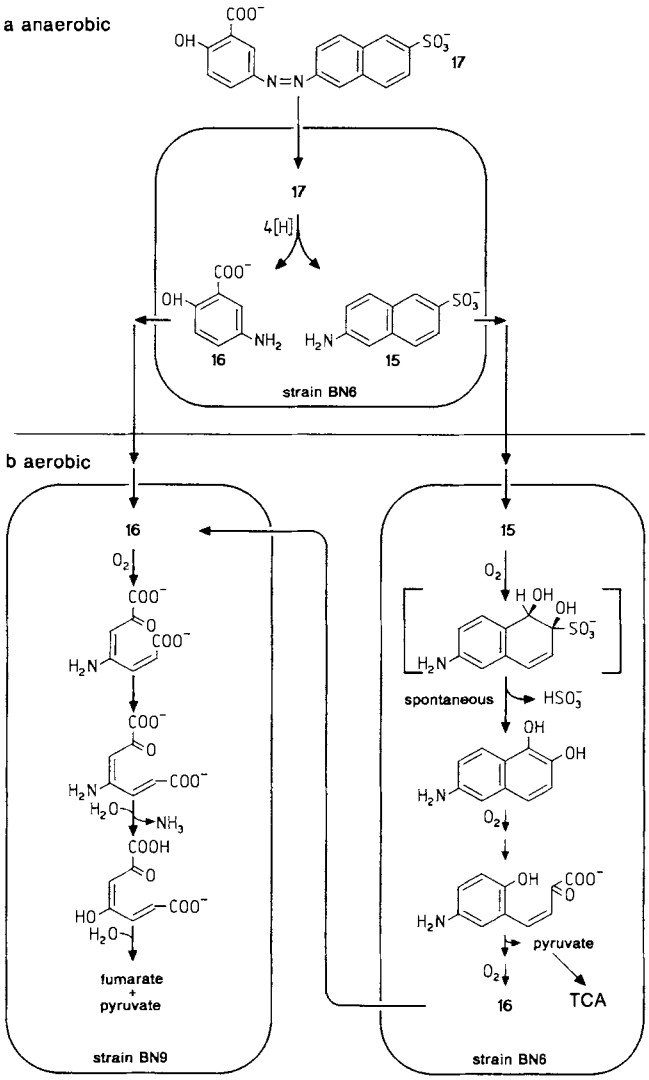

Scheme 3. Mineralization of mordant yellow (**17**) by an anaerobic–aerobic process using a syntrophic mixed culture. The reductive cleavage of **17** by cells of *Pseudomonas vesicularis* BN6 under anaerobic conditions (a) produces 6-aminonaphthalene-2-sulfonate (**15**) and 5-aminosalicylate (**16**) in a 1:1 molar ratio. These compounds are completely and productively degraded under aerobic conditions (b). After desulfonation and ring opening, strain BN6 obtains pyruvate as a utilizable metabolite. The **16** formed is excreted as a dead-end product, taken up by the accompanying *Pseudomonas* sp. BN9, and used as a growth substrate. For continuous degradation, biomass from the aerobic step must be returned to the anaerobic step.

C–S bond labile and leads to the cleavage of the sulfonic acid group generating sulfite. The reactions that follow correspond to the known degradative pathway for naphthalene and yield pyruvate, which serves as a growth substrate. On the other hand, this energy-yielding partial degradation also leads to the accumulation of toxic salicylates and their oxidation products which can damage bacteria. The complete and productive degradation of this xenobiotic is possible only when other bacteria are also present that are able to degrade

the 5-aminosalicylate (**16**) produced from **15** by using a complementary degradative pathway.

Typically, a stable continuous degradation process by this mixed culture[25] can only be achieved if the partner strains are attached to an inert support like quartz sand. The close contact of the cells attached to the support apparently facilitates the transfer of **16** from one strain of bacteria to the other. The immobilization of the bacteria completely prevents loss of substrate due to intermediates being misrouted or due to autoxidation of **16**.

Under anaerobic conditions the biomass of this mixed culture produced by the degradation of **15** is able to carry out the gratuitous reduction of sulfonated azodyes. Thus mordant yellow (**17**) is cleaved quantitatively to give **15** and **16** under anaerobic conditions (Scheme 3a), which are then completely mineralized in a final aerobic step.[26] The ability to reductively cleave the azo group is harbored only by cells of the strain BN6 when these have been grown in the presence of naphthalene sulfonates. Clearly only this organism has a transport system for sulfonates, which gratuitously also takes up **17** and thus makes the reduction possible.

7. Amino and Nitro Groups Can Serve as a Nitrogen Source

The use of a xenobiotic as a growth substrate generally requires the complete breakdown of the carbon skeleton into intermediates of basic metabolism. At some point in the degradative pathway the substituents responsible for xenobiotic character must be eliminated, mostly in the form of anions. Complex structures thus resist complete biodegradation, as this requires too many novel reaction steps. Therefore classical enrichment cultures, in which the xenobiotic is the single growth-limiting carbon and energy source for the bacteria, can fail. The xenobiotic appears to be nonbiodegradable.

However, changing the selection conditions can lead to a completely different appraisal of the biodegradability of the compound concerned. In the presence of an easily degradable substrate such as glucose or malate and under nitrogen-limiting conditions, those bacteria able to satisfy their nitrogen requirement through the elimination of amino or nitro groups have a distinct advantage. A complete degradative pathway is not necessary in this case; a single degradative enzyme, for example, an ammonia- or nitrite-eliminating dioxygenase suffices.

Sulfanilate **18**, which resists degradation under normal carbon-limiting growth conditions, is a good example here. In contrast to the metabolism of **15** (Scheme 3), **18** is first deaminated by cultures of *Hydrogenophaga palleronii* by means of a dioxygenase to provide 3,4-dihydroxybenzenesulfonate (**19**) (Scheme 4). This reaction corresponds to the deamination of the naturally occurring substance 4-aminobenzoate (**20**) to give protocatechuate (**21**). 4-Aminobenzoate serves as both a nitrogen and a carbon source for *H. palleronii* (strain S1) by assimilation by the protocatechuate-4,5-dioxygenase (P45O) pathway. Compound **19** is, however, not cleaved by this enzyme.

In contrast, *Agrobacterium radiobacter* (strain S2) is able to cleave both **21** and its structural analogue **19** between the

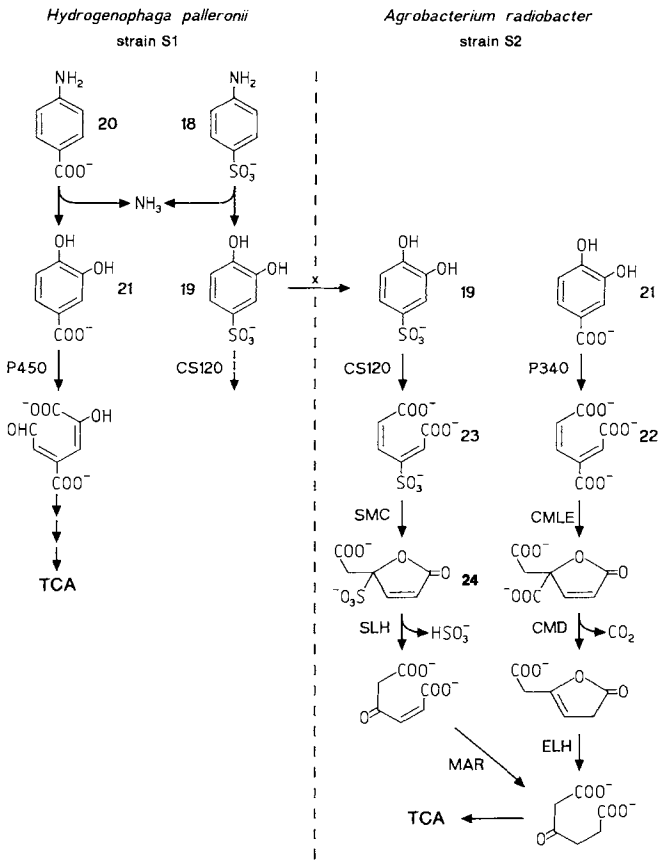

Scheme 4. Degradation of sulfanilate (**18**) by a syntrophic mixed culture: *Hydrogenphaga palleronii* (strain S1) utilizes 4-aminobenzoate (**20**) by conversion to yield protocatechuate (**21**) and deaminates **18** to give 3,4-dihydroxybenzenesulfonate (**19**). After an interspecies transfer of **19** (×), *Agrobacterium radiobacter* (strain S2) is largely responsible for the ring opening of this compound. This strain degrades **21** by the known 3-oxoadipate pathway. Compound **18** is assimilated by means of a pathway which is analogous to a large extent. However, it requires additional enzymes such as catechol-4-sulfonic acid 1,2-dioxygenase (CS12O), sulfomuconate cycloisomerase (SMC), sulfolactone hydrolase (SLH), and maleylacetate reductase (MAR). ELH = enollactone hydrolyse.

diol groups by means of a protocatechuate-3,4-dioxygenase (P34O). Subsequent mineralization of **19** and **21** takes place by a pathway analogous to the 3-oxoadipate pathway. Instead of the enzymes known from the protocatechuate pathway for ring cleavage of **21** (P34O) and cycloisomerization (CMLE) of the carboxymuconate **22**, the isoenzymes CS12O and SMC function in the transformation of the sulfur analogues substrates **19** and **23**. The elimination of sulfite from sulfolactone **24** requires the unique enzyme sulfolactone hydrolase (SLH), because the carboxymuconolactone decarboxylase (CMD) from the classical protocatechuate pathway cannot catalyze this reaction. The maleylacetate reductase (MAR) utilized in this pathway is not required in the protocatechuate pathway but is induced in the presence of **19** and is already known from degradative pathways for resorcinol and haloarenes. This enzyme allows these degradative sequences to converge with the 3-oxoadipate pathway.

When the bacterial strains S1 and S2 are cultured with **18** as the sole nitrogen, sulfur, and energy source, a stable syntrophy results.[27] Strain S2 is dependent on the initial elimination of ammonia by a regioselective dioxgenase from strain S1. In turn, strain S1 can use **18** as a nitrogen source

only because the enzyme CS12O cleaves intermediate **19** only very slowly under normal partial pressure of O_2. Exactly how *Hydrogenophaga* participates in the use of 3,4-dihydroxybenzenesulfonate as a source of carbon and energy is not yet clear.

In principle bacteria can also be isolated from nature, and under aerobic conditions they can cleave nitrite from nitroarenes and assimilate this as a nitrogen source. Under appropriate culture conditions even nitrophenols can be degraded, although they have previously been considered to be nonbiodegradable because of their high toxicity.[28] Interestingly, during selection with 2,4-dinitrophenolate (**25**) or picrate (**26**) as the sole nitrogen source, only gram-positive bacteria (mostly *Rhodococci*) grow. The strains that are isolated are found to be largely resistant to the uncoupling effect of these cell poisons.[29] Since **26** is not readily oxidized by oxygenases, the bacteria are forced to take an usual approach as shown in Scheme 5. They transfer H^- from NADPH to the aromatic ring without reducing the nitro groups.[30]

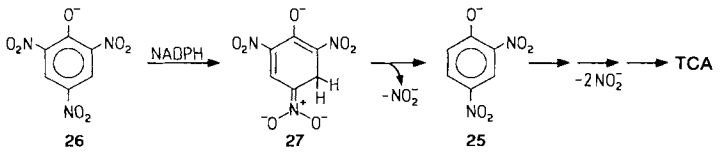

Scheme 5. *Rhodococcus erythropolis* HLPM1 utilizes picrate (**26**) and 2,4-dinitrophenol (**25**) as nitrogen source. It has been shown that the primary metabolite formed is the H^- Meisenheimer complex **27**, which is then degraded to **25** with the release of nitrite.

The resulting Meisenheimer complex **27** is stable and is cleaved by an additional enzyme to yield nitrite and simultaneously rearomatizes to yield **25**. The latter is completely degraded, and for each mole of **25** almost two moles of NO_2^- are released.

8. Tailor-Made Bacteria with Hybrid Degradative Pathways

Mixed cultures of microorganisms are almost always used in biological waste disposal technology. The wide variety of degradative potentials these mixed cultures display against organic substances of natural origin is much greater than that of a single species. However, complete mineralization and utilization of xenobiotics requires a complex interaction between partial activities within a mixed population, as in the degradations of **18** and **15**. This kind of syntrophic degradation is susceptible to many disturbing influences such as possible loss and misrouting of metabolites. Under real-world conditions a considerable portion of the xenobiotics is converted by cometabolic reactions into ill-defined, mostly dark-colored, high molecular weight products, which like humic substances are not suited for rapid biodegradation. This makes it clear that the interaction between microorganisms with complementary degradative abilities can be the weak link with regard to a complete degradation of xenobiotics. This is because xenobiotics or their metabolites can be misrouted into unproductive degradative pathways or be subject to abiotic reactions.

Bacterial cells that harbor complete degradative pathways and can degrade xenobiotics completely and productively should have a clear selective advantage. Under conditions of continuous cultivation in a sewage treatment system, the growth of such specialists that degrade xenobiotics productively, would automatically respond to the xenobiotics available, be self-regulating, and would suppress the level of unproductive degradation due to cometabolism.

In the degradation of chloronitrophenols, bacteria with complete degradative pathways readily arise under the appropriate selection conditions. Chloronitrophenols like other nitrophenols are highly toxic to bacteria because of their uncoupling effect on the respiratory electron transport chain. If the selection conditions are chosen so that 4-chloro-2-nitrophenol (**28**) is present in low concentrations ($\leq$ 0.5 mM) as the sole source of nitrogen in the presence of an readily utilizable compound (e.g. succinate), then bacteria can be easily isolated that convert **28** to 4-chlorocatechol (**29**) and nitrite by means of an oxygenation reaction (Scheme 6). Succinate already present and the nitrite produced make the growth of the bacteria possible.

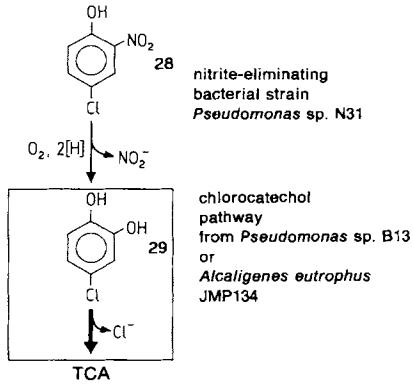

Scheme 6. Degradation of 4-chloro-2-nitrophenol (**28**) by a hybrid strain of *Pseudomonas* sp. N31 constructed in vivo.

The ability to partially degrade **28** to **29** can be easily selected for in the laboratory. However, in the real world, for example in a sewage treatment plant, this is hardly possible because nitrogen-limiting conditions necessary for its selection do not occur. In addition, the accumulating **29** is subject to autoxidation and is also toxic. In this case, bacterial strains can help that assimilate chlorocatechol and have this complementary ability (Scheme 7) on a transferable genetic element, for example on the plasmids pJP4, pWR1, or pAC25.[41] In this manner, hybrid strains with complete degradative pathways can evolve spontaneously. The bacteria produced by natural gene transfer completely degrade **28** and utilize this compound as the sole carbon, nitrogen, and energy source.[31]

As illustrated by the example of **28**, new hybrid degradative abilities for variety of other chloroarenes such as chlorobenzoates, chlorophenols, chloroanilines, chlorosalicylates, chlorobenzenes, phenoxyacetates,[41] and chlorobiphenyls[39] can be developed by natural gene transfer.[32] The basis of this evolutionary potential are natural cometabolic activities that cooxidize chloroarenes to chlorocatechols. Enzymes that degrade methylarenes are especially

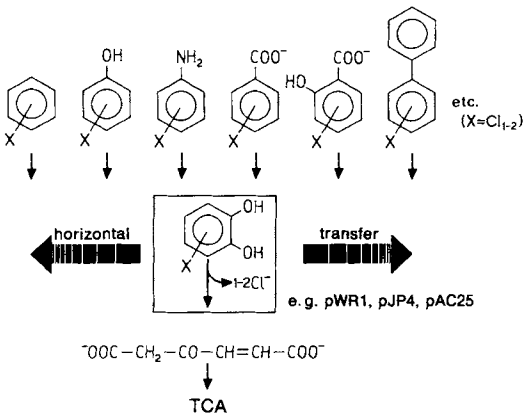

Scheme 7. The principle of the evolution of hybrid degradative pathways for chloroarenes. Chloroarenes are cometabolized by arene- or methylarene-degrading bacteria to give chlorocatechols. The acquisition of the genes for chlorocatechol degradation (see Scheme 8) can lead to the formation of hybrid degradative pathways making the complete degradation of the chloroarenes possible. Donor strains for these genes are bacteria that utilize **30** or **31** and have the catabolic information on plasmids such as pWR1, pJP4, or pAC25.

effective, since the corresponding chloro-substituted compounds are structural analogues of the natural substrates.

Bacteria with the complementary property necessary for the assimilation of chlorocatechol make up a minor part of natural populations; however, they are ubiquitous. Such specialists can be easily enriched from water and soil samples by using less toxic substrates such as 3-chlorobenzoate (**30**) and 2,4-dichlorophenoxyacetate (**31**) (Scheme 8),[33] leading to their isolation as pure cultures.

Interestingly, the catabolic sequences for **30** and **31** are analogous to the classic pathway of benzoate (3-oxadipate or *ortho* pathway, Scheme 8). Certain enzymes, for example chlorocatechol-1,2-dioxygenases (CC12O) and chloromuconate cycloisomerases (CMC and DCMC), are isoenzymes that act on the normal halogen-free substrates as well. These enzymes are only induced during growth on **30** (*Pseudomonas* sp. B13) or **31** (*Alicaligenes eutrophus*). The normal catechol-1,2-dioxygenase (C12O) and muconate cycloisomerase (MC) of the 3-oxoadipate pathway are not very effective with the chloro-substituted metabolites.

The high level of homology in the amino acid sequence of the isoenzymes indicates that they evolved from the corresponding proteins of the classical *ortho* pathway. From the frequency of the alterations in the DNA sequence which are not expressed in the amino acid sequences, it can be estimated that at least the enzymes CMC of the 3-chlorobenzoate degradative pathway and DCMC of the 2,4-dichlorophenoxyacetate degradative pathway diverged from the classical muconate cycloisomerases (MC) long before anthropogenic substrates (products of the chemical industry) could act to speed up the evolution of these proteins.[34]

The sulfolactone-hydrolyzing enzyme (SLH in Scheme 4) from the sulfocatechol pathway previously discussed has no analogue in the protocatechuate pathway with respect to its catalytic effect. The dienelactone hydrolase (DLH) of the modified *ortho* pathway (Scheme 8) is an enzyme that only attacks the dienelactones **32** and **33**, and not the corresponding lactone from the classical *ortho* pathway (benzoate route in Scheme 8).[35] The extent to which these hydrolases may be related is the subject of current investigations.

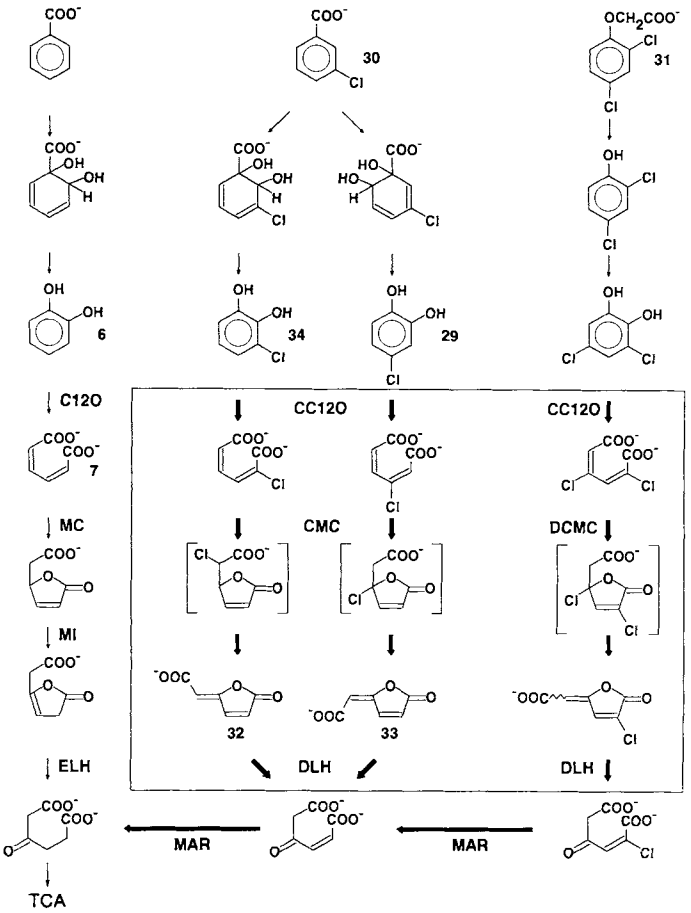

Scheme 8. Reaction sequences for the degradation of chloro- and dichloroarenes such as 3-chlorobenzoate (**30**) and 2,4-dichlorophenoxyacetate (**31**) exist in bacteria (e.g. *Pseudomonas* sp. B13 and *Alicaligenes eutrophus* JMP134). These are analogous to the known *ortho* pathway (catechol branch of the 3-oxoadipate pathway[8]). During growth on chloroarenes, specific enzymes are induced for the chlorocatechols showing high activity with the metabolites concerned. (Enzymes of the "modified *ortho* pathway" are indicated by heavy arrows).

Normally the classical[8] and the modified *ortho* pathway coexist. The genes coding for the former are usually on the chromosome, whereas the genes of the latter are plasmid encoded (shown in frames in Schemes 6, 7, and 8), and the corresponding enzymes are only induced in the presence of chlorinated compounds. In the case of substrate mixtures of arenes and chloroarenes the pathways coexist without affecting each other.

A completely different situation (and for the bacteria a fatal one) arises when chloro- and methylarenes are present at the same time.[36] The latter induce the enzymes of the *meta* pathway.[8] Because of the steric analogy, *meta*-pyrocatechase cleaves not only methyl- but chloro-substituted catechols as well (Scheme 9). Thus compound **34** is converted into acylchoride **35**, which irreversibly inactivates the ring-cleaving enzyme by acylation. The *meta* cleavage of **29** leads to the formation of stable chlorine-containing "dead-end" metabolites, primarily 5-chloro-5-formyl-2-hydroxypenta-2,4-dienoate (**36**).

It is evident that the *meta* pathway is not only unproductive for the degradation of chloroarenes but that it also loses its effectiveness for the productive degradation of methylarenes in the presence of high concentrations of chloro-

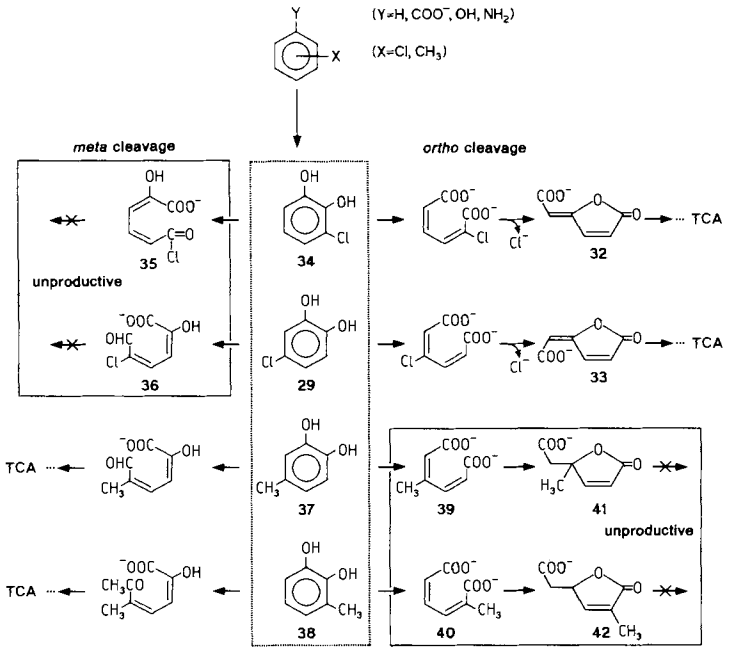

Scheme 9. Because of the relaxed specificity of the chlorocatechol-degrading enzymes (modified *ortho* pathway in Scheme 8) and the catechol-2,3-dioxygenase of the *meta* pathway[8], methyl- and chloroarenes can be misrouted into the *ortho* and *meta* pathway, respectively. This can lead to substrate incompatibilities when, for example, mixtures of chloro- and methylarenes are present and both pathways are induced at the same time.

arenes due to inactivation of catechol-2,3-dioxygenase. In addition, the incompatibility of methyl- and chloroarenes is amplified, since methylcatechols **37** and **38** can easily be misrouted to the modified *ortho* pathway for the degradation of chlorocatechol. This degradation also leads to a dead end, because the corresponding methylmuconic acids **39** and **40** cannot form dienelactones. Methyllactones **41** and **42** are thus dead-end metabolites that each accumulate as only one enantiomer by means of enzymatic cycloisomerization.

The previously mentioned evolution of new degradative pathways for chloroarenes using enzymes from the degradation of methylarenes requires the inactivation of the *meta* pathway essential for the degradation of methylarenes.[8] Thus bacterial strains that have acquired the ability to degrade chloroarenes have simultaneously lost the ability to utilize methylarenes. Typically, unstable hybrid strains are formed at first, which in the presence of chloroarenes switch off the *meta* pathway by the suicide inactivation of C23O. When the culture is incubated in the presence of chloroarenes over longer periods, rapid-growing spontaneous mutations take over. In these mutants the structural gene for C23O has been inactivated by insertion, and thus the expensive regulation by suicide inactivation of C23O is circumvented.[37]

9. The Last Resort: Degradative Strains Manipulated In Vitro

Although there are microorganisms that can degrade chloroarenes or can rapidly evolve this ability by recruiting enzymes from the methylarene degradation pathway, it is clear that the simultaneous occurrence of methyl- and chloroarenes is fatal. One approach to making the complete and productive degradation of this incompatible substrate mixture possible would be a multifunctional *ortho* pathway. Not only would arenes and chloroarenes be assimilated by such a pathway, but methylarenes would also be accessible as growth substrate by *ortho* cleavage.[36]

Pseudomonas sp. B13 is almost ideal for the development of such a multifunctional *ortho* pathway (Scheme 10), because this organism degrades catechol (**6**) and the chlorocatechols **34** and **29** by *ortho* cleavage and does not have the *meta*-cleaving activity that interfers with chloroarene degradation. For the assimilation of **37** one enzyme is missing which would transform **41** into the isomeric 3-methyllactone **43**. This lactone is then, like the muconolactone of the known *ortho* pathway (Scheme 7), isomerizable to the enol-lactone and fully degradable in an analogous reaction sequence.

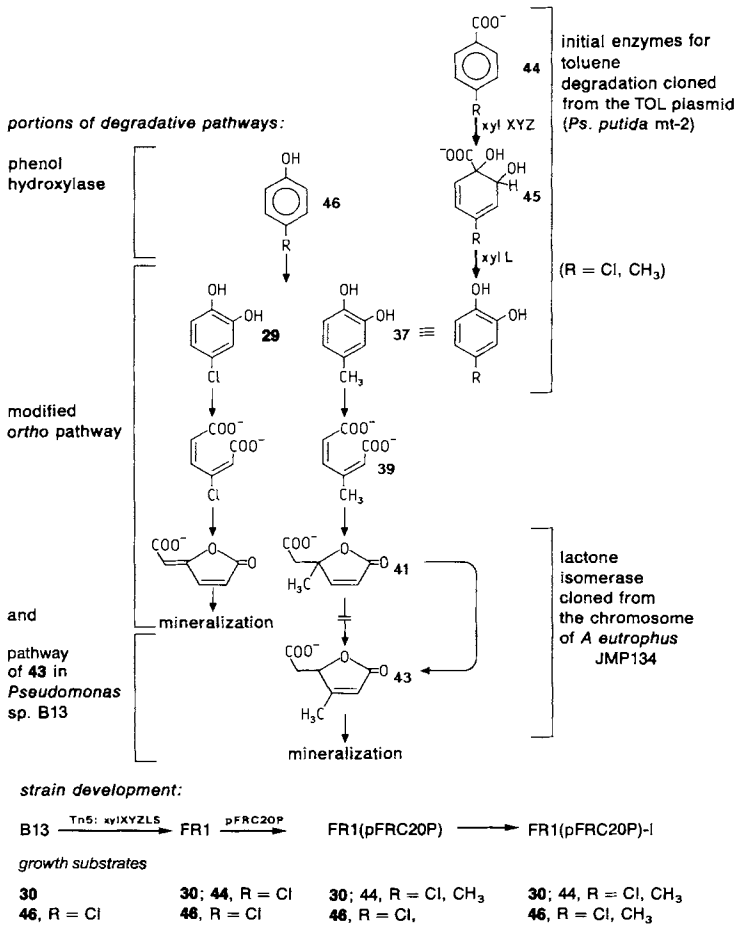

Scheme 10. The construction of a hybrid degradative pathway in vitro for the simultaneous degradation of chloro- and methylarenes. The strain *Pseudomonas* sp. B13 acquires the ability to degrade 4-chlorobenzoate (**44**, R = Cl) by the insertion of the genes for the initial enzymes of toluene degradation (TOL plasmid). The gene for lactone isomerase recruited in addition from the chromosome of *Alicaligenes eutrophus* makes the degradation of 4-methylbenzoate (**44**, R = CH_3) possible. The constructed strain FR1(pFRC20P) can simultaneously utilize 4-chlorobenzoate and 4-methylbenzoate, and after a spontaneous mutation (strain FR1(pFRC20P)-1)) 4-chlorophenol (**46**, R = Cl) and 4-methylphenol (**46**, R = CH_3) as well.

The gene for the required lactone isomerase is found on the chromosome of *Alcaligenes eutrophus* JMP134. After being cloned on the cosmid vector pFRC20P, the property was transferred by conjugation to the B13 strain. In order to

enable the new ability (assimilation of **37** by *ortho* cleavage) to be applied to a selective growth substrate, the genes for the enzymes of the initial degradation of toluene were transposed into the chromosome of the B13 strain by means of a hybrid transposon (Tn5: xylXYZLS). The gene products toluate-1,2-dioxygenase (xylXYZ), cyclohexadienediol-1-carboxylate dehydrogenase (xylL), and the regulatory gene (xylS) provide the B13 strain with initial enzymes of low substrate specificity and at the same the ability to utilize 4-chlorobenzoate (**44**, R = Cl). Through the conjugative recruitment of the isomerase the ability to degrade 4-methylbenzoate (**44**, R = CH_3) was also acquired. The derivative strain thus constructed FR1(pFRC20P) simultaneously degrades 4-chloro- and 4-methylbenzoate (**44**, R = Cl and CH_3, respectively) without any of the substrate mixture being misrouted or released as dead-end metabolites into the culture medium.

Mixtures of chlorophenols and cresols are more relevant than chloro- and methylbenzoates to actual environmental problems. Since strain B13 can completely degrade 4-chlorophenol (**46**, R = Cl), it should be able to acquire the ability to degrade cresol. This requires a spontaneous mutation (rate of mutation 10^{-7}–10^{-8}) that enables the bacterium (strain FR1(pFRC20P)-1) to recognize cresol (**46**, R = CH_3) as an inducer for chlorophenol hydroxylase.

The example of the simultaneous degradation of chloro- and methylarenes shows that the evolution of complex degradative pathways requires multiple genetic changes (see ref.[38]). Since these must occur successively and selection favors only the last evolutionary step, this process can occur only very slowly in nature. Clearly the recombination of activities already present in nature for partial degradation to provide new, active degradative sequences for xenobiotics requires a carefully drawn blueprint. Each evolutionary step must be linked to a corresponding selection principle. If this is the case, then genetic manipulation allows crucial reaction steps to be overcome. The evolution and degradative potential of natural bacterial populations against structurally related xenobiotics can be decisively increased by mobilizing specific genes and blocks of genes encoding nonspecific multifunctional degradative sequences.

A major advantage of experimental evolution of degradative pathways is that planned and targeted evolution may be possible. This, however, requires detailed knowledge of the biochemistry and regulation of xenobiotic degradation as well as the analysis of the genes involved.

Unfortunately, this basic knowledge is not available for the majority of xenobiotics relevant in practice. Thus the current application of biodegradation to problems in the real world is characterized by a pragmatic, scientifically not very demanding approach. To increase the degradative performance of natural microbial populations against xenobiotics, methods that satisfy the nutrient and energy requirements of the organisms involved, or the use of auxiliary substrates that increase the number of cometabolically active organisms and therefore favor natural gene transfer are still the methods of choice given the current state of knowledge.

Received: November 5, 1992 [A918IE]
German version: *Angew. Chem.* **1993**, *105*, 1437
Translated by Dr. M. Griffiths, Edingen (FRG)

[1] F. Bolle, *Mensch und Mikrobe*, Safari, Berlin, **1954**, pp. 12–94.
[2] M. Vasold, *Pest, Not und schwere Plagen*, C. H. Beck, Munich, **1991**.
[3] O. Günther, *Forum Mikrobiol.* **1980**, 8–10.
[4] H. G. Schlegel, *Allgemeine Mikrobiologie*, 7th ed., Thieme, Stuttgart, **1992**, pp. 1–12.
[5] S. H. Schneider, *Sci. Am.* **1989**, 38–47.
[6] A. Balows, H.-G. Trüper, M. Dworkin, W. Harder, K.-H. Schleifer, *The Prokaryotes*, Springer, Berlin, **1992**.
[7] K. Horikoshi, *Microorganisms in Alkaline Environments*, VCH, Weinheim, **1991**.
[8] G. Gottschalk, *Bacterial Metabolism*, 2nd ed., Springer, Berlin, **1986**.
[9] T. A. Krulwich, *Bacterial Energetics*, Academic Press, New York, **1990**.
[10] P. Dürre, H. Bahl, G. Gottschalk in *Handbook on Anaerobic Fermentations* (Eds.: L. E. Erickson, D. Y.-C. Fung), Dekker, New York, **1988**, pp. 187–206.
[11] A. Inoue, K. Horikoshi, *Nature* **1989**, *338*, 264–265.
[12] S. Fetzner, R. Müller, F. Lingens, *J. Bacteriol.* **1992**, *174*, 279–290.
[13] K. König, J. R. Andreesen, *Bioengineering* **1992**, *8*, 78–84.
[14] L. Johnson, K. V. Rajagopalan, O. Meyer, *Arch. Biochem. Biophys.* **1990**, *283*, 542–545.
[15] K. König, Dissertation, Universität Göttingen, **1991**.
[16] a) D. Janke, W. Fritsche, *J. Basic Microbiol.* **1985**, *25*, 603–619; b) O. Dickel, H.-J. Knackmuss, *Biodegradation* **1993**, in press.
[17] W. W. Mohn, J. M. Tiedje, *Microbiol. Rev.* **1992**, *56*, 482–507.
[18] A. H. Neilson, *J. Appl. Bacteriol.* **1990**, *69*, 445–470.
[19] J. Ewers, Dissertation, Universität Stuttgart, **1991**.
[20] a) B. Dabrock, J. Riedel, J. Bertram, G. Gottschalk, *Arch. Microbiol.* **1992**, *158*, 9–13; b) B. Dabrock, B. Averhoff, G. Gottschalk, unpublished.
[21] B. D. Ensley, *Annu. Rev. Microbiol.* **1991**, *45*, 283–299.
[22] J. Ewers, D. Freier-Schröder, H.-J. Knackmuss, *Arch. Microbiol.* **1990**, *154*, 410–413.
[23] B. G. Fox, J. G. Bornemann, L. P. Wackett, J. D. Lipscomp, *Biochemistry* **1990**, *29*, 6419–6427.
[24] B. Nörtemann, J. Baumgarten, H. G. Rast, H.-J. Knackmuss, *Appl. Environ. Microbiol.* **1986**, *52*, 1195–1202.
[25] D. C. Hempel, M. Lindert, *GWF Gas-Wasserfach: Wasser/Abwasser* **1990**, *131*, 528–535.
[26] W. Haug, A. Schmid, B. Nörtemann, D. C. Hempel, A. Stolz, H.-J. Knackmuss, *Appl. Environ. Microbiol.* **1991**, *57*, 3144–3149.
[27] B. Feigel, H.-J. Knackmuss, *Arch. Microbiol.*, **1993**, *159*, 124–130.
[28] C. Bruhn, H. Lenke, H.-J. Knackmuss, *Appl. Environ. Microbiol.* **1987**, *53*, 208–210.
[29] H. Lenke, D. H. Pieper, C. Bruhn, H.-J. Knackmuss, *Appl. Environ. Microbiol.* **1992**, *58*, 2928–2932.
[30] H. Lenke, H.-J. Knackmuss, *Appl. Environ. Microbiol.* **1992**, *58*, 2933–2937.
[31] C. Bruhn, R. C. Bayly, H.-J. Knackmuss, *Arch. Microbiol.* **1988**, *150*, 171–177.
[32] W. Reineke, H.-J. Knackmuss, *Annu. Rev. Microbiol.* **1988**, *42*, 263–287.
[33] M. L. Rochkind-Dwbinsky, G. S. Sayler, J. W. Blackburn, *Microbiological Decomposition of Chlorinated Aromatic Compounds*, Dekker, New York, **1987**.
[34] M. Schlömann, *Biologische Abwasserreinigung 1, Biologischer Abbau von Chlorkohlenwasserstoffen*, (Ed.: B. Weigert), Technische Universität Berlin, **1992**, pp. 87–109.
[35] M. Schlömann, D. H. Pieper, H.-J. Knackmuss, *Pseudomonas: Biotransformation, Pathogenesis, and Evolving Biotechnology*, (Eds.: S. Silver, A. M. Chakrabarty, B. Iglewski, S. Kaplan), Am. Soc. Microbiol., Washington, **1990**, pp. 185–196.
[36] F. Rojo, D. H. Pieper, K. H. Engesser, H.-J. Knackmuss, K. N. Timmis, *Science* **1987**, *238*, 1395–1398.
[37] W. Reineke, *J. Basic Microbiol.* **1986**, *26*, 551–567.
[38] J. R. van der Meer, W. M. de Vos, S. Harayama, A. H. B. Zehnder. *Microbiol. Rev.* **1992**, *56*, 677–694.
[39] J. Havel, W. Reineke, *FEMS Microbiol. Lett.* **1991**, *78*, 163–170.
[40] A. M. Cook, T. Leisinger in *Environmental Biotechnologie* (Eds.: H. Verachtert, W. Verstraete), Koninklijke Vlaamse Ingenieursvereiniging, Brussels, **1991**, pp. 353–367.
[41] W. M. Coco, U. M. X. Sangodkar, R. K. Rothmel, A. M. Chakrabarty in *Biotechnology and Biodegradation* (Eds.: D. Kamely, A. M. Chakrabarty, G. S. Omenn), Gulf Publishing Company, **1990**, pp. 43–59.

Triplet States in Organic Chemistry**

By *Harry Kurreck**

After the successful characterization of a hexacarbene in the tridecet ground state in 1992, the synthesis of a branched nonacarbene with an $S = 9$ ground state was recently published in this journal[1] and described as a new record on the way to supermagnetic polycarbenes. This nonacarbene is an unusual molecule with 18 unpaired electrons, if the spin pairing is considered as the basis of the chemical bonding. In carbene chemistry such systems, even though constructed from fewer carbene units, could be detected by EPR spectroscopy, that is those with four (quintet state), six (septet state), and ten (undecet state) unpaired electrons.[2]

The quite optimistic announcement of J. U. Nef in 1895 can be considered as the beginning of the history of organic triplet molecules: "It will now be my next task to prepare methylene or its derivatives".[3] Later from the investigation of the electronic properties of carbenes it was postulated that singlet carbenes are added stereospecifically to the olefinic double bond, whereas triplet carbenes are added nonstereospecifically (Skell rule).[4] After the classical optical experiments on methylene by Herzberg in 1961,[5] R. A. Bernheim et al. and E. Wasserman et al., 75 years after Nef, were able to identify the parent carbene methylene by its triplet state clearly as the expected paramagnetic species by EPR spectroscopy.[6]

Triplet molecules have become increasingly more important in many areas of organic, bioorganic, and biophysical chemistry. They can be classified according to their ground and excited states into "real" triplet molecules, characterized by a strong coupling of the unpaired electrons, and diradicals, which show a weak coupling of the unpaired electrons. The latter, in particular, can be further divided into triplet molecules with completely delocalized triplet electrons which belong to a common π-electron system, and into diradicals in which the π-electron systems of the radical fragments are localized to a great extent; in the limiting case the so-called point/dipole approximation is valid. These types of triplet states show markedly different chemical and physical (magnetic) properties.

The galvinoxyls (Coppinger radicals), named after Galvin Coppinger, derivable from phenoxyl are appropriate for the description of the diradicals.[7] According to EPR investigations, if two such components are linked, for example, by a *para*-phenylene bridge, the diradical **1** is formed with a triplet ground state, in which the unpaired electrons are weakly coupled and are located in almost completely separate π-electron systems. Thus, the point/dipole model can be used and an average distance between the unpaired electrons can be determined from the zero field splitting value which is consistent with the structure derived from molecular modeling calculations. If three galvinoxyl fragments are linked together through the 1,3,5 positions of a benzene ring, the triradical **2** in the quartet state can be identified with EPR and electron nuclear double resonance (ENDOR) spectroscopy. Finally, four *para*-positioned galvinoxyl units can be linked by a tetraphenylmethane bridge; the tetraradical **3** with tetrahedral symmetry in the quintet state is formed with properties basically the same as those of the diradical and the triradical. Other known bridged radicals are, for example, the triphenylmethyl radical derivatives (Tschitschibabin and Schlenk hydrocarbons), double cyclopentadienyl radicals (Ziegler radicals), or double nitroxide radicals.

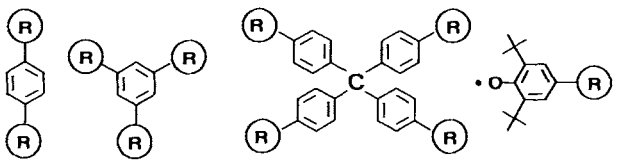

1 **2** **3** **4**

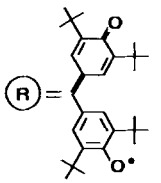

If an additional phenoxyl component is introduced into the galvinoxyl fragment, the Yang diradical **4** is obtained, which provides an interesting transition into the family of the real triplet molecules with complete delocalization of the unpaired electrons in a common π-electron system; here their coupling, however, is still classified as *weak*. Indeed, EPR and ENDOR investigations reveal a diradical with threefold symmetry in the triplet state; thus, the two unpaired electrons are delocalized over three substituted phenyl wings arranged in the form of a propeller and therefore their complete equality is retained. In this context the recent studies from the laboratory of H. Bock on the successful crystallization and X-ray structure analysis of the Yang biradical are of particular interest,[8] because these also confirm the results of the spectroscopic investigations carried out in solution and thereby the axial symmetry of the molecule with phenoxyl rings that are likewise tilted away from the plane by about 30°. Quantum mechanical calculations show that the spin density of the unpaired electrons is localized to about 50% at the outermost centers of the molecule, whereas the charges at these positions are so small that they can be neglected.

A genuine ground state triplet molecule with a triplet state more stable than the singlet state structurally related to the Yang diradical by about 110 kJ mol^{-1} is the axial symmetric trimethylenemethane **5**, whose two degenerate HOMOs, ac-

[*] Prof. Dr. H. Kurreck
Institut für Organische Chemie der Freien Universität
Takustrasse 3, D-14195 Berlin (FRG)
Telefax: Int. code + (030)838-4248

[**] I would like to thank Priv.-Doz. Dr. B. Kirste, Berlin, for constructive comments on the manuscript and for the long-time collaboration on the spectroscopy of diradicals.

cording to Hund's rule, are each occupied with one electron of the same spin.[9]

Non-Kekulé hydrocarbons, such as triangulene **6** (Clar hydrocarbon), for which no classical Kekulé structures can be formulated, are characterized by the fact that not all the spins of the electrons of the π-electron system are paired. The triangulene with two half-filled degenerate MOs should, therefore, have a triplet ground state and be paramagnetic; however, this has not been proved to date. Recently, however, a derivative, the trianion **7** of trioxytriangulene, was prepared and identified by EPR spectroscopy as a diradical triplet molecule of threefold symmetry.[10] The diradical is remarkably stable under the exclusion of oxygen, even at room temperature.

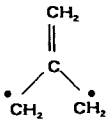

5

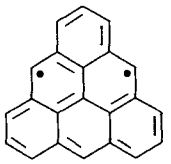

6

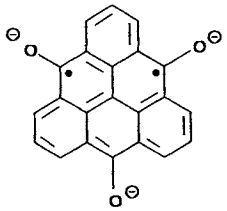

7

Triplet states have also played a role in the history of the concept of aromaticity [$(4n + 2)\pi$ electrons, Hückel's rule] with the proof of an antiaromatic molecule with $4n\pi$ electrons. Exactly 20 years ago, in a fundamental work on the chemistry and spectroscopy of the electron spin states of higher multiplicity, three research groups joined forces and proved the triplet ground state (predicted according to simple HMO concepts) for the unsubstituted cyclopentadienyl cation by EPR spectroscopy, and thus determined its "antiaromatic" character.[11] In this context the antiaromatic compound par excellence, cyclobutadiene, should not go unmentioned, for which a triplet ground state had been proposed for decades. In particular, the studies of G. Maier et al.[12] (photochemical generation and matrix isolation of cyclobutadiene at low temperatures) and of D. C. Cram et al.[13] (taming and thus stabilization of cyclobutadiene in a hemicarcerand even at room temperature) derived a singlet ground state[14] for the "Mona Lisa of organic chemistry".[13]

Hitherto only triplet ground states—resulting from the geometry of the molecule—have been considered. Triplet excited states are of significance in photochemistry both from a mechanistic and (due to their long lifetime in comparison to singlet excited states) a preparative point of view. As an example, the double photocyclization of norbornadiene (**8**) shall be discussed. Whereas on irradiation norbornadiene (**8**) reacts only slightly to give a little quadricyclane (**9**), this photoreaction proceeds in high yield by the addition of small quantities of benzophenone. Apparently, the substrate is converted into the triplet state by the sensitizer with great efficiency and with structural changes; an optimal geometry for the ring closure is employed.[15]

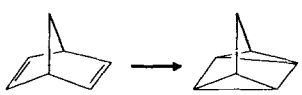

8 **9**

At present one cannot resist the temptation to include the fashionable molecules of the nineties, the fullerenes, in *Highlights*. The intensive investigations of these molecular footballs also include photochemically produced triplet states in solution, in liquid crystalline matrix, and in the solid state. The interpretation of the spectroscopic results, for example, the unequivocal identification of the triplet states and their differentiation from doublet states, is the subject of ongoing discussions. Apparently, however, due to Jahn–Teller distortion the triplet state is not of I_h symmetry, and the two Jahn–Teller states are rapidly interconverted.[16]

Triplet states are also of current significance in photobiology. Here, the light-induced charge separation taking place in the primary step in the reaction centers of the photosynthesis apparatus may be shown.[17] Today these electron transfer steps are considered to occur over singlet states, however, triplet states can occur if, for example, the electron flow in the transport chain is "blocked" by too intense light irradiation. Then under back-electron transfer the triplet state of the primary donors, and thus of chlorophyll or of bacteriochlorophyll, can be formed. This state can also be forced artificially by the prereduction of the quinone, which serves as the primary electron acceptor, because then the complete charge separation of the primary process is blocked. In the study of photosynthesis model compounds from porphyrin donors and quinone acceptors triplet states and triplet electron transfer processes could likewise be proven; the membrane orientation of native pigments can be modeled by the incorporation of the donor/acceptor systems in liquid crystals.[18]

Finally two more experiments taken from the world of curiosities deserve mention: 1. If dibenzyl ketone (advantageous in micellar systems) is irradiated, the corresponding radical pair with triplet character is formed by the homolytic bond cleavage of the bond between the carbonyl-C atom and the CH_2-C atom. If one ensures a long lifetime of these radical pairs in solvent cages—or in a micelle—the molecules with a carbonyl ^{13}C atom attain singlet character quicker by ^{13}C hyperfine interaction and can recombine. Thus, in the reformed starting material, a ^{13}C enrichment can be achieved with *sunlight and soap*.[19] 2. If a mixture of crystals of a donor (zinc tetraphenylporphyrin) and an acceptor (substituted quinones) is ground in a agate mortar, intense typical EPR powder spectra of a triplet ground state can be observed. The authors assume that this triplet ground state is generated by a mechanochemically induced electron transfer with the formation of the stable diradical zinc tetraphenylporphyrin radical cation/semiquinone-radical anion.[20]

Triplet states are not only of high diagnostic value for quantum mechanical or mechanistic studies, they are also of significance for applied fields of research. Excited states of the fullerenes in the solid state and crystalline triplet diradicals such as the described Yang diradical are of interest for material sciences, because of their possible ferromagnetism. In photosynthetic research, contributions to the understanding of the high efficiency of the photosynthesizing systems are to be expected, which, for example, could be of signifi-

cance in the development of regrowing raw materials or more generally for the use and in the storage of solar energy.

German version: *Angew. Chem.* **1993**, *105*, 1472

[1] N. Nakamura, K. Inoue, H. Iwamura, T. Fujioka, Y. Sawaki, *J. Am. Chem. Soc.* **1992**, *114*, 1484; N. Nakamura, K. Inoue, H. Iwamura, *Angew. Chem.* **1993**, *105*, 900, *Angew. Chem. Int. Ed. Engl.* **1993**, *32*, 872; Review: H. Iwamura, N. Koga, *Acc. Chem. Res.* **1993**, *26*, 346.

[2] K. Itoh, *Chem. Phys. Lett.* **1967**, *1*, 235; T. Takui, K. Itoh, *ibid.* **1973**, *19*, 120; I. Fujita, Y. Teki, T. Kinoshita, K. Itoh, F. Miko, Y. Sawaki, H. Iwamura, A. Izuoka, T. Sugawara, *J. Am. Chem. Soc.* **1990**, *112*, 4074.

[3] J. U. Nef, *Justus Liebigs Ann. Chem.* **1895**, *287*, 359.

[4] P. S. Skell, R. C. Woodworth, *J. Am. Chem. Soc.* **1956**, *78*, 4496.

[5] G. Herzberg, *Proc. R. Soc.* **1961**, *262A*, 291.

[6] R. A. Bernheim, H. W. Bernard, P. S. Wang, L. S. Wood, P. S. Skell, *J. Chem. Phys.* **1970**, *53*, 1280; E. Wasserman, W. A. Yager, V. J. Kuck, *Chem. Phys. Lett.* **1970**, *7*, 409.

[7] K. Schubert, B. Kirste, H. Kurreck, *Angew. Chem.* **1983**, *95*, 149, *Angew. Chem. Int. Ed. Engl.* **1983**, *22*, 150; M. Grimm, B. Kirste, H. Kurreck, *ibid.* **1986**, *98*, 1095 and **1986**, *25*, 1097; B. Kirste, M. Grimm, H. Kurreck, *J. Am. Chem. Soc.* **1989**, *111*, 108, and references therein.

[8] H. Bock, A. John, Z. Havlas, J. W. Bats, *Angew. Chem.* **1993**, *105*, 416, *Angew. Chem. Int. Ed. Engl.* **1993**, *32*, 416.

[9] O. Claesson, A. Lund, T. Gillbro, T. Ichikawa, O. Edlund, H. Yoshida, *J. Chem. Phys.* **1980**, *72*, 1463, and references therein.; see also G. Maier, H. P. Reisenauer, K. Lanz, R. Tross, D. Jürgen, B. A. Hess, Jr., L. J. Schaad, *Angew. Chem.* **1993**, *105*, 119; *Angew. Chem. Int. Engl.* **1993**, *32*, 74.

[10] G. Allinson, R. J. Bushby, J.-L. Paillaud, D. Oduwole, K. Sales, *J. Am. Chem. Soc.* **1993**, *115*, 2062.

[11] M. Saunders, R. Berger, A. Jaffe, J. M. McBride, J. O'Neill, R. Breslow, J. M. Hoffmann, Jr., C. Perchonock, E. Wasserman, R. S. Hutton, V. J. Kuck, *J. Am. Chem. Soc.* **1973**, *95*, 3017.

[12] G. Maier, H.-G. Hartan, T. Sayrac, *Angew. Chem.* **1976**, *88*, 252; *Angew. Chem. Int. Ed. Engl.* **1976**, *15*, 226.

[13] D. C. Cram, M. E. Tanner, R. Thomas, *Angew. Chem.* **1991**, *103*, 1048; *Angew. Chem. Int. Ed. Engl.* **1991**, *30*, 1024.

[14] See also T. Bally, S. Masamune, *Tetrahedron* **1980**, *36*, 343; and references therein.; J. Wirz, A. Krebs, H. Schmalstieg, H. Angliker, *Angew. Chem.* **1981**, *93*, 192; *Angew. Chem. Int. Ed. Engl.* **1981**, *20*, 192.

[15] G. S. Hammond, P. Wyatt, C. D. DeBoer, N. J. Turro, *J. Am. Chem. Soc.* **1964**, *86*, 2532.

[16] G. Closs, P. Gautam, D. Zhang, P. J. Krusic, S. A. Hill, E. Wasserman, *J. Phys. Chem.* **1992**, *96*, 5228; M. Terazima, N. Hirota, H. Shinohara, Y. Saito, *Chem. Phys. Lett.* **1992**, *195*, 333; H. Levanon, V. Meiklyar, A. Michaeli, S. Michaeli, A. Regev, *J. Phys. Chem.* **1992**, *96*, 6128; E. J. J. Groenen, O. G. Poluektov, M. Matsushita, J. Schmidt, J. H. van der Waals, G. Meijer, *Chem. Phys. Lett.* **1992**, *197*, 314.

[17] Recent contributions for example in *Chlorophylls* (Ed.: H. Scheer), CRC Press, Boca Raton, FL, USA, **1991**, and references therein.

[18] K. Hasharoni, H. Levanon, J. von Gersdorff, H. Kurreck, K. Möbius, *J. Chem. Phys.* **1993**, *98*, 2916, and references therein.

[19] N. J. Turro, B. Kraeutler, *J. Am. Chem. Soc.* **1978**, *100*, 7432.

[20] S. D. Chemerisov, O. Ya. Grinberg, D. S. Tipikin, Ya. S. Lebedev, H. Kurreck, K. Möbius, *Chem. Phys. Lett.*, in press.

Fast Solid-State Chemistry: Reactions under the Influence of Microwaves

By *Rüdiger Kniep**

Method: Take copper (powder), indium (powder), and sulfur (powder)—all powders with particle size between 100 and 300 mesh—in a molar ratio of 1:1:2, prepare a homogeneous mixture, load this into a quartz glass ampule, seal this under vacuum (ca. 10^{-3} Torr), place the ampule in an everyday microwave oven and "irradiate" this with 400 W at 2450 MHz. Already after 5–10 seconds, blue flashes caused by the formation of a sulfur plasma are observed in the ampule. After the light has faded, that is after about another 40–50 seconds, the ampule is removed from the microwave oven and shaken to homogenize the contents of the ampule. This procedure is performed a total of three times. Thus, the experiment lasts a little longer than 180 seconds. *Results*: Crystalline $CuInS_2$ (chalcopyrite structure); side product: small quantities of amorphous phases. *Identification/Characterization*: X-ray powder methods, scanning electron microscopy, energy dispersive X-ray analysis, and X-ray photoelectron spectroscopy. *Features*: 1. The fast reaction; 2. the fact that the ampule did not explode at temperatures, at least localized temperatures, of greater than 1000 °C (consider the vapor pressure of the (still) unreacted sulfur!). *Source of the "recipe"*: A publication by C. C. Landry and A. R. Barron[1] who extended the technique first developed by A. G. Whittacker and D. M. P. Mingos[2] for binary chacogenides to ternary semiconductor chalcogenide materials.

So what is so "exciting": "Microwaves" in the kitchen—that is already sufficiently well known. "Microwaves" in "solvent and molecular chemistry"—that is also known (here of course also the polar components are coupling).[3] "Microwaves" for the production of diamonds (e.g. microwave plasma chemical vapor deposition)[4]—that should have already been spread around. With "microwaves" even some oxides can be heated up to a good 1000 °C.[5, 6] In contrast, bulk metals or metal layers are inclined to undergo plasma discharges with microwave irradiation and are therefore, according to popular opinion, rather unsuitable to be heated by this method.

The new realization[1, 2] consists of the fact that metal *powders* can be very efficiently coupled to microwave fields (2450 MHz), so that temperatures of 1000 °C and greater can be reached within a few seconds without the occurrence of noticeable electrical discharges. Thus, the whole process resembles the "coupling" of zirconium metal (imbedded in ZrO_2 powder) to a high-frequency induction heater, a technique ("skull melting") which is used for growing large ZrO_2 single crystals.[7]

In particular, the reaction for the formation of $CuInS_2$ from the elements under the influence of microwaves apparently proceeds as follows: the dielectrical loss of the Cu powder is—in contrast to that of indium—large enough to initiate the reaction. The exothermic formation of copper

[*] Prof. Dr. R. Kniep
Eduard-Zintl-Institut der Technischen Hochschule
Hochschulstrasse 10, D-64289 Darmstadt (FRG)
Telefax: Int. code + (6151)16-4073

sulfide and/or the high temperature of the copper metal cause the indium to melt (m.p. 157 °C), so that a homogeneous ternary melt is subsequently produced, from which the ternary phase crystallizes by homogeneous nucleation during the rapid quenching. Particularly interesting in this respect is the formation of spherical particles.

Besides $CuInS_2$, the crystalline phases $CuInSe_2$ and CuInSSe, which also have the chalcopyrite structure, could be synthesized through this route.[1] The products are, however, not of "semiconductor quality", which is particularly unfortunate because these materials are of interest as solar cell materials.[8] However, the method itself is so fascinatingly simple that a greater dissemination of this solid-state synthesis by microwave irradiation is not only to be wished for but rather to be expected.

German version: *Angew. Chem.* **1993**, *105*, 1474

[1] C. C. Landry, A. R. Barron, *Science* **1993**, *260*, 1653.
[2] A. G. Whittaker, D. M. P. Mingos, *J. Chem. Soc. Salton Trans.* **1992**, 2751.
[3] D. M. P. Mingos, D. R. Baghurst, *Chem. Soc. Rev.* **1991**, *20*, 1.
[4] P. K. Bachmann, *Adv. Mater.* **1990**, *2*, 195.
[5] D. R. Baghurst, D. M. P. Mingos, *J. Chem. Soc. Chem. Commun.* **1988**, 829.
[6] T. T. Meek, C. E. Holcombe, N. Dykes, *J. Mater. Sci. Lett.* **1987**, *6*, 1060.
[7] L. Nassau, J. Nassau, *Cryst. Growth Prop. Appl.* **1980**, *2*, 1.
[8] J. Woodyard, G. A. Landis, *Sol. Cells* **1991**, *31*, 297.

The Mechanism of Fullerene Formation

By *Helmut Schwarz*

Of course there must be hundreds of mechanisms whereby a fullerene like C_{60} can form.[1]
It should be stated at the outset that almost everything in this section falls into the category of (we hope not wild) speculation. Next to nothing is known about how fullerenes actually grow and form.[2]
The data presented here unlocks the mystery of how fullerenes appear.[3]

1. The Problem

More diverse statements than the above on how fullerenes arise are hardly conceivable; though we are amazed at such contradictory quotations from renowned fullerene research scientists, we are even more astounded at the conditions under which fullerenes are formed: At plasma temperatures of over 3000 °C at which the $T\Delta S$ term should favor the existence of structurally little-organized, *highly entropic* molecules, *highly symmetric* molecules are created in carbon vapor![4] The fact that, although fullerenes are substantially destabilized relative to graphite[5] and C_{60} is distinctly less stable than C_{70} and higher fullerenes,[2, 6] C_{60} is often the major product of the graphite vaporization also precludes a thermodynamically controlled pathway. In the face of these anomalies it is not surprising that scientists wish to understand the mechanism of the formation of fullerenes, whether or not they consider the on-going fullerene activity as exaggerated or even as an expression of the lack of really important challenges.

[*] Prof. Dr. H. Schwarz
Institut für Organische Chemie der Technischen Universität
Strasse des 17. Juni 135, D-10623 Berlin (FRG)
Telefax: Int. code + (30)314-21102

2. The Facts

- Experiments using mixtures of $^{12}C/^{13}C$-labeled graphite demonstrate that the rate of carbon isotope incorporation conforms exactly to a Poisson distribution.[7] This implies that in any phase of the growth process, carbon *atoms* must be involved in the construction of fullerenes.
- If fullerenes are generated in the presence of electrostatic fields, the *neutral* carbon cluster is isolated almost exclusively from the cathode and not from the anode.[8] Apparently *cationic* intermediates play a role in the growth process.
- The coalescence of *cationic* (and not anionic) carbon rings furnish fullerenes in ion/molecule reactions that necessarily implicate a *size-selective* growth process:[9] While a reaction of C_{30}^+ with C_{30} produces predominantly C_{60}^+, the reaction of C_{18} and C_{24} with C_{18}^+ and C_{24}^+, respectively, yields mainly—via C_{72}^+—the C_{70} fullerene. Larger fullerenes can also be explained as multiples of smaller building blocks of defined size.[10] Consequently, the sequential addition of much smaller carbon fragments C_x ($x = 2, 3$) to larger fragments in the growth process does not necessarily have particular significance.
- Optimal fullerene yields during "graphite vaporization" are obtained only under a relatively narrow set of conditions, since both the temperature of the plasma and the pressure of the buffer gas are critical. Furthermore, if reactive components are mixed with the buffer gas helium, not only is the generation of fullerenes suppressed, but compounds that might be interpreted by some authors as indications for possible intermediates in the fullerene generation are also trapped. However, one has to recognize that the growth of valence-unsaturated carbon clusters can proceed differently from that of the partially derivatized clusters. A few examples suffice as illustration: Addition of H_2 to He generates polyacetylenes.[11] If the Krätschmer–Huffman conditions are modified[4] by addition of dicyanogen $(CN)_2$ instead of fullerenes, rodlike "dicyanopolyynes" $NC-(C{\equiv}C)_x-CN$ ($x = 3-7$) are formed.[12] Apparently in an early stage of

both cases, the radicals H$^{\bullet}$ or CN$^{\bullet}$ add irreversibly to the ends of *chains* of C_n species. If graphite vaporization is performed in the presence of Cl_2, beside small amounts of fullerenes (< 5%), the perchlorinated *cyclic* compounds **1**–**3** are isolated in good yields.[12] Rodlike chloroacetylene $Cl-(C\equiv C)_x-Cl$ cannot be detected. Each carbon framework of the arenes **1**–**3** represent a section of the C_{60} structure, and the occurrence of the five-membered ring in decachloroannulene (**3**), which is essential to the C_{60} structure, is particularly noteworthy. Apart from C_{60} and C_{70}, polycyclic arenes of the composition $C_{12}H_8$, C_nH_{10} ($n = 14-18$) and C_nH_{22} ($n = 20-24$) are isolated when the graphite vaporization is performed in an atmosphere of He/propene or He/methanol.[13a] Particularly interesting is the appearance of **4** and **5**, which likewise contain the structural motive of fullerenes.[13] Do the five-membered rings in the structures

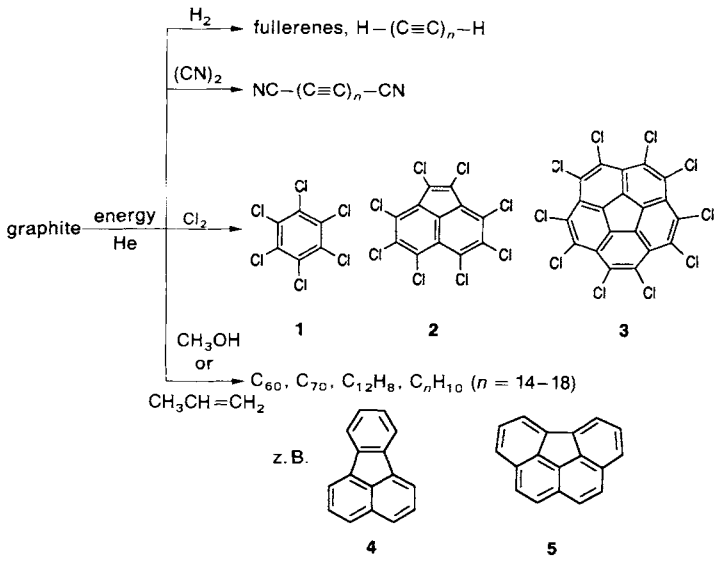

2–**5** offer support, or perhaps even confirmation, for Smalley's famous "pentagon road model", that has become widely known and that is the concept seen at present to be most consistent with the majority of the experimental data?

3. Models, Clues, and Evidence

Three criteria determine the pentagon road model: It is assumed that above a certain number of C atoms ($n \geq 30$) the energetically most favorable form of an arbitrary "graphitic sheet" is characterized by 1) only five- and six-membered rings as structural elements, 2) as many five-membered rings as possible, and 3) an avoidance of unstable pentalene units, that is, adjacent five-membered rings ("isolated pentagon rule"[16]). These surfaces have an advantage over *chainlike* C_n clusters[17] in that the average coordination numbers of the carbon atoms are higher. Furthermore, above a certain size the number of free valences on the periphery (the "dangling bonds") can be drastically reduced by the formation of closed spherical surfaces ("fullerenes"), or even completely disappear, as for the first time with C_{60}.[14b] This simple model can explain several experimental findings well: 1) The high temperature is not required only to vaporize the graphite, but is needed specifically to activate the carbon cluster thermally ("annealing") so strongly that the isomers find a pathway via the intermediate stage of graphitic sheets to optimal closed spheres that obey the Euler rule.[18] 2) The pressure of helium is likewise essential for this process, because the concentration of helium controls the diffusion of the C_n species from the hot plasma to the colder periphery. If too much buffer gas is present, the concentration of reactive C_n – and therefore the products resulting therefrom – increase so rapidly that the conditions for the annealing process are no longer optimal, and the isomerization of graphitic sheets by the pentagon road model increasingly loses its significance. How likely is the assumption of such a "self-organization" of graphite fragments?[1] It is not unfounded, since even corannulene is a higly flexible molecule already at room temperature, and thus at the higher temperatures the efficiency of annealing of larger carbon clusters will be large. But what is the experimental evidence for the intermediacy in the growth process of graphite-like molecular species with curved surfaces, which crumple to fullerenes after annealing?

The crucial experiments on this question have been performed in the past two years in the research group of M. T. Bowers.[3, 20a–c] Application of the well-established method of ion mobility (IM) in the gas phase, which in Santa Barbara[21] was developed to an "ion chromatography" led the group to fundamental insights. Despite some unexplained details, a mechanism of fullerene generation has emerged from the correlation of IM measurements with the results of ab initio and Monte Carlo calculations on the mobility of *structural types* of carbon clusters in a helium atmosphere. Initially it could be shown the C_n^+ clusters generated by laser vaporization can be attributed to different structural types depending on the cluster size n: C_5^+ and C_6^+ are linear, C_7^+ – C_{10}^+ are present both as linear species and as monocyclic cations, and C_{11}^+–C_{20}^+ exist only as monocycles. The range C_{21}^+–C_{28}^+ is characterized by planar mono- and bicyclic systems, and the first three-dimensional structure appears for C_{29}^+. Fullerenes arise for the first time at C_{30}^+ and dominate from C_{50}^+ (see Fig. 1).

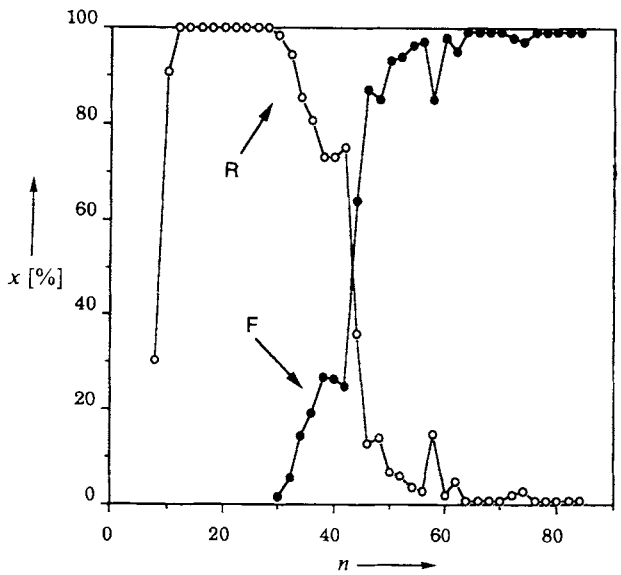

Fig. 1. The dependence of the proportion x of cationic fullerenes (F) and ring structures (R) in C_n^+ on n (according to ref. [3]).

Although for a cluster size of $n \geq 30$ several structural types coexist (see, for example, Fig. 2 for C_{30}^+ or Fig. 3a for C_{37}^+), the signals can be correlated with neither a graphitic sheet structure nor a bowl-shaped intermediate, both of which are essential for the pentagon road model. These structures cannot be detected in a cationic plasma.

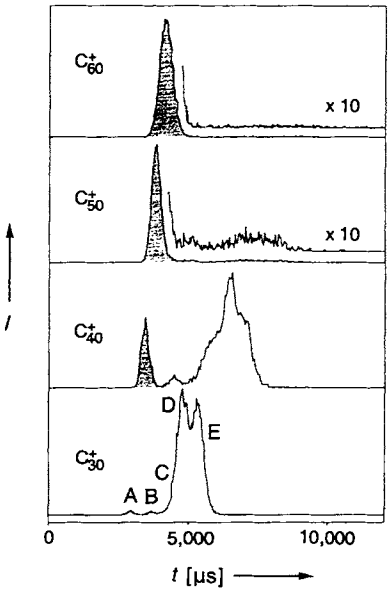

Fig. 2. Ion chromatograms for C_{30}^+, C_{40}^+, C_{50}^+, and C_{60}^+. (I is the intensity in arbitrary units.) The five isomeric families (A–E) are assigned to the following classes: A, Fullerenes (hatched region); B, three-dimensional rings; C, planar tricycles; D, planar bicycles; E, monocycles (according to ref. [20b]).

What happens when these ion mixtures are annealed by collision? The answer is contained in Figure 3 for the C_{37}^+ system. At relatively low collision energies (Fig. 3a), decomposition or isomerization is not yet observable. If the collision energy is increased (Fig. 3b), the isomer distribution for those C_{37}^+ ions that do not decompose is quite different: tri- and bicyclic species (signals C and D) disappear on annealing in favor of the monocycle (signal E). The spectra for the *decomposition products* of excited C_{37}^+ are also exceptionally instructive, because C_{36}^+ and C_{34}^+ (loss of C_1 or C_3) are undoubtedly present as fullerenes, while C_{23}^+ ("vaporization" of C_{14}^+ from C_{37}^+) again corresponds to a monocycle.

Very similar results are found for many other C_n^+ clusters with $n \geq 33$ too,[3, 20] and all experiments suggest the following scenario: deposition of energy initially causes predominantly the generation of monocyclic systems from the polycyclic C_n^+ clusters; fullerene formation does not yet occur, and no evidence for the intermediacy of graphite-like structures as discussed in the pentagon road model is found. Further excitation induces an isomerization to fullerenes. In this process the internal energy of the system increases enormously; for example, in the isomerization of a bicyclic-planar C_{36} to a C_{36}-fullerene, approximately 9 eV is released.[22] Adding the energy transferred by the collisions (5–20 eV) readily yields vibrational temperatures of about 4000 K, and the highly excited C_n^+ fullerene generated thus cools by evaporation of C_1 or C_3 (for uneven n) or C_2 (for even n). The behavior of C_{40}^+ may serve as illustration.

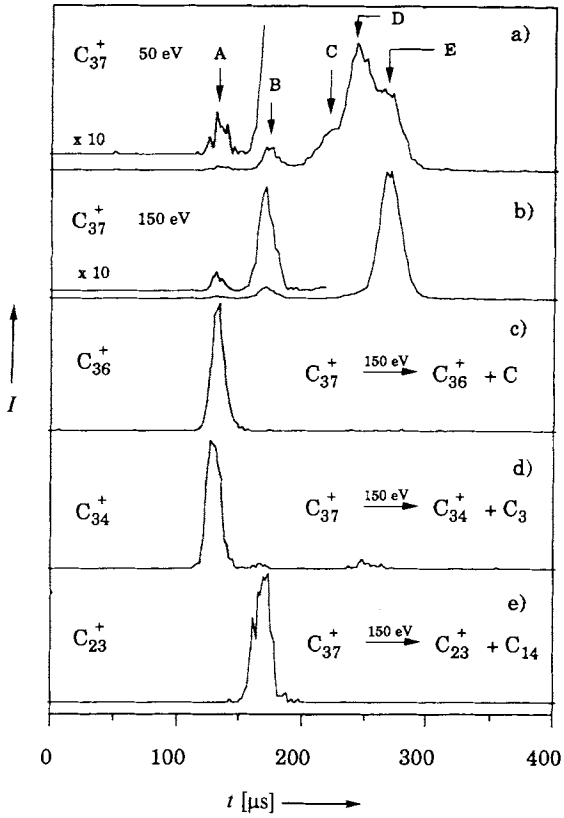

Fig. 3. Ion chromatogram for C_{37}^+ and its major decomposition products C_{36}^+, C_{34}^+, and C_{23}^+. Notation A–E as for Fig. 2. For details see text (according to ref. [20c]).

Provided that it will be possible to explain *how* the monocycles convert into fullerenes, an exciting chapter can be added to the dossier on the mechanism of fullerene formation. As spin-off of these mechanistic studies the idea arises

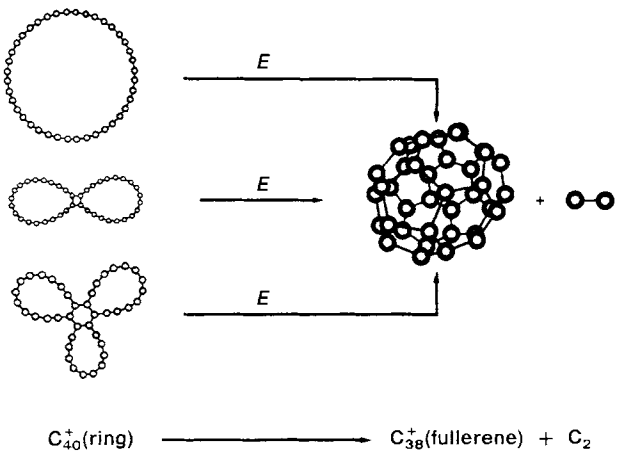

Fig. 4. Excitation of monocyclic C_{40}^+ by collision-induced heating, and generation of C_{38}^+ fullerenes.

that cyclic polyynes might be used for the tailor-made production of size-selected fullerenes:[9a, 23, 24] photochemical excitation of polymers in an inert medium may give rise to the formation of fullerenes.

German version: *Angew. Chem.* **1993**, *105*, 1475

[1] R. E. Smalley, *Acc. Chem. Res.* **1992**, *25*, 98.
[2] T. G. Schmalz, D. J. Klein in Buckminsterfullerenes (Eds.: W. E. Billups, M. A. Ciufolini), VCH, New York, **1993**, Chapter 4.
[3] G. von Helden, N. G. Gotts, M. T. Bowers, *Nature* **1993**, *363*, 60.
[4] W. Krätschmer, L. D. Lamb, K. Fostiropoulos, D. R. Huffman, *Nature* **1990**, *347*, 354.
[5] H. D. Beckhaus, C. Rüchardt, M. Kao, F. Diederich, C. S. Foote, *Angew. Chem.* **1992**, *104*, 69; *Angew. Chem. Int. Ed. Engl.* **1992**, *31*, 63.
[6] a) G. E. Scuseria, *Chem. Phys. Lett.* **1991**, *180*, 451; b) B. I. Dunlap, D. W. Brenner, J. W. Minmire, R. C. Mowrey, C. T. White, *J. Phys. Chem.* **1991**, *95*, 8737; c) D. Bakowies, W. Thiel, *J. Am. Chem. Soc.* **1991**, *113*, 3704; d) Review: H. W. Kroto, A. W. Allaf, S. P. Balm, *Chem. Rev.* **1991**, *91*, 1213.
[7] a) G. Meijer, D. S. Bethune, *J. Chem. Phys.* **1990**, *93*, 7800; b) R. D. Johnson, C. S. Yannoni, J. Salem, D. S. Bethune, *Mater. Res. Soc. Symp. Proc.* **1991**, *206*, 715; c) J. M. Hawkins, A. Meyer, S. Loren, R. Nunlist, *J. Am. Chem. Soc.* **1991**, *113*, 9394; d) T. W. Ebbesen, J. Tabuchi, K. Tanigaki, *Chem. Phys. Lett.* **1992**, *191*, 336.
[8] R. F. Bunshah, S. Jou, S. Prakash, H. J. Doerr, L. Isaacs, A. Wehosig, C. Yeretzian, H. Cynn, F. Diederich, *J. Phys. Chem.* **1992**, *96*, 6866.
[9] a) Y. Rubin, M. Kahr, C. B. Knobler, F. Diederich, C. L. Wilkins, *J. Am. Chem. Soc.* **1991**, *113*, 495; b) S. W. McElvany, M. M. Ross, N. C. Goroff, F. Diederich, *Science* **1993**, *259*, 1594.
[10] a) C. Yeretzian, K. Hansen, F. Diederich, R. L. Whetten, *Nature*, **1992**, *359*, 44; b) E. E. B. Campbell, V. Schyja, R. Ehlich, I. V. Hertel, *Phys. Rev. Lett.* **1993**, *70*, 263.
[11] a) R. J. Heath, Q. Zhang, S. C. O'Brien, R. F. Curl, H. W. Kroto, R. E. Smalley, *J. Am. Chem. Soc.* **1987**, *109*, 359; b) E. A. Rohlfing, *J. Chem. Phys.* **1990**, *93*, 7851; c) M. Broyer, A. Goeres, M. Pellarin, E. Sedlmeyer, J. L. Vialle, L. Wöste, *Chem. Phys. Lett.* **1992**, *198*, 128.
[12] T. Grösser, A. Hirsch, *Angew. Chem.* **1993**, *105*, 1390; *Angew. Chem. Int. Ed. Engl.* **1993**, *32*, 1340.
[13] a) T.-M. Chang, A. Naim, S. N. Ahmed, G. Goodloe, P. B. Shevlin, *J. Am. Chem. Soc.* **1992**, *114*, 7603. b) To what extent polycyclic arenes act as intermediates for fullerene formation in the combustion of hydrocarbons under oxygen-deficient conditions is discussed in detail in T. Baum, S. Löffler, P. Löffler, P. Weilmünster, K. H. Homann, *Ber. Bunsenges. Phys. Chem.* **1992**, *96*, 841.
[14] a) R. F. Curl, R. E. Smalley, *Sci. Am.* **1991**, *265*, No. 10, 54; b) R. E. Haufler, Y. Chai, L. P. F. Chibante, J. Conceicao, C. Jin, L.-S. Wang, S Maruyama, R. E. Smalley, *Mater. Res. Soc. Symp. Proc.* **1991**, *206*, 627.
[15] For a discussion of the most important mechanistic variations see R. F. Curl, *Philos. Trans. R. Soc. London A* **1993**, *343*, 19. In this review the following models, amongst others, which are not covered in this article, are discussed: "Nucleation model": a) Q. L. Zhang, S. C. O'Brien, J. R. Heath, Y. Liu, R. F. Curl, H. W. Kroto, R. E. Smalley, *J. Phys. Chem.* **1986**, *90*, 525; b) H. W. Kroto, K. McKay, *Nature* **1988**, *331*, 328; c) A. Goeres, E. Sedlmayer, *Chem. Phys. Lett.* **1991**, *184*, 310. "Ring stacking": d) T. Wakabayashi, Y. Achida, *ibid.* **1992**, *190*, 465; e) T. Wakabayashi, H. Shiromaru, K. Kikuchi, Y. Achiba, *ibid.* **1993**, *201*, 470; f) J. R. Dias, *ibid.* **1993**, *109*, 439. "Curling and closure of graphitic ribbons": g) H. W. Kroto, J. R. Heath, S. C. O'Brien, R. F. Curl, R. E. Smalley, *Nature* **1985**, *318*, 162; h) D. H. Robertson, W. D. Brenner, C. T. White, *J. Phys. Chem.* **1992**, *96*, 6133. "Fullerene road": i) J. R. Heath, *Fullerenes: Synthesis, Properties, and Chemistry of Large Carbon Clustrs* (Eds.: G. S. Hammond, V. J. Kuck) (*ACS Symp. Ser.* **1991**, *481*, 1).
[16] a) A. J. Stone, D. J. Wales, *Chem. Phys. Lett.* **1986**, *128*, 501; b) D. J. Klein, W. A. Seitz, T. Schmalz, *Nature* **1986**, *323*, 703; c) J.-Y. Yi, J. Bernholc, *J. Chem. Phys.* **1992**, *96*, 8634; d) Ref. [2]. e) For an experimental distinction between fullerenes with respect to the isolated pentagon rule, see: J. H. Callahan, M. M. Ross, T. Weiske, H. Schwarz, *J. Phys. Chem.* **1993**, *97*, 20.
[17] K. S. Pitzer, E. Clementi, *J. Am. Chem. Soc.* **1959**, *81*, 4477.
[18] P. Ballone, P. Milani, *Phys. Rev. B Condens. Matter* **1990**, *42*, 3201.
[19] a) L. T. Scott, M. M. Hashemi, M. S. Brateker, *J. Am. Chem. Soc.* **1992**, *114*, 1920; b) A. Borchardt, A. Fuchicello, K. V. Kilway, K. K. Baldrige, J. S. Siegel, *ibid.* **1992**, *114*, 1921.
[20] a) G. von Helden, M.-T. Hsu, P. R. Kemper, M. T. Bowers, *J. Chem. Phys.* **1991**, *95*, 3835; b) M. T. Bowers, P. R. Kemper, G. von Helden, P. A. M. von Koppen, *Science* **1993**, *260*, 1446; c) G. von Helden, N. G. Gotts, M. T. Bowers, *J. Am. Chem. Soc.* **1993**, *115*, 4363. d) For the annealing of non-fullerenoid C_{60}^+, see: J. Hunter, J. Fye, M. F. Jarrold, *Science* **1993**, *260*, 784.
[21] a) P. R. Kemper, M. T. Bowers, *J. Am. Chem. Soc.* **1990**, *112*, 3231; b) P. R. Kemper, M. T. Bowers, *J. Phys. Chem.* **1991**, *95*, 5134.
[22] a) M. Feyereisen, M. Gutowski, J. Simons, J. Almlöf, *J. Chem. Phys.* **1992**, *96*, 2926; b) see also: C. Z. Wang, C. H. Xu, C. T. Chan, K. M. Ho, *J. Phys. Chem.* **1992**, *96*, 3563.
[23] F. Diederich, Y. Rubin, *Angew. Chem.* **1992**, *104*, 1123; *Angew. Chem. Int. Ed. Engl.* **1992**, *31*, 1101.
[24] H. W. Kroto, D. R. M. Walton, *Philos. Trans. R. Soc. London A* **1993**, *343*, 103.

The Solution of the Sherman Paradox or the Successful Search for the Huntington Gene

By *Ernst-L. Winnacker**

It was Linus Pauling, the chemist, who formulated the concept of "molecular diseases" currently playing such an important role in our understanding of a variety of genetic disorders. In the late 1940s, long before the first protein sequence was established, he showed that hemoglobins from healthy people differed from those of patients with sickle cell anemia in their electrophoretic mobilities.[1] It took seven years until Vernon Ingram managed to ascribe these differences to the exchange of a single amino acid in the β-chain of hemoglobin from glutamic acid to valine.[2]

Since that time, advances in molecular biology have permitted determination of the causes of many more molecular diseases. The mutations responsible for genetic defects can be single amino acid substitutions, that is point mutations, or deletions and insertions of longer stretches of DNA. Any given gene can be subject to different types of mutations and these may lead to varying degrees of disease symptoms. A common feature however of (almost) all known hereditary diseases is their stable inheritance once a mutation has established itself. Thus, within an afflicted family the courses of a disease will not differ significantly among parents and their children. As is so often the case, exceptions should prove the rule. Well, maybe not in this case!

Human geneticists have been aware for some time of a number of genetic diseases which do not fit in with what was mentioned above. There appear to be cases in which the severity of the disease changes from generation to generation, in most cases becoming more severe. It is almost as if an initial mutation served as a basis for more and more new genetic alterations. As no explanation for this phenomenon was available, this particular situation in which the health risk of a person depends on his or her position in a pedigree was referred to as Sherman's paradox.[3]

[*] Prof. Dr. E.-L. Winnacker
Institut für Biochemie der Universität München
D-85152 Martinsried (FRG)
Telefax: Int. code + (89)8578-3795

 © VCH Verlagsgesellschaft mbH, D-69451 Weinheim, 1993 0570-0833/93/1010-1415 $ 10.00+.25/0

What exactly lies behind this paradox? Could it be a reflection of local instabilities of the genetic material? Indeed, this is the case. The nature of this new type of mutation is exemplified best by the prototype of such diseases, Huntington's chorea (often abbreviated as HD, for Huntington's Disease). Huntington's chorea, also called St. Vitus dance, was first described in 1892 by the American practioner and neurologist George Huntington who, in addition, had also already recognized the hereditary nature of the disease.[4]

This rare disease—with an incidence of 7–10 per 100000 persons—manifests itself between the ages of 35 and 50. Huntington's disease is characterized by disturbances of the neural and motor systems. The name "chorea" refers to the involuntary tremors and sudden body movements shown by afflicted individuals. Symptoms become more and more severe with time and are accompanied by a dramatic decline in mental abilities. Death inevitably follows after a few years.

It has been known for a long time that the symptoms can be ascribed to a loss of neurons in the brain; however, the biochemical causes of this phenomenon have so far remained a mystery. The classical methods of identifying genes by the isolation and characterization of a modified protein, which in cases such as sickle cell anemia can then be ascribed readily to a defective gene, could not and cannot be applied in this case. This left only the reverse procedure, fittingly known as "reverse genetics". This approach involves the direct search for the defective gene whose DNA sequence can then be used to derive the corresponding protein sequence, thus eventually allowing the biochemical properties of the protein to be investigated. Such an approach is by no means simple since the human genome contains at least 100000 genes; only one of these is the Huntington gene in question, but which one? There are two prerequisities in performing such a task. First extended families comprising as many people as possible from several generations are needed so that the hereditary course of the disease can be followed. Second characteristic markers or tags on the DNA are needed. The closer such markers are spaced along the chromosome the more accurate will be the localization of a "suspicious" DNA fragment to a specific section of the genetic material.

A large number of suitable markers are in fact available along human (and other) chromosomes in the form of DNA sequence variations known as DNA polymorphisms. These lie mostly outside of coding regions. If such markers happen to involve restriction enzyme recognition sites, this leads to DNA fragments of differing lengths that are characteristic for a particular genome and thus for an individual. These are referred to as "restriction fragment length polymorphisms" (RFLPs or RIFLIPs). Such alterations are passed on from parents to their children just like any other mutations and can be used to determine the degree of relatedness between individuals. To return to the search for the Huntington gene, if such a marker lies in close proximity to the Huntington gene it will be coinherited. Therefore it was necessary to search for a DNA fragment in Huntington pedigrees that was always present in members afflicted with the genetic disease but did not occur in disease-free individuals. To achieve this, the genome of persons from a Huntington family tree[5] is fragmented with a restriction enzyme that recognizes such polymorphic DNA cleavage sites. The resulting fragments are separated according to their sizes and hybridized with radioactively labeled human DNA fragments randomly selected from a gene library. Randomness is important because it is not known which DNA fragment will lie close to the Huntington gene. In principle it may be necessary to test thousands and thousands of DNA fragments before obtaining a fragment pattern characteristic for Huntington patients and which at the same time is not observed in healthy members of the same pedigree.

James Gusella and co-workers[6] at the Massachusetts General Hospital (MGH) in Boston were extremely lucky when they scored a hit in 1983 after having tested for eight fragments only. This particular fragment had been chosen at random, lottery-like, so to speak, from a collection of millions of cloned DNA fragments. It stemmed from chromosome 4 which established that the Huntington gene must be located on this chromosome.

Starting from this fragment, the site of the Huntington gene has been localized more and more precisely over the last ten years. By the end of 1992 it was certain that the gene was located on a 500000 base pair fragment at the end of the short arm of chromosome 4. However, even such a relatively small fragment is still large enough to accommodate 10–20 normal-sized genes. To identify their coding sequences within the plethora of noncoding sequences is no easy task. It should also be borne in mind that coding sequences are usually broken up into a large number of separate units called exons.

A variety of techniques are now available for the identification of exons. The following are of particular significance: a) the identification by sequence databank searches of evolutionarily related sequences that may have been identified previously in the genomes of other organisms; b) the detection of hypomethylated CpG islands known to be located often in promoter regions of genes; c) the identification of long open reading frames by DNA sequencing. A new technique called exon amplification was used in searching for the HD gene.[7] This involves the use of an expression vector for mammalian cells that contains a functional easily identifiable marker gene. To determine whether a piece of DNA contains an exon, it is cloned into the intron of the marker gene. If no exon is present, mRNA corresponding to the vector gene is formed after transfection of the vector into a mammalian cell; if, on the other hand, a functional exon has been inserted, the marker gene-specific mRNA formed will be extended by an amount corresponding to the length of the inserted exon. The polymerase chain reaction (PCR) is used subsequently to amplify and characterize the exon sequence.

When applied to the 500 kBp segment from the short arm of chromosome 4 this approach, among other things, identified a reading frame, designated IT15 (IT is the abbreviation for "interesting transcript"), coding for a previously unknown protein of 348 kDa.[8] This reading frame attracted the authors' attention because it had 21 copies of the triplet CAG near its 5' end which codes for the amino acid glutamine (Q) (Fig. 1). When this section of the gene was compared with the corresponding sections in other healthy persons, it was immediately apparent that there were length variations with respect to this one codon with the number of codon repetitions varying between 11 and 34. Apparently the gene was instable in this region.

```
-----AGACCCCGCCATGGCGACCCTGGAAAAGCTGATGAAGGCCTTCGAGTCCCTCAAG
                M  A  T  L  E  K  L  M  K  A  F  E  S  L  K

TCCTTCCAGCAGCAGCAGCAGCAGCAGCAGCAGCAGCAGCAGCAGCAGCAGCAGCAG
 S  F  Q  Q  Q  Q  Q  Q  Q  Q  Q  Q  Q  Q  Q  Q  Q  Q  Q  Q

CAGCAGCAGCAGCAGCCGCCACCGCCGCCGCCGCCGCCGCCTCCTCAGCTTCCTCAG
 Q  Q  Q  Q  Q  P  P  P  P  P  P  P  P  P  P  Q  L  P  G

CCG----
 P
```

Fig. 1. Part of the amino acid sequence of huntingtin and the corresponding DNA sequence. The presence of 23 glutamine residues in this sequence from a healthy individual is clearly visible. In healthy individuals the number of glutamine residues varies between 11 and 34, while it can increase to more than 80 residues in dieseased individuals.

Is it this section of the gene which perhaps is responsible for the Huntington's disease mutations? Actually it was found that patients with Huntington's disease had even longer repetitions. The largest number of repetitions found so far is 86. Furthermore, the number of repetitions appears to correlate with the age of onset of the disease; the larger the repetition number the younger the patient. Thus, not only was Sherman's paradox resolved but there was also little doubt that the gene found was the Huntington's disease gene. The corresponding protein has 3144 amino acids and was named huntingtin. It shows no homologies with other proteins, so that there is still no clue to its biochemical function.

Nevertheless, the finding is of importance in several respects. It demonstrates that reverse genetics allows individual genes to be located within large genomes without information being available about their functions. Furthermore, this work revealed the existence of a novel type of mutation not known previously, a kind of dynamic mutation characterized by increases in codon or trinucleotide repetitions. In the meantime it has been established that four other genetic diseases are based on the same kind of unstable codon repetition (see Fig. 2). Despite their differences in clinical symptoms these diseases have a number of similarities, including for example, their association with a progressive decline in motor functions and mental ability, symptoms becoming progressively more severe from generation to generation, and rising numbers of codon repetitions correlating with the onset of the age of onset of the diseases.

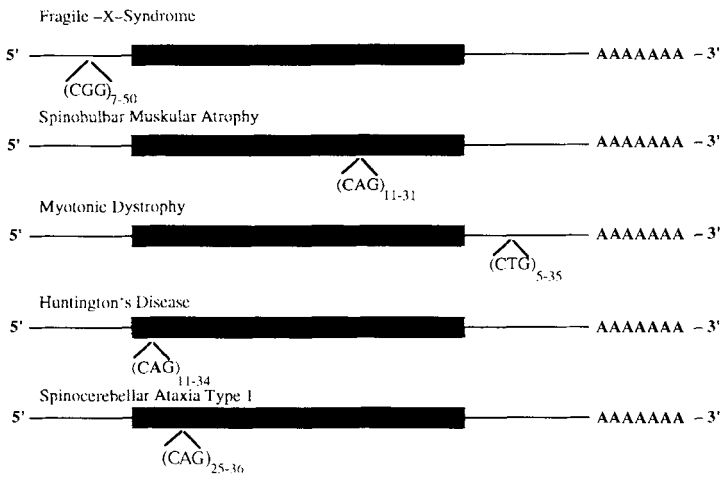

Fig. 2. Order of trinucleotide repeats in 5 different genes responsible for the occurrence of five genetic disorders which are characterized by codon instabilites (according to *Science* **1993**, *260*, 1422–1423). All five syndromes are rare hereditary diseases which are associated with neurodegenerative symptoms.

As always in cases like this progress poses more questions than it answers. For example, are there particular codons that are inherently prone to this kind of generation-dependent instability? In this context it is interesting to note that the three repetitive-prone codons observed so far, namely, CAG, CTG, and CGG (Fig. 2), have complementary bases (C and G) at positions 1 and 3. Thus, longer sections of these codons can fold back on themselves and form stable secondary structures, so-called stem–loop structures. The postulated A–A, T–T, and G–G (homo purine and homo pyrimidine) base pairs are by no means forbidden. On the contrary, they contribute significantly to the free energy of formation of such secondary structures.[9]

Why is it that trinucleotide repetitions show this instability and not di- or tetranucleotide repetitions which are also known to occur in the human genome? What effects do codon repetitions have on gene expression? Some of the codon repetitions occur outside of coding regions and therefore can "only" affect the mRNA and not the protein, as is the case in the Fragile-X-Syndrome.[10] It is easily imagined that and how such repetitions might influence the formation of mRNA secondary structures, half-life, modifications localization of the mRNA, and all the other factors which control mRNA translation. It is also possible that binding sites for mRNA binding proteins are formed in this way, which may control the efficiency of the translation process as in the case of the ferritin/transferrin receptor.[11]

The effects of codon repetitions occurring in coding regions are also easily imagined. A polyglutamine section at the N terminus of a protein must affect its folding, solubility, biological half-life, and its interactions with other proteins. However, all explanations must account for the observation that the Huntington mutation is dominant, and thus that the "defective" protein does not only cause the disease on its own but that even in the presence of the "normal" protein the mutant huntingtin must somehow have a negative effect on the normal protein as well.

These observations raise the question of the molecular causes of these instabilities. Apparently they originate in gametes which, in turn, are the product of a characteristic series of cell divisions and so-called reductive cell divisions (meiosis) of the corresponding precursor cells. During these stages of differentiation, DNA synthesis and repair processes may be accompanied by the exchange of genetic material, a process known as homologous recombination. It is conceivable that the enzymes involved in these processes may have specificities that differ from those participating in general synthetic processes. Chemistry and biochemistry are now challenged in a totally unexpected way in their endeavors to answer these and many other questions posed by these investigations.

Finally, it should be mentioned that the results discussed here also have ethical implications. Now that the gene for Huntington's disease has been identified, a diagnostic test for the disease is bound to follow. Codon repetition numbers could also be used as the basis for prognoses of life-expectancies of afflicted patients. Will it be ethically acceptable to inform an apparently healthy person that he or she will def-

initely die from Huntington's disease even if this may only happen in ten or more years's time? How can unauthorized use of such data be prevented? Such questions are not new to the field of human genetics; modern developments in molecular biology may, however, exacerbate the problem, particularly when therapeutical capabilities lag behind diagnostic means, as is so often the case. There is not sufficient space here to discuss this matter further. The identification of the gene responsible for Huntington's disease certainly is a triumph for modern genetics. The enthusiasm about this stunning achievement, however, should not prevent us from realizing that this kind of knowledge will not only benefit humanity but may also raise certain fears, worries, and social conflicts, and these will have to be properly resolved.[12]

German version: *Angew. Chem.* **1993**, *105*, 1479

[1] L. Pauling, *Science* **1949**, *110*, 543–548.
[2] V. M. Ingram, *Nature* **1957**, *180*, 326–328.
[3] Y. H. Fu, D. P. Kuhl, A. Pizutti, M. Pieretti, J. S. Sutcliff, S. Richards, A. J. M. H. Verkerk, J. A. Holden, R. G. Fenwick, S. Warren, B. A. Oostra, D. L. Nilson, C. T. Caskey, *Cell* **1991**, *67*, 1047–1058.
[4] J. F. Gusella, *Adv. Hum. Genet.* **1991**, 125–151; J. B. Martin, J. F. Gusella, *New Engl. J. Med.* **1986**, *315*, 1267–1276.
[5] Such pedigrees are known both from the US and from Venezuela. Around Lake Maracaibo, in particular, there is a cluster of about 9000 people, which can be traced back to a single woman who died in the early 19th century from HD.
[6] J. F. Gusella, N. S. Wexler, P. M. Conneally, S. L. Naylor, M. A. Anderson, R. E. Tanzi, P. C. Watkins, K. Ottina, M. R. Wallace, A. Y. Sakaguchi, A. B. Young, I. Shoulson, E. Bonilla, J. B. Martin, *Nature* **1983**, *306*, 234–238.
[7] A. J. Buckler, D. D. Chang, S. L. Graw, J. D. Brook, D. A. Haber, P. A. Sharp, D. E. Hausman, *Proc. Natl. Acad. Sci. USA* **1991**, *88*, 4005–4009.
[8] The Huntington's Disease Collaborative Research Group, *Cell* **1993**, *72*, 971–983.
[9] I. Tinoco, P. N. Borer, B. Dengler, M. D. Levine, O. C. Uhlenbeck, D. M. Crothers, J. Gralla, *Nature London New Biol.* **1973**, *346*, 40–41.
[10] C. T. Ashley, J. S. Sutcliffe, C. B. Kunst, H. A. Leiner, E. E. Eichler, D. L. Nelson, S. T. Warren, *Nat. Genet.* **1993**, *4*, 244–251.
[11] E. C. Theil, *J. Biol. Chem.* **1990**, *265*, 4771–4774.
[12] See for example: H. Markl, *Wissenschaft im Widerstreit*, VCH, Weinheim, **1990**, pp. 145–177 or E. L. Winnacker, *Am Faden des Lebens*, Piper, München, **1993**, pp. 227–256; or *The Code of Codes: Scientific and Social Issues in the Human Genome Project* (Eds. D. J. Kevles, L. Hood), Harvard University press, **1992**, p. 397.

Communications may be submitted in English *or* in German. Further details regarding the submission of communications can be found in the "Notice to Authors" reproduced in the January issue of the journal. Copies thereof may be obtained from the editorial office upon request.

Synthesis and Structure of Bis(tri-*tert*-butylphenyl)-iminohalogenphosphoranes X–P(=N*t*Bu$_3$C$_6$H$_2$)$_2$**

By *Alexander Ruban, Martin Nieger,* and *Edgar Niecke**

Dedicated to Professor Otto Scherer on the occasion of his 60th birthday

The discovery of a stable phosphorus(v) compound with a trigonal planar coordinated phosphorus atom[1] has led to a rapid development of the chemistry of this and structurally related phosphorus compounds.[2] The halogenphosphoranes, which could be obtained in a stable form[3] so far only from the bis(methylene)phosphorane system,[2c] are especially interesting as a result of their synthetic potential.

Attempts to obtain kinetically stabilized halogenbis(imino)phosphoranes XP[=N(alkyl)]=N(aryl) by N_2 elimination from halogen-4,5-dihydro-1*H*-tetraazaphospholes X–PN(aryl)N=NN(alkyl) have shown that the 2,4,6-tri-*tert*-butylphenyl group as aryl substituent combined with a sterically demanding alkyl substituent cannot stabilize the products sufficiently against subsequent reactions.[4] As we have now found, only the introduction of a second aryl substituent prevents a coordinative saturation of the reactive phosphorus center.

The reaction of (arylimino)chlorophosphanes[5] **1** with LiN(aryl)SiMe$_3$ gave the aryl(silyl)amino(arylimino)phosphane **2** (aryl = 2,4,6-*t*Bu$_3$C$_6$H$_2$), and subsequent addition of halogen (X = Cl, Br) led to the dihalogenphosphoranes **3a**,[6] **b**. From these the bis(arylimino)halogenphosphoranes **4a**, **b** were obtained thermally (110 °C) with the elimination of halogentrimethylsilane. Br/I exchange in **4b** with Me$_3$SiI affords the iodine derivative **5**. All the compounds can be isolated pure in the form as colorless to orange-red solids and can be characterized unambiguously on the basis of their analytical, NMR spectroscopic, and mass spectrometric data. Furthermore, the solid-state molecular structure of **5** was determined.[7]

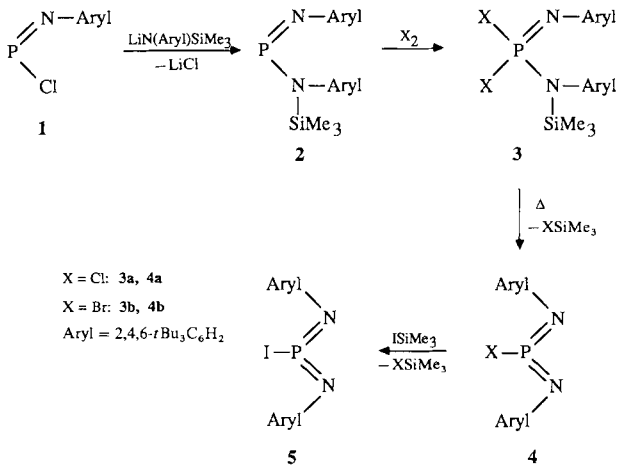

As in all structurally investigated bis(ylene)phosphoranes,[2] the phosphorus atom is in a trigonal planar environment ($\Sigma \sphericalangle 359.9°$; Fig. 1). The carbon atoms of the *t*Bu$_3$C$_6$H$_2$ substituents linked to the imine nitrogen atoms also lie in this plane; the two phenyl rings are arranged orthogonal to the central NPN π-bond system. The *exo*/*exo* conformation of

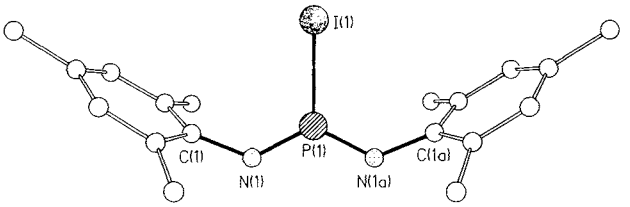

Fig. 1. Crystal structure of the bis(imino)phosphorane **5** (without peripheral methyl groups). Selected bond lengths [pm], bond angles [°], and torsion angles [°]: P(1)–I(1) 239.4(3), P(1)–N(1) 152.5(4), N(1)–C(1) 142.1(7); I(1)-P(1)-N(1) 119.0(2), N(1)-P(1)-N(1a) 121.9(2), P(1)-N(1)-C(1) 127.1(4); I(1)-P(1)-N(1)-C(1) –1.1(5), N(1a)-P(1)-N(1)-C(1) 178.9(5).

the CNPNC framework[8] in **5** is in accord with the results from an ab initio calculation of the parent chlorobis(imino)phosphane Cl–P(=NH)$_2$,[9] which also provides an explanation for the relatively small N-P-N angle (121.9(2)°). In the solid state, this conformation gives rise to a chain arrangement of the molecules (Fig. 2) due to weak I···N interactions[9] (343 pm). The P–I distance (239.4(3) pm) is significantly shorter than that in the comparable bismethylenephosphorane (253 pm in I–P[=C(SiMe$_3$)$_2$]$_2$[11]), which can be interpreted in terms of an enhancement of the positive partial charge at the phosphorus atom in **5** as compared to that in the bismethylenephosphorane system.[12] The P–N (152.5(4) pm) and N–C distances (142.1(7) pm) as well as the C-N-P (127.1(4)°) angle correspond to those of typical structural features of bis(imino)phosphoranes.[2b]

The equivalence of the resonance signals of the two *t*Bu$_3$C$_6$H$_2$ groups in the ^{1}H NMR spectra of the compounds **4** and **5** reveal their monomeric construction in solution. The sheilding of the phosphorus nucleus in the ^{31}P NMR spectrum (δ = –18.5 (**4a**), –30.2 (**4b**), –42.9 (**5**)) which is unusual for bis(imino)phosphoranes[13] is easily explained by the positive partial charge at phosphorus.[12] Further experiments will need to be carried out to determine the degree to

[*] Prof. Dr. E. Niecke, Dr. M. Nieger
Anorganisch-chemisches Institut der Universität
Gerhard-Domagk-Strasse 1, D-53121 Bonn (FRG)
Telefax: Int. code + (228) 735-327
Dr. A. Ruban
Institute for Organic Chemistry of the Academy of Sciences
252660 Kiev (Ukraine)

[**] This work was supported by the Deutsche Forschungsgemeinschaft and the Fonds der Chemischen Industrie. A. Ruban thanks the Alexander-von-Humboldt-Stiftung for a fellowship.

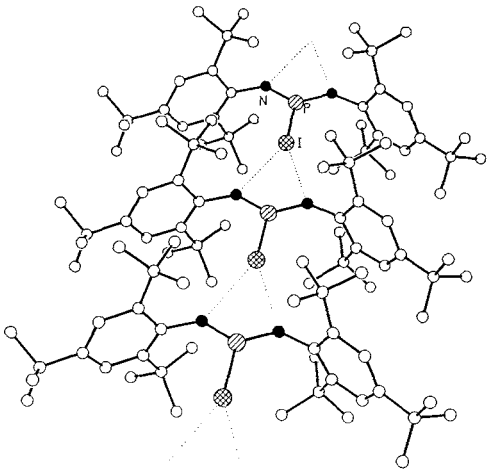

Fig. 2. Section of the chain structure of the bis(imino)phosphorane **5**. Important intermolecular distance and angle: I···N 343 pm; N···I···N 46°.

which the *exo/exo* conformation contributes to the sheilding of the ^{31}P nucleus.

Experimental Procedure

2: A solution of **1** (20 mmol) in THF (50 mL) was treated with an equimolar quantity of $LiN(tBu_3C_6H_2)SiMe_3$, dissolved in THF (40 mL) at −30 °C and stirred. The mixture was then allowed to warm to 25 °C. The solvent was removed under vacuum and the residue was taken up in hexane (40 mL), and the LiCl present was removed by filtration. The filtrate was concentrated and the residue recrystallized from toluene. Yield: 82%, m.p. 168–170 °C. ^{31}P NMR (C_6H_6): $\delta = 318.1$; ^1H NMR (C_6H_6): $\delta = -0.44$ (s, 9H, $SiMe_3$), 1.27, 1.42 (s, 9H, *p*-*t*Bu), 1.59, 1.73 (s, 18H, o-tBu), 7.59, 7.64 (s, 2H, C_6H_2).

3a [**3b**]: A solution of **2** (20 mmol) in CH_2Cl_2 at −30 °C was treated with an equimolar quantity of $Cl_2[Br_2]$, dissolved in CH_2Cl_2 (30 mL). The mixture was allowed to warm to 25 °C, stirred, and the solvent was removed under vacuum. The residue was taken up in *n*-hexane (100 mL) and recrystallized at −80 °C. Yield: 58% [74%], m.p. 74 °C (decomp) [62 °C]. ^{31}P NMR (THF): $\delta = -75.2$ [−81.4]; ^1H NMR (C_6D_6): $\delta = 0.54$ [0.62] (s, 9H, $SiMe_3$), 1.27 [1.27], 1.34 [1.35] (s, 9H, *p*-*t*Bu), 1.43 [1.42], 1.66 [1.71] (s, 18H, *o*-*t*Bu), 7.43 [7.43] (d, $J(H,P) = 3.86$ Hz [4.58 Hz], C_6H_2), 7.57 [7.58] (d, $J(H,P) = 1.59$ Hz [0.9 Hz], C_6H_2).

4a [**4b**]: A solution of **2a** [**2b**] (10 mmol) in toluene (50 mL) was heated under reflux for 2 h. The volatiles were removed under vacuum at 25 °C, and the remaining solid residue was recrystallized from toluene. Yield: 66% [82%], m.p. 156–159 °C [194–196 °C]. ^1H NMR (C_6H_6): $\delta = 1.30$ [1.31] (s, 9H, *p*-*t*Bu), 1.66 [1.69], (s, 18H, *o*-*t*Bu), 7.55 [7.74] (d, $J(H,P) = 4.40$ Hz [4.36 Hz], C_6H_2); MS (70 eV): 584 (M^+, 9%) [628 (M^+, 56%)], 290 ($tBu_3C_6H_2NP^+$, 100%) [290 ($tBu_3C_6H_2NP^+$, 100%)].

5: A solution of **2a** or **2b** (10 mmol) in benzene (15 mL) was treated with a slight molar excess of $ISiMe_3$ and stirred for 1 h at 25 °C. The solvent and the halogensilane were removed under vacuum and the residue was recrystallized from a little THF. Yield: 92%, m.p. 161–164 °C. ^1H NMR (C_6D_6): $\delta = 1.32$ (s, 9H, *p*-*t*Bu), 1.78 (s, 18H, *o*-*t*Bu), 7.54 (d, $J(H,P) = 4.28$ Hz, C_6H_2); MS (70 eV): 675 (M^+, 51%), 290 ($tBu_3C_6H_2NP^+$, 100%).

Received: May 12, 1993 [Z 6079 IE]
German version: *Angew. Chem.* **1993**, *105*, 1544

[1] E. Niecke, W. Flick, *Angew. Chem.* **1974**, *86*, 128; *Angew. Chem. Int. Ed. Engl.* **1974**, *13*, 585; O. J. Scherer, N. Kuhn, *Chem. Ber.* **1974**, *107*, 2123; S. Pohl, E. Niecke, B. Krebs, *Angew. Chem.* **1975**, *87*, 284; *Angew. Chem. Int. Ed. Engl.* **1975**, *14*, 261.

[2] a) *Multiple Bonds and Low Coordination in Phosphorus Chemistry* (Eds.: M. Regitz, O. J. Scherer), Thieme, Stuttgart, **1990**; b) E. Niecke, D. Gudat in [2a], pp. 392–404, and references therein; c) R. Appel in [2a], pp. 367–374, and references therein; d) H. Heydt in [2a], pp. 375–391, and references therein; e) M. Yoshifugi in [2a], pp. 411–414, and references therein; f) M. Meisel in [2a], pp. 415–442, and references therein; g) G. Bertrand in [2a], pp. 443–454, and references therein; h) J.-P. Majoral in [2a], pp. 455–461, and references therein.

[3] Halogen(dichalcogen)phosphoranes, $Cl-P(O,S)_2$, are known as highly unstable compounds: R. Ahlrichs, C. Ehrhardt, M. Lakenbrink, S. Schunk, H. Schnöckel, *J. Am. Chem. Soc.* **1986**, *108*, 3596–3602; M. Meisel, H. Bock, B. Soluki, M. Kramer, *Angew. Chem.* **1989**, *101*, 1378–1381; *Angew. Chem. Int. Ed. Engl.* **1989**, *28*, 1373–1377.

[4] E. Niecke, M. Nieger, V. von der Gönna, *Chem. Ber.* **1990**, *123*, 2329–2333.

[5] E. Niecke, M. Nieger, F. Reichert, *Angew. Chem.* **1988**, *100*, 1781–1782; *Angew. Chem. Int. Ed. Engl.* **1988**, *27*, 1715–1716.

[6] The iminophosphorane $(tBu_3C_6H_2)N=P(Cl_2)N=C(CtBuCH)_2C(tBu)Cl$ was formed as a by-product (17%) from the reaction of **2a** with chlorine. M.p. 126–128 °C; ^{31}P NMR (C_6H_6): $\delta = 74.1$. X-ray structural analysis of $C_{36}H_{58}N_2PCl_3$ [7b]: red crystals, crystal dimensions $0.3 \times 0.4 \times 0.5$ mm; $M_r = 656.2$; space group $P\bar{1}$ (no. 2), $a = 1025.0(1)$, $b = 1205.0(1)$, $c = 1642.7(1)$ pm, $\alpha = 69.71(1)$, $\beta = 85.07(1)$, $\gamma = 88.43(1)$°, $V = 1.896$ nm^3, $Z = 2$, $\rho_{calcd} = 1.15$ g cm^{-3}, $\mu(Mo_{K\alpha}$ radiation) = 0.31 mm^{-1}; 5940 symmetry-independent reflections ($2\theta_{max} = 48°$), of which 4674 reflections with $F > 3\sigma(F)$ were used for the structure solution (direct methods) and refinement (379 parameters), non-hydrogen atoms anisotropic, H atoms refined with a "riding" model; $R = 0.045$ ($R_w = 0.047$, $w^{-1} = \sigma^2(F) + 0.0004F^2$). (selected bond lengths [pm]): P=N 149.2(2), P–N 162.4(3), P–Cl1 204.0(1) and P–Cl2 206.1(1), N=C 128.8(4).

[7] a) X-ray structure analysis of **4** ($C_{36}H_{58}N_2PI$): orange crystals, crystal dimensions $0.15 \times 0.25 \times 0.40$ mm; $M_r = 676.7$; space group $C2/c$ (no. 15), $a = 2021.2(6)$, $b = 629.4(1)$, $c = 2992.3(16)$ pm, $\beta = 102.55(3)$°, $V = 3.716$ nm^3, $Z = 4$, $\rho_{calcd} = 1.21$ g cm^{-3}, $\mu(Mo_{K\alpha}$ radiation) = 0.92 mm^{-1}; 2413 symmetry-independent reflections ($2\theta_{max} = 45°$), of which 1761 reflections with $F > 4\sigma(F)$ were used for the structure solution (direct methods) and refinement (182 parameters), non-hydrogen atoms were refined anisotropic, H atoms with a "riding" model; $R = 0.050$ ($R_w = 0.051$, $w^{-1} = \sigma^2(F) + 0.0010F^2$). b) Further details of the crystal structure investigation may be obtained from the Fachinformationszentrum Karlsruhe, Gesellschaft für wissenschaftlich-technische Information mbH, D-76344 Eggenstein-Leopoldshafen (FRG) on quoting the depository number CSD-57372, the names of the authors, and the journal citation.

[8] Hitherto for bis(imino)phosphoranes only the *endo/endo* conformation has been proven: E. Niecke, D. Gudat in [2a], 392–404.

[9] W. W. Schoeller, C. Lerch, *Inorg. Chem.* **1986**, *25*, 576–580.

[10] For the formation of a chain structure through I···N contacts see, for example, E. O. Schlemper, D. Britton, *Acta Crystallogr.* **1965**, *18*, 419–424.

[11] V. Romanenko, L. S. Kachkovskaja, M. I. Povolotskii, A. N. Chernega, M. Yu. Antipin, Yu. T. Struchkov, L. N. Markovskii, *Zh. Obshch. Khim.* **1988**, *58*, 958–969.

[12] We thank Prof. Dr. P. R. von Schleyer, Erlangen, for providing us with the results of a population analysis on $X-P(=NH)_2$ (X = Cl, I).

[13] K. Karaghiosoff in [2a] pp. 463–471, and references therein.

The Coupled Activation of Molecular Oxygen and C–H and C–C Bonds in Gas-Phase Reactions of $[M(C_2H_4)]^+$ (M = Sc – Zn) with O_2**

By *Detlef Schröder* and *Helmut Schwarz**

Dedicated to Professor Rudolf Zahradnik

Iron compounds are essential for the transportation, activation, and storage of molecular oxygen in biological systems.[1] In addition, iron-centered proteins, like cytochromes and ferrodoxins, are of particular relevance in numerous redox-processes involving C–H and C–C bond activation.[2] With respect to biochemistry, only copper compounds mediate various oxidation processes as efficiently as iron-centered molecules do.[3]

It is a fundamental question whether the exceptional role of iron reflects an intrinsic property of this element, or whether the reactivity is due to a specific ligand environment of the reactive intermediates. Since in the gas phase intrinsic properties can be studied in the absence of additional effects caused by ligands, counterions, solvation, etc., we designed a simple gas-phase model, which, in principle, should allow

[*] Prof. Dr. H. Schwarz, Dr. D. Schröder
Institut für Organische Chemie der Technischen Universität
Strasse des 17. Juni 135, D-10623 Berlin (FRG)
Telefax: Int. code + (30)314-21102

[**] This work was supported by the Deutsche Forschungsgemeinschaft, Volkswagen-Stiftung, and Fonds der Chemischen Industrie.

us to screen the capabilities of the first-row transition metal cations with respect to the coupled activation of molecular oxygen[4] and of C–H and C–C bonds of organic substrates. Here we report the gas-phase reactions of thermalized $[M(C_2H_4)]^+$ complexes (M = Sc–Zn) with molecular oxygen under single-collision conditions by using Fourier transform ion cyclotron resonance (FT-ICR) mass spectrometry.[5, 6]

The reactivity of the $[M(C_2H_4)]^+$ complexes towards molecular oxygen[14] can be classified as follows (Table 1): 1) The complexes of the late transition metal ions Co^+–Zn^+ do not undergo O_2 or C_2H_4 activation. The same behavior is also observed for the reaction of O_2 with $C_2H_4^{\bullet+}$, $C_2H_5^+$, $[Na(C_2H_4)]^+$, or $[Mg(C_2H_4)]^+$. 2) Ligand exchange of $[M(C_2H_4)]^+$ with molecular oxygen, leading to $[M(O_2)]^+$, is observed for the early transition metal ions ($M^+ = Sc^+$–Mn^+, indicating that for these metals the binding energies $[M(O_2)]^+$ exceed that of $[M(C_2H_4)]^+$. 3) Activation of the O–O bond and product formation at the rate of collision is observed for complexes of the metal ions Sc^+, Ti^+, V^+, and Fe^+. The manganese complex $[Mn(C_2H_4)]^+$ also reacts with O_2 to form $MnOH^+$; this slow process is not yet fully understood.[4] Since rapid activation of O_2 is observed for the complexes $[M(C_2H_4)]^+$ (M = Sc, Ti, V, Fe) only, we will confine the discussion to these systems.

Table 1. Reaction efficiency and yields of the reaction products of $[M(C_2H_4)]^+$ ions with O_2 (intensities are normalized to 100%).

M	k_R/k_{ADO} [a]	M^+	MO^+	MOH^+	MO_2^+	$OMOH^+$	$OM(C_2H_4)^+$
Sc	1.0		80	<1	15		5
Ti	1.0		55	<1	25	10	10
V [b]	1.0		40	<1	15	15	30
Cr	0.8				100		
Mn	0.01			10	90		
Fe[c]	1.0	20	10	40	<1		
Co	<0.002						
Ni	<0.002						
Cu	<0.002						
Zn	<0.002						

[a] Reaction efficiency: ratio of reaction rate constant k_R versus collision rate k_{ADO} ref. [9, 15]. [b] Propene complex of vanadium cation; see text. [c] 30% are other products; see text. Small amounts of M^+, formed after several seconds reaction times, are due to incomplete thermalization of $[Fe(C_2H_4)]^+$ or reactions with the background gases.

As far as the ethylene complexes of the early transtion metal cations Sc^+, Ti^+, and V^+ are concerned, their reactions can be ascribed to the high oxophilicities of these metal ions. This is in line with the formation of MO^+ from the corresponding "bare" metal ions and O_2.[16] Therefore, we assume that the ethylene ligand remains intact in the reaction of $[M(C_2H_4)]^+$ with O_2. This conjecture is supported by the results of consecutive ligand exchange reactions of the reaction product $[OM(C_2H_4)]^+$ with other ligands (Scheme 1). Thus, these reactions of the $[M(C_2H_4)]^+$ complexes of the early transtion metal ions Sc^+, Ti^+, and V^+ can simply be ascribed to the favorable thermochemistry of M^+-O bond formation, and the organic ligand is not involved in the activation of O_2.

$$[M(C_2H_4)]^+ \xrightarrow[-O]{+O_2} [OM(C_2H_4)]^+ \xrightarrow[-C_2H_4]{+L} [OM(L)]^+$$

Scheme 1. M = Sc, Ti, V; L = C_2D_4, H_2O, O_2.

The sole products, which unequivocally establish C–H bond activation of the olefin in the course of the reaction, are the oxohydroxide cations $OMOH^+$ (M = Ti, V). However, there is no evidence for C–C bond activation in these systems. The C–H bond activation may be rationalized by invoking first the formation of the metal dioxide cations OMO^+, followed by a hydrogen abstraction process (Scheme 2). The relatively large amount of $OVOH^+$ must certainly result from the fact that only the propene complex $[V(C_3H_6)]^+$ was accessible, for which allylic C–H bond activation is facile. In conclusion, the behavior of the olefin complexes of Sc^+, Ti^+, and V^+ towards O_2 is comparable with that of the bare metal ions. Indications of a *coupled activation* of O–O, C–H, and C–C bonds do not exist for these complexes.

$$[M(C_2H_4)]^+ + O_2 \longrightarrow [O{=}\overset{+}{M}{=}O\cdots C_2H_4] \longrightarrow OMOH^+ + C_2H_3^{\bullet}$$

Scheme 2. M = Ti, V.

If $[Fe(C_2H_4)]^+$ is reacted with oxygen extensive oxidation processes occur (Scheme 3). Not only the formation of Fe^+ confirms that in the encounter complex the C_2H_4 ligand and O_2 have reacted with each other, moreover, the generation of CH_3CO^+ as well as most of the other reaction products lend support to this interpretation. Furthermore, both C–H and C–C bond activation are observed, as evidenced by the detection of $FeOH^+$, CH_3CO^+, $Fe(O_2CH)^+$, $Fe(OCH_2)^+$, and $FeCH_2^+$ ions. Although the FT-ICR experimental setup does not allow the determination of neutral products formed in the course of the reaction, thermochemical considerations as well as the observation of $Fe(OCH_2)^+$ indicate that two formaldehyde molecules accompany the formation of bare Fe^+ in the reaction of $[Fe(C_2H_4)]^+$ with O_2. Evidently, the iron cation uniquely activates three important bonds (O–O, C–H, and C–C) at the same time.

$$[Fe(C_2H_4)]^+ + O_2 \longrightarrow \begin{cases} Fe(O_2CH)^+ + CH_3^{\bullet} & 4\% \\ Fe(OCH_2)^+ + CH_2O & 10\% \\ FeOH^+ + CH_3CO^{\bullet} & 40\% \\ FeO^+ + C_2H_4O & 10\% \\ FeCH_2^+ + CH_2O_2 & 6\% \\ Fe^+ + C_2H_4O_2 & 20\% \\ CH_3CO^+ + FeOH & 10\% \end{cases}$$

Scheme 3.

A straightforward rationalization of the extraordinary reactivity of $[Fe(C_2H_4)]^+$ towards O_2 can neither be derived from a consideration of the M–O bond strengths nor from the binding energies of the corresponding ethylene complexes alone. As indicated by the data in Table 2, Fe^+ does not

Table 2. Some relevant data for MO^+, $[M(C_2H_4)]^+$, and M^+. E_D = bond dissociation energy [a].

	Sc^+	Ti^+	V^+	Cr^+	Mn^+	Fe^+	Co^+	Ni^+	Cu^+
$E_D(M^+\text{-}O)$ [b]	159	161	131	85	57	81	64	45	82
$E_D(M^+\text{-}C_2H_4)$ [c]	35	55 [e]	50 [e]	33	-	34	37	37	>28
electronic state $[M(C_2H_4)]^+$ [d]	$^1A_1^*$	$^2A_1^*$	$^5A_1^*$	$^6A_1^*$	$^7A_1$	$^4B_2$	$^3A_2$	$^2A_1$	$^1A_1$
4s occupancy [d]	0.24	0.33	0.12	0.16	1.13	0.27	0.24	0.24	0.24

[a] In kcal mol^{-1}. [b] Taken from ref. [16]. [c] Taken from ref. [17]. [d] Taken from ref. [18]. [e] A reviewer has pointed out that the E_D for Ti^+-C_2H_4 and V^+-C_2H_4 are much too high due to excited state reactions which were not taken into account when the data were analyzed. According to the reviewer, more accurate bond energies for Ti^+-C_2H_4 and V^+-C_2H_4 are 32 and 33 kcal mol^{-1}, respectively.

occupy a special position with regard to thermochemical properties, although one may speculate that in the reaction of $[Fe(C_2H_4)]^+$ with O_2 iron has just the right balance of bond energies to oxygen, hydrogen, and carbon to make a sequence of processes energetically feasible. Similarly, the 4 s occupancy is not unique for Fe^+. The only exceptional finding with respect to iron concerns the fact that the $[Fe(C_2H_4)]^+$ complex is not derived from the ground state of the corresponding bare metal ion. A phenomenological explanation for the unique behavior of the $[Fe(C_2H_4)]^+$ complex may be derived from the ease with which iron compounds are known to change their oxidation states. Similarly, one may argue that the position occupied by iron in the periodic table helps to avoid problems with the stability of filled and half-filled d shells; thus making a diverse range of intermediates accessible. Although, we do not yet have a solid theoretical model to explain the unusual reactivity of the iron complex in the activation of O_2, the present gas-phase behavior in a sense parallels the essential role of iron for oxygen activation in the condensed phase. Thus, the present findings may suggest that the unique role of iron in biochemical oxidation processes reflects an inherent property of this metal ion.

Finally, it should be mentioned that the reactivity of the iron complexes towards molecular oxygen is not limited to $[Fe(C_2H_4)]^+$. In fact, even the thermalized benzene/Fe^+ complex, generated by the ligand exchange $[Fe(C_2H_4)] + C_6H_6 \rightarrow [Fe(C_6H_6)]^+ + C_2H_4$, is oxidized efficiently by O_2 (Scheme 4).[19]

$$[Fe(C_6H_6)]^+ + O_2 \xrightarrow{k_R} \begin{cases} \xrightarrow{0.55} [Fe(C_5H_6O)]^+ + CO \\ \xrightarrow{0.45} [Fe(C_5H_4)]^+ + CO + H_2O \end{cases}$$

Scheme 4. $k_R = 6.9 \times 10^{-10}$ cm^3 molecule^{-1} s^{-1}
$k_{ADO} = 7.8 \times 10^{-10}$ cm^3 molecule^{-1} s^{-1}

We are currently exploring the iron-mediated oxidation of different organic substrates by molecular oxygen. In addition, further experimental and theoretical[20] work on the reaction of the olefin complexes is necessary to understand the reaction mechanism and the origin of the remarkable ability of iron to mediate activation of molecular oxygen for the oxidation of C–H and C–C bonds.

Received: May 22, 1993 [Z 6098 IE]
German version: *Angew. Chem.* **1993**, *105*, 1493

[1] a) *The Role of Metal Ions in the Chemistry and Biology of Oxygen* (Eds.: W. Bors, M. Saran), De Gruyter, Berlin, **1983**; b) H. Sund, V. Ullrich, *Biological Oxidations*, Springer, Berlin, **1983**; c) *The Role of Oxygen in Chemistry and Biochemistry* (Eds.: W. Ando, Y. Moka-Oka), Springer, Berlin **1988**; d) E. F. Elstner, *Der Sauerstoff: Biochemie, Biologie und Medizin*, Wissenschaftsverlag, Mannheim, **1990**; e) L. I. Simándi, *Dioxygen Activation and Homogenous Catalytic Oxidation*, Elsevier, Amsterdam, **1991**; f) D. T. Sawyer, *Oxygen Chemistry*, Oxford University Press, New York, **1991**.

[2] a) *Cytochrome P-450: Structure, Mechanism and Biochemistry* (Ed.: P. R. Ortiz de Montellano), Plenum, New York, **1986**; b) W. Kaim, B. Schwederski, *Bioanorganische Chemie*, Teubner, Stuttgart, **1991**; c) see also: R. J. P. Williams, *Nature* **1993**, *343*, 213.

[3] a) G. T. Babcock, M. Wikstrøm, *Nature* **1992**, *356*, 301; b) see also: N. P. Luneva, E. I. Knerelman, V. Y. Shafirovich, A. E. Shilov, *New. J. Chem.* **1989**, *13*, 107.

[4] D. Schröder, dissertation, Nr. D83, Technische Universität Berlin, **1992**.

[5] For recent reviews see: a) B. S. Freiser, *Chemtracts Anal. Phys. Chem.* **1989**, *1*, 65; b) K. Eller, H. Schwarz, *Chem. Rev.* **1991**, *91*, 1121.

[6] The experiments were performed with a Spectrospin CMS 47X FT-ICR mass spectrometer described previously [7]. The metal ions were formed in the external ion source by laser desorption/ionization (LD/LI) of a pure metal target with a Nd:YAG laser (Spectron Systems, 1064 nm), transferred into the analyzer cell by a system of electric potentials and lenses, and trapped in a magnetic field of a superconducting magnet (Oxford Instruments, max. field strength 7.05 Tesla). The most abundant M^+ isotopes were isolated by using the FERETS technique [8] and thermalized by collisions with argon. Reactant gases were introduced through pulsed valves; argon and molecular oxygen were introduced through leak valves at typical pressures of $2-10 \times 10^{-8}$ mbar and $2-20 \times 10^{-9}$ mbar, respectively. For the determination of the absolute rate constants, k_R, the ionization gauge was calibrated on the basis of known reaction rate constants [9, 10]. The accuracy of the absolute rate constant measurements is $\pm 25\%$ for $k_R > 10^{-12}$ cm^3 molecule^{-1} s^{-1}. The $[M(C_2H_4)]^+$ complexes were generated from the bare metal ions by one of the following methods [5]: 1) Dehydrogenation of ethane (M = Sc, Ti), 2) demethanation of propane (M = Fe, Co), and 3) dehydrohalogenation of ethylhalides (M = Cr, Mn, Fe, Co, Ni, Cu, Zn). Unfortunately, none of these methods was suitable for the generation of sufficient amounts of $[V(C_2H_4)]^+$, which under the conditions reacted further, generating oligomers of the type $[V(C_2H_4)_x]^+$; thus, the corresponding propene complex $[V(C_3H_6)]^+$ had to be used for comparison [11]. Since some of the $[M(C_2H_4)]^+$ complexes undergo ligand exchange reactions with residual background water, present in the mass spectrometer [12], all reactions described were confirmed by use of either $[M(C_2D_4)]^+$ complexes or $^{18}O_2$. Relevant bond dissociation energies and thermochemical data were taken from ref. [13].

[7] a) K. Eller, H. Schwarz, *Int. J. Mass. Spectrom. Ion Processes* **1989**, *93*, 243; b) K. Eller, W. Zummack, H. Schwarz, *J. Am. Chem. Soc.* **1990**, *112*, 621.

[8] R. A. Forbes, F. H. Laukien, J. Wronka, *Int. J. Mass. Spectrom. Ion Processes* **1988**, *83*, 23.

[9] For leading references see: Y. Lin, D. P. Ridge, B. Munson, *Org. Mass Spectom.* **1991**, *26*, 550.

[10] a) F. Nakao, *Vacuum* **1975**, *25*, 431; b) J. E. Bartmess, R. M. Georgiadis, *ibid.* **1983**, *33*, 149.

[11] M. A. Tolbert, J. L. Beauchamp, *J. Am. Chem. Soc.* **1986**, *108*, 7509.

[12] O. Blum, D. Stöckigt, D. Schröder, H. Schwarz, *Angew. Chem.* **1992**, *104*, 537; *Angew. Chem. Int. Ed. Engl.* **1992**, *31*, 603.

[13] a) S. G. Lias, J. E. Bartmess, J. F. Liebman, J. L. Holmes, R. D. Levin, W. G. Mallard, *J. Phys. Chem. Ref. Data Suppl.* 1 **1988**, *17*; b) K. R. Ervin, S. Gronert, S. E. Barlow, M. K. Gilles, A. G. Harrison, V. Bierbaum, C. H. DePuy, W. C. Lineberger, G. B. Ellison, *J. Am. Chem. Soc.* **1990**, *112*, 5750.

[14] *Anionic* transition metal complexes react with O_2. For a review, see: R. R. Squires, *Chem. Rev.* **1987**, *87*, 623.

[15] T. Su, M. T. Bowers, *Int. J. Mass Spectrom. Ion Phys.* **1973**, *12*, 347.

[16] H. Kang, J. L. Beauchamp, *J. Am. Chem. Soc.* **1986**, *108*, 5663, 7502.

[17] M. Sodupe, C. W. Bauschlicher, Jr., S. R. Langhoff, H. Partridge, *J. Chem. Phys.* **1992**, *96*, 2118 (Addendum 5670).

[18] S. K. Loh, E. R. Fisher, R. H. Schultz, P. B. Armentrout, *J. Phys. Chem.* **1989**, *93*, 3159.

[19] a) D. Schröder, H. Schwarz, *Helv. Chim. Acta* **1992**, *75*, 1281; b) D. Schröder, W. Zummack, H. Schwarz, *Organometallics* **1993**, *12*, 1079.

[20] For recent theoretical approaches towards the understanding of oxygen activation, see: a) P. K. Ross, E. I. Solomon, *J. Am. Chem. Soc.* **1991**, *113*, 3246; b) K. A. Jørgensen, P. Swanstrøm, *Acta Chem. Scand.* **1992**, *46*, 82; c) R. S. Drago, *Coord. Chem. Rev.* **1992**, *117*, 185.

Chromatographic Separation of the Four Possible Structural Isomers of a Tetrasubstituted Phthalocyanine: Tetrakis(2-ethylhexyloxy)-phthalocyaninatonickel(II)

By *Michael Hanack,* Gabriele Schmid,* and *Michael Sommerauer*

Phthalocyanines, especially those in ligand-bridged, stacked arrangements $[PcM(L)]_n$ (Pc = phthalocyanine, M = Si, L = O; M = Fe, Ru, L = pyrazine, tetrazine) are of interest because of their electrical properties; they are also gaining interest in other areas such as nonlinear optics (NLO) and Langmuir–Blodgett technology.[1] A decisive disadvantage of phthalocyanines and metal phthalocyanines is their low solubility in organic solvents; however, the solubility can be increased by introducing alkyl and alkoxy substituents into

[*] Prof. Dr. M. Hanack, G. Schmid, M. Sommerauer
Institut für Organische Chemie
Lehrstuhl für Organische Chemie II der Universität
Auf der Morgenstelle 18, D-72076 Tübingen
Telefax: Int. code + (7071)29-5244

the peripheral positions of the phthalocyanine framework. Because of their lower degree of order in the solid state, tetrasubstituted phthalocyanines are more soluble than the corresponding symmetrical octasubstituted compounds.[2]

In spite of many attempts, hitherto it has not been possible to separate and characterize all four possible structural isomers of a tetrasubstituted metal phthalocyanine.[3] Recently we separated two isomers of tetra(*tert*-butyl)phthalocyaninatonickel(II) [(*t*Bu)$_4$PcNi].[4] We report here for the first time the successful, complete separation of all four structural isomers of tetrakis(2-ethylhexyloxy)phthalocyaninatonickel [(EHO)$_4$PcNi] (Scheme 1) and their characterization by ^{1}H NMR spectroscopy.

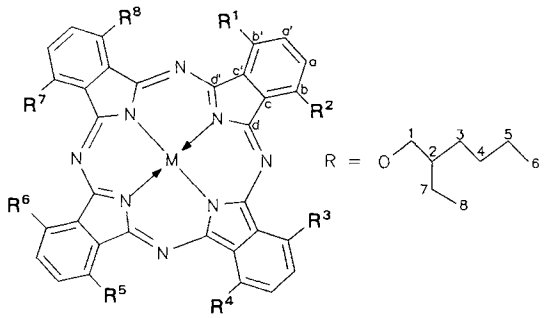

Isomer	R^1	R^2	R^3	R^4	R^5	R^6	R^7	R^8
C_{4h}	H	R	H	R	H	R	H	R
C_{2v}	H	R	R	H	R	H	H	R
C_s	H	R	H	R	H	R	R	H
D_{2h}	H	R	R	H	H	R	R	H

Scheme 1. The four structural isomers of [(EHO)$_4$PcNi] with point groups. EHO = 2-ethylhexyloxy.

The separation of the isomers of [(EHO)$_4$PcNi] was achieved analytically by high-pressure liquid chromatography (HPLC); the isomers could be isolated on a preparative scale by medium-pressure liquid chromatography (MPLC). The ^{1}H NMR spectra of the MPLC fractions allow the D_{2h}, C_s, C_{2v}, and C_{4h} isomers to be characterized unambiguously (Scheme 1). Strictly speaking, the point groups are only valid for nonchiral substituents and a completely planar phthalocyanine framework, however, the above-mentioned designation of the isomers should be retained. Figure 1 shows the

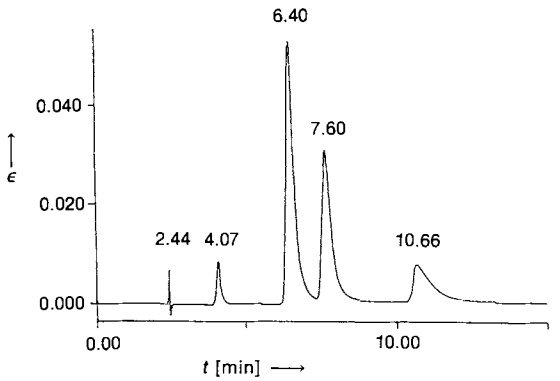

Fig. 1. HPLC chromatogram of [(EHO)$_4$PcNi]. Column: ET 250/8/4 nucleosil 5 NO_2; 5 μm; eluent: toluene/*n*-hexane (1:1); flow rate: 1 mL min^{-1}; pressure: 74.5 bar.

HPLC chromatogram of [(EHO)$_4$PcNi]. According to this, the mixture consists of 4.2% D_{2h}, 49.2% C_s, 31.3% C_{2v}, and 15.3% of the C_{4h} isomer (order of elution).

The low proportion of the D_{2h} isomer in comparison with the other three isomers is remarkable. One reason for this is the steric hindrance of the respective neighboring alkoxy groups (see Scheme 1). The individual isomers were assigned on the basis of the ^{1}H NMR signals of the H^1 alkoxy protons as well as on the basis of the aromatic protons H^a, H$^{a'}$, and H^b or H$^{b'}$ of the Pc ring system (see Scheme 1). Since nickel phthalocyanines tend to aggregate, the ^{1}H NMR spectra of [(EHO)$_4$PcNi] were recorded as very dilute solutions (0.7 mg mL^{-1}; 400 MHz). Two groups of signals are observed in the resonance region of the H^1 protons, one in the range $5.09 \leq \delta \leq 4.91$ and the other in the range $4.52 \leq \delta \leq 4.32$, that is some of the signals of the H^1 protons are shifted to low field. If the isomers D_{2h}, C_s, C_{2v}, and C_{4h} are considered as pairs of isoindolenine units, the alkoxy groups may or may not be neighbors. When alkoxy groups are neighbors,the electron density around the H^1 protons increases, explaining why the signals are shifted downfield. Accordingly, the isomer with only one group of signals, shifted downfield between $\delta = 4.99$ and 4.85 is assigned D_{2h} symmetry. The spectrum with only one group of signals between $\delta = 4.51$ and 4.41 belongs to the C_{4h} isomer. The spectra exhibiting both groups of signals, in a ratio of 1:1 are assigned to the C_s and C_{2v} isomers. The H^1 protons are magnetically nonequivalent and are located in the vicinity of the chiral centers of the ethylhexyloxy groups (C^2). Each of the four isomers exists as a mixture of diastereomers; thus, no clear multiplicity can be recognized (Table 1).

Table 1. ^{1}H NMR data of the four isomers of [(EHO)$_4$PcNi]; (400 MHz, [D$_6$]benzene $c = 0.7$ mg mL^{-1}) [a].

Isomer	D_{2h}	C_{2v}	C_s	C_{4h}
δ(H^b/H$^{b'}$)	9.46 (d, ^3J = 7.1 Hz, 4H)	9.62 (d, ^3J = 7.6 Hz, 2H) 9.24 (d, ^3J = 7.6 Hz, 2H)	9.67 (d, ^3J = 7.1 Hz, 1H) 9.45 (d, ^3J = 7.6 Hz, 2H) 9.29 (d, ^3J = 7.6 Hz, 1H)	9.49 (d, ^3J = 7.6 Hz, 4H)
δ(H^a)	7.96 (t, ^3J = 7.6 Hz, 4H)	8.17 (t, ^3J = 7.6 Hz, 2H) 7.91 (t, ^3J = 7.9 Hz, 2H)	8.16 (t, ^3J = 6.3 Hz, 1H) 8.12 (t, ^3J = 6.4 Hz, 1H) 7.98 (t, ^3J = 7.6 Hz, 1H) 7.89 (t, ^3J = 7.6 Hz, 1H)	8.13 (t, ^3J = 7.6 Hz, 4H)
δ(H^a)	7.65 (d, ^3J = 8.1 Hz; 4H)	7.75 (d, ^3J = 7.6 Hz, 2H)	7.72 (d, ^3J = 7.6 Hz, 1H) 7.68 (d, ^3J = 7.6 Hz, 1H) 7.44 (d ^3J = 7.6 Hz, 1H)	7.44 (d, ^3J = 7.6 Hz, 4H)
δ(H^1)	4.99–4.85 (m; 8H)	5.12–4.97 (m, 4H) 4.44–4.35 (m, 4H)	5.08–4.91 (m, 4H) 4.50–4.33 (m, 4H)	4.51–4.41 (m, 4H)

[a] The data of the protons H^2–H^8 were not included in the table, because an assignment, especially for the isomers with low symmetry (C_s, C_{2v}) is not possible due to the large number of signals. The signals of the H^a protons lie partly under the benzene signal.

Owing to vicinal coupling, a doublet is observed for H^a, H^b, or $H^{b'}$ (Fig. 2), in the region of the aromatic protons and a doublet of a doublet is observed for $H^{a'}$, which appears as a triplet in the spectrum. Three signals are observed for the C_{4h} and the D_{2h} isomers, (two doublets, one doublet of a doublet) for the three aromatic protons H^a, $H^{a'}$ and H^b or $H^{b'}$. It is

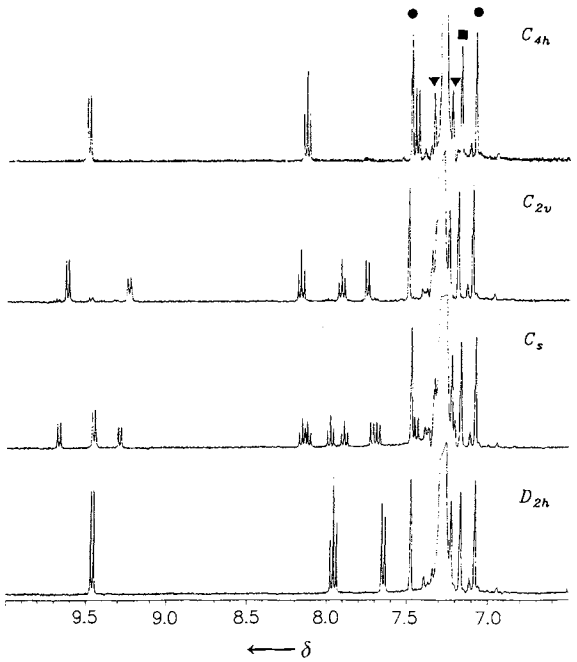

Fig. 2. ^1H NMR spectra of the four isomers (resonance range of the aromatic protons) (400 MHz, [D_6]benzene, 0.7 mg mL^{-1}). ^1J(C,H) coupling in [D_5]benzene (●), signal of [D_4]benzene (■); rotational side bands (▼).

observed that the H^a protons of the D_{2h} isomer are shifted to lower field than those of the C_{4h} isomer. In the C_s isomer, only part of the doublet is shifted. The $H^{a'}$ protons of the C_{4h} isomer are shifted downfield. The C_{2v} isomer exhibits one nonshifted group of signals and one group of signals shifted downfield, whereas the C_s isomer shows one nonshifted group of signals and two groups of signals that are shifted downfield when the triplet of the D_{2h} isomer is used as reference. One group of signals of the C_s isomer is shifted upfield in comparison with the reference. For the C_{2v} isomer, six signals (four doublets, two doublets of a doublet) are expected in the aromatic region of the spectrum. However, the spectrum exhibits two doublets for H^b or $H^{b'}$, two doublets of a doublet for $H^{a'}$, and a doublet for H^a. The second doublet expected for H^a is covered by the benzene signal. This could be proven by varying the concentration of the solution. Twelve signals are expected for the C_s isomer (eight doublets, and four doublets of a doublet). However, three doublets are observed for H^b or $H^{b'}$ whose integration corresponds to four protons. Again, by varying the concentration of the solution it could be proven that two doublets overlap. Moreover, the spectrum of the C_s isomer exhibits four doublets of a doublet for $H^{a'}$ and three doublets for H^a. The fourth doublet for H^a is likewise covered by the benzene signal.

The UV spectra of the four structural isomers of [$(EHO)_4$PcNi] do not differ significantly.[5] The IR spectra of the isomeric mixture of [$(EHO)_4$PcNi] and the isolated isomers are identical. The C_{4h} isomer is the least soluble (e.g. in benzene) and forms the last fraction on the column, whereas the D_{2h} isomer is readily soluble. One reason for the difference in solubility between the isomers might be the spatial arrangement of the substituents of the neighboring isoindolenine units.

Experimental Procedure

HPLC: Beckmann system Gold 5.1; column; Machery-Nagel; ET 250/8/4 nucleosil 5 NO_2; 5 μm; eluent: toluene/*n*-hexane (1:1); 74.5 bar; 1 mL min^{-1}.

MPLC: pump: ProMinent CfG Duramat; column: 93 × 2.54 cm packed with Merck 15–40 μm silica gel 60H.; eluent: toluene/*n*-hexane (3:2); 6 bar; 1.6 mL min^{-1}; flow detector: Büchi UV/VIS filter photometer with preparative flow cell (measuring wavelength 365 nm). For separation, [$(EHO)_4$PcNi] (50 mg), dissolved in toluene/*n*-hexane (10 mL) (3:2), was chromatographed on the MPLC column.

[$(EHO)_4$PcNi]: A solution of 1,2-dicyano-3-(2-ethylhexyloxy)benzene (racemate)[6] (2 g, 7.8 mmol) in *N*,*N*-dimethylaminoethanol (DMAE) was heated with $NiCl_2$ (260 mg) for 24 h at 140 °C. The solvent was distilled off under vacuum and the product was purified several times by column chromatography (SiO_2; toluene/*n*-hexane (7:3). A dark blue solid was obtained. Yield: 220 mg (10%). IR (KBr): ν [cm^{-1}] = 2956 (s), 2923 (s), 2869 (s), 2856 (s), 1597 (m), 1549 (w), 1528 (m), 1493 (m), 1462 (m), 1333 (m), 1271 (s), 1238 (m), 1175 (m), 1142 (m), 1128 (m), 1086 (s), 1065 (s), 947 (w), 901 (w), 808 (w), 795 (w), 758 (w), 741 (m). ^{13}C NMR (63.5 MHz, [D_6]benzene): δ = 11.48–12.05 (C^8), 14.85–14.95 (C^6), 24.22 (C^7), 24.80 (C^5), 29.53–30.54 (C^4), 31.01–31.48 (C^3), 39.85–40.88 (C^2), 71.77/76.29 (C^1), 111.23–111.59 (C^a), 113.81–117.04 (C^b/C^b), 123.62–127.20 (C^d/$C^{d'}$), 129.41–130.06 ($C^{a'}$), 139.45–141.75 (C^c), 145.29–146.32 ($C^{c'}$), 155.48–157.43 (C^b/$C^{b'}$).

Received: May 26, 1993 [Z 6108 IE]
German version: *Angew. Chem.* **1993**, *105*, 1540

[1] H. Schultz, H. Lehmann, M. Rein, M. Hanack in *Struct. Bonding (Berlin)* **1991**, *74*, 41.
[2] A. Beck, K.-M. Mangold, M. Hanack, *Chem. Ber.* **1991**, *124*, 2315.
[3] S. Gaspard, P. Maillard, *Tetrahedron* **1991**, *56*, 3501; S. Greenberg, A. B. P. Lever, C. C. Leznoff, *Can. J. Chem.* **1988**, *66*, 1059; S. M. Marcuccio, P. I. Svirskaya, S. Greenberg, A. B. P. Lever, C. C. Leznoff, K. B. Tomer, *ibid.* **1985**, *63*, 3057.
[4] M. Hanack, D. Meng, A. Beck, M. Sommerauer, L. R. Subramanian, *J. Chem. Soc. Chem. Commun.* **1993**, 58.
[5] UV/VIS (λ_{max}; Q bands; $CHCl_3$): 699 nm (C_{4h}), 700 nm (C_{2v}), 700 nm (C_s), 702.5 nm (D_{2h}).
[6] G. Schmid, dissertation, Universität Tübingen, in preparation.

Sterically Controlled, Metal-Induced Synthesis of a 1-Thia-2,4-diphosphole**

By *Ekkehard Lindner,* Cornelius Haase, Hermann A. Mayer, Martin Kemmler, Riad Fawzi,* and *Manfred Steimann*

Dedicated to Professor Jochen Ellermann on the occasion of his 60th birthday

Cyclooligomerizations of phosphaalkynes in the protective coordination sphere of transition metal complexes have been thoroughly investigated.[1] A diphosphabicyclobutane bound to [Cp_2Zr] was used by Regitz et al. for the directed synthesis of cyclic phosphorus compounds[2] and of tetraphosphacubane.[3] In contrast, the thermal cyclotetramerization of *t*BuC≡P proceeds with minimal selectively and affords the cubane only in low yield.[4] The same research group isolated derivatives of triphospha-Dewar benzene in an $AlCl_3$-medi-

[*] Prof. Dr. E. Lindner, Dipl.-Chem. C. Haase, Dr. H. A. Mayer, Dipl.-Chem. M. Kemmler, Dr. R. Fawzi, M. Steimann
Institut für Anorganische Chemie der Universität
Auf der Morgenstelle 18, D-72076 Tübingen (FRG)
Telefax: Int. code + (7071)29-5246

[**] Preparation and Properties of and Reactions with Metal-Containing Heterocycles, Part 84. This work was supported by the Volkswagen-Stiftung and the Fonds der Chemischen Industrie. The BASF AG and Schering AG are thanked for supplying starting materials, Priv.-Doz. Dr. J. Hahn, Universität Köln, for recording selective ^{31}P decoupled $^{13}C\{^1H\}$ NMR spectra. Part 83: [6d].

ated spirocyclotrimerization of *t*BuC≡P.[5] The metal-induced, regioselective cyclocotrimerization of the alkyne-like anions $R_2P{=}S^-$ with electron-poor acetylenes leads to thiophenes, phosphole complexes, and furans, which are otherwise difficult to obtain.[6] We have now achieved the direct and desired preparation of the 1-thia-2,4-diphosphole **3** in high yields (Scheme 1), by the reaction of the (η^2-thiophosphinito)manganese complex **1a** with *tert*-butylphosphaacetylene (**2**).

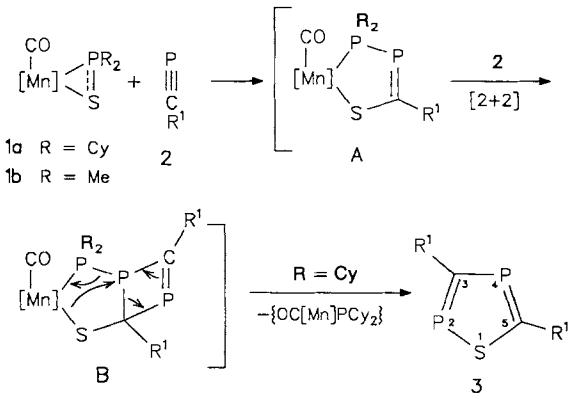

Scheme 1. [Mn] = $Mn(CO)_3$, R^1 = *t*Bu.

Recently we reported that as a result of the effect of **2** on the sterically highly strained nickel complexes [(η^5-C_5H_5)Ni-(η^2-$R_2P{\cdots}S$)] (R = *m*-xylyl, mesityl) of the type **1**, the P···S bond is cleaved with the formation of stable, nickel compounds analogous to **A**. These have been characterized by X-ray crystallography.[7] The thiadiphosphole **3** is thus formed only in traces. If the steric demand of the organometallic group in **1** is reduced by the use of a $Mn(CO)_4$ unit together with cyclohexyl groups at the phosphorus atom (⇒**Aa**), it can be assumed that this is followed by a [2 + 2] cycloaddition to give **Ba**. The latter decomposes with the elimination of the thermodynamically stable heterocycle **3**[8] (Table 1), which is obtained as a colorless liquid. The remaining metal complex fragment reacts with more **1a** to give [($OC)_3$($HPCy_2$)Mn(η^2-$PCy_2{\cdots}S$)] (Table 1) and a sparingly soluble, $Mn(CO)_x$-containing solid (IR spectrum), which could not be characterized.

Further reduction of the steric demand by the exchange of the cyclohexyl groups for methyl groups in **1** (⇒**Ab**) leads to a [2 + 2] cycloaddition of **Bb** to **2**, which via **C** affords the thermodynamically stable, orange pentacycle **4** as the final product (Table 1, Scheme 2).

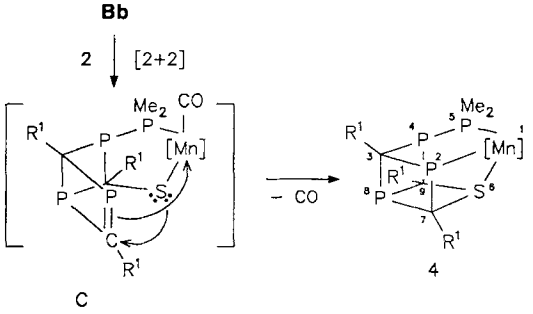

Scheme 2. [Mn] = $Mn(CO)_3$, R^1 = *t*Bu.

Table 1. Selected spectroscopic data of **3**, [($OC)_3$($HPCy_2$)Mn(η^2-$PCy_2{\cdots}S$)], **4**, and **5** [a].

3: $^{13}C\{^1H\}$ NMR: δ = 209.61 (dd, ^1J(P,C) = 66.1, ^2J(P,C) = 4.2 Hz, C5), 220.92 (dd, ^1J(P,C) = 69.6, 78.0 Hz, C3); $^{31}P\{^1H\}$ NMR: δ = 251.2 (d, ^2J(P,P) = 49.9 Hz, P4), 262.4 (d, ^2J(P,P) = 49.9 Hz, P2); MS (EI, 70 eV): *m/z* 232 (M^+, 100%)

[($OC)_3$($HPCy_2$)Mn(η^2-$PCy_2{\cdots}S$)]: IR(CH_2Cl_2): $\tilde{\nu}$[cm^{-1}] = 1895 s, 1921 vs, 2011 m (CO); ^1H NMR: δ = 4.55 (dm, ^1J(P,H) = 319.2 Hz, $HPCy_2$); $^{31}P\{^1H\}$ NMR: δ = 56.75 (s, $HPCy_2$), 95.25 (s, $PCy_2{=}S$); MS (FD, 8 kV, 65 °C): *m/z* 565.5 (M^+)

4 [b]: IR(*n*-hexane): $\tilde{\nu}$[cm^{-1}] = 1923 s, 1939 s, 2004 vs (CO); $^{13}C\{^1H\}$ NMR: δ = 17.76 (dddd, ^1J(P,C) = 10.0, 16.2, 36.4, ^2J(P,C) = 17.3 Hz, C3), 33.60 (ddd, ^1J(P,C) = 8.9, 16.5, ^3J(P,C) = 7.2 Hz, C7), 46.41 (ddd, ^1J(P,C) = 10.5, 30.5, ^2J(P,C) = 5.2 Hz, C9); $^{31}P\{^1H\}$ NMR: δ = 73.82 (ddd, ^1J(P,P) = 207.1, ^2J(P,P) = 21.8, 21.8 Hz, P4), 116.74 (ddd, ^1J(P,P) = 207.1, ^2J(P,P) = 7.6, ^3J(P,P) = 10.5 Hz, P5), 156.62 (ddd, ^2J(P,P) = 6.5, 21.8, ^3J(P,P) = 10.5 Hz, P8), 175.73 (ddd, ^2J(P,P) = 6.5, 7.6, 21.8 Hz, P2); MS (FD, 8 kV, 33 °C): *m/z* 532.4 (M^+)

5: $^{13}C\{^1H\}$ NMR: δ = 67.40 (ddd, ^1J(P,C) = 15.3, 23.2, 55.5 Hz, C5), 195.38 (dd, ^1J(P,C) = 66.5, ^3J(P,C) = 8.5 Hz, C3), 205.28 (ddd, ^1J(P,C) = 45.2, 57.4, ^3J(P,C) = 6.2 Hz, C7); $^{31}P\{^1H\}$ NMR: δ = 66.49 (dddd, ^2J(P,P) = 19.0, 54.0, ^1J(P,C) = 15.3, 45.2 Hz, P1), 219.65 (ddddd, ^2J(P,P) = 19.0, 45.0, ^1J(P,C) = 55.5, 66.5, ^3J(P,C) = 6.2 Hz, P4), 330.20 (ddddd, ^2J(P,P) = 45.0, 54.0, ^1J(P,C) = 23.2, 57.4, ^3J(P,C) = 8.5 Hz, P6); MS (FD, 8 kV, 32 °C): 332.0 (M^+)

[a] ^1H (250.13 MHz, internal standard: $CHCl_3$ relative to TMS), $^{13}C\{^1H\}$ (62.90 MHz, internal standard: $CDCl_3$ relative to TMS or [D_6]DMSO for **3**), $^{31}P\{^1H\}$ NMR spectra (32.44 MHz, 1% H_3PO_4/[D_6]acetone) in THF for **3**, in *n*-hexane for [($OC)_3$($HPCy_2$)Mn(η^2-$PCy_2{\cdots}S$)], in $CDCl_3$ for **4**, and in $CHCl_3$ for **5**. [b] For atom numbering see Scheme 2.

The $^{31}P\{^1H\}$ NMR spectrum of **4** in $CDCl_3$ shows four groups of signals, in which all four phosphorus atoms are coupling with each other. Since the X-ray structure analysis of **4** showed three possibilities for the positions of the three-coordinate P and S atoms, a ^{31}P solid-state NMR spectrum was also recorded. Likewise four signals were obtained, whose chemical shifts are in agreement with those in the $^{31}P\{^1H\}$ NMR solution spectrum. Two signals in the ^{31}P CP/MAS NMR spectrum are very broad and display a high anisotropy of the chemical shift. These effects can only be explained by the existence of a Mn–P quadrupolar interaction[9] (^{55}Mn nucleus: I = 5/2, 100%). Thus, *two* Mn–P bonds are present in **4**.

In agreement with the NMR data, the sulfur atom cannot occupy the positions P3 and P4 (large $^1J_{P,P}$ coupling between P2 and P4) in the crystal of **4** (Fig. 1).[10] The molecule has crystallographic *m* symmetry; since its constitution does not allow such symmetry, this means that in the crystal, disorder exists with respect to this mirror plane, and thus it is not possible to distinguish between P1 and S1. The pentacycle shows half of the tetraphosphacubane framework,[3, 4]

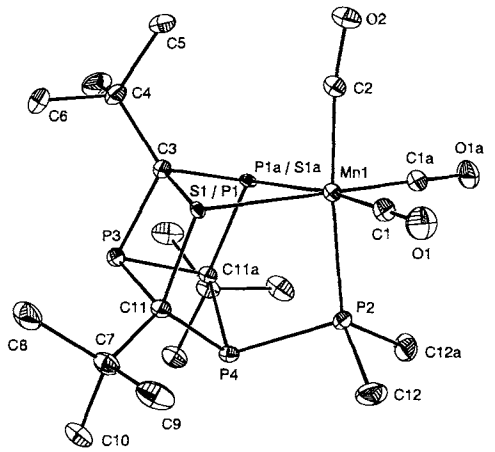

Fig. 1. Crystal structure of **4**. Selected distances [Å] and angles [°]: Mn1-P2 2.255(1), P2-P4 2.189(1), P4-C11 1.859(2), P3-C11 1.894(2), P3-C3 1.878(2), P3-P4 2.655(1); Mn1-P2-P4 105.8(1), P2-P4-C11 108.1(1), P4-C11-P3 90.0(1), C11-P3-C3 85.2(1). The atom numbering is different from that in Scheme 2.

in which one P atom is replaced by an S atom, and one edge consists of a $Mn(CO)_3-PMe_2-P$ unit. The structural parameters of the cubane section are similar to those of the parent compound.[3,4] The phosphorus atom P4 is shifted from the ideal cubic position because of the PMe_2 bridge (the interplanar angle between C11-P3-C11a and C11-P4-C11a is 147.7°). The P2–P4 distance is somewhat shorter than that of a single bond.

If reactions, in which the steric demand of the R group is between methyl and cyclohexyl, for example R = Ph, are carried out starting from **1**, in addition to **3** and the corresponding pentacycle **4** with Ph instead of Me, the metal-free, intense yellow bicyclic compound **5** is obtained (Table 1).

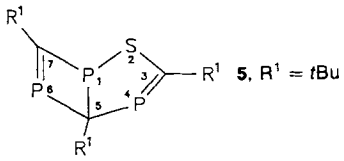

5, $R^1 = t$Bu

The described reaction can also be transferred to other phosphaalkynes such as adamantyl- and methylcyclohexylphosphaacetylenes (δ^{31}P of **3**, R^1 = adamantyl (in dimethoxyethane): 245.04 and 256.24, $^2J_{P,P} = 48.7$ Hz; of **3**, R = MeC_6H_{10} (in C_6D_6): 255.26 and 265.16, $^2J_{P,P} = 49.7$ Hz).

Experimental Procedure

3: A solution of **1a** (535 mg, 1.35 mmol) and **2** (340 mg, 3.40 mmol) was heated to 66 °C for 5 h in THF (50 mL). After the removal of the solvent at 50 mbar the residue was taken up in petroleum ether 60/90 (20 mL) and purified on a short silica gel column. The main product was separated by MPLC with petroleum ether 60/90 on a silica gel column. First fraction: **3** (122 mg, 78% yield based on 0.675 mmol **1a**), correct elemental analysis, m.p. 10 °C; third fraction: $[(OC)_3(HPCy_2)Mn(\eta^2\text{-}PCy_2\text{-}S)]$ (310 mg, 81% based on 0.675 mmol **1a**; H stems from traces of moisture), yellow powder, correct elemental analysis, m.p. 123 °C.

4: **1b** (470 mg, 0.90 mmol, exists as dimer [6c]) and **2** (640 mg, 6.40 mmol) in THF (50 mL) were mixed together and heated under reflux for 22 h. The workup was carried out as for **3** but with petroleum ether/ethyl acetate 3/1 as eluent. Third fraction: **4** (420 mg, 44%), orange single crystals from *n*-hexane, correct elemental analysis, m.p. 210 °C.

5: **1**, R = Ph, (263 mg, 0.34 mmol) was heated with **2** (200 mg, 2.00 mmol) in THF (40 mL) to 50 °C for 44 h. After the removal of the solvent under vacuum, the residue was taken up in petroleum ether/ethyl acetate (10/1) (20 mL), filtered (P4), and separated on a silica gel column with the same eluent. First fraction: **5** (12.4 mg, 11%) yellow solid.

For the assignment of the ^{31}P and ^{13}C NMR signals, **3**, **4**, and **5** were synthesized with ^{13}C-labeled **2**.

Received: June 2, 1993 [Z6116IE]
German version: *Angew. Chem.* **1993**, *105*, 1521

[1] M. Regitz in *Organic Synthesis via Organometallics* (Eds.: D. Enders, H.-J. Gais, W. Keim), Vieweg, Braunschweig, **1993**, p. 93, and references therein.

[2] P. Binger, T. Wettling, R. Schneider, F. Zurmühlen, U. Bergsträsser, J. Hoffmann, G. Maas, M. Regitz, *Angew. Chem.* **1991**, *103*, 208–211; *Angew. Chem. Int. Ed. Engl.* **1991**, *30*, 207–210.

[3] M. Birkel, J. Schulz, U. Bergsträsser, M. Regitz, *Angew. Chem.* **1992**, *104*, 870–873; *Angew. Chem. Int. Ed. Engl.* **1992**, *31*, 879–882.

[4] T. Wettling, J. Schneider, O. Wagner, C. G. Kreiter, M. Regitz, *Angew. Chem.* **1989**, *101*, 1035–1037; *Angew. Chem. Int. Ed. Engl.* **1989**, *28*, 1013–1014.

[5] B. Breit, U. Bergsträsser, G. Maas, M. Regitz, *Angew. Chem.* **1992**, *104*, 1043–1046; *Angew. Chem. Int. Ed. Engl.* **1992**, *31*, 1055–1058.

[6] a) E. Lindner, *Adv. Heterocycl. Chem.* **1986**, *39*, 237–279; b) E. Lindner, V. Käss, W. Hiller, R. Fawzi, *Angew. Chem.* **1989**, *101*, 460–462; *Angew. Chem. Int. Ed. Engl.* **1989**, *28*, 448–450; c) E. Lindner, V. Käss, H. A. Mayer, *Chem. Ber.* **1990**, *123*, 783–790; d) E. Lindner, T. Schlenker, R. Fawzi, C. Maichle, *J. Organomet. Chem.* **1993**, in press.

[7] E. Lindner, A. Nothdurft, R. Fawzi, C. Maichle, *J. Organomet. Chem.* **1992**, *435*, 213–224.

[8] A. Schmidpeter, K. Karaghiosoff in *Multiple Bonds and Low Coordination in Phosphorous Chemistry*, 1. edition, (Eds.: M. Regitz, O. J. Scherer) Thieme, Stuttgart, **1990**, p. 279, and references therein.

[9] E. Lindner, R. Fawzi, H. A. Mayer, K. Eichele, K. Pohmer, *Inorg. Chem.* **1991**, *30*, 1102–1107.

[10] Crystal structure analysis (Siemens-P4 diffractometer): **4** crystallized from *n*-hexane, $C_{20}H_{33}MnO_3P_4S$, $M = 532.3$, crystal dimensions $0.2 \times 0.5 \times 0.5$ mm^3, orthorhombic, space group *Pnma* (*Pna*2$_1$ was checked), $a = 984.7(2)$, $b = 1463.6(3)$, $c = 1744.6(3)$ pm, $V = 2514.3(8) \times 10^6$ pm^3, $\rho_{calcd} = 1.406$ g cm^{-3}, $Z = 4$ (measurement temperature 173 K), $Mo_{K\alpha}$ radiation ($\mu = 0.881$ mm^{-1}), $2\theta = 4-45°$, total number of reflections 12462, number of symmetry-independent reflections with $I \geq 2\sigma(I)$ 1623, refined parameters 160, absorption correction Ψ scan, $R = 0.022$, $R_w = 0.026$, $S = 0.94$, residual electron density 0.23 eÅ^{-3}, solution and refinement with the SHELXTL-PC program. The positions of S1/P1 and P1a/S1a were each refined with the occupation factor 0.5. The H atoms were geometrically positioned (riding model). Further details of the crystal structure investigation may be obtained from the Fachinformationszentrum Karlsruhe, Gesellschaft für wissenschaftlich-technische Information mbH, D-76344 Eggenstein-Leopoldshafen (FRG) on quoting the depository number CSD-57347, the names of the authors, and the journal citation.

Hydrolysis to a Complex with a Central, Octahedral (μ_6-O)In$_6$ Unit**

By *Kaspar Hegetschweiler,* Michele Ghisletta, Thomas F. Fässler, and Reinhard Nesper*

In a number of studies over the last two years we have been able to show that the ligand 1,3,5-triamino-1,3,5-trideoxy-*cis*-inositol (taci) is remarkably versatile in complexing metal ions.[1–4] In aqueous solution monovalent to tetravalent cations of the groups 1–15 are readily complexed. Two different chair conformations (Scheme 1) enable the binding of a metal ion to three nitrogen atoms (a), two nitrogen atoms and one oxygen atom (b), two oxygen atoms and one nitrogen atom (c) as well as three oxygen atoms (d). In the $[M(taci)_2]^{3+}$ complexes (M = Al, Ga, Tl), coordination proceeds by binding the cations at the triaxial sites (a) or (d). The oxophilic Al^{3+} is coordinated exclusively by oxygen donors, whereas Tl^{3+} shows an N_6 coordination sphere. Ga^{3+} lies in between Al^{3+} and Tl^{3+} and consequently is bound to three nitrogen atoms of one ligand and to three oxygen atoms of the other.[3] In contrast, Pb^{2+} and Bi^{3+} prefer the asymmetric coordination mode (c).[4]

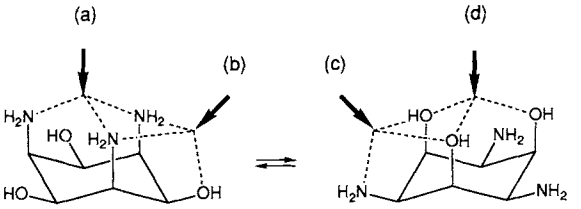

Scheme 1. Possible coordination modes of the ligand taci.

The stability constants determined in aqueous solution show that the Al, Ga, and Tl complexes are not stable with respect to the formation of solid hydroxides or oxides.[3] Indeed, the tendency to hydrolyze was confirmed by spectro-

[*] Dr. K. Hegetschweiler, Dipl.-Chem. M. Ghisletta, Dr. T. F. Fässler, Prof. R. Nesper
Laboratorium für Anorganische Chemie
ETH Zentrum, CH-8092 Zürich (Switzerland)
Telefax: Int. code + (1)252-8935

[**] 1,3,5-Triamino-1,3,5-trideoxy-*cis*-inositol, a new, ligand with a remarkable versatility for metal ions, part 6. This work was supported by the ETH Zürich. Part 5: K. Hegetschweiler, R. D. Hancock, M. Ghisletta, T. Kradolfer, V. Gramlich, H. W. Schmalle, *Inorg. Chem.*, in press.

scopic and potentiometric measurements. These measurements clearly show that the rate of hydrolysis increases dramatically in the sequence $Al^{III} < Ga^{III} < Tl^{III}$. Starting from the corresponding In^{III} complex we could isolate a hydrolysis product of the composition $[OIn_6(taci-3H)_4](NO_3)_4 \cdot 8H_2O$ from aqueous solution. Spectroscopic methods[5, 6] as well as an X-ray structural analysis[7] were used for its characterization.

Discrete $[OIn_6(taci-3H)_4]^{4+}$ ions, whose structure is shown in Figure 1, are found in the crystal. A single oxide ion in the center of the complex is surrounded by six In^{III} ions.[8]

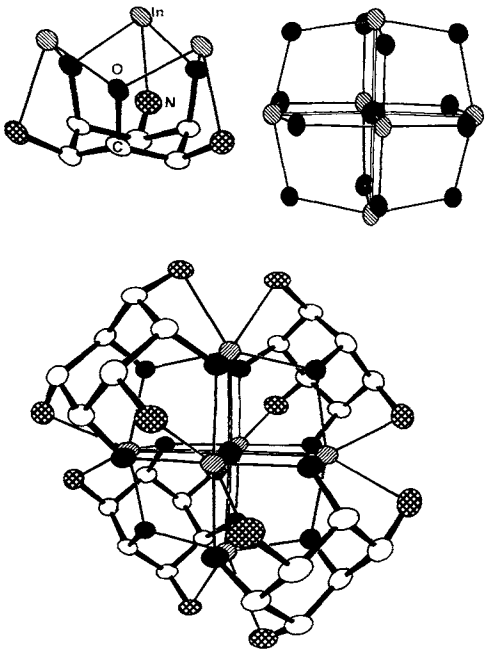

Fig. 1. Structure of $[OIn_6(taci-3H)_4]^{4+}$. $[In_3(taci-3H)]$ fragment (top left), In_6O_{13} core (top right), and perspective overall view (bottom). The vibrational ellipsoids correspond to the 50% probability level. Bond lengths [pm]: In-O_{oxo} 241.7(5)-264.3(6), In-O_{taci} 213.0(5)-220.8(5), In-N 232.3(6)-236.0(5), C-O 141.7(6)-143.7(7), C-N 145.5(8)-147.5(6), C-C 151.2(6)-154.3(8). Selected angles [°]: O-In-O (intraligand) 85.1(2)-87.0(1), O-In-O (interligand, *cis*) 89.2(1)-90.7(2), O-In-O (interligand, *trans*) 154.5(2)-161.5(5), O-In-O_{oxo} 76.7(2)-81.0(1), O-In-N (intraligand) 71.5(2)-75.4(2), O-In-N (interligand) 122.3(2)-129.0(1), N-In-O_{oxo} 141.4(2)-144.1(1), N-In-N 73.0(2)-76.4(3), In-O_{oxo}-In (*cis*) 88.6(1)-90.4(1), In-O_{oxo}-In (*trans*) 177.2(2)-180.0, C-O-In 113.4(3)-115.6(4), C-N-In 97.3(3)-98.8(4).

This OIn_6 unit is in turn encapsulated by four triply deprotonated taci molecules. All six donor atoms of each ligand molecule interact with the In^{III} ions with the hydroxyl groups deprotonated. In contrast to the terminally coordinating amino groups, these deprotonated hydroxyl groups bridge two In^{III} ions. Each ligand molecule binds three In^{III} ions, and every In^{III} ion is simultaneously coordinated by two ligand molecules, so that all six In^{III} ions obtain the coordination number 7. The In-O_{oxo} bonds are unusually long. However, the other In-O and In-N bond lengths agree well with those values found in other complexes with a sevenfold coordinated In^{III}.[9] The twelve coordinating alkoxo groups, together with the six In^{III} ions and the central oxide ion, form an In_6O_{13} core with approximate O_h symmetry.

The crystallographic symmetry of the entire complex is C_2. However, NMR spectroscopic measurements reveal that the complex has tetrahedral T_d symmetry in solution: the observation of only two signals in the ^1H NMR and ^{13}C NMR spectra, respectively, demonstrate the equivalence of the four ligands as well as that of the three O and the three N substituted CH groups within a ligand. Four C_3 axes thus pass through the central oxygen atom and the center of the cyclohexane rings, whilst the three S_4 axes correspond to the space diagonals in the OIn_6 octahedron. It is noteworthy that $[OIn_6(taci)_4\text{-}xH]$ units are also preserved in the mass spectrometer. Signals due to single monopositive ions, which are generated by multiple deprotonation and by association of NO_3^-, are observed.[6]

The reaction of taci with Tl^{III} in the ratio of 2:1 in methanol gave the mononuclear complex ion $[Tl(taci)_2]^{3+}$.[3] The analogous reaction with In^{III} gives a crude product which contains the mononuclear ion $[In(taci)_2]^{3+}$ as main component according to mass spectrometry and NMR spectroscopy. $[OIn_6(taci-3H)_4]^{4+}$ is formed subsequently in aqueous solution and can be regarded as a first intermediate in the hydrolytic polymerization of a mononuclear precursor complex. However, in the thermodynamically stable In_2O_3, the final product of this polymerization, the oxygen atoms are four- and not six-coordinate.[19]

Polynuclear metal complexes with a central OM_6 unit are well known.[11-13] In the isopoly anions of V^V, Nb^V, Ta^V, Mo^{VI}, and W^{VI}, this unit is obtained by the linking of MO_6 octahedra over common edges, resulting in the formation of the characteristic M_6O_{13} core.[12] Related structures have recently also been found for complexes of V^{IV}, Mn^{II}/Mn^{III}, and Fe^{III}. However, in these complexes, the peripheral oxo ligands are replaced by alkoxo groups.[13] To date, the M_6O_{13} core described here has only been known for transition metals. $[OIn_6(taci-3H)_4]^{4+}$ is the first main group element complex of this type. Moreover, it differs from the previously known complexes by adopting the coordination number 7 at the metal.

The formation of complexes with a M_6O_{13} core can be understood as a spontaneous self association of a mononuclear precursor complex. It is noteworthy that this core is observed in $[OIn_6(taci-3H)_4]^{4+}$, $[OFe_6(OCH_3)_{18}]^{2-}$, and $[Mo_6O_{19}]^{2-}$, that is metal ions with distinctly different chemical properties. We therefore assume that the M_6O_{13} unit, due to its particularly favorable geometry, is a common structural element in oligonuclear hydrolysis products of metal complexes with a relatively small number of metal centers.

Experimental Procedure

A solution of indium(III) nitrate (0.42 g, 1.4 mmol) in methanol (20 mL) was added dropwise with stirring to a solution of taci (0.51 g, 2.88 mmol) in methanol (20 mL). A white solid precipitated immediately. The suspension was stirred for an additional hour at room temperature and the solid was then filtered off. This residue was dissolved in water (10 mL), filtered through Celite and the colorless filtrate was layered with ethanol. After a few days colorless crystals were formed which were suitable for single-crystal X-ray analysis.

Received: May 21, 1993 [Z 6097 IE]
German version: *Angew. Chem.* **1993**, *105*, 1514

[1] H. W. Schmalle, K. Hegetschweiler, M. Ghisletta, *Acta Crystallogr. Sect. C.* **1991**, *47*, 2047-2052.
[2] K. Hegetschweiler, V. Gramlich, M. Ghisletta, H. Samaras, *Inorg. Chem.* **1992**, *31*, 2341-2346.
[3] K. Hegetschweiler, M. Ghisletta, T. F. Fässler, R. Nesper, H. W. Schmalle, G. Rihs, *Inorg. Chem.* **1993**, *32*, 2032-2041.
[4] K. Hegetschweiler, M. Ghisletta, V. Gramlich, *Inorg. Chem.* **1993**, *32*, 2699-2704.
[5] ^1H NMR (200 MHz, D_2O): $\delta = 4.00$ (t, $J = 3.2$ Hz, 12H), 3.17 (t, $J = 3.2$ Hz, 12H); ^{13}C NMR (50.4 MHz, D_2O, TSP): $\delta = 74.3$, 53.0.
[6] FAB^+ mass spectra were recorded on a double focussing VG-ZAB-VSEQ mass spectrometer. The aqueous sample solution was mixed with a glycerol matrix. Assignments in the range $1000 < m/z < 1500$; 1398.6 (100%) $[[OIn_6(taci)_4]-15H]^+$, 1461.6 (36) $[[OIn_6(taci)_4](NO_3)-14H]^+$, 1524.8 (12) $[[OIn_6(taci)_4](NO_3)_2-13H]^+$.
[7] The composition $C_{24}H_{48}In_6N_{16}O_{25} \cdot 8H_2O$ was confirmed by C, H, N analyses. The compound crystallized in the monoclinic space group $C2/c$

(no. 15) with $a = 2130(3)$, $b = 1251(2)$, $c = 2295(3)$ pm, $\beta = 125.28(9)°$, $Z = 4$, $V = 4992(12) \times 10^6$ pm^3, $Mo_{K\alpha}$ radiation, graphite monochromator, four-circle diffractometer STOE STADI4, reflections: 6474 observed, 6322 unique, of these 5141 with $I > 2.5\sigma(I)$ were used for the refinement of 358 parameters; structure solution by using direct methods, no absorption correction, $R = 0.0328$, $Rw = 0.0409$, residual electron density $+0.99$ / -1.2 $e_0/Å^3$. Further details of the crystal structure investigation are available on request from the Director of the Cambridge Crystallographic Data Centre, 12 Union Road, GB-Cambridge CB2 1EZ (UK), on quoting the full journal citation.

[8] We exclude the possibility of OH^- instead of O^{2-} being in the center for the following reasons: 1) The resulting divergence of the charge balance $O^{2-} + 6In^{3+} + 4(taci-3H)^{3-} + 4NO_3^-$ would require compensation by either a lower oxidation state for one In atom, by an additional deprotonation of a ligand, or by the occupation of a noncoordinated H_2O position by OH^-. However, the NMR spectroscopic evidence of four symmetry-equivalent ligands, the In–O and In–N distances, and the observation that the aqueous complex solution showed almost no alkaline reaction are all not in agreement with such compensations. 2) A disordered hydroxide ion in the center of the approximately octahedral complex should result in an increased temperature factor. This also is not observed.

[9] A. Riesen, T. A. Kaden, W. Ritter, H. R. Mäcke, *J. Chem. Soc. Chem. Commun.* **1989**, 460–462.

[10] M. Marezio, *Acta Crystallogr.* **1966**, *20*, 723–728.

[11] a) P. Miele, J. D. Foulon, N. Hovnanian, L. Cot, *J. Chem. Soc. Chem. Commun.* **1993**, 29–31; b) K. G. Caulton, M. H. Chisholm, S. R. Drake, J. C. Huffman, *ibid.* **1990**, 1498–1499; c) R. Schmid, A. Mosset, J. Galy, *Inorg. Chim. Acta* **1991**, *179*, 167–170.

[12] Q. Chen, J. Zubieta, *Coord. Chem. Rev.* **1992**, *114*, 107–167.

[13] a) M. I. Khan, Q. Chen, D. P. Goshorn, J. Zubieta, *Inorg. Chem.* **1993**, *32*, 672–680; b) M. Cavaluzzo, Q. Chen, J. Zubieta, *J. Chem. Soc. Chem. Commun.* **1993**, 131–133; c) K. Hegetschweiler, H. Schmalle, H. M. Streit, W. Schneider, *Inorg. Chem.* **1990**, *29*, 3625–3627; d) K. Hegetschweiler, H. W. Schmalle, H. M. Streit, V. Gramlich, H.-U. Hund, I. Erni, *ibid.* **1992**, *31*, 1299–1302.

$[AltBu]_6^-$: EPR Spectroscopic Evidence and Ab Initio Calculations**

By *Carsten Dohmeier, Mario Mocker, Hansgeorg Schnöckel,* Albert Lötz, Uwe Schneider,* and *Reinhart Ahlrichs**

Dedicated to Professor Hans Bock on the occasion of his 65th birthday

Perhalogenated *closo*-borates $[BX]_n^{2-}$ (X = Cl, Br, I) with $n = 8$–12[1–3] have been known for some time.[4] Recently, the first analogous aluminum compound, $[AlBu]_{12}^{2-}$,[5] was characterized. We report here on the second anionic aluminum cluster, the radical anion $[AltBu]_6^-$ $\mathbf{1}^{\bullet-}$.[6] After tetrahedral $[(AlCp^*)_4]$[9, 10] and icosahedral $[AlBu]_{12}^{2-}$,[5] $\mathbf{1}^{\bullet-}$ is the first aluminum cluster derived from octahedral symmetry.

The reaction of a solution of AlCl in toluene and diethyl ether[11] with *t*BuLi gave a dark red solution from which LiCl slowly precipitated.[11] A homogeneous reaction pathway is revealed by NMR spectroscopy.[12] The analysis of the product shows it to be a monovalent aluminum compound.[13] If the solution is reduced with Na/K alloy, hardly any differences in the NMR spectra can be detected. Only the proton spectrum indicates the presence of a paramagnetic species by showing a very broad resonance ($\delta = 1.4$). This was confirmed by the EPR spectrum (Fig. 1). The 31 lines

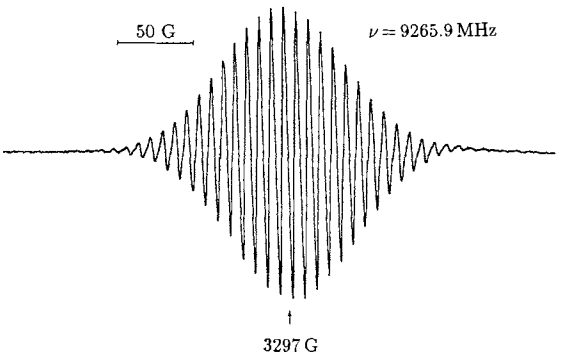

Fig. 1. EPR spectrum of $[AltBu]_6^-$ in C_6D_6 ($a(^{27}Al) = 8.2$ G, $g = 2.008$).

clearly point to a compound with six equivalent aluminum atoms (^{27}Al: 100%, $I = 5/2$). The analogous alkylation of AlBr[14] instead of AlCl, gives, without reduction, a product with the same NMR and EPR spectra.[15] The compound, evidenced by EPR, thus cannot be a species containing halogen. Since neither isomerization nor elimination of the *t*Bu substituents are observed, the conclusion is that the radical anion $[AltBu]_6^-$ ($\mathbf{1}^{\bullet-}$) must be present. The isolation of $[(AltBu)_6]$ (**1**) and $M_A^+\mathbf{1}^{\bullet-}$ [Eq. (a)] has so far not been successful.[16]

$$6AlCl \xrightarrow[-LiCl]{tBuLi} \text{“}[(AltBu)_6]\text{”} \xrightarrow{Na/K} M_A^+[AltBu]_6^- \qquad (a)$$

In order to elucidate the structure and electron distribution of $\mathbf{1}^{\bullet-}$, a quantum chemical geometry optimization[17] was carried out at the SCF level. In addition, Al*t*Bu and **1** were also studied with these methods.

Wade's rules predict a perfectly regular octahedron for Al_6 cages only for the dianion. For neutral compounds or monoanions, however, an octahedral cage leads to the occupation of the t_{2g} HOMO with four or five electrons, respectively, and thus to a Jahn-Teller distortion, which was verified in the SCF approximation. All calculations were carried out in D_{3d} symmetry (Fig. 2), since this is the highest possible symmetry consistent with *t*Bu groups as ligands, leads to six equivalent Al atoms, and, moreover, allows a continuous transition between octahedron and ring.[18] Then, from the t_{2g} HOMO

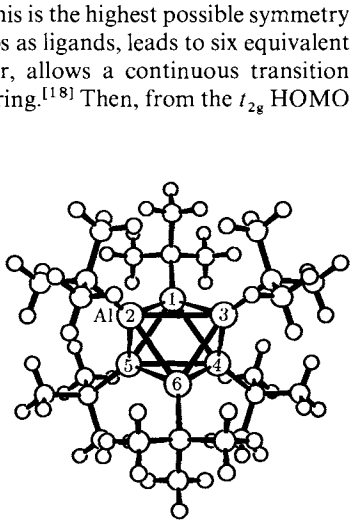

Fig. 2. Ball-and-stick model of the structure of $[AltBu]_6^-$ (D_{3d} symmetry) as calculated with ab initio methods.

[*] Prof. Dr. H. Schnöckel,[+] Dipl.-Chem. C. Dohmeier, Dipl. Chem. M. Mocker
Institut für Anorganische Chemie der Universität
Meiserstrasse 1, D-80333 München (FRG)

[+] New address: Institut für Anorganische Chemie der Universität
Postfach 6980, D-76128 Karlsruhe (FRG)
Telefax: Int. code + (721)608-4290

Priv.-Doz. Dr. A. Lötz
Institut für Physikalische Chemie der Universität München (FRG)

Prof. Dr. Ahlrichs, Dipl. Chem. U. Schneider
Lehrstuhl für Theoretische Chemie
Institut für Physikalische Chemie und Elektrochemie der Universität
Kaiserstrasse 12, D-76128 Karlsruhe (FRG)

[**] This work was supported by the Deutsche Forschungsgemeinschaft and the Fonds der Chemischen Industrie. We thank Prof. Dr. J. Voitländer for providing the EPR spectrometer.

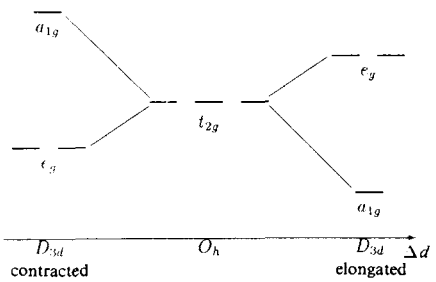

Scheme 1. Correlation diagram of the HOMOs of octahedral Al_6 compounds with distortion towards D_{3d}. Δd = change of distance.

in the octahedron, an a_{1g} and an e_g orbital result. Their energy level sequence depends on whether elongation or contraction occurred along the threefold axis (Scheme 1). We investigated all states that are obtained by assigning a total of four or five elctrons to these a_{1g} and e_g orbitals (Tables 1 and 2 for **3** and **1**, respectively).[19] The analysis of the SCF-MOs shows that these orbitals are restricted to the Al_6 cage, that is the *t*Bu ligands contribute only very little.[20]

Table 1. The configurations of [(Al*t*Bu)$_6$] in D_{3d} symmetry. Numbering of atoms as in Figure 2, energies relative to $^3A_{1g}$ ($a_{1g}^2e_g^2$, $E_{SCF} = -2389.35068$ a.u.).

State	$^1A_{1g}$ ($a_{1g}^0e_g^4$)	^3E_g ($a_{1g}^1e_g^3$)	$^3A_{2g}$ ($a_{1g}^2e_g^2$)
ΔE_{SCF} [kJ mol^{-1}]	+12	+12	0
ΔE_{Hex} [kJ mol^{-1}]	−536	−536	−548
d(Al1–Al2) [pm]	289.1	275.2	262.7
d(Al1–Al4) [pm]	258.2	267.2	281.1
d(Al–C) [pm]	201.1	201.0	201.3

Table 2. The configurations of the [Al*t*Bu]$_6^-$ anion in D_{3d} symmetry. Numbering of atoms as in Figure 2, energies and electron affinities relative to $^3A_{1g}$ ($a_{1g}^2e_g^2$, $E_{SCF} = -2389.35068$ a.u.).

State	$^2A_{1g}$ ($a_{1g}^1e_g^4$)	^2E_g ($a_{1g}^2e_g^3$)
ΔE_{SCF}/[kJ mol^{-1}] (eV)	−143 (−1.48)	−128 (−1.33)
ε(HOMO)[eV]	−2.59	−2.52
d(Al1–Al2) [pm]	275.2	263.9
d(Al1–Al4) [pm]	261.7	272.7
d(Al–C) [pm]	203.4	203.5

For the neutral system and the anion, several configurations are separated from one another by only a few kJ mol^{-1}; however, they differ considerably with respect to the structure of the Al_6 cage. The most important result is the remarkable stability of the hexamer compared to that of six monomers [Eq. (b)].[21]

$$\Delta E_{Hex} = 6\,E(\text{Al}t\text{Bu}) - E([(\text{Al}t\text{Bu})_6]) \approx 540\ \text{kJ mol}^{-1} \qquad \text{(b)}$$

The vertical electron affinity of the neutral cluster can be estimated, on the one hand, from the energy difference between the neutral species and the anion (with the same geometry as the neutral species) and on the other, from the HOMO energy of the anion, by using Koopmans' theorem.[22]

$E_A = 1.41$ eV ($a_{1g}^0e_g^4 \rightarrow a_{1g}^1e_g^4$) and $E_A = 1.24$ eV ($a_{1g}^2e_g^2 \rightarrow a_{1g}^2e_g^3$)

Even though the calculated Al–Al distances vary between 258 and 289 pm (Tables 1 and 2), the average Al–Al distances are 271 ± 3 pm for all treated cases, and fall in the range typical for AlX tetramers.[10]

$E_A = 2.14$ eV ($a_{1g}^0e_g^4 \rightarrow a_{1g}^1e_g^4$) and $E_A = 2.33$ eV ($a_{1g}^2e_g^2 \rightarrow a_{1g}^2e_g^3$)

The D_{3d} symmetry of an $[AlR]_6^-$ anion also appears plausible in view of the bonding in $[n\text{Bu}_4\text{N}][BI]_6$.[7, 8] The two (crystallographically different) anions (C_i symmetry) of the latter exhibit significantly longer B–B bonds (175–191 pm) within the B1,B2,B3 and B4,B5,B6 triangles (numbering as in Fig. 2) than those between these triangles (175–191 pm). Thus, the distorted D_{3d} structure of the $[BI]_6^-$ unit – in line with the results of the quantum chemical calculations for $\mathbf{1}^{\bullet-}$ – offers additional support for the reasoning that Al_6 clusters with D_{3d} symmetry are responsible for the hyperfine structure of the EPR spectrum.

Experimental Procedure

All operations were carried out under nitrogen. NMR spectra (C_6D_6, 25 °C): JEOL-GSX-270 spectrometer (^{1}H, ^{13}C, ^{27}Al; reference: TMS or (external) $[Al(H_2O)_6]^{3+}$), Bruker-AC-200 (^{7}Li; reference (external): LiCl/D_2O). The EPR spectra were recorded with a Varian-E-Line (E101) spectrometer.

1: A solution of *t*BuLi (2.24 mmol) in pentane (6 mL) was added dropwise at −78 °C to a solution of AlCl (2 mmol) in toluene/diethyl ether (3:1) (6.6 mL). After 18 h the mixture was warmed to room temperature and after another 24 h the dark red solution was filtered and analyzed by NMR spectroscopy. Another solution prepared analogously was treated with Na/K alloy (1:3) (90 mg) and stirred at +4 °C for 24 h. This solution, now even darker than before, was also filtered. The solvent was removed under vacuum from a sample of this solution, and the residue was taken up in C_6D_6 and used for the EPR spectroscopic analysis. The yield of **1** after a reduction time of 24 h was estimated by EPR spectroscopy to be approximately 5% (relative to 2,2,6,6-tetramethyl-piperidine-1-oxyl as a concentration standard in C_6D_6).

Received: November 11, 1992
Revised version: May 4, 1993 [Z 5675 IE]
German version: *Angew. Chem.* **1993**, *105*, 1491

[1] W. H. Knoth, H. C. Miller, J. C. Sauer, J. H. Balthis, Y. T. Chia, E. L. Meutterties, *Inorg. Chem.* **1964**, *3*, 159.
[2] E. H. Wong, R. M. Kabbani, *Inorg. Chem.* **1980**, *19*, 451.
[3] R. M. Kabbani, E. H. Wong, *J. Chem. Soc. Chem. Commun.* **1978**, 462.
[4] $[BCl]_9^{2-}$ and $[BCl]_{10}^{2-}$ can be oxidized electrochemically to give stable radical anions ($[BCl]_9^-$: [2], $[BCl]_{10}^-$: E. H. Wong, M. G. Gatter, R. M. Kabbani, *Inorg. Chim. Acta* **1982**, *57*, 25).
[5] W. Hiller, K.-W. Klinkhammer, W. Uhl, J. Wagner, *Angew. Chem.* **1991**, *103*, 182; *Angew. Chem. Int. Ed. Engl.* **1991**, *30*, 179.
[6] In the chemistry of boron, [B*t*Bu]$_9$, (S. L. Emery, J. A. Morrison, *J. Am. Chem. Soc.* **1982**, *104*, 6790), [B*t*Bu]$_4$ (T. Mennekes, P. Paetzold, R. Boese, D. Bläser, *Angew. Chem.* **1991**, *103*, 199; *Angew. Chem. Int. Ed. Engl.* **1991**, *30*, 173; T. Davan, J. A. Morrison, *J. Chem. Soc. Chem. Commun.* **1981**, 250), and [B*t*Bu]$_4^-$ are known; the latter was characterized by EPR spectroscopy (H. Klusik, A. Berndt, *J. Organomet. Chem.* **1982**, *234*, C17).
[7] A. Heinrich, H.-L. Keller, W. Preetz, *Z. Naturforsch. B* **1990**, *45*, 184.
[8] The octahedral cluster anions $[BX]_6^{2-}$ (X = Cl, Br, I) have also recently been characterized (J. Thesing, J. Baurmeister, W. Preetz, D. Thiery, H. G. von Schnering, *Z. Naturforsch. B* **1991**, *46*, 800 and [7]).
[9] C. Dohmeier, C. Robl, M. Tacke, H. Schnöckel, *Angew. Chem.* **1991**, *103*, 594; *Angew. Chem. Int. Ed. Engl.* **1991**, *30*, 564.
[10] The structures and spectroscopic properties of $[(AlCp)_4]$ (a) and $[\{Al(Si\text{Bu}_3)\}_4]$ (b) were calculated theoretically: R. Ahlrichs, M. Ehrig, H. Horn, *Chem. Phys. Lett.* **1991**, *183*, 227; (a) and (b): J. Gauss, U. Schneider, R. Ahlrichs, C. Dohmeier, H. Schnöckel, *J. Am. Chem. Soc.* **1993**, *115*, 2402; (b): U. Schneider, R. Ahlrichs, H. Horn, A. Schäfer, *Angew. Chem.* **1992**, *104*, 327; *Angew. Chem. Int. Ed. Engl.* **1992**, *31*, 353. These compounds could be authenticated spectroscopically.
[11] M. Tacke, H. Schnöckel, *Inorg. Chem.* **1989**, *28*, 2895.
[12] ^{1}H: $\delta = 1{,}21$(s), ^{13}C: $\delta = 30.5$, ^{27}Al: $\delta = 160$ ($\omega_{1/2} = 3000$ Hz). Signals at ^{1}H: $\delta = 0.69$(t), 3.52(q); ^{13}C: $\delta = 13.3$, 67.8, and ^{7}Li: $\delta = -0.4$ we assign to unseparated LiCl·(OEt$_2$)$_x$ (ratio of OEt$_2$ to *t*Bu 1:2.5).
[13] The filtered solution was protolyzed with semidilute HCl, and the amount of H_2 evolved ($Al^+ + 2\,H^+ \rightarrow Al^{3+} + H_2$) correlated with the total aluminum content. The average oxidation state for Al is 1 ± 0.3.
[14] M. Mocker, H. Schnöckel, unpublished results.
[15] Possibly in this case subvalent Al–Br species act as reducing agents.
[16] From the NMR spectra,[12] a very symmetrical structure is derived for the primary product formed from the reaction of AlCl and *t*BuLi. We consider

the formation of the hexamer **1** according to Equation (a) is plausible, since the resulting high Al–Al binding energy in the alkylated aluminum clusters (see also [10]) obtained in the quantum chemical calculations has the result that the oligomers $[(AlrBu)_n]$ with $n < 6$ are energetically disfavored in comparison with the hexamer, whereas, the cleavage of larger clusters is very unlikely under the given experimental conditions. Moreover, there are no indications in the EPR and NMR spectra of radical anions or dianions, which would be expected had reduction of other oligomers occurred.

[17] The computations were performed with the program system TURBOMOLE (R. Ahlrichs, M. Bär, M. Häser, H. Horn, C. Kölmel, *Chem. Phys. Lett.* **1989**, *162*, 165) on an IBM RISC 6000 workstation. The open-shell molecules were treated with the RHF-SCF formalism (C. C. J. Roothan, *Rev. Mod. Phys.* **1960**, *32*, 179). Basis sets: Al: (10s7p)/[4s3p] + d(η = 0.30); C (quaternary): (7s4p)/[3s2p] + d(η = 0.80), C (primary): (6s3p)/[2s1p]; H: (3s)/[1s]. The first two basis sets were fully energy optimized on the atom, and the last two basis sets on neopentane (A. Schäfer, H. Horn, R. Ahlrichs, *J. Chem. Phys.* **1992**, *97*, 2571).

[18] For the model compound $[(AlMe)_6]$, the structure obtained was verified as a local minimum by SCF force field calculations.

[19] It should be noted that for the relatively high-lying ^3E_g $(a_{1g}^1e_g^3)$ and $^2E_g(a_{1g}^2e_g^3)$ energy states the Jahn-Teller theorem predicts a further lowering of the symmetry, which leads to nonequivalent Al atoms.

[20] Mulliken population analysis shows the electrons in the high-lying a_{1g} and e_g orbitals to be 99% localized within the Al_6 cage.

[21] The inclusion of the correlation energy with single point MP2 calculations (2nd order perturbation) increases the stabilization energy for the model compound $[(AlMe)_6]$ by 320 kJ mol^{-1} from 540 kJ mol^{-1} to 860 kJ mol^{-1}. This corresponds with the AlX tetramers, where MP2 calculations result in a stabilization energy of 50 kJ mol^{-1}.

[22] Koopmanns' theorem systematically overestimates the electron affinity because it neglects orbital relaxation.

The Structures of Tris(8-dimethylamino-1-naphthyl)phosphane and Tris[2-(dimethylaminomethyl)phenyl]phosphane: Crystallographic Evidence of Seven-Coordinate Phosphorus

By *Claude Chuit, Robert J. P. Corriu,* Pascal Monforte, Catherine Reyé, Jean-Paul Declercq*, and *Antoine Dubourg*

Dedicated to Professor Hans Bock on the occasion of his 65th birthday

Following our work on the chemistry of hypercoordinate silicon compounds,[1] we are at present investigating the ability of phosphorus to expand its coordination number by intramolecular coordination. Surprisingly, with the exception of phosphoranes in which the formation of intramolecular coordination has been shown,[2–6] few studies[4, 7] have been reported in this field. While phosphanes with one N-donor group appropriately placed for intramolecular chelation[8–13] have been prepared, the possible formation of such an interaction has been suggested only rarely.[14]

We report here the preparation, structural characterization, and some observations on the reactivity of phosphanes in which increase in coordination number at the phosphorus atom is achieved by three intramolecular N–P dative bonds.

The phosphane **1** was prepared by reaction of an excess of 8-dimethylamino-1-naphthyllithium[15] with PBr_3 in 67% yield. It was identified on the basis of its mass spectrometric and NMR spectroscopic data. The ^{1}H NMR solution spectrum shows the equivalence of the three NMe_2 groups whose resonances appear as two singlets of equal intensity, which correspond to two sets of diastereotopic methyl groups resulting from the coordination of the nitrogen atoms to the phosphorus atom. Interestingly, **1** shows no change in its ^{1}H NMR spectrum at high temperature (90 °C, 250 MHz).

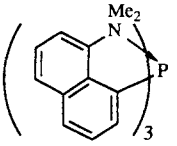

1

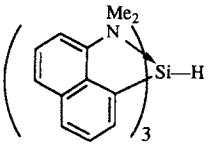

2

Confirmation of the intramolecular coordination of the three NMe_2 groups at the phosphorus atom was provided by a single-crystal X-ray structural analysis.[16] In the crystal, the molecules of **1** have a helicoidal shape (Fig. 1) with a pseudo threefold rotation axis in contrast with the lack of symmetry of the triphenylphosphane molecule.[17] The pyramidal configuration about the phosphorus atom is retained with C-P-C angles of 106.6(3), 107.2(3), and 107.8(3)° [average value 107.2(3)°], whereas for triphenylphosphane the average C-P-C angle is 103.44°. The nitrogen–phosphorus distances (2.805, 2.844, and 2.853 Å) are significantly shorter than the sum of the N and P van der Waals radii (3.4 Å),[18] but much more longer than a covalent N–P bond (1.77 Å), so that these bonds can be considered as weak coordinative bonds. Nitrogen coordination is observed *trans* to a C–P bond with an average C-P-N angle of 171.6°, and the naphthyl groups remain approximately planar as indicated by some selected torsion angles (Fig. 1).

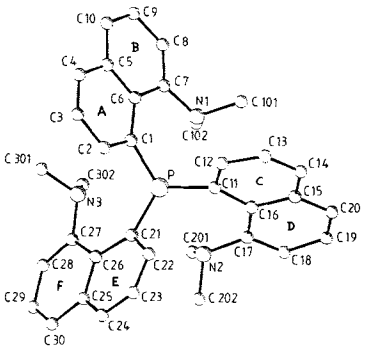

Fig. 1. Crystal structure of **1**. Selected angles [°]: C(1)-P···N(1) 75.4(3), C(1)-P···N(3) 80.2(3), C(11)-P···N(1) 78.9(3), C(21)-P···N(2) 79.5(3), C(21)-P···N(3) 74.2(3). Angle between normals to planes: A-ring–B-ring = 3 ; C-ring–D-ring = 6 ; E-ring–F-ring = 6°.

It is worth noting that the geometry of the silane **2**,[19] revealed by X-ray analysis, is the same as that of **1**, the hydrogen atom at silicon occupying the position of the phosphorus lone pair. The angles are very similar, the C-Si-C angles ranging from 104.8(4) to 107.6(4)° [average value 105.7(4)°] with Si–N distances from 2.876 to 2.928 Å.

Since intramolecular coordination by the NMe_2 groups is facilitated in **1** by the rigid geometry of the 8-dimethylamino-1-naphthyl group, we thought it might be interesting to prepare a further example of possible tris-chelated phosphane by using a coordinating ligand with a more flexible geometry, such as the [2-(dimethylaminomethyl)phenyl] ligand.[20] Phosphane **3** was prepared by the reaction of an excess of 2-(dimethylaminomethyl)phenyllithium[21] with PBr_3 in 65% yield. Its ^{1}H NMR spectrum exhibits the resonance signal of the three NMe_2 groups as a sharp singlet at room

[*] Prof. Dr. R. J. P. Corriu, Dr. C. Chuit, P. Monforte, Dr. C. Reyé
Université de Montpellier II
Sciences et Techniques du Languedoc, URA 1097
Place Eugène Bataillon, case 007
F-34095 Montpellier Cédex 5 (France)
Telefax: Int. code + (67)143888
Prof. Dr. J.-P. Declercq
Université de Louvain-la-Neuve (Belgium)
Dr. A. Dubourg
Université de Montpellier I (France)

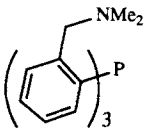

3

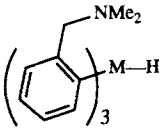

4a: M = Ge
b: M = Si

temperature and the ^{31}P (NMR) chemical shift appears at $\delta = -34$ upfield from that of triphenylphosphane ($\delta = -6$),[22] suggesting an increase in phosphorus atom coordination number. That was confirmed by the X-ray crystal structure determination of **3**[23] which indicates the same helicoidal shape observed for **1** (Fig. 2). The other main

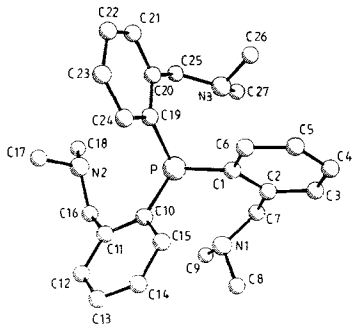

Fig. 2. Crystal structure of **3**. Selected angles [°]: C(1)-P···N(1) 72.9(3), C(1)-P···N(3) 76,4.(3), C(10)-P···N(1) 78.6(2), C(19)-P···N(2) 76.1(2), C(19)-P···N(3) 72.5(3).

features of this structure are the following: 1) The average C-P-C angle is 100.7(5)° compared with 107.2(3)° for **1** and 103.44° for triphenylphosphane; thus the basic pyramidal geometry is also retained. 2) The NMe_2 groups are directed towards the phosphorus center, *trans* to a C–P bond with N···P-C angles varying from 171.2(3) to 173.1(3)° (average value 172.1(9)°). The N···P separations (2.999 Å, 3.010 Å, 3.071 Å) are slightly longer than for **1**, but here too remain below the sum of the N and P van der Waals radii (3.4 Å), thus suggesting a weak interaction. Interestingly, the geometry of this phosphane is also similar to those of the germane **4a**[24] and the silane **4b**.[24]

It is important to emphasize that phosphanes **1** and **3** adopt the same geometry when there is no steric constraint in phosphane **3** to force the NMe_2 donor groups to interact with the phosphorus center. The flexibility of the 2-(dimethylaminomethyl)phenyl ligand compared with the rigidity of the 8-dimethylamino-1-naphthyl group explains why a) the N···P distances in **3** (2.999–3.071 Å) are slightly longer than those in **1** (2.805–2.853 Å), and b) the ^1H NMR spectrum of **3** exhibits the resonance of the NMe_2 groups as a sharp singlet, while the resonance of three NMe_2 groups in **1** appears as two singlets even at high temperature (90 °C, 250 MHz). This indicates that **1** remains coordinated in solution, while an equilibrium exists between the opened and closed forms of **3** in solution. This interpretation is corroborated by the difference of reactivity between **1** and **3** toward MeI. Phosphane **3** reacts rapidly with MeI to give the ammonium salt **5**, while **1** reacts very slowly to give the phosphonium salt **6**.

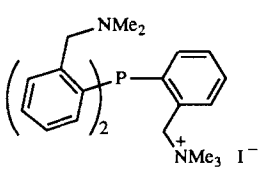

5

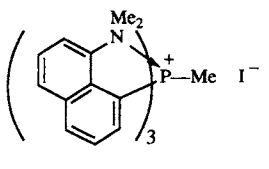

6

Thus, the P atom in compounds **1** and **3** is formally seven-coordinate with three carbon atoms, three nitrogen atoms, and its lone pair, which together form a tricapped tetrahedron. Another example of a complex with a seven-coordinate phosphorus atom results from the insertion of CS_2 in the P–N bonds of an aminophosphane.[25] The single-crystal X-ray structural analysis of this complex, the empirical molecular formula of which is $(Me_2N)_3P \cdot 3CS_2$, has shown that the phosphorus center is surrounded by six sulfur atoms, which together with the phosphorus atom lone pair form a distorted capped trigonal antiprism.

Experimental Procedure

All experiments were performed under a nitrogen atmosphere in Schlenk tubes and with predried solvents.

1: PBr_3 (2.6 g, 9.6 mmol) was added dropwise at −80 °C to a stirred suspension of yellow (8-dimethylamino-1-naphthyl)lithium [15] (6.4 g, 36 mmol) in diethyl ether (80 mL). The reaction mixture was allowed to warm to room temperature and was refluxed for 2 h. Subsequently, 10% NaOH solution (100 mL) was slowly added to the cooled yellow suspension. The yellow solid was filtered off, washed with water, acetone and diethyl ether, and dried in vacuum to give 1.55 g of crude product. After two recrystallizations from benzene, 1.15 g (67%) of pure **1** was obtained as a yellow powder: M.p. 300–303 °C; ^1H NMR (300 MHz; $CDCl_3$): $\delta = 1.4$ (s, 3H), 2.8 (s, 3H), 7.7 (m, 6H); ^{31}P NMR (250 MHz, CD_2Cl_2): $\delta = 6.07$, positive-ion FAB MS [(*m*-nitrobenzylalcohol) matrix (NOBA)]: *m/z* 542 $[M + H]^+$. Correct C,H,N analysis for $C_{36}H_{36}N_3P$.

Crystals of **1** suitable for an X-ray diffraction study could not be obtained in this way. Instead when the crude product was recovered by filtration without hydrolysis, yellow crystals of **1**, suitable for X-ray analysis were obtained after two recrystallizations in ethanol. Under these conditions, **1** crystallized with one molecule of HBr and one molecule of EtOH. M.p. 50–55 C (decomp). Correct C,H,N, analysis for $C_{38}H_{43}BrN_3OP$.

3: PBr_3 (3.7 g, 13.7 mmol) was added dropwise at −80 °C to a stirred suspension of 2-(dimethylaminomethyl)phenyllithium [21] (7.29 g, 52 mmol) in Et_2O (200 mL). The temperature was maintained at −80 °C during the addition. The reaction mixture was then allowed to warm very slowly to room temperature, and refluxed for 2 h. 10% NaOH solution (150 mL) was added to the yellow suspension. The colorless precipitate obtained was filtered off, washed with water/acetone and dried in vacuum. The powder was recrystallized from Et_2O/EtOH (1/1) to give 3.94 g (65%) of white crystals of **3**: M.p. 117–120 °C; ^1H NMR (250 MHz, CD_2Cl_2): $\delta = 2.05$ (s, 6H), 3.55 (s, 2H), 7.15 (m, 4H); ^{31}P NMR (250 MHz, CD_2Cl_2): $\delta = -34$; positive-ion FAB MS (NOBA matrix) *m/z*: 434 $(M + H)^+$; correct C,H,N analysis for $C_{27}H_{36}N_3P$.

5: A mixture of **3** (0.52 g, 1.2 mmol), methyl iodide (0.07 mL, 1.2 mmol) and toluene (20 mL) were heated in a sealed tube at 100 °C for 3 h. Then the white precipitate formed was filtered off, washed with toluene and anhydrous ether. After two recrystallizations from EtOH/benzene, 0.427 g of a white powder identified as **5** was obtained (62%): M.p. 210–213 °C. ^1H NMR (250 MHz, CD_2Cl_2): $\delta = 2.1$ (s, 12H), 3.2 (s, 9H), 3.3 (s, 4H), 5.1 (s, 2H), 6.4–8.0 (m, 12H); ^{31}P NMR (250 MHz, D_2O): $\delta = -7.85$; positive-ion FAB MS (NOBA matrix) *m/z*: 448 $(M - I)^+$; correct C,H,N analysis for $C_{28}H_{39}IN_3P$.

6: A mixture of **1** (1 g, 1.84 mmol) and MeI, (0.95 mL, 15 mmol) in toluene (5 mL) was heated in a sealed tube at 100 °C. After 10 days, the precipitate formed was filtered off and recrystallized twice from EtOH/benzene (1/3) to give 0.402 g (32%) of a pale yellow powder which was identified as **6**: M.p. 350 °C (decomp); ^1H NMR (80 MHz, $CDCl_3$): $\delta = 0.8$ (s, 9H), 2.0 (s, 9H), 2.4 (d, $^2J(P,H) = 20$ Hz, 3H), 7.0–8.6 (m, 18H); ^{31}P NMR (250 MHz, CD_2Cl_2): $\delta = 12.26$; positive-ion FAB MS (NOBA matrix): *m/z* 556 $(M - I)^+$. Correct C,H,N analysis for $C_{37}H_{39}IN_3P$.

Received: January 29, 1993
Revised version: June 23, 1993 [Z 5839 IE]
German version: *Angew. Chem.* **1993**, *105*, 1529

[1] R. J. P. Corriu, J. C. Young, *Chem. Org. Silicon Comp. 1989* **1989**, 1241; R. J. P. Corriu, *J. Organomet. Chem.* **1989**, *400*, 81; C. Chuit, R. J. P. Corriu, C. Reyé, J. C. Young, *Chem. Rev.* **1993**, *93*, 1371.
[2] K. P. John, R. Schmutzler, W. S. Sheldrick, *J. Chem Soc. Dalton Trans.* **1974**, 1841, 2466; R. Krebs, R. Schmutzler, D. Schomburg, *Polyhedron* **1989**, *8*, 731.
[3] A. Munoz, G. Gence, M. Koenig, R. Wolf, *C. R. Acad. Sci. Ser. C* **1975**, *280*, 395.
[4] C. B. Cong, G. Gence, B. Garrigues, M. Koenig, A. Munoz, *Tetrahedron* **1979**, *35*, 1825.
[5] D. Robert, H. A. Gawad, J. G. Riess, *Bull. Soc. Chim. Fr.* **1987**, 511.
[6] D. K. Kennepohl, B. D. Santarsiero, R. G. Cavell, *Inorg. Chem.* **1990**, *29*,

5081; D. K. Kennepohl, A. A. Pinkerton, Y. F.Lee, R. G. Cavell, *ibid.* **1990**, *29*, 5088.
[7] D. S. Milbrath, J. G. Verkade, *J. Am. Chem. Soc.* **1977**, *99*, 6607.
[8] G. Marr, T. Hunt, *J. Chem. Soc. C* **1969**, 1070.
[9] T. B. Rauchfuss, F. T. Patino, D. M. Roundhill, *Inorg. Chem.* **1975**, *14*, 652.
[10] L. Horner, G. Simons, *Phosphorus Sulfur Relat. Elem.* **1983**, *15*, 165.
[11] L. Horner, G. Simons, *Phosphorus Sulfur Relat. Elem.* **1984**, *19*, 65.
[12] G. K. Anderson, R. Kumar, *Inorg. Chem.* **1984**, *23*, 4064.
[13] G. P. C. M. Dekker, A. Buijs, C. J. Elsevier, K. Vrieze, P. W. N. M. van Leeuwen, W. J. J. Smeets, A. L. Spek, Y. F. Wang, C. H. Stam, *Organometallics* **1992**, *11*, 1937.
[14] G. P. Schiemenz, E. Papageorgiou, *Phosphorus Sulfur Relat. Elem.* **1982**, *13*, 41.
[15] J. T. B. H. Jastrzebski, C. T. Knaap, G. van Koten, *J. Organomet. Chem.* **1983**, *255*, 287.
[16] a) X-ray crystal structure analysis of **1**: $C_{36}H_{36}N_3P \cdot HBr \cdot C_2H_5OH$, $M_r = 668.64\ g\,mol^{-1}$. Crystal size: $0.3 \times 0.3 \times 0.4$ mm. Huber diffractometer, $Cu_{K\alpha}$ radiation, measurement at room temperature. Orthorhombic, space group, *Pbca*, $a = 17.415(4)$, $b = 25.584(4)$, $c = 15.101(2)$ Å, $V = 6728(2)$ Å^3. $Z = 8$; $\varrho_{calcd} = 1.32\ g\,cm^{-3}$; $F(000) = 2800$. No absorption correction, $\mu = 2.5\ mm^{-1}$ ($\lambda = 1.54178$ Å). $2\theta_{max} = 135°$. 6066 independent reflections for 3438 of which $I \geq 3\sigma(I)$. Structure determination: MULTAN 80 + DIRDIF. Refinement: SHELX-76 (using *F*) final values: $R = 0.069$; $R_w = 0.064$. b) Further details of the crystal structure investigation are available on request from the Fachinformations-Zentrum Karlsruhe, Gesellschaft für wissenschaftlich-technische Information mbH, D-76344 Eggenstein-Leopoldshafen (FRG), quoting the depository number CSD-57389, the name of the authors, and the journal citation.
[17] J. J. Daly, *J. Chem. Soc.* **1964**, 3799.
[18] A. Bondi, *J. Phys. Chem.* **1964**, *68*, 441.
[19] C. Brelière, F. Carré, R. J. P. Corriu, M. Wong Chi Man, J. Lappasset, unpublished results.
[20] G. van Koten, J. C. Noltes, A. L. Spek, *J. Organomet. Chem.* **1976**, *118*, 183.
[21] G. van Koten, A. J. Leusink, J. G. Noltes, *J. Organomet. Chem.* **1975**, *84*, 117.
[22] D. G. Gorenstein, D. O. Shah in *Phosphorus ^{31}P NMR. Principles and Applications*, Academic Press, New York, **1984**, p. 553.
[23] X-ray crystal structure analysis of **3**: $C_{27}H_{36}N_3P$, $M_r = 433.53\ g\,mol^{-1}$. Crystal size: $0.5 \times 0.3 \times 0.2$ mm. Huber diffractometer, $Mo_{K\alpha}$ radiation, measurement at room temperature. Monoclinic, $P2_1/c$, $a = 8.974(2)$, $b = 16.444(5)$, $c = 17.958(4)$ Å, $\beta = 102.69(2)°$; $V = 2585(1)$ Å^3; $Z = 4$; $\varrho_{calcd} = 1.11\ g\,cm^{-3}$; $F(000) = 936$. No absorption correction, $\mu = 0.13\ mm^{-1}$ ($\lambda = 0.71069$ Å). $2\theta_{max} = 52°$. 5073 independent reflections for 2222 of which $I \geq 2.5\sigma(I)$. Structure determination: MULTAN 80+ DIRDIF. Refinement: SHELX-76 (using F), final values: $R = 0.057$; $R_w = 0.067$ [16b].
[24] C. Brelière, F. Carré, R. J. P. Corriu, G. Royo, *Organometallics* **1988**, *7*, 1006.
[25] R. W. Light, L. D. Hutchins, R. T. Paine, C. F. Campana, *Inorg. Chem.* **1980**, *19*, 3597.

Synthesis and Pairing Properties of Deca-nucleotides from (3′*S*,5′*R*)-2′-Deoxy-3′,5′-ethano-β-D-ribofuranosyladenine and -thymine**

By *Markus Tarköy* and *Christian Leumann**

Sequence-specific complexation of RNA single strands and DNA duplexes by oligonucleotides provides a way of selective inhibition of protein biosynthesis.[1] Specificity in the recognition process relies on the fundaments of the Watson–Crick base pairing rules[2] and the corresponding rules for triplex formation,[3] and depends on the base sequence and the length of the oligonucleotide. With the goal of a possible therapeutic application, an extensive search for oligonucleotide analogues that exhibit stronger binding to complementary DNA and RNA and show higher enzymatic resistance towards nucleases as well as higher membrane permeability has evolved over the last decade.[4]

Recently we introduced a new type of nucleosides ("bicyclonucleosides") that differs from the natural deoxyribonucleosides by an additional ethylene bridge between the C3′ and C5′ centers (Scheme 1).[5] These bicyclonucleosides show

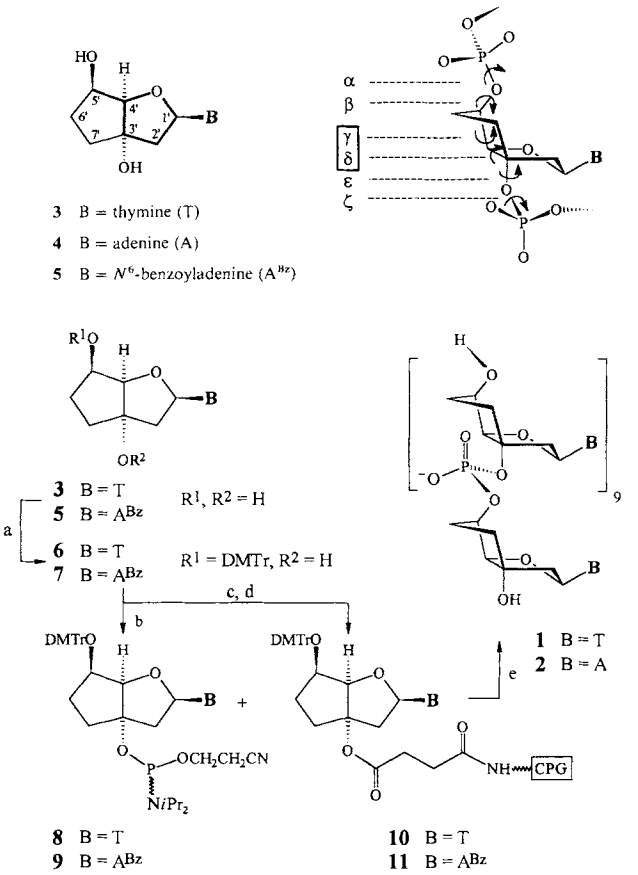

Scheme 1. Synthesis of deca-(3′*S*,5′*R*)-2′-deoxy-3′,5′-ethano-β-D-ribonucleotides **1** and **2** of the nucleobases adenine and thymine, respectively. a) $DMTr^+CF_3SO_3^-$, pyridine, 3h, room temperature (RT), 88%, **6**, (85%, **7**); b) $[(NCCH_2CH_2O)(iPr_2N)PCl]$, iPr_2EtN, THF, RT, 1 h, 63%, **8**, (76%, **9**); c) succinic anhydride, pyridine, 4-(dimethylamino)pyridine (DMAP), RT, 70 h, then *p*-nitrophenol, THF, *N*,*N*′-dicyclohexylcarbodiimide, RT, 2 h, 73%, B = T (63%, B = A^{Bz}); d) LCAA-CPG (Sigma), dioxane, dimethylformamide (DMF), Et_3N, RT, 2 d, then Ac_2O, pyridine, DMAP, RT, 30 min.; e) see [9].

less conformational flexibility in the furanose framework than the natural deoxyribonucleosides and were designed to confer, as constituents of an oligonucleotide chain, a higher degree of preorganization of a single strand for hybridization. This should lead to an entropic advantage for the pairing process and, eventually, to thermodynamically more stable complexes. Furthermore, oligonucleotides consisting of bicyclonucleosides have secondary and tertiary phosphodiester groups, and can be expected to be more resistant against enzymatic degradation by phosphodiesterases than their natural counterpart. Here we report on the synthesis of the two bicyclo-DNA decamers **1** and **2** and their pairing behavior with complementary RNA and DNA.

[*] Dr. C. Leumann,[+] M. Tarköy
Laboratorium für Organische Chemie der ETH
Universitätstrasse 16, CH-8092 Zürich (Switzerland)
[+] New address:
Institut für Organische Chemie der Universität
Freiestrasse 3, CH-3012 Bern (Switzerland)
Telefax: Int. code + (31) 631-8057

[**] Nucleic Acid Analogues with Constraint Conformational Flexibility in the Sugar-Phosphate Backbone, Part 2. This work was supported by a grant from ETH and from the Stipendienfonds der Basler Chemischen Industrie. Part 1: [5].

For automated oligonucleotide synthesis, according to standard phosphoramidite chemistry,[6] the bicyclic nucleoside derivatives **3** and **5**[5] were initially converted to the corresponding trityl derivatives **6** and **7** with 4,4'-dimethoxytriphenylmethyl (DMTr) trifluoromethanesulfonate.[7] The reactions of **6** and **7** with chloro-(β-cyanoethoxy)diisopropylaminophosphane in THF led to the phosphoramidite building blocks **8** and **9**, respectively. The supports derivatized with nucleoside (long-chain alkylamine controlled pore glass, LCAA-CPG), **10** and **11**, were obtained in analogy to standard methods in oligonucleotide chemistry[8] from the nitrophenylsuccinates of **6** and **7**, respectively; thus, loading capacities of 22–39 μmol g^{-1} (trityl assay) were achieved. The synthesis of the deca(bicyclodeoxynucleotides) **1** and **2** was performed on a DNA synthesizer with a modified synthesis protocol[9] and proceeded with coupling yields of >98% per step (trityl assay). After removal of the protecting groups and detachment from the solid support according to standard procedures (conc. NH_3, 55 °C, 10–16 h), the crude oligomers were purified by HPLC and analyzed by mass spectrometry[10] as well as by enzymatic degradation (snake venom phosphodiesterase/alkaline phosphatase), followed by identification of the mononucleosides **3** and **4**, respectively, with reversed-phase HPLC (coinjection with authentic material).

T_m values from UV melting curves of complexes of **1** and **2** with the natural DNA and RNA complements and with each other at comparable oligonucleotide concentrations are summarized in Table 1. At neutral pH values, the duplex

Table 1. T_m values [°C] (hyperchromicity [%]) from melting curves (260 nm) in 10 mM Tris·HCl (Tris = 2-amino-2-hydroxymethyl-1,3-propanediol) pH 7.0, 0.15 M NaCl (base pair concentration = 44 μM ± 10%).

	2	d(A_{10})	poly(dA)	poly(A)
1	33 (45) [a]	10 (20)	7 (30)	20 (37)
d($T)_{10}$	25 (35)	23 (27)	27 (45)	24 (40)
poly(U)	45 (50) [a]	32 (42) [a]	45 [b]	57 [b]

[a] base pair concentration = 26 μM. [b] adapted from the work of M. Riley et al. [11].

2·poly(U) is considerably more stable than the natural hybrid d(A_{10})·poly(U) (ΔT_m = 13 K, Fig. 1),[11] whereas the duplex **1**·poly(A) is slightly less stable than its natural equivalent d(T_{10})·poly(A) (ΔT_m = − 4 K). With DNA as the complex partner, duplex stability decreases in the order **2**·d(T_{10}) ≈ d(A_{10})·d(T_{10}) > **1**·d(A_{10}). Of all possible pairings in the series of decamers, the fully bicyclic duplex **1**·**2** is the most

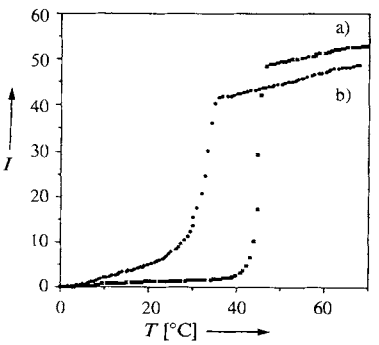

Fig. 1. UV melting curves (260 nm) of a) **2**·poly(U) and b) d(A_{10})·poly(U) in 10 mM Tris·HCl pH 7.0, 0.15 M NaCl. (base-pair concentration 26 μM). I = % hyperchromicity at 260 nm.

stable. The bicyclothymidine oligomer **1** shows preferential binding to poly(A) over poly(dA) (ΔT_m = 13 K) which is not observed in the case of its natural analogue d(T_{10}) (ΔT_m = − 3 K). In the hybrid systems **2**/d(T_{10}) and **1**/**2**, we have determined the pairing stoichiometry by recording UV mixing curves according to the method of Job.[12] It was found that (T-A-T)-type but not (A-A-T)-type triplexes were formed in both systems at the appropriate stoichiometric strand ratio under conditions (0.15 M NaCl) in which only duplex formation is found in the natural d(A_{10})/d(T_{10}) system[13] (Fig. 2, mixing curve of **1**/**2** is not shown). Oligo(bicyclodeoxy)nucleotides of adenine and thymine thus show a higher propensity for triplex formation relative to the natural sequences.

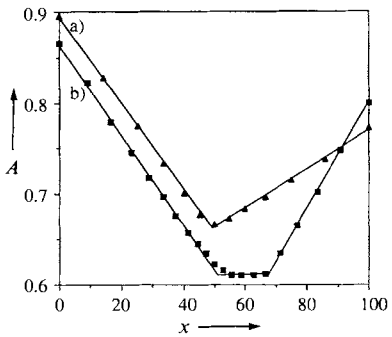

Fig. 2. UV mixing curves (260 nm, 8 °C) of a): d(A_{10})/d(T_{10}) (total strand concentration c_T = 8.4 μM) and b) **2**/d(T_{10}) (c_T = 8.3 μM) in 10 mM Tris·HCl pH 7.0, 0.15 M NaCl. A = absorption at 260 nm, x = concentration of T in mol%.

To answer the question whether the entropy change upon pairing is influenced by the structural modifications in the sugar part of the oligo(bicyclonucleotide), we determined pairing enthalpies (ΔH) and entropies (ΔS) in the series of decamers from the UV melting curves (Fig. 3) by a curve-fitting procedure as well as from a plot of T_m^{-1} against the logarithm of oligonucleotide concentration according to the method of Marky and Breslauer[14] (Table 2). From the data

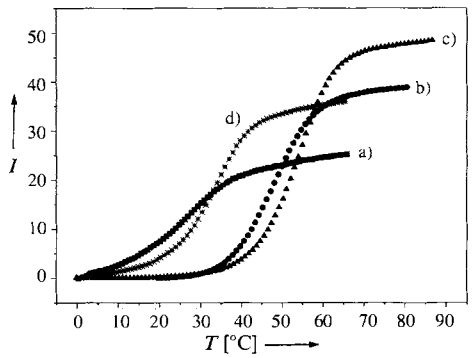

Fig. 3. UV melting curves of the duplexes a) **1**·d(A_{10}) (c_T = 8.3 μM), b) **2**·d(T_{10}) (11.9 μM), c) **1**·**2** (11.9 μM), and d) d(A_{10})·d(A_{10}) (12.2 μM) in 10 mM NaH_2PO_4, 1 M NaCl, pH 7.0.

of either method it emerges that in both hybrid duplexes **2**·d(T_{10}) and **1**·d(A_{10}), as well as in the completely bicyclic duplex **1**·**2**, the pairing entropy term (ΔS) is (numerically) reduced relative to the natural duplex d(A_{10})·d(T_{10}).[15] The pairing enthalpy term is generally affected in a way that destabilizes duplex formation. The deviation of the data for **2**·d(T_{10}) (Table 2), obtained by the two different methods,

may be an indication that the "two-state model", on which the elucidation of the thermodynamic data is based, is most likely an oversimplification in this case. It seems reasonable that the reduction of the enthalpy term in the hybrid duplexes is due to a partly "incorrect" pairing geometry or to strain within the bicyclic strand. The reduction of the entropy term can be attributed to the reduced degree of rotational freedom in the sugar-phosphate backbone of the DNA analogues, although other contributions, especially from differences in duplex and single strand solvation, may also play an important role.

Table 2. Thermodynamic data of duplex formation from UV melting curves (curve-fitting and plots of T_m^{-1} against ln[c] [14]) in 10 mM NaH_2PO_4, pH 7.0, 1 M NaCl. Estimated errors $\leq \pm 5\%$.

	curve fitting		T_m^{-1} vs. ln[c]	
	ΔH [kcal mol^{-1}]	ΔS [cal K^{-1} mol^{-1}]	ΔH [kcal mol^{-1}]	ΔS [cal K^{-1} mol^{-1}]
1 · d(A_{10})	−55.7	−160	−56.1	−161
2 · d(T_{10})	−64.9	−177	−53.3	−141
1 · **2**	−63.2	−169	−61.1	−164
d(A_{10}) · d(T_{10})	−66.3	−191	−61.8	−176

[a] Average of six measurements at six different concentrations in the range of $c_T = 1-30$ μM.

A further aspect in the design of nucleic acid analogues is concerned with their stability against enzyme-catalyzed degradation. From oligo(bicyclodeoxynucleotides), containing exclusively secondary and tertiary phosphodiester linkages between nucleosides, one would expect an enhanced stability against phosphodiesterases. This was investigated by subjecting the decamer **1** to hydrolysis catalyzed by snake venom phosphodiesterase (SVP), nuclease S1, and fetal calf serum phosphodiesterase (CSP), and determining its stability relative to that of natural d(T_{10}).[16] While **1** showed an enhanced resistance against SVP (a 3′-exonuclease) by a factor of 3, its relative stability increased to factors of 100 and 1.4×10^3 in the cases of nuclease S1 (endo- and exonuclease) and CSP (5′-exonuclease), respectively.

The concept of reducing the pairing entropy upon bimolecular duplexation by reducing the torsional flexibility of the sugar phosphate backbone, as derived from observations of the pairing properties of oligo-2′,3′-dideoxy-β-D-glucopyranonucleotides (homo-DNA) by Eschenmoser et al.,[17] can successfully be applied to structures that were designed to bind to complementary natural DNA and, therefore, opens novel routes in the design of antisense analogues.

Received: March 12, 1993
Revised version: July 1, 1993 [Z 5915 IE]
German version: *Angew. Chem.* **1993**, *105*, 1516

[1] P. C. Zamecnik, M. L. Stephenson, *Proc. Natl. Acad. Sci. USA* **1978**, *75*, 280–284; M. L. Stephenson, P. C. Zamecnik, *ibid.* **1978**, *75*, 285-288.
[2] J. D. Watson, F. H. Crick, *Nature* **1953**, *171*, 737-738.
[3] G. Felsenfeld, D. R. Davies, A. Rich, *J. Am. Chem. Soc.* **1957**, *79*, 2023–2024; H. E. Moser, P. B. Dervan, *Science* **1987**, *238*, 645–650; J.-C. François, T. Saison-Behmoaras, C. Hélène, *Nucleic Acids Res.* **1988**, *16*, 11431–11440; N. T. Thong, C. Hélène, *Angew. Chem.* **1993**, *105*, 697–723; *Angew. Chem. Int. Ed. Engl.* **1993**, *32*, 666–690; M. Cooney, G. Czernuszewicz, E. H. Postel, S. J. Flint, M. E. Hogan, *Science* **1988**, *241*, 456–459; P. A. Beal, P. B. Dervan, *ibid.* **1991**, *251*, 1360-1363.
[4] E. Uhlmann, A. Peyman, *Chem. Rev.* **1990**, *90*, 543–584; J. Goodchild, *Bioconjugate Chem.*, **1990**, *1*, 165–187; J. Engels, *Nachr. Chem. Tech. Lab.* **1991**, *39*, 1250–1254; U. Englisch, D. Gauss, *Angew. Chem.* **1991**, *103*, 629–646; *Angew. Chem. Int. Ed. Engl.* **1991**, *30*, 613–629.
[5] M. Tarköy, M. Bolli, B. Schweizer, C. Leumann, *Helv. Chim. Acta* **1993**, *76*, 481–510.
[6] M. H. Caruthers, *Acc. Chem. Res.* **1991**, *24*, 278–284.
[7] $DMTr^+CF_3SO_3^-$ was obtained in crystalline form by reaction of the corresponding chloride with CF_3SO_3Ag in THF (82%). Correct elemental analysis (C, H, F, S) for $C_{22}H_{19}O_5F_3S$.
[8] M. J. Gait, *Oligonucleotide Synthesis - a Practical Approach*, IRL Press, Oxford, **1984**.
[9] Oligonucleotide synthesis was performed on a Pharmacia Gene Assembler Plus DNA synthesizer in scales of 0.6–1.3 mmol. The only parameters changed relative to the synthesis of natural DNA oligomers were the detritylation time (extended to 60 s) and the coupling time (extended to 6 min). The last step in every synthesis was the removal of the 5′-terminal trityl group (trityl off mode).
[10] Crude **1** and **2** were purified by anion exchange HPLC (column: Nucleogen 60 DEAE Macherey-Nagel; elution with a linear KCl gradient in 20 mM KH_2PO_4, pH 6.0 in H_2O:CH_3CN 4:1). Quality of the isolated material was checked by reversed-phase HPLC (column: Aquapore Rp 300, Brownlee; elution with a linear gradient of CH_3CN in 0.1 M aqeous Et_3NHOAc, pH 7.0). Mass spectrometric analysis of **1** and **2** (NH_4^+ form) was performed by matrix-assisted laser desorption time of flight mass spectroscopy (*m/z* 3240.8 (**1**), 3330.8 (**2**)).
[11] Whereas **2**·poly(U) forms a duplex at a ratio of bases of 1:1, d(A_{10})·poly(U) disproportionates to the (U-dA-U)-triplex and unpaired d$(A)_{10}$ under the buffer conditions used for recording the UV melting curves. This is in accordance with previous findings on the pairing behavior of poly(dA) with poly(U) (M. Riley, B. Maling, M. J. Chamberlin, *J. Mol. Biol.*, **1966**, *20*, 359-389).
[12] P. Job, *Anal. Chim. Acta* **1928**, *9*, 113–134.
[13] D. S. Pilch, C. Levenson, R. H. Shafer, *Proc. Natl. Acad. Sci. USA* **1990**, *87*, 1942–1946.
[14] L. A. Marky, K. J. Breslauer, *Biopolymers* **1987**, *26*, 1601–1620.
[15] Thermodynamic data for hybridization in the mixed duplex **2**·d(T_{10}) and natural d(A_{10})·d(T_{10}) were also obtained by differential scanning calorimetry on a Microcal MC-2D instrument (1 M NaCl). A (numerical) entropy reduction of 23% in the former duplex relative to the latter was observed.
[16] Relative hydrolysis rates were estimated by incomplete digestion of each oligomer with the corresponding enzymes. Ratios of unchanged substrate over the sum of products were obtained by reversed-phase HPLC (quantification by peak integration). Stability factors were calculated as the fraction of the forementioned ratios for **1** and d(T_{10}), respectively.
[17] A. Eschenmoser, *Nachr. Chem. Tech. Lab.* **1991**, *39*, 795–806; *Nova Acta Leopold.* **1992**, *67*, 201–233; A. Eschenmoser, E. Loewenthal, *Chem. Soc. Rev.* **1992**, *21*, 1–16; A. Eschenmoser, M. Dobler, *Helv. Chim. Acta* **1992**, *75*, 218–259; M. Böhringer, H.-J. Roth, J. Hunziker, M. Göbel, R. Krishnan, A. Giger, B. Schweizer, J. Schreiber, C. Leumann, A. Eschenmoser, *ibid.* **1992**, *75*, 1416–1477; J. Hunziker, H.-J. Roth, M. Böhringer, A. Giger, U. Diederichsen, M. Göbel, R. Krishnan, B. Jaun, C. Leumann, A. Eschenmoser, *ibid.* **1993**, *76*, 259–352.

Multiring Catenanes with a Macrobicyclic Core**

By *Christiane Dietrich-Buchecker,* Bruno Frommberger, Ingo Lüer, Jean-Pierre Sauvage,** and *Fritz Vögtle**

Catenanes consist of two or more interlocking rings.[1, 2] Two templated strategies based either on interactions with transition metals[3] or on π-stacking interactions[4] have been developed and used to make catenanes with increasingly more complex structures and topologies. Furthermore, recently a hydrogen bond template synthesis was introduced.[5] Up to now, all the catenanes synthesized contain *mono*cycles, although it is easy to imagine that by applying construction

[*] Dr. C. Dietrich-Buchecker, Dr. J.-P. Sauvage
Laboratoire de Chimie Organo-Minérale, UA 422 du CNRS
Institut de Chimie, Université Louis Pasteur
F-67008 Strasbourg (France)
Telefax: Int. code + (88)607312
Prof. Dr. F. Vögtle, B. Frommberger, Dr. I. Lüer
Institut für Organische Chemie und Biochemie der Universität Bonn
Gerhard-Domagk-Strasse 1, D-53121 Bonn (FRG)
Telefax: Int. code + (228)73-5662

[**] This work was supported by the Bundesministerium für Forschung und Technologie (BMFT-03 291 209). We thank the Mass Spectrometry Laboratory (Strasbourg) for analysis, and J.-P. Kintziger and P. Maltese for recording the NMR spectra and fruitful discussions.

principles derived from the template routes mentioned above, catenanes containing polycyclic components may be obtained.[6] In other words, the molecular graphs of all the previously synthesized catenanes only contain two-order vertices.[7] The introduction of higher order vertices represents an interesting extension, in which the simplest case would be to use a *bi*cyclic skeleton as the interlocking component for which the two bridgehead atoms are three-order vertices. Indeed, the successful application of this strategy (Fig. 1) is reported herein.

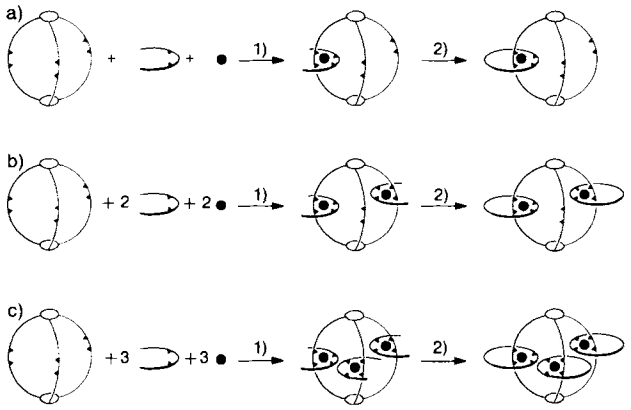

Fig. 1. The reaction pathway to catenanes starting from a bicyclic compound with three coordinating arms (the small black triangles symbolize the 1,10-phenanthroline nitrogen atoms). The metal centers (black circles) control the assembly and orientation of the components. The number of metal ions used per bicyclic molecule, in principle, determines the number of monocycles interlocked to the central organic unit. 1) Complexation, 2) cyclization.

A series of macrobicyclic endoreceptors containing three convergent 2,9-diphenyl-1,10-phenanthroline (dpp) units, which can complex three Cu^{I} ions and three open-chain dpp units, has recently been described.[8] The same assembling principle has now been applied to synthesize the precursors for catenanes (step 1 of Fig. 1). The structures of the compounds used and the reactions performed are represented in Figure 2.

The macrobicycle **1** was prepared as previously described.[8] It was allowed to react in CH_3CN/dimethylformamide (DMF) with three equivalents of $[Cu(CH_3CN)_4]BF_4$ and subsequently with three equivalents of **2** to yield $\mathbf{3}^{3+}$ almost quantitatively. The ^1H NMR spectrum of $\mathbf{3}^{3+}$ clearly shows that the three components **2** are sterically congested inside the cage cavity (strong upfield shift of the signals for the $H'_{5,6}$ protons which suggests that the three phenanthroline units of **2** overlap). The cyclization of the open-chain components **2** in $\mathbf{3}^{3+}$ in presence of Cs_2CO_3 and **4** leading to $\mathbf{5}^{+}$, $\mathbf{6}^{2+}$, and $\mathbf{7}^{3+}$ was carried out according to a method derived from the one used for making catenates[9] (see Experimental Procedure). After repeated careful chromatographic separation, $\mathbf{5}^{+}$, $\mathbf{6}^{2+}$, and $\mathbf{7}^{3+}$ were obtained in 8%, 4%, and 0.5% yield, respectively. Substantial amounts of insoluble materials were also formed. The structure and the topology of these three catenates were confirmed by FAB and electrospray mass spectrometry (see Experimental Procedure). The ^1H NMR spectra afforded valuable information regarding the structure of the catenane framework and, in particular, the level of crowding within the cavity of the macrobicyclic component. Some data are collected in Table 1.

Interesting conclusions with regard to the structure can be drawn from the chemical shift values (Table 1). Three types of dpp groups have to be considered:

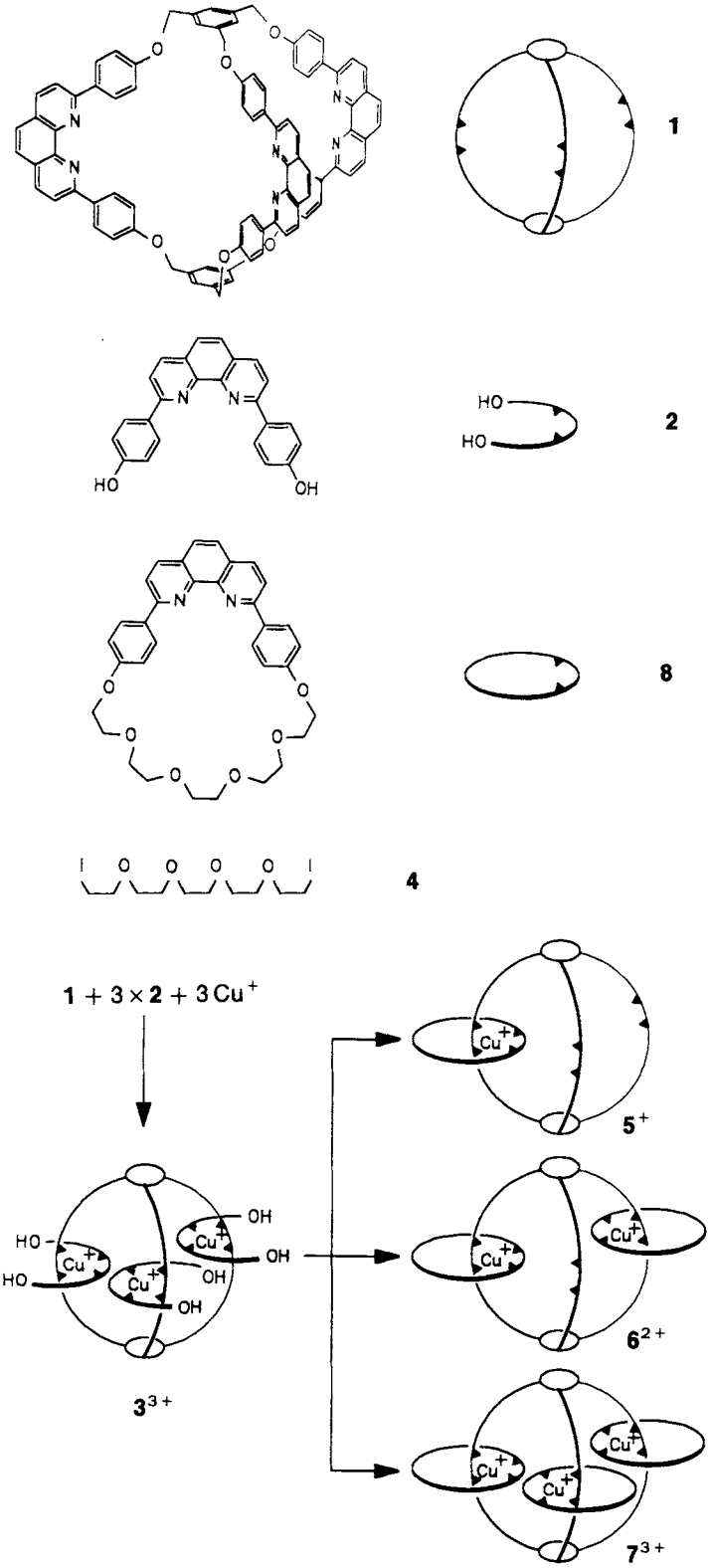

Fig. 2. Starting materials and synthesis of the catenanes $\mathbf{5}^{+}$, $\mathbf{6}^{2+}$, and $\mathbf{7}^{3+}$ as well as the precursor $\mathbf{3}^{3+}$.

1) *The complexed arms,* which belong to the bicyclic central unit and coordinate to Cu^{I} ions. Each cycle of the macrobicycle (**1**) consists of a 42-membered ring, and is thus much larger than **8**, the other components of the interlocking systems (30-membered ring; see Fig. 2). It is expected that the smaller the rings, the tighter and more entwined the catenane units. This is reflected by the H_o signal, which ap-

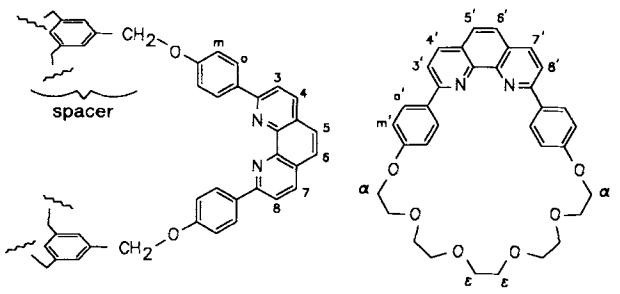

Table 1. Chemical shifts for the complexes 5^+, 6^{2+}, and 7^{3+} as well as $[Cu(8)_2]^+$ and **8** at 25 °C in $CHDCl_2$ ($\delta H = 5.320$) at 400 MHz [a].

	Cage													Macrocycle **8**					
	complexed arms						free arms						spacer						
	$H_{4,7}$	$H_{5,6}$	$H_{3,8}$	H_o	H_m	OCH_2	H_o	$H_{4,7}$	$H_{3,8}$	$H_{5,6}$	H_m	OCH_2		$H'_{4,7}$	$H'_{5,6}$	$H'_{3,8}$	H'_o	H'_m	H_ε
5^+	8.59	8.22	7.84	7.45	6.14	4.64	8.41	8.31	8.11	7.78	7.30	5.34	7.66 7.41	8.35	7.97	7.71	7.24	5.93	3.81
6^{2+} [b]	8.63	8.26	7.90	7.56	6.27	4.91	8.47	8.32	8.13	7.79	7.42	5.42	7.59 7.45	8.49	7.97 7.87	7.82	7.36 7.31	5.96	3.82
7^{3+}	8.62	8.28	7.88	7.64	6.34	5.10							7.64	8.37	7.64	7.92	7.40	5.97	3.82 [c]
			$[Cu(8)_2]^+$						**8**										
	8.66	8.28	7.87	7.37	6.02	3.62 [d]	8.44	8.30	8.10	7.79	7.23	4.37 [d]							

[a] The ^1H NMR spectra contain all the characteristic patterns of the dpp subunits present in the cage **1** as well as in the interlocked macrocycles **8**: a singlet for H_5 and H_6, an AB pattern for H_3 or H_8 and H_4 or H_7 ($J \approx 8.5$ Hz) and a AA'XX' system ($J \approx 8.7$ Hz) for H_o and H_m. [b] In complex 6^{2+}, the dpp subunits of the two interlocked macrocycles **8** present an AB pattern for their H'_5 and H'_6 protons, whereas their H'_o protons appear as two distinct doublets. [c] In $[Cu(8)_2]^+$ the signal for H_ε also occurs at $\delta = 3.82$. [d] Signal for H_ε.

pears at higher field for the simple catenate $[Cu(8)_2]^+$ than for the interlocking systems 5^+, 6^{2+} and 7^{3+}. In addition, by filling-up the cavity with more and more dpp units, the steric strain within each complex subunit increases, leading to less stacking interactions between the phenyl and phenanthroline rings, with the same consequences as the reduction in the ring size. Overall, the less and less entwined situation of the Cu^I complexes from $[Cu(8)_2]^+$ to 7^{3+} leads to significant increase of the δ values for H_o, H_m and OCH_2. Indeed, the latter protons feel less and less the shielding effect of the phenanthroline units of the macrocycle **8**. It is worth noting that, as expected, the signals of the protons outside the cage ($H_{4,7}$, $H_{5,6}$, and $H_{3,8}$ of the complexed arms) are almost completely insensitive to the filling-in of the cavity.

2) *The internal phenanthroline units*, which belong to the 30-membered rings. The ring current effect of the two capping phenylene units onto the "rear" of the phenanthroline groups is very significant. The $H'_{4,7}$ and $H'_{5,6}$ signals undergo an upfield shift when switching from $[Cu(8)_2]^{2+}$ to 5^+ ($\Delta\delta \approx -0.3$). In order to explain the large shielding of the $H'_{5,6}$ protons in 7^{3+} (upfield shift by $\Delta\delta = -0.64$ in comparison to $H_{5,6}$ in $[Cu(8)_2]^+$), two factors can be invoked: a) the ring current effect of the two phenylene units and b) the pronounced overlap of the three internal phenanthroline units, especially in the $H'_{5,6}$ region. To a lesser extent, the same is true for the $H'_{4,7}$ protons ($\Delta\delta = -0.29$ between $[Cu(8)_2]^+$ and 7^{3+}). CPK (space-filling) models show that the three phenanthroline rings inside the cavity must stack in order to accomodate the size of the bicyclic component. By contrast, all the other signals of the aromatic protons are slightly shifted downfield on going from $5^+ \rightarrow 6^{2+} \rightarrow 7^{3+}$.

3) *The free arms*, which are completely unperturbed by the complexation of their neighboring arms. It is striking that the signals of the outside $CH_{2\varepsilon}$ protons are also totally insensitive to modification occurring inside the cage ($\delta = 3.82 \pm 0.01$ for $CH_{2\varepsilon}$ of the four Cu^I complexes).

The new types of structures 5^+, 6^{2+}, and 7^{3+} should allow the study of steric and electronic interactions between transition metal complex subunits nested inside the cavities of large bicyclic cage compounds.

Experimental Procedure

3^{3+}: $[Cu(CH_3CN)_4]BF_4$ (318 mg, 1.01 mmol) in degassed CH_3CN (50 mL) was added to **1** (424 mg, 0.32 mmol) in degassed DMF (50 mL) with stirring under argon and at room temperature (RT). The solution turned dark yellow. It was stirred for a further 30 min, after which the diphenol **2** (368 mg, 1.01 mmol), dissolved in degassed DMF (40 mL), was added slowly over 30 min. The solution turned dark red. After it was stirred for about 15 h at RT, the solvents were evaporated to dryness. The black-red complex 3^{3+} was obtained quantitatively as a glassy solid (921 mg, 0.32 mmol). Compound 3^{3+} was utilized without further purification. Electrospray mass spectra confirmed the composition of precatenate 3^{3+}: m/z = 2778.7, 1346.5, and 868.8 correspond to $[3(BF_4)_2]^+$, $[3(BF_4)]^{2+}$, and 3^{3+}, respectively. ^1H NMR (CD_3CN): δ = 8.55 (d, 6H, H_4 or H_7); 8.07 (s, 6H, H_5 and H_6); 8.04 (d, 6H, H'_4, H'_7); 7.92 (d, 6H, H'_3 or H'_8); 7.73 (d, 6H, H_3 or H_8); 7.57 < m < 7.43 (24H, H_o, $H'_{5,6}$, H_{spacer}); 7.40 (d, 12H, H'_o); 6.30 (d, 12H, H_m); 5.90 (d, 12H, H'_m); 4.96 (s, 12H, H_{OCH_2}).

Macrocyclization leading to 5^+, 6^{2+}, and 7^{3+}: A degassed suspension of Cs_2CO_3 (1.6 g, 5 mmol) in DMF (150 mL) was added by the double-ended needle transfer technique (addition made by small successive batches over a 24 h period) to a solution of **3** $(BF_4)_3$ (921 mg, 0.32 mmol) and **4**, the diiodo-derivative of pentaethyleneglycol (485 mg, 1.06 mmol) in DMF (350 mL) kept under argon at 60–65 °C. The reaction was monitored by TLC which showed that **4** was consumed faster than 3^{3+}. Additional **4** (470 mg, 1.03 mmol) in DMF (50 mL) was added over a period of 4 h. After this second addition of **4**, stirring and heating was continued for 24 h at about 60 °C after which classical workup was carried out [9]. The crude reaction mixture was purified by numerous successive column chromatographic separations (silica gel, eluent: CH_2Cl_2/MeOH 100:1 to 100:5 v/v). Besides significant amounts of insoluble material and recovered cage **1**, we isolated 52.2 mg of 5^+ (8% yield, eluent: CH_2Cl_2/MeOH 100:1), 35.3 mg of 6^{2+} (4% yield, eluent: CH_2Cl_2/MeOH 100:1.5) and 5.5 mg of 7^{3+} (0.5% yield, CH_2Cl_2/MeOH 100:2–4).

5^+: Dark brown-red solid. ^1H NMR (CD_2Cl_2): (see Table 1). ES-MS: m/z = 1951.3, 976.8, and 651.2, corresponding to 5^+, 5^+H^+, and 5^+2H^+, respectively. UV/VIS (CH_2Cl_2), λ_{max} (nm, [ε]): 442 [2668]; 422 [2683]; 321 [96229]; 284 [159557]; 239 [120286].

6^{2+}: Dark purple solid. ^1H NMR (CD_2Cl_2): (see Table 1). ES-MS: m/z = 1290.7, 861.3, corresponding to 6^{2+} and $6^{2+}H^+$. UV/VIS (CH_2Cl_2), λ_{max} (nm, [ε]): 438 [5055]; 323 [97502]; 287 [151287]; 248 [151287].

7^{3+}. Dark purple solid. ^{1}H NMR (CD_2Cl_2): (see Table 1). ES-MS: m/z = 1070.5 corresponding to 7^{3+}. UV/VIS (CH_2Cl_2), λ_{max} (nm, [ε]): 444 [5870]; 325 [94 147]; 284 [126 626]; 247 [141 444].

Received: April 2, 1993 [Z 5970 IE]
German version: *Angew. Chem.* **1993**, *105*, 1526

[1] H. L. Frisch, E. Wassermann, *J. Am. Chem. Soc.* **1961**, *83*, 3789–3795.
[2] G. Schill, *Catenanes, Rotaxanes and Knots*, Academic Press, New York, **1971**.
[3] C. Dietrich-Buchecker, J.-P. Sauvage, *Bioorganic Chemistry Frontiers, Vol. 2*, Springer, Berlin, **1991**, pp. 195–248.
[4] J. Y. Ortholand, A. M. Z. Slawin, N. Spencer, J. F. Stoddart, D. J. Williams, *Angew. Chem.* **1989**, *101*, 1402–1403; *Angew. Chem. Int. Ed. Engl.* **1989**, *28*, 1394–1395; P. R. Aston, T. T. Goodnow, A. E. Kaifer, M. Reddington, A. M. Z. Slawin, N. Spencer, J. F. Stoddart, C. Vicent, D. J. Williams, *ibid.* **1989**, *101*, 1404–1408 and **1989**, *28*, 1396–1399.
[5] F. Vögtle, S. Meier, R. Hoss, *Angew. Chem.* **1992**, *104*, 1628–1631; *Angew. Chem. Int. Ed. Engl.* **1992**, *31*, 1619–1622; C. A. Hunter, *J. Am. Chem. Soc.* **1992**, *114*, 5303–5311.
[6] P. R. Ashton, A. S. Reder, N. Spencer, J. F. Stoddart, personal communication. We thank Professor J. F. Stoddart, University of Birmingham, for providing us with a copy of a manuscript on their most recent results.
[7] D. M. Walba, *Graph Theory Topol. in Chem. Collect. Pap. Int. Conf.* **1987**.
[8] F. Vögtle, I. Lüer, V. Balzani, N. Armaroli, *Angew. Chem.* **1991**, *103*, 1367–1370; *Angew. Chem. Int. Ed. Engl.* **1991**, *30*, 1333–1336.
[9] C. Dietrich-Buchecker, J.-P. Sauvage, *Tetrahedron* **1990**, *46*, 503–512.

Oxoferryl π-Cation Radical of β-Pyrrole Octachlorinated *meso*-Tetramesitylporphyrin: Electronic and Structural Properties**

By *Philippe Ochsenbein, Dominique Mandon, Jean Fischer, Raymond Weiss,* Rachel Austin, Karupiah Jayaraj, Avram Gold,* James Terner,* Eckhard Bill, Markus Müther,* and *Alfred X. Trautwein**

Iron tetraarylporphyrins with halogenated pyrrole units and protected methine positions, for example **1** or **2** (Scheme 1), are very efficient catalysts for the hydroxylation of poorly reactive alkanes.[1] The chemo- and regioselectivities of the oxidations differ considerably from those observed with "planar peripherally unsubstituted" porphyrin catalysts such as **3**, suggesting a change in the structure of the high-valent iron–oxo intermediates.[2]

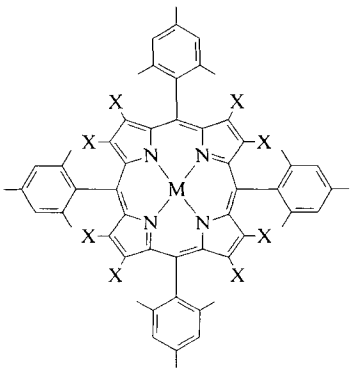

Cmpd.	M	X
1	$Fe^{III}Cl$	Cl
2	$Fe^{III}Cl$	Br
3	$Fe^{III}Cl$	H
4	$Fe^{IV}O$	H
5	2 H	Cl
6	2 H	Br
7	$Fe^{IV}O$	Cl
8	$Fe^{IV}O$	Br

Scheme 1. Structures of the porphyrins discussed in the text.

Indeed, recent structural determinations of β-pyrrole octabrominated tetraarylporphyrins and their nickel(II) derivatives have established that halogen substitution at the β positions induces severe saddle-shaped distortions of the porphyrin core.[3, 4] In this report we show that 1) the cores of the five-coordinate iron(III) derivatives of the β-pyrrole octahalogenated porphyrins **1** and **2** also adopt a saddle shape and 2) that a high-valent iron porphyrin species, with EPR spectral properties similar to those reported for the oxoferryl π-cation radicals of "planar protected" tetraarylporphyrins such as $\mathbf{4}^{\bullet+}$, can be generated in dichloromethane by reaction at −80 °C of **1** with *m*-chloroperoxybenzoic acid (*m*-CPBA).[5, 6]

Complexes **1** · H_2O and **2** · H_2O crystallize,[7, 8, 10–12] like the metal-free porphyrins **5** and **6**,[3, 9] in space group $P\bar{4}2_1c$ with two molecules per unit cell. The macrocycles lie on a crystallographic fourfold inversion axis; therefore, the Fe-Cl groups are orientationally disordered along this axis; the effective symmetry of each molecule is C_2. The high-spin iron ion is bound to the four pyrrole nitrogen atoms of the ring and to a chloride ion (Fig. 1). In both compounds, the

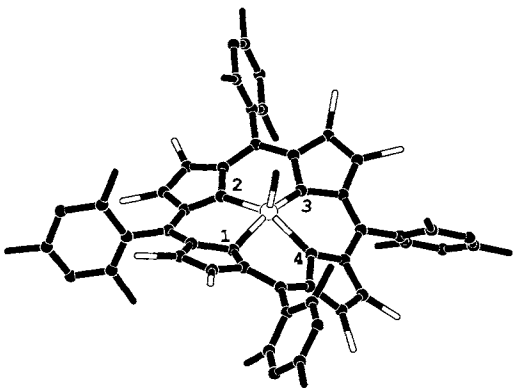

Fig. 1. Structure of **1** and **2** in the crystal (stick plot, hydrogen atoms are omitted and the orientational disorder of the Fe-Cl group is not shown.) Selected bond lengths in **1** · H_2O: Fe-Cl = 2.21(1), Fe-N_p1 = Fe-N_p3 = 2.04(1), Fe-N_p2 = Fe-N_p4 = 2.09(1) Å; selected bond lengths in **2** · H_2O: Fe-Cl = 2.30(2), Fe-N_p1 = Fe-N_p3 = 2.03(1), Fe-N_p2 = Fe-N_p4 = 2.09(1) Å.

coordination polyhedron of the iron center is a pyramid in which one set of opposing Fe–N_p bond lengths is longer than the other set (see legend to Fig. 1). In **1** and **2**, the iron atoms lie 0.55(1) Å above the 4 N_p and 24-atom core mean-planes of the porphyrins. Both molecules are severely nonplanar; however, the saddle is somewhat less pronounced in

[*] Prof. Dr. R. Weiss, Dipl.-Chem. P. Ochsenbein, Dr. D. Mandon, Prof. Dr. J. Fischer
Institut LeBel, Université Louis Pasteur
4, rue B. Pascal, F-67070 Strasbourg Cedex (France)
Telefax: Int. code + (88)41-5363
Prof. Dr. A. Gold, Dipl.-Chem. R. Austin, Dr. K. Jayaraj
Department of Environmental Sciences and Engineering
University of North Carolina
Chapel Hill, NC 27599-7400 (USA)
Telefax: Int. code + (919) 966-4711
Prof. Dr. J. Terner
Department of Chemistry
Virginia Commonwealth University
Richmond, VA 23284-2006 (USA)
Telefax: Int. code + (804) 367-8599
Prof. Dr. A. X. Trautwein, Dr. E. Bill, Dipl.-Phys. M. Müther
Institut für Physik, Medizinische Universität
Ratzeburger Allee 160, D-23538 Lübeck (FRG)
Telefax: Int. code + (451) 500-4214

[**] This work was supported by the Centre National de la Recherche Scientifique (URA-424), United States Public Health Service (USPHS) Grants ES03433 (for A. G.), GM34443 (for J. T.), and the Deutsche Forschungsgemeinschaft. R. W. thanks the Alexander-von-Humboldt Foundation for financial support. A. G. and R. W. thank NATO for a collaborative research grant. R. W. thanks also Dr. J. Fajer (Brookhaven National Laboratory) for valuable discussions. – In this article "oxoferryl" denotes the group $Fe^{IV}O$.

the iron complexes **1** and **2** than in the metal-free porphyrins **5** and **6**. Indeed, the average displacements of 0.87 and 0.90 Å of the β-C atoms from the mean-planes of the porphyrins in **1** and **2**, respectively, are slightly smaller than those of 0.90 and 0.95 Å, respectively, in the metal-free porphyrins **5** and **6**. A small ruffling is also present, with the *meso*-carbon atoms in **1** and **2**, respectively, deviating by 0.34 and 0.33 Å from the mean porphyrin planes. The dihedral angles between adjacent and opposite pyrrole rings indicate that the twist of the pyrrole rings around their central axes is slightly greater in **1** than in **5** and slightly smaller in **2** than in **6**; for opposite rings these dihedral angles average to 49.0 and 48.4° in **1** and **5**, respectively, and 49.3 and 49.8° in **2** and **6**, respectively. For adjacent rings these values are 34.1 and 33.7°, respectively for **1** and **5**, and 34.3 and 34.7°, respectively for **2** and **6**.

The chloroiron(III) octahalogenated or porphyrins were oxidized in toluene/[D_4]methanol (6:1) dichloromethane/[D_4]methanol (6:1) at -80 °C by addition of an approximately fourfold molar excess of *m*-CPBA in [D_4]methanol to an approximately 10^{-3} molar solution of iron(III) porphyrin. Techniques for obtaining UV/VIS, ^{1}H NMR, EPR, resonance Raman (rR), and Mössbauer spectra have been described elsewhere.[5, 6] In toluene, only the EPR-inactive oxoferryl complexes **7** and **8** were obtained and characterized by UV/VIS, ^{1}H NMR, rR, and Mössbauer spectroscopy.[9] In dichloromethane, **2** also led to EPR-inactive **8**; however, **1** yielded EPR-active oxoferryl porphyrin π-cation radical $\mathbf{7}^{\bullet+}$, with spectral properties similar to those of the oxoferryl porphyrin π-cation radical of the "planar" tetramesitylporphyrin **4**.[5, 6]

Indeed, the X-band EPR spectrum of $\mathbf{7}^{\bullet+}$, (Fig. 2) shows resonances at effective g values of 4.2, 3.7, and 1.99 which are typical of a quartet species $S_t = 3/2$. The fact that the average of g_x^{eff} and g_y^{eff} is less than 4 indicates that the spectrum originates from a low-spin iron(IV) center ($S = 1$) ferromagnetically coupled to a porphyrin π-cation radical ($S' = 1/2$).[13] A quantitative measure of spin coupling could be derived by inspection of the temperature dependence of the EPR signal intensities and by simulating the EPR spectrum, for example at 10 K (Fig. 2).[6] This temperature dependence is appropriately described by a three-state model of the three Kramers doublets, the energy separations of which are consistent with the spin-Hamiltonian parameters derived by simulating the EPR spectrum measured at 10 K (Fig. 2): $D_{Fe} = 18\ cm^{-1}$, $E_{Fe}/D_{Fe} = 0.063$ (zero-field parameters of Fe^{IV}), $g_{Fe} = 2.14$, 2.17, 1.995 and $J^0 = 25\ cm^{-1}$ (J^0 = isotropic exchange interaction between iron and radical spin in $-J^0(S \cdot S')$. Since it has not yet been possible to generate $\mathbf{7}^{\bullet+}$ in a form suitable for Mössbauer spectroscopy, these parameters had to be derived from EPR studies alone.

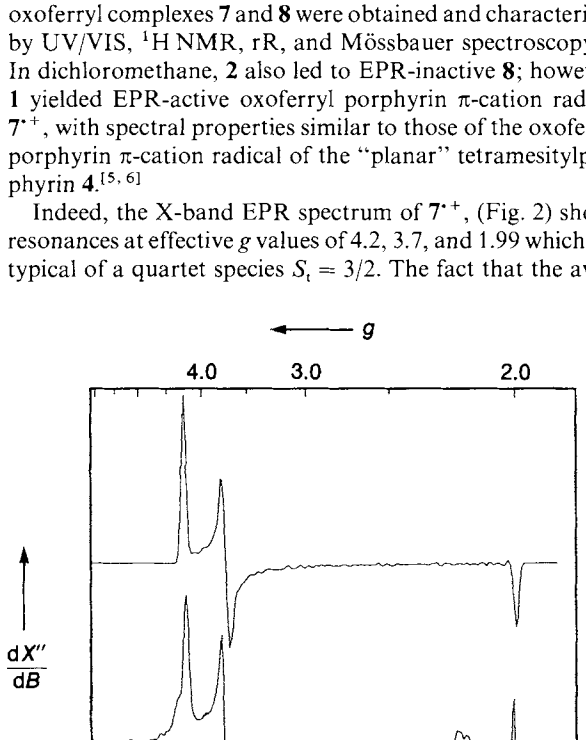

Fig. 2. Lower part: Experimental EPR spectrum of $\mathbf{7}^{\bullet+}$ at 10 K, microwave frequency 9.4316 GHz, power 20 μW, modulation amplitude 100 KHz; upper part: Simulated EPR spectrum based on the analysis of the spin-Hamiltonian operators [6] with parameters as given in the text, using a g-strain model for the line shapes, which is based on a Gaussian distribution $\sigma(E_{Fe}/D_{Fe}) = 0.08$ of the rhombicity E_{Fe}/D_{Fe} of Fe^{IV}.

However, all other spectral data of $\mathbf{7}^{\bullet+}$ are also consistent with an oxoferryl porphyrin π-cation radical: UV/VIS (CH_2Cl_2, -80 °C): λ_{max} [nm] (ε [$cm^2\,mmol^{-1}$]) = 391 (13.6; Soret), 725 (1.64); ^{1}H NMR (500 MHz, -65 °C, CD_2Cl_2/CD_3OD, TMS): $\delta = 13.5$ (12H, *p*-CH_3), 21.8 (12H, *o*-CH_3) 24.0 (12H, *o'*-CH_3) (the phenyl *meta*-proton resonances were not identified because of broadening). In the rR spectrum of **1** (CH_2Cl_2, -65 °C), porphyrin marker band assignments in the high-frequency region (wavelength of the laser 4067 Å) (based on polarization studies at 5145, 4545, 4131, 4067, and 3564 Å) are: $\nu_4 = 1345\ cm^{-1}$; $\nu_3 = 1461\ cm^{-1}$; $\nu_{11} = 1481\ cm^{-1}$, and overlapping bands $\nu_2 = 1528$ and $\nu_{10} = 1539\ cm^{-1}$. On *m*-CPBA oxidation of **1** to $\mathbf{7}^{\bullet+}$, the band intensities are markedly reduced, as expected for ring oxidation; ν_4 could not be definitively assigned but ν_2 was observed at 1538 cm^{-1}. This upfield shift of ν_2 suggests differences between the structural parameters of $\mathbf{7}^{\bullet+}$ and the oxoferryl π-cation radical of tetramesitylporphyrin ($\mathbf{4}^{\bullet+}$). In conclusion, the electronic properties of $\mathbf{7}^{\bullet+}$ are similar to those of $\mathbf{4}^{\bullet+}$, in which the oxoferryl and the π-cation radical spins are also ferromagnetically coupled;[5, 6] that is, the saddle distortion of the porphyrin does not influence the coupling of the oxoferryl center to its radical.

Received: March 29, 1993 [Z 5956 IE]
German version: *Angew. Chem.* **1993**, *105*, 1504

[1] a) T. G. Traylor, S. Tsuchiya, *Inorg. Chem.* **1987**, *26*, 1338–1339; b) T. P. Wijesekera, A. Matsumoto, D. Dolphin, D. Lexa, *Angew. Chem.* **1990**, *102*, 1073–1074; *Angew. Chem. Int. Ed. Engl.* **1990**, *29*, 1028–1029; c) D. H. Dolphin, T. Nakano, T. K. Kirk, T. E. Marone, R. L. Farrel, T. P. Wijesekera, US-A 4892941; d) S. Tsuchiya, M. Seno, *Chem. Lett.* **1989**, 263–266.

[2] a) J. F. Bartoli, O. Brigaud, P. Battioni, D. Mansuy, *J. Chem. Soc. Chem. Commun.* **1991**, 440; b) P. Battioni, O. Brigaud, H. Desvaux, D. Mansuy, T. G. Traylor, *Tetrahedron Lett.* **1991**, *32*, 2893–2896.

[3] D. Mandon, P. Ochsenbein, J. Fischer, R. Weiss, K. Jayaraj, R. N. Austin, A. Gold, P. S. White, O. Brigaud, P. Battioni, D. Mansuy, *Inorg. Chem.* **1992**, *31*, 2044–2049.

[4] H. B. Gray, California Institute of Technology, Pasadena, personal communication.

[5] E. Bill, X.-Q. Ding, E. L. Bominaar, A. X. Trautwein, H. Winkler, D. Mandon, R. Weiss, A. Gold, K. Jayaraj, W. E. Hatfield, M. L. Kirk, *Eur. J. Biochem.* **1990**, *188*, 665–672.

[6] D. Mandon, R. Weiss, K. Jayaraj, A. Gold, J. Terner, E. Bill, A. X. Trautwein, *Inorg. Chem.* **1992**, *31*, 4404–4409.

[7] **1**: The free porphyrin was metalated by using the standard $FeCl_2$/DMF/lutidine method. UV/VIS (CH_2Cl_2): λ_{max} [nm] (ε [$cm^2\,mmol^{-1}$]) = 392 (19.8), 450 (29.8; Soret), 525(4.4), 560(3.0), 747(0.6). ^{1}H NMR (500 MHz, $CDCl_3$, 20 °C, TMS): $\delta = 4.62$ (12H, *p*-CH_3) 5.50 (12H, *o*-CH_3), 7.97 (12H, *o'*-CH_3), 15.50 (4H, *m*-phenyl), 16.20 (4H, *m'*-phenyl). EPR (toluene, 10.0 K): $g \approx 6.9$, 5.1, 1.95.

[8] **2**: Metalation as for **1**. UV/VIS (CH_2Cl_2): λ_{max} [nm] (ε [$cm^2\,mmol^{-1}$]) = 404 (14.5), 455 (21.3) (Soret), 528 (5.1), 576 (3.4), 774 (1.2). ^{1}H NMR (200 MHz, $CDCl_3$, 20 °C, TMS): $\delta = 5.31$ (12H, *p*-CH_3), 6.72 (12H, *o*-CH_3), 9.03 (12H, *o'*-CH_3), 16.0 (4H, *m*-phenyl), 16.4 (4H, *m'*-phenyl). EPR (toluene, 10.0 K): $g \approx 7.0$, 5.0, 1.93.

[9] R. Weiss, D. Mandon, A. Gold, K. Jayaraj, R. Austin, J. Terner, A. X. Trautwein, E. Bill, M. Müther, unpublished results.

[10] Crystal Data for $1 \cdot H_2O$: $C_{56}H_{46}N_4OCl_9Fe$, $M_r = 1165.9$, tetragonal $P\bar{4}2_1c$, $a = b = 14.857(4)$, $c = 13.274(3)$ Å, $V = 2929.9$ Å^3, $Z = 2$, $\varrho_{calcd} = 1.32$ g cm^{-3}, $\lambda(Mo_{K\alpha}) = 0.7107$ Å (graphite monochromator), 2359 reflections ($2° < \theta < 29°$) were collected at -100 °C on a black crystal of $0.25 \times 0.30 \times 0.35$ mm, semiempirical absorption corrections were applied, 1374 reflections with $I > 3\sigma(I)$ were used in the refinements, 173 refined parameters, $R = 0.069$, $Rw = 0.091$, GOF = 1.01, final residual electron density = 0.33 e Å^{-3} [12].

[11] Crystal data for $2 \cdot H_2O$: $C_{56}H_{46}N_4OClBr_8Fe$, $M_r = 1519.6$, tetragonal $P\bar{4}2_1c$, $a = b = 14.964(4)$, $c = 13.712(4)$ Å, $V = 3070.9$ Å^3, $Z = 2$, $\varrho_{calcd} = 1.64$ g cm^{-3}, $\lambda(Mo_{K\alpha}) = 0.7107$ Å (graphite monochromator), 2486 reflections ($2° < \theta < 29°$) were collected at -100 °C on a black crystal of $0.25 \times 0.35 \times 0.35$ mm, semiempirical absorption corrections were applied, 1152 reflections with $I > 3\sigma(I)$ were used in the refinements, 173 refined parameters, $R = 0.053$, $Rw = 0.075$, GOF = 1.07, final residual electron density = 0.28 e Å^{-3} [12].

[12] Further details of the crystal structure investigations may be obtained from the Fachinformationszentrum Karlsruhe, Gesellschaft für wissenschaftlich-technische Information mbH, D-76344 Eggenstein-Leopoldshafen (FRG), on quoting the depository number CSD-57375, the names of the authors and the journal citation.

[13] R. Rutter, L. P. Hager, H. Dhonau, M. Hendrich, M. Valentine, P. G. Debrunner, *Biochemistry*, **1984**, *23*, 6809–6816.

The Dimeric Tris(lithioarsino)germane *t*BuGe[As(Si*i*Pr$_3$)Li]$_3$: A Self-Assembled, Solvent-Free Lithium–Main Group Element Aggregate with a $Ge_2As_6Li_6$ Rhombododecahedral Framework**

By *Laszlo Zsolnai, Gottfried Huttner,* and *Matthias Driess**

In memoriam Joachim Rudolph

P- and/or Si-rich silylphosphanes, that is compounds with Si–P bonds, reveal a considerable structural diversity and reactivity.[1] Whether and in how far the heavy homologues of the acyclic and cyclic silylphosphanes (silaphosphanes), that is germylarsanes (Ge–As), stannylstibanes (Sn–Sb), and plumbylbismutanes (Pb–Bi), have a similarly diverse molecular chemistry, are challenging questions of current main group element chemistry that cannot be answered at present. To date very little is known about even the simple acyclic germylarsanes of the type $R_3Ge-AsH_{2-n}R_n$ (R = H, alkyl; $n = 0-2$).[2] In the course of our investigations on germylarsanes we have also studied the synthesis of primary and secondary di- and triarsinoorganogermanes of the type **A** and **B** (Scheme 1), respectively, which may be considered as synthetic building blocks for the construction of cyclic germa- and heterogermaarsanes.

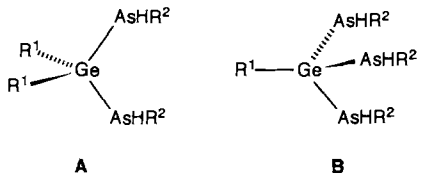

Scheme 1. R^1 = alkyl, aryl; R^2 = H, triorganosilyl.

[*] Dr. habil. M. Driess, Dr. L. Zsolnai,[+] Prof. Dr. G. Huttner[+]
Anorganisch-chemisches Institut der Universität
Im Neuenheimer Feld 270, D-69120 Heidelberg (FRG)
Telefax: Int. code + (6221)56-4197

[+] X-ray structure analysis.

[**] This work was supported by the Deutsche Forschungsgemeinschaft (SFB 247) and the Fonds der Chemischen Industrie.

We recently prepared the first compounds of type **A** by the reaction of diorganodifluorogermanes with bulky substituents with lithio(triorganosilyl)arsanes.[3] It appeared to us that the next logical step was to examine whether derivatives of type **B** could be obtained from organotrifluorogermanes and three molar equivalents of lithio(triorganosilyl)arsanes. We report here on the reaction of *tert*-butyltrifluorogermane with lithio(triisopropylsilyl)arsane, in which surprisingly the dimeric, solvent-free tris[lithio(triisopropylsilyl)arsino]*tert*-butylgermane (**1**) is formed.

*t*BuGeF$_3$ reacts with LiAsH(Si*i*Pr$_3$) already at -80 °C in Et$_2$O in the molar ratio 1:6; a clear, orange solution forms, from which **1** can be isolated in the form of yellow-orange crystals in 19% yield. Apparently, in this reaction not only the complete substitution of the F atoms at the Ge atom by arsino groups, but also the subsequent lithiation of the three As atoms in the intermediately formed *t*BuGe[As(Si*i*Pr$_3$)H]$_3$ occurs very readily. In total three equivalents of lithioarsane were required for the nucleophilic substitution and three more for the lithiation. To ensure an efficient use of the lithioarsane, however, *tert*-butyllithium can also be employed as an auxiliary base; as a result of which the yield of **1** increases to 24%.

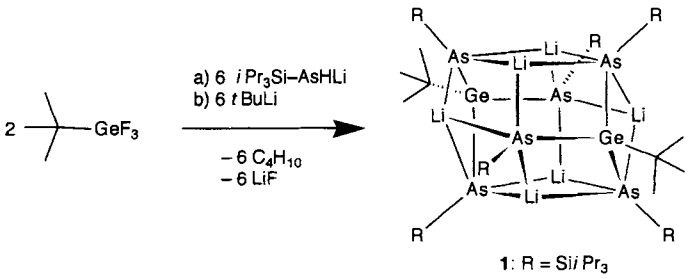

Compound **1** is the first lithioarsinoorganogermane derivative. Its molecular structure was determined by X-ray crystallography (Fig. 1).[4] Compound **1** has a $Ge_2As_6Li_6$ molecular framework with a center of symmetry; this novel

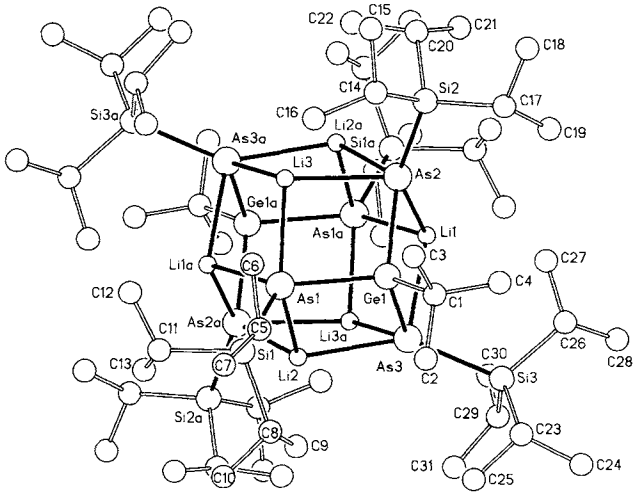

Fig. 1. Crystal structure of **1** (without H atoms). Selected distances [Å] and angles [°]: As1-Ge1 2.442(2), As1-Li1 2.59(2), As1-Li3 2.56(1), As1-Si1 2.331(3), As1-Li1a 2.62(1), As2-Ge1 2.447(1), As2-Li1 2.54(2), As2-Li2a 2.62(1), As3-Ge1 2.448(2), As3-Li1 2.59(1), As3-Li2 2.52(2), As3-Li3a 2.62(1), Ge1-C1 1.998(7); Li3-As2-Li2a 67.6(5), Li2-As3-Li3a 68.3(5), Si3-As3-Li2 147.1(2), Si3-As3-Li1 99.6(3), Si2-As2-Li2a 114.3(3), Li1-As2-Si2 145.1(3), As2-Li3-As3a 110.3(6), As1-Li3-As2 96.1(4), As3-Li2-As2a 112.2(6), As3-Li1-As1a 110.4(5), As2-Li1-As3 97.9(6), Ge1-As2-Li3 80.2(2), Ge1-As1-Li3 80.8(3), As1-Ge1-As2 102.7(1), As1-Ge1-As3 103.9(1).

lithium–main group element aggregate has the topology of a distorted rhombododecahedron. The Ge atoms are each bound to three As atoms in the molecular framework and are thus almost ideally tetrahedrally surrounded. The Ge–As distances (average 2.444(2) Å) differ very little from one another and are similar to the values found in the Zintl phase Ba_4GeAs_4[5] and in 1,3-diarsa-4-sila-2-germacyclobutanes.[3] The Ge–Li distances of 3.18–3.19 Å are considerably longer than the sum of the van-der-Waals radii (ca. 2.02 Å) and are thus not significant for the interpretation of the bonding in the aggregate. Each As atom is bound to three Li atoms, one Ge atom, and one exocyclic $SiiPr_3$ group; thus, it is five coordinated. The coordination geometry at the arsenic atom, however, does not correspond to an ideal tetragonal pyramid: the silyl group is pushed out of its ideal position as a result of the steric hindrance caused by the neighboring *tert*-butyl group at the germanium atom (Fig. 1). The Li–As distances (2.54(2)–2.62(1) Å) also differ considerably in length, probably likewise for steric reasons. In the only lithiosilylarsanes structurally characterized to date, [LiAs(SiMe$_3$)$_2$·dme] (dimeric in the crystal)[6a] and Is$_2$SiF–As(Si*i*Pr$_3$)Li(thf)$_2$ (Is = 2,4,6-*i*Pr$_3$C$_6$H$_2$) (monomeric in the crystal),[6b] the Li–As distances are 2.59(2) and 2.46(3) Å, respectively. The coordination of the lithium centers in **1** unprecedented for a lithium silylpnictogenide is particularly noteworthy. Through the self-assembly of two tris[lithio(triisopropylsilyl)arsino]*tert*-butylgermane molecules the Li centers can be stabilized electronically without additional coordination of solvent molecules (**1** is prepared in Et_2O!). However, the surprising stability of the aggregate apparently might also result from the shielding by the sterically demanding silyl and *tert*-butyl groups. The bonding of the lithium atoms can be generally described as follows: the contributions to the electronic saturation are mainly ascribed to lithium–arsenic multicenter bonds in the sense of a cluster and less importantly also to Li–H–C interactions; the latter are formed between lithium and several hydrogen atoms of the methyl groups of the $SiiPr_3$ groups close by, which is supported by the relatively short Li–H distances (2.34(7)–2.6(1) Å) observed. The positional parameters of the methyl H atoms, considered for Li–H–C interactions (at C 9, C 13, C 16, C 22, C 27, and C 30) because of their short Li–H distances, were localized in the difference Fourier synthesis and refined. The observed positions of the relevant ligand atoms to the lithium centers can be interpreted in such a way that an almost tetragonal pyramidal coordination geometry is assigned to each Li atom; each Li atom forms strong interactions with three As and two H atoms of different methyl groups. Considerably shorter Li–H distances were observed in solvent-free organolithium compounds (e.g. 2.04(2) Å in (nBuLi)$_6$),[7a] whereas in solvent-free, hexameric lithium bis(trimethylsilyl)phosphide[7b] similar values to those in **1** were found.

The relatively high stability of the "inner complexed" $Ge_2As_6Li_6$ aggregate also becomes clear in view of the solubility of **1**, depending on the donor properties of the solvent. Thus, **1** is almost insoluble in aliphatic and aromatic solvents as well as in diethyl ether, whereas it is readily soluble in highly coordinating solvent mixtures such as THF/TMEDA (tetramethylethylenediamine) and THF/PMDETA (pentamethyldiethylenetriamine). Here a complete degradation of the aggregate into two discrete tris(triisopropylsilylarsanide)*tert*-butylgermane anions and six solvent-coordinated lithium cations (chelate complexation of the lithium atoms) probably occurs. The exact molecular structures of the thus obtained complexes are not known to date. Further investigations shall determine the structures of these complexes and the reactivity of **1**, as well as establish whether the phosphorus analogue can also be synthesized.

Experimental Procedure

A solution of *t*Bu–GeF$_3$ (878 mg, 4.69 mmol) in Et_2O (20 mL) was treated at −80 °C with LiHAs–Si*i*Pr$_3$ (14.08 mmol) [dissolved in Et_2O, prepared from H_2As–Si*i*Pr$_3$ (3.296 g, 14.08 mmol) and *t*BuLi (901 mg, 14.08 mmol, 1.5 M solution in pentane) at −80 °C in Et_2O (10 mL)]. The solution was allowed to warm to about −20 °C over the course of 2 hours, then recooled to −80 °C and a solution of *t*BuLi (901 mg, 14.08 mmol) in pentane was added. After the removal of the solvent under vacuum (10^{-2} Torr), an orange, viscous oil remained, which was taken up in hexane (10 mL). Compound **1** crystallized out after about 2 weeks. Yield: 96 mg (0.59 mmol, 24%), yellow-orange crystals; correct C, H analysis.

Received: June 4, 1993 [Z 6123 IE]
German version: *Angew. Chem.* **1993**, *105*, 1549

[1] Review: D. A. Armitage, *Organosilicon Derivatives of Phosphorus, Arsenic, Antimony and Bismuth in The Silicon-Heteroatom Bond* (Eds.: S. Patai, Z. Rappoport), Wiley, New York, **1991**, Chapters 5,6, p. 151–211.

[2] J. W. Anderson, J. E. Drake, *J. Chem. Soc. A* **1970**, 3131, and references therein.

[3] M. Driess, H. Pritzkow, unpublished results.

[4] X-ray structure analysis of **1**: space group $P\bar{1}$, $a = 1378.9(6)$, $b = 1406.0(6)$, $c = 1418.2(7)$ pm, $\alpha = 91.00(4)$, $\beta = 113.52(3)$, $\gamma = 118.65(3)°$, $V = 2136.64 \times 10^{-6}$ pm^3, $Z = 1$; 5010 observed reflections (Siemens (Nicolet Syntext)R3m/V four-circle diffractometer, $Mo_{K\alpha}$ radiation, graphite monochromator, ω scan, $I > 2\sigma(I)$, T = 190 K); Structure solution with direct methods, all non-hydrogen atoms were refined anisotropicically, the Li–H–C hydrogen atoms at C 9, C 13, C 16, C 22, C 27, and C 30 were localized in the difference Fourier synthesis and refined; 460 refined parameters, one absorption correction was carried out. $R1 = 0.042$, $Rw = 0.038$. Further details of the crystal structure investigation may be obtained from the Fachinformationszentrum Karlsruhe, Gesellschaft for wissenschaftlich-technische Information mbH, D-76344 Eggenstein-Leopoldshafen (FRG) on quoting the depository number CSD-57488, the names of the authors, and the journal citation.

[5] B. Eisenmann, H. Jordan, H. Schäfer, *Angew. Chem.* **1981**, *93*, 211; *Angew. Chem. Int. Ed. Engl.* **1981**, *20*, 197.

[6] a) G. Becker, C. Witthauer, *Z. Anorg. Allg. Chem.* **1982**, *492*, 28; b) M. Driess, H. Pritzkow, *Angew. Chem.* **1992**, *104*, 350; *Angew. Chem. Int. Ed. Engl.* **1992**, *31*, 316.

[7] a) I. Craubner, *Z. Phys. Chem.* **1966**, *51*, 225; W. N. Setzer, P. von R. Schleyer, *Adv. Organomet. Chem.* **1985**, *24*, 353; T. Kottke, D. Stalke, *Angew. Chem.* **1993**, *105*, 619; *Angew. Chem. Int. Ed. Engl.* **1993**, *32*, 580; b) E. Hey-Hawkins, E. Sattler, *J. Chem. Soc. Chem. Commun.* **1992**, 775.

Relative Significance of Electrostatic- and Hydrophobic-Induced pK_a Shifts in a Model Protein: The Aspartic Acid Residue

By *Dan W. Urry*, Shao Q. Peng, Timothy M. Parker, D. Channe Gowda,* and *Roland D. Harris*

A common theme in biology is protein function that is dependent upon an amino acid residue with an unusual pK_a. In thioredoxin the amino acid residue is Asp 26 with a pK_a of 7.5,[1, 2] in chicken egg white lysozyme Glu 35 with a pK_a of 6.1,[3] in phosphofructokinase Asp 27 with pK_a values in two different functional states of 6.6 and above 9.6,[4] and in bacterial photoreaction centers Glu 212 with a pK_a of about

[*] Prof. D. W. Urry, S. Q. Peng, T. M. Parker
Laboratory of Molecular Biophysics
The University of Alabama at Birmingham
VH300 Birmingham, AL 35294-0019 (USA)
Telefax: Int. code + (205)934-4256
D. C. Gowda, R. D. Harris
Bioelastics Research, Ltd., AL 35205-3409 (USA)

[**] This work was supported in part by contracts (DAAL03-92-C-0005 (to R. D. H.) from the Department of the Army, Army Research Office, and N00014-89-J-1970 (to D. W. U.) from the Department of the Navy, Office of Naval Research.

9.[5] Most commonly these shifts are explained as arising from electrostatic interactions,[6, 7] but increasingly the role of hydrophobic effects is being appreciated.[3, 8] In this communication both electrostatic- and hydrophobic-induced pK_a shifts are observed and can be compared in a family of aspartic acid containing polypentapeptides. It is argued that the most effective means of achieving a pK_a shift in water arises not from the predominance of the coulombic interactions of electrostatics, but from a competition of hydrophobic (apolar) and charged (polar) species for hydration in which the respective hydration shells cannot be shared. This results in an apolar–polar repulsive free energy of hydration that can be calculated from the magnitude of the pK_a shift in the hydrophobic domain.

Figure 1 depicts a plot of f_D, the mole fraction of pentamers containing aspartic acid (D) for the set of protein-based polymers poly[f_V(IPGVG),f_D(IPGDG)], versus pK_a, where $f_V + f_D = 1$ and where I = Ile, P = Pro, G = Gly and V = Val. As seen in Figure 1, the minimal value, found at $f_D = 0.5$ in water and at $f_D = 1.0$ in saline, is essentially 3.9, which is the normal pK_a for the carboxyl moiety of the aspartic acid residue.[9]

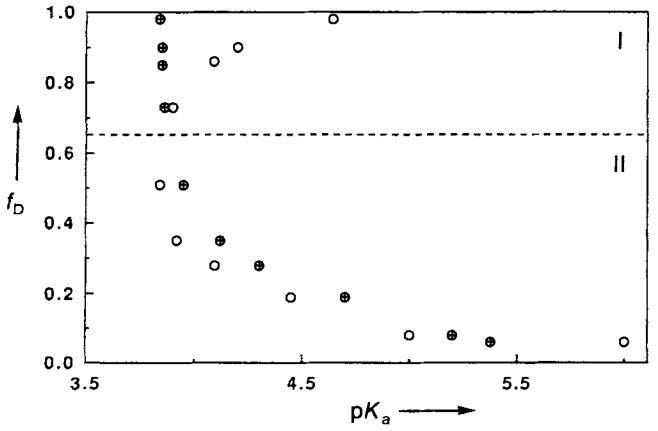

Fig. 1. The pK_a values determined by classical acid–base titrations for poly[f_V(IPGVG),f_D(IPGDG)], in which values of f_D range from 1.00 to 0.06 in water with a resistance of greater than 11 MΩ (i.e., Type 1 water) and in 0.15 M NaCl (⊕) at 37 °C (see text for further details). I: Region dominated by electrostatic interactions. II: Region dominated by hydrophobic interactions.

In water, the curve is parabolic with respect to the f_D axis; at $f_D = 1.0$ the pK_a is 4.6, and it systematically decreases to a minimum near 3.9 for $f_D = 0.5$; for values of $f_D < 0.5$ the pK_a values again increase systematically until the value of 6.0 is reached at $f_D = 0.06$. Since the positive pK_a shift decreases as the density of Asp residues (that is, negative charges) decreases to one in ten residues ($f_D = 0.5$), and as the positive shift in this region is entirely removed by the addition of 0.15 M NaCl, which can screen charge–charge interactions, the domain defined by $f_D > 0.5$ is clearly the electrostatic, or charge–charge repulsion, domain. For $f_D < 0.5$, the increase in pK_a becomes greater as the number of chargeable aspartic acid residues diminishes. Accordingly, this larger shift cannot be due to charge–charge repulsion; instead, it is proportional to the increase in hydrophobicity due to the replacement of polar aspartic acid residues with hydrophobic Val residues.

The increasing hydrophobicity as f_D decreases may be quantified using an experimental hydrophobicity scale based on the value of T_t (the temperature of the inverse temperature transition, at which hydrophobic folding, assembly, and phase transition occur on raising the temperature). The experimental value of T_t, having been determined in the polypentapeptide sequence for all of the amino acid residues,[10, 11] is seen to decrease as the hydrophobicity of the amino acid residue increases, such that a calulated mean value of T_t, i.e., $\langle T_t \rangle$, for a given polypeptide sequence, becomes a quantitative measure of hydrophobicity. In Table 1, $\langle T_t \rangle$ is seen to decrease as f_D decreases.

On the basis of this hydrophobicity scale, the domain identified by $f_D < 0.5$ is reasonably defined as the hydrophobic, or apolar–polar repulsion, domain. In 0.15 M NaCl, the charge–charge repulsion effect is entirely suppressed, and the hydrophobic-induced pK_a shift begins to appear as f_D decreases below 0.7.

Of course, the magnitude of the positive shift in pK_a due to charge–charge repulsion can be increased by increasing charge density to more than one COO^- moiety per fifteen backbone atoms of the polypentapeptide. In poly(methacrylic acid), $-(CH_3)C(COOH)CH_2-_n$, there is one COO^- moiety per two backbone atoms, a greater density than is possible for polypeptides. Here the pK_a in water is 7.3,[12] several pH units higher than that of the carboxylic acid moiety in the monomer.

In deciding the relative importance of electrostatic- and hydrophobic-induced pK_a shifts, the question becomes how large can the hydrophobic-induced shifts be in polypeptides and proteins. By using the broader family of poly(pentapeptides), poly[f_V(VPGVG),$f_{\alpha\beta}$(αPGβG)] ($f_V + f_{\alpha\beta} = 1$, where α may be one of a few hydrophobic residues, such as Val, Ile, or Phe, and β can be any of the naturally occurring amino acid residues or chemical modifications), a series of polytricosapeptides have been prepared in which a single Asp

Table 1. Amino acid analyses [a], experimental pK_a values and calculated mean hydrophobicity, $\langle T_t \rangle$, for poly[f_V(IPGVG),f_D(IPGFG)].

Amino acid or property	I	II	III	IV	V	VI	VII	VIII	IX	X
aspartic acid (D) (f_D)	0.06	0.08	0.19	0.28	0.35	0.51	0.73	0.84	0.89	0.99
glycine (G)	1.96	2.01	1.99	2.01	2.00	2.05	2.00	1.99	2.00	1.97
proline (P)	1.0	1.0	1.0	1.0	1.0	1.0	1.0	1.0	1.0	1.0
valine (V) (f_V)	0.86	0.83	0.77	0.74	0.64	0.46	0.27	0.19	0.12	···
isoleucine (I)	0.92	0.91	1.02	1.01	1.03	1.04	0.99	0.99	1.01	0.98
experimental pK_a (NaCl) [b]	5.4 ± 0.1	5.2 ± 0.08	4.7 ± 0.05	4.3 ± 0.04	4.1 ± 0.05	4.0 ± 0.02	3.9 ± 0.01	3.9 ± 0.01	3.9 ± 0.01	3.8 ± 0.01
experimental pK_a (water) [b]	6.0 ± 0.12	5.0 ± 0.1	4.5 ± 0.06	4.2 ± 0.05	3.9 ± 0.05	3.8 ± 0.03	3.9 ± 0.02	4.1 ± 0.01	4.2 ± 0.02	4.6 ± 0.02
$\langle T_t \rangle^0$ [c]	28	28	28	28	29	30	30	31	31	31
$\langle T_t \rangle^-$ [c]	29	30	33	35	37	42	49	52	53	56

[a] In the analyses all acids are quoted as a proportion relative to proline, which is taken as 1.0. This makes the value for aspartic acid identical to f_D. [b] Mean and standard derivations of more than three titrations. [c] Calculation of mean hydrophobicities according to reference [21]; D^0 stands for Asp(COOH) and D^- for Asp(COO^-).

 © VCH Verlagsgesellschaft mbH, D-69451 Weinheim, 1993 0570-0833/93/1010-1441 $ 10.00+.25/0

residue occurs with five hydrophobic phenylalanine (Phe) residues per 30-mer. When the five Phe residues were placed as far from the Asp residue as possible without changing the filamentous β-spiral molecular structure of the polypentapeptides with three pentamers per turn of helix,[13, 14] the pK_a was shifted to 6.7 from the usual value of 3.9.[9] When the five Phe residues were placed as close to the Asp residue as possible but still consistent with the retention of the molecular structure, a remarkable pK_a of 10.0 was found (D. W. Urry, D. C. Gowda, S. Peng, T. M. Parker, N. Jing, R. D. Harris, unpublished results). This is a pK_a shift of 6, twice as great as that found for the excessively charge-dense poly(methacrylic acid). Thus it would appear that the capacity to shift pK_a values is greater when the apolar–polar repulsion mechanism is employed.

Our understanding of electrostatic-induced pK_a shifts comes from Coulombs law, in which the increase in energy (i.e., repulsive energy) between a pair of like charged species, q_1 and q_2, is the product of the charges q_1q_2, divided by the distance, r, and the effective dielectric constant, ε, between the two charges: $E = q_1q_2/\varepsilon r$. Polymers have been explicitly treated by Harris and Rice[15] and by Katchalsky et al.,[16] and Honig et al. have extensively considered proteins.[7, 17] There is as yet no formal expression for the apolar–polar repulsive free energy of hydration, but, as the name intends to convey, it involves the interference that each apolar (hydrophobic) and polar (e.g., charged) moiety experiences due to the presence of the other in a structurally constrained, and thereby, hydration-limiting polymer such as a protein or polypeptide. In short, when the distance between apolar and polar moieties is sufficiently short, the intervening water molecules cannot simultaneously provide the full free energy of hydration for both the apolar and polar species.

When, in the hydrophobic domain where apolar hydration dominates, the carboxyl species, for example, cannot achieve the hydration required of the carboxylate moiety, a higher hydroxyl ion concentration is required before the COOH proton can be removed to form COO^-.[10] In this case the change in chemical potential, $\Delta\mu$, of proton, as Gibbs free energy per mole, is given by $\Delta\mu = -2.3\,RT\Delta pK_a$, where $R = 1.987\ \mathrm{cal\,K^{-1}\,mol^{-1}}$ and T is in degrees Kelvin. Under these circumstances, $\Delta\mu$ becomes a direct measure of the repulsive apolar–polar free energy of hydration. On the other hand, when the charged species does form, its pull for hydration is sufficient to destructure the water of hydrophobic hydration, the driving force for hydrophobic folding and assembly is lost, and disassociation and unfolding occur.

In fact, as the number of ionized species increases, the temperature T_t, at which the hydrophobic folding and assembly transition occurs, increases.[10, 11] When the value of T_t becomes greater than the working temperature of the polypeptide or protein, disassembly and unfolding sets in. Also, as seen by differential scanning calorimetry, the endothermic heat of the transition, which is interpreted as the heat required to destructure the more structured hydrophobic hydration to form less ordered bulk water, decreases as the degree of ionization increases, consistent with the charged species destructuring of the hydrophobic hydration.[18] A more extensive discussion of these hydrophobic effects is available in references[10, 19].

Experimental Procedures

The family of polypentapeptides, poly[f_V(IPGVG),f_D(IPGDG)] with $f_D = 1.0$–0.06 for a total of ten polypentapeptides were characterized by using classical acid–base titrations to determine the pK_a values. The specific syntheses, which will be described elsewhere, were carried out analogously to those in [20] for Glu-containing peptides but with care to avoid the α/β exchange of the Asp residue, and were verified by means of amino acid analyses and ^{13}C NMR spectroscopy, which also provided accurate values for f_D (see Table 1). The acid–base titrations for the $COOH/COO^-$ couple, carried out at 37 °C as previously described [20] under argon, allowed 45 min per data point, thus requiring approximately 24 h per titration for concentrations of Asp-containing pentamers ranging from 22 to 29 mM. In general, the samples remained in a viscoelastic state until the degree of ionization was sufficient for dissolution.

Received: April 30, 1993 [Z 6050 IE]
German version: *Angew. Chem.* **1993**, *105*, 1523

[1] K. Langetsmo, J. A. Fuchs, C. Woodward, *Biochemistry* **1991**, *30*, 7603–7609.
[2] K. Langetsmo, J. A. Fuchs, C. Woodward, K. A. Sharp, *Biochemistry* **1991**, *30*, 7609–7614.
[3] M. Inoue, H. Yamada, T. Yasukochi, R. Kuroki, T. Miki, T. Horiuchi, T. Imoto, *Biochemistry* **1992**, *31*, 5545–5553.
[4] I. Auzat, J.-R. Garel, *Protein Sci.* **1992**, *1*, 254–258.
[5] M. Y. Okamura, G. Feher, *Annu. Rev. Biochem.* **1992**, *61*, 861–896.
[6] C. Tanford, *Adv. Protein Chem.* **1962**, *17*, 69–165.
[7] K. Sharp, B. Honig, *Annu. Rev. Biophys. Biophys. Chem.* **1990**, *19*, 301–332.
[8] D. W. Urry, D. C. Gowda, S. W. Peng, T. M. Parker, R. D. Harris, *J. Am. Chem. Soc.* **1992**, *114*, 8716–8717.
[9] J. T. Edsall, J. Wyman, *Biophysical Chemistry*, Academie, New York, NY, **1958**, pp. 452–453.
[10] D. W. Urry, *Angew. Chem.* **1993**, *105*, 859–883; *Angew. Chem. Int. Ed. Engl.* **1993**, *31*, 819–841.
[11] D. W. Urry, *Prog. Biophys. Mol. Biol.* **1992**, *57*, 23–57.
[12] A. Katchalsky, *J. Polym. Sci.* **1951**, *7*, 393–412.
[13] D. W. Urry, *J. Protein Chem.* **1984**, *3*, 403–436.
[14] D. W. Urry, in *Molecular Conformation and Biological Interactions* (Eds.: P. Balaram, S. Ramaseshan), Indian Academy of Sciences, Bangalore, India, **1991**, p. 555–583.
[15] F. E. Harris, S. A. Rice, *J. Phys. Chem.* **1954**, *58*, 725–732.
[16] A. Katchalsky, S. Lifson, I. Michaeli, M. Zwick in *Size & Shape of Contractile Polymers: Conversion of Chemical & Mechanical Energy* (Ed.: A. Wasserman), Pergamon, New York, **1960**, pp. 1–40.
[17] M. E. McGrath, J. R. Vasquez, C. S. Craik, A. S. Yang, B. Honig, R. J. Fletterick, *Biochemistry* **1992**, *31*, 3059–3064.
[18] D. W. Urry, C.-H. Luan, R. D. Harris, K. U. Prasad, *Polym. Prep. Am. Chem. Soc. Div. Polym. Chem.* **1990**, *31*, 188–189.
[19] For hydrophobic hydration and hydrophobic interactions see also W. Blokzijl, J. B. F. N. Engberts, *Angew. Chem.* **1993**, *105*, No. 11; *Angew. Chem. Int. Ed. Engl.* **1993**, *32*, No. 11.
[20] D. W. Urry, S. Q. Peng, T. M. Parker, *Biopolymers* **1992**, *32*, 373–379.
[21] D. W. Urry, D. C. Gowda, T. M. Parker, C.-H. Luan, M. C. Reid, C. M. Harris, A. Pattanaik, R. D. Harris, *Biopolymers* **1992**, *32*, 1243–1250.

High-Pressure Synthesis of LiSi: Three-Dimensional Network of Three-Bonded Si^- Ions**

By *Jürgen Evers,** *Gilbert Oehlinger,* and *Gerhard Sextl*

Lithium germanide LiGe[1] crystallizes under normal pressure (NP) with MgGa[2] structure and belongs to the Zintl phases.[3] According to current textbooks,[4] several binary Li–Si compounds such as $Li_{21}Si_5$,[5] $Li_{13}Si_4$,[6] $Li_{14}Si_6$,[7] and $Li_{12}Si_7$[8] have been characterized, however, "LiSi is not known".[4]

Our investigations also confirmed the results of previous experimenters: simple fusion of equimolar amounts of Li and Si at NP always results in a phase mixture, but never in LiSi. LiSi should be stabilized with respect to a mixture

[*] Priv.-Doz. Dr. J. Evers, G. Oehlinger
Institut für Anorganische Chemie der Universität
Meiserstrasse 1, D-80333 München (FRG)
Telefax: Int. code + (89)5902-451
Dr. G. Sextl
Degussa AG
Rodenbacher Chaussee 4, D-63457 Hanau (FRG)

[**] This work was supported by the Deutsche Forschungsgemeinschaft and the Fonds der Chemischen Industrie.

consisting of 1/12 $Li_{12}Si_7$ and 5/12 Si, however, if, under sufficiently high pressure, it could be considerably more densely packed than the mixture. For this reason, a high-pressure (HP) synthesis was attempted in boron nitride and molybdenum crucibles by using the Belt apparatus according to Equation (a). Typical reaction conditions were p = 4 GPa, T = 600 °C, t = 5 min: after this time the reaction

$$Li_{12}Si_7 + 5\,Si \rightleftharpoons 12\,LiSi \qquad (a)$$

mixture was quenched to room temperature and the pressure relieved. It proved favorable to use an excess of Li (10 atom%) in the starting mixture. Due to the high sensitivity of the reactions towards both air and moisture, all preparative work with open crucibles was performed in a glove box.

The Guinier diffractogram ($Cu_{K\alpha 1}$ radiation) of the reaction product was indexed by the Dicvol method[9] and found to have a tetragonal unit cell and very good reliability indices (F_{20} = 36, M_{20} = 40).[10] The sequence of the reflections and the course of the intensities indicate that the structures of LiSi and NP-LiGe[1] are isotypic (MgGa structure[2]) (Rietveld method[11]). A single-crystal X-ray analysis[12, 13] confirmed the results of the powder experiment.

According to the Zintl–Klemm concept,[3] silicon in Li^+Si^-, like a phosphorus atom in elemental phosphorus, possesses five valence electrons and has, correspondingly, three nearest Si neighbors (241.7(6) (2×) and 250.2(6) pm). The Si-Si-Si bond angles are 107.2(2), 110.7(2), and 117.9(2)°. The Si–Si bond length of 250.2 pm in LiSi is one of the longest yet observed in binary metal silicides. Longer Si–Si distances have only been found in organometallic compounds with bulky *tert*-butyl groups, such as in hexa(*tert*-butyl)disilane (Si–Si = 269.7 pm).[14, 15] Typical Si–Si bond lengths in $Li_{14}Si_6$ and $Li_{12}Si_7$ lie in the range 233–239 pm.[7, 8]

Lithium silicide forms a three-dimensional network in which each Si^- ion is connected with three further Si^- ions (Fig. 1). A three-dimensional arrangement of Si^- ions is also

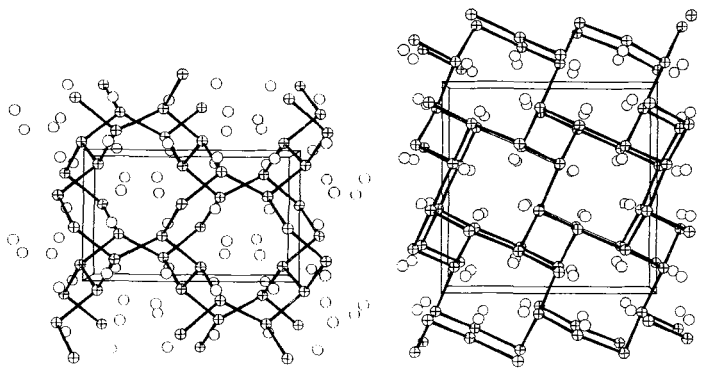

Fig. 1. Lithium silicide, LiSi (MgGa structure): three-dimensional network of three-bonded Si^- ions. Right: view along [001]; left: view along [100]. ○ = Li, ⊗ = Si.

found in $SrSi_2$[16, 17] and in α-$ThSi_2$.[18, 19] As in LiSi, the cavities in these three-dimensional networks are also filled by cations. A stabilization of this type in structures formed by elemental phosphorus requires that these disproportionate to form cations and anions. For this reason, the structures formed by elemental phosphorus that have been observed until now, all consist of isolated tetrahedra and layers of three-bonded P atoms which pack together without the formation of larger cavities. The structure of β-manganese,[20, 21] on the other hand, may be considered as a three-dimensional network of $Mn^{\delta-}$ atoms, whose cavities are filled by $Mn^{\delta+}$ atoms. In the space group $P4_332$ (a = 631.5(2) pm), the three-bonded $Mn^{\delta-}$ atoms (bond length 236.4(2) pm),[21] like the Si^- ions in NP-$SrSi_2$ (a = 653.5(3) pm, bond length 239.2(1) pm),[17, 22] occupy the 8c site with very similar site parameters.

In LiSi, the three-dimensional network contains fourfold screw axes of silicon atoms aligned along the a axis; neighboring screw axes are of opposite chirality. The two shorter Si–Si distances (241.7 pm) and the smaller Si-Si-Si bond angles (107.2, 110.7°) are found between atoms of one particular fourfold axis. Cross-linking of the fourfold screw axes with one another leads to formation of the longer Si–Si bond (250.2 pm) and the larger Si-Si-Si bond angle (117.9°). The puckered Si_8 rings formed in this manner are centered on z = 1/8, 3/8, 5/8, and 7/8. The Li^+ cations are arranged as tetrahedra and are located in the cavities formed by the Si_8 rings. The tetrahedron centers are displaced by $c/2$ with respect to the Si_8 rings. Each Li^+ ion has six Li^+ neighbors within a distance of 305 pm; three of these are in the same tetrahedron, two in the next nearest and one in the next nearest but one. The long Li–Li distances effectively rule out a discussion of tetrahedral Li_4 clusters with bonding Li–Li interactions.

Each Li^+ cation has eight Si neighbors within a distance of 326 pm (and vice versa). Five of these come from the nearest fourfold Si screw axis, two from the next nearest and one from the next nearest but one. This implies a formal 8:8 coordination in the three-dimensional network structure of LiSi. 1:1 silicides of the heavier alkali metals (Na–Cs) have lower coordination numbers. In these alkali metal silicides the three-bonded Si^- ions form isolated tetrahedra, as also found for P atoms in white phosphorus. NaSi with the NaSi structure[23] formally has a 6:6 coordination, as have NP-KSi, NP-RbSi, and NP-CsSi with the KGe structure.[24] In contrast, HP-KSi, HP-RbSi, and HP-CsSi[25] with the NaPb structure[26] achieve 7:7 coordination. NaSi could possibly be converted into another modification under HP, but a new phase has not yet been proven on quenching from pressures of up to 4 GPa.

$$5\,Li + 7\,LiSi \rightleftharpoons Li_{12}Si_7 \qquad (b)$$

$$12\,LiSi \rightleftharpoons Li_{12}Si_7 + 5\,Si \qquad (c)$$

Although it is synthesized under high-pressure conditions, LiSi is, somewhat surprisingly, not a metastable HP phase under normal conditions. This is confirmed first by coulometric titrations and second by thermal analysis. Reaction (b) (NP, 400 °C, LiCl/KCl melt) can be reversed by reversing the polarity, resulting in a negative free energy of formation.[27] The thermogram (NP, Ta crucible, Ar atmosphere) shows an endothermic signal between 470–490 °C ($\Delta H = +0.9 \pm 0.2$ kJ mol^{-1}) which may be attributed to reaction (c). A strongly endothermic signal is observed at 590 ± 10 °C, which corresponds to the melting point of the eutectic in the Li–Si phase diagram.[28] In attempting to prepare LiSi by cooling a LiSi melt, it has to be taken into consideration that NP-LiSi is thermodynamically unstable above 470 °C under NP. Thus, LiSi can only be prepared under NP at temperatures below 470 °C. The formation of LiSi from the phase mixture is extremely slow under these conditions due to kinetic hindrance. In ignorance of this, earlier experiments at NP failed due to a lack of patience. At HP (4 GPa, 600 °C, 5 min), the synthesis is achieved in a shorter time, since LiSi is about 6% more densely packed than the mixture, and thus a rise in pressure leads to its

formation in accordance with Le Chatelier's principle ($-p$, ΔV).

Received: May 4, 1993 [Z 6058 IE]
German version: *Angew. Chem.* **1993**, *105*, 1532

[1] E. Menges, V. Hopf, H. Schäfer, A. Weiß, *Z. Naturforsch. B* **1969**, *24*, 1351.
[2] K. Schubert, F. Gauzzi, K. Frank, *Z. Metallkd.* **1963**, *54*, 422. MgGa-type (*tI*32, $I4_1/a$, $a = 1053$, $c = 553$ pm, 16 Mg in 16f (0.070, 0.874, 0.129), 16 Ga in 16f (0.106, 0.948, 0.629)).
[3] H. Schäfer, B. Eisenmann, W. Müller, *Angew. Chem.* **1973**, *85*, 742; *Angew. Chem. Int. Ed. Engl.* **1973**, *12*, 694.
[4] Holleman-Wiberg, *Lehrbuch der Anorganischen Chemie*, de Gruyter, Berlin, **1985**, p. 737.
[5] R. Nesper, H. G. von Schnering, *J. Solid State Chem.* **1987**, *70*, 48.
[6] U. Frank, W. Müller, H. Schäfer, *Z. Naturforsch. B* **1975**, *30*, 10.
[7] H. G. von Schnering, R. Nesper, K.-F. Tebbe, J. Curda, *Z. Metallkd.* **1980**, *71*, 357.
[8] R. Nesper, H. G. von Schnering, J. Curda, *Chem. Ber.* **1986**, *119*, 3576.
[9] D. Louer, R. Vargas, *J. Appl. Crystallogr.* **1982**, *15*, 542.
[10] G. S. Smith, R. L. Synder, *J. Appl. Crystallogr.* **1979**, *12*, 60.
[11] D. B. Whiles, R. A. Young, *J. Appl. Crystallogr.* **1981**, *14*, 149. LiSi: 3500 measurement points, θ-range: 8–43°, $R_w = 0.071$; $R_p = 0.057$.
[12] LiSi crystal, cuboid with no well-defined surfaces ($0.5 \times 0.5 \times 0.25$ mm^3), Nicolet diffractometer, filtered $Cu_{K\alpha}$ radiation, 365 measured reflections (h: 0 + 10, k: ± 10, l: 0 + 5), 170 equivalent reflections, 153 reflections with $F > 3\sigma(F)$, internal R value = 0.0803, SHELXTL program system, 11 parameters, $R = 0.0645$, $R_W = 0.0516$, $R_G = R_M = 0.0855$, $a = 935.3(1)$, $c = 574.3(1)$ pm; 16 Li in 16f (0.082(2), 0.885(2), 0.058(4)), $U_{Li} = 0.031(7)$ Å^2; 16 Si in 16f (0.1109(3), 0.9526(3), 0.5941(5)), $U_{Si} = 0.0149(14)$ Å^2.
[13] Further details of the crystal structure investigation may be obtained from the Fachinformationszentrum Karlsruhe, Gesellschaft für wissenschaftlich-technische Information mbH, D-76344 Eggenstein-Leopoldshafen (FRG) on quoting the depository number CSD-57346, the names of the authors, and the journal citation.
[14] N. Wiberg, H. Schuster, A. Simon, K. Peters, *Angew. Chem.* **1986**, *98*, 100; *Angew. Chem. Int. Ed. Engl.* **1986**, *25*, 79.
[15] H. Bock, J. Meuret, K. Ruppert, *Angew. Chem.* **1993**, *105*, 413; *Angew. Chem. Int. Ed. Engl.* **1993**, *32*, 414.
[16] K. Janzon, H. Schäfer, A. Weiss, *Angew. Chem.* **1965**, *77*, 258; *Angew. Chem. Int. Ed. Engl.* **1965**, *4*, 245.
[17] J. Evers, G. Oehlinger, A. Weiss, *Angew. Chem.* **1978**, *90*, 562; *Angew. Chem. Int. Ed. Engl.* **1978**, *17*, 538.
[18] G. Brauer, A. Mitius, *Z. Anorg. Allg. Chem.* **1942**, *249*, 325.
[19] J. Evers, *J. Solid State Chem.* **1978**, *24*, 199; *ibid.* **1979**, *28*, 369.
[20] G. D. Preston, *Philos. Mag.* **1928**, *5*, 1207.
[21] C. B. Shoemaker, D. P. Shoemaker, T. E. Hopkins, S. Yindepit, *Acta Crystallogr. Sect. B* **1978**, *34*, 3573.
[22] J. Evers, Habilitation Thesis, Universität München, **1982**.
[23] J. Witte, H. G. von Schnering, *Z. Anorg. Allg. Chem.* **1964**, *327*, 260.
[24] E. Busmann, *Z. Anorg. Allg. Chem.* **1961**, *313*, 90.
[25] J. Evers, G. Oehlinger, G. Sextl, A. Weiss, *Angew. Chem.* **1984**, *96*, 512; *Angew. Chem. Int. Ed. Engl.* **1984**, *23*, 528.
[26] R. E. Marsh, D. P. Shoemaker, *Acta Crystallogr.* **1953**, *6*, 197.
[27] H. G. von Schnering, R. Nesper, J. Curda (Max-Planck-Institut for Festkörperforschung, Stuttgart), personal communication **1987**.
[28] C. van der Marel, G. J. B. Vinke, W. van der Lugt, *Solid State Commun.* **1985**, *54*, 917.

Vitamin D_3 Synthetic Studies: Enantiospecific Synthesis of the CD Ring Fragment**

By *Martin C. Clasby, Donald Craig,** and *Andrew Marsh*

The discovery that 1α,25-dihydroxy vitamin D_3 (**1**), the hormonally active form of vitamin D_3 (**2**),[1] induces cellular differentiation and suppresses cell proliferation[2] has aroused renewed interest in this classical synthetic target.[3] Many of the published synthetic approaches to this class of compounds involve coupling of CD-ring and A-ring fragments by olefination procedures such as the Julia[4] and Wadsworth–Emmons[5] reactions. This strategy is particularly attractive for the synthesis of semisynthetic analogs of **1** and **2** as drug candidates;[6] combination of modified A- and CD-ring fragments prepared by chemical elaboration of degradatively derived materials allows access to a wide range of unnatural vitamin D_3 mimics.

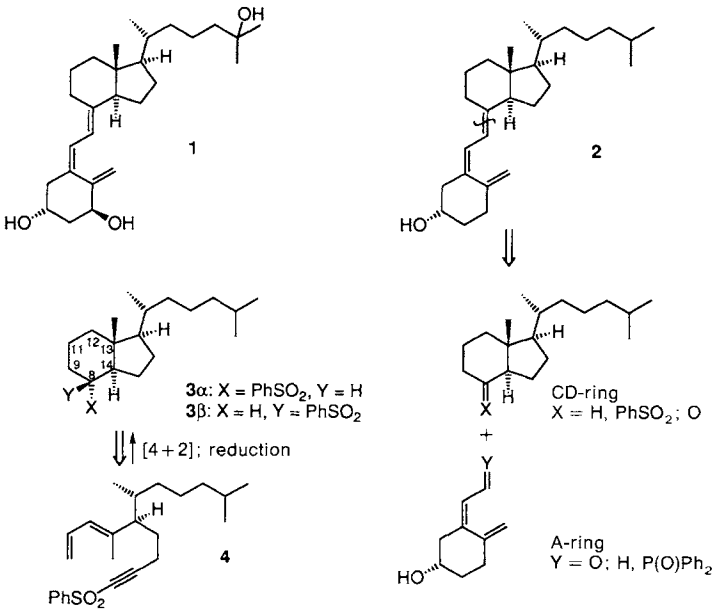

In this context, there has recently been an upsurge in research aimed at developing both new methods for A-ring assembly and improved procedures for coupling these intermediates with CD-ring units.[7] We have embarked on a program seeking on synthesize analogs of vitamin D_3 in which the CD-ring fragment is assembled by total synthesis. Such an approach is uniquely able to deliver analogs of the natural system incorporating extremely subtle structural changes, including isotopically labeled materials, which may serve as probes of the origins of biological activity.

We selected the known[4b] bicyclic sulfones **3** as the synthetic target. We envisaged that **3** would be accessible by stereoselective dihydrogenation of the product of the intramolecular Diels–Alder (IMDA) reaction[8] of dienynylsulfone **4**.[9, 10] This approach contrasts with existing IMDA-based strategies,[11] in that the C8–C9 and C13–C14 bonds rather than the C11–C12 and C13–C14 bonds are formed in the cyclization reaction. The stereocenters in IMDA substrate **4** would be installed by using a combination of the chiral pool[12] and the well-established asymmetric enolate alkylation methodology developed by Evans et al.[13]

Our synthesis of **3** started from (+)-(*R*)-citronellic acid, which was prepared on about a 1 mol scale in 61% yield from (+)-(*R*)-pulegone according to a published procedure.[14] Catalytic hydrogenation gave (+)-(*R*)-dihydrocitronellic acid, which was converted into the corresponding acid chloride **5** by thionyl chloride. Treatment of the anion of oxazolidone **6**[15] with **5** gave the crystalline[16] *N*-acyloxazolidone **7** in good yield (Scheme 1). Allylation of the sodium enolate[17] of **7** at low temperature proceeded efficiently with ≥20:1 diastereoselectivity to give alkene **8** as an oil after chromatographic separation of the diastereomers. Removal of the chiral auxiliary was attempted by several liter-

[*] Dr. D. Craig, M. C. Clasby, A. Marsh
Department of Chemistry
Imperial College of Science, Technology and Medicine
GB-London SW7 2AY (UK)
Telefax: Int. code + (71)589 3869

[**] This research was supported by the British Science and Engineering Research Council (SERC) (Quota Studentships to M. C. C. and A. M.).

ature procedures.[18] Exposure of **8** to trimethylaluminum–*O*,*N*-dimethylhydroxylamine[19] resulted in incomplete cleavage of the oxazolidone moiety. Compound **8** was poorly reactive towards lithium benzyloxide,[20] and sodium benzyloxide caused extensive (approximately 20%) epimerization at the α-stereocenter. Finally hydroboration of **8** with oxidative workup gave the expected primary alcohol, which was treated crude with *catalytic* potassium *tert*-butoxide[21] to give δ-lactone **9** in good overall yield for the two steps from **8**. Reduction of **9** mediated by diisobutylaluminum hydride to form the corresponding lactol, followed by chemoselective silylation[22] of the open-chain tautomer, gave the protected δ-hydroxyaldehyde **10**. Incorporation of the alkyne unit in readiness for diene assembly was accomplished by sequential *Z*-selective iodomethylenation,[23] potassium *tert*-butoxide induced E2 elimination, and desilylation with tetrabutylammonium fluoride to give alkynol **11**.[24] In order to ensure *E*-specificity during the formation of the 1,3-diene unit, we subjected **11** to the *syn*-specific, zirconocene dichloride mediated carbometalation procedure developed by Negishi,[25] trapping the intermediate vinylalane with iodine. Palladium(0)-mediated coupling of the resulting *E*-iodoalkene with vinylmagnesium bromide[26] and oxidation of the product alcohol with dimethylsulfoxide activated with oxalyl chloride[27] gave dienal **12** in high yield (from **11**).[28] The final phase of the synthesis of IMDA substrate **4** involved the introduction of the dienophile group, alkynylsulfone. This was effected with our recently published procedure.[29] Thus, addition of **12** to lithio(phenylsulfonyl)methane gave a mixture of diastereomeric β-hydroxysulfones, which were oxidized with pyridinium dichromate to the β-ketosulfone **13**. Treatment of **13** with triflic anhydride in the presence of Hünig's base gave dienyne **4** in excellent yield.

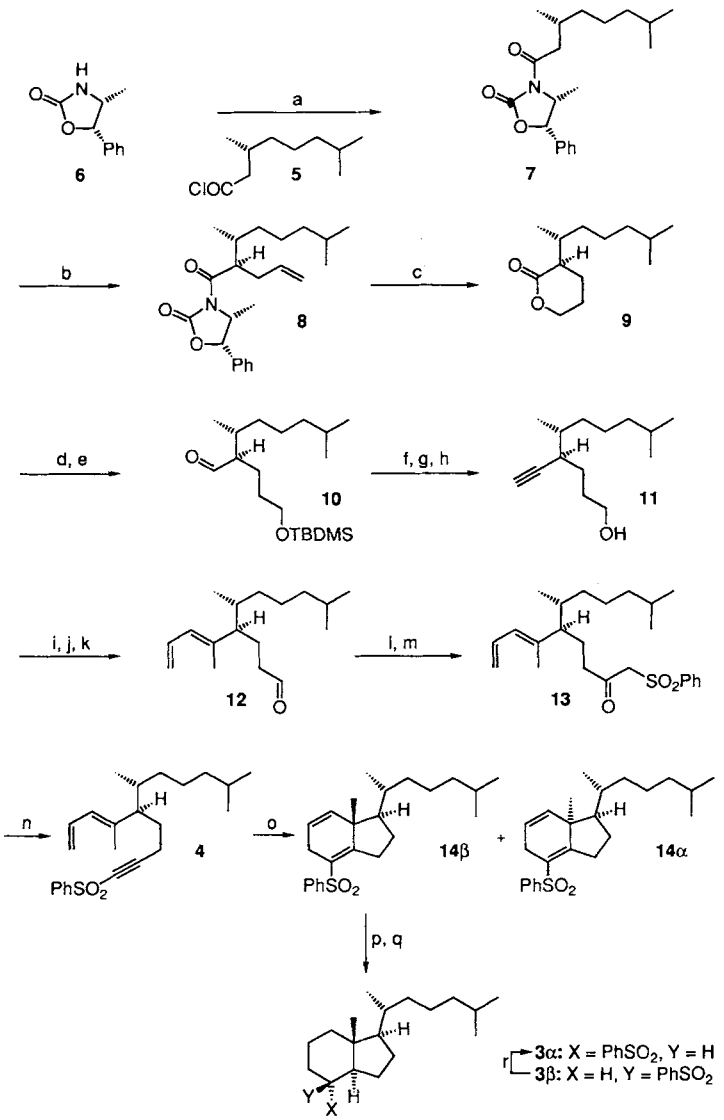

Scheme 1. a) *n*BuLi, THF, −78 °C, **+5**, −78 °C → room temperature (RT) (71%). b) $NaN(SiMe_3)_2$ (NaHMDS), THF, −78 °C; $CH_2=CHCH_2Br$, −78 °C → −50 °C, 5 h; −50 °C, 12 h (87%). c) 1: 9-Borabicyclo[3.3.1]nonane, THF, RT; NaOH, 30% w/v H_2O_2, 0 °C; 2: KO*t*Bu (0.02 equiv.), *t*BuOH (20 equiv.), THF, 0 °C (72%). d) iBu_2AlH, PhMe, −78 °C (87%). e) $TBDMSOSO_2CF_3$, Et_3N, CH_2Cl_2 (79%). f) $[Ph_3PCH_2I]I$, NaHMDS, THF, −78 °C (82%). g) KO*t*Bu (2 equiv.), THF, −78 °C (97%). h) nBu_4NF (2 equiv.), THF, RT (98%). i) Me_3Al, $[(C_5H_5)_2ZrCl_2$, $ClCH_2CH_2Cl$; I_2, THF (88%). j) $CH_2=CHMgBr$ (3 equiv.), $(Ph_3P)_4Pd$ (0.05 equiv.), PhMe–THF, RT (90%). k) $(COCl)_2$, dimethylsulfoxide, Et_3N, CH_2Cl_2, −60 °C → RT (79%). l) $PhSO_2Me$, *n*BuLi, THF, −78 °C, **+11** (90%). m) $(pyH^+)_2Cr_2O_7$, 4 Å molecular sieves, CH_2Cl_2, RT (71%). n) $(CF_3SO_2)_2O$ (1 equiv.), $EtNiPr_2$ (3 equiv.), CH_2Cl_2, 0 °C (93%). o) PhMe, 115 °C, 9 h (99%). p) H_2, 10% Pd/C, EtOAc (99%). q) $LiAlH_4$ (1 equiv.), THF, reflux, 20 min (**3α**: 76%; **3β**: 8%). r) KO*t*Bu (4 equiv.), *t*BuOH (40 equiv.), THF, RT, 1 h (99%).

The selectivity, albeit modest, of the cyclization of **4** to give **14** may be rationalized by considering the competing transition-state conformations (Scheme 2). In conformation **A**, $A_{1,3}$ strain between the diene H3 and H5 is less than that between H3 and the α-branched side chain in conformation **B**.

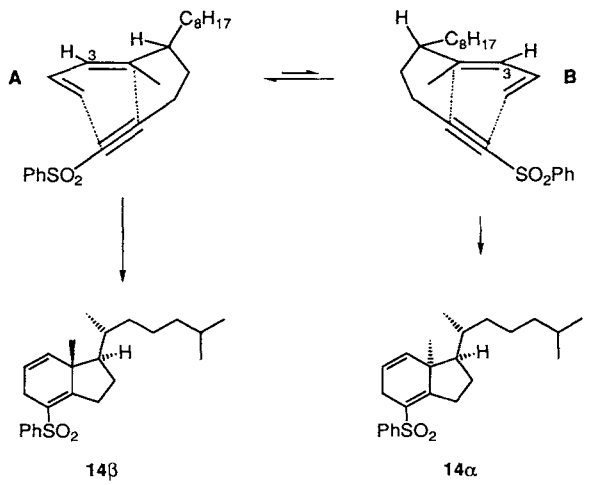

Scheme 2. **14β** is the major product.

In summary, we have accomplished the enantiospecific synthesis of the key building block **3** of vitamin D_3 in 18 steps from commercially available oxazolidone **6** and (+)-(*R*)-dihydrocitronellyl chloride. The highly convergent nature of the synthetic sequence makes it especially attractive for the synthesis of structural analogs of the natural systems that are inaccessible with semisynthetic or degradative procedures. We are currently exploring new methods for the construction of the A-ring unit, and are actively investigating novel coupling strategies. The results of these studies will be reported in due course.

Received: June 18, 1993 [Z 6147 IE]
German version: *Angew. Chem.* **1993**, *105*, 1495

[1] A. W. Norman, *Vitamin D, the Calcium Homeostatic Steroid Hormone*, Academic Press, New York, **1979**.
[2] H. F. DeLuca, *FASEB J.* **1988**, *2*, 224.
[3] B. Lythgoe, *Chem. Soc. Rev.* **1980**, *9*, 449.
[4] a) P. J. Kocienski, B. Lythgoe, S. Ruston, *J. Chem. Soc. Perkin Trans. 1* **1979**, 1290; b) H. Nemoto, H. Kurobe, K. Fukumoto, T. Kametani, *J. Org. Chem.* **1986**, *51*, 5311 (synthesis of **3α**).
[5] B. Lythgoe, T. A. Moran, M. E. N. Nambudiry, J. Tideswell, P. W. Wright, *J. Chem. Soc. Perkin Trans. 1* **1978**, 590.
[6] For example, see A. S. Leo, A. G. Schering, *Drugs of the Future* **1991**, *16*, 68.
[7] For leading references, see J. M. Nuss, M. M. Murphy, R. A. Rennels, M. H. Heravi, B. J. Mohr, *Tetrahedron Lett.* **1993**, *34*, 3079.
[8] For reviews of the IMDA reaction, see: a) W. R. Roush, in *Adv. Cycloaddition*, **1990**, *2*, 91; b) D. Craig, *Chem. Soc. Rev.* **1987**, *16*, 187; c) E. Ciganek, *Org. React.* **1984**, *32*, 1; d) A. G. Fallis, *Can. J. Chem.* **1984**, *62*, 183.
[9] For a study of IMDA reactions of sulfonyl-substituted trienes, see D. Craig, D. A. Fischer, Ö. Kemal, A. Marsh, T. Plessner, *Tetrahedron* **1991**, *47*, 3095.
[10] For a recent overview of intermolecular Diels–Alder reactions of alkynylsulfones, see N. S. Simpkins, *Sulphones in Organic Synthesis*, Pergamon, Oxford, **1993**, pp. 241–243. For an example of an IMDA reaction of an alkynylsulfone having an additional dienophile-activating group, see E. J. Corey, P. Da Silva Jardine, J. C. Rohloff, *J. Am. Chem. Soc.* **1988**, *110*, 3672.
[11] S. R. Wilson, M. S. Haque, *Tetrahedron Lett.* **1984**, *25*, 3151; S. R. Wilson, L. Jacob, *J. Org. Chem.* **1992**, *57*, 4380; K. Parker, T. I. Iqbal, *ibid.* **1987**, *52*, 4369; H. Nemoto, M. Ando, M. Fukumoto, *Tetrahedron Lett.* **1990**, *31*, 6205.
[12] S. Hanessian, *Total Synthesis of Natural Products: The 'Chiron' Approach*, Pergamon, Oxford, **1983**.
[13] D. A. Evans, R. L. Dow, T. L. Shih, J. M. Takacs, *J. Am. Chem. Soc.* **1990**, *112*, 5290.
[14] J. Plesek, *Collect. Czech. Chem. Commun.* **1957**, *22*, 644.
[15] M. S. Newman, A. Kutner, *J. Am. Chem. Soc.* **1951**, *73*, 4199.
[16] M.p. 90–93 °C (EtOH); $[\alpha]_D^{20}$ +37.7 (*c* 1.03, $CHCl_3$).
[17] The lithium enolate of **7** was found to be prohibitively unreactive towards allylation.
[18] For a comparative study of nonreductive methods for oxazolidone cleavage, see D. A. Evans, T. C. Britton, J. C. Ellman, *Tetrahedron Lett.* **1987**, *28*, 6141.
[19] D. A. Evans, S. L. Bender, *Tetrahedron Lett.* **1986**, *27*, 799. The use of two equivalents of reagent caused loss of the elements of carbon dioxide from **8** to give the corresponding oxazoline. With three equivalents, addition of *O,N*-dimethylhydroxylamine occurred with concomitant cleavage of the N–carbamoyl bond of the cyclic carbamate.
[20] D. A. Evans, M. D. Ennis, D. J. Mathre, *J. Am. Chem. Soc.* **1982**, *104*, 1737.
[21] The use of stoichiometric quantities of base led to substantial α-epimerization of **9**.
[22] The *tert*-butyldimethylsilyl (TBDMS) derivative of the cyclic tautomer was obtained as a by-product (11%) in this reaction. The use of *t*-$BuMe_2SiCl$ instead of $tBuMe_2SiOSO_2CF_3$ resulted in dehydration of the lactol to the corresponding glycal.
[23] G. Stork, K. Zhao, *Tetrahedron Lett.* **1989**, *30*, 2173.
[24] T. W. Greene, P. G. M. Wuts, *Protective Groups in Organic Synthesis*, 2nd ed., Wiley, New York, **1991**.
[25] E.-I. Negishi, *Pure Appl. Chem.* **1992**, *64*, 323.
[26] H. P. Dang, G. Linstrumelle, *Tetrahedron Lett.* **1978**, 1027.
[27] A. J. Mancuso, D. Swern, *Synthesis* **1981**, 165.
[28] Dienal **12** was contaminated with about 15% of the enal resulting from simple reduction of the iodoalkene precursor. All yields cited subsequently have accounted for this impurity.
[29] M. C. Clasby, D. Craig, *Synlett* **1992**, 825.
[30] Determined by ^1H NMR analysis (500 MHz) of the crude reaction mixture.
[31] HPLC separations were performed on a Rainin Instrument Company Dynamax® 60A column (300 × 21.4 mm) with 0.5% propan-2-olhexanes as eluant (15 mL min^{-1}) and UV (254 nm) detection; t_R (**14β**) = 14 min; t_R (**14α**) = 17 min.
[32] D. C. Dittmer, J. M. Balquist, *J. Org. Chem.* **1968**, *33*, 1364.
[33] In the present work, the thermal *syn*-elimination step in the sequence reported in reference [4a] (for vitamin D_4) was carried out (neat, 215 °C, 6 min) on the xanthate instead of the benzoate derivative.
[34] ^{13}C NMR data for **3α** (68 MHz, $CDCl_3$, 20 °C): δ = 138.6, 133.4, 129.0, 128.9, 63.9, 55.2, 48.3, 44.8, 39.5, 38.9, 36.2, 35.6, 28.1, 28.0, 27.5, 25.5, 23.9, 22.9, 22.6, 21.3, 18.8, 12.0.

Carbonyl–Metal Complexes of Diphosphadiboretane (mesB–P*t*Bu)$_2$ and of Triphosphatriborinanes (mesB–P*t*Bu)$_3$**

By *Bernhard Kaufmann, Heinrich Nöth*, Robert T. Paine, Kurt Polborn*, and *Martina Thomann*

Dedicated to Professor Hans Bock on the occasion of his 65th birthday

2,4-Bis(dialkylamino)-1,3-diorgano-1,3,2,4-diphosphadiboretanes **1** react with $[Cr(CO)_6]$ or $[Cr(CO)_5(thf)]$ to yield the mononuclear metal carbonyl complexes **2** or the binuclear complexes **3**, respectively.[1] If bulky amino groups such as the 2,2,6,6-tetramethylpiperidino group (R_2N = tmp) are bound to the B atoms, cycloreversion occurs, and allene-analogous complexes are formed, for example **4**, which contain a B–P double bond.[2] The stability of **4**, like that of the borylideneammonium ions $[R_2N{=}BX]^+$ (X = NR_2, OR, R),[3] is afforded by the BN π-bond. We, therefore expected that compounds of the types **2** or **3** would form, when tetraorgano-1,3,2,4-diphosphadiboretanes (RB-PR′)$_2$ react with metal carbonyls.

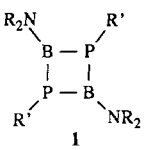

1

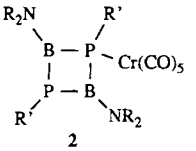

2

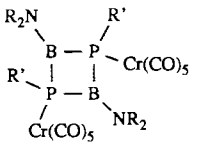

3

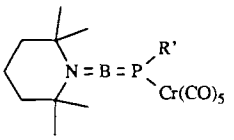

4

The diphosphadiboretane (mesB–P*t*Bu)$_2$ (**5**), obtainable from $mesBCl_2$ (mes = mesityl) and *t*BuP(H)Li at −30 °C in hexane [beside (mesB–P*t*Bu)$_3$ (**6**)],[4, 5] readily reacts with $[Cr(CO)_5(thf)]$ at ambient temperature to give the yellow tetracarbonyl complex **7** and CO gas [Eq. (a)]. When $[Fe_2(CO)_9]$ is treated with **5** in hexane/benzene, the red, light-sensitive tetracarbonyliron complex **8** forms [Eq. (b)]. This

[*] Prof. Dr. H. Nöth, Dipl.-Chem. B. Kaufmann, Dr. M. Thomann
Institut für Anorganische Chemie der Universität
Meiserstrasse 1, D-80333 München (FRG)
Telefax: Int. code + (89)590-2451
Prof. Dr. R. T. Paine
Department of Chemistry, University of Albuquerque, NM (USA)
Dr. K. Polborn
Institut für Organische Chemie der Universität München

[**] This work was supported by the Fonds der Chemischen Industrie, the BASF, and NATO.

complex when irradiated with UV light, releases one CO ligand to afford **9** [Eq. (c)]. Ligand **5** thus differs from the compounds **1** by its pronounced ability to form clusters with metal carbonyl fragments. Compound **10** is obtained [Eq. (d)] as golden yellow fine needles analogously to Equation (a) from 1,3,5,2,4,6-triphosphatriborinane (**6**). The B

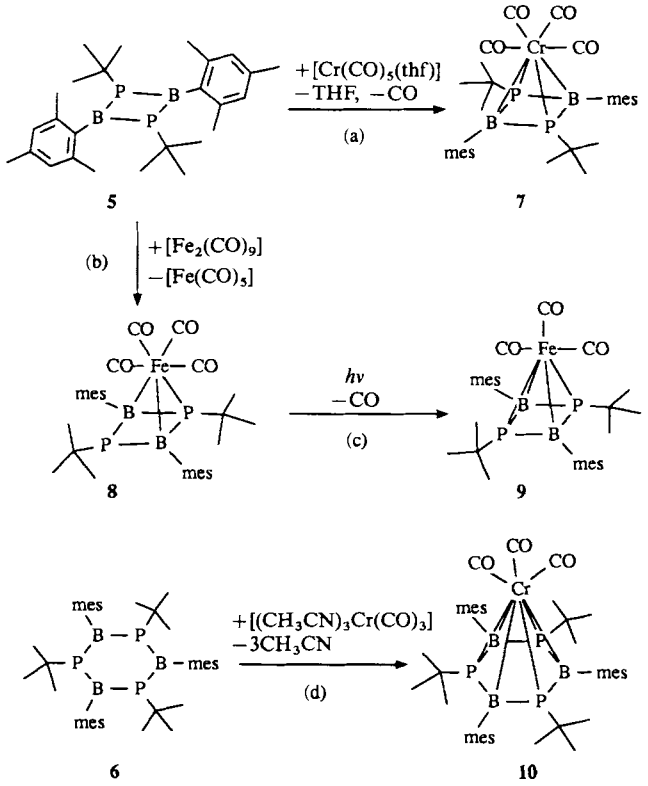

nuclei in **5** are shielded distinctly better ($\delta^{11}B = 86.2$) than those in the thexyl (tex) compound (texB–Pmes)$_2$, ($\delta^{11}B = 95.1$),[5] but they show almost the same chemical shift as those of the mesityl derivative (mesB–Pmes)$_2$ ($\delta^{11}B = 86.3$).[4] The ^{11}B NMR signals of complexes **7** and **9** are considerably shifted upfield ($\Delta\delta^{11}B = 56.5, 78.9$) in comparison to those of **5**. The improved shielding effected by a central Fe atom in a complex (e.g., in **9**) exceeds that of a central Cr atom (**7**) by $\Delta\delta > 20$, because the HOMO of the Fe(CO)$_3$ group allows for a stronger interaction between the metal d-electrons and the orbitals of the B atoms than the HOMO of the Cr(CO)$_4$ group.

The ^{31}P NMR signal of **5** is substantially shifted toward high field ($\Delta\delta^{31}P = 50.4, 64.5$) relative to that of (texB–Pmes)$_2$ ($\delta^{31}P = 80$)[5] and (mesB–Pmes)$_2$ ($\delta^{31}P = 65$).[4] The ^{31}P nuclei in the complexes **7** and **9** are much more strongly shielded, though. The ^{31}P NMR spectrum of **8** shows two downfield-shifted signals ($\Delta\delta^{31}P = -4.0, -38.4$), whereas the B atoms in **8** are shielded better than those in **5** by $\Delta\delta = 56$. Thus the bonding conditions in **7**, **8**, and **9** are mutually comparable. These data support the notion that the Fe(CO)$_4$ group in **8** is η^3-bound to a B_2P ring entity, whereas the diphosphadiboretane ligand in **7** and **9** is η^4-coordinated. This assignment is corroborated by the ^{13}C NMR spectra as well, which, in addition, display a single signal for the C atoms of the carbonyl groups. Consequently the carbonyl groups exhibit fluxional behavior at ambient temperature. The bonding parameters and conformations of **5**,[6] **7** (Fig. 1) and **9** (Fig. 2) were determined by X-ray structure analysis.

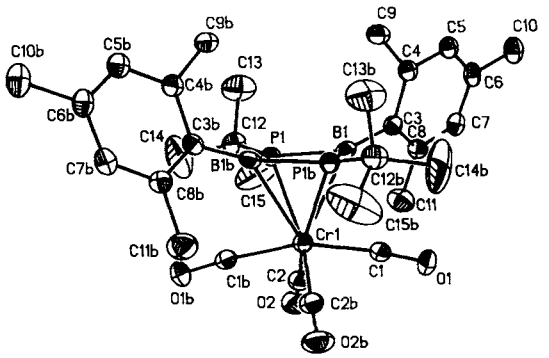

Fig. 1. Molecular structure of one of the two independent molecules **7** (ORTEP). H atoms are not shown, for clarity. Selected bond lengths [Å] and bond angles [°]: P1-B1 1.864(6), P1-B1b 1.911(7), Cr-P1 2.400(3), Cr-B1 2.542(7), Cr-C1 1.877(6), Cr-C2 1.853(7), B1-C3 1.573(9), P1-C12 1.858(7); B1-P1-B1b 93.8(3), P1-B1-P1b 85.8(3), B1-P1-C12 130.0(3), B1b-P1-C12 133.8(3), P1-B1-C3 133.6(4), C3-B1-P1b 137.0(4), P1-Cr-P1b 64.8(1), B1-Cr-B1b 65.6(3), P1-Cr-B1 44.2(1), P1-Cr-C1 113.3(2), P1-Cr-C2 99.7(2), B1-Cr-C1 71.2(2), B1-Cr-C2 109.7(3), C1-Cr-C2 85.8(3).

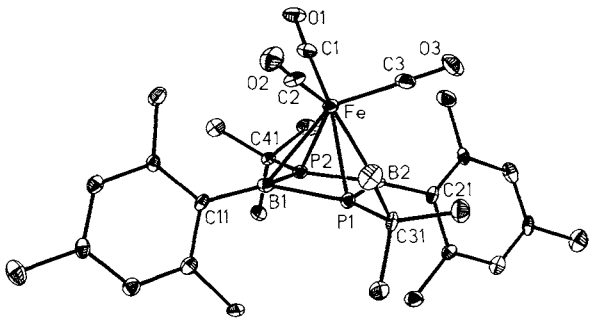

Fig. 2. Molecular structure of **9** (ORTEP). H atoms are not shown, for clarity. Selected bond lengths [Å] and bond angles [°]: P1-B1 1.94(1), P1-B2 1.910(8), P2-B1 1.888(8), P2-B2 1.872(10), Fe-P1 2.289(3), Fe-P2 2.294(2), Fe-B1 2.339(9), Fe-B2 2.325(9), Fe-C1 1.763(8), Fe-C2 1.771(9), Fe-C3 1.785(10), P1-C31 1.862(7), P2-C41 1.841(7), B1-C11 1.541(13), B2-C21 1.566(12); P1-B1-P2 83.5(4), B1-P2-B2 97.3(4), P2-B2-P1 84.7(4), B2-P1-B1 94.3(4), P1-Fe-P2 67.6(1), B1-Fe-B2 74.5(3), B1-Fe-P1 49.5(2), P2-Fe-B1 48.1(2), P1-Fe-B2 48.9(2), P2-Fe-B2 47.8(2), B1-P1-C31 136.2(4), B2-P1-C31 129.2(4), B1-P2-C41 130.1(4), B2-P2-C41 132.5(4), P1-B1-C11 136.0(5), P2-B1-C11 135.9(6), P1-B2-C21 134.1(6), P2-B2-C21 136.9(5).

The B–P bonds of the planar B_2P_2 four-membered ring in **5** [1.901(5) Å, 1.892(4) Å] are to be perceived as equally long.[7] They are, however, significantly shorter than those in most diphosphadiboretanes of the type **1** (1.94–1.97 Å).[8] On clustering to form **7** and **9**, the B_2P_2 four-membered ring of **5** is slightly deformed toward a diamond shape, which gives rise to a differentiation in the lengths of the B–P bonds [1.911(7) and 1.864(6) Å in **7**; 1.94(1), 1,910(8), 1.87(1), 1.888(8) Å in **9**]. The B atoms in **5** have a strictly planar configuration, as opposed to the B atoms in **7** (sum Σ of the bond angles at the B atoms in the B_2P_2 four-membered ring: 355.7°) and **9** (Σ = 357.5°). The formation of the clusters **7** and **9**, though, causes the P atoms in these compounds to become surrounded by the atoms B and C in an almost planar geometry (Σ = 357.5° in **7** and 359.8° in **9**), in contrast to the pyramidalized P atoms in **5** (Σ = 329.3°). There is another important difference between **5** on one hand and **7** and **9** on the other: The B_2P_2 four-membered rings in the clusters are folded: the angles between the P-B-P planes and an idealized planar structure are 10.4° in **7** and 3.9° in **9**. The B–C and P–C bonds are not significantly affected.

The P–Cr bond in **7** is distinctly longer (2.400(3) Å) than the P–Fe distances in **9** [2.289(3), 2.294(2) Å]. The boron–

metal distances are only slightly larger [2.542(7) Å in **7** and 2.339(9), 2.325(9) Å in **9**]. Although the covalent radius of a B atom ($r \approx 0.85$ Å) is smaller than that of a P atom ($r \approx 1.1$ Å), the boron–metal distances fall in the range of those in metallaboranes and metallacarboranes.[9] The B–Fe bonds in **9** are shorter than the B–Cr bonds in **7**, which is consistent with the smaller atomic radius of Fe.

While the change in the configuration of **5** on cluster formation (**7**, **9**) has been proven unambiguously, the discussion about the structure of **10** must be based on NMR data alone. The upfield shifts of $\Delta\delta \approx 40$, observed for both the ^{11}B and the ^{31}P signals, correspond to the differences between **5** and **7**. This fact justifies the proposition of an essentially planar CPB_2 configuration and of a structure analogous to **7**.[10] It also indicates some strong interaction between the Cr and the B atoms, beyond the metal-phosphorus coordination. Whether ligand **6** contains a planar six-membered ring, as $(mesB-PC_6H_{11})_3$ does,[11] remains unknown at present.

According to the Rudolph–Williams–Wade rules,[12] **8** may be considered as an *arachno* cluster, and the complexes **7**, **9** and **10** as *nido* clusters. Diazadiboretane(carbonyl)metal complexes $[(CO)_nM(RN-BR')_2]$, for example, are counted among the *nido* clusters, too.[13] Rehybridization at the N atoms does not necessarily occur when the complex is formed from the BN heterocycle and the complex fragment, because the N atoms in the free ligand are surrounded by their bonding partners in a planar geometry anyway. Attempts to convert the above *nido* clusters into *closo* clusters $[(RB-PR)_n\{M(CO)_n\}_2]$ by reactions with carbonyl complex fragments have remained unsuccessful so far.

Experimental

7: $[Cr(CO)_6]$ (1.21 g, 5.50 mmol) in 70 mL THF was converted into $[Cr(CO)_5(thf)]$ by irradiation (Hg vapor lamp, Hanovia S200W). The solution was slowly pipetted to a stirred solution of **5** (0.57 g, 1.31 mmol) in 20 mL hexane. After stirring for about 15 h, the volatiles were removed in vacuo. The residue was treated with 30 mL hexane, insolubles were fritted off, and the product crystallized at −30 °C. Yield: 0.34 g, 0.57 mmol, 52%; small yellow rods, m.p. 174 °C (decomp.; discoloration to brown above 125 °C). ^{1}H NMR (400 MHz, C_6D_6): $\delta = 1.04$ (pseudo t, N [16] = 19.0 Hz, 18 H, *t*Bu), 2.11 (s, 6 H, *p*-CH_3), 2.60 (s, 12 H, *o*-CH_3), 6.79 (s, 4 H, *m*-H); ^{13}C NMR (50 MHz, C_6D_6): $\delta = 21.0$ (s, *p*-CH_3), 25.4 (s, *o*-CH_3), 30.4 (d, $^2J(P,C) = 27.0$ Hz, $C(CH_3)_3$), 37.2 (d, $^1J(P,H) = 25.0$ Hz, $C(CH_3)_3$), 128.9 (s, *m*-C), 138.0 (s, *o*-C), 140.6 (s, *p*-C), 229.2 (t, $^2J(P,C) = 7.0$ Hz, CO); ^{31}P NMR (81 MHz, C_6D_6): $\delta = -39.8$; ^{11}B NMR (64 MHz, C_6D_6): $\delta = 29.7$, ($h_{\frac{1}{2}} = 525$ Hz); MS (70 eV): *m/z* 544 ($M^+ - 2CO$, 5%), 516 ($M^+ - 3CO$, 7%) 488 ($M^+ - 4CO$, 14%), 438 (51%), 436 ($M^+ - Cr(CO)_4$, 39%), 432 ($M^+ - 4CO$ − *iso*-butene, 34%), 379 ($M^+ - Cr(CO)_4 - t$Bu, 69%), 249 ($M^+ - Cr(CO)_4 - t$Bu − mesB, 100%); IR (Hostaflon): $\tilde{\nu}$(C≡O)[cm^{-1}] = 2000.4, 1991.3, 1918.0, 1899.4.

8: A solution of $[Fe_2(CO)_9]$ (0.38 g, 1.04 mmol) in benzene (25 mL) was slowly added dropwise to a stirred solution of **5** (0.45 g, 1.04 mmol) in hexane (20 mL), at ambient temperature. After 3 days all volatiles were removed from the dark brown solution in vacuo (oil pump). The residue was extracted with 25 mL pentane. Insolubles were removed by filtration. At −30 °C **8** crystallized in dark red platelets, which gradually decayed in daylight to yellow **9** ($\delta^{31}P = -53.7$). Yield: 0.45 g (0.74 mmol, 75%); m.p. 244 °C (decomp. > 233 °C); ^{1}H NMR (400 MHz, C_6D_6): $\delta = 0.94$ (d, $^3J(P,H) = 18.1$ Hz, 9 H, *t*Bu), 1.12 (d, $^3J(P,H) = 16.9$ Hz, 9 H, *t*Bu'), 2.14 ($N = 6.2$ Hz, 6 H, *p*-CH_3), 2.68 ($N = 14.2$ Hz, 12 H, *o*-CH_3), 6.83 ($N = 25.9$ Hz, 4 H, *m*-H); ^{13}C NMR (50 MHz, C_6D_6): $\delta = 21.0$ (s, *p*-CH_3), 25.2 (m, $N = 77.2$ Hz, *o*-CH_3), 28.5 (s, $C(CH_3)_3$), 29.6 (s, $C(CH_3)_3$), 34.4 ($N = 38$ Hz, $C(CH_3)_3$), 129.2 (s, *m*-C), 129.3 (s, *m*-C'), 139.2 (s, *o*-C), 139.6 (s, *o*-C'), 141.4 (s, *p*-C); 215.6 (s, CO); ^{31}P NMR (81 MHz, C_6D_6): $\delta = 14.6$ ($h_{\frac{1}{2}} = 180$ Hz), 49.0 ($h_{\frac{1}{2}} = 160$ Hz); ^{11}B NMR (64 MHz, C_6D_6): $\delta = 8.5$, $h_{\frac{1}{2}} = 520$ Hz; IR (Hostaflon): $\tilde{\nu}$(C≡O)[cm^{-1}] = 2022.5, 1969.7, 1957.7.

9: A solution of **7** (0.19 g, 0.31 mmol) in 5 mL toluene is irradiated (Hg vapor lamp, Hanovia S200W) in a quartz cuvette for 8 h. Addition of 5 mL of pentane effects crystallization of **9** as light yellow platelets. at −30 °C. Yield: 0.11 g (0.18 mmol, 58%); m.p. > 250 °C (decomp.); ^{1}H NMR (200 MHz, C_6D_6): $\delta = 0.98$ (pseudo-t, $N = 19.5$ Hz, 18 H, *t*Bu), 2.16 (s, 6 H, *p*-CH_3), 2.65 (s, 12 H, *o*-CH_3), 6.70 (s, 4 H, *m*-H); ^{13}C NMR (50 MHz, C_6D_6) $\delta = 21.1$ (s, *p*-CH_3), 25.9 (s, *o*-CH_3), 30.8 (s, $C(CH_3)_3$), 35.7 (pseudo-t, $N = 18.1$ Hz, $C(CH_3)_3$), 129.3 (s, *m*-C), 137.4 (s, *o*-C), 142.0 (s, *p*-C), 218.4 (s, CO); ^{31}P NMR (81 MHz, C_6D_6): $\delta = -53.9$, $h_{\frac{1}{2}} = 150$ Hz; ^{11}B NMR (64 MHz, C_6D_6): $\delta = 7.3$, $h(1/2) = 340$ Hz; IR (Hostaflon): $\tilde{\nu}$(C≡O[cm^{-1}] = 2002.9, 1946.1, 1933.9.

10: $[(CH_3CN)_3Cr(CO)_3]$ (0.35 g, 1.4 mmol) was added to a stirred solution of **6** (0.45 g, 0.69 mmol) in dioxan (150 mL). Twice a day 50 mL of dioxan was distilled off at 1 torr, and the same volume of dioxan was replenished. After 8 days the red solution was filtered, and the dioxan distilled off at 1 torr. At −30 °C the residue deposits **10** as golden yellow, very fine needles, from toluene/hexane. Yield: 0.37 g (0.47 mmol, 69%); m.p. > 250 °C (decomp.); ^{1}H NMR (400 MHz, C_6D_6): $\delta = 1.08$ (m, $N = 17$ Hz, 27 H, *t*Bu), 2.12 (s, 9 H, *p*-CH_3), 2.56 (s, 9 H, *o*-CH_3), 2.94 (s, 9 H, *o*-CH_3), 6.74 (s, 3 H, *m*-H), 6.80 (s, 3 H, *m*-H'); ^{13}C NMR (50 MHz, C_6D_6): $\delta = 21.1$ (s, *p*-CH_3), 25.5 (s, *o*-CH_3), 27.0 (s, *o*-C'H_3), 31.5 (s, $C(CH_3)_3$), 40.9 (s, $C(CH_3)_3$), 129.3 (s, *m*-C), 129.5 (s, *m*-C'), 137.7 (s, *o*-C), 142.2 (s, *p*-C), 243.9 (s, CO); ^{31}P NMR (81 MHz, C_6D_6): $\delta = 20.3$, $h_{\frac{1}{2}} = 150$ Hz; ^{11}B NMR (64 MHz, C_6D_6): $\delta = 20.9$, $h_{\frac{1}{2}} = 480$ Hz. MS (70 eV): *m/z* 790 (M^+, 11%), 706 ($M^+ - 3CO$, 100%), 649 ($M^+ - 3CO - t$Bu, 15%), 597 ($M^+ - Cr(CO)_3$, 34%), 592 ($M^+ - 3CO - 2t$Bu, 27%), 535 ($M^+ - 3Cr(CO)_3$ − mes, 13%); IR(CH_2Cl_2): $\tilde{\nu}$(C≡O)[cm^{-1}] = 1930.7, 1863.0.

Received: March 27, 1993 [Z 5951 IE]
German version: *Angew. Chem.* **1993**, *105*, 1534

[1] G. Linti, H. Nöth, R. T. Paine, *Chem. Ber.*, **1993**, *126*, 875–887.
[2] G. Linti, H.Nöth, R. T. Paine, K. Polborn, *Angew. Chem.* **1990**, *101*, 715–717; *Angew. Chem. Int. Ed. Engl.* **1990**, *29*, 682–684.
[3] H. Nöth, P. Kölle, *Chem. Rev.* **1985**, 399–418.
[4] G. Linti (Dissertation, Universität München, **1990**) obtained **6** almost exclusively by the same reaction. Ligand **5** prevails, when working at high concentrations.
[5] H. V. R. Dias, P. P. Power, *J. Am. Chem Soc.* **1989**, *111*, 144–148.
[6] An independent structure determination of **5** was carried out by P. P. Power et al. (*J. Organomet. Chem.* **1990**, *400*, 49–69). Except for selected bond lengths and angles, physical, spectroscopic, and crystallographical data are missing, though.
[7] X-ray structure analyses: Single crystals were sealed in glass capillaries under Ar. $Mo_{K\alpha}$ radiation, graphite monochromator. Data collection in ω-scan. Structure determination by direct methods (SHELXTL PC), non-hydrogen atoms were described anisotropically, H atoms incorporated in the refinement by the "riding model". **5**: $C_{26}H_{40}B_2P_2$, $M_r = 436.1$, triclinic, $a = 8.396(3)$, $b = 9.158(5)$, $c = 10.471(5)$ Å, $\alpha = 93.29(5)$, $\beta = 97.55(4)$, $\gamma = 117.23(3)°$, $V = 703.4(6)$ Å^3, space group $P\bar{1}$ (Nr. 2), $Z = 1$, $\varrho_{calcd} = 1030$ Mg m^{-3}, Nicolet–Siemens R3m diffractometer, 2θ-range: 2–48° in h, $+/-k$, $+/-l$, 0.8° scan width, scan rate = 2.5–29.3° min^{-1}, 2566 reflections measured, 2379 independent and 1755 observed ($F > 3\sigma(F)$), 136 parameter, $R = 0.071$, $R_w = 0.1168$. Selected bond lengths [Å] and bond angles [°]: B-P 1.901(5), P-B(a) 1.892(4), P-C10 1.858(5), B-C1 1.549(6); B-P-B(a) 88.6(2), P-B-P(a) 91.4(2), B-P-C10 120.5(2), P-B-C1 134.2(2), B(a)-P-C10 120.2(2). **7**: $C_{30}H_{40}B_2CrO_4P_2$, $M_r = 600.2$, monoclinic, $a = 20.51(2)$, $b = 9.001(9)$, $c = 18.12(2)$ Å, $\beta = 105.00(6)°$, $V = 3231(6)$ Å^3, space group $P2/c$ (Nr. 13), $\varrho_{calcd} = 1.234$ Mg m^{-3}, $Z = 4$, $\mu = 4.72$ cm^{-1}, Enraf Nonius CAD four circle diffractometer, $2\theta = 4–46°$ in $+/-h, k, l$, 0.8° scan width, max. scan time 180 s, 4992 reflections measured, 3963 independent and 3051 observed ($F > 4\sigma(F)$), 353 parameter, $R = 0.0575$, $R_w = 0.054$. The asymmetric unit contains two half-molecules with a diad axis. **8**: $C_{29}H_{40}B_2FeO_3P_2.C_6H_5CH_3$, $M_r = 618.1$, monoclinic, $a = 11.722(6)$, $b = 16.259(4)$, $c = 18.37(1)$ Å, $\beta = 108.24(4)°$, $V = 3325(3)$ Å^3, space group $P2_1/c$ (Nr. 14), $\varrho_{calcd} = 1.235$ Mg m^{-3}, $Z = 4$, $\mu = 5.76$ cm^{-1}, Nicolet-Siemens R3m diffractometer, $2\theta = 2–45°$ in $+/-h, k, l$, 0.65° scan width, ω scan rate = 2.4–29.3° min^{-1}, 7009 reflections measured, 4554 independent and 3281 observed ($F > 3\sigma(F)$), max./min. transmission = 0.8277/0.7773, 379 parameter, $R = 0.0757$, $R_w = 0.0811$. The crystal was photolabile. The correction for drop in intensity was performed with 3 control measured after every 48 intensity measurements. The toluene molecules intercorporated in the crystal are disordered in two orientations. Further details of the crystal structure investigation may be obtained from the Fachinformationszentrum Karlsruhe, Gesellschaft für wissenschaftlich-technische Information mbH, D-76344 Eggenstein-Leopoldshafen (FRG), on quoting the depository number CSD-57288, the names of the authors and the journal citation.
[8] P. Kölle, G. Linti, N. Nöth, G. L. Wood, C. K. Narula, R. T. Paine, *Chem. Ber.* **1988**, *121*, 871–879.
[9] O. Hollander, W. R. Clayton, S. G. Shore, *J. Chem. Soc. Chem. Commun.* **1974**, 604–605.
[10] The B_3P_3 six-membered ring in $[(mesB-PPh)_3Cr(CO)_3]$ has a very flat chair configuration. The sum of the bond angles at the P atoms fall between 357° and 358.7° for the PB_2C units (unpublished investigation, result obtained after submission of this paper).
[11] H. V. R. Dias, P. P. Power, *Angew. Chem.* **1987**, *99*, 1320–1321; *Angew. Chem. Int. Ed. Engl.* **1987**, *26*, 1270–1271.
[12] K. Wade, *J. Chem. Soc. D* **1971**, 792–793.
[13] P. Paetzold, K. Delpy, R. Boese, *Z. Naturforsch. B* **1988**, *43*, 839–845.
[14] D. Kaufmann, *Chem. Ber.* **1987**, *120*, 853–854; in analogy to $mesBBr_2$.
[15] A. Zschunke, M. Riemer, H. Schmidt, K. Issleib, *Phosphorus Sulfur Relat. Elem.* **1983**, *17*, 237–244.
[16] N describes the distance between the outermost signals of a multiplet.

Titanated Methoxyallene as Novel Homoaldol Equivalent for Diastereoselective Additions to Chiral Amino Aldehydes**

By *Stephan Hormuth, Hans-Ulrich Reissig,** and *Dieter Dorsch**

Dedicated to Professor R. W. Hoffmann on the occasion of his 60th birthday

Methoxyallene **1** is a structural unit which has found many applications in organic synthesis.[1] Thus the lithium derivative of methoxyallene can be used as synthetic equivalent of the α-acrolein anion[2] and has recently also been applied in diastereoselective reactions with α-amino aldehydes.[3] We have now investigated whether it is also possible to achieve γ-additions to produce methoxyalkyne derivatives by changing the metal. Several other research groups have already reported on such reactions for other metalated allene derivatives. Especially with allenyltitanium compounds it was hoped that in analogy to allyltitanium compounds a very high γ-selectivity could be expected; no results were available for hetero substituted allenyl titanium compounds.[5] Such addition to α-amino aldehydes would open a new, possibly diastereoselective, path to precursors of homostatine derivatives,[6] which are of major significance as the components of some inhibitors of aspartyl proteases such as renin,[7] a blood pressure regulatory enzyme, and HIV-1 protease, an enzyme which is involved in the production of infectious HIV particles.[8] We report here on the diastereoselective additions of titanated methoxyallene **2** to α-*N*,*N*-dibenzyl amino aldehydes **3**, which result in methoxyalkyne derivatives **5**. Some subsequent reactions of **5** are also described.

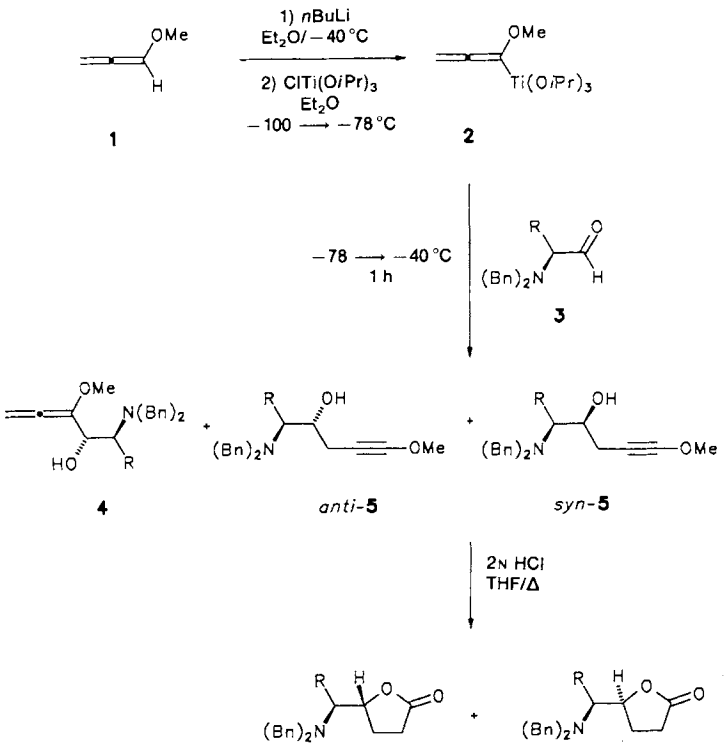

R = Me	*anti*-**6a**	94	: 6	*syn*-**6a**	53%
R = CH_2Ph	*anti*-**6b**	90	: 10	*syn*-**6b**	46%
R = CH_2CHMe_2	*anti*-**6c**	82	: 18	*syn*-**6c**	46%

Scheme 1.

Methoxyallene **1** was lithiated with *n*-butyl lithium.[2] The lithium compound was transmetalated into the titanium compound **2** by reaction at −50 °C with a molar equivalent of chlorotriisopropoxytitanium.[9, 10] Intermediate **2** was then treated with *N*,*N*-dibenzylalaninal **3a** (Scheme 1).[11] To achieve a satisfactory yield and a high γ-selectivity, the transmetalation reaction with chlorotriisopropoxytitanium needs to be carried out within 14 h at temperatures between −100 °C and −78 °C. Under these conditions the proportion of α-addition product **4a** (mainly *anti*-diastereomer) to both γ-addition products *anti*-**5a** and *syn*-**5a** was 9:91 (determined by the comparison of methoxy signals in the ^{1}H NMR spectrum).[12] The *anti* configuration of the main product was determined beyond doubt by the X-ray structural analysis of the derived compound *anti*-**6a**.[13] Similar to additions of lithiated methoxyallene to α-*N*,*N*-dibenzylamino aldehydes,[3] the stereochemical course of the reaction can be explained by the Felkin–Anh model *without* having to postulate the formation of a chelate.

As reactive carboxylic acid derivates, methoxalkynes such as **5** have great synthetic potential. For example, according to Arens et al.,[14] they can easily be hydrolyzed in acidic media to produce lactones, in this case compound **6**. It is convenient to carry out the addition and the hydrolysis as "one pot" reactions. By this procedure N-protected homostatine lactones **6** are produced in 50% yields from N-protected α-amino aldehydes in one step (Scheme 1).[15]

According to Weinreb et al.,[16] the lactones **6**, when treated with secondary amines such as pyrrolidine and piperidine

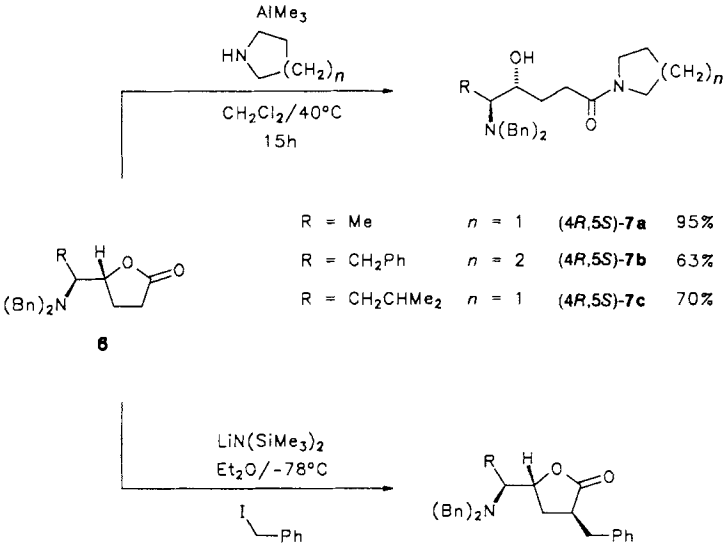

R = Me	*n* = 1	(4*R*,5*S*)-**7a**	95%	
R = CH_2Ph	*n* = 2	(4*R*,5*S*)-**7b**	63%	
R = CH_2CHMe_2	*n* = 1	(4*R*,5*S*)-**7c**	70%	

			trans : *cis*
R = Me	**8a**	67%	>99 : 1
R = CH_2Ph	**8b**	68%	81 : 19
R = CH_2CHMe_2	**8c**	73%	92 : 8

Scheme 2.

[*] Prof. Dr. H.-U. Reissig,[+] Dr. S. Hormuth
Institut für Organische Chemie der Technischen Hochschule
Petersenstrasse 22, D-64287 Darmstadt (FRG)
Dr. D. Dorsch
E. Merck, Präklinische Pharmaforschung
D-64271 Darmstadt (FRG)
Telefax: Int. code + (6151)71-0757

[+] New address: Institut für Organische Chemie und Farbenchemie der Technischen Universität
Mommsenstrasse 13, D-01062 Dresden (FRG)
Telefax: Int. code + (351)463-7030

[**] This work was supported by the Deutsche Forschungsgemeinschaft and the Fonds der Chemischen Industrie.

in the presence of trimethylaluminum, open up to the homostatine derivatives **7**. By means of chromatography hydroxycarboxylic acid amides (*4R,5S*)-**7** can be isolated in diastereomerically pure form. The yields vary between 70 to 90% (Scheme 2).

The deprotonation of the lactones **6** and subsequent alkylation with benzyl iodide[17] proceeds with high stereoselectivity to form *trans*-substituted benzyllactones **8** (Scheme 2). Their *trans* configuration has been determined by the 500 MHz 2D ROESY NMR spectrum of **8a**. These lactones are intermediates in the synthesis of stereoisomers of HIV protease inhibitors.

In addition to the reactions of titanated methoxyallene described here, a number of other applications of these homoaldol equivalents in reactions with achiral and chiral aldehydes seem possible. Also, the methoxyalkynes formed as primary products are activated carboxylic acid derivatives that can also react directly with electrophiles[14] to effect other functionalization.

Experimental Procedure:

Preparation of lactones **6** described with compound **6a** as typical example: A 1.6 M *n*-butyl lithium solution in hexane (12.0 mmol in 7.5 mL) is added to a solution of methoxyallene **1** (980 mg, 6.00 mmol) in dry ether (12 mL) at −40 °C. The reaction mixture is stirred for an additional 5 min and then cooled down to −78 °C. Then freshly distilled chlorotriisopropoxytitanium (3.12 g, 12.0 mmol) dissolved in dry ether (24 mL) is added over 1 h at −78 °C. The mixture is stirred for 14 h at −78 °C, after which the aldehyde **3a** (1.67 g, 6.00 mmol) dissolved in dry ether (12 mL) is added. The reaction mixture is allowed to warm from −78 °C to −40 °C in 1 h. Then 40 mL of a 1:1 mixture of THF and 2 N HCl is added. After hydrolysis the mixture is heated at reflux for 3 h. Thereupon it is cooled to room temperature, neutralized with a saturated $NaHCO_3$ solution, saturated with NaCl, and extracted five times with 25 mL portions of ether. The combined organic layers are dried over Na_2SO_4, and the solvents removed under vacuum. The residue is purified by chromatography on silica gel (30 cm column, petroleum ether/ethyl acetate 5:1). A light yellow oil is recovered (1.08 g, 53%), which is a mixture of the lactones *anti*-**6a** and *syn*-**6a** in the ratio of 94:6. By recrystallization from methanol, the pure diastereomer *anti*-**6a** (825 mg, 44%) is obtained as a colorless solid: m.p. 83–84 °C, $[\alpha]_D^{20} = +29.0$ ($c = 1.0$ in $CHCl_3$).

Received: April 8, 1993 [Z 5987 IE]
German version: *Angew. Chem.* **1993**, *105*, 1513

[1] Review: R. Zimmer, *Synthesis* **1993**, 165–178.
[2] First examples: S. Hoff, L. Brandsma, J. F. Arens, *Recl. Trav. Chim. Pays-Bas* **1968**, *87*, 1179–1184; see also reference [1].
[3] S. Hormuth, H.-U. Reissig, *Synlett* **1991**, 179–180.
[4] R. Gelin, S. Gelin, M. Albrand, *Bull. Chem. Soc. Fr.* **1971**, 4546–4550; G. Hahn, G. Zweifel, *Synthesis* **1983**, 883–885; R. Matsuoka, Y. Horiguchi, I. Kuwajima, *Tetrahedron Lett.* **1987**, *28*, 1299–1302; R. W. Hoffmann, J. Lanz, R. Metternich, G. Tarara, D. Hoppe, *Angew. Chem.* **1987**, *99*, 1196–1197; *Angew. Chem. Int. Ed. Engl.* **1987**, *26*, 1145–1146; R. W. Hoffmann, J. W. Lanz, R. Metternich, *Liebigs Ann. Chem.* **1988**, 161–166; M. R. Burns, J. K. Coward, *J. Org. Chem.* **1993**, *58*, 528–532.
[5] For first γ-selective reactions of allyl(trialkoxy)titanium compounds with aldehydes, see L. Widler, D. Seebach, *Helv. Chim. Acta* **1982**, *65*, 1085–1089; 1-methoxyallenyl magnesium bromide reacts with carbonyl compounds to produce mixtures of α- and γ-products: L. Brandsma, unpublished results; L. Brandsma, H. Verkruijsse, *Preparative Polar Organometallic Chemistry, Vol. 1*, Springer, Berlin, **1987**, p. 97.
[6] Several research groups previously described the reactions of titanium homoaldol reagents with various protected α-amino aldehydes, which aimed at the synthesis of homostatine derivatives: S. Kano, T. Yokomatsu, S. Shibuya, *Tetrahedron Lett.* **1991**, *32*, 233–236; A. E. DeCamp, A. T. Kawaguchi, R. P. Volante, I. Shinkai, *ibid.* **1991**, *32*, 1867–1870; J. D. Armstrong III, F. W. Hartner, Jr., A. E. DeCamp, R. P. Volante, I. Shinkai, *ibid.* **1992**, *33*, 6599–6602; F. Rehders, D. Hoppe, *Synthesis* **1992**, 859–870.
[7] B. Weidmann, *Chimia* **1991**, *45*, 367–376; R. Henning, *Nachr. Chem. Tech. Lab.* **1990**, *38*, 460–464; W. Greenlee, *J. Med. Res.* **1990**, *10*, 173–236.
[8] R. Huff, *J. Med. Chem.* **1991**, *34*, 2306–2314.
[9] Prepared according to D. Seebach in *Modern Synthetic Methods, Vol. 3* (Ed.: R. Scheffold), Salle Sauerländer, Frankfurt am Main, **1983**, p. 223.
[10] The structure of **2** is assumed to be an allenyl derivative and not a propargyl titanium derivative, which is also conceivable. This is based on the ^{13}C NMR studies of the [D_8]THF solutions of **2**. The signal for the C2 atom appears at $\delta = 195.7$, which is the typical chemical shift for allene carbon atoms, such as in methoxyallene itself ($\delta = 202.0$) and in lithiated methoxyallene ($\delta = 196.3$).
[11] M. T. Reetz, M. W. Drewes, A. Schmitz, *Angew. Chem.* **1987**, *99*, 1186–1187; *Angew. Chem. Int. Ed. Engl.* **1987**, *26*, 1141–1143.
[12] The reaction of **2** with benzaldehyde resulted in a mixture containing almost equal amounts of the α- and the γ-addition products.
[13] S. Hormuth, H.-U. Reissig, S. Foro, H. J. Lindner, *Z. Kristallogr.* **1993**, in print.
[14] H. C. Volger, J. F. Arens, *Recl. Trav. Chim. Pays-Bas* **1958**, *77*, 1170–1188.
[15] M. Meints, C. Wolff, W. Tochtermann, *Liebigs Ann. Chem.* **1993**, 527–530, and references therein.
[16] A. Basha, M. Lipton, S. M. Weinreb, *Tetrahedron Lett.* **1977**, 4171–4174.
[17] A. K. Ghosh, S. P. McKee, W. J. Thompson, *J. Org. Chem.* **1991**, *56*, 6500–6503.

Formation of Monomeric Terminal Chalcogenides by Template-Induced Disilylchalcogenide Elimination; the Crystal Structures of [ETa{$(Me_3SiNCH_2CH_2)_3N$}] (E = Se, Te)**

By *Victor Christou* and *John Arnold**

Compounds containing terminal M = E bonds are relatively common for the lighter Group 16 elements, oxygen and sulfur, and show a wide variety of interesting and unusual reactivities.[1, 2] Only recently, however, have their heavier analogues, terminal selenides and tellurides, been described.[3, 4] Because of the current interest in the chemistry of metal–chalcogenides as thin-film semiconductors,[5] and since terminal metal–chalcogenide species are implicated as intermediates in the decomposition pathway of monomeric precursors to bulk materials,[6, 7] we sought to expand the range of known terminal tellurides and selenides in an effort to probe their reactivity. Here, we report the synthesis of rare, monomeric, terminal metal–chalcogenide species and the first structural comparison of terminal M = Se and M = Te interactions in closely related compounds.

A suitable ligand to support these terminal chalcogenide species seemed to be the substituted amine $[(Me_3Si)HNCH_2CH_2]_3N$ (H_3[TMStren])[8] that has been used to prepare a wide range of complexes.[8, 9] We hoped that this ligand would engender high solubility, prevent oligomerization, and promote the elimination reaction shown in Equation 1.[6, 10]

$$[L_nM(ER)_2] \rightarrow [L_nM{=}E] + ER_2 \qquad (1)$$

Treatment of $TaCl_5$ with Li_3[TMStren][11] in Et_2O led to the formation of [$TaCl_2$(TMStren)] (**1**) in yields of 40 to 60%. Subsequent reaction of **1** with two equivalents of $(thf)_2LiESi(SiMe_3)_3$ (E = Se,[12] Te[13]) at −78 °C afforded the terminal chalcogenides **2** and **3** and one equivalent of the disilylchalcogenide $E[Si(SiMe_3)_3]_2$ upon warming to room temperature. These reactions appear to be quantitative, as judged by ^1H NMR spectroscopy; colorless **2** and orange **3** were isolated as analytically pure crystals, typically in yields ranging from 55 to 80% and were characterized by a wide range of experimental techniques including Raman, ^{125}Te and ^{77}Se NMR spectroscopy and X-ray crystallography.

[*] Prof. Dr. J. Arnold, Dr. V. Christou
Department of Chemistry, University of California
Berkeley, CA 94720 (USA)
Telefax: Int. code + (510)642-8369

[**] We thank the National Science Foundation for funding (CHE-9210406) and Joe Shiang for help with Raman spectroscopy.

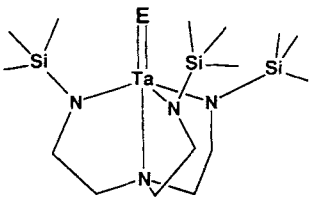

1, E = Cl_2
2, E = Se
3, E = Te

As with **1**, both the ^1H and ^{13}C NMR spectra of **2** and **3** (Table 1) show resonances that confirm the threefold symmetry of the Ta(TMStren) fragment. Compound **2** also exhibits a single resonance in its $^{77}Se\{^1H\}$ NMR spectrum ($\delta = 1518$) attributable to the terminal selenide group and close to the value reported for the terminal selenide resonance for $[PPh_4]_2[W_2Se_6]$, ($\delta = 1559$).[14] Likewise, **3** exhibits a single resonance in its $^{125}Te\{^1H\}$ NMR spectrum at $\delta = 1681$, which is assigned as the terminal telluride resonance. This value is shifted by nearly $\Delta\delta = 1000$ downfield of the resonances we reported for the terminal tellurides in the species $[M(Te)\{TeSi(SiMe_3)_3\}_2dmpe_2]$ (M = Zr, Hf; dmpe = bis(dimethylphosphino)ethane);[6] however, it lies close to the value reported by Parkin et al. for $[W(Te)_2(PMe_3)_4]$.[15] The extremely similar IR spectra of **2** and **3** support the isostructural assignment. The Raman spectrum of **2**, recorded between 100–600 cm^{-1}, shows only one peak, at 507 cm^{-1}, which we assign to the symmetrical Ta–Se stretch. A similar peak at 460 cm^{-1} was observed in the Raman spectrum of **3** and was therefore ascribed to the Ta–Te stretch. The difference in wavenumbers between these two resonances is in rough agreement with that expected on the basis of reduced mass calculations ($\Delta\nu \approx 70$ cm^{-1}) and is in line with values reported by Gibson and Siemeling from their studies of [Cp*Nb(NAr)(PMe_3)E] (Ar = 2,6-$iPr_2C_6H_3$, E = S, Se, Te).[16]

The X-ray structures of the selenide and telluride complexes[17] show both to have the central tantalum atom coordinated in a roughly trigonal bipyramidal fashion (Fig. 1). For the selenide compound there is a strict threefold axis along the Se-Ta-N vector, whilst in the telluride complex this symmetry is destroyed by the disposition of the methylene bridges in the backbone of the TMStren ligand, although overall threefold symmetry is retained. In common with other complexes chelated by related tripodal ligands,[18] the metal atoms in both **2** and **3** are displaced out of the equatorial plane, away from the basal atom of the ligand. This displacement is larger for the telluride complex (0.529 Å) than for the selenide (0.476 Å) and is presumably related to the shorter Ta–N (basal) bond in the latter (2.349 Å in **2**; 2.487 Å in **3**). We ascribe this feature to the difference in electronegativity between the two chalcogens, with the more electronegative selenium in **2** inducing a stronger N → Ta bond than does the tellerium in **3**. Steric interactions between the chalcogenide and the Me_3Si fragments on the ligand do not appear to play an important role in these two complexes, as all Ta-N-Si angles are within the normal ranges expected for an sp^2-hybridized amide nitrogen. Equatorial Ta–N bond lengths for both molecules fall within 3 σ of each other and lie in the range 2.011–1.982 Å, typical for tantalum–amide bonds.[19] Similarly all E-Ta-N bond angles fall within a narrow range (106.3–103.7°) and are close to those seen for other crystallographically characterized tren derivatives.[8, 9] The Ta–Te bond length of 2.568 Å is noticeably shorter than either of the previously reported values for terminal metal telluride species (Zr–Te, 2.650 Å und W–Te, 2.596 Å); however, this merely reflects the difference in ionic radii between the metals and is not significant. Compared to the analogous bond in **3**, the Ta–Se bond length (2.330 Å) is close to that expected, based on the 0.20 Å difference in radius between selenium and tellurium; however, it is longer than those reported in other examples of terminal selenide complexes (V–Se, 2.196 Å;[20] Mo–Se, 2.270 Å;[21] W–Se, 2.247, 2.254 Å[22]).

Table 1. Spectroscopic data for the compounds **1**–**3** [a, b].

1: M.p. 157–158 °C (decomp); ^1H NMR (400 MHz): $\delta = 3.84$ (t, $^3J(H,H) = 5$ Hz, 2H, CH_2), 2.49 (t, $^3J(H,H) = 5$ Hz, 2H, CH_2), 0.41 (s, 9H, $SiMe_3$); $^{13}C\{^1H\}$ NMR (100 MHz): $\delta = 65.82$, 55.73, 2.16; IR (Nujol/cm^{-1}): $\tilde{\nu} = 1292$ m, 1253 sh, 1244 s, 1141 m, 1129 m, 1087 s, 1077 m, 1033 s, 1001 w, 959 s, 928 s, 904 s, 838 vs, br, 785 s, br, 750 sh, 745 s, 682 m, 631 w, 604 m, 575 w; MS (70 eV): *m/z* (%): 612(15) [M^+], 597(15) [$M^+ - Me$], 575(25) [$M^+ - Cl$], 496(100) [$M^+ - Me_3SiNCH_2CH_2$].

2: M.p. 185–186 °C; ^1H NMR (400 MHz): $\delta = 3.43$ (t, $^3J(H,H) = 5$ Hz, 2H, CH_2), 1.87 (t, $^3J(H,H) = 5$ Hz, 2H, CH_2), 0.62 (s, 9H, $SiMe_3$); $^{13}C\{^1H\}$ NMR (100 MHz): $\delta = 55.27$, 51.52, 4.23; $^{77}Se\{^1H\}$ NMR (57 MHz): $\delta = 1518$(s); IR: $\tilde{\nu} = 1287$ m, 1268 m, 1253 m, 1241 s, 1143 w, 1073 s, 1027 w, 949 s, 930 s, 910 s, 845 vs, br, 789 s, br, 762 sh, 729 w, 679 w, 633 w, 589 m, 446 m, 356 m; MS: *m/z* (%): 620(20) [M^+], 605(100) [$M^+ - Me$].

3: M.p. 226–227 °C; ^1H NMR (400 MHz): $\delta = 3.39$ (t, $^3J(H,H) = 5$ Hz, 2H, CH_2), 1.70 (t, $^3J(H,H) = 5$ Hz, 2H, CH_2), 0.60 (s, 9H, $SiMe_3$); $^{13}C\{^1H\}$ NMR (100 MHz): $\delta = 58.39$, 50.40, 3.89; $^{125}Te[^1H]$ NMR (95 MHz): $\delta = 1681$(s); IR: $\tilde{\nu} = 1269$ m, 1244 m, 1146 w, 1056 s, 1018 w, 936 s, 922 sh, 905 w, 843 vs, br, 785 s, br, 777 sh, 755 w, 741 w, 725 w, 689 w, 676 w, 572 w, 353 w; MS: *m/z* (%): 670(60) [M^+], 655(70) [$M^+ - Me$], 611(100) [$M^+ - SiMe_2$], 541(50) [$M^+ - Te$].

[a] Al NMR spectra were recorded in C_6D_6 at 25 °C. [b] All compounds gave satisfactory C,H, and N analyses.

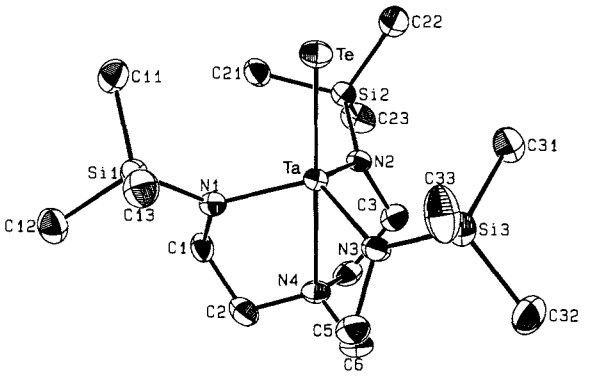

Fig. 1. Crystal structure of $[TaTe\{(Me_3SiNCH_2CH_2)_3N\}]$ (**3**) with thermal ellipsoids drawn at the 50% probability level (ORTEP). Hydrogen atoms have been omitted for clarity. The crystal structure of **2** appears identical and is not shown. Selected bond lengths [Å] and angles [°] for **3**: Ta-Te 2.568(1), Ta-N(1) 2.000(5), Ta-N(2) 1.986(5), Ta-N(3) 1.982(5), Ta-N(4) 2.487(5); Te-Ta-N(4) 178.2(1), [Te-Ta-N(1,2,3)] (averaged) 105.4(1), [Ta-N(1,2,3)-Si] (averaged) 126.5(3), [N(1,2,3)-Ta-N(4)] (averaged) 74.6(2), N(1)-Ta-N(2) 111.4(2), N(1)-Ta-N(3) 116.5(2), N(2)-Ta-N(3) 111.7(2). Selected bond lengths [Å] and angles [°] for **2**: Ta-Se 2.330(1), Ta-N(1) 2.011(4), Ta-N(2) 2.349(2): Se-Ta-N(1) 103.7(1), Se-Ta-N(2) 180.0(0), Ta-N(1)-Si 124.9(2), N(1)-Ta-N(2) 76.3(1), N(1)-Ta-N(1) 114.6(1).

Experimental Procedure

1: A mixture of $TaCl_5$ (3.70 g, 10.3 mmol) and $Li_3TMStren$ (4.00 g, 10.8 mmol) were cooled to −78 °C, and diethyl ether (150 mL), also at −78 °C, was added rapidly with vigorous stirring. The heterogeneous mixture was warmed slowly

to room temperature, the solvent removed in vacuo, and the dark brown residue extracted into Et_2O (60 mL). This ether solution was filtered and concentrated to roughly half of the original volume, at which point the product began to precipitate as yellow crystals. The solution was slowly cooled to $-40\,^{\circ}C$ over a period of 12 h to afford the product as bright orange crystals (3.24 g, 51%).

2: 50 mL of hexanes at $-78\,^{\circ}C$ was added to a mixture of **1** (1.00 g, 1.63 mmol) and $(THF)_2LiSeSi(SiMe_3)_3$ (1.56 g, 3.28 mmol), also at $-78\,^{\circ}C$. The resultant orange solution was allowed to warm to room temperature. After stirring for a further 2 h, the volatiles were removed under reduced pressure to give an orange residue, which was extracted into Et_2O, filtered, concentrated, and cooled to $-40\,^{\circ}C$. The product precipitated as colorless plates, which were recrystallized from Et_2O. The yield of analytically pure materials was 0.67 g (66%).

3: A mixture of **1** (1.00 g, 1.63 mmol) and $(thf)_2LiTeSi(SiMe_3)_3$ (1.73 g, 3.30 mmol) were dissolved in hexanes (20 mL) at $-78\,^{\circ}C$. Immediately upon addition of the hexanes, the solution became dark red. Then, over 1 h while the solution was warming to room temperature, it gradually lightened in color to yellow brown accompanied by precipitation of a colorless solid. When room temperature had been reached, the mixture was stirred for a further 2 h, upon which the volatiles were removed under reduced pressure to give a dark brown solid, which was extracted into hexanes, filtered, concentrated, and cooled to $-40\,^{\circ}C$ to give the product as red crystals. Multiple recrystallizations were necessary to remove traces of dark brown impurities (0.60 g, 55%).

Received: May 17, 1993 [Z 6088 IE]
German version: *Angew. Chem.* **1993**, *105*, 1551

[1] W. A. Nugent, J. M. Mayer, *Metal-Ligand Multiple Bonds*, Wiley Interscience, New York, **1988**.
[2] A. Muller, E. Diemann in *Comprehensive Coordination Chemistry, Vol. 2* (Eds.: G. Wilkinson, R. D. Gillard, J. A. McCleverty), Pergamon, New York, **1987**, Sections 16.1 and 16.3.
[3] U. Siemeling, *Angew. Chem.* **1993**, *105*, 70; *Angew. Chem. Int. Ed. Engl.* **1993**, *32*, 67.
[4] M. A. Ansari, J. A. Ibers, *Coord. Chem. Rev.* **1990**, *100*, 223.
[5] P. O'Brien, *Chemtronics* **1991**, *5*, 61.
[6] V. Christou, J. Arnold, *J. Am. Chem. Soc.* **1992**, *114*, 6240.
[7] D. R. Cary, J. Arnold, *J. Am. Chem. Soc.* **1993**, *115*, 2520.
[8] D. Gudat, J. G. Verkade, *Organometallics* **1989**, *8*, 2772.
[9] a) C. C. Cummins, R. R. Schrock, W. M. Davis, *Organometallics* **1992**, *11*, 1452; C. C. Cummins, J. Lee, R. R. Schrock, W. M. Davis, *Angew. Chem.* **1992**, *104*, 1510; *Angew. Chem. Int. Ed. Engl.* **1992**, *31*, 1501. Note added in proof (1.9.93). See also C. C. Cummins, R. R. Schrock, W. M. Davis, *Angew. Chem.* **1993**, *105*, 758; *Angew. Chem. Int. Ed. Engl.* **1993**, *32*, 756; and the Highlight: P. P. Power, *ibid.* **1993**, *105*, 893 or **1993**, *32*, 850.
[10] J. Arnold, J. M. Walker, K. M. Yu, P. J. Bonasia, A. L. Seligson, E. D. Bourret, *J. Cryst. Growth* **1992**, *124*, 674.
[11] Li_3TMStren was prepared by the following modification to the procedure reported in ref. [9a]: After preparation according to the reported procedure, the lithium salt was recrystallized from hot toluene, thereby removing occluded hexanes and improving crystallinity. This modification leads to improved purity and better yields of $[TaCl_2(TMStren)]$.
[12] P. J. Bonasia, V. Christou, J. Arnold, *J. Am. Chem. Soc.* **1993**, *115*, 6777.
[13] P. J. Bonasia, D. E. Gindleberger, B. O. Dabbousi, J. Arnold, *J. Am. Chem. Soc.* **1992**, *114*, 5209.
[14] Y.-J. Lu, M. A. Ansari, J. A. Ibers, *Inorg. Chem.* **1989**, *28*, 4049.
[15] D. Rabinovich, G. Parkin, *J. Am. Chem. Soc.* **1991**, *113*, 9421.
[16] U. Siemeling, V. Gibson, *J. Chem. Soc. Chem. Commun.* **1992**, 1670.
[17] Crystal data for **2**: $a = 17.178(5)$, $b = 17.193(3)$, $c = 17.197(5)$ Å, $V = 5079(2)$ Å^3, space group $Pa\bar{3}$, $Z = 8$. The structure was solved by heavy atoms methods, leaving the final residuals for the 73 variables refined against the 775 reflections for which $|F^2| > 3\sigma|F^2|$ as; $R = 0.0181$, $R_w = 0.0230$ and $GOF = 0.819$. Crystal data for **3**: $a = 10.070(2)$, $b = 17.020(2)$, $c = 14.700(2)$ Å, $\beta = 95.14(1)^{\circ}$, $V = 2509.3(7)$ Å^3, space group $P2_1/c$, $Z = 4$. The structure was solved by heavy atoms methods, leaving the final residuals for the 218 variables refined against the 2650 reflections for which $|F^2| > 3\sigma|F^2|$ as; $R = 0.0232$, $R_w = 0.0268$ and $GOF = 1.066$. Further details of the crystal structure analyses are available on request from the Director of the Cambridge Crystallographic Data Centre, University Chemical Laboratory, 12 Union Road, GB-Cambridge CB21EZ (UK), on quoting the full journal citation.
[18] G. Jia, S. D. Drouin, P. G. Jessop, A. J. Lough, R. H. Morris, *Organometallics* **1993**, *12*, 906, and references therein.
[19] See for example M. H. Chisholm, J. C. Huffman, L.-S. Tan, *Inorg. Chem.* **1981**, *20*, 1859.
[20] J. R. Nicholson, J. C. Huffman, D. M. Ho, G. Christou, *Inorg. Chem.* **1987**, *26*, 3030.
[21] S. C. O'Neal, J. W. Kolis, *J. Am. Chem. Soc.* **1988**, *110*, 1971.
[22] R. W. M. Wardle, C.-N. Chau, J. A. Ibers, *J. Am. Chem. Soc.* **1987**, *109*, 1859.

Linear Total Synthesis of (−)-ACRL Toxin III B**

By *Johann Mulzer,* Susanne Dupré, Jürgen Buschmann,* and *Peter Luger*

ACRL toxin III A (**1a**)[1] is one of a group of toxins present in the fungus *Alternaria citri* which causes crop-threatening necroses on the leaves and fruits of certain types of citrus (brown spot disease). Compound **1a** was isolated, together with other components of the toxin complex, in small quantities and in what was clearly an impure form. It also proved to be unstable; adequate characterization was only possible for the 3-methyl ether **1b** (ACRL toxin III B). Despite some recent confusion in the literature on this matter,[2] there is no ambiguity in the structure and configuration of **1a, b**. Next to nothing is known about the mechanism of action and further physiological properties of the toxins. Whereas the main active component of the toxin complex, ACRL toxin I [(5*R*)-4,5-dihydro-**1b**], has been synthesized in a multistep sequence from D-glucose,[3] compounds **1a, b** have not hitherto been prepared.

The methyl ether **1b** is an attractive synthetic target. Biogenetically, this compound is a polyketide; a distinguishing feature is the alternating, partly dehydrated, acetate (C1/2, C3/4, C5/6, C9/10, C15/16) and propionate (C7/8, C11/12, C13/14) units. These are present in saturated and unsaturated form as well as in the form of an α-pyrone ring. The hydroxymethyl units at C7/8/9 and C12/13 are *anti*-configurated and thus pose a synthetic problem which is still difficult to solve by classical aldol addition methodology.[4]

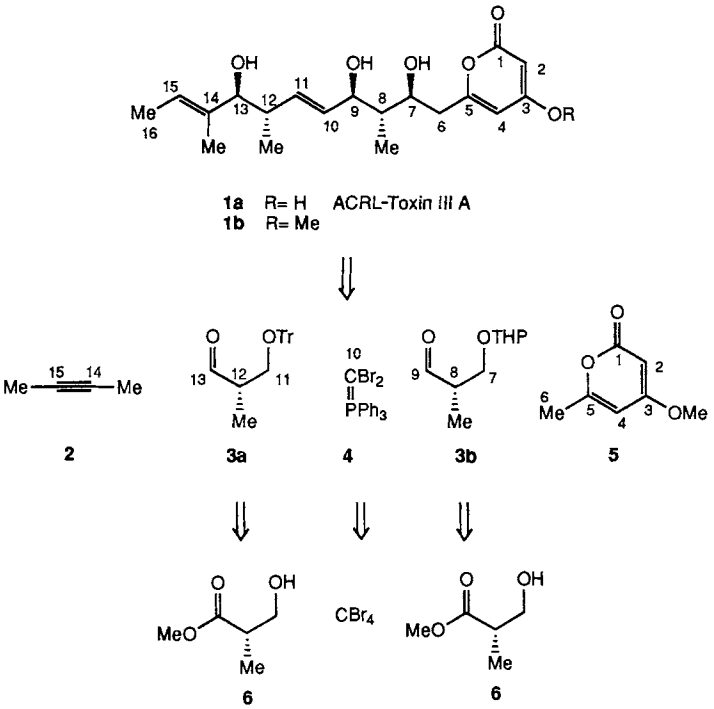

Scheme 1. Retrosynthetic analysis of compounds **1a, b**. Tr = trityl, THP = tetrahydropyranyl.

[*] Prof. Dr. J. Mulzer, Dipl.-Chem. S. Dupré
Institut für Organische Chemie der Freien Universität
Takustrasse 3, D-14195 Berlin (FRG)
Telefax: Int. code + (30)838-3412
Dr. J. Buschmann, Prof. Dr. P. Luger
Institut für Kristallographie der Freien Universität Berlin (FRG)

[**] This work was supported by the Deutsche Forschungsgemeinschaft.

Our retrosynthetic analysis (Scheme 1) is aimed at a synthesis of **1b** which proceeds linearly from C16 to C1. Of the required building blocks, **2** and **5** are commercially available. Compounds **3a, b** were prepared on a multigram scale in three steps from the ester **6** (total yield 90–95%),[5] which is the central chiral building block in the synthesis. Compound **4** was formed in situ from CBr_4 and PPh_3.

All C–C connections were achieved by addition of carbanions, generated in various ways, to aldehydes (Scheme 2).

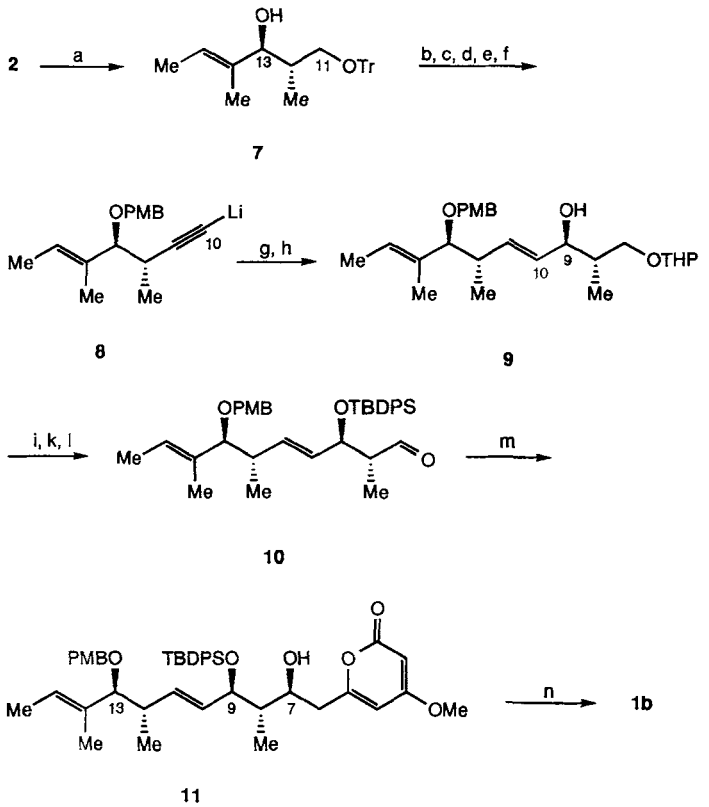

Scheme 2. Overview of the synthesis. a) *i*BuMgCl, $[Cp_2TiCl_2]$ (2 mol %), THF, **3a** 78%; b) NaH, DMF, PMBCl (*p*-methoxybenzyl chloride), 95%; c) $ZnBr_2$, CH_2Cl_2, 71%; d) $(COCl)_2$, DMSO, iPr_2NEt, CH_2Cl_2, −60 °C, 96%; e) CBr_4, PPh_3, Zn, CH_2Cl_2, 89%; f) 2 equiv *n*BuLi, 91%; g) **3b**, 57%; h) $LiAlH_4$, THF, 50 °C, quantitative; i) TBDPSCl (*tert*-butyldiphenylsilyl chloride), imidazole, CH_2Cl_2, 84%; k) EtOH, *p*-toluenesulfonic acid, 45 °C, 84%; l) $(COCl)_2$, DMSO, iPr_2NEt, CH_2Cl_2, −60 °C, 87%; m) KHMDS (K-hexamethyldisilazide), −100 °C, 55%; n) DDQ (2,3-dichloro-5,6-dicyano-1,4-benzoquinone) CH_2Cl_2, then TBAF (tetrabutylammonium fluoride), AcOH, THF, 65%.

The vinyl anion, formed in an (*E*)-selective (> 99%) hydromagnesation of **2**,[6] adds to **3a** to give the allyl alcohol **7** (a 1:1 mixture of the 13-epimers). After separation by HPLC, protection of the 13- and detritylation of the 11-hydroxyl group, alcohol **7** is subjected to a Corey–Fuchs sequence[7] to give the acetylide **8**. This is added in situ[8] to the aldehyde **3b**, and the resulting propargyl alcohol (1:1.8 mixture of the (9*S*)- and (9*R*)-epimers) is reduced to the allyl alcohol **9**. After separation of the diastereoisomers by HPLC, the (9*R*)-diastereomer is transformed into aldehyde **10**, which is then coupled with anion **5**. The regioselectivity of this addition depends critically on the reaction temperature and the cation. Only under the conditions described can formation of the 4-adduct be suppressed in favor of the desired 6-adduct.[9]

After removal of the protecting groups from positions 9 and 13, **1b** is isolated as a 96:4 mixture with its 7-epimer. After chromatographic purification, **1b** is obtained in pure crystalline form. The crystal structure analysis shows that the saturated ketide fragments C4/5 and C8–11 (positions refer to numbering in Fig. 1) are almost coplanar; the hydroxyl groups protruding on one side of the plane and the methyl groups on the other. The "upper face" is thus hydrophilic and the "lower face" hydrophobic in character. As a result of numerous 1,3-interactions (e.g. C2/4, C3/5, C6/8), the six-membered ring and the olefinic units (C6/7 and C2/3) are tilted out of the plane in the same direction and form a dihedral angle of 50–60° with the plane. The *syn*-coplanar arrangement of the hydroxyl groups at C8 and C10, which would normally be disfavored, is stabilized by an intramolecular hydrogen bond.[10]

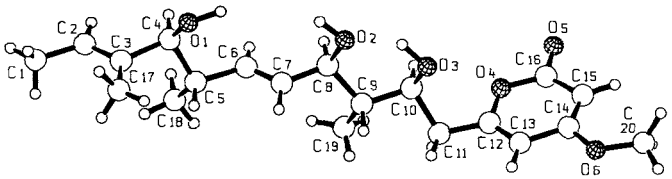

Fig. 1. Crystal structure of **1b** [16].

The synthesis comprises 16 steps—including the two straightforward HPLC separation steps—from **6** and provides the target molecule **1b** in 1.3% overall yield. The formation of the alcohols **7** and **9** is not selective; this can be rectified by employing an oxidation–reduction sequence. Ketones **12** and **13**, which are available in good yields (80 and 95% respectively) from the Swern oxidation of **7** and **9**, respectively, are reduced with very variable selectivity. In the

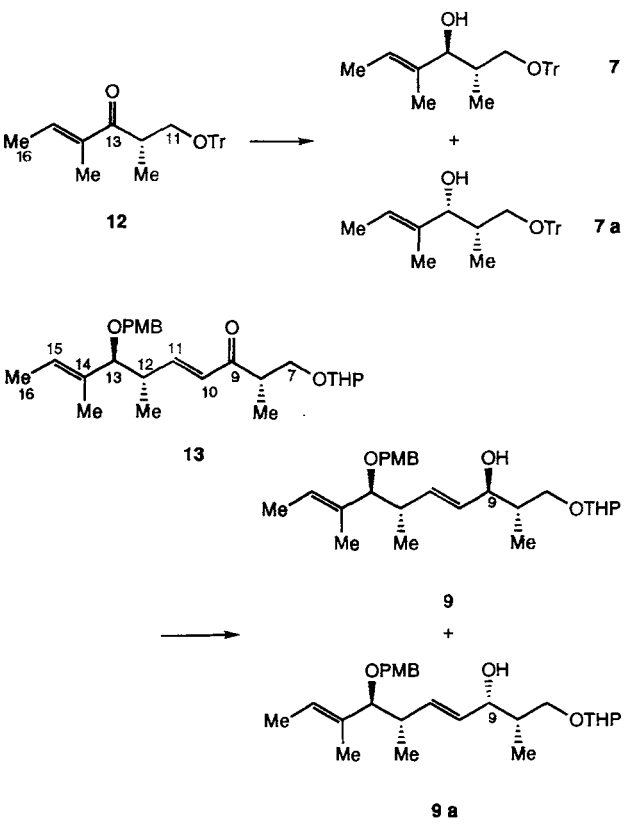

case of **12**, the highest (Felkin–Ahn) selectivity (**7**:**7a** = 96:4, overall yield 83%) is obtained with $LiBEt_3H$ (superhydride). Selective reduction of **13** to **9** (**9**:**9a** = 85:15, overall yield 84%) can only be achieved with the help of double asymmetric induction by using the reducing agent (*R*)-oxazaborolidine developed by Corey et al.[11, 12] In contrast, reduction with (*S*)-oxazaborolidine gives a 4:96 ratio of **9**:**9a** (overall yield 89%). Hydroboration does not take place at either the conjugated or the isolated double bonds during the above reaction. On reducing the 7-OTr protected ketone **13** with L-selectride, a *de* of 91% (overall yield 88%) is achieved to give 7-OTr-**9**. Thus, with a slightly modified procedure,[13] it is possible to manage with a commercially available reducing agent.

Thus two options exist for the synthesis of compound **1b**. If we accept the lack of selectivity in the two aldehyde additions and perform the two resulting HPLC separation steps, an overall yield of 1.3% over 16 steps is obtained, which corresponds to 2.3 steps per stereogenic unit (five chiral centers and two double bonds). If, on the other hand, we choose the route via the ketones **12** and **13**, 20 steps are required (overall yield 2%). This corresponds to 2.8 steps per stereogenic unit, but the selectivity of each step is now > 90%! This sequence can again be reduced to 16 steps if the corresponding Weinreb amides[14] are employed instead of the aldehydes **3**. Ketones **12** and **13** are then generated directly in the C–C bond-formation step.

Since the chiral starting material **6** is available in both (*R*)- and (*S*)-forms, the two enantiomers of **1b** are also equally accessible—an indispensable requirement for pharmacological testing. Remarkably, the purity of the synthetic product is higher than that of the isolated natural product, since compound **1b** is described as an oil in the literature.[1] The ^1H and ^{13}C NMR spectra are consistent (superimposable) with those of our synthetic material.[15] The originally assigned absolute and relative configurations of the natural product[1] have thus been confirmed.

Received: April 17, 1993 [Z 6019 IE]
German version: *Angew. Chem.* **1993**, *105*, 1538

[1] a) Y. Kono, J. M. Gardner, K. Kobayashi, Y. Suzuki, S. Takeuchi, T. Skurai, *Phythochemistry* **1986**, *25*, 69; b) Y. Kono, J. M. Gardner, Y. Suzuki, S. Takeuchi, *ibid.* **1985**, *24*, 2869; c) K. Kohomoto, R. P. Scheffer, J. O. Whiteside, *Phytopathology* **1979**, *69*, 667.
[2] H. Danda, M. M. Hansen, C. H. Heathcock, *J. Org. Chem.* **1990**, *55*, 173.
[3] F. W. Lichtenthaler, J. Dinges, Y. Fukuda, *Angew. Chem.* **1991**, *103*, 1385; *Angew. Chem. Int. Ed. Engl.* **1991**, *30*, 1339.
[4] a) M. Braun, *Adv. Carbanion Chem.* **1992**, *1*, 177; b) [2]; c) M. T. Reetz, E. Rivadeneira, C. Niemeyer, *Tetrahedron Lett.* **1990**, *31*, 3863; d) E. J. Corey, S. S. Kim, *J. Am. Chem. Soc.* **1990**, *112*, 4976; e) R. O. Duthaler, P. Herold, S. Wyler-Helfer, M. Riediker, *Helv. Chim. Acta* **1990**, *73*, 659; f) A. G. Myers, K. L. Widdowson, *J. Am. Chem. Soc.* **1990**, *112*, 9672; g) M. Braun, H. Sascha, *Angew. Chem.* **1990**, *103*, 1369; *Angew. Chem. Int. Ed. Engl.* **1990**, *30*, 1318.
[5] Starting from commercially available **6**, the primary hydroxyl group is protected (97%), the ester is reduced to the alcohol with $LiAlH_4$ (95%), and the alcohol is finally oxidized to the aldehyde under Swern reaction conditions (92%).
[6] a) F. Sato, *J. Organomet. Chem.* **1985**, *285*, 53; b) F. Sato, Y. Kobayashi, *Org. Synth.* **1990**, *69*, 106.
[7] E. J. Corey, P. L. Fuchs, *Tetrahedron Lett.* **1972**, 3769.
[8] Both the intermediate dibromide and the alkyne **8** can be isolated and characterized. Compound **8** is obtained in 75% yield by both the C_1 extension and elimination steps.
[9] W. Stahl, dissertation, Universität Bonn, **1990**.
[10] In reference [3], the crystal structure of the O-protected ACRL toxin I is described; it has a similar conformation.
[11] a) E. J. Corey, *Pure Appl. Chem.* **1990**, *62*, 1209; b) E. J. Corey, R. B. Bakshi, S. Shibata, C.-P. Chen, V. S. Singh, *J. Am. Chem. Soc.* **1987**, *100*, 7925.
[12] a) E. J. Corey, J. O. Link, *Tetrahedron Lett.* **1989**, *30*, 6275; b) D. A. Evans, *Science* **1988**, *240*, 420; c) D. K. Jones, D. C. Liotta, I. Shinkai, D. J. Mahre, *J. Org. Chem.* **1993**, *58*, 799.
[13] Coupling of **8** with **3a** and detritylation with $ZnBr_2$ in step k of Scheme 2 (62% yield).
[14] S. Nahm, S. M. Weinreb, *Tetrahedron Lett.* **1981**, *22*, 3815.
[15] All new compounds were characterized by their ^1H NMR, ^{13}C NMR, MS, and IR spectra, as well as by their elemental analyses:
[16] **1b**: Monoclinic, space group $P2_1$, $a = 5.196(5)$, $b = 10.000(10)$, $c = 20.395(40)$ Å, $\beta = 100.52(19)°$; $\rho_{calcd} = 1.168\ g\,cm^{-3}$; $Z = 2$; STOE four-circle diffractometer, monochromated $Cu_{K\alpha}$ radiation; $R = 0.080$, $wR = 0.038$; $S = 2.77$. Further details of the crystal structure investigation may be obtained from the Fachinformationszentrum Karlsruhe, Gesellschaft for wissenschaftlich-technische Information mbH, D-76344 Eggenstein-Leopoldshafen (FRG) on quoting the depository number CSD-57341, the names of the authors, and the journal citation.

$Ba_{44}Cu_{48}(CO_3)_6O_{87.9}$: The Structure of "$BaCuO_2$" from Simultaneous X-ray and Neutron Powder Diffraction**

By *Miguel A. G. Aranda** and *J. Paul Attfield*

"$BaCuO_2$" is often formed as an unwanted impurity in the synthesis of high-temperature cuprate superconductors. Previous attempts to determine the structure of this disordered material have been only partially successful, so we have taken advantage of the different relative X-ray and neutron scattering factors of Ba, Cu, and O and developed the structural model from powder X-ray and neutron diffraction profiles simultaneously. This has enabled us to identify a previously unsuspected carbonate ion within the disordered region of the structure and to show that the true stoichiometry of "$BaCuO_2$" is $Ba_{44}Cu_{48}(CO_3)_6O_{81+x}$ ($x = 6.9(3)$ for our sample). The mechanism of nonstoichiometry is similar to that in $YBa_2Cu_3O_{6+y}$. Our determination of this structure (volume of unit cell 6135 Å^3) demonstrates the power of simultaneous X-ray and neutron refinements.

Early studies showed that "$BaCuO_2$" is semiconducting and has a body-centred cubic structure with lattice parameter $a \approx 18.3$ Å,[1, 2] and a small range of nonstoichiometry up to $x = 0.12$ in "$BaCuO_{2+x}$."[3] The structure was originally solved by single-crystal X-ray diffraction,[4] and had subsequently been reexamined by using these data,[5] X-ray data from a new crystal,[6] and powder neutron diffraction profiles for two samples with differing oxygen contents.[7] All of these studies demonstrate that the structure contains two unusual clusters, $Cu_{18}O_{24}$ cages and Cu_6O_{12} rings, built from edge-sharing CuO_4 square planes, which are surrounded by the Ba atoms. However, no satisfactory models for the disordered region between these entities were found, and so the exact composition and structure remained uncertain. As the relative magnitudes of the Ba, Cu, and O scattering factors for X-rays ($f(0) = 56$, 29, and 8 electrons per atom) and neutrons ($b = 5.25$, 7.72, and 5.81 fm) are very different, they may be used together to identify the atoms present in the disordered regions of the "$BaCuO_2$" structure. We have

[*] Dr. M. A. G. Aranda, Dr. J. P. Attfield
IRC in Superconductivity, University of Cambridge
Madingley Road, Cambridge CB3 0HE (UK)
and
Department of Chemistry, University of Cambridge
Lensfield Road, Cambridge CB2 1EW (UK)
Telefax: Int. code + (223)336-362

[**] This work was supported by the Spanish Government and the European Community through a Human Capital and Mobility Fellowship (M.A.G.A.). We thank Drs. J. Rodriguez-Carvajal (Laboratoire Leon Brillouin, Saclay), A. Hewat (Institut Laue-Langevin Grenoble), and Prof. S. Bruque (University of Malaga) for their help.

collected powder X-ray and neutron diffraction data (Fig. 1) from the same polycrystalline sample to determine the crystal structure and composition of this material (see Experimental Procedure).

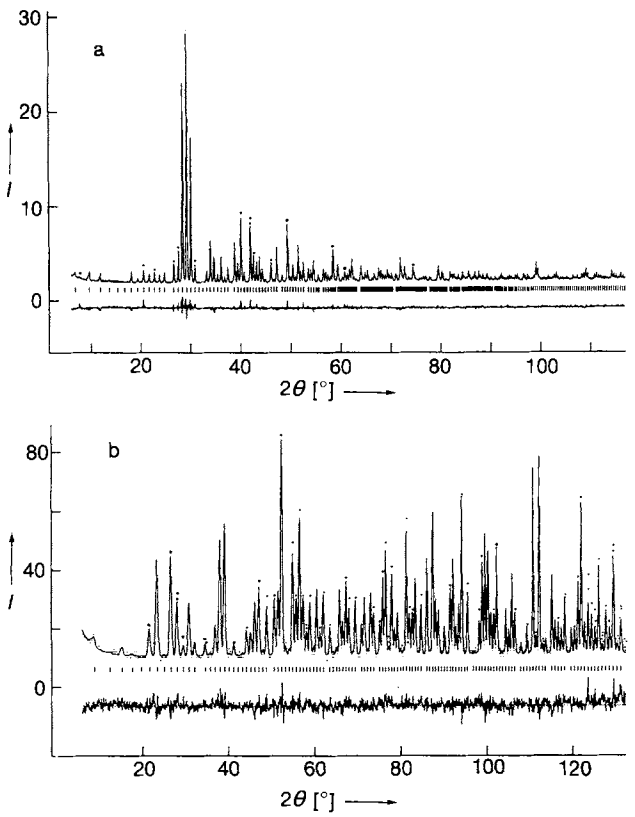

Fig. 1. Observed powder diffraction plots (points), calculated (full line), and difference profiles for $Ba_{44}Cu_{48}(CO_3)_6O_{87.9}$. a) X-ray diffraction ($\lambda = 1.54$ Å); b) neutron diffraction, ($\lambda = 1.98$ Å); positions of reflections marked. I = intensity (counts, for a) the values are multiplied by 10^3).

A view of the local geometries in the disordered part of the $Ba_{44}Cu_{48}(CO_3)_6O_{81+x}$ structure is shown in Figure 2. Each C atom is surrounded by eight O sites due to the statistical disorder of four CO_3^{2-} orientations. The carbonate group lies between two Cu_6O_{12} rings and forms a long Cu–O contact with one of them. The $Cu_{18}O_{24}$ clusters are linked by O5-Cu4-O7-Cu4-O5 bridges (see also Tables 1 and 2) in one of four possible orientations around [100], which refine to

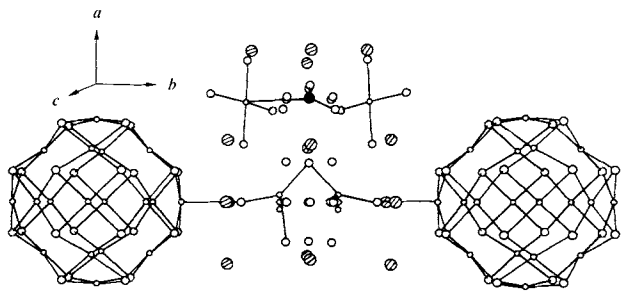

Fig. 2. The disordered region of $Ba_{44}Cu_{48}(CO_3)_6O_{87.9}$ (Cu small open circles; O medium open circles; C filled circle, Ba large hatched circles). All possible Cu and O sites are drawn with bonds showing one particular configuration for the bridge between two $Cu_{18}O_{24}$ clusters, and the carbonate group lying between two CuO_4 groups from different Cu_6O_{12} rings.

Table 1. Atomic parameter for $Ba_{44}Cu_{48}(CO_3)_6O_{87.9}$.

Atom	Position	x	y	z	U_{iso} [Å^2]	Occupancy
Ba1	48j	0.0000	0.1507(1)	0.3093(1)	0.0008(2)	1.00
Ba2	24h	0.0000	0.3649(1)	0.3649(1)	0.0008	1.00
Ba3	16f	0.1766(1)	0.1766(1)	0.1766(1)	0.0008	1.00
Cu1	48i	0.1498(1)	0.3502(1)	0.2500	0.0057(7)	1.00
Cu2	48k	0.0093(5)	0.1261(2)	0.1261(2)	0.0057	0.50
Cu3	12e	0.0000	0.0000	0.2009(3)	0.0057	1.00
Cu4	48j	0.0000	0.0171(17)	0.4313(5)	0.052(7)	0.25
C	12d	0.2500	0.0000	0.5000	0.016(3)	1.00
O1	48k	0.0747(2)	0.0747(2)	0.1892(3)	0.005(2)	1.00
O2	48k	0.1457(2)	0.1457(2)	0.3443(3)	0.004(1)	1.00
O3	48k	0.2670(2)	0.2670(2)	0.0846(3)	0.005(2)	1.00
O5	12e	0.0000	0.0000	0.3408(7)	0.020(4)	1.00
O6	48j	0.0000	0.0974(10)	0.4461(9)	0.004(7)	0.286(14)
O7	24g	0.0949(22)	0.0000	0.5000	0.04(1)	0.25
O8	48j	0.2236(7)	0.0000	0.4388(7)	0.036(4)	0.50
O9	48i	0.2500	0.0532(8)	0.4468(8)	0.004(6)	0.25

maximum (i.e. 25%) occupancy. Variable filling of the O6 sites around the Cu4 positions accounts for the range of oxygen nonstoichiometry, x, and shows local structural changes similar to those around the "chain" Cu sites in $YBa_2Cu_3O_{6+y}$ ($0 < y < 1$).[8] When the O6 sites are vacant

Table 2. Bond lengths [Å] and selected angles [°] for $Ba_{44}Cu_{48}(CO_3)_6O_{87.9}$.

Distances					
Ba1-O1 × 2	2.940(5)	Ba2-O7 × 0.5	2.58(1)	Cu2-O1 × 2	1.911(7)
Ba1-O2 × 2	2.745(4)	Ba2-O8 × 1	2.92(1)	Cu2-O1 × 2	2.141(8)
Ba1-O3 × 2	2.744(4)	Ba2-O8 × 2	3.161(8)	Cu3-O1 × 4	1.947(6)
Ba1-O5 × 1	2.819(3)	Ba2-O9 × 1	2.761(3)	Cu3-O5 × 1	2.56(1)
Ba1-O6 × 0.3	2.69(2)	Ba3-O1 × 3	2.647(6)	Cu4-O5 × 1	1.69(2)
Ba1-O8 × 0.5	2.72(1)	Ba3-O2 × 3	3.174(6)	Cu4-O7 × 1	1.89(4)
Ba1-O9 × 0.5	3.253(7)	Ba3-O3 × 3	2.884(5)	Cu4-O6 × 1.2	1.83(2)
Ba2-O2 × 2	2.863(6)	Cu1-O2 × 2	1.914(4)	C-O8 × 2	1.22(1)
Ba2-O3 × 2	2.970(6)	Cu1-O3 × 2	1.960(4)	C-O9 × 1	1.38(2)
Ba2-O6 × 1.1	2.751(8)	Cu1-O9 × 0.3	2.50(2)		
Angles					
O8-C-O8 × 1	99.1(4)	O8-C-O9 × 2	130.5(2)	Cu1-O9-C × 1	180

($x = 0$), the Cu4 sites contain Cu^+ in a typical two-coordinate environment and the other Cu sites have an average formal charge of +1.90. This is comparable to the charge distribution in $YBa_2Cu_3O_6$. The occupation of two O6 sites around one Cu4 site in each bridge ($x = 6$) gives a distorted square planar coordination (right hand side of the bridge in Fig. 2) with short Cu–O bonds, consistent with oxidation to Cu^{3+}. The mean oxidation state for the Cu atoms in the clusters is now +2.12, showing that they act as charge reservoirs during the oxidation of the Cu4 sites, as is found in $YBa_2Cu_3O_{6+y}$. Filling a third O6 site giving $x = 9$ is sterically possible and results in an unusual trigonal environment around Cu (left hand side of bridge in Fig. 2). Our refined value of $x = 6.9(3)$ does not represent a significant filling of this site.

As $Ba_{44}Cu_{48}(CO_3)_6O_{81+x}$ is stoichiometric in carbonate, and all previous structure determinations found an atom at the C site, we conclude that carbonate ions are required to stabilize this structure. Evidence that the analogous nickel compound, cubic "$BaNiO_2$," contains carbonate ions has very recently been reported,[9] although the proposed composition, $Ba_{42}Ni_{36}(CO_3)_6O_{72}$, is slightly different. The compound "$BaCuO_{2.5}$,"[1] which decomposes into cubic "$BaCuO_{2+x}$" above 800 °C,[10, 11] is probably an oxocarbonate as well. The formation of $Ba_{44}Cu_{48}(CO_3)_6O_{81+x}$

as an equilibrium phase at 850 °C in air highlights the ability of Ba and related elements to form very stable oxocarbonates. This has recently led to the development of superconducting phases such as $(Ba_{0.55}Sr_{0.45})Cu_{1.1}(CO_3)_{0.1}O_{2.2}$ (T_c = 40 K)[12] and $Tl_{0.5}Pb_{0.5}Sr_4Cu_2(CO_3)O_7$, a 70 K superconductor containing layers of carbonate groups.[13] Rigorously excluding carbon should prevent the formation of "$BaCuO_2$" during the synthesis of superconducting cuprates and may also enable new, superconducting, infinite-layer type materials $(Ba,Sr)_{1-y}CuO_2$ to be prepared with small or zero strontium contents.[14]

Our determination of the complex disorder within this large unit cell (6135 Å^3) demonstrates the power of simultaneous refinements. The combined information from powder X-ray and neutron patterns of moderate quality has proved more effective than previous individual single-crystal X-ray data sets.

Experimental Procedure

"$BaCuO_2$" was synthesized by heating an intimate, equimolar (Ba:Cu = 1:1) mixture of $BaCO_3$ (Aldrich, 99.98 %) and CuO (Aldrich, 99.99 + %) at 850 °C in air for 24 h. The sample was reground and reheated at the same temperature for a further 24 h.

Structure determination: X-ray powder diffraction data were recorded for $2\theta = 6-117°$ on a Siemens D501 diffractometer by using monochromated $Cu_{K\alpha}$ radiation, counting for 20 s per 0.03° step. Neutron powder diffraction data were collected on instrument D1A at the Laboratoire Leon Brillouin, Saclay, France, by using a wavelength of 1.9841(2) Å for $2\theta = 5-132.5°$ in 0.05° steps. Rietveld analysis [15] with the GSAS package [16] enabled the structural model to be fitted to either or both data sets. No impurity phases were observed.

Starting coordinates were those reported for "$BaCuO_{2.07}$" from powder neutron refinement [7], but this model gave a poor fit to our neutron data. Examination of the structure revealed an anomalous atom at (1/4,0,1/2), which has been reported in all previous studies as either an O atom [4, 5, 7] or a partially occupied Cu site [6]. We refined the scattering factor of this atom by using the X-ray and neutron data separately, giving $f(0) \approx 9$ electrons per atom and $b \approx 7$ fm, respectively. These values clearly rule out partial occupation by Ba or Cu, although they are consistent with O. However, the long distances (> 3.2 Å) from this site to the nearest cations make oxygen occupation chemically unrealistic. We therefore considered possible cationic impurity atoms: an obvious candidate was carbon in view of the scattering factors ($f(0) = 6$ electrons per atom, $b = 6.65$ fm) and the ability of barium to form thermally stable carbonates.

Carbon refined to full occupancy at (1/4,0,1/2) in both the X-ray and neutron refinements, and a neutron difference Fourier map revealed two partially occupied oxygen positions (O8 and O9) approximately 1.3 Å from this site. These positions define four possible orientations of a CO_3^{2-} group, pivotally disordered around the C atom. Including the carbonate group improved the profile fits and further simultaneous X-ray and neutron refinements enabled us to resolve other disordered features more clearly than in previous determinations. Disorder in the Cu2 position, which has been modeled by refining this atom off (0,x,x), reflects a slight disorder in the orientation of the near-spherical $Cu_{18}O_{24}$ cages around the symmetry axes. The final model (space group $Im3m$, $a = 18.3069(2)$ Å, $Z = 2$) shown in Table 1 has composition $Ba_{44}Cu_{48}(CO_3)_6O_{81+x}$ ($x = 6.9(3)$) and gives good fits (Fig. 1) to both X-ray ($R_{WP} = 0.040$, $R_F = 0.066$, R factors are defined in refs. [15] and [16]) and neutron ($R_{WP} = 0.081$, $R_F = 0.057$) profiles. This model gives satisfactory bond lengths and angles for all atoms (Table 2) and bond valence calculations [17] give total valence of 4.1 for C and values between 1.8 and 2.3 for all the Ba, Cu, and O sites, except Cu2 and O6 where low valences of 1.6 indicate further slight disorder. Further details of the crystal structure investigation may be obtained from Fachinformationszentrum Karlsruhe, Gesellschaft für wissenschaftlich-technische Information mbH, D-76344 Eggenstein-Leopoldshafen (FRG) on quoting the depository number CSD-57708, the names of the authors and the journal citation.

IR Spectroscopy: The presence of carbonate groups was corroborated by the IR spectrum (Perkin-Elmer 1710 FT spectrometer, CsI disk) of "$BaCuO_2$" which showed typical carbonate absorptions at 1410 and 865 cm^{-1}; those for $BaCO_3$ are at 1440 and 875 cm^{-1}.

Received: April 30, 1993 [Z 6047 IE]
German version: *Angew. Chem.* **1993**, *105*, 1511

[1] M. Arjomand, D. J. Machin, *J. Chem. Soc. Dalton Trans.* **1975**, 1061–1066.
[2] H. N. Migeon, F. Jeannot, M. Zanne, J. Aubry, *Rev. Chim. Miner.* **1976**, *13*, 440–445.
[3] H. N. Migeon, M. Zanne, F. Jeannot, C. Gleitzer, *Rev. Chim. Miner.* **1977**, *14*, 498–502.
[4] R. Kipka, H. K. Müller-Buschbaum, *Z. Naturforsch. B* **1977**, *32*, 121–123.
[5] W. Gutau, H. K. Müller-Buschbaum, *J. Less Common Met.* **1989**, *152*, L11–L13.
[6] E. F. Paulus, G. Miehe, H. Fuess, I. Yehia, U. Lochner, *J. Solid State Chem.* **1991**, *90*, 17–26.
[7] M. T. Weller, D. R. Lines, *J. Chem. Soc. Chem. Commun.* **1989**, 484–485.
[8] D. W. Murphy, S. A. Sunshine, P. K. Gallagher, H. M. O'Bryan, R. J. Cava, B. Batlogg, R. B. van Dover, L. F. Schneemeyer, S. M. Zahurak *Chemistry of High-Temperature Superconductors* (Eds.: D. L. Nelson, M. S. Whittingham, T. F. Goerge) (*ACS Symp. Ser.* **1987**, *351*, 181–191).
[9] R. Gottschall, R. Schöllhorn, *Solid State Ionics* **1993**, *59*, 93–98.
[10] M. Machida, K. Yasuoka, K. Eguchi, H. Arai, *J. Solid State Chem.* **1991**, *91*, 176–179.
[11] S. Petricek, N. Bukovec, P. Bukovec, *J. Solid State Chem.* **1992**, *99*, 58–62.
[12] K. Kinoshita, T. Yamada, *Nature* **1992**, *357*, 313–315.
[13] M Huve, C. Michel, A. Maignan, M. Hervieu, C. Martin, B. Raveau, *Physica C (Amsterdam)* **1993**, *205*, 214–224.
[14] M. Takano, M. Azuma, Z. Hiroi, Y. Bando, Y. Takeda, *Physica C (Amsterdam)* **1991**, *176*, 441–444.
[15] H. M. Rietveld, *J. Appl. Crystallogr.* **1969**, *2*, 65–71.
[16] A. C. Larson, R. B. Von Dreele, Los Alamos Laboratory Rep. No. LA-UR-86-748, **1987**.
[17] N. E. Brese, M. O'Keefe, *Acta Crystallogr. Sect. B* **1991**, 47, 192–197.

Synthesis and Reactivity of Hexafluoro-1,2-diisocyanocyclobutanechromium Complexes**

By *Dieter Lentz,* Frank Nowak, Dagmar Preugschat,* and *Markus Wasgindt*

Di- and triisocyanides have recently acquired considerable significance, owing to their interesting coordination chemistry,[1] in particular their ability to function as polydentate ligands. Fluorinated cycloalkyl isocyanides and fluorinated diisocyanides are hitherto unknown. The chemistry of perfluorinated isocyanides, inaccessible through conventional isocyanide syntheses,[2] was until recently restricted to trifluoromethyl isocyanide[3] and pentafluorophenyl isocyanide.[4] The more thoroughly investigated trifluoromethyl isocyanide is particularly noteworthy due to its unusual ligand properties[5] and reactivity.[6] As shown by Fehlhammer et al., pentacarbonyl(cyano)chromate undergoes radical-type alkylation,[7] giving rise to pentacarbonylchromium complexes of functionalized isocyanides. We recently succeeded in synthesizing the first fluorinated alkenyl isocyanide $F_2C{=}CF{-}NC$ **1** by the formation of the corresponding $[Cr(CO)_5]$ complex, followed by flash vacuum pyrolysis.[8] We now report the synthesis and preliminary reactions of the thus far unique complex-stabilized, fluorinated diisocyanide.

If pentacarbonyl(trifluorovinyl isocyanide)chromium **2** is heated to 70 °C under atmospheric pressure, cleavage of the isocyanide ligand does not take place; instead a [2 + 2] cycloaddition reaction occurs. [2 + 2] Cycloaddition reactions are thermally forbidden according to the Woodward–Hoffmann rules,[9] and do not normally occur. Fluorinated alkenes, on the other hand, display a strong tendency to undergo [2 + 2] cycloadditions,[10] from which four possible isomeric

[*] Priv.-Doz. Dr. D. Lentz, F. Nowak, Dr. D. Preugschat, M. Wasgindt
Institut für Anorganische und Analytische Chemie der Freien Universität
Fabeckstrasse 34–36, D-14195 Berlin (FRG)
Telefax: Int. code + (30)838-2424

[**] This work was supported by the Fonds der Chemischen Industrie, the Deutsche Forschungsgemeinschaft, and the Graduiertenkolleg "Synthese und Strukturuntersuchung niedermolekularer Verbindungen" of the Freie Universität and Technische Universität, Berlin. We thank Hoechst AG for a gift of 1,2-dichloro-1,1,2-trifluoroethane.

products may, in principle, arise. Head-to-head dimers of *cis* and *trans* geometry are usually observed, whose formation is explained by a stepwise diradical mechanism.[11]

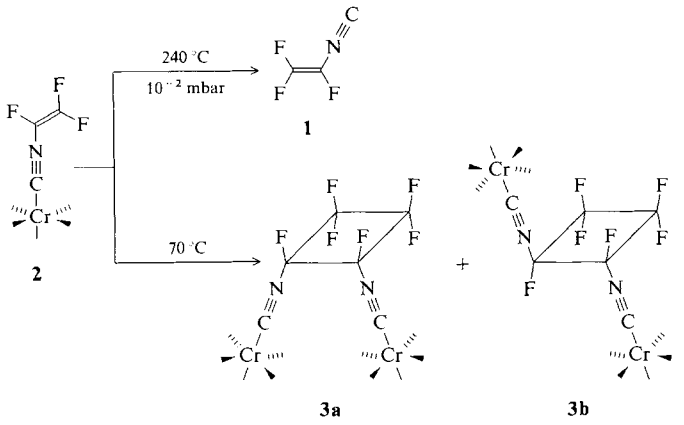

Upon dimerization of **2**, a 1:1 isomeric mixture of *cis*- and *trans*-hexafluorodiisocyanocyclobutanechromium complexes (**3a** and **3b**, respectively) is formed. The structures of both compounds were established spectroscopically; in addition an X-ray crystal structure analysis was performed for the *cis* isomer **3a**.[12] The cyclobutane ring in **3a** is distinctly puckered, as is the case for unsubstituted cyclobutane[13] and octafluorocyclobutane[14] (Fig. 1). The angles between the

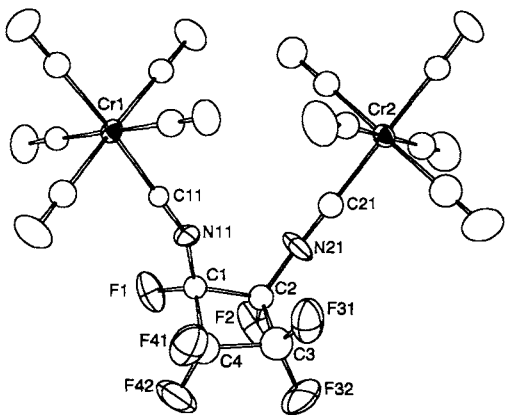

Fig. 1. Molecular structure (ORTEP [17]) of **3a**, (ellipsoids drawn at 30% probability). Selected bond lengths [pm] and angles [°]: Cr-CO 188.1(7)–191.4(6), C-O 113.0(7)–114.7(7), C11-N11 117.4(7), C21-N21 117.5(7), C1-N11 140.7(7), C2-N21 137.7(7), C-F 128.3(8)–138.0(7), C1-C2 155.8(8), C2-C3 149(1), C3-C4 155.1(9), C1-C4 153.7(9); N11-C1-C2 113.4(5), N11-C1-C4 110.3(5), N21-C2-C1 118.5(5), N21-C2-C3 119.4(7), C11-N11-C1 155.7(5), C21-N21-C2 163.8(7), C2-C1-C4 89.5(5), C1-C2-C3 88.9(5), C2-C3-C4 91.3(6), C1-C4-C3 87.5(5), C-C-F 107.9(6)–116.9(7), F-C-F 109.2(7)–112.9(6), N-C-F 111.5(6)–112.3(6).

planes C1-C2-C3/C1-C3-C4 and C1-C2-C4/C2-C3-C4 are 21.3 and 21.1°, respectively. The N-C-C bond angles at the cyclobutane ring [110.3(5)–119.4(7)°] and the bending of the isocyanide function at the nitrogen atom [C1-N11-C11 155.7(5), C2-N21-C21 163.8(7)°], allow the two bulky $(CO)_5Cr(CN)$ substituents to adopt a *cis* orientation. The two chromium atoms exhibit approximately octahedral coordination geometry, and the Cr–C distances to the carbonyl ligands [188.1(7)–191.4(6) pm] are very similar, showing, above all, no significant differences compared to those to the isocyanide carbon atoms [Cr1–C11 190.3(6), Cr2–C21 190.0(6) pm].

The isomers **3a** and **3b** do not differ appreciably in their solubility, hence separation by fractional crystallization was not possible. Attempts to separate the isomers by chromatography were likewise unsuccessful. The complexes **3**, however, crystallize in different forms; thus, the fine needles of **3a** could be separated from the intergrown mass of platelets of the *trans* isomer **3b**.

The ^{19}F NMR spectra of both isomers show the signal patterns of AA'BB'CC' spin system, which could not be analyzed completely because of the very small vicinal coupling constants. Of note are the geminal $^2J_{F,F}$ coupling constants (218 Hz), which are typical for fluorinated cyclobutane rings.[15] Analysis of the vibrational spectra was unsuccessful due to the strong coupling of the CN vibration with the CO vibrations. The location of the intense carbonyl bands in the IR spectra highlights the strong π-acceptor properties of these fluorinated isocyanide ligands.

Starting from **3**, nucleophilic attack at the isocyanide-carbon atom[16] ought to permit the synthesis of biscarbene complexes. Indeed, an isomeric mixture of **3** reacts readily with dimethylamine **4**, even at −78 °C. This gives rise to a deep blue solution, whose ^{19}F NMR spectrum at −100 °C (an ABCD spectrum with large $^2J_{F,F}$ coupling constants and unresolved $^3J_{F,F}$ couplings) indicates the presence of biscarbene complex **5**. Above −20 °C, the solution becomes yellow, and the ^{19}F NMR spectrum shows the appearance of signals due to the carbene complex **6**, generated through cleavage of $[Cr(CO)_5]$ fragment and the subsequent cyclization to give the imidazole ring system. Despite the instability,

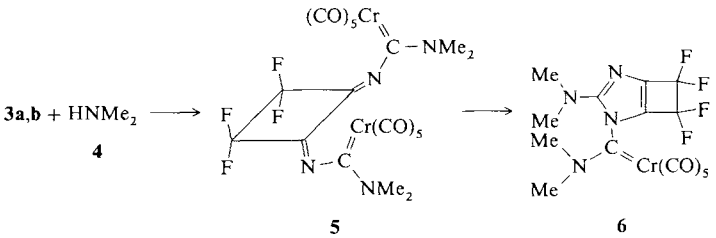

of the biscarbene complex **5**, we succeeded in obtaining single crystals, allowing us to clarify its structure by X-ray crystallography[12] (Fig. 2). The most important structural element is the tetrafluorocyclobutane ring with the iminonitrogen atoms N1 and N3 in the 1,2 positions, bonded to the carbene carbon atoms C16 and C26, respectively. The carbon atom C16 points towards, and C26 away from the neighboring fluorine atoms and the $[Cr(CO)_5]$ fragments are arranged above and below the plane of the four-membered ring, respectively. The orientation of atoms N1, C1, C4, N3, and C26 appears decisive for the reactivity, allowing nucleophilic attack at C26 by the nitrogen atom N1, which leads to carbene complex **6**, upon cleavage of a $[Cr(CO)_5]$ fragment. Compound **6** can be isolated as the final product of this reaction, and has been fully characterized on the basis of spectroscopic data and a crystal structure analysis.[12]

If this reaction can be generalized and the removal of the organometallic protecting group can be achieved successfully, this would be a convenient synthesis for imidazole deria-

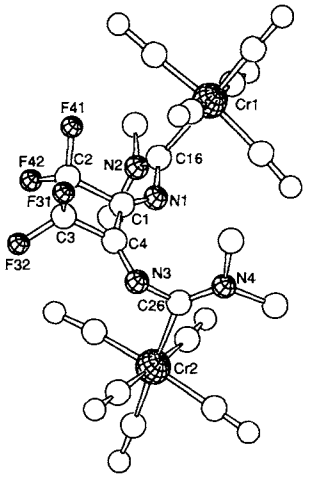

Fig. 2. Molecular structure (SCHAKAL [18])) of **5**. Selected bond lengths [pm], bond angles [°], and dihedral angles [°]: Cr1-C16 209(3), Cr2-C26 213(3), Cr-CO 181–193(3), C-O 109–120(4), C16-N1 134(3), C16-N2 132(3), C26-N3 134(3), C26-N4 128(3), C1-N1 123(3), C4-N3 128(3), C1-C2 160(4), C2-C3 154(4), C3-C4 150(4), C1-C4 146(4), C-F 131-135(3); Cr1-C16-N1 110(2), Cr1-C16-N2 135(2), N1-C16-N2 113(2), Cr2-C26-N3 108(2), Cr2-C26-N4 135(3), N3-C26-N4 117(3), C16-N1-C1 127(2), C26-N3-C4 123(2), C2-C1-N1 135(2), C4-C1-N1 137(3), C2-C1-C4 88(2), C1-C4-N3 136(3), C3-C4-N3 129(3), C1-C4-C3 94(2), F-C-F 105(2), C1-N1-C16-Cr1 96(3), C4-N3-C26-Cr2 −99(3).

tives with annelated, fluoro-substituted, four-membered rings.

Experimental Procedure

3: **2** (1.26 g, 4.2 mmol) was heated to 70 °C for 7 h. After cooling to room temperature, recrystallization from *n*-hexane gave pale yellow crystals as a mixture of **3a** and **3b**. Yield 1.02 g (81 %). **3a**: colorless crystals, m.p. 111 °C, ^{19}F NMR (376.442 MHz, $CDCl_3$, C_6F_6/$CFCl_3$) δ = 20.6/−139.4 (s, 2 F), 32.8/−127.2 (d, ^2J(F,F) = 218 Hz, 2 F), 39.7/−120.3 (d, ^2J(F,F) = 218 Hz, 2 F); MS (80 eV): *m/z* 598 [M^+], 458 [$M^+ - 5CO$], 318 [$M^+ - 10CO$], 299 [$(CO)_5Cr(CNCFCF_2)^+$] and additional smaller fragments; IR (CH_2Cl_2): $\tilde{\nu}$ = 2027(w), 1994(vs), 1975(vs), 1902(w) cm^{-1}.

3b: Light yellow crystals, m.p. 95 °C; ^{19}F NMR (376.442 MHz, $CDCl_3$, C_6F_6/$CFCl_3$) δ = 21.6/−138.4 (s, 2 F), 35.5/−124.5 (d, ^2J(F,F) = 218 Hz, 2 F), 36.7/−123.3 (d, ^2J(F,F) = 218 Hz, 2 F); MS (80 eV): *m/z* 598 [M^+], 458 [$M^+ - 5CO$], 318 [$M^+ - 10$ CO], 299 [$(CO)_5Cr(CNCFCF_2)^+$] and further smaller fragments; IR (CH_2Cl_2): $\tilde{\nu}$ = 2027(w), 2010(w), 1986(s), 1953(w), 1918(m) cm^{-1}.

5: A THF (25 mL) solution of **3** (100 mg, 0.17 mmol) in a Schlenk flask was cooled to −196 °C. Dimethylamine **4** (0.85 mmol) was condensed into the flask by using a vacuum line. Upon warming to −78 °C, the yellow solution turned deep red and then dark blue. The mixture was stirred for 1 h at −78 °C, after which the bulk of the THF was removed under high vacuum at −78 °C. The solution was layered with *n*-pentane and left to crystallize at −40 °C. After several days, **5** crystallized as deep blue plates, which decomposed slowly at room temperature. Yield: 62 mg (56 %). ^{19}F NMR (84.25 MHz, THF, $CFCl_3$, −100 °C): δ = −113.3, −129.4, ^2J(F,F) = 239 Hz, −118.3, −122.3, ^2J(F,F) = 234 Hz; ^{19}F NMR (84.25 MHz, THF, $CFCl_3$, −40 °C): −116.4, −125.9, ^2J(F,F) = 239 Hz.

6: **4** was passed into a rapidly stirred solution of **3** (97 mg, 0.16 mmol) in diethyl ether (20 mL), until the solution turned deep blue. Within 30 min, the dark blue solution turned green and then yellow. Cooling to −30 °C gave **6** (63 mg, 89 %), which was purified further by recrystallization from diethyl ether to give yellow air-stable crystals (49 mg, 70 %); decomp >110 °C. ^{19}F NMR (84.25 MHz, $CDCl_3$, $CFCl_3$) δ = −96.6, −101.2; ^{1}H NMR (89.55 MHz, $CDCl_3$) δ = 2.98 (s, 6 H), 3.29 (s, 3 H), 3.95 (s, 3 H); MS (80 eV) *m/z* 456 [M^+], 428 [$M^+ - CO$], 400 [$M^+ - 2CO$], 372 [$M^+ - 3CO$], 344 [$M^+ - 4CO$], 316 [$M^+ - 5CO$], 301 [$M^+ - 5CO\text{-}CH_3$]; IR (CH_2Cl_2): $\tilde{\nu}$ = 2061(m), 1983(sh), 1942(vs) cm^{-1}.

Received: May 4, 1993 [Z 6057 IE]
German version: *Angew. Chem.* **1993**, *105*, 1547

[1] F. E. Hahn, *Angew. Chem.* **1993**, *105*, 681; *Angew. Chem Int. Ed. Engl.* **1993**, *32*, 650.

[2] C. Grundmann, *Methoden Org. Chem. (Houben-Weyl) 4th Ed. 1952–1985*, Vol. E5.

[3] D. Lentz, *J. Fluorine Chem.* **1984**, *24*, 523, and references therein.

[4] D. Lentz, K. Graske, D. Preugschat, *Chem. Ber.* **1988**, *121*, 1445, and references therein.

[5] R. D. Adams, Y. Chi, D. D. DesMarteau, D. Lentz, R. Marschall, A. Scherrmann, *J. Am. Chem. Soc.* **1992**, *114*, 10822; R. D. Adams, Y. Chi, D. D. DesMarteau, D. Lentz, R. Marschall, *ibid.* **1992**, *114*, 1909; D. Lentz, R. Marschall, *Chem. Ber.* **1991**, *124*, 777; *Organometallics* **1991**, *10*, 1487; *Chem. Ber.* **1991**, *124*, 497; D. Lentz, B. Pötter, R. Marschall, I. Brüdgam, J. Fuchs, *Chem. Ber.* **1990**, *123*, 257, and references therein.

[6] D. Lentz, R. Marschall, *Z. Anorg. Allg. Chem.* **1992**, *617*, 1; M. Weidenbruch, J. Hamann, H. Piel, D. Lentz, K. Peters, H. G. von Schnering, *J. Organomet. Chem.* **1992**, *426*, 35; D. Lentz, *Z. Naturforsch. B* **1992**, *47*, 148; D. Lentz, I. Brüdgam, H. Hartl, *Angew. Chem.* **1987**, *99*, 951; *Angew. Chem. Int. Ed. Engl.* **1987**, *26*, 921.

[7] W. P. Fehlhammer, F. Degel, G. Beck, *Chem. Ber.* **1987**, *120*, 461.

[8] D. Lentz, D. Preugschat, *J. Chem. Soc. Chem. Commun.* **1992**, *1523*.

[9] R. B. Woodward, R. Hoffmann, *Die Erhaltung der Orbitalsymmetrie*, 1st. ed., Verlag Chemie, Weinheim, **1970**; *Angew. Chem.* **1969**, *81*, 797; *Angew. Chem. Int. Ed. Engl.* **1969**, *8*, 781.

[10] M. Hudlicky, *Chemistry of Organic Fluorine Compounds*, 2nd ed., Ellis Horwood, Chichester, **1976**.

[11] P. D. Bartlett, L. K. Montgomery, B. Seidel, *J. Am. Chem. Soc.* **1964**, *86*, 616; L. K. Montgomery, K. Schueller, P. D. Bartlett, *ibid.* **1964**, *86*, 622; P. D. Bartlett, L. K. Montgomery, *ibid.* **1964**, *86*, 628.

[12] **3a**: triclinic, $P\bar{1}$ (no. 2), a = 628.0(2), b = 1060.2(4), c = 1641.4(6) pm, α = 86.03(3), β = 85.24(3), γ = 82.85(3)°, Z = 2, ϱ_{calcd} = 1.84 gcm^{-1}, R = 0.043, R_w = 0.043, $w = [\sigma(F_0)^2 + 0.0005\,F_0^2]^{-1}$, $Mo_{K\alpha}$ radiation, λ = 71.069 pm, data collection at −60 °C, 3784 crystallographically independent reflections $4 \le 2\theta \le 50°$, 2257 of which with $F_0 > 3\sigma(F_0)$, anisotropic thermal parameters for Cr, C, F, N, and O. Starting coordinates by direct methods (SHELXS-86) [19], full-matrix least-squares refinement, (SHELX-76) [20], 274 refined parameters, final parameter shift/standard deviation (max) = 0.001, residual electron density (max/min) 0.52/−0.41 $eÅ^{-3}$. **5**: monoclinic, $C2/c$ (no. 15), a = 3085(2), b = 1038.2(8), c = 1694(2) pm, β = 107.6°, Z = 8, ϱ_{calcd} = 1.67 gcm^{-3}, R = 0.084, R_w = 0.084, w = 1, $Mo_{K\alpha}$ radiation, λ = 71.069 pm, data collection at −65 °C, 2404 crystallographically independent reflections $4 \le 2\theta \le 40°$, of which 914 with $F_0 > 3\sigma(F_0)$, isotropic thermal parameters. Starting coordinates by direct methods (SHELXS-86) [19], full-matrix least-squares refinement, (SHELX-76) [20], 161 refined parameters, final parameter shift standard deviation (max) 0.001, residual electron density/(max/min) 0.57/−0.51 $eÅ^{-3}$. **6**: orthorhombic, $Pbc2_1$ (no. 29), a = 1008.0(2), b = 1254.8(4), c = 1475.8(3) pm, Z = 4, ϱ_{calcd} = 1.62 gcm^{-3}, R = 0.044, R_w = 0.042 $w = [\sigma(F_0)^2 + 0.0005\,F_0^2]^{-1}$, $Mo_{K\alpha}$ radiation, λ = 71.069 pm, 3854 crystallographically independent reflections $4 \le 2\theta \le 54°$, of which 2484 with $F_0 > 3\sigma(F_0)$, anisotropic thermal parameters for C, Cr, F, N, and O, methyl groups refined as rigid groups with common isotropic thermal parameters (U_H = 0.081) and the H atoms in calculated positions (C–H 95 pm). Starting coordinates by direct methods (SHELXS-86) [19], full-matrix least-squares refinement (SHELX-76) [20], 274 refined parameters, final parameter shift/standard deviation (max) = 0.025, residual electron density (max/min) 0.44/−0.50 $eÅ^{-3}$. Further details of the crystal structure investigations may be obtained from the Fachinformationszentrum Karlsruhe, Gesellschaft für wissenschaftlich-technische Information mbH, D-76344 Eggenstein-Leopoldshafen, on quoting the depository number CSD-75344, the names of the authors, and the journal citation.

[13] A. Stein, C. W. Lehmann, P. Luger, *J. Am. Chem. Soc.* **1992**, *114*, 7684.

[14] C. H. Chang, R. F. Porter, S. H. Bauer, *J. Mol. Struct.* **1971**, *7*, 89.

[15] J. W. Emsley, L. Phillips, V. Wray, *Prog. Nucl. Magn. Reson. Spectrosc.* **1975**, *8*, 85.

[16] B. Crociani in *Reactions of Coordinated Ligands* (Ed.: P. S. Braterman), Plenum, New York, **1986**; G. Beck, W. P. Fehlhammer, *Angew. Chem.* **1988**, *100*, 1391; *Angew. Chem. Int. Ed. Engl.* **1988** *27*, 1344; W. P. Fehlhammer, G. Beck, *J. Organomet. Chem.* **1989**, *369*, 105, *Chem. Ber.* **1989**, *122*, 1907; W. P. Fehlhammer, W. Finck, *J. Organomet. Chem.* **1991**, *414*, 261; D. Lentz, R. Marschall, *Chem. Ber.* **1990**, *123*, 467; *ibid.* **1990**, *123*, 751, and references therein

[17] C. K. Johnson, ORTEP: A FORTRAN Thermal Ellipsoid Plot Program for Crystal Structure Illustrations, Report ORNL-3794, Oak Ridge National Laboratories, Oak Ridge Tennessee, **1970**.

[18] E. Keller, SCHAKAL-88, FORTRAN Program for the Graphical Representation of Molecular and Crystallographic Models, Freiburg, **1988**.

[19] G. M. Sheldrick: SHELXS-86, A Programm for Crystal Structure Solution, Göttingen, **1986**.

[20] G. M. Sheldrick: SHELX-76, A Programm for Crystal Structure Determination, Cambridge, **1976**.

A Light-Induced Molecular Shuttle Based on a [2]Rotaxane-Derived Triad**

By *Andrew C. Benniston* and *Anthony Harriman**

Illumination of an intimate (or tight) charge-transfer complex, as formed by close association of an electron donor with a complementary electron acceptor, results in instantaneous formation of an intimate radical ion pair (RIP).[1] Charge recombination,[2] to reform the ground state, competes with dissociation of the RIP into separated radical ions[3] and with solvent penetration to form a solvent-separated (or loose) RIP.[4] If illumination is provided by a short laser pulse, the rates of charge recombination and dissociation of the RIP can be determined and correlated with thermodynamic,[5] electrostatic,[6] or structural[7] properties of the system. Indeed, recent work[8] has established that the rate of charge recombination correlates remarkably well with the energy of the optical charge-transfer transition for a series of cyclophane-derived RIPs having well-defined molecular architecture. This study revealed, however, that the strong electronic coupling between the partners within the RIP, which is an inherent feature of such compact systems, favored rapid charge recombination. In attempting to prolong the lifetime of the redox intermediates, we have synthesized a [2]rotaxane-derived system in which the terminal stoppers are redox active and which facilitates spatial separation of the primary redox charges.[9] The resultant molecular triad mimics those prepared earlier containing a central porphyrin with appended donor and acceptor functions.[10, 11]

The ferrocenyl-stoppered [2]rotaxane **3** was synthesized by the route depicted in Scheme 1, which follows the procedure pioneered by Stoddart et al.[12] Ferrocenyl carboxylic chloride,[13] prepared from ferrocene-1-carboxylic acid and oxalyl chloride, was added to a solution of 1,4-bis[2-{2-(2-hydroxyethoxy)ethoxy}ethoxy]benzene[12] and triethylamine to form **1**. Compound **1** and 1,1′-[1,4-phenylenebis(methylene)]-bis-4,4′-bipyridinium bis(hexafluorophosphate) (**2**)[12] yielded **3** in 10% yield a a brownish-red solid, according to the template method introduced by Stoddart et al.[14] The compound was purified by gravitational chromatography followed by anion exchange.

X-ray crystallography and ^{1}H NMR spectroscopy established that for **3**, and for closely-related cyclophanes[12, 15] and [2]rotaxanes,[12, 16] the dialkoxybenzene subunit is held inside the cavity of the cyclophane. Indeed, for the corresponding [2]rotaxane possessing triisopropylsilyl groups in place of ferrocene there is sufficient interaction between the π systems of the dialkoxybenzene donor and the cyclophane-derived acceptor to cause appearance of a pronounced charge-transfer absorption band centered at 467 nm ($\varepsilon = 350\ M^{-1}cm^{-1}$) and a weak emission band centered at 548 nm in acetonitrile solution. These spectral measurements can be used to calculate[17] the reaction exergonicity for charge recombination ($\Delta G^0 = -2.46$ eV), the total reorganization energy accompanying charge recombination ($\lambda = 0.19$ eV), and the electronic matrix coupling element

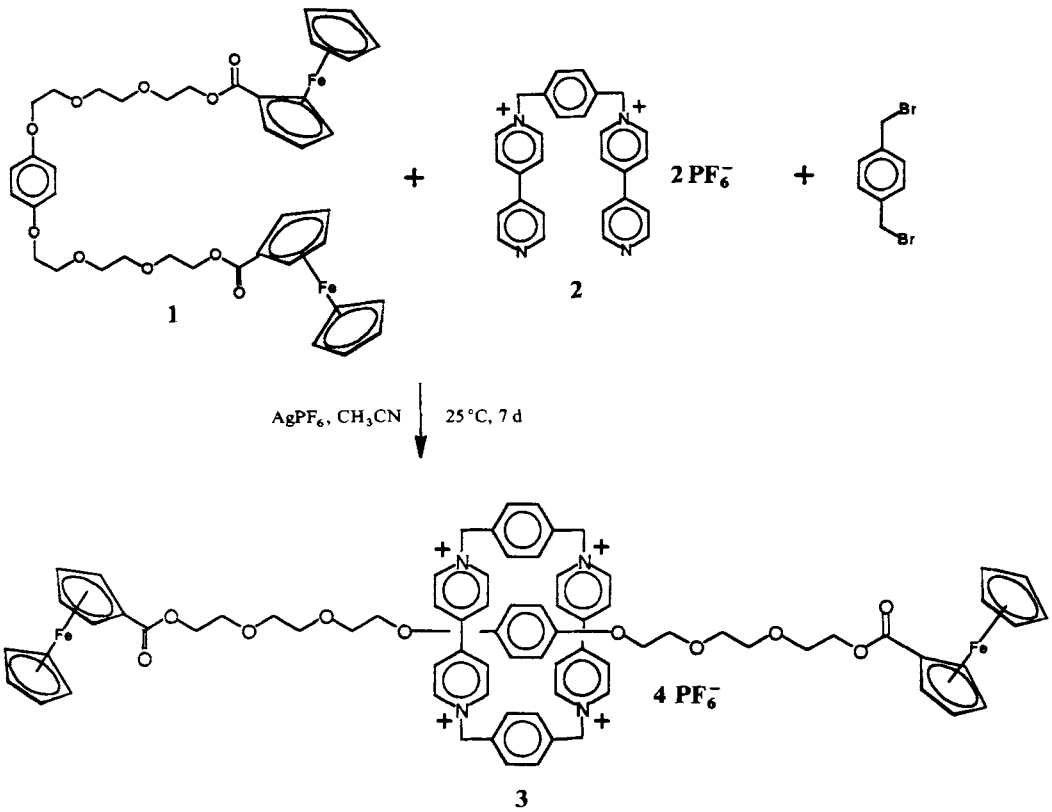

Scheme 1. Scheme for the synthesis of the [2]rotaxane **3**.

[*] Dr. A. Harriman, Dr. A. C. Benniston
Center for Fast Kinetics Research
The University of Texas at Austin
Austin, TX 78712 (USA)
Telefax: Int. code + (512)471 6095

[**] This work was supported by the National Science Foundation (CHE 9102657). The CFKR is supported jointly by the Biotechnology Research Resources Division of the National Institutes of Health (RR 00886) and by the University of Texas at Austin.

($V = 1215\ cm^{-1}$).[18] For **3**, the charge-transfer absorption band partially overlaps a weak transition associated with the ferrocene subunit, which renders calculation of the above parameters a difficult task. Consequently, we assume that the ferrocene subunits do not affect the charge-transfer characteristics of the complex; X-ray crystallography and ^1H NMR spectra provided firm evidence in support of the dialkoxybenzene subunit residing within the central cavity of the cyclophane. From CPK molecular models, the maximum edge-to-edge separation between the dialkoxybenzene and ferrocene subunits was estimated to be approximately 10 Å for a fully extended conformation. Preliminary X-ray crystal structure data, however, indicated π-stacking between the ferrocene subunits and the cyclophane implying that, in the solid state, a folded conformation is preferred.

Cyclic voltammetry studies made with **3** in deaerated acetonitrile solution containing tetra *N*-butylammonium perchlorate (0.2 M) gave one-electon redox potentials of −0.53 V vs the saturated calomel electrode (SCE) for reduction of the cyclophane and 0.46 and 1.14 V vs SCE, respectively, for oxidation of the ferrocene and dialkoxybenzene subunits. We might expect, therefore, that the dialkoxybenzene π-radical cation formed by excitation of the charge-transfer complex could oxidize one of the appended ferrocene subunits, since there is a high thermodynamic driving force for this reaction ($\Delta G^0 = -0.68$ eV).

Excitation of **3** in acetonitrile solution with a 500 fs laser pulse at 437 nm resulted in the immediate appearance of a species possessing a transient differential absorption spectrum very similar to that formed[8] by addition of a single electron to the cylophane (Fig. 1a). Therefore, this species is believed to be the RIP as formed by electron transfer from the included dialkoxybenzene to the cyclophane within the confines of a charge-transfer complex. The same absorption spectral features appear following laser excitation of the [2]rotaxane having the terminal ferrocene subunits replaced with triisopropylsilyl groups. However, whereas the transient absorption signal observed for this latter system decayed completely to the prepulse baseline with a lifetime of about 9 ps, that observed for **3** decayed with a lifetime of about 22 ps to leave a residual signal (Fig. 1a). The transient absorption spectrum of the longer lived species, as recorded following excitation at 532 nm with a 30 ps laser pulse (Fig. 1b), was very similar, if not identical, to that observed immediately after excitation of **3**, and the species decayed slowly by first-order kinetics with a lifetime of 550 ns (Fig. 1b). Excitation of the rotaxane without the cyclophane (i.e., compound **1**) under conditions identical to those described above did not give rise to any detectable transient species.

The laser flash photolysis records can be explained in terms of Scheme 2. Excitation of **3** at a wavelength corresponding to absorption into the charge-transfer transition generates the corresponding RIP. Deactivation of the RIP occurs predominantly by rapid charge recombination ($\Delta G^0 \approx -2.46$ eV), for which the rate constant is $3.4 \times 10^{10}\ s^{-1}$. This process competes with oxidation of one of the appended ferrocene subunits by the dialkoxybenzene π-radical cation ($\Delta G^0 \approx -0.68$ eV), which occurs with a rate constant of $1.1 \times 10^{10}\ s^{-1}$. The ground state system is recovered by slow electron transfer from the π-radical cation of the cyclophane to the adjacent ferrocenium cation ($\Delta G^0 \approx -1.0$ eV), for which the rate constant is $1.8 \times 10^{6}\ s^{-1}$. In this way, some 25% of the primary redox charge is preserved for 500 ns or so.

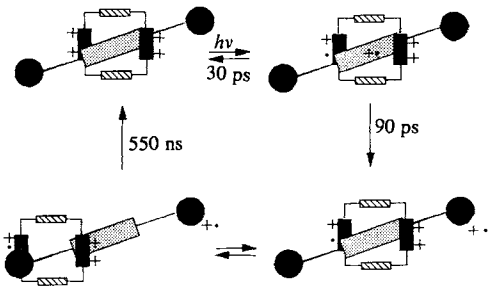

Scheme 2. Proposed scheme for the photoprocesses occurring upon excitation of the [2]rotaxane **3** into the charge-transfer absorption band.

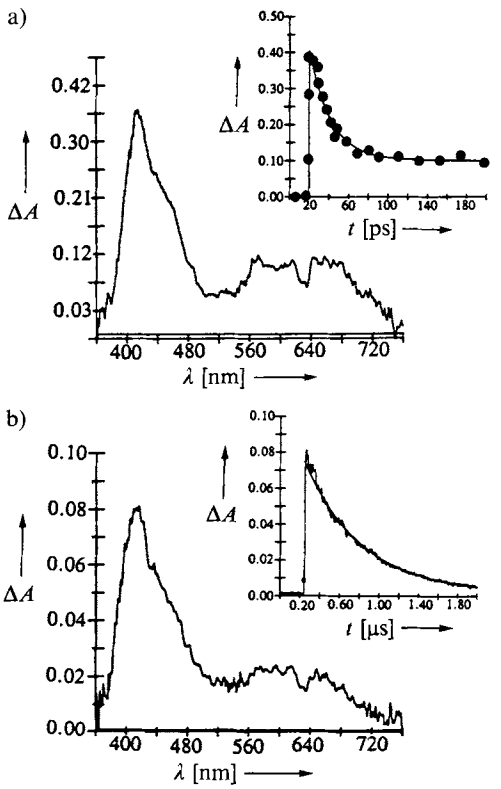

Fig. 1. Transient differential absorption spectra recorded a) 5 ps and b) 200 ps after laser excitation of the [2]rotaxane **3** in acetonitrile solution. The insert to each spectrum shows the decay profile recorded at 410 nm together with its computed best fit.

The close proximity of the threaded components ensures rapid and quantitative formation of the RIP upon illumination, and the large amount of energy that must be dissipated by this species contributes towards its relatively long lifetime. This lifetime is sufficient to permit secondary electron transfer to an appended ferrocene subunit, which separates the redox charges spatially. It should be noted that whereas there is strong electronic coupling between the reactants in the RIP, the dialkoxybenzene π-radical cation and the terminal ferrocene subunits are expected to be coupled only weakly. Thus, direct charge recombination may be under adiabatic contol,[19] whilst oxidation of the ferrocene subunit should be under nonadiabatic control.[20] Annihilation of the remote redox charges is relatively slow and is reduced by a factor of approximately 20000 with respect to the primary charge recombination process. The slowness of this reaction may permit migration of the cyclophane along the thread in

order to minimize electrostatic repulsion between the positively charged reactants. In fact, if the cyclophane is centered over the dialkoxybenzene subunit in the RIP it would require only about 10 ns for it to migrate coherently to the nonoxidized ferrocene subunit.[21] In this respect, **3** operates as a light-induced molecular shuttle, since absorption of light induces migration of the cyclophane along the thread before reverse electron transfer restores the original conformation.

Experimental Procedure

1: To a vigorously stirred solution of 1,4-bis[2-{2-(2-hydroxyethoxy)ethoxy}-ethoxy]benzene [12] (1.2 g, 3.2 mmol) in dried CH_2Cl_2 (50 mL) containing triethylamine (1 g, 9.9 mmol) was added dropwise a solution of ferrocenyl carboxylic chloride [13] (2 g, 8.0 mmol) in dried CH_2Cl_2 (25 mL). The mixture was stirred for a further 48 h before addition of water (20 mL). The organic layer was separated, washed with water, dried, and evaporated to dryness under reduced pressure to give a red oil. The oil was purified by chromatography on silica (60–200 mesh) with CH_2Cl_2 as eluent to remove unchanged starting materials and subsequently with CH_2Cl_2/CH_3OH (95/5) to elute compound **1**. Removal of the solvent gave **1** as a yellow solid. Yield: 1.6 g (62%). ^1H NMR (250 MHz, $CDCl_3$, 25 °C): $\delta = 3.71-3.85$ (m, 16H), 4.04–4.08 (t, 4H, $J = 5$ Hz); 4.20 (s, 10 H), 4.37–4.41 (m, 8 H), 4.81–4.83 (m, 4H); 6.82 (s, 4H). ^{13}C NMR (63 MHz, $CDCl_3$, 25 °C): $\delta = 63.23$, 68.00, 69.44, 69.79, 69.87, 70.17, 70.64, 70.79, 70.88, 71.30, 115.52, 153.03, 170.90. FAB-MS (nitrobenzyl alcohol matrix): 798 $[M]^+$; 585 $[M - FcCO]^+$. UV/VIS (CH_3CN): λ_{max} [nm] (ε [$M^{-1}cm^{-1}$]) = 442 (500).

3: A mixture of **2** [12] (180 mg, 0.25 mmol), 1,4-bis(bromomethyl)benzene (66 mg, 0.25 mmol), **1** (600 mg, 0.75 mmol), and $AgPF_6$ (158 mg, 0.63 mmol) in dried CH_3CN (50 mL) was stirred for 7 days at room temperature. Subsequently, the solution was filtered and evaporated to dryness under reduced pressure. The residue was washed with CH_2Cl_2 (15 mL) and centrifuged. After removal of the supernatant liquid, the residue was washed again with CH_2Cl_2 (2×15 mL) and centrifuged. The solid was dissolved in a mixture of CH_3NO_2 (15 mL) and CH_2Cl_2 (10 mL) and centrifuged once more. The liquid phase was separated, and the solid residue was extracted with a mixture of CH_3NO_2 (10 mL) and CH_2Cl_2 (10 mL). The liquid phases were combined, and the solvent removed under vacuum without heating to give a brown oil. Chromatography on silica with CH_3OH/aq. NH_4Cl (2 M)/CH_3NO_2 (7/2/1) as eluent yielded the required fraction ($R_F = 0.37$), from which the solvent was removed by freeze-drying to give a brown solid. This material was dissolved in water (20 mL), and the required product was precpitated by addition of aqueous NH_4PF_6. Yield: 31 mg (6%). ^1H NMR (250 MHz, $[D_6]$-dimethylsulfoxide, 25 °C): $\delta = 3.32-3.66$ (m, 20H); 3.89–3.93 (m, 8H), 4.21 (s, 10H), 4.39 (t, 2H, $J = 5$ Hz), 4.48 (t, 2H, $J = 5$ Hz), 4.61 (t, 2H, $J = 5$ Hz), 4.72 (t, 2H, $J = 5$ Hz), 5.75 (s, 8H), 7.88 (s, 8H), 8.21–8.24 (d, 8H, $J = 6.5$ Hz), 9.23–9.26 (d, 8H, $J = 6.5$ Hz). FAB-MS (nitrobenzyl alcohol matrix): 1898 $[M]^+$; 1753 $[M - PF_6]^+$; 1608 $[M - 2PF_6]$. UV/VIS (CH_3CN): λ_{max} [nm] (ε[$M^{-1}cm^{-1}$]) = 452 (700).

Received: May 10, 1993 [Z 6073 IE]
German version: *Angew. Chem.* **1993**, *105*, 1553

[1] T. Yabe, J. Kochi, *J. Am. Chem. Soc.* **1992**, *114*, 4491.
[2] T. Asahi, N. Mataga, *J. Phys. Chem.* **1989**, *93*, 6575.
[3] I. R. Gould, R. Moody, S. Farid, *J. Am. Chem. Soc.* **1988**, *110*, 7242.
[4] N. Mataga, Y. Kanda, T. Asahi, H. Misasaka, T. Okada, T. Kakitani, *Chem Phys.* **1988**, *127*, 239.
[5] C. Zhou, J. B. Miers, R. M. Ballew, D. D. Dlott, G. B. Schuster, *J. Am. Chem. Soc.* **1991**, *113*, 7823.
[6] H., Segawa, C. Takehara, K. Honda, T. Shimidzu, T. Asahi, N. Mataga, *J. Phys. Chem.* **1992**, *96*, 503.
[7] A. M. Brun, A. Harriman, S. M. Hubig, *J. Phys. Chem.* **1992**, *96*, 254.
[8] A. C. Benniston, A. Harriman, D. Philp, J. F. Stoddart, *J. Am. Chem. Soc.* **1993**, *115*, 5298.
[9] A. C. Benniston, A. Harriman, *Synlett* **1993**, 223.
[10] D. Gust, T. A. Moore, *Science* **1989**, *244*, 35.
[11] M. R. Wasielewski, *Chem. Rev.* **1992**, *92*, 435.
[12] P.-L. Anelli, P. R. Ashton, R. Ballardini, V. Balzani, M. Delgado, M. T. Gandolfi, T. T. Goodnow, A. E. Kaifer, D. Philp, M. Pietraszkiewicz, L. Prodi, M. V. Reddington, A. M. Z. Slawin, N. Spencer, J. F. Stoddart, C. Vicent, D. J. Williams, *J. Am. Chem. Soc.* **1992**, *114*, 193.
[13] H. J. von Lorkowski, R. Pannier, A. Wende, *J. Prakt. Chem.* **1967**, *35*, 149.
[14] B. Odell, M. V. Reddington, A. M. Z. Slawin, N. Spencer, J. F. Stoddart, D. J. Williams, *Angew. Chem.* **1988**, *100*, 1605; *Angew. Chem. Int. Ed. Engl.* **1988**, *27*, 1547.
[15] P. R. Ashton, D. Philp, M. V. Reddington, A. M. Z. Slawin, N. Spencer, J. F. Stoddart, D. J. Williams, *J. Chem. Soc. Chem. Commun.* **1991**, 1680.
[16] P. R. Ashton, M. R. Johnson, J. F. Stoddart, M. S. Tolley, J. W. Wheeler, *J. Chem. Soc. Chem. Commun.* **1992**, 1128.
[17] N. S. Hush, *Prog. Inorg. Chem.* **1967**, *8*, 391.
[18] According to this analytical treatment, both ΔG^0 and λ are obtained from the absorption and emission peak maxima, while V is calculated by fitting the charge-transfer absorption band to a Gaussian profile. Modern theory relates the rate of electron transfer to these three parameters.
[19] A. Masad, H. Huppert, E. M. Kosower, *Chem. Phys.* **1990**, *144*, 391.
[20] R. A. Marcus, *J. Chem. Phys.* **1965**, *43*, 679.
[21] Calculated according to $d = (2Dt)^{1/2}$ where d is the one-dimensional translation distance (10 Å), D is the diffusion coefficient of the cyclophane ($\approx 5 \times 10^{-7}$ $cm^2 s^{-1}$), and t is the time required for the migration.

DNA Supercoiling Imaged in Three Dimensions by Scanning Force Microscopy**

By *Bruno Samorì,* Carmelo Nigro, Valerio Armentano, Salvatore Cimieri, Giampaolo Zuccheri,* and *Carla Quagliariello*

Scanning force microscopy (SFM) is being employed ever more extensively in organic[1] and biological chemistry.[2, 3] With SFM molecules can be imaged both in water[4] and organic solvents.[2, 5, 6] Though this technique is still being developed, there is no question about the profound impact it will have on the study of molecular structure and behavior.

In essentially all organisms the DNA double strand is coiled in a right-handed fashion termed negative supercoiling.[7] Supercoiled and relaxed circular DNA molecules are now routinely imaged by SFM.[2, 4, 6] Up until now this kind of imaging provided, like electron microscopy (EM),[7] only a planar projection of the molecular shape of supercoiled circular DNA.[2, 4, 5] However, these SFM images also contain surface height information for the DNA molecules examined, although the vertical resolution attained is not high enough to allow the complete three-dimensional path of the chains to be observed directly. The image in Figure 1 shows, however, that this can indeed be achieved.

The number of turns (two) of the DNA molecule chain about the superhelical axis and the right-handedness of the winding are well distinguished. We can thus fully and directly characterize the supercoiling of this molecule because we "see" it. This high resolution has so far been obtained only for molecules with two or three turns.[8] In the other cases stratigraphic analysis can be applied[6] to obtain the third-dimension data contained in SFM images of more tightly supercoiled molecules, and the chirality of the supercoiling can be identified for most well-detected loops.

This display of the complete three-dimensional path of the axis of the DNA double strand opens up several important prospects:

1. Experiments can now be designed so that one can directly monitor the local modulations of supercoiling, which facilitate and drive many important biological processes such as DNA transcription[9, 10] and polymorphism.[11] Supercoiling stabilizes H-triple helices and cruciform and left-

[*] Prof. B. Samorì, Dr. C. Nigro, V. Armentano, S. Cimieri, G. Zuccheri
Dipartimento di Chimica, Università della Calabria
Arcavacata di Rende (CS) I-87030 (Italy)
Telefax: Int. code + (984)492044
Prof. C. Quagliariello
Dipartimento di Biologia Cellulare, Università della Calabria

[**] This work was supported by CNR (Rome), Progetto Finalizzato Biotecnologie Biostrumentazione, Regione Emilia Romagna, and Digital Instruments (Santa Barbara, CA, USA).

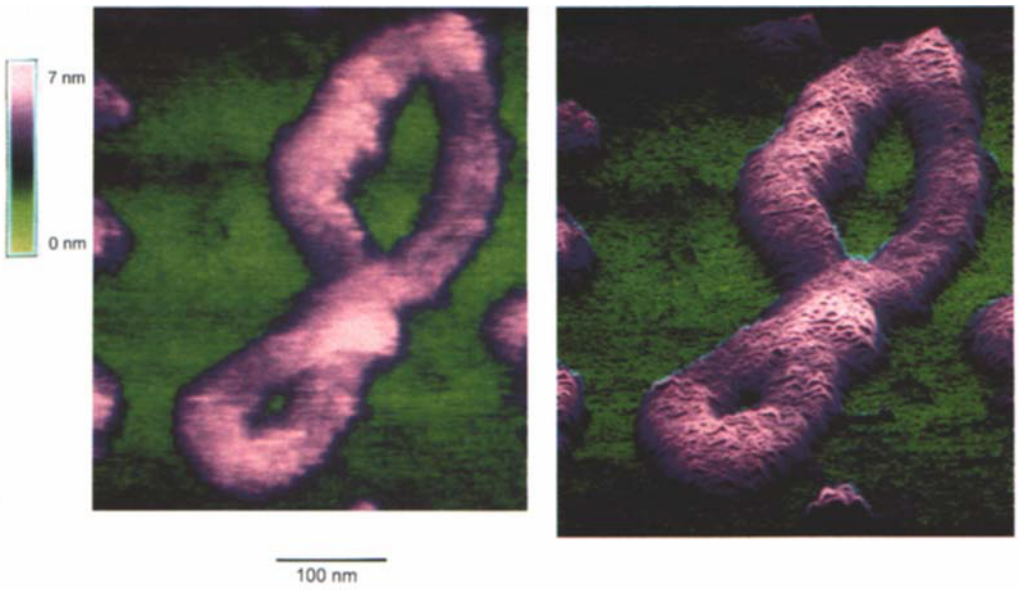

Fig. 1. SFM image of a supercoiled pBR322 DNA molecule. The three-dimensional shape of a circular DNA molecule is clearly displayed by the unfiltered image (left) in which the height information is coded by shades of purple (the lighter, the higher). In the line plot (right), which is obtained by plotting each scan line on an x,y,z scale, the path of the DNA double strand is even more distinct. The two turns of the DNA chains about the superhelical axis and the right-handedness of the supercoiling can be directly recognized by inspection.

handed Z-DNA structures.[11] The conversion from negative to positive supercoiling is reported as characterizing highly transcribed genes.[10] The modulations of supercoiling depend upon local sequences, the position of promoters, and the vectorial tracking of macromolecular complexes along the DNA.[9–12]

2. The writhing number (W_r) of coiled molecules,[7, 13] the most complete and accurate parameter for describing supercoiling and the overall hydrodynamic shape of DNA molecules, can now be determined experimentally. The most widely used descriptor of supercoiling has thus far been the "linking deficit" ($\Delta L_k = L_k - L_{k0}$), which reduces the three-dimensional intertwining of DNA strands to a single number that can be measured by two-dimensional gel electrophoresis. The linking number L_k is the sum of the signed indexes associated with the crossing between either DNA strand and the DNA axis.[3] These nodes can arise in either of two ways: from the winding of the strands about the axis of the double helix, which is related to the twisting number (T_w), or from the crossings of the helix axis itself, which are described by the writhing number (W_r). L_{k0} is the reference linking number of the relaxed circular DNA molecule.

There are at least two reasons to regard the linking deficit as a poor descriptor of supercoiling. It is a topological property defined independently of DNA geometry, whereas supercoiling is a geometric concept. Then, too, it is formally possible to have a nonzero linking deficit ΔL_k for a perfectly planar DNA molecule.[13]

By contrast, W_r is a truly geometric property of the DNA axis. It is directly proportional to the number of times the DNA winds round the supercoiling axis and equal to zero for relaxed DNA. The use of W_r in place of ΔL_k as a descriptor of supercoiling has been very limited heretofore, as W_r could not be experimentally determined. The W_r of an ideal model of the supercoiled helical winding was indirectly computed from EM-derived DNA geometric parameters.[14] Resolution like that of the image in Figure 1 allows the direct determination of the W_r of the imaged molecules as the Gauss integral of the complete three-dimensional path of the chain.[13] In simple cases like that in Figure 1 it is also possible to estimate W_r directly from the image. For this molecule deposited on mica the contribution from planar looped pieces is zero. Because of the tight interwinding of the chain in the central part of the molecule, the number of negative[7] crossings is two for almost all projections. W_r of the molecule in Figure 1 is therefore very close to -2.

3. The partition of ΔL_k between the changes in the supercoiling state (W_r) and the change in the twist of the DNA strand (T_w) can now be experimentally determined too. In fact, the measurement of W_r in plasmid samples of defined ΔL_k yields ΔT_w.

4. SFM makes it possible to study the spatial architecture, intertwining, and coiling of polymers other than DNA.

In conclusion, images like those in Figure 1 demonstrate that it is now possible to monitor local modulations in the supercoiling of single DNA molecules directly and to fully characterize their topology.

Experimental Procedure

10 μL of a solution of pBR322 plasmid DNA (10 μg mL^{-1}) in TE buffer (10 mM Tris, 1 mM EDTA, pH 8.0) was deposited on the surface of freshly cleaved mica. After 2 min the excess solution was blotted off with filter paper. The sample was immediately rinsed with 15 μL of water and then dried for 5 min under a flow of nitrogen. The sample was imaged with the NANOSCOPE III AFM (Digital Instruments) under 1-propanol with silicon nitride tips ("nanoprobes", Digital Instruments). PBR322 plasmid DNA was obtained from transformed DH5 *E. coli* cells. Large-scale plasmid purification was performed using a method employing thermal lysis, followed by two cycles of density-gradient centrifugation with ethidium bromide/CsCl to equilibrium [15]. The sample showed three bands in its agarose gel electrophoresis pattern: the fastest has been attributed to supercoiled forms, the second to nicked and relaxed, and the slowest to high molecular weight DNA.

Received: March 28, 1993 [Z 5957 IE]
German version: *Angew. Chem.* **1993**, *105*, 1482

[1] J. Frommer, *Angew. Chem.* **1992**, *104*, 1325; *Angew. Chem. Int. Ed. Engl.* **1992**, *31*, 1298–1328.
[2] H. G. Hansma, J. Vesenka, C. Siegerist, G. Kelderman, H. Morrett, R. L. Sinsheimer, V. Elings, C. Bustamante, P. K. Hansma, *Science* **1992**, *256*, 1180–1184.
[3] A. Engel, *Annu. Rev. Biophys. Chem.* **1991**, *20*, 79–108.
[4] H. G. Hansma, M. Bezanilla, F. Zenhausern, M. Adrian, R. L. Sinsheimer, *Nucleic Acids Res.*, **1993**, *21*, 505–512.
[5] F. Zenhausern, M. Adrian, B. ten Heggeler-Bordier, R. Emch, M. Jobin, M. Taborelli, P. Descouts, *J. Struct. Biol.* **1992**, *108*, 69–73.
[6] B. Samori, G. Siligardi, C. Quagliariello, A. L. Weisenhorn, J. Vesenka, C. J. Bustamante, *Proc. Natl. Acad. Sci. USA* **1993**, *90*, 3598–3601.
[7] W. R. Bauer, F. H. C. Crick, J. H. White, *Sci. Am.* **1980**, *243*, 100–113.
[8] The three-dimensional resolution of the complete path of very tightly intertwined chains appeared to be hardly achievable with the commercial tips we used in this investigation. This is likely to be due both to the decrease of the superhelix radius with the increase of the supercoiling [14] and the tip's shape and profile. In fact, in SFM images the horizontal

resolution depends on the end radius of curvature of the tip (M. J. Allen, N. V. Hud, M. Balooch, R. J. Tench, W. J. Siekhaus, R. Balhorn, *Ultramicroscopy* **1992**, *42–44*, 1095; J. Vesenka, M. Guthold, C. L. Tang, D. Keller, E. Delaine, C. Bustamante, *ibid.* **1992**, *42–44*, 1243), whereas the vertical resolution, in other words, how well steep features are visualized, is determined by the opening angle of the tip (D. Keller, D. Deputy, A. Alduino, K. Luo, *Ultramicroscopy* **1992**, *42–44*, 1481). A chain crossing profile can thus be resolved in three dimensions only if its opening angle is greater than that of the tip. The unusually large width and double-traced path of the DNA chain in Figure 1 suggest that this image was traced by a probe with two very sharp and close tips at its end. Under these conditions unusually high vertical resolutions are frequently obtained also imaging straight pieces of DNA.

[9] L. F. Liu, J. C. Wang, *Proc. Natl. Acad. Sci. USA* **1987**, *84*, 7024–7027.

[10] M. S. Lee, T. W. Garrard, *Proc. Natl. Acad. Sci. USA* **1991**, *88*, 9675–9679.

[11] M. D. Frank-Kamenetskii in *DNA Topology and its Biological Effects* (Eds.: N. R. Cozzarelli, J. C. Wang), Cold Spring Harbor Laboratory Press, New York, **1990**, pp. 185–215.

[12] H. Zhang, C. B. Jessee, L. F. Liu, *Proc. Natl. Acad. Sci. USA* **1990**, *87*, 9078–9082.

[13] N. R. Cozzarelli, T. C. Boles, J. H. White in *DNA Topology and its Biological Effects* (Eds.: N. R. Cozzarelli, J. C. Wang), Cold Spring Harbor Laboratory Press, New York, **1990**, pp. 139–184.

[14] T. C. Boles, J. H. White, N. R. Cozzarelli, *J. Mol. Biol.* **1990**, *213*, 931–951.

[15] E. F. Fritsch, J. Sambrook, T. Maniatis, *Molecular Cloning: a Laboratory Manual*, 2nd edition, Cold Spring Harbor Laboratory Press, New York, **1989**, Vol. 1, pp. 34–35 and 42–43.

Structure of a One-Dimensional Infinite Double-Helical Copper(I) Complex**

By *Riccardo F. Carina, Gérald Bernardinelli,* and *Alan F. Williams**

Dedicated to Professor Erwin Parthé on the occasion of his 65th birthday

Supramolecular chemistry, the chemistry of complicated structures formed by the controlled association of simple molecular units, is currently an area of considerable interest.[1] In supramolecular coordination chemistry the structure is assembled by the coordination of suitably structured ligands about a metal ion, and the assembly may be controlled by the disposition of binding sites within the ligand structure, and by the stereochemical preferences of the metal ion.[2] The synthesis of helical complexes has recently attracted particular attention: double-helical complexes containing up to five Cu^I ions have been reported by Lehn et al.[3] by using oligobipyridyl ligands; Constable has prepared helical complexes with a variety of metal ions by using polypyridyl ligands,[4] while we have previously reported triple-helical complexes of six-coordinate Co^{II}[5] and nine-coordinate Eu^{III}.[6] A general feature of these complexes is that the length of the helix is determined by the number of binding sites of the ligand; thus, a ligand with three bipyridyl binding sites can bind up to three cations, and will form a helical, trinuclear complex. If it is desired to extend the helix, it will be necessary to design a new ligand with additional binding sites. An alternative strategy is to form an extended helix, in the ideal case a one-dimensional infinite helical complex, in two steps: an initial formation of a helical subunit, which is followed by an association to give an extended helical structure. We report here the realization of this strategy to give a one-dimensional infinite double-helical copper(I) complex.

Some years ago we reported the synthesis and structure of the simple double-helical complex $[Cu_2(\mathbf{1})_2]^{2+}$ (**3**).[7] A feature of **3**, which is also found in many other helical complexes, is the intramolecular stacking between the aromatic planes of the heterocyclic ligands. In order to study the importance of this stacking we have prepared the ligand 2,6-bis(1-methyl-imidazol-2-yl)pyridine (**2**), in which molecular models suggested that the intramolecular stacking interactions would be greatly reduced.

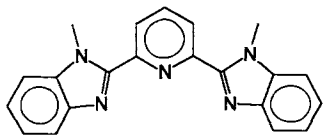

1

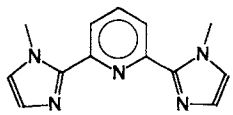

2

The X-ray crystal structure of $[Cu_2(\mathbf{2})_2](ClO_4)_2$ (**4**) shows that the basic $[Cu_2L_2]^{2+}$ unit found in **3**[7] is also observed with ligand **2**. The ligands bind in a bis-monodentate coordination mode, and form the strands of the helix that twist around the helical axis on which the copper ions lie. Each Cu^I center is essentially linearly coordinated by two imidazole units, and is slightly bent towards the second Cu^I center of the $[Cu_2L_2]^{2+}$ unit; the interaction with the two bridging pyridines is weak. The asymmetric unit is composed of two independent half molecules, and a crystallographic twofold symmetry axis passes through the Cu ions so that the two ligand strands are symmetry related. Relevant bond lengths and angles of **4** are given in Table 1, and Figures 1 to 3 show different views of the complex cations. The $Cu-N_{imidazole}$ distances in **4** are slightly shorter than the $Cu-N_{benzimidazole}$ distances in **3**; the $Cu-N_{pyridine}$ distances, however, are significantly longer in **4** than in **3**, although the Cu–Cu distances (2.821(5), 2.828(5) Å) are 0.03 Å shorter. The dihedral angles between the pyridine and the imidazole groups, which describe the twisting of the ligand, are in **4** slightly smaller than the average value for **3**, but more significantly, they show much less variation than for **3** where the variation was from 18 to 44°. As expected, the intramolecular stacking of the

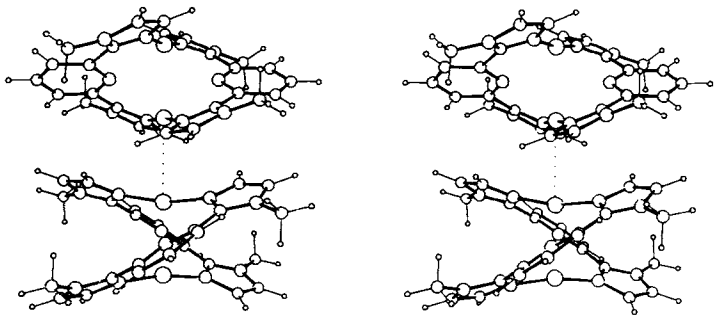

Fig. 1. ORTEP [13] stereoview of two $[Cu_2(\mathbf{2})_2]^{2+}$ units. The crystallographic twofold axis passes through all four copper ions, and the two molecules of complex are crystallographically nonequivalent.

[*] Dr. A. F. Williams, Dr. R. F. Carina
Département de Chimie Minérale Analytique
et Appliquée Université de Genève
30 quai Ernest Ansermet, CH 1211 Genève 4 (Switzerland)
Telefax: Int. code + (22)329-6102
Dr. G. Bernardinelli
Laboratoire de Cristallographie aux Rayons-X
Université de Genève, CH 1211 Genève 4 (Switzerland)

[**] This work was supported by the Swiss National Science Foundation (Grant no. 20.30129.90)

Table 1. Distances [Å] and angles [°] for $[Cu_2(\mathbf{2})_2]^{2+}$ (**4**) [a].

	1	2	3	4	average	$[Cu_2(\mathbf{1})_2]^{2+}$ (**3**)
$Cu\text{-}N_{imid}$	1.87(1)	1.85(2)	1.90(1)	1.87(2)	1.87	1.915
$Cu\text{-}N_{py}$	2.55(1)	2.49(1)	2.60(1)	2.66(1)	2.57	2.50
$N_{imid}\text{-}Cu\text{-}N_{imid}$	173.5(6)	169.3(6)	166.8(6)	167.9(6)	169.4	171.2
py-imid torsion angle	27.7(7)	25.2(7)	27.7(7)	25.1(7)	26.3	31.9

[a] py = pyridine, imid = imidazole. Columns 1 to 4 refer to the sites of the four crystallographically inequivalent copper ions. The values for **3** are averages. The torsion angle between the imidazole rings and the pyridine ring is the angle between the least-squares planes defined by the atoms of the cycle.

benzimidazoles, which was observed in **3**, is absent in **4**. In general the complex **4** is much closer than **3** to D_2 symmetry.

The major difference between **3** and **4** lies in the crystal packing; **4** contains two crystallographically distinct $[Cu_2(\mathbf{2})_2]^{2+}$ complexes which are stacked on top of each other along the twofold symmetry axis. The two distinct complexes

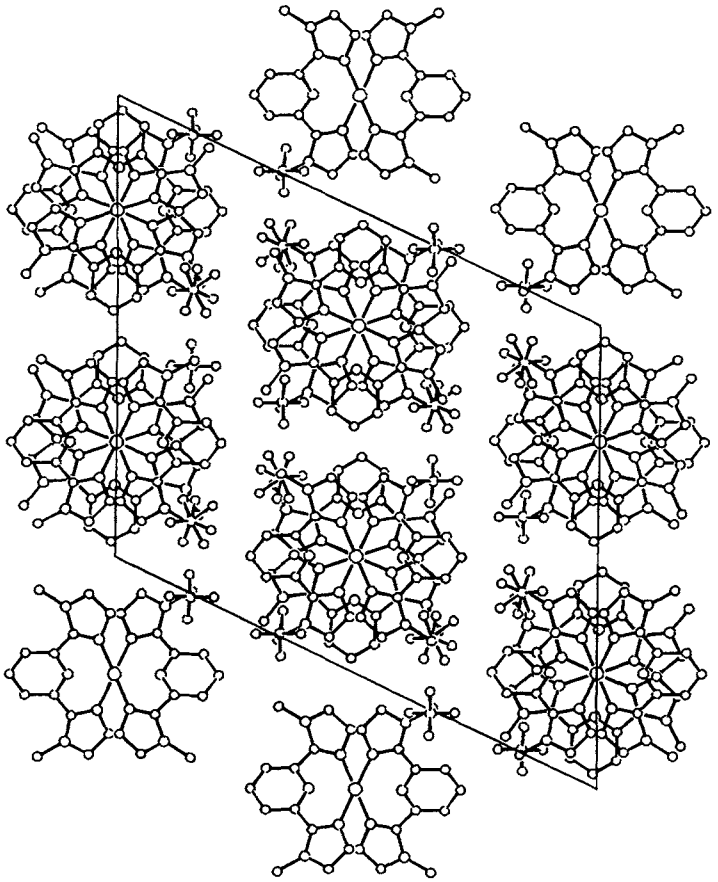

Fig. 2. ORTEP [13] view of the packing along the *b* axis. Adjacent columns are of opposite helicity.

do not differ significantly in their structure, but the second is rotated by approximately 90° about the twofold axis with respect to the first. This allows a strong stacking interaction between the imidazole planes of superposed complexes with interplanar angles of 10.7(8) and 6.8(8)° and average interplanar distances of 3.48 and 3.45 Å, respectively. The intermolecular Cu–Cu distances are 3.291(5) and 3.425(5) Å. The rotation by 90° about the Cu–Cu axis of successive complexes allows the double-helical $[Cu_2(\mathbf{2})_2]^{2+}$ units to mesh together perfectly so that the structure appears as an infinite double helix (Fig. 3). In this each strand is a series of molecules of the ligand **2**, and the strands are held together by a combination of coordination and stacking interactions.

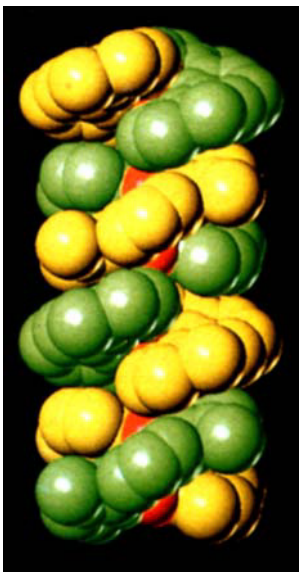

Fig. 3. MOLCAD [14] view of four $[Cu_2(\mathbf{2})_2]^{2+}$ units stacked along the *b* axis. The eight copper ions are red, and the ligands yellow and green.

The loss of the intramolecular stacking present in **3** has been compensated by the intermolecular stacking between units in **4**. The selectivity of the interaction is nicely illustrated by the complete separation of complexes with different helicity: in this racemic compound complexes of positive and negative helicity are formed in equal amounts; upon crystallization, however, the complexes stack together in parallel columns of constant but different helicity. The final structure may therefore be considered as resulting from the stereoselective assembly (by stacking interactions) of double-helical subunits formed by the coordination of **2** to copper(I) to give infinite double-helical columns. These columns are arranged in an almost ideal heaxagonal packing of rods along [010] as described by O'Keefe and Andersson,[8] although the rods show alternating chirality.

On dissolution of **4** in nonpolar solvents, the one-dimensional infinite chains dissociate; the NMR data, however, show that the double-helical $[Cu_2(\mathbf{2})_2]^{2+}$ units are maintained.[15]

Experimental Procedure

2,6-bis(2-imidazol-2-yl)pyridine was prepared by barium manganate oxidation [9] of 2,6-bis(2-imidazolin-2-yl)pyridine obtained by condensation of pyridine-2,6-dicarboxylic acid with ethylenediamine [10]. 2,6-bis(2-imidazol-2-yl)pyridine was methylated to give ligand **2** as described previously [7]. Complex **4** was obtained by reaction of ligand **2** with $[Cu(CH_3CN)_4]^+$ as for complex **3** [7].

Crystals of **4** suitable for X-ray difffraction were obtained by vapour diffusion (under nitrogen) of THF into a concentrated solution of **4** in acetonitrile:DMF (9:1). An orange-red crystal (0.12 × 0.17 × 0.31 mm) was mounted on a quartz fiber. $M_r = 804.6$, monoclinic, $I2/a$, $a = 22.369(4)$, $b = 12.365(2)$, $c = 25.421(4)$ Å, $\beta = 115.74(1)°$ based on 23 reflections ($16° < 2\theta < 28°$), $V = 6334(2)$ Å^3, $Z = 8$. Intensity data were collected at room temperature on a Philips PW1100 diffractometer with $Mo_{K\alpha}$ radiation ($\lambda = 0.71069$ Å), $6° < 2\theta < 44°$. 3858 unique reflections measured. The structure was solved by direct methods [11], other calculations were made with XTAL 3.2 [12]. The perchlorate ions lie in general positions and are disordered. Full-matrix refinement with anisotropic thermal displacement parameters for all non-hydrogen atoms (apart from two disordered oxygen atoms) and hydrogen atoms in calculated

positions gave a final R factor $R = R_w = 0.072$ for 1935 observed reflections ($|F_o| > 4\sigma(F_o)$) and 453 variables. Further details of the crystal structure are available on request from the Director of the Cambridge Crystallographic Data Centre, 12 Union Road, GB-Cambridge CB2 1EZ (UK), on quoting the full journal citation.

Received: May 3, 1993 [Z 6055 1E]
German version: *Angew. Chem.* **1993**, *105*, 1483

[1] J.-M. Lehn, *Angew. Chem.* **1990**, *102*, 1347; *Angew. Chem. Int. Ed. Engl.* **1990**, *29*, 1304-1319; F. Vögtle, *Supramolecular Chemistry*, Wiley, Chichester, England, **1991**.
[2] C. Piguet, G. Bernardinelli, B. Bocquet, A. Quattropani, A. F. Williams, *J. Am. Chem. Soc.* **1992**, *114*, 7440-7451.
[3] J.-M. Lehn, A. Rigault, J. Siegel, J. Harrowfield, B. Chevrier, D. Moras, *Proc. Natl. Acad. Sci. USA* **1987**, *84*, 2565-2569; J.-M. Lehn, A. Rigault, *Angew. Chem.* **1988**, *100*, 1121-1122; *Angew. Chem. Int. Ed. Engl.* **1988**, *27*, 1095-1097.
[4] E. C. Constable, *Tetrahedron* **1992**, *48*, 10013-10059.
[5] A. F. Williams, C. Piguet, G. Bernardinelli, *Angew. Chem.* **1991**, *103*, 1530; *Angew. Chem. Int. Ed. Engl.* **1991**, 30, 1490-1492.
[6] G. Bernardinelli, C. Piguet, A. F. Williams, *Angew. Chem.* **1992**, *104*, 1626; *Angew. Chem. Int. Ed. Engl.* **1992**, 31, 1622-1624.
[7] C. Piguet, G. Bernardinelli, A. F. Williams, *Inorg. Chem.* **1989**, *28*, 2920.
[8] M. O'Keefe, S. Andersson, *Acta Cryst., Sect. A* **1977**, *33*, 914-923.
[9] S. Knapp, T. P. Keenan, X. Zang, R. Fikar, J. A. Potenza, H. J. Schugar, *J. Am. Chem. Soc.* **1987**, *109*, 1822.
[10] A. T. Bakar, P. Singh, V. Vignevich, *Aust. J. Chem.* **1991**, *44*, 1041.
[11] P. Main, S. J. Fiske, S. E. Hull, L. Lessinger, D. Germain, J. P. Declercq, M. M. Woolfson, *MULTAN 87*, Universities of York, England, and Louvaine-La-Neuve, Belgium, **1987**.
[12] *XTAL 3.2 User's Manual* (Eds.: S. R. Hall, J. M. Stewart), Universities of Western Australia and Maryland, **1992**
[13] C. K. Johnson, ORTEP II Report ORNL-5138, Oak Ridge National Laboratory, Oak Ridge TN, USA, **1976**.
[14] J. Brickmann, *MOLCAD Molecular Modelling Package*, Technische Hochschule, Darmstadt (FRG) **1990**.
[15] Editorial note: see also the next communication in this issue: E. C. Constable, A. J. Edwards, P. R. Raithby, J. V. Walker, *Angew. Chem.* **1993**, 105, 1486; *Angew. Chem. Int. Ed. Engl.* **1993**, *32*, 1465.

The First Structurally Characterized Heterodinuclear Double-Helicate Complex**

By *Edwin C. Constable,* Andrew J. Edwards, Paul R. Raithby*, and *Juliet V. Walker*

Metal-directed self-assembly of topologically novel supramolecular arrays has attracted considerable attention in recent years.[1] We and others have shown that oligopyridines provide versatile metal-binding domains for the assembly of helicate and double-helicate complexes.[2] We have developed a strategy involving the matching together of the donor characteristics of a ligand array to the coordination requirements of metal centers. Helicates are the result of the partitioning of the donor set of an oligopyridine into two metal-binding domains; for a 2,2′:6′,2″:6″,2‴:6‴,2⁗-quinquepyridine (**1**, qpy) this involves a rotation about an interannular C–C bond to separate the ligand into a tridentate 2,2′:6′,2″-terpyridyl and a didentate 2,2′-bipyridyl part. A double-helical array of two qpy ligands presents a total of ten nitrogen donor atoms, which are usually arranged to create a six-coordinate [tpy + tpy] and a four-coordinate [bpy + bpy] metal-bonding cavity, although two five-coordinate [bpy + tpy] cavities are also possible.[2]

In the solid state, $[Co_2(\mathbf{1})_2(OAc)](PF_6)_3$ is double-helical, but upon dissolution in a donor solvent, a mononuclear seven-coordinate species $[Co(\mathbf{1})(solv.)_2]^{2+}$ (solv. = MeCN, MeOH, or H_2O) is formed.[3] We argued that this was the result of a destabilization of the cobalt in the [bpy + bpy] site, and showed that treatment of the solution species with Ag^+ ions resulted in the formation of the heterodinuclear double-helicate $[CoAg(\mathbf{1})_2]^{3+}$ in which we assumed the cobalt to be in a [tpy + tpy] and the silver in the [bpy + bpy] site. We now describe a high yield systematic synthesis of these complexes and the structural characterization of $[CoAg(\mathbf{1})_2](ClO_4)_3$.

The reaction of the two mononuclear cations $[Co(\mathbf{1})(MeOH)_2]^{2+}$ and $[Ag(\mathbf{1})]^+$[4] in a 1:1 ratio gave $[CoAg(\mathbf{1})_2]^{3+}$ in near-quantitative yield. The reactions with the substituted qpy ligands, **2**–**5** proceeded in a precisely similar manner to give the substituted analogues. In all cases,

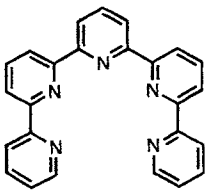

1

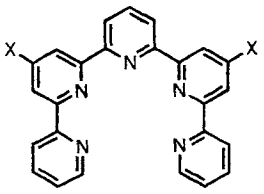

2, X = MeS
3, X = Ph
4, X = 4-ClC_5H_4
5, X = 4-ClC_6H_4

the complexes were readily purified by chromatography to yield pale yellow microcrystalline materials. Attempts to prepare specifically the heterodinuclear heteroleptic double-helicates, such as $[CoAg(\mathbf{1})(\mathbf{3})]^{3+}$, by the reaction of either $[Co(\mathbf{1})(MeOH)_2]^{2+}$ and $[Ag(\mathbf{3})]^+$ or $[Co(\mathbf{3})(MeOH)_2]^{2+}$ and $[Ag(\mathbf{1})]^+$ were unsuccessful, and gave inseparable statistical mixtures of $[CoAg(\mathbf{1})_2]^{3+}$, $[CoAg(\mathbf{3})_2]^{3+}$, and $[CoAg(\mathbf{1})(\mathbf{3})]^{3+}$ as shown by FAB mass spectrometry and also by ^1H NMR spectroscopy. The ^1H NMR spectrum indicated that these heterodinuclear complexes were the only species observable on the NMR time-scale; the mononuclear silver complexes were not observed. We attempted to obtain X-ray quality crystals of $[CoAg(\mathbf{1})_2]^{3+}$ with a variety of substituted ligands, a range of counterions, and from a variety of solvents but in all cases we obtained either powders, or small crystals which immediately lost solvent upon removal from the crystallization solvent.

We finally obtained small crystals of $[CoAg(\mathbf{1})_2](ClO_4)_3 \cdot 2\,H_2O$ (**6**) from acetone/H_2O and mounted these in perfluoropolyether oil RS3000 and determined the structure of 153 K.[5] The lattice consists of dimeric $\{CoAg(\mathbf{1})_2\}_2^{6+}$ units and hydrogen bonded, but disordered, water molecules and perchlorate anions. The structure of one of the two crystallographically independent $[CoAg(\mathbf{1})_2]$ units in the dimeric cation is shown in Figure 1. The structural determination confirms our predictions that the heterodinuclear double-helical cation has been formed, and that the cobalt is in a [tpy + tpy] and the silver in a [bpy + bpy] environment. The

[*] Dr. E. C. Constable,[+] Dr. A. J. Edwards, Dr. P. R. Raithby, J. V. Walker
University Chemical Laboratory
Lensfield Road, GB-Cambridge CB2 1EW (UK)
[+] New address:
Institut für Anorganische Chemie der Universität
Spitalstrasse 51, CH-4056 Basel (Switzerland)
Telefax: Int. code + (61) 322–1554

[**] This work was supported by the UK Science and Engineering Research Council (grant for J. V. W.). We also thank the Royal Society of Great Britain and the Isaac Newton Trust for assistance in the purchase of spectrophotometers and the Cambridge Crystallographic Data Centre for support (A. J. E.). We should also like to thank Miss Linda Crow for her assistance.

Co···Ag distances within the two independent units are 4.167 and 4.224 Å, respectively, and these are comparable to, but slightly shorter than, the Co···Co distance (4.461 Å) in $[Co_2(\mathbf{1})_2(OAc)](PF_6)_3$.[3] The Co–N and Ag–N bond lengths and angles in **6** are not unusual, although the coordination geometry about the silver differs substantially from that observed in the double-helical cation $[Ag_2(qtpy)_2]^{2+}$ (qtpy = 2,2′:6′,2″:6″,2‴-quaterpyridine).[6] A detailed comparison of the four-coordinate metal coordination spheres in the complexes $[Cu_2(\mathbf{1})_2(OAc)](PF_6)_3$, $[Ag_2(qtpy)_2](BF_4)_2$, and **6** is not particularly informative.

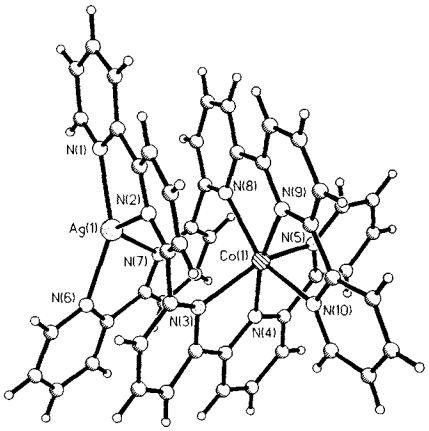

Fig. 1. Structure of one of the two $[CoAg(\mathbf{1})_2]^{3+}$ units present in **6**, showing the numbering scheme adopted. Selected bond lengths [Å] and angles [°] within the coordination sphere include: Ag(1)-N(1) 2.294(7), Ag(1)-N(2) 2.350(6), Ag(1)-N(6) 2.311(6),Ag(1)-N(7) 2.329(6), Co(1)-N(3) 2.239(6), Co(1)-N(4) 2.050(6), Co(1)-N(5) 2.161(6), Co(1)-N(8) 2.228(6), Co(1)-N(9) 2.058(6), Co(1)-N(10) 2.194(6); N(1)-Ag(1)-N(2) 71.4(2), N(6)-Ag(1)-N(7) 71.2(2), N(8)-Co(1)-N(9) 75.4(2), N(9)-Co(1)-N(10) 76.4(2), N(3)-Co(1)-N(4) 76.1(2), N(4)-Co(1)-N(5) 76.5(2). Angles and lengths within the other crystallographically independent dinuclear unit of **6** are similar.

The summation of the individual variations in interannular twisting along the oligopyridine chains results in significant but not readily explained changes in the coordination sphere. The cation exhibits the usual stacking interactions between approximately coplanar rings of the two different qpy ligands with rings 2 and 9 (numbered by the nitrogen atom they contain) with a centroid-to-centroid distance of 3.480 Å. The partitioning of the qpy ligands into bpy and tpy portions is achieved by interannular twistings of approximately 60° between rings 2 and 3 and rings 7 and 8, very similar to those observed in $[Co_2(\mathbf{1})_2(OAc)](PF_6)_3$.[3] The individual bpy and tpy domains are approximately, but not precisely, planar.

The most interesting feature of this structure is the assembly of the dimeric unit by the head-to-head interaction of two $[CoAg(\mathbf{1})_2]^{3+}$ units (Fig. 2) with a nonbonded Ag(1)···Ag(1′) contact of 3.822 Å. The long Ag···Ag contact cannot account for the formation of the head-to-head dimer. No such interactions are present between $[Ag_2(qtpy)_2]^{2+}$ units in the solid state.[6] The shortest contacts between the two double-helical $[CoAg(\mathbf{1})_2]^{3+}$ cations are those of approximately coplanar pyridine rings. Specifically, rings 6 and 6′ are stacked with a centroid-to-centroid distance of 3.663 Å whilst the corresponding rings 1 and 1′ are at 3.606 Å. These stacking interactions are undoubtedly responsible for the formation of the dimer, and unambiguously establish the importance of such interactions in determining the solid-state structures and conformations of helicates. The entire dimeric assembly is seen to exhibit a series of stacking interactions along its entire length (Fig. 2 bottom).

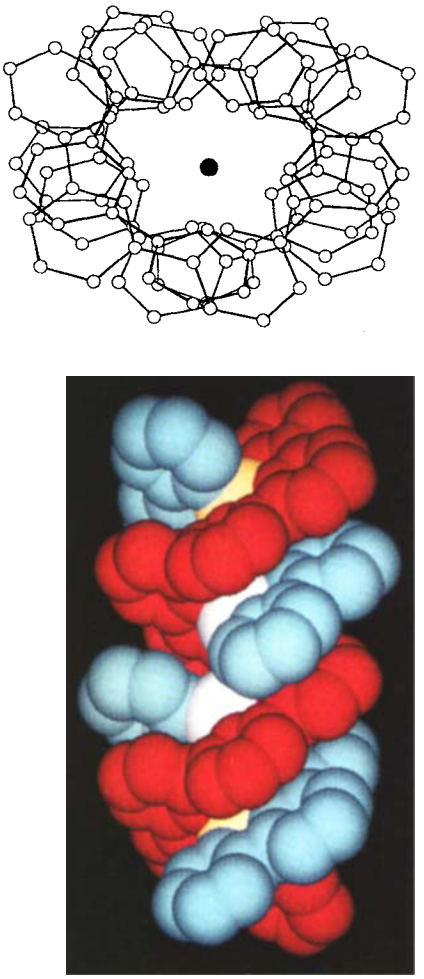

Fig. 2. The tetranuclear assembly of two $[CoAg(\mathbf{1})_2]^{3+}$ cations. Top: The view along the cobalt-cobalt vector. The metal–N bonds and hydrogen atoms have been omitted for clarity. Bottom: A space-filling representation of **6** showing the numerous stacking interactions which are present. The cobalt ions are yellow, the silver ions white, and the two ligand strands are colored red and blue. The stacking is between the red strand of one ligand and the blue strand of the other.

Experimental Procedure

The ligands **1**–**5** were prepared by the literature methods [7].

$[CoAg(\mathbf{1})_2](PF_6)_3$ and $[CoAg(\mathbf{1})_2](ClO_4)_3 \cdot 2\,H_2O$ **6**: Cobalt(II)-acetate (1 mmol, 25 mg) and **1** (1 mmol, 38 mg) were warmed in methanol (20 cm^3) and treated with ultrasound until dissolution was complete. A suspension of silver(I) acetate (1 mmol, 17 mg) and **1** (1 mmol, 38 mg) was treated similarly again to complete dissolution. The solution of the silver complex was then added dropwise with swirling to the solution of cobalt complex. The complexes were readily purified by chromatography (silica, 8:1 MeCN/saturated aqueous KNO_3 or $NaClO_4$) to yield pale yellow solutions, from which yellow microcrystalline materials were precipitated by the addition of methanolic ammonium hexafluorophosphate or sodium perchlorate. The hexafluorophosphate salt was recrystallized from acetonitrile by ether diffusion to yield yellow/orange crystals. The perchlorate salt could be recrystallized from a mixture of acetonitrile, acetone, and water by slow evaporation again to yield yellow/orange crystals. Yields were ≈65% in each case. FAB mass sepctrum, *m/z*: 1230, $[CoAg(\mathbf{1})_2](PF_6)_2$; 1085, $[CoAg(\mathbf{1})_2](PF_6)$ (based on ^{107}Ag).

A similar reaction with the ligand **5** gave the analogous complex $[CoAg(\mathbf{5})_2](PF_6)_3$ in 60% yield. FAB mass spectrum, *m/z*: 1525; $[CoAg(\mathbf{5})_2](PF_6)$; 1380, $[CoAg(\mathbf{5})_2]$ (based on ^{107}Ag, ^{35}Cl).

Received: May 10, 1993 [Z 6075 IE]
German version: *Angew. Chem.* **1993**, *105*, 1486

[1] J.-M. Lehn, *Angew. Chem.* **1990**, *102*, 1347; *Angew. Chem. Int. Ed. Engl.* **1990**, *29*, 1304; *J. Coord. Chem.* **1992**, *27*, 3.
[2] Review: E. C. Constable, *Tetrahedron* **1992**, *48*, 10013, and references therein.
[3] E. C. Constable, S. M. Elder, P. R. Raithby, M. D. Ward, *Polyhedron* **1991**, *10*, 1395; E. C. Constable, J. V. Walker, D. A. Tocher, *J. Chem. Soc. Chem. Commun.* **1992**, 768.
[4] E. C. Constable, M. G. B. Drew, G. Forsyth, M. D. Ward, *J. Chem. Soc. Chem. Commun.* **1988**, 1450.
[5] Crystal data for **6**: $C_{100}H_{76}Ag_2Cl_6Co_2N_{20}O_{28}$, triclinic, $P\bar{1}$, $a = 14.582(3)$, $b = 18.828(4)$, $c = 19.151(4)$ Å, $\alpha = 96.80(3)$, $\beta = 95.07(3)$, $\gamma = 106.00(3)°$, $V = 4978(2)$ Å^3, $M_r = 2552.15$, $Z = 2$, $\varrho = 1.697$ Mg m^{-3}, $F(000) = 2564$, $T = 153(2)$ K, $Mo_{K\alpha}$ radiation, $\lambda = 0.71073$ Å, $\mu(Mo_{K\alpha}) = 0.968$ mm^{-1}). The structure was solved by direct methods by using SHELX TL+ and refined by full-matrix-block least squares by using SHELX 92; Co, Cl, N, C atoms anisotropic; H atoms riding on appropriate carbon atoms with fixed isotropic U. Disorder was present in the perchlorate counterions and the solvent water molecules. 13448 reflections measured ($2.52 < \theta < 22.49°$), corrected for absorption, 12981 unique reflections, $R = 0.081$, $wR2 = 0.2281$. Further details on the crystal structure investigation are available on request from the Director of the Cambridge Crystallographic Data Centre, 12 Union Road, GB-Cambridge CB21EZ (UK), on quoting the full journal citation.
[6] E. C. Constable, M. J. Hannon, A. Martin, P. R. Raithby, D. A. Tocher, *Polyhedron* **1992**, *11*, 2967.
[7] F. Krohnke, *Synthesis* **1976**, 1; E. C. Constable, M. A. M. Daniels, M. G. B. Drew, D. A. Tocher, J. V. Walker, P. D. Wood, *J. Chem. Soc. Dalton Trans.*, in press; K. T. Potts, *Bull. Soc. Chim. Belg.* **1990**, *99*, 741, and references therein; K. T. Potts, M. J. Cipullo, P. Ralli, G. Theodoris, *J. Org. Chem.* **1982**, *47*, 3027; K. T. Potts, D. A. Usifer, A. Guadalupe, H. D. Abruna, *J. Am. Chem. Soc.* **1987**, *109*, 3961.
[8] Editorial Note: See also the preceeding communication in this issue: R. F. Carina, G. Bernardinelli, A. F. Williams, *Angew. Chem.* **1993**, *105*, 1483; *Angew. Chem. Int. Ed. Engl.* **1993**, *32*, 1463.

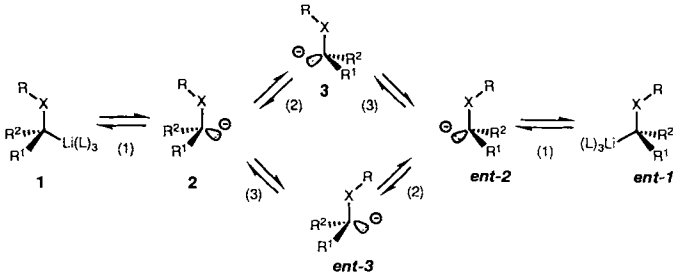

Scheme 1. L = THF or other ligand.

Rotation about the C–Se Bond as the Rate-Determining Step in the Racemization of α-Selenium-Substituted Alkyllithium Compounds**

By *Thomas Ruhland, Ruprecht Dress,* and *Reinhard W. Hoffmann**

Structural aspects of organolithium compounds have been investigated both experimentally[1] and theoretically[2] in recent years. The extent of aggregation can be determined,[3] and it is known which solvents favor contact ion pairs and which favor solvent-separated ion pairs.[4] In addition, there are reliable data on the configurational stability of organolithium compounds.[5] However, what is not yet fully elucidated is the mechanism of racemization.[6–8] In α-heterosubstituted alkyllithium compounds **1** (e.g., where X = S, Se, PR, SiR_2), the negative charge is stabilized by, amongst other effects, n → σ* delocalization (negative hyperconjugation) into the X–R bond.[9] In **1** this results in an antiperiplanar arrangement of X–R and C–Li bonds.[10] For lithium compounds of this type, a three-step racemization is postulated (Scheme 1). Step (1) is the dissociation of lithium from carbon (only the anionic parts of the contact ion pairs **2** and **3** are shown), step (2) is inversion at the pyramidal carbanion C atom, and step (3) is the rotation about the $C_{carbanion}$–heteroatom bond.

[*] Prof. Dr. R. W. Hoffmann, Dipl.-Chem. T. Ruhland, Dipl.-Chem. R. Dress
Fachbereich Chemie der Universität
D-35032 Marburg (FRG)
Telefax: Int. code + (6421)28-5547

[**] This work was funded by the Graduierten-Kolleg Metallorganische Chemie at the University of Marburg, the Deutsche Forschungsgemeinschaft (SFB 260), and the Fonds der Chemischen Industrie.

For the development of configurationally more stable organolithium compounds it is important to identify the rate-determining step for racemization in order to control it. The following results clearly show that in certain systems the rotational step (3) could be rate-determining,[11] and that sterically demanding residues at the heteroatom increase the threshold for racemization.

We studied the rate of enantiomerization of racemic arylselenoalkyllithium compounds **5** in [D$_8$]THF/[D$_6$]benzene (6:1) with ^{1}H NMR spectroscopy. The lithium compounds **5** were prepared from the selenoacetal **4** and *tert*-butyllithium at −78 °C. After irradiation of the H1 signal, the

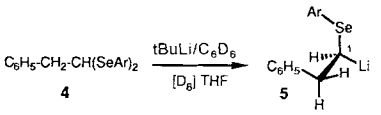

diastereotopic benzylic protons showed an AB pattern in the ^{1}H NMR spectrum, which for **5a**–**5c** coalesced on warming (see Table 1). By applying line-shape analysis (233–313 K),[12] the barrier to racemization for **5a** was calculated to be $\Delta G^{\ddagger}_{275} = 12.4$ kcal mol^{-1} ($\Delta H^{\ddagger} = 11.9 \pm 0.3$ kcal mol^{-1}, $\Delta S^{\ddagger} = -2.5 \pm 1.3$ cal K^{-1} mol^{-1}). We

Table 1. Topomerization of the diastereotopic benzylic protons in **5**.

5	Ar =	Δν [Hz]/T [K]	T_c [K]	$\Delta G^{\ddagger}$ [kcal mol^{-1}]
a	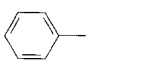	248/233	273	12.4 [a]
b	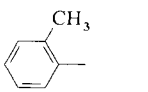	269/223	278	12.7 [b]
c	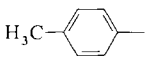	230/223	268	12.3 [b]
d	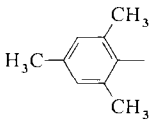	56/213	> 273	> 14.3 [b]
e	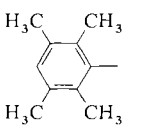	35/223	> 293	> 14.5 [b]

[a] Determined by line-shape analysis (QUABEX [12]). [b] Estimated from the coalescence temperature T_c.

deduce that **5** exists as a contact ion pair,[13] because the ^{13}C NMR spectrum of the doubly labeled 1-^{13}C, ^{6}Li-**5a** shows $^{6}Li/^{13}C$ coupling. The $^{6}Li/^{6}Li$ exchange, the rate of which is concentration-dependent, can be followed in this doubly labeled system (see ref. [7]). This process is not coupled to racemization, the rate of which does not change on altering the concentration by up to a factor of 3. The racemization of **5a** is therefore first order, in contrast to that of secondary alkyllithium compounds.[8] The extent of aggregation of a 0.15 M solution of **5a** in THF was cryoscopically determined to be 1.04 ± 0.07 at $-108\,^{\circ}C$.

The barriers to rotation scarcely altered on changing the solvent to $[D_{10}]Et_2O$ ($\Delta G^{\ddagger}_{278} = 12.7\ kcal\,mol^{-1}$, $\Delta H^{\ddagger} = 10.9 \pm 0.4\ kcal\,mol^{-1}$, $\Delta S^{\ddagger} = -6.3 \pm 1.5\ cal\,K^{-1}\,mol^{-1}$) or on addition of 1.1 equivalents of pentamethyldiethylenetriamine ($\Delta G^{\ddagger}_{275} = 12.4\ kcal\,mol^{-1}$).

At this stage it was not possible to conclude from the data whether step (1), the dissociation of lithium from carbon, an ion-pair reorganization step, was rate-determining. The magnitude of the activation barriers of processes of this type are known,[14] but more negative values ($-15\ cal\,K^{-1}\,mol^{-1}$) were reported for the entropy of activation.

Could step (2), the inversion at carbon, be rate-determining? Ab initio calculations[15] for pyramidal sulfur-substituted carbanions gave inversion barriers of approximately $3\ kcal\,mol^{-1}$. This value is well below the barrier to racemization determined for **5**. Carbanion inversion could show an α-deuterium isotope effect; for example the analogous nitrogen inversion in $(CH_3)_2ND$ has an isotope effect k_H/k_D of 24,[16] which indicates a tunnel effect. We therefore studied the isotope effect of the racemization of **5a** but found no effect, within experimental error, with 1-deuterio-**5a** ($0.87 < k_H/k_D < 1.3$). This also suggests that inversion is not the rate-determining step of racemization of **5a**.

Therefore attention is focused on the rotational step (3). This should be affected by steric hindrance. Accordingly the aryl group (Ar) bonded to selenium was varied. The results in Table 1 show that the barrier to rotation is not affected by *one* methyl group in an *ortho* or para position in the aryl moiety, but that *two ortho* methyl groups raise the rotational barrier by more than $2\ kcal\,mol^{-1}$. This may be understood if the rate-determining step, based on Scheme 1, is the rotation about the C1–Se bond (cf. **6**). In the case of **5d** and **5e** a methyl group in the *ortho* position *must* come into contact with H1.[17]

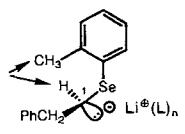

6

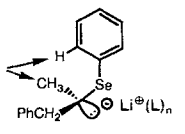

7

$\Delta G^{\ddagger}_{253} > 12.9\ kcal\,mol^{-1}$

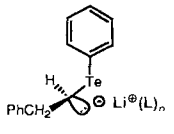

8

$\Delta G^{\ddagger}_{248} = 11.6\ kcal\,mol^{-1}$

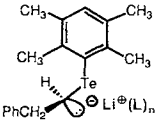

9

$\Delta G^{\ddagger}_{285} = 14.1\ kcal\,mol^{-1}$

The same steric hindrance should occur when the positions of CH_3 and H marked with arrows in **6** are interchanged. Therefore we studied the system **7**, in which no coalescence of the signals due to the diastereotopic benzylic protons within the stability range ($T < -20\,^{\circ}C$) was observed.

These results strongly suggest that, at least in **5d**, **5e**, and **7**, the rate-determining step for racemization is rotation about the C1–Se bond.[18] We can only speculate that the same may be true for compounds **5a**–**5c**. The exact fate of the lithium cation after leaving the carbon atom is still unclear. It could be coordinated to the heteroatom during the change in configuration of the carbanion system or form a solvent-separated ion pair.

The extent of the substituent-induced hindrance to rotation on the enantiomerization of **1** should also be dependent on the length of the C–X bond. This is evident on going to the analogous tellurium compounds **8** and **9**, in which the topomerization barriers calculated from the coalescence temperatures are 11.6 and 14.1 $kcal\,mol^{-1}$. If these rotational barriers crucial for the racemization are raised by $2.5\ kcal\,mol^{-1}$ or more by *ortho* substitution in an aryltellurium compound, the substituent effects in arylselenium compounds should be more pronounced. Accordingly we expect a substantial increase in the configurational stability of mesitylthio- or durylthio-substituted alkyllithium compounds.

Received: May 7, 1993 [Z 6065 IE]
German version: *Angew. Chem.* **1993**, *105*, 1487

[1] a) W. N. Setzer, P. von R. Schleyer, *Adv. Organomet. Chem.* **1985**, *24*, 353–451; b) D. Seebach, *Angew. Chem.* **1988**, *100*, 1685–1715; *Angew. Chem. Int. Ed. Engl.* **1988**, *27*, 1624; c) G. Boche, *ibid.* **1989**, *101*, 286–306 and **1989**, *28*, 277–297.

[2] a) P. von R. Schleyer, *Pure Appl. Chem.* **1984**, *56*, 151–162; b) P. von R. Schleyer, T. Clark, A. J. Kos, G. W. Spitznagel, C. Rohde, D. Arad, K. N. Houk, N. G. Rondan, *J. Am. Chem. Soc.* **1984**, *106*, 6467–6475.

[3] a) D. Seebach, R. Hässig, J. Gabriel, *Helv. Chim. Acta* **1983**, *66*, 308–337; b) O. Eppers, H. Günther, *ibid.* **1992**, *75*, 2553–2562.

[4] H. J. Reich, D. P. Green, *J. Am. Chem. Soc.* **1989**, *111*, 8729–8731.

[5] R. Hirsch, R. W. Hoffmann, *Chem. Ber.* **1992**, *125*, 975–982, and references therein.

[6] a) T. Clark, P. von R. Schleyer, J. A. Pople, *J. Chem. Soc. Chem. Commun.* **1978**, 137–138; b) E. Kaufmann, K. Raghavachari, A. E. Reed, P. von R. Schleyer, *Organometallics* **1988**, *7*, 1597–1607.

[7] J. Heinzer, J. F. M. Oth, D. Seebach, *Helv. Chim. Acta* **1985**, *68*, 1848–1862.

[8] H. J. Reich, M. A. Medina, M. D. Bowe, *J. Am. Chem. Soc.* **1992**, *114*, 11003–11004.

[9] J. M. Lehn, G. Wipff, J. Demuynck, *Helv. Chim. Acta* **1977**, *60*, 1239–1246, and references therein.

[10] H. J. Reich, M. D. Bowe, *J. Am. Chem. Soc.* **1990**, *112*, 8994–8995.

[11] a) H.-J. Gais, G. Hellmann, H. Günther, F. Lopez, H. J. Lindner, S. Braun, *Angew. Chem.* **1989**, *101*, 1061–1063; *Angew. Chem. Int. Ed. Engl.* **1989**, *28*, 1025; b) H.-J. Gais, S. Hellmann, *J. Am. Chem. Soc.* **1992**, *114*, 4439–4440.

[12] G. Binsch, *Top. Stereochem.* **1967**, *3*, 97–192.

[13] H. J. Reich, R. R. Dykstra, *J. Am. Chem. Soc.* **1993**, *115*, 7041–7042.

[14] G. Fraenkel, J. A. Cabral, *J. Am. Chem. Soc.* **1993**, *115*, 1551–1557, and references therein.

[15] W. Zarges, M. Marsch, K. Harms, W. Koch, G. Frenking, G. Boche, *Chem. Ber.* **1991**, *124*, 543–549.

[16] J. E. Wollrab, V. W. Laurie, *J. Chem. Phys.* **1968**, *48*, 5058–5066; cf. also J. D. Swalen, J. A. Ibers, *ibid.* **1962**, *36*, 1914–1918; C. C. Costain, G. B. B. M. Sutherland, *J. Phys. Chem.* **1952**, *56*, 321–324.

[17] MNDO calculations for the rotation about the aryl–Se bond and the C1–Se bond in the corresponding carbanion **2** of **5** show that the aryl ring tends to stay coplanar with the C1–Se bond during rotation about the C1–Se bond, that is, it doesn't spontaneously turn.

[18] H. J. Reich, R. R. Dykstra, *Angew. Chem.* **1993**, *105*, 1489; Angew. Chem. **1993**, *32*, 1469. This study of other α-heterosubstituted alkyllithium compounds likewise suggests that rotation about the carbanion-heteroatom bond could be rate-limiting in racemization. We thank Prof. H. J. Reich for advance information.

Effects of Ion Pair Separation on Inversion and Rotation of Sulfur-, Selenium-, and Silicon-Stabilized Organolithium Reagents**

By *Hans J. Reich** and *Robert R. Dykstra*

Most vinyl,[1] cyclopropyl,[2] and α-alkoxy[3] lithium reagents are configurationally stable. Other types racemize too rapidly for trapping experiments[4a, 5] or require very low temperatures to avoid rapid equilibration.[4a, 6] Advances in the utility of chiral organolithium reagents depend on detailed structural information[7] and mechanistic understanding of their racemization. One limiting mechanism for organolithium reagent epimerization is a bimolecular associative process through intermediate **1**.[4b] An alternative ion pair dissociation process via **2** has been frequently proposed since polar solvents usually accelerate racemization,[1a, 2a, 6a] but this has not been directly testable since the ion pair status of most organolithium reagents is not known. Our hexamethylphosphoric triamide (HMPA) titration technique[4c, d, 8] addresses this problem by allowing the unequivocal identification of contact and separated ion pairs. The correlation between ion pair structure and inversion barriers for several organolithium reagents can now be established.

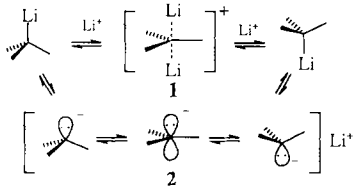

We selected compounds **3**[9] and **4** for detailed study. These and related compounds are valuable reagents[10] that are easily prepared and stable in polar solvents. The presence

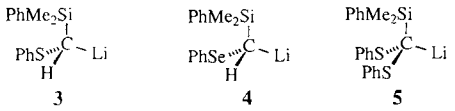

of several NMR-active nuclei (^{1}H, ^{13}C, ^{7}Li, ^{29}Si, and ^{77}Se) facilitates careful NMR investigations. Figure 1 shows the results of an HMPA titration of **3**. The ^{7}Li, ^{31}P, and ^{13}C data, as well as other spectra not shown, indicate that in THF **3** is a contact ion pair ($^1J_{Li\text{-}C}$ = 18.5 Hz) with a pyramidal carbanion center ($^1J_{C\text{-}H}$ = 132 Hz,[7, 11] $^1J_{C\text{-}Si}$ = 75 Hz).[9] The dimethyl(phenyl)silyl group served as a probe and indicated the configurational equilibration of **3**; below −100 °C **3** is chiral on the NMR timescale. The adduct **3** · 1 HMPA is also a pyramidal ($^1J_{C\text{-}H}$ = 136 Hz, $^1J_{C\text{-}Si}$ = 85 Hz), chiral contact ion pair ($^1J_{C\text{-}Li}$ = 14.4 Hz). After the addition of three equivalents of HMPA, **3** is a fully solvent-separated ion pair, as shown by the characteristic $R^-//Lih_3^+$ quartet and

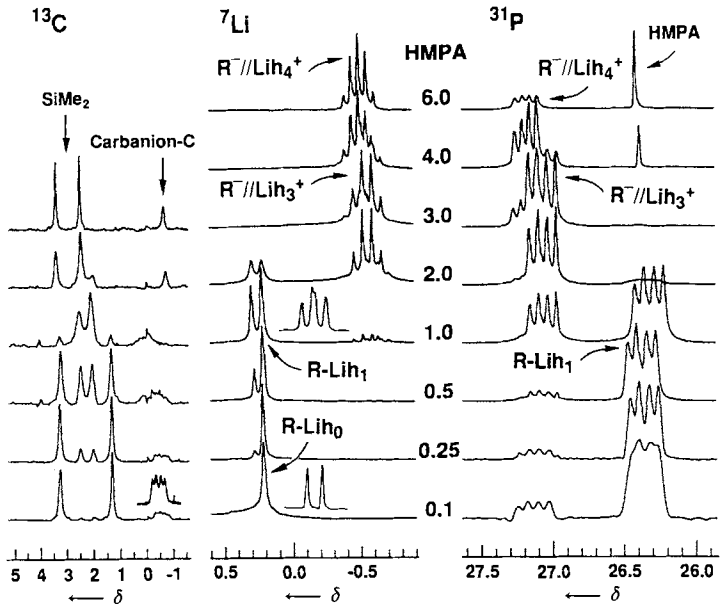

Fig. 1. ^{13}C, ^{7}Li, and ^{31}P NMR spectra of an HMPA titration of **3** in a 3:2 mixture of THF/ether at −121 °C. The insets show spectra from a ^{13}C-enriched sample (h = HMPA, // = solvent-separated ion pair).

$R^-//Lih_4^+$ quintet in the ^{7}Li NMR spectra and absence of coupling between lithium and carbon. Formation of separated ion pairs did not result in the loss of diastereotopicity of the $SiMe_2$ group even though increases in $^1J_{C\text{-}H}$ from 136 to 148 Hz and $^1J_{C\text{-}Si}$ from 85 to 106 Hz[4e] indicate significant planarization at the carbanion center.

Variable-temperature ^{13}C NMR spectra of **3** in THF, THF/1HMPA, and THF/3HMPA are shown in Figure 2. In THF, coalescence is observed at −100 °C and in THF/1HMPA at −112 °C. The slight lowering of the barrier on

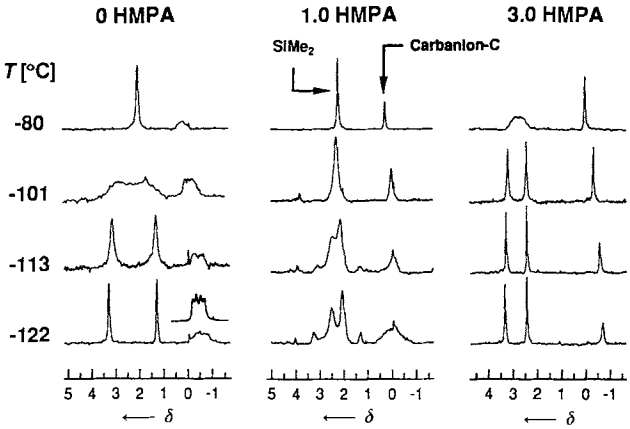

Fig. 2. Variable-temperature ^{13}C NMR spectra of **3** in a 3:2 mixture of THF/ether after addition of 0, 1, and 3 equiv of HMPA.

coordination to HMPA ($\Delta G^{\neq}$ = 8.0 to 7.8 kcal mol^{-1} for **3**, 8.2 to 7.8 kcal mol^{-1} for **4**) would seem to indicate that inversion of the pyramidal structure is accelerated by the strong donor ligand HMPA which loosens C–Li coordination. One might, therefore, expect an even lower barrier for the separated ion pair. The separated ion pair, however, racemizes more slowly (approximately 1/20 as fast at −101 °C)

[*] Prof. Dr. H. J. Reich, R. R. Dykstra
Department of Chemistry, University of Wisconsin
Madison, WI 53706 (USA)
Telefax: Int. code + (608)265-4534

[**] This work was supported by the U.S. National Science Foundation.

with a coalescence temperature above $-80\,^{\circ}C$ ($\Delta G^{\ddagger}$ = 9.1 kcal mol^{-1} for **3**, 9.5 kcal mol^{-1} for **4**). The separation of the ion pair (formation of **2**) cannot be the rate-determining step for the racemizaton of **3** and **4**. These data cannot easily be explained by an inversion process but fit well for rotation. Similar conclusions have been reached by R. W. Hoffmann et al. in a study of arylseleno- and aryltelluro-substituted alkyllithium reagents.[12] Barriers to rotation in carbanions have origins in stabilizing n-σ^* interactions when the carbanion lone pair is aligned with the S–Ph or Si–R bonds, and destabilizing repulsions between lone pairs when the carbanion is not aligned.[13] Such interactions should be stronger in a free carbanion than in a contact ion pair. When the carbanion C atom rotates away from the favored orientation, the charge density on the C atom must increase. This extra charge is more effectively stabilized by lithium in a contact rather than in a separated ion pair.

The racemization of **3** in THF is independent of concentration (0.04 to 0.64 M). In addition, the presence of 1 mol equiv of the separated ion pair lithium fluorenide[4d] had no effect on the racemization rate, so the reaction does not involve intermediate **1**. Since lithium fluorenide did lower the coalescence temperature for loss of Li-C coupling from -92 to $-112\,^{\circ}C$, Li–Li exchange may be intermolecular.

The complex behavior of **3** and **4** prompted us to examine a system in which there is no ambiguity between inversion and rotation. The organolithium reagent **5** is achiral in the absence of rotational barriers even if inversion is slow. We studied this compound, as well as the related PhS(PhSe)CLiSiMe$_2$Ph (**6**). Both are largely separated ion pairs in THF as well as in THF/HMPA, and both show diastereotopic SiMe$_2$ groups up to at least $-20\,^{\circ}C$. For **5** in a 1:3 mixture of THF/ether the SiMe$_2$ signals coalescence at $-12\,^{\circ}C$ ($\Delta G^{\ddagger}$ = 13.3 kcal mol^{-1}), whereas for **6** in a 3:2 mixture of THF/ether coalescence is reached at $7\,^{\circ}C$ ($\Delta G^{\ddagger}$ = 14.3 kcal mol^{-1}). The measured barrier probably corresponds to rotation about the C–S bond, which converts the chiral conformation of **5** to the achiral.

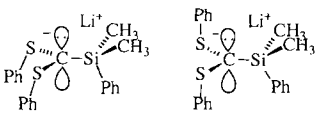

5

These findings provide a basis for understanding one odd facet of the behavior of **3**: the racemization barrier of the separated ion pair *increased* as more HMPA was added (T_c = $-98\,^{\circ}C$ at 2 equiv of HMPA, $-79\,^{\circ}C$ at 3 equiv, and $-75\,^{\circ}C$ at 6 equiv). This suggests that the racemization of the separated ion pair R$^-$//Lih$_3^+$ might actually proceed via the contact ion pair. If the rotation barrier for the separated ion pair **3** is as high as those measured for **5** and **6**, then a mechanism involving recoordination of lithium to carbon (accompanied by loss of one or more coordinated HMPA molecules) explains the rate-retarding effect of high HMPA concentrations. Clearly, the racemization is mechanistically complex. A coupled inversion–rotation process fits our data: the inversion is more significant for the contact ion pair in THF, and rotation dominates for the (probably planar) solvent-separated ion pair in THF/HMPA. We envision a mechanism in which lithium coordination to S or Se allows the lithium to move from one face of the carbanion to the other without separation of the ion pair. Coupled rotation–inversion processes have been extensively studied for sulfenamides, which are isoelectronic with phenythiocarbanions.[14]

Substantial rotation barriers have been reported for lithiated sulfones,[6d, 15] in which lithium coordinates to oxygen, but not for lithiated sulfides, selenides, or silanes.[12] However, the strong preference of Li for the equatorial position in dithianes[16] is equivalent to high rotation barriers in acyclic systems. The observation of a diastereotopic CH$_2$ group in the tetramethylethylenediamine (TMEDA) adduct of Ph$_2$PCH$_2$Li ($\Delta G^{\ddagger}$ = 7 kcal mol^{-1}),[17] interpreted as indicating a barrier to inversion, implies that there is a significant rotation barrier associated with C–P bonds as well. The relatively high epimerization barriers of α-lithio selenides,[4a, 6a] sulfides,[4a, 5] amines,[6b] and ethers[3] take on a new perspective with this information.

Received: May 12, 1993 [Z 6081 IE]
German version: *Angew. Chem.* **1993**, *105*, 1489

[1] a) E. J. Panek, B. L. Neff, H. Chu, M. G. Panek, *J. Am. Chem. Soc.* **1975**, *97*, 3996; R. Knorr, E. Lattke, *Tetrahedron Lett.* **1977**, 3969; b) D. Seyferth, L. G. Vaughan, *J. Am. Chem. Soc.* **1964**, *86*, 883; H. Neumann, D. Seebach, *Chem. Ber.* **1978**, *111*, 2785.

[2] a) G. Köbrich, D. Merkel, K. Imkampe, *Chem. Ber.* **1973**, *106*, 2017; b) D. E. Applequist, A. H. Peterson, *J. Am. Chem. Soc.* **1961**, *83*, 862; H. M. Walborsky, F. J. Impastato, A. E. Young, *ibid.* **1964**, *86*, 3283.

[3] W. C. Still, C. Sreekumar, *J. Am. Chem. Soc.* **1980**, *102*, 1201; D. Hoppe, F. Hintze, P. Tebben, *Angew. Chem.* **1990**, *102*, 1457; *Angew. Chem. Int. Ed. Engl.* **1990**, *29*, 1422.

[4] For previous papers see: a) H. J. Reich, M. D. Bowe, *J. Am. Chem. Soc.* **1990**, *112*, 8994; b) a bimolecular mechanism has been reported for a cyclohexyllithium derivative: H. J. Reich, M. A. Medina, M. D. Bowe, *ibid.* **1992**, *114*, 11003; c) H. J. Reich, D. P. Green, *ibid.* **1989**, *111*, 8729; d) H. J. Reich, J. P. Borst, *ibid.* **1991**, *113*, 1835; e) H. J. Reich, R. R. Dykstra, *ibid.* **1993**, *115*, 7041.

[5] P. G. McDougal, B. D. Condon, *Tetrahedron Lett.* **1989**, *30*, 789.

[6] a) Selenides: R. W. Hoffmann, M. Julius, K. Oltmann, *Tetrahedron Lett.* **1990**, *31*, 7419; A. Krief, G. Evrard, E. Badaoui, V. de Beys, R. Dieden, *ibid.* **1989**, *30*, 5635; b) amines: W. H. Pearson, A. C. Lindbeck, *J. Am. Chem. Soc.* **1991**, *113*, 8546; S. T. Kerrick, P. Beak, *ibid.* **1991**, *113*, 9708; c) bromides: R. W. Hoffmann, T. Ruhland, M. Bewersdorf, *J. Chem. Soc. Chem. Commun.* **1991**, 195; d) sulfones: H.-J. Gais, G. Hellmann, *J. Am. Chem. Soc.* **1992**, *114*, 4439.

[7] W. N. Setzer, P. von R. Schleyer, *Adv. Organomet. Chem.* **1985**, *24*, 353; R. Amstutz, T. Laube, W. B. Schweizer, D. Seebach, J. D. Dunitz, *Helv. Chim. Acta* **1984**, *67*, 224; G. Boche, *Angew. Chem.* **1989**, *101*, 286; *Angew. Chem. Int. Ed. Engl.* **1989**, *28*, 277.

[8] P. R. Raithby, D. Reed, R. Snaith, D. S. Wright, *Angew. Chem.* **1991**, *103*, 1040; *Angew. Chem. Int. Ed. Engl.* **1991**, *30*, 1011.

[9] H.-J. Gais, J. Vollhardt, C. Krüger, *Angew. Chem.* **1988**, *100*, 1108; *Angew. Chem. Int. Ed. Engl.* **1988**, *27*, 1092.

[10] a) E. Schaumann, C. Friese, *Tetrahedron Lett.* **1989**, *30*, 7033; b) D. J. Ager, M. B. East, *J. Org. Chem.* **1986**, *51*, 3983; J. Otera, Y. Niibo, H. Nozaki, *ibid.* **1989**, *54*, 5003; M. R. Myers, T. Cohen, *ibid.* **1989**, *54*, 1290.

[11] W. Zarges, M. Marsch, K. Harms, W. Koch, G. Frenking, G. Boche, *Chem. Ber.* **1991**, *124*, 543; G. Chassaing, A. Marquet, *Tetrahedron* **1978**, *34*, 1399; D. Seebach, J. Gabriel, R. Hassig, *Helv. Chim. Acta* **1984**, *67*, 1083.

[12] T. Ruhland, R. Dress, R. W. Hoffmann, *Angew. Chem.* **1993**, *105*, 1487; *Angew. Chem. Int. Ed. Engl.* **1993**, *32*, 1467.

[13] J.-M. Lehn, G. Wipff, *Helv. Chim. Acta* **1977**, *60*, 1239; F. Bernardi, A. Bottoni, G. S. Valli, A. Venturini, *Gazz. Chim. Ital.* **1990**, *120*, 301; P. von R. Schleyer, T. Clark, A. J. Kos, G. W. Spitznagel, C. Rohde, D. Arod, K. N. Houk, N. G. Rondan, *J. Am. Chem. Soc.* **1984**, *106*, 6467.

[14] M. Raban, D. Kost, *Tetrahedron* **1984**, *40*, 3345.

[15] H.-J. Gais, G. Hellmann, H. J. Lindner, *Ang. Chem.* **1990**, *102*, 96; *Angew. Chem. Int. Ed. Engl.* **1990**, *29*, 100.

[16] E. L. Eliel, A. A. Hartmann, A. G. Abatjoglou, *J. Am. Chem. Soc.* **1974**, *96*, 1807.

[17] G. Fraenkel, W. R. Winchester, P. G. Williard, *Organometallics* **1989**, *8*, 2308.

The Search for an Isolable Silyl Cation Must Continue**

By *Paul von Ragué Schleyer,* Peter Buzek, Thomas Müller, Yitzhak Apeloig,** and *Hans-Ullrich Siehl**

In a well-publicized new development in the over forty-year search for an isolable R_3Si^+ cation,[1, 2] Lambert, Zhang, Stern, and Huffman[1] reported the "crystal structure of a silyl cation [as the salt **1**] with no coordination to anion and distant coordination to solvent". This claim was based on the use of the very non-nucleophilic $[(C_6F_5)_4B]^-$ anion. However, their crystal structure also included the solvent, toluene, along with the $(C_2H_5)_3Si^+$ moiety. The au-

$Et_3Si[B(C_6F_5)_4]$ **1**

thors argued that the silyl cation and the toluene molecule were not involved in a possible σ complex, since the toluene moiety had a nearly planar geometry and the $Si-C_{(ring)}$ distance (2.18 Å) was relatively long. But two features argued against this interpretation. The SiR_3 moiety was not planar; the average C-Si-C angle was 114°, and the ^{29}Si NMR chemical shift ($\delta = 81.8$, measured in toluene)[1b] deviated considerably from the $\delta = 355$ computed by the IGLO method for planar Me_3Si^+.[3] The authors attributed this discrepancy to pyramidalization of the R_3Si group, which they suggested might result in a more shielded Si chemical shift. They concluded, "This structure, albeit nonplanar, is best termed a stable silyl cation because it entirely lacks coordination to the anion, the distance to the weakly coordinating toluene is unprecedented for bonding, and the toluene lacks any of the geometric characteristics of the σ complex."[4]

We dispute this interpretation and now present decisive evidence that the species observed by the authors is an $[R_3Si-toluene]^+$ σ complex—arenium ion—in which the positive charge is substantially delocalized to the aromatic ring.

Our evidence is based on ab initio calculations[5] of the $[Me_3Si-toluene]^+$ (**2**) and the $[Me_3Si-benzene]^+$ and $[H_3Si-benzene]^+$ (**3**) complexes, which are close models for the $[Et_3Si-toluene]^+$ complex in **1** · toluene. Optimization at the HF/3-21G, HF/3-21G(*), and HF/6-31G* levels were carried out, and, for $[H_3Si-benzene]^+$ (**3**) also at the MP2(fc)/6-31G* level (i.e. with inclusion of electron correlation).[*] All calculations resulted in theoretical geometries which not only are very similar among themselves, but also closely resemble the main features found in the crystal structure of **1** · toluene. Hence, it suffices to show the HF/6-31G* geometry of **2** as well as the MP2(fc)/6-31G* geometry of **3** in Figure 1. The $Si-C_{(ring)}$ separations, the 114° average

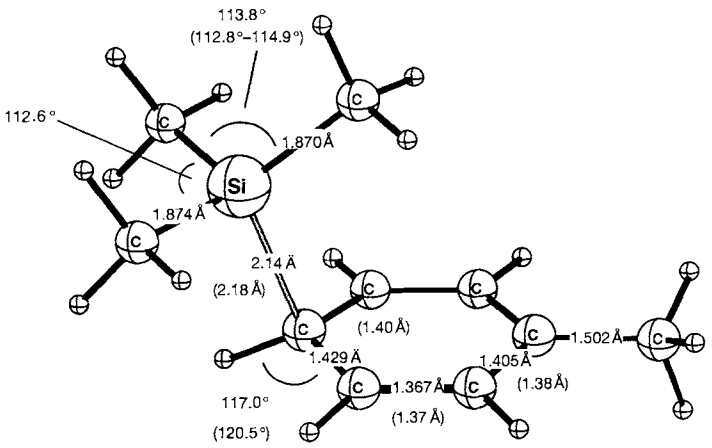

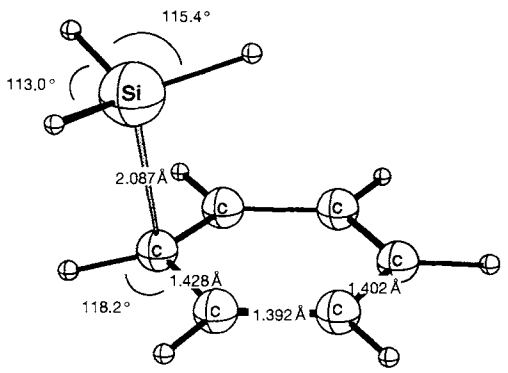

Fig. 1. The geometries of the $[Me_3Si-toluene]^+$ complex (**2**) ($E = -677.31182$ Hartree) and the $[H_3Si-benzene]^+$ complex (**3**) (MP2(fc)6-31G*, $E = -521.94073$ Hartree) determined by ab initio methods. The values for **2** in parentheses show the data from the X-ray structure analysis of **1** · toluene for comparison [1a]. Note the close correspondence of the structure **2** with the calculated structure **3** at the higher theoretical level.

bond angle at silicon in the silyl groups, and the near planarity of the six-membered rings, correspond precisely with those reported for **1** · toluene.[1a] Carbocations are stabilized strongly by vicinal silyl groups.[6, 7] Hence, the *ipso* positions of silyl-substituted arenes have enhanced proton affinities.[8, 9] Cationic Si–C hyperconjugation is also responsible for the $Si-C_{(ring)}$ bond lengths[6] (ca. 2.1 Å) in **2**, **3**, and **1** · toluene. The $C-C^+$ bonds involved in the X-C-C^+ moieties (X = R_3Si) are shortened: compare the $C_{ipso}-C_{ortho}$ separations in **2** (1.429 Å) and **3** (1.426 Å) with that in the ben-

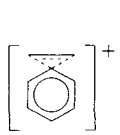

4

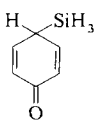

5

[*] Prof. Dr. P. von R. Schleyer, P. Buzek
Institut für Organische Chemie I der Universität Erlangen-Nürnberg
D-91054 Erlangen (FRG)
Telefax: Int. code + (9131)85 91 32
Prof. Dr. Y. Apeloig, Dr. T. Müller
Department of Chemistry
Technion–Israel Institute of Technology
32000 Haifa (Israel)
Telefax: Int. code + (4)233-735
Prof. Dr. Hans-Ullrich Siehl
Institut für Organische Chemie der Universität
Auf der Morgenstelle 18, D-72076 Tübingen (FRG)
Telefax: Int. code + (7071)29-5244

[**] Presented at the Third World Congress, World Association of Theoretical Organic Chemists (WATOC), Toyohashi, Japan, July 27, 1993, and the Tenth International Symposium on Organosilicon Chemistry, Poznan, Poland, August 15–20, 1993. This work was supported by the Deutsche Forschungsgemeinschaft, the Volkswagen-Stiftung, the Fonds der Chemischen Industrie, the Convex Computer Corporation, the Minerva Foundation, the Wolf Fund for the Promotion of the Sciences and the Arts, administered by the Israel Academy of Sciences and Humanities, and by the Alexander Goldberg Memorial Fund (Technion). We also thank Prof. G. A. Olah warmly for a preprint of his related paper which reports the same conclusions.

[*] MP2 = Møller–Plesset perturbation theory second order; fc = frozen core, that is the nonvalence electrons are not correlated.

zenium ion (1.464 Å).[10] Strong bond length alternation in the benzene ring (quinonoid distortions) is not to be expected when strongly hyperconjugating groups are present at the *ipso* position. In $C_8H_9^+$ (**4**), a phenonium ion, in which the positive charge is stabilized by strong hyperconjugative interaction with the strained three-membered ring bonds, the MP2(fc)/6-31G* six-ring C–C distances (1.401 ± 0.018 Å) are all nearly the same.[10]

High-pressure mass spectrometric measurements of silyl cation–arene complexes[8, 9] have established that the binding energies of the Me_3Si cation to benzene, toluene, and other arenes (Table 1) are nearly as large as those for the binding of water (30.1 kcal mol^{-1}) and weaker oxygen bases (e.g. CH_3OH 39.2 kcal mol^{-1}).[11] Direct aromatic substitution and other reactions have established "that σ complex intermediates are formed".[8, 9b] Our computed binding energies, relative to the separated R_3Si^+ and arene species, also summarized in Table 1, agree quite well with the measured values. Although these data pertain to the gas phase, association energies can be expected to be nearly as large in the nonpolar media employed by Lambert et al.[1] in their experiments.

Table 1. Experimental and computed association energies [kcal mol^{-1}] of silyl and *tert*-butyl cations with arenes

Arenium ion	Method	Association energy [a]
$C_6H_6SiH_3^+$	HF/3-21G(*)//3-21G(*)	− 51.1
	HF/6-31G*//6-31G*	− 47.1 [b]
3 (Fig. 1)	MP2(fc)/6-31G*//MP2/(fc)6-31G*	− 54.8 [b]
$C_6H_6SiMe_3^+$	HF/3-21G(*)//3-21G(*)	− 25.2
	HF/6-31G*//6-31G*	− 20.5
	MP2(fc)/6-31G*//HF/6-31G*	− 31.1
	exp.	− 23.9 ± 0.4 [c]
$C_6H_6CMe_3^+$ *ipso* (**6**)	MP2(fc)/6-31G*//HF/6-31G*	− 14.9
para (**8**, R = *t*Bu)	MP2(fc)/6-31G*//HF/6-31G*	− 21.1
	exp.	− (22 ± 2)[d, e]
$4\text{-}CH_3C_6H_5SiMe_3^+$	HF/3-21G(*)//3-21G(*)	− 29.7
2 (Fig. 1)	HF/6-31G*//6-31G*	− 25.1
	MP2(fc)/6-31G*//HF/6-31G*	− 34.2
	exp.	− 28.4 ± 0.4 [f]
$CD_3C_6D_5SiMe_3^+$	exp.	− 31.3 ± 0.3 [f]
$CH_3C_6H_5CMe_3^+$	exp.	− (29.1 ± 0.3)[e, f]
$CD_3C_6D_5CMe_3^+$	exp.	− (28.6 ± 0.8) [e, f]

[a] Zero point energy (ZPE) corrections (computed at HF and scaled by 0.89) are included. [b] The basis set superposition error is 1.97 kcal mol^{-1}, computed by the counterpoise method [5], for $C_6H_6SiH_3^+$ at HF/6-31G*//HF/6-31G*, and 4.72 kcal mol^{-1} at MP2/6-31G* with the same geometry. The other computed association energies may be too high by similar amounts. [c] Ref. [8a]. [d] Ref. [11]. [e] These experimental values refer to lower energy, rearrangement isomers, for example, **8** instead of **7**; see ref. [8b, 9d] and the text. [f] Ref. [8b].

According to natural population analysis[12] of the HF/6-31G* wave functions, the Si–C Wiberg bond index in **3** is 0.44, about half the size of the bond indexes found for the polar covalent Si–C bonds in neutral models, methylsilane (0.82) and phenylsilane (0.77). The positive charge on the six-membered rings is appreciable, +0.29 in **2** and +0.27 in the less strongly bound [Me_3Si–benzene]$^+$ complex. In **3** the complimentary charge on the smaller SiH_3 group is only +0.62. This is only about 36% larger than those in neutral compounds. The charge of the SiH_3 group is +0.49 in the quinoid model (**5**), +0.45 in phenylsilane, and +0.43 in methylsilane.

IGLO chemical shift computations[3d] afford even more dramatic evidence for the consequences of complexation. As has been reported for CH_3^+,[3b] pyramidalization of silyl cations results in even greater deshielding rather than the opposite effect as required by the interpretation by Lambert et al. Thus, an IGLO computation (basis II//HF/6-31G*) on the distorted Me_3Si^+ ion, by using the C-Si-C average bond angle of 114° (cf. X-ray structure from Lambert et al.), results in a ^{29}Si chemical shift of $\delta = 368$, very far from the reported experimental value for $[Et_3SiC_6H_6]^+$ ($\delta = 83.6$ in benzene[1b]). In sharp contrast, an IGLO calculation on the [Me_3Si–benzene]$^+$ complex (dz basis (C,H), basis II (Si)//HF/6-31G*) gives a chemical shift of $\delta(^{29}Si) = 80.9$, in good agreement with the experimental value for $[Et_3SiC_6H_6]^+$.[1b] The same IGLO basis gives a chemical shift of $\delta(^{29}Si) = 60$ for the [Me_3Si–toluene]$^+$ σ-complex (**2**) (HF/6-31G* geometry). These computed ^{29}Si chemical shifts are in line with the trends reported by Lambert and Zhang,[1b] as the association energies to toluene are larger than those to benzene (Table 1).

While carbocations are stabilized more strongly by α- than by β-alkyl groups, just the opposite is true for silyl substituents (see Scheme 1) where β is more effective hyperconjugatively than α attachment.[6, 7, 13, 14] Consequently, *ipso* protonation of silylarenes, that is **7** (R = SiH_3), is preferred thermodynamically, and the resulting arenium ions, like **2** and **3**, do not undergo 1,2-H shifts readily.[8, 9] The bonding and structures of the arenium ions resulting initially from the association of, for example benzene, with Me_3Si^+ (which resembles **2**, Fig. 1) and with Me_3C^+ ($C_6H_6CMe_3^+$ (**6**) Fig. 2) differ considerably. While **6** also has an elongated

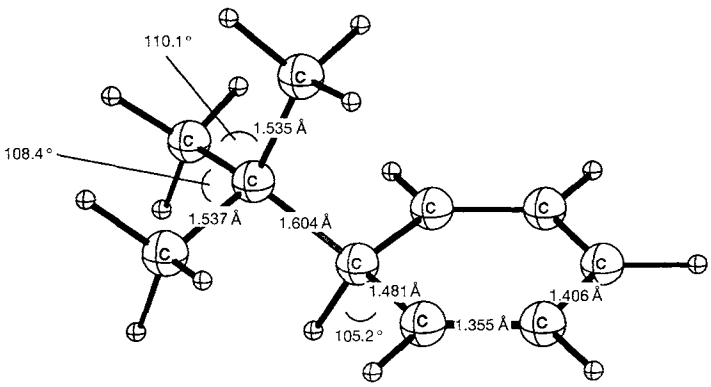

6

Fig. 2. The geometry of the [Me_3C–benzene]$^+$ complex (**6**) (HF/6-31G*, $E = -387.15397$ Hartree) determined by ab initio methods.

bond ($rC-C = 1.604$ Å at HF/6-31G*) between the substituent and the *ipso* carbon, the *tert*-butyl group has nearly tetrahedral C-C-C bond angles and the ring bond lengths show more pronounced alternation. Due to their greater degree of hyperconjugative involvement, silyl groups are bound less covalently than their alkyl counterparts. Hyperconjugation in **2** (and in **3**) results in the Si–$C_{(ipso)}$ bond lengthening and is responsible for the small distortion of the arene geometry as well as the widening of the R-Si-R angles in the R_3Si groups from 109.5° to about 114°.

The energy of the initial association of Me_3C^+ with benzene is much less than that with Me_3Si^+ (cf. the computed data in Table 1), and the same will be true of other arenes. While the carbocation and silyl cation association energies deduced from high-pressure mass spectrometry[10] appear to be comparable (see Table 1), these data refer to different overall reactions. Unlike **2**, the *ipso* species (e.g., **6**) formed

initially from Me_3C^+ and arenes, rearranges during the measurements to isomers (e.g., the *para* species **8** (R = *t*Bu)) in which the alkyl group stabilizes the cyclohexadienyl carbocation more effectively.[8, 9] We compute an exothermic **7** → **8** (R = *t*Bu) isomerization energy of 6.3 kcal mol^{-1} (Scheme 1). When the *tert*-butyl group is replaced by a methyl group, the corresponding *ipso* → *para* isomerization energy **7** → **8** (R = Me) is nearly the same (−7.5 kcal mol^{-1}). In contrast our computations show the *ipso* silyl compound **3** to be 19.5 kcal mol^{-1} more stable than its *para* isomer **8** (R = SiH_3) (Scheme 1). The benzene–SiH_3^+ π com-

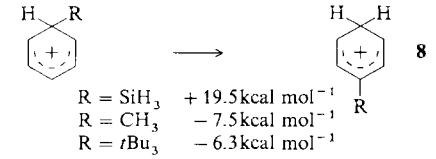

Scheme 1. Relative energies of $C_6H_6R^+$ isomers (MP2(fc)/6-31G*//HF/6-31G* + ZPE for R = *t*Bu and MP2(fc)/6-31G*//MP2(fc)/6-31G* + ZPE for R = SiH_3 and R = CH_3).

plex (**9**) with C_{3v} symmetry which was proposed as a possibility in the early literature,[8a] is even higher in energy, 28.2 kcal mol^{-1} vs **3** at MP2(fc)/6-31G*//MP2(fc)/6-31G*, and, having a degenerate pair of imaginary frequencies, is not a minimum.

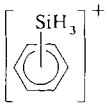

9

We conclude that the $[Et_3Si$–toluene$]^+$ X-ray structure reported by Lambert et al. is that of an arenium ion—a bound σ complex—as are the models we have calculated (see Fig. 1 and Table 1). Benzene and toluene are not weak bases towards silyl cations. These silylarenium ions are similar to the heteroatom-bound complexes described by Reed et al.[4] and the β-silyl-substituted cyclohexadienyl cations of McClelland et al.[15] generated by flash photolysis. Free silyl cations were not detected. Even a modest degree of pyramidalization at silicon is prima facie evidence for complexation, as silyl cations are inherently planar.[13] The search for these elusive species must continue.

Received: July 15, 1993
Revised version: August 23, 1993 [Z 6216 IE]
German version: *Angew. Chem.* **1993**, *105*, 1558

[1] a) J. B. Lambert, S. Zhang, C. L. Stern, J. C. Huffman, *Science* **1993**, *260*, 1917; see J. Haggin, *Chem. Eng. News* **1993**, *71* (26), 7; b) J. B. Lambert, S. Zhang, *J. Chem. Soc. Chem. Commun.* **1993**, 383; c) F. C. Whitmore, L. H. Sommer, J. Gold, *J. Am. Chem. Soc.* **1947**, *69*, 1967; F. R. Price, *ibid.* **1948**, *70*, 871; C. G. Swain, R. M. Esteve Jr., R. H. Jones, *ibid.* **1949**, *71*, 65.

[2] a) For leading references [3c, 4, 10, 13] and J. B. Lambert, W. J. Schultz, Jr. in *The Chemistry of Organic Silicon Compounds* (Eds.: S. Patai, Z. Rappoport), Wiley, Chichester, **1989**, Part 2; Chap. 16, 1007; b) P. D. Lickiss, *J. Chem. Soc. Dalton Trans.* **1992**, 1333; c) C. Eaborn, *J. Organomet. Chem.* **1991**, *405*, 173; d) G. A. Olah, L. Heiliger, X. Y. Li, G. K. S. Prakash, *J. Am. Chem. Soc.* **1990**, *112*, 5991.

[3] a) W. Kutzelnigg, U. Fleischer, M. Schindler, *NMR Basic Princ. Prog.* **1990**, *23*, 165; b) Table 24 in [3a]; c) G. A. Olah, G. Rasul, L. Heiliger, J. Bausch, G. K. S. Prakash, *J. Am. Chem. Soc.* **1992**, *114*, 7737. d) All the reported calculated chemical shifts are relative to TMS.

[4] A closely related X-ray structure involving iPr_3Si complexes, for example with the very non-nucleophilic $Br_5CB_9H_5$ anion also had similar features (long SiBr bond, 115.8(2.0)° average C-Si-C bond angles, and $\delta(^{29}Si) = 97.9$), but was interpreted as having "about one third silylenium ion character". Z. Xie, D. J. Liston, T. Jelínek, V. Mitro, R. Bau, C. A. Reed, *J. Chem. Soc. Chem. Commun.* **1993**, 384.

[5] GAUSSIAN 92: M. J. Frisch, G. W. Trucks, M. Head-Gordon, P. M. W. Gill, M. W. Wong, G. B. Foresman, B. G. Johnson, H. B. Schlegel, M. A. Robb, E. S. Replogle, R. Gomperts, J. L. Andres, K. Raghavachari, J. S. Binkley, C. Gonzalez, R. L. Martin, D. J. Fox, D. J. Defrees, J. Baker, J. J. P. Stewart, J. A. Pople, Gaussian Inc., Pittsburgh, PA, **1992**; b) W. Hehre, L. Radom, P. von R. Schleyer, J. A. Pople, *Ab Initio Molecular Orbital Theory*, Wiley, New York, **1986**.

[6] Cf. a) M. R. Ibrahim, W. L. Jorgensen, *J. Am. Chem. Soc.* **1989**, *111*, 819; b) H. Vančik, K. Percac, P. Buzek, P. von R. Schleyer, *ibid.*, submitted.

[7] a) H.-U. Siehl, F.-P. Kaufmann, Y. Apeloig, V. Braude, D. Danovich, A. Berndt, N. Stamatis, *Angew. Chem.* **1991**, *103*, 1546; *Angew. Chem. Int. Ed. Engl.* **1991**, *30*, 1479; b) H.-U. Siehl, F.-P. Kaufmann, *J. Am. Chem. Soc.* **1992**, *114*, 4937; c) H.-U. Siehl, F.-P. Kaufmann, K. Hori, *ibid.* **1992**, *114*, 9343.

[8] a) A. C. M. Wojtyniak, J. A. Stone, *Int. J. Mass Spectrum. Ion Processes* **1986**, *74*, 59 (see particularly Table 6 in this paper); b) J. M. Stone, J. A. Stone, *ibid.* **1991**, *109*, 247.

[9] a) F. Cacace, *Acc. Chem. Res.* **1988**, *21*, 215; b) S. Fornarini, *J. Org. Chem.* **1988**, *53*, 1314; c) F. Cacace, M. E. Crestoni, S. Fornarini, R. Gabrielli, *Int. J. Mass Spectrom. Ion Processes* **1988**, *84*, 17; d) F. Cacace, M. E. Crestoni, G. De Petris, S. Fornarini, F. Grandinetti, *Can. J. Chem.* **1988**, *66*, 3099. This paper reports partially optimized STO-3G computations on $C_6H_6SiMe_3^+$ and other arene ions. e) M. Attina, F. Cacace, A. Ricci, *J. Am. Chem. Soc.* **1991**, *113*, 5937; f) M. Attina, F. Cacace, *Int. J. Mass Spectrom. Ion Processes* **1992**, *120*, R1; g) F. Cacace, M. E. Crestoni, S. Fornarini, *J. Am. Chem. Soc.* **1992**, *114*, 6776.

[10] S. Sieber, P. von R. Schleyer, J. Gauss, *J. Am. Chem. Soc.* **1993**, *115*, 6987. In the C_{2v} MP2/6-31G* geometry of the parent benzenium ion ($C_6H_7^+$, protonated benzene), the C–C bond lengths (1.464 Å) to the methylene carbon atom are longer than in **3**, reflecting the strong C–Si hyperconjugation in the latter. We consider the crystallographic σ-complex model Lambert et al. employed (**I**, NR'_2 = pyrrolidinio, R = Me, F. Effenberger, F. Reisinger, K. H. Schönwälder, P. Bäuerle, J. J. Stezowski, K. H. Jogun, K. Schöllkopf, and W.-D. Stohrer, *J. Am. Chem. Soc.* **1987**, *109*, 882) to be inappropriate because of the strong stabilization by three π-donating amino substituents at all *ortho* and *para* positions.

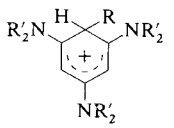

I

[11] D. K. Sen Sharma, S. Ikuta, P. Kebarle, *Can. J. Chem.* **1982**, *60*, 2325.

[12] A. R. Reed, L. A. Curtiss, F. H. Weinhold, *Chem. Rev.* **1988**, *88*, 899.

[13] Y. Apeloig, *The Chemistry of Organic Silicon Compounds* (Eds.: S. Patai, Z. Rappoport), Wiley, Chichester, **1989**, Part 1, p. 184.

[14] a) Y. Apeloig, A. Stanger, *J. Am. Chem. Soc.* **1985**, *107*, 2806; Y. Apeloig, R. Biton, A. Abu-Freih, *ibid.* **1993**, *115*, 2522.

[15] C. S. Lew, R. A. McClelland, *J. Am. Chem. Soc.* **1993**, *115*, in press.

Non-Twisted Tetrakis(organosilyl)ethene**

By *Masahiro Murakami, Michinori Suginome, Kenzo Fujimoto,* and *Yoshihiko Ito**

The change in the positions of the electronic transitions of organic chromophores caused by structural deviation and/or heteroatom-substitution has been a subject of continuing interest. Mono- or bis(organosilyl) ketones are some of the most extensively studied compounds owing to the marked bathochromic shift of the n → π* transition.[1] Tetrakis(organosilyl)ethenes **1**, synthesized by Sakurai et al., possess unusual properties.[2, 3] The compounds exhibit weak ab-

[*] Prof. Dr. Y. Ito, Dr. M. Murakami, Dr. M. Suginome, K. Fujimoto
Department of Synthetic Chemistry
Faculty of Engineering, Kyoto University
Yoshida, Kyoto 606-01 (Japan)

[**] We thank Prof. E. Nakamura and Dr. S. Yamago (Tokyo Institute of Technology) for carrying out experiments under high pressure. We also thank Dr. C. Katayama and Mr. H. Inoue (MAC Science) for collecting the diffraction data at low temperature.

sorptions at 341–434 nm together with strong $\pi \rightarrow \pi^*$ transitions in their UV spectra, and all but **1a** twist along the C–C double bond to yield a dihedral angle of between 30° and 53° in order to relieve a steric repulsion between the organosilyl groups. We now report an intramolecular bissilylation reaction under pressure leading to the efficient synthesis of a new cyclic tetrakis(organosilyl)ethene, which exhibits an analogous absorption behavior despite the non-twisted structure.

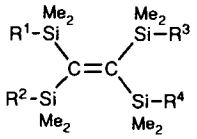

1a: $R^1 = R^2 = R^3 = R^4 = H$
1b: $R^1 = R^2 = R^3 = R^4 = Me$
1c: $R^1 = R^2 = Me$, $R^3 = R^4 = t\text{Bu}$
1d: $R^1 = R^3 = Me$, $R^2 = R^4 = t\text{Bu}$
1e: $R^1 = Me$, $R^2 = R^3 = R^4 = t\text{Bu}$

We reported recently that a catalyst of $[Pd(OAc)_2]$/*tert*-alkyl isocyanide effectively promotes the bissilylation of C–C triple bonds and that the intramolecular version renders it possible to bissilylate otherwise unreactive internal alkynes.[4] This method was next applied to 1,2-bis(organosilyl)alkyne **2** in which one organosilyl substituent is tethered to a disilanyl group (Scheme 1). Although sluggish under

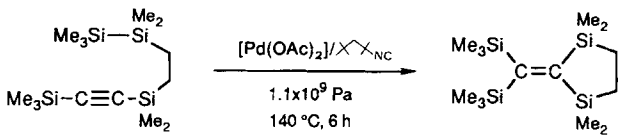

2 **3**

Scheme 1. Synthesis of **3** by an intramolecular bissilylation under high pressure.

atmospheric pressure, the bissilylation reaction did take place on heating **2** under high pressure (1.1×10^9 Pa) at 135–140 °C in the presence of $[Pd(OAc)_2]$/*tert*-alkyl isocyanide to afford a new tetrakis(organosilyl)ethene **3**, in which one of the olefinic carbon atoms is part of a heterocycle, in 66% yield.[5] Recrystallization of **3** from ethanol provided colorless crystals. When dissolved, however, **3** was slightly yellow at room temperature. Notably, in hexane the cyclic **3** exhibits UV absorptions at 228 nm ($\varepsilon = 16800$) and 361 nm ($\varepsilon = 160$), very close to those of the acyclic tetrakis(trimethylsilyl)ethene **1b** [224 nm ($\varepsilon = 17900$), 370 nm ($\varepsilon = 710$)].[2]

Next, the single crystal was subjected to X-ray crystallographic study (Fig. 1).[6] In marked contrast to the acyclic tetrakis(organosilyl)ethenes **1b–e**, neither twisting nor pyramidalization of the sp^2 carbons was observed. The four silicon atoms of **3** lie almost in a plane. The angle between the planes Si1-C11-Si2 and Si3-C12-Si4 is 3.9°. Although small, the twisting increases the intramolecular repulsive interactions; for example, the distance between C5 and C16 is only 329 pm, about 18% less than the sum of the van der Waals radii of two methyl groups (400 pm, Fig. 1c). Noteworthy is that the angle Si3-C12-Si4 is exceedingly narrow (102.72(7)°) to bring Si3 and Si4 as close as 299 pm, due to the constraints imposed by the 5-membered ring. It is conceivable that this narrow angle leads to the tolerable nonbonded distances between the peripheral methyl groups on the non-twisted C=C backbone.[7] The C=C and Si–C_{sp^2} bonds (137 and 191–192 pm, respectively) are longer than standard ones and these lengths agree well with those of the acyclic tetrakis(organosilyl)ethenes **1**.

The origin of the weak absorptions that were observed in the region of 341–434 nm with all tetrakis(organosilyl)-

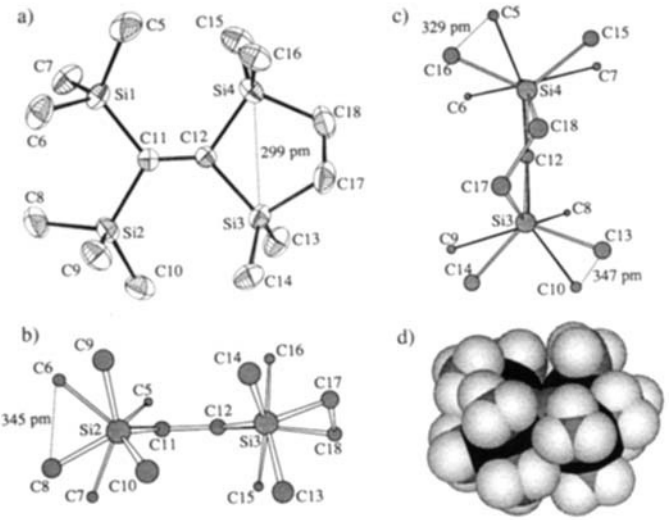

Fig. 1. Single crystal X-ray structure of **3**. Hydrogens are omitted for clarity in (a)–(c). (a) Top view (40% probability ellipsoids); b) front view; c) side view; d) space-filling model. Selected distances [pm] and angle [°]: Si1–Si2 316.65(7), Si1–Si4 364.92(7), Si2–Si3 362.80(7), C6–C9 365.0(4), C7–C8 350.7(4); Si1–C11–Si2 111.79(8).

ethenes **1** and **3** is of much interest.[8] One important deduction from a comparison of the UV spectra and crystal structures of **1** and **3** is that the weak UV absorption of tetrakis(organosilyl)ethenes is not necessarily a result of structural twisting but of the substitution with silicon. For comparison, UV spectra of tris(trimethylsilyl)ethene (**4**)[9] and 1,2-bis(trimethylsilyl)ethene (**5**) were measured; **4** absorbs at 293 nm ($\varepsilon = 690$), whereas **5** exhibits a small peak around 220 nm on the shoulder of the strong $\pi \rightarrow \pi^*$ transition [215 nm ($\varepsilon = 14000$)]. These results reveal that more silicon

4 **5**

substituents at an olefinic skeleton shift the absorption to longer wavelength. Although more precise theoretical treatment is awaited, the present experimental studies indicate that the fourfold substitution with silyl groups primarily causes the bathochromic shift of the weak absorption of tetrakis(organosilyl)ethenes.[10]

Experimental Procedure

2: To (trimethylsilyl)ethyne (3.2 g, 33 mmol) in THF (20 mL) at room temperature was slowly added MeMgBr (22 mmol) in ether. After evolution of methane ceased, 1,1,4,4,5,5-hexamethyl-1,4,5-trisilahexyl chloride (2.7 g, 11 mmol), prepared by the platinum-catalyzed hydrosilylation reaction of vinylpentamethyldisilane with chlorodimethylsilane, was added. The mixture was stirred for 2 h at room temperature, then diluted with a saturated aqueous solution of NH_4Cl, extracted with ether, and distilled to afford **2** (3.2 g, 92%). B.p. 142–143 °C/20 Torr; ^{1}H NMR ($CDCl_3$): $\delta = 0.02$ (s, 6H), 0.06 (s, 9H), 0.14 (s, 6H), 0.17 (s, 9H), 0.47–0.61 (m, 4H); ^{13}C NMR ($CDCl_3$): $\delta = -4.9$, -2.6, -2.1, -0.3, 6.5, 9.0, 113.3, 114.4.

3: A mixture of **2** (420 mg, 1.33 mmol), $[Pd(OAc)_2]$ (13 mg, 56 μmol), and 1,1,3,3-tetramethylbutyl isocyanide (114 mg, 0.84 mmol) in toluene (2.9 mL) was heated under pressure of 1.1×10^9 Pa at 135–140 °C for 6 h. The cooled reaction mixture was eluted through a short column of silica gel with hexane, and the subsequent preparative TLC (hexane) afforded **3** (278 mg, 66%). M.p. 114–115 °C; ^{1}H NMR ($CDCl_3$): $\delta = 0.23$ (s, 30H), 0.73 (s, 4H); ^{13}C NMR ($CDCl_3$): $\delta = 1.5$, 4.0, 11.6, 188.3, 188.7; MS: *m/z* 314 (M^+).

Received: May 7, 1993 [Z 6067 IE]
German version: *Angew. Chem.* **1993**, *105*, 1542

[1] A. G. Brook, P. F. Jones, G. J. D. Peddle, *Can. J. Chem.* **1968**, *46*, 2119; B. G. Ramsey, A. Brook, A. R. Bassindale, H. Bock, *J. Organomet. Chem.* **1974**, *74*, C41; A. Ricci, M. Fiorenza, A. Degl'Innocenti, G. Seconi, P. Dembech, K. Witzgall, H. J. Bestmann, *Angew. Chem.* **1985**, *97*, 1068; *Angew. Chem. Int. Ed. Engl.* **1985**, *24*, 1068; K. Narasaka, N. Saito, Y. Hayashi, H. Ichida, *Chem. Lett.* **1990**, 1411; J. A. Soderquist, E. I. Miranda, *J. Am. Chem. Soc.* **1992**, *114*, 10078, and references cited therein.

[2] H. Sakurai, Y. Nakadaira, H. Tobita, T. Ito, K. Toriumi, H. Ito, *J. Am. Chem. Soc.* **1982**, *104*, 300; H. Sakurai, H. Tobita, Y. Nakadaira, C. Kabuto, *ibid.* **1982**, *104*, 4288; H. Sakurai, K. Ebata, C. Kabuto, Y. Nakadaira, *Chem. Lett.* **1987**, 301; H. Sakurai, K. Ebata, K. Sakamoto, Y. Nakadaira, C. Kabuto, *ibid.* **1988**, 965.

[3] A different kind of tetrakis(organosilyl)ethene in which the olefinic C atoms are part of a cycle has been synthesized, and photoelectron and ESR spectroscopic studies have been carried out. H. Bock, G. Brähler, G. Fritz, E. Matern, *Angew. Chem.* **1976**, *88*, 765; *Angew. Chem. Int. Ed. Engl.* **1976**, *15*, 699; G. Fritz, E. Matern, H. Bock, G. Brähler, *Z. Anorg. Allg. Chem.* **1978**, *439*, 173.

[4] Y. Ito, M. Suginome, M. Murakami, *J. Org. Chem.* **1991**, *56*, 1948; M. Murakami, H. Oike, M. Sugawara, M. Suginome, Y. Ito, *Tetrahedron* **1993**, *49*, 3933.

[5] Recently, our procedure for an intramolecular bissilylation with $[Pd(OAc)_2]$/isocyanide under high pressure has been successfully applied to the synthesis of 2,2',5,5'-tetrasila-1,1'-bicyclopentylidene: M. Ichinohe, A. Sekiguchi, C. Kabuto, H. Sakurai, *65th Annual Meeting of the Chemical Society of Japan*, Tokyo, March **1993**.

[6] **3**: Monoclinic, $P2_1/c$, $a = 17.258(6)$, $b = 9.533(4)$, $c = 12.115(6)$ Å, $\beta = 93.13(3)°$, $V = 1990(1)$ Å^3, $Z = 4$, $\lambda(Cu_{K\alpha}) = 1.54178$ Å, $T = 203$ K, MAC Science MXC18 diffractometer. The structure was solved by direct methods and fourier synthesis with the CRYSTAN program package. $R = 0.046$, $R_w = 0.076$ for 3228 reflections. Further details of the crystal structure investigation are available on request from the Director of the Cambridge Crystallographic Data Centre, 12 Union Road, GB-Cambridge CB2 1EZ (UK), on quoting the full journal citation.

[7] In **1b** the shortest distance between the methyl carbon atoms of the vicinal organosilyl groups is 325 pm [2]. For a review on sterically overcrowded molecules, see H. Bock, K. Ruppert, C. Näther, Z. Havlas, H.-F. Herrmann, C. Arad, I. Göbel, A. John, J. Meuret, S. Nick, A. Rauschenbach, W. Seitz, T. Vaupel, B. Solouki, *Angew. Chem.* **1992**, *104*, 564; *Angew. Chem. Int. Ed. Engl.* **1992**, *31*, 550.

[8] The absorption is possibly attributable to $\sigma \rightarrow \pi^*$ transition, which is allowed by the slight deviation of the Si–C σ bond from the sp^2 plane: A. Sekiguchi, K. Ebata, C. Kabuto, H. Sakurai, *Chem. Lett.* **1990**, 539.

[9] J. Hibino, S. Nakatsukasa, K. Fugami, S. Matsubara, K. Oshima, H. Nozaki, *J. Am. Chem. Soc.* **1985**, *107*, 6416.

[10] Since a greater bathochromic shift has been reported for more twisted tetrakis(organosilyl)ethene **1**, [2] the shift is certainly influenced by twisting in the dihedral angle range of 30–53°.

A Nickel–Anthracene Complex Having η^3 and η^4 Coordination in One Crystal

By *Roland Boese,* Amnon Stanger,* Peter Stellberg,* and *Anat Shazar*

Only a few compounds are known that contain structural isomers within one crystal, and to the best of our knowledge, these compounds all contain ionic species. These systems are of special interest because the two isomers must be almost isoenergetical; therefore, there is a high probability of seeing interconvergence between the two forms in the solid state.

[*] Priv.-Doz. Dr. R. Boese, Dipl.-Chem. P. Stellberg
Institut für Anorganische Chemie der Universität-Gesamthochschule
Universitätsstrasse 5–7, D-45117 Essen (FRG)
Telefax: Int. code + (201)183-2535

Dr. A. Stanger, A. Shazar
Department of Chemistry
Technion – Israel Institute of Technology
Haifa 32000 (Israel)
Telefax: Int. code + (4)233-735

[**] This work was supported by the Volkswagenstiftung. R. B. thanks the Fonds der Chemischen Industrie, A. S. the Israeli Academy for Sciences and Humanities and Technion's V. P. R. Fund.

Nickel complexes are natural candidates for the study of such phenomena, since nickel(0) has the ability to form 16e and 18e complexes, depending on the ligand.[1] For example, $[Ni(CO)_4]$ is far more stable than $[Ni(CO)_3]$, whereas $[Ni(C_2H_4)_3]$ is more stable than $[Ni(C_2H_4)_4]$. Quantification of the bonding in Ni complexes is of prime importance for understanding catalysis in which Ni compounds play an important role.[2] Ni^0–arene complexes are particularly suitable for the investigation of the dependence of the coordination number on the type of ligands. Although all the complexes of this type which have been structurally determined (**1** and **2a**) are η^2 bound,[3] the energy difference between these 16e complexes and the corresponding η^4, 18e complexes is expected to be rather small.[4]

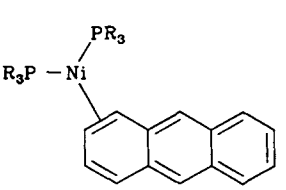

1a, R = Cy
1b, R = Bu
1c, R = Et

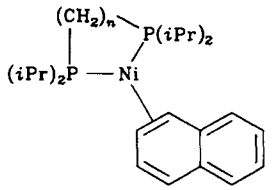

2a, $n = 2$
2b, $n = 3$

In addition, a comparison of **1a**–**1c** led to a prediction regarding the type of phosphane ligands that should be used to stabilize the η^4 18e coordination in Ni–anthracene complexes.[3b] For these reasons we prepared **3**, and we report here the results of the single-crystal X-ray investigation.

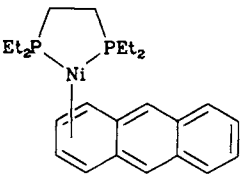

3

Compound **3** was prepared from $[Mg(C_{14}H_{10})(thf)_3]$, anthracene ($C_{14}H_{10}$), and [(depe)$NiCl_2$] (depe = 1,2-bis(diethylphosphino)ethane), in analogy to the synthesis of **1b** and **1c**.[4a, 5] Single crystals suitable for X-ray study were obtained with a slow cooling crystallization technique.[6] These crystals break when cooled below about 150 K, indicating a possible solid-state phase transition; thus, the X-ray study had to be carried out at relatively high temperature.[7] There are two independent isomeric molecules in the asymmetric unit. One is the expected[3b] η^4-complex **3a** and the other is the unique η^3-complex **3b** (Fig. 1).

In **3a** (Fig. 1 top) the Ni is bound to C1 to C4 with usual bond lengths (e.g., 2.014(8)–2.303(6) Å). The P-Ni-P angle is 91.6(1)°, significantly smaller than the corresponding angle in **1b** and **1c** (108.9 and 106.4°, respectively), but similar to that of other diphosphinoethane derivatives.[3c] The most striking difference between **1** and **3a** is, however, the interplanar angle ϕ of the plane between the atoms C1–C4 and that of the naphthalene residue. Thus, in the η^2 complexes the anthracene ligands deviate only slightly from planarity (ϕ is 6.3, 8.1, and 12.4° for **1a**, **1b** and **1c**, respectively), whereas ϕ is 26.2(3)° for **3a**. This is in accordance with the prediction[3b] based on the structures of **1** and an η^4-tantalum–anthracene complex.[8] The η^3-complex **3b** (Fig. 1 bot-

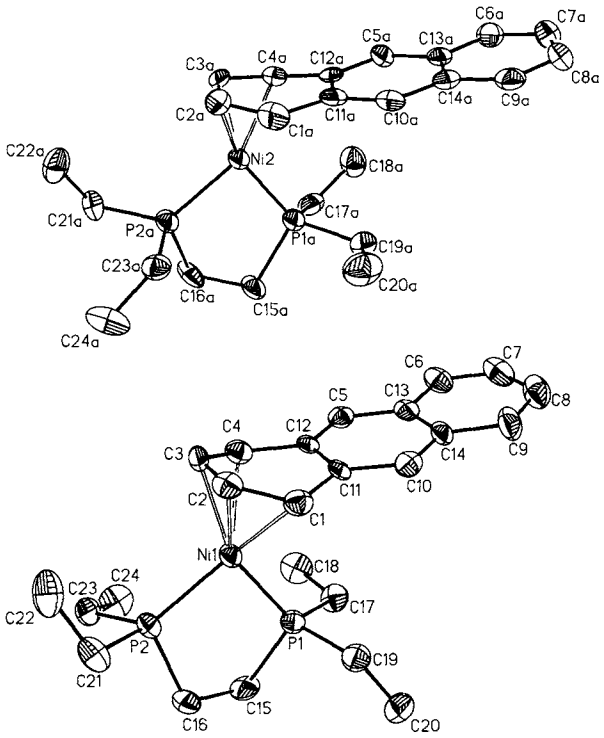

Fig. 1. The molecular structures of **3a** (top) and **3b** (bottom) (drawn at 50% probability levels of the ellipsoids) hydrogen atoms are omitted. Selected bond lengths [Å] and angles [°] (standard deviations in parentheses): **3a**: C1-C2 1.404(11), C2-C3 1.434(9), C3-C4 1.388(9); P1-C15-C16-P2 38.8(7); **3b**: C1a-C2a 1.363(11), C2a-C3a 1.411(9), C3a-C4a 1.423(10); P1a-C15a-C16a-P2a −44.8(7).

tom) has an intermediate value of $\phi = 17.3(4)°$. The comparison between the three complexes is illustrated in Figure 2 top. Table 1 gives the most relevant data for **1a–1c**, **2a**, **3a**, and **3b**; note that there is, at least qualitatively, a connection between ϕ and the P-Ni-P angle.

Table 1. The most important structural parameters of the $(PR_3)_2Ni$–arene complexes **1a–1c** and **2a** in comparison to those of the title molecules **3a** and **3b**.

	1a [a]	**1b**	**1c**	**2a** [a]	**3a**	**3b**
Ni-C1 [Å]	2.060	2.007(3)	2.013(7)	2.002	2.176(8)	2.824(8)
Ni-C2 [Å]	1.993	1.963(3)	1.961(7)	1.987	2.014(8)	2.343(8)
Ni-C3 [Å]	2.769	2.714(3)	2.698(7)	2.761	2.069(7)	1.963(9)
Ni-C4 [Å]	3.448	3.335(3)	3.337(7)	3.378	2.303(6)	2.057(8)
P-Ni-P [°]	118.3	108.9(1)	106.4(1)	92.2	91.6(1)	90.3(1)
ϕ [°]	6.3	8.1(2)	12.4(6)	5.0	26.2(3)	17.3(4)
(P,Ni,P)/ (Ni,C1,C2) [°] [b]	22.0	12.0(3)	12.3(3)	2.0	80.5(1)	42.7(1)

[a] The data taken from the literature have no standard deviations. [b] Ni1,X1, X2; Ni2,X3,X4 for **3a** and **3b**, in which X1, X2, X3, and X4 are dummy atoms in the center of the bonds C1/C2 (X1), C3/C4 (X2), C2a/C3a (X3) and C3a/C4a (X4) for the calculation of the geometry of the coordination spheres around the Ni atoms. These angles are expected to be 0° for ideal square-planar and 90° for ideal tetrahedral coordination.

Another interesting feature of the η^3 complex is the coordination sphere around the Ni atom. The ideal geometries for Ni^0 complexes with 16e and 18e are square planar and tetrahedral, respectively. The geometries of **1** and **3a** confirm this (see Table 1). The Ni atom in the η^3-complex **3b** shows an intermediate geometry (Table 1 last column, Fig. 2 bottom).

These results concerning the structure suggest that **3b** closely models an intermediate of the dynamic process

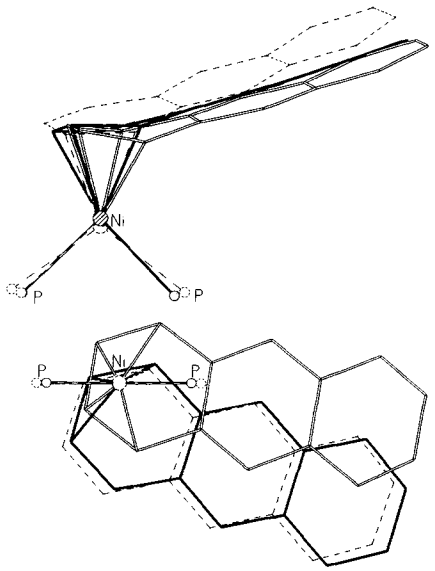

Fig. 2. Overlap pictures of **1b** (dashed lines), **3a** (open bars), and **3b** (solid bars) in a side view (top) and a top view (bottom). The overlapping features are the two Ni–P bonds. Alkyl groups and hydrogen atoms are omitted for clarity.

($\eta^2 \rightleftarrows \eta^3 \rightleftarrows \eta^4 \rightleftarrows \eta^3 \rightleftarrows \eta^2$) which was observed for **2**. To the best of our knowledge, this is the first time that all possible intermediates for such a dynamic process have been isolated and characterized in the solid state. All other structural parameters of **3b** are consistent with the η^3 coordination; for example, the C1–C2 distance for **3a** is 1.404(11) Å and 1.363(11) Å for **3b**, and the Ni2–C1a distance in **3b** (2.824(8) Å) is clearly a nonbonding distance.

Formally, the Ni center in **3b** contains 17e, thus **3b** should be a diradical which shows paramagnetic behavior.[9] We are currently investigating this point as well as the connection between ϕ, the size of the phosphane ligands, and the P-Ni-P angle. As mentioned Ni–arene complexes undergo dynamic processes.[4] In solution one observes the migration of the $(R_3P)_2Ni$ moiety between the two terminal rings of the arene.[4] This rearrangement can be intra-[4b] or intermolecular.[10] The bridged-naphthalene complexes **2** have been investigated in the solid state, and they undergo the rearrangement described in Scheme 1.[4c]

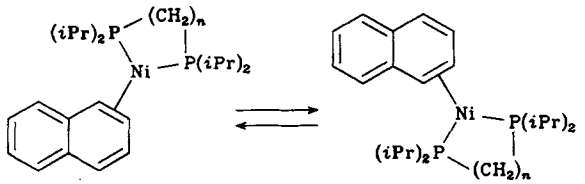

Scheme 1.

Compounds **1b** and **1c** undergo the same type of rearrangement in solution.[11] The NMR spectra of the solution of **3** show that this complex is diamagnetic. Thus, in solution **3** is only an 18e, η^4 complex. Some preliminary variable temperature NMR studies suggest that the solution behavior of **3** is rather different from that of **1**. The main difference is that **3** undergoes an intermolecular (possibly also intramolecular) process with an amazingly low activation energy. Thus, saturation transfer to a free ligand and to the uncomplexed ring can be observed already at −101 °C.[12]

Received: February 6, 1993
Revised version: July 3, 1993 [Z 5855 IE]
German version: *Angew. Chem.* **1993**, *105*, 1500

[1] For a comprehensive review on nickel chemistry see: G. Wilke, *Angew. Chem.* **1988**, *100*, 189; *Angew. Chem. Int. Ed. Engl.* **1988**, *27*, 186.
[2] W. Keim, *Angew. Chem.* **1990**, *102*, 251; *Angew. Chem. Int. Ed. Engl.* **1990**, *29*, 235.
[3] a) Solid-state structure of **1a**: D. J. Brauer, C. Krüger, *Inorg. Chem.* **1977**, *16*, 884; b) Solid-state structures of **1b** and **1c**: A. Stanger, R. Boese, *J. Organomet. Chem.* **1992**, *430*, 235; c) Solid-state structure of **2a**: F. Scott, C. Krüger, P. Betz, *ibid.* **1990**, *387*, 113. d) One η^4-Ni complex with butadiene is known, see: R. Benn, P. Betz, R. Goddard, P. W. Jolly, N. Kokel, C. Krüger, I. Topalović, *Z. Naturforsch. B* **1991**, *46*, 1395.
[4] a) A. Stanger, K. P. C. Vollhardt, *Organometallics* **1992**, *11*, 317; b) A. Stanger, *ibid.* **1991**, *10*, 2979; c) R. Benn, R. Mynott, I. Topalović, F. Scott, *ibid.* **1989**, *8*, 2299; d) see also the discussion in ref. [3c].
[5] Selected analytical data of **3**: Correct elemental analysis; ^{1}H NMR (−101 °C): δ = 7.30 (m, 2H, H(5,8)), 6.98 (m, 2H, H(6,7)), 6.89 (s, 2H, H(9,10)), 5.65 (m, 2H, H(2,3)), 5.23 (m, 2H, H(1,4)), 0.88–1.26 (m, 22H, $(Et_2P\text{-}CH_2)_2$); $^{31}P\{^1H\}$ NMR (−101 °C): δ = 58.85 (d), 28.92 (d), $J_{P,P}$ = 47.9.
[6] R. Boese, D. Bläser, *J. Appl. Crystallogr.* **1989**, *22*, 394.
[7] X-ray structure determination of **3**: A crystal (0.24 × 0.13 × 0.08 mm^3) was measured on a Nicolet R3m/V diffractometer, $Mo_{K\alpha}$ radiation at 170 K. Cell dimensions were refined from the diffractometer angles of 30 centered reflections; a = 8.922(6), b = 21.021(14), c = 12.633(7) Å, β = 106.52(5)°, V = 2272(2) Å^3; Z = 4, ϱ_{calcd} = 1.296 gm^{-3}, μ = 1.00 mm^{-1}, space group $P2_1$, data collection of 3753 unique reflections ($2\theta_{max}$ = 40°), 3407 observed ($F_0 \geq 4\sigma(F)$), structure solution with direct methods and refinement with full-matrix least squares (493 parameters) with the SHELXTL-Plus program, riding groups for hydrogen atoms; common and isotropic U values for each group, all other atoms with anisotropic ADPs, R = 0.0377, R_w = 0.0396, $w^{-1} = \sigma^2(F_0) + 0.0016F_0^2$, maximum residual electron density 0.43 eÅ^{-3}. Further details of the crystal investigation are available on request from the Fachinformationszentrum Karlsruhe, Gesellschaft für wissenschaftlich-technische Information mbH, D-76344 Eggenstein-Leopoldshafen, on quoting the depository number CSD-57711, the authors names, and the full citation of the journal.
[8] J. D. Protasiewicz, P. A. Bianconi, I. D. Williams, S. Liu, Ch. P. Rao, S. J. Lippard, *Inorg. Chem.* **1992**, *31*, 4134.
[9] The magnetic moment of **3** (**3a** and **3b**) obeys Curie Weiss Law at 200–330 K. The measured μ_{eff} is 2.00 BM. The magnetic measurements were carried out with a Quantum Design SQUID Magnetometer. We thank Dr. J. Pebler for the measurements.
[10] In dimethoxy-substituted anthracenes and 9- and 9,10-alkylanthracene complexes with $(Bu_3P)_2Ni$, the rearrangements are intermolecular or inter- and intramolecular: A. Shazar, H. Weismann, A. Stanger, unpublished results.
[11] We have developed a method (based on magnetization transfer in the presence of a free ligand) to determine the stable coordination number in solution even when the dynamic process cannot be frozen out (i.e. $\Delta G^{\neq}$ for the $\eta^2 \rightleftarrows \eta^2$ is very small): A. Stanger, A. Shazar, H. Weismann, unpublished results.
[12] A. Stanger, A. Shazar, unpublished results.

Synthesis, Structure, and Reactivity of Stable PN Heterocycles with Two and Six Methyleneamine Units: $[H_2C{=}N{-}N(Me)]_2P(S)(Ph)$ and $[H_2C{=}N{-}N(Me)]_6P_3N_3$

By *Christophe Galliot, Anne-Marie Caminade, Françoise Dahan,* and *Jean Pierre Majoral**

N-Methyleneamine type compounds $H_2C{=}N{-}R$ (R = CR'_3, NR'_2, OR', etc.) are useful reagents in organic synthesis; however, most of these compounds are unstable and dimerize,[1] trimerize,[2] or polymerize spontaneously. Consequently, only X-ray structures of some related salts or complexes have been described.[3] We report here the first single-crystal X-ray analysis of a neutral, uncomplexed compound of this type, the bis(*N*-methylenehydrazone) **4a**, as well as those of the rather unexpected cationic heterocycles **5** and **5'**, which arise from the stereoselective reaction of **4a** with $[(iPr_2N)_2P]^+[CF_3SO_3]^-$. Remarkably, this reaction can be extended to the synthesis of the cyclotriphosphazene **11** possessing six perfectly stable $H_2C{=}N$ moieties!

Various strategies have been designed to generate compounds with $H_2C{=}N$ units,[4] the most straightforward of which uses formaldehyde.[5] The reaction of aqueous formaldehyde with phosphono dihydrazide **1** leads initially to the dimer **2**, then to the bicycle **3**.[1c, 6] Completely different products are isolated when paraformaldehyde $(CH_2O)_n$ in THF and a molecular sieve are used instead of aqueous formaldehyde; thus, the bis(*N*-methylenehydrazone) derivatives **4a**, **b** are isolated in near quantitative yield (Scheme 1).

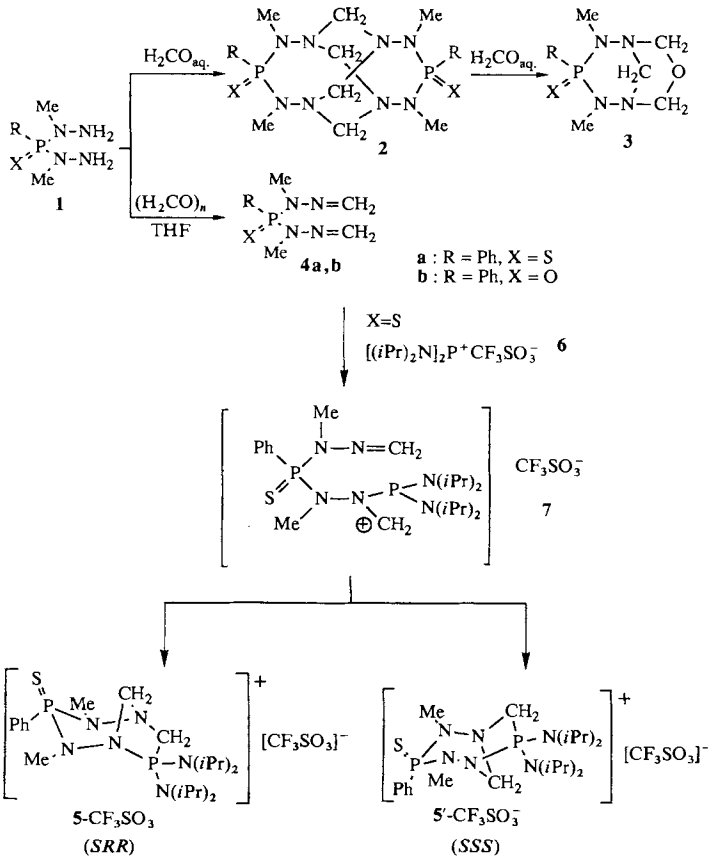

Scheme 1.

Compounds **4a**, **b** are stable at room temperature for several days in air and for several months under dry argon. Their structures were first deduced from ^{1}H NMR spectra, which exhibited an AB pattern in the range expected for the $H_2C{=}N$ group[5b, 7] (**4a**[8]: δ_{H_A} = 6.37, δ_{H_B} = 6.48, $^2J_{H_A,H_B}$ = 9.3 Hz; **4b**[8]: δ_{H_A} = 6.25, δ_{H_B} = 6.41, $^2J_{H_A,H_B}$ = 10.8 Hz), and mass spectra. These surprising results prompted us to undertake an X-ray structure determination of **4a**.[9]

The molecular structure of **4a** is consistent with NMR spectroscopic and mass spectrometric data (Fig. 1). The most interesting feature of the structure is the two slightly different $H_2C{=}N$ subunits. The bond lengths are similar to those of C-substituted imines and hydrazones:[10] (N(2)–C(7) 1.265(7) and N(4)–C(9) 1.276(7) Å), and no interaction exists between the two C=N bonds ($d_{N2\cdots N4}$ = 4.090 and $d_{C7\cdots C9}$ = 3.732 Å). The bond lengths and angles in the phosphono dihydrazide part are similar to the values previously reported for N_4P_2 macrocycles.[10]

[*] Dr. J. P. Majoral, C. Galliot, Dr. A.-M. Caminade, Dr. F. Dahan
Laboratoire de Chimie de Coordination du CNRS
205, Route de Narbonne, F-31077 Toulouse Cédex (France)
Telefax: Int. code + (61)55 30 03

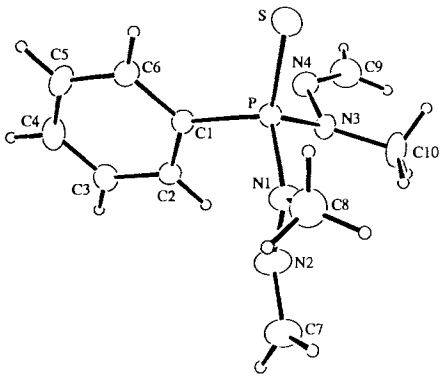

Fig. 1. Molecular structure of **4a**. Selected bond lengths [Å] and angles [°]: N2-C7 1.265(7), N4-C9 1.276(7), P-N1 1.679(4), P-N3 1.682(4), N1-N2 1.385(6), N3-N4 1.376(5); N1-P-N3 102.0(2), P-N1-N2 113.2(3), P-N3-N4 110.7(3), N1-N2-C7 118.8(4), N3-N4-C9 118.8(4).

Compounds **4a**, **b** should be interesting reagents in heterocyclic chemistry and should react differently to the corresponding C-substituted derivatives. Indeed **4a**, **b** react quantitatively (Scheme 1) with bis(diisopropylamino)phosphanylium trifluoromethanesulfonate,[11] while species like $PhP(S)(NMe-N=CHPh)_2$ do not react at all. The ^{31}P NMR spectra of the crude reaction mixture in CH_2Cl_2 reveal the presence of two singlets ($\delta = 64.4$ and 77.5) and two doublets ($\delta = 69.2$ and 81.0, $J_{P,P} = 8.5$ Hz) in a 70:30 ratio. Two compounds (**5** and **5′** as $CF_3SO_3^-$ salts) can be isolated following repeated extraction and washing with Et_2O and THF, and subsequent crystallization from toluene: the two doublets are assigned to **5** and the two singlets to **5′**. The ^{31}P NMR data of both compounds indicated the presence of a phosphonium type phosphorus (**5**: $\delta = 81.0$; **5′**: $\delta = 77.5$) in addition to the thiophosphono dihydrazide type phosphorus (**5**: $\delta = 69.2$; **5′**: $\delta = 64.4$). The ^1H and ^{13}C NMR spectra of **5** and **5′** showed no signals for sp^2 CH_2 groups, only those for sp^3 CH_2 groups.[8] Surprisingly, mass spectra (FAB^+) revealed that both compounds had the same molecular weight, corresponding to the addition of one phosphanylium ion to one bis(*N*-methylenehydrazone). Since several structures are conceivable for **5** and **5′**, two single-crystal X-ray structure determinations were carried out.

The structures of **5** and **5′** are illustrated in Figures 2 and 3, respectively. Both compounds are heterobicycles, constructed from a six- and a five-membered ring with a common $N-CH_2-N$ unit. The five-membered rings are formed by the unsymmetric addition of the phosphanylium ion on two $H_2C=N$ bonds. The six-membered rings, built from the phosphono dihydrazide part, adopt a boat type conformation, in contrast to the six-membered ring in **3** which has a chair type conformation.[6] Furthermore, the sum of angles around the nitrogen atoms of the $N-CH_2$ unit (**5**: $\Sigma N2 = 325.3$, $\Sigma N3 = 319.5$; **5′**: $\Sigma N2 = 319.6$, $\Sigma N3 = 327.9°$) shows that they are highly pyramidalized. Compounds **5** and **5′** differ mainly with regard to the position of the phosphonium group and the position of the phenyl group relative to the six-membered ring: *"cis"* in the minor compound **5**, and *"trans"* in the major compound **5′**. This gives rise to a difference in the dihedral angles between the planes P1-N4-N3 and P2-N3-N4 (109.6(1)° for **5** and 93.8(1)° for **5′**), which in turn may account for the difference observed for the $^3J_{P,P}$ coupling constant: 8.5 Hz for **5** and $\triangleq 0$ Hz for **5′**. It should be noted that no thermal equilibration between **5** and **5′** was detected by variable-temperature NMR experiments.

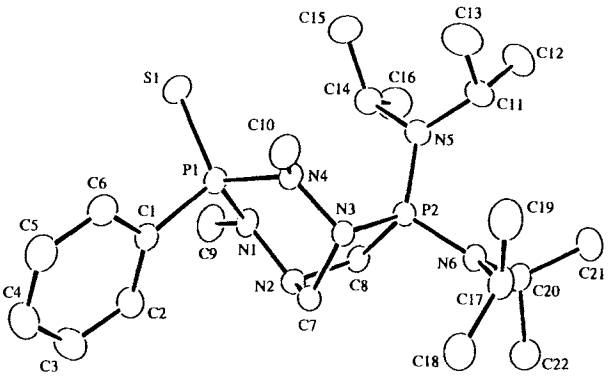

Fig. 3. Molecular structure of the cation **5′**. Selected bond lengths [Å] and angles [°]: N2-C7 1.467(3), N3-C7 1.487(3), N2-C8 1.478(3), P1-N1 1.662(2), P1-N4 1.699(2), P2-N3 1.715(2), P2-N5 1.627(2), P2-N6 1.620(2); N1-P1-N4 99.25(8), C8-P2-N3 94.46(8), C1-P1-N4 111.11(8), N3-P2-N5 117.87(9), P2-N3-N4 114.4(1).

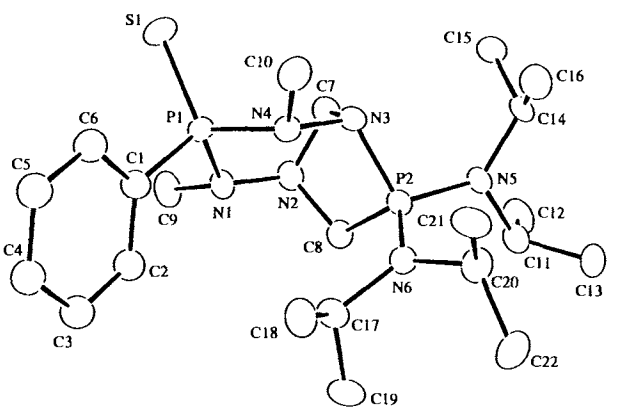

Fig. 2. Molecular structure of the cation **5**. Selected bond lengths [Å] and angles [°]: N2-C7 1.457(3), N3-C7 1.486(3), N2-C8 1.480(3), P1-N1 1.684(2), P1-N4 1.701(2), P2-N3 1.719(2), P2-N5 1.619(2), P2-N6 1.613(2); N1-P1-N4 98.61(8), C8-P2-N3 94.05(9); C1-P1-N4 105.74(9), N3-P2-N5 104.46(8), P2-N3-N4 107.7(1).

The formation of **5** and **5′** may involve two steps. The first one, initiated by the Lewis acidity of **6** led to the transient carbocation **7**, which is intramolecularly trapped to give **5** and **5′** (Scheme 1). This mechanism implies that **4a** reacts as an imine[13] and not as hydrazone in which conjugation of the C=N bond with the adjacent nitrogen atom makes the azomethine carbon atom negatively charged.

Hydrazones $R_2N-N=CHR'$ (R = Me, R′ = Et, Ph) generally react with trifluoroacetic anhydride (**8**) in the presence of base (pyridine, 2,6-lutidine) by an electrophilic substitution reaction at the azomethine carbon atom to give compounds of the type $R_2N-N=C(R')COCF_3$.[14] The addition of **8** to **4a** in the presence of pyridine, however, afforded the pyridinium salt **9** in 80% yield (Scheme 2).[15] The formation

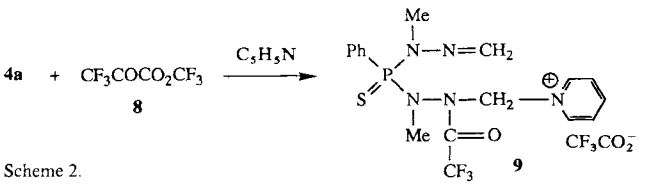

Scheme 2.

of **9** was particularly interesting since it corroborated the proposed mechanism for the generation of the transient cation **7** (Scheme 1). The synthesis of **9** involved the electrophilic attack of CF_3CO^+ at one of the imino nitrogen atoms and trapping of the resulting carbocation with pyridine (Scheme 2).[16]

Preparation of stable compounds which contain methyleneamine units is not limited to **4a, b**. Thus, treatment of hexahydrazinocyclotriphosphazene **10** with a large excess of paraformaldehyde $(CH_2O)_n$ in the presence of molecular sieves affords quantitatively compound **11** possessing six $H_2C{=}N$ units. The structure of **11** was proposed on the basis of mass spectrometric (m/z 477) and NMR spectroscopic data,[17] and confirmed by a single-crystal X-ray diffraction study.[18]

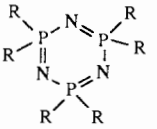

10: R = N(Me)-NH_2
11: R = N(Me)-N=CH_2

The surprising stability of **4a, b** and **11** in comparison with other $H_2C{=}N$ compounds cannot be explained satisfactorily at present. Ab initio calculations, as well as more detailed experimental studies on the synthetic potential of these new powerful reagents are underway.

Experimental Procedure

4a: A mixture of **1** (0.280 g, 1.22 mmol) and paraformaldehyde (0.260 g, 8.66 mmol) in THF (30 mL) was stirred for 10 hours in the presence of molecular sieves (4 Å). Filtration of the solution, followed by evaporation to dryness gave **4a** as a white powder, which was recrystallized in acetone or toluene.

5 and **5′**: A solution of **6** (0.483 g, 1.27 mmol) in CH_2Cl_2 (10 mL) was added by canula at −80 °C to a solution of **4a** (0.323 g, 1.27 mmol) in CH_2Cl_2 (10 mL). The mixture was stirred overnight, then the solvent was evaporated to give a residue which was washed with CH_2Cl_2/pentane (1:3) to give an oil. Treatment of this oil with Et_2O (10 mL) then THF (10 mL) gave a white powder (**5′**-CF_3SO_3) and a solution which was evaporated to give an oil. After several treatments of this oil with Et_2O then THF as above, **5** was obtained as a white powder.

Received: April 30, 1993
Revised version: June 11, 1993 [Z 6049 IE]
German version: *Angew. Chem.* **1993**, *105*, 1508

[1] a) F. G. Riddell, P. Murray-Rust, *J. Chem. Soc. Chem. Commun.* **1970**, *1075*; b) J. Hocker, D. Wendisch, *J. Chem. Res. Synop.* **1977**, 236; c) J. P. Majoral, M. Revel, J. Navech, *ibid.* **1980**, 129; *J. Chem. Res. Miniprint* **1980**, 2001.

[2] See for example: M. M. Sprung, *Chem. Rev.* **1940**, *26*, 297.

[3] a) E. W. Abel, R. J. Rowley, R. Mason, M. K. Thomas, *J. Chem. Soc. Chem. Commun.* **1974**, 72; b) D. J. Sepelak, C. G. Pierpont, E. K. Barefield, J. T. Budz, C. A. Poffenberger, *J. Am. Chem. Soc.* **1976**, *98*, 6178; c) A. D. Clauss, J. R. Shapley, S. R. Wilson, *ibid.* **1981**, *103*, 7387; d) W. A. Herrmann, L. K. Bell, M. L. Ziegler, H. Pfisterer, C. Pahl, *J. Organomet. Chem.* **1983**, *247*, 39; e) P. Legzdins, G. B. Richter-Addo, F. W. B. Einstein, R. H. Jones, *Organometallics* **1987**, *6*, 1807; f) P. Legzdins, G. B. Richter-Addo, B. Wassink, F. W. B. Einstein, R. H. Jones, A. C. Willis, *J. Am. Chem. Soc.* **1989**, *111*, 2097; g) A. B. Burg, *Inorg. Chem.* **1989**, *28*, 1295; h) R. Minkwitz, D. Bernstein, H. Preut, P. Sartori, *ibid.* **1991**, *30*, 2157.

[4] a) B. Braillon, M. C. Lasne, J. L. Ripoll, J. M. Denis, *New J. Chem.* **1982**, *6*, 121; b) J. Barluenga, A. M. Bayon, G. Asensio, *J. Chem. Soc. Chem. Commun.* **1983**, 1109; c) *ibid.* **1984**, 427; d) L. E. Overman, R. M. Burk, *Tetrahedron Lett.* **1984**, *25*, 1635.

[5] a) G. A. Harff, A. Sinnema, B. M. Wepster, *Recl. Trav. Chim. Pays-Bas* **1979**, *98*, 71; b) H. Möhrle, U. Scharf, E. Rühmann, R. Schmid, *Arch. Pharm. (Weinheim, Ger.)* **1983**, *316*, 222; c) Y. Kamitori, M. Hojo, R. Masuda, T. Fujitani, S. Ohara, T. Yokoyama, *J. Org. Chem.* **1988**, *53*, 129.

[6] J. Jaud, J. Galy, R. Kraemer, J. P. Majoral, J. Navech, *Acta Crystallogr. Sect. B* **1980**, *36*, 869.

[7] a) B. L. Shapiro, S. J. Ebersole, G. J. Karabatsos, F. M. Vane, S. L. Manatt, *J. Am. Chem. Soc.* **1963**, *85*, 4041; b) G. J Karabatsos, K. L. Krumel, *Tetrahedron* **1967**, *23*, 1097.

[8] **4a**: $^{31}P\{^1H\}$ NMR ($CDCl_3$): $\delta = 77.4$(s); ^1H NMR ($CDCl_3$): $\delta = 3.01$ (d, $^3J_{HP} = 9.4$ Hz, 6H, N-CH_3), 6.37, 6.48 (AB system, $^2J_{H_AH_B} = 9.3$ Hz, 4H, $H_2C{=}N$), 7.24–8.09 (m, 5H; C_6H_5-P); ^{13}C NMR ($CDCl_3$): $\delta = 29.6$ (qd, $^1J_{CH} = 138.8$ Hz, $^2J_{CP} = 9.5$ Hz, CH_3), 126.9–132.6 (m, N=CH_2, P-C_6H_5); MS (DCI/CH_4): m/z 255 $[M+1]^+$. **4b**: $^{31}P\{^1H\}$ NMR ($CDCl_3$): $\delta = 21.4$ (s); ^1H NMR ($CDCl_3$): $\delta = 2.90$ (d, $^3J_{HP} = 7.2$ Hz, 6H, N-CH_3), 6.25, 6.41 (AB system, $^2J_{H_AH_B} = 10.8$ Hz, 4H, $H_2C{=}N$), 7.29–7.77 (m, 5H; C_6H_5-P). **5**: $^{31}P\{^1H\}$ NMR ($CDCl_3$): $\delta = 69.2$ (d, $^3J_{PP} = 8.5$ Hz, P=S), 81.0 (d, $^3J_{PP} = 8.5$ Hz, P^+); ^1H NMR ($CDCl_3$): $\delta = 1.35$ (br.d, $^3J_{HH} = 6.3$ Hz, 24H, CH-CH_3), 2.88 (d, $^3J_{HP} = 14.3$ Hz, 3H, N-CH_3), 2.91 (d, $^3J_{HP} = 14.4$ Hz, 3H, N-CH_3), 3.62–4.37 (m, 8H, N-CH, CH_2), 7.32–7.95 (m, 5H, C_6H_5); FAB$^+$-MS m/z 485.4 $[M - CF_3SO_3]^+$. **5′**: $^{31}P\{^1H\}$ NMR ($CDCl_3$): $\delta = 64.4$ (s, P=S), 77.5 (s, P^+); ^1H NMR ($CDCl_3$): $\delta = 1.34$ (d, $^3J_{HH} = 6.4$ Hz, 6H, CH-CH_3), 1.37 (d, $^3J_{HH} = 6.3$ Hz, 6H, CH-CH_3), 1.53 (d, $^3J_{HH} = 6.9$ Hz, 12H, N-(CH-CH_3)$_2$), 2.98 (d, $^3J_{HP} = 10.6$ Hz, 3H, N-CH_3), 3.15 (d, $^3J_{HP} = 9.2$ Hz, 3H, N-CH_3), 3.27–3.85 (m, 4H, N-CH), 3.91–4.28 (m, 4H, CH_2), 7.50–7.72 (m, 5H, C_6H_5); $^{13}C\{^1H\}$ NMR ($CDCl_3$): $\delta = 21.8$ (d, $^3J_{CP} = 1.2$ Hz, N-CH-CH_3), 22.5 (d, $^3J_{CP} = 2.4$ Hz, N-CH-CH_3), 23.1 (d, $^3J_{CP} = 4.5$ Hz, N-CH-CH_3), 23.7 (d, $^3J_{CP} = 1.6$ Hz, N-CH-CH_3), 34.9 (d, $^2J_{CP} = 8.7$ Hz, N-CH_3), 38.4 (dd, $^2J_{CP} = 10.1$ Hz, $^3J_{CP} = 6.2$ Hz, N-CH_3), 49.5 (d, $^2J_{CP} = 13.9$ Hz, N-CH-CH_3), 49.6 (d, $^2J_{CP} = 14.4$ Hz, N-CH-CH_3), 56.6 (d, $^1J_{CP} = 64.3$ Hz, CH_2P); 71.2 (dd, $J_{CP} = 26.1$ Hz, $J_{CP} = 25.0$ Hz, N-CH_2-N) 128.2–130.2 (m, C_6H_5); FAB$^+$-MS: m/z 485.3 $[M - CF_3SO_3]^+$.

[9] Crystal data for **4a**: $[C_{10}H_{15}N_6PS]$, $P2_12_12_1$, (orthorhombic), $a = 6.600(1)$, $b = 7.444(1)$, $c = 26.323(3)$ Å, $Z = 4$, $V = 1293.3(5)$ Å^3, $M = 254.3$, $\varrho_{calcd} = 1.306$ g cm^{-3}, $\mu = 3.4$ cm^{-1}; 2133 unique reflections were measured and 1748 with $I > 3\sigma(I)$ were used in the refinement to $R = 0.033$, $R_w = 0.043$. Crystal data for **5**: $[C_{22}H_{43}N_6P_2S]CF_3SO_3$, $P2_1/n$, (monoclinic), $a = 11.216(1)$, $b = 15.672(2)$, $c = 18.403(2)$ Å, $\beta = 99.96(1)°$, $Z = 4$, $V = 3186(1)$ Å^3, $M = 634.7$, $\varrho_{calcd} = 1.323$ g cm^{-1}, $\mu = 3.1$ cm^{-1}; 7287 unique reflections were measured and 3929 with $I > 3\sigma(I)$ were used in the refinement to $R = 0.021$, $R_w = 0.023$. Crystal data for **5′**: $[C_{22}H_{43}N_6P_2S]CF_3SO_3$, $P2_1/n$, (monoclinic), $a = 8.839(1)$, $b = 15.745(2)$, $c = 23.052(2)$ Å, $\beta = 97.02(1)°$, $Z = 4$, $V = 3184(1)$ Å^3, $M = 634.7$, $\varrho_{calcd} = 1.324$ g cm^{-1}, $\mu = 3.1$ cm^{-1}; 5571 unique reflections were measured and 3499 with $I > 3\sigma(I)$ were used in the refinement to $R = 0.024$, $R_w = 0.026$. Further details of the crystal structure investigations are available on request from the Fachinformationszentrum Karlsruhe, Gesellschaft für wissenschaftlich-technische Information mbH, D-76344 Eggenstein-Leopoldshafen (FRG) on quoting the depository number CSD-57371, the names of the authors, and the journal citation.

[10] See for example: a) M. Badri, J. P. Majoral, A. M. Caminade, M. Delmas, A. Gaset, A. Gorgues, J. Jaud, *J. Am. Chem. Soc.* **1990**, *112*, 5618; b) F. Gonce, A. M. Caminade, J. Jaud, P. Vignaux, J. P. Majoral, *Bull. Soc. Chim. Fr.* **1992**, *129*, 237.

[11] Phosphanylium ions are known to react with dienes [12] and imines [13].

[12] A. H. Cowley, R. A. Kemp, *Chem. Rev.* **1985**, *85*, 367, and references therein.

[13] a) M. R. Mazières, C. Roques, T. Kim, J. P. Majoral, R. Wolf, M. Sanchez, *Phosphorus Sulfur and Silicon* **1990**, *49–50*, 309; b) T. Kim. M. R. Mazières, R. Wolf, M. Sanchez, *Tetrahedron Lett.* **1990**, *31*, 4459.

[14] Y. Kamitori, M. Hojo, R. Masuda, T. Fujitani, S. Ohara, T. Yokoyama, *J. Org. Chem.* **1988**, *53*, 529.

[15] **9**: $^{31}P\{^1H\}$ NMR (CD_3CN): $\delta = 81.5$ (s); ^1H NMR (CD_3CN): $\delta = 2.78$ (d, $^3J_{HP} = 10.5$ Hz, 3H, H_2C = N-N-CH_3); 3.22 (d, $^3J_{HP} = 6.5$ Hz, 3H, H_2C-N-N-CH_3), 6.44, 6.56 (AB system, $^2J_{H_A\ H_B} = 14.1$ Hz, 2H, N=CH_2), 6.92 (s, 2H, N-CH_2-N), 7.50–8.01 (m, 5H, C_6H_5), 8.12–9.06 (m, 5H, C_5H_5N); $^{13}C\{^1H\}$ NMR (CD_3CN): $\delta = 32.4$ (d, $^2J_{CP} = 8.75$ Hz, H_2C=N-N-CH_3), 40.6 (s, H_2C-N-N-CH_3), 73.2 (s, N-CH_2-NC_5H_5), 116.5 (q, $^1J_{CF} = 288.0$ Hz, CF_3), 117.9 (q, $^1J_{CF} = 289.0$ Hz, CF_3), 129.3, 146.6, 148.9 (NC_5H_5), 130.0 (d, $J_{CP} = 14.3$ Hz), 133.3 (d, $J_{CP} = 12.1$ Hz) 134.0 (d, $J_{CP} = 13.0$ Hz), 134.4 (s, C_6H_5), 154.2 (d, $^2J_{CF} = 37.4$ Hz, CO), 157.3 (d, $^2J_{CF} = 44.2$ Hz, OCO); ^{19}F NMR (CD_3CN): $\delta = 2.60$, 9.05 (br.s., N-$COCF_3$, $CF_3CO_2^-$); FAB$^+$-MS: m/z 429.9 $[M]^+$.

[16] Reaction of **4a** with **6** in the presence of pyridine failed because of Lewis acid properties of **6**, giving with pyridine the adduct $[(iPr_2N)_2P$-$NC_5H_5]CF_3SO_3$: M. Sanchez, M. R. Mazières, L. Lamandé, R. Wolf in *Multiple Bonds and Low Coordination in Phosphorus Chemistry* (Eds.: M. Regitz, J. O. Scherer), Thieme, Stuttgart, **1990**, p. 129.

[17] **11**: Selected spectroscopic data: $^{31}P\{^1H\}$ NMR (THF): $\delta = 14.9$ (s); ^1H NMR ($CDCl_3$): $\delta = 2.99$ (m, 18H, CH_3), 6.27, 6.38 (AB system, $^2J_{H_A\ H_B} = 11.2$ Hz, 12H, N=CH_2); $^{13}C\{^1H\}$ NMR ($CDCl_3$): $\delta = 29.7$ (m, CH_3), 124.8 (m, $H_2C{=}N$).

[18] X-ray data will be published elsewhere.

Carbenerhodium Complexes with Diaryl- and Aryl(alkyl)carbenes as Ligands: The Missing Link in the Series of the Double Bond Systems *trans*-[RhCl{=C(=C)$_n$RR'}(L)$_2$] Where $n = 0$, 1, and 2**

By *Peter Schwab, Norbert Mahr, Justin Wolf,* and *Helmut Werner**

Dedicated to Professor Ernst Otto Fischer on the occasion of his 75th birthday

There are but a few comparative studies concerning the reactivity of homologous trialkylphosphane and trialkylstibane transition metal complexes to date.[1] We observed a remarkable difference in the behavior of rhodium(I) compounds containing P*i*Pr$_3$ and Sb*i*Pr$_3$ as ligands, when we tried to prepare carbene complexes **A** as relatives to the known vinylidene and allenylidene complexes of type **B**[2] and **C**.[3] The missing link in the series of Rh–C double bond systems **A**–**B**–**C** is not accessible from **1** (the starting material for the synthesis of **B** and **C**), because on warming the diazoalkane complex **2** (Scheme 1), obtained from **1** and CPh_2N_2, does not eliminate N_2 but CPh_2 to give the dinitrogenrhodium compound **3**.[4] The original goal can be achieved, however, if a rhodium complex possessing two Sb*i*Pr$_3$ ligands is prepared first, and after the carbene–metal bond has been generated a subsequent ligand exchange is carried out. Crucial is the longer M–Sb distance (compared with M–P) and the weaker M–SbR$_3$ bond (compared with M–PR$_3$[1]) in the stibane rhodium compounds that open reaction pathways which for kinetic reasons are hindered in the case of the corresponding phosphane metal complexes.

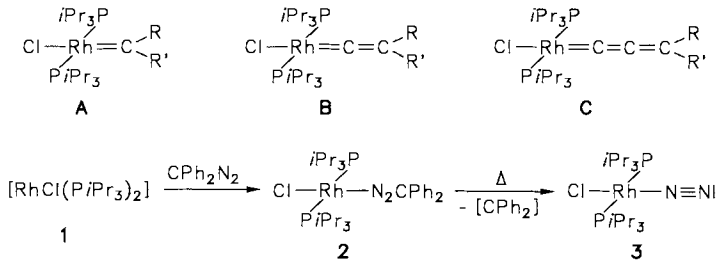

Scheme 1.

Treatment of compound **4**[5] with CPh_2N_2 in pentane at room temperature leads to a rapid displacement of ethene by the diphenylcarbene ligand. The olive-green crystals of **5** (Scheme 2), which were isolated in 96% yield, can be stored under argon at $-20\,^{\circ}C$ but decompose in solution in a few hours. The X-ray crystal structure analysis of **5** (Fig. 1)[6] reveals that the rhodium has a somewhat distorted square-planar coordination sphere. The angle Sb1-Rh-Sb2 (155.48(2)°) deviates significantly from the ideal value of 180°, which is probably due to the repulsive forces between the isopropyl and phenyl groups. The Rh–Cl bond is surprisingly short (it is, to the best of our knowledge, the shortest Rh–C(carbene) distance ever found[7]) and thus indicative of a strong Rh–C back-bonding.

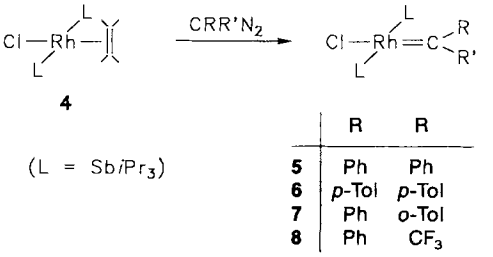

	R	R
5	Ph	Ph
6	*p*-Tol	*p*-Tol
7	Ph	*o*-Tol
8	Ph	CF_3

Scheme 2.

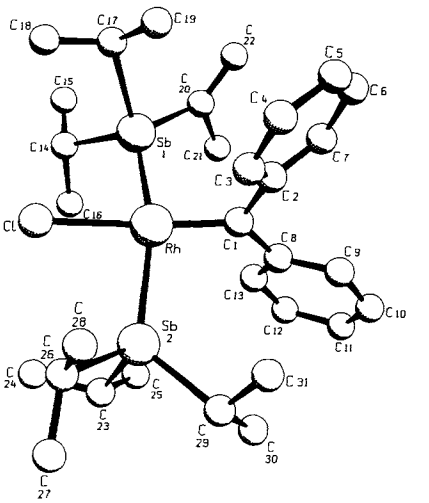

Fig. 1. Crystal structure of **5**. Selected bond distances [Å] and angles [°]: Rh–Sb1 2.5843(5), Rh–Sb2 2.5633(5), Rh–Cl 2.452(1), Rh–C1 1.863(4), C1–C2 1.489(6), C1-C8 1.497(6); Sb1-Rh-Sb2 155.48(2), Cl-Rh-C1 171.0(1), Sb1-Rh-Cl 84.15(3), Sb1-Rh-C1 96.8(1), Sb2-Rh-Cl 84.75(3), Sb2-Rh-C1 97.6(1), Rh-C1-C2 115.7(3), Rh-C1-C8 127.6(3), C2-C1-C8 116.6(4).

With di-*p*-tolyldiazomethane, phenyl-*o*-tolyldiazomethane, and even with phenyl(trifluoromethyl)diazomethane, carbene complexes **6**–**8**, structurally related to **5**, are obtained in nearly quantitative yield. In general, the rate of reaction increases considerably in the order **6** < **7** < **5** < **8**, that is, faster for alkyl(aryl) derivatives. The composition of **6**–**8** is confirmed both by elemental analysis and spectroscopic data (Table 1). Compound **4** also reacts spontaneously with benzoyldiazomethane and PhC(O)CPhN$_2$ (azibenzil) in ether at $-78\,^{\circ}C$, but in these cases a diazoalkanerhodium complex is formed instead of a carbenerhodium species.

Scheme 3 illustrates that the square-planar carbenerhodium compounds have great potential as starting materials for the synthesis of other organorhodium derivatives. Both **5** and **7** react with NaC_5H_5 in THF to give the half-sandwich type complexes (**9** and **10**), which are isolated in 70–80% yield. The fact that in contrast to **5**–**8** they are not 18-electron compounds is reflected in the high field shift of the signal of the carbene C atom, which for **9** is observed at $\delta = 260.97$ (cf. **5**: $\delta = 316.16$).

The reactions of **9** with CO and *t*BuNC lead, in pentane at room temperature, almost quantitatively to the displacement of the stibane ligand and to the formation of the corresponding carbonyl and isocyanide complexes. Half-sandwich complexes **11** and **12** are red crystalline solids which are stable under inert atmosphere (Ar). We note that carbene(carbonyl)rhodium compounds of half-sandwich type were originally prepared by Erker et al.[9] upon treatment of

[*] Prof. Dr. H. Werner, Dipl.-Chem. P. Schwab, Dipl.-Chem. N. Mahr, Dr. J. Wolf
Institut für Anorganische Chemie der Universität
Am Hubland, D-97074 Würzburg (FRG)
Telefax: Int. code + (931)888-4605

[**] This work was supported by the Deutsche Forschungsgemeinschaft (Sonderforschungsbereich 347), the Fonds der Chemischen Industrie and Degussa AG.

Table 1. Selected spectroscopic data (omitting the ^1H and ^{13}C NMR data for aryl groups). NMR spectra in C_6D_6 at 200 MHz (^1H), for **12** at 400 MHz; 50.3 MHz (^{13}C), for **8** and **12** at 100.6 MHz; 81 MHz (^{31}P); 188.3 MHz (^{19}F).

5: ^1H NMR: $\delta = 2.08$ (sept, $^3J(HH) = 7.3$ Hz, $SbCHCH_3$), 1.31 (d, $^3J(HH) = 7.3$ Hz, $SbCHCH_3$); ^{13}C NMR: $\delta = 316.16$ (d, $^1J(RhC) = 29.1$ Hz, Rh=C), 21.90 (s, $SbCHCH_3$), 19.07 (d, $^2J(RhC) = 3.4$ Hz, $SbCHCH_3$).

6: ^1H NMR: $\delta = 2.12$ (sept, $^3J(HH) = 7.3$ Hz, $SbCHCH_3$), 1.35 (d, $^3J(HH) = 7.3$ Hz, $SbCHCH_3$); ^{13}C NMR: $\delta = 316.57$ (d, $^1J(RhC) = 28.0$ Hz, Rh=C), 22.16 (s, $SbCHCH_3$), 19.06 (d, $^2J(RhC) = 3.7$ Hz, $SbCHCH_3$).

7: ^1H NMR: $\delta = 2.03$ (sept, $^3J(HH) = 7.3$ Hz, $SbCHCH_3$), 1.31 (d, $^3J(HH) = 7.3$ Hz, $SbCHCH_3$); ^{13}C NMR: $\delta = 298.07$ (d, $^1J(RhC) = 31.0$ Hz, Rh=C), 22.08 (s, $SbCHCH_3$), 18.65 (d, $^2J(RhC) = 3.6$ Hz, $SbCHCH_3$).

8: ^1H NMR: $\delta = 2.14$ (sept, $^3J(HH) = 7.3$ Hz, $SbCHCH_3$), 1.33 (d, $^3J(HH) = 7.3$ Hz, $SbCHCH_3$); ^{13}C NMR: $\delta = 293.61$ (dq, $^1J(RhC) = 17.4$, $^2J(FC) = 14.6$ Hz, Rh=C), 127.70 (q, $^1J(FC) = 259.8$ Hz, CF_3), 21.91 (s, $SbCHCH_3$), 19.66 (s, $SbCHCH_3$); ^{19}F NMR: $\delta = -57.22$ (s).

9: MS (70 eV): m/z 585 (M^+); ^1H NMR: $\delta = 5.00$ (d, $^2J(RhH) = 0.9$ Hz, C_5H_5), 1.35 (sept, $^3J(HH) = 7.0$ Hz, $SbCHCH_3$), 1.10 (d, $^3J(HH) = 7.0$ Hz, $SbCHCH_3$); ^{13}C NMR: $\delta = 260.97$ (d, $^1J(RhC) = 46.9$ Hz, Rh=C), 82.79 (d, $^1J(RhC) = 3.8$ Hz, C_5H_5), 21.62 (s, $SbCHCH_3$), 18.26 (d, $^3J(RhC) = 3.2$ Hz, $SbCHCH_3$).

10: MS (70 eV): m/z 599 (M^+); ^1H NMR: $\delta = 4.63$ (s, br, C_5H_5), 1.74 (sept, $^3J(HH) = 7.2$ Hz, $SbCHCH_3$), 1.29 (d, $^3J(HH) = 7.2$ Hz, $SbCHCH_3$); ^{13}C NMR: $\delta = 253.71$ (d, $^1J(RhC) = 45.6$ Hz, Rh=C), 88.27 (d, $^1J(RhC) = 3.8$ Hz, C_5H_5), 21.42 (s, $SbCHCH_3$), 18.26 (s, $SbCHCH_3$).

11: MS (70 eV): m/z 362 (M^+); IR (KBr): $\nu[cm^{-1}] = 1982$ (CO); ^1H NMR: $\delta = 4.92$ (d, $^2J(RhH) = 0.7$ Hz, C_5H_5); ^{13}C NMR: $\delta = 286.68$(d, $^1J(RhC) = 48.0$ Hz, Rh=CPh_2), 192.71 (d, $^1J(RhC) = 101.7$ Hz, CO), 89.68 (d, $^1J(RhC) = 3.5$ Hz, C_5H_5).

12: MS (70 eV): m/z 417 (M^+); IR (KBr): $\nu[cm^{-1}] = 2118$ (CN); ^1H NMR: $\delta = 5.14$ (d, $^2J(RhH) = 0.4$ Hz, C_5H_5), 0.78 (s, CCH_3); ^{13}C NMR: $\delta = 267.91$ (d, $^1J(RhC) = 50.3$ Hz, Rh=CPh_2), 148.17 (d, $^1J(RhC) = 98.3$ Hz, $CNCCH_3$), 86.74 (d, $^1J(RhC) = 3.9$ Hz, C_5H_5), 55.87 (s, CCH_3), 30.10 (s, CCH_3).

14: ^1H NMR: $\delta = 2.33$ (m, $PCHCH_3$), 1.18 (dvt, $N = 13.2$, $^3J(HH) = 7.1$ Hz, $PCHCH_3$); ^{13}C NMR: $\delta = 316.11$ (dt, $^1J(RhC) = 36.9$, $^2J(PC) = 8.4$ Hz, Rh=C), 25.25 (vt, $N = 17.4$ Hz, $PCHCH_3$), 20.59 (s, $PCHCH_3$); ^{31}P NMR: $\delta = 22.89$ (d, $^1J(RhP) = 169.4$ Hz).

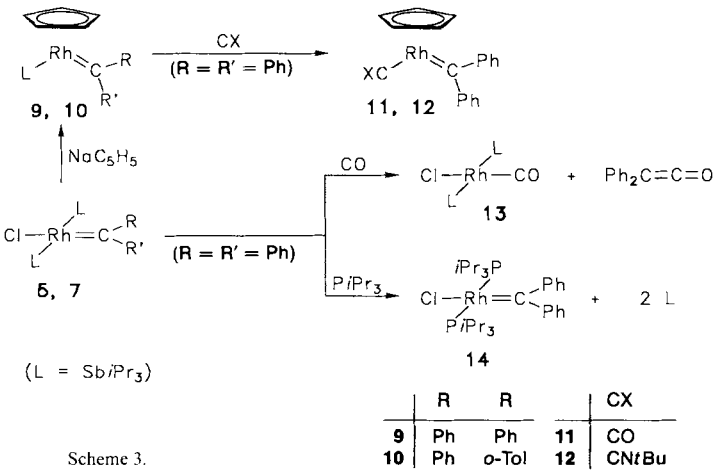

	R	R		CX
9	Ph	Ph	11	CO
10	Ph	o-Tol	12	CN*t*Bu

Scheme 3.

$[(C_5H_5)Rh(CO)_2]$ with a reactive metallocene derivative such as $[(C_5H_5)_2Zr(\eta^4\text{-}C_4H_6)]$. No carbene(isocyanide) complex similar to **12**, however, is known.

The reactions of compound **5** with CO and $PiPr_3$ take a completely different course. Whereas by passing CO through a solution of **5** in pentane the carbonylrhodium complex **13**[5] and diphenylketene (identified by the IR and ^{13}C NMR spectra) are formed, on treatment of **5** with $PiPr_3$ a substitution of the stibane by the phosphane takes place. The yield of **14**, a yellow-green crystalline solid, is 98%! A complex of type **A**, which was the main target of this work, thus can be prepared from $[\{RhCl(C_2H_4)_2\}_2]$ not on a direct but an indirect route (via **4** and **5**), and such a complex is remarkably stable.

Compounds **5**–**8**, **9**–**12**, and **14** are the first carbenerhodium(I) complexes carrying a carbene ligand that is not stabilized by linkage to a hetero atom (O or N).[10] It should be emphasized that not only the primary reaction products **5**–**8** but also the subsequently formed compounds **9**–**12** and **14** are isolated in excellent (sometimes quantitative) yields. Furthermore, in the reactions of **5** the attack of the nucleophile (with the exception of CO) is preferentially directed to the metal and not to the carbene carbon atom as in Fischer-type carbene complexes.[10a, 11] Although diphenyldiazomethane and its derivatives were already used in 1974 by Herrmann et al. for the synthesis of carbenemetal compounds,[12] more recently this source of carbenes has hardly been employed for the formation of $M=CR_2$ bonds.[10] The crucial point is that in most of these reactions diazoalkane metal complexes are formed that do not lose N_2 to give the corresponding metal carbenes at ambient temperatures.

Experimental Procedure

5: A solution of **4** (87 mg, 0.13 mmol) in pentane (10 mL) was treated at −78 °C with a solution of CPh_2N_2 (51 mg, 0.26 mmol) in pentane (2 mL). After warming to room temperature, the solution was stirred for 30 min, and then the solvent was removed. The residue was washed twice with small amounts of methanol and dissolved in hexane (2 mL). The product mixture was separated by chromatography on Al_2O_3 (neutral, activity grade V, 3 cm column) with hexane, the dark green fraction was evaporated to dryness, and the residue was recrystallized from pentane (−78 °C) to give olive-green crystals. Yield 101 mg (96%); m.p. 61 °C (decomp). Compounds **6**, **7**, and **8** were prepared in a similar way. For **6** and **7**, the reaction time at room temperature is 90 and 60 min, respectively; for **8** the reaction is performed (without warming) at −78 °C, and column chromatography is unnecessary. **6**: yield 94%; m.p. 55 °C (decomp.). **7**: yield 93%; m.p. 28 °C (decomp.). **8**: yield 91%; m.p. 43 °C (decomp.).

9: A solution of **5** (83 mg, 0.10 mmol) in THF (10 mL) was treated at room temperature with NaC_5H_5 (44 mg, 0.50 mmol). The solution was stirred for 30 min, the solvent then removed, the oily residue extracted with pentane (10 mL), and the extract concentrated to about 0.5 mL. The concentrate was chromatographed on Al_2O_3 (see **5**) with hexane, and the dark fraction was evaporated to dryness in vacuum. The residue was washed twice with methanol (−30 °C) and recrystallized from pentane (−78 °C) to give deep blue crystals. Yield 57 mg (78%); m.p. 30 °C (decomp.). Compound **10** (blue violet oil) was prepared analogously; yield 73%.

11: CO was passed through a solution of **9** (70 mg, 0.12 mmol) in pentane (10 mL) for 30 s at room temperature. After the solution had been stirred for 1 h, the solvent was removed, and the residue worked up as described for **9**: red crystals; yield 38 mg (87%); m.p. 49 °C (decomp.). Compound **12** was prepared in an analogous way. Pure material (red crystals) was obtained without column chromatography; yield 89%; m.p. 88 °C (decomp.).

13: CO was passed through a solution of **5** (81 mg, 0.10 mmol) in pentane (10 mL) for 30 s at room temperature. After the solution had been stirred for 1 h, it was concentrated to about 1 mL, and the concentrate chromatographed on Al_2O_3 (neutral, activity grade III, 6 cm column). With hexane a yellow fraction was eluted, which, after removal of the solvent, gave a solid that was characterized by IR and ^1H and ^{13}C NMR spectroscopic data as **13** [5]. With hexane/benzene a red substance was eluted, which was identified by IR and ^{13}C NMR data as $Ph_2C=C=O$.

14: A solution of **9** (81 mg, 0.10 mmol) in pentane (10 mL) was treated with $PiPr_3$ (41 µL, 0.20 mmol) and stirred for 30 min at room temperature. After removal of the solvent, the oily residue was washed twice (at 0 °C) with small amounts of methanol, then dissolved in hexane (2 mL), and the solution was worked up as described for **5**: yellow-green crystals; yield 61 mg (98%); m.p. 81 °C (decomp.).

Received: February 18, 1993 [Z 5875 IE]
German version: *Angew. Chem.* **1993**, *105*, 1498

[1] a) W. Levason, C. A. McAuliffe, *Phosphine, Arsine and Stibine Complexes of the Transition Elements*, Elsevier, Amsterdam, **1977**; b) W. Levason, C. A. McAuliffe, *Acc. Chem. Res.* **1978**, *11*, 363–368.

[2] a) H. Werner, F. J. Garcia Alonso, H. Otto, J. Wolf, *Z. Naturforsch. B* **1988**, *43*, 722–726; b) H. Werner, U. Brekau, *ibid.* **1989**, *44*, 1438–1446; c) H. Werner, T. Rappert, J. Wolf, *Isr. J. Chem.* **1990**, *30*, 377–384; d) D. Schneider, H. Werner, *Angew. Chem.* **1991**, *103*, 710–712; *Angew. Chem. Int. Ed. Engl.* **1991**, *30*, 700–702; e) T. Rappert, O. Nürnberg, N. Mahr, J. Wolf, H. Werner, *Organometallics* **1992**, *11*, 4156–4164.

[3] a) H. Werner, T. Rappert, *Chem. Ber.* **1993**, *126*, 669–678; b) T. Rappert, Dissertation, Universität Würzburg, **1992**.
[4] C. Busetto, A. D'Alfonso, F. Maspero, G. Perego, A. Zazzetta, *J. Chem. Soc. Dalton Trans.* **1977**, 1828–1834.
[5] H. Werner, P. Schwab, N. Mahr, J. Wolf, *Chem. Ber.* **1992**, *125*, 2641–2650.
[6] Crystals from pentane (−20 °C); crystal size 0.4 × 0.3 × 0.2 mm; triclinic, space group $P\bar{1}$ (no. 2), $Z = 2$; $a = 11.025(2)$, $b = 12.348(5)$, $c = 14.194(2)$ Å; $\alpha = 83.18(2)$, $\beta = 86.17(1)$, $\gamma = 63.11(2)°$; $V = 1711.3(9)$ Å^3, $\varrho_{calcd} = 1.56$ g cm^{-3}; max. $2\theta = 44°$ ($Mo_{K\alpha}$, $\lambda = 0.70930$ Å, graphite monochromator, $\omega/2\theta$-Scan, $T = 223$ K); 4447 reflections measured, 4180 independent, 3950 observed [$F_o > 3\sigma(F_o)$], Lorentzian polarization and empirical absorption corrections ($\mu = 21.4$ cm^{-1}, ψ-scan method, min. transmission 84.11%); direct methods (SHELXS-86), refinement with program package SDP (Enraf–Nonius), positions of hydrogen atoms calculated according to ideal geometry (C-H distance 0.95 Å); $R = 0.0285$, $R_w = 0.0395$; reflex/parameter ratio 12.5; residual electron density +0.582/−0.910 eÅ^{-3}. Further details of the X-ray structure analysis are available on request from the Fachinformationszentrum Karlsruhe, Gesellschaft für wissenschaftlich-technische Information mbH, D-76344 Eggenstein-Leopoldshafen (FRG), on quoting the depository number CSD-57130, the names of the authors, and the journal citation.
[7] For comparison: *trans*-[Rh(=CN(CH$_3$)CH$_2$CH$_2$NCH$_3$){N = C(CF$_3$)$_2$}-(PPh$_3$)$_2$], [*d*(Rh-C) = 2.006(15) Å] (Ref. [8a]) and *trans*-[Rh(=CN(CH$_3$)CH$_2$CH(CH$_2$CH(CH$_3$)$_2$)NCH$_3$)Cl(PPh$_3$)$_2$], [*d*(Rh-C) = 1.92(3) Å] (Ref. [8b]).
[8] a) M. J. Doyle, M. F. Lappert, G. M. McLaughlin, J. McMeeking, *J. Chem. Soc. Dalton Trans.* **1974**, 1494–1501; b) A. W. Coleman, P. B. Hitchcock, M. F. Lappert, R. K. Maskell, J. H. Müller, *J. Organomet. Chem.* **1985**, *296*, 173–196.
[9] Reviews: a) G. Erker, *Angew. Chem.* **1989**, *101*, 411–426; *Angew. Chem. Int. Ed. Engl.* **1989**, *28*, 397–412; b) *Polyhedron* **1988**, *7*, 2451–2463; c) recent publication: G. Erker, M. Mena, U. Hoffmann, B. Menjon, J. L. Petersen, *Organometallics* **1991**, *10*, 291–298.
[10] Reviews: a) K. H. Dötz, H. Fischer, P. Hofmann, F. R. Kreissl, U. Schubert, K. Weiss, *Transition Metal Carbene Complexes*, Verlag Chemie, Weinheim, **1983**; b) *Advances in Metal Carbene Chemistry* (Ed.: U. Schubert) (*NATO ASI Ser. C*, **1989**); c) P. J. Brothers, W. R. Roper, *Chem. Rev.* **1988**, *88*, 1293–1326; d) M. F. Lappert, *J. Organomet. Chem.* **1988**, *358*, 185–214.
[11] a) E. O. Fischer, *Angew. Chem.* **1974**, *86*, 651–663; *Adv. Organomet. Chem.* **1976**, *14*, 1–32; b) W. R. Roper, *J. Organomet. Chem.* **1986**, *300*, 167–190.
[12] a) W. A. Herrmann, *Angew. Chem.* **1974**, *86*, 556–557; *Angew. Chem. Int. Ed. Engl.* **1974**, *13*, 599–600; b) Review: W. A. Herrmann, *ibid.* **1978**, *90*, 855–868 and **1978**, *17*, 800–813.

Synthesis and Structure of Surprisingly Stable Tetrakis(trifluoromethyl)cuprate(III) Salts**

By *Dieter Naumann,* Thomas Roy, Karl-Friedrich Tebbe,* and *Wolfgang Crump*

Previously only a few copper(III) compounds could be characterized unequivocally.[1] The single known copper(III) compound containing a perfluoroalkyl group is $[Cu(CF_3)_2SC(S)NEt_2]$;[2] the oxidation of bis(trifluoromethyl)cuprate(I) was reported to yield $[Cu(CF_3)_4]^-$, but no further details were given.[2]

We report here on the synthesis, isolation, and structure of $[Cu(CF_3)_4]^-$ salts. These compounds were prepared by oxidation of a mixture of Cu^I-CF_3 compounds in dimethylformamide (DMF)[3] with a stoichiometric amount of XeF_2, iodine, bromine, chlorine, or ICl; when an excess of the oxidant was used, the product decomposed giving CF_3X (X = F, Cl, Br, I). The reaction mixture was then treated with a salt with a bulky cation ([Bu_4N]Br, [Ph_4P]Cl, or [PNP]Cl(PNP=Ph_3PNPPh_3)), the solvent removed by distillation, and the residue taken up in CH_2Cl_2. After chromatography and concentration of the eluate, the product was dried under vacuum to provide the salts $[cat]^+[Cu(CF_3)_4]^-$ (cat = Bu_4N, Ph_4P, PNP) as colorless crystalline solids; these were not sensitive to light, air, and moisture. The higher homologues Cu^I-C_2F_5 and Cu^I-*i*-C_3F_7 were not oxidized under these conditions. The surprisingly stable $[Cu(CF_3)_4]^-$ compounds decompose upon melting at temperatures above 140 °C,[4] roughly 50 °C higher than for the homologous Ag^{III} compound $[Ag\{Ag(CF_3)_4\}]$.[5] In contrast to the Cu^I-CF_3 compounds these cuprates(III) are soluble in almost all organic solvents without decomposition.

Examination of the Cu^{III} salts by differential thermoanalysis/thermogravimetry (DTA/TG) indicates that the mass loss at the melting point corresponds roughly to the cleavage of four CF_2 groups, as was also the case for the Ag^{III} compound.[6] The vibrational spectra are in accord with the D_{4h} symmetry expected for compounds with d^8 configuration.[7] Because of the quadrupole moment of the ^{63}Cu and ^{65}Cu isotopes, the NMR spectra do not give any definite structural information.[8] The crystal structure determination confirms the approximately square-planar arrangement of the four C atoms around the Cu atom in the complex anion[9] (Fig. 1). The neighboring CF_3 groups are staggered,

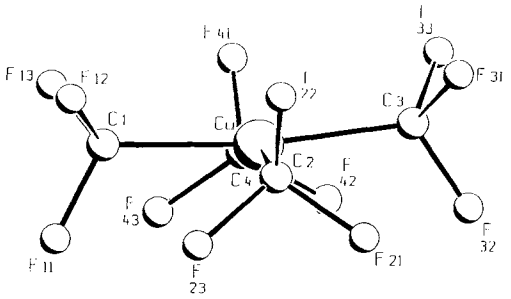

Fig. 1. Crystal structure of the $[Cu(CF_3)_4]^-$ anion in [PNP][$Cu(CF_3)_4$]. Bond lengths [pm] and angles [°]: Cu-C1 194.9(15), Cu-C2 198.3(13), Cu-C3 195.4(16), Cu-C4 198.0(17), C1-F11 130(2), C1-F12 140(2), C1-F13 136(2), C2-F21 136(1), C2-F22 131(2), C2-F23 136(2), C3-F31 136(2), C3-F32 131(2), C3-F33 139(2), C4-F41 133(2), C4-F42 136(2), C4-F43 133(2); C3-Cu-C4 91.3(7), C2-Cu-C4 165.0(7), C2-Cu-C3 90.2(6), C1-Cu-C4 89.1(7), C1-Cu-C3 172.2(6), C1-Cu-C2 91.4(6).

the *trans* groups eclipsed, and the C atoms are displaced from the ideal plane by approximately 20 pm. The two sets of six F atoms form a planar hexagon above and below the CuC_4 plane. The Cu atom is thereby shielded from nucleophilic attack. This "shielding" may explain the high chemical and thermal stability.

Experimental Procedure

All operations were conducted under nitrogen. The $[Cd(CF_3)_2]$ complexes employed in the synthesis of the Cu^I-CF_3 compounds were prepared according to ref.[10]. All other chemicals are commercially available.

cat[$Cu(CF_3)_4$]: The preparation of [Ph_4P][$Cu(CF_3)_4$] with iodine as oxidant serves as an example. The solution of Cu^I-CF_3 compounds[3] at −40 °C was treated with iodine (155 mg, 0.6 mmol) in DMF, stirred for 2 h, and slowly allowed to warm to room temperature. [Ph_4P]Cl (3.747 g, 10 mmol) in DMF was added. The solvent was removed by distillation at room temperature. The soluble residue was taken up in CH_2Cl_2 and purified by column chromatography (silica gel, eluent CH_2Cl_2/acetone (5/1)). The solvent was distilled off, and [Ph_4P][$Cu(CF_3)_4$] was obtained as a colorless, light-, air-, and moisture-insensitive crystalline solid, which does not sublime up to 80 °C/10^{-2} Torr. Total yield: 51.3% (based on $Cd(CF_3)_2 \cdot D$).

[*] Prof. Dr. D. Naumann, Dipl.-Chem. T. Roy, Prof. Dr. K.-F. Tebbe, Dipl.-Chem. W. Crump
Institut für Anorganische Chemie der Universität
Greinstrasse 6, D-50939 Köln (FRG)
Telefax: Int. code + (221)470-5196

[**] This research was supported by the Fonds der Chemischen Industrie and the Ministerium für Wissenschaft und Forschung des Landes Nordrhein-Westfalen (Arbeitsgemeinschaft Fluorchemie).

The salts [PNP][Cu(CF$_3$)$_4$] and [(nBu)$_4$N][Cu(CF$_3$)$_4$] were synthesized analogously; Br_2, Cl_2, ICl, and XeF_2 are also suitable oxidants.

Molecular masses determined in CH_3CN (calcd) for cat = PNP: 426.7 (878.2); cat = Ph_4P: 356.3 (679.0); cat = Bu_4N: 298.6 (582.0); thus in CH_3CN the salts are completely dissociated. Correct elemental analyses.

Received: May 27, 1993 [Z 6111 IE]
German version: *Angew. Chem.* **1993**, *105*, 1555

[1] See for example: N. N. Greenwood, A. Earnshaw, *Chemistry of the Elements*, Pergamon, Oxford, **1985**, p. 1371, 1379.
[2] M. A. Willert-Porada, D. J. Burton, N. C. Baenziger, *J. Chem. Soc. Chem. Commun.* **1989**, 1633–1634.
[3] D. M. Wiemers, D. J. Burton, *J. Am. Chem. Soc.* **1986**, *108*, 832–834; D. J. Burton, Z.-Y. Yang, *Tetrahedron* **1992**, *48*, 189–275; W. Strauss, Dissertation, Universität Dortmund, **1986**; B. Caeners, Dissertation, Universität Dortmund, **1990**.
[4] Melting and decomposition points: [Bu_4N][Cu(CF$_3$)$_4$] 142 °C, [Ph_4P][Cu(CF$_3$)$_4$] 146 °C, [PNP][Cu(CF$_3$)$_4$] 147 °C.
[5] W. Dukat, D. Naumann, *Rev. Chim. Miner.* **1986**, *23*, 589–603.
[6] DTA/TG of [Bu_4N][Cu(CF$_3$)$_4$]: Δm at 142.5 °C: 38.8%.
[7] [Bu_4N][Cu(CF$_3$)$_4$] (only CuC vibrations): IR (KBr): $\tilde{\nu}$ = 372 cm^{-1}, w (E_u); Raman (solid, 23 °C): $\tilde{\nu}$ = 232 cm^{-1}, vs, p, (A_{1g}), 212 sh, w, dp (B_{1g}) (cf. Ag[Ag(CF$_3$)$_4$]: IR: 325 cm^{-1}, w; Raman: 225 cm^{-1}, vs, p, 210 cm^{-1}, sh, dp[5]).
[8] ^{19}F NMR spectra (CCl_3F standard): δ(^{19}F) is concentration independent but solvent dependent: pyridine −31.5; DMSO −32.3; DMF −33.2; THF −33.8; CH_3CN −33.9; CH_3OH −34.0; CH_2Cl_2 −34.7; ^{13}C NMR spectra ([D$_6$]acetone): δ(^{13}C) = 135.7. At −30 °C ^1J(F,C) is determined to be 374 Hz.
[9] [PNP][Cu(CF$_3$)$_4$] ($C_{40}H_{30}CuF_{12}NP_2$, M = 878.15), tetragonal, space group $P4_1$ (no. 76), a = 950.9(3), c = 4245.2(10) pm, V = 3.838(3) nm^3, Z = 4, ρ_{calcd} = 1.52 g cm^{-3}, μ(Mo$_{K\alpha}$) radiation) = 6.98 cm^{-1}. In the range $2° \le \vartheta \le 25°$ 3889 reflections were measured, of which 2160 were symmetry independent, classified as observed according to $|F| \ge 4\sigma(F)$, and used for the structure determination. The complete anisotropic refinement with 506 parameters converged at R_F = 0.063 and wR_F = 0.063. The measurement was conducted at 293 K with a CAD4 diffractometer (Mo$_{K\alpha}$ radiation, λ = 0.71069 Å). For data reduction the Molen program package was employed; the structure was solved with the SHELXS86 program; other structure calculations were conducted with the SHELX76 program. Further details of the crystal structure investigation may be obtained from the Fachinformationszentrum Karlsruhe, Gesellschaft für wissenschaftlich-technische Information mbH, D-76344 Eggenstein-Leopoldshafen (FRG) on quoting the depository number CSD-57323, the names of the authors, and the journal citation.
[10] H. Lange, D. Naumann, *J. Fluorine Chem.* **1984**, *26*, 1–18.

Synthesis and Structure of a Sixteen-Membered (AlNCO)$_4$ Ring**

By *Craig M. Bird, Catherine Breheny, Matthew G. Davidson, Andrew J. Edwards, S. Clare Llewellyn, Paul R. Raithby*, and *Ronald Snaith**

We described recently the syntheses and structures of alkali and alkaline earth metal chelate complexes **A** containing ligands of type (Y-R-X)$^-$.[1, 2] In these, R is a heterocyclic framework, X and Y are two electronegative centers, and L is a neutral ligand, for example, hexamethylphosphoric triamide (HMPA). Most attention has focused on complexes with ligand **B**, the anion of 2-mercaptobenzoxazole (OxSH; X, Y = N, S). Solutions of these complexes will dissolve salts M′Z of other metals such as $PtCl_2$[2a] and $HgCl_2$.[2b] When the metal center M in complex **A** is complexed by Z, one center of its chelating ligand, for example Y, is displaced and then coordinates to the inserted metal M′ to give a cocomplex of the general type **C**. We have been interested in an Al-Ti cocomplex of this type with regard to Ziegler–Natta catalysis.[3] Here we describe the synthesis of a precursor Al complex containing the [C$_6$H$_4$OC(=O)N]$^-$ anion (OxO$^-$; X,Y = N,O). This ligand is similar to **B**, but S is replaced by O, since O coordinates better to hard cations like Ti^{3+} and Ti^{4+}.

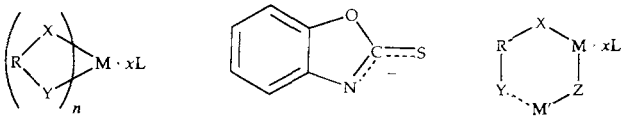

A; n = 1, 2 B C

Reaction of Me_3Al with OxOH (1:1 mol ratio) in toluene afforded a pale yellow solution, refrigeration of which gave crystals of **1** (see Experimental Procedure). Two possible

[{(OxO)AlMe$_2$}$_4$] **1**

solid-state structures were envisaged for **1**: 1) a monomer with a four-membered ring in which the OxO$^-$ ligand chelates the Me_2Al unit through its N and *exo*-O centers, or 2) a dimer in which these centers act "intermolecularly" and span two Al centers, affording an eight-membered (Al-O-C-N-Al-O-C-N) ring. A search of the Cambridge Crystallographic Data Base revealed that the second structure type is the norm for (Y-R-X)Al compounds, for example in [(PhNCPhOAlMe$_2$)$_2$] (NCO system),[4a] in the mercaptopyridine complex [NC$_5$H$_4$SAlMe$_2$SC$_5$H$_4$NAlMe$_2$] (NCS system),[4b] and in [(Me$_2$AlNMeCMeNMe)$_2$] (NCN system).[4c] No structures with larger than eight-membered rings (e.g., a trinuclear Al complex with a twelve-membered ring) are known. Indeed, in Al complexes with (Y-R-R′-X)$^-$ ligands, dimerization to give a ten-membered ring is resisted; instead monomers with five-membered rings are found, for example, [Me_2Al(CONMe)$_2$AlMe$_2$] (NCCO system)[5a] and [Me_2Al{C(NMe$_2$)$_2$}$_2$AlMe$_2$] (NCCN system).[5b] In contrast to these earlier results, an X-ray diffraction study on **1**[6] has revealed a *tetramer* with a 16-membered (AlNCO)$_4$ ring.

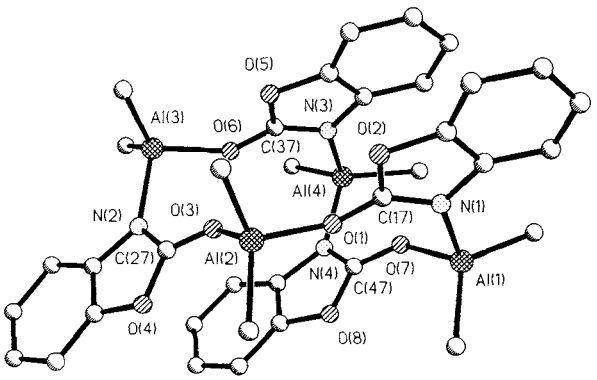

Fig. 1. Crystal structure of **1**.

[*] Dr. R. Snaith, C. M. Bird, C. Breheny, M. G. Davidson, Dr. A. J. Edwards, S. C. Llewellyn, Dr. P. R. Raithby
University Chemical Laboratory
Lensfield Road, GB-Cambridge, CB21EW (UK)
Telefax: Int. code + (223)336-362

[**] This work was supported by the Science and Engineering Research Council (all authors), the Associated Octel Co. Ltd. (M. G. D., R. S.), St. John's College, Cambridge (M. G. D.), and the Cambridge Crystallographic Data Centre (A. J. E.).

Figure 1 shows the whole tetrameric solid-state structure of **1**, and Figure 2a highlights the central core (including the uncoordinated O atoms of the heterocycle. The key feature in the structure is the alternation of OxO^- ligands and their $[N{-}C{-}O]^-$ coordinating units around the sixteen-membered ring. The resulting sequence is (Al(1)-NCO-Al(2)-OCN-Al(3)-OCN-Al(4)-NCO)], in which Al(1) and Al(3) are coordinated by N and O, Al(2) by O and O, and Al(4) by N and N. The effect of this alternation is to organize and space out the ring components of the OxO^- ligands, thus allowing the formation of such a large ring. As shown in Figure 2b (and as indicated in Fig. 1), these ring components are aligned in two nearly parallel pairs: the ring system containing N1 with that containing N3, and the ring system containing N2 with that containing N4. That this effect is steric (rather than electronic) in origin is emphasized by the fact that the distances between these aligned rings are long, >4.2 Å; this rules out graphite-like π interactions. The distances between the heterocyclic rings of neighboring tetramers are 3.6 Å or greater. Within the tetramer, distances to Al are as expected: Al–O 1.820–1.840 Å (average 1.832 Å), Al–N 1.948–1.955 (1.951 Å), Al–C 1.945–1.963 (1.953 Å). The relevant distances with the OxO^- anions are N–C 1.318–1.333 (average 1.327 Å), C–*exo*-O 1.260–1.268 (1.265 Å), and C–(ring)O 1.345–1.359 (1.351 Å). Thus the coordinating section of the anion, N-C-(*exo*)O, is best represented as $[N{-}C{-}O]^-$.

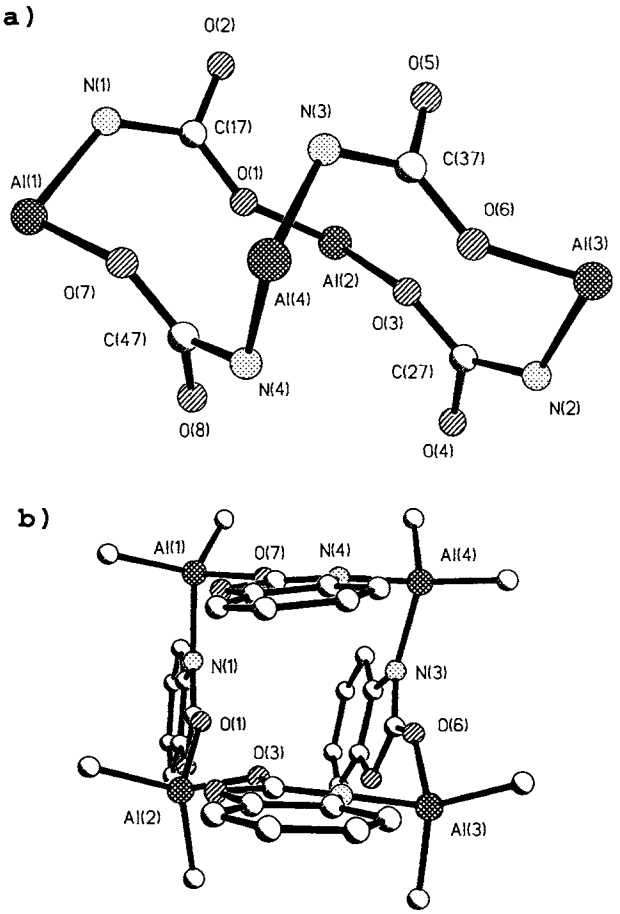

Fig. 2. a) The central 16-membered ring of **1**. b) A view of the molecular structure of **1** highlighting the two sets of aligned parallel heterocycles and the central cavity.

These findings are intriguing on two counts. Firstly, they form an interesting contrast to the widespread use of bulky ligands to *restrict* association; in **1** a *flat* bifunctional ligand allows formation of a ring of unprecedented size. Secondly, **1** could be regarded as a metallacoronand in its own right: each N is only three coordinate, and both O centers of each anion are merely two coordinate. Given this coordinative unsaturation, and the fact that the molecular structure of **1** has a cavity (Fig. 2b), we are exploring the use of **1** to coordinate other compounds including $TiCl_4$ and $[Cp_2TiCl_2]$.

Experimental Procedure

1: Me_3Al (2.5 mL of a 2.0 M solution in toluene) was added to a solution of OxOH (0.676 g, 5 mmol) in 15 mL of dry toluene at −78 °C. On warming to room temperature, a vigorous effervescence occurred, leaving a clear, pale-yellow solution. Refigeration of the solution at −5 °C afforded colorless crystals of **1** (first batch yield 0.537 g, 56%) m.p. 127–129 °C. Correct elemental analyses. ^1H NMR (250 MHz, C_6D_6, 25 °C): δ = 7.50–6.50 (series of m, 4H; OxO^-), 0.10 – 0.50 (series of s, 6H; $AlMe_2$)].

Received: April 3, 1993 [Z 5975 IE]
German version: *Angew. Chem.* **1993**, *105*, 1502

[1] a) D. Barr, P. R. Raithby, P. von R. Schleyer, R. Snaith, D. S. Wright, *J. Chem. Soc. Chem. Commun.* **1990**, 643–645; b) D. R. Armstrong, D. Barr, P. R. Raithby, P. von R. Schleyer, R. Snaith, D. S. Wright, *Inorg. Chim. Acta* **1991**, *185*, 163–167; c) P. Mikulcik, P. R. Raithby, R. Snaith, D. S. Wright, *Angew. Chem.* **1991**, *103*, 452–454; *Angew. Chem. Int. Ed. Engl.* **1991**, *30*, 428–430; d) F. A. Banbury, M. G. Davidson, A. J. Edwards, M.-I. Lopez Solera, P. R. Raithby, R. Snaith, D. Stalke, D. S. Wright, *Inorg. Chim. Acta* **1993**, *203*, 93–95.

[2] a) M. G. Davidson, P. R. Raithby, R. Snaith, D. Stalke, D. S. Wright, *Angew. Chem.* **1991**, *103*, 1696–1697; *Angew. Chem. Int. Ed. Engl.* **1991**, *30*, 1648–1650; b) M. G. Davidson, S. C. Llewellyn, M.-I. Lopez Solera, P. R. Raithby, R. Snaith, D. S. Wright, *J. Chem. Soc. Chem. Commun.* **1992**, 573–575.

[3] a) K. Ziegler, *Adv. Organomet. Chem.* **1968**, *6*, 1–17; b) R. F. Jordan, *ibid.* **1991**, *32*, 325–387, see especially pp. 327–329, and references therein.

[4] a) Y. Kai, N. Yasuoka, N. Kasai, *J. Organomet. Chem.* **1971**, *32*, 165–179; b) R. Kumar, V. S. J. de Mel, J. P. Oliver, *Organometallics* **1989**, *8*, 2488–2490; c) H. D. Hausen, F. Gerstner, W. Schwarz, *J. Organomet. Chem.* **1978**, *145*, 277–284.

[5] a) P. Fischer, R. Gräf, J. J. Stezowski, J. Weidlein, *J. Am. Chem. Soc.* **1977**, *99*, 6131–6132; b) F. Gerstner, W. Schwarz, H. D. Hausen, *J. Organomet. Chem.* **1979**, *175*, 33–47.

[6] X-ray crystal structure data on **1**: $C_{36}H_{40}Al_4N_4O_8$ + disordered solvent molecule, M_r = 764.66 + disordered solvent molecule, triclinic, space group $P\bar{1}$ (no. 2), a = 12.753(3), b = 12.818(3), c = 13.506(3) Å, α = 94.50(3), β = 105.47(3), γ = 92.78(3)°, V = 2115.7(8) Å^3, Z = 2, ϱ_{calc} = 1.238 Mg m^{-3}, $F(000)$ = 800, $\lambda(Mo_{K\alpha})$ = 0.71073 Å, $\mu(Mo_{K\alpha})$ = 0.162 mm^{-1}, T = 153(1) K. Data were collected on a Stoe four-circle diffractometer, 5812 reflections collected in the range $5.0° < 2\theta < 45.0°$. The structure was solved by a combination of direct methods and Fourier difference techniques, and refined by full-matrix least squares on F^2 (all non-hydrogen atoms except disordered solvent atoms anisotropic; all hydrogen atoms in idealized positions (C–H 0.96 Å)) to R_1 = 0.078, wR_2 = 0.239 for 4356 reflections with $I > 2\sigma(I)$, R_1 = 0.107, wR_2 = 0.309 for all data. Further details of the crystal structure investigation are available on request from the Director of the Cambridge Crystallographic Data Centre, 12 Union Road, GB-Cambridge CB2 1EZ (UK), on quoting the full journal citation.

The First Example of an Increase in the Enantioselectivity of a Chemical Reaction in the Presence of a Chiral Lewis Acid under High Pressure**

By *Lutz F. Tietze,* Christian Ott, Kerstin Gerke,* and *Michael Buback**

The development of methods for asymmetric synthesis is an important and widely investigated area of organic chemistry. Of particular interest is the use of chiral catalysts and mediators. In the last few years numerous chiral Lewis acids have been developed[1] which allow intermolecular reactions to be carried out with high enantioselectivity. More recently it has been shown that highly enantioselective intramolecular reactions are also possible.[2] The dependence of enantioselectivity on pressure has not been studied previously. Also the effect of pressure on reactions mediated by achiral Lewis acids has only been studied for a few cases.[3] For the first time we have recently shown for a hetero-Diels–Alder reaction that the diastereoselectivity can be increased significantly by applying high pressure ($\Delta\Delta V^{\neq} \approx 7\ cm^3\ mol^{-1}$).[4, 5] In this report we describe the first example of a reaction with increased enantioselectivity under high pressure.

The intramolecular hetero-Diels–Alder reaction of the benzylidene compound **1** proceeds by a *meta*-addition to give the two enantiomeric bridged cycloadducts **2** and **3** (Scheme 1).[6, 7] In the presence of the chiral titanium Lewis acid **4** (first described by K. Narasaka et al.[8] and available from natural tartaric acid) at 1 bar pressure, **2** was formed preferentially with 4.5% *ee*.[9]

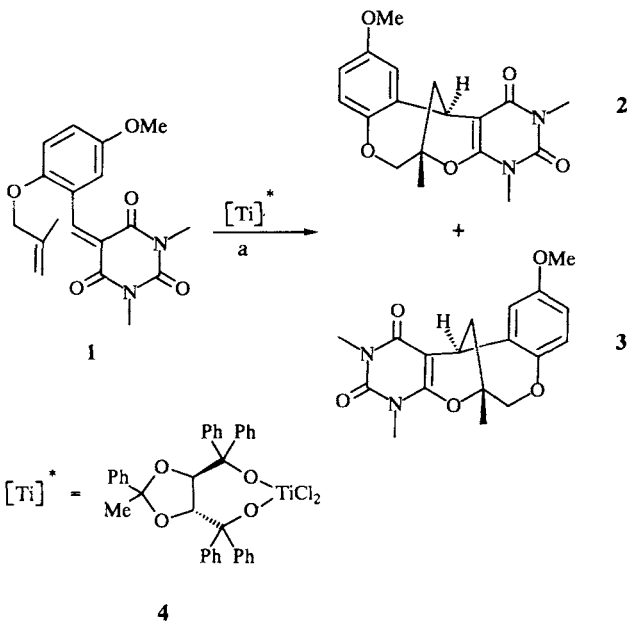

Scheme 1. a: Room temperature, 4 Å molecular sieves.

[*] Prof. Dr. L. F. Tietze, Dipl.-Chem. C. Ott
Institut für Organische Chemie der Universität
Tammannstrasse 2, D-37077 Göttingen (FRG)
Telefax: Int. code + (551)39-9476
Prof. Dr. M. Buback, Dipl.-Chem. K. Gerke
Institut für Physikalische Chemie der Universität
Tammannstrasse 6, D-37077 Göttingen (FRG)

[**] Inter- and Intramolecular Hetero-Diels–Alder Reactions, Part 43. This work was supported by the Deutsche Forschungsgemeinschaft within the Graduiertenkolleg "Kinetics and Selectivity of Chemical Transformations in Condensed Fluid Phase" and the Fonds der Chemischen Industrie. – Part 42: L. F. Tietze, P. Saling, *Chirality* **1993**, in press.

The pressure dependence of the enantioselectivity of this cycloaddition was studied by treating solutions of **1** and the chiral Lewis acid **4** (1.1 equiv) in dichloromethane, prepared under an inert atmosphere and with the exclusion of water, with powdered molecular sieves (4 Å) at −78 °C in a teflon cell. After the teflon cell was sealed, it was placed in an autoclave, where cyclization was performed at room temperature (296 K) under pressures between 1 and 5000 bar. The enantioselectivity was determined by analytical chiral reverse-phase HPLC on a sample following aqueous workup, removal of solvent under vacuum, and separation from the diol on silica. A silica-supported cellulose derivative was used as the chiral phase.[10]

This investigation shows that formation of the (−) enantiomer **2**[9] is favored at high pressure. Thus, the enantioselectivity of the cycloaddition can be increased from 4.5% *ee* at 1 bar to 20.4% *ee* at 5 kbar. In addition the chemical yield is improved (Table 1). From the plot of enantioselectivity (ln[**2**/**3**]) versus applied pressure (**P**), it can be seen that the difference in the activation volumes for the two diastereomeric transition states, $\Delta\Delta V^{\neq}$, is $-(1.7 \pm 0.2)\ cm^3\ mol^{-1}$ (Fig. 1). This value is significant; for intermolecular diasteroselective cycloadditions, however, $\Delta\Delta V^{\neq}$ values of up to $\approx 7\ cm^3\ mol^{-1}$ have been reported.[5, 11]

Table 1. Pressure dependence of the ratio of enantiomers (**2**/**3**) at 296 K in dichloromethane.

p [bar]	*t* [h]	ln (**2**/**3**) [a]	*ee* [%]	$[\alpha]_D^{20}$ [b]	Yield [%]
1	31	0.089	4.5	−13.0	50
1000	26	0.131	6.6	−22.5	85
2000	26	0.203	10.1	−26.0	81
2800	24	0.216	10.7	−33.5	89
3600	24	0.341	16.9	−54.5	95
5000	7	0.414	20.4	−61.7	89

[a] Determined by HPLC: CHIRACEL OD-R, 10 μm, 0.46 × 25 cm, Daicel Chemical Industries, Ltd.; acetonitrile/water (40:60), flow rate: 0.7 mL min^{-1}, t_r (**3**) = 21 min, t_r (**2**) = 26 min. [b] Optical rotation (c = 1 in chloroform).

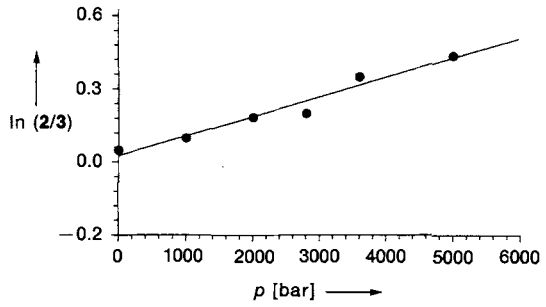

Fig. 1. Pressure dependence of the enantioselectivity of the hetero-Diels–Alder reaction of **1** in the presence of **4** at 296 K in dichloromethane. $\Delta\Delta V^{\neq} = -1.7 \pm 0.2\ cm^3\ mol^{-1}$.

Interpretation of these results is not simple, particularly because the effect of pressure on the structure of Lewis acids has not yet been examined. Dynamic effects[12] on the activation volume should be negligible, since the competing processes leading to the two enantiomers take place in the same reaction medium. The observed effect should be considered with respect to the static contribution to the activation volume, which mainly affects the equilibrium properties of the transition structures surrounded by solvent molecules. Here

it must be assumed that heterodiene **1** and Lewis acid **4** form at least two diastereomeric transition structures in which the ratio of **1** to **4** is unknown. The pressure dependence of the enantioselectivity implies that the transition structure that leads to **2** has a smaller (more negative) activation volume and thus is more compact. Therefore the preferential formation of **2** at normal pressure is enhanced at increased pressure. However, this advantageous result for the enantioselective transformation of **1** cannot be generalized. Preliminary investigations[13] on the intermolecular cycloaddition of **5** and **6** in the presence of chiral Lewis acid **4** showed a decrease in enantioselectivity when pressure was increased.

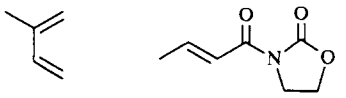

5 **6**

This is what we expected, because it can be assumed that the diene attacks the complex of the dienophile and the chiral Lewis acid from the less hindered side; the corresponding transition structure should therefore have a larger volume than that leading to the other enantiomer, and will thus be disfavored at high pressure.

The observed increase in the enantioselectivity of the intramolecular reaction of **1** at higher pressure may be due to the formation of complexes with different stoichiometry. This point will be clarified by further investigations with other substrates, and by varying the Lewis acid concentration. In particular, chiral and achiral Lewis acid/substrate complexes will be studied at high pressure by NMR spectroscopy.

Received: April 14, 1993 [Z 6008IE]
German version: *Angew. Chem.* **1993**, *105*, 1536

[1] R. O. Duthaler, A. Hafner, *Chem. Rev.* **1992**, *92*, 807–832; H. U. Blaser, *ibid.* **1992**, *92*, 935–952; H. B. Kagan, O. Riant, *ibid.* **1992**, *92*, 1007–1019; K. Mikami, M. Shimizu, *ibid.* **1992**, *92*, 1021–1050; K. Narasaka, *Synthesis* **1991**, 1–11; K. Tomoika, *ibid.* **1990**, 541–549; D. Sartor, J. Saffrich, G. Helmchen, *Synlett* **1990**, 197–198; H. C. Brown, R. S. Randad, *Tetrahedron Lett.* **1990**, *31*, 455–458; K. Mikami, M. Terada, T. Nakai, *J. Am. Chem. Soc.* **1989**, *111*, 1940–1941; N. Iwasawa, Y. Hayashi, H. Sakurai, K. Narasaka, *Chem. Lett.* **1989**, 1581–1584; N. N. Joshi, M. Srebnik, H. C. Brown, *Tetrahedron Lett.* **1989**, *30*, 5551–5554; D. Seebach, A. K. Beck, R. Imwinkelried, S. Roggo, A. Wonnacott, *Helv. Chim. Acta* **1987**, *70*, 954–974; G. Helmchen, R. Wierzchowski, *Angew. Chem.* **1984**, *96*, 59–60; *Angew. Chem. Int. Ed. Engl.* **1984**, *23*, 60–61.

[2] L. F. Tietze, P. Saling, *Synlett* **1992**, 281–282; K. Furuta, A. Kanematsu, H. Yamamoto, *Tetrahedron Lett.* **1989**, *30*, 7231–7232; K. Mikami, M. Terada, E. Sawa, T. Nakai, *ibid.* **1991**, *32*, 6571–6574.

[3] J. Jurczak, A. Golebiowski, *Synlett* **1993**, 241–245; R. W. M. Aben, L. Minuti, H. W. Scheeren, A. Taticchi, *Tetrahedron Lett.* **1991**, *32*, 6445–6448; T. A. Engler, U. Sampath, S. Naganathan, D. V. Velde, F. Takusagawa, *J. Org. Chem.* **1989**, *54*, 5712–5727; J. Jurczak, A. Golebiowski, T. Bauer, *Synthesis* **1985**, 928–929.

[4] For reviews on the effect of pressure on chemical reactions see: N. S. Isaacs, *Tetrahedron* **1991**, *47*, 8463–8497; K. Matsumoto, R. M. Acheson, *Organic Synthesis at High Pressures*, Wiley-Interscience, New York, **1991**; F. G. Klärner, *Chem. Unserer Zeit* **1989**, *23*, 53–63; R. van Eldik, T. Asano, W. J. le Noble, *Chem. Rev.* **1989**, *89*, 549–688; W. J. le Noble, *Organic High Pressure Chemistry*, Elsevier, Amsterdam, **1988**; K. Matsumoto, A. Sera, T. Uchida, *Synthesis* **1985**, 1–26; K. Matsumoto, A. Sera, *ibid.* **1985**, 999–1027; N. S. Isaacs, *Liquid Phase High Pressure Chemistry*, Wiley-Interscience, New York, **1981**.

[5] L. F. Tietze, T. Hübsch, E. Voss, M. Buback, W. Tost, *J. Am. Chem. Soc.* **1988**, *110*, 4065–4066; M. Buback, W. Tost, T. Hübsch, E. Voss, L. F. Tietze, *Chem. Ber.* **1989**, *122*, 1179–1186; L. F. Tietze, T. Hübsch, M. Buback, W. Tost, *High Pressure Res.* **1990**, *2*, 638–640; L. F. Tietze, T. Hübsch, J. Oelze, C. Ott, W. Tost, G. Wörner, M. Buback, *Chem. Ber.* **1992**, *125*, 2249–2258.

[6] L. F. Tietze, H. Stegelmeier, K. Harms, T. Brumby, *Angew. Chem.* **1982**, *94*, 868–869; *Angew. Chem. Int. Ed. Engl.* **1982**, *21*, 863.

[7] **2** and **3**: ^{1}H NMR ($CDCl_3$): δ = 1.42 (s; 3H, 6-CH_3), 2.11 (dd, J = 14 Hz, J = 2.0 Hz; 1H, 14-H), 2.20 (ddd, J = 14, 5.5, 2.5 Hz; 1H, 14-H), 3.25 (s; 3H, N-CH_3), 3.42 (s; 3H, N-CH_3), 3.58 (d, J = 13 Hz; 1H, 7-H_{ax}), 3.79 (s; 3H, O-CH_3), 3.94 (dd, J = 5.5, 2.0 Hz; 1H, 13-H), 4.26 (dd, J = 13, 2.5 Hz; 1H, 7-H_{eq}), 6.65 (dd, J = 9.0, 3.0 Hz; 1H, 10-H), 6.84 (d, J = 9.0 Hz; 1H, 9-H), 6.98 (d, J = 3.0 Hz; 1H, 12-H).

[8] Prepared according to: K. Narasaka, N. Iwasawa, M. Inoue, T. Yamada, M. Nakashima, J. Sugimori, *J. Am. Chem. Soc.* **1989**, *111*, 5340–5345. The chiral diol was purified by column chromatography.

[9] Determination of the absolute configuration has not yet been possible.

[10] CHIRACEL® OD-R, 10 μm, 0.46 × 25 cm; Daicel Chemical Industries, Ltd.

[11] F. G. Klärner, B. M. J. Dogan, O. Ermer, W. von E. Doering, M. P. Cohen, *Angew. Chem.* **1986**, *98*, 109–111; *Angew. Chem. Int. Ed. Engl.* **1986**, *25*, 108–110.

[12] J. Troe, *High Pressure Res.* **1990**, *2*, 625–628.

[13] L. F. Tietze, C. Ott, K. Gerke, M. Buback, unpublished results.

The Behavior of Cp^*MoBr/Br_2 Redox Systems: The Unusual Structure of $[(Cp^*_2Mo_2Br_4)_2(Cp^*MoBr_4)_3]$, a Compound Containing Mo^{III}, Mo^{IV}, and Mo^V**

By *Jahanvi U. Desai, John C. Gordon, Heinz-Bernhard Kraatz, Beth E. Owens-Waltermire, Rinaldo Poli,** and *Arnold L. Rheingold*

There is considerable interest in the use of cyclopentadienyl transition metal complexes having one or more halo ligands as convenient starting materials for the synthesis of a large variety of organometallic compounds.[1] Although complexes of the group 6 metals molybdenum and tungsten are well known for the III and V oxidation state, Mo^{IV} and W^{IV} complexes have received little attention. Only recently, we were able to obtain $[CpMoCl_3]$ ($Cp = \eta^5$-C_5H_5), an insoluble powder and presumably an oligomer[2] In order to obtain complexes that lend themselves to structural characterization, we have moved to the more soluble Cp* complexes ($Cp^* = \eta^5$-C_5Me_5). We report here on the synthesis and highly unusual crystal structure of **1**.

$[\{[Cp^*Mo(\mu\text{-}Br)_4MoCp^*]^+[Cp^*MoBr_4]^-\}_2][Cp^*MoBr_4]$ **1**

This compound is novel in that it is 1) the first known tetrabromo-bridged d^2-d^3 dimer, 2) the first d^2 $[Cp^*MX_4]^-$ complex to be structurally characterized, and 3) the first neutral Mo^V tetrabromide to be structurally characterized. In addition, molybdenum is found in three different oxidation states in the same crystal. This is possible because of the particular redox properties of the Cp^*MoBr/Br_2 system which we will describe here. Complex **2** has been prepared from **3**[3] and sodium amalgam in toluene as a diamagnetic

$[Cp^*Mo(\mu\text{-}Br)_4MoCp^*]$ **2** $[Cp^*MoBr_4]$ **3**

[*] Prof. R. Poli, J. U. Desai, Dr. J. C. Gordon, Dr. H.-B. Kraatz
Department of Chemistry and Biochemistry
University of Maryland
College Park, MD 20742 (USA)
Telefax: Int. code + (301)314-9121
Dr. B. E. Owens-Waltermire, Prof. A. L. Rheingold
Department of Chemistry, University of Delaware (USA)

[**] This research was supported by the U.S. Department of Energy – Office of Energy Research (grant no. 92ER14230). R. P. is a Presidential Young Investigator (1990–1995), an Alfred P. Sloan Research Fellow (1992–1994), and an Alexander von Humboldt Research Fellow (1993–1994).

crystalline complex, which is isostructural to the neutral (d^3-d^3) complex [Cp'Mo(μ-Br)$_4$MoCp'] (Cp' = η^5-1-(2,5-dimethoxyphenyl)-2,3,4,5-tetraphenylcyclopentadienyl)[4] and to [(*i*Pr)CpMo(μ-Cl)$_4$MoCp(*i*Pr)].[5] The unit cell of **2**[6] contains two independent molecules, one located at an inversion center and the second one in a general position. The two crystallographically independent molecules are chemically equivalent and can be described as two four-legged piano stool structures sharing a common square face defined by the four bridging bromo ligands (Fig. 1). Complex **2** undergoes two reversible one-electron oxidations at $E = -0.30$ V and $+0.73$ V (vs. ferrocene).

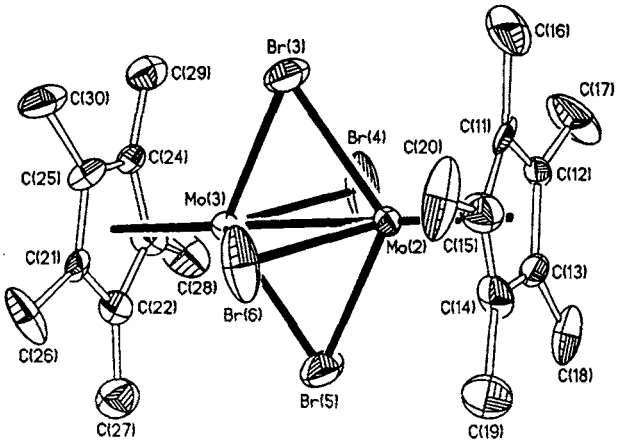

Fig. 1. Crystal structure of **2** (ORTEP plot shows the molecule in a general position). The geometry is identical to that of the molecule located at an inversion center in **2** and also to that in cation 2^+. Selected bond lengths [Å] and angles [°] (averaged over all chemically equivalent groups of atoms): **2**: Mo-Mo 2.643(2), Mo-Br 2.613(9); Mo-Br-Mo 60.8(3). 2^+: Mo-Mo 2.643(5) Mo-Br 2.64(3); Mo-Br-Mo 60.0(8).

In an attempt to prepare **4** by bromination of **2** with Br_2 (mol ratio 1:1) in benzene, we obtained a brick-red precipitate (**5**), which analyzes as Cp*MoBr$_{3.3}$ and shows a single

[{Cp*MoBr$_3$}$_2$] **4** [{Cp$^*_2$Mo$_2$Br$_4$}]$^+$[Br, Br$_3$]$^-$ **5**

broad resonance at $\delta = 4.3$ in its ^{1}H NMR spectrum in $CDCl_3$. This resonance is identical to that of the product obtained upon treatment of **2** with one equivalent of $AgBF_4$. Thus **5** is interpreted as being a salt of [Cp*Mo(μ-Br)$_4$MoCp*]$^+$ (2^+), and its anion is presumably a 1:4 mixture of Br^- and Br_3^-. According to our electrochemical investigations and the literature,[7] Br_2 does not have sufficient oxidizing power to produce the dication 2^{2+} (see Fig. 2).

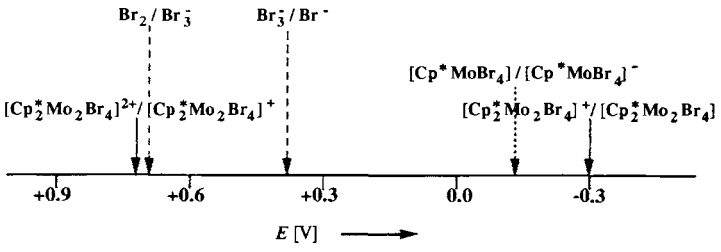

Fig. 2. Electrochemical behavior of the [Cp$^*_2$Mo$_2$Br$_4$]$^{n+}$, [Cp*MoBr$_4$]$^{n-}$, and $Br_2/Br_3^-/Br^-$ systems.

Recrystallization of **5** from CH_2Cl_2/*n*-heptane yielded the title compound **1** as a dark red, crystalline material, which is paramagnetic and displays two broad peaks at $\delta = 4.2$ and -19.5 in its ^{1}H NMR spectrum. The resonance at $\delta = -19.5$ is assigned to the anion [Cp*MoBr$_4$]$^-$ (3^-) (vide infra). The cyclic voltammogram of **1** shows, in addition to the two reversible one-electron oxidations characteristic of **2**, a reversible wave at $E = -0.14$ V (vs. ferrocene), which is due to the [Cp*MoBr$_4$]^0/[Cp*MoBr$_4$]$^-$ couple as shown by an independent study of **3** (Fig. 2). A comparison of the oxidation potentials in Figure 2 indicates that **1** consists of the mixed-valence cation [Cp*Mo(μ-Br)$_4$MoCp*]$^+$ and a 2:1 mixture of the anion [Cp*MoBr$_4$]$^-$ and the corresponding Mo^V neutral analogue. This rules out the alternative formulation of **1** as a 1:1 mixture of monocation and dication for the dinuclear complex accompanied by three negatively charged mononuclear complexes.

Compound **1** crystallizes in the monoclinic space group $P2_1/m$ with two formula units per unit cell.[8] The dinuclear monocation 2^+ is located in a general position, and its structure is practically identical to that of the neutral precursor **2** (Fig. 1). According to theoretical considerations,[9] the HOMO of **2** should be nonbonding. This explains the little change in the Mo–Mo separation upon oxidation (d(Mo–Mo): **2** = 2.645(2) Å; 2^+ = 2.691(4) Å). This is the first direct comparison of metal–metal distances in a pair of [{CpMX$_2$}$_2$]$^{n+}$ complexes and experimentally confirms the theoretical predictions by Green et al.[9] The two Mo^{IV} anions 3^- and the neutral Mo^V complex **3** are located on mirror planes. These all have the familiar four-legged piano stool structure (Fig. 3). The bond angles are not significantly

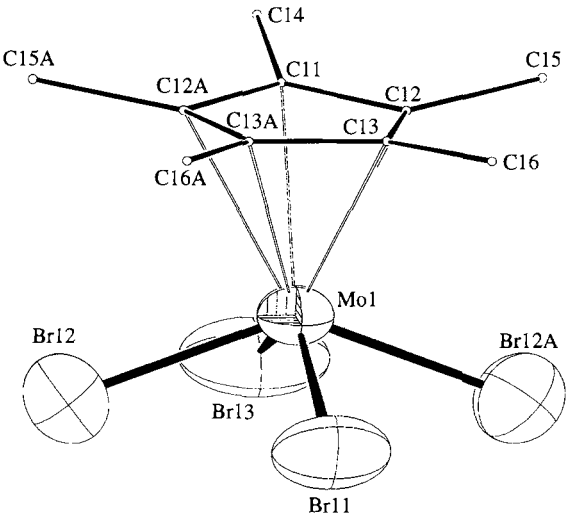

Fig. 3. Crystal structure of **3** (ORTEP). The two crystallographically independent anions 3^- have identical structural parameters. Selected bond lengths [Å] and angles [°] (averaged over all chemically equivalent groups of atoms): 3^-: Mo-Br 2.62(4), Br-Mo-Br (*cis*) 81.8(4), Br-Mo-Br (*trans*), 136(3). **3**: Mo-Br 2.48(3), Br-Mo-Br (*cis*) 82.8(4), Br-Mo-Br (*trans*) 138(2).

different in the three mononuclear complexes; however, the Mo–Br distances at atom Mo1 are significantly shorter (average 2.48(4) Å) than those at atoms Mo4 and Mo5 (Mo4: range 2.595(6)–2.616(9) Å; Mo5: range 2.591(6)–2.721(8) Å). This reflects the stronger π acidity of the neutral d^1 complex [Cp*MoBr$_4$] and allows us to identify Mo1 as the central atom in as **3**. An ORTEP representation of the unit

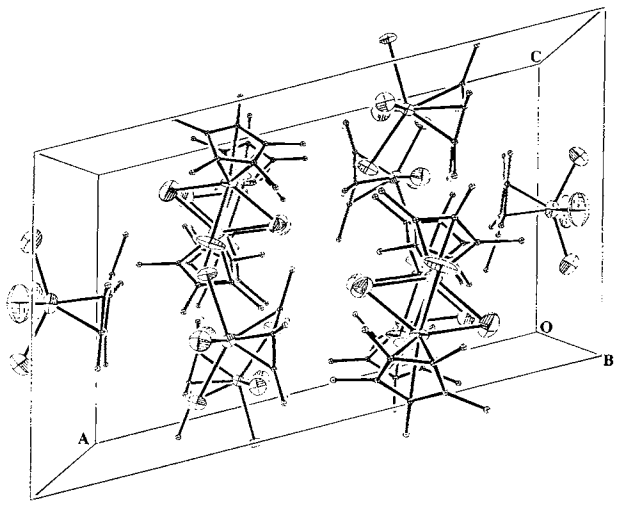

Fig. 4. Unit cell of **1** (ORTEP).

cell of **1** giving the relative orientations of all three constituents to each other is shown in Figure 4.

The formation of **1** from **2** and Br_2 can be understood in terms of their redox behaviors (see Fig. 2). Initially, Br_2 oxides **2** to give the benzene-insoluble salt **5**, which contains the cation $\mathbf{2}^+$ and a mixture of Br^- and Br_3^- as discussed above. During the crystallization from CH_2Cl_2, Br^- can add to $\mathbf{2}^+$ to give the neutral adduct **2**-Br. Oxidation with Br_3^- and subsequent reaction with Br^- via the possible intermediate $[Cp^*MoBr_3]_2$ will give the paramagnetic anion $\mathbf{3}^-$ (Scheme 1).

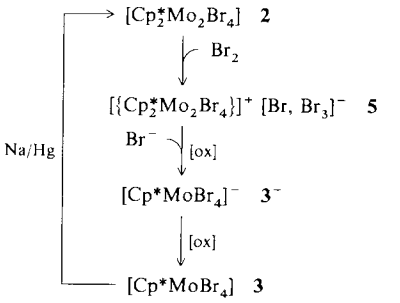

Scheme 1. [ox] = oxidation.

Any residual Br_3^-, according to the electrochemical study (Fig. 2), would be capable of oxidizing $\mathbf{3}^-$ to give neutral **3**. Thus, considering the composition of compound **5**, a mixture of **2**, $\mathbf{3}^-$ and **3** in a mol ratio of 1:1:2.1 should be produced in solution. But a mixture of the three components in a mol ratio of 2:2:1 is found in the crystal, presumably because a compound with this particular combination is the least soluble material in the solvent combination used for crystallization. Treatment of compound **5** with excess Br^- eventually leads to a product with a single broad ^{1}H NMR resonance at $\delta = -19.5$, which is attributed to $\mathbf{3}^-$ in agreement with the reactions depicted in Scheme 1. Figure 2 indicates that the two neutral complexes **3** and **2** are not stable with respect to electron transfer. In fact, mixing a stoichiometric amount of **3** and **2** produces a solution that exhibits the ^{1}H NMR resonances of the cation $\mathbf{2}^+$ and the Mo^{IV} anion $\mathbf{3}^-$.

Currently, efforts are under way to isolate $[\{Cp^*MoBr_3\}_2]$ (**4**), which requires reaction conditions under which free bromide ion cannot exist.

Experimental Procedure

3: $[Cp^*MoBr_4]$ was prepared by a procedure similar to that described for $[Cp'MoBr_4]$ [3]: $[\{Cp^*Mo(CO)_3\}_2]$ (1.03 g, 1.62 mmol) was dissolved in CH_2Cl_2 (20 mL), and the red-orange solution was transferred by cannula to a slurry of yellow PBr_5 (2.80 g, 6.52 mmol) in CH_2Cl_2 (20 mL). Vigorous gas evolution indicated an immediate reaction. The reaction mixture was then refluxed approximatly 12 h. The solution was reduced in volume to approximately 30 mL. The almost black precipitate was collected by filtration, washed with cold CH_2Cl_2 (3 × 5 mL) and dried under vaccum to yield 1.56 g (87%) of **3**. Correct elemental analysis (C, H, Br).

2: Compound **3** (3.427 g, 6.22 mmol) was placed in a Schlenk tube containing freshly prepared sodium amalgam (311 mg of Na, 13.5 mmol in 31 g Hg). Toluene (40 mL) was added, and the dark suspension was allowed to stir at room temperature (21 °C) for about 12 h, during which the solution developed a tan brown color. The reaction mixture was filtered and the precipitate washed with toluene until the washings were colorless (4 × 20 mL). The combined filtrates were reduced in volume and cooled to −20 °C to yield 2.18 g (90%) of **2**. ^{1}H NMR (200 MHz, $CDCl_3$, 25 °C): $\delta = 1.93$(s). Cyclic voltammogram (CH_2Cl_2/0.1 M nBu_4NPF_6, E[V] vs. Cp_2Fe/Cp_2Fe^+): −0.30 ($[\{Cp^*MoBr_2\}_2]$/$[\{Cp^*MoBr_2\}_2]^+$), +0.73 ($[\{Cp^*MoBr_2\}_2]^+/[\{Cp^*MoBr_2\}_2]^{2+}$). Correct elemental analysis (C, H).

1: Compound **2** (538 mg, 0.69 mmol) was dissolved in benzene (10 mL). A solution of Br_2 (35 μL, 0.69 mmol) in benzene (5 mL) was added, causing the immediate formation of a red precipitate. The product was collected by filtration, washed with *n*-heptane, and dried under vacuum (381 mg). ^{1}H NMR (200 MHz, $CDCl_3$, 25 °C): $\delta = 4.3$ (br, $w_{1/2} = 120$ Hz). Recrystallization of this product from CH_2Cl_2/*n*-heptane yielded **1** as dark red plates. ^{1}H NMR (200 MHz, $CDCl_3$, 25 °C): $\delta = 4.2$ ($w_{1/2} = 120$ Hz), −19.5 ($w_{1/2} = 137$ Hz). One of these crystals was used in the crystallographic investigation.

Reaction between **3** and **2**: To a solid mixture of **2** (17 mg; 0.022 mmol) and **3** (23 mg; 0.042 mmol) in a Schlenk tube, was added $CDCl_3$ (1 mL). The resulting orange-brown solution was transferred to an NMR tube (5 mm o.d.). ^{1}H NMR (200 MHz, $CDCl_3$, 25 °C): $\delta = 4.13$ ($w_{1/2} = 85$ Hz), −19.53 ($w_{1/2} = 137$ Hz).

Received: April 3, 1993 [Z 5977 IE]
German version: *Angew. Chem.* **1993**, *105*, 1506

[1] R. Poli, *Chem. Rev.* **1991**, *91*, 509–551.
[2] R. Poli, M. A. Kelland, *J. Organomet. Chem.* **1991**, *419*, 127–136.
[3] M. L. H. Green, J. D. Hubert, P. Mountford, *J. Chem. Soc. Dalton Trans.* **1990**, 3793–3800.
[4] C. Saadeh, S. B. Colbran, D. C. Craig, A. D. Rae, *Organometallics* **1993**, *12*, 133–139.
[5] a) M. L. H. Green, A. Izquierdo, J. J. Martin-Polo, V. S. B. Mtetwa, K. Prout, *J. Chem. Soc., Chem. Commun.* **1983**, 538–540; b) R. Poli, J. C. Gordon, J. U. Desai, A. L. Rheingold, *ibid.* **1991**, 1518–1520.
[6] Crystal structure analysis of **2**: $C_{20}H_{30}Br_4Mo_2$, $M = 782.0$, monoclinic, $a = 8.356(1)$, $b = 32.272(5)$, $c = 13.972(2)$ Å, $\beta = 98.17(1)°$, $V = 3729.3(10)$ Å^3, space group $P2_1/n$, $Z = 6$, $\mu(Mo_{K\alpha}) = 73.60$ cm^{-1}, $\varrho_{calcd} = 2.088$ g cm^{-3}, independent reflections (total reflections) 5741 (6407), 2715 reflections ($F_0 > 4\sigma(F_0)$), $R = 0.0614$ ($R_w = 0.0755$) [8].
[7] M. Mastragostino, S. Valcher, P. Lazzari, *J. Electroanal. Chem. Interfacial Electrochem.* **1981**, *126*, 189–198.
[8] Crystal structure analysis of **1**: $C_{84}H_{137}Br_{20}Mo_7$, $M = 3416.67$, monoclinic, $a = 20.218(6)$, $b = 23.332(5)$, $c = 12.093(2)$ Å, $\beta = 104.76(2)°$, $V = 5516(2)$ Å^3, space group $P2_1/m$, $Z = 2$, $\mu(Mo_{K\alpha}) = 84.62$ cm^{-1}, $\varrho_{calcd} = 2.06$ g cm^{-3}, independent reflections (total reflections) 7414 (7657), 2172 reflections ($|F_0|^2 > 3\sigma|F_0|^2$), 365 parameters refined, $R = 0.089$ ($R_w = 0.094$). The reflections were measured on an Enraf-Nonius CAD4 diffractometer with $Mo_{K\alpha}$ radiation ($\lambda = 0.71073$ Å) by using the ω-2θ scan method. The structure of **1** was solved using the TEXSAN program package. The positions of all non-hydrogen atoms were determined from difference Fourier maps. The Mo and Br atoms were refined anisotropically; the C atoms were refined isotropically. All Cp* ligands were restrained to ideal pentagons with C–C(ring) = 1.42(1) Å and C–C(Me) = 1.56 Å and the interstitial heptane molecule restrained to C–C = 1.54(2) Å (SHELX76). Some of the Cp* methyl carbon atoms refined with very a high thermal parameter, indicating fast rotation of the rings about the metal–ring axis and/or partial disorder of the rings. Further details of the crystal structure can be obtained upon request from the Director of the Cambridge Crystallographic Data Centre, University Chemical Laboratory, 12 Union Road, GB-Cambridge CB21EZ (UK), on quoting the full journal citation.
[9] J. C. Green, M. L. H. Green, P. Mountford, M. J. Parkington, *J. Chem. Soc., Dalton Trans.* **1990**, 3407–3418.

Coherence Selection by Gradients without Signal Attenuation: Application to the Three-Dimensional HNCO Experiment**

By *Jürgen Schleucher, Michael Sattler,* and *Christian Griesinger**

Pulsed field gradients, that is, short, defined inhomogeneities of the static magnetic field B_0, have recently been introduced into high-resolution NMR.[1] In multidimensional NMR experiments they offer a reduction of artifacts and can substitute phase-cycles. Spectra can therefore be recorded more quickly, provided that the experiment duration is determined by the need to suppress undesired transfer pathways rather than by S/N requirements. By the application of a gradient pulse during the evolution time of the magnetization of the heteronucleus and before acquisition of proton signals, a heteronuclear gradient echo[2] can be generated.[3] This results in excellent suppression of signals from all protons that are not bound to the heteronucleus (e.g., solvent resonances). Thus, proton signals underlying the water resonance can be observed in proton-detected ^{13}C correlations at natural abundance for millimolar concentrations.

If applied in standard pulse sequences, the excellent suppression of the water signal provided by the use of heteronuclear gradient echoes is associated with a loss in signal-to-noise ratio (S/N), as shall be explained in the following. In amplitude-modulating NMR experiments, to which all multidimensional standard pulse sequences belong, two coherence transfer pathways contribute intensity $\frac{1}{2}$ to the signal recorded.[4] These are called echo pathway ($p(t_1) = 1 \rightarrow p(t_2) = -1$) and antiecho pathway ($p(t_1) = -1 \rightarrow p(t_2) = -1$) ($p$: coherence order) (Fig. 1a). Echo and antiecho are recorded simultaneously, however, with different relative signs in two transients. Pure phases are obtained according to the method introduced by States, Haberkorn, and Ruben.[5] The signal intensity acquired in these transients is $4 \times \frac{1}{2} = 2$. Because of addition of the two free induction decays (FIDs) and of folding at $\omega_1 = 0$, the noise increases by $\sqrt{4}$. Therefore, the S/N obtained is $2/2 = 1$.

In the course of a pulse sequence, pulsed field gradients select coherence orders p according to the condition $\sum_i p_i \gamma_i G_i = 0$ (i is an index for the ith gradient pulse applied in the course of the sequence, γ_i and p_i are the gyromagnetic ratio and the coherence order of the nucleus (nuclei) affected by the gradient pulse i, and G_i is the strength of the ith gradient). If a gradient pulse is applied in an evolution time of an amplitude-modulating pulse sequence, and the magnetization to be observed is refocused by a gradient applied before the detection period, only one of the two possible coherence transfer pathways is retained. Depending on the relative sign of the gradients, either the echo or the antiecho is selected (Fig. 1b). Thus, the application of gradients for coherence selection in amplitude-modulating pulse sequences results in the recording of phase-modulated signals. The accumulated signal intensity is $2 \times \frac{1}{2} = 1$, and the noise increases to $\sqrt{2}$ as a result of summation of the transients. The S/N obtained is $1/\sqrt{2}$, that is, a factor of $\sqrt{2}$ poorer than the original amplitude-modulating pulse sequence without gradients. If gradients are applied during fixed delays (where two coherence orders of opposite sign contribute to the signal equally), such as in the mixing time of a relayed-COSY or DQF-COSY, S/N is a factor of 2 smaller than for the same sequence without gradients, since the signals sketched in Figure 1a are selected in such sequences, but their intensity is again reduced by half.

a) States–Haberkorn–Ruben method yields pure phases and sign discrimination for amplitude-modulating experiments.

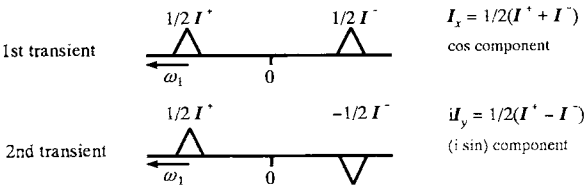

b) Gradient-selected echo and antiecho spectrum from an amplitude-modulating experiment yields pure phases with reduced intensity.

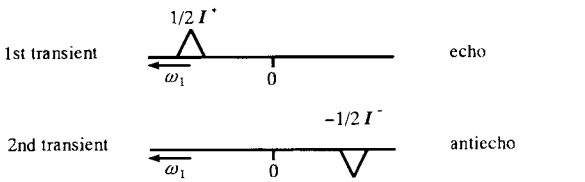

c) Gradient-selected echo and antiecho spectrum from a phase-modulating experiment yields pure phases with enhanced intensity.

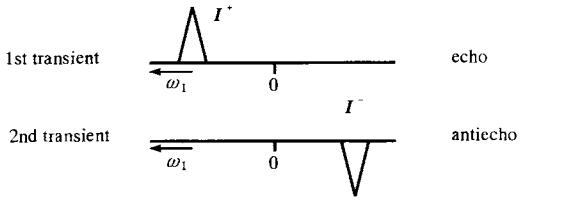

Fig. 1. Schematic drawing of the signals resulting from different NMR experiments for the evolution time: a) quadrature detection according to States, Haberkorn and Ruben in an amplitude-modulating pulse sequence; b) signals selected by the application of gradients in the evolution time and before acquisition of an amplitude-modulating sequence; c) signals obtained in a phase-modulating sequence.

The substantial drawback of reduced sensitivity, which is inherent to the application of gradients in the evolution time and before signal acquisition of amplitude-modulating NMR experiments, is overcome in phase-modulating experiments, since only one coherence order contributes to the signal in such sequences. This coherence order can be selected without attenuation, that is, with intensity 1, by the application of gradients during the evolution time (Fig. 1c). In the two transients recorded for each t_1-increment of such an experiment, the intensity $2 \times 1 = 2$ is accumulated. As the noise is $\sqrt{2}$, the optimal S/N of $\sqrt{2}$ is obtained. Whilst all conventional correlation experiments yield amplitude-modulated time signals, the advantage in sensitivity of phase-modulation in conjunction with the use of gradients for coherence selection can be exploited in the so-called "sensitivity-enhanced" HSQC experiments:[6] In the case of X–H spin systems (X: heteronucleus), these experiments yield a phase-

[*] Prof. Dr. C. Griesinger, Dipl.-Chem. J. Schleucher, Dipl.-Chem. M. Sattler
Institut für Organische Chemie der Universität
Marie-Curie-Str. 11, D-60439 Frankfurt (FRG)
Telefax: Int. code + (69)5800-9128

[**] This work was supported by the Fonds der Chemischen Industrie, the Graduiertenkolleg Gk Eg 52/3-3 (supported by the Deutsche Forschungsgemeinschaft), the state of Hessen, and the Bundesministerium für Bildung und Wissenschaft. The authors thank Prof. Dr. E. Carafoli, Dr. J. Krebs (ETH Zürich), Dr. T. Vorherr (Hoffmann-La Roche, Basel), and P. Schulte (Frankfurt) for the Calmodulin/C20W complex. We thank Dr. R. Kerssebaum and Dr. W. Bermel, BRUKER Analytische Meßtechnik, for support in the initial phase of this project.

modulated, two-dimensional data set even in the absence of gradients. From this data set, consisting of FIDs formed by echo and antiecho selection, an amplitude-modulated data set in States–Haberkorn–Ruben format can be reconstituted.[6] No additional methods for sign discrimination in ω_1, such as time-proportional phase incrementation (TPPI)[7] or States–Haberkorn–Ruben,[5] need to be applied.

One example of a HSQC experiment using gradients for coherence selection without loss in sensitivity has recently been published.[8] Here we demonstrate the application of this general principle to heteronuclear multidimensional NMR experiments. The HNCO experiment[9] is used to obtain sequential connectivities of the backbone atoms in proteins uniformly labeled with ^{15}N and ^{13}C. In this experiment coherence is transferred through ^1J couplings from the amide proton to the amide nitrogen atom and further to the carbonyl carbon resonance of the preceding amino acid. After evolution of the carbonyl chemical shift (t_1) coherence is transferred back to the amide nitrogen atoms ("constant time" evolution time t_2), and to the amide protons for detection. The pulse sequences of a conventional CT-HNCO ("constant time"-HNCO), a gradient CT-HNCO, and a sensitivity-enhanced gradient CT-HNCO experiment are shown in Figure 2. In the two gradient experiments, coherence selection is achieved by the application of a gradient pulse during t_2 and before acquisition (t_3).

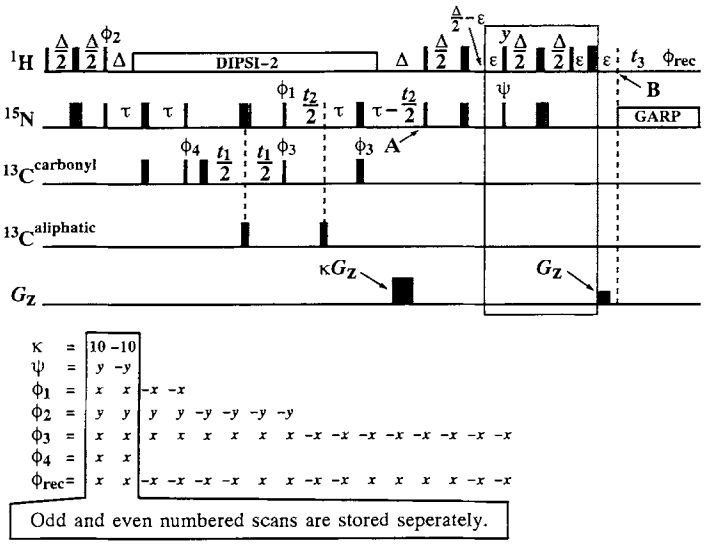

Fig. 2. Pulse sequence of the "sensitivity-enhanced" gradient CT-HNCO experiment. Narrow bars represent 90° pulses and wide bars 180° pulses. Unless stated otherwise, all pulses are applied along x. Simultaneous acquisition of complex data points is used during t_3. The nitrogen magnetization evolution must occur immediately prior to the N → H transfer for the application of sensitivity enhancement. The sign of the gradient acting on nitrogen atoms as well as the phase ψ are inverted from one scan to the other and the resulting FIDs stored separately. The echo and antiecho signals obtained in this way are converted into an amplitude-modulated data set by the following procedure: For all values of t_1 and t_2 the echo and antiecho FIDs are added (resulting in FID1) or subtracted and shifted by 90° (resulting in FID2). FID1 and FID2 have States–Haberkorn–Ruben format and can be processed by standard software. The state of the spin system at times A and B is discussed in the text. Spectra were recorded on an AMX600 spectrometer equipped with a triple resonance probe with a self-shielded gradient coil. ^{13}C pulses were delivered by a BSV-10 amplifier feeding a supplementary BLKX 300 W linear amplifier. ^{13}CO pulses were applied at 176 ppm as selective G4 or G3 pulses [11] (duration 400 μs and 250 μs, respectively). Selective inversion of the aliphatic carbon resonances was achieved with a phase-modulated G3 pulse (duration 250 μs, modulation frequency 20000 Hz). Bloch–Siegert effects of zeroth and first order occurring during t_1 and evolution of the ^{13}CO chemical shift for $t_1 = 0$ were compensated, respectively, by correcting ϕ_4 and by introduction of a delay before the ^{13}CO 180° pulse before t_1. The delays are: $\varepsilon = 2.2$ ms, $\Delta = 5.0$ ms, $\tau = 14.7$ ms. Eight scans were used to record $40(t_1) \times 36(t_2) \times 768(t_3)$ complex points. Corresponding acquisition times were 9.75 ms (t_1), 9.5 ms (t_2), and 192 ms (t_3). Total measurement time was 20 h. Omission of the pulses and delays inside the frame results in the pulse sequence of a gradient CT-HNCO experiment; omitting the gradient pulses as well and including presaturation instead leads to a conventional HNCO experiment [9c]. G_z is a pulsed field gradient along the static magnetic field B_0 of length 2 ms.

We use product operators to describe the back transfer from ^{15}N to ^1H. Operators acting on nitrogen are designated N; those acting on proton spins are designated H. We use H^-, N^-, N^+ for transverse operators and H_z for the longitudinal operator. The "double INEPT" back transfer converts heteronuclear single quantum coherence $2N^-H_z$ or $2N^+H_z$ at the end of t_2 completely into detectable proton coherence H^-. In the first transient of each t_2-increment, the echo $2N^-H_z$ (time A in Fig. 2) → H^- (time B in Fig. 2) is selected by the combination of a gradient pulse of amplitude 10 (in general $|\gamma_H/\gamma_X|$) during the evolution time of nitrogen atoms and a gradient of amplitude 1 acting on protons before acquisition. Note the reverse definition in terms of operators of echo and antiecho due to the negative γ_N/γ_H. The antiecho signal $2N^+H_z$ (time A) → H^- (time B) is detected in the second transient of each t_2-increment by the combination of gradient of strength −10 during the evolution time of nitrogen atoms and a gradient of strength 1 acting on protons before acquisition. Since selection of either $2N^+H_z$ or $2N^-H_z$ is achieved in sensitivity-enhanced sequences by an inversion of the phase ψ of the last 90° (^{15}N) pulse, the inversion of this phase and the change of the relative sign of the gradients have to occur simultaneously if gradients are to be implemented for coherence selection into such sequences. For the conventional detection of H^-, the transfer amplitudes (t_2, t_3) of the two FIDs (which are stored separately) are given in Scheme 1.

First transient (echo): $\exp(-i\Omega_N t_2)\exp(i\Omega_H t_3)$
Second transient (antiecho): $\exp(i\Omega_N t_2)\exp(i\Omega_H t_3)$

Scheme 1. Definition of transfer amplitudes.

By addition and subtraction of the two phase-modulated signals, and subsequent phase correction by 90° of the FID obtained by subtraction, two amplitude-modulated signals are obtained (Scheme 2).

FID 1 (Addition): $\cos(\Omega_N t_2)\exp(i\Omega_H t_3)$
FID 2 (Subtraction and phase-correction by 90° in t_3): $\sin(\Omega_N t_2)\exp(i\Omega_H t_3)$

Scheme 2. The two amplitude-modulated signals obtained from the phase-modulated signals.

Complex Fourier transformation of these signals results in a spectrum with pure phases in ω_2 and ω_3. In Figure 3, traces taken from the first ω_2, ω_3 spectrum ($t_1 = 0$) are shown for a) a conventional (amplitude-modulating) CT-HNCO experiment using gradients for coherence selection in t_2 (Fig. 2, neglecting the part of the pulse sequence inside the frame), b) a conventional CT-HNCO experiment[9c] (cf. legend to Fig. 2), and c) a phase-modulating CT-HNCO experiment using gradients for coherence selection in t_2 (Fig. 2).

Experiments of equal duration were recorded on a complex of uniformyl $^{13}C/^{15}N$ labeled Calmodulin und C20W, a Calmodulin recognition sequence of the plasma membrane calcium pump.[10] We choose experiment (a) as a reference for S/N with a value of $1/\sqrt{2}$ (in accordance with Fig. 1 b). Averaging eleven traces, we calculated a relative S/N of 0.78 for experiment (b) (corresponding to Fig. 1 a) and a relative

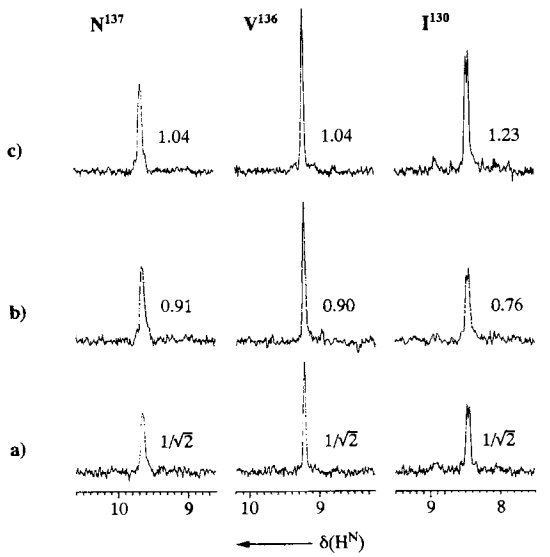

Fig. 3. Traces taken from the first ω_2, ω_3 spectra ($t_1 = 0$). For a)–c) see text. The numbers next to the traces indicate the S/N relative to experiment (a). The measurement time was the same for all experiments.

S/N of 1.11 for experiment (c) (corresponding to Fig. 1c). The enhancement for experiment (b) relative to (a) of 1.11 is smaller than the expected value of $\sqrt{2}$. The theoretical factor is not observed because of a loss of magnetization in experiment (b) due to saturation transfer from the water to the amide protons. In contrast, no presaturation is needed in experiments (a) and (c). The increase of 1.55 in S/N over experiment (a) in experiment (c) does not correspond to the theoretical gain in sensitivity either, since sequence (c) is longer and signal is therefore lost due to relaxation. Nevertheless, (c) is clearly the most sensitive sequence. Compared to the second best sequence b), a reduction of the measuring time of 50% is possible for the same signal-to-noise ratio.

We have introduced B_0-gradients into a phase-modulating three-dimensional triple-resonance NMR sequence and have demonstrated the sensitivity of this method using the sensitivity-enhanced gradient CT-HNCO experiment on a protein/peptide complex as example. Phase-modulating, heteronuclear backtransfer can be implemented in any 3D NMR sequence that detects the H^N resonances. This principle offers optimum sensitivity and at the same time uses gradients most efficiently to suppress artifacts.

Received: April 6, 1993
Revised version: June 5, 1993 [Z 5984 IE]
German version: *Angew. Chem.* **1993**, *105*, 1518

[1] a) A. Bax, P. G. De Jong, A. F. Mehlkopf, J. Smidt, *Chem. Phys. Lett.* **1980**, *69*, 567–570; b) P. Barker, R. Freeman, *J. Magn. Reson.* **1985**, *64*, 334–338; c) R. E. Hurd, *ibid.* **1990**, *87*, 422–428; d) A. L. Davis, E. D. Laue, J. Keeler, D. Moskau, J. Lohman, *ibid.* **1991**, *94*, 637–644; e) B. K. John, D. Plant, S. L. Heald, R. E. Hurd, *ibid.* **1991**, *94*, 664–669; f) G. W. Vuister, R. Boelens, R. Kaptein, M. Burgering, P. C. M. van Zijl, *J. Biomol. NMR* **1992**, *2*, 301–305.

[2] A. A. Maudsley, A. Wokaun, R. R. Ernst, *Chem. Phys. Lett.* **1978**, *55*, 9–14.

[3] a) R. E. Hurd, B. K. John, *J. Magn. Reson.* **1990**, *91*, 648–653; b) G. W. Vuister, R. Boelens, R. Kaptein, R. E. Hurd, B. K. John, P. C. M. van Zijl, *J. Am. Chem. Soc.* **1991**, *113*, 9688–9690; c) A. L. Davis, J. Keeler, E. D. Laue, D. Moskau, *J. Magn. Reson.* **1992**, *98*, 207–216; d) J. R. Tolman, J. Chung, J. H. Prestegard, *ibid.* **1992**, *98*, 462–467; e) J. Boyd, N. Soffe, J. Boban, D. Plant, R. E. Hurd, *ibid.* **1992**, *98*, 660–664; f) J. Ruiz-Cabello, G. W. Vuister, C. T. W. Moonen, P. van Geldern, J. S. Cohen, P. C. M. van Zijl, *ibid.* **1992**, *100*, 282–302; g) A. L. Davis, R. Boelens, R. Kaptein, *J. Biomol. NMR* **1992**, *2*, 395–400.

[4] G. Bodenhausen, H. Kogler, R. R. Ernst, *J. Magn. Reson.* **1984**, *58*, 370–388.

[5] D. J. States, R. A. Haberkorn, D. J. Ruben, *J. Magn. Reson.* **1982**, *48*, 286–292.

[6] a) J. Cavanagh, A. G. Palmer III, P. E. Wright, M. Rance, *J. Magn. Reson.* **1991**, *91*, 429–436; b) A. G. Palmer III, J. Cavanagh, P. E. Wright, M. Rance, *ibid.* **1991**, *93*, 151–170; c) O. W. Sørensen, *ibid.* **1992**, *100*, 431–436.

[7] D. Marion, K. Wüthrich, *Biochem. Biophys. Res. Commun.* **1983**, *113*, 967–974.

[8] L. E. Kay, P. Keifer, T. Saarinen, *J. Am. Chem. Soc.* **1992**, *114*, 10663–10665.

[9] a) M. Ikura, L. E. Kay, A. Bax, *Biochemistry* **1990**, *29*, 4659–4667; b) L. E. Kay, M. Ikura, R. Tschudin, A. Bax, *J. Magn. Reson.* **1990**, *89*, 496–514; c) S. Grzesiek, A. Bax, *ibid.* **1992**, *96*, 432–440.

[10] a) T. Vorherr, P. James, J. Krebs, A. Enyedi, D. J. McCormick, J. T. Pennington, E. Carafoli, *Biochemistry* **1990**, *29*, 355–365; b) M. Kataoka, J. F. Head, T. Vorherr, J. Krebs, E. Carafoli, *ibid.* **1990**, *30*, 6247–6251; c) M. Sattler, P. Schulte, R. Wechselberger, T. Vorherr, J. Krebs, E. Carafoli, C. Griesinger, unpublished results.

[11] L. Emsley, G. Bodenhausen, *Chem. Phys. Lett.* **1990**, *165*, 469–576.

Amination of Methane and Ethane by Mercury Photosensitization in the Presence of Ammonia**

By *Demetrius Michos, Caroline A. Sassano, Paul Krajnik,* and *Robert H. Crabtree**

Methods for the direct functionalization of saturated hydrocarbons are actively sought in connection with the problem of natural gas utilization.[1] Methane and ethane have strong C–H bonds (CH_4, 105 kcal mol^{-1}; C_2H_6, 101 kcal mol^{-1}) and are thus particularly difficult to functionalize. Overoxidation is a severe problem, because the initial oxidation products are usually more reactive than the alkanes themselves. We have looked at several alkane functionalization reactions based on mercury photosensitization. Here, the initial products are prevented from reacting further by condensation, as their vapor pressures are lower than those of the reactants.[2] The abstraction of a hydrogen atom from methane or ethane by the excited mercury atom Hg* ($^3P_1$, $d^{10}s^1p^1$, 112 kcal mol^{-1}) is not efficient because of their poor interaction. Recent studies by Soep et al.[3a] show that the Hg($^3P_1$)-NH_3 exciplex [Hg-NH_3]* has a heat of formation of 17 kcal mol^{-1}. In this exciplex NH_3 is bound to the Hg* atom like a ligand in a transition metal complex, except that the presence of three electrons, two from NH_3 and the Hg* s electron, leads to an Hg*–N bond order of 0.5. This strong interaction allows efficient energy transfer from the mercury atom to ammonia resulting in homolytic cleavage of the N–H bond to produce H$^\bullet$ and $NH_2^\bullet$ radicals.[3b] Since the H_2N–H bond strength is 107 kcal mol^{-1}, we thought that the $NH_2^\bullet$ radical should be capable of abstracting an H atom from CH_4 and C_2H_6. We therefore exposed alkane/NH_3 mixtures (mol ratio: 1:1) containing a trace of Hg vapor to UV light ($\lambda = 254$ nm). An oligomeric high-boiling liquid containing C, H, and N resulted, which is still under investigation.

[*] Prof. Dr. R. H. Crabtree, Dr. D. Michos, C. A. Sassano
Sterling Chemistry Laboratory, Yale University
225 Prospect Street, New Haven, CT 06520 (USA)
Telefax: Int. code +(203)432-6144
Dr. P. Krajnik
Current address: Institut für Theoretische Chemie und Strahlenchemie, Universität Wien
Währingerstrasse 38, A-1090 Wien (Austria)

[**] This work was supported by the Department of Energy, Amoco Corporation, Yale University, and the Fonds zur Förderung der wissenschaftlichen Forschung.

It was clear that activation was taking place, but the initial products, which are more reactive than the starting alkane and still volatile, were reacting further. To avoid this, we devised a simple reactor (Fig. 1) in which the gas mixture is cycled by a peristaltic pump through a photolysis chamber and then into a cold trap (−20 °C) to remove the initial photoproducts. We find that this leads to efficient amination

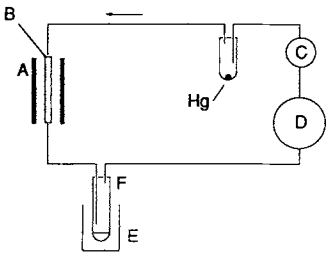

Fig. 1. Schematic representation of the apparatus used for the Hg photosensitization of CH_4 and C_2H_6. A = Hg lamps, B = photolysis chamber, C = peristaltic pump, D = gas reservoir, E = cooling bath, F = trap (see Experimental Procedure for details).

of these alkanes to give the corresponding imines. The products were hydrolyzed to give the corresponding aldehydes, converted into water-insoluble 2,4-dinitrophenylhydrazones, and identified.[4, 5] No amines were detected in the products.[6] These data are consistent with the formulation of the products as RHC=NH (R = H, Me). The proposed sequence of reactions is shown in Equations (a)–(e) for methane.

$$Hg^* + NH_3 \longrightarrow H^{\cdot} + NH_2^{\cdot} + Hg \quad (a)$$

$$CH_4 + NH_2^{\cdot} \longrightarrow CH_3^{\cdot} + NH_3 \quad (b)$$

$$CH_3^{\cdot} + NH_2^{\cdot} \longrightarrow CH_3NH_2 \quad (c)$$

$$CH_3NH_2 + Q^{\cdot} \longrightarrow {}^{\cdot}CH_2NH_2 + QH \quad (d)$$

$${}^{\cdot}CH_2NH_2 + Q^{\cdot} \longrightarrow H_2C{=}NH + QH \quad (e)$$

$MeNH_2$ is not expected as a final product because it is converted to $H_2C{=}NH$ [Eq. (d) and (e)] by Hg photosensitization;[7] $EtNH_2$ should behave similarly. The overall reaction can be expressed by Equation (f). When the gas flow rate is decreased, we see formation of higher molecular weight products, for example, MeHC=NH from CH_4/NH_3. This probably arises according to Equation (g). Hydrogen atoms are known to add to imines at the nitrogen atom.[8]

$$RCH_3 + NH_3 \xrightarrow{h\nu} RHC{=}NH + 2H_2 \quad (f)$$

$$H_2C{=}NH \xrightarrow{H^{\cdot}} {}^{\cdot}CH_2NH_2 \xrightarrow{Me^{\cdot}} MeCH_2NH_2 \longrightarrow MeHC{=}NH \quad (g)$$

Hg photosensitization reactions in the presence of NH_3 are dominated by Hg^*/NH_3 exciplex formation leading to the formation of the $NH_2^{\cdot}$ radical, a powerful $H^{\cdot}$ abstractor capable of functionalizing CH_4 and C_2H_6. These experiments show that functionalization and oligomerization of methane is possible if the initially formed products are prevented from reacting further.

Experimental Procedure

The apparatus (Fig. 1) consisted of a Rayonet photoreactor with 16 8-W low-pressure Hg lamps (254 nm). The surface of the cylindrical quartz photolysis vessel exposed to light had an area of 210 cm^2. The cooling bath was maintained at −20 °C and the peristaltic pump (Rainin, Rabbit-plus) at a circulation rate of 2.4 $mL\,s^{-1}$. The gas reservoir had a volume of 5.5 L. The gas mixture was saturated with Hg vapor by passing it over Hg before it entered the photolysis chamber. The pressure of the closed circulating system was periodically checked and adjusted to 1 atm by introducing an alkane/NH_3 mixture (1:1).

Analysis: Amines were detected with $NaBPh_4$ at pH = 2–3. The precipitated NH_4BPh_4 does not interfere with the ^1H NMR spectroscopic analysis (in C_5D_5N) of the precipitate, which did not show signals for alkyl groups. The 2,4-dinitrophenylhydrazones were prepared by acidifing the reaction product to pH = 3–4 and adding a 2 N HCl solution of 2,4-dinitrophenylhydrazine. The yellow precipitate was stirred for approximately 15 h, filtered, and washed (2 × 5 mL) with water. In a typical run (120 h, 2.4 $mL\,s^{-1}$ flow rate) 0.7 g of the corresponding pure hydrazone was isolated. A quantum yield of 0.04 was observed relative to Et_3SiH ($\Phi = 0.8$) [2a].

Received: April 24, 1993 [Z 6033 IE]
German version: *Angew. Chem.* **1993**, *105*, 1531

[1] a) *Activation and Functionalization of Alkanes* (Ed.: C. L. Hill), Wiley, New York, **1989**; b) R. A. Periana, D. J. Taube, E. R. Evitt, D. G. Loffler, P. R. Wentrcek, G. Voss, T. Masuda, *Science* **1993**, *259*, 340; c) R. H. Crabtree, *Chem. Rev.* **1985**, *85*, 245; d) N. R. Hunter, H. D. Gesser, L. A. Morton, P. S. Yarlogadda, *Appl. Catal.* **1990**, *57*, 45; e) *Methane Conversion by Oxidative Processes* (Ed.: E. E. Wolf), Van Nostrand Reinhold, New York, **1991**, p. 403; f) H. D. Gesser, N. R. Hunter, C. B. Prakash, *Chem. Rev.* **1985**, *85*, 235; g) N. R. Foster, *Appl. Catal.* **1985**, *19*, 1.

[2] a) S. H. Brown, R. H. Crabtree, *J. Am. Chem. Soc.* **1989**, *111*, 2935, 2946; b) C. M. Muedas, R. R. Ferguson, S. H. Brown, R. H. Crabtree, *ibid.* **1991**, *113*, 2233.

[3] a) M. C. Duval, B. Soep, W. H. Breckenridge, *J. Phys. Chem.* **1991**, *95*, 7145; b) J. G. Calvert, J. N. Pitts, Jr., *Photochemistry*, Wiley, New York, **1967**, p. 114.

[4] a) S. Freeman, *Anal. Chem.* **1953**, *25*, 1750; b) D. J. Curran, S. Siggia, *Carbon-Nitrogen Double Bond 1970* **1970**, 156; c) L. I. Braddoc, K. Y. Garlow, L. I. Grim, A. F. Kirkpatrick, S. W. Pease, A. J. Pollard, E. F. Price, T. L. Reissmann, H. A. Rose, M. L. Willard, *Anal. Chem.* **1953**, *25*, 301.

[5] Spectroscopic data for the 2,4-dinitrophenylhydrazones (signals for the aromatic protons are omitted). 2,4-$[(NO_2)_2C_6H_3]N(H)N=CH_2$: ^1H NMR (250 MHz, CD_2Cl_2, 25 °C, TMS): δ = 11.09 (br. s, 1H; NH), 7.16 (d, $^2J(H,H)$ = 10.8 Hz, 1H; CH), 6.72 (d, $^2J(H,H)$ = 10.8 Hz, 1H; CH); 2,4-$[(NO_2)_2C_6H_3]N(H)N=C(H)(CH_3)$ (two geometric isomers): major isomer: δ = 10.99 (br. s, 1H; NH), 7.58 (q, $^3J(H,H)$ = 5.5 Hz, 1H; CH), 2.11 (d, $^3J(H,H)$ = 5.5 Hz, 3H; CH_3); minor isomer: δ = 11.12 (br. s, 1H; NH), 7.11 (q, $^3J(H,H)$ = 5.5 Hz, 1H; CH), 2.06 (d, $^3J(H,H)$ = 5.5 Hz, 3H; CH_3).

[6] F. E. Crane, Jr., *Anal. Chem.* **1956**, *28*, 1794.

[7] a) O. C. Wetmore, H. A. Taylor, *J. Chem. Phys.* **1944**, *12*, 61; b) J. S. Watson, B. deB. Darwent, *ibid.* **1952**, *20*, 1041; c) G. DeStefano, J. Heicklen, *J. Phys. Chem.* **1986**, *90*, 4637.

[8] a) W. F. Smith, Jr., B. W. Rossiter, *J. Am. Chem. Soc.* **1967**, *89*, 717; b) A. Padwa, W. Bergmark, D. Pashayan, *ibid.* **1969**, *91*, 2653; c) T. H. Koch, R. J. Sluski, R. H. Moseley, *ibid.* **1973**, *95*, 3957; d) E. V. Donckt, G. Porter, *J. Chem. Phys.* **1967**, *46*, 1173; e) M. Fischer, *Chem. Ber.* **1967**, *100*, 3599.

A New Type of Paratungstate**

By *Hans Hartl,* Rosemarie Palm,* and *Joachim Fuchs*

Whether hexatungstate anions exist in acidified tungstate solutions has been disputed for the last 65 years;[1] up to now a salt containing such an anion, $[HW_6O_{21}]^{5-}$ or $[H_3W_6O_{22}]^{5-}$, has not been isolated.

By following the increasing acidification of an alkali metal tungstate solution through physical measurements (such as potentiometry, conductometry),[2] a distinct jump in the course of the curve is observed after the addition of about 1.15 H^+/WO_4^{2-} ($7H^+/6WO_4^{2-}$ or $8H^+/7WO_4^{2-}$), which is labeled the paratungstate step. Molar mass determinations conducted by various methods[2] indicate that hexameric anions could be present in the paratungstate solutions; however, in all of these techniques, which are performed at equilibrium, only an average molar mass or particle count can be

[*] Prof. Dr. H. Hartl, R. Palm, Prof. Dr. J. Fuchs
Institut für Anorganische und Analytische Chemie der Freien Universität
Fabeckstrasse 34/36, D-14195 Berlin (FRG)
Telefax: Int. code + (30)838-2424

[**] This work was supported by the Fonds der Chemischen Industrie.

determined. The crystallization of salts from such solutions is extremely difficult, because transformation reactions are continuously taking place. From aged solutions in which the transitions are complete or the equilibrium state has been reached, the isolation of crystals is easy. These crystals contain the dodecameric anion $[H_2W_{12}O_{42}]^{10-}$, whose structure has been known for some time.[3]

Until now, crystalline solids could be obtained from freshly acidified solutions only (paratungstate A solutions) by the precipitation with acetone and the application of appropriate organic cations. However, as shown by the X-ray crystal structure determinations of piperidinium tungstate $(C_5H_{10}NH_2)_6[W_7O_{24}]$[4] and sodium tungstate $Na_6[W_7O_{24}]\cdot 14H_2O$,[5] the heptatungstate is isolated, not the hexatungstate. The results of Raman spectroscopic studies[4] as well as ^{17}O and ^{183}W NMR measurements[6] indicate that $[W_7O_{24}]^{6-}$ is the dominating species in paratungstate A solutions. Based on the chemical reaction behavior of the solution with aging (e.g. reaction with H_2O_2[7]) and pure mechanistic considerations, it must be

$Na_5[H_3W_6O_{22}]\cdot 18\,H_2O$ **1**

assumed, as already discussed earlier,[4] that besides $[W_7O_{24}]^{6-}$ and $[H_2W_{12}O_{42}]^{10-}$ additional intermediates are formed. The anion of the sodium salt **1** may represent such an intermediate product. This compound was obtained through the reaction of $Na_2WO_4\cdot 2H_2O$ and $WO_3\cdot H_2O$ in a hydrolysis autoclave as well as at room temperature from weakly alkaline solutions. Decisive for the formation of **1** is a high tungstate concentration and the addition of only 1/8 the stoichiometric amount of $WO_3\cdot H_2O$ necessary for the theoretical equation of formation (a) (see Experimental Procedure). From the IR and Raman spectra, it is immediately

$$5\,Na_2WO_4 + 7\,WO_3 + 3\,H_2O \longrightarrow 2\,Na_5[H_3W_6O_{22}] \qquad (a)$$

recognizable that the complex generated is an unprecedented polytungstate compound. The IR spectrum of **1**, in particular, clearly differs from that of the heptatungstate (Fig. 1), although, as found in the X-ray crystal structure analysis, the anion $[H_3W_6O_{22}]^{5-}$ is a structural fragment of the heptatungstate anion (Fig. 2).

The occurrence of this particular structural unit in **1** is very interesting, because it contains two WO_6 octahedra with free octahedra faces (i.e. with three terminal oxygen atoms in *fac* configuration). Previously, it was assumed that polymetallates containing MO_6 octahedra with more than two neighboring terminal oxygen atoms ("free octahedra edges") were not stable.[9, 10] After the molybdate ions $[Mo_8O_{26}(OH)_2]^{6-}$[11] and $[Mo_{36}O_{112}(H_2O)_{16}]^{8-}$,[12] **1** represents a further example of a polymetallate structure in which the MO_6 octahedra have "free octahedra faces", however, always in "protonated" form because here the protons of the anion are coordinated to the oxygen atoms of the free octahedra faces. Only *one* significantly lengthened distance between tungsten and a terminal oxygen atom occurs (187 pm versus an average value of 176 pm); however the results of valence sum calculations[13] with respect to the Na^+ coordination by the terminal oxygen atoms suggest that a second proton is bound to the oxygen atom of the other free octahedra face. The probable positions are marked with arrows in Figure 2. The valence sums for the terminal oxygen atoms amount to 1.12 and 1.49 as compared with the expected value of 2. The position of the third proton remains in question. The sodium ions are surrounded in an octahedral environment by water molecules and oxygen atoms of the anion.

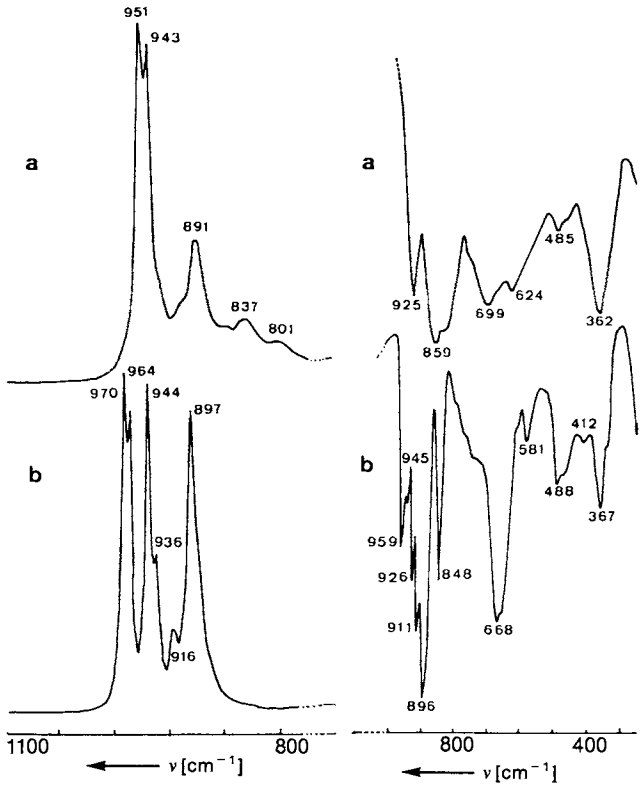

Fig. 1. IR and Raman spectra of $Na_5[H_3W_6O_{22}]\cdot 18H_2O$ **1** (a) and $Na_6[W_7O_{24}]\cdot 21H_2O$ (b) in the region for the W–O vibrational bands. Left: Raman, right: IR spectrum.

Through the construction of $Na(H_2O)_6$, $Na(H_2O)_5O$, $Na(H_2O)_4O_2$, and $Na(H_2O)_3O_3$ octahedra, the polytungstate anions of **1** are interconnected within the crystal lattice. Four of the water molecules do not have any contact to Na^+ ions, however, they do apparently interact, as evidenced by short distances, through strong hydrogen bonding with other water molecules or oxygen atoms.

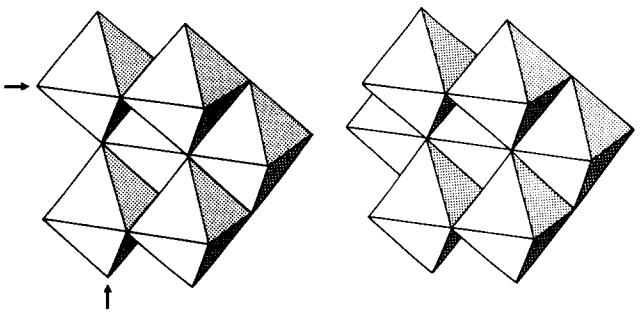

Fig. 2. Polyhedral representation of the structures of $[H_3W_6O_{22}]^{5-}$ (left) and $[W_7O_{24}]^{6-}$ (right). W–O bond lengths [pm] of **1**: W–O (terminal) 171–187, average value 176; W–μ_2O 177–227, average value 198; W–μ_3O 190–227, average value 212; W–μ_4O 214–228, average value 219; standard deviation ±3 pm.

The question of whether the anion of **1** is a precursor in the formation of $[W_7O_{24}]^{6-}$ or a hydrolysis product of the latter, still remains to be answered. Most likely both are true and in aqueous solution an equilibrium exists between the two species, which, however, as already implied, is shifted towards the side of the heptatungstate. Tytko and Glemser have compiled 18 possible geometric forms, derived from WO_6 octahedra, for hexatungstate ions and have developed probability

criteria for their existence.[14] In addition they have discussed conceivable formation mechanisms for hexatungstates and the heptatungstate ion.[15]

Experimental Procedure

$Na_2WO_4 \cdot 2H_2O$ (45 g) was stirred with $WO_3 \cdot H_2O$ (5 g) in water (50 mL) at 20 °C under argon in a closed Cautex vessel. After about 30 min, the WO_3 was completely dissolved; shortly thereafter a colorless precipitate formed, which was then filtered off. Acetone was carefully added to the filtrate until turbidity was first noted. After about 15 min the hexatungstate crystallized. The use of glass vessels should be strictly avoided because otherwise tungsten silicates are easily formed. Compound **1** cannot be recrystallized from water, but rather only from the alkaline mother liquor, in which, however, it is not indefinitely stable. On standing for some time, it was converted into a compound with the composition $Na_2W_2O_7 \cdot 4H_2O$.

The compound was originally isolated in a hydrolysis autoclave (pressure hydrolysis system II, Berghof). $WO_3 \cdot H_2O$ (0.7 g) was added to $Na_2WO_4 \cdot 2H_2O$ (1 M, 10 mL) in a PTFE insert (50 mL) and diluted with H_2O (ca. 12 mL). The mixture was heated at 150–180 °C for 24–48 h. The product mixture was subsequently worked up as described above. The yield in both cases was very low.

Received: March 31, 1993 [Z 5965 IE]
German version: *Angew. Chem.* **1993**, *105*, 1545

[1] H. Schulz, G. Jander, *Z. Anorg. Chem.* **1929**, *180*, 129–149.
[2] K. F. Jahr, H. Witzmann, *Z. Anorg. Chem.* **1932**, *208*, 145–156.
[3] R. Allmann, *Acta Crystallogr. Sect. B* **1971**, *27*, 1393–1404.
[4] J. Fuchs, E. P. Flindt, *Z. Naturforsch. B* **1979**, *34*, 412–422.
[5] K. G. Burtseva, T. S. Chernaya, M. I. Sirota, *Sov. Phys. Dokl. (Engl. Transl.)* **1978**, *23*, 784.
[6] R. I. Maksimovskaya, K. G. Burtseva, *Polyhedron* **1985**, *4*, 1559–1562; J. J. Hastings, O. W. Howarth, *J. Chem. Soc. Dalton Trans.* **1992**, 209–215.
[7] See also P. Souchay, *Ions Minéreaux Condensés*, Masson et Cie, Paris, **1969**, p. 55.
[8] Crystal structure data: triclinic, $P\bar{1}$, $a = 9.704(5)$, $b = 11.651(4)$, $c = 16.445(9)$ Å, $\alpha = 76.50(4)$, $\beta = 82.31(5)$, $\gamma = 88.41(4)°$, $Z = 2$, $V = 1791.7$ Å^3, $\rho_{calcd} = 3.52$ g cm^{-3}; Enraf–Nonius–CAD4 four-circle diffractometer, $\omega/2\theta$ scanning, $Mo_{K\alpha}$/ graphite monochromator, $2\theta_{max} = 46°$, 5328 symmetry-independent reflections, 3397 of which with $I > 2\sigma(I)$; 260 refined parameters (W and Na anisotropic, O isotropic, no H atoms), isotropic extinction correction, absorption correction DIFABS, $R = 0.059$ at unit weighting. Further details of the crystal structure investigation may be obtained from the Fachinformationszentrum Karlsruhe, Gesellschaft für wissenschaftlich-technische Information mbH, D-76344 Eggenstein-Leopoldshafen (FRG) on quoting the depository number CSD-57292, the names of the authors, and the journal citation.
[9] W. N. Lipscomb, *Inorg. Chem.* **1965**, *4*, 132–134.
[10] M. T. Pope, *Heteropoly and Isopoly Oxometalates*, Springer, Berlin, **1983**, p. 19.
[11] M. Isobe, F. Marumo, T. Yamase, T. Ikawa, *Acta Crystallogr. Sect. B* **1978**, *34*, 2728–2731.
[12] B. Krebs, I. Paulat-Böschen, *Acta Crystallogr. Sect. B* **1982**, *38*, 1710–1718.
[13] I. D. Brown, K. K. Wu, *Acta Crystallogr. Sect. B* **1975**, *32*, 1957–1957.
[14] K. H. Tytko, O. Glemser, *Z. Naturforsch. B* **1971**, *26*, 659–678.
[15] K. H. Tytko, O. Glemser, *Adv. Inorg. Chem. Radiochem.* **1976**, *19*, 239–315.

β-Na_3Hg: A Solid with a Quasi-Fluid Sodium Substructure between 36 and 60 °C

By *Hans-Jörg Deiseroth** and *Matthias Rochnia*

Na_3Hg is the outermost compound on the sodium-rich side of the binary sodium–mercury phase diagram. It is dimorphic, with an α form below 36 °C (modified Na_3As type, single-crystal structure investigation at room temperature[11]) and a β form between 36 and 60 °C (modified Li_3Bi type, powder data[1, 2]). We here report on temperature-dependent single-crystal studies of β-Na_3Hg. These studies not only clarify the hitherto puzzling deviation of the compound's true structure from the ideal Li_3Bi type. In combination with heat capacity measurements they also yield the surprising result that the sodium sublattice must be regarded as a "quasi fluid" in the temperature range between 36 and 60 °C, that is, across the full stability range of the solid β phase. β-Na_3Hg forms from α-Na_3Hg in a reversible (first-order) phase transition ($\Delta H_u = +0.3(1)$ kJ mol^{-1} based on a composition of $Na_{0.75}Hg_{0.25}$), accompanied by about 10% decrease in molar volume (α-Na_3Hg: 75.6 cm^3 mol^{-1} at 34 °C, β-Na_3Hg: 68.1 cm^3 mol^{-1} at 42 °C) and is the thermodynamically stable modification up to the melting point. On the mercury-rich side of the phase diagram, the β form is in equilibrium with solid Na_8Hg_3 (= $Na_{2.67}Hg$);[3] on the sodium-rich side it is in equilibrium with the melt. The conditions under which single crystals of β-Na_3Hg can be obtained have been described.[4] Here we note that with due care while lowering the temperature, crystals once formed can be kept in a metastable state down to a temperature of 16 °C below the phase transition temperature $T_u = 36$ °C (hysteresis). Only at even lower temperatures do we find changes in the X-ray patterns indicating retransformation.

The crystallographic data[5] show β-Na_3Hg to be a variant of the Li_3Bi type structure. The mercury atoms form a capacious cubic close-packed structure (slightly distorted towards rhombohedral symmetry) in which sodium atoms fill the octahedral and tetrahedral voids ($d_{Hg-Hg} \approx 5.5$ Å). The rhombohedral distortion of the cubic unit cell of the Li_3Bi type can also be unequivocally derived from Guinier diffractograms and increases the c/a ratio to 2.483 (42 °C, ideal value $c/a = 2.449$). Though this description apparently implies an ionic character for the compound, β-Na_3Hg is a solid with a silver metallic luster and metallic conductivity, as evidenced by preliminary conductivity measurements on pressed powders. Considering the geometrical conditions, we find that actually only the tetrahedral voids should be ideally suited to accommodate the sodium atoms Na2 ($d_{Na-Hg} = 3.3$ Å). From the incorporation of sodium atoms Na1 into the center of the octahedral voids, however, unacceptably long interatomic Na–Hg distances of 3.9 Å ensue. This observation is, in fact, essential for understanding the anomalies of the sodium substructure, as discussed in the following.

The temperature-dependent single-crystal studies clearly show the sodium atoms, especially those in the octahedral interstices, to undergo an increasingly statistical distribution with increasing temperature (Fig. 1b–1d).

At + 20 °C, substantial electron density can be detected inside the octahedral interstice. There it decreases strongly with increasing temperature and delocalizes ("smears") into the periphery. Attempts to simulate it by partially occupied split positions (Na1a–Na1d in ref. [5]) during the refinement cycles remain unsatisfactory. Concurrently, the electron density corresponding to the sodium atoms in the tetrahedral interstices also becomes delocalized, but to a much lesser degree. This is expressed in increased Debye–Waller temperature coefficients. The X-ray data, along with the split positions, only hint at possible diffusion paths through the lattice or at preferred locations of the sodium atoms. One can see, however, that the maxima of the electron density concentrate primarily in the periphery of the octahedral voids with distinct components towards the centers of the adjacent tetrahedral voids and vice versa. This effect is enhanced by increasing the temperature.

These structural features correlate directly with the specific heat capacity (c_p) curve in the stability range of the β-Na_3Hg phase (Fig. 2), which indicates melting of a sublattice below the melting point proper of the compound.

[*] Prof. Dr. H.-J. Deiseroth, Dipl.-Chem. M. Rochnia
Institut für Anorganische Chemie der Universität
Pfaffenwaldring 55, D-70569 Stuttgart (FRG)

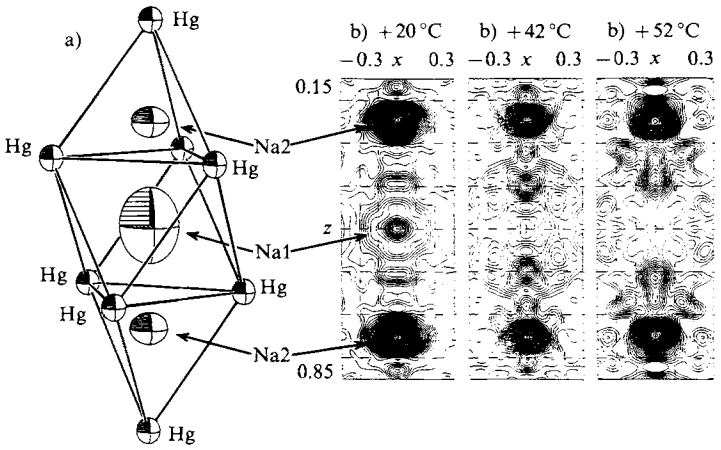

Fig. 1. a) ORTEP plot of a characteristic motif from the rhombohedral crystal structure of β-Na_3Hg. An octahedral interstice, occupied by a sodium atom Na1, and two adjacent face-sharing tetrahedral interstices along [001], occupied by sodium atoms Na2, are shown. b–d) Fourier sections $\rho(x\,0\,z)$ through a motif analogous to a), but without the mercury atoms, for different temperatures. Electronic density contours in steps of 2 e Å^{-3}. Note the obvious delocalization in the area of the octahedral interstice increases with temperature.

From the foregoing discussion, the mobility of the sodium atoms in a structure analogous to a Li_3Bi type seems inconceiveable at first, because in such a structure all octahedral and tetrahedral interstices are fully occupied. Therefore vacancies should only be available in small concentrations, depending on the thermal vacancy equilibrium. In this respect, one of our earlier observations is noteworthy.[1] Well-grown β-Na_3Hg crystals can only be obtained from samples slightly but significantly substoichiometric in sodium with composition $Na_{8.5}Hg_3$ (= $Na_{2.85}Hg$), rather than with the ideal composition of Na_9Hg_3. A corresponding sodium deficiency, and consequently a proportion of approximately 5% unoccupied sodium positions, must thus be assumed in the solid-state structure. This gives a plausible explanation of the mobility of the sodium atoms and makes the formula chosen as Na_3Hg for the title compound but a limiting, sodium-rich composition resulting from the associated structure type.

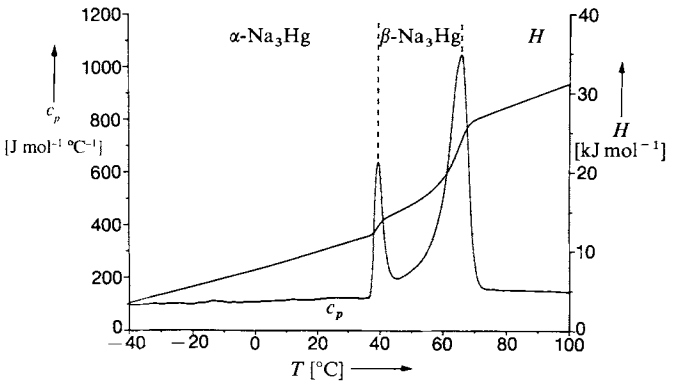

Fig. 2. Specific heat capacity c_p as a function of temperature T for β-Na_3Hg (H: total enthalpy, heating rate = 7 °C min^{-1}, sample mass 19.2 mg). The c_p curve does not return to its initial base line after the α/β phase transition.

For obvious reasons, in the present case the exact composition of the investigated crystals (with respect to sodium) cannot be determined from the X-ray occupation factors. For the 6c site (Na2, tetrahedral void), full occupation is found within experimental error, provided that the mercury positions are also fully occupied. The occupation factor for the 3b site (Na1, octahedral void), as well as the partial occupation factors for the split positions (Na1a–Na1d) introduced to simulate the delocalized electron density, however, converge during refinement at physically meaningless values, due to strong correlations.

Received: May 22, 1993 [Z6096IE]
German version: *Angew. Chem.* **1993**, *105*, 1556

[1] H. J. Deiseroth, D. Toelstede, *Z. Anorg. Allg. Chem.* **1992**, *615*, 43–48.
[2] H. J. Deiseroth, M. Rochnia, *Z. Anorg. Allg. Chem.* **1992**, *616*, 35–38.
[3] H. J. Deiseroth, D. Toelstede, *Z. Anorg. Allg. Chem.* **1990**, *587*, 103–109.
[4] Sample preparation: from preliminary experiments with samples of different net composition we found that single-crystals of β-Na_3Hg (silver metallic luster, tetrahedral habit, $\varnothing \approx 0.25$ mm, air sensitive) suitable for X-ray analysis can be obtained as follows: samples with a net composition of $Na_{2.85}Hg$ are annealed at $T = 50$ °C for 30 days and then quenched in a mixture of dry-ice/methanol. The regulus is crushed under an inert atmosphere in an agate mortar, and the crystals picked under the microscope are wedged into X-ray capillaries. From samples with a composition of Na_xHg ($x < 2.85$), Na_8Hg_3 precipitates besides β-Na_3Hg. Samples richer in sodium produce β-Na_3Hg crystals surrounded by melt.
[5] Crystal data for β-Na_3Hg: space group $R\bar{3}m$ (no.166), $Z = 3$, $a = 5.404(1)$, $c = 13.420(4)$ Å, $\mu = 340.7$ cm^{-1}, (rhombohedral cell: $a = 5.454(1)$ Å, $\alpha = 59.4°$), CAD4 diffractometer, $T = 42$ °C, $Mo_{K\alpha}$ radiation, $2\theta_{max} = 80°$, crystal size: $0.21 \times 0.18 \times 0.25$ mm^{-3}, 287 unique reflections observed, of which 154 with $I > 2.5\sigma(I)$. $R_{aniso} = 0.055$ (reflections with $I > 2.5\sigma(I)$, $R' = 0.089$ (all reflections); empirical absorption correction: Ψ-scan; maximum/minimum residual electron density: ± 1.5 e Å^{-3}. Atomic positions (with respect to the hexagonal setting in $R\bar{3}m$): Na1(3b): 0, 0, 0.5, ideal central position in the octahedral void. Split positions (see text): Na1a(6c): 0, 0, 0.401; Na1b(18h): 0.032, −0.032, 0.071; Na1c(18h): 0.425, 0.575, 0.145; Na1d(18h): 0.103, −0.103, 0.059; Na2(6c): 0, 0, 0.245, ideal central position in the tetrahedral void would be $z = 1/4$ instead of 0.245; Hg(3a): 0, 0, 0. The program system NRCVAX [6] was used for all structure calculations. Further details of the crystal structure investigation may be obtained from the Fachinformationszentrum Karlsruhe, Gesellschaft für wissenschaftlich-technische Information mbH, D-76344 Eggenstein-Leopoldshafen, on quoting the depository number CSD-57630, the names of the authors, and the journal citation.
[6] E. J. Gabe, Y. Le Page, J.-P. Charland, F. L. Lee, P. S. White, *J. Appl. Crystallogr.* **1989**, *22*, 384–387.

Tetranuclear Silver(I) Clusters Linked by Bridging Succinate Anions in a Three-Dimensional Network: Crystal Structure of Succinatodisilver(I)

By *Adonis Michaelides,* Vangelis Kiritsis, Stavroula Skoulika,* and *Andre Aubry*

In the design of new solids, weak intermolecular interactions are usually taken into account in order to engineer the desired crystal structure.[1–2] The use of metal cations to link organic molecules is an alternative method for the design of new structures. Some authors have indeed obtained two-dimensional solids,[3–4] as well as porous solids,[5–7] by combining the strongly directional coordination bonds around the metal with an appropriate multifunctional ligand (coordination polymers). In our program of crystal engineering, we plan to study the formation of coordination polymers of silver(I) with various polycarboxylato ligands. Silver (I) principally exhibits linear, trigonal, and tetrahedral coor-

[*] Dr. A. Michaelides, V. Kiritsis, Dr. S. Skoulika
Department of Chemistry, University of Ioannina
GR-45110, Ioannina (Greece)
Telefax: Int. code +(651)44112
Dr. A. Aubry
Laboratoire de Minéralogie, Cristallographie et Physique Infrarouge
Faculté des Sciences, Université de Nancy I
Vandoeuvre les Nancy (France)

dination,[8] and frequently forms polynuclear complexes (molecular or polymeric) with carboxylic acids.[9] To get initial information about the possible structural patterns in systems with complex polycarboxylato ligands, we studied complexes of silver(I) with α,ω-dicarboxylic acids. Herein we report the highly unusual crystal structure of succinatodisilver(I) **1**.[10]

Single crystals of $[Ag_2\{OOC\text{-}(CH_2)_2\text{-}COO\}]_\infty$ suitable for X-ray crystallography are formed at room temperature by slow diffusion of a solution of Ag^+ ions into a silica gel medium containing succinate anions.[11-13]

X-ray analysis[14] shows that the structure of **1** consists of planar tetranuclear silver clusters (Fig. 1) strictly parallel to the *ac* plane and bridged by succinate anions (Fig. 2). In the direction perpendicular to the *ac* plane (*b* axis), the clusters form helicoidal sequences around quasi 4_1 axes (exact 2_1).[15] All ligands lie on crystallographic inversion centers. The oligomer, represented by the Ag_4 cluster with its four succinate anions, exhibits pseudo-S_4 symmetry and is linked through its four ligands to four neighboring clusters. If we consider only the centers of the clusters that are bridged by the ligands, then we obtain an infinite structure formed by three interpenetrating, distorted diamandoid frameworks (Fig. 3).[16] Between these frameworks there are no bonds. The shortest intercluster Ag–Ag distance is 3.67 Å, too long for any metal–metal interaction (3.40 Å is the van der Waals contact distance). As far as we know, this is the first example of a three-dimensional coordination polymer containing metal clusters and might constitute a link between purely inorganic solids on the one hand, and extended cation aggregates and molecular clusters on the other.

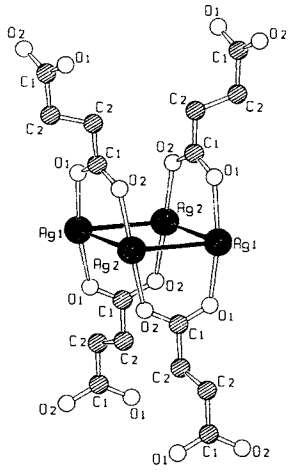

Fig. 1. SCHAKAL[21] view of the cluster and surrounding ligands. Selected distances [Å] and angles [°] are: Ag1–O1 2.211(4), Ag2–O2 2.174(4), Ag1-Ag2 2.938(1), Ag2-Ag2 3.104(1); O1-Ag1-O1 169.1(1), O2-Ag2-O2 177.6(1), Ag2-Ag1-Ag2 63.8(1), Ag1-Ag2-Ag1 116.2(1).

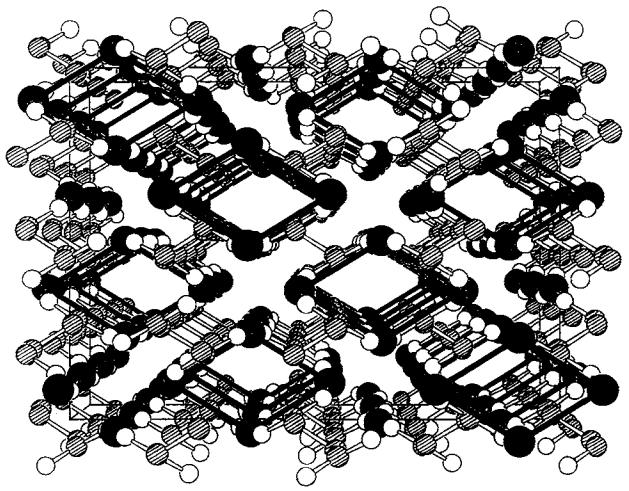

Fig. 2. SCHAKAL perspective view of the polymer **1** down the *b* axis.

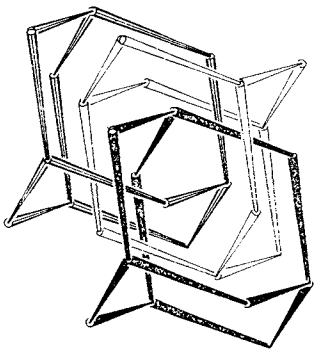

Fig. 3. SCHAKAL view of the three interpenetrating distorted diamandoid networks. The intersections represent the centers of the Ag_4 clusters while the interconnecting rods symbolize the succinate anions.

Each cluster is a Ag_4 rhombus with sides of 2.938(1) Å, interior angles of 63.8(1)° and 116.2(1)° and shortest diagonal of 3.104(1) Å (Fig. 1). These distances are within the range of weak bonding interactions.[17] The center of the rhombus is located on a *222* site, and half of these sites in the unit cell are "occupied" by clusters. The silver cations are held together by bridging carboxylato ligands that are approximately perpendicular to the Ag_4 plane; adjacent carboxylato ligands are on opposite sides of the plane. This is the first example of such unusual arrangement of carboxylato ligands around a Ag_4 cluster.[18] The coordination of silver is quasi linear ($\sphericalangle = O_1\text{-}Ag_1\text{-}O_1 = 169.1(1)°$ and $O_2\text{-}Ag_2\text{-}O_2 = 177.6(1)°$) and the Ag–O distances ($Ag_1\text{–}O_1 = 2.211(4)$ Å and $Ag_2\text{–}O_2 = 2.174(4)$ Å)[4] are similar to previously reported values.[19]

It would be interesting to see if other polyfunctional ligands can lead to similar structures. We wonder, for instance, if it is possible to reduce the intercluster distances, thus forming organometallic compounds with extended cation aggregates as in purely inorganic solids. Work in this direction is in progress.[20]

Experimental procedure

A sodium silicate solution ($\varrho = 1.1$) was slowly added to an aqueous solution of succinic acid (10 mL, 0.1 M) until the pH reached 5.6. The resulting gelling solution was poured into a test tube and was allowed to stand for about 24 h. Then, an aqueous solution of $AgNO_3$ (10 mL, 0.1 M) was carefully added at the top of the gel. Pale yellow prismatic crystals elongated along the *c* axis formed within 2 days.

Received: April 14, 1993 [Z 6003 IE]
German version: *Angew. Chem.* **1993**, *105*, 1525

[1] G. R. Desiraju, *Crystal Engineering, the Design of Organic Solids*, Elsevier, New York, **1989**.
[2] M. C. Etter, *J. Phys. Chem.* **1991**, *95*, 4601.
[3] A. Efraty, I. Feinstein, F. Frolow, L. Wackerle, *J. Am. Chem. Soc.* **1980**, *102*, 6341.
[4] J. A. Real, G. D. Munno, M. C. Munoz, M. Julve, *Inorg. Chem.* **1991**, *30*, 2701.
[5] B. F. Hoskins, R. Robson, *J. Am. Chem. Soc.* **1990**, *112*, 1546.
[6] C. Robl, *Mater. Res. Bull.* **1991**, *27*, 99.
[7] D. M. L. Goodgame, D. J. Williams, R. E. P. Winpenny, *Angew. Chem.* **1988**, *100*, 266; *Angew. Chem. Int. Ed. Engl.* **1988**, *27*, 261.
[8] F. A. Cotton, G. Wilkinson, *Advanced Inorganic Chemistry*, Wiley, New York, **1988**.

[9] X.-M. Chen, Thomas C. W. Mak, *Polyhedron* **1991**, *10*, 1723.
[10] Malonatodisilver(I) is polymeric too, but its structure is completely different to ours: F. Charbonnier, R. Faure, H. Loiseleur, *Rev. Chim. Miner.* **1981**, *18*, 245.
[11] A. Michaelides, S. Skoulika, *J. Cryst. Growth* **1989**, *94*, 208.
[12] A. Michaelides, S. Skoulika, A. Aubry, *Mater. Res. Bull.* **1988**, *23*, 579.
[13] The compound is insoluble in all common organic solvents and thermally stable up to 250 °C.
[14] Orthorhombic, $a = 16.218(3)$, $b = 11.919(3)$, $c = 11.778(2)$ Å, $V = 2276$ Å^3. *Fddd*, $\varrho_{calcd} = 3.872$ gcm^{-3}, CAD-4 diffractometer, $\omega/2\theta$ scan, graphite-monochromated $Mo_{K\alpha}$ radiation. SHELXS-86 and SHELX-76 program systems, 740 reflections with $I > 3\,\sigma(I)$, no empirical absorption correction. Anisotropic refinement $R = 0.0279$, $R_w = 0.0322$, secondary extinction correction. Further details of the crystal structure investigation are available on request from the Director of the Cambridge Crystallographic Data Centre, 12 Union Road, GB-Cambridge CB2 1EZ (UK), on quoting the full journal citation.
[15] In this respect, this structure is reminiscent of that of $[Cd(SPh)_2]$: D. Craig, I. G. Dance, R. Garbutt, *Angew. Chem.* **1986**, *98*, 178; *Angew. Chem. Int. Ed. Engl.* **1986**, *25*, 165.
[16] Interesting examples of interpenetrating diamandoid frameworks are given in a) K. W. Kim, M. G. Kanatzidis, *J. Am. Chem. Soc.* **1992**, *114*, 4878; b) O. Ermer, *ibid.* **1988**, *110*, 3747; c) O. Ermer, A. Eling, *Angew. Chem.* **1988**, *100*, 856; *Angew. Chem. Int. Ed. Engl.* **1988**, *27*, 829.
[17] M. Jansen, *Angew. Chem.* **1987**, *99*, 1136; *Angew. Chem. Int. Ed. Engl.* **1987**, *26*, 1098.
[18] This motif has recently been observed in the structure of the silver compound $[Ag(F-C_3H_4N_3C_6H_4-F)]_4$: E. Hartmann, J. Strähle, *Z. Anorg. Allg. Chem.* **1990**, *583*, 31.
[19] F. Charbonnier, R. Faure, M. Petit-Ramel, *Eur. J. Solid State Inorg. Chem.* **1992**, *29*, 93.
[20] Crystals of Ag^+ with other dicarboxylic acids have been obtained, and the structures will soon be solved.
[21] E. Keller, SCHAKAL, Universität Freiburg (FRG) **1988**.

BOOKS

This section contains book reviews and a list of new books received by the editor. Book reviews are written by invitation from the editor. Suggestions for books to be reviewed and for book reviewers are welcome. Publishers should send brochures or (better) books to the Book Editor, Dr. Gerhard Karger, Redaktion Angewandte Chemie, Postfach 101161, D-69451 Weinheim, Federal Republic of Germany. The editor reserves the right of selecting which books will be reviewed. Uninvited books not chosen for review will not be returned.

Book Reviews

Human Protein Data. 1st Instalment. Edited by *A. Haeberli*. VCH Verlagsgesellschaft, Weinheim/VCH Publishers, New York, 1992. XLV, 424 pp., looseleaf collection DM 275.00, subscription price DM 225.00.—ISBN 3-527-28211-4/1-56081-110-2

To begin compiling a collection of data on human proteins probably strikes most of us as an unending task, comparable with the rapidly growing data banks of protein sequences. It is, therefore, all the more pleasing that three years ago A. Haeberli had the courage to make a start on this, and especially that he had the good sense to delegate much of the work, in which so far 167 authors have covered 147 proteins. Anyone who sees gaps in this and feels a duty to contribute is likely to be enthusiastically recruited by the editor to join in. Thus one can envisage that the necessary continuation and updating of this looseleaf collection, which the publishers plan to extend by about 70 more proteins per year, will proceed successfully. The 147 proteins in this first instalment are mainly plasma proteins, together with a number of protein hormones and protein factors. The descriptions are concise, comprehensible to the general user and not too specialized, and contain quite enough information for a first source. Relevant literature references enable one to go into more detail.

The same clear layout is used for each protein, listing synonyms, abbreviations, classification, e.g. according to EC number or from serum electrophoresis, short description, structural features, molecular mass, sedimentation constant, isoelectric point, extinction coefficient, enzymic activity, coenzymes/cofactors, substrates, inhibitors, biological function, physiological and pathological role, breakdown behavior, genetics and mutants, biological half-life, concentration and isolation procedures, sequence, and disulfide or SH groups. In many cases the structure is illustrated at the end by a clear schematic diagram, or by three-dimensional diagrams and ribbon models where these are known. The above list is, of course, very comprehensive, and it is not surprising that in many cases not every item of information has yet been included. However, this does not indicate that the searching has been inadequate but rather that an effort has been made to present the very latest knowledge. In view of the brevity of the ID codes of proteins as given in sequence data banks, it would not have been a bad idea to include cross-references to, for example, PIR, SWISSPROT, or the protein structure data bank.

The question arises: why a growing file for our bookshelves rather than a data bank for interrogating through the VDU screen? Ten years from now the answer to this question is likely to be different. At present the proportion of biochemists and medical scientists who can gain access to a central external data bank through a computer terminal near their desk, or who wish to learn how to do so, is probably less than 10%. However, for the VDU enthusiasts among them a diskette is included in the package.

In 1990 the Gesellschaft für Biotechnologische Forschung (GBF) in Braunschweig issued an "Enzyme Handbook" consisting of five A5-size files, listing enzymes according to their EC numbers. Although the GBF files and the "Human Protein Data" collection reviewed here appear to have similar aims, they are somewhat different in style. Neither makes the other redundant: to begin with, the "Enzyme Handbook" sets out to cover all the known sources for each enzyme. It is desirable that the different approaches should be maintained, so that the two works will complement rather than duplicate each other.

The "Human Protein Data" collection will become increasingly important as the human genome project gets under way. It is only by combining information on the many possible human DNA sequences with a data bank on gene products that advances in practically useful knowledge can be achieved.

Emil Schiltz
Institut für Organische Chemie und Biochemie
der Universität Freiburg (FRG)

Organic Peroxides. Edited by *W. Ando*. Wiley, Chichester, 1992. XVI, 845 pp., hardcover £ 140.00.—ISBN 0-471-93438-0

Qinghaosu is a naturally occuring tetracyclic peroxide with high anti-malarial activity, and is extracted from *Artemisia annua*, a plant that is widely distributed in China. An unusual structure might be expected to be associated with unusual properties, and this is confirmed for many peroxides. This class of compounds has been much studied by chemists since the end of the nineteenth century. In recent decades research activity has further intensified, because peroxides are in many cases ideal reagents for the synthesis of oxyfunctionalized compounds, they play an essential role in the metabolization of chemicals by organisms, and reactive peroxides often undergo thermal or photochemical breakdown through unusual pathways. These different aspects of the subject are drawn together in this excellent book.

The editor, W. Ando, has succeeded in recruiting expert authors for all the chapters, and thereby presenting an overview of this important area of chemistry which is thoroughly up-to-date (including many literature citations from the last five years). Synthetic routes to the above mentioned compound qinghaosu alone are described in five chapters. However, the overall layout of the book is unimaginative. Thus, the first ten chapters deal with different compound classes, and only in the last five chapters is the subject matter arranged according to oxidation pathways. Consequently, although finding an answer to a question of detail should be relatively quick and straightforward, there has evidently been no attempt to unite the topics in a way that could also introduce non-specialists to the field.

In the first hundred pages Yamaguchi and co-authors give an excellent overview of theoretical aspects of organic peroxides. Modern views concerning the Sharpless epoxidation are discussed, as also are the studies by Bernardi on the addition of singlet oxygen to ethylene and by Robb on the breakdown of 1,2-dioxetanes (1990, 1991). The chapters on alkyl hydroperoxides (Ch. 2, Porter), dialkyl peroxides (Ch. 3, Matsugo and Saito), diacyl peroxides (Ch. 7, Fujimori), sulfur and phosphorus peroxides (Ch. 8, Kim), and peroxyacids and peroxyesters (Ch. 9, Sawaki) are well worth reading and of appropriate length, and give particular attention to the uses of these compounds in synthesis. In cases where chapter subjects have not been clearly defined beforehand, overlapping always results. Thus, under the heading of dialkyl hydroperoxides we find that many endoperoxides and their reactions are treated, then these appear again in the chapter with this title (Ch. 6, Clennan and Foote). Of special interest here are the important studies by Jefford on the synthesis of 1,2,4-trioxanes and by Hayes on copper(II)- and iron(III)-catalyzed cyclizations of alkyl hydroperoxides (both of which are also relevant to the synthesis of qinghaosu and its analogues). Dioxiranes and dioxetanes are treated very briefly in Chapters 4 and 5 (Adam et al.). Here one is relieved to find that the authors have avoided giving an encyclopedic list of all the available data on reactions of dioxiranes and properties of dioxetanes, which would be enough to fill another book. Dioxirane chemistry is undergoing a near-explosive phase of development, as is apparent from the bibliography, in which half the papers cited are for the period 1989–1992. In contrast, dioxetane chemistry is relatively quiet, although some interesting transformations of these highly reactive peroxides have recently been discovered. Polyoxides, a class of compounds that chemists tend to group under "exotica", are described by Plesničar in Chapter 10. The author gives a nice explanation of how these compounds have gradually emerged from being regarded as merely unstable intermediates or models for theoretical studies, and are now even used in synthesis. One of special interest is triethylsilylhydrotrioxide (Corey, Posner), which can be used as a source of singlet oxygen, or for the direct (per)oxyfunctionalization of carbon–carbon double bonds or thioethers.

Chapters 11–14 are concerned with four methods for the synthesis of peroxides. Modena et al. report on the current state of metal-catalyzed oxidation reactions. However, there is no mention of biochemical processes, and only a very inadequate treatment of applications of the Sharpless and Kagan methods to enantioselective oxidations, *cis*-hydroxylations, and the oxidation of thioethers. The photosensitized oxygenation of heteroatoms (Ch. 12, Akasaka and Ando), the ozonolysis method (Ch. 13, McCullogh and Nojima), and reactions using superoxides (Ch. 14, Nagano et al.) yield peroxides with a great variety of structures, and these methods are therefore treated very thoroughly. But here, if not earlier in the book, one notes with annoyance that there is no chapter on the synthesis of peroxides by reactions using singlet oxygen. Whereas a separate chapter is devoted to heteroatom photooxidation reactions (which are the editor's specialty), photooxidations of alkenes, alkynes, dienes, etc. are only mentioned under the corresponding compound classes, inevitably resulting in incomplete coverage. There are, of course, alternative publications such as the (now rather outdated) book by Murray (1979), or the CRC collection by Frimer (1985), but this remains a shortcoming in the present work. Lastly, with the aim of making a link with biology, a brief discussion of peroxides in biological systems has been added (Ch. 15, Niki).

Overall this is a very useful collection of articles on the current state of peroxide chemistry, and despite a few gaps in the coverage it deserves to reach a wide readership. Additional points in its favor are the high standard of production and the consistent quality of the figures.

Axel G. Griesbeck
Institut für Organische Chemie
der Universität Würzburg (FRG)

Writing Reaction Mechanisms in Organic Chemistry. By *A. Miller*. Academic Press, New York, 1992. X, 488 pp., hardcover (spiral binding) $ 34.95.—ISBN 0-12-496711-6

The title accurately describes what this book is about: writing equations that represent the "correct" (i.e. most plausible) reaction mechanisms. It is intended mainly for students beginning their first course in organic chemistry; some parts of the chapters on free radicals and pericyclic reactions will also be of interest to more advanced students.

It cannot be used as a substitute for a conventional textbook, but it includes many explanations and useful hints that make it much more than just a collection of exercises. The author summarizes in a lucid and understandable form the important principles of organic chemistry that must be observed in writing reaction mechanisms. In doing so she deals in detail with possible misunderstandings and logical errors, and discusses examples of unclear mechanistic equations picked out from the literature.

The book consists of seven chapters, each containing many exercise problems in which one is given the structures of the starting materials and products and the reaction conditions and has to derive a probable reaction mechanism. The solutions to these problems are discussed in considerable detail, sometimes in the main text and sometimes at the end of the chapter.

In the first chapter the author discusses some fundamental principles such as Lewis structures, formal charges, hybridization, charge distributions, and aromaticity. Terms such as resonance, equilibrium, tautomerism, basicity, acidity, nucleophilicity, and electrophilicity are clearly defined and discussed with the help of examples. A comprehensive table of pK_a values is included, and much use is made of these data in solving the problems in this chapter, and also in setting those of the following chapters. However, throughout the book the reader is hindered by the lack of definitions and examples to distinguish between kinetic and thermodynamic control of product formation.

The second chapter explains some further basic concepts related to chemical reactions, and discusses the stoichiometry of atoms and charges, and the use of curved arrows to indicate a redistribution of electrons (e.g., in nucleophilic attack). A method is also suggested whereby, on comparing the structures of the starting material and the product, one can most easily identify the bonds that are broken and those that are newly formed.

The next chapter is concerned with nucleophilic substitutions and additions, and with base-induced eliminations and rearrangements. These are again illustrated by a wealth of well chosen example problems. However, Exercise 3–18 raises doubts: here a Favorskii rearrangement is explained in terms of a bicyclobutanone intermediate (alternative: semibenzilic acid rearrangement).

Chapter 4 continues by discussing reactions that proceed via intermediates with electron-deficient carbon atoms or related species. These include rearrangements of carbenium ions, electrophilic additions, acid-catalyzed reactions of carbonyl compounds, electrophilic aromatic substitutions, and reactions of carbenes, nitrenes, and nitrenium ions. Here and in the following chapter the word regiospecificity is often used when what is meant is regioselectivity. Also it seems doubtful whether simple *primary* carbenium ions are formed from the reaction of alcohols with common acids (p. 213).

Chapter 5 deals with reactions that proceed via free radical intermediates. The main emphasis is on radical chain processes, but fragmentations and rearrangements of radicals are also touched on, as also are the $S_{RN}1$ reaction and the Birch reduction.

Chapter 6 is concerned with pericyclic reactions. First the author discusses the shapes of molecular orbitals from a qualitative standpoint, before going on to the question of allowed and forbidden reaction pathways and its solution, either in terms of the sum of the $[4q + 2]_s$ and $[4r]_a$ components or by considerations of frontier orbitals. In this connection electrocyclic and sigmatropic reactions, cycloadditions, and the ene reaction are all treated in detail. The many clearly understandable example problems are treated without reference to the concepts of retention and inversion in sigmatropic shifts that are usually employed; in the case of 1,3-dipolar cycloadditions the author avoids introducing the 1,3-dipolar resonance form. The statement on page 392 that thermal $[{}_\pi 2_s + {}_\pi 2_a]$-cycloadditions cannot be concerted reactions on geometrical grounds conflicts with textbook reactions of ketenes. One might also question the assumption of a concerted [1,5] hydrogen shift in the problem on the *trans* isomer of 2,4-pentadienylbenzene (Exercise 6–15a).

The last chapter contains an assortment of slightly more difficult exercises. In a few cases here (as also in the preceding chapter) the stereochemistry of the starting material and/or the product is ignored, perhaps to simplify the problem.

The book has been produced in a spiral binding which turns out to be surprisingly durable. It is written in an easily understandable style, and should present no difficulties even for students whose first language is not English. The reaction mechanisms are shown by formula diagrams that are clear, though somewhat too large, with the result that a single example can extend over several pages. The reaction equations seldom indicate yields, an omission that is not entirely made up for by the many literature citations. Printing errors are few, but unfortunately these usually occur in the formula diagrams where they can lead to some confusion: for example, students will have a hard time with Exercise 7–4 as the structural formula given for the product is wrong.

Despite a few minor shortcomings the book can be recommended for students as an accompaniment to a standard textbook. By reading it they will learn about many factors to be considered in assessing the plausibility of reaction mechanisms, and will be encouraged to search systematically for a likely reaction path, even for rather more complex reactions. For teachers too the book not only provides a collection of problems for seminars and examinations, but also identifies some misunderstandings and difficulties that students often encounter in the treatment of reaction mechanisms.

Klaus Banert
Fachbereich Chemie
der Universität-Gesamthochschule Siegen (FRG)

New Books
see next page

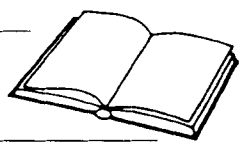

 © *VCH Verlagsgesellschaft mbH, D-69451 Weinheim, 1993* *0570-0833/93/1010-1499 $ 10.00+.25/0*

New Books

Advances in Chemical Diagnosis and Treatment of Metabolic Disorders, Vol. 1. Edited by **I. Matsumoto.** Wiley, West Sussex, Great Britain, **1992.** 184 pp., hardcover, £ 30.—ISBN 0-4719-3889-0

Guidelines for Engineering Design for Process Safety. American Institute of Chemical Engineers, New York, **1993.** ca. 500 pp., hardcover, $ 140.—ISBN 0-8169-0565-7

Dictionary of Analytical Reagents. Edited by **A. Townshend, D. T. Burns, R. Lobinski et al.** Chapman & Hall, London, **1993.** 1400 pp., hardcover, £ 595.—ISBN 0-412-35150-1

Grundlagen der Radiochemie. By **C. Keller.** Salle + Sauerländer, Frankfurt/Main, **1993.** 324 pp., hardcover, DM 68.—ISBN 3-7935-5487-2

Einführung in die Angewandte Elektrochemie. By **E. Zirngiebl.** Salle + Sauerländer, Frankfurt/Main, **1993.** 514 pp., hardcover, DM 168.—ISBN 3-7935-5534-8

The Design of Drugs to Macromolecular Targets. Edited by **C. R. Beddell.** Salle + Sauerländer, Frankfurt/Main, **1993.** 287 pp., hardcover, DM 268.—ISBN 3-7935-5547-X

Inorganic Materials. Edited by **D. W. Bruce, D. O'Hare.** Salle + Sauerländer, Frankfurt/Main, **1993.** 543 pp., hardcover, DM 165.—ISBN 3-7935-5648-4

Chemie und Umweltbelastung. By **R. Demuth.** Diesterweg, Frankfurt/Main, **1993.** 196 pp., paperback, DM 19.80.—ISBN 3-425-05431-7

Polymer Chemistry. An Introduction. (Ellis Horwood Series in Polymer Science). By **G. Challa.** Ellis Horwood, West Sussex, Great Britain, **1993.** 192 pp., paperback, £ 25.—ISBN 0-13-489691-2

Chemistry Imagined. Reflections on Science. By **R. Hoffmann, V. Torrence.** Smithsonian Institution Press, Washington, **1993.** 168 pp., hardcover, $ 23.95.—ISBN 1-56098-214-4

Comprehensive Handbook on Hydrosilylation. Edited by **B. Marciniec.** Pergamon Press, Oxford, **1992.** 754 pp., hardcover, £ 150.—ISBN 0-08-040272-0

Advances in Photochemistry, Vol. 18. Edited by **D. H. Volman, G. S. Hammond, D. C. Neckers.** Wiley, West Sussex, Great Britain, **1993.** 406 pp., hardcover, £ 103.—ISBN 0-471-59133-5

Molecular Biology and Biotechnology, 3rd Edition. Edited by **J. M. Walker, E. B. Gingold.** Royal Society of Chemistry, Cambridge, Great Britain, **1993.** 428 pp., paperback, £ 39.—ISBN 0-85186-794-4

Strukturelemente biologisch aktiver Substanzen. By **W. Perkow.** Harri Deutsch, Frankfurt, **1993.** 323 pp., DM 58.— ISBN 3-8171-1234-3

Analyses of Hazardous Substances in Air, Vol. 2. Edited by **A. Kettrup.** VCH, Weinheim/New York, **1993.** 189 pp., hardcover, DM 108.-/$ 70.—ISBN 3-527-27026-4/1-56081-275-3

Spectroscopy in Catalysis. By **J. W. Niemantsverdriet.** VCH, Weinheim/New York, **1993.** 288 pp., hardcover, DM 148.-/$ 95.—ISBN 3-527-28593-8/1-56081-792-5

Fullerene C_{60}. History, Physics, Nanobiology, Nanotechnology. By **D. Koruga, S. Hameroff, J. Withers, R. Loutfy, M. Sundareshan.** Elsevier, Amsterdam, **1993.** 381 pp., hardcover, Dfl 200.—ISBN 0-444-89833-6

Iron-Carbene Complexes. (Scripts in Inorganic and Organometallic Chemistry). Springer, Heidelberg/New York, **1993.** 202 pp., paperback, DM 68.—/$ 49.—ISBN 3-540-56258-3/0-387-56258-3

Spectroscopy of New Materials. (Advances in Spectroscopy, Vol. 22). Wiley, West Sussex, Great Britain, **1993.** 339 pp., hardcover, £ 110.—ISBN 0-471-93911-0

The World of Physical Chemistry. By **K. J. Laidler.** Oxford University Press, Oxford, **1993.** 488 pp., hardcover, £ 55.—ISBN 0-19-855597-0

Stereoselective Synthesis in Organic Chemistry. By **Atta-ur-Rahman, Z. Shah.** Springer, Heidelberg, **1993.** 522 pp., hardcover, DM 138.—ISBN 3-540-94029-4

Special Applications. (NMR Basic Principles and Progress, Vol. 29). Edited by **H. Pfeifer, P. Barker.** Springer, Heidelberg, **1993.** 178 pp., hardcover, DM 178.—ISBN 3-540-56438-1

Structure in Polymers with Special Properties. (Advances in Polymer Science, Vol. 108). Edited by **H.-G. Zachmann.** Springer, Heidelberg, **1993.** 137 pp., hardcover, DM 138.—ISBN 3-540-56579-5

GABCOM & GABMET. Acronyms of Compounds and Methods in Chemistry and Physics. Edited by **Gmelin Institute.** Springer, Heidelberg, **1993.** 381 pp., softcover, DM 98.—ISBN 3-540-93653-X

Thermostability of Enzymes. Edited by **M. N. Gupta.** Springer, Heidelberg, **1993.** 213 pp., hardcover, DM 148.—ISBN 3-540-56275-3

Structures and Biological Effects. (Structure and Bonding, Vol. 81). Edited by **D. M. P. Mingos, R. J. P. Williams.** Springer, Heidelberg, **1993.** 193 pp., hardcover, DM 168.—ISBN 3-540-56481-0

New Gmelin Volumes:
Compounds with Sulfur of Oxidation Number 2. (S Sulfur-Nitrogen Compounds, Part 9). Edited by **A. Kubny, N. Baumann, H.-J. Fachmann et al.** Springer, Heidelberg, **1993.** 336 pp., hardcover, DM 1998.—ISBN 3-540-93664-5

Natural Occurence. Minerals. (Mn Manganese, Vol. A2). Edited by **W. Töpper, R. Ditz.** Springer, Heidelberg, **1993.** 180 pp., hardcover, DM 1090.—ISBN 3-540-93665-3

Physical Methods of Chemistry, Second Edition. (Investigations of Surfaces and Interfaces, Part B, Vol. IXB). Edited by **Bryant W. Rossiter, R. C. Baetzold.** Wiley, West Sussex, Great Britain, **1993.** 745 pp., hardcover, £ 206.—ISBN 0-471-54405-1

Plant Mitochondria. Edited by **A. Brennicke, U. Kück.** VCH, Weinheim/New York, **1993.** 434 pp., hardcover, DM 178.-/$ 115.—ISBN 3-527-30033-3/1-56081-767-4

Semiconductor Surfaces and Interfaces. (Springer Series in Surface Sciences 26). By **W. Mönch.** Springer, Heidelberg, **1993.** 366 pp., hardcover, DM 120.—ISBN 3-540-54423-2

^{31}P-NMR-Spektroskopie. (NMR-Spektroskopie von Nichtmetallen, Vol. 3). By **S. Berger, S. Braun, H.-O. Kalinowski.** Thieme, Stuttgart, **1993.** 205 pp., paperback, DM 253.—ISBN 3-13-769201-6

Asymmetric Synthesis of Natural Products. By **A. Koskinen.** Wiley, Chichester, West Sussex, Great Britain, **1993.** 234 pp., paperback, £ 16.95.—ISBN 0-471-93848-3

Registered names, trademarks, etc. used in this journal, even when not marked as such, are not to be considered unprotected by law.

© VCH Verlagsgesellschaft mbH, D-69451 Weinheim, 1993. – Printed in the Federal Republic of Germany by Konrad Triltsch Druck- und Verlagsanstalt Würzburg.

All rights reserved (including those of translation into foreign languages). No part of this issue may be reproduced in any form – by photoprint, microfilm, or any other means – nor transmitted or translated into a machine language without written permission from the publishers. Only single copies of contributions, or parts thereof, may be made for personal use. This journal was carefully produced in all its parts. Nevertheless, authors, editors, and publisher do not warrant the information contained therein to be free of errors. Readers are advised to keep in mind that statements, data, illustrations, procedural details, or other items may inadvertently be inaccurate.

Valid for users in the USA: The appearance of the code at the bottom of the first page of an article (serial) indicates the copyright owner's consent that copies of the article may be made for personal or internal use, or for the personal or internal use of specific clients. This consent is given on the condition, however, that the copier pay stated per-copy fee through the Copyright Clearance Center, Inc. (CCC), for copying beyond that permitted by Sections 107 or 108 of the U.S. Copyright Law. This consent does not extend to other kinds of copying, such as copying, for general distribution, for advertising or promotional purposes, for creating new collective works, or for resale. For copying from back volumes of this journal see 'Permissions to Photo-Copy: Publisher's Fee List' of the CCC.

Editorial office: Postfach 10 11 61, D-69451 Weinheim, Federal Republic of Germany, Telephone (06201) 606 315, Telex 465 516 vchwh d, Telefax (06201) 606 328, E-Mail Z16@DHDURZ2 in Earn Bitnet.

Editor: *Peter Gölitz*

Associate editors: *N. A. Compton, R. H. Schmidt-Radde, K. J. Schneider.* **Book editor:** *G. Karger.* **Editorial assistants:** *J. Göhrig, E. Schweikart*

Publishers: VCH Verlagsgesellschaft mbH. (Managing Directors: *Hans Dirk Köhler, Dr. Karlheinz Köpfer*), Pappelallee 3, D-69451 Weinheim, Federal Republic of Germany.

Advertising office (Advertising Manager: *N. Schippel*): Postfach 10 11 61, D-69451 Weinheim, Federal Republic of Germany, Telephone (0 62 01) 606 312, Telefax (0 62 01) 606 328.

ANGEWANDTE CHEMIE
International Edition in English
Volume 32 · Number 11
November 1993
Pages 1501–1670

Structures of Organo Alkali Metal Complexes and Related Compounds

By Erwin Weiss*

Dedicated to Professor Ernst Otto Fischer on the occasion of his 75th birthday

The investigation of the reactivity and structure of organometallic compounds of alkali metals has experienced a blustering development in the last decades. This class includes compounds that are especially important for our understanding of chemical bonding and also quite simple, for example methyl alkali metal complexes, whose structures have been unequivocally determined. Organometallic compounds of alkali metals (and also magnesium) generally exist as ion aggregates whose properties can be significantly modified through solvation by, for example, ether or amines. Important advances in the synthesis of new compounds, especially those of the heavier alkali metals, have been based on these results. It was long believed that the alkali metals had little tendency to undergo coordination and that their coordination chemistry would offer few surprises. This picture has now changed completely. Results from crystal structure investigations have revealed a variety of often surprising structure types (rings, heterocubanes, chains, layers, etc.) not only with the organometallic compounds but also with the amides, imides, alkoxides, phenoxides, enolates, and even halides. A comparison reveals interesting similarities between compounds that appear to be so different and leads to a general classification of the structure types possible with C, N, O, and halo ligands.

1. Introduction

Organo alkali metal complexes were first reported in 1914, 14 years after the discovery of the Grignard compounds, in the pioneering work of Wilhelm Schlenk.[1] His name also remains associated with the development of inert gas techniques for the handling of reactive compounds. A comprehensive monograph published in 1937[2] showed that only few advances had been achieved in the study of organo alkali metal compounds up to the 1930s. A revival in organolithium chemistry occurred soon afterwards, however, which was particularly promoted through the work of Karl Ziegler, Georg Wittig, and Henry Gilman. The application of lithium compounds in preparative chemistry was the main area of interest, and this class of reagents soon achieved an importance similar to that of the Grignard compounds.

Structure investigations were first performed in the 1960s and have since then yielded many new and unexpected results on the structures and coordination modes of alkali metal and magnesium compounds involving not only carbanions but also amides, alkoxides, and other anions. Since these reagents are typically used in solution, the nature of their solvent adducts is an obvious area of interest. Structure information enables a better understanding of the reaction mechanisms and is therefore useful in synthetic chemistry. The important structure types will be presented and compared in this contribution. Because of the tremendous volume of published results and space limitations, the list of references is unfortunately rather incomplete. For this reason the reader is referred to further review articles and monographs[3–9] as well as to annual reports.[10]

[*] Prof. Dr. E. Weiss
Institut für Anorganische und Angewandte Chemie der Universität
Martin-Luther-King-Platz 6, D-20146 Hamburg (FRG)

Crystal structure analysis (X-ray diffraction and, more recently, neutron and synchrotron X-ray diffraction) is unquestionably the most important method of investigation. As such, these results will be emphasized in this report. Some of the knowledge gained from crystal studies may also allow conclusions to be drawn about the structures in solution; however, direct methods for the investigation of structures in solution are also available (NMR and IR spectroscopy, and measurements of colligative properties).

2. Simple, Unsolvated Organo Alkali Metal Compounds

2.1. Methyllithium: Structure and Bonding

The investigation of the structure of methyl alkali metal compounds began in 1964 with methyllithium.[11a] Since single crystals were not available, X-ray powder methods had to be applied. Shortly before this and independently, the structure of ethyllithium had been reported by H. Dietrich[12] as the first organo alkali metal compound (single-crystal methods). Both compounds form tetrameric aggregates having a Li_4C_4 heterocubane framework. The tetramers in $(LiCH_3)_4$ have ideal T_d symmetry and form a body-centered cubic lattice (Fig. 1). A structure refinement[11b] also provided the approximate positions of the H atoms and thus evidence for pyramidal methyl groups (C_{3v} symmetry). In this structure the C atom of each methyl group has three short contacts to three of the Li atoms of its tetramer as well as a further contact only about 5–10 pm longer to a neighboring tetramer located on a space diagonal of the body-centered cubic unit cell (coordination number of 7 for C!).

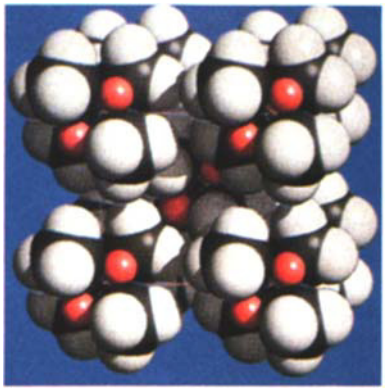

Fig. 1. Space-filling model of the body-centered cubic unit cell of $(LiCH_3)_4$[11,18]. The Li radii were chosen to be 75 pm, in accord with approximately 85% ionic character (normal ionic radius of 65 pm).

Each tetramer interacts with its eight neighbors. The very low volatility and the nonmelting character of methyllithium are direct consequences of this three-dimensional network. The strength of these interactions is drastically reduced for ethyllithium and falls off almost entirely for organolithium compounds having larger organic residues. The compounds become increasingly more volatile and have lower melting points or are even liquid as with $(LinBu)_6$. It is misleading to try to deduce covalent bonding from these properties as was often done earlier. The physical properties result from the overall structures that form from approximately spherical aggregates, which are lipophilic on the outside but can be strongly polar on the inside.

A few remarks on bonding relationships are in order at this point. These are of general interest for the organolithium compounds, and particularly for methyllithium, and have been the topic of numerous and sometimes controversial discussions. Since organolithium compounds contain only light atoms, they are well suited for theoretical studies, especially ab initio calculations. Many authors, but above all P. von R. Schleyer et al.,[4,13] have carried out these types of calculations. In the first publication on $(LiCH_3)_4$[11a] we interpreted the bonding in the tetramer based on a qualitative MO model. These ideas have been refined many times by other authors, and $(LiCH_3)_4$ has even been mentioned in textbooks as an illustration of LiC_3 two electron–four center bonds.

Initially, the covalent contribution to the Li–C bond was considerably overestimated based on the observation of ^7Li-^{13}C couplings in the NMR spectra.[14] Streitwieser et al.,[15] however, had already shown in the late 1970s that the tetrameric structure of methyllithium can also be explained with a purely electrostatic point charge model. This model was extended and generalized by describing the atoms as hard spheres (Hard Sphere Electrostatic Model).[16] Although the ionic contribution to the M–C bond is not easily determined for M = Li, recent calculations[4,13,17] estimate it to be about 80–88% and to be even greater with the heavier alkali metals. According to the current viewpoint, therefore, the alkali metal–carbon bond should be considered predominantly ionic, and the results of numerous structure investigations presented in the following discussions fully support this. The aggregates often observed are, in fact, ion aggregates having only a small covalent bonding contri-

Erwin Weiss, born in 1926 in Arzberg/Oberfranken, studied chemistry at the Technische Hochschule in Munich and received his Ph.D. in 1956 for his work with Walter Hieber on the structure of metal carbonyls and arene complexes. After conducting postdoctoral research (Massachusetts Institute of Technology, Cambridge, USA, 1956), he worked in research laboratories in Europe (European Research Institute, Brussels, 1957–1961, Cyanamide European Research Institute, Geneva, 1961–1965) and was than was appointed to the faculty of the University of Hamburg, where he remained until 1991. His research interests focus on the synthesis and structure of organometallic compounds with main group and subgroup metals. This review was written in part during a research sabbatical in Paris which was associated with the French Alexander-von-Humboldt-Preis 1992.

bution. This approach can also be reflected in the nomenclature where, for example, the methyl alkali metal compounds would be denoted as alkali metal methanides.[21, 25] In this report, however, the more conventional "-yl" nomenclature will be used.

We have recently further refined the structure of methyllithium from neutron diffraction data and have thereby also found that no phase transition occurs down to 1.5 K.[18] Since the incoherent scattering of ^1H nuclei causes a high level of background noise in the diffraction diagram, powder samples of the deuterated compound $(LiCD_3)_4$ were examined. These investigations furnished the first precise structure data for a trigonal-pyramidal methyl carbanion (we will return to this in Section 2.4). These studies also confirmed a staggered orientation of the methyl carbanion relative to the three neighboring Li atoms of the tetramer.

2.2. Methylpotassium, Methylrubidium, and Methylcesium

Since the structures of the methyl compounds of the heavier alkali metals are simpler, their descriptions will be treated before that of methylsodium. Methylpotassium was first described by Schlenk and Holtz[1c] as a black coating on potassium metal obtained upon its reaction with dimethylmercury. These samples were not suitable for X-ray investigations because of substantial amalgam impurities. Our synthesis of nearly colorless and pure methylpotassium from a metal-exchange reaction between methyllithium and potassium *tert*-butoxide allowed its structure to be determined.[19] The first preparation and investigation of the highly reactive compounds methylrubidium and methylcesium was possible in an analogous way.[20]

All three compounds display the NiAs structure type and contain CH_3^- ions with trigonal-prismatic coordination to six K ions. Although the diffraction data, which was once again obtained from powder samples, could not furnish the exact H atom positions, IR spectroscopic investigations suggested pyramidal CH_3^- ions.[19] Later, a more precise neutron diffraction analysis was carried out on the deuterated compound KCD_3 (powder samples, measurements at 290 and 1.4 K).[21]

A significant result from this structure refinement was the experimental verification of pyramidal methyl anions. Their orientations alternate within the lattice whereby, rather than the hexagonal cell previously measured, a larger orthorhombic cell results. The relation between the two unit cells is illustrated in Figure 2. Each methyl group is surrounded by six K ions in a distorted trigonal prism. This distortion is a consequence of the CH_3^- structure and also causes smaller deviations of the K ions from their ideal positions in the NiAs structure. The three K ions surrounding the lone pair of electrons on CH_3^- have shorter K–C distances (295 and 302 pm) than those of the three K atoms associated with the H atoms (330 and 344 pm). A space-filling model of the unit cell of methylpotassium is shown in Figure 3. Methylrubidium and methylcesium crystallize in the same orthorhombic structure type, as a recent reexamination[22] of the earlier powder data[20] proved.

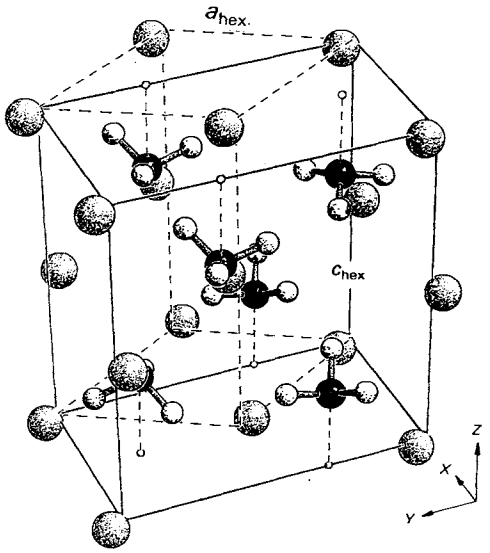

Fig. 2. Crystal structure of KCH_3 (ball-and-stick model) illustrating the relationship between the orthorhombic (*Pmcn*) and hexagonal unit cells ($b_{orthorh} \approx \sqrt{3}\,a_{hex}$)[21].

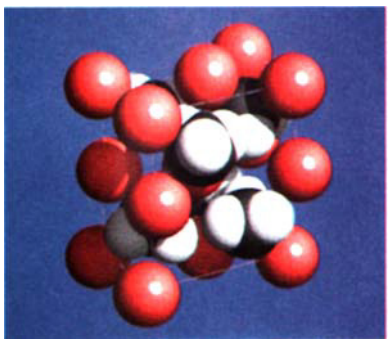

Fig. 3. Space-filling model of the unit cell of KCH_3 (K radius chosen to be 145 pm)[21].

2.3. Methylsodium

2.3.1. Methyllithium-Containing Methylsodium $(NaCH_3)_4 \cdot [(LiCH_3)_4]_x$, $x \leq 0.333$

In earlier work[23] we described the synthesis and structure of methylsodium containing variable amounts of methyllithium. Finely crystalline samples were obtained from $LiCH_3$ and sodium *tert*-butoxide by a metal-exchange reaction [Eq.(a)], and various amounts of $LiCH_3$ (mol ratios of $NaCH_3$:$LiCH_3$ from ca. 3:1 to 36:1) could be incorporated depending on the composition of the solvent.

$$LiCH_3 + NaO\,tBu \xrightarrow{\text{ether/(hexane)}} NaCH_3(LiCH_3)_x + LiO\,tBu \qquad (a)$$

In these experiments, $NaO\,tBu$ was added to a solution of $LiCH_3$. The structure of the product (Fig. 4), as determined from the powder data, is a giant cubic cell in which 24 tetrameric $(NaCH_3)_4$ aggregates build a zeolite-like host lattice. Although it is similar to the methyllithium lattice, the arrangment of the $(NaCH_3)_4$ units is more complicated. Large cavities result which firmly and selectively incorporate $(LiCH_3)_4$ units up to a structurally specified $NaCH_3$:$LiCH_3$

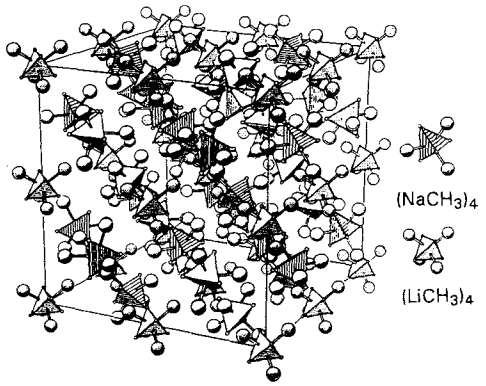

Fig. 4. The host–guest compound $(NaCH_3)_4 \cdot [(LiCH_3)_4]_x$ ($x \leq 0.333$)[23]. The host lattice (cubic cell, $a = 2020$ pm with 24 $(NaCH_3)_4$ units) contains large cavities that can incorporate a maximum of 8 $(LiCH_3)_4$ aggregates.

ratio of 3:1. To our knowledge this is the first example of an organometallic supramolecular compound. Previously obtained methyl/ethyl- and ethyl/*tert*-butyllithium compounds[24] most probably are similar types of clathrates with complicated structures.

2.3.2. *Methylsodium: Synthesis and Structure*

Only later[25] did we realize that pure methylsodium has a different, more compact structure. It is obtained when the reaction following Equation (a) is performed in the opposite sequence; that is, the $LiCH_3$ solution must be added to the NaO*t*Bu solution. Thus, the tetrameric methyllithium aggregates present in the ether solution[26] envelop the $(NaCH_3)_4$ tetramers that form upon addition of NaO*t*Bu, and thereby a special clathrate lattice is constructed. The formation of the $NaCH_3/LiCH_3$ inclusion compound is therefore template directed.

Methylsodium crystallizes as a new and complicated structure type (orthorhombic, $I222$, $Z = 16$). The structure solution was in no way trivial, for it was only possible by a combination of the complimentary methods of neutron diffraction and X-ray synchrotron diffraction on $NaCD_3$ powder samples.[27] In this new approach the Na and C positions were determined from the synchrotron data, and the D positions were subsequently obtained from the neutron diffraction data. Measurements performed at 1.5 and 293 K indicated that no phase transformation took place. Representations of the structure are shown in Figures 5 and 6 (and as stereoplots in ref.[25]).

In this structure, half of the ions form $(NaCH_3)_4$ tetramers that have slightly distorted T_d symmetry but are very similar to those in methyllithium. The remaining eight Na and eight methyl ions connect the tetramers through Na–C contacts. Depending on the orientation of the methyl ion relative to the cation, both short and long M–C distances (253 to 291 pm) are observed here, too. The distances are short within the tetramers and longer to the immediately adjoining ions ("backsides" of the methyl groups). The ions located between the tetramers also show this type of coordination: each CH_3^- ion is surrounded by three Na ions at shorter distances and one Na at a longer distance in a distorted tetrahedron. The structure of methylsodium is thus related to that of methyllithium, and its lower symmetry is a result

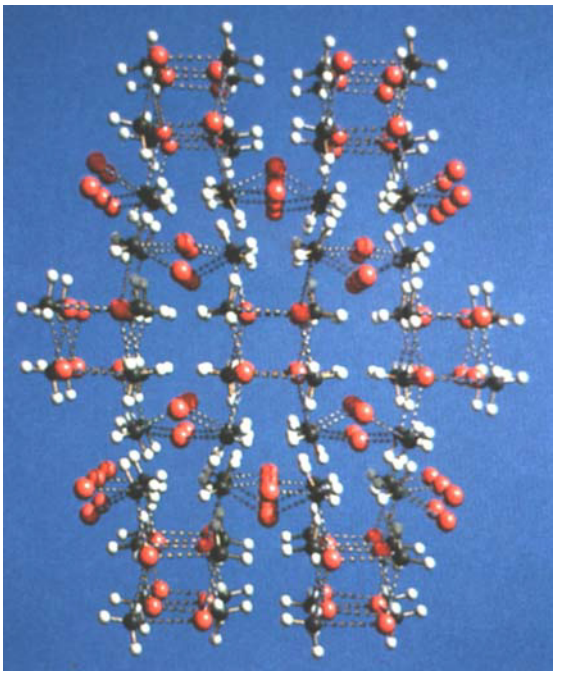

Fig. 5. Ball-and-stick model of the methylsodium lattice (Na red, C gray); adjoining unit cells of methylsodium[25]. A row of two tetrameric aggregates is found at each edge and in the middle of the picture. Dashed lines denote Na–C contacts less than 270 pm. Thus the methyl groups located between the tetramers also appear to be coordinated to three Na ions.

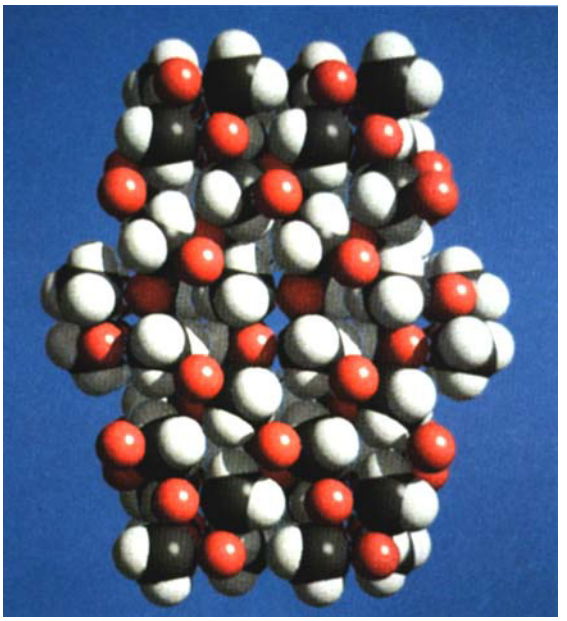

Fig. 6. Space-filling model of the crystal structure of methylsodium (orientation as in Fig. 5). The Na radii have been chosen to be 110 pm in accord with approximately 90% ionic character (standard ionic radius 97 pm).

of the different cation radii. All of the methyl ions are trigonal pyramidal with C–H bond lengths of 109 pm and H-C-H bond angles of 106° (at 1.5 K).

These results filled the gap in our knowledge on the structures of the methyl alkali metal compounds. Methylsodium takes on a median position between methyllithium and the methyl compounds of the heavier alkali metals, because its structure contains both tetrameric aggregates as well as single ions. An optimal packing in the ionic lattice is achieved through its special structure.

2.4. A Comparison of the Structures of CH_3^-, SiH_3^-, and GeH_3^-

The exact structure determinations performed with neutron diffraction that were discussed in the previous sections provide good data for the CH_3^- ion in crystalline solids.[28] It is always pyramidal (average H-C-H bond angle 107°) and isostructural with NH_3 (H-N-H bond angle 107.6°, Table 1), but the inversional bending modes known for ammonia are not possible for the CH_3^- ion in a rigid crystal lattice.

Table 1. Comparison of CH_3^-, SiH_3^-, and GeH_3^- with each other and with their analogues from the fifth main group.

$EH_3^{(-)}$	Distance E-H [pm]	Angle H-E-H [°]	Determined for
CH_3^-	107.2	108.2	$LiCD_3$ (1.5 K [18])
	109.4 (ave.)	106.2 (ave.)	$NaCD_3$ (1.5 K [25])
	109.6 (ave.)	105.1 (ave.)	KCD_3 (1.5 K [21])
NH_3	106	107.6	(2 K [33])
SiH_3^-	-	94(4)	$KSiH_3$ (NMR [30])
	143	95	$KSiH_3$ [32]
PH_3	141	93.5	
GeH_3^-	-	93(4)	$KGeH_3$ (NMR [30])
AsH_3	152	91.8	

We had previously examined a number of alkali metal silanides and germanides: $KSiH_3$, $RbSiH_3$, $CsSiH_3$,[29] $KGeH_3$, $RbGeH_3$, and $CsGeH_3$.[30, 31] We found that with the exception of $CsGeH_3$ all the compounds crystallize at room temperature in the NaCl structure type. The H-E-H bond angles for the silanide and germanide ions were determined by solid-state NMR spectroscopy and are listed for comparison in Table 1.

For the understanding of the structure of KCH_3 (distorted NiAs type), a comparison with the room-temperature modification of $KSiH_3$ (NaCl type)[29] is especially informative. The trigonal-prismatic coordination of the methyl carbanions to six alkali metal ions is a consequence of the trigonal CH_3^- structure. In contrast, the SiH_3^- ion is more spherical on account of the larger radius of Si. Thus, steric factors are less important than electrostatic factors in the alkali metal silanides (and germanides), and octahedral coordination (NaCl structure type) results, at least in the high-temperature modifications.[32]

2.5. Ethyllithium, Ethylsodium, Alkali Metal Alkynides and Acetylides, and Dilithiomethane

As already mentioned, ethyllithium forms tetramers that are similar to those of methyllithium but of lower symmetry. Very different, however, is the layered structure found for ethylsodium (Fig. 7).[34] This structure is a consequence of the larger radius of the cation and clearly indicates ionic interactions. An ABC arrangement of three sequentially staggered but identical double layers lies perpendicular to the long c axis of the crystal. The Na ions are located within the double layers, and the ethyl ions are oriented perpendicular to the layers with their methyl groups pointing outward (Na–C 263 and 268 pm).

The alkali metal ethynides $MC{\equiv}CH$ (M = Na, K, Rb)[35] and propynides $MC{\equiv}CCH_3$ (M = Na, K)[35a] (Fig. 8), as

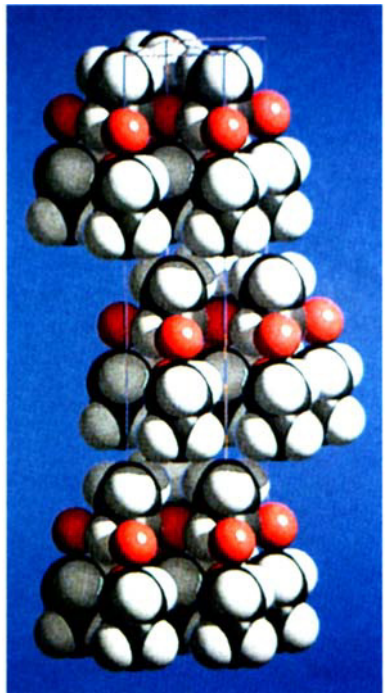

Fig. 7. The layered structure of ethylsodium (rhombohedral space group $R\bar{3}m$; Na radii chosen to be 110 pm).

well as the methoxides and ethoxides (discussed in Section 8), have related structures. As a result of their layered structures, they are neither volatile nor soluble in nonpolar solvents, and so, once again, structure investigations could only be performed on microcrystalline powder samples. The alkali metal acetylides $MC{\equiv}CM$ (M = Li, Na, K) have also been investigated (Fig. 8).[36] A distorted antifluorite structure is shown by Na_2C_2,[36b] and the K analogue is isostructural.[36c]

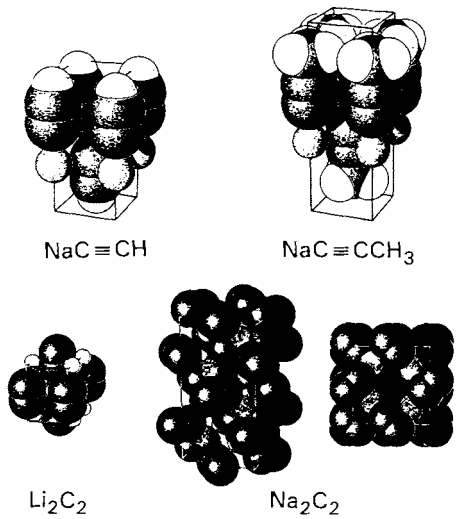

Fig. 8. Space-filling model of the layered structures of several alkynides; the structure type and the metal ions that lead to isotypic structures are given in parentheses. $NaC{\equiv}CH$ (tetragonal; K, Rb, Cs), $NaC{\equiv}CCH_3$ (tetragonal; K), Li_2C_2 (tetragonal)[36a], Na_2C_2 (tetragonal[36b]; K[36c]).

Polylithiated hydrocarbons were first structurally investigated in the early 1980s.[37] The theoretical proposition[38] that the *cis* planar structure of gas-phase dilithiomethane Li_2CH_2 is more stable than the tetrahedral structure has

drawn great attention. Unfortunately, the only experimental information available to date is for the solid phase. Following earlier, still incomplete powder X-ray diffraction investigations,[39] the structure was finally completely determined by neutron diffraction.[40] Here, bent CH_2 anions are coordinated in a complicated way to six Li ions in a strongly distorted antifluorite structure.

3. The Significance of Solvation: Base Adducts of Organolithium Compounds

3.1. Solvation

Solvation has great impact on the physical and chemical properties of organolithium compounds.[8, 9] Organolithium compounds are generally employed as ether solutions, and Grignard reagents only exist as ether adducts since dismutation to MgR_2 and MgX_2 occurs otherwise.[41] Solvation increases solubility and can also cause a drastic increase in reactivity.[42] Thus, base adducts have found important applications in synthetic chemistry. The metalation of benzene by *n*BuLi, for example, is only possible with the addition of tmeda or *tert*-butoxide ("LICKOR superbase").[42]

Solvation often lowers the degree of aggregation; nevertheless, organolithium compounds remain mostly associated even in polar solvents, as the examples in Table 2 show. Here, molar mass determinations[43] and especially NMR investigations[44] have provided important results. Since solid-state investigations are the primary source of detailed structural information, we will report exclusively on these results. Crystalline ether adducts are only slightly thermally stable and thus easily degraded. Therefore, more stable adducts with amines and especially those with the respective bidentate and tridentate chelating ligands tmeda ($Me_2NCH_2CH_2NMe_2$) and pmdta ($Me_2NCH_2CH_2N(Me)CH_2CH_2NMe_2$) are usually examined. Non-N-methylated amines such as ethylenediamine are easily metalated and therefore seldom used as donor ligands. Even ethers, in particular thf, can be attacked and cleaved,[45] which can lead to problems with the more reactive organometallic compounds of the heavier alkali metals.

Often, but not always, the structure of an amine adduct can be used to infer that of the corresponding ether adduct. Many structure investigations have revealed the specific influence of not only the carbanion but also the donor ligand on the total structure. Examples of aggregated organolithium compounds both in solution and in the solid state are listed in Table 2. Also included are some unsolvated tetramers and hexamers like $[Li(1\text{-norbornyl})]_4$[46] and $[Li(cyclohexyl)]_6$[48] (Fig. 9).

Table 2. Degree of aggregation for some organolithium compounds in solution and in the crystals[a].

Compound	Degree of association	Solvent or ref.
a) *In solution* [9, 10]		
LiMe	tetramer	Et_2O, THF
LiEt	tetramer	Et_2O, THF
LiEt	hexamer	hydrocarbon
Li*n*Bu	hexamer	hydrocarbon
Li*n*Bu	tetramer/dimer	THF
Li*t*Bu	tetramer	hydrocarbon
Li*t*Bu	dimer/monomer	Et_2O, THF
LiPh	dimer	Et_2O, THF
$LiCH_2Ph$	> monomer	Et_2O, THF
LiC_3H_5	> monomer	Et_2O, THF
b) *In crystals*		
$(LiMe)_4$	tetramer	[11, 18]
$(LiEt)_4$	tetramer	[12]
$[Li(1\text{-norbornyl})]_4$	tetramer	[46]
$(Li\,t\text{Bu})_4$	tetramer	[47]
$(Li\,n\text{Bu})_6$	hexamer, cluster	[47]
$[Li(cyclohexyl)]_n$	hexamer, cluster	[48]
$[Li(tetramethylcyclopropylmethyl)]_6$	hexamer, cluster	[49]
$[Li\{2,6\text{-}(NMe_2)_2C_6H_3\}]_3$	trimer, ring	[50]
$[Li(CH_2SiMe_3)]_6$	hexamer, ring	[51]
$[LiC(SiMe_3)_3]_2$	dimer	[52]
c) *Base adducts*		
$[(LiMe)_4(tmeda)_2]_n$	3D net of tetramers	[53]
$[Li\{CH(SiMe_3)_2\}(pmdta)]$	monomer	[54]
$[Li\,t\text{Bu}(Et_2O)]_2$	dimer	[47]
$[Li(thf)_3][Li\{C(SiMe_3)_3\}_2]$	ion pair, ate complex	[55]
$[\dot{L}iCH_2CH_2CH_2\dot{O}Me]_4$	tetramer	[56]
$[\dot{L}iCH_2CH_2CH_2\dot{N}Me_2]_4$	tetramer	[57]
$[LiPh(Et_2O)]_4$	tetramer	[58a]
$[LiPh(Me_2S)]_4$	tetramer	[58b]
$[LiPh(tmeda)]_2$	dimer	[59]
[LiPh(pmdta)]	monomer	[60]
$[Li(2,4,6\text{-}t\text{Bu}_3C_6H_2)(tmpda)]$	monomer	[61]
$[LiC{\equiv}CH(en)]_n$	double chain (ladder structure)	[62]
$[LiC{\equiv}CPh(tmpda)]_2$	dimer	[63]
$[(LiC{\equiv}CPh)_4(tmhda)_2]_n$	chain of tetramers (double helix)	[64]
$[(LiC{\equiv}C\,t\text{Bu})_4(thf)_4]$	tetramer	[65]
$[(LiC{\equiv}C\,t\text{Bu})_{12}(thf)_4]$	stack	[65]
$[Li(allyl)(tmeda)]_n$	chain	[66]
$[Li(\eta^2\text{-allyl})(pmdta)]$	monomer	[67]
$[Li(\eta^3\text{-}1,3\text{-diphenylallyl})(Et_2O)]_n$	chain	[68a]
$[Li\{\eta^3\text{-}1,3\text{-bis(trimethylsilyl)allyl}\}$-(tmeda)]	monomer	[68b]
$[Li(benzyl)(dabco)]_n$	chain	[69]
$[Li(benzyl)(Et_2O)]_n$	chain	[70a]
[Li(benzyl)(tmeda)(thf)]	monomer	[70b]
$[Li\{CH(SiMe_3)Ph\}(tmeda)]$	monomer	[70c]
$[Li(CPh_3)(tmeda)]$	monomer	[71]
$[Li(CPh_3)(Et_2O)_2]$	monomer	[72]
$[Li[12]crown\text{-}4)_2][CHPh_2]$ $[Li[12]crown\text{-}4)_2][CPh_3]$	ion pair	[73]

[a] Abbreviations: tmeda = tetramethylethylenediamine, tmpda = tetramethyl-1,3-propylenediamine, tmhda = tetramethyl-1,6-hexylenediamine, pmdta = pentamethyldiethylenetriamine, dabco = 1,4-diazabicyclo[2.2.2]octane.

3.2. Base Adducts of Organolithium Compounds

3.2.1. Methyllithium and Its Derivatives

The $LiCH_3$ tetramer is relatively stable and cannot be cleaved by either ethers or amines. In its tmeda adduct $[(LiCH_3)_4(tmeda)_2]_n$,[53] the tmeda molecules do not act as chelating ligands but rather as bridges between the tetramers and effect the formation of a three-dimensional network. Recent investigations have shown that the tetramer $(Li\,t\text{Bu})_4$ is transformed into the dimer $[Li\,t\text{Bu}(Et_2O)]_2$ upon solvation with ether.[47]

A monomer, $[Li\{CH(SiMe_3)_2\}(pmdta)]$,[54] is formed under the large steric requirements of, on the one hand, the highly substituted methyl carbanion $CH(SiMe_3)_2^-$ and, on the other hand, the tridentate base pmdta. Still greater shielding can lead to solvent-separated ion pairs as observed

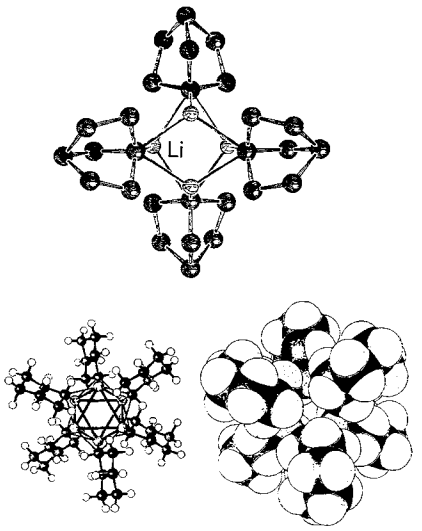

Fig. 9. Structures of $[Li(1\text{-norbornyl})]_4$ (top) and $[Li(cyclohexyl)]_6$ (bottom, ball-and-stick and space-filling models).

in the ate complex $[Li(thf)_3][Li\{C(SiMe_3)_3\}_2]$.[55] Crown ethers likewise lead to ion pairs such as $[Li([12]crown\text{-}4)_2]^+$ with the counterions $[CHPh_2]^-$ and $[CPh_3]^-$.[73] "Internal solvation" occurs when an appropriately functionalized carbanion is employed, as in $[\overline{LiCH_2CH_2CH_2OMe}]_4$[56] and $[\overline{LiCH_2CH_2CH_2NMe_2}]_4$.[57]

3.2.2. Phenyllithium

This compound is a prime example illustrating the influence that the donor ligand has on the structure: with Et_2O or Me_2S the respective heterocubane-type tetramers $[LiPh(Et_2O)]_4$[58a] and $[LiPh(Me_2S)]_4$[58b] are generated, with tmeda the dimer $[LiPh(tmeda)]_2$ having somewhat unsymmetric phenyl bridges,[59] and with the tridentate pmdta ligand the monomer [LiPh(pmdta)][60] (Fig. 10). Since the Li ion is always four coordinate, it is understandable that the degree of aggregation decreases as the hapticity of the ligands increases. Recent solid-state ^{13}C NMR investigations have also verified this.[74]

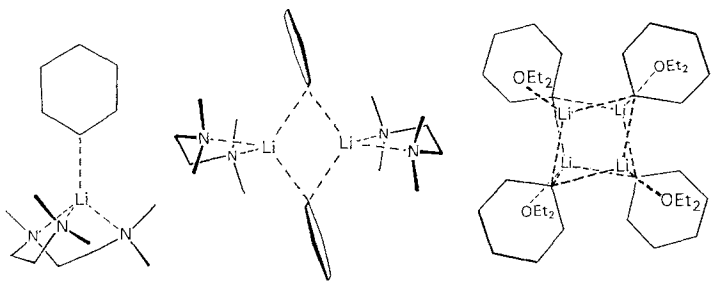

Fig. 10. The influence of the solvent on the aggregation of phenyllithium. From left to right: [LiPh(pmdta)][60], $[LiPh(tmeda)]_2$[59], and $[LiPh(Et_2O)]_4$[58]. The π electron system of the benzene rings is not indicated.

3.2.3. Alkynyllithium Compounds

Ethynyllithium is only stable as a base adduct. Our investigations[62] have shown that with ethylenediamine (en), ethynyllithium forms the polymeric compound $[LiC{\equiv}CH(en)]_n$, whose crystal structure reveals double strands connected in a ladder-like fashion by ethylenediamine bridges.

Phenylethynyllithium is solvated by the longer chained diamines tmpda ($Me_2N(CH_2)_3NMe_2$) and tmhda ($Me_2N(CH_2)_6NMe_2$). With the former, the dimer $[LiC{\equiv}CPh(tmpda)]_2$ having nearly symmetric alkynyl bridges results,[63] and with the latter, tetramers are formed that are linked by pairs of bridging tmhda ligands to make a double helix, $[(LiC{\equiv}CPh)_4(tmhda)_2]_n$.[64]

Depending on the conditions for crystallization, the thf adducts of *tert*-butylethynyllithium will form as either tetramers, $[(LiC{\equiv}CtBu)_4(thf)_4]$, or dodecamers, $[(LiC{\equiv}CtBu)_{12}(thf)_4]$ (Fig. 11).[65] These especially interesting examples illustrate an often observed structural principle: the stacking of dimers. Thus, the stacking of two dimers produces a cubane structure and that of six dimers a dodecamer. Other degrees of aggregation are also conceivable, and examples are found among the alkali metal amides (Section 7.2).

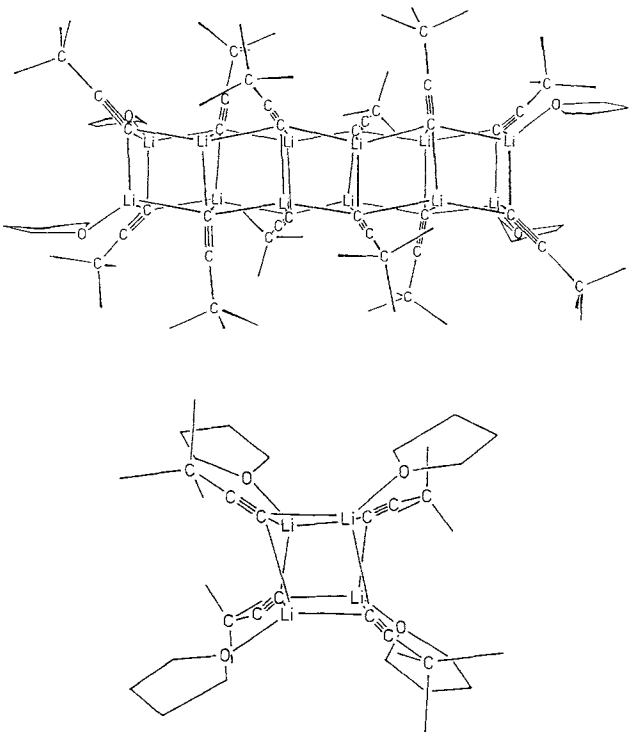

Fig. 11. Structures of $[(LiC{\equiv}CtBu)_4(thf)_4]$ (bottom) and $[(LiC{\equiv}CtBu)_{12}(thf)_4]$ (top) can be described as stacks of cyclic dimers.

3.2.4. Allyllithium

The allyl ion is particularly interesting since it is one of the simplest π electron systems. The first crystal structure investigation on a tmeda adduct revealed a chain structure $[Li(allyl)(tmeda)]_n$, in which solvated Li ions act as bridges between the terminal CH_2 groups of the allyl ions as $(\cdots Li(allyl)Li(allyl)\cdots)$.[66] A Li ion coordinated to the allyl π electron system was first found in the pmdta adduct $[Li(\eta^2\text{-}allyl)(pmdta)]$[67] which appears as a monomer as expected because of the greater hapticity of the tripod ligand. In agree-

ment with the results from model calculations,[3] the carbanion is no longer planar as a result of its (predominantly ionic) interaction with the cation. The unexpected η^2-coordination is a consequence of the very strong shielding of the Li ion by the pmdta ligand, which occupies three coordination sites on the Li. These factors are to a large extent not applicable in the compound $[Li(\eta^3\text{-}1,3\text{-diphenylallyl})(Et_2O)]_n$[68a], and the expected η^3-coordination is observed (polymer chains).

3.2.5. Benzyl- and Triphenylmethyllithium

The early X-ray structure analyses of $[Li(\eta^2\text{-benzyl})\text{-}(N(CH_2CH_2)_3N)_2]_n$ (polymer chains)[69] and $[Li(benzyl)(Et_2O)]_n$ (polymer chains)[70a] are representative of the structures of the numerous benzyllithium compounds. The benzyl ligands are planar in these chain structures, and the Li atoms lie in approximately symmetrical positions above and below the benzylic carbon atoms. The monomers [Li(benzyl)(tmeda)(thf)][70b] and $[Li\{CH(SiMe_3)Ph\}(tmeda)]$[70c] are rare examples showing benzyl C atoms with pyramidal coordination.

The monomeric triphenylmethyl compounds $[Li(CPh_3)\text{-}(tmeda)]$[71] and $[Li(CPh_3)(Et_2O)_2]$[72] contain central C atoms with planar coordination. Additional alkali metal compounds having this carbanion will be discussed in the next section.

4. Base Adducts of Organometallic Compounds of the Heavier Alkali Metals

4.1. Synthesis of Organosodium and Organopotassium Compounds

The organometallic compounds of the heavier alkali metals are more reactive and less soluble than their lithium analogues, which makes their syntheses particularly problematic. The strongly polar solvent (ether) required in these reactions is readily attacked by the reactive organometallic compounds, and even with cooling this process can be slowed but not halted. For a long time only a few representatives were known; only those derived from strong C–H acids like cyclopentadiene or alkynes were significant.

Based on the fundamental work of L. Lochmann et al.,[42a, b] we began in 1968 to use metal-exchange reactions between organolithium compounds and soluble alkali metal alkoxides (sodium and potassium *tert*-butoxide, see Section 8) to successfully prepare various compounds of the heavier alkali metals; important examples of these compounds were discussed in Sections 2.2 and 2.3). We also described the synthesis of unsolvated phenylsodium and phenylpotassium,[75] whose structure determinations are still pending.

In an alternative preparative route to these compounds, *n*-butyllithium and sodium *tert*-butoxide are used to prepare *n*-butylsodium, whose C–H acidity is strong enough to serve in the metalation of hydrocarbons. Aromatic hydrocarbons as well as amines and other compounds can be used in these reactions. Solvated organosodium compounds can be prepared in the presence of donor ligands, as was first shown with $[Na(CPh_3)(tmeda)]$.[76] In a valuable variation of this metalation reaction, [Na*n*Bu(tmeda)], an adduct soluble in hydrocarbon solvents and readily synthesized from *n*BuLi and NaO*t*Bu, is employed.[77, 78] The analogous potassium compound, [K*n*Bu(tmeda)], is likewise soluble and also an effective metalating agent.[79]

4.2. Structures of Solvated Organometallic Compounds of the Higher Alkali Metals

4.2.1. Phenylsodium and Biphenylylsodium

In contrast to the monomeric lithium compound [LiPh-(pmdta)],[60] the adduct formed from phenylsodium and pmdta, $[NaPh(pmdta)]_2$, is a dimer in the solid state (Fig. 12).[80] The difference is a consequence of the different

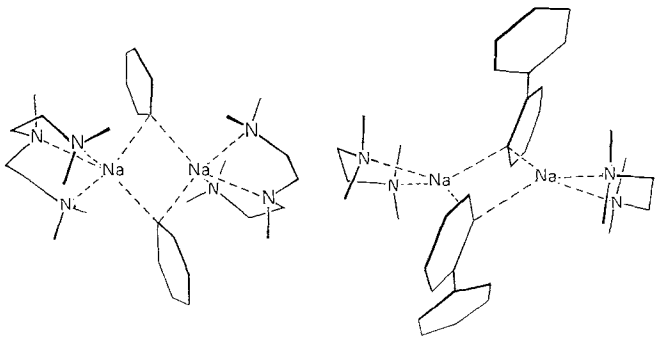

Fig. 12. Dimeric amine adducts of phenylsodium (left) and biphenylylsodium (right).

cation radii: the larger Na ion has a coordination number of 5 and thus the dimer structure is possible. A similar structure is also exhibited by the Na derivative of biphenyl having bidentate tmeda ligands, $[Na(C_6H_4Ph)(tmeda)]_2$ (Fig. 12).[81] Here, the two benzene rings of the bridging biphenylyl ligands are no longer coplanar, a result also observed in the corresponding lithium compound $[Li(C_6H_4Ph)(tmeda)]_2$.[82]

4.2.2. Benzyl, Diphenylmethyl, and Triphenylmethyl Compounds

In the following, examples containing the phenyl-substituted methyl anions benzyl, diphenylmethyl, and triphenylmethyl anion will be presented. Depending on the steric requirements of both the carbanion and the donor ligand, a number of different structure types result.

Benzyl anion: Both the benzyl and the *o*-xylyl carbanion form cyclic tetramers with the tmeda-solvated Na ion in the respective complexes $[Na(benzyl)(tmeda)]_4$[83] and $[Na(o\text{-}xylyl)(tmeda)]_4$[84] (Fig. 13 left). In contrast, with the tridentate pmdta ligand, a polymeric structure results, $[Na(\eta^1\text{-benzyl})(pmdta)]_n$,[84] in which only the *ipso* carbon atoms of the planar benzyl anions are coordinated to the Na ions and form the zigzag chains (Fig. 13 right). Similar polymer chains are also formed in the lithium compound $[Li(\eta^2\text{-benzyl})(OEt_2)]_n$[70a] (see Section 3.2.5) and in the recently re-

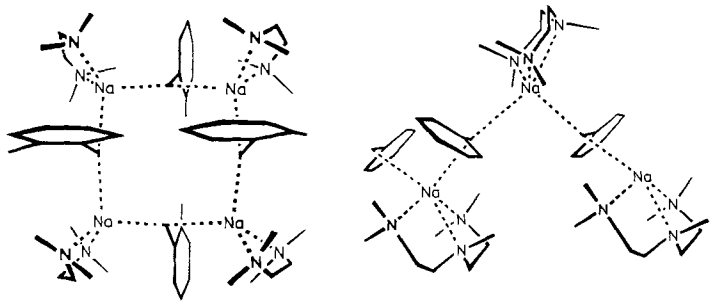

Fig. 13. Aggregation of [Na(*o*-xylyl)(tmeda)]$_4$ (left) and [Na(benzyl)(pmdta)]$_n$ (right).

ported potassium compound [K(η-benzyl)(pmdta)]$_n$,[85a] although the hapticity is different.

Diphenylmethyl anion: The diphenylmethyl ion is also planar in its sodium compounds. Its adduct with the tridentate base pmdta, [Na(CHPh$_2$)(pmdta)], is, as expected, monomeric. With tmeda, however, it forms a cyclic tetramer, [Na(CHPh$_2$)(tmeda)]$_4$[84] (Fig. 14); isotypic compounds [M(CHPh$_2$)(pmdta)]$_n$ (M = K, Rb, Cs)[85b] are polymers.

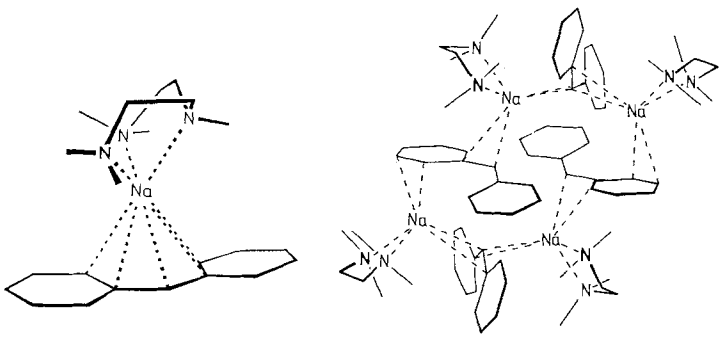

Fig. 14. The influence of the solvent on the aggregation of diphenylmethylsodium. [Na(CHPh$_2$)(pmdta) (left), [Na(CHPh$_2$)(tmeda)]$_4$ (right). The asymmetric unit of [Na(CHPh$_2$)(pmdta)] contains two very similar molecules.

Triphenylmethyl anion: The aliphatic H atom in triphenylmethane is easily replaced by a metal atom. It was already noticed in the first examples, [Li(CPh$_3$)(tmeda)][71] and [Na(CPh$_3$)(tmeda)]$_n$,[76] that the propeller-shaped carbanion contains a central planar sp^2 carbon atom. The cation takes up an asymmetrical position relative to this carbon atom in order to accommodate a maximum number of M–C contacts. Additional weak intermolecular contacts are present in the sodium compound leading to polymer chains with zigzag structures (Fig. 15 top). Since these early reports, triphenylmethyl compounds of all the alkali metals have been examined. In these, the position of the cation relative to the CPh_3^- anion can vary greatly such that it is shifted towards the peripheral phenyl groups as the cation radius increases. We have recently investigated three potassium compounds with various bases (including ethers)[86] and found that [K(CPh$_3$)(pmdta)] is monomeric, [K(CPh$_3$)(thf)]$_n$ a two-dimensional network, and [K(CPh$_3$)(diglyme)]$_n$ a polymer chain (Fig. 15 middle and bottom). The large counterions K, Rb, and Cs allow not only greater hapticity but are also particularly well suited for η^6-coordination to the phenyl groups, as recently observed in the polymeric chain compounds [Rb(CPh$_3$)(pmdta)]$_n$ and [Cs(CPh$_3$)(pmdta)]$_n$ as well as the monomeric compound [K(CPh$_3$)(pmdta)(thf)].[87]

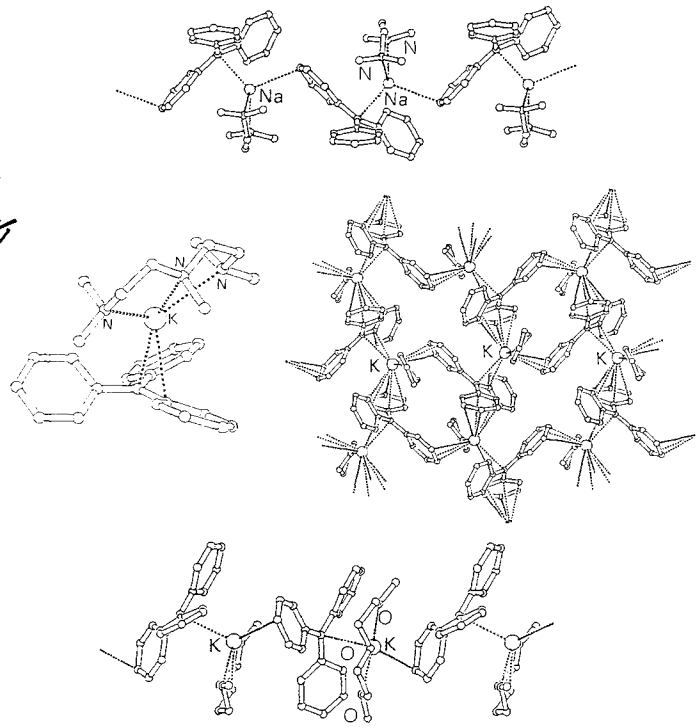

Fig. 15. Structures of some adducts of triphenylmethylsodium and -potassium. [Na(CPh$_3$)(tmeda)]$_n$ (top) [76], [K(CPh$_3$)(pmdta)] (middle left) [86], [K(CPh$_3$)(thf)]$_n$ (middle right)[86], [K(CPh$_3$)(diglyme)]$_n$ (bottom)[86].

All the compounds described in this section have been shown to be either ion pairs or complicated aggregates of carbanions and solvated counterions. The structure is determined by a combination of electrostatic interactions and steric effects (structure of the carbanion and donor ligand, cation radius). The following examples also emphasize this principle.

The metal–C distances can vary tremendously even within one compound. In such cases, the number of M–C contacts, in other words the coordination number of the cation, often cannot be definitively established. The coordination number of sodium is always greater than 4, that of potassium, rubidium, and cesium often around 8. The minimum distance for a proposed Na–C contact is roughly 265 pm; in the figures distances up to 300 pm are typically indicated with dashed lines. In general, the larger the cation radius, the greater the number of M–C contacts.

4.2.3. Allyl Compounds

The metalation of allylbenzene by butylsodium in the presence of pmdta yields the monomeric compound [Na(1-phenylallyl)(pmdta)][88] with the expected η^3-coordination (Scheme 1; compare to [Li(η^2-allyl)(pmdta)][67]). The analogous metalation of 1-phenylcyclohexene also produces a carbanion having an allyl system[88] (Scheme 1). Surprisingly, here the solvated Na ion is not coordinated to the allyl part of the carbanion but instead is centered η^6 over the phenyl group. This arrangement is analogous to that in a Na-benzene complex in which the Na ion is sandwiched between the amine and the carbanion. What is the explaination for this unusual coordination? The Na ion is so strongly shielded by its solvation shell that the allyl system of the

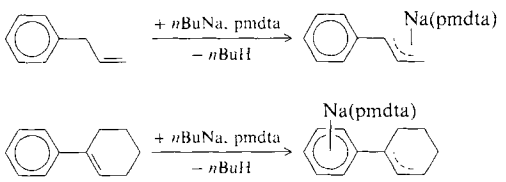

Scheme 1. Synthesis of phenylallyl compounds with η^3-allyl and η^6-phenyl coordination [88].

cyclohexenyl ion can no longer approach it (hindrance by the CH_2 groups of the carbanion). In addition, the negative charge on the carbanion is also distributed over the phenyl part by conjugation. Thus, in consideration of both steric and electrostatic interactions, the energetically most favorable position for the solvated cation is centered above the phenyl group.

Additional examples in which the alkali metal has η^6-coordination at the center of phenyl ligand are known, for example, [Na(tetraphenylallyl)(Et_2O)][89] (distorted dibenzene sodium sandwich complex) and the triple contact ions in [Na_2(tetraphenylethene)(Et_2O)$_2$][90] and [Na_2(1,1,4,4-tetraphenylbutane-1,4-diyl)(Et_2O)$_2$].[91]

The compound [Na(1-phenylethyl)(tmeda)]$_n$, obtained by the sodium metalation of ethylbenzene, is also worth mentioning in this context.[84] Here, the carbanions lie in a bridged zigzag chain and are coordinated through their CH_3CH groups as well as through the phenyl rings (η^2- and η^3-coordination).

4.2.4. Cyclopentadienyl, Indenyl, and Fluorenyl Compounds

Solvated Cyclopentadienyl Alkali Metal Compounds: The structures of these compounds have been repeatedly described and summarized.[92] A number of important examples with lithium and sodium have been known for quite some time now and include [Li(η^5-$C_5H_4SiMe_3$)(tmeda)][93] (monomer), [Li(η^5-C_5H_4Me)(tmeda)][94] (monomer), and [Na(η^5-Cp)(tmeda)]$_n$[95] (zigzag chain) (Fig. 16 left). In contrast, almost no crystal structures of the higher homologues have been described till now. Recent examples are the potassium compounds [K{η^5-C_5(CH_2Ph)$_5$}(thf)$_3$][96] ("piano-stool geometry") and [K(η^5-Cp)(OEt_2)]$_n$[97] (polymer chain) (Fig. 16 right). In the latter, the polymer chain is only slightly angled as a result of the larger radius of potassium, and the structure thus corresponds well to a "multidecker structure". The first structurally characterized cyclopentadienyl alkali metal compound that is not solvated is [K(η^5-$C_5H_4SiMe_3$)]$_n$ (chains with weak interactions between the strands).[98]

Solvated Indenyl Alkali Metal Compounds: Examples of structurally characterized indenyl compounds include [Li(η^5-indenyl)(tmeda)][99] (monomer) and [Na(indenyl)-(tmeda)]$_n$[100] (polymer chains with η^1/η^2 coordination). In the structures shown in Figure 17 it is not surprising that [Na(η^5-indenyl)(pmdta)] forms as a monomer. Also, because of the larger radius of the potassium cation, the compounds [K(η^5-indenyl)(tmeda)]$_n$ and [K(η^5-indenyl)(pmdta)]$_n$ form slightly angulated polymer chains (multidecker).[101] A detailed discussion of the factors that are structure determining in the indenyl complexes is given in ref.[100] and in the work cited therein.

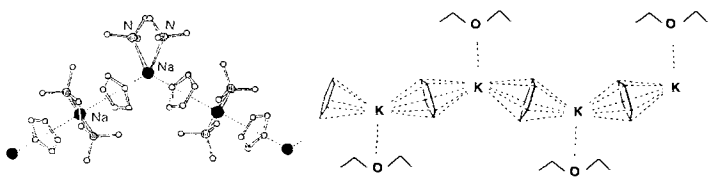

Fig. 16. Solvated cyclopentadienyl alkali metal compounds. [Na(η^5-Cp)-(tmeda)]$_n$ (left), [K(η^5-Cp)(OEt_2)]$_n$ (right).

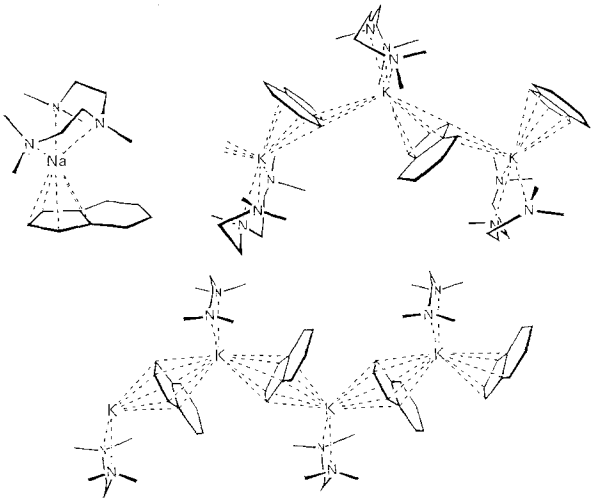

Fig. 17. Solvated indenyl alkali metal compounds[101]. [Na(η^5-indenyl)-(pmdta)] (top left). [K(η^5-indenyl)(pmdta)]$_n$ (top right). [K(η^5-indenyl)(tmeda)]$_n$ (bottom).

Solvated Fluorenyl Alkali Metal Compounds: Three different structures are found for fluorenylsodium and result from a simple variation in the donor ligands:[102] [Na(fluorenyl)L], with L = pmdta, tmeda, and tmpda. The compound is monomeric with the sterically demanding tridentate pmdta ligand, forms polymer chains with the smaller tmeda, and exists as rings constructed from four monomer units with tmpda, despite the fact that the chain lengths of tmeda and tmpda differ by only one C atom. These examples are an impressive illustration of the significance of steric effects. Monomers, polymers, and cyclic tetramers comprise the most important structure types for solvated organosodium compounds. In contrast to these, [K(fluorenyl)(pmdta)]$_2$ (Fig. 18) is a cyclic dimer, no doubt as a result of the larger radius of the cation.[101] In the complicated structure of [K(fluorenyl)(tmeda)]$_2$,[103] the tmeda can no longer coordinate the large potassium ion in a chelating fashion, and so it bridges between two cations. Chains with "square waves" are formed in [Rb(η^5-fluorenyl)(pmdta)]$_n$.[104]

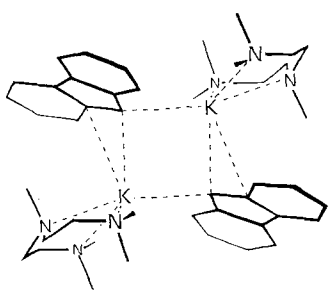

Fig. 18. Structure of [K(fluorenyl)(pmdta)]$_2$ [101].

4.2.5. The Influence of the Metal Ions on the Structure of the Carbanions

It has been repeatedly shown both experimentally and theoretically[3, 4] that the structures, reactivities, and energies of organometallic compounds are strongly influenced by the metal cations. Some carbanions, for example $C_2H_5^-$, are only stable in the presence of a counterion.[4] Numerous examples (see for example refs.[67,69,100]) illustrate the influence the cation has on the structure of the carbanion. It is noticeable that the phenyl groups bound to metal centers have regular distortions of the six-membered rings. The C2-C1-C6 angle is always less than 120° (down to ca. 112°), and the angles at C2 and C6 atoms are widened to ca. 124°. Of the many examples known, we mention here only [LiPh(pmdta)], [NaPh(pmdta)]$_2$, and [MgPh$_2$(tmeda)]. A qualitative correlation exists between the endocyclic angles and the electronegativity of the metal.[61]

5. Organomagnesium Compounds

In this section, as in the preceding, our own investigations will be highlighted. The reader is referred to the literature citations given in ref.[5] for additional examples, and to the discussion of organomagnesates in Section 6.4.

5.1. Diorganomagnesium Compounds

Four unsolvated diorganomagnesium compounds are especially important: $MgMe_2$, $MgEt_2$, $MgPh_2$, and $MgCp_2$ (Figs. 19–21). Bis(η^5-cyclopentadienyl)magnesium (magnesocene) was the first structurally characterized organomagnesium compound; its sandwich structure was first determined in 1955[105a] and later refined[105b]. Dimethylmagnesium and diethylmagnesium are obtained as fine crystalline powders by drying their thermally labile ether adducts. Their polymeric structures, $[MgMe_2]_n$[106] and $[MgEt_2]_n$,[107] were discovered by us quite some time ago. Recent investigations have shown that diphenylmagnesium is also polymeric.[108] As expected, these compounds are not volatile and only sparingly soluble in hydrocarbon solvents. Ether and other polar solvents break the polymer chains by formation of solvated monomers.

The magnesium ions in the polymer chain are each surrounded by a tetrahedron of four carbanions which form pairs of μ_2 bridges between the Mg ions similar to that found in dimethylberyllium.[109] Unsolvated monomers are obtained with more bulky carbanions as in

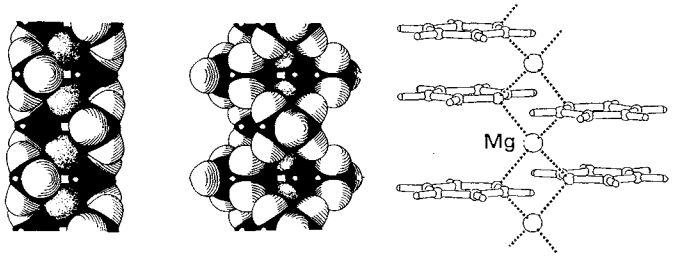

Fig. 19. Polymer chains of dimethylmagnesium (left), diethylmagnesium (middle), and diphenylmagnesium (right).

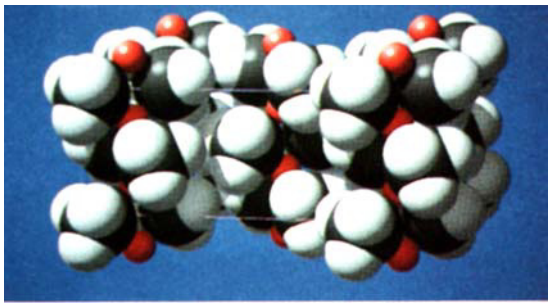

Fig. 20. Space-filling model of $[MgMe_2]_n$ (body-centered orthorhombic unit cell; Mg radius chosen to be 70 pm).

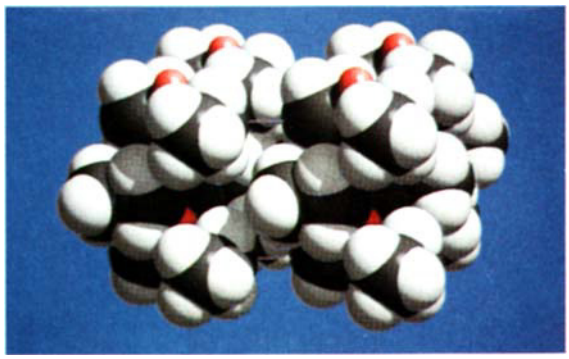

Fig. 21. Space-filling model of $[MgEt_2]_n$ (tetragonal unit cell; high-temperature modification; Mg radii chosen to be 70 pm).

$[Mg\{C(SiMe_3)_3\}_2]$.[110] in which the magnesium ion has linear coordination.

As with the methyl alkali metal compounds, there was some uncertainty as to the H positions in $[Mg(CH_3)_2]_n$ and $[Mg(C_2H_5)_2]_n$. Therefore, we recently carried out new structure determinations from neutron diffraction data on the deuterated compounds $[Mg(CD_3)_2]_n$ and $[Mg(C_2D_5)_2]_n$ at 293 and 1.5 K.[111] These structures verified the earlier results but also showed a statistical or dynamic disorder in the alkyl groups (rotation of the methyl groups). A phase transition only occurs with $[MgEt_2]_n$ (tetragonal $\rightleftharpoons$ monoclinic at ca. 260 K). As a result of the bent ethyl groups, the chains are chiral helices (right- and left-handed screw sense) in a statistical distribution, whereby a higher pseudosymmetry is attained.[107]

5.2. Solvated Diorganomagnesium Compounds

As already mentioned, because the ether adducts of the organomagnesium compounds are thermally labile, the more stable adducts of the chelating amines were examined in preference. Since improvements in instrumentation have made low-temperature measurements experimentally more accessible, the number of ether adducts investigated has increased. The structural characterization of the species involved in the Schlenk equilibrium of the Grignard compounds is especially challenging. The halo-bridged dimers belong to this group of compounds but will not be discussed here. Even though base adducts of the amines can also serve as models for the ether adducts, they are interesting in their own right. Similar to the alkali metal compounds, the reac-

tivity of the magnesium compounds can be increased through solvation, whereby the character of the carbanion is strengthened. The complexes formed from the addition of tmeda to Grignard compounds have proved to be cocatalysts in the anionic polymerization of olefins, and some yield syndiotactic polymers.[112]

Only monomeric adducts are listed in Table 3. They contain magnesium atoms with various coordination modes as illustrated in Figure 22 by selected examples. Tetrahedrally coordinated magnesium can be found in the compounds with tmeda: $[MgMe_2(tmeda)]$,[113] $[MgEt_2(tmeda)]$,[114] and $[MgPh_2(tmeda)]$.[115] The coordination number 5 (distorted trigonal bipyramid) is also possible as shown by recent examples with pmdta—$[MgMe_2(pmdta)]$,[114] $[MgEt_2(pmdta)]$[114]—and a few Grignard compounds. The "slender" alkynyl carbanions allow for even octahedral coordination in $[Mg(C{\equiv}CPh)_2(tmeda)_2]$[118] and $[Mg(C{\equiv}CtBu)_2(tmeda)_2]$.[119]

Table 3. Solvated monomeric organomagnesium compounds.

Compound	Mg C.N. [a]	Ref.	Compound	Mg C.N. [a]	Ref.
$[MgMe_2(tmeda)]$	4	[113]	$[Mg(C{\equiv}CtBu)_2(tmeda)_2]$	6	[119]
$[MgMe_2(pmdta)]$	5	[114]	$[MgPh_2(1,3\text{-xylyl-}[18]\text{-crown-}5)]$	6	[120]
$[MgEt_2(tmeda)]$	4	[114]	$[MgEtBr(Et_2O)_2]$	4	[121]
$[MgEt_2(pmdta)]$	5	[114]	$[MgPhBr(thf)_2]$	4	[122]
$[MgPh_2(tmeda)]$	4	[115]	$[MgPhBr(Et_2O)_2]$	4	[123]
$[MgPh_2(thf)_2]$	4	[116]	$[MgMeBr(furan)_3]$	5	[124]
$[Mg(p\text{-}tBuC_6H_4)_2(diglyme)]$	5	[117]			
$[Mg(C{\equiv}CPh)_2(tmeda)_2]$	6	[118]			

[a] C.N. = coordination number.

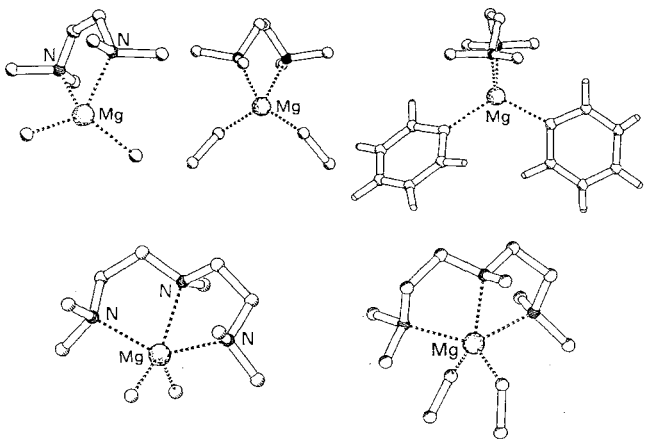

Fig. 22. Structures of $[MgMe_2(tmeda)]$ (top left), $[MgEt_2(tmeda)]$ (top middle), and $[MgPh_2(tmeda)]$, all of which have tetrahedral coordination at Mg; structures of $[MgMe_2(pmdta)]$ (bottom left) and $[MgEt_2(pmdta)]$, which both have distorted trigonal-bipyramidal coordination at Mg.

5.3. Unsymmetric Diorganomagnesium Compounds

The base adducts that are soluble in hydrocarbon solvents, for example $[MgR_2(tmeda)]$ (R = Me, Et), are suitable starting materials for the preparation of unsymmetric diorganomagnesium compounds, a class of compounds that has been hardly investigated till now. By their reaction with C–H acidic hydrocarbons R'H (alkynes, cyclopentadiene, indene, fluorene) in a 1:1 ratio, we have recently[125] synthesized the adducts $[MgMe(\eta^3\text{-Cp})(tmeda)]$, $[MgMe(\eta^3\text{-indenyl})(tmeda)]$, $[MgMe(\eta^1\text{-fluorenyl})(tmeda)]$, and $[Mg_2Et(C{\equiv}CPh)_3)(tmeda)]_2$. It is remarkable that none of the π carbanions exhibit η^5-coordination. On account of steric hindrance of the methyl groups, at most η^3-coordination can be achieved, and with the fluorenyl carbanion only η^1-coordination is attained.

6. Organometalates: Compounds with Two Different Metals

These compounds are among the organometallic compounds longest known and include, for example, $NaEt{\cdot}ZnEt_2$.[126] They are often obtained by simply mixing together stoichiometric amounts of the components and were initially considered as double compounds. The true nature of these compounds was recognized only later when G. Wittig termed them *ate complexes*.[127] In many cases their true nature could only be completely elucidated by X-ray structure analysis. We investigated compounds that contain in addition to an alkali metal the following elements in the organometalate: lithium, copper (as Cu^I), beryllium, magnesium, zinc, cadmium, boron, aluminum, gallium, indium, and thallium (Table 4; further examples in refs.[3,4] and the work cited therein). In these compounds the coordination numbers 2 (Cu, linear), 3 (Zn, trigonal planar), 4 (tetrahedral), and 5 (Mg, trigonal bipyramidal) have been observed. Sometimes the organometalate ion is di- or even trinuclear; these special cases will be discussed in more detail.

Although sometimes the partitioning of these compounds into a complex organometalate ion and a counterion is only formally possible, it is very useful as an ordering principle as well as for the nomenclature. In most cases the relation of the organic substituents to the central atom is clearly discernible from the structures. The charge localization on the carbanion is always greatest for the cation with the highest charge ($M^{3+} > M^{2+} > M^+$) and, for cations with the same charge, the one with the smaller radius ($Li^+ > Na^+$). This is then the coordination center. As far as it is sterically possible, the carbanions orient their most strongly negative polarized centers toward the coordination centers and form as many and as short contacts as possible. In this way carbanions can also become bridging ligands (e.g. μ_2-Me, μ_2-Ph), whereby both symmetric and unsymmetric bridges are possible as the examples in Figure 23 show. Solvation of the counterion is often observed, especially with the small lithium ion. Solvent-separated ion pairs are ultimately formed with sterically demanding donor ligands.

6.1. Lithates

In 1958 Wittig et al. described a sodium diphenyllithate ("diphenyllithium sodium")[156] whose structure could not

Table 4. Some organometalates structurally characterized by X-ray crystallography.

Compound	C.N. of the central atom	Ref.
Organolithates		
Tetraorganolithate: $[Na(tmeda)]_3[LiPh_4]$	4	[128]
Diorganolithate: $[Li(thf)_4][Li\{C(SiMe_3)_3\}_2]$ [a]	2	[129]
Diorganocuprates		
$[\{Li(Et_2O)\}(CuPh_2)]_2$	2	[130]
$[Li_2Cu_2Me_4]$ (ring)	2	[131]
$[Li_6(Et_2O)_3Cu(C{\equiv}CPh)_{10}]$	4	[132]
Organoberyllates		
$Li_2[BeMe_4]$	4	[133]
$Li[BetBu_3]$	3	[134]
Organomagnesates		
Triorganomagnesate: [Mg(neopentyl)([2.1.1]cryptand)]-[Mg(neopentyl)$_3$]	3	[135]
Tetraorganomagnesates: $[Li(tmeda)]_2[MgMe_4]$	4	[136]
$[Na(pmdta)]_2[MgPh_4]$	4	[137]
Hexaorganodimagnesates: $[Li(tmeda)]_2[Mg_2Ph_6]$	4	[138]
$[MgEt([2.1.1]cryptand)]_2[Mg_2Et_6]$	4	[135]
$[Mg(neopentyl)([2.1.1]cryptand)]_2[Mg_2Et_6]$	4	[135]
Octaorganotrimagnesate: $[Mg_2Me_5(tacn)_2]_2[Mg_3Me_8]$ [b]	4	[139]
Dimeric diamine(triorgano)magnesates:		
$Li_2[Mg(C{\equiv}CPh)_3(tmeda)]_2$	5	[140]
$Na_2[Mg(C{\equiv}CtBu)_3(tmeda)]_2$	5	[137]
$Na_2[Mg(C{\equiv}CtBu)_3(pmdta)]_2$	5	[137]
$[Li(tmeda)_2][tmeda)Li(benzyl)_2Mg(benzyl)_2]_2$ [a]	4	[140]
Organozincates		
Tetraorganozincates: $Li_2[ZnMe_4]$	4	[141]
$K_2[Zn(C{\equiv}CH)_4]$	4	[142]
Triorganozincate: $K[ZnMe_3]$	3	[143]
Organocadmate		
$K_2[Cd(C{\equiv}CH)_4]$	4	[142]
Organoborate		
$[Li(BMe_4)]_4$ (ring)	4	[144]
$Na[BMe_4]$, $K[BMe_4]$, $Rb[BMe_4]$, $Cs[BMe_4]$	4 A [c]	[145]
$K[BPh_4]$	4	[146]
$Rb[BPh_4]$	4	[147]
$[NMe_4][BPh_4]$	4	[148]
Organoluminates		
Tetraorganoaluminates: $K[AlMe_4]$, $Rb[AlMe_4]$, $Cs[AlMe_4]$	4 B [c]	[149]
$[LiEt_2AlEt_2]_n$ (μ_2-bridged polymer)	4	[150]
Hydridotriorganoaluminate: $K[AlHMe_3]$	4	[151]
Organogallates		
$K[GaMe_4]$, $Rb[GaMe_4]$	4 B [c]	[149]
Organoindates		
$Li[InMe_4]$, $Na[InMe_4]$	4 C [c]	[152]
$K[InMe_4]$, $Rb[InMe_4]$	4 B [c]	[153]
$Cs[InMe_3]$	4 D [c]	[153]
$Li[InPh_4]$, $Na[InPh_4]$	4	[154]
Organothallates		
$Na[TlMe_4]$	4 C [c]	[155]
$K[TlMe_4]$	4 B [c]	[155]
$Na[TlPh_4]$	4	[155]

[a] Solvent-separated ion pair. [b] tacn = *N*,*N*′,*N*″-trimethyl-1,4,7-triazacyclononane. [c] The compounds listed together on the same line are isotypical (structure types A–D).

be characterized. Under similar reaction conditions, but with tmeda, we were able to isolate the compound $[LiNa_3Ph_4(tmeda)_3]$.[128] It contains a tetrahedral tetraphenyllithate ion surrounded by three solvated sodium ions—$[Na(tmeda)]_3[LiPh_4]$ (Fig. 24). Also of note is $[Li(thf)_4][Li\{C(SiMe_3)_3\}_2]$, only the second example of an organolithate known to date. It is a solvent-separated ion pair in which a diorganolithate having a central atom with linear coordination is the anion.[129]

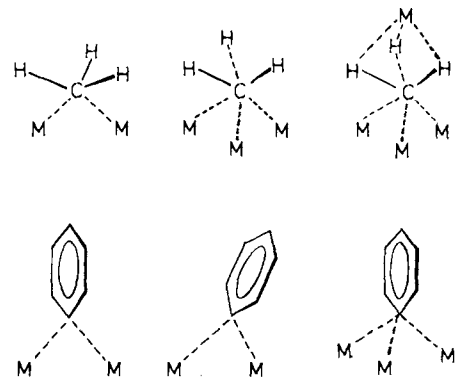

Fig. 23. Coordination modes for bridging methyl and phenyl groups.

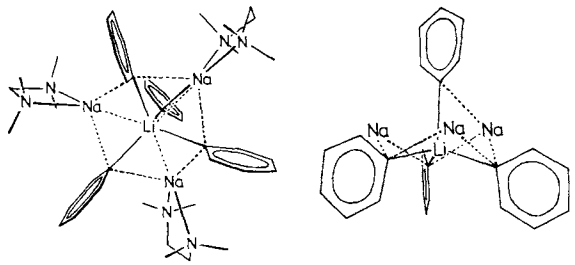

Fig. 24. $[Na(tmeda)]_3[LiPh_4]$, a tetraphenyllithate with three solvated counterions; amine ligands are not shown in the picture on the right.

6.6. Cuprates

Many examples of lithium organocuprates are known.[157] They are important in organic synthesis and in many cases even superior to the traditional Grignard and organolithium reagents. These very labile compounds are generally introduced as ether solutions and usually decompose upon attempted isolation. For this reason the first example of a simple ether-solvated lithium cuprate confirmed by X-ray crystallography is of particular significance. This dimer, $[\{Li(Et_2O)\}(CuPh_2)]_2$ (Fig. 25), is formed from two linear diphenylcuprate units held together by solvated Li ions.[130]

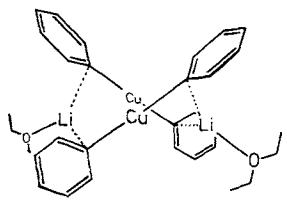

Fig. 25. $[\{Li(OEt_2)\}(CuPh_2)]_2$, a dimeric lithium diphenylcuprate.

The compound $[Li_6(Et_2O)_3Cu_4(C{\equiv}CPh)_{10}]$ is an example of the even rarer, higher order organocuprates ("HO cuprates").[132] It contains a $[Cu(C{\equiv}CPh)_4]^{3-}$ tetrahedral anion "crowned" by a cyclic $[Li_3Cu_3(C{\equiv}CPh)_6]$ unit. The Li_3Cu_3 atoms of this unit form a slightly bent six-membered ring and are bridged by the C_α atoms of the six phenylethynyl ligands. The three remaining Li atoms are solvated by Et_2O and lie below the base of the anion.

6.3. Beryllates

Organoberyllates are not very well investigated. The compound $Li_2[BeMe_4]$,[133] prepared without solvent, contains the tetrahedral tetramethylberyllate ion (see Fig. 28). In contrast, simple planar threefold coordination occurs with the voluminous *t*-butyl anion in $Li[Be(tBu)_3]$.[134]

6.4. Magnesates

Organomagnesates exist in many interesting structure types and with various coordinations (3, 4, 5) at the magnesium centers (see Table 4). The compounds $[Li(tmeda)]_2[MgMe_4]$[136] and $[Na(pmdta)]_2[MgPh_4]$[137] have tetrahedral coordination (Fig. 26 top), and the organic groups form unsymmetric μ_2 bridges between magnesium and the solvated alkali metal atom.

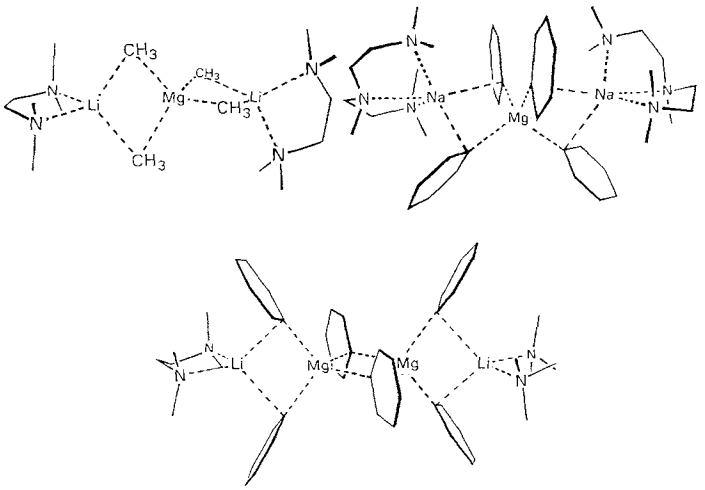

Fig. 26. Top: Tetraorganomagnesates with methyl and phenyl bridges: $[Li(tmeda)]_2[MgMe_4]$ and $[Na(pmdta)]_2[MgPh_4]$. Bottom: $[Li(tmeda)]_2[Mg_2Ph_6]$, an example of a hexaorganodimagnesate. The pairs of phenyl groups form either symmetrical or unsymmetrical bridges.

The two magnesium atoms in the dinuclear hexaorganodimagnesates $[Li(tmeda)]_2[Mg_2Ph_6]$[138] (Fig. 26 bottom) and $[Mg(neopentyl)([2,1,1]cryptand)]_2[Mg_2Et_6]$[135] have distorted tetrahedral coordination. The (formally) $[Ph_2Mg(\mu\text{-}Ph)_2MgPh_2]^{2-}$ ion is, incidentally, isoelectronic and isostructural with the neutral compound Al_2Ph_6[158] and contains symmetric phenyl bridges between Mg and Mg but unsymmetric bridges between Mg and Li (Fig. 26 bottom).

We recently found the first octaorganotrimagnesate with the compound $[Mg_2Me_3(tacn)_2]_2[Mg_3Me_8]$,[139] which is obtained from the reaction of $MgMe_2$ with the cyclic triamine tacn. Unprecedented here is also the occurrence of an organomagnesium cation with a "triple-decker structure" in which three μ_2-Me groups bridge the solvated magnesium ions—$[LMg(\mu_2\text{-}Me)_3MgL]^+$.

A few organomagnesates exist as dimers in which the pentacoordinate magnesium center is bound to three organic substituents and one bidentate diamine ligand: $Li_2[Mg(C{\equiv}CPh)_3(tmeda)]_2$,[140] $Na_2[Mg(C{\equiv}CtBu)_3(tmeda)]_2$,[137] and $Na_2[Mg(C{\equiv}CtBu)_3(pmdta)]_2$.[137] The alkali metal ions connect the two units of the dimer through contacts to the alkyne groups as shown in Figure 27.

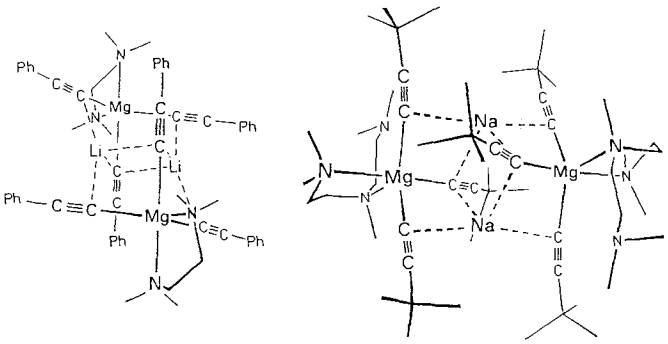

Fig. 27. Organomagnesates with pentacoordinated magnesium: $Li_2[Mg(C{\equiv}CPh)_3(tmeda)]_2$ and $Na_2[Mg(C{\equiv}CtBu)_3(pmdta)]_2$.

Finally, solvent-separated ions are found in the benzylmagnesate $[Li(tmeda)_2][(tmeda)Li(\mu_2\text{-benzyl})_2Mg(benzyl)_2]_2$.[140] The anion has a complicated structure in which two of the four benzyl groups of a strongly distorted tetrahedral $Mg(benzyl)_4$ unit are bridged at their CH_2 groups by a lithium atom.

6.5. Zincates and Cadmates

The zincates $Li_2[ZnMe_4]$[141] and $K_2[Zn(C{\equiv}CH)_4]$,[142] and the cadmate $K_2[Cd(C{\equiv}CH)_4]$[142] all contain tetrahedral anions. The simple substitution of potassium for lithium in the methyl zincate causes a change to the rarely encountered trigonal-planar coordination as found in the triorganozincate $K[ZnMe_3]$ (Fig. 28).[143]

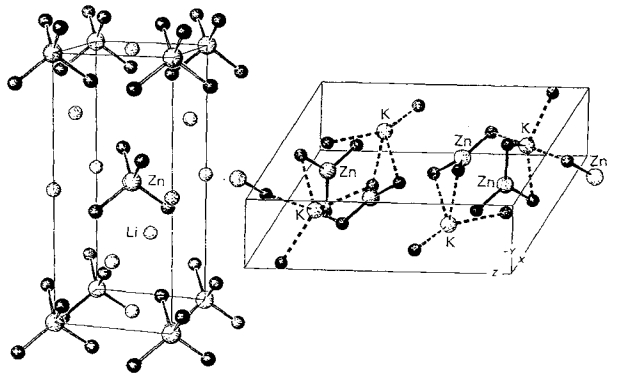

Fig. 28. Methylzincates with tetrahedral and trigonal-planar coordination at the zinc atom. Left: $Li_2[ZnMe_4]$ (isotypic to $Li_2[BeMe_4]$[133]). Right: $K[ZnMe_3]$ (monoclinic unit cell).

6.6. Borates, Aluminates, Gallates, Indates, and Thallates

All the compounds presented here are tetraorganometalates with the exception of the hydridometalate $K[AlHMe_3]$.[151] Apart from $[Li(BMe_4)]_4$ (ring structure),[144] they all contain quite distinct MR_4^- units and display a number of crystallographically different structure types. Orthorhombic (type A), tetragonal (types B and D), and cubic (type C) lattices have been observed for the methyl compounds (Figs. 29 and 30). The isotypic representatives of each type

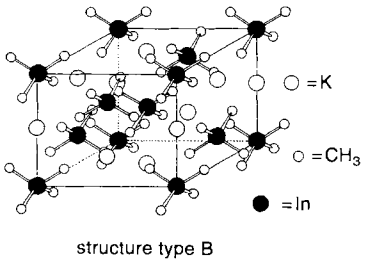

structure type B

Fig. 29. Example of a tetramethylmetalate of structure type B (tetragonal), $K[InMe_4]$.

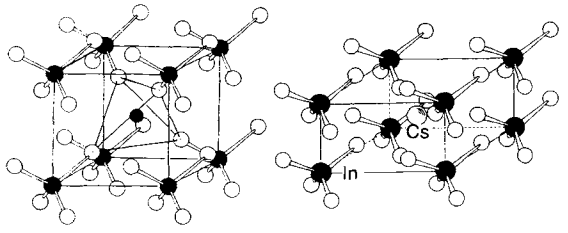

structure type C structure type D

Fig. 30. Examples of tetramethylmetalates of structure types C (cubic) and D (tetragonal), $Na[InMe_4]$ (C, cubic) and $Cs[InMe_4]$ (D, tetragonal). In structure type C both types of metal centers have tetrahedral coordination.

are summarized in Scheme 2. A few tetraphenylmetalates have also been structurally characterized (Scheme 2).

Type A
$Na[BMe_4]$, $K[BMe_4]$, $Rb[BMe_4]$, $Cs[BMe_4]$

Type B
$K[AlMe_4]$, $Rb[AlMe_4]$, $Cs[AlMe_4]$, $K[GaMe_4]$, $Rb[GaMe_4]$, $K[InMe_4]$, $Rb[InMe_4]$, $K[TlMe_4]$

Type C
$Li[InMe_4]$, $Na[InMe_4]$, $Na[TlMe_4]$

Type D
$Cs[InMe_4]$

Tetraphenylmetalates
$K[BPh_4]$, $Rb[BPh_4]$, $[NMe_4][BPh_4]$, $Li[InPh_4]$, $Na[InPh_4]$, $Na[ThPh_4]$

Scheme 2. Structurally characterized methyl- and phenylborates, -aluminates, -gallates, -indates, and -thallates.

7. Alkali Metal Amides

Together with the organometallic compounds, the alkali metal amides have established themselves as the most important metalating and deprotonating agents. For this reason a great interest in their structures has developed.

7.1. Simple Alkali Metal Amides

The structures of the simple alkali and alkaline earth metal amides $M(NH_2)_n$ ($n = 1, 2$) have been known for a long time from the investigations of R. Juza, H. Jacobs, and others.[159] The H atoms were located by either X-ray ($LiNH_2$[159b]) or neutron diffraction ($NaND_2$[159e]). Because of the difference in the anion shapes, no structural relationships exist between the methyl compounds MCH_3 and the amides MNH_2. In an X-ray refinement of the structure of sodium amide we were also able to locate the H atoms in good agreement with the neutron diffraction results (Fig. 31).[97] The structure can be understood as a three-dimensional network of dimeric $(NaNH_2)_2$ units.

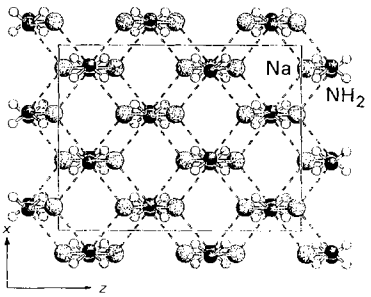

Fig. 31. Structure of $NaNH_2$. Projection is along (010) in the centrosymmetric setting of *Fddd*[97,159e].

More recently a number of solvated alkali metal amides derived from organic amines have been investigated; these will be discussed in Section 7.2. In contrast, the study of the nonsolvated compounds is only in its initial phases. Here, potassium diethylamide is one of the first examples and contains $(KNEt_2)_2$ units which build rings in a complicated arrangement.[97] An interesting "ladder structure" has been found in $[Na(2,3,4,5\text{-tetramethylpyrrolyl})]_n$ (azacyclopentadienyl ligand),[160] in which the characteristic features of amide bridges are combined with those of the π coordination of the cyclopentadienyl ligands.

7.2. Base Adducts of Alkali Metal Amides and Imides

The structural chemistry of the solvated lithium amides and imides having organic substituents on N has made great progress. Numerous original papers and some excellent reviews[6, 161, 162] attest to the multitude of structure types known for these compounds, including stacked rings and ladder structures. In the following, the amides of the heavier alkali metals, which have been less well investigated, will be highlighted. In general, alkali metal amide adducts are very often observed as dimers with four-membered M_2N_2 rings; however, other structure types are also known (Table 5). New, as yet unpublished examples of dimeric amides are shown in Figure 32. Structural investigations on their base adducts are also of interest here since the reactivity of amides can be increased by such additives.[163]

Alkali metal amides are generally obtained by the direct reaction of amines with the metals. Often, hydrides and organo alkali metal compounds such as the soluble adduct [Na*n*Bu(tmeda)] are more suitable for metalation reactions, since the synthesis can then take place in a homogeneous medium. Many of the amides listed in Table 5 have been prepared in this way. As a result of the high reactivity of butylsodium, however, cleavage of tmeda under formation of $NaNMe_2$ cannot be ruled out.[167] This product crystallizes in situ in the form of oligomeric aggregates. The interesting stacked structures of $[Na_{10}(NMe_2)_{10}(tmeda)_4]$ and $[Na_{12}(NMe_2)_{12}(tmeda)_4]$ were thus obtained in this way (Fig. 33).[167] These are decameric and dodecameric aggre-

Table 5. Solvated amide and imide complexes of the heavier alkali metals.

Compound	Degree of aggregation	Ref.	Compound	Degree of aggregation	Ref.
$[NaNMe_2(pmdta)]_2$	dimer	[97]	$[Na_4(NMe_2)_4(HNMe_2)(tmeda)]_2$	stack	[167]
$[NaNEt_2(tmeda)]_2$	dimer	[97]	$[Na_{10}(NMe_2)_{10}(tmeda)_4]$	stack	[167]
$[LiNPh_2(tmeda)]_2$	dimer	[97]	$[Na_{12}(NMe_2)_{12}(tmeda)_4]$	stack	[167]
$[NaNPh_2(tmeda)]_2$	dimer	[97]	$[Na_{12}(NMe_2)_{10}(p\text{-xylyl})_2(tmeda)_4]$	stack	[167]
$[KNPh_2(tmeda)]_2$	dimer	[97]	[Na(indolyl)$(tmeda_2]$	dimer	[168]
$[K_2(NPh_2)_2(tmeda)_3]_n$	chain [a]	[97]	$[Na(indolyl)(pmdta)]_2$	dimer	[168]
$[Li(NMePh)(tmeda)]_2$	dimer	[164]	$[Li(carbazolyl)(thf)_2]_2$	dimer	[169]
$[Na\{NPh(2\text{-pyridyl}\}(pmdta)]_2$	dimer	[165]	$[K(carbazolyl)(pmdta)]_2$	dimer	[170]
$[NaN=CtBu_2]_4[HN=CtBu_2]_2$	cubane	[166]	$[Cs(carbazolyl)(pmdta)]_2$	dimer	[170]

[a] $[K_2(NPh_2)(tmeda)_3]_n$ forms chains of $[K(NPh_2)(tmeda)]_2$ units bridged by tmeda.

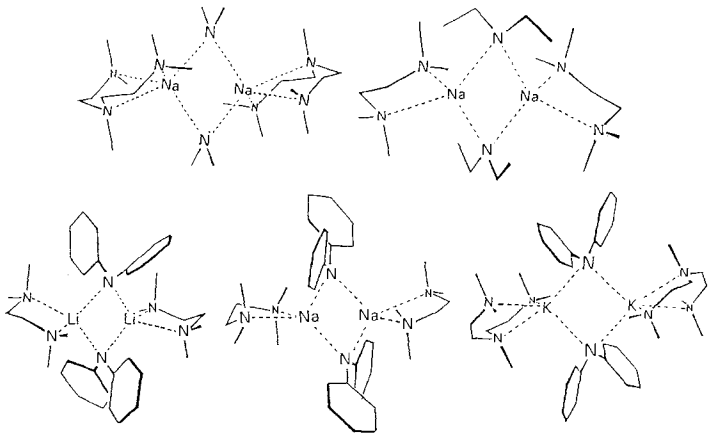

Fig. 32. Structures of dimeric base adducts of alkali metal amides. Top: $[NaNMe_2(pmdta)]_2$, $[NaNEt_2(tmeda)]_2$; bottom: $[LiNPh_2(tmeda)]_2$, $[NaNPh_2(tmeda)]_2$, and $[KNPh_2(pmdta)]_2$ [97].

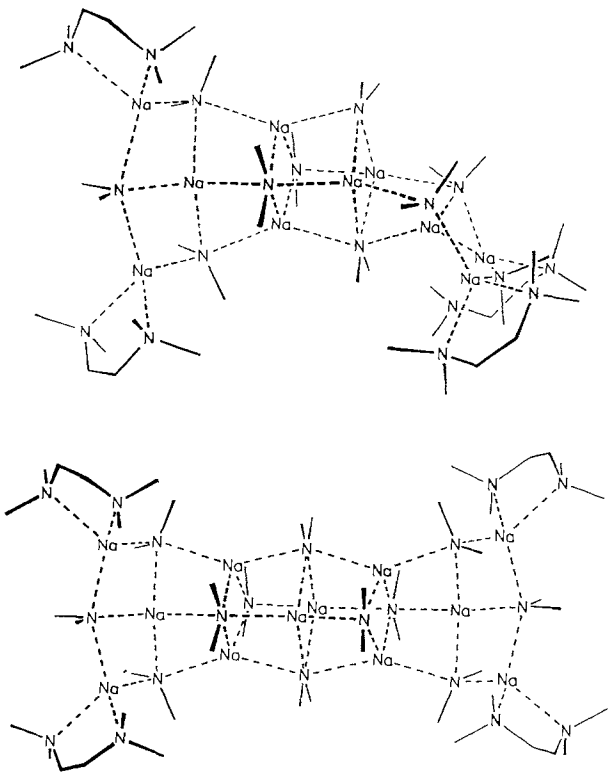

Fig. 33. The stacked structures of the amine adducts of sodium dimethylamides: $[Na_{10}(NMe_2)_{10}(tmeda)_4]$ (top) and $[Na_{12}(NMe_2)_{12}(tmeda)_4]$ (bottom).

gates, which can be considered to be constructed from ring-shaped dimers and bounded by terminal donor molecules. Thus, analogies to the organolithium compound $[(LiC\equiv CtBu)_{12}(thf)_4]$[65] discussed in Section 3.2.3 can be drawn. The occurrence of $[Na_{12}(NMe_2)_{10}(p\text{-xylyl})_2(pmdta)_4]$ indicates that carbanions can also be fitted into the amide stack.[167]

Related examples can be found under the amides listed in Table 5 which are formed from the heterocycles pyridine, carbazole, and indole. These amides also form bridges in the dimers and can exhibit both σ and π interactions. The amide bridges are unsymmetric in $[Na(indolyl)(tmeda)]_2$ and symmetric in $[Na(indolyl)(pmeda)]_2$ and thus reflect the difference in the spatial requirements of the solvate bases.[168]

8. Alkoxides, Aryloxides, Enolates, and Acetylenediolates

Investigations on the structures of alkali metal alkoxides also began relatively late, as the appearance of a monograph first in 1978 indicates.[171] A review on phenoxides is given in ref.[172]. Considering the importance of these compounds, not many structures are known even today. Table 6 contains a few simple but important examples of some unsolvated compounds.

Table 6. Unsolvated metal alkoxides, thiolates, and acetylenediolates.

Compound	Degree of aggregation	Ref.
LiOMe	layered structure	[173]
NaOMe	layered structure (LiOMe-type)	[174]
KOMe	layered structure	[175]
RbOMe, CsOMe	layered structure (KOMe-type)	[176]
KO*i*Pr, RbO*i*Pr, CsO*i*Pr	layered structure (LiOMe-type)	[177]
$(NaOtBu)_6$, $(NaOtBu)_9$	hexamer, nonamer	[178]
$(KOtBu)_4$, $(RbOtBu)_4$, $(CsOtBu)_4$	tetramer, cubane	[179]
$(KOSiMe_3)_4$, $(RbOSiMe_3)_4$, $(CsOSiMe_3)_4$	tetramer, cubane	[180]
$(CuOtBu)_4$	tetramer, ring	[181]
$Ca(OMe)_2$, $Sr(OMe)_2$, $Ba(OMe)_2$	layered structure (CaI_2-type)	[182]
LiSMe, NaSMe	layered structure (LiOMe-type)	[183]
KSMe	layered structure (KOMe-type)	[183]
NaOC≡CONa	-	[184]
KOC≡COK	-	[185]
RbOC≡CORb, CsOC≡COCs	-	[186]

8.1. Layered Structures: Methoxides, Ethoxides, Propoxides

The standard synthesis of alkali metal alkoxides from a metal and an alcohol leads to solvent adducts which are

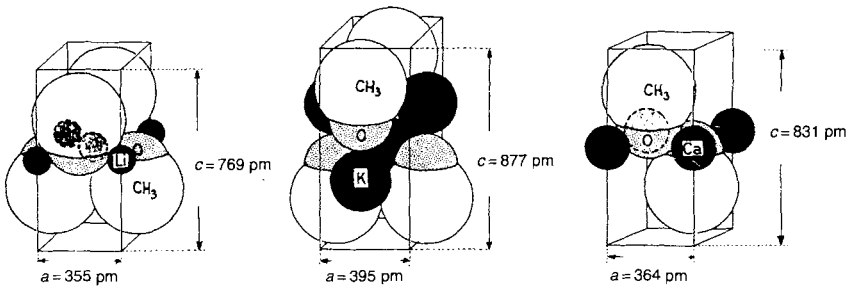

Fig. 34. The layered structures of (from left to right) LiOMe, KOMe (tetragonal), and $Ca(OMe)_2$ (hexagonal).

often crystallizable; the solvent-free compounds usually provide finely crystalline powder upon drying. Their X-ray investigations are thus more difficult, and the determination of the hydrogen atom positions is rarely possible. Disorder arising from rotomers is likely; solid-state ^1H NMR investigations[179b] have shown that the alkyl groups rotate in crystalline samples.

All of the simple alkoxides investigated so far, MOMe (M = Li–Cs),[173–176] and MO*i*Pr (M = K–Cs),[177] have layered structures (Fig. 34). The methoxides of calcium, strontium, and barium[182] as well as the thiolates MSMe (M = Li–K)[183] are also to be included here. The alkyl groups are always found on the outside of the layers, and the cations are distributed within the layer over one (Li, Na, Ca, Sr, Ba) or two (K, Rb, Cs) sites depending on the radius of the ion. The compounds are nonvolatile and insoluble in apolar solvents as a consequence of their layered structures.

8.2. Spherical and Cyclic Aggregates: *tert*-Butoxides, Enolates

Layered structures are no longer possible with large bulky alkyl groups (the lower boundary seems to lie by *t*-butyl), and so spherical or cyclic aggregates are formed in these cases. The compounds initially investigated, $(MO\,t\mathrm{Bu})_4$ (M = K, Rb, Cs; Fig. 35),[179] as well as the trimethylsilanolates $(MOSiMe_3)_4$ (M = K, Rb, Cs)[180] and the recently described imide $(CsNHSiMe_3)_4$,[187] are all tetrameric and form cubane structures in crystalline samples. The corners of the distorted cube are occupied by metal atoms alternating with O or N atoms.

The compounds are soluble and volatile as a result of their spherical structures, whereby the outer surfaces have predominantly hydrocarbon character. Molar mass determinations in aprotic solvents[188] indicate similar degrees of aggregation as found in the crystal. According to mass spectrometric investigations, tetramers—$(KO\,t\mathrm{Bu})_4$,[179b] $(MOSiMe_3)_4$ (M = K, Rb, Cs)[179b]—and hexamers—$(LiOCMe_3)_6$[189] and $(MOSiMe_3)_6$ (M = Li, Na)[189]—also exist in the gas phase.

The application of these alcoholates in the synthesis of organometallic compounds (see Sections 2.2, 2.3, and 4.1) as well as their versatility as synthetic building blocks and catalysts for organic reactions is ultimately based upon their structure-dependent solubility.[190a] Soluble alkoxides are also valuable precursors for the preparation of metal oxides under mild reaction conditions (sol–gel and MOCVD methods). The discovery of high-temperature superconductors has recently sparked a lively interest in mixed oxide systems and other ceramic materials and has thus contributed to a renaissance in the chemistry of the alkoxides.[190b,c]

The structure of sodium *tert*-butoxide (Fig. 36) is especially noteworthy. Within its unit cell, hexameric $(NaO\,t\mathrm{Bu})_6$

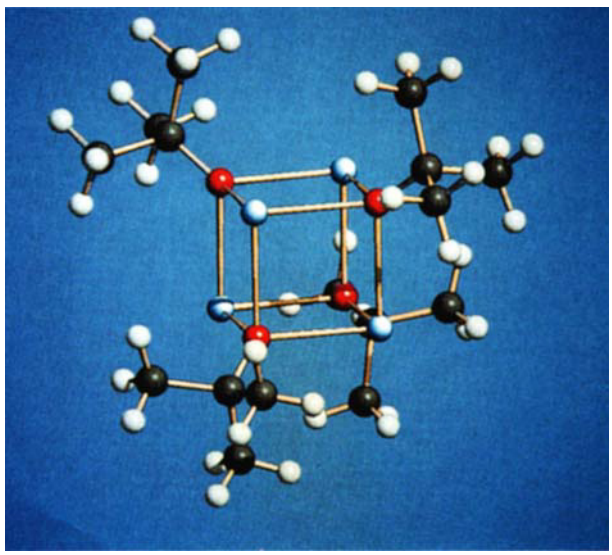

Fig. 35. The cubane structure of $(KO\,t\mathrm{Bu})_4$; isotypic structures include $(MO\,t\mathrm{Bu})_4$ (M = Rb, Cs) and $(MOSiMe_3)_4$ (M = K, Rb, Cs).

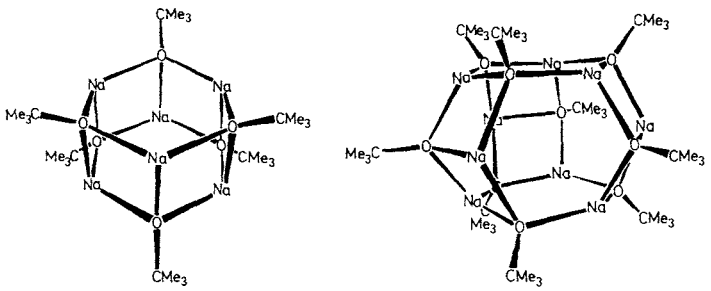

Fig. 36. The structures of $(NaO\,t\mathrm{Bu})_6$ (left) and $(NaO\,t\mathrm{Bu})_9$ (right). The central six-membered ring in the nonamer is expanded to the extent that only three Na–O contacts are possible here.

and nonameric $(NaO\,t\mathrm{Bu})_9$ aggregates (1:1 ratio) lie in very close proximity to one another, a rarity even from a crystallographic viewpoint.[178] Just as a cubane structure can result from the stacking of two ring-shaped dimers, so can the trigonal-prismatic structure of $(NaO\,t\mathrm{Bu})_6$ be regarded as a stacking of two ring-shaped trimers. Although inadequate crystal quality has prohibited a definitive investigation on

lithium *tert*-butoxide, hexamers are probably also present in its crystals.

Copper(I) can hardly be compared to the alkali metals. In its complexes the metal center strives for linear coordination, as the structures of the diorganocuprates show. Thus, copper *tert*-butoxide forms the four-membered ring structure $(CuO\,t\mathrm{Bu})_4$[181] (Fig. 37). Although the very explosive compound methylcopper has not yet been crystallographically investigated, it should have an analogous structure.

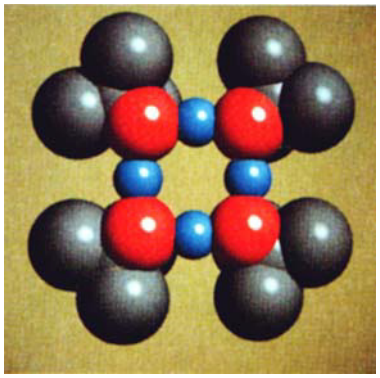

Fig. 37. The ring structure of $(CuO\,t\mathrm{Bu})_4$.

The enolates are very important members of the group of lithium compounds having O ligands. Their structures have been well investigated and included in reviews over the last decade.[191] It is sufficient to indicate here that the known structure types (dimers, tetramers, hexamers, etc.) also occur with these compounds. Most compounds have been investigated as their solvent adducts. The trimeric magnesium-acetylacetonate $Mg_3[MeC(O)CHC(O)Me]_6$ and its phosphinoyl derivative $Mg_3[(Et_2O)_2P(O)CHC(O)Me]_6$[192] are solvent-free enolates. As a consequence of the octahedral coordination preferred by the dications, these compounds contain face-sharing MO_6 polyhedra similar to those found in $[Zn_3(acac)_6]$[193] and $[Ni_3(acac)_6]$.[194]

8.3. Base Adducts of the Alkoxides and Phenoxides, Complexes from Alkoxides and Organometallic Compounds

Apart from the alkali metal enolates, there are very few structurally characterized compounds with other, even simple, alkoxides. Two examples are the dimeric phenoxides (phenolates) $[Li(p\text{-}OC_6H_4Br)(tmeda)]_2$[195] and $[Na(OPh)(pmdta)]_2$[195] which contain central M_2O_2 rings. A few compounds with more highly substituted phenoxides also have ring structures: lithium-2,6-di(*t*-butyl)phenoxide $[Li(OC_6H_3t\mathrm{Bu}_2)(Et_2O)]_2$[196] and sodium-2,4,6-tris(trifluoromethyl)phenoxide $[Na(OR)(thf)_2]_2$.[197] In $[Li\{O\text{-}2,6\text{-}(CH_2NMe_2)_2\text{-}4\text{-}MeC_6H_2\}]_3$, a cyclic trimer $(LiOR)_3$ is formed by "inner solvation" with a phenoxide having two amine substituents.[198]

Some recent investigations on soluble (oxo)alkoxides of the heavier alkali earth metals, and especially those with barium,[199] are worth mentioning with regard to the interest in superconductors noted in the previous section. The structural framework in $[Ca_6O_2(OEt_2)_8]\cdot 14Et_2O$ is made up of a stack of three Ca_2O_2 rings,[200] and $[Ca_9(OCH_2CH_2OMe)_{18}(HOCH_2CH_2OMe)_2]$[201] is the largest alkoxo complex known.

It was already mentioned in Section 3.1 that the reactivity of the organometallic compounds can often be drastically increased by the addition of amines (tmeda) or *tert*-butoxides. This very important effect is based on the formation of complexes from organometallic compounds and the base ("superbases"). The solubility of the organometallic compound usually increases parallel to this. Although crystal structure investigations on appropriate compounds are only in their initial stages at this point, the benzene-soluble tetramer $[n\mathrm{BuLi}\cdot Li\,O\,t\mathrm{Bu}]_4$[202a] and [Li(4,6-dimethyl-2-sodiomethylphenoxide)(tmeda)]$_4$,[202b] which contains a Li_4O_4 cubane framework, are the first examples. The solubilization of organosodium compounds by magnesium alkoxides[203a] is also possible and, conversely, polymeric diphenylmagnesium forms benzene-soluble complexes with alkali metal alkoxides.[203b]

8.4. Acetylenediolates

J. Liebig reported in 1834 on the formation of a black and extremely reactive "potassium carbonyl" from the reaction of CO and melted potassium in a 1:1 mol ratio.[204] The product was later formulated as $K_6C_6O_6$, since small amounts of hexahydroxybenzene (together with its oxidation products) could be obtained by careful hydrolysis (otherwise an explosive reaction occurs).

The reaction can also be performed with alkali metals dissolved in liquid ammonia. Following the introduction of CO into the blue solution of the metal, a colorless and likewise very reactive powder precipitates which, upon hydrolysis, yields small amounts of glyoxal together with other products. The "alkali metal carbonyls" prepared in this way were the subject of our systematic investigations with W. Büchner starting in 1963.[184–186] X-ray diffraction studies, among others, proved these compounds to exist as dimers. The Na, K, Rb, and Cs salts of these acetylenediolates were examined and found to be isotypic (Fig. 38). The lithium compound is

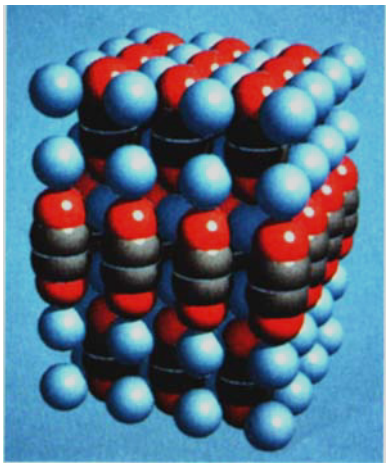

Fig. 38. Space-filling model of the crystal structure of KOC≡COK[185]. NaOC≡CONa[184], RbOC≡CORb, and CsOC≡COCs[186] are isotypic.

extremely shock sensitive and thus its structure determination has not been possible. Generally the compounds become more stable with increasing cation radius, since intermolecular reactions within the crystal are then minimized.

The following reaction steps apparently occur during the reaction of CO with alkali metals (Scheme 3). First, CO is

$$M + CO \rightarrow M^+ + CO^{\cdot -}$$
$$2\,CO^{\cdot -} \rightarrow {}^-OC{\equiv}CO^-$$

Scheme 3. Formation of acetylenediolate from the reaction of CO with an alkali metal.

reduced to the radical anion $CO^{\cdot -}$ (isoelectronic with NO), which immediately dimerizes to form the acetylenediolate (along with other compounds[205]). If the reaction is carried out in a potassium melt, then cyclotrimerization directly follows to form $K_6C_6O_6$. Such cyclization reactions are well known with the alkynes.

9. Solvated Alkali Metal Halides

Gas-phase alkali metal halide homo-complexes[206] like $(NaCl)_n$ ($n = 2-4$) have been known for a long time. Their structures usually represent sections of the crystal lattice, for example the Na_4Cl_4 heterocubane, and they can be stabilized by solvation. Appropriate bases containing N and O atoms can form adducts, a few of which are even soluble in hydrocarbon solvents. The most commonly known complexes are those formed from crown ethers, cryptands, and calixarenes and are usually solvent-separated ion pairs.[207]

In contrast, simple adducts of the alkali metal halides with amines, and particularly those with chelating amines, remain less well known, even though they display special properties[208] and despite the fact that their structure investigations were conducted as far back as the 1960s.[209] Since the small Li ion is easily solvated, most of the investigations have been performed with Li derivatives. Adducts of the heavier alkali metals, and especially their chlorides, are not very soluble in amines. Apparently their solvation enthalpies and entropies are often not sufficient to overcome the lattice energy; many adducts cannot be synthesized by simply mixing the salts with the donor ligands. They are formed more easily when the metal halides are as dry and as finely dispersed as possible. These conditions sometimes exist in the preparation of organo alkali metal compounds in the presence of halide sources. This explains the often unexpected formation of solvated alkali metal halides during the synthesis of organometallic compounds. Thus, solvated lithium complexes having both carbanions and halide ions in the same aggregate have been obtained. The compounds $[Li_4(cyclopropyl)_2Br_2(Et_2O)_4]$[210] and $[Li_4Ph_3Br(Et_2O)_3]$,[211] which crystallize as heterocubanes, are examples.

Syntheses aimed at preparing water-free solvent adducts of lithium halides of the form $[LiX \cdot x\,L]_n$ are based on the reactions of *n*BuLi with *n*BuX/L[212] or reactions of *n*BuLi (or LiH) with solid ammonium halides in the presence of bases L.[213] We have been able to prepare sodium compounds analogously by using *n*BuNa and RX/L.

Among the systematic investigations on solvent adducts of alkali metal halides carried out recently, those by R. Snaith et al. and A. H. White et al deserve particular note. We have also investigated several adducts including $[(LiCl)_8(tmeda)_7]$ (two solvated Li_4Cl_4 units connected by a tmeda bridge),[214] $[NaI(tmeda)]_4$ (heterocubane; Fig. 39),[215] $[NaI(tmeda)_2]_n$ (*catena*-μ-I[Na(tmeda)$_2$], polymer chain; Fig. 40),[216] and $[NaI(pmdta)]_2$ (dimer; Fig. 40).[217] These structures compliment those described in the literature, and in many cases the compounds were examined independently by several research groups. A surprising variety of structures is also found with these compounds; the most important types include monomers, rings (dimers, trimers), stacks (cubanes, double cubanes), and polymer chains.

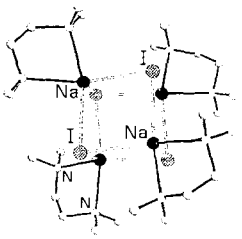

Fig. 39. The structure of $[NaI(tmeda)]_4$ (heterocubane).

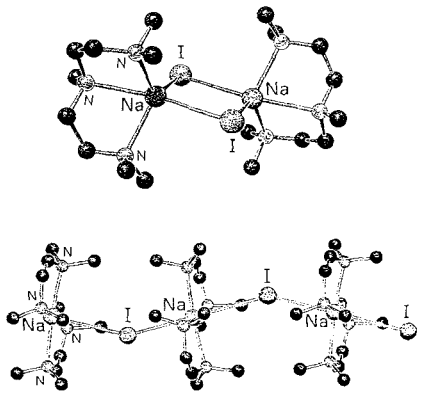

Fig. 40. The structures of $[NaI(pmdta)]_2$ (dimer) and $[NaI(tmeda)_2]_n$. A dimer structure very similar to that of $[NaI(pmdta)]_2$ is found as a component in the crystal of the mixed aggregate $[NaI(pmdta)]_2[Li(pmdta)(OH_2)I]_2$[218]. In *catena*-$\mu$-I[Na(tmeda)$_2$] the Na ions have distorted octahedral coordination.

10. Closing Remarks

The structures of organometallic compounds presented in this review display an unexpected and fascinating variety with the most diverse C, N, O, and X ligands. Many of the physical and chemical properties of these ion aggregates first became understandable through their structure determinations. For example, the solubility of many organometallic compounds is a consequence of their structure and not of "covalent bonding". The application of the structure information to the study of reaction mechanisms and to the directed control of reactions is still in its infancy.

The largest structural diversity is found with the lithium compounds. Here, almost all of the important structure

types occur: monomers, dimers (rings), trimers (rings), tetramers (heterocubanes and rings), hexamers (pseudooctahedra), decamers, dodecamers (stacked rings), and polymers (chains, double chains). The heavier alkali metal ions allow for a greater hapticity, whereby not only the formation of two- and three-dimensional ion aggregates is promoted, but also multihapto contacts to aromatic ring systems. The important structure types are presented in simplified form in Figure 41 (Lewis-basic solvent molecules are excluded).

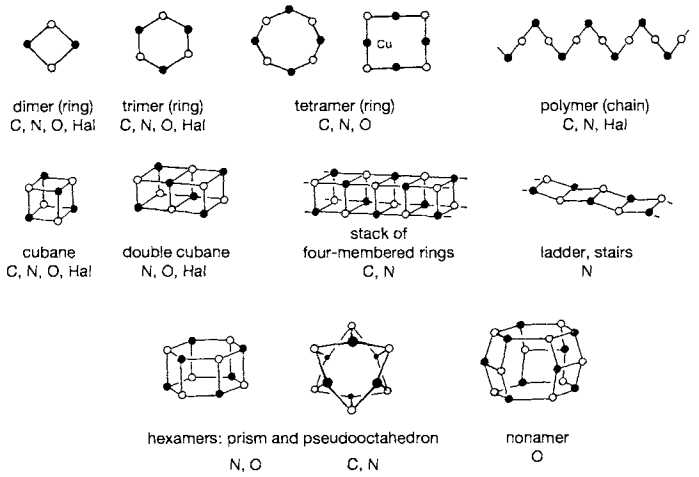

Fig. 41. Important idealized coordination types for ion aggregates of the alkali metals (●) with C, N, O, and halogen anions (○). The pseudooctahedron can also be considered a distorted hexagonal prism. The anions for which each coordination type has been found are listed for each case.

The organic compounds of the main group metals continue to be of tremendous interest. At the moment it seems that a rapid development in the compounds of the heavier alkali metals is taking place. Of the elements of the second main group, magnesium remains at the focus of interest. When will the decisive breakthrough occur for the heavier alkaline earth metals?[219] Conditional here are substantial advances in the further development of low-temperature techniques. Good progress has been made in crystal structure analysis which has enabled an increasing number of routine investigations on thermally labile substances.[220] Further surprises in this field of study may certainly be expected.

My special thanks go to the many co-workers and colleagues who have carried out or supported our work over the past nearly three decades. Since their large number prevents mentioning all their names, I can only refer to the literature citations. I would, however, like to thank especially Prof. Dr. U. Behrens and Priv.-Doz. Dr. J. Kopf for continuous and valuable help, particularly with difficult crystal structure analyses, and also Dr. J. Cockcroft for the neutron diffraction investigations. I have had the pleasure of working with many very dedicated and imaginative co-workers who have contributed substantially to the results presented here. I am grateful to the Deutsche Forschungsgemeinschaft and the Fonds der Chemischen Industrie.

Received: April 6, 1993 [A 923 IE]
German version: *Angew. Chem.* **1993**, *105*, 1565
Translated by Dr. J. R. Kennedy, Stuttgart

[1] a) W. Schlenk, J. Appenrodt, A. Michael, A. Thal, *Ber. Dtsch. Chem. Ges.* **1914**, *47*, 473; b) W. Schlenk, R. Ochs, *ibid.* **1916**, *49*, 608; c) W. Schlenk, J. Holtz, *ibid.* **1917**, *50*, 262.
[2] E. Krause, A. von Grosse, *Die Chemie der metall-organischen Verbindungen*, Bornträger, Berlin, **1937**.
[3] W. N. Setzer, P. von R. Schleyer, *Adv. Organomet. Chem.* **1985**, *24*, 353.
[4] C. Schade, P. von R. Schleyer, *Adv. Organomet. Chem.* **1987**, *27*, 159–278.
[5] P. R. Markies, O. S. Akkerman, F. Bickelhaupt, W. J. J. Smeets, A. L. Spek, *Adv. Organomet. Chem.* **1991**, *32*, 147.
[6] K. Gregory, P. von R. Schleyer, R. Snaith, *Adv. Organomet. Chem.* **1992**, *37*, 47.
[7] *Comprehensive Organometallic Chemistry, vols. 1, 2, 9* (Eds.: G. Wilkinson, F. G. A. Stone, E. W. Abel), Pergamon, Oxford, **1982**.
[8] B. J. Wakefield, *The Chemistry of Organolithium Compounds*, Pergamon, Oxford, **1974**.
[9] a) M. Schlosser, *Struktur und Reaktivität polarer Organometalle*, Springer, Berlin, **1973**; b) *Angew. Chem.* **1964**, *76*, 124, 258; *Angew. Chem. Int. Ed. Engl.* **1964**, *3*, 287, 362; c) H. F. Ebel, *Fortschr. Chem. Forsch.* **1969**, *12*, 387; d) P. West, *MTP Int. Rev. Sci. Inorg. Chem. Ser. One 1972* **1972**, *4*, 1.
[10] Yearly report: a) *Organomet. Chem.* **1972 ff**; b) *Annu. Rep. Prog. Chem.* **1950**, *47* to **1966**, *63*; *Annu. Rep. Prog. Chem. Sect. A* in subsequent years.
[11] a) E. Weiss, E. A. C. Lucken, *J. Organomet. Chem.* **1964**, *2*, 197; b) E. Weiss, G. Hencken, *ibid.* **1969**, *21*, 265.
[12] H. Dietrich, *Acta Crystallogr.* **1963**, *16*, 681; *J. Organomet. Chem.* **1981**, *205*, 291.
[13] E. Kaufmann, K. Raghavachari, A. E. Reed, P. von R. Schleyer, *Organometallics* **1988**, 1597, and references therein.
[14] a) L. D. McKeever, R. Waack, M. A. Doran, E. B. Baker, *J. Am. Chem. Soc.* **1968**, *90*, 3244; b) *ibid.* **1969**, *91*, 1057; see also c) L. M. Seitz, T. L. Brown, *ibid.* **1966**, *88*, 2174; d) T. L. Brown, *ibid.* **1966**, *88*, 4140.
[15] a) A. Streitwieser, Jr., *J. Organomet. Chem.* **1978**, *156*, 1; b) A. Streitwieser, J. E. Williams, S. Alexandratos, J. M. McKelvey, *J. Am. Chem. Soc.* **1987**, *98*, 4778.
[16] a) R. Bushby, H. L. Steel, *J. Organomet. Chem.* **1987**, *336*, C25; b) *J. Chem. Soc. Perkin Trans. 2* **1990**, 1143, 1169, and references therein.
[17] C. Lambert, P. von R. Schleyer, *Angew. Chem.* **1994**, *106*; *Angew. Chem. Int. Ed. Engl.* **1994**, *33* (planned for Issue 6).
[18] E. Weiss, T. Lambertsen, B. Schubert, J. K. Cockcroft, A. Wiedenmann, *Chem. Ber.* **1990**, *123*, 79.
[19] a) E. Weiss, G. Sauermann, *Angew. Chem.* **1968**, *80*, 123; *Angew. Chem. Int. Ed. Engl.* **1968**, *7*, 133; b) *Chem. Ber.* **1970**, *103*, 265.
[20] E. Weiss, H. Köster, *Chem. Ber.* **1977**, *110*, 717.
[21] E. Weiss, T. Lambertsen, B. Schubert, J. K. Cockcroft, *J. Organomet. Chem.* **1988**, *358*, 1.
[22] A reindexing of the earlier powder data [19] from KCH_3 (hexagonal indexing, 293 K) based on an orthorhombic cell ($a = 428.1$, $b = 740.3$, $c = 821.1$ pm, 290 K) has already been carried out [21]. The new orthorhombic parameters for $RbCH_3$ and $CsCH_3$ are: $RbCH_3$: $a = 448.8$, $b = 777.3$, $c = 856.2$ pm; $CsCH_3$: $a = 470.5$, $b = 814.9$, $c = 901.1$ pm (293 K); E. Weiss, H. Viebrock, unpublished; H. Viebrock, Diplomarbeit, Universität Hamburg, **1989**. (For the old values see ref. [20].)
[23] E. Weiss, G. Sauermann, G. Thirase, *Chem. Ber.* **1983**, *116*, 74.
[24] E. Weiss, *Chem. Ber.* **1964**, *97*, 3241.
[25] a) E. Weiss, S. Corbelin, J. K. Cockcroft, A. N. Fitch, *Angew. Chem.* **1990**, *102*, 728; *Angew. Chem. Int. Ed. Engl.* **1990**, *29*, 650; b) *Chem. Ber.* **1990**, *123*, 1629.
[26] P. West, R. Waack, *J. Am. Chem. Soc.* **1967**, *89*, 4395.
[27] See also A. K. Cheetham, A. P. Wilkinson, *Angew. Chem.* **1992**, *104*, 1594; *Angew. Chem. Int. Ed. Engl.* **1992**, *31*, 1557.
[28] It is still not known whether the CH_3^- anion has a pyramidal or a trigonal-planar structure in the gas phase. Theoretical calculations indicate that the two structures are close in energy. For further discussion see ref. [21].
[29] E. Weiss, G. Hencken, H. Kühr, *Chem. Ber.* **1970**, *103*, 2868.
[30] G. Thirase, E. Weiss, H. J. Hennig, H. Lechert, *Z. Anorg. Allg. Chem.* **1975**, *417*, 221.
[31] G. Thirase, E. Weiss, *Z. Naturforsch. B* **1974**, *29*, 800.
[32] $KSiH_3$ is transformed into an orthorhombic β modification below $-5\,^{\circ}C$: O. Mundt, G. Becker, H.-M. Hartmann, W. Schwarz, *Z. Anorg. Allg. Chem.* **1989**, *572*, 75.
[33] A. W. Hewat, C. Riekel, *Acta Crystallogr. Sect. A* **1979**, *35*, 569 (neutron diffraction investigations of ND_3 at 2 K).
[34] E. Weiss, G. Sauermann, *J. Organomet. Chem.* **1970**, *21*, 1.
[35] a) E. Weiss, H. Plass, *Chem. Ber.* **1968**, *101*, 2947; M. Atoji, *J. Chem. Phys.* **1972**, *56*, 4947 (neutron diffraction investigation of NaC≡CH).
[36] a) R. Juza, V. Wehrle, H.-U. Schuster, *Z. Anorg. Allg. Chem.* **1967**, *352*, 252; b) M. Atoji, *J. Chem. Phys.* **1974**, *60*, 3324 (neutron diffraction investigation); c) H. Föppl, *Angew. Chem.* **1958**, *70*, 401.
[37] A. Maercker, M. Theis, *Top. Curr. Chem.* **1987**, *138*, 1.
[38] J. B. Collins, J. D. Dill, E. D. Jemmins, Y. Apeloig, P. von R. Schleyer, R. Seeger, J. A. Pople, *J. Am. Chem. Soc.* **1976**, *98*, 5419.

[39] a) E. Weiss, **1964**, unpublished; b) H. Riechers, Dissertation, Universität Hannover, **1979**; b) S. Corbelin, Diplomarbeit, Universität Hamburg, **1987**.
[40] G. D. Stucky, M. M. Eddy, W. H. Harrison, R. Lagow, H. Kawa, D. E. Cox, *J. Am. Chem. Soc.* **1990**, *112*, 2425.
[41] E. Weiss, *Chem. Ber.* **1965**, *98*, 2805.
[42] For the activation or organolithium compounds and lithium amides by addition of amines or alkoxides see: a) L. Lochmann, J. Pospíšil, D. Lím, *Tetrahedron Lett.* **1966**, 257; b) L. Lochmann, J. Trekoval, *Collect. Czech. Chem. Commun.* **1988**, *53*, 76; c) M. Schlosser, *J. Organomet. Chem.* **1967**, *8*, 9; d) M. Schlosser, S. Strunk, *Tetrahedron Lett.* **1984**, *25*, 741; e) M. Schlosser, *Pure Appl. Chem.* **1988**, *60*, 1627; f) C. Agami, *Bull. Soc. Chim. Fr.* **1970**, *37*, 1620; g) T. Durst, *Stud. Org. Chem. (Amsterdam)* **1984**, *5*, 239; h) R. R. Fraser, T. S. Mansour, *Tetrahedron Lett.* **1986**, *27*, 331, and references therein; i) W. Bauer, L. Lochmann, *J. Am. Chem. Soc.* **1992**, *114*, 7482.
[43] For example ref. [9]; W. Bauer, D. Seebach, *Helv. Chim. Acta* **1984**, *67*, 1972.
[44] For example a) D. Seebach, R. Hässig, J. Gabriel, *Helv. Chim. Acta* **1983**, *66*, 308, 2269; b) H. Günther, D. Moskau, P. Bast, D. Schmalz, *Angew. Chem.* **1987**, *99*, 1242; *Angew. Chem. Int. Ed. Engl.* **1987**, *26*, 1212; c) J. F. McGarrity, C. A. Ogle, Z. Brich, H.-R. Loosli, *J. Am. Chem. Soc.* **1985**, *107*, 1811; e) D. H. O'Brien, *Stud. Org. Chem. (Amsterdam)* **1980**, *5*, 271.
[45] A. Maercker, *Angew. Chem.* **1987**, *99*, 1002; *Angew. Chem. Int. Ed. Engl.* **1987**, *26*, 972.
[46] V. Jordan, V. Dimitrov, E. Weiss, unpublished; V. Jordan, Diplomarbeit, Hamburg, **1989**. In the crystal investigated (orthorhombic, $P2_1nm$, $a = 1020$, $b = 1058$, $c = 1225$ pm, $Z = 2$, $T = 298$ K) three of the carbon atoms averted from the heterocubane were disordered, and therefore their positions could not be determined exactly.
[47] T. Kottke, D. Stalke, *Angew. Chem.* **1993**, *105*, 619; *Angew. Chem. Int. Ed. Engl.* **1993**, *32*, 580.
[48] R. Zerger, W. Rhine, G. Stucky, *J. Am. Chem. Soc.* **1974**, *96*, 6048.
[49] A. Maercker, M. Bsata, W. Buchmeier, B. Engelen, *Chem. Ber.* **1984**, *117*, 2547.
[50] S. Harder, J. Boersma, L. Brandsma, J. A. Kanters, W. Bauer, P. von R. Schleyer, *Organometallics*, **1989**, *8*, 1696.
[51] B. Tecle', A. F. M. M. Rahman, J. P. Oliver, *J. Organomet. Chem.* **1986**, *317*, 267.
[52] H. Hiller, M. Layh, W. Uhl, *Angew. Chem.* **1991**, *103*, 339; *Angew. Chem. Int. Ed. Engl.* **1991**, *30*, 324.
[53] H. Köster, D. Thoennes, E. Weiss, *J. Organomet. Chem.* **1978**, *160*, 1.
[54] M. F. Lappert, L. M. Engelhardt, C. L. Raston, A. H. White, *J. Chem. Soc. Chem. Commun.* **1982**, 1323.
[55] C. Eaborn, P. B. Hitchcock, J. D. Smith, A. C. Sullivan, *J. Chem. Soc. Chem. Commun.* **1983**, 827.
[56] G. W. Klumpp, P. J. A. Geurink, N. J. R. van Eikema Hommes, F. J. J. de Kanter, M. Vos, A. L. Spek, *Recl. Trav. Chim. Pays-Bas* **1986**, *10*, 398.
[57] K. S. Lee, P. G. Willard, J. W. Suggs, *J. Organomet. Chem.* **1986**, *299*, 311.
[58] a) H. Hope, P. P. Power, *J. Am. Chem. Soc.* **1983**, *105*, 5320; b) M. M. Olmstead, P. P. Power, *ibid.* **1990**, *112*, 8008.
[59] D. Thoennes, E. Weiss, *Chem. Ber.* **1978**, *111*, 3157.
[60] U. Schümann, J. Kopf, E. Weiss, *Angew. Chem.* **1985**, *97*, 222; *Angew. Chem. Int. Ed. Engl.* **1985**, *24*, 215.
[61] T. Maetzke, D. Seemann, *Helv. Chim. Acta* **1989**, *72*, 624.
[62] M. Geissler, E. Weiss, unpublished; M. Geissler, Diplomarbeit, Hamburg, **1984**.
[63] B. Schubert, E. Weiss, *Chem. Ber.* **1983**, *116*, 3212.
[64] B. Schubert, E. Weiss, *Angew. Chem.* **1983**, *95*, 499; *Angew. Chem. Int. Ed. Engl.* **1983**, *22*, 496; *Angew. Chem. Suppl.* **1983**, 703.
[65] M. Geissler, J. Kopf, B. Schubert, E. Weiss, W. Neugebauer, P. von R. Schleyer, *Angew. Chem.* **1987**, *99*, 569; *Angew. Chem. Int. Ed. Engl.* **1987**, *26*, 587.
[66] H. Köster, E. Weiss, *Chem. Ber.* **1982**, *115*, 3422.
[67] U. Schümann, E. Weiss, H. Dietrich, W. Mahdi, *J. Organomet. Chem.* **1987**, *322*, 299.
[68] a) G. Boche, H. Etzrodt, M. Marsch, W. Massa, G. Baum, H. Dietrich, W. Mahdi, *Angew. Chem.* **1986**, *98*, 84; *Angew. Chem. Int. Ed. Engl.* **1986**, *25*, 104; b) G. Boche, G. Fraenkel, J. Cabral, K. Harms, N. J. R. van Eikema Hommes, J. Lhorenz, M. Marsch, P. von R. Schleyer, *J. Am. Chem. Soc.* **1992**, *114*, 1562.
[69] S. P. Patterman, I. L. Karle, G. D. Stucky, *J. Am. Chem. Soc.* **1970**, *92*, 1150.
[70] a) M. A. Beno, H. Hope, M. M. Olmstead, P. P. Power, *Organometallics* **1985**, *4*, 2117; b) W. Zarges, M. Marsch, K. Harms, G. Boche, *Chem. Ber.* **1989**, *122*, 2302; c) W. Zarges, M. Marsch, K. Harms, W. Koch, G. Frenking, G. Boche, *ibid.* **1991**, *124*, 543.
[71] J. J. Brooks, G. D. Stucky, *J. Am. Chem. Soc.* **1972**, *94*, 7333.
[72] R. A. Bartlett, H. V. R. Dias, P. P. Power, *J. Organomet. Chem.* **1988**, *341*, 1.
[73] a) M. M. Olmstead, P. P. Power, *J. Am. Chem. Soc.* **1985**, *107*, 2174; b) P. P. Power, *Acc. Chem. Res.* **1988**, *21*, 147.
[74] a) D. Johnels, U. Edlund, *J. Organomet. Chem.* **1990**, *393*, C35; b) D. Johnels, *ibid.* **1993**, *445*, 1.
[75] G. Thirase, E. Weiss, *J. Organomet. Chem.* **1974**, *81*, C1.
[76] H. Köster, E. Weiss, *J. Organomet. Chem.* **1979**, *168*, 273.
[77] C. Schade, W. Bauer, P. von R. Schleyer, *J. Organomet. Chem.* **1985**, *295*, C25.
[78] Organosodium compounds can also be solubilized by complexation with magnesium alkoxides: a) C. G. Screttas, M. Micha-Screttas, *J. Organomet. Chem.* **1986**, *316*, 1; b) *Organometallics* **1984**, *3*, 904.
[79] R. Pi, W. Bauer, B. Brix, C. Schade, P. von R. Schleyer, *J. Organomet. Chem.* **1986**, *306*, C1.
[80] U. Schümann, U. Behrens, E. Weiss, *Angew. Chem.* **1989**, *101*, 481; *Angew. Chem. Int. Ed. Engl.* **1989**, *28*, 476.
[81] U. Schümann, E. Weiss, unpublished; U. Schümann, Dissertation, Hamburg, **1987**.
[82] W. Bauer, W. Neugebauer, P. von R. Schleyer, H. Dietrich, W. Mahdi, unpublished.
[83] C. Schade, P. von R. Schleyer, H. Dietrich, W. Mahdi, *J. Am. Chem. Soc.* **1986**, *108*, 2484.
[84] S. Corbelin, N. P. Lorenzen, J. Kopf, E. Weiss, *J. Organomet. Chem.* **1991**, *415*, 293.
[85] a) D. Hoffmann, N. J. R. van Eikema Hommes, P. von R. Schleyer, D. Stalke, U. Pieper, D. Wright, R. Snaith, *J. Am. Chem. Soc.*, submitted; b) D. Hoffmann, F. Hampel, W. Bauer, P. von R. Schleyer, unpublished.
[86] H. Viebrock, E. Weiss, unpublished; H. Viebrock, Dissertation, Hamburg, **1992**.
[87] a) D. Hoffmann, W. Bauer, P. von R. Schleyer, U. Pieper, D. Stalke, *Organometallics* **1993**, *12*, 1193; b) see also U. Pieper, D. Stalke, *ibid.* **1993**, *12*, 1201.
[88] S. Corbelin, J. Kopf, N. P. Lorenzen, E. Weiss, *Angew. Chem.* **1991**, *103*, 875; *Angew. Chem. Int. Ed. Engl.* **1991**, *30*, 825.
[89] H. Bock, K. Ruppert, Z. Havlas, D. Fenske, *Angew. Chem.* **1990**, *102*, 1095; *Angew. Chem. Int. Ed. Engl.* **1990**, *29*, 1042.
[90] H. Bock, K. Ruppert, D. Fenske, *Angew. Chem.* **1989**, *101*, 1717; *Angew. Chem. Int. Ed. Engl.* **1989**, *28*, 1685.
[91] a) H. Bock, K. Ruppert, Z. Havlas, W. Bensch, W. Hönle, H. G. von Schnering, *Angew. Chem.* **1991**, *103*, 1197; *Angew. Chem. Int. Ed. Engl.* **1991**, *30*, 1183; b) Review: H. Bock, K. Ruppert, C. Näther, Z. Havlas, H.-J. Herrmann, C. Arad, I. Göbel, A. John, J. Meuret, S. Nick, A. Rauschenbach, W. Seitz, T. Vaupel, B. Solouki, *Angew. Chem.* **1992**, *104*, 564; *Angew. Chem. Int. Ed. Engl.* **1992**, *31*; 550.
[92] a) P. Jutzi, *Adv. Organomet. Chem.* **1986**, *26*, 217; b) *Pure Appl. Chem.* **1989**, *61*, 1731.
[93] M. F. Lappert, A. Singh, L. M. Engelhardt, A. H. White, *J. Organomet. Chem.* **1984**, *262*, 271.
[94] A. Hammel, W. Schwartz, J. Weidlein, *Acta Crystallogr. Sect. C* **1990**, *46*, 2337.
[95] T. Aoyagi, H. M. M. Shearer, K. Wade, G. Whitehead, *J. Organomet. Chem.* **1979**, 175, 21.
[96] J. Lorberth, S.-H. Shin, S. Wocadlo, W. Massa, *Angew. Chem.* **1989**, *101*, 793; *Angew. Chem. Int. Ed. Engl.* **1989**, *28*, 735.
[97] V. Jordan, E. Weiss, unpublished; V. Jordan, Dissertation, Hamburg, **1992**.
[98] P. Jutzi, W. Leffers, B. Hampel, S. Pohl, W. Saak, *Angew. Chem.* **1987**, *99*, 563; *Angew. Chem. Int. Ed. Engl.* **1987**, *26*, 583.
[99] W. E. Rhine, G. D. Stucky, *J. Am. Chem. Soc.* **1975**, *97*, 737.
[100] C. Schade, P. von R. Schleyer, P. Gregory, H. Dietrich, W. Mahdi, *J. Organomet. Chem.* **1988**, *341*, 19.
[101] V. Jordan, E. Weiss, unpublished; V. Jordan, Dissertation, Hamburg, **1992**.
[102] S. Corbelin, J. Kopf, E. Weiss, *Chem. Ber.* **1991**, *124*, 2417.
[103] R. Zerger, W. Rhine, G. D. Stucky, *J. Am. Chem. Soc.* **1974**, *96*, 5441.
[104] D. Hoffmann, F. Hampel, P. von R. Schleyer, *J. Organomet. Chem.* **1993**, in press.
[105] a) E. Weiss, E. O. Fischer, *Z. Anorg. Allg. Chem.* **1955**, *278*, 219; b) W. Bünder, E. Weiss, *J. Organomet. Chem.* **1975**, *92*, 1.
[106] E. Weiss, *J. Organomet. Chem.* **1964**, *2*, 314.
[107] E. Weiss, *J. Organomet. Chem.* **1965**, *4*, 101.
[108] P. R. Markies, G. Schat, O. S. Akkerman, F. Bickelhaupt, W. J. J. Smeets, P. van der Sluis, A. L. Spek, *J. Organomet. Chem.* **1990**, 393, 315.
[109] A. I. Snow, R. E. Rundle, *Acta Crystallogr.* **1951**, *4*, 348.
[110] S. S. Al-Juaid, C. Eaborn, P. B. Hitchcock, C. A. McGeary, J. D. Smith, *J. Chem. Soc. Chem. Commun.* **1989**, 273.
[111] E. Weiss, H. Viebrock, K. J. Cockcroft, unpublished; H. Viebrock, Dissertation, Hamburg, **1992**.
[112] B. Wesslen, G. Mattson, *J. Polym. Sci. Part A Polym. Chem.* **1990**, *28*, 1033.
[113] T. Greiser, J. Kopf, D. Thoennes, E. Weiss, *J. Organomet. Chem.* **1980**, *191*, 1.
[114] H. Viebrock, E. Weiss, *J. Organomet. Chem.* **1993**, in press.
[115] D. Thoennes, E. Weiss, *Chem. Ber.* **1978**, *111*, 3381.
[116] See ref. [108].
[117] See ref. [4].
[118] B. Schubert, U. Behrens, E. Weiss, *Chem. Ber.* **1981**, *114*, 2640.
[119] M. Geissler, J. Kopf, E. Weiss, *Chem. Ber.* **1989**, *122*, 1395.

[120] P. M. Markies, T. Nomoto, O. S. Akkerman, F. Bickelhaupt, *J. Am. Chem. Soc.* **1988**, *110*, 4845.
[121] L. J. Guggenberger, R. E. Rundle, *J. Am. Chem. Soc.* **1964**, *86*, 5344; *ibid.* **1968**, *90*, 5375.
[122] F. A. Schröder, *Chem. Ber.* **1969**, *102*, 2035.
[123] G. D. Stucky, R. E. Rundle, *J. Am. Chem. Soc.* **1964**, *86*, 4825.
[124] M. Vallino, *J. Organomet. Chem.* **1969**, *20*, 1.
[125] H. Viebrock, D. Abeln, E. Weiss, *Z. Naturforsch. B* **1993**, submitted.
[126] J. A. Wanklin, *Justus Liebigs Ann. Chem.* **1858**, *108*, 67; *ibid.* **1859**, *111*, 234.
[127] a) G. Wittig, *Angew. Chem.* **1958**, *70*, 65; b) W. Tochtermann, *Angew. Chem.* **1966**, *78*, 355; *Angew. Chem. Int. Ed. Engl.* **1966**, *5*, 351.
[128] U. Schümann, E. Weiss, *Angew. Chem.* **1988**, *100*, 573; *Angew. Chem. Int. Ed. Engl.* **1988**, *27*, 584.
[129] C. Eaborn, P. B. Hitchcock, J. D. Smith, A. C. Sullivan, *J. Chem. Soc. Chem. Commun.* **1983**, 827.
[130] N. P. Lorenzen, E. Weiss, *Angew. Chem.* **1990**, *102*, 322; *Angew. Chem. Int. Ed. Engl.* **1990**, *29*, 300.
[131] R. G. Pearson, C. D. Gregory, *J. Am. Chem. Soc.* **1976**, *98*, 4098.
[132] F. Olbrich, J. Kopf, E. Weiss, *Angew. Chem.* **1993**, *105*, 1136; *Angew. Chem. Int. Ed. Engl.* **1993**, *32*, 1077.
[133] E. Weiss, R. Wolfrum, *J. Organomet. Chem.* **1968**, *12*, 257.
[134] I. R. Werner, D. F. Gaines, H. A. Harris, *Organometallics* **1988**, *7*, 2421.
[135] a) E. P. Squiller, R. R. Whittle, H. G. Richey, Jr., *J. Am. Chem. Soc.* **1985**, *107*, 432; b) *Organometallics* **1985**, *4*, 1154; c) see also A. D. Pajerski, M. Parvez, H. G. Richey, Jr., *J. Am. Chem. Soc.* **1988**, *110*, 2660.
[136] T. Greiser, J. Kopf, D. Thoennes, E. Weiss, *Chem. Ber.* **1981**, *114*, 209.
[137] See ref. [119].
[138] D. Thoennes, E. Weiss, *Chem. Ber.* **1978**, *111*, 3726.
[139] H. Viebrock, E. Weiss, unpublished.
[140] B. Schubert, E. Weiss, *Chem. Ber.* **1984**, *117*, 366.
[141] E. Weiss, R. Wolfrum, *Chem. Ber.* **1968**, *101*, 35.
[142] E. Weiss, H. Plass, *J. Organomet. Chem.* **1968**, *14*, 21.
[143] H. Alsdorf, E. Weiss, unpublished; H. Alsdorf, Dissertation, Hamburg, **1969**. Single-crystal data: monoclinic $P2_1/c$, $a = 780(1)$, $b = 683(1)$, $c = 1322(20)$ pm, $\beta = 117.8(2)$; $Z = 4$, 1005 reflections (film method), $R = 0.09$ (without refinement of H atoms): Zn–C 207(1) pm, ZnC_3 group is approximately trigonal planar.
[144] W. E. Rhine, G. D. Stucky, S. W. Peterson, *J. Am. Chem. Soc.* **1975**, *97*, 6401.
[145] H. Staeglich, E. Weiss, unpublished; H. Staeglich, Dissertation, Hamburg, **1976**. Single-crystal data for $K[BMe_4]$: orthorhombic *Pbcm*, $a = 858.6(8)$, $b = 876.5(9)$, $c = 925.3(7)$ pm (273 K), $Z = 4$, refined anisotropically (without H atoms), $R = 0.007$, B–C 166 pm (average). Powder data: $Na[BMe_4]$: $a = 886(2)$, $b = 843(2)$, $c = 924(3)$; $Rb[BMe_4]$: $a = 886(2)$, $b = 904(1)$, $c = 928(2)$; $Cs[BMe_4]$: $a = 898(3)$, $b = 936(3)$, $c = 942(4)$ pm.
[146] Ya. Ozol, S. Vimba, A. Ievins, *Sov. Phys. Crystallogr.* **1962**, *7*, 289.
[147] Ya. Ozol, S. Vimba, A. Ievins, *Latv. PSR Zinat. Akad. Vestis Kim. Ser.* **1975**, 517.
[148] K. Hoffmann, E. Weiss, *J. Organomet. Chem.* **1974**, *67*, 221.
[149] R. Wolfrum, G. Sauermann, E. Weiss, *J. Organomet. Chem.* **1969**, *18*, 27.
[150] R. L. Gerteis, R. E. Dickerson, T. L. Brown, *Inorg. Chem.* **1964**, *3*, 872.
[151] G. Hencken, E. Weiss, *J. Organomet. Chem.* **1974**, *73*, 35.
[152] K. Hoffmann, E. Weiss, *J. Organomet. Chem.* **1972**, *37*, 1.
[153] K. Hoffmann, E. Weiss, *J. Organomet. Chem.* **1973**, *50*, 17.
[154] K. Hoffmann, E. Weiss, *J. Organomet. Chem.* **1973**, *50*, 25.
[155] U. Joergens, E. Weiss, unpublished; U. Joergens, Dissertation, Hamburg, **1976**. Single-crystal data: a) $Na[TlMe_4]$: cubic ($P23$ or $P\bar{4}3m$), $a = 569.2(2)$, $Z = 1$, isotypic to $Li[InMe_4]$, Tl–C 226(4), Na–C 267(4) pm, refinement without H atoms and absorption correction, $R = 0.08$; b) $K[TlMe_4]$: tetragonal ($I4_1/amd$), $Z = 4$, isotypic to $K[AlMe_4]$, $a = 996.44(6)$, $c = 805.4(9)$ pm; Tl–C 231, K–C 352 and 310 pm, $R = 0.06$; c) $Na[TlPh_4]$: tetragonal ($P\bar{4}2_1c$), $a = 1202.7(20)$, $c = 682.6(8)$ pm, $Z = 2$, isotypic to $Li[InPh_4]$, Tl–C 226(4), $R = 0.09$.
[156] a) G. Wittig, R. Ludwig, R. Polster, *Chem. Ber.* **1955**, *88*, 294; b) G. Wittig, F. Bickelhaupt, *ibid.* **1958**, *91*, 865; c) G. Wittig, E. Benz, *ibid.* **1958**, *91*, 873.
[157] a) G. van Koten, J. G. Noltes in *Comprehensive Organometallic Chemistry, Vol. 4* (Eds.: G. Wilkinson), Pergamon, New York, **1982**, p. 709; b) P. P. Power, *Prog. Inorg. Chem.* **1991**, *39*, 75.
[158] J. F. Malone, W. S. McDonald, *J. Chem. Soc. Dalton Trans.* **1972**, 2646.
[159] a) Review: R. Juza, *Angew. Chem.* **1964**, *76*, 290; *Angew. Chem. Int. Ed. Engl.* **1964**, *3*, 471; b) $LiNH_2$ (new structure determination): H. Jacobs, R. Juza, *Z. Anorg. Allg. Chem.* **1972**, *391*, 271; c) $NaNH_2$: R. Juza, H. H. Weber, K. Opp, *ibid.* **1956**, *284*, 73; d) $NaNH_2$: A. Zalkin, D. H. Templeton, *J. Phys. Chem.* **1956**, *60*, 821; e) $NaND_2$ (neutron diffraction): M. Nagib, H. Kistrup, H. Jacobs, *Atomkernenergie* **1975**, *26*, 87.
[160] N. Kuhn, G. Henkel, J. Kreutzberg, *Angew. Chem.* **1990**, *102*, 1179; *Angew. Chem. Int. Ed. Engl.* **1990**, *29*, 1143.
[161] R. E. Mulvey, *Chem. Soc. Rev.* **1991**, *20*, 167.
[162] M. Veith, *Angew. Chem.* **1987**, *99*, 1; *Angew. Chem. Int. Ed. Engl.* **1987**, *26*, 1.
[163] See for example M. C. Carre, G. Ndebeka, A. Riondel, P. Bourgasser, P. Caubère, *Tetrahedron Lett.* **1984**, *25*, 1551.
[164] D. Barr, W. Clegg, R. E. Mulvey, R. Snaith, J. Wright, *J. Chem. Soc. Chem. Commun.* **1987**, 716.
[165] P. C. Andrews, W. Clegg, R. E. Mulvey, *Angew. Chem.* **1990**, *102*, 1480; *Angew. Chem. Int. Ed. Engl.* **1990**, *29*, 1440.
[166] W. Clegg, M. MacGregor, R. E. Mulvey, P. A. O'Neil, *Angew. Chem.* **1992**, *104*, 74; *Angew. Chem. Int. Ed. Engl.* **1992**, *31*, 93.
[167] N. P. Lorenzen, J. Kopf, F. Olbrich, U. Schümann, E. Weiss, *Angew. Chem.* **1990**, *102*, 1481; *Angew. Chem. Int. Ed. Engl.* **1990**, *29*, 1441.
[168] K. Gregory, M. Bremer, W. Bauer, P. von R. Schleyer, N. P. Lorenzen, J. Kopf, E. Weiss, *Organometallics* **1990**, *9*, 1485.
[169] R. Hacker, E. Kaufmann, P. von R. Schleyer, W. Mahdi, H. Dietrich, *Chem. Ber.* **1987**, *120*, 1533.
[170] K. Gregory, M. Bremer, P. von R. Schleyer, P. A. A. Klusener, L. Brandsma, *Angew. Chem.* **1989**, *101*, 1261; *Angew. Chem. Int. Ed. Engl.* **1989**, *28*, 1224.
[171] D. C. Bradley, R. C. Mehrotra, D. P. Gaur, *Metal Alkoxides*, Academic Press, London, **1978**.
[172] Metal phenoxides: K. C. Malhotra, R. L. Martin, *J. Organomet. Chem.* **1982**, *239*, 159.
[173] a) P. J. Wheatley, *J. Chem. Soc.* **1961**, 4270; b) H. Dunken, J. Krause, *Z. Chem.* **1961**, *1*, 27.
[174] a) E. Weiss, *Z. Anorg. Allg. Chem.* **1964**, *332*, 197; b) E. Weiss, W. Büchner, *Angew. Chem.* **1963**, *75*, 1116; *Angew. Chem. Int. Ed. Engl.* **1964**, *3*, 152.
[175] E. Weiss, *Helv. Chim. Acta* **1963**, *46*, 2051.
[176] E. Weiss, H. Alsdorf, *Z. Anorg. Allg. Chem.* **1970**, *372*, 206.
[177] T. Greiser, E. Weiss, *Chem. Ber.* **1979**, *112*, 844.
[178] a) T. Greiser, E. Weiss, *Chem. Ber.* **1977**, *110*, 3388; b) J. E. Davies, J. Kopf, E. Weiss, *Acta Crystallogr. Sect. B* **1982**, *38*, 2251.
[179] a) E. Weiss, H. Alsdorf, H. Kühr, *Angew. Chem.* **1967**, *79*, 816; *Angew. Chem. Int. Ed. Engl.* **1967**, *6*, 801; b) E. Weiss, H. Alsdorf, H. Kühr, H.-F. Grützmacher, *Chem. Ber.* **1968**, *101*, 3777.
[180] E. Weiss, K. Hoffmann, H.-F. Grützmacher, *Chem. Ber.* **1970**, *103*, 1190.
[181] T. Greiser, E. Weiss, *Chem. Ber.* **1976**, *109*, 3142.
[182] a) H. Staeglich, E. Weiss, *Chem. Ber.* **1978**, *111*, 901; b) N. J. Turowa, B. A. Popowkin, A. W. Nowoselowa, *Z. Anorg. Allg. Chem.* **1969**, *365*, 100; c) H. D. Lutz, *ibid.* **1967**, *353*, 207.
[183] E. Weiss, U. Joergens, *Chem. Ber.* **1972**, *105*, 481.
[184] E. Weiss, W. Büchner, *Chem. Ber.* **1965**, *98*, 126.
[185] E. Weiss, W. Büchner, *Helv. Chim. Acta* **1963**, *46*, 1121.
[186] E. Weiss, W. Büchner, *Z. Anorg. Allg. Chem.* **1964**, *330*, 251.
[187] K. F. Tesh, B. D. Jones, T. P. Hanusa, *J. Am. Chem. Soc.* **1992**, *114*, 6590.
[188] V. Halaska, L. Lochmann, D. Lim, *Collect. Czech. Chem. Commun.* **1968**, *33*, 3245.
[189] G. E. Hartwell, T. L. Brown, *Inorg. Chem.* **1966**, *5*, 1257.
[190] a) See for example D. E. Pearson, C. A. Buehler, *Chem. Rev.* **1974**, *74*, 45; b) D. C. Bradley, *ibid.* **1989**, *89*, 1317; c) K. C. Caulton, L. G. Hubert-Pfalzgraf, *ibid.* **1990**, *90*, 969.
[191] a) D. Seebach, *Angew. Chem.* **1988**, *100*, 1685; *Angew. Chem. Int. Ed. Engl.* **1988**, *27*, 1624; b) see also G. Boche, *ibid.* **1989**, *101*, 286 and **1989**, *28*, 277.
[192] E. Weiss, J. Kopf, T. Gardein, S. Corbelin, U. Schümann, M. Kirilov, G. Petrov, *Chem. Ber.* **1985**, *118*, 4059.
[193] M. J. Bennett, F. A. Cotton, R. Eiss, R. C. Elder, *Nature* **1967**, *213*, 174.
[194] G. J. Bullen, R. Mason, P. Pauling, *Inorg. Chem.* **1965**, *4*, 456.
[195] M. Geissler, E. Weiss, unpublished; M. Geissler, Dissertation, Hamburg, **1987**.
[196] B. Cetinkaya, I. Gümrükçü, M. F. Lappert, J. L. Atwood, R. Shakir, *J. Am. Chem. Soc.* **1980**, *102*, 2086.
[197] S. Brooker, F. T. Edelmann, T. Kottke, H. W. Roesky, G. M. Sheldrick, D. Stalke, K. H. Whitmire, *J. Chem. Soc. Chem. Commun.* **1991**, 144.
[198] P. A. van der Schaaf, M. P. Hogerheide, D. M. Grove, A. L. Spek, G. van Koten, *J. Chem. Soc. Chem. Commun.* **1992**, 1703.
[199] a) K. G. Caulton, M. H. Chisholm, S. R. Drake, K. Folting, *J. Chem. Soc. Chem. Commun.* **1990**, 1349; b) K. G. Caulton, M. H. Chisholm, S. R. Drake, J. C. Huffman, *ibid.* **1990**, 1498; c) K. G. Caulton, M. H. Chisholm, S. R. Drake, K. Folting, *Inorg. Chem.* **1991**, *30*, 1500; d) K. G. Caulton, M. H. Chisholm, S. R. Drake, W. E. Streib, *Angew. Chem.* **1990**, *102*, 1492; *Angew. Chem. Int. Ed. Engl.* **1990**, *29*, 1483.
[200] N. Ya. Turova, E. P. Turevskaya, V. G. Kessler, A. I. Yanovsky, Y. T. Struchkov, *J. Chem. Soc. Chem. Commun.* **1993**, 21.
[201] S. C. Goel, M. A. Matchett, M. Y. Chiang, W. E. Buhro, *J. Am. Chem. Soc.* **1991**, *113*, 1844.
[202] a) M. Marsch, K. Harms, L. Lochmann, G. Boche, *Angew. Chem.* **1990**, *102*, 334; *Angew. Chem. Int. Ed. Engl.* **1990**, *29*, 308; b) S. Harder, A. Streitwieser, *ibid.* **1993**, *105*, 1108 or **1993**, *32*, 1066.
[203] a) C. G. Screttas, M. Micha-Screttas, *J. Organomet. Chem.* **1986**, *316*, 1; b) *ibid.* **1985**, *290*, 1.
[204] J. Liebig, *Ann. Chem. Pharm.* **1834**, *11*, 182.
[205] W. Büchner, E. Weiss, *Helv. Chim. Acta* **1964**, *47*, 1415.
[206] a) See for example H. Schäfer, *Angew. Chem.* **1976**, *88*, 775; *Angew. Chem. Int. Ed. Engl.* **1976**, *15*, 713; b) Electron diffraction investigations

reveal only monomers and dimers: R. J. Mawhorter, M. Fink, J. G. Hartley, *J. Chem. Phys.* **1985**, *83*, 4418.
[207] a) B. Dietrich, P. Viout, J.-M. Lehn, *Macrocyclic Chemistry*, VCH, Weinheim, **1993**; b) Y. Inoue, G. W. Gokel, *Cation Binding by Macrocycles*, Dekker, New York, **1990**.
[208] a) W. R. Moser, A. W. Langer, Jr., *Catal. Org. Synth.* **1980**, 219; b) *Polyamine-chelated Alkali Metal Compounds* (Ed.: A. W. Langer) *Adv. Chem. Ser.* **1974**, *130*.
[209] See for example a) [LiCl(en)], [LiBr(en)]: F. Durant, P. Piret, M. van Meersche, *Acta Crystallogr.* **1967**, *23*, 789; b) $[LiCl(en)_2]$, $[LiBr(en)_2]$: S. Jamet-Delcroix, *J. Chim. Phys. Phys. Chim. Biol.* **1967**, *64*, 601; c) $[LiI(en)_3]$: H. Gillier-Pandraud, S. Jamet-Delcroix, *Acta Crystallogr. Sect. B* **1971**, *27*, 2476; d) [LiI(pmdta)] (monomer): C. L. Raston, B. W. Skelton, C. R. Whitaker, A. H. White, *J. Chem. Soc. Dalton Trans.* **1988**, 987; e) solvate of LiX (X = Cl, Br, I) with tmeda: *Aust. J. Chem.* **1988**, *41*, 1925.
[210] H. Schmidbaur, A. Schier, U. Schubert, *Chem. Ber.* **1983**, *116*, 1938.
[211] H. Hope, P. P. Power, *J. Am. Chem. Soc.* **1982**, *105*, 5320.
[212] S. R. Hall, C. L. Raston, B. W. Skelton, A. H. White, *Inorg. Chem.* **1983**, *22*, 4070.
[213] a) D. Barr, R. Snaith, D. S. Wright, R. E. Mulvey, K. Wade, *J. Am. Chem. Soc.* **1987**, *109*, 7891; b) D. Barr, M. J. Doyle, R. E. Mulvey, P. R. Raithby, R. Snaith, D. S. Wright, *J. Chem. Soc. Chem. Commun.* **1988**, 145.
[214] P. von R. Schleyer, D. Hoffmann, D. Stalke, M. Geissler, E. Weiss, G. Sheldrick, unpublished.
[215] M. Geissler, C. Hagen, E. Weiss, G. Sheldrick, unpublished. Crystal data: orthorhombic, *Pbcn*, $a = 1263.1$, $b = 2006.8$, $c = 1832.8$ pm, $Z = 4$ tetramers.
[216] a) C. L. Raston, B. W. Skelton, C. R. Whitaker, A. H. White, *Aust. J. Chem.* **1988**, *41*, 1621; b) C. Hagen, S. Corbelin, E. Weiss, unpublished.
[217] a) C. L. Raston, C. R. Whitaker, A. H. White, *Aust. J. Chem.* **1989**, *42*, 1393; b) C. Hagen, S. Corbelin, E. Weiss, unpublished.
[218] C. L. Raston, C. R. Whitaker, A. H. White, *Aust. J. Chem.* **1988**, *41*, 823.
[219] a) T. P. Hanuska, *Polyhedron* **1990**, *9*, 1345; b) M. Rieckhoff, U. Pieper, D. Stalke, F. T. Edelmann, *Angew. Chem.* **1993**, *105*, 1102; *Angew. Chem. Int. Ed. Engl.* **1993**, *32*, 1079.
[220] T. Kottke, D. Stalke, *J. Appl. Crystallogr.* **1993**, in press, and references therein.

Water-Soluble Ligands, Metal Complexes, and Catalysts: Synergism of Homogeneous and Heterogeneous Catalysis

By Wolfgang A. Herrmann* and Christian W. Kohlpaintner*

Dedicated to Professor Ernst Otto Fischer on the occasion of his 75th birthday

Rapid developments in the field of catalysis are leading to an increased demand for tailor-made catalysts. Water-soluble complex catalysts, which are being intensively investigated at the present time, combine the advantages of homogeneous and heterogeneous catalysis: simple and complete separation of the product from the catalyst, high activity, and high selectivity. From the large number of available water-soluble ligands, the appropriate catalysts can be developed for many reactions. The industrial applications in the fields of hydrogenation and hydroformylation have already indicated the wide scope of this type of catalyst. In addition, the annual production of 300000 tons of butyraldehyde through application of water-soluble rhodium complexes at Hoechst AG in Oberhausen, Germany, has demonstrated the industrial importance of the concept of complex-catalyzed reactions in aqueous two-phase systems. The efficient operation of catalytic processes increasingly requires the loss-free recycling of the noble metal catalyst, and this can be simply and economically realized in two-phase systems. Special applications in biochemical problems open up developments in the field of water-soluble transition metal complexes that far transcend the familiar kinds of homogeneous catalysis. In the near future, the investigation and application of metal complex catalysts that are compatible with the physiological, cheap, and environmentally friendly solvent, water, is likely to become a high priority in catalysis research.

1. Introduction[**]

The chemistry of water-soluble ligands and their metal complexes is presently undergoing very rapid growth. The special advantages of water-soluble catalysts are being increasingly recognized, as is borne out alone by the number of publications and patents. Following the introduction to industry of the valuable Ruhrchemie/Rhône–Poulenc process in 1984 there was spate of publications, which is still continuing (Fig. 1). Meanwhile, about a dozen research groups applied for patents, and the number of these now even surpasses the number of publications in the open literature.

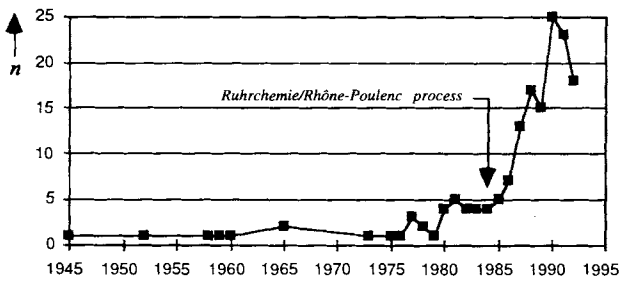

Fig. 1. Number (n) of publications annually on water-soluble complex ligands and catalysts (excluding patent applications).

What are the advantages of water-soluble catalysts? The basic problem of homogeneously catalyzed processes is the separation of the product phase from the (molecular) catalyst, which is soluble in it. The process stages necessary to achieve this usually include thermal operations such as distillation, decomposition, transformation, and rectification, which normally lead to thermal stresses on the catalyst. These can cause decomposition reactions and progressive deactivation during the lifetime of the catalyst. Furthermore, thermal separation processes seldom give quantitative recovery of the catalyst, which causes loss of productivity through loss of metal.

Product separation is simpler for two-phase systems incorporating water-soluble catalysts as shown in Figure 2. The

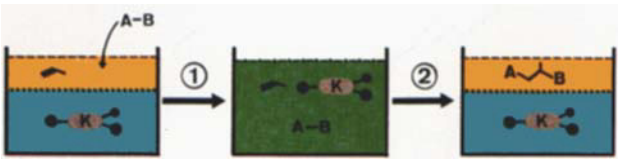

Fig. 2. General principle of two-phase catalysis in water. The metal complex catalyst (K), which is solubilized by hydrophilic ligands, converts the starting material (in this case, propene and A–B, such as CO/H_2) to the products, which can be separated from the catalyst (medium) by phase separation. Thorough mixing of the phases is necessary during the catalytic process.

hydrophilic catalyst, which is insoluble in the organic product phase, is an (organometallic) coordination complex, and as such is molecularly well defined like conventional homogeneous catalysts. It brings about the catalytic reactions (e.g., C–C coupling) in the aqueous phase or at the phase boundary, and is removed from the desired product at the end of the reaction by a simple phase separation. Thermal separation processes, which can have a detrimental ef-

[*] Prof. Dr. W. A. Herrmann
Anorganisch-chemisches Institut der Technischen Universität München
Lichtenbergstrasse 4, D-85747 Garching (FRG)
Telefax: Int. code + (89)3209-3473
Dr. C. W. Kohlpaintner
Hoechst AG, Zentralforschung (Hauptlaboratorium I)
Postfach 80 03 20, D-65926 Frankfurt am Main (FRG)
Telefax: Int. code + (69)33 1320

[**] Often used abbreviations: tpp = triphenylphosphane; tppts = trisodium salt of 3,3',3''-phosphanetriylbenzenesulfonic acid; tppms = sodium salt of 3-diphenylphosphinobenzenesulfonic acid.

fect on the active life of the catalyst, are thereby avoided. Because of the high polarity of the water-soluble catalyst and its consequent insolubility in the organic phase, the loss rate is often below the limit of detection.

Rates achievable with two-phase systems are strongly dependent on the polarity of the reacting substrate. For example, the rhodium-catalyzed hydroformylation of propene using the water-soluble complex $[HRh(CO)(tppts)_3]$ takes place with the apparent activation energy of a homogeneous reaction, whereas with 1-hexene the rate-determining step appears to be mass transfer.[1] Therefore, although overall reaction rates are lower than in homogeneous reactions, the simplicity of the process for separating the product from the catalyst compensates for this disadvantage.

Another technique, which has been practiced for a long time without any spectacular success, is to immobilize solid complex catalysts on solid ("stationary") supports. Here, the continuous loss of the metal ("bleeding", "leaching") and low reaction rates are serious disadvantages. However, the immobilization of a catalyst in a "mobile phase", that is, an aqueous solution immiscible with the product phase, represents an almost ideal combination of homogeneous and heterogeneous reaction processes.

This article reviews current developments in both research and technology, and indicates the areas where this new class of catalysts has gained acceptance within only a few years to become "state of the art". The review covers the classification of water-soluble ligands and their metal complexes to catalytic uses in the laboratory and industry, and special applications in biochemistry.

2. Concept of Two-Phase Catalysis

Under the simplified assumption that all starting materials E are in solution, three variations of the two-phase process of homogeneous catalysis can be considered (Fig. 3): In the simplest case the solubilities of the components E and of the catalyst K are so different that a perfect phase separation results (Figs. 2 and 3a). A workup step for the product P follows, depending on its properties and purity, and as a rule is a distillation. The technical desirable ideal would be a catalyst K which formed its own phase in which the components E and the products P are not in the least soluble (Fig. 2 and 3a). If the product P is partly dissolved in the catalyst phase, an extraction is necessary according to Figure 3b, and is performed with the phase of E (for example, petroleum) which is completely insoluble in K (for example, water). It is also possible that a two-phase system forms from an initially uniform phase during the reaction, because the product P is insoluble in the original medium of the catalyst (Fig. 3c). A phase separation in the skimmer enables continuous return of the catalyst to the reactor. Only when the products P are partly soluble in the catalytic medium K is a solvent extraction step (related to a distillative workup) necessary for the whole contents of the reactor (Fig. 3c).

The concept of two-phase catalysis was first realized industrially in the "*S*HELL *H*igher *O*lefins *P*rocess" (SHOP) designed by W. Keim et al.[2a-c] In this procedure ethylene is polymerized at 80–120 °C and 70–140 bar in a polar phase of 1,4-butanediol that also contains the organonickel catalyst to afford oligomers (mainly linear C_{4-20}-α-olefins).

Wolfgang A. Herrmann was born in 1948 in Kelheim/Donau (Bavaria). After studying chemistry (Diplom at the Technische Universität München) under E.O. Fischer (1971), he obtained his doctorate on a theme from early organometallic stereochemistry at the Universität Regensburg with Henri Brunner (1973). From 1975–1976 he pursued his research interests in the USA at Penn State University with P.S. Skell, and in 1978 completed his habilitation with a thesis on "Organometallic Syntheses with Diazoalkanes". He was appointed Professor at the Universities of Regensburg (1979) and full professor in Frankfurt (1982). In 1985 he accepted the chair at the Technische Universität München as successor to E.O. Fischer. His area of research is synthetic and catalytic chemistry, mainly in the field of organometallic chemistry. He is author of 350 original papers and holder of 30 patents, and has received many honours including the Karl Winnacker Fellowship (1979–1983), the Leibniz Award of the Deutsche Forschungsgemeinschaft (1986), the German/French Alexander von Humboldt Award (1988), the Otto Bayer Prize (1990), and the Max-Planck-Forschungspreis (1991). He is member of the Akademie der Wissenschaften und Literatur zu Mainz (1990) and Honorary Doctor of the University of Lyon, France (1990).

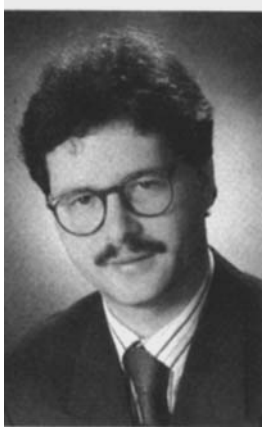

Christian W. Kohlpaintner was born in 1963 in Schloßberg, near Rosenheim (Bavaria), and began his study of chemistry at the Technische Universität München in 1984. In October 1989, he joined the research group of Prof. W.A. Herrmann. He completed his Diplom in March 1990 on new water-soluble phosphane ligands and catalysts, and received the Ph.D. students' Award from Hoechst AG. He completed his Ph.D. thesis in August 1992 following work on the Ruhrchemie/Rhône–Poulenc process, the two-phase hydroformylation process which is used on industrial scale. He then joined Hoechst AG and has worked in the Central Research Department at Frankfurt since the beginning of this year. He has coauthored 6 papers and holds 7 patents.

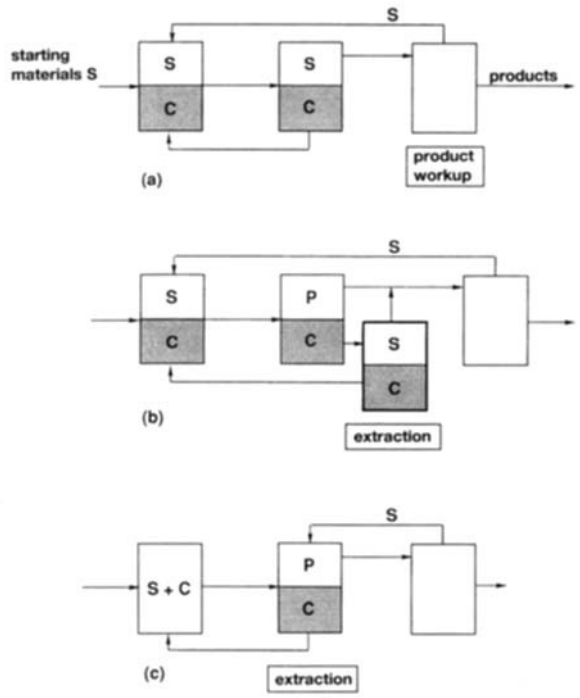

Fig. 3. Simplified flow diagram for two-phase catalysis: a) Product(s) P are completely insoluble in the medium that contains the catalyst C; b) product(s) P are soluble in the medium containing C; c) formation of the second phase occurs during catalytic process; cf. text.

The catalyst is formed from $[Ni(1,5\text{-cod})_2]$ and $(C_6H_5)_2PCH_2COOH$. The products separate as a second, transparent liquid phase above the 1,4-butanediol and can therefore be removed without difficulty. After this simple catalyst/product separation, catalyst traces are washed out of the olefin phase in the phase separator. The distillation fractions of the subsequent purification are either marketed directly or fed into the next two SHOP catalytic steps of isomerization and metathesis (cf. Fig. 4). This combination of homogeneous and heterogeneous catalytic steps now occupies a key position in olefin chemistry.

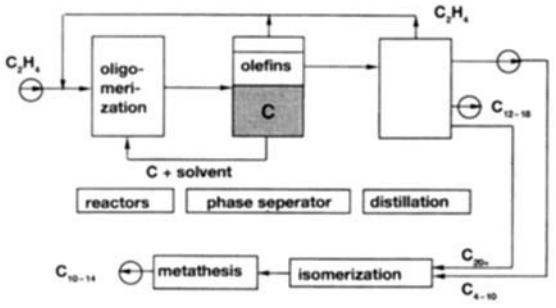

Fig. 4. Simplified flow diagram for the first catalytic stage of the *S*HELL *h*igher *o*lefins *p*rocess (SHOP). The subsequent steps of isomerization and metathesis are not given in detail.

A process for the oligomerization of butadiene developed along the lines of this technology, which has been known since 1968, likewise employs 1,4-butanediol as polar phase. Thus, Keim et al.[2d, e] describe the dimerization of 1,3-butadiene to 1,3,7-octatriene with Pd/phosphane catalysts in acetonitrile with isooctane as extractant for the product. On addition of phthalic acid this reaction yields octylphthalates. Surprisingly, no further information on the use of highly polar solvents as the second phase is available in the literature, although in many cases miscibility gaps exist with saturated hydrocarbons, for example, methanol, acetonitrile, nitromethane, dimethylsulfoxide (DMSO), dimethylformamide (DMF), ethyleneglycol, and sulfolan. Nevertheless, reactions of these solvents with homogeneous catalysts are known, and therefore the influence of the second phase on the chemical and kinetic characteristics of the catalytic cycle must be taken into account. This treatise, however, aims to concentrate on water as catalytic medium.

3. Classes of Water-Soluble Phosphanes

Phosphanes can be converted into water-soluble derivatives by the introduction of polar groups, including sulfonate, carboxylate, ammonium, phosphonium, and hydroxyl groups.[3-7] A classification based on these functional groups seems expedient and is shown in Scheme 1. Other hydrophilic substituents, for example, phosphate groups, have so far been of little importance.

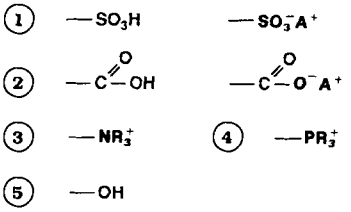

Scheme 1. Functional groups in water-soluble phosphanes (A^+ = cation).

3.1. Sulfonated Phosphanes

3.1.1. Water-Soluble Phosphanes by Direct Sulfonation

Owing to their diverse coordination chemistry, sulfonated phosphanes at present constitute the most widely used class of ligands in water-soluble metal complexes, especially in catalysis. Apart from the compound tppts (**1**), which is used in a rhodium catalyst for the production of butyraldehyde on an industrial scale, the monosulfonated derivative tppms (**2**) must be mentioned. Both these compounds (sodium salts) can be obtained by the sulfonation of triphenylphosphane with oleum and subsequent neutralization with NaOH. The technique of sulfonating water-insoluble ligand precursors can be applied to di- and polydentate, and also chiral phosphanes, for example, **3**–**9** (Scheme 2).[8-12] The sulfonate group mostly occupies the position *meta* to the phosphorus atom. Tris(*p*-fluorophenyl)phosphane can be sulfonated in the *meta* position.[13] The introduction of a sulfonate group by reaction with oleum is not limited to arylphosphanes. It can also be carried out with the tris(ω-phenylalkyl)-phosphanes $P[(CH_2)_n(C_6H_5)]_3$ ($n = 1$, 2, 3, and 6).[14] Here, the sulfonate groups, as expected, occupy the *para* and, to a lesser extent, the *ortho* positions.

The sulfoxylic derivative of 1,2-bis[di(*m*-sodium-sulfonatophenyl)phosphino]ethane (dppets) is now also available

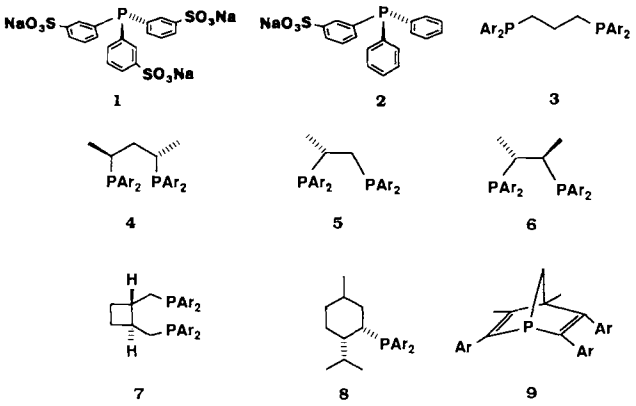

Scheme 2. Water-soluble phosphanes obtained by direct sulfonation with oleum (Ar = m-$C_6H_4SO_3Na$; for **9**, Ar = p-$C_6H_4SO_3Na$).

as a ligand for hydroformylation in the two-phase process since direct sulfonation of 1,2-bis(diphenylphosphino)-ethane(dppe) by means of oleum (20% SO_3) was successful. However, the Rh/dppets catalyst is not very active in hydroformylation.[67]

Because of the oxidizing effect of oleum, an appreciable fraction of the phosphane is converted into the phosphane oxide during the process of sulfonation, which complicates the purification of water-soluble phosphanes substantially (Section 4). Complete oxidation affords sulfonated phosphane oxides, which can be reduced by trichlorosilane after conversion to sulfonic esters.[15] The water-soluble ligands are available after hydrolysis of the ester. The use of this laborious method is meaningful only for phosphanes that are very sensitive to oxidation. It is not likely to increase in importance, however, since we discovered an efficient direct sulfonation method in which the formation of phosphane oxide is strongly inhibited.[16]

3.1.2. *Introduction of the Sulfonate Group during Synthesis of the Aryl Phosphane*

Sulfonate groups can be introduced during the course of phosphane synthesis. For example, as shown in Equation (1), the sodium salt of p-diphenylphosphinobenzenesulphonic acid (**10**) is formed from potassium diphenylphosphide and sodium p-chlorobenzenesulfonate.[17]

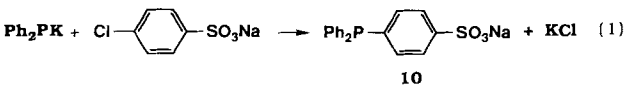

(1)

Water-soluble phosphanes of the type $R_{3-n}P$-$(p\text{-}C_6H_4SO_3K)_n$ (R = C_6H_5, 2-pyridyl, 3-pyridyl; $n = 1-3$) can be obtained by the reaction of potassium p-fluorobenzenesulfonate with PH_3 or primary or secondary phosphanes in the "superbasic" medium DMSO/KOH.[18] The unpleasant properties of PH_3 have to be mastered here, but otherwise this is a very powerful, general synthetic method. Surprisingly hydrolysis-resistant sulfonated phenylphosphites have recently been prepared.[19] The ammonium salts, in particular, are more water-stable than triphenylphosphite: whereas $P(OC_6H_5)_3$ is decomposed within 3 h, the hydrolysis of the derivative $P[p\text{-}OC_6H_4SO_3\{NH(i\text{-octyl})_3\}]_3$ is only complete after 24 h.

3.1.3. *Phosphanes with Peripheral Hydrophilic Functional Groups*

Functionalized phosphanes that carry sulfonic acid groups in one or more side chains are also known. The class of substances developed by Whitesides et al.[20] is represented by the example in Equations (2a) and (2b). The water-soluble phosphane **15** is obtained by acylation of bis(2-diphenylphosphinoethyl)amine (**11**) with the carboxylic chloride (**12**) of phthalic anhydride followed by reaction with sodium taurinate (**14**). This synthesis principle can be applied to many functionalized acid chlorides. The opening of the anhydride **13** by **14** is unspecific, so two constitutional isomers **15a** and **15b** are always obtained. The maximum attainable solubility in water is 0.3 mol L^{-1}. Further work on this class of compounds was carried out by Sinou et al.[21] The tertiary phosphane $(C_6H_5)_2PCH_2CH_2SO_3Na$ was prepared from sodium diphenylphosphide and the sodium salt of 2-bromoethylsulfonic acid.[22]

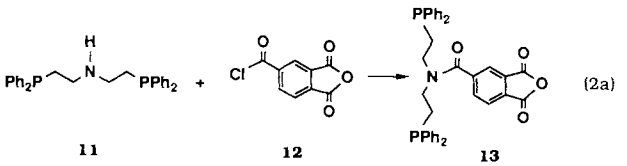

(2a)

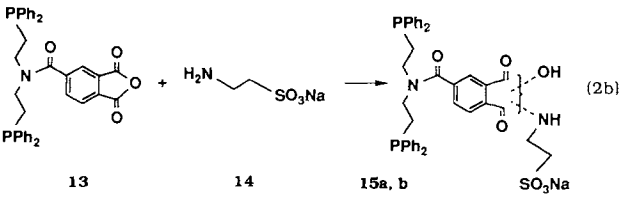

(2b)

Another route to water-soluble phosphane ligands through ring opening of sultones was established by Oehme et al.[23,24] Fell et al. extended this concept to tris-(pyridyl)phosphanes, which can be prepared in water-soluble form by sulfoalkylation with 1,2-alkanesultones.[25] This procedure results in zwitterionic sulfobetaines with n = 0, 3, 5, 7, and 11 [Eq. (3)].

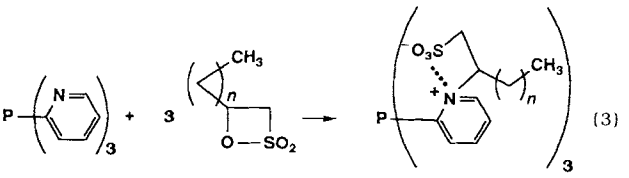

(3)

3.2. Phosphanes with Quaternized Aminoalkyl and Aminoaryl Groups

Water-soluble phosphanes can also result from the quaternization of the nitrogen atom of aminoalkyl and aminoaryl

phosphanes. However, before the nitrogen atom can be alkylated, the (more reactive) phosphorus center has to be protected, either by oxidation or by coordination to a metal. Subsequent reduction or decomplexation, respectively, yields the desired phosphane ligands. The most important example of this class of substances is "amphos" (**16**), first synthesized by Baird et al.[26-28] Tóth et al.,[29] Peiffer et al.,[30] and Nagel et al.[31] were able to extend this synthesis principle to other phosphanes (Scheme 3).

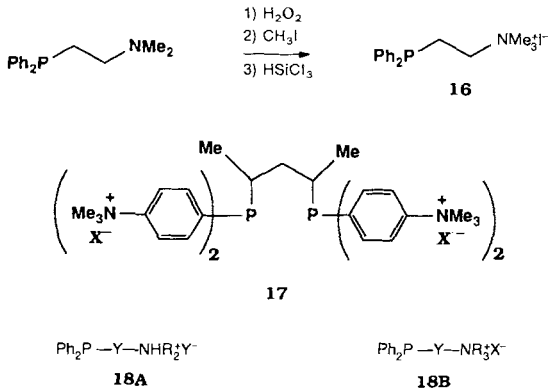

Scheme 3. Aminoalkyl- and aminoarylphosphanes (Y = $-CH_2CH_2-$, $-CH(CH_3)CH_2-$, $-CH_2CH(CH_3)CH_2-$; R = CH_3) made water-soluble by quaternization of the N atom.

3.3. Carboxylated Phosphanes

Phosphanes with carboxylic groups were some of the earliest investigated water-soluble phosphanes. The first example **19** was prepared by Mann et al.[32] in 1952 through cyanoethylation of diphenylphosphane with subsequent nitrile saponification. The development of the "carboxyalkylphosphanes" (phosphinocarboxylic acids) was carried out predominantly by the research groups of Rauhut, Issleib, and Podlahová.[33-38] The most important example is the phosphane analog of ethylenediaminetetraacetic acid (H_4edta).[39] It is obtained as an air-stable monohydrate of the tetrasodium salt (**20**). A new short review of the catalytic uses of the carboxyalkylphosphanes was published by Jegorov and Podlahová.[40]

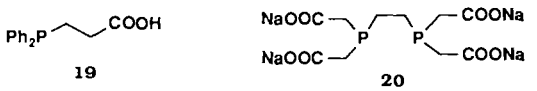

The history of the phosphinobenzoic acids **21** goes back as far as 1945. Gilman and Brown synthesized *meta*- and *para*-diphenylphosphinobenzoic acid. Not till 1977 did Luckenbach and Lorenz[42] succeed in preparing the *ortho* isomer. Further work was done by Schumann et al.,[43] and Lindner reviewed the progress.[44] A newer report refers to a phosphorylated derivative **22** of maleic acid.[45]

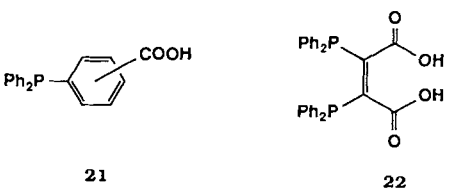

Phosphanorbornadienes with a carboxylic anhydride function can be obtained by [4 + 2] cycloaddition of 3,4-dimethylphosphol to maleic anhydride and subsequent rearrangement [Eq. (4)].[46] Alkaline hydrolysis yields the water-soluble carboxylates.

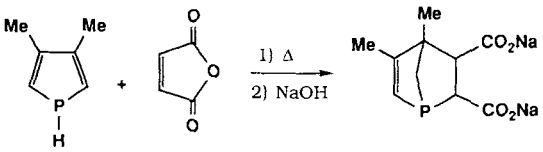

(4)

3.4. Phosphanes with Hydroxyalkyl and Polyether Substituents

By varying the length of the polyether chain of substituted phosphanes, the solubility can be deliberately adjusted. Bisphosphanes of the type **23** ($n = 5$) are insoluble in water. For $n \geq 16$ (e.g., $n = 42$), however, they are extremely soluble.[47] Other examples related to **23** are the class of compounds **24** ($n = 12$, 16, 110) and **25** ($n = 18$).[48,49] The number n gives the average "degree of polycondensation". Supplementary work was performed by Okano et al.,[50] who were the first to prepare phosphanes **26** substituted by crown ethers.[51,52]

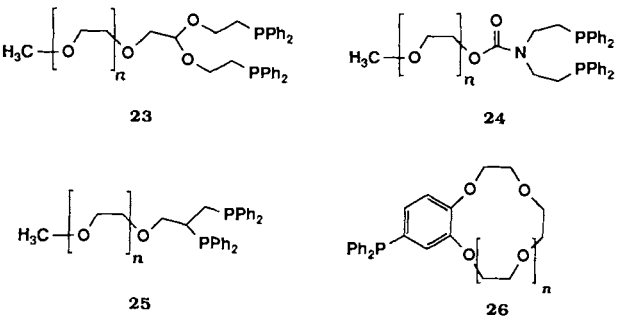

Investigations into water-soluble hydroxyalkyl-substituted phosphanes were carried out by Chatt et al. in 1973.[53] The phosphanes are significantly soluble in water only if they carry several hydroxyalkyl groups.[54] The water-soluble, commercially available trisubstituted phosphane $P(CH_2OH)_3$ is being tested in the form of metal complexes for catalytic properties in the addition of PH_3 to formaldehyde.[55] Homoleptic nickel, platinum, and palladium complexes of this phosphane were synthesized, and the elucidation of the structure of the palladium complex $[Pd\{P(CH_2OH)_3\}_4 \cdot CH_3OH]$ was carried out by single crystal X-ray structural analysis.[56]

Finally ethylene glycol derivatives react with sugar diacetonides to form monoallyl ethers that can be brominated at the double bond. Successive reaction with phenyl- and diphenylphosphanes yields hydrophilic phosphanes exhibiting a sugar function in the side chain.[57]

3.5. Phosphinoalkylphosphonium Salts

A new class of water-soluble phosphanes, named "phophos", was opened up in 1991 by Baird et al.[58] Monoquaternization of bisphosphanes yields phosphinoalkylphosphonium salts $[Ph_2P(CH_2)_nPMe_3]X$, where $n = 2$, 3, 6, or 10, and $X = NO_3^-$, Cl^-, or PF_6^-. The synthesis proceeds according to Equations (5a) and (5b). For increasing chain

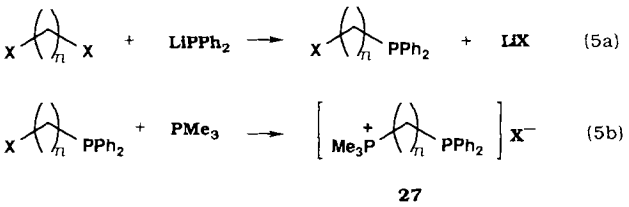

(5a)

(5b)

length n, the more reactive bromine (or iodine) derivative must be used instead of the chloro compound. The halides are converted into the more stable nitrates and hexafluorophosphates by ion exchange or salt metathesis. The rhodium-catalyzed hydrogenation of 1-hexene gave the following activity series: [6]-phophos > [10]-phophos ≥ [3]-phophos > [2]-phophos, where the numbers correspond to the chain length n. The reasons for this particular series remain unclear. The X-ray structural analytical characterization of the rhodium complex [(nbd)RhCl([2]-phophos)]PF_6 (nbd = norbornadiene) and the attachment of the free ligands to cation exchangers[59] underline the rapidly growing interest in this class of compound.

3.6. Other Ligands

As the present article concentrates on metal complexes and catalysts whose solubility in water depends on hydrophilic phosphane ligands, the following topics are not considered: phase-transfer reagents, saltlike metal catalysts such as $Pd(OAc)_2$ and Pd(edta), metal complexes of sulfonated 2,2'-bipyridine[60, 61] and alizarin,[62, 63] metal complexes of sulfonated phenanthroline derivatives,[64] water-soluble porphyrins, and cyclopentadienyl ligands.[65] A summary is given in Ref. [7].

4. Purification of tppts and its Metal Complexes

Besides their catalytic uses, the characterization of the water-soluble complexes is of interest. Firstly, their bond strengths, complex geometry, and coordination properties, for example, can be compared with those of analogous water-insoluble complexes.[83] Secondly, well-defined water-soluble model complexes are essential for the understanding of the individual steps in the catalytic cycle of two-phase systems, and in kinetic studies. For instance, the Hieber base reaction could also be successfully applied to $[Co_2(CO)_6(tppts)_2]$, the water-soluble pendant of $[Co_2(CO)_6(PPh_3)_2]$, which is converted into the carbonyl metalate $Na[Co(CO)_3(tppts)]$ in aqueous NaOH at pH > 10.[67]

The first synthesis of tppts (**1**)[66] was carried out some years after Chatt's first reports on the monosulfonation of triphenylphosphane (tpp).[68] Although it was possible to obtain the triply sulfonated arsenic compound **28**, triphenylphosphane only gave the monosulfonated tppms (**2**). In 1975, E. G. Kuntz of Rhône-Poulenc Ind., Lyon, was able to prepare the sodium salt **1** of tppts according to Equation (6) by prolonging the reaction time, obtaining it in a purity adequate for industrial use on repeated precipitation from methanol/water mixtures.

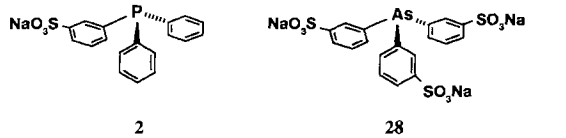

2 28

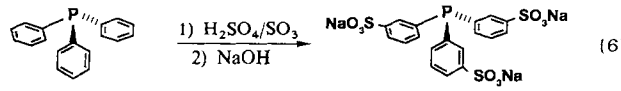

(6)

1

The excellent solubility of tppts in water (about 1100 $g\,L^{-1}$)[69] and its related insolubility in almost all organic solvents prepared the way for its use in two-phase catalytic processes on an industrial scale. However, for a long time there was no access to analytically pure tppts and its metal complexes, mainly due to problems of separation. The phosphane oxides produced during sulfonation of tpp could not be completely removed for chemical reasons ($-SO_3H$ vs. $-P{=}O$), and the separation of the various sulfonated products also presented problems. Only recently has it been possible to avoid the oxidation of the phosphane during sulfonation with oleum.[16] Optimization of temperature, reaction time, and oleum concentration can also help to reduce the extent of the oxidation of easily oxidizable phosphanes.[1]

The use of "soap chromatography" for the purification of water-soluble mono- and bisphosphanes is only useful for analysis, but not for preparative work.[70, 71] Alone the poor availability of an exactly defined ligand complicates the preparation of analytically pure metal complexes. Difficulties are caused by slight oxidation of the phosphane by atmospheric oxygen in the aqueous phase. Analytically pure metal complexes of tppts could therefore not be obtained with conventional methods of purification.[72-74] The breakthrough came from a change to the use of gel permeation chromatography, adapted to the solution of this problem, with cyclodextrane as the stationary phases.[75-77] The experimental apparatus is shown in Figure 5.[78] This was used for the first convenient preparation of analytically pure metal complexes of tppts on laboratory scale. The metal complexes were obtained by direct synthesis, by ligand exchange, and through addition methods in which the water-soluble phosphane combines with a coordinatively unsaturated complex intermediate without displacing another ligand. With this purification method over 40 metal complexes of the ligand tppts were prepared analytically pure and characterized (Fig. 6).[77] Spectroscopic data for tppts and its oxide have been published.[82]

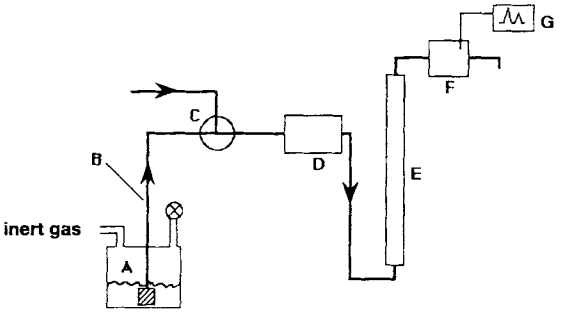

Fig. 5. Experimental equipment for gel permeation chromatography for the purification of metal complexes of tppts. The eluent water is pumped from the storage vessel A through the flexible poly(vinylidene fluoride) ("Viton", "Isoversinic") tube B, the peristaltic pump D, and the three-way valve C into the column E, which is filled with the gel. A UV/VIS detector or refractometer F fitted with a recorder G is connected to the exit of the chromatography column. As many water-soluble metal complexes and ligands absorb UV strongly, the fractions are sometimes difficult to separate with a UV detector. In these cases, a refractometer should be used, which, after compensation for water, detects very low amounts of substance. The chromatography is operated in "upside-down" mode as this gives the best separation results (no tailing). The stationary phases used are standard gels from LKB Pharmacia (Sephadex G15, G25, and G50) and Merck (Fractogel TSK HW-40F). A detailed description of the equipment and its function has been published [76, 78].

An example of the efficiency of gel permeation chromatography as a diagnostic method is the revision of the formula of the complex "[Ni(tppts)$_4$]",[69] which should be formulated as [Ni(tppts)$_3$].[77] The rhodium complexes, isolated as pure substances, were crucial in the elucidation of degradation steps occurring in the two-phase hydroformylation of propene catalyzed by Rh–tppts catalysts.[79] More recent investigations show that the purification method is not only successful for tppts, but is applicable to a wide range of water-soluble ligands and their metal complexes.[12]

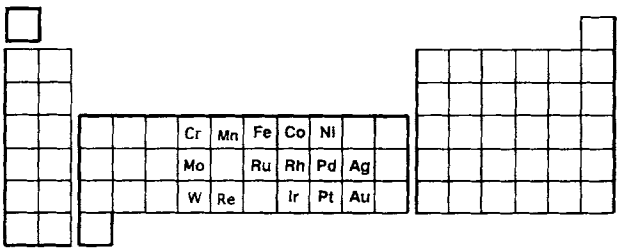

Fig. 6. Central atoms of tppts–metal complexes characterized to date.

The X-ray characterization of a tppts–metal complex was recently carried out by Darensbourg et al.[80] UV irradiation of [W(CO)$_6$] in methanol, according to Equation (7), caused the labile methanol adduct of the W(CO)$_5$ intermediate to react with solid tppts to give the desired complex [W(CO)$_5$(tppts)]. After complexation of the sodium ions by kryptofix-[2.2.1], **29** crystallizes out of the solvent mixture THF/methoxyethanol/acetonitrile. Crystallization and structural characterization of tpp, sulfonated in the *para* position, is similarly performed.[18] Bartik et al. report the molecular structure of [Co$_2$(CO)$_6$(tppts)$_2$].[67]

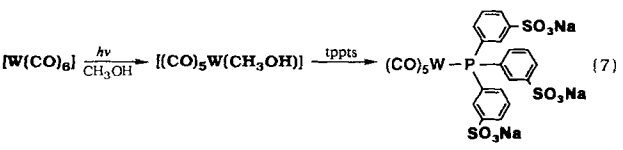

29 (with Kryptofix [2.2.1])

The steric demand of the tppts ligand is about 20% greater than that of triphenylphosphane (tpp). The cone angle θ according to Tolman[81] is 170° for tppts (tpp: $\theta = 145°$), and is the same as that of tricyclohexylphosphane (PCy_3, Table 1). This explains the tendency of tppts to form complexes in which the transition metal has a lower coordination number.[75, 76] Thus, the compound "[HRh(tppts)$_4$]", unlike [HRh(tpp)$_4$], is unknown.[77] The linear relationship between ^{31}P NMR shifts and the cone angle in [L$_2$PdCl$_2$] complexes has been stressed.[14] For steric reasons, sulfonated bisphosphane chelate ligands, for example biphenyl derivatives, can more efficiently differentiate regio- and stereospecificity if the conformative mobility of the ligand is limited. This possibility for control of a reaction has so far hardly been recognized.

Table 1. Cone angles θ according to Tolman [81] of some phosphanes.

Phosphane ligand	θ [°]	Phosphane ligand	θ [°]
PH_3	87	PPh_3	145
PF_3	104	$P(m\text{-}C_6H_4F)_3$	145
$P(OMe)_3$	107	PCy_3	170
PMe_3	118	$P(m\text{-}C_6H_4SO_3Na)_3$	170 [a]
$P(OiPr)_3$	130	$P(o\text{-Tol})_3$	194
$P(CF_3)_3$	137	$P(2,4,6\text{-}Me_3C_6H_2)_3$	212

[a] From Darensbourg et al. [80].

5. Hydrogenation with Water-Soluble Catalysts

5.1. Reduction of Achiral Unsaturated Substrates

The reduction of CC- and OC-unsaturated compounds was the first application of water-soluble catalysts.[84–87] Dror has stated that cosolvents are necessary for acceptable hydrogenation rates.[85] A large number of different catalysts and substrates have been studied (Table 2). The TOFs

Table 2. Hydrogenation of unsaturated compounds with water-soluble catalysts [a].

Catalyst	$n_{Cat.}$ [M]	Substrate	TOF [b]	Ref.
$RhCl_3$/**2**	1.3×10^{-3}	cyclohexene	3.1	[85]
[HRu(OAc)(**2**)$_3$]	1.0×10^{-5}	[c]	25–74	[86]
[RuCl$_2$(**2**)$_2$]	1.0×10^{-5}	[c]	164	[86]
[HRuCl(**2**)$_3$]	5.0×10^{-6}	[c]	92–198	[86]
[RhCl(**2**)$_3$]	2×10^{-3}	hexenes		[3]
[RuHCl(**2**)$_3$]	3×10^{-3}	hexenes		[3]
Rh/**13**	8.0×10^{-6}	**36** [d]	1.6–200	[20]
Rh/**13**	–	**36**	>275	[20]
Rh/**14**	2.5×10^{-3}	Styrene	14–71	[93]
Rh/**14**	2.5×10^{-3}	1-hexene	20–84	[93]
RhCl(**2**)$_3$	1.0×10^{-3}	**36**	1270	[94]
[PdCl$_2$(**31**)$_2$]	5.0×10^{-5}	**39** [d]	<10640	[95]
[RuCl$_2$(**2**)$_2$] [e]	1.5×10^{-5}	RCH=CHCHO	100–230	[91]
Ru/**1** [f]	4.8×10^{-5}	CH_3CH_2CHO	320–360	[96]
Ru/**1** [f]	1.0×10^{-4}	RCH=CHCHO	13–194	[89]
Rh/**1** [f]	5.0×10^{-5}	RCH=CHCHO	25–1260	[89]
Rh/**27**	6.5×10^{-5}	1-hexene	12–296	[58]

[a] $p(H_2) = 1$ bar. [b] TOF (*t*urnover *f*requency) defined as mol(product) mol(catalyst)$^{-1}$ h^{-1}. Note that TON (*t*urnover *n*umber) is defined differently: mol(product) mol(catalyst)$^{-1}$. [c] RC(O)COOH and RCH=CHCOOH. [d] See Section 5.2 for formulas. [e] Sodium formate as hydrogen source. [f] $p(H_2) = 20$–50 bar.

(*turnover frequencies*—definition in Table 2) are in general low, but can be increased by the use of cosolvents such as methanol or ethanol. The rates are limited mainly by the low solubility of the unsaturated substrate in the aqueous solution of the catalyst. However, the question where the reaction takes place—phase boundary, organic phase, or aqueous phase—has hardly been investigated and is still unclear. From the comparison of the catalysis results with $[RuHCl(tpp)_3]$ (homogeneous) and $[RuHCl(tppms)_3]$ (two phases), Wilkinson concludes that the hydrogenation of unsaturated substrates in the two-phase system proceeds considerably more slowly. The low rate of hydrogenation is due to the necessary diffusion of the hydrogen to the alkene/water interface. In this way, the isomerization, which is the substantially slower reaction, can compete with the hydrogenation. However, the hydrolytic cleavage of water-soluble ligands, for example by cleavage of the dioxolan ring in PGE-17-DIOP (**30**), does not support the low reaction rates,[47] as the reduction in reactivity applies to all water-soluble catalysts.

New work by Rhône–Poulenc Ind. with ruthenium and rhodium tppts complexes shows that hydrogenation in simple two-phase systems (aqueous/organic) is possible without cosolvents.[88, 89]

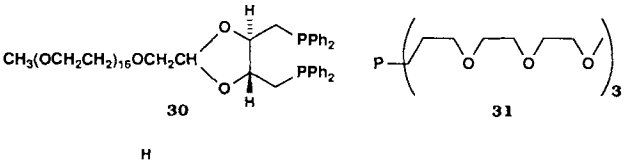

30 **31**

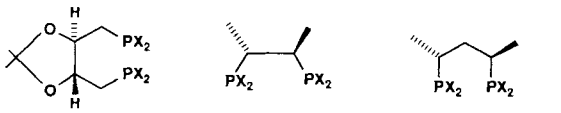

32 **33** **17**

$X = [p\text{-}C_6H_4(NHMe_2)]^+, [p\text{-}C_6H_4(NMe_3)]^+$

One valuable application is the selective reduction of α,β-unsaturated aldehydes to unsaturated alcohols according to Equation (8).[89]

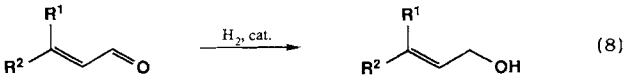

(8)

A catalyst formed from $RuCl_3$/tppts reduces 3-methyl-2-butenal to 3-methyl-2-buten-1-ol ("prenol") with 96% selectivity ($R^1 = R^2 = CH_3$) and 84–99% conversion. Other CC-unsaturated aldehydes are also efficiently reduced (selectivity ≥ 97%). Analogous iridium complexes are less active. The selectivity of ruthenium is the reverse of that observed with the Rh–tppts system, as in this case the C–C double bond in the α-position is reduced. Under 20–40 bar (2–4 MPa) pressure of hydrogen, the selectivity is >95% at 30–80 °C (conversions are mostly around 90%).

Sodium and ammonium formates are also suitable as hydride donors for the hydrogenation of α,β-unsaturated and aromatic aldehydes with water-soluble Ru complexes.[90, 91] With $[RuCl_2(tppms)_2]$, both the catalyst and the formate are in the aqueous phase; the phase-transfer problem associated with catalysts not soluble in water and aqueous formate solutions does not arise.[92] Aromatic aldehydes can be almost quantitatively hydrogenated, with the exception of aromatic aldehydes bearing in the *ortho* position substituents that can coordinate (e.g., 2-hydroxy-1-naphthaldehyde or 2-hydroxybenzaldehyde). On the whole, hydride donors such as formates in a homogeneous phase constitute an interesting situation that deserves further investigation, even though other authors[88, 89] are of the opinion that, due to their basic properties, the carbonates formed from the formates deactivate the catalysts more strongly than hydrogen, which is not associated with by-products.

5.2. Reduction of Prochiral Substrates

The enantioselective hydrogenation of prochiral substrates has been thoroughly investigated. Here, too, the reaction rates are lower than with homogeneous systems. By using chiral water-soluble Rh-catalysts, prochiral α-acetamidoacrylic esters (**36**; $R^1 = R^4 = H$; $R^2 = NHCOCH_3$; $R^3 = H, CH_3$) and α-acetamidocinnamic esters (**34**; $R^1 = H, CH_3, Na$; $R^2 = CH_3, C_6H_5$) are reduced in up to 91% *ee* (Table 3) and prochiral imines of the type **37** in 94% *ee*.[97, 98] However, the optical yields obtainable with the majority of substrates **34**–**36** are still unsatisfactory.

Table 3. Enantioselective hydrogenation of prochiral substrates with water-soluble catalysts [a].

Catalyst	n_{Cat} [M]	Substrate	*ee* [%]	TOF [b]	Ref.
Rh/**30**	1.0×10^{-3}	**34**	11–69 (*R*)	102–1608	[47]
Rh/**30**	5.0×10^{-3}	**35**	10–41 (*S*)	30–4320	[47]
Rh/**41**	1.0×10^{-3}	**34**	34–87 (*R*)	333–500	[21]
Rh/**41**	1.0×10^{-3}	**35**	16–74 (*S*)	4–500	[21]
42	6.0×10^{-6}	**34**	87–96 (*S*)	870–960	[31]
Rh/**30**	2.0×10^{-3}	**34**	10–60 (*S*/*R*)	186–1608	[49]
Rh/**30**	2.0×10^{-3}	**35**	28–68 (*S*/*R*)	366–4320	[49]
Rh/**6**	1.0×10^{-2}	**34**	72–88 (*R*)	–	[8]
Rh/**7**	1.0×10^{-2}	**34**	12–42 (*S*)	–	[8]
Rh/**4**	1.0×10^{-2}	**34**, **35**, **37**, **40**	8–65 (*R*)	–	[9]
Rh/**6**	1.0×10^{-2}	**34**	81–87 (*R*)	–	[9]
Rh/**7**	1.0×10^{-2}	**34**, **35**, **40**	20–44 (*S*)	–	[9]
Rh/**4**	2.0×10^{-3}	**36**	15–31 (*R*)	–	[107]
Rh/**6**	2.0×10^{-3}	**36**	20–61 (*R*)	–	[107]
Rh/**7**	2.0×10^{-3}	**36**	5–21 (*S*)	–	[107]
Rh/**17**	2.5×10^{-2}	**34**	40–95 (*R*)	4–50	[29]
Rh/**32**	2.5×10^{-2}	**34**	8–67 (*S*)	4–100	[106]
Rh/**33**	2.5×10^{-2}	**34**	58–94 (*R*)	4–50	[106]
Rh/**17**	2.5×10^{-2}	**34**	40–79 (*R*)	8–100	[106]
Rh/**7**	5.0×10^{-5}	**36**	10–43 (*R*/*S*)	833–2166	[104]
Rh/**4** [c]	2.5×10^{-4}	**37**	2-96 (*R*)	5–16	[97, 98]
Rh/**6**	2.0×10^{-3}	**38**	6–87 [d]	0.6–1.1	[103]
Rh/**7**	2.0×10^{-3}	**38**	7–40 [d]	0.7–1.1	[103]

[a] $p(H_2) = 1$–30 bar. Catalysts prepared from Rh^I and Rh^{III}. [b] For definition of turnover frequency see Table 2. [c] Mono- and disulfonated derivatives. [d] **de** [%] = diastereomeric excess.

Selectivities are influenced by water content and H_2 partial pressure. If the reduction is carried out in solvent mixtures (e.g., $EtOH/H_2O$), an increase in water content reduces stereoselectivity.[49, 99] Increase in pressure can in extreme cases even reverse the selectivity.[100]

An explanation for the poor optical yields in aqueous media is provided by the reaction mechanism. According to

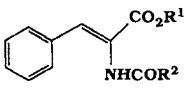

34

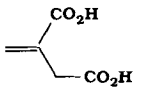

35

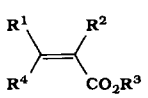

36

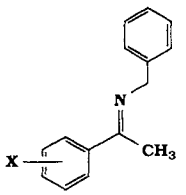

37 (X = H, OMe, Cl)

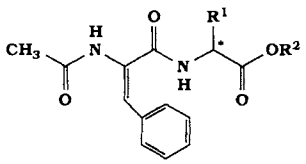

38

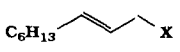

39 (X = Cl, $OC(O)CH_3$)

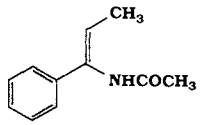

40

Scheme 4, the chiral catalyst forms diastereomeric adducts with the prochiral substrate, and these then undergo irreversible oxidative H_2 addition. According to Halpern, this step decides the enantioselection.[101] The two possible adducts react with hydrogen at rates differing by a factor of 1000. The existence of the catalyst–substrate adduct in aqueous solution has been proved.[9] The energy content of the dihydrido species **I** and **II** can be influenced by solvation. If the energy difference is very small, only a small enantiomeric excess is achievable. Amrani and Sinou have therefore postulated a small ΔE for the solvent water and a concomitant low optical yield.[49]

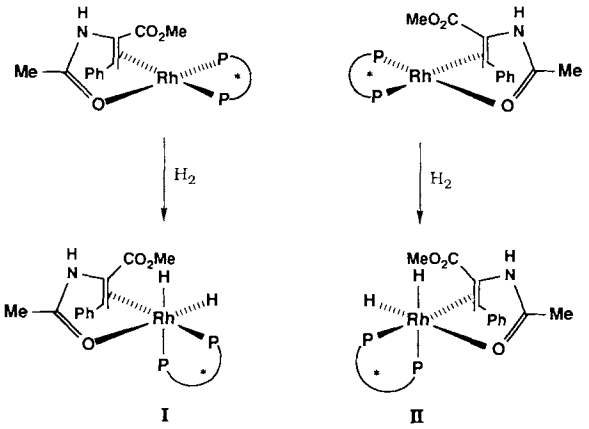

I II

Scheme 4. Oxidative H_2 addition (according to Halpern [101]) to diastereomeric catalyst–substrate adducts. All complex species are positively charged.

In a later study, a linear relationship between lg(% S/% R) and the "solvophobicity parameter" S_p is demonstrated.[99] It indicates the change in the free energy of formation ΔG_s for the transfer of a hydrocarbon from the gas phase into a given solvent.[102] Upper and lower limits are $S_p = 1$ (water) and $S_p = 0$ (hexadecane). A series of experiments with hydrophilic Rh complexes in solvent mixtures has shown that, with increasing S_p, the enantioselectivity lg(% S/% R) decreases linearly. The close relationship between stereoselectivity and the composition of the alcohol/water mixture used strongly suggests that the "two-phase hydrogenation" takes place in the polar phase and not at the phase boundary.

Sinou et al. and de Vries et al. have reported another parameter that influences enantioselectivity.[97, 98] In the reduction of prochiral imines **37** with Rh complexes of mono- or disulfonated (2*S*,4*S*)-bdpp [bdpp = 2,4-bis(diphenylphosphino)pentane], the optical yield is greater than 92% for monosulfonated ligands and only 2% for disulfonated ligands! Also, the reaction rate for the monosulfonated phosphane is many times greater. The catalytic activity of water-soluble phosphanes is apparently "tunable" by the degree of sulfonation. No explanation is yet available, and the influence of electronic and conformational effects must still be elucidated. Interestingly, the hydrolysis of imines to amines and ketones plays a subordinate role, so the imine reduction can proceed chemoselectively.

In the reduction of dehydropeptides **38** with water-soluble chiral Rh complexes of the chelating phosphanes **4**, **6**, and **7**, the diastereomeric excess (% *de*) is strongly dependent on the absolute configuration of the substrate.[103] With the tetrasulfonated bisphosphane [(*S*,*S*)-bdpp, **4**] a *de* value of only 10% can be achieved for a dehydropeptide of an *R*-configurated amino acid (Ac-Δ-Phe-(*R*)-Ala-OCH_3), but for the same peptide with an *S*-amino acid (Ac-Δ-Phe-(*S*)-Ala-OCH_3), the *de* value is as high as 72%. However, a higher diastereomeric excess for *S*-dehydropeptides is not a general feature, as, for the tetrasulfonated (*S*,*S*)-cbd (cbd = "cyclobutanediop", **7**), exactly the opposite result was obtained (higher *de* from *R*-dehydropeptide).

The choice of the reducing agent for the hydrogenation does not influence the stereoselectivity.[104] Formates of ammonium, potassium, and sodium give very similar results to molecular hydrogen. The cation has a small effect, although it is reported that the highest reaction rates and selectivities are observed with ammonium formate. This small salt effect is in contrast with the results of Basset et al., who have established a strong dependence of the reduction rate on the salt concentration.[96, 105] The addition of salts produces higher activities than in homogeneous systems for the reduction of propionaldehyde with water-soluble Ru complexes.

The fact that water is not only a solvent, but also has a chemical effect on reductions in two-phase systems is shown by the Rh-catalyzed hydrogenation of α-acetamidocinnamic ester in ethyl acetate/D_2O. Depending on the phosphane ligands used, 75% deuterium is incorporated in the reduced product.[111] The deuteration takes place selectively according to Equation (9) in the α position to the acetamido and ester function. Multiple deuteration does not occur.

Due to their negatively charged substituents, sulfonated phosphanes can compete with the unsaturated substrate at

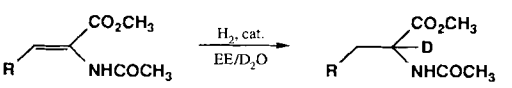

(9)

R = H, Ph
cat. = [{ Rh(cod)Cl }$_2$]/ligand; EE = $CH_3CO_2C_2H_5$

the electrophilic metal center. Various research groups have therefore synthesized cationic water-soluble Rh complexes, and have investigated their behavior in enantioselective hydrogenation. Nagel et al. reported that the cationic complex **42**[31] shows slightly improved enantioselectivity and is a factor of over 100 more reactive than a similar catalyst based on a ligand of type **41**.[21] The nucleophilic carboxylate and sulfonate groups of **41** are regarded as being responsible for the reduction in activity.[31] However, the lack of similarity in reaction conditions casts doubt on the validity of these experiments.

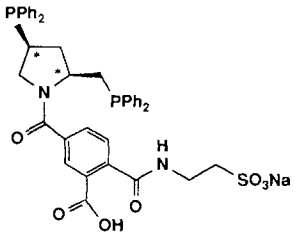

41

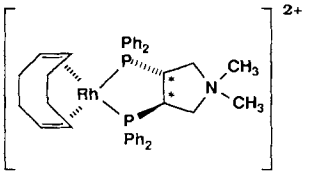

42

The substitution pattern of the P-bonded phenyl residue has little influence on the stereoselectivity. Ligands of the type **17**, **32**, and **33**, which have their hydrophilic groups *para* to the phosphorus atom, were investigated by Tóth et al.[29, 106] In the hydrogenation of dehydrocinnamic acid derivatives, the Rh-catalysts based on the cationic bisphosphanes show almost the same selectivity as those with sulfonated ligands. Chiral phosphanes sulfonated in the *para* position would unequivocally clarify the influence of the substitution pattern on the stereoselectivity, but these compounds are not yet available. The *para* isomer of tppts,[18] which has very recently been prepared and characterized by X-ray structural analysis, could serve as the starting point for the synthesis of such bisphosphanes.

The principal advantages of water-soluble catalysts—ease of separation of the product from the catalyst and long term stability—have been demonstrated in all investigations. The aqueous solutions of used catalysts show the same activity and selectivity on reuse after they have been recovered from the product phase. The industrial outlook for continuous hydrogenation processes based on water-soluble catalysts therefore seems to be full of promise.

6. C–C Coupling with Water-Soluble Catalysts

The reported CC coupling reactions include diene hydrodimerization, alkylation of CH-acidic compounds, addition reactions to the CC double bonds (hydroamination and hydroformylation), and carbonylation of allylic systems.

6.1. Hydrodimerization

The Kuraray Company in Japan is said to operate a pilot plant for the hydrodimerization of 1,3-butadiene according to Scheme 5, in which step (a) is a two-phase system with a Pd/tppms catalyst. The primary product is then isomerized

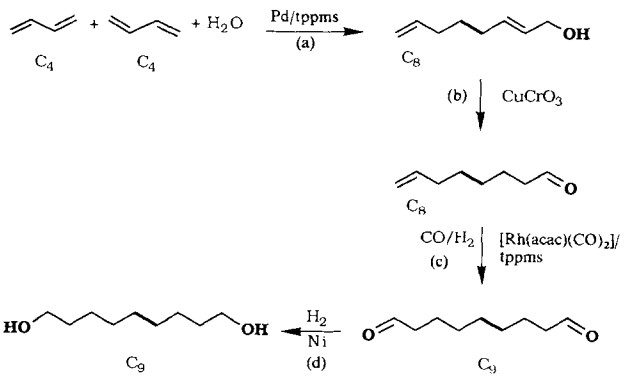

Scheme 5. The new Kuraray process for the production of 1,9-nonanediol by hydrodimerization of 1,3-butadiene.

to the C_8 aldehyde with a copper chromite heterogeneous catalyst, and the resulting product hydroformylated in a third process step (c), once again with a two-phase catalyst. The resulting ω,ω'-dialdehyde is extracted, probably with cyclohexane, and hydrogenated over molybdenum-doped Raney nickel to yield 1,9-nonanediol (step d).[1108]

6.2. Alkylation of CH-Acidic Compounds

The telomerization of dienes has been extensively investigated by Rhône-Poulenc Industries.[109] Functionalized 1,6-octadienes can be obtained from butadiene or isoprene and acidic compounds according to Equation (10). A catalyst obtained from Pd^{2+}/tppts (1/4) is very effective, while rhodium and platinum instead of palladium give poor yields. With optimized process operation, the reaction has a regioselectivity of 95/5 (Y functionality in position 1 or position 3).

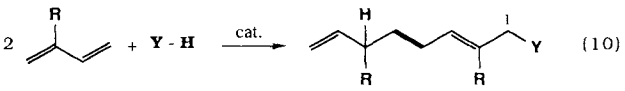

(10)

R = H, Me
Y = MeO, EtO, PhO, HO, MeCOO, Me_2N

The telomerization of dienes with N-quaternized aminophosphanes as the catalyst ligands was recently reinvestigated.[30] When $[Pd(OAc)_2]$ and **18** (fourfold excess) are used together, a water-soluble catalyst is obtained that is more active but less selective than its tppts analog (TOF = 5–26). The reaction is chemoselective; the yield of side products (e.g., 1,3,7-octatriene) is insignificant. Recycling and reuse of the catalyst are possible with only little loss of activity.

The isoprenylation of CH-acidic compounds is a similar type of reaction.[110–112] In particular, 1,3-dicarbonyl compounds can be alkylated with Rh–tppts catalysts in two-phase systems. An example is the isoprenylation of barbituric acid according to Equation (11). The two potential isomers are not always produced. When Pd catalysts are used, the terminal double bond is shifted to an inner location, as in the isomerization of Isofeprazon to Feprazon. The

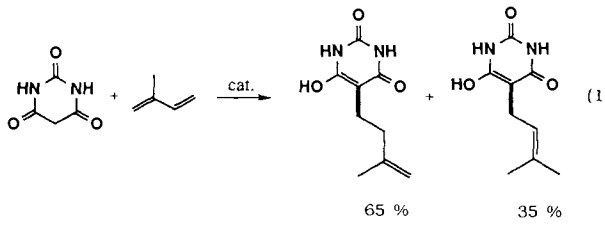

(11)

activated methylene compound adds remarkably regioselectively, and the attack takes place exclusively at the monosubstituted double bond. A twofold alkylation of the 1,3-dicarbonyl compound, only possible under drastic conditions, is not observed if conditions are normal (25 °C, 48 h). The ease of recovery and reuse of the catalyst—without loss of activity—have been convincingly demonstrated.

CC couplings can also be carried out with tppms-containing Pd catalysts.[113] The compound **43** catalyzes, in yields

$[Pd(tppms)_3]\cdot 3H_2O$ **43**

which can be greater than 99%, the arylation (biphenyl synthesis), acetylation, phosphorylation, and vinylation (Heck reaction) of halogenated arenes and heteroarenes. In solution, a rapid phosphane exchange is observed which presumably takes place through the intermediacy of a PdL_4 species. However, there is no direct proof of the existence of a complex containing tetracoordinated palladium. Compound **43** can be used for diverse functionalities, including those in unprotected nucleotides and amino acids. The good results of the Heck reaction and the cross-coupling of terminal alkynes with vinyl and aryl iodides are confirmed in an independent study.[114] Although the active catalytic species was not characterized in this case, it must nevertheless be **43**.

Water-soluble Pd compounds catalyze allyl substitutions according to Equation (12) in yields up to 95%. With acetates and carbonates of cinnamyl alcohol (R = C_6H_5), the *E* enantiomers are selectively formed.[114]

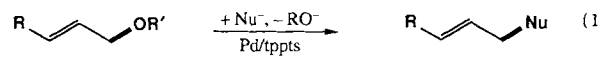

(12)

R = H, C_6H_5, CH_2OH; R′ = $CO_2C_2H_5$, $COCH_3$
Nu = $CH(COCH_3)_2$, $SO_2C_6H_4$-*p*-CH_3, $N(CH_2CH_2)_2O$ (morpholino)

The ring opening of 3,4-epoxy-1-butene by ethyl acetoacetate to give 2-acetyl-6-hydroxy-4-hexenoic acid proceeds in greater than 80% yield (*E*/*Z* = 85/15).[115] Allyl halides can be directly carbonylated by using water-soluble Pd catalysts.[116, 117] Under normal CO pressure and in the presence of sodium hydroxide or alkoxide, the β,γ-unsaturated acids or esters are obtained. Benzyl chloride can also be carbonylated to phenylacetic acid in this way.[118] The yields vary between 4 and 93%, depending on the substrate. With allyl halides, only *E* isomers are formed.

The preparation of poly(*para*-phenylene) derivatives using "Pd/tppms" is currently in progress.[119] Starting from 1,1′-biphenyl-4,4′-bis(ethylenedioxyborane) and 4,4′-dibromo-1,1′-biphenyl-2,2′-dicarbonic acid, the water-soluble polymer **44** with an average molecular weight of 50000 can be obtained according to Equation (13) (C–C coupling with elimination of the end groups $-\overline{B(OCH_2CH_2O)}$ and –Br). The polymerization process is strongly favored by the solubilities of the monomer, the growing polymer, and the catalyst. Polymerization reactions could therefore open up a new area of applications for water-soluble metal complexes that has so far been virtually ignored. Incidently, water should also be an excellent solvent for radical processes, because the OH bond enthalpy is extremely high (120 kcal mol^{-1}).[120]

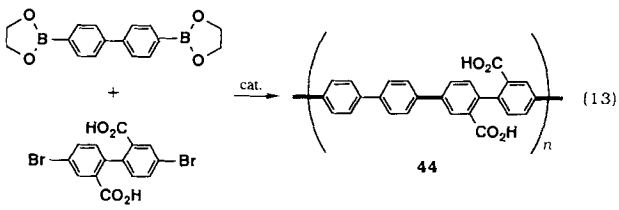

(13)

6.3. Addition of Hydrogen Cyanide

The nickel-catalyzed addition of hydrogen cyanide to CC multiple bonds is reported in a patent.[121] Adipic acid and methylglutaronitrile are obtained from 3-pentenenitrile according to Equation (14). The linear product is formed preferentially (> 10/1). In 1990, it was recognized that the correct formula of the catalyst "$[Ni(tppts)_4]$" is in fact $[Ni(tppts)_3]$.[77]

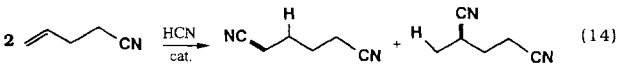

(14)

6.4. Hydroformylation

The "Oxo synthesis" (hydroformylation), which was discovered by Otto Roelen (1897–1993)[122] in 1938 at the Ruhrchemie AG, is one of the most important metal-catalyzed alkene reactions.[123] World capacity for Oxo products is about 5.6 million tons per annum (excluding 2-ethylhexanol, the most important product of a subsequent reaction). The importance of water-soluble catalysts in this type of process may be deduced from the increase in capacity (Fig. 7)[123–130] and improvement in the performance parameters of the catalytic process (Table 4). After the discovery of tppts at Rhône–Poulenc Ind. in Lyon in 1975, its implementation on an industrial scale was developed by the Ruhrchemie AG (now Hoechst AG) in Oberhausen.

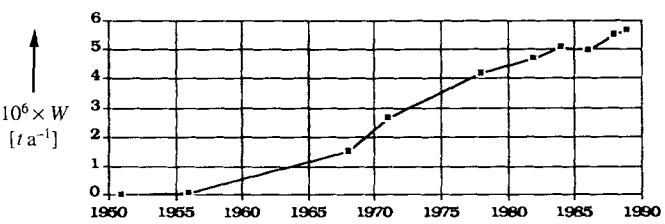

Fig. 7. Growth of worldwide Oxo capacities *W* (in million tons per annum). The sudden increase in 1968 coincides with the introduction of the Union Carbide Process (Rh catalysis). Up to that time, hydroformylation was performed with cobalt catalysts only.

Table 4. Technical parameters of the Oxo synthesis.

Catalyst parameters	Catalyst $[HCo(CO)_4]$	$[HCo(CO)_3PR_3]$ R = n-C_4H_9	$[HRh(CO)(PR_3)_3]$ R = C_6H_5	R = m-$C_6H_4SO_3Na$
p [bar]	200–350	50–100	15–20	10–100
T [°C]	110–180	160–200	85–115	50–130
n/iso ratio [a]	80/20	88/12	92/8	95/5 [b]
selectivity	medium	low	high	very high
hydrogenation activity	medium	high	low	low

[a] Depending on the position of the formyl group at the terminal or internal C of the double bond, a linear (n) or branched (iso) aldehyde arises. The desired products are linear. [b] Variants with n/iso = 99/1 are now also known.

6.4.1. Ruhrchemie/Rhône–Poulenc Process

The first patents were applied for in September 1982 for the synthesis of aldehydes,[131] the recovery of the rhodium,[132] and the production of sufficiently pure sulfonated phosphanes.[133] In particular, the elegant extraction–reextraction process[133, 134] for the tonnage production of tppts paved the way for the industrial operation of two-phase hydroformylation. The patent applications that were published afterwards describe further improvements: process optimization,[135–137] recovery of the rhodium catalyst,[138–140] reactivation of catalyst,[208] synthesis of water-soluble triarylphosphanes,[16, 133, 134] and synthesis of new ligands and metal coordination compounds for catalytic two-phase systems.[13, 141–144] These patent applications cannot be treated individually in this review, but the fact that there are so many of them bears out the extent of the research activity in this field.[204]

The Ruhrchemie/Rhône–Poulenc process went into operation in 1984. Two plants now produce 300 000 tons per annum of butyraldehyde. Depending on the quality of the propene starting material, 99 % conversion and a crude aldehyde product with an n/iso ratio (for explanation, see footnote to Table 4) of approximately 95/5 is attained. Both the hydrogenation of the alkene and the formation of condensation products by aldolization are insignificant. The loss of rhodium in the organic phase, despite the high price of this metal, is a "quantité negligeable".[145, 146] Catalysts that generate selectivities of $n/iso \geq 99/1$ have recently been discovered.

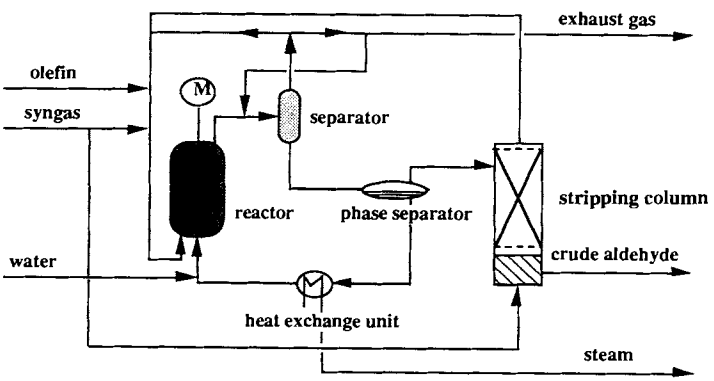

Fig. 8. Flow diagram of the Ruhrchemie/Rhône–Poulenc process for the production of n-butyraldehyde, in operation at the Ruhrchemie works of Hoechst AG (Oberhausen) [146, 151]. M = stirring device.

A flow diagram of the process is shown in Figure 8. The separation of the catalyst/product mixture is simply carried out in a phase separator, from which the aqueous catalytic solution flows back to the reactor, while the organic product continues to the stripping column. An optimized heat recovery system ensures a favorable overall energy balance for this modern process.

6.4.2. New Catalysts

The development of even better water-soluble phosphanes for two-phase hydroformylation has become a necessity in recent years. The international downward pressure on the prices of Oxo products, mainly caused by the cheap products from the "developing countries", prescribes the continuous improvement of the existing process. For the Ruhrchemie/Rhône–Poulenc process, this implies the synthesis of new, more active catalysts. To name only two examples, the sulfonated phosphanes bisbis (**45**) and norbos (**9**) enabled Rh catalysts to be produced with superior properties to those of the standard Rh–tppts system (see Fig. 9).[1, 143, 144] Jumps

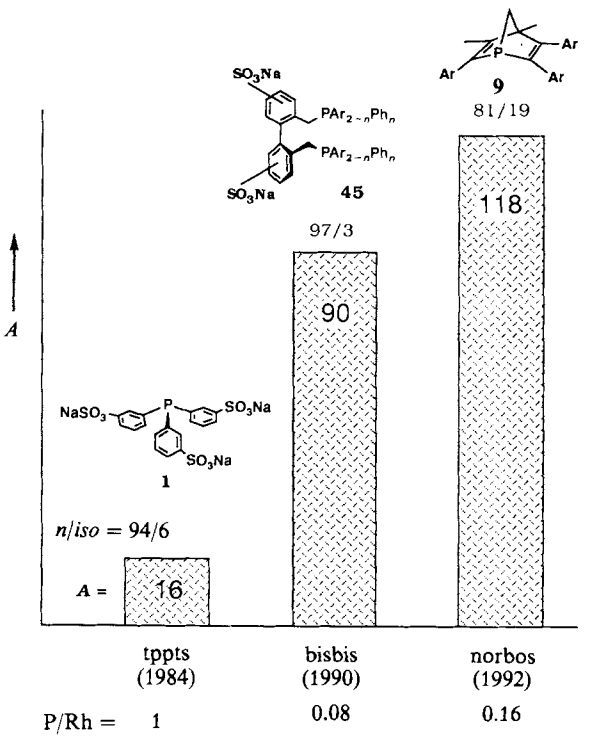

Fig. 9. Results of catalysis with water-soluble rhodium–phosphane complexes (activity A is shown on a linear scale). Activity A = n(aldehyde)n(Rh)$^{-1}$ h^{-1}, Ar = $-C_6H_4SO_3Na$, P/Rh ratios are normalized.

in activity from 16 to 90 (bisbis) or to 118 (norbos) indicate the currently attainable activity levels. The n/iso ratios in the propene hydroformylation reaction fall below 95/5 in the case of norbos only. The large phosphane excess normally required in the Rh/tppts system and many other standard catalysts (e.g. Rh/tpp) can be reduced by more than an order of magnitude without causing problems of long-term stability. Thus, the rhodium–norbos system is the most active water-soluble hydroformylation catalyst known so far.

Losses in selectivity are compensated for by the similar commercial values of *n*- and *iso*-butyraldehyde. Moreover, the ready accessibility of the norbos systems is attractive, because they allow a systematic variation of substituents.[12] Phosphane chelating ligands are attracting more attention for future industrial use, because the special phosphites of Union Carbide show extremely high activities and selectivities in *homogeneously catalyzed* hydroformylation.[148–150] However, these ligands are readily hydrolyzed, and therefore cannot be considered for aqueous systems, which was recently clearly shown in the case of sulfonated phosphites.[19] The previously mentioned sulfonated tris(ω-phenylalkyl)phosphanes P[$(CH_2)_n$*p*-$C_6H_4SO_3Na$]$_3$ ($n = 1-3$ and 6)[14] are more active in rhodium-catalyzed hydroformylation of 1-octene at low P/Rh ratios (2/1) than an analogous Rh–tppts system. In this case, the highest conversion was observed for $n = 6$. Interestingly, higher P/Rh ratios lead to a decrease in catalytic activity.[203]

Other than in the two-phase catalysis employing Rh/dppets,[67] there is a successful example of homogeneous catalysis in which the nonsulfonated parent ligand 1,2-bis(diphenylphosphino)ethane (dppe) is used. Substrates like 1,3-butadiene undergo hydroformylation to the C5-aldehyde with a TOF of 250.[205] The analogous Rh/tpp catalyst has hardly detectable activities under otherwise identical reaction conditions. An application in aqueous medium by sulfonation of the tpp ligand right be interesting.

6.4.3. Catalyst Deactivation Mechanisms

Although the standard Rh^I/tppts system has extremely good long-term stability, a slight loss of activity occurs after several years' use. The catalyst deactivation mechanism has recently been clarified in detail (Scheme 6).[78, 79, 151]

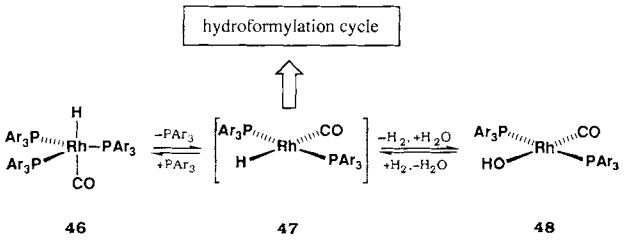

Scheme 6.

Compound **46**, which is strictly only a "precatalyst", dissociates to the active 16e species **47**. This is supported by a high-pressure NMR study by Horváth et al.,[152] which shows that **46** itself does not take up a further CO molecule from syngas, even at a pressure of 200 bar (20 MPa). The active species **47** initiates the hydroformylation cycle, which is not considered further here. The hydroxo complex **48**, which has been isolated and characterized, is formed in water under hydroformylation conditions (H_2/CO) and can be reversibly converted into **46**. The equilibrium lies almost completely on the side of **46**; accordingly, during hydroformylation there is no danger of the transformation of **46** into the catalytically inactive hydroxo complex **48**. According to Equation (15), carbon monoxide displaces a phosphane ligand from **48**. The deactivation mechanism starts with the

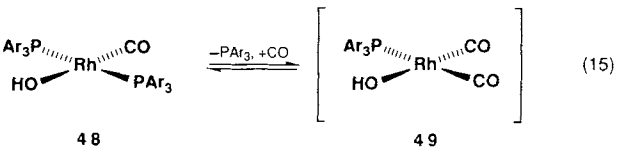

(15)

formation of the intermediate **49** (not isolable), as shown in Scheme 7.

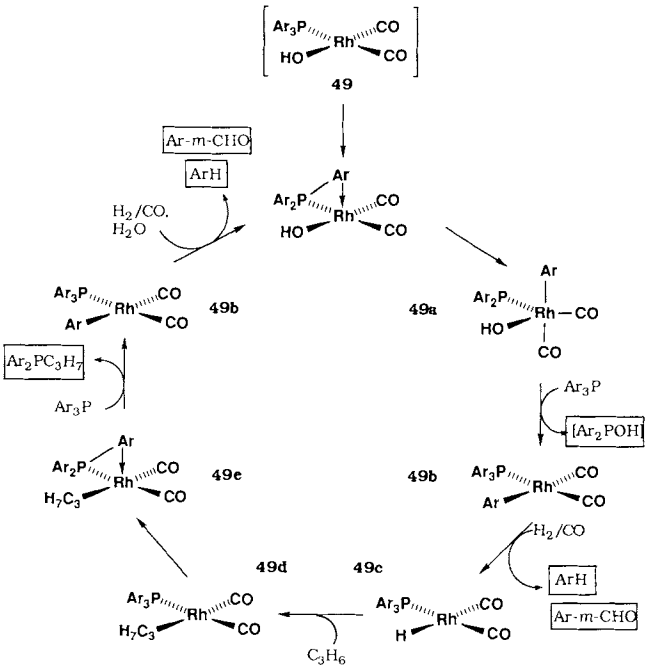

Scheme 7. Deactivation mechanism of Rh^I–tppts catalyst in the Ruhrchemie/Rhône–Poulenc process (framed products have been isolated and characterized; see text and ref. [78, 151]).

The cleavage of the P–C bond in the phosphane, which deactivates the catalyst, is caused by the oxidative addition of tppts to Rh^I with the formation of **49a**, a Rh^{III} species with a five-coordinate central atom. The cleavage of the P–C bond, combined with an aryl rearrangement, was previously recognized by Garrou et al. as the origin of the deactivation of phosphane-modified catalysts.[153] The coordination of a further molecule of tppts causes the reductive elimination of bis(*meta*-sulfophenyl)phosphinous acid as the tautomer Ar_2POH. Benzenesulfonic acid (ArH) and *meta*-formylbenzenesulfonic acid (Ar-*m*-CHO) are formed from the Rh^I intermediate compound **49b** under the given reaction conditions (and presence of syngas). Both these compounds have been detected in "exhausted" catalyst solutions.[78]

Species **49c**, which is formed by H_2 addition and product elimination, combines with propene to form the propyl complex **49d**. The later course of the reaction is determined by this intermediate stage. The insertion of CO would produce the acyl complex and finally the hydroformylation product butyraldehyde. The oxidative addition of another tppts ligand (→ **49e**), however, would mean that three products could arise from this cycle: 1) the phosphane, $Ar_2PC_3H_7$ (pdspp) by phosphido/propyl coupling; 2) benzenesulfonic acid (ArH); and 3) *meta*-formylbenzenesulfonic acid (Ar-*m*-CHO) from the intermediate compound **49b**.

The phosphane pdspp was isolated from used catalyst solutions ("contact" solutions). In an aqueous reaction medi-

um, the starting compound of the deactivation mechanism is then regenerated from **49b** under CO/H_2 pressure. The formation of *meta*-formylbenzenesulfonic acid in isolable quantities rules out the deactivation of the phosphane by *ortho*-metalation: as the formyl group is located at the position originally occupied by the phosphorus atom, the deactivation must be started off by an oxidative addition of the tppts ligand to Rh^I. Other workers confirm this observation for Rh–tpp complexes.[154–156] The subsequent fate of the reductively eliminated bis(*meta*-sulfophenyl)phosphinous acid Ar_2POH is shown in Scheme 8. For phosphinous acids,

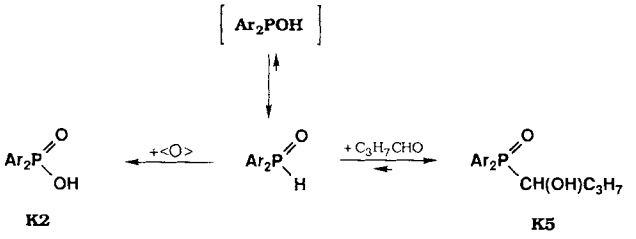

Scheme 8. Formation of the main degradation products **K5** and **K2** from bis(*meta*-sulfophenyl)phosphinous acid (Ar = m-$C_6H_4SO_3Na$, <O> from H_2O).

$R_2P(O)H$, an equilibrium between the hydroxy species Ar_2POH and the phosphane oxide $Ar_2P(O)H$ form is postulated, and in fact $(CF_3)_2POH$ is the only hydroxy tautomer that has yet been isolated. For all weakly electron-withdrawing substituents R the phosphinous acid is present as phosphane oxide. Therefore, the reductive elimination of Ar_2POH is followed by rapid tautomerization to $Ar_2P(O)H$. This compound reacts with the butyraldehyde in solution to form **K5**, and is partially oxidized to phosphinic acid **K2**. Both products were isolated from catalyst solutions originating from the plant operation.

6.4.4. Further Concepts in Catalytic Hydroformylation

Other aspects of the use of water-soluble catalysts for hydroformylation include complexes with cationic ligands,[93, 157] binuclear rhodium–tppts complexes,[158–162] immobilization of water-soluble Rh complexes on ion exchangers,[163] polymers,[164, 165] cyclodextrins,[166] and micellar two-phase hydroformylation.[25]

Some Rh^I complexes of the cationic ligand amphos **16**, $[Ph_2PCH_2CH_2NMe_3]^+$, are efficient hydroformylation catalysts when in aqueous solution or immobilized on strongly acidic cation exchangers.[93, 157] Leaching of rhodium does not occur; nevertheless, the metal can be recovered by elution from the ion exchange resin with acids.[93] In contrast, the cobalt complex $[Co(CO)_3(amphos)]_2(PF_6)_2$ suffers from considerable metal leaching. Moreover, when it is in the liquid/liquid two-phase system or immobilized on the ion exchange resin, it is less active, and gives poor *n/iso* ratios.

Recently, immobilization of water-soluble metal complexes on solid supports has been investigated,[163–166] for example, $[HRh(CO)(tppts)_3]$ on the ion exchange resin Amberlyst A-26.[163] Unlike the SAP catalysts (Section 7), the catalyst-loaded resin can be prepared with no water content. Hence, the disadvantageous oxidation of tppts to the corresponding phosphane oxide by water and Rh^{III} should be avoidable. The tppts ligand binds to the carrier by *three* sulfonate groups; hence the greater stability of the tppts system relative to the amphos systems can be explained.

1-Tetradecene, 1-dodecene, and 1-octene are hydroformylated at 100 °C and 70 bar pressure with an *n/iso* ratio of 2.3–3.4/1. The yield of aldehyde is low (seldom greater than 50%), but the extent of isomerization is high and solvent-dependent (up to 42%). The thermal instability of the resin at temperatures above 100 °C limits its use. The surprising long-term stability of this group of catalysts is more encouraging. After multiple use of the resin-supported catalyst, productivity and selectivity hardly decrease (reduction of P/Rh ratio). Rhodium leaching has not been found. After 16 cycles (corresponding to TON = 15000!), the extent of phosphane oxidation was 80%, caused by moist and oxygen-containing substrates and solvents. The exceptionally long lifetime of this class of catalysts is promising.

Polymer-fixed Rh catalysts still have a long way to go before they become industrial materials. Drawbacks are leaching and thermal instability.[167] A poly(styrenedivinylbenzene) copolymer with hydrophilic $-CH_2P(C_6H_4SO_3H)_2$ groups was investigated in Rh^I-catalyzed propene hydroformylation.[164–165] With a metal loading of 3.4 wt% Rh and P/Rh = 8.7/1, the conversion rate is 3×10^5 mol(aldehyde) per g(Rh) per min after 4 h at 100 °C and 30 bar. The selectivity (*n/iso* = 1.2/1) is very low, but this is a promising opening for asymmetric (= enantioselective) variants of hydroformylation (see ref. [206]). Again, catalyst stability is favorable.

The use of longer chain alkenes in liquid/liquid two-phase systems is limited by the solubility of the substrate in the aqueous (catalytic) phase. Cyclodextrins, which have inner lipophilic cavities and hydrophilic surfaces, offer novel possibilities. As shown in Figure 10, α-cyclodextrin can bind one molecule of 1-hexene in its cavity, and thus transfer the alkene across the phase interface. The specific orientation of the alkene in the cyclodextrin favors the formation of the linear aldehyde.[166]

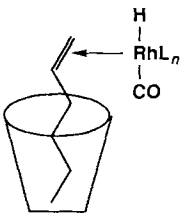

Fig. 10. Orientation and complexation of alkenes in individual cyclodextrin molecules.

The positive prognostication is not yet fulfilled with $[HRh(CO)(tppms)_3]$. By adding α-cyclodextrin, the aldehyde yield is reduced from 55% (without added dextrin) to 11%. The *n/iso* ratio, 7/3, is unaffected. The authors attribute this to hydrogen bonds between the hydroxyl groups of the α-cyclodextrin and the sulfonate groups of the tppts, which is said to hinder dissociation of a phosphane ligand and hence the coordination of the alkene. Nevertheless, modified cyclodextrins are expected to become important for the Oxo synthesis, because of their ability to cause steric orientation of substrates.[168]

Fell et al. first achieved the micellar two-phase hydroformylation of longer chain alkenes by the use of the sulfobetaine of tris(2-pyridyl)phosphane (see Eq. (3)).[125] The properties of these interfacially active compounds ($n = 0$, 3, 5, 7, 9, and 11) can be tuned. The phosphanes form complexes and promote dissolution. By suitable choice of n, they acquire surfactant properties, and, above a critical concentration, form micelles. The lipophilic alkenes can be trapped in the long alkyl groups of the micelles. The active Rh center is also inside the micelle as a result of the coordination to the phosphorus atom. For example, tetradecene can be hydroformylated, with a 79% yield of aldehyde (*n/iso* ratio $\approx 3/1$). The most suitable phosphane has a chain length n of 5. If $n > 5$, stable emulsions are formed and phase separation can become a problem. In no case is rhodium loss observed.

The binuclear rhodium complexes of the type $[Rh_2(\mu\text{-}SR)_2(CO)_2(tppts)_2]$ of Kalck et al. should also be mentioned.[158-162] They show the usual activity in the hydroformylation of 1-hexene, but unusually high selectivity (*n/iso* = 18/1). The hydroformylation can also be carried out without hydrogen, since the solvent water can function as the H_2 source through the water–gas shift reaction: $CO + H_2O \rightleftharpoons CO_2 + H_2$. 1-Hexene at pH = 4.8 can be converted into 1-heptanol with 75% yield (80 °C, $p(CO) =$ 8 bar, P/Rh = 6, 15 h, selectivity 95.8%). The use of water as a source of hydrogen makes this class of complexes especially interesting.

7. Supported Aqueous Phase Catalysts

The recent development of "*s*upported *a*queous *p*hase *c*atalysts" (SAP catalysts)[169, 170] began in 1989 with a publication in *Nature*.[171] By their work on SAP catalysts, Davis et al. opened the way to hydroformylate very hydrophobic alkenes such as oleyl alcohol, octene, or dicyclopentadiene with the water-soluble catalyst $[HRh(CO)(tppts)_3]$, using the principle sketched in Figure 11.

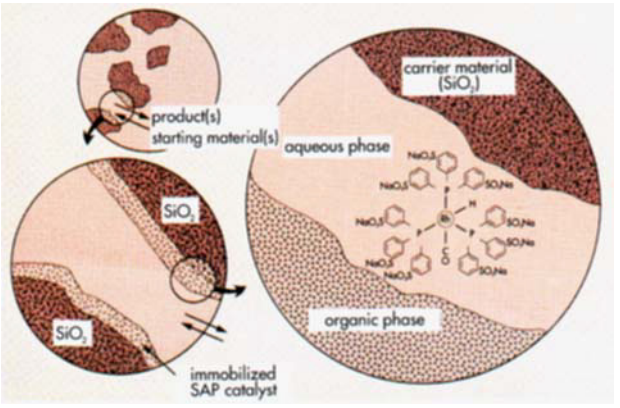

Fig. 11. Schematic diagram of a SAP catalyst according to ref. [169]. Working principle: a thin, aqueous film containing a water-soluble catalyst, for example $[HRh(CO)(tppts)_3]$, adheres to silica gel with a high surface area. These catalysts act at the liquid/liquid interface.

7.1. Preparation of SAP Catalysts

To produce SAP catalysts, a granulated, porous support material with a large inner surface is added to a stirred aqueous solution of $[HRh(CO)(tppts)_3]$ and tppts (ligand excess), and then dried under vacuum. The hydrophilic carriers consist of "*c*ontrolled-*p*ore *g*lass" (CPG) with a definite but variable large inner surface (CPG-240, CPG-350). CPG-240 has a mean pore diameter of 237 Å, a pore volume of 0.95 mL g^{-1} ($\pm 4.3\%$) and a specific surface area of 77.5 $m^2 g^{-1}$. After removal of all the solvent, a dry, yellow powder remains which still contains about 2.9 wt% water. The metal complex is homogeneously distributed on the inner and outer surface of the support. If this catalyst material is treated at 30 Torr and 30 °C with water vapor, a controlled amount of water can be added, depending on the contact time. A comprehensive account of the process is given in Ref. [172].

7.2. Hydroformylation and Hydrogenation with SAP Catalysts

The SAP catalysts were developed for the hydroformylation of liquid substrates that are completely insoluble in water, for example, oleyl alcohol.[172] In the Ruhrchemie/Rhône–Poulenc process, longer chain alkenes can only be hydroformylated in the presence of solubilizers, for example, tetraalkylammonium salts containing four long-chain alkyl groups.[151] Oleyl alcohol is converted into the C_{19} aldehyde at 100 °C, 51 bar, and a CO/H_2 ratio of 1/1, in 96.6% yield without any rhodium loss at all. Moreover, after filtering off the stationary phase, the liquid phase does not contain rhodium, either as a complex species or as a colloid. The water content of the support is important. For example, the hydroformylation of 1-octene is characterized by a reduction in activity for a water content of more than 8 wt%. Also, the *n/iso* ratio and the system stability are reduced with increasing water content. It is thought that the resulting greater mobility of $[HRh(CO)(tppts)_3]$ promotes decomposition reactions.

The site of the reaction is well established. On supports with physically different structures, the activity depends on the specific surface; that is, the reaction takes place at the phase boundary. Thus, the results are in agreement with those of solid $[HRh(CO)(tppts)_3] \cdot n H_2O$. In its isolated state, the solid contains up to 16 wt% water—it is in a sense a "primitive SAP catalyst". In the hydroformylation of 1-octene in cyclohexane, the results almost match values with SAP catalysts: 98.7% conversion, *n/iso* = 2.1–2.9. As the Rh complex is insoluble in the organic reactants, the reaction must take place at the solid/liquid interface. This conclusion is supported by comparative investigations of two-phase systems and SAP catalysts.[173] For classical liquid/liquid systems, the rate of hydroformylation decreases in the series 1-hexene > 1-octene > 1-decene; with the SAP catalytic method, these alkenes react at virtually the same rate. Typically for surface effects, the solubility of the alkene in the aqueous phase is no longer the rate-determining factor. The low *n/iso* ratio of 2.8 in the three cases is due to coordinatively unsaturated complexes such as $[HRh(CO)_2(tppts)]$, which are known for their poor regioselectivities.[152]

When the complex $[Co_2(CO)_6(tppts)_2]$[77] is immobilized on CPG-340 and used for the hydroformylation of 1-hexene, there is only negligible leaching of cobalt into the product

phase.[174] However, in a typical two-phase reaction, the metal loss is not inconsiderable. At 190 °C, 55 bar ($CO/H_2 = 1/1$) the degree of conversion reaches 68% ($n/iso \geq 2$) after 8 h, depending on the water content. Other publications describe improved methods of producing SAP catalysts, and the extension of hydroformylation to other unsaturated compounds.[175]

In variations of the SAP catalytic method, platinum/tin tppts complexes can be obtained.[176] The most active water-insoluble, homogeneous hydroformylation catalyst based on platinum is the compound $[PtCl(tpp)_2SnCl_3]$. Tin(II) chloride increases both the reaction rate and the *n/iso* ratio. However, due to the sensitivity of the platinum–tin bond to hydrolysis, a tppts-modified system cannot be used in water. As the amount of water on the SAP catalyst (as little as 3%) is required only for the solubilization of the sulfonate groups of the tppts, the hydrolysis of the metal–metal bond should be able to be kinetically limited. Therefore, CPG-350 was impregnated with $[PtCl_2(tppts)_2]$, and treated with a solution of $SnCl_2$ in CH_2Cl_2. The vacuum-dried SAP catalyst contains 1.4 wt% water (TGA data). The high selectivity (*n/iso* = ca. 12/1) compared with the tin-free system $[PtCl_2(tppts)_2]$ (*n/iso* = 3/1) indicates a stable Pt... Cl... Sn interaction. The reaction rates are low, and decrease further as the water content increases to 7.4 wt% because the active species decomposes. Hydrogenation and isomerization are strikingly dominant. In the SAP catalytic method after 120 h, $[PtCl(tppts)_2SnCl_3]$ at 100 °C, 70 bar (H_2/CO), and a P/Rh ratio of 2/1 converts 1-hexene into only 26% heptanal and 12.7% hexane, but 21.2% 2-hexene and 7.6% 3-hexene are also formed. However, as no metal loss is observed, this method of immobilization seems to have some industrial future if further optimization of the parameters can be achieved.

With SAP catalysts based on Ru–tppts complexes, the selective reduction of α,β-unsaturated aldehydes to allyl alcohols can be performed. Thus, at 100 bar pressure of H_2(!), 3-methyl-2-butenal and *all-trans*-retinal are reduced with almost quantitative yield and high selectivity (up to 89%). The reduction in activity on recycling the catalyst material is due to successive adsorption of the reactants. Metal loss only dominates when polar solvents such as methanol are used. For the first time such a decrease in activity following catalyst recycling has been clearly documented; as a result, the industrial use of SAP catalysts for this particular reaction is viewed with skepticism.[177] It remains to be seen whether the concept of SAP catalysts meets the high expectations for it.[171]

7.3. Wacker Oxidation

The Wacker process for long-chain alkenes also requires solubilizing agents. To compare performance with SAP catalysts, $PdCl_2$ and $CuCl_2$ (1/1) were immobilized on CPG-240 (15 wt% H_2O).[178] In 3 h, this catalyst converted 1-heptene at 100 °C, $p(O_2) = 4$ bar, and an alkene/Pd ratio of 210/1 into 2-heptanone (oxidation), 2-heptene, and 3-heptene (isomerization). In the conventional Wacker process, isomerization is insignificant. In the SAP catalytic process, the oxidation of Pd^0 to Pd^{2+} is probably very slow, so isomerizations at the stage of the Pd–alkene complex become more significant. The reduction in isomerization with increasing O_2 partial pressure is consistent with this conclusion and with a more rapid Cu^+ oxidation. In spite of the unfavorable product distribution, SAP catalytic technology has the advantage that use of corrosive solutions of Cu^{2+} is avoided. The latter problem affects all conventional Wacker processes.

To sum up, immobilized water-soluble complex catalysts extend the concept of two-phase reactions to a new technical dimension.[179]

8. Special Uses of Water-Soluble Ligands

In addition to their main use in catalysis, water-soluble ligands have a number of special uses.

8.1. Membrane Modification by Selective Hydrogenation

The hydrogenation of unsaturated fatty acids is an important process, because these compounds form part of the membrane structures of a wide range of lipid classes.[180–186] Water-soluble catalysts are very much more suitable than their lipophilic derivatives, as no solvent vector such as THF or DMSO is needed for the transport of the metal complex into the membrane. Furthermore, water-soluble catalysts are easier to remove from the still intact membrane at the end of the reaction, and even the polarity of the catalyst can be controlled by suitable choice of ligand. The location of the reaction can be selected by exploiting the variable extent of penetration into the membrane.

The initial research in this field was carried out by Madden et al. during 1978–1980.[180, 181] The hydrogenation activity of the catalyst $[RhCl(tppms)_3]$ on phosphatidylcholine from soya lecithin was determined for the vesicles produced by ultrasound or mechanical perturbation. The water-soluble metal complex has amphiphilic character due to its sulfonated phosphane ligands and unsubstituted phenyl groups. This bipolarity facilitates the transition between the polar aqueous phase and the lipophilic hydrocarbon phase. Approximately 85% of the catalyst is either on or in the membrane—like moths in the fold of a curtain. The membrane structure is not destroyed even if 20 mol% catalyst (based on phospholipid) is present. All the double bonds can usually be hydrogenated, even including those deep inside the membrane layer. The catalyst therefore diffuses through the membrane in a few hours. At the end of the reaction, approximately 70% of the metal complex can be recovered from the membrane by means of ion exchangers.

Further investigations of the hydrogenation of dioleylphosphatidylcholine liposomes were published, in which the hydrogenation activity of the complexes $[RhCl(tppms)_3]$ and $[RhCl(dpup)_3]$ were compared,[182] [dpup = disodium diphenylphosphinoundecylphosphate, $(C_6H_5)_2P(CH_2)_{11}P(=O)(ONa)_2$]. At 37 °C, 1.2 bar H_2, and pH = 6.9, a *cis/trans* isomerization (oleic acid to elaidic acid) takes place before the hydrogenation. The *cis* isomer is not hydrogenated, but the *trans* isomer is. The rate of hydro-

genation is independent of the catalyst concentration. The kinetics are indicated by the equilibrium in (16). If

$$[\mathrm{Cat}]_{\mathrm{micelles}} \rightleftharpoons [\mathrm{Cat}]_{\mathrm{monomer}} \rightleftharpoons [\mathrm{Cat}]_{\mathrm{membrane}} \quad (16)$$

the critical micelle concentration is exceeded, the water-soluble catalyst is present as a large reservoir in the form of micelles. The micelles are in equilibrium with the monomeric form of the catalyst, whose concentration remains constant irrespective of the initial amount used. The monomeric Rh complex diffuses to the membrane and catalyzes hydrogenation there. As the monomer concentration does not change, the rate of hydrogenation is constant. Equilibrium (16) raises the question of the self-association of water-soluble metal complexes for the first time, a subject which is also of interest in connection with colloids (see Section 9).

The phospholipids located on the outside of the membrane can be hydrogenated with $[RhCl(tppms)_3]$,[183] and the cholesteryl acids and triacylglycerides located further inside the membrane are also reduced, but with decreased activity. The hydrogenation of the "inner" compounds that can nevertheless be observed is explained by the intermingling of the CC unsaturated alkyl chains with the phospholipids bonded to the surface (Fig. 12). The sulfonate groups of the water-soluble catalyst are oriented at the hydrated surface of the lipoprotein, while the active rhodium center penetrates the alkyl chain layer of the phospholipid.

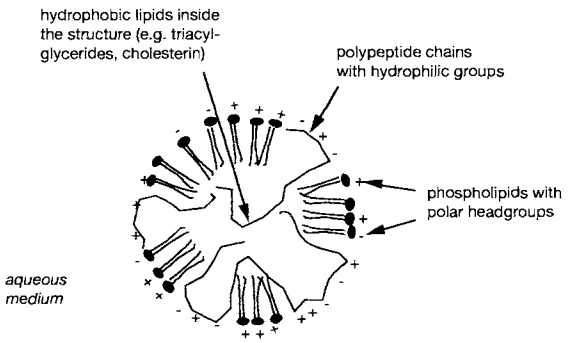

Fig. 12. Schematic diagram of a plasma lipoprotein (from ref. [184]).

Vigh et al.[185] have compared Ru and Rh catalysts for the hydrogenation of membranes. Under normal conditions, the complex $[RuCl_2(tppms)_2]$ is more active than the normally used catalyst $[RhCl(tppms)_3]$, which becomes superior to the Ru analog above 30 °C (Fig. 13).

The hydrogenation of protoplast membranes is also possible.[186] The fluidity properties of biomembranes are mainly determined by the number and position of the *cis* double bonds in the unsaturated fatty acids. Many physiological and biochemical processes are fundamentally linked to the viscosity of the cell membrane. The homogeneously catalyzed hydrogenation of the *cis* double bonds of fatty acids within an intact membrane by means of a water-soluble catalyst can therefore contribute to a deeper understanding of the modification of membrane fluidity. The complex $[RuCl_2(tppms)_2]$[87] has been used for this purpose. The catalyst is very selective at 30 °C and 7 bar H_2 for the conversion of linoleic acid (C18, three double bonds) into less unsaturated C18 acids (two to zero double bonds). If the extent of hydrogenation exceeds 30%, a serious loss of living protoplasts takes place. Destruction of intact protoplasts can be avoided by shorter contact times. From kinetic considerations, cell-like defense reactions can work against the continuing hydrogenation according to the principle of "homeoviscous adaptation".

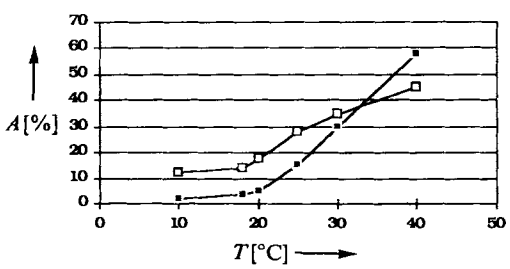

Fig. 13. Comparison of hydrogenation activities A (in % hydrogenation) of $[Ru^{II}Cl_2(tppms)_2]$ (□) and $[Rh^{I}Cl(tppms)_3]$ (■).

8.2. Light and Membrane Fluidity

Natural liposomes with a single or double layer can be hydrogenated by using the catalyst system $[RuCl_2(bpy)_3]$/$[RhCl(tppms)_3]$ (bpy = 2,2'-bipyridine)[187] with ascorbate as a light-induced hydride donor.[188] The combination of ruthenium and rhodium enables the nascent hydrogen to be produced in an ascorbate buffer. The light-collecting species is the complex $[RuCl_2(bpy)_3]$, and hydrogen transfer is performed by $[RhCl(tppms)_3]$/ascorbate.

The system is effective for the hydrogenation of ethene and ethyne and for the hydroformylation of ethene.[187] The in situ generated hydrogen enables hydrogenation even at 0.1 bar partial pressure (TON = 40 for ethene, quantum yield = 1.8). The pressureless(!) hydroformylation gives a TON of 3.5 with a quantum yield of 0.1% The mechanism of the quantum uptake by the Ru^{II} complex (Ru^{II}/Ru^{I} reduction) and the formation of the active species $[HRu(CO)(tppms)_3]$ is formulated in Equations (17–19). Despite these interesting results, the catalyst system is still somewhat unstable.

$$[Ru(bpy)_3]^{2+} + HA^- + e^- \xrightarrow{h\nu} [Ru(bpy)_3]^+ + A^{2-} + H^+ \quad (17)$$

$$2[Ru(bpy)_3]^+ + [RhCl(tppms)_3] \xrightarrow{2H^+} 2[Ru(bpy)_3]^{2+} + [H_2RhCl(tppms)_3] \quad (18)$$

$$2[Ru(bpy)_3]^+ + [RhCl(tppms)_3] \xrightarrow[-Cl^-]{H^- CO} 2[Ru(bpy)_3]^{2+} + [HRh(CO)(tppms)_3] + 2e^- \quad (19)$$

8.3. Regeneration of $NAD(P)^+$ with Water-Soluble Catalysts

$NAD(P)^+$ cofactors have important applications in biotechnological processes, for example, the conversion and storage of solar energy. According to the initial research into the regeneration of $NAD(P)^+$ cofactors,[189] $NAD(P)^+$ can be reduced in the presence of the water-soluble rhodium(III)

complex with tris(2,2'-bipyridyl-5-sulfonic acid) both electrochemically and photochemically with $[Ru(bpy)_3]^{2+}$ as a photosensitizer in aqueous alcoholic solution. However, reaction of the NAD(P)H and alcohol dehydrogenase with cyclohexanone yielded cyclohexanol in only small amounts. Only 46 catalytic cycles were performed in 33 days (based on the Rh complex). Higher conversions were achieved with $[RhCl(tppms)_3]$.[190] $NAD(P)^+$ cofactors are thermally and photochemically reduced. Formate and ascorbate were used as hydrogen sources. Kinetic investigations show that the rate-determining step is cleavage of the C–H bond and subsequent formation of a hydridorhodium species. The reaction follows Michaelis–Menten kinetics with an apparent activation energy of 20 kcal mol^{-1}. If the reduction is followed by an enzymatic reaction, such as reduction of acetaldehyde to ethanol by horse liver alcohol dehydrogenase, biologically active NAD(P)H can be produced, but the activities are inferior to reactions with conventionally regenerated NAD(P)H. Higher activities cannot be obtained, because the free ligand tppms produced by photodissociation acts as an inhibitor towards the metal complex. Reaction rates and regioselectivities of the reduction of $NAD(P)^+$ are low in comparison to enzymatic systems. A further problem is the inhibition of secondary enzymatic reactions by tppms.

9. Water-Soluble Catalysts—Colloids?

In spite of their catalytic potential, colloidal transition metals have so far attracted little attention. The preparation of stable water-soluble colloidal metals is comparatively simple, and their stability has recently been improved with the aid of sulfonated phosphane ligands such as tppms. Schmid et al. have carried out truly remarkable work on the preparation of water-soluble gold colloids (formula $[Au_x(tppms)_y]$, where $x/y = 20/1$, relative molecular weight about 40×10^6, particle diameter about 18 nm). The material has metallic properties, and can be repeatedly dissolved in and reprecipitated from water.[191, 192] Bönnemann et al. have shown that colloidal particles of various metals can be prepared from solution as a solid substance by stabilization with alkylammonium ions, can be stored in a stable condition, and subseqently redissolved. These operations leave the catalytic properties almost unchanged.[193, 194]

If the complex $[RhCl(tppts)_3]$ is prepared by the reaction of $RhCl_3 \cdot 3H_2O$ with tppts in an ethanol/water mixture, the ligand tppts is quickly and completely oxidized during the hydrogenation of an alkene (detected by ^{31}P NMR). This shows that rhodium colloids stabilized by phosphane oxide are the active species, as the rhodium remains in solution. Several publications on this theme have appeared recently, but they do not adequately explain the role of rhodium colloids in two-phase catalysis.[195–200]

Sinou et al. used the example of alkene hydrogenation to investigate the question of the homogeneous or heterogeneous nature of the active catalyst species in two-phase systems.[107] Catalysis experiments with chiral, water-soluble phosphanes and their oxides clearly showed that Rh^I forms enantioselective homogeneous catalysts with water-soluble phosphanes. On the other hand, systems containing Rh^I and phosphane oxide show the same hydrogenation activity but no optical induction, from which the existence of a colloidal "heterogeneous catalyst" is deduced. The same is true if a Rh^{III} starting complex is present. The reduction to Rh^I (preformation) is associated with the oxidation of the phosphane. The catalyst formed shows hydrogenation activity but is not enantioselective. All these findings support the view that rhodium colloids, which are stabilized by phosphane oxides and are active hydrogenation catalysts, are present in aqueous systems.

The redox chemistry of the simple system $RhCl_3 \cdot 3H_2O$/tppts in water was thoroughly investigated by Patin et al.[201] The formation of an Rh^{III}–hydroxo complex according to Equation (20) followed by coordination of a molecule of tppts according to Equation (21) leads to the reduction of Rh^{III} to Rh^I. Labeling experiments with $H_2{}^{18}O$ identified water as the source of oxygen in the concomitant phosphane oxidation. In the presence of acids or chloride-containing salts, the formation of the chloro(hydroxo) complex in Equation (20) can be suppressed. Accordingly, the addition

$$RhCl_3 + H_2{}^*O \rightleftharpoons [RhCl_2(^*OH)] + HCl \quad (20)$$

$$[Rh^{III}Cl_2(^*OH)] + P(m\text{-}C_6H_4SO_3Na)_3 \xrightarrow{-HCl} \underset{\mathbf{1}}{} \{Rh^ICl\} + {}^*O{=}P(m\text{-}C_6H_4SO_3Na)_3 \quad (21)$$

$$\{Rh^ICl\} + 3P(m\text{-}C_6H_4SO_3Na)_3 \longrightarrow \underset{\mathbf{50}}{[Rh^ICl\{P(m\text{-}C_6H_4SO_3Na)_3\}_3]} \quad (22)$$

of 0.5 M $HClO_4$ or 2 M NaCl solution reduced the extent of phosphane oxidation from 70% (without addition) to 12% or 5%.[199] The solvent-stabilized Rh^I chloride is coordinated by free unoxidized tppts, and forms the water-soluble complex **50** analogous to the Wilkinson compound [Eq. (22)]. It eliminates a molecule of tppts to form the solvated complex **51,** which dimerizes to the stable compound **52** (P = phosphane) [Equation (23)]. This study emphasizes that the situation for even simple catalyst systems in water is much more complex than for normal homogeneous catalytic systems in organic media. The findings further support the idea of catalytically active colloids. Their role is still poorly understood, but their potential is obvious.[193, 194]

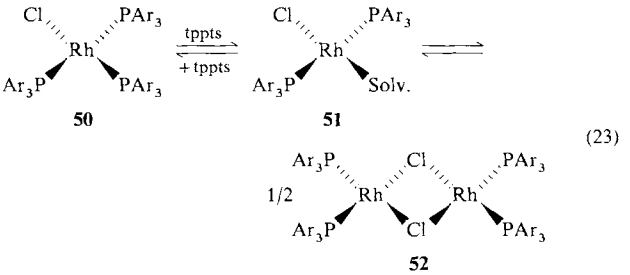

(23)

10. Perspectives

Following the technological breakthrough of the Ruhrchemie/Rhône–Poulenc process (1984), water-soluble catalysts based on coordination complexes and organo-

metallic compounds have promoted the long overdue bridging of the chasm between homogeneous and heterogeneous catalysis. The concept of stationary supports ("immobilized" homogeneous catalysts), which has to date not had any convincing success, has been overtaken by that of "mobile carriers", in which water, the catalyst medium, brings additional process advantages. Common ground first appeared in 1989 with the development of supported aqueous phase catalysts (SAP catalysts). The sometimes excellent compatibility of complex catalysts with water (up to 130 °C process temperature) was not expected even by experts in catalysis, who need to get accustomed to the idea. To ensure success, the ligands selected must have very high solubility in water. Experience suggests that 1 $kg\,L^{-1}$ is a practical guideline. However, this criterion is not met by all the ligand classes usually used in homogeneous catalysis, so synthetic chemistry is again required. Rh-catalyzed hydroformylation, the most extensively investigated process, provides convincing evidence of the advantages of the two-phase aqueous reaction system. All the phosphane ligands tested so far are more active and selective in their water-soluble (sulfonated) forms than in the homogeneously catalyzed process, often by a very large margin. Water is excellent as a reaction and catalyst medium on grounds of solubility (for example, differential solubility of starting compound and product(s)) or the thermodynamics of a desired reaction.[207] These advantages combine ideally with the techniques of separation and recycling of the noble metal, which are continuously being perfected. This young interdisciplinary field of modern catalyst research and technology belongs to the future in research at universities and in industry.[169] Even organometallic complex catalysts such as the much investigated methyltrioxorhenium(VII) ($[CH_3ReO_3]$) are soluble and stable in water.[202]

This article results from a joint research project of Hoechst AG (Werk Ruhrchemie) and the Technische Universität München. Since 1986 this project has followed the new developments in two-phase hydroformylation and its potential. As is typical for this field, the authors came into contact with the subject through practical industrial experience and must thank their colleagues in Oberhausen for numerous consultations over several years of collaboration, especially Drs. Bahrmann, Frohning, Heymanns, Konkol, Kottmann, Lappe, Peters, Reichelt, and Weber. We also acknowledge fruitful cooperation with former Doctoral students Jürgen Kulpe (Hoechst AG), Jürgen Kellner (Deutsche Shell AG), and Herbert Riepl (Klinge-Stiftung Holding GmbH) in the Munich institute as well as the present PhD students Rainer Manetsberger, Guido Albanese, and Rochus Schmid. Special thanks are due to Professor Boy Cornils and Professor Klaus Kühlein (both Hoechst AG) for their hospitality to W.A.H. and for numerous scientific discussions.

Received: May 7, 1993 [A 922 IE]
German version: *Angew. Chem.* **1993**, *105*, 1588
Translated by R. G. Leach, Basingstoke (UK)

[1] W. A. Herrmann, C. W. Kohlpaintner, H. Bahrmann, W. Konkol, *J. Mol. Catal.* **1992**, *73*, 191–201.
[2] a) W. Keim, T. M. Shryne, R. S. Bauer, H. Chung, P. W. Glockner, H. van Zwet (SHELL Int. Res.), DE-P 2054009, **1969**; b) W. Keim, *Chem. Ing. Techn.* **1984**, *56*, 850–853; c) A. Behr, W. Keim, *Arab. J. Science Eng.* **1985**, *10*, 377–385; d) A. Durocher, Dissertation, Rheinisch-Westfälische Technische Hochschule Aachen **1976**; e) A. Durocher, W. Keim, P. Voncken, *Erdöl und Kohle*, Compendium 75/76, pp. 347–354 (3. DGMK-Fachgruppentagung, 6.–8.10.1975, Hannover); W. Keim, A. Durocher, P. Voncken, *Erdoel Kohle Erdgas Petrochem.* **1976**, *29*, 31.
[3] A. F. Borowski, D. J. Cole-Hamilton, G. Wilkinson, *Nouv. J. Chim.* **1978**, *2*, 137–144.
[4] a) F. Joó, Z. Tóth, *J. Mol. Catal.* **1980**, *8*, 369–383; b) D. Sinou, *Bull. Soc. Chim. Fr.* **1987**, *3*, 480–486.
[5] T. G. Southern, *Polyhedron* **1989**, *8*, 407–413.
[6] M. Barton, J. D. Atwood, *J. Coord. Chem.* **1991**, *24*, 43–67.
[7] Up-to-date survey: P. Kalck, F. Monteil, *Adv. Organomet. Chem.* **1992**, *34*, 219–284.
[8] F. Alario, Y. Amrani, Y. Colleuille, T. P. Dang, J. Jenck, D. Morel, D. Sinou, *J. Chem. Soc. Chem. Commun.* **1986**, 202–203.
[9] Y. Amrani, L. Lecomte, D. Sinou, J. Bakos, I. Tóth, B. Heil, *Organometallics* **1989**, *8*, 542–547.
[10] L. Lecomte, D. Sinou, *Phosphorus Sulfur Silicon Relat. Elem.* **1990**, *53*, 239–251.
[11] M. Laghmari, D. Sinou, *J. Mol. Catal.* **1991**, *66*, L15–L18.
[12] R. B. Manetsberger, Diplomarbeit, Technische Universität München, **1991**.
[13] G. Papadogianakis, B. Fell, H. Bahrmann (Hoechst AG), EP-B 489330, **1992**; *Chem. Abstr.* **1992**, *117*, 131385m.
[14] T. Bartik, B. Bartik, B. E. Hanson, I. Guo, I. Tóth, *Organometallics* **1993**, *12*, 164–170.
[15] C. Larpent, H. Patin, N. Thilmont, J. F. Valdor, *Synth. Commun.* **1991**, *21*, 495–503.
[16] W. A. Herrmann, R. B. Manetsberger, (Hoechst AG), P4321512.2, **1993**.
[17] H. Schindlbauer, *Monatsh. Chem.* **1965**, *96*, 2051–2057.
[18] a) O. Herd, K. P. Langhans, O. Stelzer, N. Weferling, W. S. Sheldrick, *Angew. Chem.* **1993**, *105*, 1097–1099; *Angew. Chem. Int. Ed. Engl.* **1993**, *32*, 1058–1059; b) K. P. Langhans, N. Weferling, O. Stelzer (Hoechst AG), DE 4141299. A1, **1993**.
[19] B. Fell, G. Papadogianakis, W. Konkol, J. Weber, H. Bahrmann, *J. Prakt. Chem.* **1993**, *335*, 75–82.
[20] a) R. G. Nuzzo, D. Feitler, G. M. Whitesides, *J. Am. Chem. Soc.* **1979**, *101*, 3683–3685; b) R. G. Nuzzo, S. L. Haynie, M. E. Wilson, G. M. Whitesides, *J. Org. Chem.* **1981**, *46*, 2861–2867.
[21] R. Benhazma, Y. Amrani, D. Sinou, *J. Organomet. Chem.* **1985**, *288*, C37–C39.
[22] S. Ganguly, J. T. Mague, D. M. Roundhill, *Inorg. Chem.* **1992**, *31*, 3500–3501.
[23] E. Paetzold, A. Kinting, G. Oehme, *J. Prakt. Chem.* **1987**, *329*, 725–731.
[24] E. Paetzold, G. Oehme, *Z. Chem.* **1989**, *29*, 447–448.
[25] B. Fell, G. Papadogianakis, *J. Mol. Catal.* **1991**, *66*, 143–154.
[26] R. T. Smith, M. C. Baird, *Transition Met. Chem. London* **1981**, *6*, 197–198.
[27] R. T. Smith, R. K. Ungar, M. C. Baird, *Transition Met. Chem. London* **1982**, *7*, 288–289.
[28] R. T. Smith, M. C. Baird, *Inorg. Chim. Acta* **1982**, *62*, 135–139.
[29] a) I. Tóth, B. E. Hanson, *Organometallics*, **1993**, *12*, 1506–1513; b) I. Tóth, B. E. Hanson, M. E. Davis, *Catal. Lett.* **1990**, *5*, 183–188.
[30] G. Peiffer, S. Chhan, A. Bendayan, B. Waegell, J. P. Zahra, *J. Mol. Catal.* **1990**, *59*, 1–9.
[31] U. Nagel, E. Kinzel, *Chem. Ber.* **1986**, *119*, 1731–1733.
[32] F. G. Mann, I. T. Millar, *J. Chem. Soc.* **1952**, 4453–4457.
[33] M. M. Rauhut, I. Hechenbleikner, H. A. Currier, F. C. Schaefer, V. P. Wystrach, *J. Am. Chem. Soc.* **1959**, *81*, 1103–1107.
[34] K. Issleib, G. Thomas, *Chem. Ber.* **1960**, *93*, 803–808.
[35] K. Issleib, R. Kümmel, H. Zimmermann, *Angew. Chem.* **1965**, *77*, 172–173; *Angew. Chem. Int. Ed. Engl.* **1965**, *4*, 155–156.
[36] T. Jarolím, J. Podlahová, *J. Inorg. Nucl. Chem.* **1976**, *38*, 125–129.
[37] J. Podlahová, F. Hartl, *Collect. Czech. Chem. Commun.* **1984**, *49*, 586–591.
[38] D. Nosková, J. Podlahová, *Polyhedron* **1983**, *2*, 349–351.
[39] J. Podlahová, J. Podlaha, *Collect. Czech. Chem. Commun.* **1980**, *45*, 2049–2053.
[40] A. Jegorow, J. Podlaha, *Catal. Lett.* **1991**, *9*, 9–14.
[41] H. Gilman, G. E. Brown, *J. Am. Chem. Soc.* **1945**, *67*, 824–826.
[42] R. Luckenbach, K. Lorenz, *Z. Naturforsch. B* **1977**, *32*, 1038–1047.
[43] a) V. Ravindar, H. Hemling, H. Schumann, J. Blum, *Synth. Commun.* **1992**, *22*, 841–851; b) V. Ravindar, H. Hemling, H. Schumann, J. Blum, *ibid.* **1992**, *22*, 1453–1459.
[44] A. Badener, E. Lindner, *Coord. Chem. Rev.* **1991**, *108*, 27–110.
[45] A. Avey, D. M. Schut, T. J. R. Weakley, D. R. Tyler, *Inorg. Chem.* **1993**, *32*, 233–236.
[46] F. Mathey, Ecôle Polytechnique Paris, personal communication.
[47] Y. Amrani, D. Sinou, *J. Mol. Catal.* **1984**, *24*, 231–233.
[48] M. E. Wilson, R. G. Nuzzo, G. M. Whitesides, *J. Am. Chem. Soc.* **1978**, *100*, 2269–2270.
[49] Y. Amrani, D. Sinou, *J. Mol. Catal.* **1986**, *36*, 319–327.

[50] T. Okano, M. Yamamoto, T. Noguchi, H. Konishi, J. Kiji, *Chem. Lett.* **1982**, 977-980.
[51] T. Okano, M. Iwahara, T. Suzuki, H. Konishi, J. Kiji, *Chem. Lett.* **1986**, 1467-1470.
[52] T. Okano, M. Iwahara, H. Konishi, J. Kiji, *J. Organomet. Chem.* **1988**, *346*, 267-275.
[53] J. Chatt, G. J. Leigh, R. M. Slade, *J. Chem. Soc. Dalton Trans.* **1973**, 2021-2028.
[54] a) K. Issleib, H. M. Möbius, *Chem. Ber.* **1961**, *94*, 102-106; b) P. A. T. Hoye, P. G. Pringle, M. B. Smith, K. Worboys, *J. Chem. Soc. Dalton Trans.* **1993**, 269-274.
[55] K. N. Harrison, P. A. T. Hoye, A. G. Orpen, P. G. Pringle, M. B. Smith, *J. Chem. Soc. Chem. Commun.* **1989**, 1096-1097.
[56] J. W. Ellis, K. N. Harrison, P. A. T. Hoye, A. G. Orpen, P. G. Pringle, M. B. Smith, *Inorg. Chem.* **1992**, *31*, 3026-3033.
[57] T. N. Mitchell, K. Heesche-Wagner, *J. Organomet. Chem.* **1992**, *436*, 43-53.
[58] E. Renaud, R. B. Russell, S. Fortier, S. J. Brown, M. C. Baird, *J. Organomet. Chem.* **1991**, *419*, 403-415.
[59] E. Renaud, M. C. Baird, *J. Chem. Soc. Dalton Trans.* **1992**, 2905-2906.
[60] W. A. Herrmann, W. R. Thiel, J. G. Kuchler, *Chem. Ber.* **1990**, *123*, 1953-1961.
[61] W. A. Herrmann, W. R. Thiel, J. G. Kuchler, J. Behm, E. Herdtweck, *Chem. Ber.* **1990**, *123*, 1963-1970.
[62] L. Vigh, F. Joó, *FEBS Lett.* **1983**, *162*, 423-427.
[63] L. Vigh, Z. Gombos, F. Joó, *FEBS Lett.* **1985**, *191*, 200-204.
[64] G. Schmid, B. Morun, J. O. Malm, *Angew. Chem.* **1989**, *101*, 772-773; *Angew. Chem. Int. Ed. Engl.* **1989**, *28*, 778-780.
[65] U. Siemeling, *J. Organomet. Chem.* **1992**, *429*, C14-C18.
[66] E. G. Kuntz (Rhône-Poulenc Ind.), FR-B 2314190, **1975**.
[67] T. Bartik, B. Bartik, B. E. Hanson, K. H. Whitmire, I. Guo, *Inorg. Chem.* **1993**, *32*, in press.
[68] a) S. Ahrland, J. Chatt, N. R. Davies, A. A. Williams, *Nature* **1957**, *179*, 1187-1188; b) S. Ahrland, J. Chatt, N. R. Davies, A. A. Williams, *J. Chem. Soc.* **1958**, 276-288.
[69] E. G. Kuntz, *CHEMTECH* **1987**, *17*, 570-575.
[70] L. Lecomte, J. Triolet, D. Sinou, J. Bakos, B. Heil, *J. Chromatogr.* **1987**, *408*, 416-419.
[71] L. Lecomte, D. Sinou, *J. Chromatogr.* **1990**, *514*, 91-96.
[72] B. Fontal, J. Orlewski, C. Santini, J. M. Basset, *Inorg. Chem.* **1986**, *25*, 4320-4322.
[73] C. Larpent, R. Dabard, H. Patin, *New J. Chem.* **1988**, *12*, 907-913.
[74] C. Larpent, H. Patin, *Appl. Organomet. Chem.* **1987**, *1*, 529-534.
[75] W. A. Herrmann, J. A. Kulpe, J. Kellner, H. Riepl, H. Bahrmann, W. Konkol, *Angew. Chem.* **1990**, *102*, 408-414; *Angew. Chem. Int. Ed. Engl.* **1990**, *29*, 391-393.
[76] W. A. Herrmann, J. A. Kulpe, H. Bahrmann, W. Konkol, *J. Organomet. Chem.* **1990**, *389*, 85-101.
[77] W. A. Herrmann, J. Kellner, H. Riepl, *J. Organomet. Chem.* **1990**, *389*, 103-128.
[78] J. A. Kulpe, Dissertation, Technische Universität München, **1989**.
[79] W. A. Herrmann, C. W. Kohlpaintner, J. A. Kulpe, H. Bahrmann, W. Konkol, unpublished results.
[80] D. J. Darensbourg, C. J. Bischoff, J. H. Reibenspies, *Inorg. Chem.* **1991**, *30*, 1144-1147.
[81] C. A. Tolman, *Chem. Rev.* **1977**, *77*, 313-348.
[82] T. Bartik, B. Bartik, B. E. Hanson, T. Glass, W. Bebout, *Inorg. Chem.* **1992**, *31*, 2667-2670.
[83] E. Fache, C. Santini, F. Senocq, J. M. Basset, *J. Mol. Catal.* **1992**, *72*, 331-336.
[84] F. Joó, M. T. Beck, *React. Kinet. Catal. Lett.* **1975**, *2*, 257-263.
[85] Y. Dror, J. Manassen, *J. Mol. Catal.* **1977**, *2*, 219-222.
[86] F. Joó, Z. Tóth, M. T. Beck, *Inorg. Chim. Acta* **1977**, *25*, L61-L62.
[87] Z. Tóth, F. Joó, M. T. Beck, *Inorg. Chim. Acta* **1980**, *42*, 153-161.
[88] J. M. Grosselin, C. Mercier, *J. Mol. Catal.* **1990**, *63*, L25-L27.
[89] J. M. Grosselin, C. Mercier, G. Allmang, F. Grass, *Organometallics* **1991**, *10*, 2126-2133.
[90] F. Joó, A. Bényei, *J. Organomet. Chem.* **1989**, *363*, C19-C21.
[91] A. Bényei, F. Joó, *J. Mol. Catal.* **1990**, *58*, 151-163.
[92] R. Bar, L. K. Bar, Y. Sasson, J. Blum, *J. Mol. Catal.* **1985**, *33*, 161-177.
[93] R. T. Smith, R. K. Ungar, L. J. Sanderson, M. C. Baird, *Organometallics* **1983**, *2*, 1138-1144.
[94] F. Joó, L. Somsák, M. T. Beck, *J. Mol. Catal.* **1984**, *24*, 71-75.
[95] T. Okano, Y. Moriyama, H. Konishi, J. Kiji, *Chem. Lett.* **1986**, 1463-1466.
[96] E. Fache, F. Senocq, C. Santini, J.-M. Basset, *J. Chem. Soc. Chem. Commun.* **1990**, 1776-1778.
[97] J. Bakos, A. Orosz, B. Heil, M. Laghmari, P. Lhoste, D. Sinou, *J. Chem. Soc. Chem. Commun.* **1991**, 1684-1685.
[98] C. Lensink, J. G. de Vries, *Tetrahedron Asymmetry* **1992**, *3*, 235-238.
[99] L. Lecomte, D. Sinou, J. Bakos, I. Tóth, B. Heil, *J. Organomet. Chem.* **1989**, *370*, 277-284.
[100] I. Ojima, T. Kogure, N. Yoda, *J. Org. Chem.* **1980**, *45*, 4728-4739.
[101] J. Halpern in *Asymmetric Synthesis Vol. 5* (Ed.: J. D. Morrison), Academic Press, Orlando, FL, USA **1985**, p. 41.
[102] M. H. Abraham, P. L. Grellier, R. A. McGill, *J. Chem. Soc. Perkin Trans. 2* **1988**, 339-345.
[103] M. Laghmari, D. Sinou, *J. Organomet. Chem.* **1992**, *438*, 213-216.
[104] D. Sinou, M. Safi, C. Claver, A. Masdeu, *J. Mol. Catal.* **1991**, *68*, L9-L12.
[105] E. Fache, C. Santini, F. Senocq, J. M. Basset, *J. Mol. Catal.* **1992**, *72*, 337-350.
[106] I. Tóth, B. E. Hanson, M. E. Davis, *Tetrahedron Asymmetry* **1990**, *1*, 913-930.
[107] L. Lecomte, D. Sinou, *J. Mol. Catal.* **1989**, *52*, L21-L24.
[108] a) Y. Tokitoh, N. Yoshimura (Kuraray Co.); US-A 4808756, **1989**; N. Yoshimura, M. Tamura (Kuraray Co.), EP-B 04362226, **1990**; b) *Homogeneous Catalysis* (Eds.: G. W. Parshall, S. D. Ittel), 2nd ed., Wiley, New York, **1992**, p. 126.
[109] a) E. G. Kuntz (Rhône-Poulenc Ind.), FR-B 2366237, **1976**; b) E. G. Kuntz (Rhône-Poulenc Ind.), DE-B 2733516, **1978**; *Chem. Abstr.* **1978**, *88*, 152026t.
[110] D. Morel (Rhône-Poulenc Ind.), EP-B 8044771, **1980**.
[111] D. Morel (Rhône-Poulenc Ind.), US-A 4460786, **1984**.
[112] G. Mignani, D. Morel, Y. Colleuille, *Tetrahedron Lett.* **1985**, *26*, 6337-6340.
[113] A. L. Casalnuovo, J. C. Calabrese, *J. Am. Chem. Soc.* **1990**, *112*, 4324-4330.
[114] J. P. Genet, E. Blart, M. Savignac, *Synlett* **1992**, 715-717.
[115] M. Safi, D. Sinou, *Tetrahedron Lett.* **1991**, *32*, 2025-2028.
[116] T. Okano, N. Okabe, J. Kiji, *Bull. Chem. Soc. Jpn.* **1992**, *65*, 2589-2593.
[117] J. Kiji, T. Okano, W. Nishiumi, H. Konishi, *Chem. Lett.* **1988**, 957-960.
[118] T. Okano, I. Uchida, T. Nakagaki, H. Konishi, J. Kiji, *J. Mol. Catal.* **1989**, *54*, 65-71.
[119] T. I. Wallow, B. M. Novak, *J. Am. Chem. Soc.* **1991**, *113*, 7411-7412.
[120] a) D. M. Golden, D. F. McMillen, *Annu. Rev. Phys. Chem.* **1982**, *33*, 493-532; b) M. P. Stevens, *Polymer Chemistry*, Oxford University Press, London, **1990**.
[121] a) E. G. Kuntz (Rhône-Poulenc Ind.), FR-B 2338253, **1976**; b) E. G. Kuntz (Rhône-Poulenc Ind.), DE-B 2700904, **1977**; *Chem. Abstr.* **1977**, *87*, 117602k.
[122] B. Cornils, W. A. Herrmann, C. W. Kohlpaintner, *Nachr. Chem. Tech. Lab.* **1993**, *41*, 544-550.
[123] B. Cornils in *New Syntheses with Carbon Monoxide* (Ed.: J. Falbe), Springer-Verlag, Berlin, **1980**, Chapter 1.
[124] Dr. Kirchhoff, Hoechst AG, personal communication **1991**.
[125] O. Horn, H. Bestian, *Chem. Technol. 2nd ed.* **1959**, *3*, 744-747.
[126] *Produkte aus der Oxo-Synthese*, Technische Information Farbwerke Hoechst AG/Ruhrchemie AG, Frankfurt, **1969**, p. 11.
[127] H. Bestian, H.-J. Friedrich, O. Horn, *Chem. Technol., revised edition, 3rd ed. 1969-1975*, **1972**, *4*, 85-88.
[128] J. Falbe, W. Payer, *Ullmanns Encykl. Tech. Chem. 4th ed. 1972-1984* **1974**, *7*, 118-141.
[129] K. Weissermel, H.-J. Arpe, *Industrielle Organische Chemie*, 3rd ed., VCH, Weinheim, **1988**, p. 134.
[130] H. Bahrmann, H. Bach, *Ullmanns Encycl. Ind. Chem. 5th ed.* **1991**, *A18*, 321-327.
[131] B. Cornils, J. Hibbel, W. Konkol, B. Lieder, J. Much, V. Schmid, E. Wiebus (Ruhrchemie AG), DE-B 3234701, **1982**; *Chem. Abstr.* **1984**, *100*, 194022k.
[132] R. Gärtner, B. Cornils, L. Bexten, D. Kupies (Ruhrchemie AG), DE-B 3235029, **1982**; *Chem. Abstr.* **1984**, *100*, 198449c.
[133] R. Gärtner, B. Cornils, H. Springer, P. Lappe (Ruhrchemie AG), DE-B 3235030, **1982**; *Chem. Abstr.* **1984**, *101*, 55331t.
[134] L. Bexten, B. Cornils, D. Kupies (Ruhrchemie AG), DE-B 3431643, **1984**; *Chem. Abstr.* **1986**, *105*, 117009n.
[135] H. Bahrmann, B. Cornils, W. Konkol, W. Lipps (Ruhrchemie AG), DE-B 3412335, **1984**; *Chem. Abstr.* **1985**, *104*, 185989m.
[136] B. Cornils, W. Konkol, H. Bach, W. Gick, E. Wiebus, H. Bahrmann, H. Hahn (Ruhrchemie AG), DE-B 3546123, **1985**; *Chem. Abstr.* **1987**, *107*, 153922e.
[137] H. Bach, H. Bahrmann, B. Cornils, W. Gick, V. Heim, W. Konkol, E. Wiebus (Ruhrchemie AG), DE-B 3726128, **1987**; *Chem. Abstr.* **1989**, *111*, 156420h.
[138] G. Dämbkes, H. Hahn, J. Hibbel, W. Materne (Ruhrchemie AG), DE-B 3347406, **1983**; *Chem. Abstr.* **1985**, *103*, 127031m.
[139] B. Cornils, W. Konkol, H. Bahrmann, H. Bach, E. Wiebus (Ruhrchemie AG), DE-B 3443474, **1984**; *Chem. Abstr.* **1986**, *105*, 210764q.
[140] P. Lappe, H. Springer (Hoechst AG), DE-B 3934824, **1989**; *Chem. Abstr.* **1991**, *114*, 231481w.
[141] W. A. Herrmann, J. Kulpe, J. Kellner, H. Riepl (Hoechst AG), DE-B 3840600, **1988**; *Chem. Abstr.* **1990**, *114*, 43174z.
[142] W. A. Herrmann, J. Kulpe, J. Kellner, H. Riepl (Hoechst AG), DE-B 3921295, **1989**; *Chem. Abstr.* **1990**, *114*, 143702p.
[143] W. A. Herrmann, C. W. Kohlpaintner, H. Bahrmann (Hoechst AG), DE-B 4040314, **1990**; *Chem. Abstr.* **1992**, *117*, 151154p.

[144] W. A. Herrmann, C. W. Kohlpaintner, R. B. Manetsberger, H. Bahrmann (Hoechst AG), DE-B 4220267A, **1992**.
[145] H. Bach, H. Bahrmann, W. Gick, W. Konkol, E. Wiebus, *Chem. Ing. Tech.* **1987**, *59*, 882–883.
[146] H. Bahrmann, H. Bach, *Phosphorus Sulfur Silicon Relat. Elem.* **1987**, *30*, 611–614.
[147] B. C. Gates, *Catalytic Chemistry*, Wiley, New York, **1992**, Chapter 2.
[148] D. R. Bryant, E. Billig, *4th Int. Conf. on the Chemistry of the Platinum Group Metals*, **1990** (proceedings).
[149] E. Billig, A. G. Abatjoglou, D. R. Bryant, (Union Carbide Corp.), US-A 4769498, **1988**; *Chem. Abstr.* **1988**, *111*, 117287a.
[150] G. D. Cuny, S. L. Buchwald, *J. Am. Chem. Soc.* **1993**, *115*, 2066–2068.
[151] W. Konkol, main lecture at the GdCh-Hauptversammlung, München, **1991**; see also W. Konkol, H. Bahrmann, *Gesellschaft Deutscher Chemiker, 23. Hauptversammlung*, VCH, Weinheim, **1991**, p. 95.
[152] I. T. Horváth, R. V. Kastrup, A. A. Oswald, E. J. Mozeleski, *Catal. Lett.* **1989**, *2*, 85–90.
[153] R. A. Dubois, P. E. Garrou, K. Lavin, H. R. Allock, *Organometallics* **1984**, *3*, 649–650.
[154] A. G. Abatjoglou, E. Billig, D. R. Bryant, *Organometallics* **1984**, *3*, 923–926.
[155] A. G. Abatjoglou, D. R. Bryant, *Organometallics* **1984**, *3*, 932–934.
[156] R. M. Deshpande, S. S. Divekar, R. V. Gholap, R. V. Chaudhari, *J. Mol. Catal.* **1991**, *67*, 333–338.
[157] M. K. Markiewicz, M. C. Baird, *Inorg. Chim. Acta* **1986**, *113*, 95–99.
[158] P. Escaffre, A. Thorez, P. Kalck, *J. Chem. Soc. Chem. Commun.* **1987**, 146–147.
[159] P. Escaffre, A. Thorez, P. Kalck, *New J. Chem.* **1987**, *11*, 601–604.
[160] P. Kalck, P. Escaffre, F. Serein-Spirau, A. Thorez, *New J. Chem.* **1988**, *12*, 687–690.
[161] P. Kalck, *Pure Appl. Chem.* **1989**, *61*, 967–971.
[162] P. Kalck, *Polyhedron* **1988**, *7*, 2441–2450.
[163] I. Tóth, B. E. Hanson, I. Guo, M. E. Davis, *Catal. Lett.* **1991**, *8*, 209–214.
[164] K. S. Ro, S. I. Woo, *Appl. Catal.* **1991**, *69*, 169–175.
[165] K. S. Ro, S. I. Woo, *Catal. Sci. Technol.* **1991**, 369–372.
[166] J. R. Anderson, E. M. Campi, W. R. Jackson, *Catal. Lett.* **1991**, *9*, 55–58.
[167] a) F. R. Hartley, *Supported Metal Complexes*, Reidel, Dordrecht, **1985**; b) Y. I. Yermakov, B. N. Kuznetsov, V. A. Zakharov, *Catalysis by Supported Compounds*, Elsevier, New York, **1981**; c) *Tailored Metal Catalysis* (Ed.: Y. Iwasawa), Reidel, Boston, **1986**.
[168] J. Haggin, *Chem. Eng. News* **1992**, *70* (20), 25–26.
[169] W. A. Herrmann, *Hoechst High Chem. Magazine* **1992**, No. 13, 14–23.
[170] J. Haggin, *Chem. Eng. News* **1992**, *70* (17), 40–41.
[171] J. P. Arhancet, M. E. Davis, J. S. Merola, B. E. Hanson, *Nature* **1989**, *339*, 454–455.
[172] J. P. Arhancet, M. E. Davis, J. S. Merola, B. E. Hanson, *J. Catal.* **1990**, *121*, 327–339.
[173] I. T. Horváth, *Catal. Lett.* **1990**, *6*, 43–48.
[174] I. Guo, B. E. Hanson, I. Tóth, M. E. Davis, *J. Organomet. Chem.* **1991**, *403*, 221–227.
[175] a) J. P. Arhancet, M. E. Davis, B. E. Hanson, *J. Catal.* **1991**, *129*, 94–99; b) J. P. Arhancet, M. E. Davis, B. E. Hanson, *ibid.* **1991**, *129*, 100–105.
[176] I. Guo, B. E. Hanson, I. Tóth, M. E. Davis, *J. Mol. Catal.* **1991**, *70*, 363–368.
[177] E. Fache, C. Mercier, N. Pagnier, B. Despeyrous, P. Panster, *J. Mol. Catal.* **1993**, *79*, 117–131.
[178] J. P. Arhancet, M. E. Davis, B. E. Hanson, *Catal. Lett.* **1991**, *11*, 129–136.
[179] M. E. Davis, *CHEMTECH* **1992**, *22*, 498–502.
[180] T. D. Madden, P. J. Quinn, *Biochem. Soc. Trans.* **1978**, *6*, 1345–1347.
[181] T. D. Madden, W. E. Peel, P. J. Quinn, D. Chapman, *J. Biochem. Biophys. Methods* **1980**, *2*, 19–27.
[182] F. Farin, H. L. M. van Gaal, S. L. Bonting, F. J. M. Daemen, *Biochim. Biophys. Acta* **1982**, *711*, 336–344.
[183] C. Katagiri, J. S. Owen, P. J. Quinn, D. Chapman, *Eur. J. Biochem.* **1981**, *118*, 335–338.
[184] A. L. Lehninger, *Prinzipien der Biochemie*, de Gruyter, Berlin, **1987**, p. 348.
[185] L. Vigh, F. Joó, P. R. van Hasselt, P. J. C. Kuiper, *J. Mol. Catal.* **1983**, *22*, 15–19.
[186] L. Vigh, F. Joó, A. Cséplö, *Eur. J. Biochem.* **1985**, *146*, 241–244.
[187] I. Willner, R. Maidan, *J. Chem. Soc. Chem. Commun.* **1988**, 876–877.
[188] F. Joó, E. Csuhai, P. J. Quinn, L. Vigh, *J. Mol. Catal.* **1988**, *49*, L1–L5.
[189] M. Franke, E. Steckhan, *Angew. Chem.* **1988**, *100*, 295–297; *Angew. Chem. Int. Ed. Engl.* **1988**, *27*, 265–267.
[190] I. Willner, R. Maidan, M. Shapira, *J. Chem. Soc. Perkin Trans. 2* **1990**, 559–564.
[191] G. Schmid, A. Lehnert, *Angew. Chem.* **1989**, *101*, 733–734; *Angew. Chem. Int. Ed. Engl.* **1989**, *28*, 780–781.
[192] G. Schmid, N. Klein, L. Korste, U. Kreibig, D. Schönauer, *Polyhedron* **1988**, *7*, 605–608.
[193] H. Bönnemann, W. Brijoux, R. Brinkmann, E. Dinjus, T. Joußen, B. Korall, *Angew. Chem.* **1991**, *103*, 1344–1346; *Angew. Chem. Int. Ed. Engl.* **1991**, *30*, 1312–1314.
[194] H. Bönnemann, T. Joußen, B. Korall, *J. Mol. Catal.* **1992**, *74*, 323–333.
[195] C. Larpent, R. Dabard, H. Patin, *Tetrahedron Lett.* **1987**, *28*, 2507–2510.
[196] C. Larpent, H. Patin, *J. Mol. Catal.* **1988**, *44*, 191–195.
[197] C. Larpent, H. Patin, *J. Mol. Catal.* **1990**, *61*, 65–73.
[198] C. Larpent, F. Brisse-Le Menn, H. Patin, *New J. Chem.* **1991**, *15*, 361–366.
[199] C. Larpent, F. Brisse-Le Menn, H. Patin, *J. Mol. Catal.* **1991**, *65*, L35–L40.
[200] C. Larpent, E. Bernard, *J. Chem. Soc. Chem. Commun.* **1992**, 535–536.
[201] C. Larpent, R. Dabard, H. Patin, *Inorg. Chem.* **1987**, *26*, 2922–2924.
[202] a) W. A. Herrmann, *Angew. Chem.* **1988**, *100*, 1269–1286; *Angew. Chem. Int. Ed. Engl.* **1988**, *27*, 1297–1313; b) W. A. Herrmann, D. W. Marz, R. W. Fischer, *ibid.* **1991**, *103*, 1706–1709 or **1991**, *30*, 1638–1641; c) W. A. Herrmann, R. W. Fischer, M. U. Rauch, W. Scherer, *ibid.* **1993**, *105*, 1209–1212 and **1993**, *32*, 1157–1160; d) W. A. Herrmann, *J. Organomet. Chem.* **1990**, *382*, 1–18.
[203] T. Bartik, B. Bartik, B. E. Hanson, *J. Mol. Catal.* **1993**, in press.
[204] A just published patent covers a membrane method for the separation of up to 99% of the water-soluble noble metal catalysts from hydroformylation processes: J. R. Livingston, E. J. Mozeleski, G. Sartori (Exxon Chem. Pat. Inc.), US-A 747597, **1993**.
[205] P. W. N. M. van Leuween, C. F. Roobeek, *J. Mol. Catal.* **1985**, *31*, 345–353.
[206] C. Botteghi, S. Paganelli, A. Schionato, M. Marchetti, *Chirality* **1991**, *3*, 355–369.
[207] *Note added in proof* (21.9.1993): This prediction has meanwhile been verified in terms of hydrogenation of CO_2 with Rh/tppts complexes of F. Gassner, W. Leitner, *J. Chem. Soc. Chem. Commun.* **1993**, in press.
[208] W. Konkol, H. Bahrmann, W. A. Herrmann, C. W. Kohlpaintner (Hoechst AG), DE-B 4135050, **1993**.

Hydrophobic Effects. Opinions and Facts

By Wilfried Blokzijl* and Jan B. F. N. Engberts*

The term hydrophobic interactions denotes the tendency of relatively apolar molecules to stick together in aqueous solution. These interactions are of importance in many chemical disciplines, including the chemistry of in vivo processes. Enzyme–substrate interactions, the assembly of lipids in biomembranes, surfactant aggregation, and kinetic solvent effects in water-rich solutions are all predominantly governed by hydrophobic interactions. Despite extensive research efforts, the hydration of apolar molecules and the noncovalent interactions between these molecules in water are still poorly understood. In fact, the question as to what the driving force for hydrophobic intractions is shifts the study into a quest for a detailed understanding of the remarkable properties of liquid water. This review highlights some of the novel insights that have been obtained in the past decade. The emphasis is on both hydrophobic hydration and hydrophobic interactions since both phenomena are intimately connected. Several traditional views have been found to be deeply unsatisfactory, and courageous attempts have been made to conceptualize the driving force behind pairwise and bulk hydrophobic interactions. The review presents an admittedly personal selection of the recent experimental and theoretical developments, and when necessary, reference is made to relevant studies of earlier date.

1. Introduction

1.1. General Remarks and Outline of the Review

At moderate temperatures and pressures, apolar compounds are poorly soluble in water. Traditionally, the reluctance of apolar compounds to dissolve in water has been attributed to the hydrophobicity of these compounds, in other words, their fear of water. In fact, the term hydrophobicity is misleading. The London dispersion interactions between water and apolar compounds are favorable and quite substantial.[1] It is more appropriate to point out that the apolar compound must intrude into a liquid that is characterized by an extended network of hydrogen bonds and an extremely high cohesive energy density. Each water molecule is strongly inclined not to sacrifice any of its hydrogen bonds, leading inevitably to significant reorientation of water molecules at the surface of the nonpolar solute molecule. Water is unique among solvents, because it has not only an exceptionally small molecular volume, but also the capacity to form a molecular network with tetrahedral coordination and an extremely low isothermic compressibility. This provides water with an almost unrivaled propensity to wrap itself around an apolar solute particle and simultaneously maintain most or all hydrogen bonds. But in spite of this unique structural solution, water must be considered a notoriously poor solvent for apolar compounds.

Unabated, chemists have sought a molecular interpretation of the hydrophobicity of apolar compounds. The first explanations were based on the capricious thermodynamic parameters of the hydration of these compounds in water at room temperature. The thermodynamic parameters of the solvation of gaseous methane in various organic solvents and water at 25 °C are given in Table 1. At room temperature, the dissolution of apolar gases in water is strongly promoted by enthalpy and characterized by an anomalously large change in heat capacity (for gaseous methane, the change in heat capacity (at 25 °C) amounts to 209 kJ mol^{-1} K^{-1}[2]). In contrast, the change in heat capacity upon solvation of gaseous methane in organic solvents is generally small. The poor solubility is completely governed by an extremely large loss of entropy. The partial molar volume of an apolar gas dissolved in water is generally similar to the molar volume of the gas at the boiling point, which is remarkable since the partial molar volume of solutes in organic solvents is significantly higher. Some of these striking thermodynamic properties were first identified by Butler and Reid.[3] In 1945 Frank and Evans[4] gave a molecular interpretation for these observations which would later become the archetype for further studies on hydrophobic effects. The model, generally known as the iceberg model, explained the unusually large entropy loss upon dissolution of apolar gases in terms of the structuring of water molecules in the near vicinity of the apolar solute. The emphasis on the enhanced local structure led to overinterpretation of the original idea in later studies, and frequently the hydration

Table 1. Thermodynamic parameters of solvation for gaseous methane in various organic solvents and water at 25 °C (taken from ref. [31]) [a].

Solvent	$\Delta G^{\ominus}$ [kJ mol^{-1}]	$\Delta H^{\ominus}$ [kJ mol^{-1}]	$-T\Delta S^{\ominus}$ [kJ mol^{-1}]
n-hexadecane	12.7	−2.30	15.0
n-decane	13.0	−4.31	17.3
n-hexane	13.1	−2.26	15.4
cyclohexane	14.2	−3.01	17.2
CCl_4	14.5	−2.97	17.5
diethyl ether	13.4	−3.34	16.7
benzene	15.3	−1.25	16.6
acetone	15.6	−2.80	18.4
1-propanol	16.0	−10.3	26.3
ethanol	16.5	−8.78	25.3
methanol	17.5	−7.94	25.4
water	25.5	−13.8	39.3

[a] For gaseous methane (1 atm) → solution with 1 mol% methane.

[*] Prof. Dr. J. B. F. N. Engberts, Dr. W. Blokzijl
Department of Organic and Molecular Inorganic Chemistry
University of Groningen, Nijenborgh 4
NL-9747 AG Groningen (The Netherlands)
Telefax: Int. code + (50)634-296

shell of apolar solute particles has been pictured as a rather rigid clathrate-like structure.[5] The idea of a special kind of hydration, referred to as hydrophobic hydration, became generally accepted.

It was proposed that the tendency of water molecules to avoid entropically unfavorable interactions with apolar solutes constitutes a driving force for the aggregation of apolar solutes. The notion that the interactions between apolar species in aqueous solution are primarily entropy driven gave chemists a genuine feeling of discomfort. In 1959 Kauzmann[6] introduced the concept of hydrophobic interactions, the alleged solvent-induced attractive forces between apolar molecules or moieties in aqueous solution. He suggested that the attractive interactions between apolar molecules or moieties in aqueous solution are promoted by the solvent as a result of destructive overlap of structured hydrophobic hydration shells, involving the release of structured hydration water into the bulk. Later, the idea of a hydrophobic bond received much attention, particularly in the field of protein chemistry.

Hydrophobic effects play a pivotal role in many chemical phenomena in aqueous solution. The stability of biological membranes as well as of the tertiary structure of proteins in aqueous solution depends critically on interactions between apolar moieties. Molecular recognition also relies strongly on noncovalent interactions, for which hydrophobic regions in host and guest molecules are often crucial. Apart from their importance in biological processes, hydrophobic effects are also important for various solution phenomena such as surfactant aggregation, mineral flotation, coagulation, complexation, and detergency. In addition, hydrophobic effects play a decisive role in the formation of gas clathrates and in surface phenomena such as wetting, aggregation processes at air–water interfaces, and forces between apolar surfaces. In view of the wide interest in hydrophobic effects it is essential to have a clear understanding of the molecular nature behind these phenomena.

Although the qualitative concept of the increased structuring of water in hydrophobic hydration shells has provided a popular explanation for the unusual thermodynamic properties of aqueous solutions of apolar compounds, serious doubts have been voiced occasionally concerning the existence of hydrophobic effects. Frequent suggestions have been made to reassess the traditional ideas about hydrophobic effects and to adjust the somewhat dogmatic picture of hydrophobic hydration. More recently, rapid maturation of computational methods such as molecular dynamics and Monte Carlo calculations, the introduction of elaborated integral theories and refined versions of scaled particle theory for a description of liquids and solutions, the development of sophisticated microcalorimetry to measure highly accurate thermodynamic solvation data not only at room temperature but also at elevated temperatures, and the application of protein engineering to study the role of hydrophobic amino acid residues in protein folding and stability have yielded increasing evidence against the traditional interpretation of hydrophobic effects. In spite of growing doubts about the validity of the original models, the classic interpretation of hydrophobic effects still prevails in the recent literature. The fact that arguments against traditional ideas have been largely ignored must, at least in part, be attributed to notorious ambiguities in the nomenclature pertaining to the hydrophobic effect; this has lent recent discussions a strongly semantic flavor.

At this stage, we feel that there is a need to stand back a little and review recent experimental as well as theoretical studies of hydrophobic effects in different areas of chemistry. Because of the yearly surge of papers on hydrophobic effects, our survey can by no means be exhaustive. Our major goal is to signal remarkable results and to identify important shortcomings in current views on hydrophobic effects. Our review is therefore deliberately biased and aims at a critical reappraisal of hydrophobic effects in which the validity of the whole concept of hydrophobic hydration and hydrophobic interactions will be questioned. To avoid unnecessary ambiguities, definitions will be given for hydrophobic hydration and hydrophobic interactions in Section 1.2. Unfortunately, these definitions are as yet not unanimously accepted.

Jan B. F. N. Engberts was born in 1939 in Leiden, the Netherlands. He studied synthetic and physical organic chemistry at the University of Groningen under supervision of Prof. J. Strating and Dr. B. Zwanenburg. After graduating with a Ph.D. degree in 1967, he was a postdoctoral fellow with Prof. T. J. de Boer at the University of Amsterdam (1968–1969). He returned to Groningen in 1969 as Associate Professor and was appointed Professor of General Chemistry in 1978. Since 1992 he has held a chair in Physical Organic Chemistry at the same university. The research in his group is centered around the theme "organic chemistry in water" and includes projects in molecular recognition, surfactant aggregation, synthesis and properties of polymers and polysoaps, and vesicle fusion.

Wilfried Blokzijl received his degree in chemistry at the University of Groningen in 1987 for his research with Prof. G. Challa on the catalytic behavior of flavine-modified polyelectrolyte complexes. The same year he started as a Ph.D. student in the group of Prof. J. B. F. N. Engberts and collaborated also with Prof. M. J. Blandamer of the University of Leicester. In 1991 he completed his doctoral thesis entitled "Organic Reactivity in Mixed Aqueous Solvents", which described a quantitative link between kinetics and thermodynamics. He is currently examining the catalysis of organic reactions in homogeneous aqueous media. He will take a position at the Research Laboratories of Unilever in Vlaardingen in 1994.

This survey focuses mainly on developments reported during the past decade. Where necessary, reference is made to relevant studies of earlier date. Many experimental studies of hydrophobic effects applying nuclear magnetic resonance, ultrasound, diffraction methods, and calorimetry were reported in the sixties and seventies. For detailed accounts of this work, we refer to the series of books, *Water. A Comprehensive Treatise*, edited by Franks.[7] A short historical excursion into the field of hydrophobic effects presented by Franks[8] in 1982 showed that these experimental studies were often consistent with the molecular interpretation of hydrophobic effects as given by the traditional iceberg model. More theoretical approaches to understanding hydrophobic effects have been described in textbooks by Tanford,[9] Ben-Naim,[10] and Luck.[11] Following the classic review of Kauzmann,[6] the sixties and seventies witnessed a number of attempts to quantify the concept of hydrophobic interactions. Some important contributions, briefly reviewed in Section 1.3, set the stage for ensuing theoretical studies of hydrophobic effects.

This review has two parts comprising, respectively, experimental and theoretical studies of hydrophobic effects. The criteria for defining the separation of these sections are somewhat arbitrary, and activities can show considerable overlap. Following tradition, Part A is inaugurated by a survey of results of recent calorimetric studies as well as reinterpretations of previous data for the solvation of apolar gases and liquids in water over a broad temperature range (Section 2.1). In subsequent sections the importance of hydrophobic effects for the stability of tertiary protein structures (Section 2.2), molecular recognition (Section 2.3), aggregation of amphiphiles (Section 2.4), and surface forces (Section 2.5) will be discussed. This will be followed by a selection of recent results obtained by spectroscopic techniques (Section 2.6). Finally, Part A concludes with a section in which applications of water as a medium for organic reactions are discussed (Section 2.7).

Part B starts off with a brief introduction of theoretical descriptions of hydrophobic effects that have been presented over the years (Section 3.1). Subsequently, efforts are described for the development of rather simple molecular models to account for the thermodynamic properties of aqueous solutions of nonelectrolytes (Section 3.2). In Section 3.3 more sophisticated theories are summarized that are mainly based on virial expansions of thermodynamic excess properties of aqueous solutions to quantify interactions between apolar solutes in aqueous media. Section 3.4 contains a concise summary of applications of scaled particle theories to the problem of hydrophobic effects. Part B concludes with an extensive survey of results of computational studies of both hydrophobic hydration and hydrophobic interactions (Section 3.5).

A final summary and outlook is presented in the epilogue (Section 4) which signals inconsistencies between results of experimental and theoretical studies of hydrophobic effects and also identifies aspects that are currently unanimously accepted. On the basis of these considerations, we present a molecular interpretation of the solvation of apolar compounds in water as well as their aggregation in aqueous solution which is conceptually different from traditional ideas.

1.2. Hydrophobic Effects; The Terminology

Many of the existing definitions of hydrophobic effects reflect the lack of clarity with respect to the exact meaning of the terms that have been introduced to describe the unusual thermodynamic behavior of apolar solutes in aqueous solution (see, for example, the discussion in *Science* two to three years ago)[12-15]). Although the concept of hydrophobicity is widely used, its exact meaning is somewhat vague. We prefer to define hydrophobicity on the basis of the thermodynamics of the transfer of apolar compounds, either from their liquid state or from a solution in an apolar solvent, to water. This process involves the disruption of interactions between the apolar molecule and its apolar environment, refilling of the vacancy in the apolar medium, the creation of a cavity in water, the initiation of water–solute interactions, and the concomittant reordering of the water molecules in the near vicinity of the solute. Thus, hydrophobicity yields information about the limited solubility of apolar compounds in water and can be quantified on the basis of solubility measurements or partitioning studies.

The definition of hydrophobic hydration is even more troublesome, and several interpretations can be encountered in the literature. Hydrophobic hydration refers to the way a nonpolar solute affects the local structure of water in its immediate environment. A convenient definition of hydrophobic hydration considers the process of cavity formation in liquid water, the insertion of an apolar solute particle, the onset of solute–solvent interactions, and the concomittant reordering of the water molecules in close proximity to the solute. Unfortunately, this process is difficult to study by experimental means.

The occurrence of hydrophobic interactions is perhaps the most dramatic revelation of the limited solubility of apolar compounds in water. It is essential to make a clear distinction between pairwise and bulk hydrophobic interactions.[16] Scheme 1 shows a thermodynamic cycle taken from a paper by Wood and Thompson,[16] which illustrates the relation between these distinct phenomena. In this cycle, R stands for

$$\begin{array}{ccc} n\mathrm{R}(\mathrm{g},c^{\ominus}) & \xrightarrow{\Delta G_n(\mathrm{g},c^{\ominus})} & \mathrm{R}_n(\mathrm{g},c^{\ominus}) \\ n\Delta G_1^{\mathrm{s}} \downarrow & & \downarrow \Delta G_n^{\mathrm{s}} \\ n\mathrm{R}(\mathrm{aq},c^{\ominus}) & \xrightarrow[\Delta G_n(\mathrm{aq},c^{\ominus})]{} & \mathrm{R}_n(\mathrm{aq},c^{\ominus}) \end{array}$$

Scheme 1. Thermodynamic cycle for the transfer of n molecules R (nR) as well as of a cluster of n molecules R (R_n) from the gas phase into an aqueous solution, illustrating the difference between bulk and pairwise hydrophobic interactions (taken from ref. [16]). s denotes the solvation steps.

a hydrophobic compound, $c^{\ominus}$ is a standard or reference concentration (vide infra), g denotes the gas phase, and aq the aqueous phase. For $n = 2$, $\Delta G_2(\mathrm{aq},c^{\ominus})$ is the Gibbs energy involved in the interaction of a pair of molecules R in aqueous solution and provides a measure of the pairwise hydrophobic interaction. The solvent-induced part can be computed by comparing $\Delta G_2(\mathrm{aq},c^{\ominus})$ with $\Delta G_2(\mathrm{g},c^{\ominus})$.[17] Bulk hydrophobic interactions are characterized by large values of n. Interestingly, when $n \to \infty$, ΔG_n^{s} approaches zero. In this case $-(1/n)\Delta G_n(\mathrm{aq},c^{\ominus})$ is the Gibbs energy for the

transfer of an apolar compound from an aqueous solution to its liquid state. ΔG_1^s is the Gibbs energy for the solvation of a gaseous compound R in water. This process is sometimes incorrectly considered equivalent to hydrophobic hydration.

The magnitudes of the thermodynamic parameters of the various processes depend critically on the choice of standard states *c*.[18, 19] The most commonly used standard state assumes gaseous compounds at 1 atm that are dissolved in water at a mole fraction of one. The advantage of this particular choice is that the statistical part of the chemical potential (which is mainly entropic in origin) does not differ when solvents with different molecular weights and densities are considered. Other standard states such as 1 mol dm^{-3} and 1 mol kg^{-1} suffer from this disadvantage. When standard states are explicitly known, data can be easily interconverted.[18] As shown convincingly by Abraham,[18] the interpretation of transfer parameters or solvation data is often seriously hampered by application of erroneous reference states. In particular, the pure liquid is an often used but very hazardous reference state. Ben-Naim[20] enunciated the advantages of an alternative standard state based on the transfer of an apolar gas to a fixed position in water. In a subsequent step, the solute is released into the solvent, gains kinetic energy, and becomes indistinguishable from the other molecules in the solution. The so-called pseudochemical potential can be computed from known thermodynamic parameters of solvation but cannot be determined directly. The popularity of this particular standard state can be attributed to the fact that the solute molecule can always be distinguished from solvent molecules. This offers interesting possibilities for studying the solvation of organic compounds in mixed aqueous solvents.

1.3. Classic Models for Hydrophobic Effects

As mentioned in the introduction, Frank and Evans[4] were the first to speculate about the molecular origin of the thermodynamic behavior of aqueous solutions of nonelectrolytes. In their classic paper largely devoted to aqueous solutions of electrolytes, they stated that "when a rare gas atom or a nonpolar molecule dissolves in water at room temperature it modifies the water structure in the direction of greater crystallinity—the water, so to speak, builds a microscopic iceberg around it". The promotion of crystalline-like regions was rationalized by arguing that these structures contain more free space in which apolar solute particles could be accommodated. This model, based on well-known mixture models for liquid water, achieved great fame as the "iceberg model" and found a more sophisticated quantitative counterpart in a model developed by Némethy and Scheraga,[21, 22] in which the flickering cluster model for liquid water[*] proposed by Frank and Wen[23] was used. An important aspect of this model is the assumed cooperativity in the formation of hydrogen bonds in liquid water. This cooperativity was attributed to the fact that the formation of a hydrogen bond by a water molecule is greatly facilitated when a second hydrogen bond is already present. As a consequence, hydrogen bonds are made and broken as a collective rather than an isolated event. Thus, short-lived regions of either strongly hydrogen-bonded or isolated water molecules occur, described as flickering clusters. Insertion of an apolar solute particle causes a change in the energy levels of water molecules at the surface of the solute. A fully hydrogen-bonded water molecule will be stabilized by additional van der Waals interactions with the solute, and hence the number of these water molecules will increase in the vicinity of apolar solutes. In the original model of Frank and Wen,[23] the nonpolar solute is assumed to act as an effective wall unable to transmit disruptive forces that tend to destruct the icelike clusters.

One of the first critical evaluations of iceberglike models was reported by Miller and Hildebrand,[24] who developed a model for the loss of entropy upon solution of apolar gases without assuming the formation of more rigid structures. Instead, they suggested that hydrogen bonds are destroyed when water molecules are brought into contact with air or apolar surfaces, causing the low solubility of apolar compounds in water. An interesting alternative was offered by Howarth,[25] who reported an interpretation of the entropy of hydration of apolar compounds in terms of restricted motion of the hydrophobic parts of the solute molecules.

Classic models for hydrophobic interactions originate from the molecular interpretation given by Kauzmann.[6] Pioneering work in this area was done by Ben-Naim[10, 26] and Friedman et al.[27–29]. In an elegant approach by Ben-Naim[10, 26] the process of the hydrophobic association of two methane molecules in water is considered. The indirect part of the work associated with this process (δG^{HI} or $\delta G(R)$), the part that reflects the properties of water, is evaluated by computing the difference between the thermodynamic parameters of the hydration of gaseous methane and ethane as illustrated in Scheme 2 (see also Section 3.3.1). Here, $\Delta\mu_S^{\ominus}$ and $\Delta\mu_D^{\ominus}$ are the standard chemical potentials for the solvation of gaseous methane S and ethane D, respec-

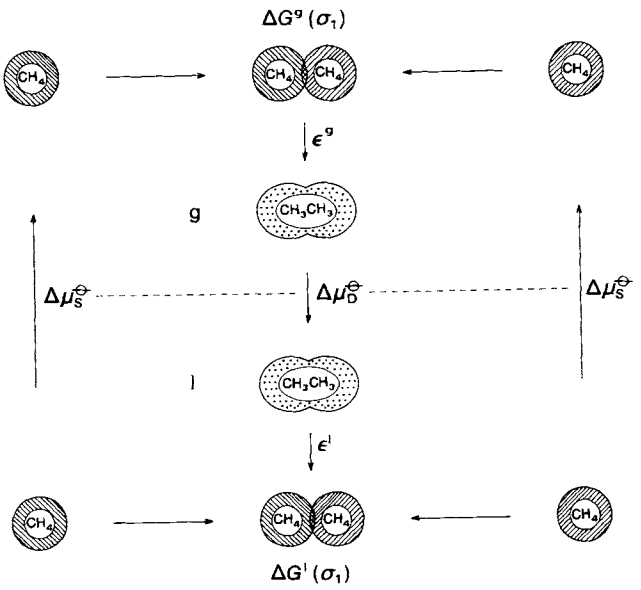

Scheme 2. Cyclic process in which two methane molecules in aqueous solution as well as in the gas phase are brought from infinite separation to a close separation σ_1 and subsequently replaced by an ethane molecule (taken from ref. [10]).

[*] In the flickering cluster approach small regions in liquid water with a given structure are assumed to undergo sudden cooperative transitions into other structures.

tively. ε^g and ε^l account for the differences between an associated pair of CH_4 molecules and a covalent bond between CH_3 moieties. The assumption is made that ε^g and ε^l are similar in magnitude. The Gibbs energy involved in the solvent-induced part of the process of hydrophobic interaction can now be expressed as $\Delta G^{HI} = \Delta\mu_D^{\ominus} - 2\,\Delta\mu_S^{\ominus}$.

Having a method to estimate the solvent-induced part of hydrophobic interactions, one can study the influence of temperature or the presence of organic cosolvents on the magnitude of hydrophobic interactions. The model developed by Friedman et al.[27-29] quantifies the thermodynamic parameters involved in the overlap of hydrophobic hydration shells upon association of apolar solute molecules and is treated in some detail in Section 3.3.3.

2. Part A. Experimental Studies

2.1. Hydrophobic Effects across a Broad Temperature Range; A Thermodynamic Approach

Traditionally, hydrophobic effects have been studied by measuring thermodynamic parameters for the solvation of gaseous or liquid organic compounds in water or, alternatively, by relating them to partition coefficients of solutes between aqueous and nonpolar phases (see, for example, Abraham et al.[30, 31] and Zaslavsky and Masimov[32]). An excellent review on previous studies of solvation of apolar gases in water is given by Wilhelm et al.[33] Since then, techniques for the measurement of solubility data on the basis of vapor–liquid equilibria have been improved significantly.[34] Furthermore, in the past decade microcalorimetry has reached a high level of sophistication. Recently, Pollack devoted an interesting discussion to the general question of why gases dissolve in liquids.[35]

The general aim of this section is twofold. First, emphasis is placed on a method to correlate thermodynamic data of solvation at 25 °C with solute parameters. This method provides a refreshing view of hydrophobic hydration and yields an interesting comparison between the thermodynamic parameters of the solution of apolar compounds in water and in organic solvents. The second part of this section describes an analysis of thermodynamic hydration parameters as a function of temperature and shows that the emphasis on the entropy-controlled nature of the solubility of apolar compounds in water cannot be maintained. Highly accurate enthalpies and heat capacities of solvation for apolar gases and liquids in water now available over a broad temperature range have seriously challenged the traditional view of hydrophobic effects.

It is notoriously difficult to correlate thermodynamic parameters of solvation with some property of the solute.[33] Correlations with the surface area[36] and molecular volume of the solute often gave satisfactory results but also revealed some remarkable discrepancies. These were explicitly noted by Cramer[37] but became more obvious in a excellent analysis of solvation data of a large series of organic compounds, presented by Abraham.[18, 31] Both approaches focused on a comparison of thermodynamic solvation data for a series of apolar gases. In Figure 1 the Gibbs energies, enthalpies, and entropies (expressed as $T\Delta S$) of solvation for a series of

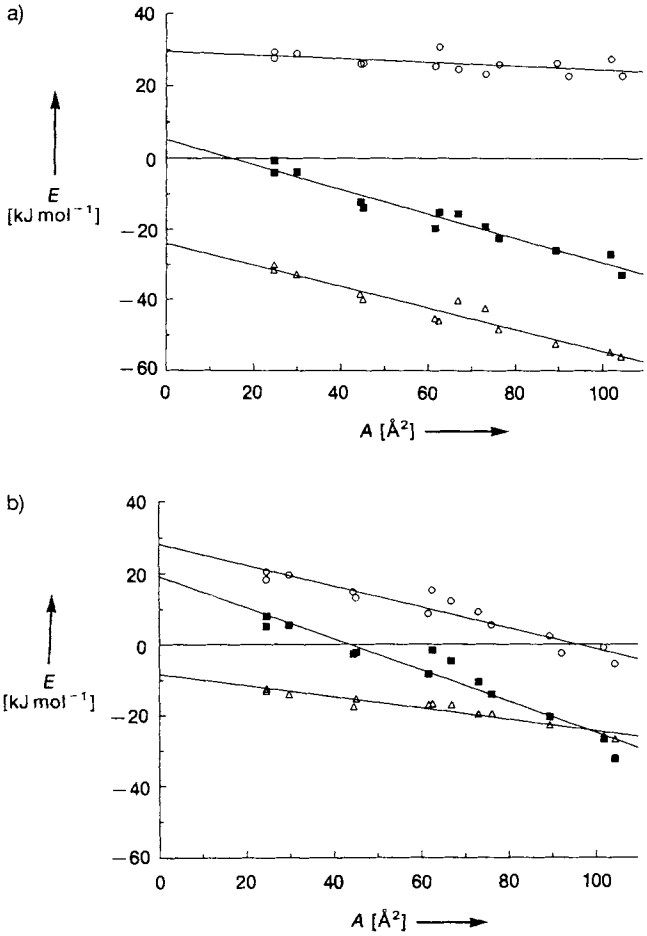

Fig. 1. $\Delta G^{\ominus}$ (○), $\Delta H^{\ominus}$ (■), and $T\Delta S^{\ominus}$ (△) of solvation for the apolar gases hydrogen (24.57 Å²), helium (24.65 Å²), neon (29.80 Å²), argon (44.41 Å²), methane (45.04 Å²), ethane (61.55 Å²), tetrafluoromethane (62.44 Å²), krypton (66.75 Å²), xenon (72.98 Å²), propane (76.08 Å²), *n*-butane (89.33 Å²), cyclopentane (92.04 Å²), *n*-pentane (101.64 Å²), cyclohexane (104.19 Å²). a) in water, b) in *n*-hexane (1 atm, 1 mol%, 298 K) as a function of the surface area *A* of the solute (in parentheses). Thermodynamic parameters are taken from ref. [31].

apolar gases in water and in *n*-hexane are plotted as a function of the surface area of the solute. Although the correlations are generally poor, the trends are obvious. Abraham developed a set of generally applicable solute parameters which are closely correlated with the surface area but have been optimized in order to correlate with thermodynamic solvation data in various organic solvents. These parameters have little physical meaning, and for the present purpose we prefer to use the surface area.

Strikingly, at 25 °C the Gibbs energy of solvation for apolar gases in water is only moderately dependent on the nature of the solute as compared to other solvents. Moreover, the dependence on the nature of the solute is quite remarkable. Helium is, for example, slightly less soluble than the larger (and more polarizable) xenon. In contrast, methane is slightly *better* soluble in water than in *n*-pentane. In organic solvents, the solubility increases rapidly with increasing size (or polarizability) of the solute. As suggested by Tanford[9] and Abraham,[18, 31] it is interesting to compare the methylene increment for the dissolution of gaseous hydrocarbons in water and in organic solvents. Table 2 lists the methylene group contributions to the Gibbs energy, enthalpy, and entropy (expressed as $T\Delta S$) of solvation for gaseous C_2–C_8

Table 2. Methylene group contributions to the Gibbs energy, enthalpy, and entropy of solvation for gaseous *n*-alkanes (C_2-C_8) in various solvents at 298.15 K (taken from ref. [31].

Solvent	$\Delta G_s^{\ominus}$ [kJ mol^{-1}]	Contribution to $\Delta H_s^{\ominus}$ [kJ mol^{-1}]	$-T\Delta S_s^{\ominus}$ [kJ mol^{-1}]
n-hexadecane	−3.10	−4.81	1.72
cyclohexane	−3.18	−4.68	1.51
n-hexane	−3.10	−5.56	2.47
benzene	−3.10	−4.48	1.38
acetone	−2.59	−3.68	1.09
propylene carbonate	−2.01	−4.14	2.13
1-butanol	−2.76	−4.98	2.22
ethanol	−2.55	−4.90	2.34
methanol	−2.34	−4.44	2.09
water [a]	0.75	−2.80	3.56

[a] Determined for *n*-alkanes C_2-C_7.

hydrocarbons in various solvents at 25 °C. The Gibbs energy increment per methylene moiety in water deviates significantly. The enhanced solubility of larger hydrocarbons in organic solvents is governed by the growing importance of the enthalpy, which is only partly counteracted by the decrease in entropy. In water, the enthalpy of solvation also increases with increasing apolar surface area, but the increase is less pronounced. In contrast, the entropy loss increases more strongly with increasing alkane size. Hence, hydrophobicity becomes more pronounced as the size of the apolar solute increases, and the slight dependence of the Gibbs energy of solvation on surface area is the most eye-catching revelation of hydrophobic hydration. This phenomenon is, however, a result of subtle differences between contributions of methylene groups to the entropy and enthalpy of solvation. The exceptionally large and positive Gibbs energy of solvation of hydrocarbons in water at 298 K finds expression in the *absolute* values of the enthalpy and entropy of solvation. Figure 1 suggests that even for a solute molecule of negligible size, the entropy of solvation in water still remains highly unfavorable.

From the methylene increments listed in Table 2 the thermodynamic parameters can be calculated for the transfer of a methylene group from an organic solvent to water. For example, the transfer of a methylene group from *n*-hexane to water is an unfavorable process (the Gibbs energy increment is +3.85 kJ mol^{-1}), and it is characterized by a loss of entropy (increment is −1.09 kJ mol^{-1}) as well as by a positive enthalpy (increment is +2.76 kJ mol^{-1}). Transfer of a methylene group from the gas phase to water is, however, *promoted* by enthalpy. This indicates that a considerable part of the unfavorable Gibbs energy involved in the transfer of an apolar methylene moiety from an organic solvent to water must be attributed to the disruption of dispersion interactions between the apolar solute and the organic solvent.

The Gibbs energies for the transfer of apolar solutes from nonpolar solvents to water have been correlated with accessible surface areas. These correlations showed that the Gibbs energy per unit surface area involved in the transfer of apolar compounds from a hydrocarbon-like solvent to water amounts to 70 to 130 J mol^{-1} Å^{-2}. The exact magnitude depends strongly on the reference solvent, the computational method used to determine the surface area, and the fitting procedure.[9, 38–43] A macroscopic measure for the hydrophobic Gibbs energy per unit surface area can be derived from liquid hydrocarbon–water surface tensions, which are about 310 J mol^{-1} Å^{-2}.[44] The discrepancy between the macroscopic and microscopic Gibbs energy relations on surfaces cannot be explained simply on the basis of differences in the curvature of the surface (see also Greco[45]). In 1991 Sharp et al.[46] reappraised the surface area dependence of the solubilities of hydrocarbons in water and showed that "hydrophobicity scales" significantly underestimate the magnitude of the hydrophobic effect. However, even in the revised estimate of the Gibbs energy per unit surface area, a considerable gap remains between macroscopic and microscopic surface tensions.[46]

During the past decade the temperature dependence of the thermodynamic parameters of solvation for many apolar gases and liquids has been determined with high accuracy. The standard molar Gibbs energy, enthalpy, and entropy ($T\Delta S$) of solvation for gaseous and liquid neopentane are represented in Figures 2a and 2b, respectively. For comparison, the temperature dependence of the thermodynamic parameters for the transfer of gaseous neopentane to its liquid state is shown in Figure 2c. The pseudo-chemical potential is used as a standard state (see Section 1.2). Using microcalorimetry, Naghibi et al. measured the heats of solution of methane,[2] ethane,[47] *n*-propane,[47] and *n*-butane[48] and showed that the enthalpy of solvation becomes less favorable with increasing temperature. This reflects the large and positive heat capacity of solvation observed near room temperature.

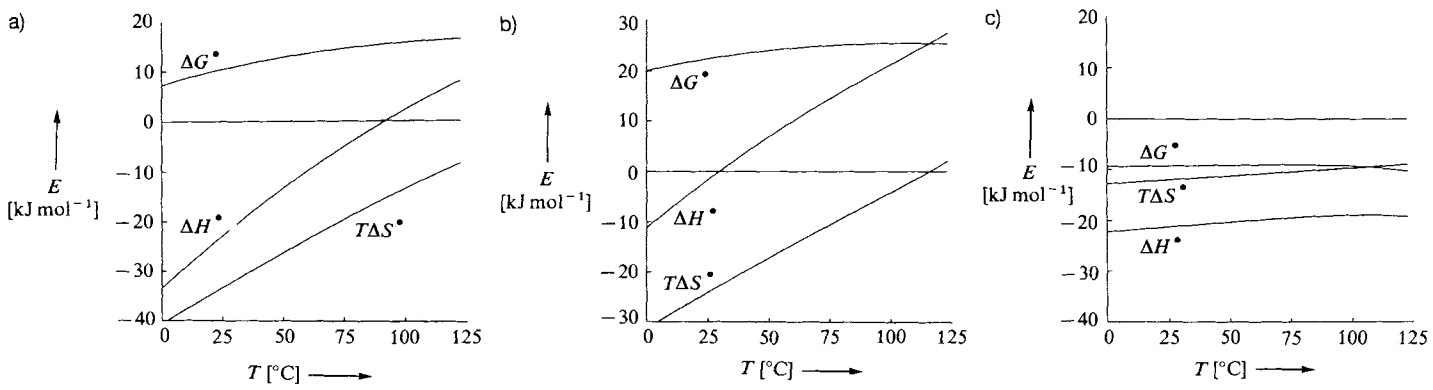

Fig. 2. Temperature dependence of ΔG°, ΔH°, and $T\Delta S^{\circ}$ of the solvation for a) gaseous neopentane and b) liquid neopentane in water, and c) gaseous neopentane in its pure liquid (taken from ref. [230]).

Solubility measurements have shown that the entropy of solvation becomes less unfavorable with increasing temperature. At elevated temperatures the solubility of apolar compounds in water is, however, still exceptionally low, since it is then governed by the unfavorable enthalpy of solvation. The Gibbs energy of solvation is only slightly dependent on temperature. The heat capacity of solvation for gaseous hydrocarbons was shown to decrease significantly with increasing temperature.[49] Unfortunately, microcalorimetric techniques did not allow accurate measurements of heats of solvation of apolar gases above 55 °C. The results, however, suggest that the heat capacity of solvation decreases continuously and eventually reaches zero at elevated temperatures. This is expected, because the hydrogen bond structure of water at these high temperatures is suggested to be completely destroyed.[36] Makhatadze and Privalov[50] determined the specific heat capacity of solvation for liquid toluene and benzene between 0 and 150 °C. Although these data confirm the decrease of the heat capacity of solvation, even at 150 °C a considerable heat capacity change was observed.

Accurate measurements of the temperature dependence of the solubility of apolar gases and liquids in water analyzed with the van't Hoff equation also yield a temperature dependence of the thermodynamic parameters of solvation. Using this approach, Shinoda[51] and Rettich et al.[52–54] found that the heat capacity of solvation decreases noticably above 80 °C and drops to zero near 160 °C. These data are in contrast with solubility data of Crovetto et al.,[55] who did observe a considerable decrease in the heat capacity of solvation for inert gases and methane between 25 and 325 °C, but even at 325 °C the heat capacity change remained quite substantial. Unfortunately, solubility measurements at high temperatures are generally subjected to large experimental errors. In later studies Biggerstaff et al.[56] used a flow calorimeter to measure directly the molar heat capacity of aqueous argon from 33 to 305 °C and found only a small decrease of the molar heat capacity when the temperature was raised to about 160 °C. Above this temperature, the heat capacity again *increases*. Near the critical point of water (about 250 °C), the heat capacity even increases extremely rapidly and goes to positive infinity.

The temperature dependences of the thermodynamic parameters of solvation for a large variety of apolar liquids in water show remarkable similarities. First, the enthalpy of solvation for apolar liquids is zero near room temperature, irrespective of the nature of the species (see Fig. 2b). Near 110 °C, the entropy of solvation for apolar liquids becomes zero. Apparently, both temperatures are universal, and are now generally referred to as T_H and T_S, respectively. The temperature dependence of the thermodynamic parameters of solvation for apolar liquids strongly resembles that for apolar gases (Fig. 2a, b). Also for the dissolution of a large series of apolar gases, temperatures can be found where $\Delta H^{\ominus}$ and $T\Delta S^{\ominus}$ reach common values but differ from zero. The occurrence of isoenthalpic and isoentropic temperatures for the thermodynamics of solvation for apolar compounds in water was rationalized by Lee.[57] His explanation is based on the assumption that the changes in enthalpy and entropy are linear functions of some property of the solute [Eq. (1)].

$$\Delta X^{\ominus} = a_X \sigma + b_X \tag{1}$$

Here $\Delta X^{\ominus}$ is the thermodynamic quantity involved, σ the property of the solute (usually the surface area), a_X a species-independent linear function of temperature, and b_X the value of $\Delta X^{\ominus}$ when a_X is zero. The molar thermodynamic quantities of solvation for apolar liquids and gases can now be expressed as functions of temperature in terms of the heat capacity change, assuming that the latter is independent of temperature,[57] according to Equations (2)–(4), where T_H^* and T_S^* are the isoenthalpic and isoentropic temperatures.

$$\Delta G^{\ominus} = \Delta G^* + \Delta C_p(T - T_H^*) - T\Delta C_p \ln(T/T_S^*) \tag{2}$$

$$\Delta H^{\ominus} = \Delta H^* + \Delta C_p(T - T_H^*) \tag{3}$$

$$\Delta S^{\ominus} = \Delta S^* + \Delta C_p(\ln T/T_S^*) \tag{4}$$

ΔH^* and ΔS^* are the values of the enthalpy and entropy of solvation at T_H^* and T_S^*, respectively. The solubility function [Eq. (5)] shows that the solubility of apolar compounds in

$$\Delta G^{\ominus}/T = \Delta G^*/T + \Delta C_p(1 - T_H^*/T) - \Delta C_p \ln(T/T_S^*) \tag{5}$$

water reaches a minimum at T_H^*. Lee[230] argued that T_H^* and T_S^* are the temperatures at which the enthalpy and the entropy of solvation, respectively, are independent of the selected property of the solute. The heat capacity change fully accounts for the temperature dependence of enthalpy and entropy of solvation,[58] and ΔH^* and ΔS^* are independent of temperature. According to Equations (3) and (4), a plot of $\Delta H^{\ominus}$ and $\Delta S^{\ominus}$ versus ΔC_p for a series of apolar gases or liquids at a selected temperature T should be linear. This has been experimentally confirmed by Sturtevant,[59] Murphy et al.,[60] and Baldwin.[61] From these plots the values of T_H^* and T_S^* have been derived.

Interestingly (vide supra), ΔS^* and ΔH^* are zero for the solvation of apolar *liquids* in water. Hence T_S^* and T_H^* equal T_S and T_H (about 110 and 25 °C, respectively), and Equation (6) applies at each temperature T.[59] Equation 6 does

$$\ln(T_S/T) = \Delta C_p/\Delta S^{\ominus} \tag{6}$$

not hold for the dissolution of apolar *gases* in water since ΔS^* and ΔH^* are *not* zero. T_S^* and T_H^* are about 124 and 94 °C, respectively.[62, 63] Apparently, the entropy of solvation is not completely proportional to the surface area, and even a mathematical point solute gives rise to an entropy of solvation of about $-80\ \mathrm{J\,K^{-1}\,mol^{-1}}$.[60] $T\Delta S^*$ is similar to the difference in translational Gibbs energy between the gas and the liquid phase. A similar phenomenon was observed in Figure 1. Although Biggerstaff et al.[56] showed that the heat capacity of an aqueous solution of argon does not depend dramatically on the temperature, T_S^* is a hypothetical temperature. Nevertheless, the variation in T_S^* for the solvation of apolar gases and liquids with temperature is surprisingly small. In contrast, the standard deviation of T_H^* is quite substantial. The existence of a unique value of T_H^* seems to be reserved only for larger liquid hydrocarbons.

The strong temperature dependence of the enthalpy and entropy of solvation for apolar gases and liquids in water

throws a different light on the analysis of thermodynamic solvation parameters measured at or near room temperature. The analysis of thermodynamic parameters of solvation for linear alkanes by means of increments (Table 2) is substantially dependent on temperature. For example, the entropy of solvation for gaseous alkanes decreases strongly with increasing temperature and eventually becomes identical for all alkanes near T_S^*. This means that the incremental methylene contribution to the entropy of solvation at T_S^* is zero. With respect to the enthalpy of solvation, the methylene contribution is zero at T_H^*. The incremental contributions to entropy and enthalpy of solvation can adopt virtually a broad range of values dependent on the temperature. In contrast, the Gibbs energy increment is hardly sensitive to temperature changes.

2.2. The Role of Hydrophobic Interactions in Protein Conformation and Stability

The stability of native protein structures and the folding of an extended protein chain have been subjects of extensive research for more than fifty years.[64, 65] Today, it is almost generally accepted that hydrophobic interactions constitute an important factor in the stability of the folded structure of water-soluble proteins.[65] The spatial distribution of α-amino acid residues in the native protein shows that, on average, α-amino acids with apolar character are found in a dense hydrophobic core in which the exposure to water is minimized.[66–68] Recently, Rose et al.[68] showed that the average spatial requirement of the α-amino acids that make up this apolar core is related to the residue hydrophobicity. Of course, Kauzmann[6] introduced the whole concept of hydrophobic interactions in connection with the interactions between apolar side chains of α-amino acid residues and their proposed importance for the stability of biopolymers. A controversy remains whether the stability of the native structure of proteins is caused by van der Waals interactions between apolar side chains or whether water actively induces the formation of an apolar core.[13, 14, 69] Obviously, this discussion strongly relates to our current understanding of the molecular basis of hydrophobic interactions. Since native structures of proteins unfold upon cooling as well as upon heating,[70] a study of both the cold and hot denaturation of native protein conformations might give valuable information about hydrophobic interactions. It must be recognized that these interactions are primarily *bulk* hydrophobic interactions.

Another topical debate centers on the question as to what extent the alleged hydrophobic interactions determine the structure of native proteins. On one hand, Dill et al.[71, 72] reported a successful theoretical analysis accounting for the temperature dependence of stability and folding of large globular proteins based on the assumption that hydrophobic interactions are the driving force for the folding of globular proteins. According to Dill,[64] hydrophobic interactions between apolar α-amino acid residues allow the extended protein chain to fold itself in only a limited number of ways. The ultimate and unique conformation is subsequently determined by more specific polar interactions. On the other hand, the theoretical analysis of solvent effects on protein folding in terms of solvation energies of individual parts of the total protein reported by Ben-Naim[73, 74] has been taken as evidence that the importance of hydrophobic interactions has generally been overestimated. The suggestion was made that correlations between hydrophilic functional groups are even more important than those between hydrophobic side chains. In particular hydrogen bonds, also at the surface of the protein, were proposed to be of paramount importance for the stability of native protein conformations.

The native structure of proteins is generally only about 50 kJ mol^{-1} more stable than the denatured state. The formation of a compact, folded protein is strongly opposed by entropic forces. A variety of intramolecular forces between α-amino acid residues in the folded state are known that contribute to the overall stability of the native protein structure. Due to the marginal stability of the folded conformation, each of these individual contributions can be decisive. Intramolecular interactions are well established, and most authors agree that these include electrostatic interactions, torsional or other "local" interactions, polar interactions (hydrogen bonds), van der Waals interactions, *and* hydrophobic interactions.[64, 75] The long-range electrostatic interactions include the classical repulsions between charged residues as well as specific electrostatic interactions due to bridging of oppositely charged α-amino acids.[76] Ion pairing is especially important at the surface of proteins.[77] Torsional and local interactions originate from preferential conformations of sequences of three or four α-amino acids, arising from short- and long-range interactions among these neighboring residues. Karplus and Holley[78] were quite successful in accounting for the architecture of proteins on the basis of these local interactions.

Hydrogen bonding is also very important in determining the structure of proteins, but if it is to be the driving force for the folding of proteins, hydrogen bonding of the unfolded protein with water must be less favorable than hydrogen bond interactions between α-amino acids in the native state of the protein. Jorgensen[79] showed on the basis of computer simulation studies that amides tend to stack in aqueous solution, but that stable amide–amide hydrogen bonds are not very likely. Dimerization of organic compounds in water has only been observed when multiple hydrogen bonds are involved. Hydrogen bonding between α-amino acids buried in the apolar core of the native protein can, nevertheless, provide additional stability for the structure.[80] Finally, interactions between permanent or induced dipoles, generally qualified as van der Waals forces, are of great importance for the stability of native protein structures.[81] This has commonly been traced back to the fact that water constitutes the natural environment for most soluble proteins. Dispersion forces between the side chains of apolar α-amino acids in the native conformation of the protein replace interactions with water in the extended conformation. As argued above, it is very difficult to make a proper distinction between van der Waals interactions and hydrophobic interactions, and the active role of the solvent is still far from clear.

α-Amino acid sequences determine the native structure of a protein. It is known that these sequences are not unique, and many different sequences can code for proteins with essentially the same native conformation. Creation of cavities in the hydrophobic core of the protein by shortening the

side chains of certain α-amino acids, the introduction of α-amino acid residues with unsatisfied hydrogen bonding, and the formation of sterically crowded regions by incorporation of bulky α-amino acids are generally not favorable for the stability of the protein, but the way in which a protein can accommodate mutations commands respect.[82]

A few years ago Sauer et al.[82, 83] elegantly showed that the sequence of α-amino acids, which plays an essential role in the formation of the core of the protein, can be replaced by alternative α-amino acids on two conditions: first, these residues must maintain the overall hydrophobicity, and second, the new packing arrangement must satisfy steric requirements. Site-directed mutagenesis combined with sophisticated calorimetric stability measurements have shown that substitution of individual α-amino acids buried in the hydrophobic interior of the protein does lead to changes in stability of the native protein.[84] The creation of a cavity in the interior of the protein destabilizes the native conformation to an extent that is strongly dependent on the actual site of the mutation.[81, 85, 86] Usually, the destabilization increases with increasing cavity size.

Kellis et al.[85, 86] and Eriksson et al.[81] studied the effects of several side-chain mutations on protein stability and focused on the response of the protein structure to cavity-creating mutations, such as the replacement of leucine residues by alanine (which is equivalent to decreasing the hydrophobicity by removing one methylene group). Eriksson et al.[81] showed on the basis of crystal structures of six mutants of T4 lysozyme that the packing of the core did not completely fill the created cavity, although side chains protruded into the cavity to some extent. Apparently, the protein interior consists of rigid parts alternating with more flexible regions. The presence of water molecules in the remaining cavities could not be determined. It is, however, extremely difficult to detect isolated water pools or water molecules. Generally, a considerable part of the volume of protein crystals is occupied by water molecules. Water molecules are found inside the protein at positions where they can form hydrogen bonds with the α-amino acids buried in the apolar interior. They may also be located in cavities and crevices created by insufficient packing. These interactions have been an important topic of research.[87] The role of these isolated water molecules for the stability of the folded protein structure can be substantial.[88]

In the last few years Monte Carlo and molecular dynamics simulations have been used to compute changes in the Gibbs energy for protein folding when a particular α-amino acid residue is replaced by another less hydrophobic moiety (e.g. leucine → alanine) by using Gibbs energy perturbation methods (see Section 3.5).[85, 89, 90] Prevost et al.[90] showed that solvation of the unfolded, unsolvated wild-type protein is hardly affected by the mutation, but that folding of the dissolved chain becomes more favorable when the more apolar residue is incorporated. This phenomenon can be reconciled with the fact that the Gibbs energy of solvation for apolar gases in water is only slightly dependent on the magnitude of the apolar surface area (see Section 2.1). This emphasizes that the interactions between apolar moieties in the core of the native protein are essentially bulk hydrophobic interactions. The conclusion given by Prevost et al.[90] that the observed decrease in stability of the mutant structure cannot be attributed to a hydration phenomenon is not correct. The decreased stability resulting from the leucine–alanine mutation is usually attributed to the loss of van der Waals interactions in the core of the protein.[81, 85, 86, 91] A remarkable result of recent simulation studies is that intrinsic side-chain terms contribute significantly to the reduced stability of mutated proteins.[90]

The packing of hydrophobic α-amino acids in a hydrophobic core leads to a highly compact conformation. Thermodynamic parameters of folding for an inactive protein chain show remarkable similarities with thermodynamic parameters of the solvation for apolar liquids in water.[12, 36, 61, 92–94] Moreover, the ratio of the entropy and heat capacity change of denaturation is constant [see Eq. (6)].[59] The heat capacity for the denaturation of proteins is linearly related to the fraction of hydrophobic residues[92] but is only slightly dependent on the temperature.[36, 70, 94] Therefore, the interior of the protein has been frequently treated as an apolar liquid or an oil drop.[95] The process of "hiding" apolar α-amino acids from water in the hydrophobic core has been modeled by determining the relative solubilities of these α-amino acids in water and in various apolar solvents.[9, 96–98]

An intriguing observation was made by Privalov,[92] who found that for the unfolding of a number of globular proteins the changes in enthalpy and entropy per amino acid residue reach a common value at 110 °C. Baldwin[61] noticed that this temperature agrees very well with the temperature at which the entropy of dissolution for apolar liquids in water becomes zero (T_S, see Section 2.1). An analogy was drawn between the thermodynamics of folding for inactive proteins in water and of the transfer of hydrocarbons from an aqueous solution to their liquid state. It was suggested[61] to estimate the hydrophobic contribution to protein stability from the characteristic temperatures T_S and T_H (the hydrocarbon model).

By using Equations (2)–(4), the Gibbs energy of protein folding can be expressed [Eq. (7)]. This relation suggests that

$$\Delta G^{\ominus}_{\text{folding}} = \Delta G^{\ominus}_{\text{nh}} + \Delta G^{\ominus}_{\text{h}} = \Delta H^{\ominus}_{\text{nh}} + T\Delta S^{\ominus}_{\text{nh}} + \Delta C_{p,\text{h}}\,(T - T_H) + \Delta C_{p,\text{h}}\,T \ln (T_S/T) \tag{7}$$

the nonhydrophobic (nh) contributions to the thermodynamics of protein folding are independent of the temperature.[61] A favorable nonhydrophobic enthalpy term is counteracted by a serious loss of entropy. At high temperatures the nonhydrophobic entropy term is large enough to cause denaturation of the protein. The analysis shows that hydrophobic interactions lead, at all temperatures, to a stabilization of the native structure of the protein. Near room temperature the stabilization is governed by a gain in entropy. Above 60 °C, however, the enthalpy becomes dominant and even prevails over the nonhydrophobic enthalpy contribution. The similarity with the solvation of apolar liquids in water is obvious.

However, much evidence indicates that it is misleading to view the interior of a protein as an apolar liquid. The packing densities of the hydrophobic core approach those of crystalline α-amino acids.[99] In addition, the interior of proteins contains several types of polar α-amino acid residues,[68] and exchange of certain core residues by more hydrophobic

counterparts does not always lead to higher protein stability.[100] In 1991 Sandberg and Terwilliger[101] showed that some polar residues reside in the core of the protein without actually interacting with each other. Apparently, the local polarity and the site-dependent packing energy are important factors for the stability of the native protein.[102]

Application of the hydrocarbon or oil-drop model to describe thermodynamic properties for the folding of proteins is also controversial for other reasons.[61] An important point of concern is that T_S^* and T_H^* are set equal to T_S and T_H, whereas Privalov et al.[12, 36] found that the entropy *and* enthalpy for the unfolding of native protein structures reach common values at T_S^*. Replacing T_S and T_H in Equation (7) by a single temperature T_S^* (or T_H^*) leads to the remarkable conclusion that hydrophobic effects *destabilize* the native protein conformation. The remaining nonhydrophobic terms show striking similarities with the thermodynamic solvation data for solid cyclic dipeptides,[12] suggesting that the structure of the interior of the folded protein is related to a solid structure.

The conclusion that hydrophobic effects destabilize the structure of proteins drawn by Privalov et al.[12, 36] contradicts a flood of experimental evidence obtained since the classical paper of Kauzmann[6] and recently sparked interesting discussions about the meaning of hydrophobicity.[13–15] Lee[57] rightfully remarked that these discussions did not provide much insight into the fundamental problem that T_S^* equals T_H^*. He argued that the assumed relation between the solvation of apolar liquids in water and the denaturation of globular proteins is based on the questionable assumption that only nonpolar groups are transferred from water to the interior of the proteins. He suggested invoking polar interaction terms as well, which would shift T_H^* without altering T_S^*. The term $\Delta G_h^{\ominus}$ introduced by Murphy et al.,[12] in which T_S equals T_H [see Eq. (7)], measures not only hydrophobic contributions but also the difference between the average contributions of polar and nonpolar interactions.

The analysis reported by Lee[57] reinforced the view of Privalov[75, 92] that cold denaturation is reflected by the fact that the favorable nonpolar, or hydrophobic terms become too small at low temperature. The temperature dependence of the Gibbs energy of hydrophobic interactions is very modest, which emphasizes the fact that native structures of proteins are only marginally stable. The cooperative effects of bulk hydrophobic interactions and polar interactions between α-amino acid residues in the interior of the protein are sufficient only over a very small temperature range to overcome the loss of configurational entropy. Indeed, the occurrence of cold and hot denaturation is indicative of opposing hydration contributions arising from the solvation of polar and nonpolar α-amino acid residues of the unfolded protein.[70]

2.3. The Role of Hydrophobicity in Molecular Recognition and Host–Guest Complexation

The specific binding of reactants in the active site of enzymes constitutes an important research topic. In these molecular recognition processes hydrophobic interactions are expected to play a major role. Originally molecular recognition was a term reserved for biochemistry and biomimetic chemistry.[103, 104] The current popularity of supramolecular chemistry has caused a shift to a more general interpretation of the term.[105, 106] Noncovalent interactions, which lie at the heart of molecular recognition, have become a fashionable topic of research.[107]

A convenient approach to studying basic aspects of noncovalent interactions is provided by synthetic host–guest chemistry. The formation of strong host–guest complexes is particularly feasible in aqueous solutions. Generally, this has been attributed to hydrophobic effects, although electrostatic interactions are also important.[107] Host–guest complexes are often stabilized by π–π or stacking interactions[108] and hydrogen bonding.[107] Stacking interactions play a dominant role in aggregation of dye molecules and hydrotropic compounds.[109, 110] In addition, a combination of stacking interactions and hydrogen bonding governs the strong binding of nucleotides to receptor sites.[111]

The role of hydrophobic interactions in host–guest chemistry and molecular recognition is still ambiguous. The arguments show remarkable similarities with those that characterize discussions in the field of protein stability and mainly center on the question whether van der Waals interactions or hydrophobic interactions govern host–guest complexation. In addition, one should recognize that host–guest complexation can involve either bulk or pairwise hydrophobic interactions. To illustrate this point we note that complexation of an apolar guest molecule in an apolar cavity of a macrocyclic host is usually accompanied by complete desolvation of the guest molecule, whereas pairwise stacking of, for example, nucleotides or dye molecules involves only local dehydration. In this section, we would like to signal a few remarkable results obtained in the field of synthetic host–guest chemistry. In the light of the feverish activities in this field, we restrict ourselves to a few examples that illustrate the current debate. For extensive surveys of synthetic host–guest chemistry in aqueous solutions we refer to reviews by Schneider[107] and Diederich.[112]

Complexation of neutral molecules with cyclic host molecules, and molecular complexation in general, involves a variety of different binding interactions, and it is difficult to separate the hydrophobic component even if one has agreed upon the exact definition of the term. In their studies of solvent and salt effects on binding constants, Schneider et al.[113] found evidence that hydrophobic interactions play a major role in the binding of apolar substrates to macrocyclic host compounds. An interesting contribution was reported by Endo et al.,[114] who studied the oxidation of associated thiols having an amide-like binding site and an alkyl recognition site (Scheme 3). A small but significant selectivity was observed in the formation of symmetrical and unsymmetrical products, which was attributed to recognition of hydrophobic moieties. Unfortunately, many of these reactions were carried out with a considerable amount of organic cosolvents and not in a dilute aqueous solution.

Thermodynamic parameters of complexation processes are sometimes difficult to interpret because of conformational changes of the host molecule upon complexation.[115] Particularly solvation of the cavity prior to complexation causes ambiguities in interpretations of thermodynamic

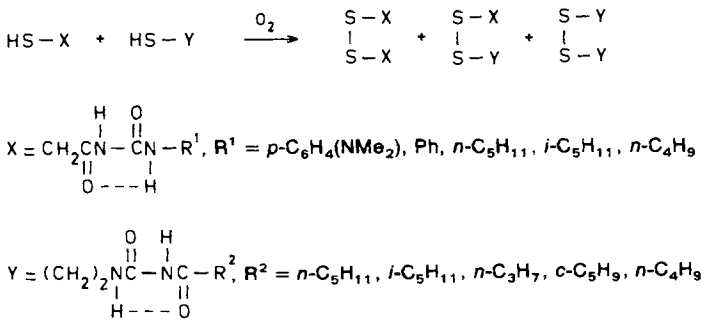

Scheme 3. Schematic representation of the oxidative coupling of thiols HSX and HSY to yield the symmetrical and unsymmetrical disulfides. The recognition sites X and Y are given as well (see ref. [114]).

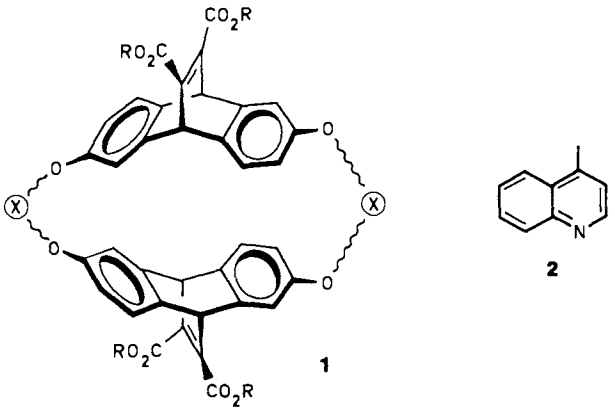

Scheme 4. Electron-rich synthetic receptor molecule **1** and electron-deficient guest molecule **2**.

parameters at the molecular level. In spite of these pitfalls, measurement of the temperature dependence of binding constants provides valuable new insights into the molecular origin of recognition processes. Frequently, a large and positive entropy change upon complexation has been found (see, for example, Stauffer et al.[116]), which is an indication for the occurrence of hydrophobic interactions. The binding efficiency of host molecules has also been successfully enhanced by increasing the hydrophobic character of the binding site.[112] The existence of a large and negative heat capacity change upon association of apolar molecules in water is generally considered to be a decisive criterion for the occurrence of hydrophobic interactions. Indeed, Harrison and Eftink[117] and Stauffer et al.[116] found a negative heat capacity change for some host–guest complexation processes.

In textbooks[118] hydrophobic contributions to molecular recognition are attributed to positive entropy changes due to the release of structured water molecules in the hydration shells of apolar moieties. More recently, some experimental results have cast serious doubt on the active role of water molecules. Diederich et al.[115] found that complexation of benzene in a cyclophane host molecule is *enthalpy* driven at room temperature. The process is even accompanied by a slightly *negative* entropy change. Enthalpically controlled complexation was also found by Harata et al.[119] These observations caused some discomfort, which tempted Diederich et al.[115] to introduce the paradoxical term "enthalpic hydrophobic effect". The molecular origin of the complexation process was attributed to London dispersion interactions between host and guest and the binding state of water molecules in the interior of the host before binding.[120]

Stauffer et al.[116] showed that the enthalpy for the binding of **2** in host **1** (Scheme 4) is extremely sensitive to temperature. These heat capacity effects are more pronounced when guest molecules of increased hydrophobicity are involved. The heat capacity effects for host–guest complexation in organic solvents such as chloroform are also considerable, though less pronounced than in water.[116] In Figure 3 the changes in Gibbs energy, enthalpy, and entropy ($T\Delta S$) are plotted as a function of temperature for the binding of compound **2** in host **1** in water. Near room temperature the complexation is governed by a favorable entropy, whereas at elevated temperatures the enthalpic contribution prevails. The striking resemblance to the data plotted in Figure 2b suggests a relation to the solvation of apolar liquids in water.[120] The gain in entropy occasionally observed for complexation of apolar guest molecules in an apolar cavity of a macrocyclic host near room temperature[116] cannot be considered the sole driving force for hydrophobic contributions to host–guest interactions and certainly cannot apply to those cases for which the enthalpy governs host–guest complexation even near room temperature.[115]

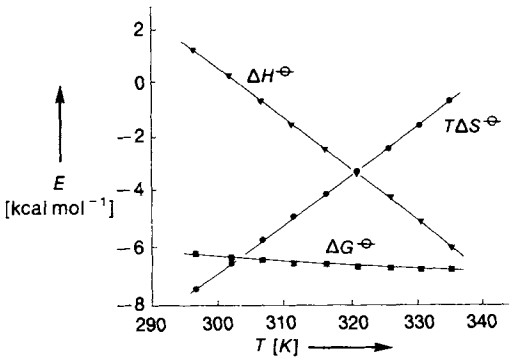

Fig. 3. Temperature dependence of $\Delta G^{\ominus}$, $\Delta H^{\ominus}$, and $T\Delta S^{\ominus}$ for the complexation of compound **2** in host molecule **1** (taken from ref. [116]).

2.4. Association of Amphiphiles

Aggregation of amphiphilic compounds in aqueous solution leads to complex supramolecular structures. Largely depending on the molecular architecture of the amphiphile, a wealth of three-dimensional structures can be formed, ranging from spherical and rodlike micelles to bilayer or multilayer structures, inverted hexagonal phases, and other sometimes very intriguing spatial arrangements. Introduction of chiral centers in the polar headgroup area can lead to beautiful structures (see, for example, Fuhrhop et al.[121, 122]). For a survey of the relation between surfactant structure and aggregation behavior we refer to a paper by Nusselder et al.;[123] for other reviews see Kunitake et al.[124] and Menger et al.[125]

It is almost generally accepted that an aqueous environment is a prerequisite for the three-dimensional assembly of amphiphilic molecules. However, examples have been found

for surfactant aggregation in other solvents such as hydrazine,[126] formamide,[127] ethylene glycol,[128] and ethylammonium nitrate.[129] Interestingly, partially fluorinated alkanes behave as amphiphilic compounds in apolar solvents in which they aggregate readily.[130, 131] Traditionally, however, hydrophobic interactions are considered to be the major driving force for amphiphile aggregation.[9] Results of studies on the micelle formation of cetyltrimethylammonium bromide (CTAB) and trimethyltetradecylammonium bromide in various solvents and at elevated temperatures urged a reappraisal of this traditional view.

As shown in Table 3, the Gibbs energies for the micelle formation of CTAB at room temperature in water and in hydrazine are not very different.[132] In contrast, the enthalpy and entropy for micelle formation differ dramatically.

Table 3. Gibbs energy, enthalpy, and entropy of micelle formation for CTAB in water and in hydrazine at different temperatures (taken from ref. [132].

Solvent	T [°C]	ΔG [kJ mol^{-1}]	ΔH [kJ mol^{-1}]	$-T\Delta S$ [kJ mol^{-1}]
water	25	−43.8	−12.6	−31.2
	95	−48.0	−51.9	3.9
	166	−44.4 [a]	−65.3	22.1
hydrazine	35	−29.7	−46.0	16.8

[a] A value of −43.2 is obtained by calculation; the values for ΔH and $T\Delta S$ may also be incorrect.

In water, micelle formation is driven by a favorable entropic contribution. As evident in Figure 4 and Table 3, the enthalpy and entropy of micelle formation of CTAB[133] and other surfactant molecules[134] are strongly dependent on temperature. At elevated temperatures the formation of micelles is governed by a favorable enthalpy and even counteracted by a loss of entropy. In fact, the thermodynamic parameters for micelle formation in water at these temperatures become similar to those found for micelle formation in hydrazine near room temperature. The aggregation number decreases with increasing temperature, and at 170 °C the aggregation number is similar to that found in polar organic solvents at room temperature.[135] Apparently, the exceptional position of water among hydrogen-bonding solvents is less evident at higher temperatures. It is furthermore remarkable that the Gibbs energy for the formation of micelles is only moderately affected by temperature, in other words, the enthalpy and entropy changes (as $T\Delta S$) are almost fully compensating. Lumry et al.[136] as well as Evans and Wightman[133] have provided a firm basis for discussions about compensation behavior of thermodynamic parameters of solvation and micelle formation in aqueous solvents (see Section 3.2).

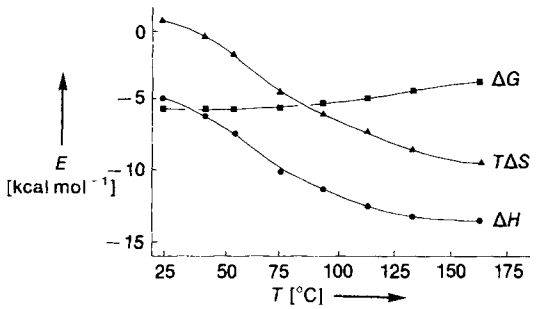

Fig. 4. Thermodynamics of micelle formation of trimethyltetradecylammonium bromide as a function of temperature, as determined by the equilibrium model (taken from ref. [133]).

The temperature dependence of the thermodynamics of micelle formation in water is remarkably similar to that of the solvation of apolar compounds in water and of the complexation of synthetic host and guest molecules (cf. Figs. 2a, b, 3, 4). This strongly suggests that these processes have a common molecular origin described by the term hydrophobic interactions. The molecular interpretation of this term in relation to aggregation of amphiphilic molecules is still a matter of debate. In 1989 Evans and Miller[135] emphasized the importance of van der Waals interactions for the aggregation of amphiphilic compounds. This, again, stresses the current dilemma centering on the distinction between dispersion interactions and hydrophobic interactions. A possible answer has been provided by Ben-Naim,[20] who clearly distinguishes the solvent-induced contribution to solute–solute interactions from the van der Waals forces. A serious disadvantage of this approach is that it is very difficult to estimate the magnitude of the solvent-induced contribution.

2.5. Surface Forces and Hydration of Flat Surfaces

In the past decade, much attention has been paid to the forces between aggregates of amphiphilic compounds in aqueous solution (for recent surveys, see Israelachvili and Wennerström[137, 138]). These so-called surface forces play an important role in biological processes as well as in a number of industrial applications such as mineral flotation, colloid stability, wetting of surfaces, and coating. In order to understand the molecular origin of surface forces between, for example, bilayer structures, forces between apolar surfaces were also considered. These forces exhibit a quite remarkable dependence on the distance between the macroscopic bodies.[139] In particular, forces between apolar surfaces show extremely long-range attractions unknown for polar surfaces.[140–145] In contrast with previous experimental results obtained by Israelachvili and Pashley[140] and Pashley et al.,[141] who found an exponential decay of attractive forces between apolar surfaces when the separation was increased from 0 to 15 nm, it has recently been shown that attractive forces between charge-free surfaces are measurable even at separations of 70–90 nm.[143–146] This means that the attractive forces are transmitted over distances corresponding to more than 300 interfacial water molecules! Claesson and Christenson[143] showed that the force between fluorocarbon surfaces in water increases exponentially until they are separated by a distance of about 10 nm. Beyond 10 nm the attractive force is even more amplified. A typical example is shown in Figure 5.

Today, much is known about the predominantly repulsive interactions between amphiphilic and polar surfaces.[137, 138, 147, 148] Despite the increasing interest in the

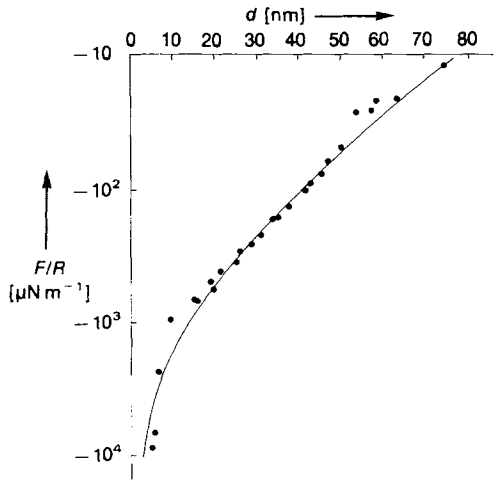

Fig. 5. Attractive surface force F/R plotted versus the separation d of fluorocarbon-covered mica surfaces (taken from ref. [167]).

anomalous forces between nonpolar surfaces in water, the origin of these forces is a matter of continuing discussions. Clearly, hydrophobicity of the surface areas is essential for the observed long-range forces. Long-range attractions have not been found between uncharged *and* nonhydrophobic surfaces such as carbohydrates[149, 150] nor between surfaces coated with a mixture of hydrophobic and hydrophilic compounds.[150] Claesson et al.[142] showed that the measured force is significantly stronger than would be expected on the basis of simple van der Waals forces. Moreover, van der Waals forces are only effective at surface separations of at most 10 nm. Some attempts have been reported to explain these amazing hydrophobic attractive forces. A possibility that has been considered is the formation of vapor cavities between the surfaces at distances less than a few hundred nanometers. The presence of such cavities has been established repeatedly.[146, 151, 152] On account of these cavities the force between the apolar surfaces is not an equilibrium force. Claesson et al.[152] showed, however, that these cavities can never give rise to the observed attractive forces. An alternative explanation is based on the possible role of electrostatic forces, but the fallacy of this view was demonstrated by Christenson et al.[145]

Several approaches focus on the properties of water present between the apolar surfaces. The hydrophobic forces are thought to arise from the alleged metastable character of water between the surface. The structure of water molecules near a large flat apolar surface has been a topic of extensive computer simulation studies. These studies[153–166] show clearly that water molecules adjacent to a hydrophobic surface are not capable of forming the optimal number of hydrogen bonds, although near the hydrophobic surface they clearly tend to form a clathrate-like structure.[157, 161] This structural response does not penetrate far into the medium, and the order in the fluid persists only over a few molecular diameters.[157, 159]

In 1989 Eriksson et al.[167] presented a phenomenological theory for the long-range attractive forces. The model was based on the variational mean-field theory developed by Marčelja et al.[168] to account for the interactions between small hydrophobic solute molecules. Eriksson et al.[167] suggested a structural mechanism based on a layer-to-layer propagation of the force due to ordering of the water molecules at the surface. Unfortunately, the question of how the force can be passed through so many water molecules remains unanswered. In the same year Attard[169] attributed the long-range attractions to van der Waals forces. Since these forces can normally not account for the observed magnitude and distance dependence of the attractive forces, he invoked an anomalous electrostatic response of the fluid between the surfaces. The large electrostatic response was assigned to the structural changes of liquid water at the surface. The molecular origin of this effect has, however, not been identified yet. In summary, although some efforts have been made to understand the inexplicably long-range action of the hydrophobic attractive forces between apolar surfaces in water, these attempts only rephrase the intriguing question of how water can mediate these forces across such a great distance.

2.6. Spectroscopy, Ultrasound, Light Scattering, and Diffraction Studies: Selected Results from the Last Few Years

The application of spectroscopic techniques to study hydrophobic effects peaked more than a decade ago. Because of the limitations of these techniques, these studies focused mainly on average changes in the organization of water molecules induced by apolar solute particles or, alternatively, on the preferential solvation or bulk hydrophobic interactions occurring at higher concentrations of the apolar solutes. Readers interested in applications of NMR spectroscopy are referred to publications of Zeidler[170] and Hertz and Leiter.[171] Results in the field of IR spectroscopy have been reviewed in detail by Walrafen[172] and Luck.[173] For more recent applications of IR spectroscopy we refer to the work of Symons et al.[174–176] and recent work of Engberts et al.[177] Most of the ultrasound studies of aqueous solutions also date from the sixties and seventies and have been reviewed thoroughly by Blandamer.[178] ESR spectroscopy has not been applied frequently, but it has been used almost exclusively to probe the environment of the solutes by inducing a spectroscopic response of the solute itself.[179] Most of these spectroscopic studies gave results that were consistent with the traditional picture of hydrophobic hydration. The question whether the structure of water is enhanced by the formation of more hydrogen bonds, stronger hydrogen bonds, or a reduction of free OH bonds has not been unambiguously answered.

In 1989 Raman scattering studies[180] confirmed the presence of bifurcated hydrogen bonds (Scheme 5), the existence

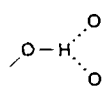

Scheme 5. Schematic representation of a bifurcated hydrogen bond.

of which had been proposed several times. Water molecules with five neighbors cause defects in the tetrahedral hydrogen bond network of liquid water and lower the energy barriers

between different arrangements of the network.[181] The "extra" water molecule acts as a catalyst by making fast restructuring possible without disrupting hydrogen bonds. Recently, Sciortino et al.[182] tentatively suggested a link with hydrophobic hydration. The inert hydrophobic solute prevents water molecules in the hydrophobic hydration shell from being approached by a fifth neighbor, thus slowing down the molecular motion of the water molecules involved. The decreased mobility of water molecules in the hydrophobic hydration shell is therefore attributed to an *increased* local density of water. The opposite, increased mobility in water of decreased density, was observed by Pottel et al. a few years ago.[183]

The most direct information about the structure of hydrophobic hydration shells can be obtained from diffraction studies, since these experiments yield the total pair correlation function $G(R)$, which is the averaged sum of a large number of partial distribution functions $g_{ij}(R)$ representing the average distribution of atom type j relative to atom type i in solution (see also Section 3.3.1).[184] Unfortunately, it is extremely difficult to obtain accurate information concerning solute–water and solute–solute interactions in hydration shells present in highly dilute aqueous solutions, since the total $G(R)$ function is dominated by the water–water terms.[185] Isotopic labeling of components of the aqueous solutions provides a possible solution of this problem.[185] In 1990 Turner et al.[186] reported a neutron diffraction study of the hydration of tetramethylammonium chloride (TMACl) in aqueous solution (0.5–2 mol kg^{-1}) with isotopic substitution of nitrogen, chlorine, and hydrogen. The results indicate that the TMA ion is surrounded by water molecules that tend to orient their OH bonds tangentially to the surface of the solute. In this respect, the results confirm the general picture of a somewhat distorted, clathrate-like solvation cage. The water correlations, however, suggest that the relative orientation of water molecules in the hydration shell is not significantly different from that in bulk water. Moreover, no evidence was found for aggregation of the TMA ions, and the structure of the hydration shell appeared to be independent on the concentration of TMACl. Results of more diffraction studies of aqueous solutions of isotopically labeled solutes are eagerly awaited.

2.7. Organic Reactions in Water

Although living organisms depend in a unique way on water as a solvent and reagent for biochemical transformations, synthetic organic chemists do no particularly like water as a solvent for chemical reactions. This "hydrophobic" attitude stems from the fact that water is a bad solvent for many organic compounds and is, in addition, highly reactive towards many organic reagents. Nevertheless, the past decade has witnessed a remarkable reappraisal of water as a solvent for organic reactions. The pioneering work of Breslow et al.,[187] who reported intriguing solvent effects of water on notoriously solvent-insensitive Diels–Alder reactions constituted a major source of inspiration.

Our interest in organic reactivity in water and mixed aqueous solvents goes back some time and was mainly excited by the unpredictable effects of the solvent on the thermodynamic parameters of activation in the water-rich region of mixed aqueous solvents.[188, 189] Solvent effects in highly aqueous media directly reflect the interactions between solute particles, in other words, the interactions between the reactant(s) and the cosolvent, and between the activated complex and the cosolvent. In dilute solutions the rate effects are mainly caused by pairwise interactions, and the results indicate that these interactions are governed by the apolar character of the reacting species and the cosolvent (from a thermodynamic point of view, it is more appropriate to speak of a cosolute). In Scheme 6 a general example is given; the rate-decreasing effect of an apolar cosolvent C on a reaction involves a loss of apolar character during the activation process, schematically represented by the transformation of reactant X into activated complex ac.

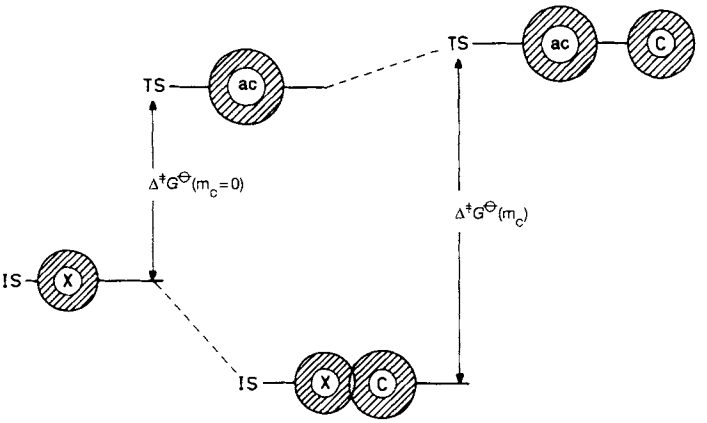

Scheme 6. Schematic representation of the effect of cosolvent molecule C on a reaction involving reactant X and activated complex ac in aqueous solution. IS = initial state, TS = transition state, $\Delta^{\ddagger}G^{\ominus}$ = standard Gibbs energy of activation.

Towards the end of the eighties Blokzijl et al.[190–194] reported a quantitative approach to explain solvent effects in dilute aqueous solvents in terms of pairwise interactions of cosolvents with reactant(s) and activated complex, respectively. By using the additivity principle developed by Savage and Wood (Section 3.3.2), contributions of functional groups in cosolvent molecules to the overall solvent effects could be determined. This approach does full justice to the complexity of intermolecular interactions in aqueous solutions. The additivity of functional group interactions was critically analyzed, and it was shown that the hydration shells of functional groups in close proximity are not independent of each other.[191] Hydrophobic methylene moieties were shown to generally retard organic reactions involving a decrease of apolar character during the activation process, whereas hydrophilic groups such as hydroxyl functionalities counteract this effect.[193] In the solvent systems examined, preferential solvation or solute aggregation does not occur. The solvent effects are therefore a consequence of hydrophobic encounters between apolar moieties in solution. These encounters are akin to molecular recognition processes but do not lead to aggregation or complexation.

Interactions between apolar groups in water are accompanied by the destructive overlap of hydrophobic hydration shells. Curiously, even apparently hydrophilic cosolutes like

carbohydrates and polyols induce a significant reduction of the rate constant of reactions involving apolar reactants and a more polar activated complex.[193, 195, 196] The hydration of polyols and carbohydrates is predominantly governed by hydrogen bonding. The rate-retarding effects suggest that apolar groups are always "noticed" by reacting species, even in the absence of hydrophobic hydration shells, whereas hydrophilic groups can be camouflaged and become almost indistinguishable from the OH groups of water.[195] Tentatively, we have made the suggestion[195, 196] that nature uses this feature in molecular recognition processes that involve polysaccharides at the surface of living cells.[197]

Diels–Alder reactions are dramatically accelerated *in* water.[198–203] The reaction of cyclopentadiene and 5-methoxynaphthoquinone (Scheme 7) has been studied in detail. The rate constants in *n*-hexane and in water are

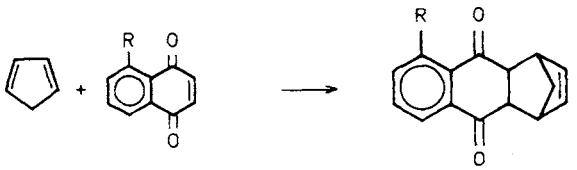

Scheme 7. Intermolecular Diels–Alder reaction of cyclopentadiene with 5-methoxy-1,4-naphthoquinone. R = OCH_3.

7.73×10^{-4} and 5.26 $dm^3 mol^{-1} s^{-1}$, respectively. An interesting aspect of a bimolecular Diels–Alder reaction of apolar reactants in water is that the formation of the activated complex necessarily models the pairwise hydrophobic interaction between the apolar reactants. According to Breslow,[198] the hydrophobic packing of diene and dienophile is the most likely explanation for the observed rate effects. This idea is mainly based on a series of kinetic experiments in solutions of "salting-in" or "salting-out" materials.[198] The enhancement or disruption of the water structure is used as a criterion for the respective promotion or inhibition of hydrophobic packing. The finding that Diels–Alder reactions are also accelerated in the presence of β-cyclodextrin by complexation of the reactants in the hydrophobic interior, appears to support this view.[198, 201] In addition, rate constants for Diels–Alder reactions in mixed aqueous solvents were successfully related to solvent parameters such as the solvophobicity parameter S_P,[201] the polarity parameter $E_T(30)$,[202, 204] and the cohesive energy density.[199, 200] These correlations strongly suggest a relation with the hydrophobicity of diene and dienophile. Schneider et al.,[201] however, did not find a correlation between the hydrophobicity of the dienophile and the observed rate effect.

These explanations for the remarkable effect of water on the rate of Diels–Alder reactions in water are doubtful and leave some important questions unanswered. On the basis of a combined quantitative and qualitative study of solvent effects in a series of Diels–Alder reactions in dilute aqueous solvents, Blokzijl et al.[205, 206] found that the rate effect arises primarily from changes in the Gibbs energy of the initial state. The activated complex appeared to be only moderately sensitive towards solvent effects. The formation of a complex between diene and dienophile could not be detected.

A study of solvent effects on a series of intramolecular Diels–Alder reactions confirmed also that hydrophobic packing of diene and dienophile in the aqueous medium cannot be held responsible for the exceptional rate effects. Therefore, the high rate constant was attributed to the fact that the hydrophobicity of diene and dienophile is considerably relieved during the activation process, a process which has been termed "enforced hydrophobic interaction".[205, 206] The term "enforced" has been introduced to stress the fact that under the employed reaction conditions diene and dienophile do not aggregate spontaneously in water. The reactive encounter is subjected to serious geometrical constraints and in water is *less unfavorable* in terms of Gibbs energy than in organic solvents. Apparently, the activated complex is a highly adaptable species that can adjust itself to the aqueous environment. Hydrogen bonding to the polarized carbonyl bond of the dienophile appears to contribute significantly to the interaction between water and the activated complex (see also Desimoni et al.[207]). A computer simulation study of Diels–Alder reactions in aqueous solution reported by Jorgensen et al.[208] suggests a similar explanation.

Other organic reactions are also accelerated when conducted in aqueous solvents.[209–214] In most cases, a reduction of the hydrophobic surface of the reactants during formation of the activated complex can largely account for the observed rate effect, although polarization effects are important as well. It is remarkable that the low solubility of the reactants enhances their reactivity, whereas complexation or aggregation only renders them less reactive. A few examples have been given, mainly photochemical processes, for which aggregation of reactants in water is favorable for the rate and product distribution.[215]

Up to this point we have discussed primarily organic reactions in dilute aqueous solvents. But mixed aqueous solvents are particularly popular reaction media in physical organic chemistry. When high proportions of an organic cosolvent are used, the preferential solvation of the reagents due to bulk hydrophobic interactions becomes a dominant factor for the observed solvent effects. The onset of bulk hydrophobic interactions is a consequence of the occurrence of highly dynamic, cosolvent-rich domains. The absolute solvent effect is then a measure of the extent of pseudo-phase separation. Recently, we have shown that these solvent effects can be analyzed quantitatively by using an inverse Kirkwood–Buff treatment[216] (see also Section 3.3.1).

3. Part B. Theoretical Studies

3.1. An Overview of the Theoretical Approaches to Explain Hydrophobic Effects

Theoretical studies of hydrophobic effects can be divided into four major categories. Most straightforward are those studies in which a model is developed that accounts for the observed thermodynamic parameters of solvation of apolar compounds in water on the basis of thermodynamic considerations; these include the liquid hydrocarbon model, multiple-step models for solvation, compensation models, and mixture models. Most of these models aim at a better under-

standing of hydrophobic hydration, and approaches along these lines will be reviewed in Section 3.2. Many of the theoretical approaches to describe hydrophobic effects center on virial expansions of thermodynamic properties of aqueous solutions containing apolar solute particles. As will be shown in some detail in Section 3.3.1, virial coefficients can be related to interactions between solute particles in aqueous media. Hence, these studies mainly deal with hydrophobic interactions either pairwise or bulk. Theoretical studies have either aimed at an empirical documentation of virial coefficients for aqueous solutions of organic solutes (Section 3.3.2), or, alternatively, have been devoted to a (semi)-quantitative description of these virial coefficients on the basis of intermolecular forces (Section 3.3.3). As will be discussed in Section 3.3.1, virial coefficients can also be interpreted in terms of the distribution of solute particles over the entire solution. Computation of these distribution functions can therefore yield both interaction potentials and virial coefficients. The accuracy of the applied methods can be tested by comparing the results with experimentally obtained virial coefficients. During the past fifteen years highly sophisticated integral theories have been developed for the solute–solute and solute–solvent distribution functions. These interaction site models (ISM) are equally suited for studying both hydrophobic hydration and hydrophobic interactions. Some approaches that have received particular attention will be described in Section 3.3.4.

A very elegant but often criticized approach to the study of hydrophobic effects uses the scaled particle theory (SPT).[*] Although the SPT is inherently a rather rigorous simplification of reality, applications of SPT yield surprisingly accurate results, and researchers in the field constantly draw attention to this remarkable fact. Some intriguing results of improved versions of SPT in the past few years are summarized in Section 3.4. The rapid maturation of theories concerning molecular liquids and solutions during the past fifteen years has made computer simulations one of the most valuable tools in the study of hydrophobic effects. Monte Carlo (MC) and molecular dynamics (MD) calculations have provided chemists with detailed information on hydrophobic effects on a molecular level that has been largely unaccessible by experimental methods. The molecular picture that has emerged from computational studies has reinforced some aspects of the traditional ideas about hydrophobic hydration, but has caused growing doubts about the validity of the whole concept of hydrophobic interactions. A detailed discussion will be given in Section 3.5.

3.2. Thermodynamic Properties of Aqueous Solutions of Apolar Compounds; Some Models

Since the introduction of the concepts of hydrophobic hydration and hydrophobic interactions, theories have been developed to account for the remarkable thermodynamic properties of aqueous solutions of apolar compounds. As will be shown in this section, thermodynamic parameters are a notoriously unspecific starting point for developing structural models. Many models can account for the thermodynamics of the solvation of apolar compounds in water, and most have a strongly qualitative character. Although each model emphasizes different aspects of hydrophobic hydration and hydrophobic interaction, most models can be categorized as mixture models. In these, water is considered to be a mixture of two or more species characterized by some differentiating property such as the number, strength, or length of hydrogen bonds. Introduction of apolar solute particles is thought to shift the equilibrium between the species. The classic models of Frank and Evans,[4] Frank and Wen,[23] Neméthy and Scheraga,[21, 22] Kauzmann,[6] and Ben-Naim[10, 26] are in fact mixture models (Section 1.2).

The geometric relaxation model developed by Lumry et al.,[217] a more recent example of a mixture model, is a hybrid of the classic model of Frank and Evans[4] and the flickering cluster model of Frank and Wen.[23] It is based on the water model of Sceats and Rice[218] and considers the water structure as composed of pairwise-bonded water molecules with continuously distributed energies, bond angles, and bond lengths. Two limiting structures are defined on the basis of bond length. One is characterized by short bonds, low entropy and enthalpy, and a large free volume available for solute particles; the other is characterized by long bonds, a large librational freedom of individual water molecules, and little free space for solute particles. Lumry et al.[217] expected small clusters of water molecules to undergo spontaneous "cluster contractions and expansions", thereby fluctuating between the limiting structures. An apolar solute particle was thought to promote the structure with short bonds by occupying the free volume and thus shifting the equilibrium.

The thermodynamic aspects of mixture models can be illustrated by a recent mixture model developed by Muller.[219] This model clearly finds its precursor in the classic model of Neméthy and Scheraga[21, 22] and is based on the assumption that every hydrogen atom in an aqueous solution can either participate in a hydrogen bond or is not involved in hydrogen bonding at all. An additional distinction is made between hydrogen atoms of bulk solvent molecules and hydrogen atoms that are perturbed by the presence of an apolar solute particle. The formation and disruption of hydrogen bonds is considered an equilibrium process, on the basis of which the enthalpy and heat capacity can be defined. A crucial aspect of the model is that it is not necessary to make any statements about the extent of structuring in the hydration shell (hs) in relation to the bulk (b) other than that $\Delta H^{\ominus}_{hs} \neq \Delta H^{\ominus}_{b}$ and $\Delta S^{\ominus}_{hs} \neq \Delta S^{\ominus}_{b}$. In this way the heat capacity of the bulk and the hydration shell can be analyzed separately. When n^h is the number of hydrogen atoms in the hydrophobic hydration shell, the heat capacity increment is given by Equation (8), in which $C^h_{p,b}$ and $C^h_{p,hs}$ are the heat

$$\Delta C^{\ominus}_{p} = n^{h}(C^{h}_{p,hs} - C^{h}_{p,b}) \qquad (8)$$

capacity contributions per mole of hydrogen atoms in the bulk and the hydration shell, respectively. The heat capacities can be quantified on the basis of the enthalpy of the equilibrium between broken and intact hydrogen bonds.

The heat capacity contribution of hydrogen atoms in the hydration shell was shown to be described by Equation (9),

[*] In the scaled particle theory all particles are assumed to be spherical with diameters defined such that thermodynamic quantities of solutions and pure liquids are reproduced.

$$C^{h}_{p,hs} = (\Delta H^{\ominus}_{hs})^2 K_{hs}/RT^2(1 + K_{hs})^2 \quad (9)$$

in which K_{hs} is the equilibrium constant. If $K_b = K_{hs}$, a positive heat capacity change can only occur when $\Delta H^{\ominus}_{hs} > \Delta H^{\ominus}_{b}$. Alternatively, if $\Delta H^{\ominus}_{hs} = \Delta H^{\ominus}_{b}$, then K_{hs} must be larger than K_b. Hence, the heat capacity effect can either be caused by increasing the strength of the hydrogen bonds or by increasing the number of broken bonds. A cooperative effect observed if $\Delta S^{\ominus}_{hs} > \Delta S^{\ominus}_{b}$ can lead to a very large heat capacity effect. A realistic choice of the parameters in Equation (9) yields a satisfactory description of the temperature dependence of the thermodynamic parameters for the solvation of apolar compounds in water. This mixture model clearly shows that statements about structure of the hydration shell with respect to bulk water are irrelevant without a proper definition of structure. Muller[219] stressed the fact that even at elevated temperatures, structural reorganization in hydrophobic hydration shells is still substantial and that the heat capacity change does not become zero; this was proven experimentally as well (see Section 2.1).

A similar but more general two-state model has been used by Gill et al. and Wadsö et al.[58, 63, 220–222] According to this model of a noncooperative hydration shell, each water molecule exists in two thermodynamic states separated by an enthalpy difference ΔH. These different states are caused by the fact that a water molecule in the solvation shell is affected by the presence of a solute boundary and cannot participate in the maximum number of hydrogen bonds. Each water molecule is assumed to behave independently of its neighbors, and cooperative effects are not taken into account. The heat capacity for the solvation process is now given by Equation (10), in which N is the number of water molecules in the solvation shell, τ the reciprocal temperature $(1/T)$, and τ_m the

$$\Delta C^{\ominus}_{p} = N\frac{(\Delta H)^2}{RT^2}\frac{\exp[-(\Delta H/R)(\tau - \tau_m)]}{[1 + \exp[-(\Delta H/R)(\tau - \tau_m)]^2} \quad (10)$$

reciprocal temperature at which the concentrations of water molecules in the two states are equal. Shinoda[51] estimated that this mean temperature is 370 K. Equation (10) is rather similar to Equation (9).

Unfortunately, thermodynamic analyses based on mixture models do not aid the molecular interpretation of hydrophobic effects, as long as water is considered as a mixture of two or more species with different characteristics. Although two-state models are somewhat simplistic, they usually do provide an adequate quantitative description of the temperature dependence of the thermodynamics of solvation of apolar compounds in water. The molecular interpretation of these mixture models remains a matter of assumptions.

Closely related to two-state or mixture models are models that we will describe as compensation models. Lumry et al.[217, 223] showed that the Gibbs energy for the transfer of argon from cyclohexane to water, hydrazine, and ethylene glycol are remarkably similar (Table 4). The low solubility of argon in the hydrogen-bonded solvents glycol and hydrazine is due to the unfavorable enthalpy change. The transfer of argon from glycol or hydrazine to water is accompanied by significant changes in enthalpy and entropy which, however, show almost complete compensation.

This observation led to the suggestion that the thermodynamics for the solvation of apolar compounds in water result

Table 4. Thermodynamic parameters for the transfer of one mole of argon from solvent I to solvent II at 298 K (taken from refs. [217, 218]).

Solvent I	Solvent II	$\Delta G^{\ominus}$ [kJ mol^{-1}]	$\Delta H^{\ominus}$ [kJ mol^{-1}]	$-T\Delta S^{\ominus}$ [kJ mol^{-1}]
cyclohexane	water	10.4	−11.2	21.6
cyclohexane	hydrazine	11.9	9.5	2.4
cyclohexane	ethylene glycol	10.3	0	10.3
ethylene glycol	water	0	−11.3	11.4
hydrazine	water	−1.5	−20.7	19.2

from two contributions. First, the low solubility of apolar compounds in water, hydrazine, and glycol is caused by the extensive hydrogen-bonded structure of the liquid;[224, 225] this contribution to the Gibbs energy of solvation is defined as the "motive" part. The second contribution is attributed to the characteristic fluctuation behavior of liquid water that distinguishes water from hydrogen-bonded organic solvents. Obviously, this aspect originates from classic mixture models (vide supra). The fluctuation of the hydrogen bond network leads to the remarkable heat capacity effects and compensation of enthalpy and entropy. This contribution is thus identified as the "compensative" part. According to Lumry,[217] the fluctuation behavior can be explained on the basis of a simple two-state, geometric relaxation model, and he attributed the low solubility of apolar compounds in water to the distortion of the hydrogen bond network. A detailed theoretical description of compensation laws was given by Grunwald[226, 227] in the mid-eighties.

In 1985 Lee[228] reported an interesting analysis of the compensation model of Lumry based on a dissection of the Gibbs energy of solvation into a contribution arising from the creation of a cavity in the solvent (G_c) and a contribution accounting for the attractive forces between the solute and the solvent (G_i). Both the cavity formation term and the interaction term were used to express the enthalpy and the entropy of the solvation process [Eqs. (11) and (12)]. The

$$\Delta h = G_i - \sigma^2_{v,H} \quad (11)$$

$$T\Delta s = -G_c - \sigma^2_{v,H} \quad (12)$$

factor $\sigma^2_{v,H}$ is a compensation term affecting both the entropy and enthalpy of solvation.[*] A statistical mechanical approach to the fluctuation behavior of liquid water has been offered by Oguni and Angell,[229] Lumry et al.,[217] and Lee.[228, 230] The compensation terms are related to the mean square fluctuations in H and S, $\langle\sigma^2_H\rangle$ and $\langle\sigma^2_S\rangle$, and can be expressed in terms of temperature and heat capacity. An important parameter determining the magnitude of the compensation term is the isothermal expansion coefficient α. The compensation term originates from the loss of solvent–solvent interactions and counteracts the favorable G_i term. For organic solvents, $\sigma^2_{v,H}$ and G_i are similar and Δh is small. The isothermal expansion coefficient α of water is extremely small, which implies that the enthalpy of water is not affected when the volume of water changes; in other words, water can accommodate large volume fluctuations without a significant enthalpy loss. Hence the compensation term for water is small, and Δh is similar to G_i, which is large and favorable.

[*] In this review the symbol σ is used in several contexts, in analogy to the literature usage.

The cavity formation term G_c results from the restricted motion of the solvent molecules in the presence of the solute particles and is governed by entropy. A large number of configurations available to the molecules in the pure solvent are unavailable in solution since they produce solvent–solute hard-core overlap. The compensation term reflects the increase in volume that leads to a loss of solvent–solvent interactions and an increase in entropy. In water the hydrogen bond network is hardly affected by the apolar solute, and the compensation term is small. According to Lee[228] it is misleading to say that apolar solute particles enhance the structure of liquid water. The low solubility of apolar compounds in water is thus mainly due to the unfavorable cavity term, which arises from the extremely small molecular volume of a water molecule (Section 3.4).[228, 230]

In the hydrocarbon model proposed by Baldwin[61] and Privalov et al.,[36, 60, 231] the thermodynamic parameters for the solvation of apolar compounds in water are also a result of two contributions—from the disruption of dispersion interactions between the hydrocarbon molecules in the liquid state and from the solvation of the hydrocarbon molecule in water. The model is based on the temperature dependence of the thermodynamic parameters of solvation for liquid hydrocarbons in water and was inspired by the role of hydrophobic effects in the folding and stability of proteins.

The crucial assumption in the hydrocarbon model is that at T_S^* (Section 2.1) water has lost its capacity to form a hydrophobic hydration shell. By applying Equation (3) the enthalpy of solvation of an apolar liquid at T_S^* can be expressed as Equation (13).[*] Combining Equations (2) and (13) provides Equation (14), in which the Gibbs energy of

$$\Delta H^{\ominus}(T_S^*) = \Delta C_p(T_S^* - T_H^*) \tag{13}$$

$$\Delta G^{\ominus} = \Delta H^{\ominus}(T_S^*) - [\Delta C_p(T_S^* - T) + T\Delta C_p \ln(T/T_S^*)] \tag{14}$$

solvation of liquid hydrocarbons is expressed as a function of T_S^*. $\Delta H^{\ominus}(T_S^*)$, the enthalpy of solvation at T_S^*, and the term in brackets are labeled as nonhydration and hydration terms, respectively. The hydration term is negative at all temperatures and counteracts the positive nonhydration term (Figs. 2a, b). In order to interpret Equation (14) in terms of a molecular model, Privalov et al.[14] introduced a somewhat artificial description of the solvation of a liquid hydrocarbon in water as a two-step process. At T_S^* the apolar liquid is first transformed into a compressed gas that has the same entropy and heat capacity properties as the liquid state but the enthalpy properties of the gas state. The second step involves the transfer of the compressed gas into water and is defined as the hydration step. The introduction of this fudged two-step process was tempting, because the nonhydration term $\Delta H^*(T_S^*)$ so beautifully equals the enthalpy of evaporation of the apolar liquid. This approach leads to the at first sight paradoxical conclusion that hydrophobic hydration increases the solubility of apolar liquids in water. The favorable Gibbs energy of hydration is small because of the compensating contributions from entropy and enthalpy. The low solubility of apolar liquids in water is fully accounted for by the nonhydration term. Hydrophobic interactions (bulk hydrophobic interactions) are most pronounced at T_S^*.

The practical value of the two-step model is questionable. It is not clear whether the contribution identified as the hydration term completely accounts for the process of hydrophobic hydration. An inherent contradiction in the approach is that the hydrocarbon model is based on the assumption that the heat capacity change is independent of temperature, whereas the two-step interpretation strongly relies on the absence of heat capacity effects at T_S^*. But the change in heat capacity of solvation at T_S^* is still considerable. In addition, at temperatures above T_S^* the entropy of solvation becomes positive, which would imply "reversed" hydrophobic hydration.

Equation (15) is a modified version of Equation (14) in which T_H^* is used instead of T_S^*. The compensative or hydration part in brackets is small and positive. The temperature-independent part describes the low solubility of apolar liquids and is comparable to the enthalpy term in Equation (14). This approach requires a different two-step model which is more difficult to interpret[36] and finds a detailed molecular expression in the scaled particle theory.[228]

$$\Delta G^{\ominus} = [\Delta C_p(T - T_H^*) - T\Delta C_p \ln(T_H^*/T)] - T_H^* \Delta S^{\ominus}(T_H^*) \tag{15}$$

Recently, Ruckenstein[232] proposed a mechanistic picture of hydrophobic hydration with a two-step model that distinguishes the process of cavity formation and the subsequent reorganization of the water molecules into "icebergs" based on earlier ideas of Shinoda.[51] The features of this model closely resemble those of the compensation models of Lumry et al.[217] and Lee.[228] Alternative two-step models for the solvation of apolar compounds in water have been proposed by Hvidt[233] and Ben-Naim.[10] From a thermodynamic point of view, two-step descriptions of solvation processes can be very convenient, but the definition of the separate steps remains an arbitrary exercise. In general, introduction of artificial intermediate states provides a deceptive sensation of clarity with respect to the molecular nature of hydrophobic effects.

3.3. Potentials of Mean Force, Virial Coefficients, Distribution Functions; Probing Hydrophobic Effects

3.3.1. Introduction

Another class of theoretical approaches to describe hydrophobic effects centers on theoretical models of molecular liquids and solutions based on statistical thermodynamics. In this section some basic terminology will be introduced to provide the context for the discussion of results in the following sections. Hydrophobic hydration is most conveniently described based on the distribution of water or, alternatively, oxygen and hydrogen atoms around a solute particle. The corresponding radial distribution function $g_{AO}(r)$ is defined as the average number of oxygen nuclei in a thin spherical shell of width Δr and radius r, which is centered on solute A [Formula (16)]. In this formula, ϱ_W is the average number of

$$4\pi r^2 \varrho_W g_{AO}(r)\Delta r \tag{16}$$

[*] In the literature T_S^* and T_H^* have been replaced by T_S and T_H, respectively, when the solvation of apolar liquids in water is considered. To avoid unnecessary confusion, we prefer to use T_S^* and T_H^* without exception.

water molecules per unit volume. The excess chemical potential of the solute particle can be computed by an integration of $g_{AO}(r)$ over a well-specified radius (at large r the integral diverges).[234] The aim is now to determine the radial dependence of the distribution function, an exercise which obviously requires detailed knowledge of the structure of liquid water. Comparison of the distribution functions of hydrogen and oxygen atoms gives insight into the orientation of the water molecules with respect to the surface of the solute particle.

When two or more apolar solute particles are present in water, the question arises as to the forces between these particles as a function of their relative distance. The chance of finding a second solute particle at a distance r from the center of the first directly measures the magnitude of the interactions between the solute particles. The potential of mean force between two solute particles A, ΔG,[*] is defined as the work required to bring two molecules of A, which were originally at infinite separation, to a separation R (which is on the order of the diameter of A). Following statistical thermodynamics, ΔG can be expressed[10, 17] by Equation (17), where $U(R)$ is the direct pair interaction between

$$\Delta G(R) = U(R) + \delta G(R) \tag{17}$$

the solute particles in the absence of solvent and $\delta G(R)$ the contribution of the solvent. The force acting between the particles is given by the first derivative of ΔG with respect to distance. Occasionally, $\delta G(R)$ is taken as a measure for hydrophobic interactions.[10, 23] Although this definition is formally more appropriate than the definition given in Section 1.2, a major disadvantage is that $\delta G(R)$ is difficult to determine experimentally.

Solvent-induced interactions result from changes in the solvation of solute particles when they approach each other. Even solute particles considered as hard spheres dissolved in a featureless solvent composed of hard spheres are subjected to solvent-induced interactions. This phenomenon is well established and is a consequence of partial shielding of solute surfaces when the particles are in close proximity.[26] When solute and solvent do not consist of hard spheres but have soft potentials, shielding leads to repulsive forces. These repulsive forces are, however, counteracted by attractive contributions caused by solvent molecules that simultaneously interact with two solute particles.

The potential of mean force acting on two solute particles is related to the distribution of the solute particles in the aqueous solution by Equation (18), where $g_{AA}(R)$ is the pair

$$g_{AA}(R) = \exp[-\Delta G(R)/k_B T] = \exp[-U(R)/k_B T] + \exp[-\delta G(R)/k_B T] \tag{18}$$

distribution function giving the chance of finding a second particle A at a distance R from the center of reference particle A [Eq. (16)]. The art of theoretical approaches to explain of hydrophobic interactions is to give a description for the behavior of either $\Delta G(R)$ or $g_{AA}(R)$.

Qualitatively, the pair distribution of spherical solute particles dissolved in a solvent containing only spherical solvent molecules can be rationalized on the basis of a number of preferred solute–solute arrangements. As shown in Figure 6, the contact arrangement and the solvent-separated arrangement give rise to well-defined maxima in the pair distribution function. More elaborate treatments also yield preferred arrangements at greater solute–solute distances.

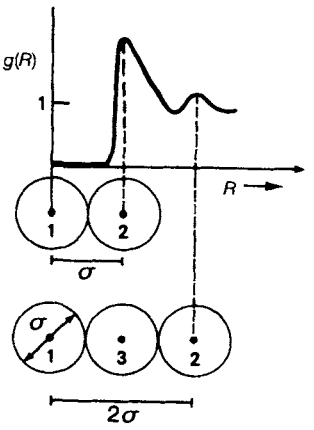

Fig. 6. Pair distribution function $g(R)$ for spherical solute particles 1 and 2 in solvent 3. Solute and solvent are shown as spherical particles with the same diameter σ. The first and second maximum in the pair distribution function correspond to the preferred arrangements (taken from ref. [17]).

Any solute–solute distribution function therefore exhibits oscillatory behavior as a function of the solute–solute distance. Unfortunately, a water molecule can hardly be taken as a spherical particle with a homogeneous charge distribution. An elegant and illustrative semiquantitative solution to this dilemma has been provided by Ben-Naim.[17] According to his approach, water is viewed as a Lennard–Jones sphere equipped with four additional binding sites, two hydrogen bond donor sites and two hydrogen bond acceptor sites. The binding energy B_W of each water molecule may be divided into a Lennard–Jones contribution and a hydrogen bond contribution [Eq. (19)].

$$B_W = B_{LJ} + B_{HB} = B_{LJ} + \sum_{l=1}^{4} B_l^{HB} \tag{19}$$

As shown in Scheme 8[17] each water molecule will be inclined to maintain hydrogen bond interactions. Thus, a water molecule near an apolar solute particle is far more likely to adopt orientation A rather than A'. Some preferred solvent-separated arrangements of two solute particles in an aqueous medium are shown by B–E. The shortest solute–

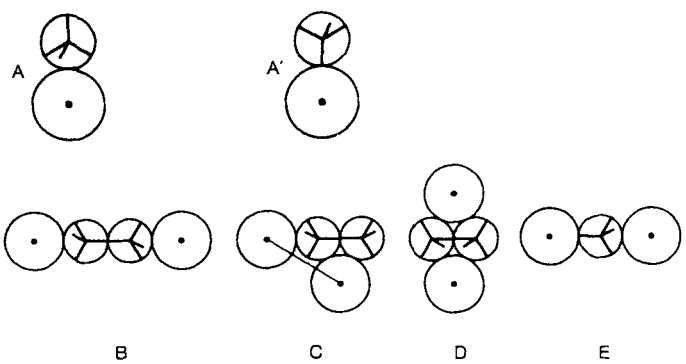

Scheme 8. Schematic representations of various arrangements of water molecules with respect to one or two apolar solute molecules (taken from ref. [17]).

[*] From this point on ΔG is used to denote the potential of mean force.

solute distance, about 6 Å, is found in arrangement C. This arrangement seems more probable than E, which has no hydrogen bonds. However, this preference has not been unambiguously confirmed by computational studies (Section 3.5). Although these qualitative and semiquantitative considerations are instructive, it remains a challenge to develop more sophisticated and quantitative molecular theories to account for the thermodynamic behavior of aqueous solutions of nonelectrolytes in terms of intermolecular potentials and distribution functions.

A convenient way of thinking about the distribution of solute particles in a solution is provided by the solution theory of McMillan and Mayer.[236] According to this theory, solutes in a solution are distributed in the same way as in a hypothetical gaseous state. The concentration of this gas equals that of the solution, and the interaction potentials in the hypothetical gas are related to the solute–solute potentials of mean force in a solution of infinite dilution. The chemical potential of the hypothetical gas is given by Equation (20), where w_2 and w_N are the pairwise and higher-

$$W(r_{1,\ldots,r_N}) = \sum w_2(r_{i,j}) + \sum w_3(r_{i,j,k}) + \ldots \quad (20)$$

order potentials of mean force acting between the solute molecules. The potentials of mean force can be calculated from the distribution at infinite dilution and used to compute the distribution of the solutes at finite concentration.

Traditionally, computer simulations only consider two-body interactions and are therefore perfectly suited for a study of pairwise hydrophobic interactions. It is, however, questionable whether the pair potential w_2 is sufficient to account for bulk hydrophobic interactions occurring in aqueous solutions of finite concentration. The theory of McMillan and Mayer[236] offers a relation between experimentally accessible thermodynamic parameters of solution and intermolecular potentials by the expression of the osmotic pressure Π in terms of a virial density expansion [Eq. (21)]. Here B_2^* is the second osmotic coefficient and directly related to the potential of mean force according to Equation (22).[236] The pointed brackets indicate that orientational averaging has been performed.

$$\Pi/kT = \rho + B_2^*\rho^2 + B_3^*\rho^3 + \ldots \quad (21)$$

$$B_2^* = 2\pi\int\langle 1 - \exp[-\Delta G(R)/kT]\rangle r^2 dr \quad (22)$$

In thermodynamic studies of aqueous solutions, thermodynamic excess functions are more widespread than osmotic pressures. The Gibbs excess function, for example, can be expressed in a molality expansion [Eq. (23)]. Here g_{AA} and

$$G^E = g_{AA}[m_A^2/m_0^2] + g_{AAA}[m_A^3/m_0^3] + \ldots \quad (23)$$

g_{AAA} are the parameters for the interaction of two and three particles, respectively; they are also known as the Lewis–Randall coefficients and should not be mixed up with $g_{AA}(R)$. Friedman[237, 238] derived a formal link between g_{AA} and the second osmotic virial coefficient B_2^* [Eq. (24)]. Here

$$g_{AA} = (RT/V_w^\ominus)(NB_2^* - V_A^\ominus + 1/2\kappa RT) \quad (24)$$

$V_w^\ominus$ is the volume of 1 kg of pure water, $V_A^\ominus$ the partial molar volume of the solute at infinite dilution, κ the isothermal compressibility, and N Avogadro's number. The second osmotic coefficient and the Lewis–Randall coefficient of aqueous solutions of nonelectrolytes are therefore a direct measure of the magnitude of pairwise hydrophobic interactions, since they reflect the number of encounters between both molecules beyond that expected statistically.

The existence of substantial triplet and higher-order terms reflects the occurrence of bulk interactions. Although it is theoretically feasible to calculate these higher-order terms from excess functions at elevated concentrations, this is not commonly done. To account for solute–solute (or solvent–solvent) interactions in more concentrated solutions or even in binary solvents, application of the theories of Kirkwood and Buff[239] is more convenient and provides insight into the molecular organization of these solutions. The crucial parameter in this theory is the Kirkwood–Buff integral G_{AA} [Eq. (25)], which is a measure of the mutual affinity of mol-

$$G_{AA} = \int_0^\infty (g_{AA}(r) - 1)4\pi r^2 dr \quad (25)$$

ecules A and yields, when multiplied with the number density of A, the excess or deficiency of particles A in the proximity of a solute particle A. The integral decays to unity beyond a certain distance R. In practice, the integral can be cut off at a distance of a few molecular diameters; the volume element is then defined as the correlation volume.[240] The integral can be related, along with other thermodynamic quantities, to the excess chemical potential of the aqueous solution (vide supra).[240] In fact, the Kirkwood–Buff integral collects all virial coefficients in the density expansion of the McMillan–Mayer theory [Eq. (21)] in one single integral function and becomes equal to the second osmotic coefficient in the limit $m_A \rightarrow 0$ [Eq. (23)]. For a recent treatment of the Kirkwood–Buff theory, see Matteoli et al.[241]

Theoretical approaches to account for structural and thermodynamic properties of aqueous solutions require knowledge of the distribution functions $g(R)$ and intermolecular potential functions. Here the previously discussed approaches run into serious difficulties.[242] First of all, various relations have been proposed to express the distribution of molecules in solution in terms of potentials of mean force acting between these molecules. In solutions in which the concentration of the solute approaches zero, the pair correlation function for the solute particles can be effectively described by Equation (18). As the density is large, which is always the case for solvent molecules, the situation is far more complicated. A number of so-called integral equations have been proposed which express the distribution of the components present in the solution in terms of potential functions. In the theoretical treatments of hydrophobic effects, the Ornstein–Zernicke equation and the Percus–Yevick equation are frequently encountered.[242] These integral equations can be solved only by numerical methods. By using computers and simple pair potential functions, such as hard-sphere potentials or Lennard–Jones potentials, solutions can be obtained[242] (see also Section 3.3.4).

3.3.2. *Virial Coefficients and Distribution Functions; (Semi)empirical Approaches*

In Figure 7 the second osmotic coefficients (at 25 °C) for homotactic interactions in aqueous solutions of noble gases and methane are plotted as a function of Henry's law constant K_H. The polarizability of the solute affects the sign and

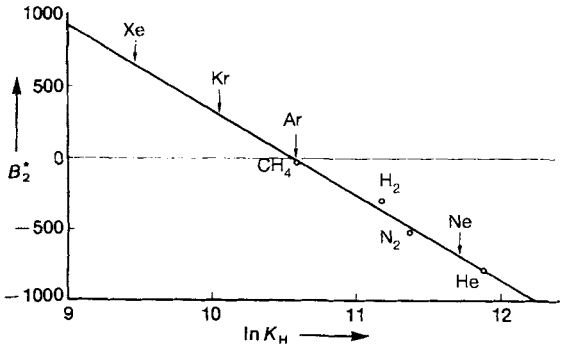

Fig. 7. Correlation between the logarithm of Henry's law constant and the osmotic virial coefficient (in Å^3) for small nonpolar solutes in water at 25 °C (taken from ref. [246]).

the magnitude of the virial coefficient. Apparently, krypton atoms repel each other in an aqueous environment, whereas methane molecules attract each other, though only slightly. On the basis of a limited number of accurate osmotic coefficients, Clark et al.[243] suggested that the association of alcohols in water is less than in the gas phase. This was also established for aqueous solutions of pure hydrocarbons such as cyclohexane and benzene[244, 245] and for noble gases such as krypton.[246] In Table 5 the second virial coefficients (at 25 °C) are given for some organic compouds in aqueous solution and in the gas phase. Remarkably, the Lewis–Randall coefficients differ quite substantially from the second osmotic coefficients and sometimes even have opposite signs; this can be reconciled by Equation (24). The results summarized in Table 5 emphasize that apolar molecules in a dilute aqueous solution show less tendency to associate than in the gas phase. Water apparently shields apolar solutes from each other and does not seem to promote their association.[16, 247] A few years ago Archer[248] studied the effect of temperature on the second virial coefficients of aqueous alcohols and showed that the "screening" effect of water weakens with increasing temperature.

Table 5. Experimental values of the second virial coefficients g_{AB} and B_{AB}^* at 25 °C (taken from ref. [16].

Solute(s)	g_{AB} [J kg mol^{-1}]	B_{AB}^* (aq) [a] [cm^3 mol^{-1}]	B_{AB}^* (g) [cm^3 mol^{-1}]
methanol	−52	17	
ethanol	−125	4	
2-propanol	−203	−11	
2-methyl-2-propanol	−277	−25	
cyclohexanol	−772	−209	
myo-inositol	−199	20	
cyclohexane		−402 to −527 [b]	−1734
benzene		−388	−1480
cyclohexanol + cyclohexane	−1163	−368	
cyclohexanol + *myo*-inositol	390	259	

[a] McMillan–Mayer standard state. [b] Strongly dependent on the method of calculation.

Second virial coefficients in the Lewis–Randall representation of thermodynamic excess functions for solvation of nonelectrolytes in water have been frequently treated by empirical models. Solute–solute interactions reflect the interactions between the functional groups that form the solute molecules and are able to interact with their surroundings. In 1976 Savage and Wood introduced a model that has received much attention during the past decade, in which the enthalpies[249] and later also Gibbs energies[273] of interaction, represented by the second Lewis–Randall coefficients h_{AB} and g_{AB}, are expressed in terms of a summation of pairwise functional group interactions [Eq. (26)]. Here $G_{i\leftrightarrow j}$ repre-

$$g_{AB} = \sum_{i,j} n_i^A n_j^B G_{i\leftrightarrow j} \tag{26}$$

sents the interaction between n_i^A groups i in solute A and n_j^B groups j in solute B in the Lewis–Randall representation. Similar equations can be set up for enthalpy and entropy. The Savage–Wood additivity of groups is based on three major assumptions: 1) Each group i of solute A interacts with each group j of solute B, 2) each of these interactions makes a characteristic contribution to the parameter for the interaction between A and B, and 3) each group interaction is independent of other groups and their relative position in the solute. A slightly different group additivity approach has been proposed by Bloemendal and Somsen.[250]

The group additivity approach can be criticized for being too simplistic.[251–253] The importance of neighboring group effects and stereochemistry have been recognized but purposefully neglected. In addition, some doubtful assumptions have been made in dissecting solute molecules into separate groups (see, for example, Tasker et al.[254] and Spitzer et al.[255]). Group additivity approaches are therefore considered to be first approximations. Theoretically, the potential of mean force acting between the solutes must be small in comparison to the thermal energy kT, since only in this case is linearization of the exponential term $\exp[W_{AB}/kT] - 1$ according to Equation (27) a valid approxima-

$$\exp[W_{AB}/kT] - 1 = \exp[(W_1/kT + W_2/kT)] \cong W_1/kT + W_2/kT \tag{27}$$

tion.[256] This exponential term expresses the solute–solute interactions as shown in Equation (18).

In spite of these shortcomings, the additivity approach has been applied to calculate pairwise interaction parameters (both Gibbs energies as well as enthalpies) for many organic compounds and functional groups (see for recent examples, Suri et al.,[257] Bloemendal et al.[258] Check et al.,[259] Borghesani et al.,[260] and Barone et al.[261, 262] and references cited therein). A selection of Gibbs energies and enthalpies of pairwise functional group interactions in aqueous solution at 25 °C is given in Table 6. In a pragmatic sense, the breakdown of the additivity rules may be used to signal atypical effects.

In studies of both heterotactic[263] and homotactic interactions[264] between a large variety of organic compounds in

Table 6. Gibbs energies and enthalpies of pairwise functional group interactions in aqueous solution at 25 °C [a].

Group i	Group j	G_{ij} [b] [J kg mol^{-2}]	H_{ij} [b] [J kg mol^{-2}]
CH_2	CH_2	−34	33
OH	OH	−24	−19
OH	CH_2	27	9
CONH	CONH	−115	−252
CONH	OH	−34	–
CONH	CH_2	55	66
CHOH	CHOH	−3	−14
CHOH	CONH	−6	−47
CHOH	CH_2	10	44

[a] Taken from refs. [254,255]. [b] Standard errors are large, often 20–40%.

aqueous solution researchers concluded that hydrophobic solutes are characterized by $g_{AB} < 0$ and $Ts_{AB} > h_{AB} > 0$. The classification of compounds as hydrophobic or hydrophilic is somewhat ambiguous, and some compounds such as carbohydrates[264] clearly show both hydrophobic and hydrophilic behavior. Because of the lack of solubility, interactions between unsubstituted hydrocarbons or noble gases can unfortunately not be studied. Hence, the approach does not provide insight into the molecular origin of pairwise hydrophobic interactions but yields a straightforward inventory of single group contributions to interactions of solutes more complex than noble gases and alkanes.

The relation between pairwise and bulk hydrophobic interactions is notoriously vague and difficult to describe in a theoretical model. To account for bulk hydrophobic interactions, Kirkwood–Buff integral functions have been frequently used.[265, 266] A typical example representing the distribution of 2-propanol and water in their binary mixture as a function of composition is shown in Figure 8. Apparently

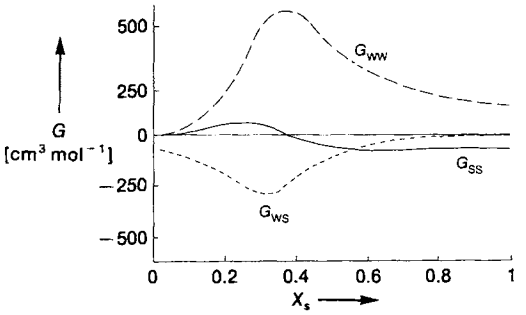

Fig. 8. Kirkwood–Buff integral functions G for mixtures of water (W) and 2-propanol (S) as a function of the mole fraction X of the organic cosolvent at 25 °C (taken from ref. [265]).

the preference of the organic component for alike molecules becomes greater with increasing concentration, and G_{SS} reaches a maximum in the water-rich region. At this concentration, the thermodynamic behavior of the mixture deviates strongly from that of an ideal mixture. A relevant question in this respect is whether the pairwise interactions predominantly present in dilute solution are additive or cooperative in more concentrated solutions. As shown above, water reduces the attractive forces between pairs of some apolar gases, but evidence suggests that it enhances the interactions between many solute particles. The molecular origin of this phenomenon is still unclear.

3.3.3. Virial Coefficients; The Models

During the past twenty years a number of approaches have been developed to calculate second osmotic coefficients on the basis of (semi)quantitative potential models for interactions between apolar solute particles in aqueous solution. A classic approach was reported by Kozak et al.,[267] who used lattice theories and the McMillan–Mayer theory to account for trends in second osmotic coefficients. Their main conclusions were that solute–solvent interactions decrease the magnitude of attractive forces between apolar solute particles and that the magnitude of the osmotic coefficient strongly depends on the size of the solute.

Friedman et al.[27–29] developed a model for solute–solute interactions on the basis of a repulsion term for hard spheres (hard-core repulsion term) and a term for the overlap of hydration spheres (cosphere overlap term) which became very popular in qualitative explanations of hydrophobic effects. The cosphere overlap term, often referred to as the Gurney contribution (in honor of Gurney[268] who first suggested the importance of overlapping hydration spheres for ion–ion interactions in aqueous solution), is estimated from the overlap volume of two solvation spheres. Following the classic ideas of Kauzmann,[6] the overlap of hydration shells leads to the release of structured water molecules into the bulk.

The basis of the model is schematically shown in Scheme 9. Water molecules in the hydrophobic hydration

Scheme 9. Schematic representation of the pairwise hydrophobic interaction between two apolar solute particles S, involving overlap of hydrophobic hydration shells and the concomittant release of structured hydration water to the bulk, according to the Gurney overlap model.

shells have a less favorable Gibbs energy than bulk water molecules; this is expressed in the Gurney coefficient. As the solute particles approach each other, the unfavorable situation of water molecules in overlapping hydration shells is gradually lost, and an attractive force increases as a function of the decreasing distance between the solute particles. The magnitude of the Gurney coefficient can be estimated from experimental data. However, it is questionable whether the Gurney overlap term measures only hydrophobic interactions, since the Gurney overlap term is a repository for all forces that are not hard-core repulsions.[269] The model has, however, been quite successful in accounting for experimental osmotic coefficients.[270, 271]

Various attempts[269, 272] to improve the cosphere overlap model have been reported. Clark et al.[269] suggested to exclude attractive solute–solute dispersion interactions from the Gurney overlap terms. The solvent-induced contribution to the solute–solute interactions was computed by compar-

ing the interactions in solution with those in the gas phase. Interestingly, the model also suggested that the attraction between apolar compounds in the gas phase and in the absence of solvent molecules appears to be stronger than in aqueous solution (vide supra).[269]

Calculation of second osmotic coefficients for interactions between hydrocarbons is hampered by the low solubility of these compounds in water and the concomittant lack of experimental data. Wood et al.[16, 273, 274] applied several additivity approaches to calculate second osmotic coefficients for interactions between medium-sized hydrocarbons such as cyclohexane. More recently Kang et al.[275–277] developed a sophisticated hydration shell concept for a quantitative description of thermodynamic parameters for the solvation of a large series of organic compounds in water. An improvement of the cosphere overlap approach was reported by Marčelja et al.[278] based on the Pople model for water. Their approach predicted a smooth exponential decay of the attraction between two apolar solutes with increasing separation.

In the late seventies and early eighties, however, it became increasingly clear that the potential of mean force between apolar solute particles is characterized by an oscillatory dependence on the separation between the particles. Using this knowledge, Wood et al.[247] developed an interaction site model (ISM) similar to that used by Clark et al.[269] However, Wood et al. employed a number of simple square-well potential functions to fit experimental osmotic coefficients. These square-well potential functions were chosen to represent both the contact arrangement and the solvent-separated arrangement, the latter by introduction of a barrier to avoid association of the solutes. In addition, nonpairwise additive contributions were introduced. The results reinforced the notion that water decreases the attractive forces that are present between (solute) particles in the gas phase under conditions of equal concentrations. Unfortunately, these models merely rephrase the question regarding the molecular origin of hydrophobic interactions.

3.3.4 Interaction Site Models; Integral Theories

One of the major problems in theoretical studies of hydrophobic effects is the description of liquid water. In water, strong attractive interactions between molecules compete with short-range repulsive forces, which is quite unusual for organic solvents. In spite of these difficulties, computer simulations of hydrophobic effects have been quite successful. To circumvent the inherent problem of having to develop a theoretical water–water potential, semiempirical approaches have been advanced that employ experimental data for liquid water. The ST2 model developed by Stillinger and Rahman[279–281] is a typical example of this approach (Section 3.5). Almost simultaneous to the appearance of the first computer simulation studies of hydrophobic effects in the literature, Pratt and Chandler[234, 282] developed an alternative microscopic theory, now known as the Pratt and Chandler theory (PC). This approach is more ambitious than the scaled particle theory and is essentially a statistical mechanical treatment using an interaction site model represented by a sum of pairwise, additive, spherically symmetric potentials acting between specified sites located on each molecule. A similar approach had already been considered useful in accounting for properties of nonassociated organic solvents. In these fluids the molecules interact predominantly through hard-core repulsions. The integral equation formulation for these solvents is generally known as the repulsive interaction site model (RISM)[283]. For a description of liquid water Pratt and Chandler[282] used the experimentally determined, orientationally averaged, pair correlation function for the oxygen–oxygen distribution. Subsequently, an Ornstein–Zernike-type integral equation (Section 3.3.1) was used to obtain the solute–solvent and solute–solute distribution functions after insertion of a solute molecule in the pure liquid.

Figure 9a shows the radial distribution of water molecules around a methane-like particle and reveals that the water molecules occupy a distinct position in the hydration shell of methane.[282, 284] As shown in Figure 9b, the PC theory predicts an oscillatory dependence of the solute–solute pair correlation function $g_{AA}(R)$ on the separation of the solute particles.[285] Simultaneously, computer simulation studies yielded similar results (see Section 3.5). The occurrence of

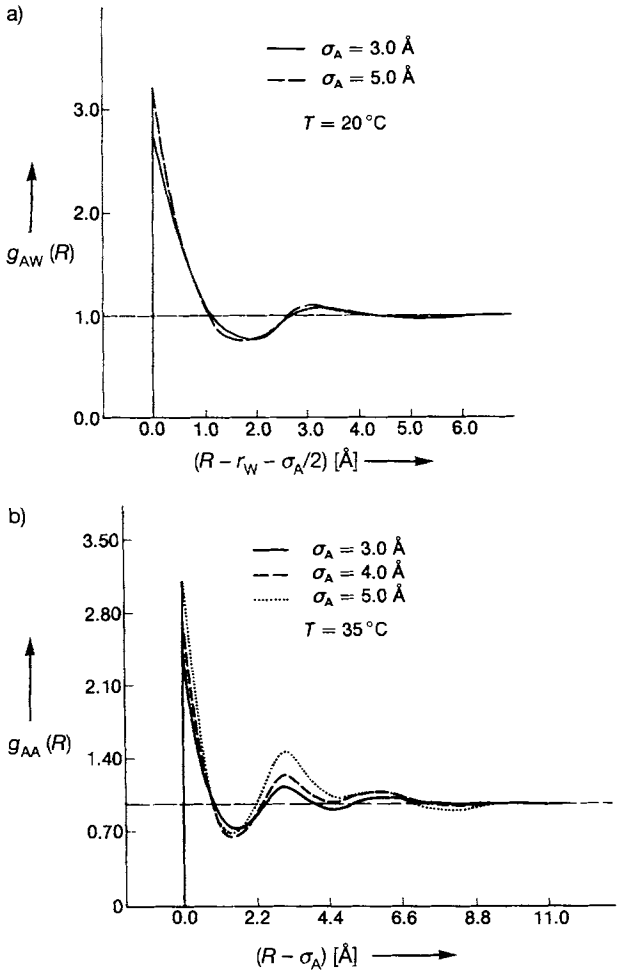

Fig. 9. Radial distribution functions $g_{AW}(R)$ (a, infinite dilution) and $g_{AA}(R)$ (b) for hard-sphere solute particles A dissolved in water W at 1 atm and 20 °C (a) and 35 °C (b). σ_A is the diameter of the solute and r_W the radius of water. g_{AA} was calculated based on the theory of Pratt and Chandler (taken from ref. [282]).

preferred arrangements of solute particles was anticipated on the basis of packing phenomena (see Section 3.3.1). Surprisingly, however, the populations of the contact and the solvent-separated arrangement appeared to be similar. The solute–solute pair correlation function was shown to be significantly altered by introducing attractive forces between the solute particles.

Unfortunately, as a result of the application of an orientationally averaged pair correlation function for water, information about the orientation of water molecules surrounding apolar solutes is lost. Tani[286] recognized this inherent weakness of the PC theory and generalized the PC model by introducing orientational aspects of water–water interactions. Application of the improved PC theory reinforced the traditional idea of clathrate-like solvation of apolar solutes in water. Tani found[286] that quantitative features of the calculated radial distribution function critically depend on the applied pair correlation function for liquid water and applied both experimental and theoretical potential models for liquid water. Generally, theoretical models for liquid water tend to exaggerate pair correlations between apolar solutes and water molecules.

Pratt and Chandler[284] and Tani[286] studied the hydration of solutes with more than one interaction site (nonspherical solutes) and found that the hydration characteristics of each site are qualitatively the same as that for an isolated interaction site. The solute–solute distribution function obtained by Tani[287] is qualitatively similar to that obtained by Pratt and Chandler.[234, 282] Remarkably, water–solute attractive forces hardly affect the quantitative features of the solute–solute distribution function. In contrast to its predecessor, the improved interaction site model[287] completely excludes the occurrence of contact interactions between apolar solutes. The size dependence of hydrophobic interactions is suggested to be small, but with increasing solute size the proportion of contact arrangements appears to be even less, which is in contrast with results obtained by other theoretical approaches (see, for example, Thompson et al.[247]).

Another extension of the PC theory was provided by Rossky et al.,[288, 289] who introduced a nonuniform charge distribution by employing an interaction site model (ISM) with charged interaction sites for dipolar and quadrupolar fluids. The extended repulsive interaction site model (XRISM) equation was used to determine the potential of mean force acting between rigid, polyatomic solutes in polar molecular solvents such as water.[290] To describe the interactions between water molecules, Rossky et al. used a theoretical model for water developed by Jorgensen et al.[291] (Section 3.5). Interestingly, Rossky et al.[290] confirmed that in both a solvent consisting of diatomic molecules and in water the potential of mean force between apolar solute particles is characterized by an oscillatory dependence on their separation. The XRISM was also used to determine internal motions of polyatomic molecules in aqueous solution.[292] More recently, Tanaka et al.[293] made a comparison between Monte Carlo simulations of aqueous solutions of apolar compounds and the results obtained by the XRISM. They confirmed the intuitively wrong result suggested by interaction site models that the solvent-separated arrangement is favored with increasing solute size.

3.4. Scaled Particle Theory (SPT); The Formation of Cavities in Liquid Water

An interesting attempt to explain thermodynamic data of solvation for apolar compounds in liquid water is the scaled particle theory (SPT). Thanks to the pioneering work of Pierotti, application of SPT to the study of hydrophobic effects should probably be considered one of the first theoretical approaches to hydrophobic effects.[294–296] In this model the dissolution of a particle is separated into two steps. The first step is the creation of a cavity in the solvent (see also Section 3.5.2) which has the appropriate size to accommodate the solute particle. The second step is the onset of interactions between the solute and the solvent. The Gibbs energies of these two processes are generally referred to as G_c and G_i respectively. The structural implications of solute–solvent interactions for the solvent in close proximity to the solute cannot be treated by the SPT. The theory uses statistical arguments based on pair distribution functions of solvent molecules in the pure liquid and yields expressions for the work that is involved in introducing a spherical particle into a solvent of spherical particles. An essential feature of the SPT is that the creation of a volume element in a liquid to accommodate a solute particle requires exclusion of solvent particles, a process that involves a certain amount of work. This can be expressed in a Boltzmann equation [Eq. (28)].[296]

$$p_o(r,\varrho) = \exp\{-W(r,\varrho)/kT\} \tag{28}$$

Here ϱ is the number of solute particles per unit volume (N/V), $W(r,\varrho)$ the work required to create a cavity of radius r, and $p_o(r,\varrho)$ the probability that such a cavity arises from statistical fluctuations in the solvent network. The second osmotic coefficient B_2^* is directly related to $p_o(r,\varrho)$. The aim of the SPT is now to determine $p_o(r,\varrho)$ as accurately as possible on the basis of statistical mechanical and geometrical arguments. Essential is that the solvent is considered to be a spherical particle with a radius σ. The general approach followed is to start off with a cavity radius of zero after which the cavity size is gradually expanded.

An important parameter for the calculation of the work involved in formation of a spherical cavity of radius R is the probability of finding a center of a spherical solvent molecule in this spherical volume element. This probability is defined in a distribution function describing the conditional distribution of solvent particles in the solution. The theory provides an expression for this conditional probability function $G(r,\varrho)$ in which experimental properties of the solvent such as the density and isothermal compressibility appear. Thus, structural information for the solvent, absent in basic forms of the SPT, is introduced and provides the theory with a semiempirical character. Nonetheless, the application of SPT to liquid water has been vigorously critized.

In a classic paper, Stillinger[297] developed methods to incorporate the strongly directional character of water–water interactions and made the SPT suitable for applications to aqueous solutions by incorporating some rudimentary aspects of the hydrogen bond structure of liquid water. This approach led to the development of the famous ST2 model

for liquid water (see Section 3.5). A pragmatic application of SPT yields very good results in calculating thermodynamic parameters for the solvation of apolar gases in water.[294, 296] In 1988 Langlet et al.[298] reported a modified SPT with excellent results for nonaqueous solvents.

During the past decades, application of the SPT to the study of the solvation behavior of apolar gases in liquid water has led to the remarkable suggestion that the low solubility of apolar gases in water is mainly due to the small molecular volume of the water molecule. In other words, because of this feature, the frequency of observing a cavity of sufficient volume to accommodate an single-atom solute or larger particle in water is much lower than in organic solvents. Lucas[299, 300] was one of the first to make this suggestion after a careful study of the role of the molecular size and the isobaric expansion coefficient α for the thermodynamics of solvation. Later Lee[228] developed a model for the solvation of apolar gases in water on the basis of cavity formation and the compensative behavior of enthalpy and entropy terms (Section 3.2) and stressed the fact that the contribution of G_i is similar for all solvents. The low solubility of apolar compounds in water is reflected almost exclusively by the G_c term, which deviates strongly from that for organic solvents. According to the SPT as well as to the theory of Pratt and Chandler (Section 3.3.4), G_c is directly correlated with the number of solvent molecules that hit the surface of the cavity during its growth. Obviously, this number is related to the size and the density of the solvent. The small molecular size of water enhances the unfavorable character of G_c, whereas the low packing density of liquid water, which is a consequence of the open hydrogen-bonded structure of liquid water, counteracts this effect. The packing density of hydrazine, whose molecular volume is somewhat larger than that of water, is considerably higher. Indeed, the solubility of apolar compounds in hydrazine is just as bad as in water and in some cases even worse. As noted by Lee,[228] the low density caused by the hydrogen bond network in liquid water promotes the dissolution of apolar gases.

Recently, Lee[230] used the experimental thermodynamic data of solvation for hydrocarbons in water and their pure liquid state in combination with solute–solvent interactions obtained from computer simulation studies to compute the enthalpy change upon solvent reorganization. In addition, the cavity term H_c was determined for the solvation of hydrocarbons in their liquid phase. These data were compared with parameters obtained from the SPT. It was shown that the thermodynamic parameters for solvent reorganization and cavity formation, in particular the enthalpy and the entropy, are strongly dependent on temperature. The SPT appeared to reproduce the temperature dependence of the Gibbs energy of cavity formation very accurately. The temperature dependence of the enthalpy and entropy of cavity formation was not reproduced as satisfactorily.

In Figure 10 the *differences* between the Gibbs energy for cavity formation G_c, the energies of the solute–water interactions E_a, and the enthalpic solvent reorganization enthalpies H_r are plotted versus temperature for the solvation of neopentane in water and in its neat phase. In addition the total Gibbs energy change ΔG^* (* indicates that the standard state advocated by Ben-Naim is used (see Section 1.2)), enthalpy change ΔH^*, and entropy change $T\Delta S^*$ for the transfer

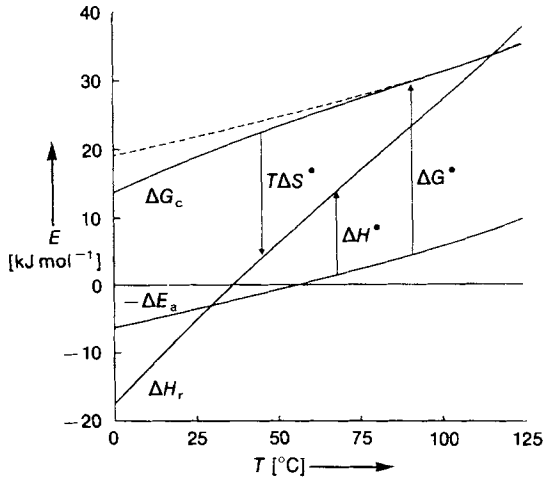

Fig. 10. Temperature dependence of changes in the Gibbs energy of cavity formation ΔG_c, the solute–solvent interaction energy ΔE_a, and the solvent reorganization enthalpy ΔH_r for the solvation of neopentane in water as opposed to in its neat phase. Thermodynamic parameters based on the Ben-Naim standard state are indicated as well (taken from ref. [230]).

of liquid neopentane to water are indicated. Figure 10 is very revealing and shows that ΔG^* is rather insensitive towards temperature, because the temperature dependence of changes in solute–solvent interactions and the changes in the cavity term are similar. By contrast, the change in the enthalpy of solvent reorganization is dramatically dependent on the temperature and causes a separation of ΔG^* into entropy and enthalpy terms that are equally temperature dependent. These terms compensate each other almost completely (see also Section 3.2). ΔH_r for the transfer of gaseous neopentane to water increases rapidly with temperature, whereas ΔH_r for the transfer of gaseous neopentane to its neat phase decreases with temperature (for solvation of apolar compounds in water, the assumption is made that $\Delta H_r = \Delta H_c$). Even near room temperature, the enthalpy of solvent reorganization is positive for both solvation processes. This observation seriously conflicts with the idea of increased solvent structure due to enhanced hydrogen bonding around the inert solute particles. In addition, solute–solvent interaction energies are remarkably similar and attractive. Thus, the low solubility of apolar compounds in water is fully governed by the Gibbs energy of cavity formation G_c, which is accurately reproduced by the SPT. According to Lee,[230] hydrophobicity must therefore be attributed to an excluded volume effect and the compensation of enthalpy and entropy to changes in the volume of the solvent.

The SPT has been criticized on various grounds, in particular for its results in applications to hydrogen-bonded solvents.[301] In fact, in addition to the SPT and the hybrid approach followed by Lee (vide supra), two other approaches are available for calculating the thermodynamic parameters of cavity formation in liquids. A semiempirical method going back to publications of Sinanoglu[302, 303] considers the formation of a cavity in a liquid in terms of the work against counteracting surface forces. The theoretical approach is based on the concept of microsurface tension in the solvent (see Section 2.1). A few years later Reisse et al.[304, 305] drew an analogy between the process of creating a molecule-sized cavity and the evaporation of the liquid.

Unfortunately, the Sinanoglu–Reisse approach is less suited for hydrogen-bonded solvents. More recently, Moura-Ramos et al.[306] showed that changes in the molecular order during the evaporation process hamper the Sinanoglu–Reisse analysis. Thus they proposed to describe the process of cavity formation in analogy to the evaporation of a disordered liquid by using the corresponding state principle.[306, 307] Entropies and enthalpies for cavity formation in various solvents, unfortunately not including water, were calculated. In contrast to the data reported by Lee[228, 230] and Sinanoglu,[303] negative entropies were found for the creation of cavities in organic solvents near room temperature.

During the past decade, computer simulations have become increasingly popular for the calculation of thermodynamic parameters for the formation of solute-sized cavities in water (see Section 3.5). Since it has been generally questioned whether the solubility of apolar compounds in water can be interpreted in terms of a packing phenomenon for spherical solvent molecules, and since even incorporation of some structural aspects of real water did not enhance the confidence in the results of SPT, the main goal of these computer simulation studies was to test the results of the SPT. The traditional idea that water is a liquid with a remarkably open structure argued against the conclusions from SPT. Computational approaches were reported by Postma et al.,[308], Jorgensen et al.,[309] Tanaka,[293] and recently by Guillot et al.[310] Particularly interesting was the approach reported by Guillot et al.[310] in which a comparison was made between the work of creating a cavity in water, described by a realistic water model, and in a liquid composed of hard spheres. The calculations show unequivocally that the Gibbs energy for the creation of cavities in liquid water is not primarily determined by the specific structure of water but by factors such as packing density, size of the solvent molecule, and the equation of state.

Recently Pohorille and Pratt[311] used molecular dynamics (MD) and Monte Carlo (MC) simulations to calculate the thermodynamics of formation of a cavity in various organic liquids and water in order to study the impact of the structure of hydrogen-bonded liquids. They found that water has a larger fractional free volume which is, however, more disperse than that of organic solvents. They also found that the work required for cavity formation predicted by the SPT is about 20% below the value obtained with the TIP4P model (see Section 3.5) for liquid water. As shown by Guillot et al.,[310] a solvent composed of hard spheres of similar size to water molecules has a significantly better capacity to accommodate apolar solute particles in its free volume. Unfortunately, the sizes of the cavities considered were still rather small. In a more detailed study of the so-called transient cavities in molecular liquids, the statistics for cavity formation in water, *n*-hexane, and *n*-dodecane were compared in relation to the density of the solvent at the surface of the spherical solutes, referred to as the contact density $\varrho_S G(\lambda)$.[312] The contact density at the surface of a hard sphere is significantly greater in water than in the organic solvents; in other words, water squeezes the solute out of solution more strongly.[312] This force reaches a maximum for cavities roughly 2.4 Å in diameter. According to Lee,[228, 230] this conclusion is essentially a different way of saying that the low solubility of apolar compounds in water is mainly an excluded-volume effect.

3.5. Computer Simulation Studies of Aqueous Solutions; An Introduction

During the past fifteen years, computer simulation studies have provided a rich source of detailed information on the molecular organization of aqueous solutions. Structural aspects of hydrophobic hydration and hydrophobic interactions became apparent that were not easily accessible by alternative methods. Results of computer simulation studies have confirmed the traditional ideas on hydrophobic effects to some extent, but have also raised a number of important questions. A typical simulation considers a limited number of water molecules (usually 100–500) at equilibrium in a box confined by periodic boundaries. One or more of these water molecules are replaced by a solute particle. The subsequent structural and thermodynamic changes are monitored by sophisticated sampling methods. The new equilibrium properties of the solution are calculated either by averaging over a large number of selected configurations (MC), or by solving the Newtonian equations of motion and taking a time average (MD). The choice of intermolecular potential functions describing the interactions between the components of the system is therefore of paramount importance.

For liquids like water with strong, attractive intermolecular interactions, the development of potential functions describing the interactions between the molecules in the liquid has been notoriously difficult. Computer simulation studies of hydrophobic effects have employed a number of well-known potential models for liquid water. Most of these potential models are (semi)empirical.[313] Charge distributions and Lennard–Jones parameters have been optimized in order to reproduce experimental properties of water with high accuracy. Stillinger and Rahman[279–281] developed a pair potential for rigid water molecules on the basis of scaled particle theory. This ST2 model became very popular and was used frequently with or without adjustments for the system investigated. Other popular mean field models are the simple point charge model (SPC) developed by Berendsen et al.[314] and the transferrable intermolecular potential functions (TIPS, TIPS2, and TIP4P) developed by Jorgensen et al.[291] A popular analytical potential model based on ab initio calculations has been advanced by Matsuoka, Clementi, and Yoshimine (MCY model).[315]

In most computer simulation studies, the total potential energy of an aqueous solution is assumed to be the sum of individual *two-body* interactions. Polarizabilities and the corresponding induced dipoles, nuclear polarization, and intramolecular flexibility are not normally included in simulations of liquid water. This is regrettable, since polarizability effects involving cooperativity of a large number of water molecules might be significant in the molecular origin of hydrophobic effects. Recently, some important progress has been made by incorporating electric polarizabilities, intramolecular degrees of freedom, and many-body effects in empirical[316, 317] as well as in nonempirical[318–321] potential models for liquid water. Unfortunately, this knowledge has not yet been employed in computer simulation studies of

hydrophobic effects. Since water–water interactions are so exceptionally strong, solute–water interactions are not a major factor for the structure of water molecules in the near vicinity of apolar solutes and are usually described by simplified interaction laws. Occasionally, quantum mechanical potentials are used to model these interactions, though ab initio calculations are not necessarily an improvement in this respect.[322]

The decisive thermodynamic quantity in chemical processes is the free energy change (either Gibbs energy or Helmholtz energy). Unfortunately, calculations of these quantities for the solvation of apolar compounds in water are still extremely difficult, and the results are subject to large errors.[79, 323–328] Alternatively, the free energy difference between two systems, for example, two aqueous solutions containing different solute particles, can be calculated by stepwise perturbations of one system by which it is slowly converted into the other. For example, aqueous solutions of propane and ethane can be compared by stepwise elimination of a methylene group. Although this might seem like a bizarre kind of alchemy to an organic chemist, it is a very convenient procedure and a valid thermodynamic path between these two states. Free energy perturbation methods are a relatively new, important improvement in the calculation of relative free energies of processes in solution on the basis of computer simulations.[79, 329]

3.5.1. Description of Hydrophobic Hydration from Computer Simulations

In hydrophobic hydration the position, orientation, mobility, and potential energy of water molecules in close proximity to single apolar solute particles all play a role. In qualitative studies of hydrophobic hydration, these parameters have been associated with the structure of water in the solvation shell. In order to determine to what extent water molecules are affected by the presence of an apolar solute particle, it is convenient to make a clear distinction between water molecules in the solvation shell and in bulk water. One useful method is the "partitioning of the configuration space". According to this method, water molecules whose oxygen nucleus is found within a certain radius R from the center of the solute particle are considered part of the hydration shell.[330, 331] The exact value of radius R is rather arbitrary and obviously depends on the diameter of the solute particle. Usually, only the first hydration shell is taken into account by including merely the first peak of the solute–solvent radial distribution function. In an alternative approach, distribution functions for the aqueous solution are simply compared to those for pure liquid water.[332] One drawback of this method is the fact that the number of water molecules that are affected by the apolar solute particles is relatively small in comparison to the total number of water molecules.

In 1974 Dashevsky and Sarkisov[333] were the first to report a MC computer simulation of a solution of methane in 64 water molecules at constant volume and temperature. The computational methods applied in this simulation study were severely criticized and the results considered unreliable.[334, 335] Three years later Owicki and Scheraga[330] performed a more sophisticated MC simulation of an aqueous solution of methane at fixed temperature and pressure. The first extensive MD simulation of an aqueous solution of two Lennard–Jones particles was published by Geiger et al.[335] almost two years later. Almost simultaneously Rossky and Karplus[331] carried out a detailed MD study of a dilute aqueous solution of an alanine dipeptide with both polar and nonpolar regions. These investigations might be considered the precursors of many computer simulation studies of the hydration of organic compounds in water.

With the aim of studying hydrophobic hydration and hydrophobic interactions simultaneously, most simulations deal with the behavior of water molecules in the presence of more than one solute particle. The solvation of prototypes of apolar solutes such as methane[163, 310, 324, 326, 330, 332, 336, 337] and noble gases[325, 334, 335, 338–343] has been studied extensively. Since *n*-butane is a popular model for studies of solvation effects on conformational equilibria, studies of the solvation of *n*-butane have been conducted frequently.[344–347] In addition to computer simulations of the solvation of other alkanes,[309, 348, 349] fundamental studies of the hydration of formaldehyde,[350] methanol,[349, 351–353] ethanol,[309, 349, 354] 2-methyl-2-propanol,[355] and a series of α-amino acids and nucleotides[356] have also been reported. Occasionally solute–water interactions have been described by potential functions based on ab initio calculations.[330, 332, 351, 352] In other cases, solute–water interactions were represented by relatively simple Lennard–Jones potentials[293] or even by merely short-range repulsive forces.[357] Recently Cramer and Truhlar[358] reported self-consistent field calculations to compute absolute free energies for the solvation of apolar organic and small inorganic molecules in water.

Although different potential functions, simulation times, and computational methods have been used, the results are qualitatively remarkably similar. Pair distribution functions representing the distribution of hydrogen and oxygen nuclei with respect to argon atoms in aqueous solution as reported by Guillot et al.[310] are shown in Figure 11. The fact that

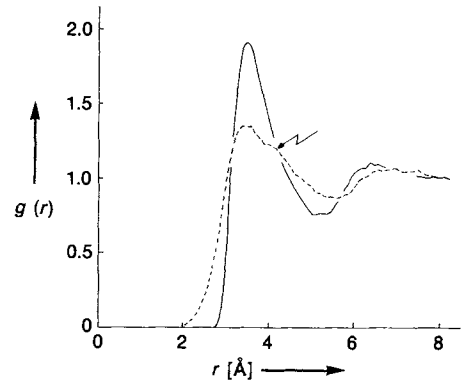

Fig. 11. Argon–oxygen and argon–hydrogen pair distribution functions $g_{AO}(r)$ (solid line) and $g_{AH}(r)$ (dashed line), respectively, for a dilute aqueous solution of argon (taken from ref. [310]). For further explanation see text.

$g_{AH}(r)$ and $g_{AO}(r)$ almost coincide indicates that water molecules adjacent to the solute particle are orientated such that their O–H bonds are tangential to the surface of the solute. This conclusion has been almost unanimously confirmed by

other computer simulation studies (see, for example refs. [310, 330, 332, 335, 338, 357]). Water molecules clearly avoid pointing their O–H bonds directly toward the nonpolar solute. The second maximum in the distribution functions shows that most water molecules in the second hydration shell point their oxygen atom toward the solute and their hydrogen atoms toward the bulk and, on average, orient themselves tangentially on the first hydration layer. An interesting feature revealed by some computer simulation studies[310, 335, 339] is the weak shoulder in the peak of the hydrogen–solute pair distribution function (see arrow in Fig. 11). The increased probability of finding hydrogen atoms of water molecules participating in the second hydration shell at a shorter distance from the solute particle gives reason to infer that some water molecules point their O–H bonds in the direction of the first hydration layer and appear to couple the two hydration shells.

The number of water molecules involved in the solvation of an apolar solute particle depends strongly on the definition of the size of the hydration shell. On the basis of "partitioning of configuration space", several computer simulation studies report hydration numbers.[330, 359] They tend to be large and vary from 20 for methane to 34 for *n*-pentane. Jorgensen et al.[359] reported an excellent correlation between the number of water molecules in the first hydration layer of a series of linear and branched alkanes and the entropy of solvation. Curiously, a Lennard–Jones solute with a diameter corresponding to the hard-sphere diameter of a water molecule is surrounded by significantly more water molecules than a water molecule itself.[357] Some evidence indicates that the coordination number of water molecules in the solvation shell is preferentially four, but differences to the coordination numbers in pure water are small.[332, 337, 348]

Although differences between binding energies of water molecules in the bulk and in the hydration shell are small, discernible shifts have been observed towards stronger binding among water molecules in the hydration shell. Most simulation studies reveal that the total binding energy distribution of water molecules generally becomes narrower after insertion of the apolar solutes and shifts towards lower energy (see, for example, refs. [330, 332, 338, 341]). In contrast, Jorgensen[346] reported a slightly lower binding energy for water molecules in the solvation shell of *n*-butane.

Okazaki et al.[348] found that the number of hydrogen bonds increases significantly when an alkane is dissolved in water, but they did not observe a relation between the size of the apolar solute particle and the observed shift in the hydrogen bonding distribution function. Geiger et al.[335] and Pangali et al.[338] observed only a modest increase in the number of hydrogen bonds in aqueous solutions of apolar compounds. Introduction of an apolar solute particle into liquid water is apparently accompanied by a small increase in the number of stronger, less distorted hydrogen bonds.[335, 341, 348]

Significant effects of an apolar solute particle on the hydrogen bonding properties of water molecules should be revealed in the librational motion of the water molecules, which can be obtained from an analysis of the dynamic pathway of these water molecules (see, for example, refs. [331, 335, 336, 342, 351, 355]). Dynamic parameters are difficult to interpret when a water molecule spends only a fraction of the total run time in the hydration shell of an apolar solute particle. The translational motion can be monitored within a very short period of time, during which relatively few water molecules exchange between the hydration shell and the bulk. Unfortunately, rotational motion of molecules in a strongly hydrogen-bonded fluid such as water is considerably slower than translational motion. The average angular reorientation of a water molecule while it is in the solvation shell is quite small, and a comparison of rotational motions of water molecules in bulk water and in a hydrophobic hydration shell is hazardous. Rossky and Karplus[331] were the first to conclude that water molecules near apolar moieties have longer translational and rotational relaxation times than bulk water molecules. A study of the shell occupancy of the hydration shell of a hard-sphere solute as a function of time showed that the exit rate of water molecules from the solvation shell is some 20% less than that from the solvation shell of bulk water.

The restricted motion of water molecules in the hydration shell was later corroborated by Zichi and Rossky,[342] who showed that the translational mobility of water molecules adjacent to Lennard–Jones particles is reduced by about 30%. The reduced translational and rotational motion was shown to be reflected in an increase of the average lifetime of hydrogen bonds. It has been suggested that structural changes in the solvation shell are more concerted than in the bulk. In contrast, Postma et al.[308] did not observe a significant reduction of the translational motion of water molecules near a hydrophobic solute. On the basis of computer simulations it has been found that molecules in the hydration shell oscillate at somewhat higher frequencies than molecules in the bulk.[360] This implies that the restoring forces following a slight perturbation of a single water molecule in the hydration shell are larger than those for a perturbed molecule in bulk water. An analysis in terms of hindered rotations and hindered translations presented by Zichi and Rossky[342] and Rossky and Karplus[331] indeed suggests a strong correlation of the movement of water molecules in close proximity to an apolar surface. However, it must be recognized that a considerable reduction in the translational motion in the hydration shell can be explained by the fact that the solute particle acts as a fixed wall.

Recently Wallqvist[163] presented evidence that the number of hydrogen bonds at the interface between an apolar phase and liquid water is significantly reduced and that the average attractive energy between the water molecules at a water–hydrocarbon interface is also reduced considerably. This observation should be considered in light of the hydration of large apolar molecules or surfaces without sufficient curvature for all hydrogen bonds of the adjacent water molecules to be maintained. Furthermore, Wallqvist showed that interactions between water and methane molecules at the interface between bulk water and a hydrocarbon phase are enhanced by the orientation of water molecules at the interface.

Computer simulations of aqueous solutions of organic compounds containing both apolar and polar goups show without exception that water molecules in close proximity to the apolar moieties exhibit characteristics similar to those of the surrounding perfectly apolar solute particles.[309, 349–355]

As indicated by Jorgensen et al.,[309, 353] the introduction of a polar hydroxyl group strongly facilitates the solvation process by increasing the solute–water interactions. This is reflected by the bimodal energy distribution function for water–alcohol interactions. Hydrogen bonding leads to a low-energy interaction band, while London dispersion interactions involving many water molecules contribute to a large interaction band with close zero energy. As might be expected, structural analysis of the solvation shell of amphiphilic molecules indicates that solvation of apolar moieties and polar functional groups is mutually obstructive.

The results obtained from computer simulations of the hydration of apolar particles in water present a coherent picture of clathrate-like hydration, and the presence of pentagonal structures has been observed.[310, 332, 361, 362] The slightly reduced mobility of the water molecules and the moderate shift to the formation of stronger hydrogen bonds reinforce the traditional idea that water molecules in the solvation shell of an apolar solute particle behave like bulk water at lower temperature. The existence of "frozen patches" can be safely excluded, since the clathrate-like solvation shell appears to be extremely labile and permits solvent exchange on a picosecond timescale.

Most computer simulation studies of hydrophobic hydration were performed to trace differences between water molecules in hydrophobic hydration shells and in the bulk near room temperature. Interestingly, Jorgensen et al.[346, 359] emphasized that the remarkable property of water molecules in the hydrophobic hydration shell is that they are almost indistinguishable from water molecules not participating in hydrophobic hydration shells. Furthermore, Jorgensen et al.[309, 359] showed that the large and favorable enthalpy of solvation of apolar gases in water near room temperature can be fully attributed to solute–water interactions. The qualitative features of the solvation shell surrounding an apolar solute particle are, however, hardly affected by removing the attractive part of the solute potential.[308, 332] Recently, Rashin et al.[363, 364] drew similar conclusions from continuum-based calculations of hydration enthalpies and entropies of a series of inert gases. Thus, the crucial question remains to what extent the thermodynamic parameters of hydration for apolar compounds in water are affected by the moderate changes in the hydrogen-bonding properties of water molecules in the hydration shell.

3.5.2. Simulations of Pairwise and Bulk Hydrophobic Interactions

Computer simulation studies of hydrophobic interactions aim at calculating the pair distribution function or, alternatively, the potential of mean force between two or more apolar solute particles in an aqueous environment. In 1974 Dashevsky and Sarkisov[333] used a MC procedure to compute the potential of mean force acting between two methane molecules in 64 water molecules and found a monotonic decay of $w_{CH_4-CH_4}(r)$ to zero as a function of the distance between the particles. The computational methods were ill-defined, and the results generally considered unreliable.

In 1979 Geiger et al.[335] reported the first MD simulation study of a system comprising two Lennard–Jones solute particles in 214 ST2 water molecules. Surprisingly, the Lennard–Jones solutes, initially placed in contact and dissolved in water, were almost immediately forced slightly apart in order to be hydrated in separate solvent "cages" that shared one layer of water molecules tangential to the surfaces of both solute particles.[335]

Swaminathan and Beveridge[365] carried out a MC simulation on a solution of two methane molecules in a similar number of water molecules but applied ab initio methods to describe the interactions between the components in solution. Their computer simulation confirmed the existence of a contact- *and* a solvent-separated hydrophobic bond.[365] Since then a series of computational studies have appeared with the aim of studying hydrophobic interactions between a variety of solute particles, for example, relatively simple Lennard–Jones solutes,[293, 334, 335, 338, 341, 342, 357, 362] noble gases,[246] and methane[163, 328, 336, 361, 365, 366] as well as more complex systems such as methanol,[351] 2-methyl-2-propanol,[355] and quinuclidine.[367] The interactions of these solute particles have been simulated by using relatively simple Lennard–Jones potentials. Incidentally, more sophisticated potentials have been applied based on ab initio calculations.[351, 355, 365] Water–water interactions have usually been modeled by empirical models such as the ST2 model,[246, 334, 335, 338, 341, 342, 362] the SPC model,[163, 366, 367] and the TIP4P model;[328, 336] the nonempirical MCY model[351, 355, 357, 361, 365] has been used as well. The run time of the simulations varied from only 7 ps (Geiger et al.[335]) to 450 ps (Andersen and Watanabe[246]).

Regardless of the computational methods and the applied potential functions, computer simulation studies generally yield potentials of mean force between apolar solute particles that oscillate as a function of the distance between the particles. Thus these results reinforce the ideas that emerged from integral theories (Section 3.3.4). A representative example, shown in Figure 12, is taken from the work of Wata-

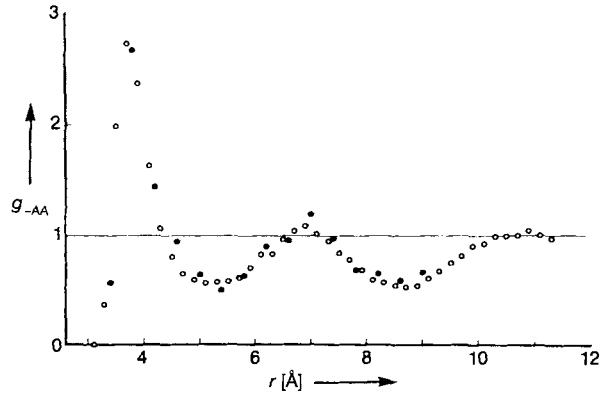

Fig. 12. Solute–solute pair distribution function $g_{AA}(r)$ for a solution of 6 solute particles (krypton-like Lennard–Jones particles; $\sigma = 3.44$ Å) in 394 water molecules (○) and for a solution of 5 solute particles in 195 water molecules (●) (taken from ref. [246]).

nabe and Andersen,[246] who carried out an extensive MD simulation of hydrophobic interactions between krypton atoms in an aqueous solution of finite concentration. The position of the first maximum corresponds to the expected contact pair, and the second maximum to an arrangement in

which the solute particles are separated by one water molecule. Even a third maximum can be distinguished, suggesting an arrangement in which the particles are separated by two layers of water molecules. The exact distance between the solute particles in the solvent-separated arrangements depends on the choice of potential models. Computer simulations by Ravishanker et al.[361] indicate that arrangement C (Scheme 8) is preferred, whereas other simulations[334] as well as the theory of Pratt and Chandler (see Section 3.3.4) suggest a preference for arrangement E.

The equilibrium solvation structure for the solvent-separated arrangement has been studied in more detail by Zichi and Rossky;[362] they placed two Lennard–Jones particles at a solvent-separated distance (arrangement E) and studied the orientation and dynamic properties of the water molecules in close proximity to the solute particles. The MD simulation revealed a variety of clathrate-like structures surrounding the two apolar particles.

Conflicting results have been reported with respect to the height of the barrier between the solvent-separated and contact pair.[342] Generally, the solvent-separated arrangement is found at higher free energy; however, this arrangement has the greater population because of the greater volume of its potential well. The relative and absolute values of the minima depend strongly on the solvent–solute interaction potential. When the interactions between solute and water decrease, the preference for the formation of hydrophobic contact pairs increases. Pangali et al.[338, 334] presented evidence that the contact and solvent-separated arrangements are equally populated, whereas Ravishanker et al.[361] and Andersen and Watanabe[246] noted a strong preference for the solvent-separated arrangement.

In order to determine the importance of attractive solute–solute interactions, Rapaport and Scheraga[357] simulated an aqueous solution of four essentially hard-sphere solutes. Solute–solute interactions were reduced to simple short-range repulsive forces by removing the long attractive tail of the full Lennard–Jones potential. The solute particles were initially not brought in contact distance. Although the solutes were shown to be highly mobile, no evidence was found for their association during a 70 ps simulation. The results of the MD simulation performed by Andersen and Watanabe[246] were similar. These authors even observed that krypton atoms tended to avoid each other in an aqueous solution of finite concentration. A compact cluster of five krypton atoms appeared to have a lifetime of about 180 ps, but this was not the dominant equilibrium arrangement. Hence, a prerequisite for reliable results are extended-time simulations.[246]

Jorgensen et al.[328] obtained the potential of mean force between two methane molecules in water by using statistical perturbation theory. The free energy for the binding of two methane molecules in water was estimated as -1.8 (± 1.4) kJ mol^{-1}, of which -1.2 kJ mol^{-1} arises from simple Lennard–Jones attractions between the solute particles. Recently, Smith et al.[366] applied traditional thermodynamic integration methods to compute the free energy and the entropy of the association of two methane molecules in water on the basis of an extensive MD simulation. They showed that the solvent-induced forces between methane molecules in water are small but attractive at short separations as a result of a favorable entropy change.[366] In contrast to Ravishanker et al.,[361] who performed a preliminary MC study of the effect of temperature on the pair distribution of methane in an aqueous solution, the results of Smith et al.[366] confirmed the experimental observation that attractive interactions between apolar solutes at short distance increase and the potential well for the contact arrangement well becomes deeper as the temperature increases.

Computational studies of pairwise hydrophobic interactions have often been frustrated by the fact that spontaneous association of two apolar solute particles has never been observed on the simulation timescale. Wallqvist and Berne[158] have shown that the stability of the solvent-separated arrangement even holds for the interaction of one apolar solute with a large flat apolar surface. A plausible explanation for this might be that the barrier between the contact arrangement and the solvent-separated arrangement is too high and the solute particles are trapped inside a solvent cage. During the simulation time, escape from this cage can be an extremely rare event. Furthermore, the formation of a contact pair from randomly distributed particles can be an unfavorable process in terms of Gibbs energy, despite substantial attractive forces between the solute particles. The existence of solvent-separated solute pairs appearing as local minima on a potential energy map is, strictly speaking, unrelated to the hydrophobic interactions. The occurrence of distinct arrangements of the solute particles is the result of a well-established packing phenomenon and occurs even in the most simple solvent systems (see Section 3.3.1). The additional arrangement of water molecules separating the solute molecules is a consequence of the directional character of the hydrogen bonds connecting the water molecules.

The fact that two apolar solute particles in dilute aqueous solution do not spontaneously aggregate on the simulation timescale has also seriously obstructed studies of bulk hydrophobic interactions. Recently Laaksonen and Stilbs[336] studied the distribution and the dynamics of methane molecules in aqueous solutions with increasing concentrations of methane. At higher concentrations more methane molecules were able to overcome the barrier between the solvent-separated and the contact arrangement and occasionally stuck together. Eventually, the solvent-separated arrangement disappeared completely.

A similar computational study was reported by Wallqvist,[163] who studied the behavior of a system comprising 18 Lennard–Jones solutes, representing methane, dispersed in 107 water molecules. Obviously, the concentration is extremely high, and spontaneous aggregation of the solute particles is inevitable. Indeed, phase separation was observed which resulted in hydrocarbon-rich domains dispersed in water. This result led Wallqvist to emphasize the necessity of invoking higher-body interactions for a successful simulation of a spontaneous aggregation of many apolar solutes.

Computer simulations of intramolecular hydrophobic interactions have generally been carried out by simulating the effect of water on the conformation of simple apolar molecules.[368] *n*-Butane is the simplest alkane for which the effect of the solvent on the conformation in solution is not a trivial problem and might be considered the prototype for conformational studies in water. Several computer simulation studies showed that the population of the more compact *gauche*

conformer increases when *n*-butane is transferred from the gas phase to an aqueous solution.[344-347] Although the applied computational methods are different, most authors find a shift of 10–35% at the expense of the extended *trans* conformer. Recently Tobias and Brooks[345] reported that the *gauche* conformer is also favored in CCl_4. In water, however, the effect is significantly larger. A thermodynamic analysis showed that the *gauche* conformer is energetically destabilized but strongly favored by entropy.

Some computer simulation studies focused on interactions between solute particles having both polar and apolar regions. MD simulations of a 3 mol% solution of 2-methyl-2-propanol and a 5 mol% solution of methanol in water using the MCY potential model for water and an ab initio description of solute–solvent interactions showed that these alcohols tend to associate in water; this is consistent with experimental findings.[351, 355] Unfortunately, it was not explicitly reported whether solvent-separated or contact pairs were formed. Hydrogen bonds between the alcohol molecules were not detected. Maliniak et al.[367] reported aggregation of quinuclidine in a 6 mol% solution using MD simulation methods. In a more dilute solution (2 mol%), the solutes did not show any tendency to form aggregates. Recently, MD methods have even been successfully applied to simulate aggregation of surfactant molecules.[369]

4. Epilogue

Traditionally, chemists have attributed a pivotal role to the structure of water in the vicinity of apolar solutes or apolar moieties in aqueous solutions as expressed in the concept of hydrophobic hydration and hydrophobic interaction. Inextricably wrapped up with the concept of hydrophobic hydration is the notion of stronger (or more) hydrogen bonds in hydrophobic hydration shells. In particular, the idea of a clathrate-like hydration layer led to the exaggerated picture of iceberg formation at the surface of apolar solute particles in water. Recent computational studies have yielded little evidence for a significant increase of either the number or the strength of hydrogen bonds in aqueous solutions of apolar compounds when compared to pure water.

The large and favorable enthalpy of solvation of apolar compounds in water, presented in classic papers as a convincing piece of evidence for enhanced hydrogen bonding in hydrophobic hydration shells, can be conveniently explained on the basis of interactions between water and the apolar solute without assuming additional interactions among water molecules. Various studies, however, have confirmed that O–H bonds of water molecules adjacent to an apolar solute are predominantly oriented tangentially to the apolar surface. Current evidence strongly indicates that water does not undergo a structural enhancement in the presence of apolar solute particles but *maintains* its original structure by accommodating the apolar solute in its original hydrogen bond network. The unique property of water is that it can dissolve an apolar solute of limited size without sacrificing a significant number of hydrogen bonds.

London dispersion interactions between water and the apolar solute create an additional source for enthalpy, resulting in a large and negative enthalpy for the solvation of apolar gases in water. The orientation of the water molecules in the first hydration layers might even give rise to a bulk polarization phenomenon induced by "proton hopping". Thus, it might be speculated that solute–water interactions are enhanced by the orientation of the water molecules in the immediate surroundings of the solute particle. Computational chemistry would be the most appropriate tool to validate or disprove this idea.

The tendency of water molecules not to sacrifice any (or only a small number) of their hydrogen bonds and to interact favorably with apolar solute particles does not mean that water is a good solvent for apolar compounds. At lower temperatures the loss of entropy hampers solvation. The interpretation in terms of "structure-making" properties of apolar solutes or related terminology is in our opinion not very elucidative and may be even wrong. As shown elegantly by applications of scaled particle theory, a large part of the negative entropy of solvation can be attributed to the small molecular volume of the water molecules; in other words, many water molecules are involved in dissolving a single solute particle. In fact, the hydrogen bond structure of water, which provides the solvent with an exceptionally low density, is even favorable for dissolving inert solutes. However, it must be noted that scaled particle theories do incorporate some structural information for the solvent such as the isothermal compressibility. As argued by Lee,[228, 230] reduction of rotational freedom and possibly compression of water molecules in the first hydration layers will contribute to the loss of entropy as well. Nonetheless, one crucial point emerges: the orientation of the water molecules in the hydration shell of apolar solute particles, generally referred to as hydrophobic hydration, *aids* the dissolution of apolar compounds in water and is not the cause for their low solubility.

At higher temperatures water gradually loses its capacity to maintain hydrogen bonds upon intrusion of apolar solute particles. This leads to less favorable solute–water interactions, expressed in a gradual reduction of the enthalpy of solvation, which even becomes positive at elevated temperatures. Since hydrogen bonds break, the entropy increases as well. At high temperatures the increase in entropy is very significant and counteracts the reduction of entropy that stems from the small molecular volume of the water molecules. Apparently, the Gibbs energy accompanying the disruption and formation of hydrogen bonds in the hydration shell of apolar solute particles is small. The entropy and enthalpy characterizing the changes due to variation in temperature are almost fully compensative. This does not necessarily imply that this compensation behavior is a result of an intrinsic property of the water structure, as is often assumed in "compensation models". Changes in the orientation and binding properties of water molecules in the hydration shell due to changes in temperature can also affect solute–water interactions. It is notoriously difficult to separate the thermodynamics of water–water interactions in hydrophobic hydrations shells from those of solute–water interactions. Although the capacity of water to dissolve apolar solutes decreases as the temperature is raised, the influence of temperature is remarkably small. This fact supports the notion that structural changes in liquid water are not the main cause for the low solubility of apolar compounds in water.

A more effective way of preventing water molecules from maintaining their hydrogen bonds upon intrusion of foreign solute particles is to increase the concentration of the solute. The hydrophobic hydration shell is apparently quite extensive. At a certain concentration of solute particles, the number of water molecules is not sufficient to form a complete hydrophobic hydration shell, which leads to interference and mutual obstruction of hydration shells and the inevitable sacrifice of hydrogen bonds. An alternative but related way of destroying hydrogen bonds is to increase the size of the apolar solute particle. In the limiting situation of a hydrophobic wall, water molecules are not able to salvage all hydrogen bond interactions, even when their O–H bonds are tangentially aligned towards the hydrophobic surface. Finally, introduction of polar functionalities leads to mutual obstruction of hydration shells. A hydroxyl group will contribute strongly to the solubility of a predominantly apolar solute particle and will considerably reduce the necessity and possibility for the formation of (local) hydrophobic hydration shells. This phenomenon governs the hydration of polyols and carbohydrates. Strikingly, the apolar methylene functionalities remain available for interactions with other apolar moieties in solution; this might be crucial for molecular recognition phenomena at the surface of living cells, in which polysaccharides play a prominent role.

Hydrophobic interactions, both pairwise and bulk, have traditionally been treated as a natural consequence of hydrophobic hydration. It was, however, alarming that computer simulations of dilute aqueous solutions of apolar solute particles do not reveal any tendency of the apolar solutes to form long-lived pairwise or higher-order aggregates on a typical simulation timescale. The concept of partial destruction of hydrophobic hydration shells involving the release of structured hydration water to the bulk, which plays a dominant role in the traditional interpretation of hydrophobic effects, has lost much of its attraction as a molecular model of hydrophobic interactions. Following the argument that hydrophobic hydration aids the dissolution of apolar compounds in water, it cannot also be considered as a cause for the association of apolar solutes in aqueous solution. In contrast, hydrophobic interactions are *counteracted* by the formation of a hydrophobic hydration shell. Apolar solute particles are "screened" in dilute aqueous solution as compared to the gas phase.

Pairwise and bulk interactions between apolar moieties do lead to partial desolvation of the apolar surface and to a concomittant reduction of the number of water molecules involved in the solvation of the solute particles. Inherently, this leads to a gain of entropy. In dilute solutions the gain in entropy is insufficient to overcome the unfavorable enthalpic effect and the loss of entropy due to the association of solute molecules and, consequently, the formation of long-lived pairs of apolar solute particles is an infrequent event. The molecular origin of the slightly unfavorable enthalpy involved in bulk hydrophobic interactions near room temperature can be explained in terms of a loss of solute–water interactions which are not completely counteracted by a gain in solute–solute interactions, while water–water interactions remain effectively unchanged. Recent computational studies of hydrophobic interactions gave rise to arguments about the preference of solvent-separated over contact solute pairs. In our opinion, this is not a very relevant question. As shown in several studies, the existence of well-defined geometrical configurations of pairs of solutes in solution is an inherent property of all solvent systems and not restricted solely to water. More interesting is the question as to the actual distance between the solute particles in the solvent-separated configuration. As shown in Section 3.3.1, the directionality of hydrogen bonds might have a significant effect on this distance.

Following the arguments given above, destruction of hydrophobic hydration shells *increases* the frequency of hydrophobic contacts. This can be accomplished by either increasing the temperature or, more effectively, by increasing the concentration of apolar compounds. Increasing temperature is not very effective in increasing hydrophobic interactions, as has been clearly demonstrated by studies of host–guest complexation and micelle formation at elevated temperatures. However, when the number of solute particles in solution prevents the formation of complete hydrophobic hydration shells, hydrogen bonds are sacrificed and an increasing number of O–H bonds will point towards the apolar surface; this is an energetically unfavorable event. As a result, the tendency to form aggregates of two or more apolar particles increases rapidly. This behavior has been repeatedly confirmed by computational studies. When the apolar solute particles can form a well-defined aggregate by means of directional bonding, for example, a micelle or an aggregate with a more complex morphology, the concentration at which aggregation takes place can be very critical. Additional factors such as surface forces, headgroup effects, and aggregate size play a decisive role, and it is too simplistic to consider only hydrophobic effects. Even aggregation of less complex organic compounds such as monohydric alcohols into small, short-lived clusters is very difficult to describe theoretically. It is still a considerable challenge to relate pairwise interactions between solutes in dilute aqueous solutions to the occurrence of bulk interactions in more concentrated solutions.

In conclusion, we believe that hydrophobic interactions are not so much a result of a structural property of the hydrophobic hydration shell of apolar compounds but rather reflect the limited capacity of liquid water to accommodate the apolar solute and maintain its original network of hydrogen bonds. It is surprising that apolar compounds dissolve in water at all; this must be attributed to the formation of a hydrophobic hydration shell.

Answers to pertinent questions regarding hydrophobic effects must be expected from either sophisticated neutron diffraction studies or from accurate computer simulatons. Incorporation of polarization effects is highly desirable if one wishes to test the proposition that solute–water interactions are enhanced by cooperative polarization effects in the hydrophobic hydration shell. Polarization effects must also be considered in investigations of the molecular origin of the exceptionally long-range interactions between large apolar surfaces.[370] Furthermore, it would be most instructive to perform an extensive comparative computational study on solutions of apolar compounds in water and in a solvent of similar size but without hydrogen bonds, for example liquid methane. In general, comparative studies of the solvation behavior of apolar compounds in various organic solvents

and water are scarce. In particular, the structural response of solvation shells to changes of temperature and concentration has been rather neglected by computational studies. Advances in this area are eagerly awaited.[371]

Received: November 30, 1992 [A 919 IE]
German version: *Angew. Chem.* **1993**, *105*, 1610

[1] J. H. Hildebrand, *Proc. Natl. Acad. Sci. USA* **1979**, *76*, 194.
[2] H. Naghibi, S. F. Dec, S. J. Gill, *J. Phys. Chem.* **1986**, *90*, 4621.
[3] J. A. V. Butler, W. S. Reid, *J.Chem. Soc.* **1936**, 1171.
[4] H. S. Frank, M. W. Evans, *J. Chem. Phys.* **1945**, *13*, 507.
[5] D. N. Glew, *J. Phys. Chem.* **1962**, *66*, 605.
[6] W. Kauzmann, *Adv. Protein Chem.* **1959**, *14*, 1.
[7] *Water Compr. Treatise 1972–1982* **1973–1979**, *1–7*.
[8] F. Franks, *Faraday Symp. Chem. Soc.* **1982**, *17*, 7.
[9] C. Tanford, *The Hydrophobic Effect*, 2nd ed., Wiley, New York, **1980**.
[10] A. Ben-Naim, *Hydrophobic Interactions*, Plenum, New York, **1980**.
[11] W. A. P. Luck, *Structure of Water and Aqueous Solutions*, Physik-Verlag, Weinheim, **1974**.
[12] K. P. Murphy, P. L. Privalov, S. J. Gill, *Science* **1990**, *247*, 559.
[13] K. A. Dill, *Science* **1990**, *250*, 297.
[14] P. L. Privalov, S. J. Gill, K. P. Murphy, *Science* **1990**, *250*, 297.
[15] J. Herzfeld, *Science* **1991**, *253*, 88.
[16] R. H. Wood, P. T. Thompson, *Proc. Natl. Acad. Sci. USA* **1990**, *87*, 946.
[17] A. Ben-Naim, *J. Chem. Phys.* **1989**, *90*, 7412.
[18] M. H. Abraham, *J. Chem. Soc. Faraday Trans. 1* **1984**, *80*, 153.
[19] A. Ben-Naim, *J. Phys. Chem.* **1978**, *82*, 792.
[20] A. Ben-Naim, *Solvation Thermodynamics*, Plenum, New York, **1987**.
[21] G. Némethy, H. A. Scheraga, *J. Chem. Phys.* **1962**, *36*, 3382, 3401.
[22] See also G. Némethy, *Angew. Chem.* **1967**, *79*, 260; *Angew. Chem. Int. Ed. Engl.* **1967**, *6*, 195.
[23] H. S. Frank, W.-Y. Wen, *Discuss. Faraday Soc.* **1957**, *24*.
[24] K. W. Miller, J. H. Hildebrand, *J. Am. Chem. Soc.* **1968**, *90*, 3001.
[25] O. W. Howarth, *J. Chem. Soc. Faraday Trans. 1* **1975**, *71*, 2303.
[26] A. Ben-Naim, *Water and Aqueous Solutions*, Plenum, New York, **1974**.
[27] P. S. Ramanathan, C. V. Krishnan, H. L. Friedman, *J. Solution Chem.* **1972**, *1*, 237.
[28] C. V. Krishnan, H. L. Friedman, *J. Solution Chem.* **1973**, *2*, 119.
[29] C. V. Krishnan, H. L. Friedman, *J. Solution Chem.* **1974**, *3*, 727.
[30] M. H. Abraham, P. L. Grellier, R. A. McGill, *J. Chem. Soc. Perkin Trans. 2* **1988**, 339.
[31] M. H. Abraham, *J. Am. Chem. Soc.* **1982**, *104*, 2085.
[32] B. Y. Zaslavsky, E. A. Masimov, *Top. Curr. Chem.* **1988**,*146*, 171.
[33] E. Wilhelm, R. Battino, R. J. Wilcock, *Chem. Rev.* **1977**, *77*, 219.
[34] E. Wilhelm, *Thermochim. Acta* **1990**, *162*, 43.
[35] G. L. Pollack, *Science* **1991**, *251*, 1323.
[36] P. L. Privalov, S. J. Gill, *Adv. Protein Chem.* **1988**, *39*, 191.
[37] R. D. Cramer III, *J. Am. Chem. Soc.* **1977**, *99*, 5408.
[38] B. Lee, F. M. Richards, *J. Mol. Biol.* **1971**, *55*, 379.
[39] C. Cothia, *J. Mol. Biol.* **1976**, *105*, 1.
[40] R. B. Hermann, *Proc. Natl. Acad. Sci. USA* **1977**, *74*, 4144.
[41] D. Eisenberg, A. D. McLachlan, *Nature* **1986**, *319*, 199.
[42] A. Radzicka, R. Wolfenden, *Biochemistry* **1988**, *27*, 1664.
[43] L. R. DeYoung, K. A. Dill, *J. Phys. Chem.* **1990**, *94*, 801.
[44] C. H. Tanford, *Proc. Natl. Acad. Sci. USA* **1979**, *76*, 4175.
[45] F. A. Greco, *J. Phys. Chem.* **1984**, *88*, 3132.
[46] K. A. Sharp, A. Nicholls, R. F. Fine, B. Honig, *Science* **1991**, *252*, 106.
[47] H. Naghibi, S. F. Dec, S. J. Gill, *J. Phys. Chem.* **1987**, *91*, 245.
[48] H. Naghibi, D. W. Ownby, S. J. Gill, *J. Chem. Eng. Data* **1987**, *32*, 422.
[49] D. Mirejovsky, E. M. Arnett, *J. Am. Chem. Soc.* **1983**, *105*, 1112.
[50] G. I. Makhatadze, P. L. Privalov, *J. Chem. Thermodyn.* **1988**, *20*, 405.
[51] K. Shinoda, *J. Phys. Chem.* **1977**, *81*, 1300.
[52] T. R. Rettich, Y. P. Handa, R. Battino, E. Wilhelm, *J. Phys. Chem.* **1981**, *85*, 3230.
[53] T. R. Rettich, R. Battino, E. Wilhelm, *Ber. Bunsenges. Phys. Chem.* **1982**, *86*, 1128.
[54] T. R. Rettich, R. Battino, E. Wilhelm, *J. Solution Chem.* **1984**, *13*, 335.
[55] R. Crovetto, R. Fernandez-Prini, M. L. Japas, *J. Chem. Phys.* **1982**, *76*, 1077.
[56] D. R. Biggerstaff, D. E. White, R. H. Wood, *J. Phys. Chem.* **1985**, *89*, 4378.
[57] B. Lee, *Proc. Natl. Acad. Sci. USA* **1991**, *88*, 5154.
[58] S. J. Gill, S. F. Dec, G. Olofsson, I. Wadsö, *J. Phys. Chem.* **1985**, *89*, 3758.
[59] J. M. Sturtevant, *Proc. Natl. Acad. Sci. USA* **1977**, *74*, 2236.
[60] See [12].
[61] R. L. Baldwin, *Proc. Natl. Acad. Sci. USA* **1986**, *83*, 8069.
[62] T. Ooi, M. Oobatake, G. Némethy, H. L. Scheraga, *Proc. Natl. Acad. Sci. USA* **1987**, *84*, 3086.
[63] S. F. Dec, S. J. Gill, *J. Solution Chem.* **1984**, *13*, 27.
[64] K. A. Dill, Biochemistry **1990**, *29*, 7133.
[65] K. A. Sharp, *Curr. Biol.* **1991**, *1*, 171.
[66] R. Wolfenden, *Science* **1983**, *222*, 1087.
[67] C. Chothia, *Annu. Rev. Biochem.* **1985**, *53*, 537.
[68] G. D. Rose, A. R. Geselowitz, G. J. Lesser, R. H. Lee, M. H. Zehfus, *Science* **1985**, *229*, 834.
[69] R. R. Matheson, H. A. Scheraga, *Macromolecules* **1978**, *11*, 819.
[70] F. Franks, R. H. M. Hatley, H. L. Friedman, *Biophys. Chem.* **1988**, *31*, 307.
[71] K. A. Dill, *Biochemistry* **1985**, *24*, 1501.
[72] D. O. V. Alonso, K. A. Dill, *Biochemistry* **1991**, *30*, 5974.
[73] A. Ben-Naim, K.-L. Ting, R. L. Jernigan, *Biopolymers* **1989**, *28*, 1309.
[74] A. Ben-Naim, *Biopolymers* **1990**, *29*, 567.
[75] A. Huidt, P. Westh, *Protein Interactions* (Ed.: H. Visser), VCH, Weinheim, **1992**, p. 327.
[76] D. Stigter, K. A. Dill, *Biochemistry* **1990**, *29*, 1262.
[77] D. E. Anderson, W. J. Becktel, F. W. Dahlquist, *Biochemistry* **1990**, *29*, 2403.
[78] L. H. Holley, M. Karplus, *Proc. Natl. Acad. Sci. USA* **1989**, *86*, 152.
[79] W. L. Jorgensen, *Acc. Chem. Res.* **1989**, *22*, 184.
[80] S. F. Sneddon, D. J. Tobias, C. L. Brooks III, *J. Mol. Biol.* **1989**, *209*, 817.
[81] A. E. Eriksson, W. A. Baase, X.-J. Zhang, D. W. Heinz, M. Blaber, E. P. Baldwin, B. W. Matthews, *Science* **1992**, *255*, 178.
[82] J. U. Bowie, J. F. Reidhaar-Olsen, W. A. Lim, R. T. Sauer, *Science* **1990**, *247*, 1306.
[83] W. A. Lim, R. T. Sauer, *Nature* **1989**, *339*, 31.
[84] T. Alber, *Annu. Rev. Biochem.* **1989**, *58*, 765.
[85] J. T. Kellis, Jr., K. Nyberg, D. Sali, A. R. Fersht, *Nature* **1988**, *333*, 406.
[86] J. T. Kellis, Jr., K. Nyberg, A. R. Fersht, *Biochemistry* **1989**, *28*, 4914.
[87] J. L. Finney, *Water Compr. Treatise 1972–1982* **1979**, Vol. 6, Chap. 2.
[88] H. J. C. Berendsen, *Water Compr. Treatise 1972–1982* **1979**, Vol. 5, Chap. 6.
[89] J. Gao, K.Kuczera, B. Tidor, M. Karplus, *Science* **1989**, *244*, 1069.
[90] M. Prevost, S. J. Wodak, B. Tidor, M. Karplus, *Proc. Natl. Acad. Sci. USA* **1991**, *88*, 10880.
[91] M. Matsumura, W. J. Becktel, B. W. Matthews, *Nature* **1988**, *334*, 406.
[92] P. L. Privalov, *Adv. Protein Chem.* **1979**, *33*, 167.
[93] R. Hawkes, M. G. Grutter, J. A. Schellmann, *J. Mol. Biol.* **1984**, *175*, 195.
[94] W. J. Becktel, J. Schellman, *Biopolymers* **1987**, *26*, 1859.
[95] See [42].
[96] G. Némethy, W. J. Peer, H. A. Scheraga, *Annu. Rev. Biophys. Bioeng.* **1981**, *10*, 459.
[97] B. Y. Zaslavsky, E. A. Masimov, *Top. Curr. Chem.* **1988**, *146*, 171.
[98] K. A. Sharp, A. Nichols, R. Friedman, B. Honig, *Biochemistry* **1991**, *30*, 9686.
[99] C. Cothia, *Nature* **1975**, *254*, 304.
[100] W. S. Sandberg, T. C. Terwilliger, *Science* **1989**, *245*, 54.
[101] W. S. Sandberg, T. C. Terwilliger, *Proc. Natl. Acad. Sci. USA* **1991**, *88*, 1706.
[102] W. S. Sandberg, T. C. Terwilliger, *Trends Biotechnol.* **1991**, *9*, 59.
[103] H. Dugas, *Bioorganic Chemistry*, 2nd ed., Springer, Berlin, **1986**.
[104] S. M. Roberts, *Molecular Recognition: Chemical and Biochemical Problems*, Royal Soc. Chem., Cambridge, **1989**.
[105] F. Vögtle, *Supramolecular Chemistry*, Wiley, Chichester, **1991**.
[106] H.-J. Schneider, H. Dürr, *Frontiers in Supramolecular Organic Chemistry and Photochemistry*, VCH, Weinheim, **1991**.
[107] H.-J. Schneider, *Angew. Chem.* **1991**, *103*, 1419; *Angew. Chem. Int. Ed. Engl.* **1991**, *30*, 1417.
[108] W. L. Jorgensen, D. L. Severance, *J. Am. Chem. Soc.* **1990**, *112*, 4768.
[109] G. H. Giles, D. G. Duff, *Water Compr. Treatise 1972–1982* **1979**, Vol. 4, Chap. 5.
[110] D. Balasubramanian, V. Srinivas, V. G. Gaikar, M. M. Sharma, *J. Phys. Chem.* **1989**, *93*, 3865.
[111] J. F. Blake, W. L. Jorgensen, *J. Am. Chem. Soc.* **1990**, *112*, 7269.
[112] F. Diederich, *Angew. Chem.* **1988**, *100*, 372; *Angew. Chem. Int. Ed. Engl.* **1988**, *27*, 362.
[113] H.-J. Schneider, R. Kramer, S. Simova, U. Schneider, *J. Am. Chem. Soc.* **1988**, *110*, 6442.
[114] T. Endo, H. Takei, T. Isago, J.-i. Kato, M. M. Ito, K. Guro, K.-y. Akiyama, Y. Nakajima, H. Kataoka, *J. Am. Chem. Soc.* **1989**, *111*, 8166.
[115] S. B. Ferguson, E. M. Seward, F. Diederich, E. M. Sanford, A. Chou, P. Inocencio-Szweda, C. B. Knobler, *J. Org. Chem.* **1988**, *53*, 5593.
[116] D. A. Stauffer, R. E. Barrans, D. E. Dougherty, *J. Org. Chem.* **1990**, *55*, 2762.
[117] J. C. Harrison, M. R. Eftink, *Biopolymers* **1982**, *21*, 1153.
[118] L. Stryer, *Biochemistry*, 2nd ed., Freeman, San Francisco, **1981**.
[119] K. Harata, K. Tsuda, K. Uekama, M. Otagiri, F. Hirayama, *J. Inclusion Phenom.* **1988**, *6*, 135.
[120] D. B. Smithrud, F. Diederich, *J. Am. Chem. Soc.* **1990**, *112*, 339.
[121] J.-H. Fuhrhop, C. Boettcher, *J. Am. Chem. Soc.* **1990**, *112*, 1768.
[122] J.-H. Fuhrhop, S. Svenson, C. Boettcher, E. Rössler, H.-M. Vieth, *J. Am. Chem. Soc.* **1990**, *112*, 4207.
[123] J. J. H. Nusselder, J. B. F. N. Engberts, *Langmuir* **1991**, *7*, 2089.
[124] T. Kunitake, *Angew. Chem.* **1992**, *104*, 692; *Angew. Chem. Int. Ed. Engl.* **1992**, *31*, 709.

[125] F. M. Menger, *Angew. Chem.* **1991**, *103*, 1104; *Angew. Chem. Int. Ed. Engl.* **1991**, *30*, 1086.
[126] M. Ramadan, D. F. Evans, R. Lumry, S. Philison, *J. Phys. Chem.* **1985**, *89*, 3405.
[127] I. Rico, A. Lattes, *J. Phys. Chem.* **1986**, *90*, 5870.
[128] H. Garibi, R. Palepu, G. J. T. Tiddy, D. G. Hall, E. Wyn-Jones, *J. Chem. Soc. Chem. Commun.* **1990**, 115.
[129] D. F. Evans, A. Yamauchi, G. J. Wei, V. A. Bloomfield, *J. Phys. Chem.* **1983**, *87*, 3537.
[130] M. P. Turnberg, J. E. Brady, *J. Am. Chem. Soc.* **1988**, *110*, 7797.
[131] Y. Ishikawa, H. Kuwahara, T. Kunitake, *J. Am. Chem. Soc.* **1989**, *111*, 8530.
[132] M. Ramadan, D. F. Evans, R. Lumry, *J. Phys. Chem.* **1983**, *87*, 4583.
[133] D. F. Evans, P. J. Wightman, *J. Colloid Interface Sci.* **1982**, *86*, 515.
[134] M. T. Bashford, E. M. Wooley, *J. Phys. Chem.* **1985**, *89*, 3173.
[135] D. F. Evans, D. D. Miller in *Water Science Reviews, Vol. 4* (Ed.: F. Franks), Cambridge University Press, Cambridge, **1989**, Chap. 1.
[136] R. Lumry, R. B. Gregory in *The Fluctuating Enzyme* (Ed.: G. R. Welsh), Wiley-Interscience, New York, **1986**.
[137] J. N. Israelachvili, H. Wennerström, *Langmuir* **1990**, *6*, 873.
[138] J. N. Israelachvili, H. Wennerström, *J. Phys. Chem.* **1992**, *96*, 520.
[139] J. N. Israelachvili, *Intermolecular and Surface Forces*, 2nd ed., Academic Press, San Diego, **1991**.
[140] J. N. Israelachvili, R. M. Pashley, *J. Colloid Interface Sci* **1984**, *98*, 500.
[141] R. M. Pashley, P. M. McGuiggan, B. W. Ninham, D. F. Evans, *Science* **1985**, *229*, 1088.
[142] P. M. Claesson, C. E. Blom, P. C. Herder, B. W. Ninham, *J. Colloid Interface Sci.* **1986**, *114*, 234.
[143] P. M. Claesson, H. K. Christenson, *J. Phys. Chem.* **1988**, *92*, 1650.
[144] Ya. I. Rabinovich, B. V. Derjaguin, *Colloids Surf.* **1988**, *30*, 243.
[145] H. K. Christenson, P. M. Claesson, J. Berg, P. C. Herder, *J. Phys. Chem.* **1989**, *93*, 1472.
[146] H. K. Christenson, P. M. Claesson, R. M. Pashley, *Proc. Indian Acad. Sci.* **1987**, *98*, 379.
[147] R. P. Rand, V. A. Parsegian, *Biochim. Biophys. Acta* **1989**, *988*, 351.
[148] G. Cevc, *J. Chem. Soc. Faraday Trans.* **1991**, *87*, 2733.
[149] J. Marra, J. N. Israelachvili, *Biochemistry* **1985**, *24*, 4068.
[150] P. M. Claesson, R. Kjellander, P. Stenius, H. K. Christenson, *J. Chem. Soc. Faraday Trans. 1* **1986**, *82*, 2735.
[151] Ya. I. Rabinovich, B. V. Derjaguin, N. V. Churaev, *Adv. Colloid Interface Sci.* **1982**, *16*, 63.
[152] H. K. Christenson, P. M. Claesson, *Science* **1988**, *239*, 390.
[153] B. Jönssen, *Chem. Phys. Lett.* **1981**, *82*, 520.
[154] M. Marchesi, *Chem. Phys. Lett.* **1983**, *97*, 224.
[155] G. Barabiono, C. Gavotti, M. Marchesi, *Chem. Phys. Lett.* **1984**, *104*, 478.
[156] R. Sonnenschein, K. Heinzinger, *Chem. Phys. Lett.* **1983**, *102*, 550.
[157] C. Y. Lee, J. A. McCammon, P. J. Rossky, *J. Chem. Phys.* **1984**, *80*, 4448.
[158] A. Wallqvist, B. Berne, *Chem. Phys. Lett.* **1988**, *145*, 26.
[159] A. Luzar, D. Bratko, L. Blum, *J. Chem. Phys.* **1987**, *86*, 2955.
[160] R. Kjellander, S. Marčelja, *Chem. Scr.* **1985**, *25*, 73.
[161] J. P. Valleau, A. A. Gardner, *J. Chem. Phys.* **1987**, *86*, 4162.
[162] P. Linse, *J. Chem. Phys.* **1987**, *86*, 4177.
[163] A. Wallqvist, *J. Phys. Chem.* **1991**, *95*, 8921.
[164] A. Ahlström, O. Teleman, B. Jönsson, *Chem. Scr.* A **1989**, *29*, 97.
[165] E. Egberts, H. J. C. Berendsen, *J. Chem. Phys.* **1988**, *89*, 3718.
[166] E. Spohr, *J. Phys. Chem.* **1989**, *93*, 6171.
[167] J. C. Eriksson, S. Ljunggren, P. M. Claesson, *J. Chem. Soc. Faraday Trans. 2* **1989**, *85*, 163.
[168] S. Marčelja, D. J. Mitchell, B. W. Ninham, M. J. Sculley, *J. Chem. Soc. Faraday Trans. 2* **1977**, *73*, 630.
[169] P. Attard, *J. Phys. Chem.* **1989**, *93*, 6441.
[170] M. D. Zeidler *Water Compr. Treatise 1972–1982* **1973**, *2*, Chap. 10.
[171] H. G. Hertz, H. Leiter, *Z. Phys. Chem. Munich* **1982**, *133*, 45.
[172] G. E. Walrafen, *Water Compr. Treatise 1972–1982* **1973**, *1*, Chap. 5.
[173] W. A. P. Luck, *Water Compr. Treatise 1972–1982* **1973**, *2*, Chap. 5.
[174] M. C. R. Symons, G. Eaton, *J. Chem. Soc. Faraday Trans. 1* **1985**, *81*, 1963.
[175] M. C. R. Symons, *Acc. Chem. Res.* **1981**, *14*, 223.
[176] G. Eaton, M. C. R. Symons, P. P. Rastogi, *J. Chem. Soc. Faraday Trans. 1* **1989**, *85*, 3257.
[177] J. B. F. N. Engberts, A. Perjéssy, M. J. Blandamer, G. Eaton, *J. Chem. Soc. Faraday Trans.* **1992**, *88*, 2493.
[178] M. J. Blandamer, *Water Compr. Treatise 1972–1982* **1973**, *2*, Chap. 9.
[179] M. C. R. Symons, G. Eaton, *Faraday Symp. Chem. Soc.* **1982**, *17*, 31.
[180] G. E. Walrafen, M. S. Hokmabadi, W.-H. Yang, Y. C. Chu, B. Monosmith, *J. Phys. Chem.* **1989**, *93*, 2909.
[181] F. Sciortino, A. Geiger, H. E. Stanley, *Phys. Rev. Lett.* **1990**, *65*, 3452.
[182] F. Sciortino, A. Geiger, H. E. Stanley, *Nature* **1991**, *354*, 218.
[183] R. Pottel, E. Asselborn, R. Eck, V. Tresp, *Ber. Bunsenges. Phys. Chem.* **1989**, *93*, 676.
[184] J. C. Dore in *Water Science Reviews, Vol. 1* (Ed.: F. Franks), Cambridge, **1985**, p. 3.
[185] J. E. Enderby, G. W. Neilson, *Water Compr. Treatise 1972–1982* **1979**, *6*, Chap. 1.
[186] J. Turner, A. K. Soper, J. L. Finney, *Mol. Phys.* **1990**, *70*, 679.
[187] D. C. Rideout, R. Breslow, *J. Am. Chem. Soc.* **1980**, *102*, 7816.
[188] J. B. F. N. Engberts, *Water Compr. Treatise 1972–1982* **1979**, *6*, Chap. 4.
[189] M. J. Blandamer, J. Burgess, J. B. F. N. Engberts, *Chem. Soc. Rev.* **1986**, *14*, 237.
[190] W. Blokzijl, J. B. F. N. Engberts, M. J. Blandamer, *J. Am. Chem. Soc.* **1986**, *108*, 6411.
[191] W. Blokzijl, J. B. F. N. Engberts, J. Jager, M. J. Blandamer, *J. Phys. Chem.* **1987**, *91*, 6022.
[192] W. Blokzijl, J. B. F. N. Engberts, M. J. Blandamer, *J. Org. Chem.* **1991**, *56*, 1832.
[193] W. Blokzijl, J. B. F. N. Engberts, M. J. Blandamer, *J. Am. Chem. Soc.* **1990**, *112*, 1197.
[194] M. J. Blandamer, J. Burgess, J. B. F. N. Engberts, W. Blokzijl, *Chem. Soc. Annu. Rep. Sect. C* **1990**, *87*, 45.
[195] S. A. Galema, M. J. Blandamer, J. B. F. N. Engberts, *J. Org. Chem.* **1992**, *57*, 1995.
[196] S. A. Galema, M. J. Blandamer, J. B. F. N. Engberts, *J. Am. Chem. Soc.* **1990**, *112*, 9665.
[197] R. U. Lemieux, *Chem. Soc. Rev.* **1989**, *18*, 347.
[198] R. Breslow, *Acc. Chem. Res.* **1991**, *24*, 159, and references therein.
[199] P. A. Grieco, S. Larsen, W. F. Fobare, *Tetrahedron Lett.* **1986**, *27*, 1975.
[200] A. Lubineau, Y. Quenau, *J. Org. Chem.* **1987**, *52*, 1002.
[201] H.-J. Schneider, N. K. Sangwan, *J. Chem. Soc. Perkin Trans. 2* **1989**, 1223.
[202] C. Cativiela, J. I. Garcia, J. A. Mayoral, A. Avenoza, J. M. Pregrina, M. A. Roy, *J. Phys. Org. Chem.* **1991**, *4*, 48.
[203] H. Waldmann, *Liebigs Ann. Chem.* **1990**, 671.
[204] I. Hunt, C. D. Johnson, *J. Chem. Soc. Perkin Trans. 2* **1991**, 1051.
[205] W. Blokzijl, J. B. F. N. Engberts, M. J. Blandamer, *J. Am. Chem. Soc.* **1991**, *113*, 4241.
[206] W. Blokzijl, J. B. F. N. Engberts, *J. Am. Chem. Soc.* **1992**, *114*, 5440.
[207] G. Desimoni, G. Faita, P. P. Righetti, L. Toma, *Tetrahedron* **1990**, *46*, 7951.
[208] J. F. Blake, W. L. Jorgensen, *J. Am. Chem. Soc.* **1991**, *113*, 7430.
[209] P. A. Grieco, E. B. Brandes, S. McMann, J. D. Clark, *J. Org. Chem.* **1989**, *54*, 5849.
[210] E. B. Brandes, P. A. Grieco, J. J. Gajewski, *J. Org. Chem.* **1989**, *54*, 515.
[211] E. T. Kool, R. Breslow, *J. Am. Chem. Soc.* **1988**, *110*, 1596.
[212] J. Light, R. Breslow, *Tetrahedron Lett.* **1990**, *31*, 2957.
[213] J. L. Luche, C. Petrier, J. Einhorn, *Tetrahedron Lett.* **1985**, *26*, 1449.
[214] J. Nokami, J. Otera, T. Sudo, R. Okawara, *Organometallics* **1983**, *2*, 191.
[215] V. Ramamurthy, *Tetrahedron* **1986**, *42*, 5753.
[216] M. J. Blandamer, J. Burgess, J. B. F. N. Engberts, P. Warrick, Jr., *J. Mol. Liq.* **1992**, *52*, 15.
[217] R. Lumry, E. Battistel, C. Jolicoeur, *Faraday Symp. Chem. Soc.* **1982**, *17*, 93.
[218] M. G. Sceats, S. A. Rice, *J. Chem. Phys.* **1980**, *72*, 3248.
[219] N. Muller, *Acc. Chem. Res.* **1990**, *23*, 23.
[220] S. F. Dec, S. J. Gill, *J. Solution Chem.* **1985**, *14*, 417.
[221] S. F. Dec, S. J. Gill, *J. Solution Chem.* **1985**, *14*, 827.
[222] G. Olofsson, A. A. Oshodi, E. Qvarnström, I. Wadsö, *J. Chem. Thermodyn.* **1984**, *16*, 1041.
[223] J.-Y. Huot, E. Battistel, R. Lumry, G. Villeneuve, J.-F. Lavalle, A. Anusiem, C. Jolicoeur, *J. Solution Chem.* **1988**, *17*, 601.
[224] R. Lumry, H. S. Frank, *Proc. 6th Int. Biophys. Congr.* **1978**, *7*, 554.
[225] R. Lumry in *Bioenergetics and Thermodynamics, Model Systems* (Ed.: Y. Braibanti), Reidel, Dordrecht, **1980**.
[226] E. Grunwald, *J. Am. Chem. Soc.* **1984**, *106*, 5414.
[227] E. Grunwald, *J. Am. Chem. Soc.* **1986**, *108*, 5726.
[228] B. Lee, *Biopolymers* **1985**, *24*, 813.
[229] M. Oguni, C. A. Angell, *J. Chem. Phys.* **1980**, *73*, 1948.
[230] B. Lee, *Biopolymers* **1991**, *31*, 993.
[231] P. L. Privalov, S. J. Gill, *Pure Appl. Chem.* **1989**, *61*, 1097.
[232] E. Ruckenstein, *Colloids Surf.* **1992**, *65*, 95.
[233] A. Hvidt, *Acta Chem. Scand. A* **1983**, *37*, 99.
[234] L. R. Pratt, *Annu. Rev. Phys. Chem.* **1985**, *36*, 433.
[235] A. Ben-Naim, *J. Chem. Phys.* **1971**, *54*, 1387.
[236] W. G. McMillan, J. E. Mayer, *J. Chem. Phys.* **1945**, *13*, 276.
[237] H. L. Friedman, *J. Solution Chem.* **1972**, *1*, 387.
[238] H. L. Friedman, *J. Solution Chem.* **1972**, *1*, 413.
[239] J. G. Kirkwood, F. P. Buff, *J. Chem. Phys.* **1951**, *19*, 744.
[240] A. Ben-Naim, *Cell Biophys.* **1988**, *12*, 255.
[241] E. Matteoli, G. A. Mansoori, *Fluctuation Theory of Mixtures*, Taylor and Francis, New York, **1990**.
[242] D. A. McQuarrie, *Statistical Mechanics*, Harper Collins, New York, **1976**.
[243] A. H. Clark, F. Franks, M. D. Pedley, D. S. Reid, *J. Chem. Soc. Faraday Trans. 1* **1977**, *73*, 290.
[244] P. J. Rossky, H. L. Friedman, *J. Phys. Chem.* **1980**, *84*, 587.
[245] E. E. Tucker, E. H. Lane, S. D. Christian, *J. Solution Chem.* **1981**, *10*, 1.
[246] K. Watanabe, H. C. Andersen, *J. Phys. Chem.* **1986**, *90*, 795.

[247] P. T. Thompson, C. B. Davis, R. H. Wood, *J. Phys. Chem.* **1988**, *92*, 6386.
[248] D. G. Archer, *J. Phys. Chem.* **1989**, *93*, 5272.
[249] R. H. Wood, J. Savage, *J. Solution Chem.* **1976**, *5*, 733.
[250] M. Bloemendal, G. Somsen, *J. Solution Chem.* **1987**, *16*, 367.
[251] F. Franks, M. D. Pedley, *J. Chem. Soc. Faraday Trans. 1* **1981**, *77*, 1341.
[252] G. M. Blackburn, T. H. Lilley, E. Walmsley, *J. Chem. Soc. Faraday Trans. 1* **1982**, *78*, 1641.
[253] G. M. Blackburn, T. H. Lilley, P. J. Milburn, *J. Chem. Soc. Faraday Trans. 1* **1986**, *82*, 2965.
[254] I. R. Tasker, R. H. Wood, *J. Solution Chem.* **1982**, *11*, 729.
[255] J. J. Spitzer, S. K. Suri, R. H. Wood, *J. Solution Chem.* **1985**, *14*, 561.
[256] J. J. Spitzer, I. R. Tasker, R. H. Wood, *J. Solution Chem.* **1984**, *13*, 221.
[257] S. K. Suri, R. H. Wood, *J. Solution Chem.* **1986**, *15*, 705.
[258] M. Bloemendal, Y. Marcus, M. Booij, R. Hofstee, G. Somsen, *J. Solution Chem.* **1988**, *17*, 15.
[259] P. J. Check, T. H. Lilley, *J. Chem. Soc. Faraday Trans. 1* **1988**, *84*, 1927.
[260] G. Borghesani, R. Pedriali, F. Pulidori, *J. Solution Chem.* **1989**, *18*, 289.
[261] G. Barone, G. Castronuovo, P. Del Vecchio, C. Giancola, *J. Chem. Soc. Faraday Trans. 1* **1989**, *85*, 2087.
[262] G. Barone, G. Castronuovo, P. Del Vecchio, V. Elia, *J. Chem. Soc. Faraday Trans. 1* **1988**, *84*, 1919.
[263] G. Barone, G. Cacace, G. Catronuovo, V. Elia, *J. Solution Chem.* **1980**, *9*, 607.
[264] C. Cascella, G. Castronuovo, V. Elia, R. Sartotio, S. Wurzburger, *J. Chem. Soc. Faraday Trans. 1* **1989**, *85*, 3289.
[265] Y. Marcus, *J. Chem. Soc. Faraday Trans.* **1990**, *86*, 2215.
[266] Y. Marcus, *J. Chem. Soc. Faraday Trans.* **1991**, *87*, 1843.
[267] J. J. Kozak, W. S. Knight, W. Kauzmann, *J. Chem. Phys.* **1968**, *48*, 675.
[268] R. W. Gurney, *Ionic Processes in Solution*, McGraw-Hill, New York, **1953**.
[269] See [243].
[270] W. H. Streng, W.-Y. Wen, *J. Solution Chem.* **1974**, *3*, 865.
[271] See [244].
[272] Q. D. Craft, R. H. Wood, *J. Solution Chem.* **1977**, *6*, 525.
[273] B. Y. Okamoto, P. T. Thompson, R. H. Wood, *J. Chem. Soc. Faraday Trans. 1* **1978**, *74*, 1990.
[274] S. K. Suri, J. J. Spitzer, R. H. Wood, E. G. Abel, P. T. Thompson, *J. Solution Chem.* **1985**, *14*, 781.
[275] Y. K. Kang, G. Némethy, H. A. Scheraga, *J. Phys. Chem.* **1987**, *91*, 4105.
[276] Y. K. Kang, G. Némethy, H. A. Scheraga, *J. Phys. Chem.* **1987**, *91*, 4109.
[277] Y. K. Kang, K. D. Gibson, G. Némethy, H. A. Scheraga, *J. Phys. Chem.* **1988**, *92*, 4739.
[278] See [168].
[279] A. Rahman, F. H. Stillinger, *J. Chem. Phys.* **1971**, *55*, 3336.
[280] F. H. Stillinger, A. Rahman, *J. Chem. Phys.* **1974**, *60*, 1545.
[281] F. H. Stillinger, A. Rahman, *J. Chem. Phys.* **1978**, *68*, 666.
[282] L. R. Pratt, D. Chandler, *J. Chem. Phys.* **1977**, *67*, 3683.
[283] D. Chandler, *J. Chem. Phys.* **1977**, *67*, 1113.
[284] L. R. Pratt, D. Chandler, *J. Chem. Phys.* **1980**, *73*, 3430.
[285] L. R. Pratt, D. Chandler, *J. Chem. Phys.* **1980**, *73*, 3434.
[286] A. Tani, *Mol. Phys.* **1983**, *48*, 1229.
[287] A. Tani, *Mol. Phys.* **1984**, *51*, 161.
[288] F. Hirata, P. J. Rossky, *Chem. Phys. Lett.* **1981**, *83*, 329.
[289] F. Hirata, B. M. Pettitt, P. J. Rossky, *J. Chem. Phys.* **1982**, *77*, 509.
[290] B. M. Pettitt, M. Karplus, *J. Chem. Phys.* **1985**, *83*, 781.
[291] W. L. Jorgensen, J. Chandrasekhar, J. D. Madura, R. W. Impey, M. L. Klein, *J. Chem. Phys.* **1983**, *79*, 926.
[292] B. M. Pettitt, M. Karplus, P. J. Rossky, *J. Phys. Chem.* **1986**, *90*, 6335.
[293] H. Tanaka, *J. Chem. Phys.* **1987**, *86*, 1512.
[294] R. A. Pierotti, *J. Phys. Chem.* **1963**, *67*, 1840.
[295] R. A. Pierotti, *J. Phys. Chem.* **1965**, *69*, 281.
[296] R. A. Pierotti, *Chem. Rev.* **1976**, *76*, 717.
[297] F. H. Stillinger, *J. Solution. Chem.* **1973**, *2*, 141.
[298] J. Langlet, P. Cleverie, J. Caillet, A. Pullman, *J. Phys. Chem.* **1988**, *92*, 1617.
[299] M. Lucas, *J. Phys. Chem.* **1973**, *77*, 2479.
[300] M. Lucas, *J. Phys. Chem.* **1976**, *80*, 359.
[301] N. Morel-Desrosiers, J. P. Morel, *Can. J. Chem.* **1981**, *59*, 1.
[302] T. Halicioglu, O. Sinanoglu, *Ann. N. Y. Acad. Sci.* **1969**, *158*, 308.
[303] O. Sinanoglu in *Molecular Association in Biology* (Ed.: B. Pullman), Academic Press, New York, **1968**, p. 427.
[304] J. J. Moura-Ramos, M. Lemmers, R. Ottinger, M. L. Stien, J. Reisse, *J. Chem. Res. Synop.* **1977**, 56.
[305] J. J. Moura-Ramos, J. Reisse, *Rev. Port. Quim.* **1984**, *26*, 61.
[306] J. J. Moura-Ramos, M. S. Dionisio, R. C. Gonçalves, H. P. Diogo, *Can. J. Chem.* **1988**, *66*, 2894.
[307] M. S. Dionísio, J. J. Moura-Ramos, R. M. Gonçalves, *Can. J. Chem.* **1990**, *68*, 1937.
[308] J. P. Postma, H. J. C. Berendsen, J. R. Haak, *Faraday Symp. Chem. Soc.* **1982**, *17*, 55.
[309] W. L. Jorgensen, C. Ravimohan, *J. Chem. Phys.* **1985**, *83*, 3050.
[310] B. Guillot, Y. Guissani, S. Bratos, *J. Chem. Phys.* **1991**, *95*, 3643.
[311] A. Pohorille, L. R. Pratt, *J. Am. Chem. Soc.* **1990**, *112*, 5066.
[312] L. R. Pratt, A. Pohorille, *Proc. Natl. Acad. Sci. USA* **1992**, *89*, 2995.
[313] G. S. Del Buono, P. J. Rossky, J. Schnitker, *J. Chem. Phys.* **1991**, *95*, 3728.
[314] H. J. C. Berendsen, J. P. M. Postma, W. F. van Gunsteren, H. J. Hermans in *Intermolecular Forces* (Ed.: B. Pullman) Reidel, Dordrecht, **1981**, p. 331.
[315] O. Matsuoka, E. Clementi, M. Yoshimine, *J. Chem. Phys.* **1976**, *64*, 1351.
[316] A. Wallqvist, *Chem. Phys.* **1990**, *148*, 439.
[317] A. Wallqvist, P. Ahlström, G. Karlström, *J. Phys. Chem.* **1990**, *94*, 1649.
[318] M. Sprik, *J. Phys. Chem.* **1991**, *95*, 2283.
[319] J. A. C. Rullman, P. T. van Duijnen, *Mol. Phys.* **1988**, *63*, 451.
[320] S. Kuwajima, A. Warshel, *J. Phys. Chem.* **1990**, *94*, 460.
[321] U. Niesar, G. Corongiu, E. Clementi, G. R. Kneller, D. K. Bhattacharya, *J. Phys. Chem.* **1990**, *94*, 7949.
[322] W. L. Jorgensen, *J. Chem. Phys.* **1981**, *75*, 2026.
[323] P. A. Bash, Y. C. Singh, F. K. Brown, R. Langridge, P. A. Kollman, *Science* **1987**, *235*, 574.
[324] W. L. Jorgensen, J. F. Blake, J. K. Buckner, *Chem. Phys.* **1989**, *129*, 193.
[325] T. P. Straatsma, H. J. C. Berendsen, J. P. M. Postma, *J. Chem. Phys.* **1986**, *85*, 6270.
[326] S. H. Fleischman, D. A. Zichi, *J. Chim. Phys.* **1991**, *88*, 2617.
[327] J. Gao, *J. Phys. Chem.* **1992**, *96*, 537.
[328] W. L. Jorgensen, J. K. Buckner, S. Boudon, J. Tirado-Rives, *J. Chem. Phys.* **1988**, *89*, 3742.
[329] D. A. Pearlman, P. A. Kollman, *J. Chem. Phys.* **1989**, *90*, 2460.
[330] J. C. Owicki, H. A. Scheraga, *J. Am. Chem. Soc.* **1977**, *99*, 7403.
[331] P. J. Rossky, M. Karplus, *J. Am. Chem. Soc.* **1979**, *101*, 1913.
[332] S. Swaminathan, S. W. Harrison, D. L. Beveridge, *J. Am. Chem. Soc.* **1978**, *100*, 5705.
[333] V. G. Dashevsky, G. N. Sarkisov, *Mol. Phys.* **1974**, *27*, 1271.
[334] C. Pangali, M. Rao, B. J. Berne, *J. Chem. Phys.* **1979**, *71*, 2975.
[335] A. Geiger, A. Rahman, F. H. Stillinger, *J. Chem. Phys.* **1979**, *70*, 263.
[336] A. Laaksonen, P. Stilbs, *Mol. Phys.* **1991**, *74*, 747.
[337] S. Okazaki, K. Nakanishi, H. Touhara, *J. Chem. Phys.* **1979**, *71*, 2421.
[338] C. Pangali, M. Rao, B. J. Berne, *J. Chem. Phys.* **1979**, *71*, 2982.
[339] W. Swope, H. C. Andersen, *J. Phys. Chem.* **1984**, *88*, 6548.
[340] H. Tanaka, K. Nakanishi, *J. Chem. Phys.* **1991**, *95*, 3719.
[341] P. J. Rossky, D. A. Zichi, *Faraday Symp. Chem. Soc.* **1982**, *17*, 69.
[342] D. A. Zichi, P. J. Rossky, *J. Chem. Phys.* **1986**, *84*, 2814.
[343] S. Okazaki, K. Nakanishi, N. Touhara, N. Watanabe, Y. Adashi, *J. Chem. Phys.* **1981**, *74*, 5863.
[344] D. A. Zichi, P. L. Rossky, *J. Chem. Phys.* **1986**, *84*, 1712.
[345] D. J. Tobias, C. L. Brooks III, *J. Chem. Phys.* **1990**, *92*, 2582.
[346] W. L. Jorgensen, *J. Chem. Phys.* **1982**, *77*, 5757.
[347] W. L. Jorgensen, J. K. Buckner, *J. Phys. Chem.* **1987**, *91*, 6083.
[348] See [343].
[349] S. H. Fleischman, C. L. Brook III, *J. Chem. Phys.* **1987**, *87*, 3029.
[350] P. K. Mehrota, D. L. Beveridge, *J. Am. Chem. Soc.* **1980**, *102*, 4287.
[351] S. Okazaki, H. Touhara, K. Nakanishi, *J. Chem. Phys.* **1984**, *81*, 890.
[352] G. Bolis, G. Corongiu, E. Clementi, *Chem. Phys. Lett.* **1982**, *86*, 299.
[353] W. L. Jorgensen, J. D. Madura, *J. Am. Chem. Soc.* **1983**, *105*, 1405.
[354] G. Alagona, A. Tani, *Chem. Phys. Lett.* **1982**, *87*, 337.
[355] H. Tanaka, K. Nakanishi, H. Touhara, *J. Chem. Phys.* **1984**, *81*, 4065.
[356] C. F. Wong, J. A. McCammon, *J. Am. Chem. Soc.* **1986**, *108*, 3830.
[357] D. C. Rapaport, H. A. Scheraga, *J. Phys. Chem.* **1982**, *86*, 873.
[358] C. J. Cramer, D. G. Truhlar, *Science* **1992**, *256*, 213.
[359] W. L. Jorgensen, J. Gao, C. Ravimohan, *J. Phys. Chem.* **1985**, *89*, 3470.
[360] H. Tanaka, K. Nakanishi, *J. Chem. Phys.* **1991**, *95*, 3719.
[361] G. Ravishanker, M. Mezei, D. L. Beveridge, *Faraday Symp. Chem. Soc.* **1982**, *17*, 79.
[362] D. A. Zichi, P. J. Rossky, *J. Chem. Phys.* **1985**, *83*, 797.
[363] A. A. Rashin, *J. Phys. Chem.* **1990**, *94*, 1725.
[364] A. A. Rashin, M. A. Bukatin, *J. Phys. Chem.* **1991**, *95*, 2942.
[365] S. Swaminathan, D. L. Beveridge, *J. Am. Chem. Soc.* **1979**, *101*, 5832.
[366] D. E. Smith, L. Zhang, A. D. J. Haymet, *J. Am. Chem. Soc.* **1992**, *114*, 5875.
[367] A. Maliniak, A. Laaksonen, J. Korppi-Tommola, *J. Am. Chem. Soc.* **1990**, *112*, 86.
[368] W. L. Jorgensen, *J. Phys. Chem.* **1983**, *87*, 5304.
[369] a) B. Smit, P. A. J. Hilbers, K. Esselink, L. A. M. Rupert, N. M. van Os, A. G. Schlijper, *Nature* **1990**, *348*, 624; b) S. Karaborni, N. M. van Os, K. Esselink, P. A. J. Hilbers, *Langmuir* **1993**, *9*, 1175.
[370] After submission of this review, a MD simulation study was reported in which, for the first time, methane hydration as well as methane association were simulated in a polarizable aqueous phase. Interestingly, the authors found that the solvent-separated arrangement almost disappeared when the polarization term was incorporated into the water potential. See D. van Belle, S. J. Wodak, *J. Am. Chem. Soc.* **1993**, *115*, 647.
[371] Added in proof: B. Guillot, Y. Guissani, *J. Chem. Phys*, in press.

Carbon(IV) Nitride C_3N_4—A New Material Harder Than Diamond?

By *Wolfgang Schnick**

The prediction of the existence and the structure of previously unknown solid-state compounds seems to be particularly difficult, because numerous complex, interacting factors must be taken into account. A simplification to a certain extent is possible with predominantly covalent polymeric solid-state compounds in which coordination numbers and geometries are unambiguously stipulated for the constituent elements.

Desired properties of new materials are, above all, extreme hardness, good thermal conduction, and high thermal stability. These properties are particularly likely in compounds with highly cross-linked structures with mainly covalent chemical bonds that are very stable. The material property, hardness, can be described by the bulk modulus B, which, on atomic scale, is influenced fundamentally by the strength and compressibility of the chemical bonds.[1] Thus logically, the highest bulk moduli have been found for covalent materials: diamond not only has the highest value (4.43 Mbar), but also is the solid with the greatest hardness.[1]

A simple empirical relationship for the estimation of the bulk modulus B of solids with the zinc blende structure was presented recently by Liu and Cohen [Eq. (a)].[1] This predicts a dependence of the magnitude of this property on the ionicity λ and the interatomic distance d. In accord with recent experiments[2] this empirical relation yields a bulk modulus for cubic boron nitride that is lower than that of diamond. Furthermore, on the basis of the expression (a), Liu and Cohen predict for a similarly constructed, covalent C–N solid an extremely high mechanical hardness.[1]

$$B = (19.71 - 2.2\,\lambda)/d^{3.5} \qquad \text{(a)}$$

Of particular significance for the development of novel inorganic materials with interesting properties is the nitride class of substances containing nitrogen as electronegative bonding partner in the oxidation state −III. As a result of its lower electronegativity, nitrogen forms bonds with stronger covalent character as compared to oxygen. Moreover, nitrogen offers more extensive structural possibilities, since it forms not only one or two, but also three or four covalent bonds to neighboring atoms.[3] In combination with light main group elements from the p block (e.g., boron, aluminum, silicon, phosphorus), highly cross-linked and predominantly covalent, polymeric solid-state compounds arise.

At present in the group of known binary nitrides of main group elements in which the group number of each corresponds to the maximum oxidation state, a carbon(IV) nitride C_3N_4 is absent. According to the double bond rule, which favors the formation of multiple bonds over the construction of polymeric structures for elements of the second row, C_3N_4 could be assumed to have a molecular structure in the form of tricyanoazane $N(CN)_3$. However, also conceivable in principle and structurally feasible is a polymeric structure analogous to one of the modifications of binary Si_3N_4 with a three-dimensional network structure of CN_4 tetrahedra, sharing corners in all directions. The carbon atoms would be bound covalently to four adjacent carbon atoms like the silicon atoms of Si_3N_4, while the nitrogen atoms would be coordinated to three tetrahedral centers (C instead of Si) in an almost trigonal-planar arrangement (Fig. 1). Although

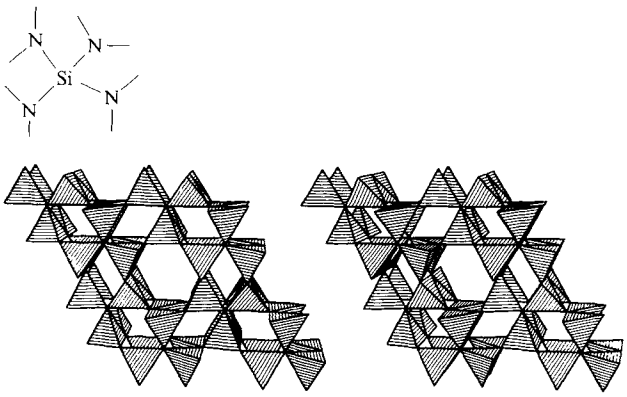

Fig. 1. Bonding and coordination of silicon and nitrogen in β-Si_3N_4 (top) and the stereoscopic representation of the crystal structure of β-Si_3N_4 viewed along [001] (bottom). The SiN_4 tetrahedra are shown as closed polyhedra. An analogous structure is postulated for β-C_3N_4 [4, 8].

no suggestion of the existence of a binary carbon nitride C_3N_4 has yet been found, the cyanamides (e.g. Na_2CN_2) are compounds that can be interpreted as ternary carbon(IV) nitrides. In accord with the double bond rule, however, carbon as an element of the second row has been shown to have a lower coordination number (CN = 2), so these compounds contain isolated, linear anions CN_2^{2-}, isosteric with CO_2.

But is there perhaps also a polymeric C_3N_4 with a structure analogous to Si_3N_4? And what material properties might be anticipated for such a compound?

The supposition formulated by Liu and Cohen that solids will have a particularly high bulk modulus when they display short bond lengths and low ionicities, that is, when the compound has a high proportion of covalent bonding, was the starting point for exact theoretical investigations into the potential stability and mechanical properties of binary carbon nitride C_3N_4. First-principles pseudopotential calculations of the structural and electronic properties (lattice constants, bulk modulus, and electronic band structure) of β-Si_3N_4 and its isotype, hypothetical β-C_3N_4, were in good agreement with experimental data obtained from silicon nitride. Two significant statements about C_3N_4 can be made: The bulk modulus of this compound should be comparable with that of diamond. Moreover, β-C_3N_4 should be able to be synthesized, at least as a metastable form under normal conditions, because of its moderately large cohesive energy.

[*] Prof. Dr. W. Schnick
Laboratorium für Anorganische Chemie der Universität
D-95440 Bayreuth (FRG)
Telefax: Int. code + (921)55-2535

As regards thermodynamic stability, β-C_3N_4 therefore fits into the series of other superhard materials, that, like diamond or cubic boron nitride, are also only metastable under normal conditions.

Efforts of various groups to synthesize a binary carbon nitride with a β-C_3N_4 structure initially yielded no indication that a polymeric solid containing carbon atoms tetrahedrally surrounded by nitrogen atoms exists.[5-7] These experiments employed, in particular, plasma deposition from CH_4/N_2 mixtures and pyrolytic decomposition of organic C–N–H compounds. Also shock wave compression in pyrolysis products of melamine–formaldehyde resins did not bring the desired success. Considerably more promising were the recently published studies of Niu, Lu, and Lieber,[8] in which synthetic methods are presented that generate both highly energetic carbon species as well as atomic and reactive nitrogen. The product was obtained by trapping of the resultant C–N products by low-temperature thin-film growth. The generation of the highly energetic carbon species takes place through the ablation of a very pure graphite target with a Nd:YAG laser. Atomic nitrogen with high kinetic energy (>1 eV) was generated by radio frequency discharge in a high-flow stream of $He-N_2$.

C–N films containing different nitrogen content were obtained with this process. Quantitative analysis of the reaction products with Rutherford back-scattering spectroscopy (RBS) revealed nitrogen contents in the studied samples of maximally 45%. This value lies distinctly below the theoretical value of 57% for β-C_3N_4. Moreover, it has been shown that a C–N solid with a nitrogen content worth mentioning can be constructed only when atomic nitrogen is introduced during the sputtering process. X-ray photoelectron spectroscopy (XPS) of the samples gave clear evidence for nonpolarized, covalent bonds between carbon and nitrogen. Transmission electron microscopic investigations (TEM) showed at first a pure crystallinity in the sputtered C–N films; however, small crystallites with grain sizes of less than 10 nm were detected. The diffraction pattern obtained under the electron microscope was readily observed to be consistent with the assumption of a structure analogous to β-Si_3N_4 having the lattice constants determined theoretically for β-C_3N_4. The remarkable material properties of β-C_3N_4 predicted by theoretical studies were able to be confirmed, at least qualitatively: the material showed a high thermal and mechanical stability.

Certainly one cannot yet speak of the synthesis of a defined, crystalline carbon nitride of composition C_3N_4 amongst the C–N layers of Niu, Lu, and Lieber. Nevertheless, the but short history of these compounds is remarkable: Whereas, for instance, in Gmelin's Handbook of Inorganic Chemistry a compound of the composition C_3N_4 is not even mentioned, simple empirical studies lead to the assumption that such a C–N solid should have particularly attractive material properties (exceptional hardness). This qualitative statement is confirmed by ab initio calculations. Simultaneously, an adequate stability is claimed that makes synthesis of C_3N_4 feasible, at least in metastable state. After some unsuccessful preparative attempts a process was finally developed to circumvent the former thermodynamic problems in the formation of C_3N_4 through the generation of highly reactive carbon species and atomic nitrogen. The solid, which is formed in a potentially metastable state is stabilized kinetically by growth at low temperatures.

Apparently the difficult prediction of the existence and structure of a previously unknown solid-state compound and its experimental verification has indeed been achieved. The results are certainly stimulating both for materials research and for solid-state chemistry. It will inspire a whole series of further preparative efforts and investigations. After all, not only is the preparative route to a new binary nitride of one of the most important main group elements attractive, but also the synthesis and applications of a new material with potentially particularly desirable properties. As with other binary nonmetal nitrides, the question of an extensive chemistry in the form of ternary and higher compounds also arises (cf. [9]).

German version: *Angew. Chem.* **1993**, *105*, 1649

[1] A. Y. Liu, M. L. Cohen, *Science* **1989**, *245*, 841.
[2] E. Knittle, R. M. Wentzcovitch, R. Jeanloz, M. L. Cohen, *Nature* **1989**, *337*, 349.
[3] Compare, for example, the coordination chemistry and bonding in SiO_2 and Si_3N_4, P_4O_{10} and P_3N_5, or B_2O_3 and BN.
[4] A. Y. Liu, M. L. Cohen, *Phys. Rev. B Condens. Matter* **1990**, *41*, 10727.
[5] H. X. Hau, B. J. Feldman, *Solid State Commun.* **1988**, *65*, 921.
[6] L. Maya, D. R. Cole, E. W. Hagaman, *J. Am. Ceram. Soc.* **1991**, *74*, 1686.
[7] M. R. Wixom, *J. Am. Ceram. Soc.* **1990**, *73*, 1973.
[8] C. Niu, Y. Z. Lu, C. M. Lieber, *Science* **1993**, *261*, 334.
[9] W. Schnick, *Angew. Chem.* **1993**, *103*, 846; *Angew. Chem. Int. Ed. Engl.* **1993**, *32*, 806.

 © *VCH Verlagsgesellschaft mbH, D-69451 Weinheim, 1993* *0570-0833/93/1111-1581 $ 10.00+.25/0*

Chiral 2-Amino-1,3-butadienes: New Reagents for Asymmetric Cycloadditions

By *Karsten Krohn**

Since its discovery over sixty years ago[1] the Diels–Alder reaction has lost none of its attraction.[2] It enables, in a one-step inter- or intramolecular reaction, the rapid preparation of cyclic compounds having a six-membered ring. During the course of the [4 + 2] cycloaddition four new stereocenters can be introduced directly, and their stereocontrol is a topic of major interest in modern synthetic chemistry. In addition, in intermolecular reactions, the relative positions of the reaction partners (regiochemistry) must be taken into account. If a concerted reaction is assumed, both a *cis* addition (suprafacial mode) and a preferred *endo* orientation (Alder Rules) can be expected. But how can the *absolute* configuration of the desired product be controlled? There are three basic possibilities: the use of a chirally modified diene, a chirally modified dienophile, or a chiral catalyst. Although the first successes resulted from the attractive, but difficult, catalytic route,[3, 4b] the majority of the investigators are concerned with the stoichiometric approach using chiral dienophiles (mostly derivatives of acrylic esters.)[4–7] Chiral dienes have been used less frequently, although Trost et al. in 1980 had achieved an attention-riveting result with the (1*S*)-butadiene derivative **2**.[8] This diene reacted regioselectively with juglone (**1**) to yield a single adduct **3** with 97% *ee*! The well-known π-stacking model was developed from this example, although it does not appear to be applicable to all reactions.[9]

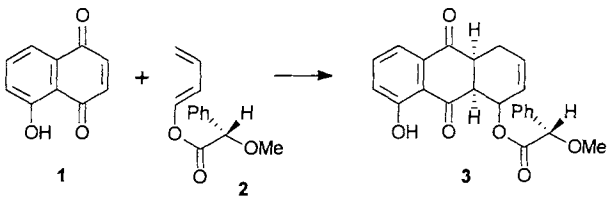

Unfortunately the result obtained by Trost et al. remained unique for more than a decade, at least in terms of enantioselectivity. The slow development in the area of chiral dienes may be ascribed to the difficulty of preparing these compounds.[4b] Recently, in quick succession and independently of one another, the research groups of Enders[10] and Barluenga[11] reported on the cycloaddition of chiral 2-aminobutadienes and described elegant solutions to the stereochemical problems (regio-, diastereo-, and enantioselectivity). The prospects of 2-aminobutadienes in this reaction were not promising, since the results of MINDO3 calculations had indicated that they would not undergo (concerted) Diels–Alder reactions.[12] Nevertheless, Valentin et al. in 1977[13] and Gompper et al. in 1979[14] obtained evidence for the cycloaddition of electron-rich methoxy- and amino-substituted dienes. Since then, the research groups of Barluenga[15–17] in Spain and Valentin[13, 18] in Italy have been able to carry out other cycloadditions with activated olefins, aldehydes, and imines. These investigations show, however, a distinct difference from reactions with the highly successful siloxydienes related to the Danishevsky diene.[19, 20] The enamine character of 2-aminodienes (or dienamines) is clearly demonstrated by non-Lewis acid catalyzed reactions, and open-chain adducts are frequently isolated alongside the cyclic adducts.[16] Nevertheless, in many cases the stereochemistry of the products indicates a concerted reaction. According to Enders et al. the stereochemistry of the final products can be explained equally plausibly by means of a concerted cycloaddition or a sequential series of ionic addition steps, and the authors leave the question of the actual mechanism open.[10a]

The chiral 2-aminobutadiene **5** was prepared in good yield from diacetyl **4** and (*S*)-2-(methoxymethyl)pyrrolidine (SMP), obtained from proline, by means of enamine formation and a Wittig reaction. The cycloaddition of **5** with five different nitrostyrenes (R = H, 4-F, 4-OMe, 4-Me, 3,4-OCH_2O) proceeded at room temperature without catalysis and yielded labile cycloadducts **6** (enamine substructure), which decomposed on silica gel to form the corresponding ketones **7**.[10a] Careful analysis of the spectra of the products

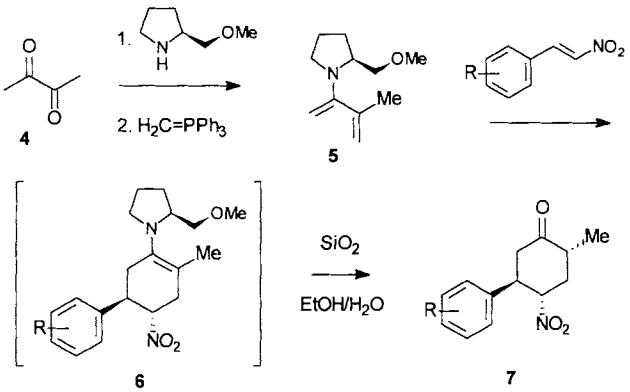

shows that the saponification of the intermediate enamines **6** ("ketonization") does not proceed in a completely uniform manner; epimers are formed at the position α to the carbonyl group. For the reaction in diethyl ether, enantioselectivities from 96 to > 99% *ee* were obtained for the main products—record values for cycloadditions not catalyzed by Lewis acids. In addition, the reaction is completely regioselective, which, in view of the strongly polarized reaction components, 2-aminobutadiene and nitrostyrene, is compatible with both the frontier orbital model for a concerted reaction and the stepwise ionic course (1,2- and 1,4-addition). The two reaction modes can be described by transition states **A** and **B**.

Barluenga et al.[11] have investigated slightly modified 2-SMP-butadienes **8** with a hydroxy- or alkoxymethyl group attached to C-4 (R = H, alkyl). The dienes can be synthesized by the addition of SMP to commercially avail-

[*] Prof. K. Krohn
Fachbereich Chemie und Chemietechnik
der Universität-Gesamthochschule
Warburgestrasse 100, D-33098 Paderborn (FRG)
Telefax: Int. code + (5251)60-3245

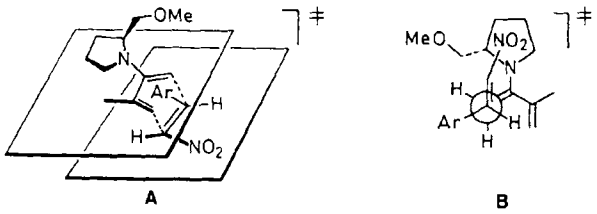

A B

able enynes. Independently of Enders et al., they also used nitrostyrenes as dienophiles in reactions with the chiral 2-aminobutadienes **8**. These workers obtained slightly lower *ee* values (82 and 90%) with the reactions in methanol, a result which the German authors had already observed with this solvent. For an unbiased observer these otherwise analogous results confirm the reproducibility of the reaction. The Spanish authors demonstrate, in addition, two highly interesting reactions which considerably extend the area of application of the new chiral 2-aminodienes. One of these is the hetero-Diels–Alder reaction with *N*-silylimines, whose products can be hydrolyzed to provide substituted piperidones **9** with a high degree of enantioselectivity (85 and 95% *ee*). Such piperidones are required for the synthesis of alkaloids and pharmaceuticals.

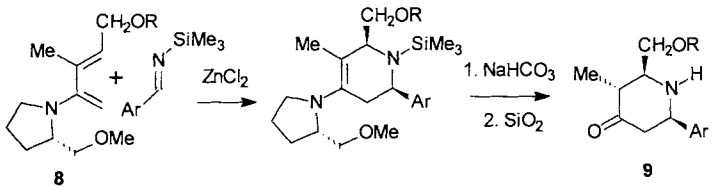

8 **9**

Recently Enders et al.[10b] treated azadienophiles such as phenyltriazoledione with (*S,S*)-2-(3,5-dimethylmorpholino)butadiene **10** (R = *n*Pr, *i*Pr, cyclohexyl, cyclopentyl, *t*Bu, Ph–C≡C) to form heterocyclic enamines which, after acid-catalyzed removal of the chiral C_2-symmetrical amine, yielded the hexahydropyridazines **12** (six examples) with an *ee* of 90–91%. The successful use of another chiral amine, [(*S,S*)-3,5-dimethylmorpholine], gives further indication of the efficiency of chiral induction by means of coupling at the C-2 position of the diene.

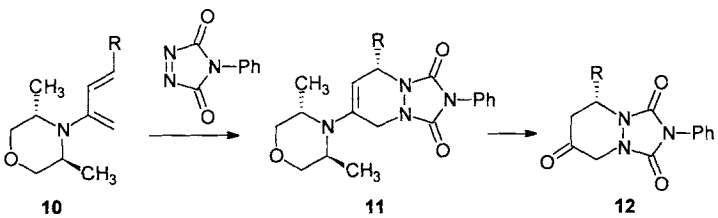

10 **11** **12**

Another example from the Spanish authors[11] is especially interesting, as the cycloaddition leads to the formation of a compound with a seven-membered ring. The literature shows that in recent years a tremendous amount of effort has been expended in trying to prepare carbocyclic five-membered rings by a route as simple and elegant as the Diels–Alder reaction for the synthesis of six membered-rings.[4c] Is a counterpart for seven-membered rings now in sight? The aminodienes **8** were allowed to react with α,β-unsaturated Fischer carbene complexes.[21] The reaction consists of two well-known concerted reactions which occur sequentially: cyclopropanation and a Cope rearrangement of the intermediate divinylcyclopropane. The principle was first demonstrated by Wulff et al.[22] with the reaction of the Danishefsky diene (1-methoxy-3-trimethylsiloxy-1,3-butadiene) and unsaturated carbene(carbonyl)chromium complexes. The Cope-type rearrangement occurs so rapidly with *cis*-oriented vinyl groups on the cyclopropane that the intermediate usually cannot be isolated. Barluenga et al. were recently able to show that the analogous reaction with 2-aminobutadienes **8** in place of the siloxybutadiene leads to the formation of seven-membered rings.[23] The decisive advantage lies, however, in the additional possibility of using a chirally modified diene component.[11] The reaction of **8** with the carbene complex **13** gave satisfactory yields (52–82% for the multistep sequence) with total regio- and diastereoselectivity and excellent enantiomeric excesses of 81 and 86% *ee*.

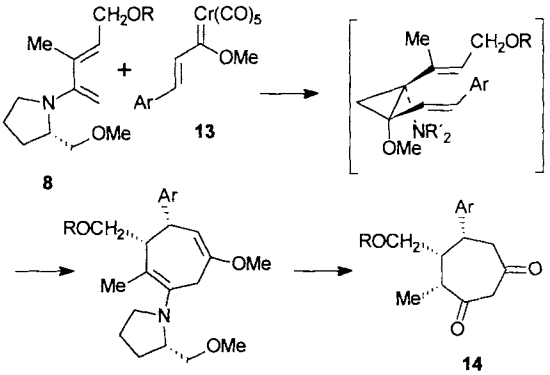

8 **13** **14**

What are the advantages of the new chiral 2-aminobutadienes? Firstly, as the well-established SMP is a commercially available chiral reagent, the chances are good that it will find broad application. Secondly, there are established methods for the coupling of SMP with other starting materials to form 2-aminobutadienes.[10c, 17] Finally, as is shown by the examples, especially the nitroolefins,[10, 13, 18] good control of the regiochemistry is possible because of the strong electron donor in the 2-position. The increased electron density of the diene increases the reactivity (for cycloadditions with "normal" electron requirements), and the reaction can be extended to compounds with, for example C=N bonds. In addition, the reaction with α,β-unsaturated Fischer carbenes opens the door to the single-pot, stereoselective synthesis of carbocyclic seven-membered rings. Especially important is the fact that the chiral component can be removed under very mild conditions and can, in principle, be recovered. Decisive, however, is the excellent enantioselectivity of the reaction which, as has been shown by Enders et al.,[10a] can be further improved by the choice of the reaction conditions.

German version: *Angew. Chem.* **1993**, *105*, 1651

[1] O. Diels, K. Alder, *Liebigs Ann. Chem.* **1928**, *460*, 98.
[2] F. Fringuelli, A. Taticchi, *Dienes in the Diels-Alder Reaction*, Wiley, New York, **1990**.

[3] For example: E. J. Corey, T.-P. Loh, T. D. Roper, M. D. Azimioara, M. C. Noe, *J. Am. Chem. Soc.* **1992**, *114*, 8290–8292.
[4] a) J. Mulzer, H.-J. Altenbach, M. Braun, K. Krohn, H.-U. Reissig, *Organic Synthesis Highlights*. VCH, Weinheim, **1991**; b) K. Krohn in [4a], pp. 54–65; c) K. Krohn in [4a], pp. 96–103.
[5] a) W. Oppolzer, *Tetrahedron* **1987**, *43*, 1969; b) W. Oppolzer, *Angew. Chem.* **1984**, *96*, 840–854; *Angew. Chem. Int. Ed. Engl.* **1984**, *23*, 876–890.
[6] G. Helmchen, A. Goeke, S. Kreisz, A. Krotz, G. H. Lauer, G. Linz, *Cyclopentanoid Natural Products via Asymmetric Diels-Alder Reactions* in *Stud. Nat. Prod. Chem.* **1991**, *8*, 139–158.
[7] M. J. Taschner, *Asymmetric Diels-Alder Reactions* (Ed.: T. Hudlicky), JAI Press, London, **1989**.
[8] B. M. Trost, D. O'Krongly, J. L. Belletire, *J. Am. Chem. Soc.* **1980**, *102*, 7595–7596.
[9] C. Siegel, E. R. Thornton, *Tetrahedron Asymmetry* **1991**, *2*, 1413–1428.
[10] a) D. Enders, O. Meyer, G. Raabe, *Synthesis* **1992**, 1242–1244; b) D. Enders, O. Meyer, G. Raabe, J. Runsink, *Synthesis*, in press; c) syntheses from α-chloroenamines and vinyllithium compounds: D. Enders, P. Hecker, unpublished.
[11] J. Barluenga, F. Aznar, C. Valdés, A. Martín, S. García-Granda, E. Martín, *J. Am. Chem. Soc.* **1993**, *115*, 4403–4404.
[12] L. N. Koikov, P. B. Terentèv, I. P. Gloriozov, Yu. G. Bundel, *J. Org. Chem. USSR* (*Engl. Transl.*) **1984**, *20*, 832.
[13] G. Pitacco, A. Risaliti, M. L. Trevisan, E. Valentin, *Tetrahedron* **1977**, *33*, 3145–3148.
[14] R. Gompper, R. Sobotta, *Tetrahedron Lett.* **1979**, 921–924.
[15] J. Barluenga, F. Aznar, M.-P. Cabal, F. H. Cano, M. Foces-Foces, *J. Chem. Soc. Chem. Commun.* **1988**, 1247–1249.
[16] J. Barluenga, F. Aznar, C. Valdés, F. López Ortiz, *Tetrahedron Lett.* **1990**, *31*, 5237–5240.
[17] Synthesis by addition of amines to β-enaminophosphonium salts followed by Wittig reaction: J. Barluenga, I. Merino, F. Palacios, *Tetrahedron Lett.* **1990**, *31*, 6713–6717.
[18] M. Mezzetti, P. Nitti, G. Pitacco, E. Valentin, *Tetrahedron* **1985**, *41*, 1415–1422.
[19] S. J. Danishefsky, M. P. DeNinno, *Angew. Chem.* **1987**, *99*, 15–23; *Angew. Chem. Int. Ed. Engl.* **1987**, *26*, 15-23.
[20] M. Petrzilka, J. I. Grayson, *Synthesis* **1981**, 753.
[21] H. K. Dötz in *Organometallic in Organic Synthesis: Aspects of a Modern Interdisciplinary Field* (Eds.: A. de Meijere, H. tom Dieck), Springer, Berlin, **1988**.
[22] W. D. Wulff, D. C. Yang, C. K. Murray, *J. Am. Chem. Soc.* **1988**, *110*, 2653–2655.
[23] J. Barluenga, F. Aznar, A. Martín, S. García-Grande, M. A. Salvadó, P. Pertierra, *J. Chem. Soc. Chem. Commun.* **1993**, 319–321.

Arene–Arene Interactions: Electrostatic or Charge Transfer?

By *Christopher A. Hunter**

Noncovalent interactions between aromatic molecules play a major role in determining the structures and properties of molecular assemblies in biology, chemistry, and materials science. However, they are not well understood. When molecular scientists obtain an unexpected result in a system which contains π systems, they tend to invoke the mythical powers of the "π–π interaction", "π-stacking", "charge transfer" (CT), "π-acid/π-base" or "electron donor acceptor (EDA) interaction". The range of terms used reflects a confusion about the precise nature of these interactions.[**] Recent experimental work shows that the concept of CT or EDA interactions is highly misleading and that π-π interactions are dominated by electrostatics.[1, 2]

Several different factors contribute to the magnitude of any noncovalent interaction between two molecules.[3]

1. The van der Waals energy; that is the sum of the dispersion energy and the repulsion energy.

2. The electrostatic interaction due to different static charge distributions in molecules.

3. The induction energy which is the interaction between the static charge distribution of one molecule and the proximity-induced change in the charge distribution of the other. It is not yet clear whether this contribution is experimentally significant.

4. CT which is a stabilization due mixing of the ground state (A B) of a molecule with an excited charge-separated state ($A^+ B^-$).

5. Desolvation of the interacting molecular surfaces.

If we are to understand the role of π-π interactions in controlling the behavior of biomolecules, and if we are to use these interactions to design synthetic receptors for small molecules, drugs for biological receptors, homogeneous catalysts or self-assembling polymolecular aggregates, then it is vital that we know the relative significance of the contributions listed above. For example, suppose we wanted to design a molecular assembly in which two π systems were held together in a face-to-face stacked orientation (this might be a self-organizing molecular material). If CT is the major factor governing the π-π interaction, then we should make one π-electron system a good electron donor and the other a good electron acceptor. On the other hand, if electrostatics dominate, then we should use two π systems with a very low π-electron density to minimize unfavorable interactions between the two closely approaching π-electron clouds (Fig. 1).[4] Perhaps tetracyanoquinodimethane (TCNQ) would be good!

Diederich et al. have carried out extensive investigations of π-π interactions in host–guest complexes between cyclophanes and aromatic compounds.[5, 6] This work has established the role played by the solvent. The association constants are up to 10^6 times larger in polar solvents like water than in nonpolar solvents like Me_2S. The strength of the interaction varies uniformly with solvent polarity and correlates well with the empirical $E_T(30)$ parameter.[5] Diederich et al. have also investigated the effect of polarizing

[*] Dr. C. A. Hunter
Department of Chemistry, University of Sheffield
GB-Sheffield S3 7HF (UK)
Telefax: Int. code + (742)738673

[**] The term used in this article is π-π interaction. This is intended as a shorthand for noncovalent interactions between π systems. It does not imply anything about the nature of the interaction.

substituents. The π-π interactions are most favorable for guest compounds with electron withdrawing (acceptor) substituents, and as the host π systems have electron donating (donor) substituents, this was taken as evidence in favor of the EDA model.[6] However, the results can also be rationalized by using an electrostatic model.[4]

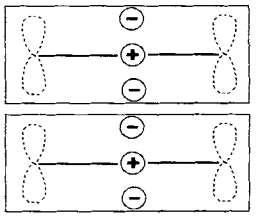

Fig. 1. A schematic representation of the charge distribution for two π systems stacked in a face-to-face orientation. There are repulsive electrostatic interactions associated with the out-of-plane π-electron density (the closest approaching charges are the negative π-electron charges). The interaction will be sensitive to substituents which change the π-electron density [4].

Flexible molecular clefts studied by Hamilton et al. provide evidence that electrostatic effects play a major role in determining the orientation of π-π interactions.[7] Hunter and Sanders have shown that the geometry of π-stacking interactions between porphyrins can be explained on the basis of electrostatic interactions involving the out-of-plane π-electron density.[4] They have used these results to develop a general model for π-π interactions based on electrostatics. A recent report by Zhang and Moore also suggests that electrostatic interactions involving the out-of-plane π-electron density may be more important than CT or EDA effects.[8]

Despite extensive literature on π-π interactions, there has not been a systematic experimental study of a simple aromatic system that has unambiguously established the relative importance of all of the contributions previously mentioned. One problem with carrying out such a study is that noncovalent interactions between small aromatic molecules are relatively weak and are highly sensitive to orientation. In order to carry out a systematic investigation, the two interacting partners must be forced together in a fixed orientation so that a change in the strength of the interaction will not lead to a change in geometry.

Cozzi, Siegel et al. have come up with a very simple and elegant way of doing this (Fig. 2).[1, 2] Naphthalene is used as

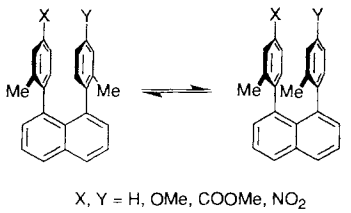

Fig. 2. Cozzi, Siegel et al. have used the energy barrier to this restricted rotation process to investigate substituent effects on π-π interactions between the two aromatic rings which are held in a face-to-face orientation [1, 2].

a covalent scaffold to hold two interacting aromatic rings in a face-to-face stacked geometry. The relative strengths of different π-π interactions are then estimated by measuring the energy barrier to the conformational exchange process shown in Figure 2. The methyl groups act as markers so that the restricted rotation can be monitored by NMR spectroscopy. The observed barrier to rotation depends markedly on the nature of the X and Y groups which polarize the π systems. The authors claim that these differences are a direct measure of the relative magnitudes of the π-π interaction energies between the aromatic rings in the ground state stacked orientation.

There are two important assumptions. The naphthalene bridge forces the interacting π systems very close together, so that the spacing of the carbon atoms connected to the *peri*-positions of the naphthalene framework is 2.8 Å, well within their van der Waals contact distance (3.4 Å). The distance dependence of electrostatic interactions between π systems varies between r^{-1} and r^{-5}, whereas orbital interactions vary as e^{-r}.[9] Thus the enforced proximity should exaggerate any CT effects over electrostatics. The second assumption is that the π-π interactions in the transition state do not depend strongly on X and Y. This would be true if orbital interactions such as CT were important but does not necessarily hold if electrostatics dominate. These limitations restrict the generality of the approach but still allow a clear experimental test of whether electrostatics or CT determines the properties of noncovalent interactions between stacked π systems.

The results suggest that it is the electrostatic interactions associated with the out-of-plane π-electron density which are the dominant factor controlling the magnitudes of the π-π interactions. The most favorable interaction is found when X and Y are both strongly electron-withdrawing: the π-electron density on the aromatic rings is lowest for these systems and therefore the π-electron repulsion is correspondingly small (Fig. 1). The least favorable interaction is found when X and Y are both strongly electron-donating: the π-electron density on the aromatic rings is highest for these systems and therefore the π-electron repulsion is correspondingly large. When X is electron donating and Y is electron withdrawing, the interaction energy lies in between these two extremes. If CT or EDA effects were significant, these systems should show the most favorable interactions. This is clearly not the case. Indeed, when the results are plotted against Hammett σ values, a straight line correlation is obtained. In other words, the only significant factor affecting the π-π interactions is the electrostatics which depend on the molecular charge distributions and π-electron density on the aromatic rings. Charge transfer effects are negligible.

Recent studies by Schwabacher et al.[10] on noncovalent interactions between charges and aromatic molecules show that electrostatic effects dominate in these systems as well. The edges of aromatic rings interact more favorably with negatively charged groups than with positively charged groups.

These experiments represent an important development in our understanding of weak intermolecular forces. They show that simple electrostatic models which allow for out-of-plane π-electron density are sufficient to explain the properties of noncovalent interactions between aromatic molecules. This provides us with a theoretical framework for modeling and interpreting these phenomena and a set of guidelines for use in molecular design. There are implications in several areas. Interactions between aromatic molecules play a role in

protein structure,[11] they determine the sequence-dependent structure of DNA,[9] and they control many molecular recognition and self-assembly processes in solution and in the solid state.[12]

German version: *Angew. Chem.* **1993**, *105*, 1653

[1] F. Cozzi, M. Cinquini, R. Annuziata, T. Dwyer, J. S. Siegel, *J. Am. Chem. Soc.* **1992**, *114*, 5729-5733.
[2] F. Cozzi, M. Cinquini, R. Annuziata, J. S. Siegel, *J. Am. Chem. Soc.* **1993**, *115*, 5330-5331.
[3] M. Rigby, E. B. Smith, W. A. Wakeham, G. C. Maitland, *The Forces Between Molecules*, Clarendon, Oxford, **1986**.
[4] C. A. Hunter, J. K. M. Sanders, *J. Am. Chem. Soc.* **1990**, *112*, 5525-5534.
[5] D. B. Smithrud, F. Diederich, *J. Am. Chem. Soc.* **1990**, *112*, 339-343.
[6] S. B. Ferguson, E. M. Sanford, E. M. Seward, F. Diederich, *J. Am. Chem. Soc.* **1991**, *113*, 5410-5419.
[7] A. V. Muehldorf, D. Van Engen, J. C. Warner, A. D. Hamilton, *J. Am. Chem. Soc.* **1988**, *110*, 6561-6562.
[8] J. Zhang, J. S. Moore, *J. Am. Chem. Soc.* **1992**, *114*, 9701-9702.
[9] C. A. Hunter, *J. Mol. Biol.* **1993**, *230*, 1025-1054.
[10] A. W. Schwabacher, S. Zhang, W. Davy, *J. Am. Chem. Soc.* **1993**, *115*, 6995-6996.
[11] S. K. Burley, G. A. Petsko, *J. Am. Chem. Soc.* **1986**, *108*, 7995-8001; C. A. Hunter, J. Singh, J. M. Thornton, *J. Mol. Biol.* **1991**, *218*, 837-846.
[12] J. F. Stoddart, *Chem. Br.* **1991**, 714-718.

 © *VCH Verlagsgesellschaft mbH, D-69451 Weinheim, 1993* *0570-0833/93/1111-1586 $ 10.00+.25/0*

Communications may be submitted in English *or* in German. Further details regarding the submission of communications can be found in the "Notice to Authors" reproduced in the January issue of the journal. Copies thereof may be obtained from the editorial office upon request.

Gas/Solid Reactions of Aliphatic Amines with Thiohydantoins: Atomic Force Microscopy and New Mechanisms**

By *Gerd Kaupp** and *Jens Schmeyers*

Gas/solid reactions involving simple aliphatic amines and ammonia are not only of interest in synthetic chemistry but could also help to reduce the undesirable introduction of ammonium compounds into woodland, which causes excessive fertilizing and thus contributes predominantly to the new type of forest damage.[1] We report here on the first reactions of thiohydantoins with gaseous amines and on atomic force microscopy (AFM) measurements from which new mechanisms for solid-phase rebuilding can be identified and explanations on the molecular level can be deduced.

Crystalline thiohydantoins **1** with at least one H substituent at position 5 react quantitatively with gaseous methylamine **2a** or dimethylamine **2b** with cleavage of the 3–4 bond to yield crystalline compounds **3** (Scheme 1).

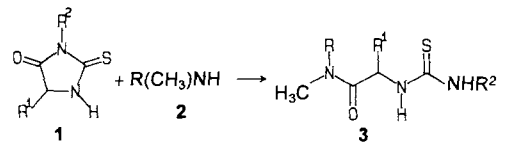

1 + $R(CH_3)NH$ (**2**) → **3**

3a: $R^1=R^2=R=H$
b: $R^1=R^2=H$, $R=CH_3$
c: $R^1=R=H$, $R^2=Ph$
d: $R^1=H$, $R^2=Ph$, $R=CH_3$
e: $R^1=CH_2Ph$, $R^2=R=H$
f: $R^1=CH_2Ph$, $R^2=H$, $R=CH_3$

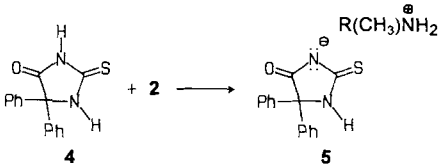

4 + **2** → **5**

Scheme 1. **1a**, $R^1=R^2=H$; **1b**, $R^1=H$, $R^2=Ph$; **1c**, $R^1=CH_2Ph$, $R^2=H$; **2a**, **5a**, $R=H$; **2b**, **5b**, $R=CH_3$.

[*] Prof. Dr. G. Kaupp, Dipl.-Chem. J. Schmeyers
FB 9 – Organische Chemie I der Universität
Postfach 2503, D-26111 Oldenburg (FRG)
Telefax: Int. code + (441)798-3409

[**] This work was supported by the Fonds der Chemischen Industrie. We would like to thank Prof. Dr. N. Karl and Dr. M. Möbus, Universität Stuttgart, as well as Dipl.-Chem. W. Saak for the determination of the Miller indices of the crystal surfaces, and BASF AG, Ludwigshafen, for supplying gaseous amines.

There are no indications for competing processes involving cleavage of the "thiourea" bonds 1–2 and 2–3. This remarkable selectivity even in the case of **1b** is substantiated by the spectra (in particular ^{13}C NMR and MS) of the uniform derivatives **3**. This is all the more surprising, as 5,5-diphenylthiohydantoin **4** does not undergo ring opening in gas/solid reactions with **2**, but instead forms quantitatively the salts **5**. Since the five-membered ring of these salts does not open even in solution (CH_3OH, [D$_6$]DMSO), it appears that the fact that **4** is more acidic than **1** is the determining factor for the reactivity (according to semiempirical PM3 calculations the deprotonation of **1a** is 1.7 kcal mol^{-1} less favorable than that of **4**). Calculations show that the significantly higher dipole moment of the anion in **5** (14.4 D) compared to the anion of **1a** (deprotonation at N3, $\mu = 6.5$ D) could lead to an additional gain in lattice energy in the salts **5**.

Neither **1** nor **4** reacts with the less nucleophilic and less basic ammonia. Up to now, ammonia can only be caused to undergo the gas/solid reaction with crystalline acids or hydrolysis-sensitive anhydrides.[2] The compounds **3**[3] are the easiest to obtain, whereas the salts **5** can *only* be prepared by the gas/solid reaction. Compound **4** has such a low acidity that **5** can be completely decomposed at room temperature in the course of one day by pumping off **2** which is released under high vacuum. Likewise, **4** can be recovered quantitatively from **5a**,**b** after dissolution in methanol or acetone and evaporation under vacuum.

The products **3** and **5** are obtained in a crystalline form without passing through a liquid phase: Powder diagrams immediately show new X-ray reflections. The true density of the crystals (DENARMAT, krypton sensor) decreases markedly with the formation of **3**, although the mass increases. This means that the volume of the crystals substantially increases during the phase rebuilding (true densities: **1a** 1.595, **3a** 1.416, **3b** 1.335, **1b** 1.376, **3c** 1.161, **3d** 1.045, **1c** 1.112, **3e** 1.053, **3f** 1.024 g cm^{-3}). The same applies to the specific surface areas: When **1a** reacts quantitatively with **2a** to yield **3a** or with **2b** to yield **3b**, the specific surface area increases by a factor of 28 from 0.0426 to 1.1914 or by a factor of 9 from 0.0426 to 0.3864 m^2 g^{-1} (2-parameter BET-analysis, DENARMAT, krypton sensor). The mechanisms of the phase rebuildings in the submicroscopic region can be determined[4, 5] by AFM, and can possibly be interpreted at a molecular level if the crystal structure of the starting material is available.[6]

Figure 1 shows remarkable differences in the reaction of methylamine **2a** on the natural face (110) and on the cleavage face (10$\bar{2}$) of **1a**, the cleavage face being inclined at 66.07° to (110). The high ridges and valleys[4] formed on (110) (also seen for **2b**) display a clear if not uniform orientation (Fig. 1b) in contrast to the "volcanos"[4] formed on (10$\bar{2}$) (Fig. 1d). The flanks of the ridges (Fig. 1b) are tilted at 26 and 41° to the mean horizontal (planefit).[7]

Particularly noteworthy is the behavior of the 9-nm-high step in Figure 1c during reaction: Despite the small height (27 molecular layers with an interlayer separation of 3.34 Å) it behaves as a crystallographic face in its own right. High ridges and valleys are formed here (inclined, of course), but without any "volcanos" as on (10$\bar{2}$). Fine details of this sort are only discernable by AFM, and allow previously unimaginable insights on the basis of the known crystal structure[8] of **1a**.

 © VCH Verlagsgesellschaft mbH, D-69451 Weinheim, 1993 0570-0833/93/1111-1587 $ 10.00+.25/0

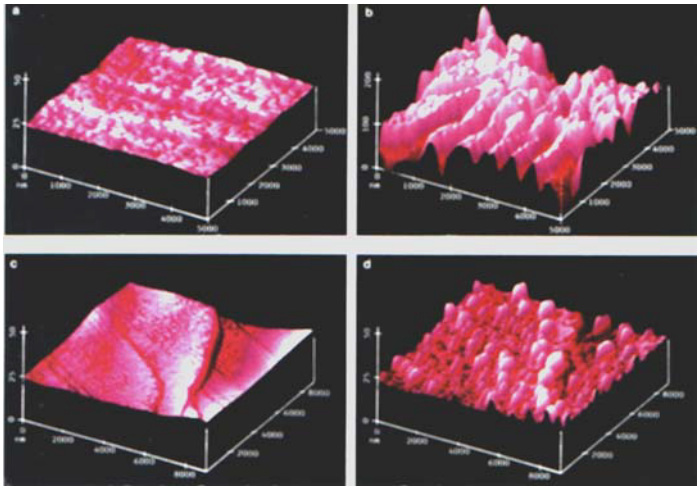

Fig. 1. AFM surfaces of **1a**. a) (110) fresh, b) (110) after a second treatment with gaseous **2a**, c) (10$\bar{2}$) before reaction, d) (10$\bar{2}$) after a second treatment with gaseous **2a**.

Figure 2 shows the layers of molecules of **1a** ($P2_1/c$) on the (110) and (10$\bar{2}$) faces. A steep layer (66°) of molecules on (110) and an almost parallel layer on (10$\bar{2}$) can be recognized. There is formation of hydrogen-bonded dimers (3-NH/4′-CO + 3′NH/4-CO). Clearly, the volume increase upon reaction on (110) causes growth in height along the cleavage face inclined at 66.07° (there are no H bonds between the layers). The finer structures on the high ridges are formed in the early stages of the reaction (not shown), but without lateral orientation. On the (10$\bar{2}$) face, the molecules of **1a** lie flat. From this position the volcano-type mounds rise continually upwards (they are approximately half as high in the early stage of the reaction (not illustrated)). Since the molecules which lie flat penetrate at a steep angle through the surface at the step in Figure 1c, it is understandable that behavior similar to that on (110) is observed, even though there are only 27 layers of molecules present.

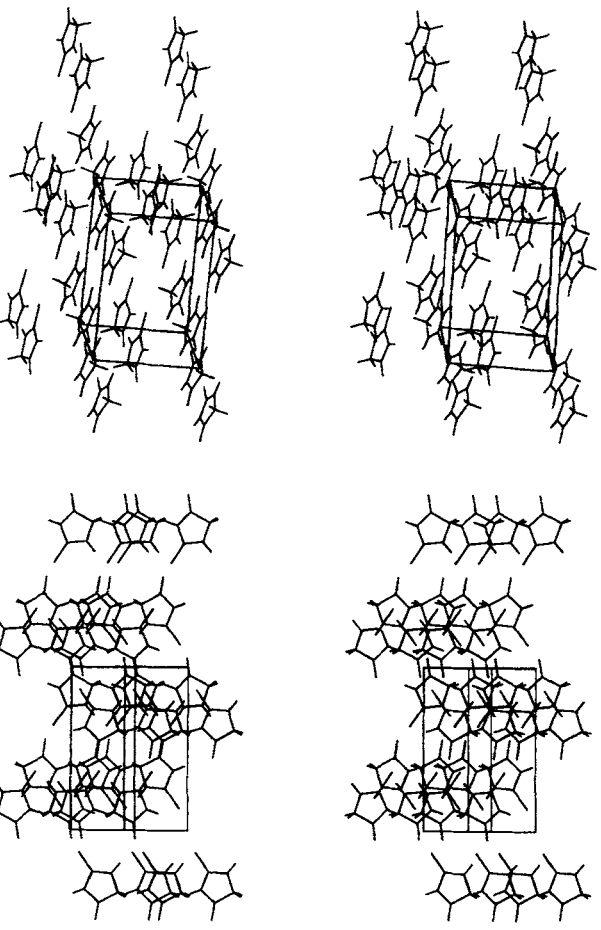

Fig. 2. Stereorepresentation of the molecular layer of **1a**. Top: view of (110); bottom: view of (10$\bar{2}$).

In the reaction with **2a**, the morphologically dominant face (10$\bar{3}$) of **1b** (platelike crystals, $P2_1/c$[9]) behaves completely differently to that of **1a**. Here, a hitherto unobserved[4, 5] *island mechanism* occurs in the phase rebuilding. The smooth surface with sharp-edged steps (Fig. 3a) does not react uniformly, but rather by the formation of widely spaced islands comprising a circular trench enclosing hills, which may surpass the 16 nm step (20 molecular layers high). The islands grow concentrically outward from smaller circular walls initially without any inner elevations, until they touch one another and merge together. Figure 3b shows several stages in the development process side by side. The reaction of **1b** with **2a** is consequently hindered. Information about this hindered reaction can actually be deduced from the crystal structure of **1b**.

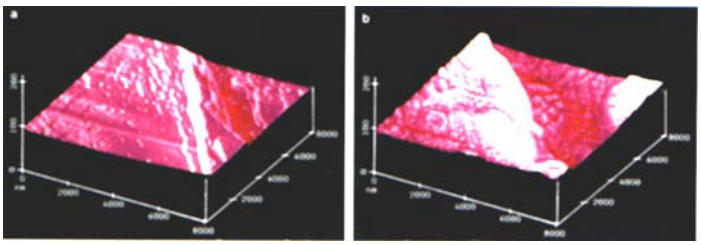

Fig. 3. AFM surfaces of **1b**. a) (10$\bar{3}$) fresh, b) (10$\bar{3}$) after a second treatment with gaseous **2a**.

Figure 4 shows a stereorepresentation of the (10$\bar{3}$) surface of **1b**.[10] The reacting amide bond never points forward, but is effectively shielded from the upward pointing methylene groups and the neighboring phenyl groups. Thus, the approach of the gas **2a** is sterically hindered, since the OC–N bond which is broken on addition of the amine lies underneath. Clearly, the chemical phase rebuilding occurring dur-

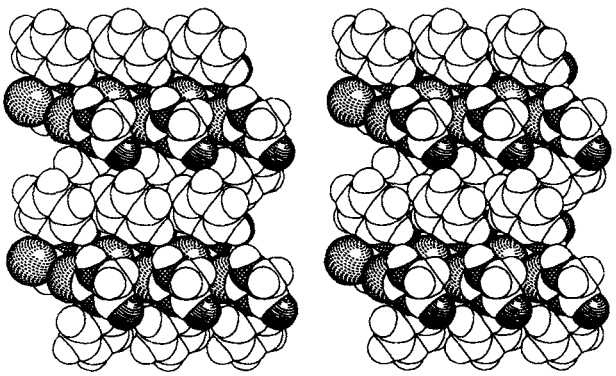

Fig. 4. Stereorepresentation of the molecular layers of **1b** on (10$\bar{3}$) using a space-filling representation to estimate the steric hindrance during the attack of a gaseous reagent on the amide bond (O: circles, N: grids, S: hatched circles).

ing the volume expansion after nucleation does not progress zonally as previously described for different reactions,[4] but rather concentrically, as long as a gas supply is available. On the inside of the wall, where the surface structure is broken up, the amine **2a** obviously has an easier route to reaction. The effects of the crystal structure on the chemical reactivity are clearly discernible. The product must rise up above the original level, as is shown in Figure 3b.

Compound **1c** behaves differently again on reaction with **2a** (morphologically dominant plane, small plates). Well-developed "volcanos"[4] of considerable height with a surrounding groove (Figs. **5a, b**) form out of the very smooth surface. A lack of crystal data means that a molecular interpretation is not possible here, however, it has been demonstrated once more just how important phase-reorganization processes[4] are in gas/solid reactions.

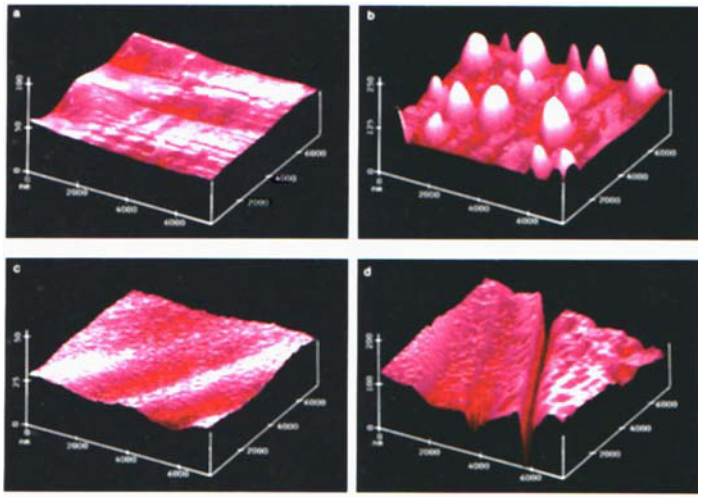

Fig. 5. Top: AFM surfaces of **1c**. a) fresh, b) after a short reaction period with gaseous **2a**. Bottom: AFM surfaces of **4**. c) fresh, d) after a second treatment with gaseous **2a**.

When studied by using AFM, the reaction of **4** with **2a** exhibits a dual mechanism. Initially craters up to 6 nm deep form on the slightly puckered, faintly undulated surface (Fig. 5c). After repeated treatment with **2a** these become only marginally deeper (7 nm), but the surface develops in addition to that deep, parallel trenches (inclination of the flanks: 22 and 32°). Figure 5d shows an already very deep channel as well as further trench formation on both sides. The ditches do not progress along the original undulations, but at an angle of approximately 55° to them. This leads once again to profound material rearrangements.

The reactions presented here indicate how free amines can be absorbed out of the gas phase without the use of solvents, through the formation of the compounds **3**, which are interesting synthetic building blocks. AFM measurements of chemical transformations have only just recently been possible.[4, 5] They provide unparalleled resolution and create the basis for the understanding of the gas/solid reactivity. A seventh mechanism for the requisite solid–phase rebuilding involving island formation has been identified and interpreted in molecular terms (for the first six mechanisms see [4, 5]).

Experimental Procedure

Thiohydantoin (2 mmol) was treated at room temperature in an evacuated 500 mL flask through a vacuum line with gaseous **2** (1 bar). After the mixture had been left to stand for about 12 hours the excess gas was pumped off. The weight increase in each case corresponded to the uptake of 1 mol equivalent of the gas **2**.

3a [3]: M.p. 157 °C (EtOH); ^{13}C NMR ([D$_6$]DMSO, in parentheses Specinfo-simulation): δ = 183.36 (173.1), 169.23 (170.8), 47.29 (48.1), 25.66 (25.8); MS (70 eV): *m/z* (%): 148 (7), 147 (100) [M^+], 130 (14), 117 (6), 116 (44), 114 (9), 88 (12), 73 (8), 60 (35).

3d: M.p. 144 °C (EtOH); ^{13}C NMR ($CDCl_3$/[D$_6$]DMSO, in parentheses Specinfo-simulation): δ = 178.35 (178.1), 166.15 (168.5), 137.57 (137.0), 127.17 (129.1, 2C), 122.97 (125.2, 2C), 121.65 (125.1), 44.74 (47.4), 34.28 (35.9), 33.78 (35.9); MS (70 eV): *m/z* (%): 237 (31) [M^+], 203 (9), 192 (32), 163 (9), 136 (25), 135 (100), 131 (36), 102 (10), 93 (52), 77 (94), 72 (52).

5a: IR(KBr): $\tilde{\nu}$ = 3138 (NH), 2504, 2198, 1663 cm^{-1}; ^{13}C NMR as **4** with **2a**.

Received: May 19, 1993 [Z 6091 IE]
German version: *Angew. Chem.* **1993**, *105*, 1656

[1] H. Flaig, H. Mohr, *Physiol. Plant.* **1992**, *84*, 568–576, and references therein.
[2] R. S. Miller, D. Y. Curtin, I. C. Paul, *J. Am. Chem. Soc.* **1974**, *96*, 6340–6349; G. Kaupp, J. Schmeyers, unpublished results.
[3] **3a**: M. R. Salem, H. A. Abdel-Hamid, A. A. Shaker, *Egypt. J. Chem.* **1983**, *26*, 323–329; **3c**: M. Pavlik, I. Kluh, F. Pavlikova, S. Vasickova, V. Kostka, *Collect. Czech. Chem. Commun.* **1989**, *54*, 1940–1955.
[4] G. Kaupp, *Mol. Cryst. Liq. Cryst.* **1992**, *211*, 1–15.
[5] G. Kaupp, *Angew. Chem.* **1992**, *104*, 606–609, 609–612; *Angew. Chem. Int. Ed. Engl.* **1992**, *31*, 592–595, 595–598.
[6] G. Kaupp, *Proc. IUPAC Symp. Photochem. 14th* **1992**, 258–259; *GIT Fachz. Lab.* **1993**, *37*, 284–294; 581–586.
[7] Under the experimental conditions used in Figure 1, angles of inclination of up to 50° could be measured, since the crystal plane was tilted by several degrees to the cantilever substrate. The quality of the tips was judged and controlled under the microscope at 400 fold magnification.
[8] L. A. Walker, K. Folting, K. L. Merritt, *Acta Crystallogr. Sect. B* **1969**, *25*, 88–93.
[9] I. A. Attia, T. Glowiak, I. Z. Siemion, *Bull. Acad. Pol. Sci. Ser. Sci. Chim.* **1976**, *24*, 781–790.
[10] Schakal 92; the next molecular layer on (10$\bar{3}$) is rotated through 90° in the plane and so on; the phenyl groups on the side face (100) along the *b*-axis [010], in the layer passing through the middle of the cell point outward as do the sulfur atoms on the layer passing through the cell surface. These correspondingly hinder the attack of **2** on the amide bond. Also the sterically shielded amide bonds on the (010) face of **1b** point inward.

Highly Branched Liquid Crystalline Polymers with Chiral Terminal Groups

By *Stephan Bauer, Hartmut Fischer*, and *Helmut Ringsdorf**

In recent years an innovative field of polymer chemistry has been the synthesis of dendrimers[1, 2] and highly branched polymers.[3, 4] These macromolecules are distinguished by their three-dimensional fractal structure. Their synthesis requires monomers with an AB$_m$ functionalization. Dendrimers can be constructed in successive synthetic steps, resulting in the formation of defined, unimolecular compounds. In an alternative and easier approach hyperbranched polymers are synthesized from AB$_m$ molecules in a one-pot reaction.[3]

Thermotropic liquid crystalline (LC) polymers constructed following this principle were first described by Percec et al.[4] The approach described here is based on the consideration that branched, liquid crystalline polymers contain numerous terminal groups, which can be functionalized in a

[*] Prof. H. Ringsdorf, Dipl.-Chem. S. Bauer
Institut für Organische Chemie der Universität
J. J.-Becher-Weg 18–20, D-55099 Mainz (FRG)
Telefax: Int. code + (6131)39-3145
Dr. H. Fischer
H. H. Wills Physics Laboratory
Tyndall Avenue, Bristol, BS8 1TL (UK)

 © VCH Verlagsgesellschaft mbH, D-69451 Weinheim, 1993 0570-0833/93/1111-1589 $ 10.00+.25/0

second reaction step (Scheme 1). We have selected a chiral functional group in order to induce a cholesteric mesophase in the highly branched polymer.

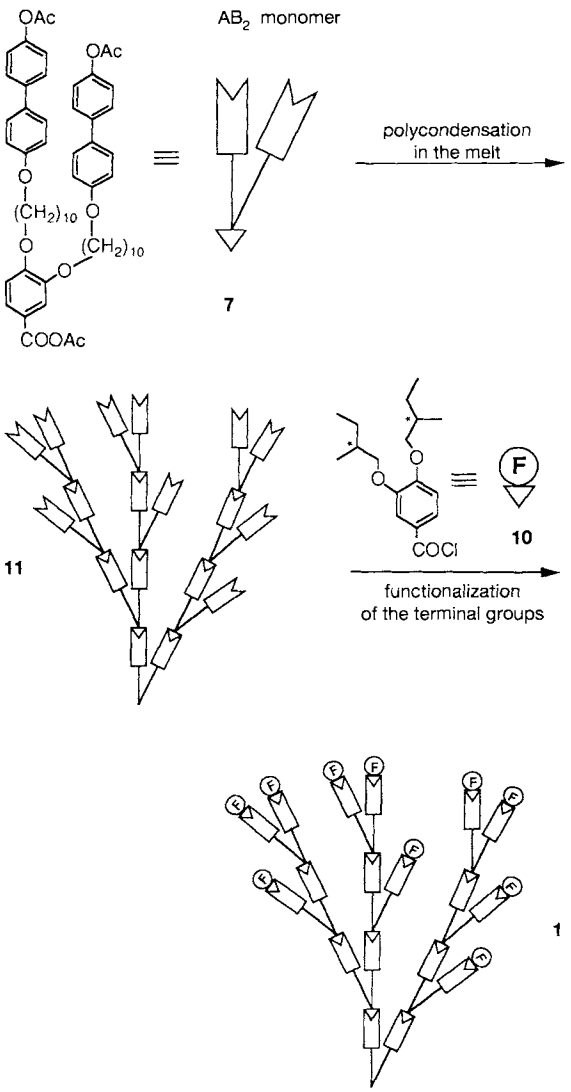

Scheme 1. Synthetic approach to polymer **1**.

The AB_2 monomer **7** chosen as the starting material consists of a mixed anhydride component and two mesogenic biphenylacetate units. The synthesis of monomer **7** and the chiral benzoyl chloride **10** is outlined in Scheme 2. Methyl 3,4-dihydroxybenzoate (**2**) was treated with excess 1,10-dibromodecane under Claisen conditions to provide ether **3**. The remaining bromine terminal groups reacted with 4-hydroxy-4′-benzyloxybiphenyl (**4**)[5] under analogous conditions yielding **5**. After cleavage of the benzyl protecting groups, ester **6** was saponified and converted into monomer **7** with acetic anhydride. In the synthesis of the chiral benzoyl chloride **10**, compound **2** was treated with 2-(*S*)-methylbutanol following the Mitsunobu method[6] to give ether **8**. Subsequent saponification and reaction with thionyl chloride provided **10**. Biphenyl benzoate mesogens linked by a spacer were then synthesized by polycondensation of the AB_2 monomer **7** in the melt (see Scheme 1). In the second reaction step, the resulting highly branched polymer **11**, with a degree of polymerization n, was then functionalized at its $(n+1)$ biphenyl acetate terminal groups by a further condensation reaction with the chiral benzoyl chloride **10**.

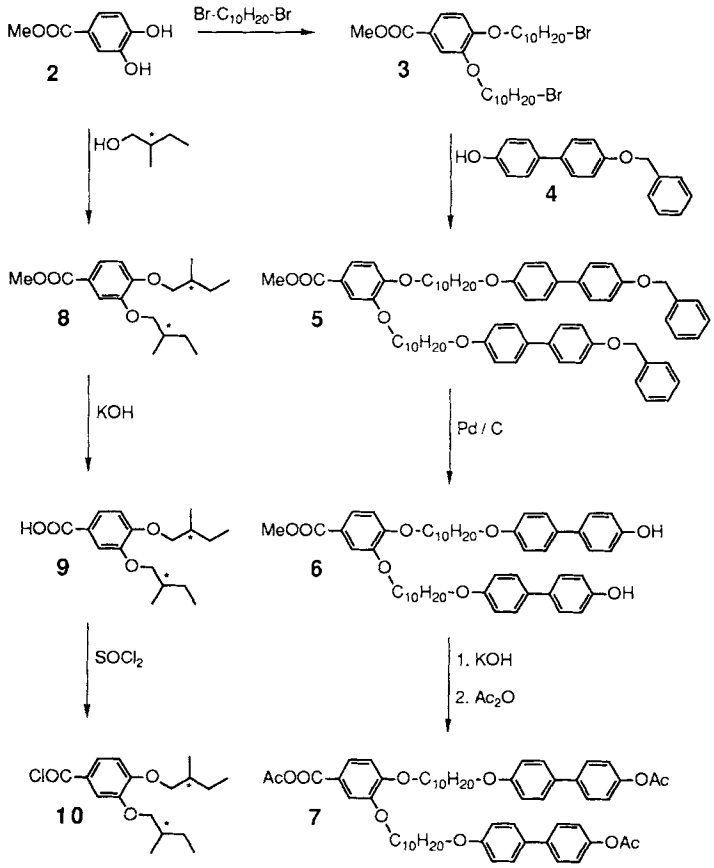

Scheme 2. Synthesis of the key components **7** and **10**.

The hyperbranched polymer thus obtained is distinguished by its good solubility, for example in chloroform, toluene, and tetrahydrofuran, and has a medium degree of polymerization ($P_n = 6$) as determined by gel permeation chromatography (GPC). The ^{1}H NMR spectrum (Fig. 1) shows the almost complete disappearance of the resonance signal of the acetate groups at $\delta = 2.3$. This proves that the coupling of the chiral carboxylic acid chloride to polymer **11** was achieved with a yield of over 95%. Polarimetric investigations verify the chirality of polymer **1**, which has an optical rotation of $[\alpha]_D^{20} = +6.8$ in dichloromethane.

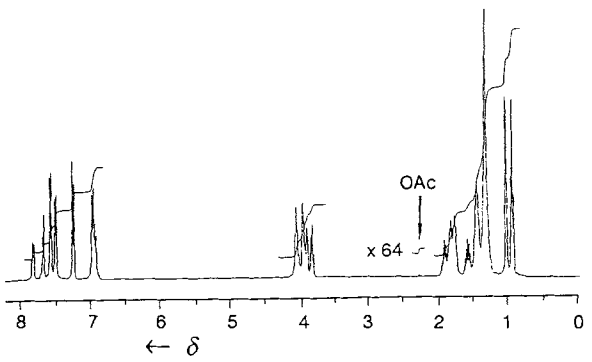

Fig. 1. ^{1}H NMR spectrum of polymer **1** ($CDCl_3$, 400 MHz). The signal indicated with OAc and an arrow is assigned to the acetate groups.

The thermal behavior of polymer **1** was characterized by polarization microscopy, differential scanning calorimetry (DSC), and X-ray scattering analysis. The DSC thermograph shows a glass transition step at 60 °C and two phase transitions at approximately 95 °C and at 151 °C in the second heating curve (Fig. 2). In the cooling curve, a phase

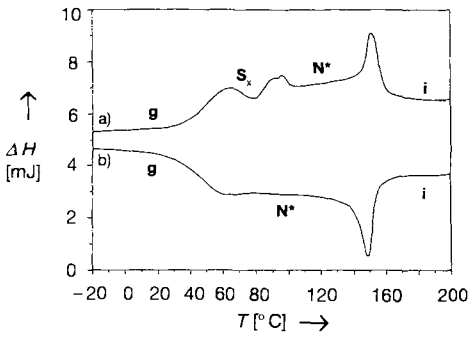

Fig. 2. DSC curve of polymer **1** (heating rate 10 K min^{-1}): a) heating curve, b) cooling curve (g = glassy, Sx = crystalline or smectic, N* = cholesteric, i = isotropic).

transition is observed only at 148 °C. Investigations of this mesophase with polarization microscopy show a typical uniform Grandjean texture,[7] which is characteristic for cholesteric phases (N*). The X-ray diffraction pattern of a fiber extruded from the polymer melt reveals a scattering diagram typical of nematic and cholesteric systems (Fig. 3).

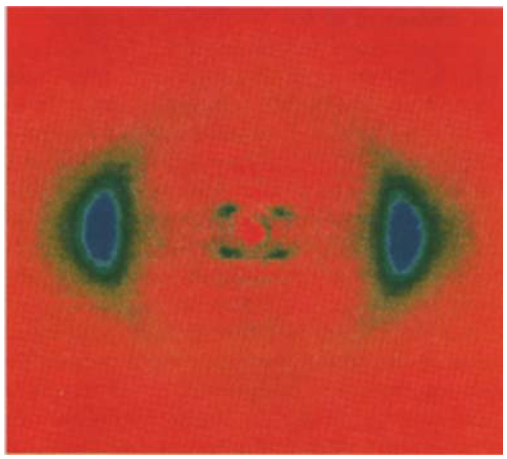

Fig. 3. X-ray diffraction pattern of polymer **1** in the cholesteric mesophase.

In the wide-angle X-ray scattering patterns a diffuse halo of high intensity is visible, which corresponds to an average distance between the mesogens of 4.4 Å. The low-intensity small-angle reflections indicates a layer structure of the cholesteric phase with a layer spacing of 28 Å. Furthermore, the small azimuthal elongation of the halo verifies that a very good unidirectional orientation was achieved during the drawing of the strand. The orientation factor $S = 0.88$ calculated from the X-ray patterns is comparable to that of main chain – side group polymers.[8] The structure of the low-temperature phase, which occurs in the heating curve between 60 and 95 °C, has not yet been elucidated. Ongoing investigations are being carried out to determine whether this is a crystalline or a smectic phase.

The introduction of functional groups in the last reaction step of the synthesis of highly branched liquid crystalline polymers opens up a large palette of possible structural variations in LC systems. Examples are the introduction of polar terminal groups for the syntheses micellar and lyotropic systems with treelike structures, and the application of these highly branched LC polymers with variable surfaces for the production of polymer blends.

Experimental Procedure

Synthesis of **7**: A mixture of **2** (10 mmol), 1,10-dibromodecane, K_2CO_3 (20 g), and KI was refluxed in anhydrous methyl propyl ketone (4 Å molecular sieves) for 24 h. After the excess dibromodecane was removed by distillation, the residue was recrystallized from acetone (yield: 92%, m.p. 30 °C). The conversion of **3** (8 mmol) into its ether derivative by treatment with **4** [5] (20 mmol) under the above conditions gave, after recrystallization in chloroform, **5** (yield: 85%, m.p. 155 °C). Compound **5** (6 mmol) was hydrogenated using Pd/C (300 mg) in methanol as catalyst, and purified by flash chromatography eluting with $CHCl_3$/MeOH 10:1 (yield: 55%, m.p. 149 °C). Ester **6** (3 mmol) was refluxed in 20 mL of EtOH/H_2O and KOH (10 mmol) for 1 h, the free acid was precipitated with 2 N HCl, dried, and refluxed in 20 mL of acetic anhydride for 20 min. The cooled reaction mixture was suction-filtered and the white precipitate recrystallized from acetone (yield: 87%, m.p. 157 °C).

7: ^{1}H NMR (200 MHz, $CDCl_3$): δ = 7.65 (d, 1H, $H_{Ph}6$), 7.48 (m, 9H, $H_{Ph}2$, $H_{biph}2$, 6, 2′, 6′), 7.10, 6.93 (2d, 8H, $H_{biph}3$, 5, 3′, 5′), 6.86 (d, 1H, $H_{Ph}5$), 3.99 (m, 8H, OCH_2), 2.34 (s, 3H, CO-O-CO-CH_3), 2.30 (s, 6H, -O-CO-CH_3), 1.78 (m, 8H, O-CH_2-CH_2), 1.5-1.2 (m, 24H, CH_2); ^{13}C NMR: (50 MHz, $CDCl_3$): δ = 169.6, 162.1, 158.7, 154.6, 149.5, 148.7, 138.6, 132.6, 128.0, 127.6, 125.0, 121.7, 120.3, 114.7, 114.6, 111.7, 69.2, 69.0, 68.0, 29.5, 29.4, 29.3, 29.0, 28.9, 26.0, 25.9, 22.3, 21.1; FD-MS: *m/z* (%) 929.2 (100), [M^+].

Synthesis of **10**: Diethyl azodicarboxylate (25 mmol) was added dropwise to a solution of **2** (10 mmol), triphenylphosphine (25 mmol), and 2-(*S*)-methylbutanol in 200 mL of anhydrous tetrahydrofuran at 0 °C and stirred at room temperature for ca. 15 h. After filtration, the solvent was distilled off and the residue purified by flash chromatography eluting with petroleum ether/acetic acid 10:1 (yield 25%, colorless oily product). Compound **8** was saponified under the previously described conditions (yield: 95%, m.p. 108 °C). The resulting acid **9** (1.5 mmol) was stirred with thionyl chloride (3 mmol), catalytic amounts of DMF, and 20 mL of benzene for ca. 15 h, freeze-dried, and used immediately in the subsequent reaction.

9: ^{1}H NMR (200 MHz, $CDCl_3$): δ = 7.70(d, 1H, $H_{Ph}6$), 7.56 (s, 1H, $H_{Ph}2$), 6.87 (d, 1H, $H_{Ph}5$), 3.85 (m, 4H, OCH_2), 1.91 (m, 2H, O-CH_2-CH), 1.58, 1.25 (2m, 4H, CH_2-CH_3), 0.99 (d, 3H, CH_3), 0.90 (t, 6H, CH_2-CH_3); FD-MS: *m/z* (%) 293.6 (100), [M^+]; $[\alpha]_D^{20}$ = +14.1 (c = 1 in CH_2Cl_2).

Synthesis of **1**: Monomer **7** (1 mmol) and *p*-toluenesulfonic acid (0.05 mmol) were stirred under vacuum at 240 °C for 8 h. The chiral benzoyl chloride **10** (1.2 mmol) and *p*-toluenesulfonic acid (0.05 mmol) were added to the cooled reaction mixture, which was then heated to 200 °C in an atmosphere of argon for 1 h. The pressure was then slowly reduced to 10^{-6} mbar. The resulting polymer was dissolved in chloroform and precipitated in methanol (yield: 89%).

1: ^{1}H NMR (200 MHz, $CDCl_3$): δ = 7.80 (d, $H_{Ph}6$), 7.64 (s, $H_{Ph}2$), 7.55, 7.48 (2d, $H_{biph}2$, 6, 2′, 6′), 7.21, 6.93 (2d, $H_{biph}3$, 5, 3′, 5′), 6.88 (d, 1H, $H_{Ph}5$), 4.1-3.8 (m, OCH_2), 2.0-1.7 (m, O-CH_2-CH_2, O-CH_2-CH), 1.7-1.2 (m, CH_2), 0.99 (d, CH_3), 0.90 (t, CH_2-CH_3); ^{13}C NMR (100 MHz, $CDCl_3$): δ = 165.1, 158.8, 154.2, 153.9, 150.1, 149.2, 148.7, 138.5, 132.8, 128.1, 127.6, 124.4, 124.3, 122.0, 121.7, 121.6, 115.6, 114.8, 114.7, 112.0, 103.8, 74.1, 73.8, 69.4, 69.1, 68.1, 34.9, 34.8, 29.5, 29.4, 29.3, 29.2, 29.1, 26.2, 26.1, 26.0, 25.9, 16.6, 16.5, 11.3; $[\alpha]_D^{20}$ = +6.8 (c = 1 in CH_2Cl_2); GPC ($CHCl_3$, polystyrene standard): M_w: 20000, M_n: 6500 g mol^{-1}.

Received: July 7, 1993 [Z 6195 IE]
German version: *Angew. Chem.* **1993**, *105*, 1658

[1] Reviews: a) D. A. Tomalia, A. M. Naylor, W. A. Goddard III, *Angew. Chem.* **1990**, *102*, 119; *Angew. Chem. Int. Ed. Engl.* **1990**, *29*, 138; b) H.-B. Mekelburger, W. Jaworek, F. Vögtle, *ibid.* **1992**, *104*, 1609 and **1992**, *31*, 1571.

[2] Dendrimers: a) C. J. Hawker, J. M. J. Fréchet, *Macromolecules* **1990**, *23*, 4726; b) J. S. Moore, Z. Xu, *ibid.* **1991**, *24*, 5893; c) T. M. Miller, E. W. Kwock, T. X. Neenan, *ibid.* **1992**, *25*, 3143; d) L.-L. Zhou, J. Roovers, *ibid.* **1993**, *26*, 963; e) K. L. Wooley, C. J. Hawker, J. M. Pochan, J. M. J. Fréchet, *ibid.* **1993**, *26*, 1514; f) G. R. Newkome, C. N. Moorefield, G. R. Baker, A. L. Johnson, R. K. Behera, *Angew. Chem.* **1991**, *103*, 1205; *Angew. Chem. Int. Ed. Engl.* **1991**, *30*, 1176; g) G. R. Newkome, C. N. Moorefield, G. R.

 © VCH Verlagsgesellschaft mbH, D-69451 Weinheim, 1993 0570-0833/93/1111-1591 $ 10.00+.25/0

Baker, R. K. Behera, G. H. Escamillia, *ibid.* **1992**, *104*, 901 and **1992**, *31*, 917; h) F. Moulines, B. Gloaguen, D. Astruc, *ibid.* **1992**, *104*, 452 and **1992**, *31*, 458; i) S. Serroni, G. Denti, S. Campagna, A. Juris, M. Ciano, V. Balzani, *ibid.* **1992**, *104*, 1540 and **1992**, *31*, 1491; j) C. J. Hawker, J. M. J. Fréchet, *J. Am. Chem. Soc.* **1992**, *114*, 8405; k) T. M. Miller, T. X. Neenan, R. Zayas, H. E. Bair, *ibid.* **1992**, *114*, 1018.

[3] Highly branched polymers: a) P. J. Flory, *J. Am. Chem. Soc.* **1954**, *74*, 2718; b) Y. H. Kim, O. W. Webster, *ibid.* **1990**, *112*, 4592; c) L. J. Mathias, T. W. Carothers, *ibid.* **1991**, *113*, 4043; d) C. J. Hawker, J. M. J. Fréchet, *ibid.* **1991**, *113*, 4583; e) K. E. Uhrich, C. J. Hawker, J. M. J. Fréchet, *Polym. Mater. Sci. Eng.* **1991**, *65*, 137; f) K. E. Uhrich, C. J. Hawker, J. M. J. Fréchet, S. R. Turner, *Macromolecules* **1992**, *25*, 4583; g) Y. H. Kim, O. W. Webster, *ibid.* **1992**, *25*, 5561. h) B. I. Voit, S. R. Turner, *Polym. Prepr.* **1992**, *33*(1), 184; i) F. Walter, S. R. Turner, B. I. Voit, *ibid.* **1993**, *34*(1), 79.

[4] Highly branched LC polymers: a) V. Percec, M. Kawasumi, *Macromolecules* **1992**, *25*, 1164; b) V. Percec, C. G. Cho, C. Pugh, D. Tomazos, *ibid.* **1993**, *26*, 963; c) Y. H. Kim, *J. Am. Chem. Soc.* **1992**, *114*, 4947.

[5] H. Kapitza, R. Zentel, *Makromol. Chem.* **1991**, *192*, 1859.

[6] O. Mitsunobu, *Synthesis* **1988**, 1.

[7] D. Demus, L. Richter, *Textures of Liquid Crystals*, Verlag Chemie, Weinheim, **1978**.

[8] B. W. Enders, M. Ebert, J. H. Wendorff, R. Reck, H. Ringsdorf, *Liq. Cryst.* **1990**, *7*, 217.

Refinement of a Model for the Nitrogenase Mo–Fe Cluster Using Single-Crystal Mo and Fe EXAFS**

By *Jie Chen, Jason Christiansen, Nino Campobasso, Jeffrey T. Bolin, Roland C. Tittsworth, Brian J. Hales, John J. Rehr*, and *Stephen P. Cramer**

The enzyme nitrogenase catalyzes the reduction of dinitrogen to ammonia.[1] Substrate conversion is thought to occur at the M clusters, which are two $MoFe_7S_9$ clusters embedded in the α subunits of the $\alpha_2\beta_2$ MoFe protein (M_r = 220000).[2] Each M cluster presumably receives electrons from a companion P cluster, an Fe_8S_8 structure located at the interface between the α and β subunit. Accurate dimensions for these clusters are important for synthetic modeling, for theoretical studies, and for the observation of possible structural changes during the catalytic cycle. The structures for MoFe proteins Cp1 and Av1 from *C. pasteurianum*[3] and *A. vinelandii*[4] respectively, are being determined by X-ray diffraction with increasing accuracy, and models for the structures of the M cluster and P cluster have been presented. However, given the limited resolution of the diffraction data (2.2 Å), it is likely that the root mean square error in the atomic positions of these models is on the order of 0.2–0.3 Å, and errors in the interatomic distances are somewhat larger. Since changes of metal–metal distances of even 0.1 Å are chemically significant, more accurate cluster dimensions are important. Now that the construction of the cluster frameworks has been established by the X-ray diffraction experiments, greatly improved metric information can be obtained from solution and especially single-crystal EXAFS spectra.

We report here the first single-crystal Fe and Mo EXAFS spectra of nitrogenase at low temperature. A new Mo–Fe component at approximately 5 Å was observed along with seven other distances between metal atoms and neighboring atoms. These data were combined with that from previous solution Fe EXAFS[5] and a new solution Mo EXAFS to refine the current model for the M cluster. The model is compared with a current electron density map for the protein from *C. pasteurianum* having a 2.3 Å resolution.[3] Although the spectroscopic results are qualitatively in complete agreement with the Kim and Rees model for the M cluster, some average distances differ by roughly 0.2 Å. The EXAFS results also suggest less variation in individual Fe–Fe and Mo–Fe distances than seen in the Kim and Rees model; in other words, the Mo–Fe cluster is more symmetrical.

Fourier transforms of the Mo and Fe K edge EXAFS for a solution of Av1, a single crystal of Cp1, and the capped-prismane model complex $(Et_4N)_3[Fe_6S_6Cl_6\{Mo(CO)_3\}_2]$[6] are shown in Figure 1. The transform of the model complex shows the expected first-shell Mo–C, Mo–S, and Mo–Fe distances (2.0, 2.6, and 2.9 Å, respectively) as well as a long-range Mo–Fe interaction at 4.28 Å. Buried under the shorter Mo–Fe component is a multiple-scattering contribution from a Mo-C-O interaction. Fitting the EXAFS yields distances within 0.05 Å of the values obtained by X-ray crystallography[6] (Table 1).

The Fourier transform of the Mo EXAFS spectrum of Av1 in solution exhibits two main peaks, which fit (Fig. 1) as Mo–S and Mo–Fe interactions at 2.37 and 2.70 Å, along with an unresolved Mo–O,N component at 2.20 Å (Table 1). The Mo–S and Mo–Fe distances, like those from previous EXAFS studies,[7–9] are clearly shorter than the corresponding distances in both the capped-prismane model and the respective average distances of 2.46 and 2.92 Å in the Kim and Rees model of the M cluster. As shown in Figure 1, the Mo EXAFS spectrum generated from the distances obtained by X-ray diffraction has different frequencies and beats (because of different distances) and damps out more rapidly (because of the greater spread in the distances between Mo and neighboring atoms). In the 3–5 Å region of the Fourier transform, a number of smaller peaks are observed, which may arise from interactions of C atoms of homocitrate and histidine ligand with Mo, as well as Fourier transform truncation ripple. We do not interpret these features at this time. There is also a modest peak at approximately 5 Å, where a second Mo–Fe interaction is expected. However, the feature is quite weak, and numerous other interactions might occur at such a distance.

We have used single-crystal EXAFS to enhance this signal at 5 Å and confirm the Mo–Fe assignment. The strength of specific metal–neighbor EXAFS components varies by $\cos^2\theta$, where θ is the angle between the photon polarization vector **E** and the metal–metal vector.[9] Although there are four M centers in the unit cell, their long axes tend to lie near the bc^* plane, as shown in Figure 1. Furthermore, the longer Mo–Fe vectors form an angle of only about 15° ($\cos^2 15° = 0.93$) with the approximately threefold symmetry axes.[3] Thus, by orienting a crystal with the **E** vector parallel to the

[*] Prof. S. P. Cramer
Department of Applied Science
University of California, Davis, CA 95616 (USA)
Telefax: Int. code + (916)752-2444
and
Energy and Environment Division, Lawrence Berkeley Laboratory
J. Chen, J. Christiansen
Department of Applied Science, University of California, Davis
N. Campobasso, J. T. Bolin
Biology Department, Purdue University
R. C. Tittsworth, B. J. Hales
Department of Chemistry, Louisiana State University
J. J. Rehr
Department of Physics, University of Washington

[**] This work was supported by the Department of Agriculture through grants 91-37305-6514 (to S. P. C.) and 91-37305-6661 (to J. T. B.), the National Institutes of Health through GM-33965 (to B. J. H.), and the Department of Energy, Office of Health and Environmental Research. We thank Prof. D. Coucouvanis (University of Michigan) for model compounds and M. Newville (University of Washington) for EXAFS analysis software. Stanford Synchrotron Radiation Laboratory (SSRL) and National Synchrotron Light Source (NSLS) are supported by the Department of Energy, Office of Basic Energy Science.—EXAFS = Extended X-ray Absorption Fine Structure.

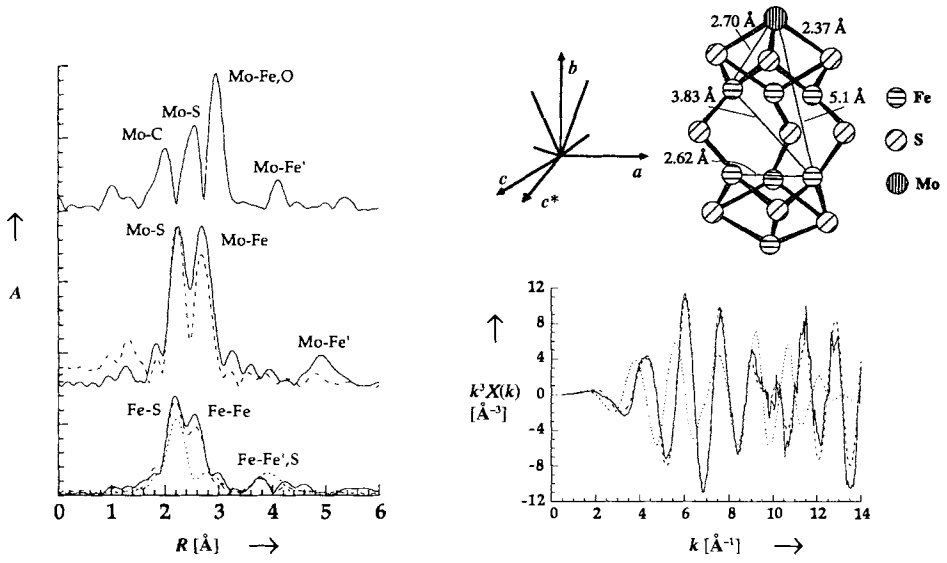

Fig. 1. Left: phase-corrected Fourier transforms (top) of the k^3 Mo EXAFS spectrum for $(Et_4N)_3[Fe_6S_6Cl_6\{Mo(CO)_3\}_2]$; Fourier transforms of the Mo (middle) and Fe EXAFS spectra (bottom) for the MoFe proteins Av1 (solution, - - -) and Cp1 (crystal, ——). Right: top: approximate orientation of the threefold symmetry axes in the M clusters of the unit cell of the MoFe protein and an assignment of EXAFS distances in the M cluster; bottom: experimental (-) and fitted (- - -) EXAFS spectra of the Mo K edge for the MoFe protein in solution. The Mo EXAFS spectrum (right bottom: dotted line) and Fourier transform of the Fe EXAFS spectrum (left bottom: dotted line) generated from crystallographic models having 2.2 Å resolution are also shown for comparison. A = amplitude.

b axis in the bc^* plane, the amplitude of the interaction at approximately 5 Å should be enhanced. In fact, a nearly twofold increase is observed (Table 1 and Fig. 1). Fourier-filtering and fitting this peak yields a good fit for several Mo–Fe interactions at 5.1 Å, close to the value of 5.2 Å obtained by X-ray crystallography. The Mo–Fe interaction at 2.7 Å also gets stronger in this orientation, while the intensity of the Mo–S signal is isotropic, consistent with three Mo–S bonds at nearly right angles to each other in each M center.

Solution EXAFS spectra of the Fe K edge reveal Fe–Fe components at 2.63 and 3.75 Å. These values change little with orientation in the single-crystal spectra, and similar Fe–Fe distances were found for the isolated FeMo cofactor.[10] The crystallographic model can be divided into two groups of Fe–Fe distances averaging 2.87 and 3.73 Å (averaging over both P and M clusters). However, the 2.87 Å group has a root mean square deviation (σ) of 0.22 Å, which does not include thermal disorder. Using the average crystallographic coordination number, the EXAFS simulation finds $\sigma = 0.09$ Å, including thermal disorder. As shown in Figure 1, larger disorder in the group with the short Fe–Fe distances would result in drastically damped Fe–Fe EXAFS. We conclude that most of the short Fe–Fe distances lie within 0.1 Å of the average distance of 2.62 Å. This is significantly shorter than the range 2.69–2.85 Å seen in Fe–S clusters with four coordinate Fe.[6, 11]

In the model obtained from X-ray diffraction, the long Fe–Fe distances average to 3.73 Å with a σ of 0.44 Å. Most of the diagonal interactions among the Fe atoms of the M cluster lie near 3.85 Å (see Fig. 1), and this is no doubt the group that the EXAFS fits find with an average distance of 3.72 Å. Although there are numerous other long Fe–Fe vectors in the range 3.0–4.4 Å, the EXAFS analysis cannot deal with a large number of minor components.

Altogether, the single-crystal Mo and Fe EXAFS studies provide eight predictions for metal–neighbor distances. Combining all the values from EXAFS and using the geometry of the M cluster proposed by Kim and Rees allows a refined model to be constructed, as shown in Figure 1. We have compared our refined model with an unbiased electron density map of Cp1 (resolution 2.3 Å) from an ongoing X-ray diffraction study.[3] The comparison was done by refining our model as a rigid body against the Cp1 diffraction data using the program TNT.[12] This process gives a very good fit to the diffraction data, as shown by Figure 2, and electron density values at the atomic positions. The mean interpolated electron density values (on an arbitrary scale) in the electron density map of Cp1 for the seven Fe and nine S atoms in the refined EXAFS model are 1886 ($\sigma = 182$) and 969 (141). For comparison, the values for the current crystallographic model for Cp1 which has been refined to $R = 0.17$ against data with 2.3 Å resolution, are 1903 (191) and 928

Table 1. Comparison of interatomic distances found by X-ray diffraction and EXAFS for nitrogenase MoFe protein and the model complex $(Et_4N)_3[Fe_6S_6Cl_6\{Mo(CO)_3\}_2]$.

Absorbing–backscattering pair	MoFe protein Av1 (solution) EXAFS [a]			Cp1 (crystal) EXAFS [b]		Diff. Av1 [c]		$(Et_4N)_3[Fe_6S_6Cl_6\{Mo(CO)_3\}_2]$ EXAFS [a]			Diff. [d]
	N	R [Å]	$\sigma_{tot.}$ [e]	N'	R [Å]	R [Å]	$\sigma_{stat.}$ [f]	N	R [Å]	$\sigma_{tot.}$ [e]	R [Å]
Mo-O,N	3.0	2.21	0.075	3.9	2.20	2.24	0.012	3.0	1.97	0.048	2.020
Mo-S	3.0	2.35	0.043	3.0	2.39	2.46	0.041	3.0	2.60	0.044	2.582
Mo-Fe	3.0	2.69	0.048	3.9	2.70	2.91	0.066	3.0	2.95	0.070	2.930
Mo-Fe'	3.0	5.09	0.066	5.8	5.10	5.22	0.095	3.0	4.28	0.073	4.241
Fe-S	2.9	2.29	0.071	2.8	2.27	2.34	0.070				
Fe-Fe	3.2	2.62	0.087	3.4	2.61	2.87	0.22				
Fe-Mo	0.2	2.74	0.035	0.4	2.71	2.91	0.066				
Fe-Fe'	1.3	3.75	0.074	1.0	3.68	3.73	0.44				

[a] The appropriate coordination number N was derived from the Kim and Rees model, averaging over both P and M clusters. [b] The relative amplitude N' was obtained by fixing $\sigma_{tot.}$ at the value derived from the solution fit and optimizing N'. This is not a coordination number, since the appropriate polarization effects have not been taken into account. [c] Crystallographic value ref. [4]. [d] Crystallographic value ref. [6]. [e] Total standard deviation $\sigma_{tot.} = \sigma_{stat.} + \sigma_{thermal}$. [f] Statistical standard deviation.

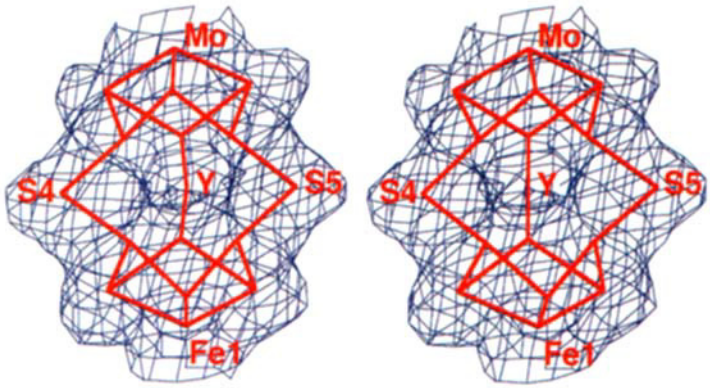

Fig. 2. Comparison of the refined EXAFS model for the M cluster in MoFe protein (red) and electron density map (blue). This stereoplot is oriented so that the Fe-Y-Fe bridge is towards the viewer. The electron density map is from a map with 2.3 Å resolution calculated with experimentally determined phases (model unbiased). The contour level of the map is set at the root mean square value of the electron density in the asymmetric unit.

(174). Clearly, the positions of atoms in our model are in excellent agreement with the electron density map and in fact fit the map as well as those in the crystallographic model.

In conclusion, the structure of the intact MoFe protein has been studied by single-crystal Mo and Fe EXAFS spectroscopy. We observed orientation dependence not only for the "well-known" Mo–Fe interaction at 2.7 Å but also for a new Mo–Fe component at 5.1 Å. Fe–Fe components at 2.6 and 3.7 Å are also stronger in the single-crystal data. Combining the Mo and Fe EXAFS results with crystallographic information allows us to propose a more symmetrical structure for the M cluster with unprecedented precision.

Experimental Procedure

Nitrogenase MoFe protein was purified from *A. vinelandii* at Louisiana State University by methods previously described [13]. Specific activities were 1800 nmol C_2H_2 reduced $min^{-1} mg^{-1}$ protein. MoFe protein crystals were prepared and mounted at Purdue University [3]. The crystals have the space group $P2_1$ with unit cell parameters $a = 69.9$, $b = 151.2$, $c = 121.8$ Å, and $\beta = 110.3°$. The experiments were performed on beamlines 7-3 and 10-2 at SSRL, X10C and X19A at NSLS. The X-ray absorption spectra were measured at 4 K in the fluorescence excitation mode using a 13-element Ge solid-state array detector [14]. The EXAFS fits were calculated using FEFF5 curved-wave multiple-scattering (MS) analysis software [15]. The geometry information was taken from the crystallographic results [4, 6]. In the capped-prismane model compound, multiple scattering is significant for the feature at approximately 3 Å because of the focusing effect arising from three almost linear Mo-C-O (ca. 177°) interactions. However, FEFF5 calculations found that multiple scattering is not significant for the Fe EXAFS in the nitrogenase cluster.

Received: May 12, 1993
Revised version: July 30, 1993 [Z 6080 IE]
German version: *Angew. Chem.* **1993**, *105*, 1661

[1] B. K. Burgess in *Advances in Nitrogen Fixation Research* (Eds.: C. Veeger, W. E. Newton), Nijhoff, Boston, **1984**, p. 103; W. Orme-Johnson, *Annu. Rev. Biophys. Biophys. Chem.* **1985**, *14*, 419.
[2] V. K. Shah, W. J. Brill, *Proc. Natl. Acad. Sci. USA* **1977**, *74*, 3249.
[3] a) J. T. Bolin, A. E. Ronco, L. E. Mortenson, T. V. Morgan, M. Williamson, N.-H. Xuong in *Nitrogen Fixation: Achievements and Objectives* (Eds.: P. Gresshoff, C. Roth, G. Stacey, W. Newton), Chapman and Hall, New York, **1990**, p. 111; b) J. T. Bolin, A. E. Ronco, T. V. Morgan, L. E. Mortenson, N.-H. Xuong, *Proc. Natl. Acad. Sci. USA*, **1993**, *90*, 1078; c) J. T. Bolin, N. Camposso, S. W. Muchmore, T. V. Morgan, L. E. Mortenson in *Molybdenum Enzymes, Cofactors and Models* (Eds.: E. Stiefel, D. Coucouvanis, W. Newton) (*ACS Symp. Ser.*), in press.
[4] a) J. Kim, D. C. Rees, *Science* **1992**, *257*, 1677; b) J. Kim, D. C. Rees, *Nature* **1992**, *360*, 553; c) M. K. Chan, J. Kim, D. C. Rees, *Science* **1993**, *260*, 792; d) J. Kim, D. C. Rees, preliminary entry 1MIN to the Brookhaven Protein Data Bank.
[5] J. Chen, J. Christiansen, R. C. Tittsworth, B. J. Hales, S. J. George, D. Coucouvanis, S. P. Cramer, *J. Am. Chem. Soc.* **1993**, *115*, 5504.
[6] D. Coucouvanis, A. Salifoglou, M. G. Kanatzidis, W. R. Dunham, A. Simopoulos, A. Kostikas, *Inorg. Chem.* **1988**, *27*, 4066.
[7] S. P. Cramer, K. O. Hodgson, W. O. Gillum, L. E. Mortenson, *J. Am. Chem. Soc.* **1978**, *100*, 3398.
[8] S. D. Conradson, B. K. Burgess, W. E. Newton, L. E. Mortenson, K. O. Hodgson, *J. Am. Chem. Soc.* **1987**, *109*, 7507.
[9] A. M. Flank, M. Weininger, L. E. Mortenson, S. P. Cramer, *J. Am. Chem. Soc.* **1986**, *108*, 1049.
[10] J. M. Arber, A. C. Flood, C. D. Garner, C. A. Gormal, S. S. Hasnain, B. E. Smith, *Biochem. J.* **1988**, *252*, 421.
[11] a) R. E. Palermo, R. Singh, J. K. Bashkin, R. H. Home, *J. Am. Chem. Soc.* **1984**, *106*, 2600; b) E. T. Adman, L. C. Sieker, L. H. Jensen, *J. Biol. Chem.* **1973**, *248*, 3987.
[12] D. E. Tronrud, L. F. Ten Eyck, B. W. Matthews, *Acta Crystallogr. Sect. A* **1987**, *43*, 489.
[13] B. J. Hales, D. J. Langosch, E. E. Case, *J. Bio. Chem.* **1986**, *261*, 15301.
[14] S. P. Cramer, O. Tench, M. Yocum, G. N. George, *Nucl. Instrum. Methods Phys. Res. Sect. A* **1988**, *266*, 586.
[15] J. J. Rehr, R. C. Albers, *Phys. Rev. B* **1991**, *41*, 8139; J. J. Rehr, J. Mustree de Leon, S. I. Zabinsky, R. C. Albers, *J. Am. Chem. Soc.* **1991**, *113*, 5153.

De Novo Design of a Novel Heterodinuclear Three-Helix Bundle Metalloprotein**

By *M. Reza Ghadiri** and *Martin A. Case*

Proteins, the epitome of molecular form and function, remain the most challenging targets for molecular design. Despite the substantial advances in the design of "small-molecule" models of enzyme active sites,[1] little progress has been made toward the construction of "large-molecule" systems that can mimic both the structural and functional properties of natural proteins.[2] Here we report the design, synthesis, and characterization of a novel three-helix bundle Ru^{II} metalloprotein which is capable of functioning as an efficient type-II copper binding protein.

The foremost problem in the de novo design of functional proteins is the availability of structurally well-defined scaffolds onto which the desired functionalities of the active site may be elaborated. Recently, we have developed a series of metal ion assisted, self-organizing processes for the design and convergent synthesis of topologically predetermined metallopeptides and artificial metalloproteins.[3] One such design, a three-helix bundle structure,[3a] was the starting point in the present study for rational modification into a heterodinuclear $Ru^{II}Cu^{II}$ metalloprotein. Our strategy is illustrated in Figure 1. As in our previous studies, the key design feature in directing the self-assembly process is the incorporation of a bipyridyl (bpy) moiety at the N-terminus of the polypeptide subunit. Metal ion complexation to the bipyridyl moieties is thought to initially sequester three peptide chains to form the putative intermediate shown. The higher coil density and the dramatically increased effective molarity of hydrophobic moieties in the intermediate species strongly bias the system toward formation of a parallel three-helix bundle ensemble. Moreover, it was hypothesized that by placing a second ligand in an appropriate position within each polypeptide sequence, a new composite metal binding site may be formed.

[*] Prof. M. R. Ghadiri, Dr. M. A. Case
Departments of Chemistry and Molecular Biology
The Scripps Research Institute
10666 North Torrey Pines Road, La Jolla, CA 92037 (USA)
Telefax: Int. code + (619)554-6656

[**] This work was supported by the Searle Scholars Program/the Chicago Community Trust and the Arnold and Mabel Beckman Foundation. We thank J. Schiffer for his contribution to the early stages of this project, Dr. D. Goodin for EPR measurements, and Drs. M. Griffith, S. Kent, and G. Siuzdak for their assistance in mass spectrometric analyses.

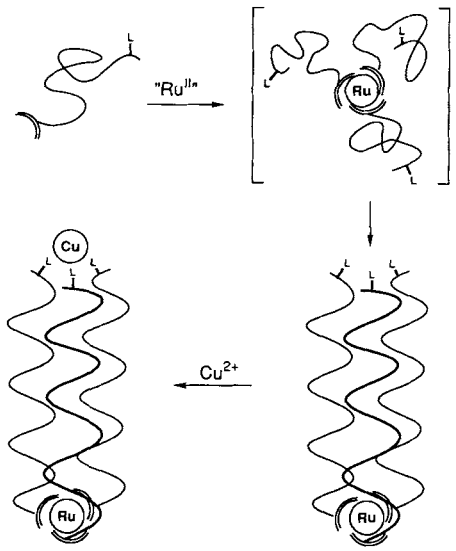

Fig. 1. Schematic representation of the hypothetical folding in the ruthenium(II)-assisted self-assembly of the three-helix bundle metalloprotein (double arcs represent the bipyridyl moieties). The peptide is designed such that upon complexation of Ru^{II} the ligands L are arranged to form a novel copper binding site.

The polypeptide sequence was designed according to previously described principles (Fig. 2).[3a] Histidine was chosen as the potential ligand in the design of the type-II copper binding site based on its natural affinity for a variety of transition metal ions as well as its high frequency of occurrence in natural copper-binding metalloproteins.[4] The optimal position for the histidine moiety within the peptide subunit was determined by the analysis of a structural model. The second metal binding site was placed near the C-termini of the peptides in the helix bundle in order to take advantage of favorable charge–helix dipole interactions and enhance the metal ion binding propensity.[5] A tyrosine residue was placed near the putative Cu^{II} binding site in order to facilitate spectroscopic analysis of copper binding.[6] Despite the simplified folding pathway illustrate in Figure 1, there are two potential ligands (imidazolyl (imd) and bpy) within each peptide subunit, thus various side reactions during the ruthenium(II)-assisted assembly process are possible. It is therefore essential that the imidazolyl side chain functionalities not interfere, in either inter- or intramolecular fashion, with the key bpyRu^{II} complex forming reaction. In other words, *the formation of the Ru^{II} complex must be exquisitely chemo- and regioselective.*

The 19-residue amphiphilic polypeptide used in this study, when reacted with the $Ru_5Cl_{12}^{2-}$ cluster anion,[7] was shown to undergo an unprecedented chemo-, regio-, and diastereoselective reaction to form the desired parallel three-helix bundle Ru^{II} metalloprotein.[8] The remarkably high selectivities observed in forming $[Ru(peptide)_3]^{2+}$, which is kinetically inert to ligand exchange, may be attributed to the following factors. The high affinity of nitrogen-containing aromatic heterocycles for ruthenium ions was expected to bias the chemical activity of the ruthenium reagent toward the bipyridyl and imidazolyl moieties.[3a, c, 9] However, the higher kinetic stability of bipyridyl- versus imidazolyl-Ru^{II} complexes may have played a significant role in the chemo- and regioselectivity of the process. Furthermore, the lack of any observable intramolecular complexation, in which the histidine and bipyridine moieties of a single subunit are both coordinated to a ruthenium ion, may be attributed to the unfavorable geometrical constraints imposed by the helical structure as well as the noncovalent interactions between the subunits of the protein. This assumption is borne out by the observed high diastereoselectivity of the process in which the *fac* isomer is formed in >95% yield suggesting strong interhelical interaction during the complex formation.[10]

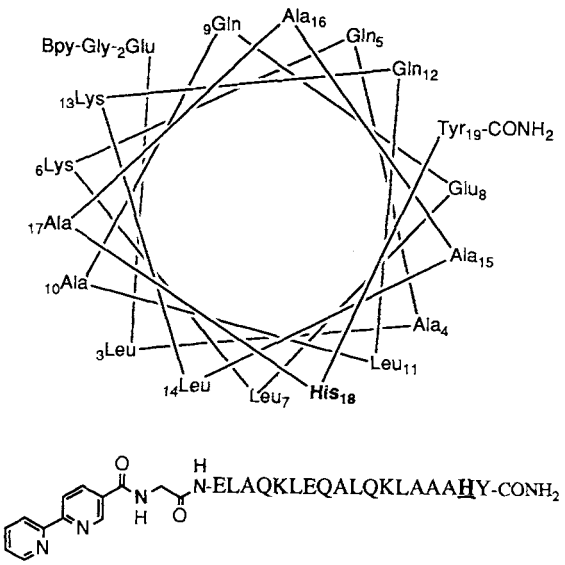

Fig. 2. Peptide sequence and the corresponding helical wheel diagram emphasizing the amphiphilic helical structure of the subunit.

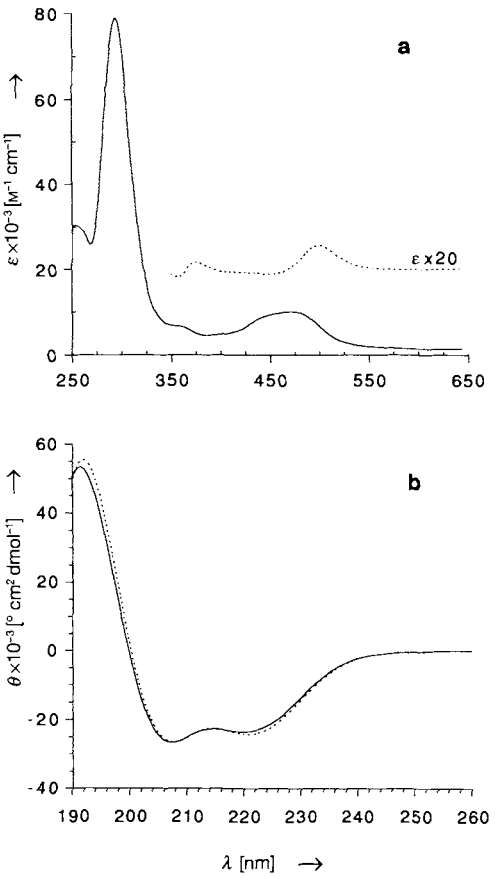

Fig. 3. UV/VIS absorption and CD spectra of the Ru^{II} and $Cu^{II}Ru^{II}$ metalloproteins. a) Room-temperature absorption spectrum of the Ru^{II} metalloprotein (solid line) and the difference spectrum (dotted line) after addition of one equivalent of Cu^{2+} (baseline is offset for clarity). b) CD spectra of the Ru^{II} (solid line) and $Cu^{II}Ru^{II}$ metalloproteins (dotted line) (1.5×10^{-6} M in 20 mM MES, pH 6.0 at 25 °C).

The overall three-helix bundle topology of the ensemble was supported by the following experimental observations. The protein displays absorption bands at $\lambda = 289$ and 475 nm characteristic of $[Ru(bpy)_3]^{2+}$ complexes (Fig. 3a).[3a, 11] Electrospray mass spectrometric analysis unequivocally establishes the trimeric nature of the ensemble (Fig. 4a). In addition, the solution properties and the hydrodynamic behavior of the complex, as judged by gel permeation chromatography, are not only consistent with the expected molecular weight, they are also indicative of the monomeric nature of the Ru^{II} metalloprotein in aqueous solutions. The absence of intermolecular aggregation is also corroborated by the lack of dependence of circular dichroism (CD) spectra on protein concentration in the measured range of 2–500 μM. Moreover, the Ru^{II} metalloprotein exhibits a CD spectrum consistent with the expected helical secondary structure of the ensemble ($\theta_{222} = -23000°\,cm^2\,dmol^{-1}$, Fig. 3b). Furthermore, the metalloprotein displays a cooperative guanidine hydrochloride (Gnd · HCl) denaturation curve with a free energy of stabilization of $\Delta G_{H_2O} = 2.0 \pm 0.2$ kcal mol^{-1} (Fig. 5).

The ruthenium(II)-assisted self-assembly of the peptide into a three-helix bundle metalloprotein has been shown to create, as anticipated, a new high-affinity type-II copper

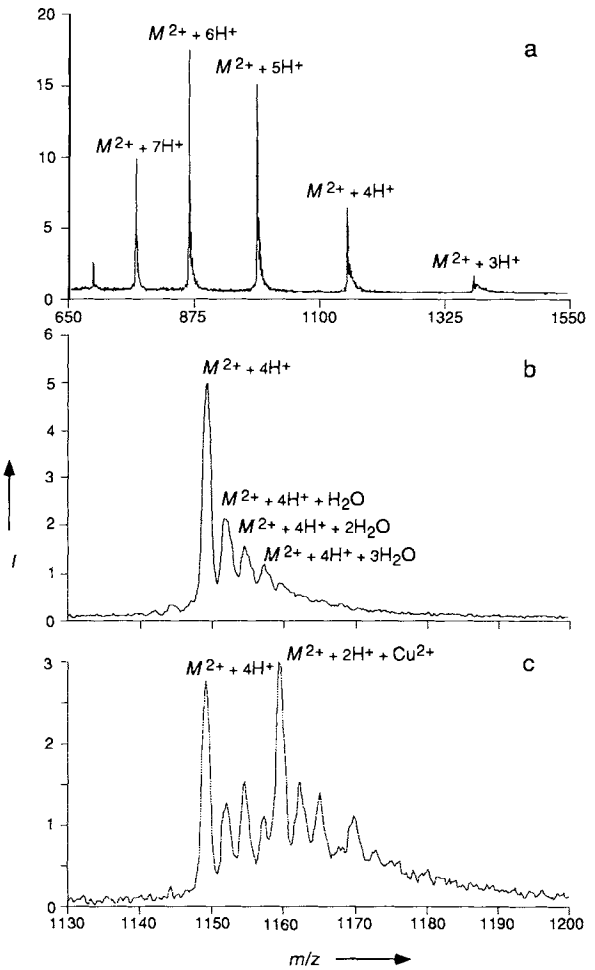

Fig. 4. Electrospray ionization mass spectra of a) the Ru^{II} metalloprotein (each peak corresponds to a detected charged state of the protein ($M_{found} = 6887 \pm 2$, $M_{calcd.} = 6887$)); b) a single charged state of the Ru^{II} metalloprotein and its hydrated forms; c) a single charged state of the dinuclear $Ru^{II}Cu^{II}$ metalloprotein. The peak corresponding to the Ru^{II} metalloprotein arises from dissociation during the gas-phase ionization process and is dependent on the applied orifice potential. Spectra were collected on Perkin-Elmer SCIEX API-3 mass spectrometer at applied orifice potential of 100 V.

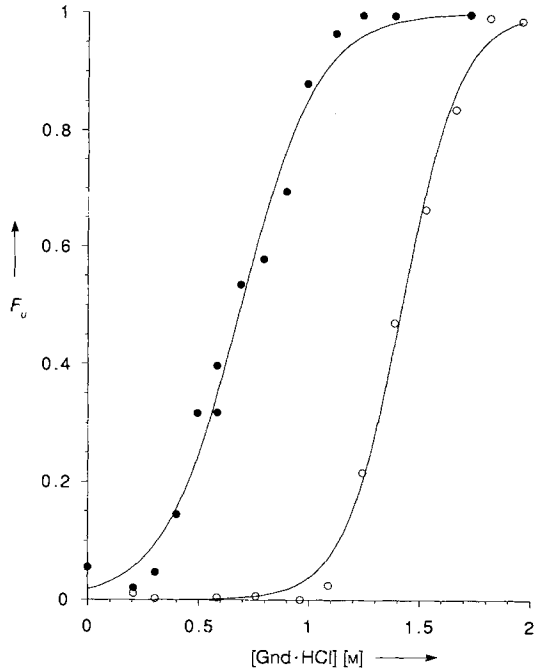

Fig. 5. Guanidine hydrochloride denaturation curves for the Ru^{II} (•) and $Cu^{II}Ru^{II}$ metalloproteins (○) (8.0×10^{-6} M, 25 mM MES, pH 6.0, 25 °C) measured by luminescence spectroscopy. Solid lines are based on parameters obtained by a nonlinear least-squares fit [3a]. F_u = proportion of denatured protein.

binding site. Site-specific Cu^{II} binding was studied spectrophotometrically by monitoring the fluorescence emission of the nearby tyrosine chromophore as a function of the concentration of Cu^{2+} ions. Least-squares fit as well as Scatchard analysis of the titration curves indicate a 1:1 copper:protein complex with an apparent dissociation constant of $K_d = 3.0 \pm 0.1 \times 10^{-7}$ M. No appreciable dimunition of the tyrosine fluorescence emission was observed under identical conditions when a control Ru^{II} metalloprotein was employed.[12] Interestingly, copper binding does not appreciably change the CD spectrum of the metalloprotein ($\theta_{222} = -24000°\,cm^2 \cdot dmol^{-1}$, Fig. 3b). Lack of a significant structural change upon copper binding as well as the high affinity of the Ru^{II} metalloprotein for copper ions suggest formation of a highly preorganized metal binding site upon assembly of the three-helix bundle. Formation of the $Ru^{II}Cu^{II}$ metalloprotein was also monitored by electrospray mass spectrometry (Fig. 4c). Interestingly, even when a 20-fold excess of Cu^{2+} was employed, a 1:1 $Ru^{II}Cu^{II}$ metalloprotein was formed, further supporting the existence of a unique high-affinity copper binding site. Moreover, the binding of Cu^{2+} at the designated site is expected to reinforce the three-helix bundle geometry by constraining the protein at both ends and further enhance the stability of the ensemble toward denaturation.[3c–d, 16a] Indeed, the $Ru^{II}Cu^{II}$ metalloprotein displays a free energy of stabilization $\Delta G_{H_2O} = 3.5 \pm 0.2$ kcal mol^{-1}, which is 1.5 kcal mol^{-1} greater than that of the corresponding uncomplexed protein (Fig. 5).

Information concerning the ligand arrangement and the environment of the copper binding site was provided by UV/VIS and EPR spectroscopy. Analysis of the difference absorption spectrum of the Ru^{II} metalloprotein before and after copper complexation reveals a $\pi(imH) \rightarrow Cu^{II}$ charge transfer band centered at $\lambda = 375$ nm ($\varepsilon = 100$ M^{-1} cm^{-1}) and a ligand field band centered at $\lambda = 495$ nm ($\varepsilon = 300$ M^{-1} cm^{-1}) consistent with tetragonal or square-planar

geometry of the copper complex (Fig. 3a).[13] Moreover, the EPR spectrum is indicative of a type-II copper binding site in a similar ligand environment with $g_{\parallel} = 2.27$ and $A_{\parallel} = 173\,(cm^{-1} \times 10^4)$. Peisach and Blumberg analysis[14] is consistent with the complexation of Cu^{II} to three nitrogen and one or more oxygen ligands which are presumably donated by water and/or buffer.

In summary, we have presented a novel approach in which two different metal ions and three peptide subunits ultimately join, through a highly selective self-assembly process, to form the first de novo designed heterodinuclear metalloprotein (Fig. 6).[15, 16] The availability of such a convergent

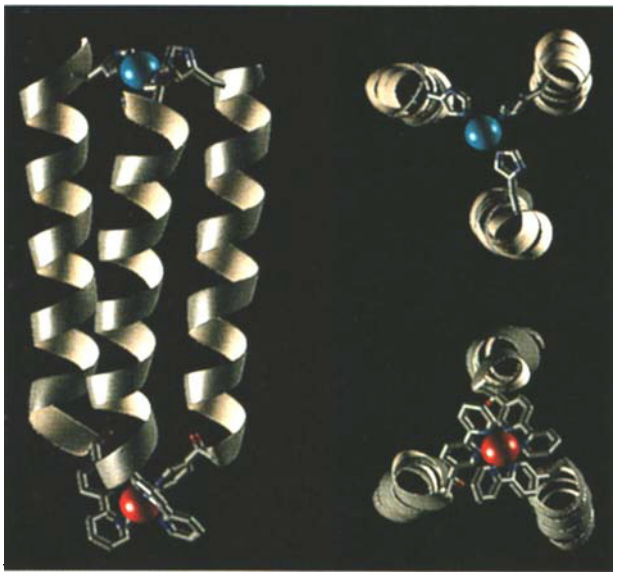

Fig. 6. Computer-generated model of the parallel three-helix bundle $Cu^{II}Ru^{II}$ metalloprotein.

synthetic process holds considerable promise for the future design of redox-active and artificial light-harvesting metalloproteins.

Received: May 13, 1993 [Z 6082 IE]
German version: *Angew. Chem.* **1993**, *105*, 1663

[1] a) H. Dugas, *Bioorganic Chemistry. A Chemical Approach to Enzyme Action*, 2nd ed., Springer, New York, **1989**; b) R. W. Hay, *Bio-Inorganic Chemistry*, Ellis Horwood, Chichester, **1984**; c) F. H. Westheimer, *Adv. Chem. Ser.* **1980**, *191*, 18–33; d) R. Breslow, *Pure Appl. Chem.* **1990**, *62*, 1859–1866; e) *Adv. Enzymol. Relat. Areas Mol. Biol.* **1986**, *58*, 1; f) J.-M. Lehn, *Angew. Chem.* **1988**, *100*, 91–116; *Angew. Chem. Int. Ed. Engl.* **1988**, *27*, 89–112; g) D. Cram, *Science* **1988**, *240*, 760–767.

[2] a) M. Mutter, *Trends Biochem. Sci.* **1988**, *13*, 260–265; b) M. Mutter, S. Vuilleumier, *Angew. Chem.* **1989**, *101*, 551; *Angew. Chem. Int. Ed. Engl.* **1989**, *28*, 535–554; c) W. F. DeGrado, Z. R. Wasserman, J. D. Lear, *Science* **1989**, *243*, 622–628; d) L. Regan, W. F. DeGrado, *ibid.* **1988**, *241*, 976–978; e) M. H. Hecht, J. S. Richardson, D. C. Richardson, R. C. Ogden, *ibid.* **1990**, *249*, 884–891; f) T. Sasaki, E. T. Kaiser, *J. Am. Chem. Soc.* **1989**, *111*, 380–381; g) K. W. Hahn, A. K. Wieslaw, J. M. Stewart, *Science* **1990**, *248*, 1544–1547; h) A. Pessi, E. Bianchi, A. Crameri, S. Venturini, A. Tramontano, M. Sollazzo, *Nature* **1993**, *362*, 367–369.

[3] a) M. R. Ghadiri, C. Soares, C. Choi, *J. Am. Chem. Soc.* **1992**, *114*, 825–831; b) *ibid.* **1992**, *114*, 4000–4002; c) M. R. Ghadiri, C. Choi, *ibid.* **1990**, *112*, 1630–1632; d) M. R. Ghadiri, K. A. Fernholz, *ibid.* **1990**, *112*, 9633–9635.

[4] a) H. B. Gray, E. I. Solomon, *Met. Ions Biol.* **1981**, *3*, 1–39; b) E. T. Adman, *Adv. Protein Chem.* **1991**, *42*, 145–197; c) P. Chakrabarti, *Protein Eng.* **1990**, *4*, 57–63.

[5] a) D. E. Blagdon, M. Goodman, *Biopolymers* **1975**, *14*, 241; b) J. S. Richardson, D. C. Richardson, *Science* **1988**, *240*, 1648; c) L. G. Presta, G. D. Rose, *ibid.* **1988**, *240*, 1632; d) K. R. Shoemaker, P. S. Kim, D. N. Brems, S. Marqusee, E. J. York, I. M. Chaiken, J. M. Stewart, R. L. Baldwin, *Proc. Natl. Acad. Sci. USA* **1985**, *82*, 2349; e) D. J. Lockhart, P. S. Kim, *Science* **1992**, *257*, 947.

[6] Tyrosine fluorescence is efficiently quenched in a distance-dependent fashion by bound copper ions. For examples, see: a) R. F. Steiner, E. P. Kirby, *J. Phys. Chem.* **1969**, *73*, 4130–4135; b) G. B. Strambini, E. Gabellieri, *ibid.* **1991**, *95*, 4347–4352.

[7] a) D. Rose, G. Wilkinson, *J. Chem. Soc. A* **1970**, 1791; b) J. D. Gilbert, D. Rose, G. Wilkinson, *ibid.* **1970**, 2765.

[8] The Ru^{II} metalloprotein was synthesized by the addition of a solution of the peptide subunit (130 mg, 13 μmol) in 300 μL of degassed water under an Ar atmosphere to a 50 °C blue solution of the $Ru_2Cl_7^{2-}$ cluster anion (prepared from 0.86 mg of $RuCl_3 \cdot xH_2O$ in a final volume of 200 μL EtOH) and refluxed for 30 min. The product is formed in 70% yield and separated from the unreacted starting peptide by C_{18} RP-HPLC according to standard procedures [3a].

[9] a) C. R. Matthews, P. M. Erickson, D. L. Van Vliet, M. Perersheim, *J. Am. Chem. Soc.* **1978**, *100*, 2260; b) R. Margalit, N. M. Kostic, C.-M. Che, D. F. Blair, H.-J. Chiang, I. Pecht, J. B. Shelton, J. R. Shelton, W. A. Schroeder, H. B. Gray, *Proc. Natl. Acad. Sci. USA* **1984**, *81*, 6554; c) S. S. Isied, H. Taube, *Inorg. Chem.* **1976**, *15*, 3070; d) I.-J. Chang, H. B. Gray, J. R. Winkler, *J. Am. Chem. Soc.* **1991**, *113*, 7056.

[10] Considering that an unsymmetrically substituted bipyridyl moiety is used in the present design, in the absence of intersubunit noncovalent interactions a statistical ratio of 3:1 *mer*-:*fac*-$[Ru(bpy)_3]^{2+}$ is expected. Indeed, in control experiments, in which a truncated subunit corresponding to the first three residues of the peptide sequence was used, no diastereoselectivity in the formation of the Ru^{II} complex was observed.

[11] S. F. Mason, *Inorg. Chem. Acta* **1968**, 89.

[12] In control experiments a three-helix bundle Ru^{II} metalloprotein in which the histidine residues have been replaced by alanine moieties does not bind copper but displays spectroscopic, hydrodynamic, and denaturation profiles similar to those of the histidine-containing Ru^{II} metalloprotein.

[13] a) H. J. Prochaska, W. F. Schwindinger, M. Schwartz, M. J. Burk, E. Bernaducci, A. Lalancette, J. A. Potenza, H. J. Schugar, *J. Am. Chem. Soc.* **1981**, *103*, 3446–3455; b) S. Knapp, T. P. Keenan, X. Zhang, R. Fikar, J. A. Potenza, H. J. Schugar, *ibid.* **1990**, *112*, 3452–3464.

[14] J. Peisach, W. E. Blumberg, *Arch. Biochem. Biophys.* **1974**, *165*, 691–708.

[15] For examples of the introduction of one metal binding site in natural peptides and protein scaffolds see: a) B. L. Iverson, S. A. Iverson, V. A. Roberts, E. D. Getzoff, J. A. Tainer, S. J. Benkovic, R. A. Lerner, *Science* **1990**, *249*, 659–662; b) F. H. Arnold, B. L. Haymore, *ibid.* **1991**, *252*, 1796; c) H. W. Hellinga, J. P. Caradonna, F. M. Richards, *J. Mol. Biol.* **1991**, *222*, 787–803; d) D. L. Merkle, M. H. Schmidt, J. M. Berg, *J. Am. Chem. Soc.* **1991**, *113*, 5450.

[16] For examples of the introduction of one metal binding sites in designed peptides and artificial proteins see ref. [3] and: a) T. Handel, W. F. DeGrado, *J. Am. Chem. Soc.* **1990**, *112*, 6710; b) F. Q. Ruan, Y. Q. Chen, P. B. Hopkins, *ibid.* **1990**, *112*, 9403; c) M. Liberman, T. Sasaki, *ibid.* **1991**, *113*, 1470; d) L. Regan, N. D. Clarke, *Biochemistry*, **1990**, *29*, 10878.

Octaethyltetraoxaporphyrin Dication—Counterpart of Octaethylporphyrin in the Tetraoxaporphyrin Series

By *Emanuel Vogel,* Joachim Dörr, Adalbert Herrmann, Johann Lex, Hans Schmickler, Peter Walgenbach, Jean Paul Gisselbrecht,* and *Maurice Gross**

The recently discovered tetraoxaporphyrin dication (as the perchlorate **1a**),[1] has a very promising chemistry, as shown by its conversion to tetraoxaisophlorin,[2] the tetraoxaporphyrin dianion,[2] and the 5-hydroxytetraoxaporphyrin dication.[3] The possibilities for the development of this new porphyrinoid become particularly obvious when one considers that as an oxonium/carbenium ion this species is related to the pyrylium ion as porphyrin is to pyridine.

[*] Prof. Dr. E. Vogel, Dipl.-Chem. J. Dörr, Dr. A. Herrmann, Dr. J. Lex, Dr. H. Schmickler, Dr. P. Walgenbach
Institut für Organische Chemie der Universität
Greinstrasse 4, D-50939 Köln (FRG)
Prof. Dr. M. Gross, Dr. J. P. Gisselbrecht
Laboratoire d'Electrochimie et de Chimie Physique du Corps Solide
Université Louis Pasteur
4, rue B. Pascal, F-67000 Strasbourg (France)

As the reaction spectrum of **1a** is impaired because of its insolubility in organic solvents, the need arose to prepare derivatives of the dication possessing solubilizing alkyl or aryl groups. Mindful of the important role played by octaethylporphyrin[4] and *meso*-tetraphenylporphyrin[5] as model compounds in porphyrin chemistry, we attempted to synthesize the corresponding tetraoxaporphyrin dications. We report here on a preparative access to the 2,3,7,8,12,13,17,18-octaethyltetraoxaporphyrin dication (as the perchlorate **1b**).

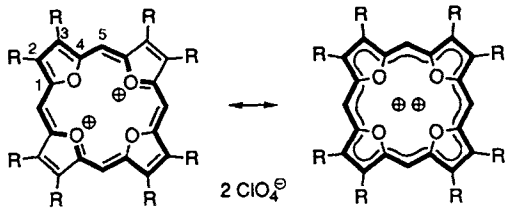

1a: R = H; **1b**: R = C_2H_5

The production of **1b** by the acid-catalyzed cyclic condensation of 2-hydroxymethyl-3,4-diethylfuran (**5**) and subsequent oxidation of the anticipated product tetraoxaporphyrinogen **6** was suggested by the routes to **1a**,[1c] as well as to porphyrin[6] and its octaethyl derivative.[4]

3,4-Diethylfuran (**4**), required as starting material and for which surprisingly no suitable preparative method existed,[7] was conveniently made by the inverse Diels–Alder reaction of 4-phenyloxazole (**2**)[8] with 3-hexyne (**3**), followed by in situ cleavage of the resulting adduct.

Heating 40 g (0.5 mol) of **3** and 91.8 g (0.65 mol) of **2** in a 500 mL autoclave (Teflon lined) for 3 d at 250 °C gave a brown, liquid mixture, from which **4** was easily separated by distillation in vacuum (colorless liquid, b.p. 51–52 °C/20 Torr; yield 43.4 g, 70%). Vilsmeier formylation of **4**, carried out by addition of the furan to a mixture of *N*,*N*-dimethylformamide (DMF) and phosphorus oxychloride in dichloromethane at 0 °C followed by heating under reflux (1 h), smoothly gave 3,4-diethyl-2-formylfuran (b.p. 96–97 °C/15 torr; yield 70%; see also Table 1), from which **5** was obtained by conventional reduction with sodium borohydride in tetrahydrofuran/water (9:1) (b.p. 108–110 °C/12 torr; yield 90%).

Based on experience in the biomimetic synthesis of porphyrins, it was anticipated that the acid-catalyzed condensation of **5** to octaethylporphyrinogen **6** could be accomplished with better yields than that of furfuryl alcohol to the parent tetraoxaporphyrinogen (hitherto only 1–2%), as the ethyl groups promote ring closure to form the macrocycle on conformational grounds (helical effect).[9] In fact, **5** could be condensed with *p*-toluenesulfonic acid in nitromethane to give **6** in 16% yield (colorless rhomboids from ethanol, m.p. 138–140 °C). Remarkably, this result was only obtained when the acid was used in equimolar (based on **5**), not catalytic amounts (see Experimental Procedure). Unlike the behavior of the pyrrole analogue, the "porphyrinogen cyclocondensation" with **5**, at least under the given reaction conditions, does not take place selectively. In addition to **6**, homologous cyclocondensation products with five or more furan components (total amount about 2–3%) are formed.

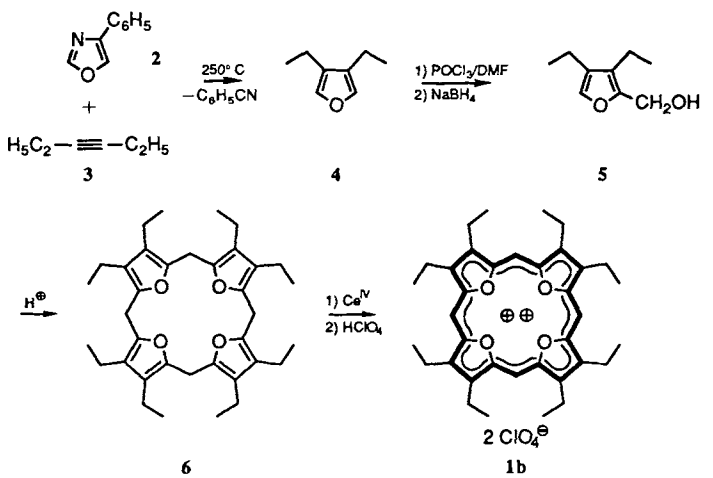

Table 1. Selected physical and spectroscopic data for 3,4-diethyl-2-formylfuran, **5**–**7**, **1b**, **8d**[a] and **9d**[a].

3,4-Diethyl-2-formylfuran: ^{1}H NMR (300 MHz, $CDCl_3$): δ = 9.66 (s, 1H; CHO), 7.32 (s, 1H; H-5), 2.69 (q, 2H; H-3a), 2.37 (q, 2H; H-4a), 1.17 (t, 3H; H-4b), 1.14 (t, 3H; H-3b); ^{13}C NMR (75.5 MHz, $CDCl_3$): δ = 177.9 (CHO), 148.4, 144.0, 139.2, 129.7, 16.6, 16.2, 14.8, 13.5; MS (EI, 70 eV): *m/z* (%): 152 (100) [M^+], 151 (36), 137 (42), 123 (42), 95 (30); IR (film): $\tilde{\nu}$ = 3363, 3134, 2969, 2936, 2875, 2771, 1674, 1599, 1520, 1463, 1416, 1379, 1341, 1299, 1263, 1222, 1144, 1116, 1058, 958, 930, 781, 762, 602 cm^{-1}.

5: ^{1}H NMR (300 MHz, $CDCl_3$): δ = 7.06 (s, 1H; H-5), 4.47 (s, 2H; CH_2OH), 2.53 (s, 1H; OH), 2.37 (m, 2H; H-3a), 2.35 (m, 2H; H-4a), 1.16 (t, 3H; H-4b), 1.09 (t, 3H; H-3b); ^{13}C NMR (75.5 MHz, $CDCl_3$): δ = 149.1, 137.5, 127.4, 123.8, 55.3, 16.8, 16.4, 15.4, 13.5; MS (EI, 70 eV): *m/z* (%): 154 (73) [M^+], 139 (25), 136 (60), 125 (100), 110 (25), 92 (30), 78 (10); IR (Film): $\tilde{\nu}$ = 3350, 2960, 2930, 2870, 1555, 1460, 1375, 1280, 1210, 1125, 1005, 908, 760 cm^{-1}.

6: ^{1}H NMR (300 MHz, $CDCl_3$): δ = 3.69 (s, 8H; H-5,10,15,20), 2.29 (q, 16H; H-2a,3a,7a,8a,12a,13a,17a,18a), 1.04 (t, 24H; H-2b,3b,7b,8b,12b,13b,17b,18b); ^{13}C NMR (75.5 MHz, $CDCl_3$): δ = 145.1, 120.7, 23.1, 16.9, 15.6; MS (EI, 70 eV): *m/z* (%): 544 (100) [M^+], 529 (6), 515 (14), 409 (8), 273 (20), 137 (18); IR (CsI): $\tilde{\nu}$ = 2962, 2928, 2870, 1583, 1462, 1408, 1374, 1230, 1124, 1060, 957, 856, 795, 692 cm^{-1}; UV/VIS (CH_2Cl_2): λ_{max} (ε) = 224 nm (22500).

1b: ^{1}H NMR (300 MHz, CD_2Cl_2): δ = 11.57 (s, 4H; H-5,10,15,20), 4.08 (q, 16H; H-2a,3a,7a,8a,12a,13a,17a,18a), 2.16 (t, 24H; H-2b,3b,7b,8b,12b,13b,17b,18b); ^{13}C NMR (75.5 MHz, CD_2Cl_2): δ = 155.6, 154.0, 98.3, 21.3, 18.0; MS (FAB): *m/z* (%): 541 (100) [(M + H$^+$ − 2 ClO_4^-)$^+$], 540 (29), 539 (12); IR (CsI): $\tilde{\nu}$ = 2976, 2938, 2877, 1505, 1451, 1084, 625 cm^{-1}; UV/VIS (CH_2Cl_2): λ_{max} (ε) = 317 (10900) sh, 351 (16500) sh, 363 (22100) sh, 377 (66000), 397 (844100), 424 (840 sh), 476 (830), 515 (2400) sh, 543 (24300), 562 (6100) sh, 589 nm (2100) sh.

7: ^{1}H NMR (300 MHz, [D_8]THF): δ = 0.16 (m, 40H; H-2a,2b,3a,3b,7a,7b,8a,8b,12a,12b,13a,13b,17a,17b,18a,18b), −0.13 (s, 4H; H-5,10,15,20); ^{13}C NMR (75.5 MHz, [D_8]THF): δ = 160.3, 133.0, 91.9, 14.6, 13.1; MS (EI, 70 eV): *m/z* (%): 540 (100) [M^+], 270 (36); IR (CsI): $\tilde{\nu}$ = 2965, 2933, 2870, 1751, 1508, 1466, 1397, 1372, 1319, 1294, 1260, 1235, 1132, 1071, 1057, 952, 902, 876, 788, 734, 670, 486 cm^{-1}; UV/VIS (THF): λ_{max} (ε) = 323 (87300) sh, 334 (107100), 351 (128400), 417 (7500) sh, 432 (9000) sh, 462 (7700), 497 (5000), 623 (460), 692 (550), 710 (550), 751 nm (510).

8d [a]: M.p. 114–120 °C (ethanol); yield 28%; ^{1}H NMR (300 MHz, $CDCl_3$): δ = 5.91 (m, 8H; H-2,3,7,8,12,13,17,18), 3.77 (t, 4H; H-5,10,15,20), 1.88 (m, 8H; H-5a,10a,15a,20a), 1.27 (m, 8H; H-5b,10b,15b,20b), 1.23 (m, 8H; H-5c,10c,15c,20c), 0.84 (m, 12H; H-5d,10d,15d,20d); ^{13}C NMR (75.5 MHz, $CDCl_3$): δ = 154.3, 105.3, 38.5, 30.6, 29.5, 22.4, 14.0; MS (EI, 70 eV): *m/z* (%): 544 (40) [M^+], 487 (100), 430 (10), 373 (45), 316 (44); IR (KBr): $\tilde{\nu}$ = 3106, 2954, 2930, 2868, 1560, 1466, 1181, 1015, 971, 947, 772, 738 cm^{-1}; UV/VIS (Cyclohexane): λ_{max} (ε) = 223 (41400), 237 nm (12900) sh.

9d: Violet needles from hot 50% $HClO_4$, yield 30%, m.p. > 300 °C (decomp.); ^{1}H NMR (300 MHz, CF_3CO_2D, CH_2Cl_2 int.): δ = 11.12 (s, 8H; H-2,3,7,8,12,13,17,18), 5.63 (t, 8H; H-5a,10a,15a,20a), 2.89 (m, 8H; H-5b,10b,15b,20b), 2.11 (Sextett, 8H; H-5c,10c,15c,20c), 1.35 (t, 12H; H-5d,10d,15d,20d); ^{13}C NMR (75.5 MHz, CF_3CO_2D, CH_2Cl_2 int.): δ = 160.9, 138.4, 124.3, 42.7, 38.7, 25.3, 14.3; MS (FAB): *m/z* (%): 541 (48) [(M + H$^+$ − 2 ClO_4^-)$^+$], 540 (100), 539 (58); IR (CsI): $\tilde{\nu}$ = 3133, 2959, 2929, 2871, 1541, 1507, 1456, 1340, 1190, 1085, 907, 816, 788, 624 cm^{-1}; UV/VIS (HCOOH): λ_{max} (ε) = 367 (15900) sh, 387 (75800) sh, 401 (715000), 423 (8200) sh, 497 (900) sh, 527 (2750) sh, 563 (15100), 571 (10900) sh, 609 nm (23500).

[a] The *n*-butyl compounds **8d** and **9d** are given as typical examples of *meso*-alkylated tetraoxaporphyrinogens **8** and tetraoxaporphyrin dications **9**. For the appropriate data for **8a–c**, **8e**, **9a–c**, and **9e** see ref.[18]. Because **8d** exists as a stereoisomeric mixture, the ^{1}H and ^{13}C NMR data are averaged.

Oxidation of **6** to the octaethyltetraoxaporphyrin dication **1b** was achieved (under anhydrous conditions) with 2,3-dichloro-5,6-dicyano-1,4-benzoquinone (DDQ), as described for the synthesis of **1a**,[1c] or with cerium(IV) ammonium nitrate in acetonitrile, in both cases with subsequent addition of perchloric acid. The cerium(IV) oxidation was given preference because of easier workup; **1b** is obtained after crystallization from formic acid or acetonitrile, each containing 1% perchloric acid, as red needles that decompose above 300 °C (yield 65 and 60%, respectively). In agreement with the intention of this work, the eight ethyl groups provide the salt **1b** with sufficient solubility in organic solvents (in particular in acids like formic and trifluoroacetic acid, or in dichloromethane, acetonitrile, and nitromethane) that the compound can be studied as a model tetraoxaporphyrin dication in homogeneous media.

In comparison with the spectra of **1a**[1a] those of **1b** show only qualitative differences (Table 1), so that further comment is unnecessary.

An X-ray crystallographic analysis of **1b**,[10] which shows the dication to be centrosymmetric in the crystal (Fig. 1), provides insight into the molecular structure. The ring

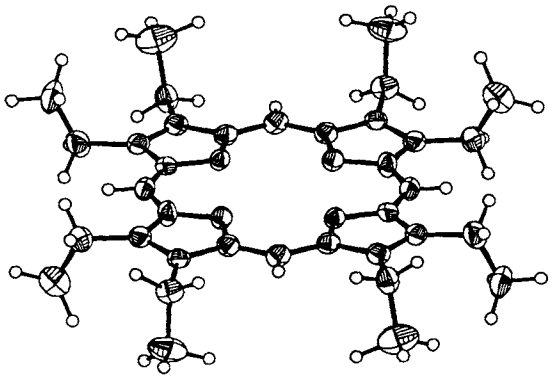

Fig. 1. Structure of **1b** in the crystal: perspective view.

framework of **1b** is planar, similar to that of the parent dication **1a**.[1a] The structural parameters of **1b** are in close agreement with those of **1a**, except for the lengths of the C_β–C_β bonds of the furan units, which are stretched (on average by 0.035 Å) as a result of the influence of the substituents. A slight deviation of the framework from the ideal D_{4h} symmetry affects the dimensions of the inner cavity in such a way as to distort the O_4 nucleus towards a rectangle (O···O distances: 2.842 and 2.944 Å). The spatial arrangement of the ethyl substituents corresponds to the situation in octaethylporphyrin.[11]

An electrochemical study of the octaethyltetraoxaporphyrin dication **1b** confirmed the existence of the tetraoxaporphyrin redox system, consisting of the 18 π dication, the radical cation, the neutral molecule ([20]annulene tetraoxaisophlorin), the radical anion, and the 22 π dianion, which was hitherto deduced mainly from chemical reduction[2] of the dication **1a** (insoluble in organic solvents) in combination with ESR studies. Polarographic investigation of **1b** in DMF with 0.1 M tetraethylammonium perchlorate (TEAP) as supporting electrolyte (accessible potential range + 0.4 to −2.9 V vs. SCE)[12] gave four half-wave potentials at + 0.24, −0.01, −1.46, and −1.73 V vs. SCE, which, as corroborated by cyclic voltammetric measurements in the same solvent, are attributable to reversible, one-electron transitions. Cyclic voltammetry of **1b** in dichloromethane with 0.1 M tetrabutylammonium hexafluorophosphate ($TBAPF_6$)[13] also shows that the compound can be reduced in four distinct one-electron steps, namely at + 0.20, −0.21, −1.63, and −1.93 V vs. SCE. The first two of these processes again are reversible transitions, whereas the third is pseudo-reversible and the fourth lies too close to the cathodic limit of measurement to be investigated in more detail.[14] Comparison of the potentials in DMF with those in dichloromethane shows that the first step in the reduction takes place at almost the same potential, whereas the three following steps are shifted to more positive potential (+ 200 mV) in DMF. This finding can be attributed to the solvating properties of this solvent. According to the results presented here, the electrochemical reduction of the dication **1b** takes place in four separate (in terms of electric potential) one-electron transitions, as shown in Scheme 1.

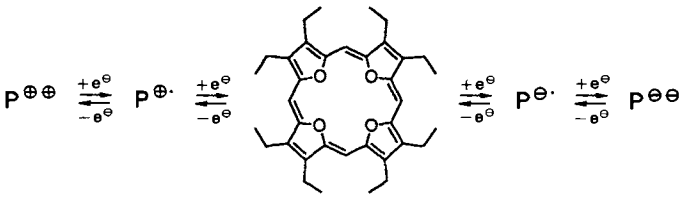

7

Scheme 1. Octaethyltetraoxaporphyrin redox system: $P^{\oplus\oplus}$ (dication **1b**), $P^{\oplus\cdot}$ (radical cation), **7** (octaethyltetraoxaisophlorin), $P^{\ominus\cdot}$ (radical anion), $P^{\ominus\ominus}$ (dianion).

The preparation of the electrochemically detected octaethyltetraoxaisophlorin (**7**) was accomplished—as for the parent compound[2]—by reduction of **1b** with potassium in THF to give the dianion, followed by partial oxidation with atmospheric oxygen. Chromatographic workup (with cooling) and crystallization from THF (−78 °C) gave **7** as a black, microcrystalline powder (yield 30%, decomposition above 0 °C).

The easy access to the 5,10,15,20-tetraalkyltetraoxaporphyrinogens **8a–e** (as stereoisomeric mixtures by the acid-induced condensation of 1,1-difurylalkanes with the appropriate aldehyde), suggested conversion of these compounds into the corresponding *meso*-alkyl-substituted tetraoxaporphyrin dications by the same process of oxidation and treatment with perchloric acid. Compounds **8a** and **8b** were already known,[15] and **8c–e** were prepared analogously here. As anticipated, the dications **9a–e** were obtained (yield 25–31%) without difficulty. The compounds were characterized by their spectra and, in the case of **9a**, moreover, by an X-ray structure analysis. All of these dications, which are stable in the crystalline state, are very soluble in formic and trifluoroacetic acid, but solubility in dichloromethane and acetonitrile is found to be adequate only for **9c–e** (the solubility increases markedly with increasing size of the alkyl group).

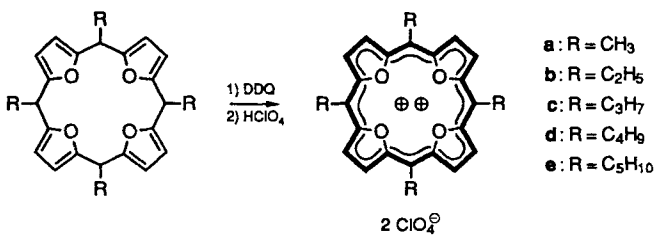

8 **9**

In striking contrast to the octaethyltetraoxaporphyrin dication **1b**, the *meso*-alkylated tetraoxaporphyrin dications **9c–e** are not stable in dichloromethane or other inert organic solvents (stability in acids, however, is retained). Relatively rapid decomposition occurs (half-lifetimes in the range 0.5–2 h), which starts, according to ^{1}H NMR experiments, by deprotonation in the side chain. Precedents for such a deprotonation exist in the case of *meso*-alkylated diprotonated porphyrins.[16] The greater stability of **1b** relative to **9c–e**, which makes **1b** a more suitable model compound for the tetraoxaporphyrin dication,[17] can be ascribed to the different substitution pattern and also to the higher degree of alkylation.

Experimental Procedure

6: To a solution of *p*-toluenesulfonic acid (4.42 g, 25 mmol) in boiling nitromethane (160 mL) was added 3,4-diethyl-2-hydroxymethylfuran (**5**, 3.85 g, 25 mmol) in nitromethane (20 mL), and the mixture heated under reflux for 15 min. After neutralization with saturated sodium bicarbonate solution the reaction mixture was extracted three times with 200 mL ether. The combined organic extracts were washed with water, dried over Na_2SO_4, and the solvent was then removed under vacuum. Chromatography of the resulting product on silica gel (3 × 70 cm column) with toluene/hexane (1:1) gave **6** as a pale yellow solid, which crystallized from ethanol as colorless rhombic crystals; m.p. 138–140 °C, yield 545 mg (16%).

1b: Porphyrinogen **6** (268 mg, 0.5 mmol) was dissolved in absolute acetonitrile (40 mL) and stirred with cerium(IV) ammonium nitrate (1.5 g, 4 mmol) at room temperature. After 45 min 0.5 mL of a 70% solution of perchloric acid was added to the reaction mixture, and the solvent removed under vacuum. The remaining amorphous residue was washed first with a little water and then with ether, and crystallized from formic acid containing 1% of a 70% perchloric acid solution. The dication **1b** was obtained as red needles, which decompose above 300 °C; yield 242 mg (65%).

Received: April 30, 1993 [Z 6053 1E]
German version: *Angew. Chem.* **1993**, *105*, 1667

[1] a) E. Vogel, W. Haas, B. Knipp, J. Lex, H. Schmickler, *Angew. Chem.* **1988**, *100*, 445; *Angew. Chem. Int. Ed. Engl.* **1988**, *27*, 406; b) W. Haas, B. Knipp, M. Sicken, J. Lex, E. Vogel, *ibid.* **1988**, *100*, 448 or **1988**, *27*, 409; c) E. Vogel, P. Röhrig, M. Sicken, B. Knipp, A. Herrmann, M. Pohl, H. Schmickler, J. Lex, *ibid.* **1989**, *101*, 1683 or **1989**, *28*, 1651.

[2] a) R. Bachmann, F. Gerson, G. Gescheidt, E. Vogel, *J. Am. Chem. Soc.* **1992**, *114*, 10855; b) E. Vogel, *Pure Appl. Chem.* **1993**, *65*, 143; c) E. Vogel, B. Knipp, J. Lex, C. Pütz, P. Röhrig, H. Schmickler, unpublished.

[3] M. Sicken, Dissertation, Universität Köln, **1991**.

[4] J. L. Sessler, A. Mozaffari, M. R. Johnson, *Org. Synth.* **1992**, *70*, 68, and references therein.

[5] J. S. Lindsey, H. C. Hsu, I. C. Schreiman, *Tetrahedron Lett.* **1986**, *27*, 4969; R. W. Wagner, D. S. Lawrence, J. S. Lindsey, *ibid.* **1987**, *28*, 3069; J. S. Lindsey, I. C. Schreiman, H. C. Hsu, P. C. Kearney, A. M. Marguerettaz, *J. Org. Chem.* **1987**, *52*, 827.

[6] H. Fischer, W. Gleim, *Liebigs Ann. Chem.* **1936**, *521*, 157; S. Krol, *J. Org. Chem.* **1959**, *24*, 2065; F. R. Longo, E. J. Thorne, A. D. Adler, S. Dym, *J. Heterocycl. Chem.* **1975**, *12*, 1305.

[7] The method of preparation described in the literature for **4** (J. Froborg, G. Magnusson, S. Thoren, *J. Org. Chem.* **1975**, *40*, 122) suffers from the disadvantage that the product contains small amounts of the structural isomer 4-methyl-3-propylfuran, which is difficult to separate.

[8] H. König, F. Graf, V. Weberndörfer, *Liebigs Ann. Chem.* **1981**, 668; M. S. Ho, H. N. C. Wong, *J. Chem. Soc. Chem. Commun.* **1989**, 1238.

[9] B. Franck, *Angew. Chem.* **1982**, *94*, 327; *Angew. Chem. Int. Ed. Engl.* **1982**, *21*, 343; G. Bringmann, B. Franck, *Liebigs Ann. Chem.* **1982**, 1272; L. F. Tietze, H. Geissler, *Angew. Chem.* **1993**, *105*, 1087; *Angew. Chem. Int. Ed. Engl.* **1993**, *32*, 1038.

[10] $C_{36}H_{44}Cl_2O_{12}$, crystals from formic acid; triclinic, space group $P\bar{1}$, $Z = 1$; $a = 7.491(1)$, $b = 9.129(1)$, $c = 14.236(3)$ Å, $\alpha = 75.25(2)$, $\beta = 72.86(2)$, $\gamma = 78.82(2)$°, $\rho_{calcd} = 1.377$ g cm^{-3}; intensity measurements were made on a four-circle Enraf-Nonius CAD-4 diffractometer (room temperature, $\lambda_{Mo} = 0.71069$ Å, $\theta_{max.} = 27$°); refinement (C, Cl, O atoms anisotropic, H atoms isotropic) taking account of 2126 reflections with $F_0 > 4\sigma(F_0)$; $R = 0.072$, $R_w = 0.079$. Further details of the crystal structure investigation may be obtained from the Fachinformationszentrum Karlsruhe, Gesellschaft für wissenschaftlich-technische Information mbH, D-76344 Eggenstein-Leopoldshafen (FRG) on quoting the depository number CSD-57312, the names of the authors, and the journal citation.

[11] J. W. Lauher, J. A. Ibers, *J. Am. Chem. Soc.* **1973**, *95*, 5148.

[12] The polarographic and cyclic voltammetric experiments in DMF were carried out with a dropping mercury electrode (flow rate 0.61 mg s^{-1}) at a scan rate of 5–100 V s^{-1}. Purification of DMF and the supporting electrolyte TEAP was as previously described: H. J. Callot, A. Giraudeau, M. Gross, *J. Chem. Soc. Perkin Trans. 2* **1975**, 1321.

[13] Dichloromethane was both dried and stored over molecular sieves (4 Å) under argon. $TBAPF_6$ (Fluka, electrochemical grade) was used without further purification as supporting electrolyte. The cyclic voltammetric measurements in dichloromethane were carried out at a Pt electrode with a scan rate of 10 mV s^{-1} - 20 V s^{-1}. The potentials were measured against a saturated calomel electrode as reference; under the prevailing experimental conditions,ferrocene (internal standard) was oxidized in dichloromethane and 0.1 M $TBAPF_6$ at + 0.4 V vs. SCE.

[14] A scan rate of 10 mV s^{-1} to 10 V s^{-1} was used for peak analysis: For the first two reductions $I_p = f(v^{1/2})$ passes through the zero point and is linear; ΔE_p varies between 60 (at rate of 10 mV s^{-1}) and 80 mV (10 V s^{-1}). For the third redox process ΔE_p increases with increasing scan rate from 80 (at 10 mV s^{-1}) to 200 mV (at 10 V s^{-1}), whereas $I_p = f(v^{1/2})$ is linear and passes through the origin.

[15] Y. Kobuke, K. Hanji, K. Horiguchi, M. Asada, Y. Nakayama, J. Furukawa, *J. Am. Chem. Soc.* **1976**, *98*, 7414; A. G. S. Högberg, M. Weber, *Acta Chem. Scand. Ser. B* **1983**, *37*, 55.

[16] R. B. Woodward, W. A. Ayer, J. M. Beaton, F. Bickelhaupt, R. Bonnett, P. Buchschacher, G. L. Closs, H. Dutler, J. Hannah, F. P. Hauck, S. Ito, A. Langemann, E. LeGoff, W. Leimgruber, W. Lwowski, J. Sauer, Z. Valenta, H. Volz, *Tetrahedron* **1990**, *46*, 7599.

[17] An investigation into the stability of **1b** in dry dichloromethane and DMF, undertaken in the light of the findings for **9c–e**, showed that the compound can be kept in these solvents for a few hours. Thereafter, decomposition becomes noticeable.

[18] P. Walgenbach, Dissertation, Universität Köln, **1992**.

New Porphycene Ligands: Octaethyl- and Etioporphycene (OEPc and EtioPc)—Tetra- and Pentacoordinated Zinc Complexes of OEPc

By *Emanuel Vogel,* Peter Koch, Xue-Long Hou, Johann Lex, Michael Lausmann, Michael Kisters, Mohamed Ally Aukauloo, Philippe Richard,* and *Roger Guilard**

The 2,7,12,17-tetrapropylporphycene ligand (TPrPc), conceived as the counterpart of octaethylporphyrin (OEP) in the porphycene series, has proved its value in metalloporphycene research on numerous occasions.[1] Although the cavity of the N_4 coordination center in porphycenes is smaller than that in porphyrins, and the lone electron pairs on the pyrrolenine nitrogen atoms as well as the N–H bonds are not strictly oriented towards the center of the molecule, TPrPc readily forms stable complexes with the common metal ions Ni^{II}, Cu^{II}, Co^{II}, Co^{III}, Fe^{III}, Mn^{III}, Al^{III}, and Sn^{IV} (each have small to medium crystal ionic radii[2]). In contrast to previous experience, TPrPc can even form complexes with the comparatively large osmium(II) ion, as recently reported by the groups of C.-M. Che and C. K. Chang.[1j]

In the light of these findings, it seemed remarkable that TPrPc shows only a relatively low tendency to coordinate to a zinc ion to form porphycenatozinc. Given the importance of zinc complexes in porphyrin chemistry, whether as photo-

[*] Prof. Dr. E. Vogel, Dr. P. Koch, Dr. X.-L. Hou, Dr. J. Lex, Dr. M. Lausmann, Dipl.-Chem. M. Kisters
Institut für Organische Chemie der Universität
Greinstrasse 4, D-50939 Köln (FRG)
Prof. Dr. R Guilard, M. A. Aukauloo, Dr. P. Richard
Université de Bourgogne
Laboratoire de Synthèse et d'Electrosynthèse Organométallique Associé au C. N. R. S. (UA 33)
Faculté des Sciences "Gabriel"
6, Boulevard Gabriel, F-21100 Dijon (France)

sensitizers,[3] as model compounds for the study of photosynthesis,[4] or as components in enzyme models,[5] there is considerable interest in porphycene ligands that are more able than TPrPc to bind zinc(II) and larger ions.

We report here on 2,3,6,7,12,13,16,17-octaethylporphycene and 2,7,12,17-tetraethyl-3,6,13,16-tetramethylporphycene (OEPc **1** and EtioPc **4**, respectively), and on the readily obtained four- and five-coordinate zinc complexes of **1**[6] (Table 1).

Table 1. Selected physical and spectroscopic data for the new compounds. ^{1}H NMR: 300 MHz; ^{13}C NMR: 75.5 MHz, $CDCl_3$; MS: EI, 70 eV; IR: CsI; UV/VIS: CH_2Cl_2.

1: M.p. 181–183 °C (methanol/chloroform); ^{1}H NMR ($CDCl_3$): δ = 9.48 (s, 4H; H-9,10,19,20), 4.02 (q, 8H; H-3a,6a,13a,16a), 3.87 (q, 8H; H-2a,7a,12a,17a), 1.65 (t, 12H; H-2b,7b,12b,17b), 1.58 (t, 12H; H-3b,6b,13b,16b), 0.65 (br. s, 2H; NH); ^{13}C NMR: δ = 143.27, 142.02, 137.23, 136.72, 109.82, 21.39, 19.94, 18.08 (2 C atoms); MS: *m/z* (%): 534 (100) [M^+], 267 (14) [M^{2+}]; IR: $\tilde{\nu}$ = 2964, 2930, 2869, 1518, 1471, 1060, 989, 946, 929, 856 cm^{-1}; UV/VIS: λ_{max} (ε) = 385 (144000), 576 (35200), 625 (19700), 665 nm (30700).

2: M.p. 263–265 °C (hexane/chloroform); ^{1}H NMR ($CDCl_3$): δ = 9.80 (s, 4H; H-9,10,19,20), 4.15 (q, 8H; H-3a,6a,13a,16a), 4.04 (q, 8H; H-2a,7a,12a,17a), 1.84 (t, 12H; H-2b,7b,12b,17b), 1.78 (t, 12H; H-3b,6b,13b,16b); ^{13}C NMR: δ = 146.91, 142.69, 140.78, 137.44, 109.78, 21.06, 20.31, 18.74, 18.69; MS: *m/z* (%): 596 (100) [M^+], 298 (19) [M^{2+}]; IR: $\tilde{\nu}$ = 2963, 2930, 2869, 1488, 1314, 1301, 1132, 1013, 994, 948 cm^{-1}; UV/VIS: λ_{max} (ε) = 375 (77500) sh, 393 (161000), 590 (21900), 638 nm (94600).

3: M.p. 243–245 °C (pyridine/dioxane); ^{1}H NMR ($CDCl_3$): δ = 9.61 (s, 4H; H-9,10,19,20), 6.49 [m, 1H; H-γ (pyridine)], 5.74 [m, 2H; H-β (pyridine)], 4.06 (q, 8H; H-3a,6a,13a,16a), 3.96 (q, 8H; H-2a,7a,12a,17a), 3.59 [m, 2H; H-α (pyridine)], 1.76 (t, 12H; H-2b,7b,12b,17b), 1.69 (t, 12H; H-3b,6b,13b,16b); ^{13}C NMR: δ = 145.87, 144.64, 142.68, 141.60, 136.51, 135.65, 122.27, 109.19, 21.04, 20.29, 18.81, 18.71; MS: *m/z* (%): 596 (100) [$M^+ - C_5H_5N$], 298 (24) [$M^{2+} - C_5H_5N$]; IR: $\tilde{\nu}$ = 2963, 2930, 2868, 1484, 1277, 1225, 1134, 1009, 995, 948 cm^{-1}; UV/VIS: λ_{max} (ε) = 371 (81000) sh, 395 (146400), 598 (22400), 644 nm (91900).

4: M.p. 268–270 °C (hexane/chloroform); ^{1}H NMR ($CDCl_3$): δ = 9.52 (s, 4H; H-9,10,19,20), 3.85 (q, 4H; H-2a,7a,12a,17a), 3.57 (s, 12H; H-3a, 6a, 13a, 16a), 1.70 (t, 12H; H-2b,7b,12b,17b), 0.86 (br. s, 2H; NH); ^{13}C NMR: δ = 143.88, 142.13, 137.32, 130.46, 109.84, 19.96, 17.23, 16.19; MS: *m/z* (%): 478 (100) [M^+], 239 (19) [M^{2+}]; IR: $\tilde{\nu}$ = 2960, 2928, 2867, 1466, 1196, 1083, 1057, 982, 938, 864, 806 cm^{-1}; UV/VIS: λ_{max} (ε) = 382 (144200), 570 (34200), 617 (18400), 657 nm (30000).

6a: M.p. 103–105 °C (ethanol); ^{1}H NMR ($CDCl_3$): δ = 9.10, 4.34, 2.75, 1.96, 1.33, 1.08. **6b**: M.p. 97–99 °C (ethanol); ^{1}H NMR ($CDCl_3$): δ = 8.87, 4.30, 2.74, 2.37, 1.33, 1.12, 1.06. **7a**: Subl. >170 °C (hexane/dichloromethane); ^{1}H NMR ($CDCl_3$): δ = 8.68, 4.33, 2.77, 2.04, 1.34, 1.14. **7b**: M.p. 161–163 °C (hexane/dichloromethane); ^{1}H NMR ($CDCl_3$): δ = 8.78, 4.28, 2.76, 2.44, 1.33, 1.17, 1.05. **8a**: decomp. >218 °C; ^{1}H NMR ([D$_6$]DMSO): δ = 10.96, 2.69, 2.49, 1.05. **8b**: decomp. >260 °C; ^{1}H NMR ([D$_6$]DMSO): δ = 11.94, 11.11, 2.69, 2.30, 1.09, 0.88. **9a**: M.p. 76–78 °C (sublimation); ^{1}H NMR ($CDCl_3$): δ = 7.68, 6.55, 2.49, 2.02, 1.22. **9b**: M.p. 90–92 °C (sublimation); ^{1}H NMR ($CDCl_3$): δ = 7.68, 6.54, 2.51, 2.42, 1.24, 1.06. **10a**: decomp. >245 °C (hexane/dichloromethane); ^{1}H NMR ($CDCl_3$): δ = 9.85, 9.65, 2.75, 2.10, 1.23. **10b**: decomp. >227 °C (hexane/dichloromethane); ^{1}H NMR ($CDCl_3$): δ = 9.64, 9.47, 2.76, 2.50, 1.26, 1.05.

Consideration of models[7] which predict that the introduction of alkyl groups to the 3,6- and 13,16-positions of the porphycene structure would cause an increase in the N1···N4 and N2···N3 distances as a result of van der Waals repulsion, was decisive for the choice of **1** and **4** as ligands. Thus with these ligands, in addition to a weakening of the N–H···N hydrogen bonds, the pronounced rectangular N_4 coordination center in the parent compound[8] and in TPrPc[1a] would now adopt an almost square arrangement. An improved tendency toward complex formation should result in both cases. The assumed deviations from planarity of the ring framework in 3,6,13,16-alkyl-substituted porphycenes, caused by steric interactions,[7] which had originally prevented us from considering **1** as a model ligand, should—as concluded from structural results with the nickel complex of TPrPc[1a]—largely if not completely cancel in the conversion of such porphycenes to metal complexes.

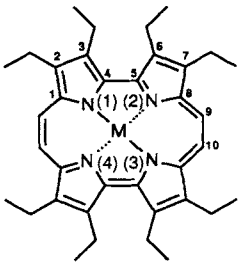

1: M = 2H **2**: M = Zn **3**: M = Zn(C_5H_5N)

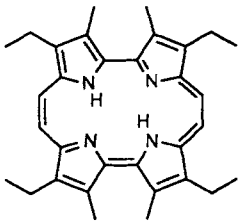

4

The synthesis of octaethylporphycene **1** was achieved according to the general method of preparation for porphycenes,[1a, 7] by subjecting 3,3′,4,4′-tetraethyl-5,5′-diformyl-2,2′-bipyrrole (**10b**), made as described in Scheme 1, to reductive carbonyl coupling with low valent titanium. After standard workup and recrystallization of the product from methanol/chloroform (5:1), **1** was obtained as violet needles (blue, nonfluorescent solutions), which melt without decomposition at 181–183 °C (yield 15%, see Experimental Procedure).

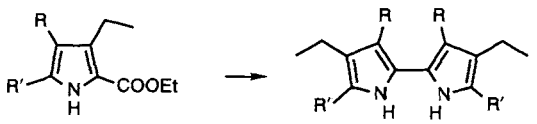

a: R = CH_3
b: R = C_2H_5

5a/5b: R′ = H[23]
6a/6b: R′ = I

7a/7b: R′ = COOEt
8a/8b: R′ = COOH
9a/9b: R′ = H
10a/10b: R′ = CHO

Scheme 1. **5a/5b** → **6a/6b**: I_2/HIO_3, CCl_4/dilute acetic acid, reflux, 45 min (85–90%); **6a/6b** → **7a/7b**: Cu, dimethylformamide (DMF), 110 °C, 3 h (45–50% for **7a**, 35–40% for **7b**); **7a/7b** → **8a/8b**: NaOH in C_2H_5OH/H_2O, reflux, 2 h (90–95%); **8a/8b** → **9a/9b**: sublimation at 195 °C/0.01 Torr (85–90%); **9a/9b** → **10a/10b**: $POCl_3$/DMF; CH_3COONa, H_2O (90–95%). For physical and spectroscopic data, see Table 1.

The ^{1}H NMR spectrum (300 MHz, $CDCl_3$) shows that **1** is an aromatic porphycene. Comparison with the signals of the corresponding protons in TPrPc reveals that the signal of H9,10,19,20 occurs at almost the same field (singlet at δ = 9.48 versus 9.62 in TPrPc), whereas that of the *N*-protons (δ = 0.65 versus 3.04) experiences a marked shift to higher field ($\Delta\delta$ = 2.39), which could be foreseen in view of the increase in the N1···N4 and N2···N3 distance (weakening of the N–H···N hydrogen bonds). The IR spectrum of **1** shows, analogous to that of TPrPc, no stretching vibration in the range 3300–3600 cm^{-1}, which indicates that the hydrogen bonds are weakened only gradually.

According to an X-ray crystallographic analysis,[9] **1** exists in the crystal as a molecule with C_2 symmetry (Fig. 1). The crystal exhibits a statistical distribution of the two *N*-hydrogen atoms with half occupancy of the four possible positions. The porphycene skeleton of **1**, in contrast to that of TPrPc, is no longer planar, but experiences a slight twist because of the van der Waals repulsions of the ethyl groups in the 3,6-

and 13,16-positions (maximum distance of the C and N atoms from the central plane of the porphycene ring structure: ±0.27 Å). Deviation of the structure from the planar arrangement is accompanied by angle deformations, in particular by contraction of the bond angles in the NCCN segments (118.5° versus 121.8° in TPrPc). Consequently, in accordance with the prediction, the N_4 coordination center adopts an approximately square arrangement. Remarkably, the N···N distance of the hydrogen bonds in **1** is now slightly larger than that between the nitrogen atoms within the bipyrrole units.

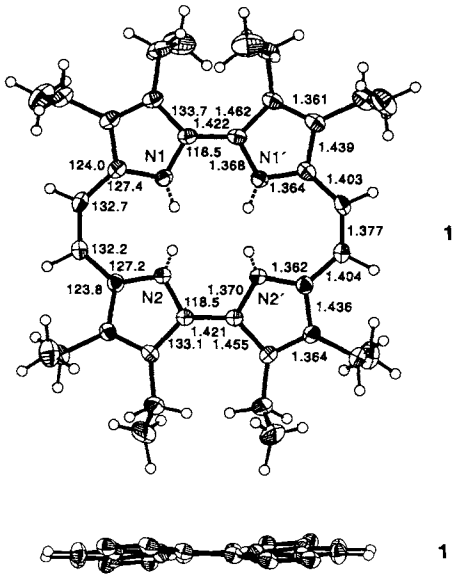

Fig. 1. Structure of **1** in the crystal (top: viewed from above; bottom: side view). Vibrational ellipsoids represent 40% probability. Also shown are selected bond lengths [Å] and angles [°] (standard deviations about 0.002 Å or 0.2°, respectively); inner hydrogen atoms in **1** disordered. The ethyl groups are not shown in the side view. N1···N2 2.799, N1···N1′ 2.732 Å.

The expectation that **1** is more suitable than TPrPc as a complexing agent for the zinc(II) ion is borne out by experiment. The new ligand can be converted quantitatively into complex **2** within 15 min by treatment with methanolic zinc acetate solution in refluxing chloroform, whereas in the case of TPrPc even extensive heating in DMF at 150 °C does not lead to complete reaction.[10] Simple workup gave **2** in the form of violet needles (from hexane/chloroform, m.p. 263–265 °C; yield 87%).[11]

Compared to that of **1**, the ^{1}H NMR spectrum (300 MHz, $CDCl_3$) of **2** exhibits a slight downfield shift for the signal of H9, 10, 19, 20 ($\Delta\delta = 0.32$) as well as for the signals of the ethyl protons. The main reason for this may be ascribed to the fact that metalation of **1** enhances the ring current effect due to the increase in symmetry of the molecular framework.[12] Apart from that, an electron transfer from the porphycene π system to the metal ion, operative in the same direction, is likely to be involved.[13] The UV/VIS spectrum shows a Soret band that is almost congruent with that of the free ligand in addition to two absorption bands in the visible range. The band positions are solvent dependent, which is linked to the ability of the zinc ion to enter into axial pentacoordination;[14] donor solvents such as pyridine cause bathochromic shifts.

According to an X-ray structural analysis,[15] complex **2** is centrosymmetric (Fig. 2); moreover, the porphycene ring system is shown to be planar (maximum distance of the heavy atoms from the central plane: ±0.05 Å). From the structural parameters of **2** it follows that the metalation of **1** with zinc profits if the bond angles in the NCCN segment—in the interests of a better alignment of the nitrogen electron pairs and bonds towards the center of the molecule—undergo further contraction (relative to TPrPc and **1**). The formation of a rectangular N_4 center must be tolerated here. The average Zn–N distance in **2** is 2.007 Å and is thus somewhat shorter than that found in tetracoordinated zinc porphyrinates (Zn–N: 2.024–2.06 Å).[16] As the metalation of **1** is associated with a considerable reduction in the nonbonding substituent interactions, the unusual situation arises that a nonplanar porphyrinoid ligand experiences a flattening effect on the incorporation of metal ions.[17]

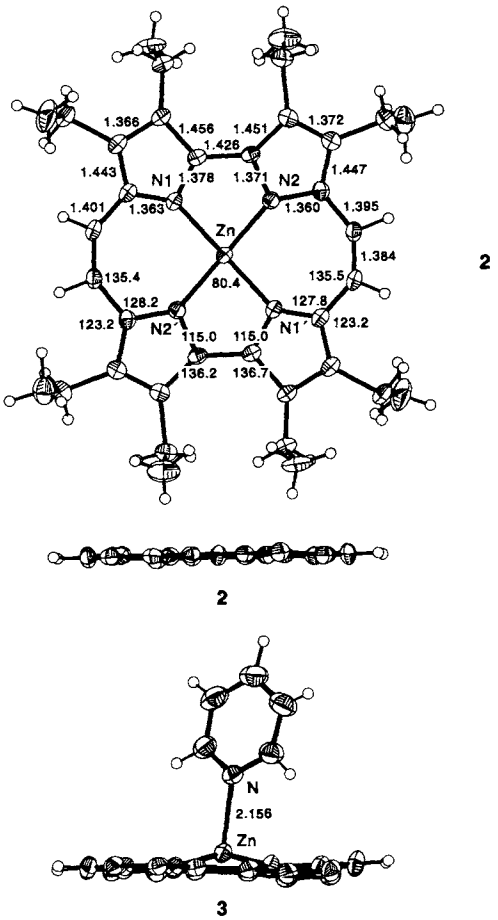

Fig. 2. Structure of the zinc complexes **2** and **3** in the crystal (top: **2** viewed from above; center: side view of **2**; bottom: side view of **3**). Vibrational ellipsoids represent 40% probability. Selected bond lengths [Å] and angles [°] are also given (standard deviations ca. 0.003 Å or 0.2°, respectively). The ethyl groups are not shown in the side views. N1···N2′ 3.066, N1···N2 2.588 Å in **2**.

By analogy with the corresponding zinc porphyrinates, **2** also shows a tendency to increase the coordination number of zinc by adding an axial donor ligand. A typical example is the formation of pyridine(octaethylporphycenato)zinc(II) (**3**) by crystallization of **2** from pyridine/dioxane (1:1). On the strength of an X-ray crystal structure analysis[18] (Fig. 2 bottom), the new complex shows great similarity with **2** in terms of bond lengths and angles, but the zinc atom resides 0.39 Å above the N_4 plane as a result of the axial ligand (corresponding distance in quinquidentate zinc porphyrin-

ates: 0.22–0.39 Å).[19] The other distances involving the zinc atom lie within normal range.

The idea of increasing the complex-forming ability of porphycenes by alkyl substitution in the 3,6,13,16-positions was followed not only in Cologne but also in Dijon. Considering the fact that many porphyrins possess the alkyl substitution pattern of etioporphyrin-II,[20] the French coauthors chose 2,7,12,17-tetraethyl-3,6,13,16-tetramethylporphycene (etioporphycene) (**4**) rather than **1** as model compound. The synthesis of **4**, using the same route as that employed for **1** (Scheme 1), is somewhat more advantageous because the Ullmann coupling of the 3,4-dialkyl-2-ethoxycarbonyl-5-iodopyrrole to afford the bipyrrole derivative gives a better yield, on evident steric grounds. Analogous to **1**, a solution of **4** is intense blue and nonfluorescent. Compound **4** is obtained as violet crystals [needles from hexane/chloroform (1:1), m.p. 268–270 °C, yield 15%].

The spectra of **4** show only slight changes relative to those of **1**, so it could not be determined whether the exchange of the 3,6,13,16-ethyl groups for methyl groups had a noticeable effect on the conformation of the ring skeleton. This is, in fact, the case. According to an X-ray crystal structure analysis,[21] the planarity of the ring framework in TPrPc is almost restored in **4** (maximum distance of the heavy atoms from the central plane of the porphycene macrocycle: ±0.15 Å, Fig. 3). As far as the other geometric features are concerned there is no major difference between **4** and **1**.

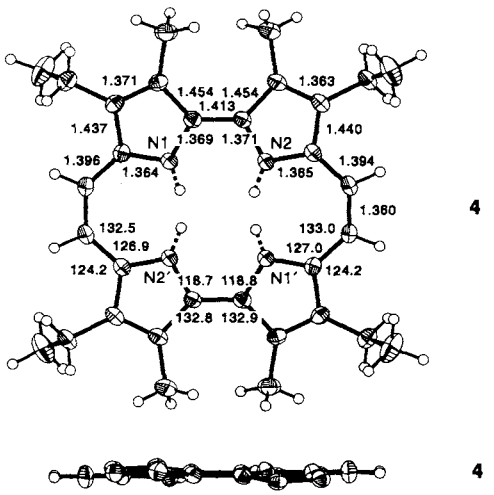

Fig. 3. Structure of **4** in the crystal (top: viewed from above; bottom; side view). Vibrational ellipsoids represent 40% probability. Selected bond lengths [Å] and angles [°] are also shown (standard deviations about 0.002 Å or 0.1°, respectively); inner hydrogen atoms in **4** disordered. The ethyl and methyl groups are not shown in the side view. N1 ··· N2' 2.791, N1 ··· N2 2.737 Å.

The two new alkyl-substituted porphycenes **1** and **4** complement TPrPc (representing the porphycene parent compound) as ligands that, on the grounds of "optimized coordinating ability", should encourage research into the metalloporphycenes—especially as they invite comparison with the corresponding metalloporphyrins.

Experimental Procedure

10a/10b: The bipyrrole dialdehydes **10a**[22]/**10b** were obtained as shown in Scheme 1.

1/4: Activated zinc (13.1 g, 200 mmol) and CuCl (2.0 g, 20 mmol) were placed in tetrahydrofuran (800 mL), $TiCl_4$ (11.0 mL, 100 mmol) added dropwise, and the resulting mixture heated at reflux for 3 h. Within 4 min (for **1**) or 15 min (for **4**) a solution of **10b** (1.5 g, 5 mmol) or **10a** (1.4 g, 5 mmol) in THF (200 mL) was added dropwise, and the reaction mixture stirred at reflux for 3 min. Finally, the resulting product was hydrolyzed with 200 mL of 10% K_2CO_3 solution and worked up.

1: After chromatography on neutral aluminum oxide (activity III, column 3 × 30 cm) with hexane/dichloromethane (1:1), **1** was obtained as the first fraction. Crystallization from methanol/chloroform (5:1) gave octaethylporphycene (**1**) as violet needles, m.p. 181–183 °C; yield 200 mg (15%).

4: After chromatography on silica gel (column 4 × 15 cm) with dichloromethane, **4** was obtained as the first fraction. Crystallization from hexane/chloroform (1:1) gave etioporphycene (**4**) as violet needles, m.p. 268–270 °C; yield 180 mg (15%).

2: Compound **1** (106 mg, 0.2 mmol) in chloroform (60 mL) was heated at reflux for 15 min with 2 mL of a saturated solution of zinc acetate in methanol. The solvent was then removed, the resulting zinc complex taken up in chloroform, and the solution filtered. Crystallization from hexane/chloroform (4:1) gave **2** as violet needles, m.p. 263–265 °C; yield 104 mg (88%).

Received: April 30, 1993 [Z 6054 IE]
German version: *Angew. Chem.* **1993**, *105*, 1670

[1] a) E. Vogel, M. Balci, K. Pramod, P. Koch, J. Lex, O. Ermer, *Angew. Chem.* **1987**, *99*, 909; *Angew. Chem. Int. Ed. Engl.* **1987**, *26*, 928; b) M. W. Renner, A. Forman, W. Wu, C. K. Chang, J. Fajer, *J. Am. Chem. Soc.* **1989**, *111*, 8618; c) M. Toporowicz, H. Ofir, H. Levanon, E. Vogel, M. Köcher, K. Pramod, R. W. Fessenden, *Photochem. Photobiol.* **1989**, *50*, 37; d) E. Vogel, *Pure Appl. Chem.* **1990**, *62*, 557; e) L. R. Furenlid, M. W. Renner, K. M. Smith, J. Fajer, *J. Am. Chem. Soc.* **1990**, *112*, 1634; f) J. Schlüpmann, M. Huber, M. Toporowicz, M. Plato, M. Köcher, E. Vogel, H. Levanon, K. Möbius, *ibid.* **1990**, *112*, 6463; g) J. P. Gisselbrecht, M. Gross, M. Köcher, M. Lausmann, E. Vogel, *ibid.* **1990**, *112*, 8618; h) W. A. Oertling, W. Wu, J. J. López-Garriga, Y. Kim, C. K. Chang, *ibid.* **1991**, *113*, 127; i) J. Waluk, M. Müller, P. Swiderek, M. Köcher, E. Vogel, G. Hohlneicher, J. Michl, *ibid.* **1991**, *113*, 5511; j) Z.-Y. Li, J.-S. Huang, C.-M. Che, C. K. Chang, *Inorg. Chem.* **1992**, *31*, 2670.

[2] *CRC Handb. Chem. Phys.*, 70th ed., **1989–1990**, F-187.

[3] K. Kalyanasundaram, M. Grätzel, E. Pelizzetti, *Coord. Chem. Rev.* **1986**, *69*, 57; W. Schuhmann, H.-P. Josel, H. Parlar, *Angew. Chem.* **1987**, *99*, 264; *Angew. Chem Int. Ed. Engl.* **1987**, *26*, 241.

[4] H. A. Staab, J. Weiser, E. Baumann, *Chem. Ber.* **1992**, *125*, 2275; H. A. Staab, J. Weiser, M. Futscher, G. Voit, A. Rückemann, C. Anders, *ibid.* **1992**, *125*, 2285; J. L. Sessler, M. R. Johnson, S. E. Creager, J. C. Fettinger, J. A. Ibers, *J. Am. Chem Soc.* **1990**, *112*, 9310.

[5] A. Hamilton, J.-M. Lehn, J. L. Sessler, *J. Am. Chem. Soc.* **1986**, *108*, 5158.

[6] For photophysical investigations on **1** and **2** see: A. Berman, A. Michaeli, J. Feitelson, M. K. Bowman, J. R. Norris, H. Levanon, E. Vogel, P. Koch, *J. Phys. Chem.* **1992**, *96*, 3041.

[7] E. Vogel, M. Köcher, J. Lex, O. Ermer, *Isr. J. Chem.* **1989**, *29*, 257.

[8] E. Vogel, M. Köcher, H. Schmickler, J. Lex, *Angew. Chem.* **1986**, *98*, 262; *Angew. Chem. Int. Ed. Engl.* **1986**, *25*, 257.

[9] **1**: $C_{36}H_{46}N_4$, crystals from hexane/dichloromethane (1:1); orthorhombic, space group *Fdd*2, $Z = 8$; $a = 14.046(3)$, $b = 28.852(6)$, $c = 15.043(4)$ Å, $\rho_{calcd} = 1.165\ g\,cm^{-3}$; intensity measurements were made on a four-circle Enraf-Nonius CAD4 diffractometer (room temperature, $\lambda_{Mo} = 0.71069$ Å, $\theta_{max.} = 27°$); refinement (C and N atoms anisotropic, H atoms isotropic) taking account of 1582 reflections with $I > 2\sigma(I)$, $R = 0.031$, $R_w = 0.039$; [24].

[10] For the isolation of dimethylformamide(2,7,12,17-tetrapropylporphycenato)zinc(II) see: M. Lausmann, Dissertation, Universität Köln, **1993**.

[11] Stability class IV after Buchler; J. W. Buchler, *Porphyrins* **1978–1979**, *1*, 389.

[12] H. Scheer, J. J. Katz, *Porphyrins Metalloporphyrins* **1975**, p. 399.

[13] D. R. Benson, R. Valentekovich, C. B. Knobler, F. Diederich, *Tetrahedron* **1991**, *47*, 2401.

[14] C. H. Kirksey, P. Hambright, C. B. Storm, *Inorg. Chem.* **1969**, *8*, 2141.

[15] **2**: $C_{36}H_{44}N_4Zn$, crystals from benzene; triclinic, space group $P\bar{1}$, $Z = 1$; $a = 5.202(1)$, $b = 12.265(3)$, $c = 12.436(3)$ Å, $\alpha = 73.47(2)$, $\beta = 89.23(2)$, $\gamma = 86.55(2)°$, $\rho_{calcd} = 1.308\ g\,cm^{-3}$; conditions of measurement as for **1**: refinement (C, N and Zn atoms anisotropic, H atoms isotropic) taking account of 3338 reflections with $I > 2\sigma(I)$, $R = 0.050$, $R_w = 0.060$; [24].

[16] For typical examples see: W. R. Scheidt, J. U. Mondal, C. W. Eigenbrot, A. Adler, L. J. Radonovich, J. L. Hoard, *Inorg. Chem.* **1986**, *25*, 795; A. Chiaroni, C. Riche, C. Bied-Charreton, J. C. Dubois, *Acta Crystallogr. Sect. C* **1988**, *44*, 429; [13].

[17] Compare on the other hand the saddlelike deformation of porphyrin ligands and hydroporphyrinoid ligands in the formation of complexes with Ni(II) ions: J. L. Hoard, *Ann. N. Y. Acad. Sci.* **1973**, *206*, 18; C. Kratky, R. Waditschatka, C. Angst, J. E. Johansen, J. C. Plaquevent, J. Schreiber, A. Eschenmoser, *Helv. Chim. Acta* **1985**, *68*, 1312.

[18] **3**: $C_{41}H_{40}N_5Zn$, crystals from pyridine/dioxan (1:1); triclinic, space group $P\bar{1}$, $Z = 2$; $a = 8.994(2)$, $b = 14.079(3)$, $c = 15.324(3)$ Å, $\alpha = 78.36(2)$, $\beta = 72.01(2)$, $\gamma = 80.70(2)°$, $\rho_{calcg} = 1.258\ g\,cm^{-3}$; conditions of measurement as for **1**; refinement (C, N, and Zn atoms anisotropic, H atoms isotropic)

 © VCH Verlagsgesellschaft mbH, D-69451 Weinheim, 1993 0570-0833/93/1111-1603 $ 10.00+.25/0

taking account of 5969 reflections with $I > 2\sigma(I)$, $R = 0.035$, $R_w = 0.040$; [24].
[19] For typical examples see: K. M. Barkigia, M. D. Berber, J. Fajer, C. J. Medforth, M. W. Renner, K. M. Smith, *J. Am. Chem. Soc.* **1990**, *112*, 8851; K. Hatano, K. Kawasaki, S. Munakata, Y. Iitaka, *Bull. Chem. Soc. Jpn.* **1987**, *60*, 1985; D. L. Cullen, E. F. Meyer, Jr., *Acta Crystallogr. Sect. B* **1976**, *32*, 2259.
[20] K. M. Smith, *Porphyrins Metalloporphyrins* **1975**, 3.
[21] **4**: $C_{32}H_{38}N_4$, crystals from hexane/chloroform (1:1); monoclinic, space group $P2_1/n$, $Z = 2$; $a = 6.884(2)$, $b = 14.183(3)$, $c = 13.684(3)$ Å, $\beta = 97.05(2)^\circ$, $\rho_{calcd} = 1.199\ g\,cm^{-3}$; conditions of measurement as for **1**: refinement (C and N atoms anisotropic, H atoms isotropic) taking account of 2706 reflections with $I > 2\sigma(I)$, $R = 0.048$, $R_w = 0.053$; [24].
[22] J. L. Sessler, M. J. Cyr, A. K. Burrell, *Synlett* **1991**, 127.
[23] D. H. R. Barton, S. Z. Zard, *J. Chem. Soc. Chem. Commun.* **1985**, 1098.
[24] Further details of the crystal structure investigations may be obtained from the Fachinformationszentrum Karlsruhe, Gesellschaft für wissenschaftlich-technische Information mbH, D-76344 Eggenstein-Leopoldshafen (FRG) on quoting the depository number CSD-57311, the names of the authors, and the journal citation.

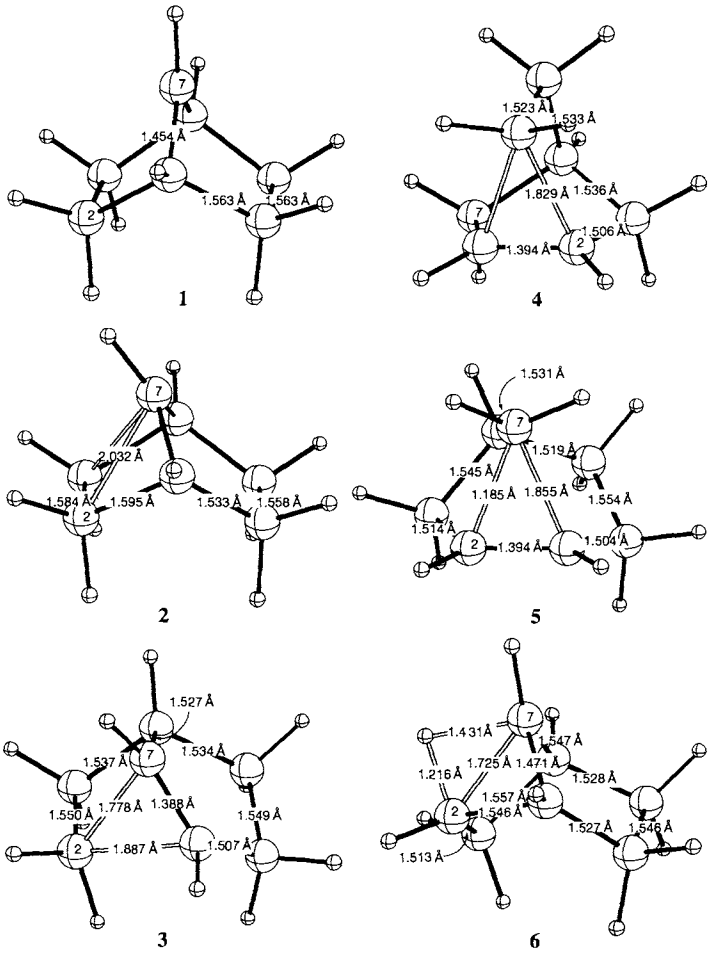

Fig. 1. MP2(full)/6-31G* optimized structures of the norbornyl cation isomers; see also [14].

The Nature of the 7-Norbornyl Cation and its Rearrangement into the 2-Norbornyl Cation**

By *Stefan Sieber, Paul von Ragué Schleyer,* Hrvoj Vančik, Milan Mesić*, and *Dionis E. Sunko*

The structure of the 7-norbornyl cation has always been an enigma.[1, 2] The exceptionally slow solvolysis rates of 7-norbornyl derivatives first suggested the absence of anchimeric assistance and the intervention of a classical cationic intermediate. However, a symmetrical C_{2v} structure (**1**, see Fig. 1) was later ruled out by the demonstration that the substitution product *retains* its stereochemistry.[1c–e] While this is also consistent with a C_s formulation (**2**), more recent interpretations favor a nonclassical, bridged structure (**3**) (Fig. 1).[1d] This is consistent with the formation of small, but significant amounts of 2-bicyclo[3.2.0]heptyl rearrangement products, as well as extensive evidence from, for example, D and CH_3 labeling experiments.

Before the present study, attempts at direct observation of the 7-norbornyl cation in superacid media all failed. In one of the earliest papers on studies in superacids, Schleyer, Olah et al. reported that ionization of 7-norbornyl derivatives led only to the 2-norbornyl cation.[1a] Subsequent attempts in our laboratories led to similar results.

Earlier computational studies were not definitive.[2] These were carried out at lower levels of theory, known now to give inadequate descriptions of such electron deficient species.[3] As part of a comprehensive examination of the $C_7H_{11}^+$ potential energy surface, we now report computations[4, 5] on the C_{2v} (**1**) and C_s (**2**) structures of the 7-norbornyl cation, the bridged ion **3**, as well as other stationary points related to the conversion into the 2-norbornyl cation (**4**)[6, 7] at the MP4(sdq,fc)/6-31G*//MP2(full)/6-31G* + ZPE(MP2(full)/6-31G*) level.[*] The vibrational frequencies, computed at the correlated level given, assist in the unambiguous identification of the $C_7H_{11}^+$ ion that we have now been able to observe experimentally.

Early ab initio calculations favored **1**, but this was due to the use of inadequate basis sets (STO-3G, 3-21G, 4-21G). Adequate searches of the carbocation potential energy surface require[3] the use at least of polarized double-ξ (DZ or split valence) basis sets with electron correlation. Thus, whereas at the HF/6-31G* level, **2** is favored over **1** by 0.4 kcal mol^{-1} and over **3** by 0.7 kcal mol^{-1}, the order changes with correlation. The (central) bridge flipping barrier (**2** ⇌ **1** ⇌ **2'**) increases to 2.3 kcal mol^{-1} at our final theoretical level. The relative stability of **2** and **3** reverses; the

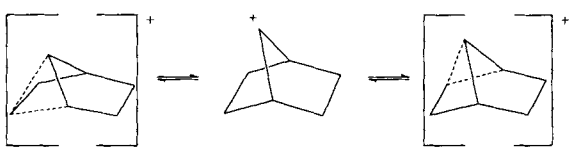

Scheme 1. The "same-side bridge-flipping" process.

[*] Prof. Dr. P. von R. Schleyer, S. Sieber
Institut für Organische Chemie der Universität Erlangen-Nürnberg
Henkestrasse 42, D-91054 Erlangen (FRG)
Telefax: Int. code +(91 31) 85-91 32
Dr. H. Vančik, Dipl.-Chem. M. Mesić, Prof. Dr. D. E. Sunko
Faculty of Natural Sciencies and Mathematics
Laboratory of Organic Chemistry, University of Zagreb
Strossmayerov trg 14, QKR-41000 Zagreb (Croatia)

[**] This work was supported in Erlangen by the Deutsche Forschungsgemeinschaft and the Fonds der Chemischen Industrie, and in Zagreb by the Ministry of Science of Croatia and the National Science Foundation (USA, Grant No. 841).

[*] MP4 = Møller-Plesset fourth-order perturbation theory; sdq: singly, doubly, and quadruply excited configurations are taken into account; fc = frozen core (that is, electrons of the inner orbitals are not considered in the generation of the configurations); full: all configurations are taken into account.

unsymmetrically bridged structure **3** is favored over **2** by 2.9 kcal mol^{-1} (Table 1); structure **2** is identified as transition state for the same-side bridge-flipping process by frequency analysis (Scheme 1).

Table 1. Relative energies of norbornyl cation isomers [kcal mol^{-1}].

	Symmetry	n [a]	HF/6-31G* //6-31G* [b]	MP2(full)/6-31G* //MP2(full)/6-31G* [c]	MP4(sdq,fc)/6-31G** //MP2(full)/6-31G* [c]
1	C_{2v}	1	14.60	26.88	21.80
2	C_s	1	14.17	22.60	19.46
3	C_1	0	14.89	18.29	16.60
4	C_s	0	0.00	0.00	0.00
5	C_1	1	10.56	13.80	12.39
6	C_1	1	32.80	33.10	30.14
7	C_1	1	–	16.92	13.64

[a] n = Number of imaginary frequencies. [b] Corrected for zero point energy at the HF/6-31G* level, scaled by 0.89 [4]. [c] Corrected for zero point energy at the MP2(full)/6-31G* level, scaled by 0.93 [4].

It is difficult to observe carbocations (like the 7-norbornyl cation) that have low rearrangement barriers.[1a] The recently developed cryogenic SbF_5 matrix IR technique[8, 9] enables otherwise elusive carbocations to be investigated. We have used this procedure to generate the 7-norbornyl cation by codepositing 7-chloronorbornane and a large excess of SbF_5 (1:500) on a CsI window at 10 K. The first spectrum, recorded at 10 K (Fig. 2a), was that of the starting chloride. During slow warming of the matrix to 100 K the signals of the chloride disappear and at the same time new signals of the 7-norbornyl cation appear (Fig. 2b). The IR spectrum at 200 K (Fig. 2c) is the same as that of the 2-norbornyl cation reported earlier.[8b]

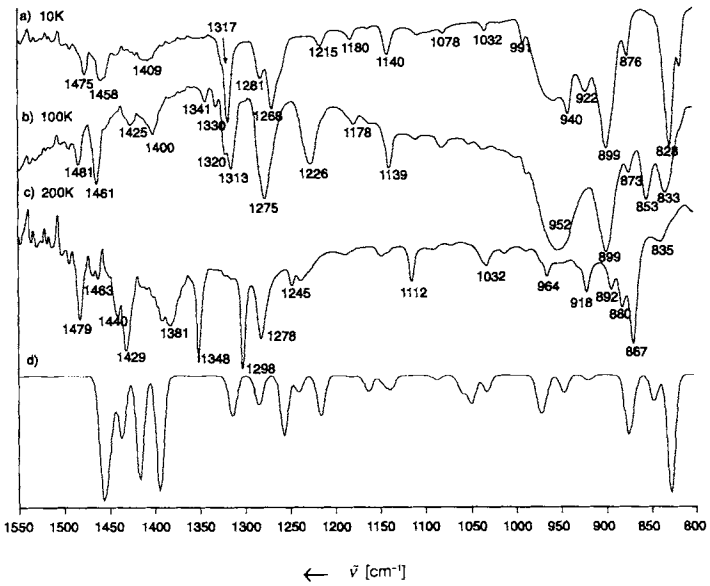

Fig. 2a)–c). Experimentally obtained spectra of 7-norbornyl chloride at 10 K, the 7-norbornyl cation **3** at 100 K, and the 2-norbornyl cation **4** at 200 K; d) the computed spectrum of **3** at the MP2(full)/6-31G* level (frequencies scaled by 0.939).

The experimental spectrum recorded at 100 K (Fig. 2b) is in very good agreement with the calculated frequencies for **3** (correlation coefficient cc = 0.9993, cf. Fig. 2d and Table 2). The intensities are reproduced with less accuracy.[10] The

Table 2. Calculated MP2(full)/6-31G* level, structure **3**, and experimental frequencies and intensities [a] (spectrum at 100 K).

Calcd [cm^{-1}] (unscaled)	Calcd [cm^{-1}] (scaled by 0.939)	Intensity [km mol^{-1}]	Experimental [cm^{-1}]	Intensity [b]
1567	1471	14.4	1481	w
1559	1464	7.6	1461	m
1545	1451	8.3	(~1450	sh)
1523	1430	13.8	1425	w
1499	1408	15.3	1400	m
1412	1326	5.4	1330	w
1381	1297	3.8	1313	s
1352	1270	0.7		
1351	1269	7.3	1275	vs
1333	1252	2.1		
1307	1227	5.3	1226	vs
1269	1192	0.2		
1250	1174	2.1	1178	w
1232	1157	0.9		
1223	1148	1.7	1139	m
1168	1097	0.5	1110	w
1139	1070	2.2	1081	w
1127	1058	3.7		
1110	1042	2.2		
1046	982	4.0		
1039	976	2.4		
1017	955	2.4	952	vs
988	928	0.7		
941	884	6.6	899	s
935	878	2.5	873	w
909	854	3.5	853	m
889	835	15.7	833	m

[a] The assignment of experimental vs. calculated frequencies is based on the best numerical agreement. Calculated frequencies outside the range of the experimental spectrum are omitted. [b] w: weak, m: medium, s: strong, vs: very strong, sh: shoulder.

slope of the correlation line (m = 0.939) is that expected, since the harmonic approximation was used in the computations.[4, 11] Although the experimental frequencies (Fig. 2b) also correlate reasonably to those computed for other isomers containing multicenter bonds (**2**, **5**, **8**;[12] $cc \approx 0.99$), these are excluded by theoretical considerations: The sym-

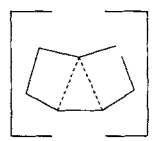

8

metrical structure **2** is a transition state; the barrier for rearrangement of the 2-norpinyl cation **5** into the 2-norbornyl cation is much too low (1.25 kcal mol^{-1}, see below) to

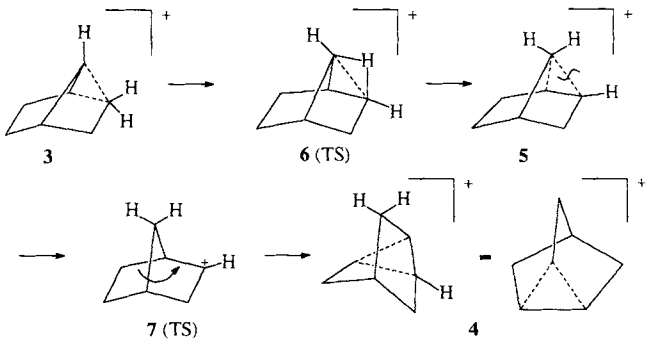

Scheme 2. Mechanism of the isomerization **3** → **4**. TS = transition state.

permit experimental detection under these conditions; the related structure **8** has been generated by Kirmse under short-lived conditions.[12] The IR spectra exclude **1** and **7** (and other isomers we have investigated).[13]

Our minimum energy reaction pathway for the rearrangement, first observed some time ago,[1a] of the 7-norbornyl cation to the 2-norbornyl cation (**4**), involves the 2-norpinyl cation **5** whose intermediacy has been postulated by Kirmse (Scheme 2).[1e]

The crucial step for the interconversion of the 7-norbornyl into the bridged 2-norbornyl cation (**4**), a 1,3 H shift from C2 to C7 (transition state **6**, Fig. 1), has a barrier of 13.5 kcal mol^{-1} to form the bridged 2-norpinyl intermediate **5**. Although **5** is 4.2 kcal mol^{-1} more stable than **3**, the high barrier between **3** and **5** allows the experimental detection of the 7-norbornyl cation. Only a 1.3 kcal mol^{-1} barrier (transition state **7**)[14] separates the 2-norpinyl cation from the global minimum of the $C_7H_{11}^+$ potential energy surface, the 2-norbornyl cation **4**. The low barrier of the latter reaction

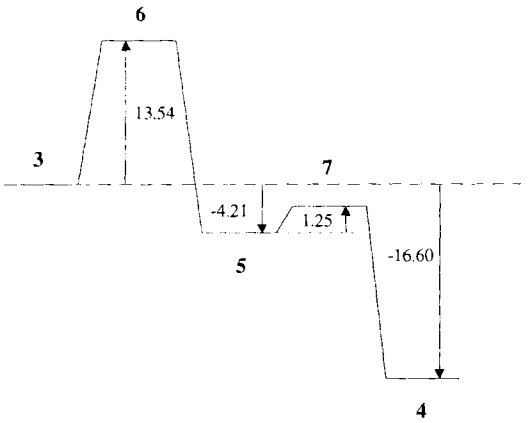

Scheme 3. Energy barriers and reaction energies associated with the isomerization **3** → **4**.

makes the experimental detection of the 2-norpinyl cation **5** (for example, in stable superacid solutions) unlikely.

Received: April 28, 1993 [Z 6043 IE]
German version: *Angew. Chem.* **1993**, *105*, 1673

[1] a) P. von R. Schleyer, W. E. Watts, R. C. Fort, M. B. Comisarow, G. A. Olah, *J. Am. Chem. Soc.* **1964**, *86*, 5679; b) R. Hoffmann, P. D. Mollère, E. Heilbronner, *ibid.* **1973**, *95*, 4860; c) D. E. Sunko, H. Vančik, V. Deljac, M. Milun, *ibid.* **1983**, *105*, 5364; d) W. Kirmse, J. Streu, *J. Org. Chem.* **1985**, *50*, 4187; e) W. Kirmse, *Acc. Chem. Res.* **1986**, *19*, 36; f) W. Kirmse, E. Herpers, *Angew. Chem.* **1991**, *103*, 989; *Angew. Chem. Int. Ed. Engl.* **1991**, *30*, 1018.

[2] a) M. J. S. Dewar, W. W. Schoeller, *Tetrahedron* **1971**, *27*, 4401; b) G. Wenke, D. Lenoir, *ibid.* **1979**, *35*, 489.

[3] See, for example, S. Sieber, P. Buzek, P. von R. Schleyer, W. Koch, J. W. de M. Carneiro, *J. Am. Chem. Soc.* **1993**, *115*, 259, and references therein.

[4] For a description of methods and basis sets employed see W. J. Hehre, L. Radom, P. von R. Schleyer, J. A. Pople, *Ab Initio Molecular Orbital Theory*, Wiley-Interscience, New York, **1986**, Chapter 7.

[5] If not given otherwise, all data (energies and geometry parameters) apply to MP4(sdq,fc)/6-31G"//MP2/full)/6-31G* + ZPE(MP2(full)/6-31G*); zero point energies (ZPEs) are scaled by 0.93 [4]. All calculations were performed with the GAUSSIAN 92 program (M. J. Frisch, M. Head-Gordon, C. W. Trucks, J. B. Foresman, H. B. Schlegel, K. Raghavachari, M. A. Robb, J. S. Binkley, G. Gonzales, D. J. Defrees, D. J. Fox, R. A. Whiteside, R. Seeger, C. F. Melius, J. Baker, R. L. Martin, L. R. Kahn, J. J. P. Stewart, S. Topiol, J. A. Pople, Gaussian Inc., Pittsburgh, PA, **1992**).

[6] a) A recent summary can be found in D. Lenoir, Y. Apeloig, D. Arad, P. von R. Schleyer, *J. Org. Chem.* **1988**, *53*, 661, and references therein; b) G. D. Sargent, *Carbonium Ions 1968–1976* **1972**, *3*, Chapter 24; c) H. C. Brown with comments by P. von R. Schleyer, *The Nonclassical Ion Problem*, Plenum, New York, **1977**, Chapter 6; d) P. Vogel, *Carbocation Chemistry*, Elsevier, Amsterdam, **1985**.

[7] Recent experimental and theoretical investigations include refs. [1e, 1f, 8b] and W. Koch, D. J. DeFrees, B. Liu, *J. Am. Chem. Soc.* **1989**, *111*, 1527; P. C. Myhre, G. G. Webb, C. S. Yannoni, *ibid.* **1990**, *112*, 8991.

[8] a) H. Vančik, D. E. Sunko, *J. Am. Chem. Soc.* **1989**, *111*, 3742; b) W. Koch, B. Liu, D. J. DeFrees, D. E. Sunko, H. Vančik, *Angew. Chem.* **1990**, *102*, 198; *Angew. Chem. Int. Ed. Engl.* **1990**, *29*, 183; c) H. Vančik, K. Percač, D. E. Sunko, *J. Am. Chem. Soc.* **1990**, *112*, 7418; d) P. Buzek, P. von R. Schleyer, S. Sieber, *Chem. Unserer Zeit* **1992**, *26*, 116.

[9] a) P. Buzek, P. von R. Schleyer, S. Sieber, W. Koch, J. W. M. Carneiro, H. Vančik, D. E. Sunko, *J. Chem. Soc. Chem. Commun.* **1991**, 671; b) P. Buzek, P. von R. Schleyer, H. Vančik, D. E. Sunko, *ibid.* **1991**, 1538.

[10] The calculation of IR intensities should be improved by the use of larger basis sets; cf. B. A. Hess, L. J. Schaad, P. Carsky, R. Zahradnik, *Chem. Rev.* **1986**, *86*, 709. Due to computational limitations this is currently not possible.

[11] R. F. Hout, B. A. Levy, W. J. Hehre, *J. Comput. Chem.* **1982**, *3*, 234.

[12] W. Kirmse, R. Siegfried, J. Streu, *J. Am. Chem. Soc.* **1984**, *106*, 2465.

[13] The details of the $C_7H_{11}^+$ potential energy surface will be published later.

[14] This structure, which resembles the classical 2-norbornyl cation closely, is discussed comprehensively in the following communication: P. von R. Schleyer, S. Sieber, *Angew. Chem.* **1993**, *105*, 1676; *Angew. Chem. Int. Ed. Engl.* **1993**, *32*, 1606.

The Classical 2-Norbornyl Cation Rigorously Defined Ab Initio**

By *Paul von Ragué Schleyer** and *Stefan Sieber*

While extensive experimental and computational data have now firmly established that the 2-norbornyl cation is the symmetrically bridged (C_s) minimum energy structure **1**,[1] most of the other intriguing features of the $C_7H_{11}^+$ potential energy surface have not been elucidated fully.[2] This applies in particular to the "classical" structure[3] of the 2-norbornyl cation (**2**). We have now been able to locate a

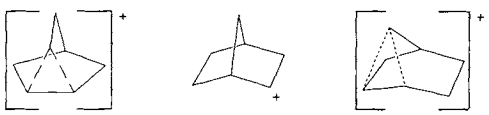

1 **2** **3**

stationary point at an adequately high ab initio level, which corresponds to the structure **2**: its geometry optimized at MP2(full)/6-31G* level is compared with that of norbornane (**3**) in Figure 1. The structures correspond well.

Earlier attempts to compute energies and bond lengths and angles for a classical 2-norbornyl geometry were either inadequate or unsuccessful. Structures have been assumed, based on the structure of the parent hydrocarbon, norbornane (**3**).[4] The classical geometries computed by semiempirical molecular orbital theory (e.g. MINDO/3, MNDO, AM1, and PM3) are artifacts arising from the failures of these methods to describe the energies of the 2-norbornyl cation and its bridged nature properly (Table 1).[2, 5] Ab initio computations with inadequate basis sets (e.g., STO-3G,

[*] Prof. Dr. P. von R. Schleyer, S. Sieber
Institut für Organische Chemie der Universität Erlangen-Nürnberg
Henkestrasse 42, D-91054 Erlangen (FRG)
Telefax: Int. code +(91 31) 85-91 32

[**] Support at Erlangen by the Deutsche Forschungsgemeinschaft, the Fonds der Chemischen Industrie, and the Convex Computer Corporation, and grants of computer time from Leibniz-Rechenzentrum, München, are appreciated. We thank J. Gauss for MP2-GIAO computations.

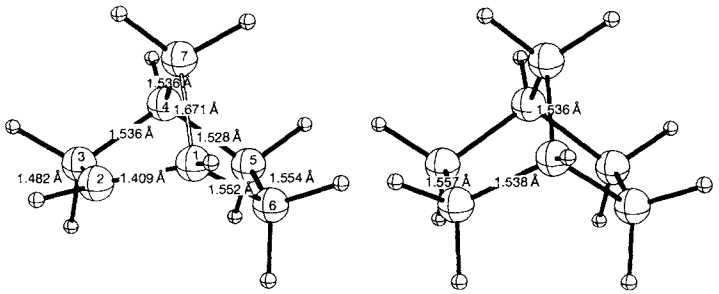

2 3

Fig. 1. The optimized geometries (at the MP2/6-31G* level) of transition structure **2** (model for the "classical" 2-norbornyl cation) and norbornane (**3**). Note the close correspondence between the structural parameters for **2** and **3**. See also structures **4** and **5** in the preceeding communication [14] for the geometries of **1** and **4**, respectively.

3-21G, 4-21G, 4-31G) find only partially bridged minima.[6, 7] The reliable investigation of carbocation potential energy surfaces require the use of flexible, basis sets that include polarization functions and electron correlation.[6-8] Searches for a minimum corresponding to a classical 2-norbornyl cation structure at such levels prior to this paper have failed.[6, 8] Optimization leads (correctly) to the symmetrical C_s minimum **1** instead.[8]

Table 1. Relative energies for the structures of **1**, **2**, and **4**, optimized with ab initio and the semiempirical MINDO/3 methods (kcal mol^{-1}).

Method	1	2	4
MP2(full)/6-31G*//MINDO/3	5.7	16.7	20.9
MP2(full)/6-31G*//MP2(full)/6-31G*	0.0	17.6	13.8
MP4(sdq,fc)/6-31G**//MP2(full)/6-31G* [a]	0.0	13.6	12.4

[a] Corrected for zero point energy at the MP2(full)/6-31G* level, scaled by 0.93 [9].

Indeed, the new $C_7H_{11}^+$ stationary point **2** that we located with considerable effort[9] is not a minimum, but rather a transition state in the rearrangement of **1** into the bridged 2-norpinyl cation, **4**.[2] The somewhat elongated C1–C7 bond (1.671 Å) in **2** reflects this character. The C–C bonds to the tricoordinated carbocation center are shortened, as expected, but the other geometric parameters differ little from those of **3** (Fig. 1). Despite the increased C1–C7 bond length, this bond may still be termed classical in the sense of a two-center, two-electron bond. According to the NPA (NPA = orbital population analysis), the natural bonding orbital for C1–C7 is occupied with 1.8 electrons, about 92% of a "normal" bond like, for example, C1–C6. Consequently, **2**, a rigorously defined stationary point, can be taken as a model for the classical 2-norbornyl cation. At the theoretical level employed, MP4sdtq/6-31G**//MP2(full)/6-31G* + ZPE(MP2(full)/6-31G*),[10] the energy of classical **2** is 13.6 kcal mol^{-1} higher than that of nonclassical **1** (see Table 1). This value is in remarkably good agreement with earlier, rough gas-phase estimates.[6, 11]

The MP2(full)/6-31G* energies computed for the MINDO/3 geometries of **1** and **4** (Table 1) are in good agreement with those obtained for the MP2(full)/6-31G* geometries, which indicates that they are similar. The energy for the MINDO/3 structure of **2** (relative to MP2(full)/6-31G*//MINDO/3 energy of **1**) is somewhat lower than that for the transition state structure calculated with ab initio methods. The MINDO/3 structure might be assigned to a point on the reaction path between **2** and **1**. (The MINDO/3, MNDO, AM1, and PM3 methods also give very similar classical minima for 2-norbornyl cations. These differ from **2** by having normal C1–C2 distances, but slightly elongated C1–C6 bonds (1.582–1.593 Å)).

Structure **2** can also be employed to predict the ^{13}C chemical shifts of the classical 2-norbornyl cation. Table 2 summarizes this data, not only for **2**, but also for **1** and **4** for comparison with the experimental measurements. Schindler's best computed (IGLO) NMR chemical shifts for a model of a classical 2-norbornyl cation[4] are provided for comparison, as are those computed using the MINDO/3 minimum energy geometry. The IGLO chemical shifts for **2** deviate considerably from those of the classical 2-norbornyl cation models of Schindler (see his "best" values in Table 2), but are much more in line with those expected for a classical carbocation (cf. the value for C2, which is close to C1 of the isopropyl cation).[12] The comparison of the chemical shifts for **1** and **2** with the experimental data confirms once again the symmetrical nonclassical structure of the 2-norbornyl cation.[1, 6-8, 12]

Although it has not been observed directly in super acidic media, the 2-norpinyl cation (**4**) also is an intriguing nonclassical species, which has been generated by solvolysis and by deamination.[7] The computed chemical shifts for **4** (Table 2) reveal shielding characteristic of hypercoordinate carbocat-

Table 2. Computed (IGLO and MP2-GIAO) ^{13}C chemical shifts for **1**, **2**, and **4** and for comparison, the experimental NMR data, for the 2-norbornyl cation (vs. TMS).

	Method [a]	C1	C2	C3	C4	C5	C6	C7	$\Sigma\delta^{13}C$ [b]
1	experimental [c]	124.8	124.8	36.6	37.9	20.2	21.3	36.6	402.2
	IGLO/DZ//MP2(full)/6-31G*	127.4	127.4	34.6	30.7	19.6	12.0	34.6	386.3
	IGLO/II//MP2(full)/6-31G*	128.7	128.7	37.2	36.9	22.7	17.0	37.2	408.4
	MP2-GIAO/DZP//MP2(full)/6-31G* [d]	121.1	121.1	38.6	39.9	21.7	22.3	38.6	403.3
	MP2-GIAO/TZP//MP2(full)/6-31G* [d]	127.0	127.0	40.5	41.5	23.5	24.0	40.5	424.0
2	IGLO/DZ//SCF [e]	78.2	423.2	72.6	32.4	22.8	22.6	42.9	694.7
	IGLO/DZ//MINDO/3	69.4	365.9	64.6	34.8	21.3	27.6	46.4	630.0
	IGLO/DZ//MP2(full)/6-31G*	77.4	317.0	46.4	28.1	21.6	25.0	56.8	572.3
4	IGLO/DZ//MINDO/3	131.8	129.3	29.6	30.3	24.2	23.4	13.9	360.5
	IGLO/DZ//MP2(full)/6-31G*	138.7	145.1	24.0	25.9	25.5	17.5	37.9	414.6

[a] DZ = double ζ basis, Tz = triple ζ basis, P with polarization functions, II = triple ζ basis with polarization functions. [b] The difference in the sums of all the ^{13}C chemical shifts between a carbocation and its corresponding alkane (norbornane: $\Sigma(\delta^{13}C) = 233$) provides an index of carbocation structure. Large differences indicate classical carbocations (e.g. **2**); values for nonclassical cations (e.g. **1** and **4**) are much smaller (200 or less): P. von R. Schleyer, D. Lenoir, P. Mison, G. Liang, G. K. S. Prakash, G. A. Olah, *J. Am. Chem. Soc.* **1980**, *102*, 683. [c] R. M. Jarret, M. Saunders, *J. Am. Chem. Soc.* **1987**, *109*, 3366. [d] MP2-GIAO calculations by J. Gauss, cf. S. Sieber, P. von R. Schleyer, J. Gauss, *J. Am. Chem. Soc.* **1993**, *115*, 6987. [e] M. Schindler's best geometry (evidently partially optimized; details were not given in ref. [3]).

ions.[2, 8, 13] The reason for the difficulty in observing **4** is now clear: the barrier to rearrangement into **1** (as represented by the energy difference between **2** and **4** is only 1.2 kcal mol^{-1}. Structure **4** also functions as a stationary point during the rearrangement of the 7-norbornyl into the 2-norbornyl cation. This has been described in the preceding communication along with other intriguing features of the $C_7H_{11}^+$ potential energy surface.[14]

Our decade-old conclusion[6] is worth repeating: "The symmetrically bridged (C_s) 2-norbornyl cation structure is expected to be the only minimum... As no minima with C_1 symmetry are found, *'classical' and partially bridged 2-norbornyl cations are not expected to exist*, at least as isolated (gas-phase) entities. The extra stabilization due to bridging of the C_s 2-norbornyl cation (the 'classical–nonclassical energy difference') is estimated approximately in two ways to be about 15 kcal mol^{-1}." We will explain in a subsequent communication why the difference in transition state energy for 2-*exo* and 2-*endo*-norbornyl solvolysis (only about 5 kcal mol^{-1})[3] is reduced to such a large extent.

Received: June 4, 1993 [Z 6124 IE]
German version: *Angew. Chem.* **1993**, *105*, 1676

[1] The latest review by D. Lenoir, Y. Apeloig, D. Arad, P. von R. Schleyer, *J. Org. Chem.* **1988**, *53*, 661 can serve as an introduction to the vast literature. Recent experimental studies include refs. [2, 7] and P. C. Myhre, G. G. Webb, C. S. Yannoni, *J. Am. Chem. Soc.* **1990**, *112*, 8991.

[2] See W. Kirmse, *Acc. Chem. Res.* **1986**, *19*, 36; W. Kirmse, E. Herpers, *Angew. Chem.* **1991**, *103*, 989; *Angew. Chem. Int. Ed. Engl.* **1991**, *30*, 1018.

[3] See H. C. Brown (with comments by P. von R. Schleyer), *The Nonclassical Ion Problem*, Plenum, New York, **1977**, p. 49–50, for definitions of "classical" and "nonclassical". Also see ref. [6] with regard to problems in applying these definitions unambiguously.

[4] For example, M. Schindler (*J. Am. Chem. Soc.* **1987**, *109*, 1020) removed an *endo* and an *exo* hydrogen, and also employed a central C2–H position for his pioneering IGLO computations of the chemical shifts of carbocations.

[5] See G. Wenke, D. Lenoir, *Tetrahedron* **1977**, *35*, 489, for an early, thorough study of the deficiencies of MINDO/3 (**4**, for example, is erroneously computed to be more stable than **1**: see M. J. S. Dewar, R. C. Haddon, A. Komornicki, H. Rzepa, *J. Am. Chem. Soc.* **1977**, *99*, 377).

[6] K. Raghavachari, R. C. Haddon, P. von R. Schleyer, H. F. Schaefer III, *J. Am. Chem. Soc.* **1983**, *105*, 5915.

[7] P. Buzek, P. von R. Schleyer, S. Sieber, *Chem. Unserer Zeit* **1992**, *26*, 116.

[8] W. Koch, D. J. DeFrees, B. Liu, *J. Am. Chem. Soc.* **1989**, *111*, 1527; see also W. Koch, B. Liu, D. J. DeFrees, D. E. Sunko, H. Vančik, *Angew. Chem.* **1990**, *102*, 198; *Angew. Chem. Int. Ed. Engl.* **1990**, *29*, 183.

[9] Optimization to the C_1-point-group transition structure **2** must be carried out directly at the MP2/6-31G* level, as it is not a stationary point at the HF/6-31G* level. Its nature was confirmed by frequency analysis at the MP2(full)/6-31G* level; an imaginary frequency of 347i cm^{-1} was found. This type of calculation uses about 100 MByte of memory, 2 GByte of disk space and 35 hours on a Cray YMP-EL.

[10] If not given otherwise, all data (energies and structure parameters) apply to MP4(sdq·fc)/6-31G**//MP2(full)/6-31G* + ZPE(MP2(full))/6-31G* (for an explanation of abbreviations, see ref. [14]); ZPE's are scaled by 0.93. This level of theory has been shown to be adequate even for demanding electronic structures: S. Sieber, P. Buzek, P. von R. Schleyer, W. Koch, J. W. M. Carneiro, *J. Am. Chem. Soc.* **1993**, *115*, 259. Larger basis sets result only in slightly different structures and energies. For a description of methods and basis sets employed, see W. J. Hehre, L. Radom, P. von R. Schleyer, J. A. Pople, *Ab Initio Molecular Orbital Theory*, Wiley Interscience, New York, **1986**, Chapter 7, and J. B. Foresman, E. Frisch, *Exploring Chemistry with Electronic Structure Methods: A Guide to Using Gaussian*, Gaussian Inc., Pittsburgh, **1993**. Absolute energies (MP4(sdq·fc)/6-31G**//MP2(full)/6-31G*) are: **1**: −272.24562, **2**: −272.22283, **4**: −272.22589 Hartree; zero point energies (MP2(full)/6-31G*, unscaled); **1**: 105.5, **2**: 104.8, **4**: 105.5 kcal mol^{-1}. All calculations were performed with the program GAUSSIAN 92 (M. J. Frisch, G. W. Trucks, M. Head-Gordon, P. M. W. Gill, M. W. Wong, J. B. Foresman, B. G. Johnson, H. B. Schlegel, M. A. Robb, E. S. Replogle, R. Gomperst, J. L. Andres, K. Raghavachari, J. S. Binkley, C. Gonzalez, R. L. Martin, D. J. Fox, D. J. Defrees, J. Baker, J. J. P. Stewart, J. A. Pople, Gaussian Inc., Pittsburgh, PA, **1992**).

[11] The estimates of the **1**/**2** energy difference in superacidic media (6–8 kcal mol^{-1}) gave lower values (see P. von R. Schleyer, J. Chandrasekhar, *J. Org. Chem.* **1981**, *46*, 225); these were, however, based on equations involving model carbocations that were assumed (erroneously) to be "classical" [6].

[12] a) P. von R. Schleyer, W. Koch, B. Liu, U. Fleischer, *J. Chem. Soc. Chem. Commun.* **1989**, 1098; b) G. A. Olah, D. J. Donovan, *J. Am. Chem. Soc.* **1977**, *99*, 5026.

[13] P. von R. Schleyer, D. Lenoir, P. Mison, G. Liang, G. K. S. Prakash, G. A. Olah, *J. Am. Chem. Soc.* **1980**, *102*, 683.

[14] S. Sieber, P. von R. Schleyer, H. Vančik, M. Mesić, D. E. Sunko, *Angew. Chem.* **1993**, *105*, 1673; *Angew. Chem. Int. Ed. Engl.* **1993**, *32*, 1604.

Tris(chlorodimethylstannyl)amine, a Molecule with a Planar Sn_3N Skeleton Stabilized by Intramolecular Sn-Cl-Sn Bridges**

By *Christian Kober, Jürgen Kroner, and Wolfgang Storch**

Dedicated to Professor Heinrich Nöth on the occasion of his 65th birthday

Structural information about the few known tristannylamines is contradictory. IR spectroscopic investigations on tris(trimethylstannyl)amine indicate a pyramidal Sn_3N skeleton,[1] electron diffraction studies in the gas phase, however, reveal a trigonal-planar arrangement of the tin atoms around the nitrogen center.[2] Especially interesting is the comparison of $N(SnR_3)_3$ compounds with the lighter homologues $N(MR_3)_3$ (M = Si, Ge), whose planar NM_3 skeleton is due in part to the π-acceptor properties of the M atoms,[3] whereas the planarity of the region around the N atom in triisopropylamine is forced by steric overcrowding.[4] Which structure tristannylamines have is of primary importance, because this determines whether or not a Sn–N π interaction can be deduced. Consequently, we are investigating the chemistry and structure of tristannylamines with varying substituents.

Tris(chlorodimethylstannyl)amine **2**,[5] the first tristannylamine functionalized at the tin atom, is synthesized by the complete exchange of the $(CH_3)_3Sn$ groups of tris(trimethylstannyl)amine **1** with $(CH_3)_2SnCl_2$ [Eq. (a)]. The NMR

$$\underset{\mathbf{1}}{[(CH_3)_3Sn]_3N} + 3(CH_3)_2SnCl_2 \longrightarrow \underset{\mathbf{2}}{[Cl(CH_3)_2Sn]_3N} + 3(CH_3)_3SnCl \qquad (a)$$

spectra of **2** (Table 1) clearly show changes in the molecular skeleton in comparison to that of the permethylated compound **1**. The exchange of one methyl group on each tin atom of **1** for a chlorine atom results in reduced shielding of the ^1H, ^{13}C, and ^{15}N nuclei in **2**. The better shielding of the ^{119}Sn nuclei is, however, unusual and indicates a higher coordination number of the Sn centers. The ^{119}Sn CP-MAS NMR spectrum of **2** in the solid state shows an even clearer high-field shift of the signal.[6] In contrast, the $\delta(^{15}N)$ signal gives no clear indication about the geometry at the nitrogen atom.[7] Due to the −I effect of the chlorine substituents and probably also due to the changed geometry at the tin atoms, the values of the coupling constants $^1J(^{119}Sn, ^{13}C)$ and $^2J(^{119}Sn, ^1H)$ are significantly larger than those of **1**. Further information about the structure of **2** is obtained by estimat-

[*] Dr. W. Storch, Dipl.-Chem. C. Kober, Dr. J. Kroner
Institute für Anorganische Chemie der Universität
Meiserstrasse 1–3, D-80333 München (FRG)
Telefax: Int. code + (89)5902-451

[**] This work was supported by the Deutsche Forschungsgemeinschaft.

Table 1. NMR data for **2** and other di- and tristannylamines (^{1}H, ^{15}N, ^{119}Sn NMR: 270 MHz, ^{13}C NMR: 400 MHz, compound : $CDCl_3$ = 30 : 70.

Compound		$\delta(^1H)$	$^2J(^{119}Sn,^1H)$ [Hz]	$\delta(^{13}C)$	$^1J(^{119}Sn,^{13}C)$ [Hz]	$\delta(^{15}N)$	$^1J(^{119/117}Sn,^{15}N)$ [Hz]	$\delta(^{119}Sn)$	$^2J(^{119}Sn,^{117}Sn)$ [Hz]
$N[Sn(CH_3)_2Cl]_3$	**2**	0.94	70.2	8.00	492.5	−335.6	66.4	83.5	−38.0 [a]
$N[Sn(CH_3)_3]_3$ [9b]	**1**	0.16	56.3	−1.10	366.0	−396.2	−83.1	86.3	−186.7
$tBuN[Sn(CH_3)_2Cl]_2$ [10]		0.89	64.3	6.80	463.5	−289.2	60.7	99.7	≈65
$tBuN[Sn(CH_3)_3]_2$ [11a]		0.29	54.8	−6.83	366.0	−326.7	−38.0	40.7	76.6

[a] To conform with previous work we assume a negative sign for $^2J(^{119}Sn,^{117}Sn)$ for **2**.

ing the C-Sn-C angle by using the $^1J(^{119}Sn, ^{13}C)$ coupling constants. Many investigations have confirmed a linear correlation between these values.[8] According to calculations based on this work,[8] the C-Sn-C angle in **2** is 122.5°, which implies a trigonal-bipyramidal geometry at the Sn atom.

Noticeable are also the very different geminal $^2J(^{119}Sn, ^{117}Sn)$ coupling constants of **1** and **2**.[9a] The value of $|^2J|$ decreases by about 150 Hz for **2**. If one assumes that the coupling constant is negative, as in **1**,[9b] the decrease in the value of the scalar coupling means an increase of the s contribution in the Sn−N bonds, which should be linked to a bond shortening and a widening of the Sn-N-Sn angle.[10, 11] This assumption is supported by the significantly smaller value of the $^1J(^{119/117}Sn, ^{15}N)$ coupling constant in **2** in comparison to that found for **1**. For the latter compound and for a large number of other mono- and distannylamines a negative sign has been observed for the ^1J value.[11] Thus here too a smaller negative value for the ^1J coupling corresponds to a larger s contribution in the Sn−N bonds.[11a] These interpretations of the NMR data of **2** are supported completely by the crystal structure (Fig. 1).[12]

The crystal data support the almost undistorted D_{3h} symmetry of **2**. The planar NSn_3Cl_3 molecular skeleton is noteworthy. The sum of the angles at the nitrogen atom is 360°. The intramolecular, almost symmetrical Sn-Cl-Sn bridges, which lead to pentacoordination of the Sn atoms are typical for **2**. The assumption, according to the Bent rule,[13] that the equatorial bonds should have more s character than the axial is supported by a clear shortening of the Sn−N bonds to 199 pm. This leads to smaller values for the $^1J(^{119/117}Sn, ^{15}N)$ and $^2J(^{119}Sn,^{117}Sn)$ coupling constants. To our knowledge **2** has the shortest Sn−N bonds observed to date.[10] The sum of the covalent atomic radii of both elements is calculated as 203.3 pm.[14] Similarly, the Sn−C bonds at 208 pm are shortened in comparison to those in tetracoordinate Sn compounds (210 pm in $(o\text{-}iPr_2C_6H_3)N[Sn(CH_3)_2Cl]_2$[15] and 213 pm in $tBuN[Sn(CH_3)_2Cl]_2$[15]). The sum of the bond angles (360°) in the equatorial region of the tin centers confirms the planar arrangement of these substituents. The observed C-Sn-C angles in **2** agree with the value calculated from the NMR data (e.g. C1-Sn1-C2 121.8°).

The Cl−Sn bonds alternate between 270 and 280 pm. The intramolecular bridging function of the Cl atoms on the one hand leads to significantly longer Sn−Cl bonds than found in pentacoordinate, nonionic Sn compounds (e.g. $(CH_3)_3SnCl\cdot py$: 246.0 pm[16]), but on the other hand it causes a distortion of the trigonal-bipyramidal coordination polyhedron of the tin atoms in **2**. The Cl-Sn-Cl bond angle is thus only 164 instead of 180°. Thus, the chlorine bridges can also partially cause the shortening of the Sn−N bonds. The molecular structure of **2** is the first example of an intramolecularly bridged tin−nitrogen compound and a further example of the importance of the Sn-Cl-Sn bridges in determining the structure. These bridges, which also exist in solution, have previously only been confirmed[17b] for the

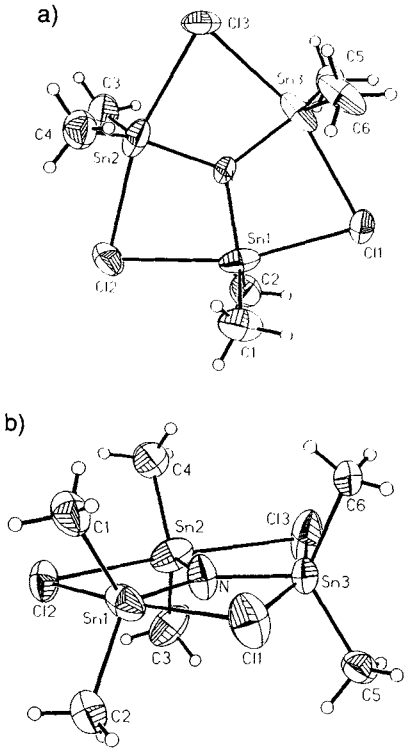

Fig. 1. a) Molecular structure of **2** (ORTEP representation). b) Structure of **2** side view. Thermal ellipsoids correspond to a 25% probability level. Selected bond lengths [pm] (standard deviations in parentheses) and angles [°]: Sn1-N 201(1), Sn2-N 198(1), Sn3-N 197(1), Sn1-C1 208(2), Sn1-C2 207(2), Sn1-Cl1 269.6(6), Sn1-Cl2 282.4(5), Sn2-Cl2 272.3(5), Sn2-Cl3 279.3(6), Sn3-Cl3 275.5(6), Sn3-Cl1 280.7(5); Sn1-N-Sn2 118.3(7), Sn1-N-Sn3 119.5(6), Sn2-N-Sn3 122.1(6), N-Sn1-C1 118.0(6), N-Sn1-C2 119.9(6), Sn1-Cl1-Sn3 77.3(1), Sn1-Cl2-Sn2 76.3(1), Sn2-Cl3-Sn3 77.2(1), Cl1-Sn1-Cl2 163.7(2), C1-Sn1-C2 121.8(7).

cyclodimeric distannylamine $[CH_3N\{Sn(CH_3)_2Cl\}_2]_2$[10] and the corresponding distannoxane $[\{Cl(CH_3)_2Sn\}_2O]_2$.[17a]

The analytical results of the unusual structure of **2** are also confirmed by geometry-optimized approximate calculations. AM1 calculations[18] for the parent compound $N(SnH_2Cl)_3$ show that a Sn-Cl-Sn bridged structure is around 104.5 kJ mol^{-1} less energetic than an unbridged structure. The potential energy surface for 13 various Sn−Cl distances and 10 N-Sn-Cl angles (Fig. 2) shows that for a simultaneous lengthening of the Sn−Cl bonds and a decrease in the N-Sn-Cl bond angles only a small barrier of <4 kJ mol^{-1} needs to be overcome to leave the extremely flat hollow of the minimum of the unbridged form and to proceed with a steady energy gain to the bridged form. The barrier to rotation about the N−Sn bond for the unbridged form is only 8.4 kJ mol^{-1} according to AM1 calculations. Compound **2**, according to these model calculations, has a trigonal-planar nitrogen center with a lone pair in a p type orbital. A planarization of the region around the nitrogen atom has been structurally confirmed for trisilyl-[3a, b] and trigermyl-

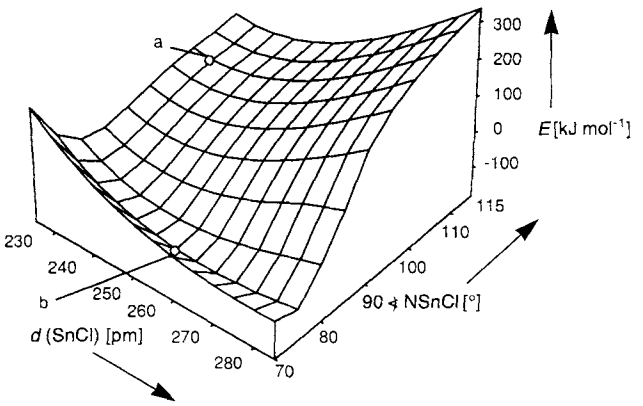

Fig. 2. AM1 potential energy surface of Sn-Cl-Sn bridged and unbridged $N(SnH_2Cl)_3$ (a: unbridged, b: bridged).

amines.[3c] The p character of the lone pair at the trigonal-planar nitrogen center was first documented for the sterically demanding triisopropylamine.[4]

A comparison of the structural data determined for **2** and the results of the AM1 calculations for $N(SnMe_2Cl)_3$ shows good agreement between the Sn–N bond lengths as well as between the Sn-N-Sn angles.[19] The energy difference between the bridged and unbridged forms is 143.5 kJ mol^{-1} according to AM1 calculations. The experimentally observed asymmetry of the Sn-Cl-Sn bridges could not be confirmed by calculations. An approximate value for the Sn-Cl-Sn bridge bond energies of about 46 kJ mol^{-1} can be estimated from the calculated energy differences. Indications of (pd)π interactions between the nitrogen and the tin atoms cannot be inferred from spectroscopic investigations (NMR and Mössbauer data[20]) or from the quantum mechanical model calculations, since these confirm the structure and bonding without including the d orbitals.

Received: 6 May, 1993 [Z 6060 IE]
German version: *Angew. Chem.* **1993**, *105*, 1693

[1] R. E. Hesters, K. Jones, *J. Chem. Soc. Chem. Commun.* **1966**, 317–319.
[2] L. S. Khaikin, A. V. Belyakov, G. S. Kcptev, A. V. Golubinskij, L. V. Vilkow, N. V. Girbasova, E. T. Bogoradovskij, V. S. Zavgorodnij, *J. Mol. Struct.* **1980**, *66*, 191–202.
[3] a) B. Beagley, A. R. Conrad, *Trans. Faraday Soc.* **1970**, *66*, 2740–2742, $[N(SiH_3)_3]$; b) D. G. Anderson, D. W. H. Rankin, H. E. Robertson, G. Gundersen, R. Seip, *J. Chem. Soc. Dalton Trans.* **1990**, 161–165, $[N(SiR_3)_3]$; c) C. Glidewell, D. W. H. Rankin, A. G. Robiette, *J. Chem. Soc. A* **1970**, 2935–2938, $[N(GeH_3)_3]$.
[4] H. Bock, I. Göbel, Z. Havlas, S. Liedle, H. Oberhammer, *Angew. Chem.* **1991**, *103*, 193–196; *Angew. Chem. Int. Ed. Engl.* **1991**, *30*, 187–191.
[5] *Experimental Procedure*: To a solution of $(CH_3)_2SnCl_2$ (68.9 g, 314 mmol) in CH_2Cl_2 (120 mL) was added dropwise at 0 °C with stirring 50 vol% of a solution of $[(CH_3)_3Sn]_3N$ **1** (52.8 g, 105 mmol) in CH_2Cl_2 (70 mL). The rest of this solution (50 vol%) was added at −35 °C. After slow warming and 12 h stirring at room temperature the solvent was condensed at about 25 °C/12 Torr into a cold trap cooled to −78 °C. Subsequently, $(CH_3)_3SnCl$ (59.5 g, 95%) was sublimed off. This process was completed by repeated dissolution of the residue in CH_2Cl_2, followed by removal of the solvent, and renewed sublimation. After recrystallization from CH_2Cl_2 53 g (90%) tris(chlorodimethylstannyl)amine **2** (m.p. 164–166 °C) was obtained. Crystals suitable for the X-ray structure analysis were obtained by slow diffusion of petroleum ether into a saturated solution of **2** in CH_2Cl_2 at room temperature. NMR data see Table 1. MS (15 eV; based on ^{120}Sn, ^{35}Cl): *m/z* (assignment), %: 567 (M^+), 1; 552 ($M^+ - CH_3$), 100; 332 ($M^+ - (CH_3)_2SnCl_2 - CH_3$), 12; 302 ($M^+ - (CH_3)_2SnCl_2 - C_2H_6 - CH_3$), 31; 282 ($M^+ - (CH_3)_2SnCl_2 - C_2H_6 - CH_3Cl - CH_3$), 22.
[6] We thank Dr. Dr. habil. A. Sebald, Universität Bayreuth, for recording the CP-MAS solid-state NMR spectra.
[7] For example the region around the N atom, according to the spectroscopic data, is planar for $(CH_3)_2B-N[Sn(CH_3)_3]_2$, $\delta(^{14}N) = -272$ [9a] and pyramidal for $CH_3N[Sn(CH_3)_3]_2$, $\delta(^{15}N) = -358.2$ [11a].
[8] a) T. P. Lockhart, W. F. Manders, J. J. Zuckerman, *J. Am. Chem. Soc.* **1985**, *107*, 4546–4547, and references therein; b) J. Holecek, A. Lycka, *Inorg. Chim. Acta* **1986**, *118*, L15-L16; calculation of the angle Φ according to an improved formula derived from [8a,b]: $\Phi(SnC_2) = 0.0874 \times |^1J(^{119}Sn^{13}C)| + 79.419$; S. Diemer, dissertation, Universität München, **1993**.
[9] a) $^2J(^{119}Sn,^{117}Sn)$ data: W. Biffar, T. Gasparis-Ebeling, H. Nöth, W. Storch, B. Wrackmeyer, *J. Magn. Reson.* **1981**, *44*, 54-61; b) B. Wrackmeyer, H. Zhou, *Magn. Reson. Chem.* **1990**, *28*, 1066-1069.
[10] S. Diemer, H. Nöth, K. Polborn, W. Storch, *Chem. Ber.* **1992**, *125*, 389-400. In (2,6-diisopropylphenyl)bis(trimethylstannyl)amine **5** with planar $CN-Sn_2$ skeleton, the Sn–N bond length is 204.4(3) pm.
[11] a) ^{15}N, ^{119}Sn NMR, and $^1J(^{119}Sn,^{15}N)$ data: B. Wrackmeyer, S. Kerschl, C. Stader, K. Horchler, *Spectrochim. Acta Part A* **1986**, *42*, 1113-1118; b) E. Kupce, B. Wrackmeyer, *Magn. Reson. Chem.* **1991**, *29*, 351-354.
[12] We thank Prof. Dr. H. Nöth for determining the crystal structure of **2**. Crystal data for **2**: Colorless prisms, 0.21 × 0.32 × 0.42 mm, monoclinic $P2_1/c$, $a = 14.639(2)$, $b = 9.351(2)$, $c = 13.381(3)$ Å, $\beta = 108.48(2)°$, $V = 1737.3(6)$ Å^3, $Z = 4$, $\rho_{calcd} = 2.166$ g cm^{-3}, $\mu(Mo_{K\alpha}) = 4.712$ mm^{-1}, $F(000) = 1048$ reflections recorded with $2° < 2\theta < 52°$, 2889 unique reflections, $R_{int} = 0.0087$, 1878 reflections with $F \leq 4.0\sigma(F)$, semiempirical absorption correction (0.169/0.105), structure solution using direct methods (SHELXTL program), refinement of 118 variables, $R = 0.0654$, $Rw = 0.0762$. Further details of the crystal structure investigation may be obtained from the Fachinformationszentrum Karlsruhe, Gesellschaft für wissenschaftlich-technische Information mbH, D-76344 Eggenstein-Leopoldshafen (FRG) on quoting the depository number CSD-57342, the names of the authors, and the journal citation.
[13] H. Bent, *Chem. Rev.* **1961**, *61*, 275-311.
[14] Determination of the sum of the covalent radii, taking into consideration the bond polarities, according to a correction by Schomaker and Stevenson: A. F. Wells, *Structural Inorganic Chemistry*, 4th ed., Clarendon, Oxford, **1975**, p. 236.
[15] C. Kober, H. Nöth, W. Storch, structural investigations on distannazanes, unpublished results.
[16] R. Hulme, *J. Chem. Soc.* **1963**, 1524-1527.
[17] a) P. G. Harrison, M. J. Begley, K. C. Molloy, *J. Organomet. Chem.* **1980**, *186*, 213-236; b) A distannylmethane, unbridged in solution, with very unsymmetrical Sn-Cl-Sn bridges in the solid state can only be compared to a limited extent: J. Meunier-Piret, M. van Meerssche, K. Jurkschat, M. Gielen, *ibid.* **1985**, *288*, 139-143.
[18] Modified MOPAC-6-Version (M. J. S. Dewar, E. G. Zoebisch, E. F. Healy, J. J. P. Steward, *J. Am. Chem. Soc.* **1985**, *107*, 3902–3902; J. J. P. Steward, *J. Comput. Chem.* **1989**, *10*, 209–220; *ibid.* **1989**, *10*, 221–264; *ibid.* **1991**, *12*, 320–341); Sn parameters: M. J. S. Dewar, E. F. Healy, D. R. Kuhn, A. J. Holder, *Organometallics* **1991**, *10*, 431–435.
[19] Comparison of calculated and experimental (in parentheses) bond lengths [pm] and angles [°]: N-Sn 201.2 (198.8), Sn-Cl 256.0/256.6 (280.8/272.5), Sn-C 209.4 (207.9), Sn-N-Sn 120.0 (120.0), N-Sn-Cl 77 (80.1/83.3), Sn-Cl-Sn 94.0 (76.9), Cl-Sn-Cl 154.1 (163.0), N-Sn-C 121.4 (118.1).
[20] $\delta_{i.s}$ [mm s^{-1}]: 0.98(2), 1.08(2), 1.29(2); Δ^{EQ} [mm s^{-1}]: 2.75(1), 3.03(1), 2.99(1); ratio of intensities 1:1:1. We thank Prof. Dr. J. Pebler, Universität Marburg, for recording the Mössbauer spectrum.

Nitrosyl Azide, N_4O, an Intrinsically Unstable Oxide of Nitrogen**

By *Axel Schulz, Inis C. Tornieporth-Oetting,** and *Thomas M. Klapötke**

Dedicated to Professor Paul von Ragué Schleyer

Nitrogen is able to form no fewer than six molecular oxides (N_2O, NO, N_2O_3, NO_2, N_2O_5, NO_3). Two (NO and NO_2) form π*–π* bound dimers, and all are thermodynamically unstable with respect to decomposition into N_2 and O_2.[1, 2] Although they all possess positive heats of formation, they are not intrinsically unstable with the exception of

[*] Dr. I. C. Tornieporth-Oetting, Priv.-Doz. Dr. T. M. Klapötke, Dipl.-Chem. A. Schulz
Institut für Anorganische und Analytische Chemie der Technischen Universität
Straße des 17. Juni 135, D-10623 Berlin (FRG)
Telefax: Int. code +(30) 31 42-2168

[**] This work was supported by the Deutsche Forschungsgemeinschaft (KL 626/2-2), the Fonds der Chemischen Industrie, and the Bundesministerium für Bildung und Wissenschaft (Graduiertenkolleg). We thank Prof. Dr. Dr. R. Hoppe for stimulating information.

the paramagnetic radical NO_3, which has not been isolated as a pure compound.[1] Moreover, prior to our work there had been some evidence for nitryl azide (NO_2N_3) and the substantially less stable nitrosyl azide (NON_3).[3] However, the identification of NON_3 was essentially based on the identification of its decomposition products (N_2 and N_2O) and four IR bands, three of which can definitely *not* be assigned to NON_3.[4, 5] The objective of our work was to establish the existence of this intriguing tetranitrogen monoxide and to elucidate its structure by a combination of low-temperature Raman spectroscopy and high-level quantum mechanical ab initio computations. As N_4O is intrinsically unstable, low-temperature techniques are more suitable than room-temperature gas-phase IR or electron diffraction studies to characterize this compound.

Reaction of activated, anhydrous NaN_3 and NOCl, followed by low-temperature vacuum sublimation, produced solid, pale yellow N_4O [Eq. (a)]. N_4O was unambiguously identified by its low-temperature Raman spectrum (Fig. 1) and, in agreement with earlier work,[4] was shown to decompose yielding N_2O and N_2 (identified by Raman spectroscopy and mass spectrometry and gas discharge—Teslar coil) [Eq. (b)].

$$NaN_3\ (\text{excess}) + NOCl \xrightarrow{-196 \le T \le -55\,^{\circ}C} NaCl + N_4O \qquad (a)$$

$$N_4O \xrightarrow{T \ge -50\,^{\circ}C} N_2O + N_2 \qquad (b)$$

To support our Raman data of N_4O, the structure and vibrational frequencies were computed with ab initio methods. The calculations were carried out with the Gaussian 92 program and the 6-31 + G* basis set.[6, 7] The geometries

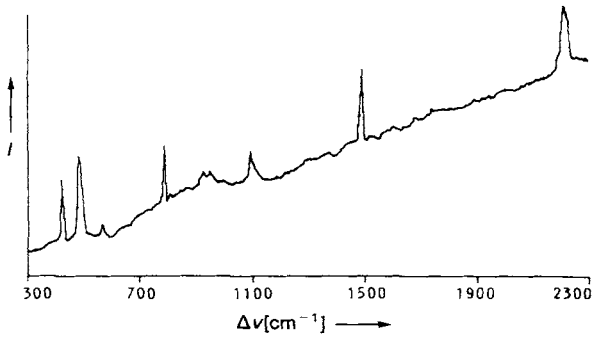

Fig. 1. Raman spectrum of N_4O in the range of 300–2300 cm^{-1} (647 nm, 30 mW, −110 °C, 3 scans, 1 s/p, 1 s integration time).

were fully optimized at the HF level and at correlated level according to Møller-Plesset second order perturbation theory (MP(FC)). Since the HF calculation predicted an unreliable, short terminal N2–N3 bond length of 1.088 Å,[8] the vibrational frequencies were computed on the correlated MP2 level (6-31 + G*). Table 1 shows the computed, scaled,[7] and observed frequencies and their assignments.

In agreement with the experimental spectroscopic results, the ab initio computation also shows a (planar, C_s) chainlike N_4O structure for nitrosyl azide. The optimized geometry and the computed structural parameters of N_4O, as well as the most likely Lewis representation, are shown in Figure 2.

As indicated by NBO analysis,[9] there is a significant interaction of one of the lone pairs on oxygen with the unoccupied, antibonding σ* orbital of the N1–N4 bond. This LP(O) → σ*(N1–N4) (negative) hyperconjugation[10] accounts for the rather long N1-N4 bond of 1.48 Å (cf. N_2F_4, d(N–N) = 1.49 Å).[11] Moreover, the ON–N_3 bond has a polarity $ON^{\delta+}$–$^{\delta-}N_3$ (cf. Fig. 2) that resembles the situation of the polarized covalent azides BrN_3 and IN_3.[12] The N_4-O distance of 1.20 Å is 0.07 Å longer than that in NOCl (1.13 Å),[1] corresponding to a bond order (b) slightly less than 2 (usual values for d(N–O): b = 1, 1.36 Å, b = 2, 1.16 Å).[1] Finally, all structural parameters of the (*trans*-bent) azide unit are in good agreement with other covalent azides.[13]

Table 1. Computed (MP2) and experimentally observed vibrational frequencies [cm^{-1}] of N_4O.

Calcd [a]	Scaled (F = 0.955) [7]	Raman (I) [b]	Assignment
2312	2208	2207 (8)	ν_{as}(N1-N2-N3)
1568	1498	1485 (8)	ν(N4-O)
1158	1106	1095 (3)	ν_s(N1-N2-N3)
818	780	784 (6)	$\delta_{\text{in plane}}$(N-N-N-N-O)
606	579	566 (2)	$\delta_{\text{in plane}}$(N_3-N-O)
506	483	484 (10)	$\gamma_{\text{out of plane}}$(N1-N2-N3)
416	397	415 (7)	ν(N_3-NO)
189	180	[c]	δ(N-N-N-N-O)
168	160	162 (1)	$\gamma_{\text{out of plane}}$(N-N-N-N-O)

[a] MP2/6-31 + G*. [b] 647 nm, 30 mW, −110 °C, 1 s/p, 1 s integration time, 3 scans. I = intensity. [c] Not observed.

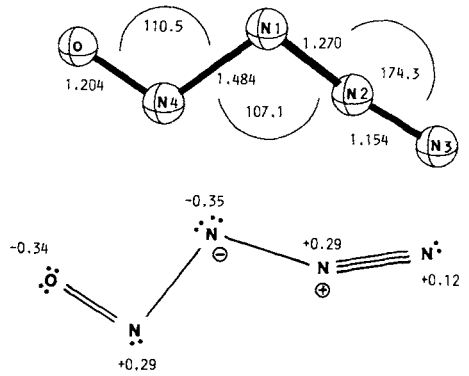

Fig. 2. Top: MP2-optimized geometry (distances in Å, angles in °); bottom: Lewis representation with natural bond order (NBO) charges for N_4O.

The dissociation of isolated, gaseous N_4O molecules into N_2O and N_2 according to Equation (b) was calculated to be strongly exothermic (after temperature correction for H by means of C_p and inclusion of the work term): ΔH^0_{298} [Eq. (b), MP2] = −91 kcal mol^{-1}.[14] It is interesting to note that N_4O is one of the few examples of an intrinsically unstable molecule that has been isolated as an essentially pure compound.

The cyclic, aromatic, 6π isomer of ON–N_3 (isoelectronic to N_5^-) was computed to be 13 kcal mol^{-1} more favorable than the observed chainlike species (MP2(FC)/6-31 + G*). The preference for the *trans*-chain form[15] can easily be explained by the reaction mechanism. The *trans* isomer formed in the first step could easily convert into the *cis* isomer (1 kcal mol^{-1} less stable); however, the cyclization requires a high activation energy (49 kcal mol^{-1}) because of the necessary bending of the azide unit.

We intend to report on the theory of the bonding in nitrogen oxides in a full paper.[16]

Experimental Procedure

Caution: Covalent azides are potentially hazardous and appropriate safety precautions should be taken.

N_4O was prepared by condensing gaseous NOCl (purified by distillation; 0.36 g, 5.54 mmol) from the calibrated, stainless steel, vacuum apparatus (the quantities of the materials were determined by volume changes at constant pressure) at −95 °C onto anhydrous NaN_3 (3.60 g, 55.38 mmol, excess) activated by recrystallization from SO_2. After the mixture was warmed to −55 °C (cf. m.p. (NOCl) = −59.6 °C) and allowed to react for 4 h, the product was sublimed into a 5 mm Raman capillary (−196 °C). Traces of N_2 and N_2O (b.p. (N_2O) = −88.5 °C) were pumped off at −85 °C leaving behind N_4O as a pale yellow solid in approximately 20% yield (0.08 g, 1.1 mmol). A mass spectrum of the sublimed and decomposed product (EI, 70 eV, 25 °C) showed N_2O to be present (m/e = 44; most intense signal beside N_2 and O_2). Subliming cold N_4O into the vacuum within an IR gas cell held at room temperature only gave evidence for the decomposition product N_2O.

Received: June 29, 1993
Revised version: July 21, 1993 [Z 6176 IE]
German version: *Angew. Chem.* **1993**, *105*, 1697

[1] N. N. Greenwood, A. Earnshaw, *Chemistry of the Elements*, Pergamon, Oxford, **1984**.
[2] N. Burford, J. Passmore, J. C. P. Sanders, *Mol. Struct. Energ.* **1989**, *11*, 53.
[3] M. P. Doyle, J. J. Maciejko, S. C. Busman, *J. Am. Chem. Soc.* **1973**, *95*, 952.
[4] H. W. Lucien, *J. Am. Chem. Soc.* **1958**, *80*, 4458.
[5] The reported IR absorptions of NON_3 are: $\tilde{\nu}$ = 2340, 1850, 2180, 1350 cm^{-1} (ref. [4]), no spectrum published, no intensities. Only the band at 2180 may correspond to N_4O according to our calculation (2208 cm^{-1}).
[6] M. J. Frisch, G. W. Trucks, M. Head-Gordon, P. M. W. Gill, M. W. Wong, J. B. Foresman, B. G. Johnson, H. B. Schlegel, M. A. Robb, E. S. Replogle, R. Gomperts, K. Andres, K. Raghavachari, J. S. Binkley, C. Gonzales, R. L. Martin, D. J. Fox, D. J. DeFrees, J. Baker, J. J. P. Stewart, J. A. Pople, GAUSSIAN 92, Gaussian Inc., Pittsburgh, PA, **1992**.
[7] W. J. Hehre, L. Radom, P. von R. Schleyer, J. A. Pople, *Ab Initio Molecular Orbital Theory*, Wiley, New York, **1986**.
[8] The HF/6-31 + G* structural parameters are: O-N4 1.165, N4-N1 1.378, N1-N2 1.276, N2-N3 1.088 Å and O-N4-N1 112.0, N1-N2-N3 173.8°.
[9] A. Reed, L. A. Curtiss, F. Weinhold, *Chem. Rev.* **1988**, *88*, 899.
[10] a) A. Reed, P. von R. Schleyer, *J. Am. Chem. Soc.* **1987**, *109*, 7362; b) *ibid.* **1990**, *112*, 1434; c) *Inorg. Chem.* **1988**, *27*, 3969.
[11] N. J. S. Peters, L. C. Allen, *Mol. Struct. Energ.* **1988**, *8*, 199.
[12] M. Otto, S. D. Lotz, G. Frenking, *Inorg. Chem.* **1992**, *31*, 3647.
[13] a) P. Buzek, T. M. Klapötke, P. von R. Schleyer, I. C. Tornieporth-Oetting, P. S. White, *Angew. Chem.* **1993**, *105*, 289; *Angew. Chem. Int. Ed. Engl.* **1993**, *32*, 275; b) M. Hargittai, I. C. Tornieporth-Oetting, T. M. Klapötke, M. Kolonitz, I. Hargittai, *ibid.* **1993**, *105*, 773 and **1993**, *32*, 759; c) I. C. Tornieporth-Oetting, T. M. Klapötke, *Comments Inorg. Chem.*, in press.
[14] Calculated absolute energies E; the first value refers to HF/6-31 + G* and the second to MP2/6-31 + G* calculations. N_4O: 292.47954, 293.32887; N_2O = 183.68528, 184.21442; N_2: 108.94702, 109.26193.
[15] Computed (MP2(FC)/6-31 + G*) IR data for the cyclic isomer (C_{2v}): 1330, 1248, 1058, 1054, 980, 814, 709, 686, 671 cm^{-1} (unscaled).
[16] I. C. Tornieporth-Oetting, T. M. Klapötke in *Combustion Efficiency and Air Quality* (Eds.: I. Hargittai, T. Vidoczy). Plenum, New York, in press.

Photo-induced *exo*-Selective Diels–Alder Reactions**

By *Bipin Pandey** and *Pramod V. Dalvi*

Dedicated to Professor Manapurathu Verghese George on the occasion of his 65th birthday

The 65-year-old Diels–Alder reaction[1] and its intramolecular,[2] inverse-electron demand,[3] hetero,[4] and asymmetric[5] variants offer many synthetic advantages in view of their simplicity and versatility. The chemo-, regio-, and stereoselectivity associated with these reactions, besides proving to be a productive testing ground for theoretical organic chemists,[6] have widely been exploited in the synthesis of natural products.[2–5, 7] Of the various levels of stereoselectivity, a particularly important feature is the predominant formation of the *endo* isomer in the thermal reaction of cyclic dienes with cyclic dienophiles.[8] The alternative possibility of exclusive *exo* selectivity is usually not achieved by conscious modification of reaction conditions,[8] although some substrate-specific exceptions are known.[9] We now report some examples, in which exclusively the *exo* isomer is obtained in Diels–Alder reactions by a suitable choice of reaction conditions.

It is known that when cyclopentadiene (**1**) is warmed with maleic anhydride (**2**), the selectivity is >98% for the *endo* isomer **3**.[8] In marked contrast, the photolysis of **1** (6.6×10^{-4} mol) and **2** (5.7×10^{-4} mol) in 5% triethylamine in dry ethanol (20 mL) furnished essentially (>98% selectivity) *exo* isomer **4** (38%) (Scheme 1 and Table 1, entry 1). The generality of *exo*-selective photo-Diels–Alder reactions is indicated in Table 1.

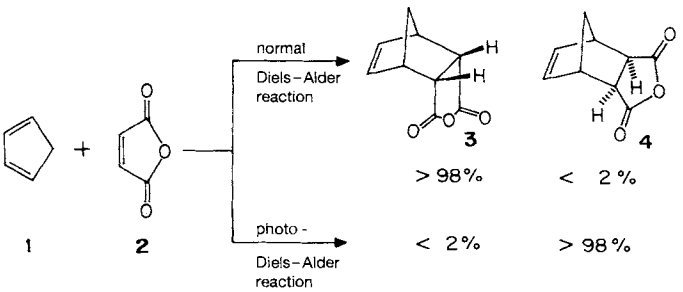

Scheme 1. *endo*- and *exo*-selective Diels–Alder reactions of **1** with **2**.

Table 1. Photo-induced, *exo*-selective Diels–Alder reactions.

Entry no	Dienophile	Molar ratio [a]	Reaction condition [b]	Photolysis duration [h]	Product (yield [%]) [c, d]
1	**2**	1:1.2	A	1	**4** (38)
2	**2**	1:1.2	A	0 [e]	**4** (0)
3	**2**	–	A	1	**2** (90)
4	**11**	1:1.2	C	2	**5a** (34) [f]
5	**12**	1:5	D	6	**6a** (26) [g]
6	**12**	1:2.3	C	6	**6a** (42) [f, g]
7	**13**	1:10	E	5	**6b** (35) [h]
8	**13**	1:5	D	5	**6b** (81)
9	**13**	1:12	B	5	**6b** (25)
10	**14**	1:10	B	4	**6c** (68)
11	**15**	1:1.3	A	2	**5b** (64) [i]
12	**15**	1:1.3	A	0 [e]	**5b** (0)
13	**2**	1:1.2	A	1	**8** (44)
14	**12**	1:2.2	B	6	**7a** (54)
15	**13**	1:2.5	C	6	**7b** (42)
16	**16**	1:1.1	C	2	**9** (70)
17	**17**	1:1	C	2	**10** (48)

[a] The molar ratio of dienophile: diene is presented. Cyclopentadiene **1** (entries 1–12 as well as 16 and 17) and cyclohexadiene (entries 13–15) were used as diene. [b] The photo-Diels–Alder reactions were carried out in the presence of different quantities of triethylamine in dry ethanol (% volume): A = 5%, B = 10%, C = 20%, D = 50%, and E = 98%. [c] The yield is for isolated pure adduct and is based on consumed dienophiles [10, 11]. The conversion of dienophiles was invariably greater than 90%. [d] The absence of *endo* isomer (i.e. >98% *exo* selectivity) was confirmed by thin-layer and/or gas chromatography [12]. [e] Control experiments (entries 2 and 12) were carried out in dark and at room temperature for the same length of time as in the corresponding photochemical experiments (entries 1 and 11). No *endo* or *exo* isomer was observed. [f] Side products due to triplet-sensitized diene dimerization, for example *exo* and *endo* dimers of **1** [13, 18]. [g] 1,4-Dihydronaphthalene as side product. [h] 1,4,5-Trihydroxynaphthalene as side product. [i] 2-Methyl-4-hydroxyphenol as side product.

[*] Dr. B. Pandey, Dipl.-Chem. P. V. Dalvi
Organic Chemistry, Technology Division
National Chemical Laboratory
Pune 411 008 (India)
Telefax: Int. code + (212)33-0233

[**] NCL Communication No. 5746. This work was supported by the Director of the National Chemical Laboratory, Dr. R. A. Mashelkar (Senior Research Fellowship for P. V. D. and a Kite Flying Grant for B. P.) and by the Department of Science & Technology, India (instrumentation support).

The *exo*-products **4**–**10** (Scheme 2)[10] have been obtained by reacting either **1** or 1,3-cyclohexadiene (CHD) with common cyclic dienophiles, for example maleic anhydride (**2**), 1,4-benzoquinone (**11**), 1,4-naphthoquinone (**12**), 5-hydroxy-1,4-naphthoquinone (**13**), 5-methoxy-1,4-naphthoquinone (**14**), 2-methyl-1,4-benzoquinone (**15**), 4-cyclopentene-1,3-dione (**16**), and 4-phenyl-1,2-dehydro-1,2,4-triazole-3,5-dione (**17**) under various photochemical conditions (Table 1).

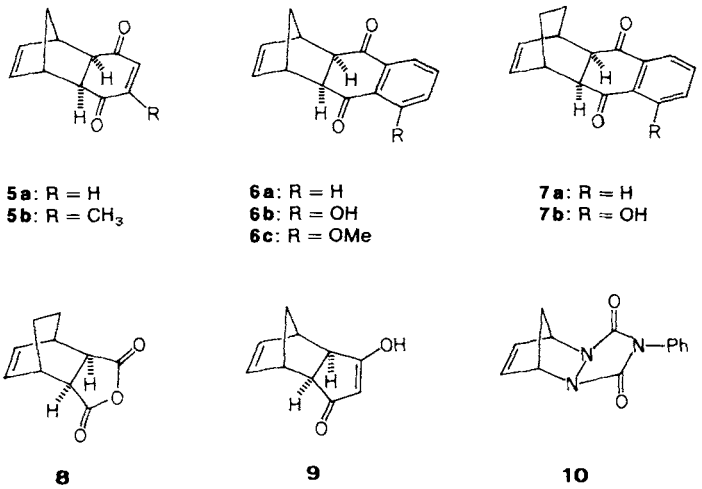

Scheme 2. *exo* Products that were prepared under different photochemical reaction conditions (see Table 1).

Several characteristic features of these reactions are summarized in the following: 1) Photo-Diels–Alder reactions are highly *exo* selective. 2) Photolysis is essential for the success of the reaction (entries 2 and 12). 3) The duration of photolysis is short, that is 1–6 h. 4) The yield of *exo* isomer ranges between 25–81%.[10, 11] 5) With naphthoquinone-type dienophiles, 20–50% of Et_3N in ethanol gives satisfactory yields of *exo* isomers (entries 6, 8, and 15). Very high concentration of Et_3N furnishes reduced products, for example 1,4-dihydroxynaphthalene and 1,4,5-trihydroxy naphthalene (entries 5 and 7). 6) Et_3N, as such, does not react with **2** under photolytic conditions (entry 3). 7) *exo*-Selective transformations can also be carried out on a gram scale (see Experimental Procedure). 8) Normally, our methodology is suitable for dienophiles containing carbonyl groups. However, photolysis of pure **1** under the reaction condition C (see Table 1) for 5 h gave a 60:40 mixture of the *exo*/*endo* dimers.

The present study unequivocally establishes the ability of triethylamine to reverse the *endo* selectivity of Diels–Alder reactions. However, one can only speculate on the electronic origin of this effect. *Endo* selectivity is generally believed to be due to secondary orbital overlap between the diene HOMO and the dienophile LUMO.[6, 14] The electron-rich Et_3N seems to disturb this secondary orbital overlap interaction in the transition state of the Diels–Alder reaction,[15] perhaps by complexing with the dienophile in the excited state.[16] An alternative explanation could be the selective isomerization of *endo* isomer under photolytic conditions.[17] But this possibility is partially valid only with highly reactive dienophiles for example **2**, **11**, and **17**. With other, less reactive dienophiles, no *endo* product was observed in control experiments. Another control experiment in which **1** and 1,4-naphthoquinone **12** in 20% Et_3N/EtOH were heated under reflux did not lead to the formation of the *exo* isomer **6a**. Additionally, photolysis of diene **1** and dienophile **12** without Et_3N is known to give triplet-sensitized diene dimers and [2 + 2] photocycloaddition products.[18, 19]

In summary, a novel photochemical methodology for *exo*-selective Diels–Alder reactions with dienophiles containing carbonyl functionality has been developed. We are currently investigating the role of triethylamine and generality of our *exo*-selective procedure for inter-, and intramolecular, asymmetric and as well as hetero-Diels–Alder reactions.

Experimental Procedure

6a (large-scale preparation): To a solution of 1,4-naphthoquinone **12** (4.0 g, 31.6×10^{-3} M) in ethanol/triethylamine (50/50; this ratio usually gave the best yield for large-scale preparations, although the 80/20 ratio led to a similar yield for small-scale reactions, see entry 6 Table 1) (800 mL) in a pyrex tube, freshly cracked cyclopentadiene **1** (3.8 g, 72.0×10^{-3} M) was added, and the reaction mixture was purged with a slow stream of nitrogen for 10 min. The solution was then irradiated at 300 nm with a Rayonet photochemical reactor with constant stirring and cooling at room temperature for 6 h. Progress of the reaction was monitored by thin-layer and gas chromatography, until more than 95% of the dienophile was consumed. After removal of the solvent and triethylamine under reduced pressure, the residue was chromatographed on a silica gel column by eluting with 5% acetone/hexane to give **6a** (2.44 g, 43%). M.p. 160 °C; IR (nujol): $\tilde{\nu}[cm^{-1}] = 1650\ cm^{-1}$ (C=O); ^1H NMR (200 MHz, $CDCl_3$, 25 °C): $\delta = 1.5$ (m, 2H, CH_2), 2.35 (m, 2H, CH), 4.15 (m, 2H, CH), 6.8 (m, 2H, vinylic H), 7.5–7.7 (m, 2H, aromatic H), 7.9–8.1 (m, 2H, aromatic H); ^{13}C NMR (50.32 MHz, $CDCl_3$): $\delta = 181.23$ (s), 162.66 (s), 142.25 (d), 132.91 (d), 132.53 (d), 125.82 (d), 73.02 (d), 48.44 (t); MS (70eV): *m/z* 224 (90%) [M^+]; correct analysis (C,H) for $C_{15}H_{12}O_2$.

Received: March 10, 1993
Revised version: May 10, 1993 [Z 5911 IE]
German version: *Angew. Chem.* **1993**, *105*, 1724

[1] O. Diels, K. Alder, *Justus Liebigs Ann. Chem.* **1928**, *460*, 98.
[2] D. Craig, *Chem. Soc. Rev.* **1987**, *16*, 187.
[3] L. F. Tietze in *Selectivity – A Goal for Synthetic Efficiency* (Eds.: W. Bartmann, B. M. Trost), Verlag Chemie, Weinheim, **1984**, p. 299.
[4] S. Danishefsky, M. P. DeNinno, *Angew. Chem.* **1987**, *99*, 15; *Angew. Chem. Int. Ed. Engl.* **1987**, *26*, 15.
[5] a) W. Oppolzer, *Angew. Chem.* **1984**, *96*, 840; *Angew. Chem. Int. Ed. Engl.* **1984**, *23*, 876; b) S. Masamune, W. Choy, J. S. Petersen, L. R. Sita, *ibid.* **1985**, *97*, 1 and **1985**, *24*, 1.
[6] a) J. Sauer, R. Sustmann, *Angew. Chem.* **1980**, *92*, 773; *Angew. Chem. Int. Ed. Engl.* **1980**, *19*, 779; b) T. Karcher, W. Sicking, J. Sauer, R. Sustmann, *Tetrahedron Lett.* **1992**, *33*, 8027.
[7] G. Desimoni, G. Tacconi, A. Barco, G. P. Pollini, *Natural Product Synthesis through Pericyclic Reactions (ACS Monogr.)*, Am. Chem. Soc., Washington, D.C., **1983**.
[8] J. Sauer, *Angew. Chem.* **1967**, *79*, 76; *Angew. Chem. Int. Ed. Engl.* **1967**, *6*, 16.
[9] Some substrate-specific exceptions to *endo* selectivity in Diels–Alder reactions are reported with unusual dienes and dienophiles. a) J. R. L. Smith, R. O. C. Norman, M. R. Stillings, *Tetrahedron* **1978**, *34*, 1381; b) J. Mattay, J. Mertes, G. Maas, *Chem. Ber.* **1989**, *122*, 327; c) R. Sustmann, W. Sicking, H. Lamy-Schelkens, L. Ghosez, *Tetrahedron Lett.* **1991**, *32*, 1401; d) W. R. Roush, B. B. Brown, *J. Org. Chem.* **1992**, *57*, 3380.
[10] All *exo* compounds exhibited satisfactory IR, ^1H NMR, ^{13}C NMR, and mass spectra as well as elemental analyses.
[11] The reported yields are not optimized. For reactions with low to moderate yields of *exo* isomers, no unreacted dienophiles were recovered. Perhaps polymerization of unreacted dienophiles occurs. However, the tarlike material does not create problems for the separation of *exo* isomers by column chromatography.
[12] Authentic samples of *endo* isomers were prepared by usual thermal Diels–Alder reactions [6, 8].
[13] For triplet-sensitized diene dimerization, see a) N. J. Turro, G. S. Hammond, *J. Am. Chem. Soc.* **1962**, *84*, 2841.
[14] I. Fleming, *Frontier Orbitals and Organic Chemical Reactions*, Wiley, New York, **1980**, pp. 106–109.
[15] The choice of amine as a tertiary amine, for example Et_3N, was governed by the high reactivity of primary and secondary amines with 1,4-naphthoquinone, and 1,4-benzoquinone during photolysis, M. Matsuoka, K. Takagi, H. Tajima, K. Ueda, T. Kitao, *J. Chem. Soc. Perkin Trans. 1* **1984**, 1297.
[16] A charge-transfer band in UV spectrum is observed, when Et_3N is mixed with either 1,4-benzoquinone or 1,4-naphthoquinone, under our experimental conditions.
[17] B. Pandey, P. V. Dalvi, A. A. Athawale, B. G. Pant, P. P. Kewale, *J. Chem. Soc. Chem. Commun.* **1990**, 1505.
[18] W. L. Dilling, *Chem. Rev.* **1969**, *69*, 845.
[19] G. O. Schenck, J. Kuhls, C. H. Krauch, *Justus Liebigs Ann. Chem.* **1966**, *693*, 20.

Crystallographic Study of a Single Crystal to Single Crystal Photodimerization and Its Thermal Reverse Reaction**

By *Kathleen Novak, Volker Enkelmann,* Gerhard Wegner,* and *Kenneth B. Wagener*

Topochemical reactions proceed in crystals under the strict control of the crystal lattice. The best studied topochemical reactions are [2 + 2] photocycloadditions[1] and the solid state polymerization of diacetylenes.[2] In their pioneering work on the [2 + 2] photodimerization of cinnamic acid derivatives, G. M. J. Schmidt et al. observed that of many possible dimers, only the one whose symmetry is already preordained in the crystal packing of the monomers is formed.[3] Photodimerizations of this type proceed heterogeneously, as do most topochemical reactions; that is, at a certain extent of conversion, phase separation occurs. This destroys the monomer crystal and results in the formation of microcrystalline aggregates. The driving force is the anisotropic changes in the lattice that occur when van der Waals forces are transformed into chemical bonds in particular directions. In contrast, homogeneous topochemical reactions, for example the solid state polymerization of diacetylenes, are characterized by the persistence of the crystal throughout the whole conversion range.[4] The monomer and polymer form a substituted mixed crystal in which monomer and polymer are statistically distributed when conversion is incomplete and occupy identical lattice positions. This is possible, because the accompanying chemical reactions, which in part involve substantial atomic shifts, are limited to only a few atoms in the center of the molecule, while the substituents form a matrix that, as a first approximation, does not alter its position during the reaction.

The system shown in Scheme 1 and first described by Hünig and Hesse,[5] does not only undergo the [2 + 2] photodimerization homogeneously, as described for individual cases in the literature,[4] but also returns thermally to a pure crystal of the monomer. It is thus possible in this case to switch between monomer and dimer state without loss of crystal quality.

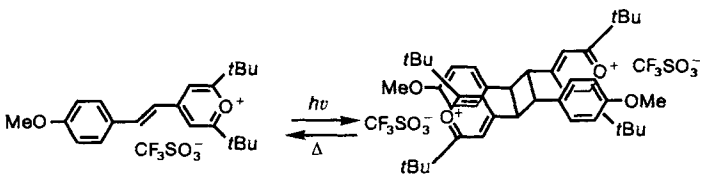

Scheme 1. Reversible [2 + 2] photodimerization in the crystal.

The key to this behavior lies in the choice of a suitable wavelength for the photodimerization. If the wavelength of the absorption maximum of the styrylpyrilium chromophore (λ_{max} = 420 nm) is used, the heterogeneous reaction typical for cinnamic acid derivatives is observed: Initially yellow microcrystalline aggregates of the dimer form on the surface of the red crystals. On further irradiation the original monomer crystals break up completely. This behavior persists for monochromatic irradiation with wavelengths up to λ = 540 nm. However, if the wavelength corresponds to the flank of the absorption, more than 150 nm longer than λ_{max} (λ > 570 nm), the crystal is preserved over the whole reaction. Nevertheless, the choice of wavelength does not influence the crystal structure of the incipient dimer. The position of the reflections and their intensities in the X-ray powder diffractogram of the microcrystals obtained on UV irradiation correspond to those from single-crystal structure analyses. Figure 1 shows projections of views of the crystal structures of the monomer and the dimer, as well as of two monomer–dimer mixed crystals that were isolated after different irradiation times.[6] In the mixed crystals, separate

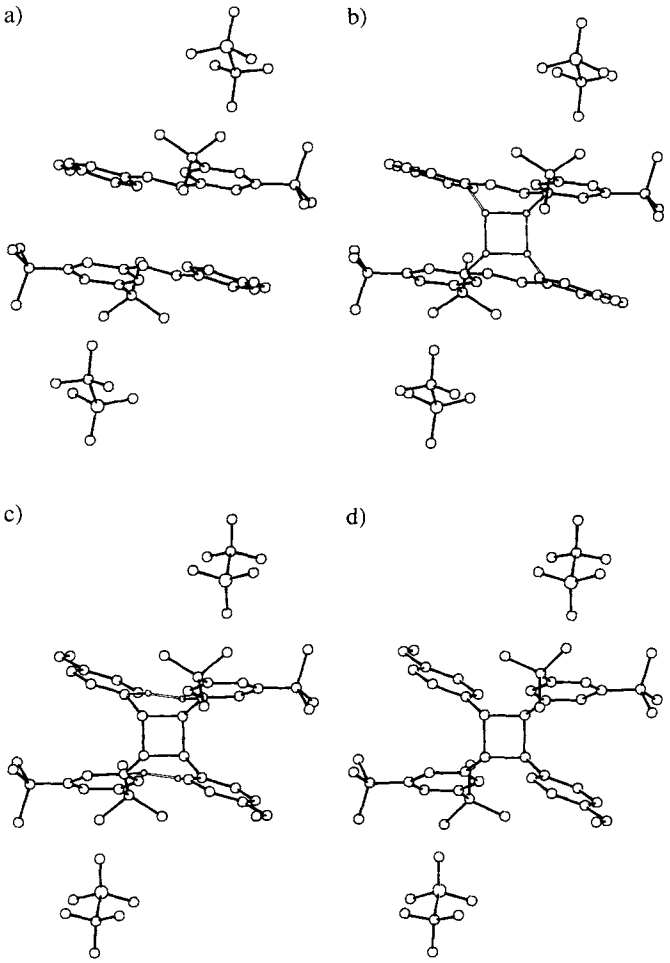

Fig. 1. Sections of the crystal structures of a) the monomer, b) a monomer–dimer mixture after 13% conversion, c) a monomer–dimer mixture after 67% conversion, and d) the dimer for the reaction in Scheme 1.

atomic coordinates are found only for those C atoms directly involved in the reaction. The occupation parameters of these atoms were optimized in the refinement and agree with the values obtained by IR spectroscopy.[7] The positions of other atoms in the mixed crystal are identical within the error limits of the structure analysis. The comparison of the crystal structures depicted in Figure 1 reveals that in the course of the reaction the positions of these atoms change substantially. For instance, the phenyl ring twists during the reaction by 18°. Similar movements of the pyrilium ring and the counterion can also be detected. The change in conformation appears to be continuous, since the dihedral angle determined from the mixed crystals lies between the two end states.

[*] Dr. V. Enkelmann, K. Novak, Prof. Dr. G. Wegner
Max-Planck-Institut für Polymerforschung
Ackermannweg 10, D-55021 Mainz (FRG)
Prof. Dr. K. B. Wagener
Department of Chemistry, University of Florida
Gainesville, FL 32611 (USA)

[**] This work was supported by the 3M Corporation of St. Paul, Minnesota. We thank Dr. Jeremy Titman for recording the ^{13}C NMR spectra.

The counterion and the *tert*-butyl groups are disordered in the monomer at room temperature, and their two orientations are statistically occupied. This is probably caused by a dynamic process. The solid state ^{13}C MAS NMR spectrum contains only one peak for the *tert*-butyl groups at room temperature.[8] Accordingly we assume that the dynamic process is a jump rotation between the two sites. This is frozen at low temperature. If the crystal structure is determined at 165 K, all disordered groups are present in only one of the two orientations. Surprisingly, in the dimer the disorder no longer occurs at room temperature. Apparently the cavities in the monomer in which these groups rotate are changed to such an extent that the movement is no longer possible after the reaction, although in the dimer no significantly smaller C–H contacts are observed.

The photochemically generated dimer is apparently in a metastable state. At temperatures greater than 100 °C the crystals of the monomer are reformed in a smooth reaction during which the unexpectedly small heat of reaction of 1.8 kcal mol^{-1} is released.[9] Preliminary experiments show that this is a reversible photochromic system. It is possible to store holograms photochemically in several cycles with a He–Ne laser (633 nm), to read them, and subsequently to delete them thermally.[10]

On recrystallization of the dimer from organic solvents another modification of the crystal is obtained. A view of the crystal structure of this form is illustrated in Figure 2.[6] In this modification of the dimer, the disorder described for the monomer is detected at room temperature. The dimer crystals formed on recrystallization can no longer be transformed back into the monomer, in contrast to the "as dimerized" form, but are stable at temperatures at which the latter are cleaved within a minute.

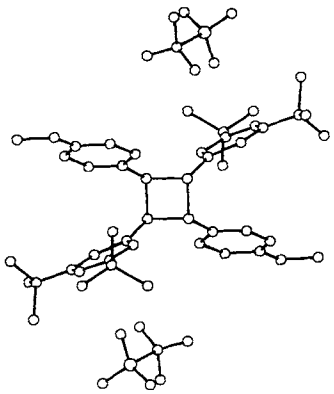

Fig. 2. Section of the crystal structure of the recrystallized dimer of the reaction in Scheme 1.

The ability to initiate a homogeneous topochemical photoreaction by irradiation into the outer absorption flank is not restricted to the system described here. Crystals of the oligomer of distyrylpyrazine have already been obtained in the same way.[4d] Some salts of styrylpyrilium monomers with counterions like ClO_4^-, BF_4^-, ReO_4^-, SbF_6^-, $AuCl_2^-$, or $SnCl_5^-$ likewise form photoreactive crystals that can be dimerized homogeneously in the same way. Preliminary experiments with α-*trans*-cinnamic acid indicate that here, too, a dimerization can take place while the crystal is retained.[11] It seems possible that further photoreactions in crystals that are heterogeneous under the usual irradiation conditions may be single crystal to single crystal transformations on irradiation into the outermost absorption flank.

It should be emphasized that topochemical control of the reaction is not affected by the homogeneous or heterogeneous course of the reaction. Every solid-state reaction is associated with anisotropic lattice changes. A steep concentration profile develops on irradiation into the absorption maximum, and the photoreaction takes place in only a thin layer on the crystal surface. As the lattices of monomer and dimer are not identical, the crystallites of the dimer detach from the surface of the crystal under these conditions. The observation of the crystal surface of heterogeneous systems therefore enables no conclusions about the mechanism of the photoreaction. The directed material transport observed by Kaupp[12] on the surface of cinnamic acid crystals under the atomic force microscope during irradiation describes the necessary structure of the crystallites under the chosen irradiation conditions, but does not support deductions on a violation of the topochemical principle.

Received: May 10, 1993 [Z 6072 IE]
German version: *Angew. Chem.* **1993**, *105*, 1678

[1] For a comprehensive literature survey see V. Ramamurthy, K. Venkatesan, *Chem. Rev.* **1987**, *87*, 433–481.

[2] V. Enkelmann, *Adv. Polym. Sci.* **1984**, *63*, 92–136.

[3] M. D. Cohen, G. M. J. Schmidt, F. I. Sonntag, *J. Chem. Soc.* **1964**, 2000–2013; G. M. J. Schmidt, *ibid.* **1964**, 2014–2021. For further work, see G. M. J. Schmidt, et al. in *Solid State Photochemistry* (Ed.: D. Ginsburg), Verlag Chemie, Weinheim, **1976**.

[4] Homogeneous solid-state reactions known formerly: a) 2-benzylidenecyclopentanone and its *p*-bromo derivative: H. Nakanishi, W. Jones, J. M. Thomas, M. B. Hursthouse, M. Motevalli, *J. Phys. Chem.* **1981**, *85*, 3636–3642; b) acridizinium salts: W. N. Wang, W. Jones, *Tetrahedron* **1987**, *43*, 1273–1279; c) photoreaction of the channel inclusion compound from deoxycholic acid and acetophenone: H. C. Chang, R. Popovitz-Biro, M. Lahav, L. Leiserowitz, *J. Am. Chem. Soc.* **1982**, *104*, 614–616; d) oligomerization of distyrylpyrazine: H. G. Braun, G. Wegner, *Makromol. Chem.* **1983**, *184*, 1103–1119; e) polymerization of butadiene in layered perovskites: B. Tieke, *J. Polym. Sci. Polym. Chem. Ed.* **1984**, *22*, 2895–2921; f) polymerization of diacetylenes: see [2] and references therein; g) solid-state reactions that form a new phase in the single crystal to single crystal process: K. Cheng, B. Foxman, *J. Am. Chem. Soc.* **1977**, *99*, 8102–8103; h) racemization of a cobaloxime complex: Y. Ohashi, K. Yanagi, T. Kurihara, Y. Sasada, Y. Ohgo, *ibid.* **1982**, *104*, 6355–6359.

[5] K. Hesse, S. Hünig, *Liebigs Ann. Chem.* **1985**, 715–739.

[6] Crystallographic data: Enraf-Nonius CAD4 diffractometer, $Cu_{K\alpha}$ radiation, ($\lambda = 1.5405$ Å). Annealing of the crystals in a stream of nitrogen. The intensity of the reflections were measured with the θ/θ probe. The scan width dependent on the scattering angle ($\Delta\omega = \Delta\omega_1 + 0.14\tan\theta$) was selected according to the reflection width of the crystals; $\Delta\omega_1$ varied only marginally and lay between 0.4 and 0.6°; structure resolved with direct methods. The parameters of the H atoms were refined in "riding mode". Programs used: SIR 88, Molen, CRYSTALS. Monomer at room temperature: $a = 10.3873(8)$, $b = 14.7855(8)$, $c = 16.4929(16)$ Å, $\beta = 103.147(8)$, $V = 2466.5$ Å^3, $P2_1/c$, $Z = 4$, $\rho_{calcd} = 1.272$ g cm^{-3}, $\mu = 15.98$ cm^{-1}; 3256 measured reflections of which 2071 observed ($I > 3\sigma(I)$), $R = 0.090$, $R_w = 0.099$. Monomer at 165 K: $a = 10.3077(9)$, $b = 14.7763(7)$, $c = 16.0772(12)$ Å, $\beta = 102.162(9)$, $V = 2393.8$ Å^3, $P2_1/c$, $Z = 4$, $\rho_{calcd} = 1.311$ g cm^{-3}, $\mu = 16.47$ cm^{-1}; 2859 measured reflections of which 1589 observed ($I > 3\sigma(I)$), $R = 0.063$, $R_w = 0.074$. Thermally regenerated monomer at 165 K: $a = 10.2845(10)$, $b = 14.7491(27)$, $c = 16.1026(27)$ Å, $\beta = 102.210(9)$, $V = 2387.3$ Å^3, $P2_1/c$, $Z = 4$, $\rho_{calcd} = 1.320$ g cm^{-3}, $\mu = 16.51$ cm^{-1}; 3294 measured reflections of which 2440 observed ($I > 3\sigma(I)$), $R = 0.031$, $R_w = 0.034$. Mixed crystal (13% conversion) at 165 K: $a = 10.2941(14)$, $b = 14.7400(12)$, $c = 16.0874(16)$ Å, $\beta = 102.328(8)$, $V = 2385$ Å^3, $P2_1/c$, $Z = 4$, $\rho_{calcd} = 1.322$ g cm^{-3}, $\mu = 16.53$ cm^{-1}; 2820 measured reflections of which 2088 observed ($I > 3\sigma(I)$), $R = 0.068$, $R_w = 0.080$. Mixed crystal (67% conversion) at 165 K: $a = 10.7497(12)$, $b = 14.2531(13)$, $c = 16.4773(15)$ Å, $\beta = 105.267(7)$, $V = 2435.5$ Å^3, $P2_1/c$, $Z = 4$, $\rho_{calcd} = 1.294$ g cm^{-3}, $\mu = 16.19$ cm^{-1}; 3215 measured reflections of which 1863 observed ($I > 3\sigma(I)$), $R = 0.090$, $R_w = 0.082$. Dimer at room temperature: $a = 10.8603(6)$, $b = 14.1449(35)$, $c = 16.4046(8)$ Å, $\beta = 106.324(8)$, $V = 2418.5$ Å^3, $P2_1/c$, $Z = 4$, $\rho_{calcd} = 1.298$ g cm^{-3}, $\mu = 16.30$ cm^{-1}; 3759 measured reflections of which 2744 observed ($I > 3\sigma(I)$), $R = 0.056$, $R_w = 0.053$. Recrystallized dimer at room temperature: $a = 14.3055(8)$, $b = 16.2259(9)$, $c = 21.5090(15)$ Å, $V = 4992.7$ Å^3, *Pcba*, $Z = 8$, $\rho_{calcd} = 1.257$ g cm^{-3}, $\mu = 15.79$ cm^{-1}; 3203 measured reflections of which 1369 observed ($I > 3\sigma(I)$), $R = 0.077$, $R_w = 0.071$. Further details of the crystal structure investigation may be obtained from the Fachinformationszentrum Karlsruhe, Gesellschaft für

wissenschaftlich-technische Information mbH, D-76344 Eggenstein-Leopoldshafen (FRG) on quoting the depository number CSD-57343, the names of the authors, and the journal citation.
[7] The monomer was prepared as described in [5]. The photodimerization was performed with a Coherent Innova ^{90}Kr laser. Eight to nine crystals 0.3–0.5 mm long were oriented so that the (100) surface was irradiated and slowly turned within a surface that was uniformly illuminated by means of a beam expander. Two to three of these crystals were subjected to crystallographic analysis, while the rest were used for IR spectroscopic studies. The calibration was achieved by irradiation of a mixture of monomer and dimer with a Xe lamp followed by establishment of the degree of conversion by ^{1}H NMR spectroscopy.
[8] The solid-state ^{13}C NMR spectra were recorded with a Bruker MSL 300 spectrometer at 75.47 MHz. The MAS (*m*agic *a*ngle *s*pinning) frequency was 3 kHz, and the CP (*c*ross *p*olarization) time 2 ms. A TOSS (*t*otal *s*uppression of *s*pinning *s*ide bands) pulse sequence was used. The detection time was 35 ms for a 90° pulse length of 4.5 μs. For a spectral width of 29.411 Hz, 2048 data points were collected.
[9] Thermoanalytical experiments were performed on a Mettler DSC 30 instrument at a heating rate of 5 K min^{-1}.
[10] A thick sinusoidal phase grating with a period of 17.3 μm was recorded on the (100) face of a crystal with two interfering beams from a 30 mW He–Ne laser. Between writing periods, one of the writing beams was blocked, and the intensity of the diffracted reading beam measured with a photomultiplier tube. After the desired diffraction intensity had been reached, the reading beam was attenuated by a factor of 2000 to avoid bleaching, and the thermal decay of the grating was monitored continuously.
[11] V. Enkelmann, G. Wegner, K. Novak, K. B. Wagener, *J. Am. Chem. Soc.*, in press. The dimerization of α-*trans*-cinnamic acid was performed at a wavelength of 360 nm and under these conditions is quantitative as a single crystal to single crystal transformation.
[12] G. Kaupp, *Angew. Chem.* **1992**, *104*, 606–609; *Angew. Chem. Int. Ed. Engl.* **1992**, *31*, 592–595.

[Ni(P*t*Bu)$_6$] and [Ni(SiH$_2$)$_6$] Are Isolobal, Related to [In{Mn(CO)$_4$}$_5$]$^{2-}$, and Have 16-Electron Counts**

By *Huang Tang, David M. Hoffman,* Thomas A. Albright,* Haibin Deng,* and *Roald Hoffmann**

Recently Ahlrichs, Fenske et al.[1] reported the isolation, structure determination, and calculations of the unique compound **1**. The nickel and six phosphorus atoms in this com-

[Ni(P*t*Bu)$_6$] **1**

plex lie nearly in a plane. There is an interesting ambiguity in the electron counting for **1**.[1, 2] In one extreme, the P*t*Bu groups can be counted as two-electron (2e) donors, leading to a 22 electron count around the metal. Alternatively, the normal P–P distances lead one to think of two-center two-electron P–P bonds (i.e., (P*t*Bu)$_6$ is electronically saturated). But then what holds the Ni(0) within the cavity of the (P*t*Bu)$_6$ ring? There are also lone pairs on the phosphorus atoms of the (P*t*Bu)$_6$ ring, sites for potential metal coordination. But these do not point to the ring center.

[*] Prof. D. M. Hoffman, Prof. T. A. Albright, H. Tang
Department of Chemistry, University of Houston
Houston, TX 77204-5641 (USA)
Telefax: Int. code + (713)743-2787
Prof. R. Hoffmann, H. Deng
Department of Chemistry, Cornell University
Ithaca, NY 14853-1301 (USA)
Telefax: Int. code + (607)255-5707

[**] This work was supported by the Robert A. Welch Foundation, the Petroleum Research Fund, administered by the American Chemical Society, the National Science Foundation, the University of Houston President's Research Enhancement Fund, and the State of Texas through the Advanced Research Program. We also acknowledge the National Science Foundation for an allocation of computer time at the Pittsburgh Supercomputing Center and the purchase of a Cray Y-MP/EL computer. D. M. H. is a 1992–1994 Alfred P. Sloan Research Fellow.

The reason why **1** is stable and does not violate electron counting rules is symmetry-based. Consider first the hypothetical molecule **2** with a D_{6h} geometry. This is isolobal[3, 4]

[Ni(SiH$_2$)$_6$] **2**

with **1** because of the relationship between PR and SiR$_2$, as shown in Scheme 1. An idealized orbital interaction diagram

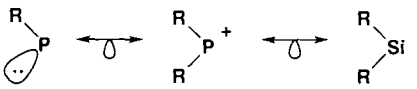

Scheme 1.

for **2** is present in Figure 1. The frontier orbitals of a carbenoid SiH$_2$ fragment consist of a radial sp^2 hybrid orbital pointing directly toward the Ni and a tangential p orbital.[4] Let us assume that intermixing between radial and tangential combinations of the same symmetry is minimal. The twelve resulting symmetry-adapted orbitals for the Si$_6$H$_{12}$ ligand are those shown on the right side of Figure 1. Three radial

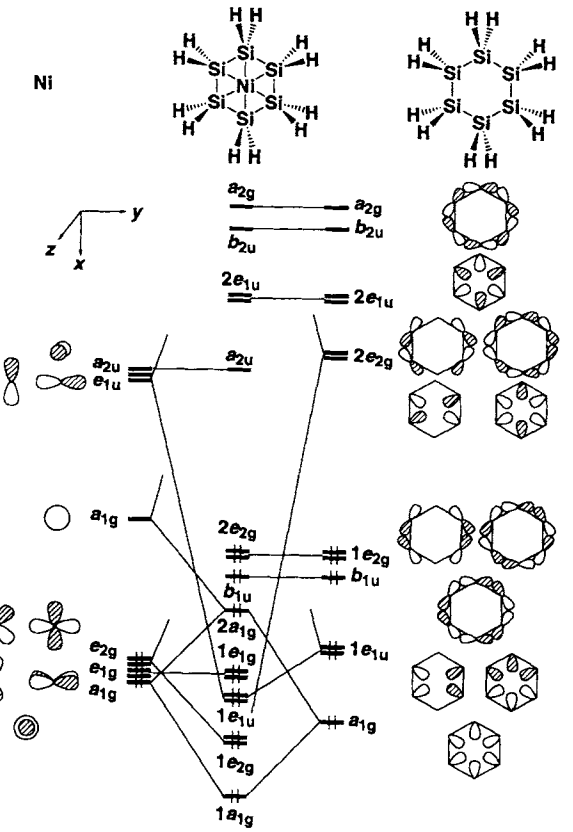

Fig. 1. An idealized orbital interaction diagram for [Ni(SiH$_2$)$_6$] (**2**) (D_{6h} symmetry).

($a_{1g} + 1e_{1u}$) and three tangential ($b_{1u} + 1e_{2g}$) combinations are Si–Si bonding and thus are at low energies. These molecular orbitals (MOs) are the delocalized equivalent of six localized Si–Si σ bonds.

When the (SiH$_2$)$_6$ MOs are interacted with the valence atomic orbitals (AOs) of a Ni atom, a simple picture emerges. The Ni s and z^2 orbital[5] interact with the Si$_6$H$_{12}$ a_{1g} orbital to form a typical three orbital pattern,[4] with the

bonding $1a_{1g}$ and nonbonding $2a_{1g}$ MOs filled. Note that the topology of the $2a_{1g}$ orbital strongly resembles that found in square- or trigonal-planar complexes;[4] namely, the $2a_{1g}$ orbital is primarily Ni z^2 and Ni s mixed in an antibonding and bonding way, respectively, with the Si_6H_{12} a_{1g} orbital. The Ni xy and $x^2 - y^2$ orbitals overlap strongly with the $2e_{2g}$ Si–Si antibonding orbital set, and are stabilized. This interaction was also noted by Ahlrichs, Fenske et al. for $[Ni(PR)_6]$ (R = *t*Bu or Me).[1] The $1e_{1u}$ orbital set on Si_6H_{12} is stabilized by interactions with the Ni x and y orbitals. All other Ni and $(SiH_2)_6$ fragment orbitals remain nonbonding. In particular, the filled b_{1u} Si_6H_{12} orbital has no symmetry match with the Ni AOs. The $1e_{2g}$ Si_6H_{12} orbital set is comprised of tangential combinations in which the electron density is concentrated at the periphery of the Si_6 ring. Therefore, the overlap with the Ni $x^2 - y^2$ and xy orbitals is small (0.11 vs. 0.23 with the $2e_{2g}$ set).

The important result from Figure 1 is that three MOs of the $(SiH_2)_6$ fragment with six electrons remain Si–Si bonding and Ni–Si nonbonding. The other eight occupied MOs are either Ni–Si bonding orbitals or nonbonding Ni orbitals. Thus, $[Ni(SiH_2)_6]$ is effectively a 16-electron complex; a valence bond construction would include the resonance structures shown in Scheme 2:[6]

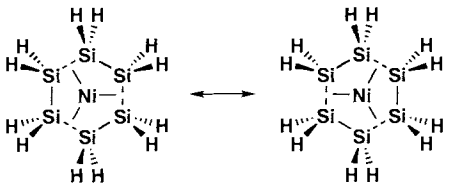

Scheme 2.

A detailed inspection of the bonding for $[Ni(SiH_2)_6]$ (**2**) and $[Ni(PH)_6]$ at the extended Hückel level[7] confirms our qualitative analysis and clearly shows that the electronic structures of both molecules are quite similar.[8] Note that the same result would be obtained for any isolobal analogue of **1** and **2**, including those with lower symmetry because the basic orbital topology does not change.

Equally interesting is the complex dianion **3**, whose potassium salt was recently synthesized by Ziegler et al.[9] In **3** the

$[In\{Mn(CO)_4\}_5]^{2-}$ **3**

indium atom and five manganese atoms lie almost in a plane. Assuming that indium is in the oxidation state III, each $[Mn(CO)_4]^-$ group could be considered a 2e donor,[3, 4] and the electron count around the indium atom would be 10 electrons. The formation of two-center two-electron Mn–Mn bonds would preclude the existence of any covalent bonding to the indium center. The relationship between the bonding in **1** and **3** is provided by the isolobal analogy (Scheme 3). $d^{10}s^0$ Ni^0 is isolobal to In^{3+}, and $[Mn(CO)_4]^-$ is isolobal to PR and CH_2.[3, 4] Thus, on the basis of the isolobal analogy, a series of compounds, such as $[Ni(PR)_5]$, $[In\{Mn(CO)_4\}_6]^{3-}$, etc., can be formulated. Moreover, because a PR fragment is isolobal to SiH_2, CH_2, S, etc., the series can be extended further. These compounds, on the surface, appear to be very electron rich and are rare examples of hexagonal- and pentagonal-planar coordinated metal centers. An interaction diagram for **3** and the isolobal **4** reveals

$[Ni(SiH_2)_5]$ **4**

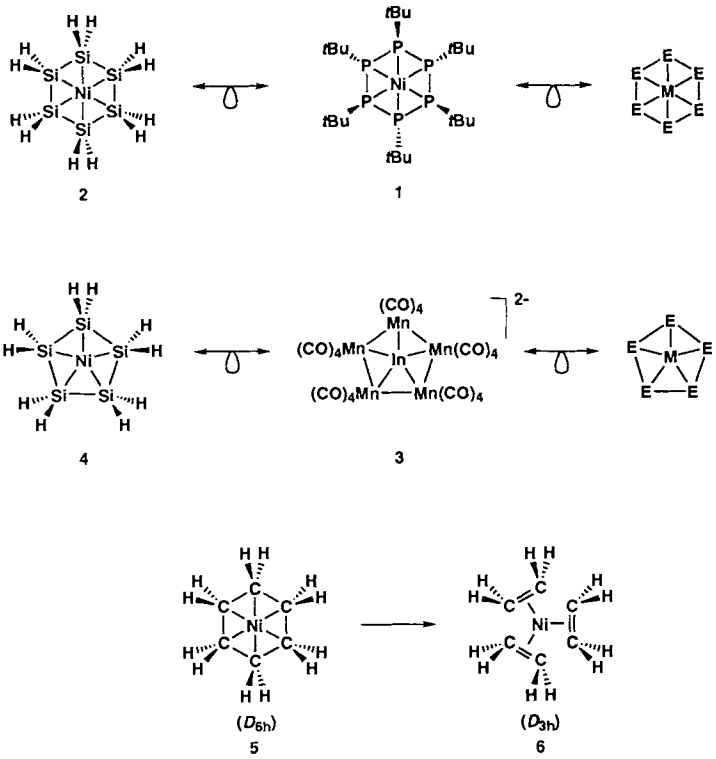

Scheme 3. The molecules considered in this study. M = d^{10} metal or metalloid. E = PR, CH_2, S, etc.

a situation analogous to that in $[Ni(SiH_2)_6]$ (**2**). There are six electrons shared between In and Mn in the former molecule and 16 electrons either localized at Ni or shared between Ni and Si for the latter molecule. There are two inter-ring orbitals, topologically identical to the $2e_{2g}$ MOs of **2** (Fig. 1), which remain nonbonding to the central atom.

To further explore the generality of this class of complexes with a hexagonal- or pentagonal-planar coordinated central atom, we have carried out a series of ab initio MO calculations[10] with basis sets at three increasing levels of complexity (BS I–III).[11] The geometry optimizations and computations of the harmonic frequencies were done at the Hartree-Fock (HF) level with BS I. For $[Ni(SiH_2)_6]$ (**2**) (Scheme 3), a D_{6h} structure is found to be a minimum on the potential energy surface. The optimized Ni–Si and Si–Si distances are 241 pm. These are 7 pm longer than the experimentally observed values for Si_6Me_{12}.[13] In **1** the P–P bond lengths are 8 pm longer than those computed for the free cyclophosphane $(PtBu)_6$.[11] The binding energies of **2** relative to the ^1S ($3d^{10}$) state of Ni and the geometry optimized Si_6H_{12} ligands (D_{3d} symmetry, chair conformation) are given in Table 1). These values also include an estimate of the basis set superposition error.[14] The values at the electron-correlated MP2 and QCISD (quadratic configuration

Table 1. The calculated binding energies [kJ mol^{-1}] for **2** and **4** which include an estimate of the basis set superposition error.

Method		2	4
BS I	HF	96	62
	MP2	515	485
	QCISD	478	453
BS II	HF	86	38
	MP2	556	538
BS III	HF	86	37
	MP2	557	539

interaction with single and double substitutions) levels are similar to those found in **1**.[1] In $[Ni(SiH_2)_5]$ (**4**), a minimum with D_{5h} structure is found. The binding energies, again relative to the ^1S state of Ni and to the geometry-optimized Si_5H_{10} ligands (C_s symmetry, envelope conformation), are only slightly smaller than those in **2**. Interestingly the Ni–Si and Si–Si distances are calculated to 220 and 259 pm, respectively. The Si–H bond lengths (147 pm) in **2** and **4** are identical. Several attempts were made to locate a D_{3h} structure as a minimum on the potential energy surface for **2**. In each instance the optimization collapsed back to the D_{6h} minimum. Note that the binding energies for **2** and **4** are greatly underestimated at the HF level; a similar situation exists for **1**.[1] Dynamical electron correlation apparently plays a critical role in setting the magnitudes.

The situation for the congener $[Ni(CH_2)_6]$ is quite different. The geometry-optimized D_{6h} structure, **5** (Scheme 3), possesses five imaginary frequencies. Furthermore, this structure lies 544 kJ mol^{-1} higher in energy than the tris-ethylene complex (**6**)[15] with D_{3h} symmetry at the HF level (BS I). The problem here is geometrical. The Ni–C and C–C distances in **5** are 185 pm. This is somewhat short for a Ni–C bond, and is much too long for an effective C–C bond; note in Figure 1 that six electrons remain in three intra-ring bonding MOs. Although geometric factors dominate, there is also an electronic component at work. That there is a striking difference in the balance between σ and π bonding for **5** and **6** on the one hand and the Si analogues on the other is not surprising—recall the similar difference between *cyclo*-O_6 and $3O_2$, and *cyclo*-S_6 and $3S_2$.

$[NiS_6]$ highlights another problem. For the D_{6h} geometry, the Ni–S and S–S bond lengths were found to be 237 pm, the latter of which is elongated by 31 pm compared to a free S_6 ring.[16] There are four imaginary frequencies associated with $[NiS_6]$. The complication here is due in part to the filled lone pairs on sulfur at the D_{6h} geometry which show both intra-ring repulsion and repulsion with the filled Ni xz, Ni yz orbitals.

In conclusion, we have shown that complexes with hexagonal- and pentagonal-planar coordinated transition metals should be regarded as 16-electron complexes. Compounds in this class will be stable provided that the interatomic distances in the ring are not too elongated in comparison to those of the free ligand and repulsions between lone pairs on the ring and filled metal d orbitals are minimized. In particular, the large binding energies associated with $[Ni(SiH_2)_6]$ (**2**) and $[Ni(SiH_2)_5]$ (**4**) strongly suggest that these compounds or their substituted derivatives should be stable. Experimental work on alkyl derivatives of **2** and **4** as well as theoretical studies on compounds with different ring sizes and atomic compositions are in progress.

Received: April 13, 1993 [Z 6000 IE]
German version: *Angew. Chem.* **1993**, *105*, 1682

[1] R. Ahlrichs, D. Fenske, H. Oesen, U. Schneider, *Angew. Chem.* **1992**, *104*, 312; *Angew. Chem. Int. Ed. Engl.* **1992**, *31*, 323.
[2] K. Dehnicke, *Angew. Chem.* **1992**, *104*, 437; *Angew. Chem. Int. Ed. Engl.* **1992**, *31*, 424.
[3] R. Hoffmann, *Angew. Chem.* **1982**, *94*, 725; *Angew. Chem. Int. Ed. Engl.* **1982**, *21*, 711.
[4] T. A. Albright, J. K. Burdett, M.-H. Whangbo, *Orbital Interactions in Chemistry*, Wiley, New York, **1985**.
[5] The notations xy, $x^2 - y^2$, x, etc. stand for d_{xy}, $d_{x^2-y^2}$, p_x, etc.
[6] We had considerable difficulty drawing these molecules with the chemist's palette of arrows, lines and dashes. Our representations of the molecules in Scheme 3 and Figure 1 should not be interpreted as implying full M–E and E–E bonds; rather, the molecules use electron deficient, multicenter bonding as implied by these resonance structures.
[7] R. Hoffmann, *J. Chem. Phys.* **1963**, *39*, 1397; R. Hoffmann, W. N. Lipscomb, *ibid.* **1962**, *36*, 3179, 3489; *ibid.* **1962**, *37*, 2872.
[8] There is some intermixing between the tangential $1e_{2g}$ and radial $2e_{2g}$ sets of orbitals on the Si_6H_{12} ligand and between the orbital counterparts on P_6H_6. This leads to a three orbital mixing pattern with Ni $x^2 - y^2$ and xy orbitals, but the middle molecular orbital (analogous to $2e_{2g}$ in Fig. 1) is still nonbonding. There are repulsive interactions between the filled lone pairs on P with the Ni xz and yz orbitals in $[Ni(PH)_6]$. We also find there to be a rather small stabilizing interation between the Ni xz and yz orbitals with Si–H or P–H σ antibonding orbitals. This interaction would increase if there were a substituent more electronegative than hydrogen or alkyl on Si or P.
[9] M. Schollenberger, B. Nuber, M. L. Ziegler, *Angew. Chem.* **1992**, *104*, 329; *Angew. Chem. Int. Ed. Engl.* **1992**, *31*, 350.
[10] M. J. Frisch, M. Head-Gordon, G. W. Trucks, J. B. Foresman, H. B. Schlegel, K. Raghavachari, M. A. Robb, J. S. Binkley, C. Gonzalez, D. J. Defrees, D. J. Fox, R. A. Whiteside, R. Seeger, C. F. Melius, J. Baker, R. L. Martin, L. R. Kahn, J. J. P. Stewart, S. Topiol, J. A. Pople, *GAUSSIAN 90*, Gaussian Inc., Pittsburgh, PA, **1990**.
[11] BS I employed an effective core potential (ECP) [12a] on Ni, Si, S, and an associated double zeta basis set for the valence orbitals 3s, 3p, 3d, 4s, and 4p on Ni, 3s and 3p on Si and S. For C and H, BS I adopted the 3-21G basis set [12b]. In BS II the same ECPs were used for Ni and Si, while the valence 3d and 4p orbitals on Ni were further split into triple zeta, and *d* polarization functions with the zeta value taken as 0.395 [12c] were added onto the Si basis set. BS III is the same as BS II except for Si where the valence 3p orbital was split into a triple zeta set.
[12] a) P. J. Hay, W. R. Wadt, *J. Chem. Phys.* **1985**, *82*, 270; W. R. Wadt, P. J. Hay, *ibid.* **1985**, *82*, 284; b) J. S. Binkley, J. A. Pople, W. J. Hehre, *J. Am. Chem. Soc.* **1980**, *102*, 936; c) M. S. Gordon, *Chem. Phys. Lett.* **1980**, *76*, 163.
[13] H. L. Carrell, J. Donohue, *Acta Crystallogr. Sect. B* **1972**, *28*, 1566.
[14] S. F. Boys, F. Bernardi, *Mol. Phys.* **1970**, *19*, 553.
[15] K. Fisch, K. Jonas, G. Wilke, *Angew. Chem.* **1973**, *85*, 620; *Angew. Chem. Int. Ed. Engl.* **1973**, *12*, 565.
[16] J. Donohue, A. Caron, E. Goldish, *J. Am. Chem. Soc.* **1961**, *83*, 3748.

Computer-Assisted Design of Chiral Boron Enolates: A Novel, Highly Enantioselective Aldol Reaction for Thioacetates and Thiopropionates**

By *Cesare Gennari,* Daniela Moresca, Siegfried Vieth,* and *Anna Vulpetti*

It is well known that the enantioselective synthesis of *syn* aldols can be achieved nowadays with high efficiency by using a plethora of methods.[1] In contrast, the methods available for the synthesis of either *anti* or unsubstituted aldols are significantly less effective.[1–3] Here we describe a new chiral boron reagent for highly enantioselective synthesis of *anti* and unsubstituted aldols.

In boron enolate chemistry, *syn* aldols are easily obtained with good enantioselectivity from chiral *Z*(OB) enolates[4] because *Z*(OB) enolates have access to a single transition structure, the chair conformation **1**.[5] High selectivity for *anti* or unsubstituted aldols is more difficult to achieve because unsubstituted enolates and (partly) *E*(OB) enolates have access to a variety of transition structures, namely the chair conformation **1**, and the boat conformations **2** and **3** (Scheme 1).[5] This competition among transition structures

[*] Prof. Dr. C. Gennari, D. Moresca, Dr. S. Vieth, A. Vulpetti
Dipartimento di Chimica Organica e Industriale
Università di Milano
Centro CNR per lo Studio delle Sostanze Organiche Naturali
via Venezian 21, I-20133 Milano (Italy)
Telefax: Int. code +(2) 236-4369

[**] This work was supported by the Commission of the European Communities [Grant SC1*.0324.C(JR)], MURST (Rome), and CNR (Rome). S. V. thanks the Deutsche Forschungsgemeinschaft for a postdoctoral stipend. We thank Dr. C. T. Hewkin, Dr. F. Molinari (Milano University) for some of the preliminary experiments, and Dr. Anna Bernardi (Milano University), Dr. Ian Paterson, and Dr. J. M. Goodman (Cambridge University, UK) for helpful discussions.

of similar energy (usually many conformers for each transition structure core-conformation **1**–**3**) makes the stereochemical control of the reaction much more difficult to obtain.

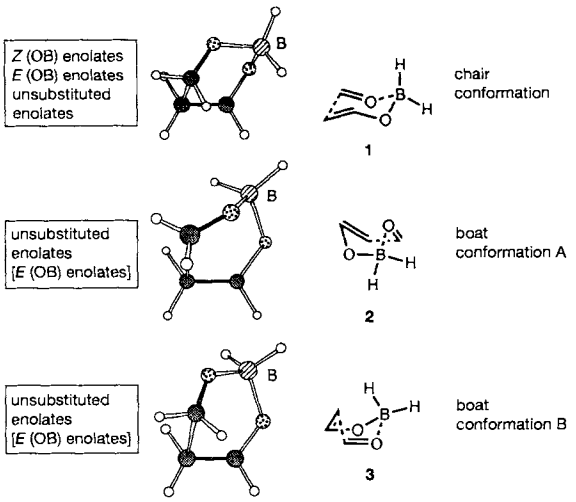

Scheme 1. Structures of the transition states (all-hydrogen substituted) determined by ab initio calculations for boron enolate aldol addition (see ref. [5a–c]).

We have recently exploited transition state computer modeling to develop a new boron reagent (**6**, X = Cl) that allows the enantioselective synthesis of *anti* and unsubstituted aldols derived from ketones.[6] The chloroborane **6** (X = Cl) is efficient and selective in the enolization of methyl and ethyl ketones at −78 °C,[6] whereas it behaves poorly (0–15% yield) in the enolization of thioesters even at room temperature (Scheme 2), although the difference in pK_a between the two substrates is quite modest (CH_3COCH_3: $pK_a = 19.0$; $CH_3COSCH_2CH_3$: $pK_a = 20.4$–21.5).[7]

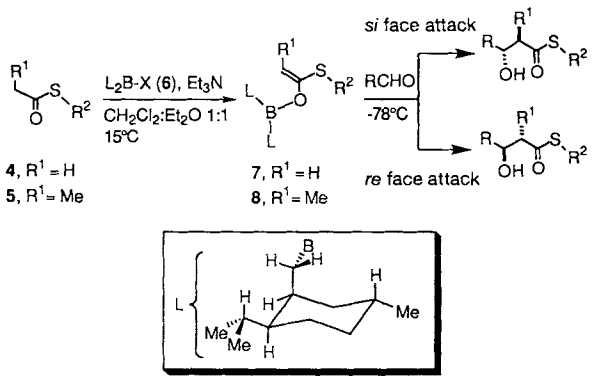

Scheme 2. Enantioselective synthesis of unsubstituted β-hydroxy thioesters and *anti* α-methyl-β-hydroxy thioesters.

Therefore a new reagent possessing a stronger Lewis acidity (**6**, X = Br) was synthesized (Scheme 3), starting with a Wittig reaction ($Ph_3P{=}CH_2$) on (−)-menthone to give (−)-(**9**) in high yield (≥90%).[6, 8] Hydroboration ($BrBH_2 \cdot Me_2S$) of (−)-(**9**) gave a mixture of diastereoisomers with a moderate preference for axial vs. equatorial -CH_2B- (**10**:**11** ≈ 3:1). Recrystallization (Et_2O, −50°/−30 °C) gave pure (**6**, X = Br) (28–30% yield; **10**:**11** ≥ 150:1).

Enolization of thioesters (**4** and **5**) proceeded smoothly at +15 °C with **6** (X = Br) and Et_3N in CH_2Cl_2/Et_2O

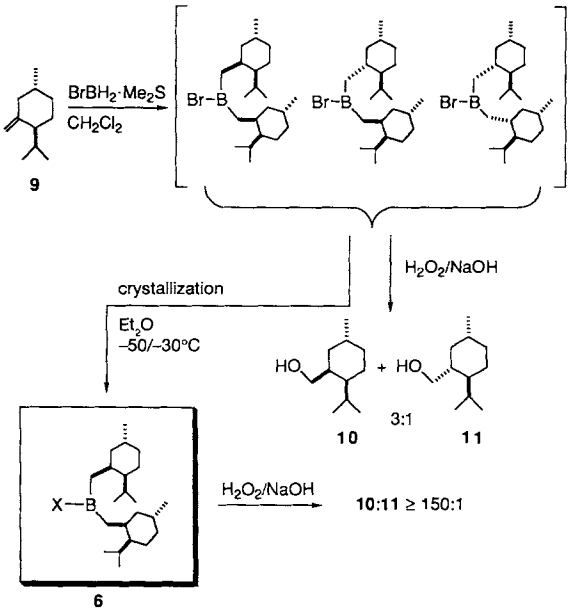

Scheme 3. Synthesis of reagent **6** (X = Br).

(Scheme 2). Addition of aldehydes at −78 °C gave the aldol products with good to excellent selectivity (Table 1). The following points are worth noting: a) The enolization of thiopropionates (**5**) preferentially results in the formation of *E*(OB) enolates **8**, as implied from the high *anti*:*syn* ratios observed in the aldol products. This preference is particularly strong for bulky substituents at sulfur (R^2) (see Table 1, entries 10, 13 (R^2 = *t*Bu) vs. 17, 18 (R^2 = Ph)). b) In the aldol reaction of thioacetates (**4**), the enantiomeric ratio is enhanced by the use of bulky substituents at sulfur (R^2) (see Table 1, entries 3 and 6 (R^2 = *t*Bu and $R^2 = CEt_3$) vs. 16 (R^2 = Ph)). Contrary to other reagents,[2o,p,r] there is no advantage in the use of the extra-large $R^2 = CEt_3$ (entries 4–

Table 1. Enantioselective synthesis of unsubstituted β-hydroxy thioesters and *anti* α-methyl-β-hydroxy thioesters.

Entry	R^1	R^2	R	*re*:*si* ratio	*anti*:*syn* ratio	yield [%]
1	H	*t*Bu	Ph	94.7:5.3 [a]	–	68
2	H	*t*Bu	*i*Pr	97.6:2.4 [b]	–	75
3	H	*t*Bu	CH_2=C(Me)-	93.6:6.4 [c]	–	71
4	H	CEt_3	Ph	93.0:7.0 [b]	–	64
5	H	CEt_3	*i*Pr	97.4:2.6 [b]	–	85
6	H	CEt_3	CH_2=C(Me)-	92.5:7.5 [c]	–	60
7	H	*t*Bu	$PhCH_2CH_2$	98.3:1.7 [a]	–	90
8	H	*t*Bu	*n*-C_3H_7	97.0:3.0 [b]	–	85
9	H	*t*Bu	*c*-C_6H_{11}	96.7:3.3 [b]	–	88
10	Me	*t*Bu	Ph	≥99:1 [b]	95:5	69
11	Me	*t*Bu	*i*Pr	99:1 [b]	96.4 [e]	61
12	Me	*t*Bu	$PhCH_2CH_2$	≥99:1 [c]	≥97:3	57
13	Me	*t*Bu	CH_2=C(Me)-	≥99:1 [c]	94:6	43
14	Me	*t*Bu	*n*-C_3H_7	99:1 [b]	≥97:3	64
15	Me	*t*Bu	PhCH=CH	99:1 [c]	≥97:3	66
16	H	Ph	CH_2=C(Me)-	80:20 [c]	–	60
17	Me	Ph	CH_2=C(Me)-	≥99:1 [d]	80:20	68
18	Me	Ph	Ph	≥99:1 [d]	74:26	65

[a] For $[\alpha]_D$ value and absolute configuration of this compound, see ref. [3s]. [b] The aldol product was reduced ($LiAlH_4$, Et_2O/THF) to the corresponding diol for correlation, according to the supplementary material of ref. [2o]. [c] Absolute configuration of this product assumed by analogy. [d] The aldol product was transformed into the corresponding β-hydroxy acid (1. LiOH, H_2O_2, H_2O/THF 2. HCl) and methyl ester (CH_2N_2), according to ref. [3k], for $Eu(hfc)_3$ NMR analysis, and optical comparison with the known methyl ester (R = Ph). [e] The ratio can be improved to 97:3 by using iPr_2EtN instead of Et_3N for the enolization.

6) over the more readily accessible *t*Bu (entries 1–3). c) The absolute configuration of the aldol products is consistent with chair transition structures featuring preferential attack on the *re* face of the aldehyde, as suggested by the computer model.[6] The boat transition structures are probably irrelevant for both the *E*(OB) enolates (**8**) and the unsubstituted enolates (**7**). d) The role of SR^2 steric hindrance in enhancing the enantioselectivity is also consistent with the computed transition state model.[6] The model suggests a distinct steric interaction between SR^2 and the pseudo-axial chiral boron ligand in the chair transition structure for the disfavored attack on the *si* face of the aldehyde.

The new bromoborane **6** (X = Br) is a very good reagent also for the enolization of ketones (Scheme 4). Diethyl ketone gave with methacrolein the aldol product with a 97.5:2.5 *anti*:*syn* ratio (enantiomeric ratio of the *anti* aldol = 7.0:1), compared to the 93:7 *anti*:*syn* ratio (enantiomeric ratio = 7.0:1) of the chloroborane **6** (X = Cl).[6] Our bromoborane is also more selective than Brown's reagents[9] in the diethyl ketone aldol addition to benzaldehyde: *anti*:*syn* 90:10 (enantiomeric ratio of the *anti* aldol = 6.1:1) vs. *anti*:*syn* 70:30 (Chx_2BBr) (Chx = cyclohexyl)[9] and 79:21 (Chx_2BCl).[9]

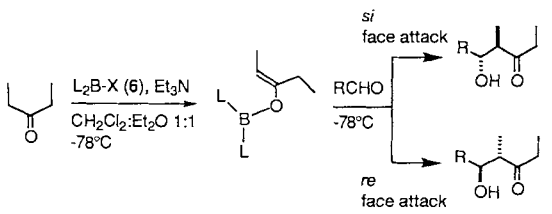

R	*re*:*si* ratio	*anti*:*syn* ratio	yield [%]
CH_2=C(Me)-	7.0:1	97.5:2.5	55
Ph	6.1:1	90:10	70

Scheme 4. Enantioselective synthesis of *anti* aldols derived from ketones.

In conclusion, we have shown that the new borane **6** (X = Br), conceived by transition state computer modeling, is an excellent reagent for the enantioselective synthesis of *anti* and unsubstituted aldols.

Experimental Procedure

6 (X = Br): A solution of (−)-(**9**) (98%, 4.2 g, 27.1 mmol) in freshly distilled dichloromethane (13.0 mL) was treated with $BrBH_2$-SMe_2 (95%, Aldrich) (1.52 mL, 13.5 mmol) at 0 °C, under argon, with stirring. The reaction mixture was stirred at room temperature (RT) overnight. The solvent dichloromethane and dimethyl sulfide liberated during hydroboration were removed under vacuum (ca. 0.1 Torr) and the residue (a thick liquid or a low melting solid) was dissolved in dry diethyl ether (7.3 mL) under argon. The solution was cooled to −50 °C and left to crystallize for 1.0 h. The solvent was removed with a double-tipped needle (cannula) under argon at −50 °C; the remaining white crystals were washed with cold diethyl ether (1.0 mL) and the solvent removed again with a cannula. The crystals were then dissolved in dry diethyl ether (4.0 mL) at RT and cannulated off of a small amount of insoluble residue (white powder) into another flask. The solution was cooled (slowly!) to −45 °C and after 1.0 h the mother liquor was removed with a cannula from the crystals formed. The solid was washed with cold diethyl ether (1 mL) at −45 °C, the solvent removed again with a cannula, and the crystals redissolved in dry ether (4.0 mL) at RT. The solution was cooled (slowly!) to −30 °C and after 1.0 h the mother liquor was removed with a cannula from the crystals formed. The crystals were weighed under argon (1.62 g, 30%). The ratio between the diastereoisomers was determined by decomposition with hydrogen peroxide and VPC analysis (OV-1 column, 70–150 °C) of alcohols **10** and **11** (≥150:1) [6]. **6** (X = Br): ^{11}B NMR (200 MHz, $CDCl_3$, 25 °C, relative to BF_3-Et_2O): δ = 78.83. Methanolysis gave **6** (X = OMe): ^{11}B NMR (200 MHz, $CDCl_3$, 25 °C, relative to BF_3-Et_2O): δ = 55.05; ^{13}C NMR ($CDCl_3$): δ = 53.30 (OCH_3), 48.39, 42.26, 35.85, 31.38, 29.57, 26.17, 24.54, 22.74, 21.41, 20.69, 16.3 (broad, C-B). Treatment of **6** (X = OMe) with $HOCH_2CH_2NH_2$ in Et_2O gave **6** (X = $OCH_2CH_2NH_2$) [6]: ^{13}C NMR ($CDCl_3$): δ = 65.52 (OCH_2), 48.86, 42.62, (CH_2NH_2), 41.93, 35.98, 31.82, 29.41, 26.24, 24.51, 22.76, 21.45, 20.71, 16 (broad, C-B). Correct C,H,N analysis.

A 0.4 M stock solution was prepared by dissolving **6** (X = Br) (1.62 g) in dichloromethane (8.4 mL) and kept for weeks in the refrigerator at 0 °C without any appreciable decomposition.

General procedure for the aldol reaction: To a stirred solution of *tert*-butyl thioester (0.40 mmol) in diethyl ether (1.41 mL for **4**; 1.80 mL for **5**) at 0 °C (ice cooling), under an argon atmosphere a solution of **6** in dichloromethane (0.4 M; 1.41 mL, 0.56 mmol for **4**; 1.80 mL, 0.72 mmol for **5**), and then Et_3N (0.084 mL, 0.60 mmol for **4**; 0.156 mL, 1.12 mmol for **5**) were added dropwise. Enol borinate was generated with concurrent formation and precipitation of $Et_3N \cdot HBr$. After 5 min at 0 °C and 2.5 h at +15 °C (for **4**; 5.0 h at +15 °C for **5**), the mixture was cooled to −78 °C and the aldehyde (1.2 mmol) was added dropwise. The resulting mixture was stirred at −78 °C for 15 h, and then quenched with Et_2O (2 mL) and pH 7 phosphate buffer (2 mL). The aqueous phase was extracted with Et_2O (3 × 5 mL), and the combined organic extracts were dried (Na_2SO_4) and evaporated. The residue was dissolved in MeOH (3.5 mL) and phosphate buffer (1 mL) at 0 °C, and treated with 30% H_2O_2 (1 mL). After 20 min stirring at RT, the mixture was diluted with water and extracted with CH_2Cl_2 (3 × 5 mL). The organic phase was washed with a pH 7 phosphate buffer solution, dried (Na_2SO_4) and evaporated. The crude product was flash chromatographed to give the desired aldol compound. The enantiomeric excesses were determined by ^{1}H NMR spectroscopy ($CDCl_3$) in the presence of Eu(hfc)$_3$, splitting the R^2 = *t*Bu singlet (Table 1, entries 1–3 and 7–15), the vinylic methyl singlet (entries 3, 6, 13, 16, 17), and the R^1 = Me doublet (entries 10–15, 17, 18), in comparison with racemic samples. Enantiomeric ratios were confirmed in selected cases (entries 4–6, 11, 12) by reaction with (*R*)-(−)-α-methoxy-α-(trifluoromethyl)phenylacetyl chloride and analysis of the resulting MTPA-esters by ^{19}F and ^{1}H NMR spectroscopy. Absolute configuration was determined by comparison with known optical rotation values (Table 1, entries 1, 7), and by chemical correlation (see footnotes of Table 1). *Anti*:*syn* ratios were determined by ^{1}H NMR spectroscopy ($CDCl_3$) (Table 1, entries 10–15, 17, 18) and by capillary VPC analysis (OV-1 column, 60–160 °C) (Table 1, entries 11, 12, 14) in comparison with authentic samples.

Received: May 29, 1993 [Z 6114 IE]
German version: *Angew. Chem.* **1993**, *105*, 1717

[1] *Comprehensive Organic Synthesis* (Eds.: B. M. Trost, I. Fleming), Pergamon Press, Oxford, **1991**, *Vol. 2* (Ed.: C. H. Heathcock): a) C. H. Heathcock, chapter 1.5, pp. 133–179; chapter 1.6, pp. 181–238; b) M. Kim, S. F. Williams, S. Masamune, chapter 1.7, pp. 239–275; c) I. Paterson, chapter 1.9, pp. 301–319.

[2] Synthesis of *anti*-α-methyl-β-hydroxy ester derivatives from silyl ketene acetals: a) C. Gennari, A. Bernardi, L. Colombo, C. Scolastico, *J. Am. Chem. Soc.* **1985**, *107*, 5812–5813; b) C. Gennari, L. Colombo, G. Bertolini, G. Schimperna, *J. Org. Chem.* **1987**, *52*, 2754–2760; c) C. Gennari, F. Molinari, P. G. Cozzi, A. Oliva, *Tetrahedron Lett.* **1989**, *30*, 5163–5166; d) G. Helmchen, U. Leikauf, I. Taufer-Knopfel, *Angew. Chem.* **1985**, *97*, 874–875; *Angew. Chem. Int. Ed. Engl.* **1985**, *24*, 874–875; e) W. Oppolzer, J. Marco-Contelles, *Helv. Chim. Acta* **1986**, *69*, 1699–1703; f) W. Oppolzer, C. Starkemann, I. Rodriguez, G. Berardinelli, *Tetrahedron Lett.* **1991**, *32*, 61–64; g) A. G. Myers, K. L. Widdowson, *J. Am. Chem. Soc.* **1990**, *112*, 9672–9674; h) E. R. Parmee, Y. Hong, O. Tempkin, S. Masamune, *Tetrahedron Lett.* **1992**, *33*, 1729–1732; from iron complexes: i) S. G. Davies, I. M. Dordor-Hedgecock, P. Warner, *ibid.* **1985**, *26*, 2125–2128; j) S. G. Davies, *Aldrichim. Acta* **1990**, *23*, 31–41; from titanium enolates: k) R. O. Duthaler, A. Hafner, P. L. Alsters, P. Rothe-Streit, G. Rihs, *Pure Appl. Chem.* **1992**, *64*, 1897–1910, and references therein; l) R. O. Duthaler, P. Herold, S. Wyler-Helfer, M. Riediker, *Helv. Chim. Acta* **1990**, *73*, 659–673; from zirconium enolates: m) M. Braun, H. Sacha, *Angew. Chem.* **1991**, *103*, 1369–1371; *Angew. Chem. Int. Ed. Engl.* **1991**, *30*, 1318–1320; from boron enolates: n) A. I. Meyers, Y. Yamamoto, *Tetrahedron* **1984**, *40*, 2309–2315; o) S. Masamune, T. Sato, B. M. Kim, T. A. Wollmann, *J. Am. Chem. Soc.* **1986**, *108*, 8279–8281; p) R. P. Short, S. Masamune, *Tetrahedron Lett.* **1987**, *28*, 2841–2844; q) M. T. Reetz, F. Kunisch, P. Heitmann, *ibid.* **1986**, *27*, 4721–4724; r) M. T. Reetz, E. Rivadeneira, C. Niemeyer, *ibid.* **1990**, *31*, 3863–3866; s) E. J. Corey, S. S. Kim, *J. Am. Chem. Soc.* **1990**, *112*, 4976–4977; *Tetrahedron Lett.* **1990**, *31*, 3715–3718; t) E. J. Corey, D. Lee *ibid.* **1993**, *34*, 1737–1740.

[3] Synthesis of unsubstituted β-hydroxy ester derivatives from titanium enolates: a) R. O. Duthaler, P. Herold, W. Lottenbach, K. Oertle, M. Riediker, *Angew. Chem.* **1989**, *101*, 490–492; *Angew. Chem. Int. Ed. Engl.* **1989**, *28*, 495–497; from magnesium enolates: b) M. Braun, R. Devant, *Tetrahedron Lett.* **1984**, *25*, 5031–5034; c) R. Devant, U. Mahaler, M. Braun, *Chem. Ber.* **1988**, *121*, 397–406; from lithium enolates: d) K. Kishikawa, M. Yamamoto, S. Kohmoto, K. Yamada, *Chem. Lett.* **1989**, 787–790; from iron acetyl complexes: e) S. G. Davies, I. M. Dordor, P. Warner, *J. Chem. Soc. Chem. Commun.* **1984**, 956–957; f) S. G. Davies, I. M. Dordor-Hedgecock, P. Warner, R. H. Jones, K. Prout, *J. Organomet. Chem.* **1985**, *285*, 213–223;

g) L. S. Liebeskind, M. E. Welker, *Tetrahedron Lett.* **1985**, *26*, 4341–4344; from zirconium enolates: h) T. Katsuki, M. Yamaguchi, *ibid.* **1985**, *26*, 5807–5810; from tin enolates: i) N. Iwasawa, T. Mukaiyama, *Chem. Lett.* **1983**, 297–298; j) Y. Nagao, Y. Hagiwara, T. Kumagai, M. Ochiai, T. Inoue, K. Hashimoto, E. Fujita, *J. Org. Chem.* **1986**, *51*, 2391–2393; from boron enolates: ref. [2o, r]; k) E. J. Corey, R. Imwinkelried, S. Pikul, Y. Bin Xiang, *J. Am. Chem. Soc.* **1989**, *111*, 5493–5495; from silyl ketene acetals: ref. [2d, e, h]; l) W. Oppolzer, C. Starkemann, *Tetrahedron Lett.* **1992**, *33*, 2439–2442; m) K. Furuta, T. Maruyama, H. Yamamoto, *Synlett* **1991**, 439–440; n) S. Kiyooka, Y. Kaneto, M. Komura, H. Matsuo, M. Nakano, *J. Org. Chem.* **1991**, *56*, 2276–2278; o) S. Kiyooka, Y. Kaneto, K. Kume, *Tetrahedron Lett.* **1992**, *33*, 4927–4930; p) S. Kobayashi, T. Mukaiyama, *Chem. Lett.* **1989**, 297–300; q) S. Kobayashi, T. Sano, T. Mukaiyama, *ibid.* **1989**, 1319–1322; r) T. Mukaiyama, S. Kobayashi, T. Sano, *Tetrahedron* **1990**, *46*, 4653–4662; s) S. Kobayashi, H. Uchiro, Y. Fujishita, I. Shiina, T. Mukaiyama, *J. Am. Chem. Soc.* **1991**, *113*, 4247–4252; t) S. Kobayashi, Y. Fujishita, T. Mukaiyama, *Chem. Lett.* **1989**, 2069–2072; u) T. Mukaiyama, A. Inubushi, S. Suda, R. Hara, S. Kobayashi, *ibid.* **1990**, 1015–1018; v) S. Kobayashi, M. Furuya, A. Ohtsubo, T. Mukaiyama, *Tetrahedron Asymmetry* **1991**, *2*, 635–638; w) T. Mukaiyama, T. Takashima, H. Kusaka, T. Shimpuku, *Chem. Lett.* **1990**, 1777–1780; x) S. Kobayashi, A. Ohtsubo, T. Mukaiyama, *ibid.* **1991**, 831–834; y) M. L. Vasconcellos, D. Desmaele, P. R. R. Costa, J. d'Angelo, *Tetrahedron Lett.* **1992**, *33*, 4921–4922.

[4] *It is more convenient to use the same stereodescriptors for the boron enolates derived from different substrates. As sequence-rule-priority changes passing from ketones (OB > alkyl) to esters (OB < O alkyl) to thioesters (OB < S alkyl), we like to define the enolates as Z(OB) enolates or E(OB) enolates, conventionally attributing to the OB substituent the highest priority.*

[5] a) Y. Li, M. N. Paddon-Row, K. N. Houk, *J. Am. Chem. Soc.* **1988**, *110*, 3684–3686; *J. Org. Chem.* **1990**, *55*, 481–493; b) A. Bernardi, A. M. Capelli, C. Gennari, J. M. Goodman, I. Paterson, *J. Org. Chem.* **1990**, *55*, 3576–3581; c) F. Bernardi, M. A. Robb, G. Suzzi-Valli, E. Tagliavini, C. Trombini, A. Umani-Ronchi, *ibid.* **1991**, *56*, 6472–6475; d) A. Bernardi, A. Cassinari, A. Comotti, C. Gennari, M. Gardner, J. M. Goodman, I. Paterson, *Tetrahedron* **1992**, *48*, 4183–4192; e) A. Vulpetti, A. Bernardi, C. Gennari, J. M. Goodman, I. Paterson, *ibid.* **1993**, *49*, 685–696.

[6] C. Gennari, C. T. Hewkin, F. Molinari, A. Bernardi, A. Comotti, J. M. Goodman, I. Paterson, *J. Org. Chem.* **1992**, *57*, 5173–5177.

[7] T. L. Amyes, J. P. Richard, *J. Am. Chem. Soc.* **1992**, *114*, 10297–10302.

[8] The other enantiomer is also easily obtainable, as (+)-menthone can be prepared in high yield (94%) by a Jones oxidation of commercially available (1*S*,2*R*,5*S*)-(+)-menthol, see A. S. Hussey, R. H. Baker, *J. Org. Chem.* **1960**, *25*, 1434.

[9] H. C. Brown, K. Ganesan, R. K. Dhar, *J. Org. Chem.* **1993**, *58*, 147–153, and references therein.

$[Mo_2(S)_2(\mu\text{-}S)(syn\text{-}Me_8[16]aneS_4)_2]^{2+}$, a Novel Sulfidomolybdenum Complex Containing a Linear S=Mo–S–Mo=S Linkage**

By *Toshikatsu Yoshida,* Tomohiro Adachi, Kazuhiko Matsumura*, and *Katsumi Baba*

Despite the extensive chemistry of transition metal sulfides, the only three 18-electron complexes containing terminal sulfido ligands known are *trans*-$[Mo(S)_2(syn\text{-}Me_8[16]aneS_4)]$, *trans*-$[W(S)_2(PMe_3)_2L_2]$ (L = PMe_3, *t*BuNC), and *trans*-$[Mo(S)(O)(dppe)_2]$.[1] The long M=S distances of these complexes compared to those of 16-electron sulfido Mo^{IV} and W^{IV} complexes suggest the significant reduction in the $p_\pi(S) \rightarrow d_\pi(M)$ interaction, which promises high nucleophilicity for the terminal sulfido ligand. However, the nucleophilicity of the terminal sulfido ligand of these electronically saturated complexes has remained virtually unexplored. Recently we reported that one of the terminal sulfido ligands in **1** is readily alkylated with alkyl halides to give sulfido(thiolato) complex *trans*-$[Mo(SR)(S)(syn\text{-}Me_8[16]aneS_4)]^+$ (R = Me, CH_2Ph).[2] We have now found that the protonation of **1** with HBF_4 proceeds with evolution of H_2S to give the salts **2** and **3**. The former contains a novel dimolybdenum

trans-$[Mo(S)_2(syn\text{-}Me_8[16]aneS_4)]$ **1**

$[Mo_2(S)_2(\mu\text{-}S)(syn\text{-}Me_8[16]aneS_4)_2](BF_4)_2$ **2**

trans-$[Mo(S)(F)(syn\text{-}Me_8[16]aneS_4)](BF_4)$ **3**

tris(sulfido) complex as cation. The X-ray structural study of **2** reveals the presence of a linear S=Mo–S–Mo=S linkage. In view of the strong propensity of sulfido ligands to bridge M-S-M in a bent fashion, linear μ-sulfido complexes are extremely rare except the well-characterized cumulated systems of the types M=S=M and M≡S≡M.[3] The cation in **2** also represents the first example of the sulfur analogue of the linear O=M–O–M=O complexes with d^0–d^2 metal centers.[4]

Addition of an equimolar amount of $HBF_4 \cdot Et_2O$ to a suspension of **1**[1a] in toluene at room temperature and subsequent recrystallization of the precipitate from acetone/toluene gave grayish green crystals of **2** together with green crystals of **3** in 7 and 40% yield, respectively. When the reaction is carried out in CH_2Cl_2, **2** was obtained as the sole product (65%). In both reactions the evolution of H_2S was detected. The ^1H NMR spectra of both compounds indicate that the $Me_8[16]aneS_4$ ligand adopts the *syn*-conformation, suggesting the retention of the *syn*-form of the macrocyclic ligand upon the protonation of **1**. The presence of both terminal (S_t) and bridging sulfido ligands (S_b) in **2** are confirmed by the observation of one IR active ν_{as} (Mo=S_t) band at 468 cm^{-1} and two Raman active ν_s (Mo=S_t) and ν_s (Mo–S_b–Mo) bands at 486 and 335 cm^{-1}, respectively. The high ν (Mo=S_t) stretching frequency in **2** compared to that found in **1** (436 cm^{-1})[1a] is consistent with the 16-electron d^2 complex in **2** and the weaker *trans* influence of a bridging sulfido ligand over a terminal sulfido ligand.

The cation in **2** (Fig. 1)[5] consists of two [Mo(S)(*syn*-$Me_8[16]aneS_4$)] moieties which are connected through the S_b atom in a face-to-face fashion. In both moieties the S_t atom occupies the congested axial site surrounded by the ring carbon atoms. The two moieties are staggered with the torsion angle S1(1)-Mo1–Mo2–S2(1) of 45.0(4)°. The angles S_t-Mo-S_b and Mo1-S_b-Mo2 are respectively 178.1(4) (average) and 177.3(3)°, thus, the S_t1-Mo-S_b-Mo-S_t2 framework is essentially linear and the cation possesses approximately D_{4d} symmetry. The mean Mo–S_t separation (2.149(9) Å) may be compared with those found for 16-electron sulfido Mo^{IV} complexes (2.126–2.149 Å),[6] but is significantly shorter than that found in **1** (2.238(9) Å). Because of the strong *trans* influence of terminal sulfido ligands, the Mo–S_b distances (average 2.407(9) Å) are considerably elongated; they are even longer than the corresponding value (2.23–2.35 Å) found for binuclear Mo^{IV} complexes with bent μ-sulfido ligands.[7] The mean nonbonded distance (4.17(5) Å) between the C atoms of axial methyl groups of the face-to-face macrocyles is comparable with twice the van der Waals radius of a methyl group (4.00 Å). Thus, the linearity of the S=Mo–S–Mo=S backbone may be rationalized by steric effects, since the van der Waals repulsions between the methyl groups should increase substantially when the molecular framework is bent.[8]

[*] Prof. Dr. T. Yoshida, T. Adachi, K. Matsumura, K. Baba
Department of Chemistry, Faculty of Integrated Arts and Sciences
University of Osaka Prefecture
Sakai, Osaka 593 (Japan)
Telefax: Int. code +(81)722-55-298

[**] This work was supported partially by a Grant-in-Aid for Scientific Research (no. 05804033) from the Ministry of Education, Science, and Culture, Japan. We are indebted to Prof. K. Tatsumi of Osaka University for extended Hückel MO calculations. $Me_8[16]aneS_4$ = 3,3,7,7,11,11,15,15-octamethyl-1,5,9,13-tetrathiacyclohexadecane.

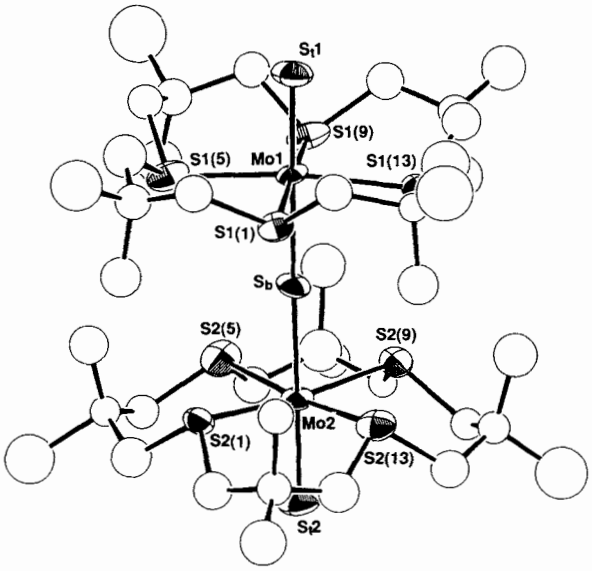

Fig. 1. Molecular structure of the cation of **2** (ORTEP, thermal ellipsoids at the 50% probability level). Selected bond lengths [Å] and angles [°]: Mo1-S_t1 2.138(9), Mo2-S_t2 2.160(9), Mo1-S_b 2.411(9), Mo2-S_b 2.404(9), Mo1-S1(1) 2.450(8), Mo1-S1(5) 2.457(11), Mo1-S1(9) 2.474(9), Mo1-S1(13) 2.471(11), Mo2-S2(1) 2.452(9), Mo2-S2(5) 2.450(10), Mo2-S2(9) 2.447(10), Mo2-S2(13) 2.491(9); S_t1-Mo1-S_b 177.3(4), S_t2-Mo2-S_b 178.9(4), Mo1-S_b-Mo2 177.3(4), S_t1-Mo1-S1(1) 95.1(3), S_t1-Mo1-S1(5) 94.2(3), S_t1-Mo1-S1(9) 92.5(3), S_t1-Mo1-S1(13) 93.7(3), S_b-Mo1-S1(1) 87.6(3), S_b-Mo1-S1(5) 86.2(3), S_b-Mo1-S1(9) 84.8(3), S_b-Mo1-S1(13) 86.0(3), S1(1)-Mo1-S1(5) 90.4(3), S1(1)-Mo1-S1(9) 172.4(3), S1(1)-Mo1-S1(13) 88.8(3), S1(5)-Mo1-S1(9) 88.8(3), S1(5)-Mo1-S1(13) 172.1(3), S1(9)-Mo1-S1(13) 90.9(3), S_t2-Mo2-S2(1) 92.9(4), S_t2-Mo2-S2(5) 93.9(3), S_t2-Mo2-S2(9) 94.4(3), S_t2-Mo2-S2(13) 92.6(3), S_b-Mo2-S2(1) 86.1(3), S_b-Mo2-S2(5) 86.4(3), S_b-Mo2-S2(9) 86.6(3), S_b-Mo2-S2(13) 87.1(3), S2(1)-Mo2-S2(5) 90.7(3), S2(1)-Mo2-S2(9) 172.6(3), S2(1)-Mo2-S2(13) 90.1(3), S2(5)-Mo2-S2(9) 89.7(3), S2(5)-Mo2-S2(13) 173.4(3), S2(9)-Mo2-S2(13) 88.7(3).

The structure of the cation in **3** (Fig. 2)[5] shows that the terminal sulfido ligand again occupies the congested axial site with the fluoro anion at the opposite readily accessible uncongested site. The results of structural studies of **2** and **3** suggest that the protonation of **1** took place stereoselectively at the sulfido ligand located on the uncongested axial site. A similar discrimination of the two sulfido ligands at the stereochemically different axial sites was observed for the monoalkylation of **1** with alkyl halides, which gave *trans*-[Mo(SR)(S)(*syn*-Me_8[16]aneS_4)]$^+$ (R = Me, CH_2Ph), in which the thiolato ligand is located at the uncongested axial site.[2]

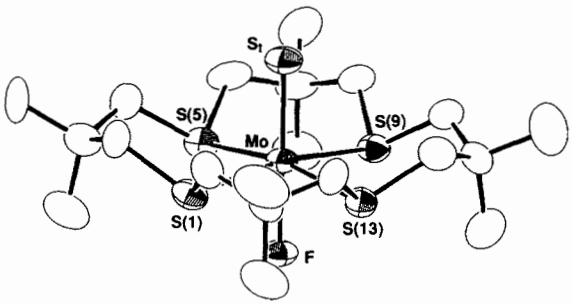

Fig. 2. Molecular structure of the cation of **3** (ORTEP, thermal ellipsoids at the 50% probability levels). Selected bond lengths [Å] and angles [°]: Mo-S_t 2.118(3), Mo-S1 2.445(4), Mo-S5 2.459(4), Mo-S9 2.451(4), Mo-S13 2.464(4), Mo-F 1.969(6); S_t-Mo-F 179.0(3), S_t-Mo-S1 95.6(1), S_t-Mo-S5 95.8(1), S_t-Mo-S9 95.3(1), S_t-Mo-S13 96.3(1), S1-Mo-S5 90.4(1), S1-Mo-S9 169.1(1), S1-Mo-S13 88.2(1), S5-Mo-S9 89.0(1) S5-Mo-S13 167.9(1), S9-Mo-S13 90.2(1), S1-Mo-F 84.3(2), S5-Mo-F 83.2(2), S9-Mo-F 84.8(2), S13-Mo-F 84.8(2).

A plausible mechanism for the protonation of **1** to afford **2** and **3** is shown in Scheme 1. The protonation of the terminal sulfido at the uncongested axial site may produce a hydrogensulfido(sulfido) species [Mo(SH)(S)(*syn*-Me_8[16]aneS_4)]$^+$, followed by a second, more facile protonation at the hydrogensulfido ligand, affording a coordinatively unsaturated monosulfido complex [Mo(S)(*syn*-Me_8[16]aneS_4)]$^{2+}$ with concomitant evolution of H_2S. The complete

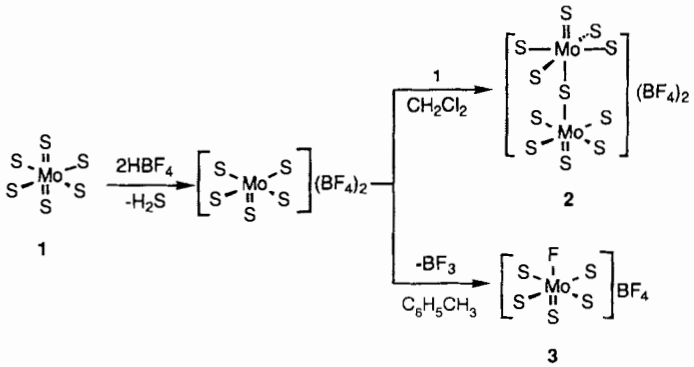

Scheme 1. Possible mechanism for the formation of **2** and **3** from **1** ($CH_2CMe_2CH_2$ units of *syn*-Me_8[16]aneS_4 were omitted for clarity).

absence of the hydrogensulfido species in the reaction mixture contrasts sharply to the alkylation of **1**, in which *trans*-[Mo(SR)(S)(*syn*-Me_8[16]aneS_4)]$^+$ is formed.[2] Subsequently the coordinatively unsaturated intermediate abstracts a F^- ion from the counterion BF_4^- to give the cation in **3**; a nucleophilic attack by **1** at the terminal sulfido ligand on the uncongested axial site produces the cation in **2**. The proposed extremely facile diprotonation of one of the terminal sulfido ligands in **1** to give the coordinatively unsaturated species is supported by the results of the protonation of **1** with 1.1 equivalents of CF_3SO_3H, which afforded **4** together

trans-[Mo(O_3SCF_3)(S)(*syn*-Me_8[16]aneS_4)](O_3SCF_3) **4**

with a recovery of unreacted **1** in 35 and 40% yields, respectively. If the reaction pathway in Scheme 1 is assumed, the solvent effect on the observed product ratio of **2** and **3** can be explained in terms of the difference in solubility of **1** in toluene and CH_2Cl_2. In the latter solvent, in which the concentration of **1** is high due to its high solubility, the coordinatively unsaturated intermediate once formed reacts preferentially with **1** to give **2**. By contrast, in toluene the concentration of **1** is low and the intermediate therefore abstracts a F^- ion from the weakly coordinating counterion BF_4^-. This is a well-documented reaction.[10] The difference in solvent polarity may also affect the product ratio. In nonpolar toluene the vacant axial site of the coordinatively unsaturated cationic species is probably blocked by the formation of a contact ion pair with BF_4^-, whereas solvent-separated ion pairs exist in CH_2Cl_2.[11]

Finally it is worth noting that the cationic 16-electron d^2 metal complex **2** is inert toward protonation with HBF_4. This was expected because the terminal sulfido ligands in **2** are less nucleophilic than that in **1**, the net charges of the former and latter assessed by Extended Hückel MO calculations are −0.81 and −1.03, respectively.[8] Two-electron reduction of the cation in **2** should give the analogous neutral 17-electron d^3 metal complex,[12] whose terminal sulfido ligands are expected to be more nucleophilic than those in the cation of **2**.

Experimental Procedure

2 and **3**: To a suspension of **1** (60 mg, 0.107 mmol) in toluene (30 ml) was added 85% ether solution of $HBF_4 \cdot Et_2O$ (22 mg, 0.115 mmol) at room temperature. The yellow suspension immediately turned orange with evolution of H_2S, which was confirmed by its characteristic odor. After the mixture was stirred for 1 h, the precipitate was filtered and recrystallized from acetone/toluene to give a mixture of **2** and **3** as grayish green and emerald green crystals, respectively. Analytical pure samples of both complexes were obtained by mechanical separation of the above crystals followed by recrystallization from acetone/toluene; the yields of **2** and **3** were 7 and 40%, respectively. When the above reaction was carried out in CH_2Cl_2, **2** was obtained as the sole product in 65% yield. **2**: M.p. 260 °C (decomp); ^{1}H NMR (200 MHz, $CDCl_3$, 25 °C, TMS): $\delta = 1.29$ (s, 3H; Me), 1.44 (s, 3H; Me), 2.51 (d, $^2J(H,H) = 11.5$ Hz, 2H, CH_2) 3.72 (d, $^2J(H,H) = 11.5$ Hz, 2H; CH_2); UV/VIS (acetone): λ_{max} (ε) = 304 (5820), 366 (7200), 4888 (37900), 672 (688), 821 nm (653); FAB-MS (3-nitrobenzyl alcohol): m/z 1106 [M^+].

3: M.p. 235 C (decomp); ^{1}H NMR (200 MHz, $CDCl_3$, 25 °C, TMS): $\delta = 1.36$ (s, 3H; Me), 1.40 (s, 3H; Me), 3.01 (br, 2H; CH_2), 3.66 (br, 2H; CH_2); IR (CsI): $\nu = 494$ cm^{-1} (Mo=S); FAB-MS (3-nitrobenzyl alcohol): m/z 557 [M^+], 538 [$M^+ - F$].

4: Treatment of **1** (33 mg, 0.058 mmol) with CF_3SO_3H (18 mg, 0.115 mmol) in toluene (10 ml) and recrystallization of the precipitate from CH_2Cl_2/toluene gave **4** as pale yellow crystals (68%). M.p. 279 °C (decomp); ^{1}H NMR (200 MHz, $CDCl_3$, 25 °C, TMS): $\delta = 1.45$ (s, 3H; Me), 3.01 (d, $^2J(H,H) = 11.6$ Hz, 2H; CH_2), 3.66 (d, $^2J(H,H) = 11.6$ Hz, 2H; CH_2); IR (CsI): $\tilde{\nu} = 519$ cm^{-1} (Mo=S). FAB-MS (3-nitrobenzyl alcohol): m/z 687 [M^+]. The reaction with 1.1 equivalents of CF_3SO_3H under the similar conditions afforded **4** (35%) together with the recovery of **1** (40%).

Received: June 1, 1993 [Z 6115 IE]
German version: *Angew. Chem.* **1993**, *105*, 1730

[1] a) T. Yoshida, T. Adachi, K. Matsumura, K. Kawazu, K. Baba, *Chem. Lett.* **1991**, 1067; b) D. Ravinovich, G. Perkin, *J. Am. Chem. Soc.* **1991**, *113*, 5904; c) I.-P. Lorenz, G. Walter, W. Hiller, *Chem. Ber.* **1990**, *123*, 979.

[2] T. Yoshida, T. Adachi, K. Matsumura, K. Baba, *Chem. Lett.* **1992**, 2447.

[3] W. A. Herrmann, *Angew. Chem.* **1986**, *98*, 57; *Angew. Chem. Int. Ed. Engl.* **1986**, *25*, 56; T. J. Greenhough, B. W. S. Kolthammer, P. Legzdins, J. Trotter, *Inorg. Chem.* **1979**, *18*, 3543; M. G. B. Drew, P. C. H. Mitchell, C. F. Pygall, *Angew. Chem.* **1976**, *88*, 855; *Angew. Chem. Int. Ed. Engl.* **1976**, *15*, 784; D. L. Lichtenberger, J. L. Hubbard, *Inorg. Chem.* **1984**, *23*, 2718; S. Lincoln, J.-L. Soong, S. A. Koch, M. Sato, J. H. Enemark, *ibid.* **1985**, *24*, 1355; J. Schiemann, P. Hübener, E. Weiss, *Angew. Chem.* **1983**, *95*, 1021; *Angew. Chem. Int. Ed. Engl.* **1983**, *22*, 980; C. Mealli, S. Midollini, L. Sacconi, *Inorg. Chem.* **1978**, *17*, 632; C. Mealli, S. Midollini, L. Sacconi, *J. Chem. Soc. Chem. Commun.* **1975**, 765.

[4] R. O. Shandles, E. O. Schlemper, R. K. Murman, *Inorg. Chem.* **1971**, *10*, 2785; S. R. Fletcher, A. C. Skapski, *J. Chem. Soc. Dalton Trans.* **1972**, 1073; J. F. Johnson, W. R. Scheidt, *Inorg. Chem.* **1978**, *17*, 1280; I. F. Jaffe, D. Gibson, J. Lippard, R. R. Schrock, A. Spool, *J. Am. Chem. Soc.* **1984**, *106*, 6305.

[5] a) X-ray structural analysis for $2 \cdot C_6H_5CH_3 \cdot Me_2CO$: triclinic, space group $P\bar{1}$ (no. 2), $a = 14.032(8)$, $b = 21.189(17)$, $c = 11.801(6)$ Å, $\alpha = 95.26(5)$, $\beta = 91.51(5)$, $\gamma = 98.74(6)°$, $V = 3450(8)$ Å^3, $Z = 2$, $\varrho_{calcd} = 1.376$ g cm^{-3}, $F(000) = 1488$, $\mu(Mo_{K\alpha}) = 7.27$ cm^{-1}, crystal dimensions $0.3 \times 0.2 \times 0.1$ mm^3. $R(R_w) = 0.076$ (0.079) for 2177 unique reflections [$I > 5\,\sigma(I)$] and 313 variables. b) X-ray structural analysis of $3 \cdot 1/2\,C_6H_5CH_3$: monoclinic, space group $P2_1/c$ (no. 14), $a = 10.865(3)$, $b = 22.259(9)$, $c = 13.181(2)$ Å, $\beta = 92.72(2)°$, $V = 3184(3)$ Å^3, $Z = 4$, $\varrho_{calcd} = 1.436$ g cm^{-1}, $F(000) = 1428$, $\mu(Mo_{K\alpha}) = 7.58$ cm^{-1}, crystal dimensions $0.8 \times 0.3 \times 0.2$ mm^3, $R(R_w) = 0.054$ (0.060) for 2357 unique reflections [$I > 9\,\sigma(I)$] and 303 variables. Data were collected with a Rigaku AFC5R diffractometer with $Mo_{K\alpha}$ radiation and both structures were solved by the Patterson method and difference Fourier syntheses and full-matrix least-squares refinement. Further details of the crystal structure investigations may be obtained from the Fachinformationszentrum Karlsruhe, Gesellschaft für wissenschaftlich-technische Information mbH, D-76344 Eggenstein-Leopoldshafen (FRG), on quoting the depository number CSD-57425, the names of the authors, and the journal citation.

[6] E. D. Simhon, N. C. Baenziger, M. Kanatzidis, M. Draganjac, D. Coucouvanis, *J. Am. Chem. Soc.* **1981**, *103*, 1218; D. Coucouvanis, M. Dranganjac, *ibid.* **1982**, *104*, 6820; C. G. Young, S. A. Roberts, R. B. Ortega, J. H. Enemark, *ibid.* **1987**, *107*, 2938.

[7] L. Ricard, J. Estienne, R. Weiss, *Inorg. Chem.* **1973**, *12*, 2182; C. J. Casewit, R. C. Haltiwanger, J. Noordik, M. R. DuBois, *Organometallics*, **1985**, *4*, 119; T. E. Burrow, A. Hills, D. L. Hughes, J. D. Lane, N. J. Lazarowyeh, M. J. Maguire, R. H. Morris, R. L. Richards, *J. Chem. Soc. Chem. Commun.* **1990**, 1757.

[8] Extended Hückel MO calculations on the model compound of the cation in **2**, $[Mo_2(S)_2(\mu\text{-}S)\{syn\text{-}(SH_2)_4\}_2]^{2+}$ with D_{4d} symmetry, where vacant sulfur d orbitals are included, indicate that the amount of electrons transferred from the occupied $p_x(p_y)$ orbital of the S_b^{2-} ion to each Mo atom is 0.337, while the corresponding value calculated for the terminal sulfido ligand is 0.791. Note that the electrons transferred through σ donation are comparable, 0.503 for each Mo–S_b bond and 0.547 for the Mo–S_t bond. The H_{ij} values and the orbital exponents for the Mo atom were taken from the reference [9], while those of other atoms are standard values. The bond lengths and angles were the average values of those found in the cation of **2** except the strict linearity of the S_t=Mo–S_b–Mo=S_t linkage and the S–H distance of 1.33 Å. Extended Hückel MO calculations of *trans*-$[Mo(S)_2\{syn\text{-}(SH_2)_4\}]$, a model compound of **1** were carried out similarly.

[9] P. Kubacek, R. Hoffmann, *J. Am. Chem. Soc.* **1981**, *103*, 4320.

[10] N. M. Doherty, N. W. Hoffman, *Chem. Rev.* **1991**, *91*, 553.

[11] We thank one of the referees for suggesting that we investigate the effect of solvent polarity on the reaction.

[12] The cyclic voltammogram of **2** (0.2 M nBu$_4$NBF$_4$ in CH_2Cl_2) shows two quasi-reversible redox potentials at -0.95 and -1.66 V (vs. Cp_2Fe^+/Cp_2Fe).

The Energetic Stabilization Caused by a Planar-Tetracoordinate Carbon Atom: A Dynamic NMR Spectroscopic Study of the Dimetallabicycle $[(Cp_2Zr)_2(\mu\text{-}C{\equiv}CCH_3)(\mu\text{-}H_3CCCCH_3)]BPh_4$**

By *Gerhard Erker** and *Dirk Röttger*

Dedicated to Professor Carl Krüger to the occasion of his 60th birthday

We recently described a new class of highly stable heterodimetallic complexes containing planar-tetracoordinate carbon atoms.[1] These compounds **3** arise, in general, by the reaction of the (η^2-alkyne)metallocene **1** generated in situ, with halide, alkyl, or alkynyl compounds of boron, aluminium, or gallium (**2**) (Scheme 1). An analogous dizirconocene complex **5a** ($R^1 = CMe_3$, $R^2 = CH_3$, $X = C{\equiv}C{-}CMe_3$) was also reported recently.[2–4]

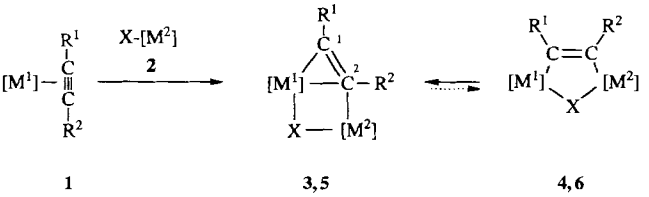

Scheme 1. $[M^1] = Cp_2Ti$, Cp_2Zr, Cp_2Hf; **3**, **4**: M^1 = Ti, Zr, Hf; M^2 = B, Al, Ga; **5**, **6**: $[M^1] = Cp_2Zr^+$, $[M^2] = Cp_2Zr$. The M^1-C-M^2 bonds in **3** and **5** are three-center, two-electron bonds.

Theoretical calculations indicate that the structures of the metallabicycles **3** with a planar-tetracoordinate carbon atom are 30–50 kcal mol^{-1} more stable than their isomers **4** with "normal" olefin structure.[5] This large difference in energy means that it is rather unlikely that **4** could be detected experimentally starting from **3**. In contrast, in compounds of type **5**, if two identical substituents were introduced at the alkyne bridge (e.g. **5b**: $R^1 = R^2 = CH_3$; $X = C{\equiv}C{-}CH_3$), the thermally induced opening of the central Zr^1–C^2 bond would then lead to a C_{2v}-symmetric dimetallamonocycle **6b**. Thus, it should be possible to detect the equilibration

[*] Prof. Dr. G. Erker, Dipl.-Chem. D. Röttger
Organisch-chemisches Institut der Universität
Corrensstrasse 40, D-48149 Münster (FRG)
Telefax: Int. code + (251)-839772

[**] This work was supported by the Fonds der Chemischen Industrie, and by the Alfried-Krupp-von-Bohlen-und-Halbach-Stiftung.

5b⇌**6b**, in contrast to that of **3**⇌**4**, by dynamic NMR spectroscopy.

Unfortunately, the synthetic procedure described by Horton et al.[2] can only be used for the preparation of the very complex **5a**, which exhibits a specific substitution pattern. With starting materials bearing different substituents, other products are obtained, rather than compounds of type **5**.[2] We have therefore prepared **5b** by a new synthetic route based on our method for the synthesis of the planar-tetracoordinate carbon compounds **3** (Scheme 2). Thus, bis(propynyl)zirconocene (**11**)[6] was allowed to react at room temperature with the methylzirconocene cation (introduced as $[Cp_2Zr(CH_3)(thf)]BPh_4$ (**12**)[7]). The σ-ligand exchange leads presumably to the intermediate **9**, which, in the presence of the intermediate (propynyl)zirconocene cation generated in the first step, affords the product **5b** in 85% yield, following reductive coupling and addition of **13**.[8]

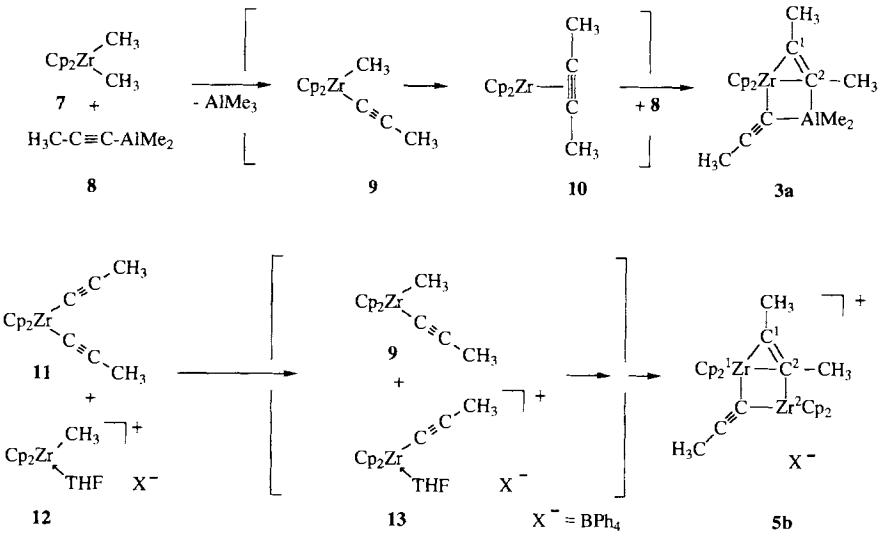

Scheme 2. Synthesis of compound **5b** in accordance with our method for the preparation of **3** with a planar-tetracoordinate C atom; $X^- = BPh_4^-$. The Zr-C-Al bonds in **3a** and the Zr-C-Zr bonds in **5b** are three-center, two-electron bonds.

Compound **5b** shows IR bands at 2070 (C≡C) and 1580 cm^{-1} (C=C). In the ^{13}C NMR spectrum at 213 K two signals are observed for the Cp ligands at $\delta = 109.8$ and 108.4. The μ-η^1:η^2-$(H_3C)CC(CH_3)$ unit gives rise to signals at $\delta = 210.4$ (C^1), 28.9 (CH_3 at C^1), 124.3 (planar-tetracoordinate C^2 atom), and −25.6 (CH_3 at C^2). In the ^1H NMR spectrum of **5b** at 200 K, two singlets are observed for the Cp ligands at $\delta = 5.84$ and 5.70 in addition to three signals at $\delta = 2.48$ (CH_3 at C^1), 2.29 (μ-C≡C-CH_3), and −0.16 (CH_3 at planar-tetracoordinate C^2) corresponding to the methyl groups.[9] Compound **5b** displays dynamic NMR spectra. Upon raising the temperature, the ^1H and ^{13}C NMR signals of the Cp ligands as well as those of the C^1CH_3 and C^2CH_3 groups rapidly broaden and pairwise coalescence is observed. The signals of the BPh_4 anion and the μ-C≡C-CH_3 ligand remain unaffected. At a sufficiently high temperature, simplified spectra are obtained, showing only one signal each for the Cp ligands [$\delta = 5.85$ (^1H NMR, 300 K), $\delta = 109.8$ (^{13}C NMR, 280 K)] and the methyl groups at C^1 and C^2 [$\delta = 1.25$ (^1H NMR, 300 K)], which have become symmetry-equivalent. It can be assumed that the observed intramolecular equilibration of **5b** is initiated by a thermally induced opening of the central Zr^1-C^2 bond (Scheme 3), which leads inevitably to the formation of the C_{2v}-symmetric compound **6b**. Starting from **6b**, it is now possible to form a stable ground-state structure by restoring an additional central Zr–C interaction. In this process, the connection of $Zr^{(A)}$ with $C^{(B)}$ and $Zr^{(B)}$ with $C^{(A)}$ is of equal probability (Scheme 3), which leads ultimately to the observed thermally induced automerization of the original compound **5b**. We have estimated a Gibbs activation energy of $\Delta G^{\ddagger}_{autom}$ (250 K) = 11.8 ± 0.5 kcal mol^{-1}[10] for this degenerate rearrangement of **5b**, based on the analysis of the temperature-dependent line shape of the ^1H NMR signals of the Cp ligands and the methyl substituents at C^1 and C^2.

Theoretical analysis of the planar-tetracoordinate Zr/Al compound **3** reveals that the dimetallamonocycle **4** is unlikely to correspond to a local minimum on the hypersurface of these systems, but is instead transformed into **3** with continual gain in energy.[5] If the **5**/**6** system behaves analogously, the activation barrier determined for the thermally induced automerization of **5b** provides an estimate of the energetic stabilization caused by the introduction of a planar-tetracoordinate carbon atom, starting from a "normal" metal-substituted olefin. However, it certainly cannot be ruled out that the cationic dimetallacycle **6** (in contrast to **4**[5]) does, in fact, correspond to a local minimum; in this case, the determined energy value of about 12 kcal mol^{-1} constitutes merely an upper limit for the stabilization of the structure containing the planar-tetracoordinate sp^2-hybridized carbon atom compared with the "normal" olefinic structural alternative of these compounds. It is evident that the value determined for the cation **5b** [$\Delta\Delta G_{plan.C}$ (obs) ≤ 12 kcal mol^{-1}] is lower than that predicted from the calculations for **3**: the Cp_2ZrX moiety is a poorer σ-donor substituent than $XAlR_2$.[11]

We have demonstrated that for specific model compounds (e.g. **5b**) with a planar-tetracoordinate sp^2-carbon atom, the

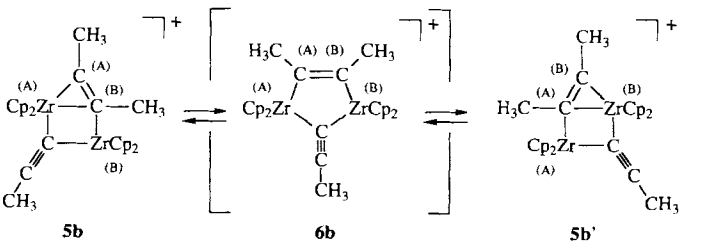

Scheme 3. The Zr-C-Zr bonds in **5** are three-center, two-electron bonds.

degree of energetic stabilization relative to that of their "conventional" isomers with trigonally planar carbon atoms can easily be approximated by experiment. This should provide a good basis from which to assess the results of quantum mechanical calculations carried out on such systems, and thus help us to obtain a realistic picture of the common factors which lead to the formation of stable compounds containing planar-tetracoordinate carbon atoms.

Received: April 14, 1993
Revised version: July 14, 1993 [Z 6006 IE]
German version: *Angew. Chem.* **1993**, *105*, 1691

[1] G. Erker, R. Zwettler, C. Krüger, R. Noe, S. Werner, *J. Am. Chem. Soc.* **1990**, *112*, 9620; G. Erker, M. Albrecht, C. Krüger, S. Werner, *Organometallics* **1991**, *10*, 3791; M. Albrecht, G. Erker, M. Nolte, C. Krüger, *J. Organomet. Chem.* **1992**, *427*, C21; G. Erker, M. Albrecht, S. Werner, M. Nolte, C. Krüger, *Chem. Ber.* **1992**, *125*, 1953; G. Erker, M. Albrecht, C. Krüger, S. Werner, *J. Am. Chem. Soc.* **1992**, *114*, 8531; G. Erker, M. Albrecht, C. Krüger, S. Werner, P. Binger, F. Langhauser, *Organometallics* **1992**, *11*, 3517; review: G. Erker, *Comments Inorg. Chem.* **1992**, *13*, 111; *Nachr. Chem. Techn. Lab.* **1992**, *40*, 1099; M. Albrecht, G. Erker, *Synlett* **1993**, 441.

[2] A. D. Horton, A. G. Orpen, *Angew. Chem.* **1992**, *104*, 912; *Angew. Chem. Int. Ed. Engl.* **1992**, *31*, 876.

[3] See also: R. H. Cayton, S. T. Chacon, M. H. Chisholm, M. J. Hampdon-Smith, J. C. Huffman, K. Folting, P. D. Ellis, B. A. Huggins, *Angew. Chem.* **1989**, *101*, 1547; *Angew. Chem. Int. Ed. Engl.* **1989**, *28*, 1523; S. T. Chacon, M. H. Chisholm, K. Folting, J. C. Huffman, M. J. Hampdon-Smith, *Organometallics* **1991**, *10*, 3722; F. A. Cotton, M. J. Millar, *J. Am. Chem. Soc.* **1977**, *99*, 7886; S. Harder, J. Boersma, L. Brandsma, A. van Heteren, J. A. Kanters, W. Bauer, P. von R. Schleyer, *ibid.* **1988**, *110*, 7802; S. L. Buchwald, E. A. Lucas, W. M. Davis, *ibid.* **1989**, *111*, 397; see also: T. Beringhelli, G. Ciani, G. D'Alfonso, A. Sironi, M. Freni, *J. Chem. Soc. Chem. Commun.* **1985**, 978; W. Uhl, M. Layh, W. Massa, *Chem. Ber.* **1991**, *124*, 1511; M. Layh, W. Uhl, *Polyhedron* **1990**, *9*, 277; F. A. Cotton, M. Shang, *J. Am. Chem. Soc.* **1990**, *112*, 1584.

[4] Theoretical studies: R. Hoffmann, R. W. Alder, C. F. Wilcox, Jr., *J. Am. Chem. Soc.* **1970**, *92*, 4992; R. Hoffmann, *Pure Appl. Chem.* **1971**, *28*, 181; J. B. Collins, J. C. Dill, E. D. Jemmis, Y. Apeloig, P. von R. Schleyer, R. Seeger, J. A. Pople, *J. Am. Chem. Soc.* **1976**, *98*, 5419; P. von R. Schleyer, A. I. Boldyev, *J. Chem. Soc. Chem. Commun.* **1991**, 1536, and references therein; A. I. Boldyrev, P. von R. Schleyer, *J. Am. Chem. Soc.* **1991**, *113*, 9045.

[5] R. Gleiter, I. Hyla-Kryspin, S. Niu, G. Erker, *Angew. Chem.* **1993**, *105*, 753; *Angew. Chem. Int. Ed. Engl.* **1993**, *32*, 754.

[6] G. Erker, W. Frömberg, R. Benn, R. Mynott, K. Angermund, C. Krüger, *Organometallics* **1989**, *8*, 911.

[7] S. L. Borkowsky, R. F. Jordan, G. D. Hinch, *Organometallics* **1991**, *10*, 1268; R. F. Jordan, *Adv. Organomet. Chem.* **1991**, *32*, 325.

[8] **5b**: Reaction of **11** with **12** (equimolar) at room temperature in bromobenzene, yield 85% (230 mg) after recrystallization from dichloromethane, m.p. (DSC) 155 C (decomp); IR(KBr): $\tilde{\nu} = 2070$ (C≡C), 1580 (C=C) cm^{-1}; ^1H NMR (CD_2Cl_2, 360 MHz, 200 K): $\delta = 5.84$ (s, 10H, Cp), 5.70 (s, 10H, Cp), 2.48 (s, 3H, CH_3 at C^1), 2.29 (s, 3H, C≡C-CH_3), −0.16 (s, 3H, CH_3 at C^2); ^{13}C NMR (CD_2Cl_2, 90 MHz, 213 K): $\delta = 210.4$ (C^1), 135.2, 125.7, 121.7 (BPh_4^-), 127.7, 124.3, 110.3 (*C*≡*C*Me, C^2), 109.8 ($^1J_{CH} = 168$ Hz, Cp), 108.4 ($^1J_{CH} = 166$ Hz, Cp), 28.9 ($^1J_{CH} = 127$ Hz, CH_3 at C^1), 10.0 ($^1J_{CH} = 133$ Hz, C≡C-*C*H_3), −25.6 ($^1J_{CH} = 130$ Hz, CH_3 at C^2).

[9] Reference data: **3a**, ^1H NMR ([D_6]benzene): $\delta = 5.67$ (Cp), 1.91, 1.66, 1.43 (CH_3) [1]. **5a**, ^1H NMR (CD_2Cl_2): $\delta = 6.09$, 5.92 (Cp), −0.30 (CH_3 at C^2); ^{13}C NMR (CD_2Cl_2): $\delta = 111.2$, 107.9 (Cp), 232.5 (C^1), −14.6 ($^1J_{CH} = 128$ Hz, *C*H_3 at C^2) [2]. In the crystal, **5a** shows an agostic interaction between a C–H bond of the methyl group at C^2 and the neighboring zirconium center. Solutions of **5b** are characterized by a high-field shift of the ^1H/^{13}C NMR resonances of this methyl group, as was similarly observed for **5a**. The ^1J(C,H) coupling constants associated with this ^{13}C NMR methyl signal were likewise within the normal range. In the ^1H NMR spectrum (360 MHz) of **5b** at 173 K, we observe, however, a pronounced broadening of this CH_3 signal, whilst all other signals maintain normal line widths.

[10] D. S. Stephenson, G. Binsch, DNMR 5; A Computer Program for Iterative Analysis of Exchange-Broadened NMR Spectra (Quantum Chemistry Program Exchange **1978**, *10*, 365); G. Binsch, *Dyn. Nucl. Magn. Reson. Spectrosc.* **1975**, 45; G. Binsch, H. Kessler, *Angew. Chem.* **1980**, *92*, 445; *Angew. Chem. Int. Ed. Engl.* **1980**, *19*, 411; M. L. H. Green, L.-L. Wong, A. Sella, *Organometallics* **1992**, *11*, 2660, and references therein.

[11] J. W. Lauher, R. Hoffmann, *J. Am. Chem. Soc.* **1976**, *98*, 1729; P. Hofmann, P. Stauffert, N. E. Shore, *Chem. Ber.* **1982**, *115*, 2153.

Lithium Di-*tert*-butylmethylsilylhydrazide, a Hexamer with Li^+ Ions Bound Side-on and End-on**

By *Sven Dielkus, Christian Drost, Regine Herbst-Irmer,* and *Uwe Klingebiel**

The only monosilylhydrazine known is $Ph_3SiNHNH_2$, described by Wannagat et al. in 1958. At 90 °C it readily condenses to *N,N'*-bis(silyl)hydrazine, while releasing N_2H_4.[1] This class of compounds is better kinetically stabilized by the use of *tert*-butylsilyl groups.[2]

By treating di-*tert*-butylmethylfluorosilane with lithiated hydrazine, we prepared the thermally stable monosilylhydrazine **1**, which can be converted into the lithium derivative **2** by *n*BuLi. When **2** reacted with trifluorosilylbis(trimethylsilyl)amine, we observed the formation of the *N,N'*- or *N,N*-bis(silyl)hydrazines **3** and **4**, respectively. The NMR data of these compounds are compiled in Table 1.

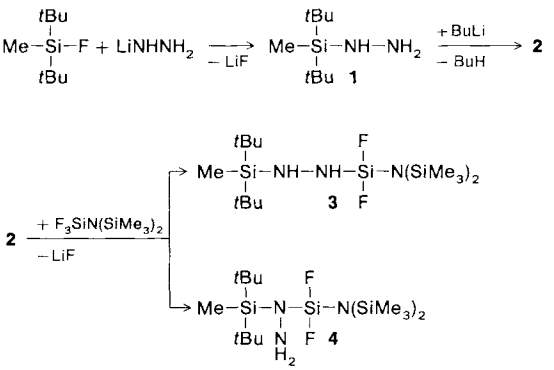

Table 1. NMR data of compounds **1**–**4**. All measurements were made at 25 C with a 250 MHz spectrometer (except ^{19}F NMR: 80 MHz instrument). Standard for ^1H, ^{13}C, and ^{29}Si NMR: TMS int., for ^{19}F NMR: C_6F_6 ext., for ^7Li NMR: LiCl ext.

1 (all measurements in $CDCl_3$): ^1H NMR: $\delta = -0.14$ (SiMe, 3H), 0.85 ($SiCMe_3$, 18H); ^{13}C NMR: $\delta = -9.44$ (SiC), 20.23 ($SiCC_3$), 28.25 ($SiCC_3$); ^{29}Si NMR: $\delta = 8.74$.

2 (measurements in C_6D_6/THF): ^7Li NMR: $\delta = 0.55$; ^{29}Si NMR: $\delta = 9.13$, 10.65.

3 (all measurements in $CDCl_3$): ^1H NMR: $\delta = 0.11$ (SiMe, 3H), 0.22 (t, ^5J(H,F) = 0.8 Hz, $SiMe_3$, 18H), 0.98 ($SiCMe_3$, 18H), 2.98 (t, ^3J(H,F) = 3.3 Hz, NH, 1H), 2.99 (NH, 1H); ^{13}C NMR: $\delta = -9.40$ (t, ^5J(C,F) = 1.2 Hz, SiC), 3.62 (t, ^4J(C,F) = 1.6 Hz, SiC_3), 20.49 ($SiCC_3$), 28.27 ($SiCC_3$); ^{19}F NMR: $\delta = 25.82$; ^{29}Si NMR: $\delta = -66.12$ (t, ^1J(Si,F) = 219.8 Hz, SiF_2), 6.27 (t, ^3J(Si,F) = 1.0 Hz, $SiMe_3$), 10.85 ($SiCMe_3$).

4 (all measurements in $CDCl_3$): ^1H NMR: $\delta = 0.04$ (t, ^5J(H,F) = 2.2 Hz, SiMe, 3H), 0.26 (t, ^5J(H,F) = 0.8 Hz, $SiMe_3$, 18H), 1.07 ($SiCMe_3$, 18H), 2.68 (NH_2, 2H); ^{13}C NMR: $\delta = -7.55$ (t, ^4J(C,F) = 3.9 Hz, SiC), 3.74 (t, ^4J(C,F) = 1.8 Hz, SiC_3), 21.14 ($SiCC_3$), 28.92 ($SiCC_3$); ^{19}F NMR: $\delta = 37.04$; ^{29}Si NMR: $\delta = -60.37$ (t, ^1J(Si,F) = 236.8 Hz, SiF_2), 5.93 (t, ^3J(Si,F) = 1.4 Hz, $SiMe_3$), 9.22 (t, ^3J(Si,F) = 1.5 Hz, $SiCMe_3$).

Formation of the isomers **3** and **4** requires prior coordination of the Li^+ ion with the two N atoms of the hydrazine unit. Side-on coordination of Li^+ has so far been predicted

[*] Prof. Dr. U. Klingebiel, S. Dielkus,[+] Dr. C. Drost, Dr. R. Herbst-Irmer[+]
Institut für Anorganische Chemie der Universität
Tammannstrasse 4, D-37077 Göttingen (FRG)
Telefax: Int. code + (551)39-3373

[+] Crystal structure analysis.

[**] This work was supported by the Fonds der Chemischen Industrie.

only by ab initio calculations for lithiated hydrazine.[3] To prove our point, we isolated single crystals of **2** and carried out an X-ray structural analysis.[4]

The crystal structure of **2** (Fig. 1)[4] exhibits two different silylhydrazide units **I** and **II**, which are bound by six Li^+ ions to form a hexameric entity. The Li^+ ions are bound to three

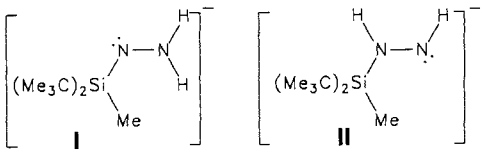

different structural units: Li1 is coordinated with one N atom and two NH groups, Li2 with one N atom, one N_2, and one NH unit, and Li3 with one NH, one N_2, and one NH_2 unit. Thus four Li^+ ions are bound side-on.

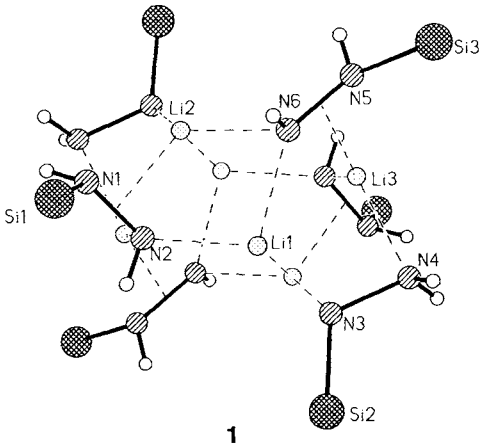

Fig. 1. Crystal structure of **2** (Me and *t*Bu groups were omitted for clarity). Selected bond lengths [pm] and angles [°]: Li1-N1 199.5(14), Li1-N3 201.6(13), Li1-N6 201.8(14), Li2-N2 200.8(14), Li2-N6 203.6(13), Li2-N3 [a] 204.0(13), Li2-N1 210.4(13), Li3-N4 201.3(14), Li3-N6 202.3(13), Li3-N5 202.4(14), Li3-N2 [a] 202.7(13), N1-N2 149.3(8), Si1-N1 174.4(6), Si2-N3 173.0(6), N3-N4 149.3(9), N5-N6 147.7(8), Si3-N5 174.4(6); N2-Li2-N1 42.5(3), N6-Li3-N5 42.8(3), N2-N1-Li2 65.3(5), N1-N2-Li2 72.2(5), N4-N3-Si2 115.4(4), N4-N3-Li1 108.4(5), Si2-N3-Li1 112.7(5), N5-N6-Li3 68.6(5), N6-N5-Li3 68.5(5); symmetry transformation for the equivalent atoms [a]: $-x+1, -y+1, -z$.

Unlike unit **II**, in the solid state **I** does not coordinate Li^+ ions side-on. The side-on bond lengths for the atoms Li2 and Li3 were determined to be 192 and 188 pm, respectively. The angles at N5 and N6, which bind Li3 side-on, are nearly identical; the angles at N1 and N2, which coordinate Li2, deviate by 7° (N5-N6-Li3 68.6, N6-N5-Li3 68.5; and N1-N2-Li2 72.2, N2-N1-Li2 65.3°). Thus Li3 is positioned centrosymmetrically above the N–N bond.

As X-ray structural analyses of Li derivatives of silyl-substituted hydrazines had been unknown so far, the structural analysis of **2** was compared with ab initio calculations for lithium hydrazide.[3] Table 2 shows a comparison of the data for the calculated $(NHNH_2)Li^+$ system (**A**) with that for the side-on units N1-N2-Li2 and N5-N6-Li3 (**B**) in **2**, derived from the X-ray structure determination.

The stuctural analysis confirms the ab initio calculations,[3] according to which Li^+ ions in hydrazides can be

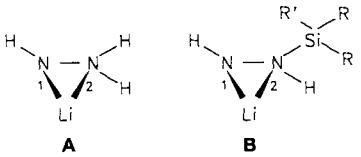

Table 2. Calculated and measured parameters in $Li(HN\text{-}NH_2)$ **A** and **2** (**B**), respectively.

Bond lengths [pm]	A	B	Bond angles [°]	A	B
N-N	145	149.3; 147.7	N-Li-N	56	42.5, 42.8
N^1-Li	161	200.8, 202.3	Li-N^1-N^2	49	72.2, 68.6
N^2-Li	189	210.4, 202.4	Li-N^2-N^1	76	65.3, 68.5

coordinated equally by both N atoms of the hydrazine. This phenomenon also accounts for the isomerizations during the secondary substitutions.

Experimental Procedure

1: N_2H_4 (0.02 mol, 0.64 g) in hexane (50 mL) was metalated with an equimolar quantity of BuLi (15% in hexane). When release of butane had ceased, THF (50 mL) and tBu_2MeSiF (0.02 mol, 3.52 g) were added. After the mixture was heated to reflux for 36 h the solvent was distilled off, and the residue was heated to 90 °C for 36 h. LiF was removed, and **1** was purified by distillation. Yield: 65%. B.p. 36 °C/0.01 mbar; MS (70 eV): *m/z* 188 (M^+, 6%).

2: To **1** (0.01 mol, 1.88 g) in hexane (20 mL) was added BuLi (0.01 mol, 15% in hexane). The suspended matter was dissolved by addition of THF at boiling temperature, and **2** was obtained in a crystalline form by slow cooling to room temperature. Yield: 95%, m.p. 68 °C (decomp) **3** and **4**: **1** (0.01 mol, 1.88 g) in hexane/THF (50 mL) was lithiated with BuLi (0.01 mol, 15% in hexane). An equimolar quantity of the fluorosilane was added rapidly to the Li derivative at −30 °C. The reaction mixture was slowly warmed to room temperature and heated to reflux for 1 h. The crude products were purified by distillation; a separation of the structural isomers was not accomplished. Yields (according to integration of the ^1H NMR data): 70% (**3**), 5% (**4**). B.p. 79 °C/0.01 mbar. MS (FI): *m/z* 413 (M^+, 100%).

Received: May 18, 1993 [Z 6090 IE]
German version: *Angew. Chem.* **1993**, *105*, 1689

[1] U. Wannagat, W. Liehr, *Z. Anorg. Allg. Chem.* **1958**, *297*, 129–136.
[2] C. Drost, U. Klingebiel, *Chem. Ber.* **1993**, *126*, 1413–1416.
[3] J. R. Dilworth, A. Rodriguez, G. L. Leigh, J. N. Murrell, *J. Chem. Soc. Dalton Trans.* **1983**, *2*, 455–461.
[4] Crystal structure of **2**: Space group $P2_1/n$, $a = 1248.1(2)$, $b = 1341.3(3)$, $c = 2327.4(5)$ pm, $\beta = 100.17(2)°$, $V = 3.835(2)$ nm^3, $Z = 4$, $\mu = 0.147$ mm^{-1} ($Mo_{K\alpha}$), 6003 measured intensities, $2\theta_{max} = 48°$, structure solution by direct methods [5], 5996 symmetry-independent reflections used for the refinement according to F^2 [6], non-H atoms anisotropic, H atoms at C atoms according to the "riding" model, H atoms at N atoms refined with distance restraints, 391 parameters, *R*1 for $F > 4\sigma(F)$ 0.0873 ($R1 = \sum||F_o| - |F_c||/\sum|F_o|$), *w*R2 for all data 0.2594 ($wR2 = [\sum[w(F_o^2 - F_c^2)^2]/\sum[w(F_o^2)^2]]^{1/2}$). The relatively high *R* values are due to a very weakly diffracting crystal. Further details of the crystal structure investigation may be obtained from the Fachinformationszentrum Karlsruhe, Gesellschaft für wissenschaftlich-technische Information mbH, D-76344 Eggenstein-Leopoldshafen (FRG), on quoting the depository number CSD-57639, the names of the authors, and the journal citation.
[5] G. M. Sheldrick, *Acta Crystallogr. Sect. A* **1990**, *46*, 467.
[6] G. M. Sheldrick, SHELXL-93, Universität Göttingen, **1993**.

New As–S Cage Structures with Organometallic Components Formed by Complex-Induced Realgar Fragmentation**

By *Henri Brunner, Bernhard Nuber, Ludwig Poll,* and *Joachim Wachter**

Dedicated to Professor Ernst Otto Fischer on the occasion of his 75th birthday

Substituent-free ligands from the elements of groups 15 and 16 are interesting primarily because of their vast structural diversity.[1, 2] Similarities exist above all in the formation of multinuclear complexes. However, the ability of P and As ligands to form ring systems is unusual; these ring systems show remarkable parallels to cyclic hydrocarbon ligands through the isolobal relationship P(As) $\leftrightarrow$ CH. Relatively little is known to date about complexes with ligands that contain elements from groups 15 and 16. A simple route to such compounds is the fragmentation of As_4S_4 with reactive transition metal complexes. Mixed realgar fragmentation products that have so far been structurally characterized are complexes with *cyclo*-As_2S,[1c] As_2S_3,[3] and As_3S_3 ligands.[4] The AsS_3 building block,[5] the first molecular example from the extensive class of sulfo salt minerals, is of particular significance.[6] Since the investigations were carried out on complexes with different structures and with various metal centers, nothing is known as yet about the fragmentation mechanism of realgar.[3, 7] We report here on the synthesis and structure determination of bi- and trinuclear Cp^xCo complexes ($Cp^x = \eta^5$-C_5Me_4Et) with AsS and As_2S_3 ligands in new modes of coordination and their reactivity relationships with one another.

The reaction of **1** with stoichiometric quantities of As_4S_4 (toluene, 80 °C) affords complexes **2**–**5** in yields between 6 and 13%. All compounds were characterized analytically[8] and conclusions about the symmetry can be drawn from the ^{1}H NMR spectra (Table 1). X-ray structure determinations were carried out for **2** and **5**. Since the properties of **3** are very similar to those of the structurally characterized complex **6** ($Cp^* = C_5Me_5$),[3] this suggests that also in **3** a chain, in which S and As atoms alternate, bridges the two Co centers. In contrast, the structure of **4** remains open because of the numerous possible isomers.

Table 1. ^{1}H NMR spectroscopic data [a] of compounds **2**–**5**.

	$\delta(CH_2CH_3)$ [b]	$\delta(CH_3)$	$\delta(CH_2CH_3)$ [b]
2	0.93 (t, 3H), 1.11 (t, 3H)	1.64 (s, 6H), 1.71 (s, 6H), 1.92 (s, 6H), 1.93 (s, 6H)	2.26 (q, 2H), 2.36 (q, 2H)
3	0.95 (t, 6H)	1.65 (s, 6H), 1.66 (s, 6H), 1.75 (s, 6H), 1,76 (s, 6H)	2.27 (q, 2H), 2.28 (q, 2H)
4	0.92 (m, 6H), 1.11 (t, 3H)	1.49 (s, 3H), 1.50 (s, 3H), 1.51 (s, 3H), 1.54 (s, 3H), 1.55 (s, 3H), 1.56 (s, 3H), 1.60 (s, 3H), 1.61 (s, 3H), 1.85 (s, 3H), 1.86 (s, 3H), 1.88 (s, 6H)	2.12 (m, 4H), 2.39 (q, 2H)
5	0.95 (m, 9H)	1.47 (s, 6H), 1.49 (s, 6H), 1.52 (s, 6H), 1.57 (s, 12H), 1.60 (s, 6H)	2.10 (m, 6H)

[a] 250 MHz, $CDCl_3$, TMS int.; [b] $^3J(H,H) = 7.6$ Hz.

$[\{Cp^xCo(CO)\}_2]$ **1**

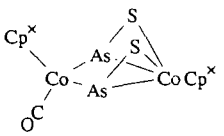

2

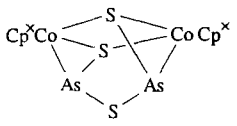

3

$[Cp^x_3Co_3As_4S_2]$

4

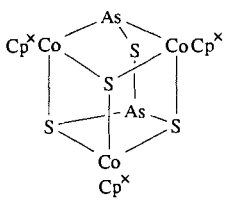

5

$[Cp^*_2Co_2As_2S_3]$ **6**

The most important feature of the crystal structure of **2**[9] is the two Co centers *syn* bridged by two $\eta^1:\eta^2$-AsS ligands (Fig. 1). A terminal CO group at Co2, also evident by an IR absorption at 1987 cm^{-1}, is responsible for the formal saturation of the two Co centers. The two As atoms come remarkably close to each other (2.717(2) Å),[10] whereas the S–S distance (3.278 Å) is greater than that for bonding interactions. The Co–S distances in the frameworks of **6** and **2** are the same length; of the two different Co–As distances ($\Delta = 0.08$ Å) in **2**, however, even the shorter ones are about 0.06 Å longer than those in **6**. The As–S distance (mean 2.169 Å) is about 0.07 Å shorter than that in the minerals As_2S_3 and As_4S_4[11] and other complexes which contain the $\eta^2:\eta^2$ AsS ligand.[7, 12]

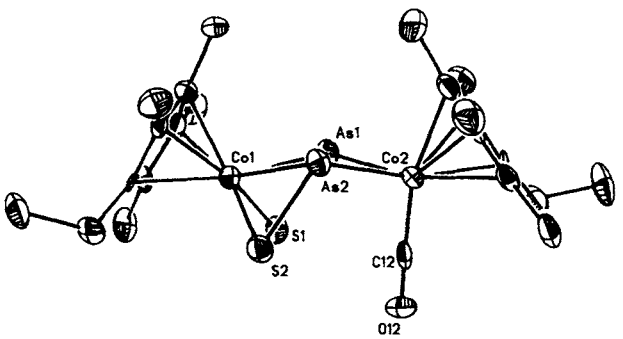

Fig. 1. Crystal structure of **2**. Selected distances [Å] and angles [°]: Co1-As1 2.473(2), Co1-As2 2.465(2), Co1-S1 2.275(4), Co1-S2 2.279(4), Co2-As1 2.383(3), Co2-As2 2.381(3), As1-S1 2.174(4), As2-S2 2.164(4), As1···As2 2.717(2), S1···S2 3.278(4); As1-Co1-As2 66.7(1), As1-Co1-S1 54.3(1), As1-Co1-S2 102.3(1), S1-Co1-S2 92.1(2), As1-Co2-As2 69.5(1), As1-Co2-C12 93.3(4), As2-Co2-C12 97.3(4), Co1-As1-Co2 107.7(1), Co1-As1-S1 58.2(1), Co2-As1-S1 110.7(1).

The crystal structure of **5**[13] is characterized by a $Co_3As_2S_4$ cage, in which one μ_3-S and one μ_3-As_2S_3 ligand form the main constituents of a distorted cube (with As1 above a plane) (Fig. 2). The construction of the As_2S_3 bridge can be seen as a molecular section from the As_nS_{2n+1} chain

[*] Dr. J. Wachter, Prof. Dr. H. Brunner, L. Poll
Institut für Anorganische Chemie der Universität
D-93040 Regensburg (FRG)
Telefax: Int. code + (941)943-4439
Dr. B. Nuber
Anorganisch-chemisches Institut der Universität Heidelberg
D-69120 Heidelberg (FRG)

[**] We thank Prof. Dr. G. Huttner, Heidelberg, for providing the facilities for the structure determination.

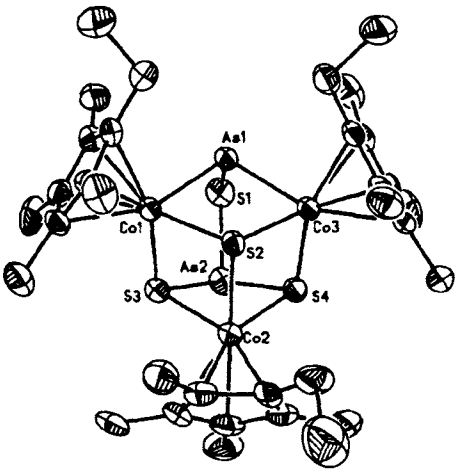

Fig. 2. Crystal structure of **5**. Selected distances [Å] and angles [ ]: Co1-As1 2.342(3), Co1-S2 2.266(4), Co1-S3 2.209(4), Co2-S2 2.274(4), Co2-S3 2.272(4), Co2-S4 2.274(4), Co3-As1 2.341(3), Co3-S2 2.263(4), As1-S1 2.318(4), As2-S1 2.196(1), As2-S3 2.292(4), As2-S4 2.292(4); As1-Co1-S2 78.5(1), Co1-As1-Co3 98.1(1), Co1-S2-Co3 102.7(1), S3-Co2-S4 89.0(1), S3-As2-S4 88.1(1), As1-S1-As2 98.0(1).

with trigonal pyramidal AsS_3 subunit[6] typical for sulfo salts; at the As1 atom two Co atoms replace two S atoms. Correspondingly, the As–S distances also vary between 2.195 and 2.318 Å. Of the noble gas-configurated Co centers, Co1 and Co3 are symmetry equivalent, which is also in accordance with the ^{1}H NMR spectrum (Table 1).

Since the reaction of **1** with As_4S_4 in boiling xylene (15 h) only affords **3** and **5** in 11 and 51% yield, respectively, it appears likely that **2** and **4** are intermediate products. Indeed, warming solutions of **2** to 110 °C affords **3** (25% yield), **4** (10%), and **5** (18-28%). Interestingly, the addition of sulfur does not cause the linkage of the two AsS ligands, rather, only the isolation of a small quantity of $[Cp^x_2Co_2S_4]$.[15]

It can be concluded that AsS units play an important role in the construction of new cage structures which are characterized by the As_2S_3 framework. A comparison with the fragmentation of the As_4 tetrahedron by **1** seems appropriate,[16] although the apparently rapid opening of the edges of the As_4S_4 framework has not been proven to date. Compound **2** is, however, structurally analogous to [Cp*Co-(μ-η^4:η^1:η^1-As_4)Co(CO)Cp*], an intermediate from this reaction, when the two S-"wing tips" are replaced by an As–As building block. Also this complex is thermally unstable. However, it rearranges into a Co_3As_6 framework, which can be described as a strongly distorted As_6 prismane constructed from three As_2 units.

Experimental Procedure

The suspension from **1** (902 mg, 1.91 mmol) and As_4S_4 (817 mg, 1.91 mmol) in toluene (50 mL) was stirred for 15 h at 80 °C. After the solvent had been removed, the oily brown residue was taken up in toluene and prepurified on SiO_2 (column 10 × 3 cm). With toluene/ether 10:1 first a very broad red-brown zone was eluted and then a brown zone which contained **2** in 10% yield. The first zone was then chromatographed on SiO_2 (column 84 × 2.5 cm). With toluene/pentane 1:1 a series of compounds was eluted: orange-red $[Cp^*Co(CO)_2]$, green-brown **4**, red-brown **5**, and finally violet **3** (yields: 13 (**4**), 11 (**5**), 6 (**3**)%). Recrystallization at −20 °C from toluene/pentane mixtures afforded brown (**2**.**4**.**5**) and dark violet (**3**) crystals, respectively.

Received: May 18, 1993 [Z 60891E]
German version: *Angew. Chem.* **1993**, *105*, 1699

[1] The most current review articles: O. J. Scherer, *Angew. Chem.* **1990**, *102*, 1137; *Angew. Chem. Int. Ed. Engl.* **1990**, *29*, 1104; b) A.-J. DiMaio, A. L. Rheingold, *Chem. Rev.* **1990**, *90*, 169; c) M. Di Vaira, P. Stoppioni, *Coord. Chem. Rev.* **1992**, *120*, 259.

[2] J. Wachter, *Angew. Chem.* **1989**, *101*, 1645; *Angew. Chem. Int. Ed. Engl.* **1989**, *28*, 1613.

[3] H. Brunner, H. Kauermann, B. Nuber, J. Wachter, M. L. Ziegler, *Angew. Chem.* **1986**, *98*, 551; *Angew. Chem. Int. Ed. Engl.* **1986**, *25*, 557.

[4] M. Di Vaira, P. Stoppioni, M. Peruzzini, *Inorg. Chim. Acta* **1987**, *132*, 37.

[5] G. A. Zank, T. B. Rauchfuss, S. R. Wilson, *J. Am. Chem. Soc.* **1984**, *106*, 7621.

[6] For the obtained rings, chains, and networks from anionic, pyramidal XE_3 subunits (X = As, Sb, Bi; E = S, Se, Te) see: W. Nowacki, *Schweiz. Mineral. Petrogr. Mitt.* **1969**, *49*, 109; E. Hellner, *J. Geol.* **1958**, *66*, 503; Y. Takeuchi, R. Sadanaga, *Z. Kristallogr.* **1969**, *130*, 346.

[7] The 48 e cluster $[Cp^*_2Mo_2AsS_3Co(CO)_2]$ contains a μ_2,η^2-AsS ligand, however this ligand is derived from the compound $[Cp^*_2Mo_2As_2S_3]$, which has not yet been confirmed structurally (H. Brunner, H. Kauermann, U. Klement, J. Wachter, T. Zahn, M. L. Ziegler, *Angew. Chem.* **1985**, *97*, 122; *Angew. Chem. Int. Ed. Engl.* **1985**, *24*,132).

[8] Correct C, H, S elemental analyses. FD mass spectra (toluene) **2**: *m/z* 658.2 ($M^{\oplus}$); **3**: *m/z* 662.3 ($M^{\oplus}$); **4**: *m/z* 988.7 ($M^{\oplus}$); **5**: *m/z* 902.5 ($M^{\oplus}$).

[9] Compound **2** crystallizes in the form of brown plates, which contain half a molecule of toluene (disordered) per formula unit. Space group $C2h/5.P2_1/n$ (no. 14), a = 9.046(4), b = 26.01(1), c = 12.636(5) Å, β = 99.59(3)°, V = 2931.5 Å^3 (25 reflections ($3.0 < 2\theta < 19.0$°)); Z = 4. Syntex-R3 diffractometer ($Mo_{K\alpha}$), $3.0 < 2\theta < 52.5$°; 6069 reflections, of which 2537 with $I > 2.5\sigma(I)$ were used for the refinement. Decrease in intensity of the reference reflections during the measurement balanced up to 55% by corresponding correction of the intensities. Patterson and Fourier methods, anisotropic refinement to R = 0.073, R_w = 0.055 [14].

[10] As–As bonds in transition metal complexes lie in the range 2.273(3)–2.445(4) Å [1a]. However, distances of 2.57 and 2.76 Å have also previously been discussed as being of bonding nature (A. L. Rheingold, M. J. Foley, P. J. Sullivan, *J. Am. Chem. Soc.* **1982**, *104*, 4727).

[11] D. J. E. Mullen, W. Nowacki, *Z. Kristallogr. Kristallgeom. Kristallphys. Kristallchem.* **1972**, *136*, 48, and references therein.

[12] A.-J. DiMaio, A. L. Rheingold, *Inorg. Chem.* **1990**, *29*, 798.

[13] **5** crystallizes in the form of thin, long plates of the dimensions 0.05 × 0.15 × 0.7 mm^3. Space group $C2h/5$, $P2_1/n$ (no. 14), a = 8.849(3), b = 21.81(2), c = 19.54(2) Å, β = 96.24(6)°, V = 3748.8 Å^3 (16 reflections ($4.3 < 2\theta < 14.8$°)), Z = 4. Syntex-R3 diffractometer ($Mo_{K\alpha}$), $3.0 < 2\theta < 47.5$°; 5878 reflections, of which 2867 with $I < 2.5\sigma(I)$ were used for the refinement. Empirical absorption correction. Patterson and Fourier methods, anisotropic refinement to R = 0.060, R_w = 0.048 [14].

[14] Further details of the crystal structure investigation may be obtained from the Fachinformationszentrum Karlsruhe, Gesellschaft für wissenschaftlich-technische Information mbH, D-76344 Eggenstein-Leopoldshafen (FRG) on quoting the depository number CSD-57465, the names of the authors, and the journal citation.

[15] H. Brunner, N. Janietz, W. Meier, G. Sergeson, J. Wachter, T. Zahn, M. L. Ziegler, *Angew. Chem.* **1985**, *97*, 1056; *Angew. Chem. Int. Ed. Engl.* **1985**, *24*, 1060.

[16] O. J. Scherer, K. Pfeiffer, G. Wolmerhäuser, *Chem. Ber.* **1992**, *125*, 2367.

The First Heteroallyl Metal Complexes of Arsenic with the Coordination Number 2**

By *Uwe Wirringa, Herbert W. Roesky,** *Mathias Noltemeyer,* and *Hans-Georg Schmidt*

Dedicated to Professor Helmut Werner on the occasion of his 60th birthday

The chemistry of low-coordinate group 15 elements of the periodic table has already been the subject of numerous investigations. Particular emphasis was focused on phosphorus compounds such as phosphaalkynes and -alkenes,[1] diphosphenes,[2] and iminophosphanes.[3] These compounds have already been used as synthetic building blocks.[1–4] In contrast, the chemistry of compounds containing low-coor-

[*] Prof. Dr. H. W. Roesky, Dipl.-Chem. U. Wirringa, Dr. M. Noltemeyer, H.-G. Schmidt
Institut für Anorganische Chemie der Universität
Tammannstrasse 4, D-37077 Göttingen
Telefax: Int. code + (551)393373

[**] This work was supported by the Deutsche Forschungsgemeinschaft and the Fonds der Chemischen Industrie.

dinate arsenic and higher homologues is only in its infancy.[5–9] Attempts to synthesize heteroallyl metal complexes by deprotonation were only partially successful.[10–12] Structural investigations of corresponding arsenic systems were completely unknown. Our aim was to coordinate metal atoms to aryl imides of arsenic by deprotonation reactions, and, moreover, to use these systems for additional metal complexation.

The starting material **2** was prepared by using the method described by M. F. Lappert et al.[7] Instead of 2,4,6-tri-*tert*-butylaniline, we used 2,6-diisopropylaniline **1**, which yielded the dimeric arsazene **2** [Eq. (a)]. Mass spectrometric investigations confirmed the dimeric nature of the product ((FI MS): *m/z* 853).

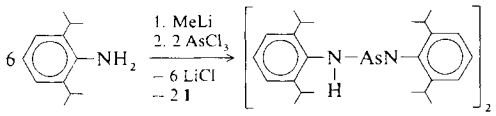

(a)

1 **2**

The reactions of **2** with bis(bis(trimethylsilyl)amido)zinc **3a**[13] and bis(bis(trimethylsilyl)amido)cadmium **3b**[13] led to the heteroallyl complexes **4** and **5**, respectively, which formed orange powders [Eq. (b)]. This indicates that the nitrogen-bonded hydrogen atom of **2** is reactive enough to generate the readily separable hexamethyldisilazane. It is expected that the method described here is generally suitable for the synthesis of heteroallyl metal complexes.

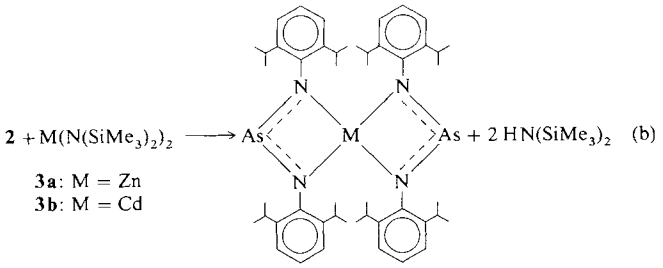

(b)

The structures of compounds **4** and **5** are isotypical (Fig. 1), which was already to be expected based on the spectroscopic data and the almost identical melting points (304 °C (**4**) and 302 °C (**5**)). The molecules of both complexes are arranged chainlike in the crystal (Fig. 2). The intermolecular As–As distances (**4**: 387.4; **5**: 382.5 pm) are, however, too long to assume interactions between the molecules.

The molecules consist of two four-membered rings spirocyclically linked through the central atom.[14] In contrast to **4**, the rings in **5** have different sizes. The NMR data in solution are in agreement with the structures in the solid state. The rings consisting of arsenic, nitrogen, and the corresponding metal are planar, forming a torsion angle of 62.9° in **4** and one of 51.8° in **5**. The more distorted tetrahedral geometry at the metal center in **5** cannot be explained by steric influences; similar tendencies are observed in aluminum-, gallium-, and indium–nitrogen systems.[15] This might be explained by the decreasing degree of hybridization, parallel to the increasing atomic number within a group.

The remarkably strong exposition of the arsenic atoms can be deduced from the N-As-N angles (**4**: 92.47(14) and 92.73(14)°; **5**: 94.7(3) and 91.9(2)°). As a result of this, a strong nucleophilic character for these centers can be assumed. This can only be explained by a reduction of the electron density at the central atom. In contrast, the steric influence of the 2,6-diisopropylphenyl substituents is very small. This is already demonstrated by the dimeric structure of compound **2**.

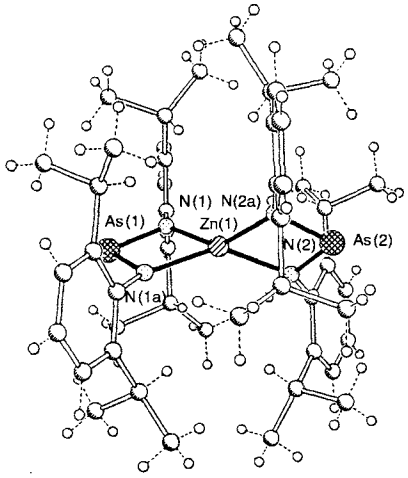

Fig. 1. Crystal structure of **4**, which is isotypical to that of **5**. Selected bond lengths [pm] and angles [°] of **4**: Zn(1)-N(2) 203.5(2), Zn(1)-N(2a) 203.5(2), Zn(1)-N(1a) 204.0(2), Zn(1)-N(1) 204.0(2), As(1)-N(1) 174.4(2), As(1)-N(1a) 174.4(2), As(2)-N(2a) 174.2(2), As(2)-N(2) 174.2(2); N(2)-Zn(1)-N(2a) 76.36(12), N(2a)-Zn(1)-N(1a) 116.32(9), N(2a)-As(2)-N(2) 92.47(14), As(2)-N(2)-Zn(1) 95.58(9), N(1)-As(1)-N(1a) 92.73(14), N(1a)-Zn(1)-N(1) 76.42(12); of **5**: Cd(1)-N(1a) 219.7(4), Cd(1)-N(1) 219.7(4), Cd(1)-N(2) 222.9(4), Cd(1)-N(2a) 222.9(4), As(1)-N(1) 169.5(3), As(1)-N(1a) 169.5(3), As(2)-N(2) 173.9(4), As(2)-N(2a) 173.9(4); N(1a)-Cd(1)-N(1) 67.4(2), N(1)-Cd(1)-N(2) 122.51(14), N(1)-Cd(1)-N(2a) 145.7(2), N(2)-As(2)-N(2a) 94.7(3), As(2)-N(2)-Cd(1) 97.6(2), N(2)-Cd(1)-N(2a) 70.0(2), N(1)-As(1)-N(1a) 91.9(2), As(1)-N(1)-Cd(1) 100.4(2).

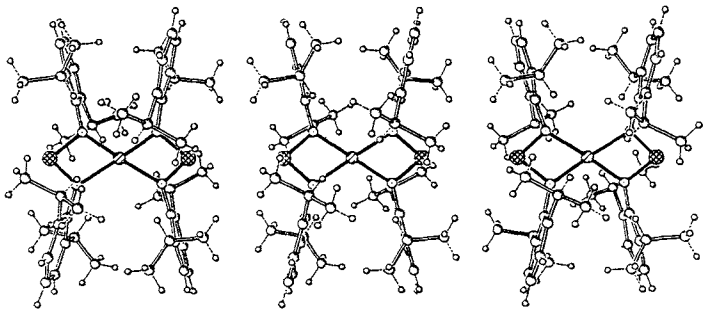

Fig. 2. Representation of the arrangement of the molecules of **4** and **5** in the crystal.

The metal–nitrogen bond lengths in both compounds are in the range of those expected for single bonds (**4**: 203.5(2) and 204.0(2) pm; **5**: 219.7(4) and 222.9(4) pm). The As–N distances within the heteroallyl ligands of the two compounds are the same (**4**: 174.4(2) and 174.2(2) pm, **5**: 169.5(3) and 173.9(4) pm). M. F. Lappert et al. determined As–N bond lengths of 174.5(7) and 171.4(7) pm[7] for their arsazene. According to L. Pauling's calculations the length of an As–N double bond is 173 pm and that of an As–N single bond 195 pm.[16]

Interestingly, in both compounds, the phenyl rings are arranged almost parallel, and perpendicular to the As-M-As axis. This arrangement leads to a tube formed by the organic substituents enclosing the As-M-As axis and results in unprotected As atoms. This becomes important if metal fragments are to be coordinated to the arsenic atoms.

Experimental Procedure

2: **1** (15.9 g, 90 mmol) was dissolved in hexane (100 mL) and subsequently treated with methyllithium (2.0 g, 90 mmol) dissolved in diethyl ether (57 mL) at room temperature; thus, the reaction mixture heated up to almost boiling. After the addition of MeLi was completed, the mixture was stirred at room temperature for about 1.5 h. Subsequently, arsenic trichloride (5.4 g, 30 mmol) was added dropwise; again the reaction mixture heated to almost boiling. The solution turned orange immediately. The reaction mixture was then heated under reflux for 14 h. The lithium chloride was recovered by filtration. The remaining deep red solution was concentrated in vacuo and the product was precipitated at −18 °C. To separate **2** from adhesive **1**, after filtration, the solid was washed three times with hexane (ca. 10 mL). Yield 8.4 g (23 mmol, 77%). M.p. 164 °C; MS(FI): *m/z* (%): 853 (100) $[M^+]$; ^{13}C NMR (63 MHz, [D$_8$]toluene, 25 °C, TMS): δ = 22.5 (Me), 28.2 (*C*HMe$_2$), 119.0 (aryl-C), 123.1 (aryl-C), 132.4 (aryl-C), 140.8 (aryl-C); ^1H NMR (250 MHz, [D$_8$]toluene, 25 °C, TMS): δ = 1.15 (d, ^3J(H,H) = 7 Hz, 48 H; CH*Me*$_2$), 2.63 (sept., ^3J(H,H) = 7 Hz, 8 H; *CH*Me$_2$), 3.21 (s, 2H; NH), 6.99 (m, 12 H; aryl-H); IR (nujol): $\tilde{\nu}$ = 3397 cm^{-1} (N–H).

4: **2** (0.856 g, 2 mmol) was dissolved in toluene (30 mL) and treated with **3a** (0.385 g, 1 mmol). Subsequently, the mixture was heated under reflux for 14 h. The solution turned red and an orange solid precipitated. Some of the solvent was removed in vacuo, the solid was filtered off and finally recrystallized from hot toluene. Yield: 0.61 g (67%). M.p. 304 °C; MS(FI): *m/z* (%): 914 (30) $[M^+]$, 739 (100) $[M^+ - C_{12}H_{17}N]$; ^{13}C NMR (63 MHz, [D$_8$]toluene, 25 °C, TMS): δ = 22.5 (Me), 28.2 (*C*HMe$_2$), 118.9 (aryl-C), 123.0 (aryl-C), 132.2 (aryl-C), 140.7 (aryl-C); ^1H NMR (250 MHz, [D$_8$]toluene, 25 °C, TMS): δ = 1.15 (d, ^3J(H,H) = 7 Hz, 48 H; CH*Me*$_2$), 2.63 (sept., ^3J(H,H) = 7 Hz, 8 H; *CH*Me$_2$), 7.02 (m, 12 H; aryl-H); correct elemental analysis.

5: The experimental procedure was similar to that for the synthesis of **4**. Compound **2** (0.856 g) was treated with **3b** (0.433 g). The orange product **5** was obtained in 83% yield (0.80 g). M.p. 302 °C; MS(FI): *m/z* (%): 964 (10) $[M^+]$, 788 (100) $[M^+ - C_{12}H_{17}N]$; ^{13}C NMR (63 MHz, [D$_8$]toluene, 25 °C, TMS): δ = 22.5 (Me), 28.2 (*C*HMe$_2$), 118.9 (aryl-C), 123.0 (aryl-C), 124.0 (aryl-C), 132.2 (aryl-C), 140.8 (aryl-C), 144.3 (aryl-C); ^1H NMR (250 MHz, [D$_8$]toluene, 25 °C, TMS): δ = 1.08 (d, ^3J(H,H) = 7 Hz, 24 H; CH*Me*$_2$), 1.15 (d, ^3J(H,H) = 7 Hz, 24 H; CH*Me*$_2$), 2.63 (sept., ^3J(H,H) = 7 Hz, 4 H; *CH*Me$_2$), 3.33 (sept., ^3J(H,H) = 7 Hz, 4 H; *CH*Me$_2$), 7.02 (m, 12 H; aryl-H); correct elemental analysis.

Received: June 19, 1993 [Z6151IE]
German version: *Angew. Chem.* **1993**, *105*, 1680

[1] R. Appel, F. Knoll, I. Ruppert, *Angew. Chem.* **1981**, *93*, 771; *Angew. Chem. Int. Ed. Engl.* **1981**, *20*, 731.
[2] L. Weber, *Chem. Rev.* **1992**, *92*, 1839.
[3] E. Niecke, D. Gudat, *Angew. Chem.* **1991**, *103*, 251; *Angew. Chem. Int. Ed. Engl.* **1991**, *30*, 217.
[4] C. M. Angelov, R. H. Neilson, *Inorg. Chem.* **1993**, *32*, 2279.
[5] O. J. Scherer, *Angew. Chem.* **1990**, *102*, 1137; *Angew. Chem. Int. Ed. Engl.* **1990**, *29*, 1104; O. J. Scherer, R. Winter, G. Heckmann, G. Wolmershäuser, *ibid.* **1991**, *103*, 860 and **1991**, *30*, 850.
[6] M. Drieß, H. Pritzkow, M. Sander, *Angew. Chem.* **1993**, *105*, 273; *Angew. Chem. Int. Ed. Engl.* **1993**, *32*, 283.
[7] P. B. Hitchcock, M. F. Lappert, A. K. Rai, H. D. Williams, *J. Chem. Soc. Chem. Commun.* **1986**, 1633.
[8] G. Märkl, H. Sejpka, *Angew. Chem.* **1986**, *98*, 286; *Angew. Chem. Int. Ed. Engl.* **1986**, *25*, 264.
[9] P. B. Hitchcock, J. A. Johnson, J. F. Nixon, *Angew. Chem.* **1993**, *105*, 86; *Angew. Chem. Int. Ed. Engl.* **1993**, *32*, 103.
[10] P. B. Hitchcock, H. A. Jasim, M. F. Lappert, H. D. Williams, *J. Chem. Soc. Chem. Commun.* **1986**, 1634.
[11] P. Jutzi, U. Meyer, *Phosphorus Sulfur Relat. Elem.* **1988**, *40*, 275.
[12] R. Detsch, E. Niecke, M. Nieger, W. W. Schoeller, *Chem. Ber.* **1992**, *125*, 1119.
[13] H. Bürger, W. Sawodny, U. Wannagat, *J. Organomet. Chem.* **1965**, *3*, 113.
[14] a) X-ray structure analysis of **4**: monoclinic, space group *C*2/*c*, a = 2366.5(3), b = 948.5(2), c = 2417.2(3) pm, β = 116.710(10)°, V = 4.8467(13) nm^3; measured reflections: 6316; final R Values [$I > 2\sigma(I)$]: R_1 = 0.0271, wR_2 = 0.0679; b) X-ray structure analysis of **5**: monoclinic, space group *C*2/*c*, a = 2359.3(5), b = 983.6(3), c = 2514.8(7) pm, β = 120.62(2)°, V = 5.022(2) nm^3; measured reflections: 4696; final R Values [$I > 2\sigma(I)$]: R_1 = 0.0375, wR_2 = 0.0803; both structures were refined with SHELXL-92 against F^2. Further details of the crystal structure investigations may be obtained from the Fachinformationszentrum Karlsruhe, Gesellschaft für wissenschaftlich-technische Information mbH, D-76344 Eggenstein-Leopoldshafen (FRG) on quoting the depository number CSD-57447, the names of the authors, and the journal citation.
[15] T. Belgardt, H. W. Roesky, M. Noltemeyer, H.-G. Schmidt, *Angew. Chem.* **1993**, *105*, 1101; *Angew. Chem. Int. Ed. Engl.* **1993**, *32*, 1056.
[16] L. Pauling, *Die Natur der chemischen Bindung*, 3rd ed., Verlag Chemie, Weinheim, **1973**, p. 217.

Comparison of the Electrophilicities of Cationic Metal π Complexes and of Ordinary Carbenium Ions**

By *Herbert Mayr*,* *Karl-Heinz Müller*, and *Doris Rau*

The terms nucleophilicity and electrophilicity play a central role in the discussion of reaction mechanisms, and there have been numerous attempts to gauge these kinetic quantities.[1, 2]

Kane-Maguire, Sweigart et al. elaborated one of the most extensive sets of data by kinetic investigation of the reactions of cationic metal π complexes with phosphanes, phosphites, and amines.[2] The relative reactivities of these electrophiles were independent of the nature of the reference nucleophiles, and it was thus possible to formulate a uniform electrophilicity scale. From kinetic investigations of the reactions of these π complexes with electron-rich arenes it has been deduced that carbon nucleophiles do not obey these so-called "constant selectivity relationships", and the electrophilicity scale of Kane-Maguire, Sweigart et al. appeared to be applicable only to *n*-nucleophiles (*n* = amines, phosphanes).[2]

We have now studied the kinetics of the reactions of the three electrophilic metal complexes (**1a–c**)[3] with electron-rich vinyl derivatives and the hydride donor tributylstannane, and we found also in these reactions the relative reactivities of **1a–c** to be independent of the nature of the nucleophile. Since the rates of the reactions of these nucleophiles with diarylcarbenium ions are already known,[6] one can now link the electrophilicity scale of the metal π complexes to that of ordinary carbenium ions.

The dienylium complexes **1a–c** react with silylated enol ethers[7a, b] and allylstannes[7c] in the typical way to give the 5-*exo*-substituted cycloalkadiene complexes regio- and stereoselectively (Scheme 1). Some of these products had already been synthesized in different ways.[8, 9] The cycloheptadienylium complex **1c** also reacts with carbon nucleophiles in this way, though it has been reported that under certain circumstances triphenylphosphane initially attacks these complexes at the metal atom and finally ends up at the 5-

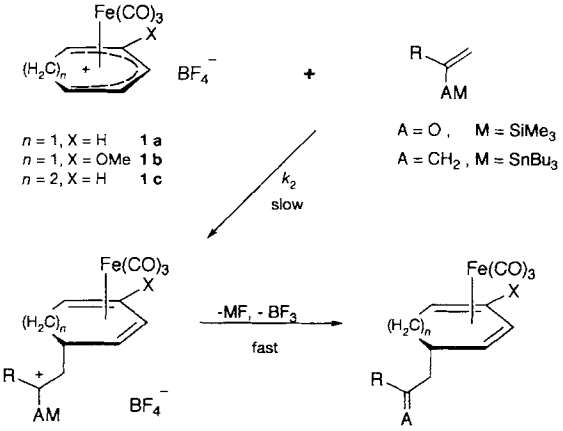

Scheme 1.

[*] Prof. Dr. H. Mayr, Dipl.-Ing. K.-H. Müller, Dr. D. Rau
Institut für Organische Chemie der Technischen Hochschule
Petersenstrasse 22, D-64287 Darmstadt (FRG)
Telefax: Int. code + (6151)16-5591

[**] This work was supported by the Volkswagen-Stiftung and the Fonds der Chemischen Industrie. We thank Mr. A. Hodapp for experimental collaboration, one referee for assistance with the graphical presentations, and the BASF AG for gifts of chemicals.

endo position of the seven-membered ring.[10] The reaction of **1a–c** with tributylstannane proceeds with hydride transfer to yield the cycloalka-1,3-diene complexes, from which **1a–c** is usually generated by hydride abstraction.

Table 1. Rate constants (20 °C, acetone) and activation parameters for the reactions of tricarbonyl(dienylium)iron complexes with various nucleophiles.

Nucleophile	Electrophile	k_2 [L mol^{-1} s^{-1}]	$\Delta H^{\neq}$ [kJ mol^{-1}]	$\Delta S^{\neq}$ [J mol^{-1} K^{-1}]
	1a	9.16×10^{-3}	58.4 ± 3.2	-84 ± 11
	1a	8.56×10^{-2}	49.3 ± 1.0	-97 ± 4
	1a	2.55×10^{-2}	50.5 ± 1.5	-103 ± 5
	1b	3.35×10^{-3}	51.6 ± 0.7	-116 ± 3
	1c	2.78×10^{-3}	-	-
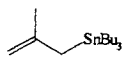	**1a**	2.36×10^{-1}	44.7 ± 1.0	-104 ± 4
	1b	5.50×10^{-2}	42.3 ± 0.5	-124 ± 2
	1c	4.58×10^{-2}	33.1 ± 0.3	-158 ± 1
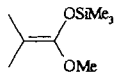	**1a**	6.59	31.6 ± 0.2	-121 ± 1
	1b	7.66×10^{-1}	37.9 ± 0.8	-118 ± 3
	1c	2.05×10^{-1}	31.2 ± 1.5	-152 ± 6
	1a	4.87	43.8 ± 0.9	-82 ± 3
$HSnBu_3$	**1b**	8.31×10^{-1}	44.1 ± 1.0	-96 ± 4
	1c	5.98×10^{-1}	46.9 ± 0.7	-89 ± 1

Photometric monitoring of the reaction kinetics, as described for the reactions of diarylcarbenium ions with alkenes,[11] revealed a second-order rate law. Eyring activation parameters were determined from the temperature dependence of the rate constants (Table 1); for the reactions of **1a** and **1b**, the activation entropies were of similar order of magnitude as for the corresponding reactions of diarylcarbenium ions.[6d] Considerably more negative values of $\Delta S^{\neq}$ were observed for the reactions of **1c** with π systems possibly because of steric shielding of the reaction center in the seven-membered ring.

According to Figure 1 the reactivities of all nucleophiles toward the cyclohexadienyl complex **1a** correlate linearly with their reactivities toward the bis(*p*-dimethylaminophenyl)carbenium ion.[6d] Accordingly Sweigart et al. reported that the reactivity order of *n*-nucleophiles toward metal π complexes is also valid toward ordinary carbenium ions.[12] Figure 1 unambiguously proves that C-nucleophiles behave analogously.

Figure 2 shows for five selected nucleophiles that the nucleophilicity order $PPh_3 > Me_2C{=}C(OMe)OSiMe_3 \approx HSnBu_3 > H_2C{=}C(Me)CH_2SnBu_3 > H_2C{=}C(Ph)OSiMe_3$ holds for all electrophiles examined. The small differences of the slopes of the various correlations imply that a reversal of relative reactivities of nucleophiles upon variation of electrophiles only has to be taken into consideration when nucleophiles with very similar reaction rates are compared.

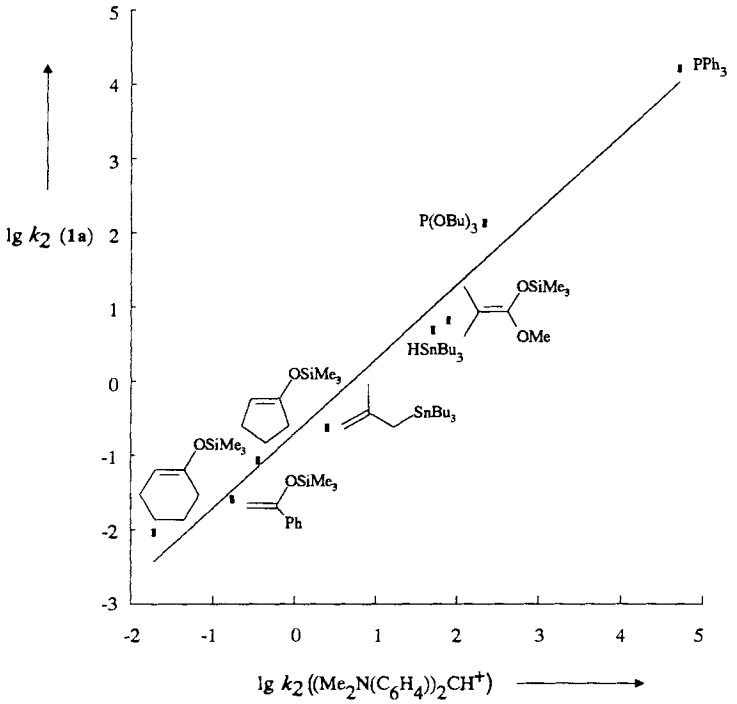

Fig. 1. Correlation of the reactivities of tricarbonyl(η^5-cyclohexadienyl)iron (1+) (**1a**, 20 °C, acetone) toward various nucleophiles with the corresponding reactivities of the bis(*p*-dimethylaminophenyl)carbenium ion [6d] (20 °C, CH_2Cl_2). Data for **1a** + PR_3 from ref. [2].

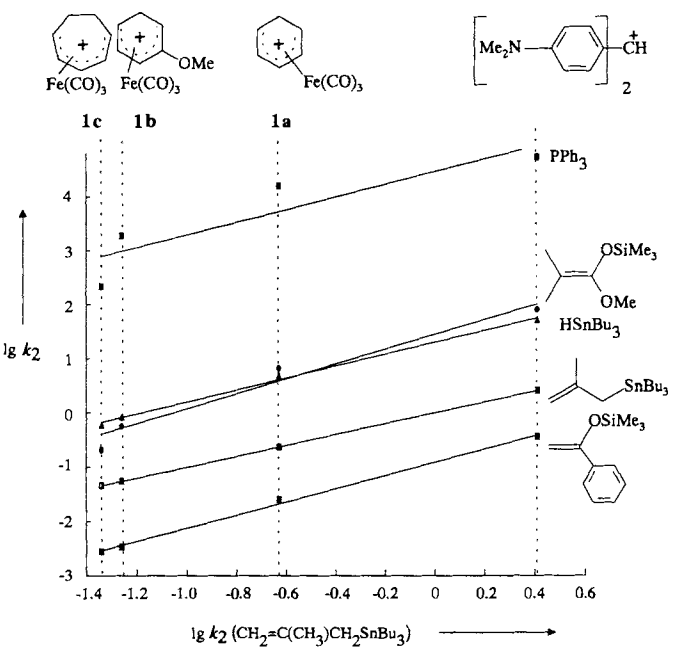

Fig. 2. Correlation of the reactivities of π-, σ-, and *n*-nucleophiles toward various electrophiles with the corresponding reactivities of the tributyl(2-methylallyl)stannane.

Knowing rate constants for the reactions of three electrophiles from the listing of Sweigart, Kane-Maguire et al.[2] with some nucleophiles whose reactivities towards diarylcarbenium ions we had determined previously,[6] we can now combine these two electrophilicity scales to render a direct comparison of the electrophilicities of metal π complexes and of ordinary carbenium ions (Fig. 3). In combination with the reactivity scale for nucleophiles published recent-

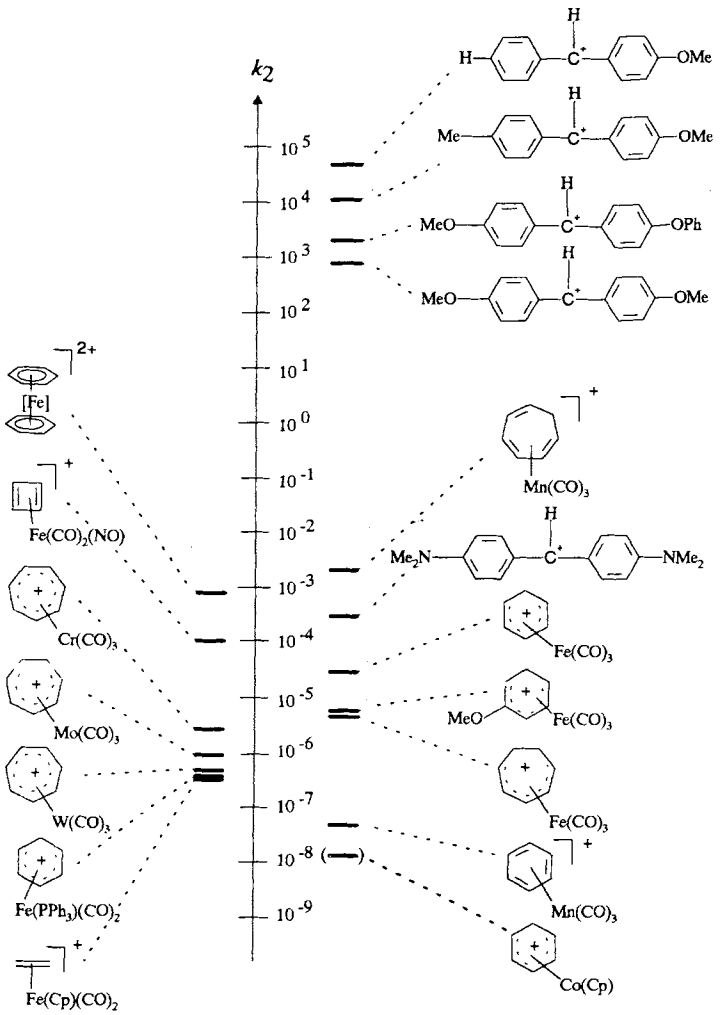

Fig. 3. Averaged reactivities of diarylcarbenium ions [6] and metal π complexes [2] toward nucleophiles (20 °C). Values in parentheses indicate electrophiles that have only been investigated with respect to one nucleophile.

ly,[13] predictions of reactivities in a wide field of organometallic chemistry are now possible.

Received: July 2, 1993 [Z 6184 IE]
German version: *Angew. Chem.* **1993**, *105*, 1732

[1] a) C. G. Swain, C. B. Scott, *J. Am. Chem. Soc.* **1953**, *75*, 141–146; b) J. O. Edwards, *ibid.* **1954**, *76*, 1540–1547; c) *ibid.* **1956**, *78*, 1819–1820; d) J. F. Bunnett, *Annu. Rev. Phys. Chem.* **1963**, *14*, 271–290; e) R. G. Pearson, H. Sobel, J. Songstad, *J. Am. Chem. Soc.* **1968**, *90*, 319–326; f) A. J. Parker, *Chem. Rev.* **1969**, *69*, 1–32; g) *Nucleophilicity* (Eds.: J. M. Harris, S. P. McManus) (*Adv. Chem. Ser.* **1987**, *215*).

[2] L. A. P. Kane-Maguire, E. D. Honig, D. A. Sweigart, *Chem. Rev.* **1984**, *84*, 525–543.

[3] The complexes **1a–c** are synthesized by hydride abstraction from the corresponding diene complexes [4], which are either prepared conventionally from iron carbonyl complexes and the corresponding diene [4], or preferentially according to a recent procedure by Knölker [5], which uses a 1-aza-1,3-butadiene as the catalyst for the transfer of the tricarbonyliron fragment to 1,3-dienes.

[4] a) B. F. Hallam, P. L. Pauson, *J. Chem. Soc.* **1958**, 642–645; b) T. H. Whitesides, R. A. Budni, *Inorg. Chem.* **1975**, *14*, 664–676; c) H. J. Dauben, D. J. Bertelli, *J. Am. Chem. Soc.* **1961**, *83*, 497–498.

[5] H.-J. Knölker, P. Gonser, *Synlett* **1992**, 517–520.

[6] a) G. Hagen, H. Mayr, *J. Am. Chem. Soc.* **1991**, *113*, 4954–4961; b) H. Mayr, N. Basso, *Angew. Chem.* **1992**, *104*, 1103–1105; *Angew. Chem. Int. Ed. Engl.* **1992**, *31*, 1046–1048; c) J. Bartl, S. Steenken, H. Mayr, *J. Am. Chem. Soc.* **1991**, *113*, 7710–7716; d) M. Patz, H. Mayr, *Tetrahedron Lett.* **1993**, *34*, 3393–3396.

[7] a) A. J. Birch, L. F. Kelly, A. S. Narula, *Tetrahedron* **1982**, *38*, 1813–1823; b) *Tetrahedron Lett.* **1979**, 4107–4110; c) C. Eaborn, G. R. John, T. I. Odiaka, L. A. P. Kane-Maguire, *J. Chem. Soc. Dalton Trans.* **1983**, 1721–1727.

[8] a) A. J. Birch, K. B. Chamberlain, M. A. Haas, D. J. Thompson, *J. Chem. Soc. Perkin Trans. 1* **1973**, 1882–1891; b) B. F. G. Johnson, J. Lewis, D. G. Parker, G. R. Stephenson, *J. Organomet. Chem.* **1980**, *197*, 67–75.

[9] All products not described in ref. [7] and [8] have been completely characterized by us (^{1}H and ^{13}C NMR spectroscopy, elemental analysis).

[10] D. A. Brown, W. K. Glass, F. M. Hussein, *J. Organomet. Chem.* **1981**, *218*, C15–C17.

[11] H. Mayr, R. Schneider, C. Schade, J. Bartl, R. Bederke, *J. Am. Chem. Soc.* **1990**, *112*, 4446–4454.

[12] D. A. Sweigart, T. J. Alavosus, *J. Am. Chem. Soc.* **1985**, *107*, 985–987.

[13] H. Mayr, J. Bartl, G. Hagen, *Angew. Chem.* **1992**, *104*, 1689–1691; *Angew. Chem. Int. Ed. Engl.* **1992**, *31*, 1613–1615.

Bromine Bromate Br_2O_3**

By *Raimund Kuschel* and *Konrad Seppelt**

Dedicated to Professor Wolfgang Sundermeyer on the occasion of his 65th birthday

Oxides of the halogens have been known for a long time.[1] However, much of the knowledge about them has only been gained over the past few years. Chloryl chloride (ClO_2–Cl)[2] and solid Cl_2O_6 as $ClO_2^+ClO_4^-$,[3] for example, were described only recently, as were the structure of solid Cl_2O_7[4] and the paramagnetic-diamagnetic transformation of ClO_2 in the solid state.[5] Whereas also most of the oxygen fluorides and the iodine oxides are well characterized, our knowledge about bromine oxides is limited. The only bromine oxide which could be identified with certainty, and of which the structure could be determined, is Br_2O.[6, 7]

There have been reports of another bromine oxide ("BrO_2"), which supposedly forms in a Br_2/O_2 gas (1:3) high-voltage discharge,[8] as well as during the ozonization of bromine in $CFCl_3$ at low temperatures.[9] In both cases, a yellow powder is obtained which decomposes when warmed to room temperature. From its Raman spectrum, "BrO_2" produced by ozonization was assumed to be $O_2Br–BrO_2$ with a $S_2O_4^{2-}$ or hydrazine structure.[10] Recently, "BrO_2" produced by the discharge route was reported to be really $Br–O–BrO_3$.[11] The main arguments for this assignment were 1) the EXAFS (*E*xtended *X*-ray *A*bsorption *F*ine *S*tructure) data 2) the Raman spectrum (though distinctly different from the one described in ref. [10]), and 3) the fact that BrO_4^- can be identified as one of the hydrolysis products.

It was our aim to characterize the "BrO_2" products unambiguously by single-crystal structure investigations. Ozonization of bromine in $CFCl_3$ yields a lemon-yellow precipitate which dissolves partly in CH_2Cl_2, forms an orange solution, and leaves an insoluble colorless solid. From the solution, orange needles crystallize at −90 °C. The crystals decompose above −40 °C and detonate if warmed rapidly to approximately 0 °C. The crystal structure investigation gave $Br–O–BrO_2$ **1** as the molecular composition (Fig. 1). Bromine bromate **1** is formally the anhydride of hypobromous and bromic acid. Some covalent hypobromites such as $BrO–SO_2F$,[12] $BrOSeF_5$,[13] $BrOTeF_5$,[13] $(BrO)_2TeF_4$,[14] $BrONO_2$,[15] $BrO–ClO_3$,[16] and only very

[*] Prof. Dr. K. Seppelt, Dr. R. Kuschel
Institut für Anorganische und Analytische Chemie der Freien Universität
Fabeckstrasse 34–36, D-14195 Berlin
Telefax: Int. code + (30)838-2424

[**] This work was supported by the Fonds der Chemischen Industrie.

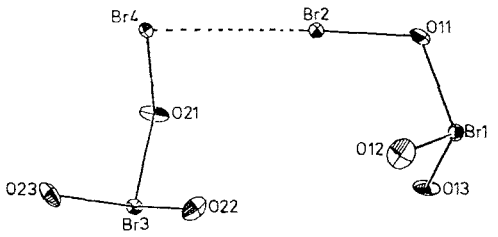

Fig. 1. The structure of $Br-O-BrO_2$ **1**. (ORTEP plot, thermal ellipsoids at 50% probability level). Distances [pm] and angles [°]: Br1-O11 184.9(5), Br1-O12 161.2(5), Br1-O13 162.0(5), Br2-O11 184.9(5), Br3-O21 186.0(5), Br3-O22 161.0(4), Br3-O23 160.5(4), Br4-O21 184.1(4), Br2···Br4 299.5(1); O11-Br1-O12 103.0(2), O11-Br1-O13 103.2(2), O12-Br1-O13 106.4(3), Br1-O11-Br2 111.2(2), O21-Br3-O22 103.5(2), O21-Br3-O23 102.8(2), O22-Br3-O23 108.8(2), Br3-O21-Br4 112.1(2), O11-Br2···Br4 175.9(2), O21-Br4···Br2 86.4(2).

few covalent bromates like O_2BrONO_2,[16] $O_2BrOClO_3$,[17] and $C_6F_5BrO_2$[18] are known. Crystal structure analyses of these compounds have not yet been reported.

The new bromine oxide **1** has bond lengths and bond angles in accord with the formula $Br-O-BrO_2$, that is, **1** has Br^V in a pyramidal environment with two short Br=O bonds and an angled Br-O-Br unit. The two crystallographically different but chemically identical molecules both have a *syn* conformation. Of particular note are the dimers of **1** in the crystalline solid with a Br···Br distance of 299.5(1) pm. This distance is even somewhat shorter than the intramolecular Br···Br distance of 305.0(1) pm. The directionality of this interaction is also indicated by the angles in the -O-Br···Br-O- bridge, which are 175.9(2) and 86.4(2)°.

A comparison between the structural data of **1** and those of the compound recently described as $Br-O-BrO_3$[11] reveals a striking resemblance. The latter was prepared with the discharge method and characterized by EXAFS as $BrO-BrO_3$. The EXAFS method determines fairly accurate bond lengths only if multiple scattering effects can be excluded or if they are properly considered. Moreover, the determination of the number of neighboring backscatterers (which is generally not very accurate) becomes impossible if perhaps polymorphic products or even product mixtures are investigated. A comparison of the Raman spectra also fails to decide if we have identical or different products. If we restrict ourselves to the prominent bands above 400 cm^{-1}, **1** absorbs at 449, 588, and 849 cm^{-1}. The postulated[11] $BrOBrO_3$ absorbs at 453, 582, and 842 cm^{-1}. If it is assumed that the local C_{3v} symmetry of the BrO_3 part of the molecule dominates the Raman spectrum, the spectra of the compounds could be indeed very similar. The detection of BrO_4^- among the hydrolysis products is only meaningful for a uniform product. The existence of $BrOBrO_3$ is therefore questionable.

None of our experiments resulted in a product with a prominent Raman band at $\tilde{\nu} = 205\ cm^{-1}$. The occurrence of this band had been the main argument for the existence of a bromine oxide formulated as $O_2Br-BrO_2$, which should now be regarded as a totally hypothetical entity.[10]

For the colorless residual bromine oxide, which precipitates on dissolution in CH_2Cl_2, we have as yet not found a suitable solvent. Its Raman spectrum shows it to be a new compound, and it seems to be more strongly oxidized, since the colorless-residue/Br_2O_3 ratio increases with increasing ozonization time. Its lack of coloration excludes the presence of a hypobromite group. We refrain from speculating about its structure at this point.[19] At any rate, if $Br-O-BrO_2$ **1** is the first traceable product during ozonization, it is fascinating to think that it might have been formed by a bimolecular reaction $Br_2 + O_3 \rightarrow Br_2O_3$.

Experimental Procedure

Ozone adsorbed on silica gel at −78 °C was passed very slowly between −50 − −60 °C through a solution of Br_2 in $CFCl_3$ with a stream of argon, until the brown color of the bromine in solution had almost disappeared. The lemon-yellow solid was freed from solvent and ozone under vacuum and dissolved in a little CH_2Cl_2 at −78 °C. The undissolved colorless bromine oxide was removed by low-temperature centrifugation. When the orange solution was cooled to −90 °C, Br_2O_3 crystallized in needles of the same color. Raman spectrum (solid, krypton ion laser, 647.0 nm): $\tilde{\nu}$ = 156, 167 m, sh, 325 $\delta_s(BrO_2)$ s, 387 w, 449 ν(BrOBr) s, 588 ν(BrOBr) s, 849 $\nu_s(BrO_2)$ s, 890 $\nu_{as}(BrO_2)$ w cm^{-1}. Crystal structure analysis: a = 1186.6(2), b = 762.9(1), c = 869.3(2) pm, β = 106.4(1)°, T = −145 °C, $P2_1/c$, Z = 8, μ = 208 cm^{-1}, 3029 measured reflections in the range θ = 2–35°, $\pm h, +k, +l$, 2800 unique reflections. R_{int} = 0.020, 2302 reflections with $I \geq 3\sigma(I)$. R = 0.046, R_w = 0.039. Further details of the crystal structure investigation may be obtained from the Fachinformationszentrum Karlsruhe, Gesellschaft für wissenschaftlich-technische Information mbH, D-76344 Eggenstein-Leopoldshafen (FRG), on quoting the depository number CSD-57429, the names of the authors, and the journal citation.

Received: June 5, 1993 [Z6126IE]
German version: *Angew. Chem.* **1993**, *105*, 1734

[1] H. Davy, *Philos. Trans.* **1811**, 155.
[2] H. S. P. Müller, H. Willner, *Inorg. Chem.* **1992**, *31*, 2527–2534.
[3] K. M. Tobias, M. Jansen, *Z. Anorg. Allg. Chem.* **1987**, *550*, 16–26.
[4] A. Simon, H. Borrmann, *Angew. Chem.* **1988**, *100*, 1386–1388; *Angew. Chem. Int. Ed. Engl.* **1988**, *27*, 1339–1341.
[5] A. Rehr, M. Jansen, *Inorg. Chem.* **1992**, *31*, 4740–4742.
[6] C. Campbell, J. P. M. Jones, J. J. Turner, *J. Chem. Soc. Chem. Commun.* **1968**, 888–889.
[7] W. Levason, J. S. Ogden, M. D. Spicer, N. A. Young, *J. Am. Chem. Soc.* **1990**, *112*, 1019–1022.
[8] R. Schwarz, M. Schmeisser, *Chem. Ber.* **1937**, *70*, 1163–1166.
[9] M. Schmeisser, K. Joerger, *Angew. Chem.* **1959**, *71*, 523–524.
[10] J.-L. Pascal, J. Potier, *J. Chem. Soc. Chem. Commun.* **1973**, 446–447.
[11] T. R. Gilson, W. Levason, J. S. Ogden, M. D. Spicer, N. A. Young, *J. Am. Chem. Soc.* **1992**, *114*, 5469–5470.
[12] D. D. DesMarteau, *Inorg. Chem.* **1968**, *7*, 434–437.
[13] K. Seppelt, *Chem. Ber.* **1973**, *160*, 157–164.
[14] B. Pötter, D. Lentz, H. Pritzkow, K. Seppelt, *Angew. Chem.* **1981**, *93*, 1095–1096; *Angew. Chem. Int. Ed. Engl.* **1981**, *20*, 1036–1037.
[15] M. Schmeisser, L. Taglinger, *Chem. Ber.* **1961**, *94*, 1533–1539.
[16] C. J. Schack, K. O. Christe, R. D. Wilson, *Inorg. Chem.* **1971**, *10*, 1078–1081.
[17] C. J. Schack, K. O. Christe, *Inorg. Chem.* **1974**, *13*, 2378–2381.
[18] W. Breuer, H. J. Frohn, *Z. Anorg. Allg. Chem.* **1993**, *619*, 209–214.
[19] M. Schmeisser, K. Brändle, *Adv. Inorg. Chem. Radiochem.* **1963**, *5*, 41–89. A summary of earlier work on $(Br_2O_5)_x$, $(Br_3O_8)_x$ and $(BrO_3)_x$. None of these bromine oxides is characterized unambiguously.

Double Lewis Acid Activation in Phosphate Diester Cleavage**

By *Mark Wall, Rosemary C. Hynes*, and *Jik Chin**

It has recently been shown that a number of important enzymes that hydrolyze phosphate diesters are activated by two metal ions. They include 3′-5′ exonuclease from DNA polymerase[1] as well as RNase H from HIV reverse transcriptase.[2] In order to investigate the cooperativity between adjacent metal ions for cleaving phosphate diesters, we compared the reactivities of a simple mononuclear and a simple dinuclear copper(II) complex, using 2-[bis(2-benzimidazolylmethyl)aminomethyl]-4,6-dimethylphenol (HL-1) and 2,6-bis[bis(2-benzimidazolylmethyl)aminomethyl]-4-methylphenol (HL-2), which are mono- and dinucleating ligands respectively (Fig. 1).[3] Here we report on the reactivity of the

[*] Prof. J. Chin, M. Wall, Dr. R. C. Hynes
Department of Chemistry, McGill University
801 Sherbrooke Street West, Montreal, Quebec H3A 2K6 (Canada)
Telefax: Int. code + (514)398-3797

[**] Financial support was provided by the National Science and Engineering Council of Canada and the US Army Research Office.

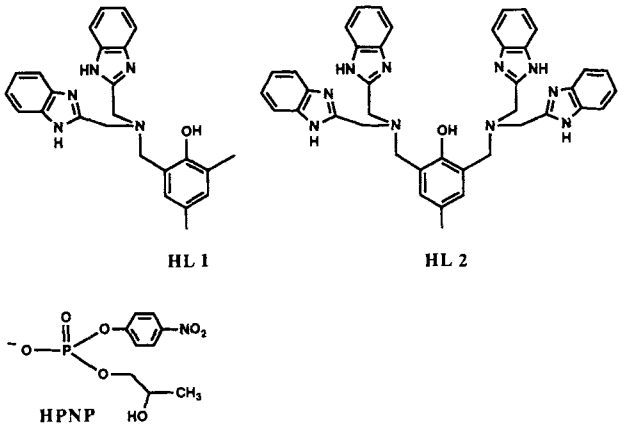

Fig. 1. Structures of HL-1, HL-2, and HPNP.

mononuclear copper (II) complex **1** and the dinuclear copper (II) complex **2** for cleaving 2-hydroxypropyl-*p*-nitrophenylphosphate (HPNP).

[(L-1)CuCl] **1**
[(L-2)Cu_2Cl_2]Cl **2**

There is considerable interest in developing catalysts that hydrolyze RNA. Many artificial enzymes that hydrolyze RNA or simple RNA models (e.g. HPNP) have been reported to date. They include nonmetallic compounds,[4] as well as mononuclear transition metal[5] complexes and lanthanide complexes.[6] In nature there are many DNases and RNases that are activated by two metal ions. Crystal structures reveal that both 3′-5′ exonuclease[1] and RNase H from HIV reverse transcriptase[2] contain two metal ions at the active site. There is evidence that the *Tetrahymena* ribozyme is also activated by two metal ions.[7] Site-directed mutagenesis may shed some light into the role of each metal ion in the enzymes. However, it would be easier to evaluate whether two metals could be better than one as catalysts in simple chemical systems rather than in complex biological systems. Interestingly, **2** is more reactive than **1** for cleaving HPNP. The pseudo first-order rate constants for cleavage of HPNP (50 μM) catalyzed by **1** or **2** (1 mM) at 25 °C and pH 7 are $4.0 \times 10^{-5}\,s^{-1}$ and $2.1 \times 10^{-3}\,s^{-1}$, respectively. The dinuclear **2** cleaves HPNP by intramolecular transesterification rather than by oxidation. The products of the cleavage of HPNP catalyzed by **2**, as detected by ^1H and ^{31}P NMR, are *p*-nitrophenol and the cyclic phosphate.

To gain some insight into the mechanistic role of the dinuclear complex in cleaving HPNP we obtained a crystal structure of dibenzyl phosphate (DBP) coordinated to the copper complex **3**.[8] The crystal structure reveals that both oxygen atoms of the phosphate diester are coordinated to metal centers of the dinuclear complex to form a bridged structure (Fig. 2). The distance between the two metal centers in **3** (3.67 Å) is comparable to that in 3′-5′ exonuclease (3.8 Å) and HIV RNase H (4 Å). We propose that the key to the reactivity of **2** for cleaving HPNP is double Lewis acid activation of the phosphate diester (Fig. 3). Double Lewis acid activation should be particularly effective for cleaving phosphate diesters bound to a nucleophile (for instance, RNA or HPNP).[9] Single Lewis acid activation in combination with intramolecular metal hydroxide activation has been shown to be effective for hydrolyzing phosphate diesters not bound to a nucleophile (dimethyl phosphate, bis(*p*-nitrophenyl)phosphate).[10] Intramolecular metal-hydroxide activation should not provide much rate-acceleration for cleaving phosphate diesters that are already bound to a nucleophile.

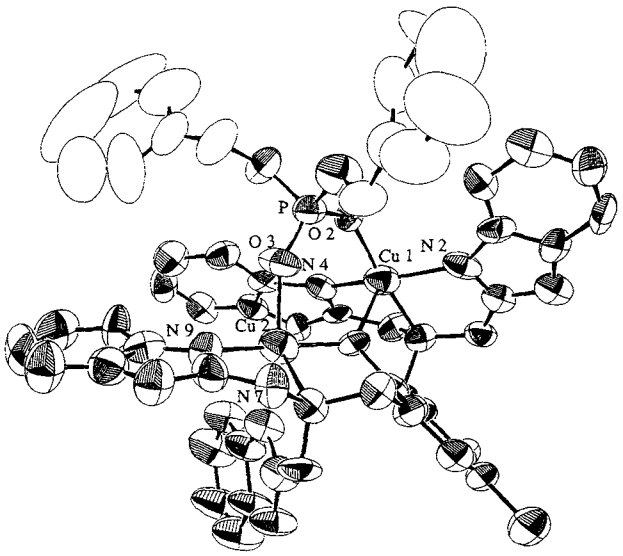

Fig. 2. View of cation in **3** (ORTEP ellipsoids at the 50% probability level). Selected bond lengths [Å] and angles [°]: Cu1–Cu2 3.670(4), O2–O3 2.496(18); N2–Cu1–N4 152.8(6), N7–Cu2–N9 91.1.

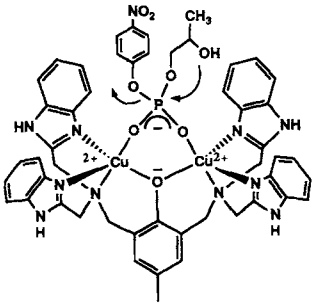

Fig. 3. Proposal for the mechanism of double Lewis acid activation for HPNP cleavage.

([(L2)Cu_2(DBP)]$(ClO_4)_2$ **3**

Over the years, many elegant dinuclear metal complexes with bridging carboxylates or phosphates have been synthesized as spectroscopic models for dimetallic enzymes.[11] In contrast, functional models of dimetallic enzymes are scarce. Dinuclear **2** is not only more reactive for cleaving HPNP than mononuclear **1**, but also significantly more reactive than previously reported nonmetallic catalysts,[4e] and than mononuclear transition metal complexes[5g] and lanthanide complexes.[6c, d]

Experimental Procedure

Compound **3** was prepared by adding sodium dibenzyl phosphate (10 μmol) to an ethanolic solution of HL-2 (10 μmol) and $Cu(ClO_4)_2$ (20 μmol). The crude product was recrystallized from ethanol by slow evaporation to yield thin greenish plates.

The cleavage of the barium(II) salt of HPNP was followed by monitoring the increase in the visible absorbance at 400 nm caused by release of the *p*-nitrophenolate ion. In a typical kinetic experiment, 5 mL of a 0.01 M stock solution of HPNP in water was added to 1 mL of a solution of **1** or **2** (0.5 to 1 mM) at 25 °C and pH 7.0. The rate constants were obtained by fitting the first three half-lives of the reaction to a first-order rate low (correlation coefficient >0.996). Each kinetic run was reproducible to within 3% error. The pH of the reaction solution did not change appreciably during the course of the hydrolysis as a result of the buffering effect of the metal complex solution. In water, the coordinated

chloride atoms are replaced by solvent molecules. Potentiometric titration reveals that the pK_a values of the two bound water molecules in $[(L\text{-}2)Cu_2(H_2O)_2]^{3+}$ are 6.7 and 7.2. The pK_a value of the bound water molecule in $[(L\text{-}1)Cu(H_2O)]^+$ is 6.6.

Received: June 23, 1993 [Z 6160 IE]
German version: *Angew. Chem.* **1993**, *105*, 1696

[1] L. S. Beese, T. A. Steitz, *EMBO J.* **1991**, *10*, 25.
[2] J. F. Davies, Z. Hostomska, Z. Hostomsky, S. R. Jordan, D. A. Mathews, *Science* **1991**, *252*, 88.
[3] P. B. Hilde, D. W. Stephan, *Inorg. Chem.* **1987**, *26*, 749.
[4] a) J. Smith, K. Ariga, E. V. Anslyn, *J. Am. Chem. Soc.* **1993**, *115*, 362; b) R. Breslow, M. Labelle, *ibid.* **1986**, *108*, 2655; c) B. Barbier, A. Brack, *ibid.* **1992**, *114*, 3511; d) M. W. Göbel, J. W. Bats, G. Dürner, *Angew. Chem.* **1992**, *104*, 217; *Angew. Chem. Int. Ed. Engl.* **1992**, *31*, 207; e) V. Jubian, R. P. Dixon, A. Hamilton, *J. Am. Chem. Soc.* **1992**, *114*, 1120.
[5] a) J. Chin, *Acc. Chem. Res.* **1991**, *25*, 145; b) M. K. Stern, J. K. Bashkin, E. D. Sall, *J. Am. Chem. Soc.* **1990**, *112*, 5357; c) W. R. Farkas, *Biochim. Biophys. Acta* **1968**, *155*, 401; d) M. Sundaralingam, J. R. Rubin, J. F. Cannon, *Int. J. Quantum Chem. Quantum Biol. Symp.* **1984**, *11*, 355; e) Y. Matsumoto, M. Komiyama, *J. Chem. Soc. Chem. Commun.* **1990**, 1050; f) J. J. Butzow, G. L. Eichhorn, *Biopolymers* **1965**, *3*, 95. g) R. Breslow, D. L. Huang, E. Anslyn, *Proc. Natl. Acad. Sci. USA* **1989**, *86*, 1746.
[6] a) G. L. Eichhorn, J. J. Butzow, *Biopolymers* **1965**, *3*, 79; b) J. R. Morrow, L. A. Buttrey, V. M. Shelton, K. A. Berback, *J. Am. Chem. Soc.* **1992**, *114*, 1903; c) R. Breslow, D. L. Huang, *Proc. Natl. Acad. Sci. USA* **1991**, *88*, 4080; d) J. R. Morrow, L. A. Buttrey, K. A. Berback, *Inorg. Chem.* **1992**, *31*, 16.
[7] T. Cech (University of Colorado), private communication.
[8] Crystal structural data of **3**: triclinic, $P\bar{1}$, $a = 14.402(3)$, $b = 15.635(3)$, $c = 15.634(3)$ Å, $\alpha = 94.819(17)$, $\beta = 96.546(16)$, $\gamma = 117.213(12)°$, $V = 3073.3(10)$ Å^3, $Z = 2$; 6681 measured reflections, 2931 with $I > 2.5\,\sigma(I)$, 322 refined parameters, $R = 0.089$. Futher details of the crystal structure investigation may be obtained from the Fachinformationszentrum Karlsruhe, Gesellschaft für wissenschaftlich-technische Information mbH, D-76344 Eggenstein-Leopoldshafen (FRG), on quoting the depository number CSD-57635, the names of the authors, and the journal citation.
[9] The difference in the reactivity of **1** and **2** may also be in part due to the difference in the equilibrium constant for coordination of the substrate to the catalysts.
[10] a) J. H. Kim, J. Chin, *J. Am. Chem. Soc.* **1992**, *114*, 9792; b) B. K. Takasaki, J. H. Kim, E. Rubin, J. Chin, *ibid.* **1993**, *115*, 1157; c) J. H. Kim, J. Britten, J. Chin, *ibid.* **1993**, *115*, 3618; d) J. Chin, M. Banaszczyk, V. Jubian, X. Zou, *ibid.* **1989**, *111*, 186.
[11] a) K. Schepers, B. Bremer, B. Krebs, G. Henkel, E. Althaus, B. Mosel, W. Müller-Warmuth, *Angew. Chem.* **1990**, *102*, 582; *Angew. Chem. Int. Ed. Engl.* **1990**, *29*, 531. b) S. Uhlenbrock, B. Krebs *ibid.* **1992**, *104*, 1631 and **1992**, *31*, 1647; c) M. Suzuki, H. Kanatomi, I. Murase, *Chem. Lett.* **1983**, 185; d) W. H. Armstrong, A. Spool, G. C. Papaefthymiou, R. B. Frankel, S. J. Lippard, *J. Am. Chem. Soc.* **1984**, *106*, 4632.

catalytic cycle of iron-containing heme peroxidases.[4] Notably all structurally characterized iron(IV) model complexes to date have the t_{2g}^4 low-spin configuration with a triplet ground state ($S = 1$) regardless of the coordination number at the iron(IV) center (five or six).[11]

Inspired by the work of Gerbeleu et al. and Leovac et al.,[3] who showed that the trianionic pentane-2,4-dione-bis(*S*-alkylisothiosemicarbazonate), a porphyrin-like, four-coordinate ligand L^{3-}, can form stable square-pyramidal iron(IV) complexes $[Fe^{IV}(L^{3-})X]$ (X = Cl, Br, I, NCO, NCS[3a]) and $[(Fe^{IV}L)_2(\mu\text{-}O)]$,[3b] we determined the crystal structure of the *S*-methyl derivative $[Fe^{IV}(L^{3-})I]$ (**1**, Scheme 1 and Fig. 1, top). The structure is very similar to the

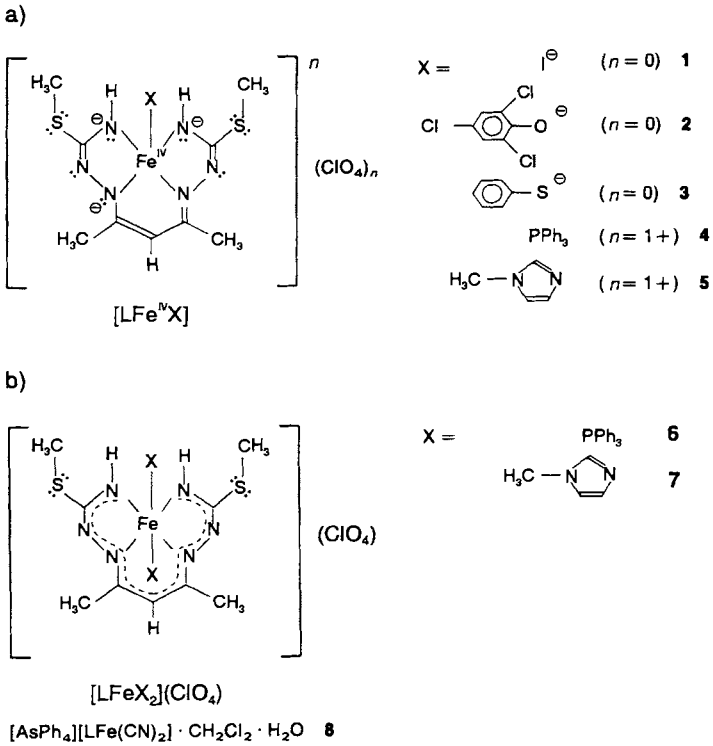

Scheme 1. Synthesized square-pyramidal (a) and octahedral (b) iron complexes **1**–**8**.

How "Innocent" Are Pentane-2,4-dione-bis(*S*-alkylisothiosemicarbazonato) Ligands in Biomimetic Fe^{II} and Fe^{IV} Complexes?**

By *Ulrich Knof, Thomas Weyhermüller, Thomas Wolter, Karl Wieghardt,* Eckhard Bill, Christian Butzlaff,* and *Alfred X. Trautwein*

In recent years a few square-pyramidal and octahedral iron(IV) complexes have been isolated and structurally characterized.[1–3] Complexes of this type have been studied in detail, as compounds with iron in the +IV oxidation state have been shown by spectroscopy to be intermediates in the analogous S-ethyl complex.[3a, 5] The iodide ion in **1** was then exchanged for the biomimetic ligands, thiophenolate and *N*-methylimidazole, as well as 2,4,6-trichlorophenolate and triphenylphosphane, to form **2**–**5** (Scheme 1). The new five-coordinate complexes **2**–**5** were isolated as analytically pure species; as expected they have an $S = 1$ ground state (see Table 1).

We then noticed that the reaction of $[(Fe^{IV}L)_2(\mu\text{-}O)]$[3b] in $CHCl_3$ with a large excess of PPh_3 or *N*-methylimidazole gave the octahedral complexes **6** and **7** after the addition of some aqueous $HClO_4$ [Eq. (a)]. Treatment of **1** with KCN in

$$[(LFe^{IV})_2(\mu\text{-}O)] + 4X + 2H^+ \longrightarrow 2[FeL(X)_2]^+ + H_2O \qquad (a)$$

6: X = PPh_3
7: X = $CH_3\text{–}C_3H_3N_2$ (in CH_2Cl_2)

a two-phase CH_2Cl_2/H_2O mixture, followed by addition of $[AsPh_4]Cl$, gave black crystals of **8**, the structure of which has been determined by X-ray crystallography (Fig. 1 bottom).[5]

The complexes **6** and **7** can also be obtained from solutions of **4** and **5** in CH_2Cl_2 with an excess of PPh_3 or *N*-methylim-

[*] Prof. Dr. K. Wieghardt, Dipl.-Chem. U. Knof, Dipl.-Chem. T. Weyhermüller, Dipl.-Chem. T. Wolter
Lehrstuhl für Anorganische Chemie I der Universität
Postfach 102148, D-44780 Bochum (FRG)
Telefax: Int. code + (234)7094-201
Dr. E. Bill, Dipl.-Phys. C. Butzlaff, Prof. Dr. A. X. Trautwein
Institut für Physik der Medizinischen Universität
Ratzeburger Allee 160, D-23538 Lübeck (FRG)

[**] This work was funded by the Fonds der Chemischen Industrie and the Deutsche Forschungsgemeinschaft.

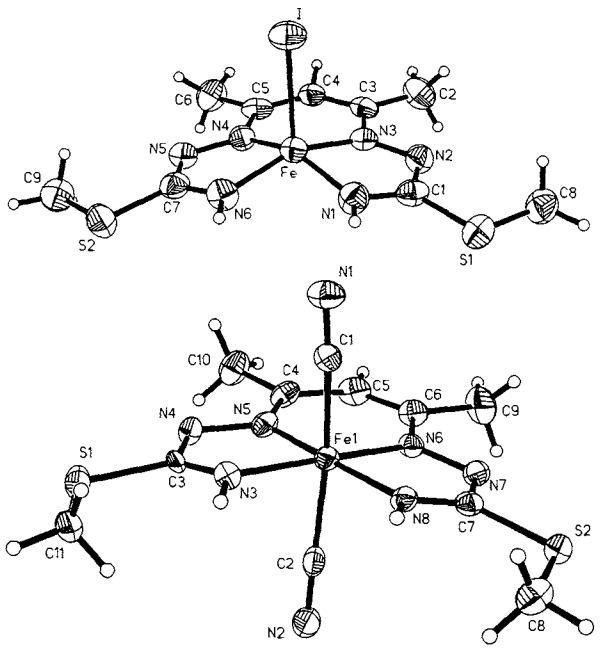

Fig. 1. The structure of the neutral complex in **1** (above) and one of the crystallographically independent monoanions in **8** (below). Selected bond distances [Å] and angles [°]: **1**: Fe-I 2.593(2), Fe-N1 1.87(1), Fe-N3 1.890(9), Fe-N4 1.882(9), Fe-N6 1.860(9), N1-C1 1.32(1), C1-N2 1.32(2), N2-N3 1.37(1), N3-C3 1.37(2), C3-C4 1.40(2), C4-C5 1.36(2), N4-C5 1.36(2), N4-N5 1.36(1), N5-C7 1.34(2), C7-N6 1.32(1), C1-S1 1.73(1), C7-S2 1.75(1); N1-Fe-N3 79.1(4), N3-Fe-N4 93.2(4), N3-Fe-N6 153.3(4), N1-Fe-N4 152.2(4), N1-Fe-N6 95.5(4), N4-Fe-N6 79.4(4), Fe-N1-C1 115.2(9), N1-C1-N2 118.4(10), C1-N2-N3 108.8(9), N2-N3-C3 116.7(9), N3-C3-C4 118.9(10), C3-C4-C5 130.0(10), C4-C5-N4 121.1(10), C5-N4-N5 115.9(9), N4-N5-C7 106.5(8), N5-C7-N6 120.0(10).—**8**: C1-N1 1.154(8), C2-N2 1.151(9), Fe-C1 1.955(6), Fe-C2 1.947(7), Fe-N3 1.969(5), Fe-N5 1.874(5), Fe-N6 1.839(5), Fe-N8 1.965(5), S1-C3 1.764(6), S1-C11 1.799(7), S2-C7 1.757(7), S2-C8 1.790(7), N3-C3 1.295(8), N4-C3 1.330(9), N4-N5 1.374(7), N5-C4 1.329(8), C4-C5 1.396(10), C5-C6 1.37(1), N6-C6 1.362(8), N6-N7 1.364(7), N7-C7 1.354(8), N8-C7 1.285(8), C6-C9 1.513(10), C4-C10 1.51(1); C1-Fe1-C2 166.5(3), C1-Fe1-N3 85.8(2), C2-Fe1-N3 82.9(2), C1-Fe1-N5 91.2(2), C2-Fe1-N5 94.1(2), N3-Fe1-N5 80.5(2), C1-Fe1-N6 96.8(2), C2-Fe1-N6 94.9(2), N3-Fe1-N6 176.4(2), N5-Fe1-N6 96.9(2), C1-Fe1-N8 90.6(2), C2-Fe1-N8 84.7(2), N3-Fe1-N8 102.2(2), N5-Fe1-N8 176.8(2), N6-Fe1-N8 80.3(2), Fe1-C1-N1 177.3(5), Fe1-C2-N2 175.2(6).

idazole. The formation constants of **6** ($K(\mathbf{6}) = 200\ \mathrm{M}^{-1}$) and **7** ($K(\mathbf{7}) = 1400\ \mathrm{M}^{-1}$) [Eq. (b)] were determined spectrophotometrically at 20 °C (inset, Fig. 2). The cyanoiron complex **8** is so stable in CH_2Cl_2 that no dissociation could be detected by spectrophotometry.

$$\underset{\mathbf{4,5}}{[FeLX]^+ + X} \rightleftharpoons \underset{\mathbf{6,7}}{[FeL(X)_2]^+} \qquad \text{(b)}$$

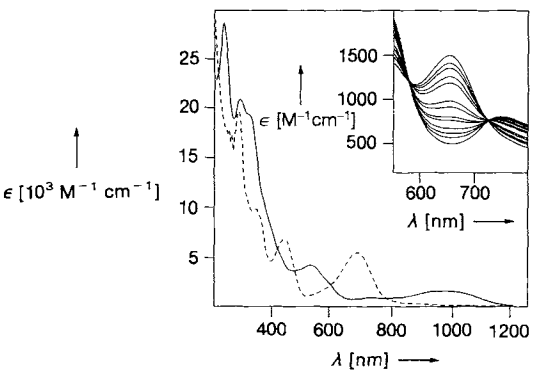

Fig. 2. Electronic spectra of **1** (–) and **8** (···) in CH_3CN. The inset shows the conversion **4** + PPh_3 ⇄ **6**, monitored by spectrophotometry ([**4**] = 3×10^{-4} M, [PPh_3] = $(0.08 \cdots 6.9) \times 10^{-2}$ M).

Magnetic susceptibility values (Fig. 3) measured as a function of temperature, as well as Mössbauer spectra (Fig. 4) recorded with and without an applied external field (4.96–2.45 T) clearly show that complexes **1**–**5** have a triplet ground state ($S = 1$). Adjusted calculations for **1** for both

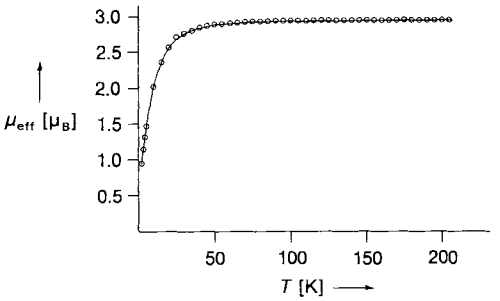

Fig. 3. Temperature dependence of the effective magnetic moment (μ_{eff}) of **1**. The curve represents the fitted ligand-field model described in the text for a $3d^4$ electron configuration ($S = 1$).

methods by using the spin-Hamiltonian operator $\mathcal{H}_e = D[S_z^2 - {}^2/_3 + E/D(S_x^2 - S_y^2)] + \mu_{Bohr}\vec{S}g\vec{B}$ for $S = 1$ gave the following parameters: zero-field splitting $D = +30\ \mathrm{cm}^{-1}$ and rhombicity $E/D = 0.28$. Due to the size of the zero-field splitting the g values of iron are correlated with the zero-field parameters in the spin-Hamiltonian simulation. On the basis of the ligand-field model for the low-spin t_{2g}^4 ($S = 1$) configuration,[6] the g values are found to be (2.19, 2.35, 1.99) if a one-electron spin-orbit coupling constant $\zeta = 500\ \mathrm{cm}^{-1}$ is assumed.

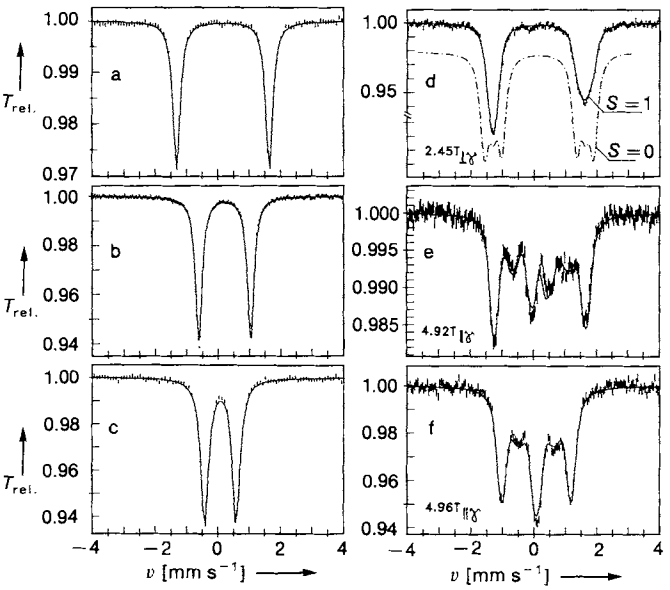

Fig. 4. Mössbauer spectra of **1** (a, d), **6** (b, e) and **8** (c, f) at 4.2 K with (d, e and f) and without (a, b, and c) an external field. The solid lines in a, b, and c are fitted Lorentz curves. In d the solid line is obtained from a simulation with the spin-Hamiltonian operator with $S = 1$ and the parameters given in the text and in Table 1, together with the asymmetry parameter $\eta = 1$ and the hyperfine coupling constant $A = (-20, -12, -20)$ T. The dashed line in d and the solid lines in e and f fit the usual nuclear-Hamiltonian operator for an external field with quadrupolar splittings as in Table 1 ($\eta = 0.8$ for e and $\eta = 1$ for f); in this case the valence shell of the iron center does not contribute to the magnetic splitting. The simulation in f was calculated with an effective outer field of 4.6 T, which is reduced by 0.36 T compared to the actual applied field of 4.96 T [7].

In stark contrast to this, the six-coordinate complexes **6**, **7**, and **8** have a singlet ground state ($S = 0$) and are diamagnetic (a small residual magnetism remains, which is caused either by small amounts of an impurity that is five-coordinate ($S = 1$), or by a weak orbital moment). The Mössbauer spectra measured with an externally applied field prove that **6**–**8** have singlet ground states[7] (Fig. 4).

The quadrupolar splitting of all complexes is practically temperature independent, which rules out energetically low-lying excited electron states; the splitting is smaller for the more symmetric octahedral complexes **6**–**8** than for the square-pyramidal complexes **1**–**5**. The low isomer shifts, similar for all complexes, in the region 0.06–0.18 mm s^{-1} are in agreement with known Fe^{IV} complexes.[1–3]

Although it seems theoretically possible for the complexes **6**–**8** to have a diamagnetic ground state with an iron(IV) t_{2g}^4 electron configuration (low low spin), which would be in agreement with the Mössbauer spectra and magnetic properties, the fact that the neutral octahedral Fe^{IV} complexes **9** of Collins et al.[2b] and also Sellmann's complex **10**[1b] have a triplet ground state must cast some doubt on this. Instead of Fe^{IV} complexes, **6**–**8** might be low-spin Fe^{II} complexes with $S = 0$. The question then is whether L^{3-} is an electronically 'innocent ligand', or whether it can also be thought of as the monoanion L^-.[8]

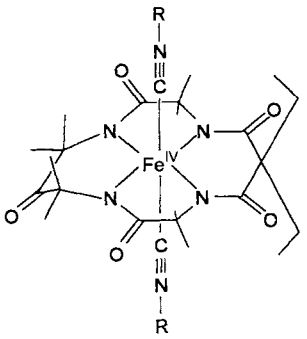

9

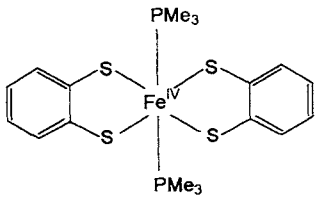

10

The two resonance forms L^{3-} and L^- in Scheme 2 show that L^{3-} is a 14π-electron system, and L^-, its oxidized form, is a 12π electron system. The trianion L^{3-} has four delocalized double bonds, whilst the monoanion L^- has five. It is therefore to be expected that the sum of the C–N, N–N, and C–C bond lengths of the ligand π-electron system in ML^{3-} and ML^- complexes will be different; the sum for the former should be somewhat greater than the sum for the latter. For calibration we used the complex $[Cu^{III}(L^{3-})]$,[9] which we recently reported and which is diamagnetic with an essentially square-planar CuN_4 coordination geometry. Formulation as $[Cu^{I}(L^-)]$ is out of the question, as this would be expected to have tetrahedral CuN_4 geometry. The sum of the distances $\Sigma[6(C-N) + 2(N-N) + 2(C-C)]$ comes to 13.546 Å for this complex. For **1**, its *S*-ethyl derivatives,[3a] and $[\{Fe^{IV}(L^{3-})\}_2(\mu\text{-O})]$,[3b] these sums are 13.503, 13.491, and 13.495 Å, respectively, and for the two crystallographically independent anions in **8**, the average value is 13.470 Å. Remarkably, **8** has the smallest and $[Cu^{III}L]$ the largest total. We therefore suggest that **8** may be written as $[Fe^{II}(L^-)(CN)_2]^-$. A similar trend is found on considering only the C–NH bond lengths, which should have more single-bond character in L^{3-} than in L^-. In $[Cu^{III}L]$, **1**, its *S*-ethyl derivatives, and $[\{Fe^{IV}(L^{3-})\}_2(\mu\text{-O})]$, these distances are 1.319, 1.314, 1.332 and 1.318 Å, respectively, whilst in **8** this distance is significantly shorter (1.285 Å).

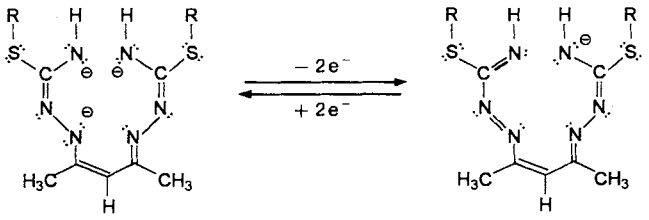

Scheme 2. Resonance forms of the trianion L^{3-} and the monoanion L^-.

These considerations all suggest that the structures **1**–**5** are correctly described as Fe^{IV} complexes, whilst **8** (and because of their similar electronic spectra (Table 1) **6** and **7**, too) should be considered to be octahedral, low-spin Fe^{II} complexes.

Cyclic voltammetry and coulometry of **8** gave further evidence for the validity of the above hypothesis.[10] A quasi-reversible one-electron *oxidation* is observed at a redox potential of 0.30 V vs. the standard hydrogen electrode (SHE), which is attributed to the redox pair $[Fe^{II}(L^-)(CN)_2]^-/$

Table 1. UV/VIS and Mössbauer spectra together with magnetic properties of the iron complexes **1**–**8** [a, b].

Complex	CN [c]	λ_{max} [nm] (ε[10^3 L mol^{-1} cm^{-1}])	δ [mm s^{-1}]	ΔE_q [mm s^{-1}]	Γ [mm s^{-1}]	μ_{eff} μ_B(295 K)
1	5	256 (26.2), 308 (18.8), 330 (16.3), 376 (10.0; sh), 526 (4.1), 580 (2.4; sh), 737 (1.0), 956 (1.6),	0.17	2.96	0.27	2.91
2	5	249 (14.8), 295 (13.9), 336 (6.8; sh), 380 (4.1; sh), 520 (2.9; sh), 549 (2.9), 704 (0.9), 921 (1.1),	0.18	2.37	0.32	2.89
3	5	233 (19.2), 339 (16.9), 418 (5.4; sh), 490 (4.1; sh) 515 (4.1), 628 (1.8), 736 (1.7), 881 (1.2)	0.10	2.70	0.26	2.92
4	5	258 (15.6), 349 (7.6), 429 (3.6; sh), 521 (2.0; sh) 764 (0.7), 952 (0.7)	0.06	2.92	0.26	2.75
5	5	257 (16.9), 299 (12.5), 335 (11.8), 409 (6.1; sh), 508 (2.5; sh), 525 (2.6), 723 (0.7), 986 (1.4)	[d]	[d]	[d]	2.9
6	6	352 (9.5; sh), 449 (2.7; sh), 542 (1.2; sh), 580 (2.4; sh), 652 (1.4)	0.22	1.66	0.26	1.1
7	6	269 (17.5), 303 (8.7; sh), 372 (4.9), 494 (2.6) 672 (0.8), 814 (1.8)	0.22	1.82	0.28	1.2
8	6	294 (17.8), 354 (8.5), 446 (6.2), 687 (5.0)	0.08	1.01	0.29	0.75

[a] UV/VIS spectra: solvent CH_2Cl_2. [b] Mössbauer spectra: measured at 4.2 K in zero-field; the isomer shift δ is relative to α-Fe at 298 K; ΔE_Q = quadrupolar splitting; Γ = line width at half height. [c] CN = coordination number. [d] Not measured.

$[Fe^{III}(L^-)(CN)_2]$. However complexes **9**[2b] and **10**[1b] showed quasi-reversible *reductions* at 1.16 V and −0.28 V vs. SHE, as did **1**–**5**[10] ($E_{1/2}(Fe^{IV}/Fe^{III})$: **1**, −0.37; **2**, −0.33; **3**, −0.66; **4**, −0.10; **5**, −0.19 V vs. SCE).

If **6**, **7**, and **8** are indeed Fe^{II} complexes and **4** and **5** Fe^{IV} complexes, then the formation (b) of octahedral complexes from square-pyramidal substrates can be described as reductive addition and the reverse reaction as oxidative elimination. Finally, in answer to the question posed in the title we have shown that the ligand can coordinate as a 14π- or 12π-electron system; it is therefore definitely not electronically 'innocent'.

Experimental Procedure

Complex **1** and $[(FeL)_2(\mu\text{-}O)]$ were synthesized according to literature methods [3]. All following syntheses were carried out in an argon atmosphere. All complexes gave good elemental analyses for C, H, N and Fe.

2 and **3**: A solution of $[(FeL)_2O]$ (0.10 g; 0.15 mmol) in $CHCl_3$ (10 mL) was treated with either 2,4,6-trichlorophenol (0.30 mmol) or thiophenol (0.75 mmol) and stirred for 3 h at 20 °C, whereupon the green solution turned red-brown. After separation of the $CHCl_3$ layer and overlaying with *n*-pentane (10 mL) for 12 h at −20 °C, red-brown microcrystals of **2** or **3** separated (56 and 38% yield, respectively). IR(KBr): ν(N–H) [cm^{-1}]: **2**, 3310(s); **3**, 3330(s).

4 and **5**: To a solution of $[(FeL)_2O]$ (0.10 g, 0.15 mmol) in $CHCl_3$ (10 mL) were added either PPh_3 (0.30 mmol) or *N*-methylimidazole (0.30 mmol). After addition of 5 mL of a 6 mM aqueous solution of $HClO_4$ containing $NaClO_4$ (0.20 g), the solution was stirred vigorously for 1 h at 20 °C. The resulting red-brown $CHCl_3$ layer was separated off, overlaid with *n*-pentane (10 mL), and left to stand for 12 h at −20 °C, whereupon red-brown microcrystals formed (yield: **4**, 51%; **5**, 45%). IR(KBr): ν(N–H) [cm^{-1}]: **4**, 3340(s); **5**, 3300(s).

6 and **7**: Both complexes were synthesized similarly to **4** and **5**, by addition of PPh_3 or *N*-methylimidazole, respectively, (5 mmol) and enough 6 mM $HClO_4$ solution to make the aqueous phase slightly acidic. Green microcrystals formed in 42% (**6**) and 68% (**7**) yield. IR(KBr): ν(N–H) [cm^{-1}]: **6**, 3350(s) and 3340; **7**, 3350(s).

8: A solution of **1** (0.20 g; 0.44 mmol) in CH_2Cl_2 (100 mL) was overlaid with H_2O (50 mL) and treated with KCN (1.0 g, 15 mmol) with vigorous stirring at 20 °C. Initially the organic layer, and then after a few minutes, also the aqueous layer, turned dark green. After 30 min the aqueous layer was separated off and treated with $[AsPh_4]Cl$ (0.5 g, 1.2 mmol), whereupon black-green microcrystals of **8** separated in 72% yield. The CH_2Cl_2 layer could be extracted further by addition of H_2O. Single crystals were obtained by slow diffusion of *n*-pentane into a CH_2Cl_2 solution of **8**. IR(KBr) [cm^{-1}]: $\nu(OH_2)$: 3440, 3527; ν(NH) = 3366; ν(CN) = 2098. ^1H NMR (80 MHz, $CDCl_3$): δ = 6.17 (s, 2H), 5.26 (s, 1H), 2.53 (s, 6H), 2.47 (s, 6H).

Received: May 26, 1993 [Z 6107 IE]
German version: *Angew. Chem.* **1993**, *105*, 1701

[1] Fe^{IV} complexes with S-donor ligands: a) D. Petridis, D. Niarchos, B. Kanellakopulos, *Inorg. Chem.* **1979**, *18*, 505; b) D. Sellmann, M. Geck, F. Knoch, G. Ritter, J. Dengler, *J. Am. Chem. Soc.* **1991**, *113*, 3819.

[2] Fe^{IV} complexes with macrocyclic N_4-donor ligands: a) T. J. Collins, K. L. Kostka, E. Münck, E. S. Uffelmann, *J. Am. Chem. Soc.* **1990**, *112*, 5637; b) T. J. Collins, B. G. Fox, Z. G. Hu, K. L. Kostka, E. Münck, C. E. F. Rickard, L. J. Wright, *ibid.* **1992**, *114*, 8724; c) W. Hiller, J. Strähle, M. Hanack, W. E. Hatfield, L. W. Haar, P. Gütlich, *ibid.* **1984**, *106*, 329; d) G. T. Groves, R. C. Haushalter, M. Nakamura, T. E. Nemo, B. J. Evansk, *ibid.* **1981**, *103*, 2884.

[3] Fe^{IV} complexes with bis(*S*-alkylthiosemicarbazonate) ligands. a) N. V. Gerbeleu, Y. A. Simonov, V. B. Arion, V. M. Leovac, K. I. Turta, K. M. Indrichan, D. I. Gradinaru, V. E. Zavodnik, T. I. Malinovskii, *Inorg. Chem.* **1992**, *31*, 3264; b) V. M. Leovac, R. Herak, B. Prelesnik, S. R. Niketic, *J. Chem. Soc. Dalton Trans.* **1991**, 2295; c) V. M. Leovac, L. S. Jovanovic, V. I. Cesljevic, L. J. Bjelica, N. J. Evic, *Polyhedron* **1992**, *11*, 1029.

[4] a) *Cytochrome P-450. Structure, Mechanism and Biochemistry* (Ed.: P. R. Ortiz de Montellano), Plenum, New York, **1986**; b) *Molecular Mechanisms of Oxygen Activation* (Ed: O. Hayaishi), Academic Press, New York **1974**.

[5] Crystal structures: **1**: a = 13.966(3), b = 11.871(2), c = 19.367 Å, space group *Pbca*, Z = 8, R = 0.059, R_w = 0.058; measurements were carried out on a Siemens P4 diffractometer at 293 K using monochromatized (graphite single crystal) $Mo_{K\alpha}$ radiation, ω-scan $3° \le 2\theta \le 50°$, 2760 independent reflections ($F > 4.0\sigma(F)$), all non-hydrogen atoms anisotropic, structure solution and refinement by SHELXTL-PLUS (VMS). All H atoms were located and their positions refined with isotropic thermal parameters. **8**: a = 10.969(2), b = 16.346(3), c = 22.382(4) Å, α = 78.74(3), β = 88.92(3), γ = 85.20(3)°, space group $P\bar{1}$, Z = 4, R = 0.056, R_w = 0.058; Siemens P4 diffractometer, intensity measurement at 173 K with $Mo_{K\alpha}$ radiation (graphite monochromator), ω-scan, $3° \le 2\theta \le 50°$, 8717 independent reflections ($F > 4.0\sigma(F)$), all non-hydrogen atoms anisotropic. All H atoms were located and their positions refined with isotropic thermal parameters. Further details of the crystal structure determinations may be obtained from the Fachinformationszentrum Karlsruhe, Gesellschaft für wissenschaftlich-technische Information mbH, D-76344 Eggenstein-Leopoldshafen on quoting the depository number CSD-57428, the authors, and the journal citation.

[6] W. T. Oosterhuis, G. Lang, *J. Chem. Phys.* **1983**, *58*, 4757.

[7] For a satisfactory simulation of the 4.96 T spectrum of **8** we had to assume a small, internal field of 0.36 T acting in the opposite direction to the applied field (Fig. 4). We presume that this field is due to the orbital moment of the diamagnetic iron center, in accord with the observed weak residual magnetism of **8** (Table 1).

[8] C. K. Jørgensen, *Struct. Bonding* **1966**, *1*, 234.

[9] U. Knof, T. Weyhermüller, T. Wolter, K. Wieghardt, *J. Chem. Soc. Chem. Commun.* **1993**, 726.

[10] Measurement conditions: complexes dissolved in CH_3CN (about 10^{-3} M) with tetra-*n*-butylammonium hexafluorophosphate (0.10 M) as electrolyte; glassy carbon disk electrodes; Ag/AgCl (saturated LiCl C_2H_5OH solution) reference electrode; scan speed 100 mV s^{-1}.

[11] Very recently the first five-coordinate Fe(IV) complex with an $S = 2$ ground state has been described: K. L. Kostka, B. G. Fox, M. P. Hendrich, T. J. Collins, C. E. F. Rickard, L. J. Wright, E. Münck, *J. Am. Chem. Soc.* **1993**, *115*, 6746.

Metallacyclic Interconversions in the Chemistry of Palladium with Phenyl Isocyanate**

By *Frédéric Paul, Jean Fischer, Philippe Ochsenbein,* and *John A. Osborn**

The palladacycle **1** was isolated[1] from solutions of the homogeneously catalyzed palladium/*o*-phenanthroline carbonylation of nitrobenzene, which yields phenyl carbamate in excellent yield (90%) when ethanol is present (Scheme 1).[2] We proposed that **1** and similar metallacyclic

$$PhNO_2 \longrightarrow PhNHCO_2Et$$

Scheme 1. Carbonylation of introbenzene. Reaction conditions: 1 equiv $[Pd(OAc)_2]_3$ + 3 equiv *o*-phen, 8 equiv CF_3COOH, 180 °C, 120 bar CO, EtOH, 30 min. $c(PhNO_2)/c(Pd)$ = 360; 100% conversion; 90% selectivity.

species may be involved as intermediates in this multistep catalytic process.

Using conditions similar to those previously[1] described, $[Pd(OAc)_2]$, *o*-phen (3 equiv), CO (40 bar, 80 °C, 1 h) but with only nitrobenzene (200 equiv) as solvent (thus omitting alcohol), we obtained a yellow complex **2** (40% yield) along with **1** (30% yield). In the presence of protons (8 equiv of 2,3,5,6-tetramethylbenzoic acid), the yield of **2** after several hours is nearly quantitative. Analysis and spectroscopic studies indicate that **2** contains, in addition to a Pd(*o*-phen) moiety, two C_6H_5NCO units. Thus, the FAB-MS analyses (*o*-nitrobenzyl alcohol as matrix) of **2** shows peaks at

[*] Prof. J. A. Osborn, Dipl.-Chem. F. Paul
Laboratoire de Chimie des Métaux de Transition et de Catalyse
U.R.A. 424 C.N.R.S., Institut Le Bel
4 rue Blaise Pascal, F-67070 Strasbourg Cedex (France)
Telefax: Int. code +(88)416171
Prof. J. Fischer[+], Dipl.-Chem. P. Ochsenbein[+]
Laboratoire de Cristallochimie et de Chimie Structurale
[+] X-Ray structure analysis

[**] We thank Rhône-Poulenc Recherches and the Centre National de la Recherche Scientifique (C.N.R.S.) for financial support of this research. For related research see ref. [1].

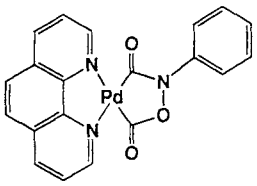

1

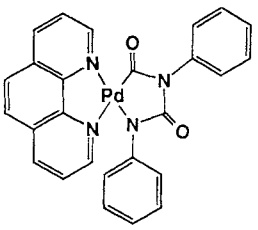

2

m/z (%) 525 ($M+1$), 497 ($M+1-CO$), 406 ($M+1-C_6H_5NCO$), 377 ($M-C_6H_5NCO-CO$), and 286 ($M-2C_6H_5NCO$). The IR spectrum shows two intense absorptions at 1675 and 1610 cm^{-1}, characteristic of carbonyl groups. A five-membered metallacyclic structure resulting from an *apparent* head-to-tail coupling of two isocyanate molecules was indicated (Scheme 1), which has been confirmed in an X-ray structure determination[3, 4] (Fig. 1).

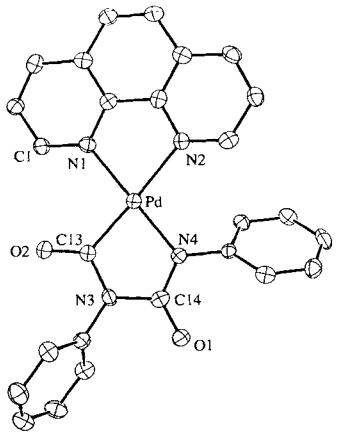

Fig. 1. ORTEP plot of **2** (50% probability level), showing part of the labeling scheme used. Hydrogen atoms are omitted for clarity. Selected distances [Å] and angles [°]: Pd–N1 2.062(4), Pd–N2 2.169(3), Pd–C13 1.963(4), Pd–N4 1.996(3), N3–C13 1.383(6), N3–C14 1.420(6), N4–C14 1.327(6), O1–C14 1.230(5), O2–C13 1.213(5), O2–C1 2.976(5), N1–Pd–N2 78.9(1), C13–Pd–N4 80.1(2), N2–Pd–N4 102.3(1), N1–Pd–C13 99.8(2).

Compound **2** is extremely stable (decomposition only at 290 °C) and unlike **1** does not react with alcohol in the presence or absence of protons. We surmised that **2** might be formed in the reaction of **1** with C_6H_5NCO, but heating **1** with C_6H_5NCO (40 equiv) at 140 °C for 7 h in nitrobenzene or *o*-dichlorobenzene yields a orange-yellow complex **3** in about 90% yield. Spectroscopic studies (^1H NMR, FAB-MS) indicate that **3** contains a six-membered metallacyclic structure. The X-ray structure[5] of the *p*-tolyl derivative **3a** is very similar to that of an analogous nickellacycle,[6] which has been isolated from the reaction of Ni^0 with C_6H_5NCO. Indeed, we find that on refluxing [Pd(*o*-phen)(dba)] (dba = dibenziliden acetone), with C_6H_5NCO (20 equiv) in benzene, **3** is formed in about 30% yield. Under milder conditions (25 °C, CH_2Cl_2) and a large excess of C_6H_5NCO, **2** is formed in approximately 50% yield along with extensive formation of the cyclic trimer of C_6H_5NCO, triphenylisocyanurate.

However, **2** is unexpectedly neither a catalyst for this trimerization process nor an intermediate in the formation of **3**; no reaction occurs on prolonged heating on **2** with excess C_6H_5NCO at 140 °C. Although **3** is quite stable (decomposition in the solid only at 250 °C), it undergoes two reactions of note: a) treatment with CO (1 bar) in $C_6H_5NO_2$ at 140 °C for 5 h produces **2** along with the precipitation of some Pd metal and b) heating **3** in solution with a labeled isocyanate (e.g. *p*-tolyl isocyanate) causes total exchange of the phenyl isocyanate groups to yield quantitatively the *p*-tolyl analogue (**3a**) of **3**.

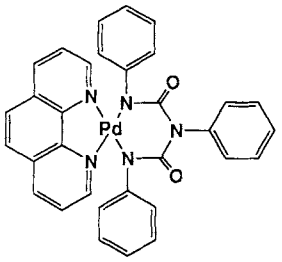

3

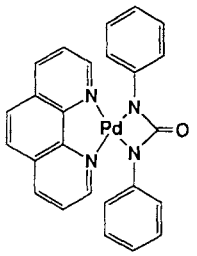

4

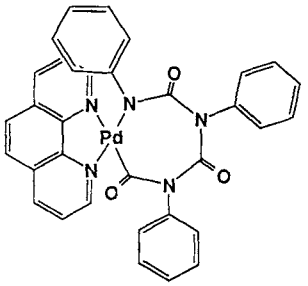

5

Since a sequence of ring expansion and contraction (or the reverse) could be envisaged for these reactions, we heated **3** in *o*-dichlorobenzene at 140 °C for 1 h. The ^1H NMR, IR ($\nu = 1615\ cm^{-1}$ (C=O)), and FAB-MS data of the resulting red compound showed that a four-membered metallacycle **4** was formed with the concomitant extrusion of C_6H_5NCO.[7] The structure determined by X-ray methods is shown[8] (Fig. 2) and will be described in detail elsewhere.[9] Further, mild treatment of **4** with excess C_6H_5NCO (50 equiv) regenerates **3** quantitatively (80% yield). Thus we propose that the isocyanate exchange reaction occurs by a reversible six- to four- to six-membered palladacycle interconversion. Furthermore, since **4** also reacts with CO (40 bar) in CH_2Cl_2 to yield **2** (85% yield), formation of **2** from **3** is thus seen to result from a six- to a four-membered ring contraction with

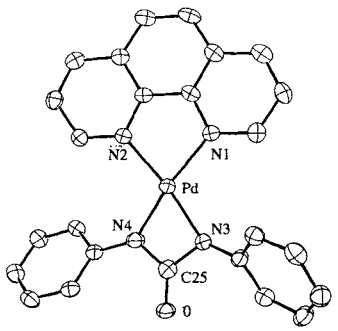

Fig. 2. ORTEP plot of **4** (50% probability level) showing part of the labeling scheme used. Hydrogen atoms are omitted for clarity. Selected distances [Å] and angles [°]: Pd–N1 2.066(3), Pd–N2 2.034(3), Pd–N3 1.992(3), Pd–N4 2.001(3), N3–C25 1.376(5), N4–C25 1.373(5), O–C25 1.238(5), N1–Pd–N2 80.3(1), N3–Pd–N4 65.6(1), N2–Pd–N4 107.1(1), N1–Pd–N3 107.2(1).

loss of isocyanate followed by a four- to a five-membered ring expansion upon insertion of CO. The detailed mechanism of formation of **3** (as well as **2**) from aryl isocyanate and Pd^0 is not evident, although decarbonylation of the 7-membered palladacycle **5**, formed by the head to tail coupling of three isocyanates and Pd^0, is probably the last step. Note, however, that a classical coupling process of two C_6H_5NCO ligands on Pd^0 to form a five-membered palladacycle such **2**, followed by a further insertion of isocyanate to give **5**, can be excluded since **2** does not react with isocyanate.

Although the above reactions are not directly implicated in the catalytic carbonylation of nitrobenzene[11], the pervasiveness and stability of the palladacycles **1**–**4** and their interconversions would offer credence to the intermediacy of analogous cycles in this catalytic process, particularly if the isoelectronic and isolobal nature of certain entities involved, e.g. RNCO and CO_2, are considered.[10] Furthermore, considering the relationship of **2** and **3** to diphenylurea and triphenylbiuret, which are undesirable by-products[12] in the carbonylation process, our results indicate that such metallacycles, however, may indeed play a subsidiary perhaps even detrimental, role in this catalytic reaction. Finally the formation of both **1** and **2** under the catalytic conditions described above in the absence of a proton source or alcohol would seem to argue against the existence of intermediates such as aniline in the formation of carbamates in this palladium system.[10b]

Received: June 26, 1993 [Z 6170 IE]
German version: *Angew. Chem.* **1993**, *105*, 1687

[1] P. Leconte, F. Metz, A. Mortreux, J. A. Osborn, F. Paul, F. Petit, *J. Chem. Soc. Chem. Commun.* **1990**, 1616–1617. A recent X-Ray determination has confirmed the assigned structure of **1** (J. Fischer and P. Ochsenbein; unpublished work).

[2] a) S. Cenini, F. Ragaini, M. Pizzotti, F. Porta, G. Mestroni, E. Allessio, *J. Mol. Catal.* **1991**, *64*, 179–190, and references therein; b) E. Drent, *Eur. Pat. Appl.* EP 224292, **1987** (*Chem. Abstr. 107*, 199074h).

[3] a) Crystal data for **2**: $C_{26}H_{18}N_4O_2Pd \cdot CH_2Cl_2$, $M_r = 609.8$ g, triclinic, space group $P\bar{1}$, $a = 10.899(3)$ Å, $b = 11.937(3)$ Å, $c = 10.539(3)$ Å, $\alpha = 116.06(2)^\circ$, $\beta = 91.72(2)^\circ$, $\gamma = 100.96(2)^\circ$, $V = 1199.3$ Å^3, $Z = 2$, $\varrho_{calcd} = 1.689$ g cm^{-3}, $\lambda(Cu_{K\alpha}) = 1.5418$ Å (graphite monochromator), $T = -100$ °C. A Philips PW1100/16 diffractometer, equipped with a locally built low-temperature device, was used to collect 2642 reflections ($3^\circ < \theta < 52^\circ$) on a yellow crystal $0.15 \times 0.25 \times 0.25$ mm. Of these, 2513 were observed [$I > 3\,\sigma(I)$]. The hydrogen atoms were included as idealized contributions. $R = 0.040$, $R_w = 0.067$, GOF = 1.683, final residual = 0.31 e Å^{-3}; b) empirical absorption corrections and Lorentz and polarization corrections were applied to the data. All non-hydrogen atoms were located by the heavy atom method, and were refined anisotropically. All computations used the program MOLEN on a VAX computer: B. A. Frenz in *"The Enraf-Nonius CAD4-SDP" in Computing in Crystallography* (Eds.: H. Schenk, R. Olthof-Hazekamp, H. Van Koningveld, G. C. Bassi), Delft University Press, **1978**, pp. 64–71. See also [4].

[4] Further details of the crystal structure investigations may be obtained from the Fachinformationszentrum Karlsruhe, Gesellschaft für wissenschaftlich-technische Information mbH, D-76344 Eggenstein-Leopoldshafen (FRG), on quoting the depository number CSD-57482, the names of the authors and the journal citation.

[5] Crystal data for **3a**: $C_{35}H_{29}N_5O_2Pd \cdot C_4H_{10}O$, $M_r = 732.18$ g, monoclinic, $P2_1/n$, $a = 20.172(6)$ Å, $b = 12.922(3)$ Å, $c = 12.797(3)$ Å, $\beta = 100.67(2)^\circ$, $V = 3278$ Å^3, $Z = 4$, $\varrho_{calcd} = 1.483$ g cm^{-3}, $\lambda(Cu_{K\alpha}) = 1.5418$ Å (graphite monochromator), $T = -100$ °C. A Philips PW1100/16 diffractometer, equipped with a locally built low-temperature device, was used to collect 4407 reflections ($3^\circ < \theta < 54^\circ$) on a yellow crystal $0.20 \times 0.30 \times 0.40$ mm. Of these, 3528 were observed [$I > 3\,\sigma(I)$]. The hydrogen atoms were included as idealized contributions. $R = 0.049$, $R_w = 0.078$, GOF = 1.86, final residual = 0.28 e Å^{-3}. See refs. [3b, 4].

[6] For extensive studies on the Ni^0 coupling of isocyanates see: a) H. Hoberg, *J. Organomet. Chem.* **1988**, *358*, 507–517, and references therein; b) H. Hoberg, B. W. Oster, C. Krüger, Y. H. Tsay, *ibid.* **1983**, *252*, 365–373.

[7] For related four-membered palladacycles made from Pd^0 see: W. Beck, W. Rieber, S. Cenini, F. Porta, G. La Monica, *J. Chem. Soc. Dalton Trans.* **1974**, 298–304.

[8] Crystal data for **4**: $C_{28}H_{18}N_4OPd \cdot CH_2Cl_2$, $M_r = 581.8$ g, monoclinic, $C2/c$, $a = 16.201(3)$ Å, $b = 15.147(3)$ Å, $c = 19.432(3)$ Å, $\beta = 102.67(2)^\circ$, $V = 4652.5$ Å^3, $Z = 8$, $\varrho_{calcd} = 1.661$ g cm^{-3}, $\lambda(Cu_{K\alpha}) = 1.5418$ Å, (graphite monochromator), $T = -100$ °C. A Philips PW1100/16 diffractometer, equipped with a locally built low-temperature device, was used to collect 2838 reflections ($3^\circ < \theta < 52^\circ$) on a red crystal $0.08 \times 0.16 \times 0.30$ mm. Of these, 2247 were observed [$I > 3\,\sigma(I)$]. The hydrogen atoms were included as idealized contributions. $R = 0.025$, $R_w = 0.038$, GOF = 1.155, final residual = 0.30 e Å^{-3}. See ref. [3b].

[9] Compound **4** can also be simply synthesized from treating [(*o*-phen)Pd(OAc)$_2$] with the dilithio salt of the diphenylurea dianion. Surprisingly, complexes containing the diphenylurea dianion as ligand are not as widespread as may have been anticipated, but see for example: a) R. I. Michelman, R. A. Andersen, R. G. Bergman, *J. Am. Chem. Soc.* **1991**, *113*, 5100–5102; b) P. Legzdins, E. C. Phillips, S. J. Rettig, J. Trotter, J.E. Veeltheer, V. C. Yee, *Organometallics* **1992**, *11*, 3104–3110; c) H.-W. Lam, G. Wilkinson, B. Hussain-Bates, M. B. Hursthouse, *J. Chem. Soc. Dalton Trans.* **1993**, 781–788 and references cited in [1]. Further details of the structure of **4** will be published separately.

[10] Metallacyclic intermediates for these conversions have been increasingly postulated: a) F. Ragaini, S. Cenini, F. Demartin, *J. Chem. Soc. Chem. Commun.* **1992**, 1467–1468; b) J. D. Gargulak, A. J. Berry, M. D. Noirot, W. L. Gladfelter, *J. Am. Chem. Soc.* **1992**, *114*, 8933–8945; c) K. Unverferth, R. Höntsch, K. Schwetlick, *J. Prakt. Chem.* **1979**, *321*, 928–934.

Tautomer-Specific Anti-(N-3-Substituted)-Adenine Antibodies: New Tools in Molecular Dosimetry and Epidemiology**

By *Karl-Heinz Glüsenkamp,* Kai Krüger, Gertrud Eberle, Wolfgang Drosdziok, Eckhard Jähde, Oliver Gründel, Andrea Neuhaus, Roland Boese, Peter Stellberg,* and *Manfred F. Rajewsky*

Mutagenic and carcinogenic substances are found in the environment (including foodstuffs) and are produced endogenously within organisms.[1] Such compounds cause structural modifications of the deoxyribonucleic acid (DNA) in exposed cells, often leading to the formation of covalent DNA-base adducts.[1–8] Of particular importance in this context is the class of alkylating agents, which includes many N-nitroso compounds,[2, 3, 6] polycyclic hydrocarbons,[7] some fungal metabolites,[8] and numerous chemotherapeutic agents.[4] Among the functional groups of DNA that are reactive towards alkylating agents, the nucleophilic N-3 atom of deoxyadenosine is of special interest, because its alkylation destabilizes the N-glycosidic bond[9] and may thus lead to the release of N-3-substituted adenines, resulting in the formation of apurinic ("abasic") sites. In addition, 3-alkyladenines are removed from DNA by DNA-repair enzymes (3-alkyladenine-DNA-glycosylase).[10] Many modified bases are not further metabolized and hence appear unchanged in the body fluids (urine, blood plasma).[11] Besides DNA, RNA is a potential target for alkylating agents, too; however, after exposure of cells to alkylating agents 3-alkyladenines are formed mainly in DNA.[12]

[*] Dr. K.-H. Glüsenkamp, Dipl.-Chem. K. Krüger, Dr. G. Eberle, Dipl.-Ing. W. Drosdziok, Dr. E. Jähde, A. Neuhaus, Prof. Dr. M. F. Rajewsky
Institut für Zellbiologie (Tumorforschung),
Westdeutsches Tumorzentrum Essen, Universitätsklinikum Essen,
Virchow-Strasse 173, D-45122 Essen (FRG)
Telefax: Int. code + (201)723-5904
Dr. O. Gründel
Elisabeth-Krankenhaus, Essen (FRG)
Priv.-Doz. Dr. R. Boese, Dipl.-Chem. P. Stellberg
Institut für Anorganische Chemie
der Universität-Gesamthochschule, Essen (FRG)

[**] This work was supported by the European Community as part of the program "Science and Technology for Environmental Protection (S. T. E. P.)" (EV5V-CT91-0012), and by the Kind-Phillipp-Stiftung für Leukämieforschung im Stifterverband für die Deutsche Wissenschaft.

A variety of N-3-substituted adenines may be produced in cellular DNA, depending on the molecular nature of the alkylating reactant. Many alkyl and allyl substituents, some bearing aromatic groups, have been found at the N-3 position of adenine in vivo and in vitro.[13] To determine N-3-adenine adducts by immunoanalytical methods in cellular DNA for "molecular dosimetry" of a broad spectrum of endogenous and exogenous DNA-reactive compounds, we have produced novel anti-(N-3-*R*-adenine) monoclonal antibodies (mab). These mabs bind to modified adenines with high affinity, regardless of the size of the substituents at position N-3.

We describe here the design and synthesis of the haptens used for coupling to carrier proteins for the immunization of BALB/c mice.[11b] The aim of our studies was the production of antibodies with very high specificity for the entire family of N-3-substituted adenines and with very low cross-reactivity with other, naturally occurring purine derivatives.

AM1-calculations[14] and spectroscopic studies[15] on the tautomerization equilibria (Fig. 1) of several N-3-substituted adenines revealed that the tautomeric structure **1** is energetically preferred, regardless of the substituent at the position N-3. Analogous considerations for the parent

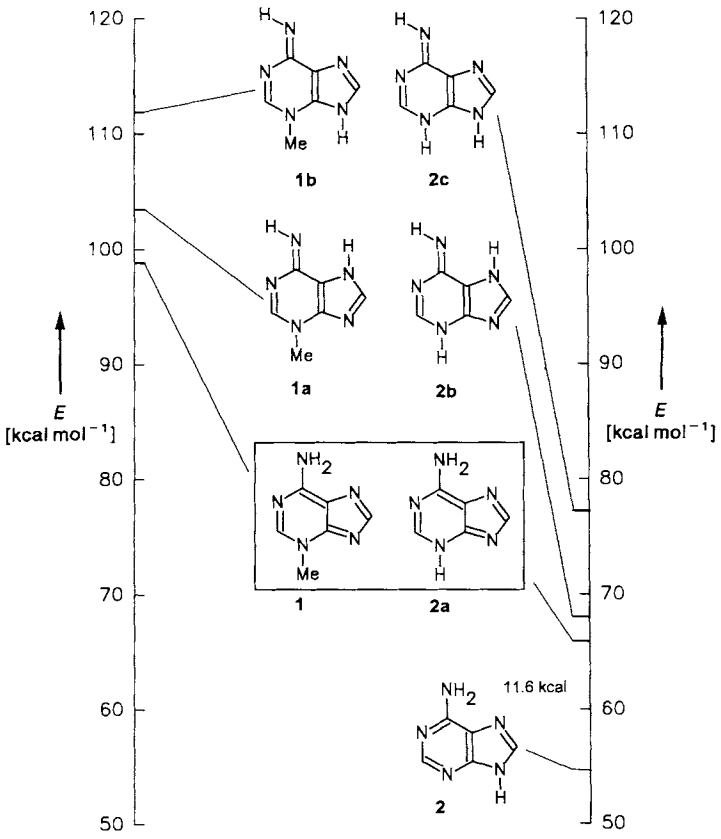

Fig. 1. Comparison of the enthalpy of formation for selected tautomeric structures of 3-methyladenine (**1**) (left) and adenine (**2**) (right), determined by using the AM1 method[14-16]. Structures **1** and **2a** show the tautomeric forms of the adenine skeleton (in the box), which are recognized by mab EM-6-47. In the case of unsubstituted adenine, the tautomeric form **2** is 11.6 kcal mol^{-1} lower in energy.

compound, adenine, show that the tautomeric structure **2** is 11.6 kcal mol^{-1} more stable than the tautomer **2a**, which represents the lowest energy structure of the family of N-3-substituted adenines. Based on this large energy difference, it seemed possible to develop mabs that would specifically recognize the favored tautomeric structure **1** induced by a substituent at the N-3 position.

For the production of mabs directed against low molecular weight compounds these must first be conjugated to an immunogenic carrier protein (e.g., keyhole limpet hemocyanin[11b]). To obtain tautomer-specific anti-(N-3-R-adenine) mabs, the tautomerization equilibrium of the 3-substituted adenines must remain unaffected by the coupling of haptens to carrier proteins. By using AM1-calculations on 3,8-disubstituted adenines we were able to show that the tautomer equilibria of N-3-substituted adenines are not influenced significantly by 8-alkyl substituents.[14c] For the production of a tautomer-specific anti-(N-3-R-adenine) mabs the key haptens **3**–**5** were synthesized in three steps.[17]

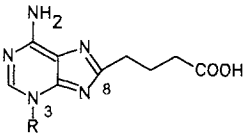

3: R = Me
4: R = Et
5: R = *n*Bu

The carboxypropyl substituent in position 8 served both as a coupling group to the carrier protein and as a spacer for optimal presentation of the antigen on the protein surface.[19]

Figure 2 shows the result of an X-ray structure analysis[20] of 3-methyl-8-(3-carboxypropyl)adenine (**3**), which crystallized with four molecules of water per formula unit.

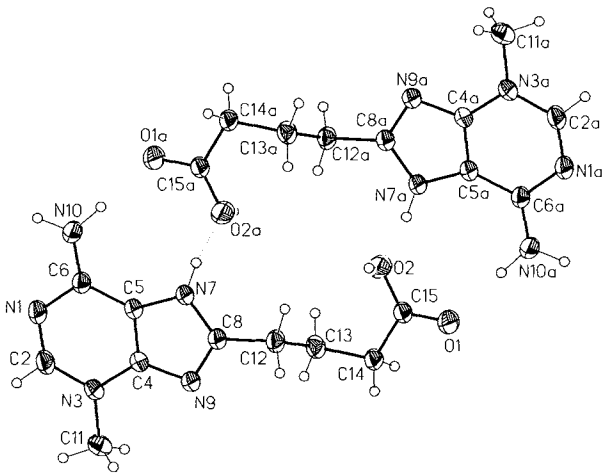

Fig. 2. The crystal structure of **3**. The thermal ellipsoids are drawn at the 50% probability level.

Whereas the protein conjugates of **3** and the corresponding *n*-butyl derivative **5** gave no satisfactory immune response, the conjugate bearing an ethyl substituent in the 3-position induced a large number of high-affinity mabs (affinity constants for 3-ethyladenine of the order of 10^{10} L mol^{-1}[11a, b]). As expected, binding studies with these mabs and the purine derivatives shown in Scheme 1 revealed high specificity and affinity for 3-substituted adenines. The adenine N-3 substituents can range from methyl to sterically demanding diphenylmethyl groups without causing significant changes in the affinity. In contrast, the observed binding constants of naturally occurring purine derivatives such as adenine (**2**), adenosine (**11**), and theophylline (**14**) is more than five orders of magnitude lower. Table 1 shows a selec-

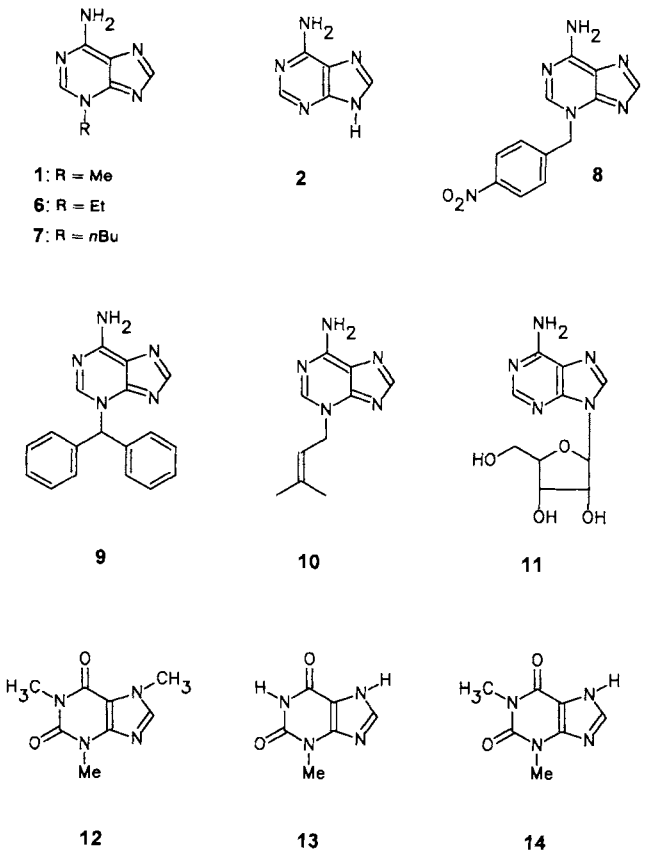

Scheme 1. 3-Substituted adenines and naturally occurring purines as competitors of 3-ethyladenine (**6**) in the radioimmunoassay with mab EM-6-47.

tion of purines tested and summarizes the binding characteristics of a representative mab (mab EM-6-47). In accordance with the earlier theoretical considerations, the binding studies indicate tautomer-specific, high-affinity, antigen–antibody binding.

Table 1. Cross-reactivity[a] of the monoclonal antibody EM-6-47 with alkylated adenines and naturally occurring purines (competitors).

Competitor		Binding of competitor relative to **6** in competitive radioimmunoassays [a]
3-ethyladenine	**6**	1
3-methyladenine	**1**	0.04
3-methyl-8-(3-carboxypropyl)adenine [17]	**3**	0.05
3-ethyl-8-(3-carboxypropyl)adenine [17]	**4**	0.6
3-butyl-8-(3-carboxypropyl)adenine [17]	**5**	5.2
3-butyladenine	**7**	2.5
triacanthin [23]	**10**	0.2
3-(*p*-nitrobenzyl)adenine	**8**	0.9
3-(diphenylmethyl)adenine	**9**	0.1
adenine	**2**	<0.00001
adenosine	**11**	<0.00001
coffeine	**12**	<0.00001
3-methylxanthine	**13**	<0.00001
theophylline	**14**	<0.00001

[a] The competitive radioimmunoassays were carried out as described in ref. [21]. All compounds except **3**–**5** are described [22].

Until now, we have been able to quantify 3-methyladenine and 3-ethyladenine at fmol levels in the urine of experimental animals and human individuals.[11b] On the basis of a recently developed conjugation method,[24] immunoaffinity columns have been prepared with anti-(N-3-R-adenine) mabs, allowing the quantitative isolation of 3-substituted adenines from body fluids.[25] By using these mabs as an efficient tool in combination with separation by HPLC (HPLC = high-performance liquid chromatography) we will be able to measure individual exposures to environmental alkylating agents and hence gain access to novel markers for exposure studies.

Another potential application for anti-(N-3-adenine) mabs is in monitoring during chemotherapeutic treatment with anti-cancer drugs. These mabs can be employed for dosimetry at the level of target cell DNA by measuring the rate of formation of N-3-substituted adenines, which can vary dramatically among individuals.

Received: June 21, 1993 [Z 6153 IE]
German version: *Angew. Chem.* **1993**, *105*, 1710

[1] B. N. Ames, L. S. Gold, *Angew. Chem.* **1990**, *102*, 1233–1246; *Angew. Chem. Int. Ed. Engl.* **1990**, *29*, 1197; P. L. Grover, *Chemical Carcinogens and DNA*, CRC, Boca Raton, FL, USA, **1979**.
[2] M. F. Rajewsky, *Molecular and Cellular Aspects of Carcinogen Screening Tests* (Eds.: R. Montesano, H. Bartsch, L. Tomatis) (*IARC Sci. Publ.* **1980**, *27*, 41).
[3] B. Singer, D. Grunberger, *Molecular Biology of Mutangens and Carcinogens*, Plenum, New York, **1983**.
[4] K. Hemminki, D. B. Ludlum, *J. Natl. Cancer Inst.* **1984**, *73*, 1021–1023.
[5] R. Preussmann, G. Eisenbrand, *Chemical Carciogens* (Ed.: C. E. Searle) (*ACS Monogr.* **1984**, *182*, 829).
[6] B. Singer, W. J. Bodell, J. E. Cleaver, G. H. Thomas, M. F. Rajewsky, W. Thon, *Nature* **1978**, *276*, 85–88.
[7] M. C. MacLeod, B. K. Mansfield, J. K. Selkirk, *Carcinogenesis* **1982**, *3*, 1031–1037.
[8] L. H. Hurley, V. L. Reynolds, D. H. Swenson, G. L. Petzold, T. A. Scahill, *Science* **1984**, *226*, 843–844.
[9] T. Lindahl, B. Nyberg, *Biochemistry* **1972**, *11*, 3610–3618; T. Fujii, T. Saito, T. Nakasaka, *J. Chem. Soc. Chem. Commun.* **1980**, 758–759.
[10] T. Lindahl, *Annu. Rev. Biochem.* **1982**, *51*, 61–87.
[11] a) G. Eberle, dissertation, Universität Essen, **1989**; b) G. Eberle, K.-H. Glüsenkamp, W. Drosdziok, M. F. Rajewsky, *Carcinogenesis* **1990**, *11*, 1753–1759; c) C. Hanski, P. D. Lawley, *Chem. Biol. Interact.* **1985**, *55*, 225–234; d) D. E. G. Shuker, E. Bailey, S. M. Gorf, J. Lamb, P. B. Farmer, *Anal. Biochem.* **1984**, *140*, 270–275; e) D. E. G. Shuker, P. B. Farmer, *Chem. Res. Toxicol.* **1992**, *5*, 450–460; f) V. Prevost, D. E. G. Shuker, H. Bartsch, R. Pastorelli, W. G. Stillwell, L. J. Trudel, S. R. Tannenbaum, *Carcinogenesis* **1990**, *11*, 1747–1751.
[12] B. Singer, *Prog. Nucleic Acid Res. Mol. Biol.* **1975**, *15*, 219–285; D. T. Beranek, C. C. Weis, D. H. Swenson, *Carcinogenesis* **1980**, *1*, 595–606; R. H. Hall, *Modified Nucleosides in Nucleic Acids*, Columbia University Press, New York, **1971**.
[13] a) B. Singer, L. Sun, H. Fraenkel-Conrat, *Biochemistry* **1974**, *13*, 1923–1920; b) P. D. Lawley, D. J. Orr, M. Jarman, *Biochem. J.* **1975**, *145*, 73–84; c) E. Eder, D. Lutz, M. Jörns, *Chem. Biol. Interact.* **1987**, *61*, 97–108; d) N.-C. C. Yang, C.-W. Chang, *Prog. Natl. Acad. Sci. USA* **1985**, *82*, 5250–5254.
[14] a) M. J. S. Dewar, E. G. Zoebisch, E. F. Healy, J. J. P. Stewart, *J. Am. Chem. Soc.* **1985**, *107*, 3902-3909; b) The calculations were carried out with Hyperchem (Version 2.0, Autodesk, D-80686 Munich); c) K.-H. Glüsenkamp, M. F. Rajewsky, unpublished.
[15] a) B. Pullman, A. Pullman, *Quantum Biochemistry*, Wiley, New York, **1963**; b) M. Dreyfus, G. Dodin, O. Bensaude, J. E. Dubois, *J. Am. Chem. Soc.* **1977**, *99*, 7027–7037; c) N. C. Gonella, H. Nakanishi, J. B. Holtwick, D. S. Horowitz, K. Kanamori, N. J. Leonard, J. D. Roberts, *ibid.* **1983**, *105*, 2050–2055.
[16] a) B. Pullman, H. Berthod, M. Dreyfus, *Theor. Chim. Acta* **1969**, *15*, 265–268; b) W. M. F. Fabian, *J. Comput. Chem.* **1991**, *12*, 17–35; c) U. Norinder, *J. Mol. Struct.* **1987**, *151*, 259–269.
[17] The synthesis of the 8-substituted adenine ring skeleton was carried out by condensation of triaminopyridine and glutaric anhydride in the melt at 180 °C, according to ref. [18]. Selective alkylation at the N-3 position to yield the crystalline 3,8-disubstituted adenines was done in dry *N,N*-dimethylformamide (DMF) using the corresponding alkylhalides. – **3**: M.p. 230–245 °C (decomp), ^{1}H NMR (200 MHz, [D$_6$]DMSO, D$_2$O, 25 °C, TMS): δ = 2.20 (m, 2H; CH$_2$), 2.41 (m, 2H; CH$_2$), 3.05 (m, 2H; CH$_2$), 4.18 (s, 3H; CH$_3$), 8.25 (s, 1H; CH). UV/VIS (MeOH): λ_{max} (ε) = 273 nm (10600). – **4**: M.p. 218–230 °C (decomp). ^{1}H NMR (200 MHz, [D$_6$]DMSO, 25 °C, TMS): δ = 1.45 (t, J(H,H) = 8.0 Hz, 3H; CH$_3$), 1.95 (m, 2H; CH$_2$), 2.30 (m, 2H; CH$_2$), 2.80 (m, 2H; CH$_2$), 4.30 (m, 2H; CH$_2$), 7.60 (s, 2H; NH$_2$), 8.27 (s, 1H, CH). UV/VIS (MeOH): λ_{max} (ε) = 275 nm (12900). – **5**: M.p. 245–248 °C (decomp). ^{1}H NMR

(200 MHz, [D$_6$]DMSO, 25 °C, TMS): δ = 1.29 (m, 3H; CH_3), 1.90 (m, 6H; CH_2), 2.95 (m, 2H; CH_2), 2.77 (m, 2H, CH_2), 4.25 (m, 2H; CH_2), 7.60 (s, 2H; NH_2), 8.25 (s, 1H, CH). UV/VIS (MeOH): λ_{max} (ε) = 277 nm (16100). The radioactively labelled 3-alkyladenine tracers for the competitive radioimmunoassay were synthesized by alkylation of the corresponding radioactively labelled [8-^{3}H]adenines (up to 100 Ci mmol^{-1}, Amersham-Buchler, D-38110 Braunschweig) with the corresponding alkylhalides.

[18] N. J. Leonard, K. Ito, *J. Am. Chem. Soc.* **1973**, *95*, 4010–4016.

[19] Conjugation of haptens **3**–**5** with the carrier protein was carried out with water-soluble carbodiimides, and the degree of coupling was measured by UV spectroscopy.

[20] A crystal (0.46 × 0.37 × 0.23 mm) was measured with an R3m/V-Nicolet four-circle diffractometer ($Mo_{K\alpha}$ radiation, graphite monochromator) at room temperature. Crystal system triclinic, cell dimensions refined from the diffractometer angles from 25 reflections in the 2Φ region 20–25, a = 7.056(2), b = 9.078(3), c = 12.910(3) Å, α = 97.23(2), β = 102.28(2), γ = 106.95(2)°, V = 753.1(4) Å^3, space group $P\bar{1}$ (no. 2), Z = 2, ρ_{calcd} = 1.360 g cm^{-3}, μ = 0.11 mm^{-1}, $2\Phi_{max}$ = 50, 3453 independent reflections (R_{merg} = 0.028), of which 2729 were observed ($F_0 \geq 4\sigma(F)$). The structure was solved by direct methods, and was refined for F in the complete matrix using the SHELXTL-Plus program package (Version 4.11/V), 257 parameters in the refinement with anisotropic factors for C, O, and N, and isotropic factors for the hydrogen atoms. R = 0.0473, Rw = 0.0547, $w^{-1} = (\sigma^2(F_0) + 0.00103F_0^2$, maximal residual electron density 0.34 e Å^3. Further details of the crystal structure investigation may be obtained from the Fachinformationszentrum Karlsruhe, Gesellschaft für wissenschaftlich-technische Information mbH, D-76344 Eggenstein-Leopoldshafen (FRG) on quoting the depository number CSD-400257, the names of the authors, and the journal citation.

[21] a) R. Müller, M. F. Rajewsky, *Z. Naturforsch. C* **1978**, *33*, 897–901; R. Müller, *J. Immunol. Methods* **1980**, *34*, 345–352.

[22] J. A. Montgomery, J. Thomas, *J. Heterocycl. Chem.* **1964**, *1*, 115–120; C. J. Abshire, L. Berlinguet, *Can. J. Chem.* **1964**, *42*, 1599–1604; T. Fujii, G. C. Walker, N. J. Leonard, *J. Med. Chem.* **1979**, *22*, 125–129.

[23] N. J. Leonard, J. A. Deyrup, *J. Am. Chem. Soc.* **1962**, *84*, 2148–2160.

[24] K.-H. Glüsenkamp, W. Drosdziok, G. Eberle, E. Jähde, M. F. Rajewsky, *Z. Naturforsch. C* **1991**, *46*, 498–501; L. F. Tietze, M. Arlt, M. Beller, K.-H. Glüsenkamp, E. Jähde, M. F. Rajewski, *Chem. Ber.* **1991**, *124*, 1215–1221.

[25] G. Eberle, K.-H. Glüsenkamp, M. F. Rajewsky, unpublished.

Rigid Rodlike Metal Complexes of Nanometric Dimension: Synthesis, Luminescence Properties, and Long-Range Energy Transfer**

By *Fritz Vögtle,* Michael Frank, Martin Nieger, Peter Belser,* Alex von Zelewsky, Vincenzo Balzani,* Francesco Barigelletti, Luisa De Cola,** and *Lucia Flamigni*

The development of photochemical molecular devices[1–3] for a variety of applications (e.g., artificial photosynthesis[3–7] and information processing[8–11]) is largely based on the design of supramolecular species in which photoinduced energy or electron transfer processes can take place over a long distance with high efficiency. An important requirement for the usefulness of such supramolecular species is their degree of spatial organization. Species in which the active components are linked by nonrigid bridges are of little applicative interest because practical devices require vectorial energy or electron transfer over long distances. Furthermore, when the geometry of the system is not strictly defined, the results obtained are of limited basic interest since they cannot be compared with the predictions of energy and electron transfer theories.[3–5, 12–17]

Because of their outstanding excited state and redox properties,[18] Ru^{II} and Os^{II} bpy-type complexes (bpy = 2,2′-bipyridine) are excellent components for building supramolecular species capable of exhibiting photoinduced energy and electron transfer processes.[3, 19] For synthetic reasons, however, it is difficult to assemble these metal-containing building blocks in *extended and rigid* supramolecular structures.[20]

We have synthesized the novel bridging ligand 1,4-bis[2-(2,2′-bipyridine-5-yl)ethynyl]bicyclo[2.2.2]octane (hereafter indicated by b-Z-b, in which two bipyridine units (b) are separated by a 1.0 nm long spacer (Z) made of a rigid bicyclooctane component and two linear acetylene-type units. Such a rigid bridging ligand has allowed us to prepare the mono- and dinuclear complexes of Ru^{II} and Os^{II} shown in Scheme 1. In the dinuclear species, the distance between the two metal centers (ca. 1.7 nm) changes only slightly on rotation around the single bonds that connect the bridge (spacer) to the bpy units. These rodlike, nanoscale supramolecular species exhibit interesting excited state and redox properties.

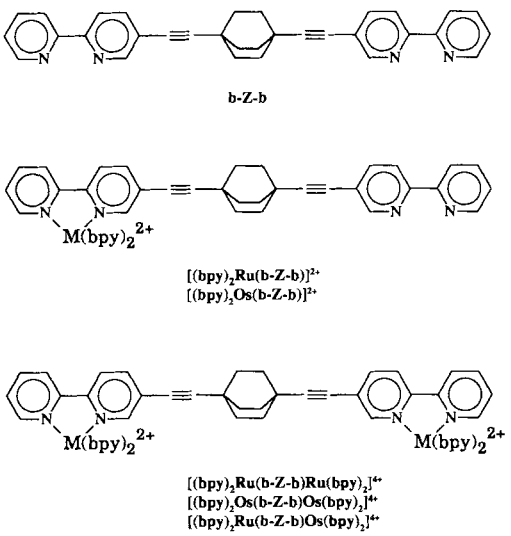

Scheme 1. Structural formulas of the bridging ligand b-Z-b and of the complexes it has been used to prepare.

The novel ligand b-Z-b has been synthesized via the corresponding bis-alkene **3** (Scheme 2). Phosphonate ester **1** was readily obtained by an Arbuzov rearrangement from 5-bromomethyl-2,2′-bipyridine.[23] Bicyclo[2.2.2]octane-1,4-dicarboxaldehyde **2**[24] and **1** were coupled by a Wadsworth–Emmons reaction to give the (*E*,*E*) diene **3**. Bromination at room temperature gave **4** and subsequent dehydrobromination by refluxing with excess potassium hydroxide yielded the diyne b-Z-b, which was isolated as a colorless, crystalline solid. An X-ray structure of the bridg-

[*] Prof. Dr. F. Vögtle, Dr. M. Frank
Institut für Organische Chemie und Biochemie der Universität
Gerhard-Domagk-Strasse 1, D-53121 Bonn (FRG)
Telefax: Int. code + (228)73-5662

Prof. Dr. P. Belser, Prof. Dr. A. von Zelewsky
Institut für Anorganische und Analytische Chemie der Universität
Pérolles, CH-1700 Freiburg (Switzerland)
Telefax: Int. code +(37)826531

Prof. V. Balzani, Dr. L. De Cola
Dipartimento di Chimica "G. Ciamician", Università di Bologna
Via Selmi 2, I-40126 Bologna (Italy)
Telefax: Int. code + (51)259-456

Dr. F. Barigelletti, Dr. L. Flamigni
Istituto FRAE-CNR, Bologna (Italy)

Dr. M. Nieger
Anorganisch-chemisches Institut der Universität Bonn (FRG)

[**] This work was supported by Bundesministerium für Forschung und Technologie (Project no. 03291 20A) (FRG), Swiss National Science Foundation, and Ministero dell'Università e della Ricerca Scientifica e Technologica (MURST) and Consiglio Nazionale della Ricerche (CNR) (Italy).

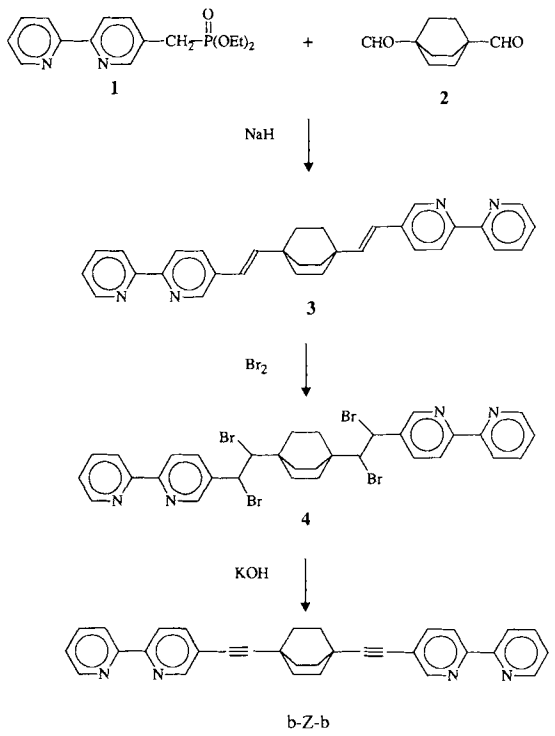

Scheme 2. Synthesis of the ligand b-Z-b.

ing ligand b-Z-b proved the assumed, rodlike structure (Fig. 1).[25]

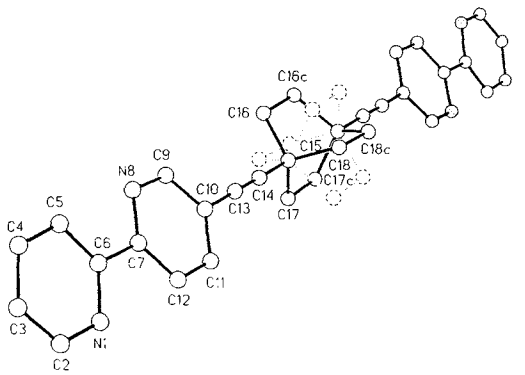

Fig. 1. Crystal structure of the bridging ligand b-Z-b; the bicyclooctane unit is disordered.

The mono- and dinuclear complexes of the bridging ligand b-Z-b were prepared and purified according to a previously reported procedure.[26] Characterization was performed by elemental analysis, FAB mass spectrometry, ^{1}H NMR, UV/VIS, spectroscopy. The equipment used to measure the absorption spectra, luminescence properties, and oxidation potentials have been previously described.[26] Some of the results obtained have been gathered in Table 1, in which data on the "parent" $[Ru(bpy)_3]^{2+}$ and $[Os(bpy)_3]^{2+}$ compounds[18] are also shown for comparison purposes.

The absorption spectra in the visible region and the luminescence spectra of the dinuclear compounds are displayed in Figure 2. Particularly noteworthy are the isosbestic

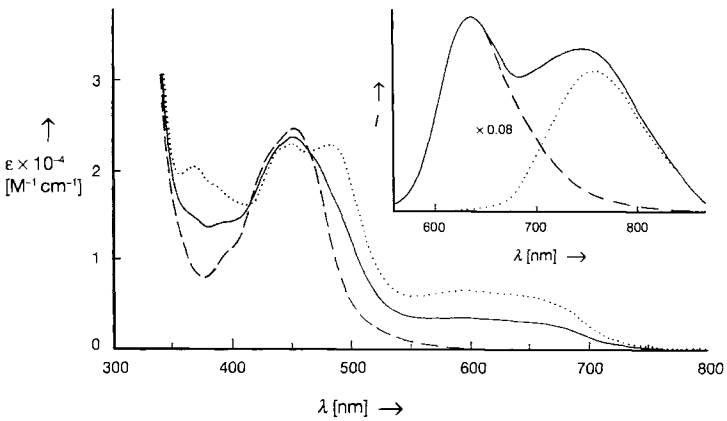

Fig. 2. Absorption and (inset) uncorrected luminescence spectra of $[(bpy)_2Ru(b\text{-}Z\text{-}b)Ru(bpy)_2]^{4+}$ (– –) multiplied by 0.08, $[(bpy)_2Os(b\text{-}Z\text{-}b)Os(bpy)_2]^{4+}$ (· · ·), and $[(bpy)_2Ru(b\text{-}Z\text{-}b)Os(bpy)_2]^{4+}$ (–).

points at 416 and 466 nm. When excitation is performed at one of these wavelengths on the Ru–Os complex (as was the case for the luminescence experiments), each metal-based unit absorbs 50% of the incident light.

From Table 1 and Figure 2 one can see that in the novel compounds each metal-based unit displays its own electrochemical properties and absorption spectrum regardless of the presence and nature of a second metal-based unit. Furthermore, the dinuclear homometallic compounds exhibit the same luminescence properties as the corresponding mononuclear species (Table 1). These results indicate that the electronic interaction between the metal-containing units in the dinuclear compounds is very weak.

Table 1. Spectroscopic and electrochemical data of Ru and Os(bpy) complexes [a].

	Absorption [b]	Luminescence [c]			Electrochemistry [d]
	λ_{max}	λ_{max}	τ	$\Phi \times 10^2$ [e, f]	$E_{1/2}$ [V]
$[(bpy)_2Ru(b\text{-}Z\text{-}b)]^{2+}$	453	635	226	1.5	+1.25 (1)
$[(bpy)_2Os(b\text{-}Z\text{-}b)]^{2+}$	484	787	28	0.18	+0.84 (1)
$[(bpy)_2Ru(b\text{-}Z\text{-}b)Ru(bpy)_2]^{4+}$	452	635	231	1.5	+1.28 (2)
$[(bpy)_2Os(b\text{-}Z\text{-}b)Os(bpy)_2]^{4+}$	484	787	29	0.18	+0.84 (2)
$[(bpy)_2Ru(b\text{-}Z\text{-}b)Os(bpy)_2]^{4+}$	452/(484) [g]	638/787	22 [h]/29 [i]	0.13/0.18 [h]	+1.27 (1)/+0.84 (1)
$[Ru(bpy)_3]^{2+}$	452	615	170	1.5	+1.26 (1)
$[Os(bpy)_3]^{2+}$	478	743	49	0.32	+0.83 (1)

[a] Acetonitrile solution, room temperature; λ_{max} in nm, τ in ns. For $[(bpy)_2Ru(b\text{-}Z\text{-}b)Os(bpy)_2]^{4+}$ the first value is for the Ru-based and the second for the Os-based units. [b] Maximum of the lowest energy spin-allowed charge-transfer band. [c] Air-equilibrated acetonitrile solution. Excitation was performed at $\lambda = 466$ nm, which is an isosbestic point between the Ru-based and Os-based units. λ_{max} has been corrected for photomultiplier response. [d] $E_{1/2}$ values vs SCE and, within parentheses, relative current intensities. All the oxidation peaks are reversible. [e] Standard: $[Ru(bpy)_3]^{2+}$ in deaerated CH_3CN, $\Phi = 0.062$ (J. M. Calvert, J. V. Caspar, R. A. Binstead, T. D. Westmoreland, T. J. Meyer, *J. Am. Chem. Soc.* **1982**, *104*, 6620). [f] Standard: $[Os(bpy)_3]^{2+}$ in deaerated CH_3CN, $\Phi = 0.005$ (E. M. Kober, J. V. Caspar, R. S. Lumpkin, T. J. Meyer, *J. Phys. Chem.* **1986**, *90*, 3722). [g] Shoulder, see Figure 2. [h] 1:1 mixture of $[(bpy)_2Ru(b\text{-}Z\text{-}b)Ru(bpy)_2]^{4+}$ and $[(bpy)_2Os(b\text{-}Z\text{-}b)Os(bpy)_2]^{4+}$ having the same concentration of $[(bpy)_2Ru(b\text{-}Z\text{-}b)Os(bpy)_2]^{4+}$ shows the luminescence properties expected in the absence of any interaction. [i] Part of the luminescence signals shows a rise time of 21 ns.

In the dinuclear heterometallic species $[(bpy)_2Ru(b\text{-}Z\text{-}b)Os(bpy)_2]^{4+}$ the quantum yield of the Ru-based luminescence (after correction for the 50% light absorption by the Os-based unit) is about ten times smaller than that of the reference compounds $[(bpy)_2Ru(b\text{-}Z\text{-}b)]^{2+}$ and $[(bpy)_2Ru(b\text{-}Z\text{-}b)Ru(bpy)_2]^{4+}$, whereas the quantum yield of the Os-based luminescence is about the same as that observed for the reference compounds $[(bpy)_2Os(b\text{-}Z\text{-}b)]^{2+}$ and $[(bpy)]_2Os(b\text{-}Z\text{-}b)Os(bpy)_2]^{4+}$ (Table 1; Fig. 2, inset). Under the experimental conditions used (complex concentration 1×10^{-5} M), intermolecular energy transfer can be excluded. Therefore the results demonstrate that in $[(bpy)_2Ru(b\text{-}Z\text{-}b)Os(bpy)_2]^{4+}$ an *intramolecular* (intercomponent) energy transfer process takes place, which quenches the luminescent excited state of the Ru-based unit and sensitizes the luminescent excited state of the Os-based one. This is confirmed by the decrease in the excited state lifetime of the Ru-based unit (from 231 nm in $[(bpy)_2Ru(b\text{-}Z\text{-}b)Ru(bpy)_2]^{4+}$ to 22 ns in $[(bpy)_2Ru(b\text{-}Z\text{-}b)Os(bpy)_2]^{4+}$) and by the rise time (21 ns) observed for part of the luminescence of the Os-based unit (Table 1).

The rate constant for energy transfer from the Ru-based to the Os-based unit of $[(bpy)_2Ru(b\text{-}Z\text{-}b)Os(bpy)_2]^{4+}$ can be obtained from Equation (a), in which τ and τ^0 are the luminescence lifetimes of the Ru-based component in $[(bpy)_2Ru(b\text{-}Z\text{-}b)Os(bpy)_2]^{4+}$ and $[(bpy)_2Ru(b\text{-}Z\text{-}b)Ru(bpy)_2]^{4+}$, respectively (Table 1). Energy transfer processes can take place by Förster-type (dipole–dipole resonance)[27] and/or Dexter-type (electron exchange)[28] mechanisms.[3] The expected rate constant for energy transfer according to the Förster mechanism can be estimated on the basis of spectroscopic quantities by Equation (b).

$$k_{en} = \frac{1}{\tau} - \frac{1}{\tau^0} = 4.1\times10^7\ s^{-1} \qquad (a)$$

$$k_{en} = 5.9\times10^{-25}\,(\Phi_D/n^4\tau_D r^6)\int_0^\infty F_D(\tilde{\nu})\varepsilon_A(\tilde{\nu})d\tilde{\nu}/\tilde{\nu}^4 \qquad (b)$$

For $[(bpy)_2Ru(b\text{-}Z\text{-}b)Os(bpy)_2]^{4+}$, $\Phi_D = 0.015$, $\tau_D = 226$ ns, $r = 1.7$ nm (n = refractive index of the solvent, $\tilde{\nu}$ = wavenumber, ε_A = molar extinction coefficient) and the value of the overlap integral is $4.7\times10^{-14}\ M^{-1}\,cm^{-3}$. The value obtained for k_{en} ($2.4\times10^7\ s^{-1}$) is somewhat smaller (but of the same order of magnitude) than the experimental value ($4.1\times10^7\ s^{-1}$). In view of the approximations involved, it could well be that the Förster mechanism can account for most of the observed energy transfer. It cannot be excluded, however, that exchange energy transfer is also involved and even plays a major role. For an exchange energy transfer mechanism, the rate constant in the nonadiabatic limit can be expressed as in Equation (c);[3, 14, 17, 29] ν_{en} and $\Delta G^{\neq}$ can be obtained from Equations (d) and (e), respectively.

$$k_{en} = \nu_{en}\exp(-\Delta G^{\neq}/RT) \qquad (c)$$

$$\nu_{en} = \frac{2(H_{en})^2}{h}\left(\frac{\pi^3}{\lambda_{en}RT}\right)^{1/2} \qquad (d)$$

$$\Delta G^{\neq} = \left(\frac{\lambda}{4}\right)\left(1+\frac{\Delta G^0}{\lambda}\right)^2 \qquad (e)$$

Following usual assumptions,[29–31] the free energy change ΔG^0 can be expressed by the difference between the spectroscopic energies of the donor and acceptor (− 0.33 eV, as estimated from the energy of the emission maxima of the Ru-based and Os-based luminescence at 77 K), and the reorganizational energy λ (ca. 0.2 eV) can be obtained from the spectroscopic Stokes shift.[29–31] This yields a value of about 0.4 for the exponential term of Equation (c), which means than ν_{en} must be about $1\times10^8\ s^{-1}$ to account for the experimental rate constant. From Equation (d) a value of $0.4\ cm^{-1}$ can thus be obtained for the through-bond electronic interaction energy H_{en} between the two metal-containing units, under the assumption that the observed energy transfer process only takes place by an exchange mechanism.[32]

In conclusion, we have synthesized a rigid bis(bipyridine) bridging ligand, b-Z-b, which has been used to construct rodlike dinuclear metal complexes of nanometric dimension. In spite of the long metal–metal distance (1.7 nm), in the dinuclear, heterometallic $[(bpy)_2Ru(b\text{-}Z\text{-}b)Os(bpy)_2]^{4+}$ compound light excitation of the Ru-based unit is followed by a very efficient (>90%) energy transfer process ($k_{en} = 4.1\times10^7\ s^{-1}$), which causes the sensitized emission of the Os-based unit. To our knowledge, the b-Z-b ligand described here is the first example of a bis(bipyridine) bridging ligand in which two chelating units are separated by a rigid rodlike spacer. The new ligand might be used to build up rigid, dendrimer-type polymetallic compounds,[33] and self-assembled multicomponent supramolecular structures.[34] More generally, this novel rodlike ligand represents a useful component for the construction of nanodevices[35] based on transition metal complexes.

Experimental Procedure

(*E,E*)-1,4-Bis[2-(2,2′-bipyridine-5-yl)ethenyl]bicyclo[2.2.2]octane **3**: Under an argon atmosphere a solution containing phosphonate **1** (5.52 g, 18 mmol) in dry THF (100 mL) was added at room temperature to a suspension of sodium hydride (0.57 g, 19 mmol, 80% in an oil suspension) in dry THF (50 mL). The mixture was stirred for 10 min. Aldehyde **2** (1.36 g, 8.2 mmol) was dissolved in dry THF (50 mL) and added dropwise over a period of 1 h. The mixture was stirred for a further 2 h, ice (200 g) was added and a solid precipitated. The crude product was filtered off and washed with water and *n*-hexane. For purification the residue was chromatographed on silica gel (eluent: $CHCl_3/CH_3OH$/aqueous ammonia, 300:10:1; R_f value: 0.55) and recrystallized from toluene. Yield of **3**: 2.9 g (76%), m.p. 310–312 °C. ^1H NMR (200 MHz, $CDCl_3$): $\delta = 1.7$ (s, 12H, CH_2), 6.3 (s, 4H, CH), 7.28 (ddd, 2H, CH), 7.78 (td, 2H, CH), 7.8 (td, 2H, CH), 8.35 (m, 2H, CH), 8.36 (m, 2H, CH), 8.6 (d, 2H, CH), 8.66 (dm, 2H, CH). MS (70 eV): m/z 470.2467 $[M]^+$ (calcd. 470.2470). Satisfactory C,H,N analysis for $C_{32}H_{30}N_4$.

1,4-Bis[2-(2,2′-bipyridine-5-yl)ethynyl]bicyclo[2.2.2]octane (b-Z-b). To the diene **3** (2.35 g, 5.0 mmol) in CCl_4 (200 mL) bromine (11 mmol) in CCl_4 was added. The reaction mixture was stirred for 12 h and evaporated to dryness. The crude product was washed with diluted aqueous $NaHSO_3$ and ether. The stereoisomeric mixture of the tetrabromide **4** was directly used in the subsequent dehydrobromination. Tetrabromide **4** (1.6 g, 2.12 mmol) was dissolved in dry ethanol (100 mL) and anhydrous dioxane (50 mL); excess potassium hydroxide (ca. 25 g) was added. The mixture was allowed to reflux for 40 h, poured on ice water and extracted with dichloromethane. The combined extracts were treated with diluted aqueous NH_4Cl and water and dried over magnesium sulfate. After evaporation of the solvent the residue was chromatographed on silica gel (eluent: $CHCl_3/CH_3OH$/aqueous ammonia, 300:10:1; R_f value: 0.78) and recrystallized from toluene. Yield of b-Z-b: 0.50 g (51%), m.p. 290–293 °C. ^1H NMR (200 MHz, $CDCl_3$): $\delta = 1.95$ (s, 12H, CH_2), 7.3 (ddd, 2H, CH), 7.79 (dd, 2H, CH), 7.8 (td, 2H, CH), 8.3–8.42 (m, 4H, CH), 8.6–8.7 (m, 4H, CH); MS (70 eV): m/z 466.2157 $[M]^+$ (calcd. 466.2158).

The metal complexes were prepared by using $[M(bpy)_2Cl_2]$ (M = Ru, Os) and the ligand b-Z-b in refluxing methoxyethanol. Upon addition of excess NH_4PF_6, the PF_6^- salts of the complexes were precipitated and purified as previously described [26]. Characterization for $[(bpy)_2Ru(b\text{-}Z\text{-}b)Os(bpy)_2]^{4+}$: Elemental analysis: (calcd. for $C_{73}H_{66}Cl_2F_{24}N_{12}O_3OsP_4Ru$ including 3 mol water and 1 mol dichloromethane): C, 43.02 (43.18); H, 3.23 (3.28); N, 7.91 (8.28). FAB-MS: m/z = 1817 (75%) $[M^+PF_6^-]$, 1672 (100%) $[M^+ - 2PF_6^-]$. ^1H NMR (300 MHz, CD_3CN): $\delta = 1.73$ (s, 12H, CH_2), 7.26–8.51 (m, 46H, bpy and (b-Z-b)-H). UV/VIS spectral and electrochemical data: see Table 1. The homometallic complexes gave similar results in accordance with the expected values.

Received: May 25, 1993 [Z 6106 IE]
German version: *Angew. Chem.* **1993**, *105*, 1706

[1] V. Balzani, L. Moggi, F. Scandola, *Supramol. Photochem. 1987* (Ed.: V. Balzani), *NATO ASI Ser. Ser. C* **1987**, *214*, 1.
[2] J.-M. Lehn, *Angew. Chem.* **1990**, *102*, 1387; *Angew. Chem. Int. Ed. Engl.* **1990**, *29*, 1304.
[3] V. Balzani, F. Scandola, *Supramolecular Photochemistry*, Horwood, Chichester, **1991**.
[4] M. R. Wasielewski in *Photoinduced Electron Transfer, Part D* (Eds.: M. A. Fox, M. Channon), Elsevier, New York, **1988**, p. 161.
[5] D. Gust, T. A. Moore, *Science* **1989**, *244*, 35.
[6] B. O'Regan, M. Grätzel, *Nature* **1991**, *353*, 738.
[7] G. Denti, S. Campagna, S. Serroni, M. Ciano, V. Balzani, *J. Am. Chem. Soc.* **1992**, *114*, 2944.
[8] *Molecular Electronic Devices* (Eds.: F. L. Carter, R. E. Siatkowsky, H. Woltijen), North Holland, Amsterdam, **1988**.
[9] J. J. Hopfield, J. N. Onuchic, D. N. Beratan, *J. Phys. Chem.* **1989**, *93*, 6350.
[10] R. A. Bissel, A. P. de Silva, H. Q. N. Gunaratne, P. L. M. Lynch, G. E. M. Maguire, K. R. A. S. Sandanayake, *Chem. Soc. Rev.* **1992**, *21*, 187.
[11] R. Ballardini, V. Balzani, M. T. Gandolfi, L. Prodi, M. Venturi, D. Philp, H. G. Ricketts, J. F. Stoddart, *Angew. Chem.* **1993**, *105*, 1362; *Angew. Chem. Int. Ed. Engl.* **1993**, *32*, 1301.
[12] R. A. Marcus, *Annu. Rev. Phys. Chem.* **1964**, *15*, 155; R. A. Marcus, N. Sutin, *Biochim. Biophys. Acta* **1985**, *811*, 265.
[13] J. Jortner, *J. Phys. Chem.* **1979**, *64*, 4860.
[14] G. Orlandi, S. Monti, F. Barigelletti, V. Balzani, *Chem. Phys.* **1980**, *52*, 313.
[15] J. R. Miller, J. V. Beitz, *J. Phys. Chem.* **1981**, *74*, 6746.
[16] H. Oevering, M. N. Paddon-Row, M. Hoppener, A. M. Oliver, E. Cotsaris, J. W. Verhoeven, N. S. Hush, *J. Am. Chem. Soc.* **1987**, *109*, 3258.
[17] G. L. Gloss, J. R. Miller, *Science* **1989**, *244*, 35.
[18] A. Juris, V. Balzani, F. Barigelletti, S. Campagna, P. Belser, A. von Zelewsky, *Coord. Chem. Rev.* **1988**, *84*, 85; E. M. Kober, J. V. Caspar, B. P. Sullivan, T. J. Meyer, *Inorg. Chem.* **1988**, *27*, 4587; V. Balzani, F. Barigelletti, L. De Cola, *Top. Curr. Chem.* **1990**, *158*, 31.
[19] F. Scandola, M. T. Indelli, C. Chiorboli, C. A. Bignozzi, *Top. Curr. Chem.* **1990**, *158*, 73.
[20] Linear rigid structures can more easily be obtained by using the tridentate 2,2′:6′,2″-terpyridine (tpy) ligand [21]. However, the Ru^{II} complexes of tpy-type ligands are only weakly or not at all luminescent at room temperature and the lifetime of their lowest excited state is very short [22].
[21] E. C. Constable, A. M. W. Cargill Thompson, *J. Chem. Soc. Dalton Trans.* **1992**, 3467; J.-P. Collin, S. Guillerez, J.-P. Sauvage, F. Barigelletti, L. De Cola, L. Flamigni, V. Balzani, *Inorg. Chem.* **1992**, *31*, 4112; V. Grosshenny, R. Ziessel, *J. Chem. Soc. Dalton Trans.* **1993**, 817; F. Barigelletti, L. Flamigni, V. Balzani, J.-P. Collin, J.-P. Sauvage, A. Sour, E. C. Constable, A. M. W. Cargill Thompson, *J. Chem. Soc. Chem. Commun.* **1993**, 942.
[22] E. C. Constable, A. M. W. Cargill Thompson, N. Armaroli, V. Balzani, M. Maestri, *Polyhedron* **1992**, *20*, 2707, and references therein.
[23] J. G. Eaves, H. S. Munro, D. Parker, *J. Chem. Soc. Chem. Commun.* **1985**, 684.
[24] K. Kumar, S. S. Wang, C. N. Sukenik, *J. Org. Chem.* **1984**, *49*, 665.
[25] Crystal structure analysis of b-Z-b: colorless crystals: crystal dimensions: $0.4 \times 0.5 \times 0.8$ mm; $M_r = 466.6$, space group $P2_1/c$ (no. 14), $a = 6.269(1)$, $b = 15.959(2)$, $c = 12.628(3)$ Å, $\beta = 99.49(1)^\circ$, $V = 1245.3(4)$ Å^3, $Z = 2$, $\varrho_{calcd} = 1.24$ g cm^{-3}, $F(000) = 492$. $T = 193$ K, $Mo_{K\alpha}$ ($\kappa = 0.71073$ Å), $\mu(Mo_{K\alpha}) = 0.07$ mm^{-1}, Enraf-Nonius CAD4 diffractometer, $4^\circ < 2\theta < 50^\circ$, 2195 symmetry-independent reflections; 1744 reflections with $|F| > 3\,\sigma(F)$ were used for the structure solution (direct methods) and refinement (190 parameters); non-hydrogen atoms anisotropically [disordered bicyclooctane unit (SOF (C16, C17, C18) = 0.50)], H atoms refined with a riding model, $R = 0.048$ ($R_w = 0.048$, $w^{-1} = \sigma^2(F) + 0.0005\,F^2$). Further details of the crystal structure investigation are available on request from the Fachinformationszentrum Karlsruhe, D-76344 Eggenstein-Leopoldshafen (FRG) on quoting the depository number CSD-57464, the names of the authors, and the journal citation.
[26] P. Belser, A. von Zelewsky, M. Frank, C. Seel, F. Vögtle, L. De Cola, F. Barigelletti, V. Balzani, *J. Am. Chem. Soc.* **1993**, *115*, 4076.
[27] T. H. Förster, *Discuss. Faraday Soc.* **1959**, *27*, 7.
[28] D. L. Dexter, *J. Chem. Phys.* **1953**, *21*, 836.
[29] V. Balzani, F. Bolletta, F. Scandola, *J. Am. Chem. Soc.* **1980**, *102*, 2552; V. Balzani, F. Scandola, *J. Chem. Educ.* **1983**, *60*, 814.
[30] C. K. Ryu, R. H. Schmehl, *J. Phys. Chem.* **1989**, *93*, 7961.
[31] N. Sutin, *Acc. Chem. Res.* **1982**, *15*, 275.
[32] If the exchange mechanism is responsible for 50% of the observed energy transfer process, the electronic interaction energy H_{en} would be 0.3 cm^{-1}.
[33] For a recent example of dendrimer-type polymetallic compounds, see: S. Serroni, G. Denti, S. Campagna, A. Juris, M. Ciano, V. Balzani, *Angew. Chem.* **1992**, *104*, 1540; *Angew. Chem. Int. Ed. Engl.* **1992**, *31*, 1495.
[34] For a recent example of multicomponent self-assembly involving bpy-type ligands, see: P. Baxter, J.-M. Lehn, A. DeCian, J. Fischer, *Angew. Chem.* **1993**, *105*, 92; *Angew. Chem. Int. Ed. Engl.* **1993**, *32*, 69.
[35] K. E. Drexler, *Nanosystems: Molecular Machinery, Manufacturing, and Computation*, Wiley, New York, **1992**.

Electrochemical Synthesis of New Sb–Te Zintl Anions by Cathodic Dissolution of Sb_2Te_3 Electrodes: Structures of $[Sb_4Te_4]^{4-}$ and $[Sb_9Te_6]^{3-}$**

By *Christopher J. Warren, Douglas M. Ho, Robert C. Haushalter,** and *Andrew B. Bocarsly**

Dedicated to Professor Josef Zemann on the occasion of his 70th birthday

In the early 1930s Eduard Zintl showed that the electrolysis of certain main group, main group alloy, and intermetallic phases could produce metal polyanions in the catholyte.[1] Through the use of potentiometric titrations of liquid ammonia solutions of these saltlike intermetallic compounds, and exhaustive extractions of alkali metal alloys of the heavier elements of groups 14 and 15, Zintl et al. were able to deduce the existence of Sn_9^{4-}, Pb_9^{4-}, Pb_7^{4-}, As_3^{3-}, As_5^{3-}, As_7^{3-}, Sb_7^{3-}, Sb_3^{3-}, Bi_7^{3-}, Bi_5^{3-}, and Bi_3^{3-}, but were unable to isolate and structurally characterize corresponding crystalline salts to confirm their findings. Since the initial report by Kummer and Diehl[2] on the ethylenediamine (en) extraction of Na_4Sn_9 and isolation of Sn_9^{4-} from Na_4Sn_9, many homopolyatomic[3] and heteropolyatomic anions[3] have been isolated by the solvent extraction of Zintl phases. The electrolytic generation of Zintl anions, however, has not been thoroughly investigated and is limited to the early work of Zintl himself and two more recent, brief communications.[4, 5] We previously reported the novel electrochemical synthesis of the gold tellurides $(n\mathrm{Bu_4N})_3[Au_3Te_4]$[6] and $(Ph_4P)_2[Au_2Te_4]$[6] by the cathodic dissolution of $AuTe_2$ alloy electrodes. This technique, which was inspired by the early electrolyses of Zintl, has allowed us to prepare and structurally characterize solids that may not be accessible by standard hydrothermal and high-temperature elemental fusion techniques. In many cases our technique, which relies on the constantly increasing concentration of polyanions as they are discharged from the cathode to crystallize with cations of the electrolyte, provides single crystals suitable for X-ray analysis in three to four days. Here we report the electrochemical synthesis of two new antimony tellurides **1** and **2**, both of which contain discrete polyanions in the solid

$(TPA)_4[Sb_4Te_4]$ **1**
$(TPA)_3[Sb_9Te_6]$ **2**
$TPA = (n\text{-}C_3H_7)_4N^+$

state and are synthesized concurrently from the cathodic dissolution of a Sb_2Te_3 alloy electrode.

In contrast to the numerous known antimony sulfides[7] and selenides,[8] only very few antimony telluride compounds are found in the literature. Apart from the known binary phase Sb_2Te_3, there appears to be only four other known compounds containing Sb–Te polyanions: $BaSbTe_3$,[9] $LiSbTe_2$,[10a] K_3SbTe_3,[10b] and $AgSbTe_2$.[11] Several mixed antimony germanium telluride compounds such as $GeSb_4Te_7$,[12] $GeSb_2Te_4$,[12] and $Ge_2Sb_2Te_5$[12] also exist and have been studied for their potential semiconduct-

[*] Dr. R. C. Haushalter, C. J. Warren
NEC Research Institute
4 Independence Way, Princeton, NJ 08540 (USA)
Telefax: Int. code + (609)951-2483
Prof. A. B. Bocarsly, Dr. D. M. Ho, C. J. Warren
Department of Chemistry, Princeton University
Princeton, NJ 08544 (USA)
Telefax: Int. code + (609)258-2383

[**] This work was supported by the NEC Research Institute.

ing properties. All of these compounds have been prepared by the high-temperature fusion of the elements.

Tellurides **1** and **2** were prepared by the cathodic dissolution of a Sb_2Te_3 electrode, which was made by melting stoichiometric amounts of the elements under N_2 in a quartz tube. The resulting silver solid was then crushed into a fine powder and fabricated into electrodes in accordance with the procedure reported for the Au–Te system.[6] The synthesis was conducted in a two-compartment, liquid junction, airtight electrochemical cell equipped with a nickel plate counter electrode. The use of nickel as a counter electrode is advantageous, since an insoluble purple precipitate (the qualitative microprobe analysis of which showed Ni and Br in a 1:2 molar ratio) is then generated in the anode chamber. Cross-contamination of the cathode chamber with oxidation products from the anode chamber is thus prevented, allowing longer reaction times. The cell was filled with a 0.56 M solution of tetrapropylammonium bromide (TPABr) in ethylenediamine (en) which served as both the supporting electrolyte and a source of cations for the crystallization process. The ethylenediamine was purified by distillation from a red solution of K_4Sn_9, and all manipulations were performed in a high-purity (<1 ppm O_2) He atmosphere.

The cathodic dissolution of a Sb_2Te_3 alloy electrode running at a current density of approximately 300 $\mu A\,cm^{-2}$ immediately gave rise to a deep brown stream of anions which surrounded the cathode and then slowly sank to the bottom of the cathode chamber. After one day a red-brown crystalline solid, which was later identified as **1**, was observed growing on the Sb_2Te_3 cathode. After approximately two days the deep brown catholyte solution also yielded brown spear-shaped crystals of **2**, which were found growing on the bottom of the chamber. The reaction was halted after five days to yield **1** and **2** in an approximately 80:20 ratio. The chemical and electrochemical yields calculated based on moles of Sb were 29% and 17% for **1**, and 12% and 2% for **2**.[13] These two compounds appear to be the only solid products of the electrochemical dissolution reaction and are not obtained from a control experiment with powdered Sb_2Te_3 and TPABr in en. Independent experiments have also shown that **1** is not converted into **2** on standing in the electrolyte solution, which suggests that the anions are formed independently during the dissolution of the electrode.

Telluride **1** crystallizes in space group *Pbcn* with eight $[Sb_4Te_4]^{4-}$ anions in the unit cell.[14] The structure of the anion is shown in Figure 1. The anion displays approximate, but not crystallographically imposed, *2mm* point group symmetry in the solid state and consists of a folded Sb_4 ring to which four terminal Te atoms are attached in the equatorial positions. This geometry is quite different from that of the bare, square-planar Sb_4^{2-} anion[15] but more closely resembles that of $(t\mathrm{Bu})_4Sb_4$,[16] in which the *t*Bu groups are bonded to a folded Sb_4 ring in equatorial positions. The Sb–Sb distances in **1** are in the range 2.836(4)–2.883(4) Å and can be compared to those in the *t*Bu-substituted Sb_4 ring (2.814(2)–2.821(2) Å). The average transannular nonbonded Sb–Sb distance in **1** is 3.916 Å. For comparison the average Sb–Sb distance in the Sb_4^{2-} anion is 2.750 Å, and it has an average transannular nonbonded Sb–Sb distance of 3.889 Å. The Sb–Te bond lengths in $[Sb_4Te_4]^{4-}$ are in the range 2.722(4)–2.761(4) Å. Paucity of structurally characterized Sb–Te compounds makes extensive comparisons with these Sb–Te bond lengths difficult. The ternary Zintl phase compound K_3SbTe_3 contains discrete, trigonal-pyramidal, anionic units having three equivalent Sb–Te bond lengths of 2.7831(7) Å. The Sb–Te bond length in the solid-state phase Sb_2Te_3 is 2.974 Å, and Sb–Te distances in $BaSbTe_3$ are in the range 2.832–3.090 Å.

Telluride **2** crystallizes in the monoclinic space group $P2_1/c$ with four $[Sb_9Te_6]^{3-}$ anions in the unit cell.[14] The structure of the $[Sb_9Te_6]^{3-}$ anion is shown in Figure 2. The assignment of Sb and Te atoms in this anion was based on their chemically reasonable connectivities and a microprobe analysis, which yielded an Sb:Te ratio of 1.5:1. The $[Sb_9Te_6]^{3-}$ anion can be thought of as the fusion product of two well-known structure types: a bicyclic Sb_6Te_2 moiety (Fig. 3a) with a Sb–Sb transannular closure and a geometry closely resembling that of Se_8^{2+},[17] and an Sb_6Te_2 cage, (Fig. 3b), which resembles the cages found in X_4N_4 (X = As, S, Se),[18–20] X_4S_4 (X = P, Te),[21, 22] and As_4Se_4.[23]

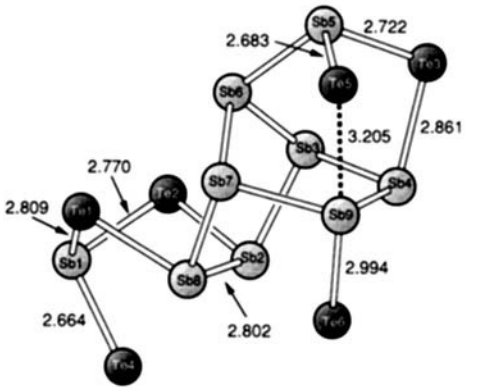

Fig. 2. Structure of the $[Sb_9Te_6]^{3-}$ anion in **2** [14]. The dashed line represents a long Sb–Te contact of 3.205(6) Å. Some other Sb–Sb and Sb–Te distances [Å] are noted.

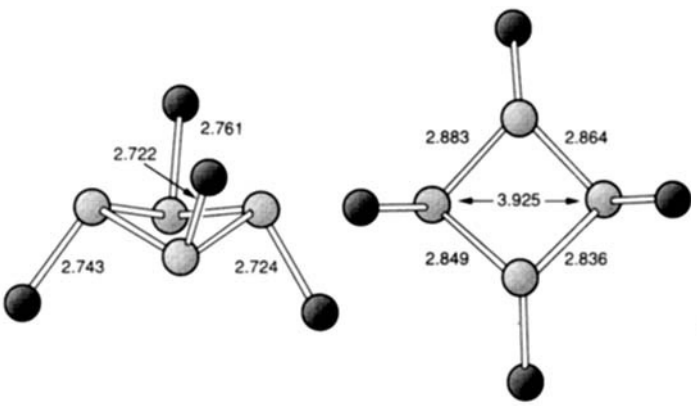

Fig. 1. Two views of the structure of the $[Sb_4Te_4]^{4-}$ anion in **1** [14]. Left: projection approximately down one of the two transannular Sb–Sb vectors in the molecule; right: view perpendicular to the plane defined by the four Sb atoms. The Te atoms have darker shading.

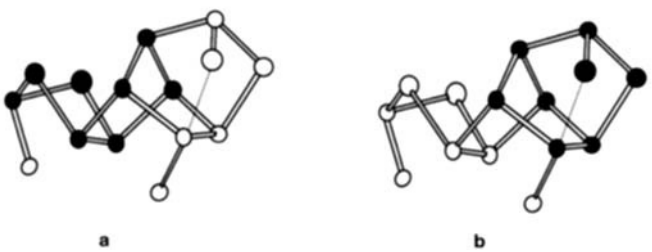

Fig. 3. Structure types found in the $[Sb_9Te_6]^{3-}$ anion in **2**.

An interesting feature of the structure of $[Sb_9Te_6]^{3-}$ is the pseudo-four-coordinate Sb9 atom, which is bonded to Sb4 and Sb7 (2.756(5) and 2.803(5) Å, respectively), but displays an abnormally long Sb9–Te6 contact of 2.994(5) Å. The other two terminal Te–Sb contacts in the anion are much shorter (Sb5–Te5 2.683(6) Å, Sb1–Te4 2.664(5) Å). The lengthening of the terminal Sb9–Te6 contact is most likely due to the weak coordination of Sb9 to Te5 (distance 3.205(6) Å) making Sb9 pseudo-four-coordinate. It is interesting to note that all three terminal Sb–Te bonds are *"endo"* relative to the cluster. It is not clear if this is simply due to packing forces in the crystal, or if the effect is driven by weak Sb–Te interactions like those involving Te4 and Sb2 and Sb8 (corresponding Te–Sb distances 3.671 and 3.720 Å, respectively) or Te6 and Sb4 (3.327 Å). Sb–Sb distances in $[Sb_9Te_6]^{3-}$ are in the range 2.756(5)–2.871(5) Å, and internal Sb–Te distances vary from 2.722(7) to 2.878(5) Å; these separations are all comparable to those in the $[Sb_4Te_4]^{4-}$ anion and in other structurally characterized antimony tellurides.

Our continuation of the early investigations of Zintl has shown that polyanion synthesis from the cathodic dissolution of alloy electrodes is very useful for the preparation of a wide variety of solids. In addition to the novel Sb–Te polyanions described here, we have also prepared and structurally characterized others such as $[GaTe_2(en)_2]^-$[24] and $[In_2Te_4]^{4-}$,[25] as well as tellurides from the As and Hg systems.

Received: June 28, 1993 [Z 6174 IE]
German version: *Angew. Chem.* **1993**, *105*, 1684

[1] E. Zintl, A. Harder, *Z. Phys. Chem. Abt. A* **1931**, *154*, 47; E. Zintl, J. Goubeau, W. Dullenkopf, *ibid.* **1931**, *154*, 1; E. Zintl, W. Dullenkopf, *Z. Phys. Chem. Abt. B* **1932**, *16*, 183, 195; E. Zintl, H. Kaiser, *Z. Anorg. Allg. Chem.* **1933**, *211*, 113; E. Zintl, S. Neumayr, *Z. Phys. Chem. Abt. B* **1933**, *20*, 272; E. Zintl, S. Neumayr, *Z. Elektrochem.* **1933**, *39*, 86; E. Zintl, G. Brauer, *Z. Phys. Chem. Abt. B* **1933**, *20*, 245; E. Zintl, E. Husemann, *ibid.* **1933**, *21*, 138; E. Zintl, A. Harder, B. Dauth, *Z. Elektrochem.* **1934**, *40*, 588; E. Zintl, G. Woltersdorf, *ibid.* **1935**, *41*, 876; E. Zintl, G. Brauer, *ibid.* **1935**, *41*, 297; E. Zintl, A. Harder, *Z. Phys. Chem. Abt. B* **1936**, *34*, 238.

[2] D. Kummer, L. Diehl, *Angew. Chem.* **1970**, *82*, 881; *Angew. Chem. Int. Ed. Engl.* **1970**, *9*, 895.

[3] For a review of these see: H. G. von Schnering, W. Hönle, *Chem. Rev.* **1988**, *88*, 243; J. D. Corbett, *ibid.* **1985**, *85*, 383; H. Schäfer, *Annu. Rev. Mater. Sci.* **1985**, *15*, 1; H. G. von Schnering, *Angew. Chem.* **1981**, *93*, 44; *Angew. Chem. Int. Ed. Engl.* **1981**, *20*, 33; H. Schäfer, B. Eisenmann, *Rev. Inorg. Chem.* **1981**, *3*, 29; H. Schäfer, B. Eisenmann, W. Müller, *Angew. Chem.* **1973**, *85*, 742; *Angew. Chem. Int. Ed. Engl.* **1973**, *12*, 694, and references therein.

[4] E. Garcia, A. H. Cowley, A. J. Bard, *J. Am. Chem. Soc.* **1986**, *108*, 6082.

[5] B. S. Pons, D. J. Santure, R. C. Taylor, R. W. Rudolph, *Electrochem. Acta* **1981**, *26*, 365.

[6] C. J. Warren, D. M. Ho, A. B. Bocarsly, R. C. Haushalter, *J. Am. Chem. Soc.* **1993**, *115*, 3316.

[7] Examples: a) $[Mg(N\text{-MeIm})_6]Sb_{12}S_{15}$ (*N*-MeIm = *N*-methylimidazole): P. P. Paul, T. B. Rauchfuss, S. R. Wilson, *J. Am. Chem. Soc.* **1993**, *115*, 3316; b) $(C_3H_7)_4NSb_3S_5$ and $C_4H_8N_2Sb_4S_7$: J. B. Parise, Y. Ko, *Chem. Mater.* **1992**, *4*, 1446; c) $CaSb_2S_4$, $Ca_2Sb_2S_5$ and $CaSb_4S_7$: T. N. Guliev, P. G. Rustamov, M. I. Chiragov, *Izv. Vyssh. Uchebn. Zaved. Khim. Khim. Tekhnol.* **1988**, *31*, 20; d) $SrSb_4S_7 \cdot 6H_2O$: G. Cordier, H. Schäfer, C. Schwidetzky, *Z. Naturforsch. B* **1984**, *39*, 131; e) $RbSb_3S_5 \cdot H_2O$: K. Volk, H. Schäfer, *ibid.* **1979**, *34*, 172; f) $Rb_2Sb_4S_7 \cdot H_2O$: G. Dittmar, H. Schäfer, *Z. Anorg. Allg. Chem.* **1978**, *441*, 93; g) $KSbS_2$: H. A. Graf, H. Schäfer, *ibid.* **1975**, *414*, 211; h) $K_2Sb_4S_7$: H. A. Graf, H. Schäfer, *Z. Naturforsch. B* **1972**, *27*, 735.

[8] Examples: a) $RbSb_3Se_5$: W. S. Scheldrick, H. J. Häusler, *Z. Anorg. Allg. Chem.* **1988**, *557*, 98; b) $CsSbSe_2$: A. S. Kanishcheva, Y. N. Mikhailov, V. B. Lazarev, N. A. Moshchalkova, *Dokl. Akad. Nauk SSSR* **1980**, *252*, 872; c) $BaSb_2Se_4$: G. Cordier, H. Schäfer, *Z. Naturforsch. B* **1979**, *34*, 1053; d) $KSbSe_2$: G. Dittmar, H. Schäfer *ibid.* **1977**, *32*, 1346.

[9] K. Volk, G. Cordier, R. Cook, H. Schäfer, *Z. Naturforsch. B* **1980**, *35*, 136.

[10] a) M. Evain, F. Boucher, R. Brec, J. Rouxel, J. S. Jung, C. J. O'Connor, *Eur. J. Solid State Inorg. Chem.* **1992**, *29*, 1055; b) J. S. Jung, B. Wu, E. D. Stevens, C. J. O'Connor, *J. Solid State Chem.* **1991**, *94*, 362.

[11] S. Geller, J. H. Wernick, *Acta Crystallogr.* **1959**, *12*, 46.

[12] A. S. Skoropanov, V. F. Skums, S. A. Al'fer, E. A. Gusev, A. A. Vecher, *Z. Phys. Chem. Leipzig* **1987**, *268*, 545.

[13] The yield calculations were based on 0.2475 g (0.3952 mmol) of Sb_2Te_3 electrode which dissolved after five days giving 0.1255 g of crystals that were collected from the cathode chamber. The percent yields were based on the assumption that the product was 80% **1** (0.1004 g, 0.0576 mmol) and 20% **2** (0.0251 g, 0.0137 mmol), and were calculated based on moles of Sb. Electrochemical yield = moles product per moles e^- passed. The deep brown color of the catholyte suggests that some fraction of the polyanions produced are soluble and remain in solution. The difference in stoichiometry of the reactant and products requires the existence of excess Te, which could also be present in the catholyte solution in the form of soluble polytellurides.

[14] Crystal data for **1**: orthorhombic, *Pbcn* (no. 60), $a = 41.790(9)$, $b = 17.978(2)$, $c = 18.132(4)$ Å, $V = 13{,}623(5)$ Å^3, $Z = 8$; 8964 unique reflections, 2671 with $F > 3.0\,\sigma(F)$, 281 parameters. $R(R_w) = 0.0692$ (0.0612). **2**: monoclinic, $P2_1/c$ (no. 14), $a = 23.580(5)$, $b = 13.446(3)$, $c = 20.427(4)$ Å, $\beta = 92.87(2)^\circ$, $V = 6{,}468(2)$ Å^3, $Z = 4$; 11455 unique reflections, 2503 with $F > 3.0\,\sigma(F)$, 292 parameters. $R(R_w) = 0.0629$ (0.0574). The data for both samples was collected on a Siemens P4 diffractometer ($Mo_{K\alpha}$ radiation) at 235 K. Structures were solved by direct methods and refined by full-matrix least-squares using the Siemens SHELXTL PLUS program package. Further details of the crystal structure determinations may be obtained from the Fachinformationszentrum Karlsruhe, Gesellschaft für wissenschaftlich-technische Information mbH, D-76344 Eggenstein-Leopoldshafen (FRG), on quoting the depository number CSD-57483, the names of the authors, and the journal citation.

[15] S. C. Critchlow, J. D. Corbett, *Inorg. Chem.* **1984**, *23*, 770.

[16] V. O. Mundt, G. Becker, H. J. Wessely, H. J. Breunig, H. Kischkel, *Z. Anorg. Allg. Chem.* **1982**, *486*, 70.

[17] R. K. McMullan, D. J. Prince, J. D. Corbett, *Inorg. Chem.* **1971**, *10(8)*, 1749.

[18] D. B. Sharma, J. Donohue, *Acta Crystallogr.* **1963**, *16*, 891; A. G. Turner, F. S. Mortimer, *Inorg. Chem.* **1966**, *5*, 906.

[19] H. Bärnighausen, T. von Volkmann, J. Jander, *Acta. Crystallogr.* **1966**, *21*, 571.

[20] a) T. Ito, N. Morimoto, S. Sadanaga, *Acta. Crystallogr.* **1952**, *5*, 775; b) E. J. Porter, G. M. Sheldrick, *J. Chem. Soc. Dalton Trans.* **1972**, 1347.

[21] A. M. Griffin, P. C. Minshall, G. M. Sheldrick, *J. Chem. Soc. Chem. Commun.* **1976**, 809.

[22] R. Faggiani, R. J. Gillespie, J. E. Vekris, *J. Chem. Soc. Chem. Commun.* **1988**, 902.

[23] T. J. Bastow, H. J. Whitfield, *J. Chem. Soc. Dalton Trans.* **1973**, 1739.

[24] C. J. Warren, D. M. Ho, R. C. Haushalter, A. B. Bocarsly, *J. Chem. Soc. Chem. Commun.*, in press.

[25] C. J. Warren, S. S. Dhingra, R. C. Haushalter, A. B. Bocarsly, unpublished results.

Substrate-Specific Catalysis by Ion Pairs**

By *Paul J. Smith, Eun-il Kim*, and *Craig S. Wilcox**

The electrostatic fields associated with charged and dipolar functional groups in the active sites of enzymes may well be essential to the rate accelerations achieved by these complex molecules. The electric fields generated by the spatially fixed polar groups of the protein can be properly positioned to complement the field of the transition state and in this way lower the activation energy for reaction.[1] To evaluate the magnitude of such effects and to contribute to current efforts to develop selective molecular recognition based catalysts,[2] we have examined the effects of ion pairs on the reactivity of some simple molecules in chloroform. Those

[*] Prof. Dr. C. S. Wilcox, P. J. Smith, E.-il Kim
Department of Chemistry
University of Pittsburgh
Pittsburgh, PA 15260 (USA)
Telefax: Int. code + (412)624-8552

[**] Chemistry of Synthetic Receptors and Functional Group Arrays, Part 22. This work was supported by the U.S. Health Service (National Institute of General Medical Sciences), the Alfred P. Sloan Foundation, and the University of Pittsburgh Faculty of Arts and Sciences. We thank Prof. Robert D. Coalson and Prof. David H. Waldeck for their thoughtful comments concerning this project. Part 21: C. S. Wilcox, T. H. Webb, F. J. Zawacki, N. Glagovich, H. Suh, *Supramolecular Chem.* **1993**, *1*, 129–137.

experiments have shown that covalently attached ion pairs can substantially accelerate chemical reactions in nonpolar solvents.[3] This suggests that the reversible binding of ion pairs to organic reactants could lead to significant rate enhancements in processes whose rate-determining step proceeds through a polar transition state (Fig. 1).[3b, 4] In this paper we illustrate the idea and confirm that the noncovalent binding of ion pairs can be used for selective and reversible activation of functional groups.

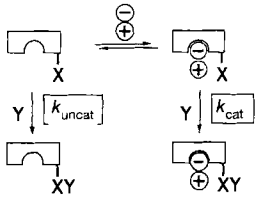

Fig. 1. Generalized example of ion pair catalysis. k_{cat} = rate constant for the catalyzed reaction, k_{uncat} = rate constant for the uncatalyzed reaction.

Amine **1** was synthesized because the urea group can serve as a strong binding site for ion pairs in chloroform.[5] Imidazolidinone **2** was prepared to serve as a control compound for **1** containing a blocked binding site. The measured association constant for **1** with zwitterion **3** in chloroform (determined by UV spectroscopic methods) is $1350 \pm 240\ M^{-1}$. Binding to ion pairs was also evaluated: tetrabutylammonium tosylate (**4**, $K_a = 1290\ M^{-1}$) and tetrabutylammonium benzoate (**5**, $K_a = 5800\ M^{-1}$) both bind to the urea derivative **1**.

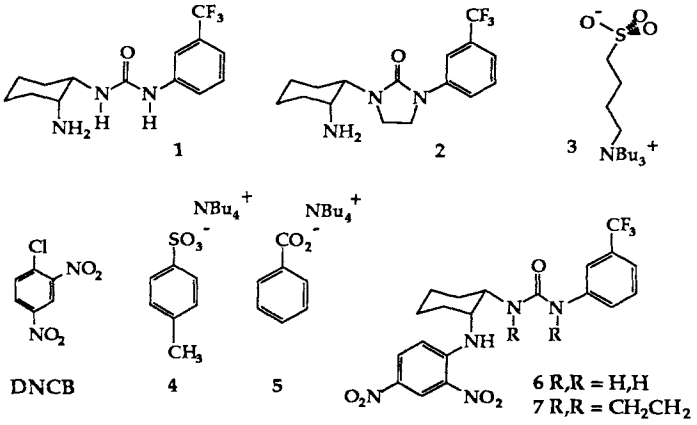

The reactions of amines **1** and **2** with 1-chloro-2,4-dinitrobenzene (DNCB) in the presence of various concentrations of ionic compounds **3**–**5** were examined. This reaction was chosen because its rate-determining step proceeds through a polar transition state, and it can be conveniently followed by UV/VIS spectrophotometry.[6] The initial rates for the reaction of 1.0 mM amine **1** or **2** with 20.0 mM DNCB in the presence of 0 to 5 mM **3** were measured in chloroform at 298 K. Absorbance at $\lambda = 420$ nm was used to monitor the appearance of products **6** or **7**, and data up to 2.0% conversion were used.

The results from the reactions of **1** and **2** with **3** are shown in Figure 2. The rate of reaction of **1** increased with increasing salt concentration, asymptotically approaching a limiting value. The initial rates for imidazolidinone **2**, which contains a blocked binding site, were found to increase only slightly and linearly in the range of zwitterion concentrations employed, as is usually the case for an intermolecular salt effect.[3b, 7] The binding site is therefore required for significant catalysis of this reaction by **3** in chloroform. Similar results were obtained with ion pairs **4** and **5**.

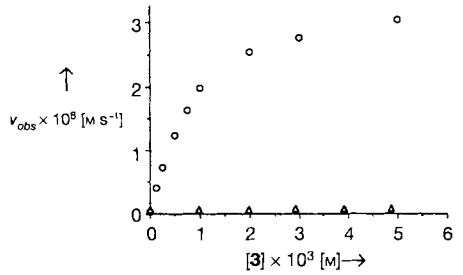

Fig. 2. Initial rates for the reactions of 1.0 mM **1** (○) and **2** (△) with 20.0 mM DNCB as a function of the concentration of added **3**. Each point represents the average value of two determinations. The measured initial rate in the absence of **3** is 2.64×10^{-10} M s^{-1}. The equation of the regression line (least squares) for these data is: reaction rate $v = 6.4 \times 10^{-10} + 3.0 \times 10^{-8} \times [3]$. All experiments were conducted in chloroform at 298 ± 1 K.

The observed catalysis of the reaction of **1** and DNCB by **3**, **4**, and **5** may be analyzed in terms of the Michaelis–Menten model for enzyme kinetics. The reaction process is mathematically equivalent to the "random BI-BI" enzyme reaction mechanism.[8] Nucleophilic attack is the rate-determining step for the reaction of DNCB with aliphatic amines in solvents with low dielectric constants ($k_3 \gg k_{-2}$, Scheme 1).[9] The absence of base catalysis by the nucleophile and by added bases is evidence that conversion of the σ complex to products is much faster than the back-reaction of this intermediate to give starting materials.[9] If this were the case for the catalyzed reaction (or more explicitly, if

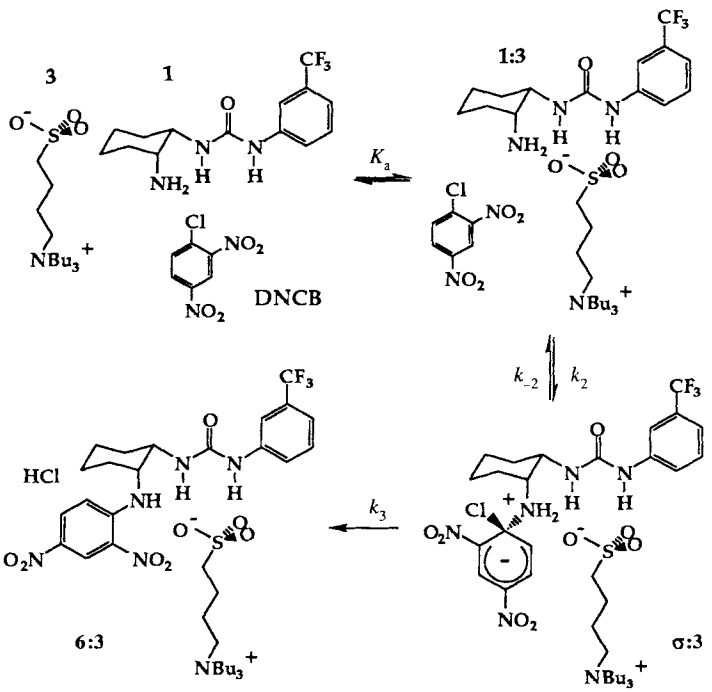

Scheme 1.

 © VCH Verlagsgesellschaft mbH, D-69451 Weinheim, 1993 0570-0833/93/1111-1649 $ 10.00+.25/0

$k_3 + k_{-2}$ were much larger than [DNCB] · k_2), then the value of K_M^{-1} (K_M = Michaelis constant) obtained from this plot should equal our measured value of K_a. A plot of $(v_{obs} - v_{uncat})^{-1}$ versus the reciprocal of concentration of the unbound salt (Fig. 3) allows K_M and k_{cat} to be determined. Since

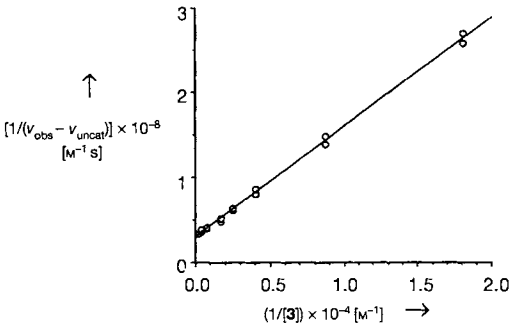

Fig. 3. Another plot of the data used in Figure 2. The reciprocal of the observed rate minus the uncatalyzed rate for the reaction of **1** and DNCB is plotted as a function of the reciprocal of initial concentration of unbound salt [14]. Sixteen data points are included. The equation of the regression line (least squares) for these data is: $(v_{obs} - v_{uncat}^{-1})^{-1} = 3.01 \times 10^7 + 1.30 \times 10^4$ ($[\mathbf{3}]^{-1}$).

k_{uncat} is known, the rate acceleration due to the presence of the ion pair ($k_{cat} \cdot k_{uncat}^{-1}$) can be calculated. For **4**, $K_M = 6.76 \times 10^{-4}$ M ($K_M^{-1} = 1480$ M^{-1}) and $k_{cat} \cdot k_{uncat}^{-1} = 84$; for **5**, $K_M = 1.85 \times 10^{-4}$ M ($K_M^{-1} = 5400$ M^{-1}) and $k_{cat} \cdot k_{uncat}^{-1} = 390$; and for the zwitterion **3**, $K_M = 4.33 \times 10^{-4}$ M ($K_M^{-1} = 2300$ M^{-1}) and $k_{cat} \cdot k_{uncat}^{-1} = 130$. Because the association constants K_a are used to calculate the concentration of unbound salt for the double-reciprocal plot, if the catalyst and substrate do not aggregate or follow alternative kinetic pathways under the reaction conditions, then the value of K_M^{-1} for these ion pairs will be in agreement with the measured association constants. Ion pairs **4** and **5** are freely soluble in chloroform (>1 M). At present we think that the discrepancy between K_M^{-1} and K_a observed for zwitterion **3** is best explained by aggregation of this marginally soluble species. In any case, the value of $k_{cat} \cdot k_{uncat}^{-1}$ would not be much affected by errors in K_a: for **4**, using the observed value of $K_a = 1290$ M^{-1}, $k_{cat} \cdot k_{uncat}^{-1} = 84$; using $K_a = 2590$ M^{-1}, $k_{cat} \cdot k_{uncat}^{-1} = 90$; using $K_a = 645$ M^{-1}, $k_{cat} \cdot k_{uncat}^{-1} = 110$.

What is the mechanism of catalysis? For the addition step, the bound salt would stabilize the polar intermediate reaction states and lower the standard free energy of the σ complex. Coulombic forces, including hydrogen bonding and dipole–dipole interactions, are likely to be the dominant forces. General base catalysis of this step by bound sulfonate is not possible, because the sulfonate is not basic enough to deprotonate the σ complex.[10] (The equilibrium constant for formation of a hydrogen-bonded ion pair between methanesulfonic acid and *n*-butylamine in chloroform is 4.5×10^9 M^{-1}.[11]) In aqueous solutions, Meisenheimer complexes of 1,3,5-trinitrobenzene and primary and secondary amines are 100–400 times less basic than the amines from which they are formed.[12]) These experiments cannot reveal the role the bound ion may have in the transformation of the intermediate σ complex to the product. The pathway from the σ complex to product could follow any of three pathways: 1) a direct loss of chloride ion, 2) a concerted general base mechanism, or 3) a nonconcerted general base/general acid mechnism in which bound sulfonic acid promotes the rate-determining loss of chloride ion.[6, 13]

The rate accelerations caused by these simple ion pairs are substantial and approach levels of catalysis that could afford practical control of reaction rates and selectivity. This work demonstrates that a simple ion pair can act as a potent substrate-specific catalyst for a complex chemical reaction in chloroform. The potential utility of ion pair catalysis for any given reaction may be reasonably predicted based on knowledge of the ground state and transition state character for the reaction. Enantioselective and diastereoselective processes can be proposed based on such ion pair catalysis, and experiments to demonstrate such selectivity are underway.

Received: June 14, 1993 [Z 6140 IE]
German version: *Angew. Chem.* **1993**, *105*, 1728

[1] A. Warshel, *Acc. Chem. Res.* **1981**, *14*, 284–290; A. Warshel, G. Naray-Szabo, F. Sussman, J.-K. Hwang, *Biochemistry* **1989**, *28*, 3629–3637.

[2] Selected recent examples from host–guest chemistry: aromatic substitution and eliminations: H.-J. Schneider, I. Theis, *J. Org. Chem.* **1992**, *57*, 3066–3070; F. P. Schmidtchen, *Top. Curr. Chem.* **1986**, *132*, 101–133; S_N2 reactions: T. R. Kelly, G. J. Bridger, C. Zhao, *J. Am. Chem. Soc.* **1990**, *112*, 8024–8034; A. McCurdy, L. Jimenez, D. A. Stauffer, D. A. Dougherty, *ibid.* **1992**, *114*, 10314–10321; oxidations: D. R. Benson, R. Valentekovich, F. Diederich, *Angew. Chem.* **1990**, *102*, 213–215; *Angew. Chem. Int. Ed. Engl.* **1990**, *29*, 191–193; C. J. Burrows in *Inclusion Phenonena and Molecular Recognition* (Ed.: J. L. Atwood), Plenum, New York, **1990**, pp. 199–207; S.-W. Tam, L. Jimenez, F. Diederich, *J. Am. Chem. Soc.* **1992**, *114*, 1503–1505; hydrogen abstraction: R. Breslow, P. J. Duggan, J. P. Light, *ibid.* **1992**, *114*, 3982–3983; ester hydrolysis: P. Scrimin, P. Tecilla, U. Tonellato, N. Vignaga, *J. Chem. Soc. Chem. Commun.* **1991**, 449–451; R. Breslow, B. Zhang, *J. Am. Chem. Soc.* **1992**, *114*, 5882–5883; phosphate ester hydrolysis: S. Shinkai, Y. Shirahama, T. Tsubaki, O. Manabe, *J. Chem. Soc. Perkin Trans. 1* **1989**, 1859–1860; M. Komiyama, K. Isaka, S. Shinkai, *Chem. Lett.* **1991**, 937–940; M. W. Göbel, J. W. Bats, G. Dürner, *Angew. Chem.* **1992**, *104*, 217–219; *Angew. Chem. Int. Ed. Engl.* **1992**, *31*, 207–209; V. Jubian, R. P. Dixon, A. D. Hamilton, *J. Am. Chem. Soc.* **1992**, *114*, 1120–1121; K. Ariga, E. V. Anslyn, *J. Org. Chem.* **1992**, *57*, 417–419; acyl transfer: L. E. Fikes, D. T. Winn, R. W. Sweger, M. P. Johnson, A. W. Czarnik, *J. Am. Chem. Soc.* **1992**, *114*, 1493–1495; T. K. Park, Q. Feng, J. Rebek, *ibid.* **1992**, *114*, 4529–4532; phosphate ester formation: M. W. Hosseini, J.-M. Lehn, *J. Chem. Soc. Chem. Commun.* **1991**, 451–453; pericyclic reactions: T. R. Kelly, P. Meghani, V. S. Ekkundi, *Tetrahedron Lett.* **1990**, 3381–3384; S. C. Hirst, A. D. Hamilton, *J. Am. Chem. Soc.* **1991**, *113*, 382–383; K. Harano, H. Kiyonaga, T. Hisano, *Tetrahedron Lett.* **1991**, 7557–7558; additions to aldehydes: F. Diederich, H.-D. Lutter, *J. Am. Chem. Soc.* **1989**, *111*, 8438–8446; K. Tanaka, A. Mori, S. Inoue, *J. Org. Chem.* **1990**, *55*, 181–185; A. Terfort, G. von Kiedrowski, *Angew. Chem.* **1992**, *104*, 626–628; *Angew. Chem. Int. Ed. Engl.* **1992**, *31*, 654–656.

[3] a) P. J. Smith, C. S. Wilcox, *J. Org. Chem.* **1990**, *55*, 5675–5678; b) P. J. Smith, C. S. Wilcox, *Tetrahedron* **1991**, *47*, 2617–2628; c) P. J. Smith, D. J. Soose, C. S. Wilcox, *J. Am. Chem. Soc.* **1991**, *113*, 7412–7414.

[4] Rate effects of proximate charges on reactions conducted in aqueous media: B. G. Cox, P. DeMaria, A. Fini, A. F. Hassan, *J. Chem. Soc. Perkin Trans. 2* **1981**, 1351–1357; D. B. Dahlberg, M. L. Kuzemko, Y. Chiang, A. J. Kresge, M. F. Powell, *J. Am. Chem. Soc.* **1983**, *105*, 5387–5390; P. Haberfield, *Mol. Struct. Energ.* **1988**, *10*, Chap. 4.

[5] P. J. Smith, M. V. Reddington, C. S. Wilcox, *Tetrahedron Lett.* **1992**, 6085–6088.

[6] F. Terrier, *Nucleophilic Aromatic Displacement: The Influence of the Nitro Group*, VCH, New York, **1991**.

[7] C. L. Perrin, J. Pressing, *J. Am. Chem. Soc.* **1971**, *93*, 5705–5710.

[8] I. H. Segel, *Biochemical Calculations*, Wiley, New York, **1976**, pp. 293–299.

[9] C. F. Bernasconi, *MTP Int. Rev. Sci. Org. Chem. Ser. One 1973* **1973**, *3*, 33–63.

[10] W. P. Jencks, *Acc. Chem. Res.* **1976**, *12*, 425–432.

[11] M. Rumeau, *Ann. Chim.* **1973**, *8*, 131–138.

[12] C. F. Bernasconi, M. C. Muller, P. Schmid, *J. Org. Chem.* **1979**, *44*, 3189–3196.

[13] J. A. Orvik, J. F. Bunnett, *J. Am. Chem. Soc.* **1970**, *92*, 2417–2427.

[14] M. L. Bender, R. J. Bergeron, M. Komiyama, *The Bioorganic Chemistry of Enzymatic Catalysis*, Wiley, New York, **1984**, p. 287.

Parallels and Decisive Differences in Vitamin B_{12} Biosyntheses**

By *Francis Blanche,** *Dennis Thibaut, Laurent Debussche, Ralf Hertle, Franz Zipfel,* and *Gerhard Müller**

Studies on the chemical nature of the microbial biosynthesis of vitamin B_{12}[1,14] have revealed that the organization of the individual reactions in the aerobe *Pseudomonas denitrificans* and the anaerobe *Propionibacterium shermanii* differs significantly, and that these differences could be evolutionary in their origins. The work of Blanche, Crouzet et al.[1a-c] has provided deep insight into the molecular nature of vitamin B_{12} synthesis. Their construction and efficient application of recombinant strains of *P. denitrificans* led to the discovery and isolation of new and spectacular vitamin B_{12} precursors with the responsible cloned enzymes.

It was shown that the tetrapyrrolic vitamin B_{12} ligand hydrogenobyrinic acid **7**[2] is synthesized without cobalt via the precorrins 2(**1**) and 3(**2**)[2a,14] as well as the newly discovered ring-contracted precorrins 4(**3**)[3], 6x(**4**),[4] 6y(**5**),[5] and 8x(**6**)[6] (Scheme 1). After two obligatory amidations leading to **7**-*a*,*c*-diamide,[7] cobalt is inserted by the cobaltchelatase responsible for vitamin B_{12} formation.[8] In the case of *P. shermanii* neither **7** nor **7**-*a*,*c*-diamide are precursors of vitamin B_{12}.[2,9a] Instead cobyrinic acid (**8**), the cobalt-containing analogue of **7**, and **8**-*a*,*c*-diamide appear in the biosynthetic pathway.[9a,10] Enzyme preparations from *P. shermanii* are able to transform in vitro not only the oxidized and aromatized precorrins 2(**1a**) and 3(**2a**)[2a,14] (known as factors II and III, respectively) into **8**, but also the cobalt complexes of **1a** and **2a**.[9] In contrast, the enzyme systems from *P. denitrificans* that produce **7** are able to use only **1a** and **2a** but not the corresponding cobalt complexes.

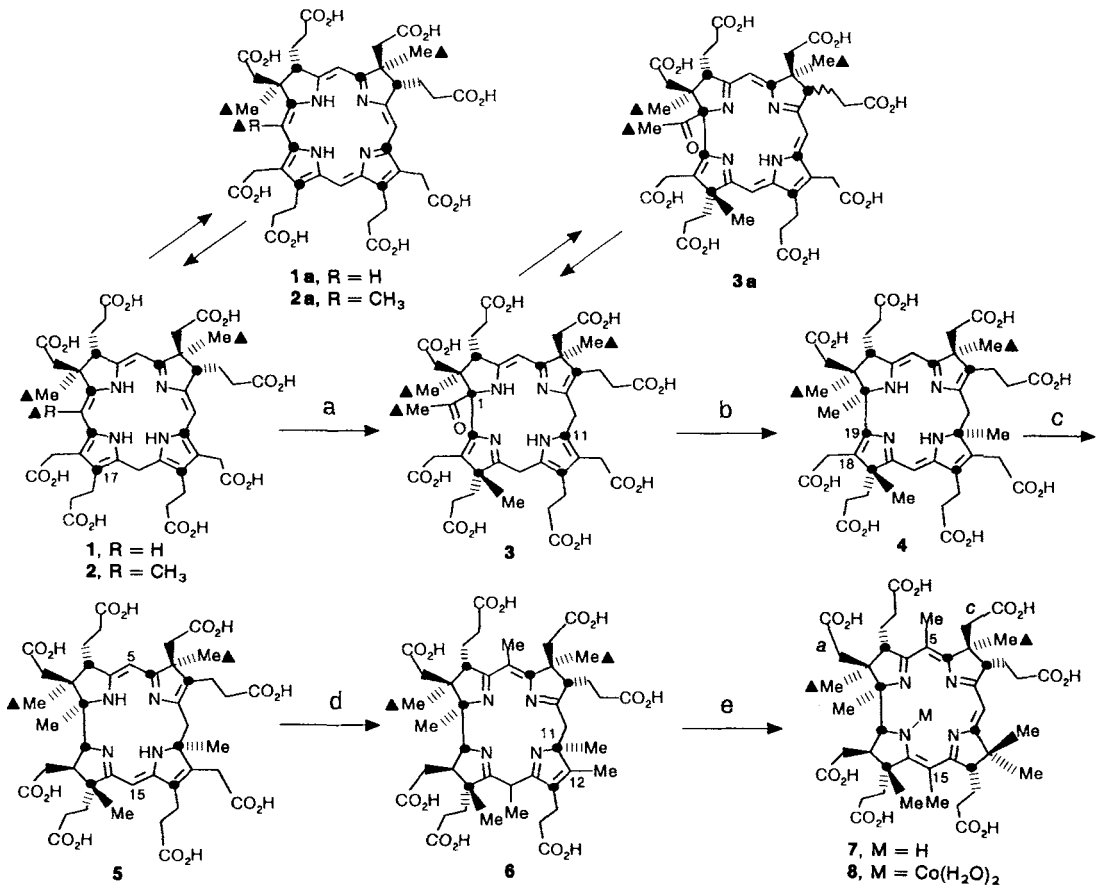

Scheme 1. Reaction steps and individual reactions of the biosynthetic pathway precorrin 3(**2**) → hydrogenobyrinic acid (**7**) and the gene products responsible [1c] (in brackets) in *Pseudomonas denitrificans*: a) ring contraction, C17 methylation (CobG and CobJ); b) elimination of the C20 acetate group and C11-, C1-methylation (CobM and CobF); c) NADPH-dependent C18/C19 reduction (CobK); d) C5-, C15-methylation + C12-acetate decarboxylation (CobL); e) C12-methylation by C11 → C12 methyl group migration (CobH), as well as regiospecific $^3H/^{14}C$ labeling via precorrin 3(**2**), biosynthesized from [4-^{14}C]5-aminolevulinate and *S*-adenosyl-L-[methyl-$^3H_3$]methionine • = ^{14}C and ▲ = ^{3}H. **1a**, **2a**, and **3a** are oxidation products or isolates from the corresponding precorrins 2–4 and can be channeled into the pathway of **7** [2a, 3]. **1a** and **2a** are utilized in the formation of **8** [2a, 14].

[*] Dr. G. Müller, Dipl.-Biol. R. Hertle, Dr. F. Zipfel
Institut für Organische Chemie und Isotopenforschung der Universität
Azenbergstrasse 18, D-70174 Stuttgart (FRG)
Dr. F. Blanche, Dr. D. Thibaut, Dr. L. Debussche
Département Analyse
Centre de Recherche de Vitry-Alfortville
Rhône-Poulenc Rorer S.A.
BP 14, F-94403 Vitry-sur-Seine (France)

[**] This work was supported by the Deutsche Forschungsgemeinschaft. We would like to thank Dr. J. Lunel (Rhône-Poulenc Rorer) for supporting this collaboration.

These and other results demonstrated that in *P. shermanii* cobalt insertion must occur at the latest after the third methylation step.[9a,b] Our latest investigations using $^{57}Co^{2+}$ have shown then that weakly enriched enzyme preparations from *P. shermanii* catalyze a cobalt insertion after the addition of either **1a** or **2a**. However, if the incubation conditions are such that [edta] ≫ [Co^{2+}], then the enzymatic insertion of cobalt is only observed with **1a**. As expect-

ed in in-vitro investigations into the formation of **8** at high concentrations of edta, only **1a** (and not **2a**) is converted to **8**. From these results it is concluded that in *P. shermanii* the true substrate for the relevant cobaltchelatase must be a dimethylated precursor. Interestingly, Co^{III}-**1a** has been previously converted into Co^{III}-**2a** under in-vitro conditions.[9a, b] Additional precursors of **8** or the enzymes responsible for their formation are not known. However, the sequence of methylation that begins with uroporphyrinogen III is the same in both organisms.[2a] To try and answer the question of the role the ring-contracted precursors of **7** (formed by *P. denitrificans*) play in the synthesis of **8**, incorporation studies based on tried-and-true procedures using $^3H/^{14}C$ doubly labeled substrates **3a**, **4**, **5**, and **6** and the enzyme systems from *P. shermanii* leading to **8** were carried out.[2, 9] Although with the known substrates **2a** and Co^{III}-**1a** (experiments 1 and 2) markedly higher levels of incorporation were achieved, the results summarized in Table 1 demonstrate unequivocally that precursors **4**, **5**, and **6** from the pathway leading to **7** can be converted into **8** by enzyme preparations from *P. shermanii*.

Table 1. Formation of cobyrinic acid (**8**) with enzyme preparations from *P. shermanii* [2] and the radioactively [$^3H/^{14}C$] doubly labeled substrates factor III (**2a**), Co^{III} factor II (Co^{III}-**1a**), precorrin 6x(**4**), precorrin 6y(**5**), and precorrin 8x(**6**) [a].

Exp.		Substrate		**8** isolated and analyzed as its heptamethyl ester [2]			
		[Bq nmol^{-1}] [e]	^3H:^{14}C [g]	[Bq] [e]	^3H:^{14}C [g]	[nmol] [f]	[%] [h]
1 [i]	**2a** [b]	45.7	4.5	3729	3.4	81.6	16.32
2 [i]	Co^{III}-**1a** [c]	28.9	4.96	1176	4.93	40.7	8.14
3	**4** [d]	74.9	3.2	659	3.1	8.8	1.74
4	**5** [d]	74.9	3.2	329	3.0	4.4	0.88
5	**6** [d]	57.2	2.7	766	2.55	13.4	2.68

[a] In each case the same enzyme preparation was used: 70 g (wet weight) of bacterial cells in 140 mL of 52 mM phosphate buffer (pH 7.7) per experiment [2] + 285 μM *S*-adenosyl-L-methionine + 58 μM Co^{2+} + 70 μM reduced nicotinamide-adenine dinucleotide phospate (NADPH) + 42 μM ethylenediaminetetraacetic acid (edta) + 500 nmol [$^3H/^{14}C$] doubly labeled substrate [g]. [b] Synthesized by in-vitro biosynthesis from [4-^{14}C]5-aminolevulinate + *S*-adenosyl-L-[methyl-$^3H_3$]methionine [2]. [c] In the same manner as [b] followed by chemical incorporation of cobalt. [d] Synthesized by in-vitro biosyntheses from **2a** via **3** + *S*-adenosyl-L-methionine: **4** [4a], **5** [5a], **6** [6b], and **3a** [3]. [e] Based only on ^{14}C radioactivity. [f] Based on radiochemical yields of the substrate/product transformation. [g] Refers to the regiospecific labeling, see Scheme 1. [h] Incorporation rates based on the radioactive substances used. [i] Control experiments with known substrates.

A plausible explanation based on these and earlier results[9] is that cobalt complexes of the tetrapyrrolic ligands **4**, **5**, and **6** occur in the biosynthesic pathway of **8**, and that these formed spontaneously from added substrates during the incorporation experiments. Indeed, this would explain the relatively low levels of incorporation observed. Direct evidence that cobalt-coordinated ligands were present during the in-vitro transformations to **8** came from the additional results of these experiments. Because of low substrate specifity of the mutase in *P. shermanii* responsible for the transfer of a methyl group from C11 to C12 (reaction step e in Scheme 1), enzyme preparations of *P. shermanii* convert **6** not only into **8** but also into **7** (e.g. 10 nmol **7** in experiment 5, isolated and analyzed as the heptamethyl ester[2]), which is not a precursor of **8** and in fact inhibits its formation.[2] But considering that **6** is the only substrate investigated that was transformed into **7**, cobalt complexes of **4** and/or **5** must have been present during the in-vitro transformation into **8**. In this context the results achieved with **4** and **5** (experiments 3 and 4) are of special interest. With these two substrates it was possible for the first time to biosynthetically prepare the 5-noranalogue of **8**[11] (10 nmol in experiment 3 and 4.2 nmol in experiment 4), whose cobalt-free ligand does not occur in *P. denitrificans*. Since the order of the *meso* methylation in *P. shermanii* is C5 > C15,[2a] the occurrence of this norcobyrinate, which has been shown not to be a precursor of **8**,[9a, 12] must be attributed to a regiospecifically incorrect primary methylation at C15 of **5**.

The conclusions based on the results can be summarized as follows: a) the pentamethylated ligand **4** with its characteristic structural features also occurs in *P. shermanii*; b) the individual reactions in the synthesis of **7** outlined in c, d, and e in Scheme 1 are also carried out in principle in the synthesis of **8**; c) in *P. shermanii*, however, cobalt-coordinated ligands are used instead; and d) the mutase enzyme from *P. shermanii* responsible for a sigmatropic 1,5 methyl shift is not very specific with respect to the central ion and *meso*-methyl groups already present.

Experiments with the didehydroisolate of unstable **3**, factor IV (**3a**), were negative. Although **3a** was transformed into **7** by means of reaction steps b, c, d, and e by using the enzyme systems from *P. denitrificans* leading to **7**, it proved impossible to convert $^3H/^{14}C$ doubly labeled **3a**[3] into **8** with the corresponding enzyme preparations from *P. shermanii*. It remains unclear if the reaction steps following the third methylation, for example the C17 methylation and/or the nature of the ring contraction, differ in *P. shermanii* and *P. denitrificans*. Experiments to clarify this point will be undertaken as soon as the corresponding substrates become available. Of special interest is a tetramethylated cobalt corphinoid that was recently isolated in minute quantities from *P. shermanii* and was found to be protein bound.

Received: July 7, 1993 [Z 6193 IE]
German version: *Angew. Chem.* **1993**, *105*, 1704

[1] a) B. Cameron, K. Briggs, S. Pridmore, G. Brefort, J. Crouzet, *J. Bacteriol.* **1989**, *171*, 547; b) J. Crouzet, S. Levy-Schil, B. Cameron, L. Chauchois, S. Rigault, M.-C. Rouyez, F. Blanche, L. Debussche, D. Thibaut, *ibid.* **1991**, *173*, 6074; c) L. Debussche, D. Thibaut, B. Cameron, J. Crouzet, F. Blanche, *ibid.*, in press.

[2] a) F. Blanche, D. Thibaut, D. Fréchet, M. Vuilhorgne, J. Crouzet, B. Cameron, K. Hlineny, U. Traub-Eberhard, M. Zboron, G. Müller, *Angew. Chem.* **1990**, *102*, 947; *Angew. Chem. Int. Ed. Engl.* **1990**, *29*, 884 and references therein; b) T. E. Podschun, G. Müller, *ibid.* **1985**, *97*, 63 or **1985**, *24*, 46.

[3] D. Thibaut, L. Debussche, D. Fréchet, F. Herman, M. Vuilhorgne, F. Blanche, *J. Chem. Soc. Chem. Commun.* **1993**, 513.

[4] a) D. Thibaut, L. Debussche, F. Blanche, *Proc. Natl. Acad. Sci. USA* **1990**, *87*, 8795; b) D. Thibaut, F. Blanche, L. Debussche, F. J. Leeper, A. R. Battersby, *ibid.* **1990**, *87*, 8800.

[5] a) F. Blanche, D. Thibaut, A. Famechon, L. Debussche, B. Cameron, J. Crouzet, *J. Bacteriol.* **1992**, *174*, 1036; b) D. Thibaut, F. Kuichi, L. Debussche, F. J. Leeper, F. Blanche, A. R. Battersby, *J. Chem. Soc. Chem. Commun.* **1992**, 139.

[6] a) F. Blanche, A. Famechon, D. Thibaut, L. Debussche, B. Cameron, J. Crouzet, *J. Bacteriol.* **1992**, *174*, 1050; b) D. Thibaut, M. Couder, A. Famechon, L. Debussche, B. Cameron, J. Crouzet, F. Blanche, *ibid.* **1992**, *174*, 1043.

[7] L. Debussche, D. Thibaut, B. Cameron, J. Crouzet, F. Blanche, *J. Bacteriol.* **1990**, *172*, 6239.

[8] L. Debussche, M. Couder, D. Thibaut, B. Cameron, J. Crouzet, F. Blanche, *J. Bacteriol.* **1992**, *174*, 7745; F. Blanche, L. Moton, L. Debussche, D. Thibaut, *ibid.* **1992**, *174*, 7452.

[9] a) G. Müller, K. Hlineny, E. Savvidis, F. Zipfel, J. Schmiedl, E. Schneider, *Chemical Aspects of Enzyme Biotechnology Fundamentals* (Eds.: T. B. Baldwin, F. M. Rushel, A. I. Scott), Plenum, New York, **1990**, p. 281; b) G. Müller, F. Zipfel, K. Hlineny, E. Savvidis, R. Hertle, U. Traub-Eberhard, A. I. Scott, H. J. Williams, N. J. Stolowich, P. J. Santander, M. Warren, F. Blanche, D. Thibaut, *J. Am. Chem. Soc.* **1991**, *113*, 9893.

[10] K. Bernhauer, F. Wagner, H. Michna, P. Rapp, H. Vogelmann, *Hoppe-Seyler's Z. Physiol. Chem.* **1968**, *349*, 1297.
[11] Spectroscopic data for the isolated dicyano-5-nor-**8** heptamethylester with correct $^3H/^{14}C$ ratio: UV/VIS (CH_2Cl_2): λ_{max} [nm] (rel. int.) = 278 (0.79), 310 (0.69), 325 (sh, 0.67), 350 (sh, 0.80), 368 (1.0), 420 (0.50), 505 (0.51), 542 (0.59), 580 (0.62); MS(FAB): *m/z* 1023 (M^+ + H). Consistent with authentic substance: M. Zboron, Dissertation, Universität Stuttgart, **1990** and ref. [12a].
[12] a) C. Nussbaumer, D. Arigoni, *Angew. Chem.* **1983**, *95*, 746; *Angew. Chem. Int. Ed. Engl.* **1983**, *22*, 736; b) J. Kulka, C. Nussbaumer, D. Arigoni, *J. Chem. Soc. Chem. Commun.* **1990**, 1512; c) I. Grgurina, S. Handa, G. Weaver, P. Cole, A. R. Battersby, *ibid.* **1990**, 1514.
[13] A. I. Scott, H. J. Williams, N. J. Stolowich, P. Karuso, M. D. Gonzales, G. Müller, K. Hlineny, E. Savvidis, E. Schneider, U. Traub-Eberhard, G. Wirth, *J. Am. Chem. Soc.* **1989**, *111*, 1898.
[14] Reviews: a) A. I. Scott, *Angew. Chem.* **1993**, *105*, 1281; *Angew. Chem. Int. Ed. Engl.* **1993**, *32*, 1223; b) A. R. Battersby, *Pure Appl. Chem.* **1993**, *65*, 1113; c) F. J. Leeper, *Nat. Prod. Rep.* **1985**, *2*, 19; *ibid.* **1987**, *4*, 441; *ibid.* **1989**, *6*, 171.

The First Complex with a Tetraethynylcyclobutadiene Ligand**

By *Uwe H. F. Bunz** and *Volker Enkelmann*

Dedicated to Dr. Manfred Kämper on the occasion of his 60th birthday

Perethynylated arenes and π perimeters such as **1**–**4** have not been widely investigated. The benzene derivative **1** was synthesized in 1986 by Vollhardt et al. by reacting hexabromobenzene with trimethylsilylacetylene in the presence of a palladium catalyst.[1] The interest in compounds such as **1**–**4** arises from their aesthetic structure, their potential applicability as multidentate ligands in organometallic chemistry,[2] and their use as potential building blocks for carbon-rich molecular entities.[3] Compound **1** was used as starting material for the synthesis of triangulane.[4] The multiple alkynylation of arenes was demonstrated by Whitesides et al., Stille et al., and Präfcke et al.; they found that some polyalkynylated arenes form discotic phases[5] or, as in the case of tetraethynylthiophene, produce glassy carbon fibers upon controlled pyrolysis.[4a, b]

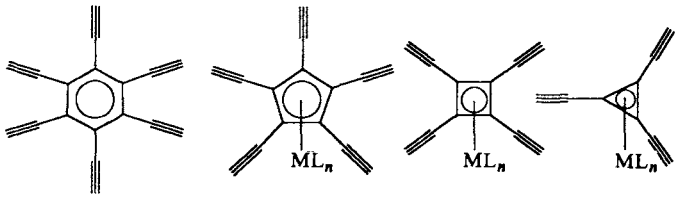

1 **2** **3** **4**

In contrast to **1**, nothing is known about the complexed smaller homologues **2**–**4** and perethynylcyclooctatetraene. In view of their high density of functional groups as well as the ease of derivatization and the complexing ability of the alkyne groups, such compounds are attractive synthetic targets. We report here the preparation of several derivatives of **3** [$ML_n = Fe(CO)_3$].

To synthesize a tetraalkyne such as **3**, its inherent sensitivity has to be taken into consideration. Neither the starting material **5** nor the expected product would survive heating with CuI and amine at 100 °C for several days, the conditions used by Vollhardt[1] to prepare **1**. An alternative approach, based on the coupling of stannylated alkynes with iodoarenes and iodocyclopentadienyl complexes, was successfully applied by Stille; this reaction leads to complete conversion of the corresponding starting materials within a day at room temperature under neutral conditions.[6] However, it was not clear if this method was suitable for multiple substitution of the tetraiodide **5**.[7]

We first attempted to react **5** with an excess of *tert*-butyl(trimethylstannyl)acetylene **6a** in dimethylformamide (DMF) using the catalyst system described by Farina et al.[8] (Scheme 1). Removal of the solvent under high vacuum fol-

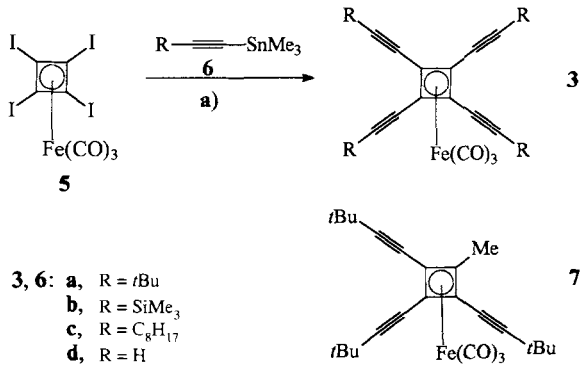

Scheme 1. a) 5 equivalents of stannane, 5.5 mol% $[Pd_2(dba)_3]$, 22 mol% triphenylarsine, about 60 mL DMF, 18 h at 20 °C, column filtration over Al_2O_3. **3a**: 40%; **7**: 20%; **3b**: 83%; **3c**: 25%.

lowed by flash chromatography on silica gel (pentane/dichloromethane 95:5) afforded the two compounds **3a** and **7** as pale yellow, somewhat light-sensitive, but otherwise stable crystalline powders in 40 and 20% yields, respectively. We assume that **7** was formed by the transfer of a methyl group from **6a** to **5**, because the high steric demand of the *t*Bu substituent at the alkyne should reduce its reactivity.

If the trimethylsilyl-protected stannylacetylene **6b** is used, **3b** can be isolated after filtration of the crude product over neutral aluminum oxide in 83% yield. In this reaction no methyl derivative analogous to **7** can be detected. The octyl-substituted tin alkyne **6c** can be used to give **3c** in 25% yield after chromatography over aluminum oxide. While solid **3b** is only slightly sensitive to light, the oil **3c** has to be stored under exclusion of light in a freezer.

Treatment of **3b** with potassium carbonate in methanol gave the parent compound **3d** in 79% yield. The complex with unprotected tetraalkyne ligand is stable in chloroform at −30 °C for several weeks; however, it can only be isolated for a short period of time at low temperature (below 0 °C) and under an inert atmosphere. Solid **3d** polymerizes at room temperature even with the exclusion of air within minutes to give an insoluble dark brown material.

The structures of the compounds **3a**–**d** and **7** follow from spectroscopic data (Table 1). The NMR spectrum of **3d**, which as a result of the high molecular symmetry only has a few lines, will serve as an example. The ^{13}C NMR spectrum

[*] Dr. U. H. F. Bunz, Priv.-Doz. Dr. V. Enkelmann
Max-Planck-Institut für Polymerforschung
Ackermannweg 10, D-55021 Mainz (FRG)
Telefax: Int. code + (6131)379-100

[**] We thank BASF for a generous donation of cyclooctatetraene and trimethylstannyl chloride. U. H. F. B. thanks the Fonds der Chemischen Industrie for a Justus-von-Liebig-Stipendium and Prof. Dr. Klaus Müllen for generous support. According to the IUPAC rules the compound **3d** would be named tricarbonyl [(1,2,3,4-η)-1,2,3,4-tetraethynyl-1,3-cyclobutadiene]iron.

Table 1. Physical data of **3a–d** and **7** [a].

3a: M.p. 137 °C; IR (KBr): $\tilde{\nu}$[cm^{-1}] = 2970, 2217, 2045, 1992; ^{1}H NMR ($CDCl_3$): δ = 1.28 (s, 36H; *t*Bu); ^{13}C NMR ($CDCl_3$): δ = 28.41 (s, $C(CH_3)_3$), 30.67 (q, $C(CH_3)_3$), 68.46, 69.12, 103.99 (3 s, ring-C/alkyne-C), 212.48 (s, CO); MS (70 eV): *m/z* 512 (M^+, 2%), 484 (M − CO, 12%), 456 (M − 2CO, 7%), 427 (M − 3CO, 100%); correct elemental analysis.

7: Sublimation 60 °C, 0.001 Torr; IR (KBr): $\tilde{\nu}$[cm^{-1}] = 2972, 2952, 2931, 2215, 2039, 1991, 1960, 1920; ^{1}H NMR ($CDCl_3$): δ = 1.22 (s, 18H; *t*Bu), 1.24 (s, 9H; *t*Bu), 1.85 (s, 3H, Me); ^{13}C NMR ($CDCl_3$): δ = 10.43 (q, Me), 28.35, 28.51 (2 s; $C(CH_3)_3$), 30.70, 30.75 (2 q, $C(CH_3)_3$), 65.22, 67.32, 69.20, 69.39, 88.33, 103.31, 103.48 (7 s, ring-C/alkyne-C), 213.18 (s, CO); MS (70 eV): *m/z* 446 (M^+, 2%), 418 (M − CO, 6%), 390 (M − 2CO, 5%), 362 (M − 3CO, 100%); high-resolution MS: *m/z* 444.1599 (found for M^+) 444.1591 (calcd).

3b: M.p. 128 °C; IR (KBr): $\tilde{\nu}$[cm^{-1}] = 2961, 2155, 2055, 2006, 1251; ^{1}H NMR ($CDCl_3$): δ = 0.19 (s, 36H; $SiMe_3$); ^{13}C NMR ($CDCl_3$): δ = −0.31 (q, $SiMe_3$), 67.37 (s, ring-C), 94.05, 102.11 (s, alkyne-C), 210.95 (s, CO); MS (FD): *m/z* 576 (M^+, 28%), 548 (M − CO, 75%), 492 (M − 3CO, 100%); high-resolution MS: *m/z*: 574.1146 (found for M^+) 574.1138 (calcd).

3c: Yellow oil; IR (KBr): $\tilde{\nu}$[cm^{-1}] = 2955, 2928, 2856, 2227, 2048, 1988, 1983, 1953, 1466; ^{1}H NMR ($CDCl_3$): δ = 0.86 (t, ^3J(H,H) = 6.6 Hz, 3H; CH_3); 1.26–1.40 (m, 10H; 5 CH_2), 1.53 (quint, ^3J(H,H) = 7.3 Hz; 2H; CH_2), 2.30 (t, ^3J(H,H) = 7.0 Hz, 2H; propargyl-H); ^{13}C NMR ($CDCl_3$): δ = 14.07 (q, CH_3), 19.89, 22.66, 28.34, 28.77, 29.07, 29.20, 31.84 (t, $(CH_2)_7$), 68.28, 70.57, 96.29 (3 s, ring-C/alkyne-C), 212.19 (s, CO).

3d: IR (KBr): $\tilde{\nu}$[cm^{-1}] = 3296, 3283, 2075, 2063, 2024, 2016, 1997, 1965, 1223, 833.94; ^{1}H NMR ($CDCl_3$): δ = 3.27 (s, 4H; alkyne-H); ^{13}C NMR ($CDCl_3$): δ = 65.51 (s, ring-C), 72.64 (s, -*C*≡C-H), 83.58 (d, -C≡*C*-H), 209.91 (s, CO).

[a] The ^{1}H NMR spectra were recorded at 300 MHz, the ^{13}C NMR spectra at 75 MHz.

of **3d** has a characteristic signal at δ = 209.91 for the CO groups bonded to the iron center and other signals at δ = 83.58 and 72.64 for the alkyne carbon atoms. A singlet shifted to high field at δ = 65.51 can be assigned to the C atoms in the four-membered ring. This interpretation is supported by the value of the J(C,H) coupling constants. The ^{1}H NMR spectrum shows, as expected, one singlet at δ = 3.27. In the IR spectrum only bands in the region around 3300 and from 1900 to 2100 cm^{-1} are observed.

The remarkable tetragonal topology was verified by the crystal structure of complex **3b**[9] (Fig. 1). It is noteworthy

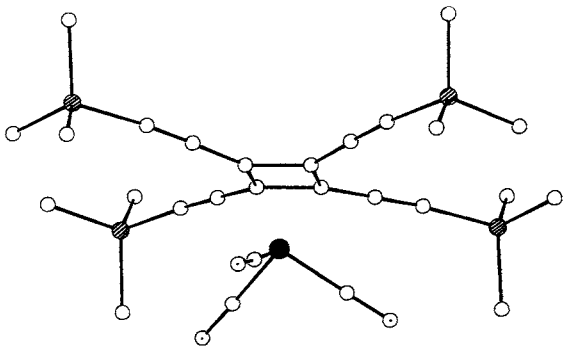

Fig. 1. Crystal structure of **3b**. The hydrogen atoms are omitted for clarity. Important bond lengths [pm]: C–C bonds in the four-membered ring: 144.2(7), 145.5(6), 147.4(7), 148.3(6). C(four-membered ring)–Fe: 203.2(9); -C≡C- (average): 121.0(7). White circles are C atoms, hatched circles are Si atoms, circles with a dot are O atoms, and the black circle is the Fe atom.

that the structure **3b** has a distinctly lower symmetry than that of the unsubstituted tricarbonyl (cyclobutadiene) iron **8**:[10] the four C–C bonds of the cyclobutadiene ligand

$(C_4H_4)Fe(CO)_3$ **8**

lie in the range 144–148 pm and are therefore about 4 pm longer than those obtained for the parent compound **8**. The average length of the triple bonds is 121 pm and thus consistent with reported values.[11] Also noteworthy is the distortion of the expected square arrangement of the alkyne substituents: the distances of the silicon atoms from one another lie in the range 690–850 pm, and are therefore not equidistant. This distortion results from packing effects; a trimethylsilyl and a tricarbonyliron group of neighboring molecules lie between two acetylene arms each of the molecule considered and thus widen the corresponding bond angles (Fig. 2). Such a ring distortion was not observed in the hexaethynylbenzene **1**.[1]

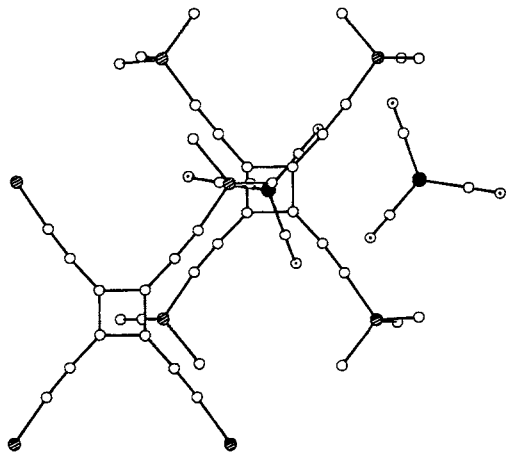

Fig. 2. The interaction of a Me_3Si and a $Fe(CO)_3$ group with the alkyne substituents in **3b** causes an unexpected distortion (labeling of the atoms as in Fig. 1).

We describe here the synthesis of new tetraethynylated-cyclobutadiene iron tricarbonyl complexes by palladium-catalyzed fourfold Stille coupling. These perethynylated compounds are fascinating monomers for the construction of carbon networks.

Experimental Procedure

3b: Tetraiodide **5** (936 mg, 1.35 mmol), stannane **6b** (1.76 g, 6.73 mmol), $[Pd_2(dba)_3]$ (68.7 mg, 75.0 μmol), and triphenylarsine (91.9 mg, 300 μmol) were dissolved in anhydrous DMF (60 mL) with exclusion of air and moisture. After the mixture had been stirred for 18 h, DMF was removed under high vacuum and the residue was filtered over neutral aluminum oxide. In this manner 641 mg (83%) of **3b** were obtained. Analogous reactions of **6a, c** gave **3a** (40%) and **7** (20%) as a mixture as well as **3c** (25%).

3d: Silane **3b** (205 mg, 355 μmol) was dissolved in methanol (20 mL), potassium carbonate (400 mg, 2.89 mmol) was added, and the mixture was stirred for 15 min. Partition between water and diethyl ether, drying of the organic phase and removal of the solvent at −10 °C/0.01 Torr gave 81 mg (79%) of **3d**.

Received: June 16, 1993 [Z 6144 IE]
German version: *Angew. Chem.* **1993**, *105*, 1712

[1] a) R. Diercks, J. C. Armstrong, R. Boese, K. P. C. Vollhardt, *Angew. Chem.* **1986**, *98*, 270; *Angew. Chem. Int. Ed. Engl.* **1986**, *25*, 268; b) butadiyne-substituted benzene derivatives: R. Boese, J. R. Green, J. Mittendorf, D. L. Mohler, K. P. C. Vollhardt, *Angew. Chem.* **1992**, *104*, 1643; *Angew. Chem. Int. Ed. Engl.* **1992**, *31*, 1643.
[2] R. Diercks, K. P. C. Vollhardt, *J. Am. Chem. Soc.* **1986**, *108*, 3150.
[3] A. D. Schlüter, K. P. C. Vollhardt, unpublished results.
[4] a) T. X. Neenan, G. M. Whitesides, *J. Org. Chem.* **1988**, *53*, 2489; T. X. Neenan, M. R. Callstrom, L. M. Scarmoutzos, K. R. Stewart, G. M. Whitesides, V. R. Howes, *Macromolecules* **1988**, *21*, 3525; M. R. Callstrom, T. X. Neenan, G. M. Whitesides, *ibid.* **1988**, *21*, 3528; b) D. R. Rutherford, J. K. Stille, *ibid.* **1988**, *21*, 3530; c) Review on the synthetic approaches toward molecular and polymeric carbon allotropes: F. Diederich, Y. Rubin, *Angew. Chem.* **1992**, *104*, 1123; *Angew. Chem. Int. Ed. Engl.* **1992**, *31*, 1101.

[5] a) J. A. Hyatt, *Org. Prep. Proced. Int.* **1992**, *23*, 460; b) K. Präfcke, B. Kohne, D. Singer, *Angew. Chem.* **1990**, *102*, 200; *Angew. Chem. Int. Ed. Engl.* **1990**, *29*, 177; M. Ebert, D. A. Jungbauer, R. Kleppinger, J. H. Wendorff, B. Kohne, K. Präfcke, *Liq. Cryst.* **1989**, *4*, 53; K. Präfcke, B. Kohne, K. Gutbier, N. Johnen, D. Singer, *ibid.* **1989**, *5*, 233; c) A. Laschewsky, *Angew. Chem. Adv. Mater.* **1989**, *101*, 1606; *Angew. Chem. Adv. Mater. Int. Ed. Engl.* **1989**, *28*, 1574.

[6] C. L. Sterzo, J. K. Stille, *Organometallics* **1990**, *9*, 687, and references therein.

[7] G. Amiet, K. Nicholas, R. Pettit, *J. Chem. Soc. Chem. Commun.* **1970**, 161.

[8] V. Farina, B. Krishnan, *J. Am. Chem. Soc.* **1991**, *113*, 9585.

[9] Crystal data for $C_{27}H_{36}FeO_3Si_4$: Enraf-Nonius-CAD4 diffractometer, $Cu_{K\alpha}$ radiation. Structure solution with direct methods. Parameters of the H atoms were refined in the "riding mode". Programs used: SIR 88, Molen. $a = 1049.7(1)$, $b = 1254.08(6)$, $c = 1477.70(9)$ pm, $\alpha = 105.169(4)$, $\beta = 103.028(7)$, $\gamma = 106.850(6)^\circ$, $P\bar{1}$, $Z = 2$, $V = 1.6986\ 10^9$ pm^3, $\varrho_{calcd} = 1.128$ g cm^{-3}, $\mu = 51.33$ cm^{-1}; 3792 measured reflections, of which 2836 observed ($I > 3\sigma(I)$), $R = 0.038$, $R_w = 0.045$. Further details of the crystal structure investigation may be obtained from the Fachinformationszentrum Karlsruhe, Gesellschaft für wissenschaftlich-technische Information mbH, D-76344 Eggenstein-Leopoldshafen (FRG) on quoting the depository number CSD-57427, the names of the authors, and the journal citation.

[10] P. D. Harvey, W. P. Schaefer, H. B. Gray, F. R. Gilson, I. S. Butler, *Inorg. Chem.* **1988**, *27*, 57.

[11] J. L. Hencher in *The Chemistry of the Functional Groups, The Chemistry of the Carbon-Carbon Triple Bond, Part 1* (Ed.: S. Patai), Wiley, New York, **1978**, p. 57.

Decamethylaluminocenium, a π-Stabilized R_2Al^+ Cation**

By *Carsten Dohmeier, Hansgeorg Schnöckel,* Christian Robl, Uwe Schneider*, and *Reinhart Ahlrichs**

Numerous reactions of organoaluminum compounds and their IR and NMR spectroscopic investigations have given hints for the existence of π complexes containing a three-coordinate aluminum center and three unsaturated organic ligands.[1] However, only a small number of these compounds could be characterized by X-ray or electron diffraction methods. Among these are complexes with π interations between Al and one C atom of an unsaturated ligand[2] with the structural unit **A**[3] and with η^3-bound Cp* groups (Cp* = C_5Me_5).[4]

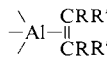

A

Only recently η^5-bound Cp* ligands could be identified in both $[(Cp^*Al)_4]$ (**1**)[5] and in $[(Cp^*AlCl_2)_2]$.[6] This coordination type is especially suited for stabilizing Al^I centers because of a strong π bond.[7] This stabilization raises the questions whether even the strongly Lewis-acidic aluminum atom of an R_2Al^+ cation can be stabilized by Cp* ligands, and if the small central ion in a $[Cp^*_2Al]^+$ complex leads to a ferrocene-like sandwich structure.[8] We report here on the synthesis and characterization of a compound containing cation **2**.

$[(\eta^5\text{-}Cp^*)_2Al]^+$ **2**

A solution of **1** was heated in toluene at 110 °C for 20 days then cooled to room temperature to provide (apart from metallic aluminum) a colorless substance, which shows a sharp signal in its ^{27}Al NMR spectrum at $\delta = -114.5$ ($\omega_{1/2} = 50$ Hz, benzene). Comparison of these results with those from the ^{27}Al NMR investigations of a reaction product formed from $AlCl_3$ and Cp*Li implies that the observed signal arises from an Al^{III} compound.[9] This NMR chemical shift, which is the furthest upfield yet reported for an Al^{III} compound (diamagnetic ring current effect of the aromatic rings), indicates η^5-bound Cp* groups with enhanced Al–Cp* bonding as a result of π contributions.[10] The narrow peak-width, which results from a highly symmetric charge distribution at the aluminum nucleus, is in accordance with the proposed ferrocene analogue $[(\eta^5\text{-}Cp^*)_2Al]^+$ **2**.

To check this hypothesis we performed ab initio calculations for **3** and **2**. The SCF geometry optimization[11] yielded

$[Cp_2Al]^+$ **3**

the following results (X denotes the center of the C_5 rings): **3**: $d(Al\text{–}C) = 220.4$, $d(Al\text{–}X) = 184.3$, $d(C\text{–}C) = 142.1$ pm; **2**: $d(Al\text{–}C) = 220.8$, $d(Al\text{–}X) = 183.6$, $d(C_{ring}\text{–}C_{ring}) = 142.9$, $d(CH_3\text{–}C_{ring}) = 151.0$ pm. The conformer of **2** with staggered Cp* ligands (D_{5d}) is more stable than that having eclipsing ligands by 1.9 kJ mol^{-1}. The rotational barrier is even smaller for **3** (0.47 kJ mol^{-1}[12]). In addition we performed MP2 calculations[13] for **3** to investigate the influence of electron correlation on the structure. Configuration interaction leads to a shortening of the Al–C distance by 3 pm and to an elongation of the C–C bond by 1 pm. We expected similar trends for the homologous compound **2**: **2** ["MP2"]: $d(Al\text{–}C) = 217.4$ pm and $d(C_{ring}\text{–}C_{ring}) = 143.9$ pm.

Subsequent calculations of the ^{27}Al NMR chemical shifts by the GIAO-SCF method[14, 15] provided a value of $\delta = -130.0$ for the MP2 geometry of **3** and $\delta = -119.8$ for the corrected structure of **2**.[16] The expected maximum error amounts to $\Delta\delta \approx 15$.[10] We thus obtained close agreement between the measured signal ($\delta = -114.5$) and the predicted value, which confirms our structural hypothesis.

Since the product of the thermal disproportionation of **1**[17] was not suitable for X-ray structure determination, we attempted to isolate cation **2** with other counterions. The reaction of [Cp*Al] with $AlCl_3$ leads to precipitation of Al and formation of the colorless, extremely air- and moisture-sensitive complex **4** [Eq. (a)]. The mass spectrum (positive and negative ions) confirms the reaction product. Compound **4** forms triclinic crystals in the space group $P\bar{1}$ with two formula units per unit cell. The $[(\eta^5\text{-}Cp^*)_2Al]^+$ ions occupy two crystallographically independant inversion cen-

$$3[Cp^*Al] + AlCl_3 \longrightarrow 2\,Al + [(\eta^5\text{-}Cp^*)_2Al][\eta^1\text{-}Cp^*AlCl_3] \quad \text{(a)}$$

4

[*] Prof. Dr. H. Schnöckel, Dipl.-Chem. C. Dohmeier
Institut für Anorganische Chemie der Universität
Kaiserstrasse, D-76128 Karlsruhe (FRG)
Telefax: Int. code + (721)608 4854

Prof. Dr. R. Ahlrichs, Dipl.-Chem. U. Schneider
Lehrstuhl für Theoretische Chemie
Institut für Physikalische Chemie und Elektrochemie der Universität
Kaiserstrasse 12, D-76128 Karlsruhe (FRG)

Priv.-Doz. Dr. C. Robl
Institut für Anorganische Chemie der Universität
Meiserstrasse 1, D-80333 München (FRG)

[**] This work was supported by the Deutsche Forschungsgemeinschaft and the Fonds der Chemischen Industrie. We thank Prof. Dr. F. Kreissl for giving us access to a mass spectrometer and R. Dumitrescu for recording the mass spectra.

ters. The X-ray structure[18] is shown in Figure 1. The average Al–C distance in the staggered conformation found here amounts to 215.5 pm, in good agreement with the MP2-corrected value of 217.4 pm. Even the calculated structure of the Cp* groups is confirmed by the X-ray results. Both predict a slight bend of the methyl groups out of the ring plane and away from the metal atom (expt. $\approx 1.8°$, calc. $= 4.0°$).

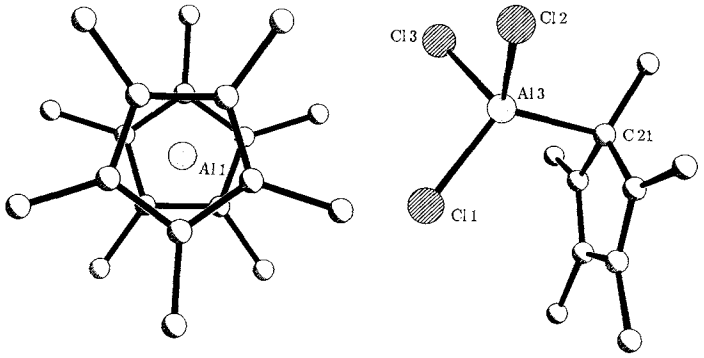

Fig. 1. Molecular structure of one of the two crystallographically independant $[(\eta^5\text{-Cp*})_2\text{Al}]^+$ (left) and $[\eta^1\text{-Cp*AlCl}_3]^-$ (right) ions in **4**. Selected distances and angles ([pm] and [°], $(d_{min}|d_{max}|\bar{d})$, standard deviations in parentheses): $[(\eta^5\text{-Cp*})_2\text{Al}]^+$: (X denotes the center of the C_5 ring) Al-C_{ring} (213.7(8)|218.4(8)|215.5), CH_3-C_{ring} (150.7 (11)|153.4(9)|152.0), C_{ring}-C_{ring} (140.9(11)|145.0(9)|142.9); X-Al-X (180.0(1)), CH_3-C-X (0.8|2.6|1.8). $[\eta^1\text{-Cp*AlCl}_3]^-$: Al3-C21 202.0(6), Al3-Cl1 214.2(3), Al3-Cl2 217.2(3), Al3-Cl3 217.1(3).

The anion $[\eta^1\text{-Cp*AlCl}_3]^-$ in **4** is nearly C_s symmetric. The η^1-coordination of the Cp* ligand to the Al center seems reasonable when one considers the increased negative charge on the metal atom compared to that in the dimer $[(\eta^5\text{-Cp*AlCl}_2)_2]$.[6] The Al–C bond length in **4** amounts to 202.0 pm; the Al–Cl distances are all nearly the same (217.2 and 214.2 pm) and lie within the range observed for $AlCl_4^-$ ions.

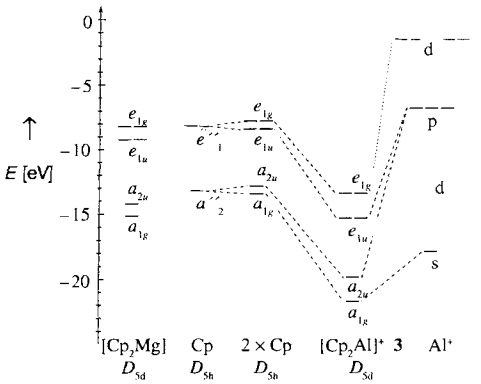

Fig. 2. MO diagram of **3** compared to Cp, Al^+ and $[Cp_2Mg]$ [26].

The π interactions that contribute to Al–Cp* bonding in the decamethyl aluminocenium ion **2** are a new contribution to stabilizing cationic aluminum compounds. The MO diagram in Figure 2 shows the energetic order of the high-lying molecular orbitals of **3**, which arise from linear combinations of the π orbitals of the C_5H_5 rings and 3s, 3p, and 3d atomic orbitals of the Al^+ ion. In comparison with the MOs of the isoelectronic complex $[Cp_2Mg]$,[19] the pronounced stabilization of all MOs in **3** by the net positive charge is evident. The splitting of ligand group orbitals in **3** ($a_{1g} + a_{2u}$ from $2a_2''$ and $e_{1u} + e_{1g}$ from $2e_1''$) is determined by the energetic position of the Al atomic orbitals: the stabilizing influence of the 3s orbital is greater than that of the 3p AOs, and the high-lying 3d AOs contribute even less to bonding. The MO diagram is in accordance with the Mulliken population analysis (MPA)[20] applied to **3**, which ascribes to the Al^+ ion a 3s occupation of 0.55, a $3p_{x,y}$ population of 0.34 each, a $3p_z$ occupation of 0.17 and a total d population of only 0.45.

If one considers the Al–Cp bond based on the purely ionic formulation $[Al^{3+}(Cp^-)_2]$, the charges are equalized by both σ-type bonding (0.76 electrons in 3s, $3p_z$, and $3d_{z^2}$) and π-type bonding (1.08 electrons in $3p_{x,y}$ and $3d_{xz,yz}$). The resulting net charges ($Al^{+1.14}$, $Cp^{-0.07}$) indicate strongly covalent contributions to the Al–Cp bonding.

Until now R_2Al^+ ions were known only in the gas phase[21] or as Lewis acid/base complexes. The latter can be donor-stabilized either intermolecularly as in $[AlMe_2 \cdot [15]\text{crown-5}]^+$ [22] or intramolecularly as in $[Al\{2\text{-C}(SiMe_3)_2C_5H_4N\}_2]^+$.[23] The boron-containing cation $[Cp_2^*B]^+$ prepared by Jutzi et al. was found to have the structure $[(\eta^5\text{-Cp*})(\eta^1\text{-Cp*})B]^+$ in NMR spectroscopic studies.[24] This means that **2** is as yet the only known sandwich complex of an element from the third main group. The higher positive charge on the Al center in **2** leads to a pronounced decrease in the metal–ring distance relative to that in $[Cp_2^*Mg]$ ($d(Mg-C) = 234.1$ pm[25]). This forces the Cp* rings closer together, and the energetic gap between eclipsed and staggered conformations increases ($\Delta E(Cp_2Mg) = 0.13$ kJ mol^{-1};[26] $\Delta E(\mathbf{3}) = 0.47$ kJ mol^{-1}; $\Delta E(\mathbf{2}) = 1.9$ kJ mol^{-1}).

Experimental Procedure

All reactions were carried out under nitrogen in pre-dried vessels. NMR spectra were recorded on a Joel GSX-270 spectrometer, TMS (^{1}H) and $[Al(H_2O)_6]^{3+}$ (^{27}Al, 70.4 MHz) served as external standards. MS: (CI, isobutane, Finnigan (MAT 90)), fragments with intensities less than 5% not listed.

4: [Cp*Al] (50 mg, 0.309 mmol) and $AlCl_3$ (15 mg, 0.115 mmol, resublimed prior to use) were suspended in 3.5 mL toluene, whereupon elimination of aluminum began. The originally yellow solution faded after the starting materials had completely dissolved. After 3 d the reaction tube was heated to 100 °C for 15 h. By slowly cooling, colorless extremely air- and moisture-sensitive **4** was obtained (29 mg, ≈ 50%). M.p. 232 °C (decomp). – Since **4** is poorly soluble in aromatic hydrocarbons, NMR spectra were recorded in $CDCl_3$. This solvent reacts with **4**, and $[Cp_2^*Al][AlCl_4]$ is formed. ^{1}H NMR ($CDCl_3$): $\delta = 2.20$ (br.); ^{27}Al NMR ($CDCl_3$): $\delta = 103.0$ ($\omega_{1/2} = 8$ Hz), $\delta = -115.2$ ($\omega_{1/2} = 8$ Hz). MS [*m/z* (%)]: positive ions: 429 $[Cp_2^*Al_2Cl_3]^+$ (5.4), 297 $[Cp_2^*Al]^+$ (100); negative ions: 367 $[Cp_2^*AlCl_2]^-$ (15.8), 267 $[Cp^*AlCl_3]^-$ (100).

Received: May 29, 1993 [Z 6113 IE]
German version: *Angew. Chem.* **1993**, *105*, 1714

[1] J. J. Eisch in *Comprehensive Organometallic Chemistry, Vol. 1* (Eds.: G. Wilkinson, F. G. A. Stone, E. W. Abel), Pergamon, London, **1982**, p. 555.
[2] For example: G. D. Stucky, A. Mootz McPherson, W. E. Rhine, J. J. Eisch, J. L.Considine, *J. Am. Chem. Soc.* **1974**, *96*, 1941; A. Almenningen, L. Fernholt, A. Haaland, *J. Organomet. Chem.* **1978**, *155*, 245; B. Teclé, P. W. R. Corfield, J. P. Oliver, *Inorg. Chem.* **1982**, *21*, 458.
[3] H. Schnöckel, M. Leimkühler, R. Lotz, R. Mattes, *Angew. Chem.* **1986**, *98*, 929; *Angew. Chem. Int. Ed. Engl.* **1986**, *25*, 921; D. Drew, A. Haaland, *Acta Chem. Scand.* **1973**, *27*, 3735.

[4] P. R. Schonberg, R. T. Paine, C. F. Campana, *J. Am. Chem. Soc.* **1979**, *101*, 7726; P. R. Schonberg, R. T. Paine, C. F. Campana, E. N. Duesler, *Organometallics* **1982**, *1*, 799.
[5] C. Dohmeier, C. Robl, M. Tacke, H. Schnöckel, *Angew. Chem.* **1991**, *103*, 594; *Angew. Chem. Int. Ed. Engl.* **1991**, *30*, 564.
[6] H.-J. Koch, S. Schulz, H. W. Roesky, M. Noltemeyer, H.-G. Schmidt, A. Heine, R. Herbst-Irmer, D. Stalke, G. M. Sheldrick, *Chem. Ber.* **1992**, *125*, 1107.
[7] R. Ahlrichs, M. Ehrig, H. Horn, *Chem. Phys. Lett.* **1991**, *183*, 227.
[8] Until now our attempts to prepare $[Cp^*_2Al]^-$ with an Al^I central atom, which is isoelectronic to $[Cp^*_2Si]$, have not been successful.
[9] When 1.0 mmol $AlCl_3$ and 1.0 mmol Cp*Li were allowed to react at 25 °C in toluene/diethyl ether, the following ^{27}Al NMR signals were observed after 4 d: $\delta(C_6D_6) = 101.2$ and 115.0. The sample thus contains the previously described compound among others.
[10] J. Gauss, U. Schneider, R. Ahlrichs, C. Dohmeier, H. Schnöckel, *J. Am. Chem. Soc.* **1993**, *115*, 2402.
[11] All calculations were performed with TURBOMOLE program package (R. Ahlrichs, M. Bär, M. Häser, H. Horn, C. Kölmel, *Chem. Phys. Lett.* **1989**, *162*, 165) on IBM RISC/6000 workstations. Basis sets for geometry optimization: Al: (10s7p)/[4s3p] + d ($\eta = 0.30$); C: (7s3p)/[3s2p] + d ($\eta = 0.80$); H: (3s)/[2s]. All basis sets were fully optimized (A. Schäfer, H. Horn, R. Ahlrichs, *J. Chem. Phys.* **1992**, *97*, 2571). SCF total energy: **2**: −1015.49175 a.u.; **3**: −625.66939 a.u.
[12] For **3**, the D_{5d} structure was proved to correspond to a local minimum on the potential energy surface by calculating the geometry hessian of the SCF energy.
[13] In MP2 calculations electron correlation is treated with second-order perturbation theory (C. Møller, M. S. Plesset, *Phys. Rev.* **1934**, *46*, 618).
[14] GIAO (Gauge-Including Atomic Orbitals): R. Ditchfield, *Mol. Phys.* **1974**, *27*, 789.
[15] M. Häser, R. Ahlrichs, H.-P. Baron, P. Weis, H. Horn, *Theor. Chim. Acta* **1992**, *83*, 455.
[16] For GIAO-SCF calculations the basis sets must have more flexibility than for structure calculations. Following ref. [10] we chose the following contraction schemes: Al: (11s7p1d)/[6s5p1d], C: (8s4p1d)/[4s3p1d], and H: (4s1p)/[2s1p]. The conversion from the calculated nuclear shieldings to NMR chemical shifts is done according to the formula $\delta_{subst} = \delta_{ref} + \sigma_{ref} - \sigma_{subst}$, which implies that the results depend on the choice of the reference molecule. We chose AlH_4^- as a standard, because it can easily be treated with theoretical methods, and its chemical shift has been measured several times (see, for example, H. Nöth, *Z. Naturforsch. B* **1980**, *35*, 119 and referenes therein).
[17] The hitherto obtained spectroscopic results indicate a multistep reaction. Probably [Cp*Al] first forms $[(Cp^*_2Al)Cp^*]$, which reacts to give a compound with the structural element $[Cp^*(C_5Me_4CH_2)Al]$ and to Cp*H. To clarify this reaction sequence further experiments will be necessary.
[18] X-ray structure analysis: $C_{30}H_{45}Al_2Cl_3$, $M = 566.0$, triclinic, space group $P\bar{1}$, $a = 910.6(3)$, $b = 970.5(3)$, $c = 1872.7(5)$ pm, $\alpha = 99.73(2)$, $\beta = 90.76(2)$, $\gamma = 92.24(2)°$, $V = 1629.5 \times 10^6$ pm^3, $Z = 2$, $\varrho_{calcd.} = 1.153$ g cm^{-3}, F(000) = 604, $\mu = 3.5$ cm^{-1} ($Mo_{K\alpha}$), 295 K, ω-Scan, $\theta_{max} = 22°$, scan velocity 1.30–14.65° min^{-1}, scan width 1.3°, Siemens R3m/V diffractometer, graphite monochromator, 4398 reflections recorded, of which 4002 were symmetry-independant, $R_{int} = 0.0206$; 2439 reflections with $|F| > 3\sigma_{|F|}$ classified as observed. Calculations with SHELXTL-Plus, 320 parameters, hydrogen atoms geometrically positioned. Non-hydrogen atoms anisotropically refined, numerical absorption correction; $R = 0.0789$, $R_w = 0.0505$, $R_g = 0.0365$, $w = \sigma^{-2}_{|F|}$. Extremes of the final difference Fourier synthesis: +0.37/−0.32 e × 10^{-6} pm^3. Further details of the crystal structure determination may be obtained from the Fachinformationszentrum Karlsruhe, Gesellschaft für wissenschaftlich-technische Information mbH, D-76344 Eggenstein-Leopoldshafen on quoting the depository number CSD-57426, the names of the authors, and the journal citation.
[19] If no Al basis functions of d type are included in the calculation, then **3** is destabilized by 81 kJ mol^{-1}. Calculations without valence p functions lead to an increase in energy by 216 kJ mol^{-1} (see: H. Horn, R. Ahlrichs, *J. Am. Chem. Soc.* **1990**, *112*, 2121).
[20] R. Mulliken, *J. Chem. Phys.* **1955**, *23*, 1833.
[21] R. Srinivas, D. Sülzle, H. Schwarz, *J. Am. Chem. Soc.* **1990**, *112*, 8334.
[22] S. G. Bott, A. Alvanipour, S. D. Morley, D. A. Atwood, C. Mitchell Means, A. W. Coleman, J. L. Atwood, *Angew. Chem.* **1987**, *99*, 476; *Angew. Chem. Int. Ed. Engl.* **1987**, *26*, 485.
[23] L. M. Engelhardt, U. Kynast, C. L. Raston, A. H. White, *Angew. Chem.* **1987**, *99*, 702; *Angew. Chem. Int. Ed. Engl.* **1987**, *26*, 681.
[24] P. Jutzi, A. Seufert, *J. Organomet. Chem.* **1978**, *161*, C5.
[25] R. A. Andersen, R. Blom, J. M. Boncella, C. J. Burns, H. V. Volden, *Acta Chem. Scand. Ser. A* **1987**, *41*, 24; R. A. Andersen, J. M. Boncella, C. J. Burns, R. Blom, A. Haaland, H. V. Volden, *J. Organomet. Chem.* **1986**, *312*, C49.
[26] K. Faegri, Jr., J. Almlöf, H. P. Lüthi, *J. Organomet. Chem.* **1983**, *249*, 303.

Synthesis of a Nine-Membered Cyclic Analogue of the Neocarzinostatin Chromophore and Its DNA-Cleaving Activity**

By *Takashi Takahashi,* Hiroshi Tanaka, Yoshimasa Hirai, Takayuki Doi, Haruo Yamada, Takashi Shiraki,* and *Yukio Sugiura*

Neocarzinostatin (NCS)[1] is a naturally occurring antitumor antibiotic complex consisting of a protein component (NCS apo-protein) and a chromophoric molecule (NCS-chr, **1**). The antitumor activity of NCS is attributed primarily to the NCS-chr **1**, which is proposed to undergo a thiol-triggered epoxide opening followed by a Myers' type cyclization[2] of enynecumulene **2** leading to a highly reactive biradical **3**, which abstracts hydrogen atoms from the sugar phosphate backbone of DNA[3] (Scheme 1).

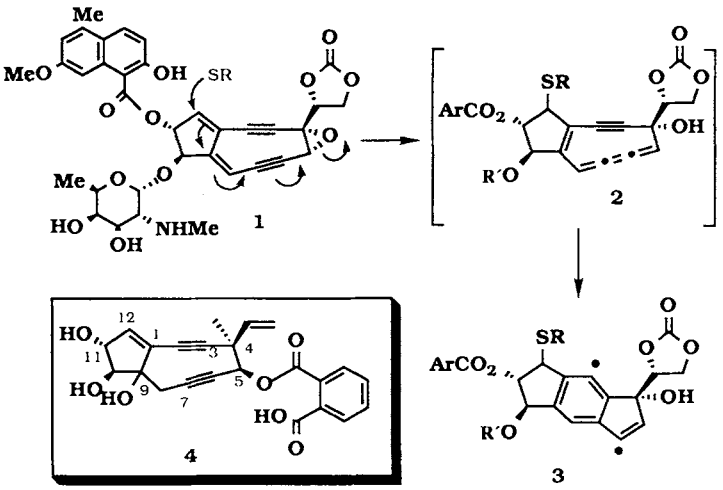

Scheme 1. Mechanism for the generation of the biradical of the NCS-chr **1** and the structure of the nine-membered analogue NCS analogue **4**. The $ArCO_2$ group corresponds to the substituted naphthoic acid residue, R'O the sugar residue in **1**.

The design and synthesis of DNA-cleaving molecules is currently a topic of intense research.[4] So far, four groups[5] have succeeded in synthesizing nine-membered analogues of NCS-chr **1**. Of these, two groups[5a,b] have demonstrated cycloaromatization of their analogues, but no group has achieved DNA cleavage. In this communication we report the first synthetic nine-membered analogue **4** which is sufficiently stable at ambient temperature to allow its handling and shows strong DNA-cleaving activity.[6]

In our synthetic plan, the first key reaction is the transannular [2,3]-Wittig rearrangement[7] of the twelve-membered cyclic ether **6**, prepared by the intramolecular O-alkylation of bromoalcohol **7** (Scheme 2). In this way we are able to construct a highly strained nine-membered diyne **5**, in which

[*] Prof. Dr. T. Takahashi, H. Tanaka, Y. Hirai, Dr. T. Doi, Dr. H. Yamada
Department of Chemical Engineering
Tokyo Institute of Technology
Meguro, Tokyo 152 (Japan)
T. Shiraki, Prof. Dr. Y. Sugiura
Institute for Chemical Research
Kyoto University
Uji, Kyoto 611 (Japan)

[**] We would like to thank Dr. Nancy I. Totah (Columbia University) for helpful discussions that have made this publication possible.

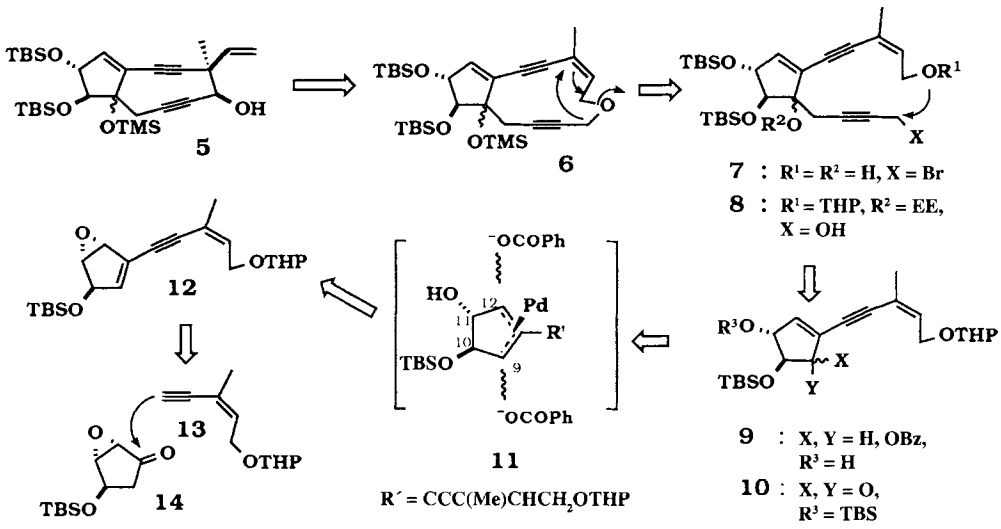

Scheme 2. The strategy for the synthesis of diyne **5**. TBS = tBuMe$_2$Si, TMS = Me$_3$Si, THP = tetrahydropyranyl, EE = ethoxyl ethyl. In Pd complex **11** only one of the two benzoate groups are bound at either C9 or C12.

the newly formed secondary alcohol and vinyl groups can be used to introduce a phthalic acid "trigger" and a cyclic carbonate group, respectively. MM2 calculations[8] of the possible conformations of **6** (Fig. 1) suggest that its [2,3]-Wittig rearrangement should proceed smoothly.

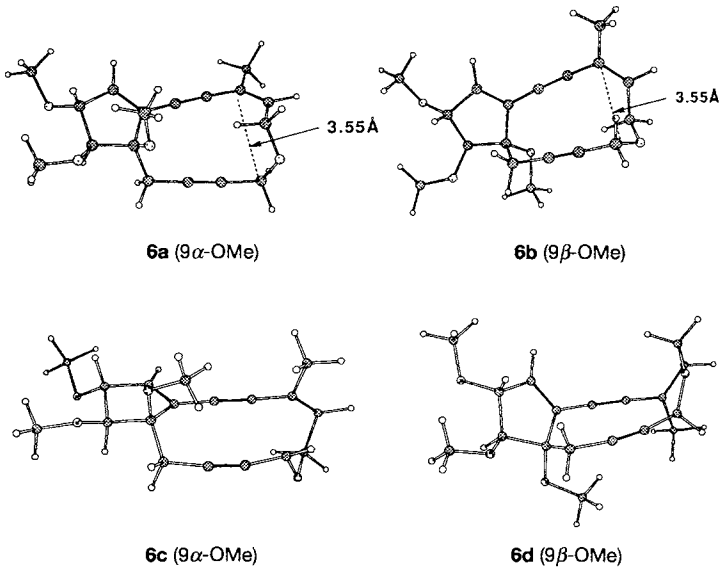

Fig. 1. Conformational analyses of the twelve-membered cyclic ether **6** based on MM2 models of the ground state (**6a**, **6b**) and MM2 models (**6c**, **6d**) of the transition state.

A second key reaction is the nucleophilic ring-opening of the unsaturated epoxide **12** with benzoic acid, which is promoted by a palladium complex.[9] This process results in a "*trans*" relative stereochemistry between the siloxy groups at C10 and C11, and introduces the $\Delta^{1(12)}$ double bond in **9** at the same time. While this palladium-catalyzed reaction could produce up to four possible regio- and stereoisomers via the π-allyl palladium complex **11** (α and β displacement at C9 and C12), all isomers can be converted into enone **10** in three steps. This methodology, if successful, offers an enantioselective approach to **4** starting from the optically active epoxide **14**, which is easily derived from the (4*S*)-hydroxy-2-cyclopentenone.[10] We describe herein a route to racemic **4**.

Molecular modeling based on MM2 calculations and MM2 transition state models[11] has proven to be useful in the design of key synthetic intermediates as well as in the prediction of stereoselectivity in reactions of macrocyclic compounds.[12] Initial conformational analyses of **6** were conducted using MacroModel[13] to predict whether the [2,3]-Wittig reaction of **6** would be likely to proceed. These analyses showed that in all lower energy conformers[14] of **6** (Fig. 1) the two reactive centers are separated by only a short distance (about 3.5 Å) and the orbitals at the reactive centers overlap well with the π orbitals oriented horizontally to the plane of the ring. Moreover, MM2 models of the transition state[15] based on Houk's ab initio calculations for the reactive centers and MM2 calculations for the rest of the molecule suggest[16] that the product of the [2,3]-Wittig reaction of **6** should have a "*cis*" relative stereochemistry between the newly formed vinyl and hydroxy groups.

The synthesis of the cyclic ether **6** was carried out as follows. Addition of the lithium derivative of **13** (*n*-BuLi/THF, −70 °C; 71 %) to ketone **14**, which is prepared from (±)-4-*tert*-butyldimethylsiloxy-2-cyclopentenone, and dehydration of the resultant tertiary alcohol ($(CF_3SO_2)_2O$/2,6-lutidine; 60 %) afforded the unsaturated epoxide **12**. Palladium-catalyzed epoxide opening of **12** ($[Pd(OAc)_2]$/PPh_3, benzoic acid, THF, 25 °C) gave a 85:15 mixture of C9-benzoate **9** (α:β benzoate = 80:20) and its C12 isomer in 80 % combined yield. The allylic alcohols thus obtained were used without separation; protection of the allylic alcohol (TBSCl/imidazole), hydrolysis of the benzoate group (K_2CO_3/MeOH), and oxidation (pyridinium chlorochromate) provided enone **10** in 50 % overall yield. 1,2-Addition of propargylmagnesium bromide to **10** (80 % yield), protection of the resultant tertiary alcohol (ethyl vinyl ether/H^+), and condensation of metalated terminal alkyne (EtMgBr/THF) with paraformaldehyde afforded the propargyl alcohol **8** in 40 % yield for the three steps. Alcohol **8** was then converted into its propargyl bromide derivative in 74 % yield by mesylation and displacement with lithium bromide. Simultaneous removal of the tetrahydropyranyl and ethoxy ethyl ethers under mild acidic conditions (AcOH:THF:H_2O = 4:1:1, at 25 °C) gave bromoalcohol **7** in 54 % yield. Cyclization of **7** was achieved under high-dilution conditions. A solution of diol **7** (10^{-2} M in THF) was added with a syringe pump to a suspension of NaH and HMPA at room temperature to give the cyclized product in 54 % yield. This compound was converted into trimethylsilyl ether **6**.[17]

The [2,3]-Wittig rearrangement of **6** promoted by *tert*-butyllithium at −100 °C in THF was complete within

10 min, and the product **5**[18] was isolated in 62% yield. In this rearrangement, as expected, a high degree of "*cis*" stereoselectivity (>99%)[19] between the newly formed vinyl and hydroxy groups was observed. Neither the corresponding *trans* isomer nor the 1,2-rearrangement product were obtained. Esterification of **5** (phthalic anhydride, pyridine, dimethylaminopyridine, room temperature; 51%) and acid hydrolysis (40% aq. HF:CH_3CN = 5:95, room temperature; 60%) gave the desired diyne **4**.[20] At ambient temperature diyne **4** was sufficiently stable for purification on silica gel and characterization.

The DNA-cleaving activity of **4** was analyzed with supercoiled pBR322 DNA (Form I) in the presence of methyl thioglycolate, and clean scission was observed. As shown by gel electrophoresis (Fig. 2), incubation of **4** (200 μM, 1 mM) with DNA Form I (0.4 mg) and methyl thioglycolate (20 mM) in 10% DMF/Tris-HCl buffer (pH 7.5) for 18 h at 37 °C cleanly produced a nicked circular Form II and finally the linear Form III. As expected, in the absence of methyl

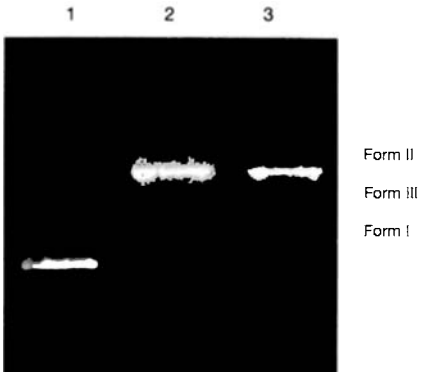

Fig. 2. Agarose gel electrophoretic patterns of DNA before and after nicking by the NCS-chr analogue **4** (lane 2, 200 μM; lane 3, 1 mM). Lane 1 shows intact DNA.

thioglycolate, incubation of **4** with Form I did not cause any cleavage. At present, the mechanism for thiol-triggered cycloaromatization of **4** is not clear. Further studies to elucidate the mechanism are currently underway in our laboratory.

In summary, we have succeeded in synthesizing the first nine-membered NCS-chr analogue possessing DNA-cleaving activity. The introduction of sugar and naphthoic acid residues at C10 and C11, respectively, as found in natural NCS-chr **1** is currently under investigation in our laboratory.

Received: June 9, 1993 [Z 6133 IE]
German version: *Angew. Chem.* **1993**, *105*, 1719

[1] a) N. Ishida, K. Miyazaki, K. Kumagai, M. Rikimaru, *J. Antibiot.* **1965**, *18*, 68; b) M. A. Napier, B. Holmquist, D. J. Strydom, I. H. Goldberg, *Biochem. Biophys. Res. Commun.* **1979**, *89*, 635; c) Y. Koide, F. Ishii, K. Hasuda, Y. Koyama, K. Edo, S. Katamine, F. Kitame, N. Ishida, *J. Antibiot.* **1980**, *33*, 342; d) K. Edo, M. Mizugaki, Y. Koide, H. Seto, K. Furihata, N. Otake, N. Ishida, *Tetrahedron Lett.* **1985**, *26*, 331; e) A. G. Myers, P. J. Proteau, T. M. Handel, *J. Am. Chem. Soc.* **1988**, *110*, 7212.

[2] a) A. G. Myers, *Tetrahedron Lett.* **1987**, *28*, 4493; b) A. G. Myers, P. J. Proteau, *J. Am. Chem. Soc.* **1989**, *111*, 1146; c) T. Tanaka, K. Fujiwara, M. Hirama, *Tetrahedron Lett.* **1990**, *31*, 5947.

[3] a) D. H. Chin, L. S. Kappen, I. H. Goldberg, *Proc. Natl. Acad. Sci. USA* **1987**, *84*, 7070; b) L. S. Kappen, I. H. Goldberg, S. H. Wu, J. Stubbe, L. Worth, Jr., J. W. Kozarich, *J. Am. Chem. Soc.* **1990**, *112*, 2797; c) L. S. Kappen, I. H. Goldberg, B. L. Frank, L. Worth, Jr., D. F. Christner, J. W. Kozarich, J. Stubbe, *Biochemistry* **1991**, *30*, 2034; d) I. Saito, H. Kawabata, T. Fujiwara, H. Sugiyama, T. Matsuura, *J. Am. Chem. Soc.* **1989**, *111*, 8302; e) B. L. Frank, L. Worth, Jr., D. F. Christner, J. W. Kozarich, J. Stubbe, L. S. Kappen, I. H. Goldberg, *ibid.* **1991**, *113*, 2271.

[4] a) P. B. Dervan, *Science* **1986**, *232*, 464; b) K. C. Nicolaou, W.-M. Dai, *Angew. Chem.* **1991**, *103*, 1453; *Angew. Chem. Int. Ed. Engl.* **1991**, *30*, 1387.

[5] a) T. Doi, T. Takahashi, *J. Org. Chem.* **1991**, *56*, 3465; b) A. G. Myers, P. M. Harrington, B.-M. Kwon, *J. Am. Chem. Soc.* **1992**, *114*, 1086; c) P. Magnus, M. Davies, *J. Chem. Soc. Chem. Commun.* **1991**, 1522; d) P. A. Wender, J. A. McKinney, C. Mukai, *J. Am. Chem. Soc.* **1990**, *112*, 5369.

[6] a) K. C. Nicolaou, Y. Ogawa, G. Zuccarello, H. Kataoka, *J. Am. Chem. Soc.* **1988**, *110*, 7247; b) K. C. Nicolaou, W.-M. Dai, S.-C. Tsay, V. A. Esterez, W. Wrasidlo, *Science* **1992**, *256*, 1172.

[7] Reviews on the acyclic [2,3]-Wittig reaction: T. Nakai, K. Mikami, *Chem. Rev.* **1986**, *86*, 885.

[8] a) N. L. Allinger, *J. Am. Chem. Soc.* **1977**, *99*, 8127; b) C. Jamie, E. Osawa, *Tetrahedron* **1983**, *39*, 2769.

[9] a) T. Takahashi, H. Kataoka, J. Tsuji, *J. Am. Chem. Soc.* **1983**, *105*, 147; b) D. R. Deardorff, D. C. Myles, K. D. MacFerrin, *Tetrahedron Lett.* **1985**, *26*, 5615.

[10] M. Suzuki, T. Kawagishi, T. Suzuki, R. Noyori, *Tetrahedron Lett.* **1982**, *23*, 4057.

[11] K. N. Houk, M. N. Paddon-Row, N. G. Ronda, Y.-D. Wu, F. K. Brown, D. C. Spellmeyer, J. T. Metz, Y. Li, R. J. Loncharich, *Science* **1986**, *231*, 1108.

[12] a) T. Takahashi, H. Nemoto, Y. Kanda, J. Tsuji, Y. Fujise, *J. Org. Chem.* **1986**, *51*, 4315; b) T. Takahashi, H. Nemoto, Y. Kanda, J. Tsuji, Y. Fukazawa, T. Okajima, Y. Fujise, *Tetrahedron* **1987**, *43*, 5499; c) T. Takahashi, K. Shimizu, T. Doi, J. Tsuji, *J. Am. Chem. Soc.* **1988**, *110*, 2674; d) T. Takahashi, Y. Yamashita, T. Doi, J. Tsuji, *J. Org. Chem.* **1989**, *54*, 4273; e) T. Takahashi, Y. Sakamoto, T. Doi, *Tetrahedron Lett.* **1992**, *33*, 3519; f) T. Takahashi, T. Harada, T. Doi, *Nat. Prod. Lett.* **1992**, *1*, 129; g) T. Takahashi, H. Yokoyama, T. Haino, H. Yamada, *J. Org. Chem.* **1992**, *57*, 3521.

[13] The program MacroModel (version 3.5) was employed for these calculations. We are grateful to Professor W. Clark Still for providing a copy of this program; F. Mohamadi, N. G. J. Richards, W. C. Guida, R. Liskamp, M. Lipton, C. Caufield, G. Chang, T. Hendrickson, W. C. Still, *J. Comput. Chem.* **1990**, *11*, 440.

[14] MM2 calculations on **6a** and **6b** showed 30 and 39 optimized structures, respectively, with energies within 3 kcalmol^{-1} of the global minimum.

[15] Y.-D. Wu, K. N. Houk, J. A. Marshall, *J. Org. Chem.* **1990**, *55*, 1421.

[16] The MM2 model of the transition state was obtained as follows: the geometries of the reactive sites were taken from the geometry of the transition state in the [2,3]-Wittig rearrangements of the (allyloxy)methyllithium obtained by ab initio calculations, and the rest of molecule was constructed by using the Monte Carlo submode of the MacroModel, followed by energy optimization with the MM2 force field.

[17] **6**: IR ($CHCl_3$): $\tilde{\nu}$ = 2952, 2926, 2854, 2390, 1470, 1373, 1358, 1252 cm^{-1}; ^1H NMR (270 MHz, $CDCl_3$): δ = 5.97 (d, 1H, J = 2.0 Hz), 5.84–5.92 (m, 1H), 4.28 (dd, 1H, J = 2.0, 5.0 Hz), 4.04–4.67 (m, 5H), 2.80, 2.13 (AB, q, 2H, J = 17.2 Hz), 1.98 (s, 3H), 0.90 (s, 18H), 0.08–0.16 (m, 21H); ^{13}C NMR (67.5 MHz, $CDCl_3$): δ = 137.54, 132.51, 131.09, 126.65, 92.98, 90.28, 84.80, 84.75, 81.87, 79.43, 78.83, 64.48, 56.34, 28.79, 25.82, 22.37, 18.04, 17.88, 2.43, −3.88, −3.99, −4.18, −4.44; FAB-MS: m/z 583 [M + Na], 561 [M + H].

[18] **5**: IR ($CHCl_3$): $\tilde{\nu}$ = 3574, 2952, 2926, 2854, 1469, 1461, 1254 cm^{-1}, ^1H NMR (300 MHz, $CDCl_3$): δ = 5.85 (dd, 1H, J = 11.0, 16.0 Hz), 5.80 (d, 1H, J = 2.0 Hz), 5.44 (d, 1H, J = 16.0 Hz), 5.22 (d, 1H, J = 11.0 Hz), 4.34 (dd, 1H, J = 2.0, 4.0 Hz), 4.21 (d, 1H, J = 4.0 Hz), 4.05 (d, 1H, J = 10.0 Hz), 2.26, 2.60 (AB, q, 2H, J = 16.0 Hz), 1.84 (d, 1H, J = 10.0 Hz), 1.34 (s, 3H), 0.89 (s, 18H), 0.05–0.25 (m, 21H); ^{13}C NMR (67.5 MHz, $CDCl_3$): δ = 137.77, 133.68, 131.29, 116.57, 93.48, 89.42, 89.13, 87.71, 86.31, 80.83, 73.57, 52.78, 29.54, 25.12, 18.01, 17.86, 2.41, −3.97, −4.44, −4.56; FAB-MS: m/z 583 [M + Na], 561 [M + H]; high-resolution MS: 583.110 (calc.: 583.3072, $C_{30}H_{52}O_4Si_3Na$).

[19] The *cis* stereochemistry between the vinyl and hydroxy groups in **5** was confirmed by NOE experiments.

[20] **4**: IR ($CHCl_3$): $\tilde{\nu}$ = 3404, 2996, 2974, 2870, 2250, 1712, 1382 cm^{-1}, ^1H NMR (270 MHz, $CDCl_3$): δ = 7.53–7.70 (m, 4H), 5.90–5.91 (m, 1H), 5.61 (dd, 1H, J = 10.6, 17.2 Hz), 5.38 (d, 1H, J = 17.2 Hz), 5.08 (s, 1H), 5.02 (d, 1H, J = 10.6 Hz), 4.54–4.56 (m, 1H), 4.27–4.29 (m, 1H), 2.49, 2.82 (AB, q, 2H, J = 18.8 Hz), 1.44 (s, 3H); ^{13}C NMR (67.5 MHz, $CDCl_3$): δ = 169.97, 167.22, 135.83, 132.79, 131.86, 131.50, 131.32, 130.71, 129.29, 116.98, 104.19, 102.09, 91.81, 87.17, 86.09, 83.79, 67.40, 65.84, 63.78, 50.82, 27.21, 26.63, 17.86, 5.33, 15.24.

 © VCH Verlagsgesellschaft mbH, D-69451 Weinheim, 1993 0570-0833/93/1111-1659 $ 10.00+.25/0

Liquid-Crystalline Perylene Derivatives as "Discotic Pigments"**

By *Christine Göltner, Dietmar Pressner, Klaus Müllen,** and *Hans Wolfgang Spiess**

Pigments based on perylene are industrially important.[1] The wider application of their chromophoric properties, however, is often restricted by their poor processibility, for example, because of their high melting and softening temperatures. Our aim was to synthesize liquid-crystalline derivatives based on the planar perylene molecule. We expected these to show advantages in terms of good solubility and meltability as well as to exhibit the ability to self assemble into columnar superstructures of discotic mesogens. In the following we report on the twofold cycloaddition of 3,5-dioxotriazoles to alkyl-substituted perylenes and the characterization of the liquid-crystalline perylene derivatives thus obtained.

Attempts to carry out cycloadditions of dienophiles at the "bay" positions of **1** (R = H), reported so far, have resulted in the addition of a single dienophile only.[2] A diaddition product was obtained in low yields only under more drastic reaction conditions.[3] This observation can be explained by the low enophilicity of the respective monoaddition products as well as their poor solubility. Treating 3,10-dialkyl perylenes **1**[4] with an excess of commercially available 4-phenyl-3,5-dioxotriazole (**2**), however, yields the aromatized diaddition product, 2,9-dialkyl-5,6,11,12-tetraaza-5,6,11,12-tetrahydrocoronene-5,6,11,12-tetracarboxylic acid bisphenylimide **3** (R = phenyl), quantitatively. Since the basic structure of this compound is disc-shaped (discoid), it seemed obvious that the reaction of 3,10-dialkyl perylenes with alkyl-substituted 3,5-dioxotriazoles might afford discotic mesogens.

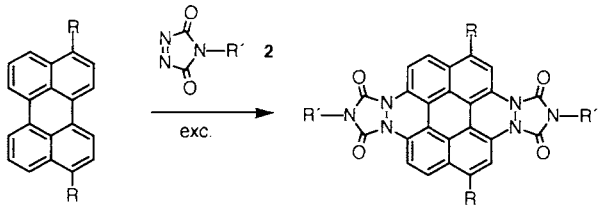

1 R = *n*-C_5H_{11}, *n*-$C_{12}H_{25}$, *n*-$C_{18}H_{37}$ **3**

R' = C_6H_5, *n*-C_5H_{11}, *n*-$C_{11}H_{23}$, *n*-$C_{17}H_{35}$, *n*-$C_{21}H_{43}$

The reaction of **1** with 4-*n*-alkyl-3,5-dioxotriazoles of different chain length also resulted in soluble compounds **3** in excellent yields. For simplicity these are defined in the following as **Px-y** (x = length of the alkyl chain attached to the perylene ring and y = length of the alkyl chain linked with the urazole unit). The materials obtained are thermally stable up to 350 °C and also stable to protonic acids (e.g. trifluoroacetic acid, 1 d reflux). Treatment with NaOH at temperatures above 90 °C causes cleavage of the imide moiety. On acidification, spontaneous decarboxylation yields the previously unknown, readily soluble tetraazacoronene **4**.[3]

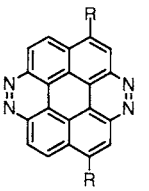

4

R = *n*-$C_{12}H_{25}$

Comparing the UV spectra of **3** with the ones obtained from the corresponding perylenes (λ_{max} = 453 nm), the longest wavelength absorption is found to be bathochromically shifted by 130 nm. The typical line shape of the UV spectra of **3** indicate that despite chemical modification the perylene chromophore is intact.

As expected, the derivatives **3** form mesophases, which qualitatively was detected by optical microscopy. The materials show birefringence and shearability, both typical of liquid crystals. The structure of the mesophases, however, could not be assigned, because the derivatives **3** show diffuse textures, and the extraordinarily high phase width generally did not allow for heating the substances above their clearing temperatures (e.g. **P11-12**: c – 20 °C D_{ho} 373 °C i). The transition temperatures could be determined by calorimetric (DSC) measurements. The clearing temperatures (T_c) significantly depend on the substitution pattern of **3**. The higher the symmetry of the molecule, that is, the more similar the chain lengths ($x \approx y$) of the alkyl substituents R(x) and R'(y), the higher is the clearing temperature (Table 1).

Table 1. Influence of the molecular shape on the phase transition temperatures [°C] of selected perylene derivatives.

Compound	Phase transition temperatures	Shape
P18-05	c 69 D_{col} 261 i	⬯
P18-17	c 45 D_{ho} 305 i	◯
P12-11	c -20 D_{ho} 373 i	◯
P05-17	c 85 D_{col} 202 i	⬭

Small-angle X-ray diffractograms allowed for an unambiguous elucidation of the phase structures of most derivatives of **3**. Long-chain substituted, symmetrical derivatives show an ordered columnar alignment of the molecules with a hexagonal superstructure (D_{ho}),[5] while more unsymmetrically substituted compounds exhibit a strong disturbance of the hexagonal lattice. The latter corresponds qualitatively to the observed decrease of the clearing temperatures determined by calorimetric measurements. As an example, Figure 1 shows the diffractogram of **P18-17**, in which the reflections, which prove the columnar, hexagonal structure of the mesophase, are labeled.

The number of lateral alkyl chains attached to the skeleton of **3** is surprisingly low in comparison to that of the "classical" discotic mesogen hexabutyloxy triphenylene **5a** (c 88 °C D_{ho} 145 °C i). The latter is the liquid-crystalline derivative of the series of hexaalkyloxy triphenylenes with the shortest possible length of alkyl chains, and it shows a significantly smaller width of the mesophase than **P5-5**, the "shortest" derivative of **3** synthesized so far. The ratio of aliphatic to aromatic carbon atoms in the triphenylene **5a** is 8:6, while it

[*] Prof. Dr. K. Müllen, Prof. Dr. H. W. Spiess, Dipl.-Chem. C. Göltner, Dipl.-Chem. D. Pressner
Max-Planck-Institut für Polymerforschung
Ackermannweg 10, D-55021 Mainz (FRG)
Telefax: Int. code + (6313)379-100

[**] This work was supported by the Bundesministerium für Forschung und Technologie, the BASF AG, and the Deutsche Forschungsgemeinschaft (SFB 262).

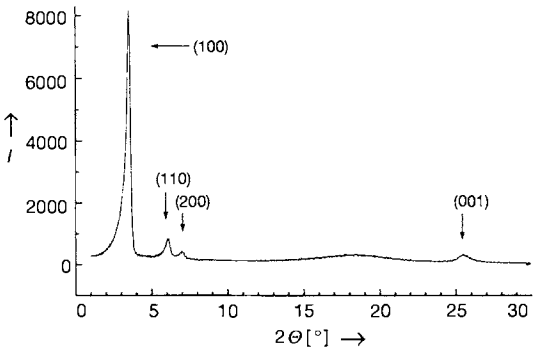

Fig. 1. X-ray diffractogram of the **P18-17** derivative at 130 °C.

is 5:6 for **P5-5**, which nevertheless forms a mesophase of more than 250 °C width (c 27 °C D 319 °C i). It can be expected that even further shortening of the lateral alkyl chains in **3** will not obstruct the formation of a mesophase.

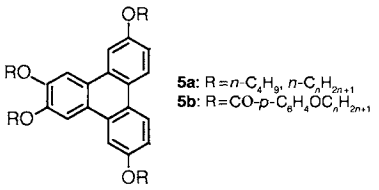

The mesophases of compounds **3** with longer alkyl substituents, however, still are extraordinarily stable (**P18-17**: c 45 °C D_{ho} 305 °C i; **P12-17**: c 15 °C D_{ho} 316 °C i). In contrast to this, triphenylenes with side chains longer than 14 carbon atoms are not liquid crystalline any more.[6] The mesophases of the parent triphenylene core can be stabilized by substitution with alkoxyaryl esters, but the hexaalkyloxy triphenylene benzoates of the type **5b** still exhibit clearing temperatures far below the ones of **3**, as shown in Figure 2.[7]

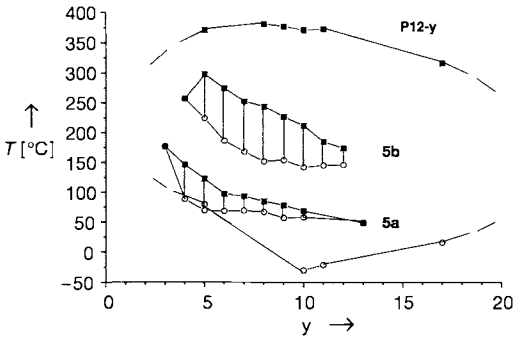

Fig. 2. Phase transition temperatures (melting point T_m (—○—) and clearing temperatures T_c (—■—) °C) of **3** compared with classical discotic mesogens [6, 7].

Since the unusual stability of the mesophases of **3** cannot only be explained by the ratio of aliphatic to aromatic carbon atoms, more specific interactions must be taken into account. Decisive indications of those and the mechanisms of dynamic processes can be obtained from solid-state ^{2}H NMR spectra. For this purpose, three derivatives of **P12-17**, selectively deuterated at different positions (**6a**, **6b**, and **6c** in Fig. 3) were synthesized. In all cases, the degree of deuteration was determined by ^{1}H NMR spectroscopy to be higher than 85%.

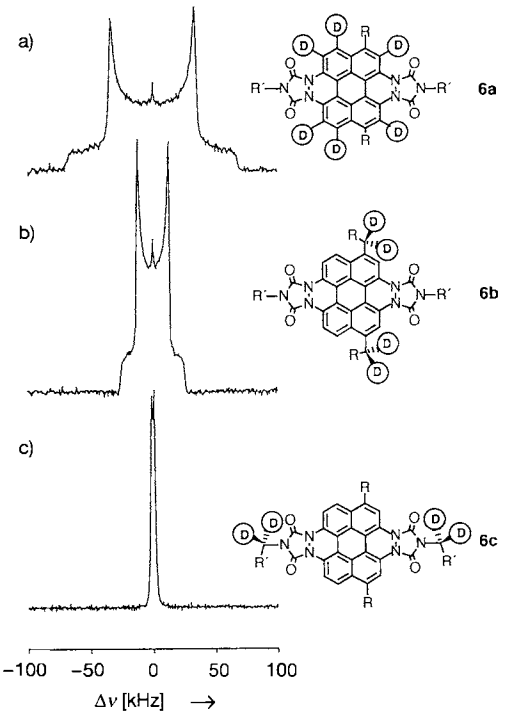

Fig. 3. Solid-state ^{2}H NMR spectra of **6a–c** at 130 °C.

In many cases reported previously, one- and two-dimensional ^{2}H NMR spectroscopy has proven to be a successful method for the elucidation of dynamic processes and structural properties of columnar mesophases.[8] The ^{2}H NMR spectra of the isotropic solid, recorded under conditions, in which the molecules can be considered rigid on the NMR time scale (rigid Pake spectra), show characteristic changes of the line shape during the transition into the mesophase. Defined motions result in defined spectra. Especially the uniaxial rotation of the disc-shaped molecule around the main columnar axis causes a characteristic, motion-averaged spectrum, the quadrupolar splitting of which is reduced by a factor of 2. This could be shown for the derivative **6a**, deuterated in the aromatic positions (Fig. 3; 131 kHz at −70 °C, 66 kHz at 130 °C). The nature of the main dynamic process of the mesogen could thus be determined unambiguously.

For the alkyl chains attached to the perylene core and to the urazole unit, respectively, a remarkably different dynamic behavior was found (cf. Figs. 3b, c). The motion-averaged, reduced spectrum observed for **6b** corresponds to the ones obtained from α-deuterated triphenylene side chains.[9] These indicated a planar *trans* conformation at the α-carbon atom of the alkyl chain. In the ^{2}H NMR spectrum of **6c** a further reduction of the quadrupolar splitting by a factor of 5 is observed. This change in the width of the spectrum is ascribed to the internal mobility of the molecule, which could be caused by a flip process of the urazole rings between the two nonplanar conformations relative to the perylene skeleton as well as an enhanced conformational freedom of the adjacent alkyl chain. The results of the ^{2}H spectra indicate that the five-membered, heterocyclic ring clearly deviates from a coplanar conformation. This nonplanarity could cause an "entanglement" between neighboring perylene

units, resulting in an increased phase width of **3**. In fact, such an entanglement was found to be the reason for the increased stability of the mesophases formed by ester-substituted triphenylenes.[10]

Further investigations will reveal, if additional dynamic processes or electronic interactions among the molecules are responsible for the extraordinary stability of the mesophases formed by **3**.

The synthesis and characterization of the novel discotic mesogen **3** allowed for the assembly of perylene as a liquid-crystalline material, not just in a liquid-crystalline matrix.[11] This extends the possibilities of processing and application of perylene pigments, and in fact, preliminary experiments show that some derivatives of **3** can be oriented in a magnetic field and that highly oriented fibers can be drawn.

Experimental Procedure

P5-17: 3,10-dipentylperylene (250 mg, 0.5 mmol) was dissolved in xylene (30 mL) under gentle heating. This solution was treated with 4.4 equivalents of 4-*n*-heptadecyl-3,5-dioxotriazole (750 mg, 2.2 mmol) [12] and heated to reflux for two minutes. Additional small portions of dioxotriazole were then added until neither the yellow starting material nor the red monoaddition product could be detected by chromatography (tlc). The reaction mixture was worked up by first pouring it into cold methanol (150 mL) followed by filtration. The residue was purified by column chromatography on silica gel (petroleum ether/toluene), yield: 470 mg (82%).

^{1}H NMR (300 MHz, [D$_2$]tetrachloroethane, 110 °C): δ = 7.93 (d, J = 9 Hz, 2H, Ar-H), 7.86 (s, 2H, Ar-H), 7.17 (d, br., 2H, Ar-H), 3.65 (t, J = 7 Hz, 4H, 2 α-urazole chains-CH$_2$), 2.58 (m, 4H, 2 benzylic CH$_2$), 1.77 (m, 4H, 2 CH$_2$), 1.56 (m, 4H, 2 CH$_2$), 1.59–1.10 (m, 64H, 16 CH$_2$), 0.93–0.82 (m, 12H, 4 CH$_3$); ^{13}C NMR (75 MHz, [D$_2$]tetrachloroethane, 110 °C): δ = 144.70, 144.64, 144.46, 141.13, 129.96, 129.81, 126.40, 125.02, 124.94, 113.85, 113.68, 113.14, 110.90, 41.34, 40.15, 32.88, 32.11, 29.90, 29.50, 29.15, 28.10, 28.00, 27.62, 27.19, 26.71, 22.84, 22.71, 14.23. IR(KBr): $\tilde{\nu}$ = 2905, 2830, 1740, 1685, 1580, 1410, 1385 cm^{-1}; UV(CHCl$_3$): λ_{max} (log ε):586 (4.01), 541 (3.94), 505 (3.64); FD-MS (70 eV): m/z (rel. intensity): 1062.98 (100%).

4: **3** (R′ = Ph, R = n-C$_{12}$H$_{25}$) (500 mg, 0.54 mmol) was suspended in benzyl alcohol (30 mL) and heated to 90 °C. This mixture was treated with solid NaOH (500 mg, 12.5 mmol) and stirred at this temperature until the solution became homogeneous and no longer showed red fluorescence. The reaction mixture was then added dropwise to a well-stirred mixture of methanol (200 mL) and concentrated hydrochloric acid (5 mL). After filtration the crude product was purified by recrystallization from isopropyl alcohol; yield: 300 mg (87%).

4: ^{1}H NMR (200 MHz, CDCl$_3$): δ = 9.00 (d, 2H, J = 9 Hz, Ar-H), 8.80 (s, 2H, Ar-H), 8.66 (d, J = 9 Hz, 2H, Ar-H), 3.52 (t, J = 8 Hz, 4H, 2 α-CH$_2$), 2.06 (m, 4H, 2 β-CH$_2$), 1.68–1.26 (m, 36H, 18 CH$_2$), 0.86 (t, J = 8 Hz, 6H, 2 CH$_3$); ^{13}C NMR (50 MHz, CDCl$_3$): δ = 142.22, 141.83, 141.48, 129.98, 128.42, 127.34, 125.53, 115.07, 111.35, 109.75, 39.38, 33.57, 31.96, 31.16, 31.16, 29.97, 29.76, 29.70, 29.40, 22.70, 14.10; IR (KBr) $\tilde{\nu}$ = 3471, 3449, 3432, 3418, 2849, 1041, 8287 cm^{-1}; UV (CH$_2$Cl$_2$): λ_{max} (log ε): 453 (4.27), 426 (3.95), 403 (3.58); EI-MS: m/z (rel. intensity): 640.38 (4.3%).

Received: June 2, 1993 [Z 6117 IE]
German version: *Angew. Chem.* **1993**, *105*, 1722

[1] a) H. Zollinger, *Color Chemistry*, VCH, Weinheim, **1987**, p. 184; b) C. I. Solvent, Green 5, Colour Index No. CI 59075, *Colour Index*, **1871**, *3*, 3632; c) Hoechst, EP-B 176900, 176901, 176902, **1985**; d) *Lumogen F-Dyes*, BASF AG, Ludwigshafen, **1985**; e) Bayer, DE-B 281513, **1986**.
[2] E. Clar, M. Zander, *Chem. Ber.* **1932**, *65*, 846.
[3] S. Tokita, K. Hiruta, K. Kitahara, H. Nishi, *Synthesis* **1982**, 229.
[4] U. Anton, C. Göltner, K. Müllen, *Chem. Ber.* **1992**, *125*, 2325–2330.
[5] C. Destrade, P. Foucher, H. Gasparoux, N. H. Tinh, *Mol. Cryst. Liq. Cryst.* **1984**, *106*, 121–146.
[6] C. Destrade, M. D. Mondon, J. Malthete, *J. Phys. (Paris)* **1979**, *4–40*, C3–17.
[7] N. H. Tinh, H. Gasparoux, C. Destrade, *Mol. Cryst. Liq. Cryst.* **1981**, *68*, 101–111.
[8] a) M. Werth, J. Leisen, C. Boeffel, R. Y. Dong, H. W. Spiess, *J. Phys. II* **1993**, *3*, 53–67; b) J. Leisen, M. Werth, C. Boeffel, H. W. Spiess, *J. Chem. Phys.* **1992**, *97*, 3749–3759.
[9] See [8 b].
[10] M. Werth, S. U. Vallerien, H. W. Spieß, *Liq. Cryst.* **1991**, *10*, 759.
[11] S. Imazeki, A. Muko, T. Yoneyama, N. Kaneko, *Mol. Cryst. Liq. Cryst.* **1987**, *145*, 79–93.
[12] B. Saville, *J. Chem. Soc. D* **1971**, 635.

Preparative Enantiomer Separation of the Anesthetic Enflurane by Gas Inclusion Chromatography**

By *Volker Schurig*,* *Heiko Grosenick*, and *Bernard S. Green*

Chiral enflurane [C*HFCl–CF$_2$OCF$_2$H] is used as an inhalation anesthetic in clinical practice. The achiral chemical synthesis yields a racemate, which is clinically administered as a 1:1 mixture of enantiomers. Because enantiomers generally have different pharmacological and toxicological properties and may differ greatly in their spectrum of activity, the preparation of the pure enantiomers is of considerable interest. A multistep enantioselective synthesis of enflurane has been described,[1] and approaches to the resolution of the racemate by formation of inclusion complexes have been presented ((−)-brucine, 8% *ee*;[1] tri-*o*-thymotide (TOT, cyclic trilactone of 3-isopropyl-6-methylsalicylic acid), 38% *ee*[2]). The analytical enantiomer separation of enflurane by gas chromatography has also been achieved.[2, 3]

We describe here the preparative-scale separation of the enflurane enantiomers by inclusion gas chromatography on octakis-(3-*O*-butanoyl-2,6-di-*O*-*n*-pentyl)-γ-cyclodextrin (**1**)[4] diluted with polysiloxane SE-54 [(poly(dimethylsilanol-*ran*-phenylmethylsilanol-*ran*-vinylmethylsilanol *ran* = random)(0.94:0.05:0.01 mol%)];[5] the antipodes are obtained in almost enantiomerically pure form (*ee* ≥ 99%, cf. Fig. 1 b,c).

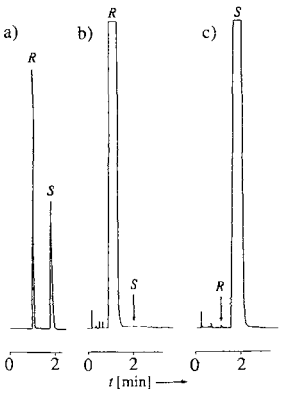

Fig. 1. Analytical enantiomer separation of enflurane on **1** [4] in OV-1701 (38 wt%) [5]. Quartz capillary column (6 m × 0.25 mm internal diameter), 25 °C, 55 cm s^{-1} hydrogen (flame ionization detector, FID). a) racemic; b) (*R*)-(−)-enflurane 99.9% *ee*; c) (*S*)-(+)-enflurane 99.9% *ee*.

Enflurane is separated into its enantiomers on an analytical capillary column coated with **1** in OV-1701, as shown in Figure 1 a. The surprisingly high separation factor $\alpha > 2$ permits a quantitative enantiomer separation in only 20 s (50 °C, 60 cm s^{-1} hydrogen). The transfer of this procedure to a preparative scale is achieved by using a 4 m × 7 mm (internal diameter) packed column filled with 10 wt% (**1**) in SE-54 (20 wt% on Chromosorb) (Fig. 2). Enflurane can be separated from the carrier gas helium without any difficulty. Since the enantiomer separation is achieved in 45 min, larger quantities of separated enantiomer can be recovered by re-

[*] Prof. Dr. V. Schurig, Dipl.-Chem. H. Grosenick
Institut für Organische Chemie der Universität
Auf der Morgenstelle 18, D-72076 Tübingen (FRG)
Prof. Dr. B. S. Green
The School of Pharmacy, Hebrew University
Jerusalem, 91120 (Israel)

[**] This work was supported by the Deutsche Forschungsgemeinschaft and the Fonds der Chemischen Industrie. We thank Wacker Chemie, Burghausen, for a generous gift of γ-cyclodextrin.

peating the separation cycle. The amount of mobile phase consumed during this process can be minimized by recycling, and the time required for separation can be reduced further by using hydrogen as carrier gas. The absolute configuration of the enantiomers were assigned according to published data.[1] Although the separation factor is smaller, the preparative separation of 8 mg of isoflurane into its enantiomers can be achieved by using the above set-up. Halothane, on the other hand, cannot be resolved on a preparative scale.

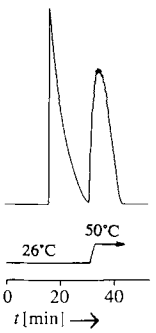

Fig. 2. Preparative enantiomer separation of 47 mg of enflurane (for conditions see Experimental Procedure).

Whereas the application of cyclodextrin derivatives in gas chromatograpy has mainly been in analytical enantiomer separations,[6, 7] our investigations demonstrate their potential in preparative separations. Native α-cyclodextrin in aqueous formamide was previously suggested as a possible stationary phase for this purpose in 1983,[8] and camphene was later separated on a preparative scale by using this system.[9] The dilution of derivatized cyclodextrins with polysiloxanes that has proved to be especially valuable in analytical work[5] is also the method of choice for preparative-scale separations, since it combines chemical selectivity with chromatographic efficiency in an optimal way.

Experimental Procedure

Polysiloxane SE-54 (WGA, Düsseldorf) (22.95 g) was placed in a round-bottomed flask and dissolved under reflux in anhydrous chloroform (600 mL). The γ-cyclodextrin derivative **1** [4] (2.55 g) was added to this mixture. Chromosorb P-AW-DMCS (80/100 mesh, Alltech, Arlington Heights, Ill., USA) (100 g) was then added to the resulting solution. The flask was shaken until the Chromosorb formed a slurry with the solution. The resulting suspension was carefully concentrated on a rotary evaporator over several hours by rotating the flask at a moderate speed, at 40 °C, and under a weak vacuum. Finally, the granular, impregnated Chromosorb was dried at 70 °C and 0.004 Torr for 24 h (the Chromosorb impregnated in this way is coated with a 20.3 wt% layer of the enantioselective stationary phase; the stationary phase itself consists of 10.0 wt% **1** in SE-54).

A glass column (4.04 m × 7 mm internal diameter) was filled with the stationary phase (ca. 95 g). In order to ensure a compact, uniform, dead-volume-free packing, the column was tapped and shaken continuously and was then placed in an ultrasonic bath for 1 min. A modified gas chromatograph (MEGA, Fisons, Mainz, FRG) was used for the preparative-scale separation of the enflurane enantiomers (carrier gas helium (4.6), inlet pressure 4 bar, 8.4 $cm\,s^{-1}$; injector block: 150 °C, on-column injection; detector: FID). Enflurane was supplied by a local clinic. The eluate from the column was led through a splitter (1:1500) into two parallel lines, one leading to the FID and the other to a U-shaped cold trap. The connection to the cold trap (dry ice/acetone) can be heated and was maintained at the column temperature. The enflurane enantiomers were recovered by condensation. The enantiomeric purity was determined by analytical enantioselective capillary gas chromatography, by using the same separation phase as above (Fig. 1). The column temperature was held constant at 26 °C until elution of the first peak and was then raised to 50 °C. A quantitative (base-line separation) resolution of 31 μL = 47 mg of racemic enflurane into its antipodes was achieved in an analysis time of 45 min (cf. Fig. 2) by using the above set-up. The percentage recovery (not optimized) was: first peak: (*R*)-(−)-enflurane (enantiomeric purity $ee \geq 99.9\%$, chemical purity: 99.5%), yield 60% with respect to the *R* enantiomer in the racemate (isolated and transferred into an ampoule); second peak: (*S*)-(+)-enflurane (enantiomeric purity $ee \geq 99.9\%$, chemical purity: 99.7%), yield 52% with respect to the *S* enantiomer in the racemate (isolated and transferred into an ampoule). The enflurane enantiomers were characterized by NMR spectroscopy and by their chiroptical data (cf. ref. [1]).

Received: June 5, 1993 [Z6127IE]
German version: *Angew. Chem.* **1993**, *105*, 1690

[1] D. L. Pearson, Thesis, Cornell University, Ithaca, NY, USA, **1990**; *Diss. Abstr. Int. B* **1992**, *52*, 6400–6401; *Chem. Abstr.* **1993**, *118*, 147168z.
[2] J. M. Gnaim, V. Schurig, H. Grosenick, B. S. Green, *J. Chem. Soc. Chem. Commun.*, submitted.
[3] J. Meinwald, R. Thompson, D. L. Pearson, W. A. König, T. Runge, W. Francke, *Science* **1991**, *251*, 560–561.
[4] W. A. König, R. Krebber, P. Mischnick, *J. High Resolut. Chromatogr.* **1989**, *12*, 732–738.
[5] V. Schurig, H.-P. Nowotny, *J. Chromatogr.* **1988**, *441*, 155–163.
[6] V. Schurig, H.-P. Nowotny, *Angew. Chem.* **1990**, *102*, 969–986; *Angew. Chem. Int. Ed. Engl.* **1990**, *29*, 939–957.
[7] W. A. König, *Gas Chromatographic Enantiomer Separation with Modified Cyclodextrins*, Hüthig, Heidelberg, **1992**.
[8] T. Koscielski, D. Sybilska, J. Jurczak, *J. Chromatogr.* **1983**, *280*, 131–134.
[9] M. Lindstroem, T. Norin, J. Roeraade, *J. Chromatogr.* **1990**, *513*, 315–320.

Synthesis, Structure, and Optical Properties of Cd_4S^{6+} Clusters Encapsulated in an Aluminate Cage**

By *Matthew E. Brenchley* and *Mark T. Weller**

Small-particle semiconductors that demonstrate a blue shift from the bulk (macrocrystalline) material in the optical spectra have been the subject of intense recent interest as a result of their physical properties.[1] Several preparative techniques have been used to prepare small-particle semiconductors including colloidal[2] and porous host methods;[3] however, with these techniques the particle size and distribution is not easily controllable. The size of the particles controls the extent of the blue shift and, hence, a preparative technique which provides greater control of particle size has been sought.

Wang and Herron[4] found that zeolites with various-sized cavities and channels could be used to entrap II–VI semiconductor units of known dimension and composition. Later Moran et al.[5] found that discrete M_4X^{6+} units could be prepared in situ within borate and beryllosilicate frameworks possessing the sodalite structure. With precise control of semiconductor unit stoichiometry and the inter-connectability of these units through the sodalite cage, exceedingly sharp absorption edges in the optical sepctrum could be obtained. However, Moran et al. were not able to synthesize the ZnS/borate sodalites in a pure form, and structural results for the cadmium sulfide helvite were not presented. We report here on the discovery of a compound of the aluminate sodalite family[6] with discrete Cd_4S^{6+} units.

$Cd_8[AlO_2]_{12}S_2$ was prepared by a two-stage process[7] via a parent sulfate sodalite synthesized at high temperatures. First CdO, $CdSO_4$, and Al_2O_3 in the molar ratio 3:1:3 were finely ground and sealed under vacuum in a silica glass tube. The tube was fired at 1000 °C for two days and then cooled to yield a white crystalline powder. The product was shown

[*] Dr. M. T. Weller, M. E. Brenchley
Department of Chemistry, The University of Southampton
GB-Southampton SO9 5NH (UK)
Telefax: Int. code + (703)59-3781

[**] This work was partially supported by A. E. A. Technology, Winfrith.

to be a single phase by powder X-ray diffraction (Siemens D5000, $Cu_{K\alpha 1}$) and all reflections were indexed on a body-centred cubic cell, sodalite structure, with $a = 9.0994(1)$ Å. IR spectroscopic measurements helped confirm this product as cadmium sulfate aluminate sodalite, $Cd_8[AlO_2]_{12}(SO_4)_2$.

The sulfate sodalite was then reduced under pure hydrogen at 600 °C for 8 hours to yield a bright yellow material. Powder X-ray diffraction measurements showed this to be a single-phase body-centred sodalite with $a = 8.8181(1)$ Å except for a very minor contribution from Al_2O_3 ($I/I_o = 0.05\%$). IR spectroscopic measurements showed no S–O vibrational modes, which is consistent with reduction of sulfate to sulfide and the formation of cadmium sulfide aluminate sodalite, $Cd_8[AlO_2]_{12}S_2$.

The powder X-ray diffraction data for the Rietveld refinement of the structure of $Cd_8[AlO_2]_{12}S_2$ were collected over the angular range 22–127° 2 θ with $Cu_{K\alpha 1}$ radiation on a Siemens D5000 diffractometer over 15 hours. The starting model for the refinement was the structure of the calcium analogue[7] in the space group $I\bar{4}3m$ adopted by sodalites with no ordering of the cage anions. Refinement was undertaken by using the DBWS-9006PC package of Wiles and Young.[8] The small amount of alumina found in the sample was included into the profile as a second phase. The refinement proceeded smoothly and final cycles included all profile and atomic parameters with χ^2 converging to 2.40. The final coordinates and isotropic temperature factors are listed in Table 1; Figure 1 shows the final profile fit to the data.

Table 1. The atomic coordinates and isotropic temperature factors of $Cd_8[AlO_2]_{12}S_2$ ($R_{wp} = 13.62$, $R_{ex} = 8.79$) derived from the powder X-ray data.

Atom	x	y	z	B_{iso}
Al	0.25	0.5	0.0	0.12(8)
O	0.1397(5)	0.1397(5)	0.4125(7)	0.24(16)
Cd	0.1660(1)	0.1660(1)	0.1660(1)	0.42(3)
S	0.0	0.0	0.0	0.55(16)

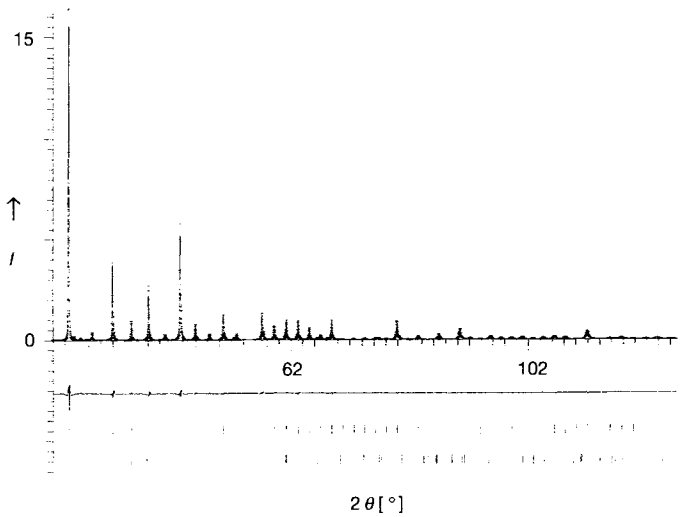

Fig. 1. Profile fit to the powder X-ray data from $Cd_8[AlO_2]_{12}S_2$. Horizontal bars are observed data and the upper full line the fit to the data. Lower full line is the difference; the upper tick marks show reflection positions for the sodalite and lower tick marks for Al_2O_3. I in units of 1 000 counts.

Bond lengths and angles calculated from the final parameters are presented in Table 2: the aluminate sodalite structure has been discussed in detail by Depmeier.[9] The central tetrahedral Cd_4S group has Cd–S bond lengths of 2.535(2) Å, somewhat larger than bulk CdS, which adopts the wurtzite structure. The next nearest neighbor cadmium to sulfide distances which represent the interaction of Cd_4S groups between cages is 5.101(4) Å. Figure 2 illustrates the relative orientations of the Cd_4S clusters to one another; the sodalite cages have been omitted for clarity.

Table 2. Bond lengths and angles of $Cd_8[AlO_2]_{12}S_2$ derived from the powder X-ray data.

Bond lengths [Å]		Bond	Angles [°]
Al-O	1.749(9)	Al-O-Al	126.1(12)
Cd-S	2.535(2)	O-Al-O (4 ×)	112.4(8)
Cd-S [a]	5.101(4)	O-Al-O (2 ×)	108.0(8)
Cd-O (3 ×)	2.198(10)		
Cd-O (3 ×)	3.297(10)		

[a] Next nearest neighbor.

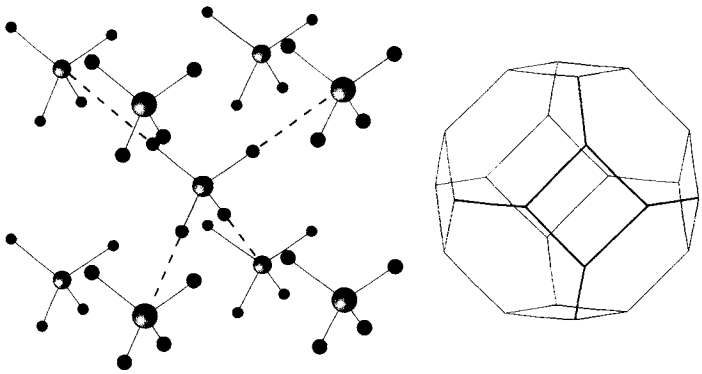

Fig. 2. Left: Spatial arrangement of the Cd_4S tetrahedra in $Cd_8[AlO_2]_{12}S_2$; interactions between the tetrahedra are shown by dotted lines. Right: The Al framework of the sodalite is shown to scale in the same orientation as the Cd_4S units.

A diffuse-reflectance UV/VIS spectrum obtained from the sodalite is shown in Figure 3. The sharp absorption edge at 505 nm is blue shifted by approximately 100 nm from the bulk material for which an absorption edge trail is observed. The sodalite does in fact behave much more like colloidal CdS with 1 μm particles which show a similar shift but preserve a gentle absorption edge. These colloid particles are some 2000 times larger than the individual Cd_4S units in the sodalite but the latter interact between cages over the so-

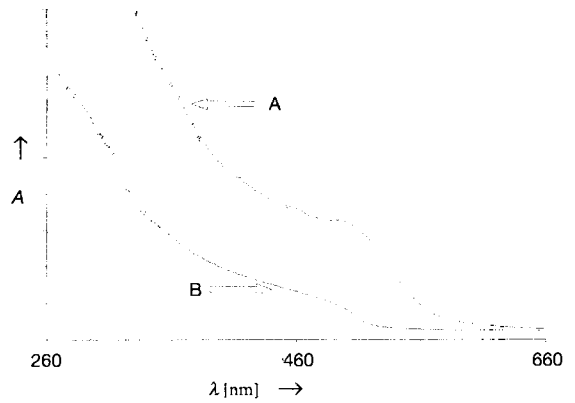

Fig. 3. UV/VIS diffuse-reflectance spectrum of bulk (macrocrystalline) CdS(A) and $Cd_8[AlO_2]_{12}S_2$ (B) in the wavelength range 260–660 nm. A = absorbance.

dalite particle size through the next nearest neighbor Cd–S interactions. The UV/VIS spectrum is not consistent with a small amount of surface CdS, since the intensity of the absorption observed for the sodalite is of a similar magnitude to that of pure bulk CdS. In addition any CdS particles would be lost from the surface at the high temperatures used in the synthesis of CdS–sodalite.

Received: March 18, 1993
Revised version: May 18, 1993 [Z 5935 IE]
German version: *Angew. Chem.* **1993**, *105*, 1726

[1] Y. Wang, N. Herron, W. Mahler, A. Suna, *J. Opt. Soc. Am. B* **1989**, *6*, 808.
[2] L. E. Brus, *J. Phys. Chem.* **1986**, *90*, 2555.
[3] J. E. MacDougal, H. Eckert, G. D. Stucky, N. Herron, Y. Wang, K. Moller, T. Bein, D. Cox, *J. Am. Chem. Soc.* **1989**, *111*, 8006.
[4] Y. Wang, N. Herron, *J. Phys. Chem.* **1987**, *91*, 257.
[5] K. L. Moran, W. T. A. Harrison, T. E. Gier, J. E. MacDougal, G. D. Stucky, *Mater. Res. Soc. Symp. Proc.* **1990**, *164*, 123.
[6] R. Kondo, *Yogyo Kyokaishi* **1965**, *71*, 1.
[7] M. E. Brenchley, M. T. Weller, *J. Mater. Chem.* **1992**, *2*, 1003.
[8] D. B. Wiles, R. A. Young, *J. Appl. Crystallogr.* **1981**, *14*, 149.
[9] W. Depmeier, *Acta Crystallogr. Sect. B* **1984**, *40*, 185.

BOOKS

This section contains book reviews and a list of new books received by the editor. Book reviews are written by invitation from the editor. Suggestions for books to be reviewed and for book reviewers are welcome. Publishers should send brochures or (better) books to the Book Editor, Dr. Gerhard Karger, Redaktion Angewandte Chemie, Postfach 101161, D-69451 Weinheim, Federal Republic of Germany. The editor reserves the right of selecting which books will be reviewed. Uninvited books not chosen for review will not be returned.

Book Reviews

The Organic Chemistry of Polycoordinated Iodine. By *A. Varvoglis*. VCH Verlagsgesellschaft, Weinheim/VCH Publishers, New York, 1992. XII, 414 pp., hardcover DM 196.00.—ISBN 3-527-89538-8/1-56081-538-8

Iodine is the most polarizable, largest, but least electronegative, of the common halogens. As a consequence it can readily polycoordinate by forming bonds with 2–5 ligands and acquire an oxidation state of 3, 5, or 7. The first polycoordinated organic species, the stable crystalline $PhICl_2$, was reported by Willgerodt in 1886. Nearly one hundred years later polycoordinated organoiodine chemistry is undergoing a renaissance. This monograph is a welcome contribution by one of the major contributors and experts in the field. It is divided into eight chapters with extensive, up-to-date references to the original literature.

The first chapter deals with general aspects and discusses nomenclature, structural types, bonding, structure, spectra, preparation, stability, and reactivity patterns. The majority of organic polycoordinated iodine compounds are λ^3-iodanes and iodonium salts of various types: the most important, common and widely used being PhIO, $PhICl_2$, $PhI(OAc)_2$, $PhI(OOCCF_3)_2$, and PhI(OH)(OTs), along with diaryliodonium salts $Ar_2I^{\oplus}X^{\ominus}$.

The second chapter covers dichloro- and difluoroiodanes. Although such inorganic species as IF_3, IF_5, IF_7, and ICl_3 are stable and well known, this chapter focuses on organic iodine(III) compounds with at least one carbon ligand, i.e. RIX_2. $ArICl_2$ and $ArIF_2$, for example, are useful in chlorinations and fluorinations, respectively.

Chapter 3 discusses the properties and extensive chemistry of [bis(acyloxy)iodo]arenes, $ArI(O_2CR)_2$, and related compounds. The great majority of reactions of these compounds involve oxidations, many of which are analogous to the reactions of $Pb(OAc)_4$ without the concomitant toxic and environmental problems of lead.

Chapter 4, "Iodosyl Compounds and their Derivatives", deals with the chemistry and properties of derivatives of the nonisolable $ArI(OH)_2$, such as $ArI(OR)_2$, $ArI(ONO_2)_2$, $ArI(OSO_2R)_2$, ArI(OH)(OSO_2R), and the amorphous PhIO. Iodosylbenzene, PhIO, is an extensively employed, very useful, oxidant, both in the presence and absence of Lewis acids, including its extensive use in Cytochrome P-450 model studies. More recent examples include the widely used "Koser's reagent" $PhI(OH)(OSO_2C_6H_4CH_3)$ and "Zefirov's reagent" $PhI^{\oplus}$-O-$I^{\oplus}Ph \cdot 2X^{\ominus}$ (X = BF_4 or CF_3SO_3).

The longest and most extensive chapter (Ch. 5) treats iodonium salts. These include the classical diaryliodonium salts, $Ar_2I^{\oplus} \cdot X^{\ominus}$, as well as more recent members of the family such as alkynyl aryliodonium salts $RC{\equiv}CI^{\oplus}Ph \cdot X^{\ominus}$. These latter species are particularly useful as synthetic equivalents of "$RC{\equiv}C^{\oplus}$", namely electrophilic acetylenes, allowing for Umpolung of the more conventional and traditional acetylide, $RC{\equiv}C^{\ominus}$, chemistry. Alkynyl(phenyl)iodonium salts were successfully employed as progenitors to the hitherto unknown, novel alkynyl esters $RC{\equiv}COC(O)Ar$, $RC{=}COP(O)(OR')_2$, and $RC{\equiv}COSO_2Ar$. They also serve as alkynylating agents in reactions with a wide variety of nucleophiles including organometallic nucleophiles. Similarly, the perfluoroalkyl aryliodonium salts, $R_FI^{\oplus}Ph \cdot X^{\ominus}$, serve as a ready means of perfluoroalkylation and hence simple introduction of the R_F group into a variety of organic compounds.

The last three chapters cover: zwitterionic iodonium compounds (Ch. 6), including iodonium ylides as well as various dipoles; organoiodates (Ch. 7), i.e. anionic species of the type $IL_n^{\ominus}$ (where n may be 2, 4, 6, or 8) such as I_3, ICl_2 etc., and the compounds of pentavalent iodine (Ch. 8) dealing

 © VCH Verlagsgesellschaft mbH, D-69451 Weinheim, 1993 0570-0833/93/1111-1665 $ 10.00+.25/0

with species such as $PhIO_2$, $PhIOF_2$, $PhIF_4$, $PhI(O_2CR)_4$, and related molecules.

What makes polycoordinated iodine chemistry particularly useful and attractive is that it closely parallels the chemistry of such familiar species as Pb^{IV}, Te^{IV}, Se^{II}, Se^{IV}, Hg^{II}, and Hg^{IV} without the problems associated with the handling and safety of these mostly toxic heavy metal analogues. Moreover, the chemistry of organic polycoordinated iodine compounds, along with other main group polycoordinated species, partly resembles that of transition metal complexes, making possible a wide variety of useful transformations like those known for transition metal compounds.

This is a superbly written monograph. It maintains a good balance between structural and mechanistic information and synthetic uses and applications of organic polycoordinated iodine compounds. The text is easy to read, well illustrated and well referenced. The book can be strongly recommended to connoisseurs of iodine chemistry as well as novices. It should also serve as a nice supplementary text in graduate courses in both mechanistic and synthetic organic chemistry, although its cost is unfortunately likely to discourage wide use in this area.

Peter J. Stang
Department of Chemistry
University of Utah
Salt Lake City (USA)

Homogeneous Catalysis. The Applications and Chemistry of Catalysis by Soluble Transition Metal Complexes. By *G. W. Parshall* and *S. D. Ittel*. Wiley, New York, 1992. XII, 342 pp., hardcover £ 39.95.—ISBN 0-471-53829-9

This book, now in its second edition, describes the current state of knowledge on homogeneous catalysis by transition metals. The subject matter is arranged according to reaction types, but the emphasis is mainly on the wide variety of applications of this chemistry rather than on mechanisms. The book not only gives a wealth of information on useful and elegant methods for the laboratory-scale synthesis of organic compounds that one could not easily prepare in other ways, but also includes an extensive compilation of all types of industrial applications of homogeneous catalysis.

The authors have the advantage of many years of experience in senior positions in Du Pont's central research laboratories. The benefits of this are evident in their coverage of the relevant patent literature, and in the almost encyclopedic treatment of commercial applications and assessment of their relative importance. These range from large-scale applications such as the SHOP process developed by Shell (ethene oligomerization, metathesis) and the Du Pont adiponitrile process (hydrocyanation of butadiene, isomerization), through processes for manufacturing intermediates such as 1,4-butandiol (hydroformylation of allyl alcohol by the Kuraray method), to those used for making specialty chemicals and pharmaceuticals, e.g. the synthesis of Vitamin A (by hydroformylation and isomerization, BASF), of L-menthol (enantioselective isomerization, Takasago Perfumery), or Monsanto's new method for *S*-Naproxen® (enantioselective hydrogenation).

The authors describe how homogeneous catalytic methods, following their spectacular successes for large-scale processes in the 1970s and 1980s, are now increasingly finding new applications in fine chemicals manufacture. They illustrate this trend by describing industrial processes for synthesizing pharmaceuticals, plant protection chemicals, fragrances, and chemicals for the electronics industry. Moreover, the armory of methods is being continually refined. Thus, enantioselective syntheses, especially those involving hydrogenations and isomerizations, have now developed to the status of routine methods, as also have homogeneously catalyzed reactions carried out in two liquid phases so that the catalyst can be removed by phase separation.

The book's most important contribution is in providing a broad overview of developments in this field. The extensive bibliographies attached to each chapter, with review articles and more specific papers listed separately, are a pleasing and very useful feature. They are not only comprehensive but also commendably up-to-date, covering publications up to the end of 1991. Also the keyword index provides an easy way into the contents, enabling one to quickly find a required reaction on the basis of educt, product, catalyzing metal, and reaction type.

The individual chapters are packed with information, are readable, and contain a wealth of useful hints. The lucid and well arranged text and clear formula diagrams will be much appreciated by the reader who wants a quick overview of one of the areas covered. On the other hand, the reader wishing to go into greater detail on a certain topic will find the background information and literature references a valuable resource.

This is a soundly written book which can be recommended unreservedly, not only for synthetic organic and organometallic chemists in universities and industry but also for advanced students who wish to learn about this increasingly important field.

Michael Röper
BASF AG
Ludwigshafen (FRG)

Cycloaddition Reactions in Carbohydrate Chemistry. (ACS Symposium Series, Vol. 494. Series editor: *M. J. Comstock*.) Edited by *R. M. Giuliano*. American Chemical Society, Washington DC, 1992. X, 181 pp., hardcover $ 49.95.—ISBN 0-8412-2429-3

How many chemists immediately associate the word carbohydrates with cycloadditions? Probably very few, since from a synthetic standpoint carbohydrates, with their important structural and information-carrying roles in biological systems, are much more likely to be associated with ideas such as glycosidation, the chiral pool, and the use of protecting groups. Thus one cannot deny that this book has a certain degree of interdisciplinary character. In fact the use of cycloaddition reactions introduces some interesting novel aspects into carbohydrate chemistry. The converse is also true, of course: the field of cycloaddition reactions is already quite extensive, and the combination with carbohydrates increases the range of possibilities still further. Moreover, such reactions can have a very wide variety of uses: carbohydrates can serve either as chiral auxiliaries or as building blocks that are incorporated into the product molecule.

All these aspects are covered in the book reviewed here. The eleven articles are based on a symposium held by the American Chemical Society. In the introductory article R. M. Giuliano presents an overview of the topic, with separate sections on Diels–Alder reactions, hetero-Diels–Alder reactions, dipolar cycloadditions, and photochemical reactions, each including examples in which one of the partners in the cycloaddition is derived from a carbohydrate. The following articles treat individual topics in detail, in the form

of progress reports. R. W. Franck deals with the use of dienophiles derived from carbohydrates, describing cycloadditions involving both electron-rich and electron-deficient dienophiles. The preparation of α,β-unsaturated aldehydes and dienes from pyranoses and their use in cycloaddition reactions is described by J. C. Lopez et al. Such α,β-unsaturated aldehydes can act not only as dienophiles but also as diene components in hetero-Diels–Alder reactions. The article by M. Chmielewski describes the use of glycals in [2 + 2]-cycloadditions with isocyanates. The cycloadducts obtained in this way can serve as educts for the synthesis of β-lactam derivatives. D. Horton discusses the control of stereospecificity in the cycloaddition of cyclopentadiene to α,β-unsaturated esters prepared from aldopentoses. Not surprisingly, it is found that the facial selectivity in the cycloaddition reaction is controlled mainly by the allylic substituent. Y. Leblanc describes the hetero-Diels–Alder reaction of glycals with azodicarboxylates. This proceeds regiospecifically, yielding heterocyclic adducts that can be used for direct glycosidation with glycosyl acceptors. The effectiveness of this method has been demonstrated by synthesizing a number of complex 2-aminosaccharides. In the following article P. DeShong describes the use of glycosyl-manganese pentacarbonyl complexes for synthesizing C-glycosides. The glycosylmanganese pentacarbonyl complexes for this purpose can easily be prepared from a glycosyl bromide and a salt of the manganese pentacarbonyl anion. By means of insertion reactions these complexes can then be converted to C-glycosides in a wide variety of ways. However, this very interesting contribution has little relevance to the subject of cycloadditions. That criticism certainly does not apply to the next article, in which P. Herzegh et al. start by describing how a thiocarbonyl derivative prepared from a carbohydrate can undergo a hetero-Diels–Alder reaction with a 1,3-diene to yield a chiral thiopyran derivative. They then go on to describe intramolecular Diels–Alder reactions in which a diene and a dienophile are linked through a chain derived from a sugar, yielding various highly functionalized hexahydroindenes and octahydronaphthalenes. The next article, by H. Kunz, is concerned with a different application of carbohydrates, namely as chiral auxiliaries. For example, acrylates derived from carbohydrates can be reacted with 1,3-dienes in the presence of a Lewis acid catalyst to give the corresponding cycloadducts with a high degree of selectivity. Similarly, imines prepared from glycosyl amines can be reacted with electron-rich dienes, again with high selectivity. In all these cases it appears that the choice of the pivaloyl protecting group at the positions of the OH groups of the sugar is crucial. Next A. Lubineau discusses the effect of using water as the solvent for the Diels–Alder reaction between water-soluble dienes and electron-deficient dienophiles. Typical dienes that can be used here are 1,3-butadienylethers of carbohydrates without protecting groups. For these cycloaddition reactions the *endo*-selectivity is practically 100%, and the reaction rates are higher than in the usual organic solvents. In the last article L. Fisera describes 1,3-dipolar cycloadditions in which various nitrones derived from sugar aldehydes are reacted with *N*-aryl maleic imides. I feel that 1,3-dipolar cycloadditions could have been given more space in this book. One important topic, the de-novo synthesis of carbohydrates by means of cycloadditions, is even omitted entirely. However, this may have been a deliberate decision, as there is already a volume on this topic in the ACS Symposium Series.

In summary, this book offers a representative collection of articles on recent work in the area of cycloaddition reactions of carbohydrates. In each article the stereochemical aspects of the results are discussed in detail using appropriate transition state models. The book includes subject and author indexes which make it easy to locate a specific topic. However, one can also enjoy simply leafing through the book and admiring the illustrations. The way in which the book has come about inevitably means that there is some overlapping between individual articles. Also some readers may be somewhat displeased by the presentation, as there are differences in the typefaces used by the individual authors, and the line spacing is not uniform throughout. Despite this, the book can be recommended for everyone whose work is concerned with carbohydrates, cycloadditions, or stereoselective syntheses in general. It should provide many stimulating new ideas.

Martin E. Maier
Fakultät für Chemie
der Universität Konstanz (FRG)

Catalytic Chemistry. By *B. Gates*. Wiley, Chichester, 1992. XXI, 458 pp., paperback £ 14.95.—ISBN 0-471-55914-8

The literature on chemical catalysis has up to now suffered from being divided, according to the catalytic principles used, into homogeneous and heterogeneous catalysis. Since it is, to a greater extent than any other area of chemistry, an interdisciplinary field between pure science and technology, the recent publication by Wiley of a textbook on "Catalytic Chemistry" for students and teachers is welcome news. This conveniently-sized book attempts to cover all the important aspects of catalysis, a difficult but worthwhile task, even if it cannot be fully achieved.

The division into chapters is essentially along the lines of types of catalysts and processes, which is sensible from a teaching standpoint. Thus the main chapters cover: catalysis in solutions (Ch. 2, 128 pp.), catalysis by enzymes (Ch. 3, 47 pp.), catalysis by polymers (Ch. 4, 71 pp.), catalysis in cavities of molecular dimensions (Ch. 5, 55 pp.), and catalysis at surfaces (Ch. 6, 106 pp.). The short first chapter (14 pp.) introduces some important concepts (amplified where necessary in a glossary at the end of the book), emphasizes the importance of the mass balance laws and kinetic relationships (which other textbooks usually neglect), discusses catalytic cycles taking as an example the production of 1,4-hexadiene by the ethylene–butadiene coupling reaction, and ends with a "Problems Section" aimed at involving the reader in some learning activity.

The merits of this book are that it gives a quick overview of the most important types of (industrially relevant) catalytic processes, discusses some problems that remain to be solved by further research, and frequently compares kinetic data with mechanistic models and hypotheses. All the important modern catalytic processes are treated and, wherever possible, discussed in the context of kinetics laws. The reader interested in the practical details of industrial catalytic processes should find the clearly set out flow schemes especially useful. The author has incorporated results from recently published work, and always makes a point of relating the discussions to practical situations; this is shown, for example, by the description in mechanistic terms of the osmium tetraoxide catalyzed *cis*-hydroxylation of olefins (p. 141 f.). Here his wide experience of catalytic research, particularly in the field of surface organometallic chemistry, shows up to advantage.

The boldness to attempt a comprehensive treatment, always a good feature in a textbook, inevitably involves the

 © VCH Verlagsgesellschaft mbH, D-69451 Weinheim, 1993 0570-0833/93/1111-1667 $ 10.00+.25/0

risk of shortcomings. Three examples of these are the following: 1) Hydroformylation (p. 91 ff.). Although the Halpern mechanism is shown by formulas, readers (who are likely to include advanced students of chemistry and process technology) are not told about the problem of regioselectivity. Consequently there is also no reference to the possibility of achieving stereoselective hydroformylation of prochiral olefins. It is pleasing that the highly topical two-phase hydroformylation process and the Aldox process are included, but there should also have been a brief discussion of the advantages and disadvantages of some more commonly used catalysts, such as the Shell and UCC systems. 2) Olefin metathesis. Leaving aside the fact that Eleuterio (1960) was not the discoverer of this reaction (it originated much earlier as a spin-off from work on olefin polymerization), no information is given about catalysts suitable for industrial use. Also the treatment of the reaction mechanism is dubious from the standpoint of organometallic chemistry. Here the description of important industrial processes (e.g., SHOP, Norsorex, Vestenamer, cf. *Kontakte* **1991** (3), 29 ff.) is quite unsatisfactory, and consequently this chapter is not convincing. 3) Propene oxidation (p. 403 ff.). The essentials of bimetallic catalysis, of which the Sohio process for the ammoxidation of propene is an important industrial example, are well described. However, although the discussion of the mechanism is up-to-date so far as the (meager) literature is concerned, it fails to convey a picture of the molecular reaction steps that might be involved. Here there was a good opportunity to relate heterogeneously catalyzed processes to organometallic model systems!

This book may well provide the advanced student of chemistry with an impression of the wide-ranging nature of chemical catalysis, but this is achieved at the cost of superficiality in some important areas. I therefore feel that work using this book needs to be accompanied, or still better preceded, by a good lecture course providing a thorough grounding in the fundamentals. Under these circumstances it would prove its worth, since a lecture course cannot include the same amount of detail on reaction kinetics and process technology. Thus the book can be recommended to everyone who has to spend a period of time concentrating on the study of catalytic chemistry and, as a chemist or chemical engineer in industry, needs to read up on the subject to extend or refresh his or her knowledge. The book is well worth its price.

Wolfgang A. Herrmann
Anorganisch-chemisches Institut
der Technischen Universität München
Garching (FRG)

Accurate Molecular Structures. Their Determination and Importance. (Series: IUCr Monographs on Crystallography, Vol. 1.) Edited by *A. Domenicano* and *I. Hargittai*. International Union of Crystallography, Oxford University Press, Oxford, 1992. XXI, 590 pp., hardcover £ 60.00.—ISBN 0-19-855556-3

With this book the International Union of Crystallography (IUCr) begins a series in which various special areas of crystallography will be treated in detail. However, rather than limiting the series strictly to crystallography, the editors (A. Domenicano and I. Hargittai) are sensibly extending the scope so as to acquaint readers with other methods of structure determination and their applications.

The determination and interpretation of the structures of molecules is an important area of chemical research, which is also interdisciplinary. To carry it out effectively it is essential to have a knowledge of the accuracy and limitations of the methods with regard to systematic and random experimental errors. This book summarizes the capabilities of the various methods used for precise molecular structure determination, as well as their use in combination and the significance of accurate structural data in modern chemical research (in the preface). The 22 chapters have been written by recognized experts. A bibliography is given at the end of each chapter, and the book concludes with author, subject, and formula indexes (although the last is very incomplete). The editors have set out to cover the whole of the field, but it is not possible for a single book to fulfill this ambitious aim. Nevertheless, it is a mine of information that will be of considerable interest to every structural chemist who wants to look beyond the immediate confines of his or her particular method.

The first chapter gives an excellent general introduction to the subject. After a short account of the historical background, experimental and theoretical methods used for structure determination are briefly sketched, and the importance of obtaining precise structural data is illustrated by a few well chosen examples.

Chapter 2 is concerned with the derivation and significance of potential functions for di- and polyatomic molecules; here the reader is assumed to have extensive mathematical knowledge in the area of group theory. Included here is a survey of the different ways of defining interatomic distances which is especially important. The chapter ends with a table listing experimentally measured data on equilibrium structures and anharmonic potential constants for polyatomic molecules; unfortunately, though, the literature references given here extend only to 1988, which does not entirely fulfill the book's declared aim of presenting "current chemical research".

Chapter 3 deals with microwave spectroscopy. The fundamental principles are derived and discussed, and their application is illustrated by describing a structure determination carried out using this method.

Chapter 4 is devoted to structure determination by vibrational-rotational spectroscopy. The author confines his discussion mainly to IR spectroscopy, and describes the mathematical formalism and procedures for di- and polyatomic molecules.

The treatment of gas phase electron diffraction (Chapter 5) begins with the development of the method, followed by the theoretical fundamentals and the experimental details. An example of a structural analysis is then described, together with a discussion of the uncertainties in the information yielded by the method. Chapter 6 gives an easily understandable introduction to the basic principles of single crystal structure analysis by X-ray diffraction. Subject matter which normally fills thick textbooks is here compressed into about 30 pages. One is prompted to wonder for whom this chapter has been written. The reader already familiar with these matters can either miss it out or use it as a source of ideas on how best to teach the subject. For the novice, however, it is so elementary that it requires too great a jump to Chapters 7–11 that follow. Even the ten-page glossary at the end of the chapter, a feature that is unfortunately missing from most textbooks, is not enough to put this right. For any structure determination by X-ray diffraction that is more than just a routine measurement, to obtain precise data one must not only have a suitable crystal, but must also make measurements at as many angles as possible, repeated as

risk of shortcomings. Three examples of these are the following: 1) Hydroformylation (p. 91 ff.). Although the Halpern mechanism is shown by formulas, readers (who are likely to include advanced students of chemistry and process technology) are not told about the problem of regioselectivity. Consequently there is also no reference to the possibility of achieving stereoselective hydroformylation of prochiral olefins. It is pleasing that the highly topical two-phase hydroformylation process and the Aldox process are included, but there should also have been a brief discussion of the advantages and disadvantages of some more commonly used catalysts, such as the Shell and UCC systems. 2) Olefin metathesis. Leaving aside the fact that Eleuterio (1960) was not the discoverer of this reaction (it originated much earlier as a spin-off from work on olefin polymerization), no information is given about catalysts suitable for industrial use. Also the treatment of the reaction mechanism is dubious from the standpoint of organometallic chemistry. Here the description of important industrial processes (e.g., SHOP, Norsorex, Vestenamer, cf. *Kontakte* **1991** (3), 29 ff.) is quite unsatisfactory, and consequently this chapter is not convincing. 3) Propene oxidation (p. 403 ff.). The essentials of bimetallic catalysis, of which the Sohio process for the ammoxidation of propene is an important industrial example, are well described. However, although the discussion of the mechanism is up-to-date so far as the (meager) literature is concerned, it fails to convey a picture of the molecular reaction steps that might be involved. Here there was a good opportunity to relate heterogeneously catalyzed processes to organometallic model systems!

This book may well provide the advanced student of chemistry with an impression of the wide-ranging nature of chemical catalysis, but this is achieved at the cost of superficiality in some important areas. I therefore feel that work using this book needs to be accompanied, or still better preceded, by a good lecture course providing a thorough grounding in the fundamentals. Under these circumstances it would prove its worth, since a lecture course cannot include the same amount of detail on reaction kinetics and process technology. Thus the book can be recommended to everyone who has to spend a period of time concentrating on the study of catalytic chemistry and, as a chemist or chemical engineer in industry, needs to read up on the subject to extend or refresh his or her knowledge. The book is well worth its price.

Wolfgang A. Herrmann
Anorganisch-chemisches Institut
der Technischen Universität München
Garching (FRG)

Accurate Molecular Structures. Their Determination and Importance. (Series: IUCr Monographs on Crystallography, Vol. 1.) Edited by *A. Domenicano* and *I. Hargittai*. International Union of Crystallography, Oxford University Press, Oxford, 1992. XXI, 590 pp., hardcover £ 60.00.—ISBN 0-19-855556-3

With this book the International Union of Crystallography (IUCr) begins a series in which various special areas of crystallography will be treated in detail. However, rather than limiting the series strictly to crystallography, the editors (A. Domenicano and I. Hargittai) are sensibly extending the scope so as to acquaint readers with other methods of structure determination and their applications.

The determination and interpretation of the structures of molecules is an important area of chemical research, which is also interdisciplinary. To carry it out effectively it is essential to have a knowledge of the accuracy and limitations of the methods with regard to systematic and random experimental errors. This book summarizes the capabilities of the various methods used for precise molecular structure determination, as well as their use in combination and the significance of accurate structural data in modern chemical research (in the preface). The 22 chapters have been written by recognized experts. A bibliography is given at the end of each chapter, and the book concludes with author, subject, and formula indexes (although the last is very incomplete). The editors have set out to cover the whole of the field, but it is not possible for a single book to fulfill this ambitious aim. Nevertheless, it is a mine of information that will be of considerable interest to every structural chemist who wants to look beyond the immediate confines of his or her particular method.

The first chapter gives an excellent general introduction to the subject. After a short account of the historical background, experimental and theoretical methods used for structure determination are briefly sketched, and the importance of obtaining precise structural data is illustrated by a few well chosen examples.

Chapter 2 is concerned with the derivation and significance of potential functions for di- and polyatomic molecules; here the reader is assumed to have extensive mathematical knowledge in the area of group theory. Included here is a survey of the different ways of defining interatomic distances which is especially important. The chapter ends with a table listing experimentally measured data on equilibrium structures and anharmonic potential constants for polyatomic molecules; unfortunately, though, the literature references given here extend only to 1988, which does not entirely fulfill the book's declared aim of presenting "current chemical research".

Chapter 3 deals with microwave spectroscopy. The fundamental principles are derived and discussed, and their application is illustrated by describing a structure determination carried out using this method.

Chapter 4 is devoted to structure determination by vibrational-rotational spectroscopy. The author confines his discussion mainly to IR spectroscopy, and describes the mathematical formalism and procedures for di- and polyatomic molecules.

The treatment of gas phase electron diffraction (Chapter 5) begins with the development of the method, followed by the theoretical fundamentals and the experimental details. An example of a structural analysis is then described, together with a discussion of the uncertainties in the information yielded by the method. Chapter 6 gives an easily understandable introduction to the basic principles of single crystal structure analysis by X-ray diffraction. Subject matter which normally fills thick textbooks is here compressed into about 30 pages. One is prompted to wonder for whom this chapter has been written. The reader already familiar with these matters can either miss it out or use it as a source of ideas on how best to teach the subject. For the novice, however, it is so elementary that it requires too great a jump to Chapters 7–11 that follow. Even the ten-page glossary at the end of the chapter, a feature that is unfortunately missing from most textbooks, is not enough to put this right. For any structure determination by X-ray diffraction that is more than just a routine measurement, to obtain precise data one must not only have a suitable crystal, but must also make measurements at as many angles as possible, repeated as

many times as possible, as slowly as possible, and at the lowest possible temperature. Chapter 7 explains all this in an impressive way, together with the necessary systematic procedures and corrections that can be applied.

It cannot be emphasized too often that the refinement of structural parameters from X-ray diffraction data can yield as an extra bonus valuable information about the dynamics of molecules and of the crystal lattice. Too few research groups make use of this capability, even though suitable programs are available and the information is obtainable at no extra cost, in the form of the anisotropic temperature parameters (or, better still, displacement parameters). Although Chapters 8 and 9 describe the background and methematical formalism of procedures such as the "rigid body test" and the determination of rotational barriers, they are not sufficient to save the user the bother of consulting the original literature. More detail and more examples would have been useful here.

The next chapter explains clearly that experimentally determined distribution functions for deformation density and residual electron density are greatly dependent on the method used and on how one defines the pro-molecule. However, the objective seems to be always that of bringing the experimental deformation density distribution into as close agreement as possible with that calculated from theory, and this must always come up against difficulties in view of the wide variety of methods. Unfortunately not enough attention is given here to the importance of the integrity or self-sufficiency of the chosen method, despite the fact that the author of this chapter, who has since died, was a leading pioneer in this field. Neutron diffraction excels where X-ray diffraction is weakest, namely in determining the positions and anisotropic displacement factors of hydrogen atoms. Consequently Chapter 11 is concerned not only with comparing the two methods but also especially with hydrogen bonding. The subject of hydrogen bonds is in turn closely related to the effects of crystal packing, and this leads one into making comparisons with quantum mechanical calculations. Many examples are presented to show that, despite the high cost of neutron diffraction experiments, this method will continue to have a secure place among methods of structure determination. Chapter 12 deals with NMR spectroscopy in liquid crystalline solvents. The basic principles and experimental details are explained, an example of a structure determination by this method is described, and factors affecting the accuracy of the measurements are discussed.

Quantum mechanical methods for calculating static and dynamic structures are described in Chapter 13 in a clearly understandable way. Chapter 14 is concerned with the methods of molecular mechanics. However, the discussion is mainly confined to the basic principles, which are generally well known, whereas relatively little space is given to applications and problem areas. Chapter 15 is mainly concerned with the Cambridge Structural Database (CSD) and with its design features, the search strategies used, and examples of applications. An updated account is given of examples that are already familiar from the author's earlier publications.

Chapters 16 and 17 use selected examples to illustrate how results from structure determinations can be applied to chemical problems. As well as describing stereoelectronic effects, examples are given to show the importance of structural correlations for determining reaction pathways and energy hypersurfaces.

Chapter 18 reviews numerous studies on the effects of substituents in distorting the benzene ring, comparing and interpreting experimental and theoretical methods of structure determination. The following chapter discusses the difficulties in estimating the packing effect, which describes the extent to which the molecular conformation in a single crystal departs from that corresponding to a global energy minimum. Here considerations based on polymorphic structures are useful, and so especially are theoretical methods. Up to this point one might have the impression that insufficient attention is devoted to structure determinations for inorganic molecules. This is remedied in Chapters 20 to 22, which discuss the particular role of structure determination in inorganic chemistry and the special problems that arise, especially with regard to single crystal structural studies. The examples described illustrate that when one attempts to determine the positions of light atoms adjacent to heavy atoms or to determine space groups or occupancy numbers, one quickly comes up against the limitations of the method.

The level of previous knowledge that is assumed varies greatly from chapter to chapter, due to the difficulty of coordinating the work of such a team of authors. However, it is pleasing to find that there are cross-references between the chapters.

This book can be emphatically recommended for the structural chemist who cannot afford to simply restrict himself to his own method, but must instead seek opportunities for interdisciplinary collaboration. However, it is less suitable for students owing to the wide differences between chapters in the level of previous knowledge needed. Further volumes in this series should, if possible, be more correctly matched to the needs of the intended readership.

Roland Boese, Waldemar A. Brett
Institut für Anorganische Chemie
der Universität-Gesamthochschule Essen (FRG)

New Books
see next page

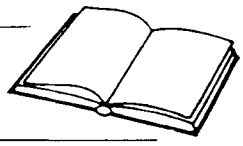

New Books

RÖMPP Lexikon Umwelt. Edited by **J. Falbe, M. Regitz.** Thieme, Stuttgart, **1993.** 770 pp., hardcover, DM 298.—ISBN 3-13-736501-5

Photosensitization and Photocatalysis Using Inorganic and Organometallic Compounds. Edited by **K. Kalyanasundaram.** Kluwer, Dordrecht, The Netherlands, **1993.** 484 pp., hardcover, Dfl. 330.—ISBN 0-7923-2261-4

Chromatography in Biotechnology. (ACS Symposium Series 529). Edited by **C. Horváth, L. S. Ettre.** American Chemical Society, Washington, **1993.** 189 pp., hardcover, $ 49.95.—ISBN 0-8412-2669-5

Control Methods in Polymer Processing. (Studies in Polymer Science, Vol. 10). By **L. Halász.** Elsevier, Amsterdam, The Netherlands, **1993.** 486 pp., hardcover, Dfl. 400.—ISBN 0-444-98741-X

Horizonte. Wie weit reicht unsere Erkenntnis heute? Edited by **G. Wilke.** Wissenschaftliche Verlagsgesellschaft, Stuttgart, **1993.** 364 pp., paperback, DM 48.—ISBN 3-8047-1280-0

Food and Cancer Prevention: Chemical and Biological Aspects. Edited by **K. W. Waldron, I. T. Johnson, G. R. Fenwick.** The Royal Society of Chemistry, Cambridge, **1993.** 462 pp., hardcover, £ 55.—ISBN 0-85186-455-4

Ion Exchange Processes: Advances and Applications. Edited by **A. Dyer, M. J. Hudson, P. A. Williams.** The Royal Society of Chemistry, Cambridge, **1993.** 372 pp., hardcover, £ 52.50.—ISBN 0-85186-445-7

Applications of Plasma Source Mass Spectrometry II. Edited by **G. Holland, A. N. Eaton.** The Royal Society of Chemistry, Cambridge, **1993.** 245 pp., hardcover, £ 45.—ISBN 0-85186-465-1

Quantities, Units and Symbols in Physical Chemistry. (Second Edition). By **I. Mills et al.** Blackwell Scientific Publications, Oxford, **1993.** 166 pp., paperback, £ 14.95.—ISBN 0-632-03583-8

Chemical Vapor Deposition. Principles and Applications. Edited by **M. L. Hitchman, K. F. Jensen.** Academic Press, London, **1993.** 677 pp., hardcover, £ 75.—ISBN 0-12-349670-5

Dictionary of Common Names. Trivialnamen-Handbuch, Vol. 1-3. Edited by **FIZ Chemie, Berlin.** VCH, Weinheim/New York, **1993.** 1008 pp., hardcover, Prepublication Prize: DM 1760.-/$ 1135.- valid until December 31, 1993, regular price: DM 2100.—/$ 1355.—ISBN 3-527-29020-0

Umweltbelastungen und Ängste. Erkennen – Bewerten – Vermeiden. Edited by **K. Aurand, B. P. Hazard, F. Tretter.** Westdeutscher Verlag, Opladen, **1993.** 424 pp., paperback, DM 59.—ISBN 3-531-12508-7

Vom Wasser. Sammelregister zu den Bänden 61-80 (1983-1993). Edited by **Gesellschaft Deutscher Chemiker.** VCH, Weinheim, **1993.** 150 pp., hardcover, DM 198.—ISBN 3-527-28607-1

Cyclitols and their Derivatives. A Handbook of Physical, Spectral, and Synthetic Data. By **T. Hudlicky, M. Cebulak.** VCH, Weinheim/New York, **1993.** 315 pp., hardcover, DM 148.-/$ 85.—ISBN 3-527-89633-3/1-56081-633-3

Laserspektroskopie. Grundlagen und Techniken. By **W. Demtröder.** Springer, Heidelberg, **1993.** 489 pp., hardcover, DM 98.—ISBN 3-540-56404-7

Recent Progress in the Chemical Synthesis of Antibiotics and Related Microbial Products, Vol. 2. Edited by **G. Lukacs.** Springer, Heidelberg, **1993.** 970 pp., hardcover, DM 348.—ISBN 3-540-56754-2

Explosionsschutz. Grundlagen und Anwendungen. By **W. Bartknecht, G. Zwahlen.** Springer, Heidelberg, **1993.** 915 pp., hardcover, DM 298.—ISBN 3-540-55464-5

Marine Natural Products - Diversity and Biosynthesis. (Topics in Current Chemistry, Vol. 167). Edited by **P. J. Scheuer.** Springer, Heidelberg, **1993.** 185 pp., hardcover, DM 148.—ISBN 3-540-56513-2

New Trends and Approaches in Electrochemical Technology. Edited by **N. Masuko, T. Osaka, Y. Fukunaka.** VCH, Weinheim/New York, Kodansha, Tokyo, **1993.** 255 pp., hardcover, DM 198.—/$ 130.—ISBN 3-527-28574-1/1-56081-781-X/4-06-206137-6

Fiber and Whisker Reinforced Ceramics for Structural Applications. By **D. Belitskus.** Marcel Dekker, New York, **1993.** 360 pp., hardcover, $ 145.—ISBN 0-8247-9111-8

Micromechanics of Concrete and Cementitious Composites. Edited by **C. Huet.** Presses Polytechniques et Universitaires Romandes, Lausanne, **1993.** 252 pp., paperback, SF 78.—ISBN 2-88074-260-9

The Measurement of Grain Boundary Geometry. (Electron Microscopy in Materials Science Series). Edited by **V. Randle.** Institute of Physics Publishing, Bristol, **1993.** 169 pp., hardcover, £ 60.—ISBN 0-7503-0235-6

Laser Chemistry of Organometallics. (ACS Symposium Series 530). Edited by **J. Chaiken.** American Chemical Society, Washington, **1993.** 313 pp., hardcover, $ 74.95.—ISBN 0-8412-2667-3

Photochemistry of Lignocellulosic Materials. (ACS Symposium Series 531). Edited by **C. Heitner, J. C. Scaiano.** American Chemical Society, Washington, **1993.** 228 pp., hardcover, $ 64.95.—ISBN 0-8412-2692-X

Semiconductor Interfaces, Microstructures and Devices. Properties and Applications. Edited by **Z. C. Feng.** Institute of Physics Publishing, Bristol, **1993.** 293 pp., hardcover, £ 67.50.—ISBN 0-7503-0180-5

Structure and Properties of Polymers. (Materials Science and Technology, Vol. 12). Edited by **E. L. Thomas.** VCH, Weinheim/New York, **1993.** 785 pp., hardcover, DM 430.—/$ 295.—ISBN 3-527-26825-1/0-89573-700-0

High Energy Non-Aqueous Batteries. (Ellis Horwood Series in Physical Chemistry). By **A. Cisak, L. Werblan.** Ellis Horwood, Chichester, **1993.** 262 pp., hardcover, £ .....—ISBN 0-13-388596-8.

Scanning Tunneling Microscopy III. (Springer Series in Surface Sciences, Vol. 29). Edited by **R. Wiesendanger, H.-J. Güntherodt.** Springer, Heidelberg, **1993.** 375 pp., hardcover, DM 118.—ISBN 3-540-56317-2

Colloid-Polymer Interactions. Particulate, Amphiphilic, and Biological Surfaces. (ACS Symposium Series 532). Edited by **P. L. Dublin, P. Tong.** American Chemical Society, Washington, **1993.** 300 pp., hardcover, $ 74.95.—ISBN 0-8412-2696-2

B-Glucosidases: Biochemistry and Molecular Biology. (ACS Symposium Series 533). Edited by **A. Esen.** American Chemical Society, Washington, **1993.** 249 pp., hardcover, $ 74.95.—ISBN 0-8412-2697-0

Registered names, trademarks, etc. used in this journal, even when not marked as such, are not to be considered unprotected by law.

© VCH Verlagsgesellschaft mbH, D-69451 Weinheim, 1993. – Printed in the Federal Republic of Germany by Konrad Triltsch Druck- und Verlagsanstalt Würzburg.

All rights reserved (including those of translation into foreign languages). No part of this issue may be reproduced in any form — by photoprint, microfilm, or any other means — nor transmitted or translated into a machine language without written permission from the publishers. Only single copies of contributions, or parts thereof, may be made for personal use. This journal was carefully produced in all its parts. Nevertheless, authors, editors, and publisher do not warrant the information contained therein to be free of errors. Readers are advised to keep in mind that statements, data, illustrations, procedural details, or other items may inadvertently be inaccurate.

Valid for users in the USA: The appearance of the code at the bottom of the first page of an article (serial) indicates the copyright owner's consent that copies of the article may be made for personal or internal use, or for the personal or internal use of specific clients. This consent is given on the condition, however, that the copier pay stated per-copy fee through the Copyright Clearance Center, Inc. (CCC), for copying beyond that permitted by Sections 107 or 108 of the U.S. Copyright Law. This consent does not extend to other kinds of copying, such as copying, for general distribution, for advertising or promotional purposes, for creating new collective works, or for resale. For copying from back volumes of this journal see 'Permissions to Photo-Copy: Publisher's Fee List' of the CCC.

Editorial office: Postfach 10 11 61, D-69451 Weinheim, Federal Republic of Germany, Telephone (06201) 606 315, Telex 465 516 vchwh d, Telefax (06201) 606 328, E-Mail Z16@DHDURZ2 in Earn Bitnet.

Editor: *Peter Gölitz*

Associate editors: *N. A. Compton, R. H. Schmidt-Radde, K. J. Schneider.* **Book editor:** *G. Karger.* **Editorial assistants:** *J. Göhrig, E. Schweikart*

Publishers: VCH Verlagsgesellschaft mbH. (Managing Directors: *Hans Dirk Köhler, Dr. Karlheinz Köpfer*), Pappelallee 3, D-69451 Weinheim, Federal Republic of Germany.

Advertising office (Advertising Manager: *N. Schippel*): Postfach 10 11 61, D-69451 Weinheim, Federal Republic of Germany, Telephone (0 62 01) 606 312, Telefax (0 62 01) 606 328.

ANGEWANDTE CHEMIE
International Edition in English
Volume 32 · Number 12
December 1993
Pages 1671–1818

The Unique Antithrombin III Binding Domain of Heparin: A Lead to New Synthetic Antithrombotics

By Constant A. A. van Boeckel* and Maurice Petitou*

Heparin, a sulfated glycosaminoglycan, is well known for its anticoagulant effect mediated by the serine protease inhibitor antithrombin III (AT III). Heparin has been used clinically for more than half a century for the prophylaxis and treatment of venous thrombosis and thromboembolism. Up until the 1980s it was assumed that the biological activity of heparin was mainly caused by its polyanionic character. However, this paradigm was contradicted when it was discovered that part of the heparin polysaccharides contains a well-defined pentasaccharide domain that specifically binds and activates AT III. The specificity of the interaction between the characteristic pentasaccharide and AT III has become more obvious after the synthesis and biological testing of various heparin analogues. This article reviews the synthesis of the heparin pentasaccharide, some closely related counterparts, and some highly modified analogues. With the aid of molecular modeling and through "tailored" molecular modifications of the pentasaccharide, much knowledge has been gained concerning structure–activity relationships. On this basis not only have more potent and simplified derivatives been developed, but also the recognition between heparin and AT III can now be understood in greater detail at the molecular level.

1. Introduction[**]

The chemically closely related polysaccharides heparin and heparan sulfate are present in many living organisms.[1–3] Whereas heparan sulfate is widely distributed in different cell types and tissues, heparin is confined to one cell type only, the mastocytes, where it is complexed to histamine. Heparin has attracted considerable attention because of its anticoagulant properties, which are at the origin of its clinical use in preventing venous thrombosis (the clotting of blood in veins).[3]

From a chemical standpoint, heparin is a glycosaminoglycan. This family of complex anionic polysaccharides includes glucosaminoglycans (heparin, heparan sulfate), galactosaminoglycans (chondroitin 4-sulfate, chondroitin 6-sulfate, dermatan sulfate), hyaluronic acid, and keratan sulfate. The structure of heparin[4] is shown schematically in Figure 1. It consists of a carbohydrate backbone made up of alternating 1,4-linked uronic acid (D-glucuronic or L-iduronic) and glucosamine residues. A standard heparin preparation consists of a mixture of linear polysaccharides composed of approximately 20 to 100 monosaccharides. Most of the monosaccharides bear one or several substituents at different positions, as shown in Figure 1.

Heparin inhibits blood coagulation[5] through activation of antithrombin III (AT III), a physiological inhibitor of coagulation. AT III belongs to the serin protease inhibitors superfamily (serpins). This glycoprotein constructed of 432

[*] Dr. C. A. A. van Boeckel
Organon International B. V.
Kloosterstraat 6, NL-5340 BH Oss (The Netherlands)
Telefax: Int. code +(4120)62546
Dr. M. Petitou
Sanofi Recherche
9, Rue du President Allende
F-94256 Gentilly Cedex (France)

[**] All = allyl, Ac = acetyl, Bn = benzyl, Bz = benzoyl, Z = benzyloxycarbonyl, MCA = monochloroacetyl, Lev = levulinoyl, Tf = trifluoromethylsulfonyl, TBDMS = *tert*-butyldimethylsilyl.

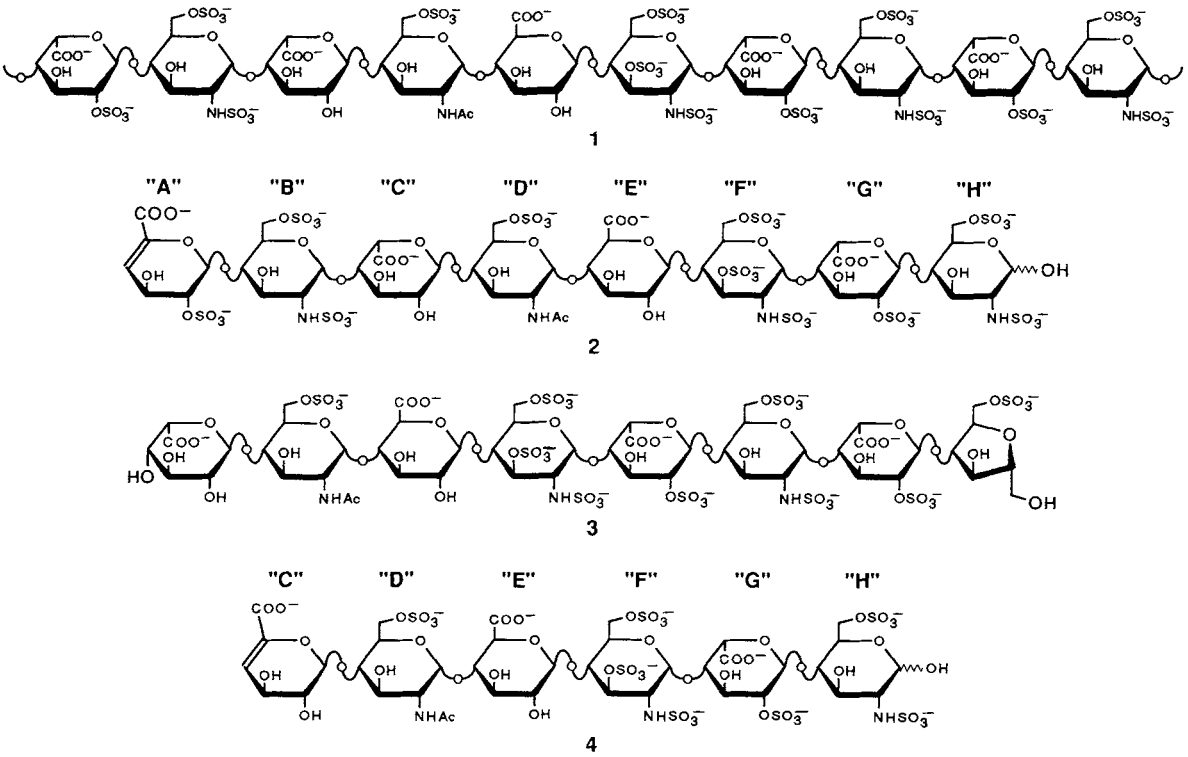

Fig. 1. Oligosaccharide **1** in the top row represents a hypothetical fragment of a heparin molecule. Heparin chains consist of alternating 1 → 4 linked uronic acid and glucosamine residues. The former may be β-D-glucuronic acid (e.g., unit E), α-L-iduronic acid (e.g., unit C), or α-L-iduronic acid-2-sulfate (e.g., unit G), while the latter may be *N*-acetyl-α-D-glucosamine-6-sulfate (e.g., unit D), α-D-glucosamine-N-sulfate-6-sulfate (e.g., unit H; see the footnote on p. 1673 for the term N-sulfate), or α-D-glucosamine-N-sulfate-3,6-disulfate) (e.g., unit F). Glucosamine units can also be present as counterparts not sulfated at position 6. The largest part of the structure of a heparin preparation is accounted for by the repeating unit consisting of the disaccharide sequence α-L-iduronic acid-2-sulfate(1 → 4)α-D-glucosamine-N-sulfate-6-sulfate (e.g. disaccharide moiety GH), which forms "regular regions" [4]. The rest of the structure contains in various proportions the other monosaccharide residues that form "irregular regions" which could be of major importance for the biological function of these complex molecules. Octasaccharides **2** and **3** result from controlled degradation of heparin by heparinase or nitrous acid, respectively [12]. Hexasaccharide **4** was obtained in the same way after prolonged enzymatic digestion [12]. The pentasaccharide sequence DEFGH (the variant in which unit D is N-sulfated), shared by all these biologically active oligosaccharides, was selected as the first target for total synthesis.

amino acids (in humans) forms tight complexes with several blood coagulation factors—we will focus here on blood coagulation factors Xa and IIa (also called thrombin)—which are thereby inactivated (see Figs. 2a, 2b). The rate of protease inactivation is increased by several orders of magnitude when ATIII is bound to a heparin molecule.[6]

Constant A. A. van Boeckel was born in 1956 in Brunei (formerly British Borneo) and studied chemistry at the University of Leyden. He received a doctorate in chemistry in 1979 and his Ph.D. degree in 1982 under J. van Boom. He then moved to the pharmaceutical industry (Organon Int. B. V., Oss). In 1988 he was appointed part-time Professor at the University of Leyden. He was awarded the Unilever Chemistry Prize (1978), the Professor Oosterhoff Prize (1981), the Akzo Chemistry Prize (1988), and the Golden Medal of the Royal Dutch Chemical Society (1988). Presently he is departmental head of the Medicinal Chemistry Department at Organon Int. His areas of interest include carbohydrate chemistry, nucleotide chemistry, protease inhibitors, and drug design.

Maurice Petitou was born in 1949 in France and studied chemistry in Clermont-Ferrand and Orléans, where he received a master's degree in 1971 and a doctorate in chemistry in 1974. He then worked for three years as a Fellow of the Ligue Nationale Française Contre le Cancer (LNFC) studying membrane glycoproteins of leukemic cells. In 1978 he joined the Institut Choay, the research branch of Laboratoires Choay, to work on the chemistry of heparin; he received his Ph.D. in 1984. He received the Groupe Français des Glucides Prize in 1985 and the Galien Prize for Pharmaceutical Research in 1986. He was appointed Research Associate Director of the Centre National de la Recherche Scientifique (CNRS) in 1988. Since 1989 he has been head of the Carbohydrate Chemistry Department at Sanofi Recherche, where he is in charge of research on the chemistry of glycosaminoglycans.

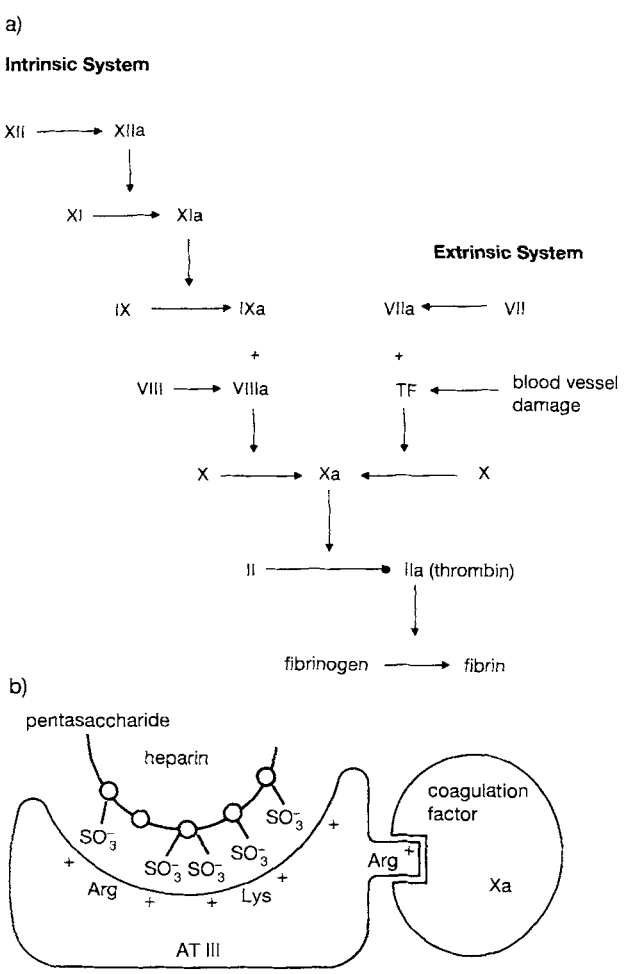

Fig. 2. a) Overview of the blood coagulation system. Blood coagulation is a complex process involving several enzymes (activated coagulation factors) present in plasma as their precursors (zymogens). Activation of these proenzymes occurs in a cascade and can be initiated by contact of blood with foreign surfaces and presumably also by subendothelial structures exposed during blood vessel damage (intrinsic pathway). These proenzymes can also be activated by thromboplastin and tissue factor (TF) excreted or released by injured cells (extrinsic pathway). The two pathways converge at the level of factor X activation. An imbalance in the system leads to a prohemorragic or to a prothrombotic state. Natural inhibitors like AT III are supposed to oppose prothrombotic states. When it is complexed to heparin, AT III can inhibit several activated blood coagulation factors, but when it is bound to a pentasaccharide it selectively inactivates factor Xa. b) A characteristic pentasaccharide domain of heparin selectively binds to AT III. During the interaction, AT III changes its conformation and a remote loop fragment of AT III becomes exposed to facilitate the inactivation of blood coagulation factor Xa.

Owing to its anticoagulant properties, heparin has been used in clinics since 1937. However, its true mechanism of action is not necessarily connected to its whole anticoagulant activity, but, possibly, to its ability to catalyze the inactivation of a particular serin protease in blood coagulation. This was recognized when clinicians began to use low doses of heparin that hardly affected the coagulation parameters (e.g. blood coagulation time) but nevertheless sufficed to prevent thrombosis. Pharmacologists then proposed that inhibition of blood coagulation factor Xa could be more relevant than inhibition of thrombin (factor IIa) for achieving optimal clinical efficacy (i.e. the best benefit/risk ratio). Since then, the scientific community has devoted efforts to obtaining heparin preparations with increased factor Xa activity and/or decreased anti-factor IIa activity, in other words, with an increased anti-Xa/anti-IIa ratio.[7]

2. Background

2.1. Fractionation and Degradation of Heparin

Following the above hypothesis that heparin preparations with increased anti-factor Xa/anti-factor IIa ratios could be better antithrombotic drugs than standard heparin itself, programs were launched aiming at the preparation of such drugs. Two crucial observations were made in 1976. The first was that only some of the heparin molecules bind to AT III when heparin is fractionated by affinity chromatography on immobilized AT III.[8-10] The second finding was that heparin molecules having affinity for AT III achieved the same degree of factor Xa inhibition, whatever their size, while thrombin inhibition was size dependent.[8] (A rational explanation based on chemical structure is discussed in Section 7.) In summary, any heparin preparation contains at least three kinds of molecules: those that can promote AT III inhibition of factor Xa and of thrombin (type 1), those that can only promote inhibition of factor Xa (type 2), and those that are unable to promote any significant inhibition (type 3). Standard heparin preparations are made up of about one-third of type 1 molecules and two-thirds of type 3. The simplest way to favor inhibition of factor Xa over that of factor IIa is to decrease the molecular weight of the preparation. This has been achieved both by chemical as well as enzymatic cleavage of heparin chains and has led[7, 11] to the widely used "low molecular weight heparin" class of drugs.[12]

2.2. Discovery of a Characteristic Antithrombin-Binding Pentasaccharide Domain

Since the ability of heparin fragments to reinforce AT III mediated inhibition of factor Xa appeared independent of their size, it was logical to look for the smallest fragments able to catalyze inhibition of factor Xa. The experimental approach consisted in controlled cleavage of heparin by chemical (nitrous acid) or enzymatic (heparinase from *flavobacterium heparinum*) means, separating the fractions having AT III affinity by affinity chromatography, and finally gel filtration of these fractions. By using this approach biologically active octasaccharides were identified, and their structures determined (Fig. 1).[*] Comparison of **2** and **3** suggests that the common hexasaccharide CDEFGH **4** contains the active sequence. This was proved after isolation of the corresponding hexasaccharide after treatment of **2** by heparinase. In hexasaccharide **4** the molecular identity of unit C has been altered without loss of biological activity. This strongly suggested that the pentasaccharide sequence DEFGH is the active sequence. It is particularly noteworthy that the active structures contain the trisaccharide sequence DEF—*N*-acetyl-6-sulfated glucosamine (D) (note that an N-sulfated glucosamine[**] has also been found in this position), glucuronic acid (E), and N-sulfated, 3,6-disulfated glucosamine (F)—since all three monosaccharides are minor

[*] The same sequences were independently found to correspond to the AT III binding site of heparin.

[**] In this review the $NHSO_3^-$ group is referred to as N-sulfate and the OSO_3^- group as sulfate.

constituents of heparin. Most remarkable is the sulfate group at position 3 of the central glucosamine unit.[13, 14] The presence of these structural features together in a short active oligosaccharide sequence suggests that DEFGH is the most characteristic domain of heparin. This hypothesis is supported further by studies of the interaction of well-defined synthetic analogues of pentasaccharide DEFGH with AT III. It is worth mentioning that in vivo studies in animals provided evidence that heparan sulfate in endothelial cells contains similar pentasaccharide domains which probably contribute to the nonthrombogenic properties of the vessel wall[15] (Fig. 3).

Since no biochemical tool for further controlled degradation has been available to obtain the pentasaccharide DEFGH, chemical synthesis has been required. Moreover, organic synthesis is the only way to obtain well-defined counterparts and simplified analogues.

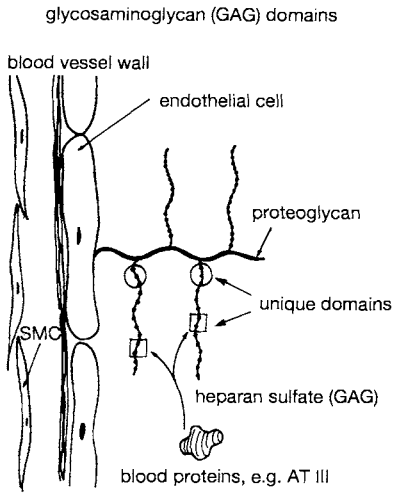

Fig. 3. There is much evidence that heparan sulfate proteoglycans are present on the luminal surface of endothelial cells of blood vessels. Heparan sulfate has been shown to endow the blood vessels with nonthrombogenic properties [15]. Furthermore this heparan sulfate contains unique domains that closely resemble the active pentasaccharide sequence of heparin. So it is assumed that a fraction of plasma ATIII is activated by heparan sulfate glycosaminoglycans located close to the surface of the blood vessels. This means that the characteristic pentasaccharide fragment of heparin is also an endogenous antithrombotic agent. SMC = smooth muscle cell.

3. Synthesis of Antithrombin-Binding Pentasaccharides

3.1. Initial Syntheses of Pentasaccharides with a Natural Sequence

In the early 1980s the synthesis of the biologically active pentasaccharide **5** was carried out according to the strategy depicted in Figure 4a, in which a fully protected pentasaccharide **6** was first prepared and then converted into **5**.[17, 18] In the selection of the protective groups of **6** the following factors were considered: 1) the need for introduction of sul-

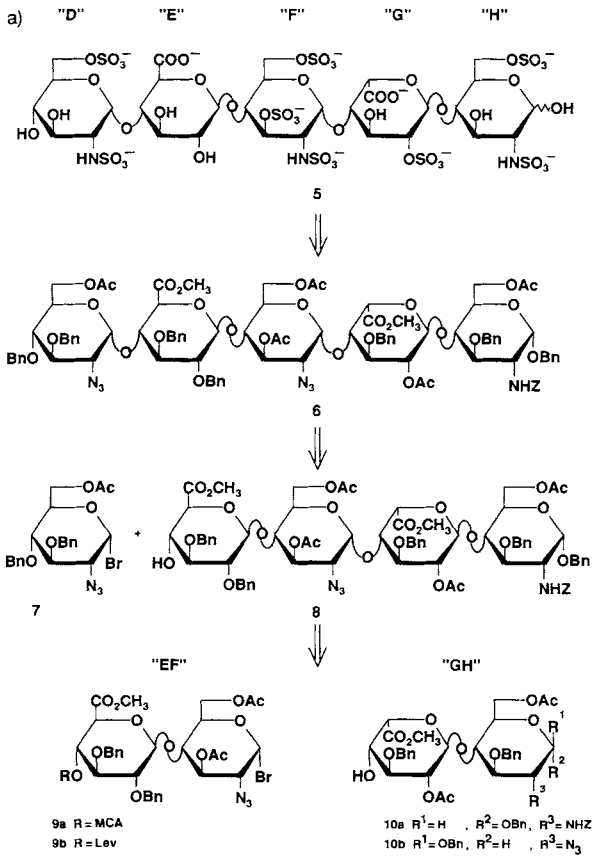

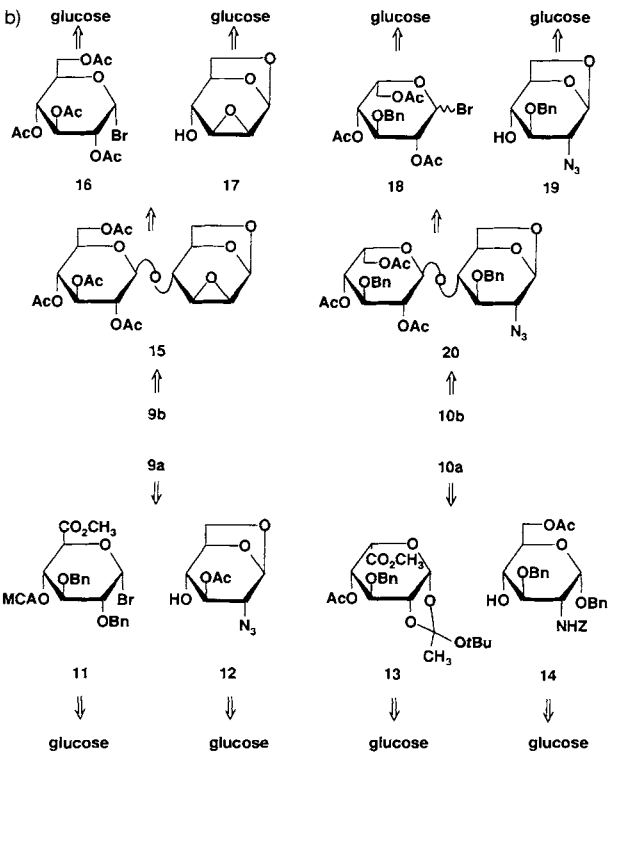

Fig. 4. a) Retrosynthetic pathway for pentasaccharide **5**. Two strategies were developed for the preparation of and the disaccharide building blocks **9** (EF) and **10** (GH), as shown in Figure 5a. b) In one route (lower part) glucose and idose derivatives, both obtained from glucose, are oxidized at the monosaccharide level to provide the corresponding uronic acid derivatives **11** and **13**, which are then coupled to glucosamine derivatives **12** and **14**, respectively. In the other route (upper part) the glucose and idose derivatives **16** and **18**, respectively, are first coupled with glucosamine derivatives or precursors yielding disaccharides **15** and **20**, respectively. Final functionalization and oxidation to give building blocks containing uronic acid is then performed at the disaccharide stage (for details see Fig. 5a and b).

fate and N-sulfate substituents, and the presence of carboxylate and hydroxyl groups in the proper positions on the target molecule **5**, and 2) the state of the art in oligosaccharide synthesis at the time, for instance the use of 2-azido glucose derivatives[16] to introduce 1,2-*cis*-linked glucosamine units (such a glycosylation requires a nonparticipating group at position 2 of the glycosyl donor) and the use of glycosyl donors having a participating group at position 2 to control the introduction of 1,2-*trans* interglycosidic bonds (as required for the two uronic acid units.)

In the first reported synthesis[17] the disaccharide building blocks **9a** and **10a**, the respective precursors of the EF and GH parts of the molecule, were obtained by condensing suitably protected glucuronic acid and iduronic acid monosaccharide derivatives with glucosamine precursors. All the monosaccharide units were obtained from glucose or from glucosamine, as illustrated in Figure 4b.

In another synthesis,[18] following a different approach but applying the same protective group strategy, similar building blocks **9b** and **10b** were prepared by condensation of the glucose and idose derivatives **16** and **18**, respectively, with the Cerny epoxide **17** and the glucosamine precursor **19**, respectively (Fig. 4b). Subsequent Jones oxidation of the function at the 6'-position then yielded disaccharides containing the corresponding uronic acids (Fig. 5b).

The protected pentasaccharide **6** was converted into **5** with the following sequence of reactions (Fig. 4a)[17]: 1) saponification of the ester groups of the molecule, 2) sulfation of the resulting free hydroxyl groups, 3) hydrogenolysis to generate the amino groups of the glucosamine units and to liberate

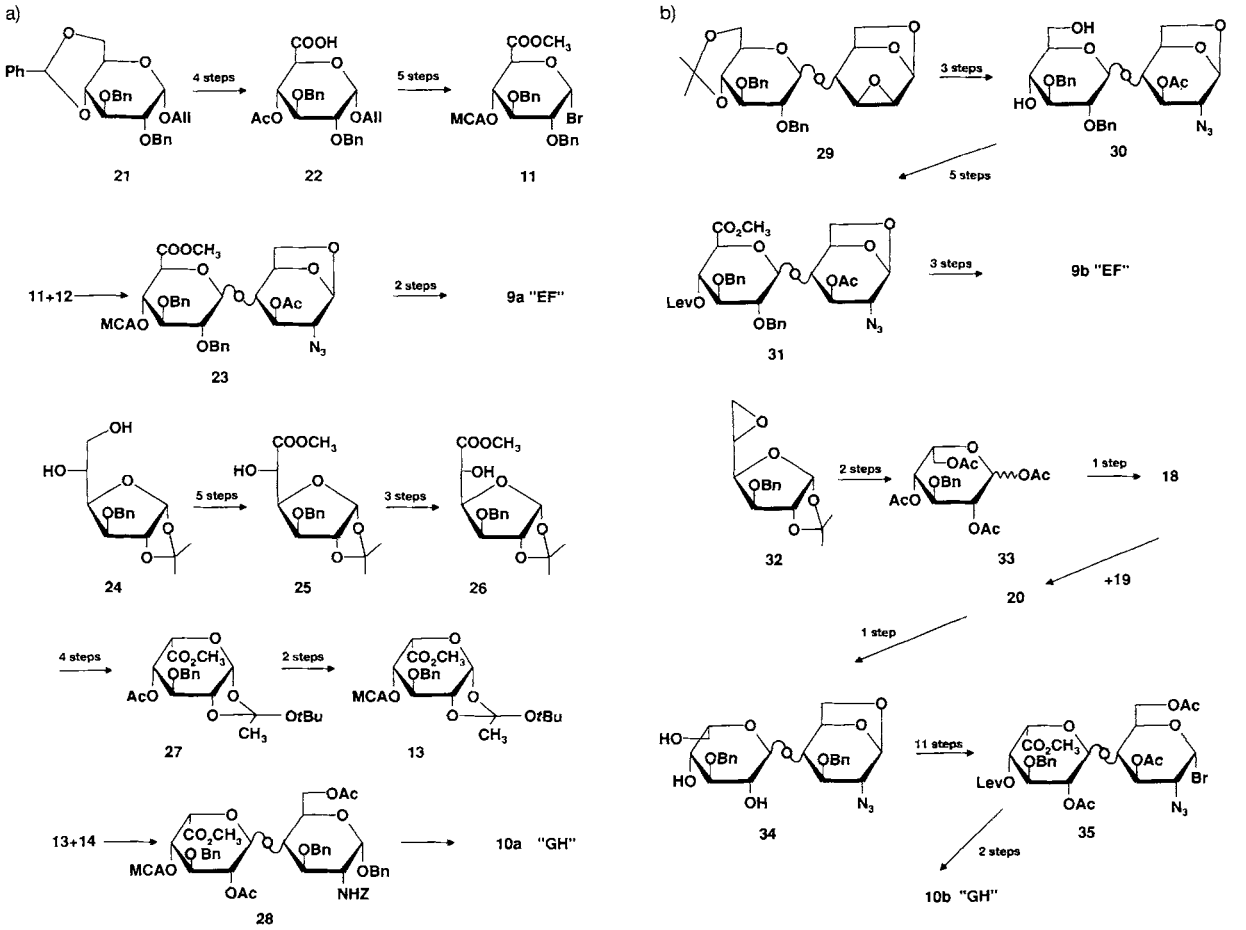

Fig. 5. a) Preparation of the disaccharide building blocks **9a** (EF), and **10a** (GH), by coupling monosaccharide derivatives of uronic acid and glucosamine, respectively [17]. 1-*O*-allyl-4,6-*O*-benzylidene-α-D-glucopyranoside [34] was benzylated to give **21** (71%, crystalline), which was converted to the glucuronic acid derivative **22** (acid hydrolysis, tritylation, acetylation, Jones oxidation; 50% overall yield). The potassium salt of compound **22** was isomerized to the prop-1'-enylglycoside (*t*BuOK, dimethyl sulfoxide (DMSO)), methylated, and monochloroacetylated. Cleavage of the glycoside and bromination using the Vilsmeier reagent then gave **11** (57% from **22**). Condensation with **12** (easily obtained from 1,6-anhydroglucose) gave **23** (70% from **11**), which was transformed into **9a** (acetolysis, bromination; 52%). For the preparation of **10a**, 3-*O*-benzyl-1,2-*O*-isopropylidene-D-glucofuranose (**24**) [33] was converted into **25** (tritylation, acetylation, Jones oxidation, saponification, methylation; 35% overall yield). Compound **25** was epimerized to provide **26** (Tf_2O, CF_3COONa or HCOONa, MeOH or $KHCO_3$; 90% overall yield), which was converted into **27** (acid hydrolysis, acetylation, bromination, formation of the ortho ester; 41% overall yield). Replacement of the acetyl group at position 4 by a monochloroacetyl group provided **13** (K_2CO_3/MeOH then MCACl/pyridine; 79%). Coupling of **13** and **14** (45% from **13**) and removal of the monochloroacetyl group gave the GH building block **10a**. b) Preparation of the disaccharide building blocks **9b** (EF) and **10b** (GH) by oxidation at the disaccharide stage [18]. Acetobromoglucose **16** was condensed with the Cerny epoxide **17** (see Fig. 4b) to give disaccharide **15** (62%, see Fig. 4b), which was converted in three steps (deacetylation, isopropylidenation, benzylation; 70% overall yield) into **29**. Compound **29** was converted into **30** (lithium azide/*N*,*N*-dimethylformamide (DMF), acetylation, acid hydrolysis; 95% overall yield). Compound **31** was obtained from **30** (dimethoxytritylation of the primary hydroxyl group, levulinoylation, acid hydrolysis, Jones oxidation, methylation; 43% overall yield) and converted into **9b** (acetolysis, removal of the acetate group at the anomeric center, bromination; 92% from **31**). For the preparation of **10b**, 3-*O*-benzyl-1,2-*O*-isopropylidene-α-D-glucofuranose (**24**) [33] was converted into **32** (dimesylation, selective substitution at C6 by an acetate, epoxidation; 71% from **30**). Compound **32** was converted into **33** (acid hydrolysis, acetylation; 54%), which was then brominated at C1 to give **18** (see Fig. 4b) and condensed with the glucosamine derivative **19** to give, after deacetylation of **20**, compound **34** (41% from **33**). **34** was converted into bromide **35** (essentially as described for the preparation of **9b** from **30**; 38% yield over 11 steps) which then was transformed into **10b** (two steps, 54%).

hydroxyl groups, and 4) selective N-sulfation of amino groups.

Other syntheses of **5** or similar compounds using either cellobiose[19] or maltose[20] as starting material have been described but again the same protective group strategy was adopted.

3.2. Synthetic Analogues of the Naturally Occurring Pentasaccharide

The conversion of the previously mentioned fully protected pentasaccharides, for example conversion of compound **6** into **5**, requires hydrogenolysis (step 3). However, under these conditions amino groups are generated very rapidly and may react with the reducing end of the pentasaccharide (aldehyde function), which is obtained after cleavage of the benzyl group at the anomeric position. The side reaction yields stable products (particularly after reduction of the intermediate Schiff base) corresponding to a mixture of dimers and trimers of the initial pentasaccharide.[21] In order to circumvent this undesired side reaction, the corresponding methyl glycoside derivative is used. Here, the reducing end is protected and the α linkage present at this position in heparin is mimicked, thus yielding analogue **39**[21] (Fig. 6). Compound **39** displays the same biological properties as **5**. Initially pentasaccharide **39** was prepared in the same way described for **5**; however, more recently the synthesis has been improved by using the trisaccharide imidate **36**[22] as a precursor for the DEF part of the molecule (Fig. 6). This reduced the amount of intermediate **37**, the expensive iduronic acid containing building block, required for the synthesis.

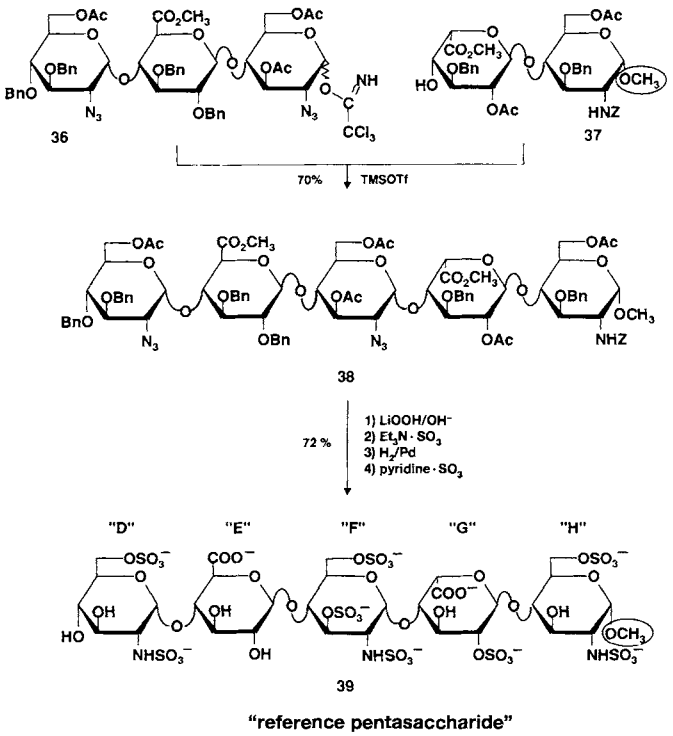

Fig. 6. In the synthesis of **39**, the α-methyl glycoside derivative of **5**, a 3 + 2 coupling approach is employed. In our studies compound **39** is referred to as the "reference pentasaccharide" or "natural product".

The preparation of **39** has been scaled up, and this synthetic heparin fragment is now the reference for studies of the series of antithrombotic oligosaccharides that selectively inhibit blood coagulation factor Xa through activation of AT III. Compound **39** displays a potency of 700 anti-Xa units (U) mg^{-1} in the Sanofi/Organon reference assay.[44]

We mentioned in Section 2.2 that in the pentasaccharide sequence responsible for the binding of heparin to AT III the D unit could be either an N-sulfated or an *N*-acetylated glucosamine residue. In the first syntheses, the N-sulfated variant was chosen because of the simpler chemistry; however; the approach starting from trisaccharide **40** (Fig. 7) allowed differentiation of the D unit at the trisaccharide level. The key reaction was the selective reduction of the azido group at position 2 of the nonreducing terminal monosaccharide unit of **40**, which could be performed by catalytic hydrogenation using either the Lindlar catalyst or hydrogen transfer conditions.[23] Afterwards the methyl glycoside analogue **42** of the natural *N*-acetylated pentasaccharide sequence could be obtained following the procedures used for the preparation of **39**. Surprisingly pentasaccharide **42** was a less potent stimulator of AT III than its N-sulfated counterpart **39** (350 anti-Xa U mg^{-1} versus 700 anti-Xa U mg^{-1}).

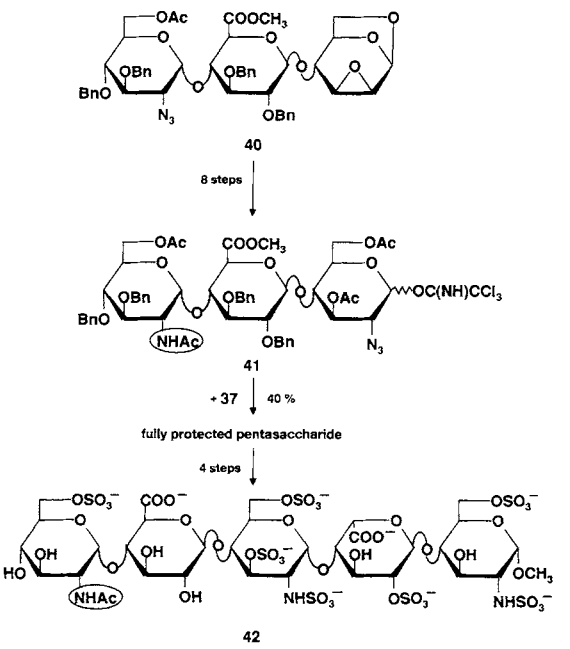

Fig. 7. Synthesis of the *N*-acetylated pentasaccharide representing the AT III binding site of porcine heparin. The azido group of **40** was reduced to give an amine which could be selectively acetylated. Further processing delivered the trisaccharide donor **41**, which was coupled with **37** to give compound **42**, following the standard transformations.

4. Conformational Analysis of the Pentasaccharide

The interaction of heparin oligosaccharides with antithrombin requires, at the level of the oligosaccharide, a

precise three-dimensional positioning of the sulfate and carboxylate groups involved (see Section 7). The orientation of these groups is mainly governed by the conformation of the carbohydrate backbone of the molecule, which in turn depends on the conformation adopted by the individual sugar residues and the conformational relationships between adjacent residues. We will first examine the conformational behavior of individual monosaccharides.

In all the heparin oligosaccharides studied so far,[17] the glucosamine and glucuronic acid residues have invariably been found to adopt the $^4C_1$ conformation[*] (Fig. 8), as supported by analysis of the coupling constants in their ^{1}H NMR spectra. In contrast, the conformation of the iduronic acid residues is highly dependent both on the substitution pattern (e.g. sulfate groups at the 2-position) and on the precise nature of the adjacent residues. Calculations on the conformational behavior of iduronic acid showed that the three conformations $^1C_4$, $^4C_1$, and $^2S_0$ (skew boat con-

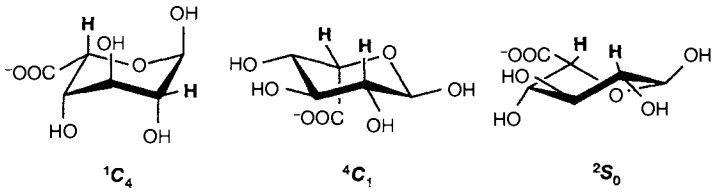

Fig. 8. The three conformers ($^1C_4$, $^4C_1$, $^2S_0$) of L-iduronic acid that may be present in heparin-like pentasaccharides. Protons H2 and H5 are close to each other in the $^2S_0$ conformer as indicated by ^{1}H NMR NOE experiments.

formation) must be considered, not just $^1C_4$ and $^4C_1$ as was previously assumed (Fig. 8). The occurrence of the third conformation, $^2S_0$, similar in energy to the other two, was also confirmed by the observation of a nuclear Overhauser enhancement (NOE) effect between protons H2 and H5, which only in this particular conformation are in close proximity (2.3 Å). Comparison of ^{1}H NMR data, particularly vicinal coupling constants (Fig. 9A), obtained for pentasaccharide **39** and its analogue **45**[25] (in which the N-sulfated, 6-sulfated glucosamine unit F is present) reveals differences in the conformations of the 2-sulfated α-L-iduronic acid residues.[26, 27] For example, replacement of the terminal reducing unit of **39** (i.e. N-sulfated, 6-sulfated glucosamine) by an N-sulfated, 3,6-disulfated glucosamine residue (**57**) favors the $^2S_0$ conformation.[28] Different conformations for iduronate residues, depending on their location in the oligosaccharide chains, were also observed in isolated heparin fragments. Similar observations were made for model trisaccharides (Fig. 9B). In these studies[29] it was also observed that at high salt concentrations (3 M NaCl) iduronic acid relaxes fully into the $^1C_4$ conformation. This phenomenon led us to postulate that the $^1C_4$ conformation predominates when the pentasaccharide is bound to ATIII.[29]

The conformations of the synthetic pentasaccharides **39** and **45** have been studied[30–32, 66] by combining computational techniques (using force fields) and NMR experiments.

[*] For pyranoses in the chair conformation, $^4C_1$ refers to the conformation in which C1 is below and C4 is above the plane formed by C2, C3, C5, O5; in the inverse $^1C_4$ conformation, C1 is above and C4 below this plane. See R. E. Reeves, *Adv. Carbohydr. Chem.*, **1951**, *6*, 107.

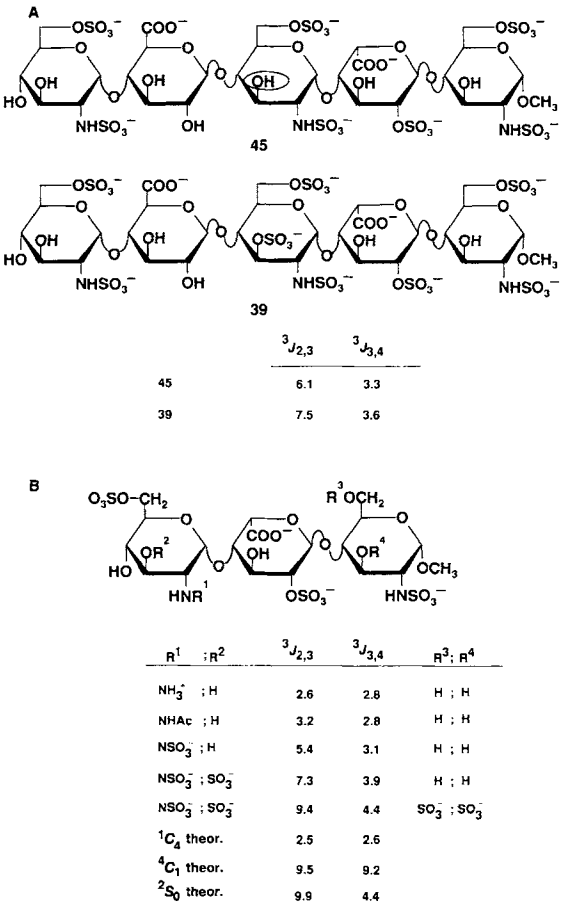

	$^3J_{2,3}$	$^3J_{3,4}$
45	6.1	3.3
39	7.5	3.6

R^1 ; R^2	$^3J_{2,3}$	$^3J_{3,4}$	R^3; R^4
NH_3^+ ; H	2.6	2.8	H ; H
NHAc ; H	3.2	2.8	H ; H
NSO_3^- ; H	5.4	3.1	H ; H
NSO_3^- ; SO_3^-	7.3	3.9	H ; H
NSO_3^- ; SO_3^-	9.4	4.4	SO_3^- ; SO_3^-
$^1C_4$ theor.	2.5	2.6	
$^4C_1$ theor.	9.5	9.2	
$^2S_0$ theor.	9.9	4.4	

Fig. 9. Conformational analysis of a series of synthetic pentasaccharides (A) and trisaccharides (B) by ^{1}H NMR spectroscopy revealed that the conformational behavior of α-L-iduronic acid-2-sulfate is governed by substituents on the neighboring D-glucosamine units. The conformations of the α-L-iduronic acids can be differentiated best by their 2,3 and 3,4 vicinal coupling constants (^3J), as can be seen from the corresponding calculated coupling constants (lower part). An ammonium or *N*-acetyl (R^1) group on the neighboring glucosamine unit (B) stabilizes the $^1C_4$ conformation of α-L-iduronic acid. Sulfate groups (R^2) in the same unit destabilize the $^4C_1$ conformation, thereby allowing a considerable contribution of the $^2S_0$ (skew boat) conformer in the equilibrium. As a consequence of this last conformational change, the distances among various sulfate groups increase and their mutual electrostatic repulsions decrease. When both glycosamine neighbors have sulfate substituents, the $^2S_0$ conformation is almost exclusively present.

As previously mentioned, glucosamine and glucuronic acid residues adopt the $^4C_1$ conformation, whereas iduronic acid moieties exist in an equilibrium between $^1C_4$ and $^2S_0$ conformers. Sulfate substituents bound to tertiary carbon atoms by either an O or a N atom adopt a conformation in which the sulfur atom is in an eclipsed arrangement with respect to the ring proton. When linked to secondary carbon atoms (6-position of glucosamines), the sulfate group prefers the *trans* conformation at the C6–O6 bond; force field calculations reveal *gt* and *gg* conformations, but *gg* is strongly predominant according to ^{1}H NMR data. Free hydroxyl groups may adopt three conformations, whereas the carboxylate groups of uronic acids show great rotational freedom. In the most stable conformations of pentasaccharides **39**, **45**, and **57** (Fig. 17) the iduronic acid residues have either the $^1C_4$ or the $^2S_0$ conformation (Fig. 10).

Inspection of the models depicted in Figure 10 reveals an asymmetric distribution of the charges that are relevant for the interaction with ATIII (see Fig. 16 and Section 7). The

effect of a conformational change at the iduronic acid residue during the binding and activation of ATIII is not yet known.

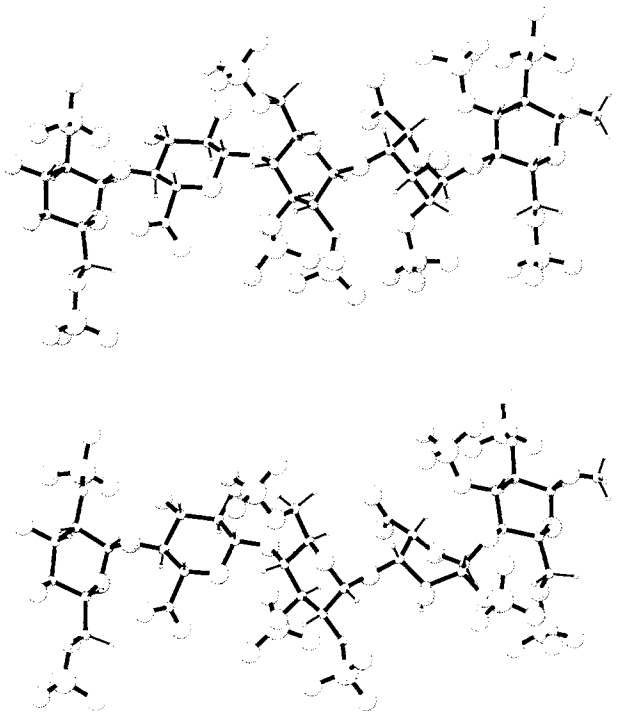

Fig. 10. Three-dimensional representation of compound **57** with an iduronic acid residue in $^1C_4$ (top) and $^2S_0$ (bottom) conformation.

5. Other Synthetic Analogues

5.1. Synthetic Analogues Lacking Charged Groups at Defined Positions

5.1.1. Analogues Lacking Certain Sulfate Groups

After the synthesis of the synthetic counterparts of the naturally occurring pentasaccharide, compounds **5** and **39**, a major question was whether all the charged groups of the pentasaccharide are required for ATIII activation. Although some important information about the role of sulfate groups was available from studies[35b] with (bio)chemically modified heparin fragments, the ultimate answer to this question was obtained by the synthesis of analogues lacking charged groups at defined positions (Fig. 11). For instance, the definitive proof that the characteristic 3-sulfate group at unit F is essential for ATIII activation came after synthesis[36] of the biologically inactive analogue **45** which lacked only this particular sulfate group. Obviously, the synthesis of analogue **45** closely resembles that of our lead compound **39**. The major difference is in the preparation of the EF disaccharide building block **43** which, according to our strategy, should contain a 3-*O*-benzyl group at unit F instead of the 3-*O*-acetyl group (as in EF building block **9b**). Apart from the 3-sulfate group at unit F it was also established[37] that the 6-sulfate group of the nonreducing D unit is absolutely required for biological activity. A similar strategy provided two synthetic pentasaccharides[38] lacking the 6-sulfate

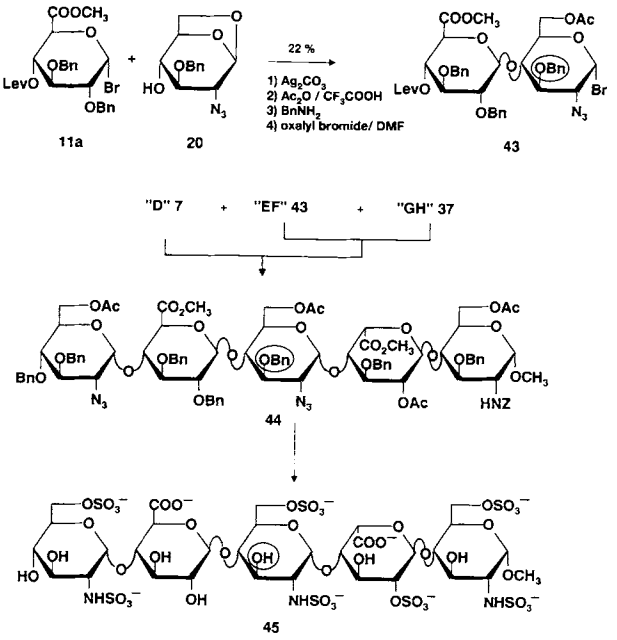

Fig. 11. Preparation of analogue **45**, which lacks the characteristic 3-sulfate group (circled) at glucosamine unit F. Compound **45** is biologically inactive, thus proving the importance of this particular sulfate group in the activation of ATIII.

group at unit H and the 2-sulfate group at unit G, respectively. Both analogues displayed about 25% of the activity of the reference pentasaccharide **39**, pointing to the importance of the sulfate groups at units G and H.

Surprisingly, a pentasaccharide lacking both the 2-sulfate group in unit G and the 6-sulfate group in unit H was almost as active as the two analogues in which only one sulfate group is absent.

The analogue without the 6-sulfate group at unit F has not yet been synthesized, but studies with naturally occurring heparin fragments lacking this group revealed that this substituent does not contribute considerably in the activation of ATIII.

5.1.2. Analogues Lacking Certain N-Sulfate Groups

With regard to the role of the N-sulfate groups at units D, F, and H, Riesenfeld et al.[39] demonstrated that removal of this substituent in either unit F or H gives rise to inactive heparin fragments. In contrast, heparin fragments with an *N*-acetyl instead of an N-sulfate group at unit D are still active. More precise information was obtained from synthetic derivatives. The synthetic analogue **42**, *N*-acetylated in unit D (see Section 3.2), which represents the most widespread ATIII binding domain of porcine heparin, was only half as active in an anti-factor Xa assay as the corresponding N-sulfated derivative **39**. The activity of a synthetic analogue with a 2-hydroxyl group at unit D was virtually the same as that of the pentasaccharide with an *N*-acetyl group (**42**).[43]

The very low activity (ca. 5%) of the synthetic analogue **46**[43] containing a 2-hydroxyl group at unit H is consistent with the studies of Riesenfeld et al.,[39] who found that the N-sulfate group at this position is essential. For the synthesis of the hydroxyl analogue **46** (Fig. 12) the suitably protected

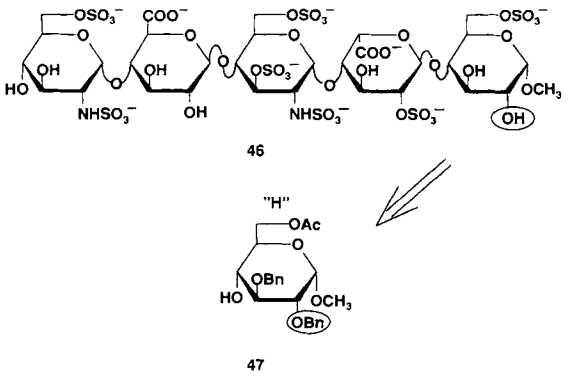

Fig. 12. In analogue **46** the N-sulfate functionality at the reducing end (H) is replaced by a hydroxyl group. According to the general strategy, the 2,3-di-*O*-benzyl-protected glucose unit **47** is required as the building block for the reducing terminal unit.

H building block **47** containing a 2-*O*-benzyl protective group had to be incorporated.[40]

5.1.3. *Analogues Lacking Certain Carboxylate Groups*

Synthetic model compounds were also used to examine the role of the two carboxylate groups in the active heparin fragment. Compound **51**, the first synthetic analogue prepared for this purpose, lacks the carboxylate group of iduronic acid; a 2-sulfate-β-D-xylopyranose unit is present instead of a 2-sulfate-α-L-idopyranuronate unit. Consequently, the GH disaccharide **49** had to be synthesized from

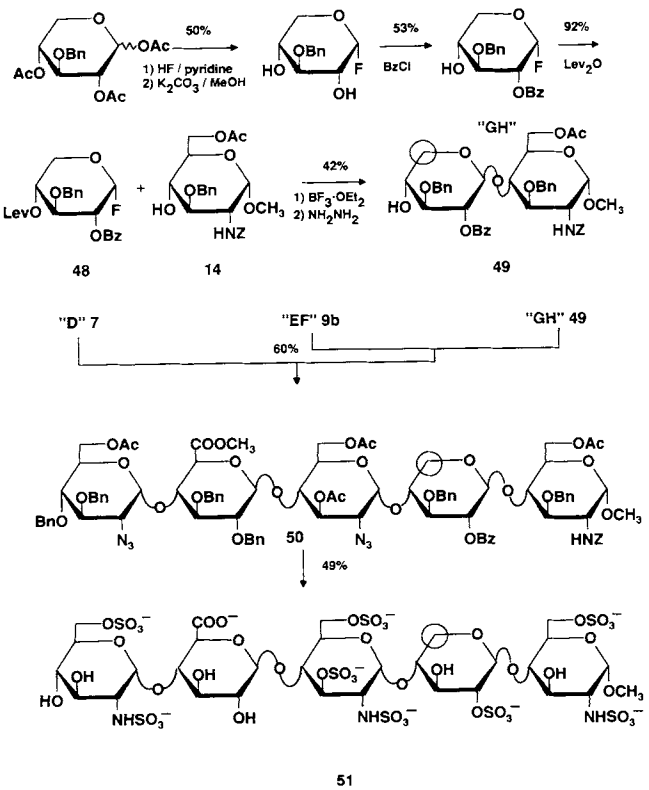

Fig. 13. Synthesis of analogue **51**, which lacks the essential carboxylate group (circled) of α-L-iduronic acid. For the preparation of compound **51** a properly protected D-xylopyranosyl derivative (compound **48**) had to be prepared as the G unit. The carboxylate group of α-L-iduronic acid is not only required for interaction with ATIII, but also governs the conformation of the G unit.

the xylopyranosyl donor **48** and the known acceptor **14** (Fig. 13). The fully protected pentasaccharide **50** was assembled by coupling **49** with the known disaccharide **9b** and monosaccharide **7**. Subsequent deprotection and sulfation delivered the inactive analogue **51**. Most likely this sharp decrease in biological activity should be ascribed to the loss of an essential carboxylate group that interacts with the protein; however, we also found[41] that the xylopyranosyl moiety in the analogue has a different conformation than that of the iduronic acid moiety ($^4C_1$ conformation instead of the $^2S_0/^1C_4$ equilibrium found for iduronic acid).

The carboxylate group of the glucuronic acid moiety (unit E) was also shown[42] to be a key charged group in the activation process, since pentasaccharide **52** (Fig. 14), which has a methyl carboxylate group at unit E, elicits only 5% of the activity of the natural product. Pentasaccharide **52** was not the result of a planned total synthesis but merely a side product that occurred during the preparation of the reference compound **39**.

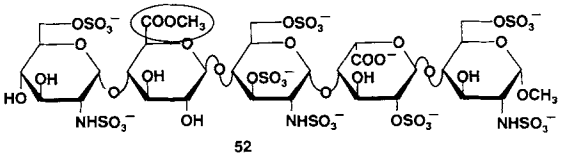

Fig. 14. Compound **52**, which contains a methyl ester at the D-glucuronic acid moiety, is hardly active, thus showing that the carboxylate group at this position plays an important role in the activation of ATIII.

The very low activity of pentasaccharides **51** and **52** indicates that the two carboxylate groups of the uronic acid moieties (units E and G) are essential for ATIII activation. In Section 5.5 it will be demonstrated that replacement of the charged group at C5 of uronic acid by another charged functionality ($CH_2SO_3^-$ instead of COO^-) is also detrimental.

In conclusion, the role of all sulfate and carboxylate groups of the active heparin pentasaccharide in ATIII activation is known from studies with well-defined synthetic analogues. The influence of the individual charged groups on the biological activity is indicated schematically in Figure 15.

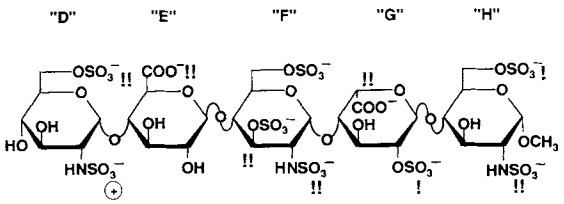

Fig. 15. The role of the individual charged groups in the activation of ATIII. Exclamation marks denote groups that are crucial, since their removal leads to loss of anti-Xa activity by more than 95% (!!) or by about 75% (!). The N-sulfate group marked with + contributes significantly (about 50% loss of anti-Xa activity after removal).

5.2. The Discovery of More Potent Derivatives

By 1987 we had assessed the role of the individual charged groups of the heparin pentasaccharide (see Section 5.1), and a reliable molecular model was available from ^{1}H NMR

spectroscopic studies and molecular modeling (see Section 4). Most remarkably, two distinct ATIII binding sites were implicated[43] based on the molecular model of the pentasaccharide as shown in Figure 16. It can be seen that

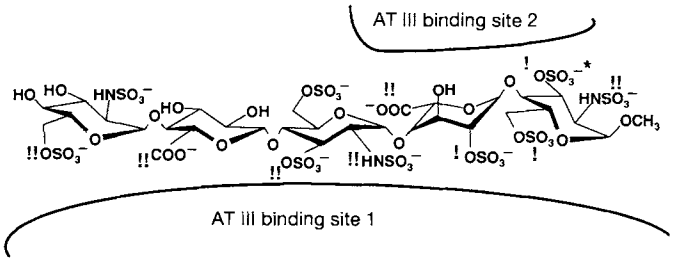

Fig. 16. When the role of the essential charged groups (!! and !) became known, the interaction model depicted, which has two ATIII/pentasaccharide binding sites, was postulated. Based on this model it was decided to introduce an extra sulfate group at the 3-position of the reducing terminal unit (*). Indeed, this "supersulfated" analogue **57** proved to be more active and to interact more strongly with the ATIII protein than the natural compound. Other supersulfated analogues were less active.

the potential interaction points should be located on the top ("north") face and the bottom ("south") face of the pentasaccharide. The essential charged groups of the DEF fragment are directed towards the southern binding region, whereas the important carboxylate and N-sulfate groups of the GH fragment are pointed towards the northern binding region. This ATIII heparin interaction model inspired us to synthesize an analogue (**57** in Fig. 17) containing an extra 3-sulfate group at unit H (see starred group in Fig. 16) which according to the model should enhance the binding capacity in the northern binding site. Indeed the derivative with the additional sulfate group (**57**) displayed a higher ATIII

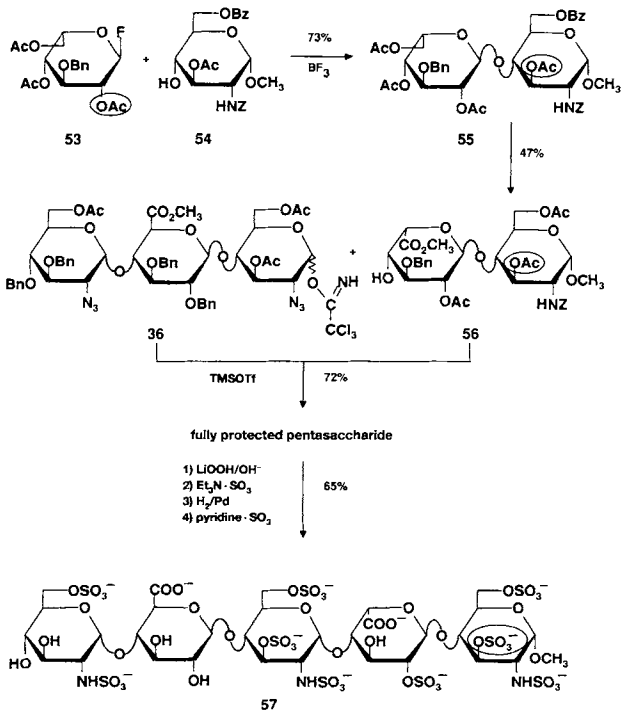

Fig. 17. Synthesis of the more active analogue **57** containing an extra 3-sulfate group at the reducing end. Following the general synthetic strategy, a suitably protected GH moiety (**56**) is required containing a 3-*O*-acyl instead of a 3-*O*-benzyl protective group (circled groups).

mediated anti-factor Xa activity than the reference compound **39** (1250 U mg^{-1} versus 700 U mg^{-1}), and analogue **57** binds to ATIII one order of magnitude stronger (see Section 7.1). Moreover, in pharmacokinetic studies[44] it was found that **57** displays a longer biological half-life, probably due to a stronger interaction with ATIII in circulation.

The synthesis of the "supersulfated" pentasaccharide **57** was based on the general strategy outlined previously. The additional 3-sulfate group at unit H required a glucosamine building block containing a 3-*O*-acetyl group instead of a 3-*O*-benzyl group. To this end, monosaccharide acceptor **54** was synthesized (Fig. 17). Coupling of **54** with the idopyranosyl fluoride donor **53** gave the fully protected disaccharide **55**, which was processed further in analogy to the preparation of **35** from **20** (see Fig. 5 b) to deliver the desired GH building block **56**.

Preparation of the fully protected pentasaccharide could be achieved most conveniently by coupling the GH acceptor **56** with an equimolar amount of the imidate-activated DEF donor **36**. However, the first attempts to convert the fully protected pentasaccharide into the required product **57** were disappointing. In the first deprotection step, saponification with sodium hydroxide, approximately 40% cleavage occurred owing to a 4,5-elimination at iduronic acid. Fortunately, this undesired side reaction could be suppressed by conducting the saponification with lithium hydroperoxide. The subsequent sulfation and deprotection steps could be conducted with good yields.

The potency of the supersulfated analogue **57** led us to turn our attention to some of its analogues. We wondered whether introduction of additional sulfate groups would render the pentasaccharide even more active, as the interaction with the positively charged ATIII may strengthen when the negative charge of the carbohydrate increases. However, the opposite was found. For instance, analogues **58** and **59** (Fig. 18) which contain an extra 3-sulfate group at glucuronic acid[45] and iduronic acid,[46] respectively, are less active than compound **57** by roughly 35% and 60%, respectively.

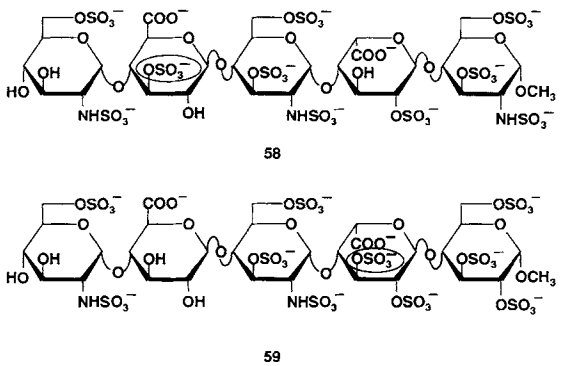

Fig. 18. Other supersulfated analogues such as compounds **58** and **59**, which contain 3-sulfated uronic acid moieties, are considerably less active than their counterpart **57** which lacks these extra sulfate substituents. This phenomenon indicates that the interaction between pentasaccharide and ATIII cannot be explained simply by the electrostatic attraction of two oppositely charged entities.

Analogues with extra sulfate groups at the D unit are approximately 10% less active.[46] At the extreme, the fully sulfated pentasaccharide is not active.[47] Apparently the in-

teraction between the characteristic heparin fragment and the protein is much more complex in nature than just the simple electrostatic attraction of two oppositely charged biomolecules.

5.3. Some Flexible Analogues

As described in Section 5.1, the carboxylate functions of the uronic acid residues E and G are strictly required for AT III activation. The next question was whether the pyran rings of the uronic acid moieties are essential. To answer this question we synthesized[48] the "ring-opened" analogues **63** and **64** (Figs. 19–21). In analogue **63** the α-L-iduronic acid

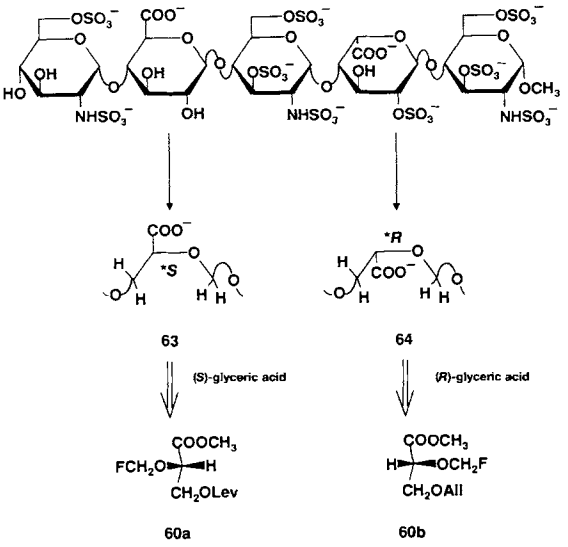

Fig. 19. We wondered if the uronic acid moieties of the pentasaccharide could be replaced by flexible "opened" pyranose moieties containing the essential carboxylate groups in the appropriate configuration. To this end the suitably protected (*S*)- and (*R*)-glyceric acid building blocks **60a** and **60b**, respectively, were synthesized.

unit is replaced by an (*R*)-glyceric acid-2-O-CH_2 moiety, while in analogue **64** the β-D-glucuronic acid unit is replaced by an (*S*)-glyceric acid-2-O-CH_2 moiety (Fig. 19). These analogues still comprise the essential carboxylate substituents in the appropriate configuration, but obviously their conformational flexibility is increased.

The key steps in the synthesis of these analogues were the preparation and incorporation of the glyceric acid-O-CH_2 residues. To this end, two suitably protected and activated building blocks **60a** and **60b** were prepared from (*S*)- and (*R*)-glyceric acid, respectively. In Figure 20 the synthesis of **63** is outlined; analogue **64** was prepared in a similar fashion (Fig. 21). Analogue **63** with the ring-opened α-L-iduronic acid unit displays about 25% of the activity of the reference compound, thus proving that the ring structure of α-L-iduronic acid is not strictly required. This phenomenon is not that surprising when one takes into account that this part of the molecule displays considerable conformational freedom[49] (see Section 4).

In contrast, analogue **64** (Fig. 21) with the ring-opened β-D-glucuronic acid moiety is virtually inactive, although all essential charged groups are present in the molecule. Probably, the rigid D-glucuronic acid moiety (unit E) is necessary in arranging the essential charged groups appropriately in space. Highly simplified analogues with two ring-opened iduronic acid moieties at positions E and G are biologically inactive.[50]

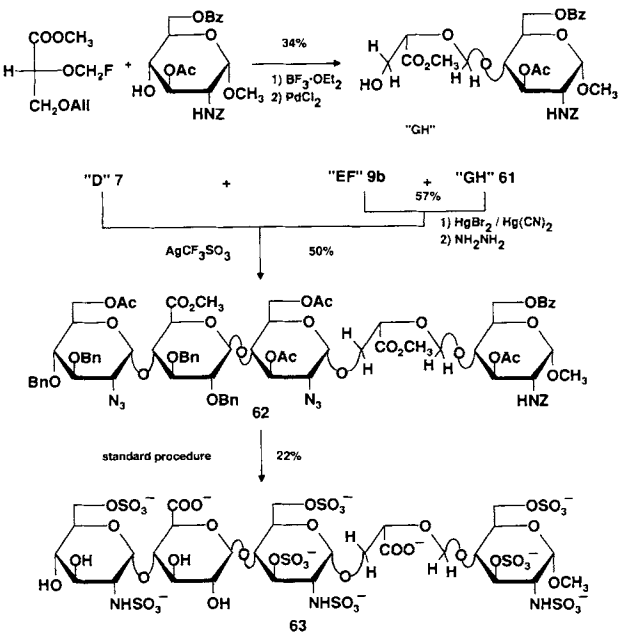

Fig. 20. Synthesis of analogue **63** containing "ring-opened" α-L-iduronic acid moiety. Analogue **63** elicits about 25% of the biological activity of the reference compound **39**. Apparently the flexible α-L-iduronic acid moiety (G) may be substituted by a linear chain exposing the carboxylate group in the appropriate configuration.

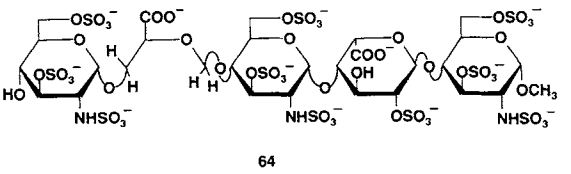

Fig. 21. Analogue **64** containing a ring-opened D-glucuronic acid moiety is not active although all essential charged groups are present. It may be concluded that the rigid D-glucuronic acid moiety (in $^4C_1$ conformation) is necessary for the activation of AT III.

5.4. Some Epimeric Analogues

In order to understand the specificity of the heparin/AT III interaction in even greater detail we examined some synthetic analogues containing all essential charged groups but in which only one of the twenty-five chiral centers has been inverted, in other words, epimeric analogues.

Compound **65** (Fig. 22) contains a β-coupled glucosamine (unit D) and is hardly active,[47] whereas compound **66** contains a β-D-glucuronic acid moiety instead of an α-L-iduronic acid residue (unit G) and is not active at all.[47] In the latter analogue, epimerization at C5 of α-L-iduronic acid to give β-D-glucuronic acid is accompanied by a drastic change in the conformational behavior of unit G, since the flexible iduronic acid ($^1C_4$ and $^2S_0$ conformations occur) is converted into a rigid glucuronic acid, which adopts solely the $^4C_1$ conformation.

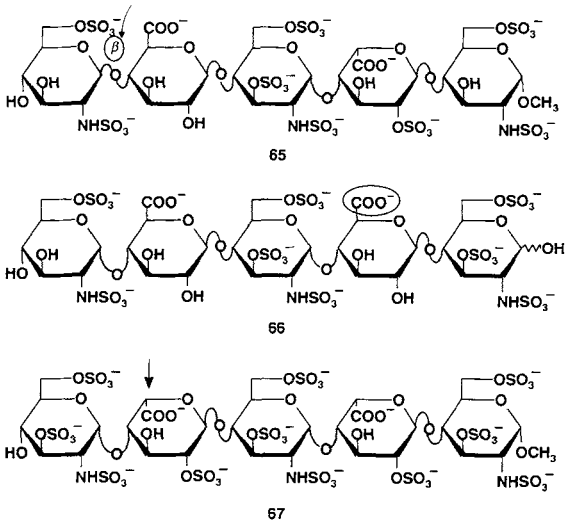

Fig. 22. The epimeric analogues **65** and **66** are hardly active, whereas analogue **67** displays about 10% of the activity of its epimer. Apparently the biological activity decreases drastically when the orientation of essential charged groups in space is changed.

Analogue **67**[51] in which D-glucuronic acid is epimerized at C5, contains two L-iduronic acid moieties, and still displays about 10% of the anti-factor Xa activity of the potent derivative **57**. From a synthetic point of view compound **67** is an attractive target molecule because it is constructed from an alternating sequence of saccharides. Units D, F, and H are alike, as well as units E and G, meaning that in principle only two building blocks are required. Interestingly, similar alternating sequences of the type [IdoA(2-SO_4)α1 → 4GlcNSO_3(3-SO_4)α1 → 4] have been identified in heparan sulfate of the glomerular basement membrane.[52]

Two epimeric analogues were also synthesized in a related series (see Section 6). One of them containing a nonreducing terminal D-mannopyranosyl unit (unit D) is only half as active as the corresponding pentasaccharide with the D-glucopyranosyl unit.[42] The other analogue with the D-galactopyranosyl unit[42] at the reducing end (unit D) had the same activity as the parent compound.

Another research group[19] showed that the biological activity of an analogue with a β-*O*-methyl group at the anomeric center (unit H) is identical to that of the reference compound. Since only a few of the possible epimeric analogues have been investigated so far, conclusions should not be drawn. Nevertheless, the results strongly suggest that the biological activity decreases when the location of essential charged substituents is changed.

5.5. Analogues with Other Charged Groups

Another aspect of the structure–activity studies of the characteristic heparin fragment is the significance of the type of charged groups in the molecule; in other words does the molecule need sulfate and carboxylate groups in the AT III activation process? We replaced,[53] for instance, the essential 6-sulfate group at unit D by a more highly charged phosphate group (compound **69** in Fig. 23). For the synthesis of this analogue a levulinoyl ester was employed for the temporary protection of the 6-position of unit D. After controlled hydrazinolysis of **68a**, the corresponding derivative **68b** with the free hydroxyl group was phosphorylated using standard phosphoramidite chemistry. Suitable phosphate protecting groups were required that are compatible with the subsequent deprotection and sulfation steps. In our hands a 2-cyanoethyl protective group in combination with a benzyl protective group gave the best results: the 2-cyanoethyl group is cleaved in the first deprotection step (saponification), and the benzyl group is removed during hydrogenolysis. To our surprise the monophosphorylated derivative **69** displays no significant activity. It is hard to explain that AT III does not recognize the phosphate group. It may be argued that the interaction of the phosphorylated derivative with AT III is weak because of the large free energy of dehydration of the phosphate group.

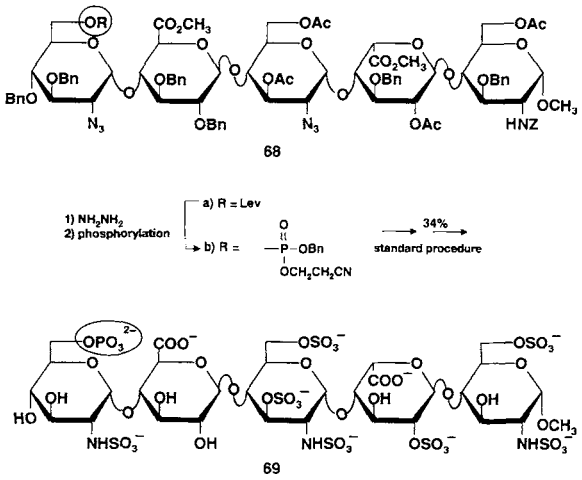

Fig. 23. Strategy for the synthesis of the 6-*O*-phosphorylated analogue **69**. To our surprise compound **69** is biologically inactive. This finding suggests that even the type of negatively charged groups of heparin (sulfate and carboxylate) is important in the specific recognition process between heparin and AT III.

Other groups[54] have found evidence that proteins may discriminate between phosphate and sulfate groups by different networks of hydrogen bonds (Fig. 24).

Since the two carboxylate groups of the pentasaccharide are involved in AT III activation, we sought to place other

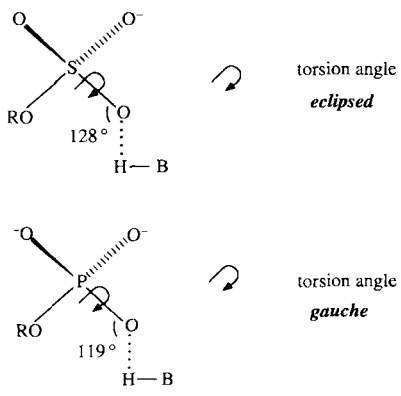

Fig. 24. X-ray crystal structures and ab initio calculations demonstrate that the formation of a hydrogen bond to a sulfate or a phosphate group results in markedly different orientations. The data shown were collected from crystal structure analysis [20a].

charged functionalities at these positions. For this purpose analogues **70** and **71**[55] (Fig. 25) were synthesized in which the COO^- groups are replaced by $CH_2OSO_3^-$ groups. Both analogues **70** and **71** are almost inactive, although they display similar conformational behavior to that of natural product. Thus, it should be concluded that also the type of charged group (i.e. carboxylate) at the 5-position of the uronic acid residue is crucial.

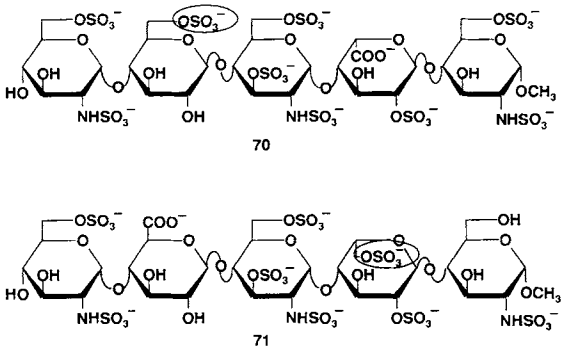

70

71

Fig. 25. Analogues **70** and **71**, containing methylsulfate instead of carboxylate groups, show only very low anti-Xa activity. This observation indicates that the carboxylate groups of the uronic acid moieties E and G have highly specific binding interactions with the positively charged complementary binding site of ATIII.

It is likely that the sulfate and carboxylate groups of heparin are deliberately selected in nature because of their distinct properties in molecular recognition. Presumably the protein–carbohydrate interaction involves highly ordered networks of hydrogen bonds (salt bridges),[54] in particular between defined, positively charged amino acid residues of ATIII and the essential charged groups of the characteristic heparin domain (see also Section 7).

6. The Development of Biologically Active "Non-Glycosamino"glycan Analogues

6.1. Replacement of N-sulfate by Sulfate

Compound **75** (Fig. 26) is an analogue of the highly potent pentasaccharide **57** (see Section 5.2) and contains a glucose moiety (unit H) instead of a glucosamine unit.[56] Since this modification did not decrease the biological activity, we developed derivatives in which all N-sulfate groups are replaced by sulfate groups, which also allowed a much simpler synthesis. We achieved this goal with a completely new series of methylated heparin fragments (see Section 6.3), which we call "non-glycosamino"glycan fragments. For the preparation of analogue **75** the new GH acceptor **74** was synthesized by coupling idopyranosyl derivative **72** with acceptor **73** followed by further reactions.

6.2. *O*-Methylated Pentasaccharides

In order to broaden our scope of our studies on structure–activity relationships we synthesized several partially O-methylated derivatives and a fully *O*-methylated derivative

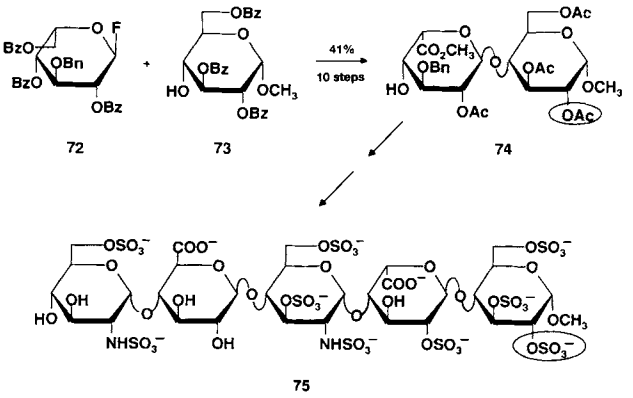

72 **73** **74**

75

Fig. 26. Strategy for the preparation of a supersulfated analogue containing a 2-sulfate group instead of N-sulfate group at the reducing end. This modification did not affect the anti-Xa activity (with respect to **57**), and therefore analogue **75** has been an important lead structure in the development of non-glycosaminoglycan analogues.

of the potent pentasaccharides **75** and **57** (Fig. 27).[57] Quite remarkably, these analogues were found to be almost as active as the corresponding nonmethylated pentasaccharides, indicating that the hydroxyl groups are not involved in the carbohydrate–protein interaction. However, in all protein–carbohydrate interactions studied so far at least a few "key polar" hydroxyl groups of the carbohydrate have been shown to interact strongly with the protein. Therefore it should be assumed that the most important feature of heparin is the exposure of key polar carboxylate and sulfate groups to AT III. This hypothesis is further supported by the biologically active analogues described in the next section.

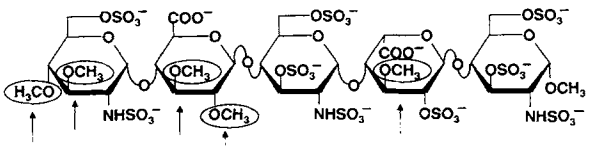

Fig. 27. Several synthetic *O*-methylated analogues have shown that no essential hydroxyl groups are present in the unique pentasaccharide domain of heparin. Subsequently non-glycosaminoglycan pentasaccharides were prepared containing solely sulfate and *O*-alkyl groups; some of these analogues have been found to be even more active than their natural counterparts.

6.3. *O*-Alkylated, Sulfated Pentasaccharides (Non-Glycosaminoglycan Analogues)

As neither methylation of free hydroxyl groups, nor replacement of the N-sulfate group of unit H by a sulfate group affected the biological activity, we prepared the non-glycosaminoglycan analogue **83** (Fig. 29), which contains solely sulfate esters and *O*-methyl ethers.[58] The synthesis of such analogues is much easier than that of heparin-like fragments (Sections 1–5), which is a distinct advantage in economically feasible drug development. The synthetic advantages of the non-glycosaminoglycans: 1) the synthetic strategy is more flexible because both acyl esters and benzyl ethers can be used to protect the hydroxyl groups to be sulfated; 2) no α-coupled glucosamines must be introduced, which would require elaborate synthetic routes towards azide-containing building blocks; 3) selective N-sulfation is

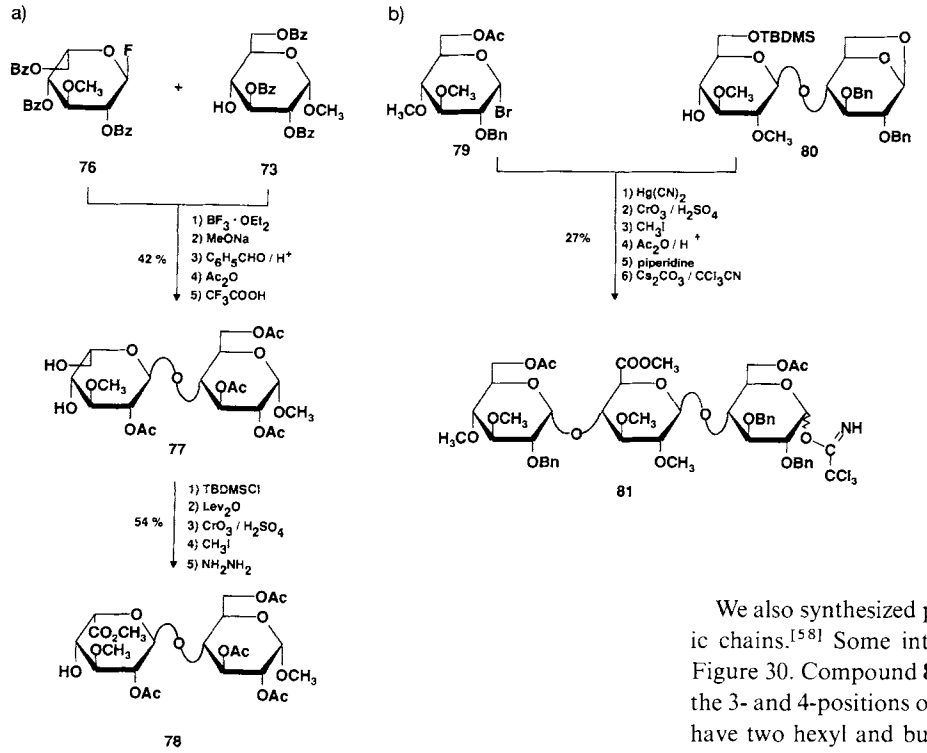

Fig. 28. a) Synthesis of the suitably protected GH disaccharide moiety **78** for the preparation of fully sulfated, *O*-methylated non-glycosaminoglycan analogues. b) Synthesis of the suitably protected DEF trisaccharide moiety **81** for the preparation of fully sulfated, *O*-methylated non-glycosaminoglycan analogues.

not necessary; 4) the scope of possible chemical modifications is broadened (carboxylates can be protected as benzyl esters, iduronic acid units can be epimerized, vide infra).

The first non-glycosaminoglycan analogue we synthesized[58] was compound **83**, which has a similar sulfation pattern as the potent derivative **57**. The syntheses of the methylated GH acceptor **78** and the methylated DEF donor **81** required for the preparation of **83** are shown in Figures 28a and 28b, respectively. The condensation of donor **81** with an equimolar amount of the acceptor **78** catalyzed by trimethylsilyl triflate afforded the required fully protected pentasaccharide in 70% yield (Fig. 29). Conversion of **82** into the final product **83** was achieved in 60% yield by a three-step procedure involving successive saponification, hydrogenolysis, and sulfation.

In order to circumvent side reactions (α,β-elimination, epimerization) at the uronic acid moieties during saponification of the protected pentasaccharide, we protected the carboxylate groups as benzyl esters;[42, 51] for example, pentasaccharide **84** was prepared instead of **82** (Fig. 29). The first deprotection step was hydrogenolysis to release (apart from the hydroxyl groups) the carboxylate groups, the presence of which suppresses α,β-elimination and epimerization in the subsequent saponification. Accordingly, the yields were higher (up to 96%), and the chemical purity of the end products was excellent. Consequently no ion-exchange chromatography was required to obtain pure final products. It should be stressed that this alternative protective group strategy is not possible in the synthesis of heparin fragments closely related to the natural product.

The sulfated, *O*-methylated analogue **83** displays even a somewhat higher ATIII mediated anti-factor Xa activity (1323 αXa U mg^{-1}) and a somewhat stronger binding with ATIII than the potent heparin analogue **57** (see Fig. 35).

We also synthesized pentasaccharides with longer aliphatic chains.[58] Some interesting examples are illustrated in Figure 30. Compound **85** has two linear tetradecyl groups at the 3- and 4-positions of unit D, while compounds **86** and **87** have two hexyl and butyl groups, respectively, at the same positions. To our surprise the introduction of tetradecyl groups is accompanied by a nearly complete loss of anti-factor Xa activity, whereas the corresponding butylated derivative **87** is even more active (1529 αXa U mg^{-1}) than the previously mentioned methylated pentasaccharide **83** (1323 αXa U mg^{-1}). Analogue **86** with two hexyl chains displays an intermediate activity (910 αXa U mg^{-1}).

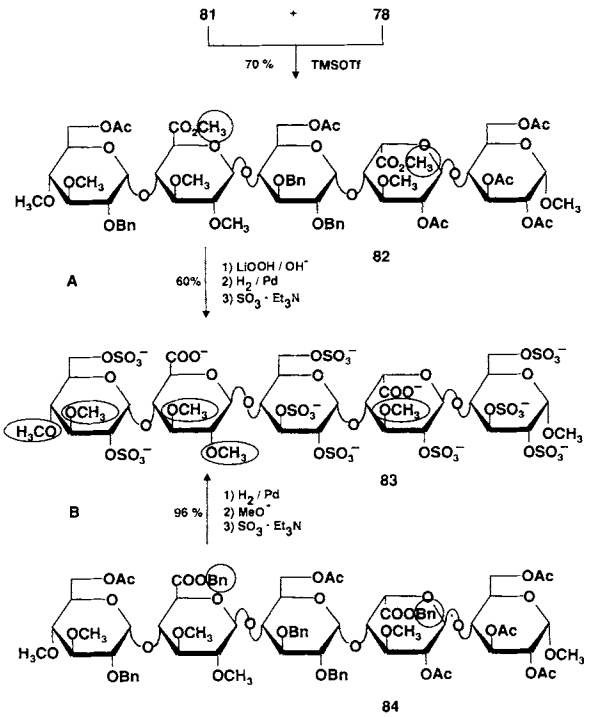

Fig. 29. Two strategies (A and B) for the preparation of non-glycosaminoglycan analogues **83**. For the synthesis of such analogues benzyl protection of the carboxylate groups is also possible (B). Deprotection of the benzyl esters by hydrogenolysis is more convenient than saponification of the corresponding methyl esters (A), because the latter deprotection conditions may cause elimination and epimerization.

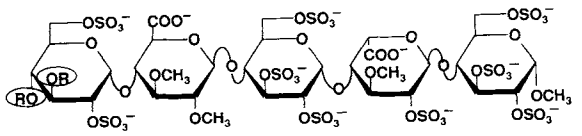

83 : R = CH_3 (1323 αXa U mg^{-1})
85 : R = $(CH_2)_{13}CH_3$ (<1 αXa U mg^{-1})
86 : R = $(CH_2)_5CH_3$ (910 αXa U mg^{-1})
87 : R = $(CH_2)_3CH_3$ (1529 αXa U mg^{-1})

Fig. 30. Some *O*-alkylated, sulfated analogues with longer alkyl chains at the D unit. When two hexyl or longer chain alkyl groups are present at the D unit, a drop in biological activity is observed. Presumably longer aliphatic chains hamper optimal interaction with AT III.

Thus, lipophilic groups of intermediate size (in the range methyl to butyl) at unit D increase the affinity of the pentasaccharide to AT III (see Fig. 35), probably owing to favorable hydrophobic interactions, but longer alkyl chains hamper an optimal binding. However, a stronger binding of an alkylated pentasaccharide with AT III does not necessarily imply increased specific activity (higher αXa activity); some hydrophobic interactions only strengthen the binding, while others also contribute to the AT III activation process (see example in Section 6.4). Furthermore, we observed that analogues with larger lipophilic groups readily adhere to other serum proteins as well, causing substantial loss of selectivity.[59]

6.4. Pentasaccharides with a "Pseudo-Alternating" Sequence; A Short Route to Simplified Analogues

The series of the sulfated, *O*-alkylated pentasaccharides provides promising candidates for drug development, because they are not only easier to synthesize, many of them display high AT III mediated αXa activity.

We wondered whether analogues could be designed for which even shorter synthetic routes could be devised. A particular appealing prospect was found[60] for derivatives with a semialternating sequence such as compound **88** in Figure 31. The EF and GH disaccharide fragments of this analogue have the same substitution pattern and differ only in configuration at C5 of the uronic acid moieties.

Taking into account the similarity between EF and GH, a route was developed in which an EF disaccharide is obtained by epimerization of a suitably protected GH disaccharide (Fig. 31). For instance epimerization of GH derivative **89** with sodium methoxide gave the corresponding EF moiety **90** in good yield. However, the EF disaccharide **90** thus obtained still contains a persistent methyl blocking group at its anomeric center. Conversion of **90** into an appropriate EF glycosyl donor requires (after protection of the 4'-hydroxyl group) acetolysis of the locked anomeric center to afford **91** in high yield. It should be stressed that both the 3-*O*- and 6-*O*-benzyl ethers were quantitatively cleaved during this last acetolysis step. One should note that this reaction sequence is only applicable in the non-glycosaminoglycan series and not in the series of heparin fragments. For the methanolate-catalyzed epimerization of GH, ether protective groups are required exclusively, whereas acetyl protective groups are required in the synthesis of heparin-like fragments. One should realize that after acetolysis of **90** to give **91** both acetyl and benzyl protective groups block the hydroxyl groups to be sulfated and that such a combination of different protective groups would not be applicable in the series of heparin-like compounds (Sections 1–5).

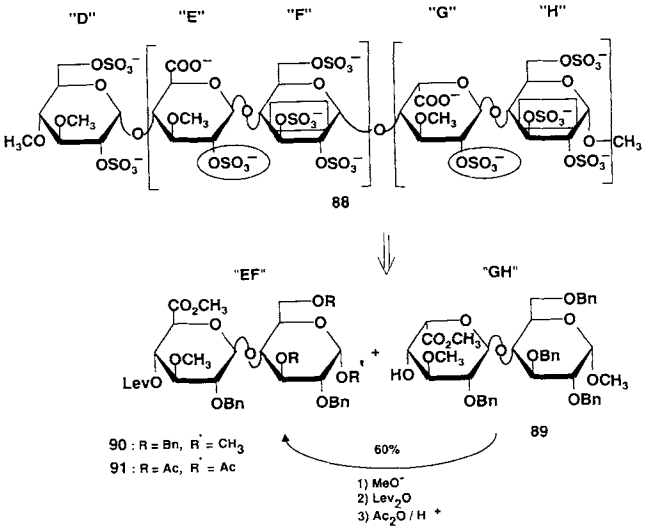

Fig. 31. By introduction of an extra 3-sulfate group at unit H and an extra 2-sulfate group at unit E, derivatives have been designed with a pseudo-alternating sequence. Thus units EF and GH of **88** are almost identical except for the configuration at C5 of the uronic acid moieties. Consequently, the suitably protected EF disaccharide building block **90** can be obtained by epimerization of the corresponding GH block **89**. This strategy can only be followed in the highly modified series of fully *O*-alkylated, sulfated analogues.

Analogue **88** displays an anti-factor Xa activity of 1150 U mg^{-1} implying that the presence of a 2-sulfate instead of 2-*O*-methyl group at glucuronic acid (unit E) reduces the activity slightly.

Another possibility for constructing a pentasaccharide with a pseudo-alternating sequence out of the lead compound **83** is the replacement of the 2-sulfate group of iduronic acid by a 2-*O*-methyl group, as seen in compound **92** (Fig. 32). Following a similar synthetic route as that described for pentasaccharide **88**, we prepared[61] several analogues methylated at the 2-O- and 3-O-positions of both uronic acid moieties (units E and G). We expected that the biological activity of these analogues would be less than half

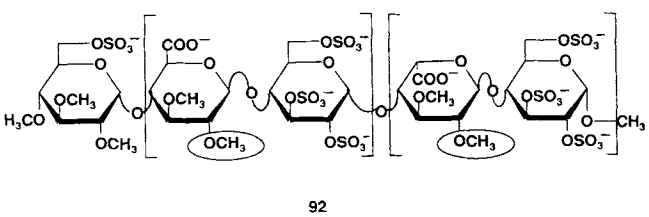

Fig. 32. In analogy to pentasaccharide **88**, a derivative with a pseudo-alternating sequence (**92**) can be designed by replacement of the 2-sulfate group of α-L-iduronic acid by a 2-*O*-methyl group. To our surprise compound **92** is the most active pentasaccharide found so far. Since removal of the 2-sulfate group of unit G in the natural compound would reduce the anti-Xa activity about fivefold, it may be concluded that methylation facilitates other favorable interactions, for example hydrophobic interactions.

of that observed for compounds in the series of heparin-like fragments lacking the 2-sulfate group of iduronic acid. However, quite unexpectedly, the methylated analogues turn out to be highly potent. Analogue **92**, which contains a 2,3,4-tri-*O*-methylated D unit, is the most active pentasaccharide identified so far with an anti-factor Xa of 1611 U mg^{-1}, notwithstanding the fact that two sulfate groups present in the natural product (at the 2-O-positions of units D and G) are lacking. The methyl groups at these positions may possibly interact even better with AT III than the corresponding sulfates, implying that the loss of electrostatic interactions may be compensated by favorable hydrophobic or van der Waals interactions. Alternative explanations for this phenomenon may be found in a reduced free energy of dehydration of permethylated analogues with respect to nonalkylated derivatives, or by assuming a decreased dielectric constant in the pentasaccharide binding region of AT III.

7. The Role of the Pentasaccharide in Antithrombin Activation

7.1. Kinetic Data and Binding Constants

As mentioned in Section 1 the characteristic heparin pentasaccharide and larger heparin fragments containing this sequence accelerate reactions of AT III with some serine proteases such as blood coagulation factor Xa. For the inactivation of other serine proteases, for instance thrombin, is not only the presence of the unique pentasaccharide a prerequisite but in addition the heparin chain should be at least 18 saccharides in length.[62] This phenomenon has been explained by a reaction that is composed of two distinct mechanisms: a conformational change of AT III (brought about by the pentasaccharide; see Figs. 2b and 34) and the bridging of AT III and thrombin by the same heparin chain (Fig. 33; a longer heparin chain is required as a bridge).[62, 63]

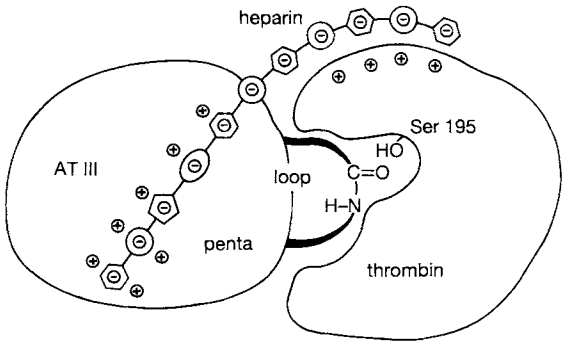

Fig. 33. For accelerating the AT III mediated inactivation of thrombin not only the unique pentasaccharide domain is required to interact with AT III but the heparin chain should also be long enough (about eighteen sugar units) to form a bridge between AT III and thrombin.

The mechanism of action of heparin was revealed by several kinetic studies.[62–64] In Figure 34 the role of the pentasaccharide in the AT III mediated inactivation of factor Xa is shown in greater detail. The pentasaccharide acts in a two-step process: first it binds to AT III (formation of the weak complex B) and achieves equilibrium quickly; then the protein undergoes a conformational change to give the activated form of AT III (C).[64] During this conformational change the interaction of the pentasaccharide with AT III strengthens. The activated form of AT III binds with factor Xa to give a stable AT III/Xa complex (D), while the pentasaccharide—the catalyst in this reaction—is released.

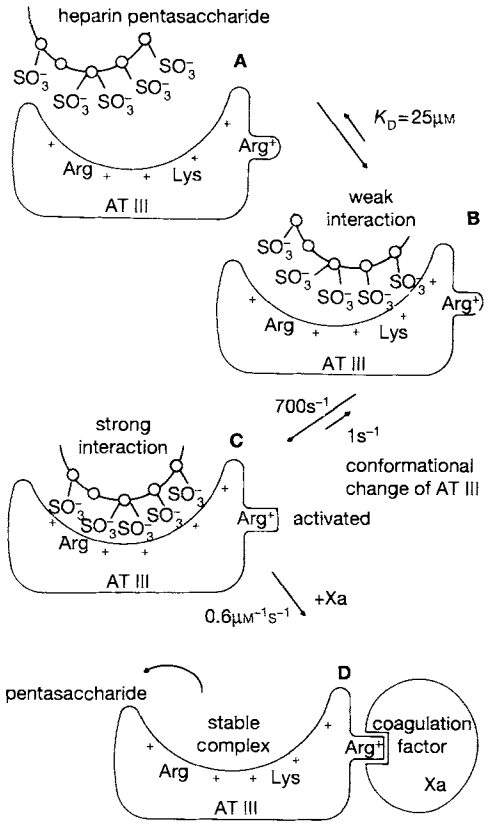

Fig. 34. Mechanism of action of the pentasaccharide as derived from kinetic studies. Initially the pentasaccharide binds to AT III (conversion of A to B), reaching equilibrium rapidly. The weak complex B changes conformation to deliver the activated pentasaccharide/AT III complex C. The active complex C then reacts with factor Xa to give a stable AT III/Xa complex D. During the formation of D another conformational change takes place, which amongst others causes the release of the pentasaccharide. When we discuss binding (dissociation) constants of the various AT III/pentasaccharide complexes, the formation of complex C is meant. In measurements of the anti-factor Xa activity, complex C and a chromogenic substrate (S2222) complete for binding with Xa.

The dissociation constant K_D for the AT III/pentasaccharide complex (C) has been determined by several groups with values between 36 and 300 nM. Obviously the value depends on the conditions, for example the pH value, and the type of AT III used. Similar studies performed with various pentasaccharide analogues have proved to be of great value in understanding the AT III activation process. For instance Atha et al. reported[35b] that tetrasaccharides comprising the DEFG and EFGH part of the pentasaccharide show 100-fold and 1000-fold lower affinity, respectively, for AT III than the pentasaccharide. These results are in line with the observation that the 6-sulfate at unit D is absolutely essential. Pentasaccharide **45**, which is not sulfated in the 3-position, binds AT III very weakly ($K_D = 5 \times 10^5$ nM), and shows essentially no capacity for effecting a conformational change in AT III.

Visser et al. studied[65] the influence of the sulfate groups at unit H (Fig. 35a). Introduction of an extra 3-sulfate group giving the potent analogue **57** leads to roughly 15-fold increase of the binding affinity for AT III, whereas removal of the 6-sulfate group from unit H (compound **93**) gives a four- to fivefold decrease. It was also shown that the decreased anti-factor Xa activity derivative **58**, which has an extra sulfate group at unit E, corresponds to a higher dissociation constant of the pentasaccharide/AT III complex.

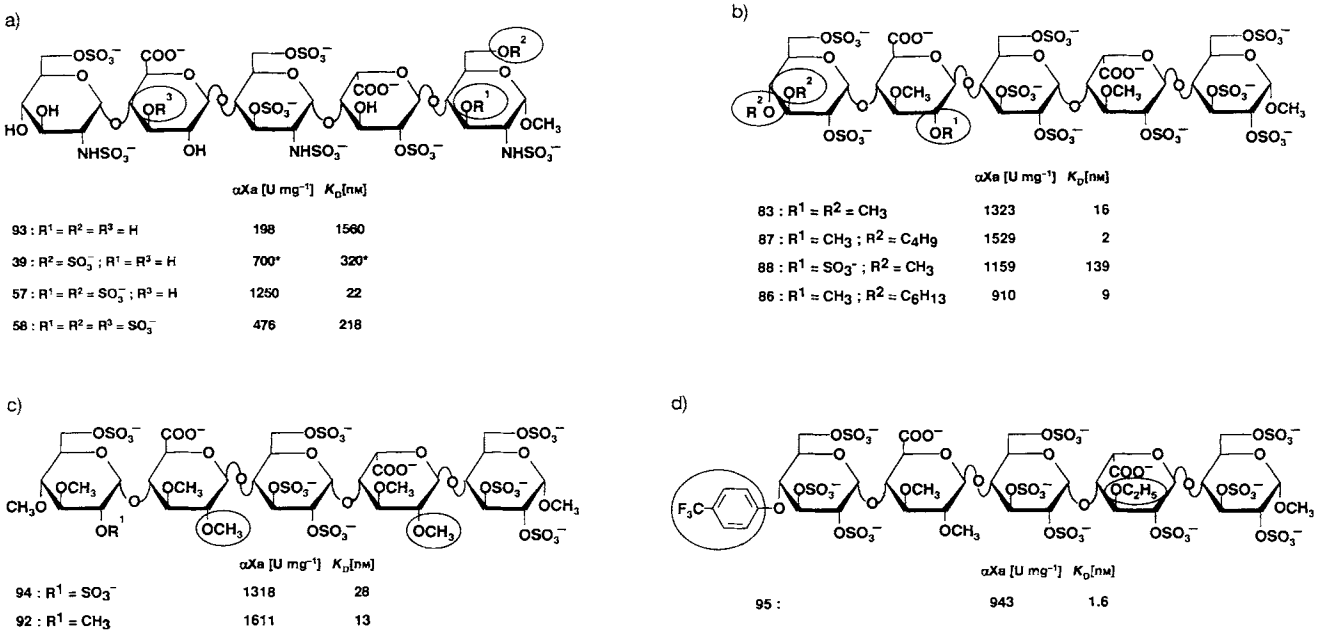

Fig. 35. Synthetic pentasaccharides and their anti-factor Xa activities and dissociation constants K_D with AT III. For a discussion see the text.

In Figures 35b and 35c the highly potent alkylated analogues **83**, **87**, **92**, and **94** are shown, which have not only improved anti-factor Xa activity but also increased affinity with AT III. Several non-glycosaminoglycan derivatives containing lipophilic, aliphatic, and aromatic residues (Fig. 35d) have also been synthesized. Most of these derivatives display strong binding with AT III (K_D up to 1.6 nM for compound **95**) but relatively low anti-factor Xa activity (< 1000 αXa U mg^{-1} for compound **95**). Moreover, the alkylated analogues also bind to other plasma proteins. These results may indicate that the derivatives are amphiphilic and therefore readily stick nonspecifically to positively charged domains of any protein.[59]

7.2. A Model of the Antithrombin–Pentasaccharide Complex

More detailed information about the interaction of the pentasaccharide with AT III was obtained after construction of a three-dimensional molecular model of the complex.[66] First a molecular model of AT III was built based on the crystal structure of cleaved α_1-antitrypsin (a member of the serpin superfamily to which AT III also belongs). Then the positively charged amino acid residues of AT III that have been identified to be essential in the interaction process (Lys 125, Arg 129, Arg 132, Lys 133, Lys 136, Arg 46, Arg 47) were highlighted. Since these amino acids display an asymmetric assembly of interaction points complementary to the essential charged groups of the pentasaccharide (Figs. 36b and 36c), the orientation of AT III and pentasaccharide toward each other could be established unambiguously in a docking trial. The model was optimized by molecular dynamics calculations in which water was assumed as solvent (Fig. 36d). The important AT III/pentasaccharide interactions are schematically depicted in Figure 37. Other reports also indicated the heparin binding region by using crystal structures of cleaved α_1-antitrypsin,[67] cleaved AT III,[68] and ovalbumin,[69] but neither the orientation of the pentasaccharide toward the binding region nor the possible interactions between complementary groups were outlined.

Recently, we performed a similar study using the crystal structure of intact AT III.[70] Although the two interaction schemes resemble each other closely, some binding characteristics differ significantly. It is interesting to note that in the crystal structure of AT III, Lys 125 and Arg 129 are located on one face of an α-helix denoted helix D, whereas the region Arg 132, Lys 133, Lys 136 possesses a coil-like conformation. During the molecular dynamics simulation in the presence of the pentasaccharide, helix D has a tendency to extend (or "elongate"). This coil–helix conformational change allows the basic side chains to interact better with the essential charged groups of heparin.

It should be recalled that there is much experimental evidence indicating that heparin stabilizes α-helical conformations by reducing detrimental electrostatic interactions between Lys and/or Arg side chains.[71] In this respect it is tempting to speculate that the pentasaccharide-induced elongation of helix D is the trigger for the well-known conformational change in AT III. Nevertheless, it is recognized that the overall conformational transition of AT III is much

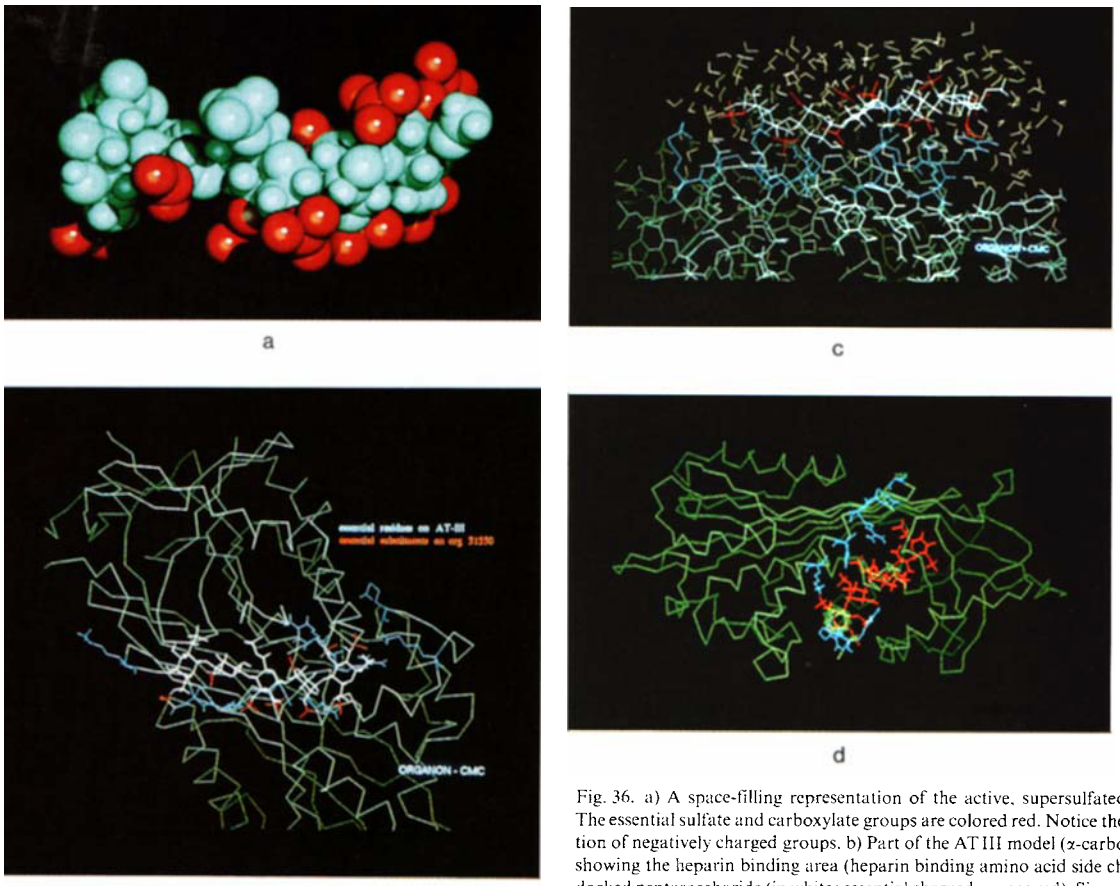

Fig. 36. a) A space-filling representation of the active, supersulfated pentasaccharide **57**. The essential sulfate and carboxylate groups are colored red. Notice the asymmetric distribution of negatively charged groups. b) Part of the AT III model (α-carbon backbone in green) showing the heparin binding area (heparin binding amino acid side chains in blue) with the docked pentasaccharide (in white; essential charged groups red). Since both the pentasaccharide and the protein have an unsymmetric assembly of interaction points, their relative orientation could be established unambiguously. c) Part of the complex of AT III and pentasaccharide **57** after hydration and further optimization by molecular dynamics calculations. d) Model of the complex of AT III and pentasaccharide **57** after molecular dynamics (30 ps). For the sake of clarity the water molecules have been omitted (pentasaccharide in red; essential amino acid side chains in blue). This complex is shown schematically in Figure 37.

more complex, since the protease binding loop of AT III becomes either more or less exposed by its partial insertion between strands S3 and S5 of "A" sheet of the protein.[71] A crystal structure of the AT III/pentasaccharide complex should give a definitive answer to the question as to how heparin activates AT III.

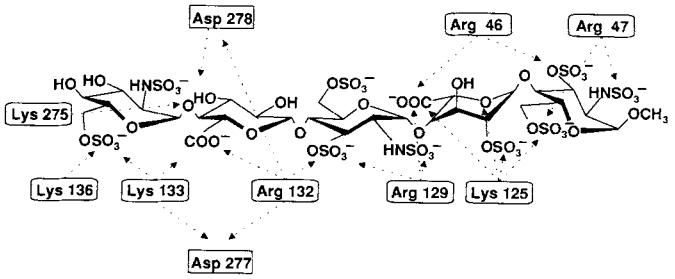

Fig. 37. Schematic diagram of the hydrogen-bonding network in an energy-minimized model of the complex of AT III and pentasaccharide **57**.

8. Summary

It is now assumed that the anticoagulant drug heparin interacts with various proteins through either cooperative or specific binding or both types of interactions. Numerous examples[2, 71a] have been described for heparin–protein interactions in which cooperative interactions appear to dominate; the longer the polysaccharide (and the higher the charge density), the higher the apparent affinity, because more positively charged areas can fit along the heparin chain. That highly specific interactions may occur became apparent when the heterogenous pentasaccharide domain of heparin was discovered, which accelerates the interaction of AT III with coagulation factor Xa. Indeed, other polyanions cannot substitute for the pentasaccharide in the binding and activation of AT III. In our opinion the discovery that a unique domain of a glycosaminoglycan, here the heparin pentasaccharide, is associated with a specific biological activity is a breakthrough in a hardly explored area of molecular biology. Unfortunately up to now only a few other examples of specific structural units in glycosaminoglycans are known.[72] For the AT III mediated inactivation of factor Xa the characteristic pentasaccharide represents the minimum chain length, but for the inactivation of thrombin (IIa) by the same serpin the heparin chain should be much longer (at least 18 carbohydrate units in length). Concerning the latter example there is good evidence that the heparin chain interacts specifically and strongly with AT III but only weakly and less specifically with thrombin.[63b]

A series of about fifty synthetic analogues of the unique pentasaccharide has provided significant advances in our

understanding of the heparin-mediated activation of AT III. The various aspects of this interaction and activation are summarized as follows:

1) The heterogenous pentasaccharide domain of heparin is the only polyanion identified so far that is able to trigger the conformational change in AT III.

2) The pentasaccharide possesses two essential sulfate groups, two essential N-sulfate groups, and two essential carboxylate groups. Removal of one of these key sulfate or carboxylate groups leads to a nearly complete loss of activity, while the presence of two to three more sulfate groups in the molecule appears to increase the activity.

3) The sulfation of the 3-hydroxyl group of the reducing unit (H) improves the biological activity, whereas sulfation of other hydroxyl groups is accompanied by a drop in activity. The persulfated pentasaccharide displays no significant activity.

4) The orientation of the key charged groups in space is important, since epimers display reduced activity.

5) The type of charge is crucial. Thus an essential sulfate group cannot be replaced by a phosphate group, and the carboxylate groups of the uronic acid moieties may not be exchanged for $CH_2OSO_3^-$ residues. These results suggest that the essential charged groups of heparin interact with the complementary residues of AT III through ordered hydrogen bonds.

6) The rigidity of some carbohydrate units such as glucuronic acid (unit E) is required, whereas flexibility of others such as iduronic acid (unit G) is allowed or even necessary.

7) AT III exposes also some negatively charged amino acid side chains in the heparin binding site which may repel charged residues of other polyanions, thereby increasing the selectivity.

8) The hydroxyl groups of the pentasaccharide do not function as hydrogen bond donors in the interaction process, since methylation of the hydroxyl groups does not reduce the activity. Neither are the hydrogen atoms of the sulfated amino groups important hydrogen bond donors, because N-sulfate can be replaced by sulfate.

9) Hydrophobic interactions may improve the binding and may increase the specific activity. In the most active derivative found so far, compound **92** (Fig. 32), two contributing sulfate ester groups are replaced by methoxy groups. However, larger hydrophobic substituents may hamper the AT III activation, while amphiphilic derivatives tend to bind nonspecifically with other proteins.

9. Outlook

The importance of the biological function of glycosaminoglycans in the control of key processes like cell growth, cell migration, cell differentiation, and cell adhesion is becoming more clearly recognized. For a long time investigation of these phenomena at the molecular level has been frustrated by a lack of suitable physico-chemical methods. Therefore it is not yet clear how many of these biological functions are associated with relatively short, well-defined domains of the complex, high molecular weight glycosaminoglycans. We feel that the example of heparin, in which a characteristic partial structure is associated with the known antithrombotic properties, should stimulate research in identifying the structures of other important domains of glycosaminoglycans. Finally, application of the preparative methods discussed in this article should offer opportunities for the development of new drugs.

We wish to thank Sjoerd van Aelst, Jan Basten, T. Bârzu, Tom Beetz, Rein van de Bosch, Jean Choay, Marcel Derrien, Theo van Dinther, Philippe Duchaussoy, Peter Grootenhuis, Françoise Gourvenec, Henk van der Heijden, Guy Jaurand, Isodore Lederman, Jean-Claude Lormeau, Hans Lucas, Jan-Remt Mellema, Dick Meuleman, Bertus Olde Hanter, Anita Rood, Pierre Sinay, Jean-Marc Strassel, Arie Visser, Jan Vos, and Pieter Westerduin for their contributions to the work described in this article and Janine Spit for preparing the figures. Part of the research has been sponsored by the European Community Eurêka programme (project EU237).

Received: January 26, 1993 [A 925 IE]
German version: *Angew. Chem.* **1993**, *105*, 1741

[1] D. A. Lane, I. Björk, U. Lindahl, *Adv. Exp. Med. Biol.* **1992**, *313*, 1–364.
[2] F. A. Ofosu, I. Danishefsky, J. Hirsch, *Ann. N. Y. Acad. Sci.* **1989**, *556*, 1–499.
[3] *Heparin* (Eds.: D. A. Lane, U. Lindahl), Edward Arnold, London, **1989**.
[4] B. Casu, *Adv. Carbohydr. Chem. Biochem.* **1985**, *43*, 51–134.
[5] R. D. Rosenberg, P. S. Damus, *J. Biol. Chem.* **1973**, *248*, 6490–6505.
[6] I. Björk, S. T. Olson, J. D. Shore, in ref. [3] p. 229–255.
[7] a) J. C. Lormeau, J. Goulay, J. Choay, (Institute Choay), FR-B 7831357; b) J. Choay, J. C. Lormeau, M. Petitou, P. Sinay, B. Casu, P. Oreste, G. Torri, G. Gatti, *Thromb. Res.* **1980**, *18*, 573–578.
[8] L. O. Andersson, T. W. Barrowcliffe, E. Holmer, E. A. Johnson, G. E. C. Sims, *Thromb. Res.* **1976**, *9*, 575–583.
[9] M. Höök, I. Björk, J. Hopwood, U. Lindahl, *FEBS Lett.* **1976**, *66*, 90–93.
[10] L. H. Lam, J. E. Silbert, R. D. Rosenberg, *Biochem. Biophys. Res. Commun.* **1976**, *69*, 570–577.
[11] V. V. Kakkar, B. Djazaeri, J. Fok, M. Fletcher, M. F. Scully, J. Westwick, *Br. Med. J.* **1982**, *284*, 375–379.
[12] M. Verstraete, *Drugs* **1990**, *40*, 498–530.
[13] a) J. Choay, J. C. Lormeau, M. Petitou, *Ann. Pharm. Fr.* **1981**, *39*, 37–44; b) J. Choay, J. C. Lormeau, M. Petitou, P. Sinay, J. Fareed, *Ann. N. Y. Acad. Sci.* **1981**, *370*, 644–649; c) B. Casu, P. Oreste, G. Torri, G. Zoppetti, J. Choay, J. C. Lormeau, M. Petitou, P. Sinay, *Biochem. J.* **1981**, *197*, 599–609.
[14] a) U. Lindahl, G. Bäckström, L. Thunberg, I. G. Leder, *Proc. Natl. Acad. Sci. USA* **1980**, *77*, 6551-6555; b) L. Thunberg, G. Bäckström, U. Lindahl, *Carbohydr. Res.* **1982**, *100*, 393–410.
[15] a) J. A. Marcum, R. D. Rosenberg in ref. [3], p. 275–294; b) G. Mertens, J. J. Cassiman, H. van den Berghe, J. Vermylen, G. David, *J. Biol. Chem.* **1992**, *267*, 20435–20443.
[16] H. Paulsen, *Angew. Chem.* **1982**, *94*, 184–201; *Angew. Chem. Int. Ed. Engl.* **1982**, *21*, 155–173.
[17] a) P. Sinay, J. C. Jacquinet, M. Petitou, P. Duchaussoy, I. Lederman, J. Choay, G. Torri, *Carbohydr. Res.* **1984**, *132*, C5–C9; b) M. Petitou, P. Duchaussoy, I. Lederman, J. Choay, P. Sinay, J. C. Jacquinet, G. Torri, *ibid.* **1986**, *147*, 221–236.
[18] C. A. A. van Boeckel, T. Beetz, J. N. Vos, A. J. M. de Jong, S. F. van Aelst, R. H. van den Bosch, J. M. R. Mertens, F. A. van der Vlugt, *J. Carbohydr. Chem.* **1985**, *4*, 293–321.
[19] Y. Ichikawa, R. Monden, H. Kuzuhara, *Tetrahedron Lett.* **1986**, *27*, 611–614.
[20] J. N. Glushka, A. S. Perlin, *Carbohydr. Res.* **1990**, *205*, 305–321.
[21] M. Petitou, P. Duchaussoy, I. Lederman, J. Choay, J. C. Jacquinet, P. Sinay, G. Torri, *Carbohydr. Res.* **1987**, *167*, 67–75.
[22] M. Petitou, G. Jaurand, M. Derrien, J. Choay, *Bioorg. Med. Chem. Lett.* **1991**, *1*, 95–98.
[23] a) M. K. Anwer, A. F. Spatola, *Synthesis* **1980**, 929–932; b) M. K. Anwer, A. F. Spatola, *Tetrahedron Lett.* **1981**, *22*, 4369–4372.
[24] P. Duchaussoy, P. S. Lei, M. Petitou, P. Sinay, J. C. Lormeau, J. Choay, *BioMed. Chem. Lett.* **1991**, *1*, 99–102.
[25] M. Petitou, P. Duchaussoy, I. Lederman, J. Choay, P. Sinay, *Carbohydr. Res.* **1988**, *179*, 163–172.
[26] G. Torri, B. Casu, G. Gatti, M. Petitou, J. Choay, J. C. Jacquinet, P. Sinay, *Biochem. Biophys. Res. Commun.* **1985**, *128*, 134–140.
[27] D. R. Ferro, A. Provasoli, M. Ragazzi, B. Casu, G. Torri, V. Bossennec, B. Perly, P. Sinay, M. Petitou, J. Choay, *Carbohydr. Res.* **1990**, *195*, 157–167.

[28] C. A. A. van Boeckel, T. Beetz, S. F. van Aelst, *Tetrahedron Lett.* **1988**, *29*, 803–806.
[29] C. A. A. van Boeckel, S. F. van Aelst, G. N. Wagenaars, J. R. Mellema, H. Paulsen, T. Peters, A. Pollex, V. Sinnwell, *Recl. Trav. Chim. Pays-Bas* **1987**, *106*, 19–29.
[30] D. R. Ferro, A. Provasoli, M. Ragazzi, G. Torri, B. Casu, G. Gatti, J. C. Jacquinet, P. Sinay, M. Petitou, J. Choay, *J. Am. Chem. Soc.* **1986**, *108*, 6773–6778.
[31] M. Ragazzi, D. R. Ferro, A. Provasoli, *J. Comput. Chem.* **1986**, *7*, 105–112.
[32] M. Ragazzi, D. R. Ferro, B. Perly, P. Sinay, M. Petitou, J. Choay, *Carbohydr. Res.* **1990**, *195*, 169–185.
[33] R. L. Whistler, W. C. Lake, *Methods Carbohydr. Chem.* **1972**, *6*, 286–291.
[34] P. M. Collins, V. R. N. Munasinghe, N. N. Oparaeche, *J. Chem. Soc. Perkin Trans. 1*, **1977**, *1*, 2433.
[35] a) U. Lindahl, G. Bäckström, L. Thunberg, *J. Biol. Chem.* **1983**, 9826–9830; b) D. H. Atha, J. C. Lormeau, M. Petitou, R. D. Rosenberg, J. Choay, *Biochemistry* **1985**, *24*, 6723–6729.
[36] a) M. Petitou, P. Duchaussoy, L. Lederman, J. Choay, P. Sinay, *Carbohydr. Res.* **1988**, *179*, 163–172; b) M. Petitou, *Nouv. Rev. Fr. Hematol.* **1984**, *26*, 221–226.
[37] a) J. Choay, *Semin. Thromb. Hemostasis* **1985**, *11*, 81–85; b) D. H. Atha, J. C. Lormeau, M. Petitou, R. D. Rosenberg, J. Choay, *Biochemistry* **1987**, *26*, 6454–6461.
[38] a) T. Beetz, C. A. A. van Boeckel, *Tetrahedron Lett.* **1986**, *27*, 5889–5892; b) M. Petitou, J. C. Lormeau, J. Choay, *Eur. J. Biochem.* **1988**, *88*, 637–640.
[39] J. Riesenfeld, L. Thunberg, M. Höök, U. Lindahl, *J. Biol. Chem.* **1981**, *256*, 2389–2394.
[40] C. A. A. van Boeckel, unpublished.
[41] C. A. A. van Boeckel, H. Lucas, S. F. van Aelst, M. W. P. van den Nieuwenhof, G. N. Wagenaars, J.-R. Mellema, *Recl. Trav. Chim. Pays-Bas* **1987**, *106*, 581–591.
[42] M. Petitou, unpublished.
[43] C. A. A. van Boeckel, S. F. van Aelst, T. Beetz, D. G. Meuleman, T. G. van Dinther, H. C. T. Moelker, *Ann. N. Y. Acid. Sci.* **1989**, *56*, 489–491.
[44] D. G. Meuleman, P. M. J. Hobbelen, T. G. van Dinther, G. M. T. Vogel, C. A. A. van Boeckel, H. C. T. Moelker, *Semin. Thromb. Hemostasis* **1991**, *17*, 112–117.
[45] M. Petitou, G. Jaurand, M. Derrien, P. Duchaussoy, J. Choay, *Abstr. Fifth European Symp. Carbohydr. EuroCarb V*, Prag, **1989**, p. A-68.
[46] M. W. P. Kat van den Nieuwenhof, J. E. M. Basten, H. Lucas, C. A. A. van Boeckel, *Abstr. Fifth European Symp. Carbohydr., EuroCarb V*, Prag, **1989**, p. A-39.
[47] J. N. Vos (Organon), unpublished.
[48] a) C. A. A. van Boeckel, J. E. M. Basten, H. Lucas, S. F. van Aelst, *Angew. Chem.* **1988**, *100*, 1217–1218; *Angew. Chem. Int. Ed. Engl.* **1988**, *27*, 1177–1178; b) H. Lucas, J. E. M. Basten, T. G. van Dinther, D. G. Meuleman, S. F. van Aelst, C. A. A. van Boeckel, *Tetrahedron*, **1990**, *46*, 8207–8228.
[49] C. A. A. van Boeckel, G. N. Wagenaars, J.-R. Mellema, *Recl. Trav. Chim. Pays-Bas* **1988**, *107*, 649–651.
[50] T. Nukada, H. Lucas, P. Konradsson, C. A. A. van Boeckel, *Synlett* **1991**, 365–367.
[51] J. E. M. Basten, unpublished.
[52] A.S. B. Edge, R. G. Spiro, *J. Biol. Chem.* **1990**, *265*, 15784–15881.
[53] J. N. Vos, P. Westerduin, C. A. A. van Boeckel, *Bioorg. Med. Chem. Lett.* **1991**, *1*, 143–146.
[54] a) Z. F. Kanyo, D. W. Christianson, *J. Biol. Chem.* **1991**, *266*, 4264–4268; b) H. Luecke, F. A. Quiocho, *Nature* **1990**, *347*, 402–406; c) G. R. J. Thatcher, D. R. Cameron, R. Nagelkerke, J. Schmitke, *J. Chem. Soc. Chem. Commun.* **1992**, 386–388.
[55] S. F. van Aelst, C. A. A. van Boeckel, *Recl. Trav. Chim. Pays-Bas*, **1987**, *106*, 593–595.
[56] a) P. Duchaussoy, P. S. Lei, M. Petitou, P. Sinay, J. C. Lormeau, J. Choay, *Bioorg. Med. Chem. Lett.* **1991**, *1*, 1–4; b) M. Petitou, J. C. Lormeau, J. Choay, *Semin. Thromb. Hemostasis* **1991**, *17*, 143–146.
[57] a) G. Jaurand, J. Basten, I. Lederman, C. A. A. van Boeckel, M. Petitou, *Bioorg. Med. Chem. Lett.* **1992**, *2*, 897–900; b) J. E. M. Basten, G. Jaurand, B. Olde-Hanter, M. Petitou, C. A. A. van Boeckel, *ibid.* **1992**, *2*, 901–904.
[58] J. E. M. Basten, G. Jaurand, B. Olde-Hanter, P. Duchaussoy, M. Petitou, C. A. A. van Boeckel, *Bioorg. Med. Chem. Lett.* **1992**, *2*, 905–908.
[59] D. G. Meuleman, unpublished.
[60] H. Lucas, J. E. M. Basten, P. Konradsson, C. A. A. van Boeckel, *Angew. Chem.* **1993**, *105*, 462–464; *Angew. Chem. Int. Ed. Engl.* **1993**, *32*, 434–436.
[61] P. D. J. Grootenhuis, C. A. A. van Boeckel, A. M. M. Rood, A. Visser, T. G. van Dinther, D. Meuleman in *Trends in QSAR and Molecular Modelling* (Ed.: C. G. Wermuth), ESCOM, Leiden, The Netherlands, **1993**, pp. 169–174.
[62] a) P. L. Lane, J. Denton, A. Flynn, L. Thunberg, U. Lindahl, *Biochem. J.* **1984**, *218*, 732–735; b) S. T. Olson, H. R. Halvorson, I. Björk, *J. Biol. Chem.* **1991**, *266*, 6342–6352.
[63] a) S. T. Olson, I. Björk, *J. Biol. Chem.* **1991**, *266*, 6353–6364; b) S. T. Olson, I. Björk, R. Sheffer, P. A. Graig, J. D. Shore, J. Choay, *ibid.* **1992**, *267*, 12528–12538.
[64] P. A. Graig, S. T. Olson, J. D. Shore, *J. Biol. Chem.* **1989**, *264*, 5452–5461.
[65] A. Visser, M. T. Buiting, T. G. van Dinther, C. A. A. van Boeckel, P. D. J. Grootenhuis, D. G. Meuleman, *Thromb. Haemost.* **1991**, *17*, 143; *J. Biol. Chem.*, submitted. The rate of factor Xa inactivation by ATIII is determined by using several concentrations of pentasaccharide at 37 °C at a pH of 8.4 and with the chromogenic substrate S2765. The dissociation constant K_D can be calculated from the apparent second-order rate constant of factor Xa inactivation. When a fluorescence assay (T. Bârzu (Sanofi Recherche), unpublished) at pH 7.4 was used, lower dissocation constants (K_D (**57**) = 1.3 nM instead of 22 nM; K_D (**39**) = 50 nM instead of 320 nM) were recorded. The differences in K_D may be brought about by the different pH values in these assays.
[66] a) P. D. J. Grootenhuis, C. A. A. van Boeckel, *J. Am. Chem. Soc.* **1991**, *113*, 2743–2747; b) C. A. A. van Boeckel, P. D. J. Grootenhuis, C. A. G. Haasnoot, *Trends Pharmacol. Sci.* **1991**, *12*, 241–243.
[67] R. Huber, R. W. Carrell, *Biochemistry*, **1989**, *28*, 8951–8966.
[68] L. Mourey, J. P. Samama, M. Delarue, J. Choay, J. C. Lormeau, M. Petitou, D. Moras, *Biochimie*, **1990**, *72*, 599–608.
[69] R. W. Carrell, D. L. I. Evans, *Curr. Opin. Struct. Biol.* **1992**, *2*, 438–446.
[70] a) H. Schreuder, unpublished. b) P. D. J. Grootenhuis, unpublished.
[71] a) R. L. Jackson, S. J. Busch, A. D. Cardin, *Physiol. Rev.* **1991**, *71(2)*, 481–539; b) D. S. Ferran, M. Sobel, R. B. Harris, *Biochemistry* **1992**, *31*, 5010–5016.
[72] For an example of a characteristic heparan sulfate domain that is involved in the binding of fibroblast growth factor see: J. T. Gallagher, J. E. Turnbull, *Glycobiology* **1992**, *2*, 523–528. For the structural determinant of dermatan sulfate that is involved in binding to the serpin heparin cofactor II (HC II) see: M. M. Maimone, D. M. Tollefsen, *J. Biol. Chem.* **1990**, *265*, 18263–18271.

Got the Flu? Try a Designer Agent Derived from a Sugar

By *Carlo Unverzagt**

When we get the flu, all we can do besides reaching for the next handkerchief is hope that it will be over within a few weeks. Afterwards we are usually protected against a new infection for a while. However, the chances of catching the flu several times a year are high, even after an influenza vaccination. The flu caused by the influenza virus can be particularly dangerous for older people and those afflicted with diseases of the respiratory tract. A group of Australian researchers examined this problem and developed a synthetic antiinfluenza drug derived from *N*-acetylneuraminic acid (**1a**),[1] which is currently being tested as a nasal spray by Glaxo. This compound was designed based on the protein structure data from a complex of the influenza sialidase with an inhibitor.

Why doesn't our immune system give us permanent protection against influenza? The virus is capable of rapidly changing its surface antigens, thus outwitting the body's defense system which posesses no antibodies against the new virus forms. Animals can also contract influenza, and most likely the infection of an organism with two different types of influenza viruses leads to new highly pathogenic strains that may give rise to a pandemic.[2] Despite the variability of the two influenza surface antigens hemagglutinin and sialidase (neuraminidase), their functions remain conserved. Both proteins bind to the sugar *N*-acetylneuraminic acid (Neu5Ac, **1a**; Scheme 1), a member of the family of sialic acids. The sialic acids constitute an important part of the cell surface where they are mostly exposed at the termini of the carbohydrate chains on glycoproteins and glycolipids. Sialic acid (**1b**), located on the cell surface of the respiratory tract epithelium, is recognized by hemagglutinin. This allows the virus to adhere and promotes the following infection. With a function opposite to that of the hemagglutinin, sialidase enzymatically cleaves the glycosidic bond of sialic acid. It is thought that this allows release of the newly formed virus particles from the host cells. The cycle of infection and replication of the influenza virus is based on the recognition of terminal *N*-acetylneuraminic acid, thus offering a good lead in the development of a drug.

The X-ray crystallographic data of hemagglutinin and sialidase have been known for more than a decade; however, those data were unsatisfactory. Only recently X-ray structure analyses with good resolution have been published for complexes with the ligand *N*-acetylneuraminic acid.[3] A well-studied inhibitor of influenza sialidase is the glycal 2-deoxy-2,3-dehydro-*N*-acetylneuraminic acid (Neu5Ac2en) **3**,[4] which can be regarded as an analogue of neuraminyl cation **2**. In the sialidase reaction this type of cation has been proposed[5] for the conversion of the glycosidically bound (**1b**) into free *N*-acetylneuraminic acid (**1a**). Sialidase binds

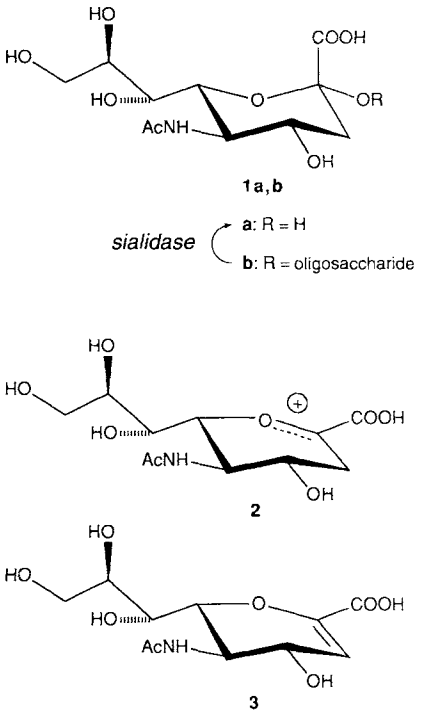

Scheme 1.

to inhibitor **3** with higher affinity ($K_i \approx 1 \times 10^{-6}$ M) than to its natural substrate *N*-acetylneuraminic acid (**1a**) ($K_i = 6.9 \times 10^{-4}$ M). Glycal **3** is a competitive inhibitor, and it is slowly hydrated by sialidase to give **1a**,[6] which supports the assumption that **3** binds as a transition state analogue. Starting from **3** as a lead structure, von Itzstein et al. have now succeeded in designing a significantly more potent inhibitor.[1] They relied mainly on a crystal structure of the influenza sialidase carrying **3** in the binding pocket.[3a] By molecular modeling they screened the surface of the enzyme's binding pocket for sites that might allow additional interactions with the protein after replacement of functional groups in **3**. What they found was a groove next to OH-4 lined by acidic amino acids. According to this analysis, a particularly favorable interaction of the 4-amino group of 4-amino-Neu5Ac2en **4a** with the carboxylate of Glu-119 was predicted. An even stronger salt bridge was anticipated for 4-guanidino-Neu5Ac2en **4b** (Scheme 2).

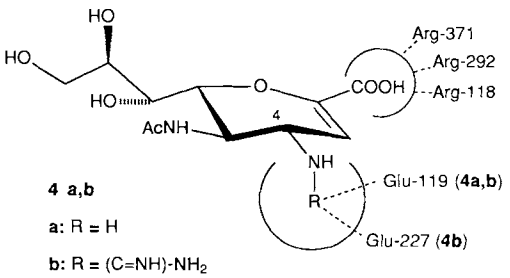

Scheme 2.

[*] Dr. C. Unverzagt
Organisch-chemisches Institut der
Technischen Universität München
Lichtenbergstrasse. 4, D-85748 Garching (FRG)
Telefax: Int. code + (89)3209-3210

 © VCH Verlagsgesellschaft mbH, D-69451 Weinheim, 1993 0570-0833/93/1212-1691 $ 10.00+.25/0

The inhibitors **4a, b** proposed in the preceding analysis were synthesized, and the crystal structure of their complexes with influenza sialidase showed that the predicted ionic interactions indeed formed. The 1-carboxylate residue keeps the molecule in place by contacts with the basic arginine residues 118, 292, and 371. The 4-amino group of **4a** is part of a salt bridge to Glu-119, whereas the 4-guanidino moiety of **4b** is bound by two glutamic acids (119 and 227). This additional ionic attraction of compounds **4a, b** through the substituents at C-4 explains their high potency as sialidase inhibitors. The amino compound **4a** has an inhibition constant of $K_i = 5 \times 10^{-8}$ M, **4b** has $K_i = 2 \times 10^{-10}$ M. Compounds **4a** and **4b**, which have in vitro activities in the nanomolar and subnanomolar range, are the most potent inhibitors of the influenza sialidase known to date.

How significant is the high activity of the new inhibitors? Will they stop an influenza infection in the organism? To answer these questions it is necessary to take a look at their selectivity. Sialidases are ubiquitous,[7] and interference of human sialidases as a part of influenza treatment might lead to complications. Probing of human and bacterial sialidases with the analogues modified at C-4 showed that those enzymes are inhibited only weakly.[8] It is likely that the high selectivity observed is related to the special groove within the binding pocket of the influenza sialidase. Large substituents at C-4 are tolerated by the influenza enzyme; this cleft is apparently not found on the other sialidases examined.

Initial experiments in tissue cultures and in the animal model (ferret) revealed that **4b** is much more active than amantadine and rimantidine; however, the latter inhibitors operate through a different mechanism of action. Interestingly, the parent compound **3** is nearly inactive in the animal model, but **4b** inhibits viral replication in the organism very efficiently.[1] It was thus shown for the first time that efficient and selective inhibition of influenza sialidase by the high affinity inhibitor **4b** can suppress an outbreak of influenza.

With their high rate of mutations, the influenza viruses might be selected by **4b** for sialidase variants lacking the groove for bulky substituents at C-4. In principle this cannot be ruled out entirely, but it would contradict the observed conservation of amino acids in the catalytic center and the scaffolding region surrounding it. Under conditions favoring the rapid occurrence of amantadine-resistant strains, no variants with resistance to **4b**[1] were observed. If the preliminary results are confirmed and the activity of **4b** proves to be equally high in humans as in animals, the question of availability arises before the drug goes into clinical trials. Chemical synthesis of **4b** (Scheme 3) begins with *N*-acetylneuraminic acid (**1a**),[9] an expensive starting material currently offered at a significantly lowered price of about \$35000 per kg.

N-acetylneuraminic acid (**1a**) is esterified with methanol followed by acetylation under acidic conditions to give the protected glycal **5**. In an intramolecular reaction, the allylic acetate moiety at C-4 is substituted by the neighboring acetamide. The conversion of **5** catalyzed by borontrifluoride–ether provides intermediate **6**[10] with an inverted configuration at C-4. Opening of the oxazoline ring activated by an allylic system readily occurs with nucleophiles such as azide, furnishing the 4-azido compound **7** with the configuration of 2,3-dehydro-*N*-acetylneuraminic acid. Starting

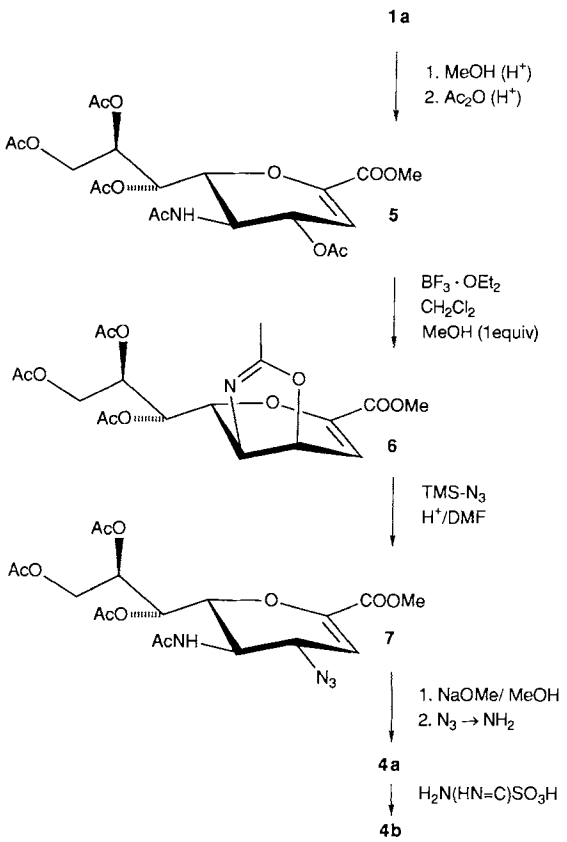

Scheme 3. DMF = *N*,*N*-dimethylformamide, TMS = trimethylsilyl.

from *N*-acetylneuraminic acid (**1a**), each reaction step can be performed in high yields. Subsequent cleavage of the acetate groups and the methyl ester, reduction of the azido group, and reaction of the resulting amine **4a** with aminoiminomethanesulfonic acid gives the guanidino compound **4b** in "reasonable" yield.[1, 10c] The synthesis, which appears laborious at first glance, leads to a compound whose price is likely to be high owing to the expensive starting material and the number of steps needed; nevertheless, economical production is mainly dependant on the cost of *N*-acetylneuraminic acid (**1a**) (vide supra).

For clinical trials and the approval of a compound it is crucial to produce "buckets" of inhibitor.[11] A pharmaceutical "glyco" industry has existed for only a few years, and solutions to such problems need to be developed. Other projects for pharmaceuticals based on carbohydrates are also promising and have stimulated the chemical industry.[11] Sugar chemistry, once considered too difficult to find application, has finally received the attention deserved, in part because of the rapidly increasing knowledge about the numerous biological functions of carbohydrates.[12]

In summary inhibitors **4a, b** of influenza sialidase are the results of more than a decade of work. Data obtained from protein crystallography led to the rational design of a tailor-made inhibitor with unequaled activity.

German version: *Angew. Chem.* **1993**, *105*, 1762

[1] M. von Itzstein, W.-Y. Wu, G. B. Kok, M. S. Pegg, J. C. Dyason, B. Jin, T. V. Phan, M. L. Smythe, H. F. White, S. W. Oliver, P. M. Colman, J. N. Varghese, D. M. Ryan, J. M. Woods, R. C. Bethell, V. J. Hotham, J. M. Cameron, C. R. Penn, *Nature* **1993**, *363*, 418–423.

[2] C. Scholtissek, *Angew. Chem.* **1986**, *98*, 47–56; *Angew. Chem. Int. Ed. Engl.* **1986**, *25*, 47–56.
[3] a) J. N. Varghese, J. L. McKimm-Breschkin, J. B. Caldwell, A. A. Kortt, P. M. Colman, *Proteins* **1992**, *14*, 327–332; b) W. P. Burmester, R. W. H. Ruigrok, S. Cusack, *EMBO J.* **1992**, *11*, 49–56; c) W. Weiss, J. H. Brown, S. Cusak, J. C. Paulson, J. J. Skehel, D. C. Wiley, *Nature* **1988**, *333*, 426–431.
[4] P. Meindl, G. Bodo, P. Palese, J. Schulman, H. Tuppy, *Virology* **1974**, *58*, 457–463.
[5] A. K. J. Chong, M. S. Pegg, N. R. Taylor, M. von Itzstein, *Eur. J. Biochem.* **1992**, *207*, 335–343.
[6] M. Flashner, J. Kessler, S. W. Tanenbaum, *Arch. Biochem. Biophys.* **1983**, *221*, 188–196.
[7] Y. Pilatte, J. Bignon, C. R. Lambré, *Glycobiology* **1993**, *3*, 201–217.
[8] C. T. Holzer, M. von Itzstein, B. Jin, M. S. Pegg, W. P. Stewart, W.-Y. Wu, *Glycoconjugate J.* **1993**, *10*, 40–44.
[9] U. Kragl, D. Gygax, O. Ghisalba, C. Wandrey, *Angew. Chem.* **1991**, *103*, 854–855; *Angew. Chem. Int. Ed. Engl.* **1991**, *30*, 827.
[10] a) E. Schreiner, E. Zbiral, R. G. Kleineidam, R. Schauer, *Liebigs Ann. Chem.* **1991**, 129–134; b) M. von Itzstein, B. Jin, W.-Y. Wu, M. Chandler, *Carbohydr. Res.* **1993**, *244*, 181–185; c) M. von Itzstein, W.-Y. Wu, T. V. Phan, B. Danylec, B. Jin, (Biota Scientific Management Pty. Ltd.), WO-P 91 16320; *Chem. Abstr.* **1992**, *117*, 49151y.
[11] S. Borman, *Chem. Eng. News* **1993**, *71*(26), 27–34.
[12] A. Varki, *Glycobiology* **1993**, *3*, 97–130.

Electrochemical Production of Zintl Anions: Renaissance of a Synthesis Route**

By *Brigitte Eisenmann*

Among the three large classes of compounds, saltlike, covalent, and metallic, the intermetallic compounds are to a chemist's way of thinking the least accessible and developed. This holds true for both the conformity to stoichiometric laws, which so far have only be derived for a few compounds, and for the crystal structures, whose packing of large, interpenetrating coordination polyhedra do not allow for an obvious recognition of the distribution of valence electrons and thereby their bonding strength. Comparative analyses of the dominating structural elements, geometric factors, and valence-electron concentrations as well as model and band structure calculations, like that recently, comprehensively discussed by Nesper,[1] have led to a closer approach to this class of compounds.

The goal of the investigation that Haushalter et al. reported in the November issue of *Angewandte Chemie*[2] was to generate reactive intermetallic building units from which conducting or semiconducting films and solids for various applications could be constructed by chemical methods.

The preliminary attempts to find an experimental route to intermetallic phases starting from known terrain were carried out by Eduard Zintl. Already in the first communication about metals and alloys in 1931, the main emphasis was the transition between salts and metals, and dealt with saltlike and intermetallic compounds of sodium in liquid ammonia.[3] Zintl took into consideration the observations of Joannis in which solutions of sodium in liquid ammonia were found to react with a series of metals and semimetals such as lead or antimony to give intensely colored solutions.[4] According to the investigations by Kraus, the deep green Na–Pb solutions are electrolytes from which lead can be anodically deposited and anionically dissolved lead can be precipitated through the addition of Pb^{2+} salts, and in which lead can be cathodically dissoluted.[5]

Zintl took these individual observations and placed them in a wider context by performing these reactions systematically with the elements of the main and subgroups, starting with the chalcogenides and progressing to the left, and monitored the reactions by potentiometric titrations. The elements were initially placed in liquid NH_3, either as suspensions or in the form of the corresponding sulfides or iodides which dissolve. These were then titrated under rigorous exclusion of air with a solution of Na in liquid NH_3. Conversely, the latter can also be treated with solutions of the element halides. This experimental procedure gives the composition of the compounds formed in solution, detectable as the turning points of the titration curves, and leads to the formulation of polyanionic compounds such as Na_4Pb_9, Na_4Pb_7, Na_3Sb_3, Na_3Sb_7, or Na_3Bi_5. The finding that elements of the fourth main group are still anionically dissoluted but those of the third group are not, formed the basis for drawing a border between the anion and cation constituents; thus between the third and fourth main groups (Zintl border). Experiments concerning the cathodic dissolution of Pb, Tl, Sn, and Ge in solutions of alkali metal halides in water-free ammonia were successful only with lead as the cathode, already with Sn the electrodes remained clean, so this synthesis route was not further pursued.[6] In order to prevent the contamination of solutions with alkali metal halides, subsequently a reaction course was preferred in which alloys preprepared in fusion reactions were investigated with respect to their solubility in liquid NH_3.[7]

The polyanionic salts like $Na_4Pb_9 \cdot x NH_3$ are only stable as ammoniates. They separate from these solutions at low temperatures on concentration as X-ray amorphous, green-black residues. As the ammonia is removed, the salts lose solvent molecules and transform into alloy-like compounds such as $NaPb_{3-x}$, which correspond to the products of melt reactions.

The structure of these polyanions, which today are often termed as Zintl anions, remained unexplained at the time. In 1970, Kummer and Diehl first succeeded in preparing a crystalline compound, $[Na_4(en)_7]Sn_9$ (en = ethylenediamine).[8] The exchange of the solvent ammonia with en also proved to be a significant step with respect to the synthesis of other new compounds. The crystal structure determination of $[Na_4(en)_7]Sn_9$—reported for the first time in 1973—revealed that the cluster anion Sn_9^{4-} exists in the form of a square antiprism with one square face capped; the electron

[*] Priv.-Doz. Dr. B. Eisenmann
Eduard-Zintl-Institut
Abteilung II für Anorganische Chemie der Technischen Hochschule
Hochschulstrasse 10, D-64289 Darmstadt (FRG)
Telefax: Int. code + (6151)16-4073

count is consistent with Wade's rules for a *nido* cluster.[8] According to investigations by Corbett, the dissolution of such pre-prepared alloys is noticeably facilitated through the addition of macrobicyclic aminopolyethers, such as [2.2.2]cryptate. These exhibit high ionic selectivities and complex formation constants for alkali metal and alkaline earth cations. By using complexed cations as counterions, it became possible to crystallize and characterize additional Zintl anions such as Bi_4^{2-}, Pb_5^{2-}, Sn_9^{3-}, and Ge_9^{2-}, and others which are like Sn_9^{4-} cluster anions with multicenter bonds.[9]

The main route for the preparation of alkali metal and alkaline earth compounds with metals, semimetals, and heavy nonmetals of the third to sixth main groups, which comprise the class of Zintl compounds, proceeds through the reaction of mixtures of the elements in melts or high-temperature syntheses. The phase diagrams of the systems under consideration often consist of many phases, thus presenting problems for the production of single-phase products. The high heat of reaction can be controlled by meticulous regulation of the heating rates. If the starting materials show considerably different vapor pressures, the reactants can be placed in zones of differing temperatures, and the more volatile components can be slowly sublimed. This synthesis technique has proven effective, especially for the production of phosphides.[10]

The stoichiometries and structures of the intensely colored to metallic gray, air-sensitive compounds obtained by this method show considerable possibilities of variation. Their polarity and thus their classification in the transitional "ionic–metallic–covalent" domain with respect to structure, reactivity, and physical properties are clearly recognizable. The structures can be interpretated on the basis of an ionic approach (Zintl–Klemm concept), which is supported by results of Zintl's experiments. The anionic substructures obey the $(8-N)$ rule, in which N corresponds to the number of valence electrons, including those taken up. Each atom therefore reaches a complete shell of eight electrons by picking up electrons and/or through bond formation. The one-, two-, or three-dimensional atomic units are not limited to anions analogous to elemental entities like the P_4 analogue $[Si_4]^{4-}$, the As analogue $^2_\infty[Si^-]_n$, or the Se analogue $^1_\infty[As^-]_n$. Such units have been found in which the atoms exhibit different coordination numbers; these include chain fragments like $[As_4]^{6-}$ or nets with two- or three-coordinate atoms like $^2_\infty[Sb_3^{3-}]_n$ and many others.[11]

The existence of these anionic moieties containing atoms with various coordination numbers leads to the question of whether it is possible to prepare the corresponding alkali metal and alkaline earth compounds having heteroanions of metalloids. The structural characterization of such heteroanions is of special interest in cases in which the tendency towards the completion of an electron octet is not structurally determining in the binary parent compounds—as apparent from their structural organization. This applies to Sb_2Se_3, whose structure reveals both pseudo-tetrahedral and also pseudo-octahedral coordination for Sb, and to Sb_2Te_3 and Bi_2Te_3 (Fig. 1) as well as Sn_4As_3, whose atomic arrangement is dominated by octahedral and pseudo-octahedral coordination.

High-temperature reactions starting from mixtures of the elements have been shown to be the most suitable synthesis

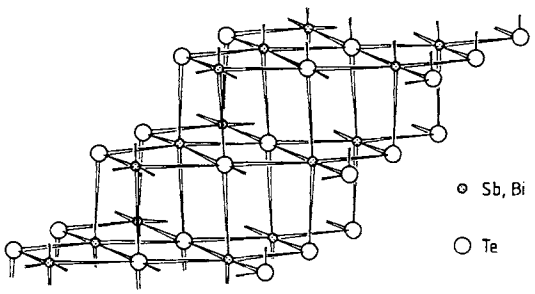

Fig. 1. A section of the crystal structure of Sb_2Te_3 and Bi_2Te_3.

route for these compounds. Difficulties arising from the strong formation tendencies and high melting points of some of the binary compounds formed, can be avoided, at least sometimes, by reacting suitable compounds with one another or with the appropriate element.

The structures of the compounds prepared by high-temperature reactions reflect the influence of the additional valence electrons and the different electronegativities. There is a clear tendency toward the formation of anionic subunits analogous to those anions of complex acids like silicates or phosphates, in which the less electronegative elements are saturated primarily through bonding and are either tetrahedrally or pseudo-tetrahedrally coordinated, as for example $[SnSb_4]^{8-} = [SiO_4]^{4-}$, $^1_\infty[SnAs_3^{5-}]_n = {}^1_\infty[SiO_3^{2-}]_n$, and $[SbTe_3]^{3-} = [AsO_3]^{3-}$.[11] Also groups in which the central atom is in a low oxidation state have been realized, such as $[As_2Te_4]^{4-}$ or $[Sn_2P_6]^{12-}$. Antimony and bismuth chalcogenide anions, like the $^2_\infty[BiTe_2]$ layer (Fig. 2) in $SrBiTe_3$, often show, corresponding to that observed in the binary compounds, high coordination numbers.[12]

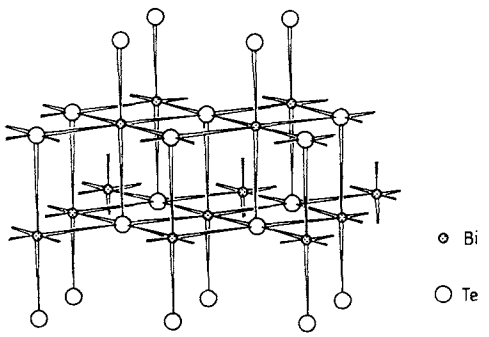

Fig. 2. A section of the $[BiTe_2]$ substructure in $SrBiTe_3$.

Here again the solubility of such compounds as well as the type and structure of solubilized species must be taken into account when considering their suitability as building units. By reacting an alloy of the net composition KTlTe with [2.2.2]cryptate and en, Corbett in 1981 was able to isolate for the first time the ternary compound $[K\text{-}([2.2.2]\text{cryptate})]_2Tl_2Te_2$ whose structure contains a $[Tl_2Te_2]^{2-}$ anion in the form of a folded four-membered ring.[9] Schäfer et al. demonstrated in 1983 that it is possible to react elements directly in en. The reaction of Ba, Sb, and Se in molar ratio 1:1:2 in boiling en afforded compounds possessing ortho anions of antimony in oxidation states of V and III, $[Ba(en)_x]_3(SbSe_4)_2 \cdot y\,en$ and $[Ba(en)_2]_3(SbSe_3)_2$, respectively. These compounds crystallize successively out of solution.

The reaction of Ba with Sb_2Se_3 in boiling en yielded, besides the two compounds mentioned above, an additional reaction product namely the polyselenidoantimonate(III) $[Ba(en)_4](SbSe_2)_2$.[13] The extraction of $Ba_4Sb_4Se_{11}$, a compound whose structure contains discrete $[SbSe_3]^{3-}$ and dimeric $[Sb_2Se_4]^{2-}$ anionic groups as well as Se_2^{2-} ions, with en at room temperature generated the same product mixture. These results show that the anionic or neutral groups present in the starting materials have little influence on the nature of the reaction products even under mild reaction conditions; the addition of cryptates also does not have any effect in the latter reactions. Since, as always, only the crystalline products are identified, the reactions are incompletely characterized. The influence of reaction parameters such as temperature and time have also not yet been analyzed. The complexity of the reactions, caused by, inter alia, differing solvating and binding energies, can be illustrated by several examples.

The reaction of the elements Ba, As, and Te in the ratio 1:1:2 under the same conditions as above, leads to a red crystalline compound $[Ba(en)_4]_2As_4Te_6$, whose anion is shown in Figure 3.[14] So far only the binary selenide [Ba-

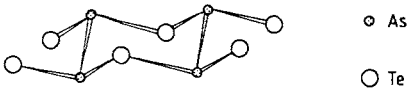

Fig. 3. The structure of the $[As_4Te_6]^{4-}$ anion.

([2.2.2]cryptate]η^1-en]Se_4[13] has been isolated from the extraction of $BaBiSe_3$ with en and addition of [2.2.2]cryptate, whereas the corresponding extraction of an alloy with the formal composition KPbSe yields the compound $[K\text{-}([2.2.2]\text{-cryptate})]_2Pb_2Se_3$.[15] These examples are not limited to chalcogenide anions. From KSnAs, whose structure is dominated by a $^2_\infty[SnAs^-]$ net, it is not possible to extract any soluble species with en. The soluble compound $[K\text{-}([2.2.2]\text{-cryptate})]_4SnAs_{14}$ can be produced, and deposited as dark orange crystals, only from a starting material obtained from a melt consisting of K_3As_7 and 2 Sn.[16] $[K\text{-}([2.2.2]\text{-cryptate})]_2Sn_2Bi_2$ is isolated from the solution reaction of "KSnBi", the composition of which does not correspond to a defined ternary compound. $[Sn_2Bi_2]^{2-}$ cluster anions analogous to P_4 exist in the crystal structure.[9]

The considerable number of fundamental and stimulating results is balanced by the number of unsolved problems. The amount of time necessary to obtain sufficiently crystalline products should also not be underestimated.

In this context, the synthesis of the new Zintl anions $[Sb_4Te_4]^{4-}$ and $[Sb_9Te_6]^{3-}$ by Haushalter et al. is especially relevant.[2] Not only the addition of two new Sb–Te anions in which antimony coordinates in different ways to tellurium, generating structures completely different from those previously reported for the handful of known Sb–Te compounds, deserves mention, but more importantly also the synthesis route. Here an "old" observation is adopted—in Zintl's experiments only the cathodic dissolution of Pb was successful—and in a cleverly simple way modified. The authors now use the binary compound Sb_2Te_3 as the cathode, and tetraalkylammonium ions in en solution serve as the counterions for the crystallization process. On the cathode as well as in the cathodic chamber, crystals of the two compounds grow, one after a short electrolysis time and the second after a short interval of a couple of days. It is evident that continuity of the cathodic process is decisive for crystal growth. The reaction route remains preparatively demanding, requiring the careful exclusion of O_2 and H_2O, since the products are sensitive to oxidation and hydrolysis. The cathodic reaction leads to anions—similar to those isolated by extraction reactions or reactions in en—which do not show any structural relationship to the starting materials, but in which for the first time besides heteronuclear Sb–Te bonds, homonuclear Sb–Sb bonds are also formed and even dominate the structure. The coordination numbers observed in the anions obey the $(8-N)$ rule, the moieties can be considered as low-valent units, like $[Sb_4Te_4]^{4-}$ or as mixed-valent units, like $[Sb_9Te_6]^{3-}$. The very recent publication by Haushalter et al. on the synthesis of a new Au–Te polyanion by cathodic dissolution of an $AuTe_2$ electrode,[17] as well as the results announced shortly thereafter concerning $[GaTe_2(en)_2]^-$ and $[In_2Te_4]^{2-}$ anions rouse expectations for the extended application of this electrochemical method.

Similar to the situation with the extraction reaction, the synthesis cannot be directed systematically with respect to the products at present, because the initially generated species are not yet known. Noteworthy is the discussion in reference [17] about the influence of the cations, up to now little has been said about the role of the composition of the cathodes. Here further investigations should certainly be initiated. The elegant and relatively quick synthesis approach presented here has, however, provided an entry to a group of highly sensitive anions, about which there is surprisingly little known concerning the potential for varying composition and structure, but which have fundamental meaning.

German version: *Angew. Chem.* **1993**, *105*, 1764

[1] R. Nesper, *Angew. Chem.* **1991**, *103*, 805; *Angew. Chem. Int. Ed. Engl.* **1991**, *30*, 789.
[2] C. J. Warren, D. M. Ho, R. C. Haushalter, A. B. Bocarsly, *Angew. Chem.* **1993**, *105*, 1684; *Angew. Chem. Int. Ed. Engl.* **1993**, *32*, 1646.
[3] E. Zintl, J. Goubeau, W. Dullenkopf, *Z. Phys. Chem. Abt. A* **1931**, *154*, 1.
[4] A. Joannis, *C. R. Hebd. Seances Acad. Sci.* **1891**, *113*, 795; *ibid.* **1892**, *114*, 587; *Ann. Chim. Phys.* **1906**, *7*, 75.
[5] C. A. Kraus, *J. Am. Chem. Soc.* **1907**, *29*, 1571; *Trans. Am. Electrochem. Soc.* **1924**, *45*, 183.
[6] E. Zintl, H. Kaiser, *Z. Anorg. Allg. Chem.* **1993**, *211*, 113.
[7] E. Zintl, A. Harder, *Z. Phys. Chem. Abt. A* **1931**, *154*, 47.
[8] D. Kummer, L. Diehl, *Angew. Chem.* **1970**, *82*, 881; *Angew. Chem. Int. Ed. Engl.* **1970**, *9*, 895; L. Diehl, K. Khodadeh, D. Kummer, J. Strähle, *Z. Naturforsch. B* **1976**, *31*, 522.
[9] Review: J. D. Corbett, *Chem. Rev.* **1985**, *85*, 383.
[10] Review: H. G. von Schnering, W. Hönle, *Chem. Rev.* **1988**, *88*, 243.
[11] Review: H. Schäfer, W. Müller, B. Eisenmann, *Angew. Chem.* **1973**, *85*, 742; *Angew. Chem. Int. Ed. Engl.* **1973**, *12*, 694; H. Schäfer, B. Eisenmann, *Rev. Inorg. Chem.* **1981**, *3*, 29; H. Schäfer, *Annu. Rev. Mater. Sci.* **1985**, *15*, 1.
[12] R. Cook, H. Schäfer, *Solid State Chem. 1982, Proc. 2nd. Europ.* Conf., Veldhoven, **1982**; *Studies in Inorganic Chemistry Vol. 3* (Eds.: R. Metselaar, H. J. M. Heijligers, J. Schoonman), Elsevier, Amsterdam, **1983**.
[13] K. T. König, B. Eisenmann, H. Schäfer, *Z. Anorg. Allg. Chem.* **1982**, *488*, 126; *Rev. Chim Minér.* **1984**, *21*, 638; *Z. Anorg. Allg. Chem.* **1983**, *498*, 99; K. T. König, Dissertation, Technische Hochschule Darmstadt **1983**.
[14] B. Eisenmann, R. Zagler, *Z. Naturforsch. B* **1987**, *42*, 1079.
[15] M. Bjorgvinsson, J. F. Sawyer, G. J. Schrobilgen, *Inorg. Chem.* **1987**, *26*, 741.
[16] R. C. Haushalter, B. W. Eichhorn, A. L. Rheingold, S. J. Geib, *J. Chem. Soc. Chem. Commun.* **1988**, 1027.
[17] C. J. Warren, D. M. Ho, A. B. Bocarsly, R. C. Haushalter, *J. Am. Chem. Soc.* **1993**, *115*, 6416.

Communications may be submitted in English *or* in German. Further details regarding the submission of communications can be found in the "Notice to Authors" reproduced in the January issue of the journal. Copies thereof may be obtained from the editorial office upon request.

Regiospecific Alkylation of 6-Chloropurine and 2,6-Dichloropurine at N7 by Transient Protection of N3/N9 by Methylcobaloxime**

By *Christine Dalby, Christine Bleasdale, William Clegg, Mark R. J. Elsegood, Bernard T. Golding,** and *Roger J. Griffin*

We have found that protection by methylcobaloxime at N3 and N9 of 6-chloropurine and 2,6-dichloropurine enables regiospecific alkylation at N7. This is in contrast to direct alkylation of these purines, which gives a mixture of materials alkylated at N7 and (predominantly) N9. The 2- and 6-chloro-substituted purines are useful starting materials for preparing 2- and 6-substituted or 2,6-disubstituted analogues of adenine and guanine (e.g., 6-alkoxypurines), which are potential enzyme inhibitors.[1] We required an efficient route to such analogues that are specifically alkylated at N7.

Marzilli et al.[2] reported that selective alkylation at N7 of xanthine and hypoxanthine could be achieved by coordination of the purine as its anion to cobalt(III) of the cation bis(dimethylglyoximato)(tributylphosphane)cobalt ("tributylphosphinecobaloxime"). The resulting cobalt complex was either methylated or benzylated to give an alkylated xanthine or hypoxanthine. For seven examples studied, the structure of the only alkylated product obtained from each reaction was based on ^{1}H NMR analysis. Unfortunately, Marzilli et al. were not entirely confident about their structural assignments, because reference samples or literature NMR data were not available for all possible alkylation products. We have found that the Marzilli strategy applied to 6-chloropurine (**1**) and 2,6-dichloropurine (**2**) does indeed yield 7-alkylated products, usually exclusively, and therefore constitutes an excellent synthetic route to 7-alkylated purines.

Marzilli et al.[2] used the aqua(tributylphosphane)-cobaloxime cation (**3a**), prepared in situ (as its acetate) by treating the corresponding chloro complex (**3b**) with silver acetate, for protection of xanthine and hypoxanthine at N7. However, **3b**[3] is not as readily available as aqua(methyl)-cobaloxime (**3c**),[4, 5] which we have examined as an alternative reagent for purine complexation. Cobaloxime **3c** is soluble in weakly coordinating solvents like dichloromethane and acetonitrile, and its water ligand is easily displaced by other Lewis bases, including nitrogen heterocycles.[6] Thus, on stirring a solution of either chloropurine **1** or **2** with **3c** in acetonitrile a purine–cobaloxime complex soon precipitates.

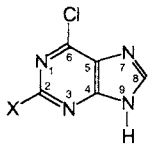

1 X = H
2 X = Cl

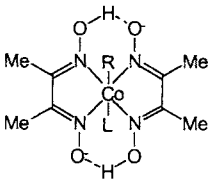

3a R = OH_2^+, L = PBu_3
3b R = Cl, L = PBu_3
3c R = Me, L = OH_2

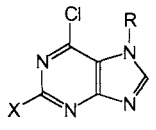

4a X = H, R = $PhCH_2$
4b X = H, R = $PhCOCH_2$
4c X = H, R = $CH_2CH{=}CH_2$
4d X = H, R = CH_2COCH_3

5a X = Cl, R = $PhCH_2$
5b X = Cl, R = $PhCOCH_2$

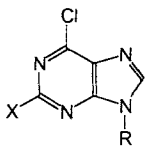

6a X = H, R = $PhCH_2$
6b X = H, R = $PhCOCH_2$
6c X = H, R = $CH_2CH{=}CH_2$
6d X = H, R = CH_2COCH_3

7a X = Cl, R = $PhCH_2$
7b X = Cl, R = $PhCOCH_2$

To the resulting suspension was added potassium carbonate and an alkyl halide, and the mixture was stirred at room temperature for several hours. Chromatography of the reaction mixture on silica led to decomposition of the alkylpurine–cobaloxime complex presumably present in the mixture and afforded the *N*7-alkylated purine (**4a–4d** from **1**, **5a–5b** from **2**) in excellent yield, obtained analytically pure after one recrystallization (Table 1). Reference samples of *N*7-alkylated purines **4a–4d**, **5a**, **5b**, and *N*9-alkylated purines **6a–6d**, **7a**, and **7b** were generated by direct alkylations[7] of **1** or **2** in acetonitrile (that is, essentially the same conditions as those just described, but with omission of the cobaloxime), which gave an approximately 1:2 ratio of *N*7- and *N*9-alkylated purine, separable by silica chromatography. The presence of (aquamethyl)cobaloxime **3c** therefore provides a remarkable control over the site of purine alkylation. (Alkylations in dimethylformamide (DMF) or dimethyl sulphoxide (DMSO)[7] give a lower *N*7- to *N*9-alkylation ratio than those in acetonitrile; we have determined a ratio of 1:9 for benzylation of **1** in DMF.)

Marzilli et al.[2] rationalized cobalt-mediated alkylation at N7 by postulating preferential ligation of N9 to cobalt in the intermediate purine–cobaloxime complex. They proved coordination of cobalt to purine N9 in the structure of bis(dimethylglyoximato)(tributylphosphane)(xanthinato)-cobalt(III) by X-ray analysis.[2] Coordination to purine N9 rather than N7 was ascribed to steric shielding of N7 by the O^6 atom. Combustion analysis of the crystalline complex isolated from mixing 6-chloropurine with **3c** supports its formulation as a 1:1 complex. The crystal structure determi-

[*] Prof. Dr. B. T. Golding, C. Dalby, Dr. C. Bleasdale, Prof. Dr. W. Clegg, Dr. M. R. J. Elsegood, Dr. R. J. Griffin
Department of Chemistry, Bedson Building
University of Newcastle
Newcastle upon Tyne NE1 7RU (United Kingdom)

[**] This research was supported by the North of England Cancer Research Campaign and the British Science and Engineering Research Council.

Table 1. Alkylations of purine–cobaloxime complexes [a].

Substrate	Reagent	Direct alkylation at N9	Direct alkylation at N7	Cobaloxime methodology
1	benzyl bromide	**6a**, 70% m.p. 87–88 °C λ_{max} (ε) = 265 nm (8200)	**4a**, 30% m.p. 151–153 °C λ_{max} (ε) = 270 nm (6800)	**4a**, 63% m.p. 151–152 °C λ_{max} (ε) = 270 nm (8000)
2	benzyl bromide	**7a**, 61% m.p. 153–154 °C λ_{max} = 274 nm	**5a**, 23% m.p. 152–153 °C λ_{max} (ε) = 283 nm (5200)	**5a**, 54% m.p. 151–152 °C [b] λ_{max} (ε) = 283 nm (5400)
1	ω-bromo-aceto-phenone	**6b**, 75% m.p. 177–178 °C λ_{max} (ε) = 249 nm (13200), $\lambda_{sh.}$ = 263 nm (9000)	**4b**, 23% m.p. 195–196 °C λ_{max} (ε) = 248 (23300), 268 nm (11700)	**4b**, 66% m.p. 196–197 °C λ_{max} (ε) = 247 (21000), 270 nm (10500)
2	ω-bromo-aceto-phenone	**7b**, 84% m.p. 140–142 °C λ_{max} (ε) = 241 (22800), 274 nm (14200)	**5b**, 15% m.p. 211–213 °C λ_{max} (ε) = 246 (15900), 282 nm (7000)	**5b**, 50% m.p. 219–220 °C λ_{max} (ε) = 246 (16300), 284 nm (7900)
1	allyl bromide	**6c**, 54% m.p. 78–79 °C λ_{max} (ε) = 265 nm (8400)	**4c**, 24% m.p. 93–94 °C λ_{max} (ε) = 270 (7700)	**4c**, 68% m.p. 89–90 °C λ_{max} (ε) = 270 nm (8500)
1	chloro-acetone	**6d**, 70% m.p. 170–171 °C λ_{max} (ε) = 265 nm (10600)	**4d**, <3% not characterized	**4d**, 30% [c]

[a] All ultraviolet spectra were recorded in ethanol. Substances were also characerized by ^{1}H NMR spectroscopy, mass spectrometry, and combustion analysis. [b] Mixed m.p. 122–126 °C with authentic N9 isomer, 152–153 °C with authentic N7 isomer. [c] Isolated as dinitrophenylhydrazone: m.p. 199–201 °C; λ_{max} (ε) = 265 (20700), 350 nm (25000).

nation[8] of this complex (Fig. 1) supports the hypothesis of Marzilli et al.[2] that the C6 substituent prevents cobalt ligation to N7. Coordination is not, however, to purine N9 in this case, but rather to N3. The complex also contains an intramolecular hydrogen bond from the hydrogen atom on the purine N9 atom to the dimethylglyoximato O1 atom. Thus, if this structure persists in acetonitrile N9 is not alkylated because of this indirect protection. The mechanism of the alkylation step could either involve direct attack at N7 (to give an intermediate that loses the N9 proton) or prior deprotonation at N9, followed by attack of alkylating agent. The latter possibility is supported by the observation that omission of potassium carbonate from a mixture containing **3c**, **1**, and benzyl bromide in acetonitrile gave no **4a** or **6a** (note: addition of base is preferred for alkylations done in the absence of **3c**, and without **3c** the chloropurine remains in solution).

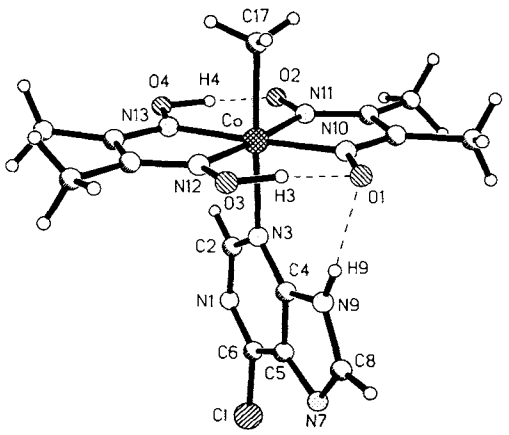

Fig. 1. Crystal structure of the methylcobaloxime complex of **1**.

Experimental Procedure

To a vigorously stirred solution of **3c** (500 mg, 1.55 mmol) in dry acetonitrile (10 mL), protected from light, was added the chloropurine (**1** or **2**, 1.55 mmol). An orange precipitate formed immediately. Dry acetonitrile (10 mL) was added followed by K_2CO_3 (214 mg, 1.55 mmol), and the mixture was stirred for 30 min. After adding the alkylating agent (1.55 mmol), the mixture was stirred at room temperature until no chloropurine remained [1–4 days, monitored by thin-layer chromatography (TLC)]. The solvent was removed and either aqueous 4 M sodium hydroxide (20 mL) (for 6-chloropurine reactions) or water (20 mL) for 2,6-dichloropurine reactions) was added. The product was extracted into dichloromethane (3 × 30 mL) and the combined extracts were washed with water and dried (Na_2SO_4). The solvent was removed and the crude product was chromatographed on silica, typically with ethyl acetate as eluent. The products were pure according to TLC and ^{1}H-NMR spectroscopy. Analytically pure samples were obtained by recrystallization, which gave white crystalline products.

Received: May 24, 1993 [Z 6102 IE]
German version: *Angew. Chem.* **1993**, *105*, 1822

[1] R. C. Moschel, M. G. McDougall, M. E. Dolan, L. Stine, A. E. Pegg, *J. Med. Chem.* **1992**, *35*, 4486.
[2] L. G. Marzilli, L. A. Epps, T. Sorrell, T. J. Kistenmacher, *J. Am. Chem. Soc.* **1975**, *97*, 3351.
[3] G. Costa, G. Tauzher, A. Puxeddu, *Inorg. Chim. Acta* **1969**, *3*, 45.
[4] G. N. Schrauzer, *Inorg. Synth.* **1968**, *11*, 61.
[5] B. T. Golding, T. J. Kemp, P. J. Sellars, E. Nocchi, *J. Chem. Soc., Dalton Trans.* **1977**, 1266.
[6] K. L. Brown, D. Lyles, M. Pencovici, R. G. Kallen, *J. Am. Chem. Soc.*, **1975**, *97*, 7338.
[7] J. A. Montgomery, C. Temple, *J. Am. Chem. Soc.* **1961**, *83*, 630.
[8] $C_{14}H_{20}ClCoN_8O_4$, $M_r = 458.76$, monoclinic, space group $P2/c$, $a = 16.115(4)$, $b = 7.570(2)$, $c = 15.168(4)$ Å, $\beta = 93.97(5)°$, $V = 1845.9(8)$ Å^3, $Z = 4$, $\varrho_{calcd.} = 1.651$ g cm^{-3}, $F(000) = 944$, $Mo_{K\alpha}$-radiation, $\lambda = 0.71073$ Å, $\mu = 1.116$ mm^{-1}. The structure was determined by direct methods and refined on F^2 using all 3206 independent reflections measured at 160 K with a Stoe–Siemens diffractometer ($2\theta_{max.} = 50°$), with anisotropic atomic displacement parameters, and with isotropic H atoms in calculated positions: $\omega R2 = [\sum\omega(F_o^2 - F_c^2)^2/\sum\omega(F_o^2)^2]^{1/2} = 0.1310$, conventional R [on F values for 2738 reflections with $I > 2\sigma(I)$] = 0.0333, S (on F^2) = 1.087 for 264 parameters. Further details of the crystal structure investigation are available on request from the Director of the Cambridge Crystallographic Data Centre, 12 Union Road, GB-Cambridge CB2 1EZ (UK), on quoting the full journal citation.

A Novel Complex with Boat-Shaped, Synfacially Bound η^3:η^3-Benzene Bridges and the First μ_3-η^2:η^2:η^2-Arenetrirhodium Complex**

By *Jörn Müller,* Petra Escarpa Gaede,* and *Ke Qiao*

Dedicated to Professor Otto Scherer on the occasion of his 60th birthday

The number of molecular complexes in which an arene is bound in a π fashion to several metal atoms has increased greatly in recent years.[1] However, the structurally diverse examples, especially those with synfacial arrangement of metal atoms, remained at first restricted to a few transition metals. In the case of rhodium, such a coordination type was

[*] Prof. Dr. J. Müller, Dr. P. Escarpa Gaede, Dipl.-Chem. K. Qiao
Institut für Anorganische und Analytische Chemie der
Technischen Universität
Strasse des 17. Juni 135, D-10623 Berlin (FRG)
Telefax: Int. code + (30)314-22168

[**] This work was supported by the Deutsche Forschungsgemeinschaft and the Fonds der Chemischen Industrie.

observed only in chemisorption of benzene, for example, on a (111) metal surface.[2] Now for the first time, we have been able to synthesize multinuclear rhodium complexes containing benzene bridges and characterize them by crystallography. At the same time we have realized a novel way of coordination for arenes.

In contrast to the analogous cobalt compound, cyclopentadienylbis(ethene)rhodium (**1**) is thermally quite stable, but eliminates the ethene ligands on illumination with UV light.[3] Irradiation of **1** in hexane in the presence of benzene gives rise to complexes **3** and **4**, probably via the intermediate **2**. Monitoring by mass spectrometry confirms the stepwise course of the reaction according to Scheme 1; with increasing irradiation times, the concentration of the trinuclear complex **4** increases at the expense of **3**; that is, the multinuclear complexes are formed by successive coordination of the photolytically generated [CpRh] fragments (Cp = η^5-C_5H_5) to the arene. The quite low overall yields are attributable to the formation of higher nuclearity decomposition products that prevent the photolysis of more **1** by absorbing UV light strongly. Consequently the formation of **4** also comes to a standstill. The actual presence of the intermediate **2** is indicated by an ion in the mass spectrum with $m/z = 246$. The concentration of **2**, however, always remains very low (no isolation was possible), from which one can deduce that the rate of the second reaction step in Scheme 1 is distinctly faster than that of the first. An additional pointer to the

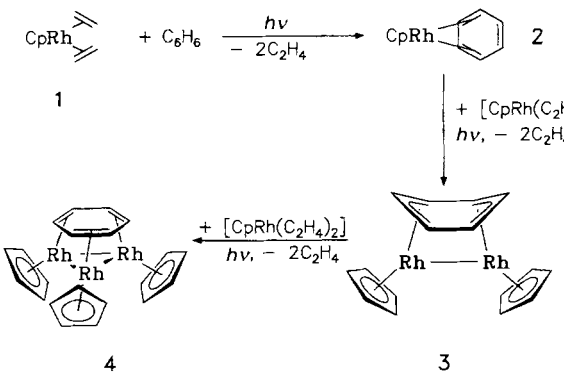

Scheme 1.

possible role of **2** as intermediate is provided by the irradiation of **1** in the presence of [CpRh(η^4-C_6Me_6] synthesized along other routes, which produces analogous hexamethylbenzene complexes to **3** and **4** in substantially higher yields.[4]

The direct attack of [CpM] units on an arene, which leads to compounds like **3** and **4**, is restricted to M = Rh in the triad Co/Rh/Ir. In the case of cobalt, the thermal reaction of [$CpCo(C_2H_4)_2$] with benzene to form a complex analogous to **4** requires a suitable vinyl substituent on the benzene ring that directs the attack of the [CpCo] fragment; however, no intermediates of the type **2** or **3** can be detected.[5] The photolysis of [$CpIr(C_2H_4)_2$] in the presence of benzene, which we studied, took a different course; only with hexafluorobenzene could the successive formation of [$CpIr(C_2H_4)(\eta^2$-$C_6F_6)$] and [$CpIr(\eta^4$-$C_6F_6)$] be observed.[6]

The synfacial arrangement of the metal atoms relative to the benzene ligands and the presence of Rh–Rh bonds in **3** and **4** is deduced from the mass spectrum, because no [M^+ – CpRh] fragment appears; in both cases the loss of the benzene ligands is the preferred primary decomposition step. The base peak in the mass spectrum of **3** is the ion [$Cp_2Rh]^+$, formed by rearrangement; for **4** it is the [$M^+ - C_6H_6 - H_2$] ion.

The X-ray diffraction analysis of **3**[7] reveals that this compound is the first η^3:η^3-arene complex with a six-membered ring arranged synfacially over a metal–metal bond (Fig. 1); it therefore represents one of the few pieces still missing in the mosaic of the structural diversity of bridged arene complexes. The μ_2 benzene ligand is in boat form and can be

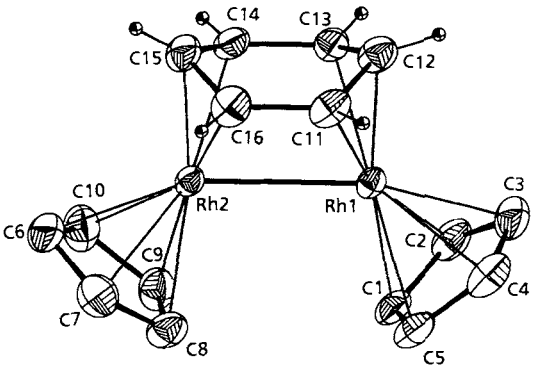

Fig. 1. Crystal structure of **3** (ORTEP). The H atoms of the Cp rings were omitted. Selected bond distances [pm] (standard deviations Rh-Rh 0.1, Rh-C 0.5, C-C 0.8): Rh1-Rh2 266.8, Rh1-C11 217.4, Rh1-C12 206.2, Rh1-C13 216.0, Rh2-C14 216.5, Rh2-C15 204.6, Rh2-C16 216.1, C11-C12 142.7, C12-C13 141.5, C13-C14 147.1, C14-C15 141.6,C15-C16 143.6, C16-C11 145.6.

described as a bis(enyl) ligand system. The angle between the two η^3-enyl planes is 127°. Within the ring the average bond lengths are shorter for the enyl structural units (142 pm) than for the remaining C13–C14 and C11–C16 distances (146 pm). The central atoms C12 and C15 of the enyl units lie closer to the rhodium atoms; these Rh–C distances of about 206 pm are distinctly shorter than the other bonds between rhodium and the benzene ring, whose length of about 216 pm lie within the usual range. The metal–metal distance (266.8 pm) is in accord with published values for Rh–Rh single bonds.[8]

Similar to the synfacial η^4:η^4-bridging arene ligands in [$(CpVH)_2(\mu$-$C_6H_6)$] and [$(CpFe)_2(\mu$-$C_6R_6)$][11], the benzene ring in **3** displays fluctional behavior. In the ^{1}H NMR spectrum (80 MHz, [D_6]acetone) at room temperature it yields only one signal at $\delta = 3.73$, a triplet with two equivalent ^{103}Rh couplings of 1 Hz. If the spectrum is recorded at lower temperatures, the signal broadens and finally splits into two resonance lines at $\delta = 4.00$ (4H) and 3.30 (2H); the coalescence temperature is −10 °C. Irrespective of the recording temperature, the Cp rings give rise to a common doublet at $\delta = 5.17$ ($J_{Rh,H} = 0.5$ Hz).

Also the trinuclear compound **4** is as first μ_3-η^2:η^2:η^2-arenerhodium complex a novelty. The crystal structure analysis[7] shows that the three Rh atoms span an equilateral triangle, which is approximately parallel to the benzene ring directly above it (Fig. 2). As in isostructural clusters,[11] the bond lengths within the arene ligands alternate slightly according to a Kekulé distortion. The crystallographically determined bending of the arene C–H bonds away from the metal centers is necessitated by the coordination and can be explained by MO theory.[9] The Rh–Rh distance of 262.5 pm is slightly less than in **3**. During the structure solution, the Cp ligand C9–C11 was found to be disordered in the crystal; this disorder is attributable to a statistical distribution of the Cp ring between two rotamers ($\Delta\phi = 36°$) in the ratio 1:1. Figure 2 depicts the ORTEP representation of one of the rotamers. The rotation of the arene ligand in

solution, already known for other compounds of this type,[1] can also be observed here; through equal coupling with the three ^{103}Rh nuclei, the isochronous benzene protons give rise to a quartet at $\delta = 4.06$, $J_{Rh,H} = 0.7$ Hz in the ^{1}H NMR spectrum (C_6D_6) at room temperature, whereas the Cp protons appear as singlet at $\delta = 5.11$.

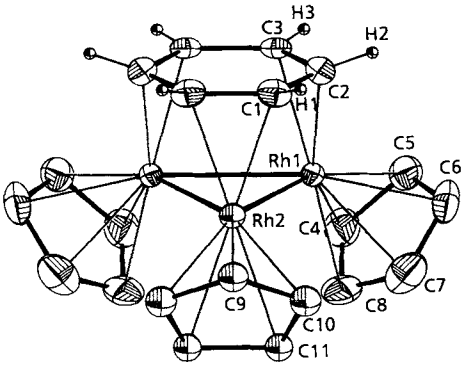

Fig. 2. Crystal structure of **4** (ORTEP). The H atoms of the Cp rings were omitted. Selected bond distances [pm] (standard deviations Rh-Rh 0.1, Rh-C 0.9, C-C 1.3): Rh1-Rh1′ 262.5, Rh1-Rh2 262.5, Rh1-C2 215.9, Rh1-C3 215.3, Rh2-C1 214.4, C1-C1′ 140.0, C1-C2 144.6, C2-C3 143.6, C3-C3′ 146.8.

As the ongoing experiments have already shown, the reactions according to Scheme 1 can be extended to other systems, for example condensed arenes. These results will be reported soon.

Experimental Procedure

All manipulations must be performed under inert atmosphere with dry solvents. Basic aluminum oxide (63–200 μm) with 7.5% water content was used as chromatographic medium.

$[CpRh(C_2H_4)_2]$ (**1**, 740 mg, 3.3 mmol) was dissolved in a mixture of hexane (170 mL) and benzene (30 mL) and irradiated by means of a mercury high-pressure lamp in a falling film apparatus for 5 h. A little Al_2O_3 was added, the solvent was removed under reduced pressure, and the mixture was transferred to the top of a chromatographic column. The separation was performed at −20 °C with hexane as eluent. First the broad, yellow band of unchanged starting material (255 mg, 1.14 mmol, 35%) was eluted. The next adjoining orange-red fraction contained, apart from very small amounts of **2**, a series of unidentified compounds. A clearly separated red zone followed, from which dark red, air-sensitive **3** (39 mg, 0.094 mmol, 8.7% based on converted **1**) was recovered after concentration of the solution and crystallization at −50 °C: m.p. 208 C (decomp.), correct elemental analysis. For further elution, 3% of ether was added to the eluent. A green zone was obtained, which yielded, when treated as above, dark green, crystalline **4** (11 mg, 0.019 mmol, 2.6% based on converted **1**), which is, to a large extent, stable to air in the solid state: m.p. 212 °C (decomp.), satisfactory elemental analysis. When the duration of irradiation is 3 h, 60% of **1** is recovered, and the yields are 15% (**3**) and 2% (**4**), in each case based on converted **1**.

Received: July 5, 1993 [Z6188IE]
German version: *Angew. Chem.* **1993**, *105*, 1809

[1] H. Wadepohl, *Angew. Chem.* **1992**, *104*, 253; *Angew. Chem. Int. Ed. Engl.* **1992**, *31*, 247.
[2] a) M. Neumann, J. U. Mack, E. Bertel, F. P. Netzer, *Surf. Sci.* **1985**, *155*, 629; b) F. P. Netzer, G. Rosina, E. Bertel, H. Saalfeld, *ibid.* **1987**, *184*, L379.
[3] D. M. Haddleton, R. N. Perutz, *J. Chem. Soc. Chem. Commun.* **1985**, 1372.
[4] J. Müller, A. Guo, T. Akhnoukh, unpublished.
[5] H. Wadepohl, K. Büchner, H. Pritzkow, *Angew. Chem.* **1987**, *99*, 1294; *Angew. Chem. Int. Ed. Engl.* **1987**, *26*, 1259.
[6] T. W. Bell, M. Helliwell, M. G. Partridge, R. N. Perutz, *Organometallics* **1992**, *11*, 1911.
[7] Crystal structure analyses: Syntex $P2_1$ diffractometer, $Mo_{K\alpha}$ radiation, ω scan, $T = 170$ K; DIFABS absorption correction; structure resolution with SHELX-76 and SHELXS-86. Data of **3**: triclinic, space group $P\bar{1}$, $a = 7.598(6)$, $b = 9.177(5)$, $c = 11.129(6)$ Å, $\alpha = 66.98(4)$, $\beta = 70.01(5)$, $\gamma = 68.96(5)°$, $V = 647.99$ Å^3, $Z = 2$; 2486 reflections measured, of which 1994 were used for the refinement ($F_0 > 4\sigma(F_0)$), 277 refined parameters (Rh, C anisotropic, H isotropic), $R = 0.0258$. Data of **4**: orthorhombic, space group $P2_1nm$, $a = 7.613(3)$, $b = 8.757(3)$, $c = 13.122(5)$ Å, $V = 874.77$ Å^3, $Z = 2$; 1784 reflections measured, of which 819 were used for the refinement ($F_0 > 4\sigma(F_0)$), 118 refined parameters (Rh, C anisotropic, H isotropic), $R = 0.0215$, $R_w = 0.0206$. Further details of the crystal structure investigation may be obtained from the Fachinformationszentrum Karlsruhe, Gesellschaft für wissenschaftlich-technische Information mbH, D-76344 Eggenstein-Leopoldshafen (FRG) on quoting the depository number CSD-57480, the names of the authors, and the journal citation.
[8] a) H. Werner, H. J. Scholz, R. Zolk, *Chem. Ber.* **1985**, *118*, 4531; b) T. E. Bitterwolf, A. L. Rheingold, *Organometallics* **1991**, *10*, 3856; c) W. A. Herrmann, C. Krüger, R. Goddard, I. Bernal, *J. Organomet. Chem.* **1977**, *140*, 73.
[9] H. Wadepohl, L. Zhu, *J. Organomet. Chem.* **1989**, *376*, 115.

A Synthetic Cavity Assembles Through Self-Complementary Hydrogen Bonds**

By *René Wyler, Javier de Mendoza*, and *Julius Rebek, Jr.**

Complementarity of shape, size, and chemical surface drives molecular recognition, and self-complementarity is the singular feature of biological molecules capable of assembly. Allosteric enzymes, palindromic nucleic acids, and viral capsids[1] all reveal an economy of information;[2] held together by weak intermolecular forces, these structures consist of interlocking, identical subunits. The instructions for assembly are written within the shapes of the subunits and the orientation of their recognition surfaces.[3] We have now synthesized a synthetic molecule that models these notional and structural features. The compound undergoes reversible dimerization to form a closed-shell cavity.

A tennis ball provides a minimalist, macroscopic analogy. Cut along its seam, the ball gives two identical pieces; in shape, the ends are complementary to the middle, and the subunits feature curvatures that dictate the overall spherical shape of the dimer (Fig. 1). Similar spacing and appropriate

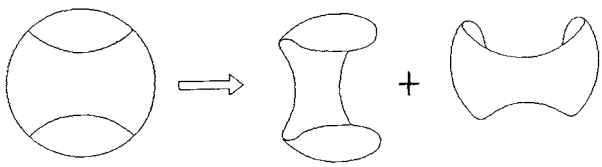

Fig. 1. Tennis ball assembly from self-complementary, interlocking subunits.

curvatures in the molecular subunit structure are required for the assembly to present a cavity.

Compound **1** (Fig. 2) presents these features at the molecular level. The lactam functions of **1** provide self-complementary hydrogen bond donors and acceptors (indicated by

[*] Prof. J. Rebek, Jr., Dr. R. Wyler
Department of Chemistry, Massachusetts Institute of Technology
Cambridge, MA 02139 (USA)
Telefax: Int. code + (617)253-7929
Prof. J. de Mendoza
Departamento de Química, Universidad Autónoma de Madrid
Cantoblanco, E-28049 Madrid (Spain)

[**] We thank the National Institutes of Health (NIH), and the Hoechst-Celanese Corporation for supporting this research, and the Swiss National Science Foundation for a fellowship to R. W. We are grateful to Profs. R. Cohen and G. M. Whitesides (Harvard University) for use of the vapor pressure osmometer, to Drs. Carolyn Knobler and William Davis for preliminary X-ray analysis, and to Mr. Edward Wintner for illustrations. Mass spectrometric data were provided by the MIT Mass Spectrometry Facility which is supported by the N.I.H. (grant. no. RR00317 to Prof. K. Biemann).

arrows). The curvature of the molecule along its length is a consequence of the folding caused by the 7-membered rings when the phenyl units are all on the same face of the structure. The curvature along its width is caused by the *cis* fusion of the 5-membered rings. The compound was prepared by condensing two molecules of diphenyl glycoluril[4] (**2**) with durene tetrabromide (**3**) using KOH in hot dimethyl sulfoxide[5] (DMSO). A congener (**5**) was prepared by similar methods for spectroscopic comparisons.

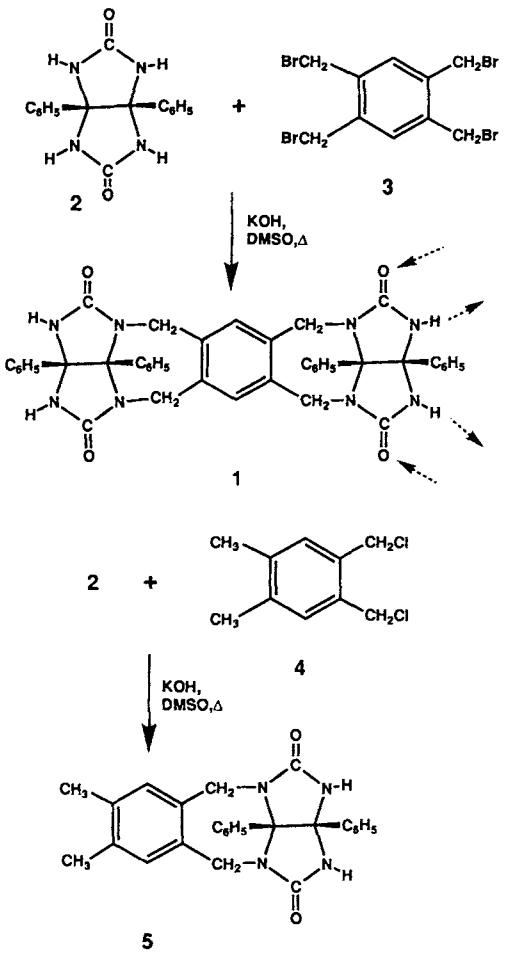

Fig. 2. Syntheses of the self-complementary compound **1** and structural congener **5**.

Two self-complementary molecules of **1** assemble to form a closed-shell, three-dimensional surface through a network of hydrogen bonds.[6] This behavior was established by the following physical measurements. Vapor pressure osmometry in $CHCl_3$ gave an average molecular weight of 1500–2000, a range which is in agreement with a dimeric structure containing a $CHCl_3$ guest. Electron impact (EI) mass spectrometry and fast atom bombardment (FAB) mass spectrometry (nitrobenzylalcohol matrix) gave sizable (25–30%) peaks at 1429 μ, while laser desorption mass spectrometry gave this value as the most intense peak. The calculated molecular weight of the dimeric structure (Fig. 3) is 1429.58.

The chemical shifts of the N–H resonances in the proton NMR spectrum in various media are recorded in Table 1. The downfield shifts indicate extensive intermolecular hydrogen bonding in $CDCl_3$ and benzene solutions when compared to the corresponding signals for **2** and congener **5**,

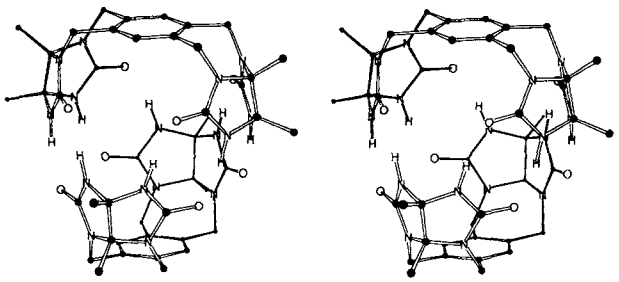

Fig. 3. Stereoscopic view of the assembly of **1** into the dimeric structure. Only those H, N, O atoms involved in the hydrogen bonding seam are labeled, and the eight phenyl groups have been replaced by carbon atoms for clarity.

which suggests the dimerization of **1**. The network of hydrogen bonds in $CDCl_3$ remains intact with up to 20% DMSO as cosolvent. These bonds are disrupted in 100% DMSO, in which the solvated monomeric **1** predominates.

Table 1. N–H Resonances (δ values) in various solvents

Compound	$CDCl_3$	$[D_6]$DMSO	C_6D_6
1	9.28	8.22	10.23
2	insoluble	7.74	insoluble
5	5.4–5.5	8.14	5.15

These data indicate an equilibrium between the dimer and its monomeric form **1**. Molecular modeling[7] suggests that the hydrogen bonds of the dimer (Fig. 3) can be nearly linear (164° for the N-H···O angles), have reasonable length (2.8 Å), and feature favorable secondary interactions.[8] In addition, one molecule of $CHCl_3$ is easily accommodated within the cavity when the Cl atoms of the guest are directed to the openings of the host. While the structure of **1** in the solid state (which may differ from that in solution) awaits X-ray crystallographic analysis, the dominant state in $CDCl_3$, benzene, and the gas phase appears to be dimeric.

Related modules that feature larger cavities have been identified, and we are pursuing their synthesis. It is perhaps not coincidental that self-complementarity is a key feature of self-replicating molecules;[9, 10] our intent is to provide chemical structures with interiors large enough to accommodate and transport synthetic replicators.

Experimental Procedure

A mixture of diphenylglycoluril **2** (26.4 g, 89.7 mmol), finely powdered KOH (10 g, 178 mmol), and DMSO (250 mL) was rapidly heated to 120 °C with vigorous stirring. Durene tetrabromide **3** (2.0 g, 4.44 mmol) was added in one portion, and stirring was continued for 1 h. The reaction mixture was poured into H_2O (3 L), and the precipitate filtered and thoroughly washed with water. The crude residue (26.2 g) was treated with boiling CH_2Cl_2 (500 mL) for 10 min. The suspension was filtered, and the treatment was repeated three more times. The combined CH_2Cl_2 extracts were evaporated to give crude **1** (1.05 g, 33%; m.p. >400 °C). IR (KBr): $\tilde{\nu}$[cm^{-1}] = 3400 (NH), 3200 (NH), 1713 (C=O); UV ($CHCl_3$): λ_{max} [nm] = 241, 254, 260, 265, 270. ^{1}H NMR (250 MHz, $CDCl_3$): δ = 9.27 (s, 4H, NH), 7.50–7.00 (m, 22H, arom. H), 4.68 (d, J = 15.4 Hz, 4H, N–CH), 3.95 (d, J = 15.2 Hz, 4H, N–CH); ^{1}H NMR (250 MHz; d_6-DMSO): δ = 8.22 (s, 4H, NH), 7.28 (s, 2H, arom. H), 7.20–6.90 (m, 20H, arom. H), 4.71 (d, J = 15.7 Hz, 4H, N-CH), 3.96 (d, J = 15.5 Hz, 4H, N-CH); ^{1}H NMR (250 MHz, C_6D_6): δ = 10.23 (s, 4H, NH), 7.70–6.80 (m, 22H, arom. H), 4.74 (d, J = 15.6 Hz, 4H, N-CH), 3.70 (d, J = 15.6 Hz, 4H, N-CH); ^{13}C NMR (125 MHz, $CDCl_3$): δ = 160.62 (s, 4C, C=O), 140–120 (m, 30C, arom. C), 87.84 (s, 4C), 79.59 (s, 4C), 43.79 (t, 4C, N-CH_2); MS (EI): m/z 1429 ($[2M]^{\cdot+}$, 22), 715 ($[M]^{\cdot+}$, 100); MS (FAB): m/z 1430 ($[2M]^{\cdot+}$, 26), 715 ($[M]^{\cdot+}$, 100); MS (laser desorption): m/z 1429 ($[2M]^{\cdot+}$, 100), 714 ($[M]^{\cdot+}$, 50). Elemental analysis: $C_{42}H_{34}N_8O_4 \cdot 1.5H_2O$: calcd. C 68.00, H 5.03, N 15.11, found C 68.18, H 4.94, N 15.14.

Received: July 6, 1994 [Z 6194 IE]
German version: *Angew. Chem.* **1993**, *105*, 1820

[1] D. Brandon, J. Tooze, *Introduction to Protein Structure*, Garland Publ., New York, **1991**, Chapter 11, pp. 161–176.
[2] For Francis Crick's predictions on this point, see H. F. Judson, *The Eighth Day of Creation*, Simon & Schuster, New York, **1980**, p. 317.
[3] J. S. Lindsey, *New J. Chem.* **1991**, *15*, 153–180; G. M. Whitesides, J. P. Mathias, C. T. Seto, *Science*, **1991**, *254*, 1312–1219.
[4] R. P. Sijbesma, L. van Dalen, A. L. Spek, W. J. J. Smeets, R. J. M. Nolte, *J. Org. Chem.* **1989**, *54*, 3710–3717.
[5] All new compounds were fully characterized.
[6] A few examples of 3-dimensional supramolecular aggregates exist: M. Simard, D. Su, J. D. Wuest, *J. Am. Chem. Soc.* **1991**, *113*, 4696–4698; P. Baxter, J.-M. Lehn, A. DeCian, J. Fischer, *Angew. Chem.* **1993**, *105*, 92–95; *Angew. Chem. Int. Ed. Engl.* **1993**, *32*, 69-72; R. P. Bonar-Law, J. K. M. Sanders, *Tetrahedron Lett.* **1993**, 1677–1680; C. Seto, G. M. Whitesides, *J. Am. Chem. Soc.* **1991**, *113*, 712–713; see also J. P. Mathias, E. Simanek, C. T. Seto, G. M. Whitesides, *Angew. Chem.* **1993**, *105*, 1848; *Angew. Chem. Int. Ed. Engl.* **1993**, *32*, 91766; J. Yang, E. Fan, S. Geib, A. D. Hamilton, *J. Am. Chem. Soc.* **1993**, *115*, 5314–5315; while 2-dimensional systems abound: C. Fouque, J.-M. Lehn, A. M. Levelut, *Adv. Mater.* **1990**, *2*, 254–257; F. Garcia-Tollado, S. J. Geib, S. Goswami, A. D. Hamilton, *J. Am. Chem. Soc.* **1991**, *113*, 9265–9269; Y. Ducharme, J. D. Wuest, *J. Org. Chem.* **1988**, *53*, 5787–5789; J. L. Sessler, D. Magda, H. Furuta, *ibid.* **1992**, *57*, 818–826; S. C. Zimmerman, B. F. Duerr, *ibid.* **1992**, *57*, 2215–2217; J. A. Zerkowski, C. T. Seto, D. A. Wierda, G. M. Whitesides, *J. Am. Chem. Soc.* **1990**, *112*, 9025–9026.
[7] MacroModel, 3.5 ×, W. C. Still, Columbia University, **1992**.
[8] W. L. Jorgensen, J. Pranata, *J. Am. Chem. Soc.* **1990**, *112*, 2008–2010.
[9] Q. Feng, T. K. Park, J. Rebek, Jr. *Science* **1992**, *256*, 1179–1180.
[10] J. Rebek, Jr. *Chem. Ind. (London)*, **1992**, 171–174.

A Hexanuclear Organogallium Fluoride Oxide**

By *Bernhard Neumüller** and *Frank Gahlmann*

Dedicated to Professor Dietmar Seyferth on the occasion of his 65th birthday

Diorganogallium fluorides can be obtained by the reaction of triorganogallium compounds with $BF_3 \cdot OEt_2$.[1–4] The degree of association of diorganogallium fluorides, as indicated by spectroscopic data and molar mass determinations, is mainly dependent on the steric bulk of the substituents.[4] None of the derivatives had yet been structurally characterized, however.

We have now performed an X-ray structure analysis[5] of Mes_2GaF **1**[4] (Mes = 2,4,6-trimethylphenyl), the result of which confirms the degree of association, $n = 2$, that we had previously postulated. Compound **1** crystallizes with one THF molecule and lies on the intersection of the twofold symmetry axes. The GaF framework forms a planar, distorted rhombus with a Ga–F bond length of 194.7(2) pm (Fig. 1). The internal angles are 78.9(1)° (F1–Ga1–F1A) and 101.1(2)° (Ga1–F1–Ga1A).

After workup, the reaction of **1** with H_2O in the molar ratio 1:1 affords the hexanuclear gallium fluoride oxide $Mes_6Ga_6F_4O_4$ [**2**, Equation (a)], which also crystallizes with one THF molecule.[6] It can be seen from Equation (a) that, under the chosen conditions, only four equivalents of H_2O are required to react with six equivalents of **1**.

$$\underset{\mathbf{1}}{6\,Mes_2GaF} + 4\,H_2O \xrightarrow{THF,\ 25\,^{\circ}C} \underset{\mathbf{2}}{Mes_6Ga_6F_4O_4} + 2\,HF + 6\,MesH \quad (a)$$

[*] Dr. B. Neumüller, Dr. F. Gahlmann
Fachbereich Chemie der Universität
Hans-Meerwein-Strasse, D-35032 Marburg (FRG)
Telefax: Int. code + (6421)28-8917

[**] This work was supported by the Deutsche Forschungsgemeinschaft and the Fonds der Chemischen Industrie. We thank Prof. Dr. W. Massa for the calculations and for his valuable contributions to discussions.

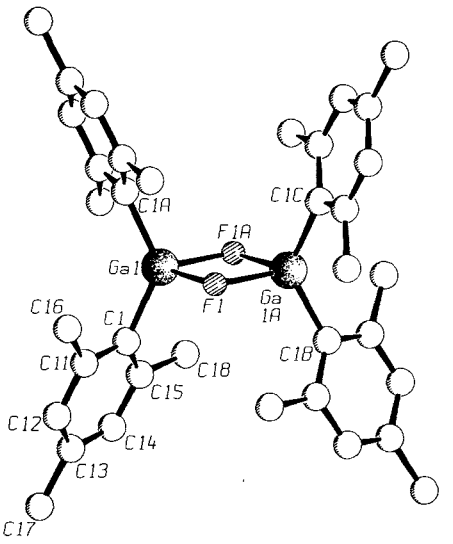

Fig. 1. Structure of **1** in crystals of **1**·THF (H atoms not shown.) Selected distances [pm] and angles [°]: Selected distances [pm] and angles [°]: Ga1-F1 194.7(2), Ga1-C1 194.9(5), Ga1···Ga1A 300.8(2); F1-Ga1-F1A 78.9(1), Ga1-F1-Ga1A 101.1(2), F1-Ga1-C1 104.5(2), F1-Ga1-C1A 113.1(2), C1-Ga1-C1A 130.8(2).

Little is known about the association of organogallium compounds to form larger aggregates,[7] although Barron et al. were recently able to demonstrate that $[t\mathrm{Bu_2GaOH}]_3$[8, 9] reacts in refluxing xylene to form $[t\mathrm{BuGaO}]_9$. The proposed structure for this oligomer was deduced mainly from ^{17}O NMR investigations. Analogously, $[t\mathrm{BuGaS}]_4$[10–12] can be converted to $[t\mathrm{BuGaS}]_n$ (n = 6-8) under the combined effect of base and heat.[8]

Hexanuclear **2** possesses threefold point symmetry, that is, the atoms O1 and F2 lie on a threefold axis (Fig. 2). The six

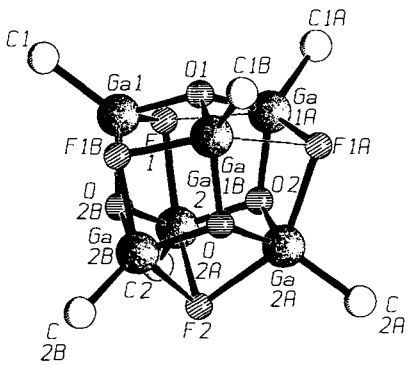

Fig. 2. Structure of **2** in crystals of **2**·THF (H atoms not shown.) Selected distances [pm] and angles [°]: Ga1-F1 197.3(3), Ga1···F1B 252.1(3), Ga1-O1 187.9(1), Ga1-O2B 186.9(3), Ga1-C1 193.0(4), Ga2-F1 222.3(2), Ga2-F2 221.9(2), Ga2-O2 186.6(3), Ga2-O2B 186.6(1), Ga2-C2 193.5(4); G1-Ga1-O1 87.2(1), F1-Ga1-O2B 84.0(1), O1-Ga1-O2B 104.3(2), F1-Ga1-F1B 144.7(1), F1-Ga2-F2 144.8(1), F1-Ga2-O2 81.6(1), F1-Ga2-O2B 77.4(1), F2-Ga2-O2 79.3(1), O2-Ga2-O2B 104.8(1), Ga1-F1-Ga2 90.3(1), Ga2-F2-Ga2A 88.0(1), Ga1-F1-Ga1A 86.5(1), Ga2-F1-Ga1A 84.5(1), Ga1-O1-Ga1A 111.5(1), Ga1A-O2-Ga2B 105.9(1), Ga1A-O2-Ga2 117.7(2), Ga2-O2-Ga2A 111.4(1).

Ga atoms form a distorted octahedron, all eight faces of which are capped by electronegative heteroatoms. The distortion arises because the Ga-O-Ga angles are larger than the Ga-F-Ga angles. The IR spectrum of **2** indicates quite clearly that the complex framework contains no OH groups. The assignment of the atomic positions of the electronegative heteroatoms can be carried out by a comparison of the

Ga–X distances, and by an estimation of the valency of X according to Donnay and Allmann.[13, 14] With the exception of F1 and its symmetry equivalent atoms, the O and F atoms are μ_3-bridging. F1 is pseudo μ_3-bridging. Two of the Ga–F distances are short (Ga1–F1 197.3(3) pm, Ga2–F1 222.3(2) pm); the remaining weaker Ga–F contact of 252.1(3) pm is between Ga1 and F1B. The solvent molecules in **1**·THF and **2**·THF are not coordinated to the metal atoms. The linking of the six Ga atoms through F and O atoms causes an approach of neighboring metal atoms to 298.05(9) pm (Ga1···Ga2) and 319.6(1) pm (Ga1···Ga2B); some 70 pm shorter than the sum of their van der Waal's radii (380 pm).[15] However, bonding Ga–Ga interactions in **2** can be discounted.[16]

Topologically related clusters can be found, for example, in organotitanium oxides: $[(MeC_5H_4)_6Ti_6Cl_4O_4]$,[17] $[Cp_6Ti_6Cl_2O_6]$,[17] and $[Cp_6Ti_6O_8]$[18] all have the same construction principle as **2**, regardless of the oxidation state of the titanium. As the space-filling model shows, the central gallium fluoride oxide unit is sterically shielded by the mesityl ligands, and this explains the kinetic inertness of **2** towards attack by water.

On the basis of cryoscopic molar mass determinations in benzene, and from NMR spectroscopic investigations, we assume that **2** does not dissociate in THF or toluene (1311, $n = 1.03$). The ^{19}F NMR spectrum shows two signals at $\delta = -90.7$ (three F) and -104.0 (one F). The ^1H and ^{13}C NMR spectra support this conclusion; two sets of signals were found, one for each of the groups of mesityl substituents in different environments, with an intensity ratio of 1:1.

Experimental Procedure

1: Synthesis according to ref. [4].

2: 0.54 g (1.65 mmol) of **1** was dissolved in a mixture of toluene (20 mL) and THF (2 mL). H_2O (0.02 mL, 1.10 mmol) were added. The solution was stirred at room temperature for three hours and then allowed to stand. The product **2**·THF separated from the solution in the form of colorless, rectangular prismatic crystals. Yield: 0.27 g (73% with respect to **1**; scaled-up reactions give corresponding yields). M.p. > 250 °C.

Cryoscopic molar mass determination (benzene, $c = 0.0054$ M): $M_r = 1311$, $n = 1.03$. ^1H NMR (C_6D_6, TMS ext.): $\delta = 2.09$, 2.15 (s, 18H, C4-CH_3), 2.51, 2.54 (s, 36H, C2/6-CH_3), 6.60, 6.67 (s, 12H, C3/5-H); ^{13}C NMR (C_6D_6, TMS ext.): $\delta = 21.0$, 21.2 (C4-CH_3), 24.5, 24.8 (C2/6-CH_3), 127.5, 127.7 (C3/5), 138.8, 139.0 (C4), 145.2, 145.4 (C2/6), 145.6, 145.7 (C1); ^{19}F NMR ([D$_8$]THF, $CFCl_3$ ext.): $\delta = -98.7$ (s, 3F), -104.0 (s, 1F). IR (Nujol): $\tilde{\nu}$[cm^{-1}] = 2728, 1600, 1558, 1495, 1412, 1292, 1238, 1030, 948, 849, 843, 688, 634, 590, 492, 437, 407, 293. EI-MS (70 eV): *m/z* (%) 1238 (4) [$(M-2Me^+$], 1142 (3) [$(M-GaF_3)^+$], 1041 (10) [$(M-Mes-3O-4Me)^+$], 925 (16) [$(Mes_5Ga_5F_3O_2-C_8H_8)^+$], 819 (7) [$Mes_4Ga_4FO_3)^+$], 207 (7) [$(MesGaF)^+$], 119 (38) [$(Mes)^+$], 105 (100) [$(C_8H_9)^+$], 69 (20) [$Ga^+$]. Elemental analysis correct.

Received: June 24, 1993 [Z61641E]
German version: *Angew. Chem.* **1993**, *105*, 1770

[1] H. Schmidbaur, H.-F. Klein, K. Eiglmeier, *Angew. Chem.* **1967**, *79*, 821; *Angew. Chem. Int. Ed. Engl.* **1967**, *6*, 806.
[2] H. Schmidbaur, J. Weidlein, H.-F. Klein, K. Eiglmeier, *Chem. Ber.* **1968**, *101*, 2268.
[3] H. Schmidbaur, H.-F. Klein, *Chem. Ber.* **1968**, *101*, 2278.
[4] B. Neumüller, F. Gahlmann, *Z. Anorg. Allg. Chem.* **1992**, *612*, 123.
[5] Crystal data for **1**·THF (−70 °C): space group *Ccca*, $a = 1173.1(2)$, $b = 2103.1(2)$, $c = 1503.6(2)$ pm, $V = 3710(1) \times 10^6$ pm^3, $Z = 4$, $\rho_{calcd} = 1.300$ g cm^{-3}, ω scan, $2\theta = 4-50°$, 1037 observed independent reflections ($F_o > 3\sigma(F_o)$), atomic positions of H atoms refined with common temperature factors (H atoms of the disordered THF molecule were not refined), numerical absorption correction ($\mu = 14.91$ cm^{-1}), $R = 0.044$, $R_w = 0.042$. Siemens R3/P3 four circle diffractometer, $Mo_{K\alpha}$ radiation, graphite monochromator.
[6] Crystal data for **2**·THF (−80 °C): space group $R\bar{3}$, $a = b = 2255.0(1)$, $c = 2120.3(2)$ pm, $V = 9337(1) \times 10^6$ pm^3, $Z = 6$, $\rho_{calcd} = 1.436$ g cm^{-3}, ω scan, $2\theta = 4-120°$, 3069 observed independent reflections ($F_o > 3\sigma(F_o)$), atomic positions of H atoms refined with common temperature factors (H atoms of C31 on the disordered THF molecule were not refined), numerical absorption correction ($\mu = 33.6$ cm^{-1}), $R = 0.046$, $R_w = 0.045$. Enraf Nonius CAD4 four-circle diffractometer, $Cu_{K\alpha}$ radiation, graphite monochromator. Further details of the crystal structure investigations may be obtained from the Fachinformationszentrum Karlsruhe, Gesellschaft for wissenschaftlich-technische Information mbH, D-76344 Eggenstein-Leopoldshafen (FRG) on quoting the depository number CSD-57903, the names of the authors, and the journal citation.
[7] Overview of organogallium compounds in *Organogallium Compounds*, *Gmelin, Handbook of Inorganic Chemistry, Gallium, Part 1*, Springer, Berlin, **1987**.
[8] M. B. Power, J. W. Ziller, A. R. Barron, *Organometallics* **1992**, *11*, 2783.
[9] D. A. Atwood, A. H. Cowley, P. R. Harris, R. A. Jones, S. U. Koschmieder, C. M. Nunn, J. L. Atwood, S. G. Bott, *Organometallics* **1993**, *12*, 24.
[10] A. H. Cowley, R. A. Jones, P. R. Harris, D. A. Atwood, L. Contreras, C. J. Burek, *Angew. Chem.* **1991**, *103*, 1164; *Angew. Chem. Int. Ed. Engl.* **1991**, *30*, 1142.
[11] M. B. Power, A. R. Barron, *J. Chem. Soc. Chem. Commun.* **1991**, 1315.
[12] M. B. Power, J. W. Ziller, A. N. Tyler, A. R. Barron, *Organometallics* **1992**, *11*, 1055.
[13] G. Donnay, R. Allmann, *Am. Mineral.* **1970**, *55*, 1003; R. Allmann, *Monatsh. Chem.* **1975**, *106*, 779.
[14] Examples for the use of the Donnay and Allmann relationship can be found in: W. Massa, D. Babel, *Chem. Rev.*, **1988**, *88*, 275.
[15] J. E. Huheey, *Anorganische Chemie*, de Gruyter, Berlin, **1988**.
[16] P. Alemany, S. Alvarez, *Inorg. Chem.* **1992**, *31*, 4266.
[17] A. Roth, C. Floriani, A. Chiesi-Villa, C. Guastini, *J. Am. Chem. Soc.* **1986**, *108*, 6823.
[18] C. J. Huffman, J. G. Stone, W. C. Krussel, K. G. Caulton, *J. Am. Chem. Soc.* **1977**, *99*, 5829.

Dicyanononasulfane $S_9(CN)_2$—An Unbranched Chain of Thirteen Atoms**

By *Ralf Steudel*,* *Klaus Bergemann*, *Jürgen Buschmann*, and *Peter Luger*

Acyclic polysulfanes X–S_n–X form extensive homologous series.[1–7] Both ^1H NMR spectra[2] and HPLC analyses[1, 3, 7] show that n can have values of 35 and above. Only compounds of up to eleven S atoms have been isolated in pure form, however,[4] and structure determinations have only been carried out on sulfanes of up to six S atoms.[1, 5] This is because longer acyclic sulfanes are difficult to isolate and crystallize, since such compounds are thermally labile and tend to form oils, honeylike solids, and microcrystalline powders because of the many possible torsional isomers. We report here on the first synthesis of dicyanononasulfane $S_9(CN)_2$, as well as on its crystal packing and molecular structure, which shows a chainlike molecule of 13 atoms.

$S_9(CN)_2$ was prepared analogously to the synthesis of the short-chained members $S_n(CN)_2$ (n = 3-8)[6] from S_7Cl_2[7] and $Hg(SCN)_2$ [Eq. (a)]. Monoclinic crystals are formed,

$$S_7Cl_2 + Hg(SCN)_2 \longrightarrow S_9(CN)_2 + HgCl_2 \qquad (a)$$

which melt at 36–38 °C and decompose at 20 °C within 24 hours to form a red polymer, but which can be stored at −50 °C without decomposition. The X-ray analysis,[8] car-

[*] Prof. Dr. R. Steudel, Dipl.-Chem. K. Bergemann
Institut für Anorganische und Analytische Chemie
der Technischen Universität
Straße des 17. Juni 135, Sekr. C2, D-10623 Berlin (FRG)
Telefax: Int. code + (30)3142-6519
Dr. J. Buschmann, Prof. Dr. P. Luger
Institut für Kristallographie der Freien Universität
Takustraße 6, D-14195 Berlin (FRG)

[**] Sulfur Compounds, Part 171. This work was supported by the Deutsche Forschungsgemeinschaft, the Fonds der Chemischen Industrie, and the Graduiertenkolleg Freie Universität–Technische Universität. Part 170: [1]

ried out at −110 °C showed that the $S_9(CN)_2$ molecule has C_1 symmetry. The terminal SCN groups are almost antiparallel to each other (Fig. 1). The S_9 chain does not have the

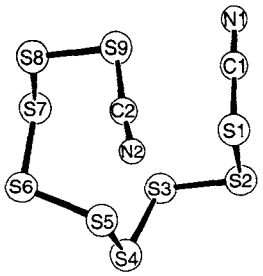

Fig. 1. Conformation of the $S_9(CN)_2$ molecule (the angle between the lines through S1 and N1 and through S9 and N2 is 170.7°). Nuclear distances [pm]: N1-C1 113(1), C1-S1 171.1(8), S1-S2 207.8(2), S2-S3 204.1(2), S3-S4 206.2(4), S4-S5 205.7(3), S5-S6 205.5(3), S6-S7 205.5(4), S7-S8 204.1(3), S8-S9 207.6(3), S9-C2 170.6(8), C2-N2 114(1); valence angles [°]: N1-C1-S1 177.2(8), C1-S1-S2 98.8(3), S8-S9-C2 100.1(3), S9-C2-N2 177.2(7); torsion angles [°]: N1-C1-S1-S2 −173(15), C1-S1-S2-S3 84.3(3), S1-S2-S3-S4 85.7(1), S2-S3-S4-S5 −80.2(1), S3-S4-S5-S6 −86.3(1), S4-S5-S6-S7 87.3(2), S5-S6-S7-S8 94.8(1), S6-S7-S8-S9 −94.2(1), S7-S8-S9-C2 82.1(3), S8-S9-C2-N2 −151(13).

expected stretched (helical) conformation, but resembles a part of the molecular structure of the S_{12} ring:[9a] the signs of the torsion angles τ of the S–S bonds, which would all be the same for a helix, are + + − − + + − + (S_{12}: + + − − + + − −...). The values of the torsion angles $|\tau|$ are in the usual region of 80–95°. The S_9 unit has approximate C_s symmetry; the S-S-S valence angles lie between 104.3(1) and 106.8(1)°. The S–S internuclear distances vary between 204.1 and 207.8 pm (average value 205.8 pm; average value for S_{12} 205.2 pm[9b]). Noticeable is that the "terminal" S–S bonds are the longest (207.7 pm) and the two neighboring ones are the shortest (204.1 pm). Similar observations were made for $S_4(CN)_2$, and the resonance structures shown in Scheme 1 were proposed.[10]

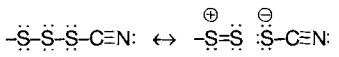

Scheme 1.

The low melting point $T_m = 310 \pm 1$ K of $S_9(CN)_2$ shows on the one hand that the intermolecular interactions can only be weak, but on the other hand that the melting entropy ΔS_m must be exceptionally large since $T_m = \Delta H_m/\Delta S_m$ (ΔH_m = melting enthalpy). The large entropy increase can be explained by the torsional isomerism of the S–S bonds, because each τ value can be about + 90° or −90° and thus for eight S–S bonds $2^8 = 256$ conformational isomers of similar energy (including enantiomers) exist.[11] The rotational barrier[12] for cumulative S–S bonds is only approximately 24 kJ mol^{-1}, so that a mixture of conformers can occur on melting.

The shortest contact distances in $S_9(CN)_2$ (S···N: 307, C···N: 318 pm) correspond roughly to van der Waals distances, yet all the SCN groups in the crystal arrange themselves parallel or antiparallel to the *b* axis of the monoclinic unit cell, which points to weak dipole–dipole interactions (Fig. 2). Since the CN groups are neither bulky nor particularly electronegative, the structure of $S_9(CN)_2$ can serve as model for the structure of other acyclic polysulfanes with small substituents, for example H_2S_n, S_nCl_2 or $(CH_3)_2S_n$, for which a compact structure in the solid state is possibly energetically more favorable than a helical conformation. Furthermore, the structure determination of $S_9(CN)_2$ yields for the first time information about the possible conformation of polymeric sulfur obtained by extraction from quenching of sulfur vapor or melts (random coil polymer). This sulfur is used in large quantities for rubber vulcanization.

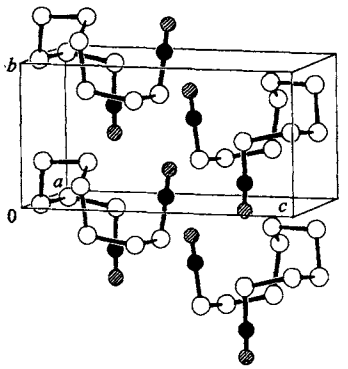

Fig. 2. Packing of $S_9(CN)_2$ molecules in the crystal. Open spheres correspond to the S atoms, solid spheres to the C atoms, and shaded spheres to the N atoms.

Experimental Procedure

Freshly prepared S_7Cl_2 [7] (1.25 mmol) was dissolved in 20 mL anhydrous CS_2, cooled to −10 °C, and $Hg(SCN)_2$ (1.56 mmol) was added with stirring. After 2 h the solvent was decanted from the $HgCl_2/Hg(SCN)_2$ mixture, cooled to −50 °C (12 h), decanted again, and warmed to 20 °C. *n*-Hexane was added until the mixture became cloudy. On cooling to −50 °C pure $S_9(CN)_2$ crystallizes (yield 21 %). Correct C, N, S analyses; ^{13}C NMR (67.69 MHz, $CDCl_3$, 25 °C): $\delta = 109.9$; FT Raman: $\tilde{\nu}$ [cm^{-1}] = 2153/2145 (C≡N), 666 (C–S), 483/466/454/438/427/402 (S–S and δ_{SCN}).

Received: 2 July, 1993 [Z 6186 IE]
German version: *Angew. Chem.* **1993**, *105*, 1781

[1] Review: R. Steudel, M. Kustos in *Encyclopedia of Inorganic Chemistry, Vol. 7* (Ed. R. B. King), Wiley, Sussex, in press.
[2] J. Hahn, *Z. Naturforsch. B* **1985**, *40*, 263.
[3] N. Etzenbach, J. Hahn, F. Rabet, *Bruker Report* **1990**, 44.
[4] H. Schmidt, R. Steudel, *Z. Naturforsch. B* **1990**, *45*, 557; H. Schmidt, Dissertation, Technische Universität Berlin, **1992**.
[5] M. Kustos, J. Pickardt, J. Albertsen, R. Steudel, *Z. Naturforsch. B* **1993**, *48*, 928.
[6] H. Lecher, A. Goebel, *Ber. Dtsch. Chem. Ges.* **1922**, *55*, 1481, 1483; F. Fehér, H. Weber, *Chem. Ber.* **1958**, *91*, 642 [The compounds $S_n(CN)_2$ with $n = 5, 7, 8$ described in this work were obtained as oils which still contained 3–7% $HgCl_2$].
[7] R. Steudel, R. Strauss, D. Jensen, *Chem. Ztg.* **1985**, *109*, 349.
[8] Crystal data for $S_9(CN)_2$ (crystallized from CS_2/*n*-hexane): M_r = 340.6 g mol^{-1}, monoclinic, space group $P2_1$, $a = 835.9(3)$, $b = 590.6(1)$, $c = 1222.0(4)$ pm, $\beta = 102.30(1)°$, $V = 589.43 \times 10^6$ pm^3, $Z = 2$, $\rho_{calc.} = 1.919$ g cm^{-1}, $\mu(Mo_{K\alpha}) = 15.74$ cm^{-1}. Data collection at −110 °C on a Siemens four-circle diffractometer ($Mo_{K\alpha}$ radiation, $\lambda = 71.069$ pm) with open 110°-χ circle and a cold gas stream for temperature adjustment. Crystal dimension: 0.3 × 0.14 × 0.11 mm. 1565 independent reflections with $I > 3\sigma(I)$, $4° < 2\theta < 58°$, 117 parameters refined, $R = 0.037$. Further details of the crystal structure investigation may be obtained from the Fachinformationszentrum Karlsruhe, Gesellschaft für wissenschaftlich-technische Information mbH, D-76344 Eggenstein-Leopoldshafen (FRG) on quoting the depository number CSD-57493, the names of the authors, and the journal citation.
[9] a) A. Kutoglu, E. Hellner, *Angew. Chem.* **1966**, *78*, 1021; *Angew. Chem. Int. Ed. Engl.* **1966**, *5*, 965; b) J. Steidel, R. Steudel, A. Kutoglu, *Z. Anorg. Allg. Chem.* **1981**, *476*, 171.
[10] R. Steudel, K. Bergemann, M. Kustos, *Z. Anorg. Allg. Chem.*, in press.
[11] In reality the number of conformers is slightly smaller, since certain torsion angle combinations would lead to a too close approach of nonbonded atoms.
[12] R. Steudel, *Z. Naturforsch. B* **1983**, *38*, 543, and references therein.

Lipophilic 5′,5′-*O*-Dinucleoside-α-hydroxybenzylphosphonic Acid Esters as Potential Prodrugs of 2′,3′-Dideoxythymidine (ddT)**

By *Chris Meier**

Nucleoside analogues are widely used in antiviral chemotherapy. Inside the cell the nucleoside analogues must be metabolized into their nucleoside triphosphates by three phosphorylation steps (Scheme 1),[1] since only the triphosphates act as inhibitors of the viral polymerases or initiate elongation termination after incorporation into a growing viral DNA chain.[2] The structural differences between the nucleoside analogues and the natural substrate could result in the inhibition of the phosphorylating enzymes (kinases). For this reason the conversion of the anti-HIV-active nucleoside analogue 2′,3′-dideoxythymidine (ddT **1**) into its 5′-monophosphate (ddTMP) by thymidine kinase is the rate limiting step: once the ddTMP is formed, the subsequent conversions are not inhibited.

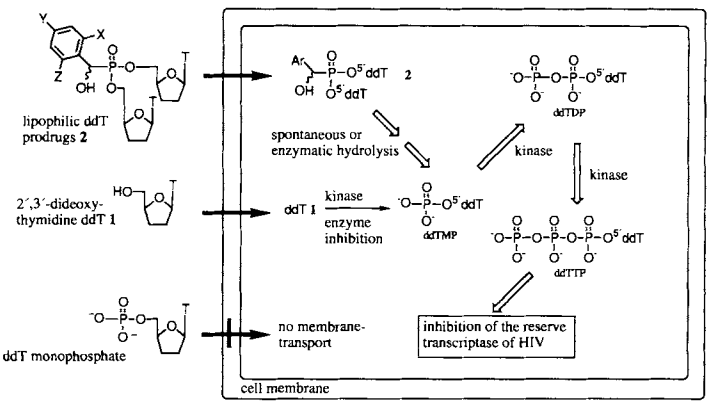

Scheme 1. In vivo activation of 2′,3′-dideoxythymidine (ddT, **1**). Ar = aryl.

Hence, for nucleoside analogues like **1**, intracellular delivery as their 5′-monophosphates from prodrugs should bypass this metabolic limitation and consequently improve their biological activity. Lipophilic nucleoside phosphotriesters were studied with the aim of releasing the nucleoside monophosphate by spontaneous or enzymatic degradation.[3] In all reported cases the controlled cleavage of the masking groups of the prodrugs is not be satisfactorily solved. Apart from the controlled hydrolysis, the lipophilicity of the prodrugs is important for passive transport through biomembranes and through the blood–brain barrier. Only one prodrug form has been described for ddT recently.[4]

This communication reports on the synthesis of di-5′,5′-*O*-(2′,3′-dideoxythymidine)-α-hydroxybenzylphosphonate esters (**2**) with different substituents at the aromatic ring, on their partition coefficients in an octanol/water mixture, and on hydrolysis studies in phosphate buffer solution (pH 7.5) at 37 °C. Starting from **2**, two completely different mechanisms should lead to phosphorylated or phosphonylated products under alkaline conditions: a) α-Hydroxybenzylphosphonates (**2**) may undergo phosphonate–phosphate rearrangement to the corresponding phosphotriester derivatives (**3**) in alkaline medium. Carbanion-stabilizing substituents in the aromatic system promote this rearrangement.[5] In **3** the $ArCH_2$–O bond is the most labile phosphate ester bond, and hydrolysis leads to the nucleoside phosphodiester **4** (Scheme 2).[6] Diester **4** is enzymatically degradable into the 5′-monophosphate **5** and **1**. b) In competition with the phosphonate–phosphate rearrangement, a direct cleavage mechanism of the α-hydroxybenzylphosphonates (**2**) leading to the ddT-H-phosphonate diester **6** and the aldehydes **7** occurs. This direct cleavage should be dominant if the aromatic ring bears a carbanion-destabilizing, electron-donating substituent. The H-phosphonate diester **6** is easily hydrolyzable into the H-phosphonate monoester **8** and **1**.[7] Alternatively, **6** might be oxidized intracellularly to give the phosphodiester **4**[8] (Scheme 2).

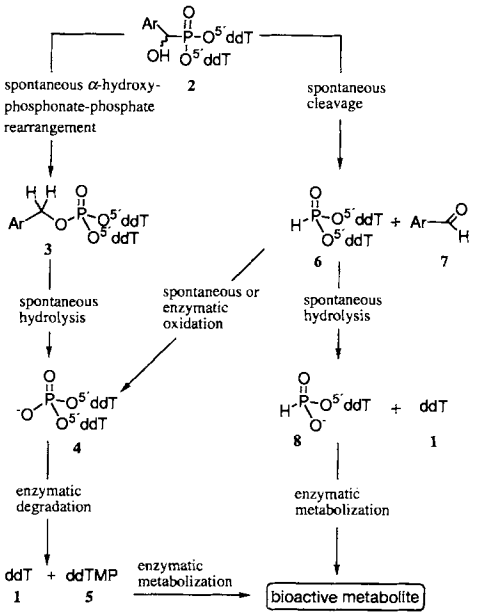

Scheme 2. Hydrolytic degradation pathways of α-hydroxyphosphonate diesters (**2**). Ar = aryl.

Consequently, the two mechanisms would lead in three and two steps to phosphorylated or phosphonylated nucleoside analogues, respectively, and both precursors (the α-hydroxy-benzylphosphonates **2** as well as the benzylphosphotriesters **3**) could act as lipophilic prodrugs. Is it possible to control the two different reaction pathways under physiological conditions by changing the substituent at the aromatic ring?

The 5′,5′-*O*-(2′,3′-dideoxythymidine)-H-phosphonate diester **6**, used as starting material for the synthesis of **2**,[7] was obtained in 60–80% yield in a one-pot reaction with iPr_2NPCl_2 (**9**) and two equivalents of ddT (**1**) via the phosphoramidite **10** as intermediate, which was directly hydrolyzed by tetrazole activation (Scheme 3).[7] Alternatively, **6** was synthesized in the same yield by esterification of 5′-*O*-(2′,3′-dideoxythymidine)-H-phosphonate monoester (**8**) with a second equivalent of ddT **1** through the pivaloylchloride activation procedure described previously.[9] Precursor **8** was obtained by reacting phosphorus trichloride with imidazole to yield the phosphotriimidazolide, followed by reaction with **1** and subsequent hydrolysis (Scheme 3).[10]

[*] Dr. C. Meier
Institut für Organische Chemie der Universität
Marie-Curie-Straße 11, D-60439 Frankfurt am Main (FRG)
Telefax: Int. code +(69)5800-9148

[**] This work was supported by the Deutschen Forschungsgemeinschaft (ME 1161/1-2), the Fonds der Chemischen Industrie, and the Otto-Röhm-Stiftung. I am grateful to Prof. Dr. Joachim Engels for his encouragement and his support.

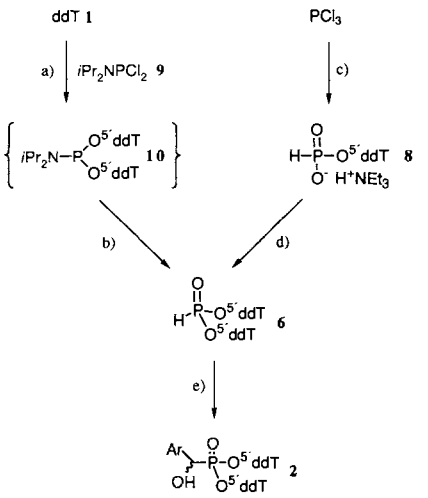

Scheme 3. Synthesis of α-hydroxybenzylphosphonates **2a–j**. a) $iPr_2NP(Cl)_2$ **9**, iPr_2NEt, CH_3CN, 0 °C, 15 min; b) tetrazole, water, CH_3CN, 25 °C, 30 min; c) 1. imidazole, NEt_2, CH_3CN, 0 °C, 4 h; 2. water, CH_3CN, 20 °C, 1 h; d) pivaloyl chloride, **1**, THF, 0 °C, 5 min; e) **7**, NEt_3, 85 °C, 30 min or **7**, THF, NEt_3 (cat.), 20 °C, 3 h.

The title compounds **2** were synthesized by two procedures (Scheme 3): a) reaction of **6** with the benzaldehyde derivatives **7** in anhydrous triethylamine (NEt_3) at 90 °C (yield: 40–60%),[11] or b) reaction of **6** and **7** in anhydrous THF in presence of catalytic amounts of NEt_3 at 20 °C (yield: 90%) (Table 1).[12] Method b was the more convenient procedure.

Table 1. Synthesized α-hydroxyphosphonates **2**, their partition coefficients (x) in octanol/water, the half-lives of **2** in 10 mmol phosphate buffer (pH 7.5), and the dependence of the hydrolysis products on the substituents.

	Substituents			$t_{1/2}$ [h]	Products		
2	X	Y	Z	x		**1** + **8** [%]	**3** [%]
a	H	NMe_2	H	0.61	23	100	-
b	H	OCH_3	H	0.45	31	100	-
c	H	CH_3	H	1.32	47	100	-
d	H	H	H	0.69	57	10	-
e	H	Cl	H	2.06	43	100	-
f	Cl	H	Cl	1.69	18	100	-
g	H	CN	H	0.26	40	60	40
h	H	NO_2	H	0.63	25	60	40
i	NO_2	H	H	0.58	12	15	85
j	NO_2	NO_2	H	0.86	0.5	2	98
1				0.23			

The first method allows the synthesis of the donor substituted compounds **2a–f** but failed to yield acceptor-substituted benzaldehydes **7g–k**. In all reactions the title compounds **2** were isolated as 1:1 diastereomeric mixtures with respect to the configuration at the C_α atom after purification by silica gel chromatography on a Chromatotron (Harrison Research). The diastereomers were not separable by chromatography but could be distinguished by ^1H, ^{13}C, and ^{31}P NMR spectroscopy. The use of the chiral base quinidine instead of triethylamine had no effect on the diastereomeric ratio formed in the reaction. In no reaction was the formation of the corresponding phosphotriester observed. Consequently, these reaction conditions avoid rearrangement as a side reaction during the synthesis.

The partition coefficients of the new compounds (**2**) in octanol/water mixture[13] allows an estimation of their lipophilic properties (Table 1). All compounds showed partition coefficients a factor 1.13 to 9 higher than that of **1** (0.23).[14] Consequently, the passive transport across a membrane should be easier for these compounds than for the free nucleoside.

In hydrolysis studies in which the disappearance of the α-hydroxybenzylphosphonates (**2**) in 10 mmolar phosphate buffer (pH 7.5) was monitored at 37 °C, a striking effect of the different substituents was observed (Table 1).[15] All α-hydroxyphosphonates disappeared following pseudo-first-order kinetics. Derivatives containing strong electron-withdrawing substituents in the aromatic residue rearranged in aqueous solution into the corresponding *O*-benzyl-*O*,*O*-dinucleosidephosphates **3** (Table 1, Scheme 2). To my knowledge, this is the first time that compounds of type **2** rearranged into **3** under aqueous, physiological conditions without enzyme mediation. Benzylphosphotriesters **3** showed further selective degradation into the 5′,5′-dinucleosidephosphodiester **4**. In this case the rate-determining step is the hydrolysis of the formed phosphotriester **3** to yield **4**. Phosphodiesters of type **4** are degraded in vivo enzymatically to yield the monophosphate **5** and ddT (**1**). Thus, α-hydroxyphosphonates (**2**) can, in principle, act as lipophilic prodrugs of 5′-nucleoside monophosphates.

Furthermore, it was shown that compounds **2a–2f** bearing weak electron-withdrawing groups or electron-donating substituents were selectively cleaved to form the 5′,5′-dinucleoside-H-phosphonate diesters **6** and the aldehydes **7** under the same conditions (Table 1, Scheme 2). The rate of this direct cleavage was controlled by the substituent: the stronger the electron-donating properties of the substituent, the faster the direct cleavage. Under the studied reaction conditions **6** was rapidly hydrolyzed into the 5′-ddT-phosphonate monoester **8** and ddT.[7] In this degradation pathway the direct cleavage is the rate-determining step. This pathway, which competes with the rearrangement, opens the possibility of the design of lipophilic prodrugs of 5′-nucleoside-H-phosphonate monoesters of type **8**. This result is important because recently it was shown that compounds of type **8** exhibit selectivity indices comparable with and even better than their parent nucleoside analogues in anti-HIV tests.[16]

In conclusion, these results show that it should be possible to deliver products with biological activity by spontaneous hydrolysis from **2a–j**. Furthermore, it is possible to control the reaction pathway (rearrangement versus direct cleavage) and the rate of the reaction with the substituents at the aromatic ring. Consequently, the new 5′,5′-dinucleoside-α-hydroxybenzylphosphonate esters **2** are potential prodrugs of phosphorylated or phosphonylated derivatives of antiviral nucleoside analogues like **1**. We are currently investigating the hydrolysis of **2** in 10% fetal calf serum (RPMI-culture medium) and their antiviral activity against HIV-1 and HIV-2.

Experimental Procedure

6: Dried 2′,3-dideoxythymidine (**1**, 4.0 mmol) was dissolved in anhydrous acetonitrile (60 mL). After addition of diisopropyl(ethyl)amine (6.0 mmol), the solution was cooled in an ice bath. iPr_2NPCl_2 (3.0 mmol) was added to the stirred solution within 5 min. After this mixture had been stirred at room temperature for 10 min, tetrazole (4.0 mmol) and water (80 μL) were added. After 15 min the solvent was evaporated under high vacuum. The reaction mixture was purified on a Chromatotron on silica gel plates (solvent gradient of ethyl acetate and methanol; 0% to 30% methanol). The 2′,3′-ddT-H-phosphonate diester **6** was isolated as a colorless solid in 80% yield.

2: **6** (1.6 mmol) and **7** (4.8 mmol) were dissolved in anhydrous THF (40 mL). While stirring freshly distilled triethylamine (20 μL) was added. After 4 h at room temperature no starting material **6** could be detected by TLC. The reaction mixture was neutralized by addition of acetic acid (20 μL), and the solvent was evaporated. The crude product was purified on a Chromatotron on silica gel plates (gradient of dichloromethane and methanol; 0% to 15% methanol).

The bis-(5',5'-*O*-2',3'-dideoxythymidine) α-hydroxybenzylphosphonate esters **2** were obtained after lyophilization, as colorless solids in 95% yield.

Received: July 8th, 1993 [Z 6197IE]
German version: *Angew. Chem.* **1993**, *105*, 1854

[1] P. A. Furman, J. A. Fyfe, M. H. St.Clair, K. Weinhold, J. L. Rideout, G. A. Furman, S. N. Lehrman, D. P. Bolognesi, S. Broder, H. Mitsuya, D. W. Barry, *Proc. Natl. Acad. Sci. USA* **1986**, *83*, 8333–8337.
[2] a) H. Mitsuya, K. J. Weinhold, P. A. Furman, M. H. St.Clair, S. Usinoff-Lehrman, R. C. Gallo, D. Bolognesi, D. W. Barry, S. Broder, *Proc. Natl. Acad. Sci. USA* **1985**, *82*, 7096; b) O. Heidenreich, F. Eckstein, *Nucleosides Nucleotides* **1991**, *10*, 535.
[3] a) D. Farquhar, *Bioorg. Chem.* **1984**, *12*, 118–123; b) C. McGuigan, R. N. Pathirana, J. Balzarini, E. DeClercq, *J. Med. Chem.* **1993**, *36*, 1048–1052; c) E. F. Hahn, M. Buddo, A. M. Mian, L. Resnik in *Nucleoside Analogues as Antiviral Agents (ACS Symp. Ser. 401*, Ed.: J. C. Martin), Am. Chem. Soc., Washington DC, **1989**, pp. 156–169; d) F. Puech, A. Pompon, I. Lefebvre, G. Gosselin, J. L. Imbach, *Bioorg. Med. Chem. Lett.* **1992**, *2*, 603–606; e) A. Namane, C. Gouyette, M. P. Fillion, G. Fillion, T. Huynh-Dinh, *J. Med. Chem.* **1991**, *34*, 1830–1837; f) C. Meier, T. Huynh-Dinh, *Bioorg. Med. Chem. Lett.* **1991**, *1*, 527–530; g) C. Meier, J. M. Neumann, F. André, Y. Henin, T. Huynh-Dinh, *J. Org. Chem.* **1992**, *57*, 7300–7307.
[4] S. I. Shimizu, J. Balzarini, E. DeClercq, R. T. Walker, *Nucleosides Nucleotides* **1992**, *11*, 583–594.
[5] a) F. Hammerschmidt, E. Schneyder, E. Zbiral, *Chem. Ber.* **1980**, *113*, 3891–3897; b) A. F. Janzen, O. C. Vaidya, *ibid.* **1973**, *51*, 1136–1138; c) I. J. Borowitz, *J. Am. Chem. Soc.* **1972**, *94*, 1623–1628; d) W. F. Barthel, P. A. Giang, S. A. Hall, *ibid.* **1955**, *77*, 2424–2427.
[6] J. W. Engels, E.-J. Schläger, *J. Med. Chem.* **1982**, *20*, 907–911.
[7] C. Meier, *Bioorg. Med. Chem. Lett.*, submitted.
[8] H-phosphonate diesters are easily converted chemically into the phosphodiesters (see H-phosphonate methodology for oligonucleotide synthesis). Cytochrome P450 oxidase might be responsible for an intracellular oxidation, but no detailed studies about this possibility have been published yet.
[9] P. J. Garegg, I. Lindh, T. Regberg, J. Stawinski, R. Strömberg, *Tetrahedron Lett.* **1986**, *27*, 4051–4054.
[10] a) P. J. Garegg, T. Regberg, J. Stawinski, R. Strömberg, *Chem. Scr.* **1985**, *25*, 280–282; b) *ibid.* **1986**, *26*, 59–62.
[11] J. Jacques, M. Leclercq, M.-J. Brienne, *Tetrahedron* **1981**, *37*, 1727–1733.
[12] K. Kondo, N. Ohnishi, K. Takemoto, H. Yoshida, K. Yoshida, *J. Org. Chem.* **1992**, *57*, 1622–1625.
[13] S. Rim, K. L. Audus, R. T. Borchardt, *Int. J. Pharm.* **1986**, *32*, 79–85.
[14] J. Balzarini, J. M. Cools, E. DeClercq, *Biochem. Biophys. Res. Commun.* **1989**, *158*, 413–422.
[15] For the hydrolysis studies **2** (1 mg) was dissolved in phosphate buffer, pH 7.5 (4 mL) and incubated at 27 °C. The composition of hydrolysis aliquots (150 μL samples) was determined after acidification by reversed-phase-HPLC (UV detection at 269 nm).
[16] A. A. Krayevsky, N. B. Tarussova, Q.-Y. Zhu, P. Vidal, T. C. Chou, P. Baron, B. Polsky, X.-J. Jiang, J. Matulic-Adamic, I. Rosenberg, K. A. Watanabe, *Nucleosides Nucleotides* **1992**, *11*, 177–196.

Tricyclo[6.2.0.0^{3,6}]deca-1,3,6,8-tetraene: A Remarkably Stable *para*-Quinodimethane from a Novel Rearrangement Reaction**

By *Jan-Dirk van Loon, Paul Seiler*, and *François Diederich**

In the course of our studies towards the development of new carbon networks,[1] we recently became interested in the synthesis of peralkynylcumulenes.[2] A possible route towards tetraethynylallene **3**, a molecule that could serve as a building block for a three-dimensional carbon lattice,[1] comprises the conversion of alcohol **1** into haloallene **2**, followed by a palladium-mediated coupling with a silyl-protected acetylene and exhaustive terminal deprotection (Scheme 1).

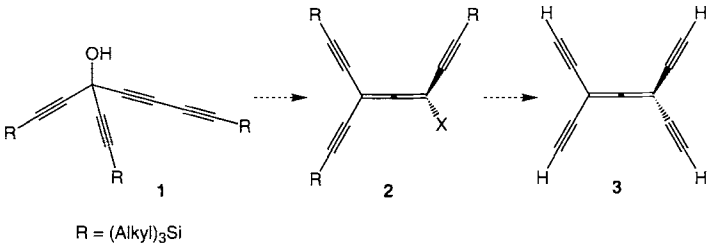

Scheme 1. Possible synthesis of tetraethynylallene **3**.

As a model for the first step, we investigated the reaction of the trialkynyl alcohols **4a**, **b**, which were readily prepared by treatment of the corresponding dialkynylketones with monoprotected lithium acetylides in hexane at 20 °C.[3] Reaction of triisopropylsilyl (TIPS)-protected **4a** with $SOCl_2$ in CH_2Cl_2 at −78 °C for 20 min afforded dialkynylchloroallene **5** in 86% yield. However, in a similar reaction with trimethylsilyl (TMS)-protected **4b**, the corresponding chloroallene **7a** could not be isolated because it rapidly dimerized to give **6a** in 76% yield. Similarly, reaction of **4b** with HBr in hexane at 20 °C (5 h) in the presence of one equivalent of CuBr[4] gave the brominated dimer **6b** in 70% yield. The different reactivity of **4a** and **4b** can be explained by the bulkiness of the TIPS groups, which prevent the dimerization of chloroallene **5**.

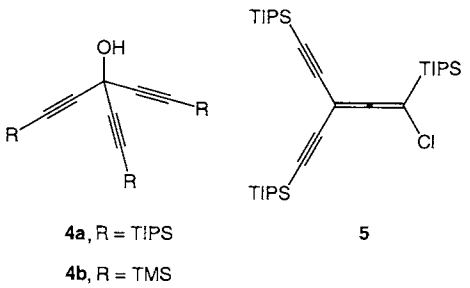

4a, R = TIPS
4b, R = TMS
5

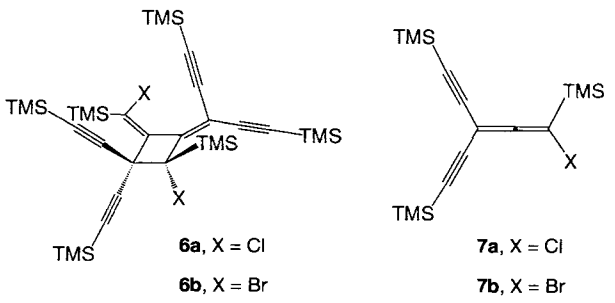

6a, X = Cl
6b, X = Br
7a, X = Cl
7b, X = Br

In order to determine the structure of the dimer, a low-temperature X-ray analysis was performed on crystals of **6b** (Fig. 1).[5] All bond lengths and angles are within the expected range, except the very long C(1)–C(2) bond (1.626(5) Å) in the cyclobutane ring.[6] In the puckered four-membered ring the torsional angle between the two exocyclic C=C bonds is 44.3°. As a result the dienyne system C(18)=C(3)–C(4)=C(22)–C(23)≡C(24) is arranged in a helix, the handedness of which is determined by the configuration at the

[*] Prof. F. Diederich, Dr. J.-D. van Loon, P. Seiler
Laboratorium für Organische Chemie
ETH-Zentrum
Universitätstrasse 16, CH-8092 Zürich (Switzerland)
Telefax: Int. code + (1)261-3524

[**] This work was supported by the Schweizerischen Nationalfonds zur Förderung der Wissenschaftlichen Forschung. J.-D. v. L. thanks the Dutch National Science Foundation (NWO) for a postdoctoral fellowship.

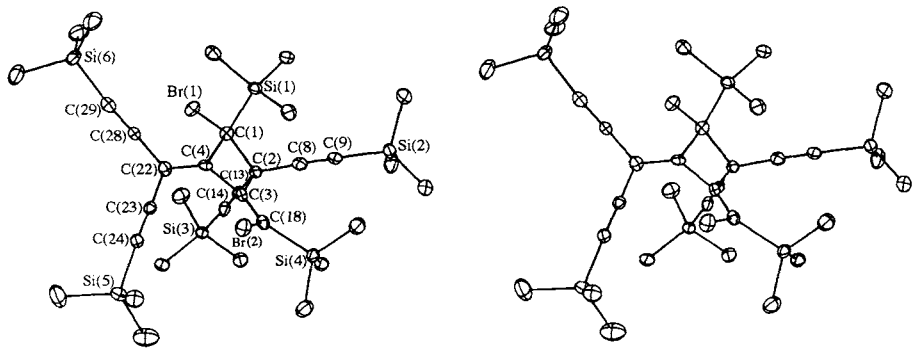

Fig. 1. X-ray crystal structure of **6b**. Selected bond lengths [Å] and angles [°]: C(1)-C(2) 1.626(5), C(1)-C(4) 1.505(5), C(2)-C(3) 1.564(6), C(2)-C(8) 1.471(6), C(2)-C(13) 1.464(5), C(3)-C(18) 1.336(6), C(4)-C(22) 1.363(5), C(8)-C(9) 1.203(6), C(13)-C(14) 1.215(5), C(22)-C(28) 1.432(5), C(22)-C(23) 1.431(6), C(23)-C(24) 1.200(6), C(28)-C(29) 1.213(5); C(1)-C(2)-C(3) 83.9(3), C(1)-C(2)-C(8) 116.8(3), C(1)-C(4)-C(3) 91.8(3), C(1)-C(4)-C(22) 134.5(4), C(2)-C(3)-C(4) 90.6(3), C(2)-C(3)-C(18) 130.8(4), C(2)-C(8)-C(9) 177.3(4), C(2)-C(13)-C(14) 178.9(4), C(4)-C(22)-C(28) 122.6(3), C(4)-C(22)-C(23) 121.6(4), C(22)-C(28)-C(29) 173.7(4), C(22)-C(23)-C(24) 179.2(4), Br(1)-C(1)-C(2) 114.7(3), Br(1)-C(1)-C(4) 116.8(3).

stereocenter. The formation of the racemic dimer **6b** can be explained by the reaction of two bromoallenes **7b** generated in situ, which approach each other orthogonally in the sterically most favorable manner.[7-9]

As the very long C(1)-C(2) bond in the cyclobutane ring of **6b** should be relatively weak, we were prompted to investigate the possible thermal rearrangement of **6b** to provide the more symmetrical cyclobutane **9** (Scheme 2). Compound **9** would be an interesting starting material for the synthesis of peralkynyl[4]radialenes by two Peterson olefination reactions. When a solution of **6b** in [D_8]toluene was heated at 90 °C, rapid rearrangement to give **9** indeed took place as was indicated by ^{1}H and ^{13}C NMR spectroscopy (Table 1). Surprisingly, however, before a thermodynamic equilibrium between **6b** and **9** could be established, **6b** reacted by a second pathway to yield the thermodynamically more stable *para*-quinodimethane **13**. The NMR signals of both **6b** and **9** disappeared, and an almost pure sample of **13** was obtained after 45 min (Scheme 2).[9] The kinetics for both pathways were followed by ^{1}H NMR spectroscopy and pseudo-first-order rate constants calculated as $k_{(\mathbf{6b}\rightarrow\mathbf{9})} = (5.7 \pm 0.5) \times 10^{-4}\ s^{-1}$, $k_{(\mathbf{9}\rightarrow\mathbf{6b})} = (2.2 \pm 0.2) \times 10^{-3}\ s^{-1}$, $k_{(\mathbf{6b}\rightarrow\mathbf{13})} = (9.8 \pm 0.8) \times 10^{-4}\ s^{-1}$, $k_{(\mathbf{13}\rightarrow\mathbf{6b})} \approx 0\ s^{-1}$ (Fig. 2).[10]

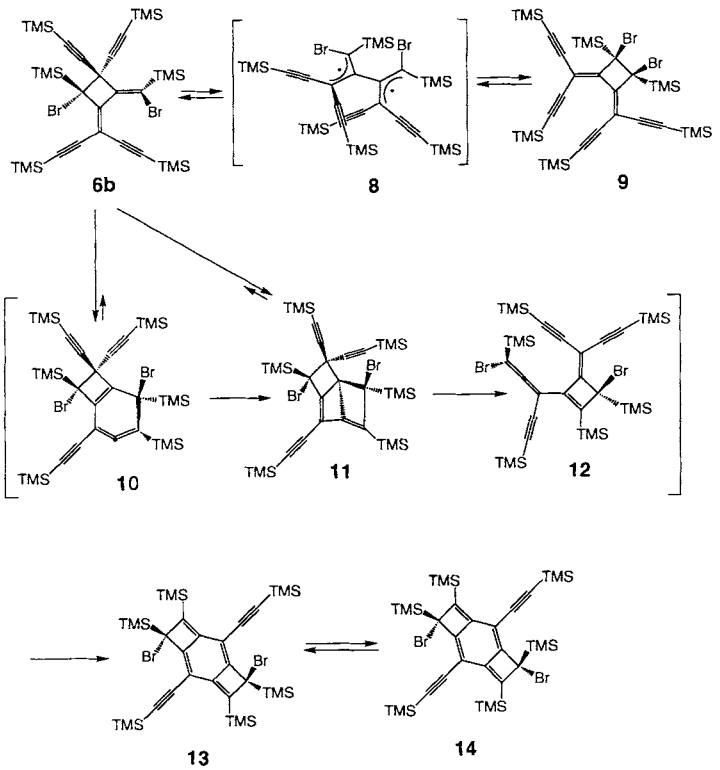

Scheme 2. Postulated mechanism of formation of **9** and **13** from **6b**.

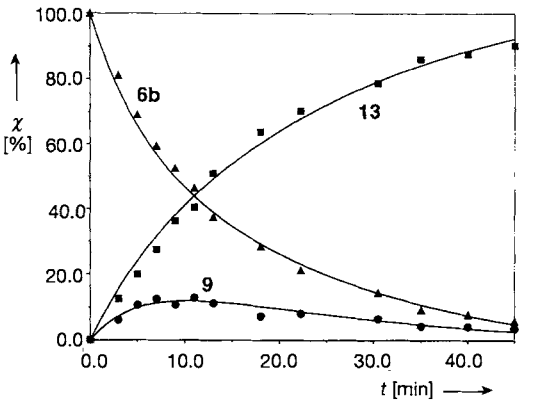

Fig. 2. Changes in the concentrations of **6b**, **9**, and **13** upon heating a solution of **6b** in toluene at 90 °C as a function of time. The fitting of the kinetic equations to the experimental data is shown.

Unambiguous structural proof of **13** was provided by a low-temperature X-ray analysis (Fig. 3).[5] The bond lengths and angles clearly show a *para*-quinodimethane bonding pattern. The inner bond angles of the four-membered rings in **13** are almost 90°, but in the six-membered ring the inner bond angles deviate significantly from 120°, with a value of 110.5° for the angle in fragment C(4A)-C(11)=C(3). The tricyclic ring system is almost planar (within 0.06 Å), and the crystal structure shows that **13** is the (*R,S*) or *meso* stereoisomer, in which the Br substituents adopt a *trans* orientation with respect to the planar ring system. The racemic mixture (*R,R*)- and (*S,S*)-**14**, in which the Br substituents adopt a *cis* orientation, eventually forms after prolonged heating of **13**, and gives ^{1}H and ^{13}C NMR spectra in which all resonances show only minor shifts compared to those in **13** (Table 1). Only after **13** is heated for several hours at 90 °C does decomposition take place, which is highly remarkable, since *para*-quinodimethanes are usually very reactive and stable only as transition metal complexes.[11,12] Compounds **13** and **14** possess the rare tricyclo[6.2.0.0^{3,6}]-deca-1,3,6,8-tetraene framework, of which only a few polyaryl-substituted derivatives have been reported so far.[13]

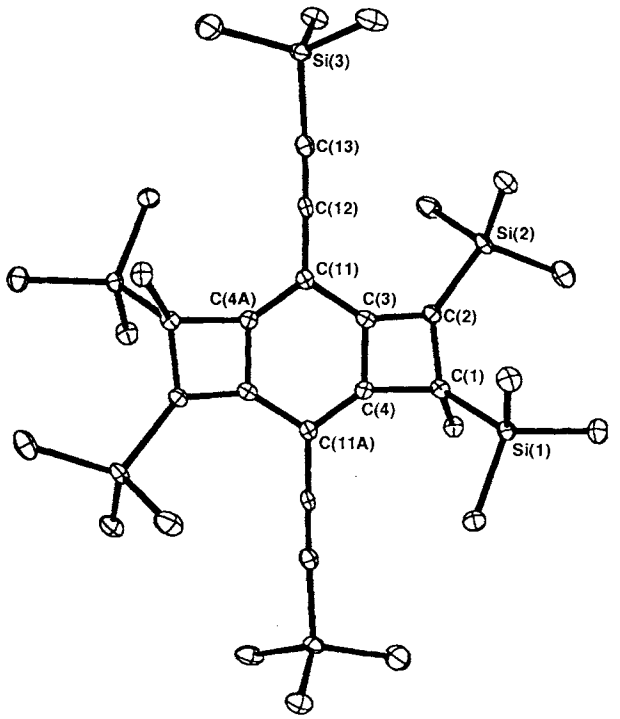

Fig. 3. X-ray crystal structure of **13**. Selected bond lengths [Å] and angles [°]: C(1)-C(2) 1.552(4), C(1)-C(4) 1.523(4), C(2)-C(3) 1.376(4), C(3)-C(4) 1.445(4), C(3)-C(11) 1.458(4), C(4)-C(11A) 1.366(4), C(11)-C(12) 1.425(4), C(12)-C(13) 1.212(4); C(1)-C(2)-C(3) 90.9(2), C(1)-C(4)-C(3) 89.5(2), C(2)-C(1)-C(4) 84.6(2), C(2)-C(3)-C(4) 94.4(2), C(2)-C(3)-C(11) 143.1(3), C(4)-C(3)-C(11) 122.3(3), C(1)-C(4)-(11A) 143.4(3), C(3)-C(11)-C(4A) 110.5(2), C(11)-C(12)-C(13) 178.0(3), Br(1)-C(1)-C(2) 114.2(2), Br(1)-C(1)-C(4) 111.8(2).

The reversible isomerization of **6b** to give **9** can be rationalized by assuming an orthogonal diradical intermediate **8**, which is formed from **6b** or **9** by a conrotatory opening of the cyclobutane ring,[7] in which one of the bulky TMS groups takes a sterically favorable inward position (Scheme 2). Diradical **8** presumably is also the intermediate in the dimerization of **7b** to give **6b**. In order to account for the selective formation of the *meso* stereoisomer **13** from **6b**, we propose a cascade pericyclic reaction mechanism. In the first step **6b** reacts in a $[2\pi_s + 2\pi_a]$ cycloaddition to provide the strained intermediate **11**. Alternatively, intermediate **11** can also be generated from **6b** by a 6π electrocyclic reaction to give the cyclic allene **10**,[14, 15] followed by a 4π conrotatory ring closure leading to **11**. In both pathways the stereochemistry at the newly formed stereocenters of **11** is controlled by the helical arrangement of the dienyne system in **6b** (vide supra), which in turn is induced by the stereocenter in the cyclobutane ring. The strained intermediate **11** opens by a $[2\pi_s + 2\pi_a]$ retrocycloaddition to give the chiral allene **12**, the configuration of which is determined by the fused ring system in **11**. Subsequent intramolecular $[2\pi_s + 2\pi_a]$ cycloaddition of the allene moiety in **12** with one of the C≡C bonds gives the *meso* form **13**. The epimerization of **13** to **14** most likely occurs through heterolytic rather than through homolytic C–Br bond cleavage, since a change of solvent from the less polar toluene to the more polar dimethylformamide accelerates the reaction significantly (roughly threefold).

Table 1. Yields and selected physical data of compounds **5**, **6b**, **9**, **13**, and **14**. ^{1}H and ^{13}C NMR spectra were recorded at 500 MHz and 125.6 MHz, respectively [a].

5: Yield 86%; yellow oil. IR (neat): $\tilde{\nu}$ = 2156 (C≡C), 1917 cm^{-1} (C=C=C); ^{13}C NMR ($CDCl_3$): δ = 216.9 (s, =C=), 97.9, 96.1 (2 × s, C=C), 96.8 (s, C=*C*Cl), 80.7 (s, *C*=C=CCl), 18.5, 18.3 (2 × q, CH_3), 11.5, 11.3 (2 × d, CH).

6b: Yield 70%. M.p. 125–126 °C; IR (KBr): $\tilde{\nu}$ = 2166 cm^{-1} (C≡C); ^{1}H NMR ([D$_8$]toluene): δ = 0.65, 0.57, 0.19, 0.18, 0.15, 0.13 (6 × s, 9H each); ^{13}C NMR ([D$_8$]toluene): δ = 157.1, 147.4 (2 × s, C=*C*-*C*=C), 130.4 (Br-*C*=C), 108.7 (s, (C≡C)$_2$*C*=C), 105.8, 104.4, 104.3, 103.5 (4 × s, Si-*C*≡C), 103.2, 102.2 (2 × s, (C≡*C*)$_2$C=C), 92.9, 91.8 (2 × s, (C≡*C*)$_2$*C*C$_2$), 62.5 (s, Br(TMS)*C*C$_2$), 50.5 (s, (C≡C)$_2$*C*C$_2$), 0.67, 0.38, 0.14, −0.19, −0.55, −0.57 (6 × q, CH_3).

9: ^{1}H NMR ([D$_8$]toluene): δ = 0.60, 0.24, 0.17 (3 × s, 18H each); ^{13}C NMR ([D$_8$]toluene): δ = 153.2 (s, C≡C-C=*C*), 107.6 (s, C≡C-*C*=C), 105.2, 105.2 (2 × s, Si-*C*≡C), 102.7, 101.6 (2 × s, Si-C≡*C*), 63.9 (s, CBr), 0.72, 0.40, −0.59 (3 × q, CH_3).

13: M.p. 219–220 °C (decomp); ^{1}H NMR ([D$_8$]toluene): δ = 0.50, 0.30, 0.29 (3 × s, 18H each); ^{13}C NMR ([D$_8$]toluene): δ = 159.3 (s, C≡C-C=*C*), 155.0 (s, Si-C=*C*), 152.3 (Si-*C*=C), 104.6 (s, Si-*C*≡C), 100.6 (s, C≡C-*C*=C), 99.2 (s, Si-C≡*C*), 62.2 (s, CBr), 0.78, −0.08, −1.36 (3 × q, CH_3); UV/VIS (hexane): λ_{max} [nm] = 399 sh (ε = 21400), 386 (27500), 373 sh (22400), 324 (6200), 264 (20500), 231 (32900).

14: ^{1}H NMR ([D$_8$]toluene): δ = 0.39, 0.26, 0.22 (3 × s, 18H each); ^{13}C NMR ([D$_8$]toluene): δ = 158.4 (s, C≡C-C=*C*), 155.5 (s, Si-C=*C*), 152.3 (Si-*C*=C), 104.3 (s, Si-*C*≡C), 100.2 (s, C≡C-*C*=C), 99.1 (s, Si-C≡*C*), 61.0 (s, CBr), 0.53, −0.07, −1.58 (3 × q, CH_3).

[a] All new compounds, except **9** and **14**, which were not isolated, were fully characterized by ^{1}H and ^{13}C NMR, IR, and UV spectroscopy, and high-resolution mass spectrometry or elemental analysis.

Received: July 27, 1993 [Z 6239 IE]
German version: *Angew. Chem.* **1993**, *105*, 1817

[1] F. Diederich, Y. Rubin, *Angew. Chem.* **1992**, *104*, 1123–1146; *Angew. Chem. Int. Ed. Engl.* **1992**, *31*, 1101–1123.

[2] J.-D. van Loon, P. Seiler, F. Diederich, *Angew. Chem.* **1993**, *105*, 1235–1238; *Angew. Chem. Int. Ed. Engl.* **1993**, *32*, 1187–1189.

[3] A. H. Alberts, H. Wynberg, *J. Chem. Soc. Chem. Commun.* **1988**, 748–749.

[4] S. R. Landor, A. N. Patel, P. F. Whiter, P. M. Greaves, *J. Chem. Soc. (C)* **1966**, 1223–1226.

[5] Single crystals of **6b** ($C_{32}H_{54}Si_6Br_2$, M_r = 767.10) were first grown from methanol at 293 K. The scattering behavior of these crystals was very poor. Moreover, a phase transition occurred around 265 K, and cooling the compound below 260 K produced twinned crystals with a large mosaic spread; at very low temperature the crystals were transformed into a powder. Thus, a first data set was measured at 295 K using $Cu_{K\alpha}$ radiation and a nearly spherical crystal specimen with a diameter of ca. 0.6 mm. The structure could be solved by the Patterson method and refined by least-squares analysis to $R(F)$ = 0.08 (details are not given here). Owing to static and dynamic disorder of the TMS groups, the derived atomic parameters are very inaccurate. To avoid the phase transition and the disorder problem, a crystal specimen of good optical quality (size ca. 0.25 × 0.20 × 0.25 mm) was grown from methanol just below the transition temperature, mounted on the diffractometer without rewarming, and cooled slowly to 85 K. A second data set was then measured with $Mo_{K\alpha}$ radiation out to H = 1.19 Å^{-1} (7735 unique reflections, 4389 reflections with $I_o > 3\,\sigma(I_o)$). Crystal data: monoclinic space group $P2_1/c$ (No. 14), ϱ_{calcd} = 1.20 g cm^{-3}, Z = 4; a = 11.3870(10), b = 18.847(2), c = 22.468(4) Å, β = 118.27(2)°, V = 4247(1) Å^3. The structure was solved by the Patterson method (SHELXS86) and refined by full-matrix least-squares analysis (SHELXL 92), using a isotropic extinction correction and experimental weights. Final $R(F)$ = 0.024, $wR(F^2)$ = 0.061 for 416 variables and 4389 observed reflections (heavy atoms anisotropic, H atoms isotropic; H positions are based on stereochemical considerations, C–H = 0.96 Å, H-C-H = 109.5°). The results discussed in this paper are based only on this low-temperature analysis. – Single crystals of **13** ($C_{32}H_{54}Si_6Br_2$, M_r = 767.10) were grown from toluene at 293 K. A crystal specimen with linear dimensions of ca. 0.3 × 0.3 × 0.3 mm was cooled very slowly (ca. 3 K h^{-1}) to 85 K, in order to keep the mosaic spread as small as possible. A data set was measured with $Mo_{K\alpha}$ radiation out to H = 1.1 Å^{-1} (2803 unique reflections, 2203 reflections with $I_o > 3\,\sigma(I_o)$). Crystal data: monoclinic space group $P2_1/c$ (No. 14), ϱ_{calcd} = 1.26 g cm^{-3}, Z = 2; a = 12.868(3), b = 12.519(3), c = 12.905(3) Å, β = 103.15(3)°, V = 2024(1) Å^3. The structure was solved by the Patterson method and refined by full-matrix least-squares analysis (SHELXTL PLUS), using an isotropic extinction correction and a modified weight factor r = 5 Å^2 (J. D. Dunitz, P. Seiler, *Acta Crystallogr. Sect. B.* **1973**, *29*, 589–595). Final $R(F)$ = 0.027, $wR(F)$ = 0.032 for 210 variables and 2203 observed reflections (heavy atoms anisotropic, H atoms isotropic; H positions are based on stereochemical considerations, C–H = 0.96 Å, H-C-H = 109.5°). Further details of the crystal structure investigations are available on request from the Director of the Cambridge Crystallographic Data Centre, 12 Union Road, GB-Cambridge CB2 1EZ (UK), on quoting the full journal citation.

[6] In a seven-membered-ring allene dimer, an even longer C–C bond of 1.652(5) Å was observed in the cyclobutane ring: H. Jelinek-Fink, M.

Christl, E.-M. Peters, K. Peters, H. G. von Schnering, *Chem. Ber.* **1991**, *124*, 2569–2575.
[7] H. Hopf in: *The Chemistry of the Allenes*, (Ed.: S. R. Landor), Academic Press, New York, **1982**, p. 539.
[8] A. J. Brattesani, E. Maverick, O. J. Muscio, Jr., T. L. Jacobs, *J. Org. Chem.* **1992**, *57*, 7346–7349.
[9] K. G. Migliorese, S. I. Miller, *Tetrahedron*, **1974**, *30*, 385–392. These authors reported on the stereospecific thermal isomerization of a tetraethynyldimethylenecyclobutane similar to **6a**. In light of our results, however, it is likely that as a product they had isolated a *para*-quinodimethane similar to **13** rather than the reported isomerized cyclobutane.
[10] The kinetic experiment was performed by addition of a solution of **6b** (100 mg) in [D_8]toluene (0.5 ml) to 20 mL of [D_8]toluene, that was thermostated at 90.0 ± 0.1 °C. Aliquots (0.5 mL) taken at this temperature were rapidly cooled and measured by ^{1}H NMR spectroscopy. The rate equations for the curve fitting were obtained by considering the equilibrium **9** ⇌ **6b** ⇌ **13**, with the corresponding (first-order) kinetic matrix which

$$\begin{pmatrix} k_{(9\to 6b)} & -k_{(6b\to 9)} & 0 \\ -k_{(9\to 6b)} & k_{(6b\to 9)}+k_{(6b\to 13)} & -k_{(13\to 6b)} \\ 0 & -k_{(6b\to 13)} & k_{(13\to 6b)} \end{pmatrix}$$

was solved by the program "Maple". We thank Ms. Tiziana Mordasini and Prof. Alfred Bauder, ETH Zürich, for their contributions.
[11] a) A. R. Koray, C. Krieger, H. A. Staab, *Angew. Chem.* **1985**, *97*, 513–514; *Angew. Chem. Int. Ed. Engl.* **1985**, *24*, 521–522; b) D. T. Glatzhofer, Y. Liang, M. A. Khan, *Organometallics* **1993**, *12*, 624–632.
[12] M. Toda, M. Hattori, K. Okada, M. Oda, *Chem. Lett.* **1987**, 1263–1266.
[13] a) F. Toda, K. Tanaka, T. Yoshioka, *Chem. Lett.* **1976**, 657–658; b) Y. Takehira, K. Tanaka, F. Toda, *ibid.* **1976**, 1323–1324.
[14] 1,2,4-Cyclohexatrienes: a) M. Christl, M. Braun, G. Müller, *Angew. Chem.* **1992**, *104*, 471–473; *Angew. Chem. Int. Ed. Engl.* **1992**, *31*, 473–476; b) R. Janoschek, *ibid.* **1992**, *104*, 473–475 and **1992**, *31*, 476–478.
[15] *cis*-1,3-Hexadien-5-yne forms benzene via 1,2,4-cyclohexatriene at 274 °C with a half-life >90 min (H. Hopf, H. Musso, *Angew. Chem.* **1969**, *81*, 704; *Angew. Chem. Int. Ed. Engl.* **1969**, *8*, 680; we thank one reviewer for pointing out this reference to us.). The conversion **6b** → **10** occurs at a faster rate already at 90 °C since the reacting *cis*-1,3-hexadien-5-yne system in **6b** is perfectly preorganized for 6π electrocyclic ring closure.

Organometallic Ferrocenyl Polymers Displaying Tunable Cooperative Interactions between Transition Metal Centers**

By *Daniel A. Foucher, Charles H. Honeyman, James M. Nelson, Ben Zhong Tang,* and *Ian Manners**

Molecular or macromolecular materials which contain atoms of transition elements in close proximity are attracting increasing attention because of their potentially interesting electrical, redox, optical, and magnetic characteristics.[1] Organometallic polymers such as poly(vinylferrocene), which possess electroactive ferrocenyl side groups that are separated from one another by insulating organic units have been well studied. In such materials the ferrocenyl moieties are essentially noninteracting and a single oxidation wave is detected by cyclic voltammetry.[2] We have previously reported that the ring-opening polymerization of strained, ring-tilted [1]metallocenophanes provides a route to high molecular weight polymers **1**–**3** which possess backbones containing ferrocene groups alternating with either silicon, germanium, or phosphorus atoms.[3–5] We have also described an extension of this synthetic approach to the polymerization of [2]ferrocenophanes with a hydrocarbon bridge, which provided access to poly(ferrocenylethylene)s (**4**).[6] In this paper we present details of our comparative electrochemical studies of **1**–**4**, which show that they exhibit redox behavior which is markedly different from that of poly(vinylferrocene) and related polymers. Thus, we provide

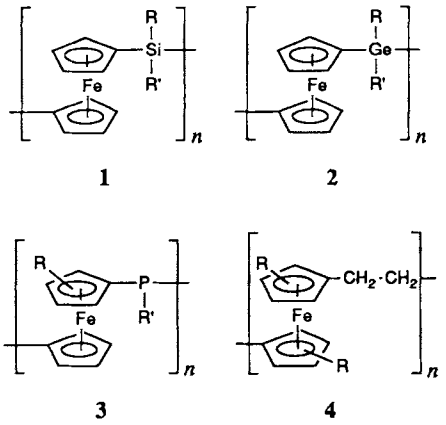

evidence that in these materials the ferrocenyl units interact with one another and, moreover, that the extent of interaction is tunable, since it is dependent on the nature of the side groups and the bridge linking the adjacent ferrocenyl centers.

The poly(ferrocenylsilane)s **1** (R = R′ = Me, Et, *n*Bu, or *n*-hexyl) yield cyclic voltammograms in CH_2Cl_2 that show two reversible oxidation waves (Table 1).[7] Representative examples for polymer **1** (R = R′ = Me) at different scan rates are shown in Figure 1. The qualitative features of the cyclic voltammograms can be understood in the light of the extensive studies on low molecular weight compounds containing two or more ferrocenyl units linked together by a bridging group.[8] For example, biferrocene **5** ($x = 0$), in which the ferrocene units are in close proximity, shows two reversible oxidation waves at $E_{1/2} = 0.31$ V and $E_{1/2} = 0.64$ V as oxidation of the first ferrocenyl moiety makes subsequent removal of an electron from the other more difficult. The difference in these redox potentials ($\Delta E = 0.33$ V for biferrocene) is indicative of the extent of the interaction between the ferrocenyl units. Thus, as would be expected, the

Table 1. Electrochemical data for selected organometallic polymers **1**–**4** and **7**.

	R	R′	M_w [a]	M_n [a]	$^1E_{1/2}$ [b] [mV]	$^2E_{1/2}$ [b] [mV]	ΔE
1	Me	Me	5.2×10^5	3.4×10^5	−0.04	0.17	0.21
1	Et	Et	7.4×10^5	4.8×10^5	−0.04	0.23	0.27
1	*n*Bu	*n*Bu	8.9×10^5	3.4×10^5	0.00	0.29	0.29
1	*n*Hex	*n*Hex	1.2×10^5	7.6×10^4	0.02	0.31	0.29
2	Me	Me	2.3×10^5	5.2×10^4	−0.01	0.19	0.20
3	*n*Bu	Ph	[c]	[c]	−0.04	0.15	0.19
7	*n*Bu	*n*Bu	1.5×10^4	3.0×10^3	−0.06	0.18	0.24
4	Me	–	8.1×10^4	6.6×10^4	−0.27	–	ca 0.06

[a] Molecular weights were determined by gel permeation chromatography (GPC) in THF containing 0.1% by weight of [NBu_4]Br using polystyrene standards. [b] $^1E_{1/2}$ and $^2E_{1/2}$ refer to the half-wave potentials for the first and second oxidation waves, respectively, and are relative to the ferrocene/ferrocenenium ion couple at 0.00 V, which was used as an internal reference. All potentials quoted refer to measurements at 250 mVs^{-1}. [c] The molecular weight was not determined because of adsorption to the GPC column.

[*] Prof. I. Manners, D. A. Foucher, C. H. Honeyman, J. M. Nelson, B. Z. Tang
Department of Chemistry, University of Toronto
80 St. George Street, Toronto, Ontario M5S 1A1 (Canada)

[**] This work was supported by the Natural Science and Engineering Research Council of Canada (NSERC). We thank Prof. R. H. Morris and Dr. T. Burrow for use of the electrochemical equipment and Prof. W. E. Geiger (University of Vermont) for helpful discussions concerning aspects of the work.

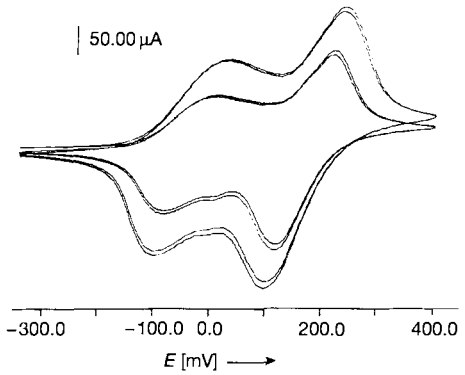

Fig. 1. Cyclic voltammogram of **1** (R = R′ = Me) in CH_2Cl_2 at scan rates of 500 and 1000 mVs^{-1}.

presence of an insulating CH_2 unit between the ferrocene groups as in diferrocenylmethane **5** (E = C, R = R′ = H, $x = 1$) leads to a decrease in ΔE to 0.1 V. Moreover, for species **5** (E = C, R = R′ = H, $x > 1$) with more than one CH_2 unit between the ferrocenyl groups, only one oxidation wave is detected ($\Delta E \approx 0$ V). Ferrocene oligomers without spacer groups such as terferrocene **6** ($x = 1$) and quaterferrocene **6** ($x = 2$) display cyclic voltammograms with a one-electron oxidation wave for each ferrocenyl unit present ($\Delta E \approx 0.2$ V).[9] These observations suggest that the first oxidations of poly(ferrocenylsilane)s occur randomly along the polymer chain at nonadjacent ferrocene sites. Subsequent oxidations would remove electrons from ferrocene groups that are adjacent to those already oxidized and would therefore be expected to occur at more positive potentials.[10] The difference (ΔE) in the oxidation potentials detected varies from 0.21 V (for **1**, R = R′ = Me) to 0.29 V (for **1**, R = R′ = *n*Bu or *n*-hexyl). For comparison, the value of ΔE for bis(ferrocenyl)dimethylsilane **5** (E = Si, R = R′ = Me, $x = 1$) is 0.145 V.[11] The results indicate that the extent of the interaction between the ferrocenyl units in poly(ferrocenylsilane)s depends significantly on the nature of the substituents at silicon. This may be caused by, for example, changes in the electronic structure of the bridge due to increased inductive effects as the length of the alkyl chain increases from Me to *n*Bu, or conformational effects which promote closer proximity of the metal centers in the case of the bulkier substituents.

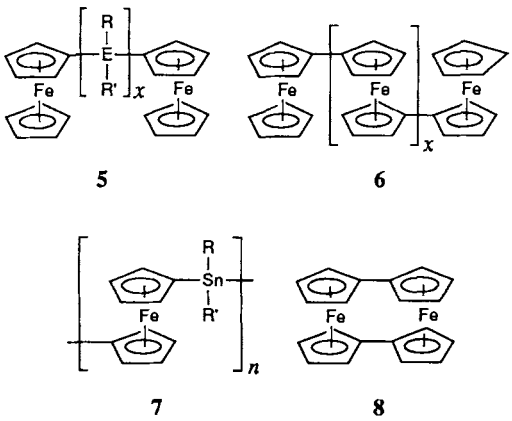

To determine whether similar interactions would be present with other elements instead of silicon, the electrochemical behavior of a selected poly(ferrocenylgermane) (**2**, R = R′ = Me) and a selected poly(ferrocenylphosphane) (**3**, R = *n*Bu, R′ = Ph) was investigated. These polymers indeed showed similar electrochemical behavior to the poly(ferrocenylsilane)s **1**. For example, the cyclic voltammograms of **2** and **3** showed two reversible oxidation waves separated by 0.20 V and 0.19 V, respectively. The comparable values for the selected germanium-containing polymer and the analogous poly(ferrocenylsilane) (**1**, R = R′ = Me) indicate that the ferrocenyl groups interact to a similar extent. In order to investigate the effect of a tin bridge on the interactions, the low molecular weight poly(ferrocenylstannane) **7** (R = R′ = *n*Bu) was synthesized by the previously reported condensation route.[12] This material gave a cyclic voltammogram with two waves separated by 0.24 V, which is slightly less than for the silicon analogue **1** (R = R′ = *n*Bu) as might be expected from the larger size of the tin atom which would lead to a larger distance between the iron centers.

In contrast to the situation for organometallic polymers derived from the ring-opening polymerization of [1]ferrocenophanes, poly(ferrocenylethylene)s (**4**), prepared from [2]ferrocenophanes containing a hydrocarbon bridge, show electrochemical behavior indicative of minor interactions between the iron centers. Representative cyclic voltammograms for **4** (R = Me) show essentially one oxidation wave, which has an only partially resolved shoulder (Fig. 2, $\Delta E \approx 0.06$ V); this implies that only very weak interactions between the metallocene units are present. The behavior is in stark contrast to that recently reported for poly(ferrocenylene persulfide)s in which the ferrocene groups are linked by two sulfur atoms, for which a ΔE value of 0.32 V has been reported. This indicates that a disulfide bridge promotes much greater interactions between the ferrocene groups.[10]

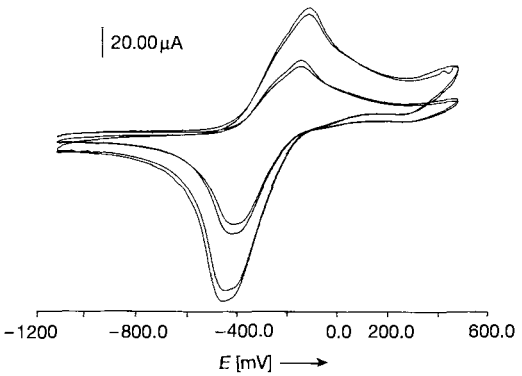

Fig. 2. Cyclic voltammogram of **4** (R = Me) in CH_2Cl_2 at scan rates of 500 and 1000 mVs^{-1}.

Further work will be directed towards obtaining a detailed understanding of the relationship between the structure of the polymer main chain and the type of side group, and the nature and extent of the interactions between the ferrocenyl groups. With this in mind, it is worth noting that in biferrocenylene **8**, which shows two reversible oxidation waves by cyclic voltammetry with $\Delta E = 0.63$ V, the extent of interaction between the ferrocene groups is so large that one-electron oxidation yields a radical cation with completely delocalized charge.[13] Clearly, an understanding of how the interactions between the ferrocenyl groups in organometallic polymers such as **1**–**3** can be maximized might allow the preparation of materials with appreciable electron mobility and therefore novel electrical and optical properties.

Received: June 28, 1993 [Z 6178 IE]
German version: *Angew. Chem.* **1993**, *105*, 1843

[1] Examples: a) P. Bergerat, J. Blumel, M. Fritz, J. Hiermeier, P. Hudeczek, O. Kahn, F. H. Köhler, *Angew. Chem.* **1992**, *104*, 1285; *Angew. Chem. Int. Ed. Engl.* **1992**, *31*, 1258; b) M. Peuckert, T. Vaahs, M. Bruck, *Adv. Mater.* **1990**, *2*, 398; c) H. W. Roesky, M. Lucke, *Angew. Chem.* **1989**, *101*, 480; *Angew. Chem. Int. Ed. Engl.* **1989**, *28*, 493; d) S. J. Davies, B. F. G. Johnson, M. S. Khan, J. Lewis, *J. Chem. Soc. Chem. Commun.* **1991**, 187; e) H. B. Fyfe, M. Mlekuz, D. Zargarian, N. J. Taylor, T. B. Marder, *ibid.* **1991**, 188; f) P. F. Brandt, T. B. Rauchfuss, *J. Am. Chem. Soc.* **1992**, *114*, 1926; g) H. R. Allcock, J. A. Dodge, I. Manners, G. H. Riding, *ibid.* **1991**, *113*, 9596; h) M. E. Wright, M. S. Sigman, *Macromolecules* **1992**, *25*, 6055; i) A. A. Dembek, P. J. Fagan, M. Marsi, *ibid.* **1993**, *26*, 2992.

[2] a) J. B. Flanagan, S. Margel, A. J. Bard, F. C. Anson, *J. Am. Chem. Soc.* **1978**, *100*, 4248; b) T. W. Smith, J. E. Kuder, D. Wychick, *J. Polym. Sci. Part A Polym. Chem.* **1976**, *14*, 2433.

[3] D. A. Foucher, B. Z. Tang, I. Manners, *J. Am. Chem. Soc.* **1992**, *114*, 6246.

[4] a) D. A. Foucher, R. Ziembinski, B. Z. Tang, P. M. Macdonald, J. Massey, R. Jaeger, G. J. Vancso, I. Manners, *Macromolecules* **1993**, *26*, 2878; b) W. Finckh, B. Z. Tang, D. A. Foucher, D. B. Zamble, A. Lough, I. Manners, *Organometallics* **1993**, *12*, 823; c) B. Z. Tang, R. Petersen, D. A. Foucher, A. Lough, N. Coombs, R. Sodhi, I. Manners, *J. Chem. Soc. Chem. Commun.* **1993**, 523; d) R. Ziembinski, C. Honeyman, O. Mourad, D. A. Foucher, R. Rulkens, M. Liang, Y. Ni, I. Manners, *Phosphorus Sulfur Silicon Rel. Elem.* **1993**, *76*, 219; e) C. Honeyman, D. A. Foucher, O. Mourad, R. Rulkens, I. Manners, *Polymer Prepr. (Am. Chem. Soc. Div. Polym. Chem.)* **1993**, *34(1)*, 330; f) D. A. Foucher, I. Manners, *Makromol. Chem. Rapid Commun.* **1993**, *14*, 63.

[5] Seyferth et al. have previously reported the synthesis of the poly(ferrocenylphosphane) **3**, (R = H, R' = Ph) by a condensation route: H. P. Withers, D. Seyferth, J. D. Fellmann, P. Garrou, S. Martin, *Organometallics* **1982**, *1*, 1283.

[6] J. M. Nelson, H. Rengel, I. Manners, *J. Am. Chem. Soc.* **1993**, *115*, 7035.

[7] Electrochemical experiments were carried out on a PAR model 273 potentiostat with a Pt working electrode, a W secondary electrode, and an Ag wire reference electrode in a Luggin capillary. The concentration of the polymer was 5×10^{-4} M in CH_2Cl_2; 0.1 M $[Bu_4N][PF_6]$ served as a supporting electrolyte. Peak currents were proportional to the square root of the scan rate over the range studied (25 mVs^{-1} to 1000 mVs^{-1}), which indicates that charge transfer is similar to a semi-infinite linear diffusion process. We attribute the slight difference in wave shapes to slight adsorption of the fully oxidized polymer to the electrode.

[8] a) U. T. Müller-Westerhoff, *Angew. Chem.* **1986**, *98*, 700; *Angew. Chem. Int. Ed. Engl.* **1986**, *25*, 702; b) T. Y. Dong, M. Y. Hwang, Y. Wen, W. S. Hwang, *J. Organomet. Chem.* **1990**, *391*, 377, and references therein; c) V. V. Dement'ev, F. Cervantes-Lee, L. Parkanyi, H. Sharma, K. H. Pannell, M. T. K. Nguyen, A. F. Diaz, *Organometallics* **1993**, *12*, 1983.

[9] G. M. Brown, T. J. Meyer, D. O. Cowan, C. Levanda, F. Kaufman, P. V. Roling, M. D. Rausch, *Inorg. Chem.* **1975**, *14*, 506.

[10] The presence of two oxidation waves for poly(ferrocenylene persulfide)s was attributed to oxidation at alternate iron atoms (ref. [1f], which is similar to our explanation.

[11] A. B. Bocarsly, E. G. Walton, M. G. Bradley, M. S. Wrighton, *J. Electroanal. Chem. Interfacial Electrochem.* **1979**, *100*, 283.

[12] D. Seyferth, H. P. Withers, *Organometallics* **1982**, *1*, 1275.

[13] For an excellent discussion of properties and redox chemistry of compounds of general structure **8**, see ref. [8a], S. 706–708.

Phenothiazine–Bipyridinium Oligooxacyclophanes**

By *Christoph Petry, Martina Lang, Heinz A. Staab,* and *Helmut Bauer**

Intermolecular electron donor–acceptor interactions of phenothiazine with acceptors, for example 1,3,5-trinitrobenzene,[1] tetracyanoquinodimethane,[2] tetracyanobenzene,[3] tetracyanoethylene,[3] quinones,[3] pyromellitic dianhydride,[4] and 1,1'-dimethyl-4,4'bipyridinium dication (methylviologen),[5] have been known for some time. However, compounds in which a phenothiazine and a dicationic bipyridinium unit are covalently linked by an oligomethylene chain have been studied only in the last few years.[6–8] These investigations focused on complexation with cyclodextrins and the electron transfer between the phenothiazine and the bipyridinium components.

We report here on the first doubly bridged phenothiazine–bipyridinium diiodide systems **1**–**5** having an oligooxacyclophane structure and on the remarkable finding that the donor and acceptor groups in the 38-membered macrocycle **2** may approach each other in solvents like dichloromethane and acetonitrile. Oligoethyleneglycol fragments of various lengths were used as bridges in the cyclophanes. Since the compounds with a large cavity should be able to coordinate metal ions, a metal ion induced approach of the donor and acceptor should be possible.

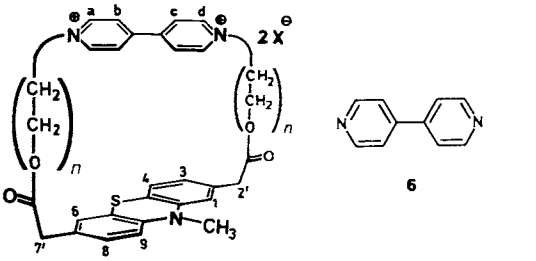

1–5 : n = 2–6 , X = I

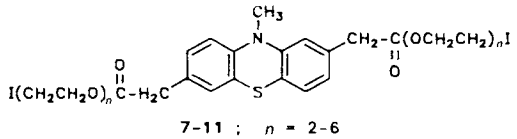

7–11 ; n = 2–6

Double alkylation of 4,4'-bipyridine (**6**) with the appropriate 2,7-bis(ω-iodo-oligooxaalkylcarbonylmethyl)-10-methylphenothiazines **7**–**11** in refluxing nitromethane (3–7 days) employing the dilution principle provided the oligooxa[3n + 2]cyclophanes **1**–**5** in yields of 8, 12, 20, 13, and 9%, respectively. Tetraoxa[8.8]cyclophane **1** was recrystallized from water to give small black plates (m.p. 262 °C, decomp), hexaoxa[11.11]cyclophane **2** forms fine black needles (m.p. 138–139 °C), and octaoxa[14.14]cyclophane **3** was recrystallized from methanol to furnish deep red plates (gradual softening starting at 75 °C). Decaoxa[17.17]- and dodecaoxa[20.20]cyclophanes **4** and **5** were purified by chromatography on P2-Gel (BIO-RAD) eluting with an aqueous buffer of 0.11 M acetic acid and 0.1 M triethylamine. After ion exchange on DOWEX 1 × 8 (iodide form), **4** and **5** were obtained as red-brown amorphous powders (softening starting at 70 and 60 °C, respectively). Each cyclophane takes up about two equivalents of triethylammonium iodide.

The syntheses of the phenothiazine cyclization components **7**–**11** all start with the known 2,7-diacetyl-10-methylphenothazine (**15**),[9] which is prepared from 2-acetyl-10-methylphenothiazine (**14**) by Friedel–Crafts acylation (Scheme 1). **Caution:** We recommend that compound **14** not be prepared as described by N-methylation of commercially available 2-acetylphenothiazine (**12**) with methyliodide in a sealed tube.[10] During one of the many reactions of this type that we carried out, tremendous pressure built up in the glass vessel leading to an **explosion**. The roundabout synthesis via ketal **13** followed by methylation at −20 °C is safer.

[*] Prof. Dr. H. Bauer, Dr. C. Petry, M. Lang, Prof. Dr. H. A. Staab
Max-Planck-Institut für medizinische Forschung
Abteilung Organische Chemie
Jahnstrasse 29, I-69120 Heidelberg (FRG)

[**] Electron Donor–Acceptor Compounds, Part 49. Part 48: H. A. Staab, A. Döhling, C. Krieger, *Tetrahedron Lett.* **1991**, *32*, 2215–2218.

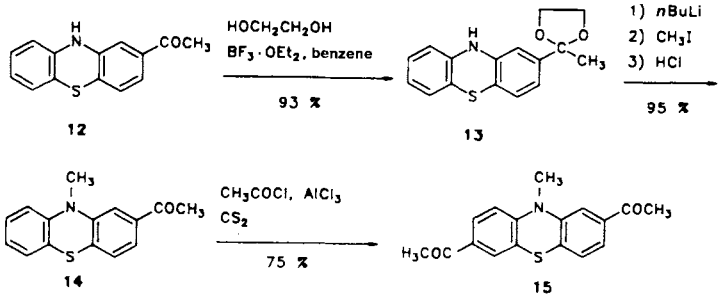

Scheme 1. Synthesis of 2,7-diacetyl-10-methylphenothiazine.

Linkage of phenothiazine with 4,4'-bipyridine by $(CH_2OCH_2)_n$ bridges could not be realized, since bis-(2,7-alkoxymethyl)-10-methylphenothiazine could not be prepared as a model compound and the ether groups of bis(2,7-methoxyethyl)-10-methylphenothiazine are cleaved even in water to give the diol. Thus, the oligooxa bridges were connected with the phenothiazine framework through ester functions. For this purpose, **15** was converted into dicarboxylic acid **16** by a Willgerodt–Kindler reaction, and the phenothiazine cyclization components **7**–**11** were subsequently obtained by two routes (Scheme 2). The first route proceeds via dimethylester **17** by transesterification with monochlorooligoethyleneglycols, the second route by esterification of **16** with monoiodo- or mono-*p*-toluenesulfonyloligoethyleneglycols employing the azolide 1,1-carbonylbis(methylimidazolium)trifluoromethanesulfonate[11] as condensation agent. Dichlorides **18**–**20** and ditoluenesulfonates **21** and **22** were readily converted into the more reactive diiodides **7**, **8**, **23**, and **10**, **11**, respectively, by reaction with sodium iodide. Diiodide **23** and bipyridine did not undergo cyclization.

In water and in acetonitrile cyclophanes **1**–**5** show only a weak, broad charge transfer (CT) absorption, but in dichloromethane this band is quite distinct: $\lambda_{CT}(\varepsilon)$ of **2** in CH_2Cl_2: 485 nm (1200), **3**: 477 nm (1000), **4**: 457 nm (920), and **5**: 475 nm (1050). A UV/VIS spectrum of [8.8]cyclophane **1** in dichloromethane could not be measured because of poor solubility. The CT absorptions can be attributed primarily to the CT interaction between the iodide ions and the bipyridinium components of the cyclophanes, since the red compound 1,1'-didodecyl-4,4'-bipyridinium diiodide[12] has a similar VIS spectrum ($\lambda_{CT}(\varepsilon)$ in CH_2Cl_2: 506 nm (1276)).

Fluorescence measurements of solutions of cyclophanes **1**–**5** in dichoromethane and acetonitrile show 95% quenching of the phenothiazine fluorescence relative to the reference compounds **17** and **11**.

The reaction of [20.20]cyclophane **5** with barium diiodide in acetone furnished the barium complex **24** as a red-brown powder in 22% yield. In analogy to previous findings[13] for cation complexes of donor–acceptor oligooxacyclophanes, the barium ion may be coordinated as shown in structure **24**.

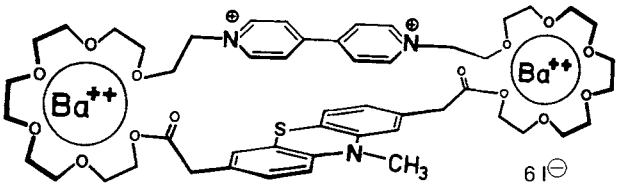

24

The red-shift of the IR band for the ester by approximately 30 cm^{-1} relative to that of [20.20]cyclophane **5** indicates that this group is also coordinated to Ba^{2+}.

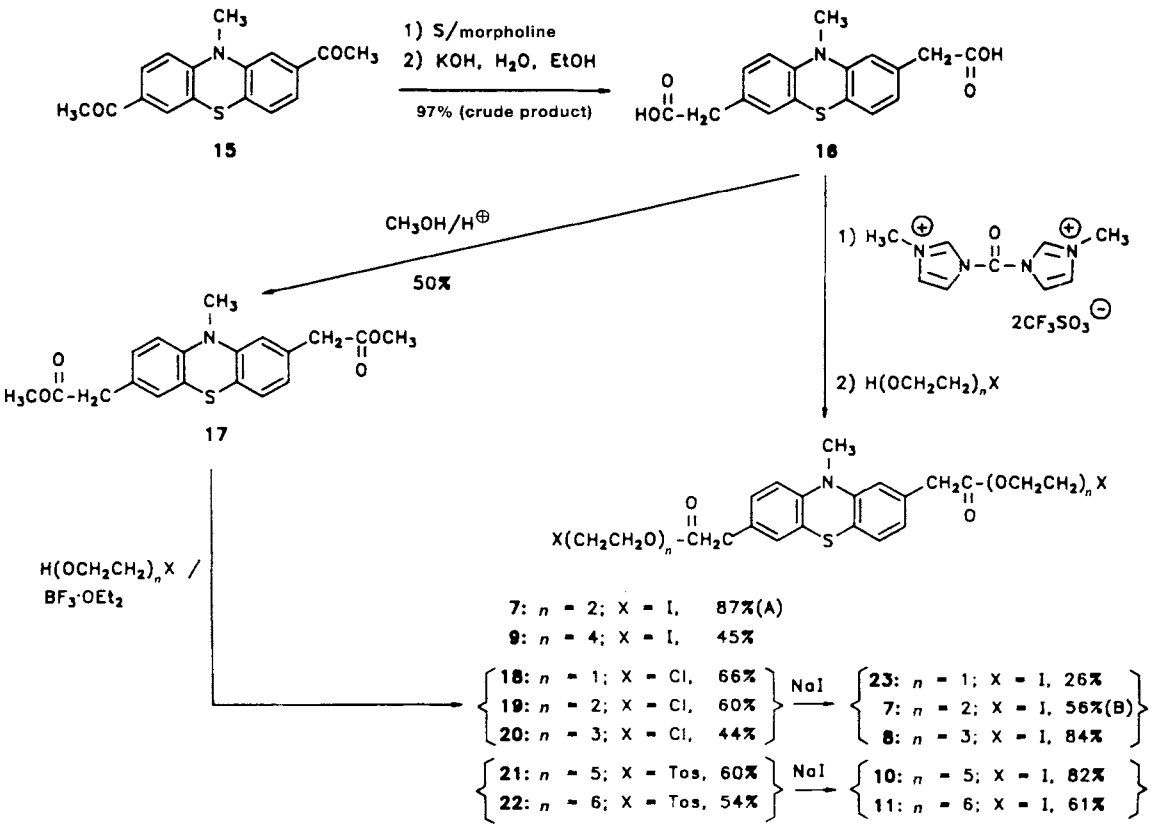

Scheme 2. Preparation of the phenothiazine cyclization components.

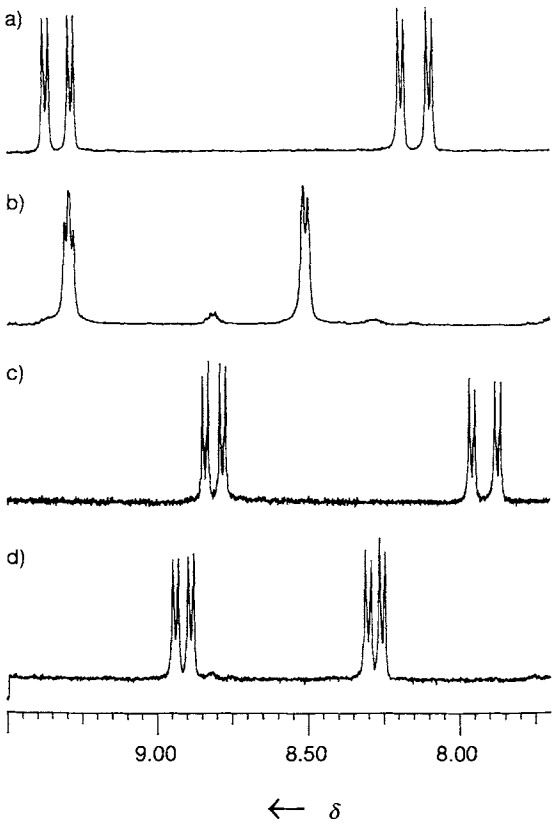

Fig. 1. Sections of the ^{1}H NMR spectra of a) **2** in CD_2Cl_2, b) **5** in CD_2Cl_2, c) **2** in CD_3CN, and d) **24** in CD_3CN.

In the ^{1}H NMR spectra of **2** and **5** in CD_2Cl_2 the signal patterns for the bipyridinium hydrogen atoms differ significantly (Fig. 1). In the spectrum of **2** the signals of both the inner and the outer hydrogen atoms of the bipyridinium unit are clearly resolved as two sets of doublets at $\delta = 9.39/9.37$, 9.29/9.27 and 8.18/8.16, 8.07/8.05, as would be expected owing to the proximity of the unsymmetric phenothiazine unit. In contrast, in the spectrum of the larger macrocycle **5** practically only the signals of the unperturbed bipyridinium unit are evident. The signal resolution observed for the Ba_2 complex **24** is similar to that for **2** (Fig. 1), which indicates that complexation brings the bipyridinium and phenothiazine units closer together.

The approach of the donor and acceptor units of cyclophane **2** in dichloromethane is proven unequivocally by rotating frame nuclear Overhauser effect (ROE) experiments (Fig. 2). Upon irradiation of the signals for the b and c hydrogen atoms of the bipyridinium component, not only the signals of the a/c and b/d hydrogen atoms are enhanced as expected, but also the signals of all the protons of the phenothiazine component including the N-CH_3 group, the benzylic CH_2 groups, and the CO_2CH_3 groups. This indicates that the donor and acceptor units of cyclophane **2** in dichloromethane are separated by only 3.5–4 Å for at least several hundred ms. Irradiation of the signals of the a/d hydrogen atoms also results in transannular nuclear Overhauser effects (NOEs). The NOEs in acetonitrile are analogous to those in dichloromethane but are weaker in dimethyl sulfoxide. NMR spectra measured in dichloromethane at low temperatures indicate that the donor and acceptor approach each other even closer: at $-90\,^\circ$C the a/d and b/c doublets are shifted further apart (from $\Delta\delta = 0.1$ to $\Delta\delta = 0.25$); moreover, the signals of the doublets of the inner bipyridinium hydrogen atoms at $\delta = 8.17$ and 8.07 are shifted upfield by $\Delta\delta = 0.34$ and $\Delta\delta = 0.22$, respectively, as a result of the transannular anisotropy of the neighboring aromatic ring.

In CD_2Cl_2 [17.17]cyclophane **4** also shows transannular NOEs, though weak, between the b/c hydrogen atoms and the signals of H(1), H(9), H(3), H(4), and H(6) of the phenothiazine.

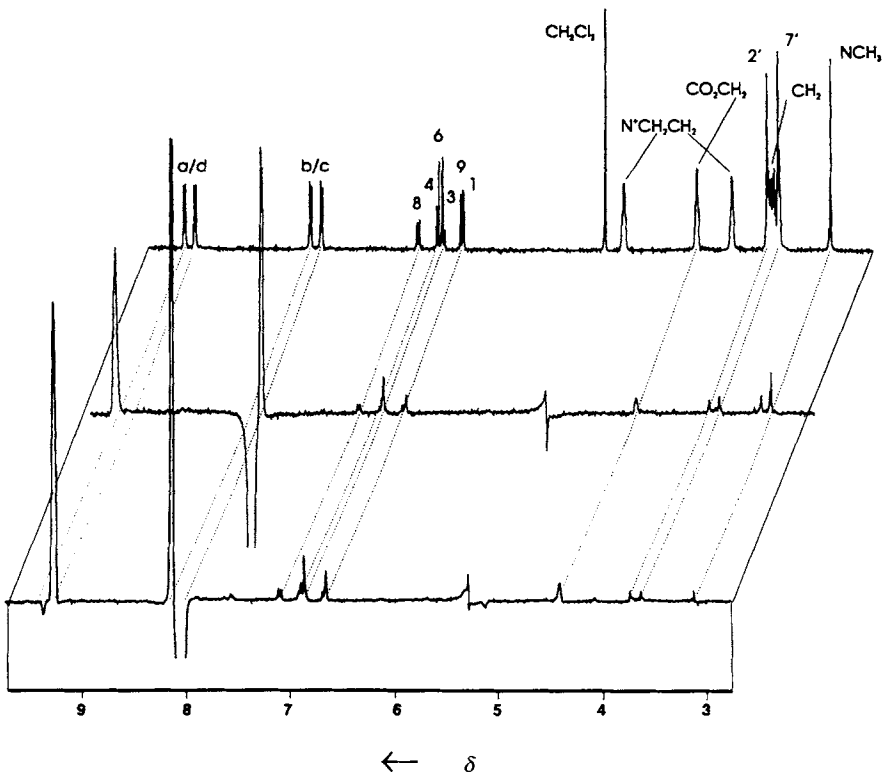

Fig. 2. ^{1}H NMR spectrum and ROE difference spectra of [11.11]cyclophane **2** in CD_2Cl_2, irradiation of signals b and c, 303 K, 360 MHz.

Table 1. Physical data of compounds **1**–**5**, 1,1′-didodecyl-4,4′-bipyridinium diiodide, and **24**.

1: ^{1}H NMR ([D$_6$]DMSO): δ = 3.11 (s, 3H, NCH_3), 3.55 (s, 2H, 7′-CH_2), 3.63 (s, 2H, 2′-CH_2), 3.73 (m, 4H, $N^+CH_2CH_2OCH_2$), 3.94 (m, 4H, $N^+CH_2CH_2$), 4.18 (m, 4H, CO_2CH_2), 4.75 (t, ^3J = 4.7 Hz, 2H, N^+CH_2), 4.84 (t, ^3J = 4.7 Hz, 2H, N^+CH_2), 6.70 ("d", 1H, ArH, pos. 1), 6.76 (d, ^3J = 8.2 Hz, 2H, ArH pos. 3 and pos. 9), 6.86 (d, ^4J = 2.0 Hz, 1H, ArH, pos. 6), 6.96 (d, ^3J = 7.6 Hz, 1H, ArH, pos. 4), 7.00 (dd, ^3J = 8.2 Hz, ^4J = 1.8 Hz, 1H, ArH, pos. 8), 8.49 (m, 4H, PyH), 9.02 (d, ^3J = 6.9 Hz, 2H, PyH), 9.08 (d, ^3J = 6.9 Hz, 2H, PyH); IR (KBr): $\tilde{\nu}$ = 1740 cm^{-1} [ν (C=O)]; MS (FAB): *m/z* 627 (100%) [$M^+ - 2I$]; correct elemental analysis for $C_{35}H_{37}I_2N_3O_6S$.

2: ^{1}H NMR (CD_2Cl_2): δ = 3.11 (s, 3H, NCH_3), 3.60–3.75 (m, 16H, CH_2, therein 3.64, s for 7′-CH_2 and 3.74, s for 2′-CH_2), 4.08 (m, 4H, $N^+CH_2CH_2$), 4.42 (m, 4H, CO_2CH_2), 5.12 (m, 4H, N^+CH_2), 6.69 (d, ^4J = 1.4 Hz, 1H, ArH, pos. 1), 6.71 (d, ^3J = 8.4 Hz, 1H, ArH, pos. 9), 6.89 (dd, ^3J = 7.8 Hz, ^4J = 1.4 Hz, 1H, ArH, pos. 3), 6.90 (d, ^4J = 1.9 Hz, 1H, ArH, pos. 6), 6.95 (d, ^3J = 7.8 Hz, 1H, ArH, pos. 4), 7.13 (dd, ^3J = 8.3 Hz, ^4J = 2.0 Hz, 1H, ArH, pos. 8), 8.06 (d, ^3J = 6.9 Hz, 2H, PyH), 8.17 (d, ^3J = 6.9 Hz, 2H PyH), 9.28 (d, ^3J = 6.9 Hz, 2H, PyH), 9.38 (d, ^3J = 6.9 Hz, 2H, PyH); IR (KBr): $\tilde{\nu}$ = 1730, 1712 cm^{-1} [ν(C=O)]; MS (FAB): *m/z* 715 (100%) [$M^+ - 2I$]; correct elemental analysis for $C_{39}H_{45}I_2N_3O_8S \cdot H_2O$.

3: ^{1}H NMR ([D$_6$]DMSO): δ = 3.16 (s, 3H, NCH_3), 3.30–3.65 (m, 24H, CH_2), 3.96 (m, 4H, $N^+CH_2CH_2$), 4.15 (m, 4H, CO_2CH_2), 4.85 (m, 4H, $N^+CH_2CH_2$), 6.74 (d, ^3J = 8.4 Hz, 1H, ArH, pos. 9), 6.77 ("d", 1H, ArH, pos. 1), 6.79 (dd, ^3J = 7.7 Hz, ^4J = 1.5 Hz, 1H, ArH, pos. 3), 6.93 (d, ^3J = 7.7 Hz, 1H, ArH, pos. 4), 6.96 (d, ^4J = 2.0 Hz, 1H, ArH, pos. 6), 7.03 (dd, ^3J = 8.3 Hz, ^4J = 2.0 Hz, 1H, ArH, pos. 8), 8.50 (m, 4H, PyH), 9.21 (m, 4H, PyH); IR (KBr): $\tilde{\nu}$ = 1726 cm^{-1} [ν(C=O)]; MS (FAB): *m/z* 803 (100%) [$M^+ - 2I$]; correct elemental analysis for $C_{43}H_{53}I_2N_3O_{10}S \cdot 1/2\ H_2O$.

4: ^{1}H NMR (CD_2Cl_2): δ = 3.23 (s, 3H, NCH_3), 3.50–3.75 (m, 32H, CH_2), 4.10 (m, 4H, $N^+CH_2CH_2$), 4.37 (m, 4H, CO_2CH_2), 5.02 (m, 4H, $N^+CH_2CH_2$), 6.73 (d, ^3J = 8.4 Hz, 1H, ArH, pos. 9), 6.80 (d, ^4J = 1.5 Hz, 1H, ArH, pos. 1), 6.86 (dd, ^3J = 7.8 Hz, ^4J = 1.6 Hz, 1H, ArH, pos. 3), 6.93 (d, ^3J = 7.8 Hz, 1H, ArH, pos. 4), 6.99 (d, ^4J = 2.0 Hz, 1H, ArH, pos. 6), 7.12 (dd, ^3J = 8.3 Hz, ^4J = 2.0 Hz, 1H, ArH, pos. 8), 8.35 (m, 4H, PyH), 9.31 (d, ^3J = 6.0 Hz, 2H, PyH), 9.35 (d, ^3J = 6.6 Hz, 2H, PyH); triethylammonium iodide at δ = 1.43 (t, ^3J = 7.3 Hz) and 3.13 (q, ^3J = 7.3 Hz); IR (KBr): $\tilde{\nu}$ = 1724 cm^{-1} [ν (C = O)]; MS (FAB): *m/z* 891 (100%) [$M^+ - 2I$]; correct elemental analysis for $C_{41}H_{61}I_2N_3O_{12}S \cdot 1.2(C_2H_5)_3NHI$.

5: ^{1}H NMR (CD_2Cl_2): δ = 3.28 (s, 3H, NCH_3), 3.50–3.60 (m, 30H, CH_2), 3.64–3.69 (m, 10H, CH_2), 4.07 (m, 4H, $N^+CH_2CH_2$), 4.27 (m, 4H, CO_2CH_2), 5.00 (br, 4H, $N^+CH_2CH_2$), 6.79 (d, ^4J = 1.5 Hz, 1H, ArH, pos. 1), 6.79 (d, ^3J = 8.2 Hz, 1H, ArH, pos. 9), 6.86 (dd, ^3J = 7.9 Hz, ^4J = 1.5 Hz, 1H, ArH, pos. 3), 6.98 (d, ^3J = 8.3 Hz, 1H, ArH, pos. 4), 7.00 (d, ^4J = 2.5 Hz, 1H, ArH, pos. 6), 7.12 (dd, ^3J = 8.2 Hz, ^4J = 2.0 Hz, 1H, ArH, pos. 8), 8.53 (d, ^3J = 5.2 Hz, 4H, PyH), 9.32 (m, 4H, PyH); triethylammonium iodide at δ = 1.43 (t, ^3J = 7.3 Hz) and 3.15 (q, ^3J = 7.3 Hz); IR (KBr): $\tilde{\nu}$ = 1728 cm^{-1} [ν(C=O)] ; MS (FAB): *m/z* 980 (100%) [$MH^+ - 2I$]; correct elemental analysis for $C_{51}H_{69}I_2N_3O_{14}S \cdot 1.8\ (C_2H_5)_3NHI$.

1,1′-Didodecyl-4,4′-bipyridinium diiodide: ^{1}H NMR ([D$_6$]DMSO): δ = 0.85 (t, ^3J = 6.7 Hz, 6H, CH_3), 1.15–1.45 (m, 40H, CH_2), 1.98 ("t" br, 4H, CH_2), 4.71 (t, ^3J = 7.3 Hz, 4H, CH_2), 8.81 (d, ^3J = 6.7 Hz, 4H, PyH), 9.42 (d, ^3J = 6.7 Hz, 4H, PyH).

24: ^{1}H NMR (CD_3CN): δ = 3.22 (s, 3H, NCH_3), 3.50–3.80 (m, 40H, CH_2), 4.05 ("t", br, 2H, NCH_2CH_2), 4.09 ("t", br, 2H, NCH_2CH_2), 4.46 (br, 4H, CO_2CH_2), 4.64 (t, ^3J = 4.6 Hz, 2H, NCH_2CH_2), 4.70 (t, ^3J = 4.7 Hz, 2H, NCH_2CH_2), 6.77 (d, ^3J = 8.4 Hz, 1H, ArH, pos. 9), 6.80 ("d", 1H, ArH, pos. 1), 6.88 (dd, ^3J = 7.9 Hz, ^4J ill-defined, 1H, ArH, pos. 3), 6.97 (d, ^3J = 7.7 Hz, 1H, ArH, pos. 4), 6.98 (s, 1H, ArH, pos. 6), 7.11 (dd, ^3J = 8.3, ^4J = 1.9 Hz, 1H, ArH, pos. 8), 8.26 (d, ^3J = 6.8 Hz, 1H, PyH), 8.30 (d, ^3J = 6.8 Hz, 1H, PyH), 8.89 (d, ^3J = 6.7 Hz, 1H, PyH), 8.94 (d, ^3J = 6.7 Hz, 1H, PyH); IR (KBr): $\tilde{\nu}$ = 1699 cm^{-1} [ν(C = O)]; MS (FAB): *m/z* 1891 (24%, $MH^+ - I$), 1764 (89%, $MH^+ - 2I$), 1637 (27%, $MH^+ - 3I$), 1372 (27%, $MH^+ - BaI_4$; 980 (100%, $MH^+ - Ba_2I_6$); correct elemental analysis for $C_{51}H_{69}I_2N_3O_{14}S \cdot 2BaI_2$.

Exchange of the iodide ions in **2** for hexafluorophosphate provides violet crystals that are insoluble in dichloromethane. A solution of this salt in acetonitrile gives rise to two weak VIS absorptions at λ = 484 nm (ε = 95) and 564 nm (ε = 105), which are attributed to the CT effect between the phenothiazine and the bipyridinium components.

Received: May 8, 1993
Revised version: August 21, 1993 [Z 6071 IE]
German version: *Angew. Chem.* **1993**, *105*, 1791

[1] C. J. Fritchie, Jr., *J. Chem. Soc. A* **1969**, 1328–1334.
[2] H. Kobayashi, *Acta Crystallogr. Sect. B* **1973**, *30*, 1010–1017.
[3] P. C. Dwivedi, K. Gurudath Rao, S. N. Bhat, C. N. R. Rao, *Spectrochim. Acta* **1975**, *31 a*, 129–135; S. N. Bath, *Indian J. Chem.* **1976**, *14 A*, 791–792.
[4] R. Anthonj, N. Karl, B. E. Robertson, J. Stezowski, *J. Chem. Phys.* **1980**, *72*, 1244–1255.
[5] Y. Kawanishi, N. Kitamura, S. Tazuke, *J. Phys. Chem.* **1986**, *90*, 2469–2475; *ibid.* 6034–6037.
[6] H. Yonemura, H. Nakamura, T. Matsuo, *Chem. Phys. Lett.* **1989**, *155*, 157–161.
[7] H. Yonemura, H. Saito, S. Matsushima, H. Nakamura, T. Matsuo, *Tetrahedron Lett.* **1989**, *30*, 3143–3146.
[8] H. Yonemura, H. Nakamura, T. Matsuo, *Chem. Phys.* **1992**, *162*, 69–78.
[9] G. Cauquil, A. Casadevall, *Bull. Soc. Chim. Fr.* **1955**, 1061–1075.
[10] G. Cauquil, A. Casadeval, *C. R. Acad. Sci.* **1954**, *238*, 908–911.
[11] A. K. Saha, P. Schultz, H. Rapaport, *J. Am. Chem. Soc.* **1989**, *111*, 4856–4859.
[12] H. Kourai, H. Takechi, M. Kume, K. Takeichi, I. Shibasaki, *Bokin Bobai [Antibacteriol and Antifungal Agents]* **1986**, *14*, 55–63.
[13] H. A. Staab, H. Bauer: Structures of Metal-Complexes of Oligooxa[3n.3]Paracyclophane Quinhydrones, unpublished; see also: H. Bauer, J. Briaire, H. A. Staab, *Angew. Chem.* **1983**, *95*, 330–331; *Angew. Chem. Int. Ed. Engl.* **1983**, *22*, 334–335; *Tetrahedron Lett.* **1985**, *26*, 6175–6178.

Heterolysis of Re_2O_7: Generation and Stabilization of the Cation $[ReO_3]^+$ **

By *Wolfgang A. Herrmann,* Peter W. Roesky, Fritz E. Kühn, Wolfgang Scherer,* and *Matthias Kleine*

Many alkyl, cyclopentadienyl, and aryl complexes of the type $[R\text{–}ReO_3]$ can be prepared from dirhenium heptaoxide and organotin or organozinc reagents.[1] Alkylation—as typical example $[CH_3ReO_3]$ of Equation (1a)—and arylation can formally be classified as heterolysis of Re_2O_7 into "rhenyl" and a "perrhenate" ion according to Equation (1b) (correct IUPAC nomenclature: trioxorhenate(VII) and tetraoxorhenate(VII) ions, respectively). We now show that a redox neutral cleavage (i.e., not accompanied by a change of oxidation number of the metal) of Re_2O_7 is indeed possible if the $[ReO_3]^+$ ion is generated and stabilized by amines.

$$Re_2O_7 + {}^1/_2\ Zn(CH_3)_2 \longrightarrow [CH_3ReO_3] + {}^1/_2\ Zn(ReO_4)_2 \quad (1a)$$

$$Re_2O_7 \longrightarrow [ReO_3]^+ + [ReO_4]^- \quad (1b)$$

Addition of 1,4,7-triazacyclononane (tcan) to a solution of dirhenium heptaoxide in THF causes immediate and quantitative precipitation of the metal complex **2a** [Eq. (2)] as a white solid, insensitive to air and water, which has salt-like properties and is a 1/1 electrolyte (Λ = 100 S cm^2 mol^{-1}; $c = 1 \times 10^{-3}$ mol L^{-1}). It is almost insoluble in organic solvents, but can be recrystallized from water. A crystallo-

[*] Prof. Dr. W. A. Herrmann, P. W. Roesky, F. E. Kühn, W. Scherer, M. Kleine
Anorganisch-chemisches Institut der Technischen Universität München
Lichtenbergstrasse 4, D-85747 Garching (FRG)
Telefax: Int. code + (89)3209-3473

[**] Multiple Bonds between Main Group Elements and Transition Metals, Part 127. This work was supported by the Fonds der Chemischen Industrie (doctoral grant for P. W. R.) and the Hermann Schlosser Foundation (doctoral grant for F. E. K.). We thank Professor K. Wieghardt, University of Bochum, for the ligand **1a**. Part 126: K. Öfele, W. A. Herrmann, D. Michalios, M. Elison, E. Herdtweck, W. Scherer, J. Mink, *J. Organomet. Chem.*, **1993**, *459*, 177–184.

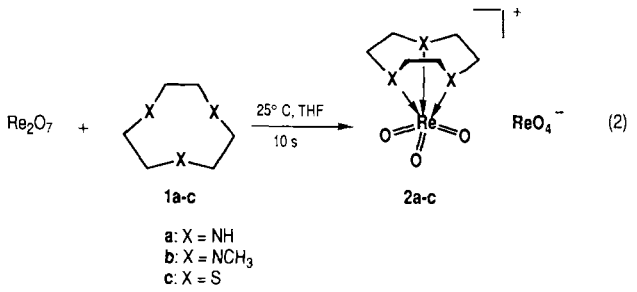

graphic study[2] analysis substantiated the ionic structure: two separate ions, the N,N,N-coordinated rhenyl ion and the perrhenate ion, are present (Fig. 1). The cation is isovalent with the crystallographically characterized half-sandwich complexes $[(\eta^5\text{-}C_5H_5)ReO_3]$ and $[(Hbpz_3)ReO_3]$ ($Hbpz_3$ = hydrotris(pyrazolyl)borate).[3] Complex **2a** forms a three-dimensional network of cations and anions that are linked together through linear $N-H\cdots O-ReO_3$ hydrogen bonds.

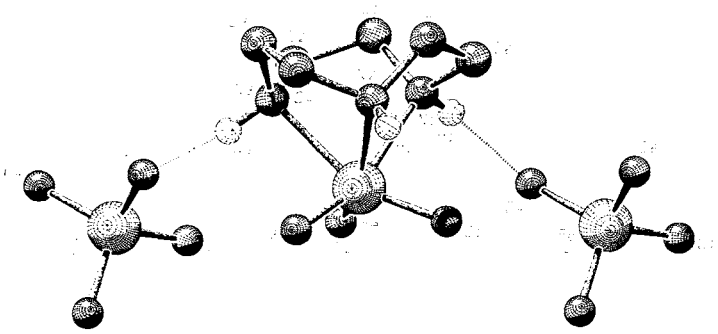

Fig. 1. Molecular structure of **2a** in the crystal (cross-section of the three-dimensional network structure; SCHAKAL representation). Shown are two typical linear hydrogen bonds between cations and anions. Selected distances [pm] and angles [°]: Re1-O1 172.4(3), Re1-O2 173.0(3), Re1-O3 171.9(3), Re2-O4 172.1(3), Re1-N1 223.1(3), Re1-N2 224.1(3), Re1-N3 225.4(1), H1-O4 214(4), H(3)-O(6) 190(4); O1-Re1-O2 106.0(1), O2-Re1-O3 106.4(1), N1-Re1-O1 86.0(1), N1-Re1-N2 74.1(1). – For comparison, selected bond distances [pm] and angles [°] of **2b**: Re1-O1 172.5(2), Re1-O2 172.1(2), Re1-O3 170.3(2), Re2-O4 173.1(2), Re1-N1 227.3(2), Re1-N2 228.9(3), Re1-N3 226.7(2); O1-Re1-O2 105.8(1), O2-Re1-O3 106.2(1), N1-Re1-O1 87.9(1), N1-Re1-N2 75.4(1).

An X-ray structure analysis was also performed on **2b**, the analogous complex containing the N-methylated ligand.[4] The most important bond lengths and angles are given in the legend of Figure 1 for comparison with those of **2a**. These complexes do not differ fundamentally in molecular structure, but **2b**, in contrast to **2a**, contains one water of crystallization per formula unit, which links the perrhenate ions into chains through hydrogen bonds.

Complex **2a** was prepared by Wieghardt et al. by nitric acid or H_2O_2 oxidation of $[(tacn)Re(CO)_3]Cl$.[5] The new route, however, enables the ligand to be varied: the derivatives containing *N*-methylated ligands (**2b**) or S-donor ligands (**2c**) can be synthesized directly by treatment of Re_2O_7 with the ligands **1b** and **1c**, respectively.[6]

Also open-chain ligands like $[(CH_3)_2NCH_2CH_2]_2NCH_3$ form ionic compounds with Re_2O_7, which are, however, sensitive to moisture. The driving force for this heterolysis is the stabilization of the $[ReO_3]^+$ ion by the tridentate donor ligands, which help the metal attain its preferred octahedral coordination and valence saturation. Recombination of $[ReO_3]^+$ and $[ReO_4]^-$ is thus impossible. Potential mono- and bidentate ligands are not adequate for this purpose: they form only covalent adducts with the formula $[Re_2O_7\cdot L_2]$, which can be isolated as pure compounds. An example is the 2,2′-bipyridine (bpy) complex **3a**.[7]

$[Re_2O_7\cdot bpy]$ **3a**

The spectroscopic data of the cation of **2a** resembles those of the known complexes $[R\text{–}ReO_3]$ (R = aryl, alkyl): $\nu(ReO) = 935\ cm^{-1}$ (typical 920–960[3a]); $\delta(^{17}O) = 1019$ (D_2O). The perrhenate ion has its characteristic band at $909\ cm^{-1}$ (KBr) and an ^{17}O NMR signal at $\delta = 562$ (D_2O).

Thermogravimetric mass spectrometric (TG-MS) studies on **2a** and **2c** confirm the strong bonding between the ligand and the $[ReO_3]^+$ fragment.[8] Though a mass loss can be detected in the case of **3a** even at low temperatures,[7] this is attributable to the greater thermal lability of the ligands relative to bpy and not to a weaker bond to the Re atom. Consequently, for **2a** and **2c** a multistep decomposition by water and carbon dioxide expulsion (and in the case of **2c** ethene) is observed, which suggests a redox reaction between ligand and oxygen (from $[ReO_3]^+$). Only the intact ligand is eliminated from **3a** and other Re_2O_7 base adducts.[9]

The unsymmetrical cleavage of Re_2O_7 is predictable from the structure: whereas the compound displays a symmetrical Re-O-Re′ bridge in the gas phase,[10] the solid state structure reveals $[ReO_4]$ tetrahedra surrounded by chains of octahedrally coordinated rhenium atoms.[11] This polymeric structure is broken up by donor solvent molecules like water, pyridine, acetonitrile, or ether:[9, 10, 12] The structure of **3b** in solution consists of discrete Re_2O_7 molecules to which two solvent molecules coordinate unsymmetrically, that is, to one of the metal atoms according to Equation (3).[10] As a

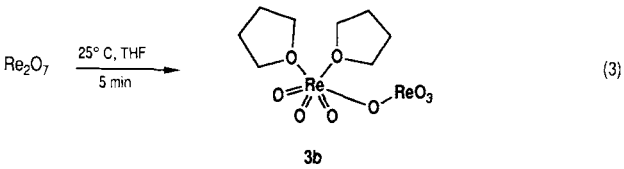

result, in contrast to the structure in the gas phase,[10] the Re–O bonds of the Re-O-Re′ bridge are different lengths, which anticipates the decomposition into $[ReO_4]^-$ and $[ReO_3]^+$ ions [Eq. (3)]. The situation resembles that in chlorine(VI) oxide Cl_2O_6, which is present in the solid as $[ClO_2]^+[ClO_4]^-$.[13]

Our results show that dinuclear, covalent metal oxides are set up for a separation into ions by unsymmetric solvation, for instance in $[Re_2O_7\cdot L_2]$, which is then executed by suitable chelating ligands. This simple method of enhancing the reactivity of metal oxides by dissolving them in polar coordinating solvents seems to have far-reaching preparative consequences for their coordination chemistry and their organometallic chemistry.[1, 14]

Experimental Procedure

2a: Re_2O_7 (245 mg, 0.5 mmol) were dissolved in THF (10 mL), and tacn (70 mg, 0.5 mmol) was added. The complex **2a** precipitates immediately as a white substance that is analytically pure after washing with THF and drying in vacuum. Yield: 300 mg (98%); *IR (KBr)*: $\tilde{\nu}$ [cm^{-1}] = 3038(w), 2844(m), 935(vs, ν(ReO) of $[ReO_3]^+$), 912(vs, ν(ReO) of $[ReO_4]^-$). ^1H NMR (D_2O, 400 MHz, 20 °C): δ = 3.07 (s, 12H, CH_2); $^{13}C\{^1H\}$ NMR (D_2O, 100.53 MHz,

20 °C): $\delta = 42.04$ (CH_2); $^{17}O\{^1H\}$ NMR (D_2O, 54.21 MHz, 20 °C): $\delta = 562.9$ ($[ReO_4]^-$), 1019.2 ($[ReO_3]^+$). Correct elemental analysis.

Complexes **2b** and **c** were prepared analogously.

Received: July 2, 1993 [Z 6185 1E]
German version: *Angew. Chem.* **1993**, *105*, 1768

[1] a) W. A. Herrmann, *Angew. Chem.* **1988**, *100*, 1269–1286; *Angew. Chem. Int. Ed. Engl.* **1988**, *27*, 1297–1313; b) W. A. Herrmann, J. G. Kuchler, G. Weichselbaumer, E. Herdtweck, P. Kiprof, *J. Organomet. Chem.* **1989**, *372*, 351–370; c) W. A. Herrmann, M. Ladwig, P. Kiprof, J. Riede, *ibid.* **1989**, *371*, C13–C17; d) W. A. Herrmann, C. C. Romão, R. W. Fischer, P. Kiprof, C. de Méric de Bellefon, *Angew. Chem.* **1991**, *103*, 183–185; *Angew. Chem. Int. Ed. Engl.* **1991**, *30*, 185–187.

[2] Complex **2a** crystallizes from water at 25 °C in the triclinic space group $P\bar{1}$ (no. 2) with $a = 685.1(2)$, $b = 880.6(4)$, $c = 1108.4(3)$ pm, $\alpha = 109.77(1)$, $\beta = 96.36(2)$, $\gamma = 93.45(2)$°, $Z = 2$, $V = 622 \times 10^6$ pm^3, $\rho_{calcd} = 3.276$ g cm^{-3}, $F(000) = 556$; $Mo_{K\alpha}$ radiation, CAD4 Enraf-Nonius, ω scan, max. 90 s, 2383 measured reflections ($1° < \theta < 25°$), $h(0/8)$, $k(-10/10)$, $l(-13/13)$, 2102 independent reflections, of which 2066 with $I > 1.0\sigma(I)$ used in the refinement, structure solution with Patterson methods. All hydrogen atoms were detected from difference Fourier syntheses and were freely refined. No intensity correction, empirical absorption correction on the basis of Psi scan data ($\mu = 197$ cm^{-1}), Larson's extinction parameter 21.39, $R = \sum(||F_o| - |F_c||/\sum|F_o| = 0.015$; $R_w = [\sum w(|F_o| - |F_c|)^2/\sum w|F_o|^2]^{1/2} = 0.016$, residual electron density $+0.64/-0.72$ e$_0$ Å^{-3}. Further details of the crystal structure investigation may be obtained from the Fachinformationszentrum Karlsruhe, Gesellschaft für wissenschaftlich-technische Information mbH, D-76344 Eggenstein-Leopoldshafen (FRG) on quoting the depository number CSD-57636, the names of the authors, and the journal citation.

[3] a) W. A. Herrmann, P. Kiprof, K. Rypdal, J. Tremmel, R. Blom, R. Alberto, J. Behm, R. W. Albach, H. Bock, B. Solouki, J. Mink, D. Lichtenberger, N. Gruhn, *J. Am. Chem. Soc.* **1991**, *113*, 6527–6537; b) I. A. Degnan, W. A. Herrmann, E. Herdtweck, *Chem. Ber.* **1990**, *123*, 1347–1349.

[4] **2b** crystallized from water at 25 °C in the triclinic space group $P\bar{1}$ (no. 2) with $a = 738.9(2)$, $b = 914.3(2)$, $c = 1229.4(3)$ pm, $\alpha = 83.68(2)$, $\beta = 77.99(2)$, $\gamma = 89.29(2)$°, $Z = 2$, $V = 807 \times 10^6$ pm^3, $\rho_{calcd} = 2.785$ g cm^{-3}, $F(000) = 624$; $Mo_{K\alpha}$ radiation, CAD4 Enraf-Nonius, ω scan, max. 50 s, 6045 measured reflections ($1° < \theta < 25°$), $h(-8/8)$, $k(-10/10)$, $l(-14/14)$, 2785 independent reflections, of which 2506 with $I > 3.0\sigma(I)$ used for the refinement, structure solution with Patterson methods. All hydrogen atoms detected from difference Fourier syntheses and were freely refined. No intensity correction, empirical absorption correction on the basis of Psi scan data ($\mu = 153$ cm^{-1}), Larson's extinction parameter 23.15, $R = \sum(||F_o| - |F_c||/\sum|F_o| = 0.018$; $R_w = [\sum W(|F_o| - |F_c|)^2/\sum w|F_o|^2]^{1/2} = 0.019$, residual electron density $+0.92/-0.85$ e$_0$ Å^{-3}. For further details of the crystal structure investigation see ref. [2].

[5] a) K. Wieghardt, C. Pomp, B. Nuber, J. Weiss, *Inorg. Chem.* **1986**, *25*, 1659–1661; b) C. Pomp, K. Wieghardt, *Polyhedron* **1988**, *7*, 2537–2542; c) G. Böhm, K. Wieghardt, B. Nuber, J. Weiss, *Angew. Chem.* **1990**, *102*, 832–834; *Angew. Chem. Int. Ed. Engl.* **1990**, *29*, 787–790.

[6] Preparation as for **2a**, yield >95%, colorless crystals. Spectroscopic data for **2b**: IR (KBr): $\tilde{\nu}$[cm^{-1}] = 3345(m), 3400(m), 1471(m), 921(vs, ν(ReO) of $[ReO_3]^+$), 912(vs, ν(ReO) of $[ReO_4]^-$), 800(m). ^1H NMR (D_2O, 400 MHz, 20 °C): $\delta = 2.70$ (s, 9H, CH_3), 3.15–3.50 (m, 12H, CH_2); $^{17}O\{^1H\}$ NMR (D_2O, 54.21 MHz, 20 °C): $\delta = 562.4$ ($[ReO_4]^-$), 751.7 ($[ReO_3]^+$). Spectroscopic data for **2c**: IR (KBr): $\tilde{\nu}$[cm^{-1}] = 2980(m), 2920(m), 1620(m), 1449(m), 1413(m), 927(vs, ν(ReO) of $[ReO_3]^+$), 910(vs, ν(ReO) of $[ReO_4]^-$), 583(m, br, ν(CS)). ^1H NMR ([D$_6$]DMSO, 400 MHz, 20 °C): $\delta = 3.51$ (s, 12H, CH_2); $^{17}O\{^1H\}$ NMR ([D$_6$]DMSO, 54.21 MHz, 20 °C): $\delta = 569.5$ ($[ReO_4]^-$), 781.5 ($[ReO_3]^+$). Correct elemental analyses for **2b** and **2c**. The analogous complex $[(C_6H_{12}S_3)ReO_3][BF_4]$ was prepared from $[NH_4][ReO_4]$: H. J. Küppers, B. Nuber, J. Weiss, S. R. Cooper, *J. Chem. Soc. Chem. Commun.* **1990**, 979–980.

[7] Despite the covalent structure, here too, a partial ReO_4 structure is already evident in the IR spectrum: IR (KBr): $\tilde{\nu}$[cm^{-1}] = 909(vs, ν(ReO)) typical of free $[ReO_4]^-$): W. A. Herrmann, F. E. Kühn, C. C. Romão, M. Kleine, J. Mink, *Chem. Ber.*, in press.

[8] Complexes **2a**,**c** were heated in a dynamic He atmosphere from 50 to 700 °C at a rate of 10 K min^{-1} in a thermobalance TGA 7 (Perkin Elmer). The gaseous decomposition products were analysed with a mass spectrometer QMG 420 (Balzers). **2a**: extrapolated onset of the first step: 217 °C; weight loss from 191 to 244 °C: 1.7% (H_2O); from 244 to 337 °C: 12.1% (H_2O); from 337 to 522 °C: 17.5% (CO_2); **2c**: extrapolated onset of the first step: 185 °C; weight loss from 156 to 247 °C: 8.8% (H_2O, CO_2, CH_2CH_2, CH_2S); from 247 to 352 °C: 9.4% (H_2O, CH_2CH_2); from 352 to 559 °C: 8.4% (CO_2). For comparison: Re_2O_7·bpy: extrapolated onset of the first step: 332 °C; weight loss from 221 to 445 °C: 16.7% (bpy); from 445 to 690 °C: 25.3% (CO_2, CO). Re_2O_7: extrapolated onset: 240 °C.

[9] W. A. Herrmann, W. R. Thiel, F. E. Kühn, R. W. Fischer, M. Kleine, E. Herdtweck, W. Scherer, J. Mink, *Inorg. Chem.*, in press.

[10] P. Kiprof, W. A. Herrmann, F. E. Kühn, W. Scherer, M. Kleine, M. Elison, K. Rypdal, H. V. Volden, S. Gundersen, A. Haaland, *Bull. Soc. Chim. Fr.* **1992**, *129*, 655–662.

[11] a) B. K. Krebs, A. Müller, H. H. Beyer, *Inorg. Chem.* **1969**, *8*, 436–443; b) B. K. Krebs, A. Müller, H. H. Beyer, *J. Chem. Soc. Chem. Commun.* **1968**, 263–264.

[12] a) H. H. Beyer, O. Glemser, B. K. Krebs, *Angew. Chem.* **1968**, *80*, 286–287; *Angew. Chem. Int. Ed. Engl.* **1968**, *7*, 295–296; b) H. W. Roesky, D. Hesse, M. Noltemeyer, *Eur. J. Solid State Inorg. Chem.* **1991**, *28*, 809–814; c) H. H. Beyer, O. Glemser, B. K. Krebs, G. Wagner, *Z. Anorg. Chem.* **1970**, *376*, 87–100; d) J. W. Johnson, J. F. Brody, G. B. Ansell, S. Zentz, *Acta Crystallogr. Sect. C* **1984**, *40*, 2024–2026.

[13] M. Tobias, M. Jansen, *Angew. Chem.* **1986**, *98*, 994–995; *Angew. Chem. Int. Ed. Engl.* **1986**, *25*, 993–994.

[14] W. A. Herrmann, F. E. Kühn, R. W. Fischer, W. R. Thiel, C. C. Romão, *Inorg. Chem.* **1992**, *31*, 4431–4432.

Catalysis of the Hydrolysis of Phosphoric Acid Diesters by Lanthanide Ions and the Influence of Ligands

By *Hans-Jörg Schneider,* Jörg Rammo,* and *Ronald Hettich*

Since Bamann discovered the catalytic effectiveness of lanthanide ions in the hydrolysis of glycerol phosphates,[1] these and transition metal ions have also been used as catalysts for the cleavage of ribose phosphates, which are structurally related through their vicinal hydroxy groups.[2–4] The hydrolysis of normal phosphoric acid esters or of DNA (**1**) requires much more drastic conditions than that of RNA (**2**) due to the absence of the 2′-OH group. Considerable acceleration of the reactions can be achieved with more highly charged transition metal ions.[5, 6] In particular, Chin et

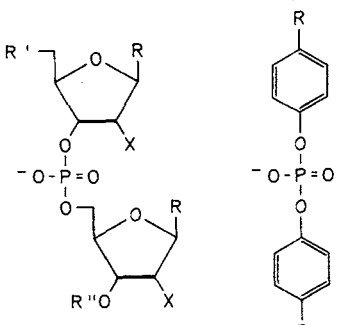

1 (X = H) **3a** (R = H)
2 (X = OH) **3b** (R = NO_2)

al.[5b] have shown that with specific cobalt complexes even nonactivated esters such as dimethyl phosphate react up to 10^{10} times faster.[7] However, it appears that the—sometimes not very stable—metal complexes are used up during the reaction, that is they are not functioning as catalysts and Michaelis–Menten kinetics (as found with enzymes) were not observed. Recently Komiyama et al.[8a] showed for the

[*] Prof. Dr. H.-J. Schneider, Dipl.-Chem. J. Rammo, Dipl.-Chem. R. Hettich
Fachrichtung Organische Chemie der Universität
D-66041 Saarbrücken (FRG)
Telefax: Int. code + (681)302-4105

[**] Supramolecular Chemistry, Part 38. Part 37: H.-J. Schneider, V. Rüdiger, O. A. Raevsky, *J. Org. Chem.*, in press.

first time that the cleavage of plasmid DNA could also be accelerated by lanthanide ions. The conditions, however, are so drastic, in comparison to those of well-known radical DNA cleavage with redox metals,[8b] that the participation, at least in part, of a radical mechanism cannot be excluded.

We report here on the highly efficient catalysis of the saponification of the phosphoric acid diaryl ester **3** by lanthanide ions, characterized by saturation kinetics and "turnover", and on the main possibilities of controlling the hydrolysis with complex ligands. The most important factor in the potential use of synthetic reagents for the hydrolysis of phosphoric acid esters—be they insecticides, chemical weapons, or nucleic acids—is that the catalytic center is located in a kinetically stable complex. This should, for example, make it possible to immobilize catalysts, to raise their affinity for DNA (thus, for example, concentrations of drugs can be reduced to levels suitable for therapy), and to selectively cleave DNA strands (through the formation of a triple helix containing oligonucleotide complex conjugation [9]). This was realized—apart from a few exceptions[10]—largely with *oxidatively* active reagents,[11] of which the iron–EDTA oligonucleotides of Dervan et al.[12] are the best known. The very reactive oxygen-containing radicals that are formed have the disadvantage of not being very selective and of producing unnatural cleavage products; this can be avoided by the hydrolysis of phosphoric acid esters—as occurs in nature.

Initially, we tried to use strong nucleophiles such as thiolates, oximates, etc. (thiophenol, salicylaldoxim, iodosobenzene) with the aim of accelerating the hydrolysis of model phosphates such as **3b**, since their affinity for DNA can be raised almost without limit by combining such ligands with polyamines.[13a] After a preliminary test of this method with plasmid DNA had led to hardly any detectable effect,[13b] we measured, photometrically, the release of nitrophenolate from the model ester **3b** in the presence of different concentrations of europium(III) chloride at pH 7.0. At $[Eu^{3+}] = 5 \times 10^{-3}$ M, for example, $k_{obs} = 1.67 \times 10^{-4}\ s^{-1}$ was measured which corresponds to an acceleration of $k_{rel}/k_0 = 1.1 \times 10^8$.[7] Under the same conditions Yb^{3+} gave $k_{obs} = 3.7 \times 10^{-5}\ s^{-1}$; addition of Pb^{2+} salts produced cloudiness. All the reactions were (pseudo)-first order with up to 95% reaction with a linear correlation coefficient of $r > 0.997$; generally an excess of catalyst was used. The measured final extinction shows that hydrolysis under normal conditions ($[\mathbf{3b}] < [Eu^{3+}]$) leads to the removal of *both* phenoxy groups. This means that the corresponding monophenyl ester, as in noncatalyzed hydrolysis, reacts faster than the diester.[5a]

To ascertain that the catalyst retained its activity under "turnover conditions", measurements were made with a tenfold excess of substrate. These could again be evaluated with a first order kinetic equation. The observed rate of nitrophenolate release, $k_{obs} = 3.9 \times 10^{-6}\ s^{-1}$ (50 °C, $[Eu^{3+}] = 1 \times 10^{-4}$ M), was about half of that found with an excess of $[Eu^{3+}]$ ($k = 8.6 \times 10^{-6}\ s^{-1}$). Here the monoester was present at a much lower concentration than the starting material which released only *one* phenolate ion. In addition, when $[\mathbf{3}] > [Eu^{3+}]$, the concentration of active, free Eu^{3+} is reduced by binding to **3**. The saturation kinetics (Fig. 1) observed for the first time with Eu^{3+} yielded, by nonlinear curve-fitting for a 1:1 complex, a Michaelis–Menten constant of $K_M = 2.9 \times 10^{-3}$ M (the order of magnitude of this is in accord with the binding constants of lanthanide ions with phosphates[14]), and a catalytic constant of $k_{cat} = 2.6 \times 10^{-4}\ s^{-1}$. The rate constant for hydrolysis without a catalyst can be estimated from known data at 50 °C[5d] as $k = 3 \times 10^{-10}\ s^{-1}$.

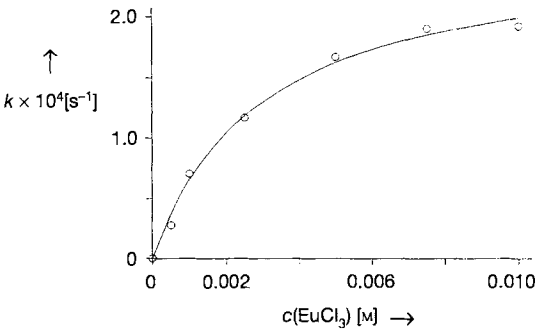

Fig. 1. Dependence of the kinetics of hydrolysis of bis(4-nitrophenyl)phosphate **3b** ($[\mathbf{3b}] = 3.76 \times 10^{-5}$ M) on catalyst concentration $[Eu^{3+}]$ (in 0.01 M EPPS buffer; 50.0 °C; pH 7.00); experimental points and a simulated Michaelis–Menten curve.

Although the rate of hydrolysis of nitrophenyl esters can be easily measured, the hydrolysis mechanism may be different from that of unactivated derivatives.[5, 10a] We have, therefore, investigated the effectiveness of lanthanide ions in the hydrolysis of the diphenylphosphate **3a**. This ester is so inert that the necessary constants for comparison of the hydrolysis at pH 7.0 are, as with dimethylphosphate,[5b] only obtainable by extrapolation from the correlations described by Kirby et al.[15] Assuming that the activation entropy for the hydrolysis in water is largely independent of the diester,[5b] an activation energy of about 30 kcal mol^{-1} is obtained. The calculated rate constant would then be $k_0 = 3.6 \times 10^{-12}\ s^{-1}$ (at 70 °C). The observed value with $[Eu^{3+}] = 4.3 \times 10^{-3}$ M is $k_{obs} = 3.95 \times 10^{-6}$ which, with $k_{obs}/k_0 \approx 10^6$ (at 70 °C), shows even a somewhat greater catalytic effect than with the nitrophenyl ester **3b** ($k_{obs}/k_0 = 0.56 \times 10^6$, 50 °C).

The effect of ligands on the catalytic effect of the Eu^{3+} ion was investigated with ligands **4**–**17** (Scheme 1) under the same conditions. From reactions with DNA it is known that with EDTA, for example, the metal effect may be completely suppressed.[4] With a series of nitrogen-containing ligands (**4**–**8**) we do indeed find a reduced rate of hydrolysis (see Scheme 1). It can be estimated from known complexing constants[14] how many "free", that is aqua-complexed, metal ions are still available at each concentration. Comparison with the values predicted from the saturation curve (Fig. 1) shows that even when they are complexed the metal ions are almost always still catalytically effective. In the presence of most ligands the activity drops only to 10–50% of that of the ligand-free solution, although with **8** and **9**, for example, only about one percent of "free" metal ion is present. The two hydroxycarboxylic acids **16** and **17** are exceptions; here, the residual activity is close to the detection limits. The Eu^{3+} complex with [2,2,2]cryptand (**9**) proved to be particularly promising. In spite of its high complexation constant, this was the only one that almost retained the activity of the free metal ion. Even the cryptands form complexes with trivalent lanthanide ions sufficiently fast under the measurement conditions,[16] whereas their dissociation, for example at 25 °C with $k_D = 10^{-3}\ s^{-1}$, is already relatively slow.[16] With their thermodynamic and kinetic stability, coupled with the retention of their activity, the most important prerequisites for the future use of such complexes are fulfilled.

In order to get closer to the typically high RNA rates of hydrolysis by varying the ligands in the complexes, a new concept was investigated. The generally accepted reason for the high reactivity of RNA is the formation of the cyclic ester *cyclo*-**2** through the participation of the neighboring 2′-OH

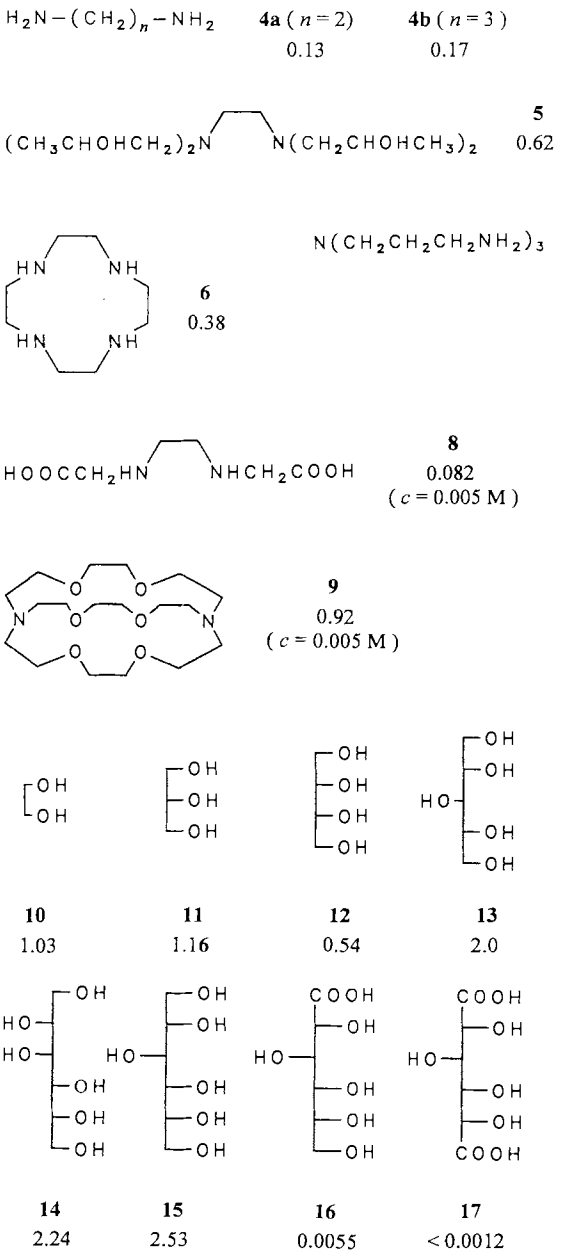

Scheme 1. Complex ligands L and their effect on the catalytic activity of Eu^{3+}; the values show the ratio of the rate constants with and without additional ligand ($[\mathbf{3b}] = 3.76 \times 10^{-5}$ M and $[\mathbf{L}] = 5 \times 10^{-2}$ M. With **8** and **9** $[\mathbf{L}] = 5 \times 10^{-3}$ M because of their low solubilities). The following compounds were also added but were unsuitable because of precipitation or clouding: spermine, *N*,*N*'-bis(3-aminopropyl)piperazine, 3,4-dihydroxyphenylalanine, m-hydroxybenzoic acid, 3,5-dihydroxybenzoic acid, pyrogallol.

group. In principle it should be possible to replace this group with a nucleophile attached to a metal complex instead of to the substrate (Scheme 2). The results of preliminary experiments with polyols, which bind—even though weakly[14a]—with the catalytically effective metal ions and, in addition, bear nucleophilic OH groups on their peripheries, support

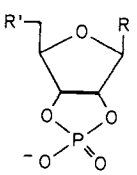

cyclo-**2**

this hypothesis (see Scheme 1). The advantage of such polyols is that—as in RNA—they contain an additional vicinal OH group next to the already phosphorylated OH group, so that in a second (faster) step a cyclic phosphate analogous to *cyclo*-**2** can be formed. The observed effects enable an *additional* acceleration of catalysis by a factor of 2.5. More importantly this acceleration is clearly dependent on the structure of the polyols; a minimum distance is obviously required from the metal binding center to the OH group which serves as a nucleophile towards the phosphate. In view of the known small complexing constants of lanthanide ions with polyhydroxy compounds containing vicinal OH groups[14a] and the resulting minimum concentration of active complex in water the observed accelerations are considerable: The addition of, for example, 5×10^{-2} M **15** under realistically observable conditions (with $[Eu^{3+}] = 5 \times 10^{-3}$ M) leads to a total increase in the hydrolysis rate of 1.4×10^6.

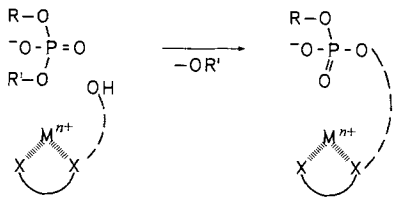

Scheme 2. The mechanism of the hydrolysis of phosphoric acid diesters when the OH group in RNA-derived substrates is replaced by the OH group from a metal catalyst complex.

In summary, it has been shown that 1) phosphoric acid ester hydrolyses can be catalyzed with turnover and Michaelis–Menton kinetics analogous to those observed for enzymes by stable and readily available lanthanide complexes; even with only slightly activated leaving groups accelerations up to a factor of 10^6 are possible, 2) the catalytic activity is retained even in thermodynamically and kinetically very stable complexes so that it should be possible, through modification of the ligands, to further raise their effectiveness and selectivity with respect to biopolymers such as DNA, and 3) through the introduction of additional nucleophilic groups in the metal complexes, instead of the 2'-OH groups which are available on the ribophosphates in the substrate, a further raising of the catalytic activity is possible.[17]

Received: May 7, 1993
Revised version: July 24, 1993 [Z 6064 IE]
German version: *Angew. Chem.* **1993**, *105*, 1773

[1] a) E. Bamann, *Angew. Chem.* **1939**, *52*, 186; b) E. Bamann, E. Nowotny, *Chem. Ber.* **1948**, *81*, 455; c) E. Bamann, F. Fischler, H. Trapmann, *Biochem. Z.* **1951**, *325*, 413, and references therein.; d) see also: W. W. Butcher, F. Westheimer, *J. Am. Chem. Soc.* **1955**, *77*, 2420.
[2] R. Breslow, D.-L. Huang, *Proc. Natl. Acad. Sci. USA* **1991**, *88*, 4080.
[3] a) M. Komiyama, K. Matsumura, Y. Matsumoto, *J. Chem. Soc. Chem. Commun.* **1992**, 640; b) Y. Matsumoto, M. Komiyama, *ibid.* **1990**, 1050; see also J. Sumaoka, M. Yashiro, M. Komiyama, *ibid.* **1992**, 1707 (hydrolysis of a cyclic phosphate).
[4] J. L. Morrow, L. A. Buttrey, V. M. Shelton, K. A. Berback, *J. Am. Chem. Soc.* **1992**, *114*, 1903, and references therein.
[5] a) J. Chin, *Acc. Chem. Res.* **1991**, *24*, 145; b) J. H. Kim, J. Chin, *J. Am. Chem. Soc.* **1992**, *114*, 9792; c) K. A. Browne, T. C. Bruice, *ibid.* **1992**, *114*, 4951, and references therein.; d) J. Chin, M. Banaszczyk, V. Jubian, X. Zou, *ibid.* **1989**, *111*, 186, and references therein.
[6] a) P. Hendry, A. M. Sargeson, *Prog. Inorg. Chem.* **1990**, *38*, 201; b) M. A. DeRosch, W. C. Trogler, *Inorg. Chem.* **1990**, *29*, 2409; c) J. R. Morrow, L. A. Buttrey, K. A. Berback, *ibid.* **1992**, *31*, 16.
[7] For a better comparison of the efficiency of the systems referred to in the literature we define: $k_{rel} = k_{obs}[\text{catalyst}]^{-1}$. With $k_{rel} = 10^9$ to 10^{10}, only

the (not catalytically effective) Co complexes of Chin et al. [5b,d] are faster than those presented here with $k_{rel} = 10^8$: complexes described earlier with $k_{rel} = 10^3$ to 10^6 are considerably less reactive [6b,c].
[8] a) Y. Matsumoto, M. Koyiyama, *Nucleic Acids Symp. Ser.* **1992**, *27*, 33; b) P. Tachon, *Free Radical Res. Commun.* **1989**, *7*, 1.
[9] Review: N. T. Thuong, C. Hélene *Angew. Chem.* **1993** *105*, 697; *Angew. Chem. Int. Ed. Engl.* **1993**, *32*, 666, and references therein.
[10] a) L. A. Basile, A. L. Raphael, J. K. Barton, *J. Am. Chem. Soc.* **1987**, *109*, 7550; b) concerning the lanthanide-ion-catalyzed hydrolysis of a phosphoric acid triester (which generally react faster than the DNA analogous phosphoric acid diesters [5a]) see: R. W. Hay, N. Govan, *J. Chem. Soc. Commun.* **1990**, 714.
[11] D. S. Sigman, *Biochemistry* **1990**, *29*, 9097; D. S. Sigman, C. B. Chen, *Annu. Rev. Biochem.* **1990**, *59*, 207; C. J. Burrows, J. G. Muller, X. Chen, A. C. Dadiz, S. E. Rokita, *Pure Appl. Chem.* **1993**, *65*, 545 (Ni complexes); B. Meunier, *Chem. Rev.* **1992**, *92*, 1411 (porphyrins).
[12] a) R. P. Hertzberg, P. B. Dervan, *J. Am. Chem. Soc.* **1982**, *104*, 313; for most recent applications see for example W. S. Wade, M. Mrksich, P. B. Dervan, *ibid.* **1992**, *114*, 8783; b) see also X. Chen, S. E. Rokita, C. J. Burrows, *ibid.* **1991**, *113*, 5884; N. Gupta, N. Grover, G. A. Neyhart, P. Singh, H. H. Thorp, *Inorg. Chem.* **1993**, *32*, 310; J. R. Morrow, K. A. Kolossa, *Inorg. Chim. Acta* **1992**, *195*, 245, and references therein.
[13] a) Cf. H.-J. Schneider, T. Blatter, *Angew. Chem.* **1992**, *104*, 1244; *Angew. Chem. Int. Ed. Engl.* **1992**, *31*, 1207, and references therein.; b) H.-J. Schneider, J. Rammo, A. E. Eliseev, B. Schu, unpublished results.
[14] a) *Gemlin, Handbook of Inorganic Chemistry* **1980**-, 8th edition, *Part D1* **1980**, p. 159 ff; *Part D2*, **1982**, p. 314 ff; *Part D3*, **1981**, p. 31 ff; b) G.-y. Adachi, Y. Hirashima in *Cation Binding by Macrocycles* (Eds.: Y. Inoue, G. W. Gokel), Dekker, New York, **1990**, p. 701 (lanthanoid complexes); c) E. M. Eyring, S. Petrucci, *ibid.* p. 179 (the discrepancies in the kinetic parameters, due to the measurement technique, discussed here and also, in part, sometimes different, complexing constants [14a,b,d] are of lesser importance for our interpretation); d) F. Vögtle, E. Weber in *Crown Ehers and Analogs* (Eds.: S. Patai, Z. Rappoport), Wiley, Chichester, England **1989**, p. 216 ff.
[15] A. J. Kirby, M. Younas, *J. Chem. Soc. B* **1970**, 510.
[16] E. L. Lee, O. A. Gansow, M. J. Weber, *J. Am. Chem. Soc.* **1980**, *102*, 2278; from the data given here it turns out that for Eu^{3+} + [2.2.2]cryptand (**9**) at 25 °C for the association under the conditions used by us a half-life of about 80 s was obtained. For this, as probably also for the even higher catalytic activity of the complex, it is important that some hydrated metal ions can still exist even inside the cryptands [14c,d].
[17] The reaction rates were measured photometrically at 400 nm (**3b**) and 275 nm (**3a**) (50 °C; pH 7.0; buffer: 0.01 M EPPS); other conditions are given in the legends to Figure 1 and Scheme 1. The nonlinear curve-fitting for (pseudo)-first order reactions, usually over two or three half-life times, had excellent correlation coefficients (> 0.997). The observed spread of the reaction rate constants obtained from the regression was ± 1%; the same spread was observed in duplicate runs.

Palladium-Catalyzed Enantioselective Bis-alkoxycarbonylation of Olefins**

By *Sylvia C. A. Nefkens, Martin Sperrle,* and *Giambattista Consiglio**

The bis-alkoxycarbonylation of olefins to give succinates as the products (Scheme 1, $n = 1$) is generally carried out with $PdCl_2$ in the presence of hydrogen acceptors.[1] Succinates have been prepared with high selectivities from various olefins by using $CuCl_2$ in the presence of sodium butyrate.[2] Other suitable catalyst systems for this reaction include $PdCl_2$ in combination with butyl nitrite,[3] $Pd(OAc)_2$ in the presence of benzoquinone and oxygen,[4] and $[Pd(acac)_2]$ (Hacac = 2,4-pentanedione) in the presence of di-*tert*-butyl peroxide.[5] Complexes of the type $[PdL_2X_2]$ with modified ligands have not been used for this reaction, despite their catalytic activity in many other carbonylation reactions.[6-9] When styrene is the substrate and either [(1,10-phenanthroline)$Pd(p\text{-}CH_3C_6H_4SO_3)_2$] or [(1,2-bipyridine)$Pd(CF_3COO)_2$] is employed as the catalyst precursor, poly(1-oxo-2-phenyltrimethylene) is formed. It was recognized that when the reaction is conducted in methanol some of the macromolecules formed contain two terminal methoxycarbonyl groups (Scheme 1).[6e] Oligomers (Scheme 1, $n = 1$, 2 up to 10) were obtained by increasing the amount of the oxidant.[10] When the catalyst precursor had diphosphane ligands, mainly saturated monoesters and α,β-unsaturated esters were observed; however, some succinate was formed as well.[11] The *syn* stereochemistry of the dicarbonylation reaction products[10] prompted us to attempt enantioselective bis-methoxycarbonylation to give optically active succinates.[12]

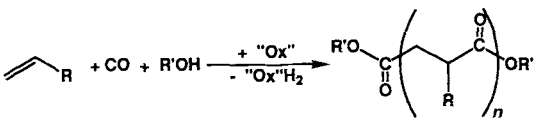

Scheme 1.

When the previously reported complex [Pd((*R,R*)-diop)$(O_2CCF_3)_2$][10] (diop = 3,4-bis[(diphenylphosphino)-methyl]-(2,2-dimethyl-1,3-dioxolane) was used as the catalyst precursor in the presence of $Sn(O_3SCF_3)_2$, (*R*)-dimethyl phenylsuccinate could in fact be isolated in 29% yield and with 30% *ee*. Similar results were obtained with an "in situ" system composed of $[Pd(acac)_2]$, (*R,R*)-diop, and two equivalents of trifluoroacetic or *para*-toluenesulfonic acid. With a similar "in situ" system, in which (*R*)-*N,N*-dimethyl-1-[(*S*)-1′,2-bis(diphenylphosphino)ferrocenyl]ethylamine served as the chiral ligand, comparable results (< 29% *ee*) were obtained. Analogously, dimethyl propylsuccinate was obtained with 17% *ee*[13] and 4% yield from the bis-methoxycarbonylation of 1-pentene with the diop-containing catalytic system.

The excellent stereochemical control achieved in the copolymerization of propene with carbon monoxide[6g, 14] (Scheme 1, $R = CH_3$) by using atropoisomeric diphosphanes prompted us to test this type of ligand (Scheme 2) for the enantioselective bis-methoxycarbonylation.

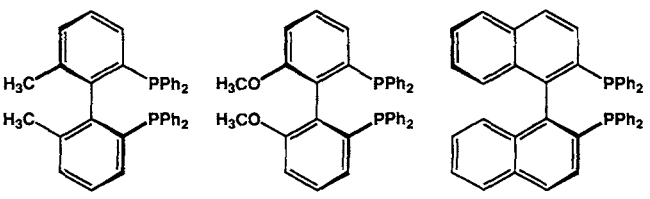

Scheme 2.

In a series of bis-methoxycarbonylations of styrene using the "in situ" system $[Pd(acac)_2]$/L–L/$p\text{-}CH_3C_6H_4SO_3H$ (1:1:2 mol ratio) the chiral diphosphane ligand (L–L) was varied. We found that the optical purity of the dimethyl phenylsuccinate obtained could be improved to 82–93% by employing the optically pure atropisomeric ligands **1**–**3** (Table 1). A maximum of 93% *ee* was obtained with 2,2′-dimethoxy-6,6′-bis(diphenylphosphino)biphenyl **2** (biphemp-OMe) as the ligand. The yield with respect to the

[*] Prof. Dr. G. Consiglio, Dr. S. C. A. Nefkens, Dipl.-Chem. M. Sperrle
Eidgenössische Technische Hochschule
Laboratorium für Technische Chemie, ETH-Zentrum
Universitätsstrasse 6, CH-8092 Zürich (Switzerland)
Telefax: Int. code + (1)262-1746

[**] This research was supported by the Schweizerischen Nationalfonds zur Förderung der wissenschaftlichen Forschung. We thank Hoffmann-La Roche AG (Dr. E. Broger) for the generous gift of the ligands **1** and **2**.

Table 1. Enantioselective bis-methoxycarbonylation of styrene with the catalyst system $[Pd(acac)_2]$/L-L/2 *p*-$CH_3C_6H_4SO_3H$ [a].

L–L	Conv. [%]	MP [b] [%]	MC [c] [%]	DMPS [d] [%]	Other [e] [%]	*ee* DMPS [f] [%] (abs. conf.)
(*R*)-**1**	51	2	6	37	55	82 (*R*)
(*S*)-**2**	48	3	8	40	49	93 (*S*)
(*S*)-**3**	36	4	6	58	32	90 (*S*)

[a] For the reaction conditions see Experimental Procedure. [b] Methyl 2-phenylpropionate and methyl 3-phenylpropionate. [c] Methyl cinnamate. [d] Dimethyl phenylsuccinate. [e] Oligomeric products. [f] Enantiomeric excess determined by gas chromatography (see Experimental Procedure).

styrene consumed (chemoselectivity) of the reaction remained, however, modest (37–58%).

The enantioselectivity in the concomitant formation of methyl 2-phenylpropanoate was much lower (ca. 50% *ee* with **2**). With all ligands tested, however, the same enantiotopic face of styrene reacted prevailingly in both hydroalkoxycarbonylation and bis-methoxycarbonylation.

The chemoselectivity of the reaction towards dicarbonylation could be improved by using $[Pd(OSO_2CF_3)_2\{(S)\text{-biphemp-OMe}\} \cdot 2\,H_2O]$ as the catalyst precursor. Under reaction conditions similar to those reported in the experimental procedure (but with styrene/Pd 1000:1; and styrene/benzoquinone 1:1 in 20 mL CH_3OH[15]) dimethyl phenylsuccinate was obtained with 92% *ee* (69% conversion, 78% chemoselectivity). The chemoselectivity is even higher considering that some *p*-hydroxyphenyl methyl 2-phenylsuccinate is formed as a coproduct. By lowering the carbon monoxide pressure to 50 bar, similar selectivities (83%, 91% *ee*) are observed at 85% conversion. Under these conditions the main coproduct appears to be methyl cinnamate. The fact that of the two possible α,β-unsaturated esters only methyl cinnamate was formed, suggests that a β-(alkoxycarbonyl)-alkyl-palladium complex is a common intermediate in the formation of both the α,β-unsaturated ester and the diester.[11] Control experiments showed that the unsaturated esters are not intermediates in the formation of succinates.[8c]

The development of catalysts showing complete regioregularity coupled with high enantiofacial selection in the copolymerization of propene with carbon monoxide[6f–h] suggests possibilities for achieving high enantioselectivities in the synthesis of aliphatic succinic acid derivatives as well. Experiments in this direction are in progress.

Experimental Procedure

A 250 mL stainless steel autoclave equipped with a glass insert was charged under an atmosphere of N_2 with 0.14 mmol catalyst precursor, 18 mmol benzoquinone, and 36 mmol styrene in 15 mL methanol, then pressurized with 350 bar of CO, and heated to 50 °C. After 20 h the autoclave was cooled to room temperature and the residual gas released. Immediate quantitative gas chromatographic analysis was carried out on Hewlett Packard HP1 (50 m) and Macherey-Nagel OV1 (10 m) columns using acetophenone as the internal standard. After removal of the methanol from the reaction mixture under reduced pressure, approximately 50 mL toluene was added causing most of the hydroquinone to precipitate. The filtrate was evaporated and the residue fractionally distilled (Kugelrohr). Each fraction was purified by column chromatography over silica (70–230 mesh) eluting with hexane/ether (3:1). The products were characterized by NMR spectroscopy and GC-MS [10]. The enantiomeric excess was determined by gas chromatography with a cyclodextrin as the stationary phase [Macherey-Nagel Lipodex E (50 m column)].

Received: July 10, 1993 [Z 6203 IE]
German version: *Angew. Chem.* **1993**, *105*, 1837

[1] a) D. M. Fenton, P. J. Steinwand, *J. Org. Chem.* **1972**, *37*, 2034–2035; b) R. F. Heck, *J. Am. Chem. Soc.* **1972**, *94*, 2712–2716; c) S. Toda, M. Miyamoto, H. Kinoshita, K. Inomata, *Bull. Chem. Soc. Jpn.* **1990**, *64*, 3600–3606; d) Review: J. Tsuji, *Synthesis* **1990**, 739–749.

[2] a) D. E. James, J. K. Stille, *J. Am. Chem. Soc.* **1976**, *98*, 1810–1823; b) D. E. James, L. F. Hines, J. K. Stille, *ibid.* **1976**, *98*, 1806–1809; c) J. K. Stille, R. Divakaruni, *J. Org. Chem.* **1979**, *44*, 3474–3482.

[3] P. Bréchot, Y. Chauvin, D. Commereuc, L. Saussine, *Organometallics* **1990**, *9*, 26–30.

[4] E. Drent (Shell), EP-B 231044, **1986**; *Chem. Abstr.* **1988**, *108*, 166984.

[5] G. E. Morris, D. Oakley, D. A. Pippard, D. J. H. Smith, *J. Chem. Soc. Chem. Commun.* **1987**, 410–411.

[6] a) A. Sen, T.-W. Lai, *J. Am. Chem. Soc.* **1982**, *104*, 3520–3522; b) T.-W. Lai, A. Sen, *Organometallics* **1984**, *3*, 866–870; c) E. Drent, J. A. M. van Broekhoven, M. J. Doyle, *J. Organomet. Chem.* **1991**, *417*, 235–251; d) P. Corradini, C. De Rosa, A. Panunzi, G. Petrucci, P. Pino, *Chimia* **1990**, *44*, 52–54; e) M. Barsacchi, G. Consiglio, L. Medici, G. Petrucci, U. W. Suter, *Angew. Chem.* **1991**, *103*, 992–994; *Angew. Chem. Int. Ed. Engl.* **1991**, *30*, 989–991; f) A. Batistini, G. Consiglio, U. W. Suter, *ibid.* **1992**, *104*, 306–307 and **1992**, *31*, 303–305; g) M. Barsacchi, A. Batistini, G. Consiglio, U. W. Suter, *Macromolecules* **1992**, *25*, 3604–3606; h) A. Batistini, G. Consiglio, *Organometallics* **1992**, *11*, 1766–1769; i) M. Brookhart, F. C. Rix, J. M. DeSimone, J. C. Barborak, *J. Am. Chem. Soc.* **1992**, *114*, 5894–5895; j) J. C. W. Chien, A. X. Zhao, F. Xu, *Polym. Bull (Berlin)* **1992**, *28*, 315–318.

[7] a) C. Pisano, G. Consiglio, A. Sironi, M. Moret, *J. Chem. Soc. Chem. Commun.* **1991**, 421–423; b) V. N. Zudin, G. N. Il'inich, V. A. Likholobov, Y. I. Yermakov, *ibid.* **1992**, 545–546; c) C. Pisano, Dissertation Nr. 10076, ETH Zürich, **1993**; d) C. Pisano, A. Mezzetti, G. Consiglio, *Organometallics* **1992**, *11*, 20–22.

[8] a) F. J. Waller, *Prepr. Am. Chem. Soc. Div. Pet. Chem.* **1982**, *27*, 611–613; b) G. Cometti, G. P. Chiusoli, *J. Organomet. Chem.* **1982**, *236*, C31-C32; c) S. C. A. Nefkens, Dissertation Nr. 9939, ETH Zürich, **1992**.

[9] a) J. J. Mrowca (Dupont), US-B 3876672, **1972**; *Chem. Abstr.* **1976**, *84*, 30432; see also BE-B 825835, **1975**; b) E. Drent (Shell), EP-B 220767, **1986**; *Chem. Abstr.* **1987**, *107*, 39199.

[10] C. Pisano, S. C. A. Nefkens, G. Consiglio, *Organometallics* **1992**, *11*, 1975–1978.

[11] The formation of saturated monoesters does not require the presence of an oxidant. A catalytic cycle starting with a hydridopalladium or an alkoxycarbonylpalladium intermediate may be suggested for the formation of these products. The α,β-unsaturated ester and diester can only be formed starting with an alkoxycarbonylpalladium intermediate: D. Milstein, *Acc. Chem. Res.* **1988**, *21*, 428–434.

[12] For literature related to optically active succinic acid derivatives see: a) H. Jendralla, *Tetrahedron Lett.* **1991**, *32*, 3671–3672; b) J. J. Talley (Monsanto), US-B 4939288, **1989**, *Chem. Abstr.* **1990**, *113*, 211382. For a possible application of optically active phenylsuccinic acid see: A. Kleemann, J. Engel, *Pharmazeutische Wirkstoffe*, 2nd ed., Thieme, Stuttgart, **1982**, p. 718.

[13] Determined by ^1H NMR spectroscopy with $[Eu(hfc)_3]$ as the chiral shift reagent.

[14] A. Batistini, unpublished results, ETH Zürich.

[15] The completely selective formation of succinic esters theoretically requires a 1:1 ratio of oxidant to olefin. To avoid having a large excess of unreacted benzoquinone at the end of the reaction, a 2:1 ratio of styrene/benzoquinone was used in the first experiments which yielded succinic esters with only moderate selectivities.

Phosphinic Acid-Based C_2-Symmetrical Inhibitors of HIV-Protease**

By *Anusch Peyman,* Karl-Heinz Budt, Jörg Spanig,* and *Dieter Ruppert*

One of the most interesting targets for AIDS chemotherapy is the virally encoded protease of the Human Immunodeficiency Virus (HIV).[1] The HIV-protease is an enzyme of the aspartylprotease family, and plays a key role in processing the HIV-polyproteins produced directly after translation.[1] If this processing step does not take place, only im-

[*] Dr. A. Peyman, Dr. K.-H. Budt, Dr. J. Spanig, Dr. D. Ruppert,
Pharma Forschung der Hoechst AG
Postfach 800320
D-65926 Frankfurt (FRG)
Telefax: Int. code + (69)331-399

mature, uninfectious viral particles are produced.[2] The HIV-protease is a C_2-symmetrical, homodimeric protein.[3] This fact prompted several research groups simultaneously to synthesize inhibitors whose geometry was not derived from that of the natural substrate, but which instead was inspired by the symmetry of the enzyme.[4, 5] We recently reported the synthesis of bis(α-aminoalkyl)phosphinic acids,[6] which allow the placement of the phosphinic acid group into a C_2-symmetrical peptide environment, where it acts as a transition state analogue of peptide hydrolysis. This approach leads to effective inhibition of HIV-protease. Here we report on the effect the stereochemistry and substituents have on these inhibitors, and present a new synthetic approach to this class of compounds.

The synthesis of inhibitors **5** is shown in Scheme 1. The initial, decisive step in this synthesis was the alkylation of the bisimino compound **1** with benzyl bromide. The resulting

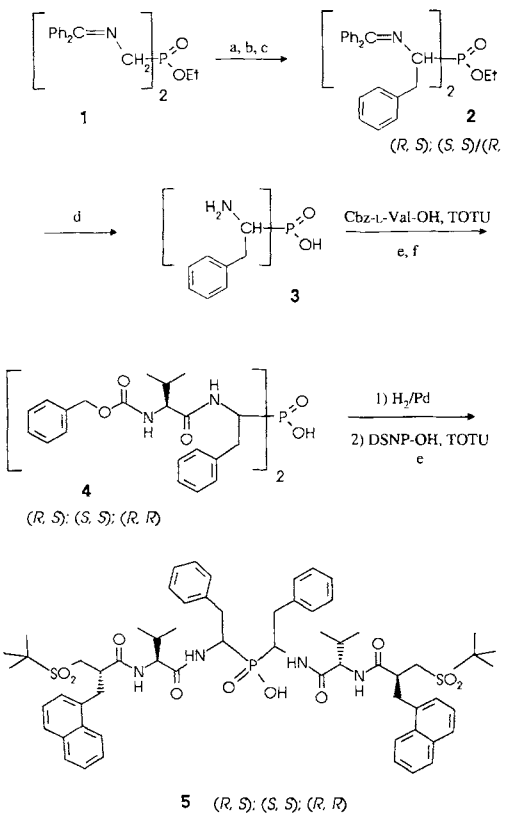

Scheme 1. Synthesis of C_2-symmetrical phosphinic acid inhibitors of HIV-protease by electrophilic substitution and separation of diastereomers: a) *n*BuLi, −78 °C. b) $PHCH_2Br$, 24 h, −78 °C, 95%. c) Chromatographic separation of (*R,S*) from (*R,R*)/(*S,S*): silica gel, ethyl acetate/*n*-heptane 4/6, R_f: (*R,S*) 0.8; (*R,R*)/(*S,S*) 0.7; yield 1:1. d) 30% HBr/AcOH, 95%. e) TOTU [7], DMF, 25 °C/2 h, 80%. f) HPLC separation of (*R,R*)/(*S,S*): C_{18}-Nucleosil 5U, CH_3CN, H_2O, NH_4OAc 4/6/0.05, pH 7.2, 1 mL min^{-1}, 40 °C, R_t(min): 11.2 (*R,R*), 19.5 (*S,S*). NBS = *N*-bromosuccinimide.

diastereomeric mixture of substitued bis(α-iminoalkyl)-phosphinic acids **2** may be separated by chromatography into an (*R,S*) and an (*R,R*)/(*S,S*) fraction, in a ratio of 1:3. After deprotection of the amino group by acid hydrolysis to give **3**, these fractions were condensed separately with *N*-benzyloxycarbonyl-L-valine (Cbz-L-Val-OH). Because of the limited solubility of **3** in organic solvents, TOTU[7] was utilized as a coupling reagent, and was found most effective in peptide condensations in aqueous organic solvents. The conversion of (*R,S*)-**2** to (*R,S*)-**4** afforded only one product, whereas conversion of the racemate (*R,R*)/(*S,S*)-**2** to (*R,R*)/(*S,S*)-**4** yielded two diastereomeric compounds. The latter could be separated by preparative high-performance liquid chromatography (HPLC).[8] After removal of the Cbz protecting group with H_2/Pd, all three fractions were coupled separately with DSNP-OH,[9] a particularly suitable N-terminal residue for inhibition of the HIV-protease.[5]

Since substituted bis(α-aminoalkyl)phosphinic acids are an interesting class of compounds with potential biological activity in a variety of areas,[10] we investigated alternative methods for their synthesis. Following studies by Steglich et al.[11] on α-aminophosphonic acids, we synthesized **3** by the method shown in Scheme 2, by nucleophilic substitution of the bis(α-acylamino-α-bromomethyl)phosphinic ester **7** with benzyl magnesium bromide. The unstable dibromo com-

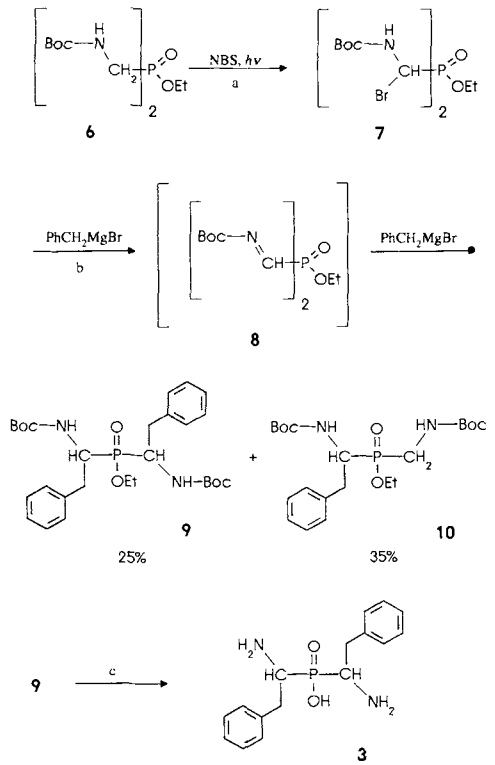

Scheme 2. Alternative synthesis of the bis(α-aminoalkyl)phosphinic acids **3** by nucleophilic substitution: a) CCl_4, 20 °C, 2 h, 96% crude yield. b) 4 equiv $PhCH_2MgBr$, −70 °C, 3 h. c) 30% HBr/AcOH, 95%.

pounds **7** were not isolated, but reacted further in situ. The first equivalent of the Grignard reagent presumably acts as a base, and the reaction proceeds via intermediate formation of the bis(α-acyliminomethyl)phosphinic ester **8**, to which the Grignard reagent then adds as a nucleophile. The yield of bis-alkylated **9** was rather low (ca. 20%, diastereomeric mixture). The major product was the monoalkylated compound **10**, in about 35% yield. However, with the two synthetic procedures presented here, both electrophilic and nucleophilic substitution are available for derivatization of the bis(α-aminomethyl)phosphinic acid, allowing access to a large palette of compounds.

The results of studies on the inhibition of the HIV-protease by compounds **4** and **5** and by several other derivatives with an unsubstituted central moiety are summarized in Table 1. The most obvious point here is that the free acid is essential for effective inhibition; the ester **12** proved to be less effective. Comparison of the unsubstituted compounds

Table 1. IC_{50} values for inhibition of the HIV-protease [13] by bis-(α-aminoalkyl)phosphinic acids and esters of type **A**.

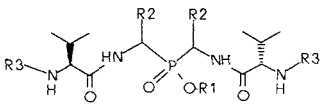

Compd.	R^1	R^2 (conf.)	R^3	IC_{50} [nM]
4a	H	$PhCH_2$ (*R,S*)	Cbz	500
4b	H	$PhCH_2$ (*S,S*)	Cbz	180
4c	H	$PhCH_2$ (*R,R*)	Cbz	1.1
5a	H	$PhCH_2$ (*R,S*)	DSNP	1.4
5b	H	$PhCH_2$ (*S,S*)	DSNP	85
5c	H	$PhCH_2$ (*R,R*)	DSNP	0.5
11	H	H	DSNP	1.1
12	CH_3	H	DSNP	950
13	H	H	Cbz	10000
14	H	H	H-Phe	12
15	H	H	H	>10000

(R^2 = H) revealed a strong dependence on the terminal residue R^3. The DSNP group in **11** proved to be ten times more effective than the phenylalanyl group in **14**, whereas the latter was far superior to the Cbz group in **13**. In the absence of a terminal residue (compound **15**), no activity was observed. Interestingly, these differences were significantly reduced after the introduction of the central benzyl groups. Thus, compounds **5b** and **5c** with a terminal DSNP unit were only twice as effective as those with a terminal Cbz unit (**4b** and **4c**). Correspondingly, introduction of the central benzyl groups in the presence of the DSNP group (from **11** to **5c**) afforded only a slight improvement. This "saturation" possibly arose from the method used for the assay, in which the enzyme was titrated with very strong inhibitors. As expected, the inhibitory action was also strongly dependent on the configuration at the C atom bearing the benzyl groups; inhibition decreased in the DSNP series **5** in the order (*R,R*) > (*R,S*) > (*S,S*), and in the Cbz series **4** in the order (*R,R*) > (*S,S*) > (*R,S*). This change in the activity dependence could be interpreted as an indication of different modes of binding.

The combination of a central phosphinic acid unit with a symmetrical peptide arrangement proved to be most successful. Compound (*R,R*)-**5c** displays an IC_{50} value of 0.5 nM[12] and is hence an extremely potent inhibitor of the HIV-protease. The new procedures for synthesis of this class of compounds give us the opportunity to elucidate their structure–activity relationships in more detail, and thereby to discover further, highly active HIV-protease inhibitors.

Received: June 23, 1993 [Z 6162 IE]
German version: *Angew. Chem.* **1993**, *105*, 1852

[1] H. Mitsuya, R. Yarchoan, S. Broder, *Science* **1990**, *249*, 1533–1544; A. G. Tomasselli, W. J. Howe, A. Wlodawer, R. L. Heinrikson, *Chim. Oggi* **1991**, May issue pp. 6–27; D. W. Norbeck, D. J. Kempf, *Annu. Rep. Med. Chem.* **1991**, *26*, 141.

[2] N. E. Kohl, E. A. Emini, W. A. Schleif, L. J. Davis, J. C. Heimbach, R. A. F. Dixon, E. M. Scolnick, I. S. Sigal, *Proc. Natl. Acad. Sci. USA* **1988**, *85*, 4686.

[3] A. Wlodawer, M. Miller, M. Jaskolski, B. K. Sathyanarayana, E. Baldwin, I. T. Weber, L. M. Selk, L. Clawson, J. Schneider, S. B. H. Kent, *Science* **1989**, *245*, 616.

[4] K.-H. Budt, A. Peyman (Hoechst AG), EP-A 0435059, **1990**; *Chem. Abstr.* **1991**, *115*, P163862u; K.-H. Budt, J. Knolle, C. Meichsner, D. Ruppert, B. Stowasser, I. Winkler, A. Paessens, J. Hansen (Hoechst AG), EP-A 0428849, **1990**; *Chem. Abstr.* **1992**, *116*, P214912m; J. Erickson, D. J. Neidhart, J. Van Drie, D. J. Kempf, X. C. Wang, D. W. Norbeck, J. J. Plattner, J. W. Rittenhouse, M. Turon, N. Wideburg, W. E. Kohlbrenner, R. Simmer, R. Helferich, D. A. Paul, M. Knigge, *Science* **1990**, *249*, 527; R. Bone, J. P. Vacca, P. S. Anderson, M. K. Holloway, *J. Am. Chem. Soc.* **1991**, *113*, 9382; D. Enders, K.-J. Heider, G. Raabe, *Angew. Chem.* **1993**, *32*, 592; *Angew. Chem. Int. Ed. Engl.* **1993**, *32*, 598; G. B. Dreyer, J. C. Boehm, B. Chenera, R. L. DesJarlais, A. M. Hassell, T. D. Meek, T. A. Tomaszek, Jr., *Biochemistry* **1993**, *32*, 937.

[5] K.-H. Budt, J. Hansen, J. Knolle, C. Meichsner, A. Paessens, D. Ruppert, *IXth Int. Conf. AIDS-IVth World Congress*, Berlin, **1993**, PO-A25-0613.

[6] A. Peyman, K.-H. Budt, J. Spanig, B. Stowasser, D. Ruppert, *Tetrahedron Lett.* **1992**, *33*, 4549; B. Stowasser, K.-H. Budt, L. Jian-Qi, A. Peyman, D. Ruppert, *ibid.* **1992**, *33*, 6625.

[7] TOTU: *O*-[cyano(ethyoxycarbonyl)methylenamino]-*N,N,N',N'*-tetramethyluronium tetrafluoroborate: W. König, G. Breipohl, P. Pokorny, M. Birkner, *Proc. 21st Europ. Peptide Symp.* **1990** (Eds.: E. Giralt, D. Andreu), ESCOM, Leiden, **1991**, p. 143.

[8] The configurations (*R,R*) and (*S,S*) have so far only been assigned with reference to the activity found with the HIV-protease. For related inhibitors bearing a bishydroxyethyl group instead of the phosphinic acid unit, activity decreases in the order (*S,S*) > (*R,R*) [5]. We have therefore assigned the more active compound **4c** the configuration (*R,R*) (the introduction of a phosphorus atom changes the priorities for the configuration assignment). A suitable derivatization and an X-ray structural analysis are still outstanding.

[9] (2*S*)-(1,1-dimethylethylsulfonylmethyl)-3-(1-naphthyl)propionic acid DSNP-OH, synthesis analogous to the phenyl derivative (2*S*)-(1,1-dimethylethylsulfonylmethyl)-3-(1-phenyl)propionic acid: P. Bühlmayer, A. Caselli, W. Fuhrer, R. Göschke, V. Rasetti, H. Rüeger, J. L. Stanton, L. Criscione, J. M. Wood, *J. Med. Chem.* **1988**, *31*, 1839.

[10] P. Kafarski, B. Lejzak, *Phosphorus, Sulfur Silicon Relat. Elem.* **1991**, *63*, 193.

[11] T. Schrader, W. Steglich, *Synthesis* **1989**, 97; T. Schrader, R. Kober, W. Steglich, *ibid.* **1986**, 372.

[12] IC_{50}: Inhibitor concentration causing a 50% reduction in enzyme activity.

[13] Inhibition of the HIV-protease was measured at pH 5.5 with an HPLC assay and the specific substrate SFNF'Opr'QI. Opr stands for 5-oxaproline, and replaces the proline in the natural substrate SFNFPQI (N terminus of the HIV-protease). The Opr-containing peptide is cleaved more rapidly, and a greatly reduced amount of enzyme is therefore required for the assay: S. Henke, G. Breipohl, W. König, K. Mölling, (Hoechst AG), EP-A 0373576, **1989**; *Chem. Abstr.* **1990**, *114*, P825535s.

The Pagodane Route to Dodecahedranes: An Improved Approach to the $C_{20}H_{20}$ Parent Framework; Partial and Total Functionalizations—Does C_{20}-Fullerene Exist?**

By *Fabian Wahl, Jürgen Wörth,* and *Horst Prinzbach**

The I_h-symmetrical pentagonal dodecahedrane (**1**) is an appealing hydrocarbon;[1] the increasing chemical modification of this molecule greatly enhances its appeal by opening a range of novel preparative and theoretical perspectives.[2] Monofunctionalizations of **1** (**A**) and directed 1,16-difunctionalizations (**B**) can be easily achieved following work of Paquette et al. and Olah et al.[3] Two to eight pairs of symmetrically positioned functionalities (**C**,[4] **D**[5]) are introduced through our pagodane → dodecahedrane route[6] by means of appropriately functionalized pagodane precursors. In this context the replacement of all the H atoms (**F**, e.g. the $C_{20}Br_{20}$ "bromine ball" **2** and the $C_{20}(OH)_{20}$ "vesicle" **3**)

[*] Prof. Dr. H. Prinzbach, Dipl.-Chem. F. Wahl, Dr. J. Wörth
Chemisches Laboratorium der Universität
Institut für Organische Chemie und Biochemie
Albertstrasse 21, D-79104 Freiburg (FRG)
Telefax: Int. code + (761) 203-5987

[**] This research was supported by the Deutsche Forschungsgemeinschaft, the Fonds der Chemischen Industrie, and BASF AG. We thank Dr. H.-D. Beckhaus (Freiburg) for help with the calculations, Doz. Dr. E. Campbell (Max-Born-Institut für Nichtlineare Optik und Kurzzeitspektroskopie (MBI), Berlin-Adlershof (FRG)) for the laser desorption time of flight (TOF) mass spectra, and Dr. W. Vetter (Ciba-Geigy, Basel) for the FAB/FD MS analyses (FAB = fast atom bombardment, FD = field desorption, MS = mass spectrometry).

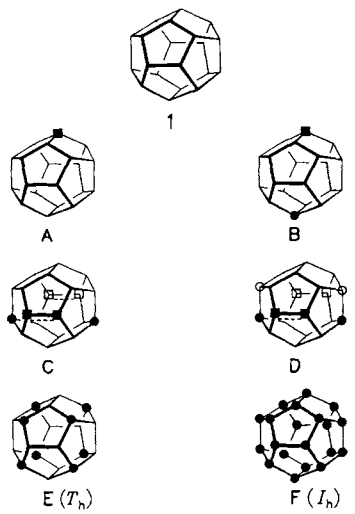

and the total dehydrogenation to provide the extremely energy-rich 20 π electron polyene **4** (C_{20}-fullerene) are fascinating extensions. Compound **4**, in particular, is of current interest, as it is the smallest fullerene according to Euler's theorem and as recent calculations have identified it as the lowest energy structure in a series of C_{20} isomers.[7, 8] Still, **1** has not entered the fullerene literature as perhydro-**4**. In this communication we report on an improved route to **1** and on the first results in multiple (e.g. **E**) and total functionalization (**F**).[12]

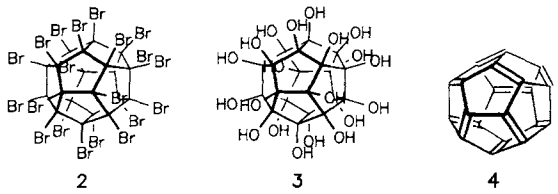

Given the efficiency of the pagodane route it was tempting to base an improved approach to **1** on products of this route (Scheme 1). The reaction sequence that turned out to be highly expeditious started from dimethyl dodecahedrane-1,6-dicarboxylate (**7a**, R = OCH_3),[4] efficiently prepared from isodrin (**5**) via diketodinitrile **6**, and consisted of saponification, Barton degradation[13] to give 1,6-dibromide **9**, and reduction.[14] Apparently in both stages the intermediate dodecahedryl radicals (e.g. 1,6-diradical **8**)[15] are trapped efficiently, despite considerable frontal shielding. The yield of 90% based on **7a** met our expectations.

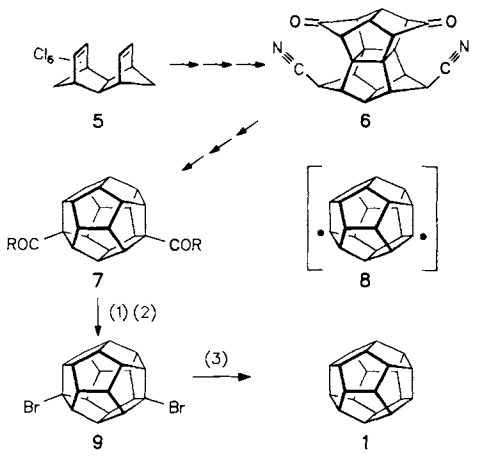

Scheme 1. (1) KOH, CH_3OH, H_2O; 8 h reflux, 99% **7b** (R = OH); (2) $(COCl)_2$, C_6H_6, 3 h reflux, **7c** (R = Cl); $BrCCl_3$, mercaptopyridine-1-oxide sodium salt, 4-dimethylaminopyridine (DMAP), 1 h reflux, 89% **9**; (3) tris(trimethylsilyl)silane, C_6H_6, low-pressure Hg lamp (254 nm), room temperature, 2 h, 99% **1**.

The dilemma in the multifunctionalization of **1** is expressed quantitatively (Polya theorem)[16] by the number of isomers (N_i) which increases rapidly even for the same X group (Table 1). Accordingly, only the preparation of

Table 1. Number of isomers (N_i) with the same substituent X and without vicinal X,X arrangements (A_i), and number of isomers of A_i (C_i) leading to **E**.

$C_{20}H_{20}$ → $C_{20}H_{20-n}X_n$

n =	1	2	3	4	5	6	7	8	9	10
N_i	1	5	15	58	149	371	693	1135	1466	1648
A_i	1	4	9	20	20	16	5	1	0	0
C_i	1	3	3	5	3	3	1	1	0	0

$C_{20}H_{19}X$, $C_{20}HX_{19}$, and $C_{20}X_{20}$ statistically makes sense. When vicinal X,X arrangements are excluded, the number of isomers N_i is reduced to A_i; for $n = 8$ this corresponds to a single, T_h-symmetrical isomer (**E**). However, **E** is directly accessible only from C_i subsets of A_i (statistical yield 0.4%).[17]

The strain energies (MM2 calculations)[18] listed in Table 2 are revealing with regard to the steric compression on the molecular surface, which is associated with increasing functionalization, and to the possibility of sterically steering multisubstitutions of **1**. This data implies that 1,2-dibromination and 1,2,3-tribromination cause an increase in strain approximately 3.4 and 11.7 kcal mol^{-1}, respectively, greater than that associated with 1,3-dibromination; in contrast perhydroxylation (→ **3**) leads to a decrease, perbromination (→ **2**) to a tremendous increase in strain (according to this **2** is more strained than **4**).

Table 2. Strain energies (MM2 calculations) E_{str} [kcal mol^{-1}] of some dodecahedrane derivatives. **1** = 68.9, **4** = 350.1 kcal mol^{-1}.

X	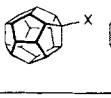	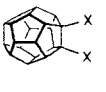	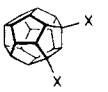	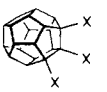	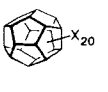
OH	69.0	69.1	69.0	69.1	64.5
F	72.7	75.8	76.5	78.8	121.6
Cl	70.9	74.9	72.8	79.3	234.6
Br	73.3	80.9	77.5	89.2	383.5

Preliminary experiments on the steric control of the multisubstitution of **1** were directed towards the synthesis of the T_h-symmetrical octabromide **10** (**E**). When **1** was subjected to conditions for irreversible radical bromination (Scheme 2), which should not enforce vicinal dibromination, a red-brown, crystalline product was isolated, which was poorly soluble in $CHCl_3$ and consisted of a mixture of brominated derivatives $C_{20}H_{15}Br_5$ to $C_{20}H_{12}Br_8$ [IR (KBr): $\tilde{\nu}$ = 2948, 2920, 2848 (C–H), 1724, 1449, 1283, 864, 818,

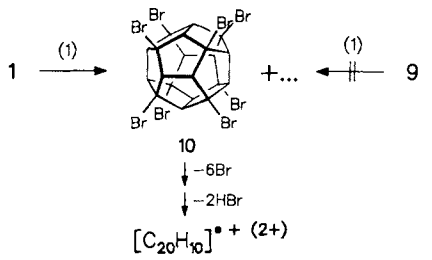

Scheme 2. (1) **1** (10 mg, 3.85×10^{-5} mol) or **9** (10 mg, 2.39×10^{-5} mol) in 5 mL bromine/CCl_4 (2:1; 0.065 mol bromine), 4h irradiation with a 300W daylight lamp, reflux.

734, 655 cm^{-1}]. In the ^1H NMR spectrum (250 MHz, $CDCl_3$; series of multiplets between $\delta = 3.4$ and 5.0) a dominant singlet is observed at $\delta = 4.49$ which is in the anticipated range for T_h-symmetrical **10** (with ca. 5% the proportion is higher than expected statistically). In the electron ionization (EI) mass spectrum of the mixture (Fig. 1) the fragmentation cascade begins with the M^+ envelope of **10** (*m/z* 884–900 (1%)) and ends after a series of HBr/Br eliminations with the bromine-free $C_{20}H_{10}$ cluster (*m/z* 250 (60%)). The $C_{20}H_{10}$ cluster provides the base peak (*m/2e* 125 (100%)), which is regarded as an indication that multiply conjugated pentaenes (cf. **13**) are present.

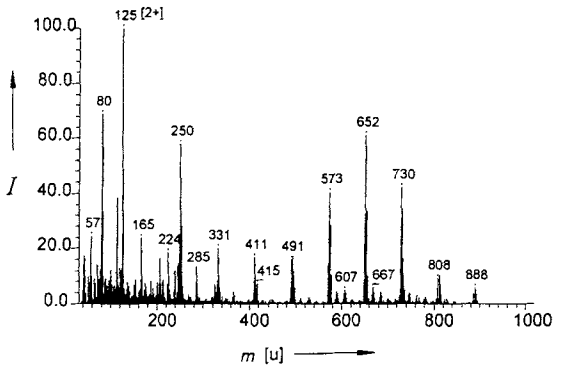

Fig. 1. EI mass spectrum (70 eV) of **10** and other products from the bromination of **1** according to Scheme 2. *I* = relative intensity, *m* = mass in atomic mass units u.

Control experiments on the irreversibility and the 1,3-selectivity of the substitutions were conducted with 1,6-dibromide **9**, as it is the only one of the four nonvicinal $C_{20}H_{18}Br_2$ isomers (A_1) that cannot lead directly to **10**. Analysis of the IR spectrum, EI mass spectrum, and ^1H NMR spectrum (series of multiplets between $\delta = 3.4$ and 5.0) of the reaction products indicates a mixture of penta- to heptabrominated dodecahedranes similar to the mixture obtained from **1** but definitely lacking octabromide **10**.

Analogous control was not evident in the initial attempts at the directed chlorination under "mild" ionic (reversible) conditions (Scheme 3). MS analyses of the readily soluble (in dimethylformamide (DMF) and $CHCl_3$) product mixtures confirm that up to 14 hydrogen atoms have been exchanged statistically for chlorine atoms [IR (KBr): $\tilde{\nu} = 2956$ (C–H),

Scheme 3. (1) **1** (10 mg, 3.85×10^{-5} mol), 20 mL CCl_4, $AlCl_3$ (100 mg, 0.75 mmol), dry chlorine gas, 5h–3d reflux.

1737, 1398, 1340, 1289, 1260, 1188, 1112, 876, 846, 801, 733, 707 cm^{-1}; ^1H NMR ($CDCl_3$, 400 MHz): $\delta = 4.20-4.72$ (series of m); ^{13}C NMR ($CDCl_3$, 100.6 MHz): $\delta = 99.1-97.2$ (20 signals for C-Cl), 90.7–82.6 (36 signals for α-C), 62.9–58.2 (17 signals for β-C))]. In the EI mass spectra (70 eV) of a number of samples, fragmentation of the framework is not evident besides the successive elimination of HCl/Cl, as was noticed for **10**; the signals at *m/z* 248 (60%) and *m/z* 246 (26%) could arise from dodecahexaenes ($C_{20}H_8$) and dodecaheptaenes ($C_{20}H_6$).

Reactions under "extreme" conditions (Scheme 4) intended to bring about total chlorination yielded a colorless, air-stable product, which crystallized from the hot reaction mixture(s) and was insoluble in all solvents tested (CH_2Cl_2, $CHCl_3$, CCl_4, tetrachloroethane, C_4Cl_6, C_6H_6, $C_6H_3Cl_3$, CH_3OH, C_5H_5N, CS_2, CF_3COOH, toluene, THF, isopropyl alcohol) even when heated. The vaporization curve (mass

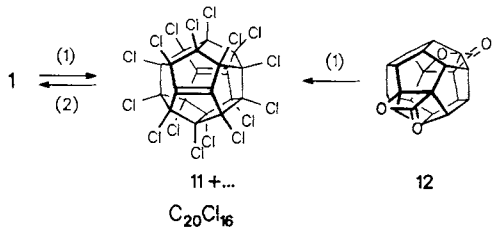

Scheme 4. (1) **1** (10 mg, 3.85×10^{-5} mol) or **12** (10 mg, 2.91×10^{-5} mol) in 30 mL CCl_4 saturated with dry chlorine gas (ca. 0.11 mol); the reaction mixture was heated for 16h at ca. 130 °C in a glass ampule (60 mL) with a safety valve by irradiation with a 300W daylight lamp; (2) Pt/H_2; ethyl acetate/methanol, room temperature, 3d.

spectrum) indicates that the product is uniform (m.p. > 330 °C). No C–H bands are seen in the IR spectrum (KBr; $\tilde{\nu} = 1782$, 1636, 1341, 1161, 1027, 993, 970, 957, 940, 885, 800, 786, 665 cm^{-1}). The EI mass spectrum (70 eV; Fig. 2, Scheme 5) supports the composition $C_{20}Cl_{16}$ (e.g. **11**) and manifests the successive loss of all Cl substituents [path (a), noteworthy signals are *m/z* 594 (97%, $C_{20}Cl_{10}$ pentaenes (e.g. **13**)) and in particular *m/z* 240 (30%, C_{20} decaene **4** (?)] and two characteristic fragmentations of the framework [path (b), *m/z* 452 (36%, $C_{11}Cl_9$) and *m/z* 355 (88%, C_9Cl_7):

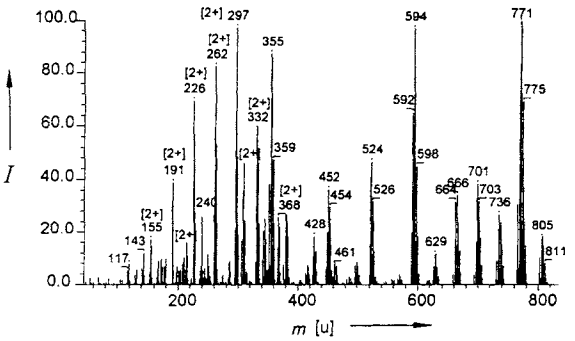

Fig. 2. EI mass spectrum (70 eV) of **11** and other products from the chlorination according to Scheme 4. *I* = relative intensity, *m* = mass in atomic mass units u.

the cleavage $C_{20} \rightarrow C_{11} + C_9$ observed for the 1,16-dodecahedradiene and bislactone **12**; path (c), *m/z* 499 (6%, $C_{15}Cl_9$) and *m/z* 308 (20%, C_5Cl_7): the cleavage $C_{20} \rightarrow C_{15} + C_5$ observed for 1,7,16-dodecahedratriene[4, 10]. The

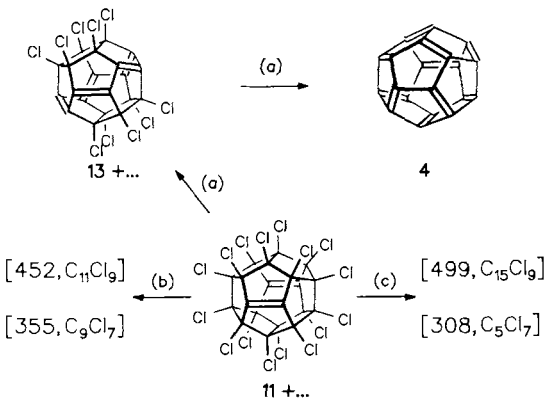

Scheme 5.

three fragmentation pathways are easier to trace in the mass spectrum recorded at 28 eV (Fig. 3), which does not have the signals of the doubly charged fragments. Under these conditions path (a) terminates at $C_{20}Cl_{10}$ with m/z 594 (15%). We can only speculate as to why the chlorination halts at $C_{20}Cl_{16}$ and which isomers are formed other than (most likely) 1,16-diene **11**. That $C_{20}Cl_{16}$ is remarkably stable to

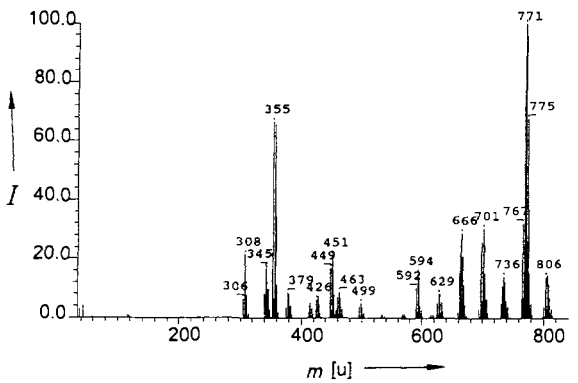

Fig. 3. EI mass spectrum (28 eV) of **11** and other products from the chlorination according to Scheme 4. I = relative intensity, m = mass in atomic mass units u.

oxygen relative to the corresponding unsubstituted dodecahedradiene[4, 5] reflects the interplay of electronic and steric factors. Attempts at recording the $^1H/^{13}C$ NMR spectra and FAB/FD mass spectra of these perchlorinated dodecahedranes as well as of their chemical modifications have failed so far because of extremely poor solubility. It is unlikely that $C_{20}Cl_{16}$ is formed from $C_{20}Cl_{20}$ under measurement conditions. $C_{20}Cl_{16}$ can be reduced very cleanly by catalytic hydrogenation to provide **1**, proof that the dodecahedrane skeleton is unchanged in $C_{20}Cl_{16}$. According to mass spectrometry, the mother liquor from the chlorination reaction contains traces of derivatives that are more soluble because their symmetry is reduced by other substituents (e.g. $C_{20}Cl_{15}CCl_3$ from the reaction with CCl_3 radicals arising from CCl_4).[19] This observation could prove useful for the future preparation of more readily soluble polyhalogenated dodecahedranes.

In attempts to prepare the perchlorinated 1,16-diene **11** in a directed manner, bislactone **12**[20] was chlorinated under "extreme" conditions (Scheme 4; **12** was previously observed to give the 1,16-diene in gas-phase thermolyses). The solid isolated after a reaction time of 16 h is identical in every respect to the $C_{20}Cl_{16}$ cluster obtained from **1**.

The "extreme" bromination of **1** (Scheme 6) yields a deep brown, crystalline, high-melting (m.p. > 330 °C, decomp), and insoluble mixture of hydrogen-free bromides (IR (KBr): $\tilde{\nu}$ = 1627, 1598, 1479, 1365, 1191, 1160, 886, 775, 740, 694, 671 cm^{-1}), which most certainly contains the $C_{20}Br_{20}$ "bromine ball" **2**. This product is supported by signals in the

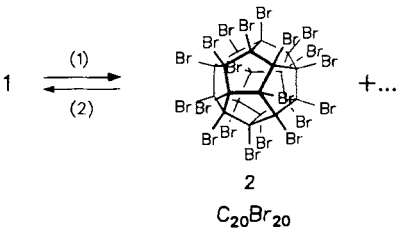

Scheme 6. (1) **1** (10 mg, 3.85×10^{-5} mol) in 10 mL bromine (0.20 mol) was heated for 8 h at ca. 130 °C in a glass ampule (60 mL) with a safety valve by irradiation with a 300 W daylight lamp; (2) Pt/H_2; ethyl acetate/methanol, room temperature, 3 d.

LD-TOF mass spectrum (Fig. 4), $M(C_{20}{}^{79}Br_{20}) = 1820$, $M(C_{20}{}^{81}Br_{20}) = 1860$. Here, too, more definitive characterization by ^{13}C NMR spectroscopy has not been possible yet. Dodecahedrane **1** can be recovered to a large extent (> 90%) from catalytic hydrogenation of the crude product of the bromination.

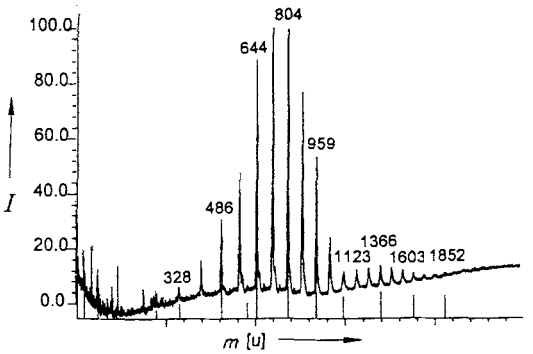

Fig. 4. LD-TOF mass spectrum of **2** and other products from the chlorination according to Scheme 6. I = relative intensity, m = mass in atomic mass units u.

The behavior of the poly- and perfunctionalized dodecahedranes, in particular the polyhalides,[21] in their mass spectra has interesting parallels and differences to that of the poly- and perfunctionalized (chlorinated,[22] brominated,[23] fluorinated[24]) C_{60}-fullerenes. The possibilities in the directed polyfunctionalization of **1** and its derivatives lend new dimensions to the chemistry of these cage molecules. In particular, routes to multiply unsaturated dodecahedranes, ultimately to C_{20}-fullerene (**4**), renders many attractive preparative and theoretical topics open to experimental study.

Received: July 15, 1993 [ZZ6214IE]
German version: *Angew. Chem.* **1993**, *105*, 1788

[1] R. Hoffmann, *Sci. Am.* **1993**, *268*, No. 2, p. 40; *Spektrum Wissensch.* **1993**, No. 4, p. 68.

[2] K. Weber, H. Prinzbach, R. Schmidlin, F. Gerson, G. Gescheidt, *Angew. Chem.* **1993**, *105*, 907; *Angew. Chem. Int. Ed. Engl.* **1993**, *32*, 875, and references therein.

[3] L. A. Paquette, *Chem. Rev.* **1989**, *89*, 1051; L. A. Paquette, J. C. Weber, T. Kobayashi, Y. Miyahara, *J. Am. Chem. Soc.* **1988**, *110*, 8591; G. A. Olah, G. K. Surya Prakash, W.-D. Fessner, T. Kobayashi, L. A. Paquette, *ibid.* **1988**, *110*, 8599.

[4] R. Pinkos, J.-P. Melder, H. Fritz, H. Prinzbach, *Angew. Chem.* **1989**, *101*, 319; *Angew. Chem. Int. Ed. Engl.* **1989**, *28*, 310; R. Pinkos, J.-P. Melder, K. Weber, D. Hunkler, H. Prinzbach, *J. Am. Chem. Soc.* **1993**, *115*, 7173.

[5] J.-P. Melder, R. Pinkos, H. Fritz, J. Wörth, H. Prinzbach, *J. Am. Chem. Soc.* **1992**, *114*, 10213.

[6] W.-D. Fessner, H. Prinzbach (*The Pagodan Route to Dodecahedranes*) in *Cage Hydrocarbons* (Ed.: G. A. Olah), Wiley, New York, **1990**, p. 353.

[7] D. Bakowies, W. Thiel, *J. Am. Chem. Soc.* **1991**, *113*, 3704; V. Parasuk, I. Almof, *Chem. Phys. Lett.* **1991**, *184*, 187; C. J. Brabec, E. Anderson, B. N. Davidson, S. A. Kajihara, Q. M. Zhang, J. Bernholc, D. Tomanec, *Phys. Rev. B Rapid Commun.* **1992**, *46*, 7326; G. van Helden, M. T. Hsu, N. G. Gotts, P. R. Kemper, M. T. Bowers, *Chem. Phys. Lett.* **1992**, *204*, 15; R. C. Haddon, *Science* **1993**, *261*, 1545.

[8] Compound **4** is the final member in the series of dodecahedrapolyenes. Contrary to early calculations and expectations[9] the dodecahedrenes and nonconjugated dodecahedradienes[4,5,12] proved to have surprising thermal stability; owing to the steric shielding of the highly bent C=C bonds ($\varphi = 43-50°$), dimerization only occurs at high temperatures[10]. The existence of $C_{20}H_{14}$ trienes and $C_{20}H_{12}$ tetraenes was deduced previously from intense signals in the mass spectra of multifunctionalized dodecahedranes[4,5,10,12]. Multiple *cis*-HX elimination and release of multiply unsaturated dodecahedranes were recently achieved with Schwesinger bases[11].

[9] A. B. McEwen, P. von R. Schleyer, *J. Org. Chem.* **1986**, *51*, 4357.

[10] K. Weber, Dissertation, Universität Freiburg, **1993**.

[11] R. Schwesinger, R. Link, G. Thiele, H. Rotter, D. Honert, H.-H. Limbach, F. Männle, *Angew. Chem.* **1991**, *103*, 1376; *Angew. Chem. Int. Ed. Engl.* **1991**, *30*, 1372, and references therein

[12] F. Wahl, Dissertation, Universität Freiburg, **1993**.

[13] D. H. R. Barton, D. Crich, W. B. Motherwell, *Tetrahedron* **1985**, *41*, 3901; E. W. Della, J. Tsanaktsidis, *Aust. J. Chem.* **1989**, *42*, 61; D. H. R. Barton, J. C. Jaszberenyl, D. Tang, *Tetrahedron Lett.* **1993**, *34*, 3381.

[14] C. Chatgilialoglu, D. Griller, M. Lesage, *J. Org. Chem.* **1988**, *53*, 3641.

[15] K. Weber, H. Fritz, H. Prinzbach, *Tetrahedron Lett.* **1992**, *33*, 619; cf. L. A. Paquette, D. R. Lagerwall, H.-G. Korth, *J. Org. Chem.* **1992**, *57*, 5413.

[16] G. Polya, *Act. Math.* **1937**, *68*, 145; J. M. Schulman, T. Venanzi, R. L. Disch, *J. Am. Chem. Soc.* **1975**, *97*, 5335; J. S. Garavelle, J. E. Leonhard, *J. Comput. Chem.* **1985**, *9*, 133; L. A. Paquette, R. J. Ternansky, D. W. Balogh, W. J. Taylor, *J. Am. Chem. Soc.* **1983**, *105*, 5441.

[17] G. Rücker, C. Rücker, *Chimia* **1990**, *44*, 116; *J. Chem. Inf. Comput. Sci.* **1990**, *30*, 187.

[18] U. Burkert, N. L. Allinger, *Molecular Mechanics* (*ACS Monogr. 177*), American Chemical Society, Washington D.C., **1982**.

[19] The polychlorides generated in recent chlorination reactions with **7a** under "extreme" conditions (including $C_{20}Cl_{14}(CCl_3)_2$) are also soluble in standard solvents.

[20] J.-P. Melder, R. Pinkos, H. Fritz, H. Prinzbach, *Angew. Chem.* **1990**, *102*, 105; *Angew. Chem. Int. Ed. Engl.* **1990**, *29*, 95.

[21] The fluorination of **1** is being studied by Prof. A. Haas and Dr. M. Lieb (Universität Bochum).

[22] F. N. Tebbe, R. L. Harlow, D. B. Chase, D. L. Thorn, G. C. Campbell, Jr., J. C. Calabrese, N. Herron, R. Y. Young, E. Wassermann, *Science* **1992**, *256*, 822; G. A. Olah, I. Bucsi, C. Lambert, R. Aniszfeld, N. J. Trivedi, D. K. Sensharma, G. K. S. Prakash, *J. Am. Chem. Soc.* **1991**, *113*, 9385; G. K. S. Prakash, I. Bucsi, R. Aniszfeld, G. A. Olah (*Improved Preparation, Chemical Reactivity, and Functionalization of C_{60} and C_{70} Fullerenes*) in *Buckminsterfullerenes* (Eds.: W. E. Billups, M. A. Ciufolini), VCH, Weinheim, **1993**, p. 301.

[23] P. R. Birkett, P. B. Hitchcock, H. W. Kroto, R. Taylor, D. R. M. Walton, *Nature* **1992**, *357*, 479; F. N. Tebbe, R. L. Harlow, D. B. Chase, D. L. Thorn, G. C. Campbell, J. C. Calabrese, N. Herron, R. J. Young, E. Wassermann, *Science* **1992**, *256*, 822.

[24] R. Taylor, G. J. Langley, A. K. Brisdon, J. H. Holloway, E. G. Hope, H. W. Kroto, D. R. Walton, *J. Chem. Soc. Chem. Commun.* **1993**, 875.

Formation of Alkynyltrithiocarbonato Ligands from Alkylidyne Ligands and Carbon Disulfide**

By *Andreas Mayr** and *Tsung-Yi Lee*

Dedicated to Professor Ernst Otto Fischer on the occasion of his 75th birthday

Coupling reactions of alkylidyne ligands with carbonyl,[1] isocyanide,[2] and alkylidyne ligands[3] are well established.[4] A simple qualitative molecular orbital model for these reactions suggests that alkylidyne–thiocarbonyl coupling should also be feasible and even more facile than alkylidyne–carbonyl coupling.[4] However, no alkylidyne thiocarbonyl metal complexes are available to test this prediction. A proven method for the synthesis of thiocarbonyl ligands is the abstraction of sulfur from coordinated carbon disulfide by phosphanes.[5] Tris-trimethylphosphane-substituted tungsten alkylidyne complexes of type **2** [see Eq. (1)] appeared to be suitable precursors for alkylidyne thiocarbonyl tungsten complexes of type **1**. Dissociation of one phosphane ligand from **2** would provide an empty site for coordination of carbon disulfide and free phosphane for sulfur abstraction. The results described in this communication indicate that alkylidyne thiocarbonyl tungsten complexes can be obtained as intermediates by this strategy and that these undergo alkylidyne–thiocarbonyl coupling.

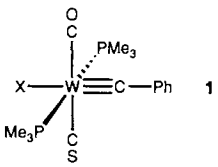

1

Alkylidyne complexes **2**[6] react slowly in THF with an excess of carbon disulfide to give the green complexes **3a–e** in moderate yields [Eq. (1)]. Trimethylphosphane sulfide is formed as a by-product.[7] The ^{13}C NMR spectra of complexes **3a–e** exhibit four signals in the low-field region at $\delta = 245-180$ (Table 1) and the expected number of signals for a phenyl group and two *trans* trimethylphosphane ligands. The ^{13}C NMR spectra thus contain one signal more than expected for complexes of type **1**. When **2b** is allowed to react with labeled $^{13}CS_2$, two ^{13}C NMR signals of complex **3b**, namely those at $\delta = 241$ and 218, are enhanced. Except for the signal at $\delta = 241$, the ^{13}C NMR data of complexes **3a–c** are similar to those of a class of tungsten

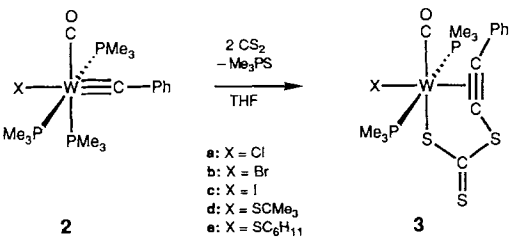

2 **3** (1)

[*] Prof. A. Mayr, T.-Y. Lee
Department of Chemistry
State University of New York at Stony Brook
Stony Brook, NY 11794-3400 (USA)
Telefax: Int. code + (516)632-7960

[**] This work was supported by the National Science Foundation. We thank Michael P. Rickenbach and Prof. Stephen A. Koch for conducting the X-ray crystallographic study.

Table 1. Characteristic ^{13}C NMR (62.9 MHz, $CDCl_3$, 25 °C) and IR (THF) data of complexes **3a–e**.

3a: δ = 240.0 (CS_3), 224.4 (CO), 219.4 (PhC*C*S), 206.2 (Ph*C*CS); $\tilde{\nu}$ = 1959 cm^{-1} (s, CO).
3b: δ = 241.2 (CS_3), 223.9 (CO), 218.1 (PhC*C*S), 205.6 (Ph*C*CS); $\tilde{\nu}$ = 1960 cm^{-1} (s, CO).
3c: δ = 243.9 (CS_3), 223.1 (CO), 216.1 (PhC*C*S), 204.0 (Ph*C*CS); $\tilde{\nu}$ = 1957 cm^{-1} (s, CO).
3d: δ = 242.1 (CS_3), 231.8 (CO), 192.7 (PhC*C*S), 180.0 (Ph*C*CS); $\tilde{\nu}$ = 1924 cm^{-1} (s, CO).
3e: δ = 243.3 (CS_3), 231.1 (CO), 193.7 (PhC*C*S), 181.8 (Ph*C*CS); $\tilde{\nu}$ = 1927 cm^{-1} (s, CO).

alkynol, alkynolester, and alkynol silyl ether complexes $[WCl_2(EOCCPh)(CO)_2(PMe_3)_2]$ (E = H, RCO, R_3Si), which were obtained by photoinduced alkylidyne–carbonyl coupling of $[W(CPh)Cl(CO)_2(PMe_3)_2]$ in the presence of ECl (E = H, Cl, and R_3Si, respectively).[8] The presence of an alkyne unit in complexes **3** is also indicated by the upfield shift of the signals at δ = 218 and 205 for complexes **3a–c** to δ = 193 and 180 for **3d**, **e**, which have thiolate ligands. These signals lie in the range characteristic for four-electron donor alkyne ligands.[9] In **3d** and **3e** π donation by the alkyne unit is reduced by competition with the strong thiolato π donor ligands, thus causing the shift of the alkyne NMR signals to higher field.

The solid-state structure of **3b** was determined by X-ray crystallography and is shown in Figure 1.[10] The newly formed alkynyltrithiocarbonato ligand is coordinated to the tungsten atom through the acetylene group and one sulfur atom. The bond lengths and angles of **3b** exhibit no unusual features.

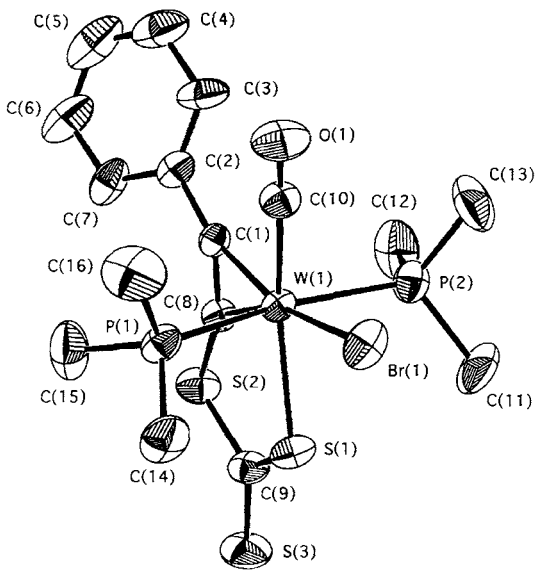

Fig. 1. Crystal structure of **3b**. Selected bond lengths [Å] and angles [°]: W1-C1 2.034(6), W1-C8 1.964(6), W1-C10 2.002(7), W1-Br1 2.6050(8), W1-P1 2.521(2), W1-P2 2.517(2), W1-S1 2.541(2), C1-C8 1.328(8), C8-S2 1.694(6), C9-S2 1.785(7), C9-S3 1.646(6), C9-S1 1.689(7); C2-C1-C8 136.9(6), C1-C8-S2 147.8(5), C8-S2-C9 98.7(3), S1-C9-S2 117.5(4), S2-C9-S3 115.3(4).

The mechanism of formation of complexes **3** is proposed to involve complexes **1** as the immediate coupling precursors.[11] An interesting question, which still remains open, is how the alkylidyne–thiocarbonyl coupling step is induced. Alkylidyne–carbonyl couplings are induced primarily by nucleophiles, whereas alkylidyne–isocyanide couplings are initiated exclusively by electrophiles.[4] Alkylidyne–thiocarbonyl couplings are expected to be susceptible to induction by both nucleophiles and electrophiles.[4] The nature of the products **3** suggests electrophilic attack of carbon disulfide at the thiocarbonyl ligand as a mechanistic possibility.[12] However, coupling could also be induced by nucleophilic attack of Me_3PS at the metal center to give an intermediate with a thioketenyl ligand. Further reaction of the thioketenyl ligand with carbon disulfide and displacement of Me_3PS from the metal center by the resulting trithiocarbonate group could also account for the formation of the products. Regardless of the actual coupling mechanism, if the alkylidyne thiocarbonyl complexes **1** are indeed intermediates in the reaction shown in Equation (1), then the results imply that alkylidyne–thiocarbonyl coupling is more facile than alkylidyne–carbonyl coupling, since the prerequisite structural components for both are present in complexes **1**.

Experimental Procedure

In a typical experiment a solution of **2b** (98 mg, 0.161 mmol) and CS_2 (50 µL, 0.831 mmol) in 30 mL THF was stirred at room temperature until most of the starting material had reacted (reaction was monitored by IR spectroscopy). During this time, the color of the solution changed from orange to brown-green. All volatile components were removed under vacuum. The product was purified by chromatography on silica gel at room temperature eluting with CH_2Cl_2/hexane (2:1). Recrystallization from CH_2Cl_2/hexane gave air-stable, green crystals. (Reaction times and yields, **3a**: 18 h, 14.7%; **3b**: 44 h, 41.9%; **3c**: 14 d, 38.0%; **3d**, 17 h, 32.7%; **3e**, 18 h, 16.9%.) Satisfactory C,H analyses were obtained for complexes **3a** and **3c–e**.

Received: June 17, 1993 [Z 6146 IE]
German version: *Angew. Chem.* **1993**, *105*, 1835

[1] F. R. Kreissl, A. Frank, U. Schubert, T. L. Lindner, G. Huttner, *Angew. Chem.* **1976**, *88*, 649; *Angew. Chem. Int. Ed. Engl.* **1976**, *15*, 632.
[2] A. C. Filippou, W. Grünleitner, *Z. Naturforsch. B* **1989**, *44*, 1023.
[3] A. Mayr, C. M. Bastos, N. Daubenspeck, G. A. McDermott, *Chem. Ber.* **1992**, *125*, 1583.
[4] A. Mayr, C. M. Bastos, *Prog. Inorg. Chem.* **1992**, *40*, 1.
[5] P. V. Broadhurst, *Polyhedron* **1985**, *4*, 1801.
[6] a) A. Mayr, M. F. Asaro, M. A. Kjelsberg, K. S. Lee, D. Van Engen, *Organometallics* **1987**, *6*, 432; b) A. Mayr, T.-Y. Lee, M. A. Kjelsberg, unpublished.
[7] PMe_3S: ^1H NMR (250 MHz, $CDCl_3$, 25 °C): δ = 1.77 (J(P,H) = 13.1 Hz) (J. B. Hendrickson, M. L. Maddox, J. J. Smis, H. D. Kaesz, *Tetrahedron* **1964**, *20*, 449).
[8] A. Mayr, C. M. Bastos, R. T. Chang, J. X. Haberman, K. S. Robinson, D. A. Belle-Oudry, *Angew. Chem.* **1992**, *104*, 802; *Angew. Chem. Int. Ed. Engl.* **1992**, *31*, 747.
[9] J. L. Templeton, *Adv. Organomet. Chem.* **1989**, *29*, 1.
[10] Crystals of **2b** suitable for X-ray structure analysis were obtained by recrystallization from CH_2Cl_2/hexane. Crystal data for **2b**: $C_{16}H_{23}OP_2S_3W$, M_r = 653.24, $P2_1/n$ (no. 14), a = 8.955(4), b = 28.571(4), c = 9.183(1) Å, β = 99.20(2)°, V = 2319(2) Å^3, Z = 4, ϱ_{calcd} = 1.871 g cm^{-3}, $\mu(Mo_{K\alpha})$ = 71.929 cm^{-1}, 3291 unique observed data, 0° < 2θ < 60.8°, 217 final variables, R = 0.033, R_w = 0.032. All intensity measurements at room temperature, $Mo_{K\alpha}$ radiation, graphite monochromator (λ = 0.71069 Å), θ-2θ scan mode. The structure was solved by direct methods and refined by full-matrix least squares. All calculations were performed using the TEXSAN programs. Further details of the crystal structure investigation may be obtained from the Fachinformationszentrum Karlsruhe, Gesellschaft für wissenschaftlich-technische Information mbH, D-76344 Eggenstein-Leopoldshafen (FRG), on quoting the depository number CSD-57807, the names of the authors, and the journal citation.
[11] An alternative mechanism could involve dissociation of PMe_3 and direct addition of CS_2 across the metal–carbon triple bond as the C–C bond-forming step. A precedent for this step is the cycloaddition of CO_2 to the aminomethylidyne complex $NEt_4[W(CNEt_2)(CO)_2(\mu\text{-}PPh_2)_2Mo(CO)_4]$: E. O. Fischer, A. C. Filippou, H. G. Alt, U. Thewalt, *Angew. Chem.* **1985**, *97*, 215; *Angew. Chem. Int. Ed. Engl.* **1985**, *24*, 203. We consider this possibility less likely. The cycloadduct $[X(CO)(PMe_3)_2W{=}C(Ph)\text{-}C(S)S]$ would be a 16-electron complex without significant stabilization of the metal center by π donation. Formation of the products from this type of intermediate would require the formulation of additional unprecedented steps.
[12] For reactions of thiocarbonyl ligands with electrophiles, see: B. D. Dombek, R. J. Angelici, *J. Am. Chem. Soc.* **1975**, *97*, 1261. For an electrophile-induced coupling of alkylidyne and carbonyl ligands, see: J. D. Protasiewicz, A. Masschelein, S. J. Lippard, *J. Am. Chem. Soc.* **1993**, *115*, 800.

Unprecedented Cage-Opening of P_4S_3 Initiated by an Organometallic Radical: Synthesis and Structure of $[Cp_4Cr_4(CO)_9(P_4S_3)]$**

By *Lai Yoong Goh,* Wei Chen,* and *Richard C. S. Wong*

We recently found that $[CpCr(CO)_3]$ radical-induced cleavage of P_4 and As_4 tetrahedra leads to the abstraction of $(\mu\text{-}\eta^2\text{-}E_2)$ and $(\eta^3\text{-}E_3)$ moieties (E = P, As) as ligands,[1, 2] and more interestingly, to a unique aggregation of P atoms to yield the novel $[\{CpCr(CO)_2\}_5P_{10}]$ complex.[3] We have now extended our study to cage compounds like P_4S_3, and we describe here the reaction of $[\{CpCr(CO)_3\}_2]$ with P_4S_3 which proceeds without fragmentation to form the title compound **1**, a new polyphosphido-sulfido complex.

$[Cp_4Cr_4(CO)_9(P_4S_3)]$ **1**

Previous examples of P_4X_3 (X = S, Se) as a ligand in transition metal complexes involve the coordination of intact P_4X_3 cages (through the apical P atom) with the metal center (Fig. 1), for example in *cis*-$[(P_4S_3)_2M(CO)_4]$ (M = Cr, Mo, W) and *cis*-$[(P_4S_3)_3M'(CO)_3]$ (M' = Cr, Mo),[4] $[Mo(CO)_5(P_4S_3)]$,[5] and $[(np_3)Ni(P_4X_3)]$ (X = S, Se; np_3 = $[N(CH_2CH_2PPh_2)_3]$).[6] In contrast, in the presence of the

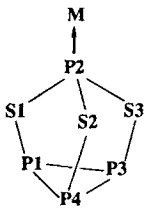

Fig. 1. Coordination of P_4S_3 to a metal complex fragment M.

chelating ligand triphos (triphos = 1,1,1-tris(diphenylphosphinomethyl)ethane), the reaction of P_4X_3 (X = S, Se) with $Co(BF_4)_2 \cdot 6H_2O$[7, 8] and $[RhCl(cod)]_2$ (cod = cycloocta-1,5-diene),[9] resulted in fragmentation of the P_4X_3 cage, yielding the complexes $[(triphos)Co(P_2X)]BF_4$ and $[(triphos)Rh(P_3X_3)]$, respectively. In its reaction with $[\{Cp^*Mo(CO)_2\}_2]$ (*Mo*≡*Mo*) ($Cp^* = \eta^5\text{-}C_5Me_5$), the P_4S_3 cage likewise underwent fragmentation giving a mixture of $[Cp^*Mo(CO)_2P_3]$, $[Cp^*_2Mo_2(CO)_4P_2]$, $[Cp^*_2Mo_2P_2S_3]$, and $[Cp^*_2Mo_2P_4S]$.[10] In reactions with the square-planar d^8 metal complexes $[IrCl(CO)(PPh_3)_2]$ (Vaska's complex) or $[Pt(C_2H_4)(PPh_3)_2]$, cleavage of a single P–P bond in the basal P_3 triangle of the cage led to the $[\mu\text{-}P_4S_3]$-bridged binuclear $[\{Ir(\mu\text{-}P_4S_3)(PPh_3)Cl(CO)\}_2]$[11] and trinuclear $[\{Pt(\mu\text{-}P_4S_3)(PPh_3)\}_3]$[12] complexes, respectively.

$[\{CpCr(CO)_3\}_2]$ and P_4S_3 (1 molequiv) in toluene were allowed to react at ambient temperature for 13 days. The compounds **1** (66%), $[\{CpCr(CO)_2\}_2S]$ (8%; yields based on $[\{CpCr(Co)_3\}_2]$ employed), unreacted P_4S_3 (38%), and an as-yet-unidentified yellow crystalline complex were isolated from the reaction mixture following column chromatography on silica gel. Complex **1** was eluted with toluene/hexane (7:3) as a reddish brown fraction, and isolated as a dark brown crystalline solid which has been characterized by analytical and spectroscopic methods.[13] Dark brown platelets of **1** suitable for a single-crystal X-ray structural analysis[14] (Fig. 2) were obtained from a THF/Et_2O solution, after three weeks at −30 °C.

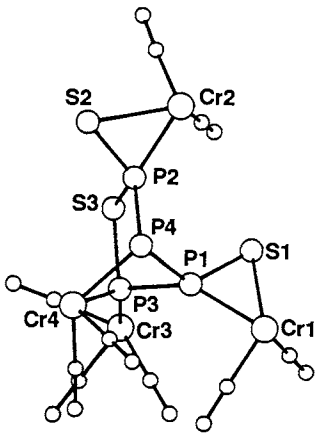

Fig. 2. Molecular structure of **1** (Cp rings omitted for clarity).

From Figure 2, it is apparent that the cleavage of the P2–S1, P4–S2, and P3–P4 bonds, with concomitant bond formation between P2 and P4, gives a five-membered P_4S ring with two external sulfur atoms as substituents, namely S1 at P1 and S2 at P2, as found in the structure of **1**. Together with Cr4, this five-membered ring forms a bicyclo[2.1.1] system, possessing common vertices at P3 and P4. In fact, the P_4S ring bridges four $[CpCr(CO)_n]$ ($n = 2$ or 3) fragments through its four P atoms; the S atom of the five-membered ring is not coordinated to a metal center. With the exception of Cr3, the other three Cr atoms are coordinated to two atoms of the P_4S_3 ligand. It should be noted that P3 is the only P atom that bridges two Cr atoms (Cr3 and Cr4), the Cr4–P3 distance is 0.084 Å shorter than that between P3 and Cr3. Cr1 and Cr2 have similar ligand environments, both possessing a pseudo η^2-PS ligand. An earlier example of η^2-PS coordination was established for the $Cr(CO)_5$ adduct of $[Cp^*_2Mo_2P_4S]$.[10] Each of the five-coordinate Cr atoms assumes a four-legged piano-stool geometry.

The P–P bond lengths (mean 2.201 Å) in **1** are significantly shorter than those in the P_4S_3 cage (mean 2.235 Å),[15] and are very close to the value for the single bond (2.21 Å) in P_4 vapor.[16] The P–S distances (mean 2.0067 Å) in **1** are also shorter than in the intact cage (mean 2.090 Å).[15] The Cr–P distances (mean 2.282 Å) in the CrPS rings for Cr1 and Cr2 are significantly shorter than the other three Cr–P bonds (mean 2.440 Å), which fall within the range 2.341–2.494 Å observed for other CpCr complexes with phosphorus ligands.[1, 3] The Cr–S distances (2.486 and 2.517 Å) in **1** are longer than those observed in $Cr(\mu\text{-}\eta^2\text{-}S_2)$ and $Cr(\mu\text{-}\eta^1, \eta^2\text{-}S_2)$ complexes (range 2.348–2.466 Å).[17]

In summary, this is the first example of multiple bond cleavage without fragmentation of the P_4S_3 cage by a transition metal complex. Slight cage rearrangement has been observed before in the insertion of a $Cr(CO)_5$ fragment into the isostructural nortricyclic homopolyatomic Zintl ion As_7^{3-}.[18] A very recent example of this reaction type is the insertion of three Ni(CO) fragments into Sb_7^{3-}.[19] The extensive cage opening cum structural rearrangement of the neutral P_4S_3 cage described here is unprecedented and may be attributed to the unusual reactivity of the radical-like

[*] Prof. Dr. L. Y. Goh, Dr. W. Chen, R. C. S. Wong (M.Sc)
Department of Chemistry, University of Malaya
59100 Kuala Lumpur (Malaysia)
Telefax: Int. code + (3)75-66343

[**] This work was supported by the University of Malaya and Malaysian IRPA (Intensification of Research in Priority Areas, Grant No. 04-07-04-211).

17-electron $[CpCr(CO)_3]$ fragment, as was observed in the formation of the polyphosphidochromium cluster $[\{CpCr(CO)_2\}_5P_{10}]$ from elemental P_4.[3]

Received: June 24, 1993 [Z 6163 IE]
German version: *Angew. Chem.* **1993**, *105*, 1838

[1] L. Y. Goh, R. C. S. Wong, C. K. Chu, T. W. Hambley, *J. Chem. Soc. Dalton Trans.* **1989**, 1951.
[2] L. Y. Goh, R. C. S. Wong, T. C. W. Mak, W.-H. Yip, *Organometallics* **1991**, *10*, 875.
[3] L. Y. Goh, R. C. S. Wong, E. Sinn, *J. Chem. Soc. Chem. Commun.* **1990**, 1484; *Organometallics* **1993**, *12*, 888.
[4] R. Jefferson, H. F. Klein, J. F. Nixon, *Chem. Commun.* **1969**, 536.
[5] A. W. Cordes, R. D. Joyner, R. D. Shores, E. D. Dill, *Inorg. Chem.* **1974**, *13*, 132.
[6] M. Di Vaira, M. Peruzzini, P. Stoppioni, *Inorg. Chem.* **1983**, *22*, 2196; *J. Organomet. Chem.* **1983**, *258*, 373.
[7] M. Di Vaira, M. Peruzzini, P. Stoppioni, *J. Chem. Soc. Chem. Commun.* **1982**, 894; *J. Chem. Soc. Dalton Trans.* **1984**, 359.
[8] M. Di Vaira, F. Mani, S. Moneti, M. Peruzzini, L. Sacconi, *Inorg. Chem.* **1985**, *24*, 2230.
[9] M. Di Vaira, M. Peruzzini, P. Stoppioni, *J. Chem. Soc. Chem. Commun.* **1983**, 903.
[10] H. Brunner, U. Klement, W. Meier, J. Wachter, O. Serhadle, M. L. Ziegler, *J. Organomet. Chem.* **1987**, *335*, 339.
[11] C. A. Ghilardi, S. Midollini, A. Orlandini, *Angew. Chem.* **1983**, *95*, 800; *Angew. Chem. Int. Ed. Engl.* **1983**, *22*, 790.
[12] M. Di Vaira, M. Peruzzini, P. Stoppioni, *J. Chem. Soc. Dalton Trans.* **1985**, 291.
[13] Satisfactory elemental analysis. ^1H NMR (300 MHz, C_6D_6, 25 °C, residual C_6H_6): The spectrum indicates a 2:1 molar mixture of isomers A and B. Isomer A: δ(Cp) = 4.58(s), 4.61(s), 4.76(s), 4.77(d, J = 1.5 Hz) and isomer B: δ(Cp) = 4.61(s), 4.70(s), 4.79(d, J = 1.5 Hz) and 4.86(s). A variable-temperature ^1H NMR study in $C_6D_5CD_3$ shows that isomer A is the predominant species below −30 °C (δ(Cp) = 4.39, 4.53, 4.63 and 4.71), and that rapid exchange of the four Cp rings at 90 °C gives rise to a singlet at δ = 4.77. ^{13}C NMR (67.80 MHz, C_6D_6): δ(Cp) = 91.71, 92.07, 92.72, 93.15. IR(toluene): $\tilde{\nu}$[cm^{-1}] = 2028vs, 1983vs, 1969vs, 1950vs, 1942vs, 1899s, 1882sh s, 1874vs (CO).
[14] Crystal data for **1**: M_r = 1012.66, triclinic, space group $P\bar{1}$, a = 12.074(1), b = 12.880(3), c = 14.451(5) Å, α = 73.05(2), β = 73.21(1), γ = 78.67(1)°, V = 2042.5(9) Å^3, Z = 2, ϱ = 1.646 Mg m^{-3}, $F(000)$ = 1020, $\lambda(Mo_{K\alpha})$ = 0.71073 Å, μ = 13.65 cm^{-1}, T = 27 °C, crystal dimensions: 0.1 × 0.2 × 0.15 mm. Enraf-Nonius CAD4 diffractometer, ω-2θ scan mode. Of 6208 reflections measured, 3221 ($I > 3\sigma(I)$) were used in refinement. The crystal used for unit cell determination and data collection was coated with epoxy glue to prevent decomposition in air. Twenty-five strong reflections were used for accurate determination of the unit cell parameters. The measured intensities were processed for Lorentz-polarization effects and decay, and corrected for absorption [20]. The structure was solved by direct methods (MULTAN). All non-hydrogen atoms were subjected to anisotropic refinement. The hydrogen atoms were generated geometrically with a distance of 0.95 Å to the carbon atoms and were allowed to "ride" with B = 1.3. A THF solvent molecule was found at a general position in the unit cell and was disordered. The positional parameters for the THF ring were fixed, while their displacement parameters were refined as carbon atoms. Residual peaks in the final difference map account mainly for peaks around the THF molecule. Computations were performed by using the MolEN [21] package on a DEC MicroVAX-II computer. Analytic expressions of atomic scattering factors were employed and anomalous dispersion corrections were incorporated [22]. Final R = 0.048, (R_w = 0.057). Further details of the crystal structure investigation are available from the Director of the Cambridge Crystallographic Data Centre, 12 Union Road, GB-Cambridge CB2 1EZ (UK), on quoting the full journal citation.
[15] Y. C. Leung, J. Waser, S. Van Houten, A. Vos, G. A. Wiegers, E. H. Wiebenga, *Acta Crystallogr.* **1957**, *10*, 574.
[16] L. R. Maxwell, S. B. Hendricks, V. M. Mosley, *J. Chem. Phys.* **1935**, *3*, 699.
[17] L. Y. Goh, T. W. Hambley, G. B. Robertson, *Organometallics* **1987**, *6*, 1051.
[18] B. W. Eichhorn, R. C. Haushalter, J. C. Huffman, *Angew. Chem.* **1989**, *101*, 1081; *Angew. Chem. Int. Ed. Engl.* **1989**, *28*, 1032.
[19] S. Charles, B. W. Eichhorn, S. G. Bott, *J. Am. Chem. Soc.* **1993**, *115*, 5837.
[20] A. C. T. North, D. C. Phillips, F. S. Mathews, *Acta Crystallogr. Sect. A* **1968**, *24*, 351.
[21] MolEN, an Interactive Structure Solution Procedure, Delft Instruments, Delft, The Netherlands, **1990**.
[22] International Tables for X-ray Crystallography, Vol. IV, Kynoch Press, Birmingham, **1974**. Tables 2.2B and 2.3.1. (now distributed by Kluwer, Dordrecht).

A Simple Synthesis of $[(Cp^*Al)_4]$ and Its Conversion to the Heterocubanes $[(Cp^*AlSe)_4]$ and $[(Cp^*AlTe)_4]$ ($Cp^* = \eta^5$-$C_5(CH_3)_5$)**

By *Stephan Schulz, Herbert W. Roesky,* Hans Joachim Koch, George M. Sheldrick, Dietmar Stalke,* and *Annja Kuhn*

Dedicated to Professor Harry Emeléus on the occasion of his 90th birthday

Aluminum occurs preferably in the oxidation state III in its compounds. In addition, there are several compounds with aluminum in the oxidation state II[1–3] and only a few containing aluminum in the oxidation state I.[4–6] One of these is the $[(Cp^*Al)_4]$ tetrahedron (**1**) synthesized by Schnöckel et al. from AlCl and $[MgCp^*_2]$ ($Cp^* = \eta^5$-$C_5(CH_3)_5$) in 1991.[4] The synthesis of the starting material AlCl from HCl and Al at 1200 K is rather difficult.[7] We report here on a simple alternative synthetic route to **1** as well as the first reactions of this compound.

Freshly prepared $[Cp^*AlCl_2]$[8] is allowed to react with a small excess of potassium in toluene under reflux [Eq. (a)]. After filtration of all the insoluble material from the hot solution, **1** is obtained in form of yellow crystals in a yield of 20 %.

$$4[Cp^*AlCl_2] + 8\,K \longrightarrow \underset{\mathbf{1}}{[(Cp^*Al)_4]} + 8\,KCl \qquad (a)$$

Compound **1** is extremely thermally stable and decomposes at 205 °C turning to a brown solid.[9] Only one signal with 100% intensity for monomeric Cp*Al (M = 162 g mol^{-1}) occurs in the mass spectrum. We were not able to detect the molecular ion in the mass spectrum by field ionization (FI) methods. Compound **1** is only slightly air- and moisture-sensitive. Exposure of the crystalline material to air or even water for about 20 min leads to a white amorphous layer, presumably consisting of aluminum oxo and/or aluminum hydroxo compounds. This chemical inertness is a result of the steric shielding of the Al_4 tetrahedron by interlocked Cp* rings.[10] Because of the poor solubility of **1** NMR investigations in C_6D_6 were performed in the temperature range + 40 to + 78 °C. In the ^1H NMR spectrum a singlet appears for the methyl protons at δ = 1.89 and two signals occur in the ^{13}C NMR spectrum for the methyl-C and for the ring-C atoms at δ = 11.35 and 114.21, respectively. The ^{27}Al NMR spectrum shows, in contrast to the previously published results,[11] only one signal at $\delta = -78.3$,[12] whose position does not change on raising or lowering the temperature. We were not able to detect a second signal that should appear above 30 °C (at $\delta = -145$) corresponding to monomeric Cp*Al.[13, 14] In addition to finding a facile access to $[(Cp^*Al)_4]$ **1**, we were also interested in the reactivity of this compound. It should undergo redox reactions in which the aluminum proceeds from the oxidation state I to its preferred oxidation state III. Hitherto, apart from reactions with AlCl, no reactions of aluminum(I) compounds have been described. We report here for the first time about reactions of **1** with elements from group 16. These reactions lead to the

[*] Prof. Dr. H. W. Roesky, Dipl.-Chem. S. Schulz, Dr. H. J. Koch, Prof. G. M. Sheldrick, Dr. D. Stalke, A. Kuhn
Institut für Anorganische Chemie der Universität
Tammannstrasse 4, D-37077 Göttingen (FRG)
Telefax: Int. code + (551)39-3373

[**] This work was supported by the Deutsche Forschungsgemeinschaft, the Volkswagen-Stiftung, and the Fonds der Chemischen Industrie.

formation of the Al–Se and Al–Te heterocubanes, **2** and **3**, respectively. Moreover, **3** is the second organometallic

$[(Cp^*AlSe)_4]$ **2**

$[(Cp^*AlTe)_4]$ **3**

Al–Te compound characterized by X-ray crystallography.[23] Compounds of the type RAlE (E = Se, Te) are isolobal with those of the type RAlXR (X = N, P, As); the latter have been thoroughly investigated during the last few years, since they are potential precursors for industrially interesting AlX materials. In our opinion the compounds RAlE and AlE also have very promising material properties.

When a solution of **1** in toluene is treated with an excess of Se or Te [see Eq. (b)], yellow-green solutions are obtained

$$[(Cp^*Al)_4] + 4\,E \longrightarrow [(Cp^*AlE)_4] \qquad \text{(b)}$$
$$\mathbf{1} \qquad\qquad \mathbf{2},\ E = Se;\ \mathbf{3},\ E = Te$$

following the removal of the insoluble material by filtration. From these solutions **2** can be obtained in the form of colorless, octahedral crystals and **3** in the form of pale green shiny octahedral crystals by slow evaporation of the solvent.

Both compounds are extremely sensitive to air and moisture. Thus, they decompose with an accompanying change in color (red (**2**) or black (**3**)) and concomitant formation of H_2Se and H_2Te, respectively. Compound **2** decomposes at 244 °C and **3** does not melt until 350 °C.

Crystals of **2** are obtained from a THF solution of **2** by very slow evaporation of the solvent. Figure 1 shows the molecular structure of **2**. Suitable crystals for a single-crystal

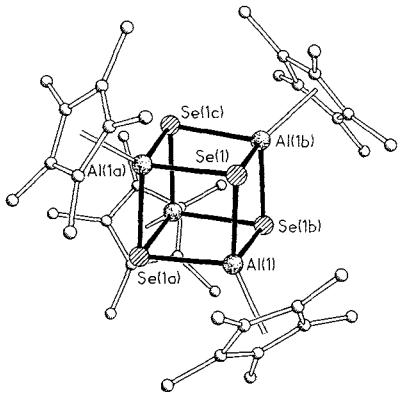

Fig. 1. Crystal structure of **2**. Selected bond lengths [pm] and angles [°]: Al(1)-Se(1) 249.70(10), Al(1)-Se(1a) 246.16(10), Al(1)-Se(1b) 247.13(10); Al(1b)-Se(1)-Al(1a) 85.38(4), Al(1b)-Se(1)-Al(1) 84.62(3), Al(1)-Se(1)-Al(1a) 85.57(4), Se(1b)-Al(1)-Se(1) 94.39(4), Se(1b)-Al(1)-Se(1a) 95.28(4), Se(1a)-Al(1)-Se(1) 94.16(4).

X-ray structural analysis of **3** can be obtained from toluene by slow evaporation of the solvent over a week. Figure 2 shows the molecular structure of **3**, which is isostructural to **2**. Both compounds are tetrameric; the parent skeleton comprises an Al–E heterocubane (E = Se, Te). The Al–Se bond lengths present in **2** vary from 246.2 to 249.7 pm. The Al–Se bond lengths thus lie in the range of those found in $[Ph_3PSe\cdot AlCl_3]$[15] and in $[CH_3Se\{Al(CH_3)_3\}_3]^-$.[16] The Al–Te bonds in **3** range from 268.8 to 275.0 pm and are thus slightly longer than those in Al_7Te_{10} (263.7–266.2 pm for the bonds from the three-coordinate Te atoms).[17] Since the atomic distances lie in a relatively narrow range and also the bond angles at Al and Se and Te, respectively, deviate very little from the ideal 90° angle (average Se-Al-Se: 94.61°, Te-Al-Te: 95.06°, Al-Se-Al: 85.19°, Al-Te-Al: 84.68°), **2** and **3** form almost ideal cubes. In both compounds, each Al atom is additionally coordinated to an η^5-Cp* ligand[18] (Al-Cp*(center) [pm]: 194.9 in **2** and 196.5 in **3**; 201.5 in $[(Cp^*Al)_4]$).

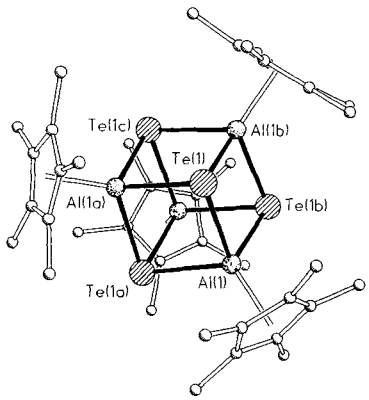

Fig. 2. Crystal structure of **3**. Selected bond lengths [pm] and angles [°]: Al(1)-Te(1) 275.00(9), Al(1)-Te(1a) 268.83(9), Al(1)-Te(1b) 269.17(9); Al(1b)-Te(1)-Al(1a) 84.86(2), Al(1b)-Te(1)-Al(1) 83.68(2), Al(1)-Te(1)-Al(1a) 85.51(2), Te(1b)-Al(1)-Te(1) 94.84(2), Te(1b)-Al(1)-Te(1a) 96.29(2), Te(1a)-Al(1)-Te(1) 94.06(2).

Noteworthy is the analogous construction of these Al heterocubanes to the $[RAlNR']_4$ compounds described by Veith[19] in a review on cage molecules. These compounds exhibit a cubic Al_4N_4 framework. The facile formation of this organometallic Al–Te compound under very mild reaction conditions in good yield is quite surprising. It illustates again the strong desire of aluminum in the oxidation state I (as occurs in **1**) to attain the more stable oxidation state III. The new facile synthesis of **1** accompanied by the high reactivity of **1** in solution should allow the access to other interesting Al compounds.

Experimental Procedure

All reactions were carried out under a nitrogen atmosphere and with dry solvents.

1: $AlCl_3$ (4.00 g, 30 mmol) was dissolved in hexane (60 mL), treated with $[Cp^*SiMe_3]$ (6.25 g, 30 mmol), and heated under reflux for 3 h. Subsequently the solvent and the Me_3SiCl formed were removed under vacuum. The white solid residue was then dissolved in toluene (60 mL) and treated with K (2.75 g, 70 mmol) and heated for 1.5 h. The insoluble material was then quickly filtered off from the hot solution; the temperature of the solution must not be allowed to drop below 80–90 °C. Compound **1** crystallized from the hot solution on cooling in the form of yellow crystals. Yield: 0.95 g (1.5 mmol)(20%). IR (nujol, CsI): $\tilde{\nu}$[cm^{-1}] = 1480, 1370, 1307, 1261, 1169, 1094, 1019, 800, 733, 595, 585, 352.

2: A mixture of **1** (0.32 g, 0.5 mmol) and Se (0.31 g, 4 mmol) in toluene (60 mL) was stirred for 4 d at room temperature. Subsequently all insoluble material was filtered off and the solvent was slowly removed under vacuum over a period of 2 d to afford **2**. Yield: 0.38 g (0.39 mmol) (78%). ^{1}H NMR (400 MHz, C_6D_6, 25 °C, TMS): δ = 1.99; ^{13}C NMR (100 MHz, C_6D_6, 25 °C, TMS): δ = 12.07, 115.68; ^{27}Al NMR (100 MHz, C_6D_6, 25 °C, $AlCl_3$): δ = −36.40. IR (nujol, CsI): $\tilde{\nu}$ [cm^{-1}] = 1261, 1095, 1064, 1021, 800, 727, 694, 661, 627, 591, 451, 425, 387. MS (EI): *m/z* 966 (M^+, 2%), 831 (M^+ −Cp*, 8), 162 (AlCp*, 100). Correct elemental analysis.

3: **1** (0.32 g, 0.5 mmol) and Te (0.50 g, 4 mmol) were stirred for 6 d in toluene (60 mL) at room temperature. After removal of the insoluble material by filtration, the solvent was slowly removed under vacuum. Compound **3** precipitated in the form of octahedral crystals. Yield 0.50 g (0.43 mmol) (86%). ^{1}H NMR (400 MHz, C_6D_6, 25 °C, TMS): δ = 1.96; ^{13}C NMR (100 MHz, C_6D_6, 25 °C, TMS): δ = 12.91, 116.44; ^{27}Al NMR (100 MHz, C_6D_6, 25 °C, $AlCl_3$): δ = −112.69 IR (nujol, CsI): $\tilde{\nu}$ [cm^{-1}] = 1262, 1168, 1019, 949, 799, 589, 446,

373, 350, 272. MS (EI): *m/z* 1025 (M^+−Cp*, 2%), 580 ($M/2^+$, 25), 135 (Cp*, 100). Correct elemental analysis.

Received: July 16, 1993 [Z 6219 IE]
German version: *Angew. Chem.* **1993**, *105*, 1828

[1] W. Uhl, *Z. Naturforsch. B* **1988**, *43*, 1113.
[2] W. Uhl, A. Vester, *Chem. Ber.* **1993**, *126*, 941.
[3] H. Hoberg, S. Krause, *Angew. Chem.* **1976**, *88*, 760; *Angew. Chem. Int. Ed. Engl.* **1976**, *15*, 694; H. Hoberg, S. Krause, *ibid.* **1978**, *90*, 1013 and **1978**, *17*, 949.
[4] C. Dohmeier, C. Robl, M. Tacke, H. Schnöckel, *Angew. Chem.* **1991**, *103*, 594; *Angew. Chem. Int. Ed. Engl.* **1991**, *30*, 564.
[5] W. Hiller, K.-W. Klinkhammer, W. Uhl, J. Wagner, *Angew. Chem.* **1991**, *103*, 182; *Angew. Chem. Int. Ed. Engl.* **1991**, *30*, 179.
[6] N. Wiberg in *Frontiers of Organosilicon Chemistry* (Eds.: A. R. Bassindale, P. P. Gaspar), The Royal Society of Chemistry, Cambridge, **1991**, p. 263; U. Schneider, R. Ahlrichs, H. Horn, A. Schäfer, *Angew. Chem.* **1992**, *104*, 327; *Angew. Chem. Int. Ed. Engl.* **1992**, *31*, 353.
[7] M. Tacke, H. Schnöckel, *Inorg. Chem.* **1989**, *28*, 2895.
[8] S. Schulz, H. J. Koch, H. W. Roesky, M. Noltemeyer, H.-G. Schmidt, A. Heine, R. Herbst-Irmer, D. Stalke, G. M. Sheldrick, *Chem. Ber.* **1992**, *125*, 1107.
[9] The physical and chemical properties of **1** described by Schnöckel et al. are slightly different from those found by us.
[10] A single-crystal X-ray structure analysis at −120 °C confirms the existence of **1**. Crystal data: $C_{40}H_{60}Al_4$, M_r = 648.85, triclinic, space group $P\bar{1}$, a = 10.759(4), b = 10.913(3), c = 18.027(5) Å, α = 82.94, β = 81.82, γ = 66.88°, V = 2116.6(12) Å^3, Z = 2.
[11] J. Gauss, U. Schneider, R. Ahlrichs, C. Dohmeier, H. Schnöckel, *J. Am. Chem. Soc.* **1993**, *115*, 2402.
[12] The measurements were carried out at +40, +70, and +78 °C.
[13] If the NMR sample tube is left open for 1 h, and then the sample is remeasured at +70 °C, two additional signals at δ = −9.3 and −148.2 appear in the ^{27}Al NMR spectrum. The latter signal is consistent with the values postulated for monomeric Cp*Al.
[14] Because of the poor solubility of **1**, it is not possible to carry out a molar mass determination.
[15] N. Burford, B. W. Royan, R. E. v. H. Spence, R. D. Rogers, *J. Chem. Soc. Dalton Trans.* **1990**, 2111–2117.
[16] J. L. Atwood, S. K. Seale, *J. Organomet. Chem.* **1976**, *114*, 107–118.
[17] R. Nesper, J. Curda, *Z. Naturforsch. B* **1987**, *42*, 557.
[18] Crystal data of **2**: $C_{10}H_{15}AlSe$, M_r = 241.16, tetragonal, space group $I\bar{4}$, $a = b$ = 12.144(1), c = 14.373(2) Å, V = 2119.7(4) Å^3, Z = 8, ρ_{calcd} = 1.511 Mgm^{-3}, $F(000)$ = 976, λ = 0.71073 Å, $\mu(Mo_{K\alpha})$ = 0.397 mm^{-1}. The data were collected on a Stoe-Siemens-Huber diffractometer. Intensities of a rapidly cooled crystal with dimensions 0.6 × 0.5 × 0.4 mm in an oil drop [20] were collected at −120 °C by the $2\theta/\omega$ method in the range $8 \le 2\theta \le 50$°. Of the 1403 reflections collected, 1367 were unique and these were corrected for absorption by using a semiempirical procedure; highest minimum and maximum of the final difference Fourier synthesis: 0.32 and −0.28 eÅ^{-3}, respectively. $R1$ = 0.021, $wR2$ = 0.050 (all data). The absolute structure was determined to 0.00(14) by a refinement of the Flack parameter (H. D. Flack, *Acta Crystallogr. Sect. A* **1983**, *39*, 876). Crystal data of **3**: $C_{10}H_{15}AlTe$, M_r = 289.80, tetragonal, space group $I\bar{4}$, $a = b$ = 12.430(2), c = 14.546(3) Å, V = 2247.4(7) Å^3, Z = 8, ρ_{calcd} = 1.713 Mgm^{-3}, $F(000)$ = 1120, λ = 0.71073 Å, $\mu(Mo_{K\alpha})$ = 0.397 mm^{-1}. The data were collected on a Stoe-Siemens-Huber diffractometer. Intensities of a rapidly cooled crystal with the dimensions 0.5 × 0.4 × 0.4 mm in an oil drop [20] were collected at −120 °C by the $2\theta/\omega$ method in the range $8 \le 2\theta \le 55$°. Of the 2370 reflections collected, 2278 were unique and these were corrected for absorption by using a semiempirical procedure; highest minimum and maximum of the final difference Fourier synthesis: 0.39 and −0.44 eÅ^{-3}, respectively. $R1$ = 0.017, $wR2$ = 0.042 (all data). The absolute structure was determined to 0.03(2) by a refinement of the Flack parameter (H. D. Flack, *Acta Crystallogr. Sect. A* **1983**, *39*, 876). The values of $R1$ and $wR2$ were defined as $R1 = \Sigma||F_o| - |Fc||/[\Sigma|F_o|]$; $wR2 = \{[\Sigma w(F_o^2 - F_c^2)^2]/[\Sigma w(F_o^2)]\}^{1/2}$. The structures were solved by direct methods (SHELXS-90) [21] and refined by least-squares procedures (SHELXL-93) [22]. The hydrogen positions were refined according to a riding model in which the CH_3 groups were allowed to rotate about their local threefold axis. Further details of the crystal structure investigations are available on request from the Director of the Cambridge Crystallography Data Centre, 12 Union Road, GB-Cambridge CB2 1EZ (UK), by quoting the full journal citation.
[19] M. Veith, *Chem. Rev.* **1990**, *90*, 3–16; see also T. Belgardt, H. W. Roesky, M. Noltemeyer, H.-G. Schmidt, *Angew. Chem.* **1993**, *105*, 1101, *Angew. Chem. Int. Ed. Engl.* **1993**, *32*, 1056; K. M. Waggoner, P. P. Power, *J. Am. Chem. Soc.* **1991**, *113*, 3385.
[20] T. Kottke, D. Stalke, *J. Appl. Crystallogr.* **1993**, *26*, 615.
[21] G. M. Sheldrick, *Acta Crystallogr. Sect. A* **1990**, *46*, 467–473.
[22] G. M. Sheldrick, *SHELXL-93*, Universität Göttingen, **1993**.
[23] A. H. Cowley, R. A. Jones, P. R. Harris, D. A. Atwood, L. Contreras, C. J. Burek, *Angew. Chem.* **1991**, *103*, 1164; *Angew. Chem. Int. Ed. Engl.* **1991**, *30*, 1143.

A Molecular Heterometal Amide with High Molecular Dynamics: Does the Lithium Atom Orbit?**

By *Michael Veith,* Michael Zimmer,* and *Stefan Müller-Becker*

Dedicated to Professor Ulrich Wannagat on the occasion of his 70th birthday

Whilst the motion of lithium atoms in solids, such as, for example, in solid Li_3N, has been thoroughly investigated and is generally accepted,[1] many indications, but little concrete evidence for such a motion in molecules exists, in spite of much effort (see e.g. ref. [2]). Here we report on our studies of the heterometal amide $[Me_2Si(NSiMe_3)_2]_2InLi$ (**1**), an example of a class of molecular complexes that has still not been investigated in detail.[3] Compound **1** can easily be prepared according to Equation (a).

$$2\,Me_2Si(NSiMe_3)_2Li_2 + InCl_3 \longrightarrow 3LiCl + \underset{\mathbf{1}}{[Me_2Si(NSiMe_3)_2]_2InLi} \quad (a)$$

According to the X-ray crystal structure analysis,[4] (Fig. 1) the trivalent indium and the monovalent lithium atom in **1** are bound close together in a tricycle of four-membered rings (In···Li = 2.748(9) Å). The ^{1}H, ^{13}C, ^{15}N, and ^{29}Si NMR spectra of **1** at room temperature in toluene (see Experimental Procedure) are not consistent with the molecular structure represented in Figure 1. Thus, only one resonance signal is found for both the dimethylsilylene and trimethylsilyl groups in the ^{13}C NMR spectrum, whereas a double set of signals would be expected because of the low C_2 symmetry of the molecule (the twofold axis passes through the two metal atoms).

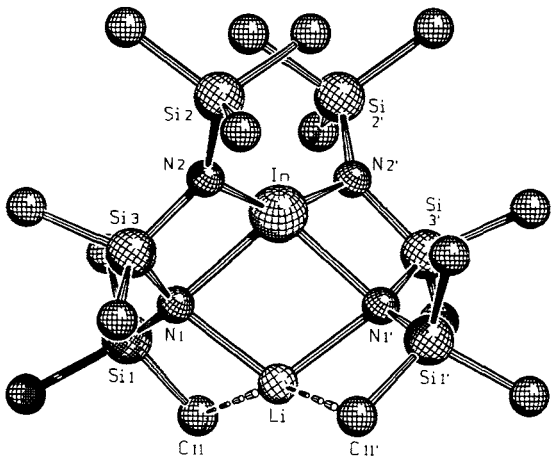

Fig. 1. Molecular structure of **1**. Some important distances [Å] and angles [°]: N1–In 2.223(3), N2–In 2.055(3), N1–Li 2.064(6), N1–Si1 1.720(3), N1–Si3 1.737(3), N2–Si2 1.714(3), N2–Si3 1.717(3), Li···C11 2.635(7); N1-In-N1' 95.2(1), N2-In-N2' 148.4(1), N1-In-N2 76.2(1), N1-In-N2' 127.3(1), N1-Li-N1' 105.4(3).

If a toluene solution of **1** is cooled, ^{1}H, ^{13}C, and ^{29}Si NMR spectra are obtained at lower temperature (as an ex-

[*] Prof. Dr. M. Veith, M. Zimmer, Dr. S. Müller-Becker
Institut für Anorganische Chemie der Universität
Postfach 11 50, D-66041 Saarbrücken (FRG)
Telefax: Int. code + (681)302-3995

[**] This work was supported by the Deutsche Forschungsgemeinschaft and the Fonds der Chemischen Industrie.

ample ^{13}C NMR spectra are reproduced in Fig. 2) with twice (or one and a half times) the number of signals as expected from the crystal structure. An activation energy of 44.3 kJ mol^{-1} can be determined from analysis of the coalescence temperature and the signal splitting derived from heteronuclear NMR spectra.[5] The signal of the trimethylsilyl groups shifted to high field shows unusual behavior: With decreasing temperature a selective broadening is found, a phenomenon that can be explained by a rotation barrier about the Si–N bond, which is also found for trimethylsilyl groups of other molecules.[6] On examination of the solid-state molecular structure (Fig. 1), it becomes apparent that the reason for the rotational barrier of this one trimethylsilyl group is due to lithium methyl contacts (dotted lines); at the same time, this finding allows the assignment of the resonance signals.

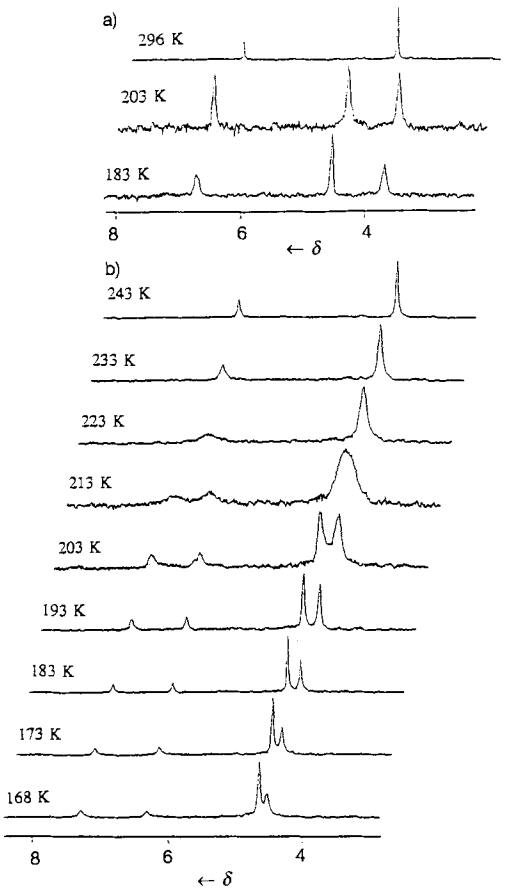

Fig. 2. ^{13}C NMR spectra (50.3 MHz) of **1** a) in hexane at three temperatures and b) in toluene between 243 and 168 K .

Temperature-dependent measurements of the spin-lattice relaxation T_1 of the ^{7}Li isotope give the expected curve shape on plotting the graph with a minimum at 203 K. Analysis of the Arrhenius plot gives a value of 13.8 kJ mol^{-1} for the high-temperature end; this value is typical for methyl and trimethylsilyl rotations about threefold axes.[7] It implies several coupled migrations in the molecule and suggests that the lithium atom is involved in these.

The series of temperature-dependent ^{13}C NMR spectra shown in Figure 2 were also repeated for significantly higher and lower concentrations of **1** in toluene (about five- and tenfold), without any observable changes occurring in the comparable spectra. We conclude from this that an intermolecular process is unlikely to be the reason for the observed spectra at room temperature. Clearly all findings are consistent with a higher "average" point symmetry of the molecule at room temperature. Instead of the $C_2(2)$ symmetry in the crystal lattice, in which the molecules are exclusively bound by van der Waals contacts, $D_{2d}(\bar{4}2m)$ symmetry must be ascribed to the whole molecular unit in solution. The increase in symmetry is clearly determined by dynamic phenomena in which lithium, as the lightest of the atoms (if one neglects the covalently bonded hydrogen atoms), plays a special role.

After exclusion of an intermolecular process only an intramolecular and a dissociative mechanism remain. We consider the formation of an ion pair of the type $Li^{+}[\{Me_2Si(NSiMe_3)_2\}_2In]^{-}$ in solution, which would involve an anion with D_{2d} symmetry, to be unlikely in toluene due to the large amount of energy required to break the Li–N bond and to the relatively low expected solvation energy. Furthermore, analogous ^{1}H and ^{13}C NMR spectra with few signals are obtained when **1** is dissolved in nonpolar hexane (Fig. 2a). Here too, a splitting of the Me_3Si signal is observed at lower temperatures. Thus, identical activation energies (44.3 kJ mol^{-1}) to those in toluene are determined. In contrast to the spectra in toluene (dipole moment: 0.36 D), in hexane the signal for the dimethylsilyl group does not split up to the freezing point of the solvent. The molecule must therefore retain a residual mobility in nonpolar solvents, which is suppressed in polar toluene, because the static molecule itself is strongly dipolar.

We believe that the observed spectra can best be explained by an *intramolecular* dynamic process. In this context, two processes can be discussed: One possibility is an essentially oscillating motion of the lithium atom in an orbit around the center of the molecule, which can be described as a indium-centered N_4-bisphenoid (Fig. 3). A conceivable alternative

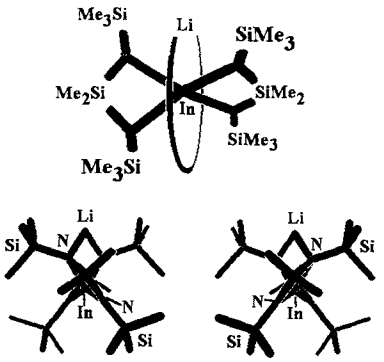

Fig. 3. Top: An intramolecular model for the "lithium migration". Bottom: The two structures of **1** found in the crystal (view orthogonal to the upper drawing). Their interconversion could explain the "residual mobility" of **1** in hexane.

would be that the $Me_2Si(NSiMe_3)_2$ ligands move disrotatory around a pseudo Si3-Si3′ axis (see Fig. 1); thus, the two metal atoms remain in their positions. Molecular dynamic model calculations[8] and the consideration of group vibrations show, however, that both processes are basically the same and that only a different reference point has been chosen. Moreover, this model explains the nature of the above-mentioned residual mobility in hexane below 220 K. In this

case the lithium atom is now only in contact with two nitrogen atoms at which inversions take place. In the extreme case this leads to the two molecules represented in the lower half of Figure 3. These are enantiomers and both crystallize together (in the crystal structure they are connected by inversion centers).

Solid-state NMR spectra were also obtained for **1**. The central line of the Magic Angle Spinning (MAS) ^{7}Li NMR spectrum (77.7 MHz) of **1** at room temperature consists of two components: a broad resonance signal showing the typical quadrupolar splitting obtained in MAS experiments for quadrupolar nuclei[9] (586 Hz), as well as a quasi-superimposed relatively sharp resonance with a half-width of about 120 Hz. If a second spectrum of the same sample is recorded at 116.5 MHz, the peak separation of the outer peaks is reduced, which is consistent with a quadrupolar effect. The sharp resonance signal at 296 K combines about 8% of the total intensity including the side bands and should be due to "readily mobile" lithium atoms.[10] Whether the signal is due to a partial "lithium dynamic" as a result of lattice vibrations in **1** or whether it is caused by a small amount of some impurity still needs to be clarified by further investigations.

Experimental Procedure

Indium chloride (0.7 g, 3.2 mmol) in diethyl ether (5 mL) was added to two molar equivalents of $Me_2Si(NSiMe_3)_2Li_2$ [11] in *n*-hexane (25 mL) and stirred for 6 h at room temperature. The suspension was filtered and the solution concentrated; during this process crystals of the ether adduct of **1** formed. The ether was eliminated from the compound in the subsequent sublimation (70–80 °C bath temperature/10^{-3} Torr) and 1.37 g (73%) of **1** were obtained as colorless crystals (m.p. 142 °C). Correct analyses and mass spectra. Chemical shifts of **1** in solution (200 MHz [D_8]toluene, 296 K, TMS): ^{1}H NMR: $\delta = 0.18$ (s, 36H, $SiMe_3$), 0.33 (s, 12H, $SiMe_2$); ^{13}C NMR ([D_8]toluene): $\delta = 4.2$ (s, 12C, $SiMe_3$), 6.6 (s, 4C, $SiMe_2$); ^{13}C NMR (hexane): $\delta = 3.9$ (s, $SiMe_3$), 6.4 (s, $SiMe_2$); ^{29}Si NMR: $\delta = -0.55$ (s, $SiMe_2$), -5.80 (s, $SiMe_3$); ^{15}N NMR (CH_3NO_2 ext.): $\delta = -308.5$ (s, $b_{1/2} = 10$ Hz); ^{7}Li NMR (ext. standard: LiCl/D_2O): $\delta = 3.0$ (s, $b_{1/2} = 5.7$ Hz). Chemical shifts of **1** in the solid state (200 MHz, 296 K, sec. standard: adamantane, TMS = 0), ^{13}C NMR: $\delta = 5.8$ ($b_{1/2} = 85$ Hz), ^{7}Li NMR (ext. standard: LiCl): $\delta = 1.0$ [12].

Received: May 3, 1993
Revised version: June 28, 1993 [Z 6051 IE]
German version: *Angew. Chem.* **1993**, *105*, 1771

[1] A. Rabenau, *Nachr. Chem. Tech. Lab.* **1978**, *26*, 310; P. Hartwig, W. Weppner, W. Wichelhaus, A. Rabenau, *Angew. Chem.* **1980**, *92*, 72; *Angew. Chem. Int. Ed. Engl.* **1980**, *19*, 74.

[2] F. Pauer, J. Rocha, D. Stalke, *J. Chem. Soc. Chem. Commun.* **1991**, 1477.

[3] M. Veith, S. Müller-Becker in *The Chemistry of Inorganic Ring Systems* (Ed.: R. Steudel), Elsevier, Amsterdam, **1992**, p. 125.

[4] Crystal data for **1**: monoclinic, space group $C2/c$, $a = 11.814(9)$, $b = 16.986(20)$, $c = 16.719(20)$ Å, $\beta = 104.63(9)°$, $V = 3246$ Å^3, $Z = 4$, $\mu = 9.14$ cm^{-1}. Siemens-AED2 diffractometer, ω-θ scan, 2109 reflections of which 81 with $F_0 < MK > 2\sigma_F$, $2\theta_{max} = 45°$; measurement temperature: 293 K. Structure solution by Patterson methods, H atom positions idealized (C–H = 1.08 Å, H-C-H = 109.5°); 153 parameters (all non-hydrogen atoms with anisotropic temperature factors). $R = 0.033$ ($R_w = 0.038$; weighting scheme: $w = 1.00/(\sigma_F^2 + 0.006384F^2)$). Maximum and minimum residual electron density: 0.27 and -0.80 e Å^{-3}. Programs used: SHELX 86 [13] and SCHAKAL [14]. Further details of the crystal structure investigation may be obtained from the Fachinformationszentrum Karlsruhe, Gesellschaft für wissenschaftlich-technische Information mbH, D-76344 Eggenstein-Leopoldshafen (FRG) on quoting the depository number CSD-57682, the names of the authors, and the journal citation.

[5] J. Sandström, *Dynamic NMR Spectroscopy*, Academic Press, New York, **1982**, p. 96.

[6] M. Zimmer, dissertation, Universität des Saarlandes, **1993**.

[7] D. W. Aksnes, K. Ramstad, *Magn. Reson. Chem.* **1988**, *26*, 1086.

[8] HYPERCHEM 3.0, Autodesk, Inc. USA 1993, parameters modified by M. Veith.

[9] R. K. Harris, A. C. Olivieri, *Progr. Nucl. Magn. Reson. Spectrosc.* **1992**, *24*, 435.

[10] A selective representation of the two components can be obtained by inversion–recovery experiments because of the very different relaxation behavior.

[11] W. Fink, *Chem. Ber.* **1963**, *96*, 1071.

[12] The ^{1}H, ^{7}Li, ^{13}C, ^{15}N, and ^{29}Si NMR spectra were recorded with a Bruker 200 MHz spectrometer, the solid-state NMR spectra were recorded on a MSL 200 (Bruker). Airtight Kel-F inserts were used in 7-mm-MAS rotors for the sample preparation. The T_1 measurements were carried out according to standard inversion–recovery methods.

[13] G. M. Sheldrick, *Program for Crystal Structure Determination*, Universität Göttingen, **1986**.

[14] E. Keller, *SCHAKAL-88, Fortran Program for the Graphical Representation of Molecular and Crystallographic Models*, Freiburg, **1988**.

Palladium-Catalyzed Arylation of Tetrasubstituted Double Bonds: A Simple Synthesis of Annelated Propellanes**

By *Gerald Dyker,* Jutta Körning, Peter G. Jones,* and *Peter Bubenitschek*

As a result of their special topology propellanes have stimulated a multitude of syntheses and investigations into their chemical and physical properties.[1] The benzoannelated [4.4.4]propellane **1**[2] is of particular interest in this respect, as in this compound a hexaarylethane[3] structure is stabilized by triple clamping. However, the increased ring strain caused by reducing the size of the propellane rings can cause destabilization of the central single bond to reoccur. The highly strained dehydrotriptycene **2**—a [2.2.2]propellane—represents an extreme example and so far all attempts at its synthesis have been unsuccessful.[4] We report here on a rational entry to aryl-annelated [3.3.*n*]propellanes with $n = 2$, 3, and 4.

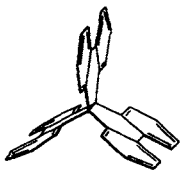

1

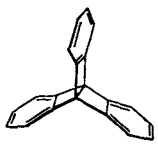

2

The hexacyclic hydrocarbon **7** is the key compound in the synthesis of the desired propellanes and can be prepared in one step from acenaphthylene and 1,8-diiodonaphthalene by a palladium-catalyzed annelation.[5] Formation of the [3.3.3]propellane **3**, which contains a threefold symmetry axis, was achieved in a single step by way of a second palladium-catalyzed annelation, this time with monoiodonaphthalene **5** (Scheme 1).[6] The use of 1,8-diiodonaphthalene in

[*] Dr. G. Dyker, Dipl.-Chem. J. Körning
Institut für Organischen Chemie der Technischen Universität
Hagenring 30, D-38106 Braunschweig (FRG)
Telefax: Int. code + (531)391-5388
Prof. Dr. P. G. Jones, Dipl.-Chem. P. Bubenitschek
Institut für Anorganische und Analytische Chemie
der Technischen Universität Braunschweig (FRG)

[**] Transition Metal-Catalyzed Annelation Reactions, Part 6. This work was supported by the Deutsche Forschungsgemeinschaft and the Fonds der Chemischen Industrie. Part 5: *Angew. Chem.* **1994**, 106, No. 1; *Angew. Chem. Int. Ed. Engl.* **1994**, *33*, No. 1.

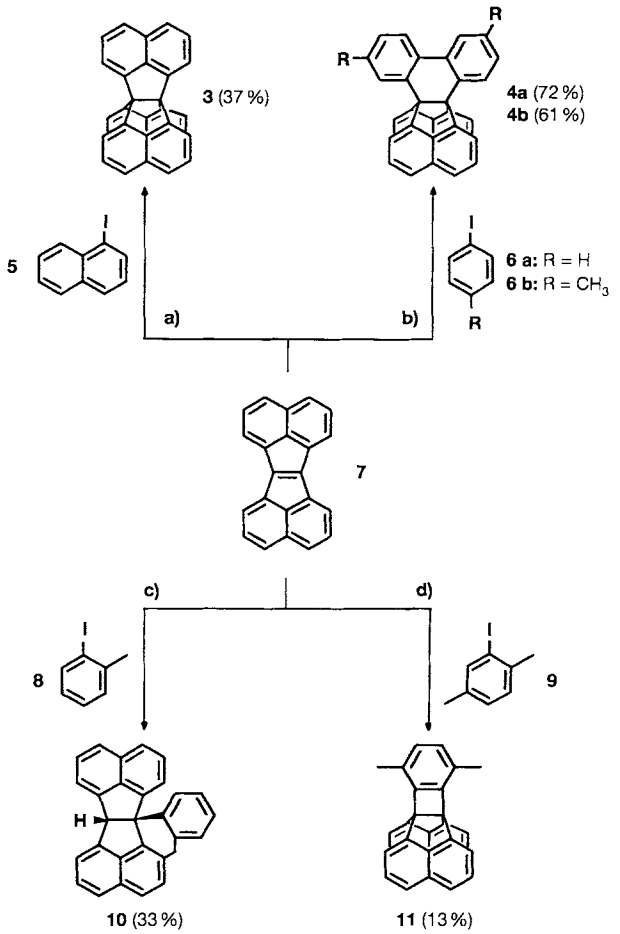

Scheme 1. Palladium-catalyzed annelation of **7**. Reaction conditions: 5 mol% $Pd(OAc)_2$, 30 equiv aryl iodide **5**, **6**, **8**, or **9**, K_2CO_3, nBu_4NBr, dimethylformamide, N_2, 100 °C, reaction times: a) 21 d, b) 14 d for **4a**, 7 d for **4b**, c) 7 d, d) 7 d.

place of **5** led exclusively to Ullmann products.[5b] As far as we are aware, examples of the intermolecular[7] palladium-catalyzed arylation of tetrasubstituted double bonds is unknown, since the reactivity of the olefins generally decreases with increasing degree of substitution.[8]

In order to investigate the range of application of such annelations on **7**, other aryl iodides were examined as coupling components. Iodobenzene **6a** and 4-iodotoluene **6b** led to good yields of the [4.3.3]propellanes **4a** and **4b**, respectively, as 1:2 products. The methyl substituents in **4b** allow the regiochemical course of the annelation process, which corresponds to similar reactions with norbornene, to be identified.[9] The X-ray crystal structure analysis[10] of **4a** revealed the twisting about the biphenyl unit and the pronounced elongation of the central single bond C8b-C14b with a bond length of 161.2(4) pm (Fig. 1).

The reaction of **7** with 2-iodotoluene **8** took a surprising course. The octacyclic hydrocarbon **10** was isolated as main product, apparently the result of activation of a C–H bond in the benzylic position. In the reaction with 2,5-dimethyliodobenzene **9**, the [3.3.2]propellane **11** was obtained as the only isolable product. In this case [4.3.3]propellanes as 1:2 products with methyl substituents in sterically demanding positions could not be demonstrated: it is possible that a methyl group sterically hinders formation of the octahedral Pd^{IV} intermediate, which has been postulated for such domino couplings.[11]

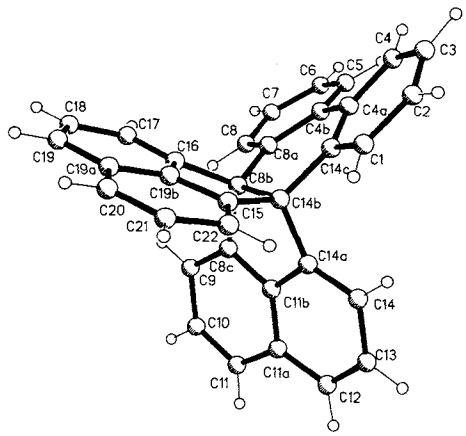

Fig. 1. Molecular structure of **4a** in the crystal (arbitrary radii) [10].

As tetrasubstituted olefin components dibenzo[*g*,*p*]-chrysene[12] and 9,9′-bifluorenylidene[13] have been shown to be too unreactive. In contrast, buckminsterfullerene C_{60} reacts with iodobenzene **6a** (5 equiv) under these reaction conditions; according to the mass spectrum[14] the resulting products were polyphenylfullerenes.[15]

The results described here prove that palladium-catalyzed arylations are also possible with tetrasubstituted olefins, providing that a strain activation is present. Thus, interesting propellanes can be rationally synthesized in annelation processes. The chemical reactivity and in particular the photochemical properties of the propellanes described here are the subject of investigations that are currently in progress.

Table 1. Selected physical and spectroscopic data [a] for the compounds **3**, **4a**, **4b**, **10**, and **11** [6]. ^1H NMR measurements: 400.1 MHz, $CDCl_3$, TMS; ^{13}C NMR measurements: 100.6 MHz, $CDCl_3$.

3: Colorless needles up to 400 °C unchanged; ^1H NMR: $\delta = 7.53$ (m, 1H), 7.60 ("d", "J" = 8.1 Hz, 1H), 8.03 ("d", "J" = 6.8 Hz, 1H); ^{13}C NMR: $\delta = 79.92$ (s), 119.14 (d), 124.20 (d), 128.50 (d), 132.46 (s), 137.20 (s), 146.65 (s); MS (70 eV): *m/z* (%): 403 (32), 402 (86, M^+), 401 (32), 400 (27), 277 (30), 276 (100), 252 (34), 57 (33); correct elemental analysis for $C_{32}H_{18}$ (402.49).

4a: Colorless solid, m.p. 338 °C; ^1H NMR: $\delta = 7.31$ (m_t, 2H; H-3,6), 7.43 (m_t, 2H; H-2,7), 7.46 (m_t, 4H; H-10, 13, 18, 21), 7.56 ("d", 4H; H-11,12,19,20), 7.65 ("d", 4H; H-9,14,17,22), 7.94 (m_d, 2H; H-4,5), 8.34 (m_d, 2H; H-1,8); ^{13}C NMR: $\delta = 67.59$ (s; C-8b,14b), 120.58 (d; C-9,14,17,22), 123.68 (d; C-11,12,19,20), 123.96 (d; C-4,5), 127.39 (d; C-3,9), 127.92 (d; C-10,13,18,21), 128.06 (d; C-2,7), 128.83 (d; C-1,8), 131.32 (s; C-4a,4b), 131.67 (s; C-8c,14a,15,16), 136.08 (s; C-8a,14c), 136.43 (s; C-8d,15a), 148.19 (s; C-11a,19a).

4b: Colorless solid, m.p. 341–342 °C; ^1H NMR: $\delta = 2.36$ (s, 3H; 6-CH_3), 2.47 (s, 3H; 2-CH_3), 7.12 (dd, J = 8.2, 1.7 Hz, 1H; H-3), 7.22 (dd, J = 8.0, 1.7 Hz, 1H; H-7), 7.43–7.48 (m, 4H; H-10,13,18,21), 7.53–7.56 (m, 4H; H-11,12,19,20), 7.62–7.65 (m, 4H; H-9,14,17,22), 7.73 (br. s, 1H; H-5), 7.84 (d, J = 8.2 Hz, 1H; H-4), 8.10 (br. s, 1H; H-1), 8.20 (d, J = 8.0 Hz, 1H; H-8); ^{13}C NMR: $\delta = 21.35$ (q; 6-CH_3), 21.65 (q; 2-CH_3), 67.48 (s; C-8b), 67.59 (s; C-14b), 120.44, 120.54 (d; C-9,14,17,22), 123.56, 123.60 (d; C-11,12,19,20), 123.88 (d; C-4), 124.26 (d; C-5), 127.87, 127.90 (d; C-10,13,18,21), 128.28 (d; C-3), 128.55 (d; C-7), 128.71 (d; C-8), 128.71 (s; C-4a), 129.28 (d; C-1), 131.21 (s; C-4b), 131.67 (s), 132.96 (s; C-8a), 136.05 (s; C-14c), 136.41 (s), 136.73 (s; C-6), 137.60 (s; C-2), 148.28 (s), 148.41 (s).

10: Colorless solid, m.p. 260–261 °C; ^1H NMR: $\delta = 4.16$ (d, J = 19.1 Hz, 1H), 4.90 (d, J = 19.1 Hz, 1H), 5.97 (s, 1H), 7.12 ("t", 1H), 7.17–7.21 (m, 2H), 7.27 (m_t, 1H), 7.39 (m_t, 1H), 7.48–7.68 (m, 9H), 7.89 ("d", 1H); ^{13}C NMR: $\delta = 36.05$ (t), 63.03 (d), 66.22 (s), 119.26 (d), 119.49 (d), 119.95 (d), 123.29 (d), 123.69 (d), 123.73 (d), 123.78 (d), 125.83 (d), 126.39 (d), 126.99 (d), 127.57 (d), 127.74 (d), 128.30 (d), 128.42 (d), 128.99 (s), 129.62 (d), 130.57 (s), 132.14 (s), 136.01(s), 136.27(s), 143.67 (s), 144.40 (s), 144.76 (s), 145.01 (s), 151.50 (s), a singlet is superimposed.

11: Colorless solid, m.p. 320 °C (decomp.); ^1H NMR: $\delta = 2.47$ (s, 6H), 6.81 (s, 2H), 7.54 (m, 4H), 7.66 ("d", 4H), 7.91 ("d", 4H); ^{13}C NMR: $\delta = 16.62$ (q), 75.48 (s), 120.23 (d), 124.50 (d), 128.07 (d), 129.56 (d), 130.68 (s), 133.13 (s), 140.09 (s), 142.27 (s), 145.31 (s).

Experimental Procedure

4a: A mixture of **7** (110.5 mg, 0.4 mmol), **6a** (2.45 g, 12.0 mmol), $Pd(OAc)_2$ (4.5 mg, 0.02 mmol), K_2CO_3 (440 mg, 3.2 mmol), and nBu_4NBr (258 mg, 0.8 mmol) in dimethylformamide (4 mL) was stirred under nitrogen for 14 d at 100 °C in a sealed reaction vessel. After the addition of water (100 mL), the mixture was extracted twice with dichloromethane (75 mL), the organic phase filtered through silica gel, and the solvent distilled off. More volatile by-products were removed by Kugelrohr distillation at 220 °C/0.1 Torr. Flash chromatography of the residue (silica gel, petroleum ether) gave 124 mg (72%) **4a**.

Received: July 6, 1993 [Z 6191 IE]
German version: *Angew. Chem.* **1993**, *105*, 1805

[1] Y. Tobe in *Carbocyclic Cage Compounds: Chemistry and Applications* (Eds.: E. Osawa, O. Yonemitsu), VCH, Weinheim, **1992**, p. 125–153.
[2] G. Wittig, W. Schoch, *Justus Liebigs Ann. Chem.* **1971**, *749*, 38–48; the unsaturated propellanes are described therein as propellamancenes.
[3] a) M. Stein, W. Winter, A. Rieker, *Angew. Chem.* **1978**, *90*, 737–738; *Angew. Chem. Int. Ed. Engl.* **1978**, *17*, 692–693; b) W. D. Hounshell, D. A. Dougherty, J. P. Hummel, K. Mislow, *J. Am. Chem. Soc.* **1977**, *99*, 1916–1924.
[4] a) H. Bohm, J. Kalo, C. Yarnitzky, D. Ginsburg, *Tetrahedron* **1974**, *30*, 217–219; b) G. Märkl, A. Mayr, *Tetrahedron Lett.* **1974**, 1817–1820; c) P. Gölitz, Dissertation, Göttingen, **1978**.
[5] a) G. Dyker, *Tetrahedron Lett.* **1991**, *32*, 7241–7242; b) *J. Org. Chem.* **1993**, *58*, 234–238.
[6] The new compounds **3**, **4a**, **4b**, **10**, and **11** were fully characterized by using spectroscopic methods (IR, UV, ^1H NMR, ^{13}C NMR), mass spectrometry, and elemental analysis (high-resolution mass determination for **10**); the NMR signals of **4a** and **4b** could be assigned on the basis of 2D NMR spectra (HH-COSY, CH-COSY, COLOC) and by NOE experiments (selected data are presented in Table 1).
[7] There are a few examples of the intramolecular palladium-catalyzed arylation of tetrasubstituted double bonds: a) R. Grigg, V. Sridharan, P. Stevenson, T. Worakun, *J. Chem. Soc. Chem. Commun.* **1986**, 1697–1699; b) M. M. Abelman, T. Oh, L. E. Overman, *J. Org. Chem.* **1987**, *52*, 4130–4133.
[8] R. F. Heck, *Org. React.* **1982**, *27*, 345–390.
[9] M. Catellani, G. P. Chiusoli, *J. Organomet. Chem.* **1985**, *286*, C13–C16.
[10] Crystal structure data: **4a** at −130 °C; orthorhombic, *Pbca*, $a = 1633.6(5)$, $b = 1517.7(5)$, $c = 1701.1(5)$ pm, $V = 4.218(2)$ nm^3, $Z = 8$, $\theta_{max} = 25°$, $wR(F^2) = 0.197$ for 3719 reflections, $R(F) = 0.071$. Colorless block, $0.5 \times 0.5 \times 0.3$ mm mounted in inert oil (type RS3000, gift from Riedel de Häen), $Mo_{K\alpha}$ radiation, Stoe-Stadi-4 diffractometer (program SHELXL-92). The structure was solved with direct methods and refined anisotropically to F^2; hydrogen atoms were taken into account with a "riding" model. Further details of the crystal structure investigation may be obtained from the Fachinformationszentrum Karlsruhe, Gesellschaft für wissenschaftlich-technische Information GmbH, D-76344 Eggenstein-Leopoldshafen (FRG) on quoting the depository number CSD-400260, the names of the authors, and the journal citation.
[11] A. J. Canty, *Platinum Metals Rev.* **1993**, *37*, 2–7.
[12] S. K. Talapatra, S. Chakrabarti, A. K. Mallik und B. Talapatra, *Tetrahedron* **1990**, *46*, 6047–6052.
[13] R. C. Fuson, H. D. Porter, *J. Am. Chem. Soc.* **1948**, *70*, 895–897.
[14] Signals in the mass spectrum of the product from the Pd-catalyzed reaction of C_{60} with iodobenzene; relevant signals with more than 720 mass units are normalized with the signal $m/z = 720$ (100%); MS (70 eV): m/z (%) 797 (6), 798 (6), 874 (2.8), 875 (2.4), 952 (2.6), 1030 (1.3), 1106 (1.8), 1108 (1.6), 1184 (0.3), 1261 (0.10), 1262 (0.13), 1339 (0.05), 1340 (0.05). The mass differences of 78 (C_6H_6) and 154 (twice C_6H_5) units prove phenylation and not annelation, for which a mass difference of 152 is expected. An explanation for this observation could be a mobile palladium atom attached to the fullerene surface by a π-allyl complex.
[15] G. A. Olah, I. Bucsi, C. Lambert, R. Aniszfeld, N. J. Trivedi, D. K. Sensharma, G. K. S. Prakash, *J. Am. Chem. Soc.* **1991**, *113*, 9387–9388.

Reverse Hydrozirconation Reaction: A Regio- and Diastereospecific Route to New Diphosphanes**

By *Maria Zablocka, Florence Boutonnet, Alain Igau, Françoise Dahan, Jean Pierre Majoral,** and *K. Michal Pietrusiewicz**

Organozirconium compounds resulting from hydrozirconation of alkenes and alkynes effect a wide variety of useful synthetic transformations.[1, 2] It is also well established that hydrozirconation of carbon–carbon multiple bonds always leads to *cis* addition products in which the zirconocene moiety is linked to the less hindered carbon atom. In this report we demonstrate for the first time that both α- and β-zirconated products can be prepared by direct hydrozirconation of dihydrophospholes in a completely regio- and diastereoselective fashion. Remarkably also, transmetalation reactions of the zirconated phospholanes with chlorophosphanes also occur diastereoselectively and afford the same diphosphane in both cases.

Hydrozirconation of dihydrophosphole **2** with $[Cp_2ZrHCl]$ (**1**) afforded quantitatively a stable α-substituted phospholane **3** (one diastereomer), which was characterized by NMR spectroscopy (Table 1), mass spectrometry, and elemental analysis. The ^1H NMR signals of the Cp protons of **3** appeared as two doublets at $\delta = 6.37$ and 6.45, each with a $^3J(C,P)$ coupling constant of 0.6 Hz, consistent with a Cp-Zr-P skeleton.[3] Similarly, two doublets ($^2J_{C,P} = 2.7$ and 2.8 Hz) were observed for the Cp carbons in the ^{13}C NMR spectrum and a large one-bond coupling constant ($^1J_{C,P} = 51.7$ Hz), typical for three-membered cyclic phosphanes,[4] for the α carbon that is part of the three-membered chelate ring. In marked contrast to other studies,[1] the formation of the less hindered β-zirconated product **5** was not observed in the reaction of **2**.[5] All these data suggest strongly that the observed reversal of regioselectivity is most likely

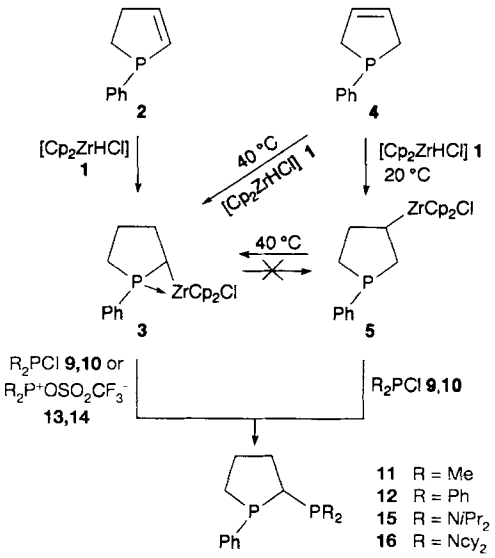

[*] Dr. J. P. Majoral, F. Boutonnet, Dr. A. Igau, Dr. F. Dahan
Laboratoire de Chimie de Coordination du CNRS
205, route de Narbonne, F-31077 Toulouse Cédex (France)
Dr. K. M. Pietrusiewicz, Dr. M. Zablocka
Centre of Molecular and Macromolecular Studies
Polish Academy of Sciences
Sienkiewicza 112, PL-90-362 Lodz (Poland)

[**] This work was supported by the CNRS (France) and the Committee for Scientific Research (Poland), Grant no. 2 1307 91 01.

due to the coordination of zirconium to the phosphane site, which provides extra stabilization of the α-metalated phospholane.

Addition of **1** (1 equiv) to a solution of the isomeric dihydrophosphole **4** (1 equiv) in THF at room temperature also resulted in a regioselective reaction, but yielded exclusively the β-zirconated phospholane **5**, which was again stable enough to be isolated and fully characterized (Table 1). On the other hand, addition of **1** to a solution of **4** in THF maintained at +40 °C afforded the thermodynamically more stable product **3**. Migration of the metal along the carbon chain—which is reported to be facile for hydrozirconations proceeding "normally"[1b]—is also observed but the direction is reversed because of the effect of coordination at P.

During hydrozirconation of **2** neither the formation of **5** nor the conversion of **3** into **5** was observed. In addition, a ^{31}P NMR spectrum recorded on a solution of **5** in THF, kept at room temperature for three days, did not reveal any detectable signal of **3** and showed instead signals at $\delta = -10.3$ (90%, unchanged **5**) and at $\delta = -11.5$ (10%), attributable probably to the second possible diastereomer of **5**.

To confirm the key role of the phosphorus lone pair, hydrozirconation reactions on the corresponding dihydrophosphole borane adducts **6** and **7** (Scheme 2) were performed. In both cases exclusive formation of the β-zirconated phospholane **8** was observed. Interestingly, treatment of the α-substituted phospholane **3** with $BH_3 \cdot SMe_2$ at 0 °C also led to the formation of **8** (Scheme 2), apparently through cleavage of the phosphorus zirconium dative bond followed by complexation of the phosphorus lone pair with BH_3 and migration of the $ZrCp_2Cl$ moiety to the less hindered position. Compound **8** was obtained as one diastereomer as demonstrated by ^{13}C NMR (Table 1).

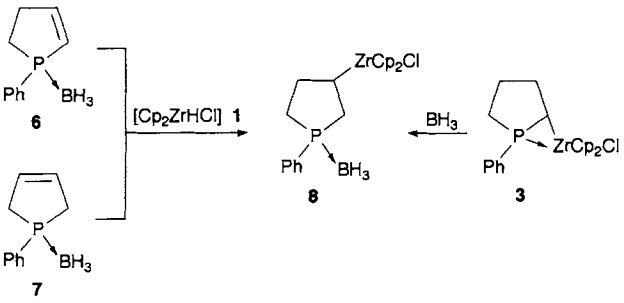

The synthetic utility of the organozirconium complex **3** will now be illustrated. Treatment of **3** with chlorophosphanes R_2PCl (**9**, R = Me; **10**, R = Ph) gave rise to the new diphosphanes **11** and **12** formed quantitatively in each case as a single diastereoisomer (Table 1). Similarly, addition of the salts $(iPr_2N)_2P^+CF_3SO_3^-$ (**13**) or $[(cyclohexyl)_2N]_2P^+CF_3SO_3^-$ (**14**) to **3** afforded other previously unknown α-diphosphanes **15** and **16** in high yield (>90%). As determined by an X-ray structure analysis of **12**[6] (Fig. 1), *cis*

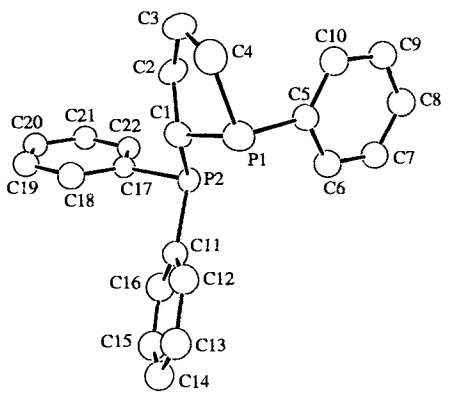

Fig. 1. Molecular structure of **12** in the crystal. Selected bond lengths [Å] and angles [°]: P(1)-C(1) 1.860(4), P(2)-C(1) 1.865(5), P(1)-C(4) 1.839(6); C(1)-P(1)-C(4) 88.8(2), C(1)-P(1)-C(5) 103.1(2), C(4)-P(1)-C(5) 103.8(2). Torsion angle [°]: P(2)-C(1)-P(1)-C(5) 56.0(3).

Table 1. Selected spectroscopic data of the compounds **3**, **5**, **8**, **11**, **12**, **15**, and **16** [a, b].

3: $^{31}P\{^1H\}$ NMR (THF): $\delta = 1.4$; ^1H NMR ([D$_8$]THF): $\delta = 1.90$ (m, 2H; CH_2), 2.09 (m, 2H; CH_2), 2.36 (m, 2H; CH_2), 2.64 (ddd, $^3J(H,H) = 7.2$, $^3J(H,H) = 10.5$, $^2J(H,P) = 4.1$ Hz, 1H; CHZr), 6.37 (d, $^3J(H,H) = 0.6$ Hz, 5H; Cp), 6.45 (d, $^3J(H,H) = 0.6$ Hz, 5H; Cp), 7.31–7.57, 7.70–7.76 (m, 5H; Ph); $^{13}C\{^1H\}$ NMR ([D$_8$]THF): $\delta = 30.77$ (d, $^2J(C,P) = 1.2$ Hz, γ-CH_2), 32.21 (d, $^1J(C,P) = 19.5$ Hz, ω-CH_2), 41.89 (d, $^2J(C,P) = 2.4$ Hz, β-CH_2), 59.89 (d, $^1J(C,P) = 51.7$ Hz, α-CH), 114.42 (d, $^2J(C,P) = 2.8$ Hz, Cp), 114.73 (d, $^2J(C,P) = 2.7$ Hz, Cp), 128.94 (s, *p*-Ph), 129.36 (d, $^3J(C,P) = 5.5$ Hz, *m*-Ph), 132.95 (d, $^2J(C,P) = 18.3$ Hz, *o*-Ph), 147.26 (d, $^1J(C,P) = 37.3$ Hz, *ipso*-Ph)

5: $^{31}P\{^1H\}$ NMR (THF): $\delta = -10.3$; $^{13}C\{^1H\}$ NMR ([D$_8$]THF): $\delta = 30.68$ (d, $^1J(C,P) = 11.8$ Hz; ω-CH_2), 39.16 (d, $^2J(C,P) = 1.3$ Hz; γ-CH_2), 40.20 (d, $^1J(C,P) = 16.9$ Hz; α-CH_2), 66.22 (d, $^2J(C,P) = 6.6$ Hz; β-CH), 115.39 (s; Cp), 127.77 (s; *p*-Ph), 129.24 (d, $^3J(C,P) = 6.8$ Hz; *m*-Ph), 131.54 (d, $^2J(C,P) = 14.8$ Hz; *o*-Ph), 145.45 (d, $^1J(C,P) = 25.7$ Hz; *ipso*-Ph)

8: $^{31}P\{^1H\}$ NMR (THF): $\delta = 37.5$ (q, $^1J(P,B) = 48.3$ Hz); $^{13}C\{^1H\}$ NMR ([D$_8$]THF): $\delta = 30.63$ (d, $^1J(C,P) = 6.9$ Hz; ω-CH_2), 32.22 (d, $^2J(C,P) = 32.4$ Hz; α-CH_2), 41.84 (s; γ-CH_2), 54.70 (s; β-CH), 115.59 (s; Cp), 130.05 (d, $^3J(C,P) = 7.6$ Hz; *m*-Ph), 132.29 (s; *p*-Ph), 133.5 (d, $^2J(C,P) = 8.3$ Hz; *o*-Ph) 137.72 (d, $^1J(C,P) = 39.1$ Hz; *ipso*-Ph)

11: $^{31}P\{^1H\}$ NMR (C_6D_6): $\delta = -5.5$ (d, $^2J(P,P) = 37.5$ Hz; PPh), −47.8 (d, $^2J(P,P) = 37.5$ Hz; PMe_2); ^1H NMR ([D$_8$]THF): $\delta = 0.67$ (d, $^2J(H,P) = 3.8$ Hz, 3H; PCH_3), 1.02 (dd, $^2J(H,P) = 3.5$, $^4J(H,P) = 0.7$ Hz, 3H; PCH_3), 1.97 (m), 1.50, 1.72, 1.97 (m, 5H; CH, CH_2), 7.16 (m, 3H; Ph), 7.61 (m, 2H; Ph); $^{13}C\{^1H\}$ NMR (C_6D_6): $\delta = 14.75$ (dd, $^1J(C,P) = 18.3$, $^3J(C,P) = 2.7$ Hz; CH_3), 15.5 (dd, $^1J(C,P) = 14.0$, $^3J(C,P) = 5.3$ Hz; CH_3), 27.00 (d, $^1J(C,P) = 14.4$ Hz; γ-CH_2), 28.75 (d, $^2J(C,P) = 8.1$ Hz; β-CH_2), 31.58 (dd, $^1J(C,P) = 13.6$, $^3J(C,P) = 2.0$ Hz; ω-CH_2), 44.42 (dd, $^1J(C,P) = 21.5$, $^1J(C,P) = 23.3$ Hz; α-CH), 129.34 (br. s, *p*-/*m*-Ph), 135.04 (d, $^2J(C,P) = 16.8$ Hz; *o*-Ph), *ipso*-Ph not found

12: $^{31}P\{^1H\}$ NMR (THF): $\delta = -4.5$ (d, $^2J(P,P) = 31.5$ Hz; PPh), −13.5 (d, $^2J(P,P) = 31.5$ Hz; PPh_2); ^1H NMR (C_6D_6): $\delta = 1.34$ (m, 2H; CH_2), 1.73 (m, 2H; CH_2), 2.04 (m, 2H; CH_2), 2.59 (dddd, $^3J(H,H) = 11.4$, $^3J(H,H) = 6.7$, $^2J(H,P) = 3.8$, $^2J(H,P) = 13.7$ Hz, 1H; PCH), 7.70–7.65, 7.49–7.34, 7.16–6.96 (m, 15H; Ph); $^{13}C\{^1H\}$ NMR (C_6D_6, 25 °C): $\delta = 26.76$ (d, $^2J(C,P) = 12.5$ Hz; γ-CH_2), 28.37 (d, $^2J(C,P) = 13.4$ Hz; β-CH_2), 33.08 (d, $^1J(C,P) = 22.2$ Hz; ω-CH_2), 38.88 (dd, $^1J(C,P) = 24.6$, $^1J(C,P) = 24.6$ Hz; α-CH)

15: $^{31}P\{^1H\}$ NMR (C_6D_6): $\delta = -5.3$ (d, $^2J(P,P) = 40.1$ Hz; PPh), 49.8 (d, $^2J(P,P) = 40.1$ Hz; $PNiPr_2$); ^1H NMR (C_6D_6): $\delta = 1.15$ (d, $J(H,P) = 6.7$ Hz, 12H; CH_3), 1.20 (d, $J(H,P) = 6.7$ Hz, 12H; CH_3), 2.06 (m, 6H; CH_2), 2.65 (m, 1H; HCP), 3.35 (m, 4H; HCN), 7.15 (m, 3H; Ph), 7.85 (m, 2H; Ph); $^{13}C\{^1H\}$ NMR (C_6D_6): $\delta = 24.85$ (d, $^3J(C,P) = 6.8$ Hz; CH_3), 25.31 (d, $^3J(C,P) = 6.1$ Hz; CH_3), 28.05 (dd, $^2J(C,P) = 14.8$, $^3J(C,P) = 2.0$ Hz; γ-CH_2), 31.68 (d, $^2J(C,P) = 14.8$ Hz; β-CH_2), 33.95 (dd, $^1J(C,P) = 23.0$, $^3J(C,P) = 3.5$ Hz; ω-CH_2), 40.28 (dd, $^1J(C,P) = 23.6$, $^1J(C,P) = 23.6$ Hz; α-CH), 46.18 (d, $^1J(C,P) = 14.7$ Hz; HCN), 48.01 (d, $^1J(C,P) = 9.3$ Hz; HCN), 134.99 (s; *p*-Ph), 135.35 (d, $^2J(C,P) = 18.7$ Hz; *o*-Ph), 135.38 (s; *m*-Ph), 141.21 (d, $^1J(C,P) = 27.7$ Hz; *ipso*-Ph)

16: $^{31}P\{^1H\}$ NMR (C_6D_6): $\delta = -5.9$ (d, $^2J(P,P) = 33.7$ Hz; PPh), 56.8 (d, $^2J(P,P) = 33.7$ Hz; PN); $^{13}C\{^1H\}$ NMR (C_6D_6): $\delta = 25.60$, 26.23, 26.44, 27.45, 27.62, 27.75, 27.96 (s; CH_2-cy), 30.71 (d, $^2J(C,P) = 16.5$ Hz; ω-CH_2), 31.92 (d, $^2J(C,P) = 13.0$ Hz; β-CH_2), 41.0 (dd, $^1J(C,P) = 24.8$, $^1J(C,P) = 25.1$ Hz; α-CH), γ-CH_2 obscured, 54.10 (d, $^2J(C,P) = 63.6$ Hz; CH-cy), 58.15 (d, $^2J(C,P) = 63.7$ Hz; CH-cy), 134.85 (s; *p*-Ph), 135.36 (d, $^2J(C,P) = 18.4$ Hz; *o*-Ph), 135.41 (s; *m*-Ph), 141.19 (d, $^1J(C,P) = 27.9$ Hz; *ipso*-Ph)

[a] All NMR spectra were recorded at 25 °C on Bruker AC 80, AC 200, or WM 250: standards: ^{31}P, 85% H_3PO_4 external; ^1H and ^{13}C, $(CH_3)_4Si$ external. [b] Carbon atoms of the phospholane ring were assigned so that the substituted C atom adjacent to the P atom is the α carbon.

diphosphanes were formed in these reactions. This *cis* arrangement appears to be inconsistent with all the previous observations on stereochemistry of reactions involving alkyl- and alkenylzirconium complexes (protodezirconation, cleavage by halogens, transmetalations, etc.), which were reported to proceed with complete retention of configuration.[1b] The reasons for this apparent discrepancy are not clear at the moment. Noteworthy is the fact that the reactions of the β-zirconated **5** with chlorophosphanes **9** and **10** at -20 °C also afforded diphosphanes **11** and **12**, the same isomers as those obtained from **3**.

To summarize, the hydrozirconation and transmetalation reactions were both diastereospecific and gave α-diphosphanes otherwise difficult to obtain. In contrast the corresponding β-diphosphanes **17**, required for comparative purposes, could be readily prepared by conjugate addition of $Ph_2P(O)H$ to the oxide of **2** followed by isomer separation and stereoretentive reduction with $PhSiH_3$ (^{31}P NMR: **17a** $\delta = -4.0$ and 8.9, $^3J_{P,P} = 8.9$ Hz (*trans*); **17b** $\delta = -2.3$ and -10.0, $^3J_{P,P} \approx 0$ Hz (*cis*)).[7]

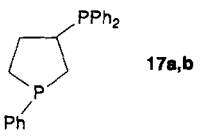

17a,b

Extension of this work to the synthesis of optically active diphosphanes[8] as well as the preparation of phosphanes containing main group elements is underway.

Experimental Procedure

All manipulations were performed in an inert atmosphere (argon).

Preparation of **3**: To a magnetically stirred solution of **2** [10] (0.146 g, 0.9 mmol) in THF (5 mL), cooled at -20 °C, was added a suspension of [Cp_2ZrHCl] (**1**, 0.232 g, 0.9 mmol) in THF (5 mL). The mixture was stirred for 15 minutes at -20 °C, then allowed to warm up slowly to room temperature, and stirred for a further 3 hours. During this time, the solution turned dark brown and became homogeneous. Evaporation of THF gave **3** quantitatively as a dark brown powder.

General procedure for transmetalations: To a magnetically stirred solution of **3** (0.9 mmol) in THF (10 mL) cooled at -20 °C was added **9** or **10** (0.9 mmol) [or a solution of **13** or **14** (0.9 mmol) in CH_2Cl_2 (3 mL)] by syringe. The mixture was kept at -20 °C for 30 min and then warmed up slowly to room temperature. The resulting colorless solution was evaporated to dryness, and the residue was extracted twice with pentane (20 mL). Diphosphanes **11**, **12**, **15**, and **16** were obtained as white powders (68–90% isolated yield).

Received: June 28, 1993 [Z 6171 IE]
German version: *Angew. Chem.* **1993**, *105*, 1846

[1] Reviews: a) E. Negishi, T. Takahashi, *Synthesis* **1988**, 1; b) J. A. Labinger in *Comprehensive Organic Synthesis, Vol. 8* (Eds.: B. M. Trost, I. Fleming), Pergamon, **1991**, p. 667.

[2] I. Hyla-Kryspin, R. Gleiter, C. Krüger, R. Zwettler, G. Erker, *Organometallics* **1990**, *9*, 517; G. Erker, R. Zwettler, C. Krüger, I. Hyla-Kryspin, R. Gleiter, *ibid.* **1990**, *9*, 524, and references therein.

[3] H. H. Karsch, B. Denbelly, J. Hofmann, U. Pieper, G. Müller, *J. Am. Chem. Soc.* **1988**, *110*, 3654; J.-P. Majoral, N. Dufour, F. Meyer, A.-M. Caminade, R. Choukroun, D. Gervais, *J. Chem. Soc. Chem. Commun.* **1990**, 507; N. Dufour, J.-P. Majoral, A.-M. Caminade, R. Choukroun, *Organometallics* **1991**, *10*, 45; N. Dufour, A.-M. Caminade, M. Bassoo-Bert, A. Igau, J.-P. Majoral, *ibid.* **1992**, *11*, 131; A. Igau, N. Dufour, A. Mahieu, J.-P. Majoral, *Angew. Chem.* **1993**, *105*, 76; *Angew. Chem. Int. Ed. Engl.* **1993**, *32*, 95.

[4] G. A. Gray, S. E. Cremer, K. L. Marsi, *J. Am. Chem. Soc.* **1976**, *98*, 2109.

[5] Hydrozirconation of 2-vinylfuran was postulated to give the terminally substituted product, but it was not detected. O-coordination, aromatic stabilization, or reduced steric effect of the flat furan ring or a combination of these were proposed to account for the formation of the product substituted at the C2 vinyl atom [9].

[6] Crystal data for **12**: $C_{22}H_{22}P_2$, $P2_1/c$, (monoclinic), $a = 10.072(1)$, $b = 11.655(1)$, $c = 16.697(2)$ Å, $\beta = 102.99(2)$°, $Z = 4$, $V = 1909.9(7)$ Å^3, $M = 348.4$, $\varrho_{calcd} = 1.211$ g cm^{-3}, $\mu = 2.2$ cm^{-1}; 2644 unique reflections were measured and 1736 with $I > 3\sigma(I)$ were used in the refinement to $R = 0.048$, $R_w = 0.023$. Further details of the crystal structure investigations are available on request from the Fachinformationszentrum Karlsruhe, Gesellschaft für wissenschaftlich-technische Information mbH, D-76344 Eggenstein-Leopoldshafen (FRG) on quoting the depositary number CSD-57481, the names of the authors, and the journal citation.

[7] M. Koprowski, K. M. Pietrusiewicz, unpublished results.

[8] Phospholane ligands: M. J. Burk, *J. Am. Chem. Soc.* **1991**, *113*, 8518; M. J. Burk, J. E. Feaster, *ibid.* **1992**, *114*, 6266; J. C. Fiaud, J. Y. Legros, *Tetrahedron Lett.* **1991**, *38*, 5089.

[9] S. L. Buchwald, S. J. LaMaire, *Tetrahedron Lett.* **1987**, *28*, 295.

[10] The starting 1-phenyl dihydrophospholes **2** ($\delta^{31}P = -2.0$) and **4** ($\delta^{31}P = -25.6$) were obtained from the corresponding oxides [11] by reduction with $PhSiH_3$ in C_6H_6 at 60 °C.

[11] L. D. Quin, *The Heterocyclic Chemistry of Phosphorus*, Wiley-Interscience, New York, **1981**.

Enzyme-Catalyzed Asymmetric Synthesis: Kinetic Resolution of Chiral Hydroperoxides by Enantioselective Reduction to Alcohols with Horseradish Peroxidase**

By *Waldemar Adam*,* *Ute Hoch*, *Chantu R. Saha-Möller*, and *Peter Schreier*

Dedicated to Professor Guiseppe Cilento on the occasion of his 70th birthday

The enzyme-catalyzed, enantioselective synthesis of organic substances has become increasingly important.[1] For example, heme-type enzymes such as peroxidases have been employed for the oxidation of numerous substrates with hydrogen peroxide and hydroperoxides.[2] Chloroperoxidase (CPO)[3] from *Caldariomyces fumago* effects the enantioselective oxidation of prochiral sulfides with H_2O_2 or *t*BuOOH to give sulfoxides in 13–99% *ee*.[3c] This peroxidase also mediates the regio- and stereoselective halogenation of glycals.[3c] Recently it was reported that CPO/H_2O_2 epoxidizes disubstituted alkenes efficiently and enantioselectively.[4]

For horseradish peroxidase (HRP), merely the asymmetric sulfoxidation of prochiral sulfides is known; however, the enantioselectivities (30–70% *ee*) are much lower.[5] While the CPO-catalyzed sulfoxidation with racemic 1-arylethyl hydroperoxides shows high affinity for the (*R*) enantiomer, such substrate selectivity has not been reported for HRP-catalyzed transformations. Moreover, besides the optically active (*R*) sulfoxides (13–99% *ee*), the corresponding (*R*) alcohols (17–80% *ee*) and the (*S*) hydroperoxides (24–91% *ee*) were isolated from the same CPO-catalyzed reaction.[3c] We report here on the kinetic resolution of chiral hydroperoxides by enantioselective HRP (Sigma, Type II, RZ 1.5–2.0) catalyzed reduction in the presence of guaiacol to provide alcohols (Scheme 1). With this enzyme-catalyzed route, we have succeeded in obtaining hydroperoxides and their alcohols simultaneously in high optical purity (>95% *ee*) (Table 1).

[*] Prof. Dr. W. Adam, Dr. C. R. Saha-Möller
Institut für Organische Chemie der Universität
Am Hubland, D-97074 Würzburg (FRG)
Lebensmittelchemikerin U. Hoch, Prof. Dr. P. Schreier
Institut für Pharmazie und Lebensmittelchemie
der Universität Würzburg

[**] This research was supported by the Deutsche Forschungsgemeinschaft (SFB 347 "Selektive Reaktionen Metall-aktivierter Moleküle") and the Fonds der Chemischen Industrie.

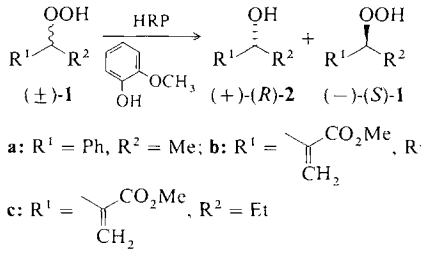

a: R^1 = Ph, R^2 = Me; **b**: R^1 = CH_2–$CH(CO_2Me)$–, R^2 = Me;

c: R^1 = CH_2–$CH(CO_2Me)$–, R^2 = Et

Scheme 1. HRP-catalyzed kinetic resolution of chiral hydroperoxides.

Table 1. Kinetic resolution of chiral hydroperoxides (±)-1 [a] by horseradish peroxidase in the presence of guaiacol [b].

Entry	(±)-1	[mmol]	(±)-1:HRP	t [min] [c]	ee [%] (S)-1	ee [%] (R)-2
1	1a	0.03	12000:1	5	>99	>99
2	1a	1.50	60000:1	120	>99	>99
3	1b	0.03	12000:1	5	97	>99
4	1b	1.50	60000:1	120	95	98
5	1c	0.03	21000:1	10	>99	>99
6	1c	1.50	12000:1	120	91	95

[a] The hydroperoxides were prepared according to literature procedures: (±)-1a [7a], (±)-1b,c [7b]. [b] Guaiacol was employed in equimolar amounts with respect to (±)-1. [c] The reaction was halted after complete consumption of guaiacol.

To assess optimal substrate concentrations for the enzymatic transformations of the racemic hydroperoxides, the kinetic parameters were determined (Table 2). At constant guaiacol concentration the K_M and V_{max} values were measured for each hydroperoxide. The data shows (Table 2) that these enzyme parameters depend notably on the R^1 and R^2 substituents of **1**. Consequently, (±)-**1** (0.03 mmol) in 5 mL 0.1 M phosphate buffer (pH 6) and (±)-**1b,c** (0.03 mmol) in 1 mL buffer solution were employed. Fortunately, the hydroperoxides (±)-**1a–c** do not react at room temperature with guaiacol in the absence of HRP, so that the enzyme-catalyzed kinetic resolution could be conducted at about 20 °C. Since it is known that the stoichiometric ratio of oxidant to substrate for the peroxidase-catalyzed oxidation of phenols is 1:2,[1a] a guaiacol:hydroperoxide ratio of 1:1 was chosen, in order to limit the hydroperoxide consumption to at most 50%. The results in Table 1 demonstrate that guaiacol was completely consumed under simultaneous formation of nearly enantiomerically pure hydroperoxides (*S*)-**1a–c** and the corresponding alcohols (*R*)-**2a–c**.

Table 2. Kinetic parameters [a] for the horseradish peroxidase catalyzed oxidation of guaiacol with hydroperoxides (±)-1.

Substrate	K_M [mM]	V_{max} [b] [mmol mg^{-1} min^{-1}]	V_{max}/K_M [L mg^{-1} min^{-1}] × 10^{-3}
guaiacol	0.2 ± 0.06	19.0 ± 0.1	95
(±)-1a	0.6 ± 0.04	18.0 ± 0.1	30
(±)-1b	37.2 ± 2.5	18.0 ± 0.6	0.48
(±)-1c	63.0 ± 2.3	8.3 ± 0.4	0.13

[a] The kinetic parameters for guaiacol were determined with 1.25 mM hydroperoxide (±)-1a; for the hydroperoxides (±)-1a–c a guaiacol concentration of 500 mM was used. [b] The initial rates were monitored by following the appearance of the guaiacol oxidation product (ε = 2.66 × 104 M^{-1}cm^{-1}) [9] at 470 nm in 0.1 M phosphate buffer (pH 6). V_{max} and K_M were calculated with the Duggleby program on an IBM computer.

The absolute configuration of (*S*)-**1a** and (*R*)-**2a** was determined by comparison of the HPLC data with those of the authentic substances.[3c, 6] The absolute configurations of (*S*)-**1b,c** and (*R*)-**2b,c** were assigned analogously. The enantiomeric excesses of the hydroperoxides (*S*)-**1** and alcohols (*R*)-**2** were determined from the ratio of areas corresponding to the two enantiomers in the HPLC (Chiracel OD column) chromatogram. A representative chromatogram is given in Figure 1 for hydroperoxide **1b** and alcohol **2b**. As can be seen for the present examples, the HRP enzyme selectively recognizes the (+)-(*R*)-hydroperoxides. Consequently, the kinetic resolution affords the optically pure (−)-(*S*)-hydroperoxides and (+)-(*R*)-alcohols. A control experiment confirmed that when sufficient guaiacol was employed to reduce all of the racemic hydroperoxide (i.e. guaiacol:hydroperoxide 2:1), the optically pure (>95% *ee*) alcohol and hydroperoxide were still obtained. This selectivity of the HRP for the oxidant, which resulted in the exclusive reduction of the (+)-(*R*) enantiomer, is unprecedented.[11] For the synthetic exploitation of this novel HRP-catalyzed, enantioselective reduction of racemic hydroperoxides to the corresponding alcohols, the enzymatic reaction was conducted on a semipreparative scale. The results in Table 1 (entries 2,4, and 6) demonstrate convincingly that the HRP-catalyzed kinetic resolution serves for the preparation of enantiomerically pure hydroperoxides and their alcohols on a 1.5 mmol scale. After conventional workup and purification by column chromatography, the optically pure hydroperoxides (80–98%, relative to 50% conversion) and the corresponding alcohols (72–88%, relative to 50% conversion) were isolated in good yields.

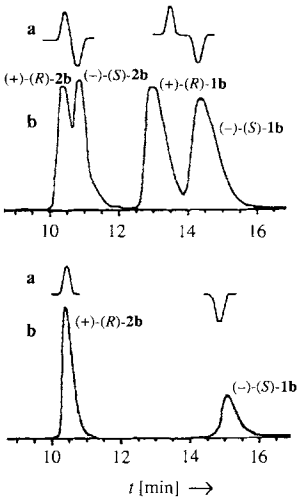

Fig. 1. HPLC chromatograms from the HRP-catalyzed reaction of (±)-**1b** with guaiacol. Top: authentic racemic samples of alcohol (±)-**2b** and hydroperoxide (±)-**1b**. Bottom: reaction products after resolution of (±)-**1b**. The polarimetric detection with the ChiraLyser (a) is placed above the UV signals (b) at 220 nm. Column: Daicel-Chiralcel OD, 250 × 4 mm; eluent: *n*-hexane/isopropyl alcohol (90:10); flow rate: 0.6 mL min^{-1}

In summary, horseradish peroxidase is highly selective for (*R*) hydroperoxides, which allows kinetic resolution of racemic hydroperoxides by means of enantioselective reduction to furnish the corresponding alcohols. This enzyme-catalyzed reduction can be performed on preparative scale and provides optically pure alcohols and hydroperoxides conveniently. In contrast, the preparation of enantiomerically pure hydroperoxides by nonenzymatic means is quite cumbersome.[8]

Experimental Procedure

In the preparative-scale reaction, 1.50 mmol hydroperoxide (±)-**1** and 1.50 mmol guaiacol were dissolved in 10 mL 0.1 M phosphate buffer (pH 6) and subsequently 0.25–1.25 × 10^{-4} mmol HRP was added. The reaction mixture was allowed to stand at 20 °C for 2 h and then extracted with CH_2Cl_2 (3 × 20 mL). The combined organic phases were dried over Na_2SO_4 and the solvent removed on the rotary evaporator (ca. 20 °C/17 Torr). Hydroperoxide (*S*)-**1** and alcohol (*R*)-**2** were separated by column chromatography (silica gel, 0.032–0.62 mmol eluting with petroleum ether/diethyl ether (4:1).

Received: September 7, 1993 [Z 6346 IE]
German version: *Angew. Chem.* **1993**, *105*, 1800

[1] a) H. L. Holland, *Organic Synthesis with Oxidative Enzymes*, VCH, New York, **1992**; b) S. M. Roberts, K. Wiggins, G. Casy, *Preparative Biotransformations: Whole Cell and Isolated Enzymes in Organic Synthesis*, Wiley, Chichester, **1992**.
[2] J. H. Dawson, *Science* **1988**, *240*, 433–439.
[3] a) S. Colonna, N. Gaggero, A. Manfredi, L. Casella, M Gullotti, G. Carrea, P. Pasta, *Biochemistry* **1990**, *29*, 10465–10468; b) S. Colonna, N. Gaggero, L. Casella, G. Carrea, P. Pasta, *Tetrahedron: Asymmetry* **1992**, *3*, 95–106; c) H. Fu, H. Kondo, Y. Ichikawa, G. C. Look, C.-H. Wong, *J. Org. Chem.* **1992**, *57*, 7265–7270.
[4] E. J. Allain, L. P. Hager, Li Deng, E. N. Jacobsen, *J. Am. Chem. Soc.* **1993**, *115*, 4415–4416.
[5] a) S. Colonna, N. Gaggero, G. Carrea, P. Pasta, *J. Chem. Soc. Chem. Commun.* **1992**, 357–358; b) R. Z. Harris, S. L. Newmyer, P. R. Ortiz de Montellano, *J. Biol. Chem.* **1993**, *268*, 1637–1645.
[6] A. Kunath, E. Höft, H.-J. Hamann, J. Wagner, *J. Chromatogr.* **1991**, *588*, 352–355.
[7] a) A. G. Davies, R. V. Foster, A. M. White, *J. Chem. Soc.* **1953**, 1541–1547; b) W. Adam, A. Griesbeck, *Synthesis* **1986**, 1050–1051.
[8] a) P. Dussault, N. A. Porter, *J. Am. Chem. Soc.* **1988**, *110*, 6276–6277; b) P. Dussault, I. Q. Lee, S. Kreifels, *J. Org. Chem.* **1991**, *56*, 4087–4089.
[9] J. Pütter, R. Becker, *Methods Enzym. Anal. 3rd ed. 1983–1986*, **1983**, *3*, 286–293.

Highly Coordinated Lanthanoid–Phosphane Complexes**

By *Hans H. Karsch,* Gunter Ferazin, Oliver Steigelmann, Huub Kooijman,* and *Wolfgang Hiller*

Dedicated to Professor Ernst Otto Fischer on the occasion of his 75th birthday

Phosphane ligands are almost indispensible in transition metal chemistry. Complexes with high numbers of coordinated phosphanes are known and are very important in many catalytic processes. Although lanthanoid complexes also have notable catalytic properties, there are only few structurally characterized examples of compounds in which the metal center is coordinated by a number of phosphane ligands. Only with heteroatom–phosphane chelating ligands, for example $[N(SiMe_2CH_2PR_2)_2]^-$, can up to four lanthanoid–phosphorus bonds be formed.[1] The electrophilicity of lanthanoid centers generally resembles that of "hard" main group metal centers such as Al^{3+}.[2] With diphosphinomethanides as chelating ligands, metal centers can attain high phosphane coordination numbers by forming covalent and ionic bonds (**I**), as in the case of Al^{3+} (**II**).[3]

In fact the corresponding lanthanum diphosphinomethanide complex **III** could also be synthesized;[4] however, the coordination modes in **II** (σ) and **III** (π) are completely different. This can be attributed at least in part to the exocyclic carbanion substituent (Me_3Si in **II**, H in **III**), which in **II** markedly reduces the nucleophilic nature of the carbanion. We have now succeeded in synthesizing highly coordi-

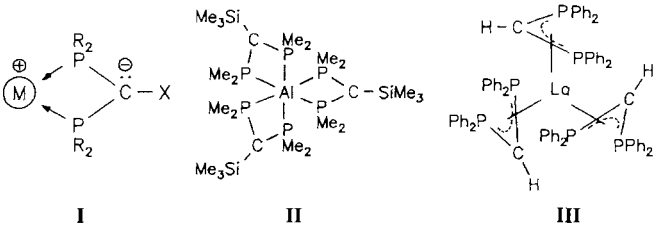

I **II** **III**

nated lanthanoid–phosphane complexes in which the ligands are bound as in **II**. The methanide **1** acts as a source of anionic diphosphinomethanide ligands. For the syntheses of these complexes metal halides are not appropriate starting materials, since only mixtures containing substantial amounts of lithium halide are formed. Evidently addition and only partial substitution occurs, as is established by the isolation and structural characterization of **2** (violet crystals from pentane) [Eq. (1)].

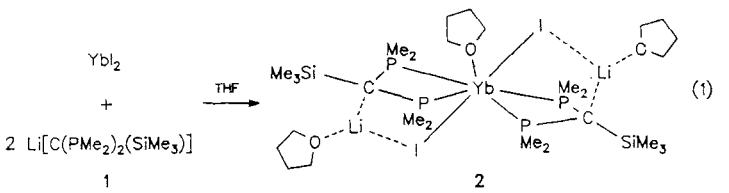

1 **2** (1)

In **2** (Fig. 1) a $YbI_2 \cdot THF$ moiety has been inserted into the framework of **1** · THF, which exists as the dimer $[(THF)Li\{C(PMe_2)_2(SiMe_3)\}]_2$,[5] whereby all Li–P bonds are broken and replaced by four Yb–P bonds. This results in a seven-coordinate Yb^{2+} ion and the formation of Li–I bonds.[6]

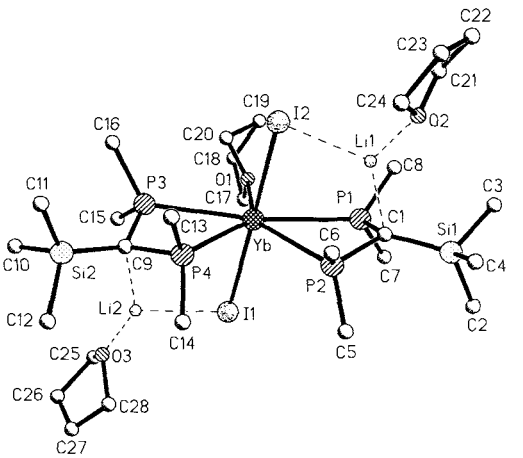

Fig. 1. Crystal structure of **2**. Important distances [Å] and angles [°]: Yb-I1 3.131(5), Yb-I2 3.114(3), Yb-P1 3.08(1), Yb-P2 2.99(2), Yb-P3 3.03(2), Yb-P4 2.96(1), Yb-O1 2.44(4), Li1-I2 2.67(7), Li1-C1 2.22(8), Li1-O1 1.93(8), Li2-I2 2.87(10), Li2-C9 2.20(10), Li2-O3 1.72(10); I1-Yb-I2 176.5(2), P1-C1-P2 103(2), Yb-P2-C1 98(1), P1-Yb-P2 55.7(3), Yb-P1-C1 96(1), P3-C9-P4 101(2), P3-Yb-C4 54.9(4), Yb-P4-C9 98(1), Yb-P3-C9 100(2).

In order to achieve complete substitution, lanthanoid complexes containing a better leaving group are needed.

[*] Prof. Dr. H. H. Karsch, Dr. G. Ferazin, Dr. O. Steigelmann, Dr. H. Kooijman, Prof. Dr. W. Hiller
Anorganisch-chemisches Institut der Technischen Universität München
Lichtenbergstrasse 4, D-85747 Garching (FRG)
Telefax: Int. code + (89)3209-3125

[**] This work was funded by the Fonds der Chemischen Industrie.

Lanthanoid triflates[7] have now been shown to be successful reagents. Complex **3** was obtained according to Equation (2) as yellow crystals (pentane).[8]

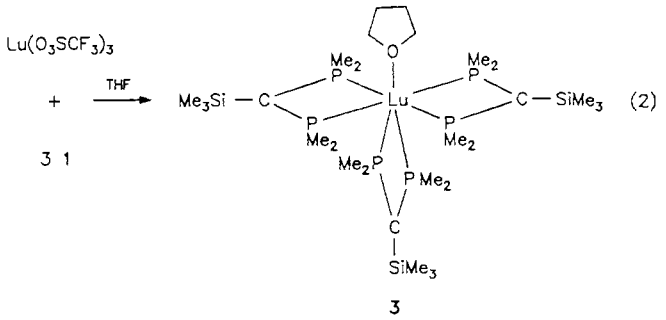

(2)

3

In **3** (Fig. 2) the lanthanoid center is also seven-coordinate: one THF and three planar diphosphinomethanide ligands surround the lutetium ion in a distorted pentagonal-bipyramidal arrangement. Thus the ion is coordinated by six phosphane donor units. The four-membered chelate rings are also planar. The THF ligand can be removed in vacuo; however, the resulting yellow solid could not be recrystallized.

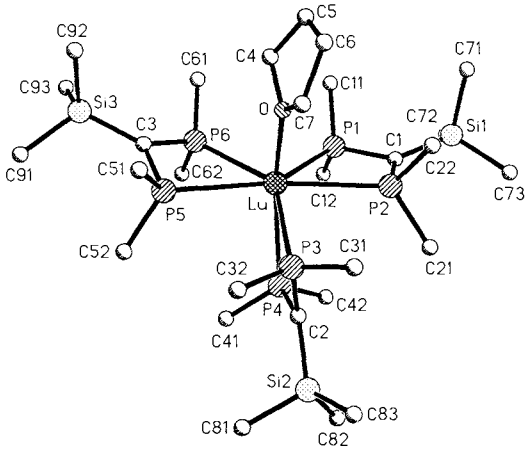

Fig. 2. Crystal structure of **3**. Important distances [Å] and angles [°]: Lu-P 2.814(2)-2.922(2), Lu-O 2.271(5); P1-C1-P2 106.1(3), C1-P1-Lu 99.4(2), C1-P2-Lu 96.8(2), P1-Lu-P2 57.7(1), P3-C2-P4 107.5(3), C2-P4-Lu 96.3(2), P3-Lu-P4 59.8(1), Lu-P3-C2 95.0(2), P5-C3-P6 104.3(3), C3-P6-Lu 97.3(2), P5-Lu-P6 57.7(1), Lu-P5-C3 95.9(2).

Lutetium, the smallest lanthanoid, is obviously coordinatively saturated in **3**. Even in the complexes with the only slightly larger erbium,[9] as well as with yttrium[9] or lanthanum, the coordination changes dramatically. The lanthanum complex **4**, which was formed as orange crystals according to Equation (3),[10] is a representative example.

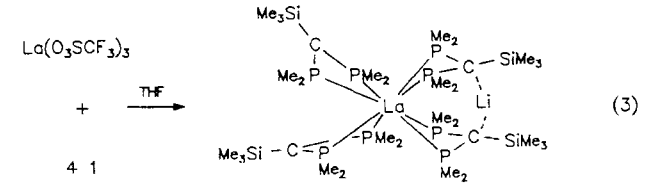

(3)

4

Not less than four diphosphinomethanide chelating ligands (regardless of the stoichiometry) are arranged around the lanthanum ion such that the eight P atoms form one almost square-planar and one tetrahedral P_4 ligand arrangement (Fig. 3). The resulting distorted dodecahedral coordination is sterically favorable. The centers of the four chelating ligands are at the corners of a tetrahedron, such that the two sets of four phosphorus atoms form together with the lanthanum center two mutually orthogonal planes. The resulting complex has "ate" character; in other words, an excess anionic charge must be compensated for. This is achieved intramolecularly by the inclusion of a lithium ion between the carbanionic atoms of two diphosphinomethanide ligands which results in a significant folding of the four-membered chelate rings. The lithium ion shows additional contacts to two P atoms and also to a PCH_3 and $SiCH_3$ group (Li···H···C), so that on the one hand it is coordinatively saturated and on the other hand so well protected, especially by the $SiCH_3$ group, that it neither coordinates additional THF nor is it released from its "basket" by, for example, crown ethers. Consider going from the largest to the smallest metal: if the lighter homologue scandium is

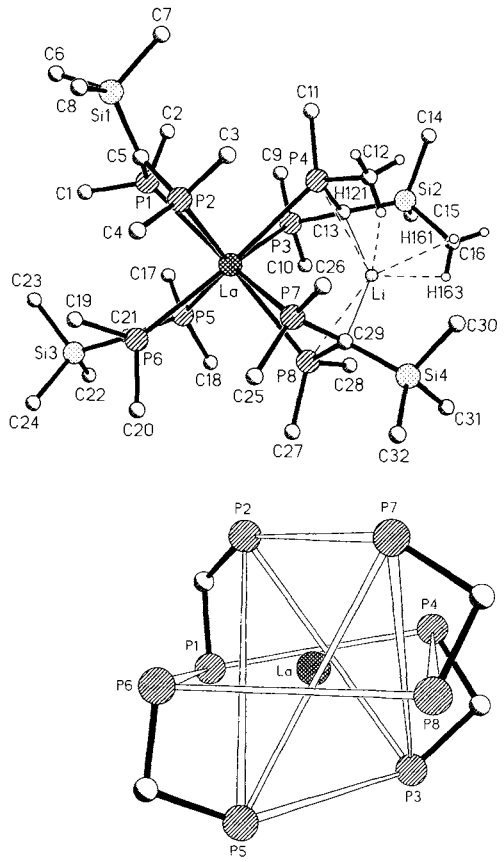

Fig. 3. Top: crystal structure of **4**. Important distances [Å] and angles [°]: La-P1 3.105(2), La-P2 3.068(2), La-P3 3.051(2), La-P4 3.145(2), La-P5 3.039(2), La-P6 3.121(2), La-P7 3.046(2), La-P8 3.234(2), Li1-C13 2.243(9), Li1-P4 2.879(8), Li1-C29 2.208(8), Li1-P8 2.814(7), Li1-Si2 2.946(8), Li1-C16 2.541(9), Li1-H121 2.419(8), Li1-H161 2.339(9), Li1-H163 2.386(9), Si2-C16 1.889(6); La-P3-C13 90.1(1), P3-C13-P4 102.6(2), C14-P4-La 87.2(1), P3-La-P4 53.75(3), P4-C13-Si2 123.3(2), P3-C13-Si2 125.7(2), La-P8-C29 90.6(1), P7-C29-P8 100.9(2), La-P7-C29 96.8(1), P7-La-P8 52.14(3), P7-C29-Si4 120.8(2), P8-C29-Si4 126.9(2), La-P5-C21 98.5(1), P5-C21-P6 107.1(2), La-P6-C21 95.6(1), P5-La-P6 54.41(5), La-P1-C5 97.8(1), P1-C5-P2 107.5(2), La-P2-C5 99.5(1), P1-La-P2 54.62(5), La-P3-C13-P4 30.3(1), La-P7-C29-P8 27.01(1), La-P5-C21-P6 13.0(1), La-P1-C5-P2 4.55(1). Bottom: structure of the $La(P_2C)_4$ fragment in **4**.

used ($r(Sc^{3+})$: 0.75 Å) instead of lanthanum ($r(La^{3+})$: 1.03 Å), the coordination number changes again. Compound **5** is obtained as yellow needles[11] according to Equation (4).

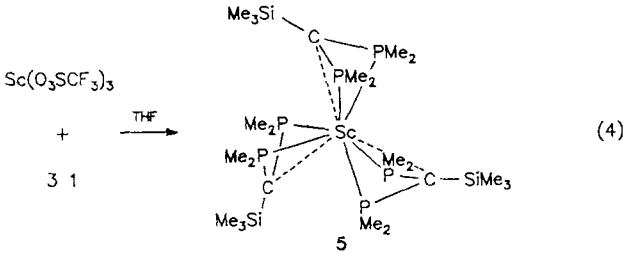

(4)

Unlike the arrangement in **3**, but similar to that in **III** the scandium center in **5** is not coordinated by a solvent molecule, and, just as in **III** the M-P-C-P four-membered rings are not planar. The CP_2 and ScP_2 planes form an angle of 121°, which is intermediate between that in **II** and **3** (180°) and in **III** (80°) (Fig. 4). As a result of the trigonal symmetry in **5** the

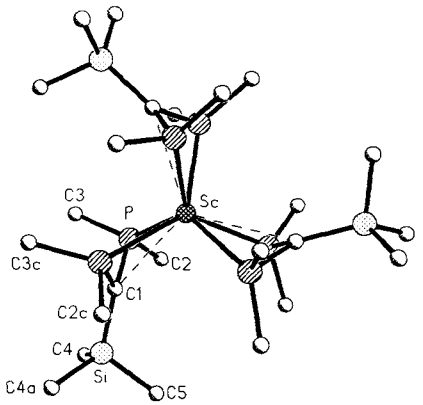

Fig. 4. Crystal structure of **5**. Important distances [Å] and angles [°]: Sc-P 2.617(1), Sc-C1 2.908(2); Sc-P-C1 80.8(2), P-C1-P 105.4(3), P-Sc-P 94.13(3), P-C1-Si 126.5(1).

P atoms are arranged in a trigonal-prismatic fashion. The planar carbanionic C atoms approach the scandium center without forming a bond (Sc···C: 2.908 Å). The coordination mode of the diphosphinomethanide ligands in **5**, intermediate between a σ-chelating (as in **3**) and a π coordination mode (as in **III**), appears almost like a snapshot of the mutual conversion of either type of coordination into the other. This accounts for the facile change in hapticity and for rearrangement reactions as, for example in silicon[12] and zirconium[13] disphosphinomethanide compounds; here we have observed this structurally for the first time. The folding of the four-membered chelates in the scandium complex can be attributed to the additional Sc···C d-orbital interactions. The reduced nucleophilicity of the Me_3Si-protected carbanion compared to that in **III** and the steric hindrance at the small Sc^{3+} ion prevents a closer approach of the carbanions to the coordination center. The four-, six-, and especially eight-coordinate phosphane–lanthanoid complexes presented here demonstrate that the disinclination of lanthanoids to coordinate phosphanes can be reversed and even transposed into a marked affinity by an appropriate choice of ligands, namely phosphinomethanides.

Experimental Procedure

All reactions were carried out under purified and dried nitrogen using conventional vacuum techniques. The glassware was dried by heating, evacuated several times, and flushed with inert gas. NMR spectra in [D_8]toluene; standards: ^1H, ^{13}C: TMS; ^{31}P: H_3PO_4.

2: To 50 mL YbI_2 (36.7 mM in THF, 1.84 mmol) was added **1** (0.84 g, 3.92 mmol) at −78 °C. The mixture was allowed to warm to room temperature, and after 12 h stirring the solvent was removed in vacuo. The remaining solid was extracted twice with 40 mL pentane. On evaporation of the pentane in vacuo violet crystals formed (1.31 g, yield 97.2%). Correct C,H,I analysis.

$^{31}P\{^1H\}$ NMR (109 MHz): δ −24.27 (s), −24.20 (d, $^1J(^{31}P, ^{171}Yb)$ = 497.3 Hz); ^1H NMR (270 MHz): δ = 1.38 (s, 24H; PMe_2), 0.32 (s, 18H; $SiMe_3$), 3.28 (s, br, 12H; THF); $^{13}C\{^1H\}$ NMR (67.8 MHz): δ = 20.21 ("t", N (separation of the outermost signals) = 21.3 Hz, PMe_2), 7.54 (s, $SiMe_3$), 25.19 (s, THF), 68.23 (s, THF).

3: $Lu(O_3SCF_3)_3$ (0.65 g, 1.05 mmol) and **1** (0.75 g, 3.50 mmol) were added together, and 40 mL THF was condensed into the mixture at −78 °C. The solution was allowed to warm to room temperature and stirred for 12 h. After removal of the solvent the residue was dried in vacuo and extracted three times with pentane. During evaporation of the solvent from the combined filtrates in vacuo **3** precipitated as a yellow, crystalline solid (0.49 g, yield: 60.3%). Correct C,H analysis.

$^{31}P\{^1H\}$ NMR (109.4 MHz, 25 °C): δ = −26.60 (br), (−110 °C): two AB patterns (2:1): δP_{A1} = −25.41, δP_{B1} = −31.72, $J_{(AB)1}$ = 245.2 Hz, δP_{A2} = −27.78, δP_{B2} = −30.13, $J_{(AB)2}$ = 240.0 Hz; ^1H NMR (270 MHz): δ = 1.35 (s, br, 36H; PMe_2), 0.37 (s, 27H; $SiMe_3$), 3.62 (s, br, 4H; THF), 1.45 (s, br, 4H; THF); $^{13}C\{^1H\}$ NMR (67.8 MHz): δ = 22.29 ("t", N = 25.3 Hz, PMe_3), 6.43 (s, $SiMe_3$), 68.48 (s, THF), 25.66 (s, THF).

4: To a mixture of $La(O_3SCF_3)_3$ (0.78 g, 1.33 mmol) and **1** (0.96 g, 4.48 mmol) at −78 °C was added 40 mL THF by condensation. After warming to room temperature the mixture was stirred for 3 d. The solvent was evaporated and the residue dried in vacuo and extracted with pentane (3 × 30 mL). When the solvent from the combined pentane extracts was removed under vacuum, the product precipitated as an orange, crystalline solid. (0.71 g, yield: 65.0%). Correct C,H analysis.

$^{31}P\{^1H\}$ NMR (109.4 MHz, 25 °C): δ = −29.0 (s, br), −30.8 (s, br), (−100 °C): δ = −22 to −48 (m); ^1H NMR (270 MHz): δ = 1.31 (s, br, 48H; PMe_2), 0.32 (s, 36H; $SiMe_3$); $^{13}C\{^1H\}$ NMR (67.8 MHz): δ = 22.95 ("t", N = 25.9 Hz, PMe_2), 7.10 (s, $SiMe_3$).

5: To a mixture of $Sc(O_3SCF_3)_3$ (0.85 g, 1.73 mmol) and **1** (1.17 g, 5.46 mmol) at −78 °C was added 40 mL THF by condensation. The resulting solution was allowed to warm to room temperature and stirred for 3 h before the solvent was evaporated. The residue was dried in vacuo and extracted with pentane (3 × 30 mL). During evaporation of the pentane from the combined extracts orange needles precipitated (0.91 g, yield: 79.3%). Correct C,H analysis.

$^{31}P\{^1H\}$ NMR (109.4 MHz, 25 °C): δ = −11 to −23 (br), (−100 °C): δ = −12.82 (s), (+70 °C): δ = −17 to −23 (br); ^1H NMR (270 MHz): δ = 1.25 (s, br, 36H; PMe_2), 0.33 (s, 27H; $SiMe_3$); $^{13}C\{^1H\}$ NMR (67.8 MHz): δ = 20.36 ("t", N = 30.2 Hz, PMe_2), 6.11 (s, $SiMe_3$).

Received: July 20, 1993 [Z 6220 IE]
German version: *Angew. Chem.* **1993**, *105*, 1814

[1] M. D. Fryzuk, T. S. Haddad, S. J. Rettig, *Organometallics* **1991**, *10*, 2026–2036.
[2] H. Schumann, *Angew. Chem.* **1984**, *96*, 475–493; *Angew. Chem. Int. Ed. Engl.* **1984**, *23*, 474–493.
[3] H. H. Karsch, A. Appelt, J. Riede, G. Müller, *Organometallics* **1987**, *6*, 316–323.
[4] H. H. Karsch, A. Appelt, G. Müller, *Angew. Chem.* **1986**, *98*, 832–834; *Angew. Chem. Int. Ed. Engl.* **1986**, *25*, 823–824.
[5] H. H. Karsch, B. Deubelly, G. Müller, *J. Organomet. Chem.* **1988**, *352*, 47–59.
[6] Crystallographic data [14] of **2** at 293 K ($Mo_{K\alpha}$ radiation, λ = 0.71073 Å): $P2_1/n$, a = 23.497(2), b = 24.864(5), c = 24.470(3) Å, β = 95.33(1)°, V = 14234(4) Å^3, Z = 4, $\varrho_{calcd.}$ = 1.500 g cm^{-3}, $\mu(Mo_{K\alpha})$ = 34.6 cm^{-1}, 6928 reflections with $I > 2.5\,\sigma(I)$, 352 parameters, R = 0.084.
[7] a) R. D. Howells, J. D. McCown, *Chem. Rev.* **1977**, *77*, 69–92; b) H. Schumann, J. A. Meese-Marktscheffel, A. Dietrich, *J. Organomet. Chem.* **1989**, *377*, C5–C8.
[8] Crystallographic data [14] of **3** at 293 K ($Mo_{K\alpha}$ radiation, λ = 0.71073 Å): $P2_1/n$, a = 10.089(1), b = 12.026(2), c = 36.693(4) Å, β = 94.55(1)°, V = 4438(2) Å^3, Z = 4, $\varrho_{calcd.}$ = 1.30 g cm^{-3}, $\mu(Mo_{K\alpha})$ = 25.4 cm^{-1}, 5649 reflections with $F > 4\sigma(F)$, 352 parameters, R = 0.033.
[9] Analogues of **4** have been obtained; however, the crystals are disordered.

[10] Crystallographic data [14] of **4** at 293 K ($Mo_{K\alpha}$ radiation $\lambda = 0.71073$ Å): $P\bar{1}$, $a = 17.972(2)$, $b = 18.099(3)$, $c = 19.241(3)$ Å, $\alpha = 70.71(1)$, $\beta = 78.09(1)$, $\gamma = 69.76(1)°$, $V = 5512(2)$ Å^3, $Z = 4$, $\varrho_{calcd.} = 1.196$ g cm^{-3}, $\mu(Mo_{K\alpha}) = 11.1$ cm^{-1}, 14705 reflections with $I > 2.5\sigma(I)$, 1011 parameters, $R = 0.0291$.

[11] Crystallographic data [14] of **5** at 293 K ($Mo_{K\alpha}$ radiation, $\lambda = 0.71073$ Å): $P6_3/m$, $a = 13.146(2)$, $c = 14.965(2)$, $V = 2239.7(7)$ Å^3, $Z = 2$, $\varrho_{calcd.} = 0.989$ g cm^{-3}, $\mu(Mo_{K\alpha}) = 4.7$ cm^{-1}, 908 reflections with $F > 4\sigma(F)$, 60 parameters, $R = 0.058$.

[12] H. H. Karsch, R. Richter, A. Schier, *Z. Naturforsch. B*, in press.

[13] a) H. H. Karsch, G. Grauvogl, B. Deubelly, G. Müller, *Organometallics* **1992**, *11*, 4238–4245; b) H. H. Karsch, G. Grauvogl, M. Kawecki, P. Bissinger, *Organometallics*, **1993**, *12*, 2757–2766.

[14] a) Further details on the crystal structure determinations can be obtained form the Fachinformationszentrum Karlsruhe, Gesellschaft für wissenschaftlich-technische Information mbH, D-76344 Eggenstein-Leopoldshafen (FRG), on quoting the deposition number CSD-56536, the authors and the journal citation; b) program used: SHELXS-86, G. M. Sheldrick, *Acta Crystallogr. Sect. A* **1990**, 46, 467–473; SHELXL-93, G. M. Sheldrick, *J. Appl. Crystallogr.* **1993**, submitted.

The Mechanism of Anaerobic, Radical-Induced DNA Strand Scission**

By *Bernd Giese*,* *Xenia Beyrich-Graf*, *Jutta Burger*, *Christoph Kesselheim*, *Martin Senn*, and *Thomas Schäfer*

Radicals generated either radiolytically or chemically may cleave the DNA strand by H abstraction. An important intermediate in this process is the 4′-deoxyribonucleotide radical **1**[1] (Scheme 1). This reactive intermediate can lead to strand breakage either by direct fragmentation or by reaction with O_2. In order to account for the cleavage products that are observed under anaerobic conditions, Schulte-Frohlinde et al. have proposed that the radical cation **2** is an intermediate, and have demonstrated analogous heterolytic β-bond cleavage in simple radicals.[2, 3]

By selective generation of 4′-nucleotide radicals, we have now been able to prove that nucleotide radical cations are produced and have studied their reactivity. Alkene **3a** and selenide **4b** were both utilized as precursors of the 4′-nucleotide radical **5**. As we recently showed, radical addition of PhSH to alkene **3a** leads via the 4′-nucleotide radical **5a** to the cyclic enol ether **7a**.[4]

If the radical cation **6a** is indeed an intermediate, then breakage of the C–O bond ought to be strongly accelerated by increasing either the polarity of the solvent or the acidity of the phosphoric dialkylester which is released as an anion.[5] We measured the ratio of the rate constants for H abstraction (k_H) and for C–O bond cleavage (k_E) under pseudo-first-order conditions, using thiophenol as the source of the radical X$^\cdot$ and as H donor.[6] Since k_H ought to be largely independent of both the nature of the solvent[7] and the type of substituent R on the phosphate group, the change in the ratio k_E/k_H is a measure of the change of the rate of C–O bond cleavage.

The data in Table 1 show that the rate of cleavage of the C–O bond (**5a** → **7a**) increases by a factor of about 100 on changing from toluene to ethanol/water (4:1) as solvent.

Table 1. Influence of the solvent and the alkyl substituent R of the leaving group $(RO)_2PO_2^-$ on the competition constant k_E/k_H of radical **5a** at 30 °C.

Solvent		K_a of $(RO)_2PO_2H$ [a]	k_E/k_H
C_2H_5OH/H_2O (4:1)	Me	9.77×10^{-4}	14.2
	Et	7.08×10^{-4}	7.7
	*n*Pr	5.13×10^{-4}	6.5
	*i*Pr	2.19×10^{-4}	1.7
$C_6H_5CH_3$	Me		0.17
	Et		0.077
	*n*Pr		0.056
	*i*Pr		0.021

[a] Values in $EtOH/H_2O$ (4:1) at 25 °C.

When the selectivity $\lg k_E/k_H$ was plotted against the acidity $\lg K_a$ of the phosphoric dialkylester in the two solvents, a linear correlation was observed with a gradient β of about 1.3 (Fig. 1). The solvent effect, which is unusually large for neutral radicals, and the high value for the slope of the Brönsted relationship are clear indications of heterolytic C–O bond cleavage in the reaction **5a** → **6a**.

Interestingly, radical cation **6a** is not trapped nucleophilically in the presence of thiophenol, because electron transfer

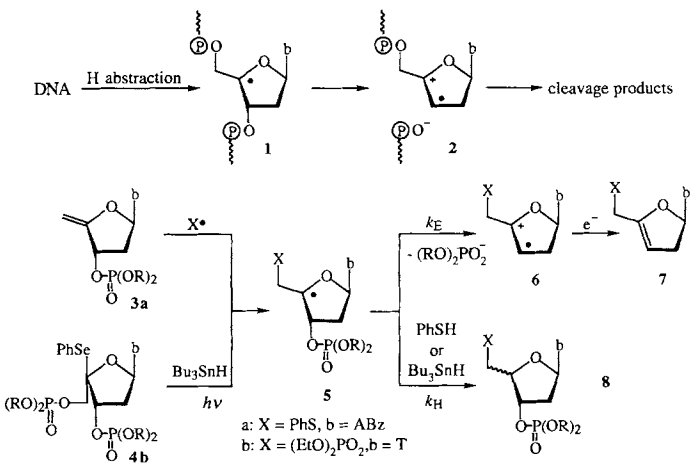

Scheme 1. ABz = 6-*N*-benzoyladenin-9-yl.

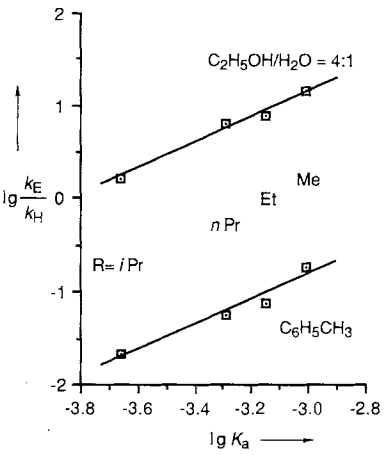

Fig. 1. Dependence of the C–O bond breakage in radical **5a** ($\lg k_E/k_H$) on the acidity ($\lg K_a$) of the phosphoric dialkylester $(RO)_2PO_2H$.

[*] Prof. Dr. B. Giese, Dipl.-Chem. X. Beyrich-Graf, Dr. J. Burger, Dipl.-Eng. C. Kesselheim, Dipl.-Chem. M. Senn, Dipl.-Eng. T. Schäfer
Departement Chemie der Universität
St.-Johanns-Ring 19, CH-4056 Basel (Switzerland)
Telefax: Int. code + (61)-3226017

[**] This work was supported by the Schweizerische Nationalfonds zur Förderung wissenschaftlichen Forschung.

from thiophenol is faster than attack by the nucleophilic solvent.[4] Different reactivity is seen when radical **5b** is generated from the selenide **4b**.[8] Photolysis of a methanolic solution of **4b** in the presence of various amounts of Bu_3SnH yields the methanol trapping products **12**–**15**, in yields of 85–91 %[9] (Scheme 2).

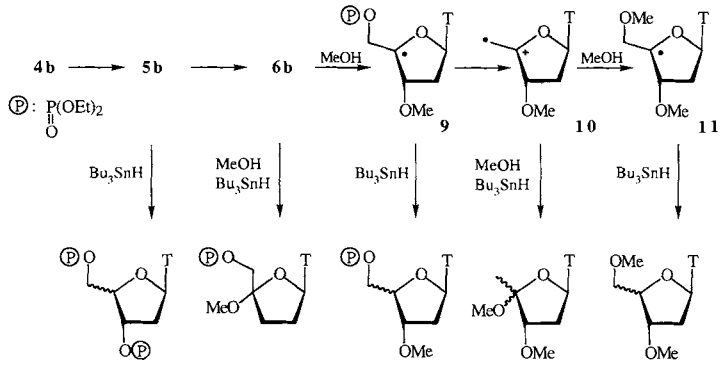

	8b	12	13	14	15
1.2 equiv Bu_3SnH:	<2%	28%	34%	~2%	27%
7.5 equiv Bu_3SnH:	9.5%	22%	55%	~1%	7.5%

Scheme 2.

Compounds **12** and **13** are produced by the trapping of radical cation **6b**. In contrast, **14** and **15** are trapping products from radical cation **10**, which arises from radical **9** after cleavage of a second C–O bond. As expected, the yield of **14** and **15** drops with increasing concentrations of Bu_3SnH. When a 7.5-fold excess of Bu_3SnH is employed (pseudo-first-order conditions), then the competition constants may be determined from the product yields. The product ratio **(13 + 14 + 15)/12**, reveals that attack of methanol on the secondary C atom of radical cation **6b** is about 2.5 times faster than attack on the tertiary C atom. The primary C atom in radical cation **10** is attacked even more selectively. Ionic methanol attack on **6b** occurs stereoselectively *trans* to the thymine unit. In contrast, radical H abstraction is unselective, because the thymine and methoxy groups are *trans* to each other. From the product ratios **(12–15)/8b** = 9.0 and **(14–15)/13** = 0.15 (7.5 equivalents of Bu_3SnH), one can conclude that the bond between the secondary C atom and the O atom in radical **5b** is broken about 60 times faster than the bond between the primary C atom and the O atom in radical **9**. This large difference in reactivity also points to heterolytic C–O bond cleavage.

In contrast to methanol, which is a good cation trap, allyl alcohol ought to be able to trap both cations and radicals. Indeed, reaction of selenide **4b** in allyl alcohol yields the bicyclic products **16** and **17** (Scheme 3). They arise from radical cation **6b**, which reacts nucleophilically with a regioselectivity of about 2.5:1 to yield the radicals **19** and **20**.

In the presence of a large excess of Bu_3SnH, radical **20** is partially converted to the reduction product **18** by intermolecular reaction. However, the majority of the radicals **19** and **20** cyclize to give the bicyclic products **16** and **17**, respectively.[10] The formation of **16** and **17** as the major products is unambiguous evidence for the presence of radical cations.

In the case of radical-induced DNA cleavage under anaerobic conditions in H_2O, Schulte-Frohlinde et al. observed analogous open-chain hydrolysis products of **12**–**15**.[2] Our studies with mononucleotide radicals in alcohols made it

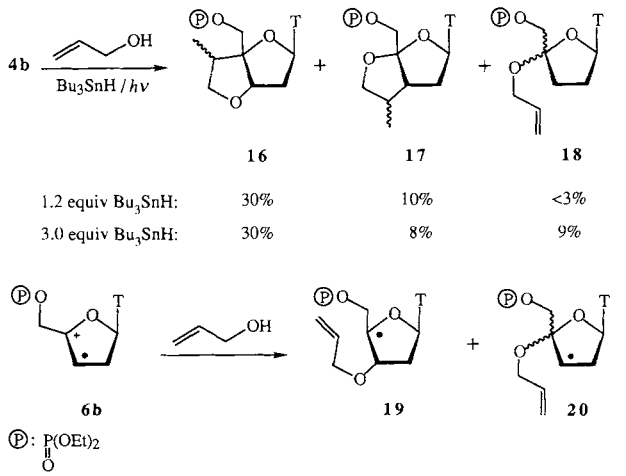

	16	17	18
1.2 equiv Bu_3SnH:	30%	10%	<3%
3.0 equiv Bu_3SnH:	30%	8%	9%

Scheme 3.

possible to trap the postulated intermediates and to prove that the reaction mechanism of DNA strand cleavage proceeds via 4′-deoxyribonucleotide radicals.

Received: August 4, 1993 [Z 6261 IE]
German version: *Angew. Chem.* **1993**, *105*, 1850

[1] General reviews: C. von Sonntag, U. Hagen, A. Schön-Bopp, D. Schulte-Frohlinde, *Adv. Radiat. Biol.* **1981**, *9*, 109; H. Sies, *Angew. Chem.* **1986**, *98*, 1061; *Angew. Chem. Int. Ed. Engl.* **1986**, *25*, 1058; J. Stubbe, J. W. Kozarich, *Chem. Rev.* **1987**, *87*, 1107; K. C. Nicolaou, W.-M. Dai, *Angew. Chem.* **1991**, *103*, 1453; *Angew. Chem. Int. Ed. Engl.* **1991**, *30*, 1387; I. H. Goldberg, *Acc. Chem. Res.* **1991**, *24*, 191; P. C. Dedon, I. H. Goldberg, *Chem. Res. Toxicol.* **1992**, *5*, 311.

[2] G. Behrens, G. Koltzenburg, D. Schulte-Frohlinde, *Z. Naturforsch. C* **1982**, *37*, 1205.

[3] G. Koltzenburg, G. Behrens, D. Schulte-Frohlinde, *J. Am. Chem. Soc.* **1982**, *104*, 7311.

[4] B. Giese, J. Burger, T. W. Kang, C. Kesselheim, T. Wittmer, *J. Am. Chem. Soc.* **1992**, *114*, 7322.

[5] T. A. Mastryukova, T. A. Melent'eva, A. E. Shipov, M. I. Kabachnik, *Zh. Obshch. Khim.* **1959**, *29*, 2178. The K_a value for $(i\text{PrO})_2PO_2H$ was measured potentiometrically with a glass electrode in $EtOH/H_2O$ (4:1).

[6] For competition experiments, a solution of 0.05 mmol of the starting material **3a** and 0.5–1.7 mmol PhSH was diluted up to 0.5 mL with the relevant solvent under Ar, degassed by freezing and evacuating twice, and irradiated for 1–2 h at 30 °C (Heraeus TQ, 150 W). After the reaction mixture was concentrated and the residue dissolved in $CDCl_3$, NMR spectroscopy was used to analyze the products **7a** and **8a** (β-D-*erythro*:α-L-*threo* = 3:1, the R group had only a minor effect on the stereoselectivity). **7a** and β-D-*erythro*-**8a** were also independently synthesized.

[7] D. V. Avila, C. E. Brown, K. U. Ingold, J. Lusztyk, *J. Am. Chem. Soc.* **1993**, *115*, 466.

[8] Selenide **4b** was synthesized from the 5′-aldehyde of deoxythymidine (see C. O. Yang, H. Y. Wu, E. B. Fraser-Smith, K. A. M. Walker, *Tetrahedron Lett.* **1992**, *33*, 37) by selenation at C-4′ ($PhSeCl/NEt_3$) followed by reduction (diisobutylaluminum hydride, DIBAH) and phosphorylation ($(EtO)_2POCl$).

[9] For the trapping experiments, 0.3 mmol of selenide **4b** and 1.2–7.5 equivalents of Bu_3SnH were dissolved in 5 mL MeOH and irradiated for 3–5 h at 20 °C (Osram HQI-T250W/D). After the reaction mixture was concentrated and the residue dissolved in CH_3CN, the tin-containing by-products were removed with pentane. The products **8b** (1:1 mixture), **12**, **13** (1:1 mixture), and **15** (1:1 mixture) were isolated by flash chromatography, and the structures elucidated by NMR spectroscopy (^1H, ^{13}C, ^{31}P, NOE) and by independent synthesis (**8b**, **15**). Compound **14** could only be analyzed in the mixture in solution.

[10] The trapping experiments followed the procedure in ref. [9]. Allyl alcohol was used as the alcohol, and 1.2–3.0 equivalents of Bu_3SnH were employed. Flash chromatography afforded **16** (2:1 mixture), **17** (only one isomer was isolated, other possible isomers of **17** were below the detection limit of 2%), and **18** (4.5:1 mixture). When the reaction was carried out with 1.2 equivalents of Bu_3SnD, the methyl group of **16** and **17** was monodeuteriated (deuteriation level 75% and 90%, determined by mass spectroscopy and NMR spectroscopy, respectively).

A Stable η^5-Germacyclopentadienyl Complex: $[(\eta^5\text{-}C_5Me_5)Ru\{\eta^5\text{-}C_4Me_4GeSi(SiMe_3)_3\}]$**

By *William P. Freeman, T. Don Tilley,* Arnold L. Rheingold,* and *Robert L. Ostrander**

The chemistry of compounds containing multiple bonds to the heavier group 14 elements (Si, Ge, Sn, and Pb) has advanced significantly over the past few years.[1] It is therefore of interest to consider extensions to delocalized π systems containing these bonds, which could exhibit new chemical and electronic properties. Much attention has previously focused on low-temperature observation of unstable silabenzene (SiC_5H_6) and its derivatives, which appear to have some aromatic character.[2] Chemical and theoretical studies indicate that stable sila- and germacyclopentadienide anions, which have been generated in solution, possess some degree of resonance stabilization.[3] However, numerous attempts to prepare η^5-sila- and η^5-germacyclopentadienyl transition metal complexes, usually from the corresponding η^4-silole or η^4-germole derivatives, have proven unsuccessful.[3] Jutzi et al. have synthesized the $[(C_4Ph_4GeMe)Fe(CO)_3]^+$ cation, which was characterized on the basis of ^{13}C NMR shift data as an η^4-diene complex with the positive charge localized on the germanium atom.[4] Here we report the first isolation and complete characterization of an η^5-germacyclopentadienyl transition metal complex.

The η^4-germole complex **1** was obtained simply by addition of the free germole to $[\{Cp^*Ru(\mu\text{-}Cl)\}_4]$[5] ($Cp^* = \eta^5\text{-}C_5Me_5$). The structure of **1** (Fig. 1)[6] contains a folded germole ring, in which the germanium atom is displaced out of the least-squares plane of the C_4 diene by 0.97 Å. The ruthenium atom is 1.76 Å from this plane, and 1.89 Å from the least-squares plane of the Cp* ring carbon atoms. Although it appears that there is little bonding between Ru and Ge (the interatomic distance is 2.985(2) Å), a significant lengthening of the Ge–Cl2 bond (2.246(2) Å) relative to the Ge–Cl3 bond (2.151(3) Å) suggests that a Ru → Ge dative interaction operates primarily through donation of electron density from the Ru atom to the Ge–Cl2 σ^* orbital.

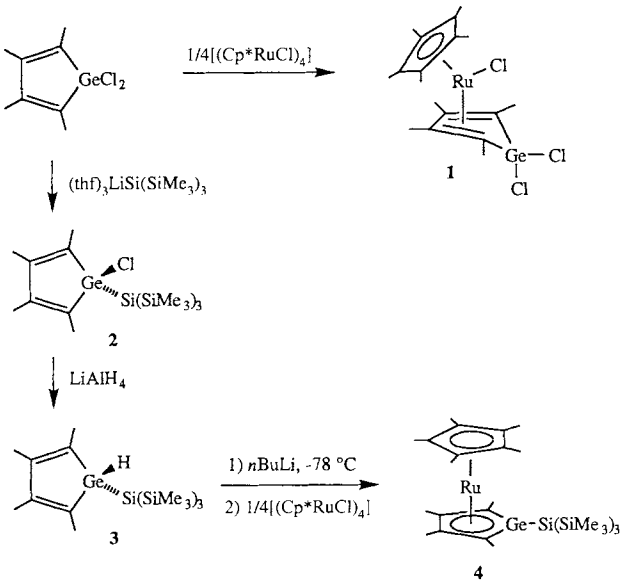

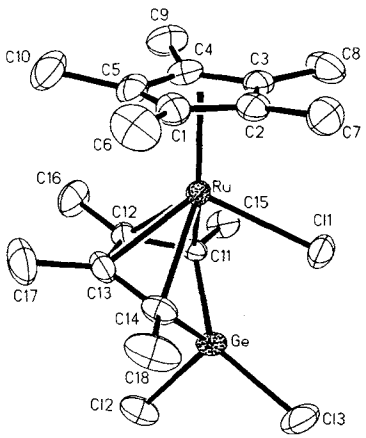

Fig. 1. Molecular structure of **1** drawn with 35% probability ellipsoids. Selected interatomic distances [Å] and angles [°]: Ru-Ge 2.985(2), Ru-Cl1 2.424(3), Ru-C1 2.278(7), Ru-C2 2.242(7), Ru-C3 2.233(7), Ru-C4 2.242(7), Ru-C5 2.235(9), Ru-C11 2.197(6), Ru-C12 2.199(6), Ru-C13 2.194(7), Ru-C14 2.218(6), Ge-Cl2 2.246(2), Ge-Cl3 2.151(3), Ge-C11 1.936(6), Ge-C14 1.925(7), C11-C12 1.421(9), C12-C13 1.458(9), C13-C14 1.412(11); C11-Ge-C14 86.2(3), C11-Ge-Cl2 102.9(2), C11-Ge-Cl3 134.7(2), C14-Ge-Cl2 108.3(2), C14-Ge-Cl3 127.1(2), Cl2-Ge-Cl3 94.8(1).

Addition of *n*BuLi to a THF solution of **3** at −78 °C generates the (germacyclopentadienyl)lithium $Li[C_4Me_4GeSi(SiMe_3)_3]$, as indicated by formation of a yellow solution (the related $Li[C_4Me_4GePh]$ species is also yellow in THF[7]). The reaction of the $Li[C_4Me_4GeSi(SiMe_3)_3]$ solution with $[\{Cp^*Ru(\mu\text{-}Cl)\}_4]$ produces the amber, η^5-germacyclopentadienyl complex **4** which was purified by crystallization from pentane. Compound **4** is thermally stable, but benzene solutions of the compound are air- and moisture-sensitive. The $^{13}C\{^1H\}$ NMR spectrum of **4** contains two resonances for the germacyclopentadienyl ring carbon atoms with similar chemical shifts, at $\delta = 80.23$ and 87.82. This would seem to reflect "aromatic" character in the coordinated C_4Ge ring, since the Cp* ring carbon atoms in the same molecule resonate at $\delta = 85.38$. In addition, the chemical shifts for ring carbon atoms in η^4-germole complexes usually differ more considerably. For example, the corresponding chemical shift values for the ring carbon atoms of **1** appear at $\delta = 80.50$ and 95.77.

X-ray quality crystals of **4** were obtained by cooling a concentrated hexamethyldisiloxane solution to −40 °C. The molecular structure of **4** (Fig. 2)[8] consists of two planar five-membered rings bound in a "sandwich" fashion to the ruthenium atom. The least-squares planes for the two five-membered rings form an angle of 8.6°, and the ruthenium atom is symmetrically positioned between these two planes (1.81 Å from the C_4Ge plane and 1.82 Å from the Cp* plane). The germanium atom deviates by only 0.02 Å from the C_4Ge ring's least-squares plane, and summation of the angles about the Ge atom (358.1°) further reflects sp^2 hybridization. Also consistent with greater s character at the germanium center are the Ge–C distances in **4** (average

[*] Prof. Dr. T. D. Tilley, W. P. Freeman
Department of Chemistry, 0506
University of California at San Diego
9500 Gilman Drive, La Jolla, CA 92093-0506 (USA)
Telefax: Int. code + (619)534-4864
Dr. R. L. Ostrander, Prof. Dr. A. L. Rheingold
Department of Chemistry
University of Delaware
Newark, DE 19716 (USA)

[**] This research was supported by the National Science Foundation.

1.90 Å), which are slightly shorter (by 0.03–0.04 Å) than the corresponding distances in **1**. Similarly, the Ru–C bond lengths involving the η^5-germacyclopentadienyl ligand (average 2.21 Å) are very similar to the Ru–C(Cp*) distances (average 2.17 Å). As expected the bulky $Si(SiMe_3)_3$ group is bent out of the C_4Ge plane, by 12.9°. For comparison, the methyl groups in **1** and **4** bend out of their ring planes by −2 to +10°. Finally the Ru–Ge distance (2.493(1) Å) is clearly bonding given that the four known structures with Ru–Ge single bonds have Ru–Ge distances that average to 2.46 Å.[9]

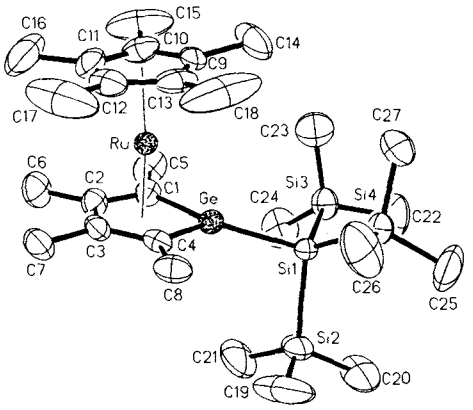

Fig. 2. Molecular structure of **4** drawn with 35% probability ellipsoids. Selected interatomic distances [Å] and angles [°]: Ru-Ge 2.493(1), Ru-C1 2.245(8), Ru-C2 2.172(8), Ru-C3 2.174(8), Ru-C4 2.252(7), Ru-C9 2.187(11), Ru-C10 2.169(9), Ru-C11 2.172(8), Ru-C12 2.166(11), Ru-C13 2.172(10), Ge-Si1 2.357(2), Ge-C1 1.900(6), Ge-C4 1.899(7), C1-C2 1.425(11), C2-C3 1.415(11), C3-C4 1.424(9); C1-Ge-C4 89.1(3), C1-Ge-Si1 136.4(2), C4-Ge-Si1 132.6(2), Ge-Si1-Si2 103.1(1),Ge-Si1-Si3 106.7(1), Ge-Si1-Si4 113.8(1).

Interestingly, it appears that the η^5-$C_4Me_4GeSi(SiMe_3)_3$ and Cp* ligands in **4** are bonded similarly to the Ru center. An irreversible oxidation wave was observed for **4** at $E_{1/2}$ = 0.25 V (vs SCE) by cyclic voltametry (dichloromethane, 0.1 M $[N(nBu)_4]ClO_4$ as the supporting electrolyte). For comparison, decamethylruthenocene displays a reversible oxidation wave at 0.42 V (vs SCE) under comparable conditions.[10] The electrochemical data therefore suggests that the η^5-$C_4Me_4GeSi(SiMe_3)_3$ ligand is more electron-donating than η^5-C_5Me_5. We are currently characterizing additional chemical and electronic properties for the η^5-germacyclopentadienyl ligand in **4**.

Experimental Procedure

Manipulations were performed under anaerobic and anhydrous conditions. NMR spectra were recorded for [D_6]benzene solutions (unless indicated otherwise) on a GE QE-300 instrument at 300 (^{1}H) and 75.5 (^{13}C) MHz.

1: Benzene (20 mL) solutions of the germole $C_4Me_4GeCl_2$ [11] (0.708 g, 2.81 mmol) and $[(Cp^*RuCl)_4]$ (0.765 g, 2.81 mmol) were combined at 5 °C. After stirring the reaction mixture for 1 h at room temperature, the volatiles were removed and the product was extracted into diethyl ether (8 × 50 mL) to give an orange solution. Concentration and cooling (−40 °C) of this solution gave **1** as orange crystals in 70% yield. Correct elemental analysis for $C_{18}H_{27}Cl_3GeRu$. ^{1}H NMR: δ = 1.10 (s, 15H, Cp*), 1.51, 1.59 (s, 6H, CMe). $^{13}C\{^1H\}$ NMR: δ = 8.92 (C_5Me_5), 11.26, 13.62 (*C*Me), 80.50, 95.77 (*C*Me), 96.78 (C_5Me_5).

2: To $C_4Me_4GeCl_2$ (0.998 g, 3.97 mmol) in benzene (75 mL) was added $(thf)_3LiSi(SiMe_3)_3$ [12] (1.68 g, 3.97 mmol) in benzene (10 mL) at 5 °C. After stirring the reaction mixture for 1 h at room temperature, the volatiles were removed and the product was extracted into pentane (3 × 50 mL), and crystallized from a concentrated solution at −78 °C. Yield 70%. Correct elemental analysis for $C_{17}H_{39}ClGeSi_4$. ^{1}H NMR: δ = 0.32 (s, 27H, $SiMe_3$), 1.59, 2.07 (s, 6H, CMe). $^{13}C\{^1H\}$ NMR (CD_2Cl_2): δ = 2.42 ($SiMe_3$), 14.53, 15.47 (*C*Me), 133.63, 146.02 (*C*Me).

3: A solution of **2** (0.30 g, 0.63 mmol) in THF (20 mL) was added to $LiAlH_4$ (0.024 g, 0.630 mmol) in THF (50 mL) at 0 °C. The resulting solution was stirred at 0 °C for 5 min, and then at room temperature for 1.5 h. The product was extracted into pentane (2 × 20 mL) and crystallized from a concentrated solution at −78 °C. Yield 80%. Correct elemental analysis for $C_{17}H_{40}GeSi_4$. ^{1}H NMR: δ = 0.29 (s, 27H, $SiMe_3$), 1.77, 2.13 (s, 6H, CMe), 4.96 (s, 1H, GeH). $^{13}C\{^1H\}$ NMR (CD_2Cl_2): δ = 2.46 ($SiMe_3$), 14.80, 17.36 (*C*Me), 132.89, 146.45 (*C*Me).

4: To a cold (−78 °C) solution of **3** (0.980 g, 2.28 mmol) in THF (25 mL) was added *n*BuLi (1.43 mL, 1.6 M in hexane). To the resulting yellow solution was then added $[(Cp^*RuCl)_4]$ (0.62 g, 2.28 mmol) in THF (25 mL), also cooled to −78 °C. Stirring was continued for 15 min at −78 °C, and then for 90 min at room temperature. After removal of the volatiles by vacuum transfer, the oily residue was extracted into pentane (2 × 50 mL). Concentration and cooling (−78 °C) of the solution gave amber crystals in 50% yield. Correct elemental analysis for $C_{27}H_{54}GeRuSi_4$. ^{1}H NMR: δ = 0.36 (s, 27H, $SiMe_3$), 1.78 (s, 6H, CMe), 1.80 (s, 21H, Cp* + CMe). $^{13}C\{^1H\}$ NMR: δ = 2.54 ($SiMe_3$), 11.61 (C_5Me_5), 13.05, 17.87 (*C*Me), 80.23, 87.82 (*C*Me), 85.38 (C_5Me_5).

Received: July 13, 1993 [Z 6209 IE]
German version: *Angew. Chem.* **1993**, *105*, 1841

[1] a) G. Raabe, J. Michl, *Chem. Rev.* **1985**, *85*, 419; J. Barrau, J. Escudié, J. Satgé, *ibid.* **1990**, *90*, 283; A. H. Cowley, N. C. Norman, *Prog. Inorg. Chem.* **1986**, *34*, 1; A. G. Brook, K. M. Baines, *Adv. Organomet. Chem.* **1986**, *25*, 1; A. Berndt, H. Meyer, G. Baum, W. Massa, S. Berger, *Pure Appl. Chem.* **1987**, *59*, 1011; R. West, *Angew. Chem.* **1987**, *99*, 1231; *Angew. Chem. Int. Ed. Engl.* **1987**, *26*, 1201; N. Wiberg, *J. Organomet. Chem.* **1984**, *273*, 141.

[2] a) G. Maier, G. Mihm, H. P. Reisenauer, *Angew. Chem.* **1980**, *92*, 58; *Angew. Chem. Int. Ed. Engl.* **1980**, *19*, 52; P. Jutzi, M. Meyer, H. P. Reisenauer, G. Maier, *Chem. Ber.* **1989**, *122*, 1227; G. Märkl, W. Schlosser, *Angew. Chem.* **1988**, *100*, 1009; *Angew. Chem. Int. Ed. Engl.* **1988**, *27*, 963; J. D. Rich, R. West, *J. Am. Chem. Soc.* **1982**, *104*, 6884; H. B. Schlegel, B. Coleman, M. Jones, Jr., *ibid.* **1978**, *100*, 6499.

[3] E. Colomer, R. J. P. Corriu, M. Lheureux, *Chem. Rev.* **1990**, *90*, 265.

[4] P. Jutzi, A. Karl, P. Hofmann, *Angew. Chem.* **1980**, *92*, 496; *Angew. Chem. Int. Ed. Engl.* **1980**, *19*, 484.

[5] P. J. Fagan, M. D. Ward, J. C. Calabrese, *J. Am. Chem. Soc.* **1989**, *111*, 1698.

[6] X-ray structure analysis of **1**: $C_{18}H_{27}Cl_3GeRu$, M_r = 523.4, monoclinic, *Cc*, a = 8.345(2), b = 17.831(4), c = 14.612(4) Å, β = 103.90(2)°, V = 2110.5(10) Å^3, Z = 4, ϱ_{calcd} = 1.647 g cm^{-3}, $\mu(Mo_{K\alpha})$ = 25.17 cm^{-1}, T = 296 K; 2518 independent reflections with $4° \le 2\theta \le 55°$ were collected, of which 2219 reflections with F_o greater than $5\sigma(F_o)$ were used in refinement. $R(F)$ = 0.0277, $R_w(F)$ = 0.0353, GOF = 0.89. The acentric space group was chosen on the initial basis of E values and retained on the basis of the refinement statistics and the symmetry of the molecule. A Rogers test indicated the choice of absolute configuration was correct, η = 1.05(6). A semiempirical absorption correction based on 216 data (6 reflections, 10° increments) was applied, $T(max)/T(min)$ = 1.30. All the non-hydrogen atoms were refined anisotropically with the hydrogen atoms treated as idealized isotropic contributions. Further details of the crystal structure investigation are available on request from the Director of the Cambridge Crystallographic Data Centre, 12 Union Road, GB-Cambridge CB2 1EZ (UK), on quoting the full journal citation.

[7] P. Dufour, J. Dubac, M. Dartiguenave, Y. Dartiguenave, *Organometallics* **1990**, *9*, 3001.

[8] X-ray structure analysis of **4**: $C_{27}H_{27}Cl_3GeRu$, M_r = 664.7, triclinic, $P\bar{1}$, a = 9.848(6), b = 12.192(7), c = 15.854(9) Å, α = 93.83(5)°, β = 90.54(5)°, γ = 107.89(4)°, V = 1806.5(18) Å^3, Z = 2, ϱ_{calcd} = 1.222 g cm^{-3}, $\mu(Mo_{K\alpha})$ = 13.95 cm^{-1}, T = 295 K; 6370 independent reflections with $4° \le 2\theta \le 55°$ were collected (Siemens P4), of which 3684 reflections with F_o greater than $6\sigma(F_o)$ were used in refinement. $R(F)$ = 0.0443, $R_w(F)$ = 0.0539, GOF = 1.13. The centrosymmetric space group was chosen on the initial basis of E values and retained on the basis of the refinement statistics and the molecular symmetry. The absorption coefficient was small and the crystal well-shaped, therefore no absorption correction was applied. All other non-hydrogen atoms were refined anisotropically with the hydrogen atoms treated as idealized isotropic contributions. Further details of the crystal structure investigation are available on request from the Director of the Cambridge Crystallographic Data Centre, 12 Union Road, GB-Cambridge CB2 1EZ (UK), on quoting the full journal citation.

[9] a) R. Ball, M. J. Bennett, *Inorg. Chem.* **1972**, *11*, 1806; J. Howard, P. Woodward, *J. Chem. Soc. (A)* **1971**, 3648; J. A. K. Howard, P. Woodward, *J. Chem. Soc. Dalton Trans.* **1978**, 412; L. Y. Y. Chan, W. A. G. Graham, *Inorg. Chem.* **1975**, *14*, 1773.

[10] P. G. Gassman, C. H. Winter, *J. Am. Chem. Soc.* **1988**, *110*, 6130.

[11] P. J. Fagan, W. A. Nugent, *J. Am. Chem. Soc.* **1988**, *110*, 2310.

[12] G. Gutekunst, A. G. Brook, *J. Organomet. Chem.* **1982**, 225, 1.

Structures and Reactions of the Oxidation Products of Dimeric Ketenylidene(triphenyl)phosphorane**

By *Hans Jürgen Bestmann,* Thomas G. Fürst,* and *Annette Schier*

Ketenylidene(triphenyl)phosphorane (**3**), readily accessible[1] from methoxycarbonyl(triphenyl)phosphorane (**1**) and sodium bis(trimethylsilyl) amide (**2**), is a monomeric crystalline compound, the structure of which has long been known.[2] When **3** is treated with HCl, the ketenylphosphonium salt **6** is formed initially; it immediately undergoes cycloaddition with another molecule of **3** to give the salt **5**. When **5** is exposed to base, **7**, a dimer of **3** forms,[3] which can be depicted by the mesomeric resonance structures **7a** ↔ **7b**, where **7b** is a push-pull-substituted cyclobutadiene.

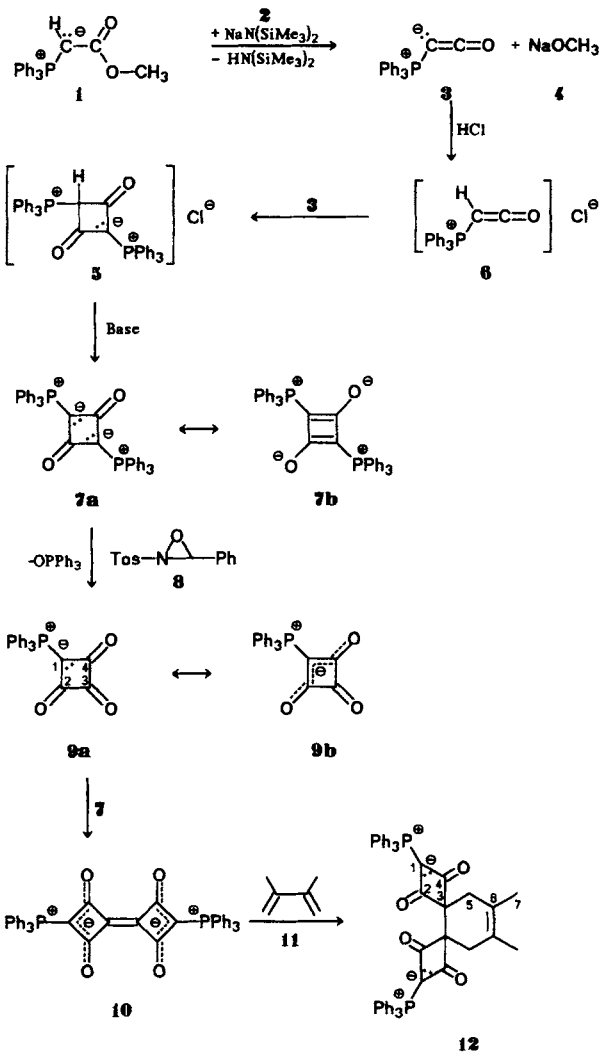

Oxidation of **7** provides trione **9** (Table 1).[3, 4] *N*-*p*-tolylsulfonyl(phenyl)oxaziridine (**8**) has been proven recently to be a particularly well-suited oxidizing agent.[5] When a solution of two equivalents of **8** is added to one equivalent of **7** suspended in ether, cyclobutanetrione **9** is collected in 75% yield. The X-ray structure analysis of **9** is the first obtained for a neutral cyclobutanetrione.[6, 7]

Table 1. Selected spectroscopic and physical data for **9**, **10**, and **12**.

9: Yellow crystals; m.p. 273–275 °C (decomp); IR (KBr): $\tilde{\nu}$ = 1770, 1755, 1650, 1630 cm^{-1}; ^{13}C NMR (100.4 MHz, $CDCl_3$, 26 °C): δ = 214.61 (d, $^3J(C,P)$ = 56.4 Hz; C3), 194.62 (d, $^2J(C,P)$ = 12.2 Hz; C2 and C4), 141.85 (d, $^1J(C,P)$ = 83.9 Hz; C1); ^{31}P NMR (161.7 MHz, $CDCl_3$, 25 °C, H_3PO_4 ext.): δ = +8.34.

10: Faintly yellow crystals which do not have a sharp melting point but char between 300 and 360 °C; IR (KBr): $\tilde{\nu}$ = 1650, 1640 cm^{-1}; ^{31}P NMR (161.7 MHz, $CDCl_3$, 25 °C, H_3PO_4 ext.): δ = +1.20.

12: Colorless crystals; m.p. 288 °C (decomp); ^1H NMR (400 MHz, $CDCl_3$, 25 °C): δ = 2.61 (s; CH_2), 1.64 (s; CH_3); ^{13}C NMR (100.4 MHz, $CDCl_3$, 25 °C): δ = 193.17 (d, $^2J(C,P)$ = 3.0 Hz; C2 and C4), 123.04 (s; C6), 76.32 (s; C3), 73.24 (d, $^1J(C,P)$ = 39.7 Hz; C1), 18.70 (s; C7); ^{31}P NMR (40.48 MHz, $CDCl_3$, 25 °C, H_3PO_4 ext.): δ = −5.02.

All C atoms of the four-membered ring of **9** lie in one plane. The bonds between two carbonyl groups in the distorted rectangle are longer (C2–C3 = 152.5(3) pm, C3–C4 = 153.8(3) pm), C1–C2 and C1–C4 substantially shorter (143.7(3) pm and 145.1(3), respectively). The distance

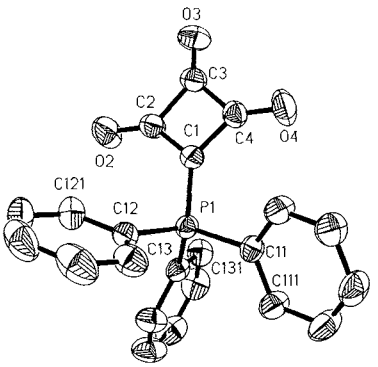

Fig. 1. Crystal structure of **9** with selected bond lengths [pm] and angles [°]: C1-C2 143.7(3), C2-C3 152.5(3), C3-C4 153.8(3), C4-C1 145.1(3), C1-P1 175.3(2), C2-O2 121.6(3), C3-O3 119.4(2), C4-O4 120.6(3); C2-C1-P1 129.0(1), C4-C1-P1 136.2(1), C4-C1-C2 94.6(1), C3-C2-C1 89.4(1), O2-C2-C1 137.9(2), O2-C2-C3 132.7(2), C4-C3-C2 87.7(1), O3-C3-C2 134.8(2), O3-C3-C4 137.4(2), C3-C4-C1 88.3(1), O4-C4-C1 138.3(2), O4-C4-C3 133.4(2).

C3–O3 (119.4(2) pm) is shorter than C4–O4 (120.6(3) pm) and C2–O2 (121.6(3) pm). These data indicate the predominance of resonance structure **9b**. The interior angle is largest at C1, 94.6(1)°, to which the P atom is bound, while the remaining three fall short of 90°. The dihedral angles (P1-C1-C2-O2: 2.67°, P1-C1-C4-O4: 2.74°, O2-C2-C3-O3: 1.14°, and O3-C3-C4-O4: 0.84°) indicate that the four substituents project out of the plane of the ring and are all on the same face (*Z* arrangement), despite the sp^2 character of the C atoms in the four-membered ring.

In the ^{13}C NMR spectrum of **9** the signal of C3 (δ = 214.61) appears as expected downfield from the signals of the CO groups adjacent to the ylide function (δ = 194.62). Remarkably the C1 signal (δ = 141.85) is found at considerably lower field than those of all other ylidic C atoms of cyclic acyl ylides such as **12** (see also analogous compounds in the following communication). The ^{31}P NMR signal appears at δ = +8.34, substantially below that of other acyl ylides hav-

[*] Prof. Dr. H. J. Bestmann, Dipl.-Chem. T. G. Fürst
Institut für Organische Chemie der Universität Erlangen-Nürnberg
Henkestrasse 42, D-91054 Erlangen (FRG)
Telefax: Int. code + (9131)85 68 64
Dr. A. Schier
Anorganisch-chemisches Institut der Technischen Universität München
Lichtenbergstrasse 4, D-85747 Garching (FRG)

[**] We thank J. Riede for recording the crystallographic data.

ing a four-membered ring structure (see **10** and **12**, as well as refs. [8, 9]).

The central CO group of **9** is very reactive.[4] We could therefore oxidize **7** with just one equivalent of **8**. As soon as **9** forms, it reacts with unoxidized **7** to give **10** (95–98% yield, Table 1).[10] Logically **10** is also obtained by reaction of **9** with **7**. Formally a derivative of ethylenetetracarboxylic acid, **10** is a bicyclic, double bis(acyl)ylide and can described by several mesomeric resonance structures.

According to an X-ray structure analysis of **10** (Fig. 2),[11] the C atoms in either of the four-membered rings lie in the same plane and are related to one another through an inversion center. Their planes, however, are shifted parallel by

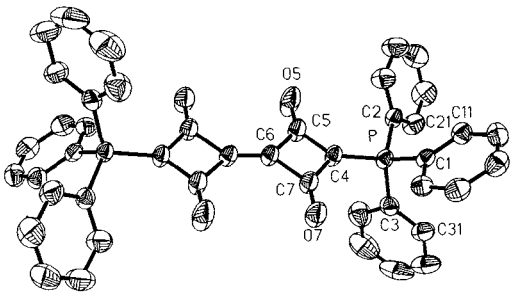

Fig. 2. Crystal structure of **10** with selected bond lengths [pm] and angles [°]: C4-C5 144.6(2), C4-C7 145.4(2), C5-C6 151.0(2), C6-C7 151.3(2), C6-C6a 132.8(3), C7-O7 121.6(2), C5-O5 120.9(2), C4-P 173.9(2); P-C4-C5 135.5(1), P-C4-C7 132.4(1), C5-C4-C7 91.9(1), C4-C5-C6 90.7(1), C4-C5-O5 136.4(2), C6-C5-O5 132.9(2), C5-C6-C7 87.1(1), C4-C7-C6 90.3(1), C4-C7-O7 136.0(2), C6-C7-O7 133.8(2).

3.2 pm. Atoms C6 and C6a are separated by 132.8(3) pm (normal length of a double bond).[12] The C–C distances and interior angles in the four-membered ring are comparable to those of **9**. The distances from the P-substituted C atoms to the adjacent O-substituted atoms are almost identical, which indicates a complete delocalization of the ylidic electron pair. The bonds C5–C6 and C7–C6 have the same length within standard error limits. Here again, the substituents of the four-membered ring project from the plane of the ring in an all-*Z* arrangement (dihedral angles: P-C4-C7-O7 4.8°, P-C4-C5-O5 4.4°, O5-C5-C6-C6a 1.3°, O7-C7-C6-C6a 2.0°).

Compound **10** is suitable as a dienophile in Diels–Alder reactions. When **10** is heated with 2,3-dimethylbutadiene (**11**) in nitrobenzene for 24 h, the bis-spirocyclic compound **12** forms in 58% yield (Table 1), the two adjacent cyclobutanedione rings of which have the characteristics of a bis(acyl) ylide. We are currently studying the photochemistry and the complex-forming behavior of the cyclobutanediones and -triones.

Received: June 30, 1993 [Z 6179 IE]
German version: *Angew. Chem.* **1993**, *105*, 1783

[1] H. J. Bestmann, D. Sandmeier, *Chem. Ber.* **1980**, *113*, 274–277.
[2] J. J. Daly, P. Weathley, *J. Chem. Soc. A* **1966**, 1703.
[3] H. J. Bestmann, G. Schmid, D. Sandmeier, L. Kisielowski, *Angew. Chem.* **1977**, *89*, 275–276; *Angew. Chem. Int. Ed. Engl.* **1977**, *16*, 268.
[4] A. H. Schmidt, A. Aimene, M. Hoch, *Synthesis* **1984**, 436.
[5] F. A. Davis, B. Chen, *J. Org. Chem.* **1990**, *55*, 360–363.
[6] Crystal structure analysis of **9**: $C_{22}H_{15}O_3P$, $M_r = 358.37$; Enraf-Nonius CAD4 diffractometer; $Mo_{K\alpha}$ radiation ($\lambda = 71.069$ pm); graphite monochromator; $T = 22$ °C; the lattice constants were determined from 25 reflections: monoclinic unit cell, $a = 1281.5(1)$, $b = 1067.6(1)$, $c = 1298.3(1)$ pm, $\beta = 92.24(1)°$, $V = 1774.9 \times 10^6$ pm^3, space group $P2_1/n$ [no. 14], $Z = 4$, $\varrho_{calcd} = 1.341$ g cm^{-3}, $F(000) = 744$ e, $\mu(Mo_{K\alpha}) = 1.67$ cm^{-1}, θ-2θ scan mode, hkl range: $-16 \le h \le 16$, $0 \le k \le 13$, $0 \le l \le 16$; of 3510 independent reflections 2963 were considered "observed" [$F_o \ge 4\sigma(F_o)$]; structure solution by direct methods (SHELXTL-PLUS), refinement by the method of least squares and difference Fourier synthesis (SHELXTL-PLUS); all non-hydrogen atoms were refined with anisotropic displacement parameters; all H atom could be located and were refined isotropically. $R(R_w) = 0.0357$ (0.0357, with $w = 1/\sigma^2(F_o)$); 295 parameters; maximum residual electron densities: $+0.29/-0.29 \times 10^6$ e pm^{-3}. See also [11 b].
[7] For X-ray structure analyses of charged derivatives of squaric acid see G. Seitz, P. Imming, *Chem. Rev.* **1992**, *92*, 1227–1260.
[8] H. J. Bestmann, B. Siegel, G. Schmid, *Chem. Lett.* **1986**, *9*, 1529–1530.
[9] G. H. Birum, C. N. Matthews, *J. Am. Chem. Soc.* **1968**, *90*, 3842.
[10] See also the oxidation of ylides with oxygen: H. J. Bestmann, O. Kratzer, *Chem. Ber.* **1963**, *96*, 1899–1908.
[11] a) Crystal structure analysis of **10**: $C_{44}H_{30}O_4P_2$, $M_r = 684.67$; Enraf-Nonius CAD4 diffractometer; $Mo_{K\alpha}$ radiation ($\lambda = 71.069$ pm); graphite monochromator; $T = 22$ °C; the lattice constants were determined from 25 reflections: triclinic unit cell, $a = 928.1(1)$, $b = 931.3(1)$, $c = 995.5(1)$ pm, $\alpha = 81.62(1)$, $\beta = 86.93(1)$, $\gamma = 88.03(1)°$, $V = 849.73 \times 10^6$ pm^3, space group $P(-1)$ [no. 2], $Z = 1$, $\varrho_{calcd} = 1.338$ g cm^{-3}, $F(000) = 356$ e, $\mu(Mo_{K\alpha}) = 1.67$ cm^{-1}, θ-2θ scan mode, hkl range: $-11 \le h \le 11$, $-11 \le k \le 11$, $0 \le l \le 11$; of 2977 independent reflections 2608 were considered "observed" [$F_o \ge 4\sigma(F_o)$]; structure solution by direct methods (SHELXS-86), refinement by the method of least squares and difference Fourier synthesis (SHELX-76); all non-hydrogen atoms were refined with anisotropic displacement parameters; all H atoms could be located and were refined isotropically. R (R_w) = 0.0356 (0.0341, with $w = 1.766/\sigma^2(F_o)$); 286 parameters; maximum residual electron densities: $+0.25/-0.27 \times 10^6$ e pm^{-3}. b) Further details of the crystal structure investigations may be obtained from the Fachinformationszentrum Karlsruhe, Gesellschaft für wissenschaftlich-technische Information mbH, D-76344 Eggenstein-Leopoldshafen (FRG), on quoting the depository number CSD-57477, the names of the authors and the journal citation.
[12] F. H. Allen, O. Kennard, D. G. Watson, *J. Chem. Soc. Perkin Trans. 2* **1987**, S1–S19.

Trimeric Ketenylidene(triphenyl)phosphorane: A Hybrid between an Arene and an Ylide**

By *Hans Jürgen Bestmann,* Thomas G. Fürst,* and *Annette Schier*

Studies on the dimer of ketenylidene(triphenyl)phosphorane **1**[1, 2] have led to the question whether a cyclic trimer **6** can also be prepared. Such a compound would be of interest, because it could be a tris-ylide, **6a**, a cyclohexatriene with alternating double bonds, **6b**, or a push–pull arene, **6c**. Or could all three forms be mesomeric resonance structures of **6**?

We prepared **6** in the following way: the salt **3**, accessible from **1** and HCl (**2**), was refluxed with **1** (eightfold excess) in dichloromethane for 16 h. Faintly yellow crystals of the desired trimer **1** were collected in 30% yield. We assume that **1** reacts with **3** to initially give **4**, which is converted to **5** by 1,6-cyclization. Excess ylide **1** deprotonates **5** to form **6**.

According to an X-ray structure analysis[13] (Figs. 1 and 2), **6** crystallizes with one equivalent of dichloromethane in the triclinic space group $P(-1)$, lacking any crystallographical symmetry. The average C–C bond length in the central six-membered ring (C1 through C6) is 144.1 pm; the C–C distances increase from C1–C2 to C6–C1 by a total of 2.5 pm. Alternation of bond lengths, as expected from the mesomeric formula **6b**, is not observed. The lengths of the C–O bonds

[*] Prof. Dr. H. J. Bestmann, Dipl.-Chem. T. G. Fürst
Institut für Organische Chemie der Universität Erlangen-Nürnberg
Henkestrasse 42, D-91054 Erlangen (FRG)
Telefax: Int. code + (9131)85 68 64
Dr. A. Schier
Anorganisch-chemisches Institut der Technischen Universität München
Lichtenbergstrasse 4, D-85747 Garching (FRG)

[**] We thank J. Riede for recording the crystallographic data.

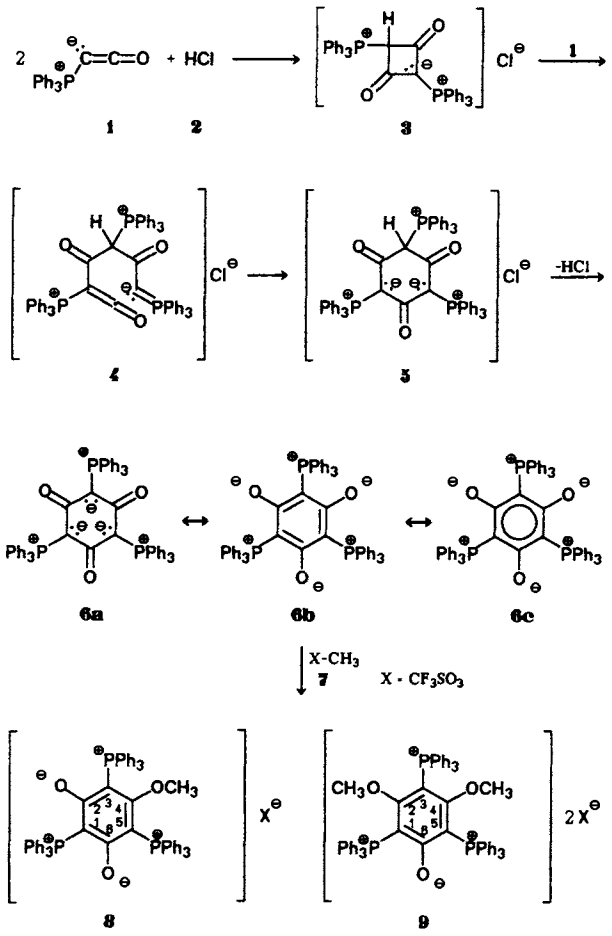

decrease from C2–O through C4–O to C6–O by 2.1 pm, whereas the C–P bonds vary only minimally.

The central six-membered ring is not planar but has a twisted boat conformation when the O and P atoms are included. C2 and C5 deviate from the plane established by C1, C3, C4, and C6, C5 much more than C2. The fold angles amount to 21.3° and 2.5°, respectively.[4] The dihedral angles shown in Figure 2 reflect the deviations from planarity. The two torsion angles involving C5 have the greatest absolute values, −20.2° and +21.6°. The sum of the six interior angles comes to 716.6°. The interior angles at C4, C5, and C6 show the most significant deviations from 120°, that is, again those angles involving C5.

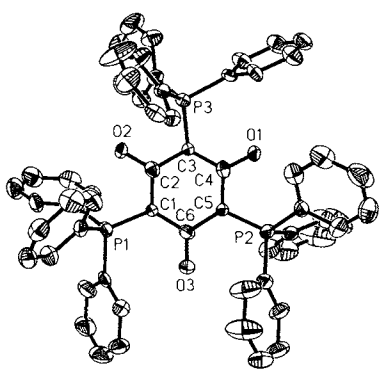

Fig. 1. Crystal structure of **6** with selected bond lengths [pm] and angles [°]: C1-C2 143.1(1), C2-C3 143.6(1), C3-C4 143.8(1), C4-C5 143.8(1), C5-C6 144.7(1), C6-C1 145.6(1), C2-O2 127.7(1), C4-O1 126.6(1), C6-O3 125.6(1), C1-P1 173.8(1), C3-P3 173.9(1), C5-P2 173.2(1); C2-C1-C6 121.8(1), P1-C1-C2 112.5(1), P1-C1-C6 125.7(1), C3-C2-C1 119.5(1), O2-C2-C1 120.5(1), O2-C2-C3 120.0(1), C2-C3-C4 121.2(1), P3-C3-C2 111.8(1), P3-C3-C4 126.1(1), C3-C4-C5 115.9(1), O1-C4-C3 124.0(1), O1-C4-C5 120.0(1), C4-C5-C6 123.5(1), P2-C5-C4 114.7(1), P2-C5-C6 121.5(1), C1-C6-C5 114.7(1), O3-C6-C1 122.9(1), O3-C6-C5 122.3(1).

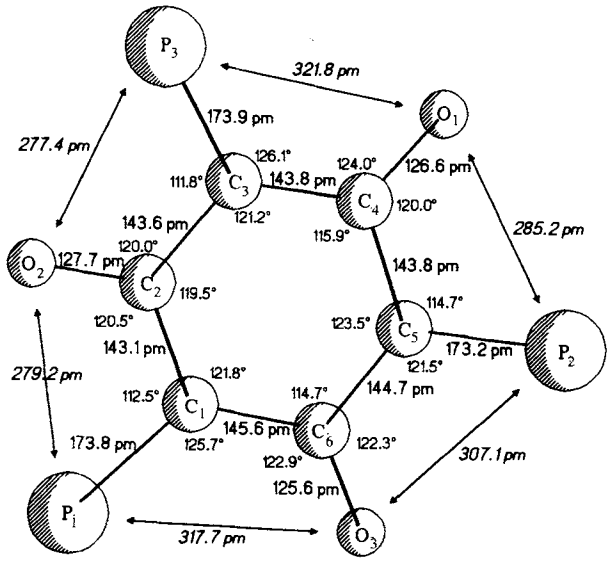

Fig. 2. Bond lengths and angles of trimer **6** (P-O distances in italics). Dihedral angles of the central six-membered ring [°]: C1-C2-C3-C4 −2.3, C2-C3-C4-C5 +9.5, C3-C4-C5-C6 +21.6, C4-C5-C6-C1 −20.2, C5-C6-C1-C2 +7.0, C6-C1-C2-C3 +3.6.

The mean bond length within the six-membered ring (144.1 pm) is distinctly greater than that in typical arenes (138.4 pm).[5] It definitely falls into the range of bond lengths found in tris-donor–tris-acceptor-substituted push–pull arenes.[6] The structure of **6** can be compared to those of the potassium salts of trinitrophloroglucinol, which closely resemble **6**. Here the mean bond lengths are 141.5 and 142.4 pm for the mono-K salt, 143.8 pm for the di-K salt, and 145.2 pm for the tri-K salt. In all of these compounds the benzene ring is likewise nonplanar.[7] The mean C–O distance in **6** (126.6 pm) is comparable to the corresponding distance in the potassium trinitrophloroglucinolates (mono 129.5, di 126.7, tri 124.5 pm). Based on its structure parameters, the trimeric ketenylidene(triphenyl)phosphorane **6** can be considered an electronically perturbed and sterically distorted push–pull arene.

The ^{13}C NMR spectrum of **6** (in CD_2Cl_2) shows two signals with greatly different chemical shifts for alternating C atoms in the central six-membered ring (Table 1). The positions of the two signals indicate a strong delocalization of the ylidic lone pairs of electrons, which is known for cyclic acyl ylides.[2] The high-frequency ν(CO) bands in the IR spectrum indicate the same.

Methylation of **6** with one to three equivalents of methyl trifluoromethylsulfonate (**7**) resulted in mono- and di-O-methylations affording **8** and **9**. Trimethylation was not possible even with a great excess of **7**. The ^{13}C NMR signals of the C atoms in **8** and **9** bearing O-methyl groups are shifted upfield by $\Delta\delta = 5-6$ relative to the related C atoms in **6**, whereas the ^{13}C resonances due to C–O groups are shifted somewhat less. The signals of the ylidic C atoms are shifted in the opposite direction and more strongly so, which is indicative of the expected decreased charge density at these atoms (Table 1).

We were especially interested in the extent of ylidic character in **6**. Although **6** undergoes Wittig reaction with aromatic

Table 1. Physical and spectroscopic data for compounds **6**, **8**, **9**, **11**, **13**, **16**, **18**, and **19**.

6: Colorless needles; m.p. 300 °C (decomp); ^{13}C NMR (100.4 MHz, CD_2Cl_2, 25 °C): $\delta = 184.4$ (s; C2, C4, C6), 74.4 (dt, $^1J(C,P) = 116.0$ Hz, $^3J(C,P) = 9.9$ Hz; C1, C3, C5); ^{31}P NMR (161.7 MHz, $CDCl_3$, 25 °C, H_3PO_4 ext.): $\delta = +13.73$.

8: M.p. 262–265 °C (decomp); ^{13}C NMR (100.4 MHz, CD_2Cl_2, 25 °C): $\delta = 182.69$ (s; C2, C6), 179.83 (s; C4), 84.74 (dt, $^1J(C,P)$ 108.3 Hz, $^3J(C,P) = 7.6$ Hz; C3, C5), 84.36 (dt, $^1J(C,P) = 119.0$ Hz, $^3J(C,P) = 9.2$ Hz; C1), 64.23 (s; CH_3); ^{31}P NMR (40.48 MHz, $CDCl_3$, 25 °C, H_3PO_4 ext.): $\delta = +13.56$.

9: M.p. 230–240 °C (decomp); ^{13}C NMR (100.4 MHz, [D$_6$]DMSO, 25 °C): $\delta = 180.01$ (s; C6), 178.01 (s; C2, C4), 97.45 (dt, $^1J(C,P) = 105.3$ Hz, $^3J(C,P) = 6.1$ Hz; C1, C5), 88.00 (dt, $^1J(C,P) = 111.4$ Hz, $^3J(C,P) = 9.2$ Hz; C3), 64.68 (s; CH_3); ^{31}P NMR (40.48 MHz, [D$_6$]DMSO, 25 °C, H_3PO_4 ext.): $\delta = +14.86$ (t, $^4J(P,P) = 5.1$ Hz), +14.26 (d, $^4J(P,P) = 5.1$ Hz).

11: Yellow crystals; m.p. 287 °C (decomp); IR(KBr): $\tilde{\nu} = 1635$, 1570, 1545, 1496 cm^{-1}; ^{13}C NMR (100.4 MHz, CD_2Cl_2, 25 °C): $\delta = 186.01$ (t, $^2J(C,P) = 6.1$ Hz; C2), 183.89, 181.84 (d, $^2J(C,P) = 6.1$ Hz; C4, C6), 138.43 (t, $^3J(C,P) = 11.4$ Hz; C5), 137.33 (s; C7), 80.19, 77.77 (dd, $^1J(C,P) = 109.8$ Hz, $^3J(C,P) = 7.6$ Hz, C1, C3); ^{31}P (161.7 MHz, $CDCl_3$, 25 °C, H_3PO_4 ext.): $\delta = +14.39$ (d, $^4J(P,P) = 9.2$ Hz), +14.22 (d, $^4J(P,P) = 9.2$ Hz).

13: Orange-red crystals; m.p. 320–340 °C (decomp); ^{13}C NMR (100.4 MHz, CD_2Cl_2 + CD_3OD, 25 °C): $\delta = 186.94$ (t, $^2J(C,P) = 5.3$ Hz; C2), 184.36 (t, $^3J(C,P) = 14.5$ Hz; C5), 175.15 (s; C6, C6a), 83.05 (dd, $^1J(C,P) = 105.3$ Hz, $^3J(C,P) = 9.2$ Hz; C1, C1a); ^{31}P NMR (40.48 MHz, $CDCl_3$, 25 °C, H_3PO_4 ext.): $\delta = +13.83$.

16: Colorless crystals; m.p. 240 °C (decomp); ^{13}C NMR (100.4 MHz, $CDCl_3$, 25 °C): $\delta = 191.77$ (s; C2, C4), 186.93 (t, $^3J(C,P) = 6.1$ Hz; C6), 78.81 (dd, $^1J(C,P) = 112.9$ Hz, $^3J(C,P) = 7.7$ Hz; C1,C5), 36.85 (t, $^3J(C,P) = 12.2$ Hz; C3) 22.72 (s; C7); ^1H NMR (400 MHz, 4 $CDCl_3$ + CD_3OD, 25 °C): $\delta = 1.41$ (s; CH_3); ^{31}P NMR (161.7 MHz, $CDCl_3$, 25 °C, H_3PO_4 ext.): $\delta = +13.58$.

18: Colorless crystals; m.p. 245 °C (decomp); ^{13}C NMR (100.4 MHz, $CDCl_3$, 25 °C): $\delta = 185.50$, 185.56 (s; C2, C4), 186.06 (t, $^2J(C,P) = 6.1$ Hz; C6), 78.33, 78.10 (2 × dd, $^1J(C,P) = 112.9$ Hz, $^3J(C,P) = 7.6$ Hz, $^1J(C,P) = 111.4$ Hz, $^3J(C,P) = 9.2$ Hz; C1, C5), 51.30 (t, $^3J(C,P) = 12.2$ Hz; C3), 38.74, 41.44 (2 s; C7, C8); ^1H NMR (400 MHz, $CDCl_3$, 25 °C): $\delta = 4.02$ (d, $^3J(H,H) = 8.9$ Hz), 3.96 (d, $^3J(H,H) = 8.9$ Hz); ^{31}P NMR (40.48 MHz, $CDCl_3$, 25 °C, H_3PO_4 ext.): $\delta = +13.05$.

19: Colorless crystals; m.p. 301–302 °C (decomp); IR(KBr): $\tilde{\nu} = 1660$, 1595, 1570 cm^{-1}; ^{13}C NMR (100.4 MHz, $CDCl_3$, 25 °C): $\delta = 196.08$ (t, $^2J(C,P) = 9.1$ Hz; C5), 187.39 (dd, $^3J(C,P) = 19.9$ Hz, $^2J(C,P) = 6.1$ Hz; C2, C3), 67.32 (dd, $^1J(C,P) = 112.2$ Hz, $^3J(C,P) = 3.8$ Hz; C1, C4); ^{31}P NMR (40.48 MHz, $CDCl_3$, 25 °C, H_3PO_4 ext.): $\delta = 8.77$.

aldehydes (several days in boiling toluene), multiple carbonyl olefinations proved to be impracticable. The reaction of **6** with 3,4-dichlorobenzaldehyde (**10**), for instance, furnished compound **11** (91% yield), which can be represented by the resonance structures **11b** or **11c** (i.e. as a *p*- or an *o*-quinone methide).

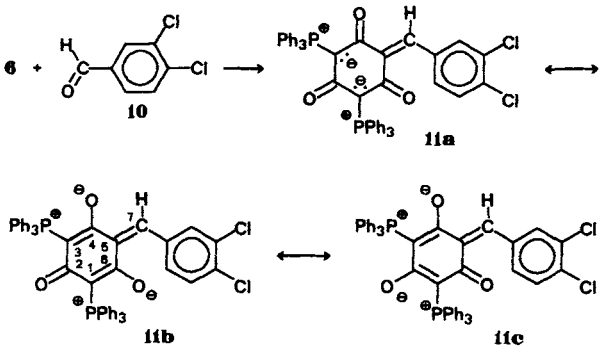

N-*p*-tolylsulfonyl(phenyl)oxaziridine **12** oxidized **6** to give **13** (92% yield),[8] which can be considered either a *p*- or an *o*-quinone **13b**↔**13c**. Figure 3 shows the result of an X-ray structure analysis.[9]

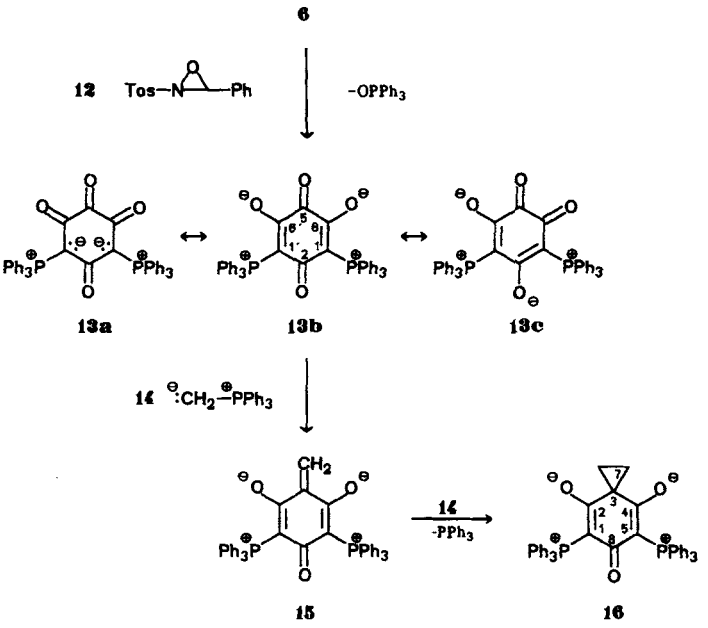

The orange-red compound **13**, also crystallizing with one equivalent of CH_2Cl_2, displays C_s symmetry and distinctly *p*-quinoid character (**13b**). The C1–C6 bond (140.3(4) pm) is significantly shorter than C1–C2 and C5–C6 though longer than the corresponding bonds in substituted benzoquinones (134.9 pm).[5] C1–C2 (144.4(3) pm) is comparable to the corresponding bond in **6**, whereas C5–C6 (155.6(3) pm) is longer than the pertinent bonds in *p*-quinone (147.8 pm). Such long C_{sp^2}–C_{sp^2} bonds are also found in the salts of oxalic acid (mono-salt 154.9, di-salt 156.4 pm).[5]

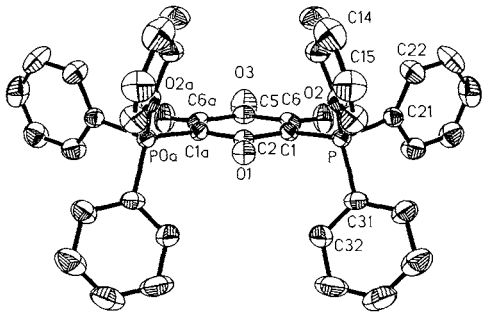

Fig. 3. Crystal structure of **13** with selected bond lengths [pm] and angles [°]: C1-C2 144.4(3), C1-C6 140.3(4), C5-C6 155.6(3), C2-O1 125.2(4), C5-O3 119.1(5), C6-O2 123.6(3), P-C1 175.1(3); P-C1-C6 123.0(2), P-C1-C2 114.2(2), C2-C1-C6 122.8(3), C1-C2-C1a 121.6(4), C1-C2-O1 119.2(3), C6-C5-C6a 120.3(4), C6-C5-O3 119.8(2), O2-C6-C1 129.0(3), O2-C6-C5 114.8(3), C1-C6-C5 116.1(3).

The central six-membered ring in **13** is approximately planar. The sum of the interior angles is 719.7°. The fold angles of the planes C1, C2, C1a and C6, C5, C6a with the reference plane C1, C6, C1a, C6a amount to a mere 3.6° and 2.2°, respectively.

The ^{13}C NMR data of **13** (Table 1) show a high-field shift of the signals of the carbonyl groups from C2 through C5 to C6/C6a, as expected. The signals of C1/C1a are shifted downfield (as in **11**) relative to those of **6**. The X-ray structure analysis and the ^{13}C NMR spectrum indicate the dominance of the mesomeric resonance form **13b**.

As expected, the carbonyl group at C5 in **13** is very reactive. It undergoes a Wittig reaction with methylene(tri-

phenyl)phosphorane **14** to give, rather than **15**, product **16** (92% yield) upon loss of triphenylphosphane. The presumed initial product **15**, a quinone methide with a very electron-poor double bond, reacts with another molecule of **14** to provide **16** in a precendented conversion.[10] As a logical consequence we found that **11** and ylide **17** react to give **18** (83% yield) as one diastereomer. Based on the ^{1}H NMR coupling constants of the protons at the three-membered ring (^3J(H,H) = 8.85 Hz), we have assigned it the *trans* configuration.

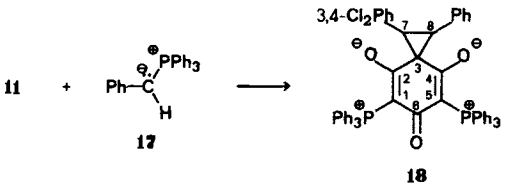

When **13** is oxidized with H_2O_2 + KOH, the bis(ylidic) cyclopentanetrione **19** (92% yield) forms, which can be described by the mesomeric forms **19a**–**19c**. According to an

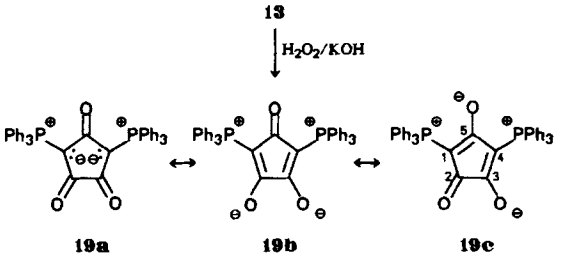

X-ray structure analysis and the ^{13}C NMR signals, **19b** seems to prevail.[11] The bonds C1–C2 (141.6(5) pm) and C3–C4 (143.0(5) pm) are shortest yet still longer than C1–C6 (140.3(4) pm) in **13**. The distances C1–C5 and C5–C4, (145.4(5) and 144.4(5) pm respectively) are comparable with those of C5–C6 (144.7(1) pm) and C6–C1 (145.6(1) pm) in **6**. Once more the distance C2–C3 (156.5(5) pm) between the vicinal carbonyl groups is strikingly different and even longer than that in **13** (155.6(3) pm).

The "cyclic acyl ylides" described here decompose upon melting. We are currently studying their thermolyses in detail. Decomposition of trimer **6** should be of particular interest to us, because release of three equivalents of triphenylphosphane oxide could lead to a C_6 compound or its subsequent reaction products.

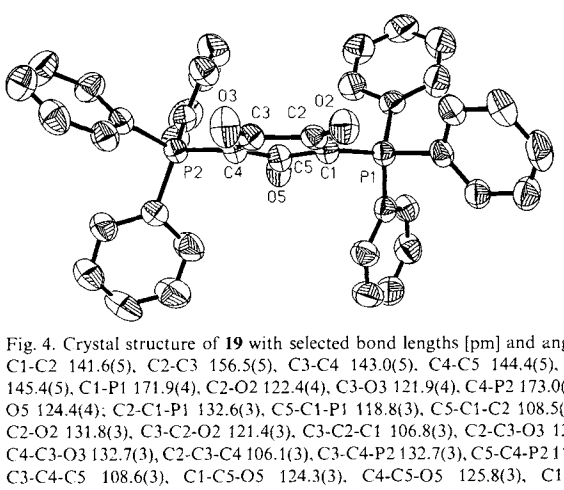

Fig. 4. Crystal structure of **19** with selected bond lengths [pm] and angles [°]: C1-C2 141.6(5), C2-C3 156.5(5), C3-C4 143.0(5), C4-C5 144.4(5), C1-C5 145.4(5), C1-P1 171.9(4), C2-O2 122.4(4), C3-O3 121.9(4), C4-P2 173.0(4), C5-O5 124.4(4); C2-C1-P1 132.6(3), C5-C1-P1 118.8(3), C5-C1-C2 108.5(3), C1-C2-O2 131.8(3), C3-C2-O2 121.4(3), C3-C2-C1 106.8(3), C2-C3-O3 121.2(3), C4-C3-O3 132.7(3), C2-C3-C4 106.1(3), C3-C4-P2 132.7(3), C5-C4-P2 118.5(3), C3-C4-C5 108.6(3), C1-C5-O5 124.3(3), C4-C5-O5 125.8(3), C1-C5-C4 109.9(3).

Received: June 30, 1993 [Z 6180 IE]
German version: *Angew. Chem.* **1993**, *105*, 1784

[1] H. J. Bestmann, G. Schmid, D. Sandmeier, L. Kisielowski, *Angew. Chem.* **1977**, *89*, 275–276; *Angew. Chem. Int. Ed. Engl.* **1977**, *16*, 268.
[2] H. J. Bestmann, T. G. Fürst, A. Schier, *Angew. Chem.* **1993**, *105*, 1783; *Angew. Chem. Int. Ed. Engl.* **1993**, *32*, 1747.
[3] Crystal structure analysis of **6**: $C_{60}H_{45}O_3P_3 \cdot CH_2Cl_2$, M_r = 991.88; Syntex P2$_1$ diffractometer; $Mo_{K\alpha}$ radiation (λ = 71.069 pm); graphite monochromator; T = −50 °C; the lattice constants were determined from 25 reflections: triclinic unit cell, a = 905.8(1), b = 1432.3(2), c = 1950.0(2) pm, α = 93.85(1), β = 90.10(1), γ = 92.10(1)°, V = 2522.46 × 10^6 pm^3, space group $P(-1)$ [no. 2], Z = 2, ϱ_{calcd} = 1.306 g cm^{-3}, $F(000)$ = 1032 e, $\mu(Mo_{K\alpha})$ = 2.66 cm^{-1}, ω scan mode, hkl range: $0 \le h \le 9$, $-15 \le k \le 15$, $-20 \le l \le 20$; of 6190 independent reflections 4526 were considered "observed" [$F_o \ge 4\sigma(F_o)$]; structure was solved by direct methods (SHELXS-86), refinement by method of least squares and difference Fourier synthesis (SHELX-76); all non-hydrogen atoms were refined with anisotropic displacement parameters; all H atoms (except those of the solvent molecule) could be located and were included in the refinement with fixed isotropic displacement parameters [$U_{iso(fix)}$ = 0.05 Å^2]; R (R_w) = 0.0615 (0.0550, with $w = 2.681/\sigma^2(F_o)$); 622 parameters; maximum residual electron densities: +0.72/−0.70 × 10^6 e pm^{-3}. See also ref. [11b].
[4] For definition of the term fold angle see G. Maas, J. Fink, H. Wingert, K. Blatter, M. Regitz, *Chem. Ber.* **1987**, *120*, 819–824.
[5] F. H. Allen, O. Kennard, D. G. Watson, *J. Chem. Soc. Perkin Trans. 2* **1987**, S1–S19.
[6] J. J. Wolff, S. F. Nelsen, D. R. Powell, *J. Org. Chem.* **1991**, *56*, 5908–5911; J. J. Wolff, S. F. Nelsen, P. A. Petillo, D. R. Powell, *Chem. Ber.* **1991**, *124*, 1719–1725.
[7] J. J. Wolff, S. F. Nelsen, D. R. Powell, J. M. Desper, *Chem. Ber.* **1991**, *124*, 1727–1731.
[8] F. A. Davis, B. Chen, *J. Org. Chem.* **1990**, *55*, 360–363.
[9] Crystal structure analysis of **13**: $C_{42}H_{30}O_4P_2 \cdot CH_2Cl_2$, M_r = 745.58; Enraf-Nonius CAD4 diffractometer; $Mo_{K\alpha}$ radiation (λ = 71.069 pm); graphite monochromator; T = 22 °C; the lattice constants were determined from 25 reflections: orthorhombic unit cell, a = 2083.5(1), b = 949.9(1), c = 917.0(1) pm, V = 1814.8 × 10^6 pm^3, space group $Pmn2_1$ [no. 31], Z = 2, ϱ_{calcd} = 1.364 g cm^{-3}, $F(000)$ = 772 e, $\mu(Mo_{K\alpha})$ = 3.06 cm^{-1}, θ-θ-scan mode, hkl range: $0 \le h \le 26$, $-11 \le k \le 11$, $-11 \le l \le 11$; of 2156 independent reflections 1981 were considered "observed" [$F_o \ge 4\sigma(F_o)$]; structure solution and refinement see [3]; all non-hydrogen atoms (except those of the disordered solvent molecule) were refined with anisotropic displacement parameters; all H atoms (except those of the solvent molecule) could be located and were refined with fixed isotropic displacement parameters [$U_{iso(fix)}$ = 0.05 Å^2]; R (R_w) = 0.0523 (0.0509, with $w = 3.908/\sigma^2(F_o)$), [R (R_w) = for the inverse model 0.0527 (0.0515)]; 235 parameters; maximum residual electron densities: +1.16/−1.69 × 10^6 e pm^{-3} (located at the disordered solvent molecule). See also [11b].
[10] H. J. Bestmann, F. Seng, *Angew. Chem.* **1962**, *74*, 154–155; H. J. Bestmann, G. Schmid, L. Kisielowski, *Isr. J. Chem.* **1981**, *22*, 45–52.
[11] a) Crystal structure analysis of **19**: $C_{41}H_{30}O_3P_2 \cdot CH_2Cl_2$, M_r = 717.57; Enraf-Nonius CAD4 diffractometer; $Mo_{K\alpha}$ radiation (λ = 71.069 pm); graphite monochromator; T = 22 °C; the lattice constants were determined from 25 reflections: triclinic unit cell, a = 885.0(1), b = 1078.0(1), c = 1906.7(1) pm, α = 93.67(1), β = 93.46(1), γ = 90.62(1)°, V = 1811.81 × 10^6 pm^3, space group $P(-1)$ [no. 2], Z = 2, ϱ_{calcd} = 1.315 g cm^{-3}, $F(000)$ = 744 e, $\mu(Mo_{K\alpha})$ = 3.02 cm^{-1}, ω scan mode, hkl range: $-10 \le h \le 10$, $-13 \le k \le 13$, $0 \le l \le 23$; of 6230 independent reflections 4938 were considered "observed" [$F_o \ge 4\sigma(F_o)$]; structure solved by direct methods (SHELXTL-PLUS), refinement by the method of least squares and difference Fourier synthesis (SHELXTL-PLUS); all non-hydrogen atoms (except those of the disordered solvent molecule) were refined with anisotropic displacement parameters; all H atoms (except those of the solvent molecule) could be located and were included in the refinement with fixed isotropic displacement parameters [$U_{iso(fix)}$ = 0.05 Å^2]; R (R_w) = 0.0590 (0.0590, with $w = 1.00/\sigma^2(F_o)$); 286 parameters; maximum residual electron densities: +0.34/−0.43 × 10^6 e pm^{-3}. b) Further details of the crystal structure investigations may be obtained from the Fachinformationszentrum Karlsruhe, Gesellschaft für wissenschaftlich-technische Information mbH, D-76344 Eggenstein-Leopoldshafen (FRG) on quoting the depository number CSD-57478, the names of the authors and the journal citation.

$[(I_6Te_2)Nb(Te_2)_2Nb(Te_2I_6)]$, a Metal Complex with Halochalcogenate Ligands**

By *Astrid Leist* and *Wolfgang Tremel**

Polycations of the main group elements have been known for almost thirty years.[1] In some cases, they have been isolated as their AsF_6^-, SbF_6^-, $Sb_2F_{11}^-$,[2] $AlCl_4^-$, or $Al_2Cl_7^-$ salts from superacid media or melts.[3] Moreover, recent investigations have shown that the halides of electron-poor transition metals, such as WCl_6 or $ZrCl_4$, are suitable oxidizing agents for the preparation of polycations of tellurium.[4, 5] Whereas a wealth of information is known about discrete polycations of the main group elements, and also the corresponding Zintl polyanions,[6] very little is known about polycations that are bound to transition metal complex fragments. Thus, the complexes $[M(CO)_4(\eta^3\text{-}Te_3)][SbF_6]$ (M = Mo, W)[7, 8] and $[(Te_4)Nb_3O(Te_2)_2I_7]$[9] are the only three compounds known in which polycations of tellurium are bound to metals. With only a few exceptions (e.g. $[Pb_9Cr(CO)_3]^{4-}$,[10] $[Sn_6\{Cr(CO)_5\}_6]^{2-}$,[11] or $[Sb_7Mo(CO)_3]^{3-}$[12]), the binding of transition metal complex fragments to Zintl polyanions is likewise a rarity. It was already apparent from the synthesis of $[(Te_4)Nb_3O(Te_2)_2I_7]$[9] that the formation of transition metal complexes with unusual ligands is possible from high-temperature reactions. We report here on a further example of this; the title compound, $Nb_2Te_8I_{12}$, has two $Te_2I_6^{2-}$ ligands coordinated to a $Nb_2Te_4^{2+}$ center.

The title compound $Nb_2Te_8I_{12}$[13] is formed by the reaction of the elements at 620 °C. The crystal structure[14] consists of discrete $Nb_2Te_8I_{12}$ molecules (Fig. 1) each of which has idealized D_{2h} and crystallographic C_i symmetry. In each molecule, the Nb atoms of the $Nb_2(Te_2)_2$ central unit are bridged by two Te_2 groups. The Te–Te distance within the Te_2 groups is 2.682(1) Å. This value is in accord with the 2.74 Å[15] reported for twice the covalent radius of tellurium and is similar to the corresponding values from compounds with typical Te–Te single bonds like diphenylditelluride Ph_2Te_2 (2.712 Å)[16] and $[Ta(Te_2)_2I_4][PtI_6]I_2$ (2.781 Å).[17] The range of Nb–Te distances (2.814(2)–2.934(1) Å) within the Nb_2Te_4 center are in agreement with the values found in $Nb_2Te_2I_6$,[18] $NbTe_4I$,[19] and Nb_2Te_6I.[20]

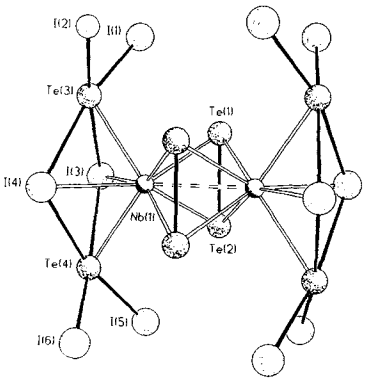

Fig. 1. The molecular structure of $Nb_2Te_8I_{12}$ in the crystal. Selected interatomic distances [Å]: Nb(1)-Te(1) 2.817(2), Nb(1)-Te(2) 2.814(1), Nb(1)-Te(3) 2.920(2), Nb(1)-Te(4) 2.934(1), Nb(1)-I(3) 2.960(1), Nb(1)-I(4) 2.951(2), Nb-Te(1A) 2.814(1), Nb(1)-Te(2A) 2.811(1), Te(1)-Te(2) 2.682(1), Te(1)···Te(2A) 3.871(1), Te(3)-I(1) 2.760(2), Te(3)-I(2) 2.789(1), Te(3)-I(3) 3.167(1), Te(3)-I(4) 3.210(1), Te(4)-I(3) 3.211(2), Te(4)-I(4) 3.217(1), Te(4)-I(5) 2.769(1), Te(4)-I(6) 2.755(2)), I(1)···Te(1) 3.705(1), I(2)···Te(2A) 3.738(1), I(5)···Te(2) 3.646(1), I(6)···Te(1A) 3.803(1). Shortest intermolecular distances: I(2)···I(2B), 3.674(1); I(2)···I(5C), 3.718(1).

The Nb–Nb distance of 3.083(2) Å is about 0.1 Å longer than the corresponding metal–metal distances in related compounds such as Nb_2Te_6I (d_{Nb-Nb}: 2.834(2) Å),[20] $Nb_2Te_2I_6$ (d_{Nb-Nb}: 2.932(2) Å),[13] and $Nb_2Cl_4S_2 \cdot 4tht$ (tht = tetrahydrothiophene, d_{Nb-Nb}: 2.888(2) Å),[21] in which formal Nb–Nb single bonds are present. An obvious question is, therefore, whether the Nb–Nb distance of 3.083(2) Å corresponds to a formal Nb–Nb single bond. Extended Hückel calculations[22] for $Nb_2Te_8I_{12}$ have shown that the HOMO–LUMO energy gap is only mildly influenced by variations in the Nb–Nb distances over the region between 2.9 Å and 3.1 Å. In contrast, larger changes in the metal–metal distances lead to either strong Van der Waals repulsions of the ligands or bond breaking within the Te_2 groups of the Nb_2Te_4 center.[23] The sum of the restraints imposed by the ligand–ligand, ligand–metal, and metal–metal bonds in this group of compounds permits changes in the molecular geometry to occur only within narrow limits if the structure type is to be retained. Hence, the structure of the title compound should also contain a dimetal center with a formal Nb–Nb single bond.

The tetragonal antiprismatic surroundings of the Nb atoms are completed with the two slightly tilted Te_2I_6 groups, each bound to a metal through the central Te and bridging I atoms. The distances between the Nb and Te atoms of the Te_2I_6 group (2.920(2) and 2.934(2) Å) as well as the Nb–I distances (2.951(2)–2.960(2) Å) are enlarged compared to the sums of their respective covalent radii. It is possible then to formally describe the bonding as $[((Nb^{4+})_2(Te_2^{2-})_2)((Te^{2+})_2(I^-)_6)_2]$. The dinuclear $Te_2I_6^{2-}$ groups are thus isoelectronic with I_2Cl_6 and isostructural to Au_2Cl_6.

The bond lengths and angles of the Te_2I_6 groups coordinated to the metal center in $Nb_2Te_8I_{12}$ are significantly different from those in the free $Te_2I_6^{2-}$ anion[25] ($Te_2I_6^{2-}$: $\bar{d}_{Te-I}$ (terminal) 2.827 Å; $Nb_2Te_8I_{12}$: $\bar{d}_{Te-I}$ (terminal) 2.768 Å; $Te_2I_6^{2-}$: $\bar{d}_{Te-I}$ (bridging) = 3.138 Å; $Nb_2Te_8I_{12}$: $\bar{d}_{Te-I}$ (bridging) = 3.201 Å). The next notable facet is that the asymmetry found in the four-membered Te_2I_2 ring of the free $Te_2I_6^{2-}$ anion[25] is virtually absent in the complexed species. Further differences are apparent, in particular, in the Te–I bond lengths of the central Te_2I_2 four-membered ring as well as the terminal Te–I bond lengths. Whereas the Te–I distances ($d_{Te(3)-I(3)}$: 3.167(1) Å) to the bridging I atoms are up to about 0.1 Å longer, the terminal Te–I distances ($d_{Te(3)-I(1)}$: 2.760(1) Å, $d_{Te(3)-I(2)}$: 2.789(1) Å) are about 0.04 Å shorter. That the shorter terminal Te–I bonds lie transverse to the longer bridging bonds can be understood as an effect of the hypervalency in the Te_2I_6 unit. The changes which occur as a result of the coordination of the $Te_2I_6^{2-}$ group to the $Nb_2Te_4^{4+}$ center therefore lead to a significant lengthening in the bridging Te–I bonds. Thus, the bonding situation changes in the transition from a free to a complex-bound ligand $[((Nb^{4+})_2(Te_2^{2-})_2)((I^-)_4(TeI_2)_4)]$ (i.e. now with the donor ligands I^- and TeI_2).

Figure 2 shows a [100] projection of the unit cell. As a result of their nearly spherical shape, the $Nb_2Te_8I_{12}$ molecules are ordered as close-packed layers in the crystal lattice. Although $Nb_2Te_8I_{12}$ exists as discrete molecules, it does not remain intact when dissolved in organic solvents like chloroform or acetonitrile. The stable decomposition product was shown to be TeI_4.

[*] Prof. Dr. W. Tremel, Dipl.-Chem. A. Leist
Institut für Anorganische Chemie und Analytische Chemie der Universität
J.-J.-Becher-Weg 24, D-55128 Mainz (FRG)
Telefax: Int. code + (6131)39-5380

[**] This work was supported by the Bundesministerium für Forschung und Technologie (grant no. 05 5UMGAB) and the Deutsche Forschungsgemeinschaft. We thank the Heraeus Quarzschmelze Co. (Dr. Höfer) and the H. C. Starck Co. (Dr. Peters) for material support.

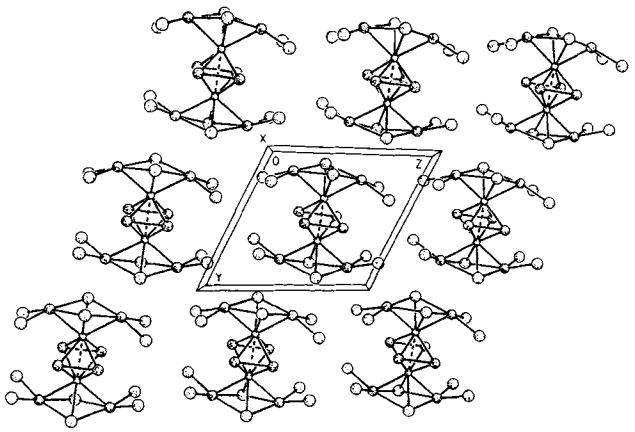

Fig. 2. [100] projection of the unit cell of $Nb_2Te_8I_{12}$.

It is not only remarkable, but also surprising, that halotellurate(II) ions, which have so far only been known to exist in free form, can be obtained in complexed form from high-temperature reactions. In compounds of tellurium and selenium with halogens, the chalcogens usually have an oxidation state IV; the most well-known examples of this class of compounds are the tetrameric molecular halides X_4Y_{16} (X = Se, Te; Y = Cl, Br, I)[26] and their solution decomposition products $[X_3Y_{13}]^-$,[27] $[X_2Y_{10}]^{2-}$,[28] and $[X_2Y_9]^-$.[29] The halides of Se^{II} and Te^{II} are much less stable; chalcogen(II) halides are not known in the solid state, but do exist in solution and in the gas phase.[30] Chalcogen(II) halides can be stabilized in solution through the formation of adducts with electron donors. The synthesis of halogeno anions like $[Se_2Cl_6]^{2-}$[31] and $[Se_5Br_{12}]^{2-}$ as well as a few mixed-valent species (such as $[Se_3Br_{10}]^{2-}$) has only recently been possible.[32] These compounds are generally prepared from organic solvents by the disproportionation of the tetrahalide with subsequent addition of halide. Whereas the chemistry of the free halogeno anions has been well described, there is to date no information on their complexation properties.[33] Since unstable or short-lived compounds appearing in the solvolysis equilibium might possibly be trapped and characterized through complex formation, the investigation of transition metal complexes having halochalcogenate ligands is of special interest.

Received: April 21, 1993 [Z 6024 IE]
German version: *Angew. Chem.* **1993**, *105*, 1798

[1] R. J. Gillespie, J. Passmore, *Acc. Chem. Res.* **1971**, *4*, 413.
[2] J. Barr, R. J. Gillespie, R. Kapoor, K. C. Malhorn, *Can. J. Chem.* **1968**, *46*, 149.
[3] T. W. Couch, D. A. Lokken, J. D. Corbett, *Inorg. Chem.* **1972**, *11*, 357.
[4] J. Beck, *Angew. Chem.* **1990**, *102*, 301; *Angew. Chem. Int. Ed. Engl.* **1990**, *29*, 293.
[5] J. Beck, *Chem. Ber.* **1991**, *124*, 677.
[6] E. Zintl, J. Goubeau, W. Dullenkopf, *Z. Phys. Chem. Abt. A* **1931**, *154*, 1; E. Zintl, A. Harder, *ibid.* **1931**, *154*, 47; E. Zintl, W. Dullenkopf, *Z. Phys. Chem. Abt. B* **1932**, *16*, 183; J. D. Corbett, *Chem. Rev.* **1985**, *85*, 383, and references therein.
[7] R. Faggiani, R. J. Gillespie, C. Campana, J. W. Kolis, *J. Chem. Soc. Chem. Commun.* **1987**, 485.
[8] A. Seigneurin, T. Makani, D. J. Jones, J. Rozière, *J. Chem. Soc. Dalton. Trans.* **1987**, 2111.
[9] W. Tremel, *J. Chem. Soc. Chem. Commun.* **1992**, 126.
[10] R. C. Haushalter, B. W. Eichhorn, *J. Chem. Soc. Chem. Commun.* **1990**, 937.
[11] B. Schiemenz, G. Huttner, *Angew. Chem.* **1993**, *105*, 295; *Angew. Chem. Int. Ed. Engl.* **1993**, *32*, 297.
[12] U. Bolle, W. Tremel, *J. Chem. Soc. Chem. Commun.* **1993**, in press.
[13] Niobium powder, finely powdered tellurium, and iodine in a molar ratio of 1:4:6.1 were placed in a dried quartz ampule. The ampule was flame-sealed under vacuum and heated to 620 °C. After about one week, blue-black, platelike crystals of $Nb_2Te_8I_{12}$ formed which were easily separated from the adhering powdery material. The composition of the latter product is still unknown.
[14] X-ray structure analysis: Space group $P\bar{1}$ (no. 2), $Z = 1$, $a = 7.818(2)$, $b = 10.859(2)$, $c = 12.069(2)$ Å, $\alpha = 111.71(1)$, $\beta = 106.68(2)$, $\gamma = 98.99(2)°$, $T = 170$ K, Siemens P2$_1$, $Mo_{K\alpha}$, $\mu = 17.52$ mm^{-1}, crystal dimensions $0.08 \times 0.06 \times 0.09$ mm, θ–2θ scan, $2\theta_{max} = 60°$, 3820 symmetry-independent reflections from which 3204 had $I > 2\sigma(I)$, empirical absorption correction (XEMP), $R(R_w) = 0.036(0.035)$. Further details of the crystal structure investigation may be obtained from the Fachinformationszentrum Karlsruhe, Gesellschaft for wissenschaftlich-technische Information mbH, D-76344 Eggenstein-Leopoldshafen (FRG), on quoting the depository number CSD-57500, the names of the authors, and the journal citation.
[15] L. Pauling, *The Nature of the Chemical Bond*, Cornell University Press, Ithaca, **1960**; *Die Natur der Chemischen Bindung*, Verlag Chemie, Weinheim, **1962**.
[16] G. Llabres, O. Dideberg, L. Dupont, *Acta Crystallogr. Sect B* **1972**, *28*, 2438.
[17] K.-L. Stork, W. Tremel, *Z. Naturforsch. B* **1993**, *48*, 1155.
[18] H. F. Franzen, W. Hönle, H.-G. von Schnering, *Z. Anorg. Allg. Chem.* **1983**, *497*, 13.
[19] W. Tremel, *Chem. Ber.* **1992**, *125*, 2165.
[20] W. Tremel, *Inorg. Chem.* **1992**, *31*, 755.
[21] M. G. B. Drew, D. A. Rice, D. M. Williams, *J. Chem. Soc. Dalton Trans.* **1985**, 417.
[22] a) R. Hoffmann, W. N. Lipscomb, *J. Chem. Phys.* **1962**, *36*, 2179, 3489; *ibid.* **1962**, *37*, 2872; b) R. Hoffmann, *ibid.* **1963**, *39*, 1397; c) J. H. Ammeter, H.-B. Bürgi, J. C. Thibeault, R. Hoffmann, *J. Am. Chem. Soc.* **1978**, *100*, 3686.
[23] Bond lengths [Å]: Nb–Te_{br} 2.799, Nb–Te, 2.92, Nb–I_4 2.96, Te–I_{br} 3.215, Te–I, 2.761. Parameters for Nb, Te, and I from ref. [24].
[24] A similar situation has been found in compounds of the type $[L_3Mo(S_2)(S)_2MoL_3]$; compare W. Tremel, R. Hoffmann, E. D. Jemmis, *Inorg. Chem.* **1989**, *28*, 1213.
[25] K. Erpenstein, Dissertation, Universität Münster, **1986**, cited in: B. Krebs, F.-P. Ahlers, *Adv. Inorg. Chem.* **1990**, *35*, 235.
[26] V. Paulat, B. Krebs, *Angew. Chem.* **1979**, *91*, 28; *Angew. Chem. Int. Ed. Engl.* **1979**, *18*, 39.
[27] B. Krebs, V. Paulat, *Angew. Chem.* **1973**, *85*, 662; *Angew. Chem. Int. Ed. Engl.* **1973**, *12*, 666.
[28] B. Krebs, V. Paulat, *2nd Europ. Crystallogr. Meet.*, Keszthely, **1974**.
[29] B. Krebs, N. Rieskamp, A. Schäffer, *Z. Anorg. Allg. Chem.* **1986**, *532*, 118.
[30] B. Krebs, A. Schäffer, S. Pohl, *Z. Naturforsch. B* **1984**, *39*, 1633.
[31] L. Fernholt, A. Haaland, H. V. Volden, R. Kniep, *J. Mol. Struct.* **1985**, *128*, 29.
[32] B. Krebs, E. Lührs, F.-P. Ahlers, *Angew. Chem.* **1989**, *101*, 190; *Angew. Chem. Int. Ed. Engl.* **1989**, *28*, 187.
[33] The compounds $[PtCl_4(SCl_2)_2]$ and $[PdCl_2(SCl_2)_2]$ represent the only two examples described to date in which SCl_2 acts as a ligand: M. Paulus, G. Thiele, *Z. Anorg. Chem.* **1990**, *588*, 69.

Tetrahedral Coordination of Palladium in $Ta_2Pd_3Te_5$: A Compound with a "Stuffed" Ta_2NiSe_5 Structure**

By *Wolfgang Tremel**

Chalcogenides of the early transition metals are very attractive solid-state materials both in terms of their chemical and physical properties. From the chemical point of view, layered structure compounds of the type MQ_2 (M = Ti, Nb, Ta; Q = S, Se) should be mentioned first in relation to investigations on their charge storage reactions and for use in photovoltaic cells.[1, 2] The Chevrel phases, such as AMo_6Q_8 (A = Pb, Sn, Ba, Au, Cu, Li, etc.; Q = S, Se, Te), with their

[*] Prof. Dr. W. Tremel
Institut für Anorganische Chemie und Analytische Chemie der Universität
J.-J.-Becher-Weg 24, D-55128 Mainz (FRG)
Telefax: Int. code + (6131)39-5380

[**] This work was supported by the Bundesministerium für Forschung und Technologie (grant no. 05 5UMGAB) and the Deutsche Forschungsgemeinschaft. We thank the Heraeus Quarzschmelze Co. (Dr. Höfer) and the H. C. Starck Co. (Dr. Peters) for material support.

associated metal clusters have become, in the meantime, textbook material.[3] The superconducting properties of many of the Chevrel phases[4] and the charge density waves in compounds of the type MQ_2 or MQ_3 (M = Nb, Ta; Q = S, Se)[5] are especially interesting from a material science point of view.

Sulfides and selenides have been extremely well investigated, whereas tellurides have remained rather neglected since it was assumed that their structures and properties would be analogous to those of the group's lighter homologues. As recent investigations have shown, however, this assumption is not justified. The compounds $CsTe_4$,[6] $[NbTe_{10}]^{3-}$,[7] Al_7Te_{10},[8] Ta_4SiTe_4,[9] M_3ATe_6 (M = Nb, Ta; A = Si, Ge),[10a-c] $Ta_{13}Ga_3Te_{24}$,[10d] and $TaNi_2Te_2$[11] are only a few particularly prominent examples which illustrate the nonconformitive behavior of the tellurides. None of these compounds has a stoichiometric counterpart among the sulfides and selenides, and each exhibits unusual chemical properties and structural features. Thus, Te–Te distances are found in the structures of $CsTe_4$[6] and $NbTe_{10}^{3-}$[7] which correspond to fractional Te–Te bond orders. Aluminum occurs in the oxidation state II in Al_7Te_{10}.[8] The silicon atoms in the structure of Ta_4SiTe_4[9] are surrounded by a square antiprismatic arrangement of eight metal atoms. The main group elements in the structures of M_3ATe_6 (M = Nb, Ta; A = Si, Ge)[10a-c] and $Ta_{13}Ga_3Te_{24}$[10d] are coordinated in a square-planar fashion to four tellurium atoms. An obvious question is therefore: Can unusual coordination geometries of transition metals also be stabilized in chalcogenides, particularly in tellurides, of niobium and tantalum? Our investigations have led to the synthesis of the title compound $Ta_2Pd_3Te_5$, in which the palladium is not coordinated in a square-planar fashion, but *tetrahedrally* to the chalcogenides.

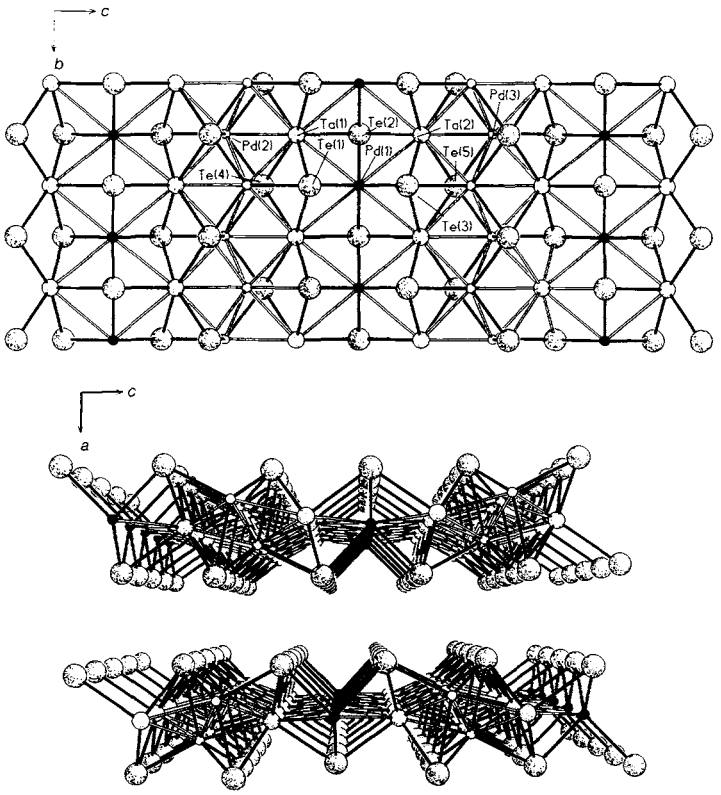

Fig. 1. Top: Structure of $Ta_2Pd_3Te_5$ (ball-and-stick representation): parallel projection of a layer along [100]. Bottom: parallel projection of the structure along [010]. Large, heavily dotted circles: Te; medium, lightly dotted circles: Ta; small, filled black circles: Pd(1); small, open circles: Pd(2) and Pd(3). Selected interatomic distances [Å]: Ta-Te 2.820(2)–2.854(2), Pd(1)-Te 2.623(2)–2.665(2), Pd(2)-Te 2.653(2), 2.716(2) (2 ×), 3.059(2), Pd(3)-Te 2.639(2), 2.716(2) (2 ×), 3.059(2), Ta-Pd(1) 2.990(2) (2 ×) and 2.990(2) (2 ×), Ta-Pd(2)2.845(2) and 2.888(2) (2 ×), Ta-Pd(3)2.853(2) (2 ×) and 2.813(2), Pd(2)-Pd(3)2.701(2) (2 ×).

Each $Ta_2Pd_3Te_5$ layer is composed of three atomic layers: tellurium atoms form the top and bottom layers (not close packed), and the middle layer contains tantalum and palladium atoms. The Pd atoms are each surrounded by a distorted tetrahedron of Te atoms. The Ta atoms are coordinated to five Te neighbors in an approximate square pyramid at distances between 2.7 and 2.8 Å, with an additional sixth Te atom at a nonbonding Ta–Te distance of 4.137 Å. Although the description of the coordination around Ta as a distorted octahedron is not chemically justified, it simplifies the discussion and emphasizes the structural relationship between Ta_2NiQ_5 (Q = S, Se)[14] and $Ta_2Pd_3Te_5$. An idealized polyhedral representation of one such layer from the $Ta_2Pd_3Te_5$ structure is shown in Figure 2. Accordingly, each $Ta_2Pd_3Te_5$ layer can be described as being based on double chains of edge-sharing Ta_2Te_6 octahedra which are condensed over their apical Te atoms to give Ta_2Te_5 layers. The unit cell contains two double chains per layer, which are displaced from one another by $a/2$.

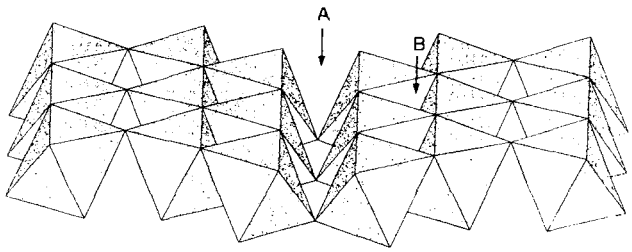

Fig. 2. Polyhedral representation of a $Ta_2Pd_3Te_5$ layer.

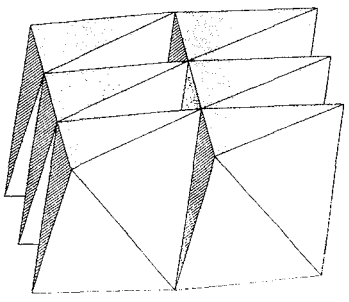

Scheme 1. Polyhedral representation of the double chains of edge-sharing Ta_2Te_6 octahedra.

The environment of the palladium atoms in this structure is rather unusual. Whereas the metal atoms in practically all known four-coordinate palladium and platinum complexes are square-planar coordinated as a result of the strong ligand-field splitting, the palladium atoms in the title compound show tetrahedral Te coordination. Each of the layers illustrated in Figures 1 and 2 contain two types of tetrahedral voids which are capable of accepting "interstitial" Pd

atoms. The tetrahedral voids A (Fig. 2) are situated between the double chains and are built from the corner- and edge-shared Te atoms of four octahedra. The tetrahedral voids B lie within the double chains; thus, their formation involves the edge-shared Te atoms from three octahedra. The ratio of A to B sites is 1:2. The complete occupation of only the A sites leads to the Ta_2NiQ_5 structure (Q = S, Se),[14] whereas filling both the A and B sites gives the $Ta_2Pd_3Te_5$ structure. The Pd(1) atoms occupy the A, and Pd(2) and Pd(3) occupy the B sites. Consequently, the $Ta_2Pd_3Te_5$ structure can be viewed as a "stuffed" Ta_2NiQ_5 structure. A structure type in which only the B holes are occupied is not known.

The most important differences between the parent and the derivative structures can be summarized: 1) While the Ta atoms in the Ta_2NiQ_5 structure are surrounded by an octahedron of Q atoms, they have only five Te neighbors in the $Ta_2Pd_3Te_5$ structure (the sixth Ta–Te distance, as mentioned earlier, is 4.137(2) Å and should therefore be considered as nonbonding). 2) Conversely, the Ta atoms in the $Ta_2Pd_3Te_5$ structure have five Pd neighbors, whereas in the Ta_2NiQ_5 structure only two Ni neighbors are found. The decrease in the number of Te neighbors is formally compensated for by an increase in the number of adjacent metal atoms.

At present, the Pd coordination cannot be fully explained. Whereas nickel is tetrahedrally coordinated to the chalcogenide ligands in, for example, the Ni analogue $Ta_2Ni_3Te_5$,[15] Ta_2NiQ_5,[14,16] and numerous other complexes,[17] examples exhibiting the coordination geometry found here for Pd are limited to only a few unstable phosphane complexes like $[Pd(PF_3)_4]$[18] and clusters of the type $[Pd_9E_6(PPh_3)_8]$ (E = As, Sb).[19] Moreover, there are no known tetrahedrally coordinated palladium or platinum chalcogenides and halides. Even in related solid-state compounds like $TlPd_2Te_3$[20] or $Ta_4Pd_3Te_{16}$[21] palladium is bound in either square-planar or an octahedral fashion.

As illustrated in Scheme 2, square-planar Pd coordination is energetically preferred, based on ligand field arguments.

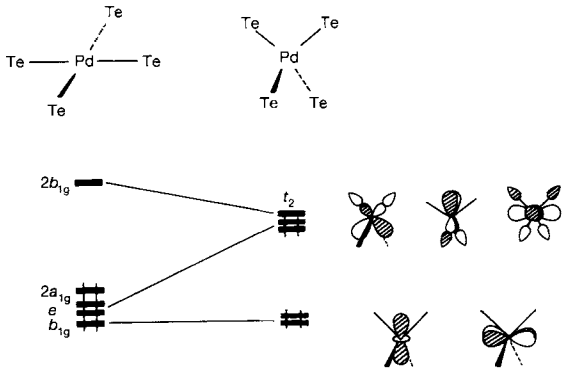

Scheme 2. Molecular orbitals of a $PdTe_4$ unit with a square-planar (left) and a tetrahedrally (right) coordinated central atom.

The occurrence of tetrahedral coordination in the present case must therefore be a result of other factors. Scheme 2 shows that each tetrahedral $PdTe_4$ unit does in fact have several metal-centered orbitals which are oriented in such a way as to allow overlap with the 5d orbitals of neighboring tantalum atoms through the shared faces of adjoining $TaTe_6$ octahedra as well as with the 4d orbitals of neighboring Pd atoms over their common tetrahedra edges. The resulting metal–metal interactions are strong.

The calculated[22] density of states (DOS) for $Ta_2Pd_3Te_5$ is illustrated in Figure 3 together with the partial densities for tantalum, palladium, and tellurium (Figs. 3a–c). The mean Ta–Ta, Ta–Pd, and Pd–Pd overlap populations are reproduced as a function of energy in Figure 4. The Fermi level is indicated in both figures by a horizontal line. For comparison, the position of the 4d levels of an isolated palladium atom has also been illustrated in Figure 3b to show that the stabilization of the Pd states is clearly a result of the metal–metal interactions. The formation of metal–metal bonds is also a reason for the tetrahedral coordination of the palladium atoms in the previously mentioned $[Pd_9E_6(PPh_3)_8]$ clusters.[23] Since the Fermi level is found in the region of a finite density of states, $Ta_2Pd_3Te_5$ is expected to have metallic properties. Investigations by photoemission spectroscopy have provided evidence for the metallic character in the corresponding Ni compound $Ta_2Ni_3Te_5$.[24]

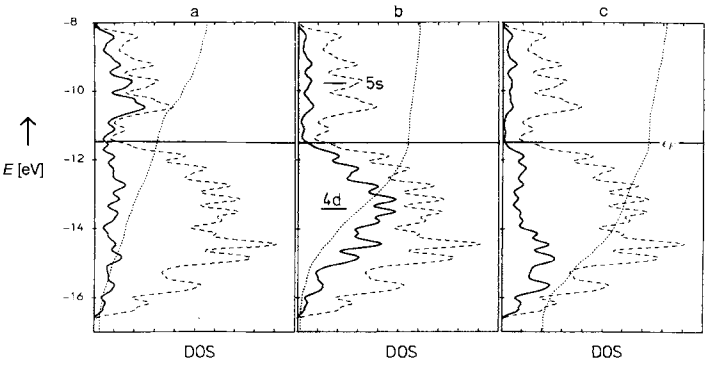

Fig. 3. Density of States (DOS) in $Ta_2Pd_3Te_5$. Dashed lines: total density; solid lines: a) Ta partial density, b) Pd partial density, c) Te partial density; dotted lines: integration curves for the respective partial densities. The Fermi level is marked by a horizontal line.

The COOP (Crystal Orbital Overlap Population) diagrams in Figure 4 further illustrate the significance of the metal–metal interactions to the stability of the structure.

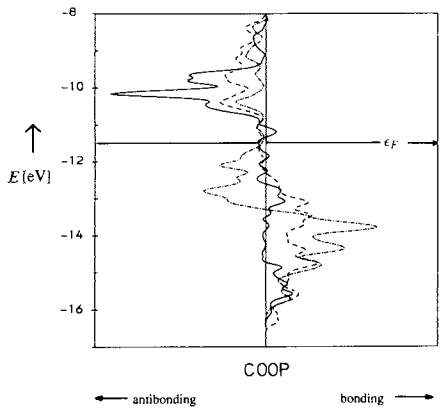

Fig. 4. COOP diagram for $Ta_2Pd_3Te_5$. Solid line: Ta–Ta, dashed line: Pd–Ta (averaged), dot-dashed line: Pd–Pd.

The strong bonding interactions between tantalum and palladium are to be noted first.[25] Interactions between electron-poor and electron-rich transition metals are an important factor for the electronic stability of the structure. It is furthermore remarkable that a large portion of the Pd–Pd antibonding states is occupied. The Pd–Pd interactions should therefore be only weakly bonding, despite the short Pd–Pd distances. In accord with this formulation is the ob-

servation of only a small calculated Pd–Pd overlap population.[25] A structural indication for the existence of Pd–Pd bonding interactions is the fact that the Pd(2) and Pd(3) atoms are not centered in the tetrahedral B sites of the Ta_2NiS_5 parent structure, but instead are displaced from the centers of these tetrahedral voids towards the two respective neighboring Pd atoms. The Ta–Ta interactions are weak, as expected from their large Ta–Ta distances (d_{Ta-Ta}: 3.713 Å).

The reasons for the preferential formation of the "filled-in" Ta_2NiQ_5 structure type with the tellurides are not yet clear. Geometric conditions cannot be the only cause since the respective radius relationships with the sulfides would also allow an occupation of the tetrahedral sites within the layers. A possible argument for the occurrence of the lattice distortions associated with the incorporation of the interstitial atoms as well as for the strong tendency for formation of the "filled-in" structure with the tellurides is the high polarizability of Te^{2-} anions. Thus, lattice distortions should preferentially occur with "soft" lattices.

Received: April 21, 1993 [Z6025IE]
German version: *Angew. Chem.* 1993, 105, 1795

[1] a) R. H. Friend, A. D. Yoffe, *Adv. Phys.* **1987**, *36*, 1; b) J. Rouxel, R. Brec, *Annu. Rev. Mater. Sci.* **1986**, *16*, 137; c) F. Hulliger, *Physics and Chemistry of Materials with Layered Structures, Vol. 5: Structural Chemistry of Layer-Type Phases* (Ed.: F. Lévy), Reidel, Dordrecht, **1976**.
[2] G. Betz, H. Tributsch, *Prog. Solid State Chem.* **1985**, *16*, 195.
[3] R. Chevrel, P. Gougeon, M. Potel, M. Sergent, *J. Solid State Chem.* **1985**, *57*, 25.
[4] K. Yvon, *Curr. Top. Mater. Sci.* **1979**, *3*, 53.
[5] a) J. A. Wilson, F. J. DiSalvo, S. Mahajan, *Adv. Phys.* **1975**, *24*, 117; b) *Electronic Properties of Inorganic Quasi One-Dimensional Compounds, Part 1 and 2* (Ed.: P. Monceau), Reidel, Dordrecht, **1985**; c) *Crystal Chemistry and Properties of Materials with Quasi One-Dimensional Structures* (Ed.: J. Rouxel), Reidel, Dordrecht **1986**.
[6] P. Böttcher, U. Kretschmann, *Z. Anorg. Allg. Chem.* **1985**, *528*, 145.
[7] a) W. A. Flomer, J. W. Kolis, *J. Am. Chem. Soc.* **1988**, *110*, 3682; b) W. Tremel, *Inorg. Chem.* **1992**, *31*, 1030.
[8] R. Nesper, J. Curda, *Z. Naturforsch. B* **1987**, *52*, 557.
[9] M. E. Badding, F. J. DiSalvo, *Inorg. Chem.* **1990**, *29*, 3952.
[10] a) $Nb_3Ge_{0.9}Te_6$: L. Monconduit, M. Evain, F. Boucher, R. Brec, J. Rouxel, *Z. Anorg. Allg. Chem.* **1992**, *616*, 177; b) Nb_3SiTe_6: J. Li, P. J. Carroll, *Mater. Res. Bull.* **1992**, *27*, 1073; c) Ta_3ATe_6 (A = Si, Ge): H. Kleinke, V. Evstafyev, W. Tremel, unpublished results; d) H. Kleinke, W. Tremel, unpublished results.
[11] W. Tremel, *Angew. Chem.* **1992**, *104*, 230; *Angew. Chem. Int. Ed. Engl.* **1992**, *31*, 217.
[12] $Ta_2Pd_3Te_5$: Pure phase samples of thin needle-shaped, metallic lustrous crystals (ca. 0.1 mm long) were prepared by reaction of stoichiometric amounts of the respective elements with the addition of iodine as transport agent (quartz ampule, 1–3 mg cm^{-3}, V = 7–10 cm^3, transport from 850 → 800 °C). In a typical synthesis of $Ta_2Pd_3Te_5$, a quartz ampule (ca. 12 mm diameter) was heated under vacuum, then charged with tantalum powder (0.181 g, 1 mmol), palladium powder (0.160 g, 1.5 mmol), tellurium powder (0.319 g, 2.5 mmol), and an appropriate amount of iodine (ca. 2 mg cm^{-3} ampule volume), and finally flame-sealed. The ampule was then slowly heated to 500 °C in a two-zone furnace, after which time the temperatures in the respective heating zones were raised to 800 and 850 °C. The polarity of the temperature gradient was reversed after one week. Long, flat, metallic lustrous needles were formed on the cooler side of the ampule after an additional two weeks. Energy-dispersive X-ray microanalysis (EDAX): Ta/Pd/Te = 2.13/2.88/4.92.
[13] X-ray structure analysis: Space group *Pnma* (no. 62), Z = 2, a = 13.989(3), b = 3.713(1), c = 18.630(4) Å, Siemens P3, $Mo_{K\alpha}$, μ = 42.44 mm^{-1}, crystal dimensions 0.002 × 0.006 × 0.08 mm, θ–2θ scan, $2\theta_{max}$ = 65°, 1992 reflections, empirical absorption correction (XEMP), 1446 symmetry-independent reflections, $R(R_w)$ = 0.038(0.038). Further details of the crystal structure investigation may be obtained from the Fachinformationszentrum Karlsruhe, Gesellschaft für wissenschaftlich-technische Information mbH, D-76344 Eggenstein-Leopoldshafen (FRG), on quoting the depository number CSD-57345, the names of the authors, and the journal citation.
[14] S. A. Sunshine, J. A. Ibers, *Inorg. Chem.* **1985**, *24*, 3611.
[15] W. Tremel, *Angew. Chem.* **1991**, *103*, 900; *Angew. Chem. Int. Ed. Engl.* **1991**, *30*, 840.
[16] Compounds having the compositions $Nb_2Pd_{0.71}Se_5$, $Ta_2Pd_{0.89}Se_5$, and $Nb_2Pd_{0.74}Cu_{0.22}Se_5$ have been described, but in these the coordination at palladium is also either octahedral or square planar. a) D. A. Keszler, J. A. Ibers, M. Shang, J. Lu, *J. Solid State Chem.* **1985**, *57*, 68. b) P. J. Squattrito, S. A. Sunshine, J. A. Ibers, *ibid.* **1986**, *64*, 261; c) P. J. Squattrito, S. A. Sunshine, J. A. Ibers, *J. Solid State Ionics* **1986**, *22*, 53.
[17] B. Krebs, G. Henkel, *Angew. Chem.* **1991**, *103*, 785; *Angew. Chem. Int. Ed. Engl.* **1991**, *30*, 769.
[18] C. A. Tolman, *Chem. Rev.* **1977**, *77*, 313.
[19] a) D. Fenske, H. Fleischer, C. Persau, *Angew. Chem.* **1989**, *101*, 1740; *Angew. Chem. Int. Ed. Engl.* **1989**, *28*, 1665; b) D. Fenske, C. Persau, *Z. Anorg. Allg. Chem.* **1991**, *593*, 61.
[20] H. Kleinke, W. Tremel, *J. Solid State Chem.*, submitted.
[21] A. Mar, J. A. Ibers, *J. Chem. Soc.* **1991**, 639.
[22] Extended-Hückel(EH) approximation: R. Hoffmann, *J. Chem. Phys.* **1963**, *39*, 1397. H_{ij} matrix elements: J. H. Ammeter, H.-B. Bürgi, J. C. Thibeault, R. Hoffmann, *J. Am. Chem. Soc.* **1978**, *100*, 3686. Tight-binding approach: M.-H. Whangbo, R. Hoffmann, *J. Am. Chem. Soc.* **1978**, *100*, 6093; M.-H. Whangbo, R. Hoffmann, R. B.Woodward, *Proc. R. Soc. London, Ser. A* **1979**, *366*, 23. parameters for Ta: J. Li, R. Hoffmann, M. E. Badding, F. J. DiSalvo, *Inorg. Chem.* **1990**, *29*, 3943; parameters for Ni and Te: J.-F. Halet, R. Hoffmann, W. Tremel, E. Liimatta, J. A. Ibers, *Chem. Mater.* **1989**, *1*, 351. Special k points: R. Ramirez, M. C. Böhm, *Int. J. Quantum Chem.* **1986**, *30*, 391; *ibid.* **1988**, *34*, 571.
[23] Wheeler could show, based on EH calculations, that the underlying M_8E_6 frame in the structures of the $[Pd_9E_6(PPh_3)_8]$ clusters (E = As, Sb) will be stabilized through the bonding of an additional "interstitial" (metal) atom.
[24] J. Neuhausen, R. Schlögl, R. K. Kremer, W. Tremel, unpublished results.
[25] Calculated Ta–Te and Pd–Te overlap populations (tight-binding calculations, EH approximation, parameters from ref. [23]): Ta–Te (4.137 Å) = –0.017; Pd–Te (2.716 Å) = 0.137; Pd–Te (3.000 Å) = 0.067; Pd–Te (3.059 Å) = 0.063. Additional values for Ta–Ta, Ta–Pd, and Pd–Pd overlap populations: Ta–Ta = 0.051; Ta–Pd(1) = 0.095; Ta–Pd(2,3) = 0.136; Pd(2,3)–Pd(2,3) = 0.072.

Monoclinic and Triclinic Tetraisopropyl-*p*-phenylenediamine: To what Extent do n_N/π Interactions Determine Structures?**

By *Hans Bock,* Ilka Göbel, Christian Näther, Zdenek Havlas, Angelo Gavezzotti,* and *Giuseppe Filippini*

Dedicated to Professor Robert Corriu

The structure of polymorphic modifications of the same compound provide multifaceted information on weak interactions in and between organic molecules.[1] In the following, we report on the serendipitously discovered monoclinic and triclinic crystals of tetraisopropyl-*p*-phenylenediamine,[2] which contain different conformers with and without n_N/π interactions between the nitrogen electron pairs n_N and the benzene π system (Fig. 1. center: dihedral angles $\omega(C_2N-C_6)$ = 28 or 74°).[3, 4]

The molecular structures (Fig. 1 top and center) demonstrate that in the conformer giving monoclinic crystals the axes of the lone pairs on the nitrogen centers deviate from those of the π system perpendicular to the six-membered ring plane by only 28° and thus allow a tenfold stronger n_N/π delocalization [$\cos^2$ (28°) = 0.78] relative to the triclinic one

[*] Prof. Dr. H. Bock, Dipl.-Chem. I. Göbel, Dipl.-Chem. C. Näther
Institut für Anorganische Chemie der Universität
Marie-Curie-Strasse 11, D-60439 Frankfurt am Main (FRG)
Dr. Z. Havlas
Institute of Organic Chemistry and Biochemistry of the
Czech Academy of Sciences
Flemingova Nam 2, CS-1160 Prag (Czech Republic)
Prof. Dr. A. Gavezzotti, Dr. G. Filippini
Institute of Physical Chemistry of the University
Via Golgi, I-20133 Milano (Italy)

[**] Structure of charge-perturbed and sterically overcrowded molecules as well as interactions in crystals. Part 30. This research project has been supported by the Deutsche Forschungsgemeinschaft, the state of Hesse, and the Fonds der Chemischen Industrie.—Part 29.: Ref. [4].

with dihedral angles of 74° [$\cos^2(74°) = 0.08$]. The lattice-enforced effects of the diisopropylamino donor substituents cause significant structural changes: the NC_3 pyramids are flattened by 12° to 353°, the NC_{ring} bonds are shortened by 4 pm to 141 pm, and the *ipso* angles at the substituted centers are reduced by 3° to 115°.[5, 6]

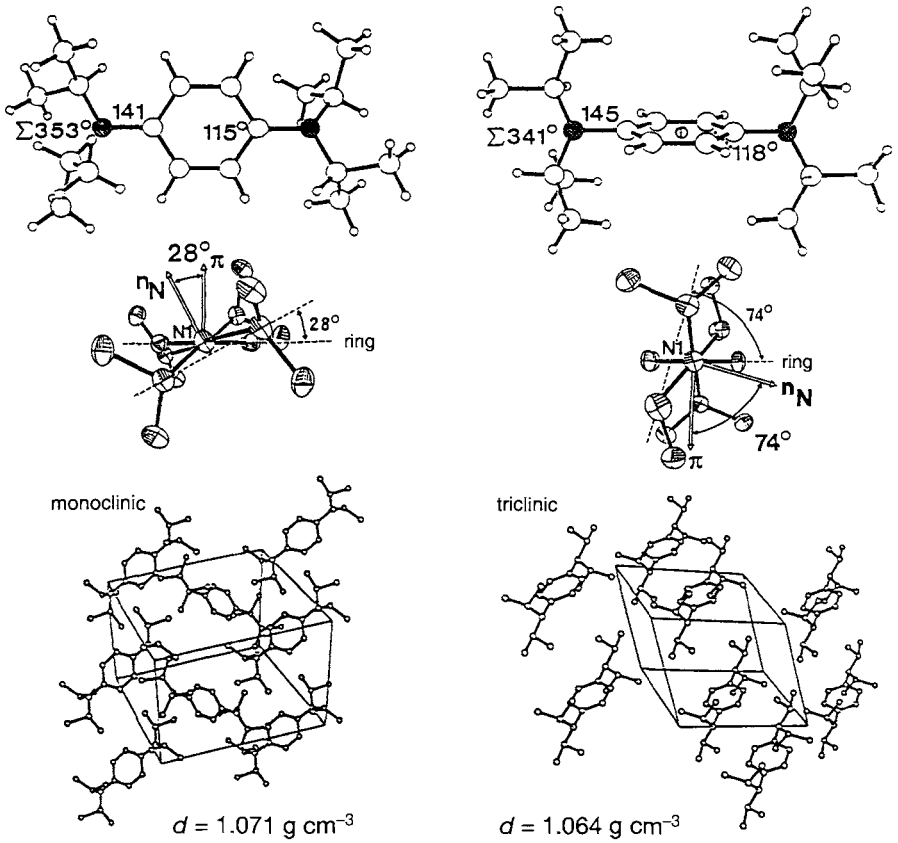

Fig. 1. Top and center: molecular structures of the tetraisopropyl-*p*-phenylenediamine conformers exhibiting skeletal symmetry C_1 and C_i in side and axial view (50% thermal ellipsoids) [3]. Significant differences between the monoclinic and triclinic conformers (bond lengths in pm and angles in °): dihedral angles $\omega(C_2N-C_6)$ 28/74, distances d_{CN} 141/145, angles α_{ipso}(ring) 115/118, and angle sums $\Sigma(\sphericalangle CNC)$ 353/341. Bottom: lattice packing in the polymorphic monoclinic ($P2_1/c$, unit cell with $Z = 4$ in x direction) [3a] and triclinic modifications ($P\bar{1}$, unit cell with $Z = 1$ in x direction and arrangement of the molecule around a crystallographic inversion center) [3b].

The molecular dynamics has been approached first for the spatially not yet overcrowded tetramethyl derivative by PM3 enthalpy hypersurface calculations (Scheme 1). For an assumed uncoupled rotation and inversion, rotation with a barrier of only 16 kJ mol^{-1} should be favored and, therefore, activated at room temperature (o: transition states). The enthalpy surface for the tetramethyl derivative (Scheme 1) reproduces all structural trends observed for the tetraisopropyl-*p*-phenylendiamine conformers (Fig. 1 top and center): the n_N/π delocalization, which sets in with the decrease of the dihedral angle $\omega = 90° \rightarrow 0°$, flattens the NC_3 pyramids, shortens the NC_{ring} bonds, and reduces the *ipso* ring angles.

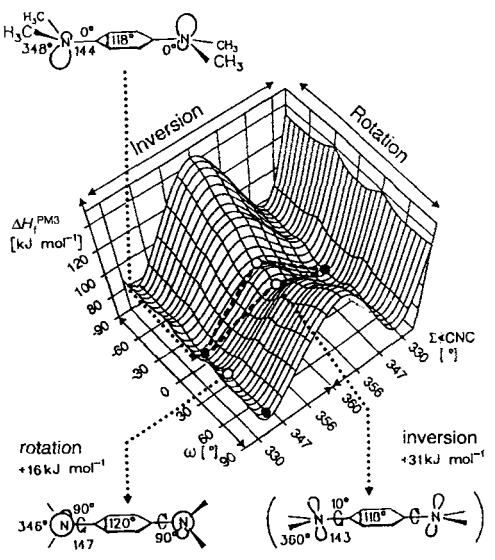

Scheme 1.

According to analogous PM3 calculations, in tetraisopropyl-*p*-phenylendiamine a complete rotation of the bulky $[(H_3C)_2HC]_2N$ substituents around the NC_{ring} bonds is no longer possible because of steric hindrance from the *ortho* ring hydrogens (van der Waals radius $r_H^{vdW} \approx 120$ pm[6]) without deformation of the isopropyl groups, which can be calculated on geometry optimization. An analysis of the wave functions for the resulting conformer set[7] shows that the maximum possible stabilization by n_N/π delocalization of about -15 kJ mol^{-1} at a dihedral angle of $\omega = 0°$ is compensated on increased twisting of ω to 90° by a fourfold H/H repulsion of a total of up to 16 kJ mol^{-1} (Scheme 2). This is in accord with the almost identical enthalpies of formation for the rather different monoclinic and triclinic crystalline conformers of tetraisopropyl-*p*-phenylenediamine, $\Delta H_f^{PM3} = -46$ and -47 kJ mol^{-1} (Scheme 2), calculated based on the experimental molecular structure data (Fig. 1).

The repulsive H/H interactions are in accord with the crystal structure data for both polymorphs (Fig. 1 top and center): In the monoclinic modification, the shortest intramolecular H···H distances amount to only 200 and 221 pm (rest > 323 pm) in contrast to 254 and 296 pm (rest > 359 pm) in the triclinic one. The almost identical en-

thalpies of formation, ΔH_f^{PM3} are in addition an essential precondition for the crystallization of polymorphic modifications, the lattice energies of which usually differ only by $< 20\ kJ\ mol^{-1}$.[1a, b, f]

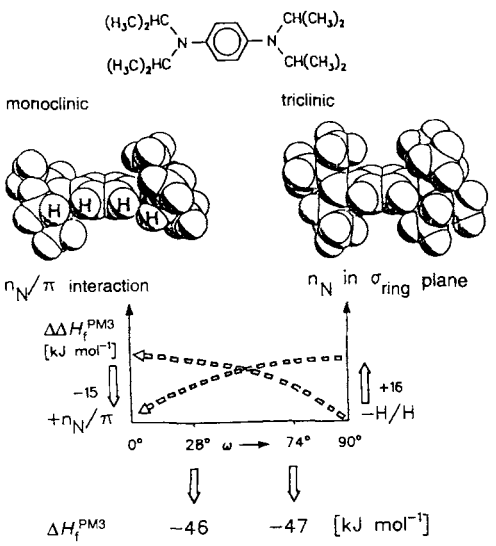

Scheme 2.

The lattice energies of nondisordered polymorphic modifications, according to an often successfully tested empirical rule,[8] can be correlated with their crystallographically determined densities. Therefore, the monoclinic crystals grown by sublimation with $\varrho = 1.071\ g\,cm^{-3}$[3a] should possess a more negative lattice energy that the triclinic ones crystallized from petroleum ether solution $\varrho = 1.064\ g\,cm^{-3}$.[3b] In the monoclinic crystal, the n_N/π interacting conformers are packed crosswise with shortest intermolecular H···H distances of 242 pm (Fig. 1 bottom left), whereas in the triclinic crystal the n_N/σ-planarized ones are stacked perpendicularly to the aligned molecular long axes with shortest intermolecular H···H distances of 240 pm (Fig. 1 bottom right). Because their difference in densities of only 0.7% borders on the precision of measurement, in addition total lattice energies have been calculated by the atom/atom potential approximation[9a] from a parameter set[9b] that recently has been optimized for a large data base of organic molecular crystals, by using either the crystallographically determined torsion angles of all methyl groups or by imposing a constant value of 60°.[10] The two resulting lattice (sublimation) energies for each of the modifications of tetraisopropyl-*p*-phenylenediamine are -115.5 or $-114.7\ kJ\,mol^{-1}$ (monoclinic) and -108.8 or $-109.4\ kJ\,mol^{-1}$ (triclinic) and indicate that, as inferred from the rather small density difference, the monoclinic modification should always be the thermodynamically more stable one, irrespective of the selected methyl group torsion angles.

The monoclinic crystals have been grown by slow vacuum sublimation of the triclinic melt over a period of about one week,[3a] whereas the triclinic ones crystallize "in a flash" (within a few minutes) from the saturated petroleum ether solution. The band pattern at low ionization energies in the photoelectron spectrum[2] and its agreement with the superposed PM 3 eigenvalue sequences for the different tetraisopropyl-*p*-phenylenediamine conformers exhibiting comparable PM 3 enthalpies of formation (Scheme 2) suggests a rotamer mixture in the gas phase as well as in solution at room temperature. Possibly, therefore, the thermodynamically based Oswald's step rule[11] should be supplemented—if surface effects could be excluded in the growth of the monoclinic crystals by vacuum sublimation—with a kinetic component: The monoclinic modification, which is more stable according to both its density and the lattice energy calculation, must have been formed by slow crystallization from the gaseous rotamer mixture and the somewhat less favored triclinic one possibly by a kinetically controlled rapid growth from solution. This speculative assumption further illustrates the subtle energy balance that enables the isolation of two rather dissimilar conformers of tetraisopropyl-*p*-phenylenediamine by crystallization in different local total energy minima.

Received: February 13th, 1993 [Z 5869 IE]
German version: *Angew. Chem.* **1993**, *105*, 1823

[1] Summaries a) J. Bernstein, (Conformational polymorphism) in *Organic Solid State Chemistry, Studies in Organic Chemistry Vol. 32* (Ed.: G. R. Desiraju), Elsevier, Amsterdam, **1987**, pp. 471–517 and 146 references therein; b) G. R. Desiraju in *Crystal Engineering* (*Mater. Sci. Monogr.* **1989**, *54*, 285–301; c) J. D. Dunitz, in *X-Ray Analysis and the Structure of Organic Molecules*, Cornell University Press, Ithaca, **1979**, p. 321 ff. Further recommended reading: d) M. Egli, J. D. Wallis, J. D. Dunitz, *Helv. Chim. Acta* **1986**, *69*, *225* (seven conformers of 1-dimethylamino-8-nitronaphthalene in three polymorphic modifications); e) I. Bar, J. Bernstein, *Tetrahedron* **1987**, *43*, 1299 and references therein (poly- and isomorphic *p*-substituted benzylideneanilines); f) J. Bernstein, J. A. R. P. Sarma, A. Gavezzotti, *Chem. Phys. Lett.* **1990**, *174*, 361 (lattice energy calculations for monoclinic and orthorhombic modifications of benzene, naphthalene, and anthracene); g) S. K. Burley, G. A. Petsko, *Science* **1985**, *229*, 23 (stabilizing interactions between unsaturated rings in proteins).

[2] I. Göbel, Ph.D. thesis, University of Frankfurt, **1993**; contains all details of the investigations: Tetraisopropyl-*p*-phenylenediamine was prepared by heating of *p*-phenylenediamine with a threefold excess of 2,2-dimethoxypropane in acetone/acetic acid in presence of Pt_x/Al_2O_3 under a pressure of 100 bar H_2 in an autoclave (A. Gaydash, J. T. Arrigo, US-A 3 234 281, **1966**; *Chem. Abstr.* **1966**, *64*, 11 125 h). Fractional distillation at 10^{-2} mbar yielded about 20% yield of a yellow oil from which at 277 K a clorless solid with m.p. 308 K crystallized (correct elemental analysis; ^1H NMR ($DCCl_3$, TMS) δ: 1.09–1.20 (d, 24H), 3.4–3.9 (m, 4H); *m/e* = 276 (M^+), 261 ($M^+ - CH_3$), 246 ($M^+ - 2CH_3$), 233 ($M^+ - CH(CH_3)_2$), 218 ($M^+ - CH_3 - CH(CH_3)_2$, 203 ($M^+ - 2CH_3 - CH(CH_3)_2$). Crystal growth: 200 mg was dissolved in 5 mL petroleum ether at 20 °C, the solvent evaporated at 20 °C and 10^{-2} mbar until crystallization began, and the oily solution kept in a refrigerator at 277 K. Under petroleum ether the triclinic modification crystallized. After evaporation almost to dryness, the monoclinic modification recrystallized at the glass wall, but it can be better synthesized by sublimation of a melt of the triclinic modification at 10^{-2} mbar to a cooler glass wall. All crystalline products were characterized by an X-ray determination of the unit cell; the polymorphic modifications were unexpectedly discovered on selection of crystals with an optimum reflection profile from different crystallizations. Differential scanning calorimetry investigations of the polymorphic modifications by slow warming (1 K/min) of a melt at 110 K to 320 K did not indicate any solid phase transitions. Investigations with photoelectron spectroscopy in the gas phase [4] showed two broad ionization bands between 6 and 9.4 eV; the peak of the first one begins at 6.6 eV, increases slowly to the maximum at 7.83 eV and dros steeply to 8.1 eV; that of the second one increases steeply from 8.2 eV to a double maximum at 8.64 and 8.92 eV and then drops slowly to about 9.6 eV. Band analysis based on MNDO eigenvalue correlation suggests the assignmet $(n_N\text{-}\pi_s) < \pi_{as} < (\pi_s\text{-}n_N)$ and can be rationalized by assuming different propotions of the doubly twisted (dihedral angle $\omega(C_2N\text{–}C_6) \approx 80°$, $\Delta IE_{1,2} \approx 0.8$ eV), the singly twisted ($\omega_1 \approx 80°$, $\omega_2 \approx 10°$, $\Delta IE_{1,2} \approx 2$ eV), and the planarized ($\omega \approx 10°$, $\Delta IE_{1,2} \approx 2{,}9$ eV) conformers in a mixture.

[3] Crystal structures $C_{18}H_{32}N_2$ (276.46): a) Monoclinic modification: a = 1014.8(1), b = 1236.9(1), c = 1415.4(1) pm, β = 105.18(1)°, V = 1714.62 × 10^6 pm^3 (150 K), $Z = 4$, $\varrho_{calcd} = 1.071\ g\,cm^{-3}$, $\mu = 0.06\ mm^{-1}$, monoclinic, space group $P2_1/c$ (no. 14), Siemens AED-II four-cirlce diffractometer, $Mo_{K\alpha}$ radiation, 5988 measured reflections with $3° < 2\theta < 53°$, of which 3502 are independent and 2619 with $I > 1\sigma(I)$, $R_{int} = 0.0238$. Structure

solution by direct method and difference Fourier technique (SHELXTL-Plus); $R = 0.0474$, $R_w = 0.0435$ for 310 parameters, $w = 1/(\sigma^2(F) + 0.0003F^2)$; GOF: 4.616, shift/error < 0.001; extinction correction, residual electron density: +0.23/−0.21 $e_o/Å^3$. All C and N atoms are anisotropically refined, all H atoms are unconditionally refined with isotropic temperature factors. b) Triclinic modification: $a = 698.2(2)$, $b = 746.3(2)$, $c = 970.5(4)$ pm, $\alpha = 70.77(2)$, $\beta = 87.25(2)$, $\gamma = 65.35(2)°$, $V = 431.58 \times 10^6$ pm^3 (150 K), $Z = 1$, $\varrho_{calcd} = 1.064$ g cm^{-3}, $\mu = 0.06$ mm^{-1}, triclinic, space group $P\bar{1}$ (no. 2), Siemens-AED four-circle diffractometer, $Mo_{K\alpha}$ radiation, 2550 measured reflections within $3° < 2\theta < 55°$, of which 1983 are independet and 1950 with $I > 0.5\,\sigma(I)$, $R_{int} = 0.0143$. Structure solution with direct methods and difference Fourier technique (SHELXTL-Plus); $R = 0.0432$, $R_w = 0.0451$ for 156 parameters, $w = 1/(\sigma^2(F) + 0.00002F^2)$; GOF: 4.93, shift/error < 0.001; extinction corrections; residual electron density: +0.27/−0.21 $e_o/Å^3$. All C and N atoms anisotropically, all H atoms unconditionally refined with isotropic temperature factors. The molecule is centered at a crystallographic inversion center. Further details of the crystal structure investigation may be obtained from the Fachinformationszentrum Karlsruhe, Gesellschaft für wissenschaftlich-technische Information mbH, D-76344 Eggenstein-Leopoldshafen (FRG) on quoting the depository number CSD-57768, the names of the authors and the journal citation.

[4] Additional investigations on conformers of *p*-phenylenediamine derivatives that like the benzylidenanilines [1a, 3] exhibit two energetically favored rotational degrees of freedom around both of the $N-C_{ring}$ bonds concern inter alia *N,N'*-bis(trimethylsily)- and tetrakis(trimethylsily)phenylenediamines (H. Bock, J. Meuret, C. Näther, *Tetrahedron Lett.* **1993**, *34*, in press.). The tetrasubstituted molecule can be reduced in ether solution to its blue radical anion(!)—in addition to the usual oxidation to Wurster's Blue radical cation (F. Gerson, U. Krynitz, H. Bock, *Angew. Chem.* **1969**, *81*, 786, *Angew. Chem. Int. Ed. Engl.* **1969**, *8*, 767). This surprising discovery can be rationalized from the different band patterns at low ionization energies of PE spectra and their assignment by Koopman's correlation with eigenvalues from geometry-optimized AM1 calculations, by assuming that the disubstituted derivative must possess an approximately planar skeleton $SiN-C_6H_4-NSi$, whereas the tetrasubstituted one should exhibit dihedral angles $\omega(Si_2N-C_6) \approx 90°$. Single crystal structures confirm the gas phase measurements: contrary to the situation in the largely planar *N,N'*-substituted derivative, the steric overcrowding by four bulky $(H_3C)_3Si$ substituents causes the H/H repulsion from the *ortho*-ring hydrogens to exceed the stabilizing n_N/π interactions, which results in a dihedral angle $\omega(Si_2N-C_6) = 83°$.

[5] Cf., for example, a) M. Kaftory in *Acyclic Organonitrogen Stereodyn.* 263; b) A. Domenicano, A. Vaciago, *Acta Crystallogr. Sect. B* **1979**, *35*, 1382; A. Hoekstra, A. Vos, *ibid.* **1975**, 1716, 1722.

[6] H. Bock, K. Ruppert, C. Näther, Z. Havlas, H.-F. Herrmann, C. Arad, I. Göbel, A. John, J. Meuret, S. Nick, A. Rauschenbach, W. Seitz, T. Vaupel, B. Solouki, *Angew. Chem.* **1992**, *104*, 565–595; *Angew. Chem. Int. Ed. Engl.* **1992**, *31*, 550–581 and references therein.

[7] The PM 3 potential energy surface calculations (J. J. P. Stewart, *J. Comput. Chem.*, **1989**, *10*, 209, 221) have been performed based on the experimental structural data [3] and partly geometry optimized (tetramethyl derivative) using the program version MOPAC 6.0/QCPE no. 455 with an IBM RISC 6000/320. Additional data (cf. Scheme 1): Inversion transition state $\Delta H_f^{PM3} = 104$ kJ mol^{-1}, $d_{CN} = 147$, $d_{CC} = 138$, 140 pm, $\sphericalangle CCC = 121°$; conformer ($\omega = 0°$) $\Delta H_f^{PM3} = 73$ kJ mol^{-1}, $d_{CN} = 148$, $d_{CC} = 139$, 140 pm, $\sphericalangle CCC = 121°$; conformer ($w = 90°$) $\Delta H_f^{PM3} = 87$ kJ mol^{-1}, $d_{CN} = 149$, $d_{CC} = 139$, 140 pm, $\sphericalangle CCC = 120°$. Estimate of the H···H repulsion between isopropyl groups and H_{ortho} (cf. Scheme 2): $\Delta\Delta H_f^{PM3}$ (kJ mol^{-1})/$d_{H\cdots H}$ (pm): 0/277, 1/250, 2.5/222, 6/195, 9.5/170, 22/149, 36/135.

[8] Cf., for example, I. Bar, J. Bernstein, *J. Phys. Chem.* **1984**, *88*, 243 and references therein.

[9] a) Summary/Survey: A. J. Pertsin, A. I. Kitaigorodsky, *The Atom-Atom Potential Method*, Springer, Berlin, **1987**; b) G. Filippini, A. Gavezzotti, *Acta Crystallogr. Sect. B* **1993**, *49*, 868 (optimized parameter set for approximate atom/atom-potential calculations of lattice (sublimation) energies).

[10] The H positions were readjusted by setting all CH bond lengths to 108 pm and, partly, by inserting torsional angles of 60° for all methyl groups. The potential is defined as an intermolecular one, and no corrections for the intramolecular energy differences have been made. Additional lattice vibration calculations yielded reasonable lattice vibration frequencies.

[11] Cf. the summary N. N. Sirota, in *Cryst. Res. Technol.* **1987**, *22*, 1343–1381.

aci-Nitrodiphenylmethane: A Hydrogen-Bonded Dimer**

By *Hans Bock**, *Rüdiger Dienelt*, *Holger Schödel*, *Zdenek Havlas*, *Eberhardt Herdtweck*, and *Wolfgang A. Herrmann*

Dedicated to Professor Helmut Schwarz on the occasion of his 50th birthday

A recent report[2] offered a summary on the nitro ⇄ *aci*-nitro tautomerism for prototype nitromethane as well as predictions from highly correlated calculations, which largely reproduce the known experimental data sketched in Scheme 1.

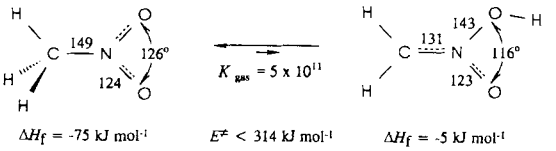

Scheme 1.

The thermally forbidden[1, 3] H transfer has a prohibitively high barrier $E^{\neq}$, and a gas-phase equilibrium constant of 5×10^{11}, which can be estimated from the difference in the enthalpies of formation $\Delta\Delta H_f$ of 70 kJ mol^{-1}, overwhelmingly favors the nitro tautomer.[2] The tautomerization should predominantly shorten the CN bond length and close the ONO angle. However, consideration of potential aggregation through hydrogen bonding, which was previously neglected, as well as a CSD search that revealed that the compounds containing *C*-phenyl and *C,C*-diphenyl-*O*-(*t*-butyl)dimethylsilyl groups are the only structurally characterized covalent *aci*-nitromethane derivatives prompted further investigations.[3] We now report on the successful crystal growth[4] of the title compound, prepared from nitrodiphenylmethane (Scheme 2) and characterized by structure determination at both 163 and 238 K[5] (Fig. 1).

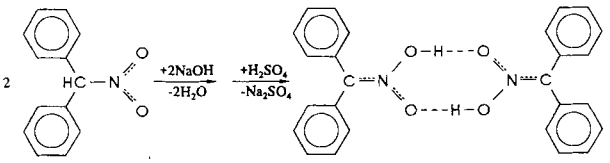

Scheme 2.

The *aci*-nitrodiphenylmethane dimers are packed perfectly in the crystal lattice (Fig. 1 top). Obviously, this is favored by the chair conformation of the H-bonded eight-membered

[*] Prof. Dr. H. Bock, Dipl.-Chem. R. Dienelt, Dipl.-Chem. H. Schödel
Institut für Anorganische Chemie der Universität
Marie-Curie-Strasse 1, D-60439 Frankfurt am Main (FRG)
Dr. Z. Havlas
Institute for Organic Chemistry and Biochemistry
of the Czech Academy of Sciences
Flemingova Nam 2, CS-16610 Prague (Czech Republic)
Prof. Dr. W. A. Herrmann, Dr. E. Herdtweck
Institut für Anorganische Chemie der Technischen Universität München
Lichtenbergstrasse 4, D-85748 Garching (FRG)

[**] Interactions in Molecular Crystals, Part 33. This research project has been supported by the Deutsche Forschungsgemeinschaft, the State of Hesse, the Fonds der Chemischen Industrie, and the A. Messer Foundation. Part 32: Ref. [1].

ring $N(OHO)_2N$, exhibiting fold angles of 40° through the oxygen centers of the planar nitro groups. Accordingly, the phenyl rings in their Y-shaped arrangement stacked with parallel axes are packed so close that the distance between their centroids is about 500 pm. At this distance substantial, attractive $>CH\cdots\pi$ interactions are evident, for instance, in the folding of phenyl group containing proteins[6a] or in the "herringbone"-motif of crystallization of unsaturated six-membered ring hydrocarbons.[6b]

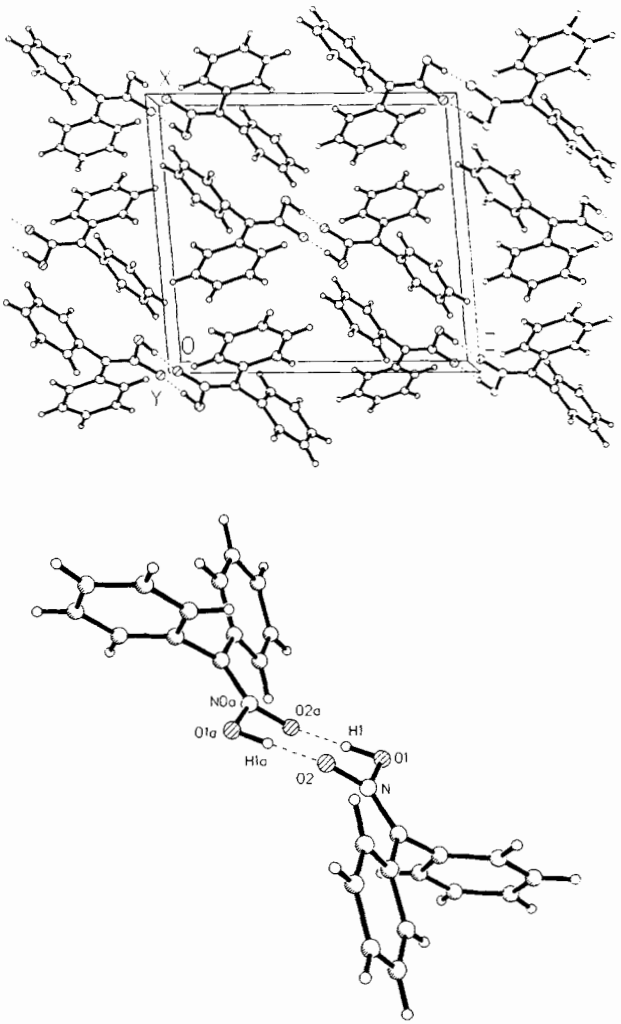

Fig. 1. Single crystal structure of the *aci*-nitrodiphenylmethane dimer at 163 K. Top: unit cell (monoclinic, $Z = 4$, $\varrho_{calc} = 1.324\ g\,cm^{-3}$) viewed along the y direction. Bottom: side view of the chair conformation of the H-bonded pair. Essential distances (pm) and angles (°): C···N 130, N···O 138, O–H 97, O(H)···O 261, C···N···O 127, C···N–O 118, O···N–O 115, O(H)O 172, φ(CC–CN) 24° and 67°, $\tilde{\omega}$ ($C_2C=NO_2$) 4°.

The hydrogen bonds are relatively short (261 pm between the O centers),[7] unsymmetrical (uncorrected distances O–H 97 pm and O···H 164 pm) and slightly bent (172°) (Fig. 1). The NO distances, ···N···O···(H) and ···N–O(H) of 130 and 138 pm are different as expected and comparable to those in the *C,C*-diphenyl-*O*-trialkylsilyl derivative (127 and 140 pm) and in part considerably stretched relative to nitroalkanes (*aci*-nitromethane:[2] N···O 123 pm). Moreover, the ONO angles are reduced by 10° as predicted in Scheme 1. The largest change (more than 20 pm) is observed for the bond shortening C–N → C···N (Scheme 1 and [3]), which accompanies the planarization of the tetrahedral methane C center.

Additional ab initio calculations (cf. Scheme 1) with a uniform 6-31G** basis set[8] have been performed on the *aci*-nitromethane tautomers (Fig. 2). Geometry optimization yields a total energy minimum structure[8] for the dimer with a doubly folded eight-membered ring $N(OHO)_2N$, which agrees satisfactorily with the experimental structure determined for the diphenyl derivative (Fig. 1 bottom). A rather small enthalpy difference of only 0.4 kJ mol^{-1} is calculated for the folding of the H-bonded ring at the O···O axes by 30°, which deviates from the usual planar arrangements in carbonic acid dimers $C(OHO)_2C$.[7] The chair conformation $N(OHO)_2N$, therefore, should be predominantly determined by the CH···π interactions between the phenyl rings in the monoclinic lattice[6] (Fig. 1 top). The H-bonded pair $N(OHO)_2N$ can be rationalized by a symmetrical double minimum potential[8] with a barrier of only 12 kJ mol^{-1} (Fig. 2). The cooperative effect on its formation, $2\,OH\cdots O \rightarrow (OH\cdots O)_2$, should amount to a considerable 40% according to the PM3 enthalpy difference of $\Delta\Delta H_f = 2(-11) - (-36) = 14$ kJ mol^{-1}, and therefore play an essential role in the stabilization of the *aci*-dimer relative to nitromethane by a total of $2 \times 71 - 73 = 69$ kJ mol^{-1} (Fig. 2).

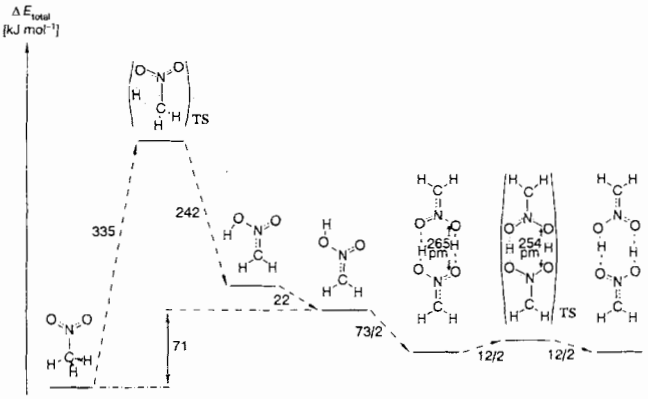

Fig. 2. Ab initio energy profile for the tautomerization of nitromethane to *anti*- and *syn-aci*-nitromethane and its H-bonded dimer.

The extremely high tautomerization barrier of the ab initio energy profile (Fig. 2) also demonstrates, why *aci*-nitro compounds can be obtained, in general, only by acidification of their salts (Scheme 2). The *aci*-nitrodiphenylmethane dimer prepared this way is also a remarkable example both for the stabilization of a thermodynamically unfavorable tautomer by H-bonded pairs,[9] as well as for molecular self-organization by their cooperative effect.[1]

Experimental Procedure[4]

Sodium methyldiphenylnitronate: 65% HNO_3 (20 mL), H_2O (80 mL), and diphenylmethane (20 mL, 0.12 mol) were mixed in a 250 mL flask and heated for 15 h at 108 °C under reflux. After cooling, the reaction solution was extracted with diethyl ether (3 × 50 mL). The combined ether phase was washed three times with H_2O (20 mL portions), cooled to 0 °C after separating from the aqueous layer, and poured slowly into a stirred solution of 33% NaOH (50 mL) cooled at 0 °C. During the strongly exothermic reaction a white amorphous precipitate formed, was filtered off, washed three times with *n*-hexane, and dried at 10^{-2} mbar; yield 20.04 g (53.6 mmol, 78%); ^1H NMR (D_2O): $\delta = 7.3-7.5$ (m,H).

aci-Nitrodiphenylmethane: Sodium methyldiphenylnitronate (0.5 g, 2.1 mmol) was dissolved in H_2O (25 mL), cooled with ice, and acidified while stirring with

5% H_2SO_4 to pH 2. The white solid with a pink luster, which precipitated immediately was filtered off at 10 mbar, washed three times with 25 mL portions of ice water, three times with 25 mL portions of *n*-hexane, and dried for 3 h at 5×10^{-3} mbar. Yield: 0.25 g (1.2 mmol, 57%). M.p. 93 °C (decomp.). ^{1}H NMR [$(D_5C_2)_2O$]: $\delta = 7.2-7.6$ (m, 10H), 4.35 (s, OHO). IR(film): $\nu = 3400\ cm^{-1}$ (hydrogen bonds), $3000\ cm^{-1}$ (C–H), $1650\ cm^{-1}$ (C=N), 1550, $1450\ cm^{-1}$ (C=C), $1300\ cm^{-1}$ (C=N). Single crystal growth: *aci*-Nitrodiphenylmethane, precipitated by acidification of the nitronate, was dissolved in diethyl ether (20 mL) and dried at 273 K by stirring for 2 h with Na_2SO_4. After filtration, the ether solution was concentrated at 273 K by slow evaporation until colorless plates crystallized, which have to be stored at 0 °C under argon and aprotic ($c_{H_2O} < 1$ ppm) *n*-hexane because of their temperature- and moisture-sensitivity.

Received: May 27, 1993 [Z 6110 IE]
German version: *Angew. Chem.* **1993**, *105*, 1826

[1] H. Bock, *Jahrb. Dtsch. Akad. Naturforsch. Leopoldina* **1993**, *38*, 221–233.

[2] K. Lammertsma, B. V. Prasad (*J. Am. Chem. Soc.* **1993**, *115*, 2348) summarize, in addition, the chemical and biological importance of nitronic acids, both the X-ray and the neutron diffraction structures of solid H_3CNO_2, and its microwave gas-phase structure, and the gas-phase detection of *aci*-nitromethane (cf. H. Egsgaard, L. Carlsen, H. Florencio, T. Drewello, H. Schwarz, *Ber. Bunsenges. Phys. Chem.* **1989**, *93*, 76). The experimentally determined rotational barrier in nitromethane is below 25 J mol^{-1} (!); for the barrier between *E* and *Z* conformers of *aci*-nitromethane, 28 kJ mol^{-1} are calculated. For ab initio calculations cf. also M. L. McKee, *J. Phys. Chem.* **1986**, *90*, 369 and references therein.

[3] E. W. Colvin, A. K. Beck, B. Bastani, D. Seebach, Y. Kai, J. D. Dunitz, *Helv. Chim. Acta* **1980**, *63*, 697. Selected structural data for the diphenyl derivative (pm und °): C=N 131, N=O 127, N–O 140, C=N=O 130, C=N–O 115, O=N–O 115, NOSi 119. For comparison, the gas-phase structure of 2-nitromethane (F. Shishkov, N. I. Sadova, L. V. Vilkev, Y. A. Panktushev, *Zh. Strukt. Khim. (engl.)* **1983**, *24*, 189) is quoted: C–N 152, N=O 123, C–N=O 117, C=N=O 125, $\bar{\omega}$(ON–CC) 18.

[4] R. Dienelt, Master's thesis, University of Frankfurt, **1993**. *aci*-Nitrodiphenylmethane ("diphenylmethylnitronic acid") was first prepared 1893 by acidification of the aqueous solution of the potassium salt with diluted sulfuric acid (M. Konowalow, *Ber. Dtsch. Chem. Ges.* **1896**, *29*, 2193; cf. also A. Hantzsch, O. W. Schulze *ibid.* **1896**, *29*, 863). For a survey of other isolated *aci*-nitro compounds cf. D. Döpp, H. Döpp in *Houben/Weyl Methoden der Organischen Chemie*, 4th edition, Vol. X, Thieme, Stuttgart, **1990**, p. 780 ff. and references therein.

[5] Crystal structure determinations of $C_{13}H_{11}NO_2)_2$. $M_r = 426.4$: crystal dimensions $0.41 \times 0.66 \times 0.51$ mm, $T = 163 \pm 5$ K and 238 ± 2 K [values in brackets]: $a = 1140.2(1)$ [1144.8(1)], $b = 739.84(3)$ [743.54(3)], $c = 1273.1(1)$ [1277.3(1)] pm, $\beta = 94.969(4)$ [94.815(4)]°, $V = 1069.6(6) \times 10^6$ [1083.4(6) $\times 10^6$] pm^3, $Z = 4$, $\varrho_{calcd} = 1.324$ [1.307] g cm^{-3}, $\mu(Cu_{K\alpha}) = 154.2$ pm, monoclinic, space group $P2_1/n$ (no. 14), Enraf-Nonius CAD4 four-circle diffractometr, 2282 [2097] measured reflections within $1° < \theta < 70°$ [65], of which 1884 [1704] are independent with $I > 0.01$. Structure solutions by direct methods (SHELXS), $N = 1884$ [1704], $NP = 189$ [190], $R = 0.045$ [0.047], $R_w = 0.041$, $\omega = 1/\sigma^2(F_0)$, residual electron density $+0.20/-0.19$ [$+0.16/-0.19$] $e_0 A^{-3}$, GF = 4.639 [4.335] ($p = 0.00$). C,N,O centers anisotropically refined, H isotropically refined. The H-bonded dimer is positioned around a crystallographic symmetry center. The differences observed at the two temperatures are the change of the dihedral angle of the phenyl rings relative to the plane C-NO1(O2) by 0.6° and of the distances O–(H)···O by 7 pm; only the low temperature structure determination is discussed. Further details of the crystal structure investigation are available from the Fachinformationszentrum Karlsruhe, Gesellschaft für wissenschaftlich-technische Information mbH, D-76344 Eggenstein-Leopoldshafen (FRG) on quoting the deposit number CSD-57805, the authors and the journal citation.

[6] Cf. a) S. K. Burley, G. A. Petsko, *Science* **1985**, *229*, 23; C. A. Hunter, J. Singh, J. M. Thornton, *J. Mol. Biol.* **1991**, *218*, 837; b) G. R. Desiraju, A. Gavezzotti, *Acta Crystallogr. Sect. B.* **1989**, *45*, 473.

[7] Cf., for example, A. F. Wells, *Structural Inorganic Chemistry*, Clarendon, Oxford, **1987**, p. 367 ff and references therein, or J. Emsley, *Chem. Soc. Rev.* **1980**, *9*, 41 and references therein. Hydrogen bonds O(H)···O with interoxygen distances between 240 and 260 pm are considered strong: examples $(N\text{-}O\cdots H\cdots O\text{-}N)_2$ in Ni(II)diacetyldioxime, 241 pm; $(RO_2P(O\cdots H\cdots O)_2P(OR_2)$, 249 pm. In contrast, the O···O distance in the benzoic acid dimer exhibiting a planar eight-membered ring $H_5C_6\text{-}CO(O\cdots H\cdots O_2)OC\text{-}C_6H_5$ are only 263 pm long (G. Bruno, L. Randaccio, *Acta Crystallogr. Sect. B.* **1980**, *36*, 1711).

[8] The ab initio calculations for nitromethane have been performed with the program GAMESS (M. W. Schmidt, J. A. Boatz, K. K. Baldridge, S. Koseki, M. S. Gordon, S. T. Elbert, B. Lam, *QCPE Bulletin* **1987**, *7*, 115). All minima and saddle points are confirmed by second derivatives and exhibit none or only one negative eigenvalue of the Hessian matrix. Selected results for H-bonded, dimeric *aci*-nitromethane: structure (bond lengths in pm, angles in °): $E_{total} = -487.30736$ a.u., C=N 129, N=O 129, N–O 136, O(H)···O 265, O–H 97, H···O 167, C=N=O 126, C=N–O 117, O=N–O 117, O(H)O 173. Charge distribution: C −0.12, N +0.44, O −0.61, O(H) −0.46, H(O) +0.38. The *aci*-nitrodiphenylmethane dimer has been calculated from the data by PM3 (J. J. Stewart, *J. Comput. Chem.* **1989**, *10*, 209, 221; version MOPAC 6), and the cooperative effect has been estimated by turning one molecular half around one of the O(H)O hydrogen bonds [9b]; for ΔH_f values, see text.

[9] Cf. a) H. Bock, T. Vaupel, C. Näther, K. Ruppert, Z. Havlas, *Angew. Chem.* **1992**, *104*, 348; *Angew. Chem. Int. Ed. Engl.* **1992**, *31*, 299 and references therein; b) H. Bock, W. Seitz, Z. Havlas, J. W. Bats, *ibid.* **1993**, *105*, 410 and **1993**, *32*, 411 and references therein.

Elimination of the Barrier to Cope Rearrangement in Semibullvalene by Li^+ Complexation**

By *Haijun Jiao* and *Paul von Ragué Schleyer**

Substituents that reduce or eliminate the already quite small barrier to valence isomerization (Cope rearrangement) in semibullvalene have been sought in many theoretical[1] and experimental[2] studies. Based on extended Hückel calculations, Hoffmann et al.[1a] predicted that the barrier can be lowered by π-donor substituents at C1,5 and π-acceptors at C2,4,6,8. Similar conclusions were reached both by Dewar et al.[1b,c] and by Dannenberg et al.,[1d] who employed semiempirical methods (MINDO/2, AM1, and MNDO-CI). The transition state for the rearrangement might even be stabilized by substituents to such an extent that the "bishomoaromatic" symmetric structure **1b** would become more stable than the classical structure **1a**!

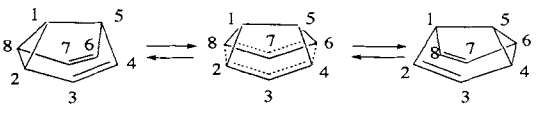

The isomerization barriers of many substituted semibullvalenes have now been measured using dynamic ^{13}C NMR spectroscopy,[2] particularly by Quast et al. The lowest measured barrier is approximately 4.5 kcal mol^{-1} for 1,5-dimethylsemibullvalene, but the barrier actually increases with some substituents, for example, to roughly 10 kcal mol^{-1} for 3,7-dicyano-2,6-dimethoxy-1,5-dimethylsemibullvalene. We now describe a new strategy which might eliminate the barrier to the Cope rearrangement in semibullvalene. According to ab initio calculations, complexation of a Li^+ ion stabilizes **1b** more effectively than **1a**. The evidence from our computations establishes that the transition state **1b** does have bishomoaromatic character.

Geometries were fully optimized first at the RHF/6-31G* level using the Gaussian 92 program package.[3] The stationary points were characterized as minima or saddle points by calculation of the vibrational frequencies. The geometries

[*] Prof. Dr. P. von R. Schleyer, Dipl.-Chem. H. Jiao
Institut für Organische Chemie der Universität Erlangen-Nürnberg
Henkestrasse 42, D-91054 Erlangen (FRG)
Telefax: Int. code + (9131)85-9132

[**] This work was supported by the Fonds der Chemischen Industrie, the Convex Computer Corporation, and the Deutsche Forschungsgemeinschaft. We also thank Prof. Dr. H. Quast, Würzburg (FRG), for his helpful suggestions and the Shanxi Normal University (People's Republic of China) for a scholarship (to H. J.).

were then refined at the correlated RMP2(full)/6-31G*[4] level. Our final relative energies (Table 1) were computed at RMP2(full)/6-31G* + ZPE (i.e. with zero-point energy correction, RHF/6-31G*, scaled by 0.89).[3] Atomic charges

Table 1. Calculated total energies [a.u.], zero-point energies (ZPE) [kcal mol^{-1}], the number and values of the imaginary frequencies [cm^{-1}], and the activation enthalpy $\Delta H^{\neq}$ [kcal mol^{-1}] of semibullvalene **1a**, the transition structure for the Cope rearrangement **1b**, and their Li^+ complexes **2a** and **2b**, respectively.

	Symmetry	ZPE [a]	RMP2(full)/6-31G*	$\Delta H^{\neq}$ [b]
1a	C_s	80.9/(0)	−308.57882	0.0
1b	C_{2v}	79.7/(1, −606)	−308.57052	4.1
2a	C_s	82.1/(0)	−315.89057	0.0
2b	C_{2v}	81.3/(1, −427)	−315.89040	−0.7 [c]
Li^+			−7.23594	

[a] RHF/6-31G* value, scaled by 0.89; in parentheses: number and value of imaginary frequencies. [b] Relative energies [RMP2(full)/6-31G* + ZPE (RHF/6-31G*)]. [c] See ref. [14].

and bond orders, derived from the natural population analysis of Reed et al.,[5] characterize the ground and transition states (Tables 2 and 3). The chemical shifts of Li^+ in **2a** and **2b** were computed using the IGLO (Individual Gauge for Localized Orbitals) method[6] employing the DZ basis sets[7] and the RMP2(full)/6-31G* geometries.

Table 2. NPA charges [a] (see text).

Atoms	**1a**	**1b**	**2a**	**2b**
C3,C7	−0.225	−0.263	−0.393	−0.408
C2,C8	−0.264	−0.224	−0.293	0.217
C4,C6	−0.206	−0.224	−0.163	−0.217
C1	−0.288	−0.251	−0.293	−0.259
C5	−0.214	−0.251	−0.203	−0.259
Li	-	-	+0.959	+0.947

[a] RMP2(full)/6-31G* geometries were used.

Table 3. Wiberg bond indexes [a] (see text).

Bond	**1a**	**1b**	**2a**	**2b**
C3-C4	1.874	1.453	1.785	1.442
C7-C8	1.066	1.453	1.114	1.442
C1-C2	0.968	0.990	0.973	0.991
C5-C4	0.993	0.990	0.995	0.991
C2-C8	0.875	0.368	0.790	0.370
C1-C5	0.998	0.984	0.986	0.984
C3-C7	0.023	0.056	0.040	0.059
C4-C6	0.046	0.368	0.093	0.370

[a] RMP2(full)/6-31G* geometries were used.

Possible mechanisms of the prototypical degenerate Cope rearrangement in 1,5-hexadiene have been investigated experimentally[2, 8] and theoretically.[1, 9–11] Because of the constrictions of the polycyclic structure, the Cope rearrangement in semibullvalene must take place via a boatlike transition state. This is facilitated by the proximity of C4 and C6.

The RMP2(full)/6-31G* optimized structural parameters for C_s semibullvalene **1a** are shown in Figure 1. The optimized bond lengths agree with those obtained by electron diffraction (values given in parentheses in Fig. 1, top[12]). The elongation of the C2–C8 bond (to ca. 1.60 Å) is noteworthy. The Wiberg bond orders for **1a** (Table 3) indicate a largely localized structure, except for the C2–C8 bond.

Transition structure **1b** (C_{2v}, Fig. 1 bottom) has one imaginary frequency (− 606 cm^{-1}). The calculated activation enthalpies, 5.2 kcal mol^{-1} at RMP2(full)/6-31G* and 4.1 kcal mol^{-1} with the RHF/6-31G* zero-point energy correction, agree well with the measured value of 4.8 ± 0.2 kcal mol^{-1}.[2] The separation of 2.036 Å and bond order of 0.368 for C2–C8 and C4–C6 in **1b** show that this transition structure may indeed be designated as homoconjugated.[1] The bond orders of 1.453 and bond lengths of 1.391 Å for the delocalized, allyl-like bonds in **1b** are close to those in the allyl radical, anion, and cation as well as in benzene and many homoaromatic systems.[13]

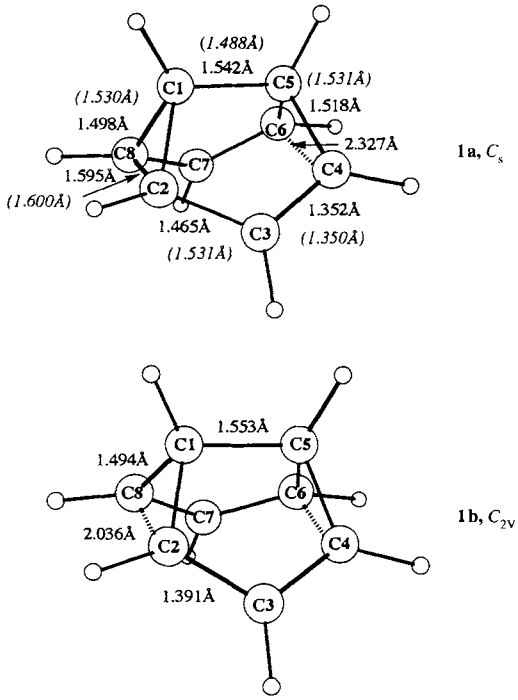

Fig. 1. The RMP2(full)/6-31G* optimized structures for the ground state of semibullvalene **1a** and the rearrangement transition state **1b**.

The effects of Li^+ complexation of **1a** and **1b** are remarkable! Although the C_s-symmetric structure **2a** (MP2(full)/6-31G*) (Fig. 2 top) is a minimum, the C_{2v} structure **2b** (Fig. 2 bottom) is only 0.1 kcal mol^{-1} less stable at this level! The C2–C8 bond length in **2a** increases to 1.711 Å (from 1.595 Å in **1a**); the corresponding bond orders, 0.790 in **2a** and 0.875 in **1a**, reflect this difference. The changes due to Li^+ complexation in the lengths of the other C–C bonds involved in the rearrangement of **1a** are smaller, but also point to the more delocalized character of the electron system of **2a**. C3,7 and C2,8 are more negatively charged and C4,6 more positive in **2a** than in **1a**. Li^+ complexation polarizes **2a** and results in a partially delocalized structure.

The C–C bond orders in the Li^+ complexed transition structure **2b** are nearly the same as in **1b**. The Li^+ ion has a charge of 0.959 in **2a** and 0.947 in **2b**. The binding of Li^+ is largely electrostatic and involves polarization of the π-electron systems. The Li^+ complexation energies for **2a** and **2b**, −47.6 and −52.7 kcal mol^{-1}, respectively, are even somewhat larger than that for benzene (− 44.8 kcal mol^{-1}, RMP2(full)/6-31G*). (This is due to the shorter Li–C3,7

distances in **2a** and **2b** than the corresponding distance in the Li^+–benzene complex (2.371 Å)).

Note that Li^+ complexes the transition state **1b** to a greater extent than semibullvalene **1a**. This essentially eliminates the activation barrier even before correction for the zero-point energies. When this ZPE correction is applied, the computed energy for **2b** at 0 K is 0.7 kcal mol^{-1} lower than for **2a**![14] The bishomoaromatic **2b** is indicated to be more stable than **2a** (Table 1). This result, which has long been sought by the introduction of substituents, is achieved by Li^+ complexation (at least at the level of theory employed here).

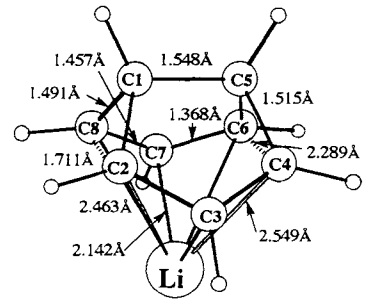

2a, C_s

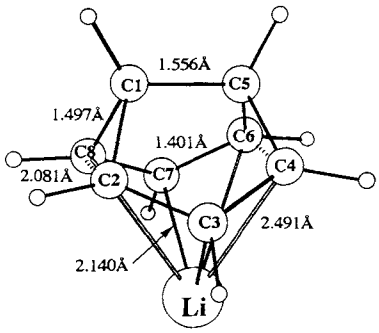

2b, C_{2v}

Fig. 2. The RMP2(full)/6-31G* optimized structures for the Li^+ complexes **2a** and **2b**.

The presence of a Li^+ ion in **2a** and **2b** affords a means of assessing the "aromaticity" of these species. Normally, lithium NMR chemical shifts have a small range (δ = ca. ± 2 relative to the standard) $\delta(Li^+)$ used as a reference in calculations). The most conspicuous experimental exceptions have been noted for lithium cyclopentadienide and its derivatives, as well as Li^+ π-complexed aromatic compounds.[15] The large shieldings observed are attributed to ring current effects (although this conclusion may be premature). IGLO chemical shift computations provide a convenient means of assessing the influence of various complexed π systems on Li NMR chemical shifts. It does appear from the data gathered in Table 4 that $\delta(Li^+)$ can be employed as an aromaticity probe.

The homoaromaticity of **2b** and the partial homoaromaticity in **2a** are indicated by the upfield chemical shifts, $\delta(Li^+) = -10.8$ and -5.7, respectively [$\sigma(Li^+) = 95.4$, $\sigma(Li^+[\mathbf{2b}] = 106.2$ and $\sigma(Li^+[\mathbf{2a}]) = 101.1$, IGLO/DZ//RMP2(full)/6-31G*]. For comparison, the computed Li NMR shifts are $\delta = -7.4$ for the C_{6v} Li^+–benzene complex, -6.9 for cyclopentadienyllithium, and -10.8 for the biscyclopentadienyllithium anion.[15] In contrast, the influence on $\delta(Li^+)$ by complexation with ethene, ethyne, and even allyl anion is much less, and the antiaromatic cyclobutadiene produces a downfield shift (Table 4).

Table 4. Absolute lithium shielding constants (σ) and chemical shifts (δ, relative to $Li^+ \equiv 0.0$) calculated by the IGLO method (IGLO/DZ//RMP2(full)/6-31G*) [a].

Complex	Point group	σ	δ
Li^+	K_h	95.4	0.0
Li^+–C_4H_4 (cyclobutadiene)	C_{2v}	92.3	+3.1
Li^+–$C_3H_5^-$ (allyl anion)	C_s	95.5	−0.1
Li^+–C_4H_6 (*cis*-1,3-butadiene)	C_s	96.9	−1.5
Li^+–HC≡CH	C_{2v}	97.2	−1.8
Li^+–H_2C=CH_2	C_{2v}	97.3	−1.9
2a	C_s	101.1	−5.7
Li^+–$C_5H_5^-$ (Cp^-)	C_{5v}	102.3	−6.9 [b]
Li^+ C_6H_6 (benzene)	C_{6v}	102.8	−7.4
2b	C_{2v}	106.2	−10.8
$LiCp_2^-$	D_{5d}	106.2	−10.8 [b]

[a] For additional data see ref. [5c]. [b] See ref. [15].

The very low activation enthalpy of 4.1 kcal mol^{-1} [RMP2(full)/6-31G* + ZPE(RHF/6-31G*)] for the degenerate Cope rearrangement of semibullvalene can be eliminated by Li^+ complexation. The C_{2v} delocalized bishomoaromatic structure **2b** is computed to be slightly more stable than the unsymmetrical form **2a**, but even the latter shows pronounced delocalization. The Li^+ ion stabilizes the more polarizable C_{2v} transition state to a greater extent than the C_s. We find such electrostatic acceleration of electrocyclic process to be general, and will report further examples subsequently. The aromaticity of **2b** is reflected by its geometry and population analysis, as well as the upfield chemical shift of Li^+ due to ring current effects. The partial delocalization of **2a** also is apparent from the same criteria.

Received: June 2, 1993 [Z 6119 IE]
German version: *Angew. Chem.* **1993**, *105*, 1830

[1] a) R. Hoffmann, W. D. Stohrer, *J. Am. Chem. Soc.* **1971**, *93*, 6941–6948; b) M. J. S. Dewar, D. H. Lo, *ibid.* **1971**, *93*, 7201–7207; c) M. J. S. Dewar, C. Jie, *Tetrahedron* **1988**, *44*, 1351–1358; d) L. S. Miller, K. Grohmann, J. J. Dannenberg, *J. Am. Chem. Soc.* **1983**, *105*, 6862–6865; e) K. N. Houk, Y. Li, J. D. Evanseck, *Angew. Chem.* **1992**, *104*, 711–739; *Angew. Chem. Int. Ed. Engl.* **1992**, *31*, 682–708; f) K. Bergmann, S. Görtler, J. Manz, H. Quast, *J. Am. Chem. Soc.* **1993**, *115*, 1490–1495.

[2] a) A. K. Cheng, F. A. L. Anet, J. Mioduski, J. Meinwald, *J. Am. Chem. Soc.* **1974**, *96*, 2887–2891; b) D. Moskau, R. Aydin, W. Leber, H. Günther, H. Quast, H. D. Martin, K. Hassenrück, L. S. Miller, K. Grohmann, *Chem. Ber.* **1989**, *122*, 925–931; c) H. Quast, J. Christ, E.-M. Peters, K. Peters, H. G. von Schnering, *ibid.* **1985**, *118*, 1154–1175; d) H. Quast, C. A. Klaubert, L. M. Jackman, A. J. Freyer, *ibid.* **1988**, *121*, 1081–1086; e) H. Quast, Y. Görlach, E.-M. Peters, K. Peters, H. von Schnering, L. M. Jackman, G. Ibar, A. J. Freyer, *ibid.* **1986**, *119*, 1801–1835; f) H. Quast, A. Mayer, E.-M. Peters, K. Peters, H. G. von Schnering, *ibid.* **1989**, *122*, 1291–1306; g) R. Iyengar, R. Pina, K. Grohmann, *J. Am. Chem. Soc.* **1988**, *110*, 2643–2644.

[3] GAUSSIAN 92, Revision B, M. J. Frisch, G. W. Trucks, M. Head-Gordon, P. M. W. Gill, M. W. Wong, J. B. Foresman, B. G. Johnson, H. B. Schlegel, M. A. Robb, E. S. Replogle, R. Gomperts, J. L. Andres, K. Raghavachari, J. S. Binkley, C. Gonzalez, R. L. Martin, D. J. Fox, D. J. Defrees, J. Baker, J. J. P. Stewart, J. A. Pople, Gaussian Inc., Pittsburgh, PA, USA, **1992**.

[4] W. J. Hehre, L. Radom, P. von R. Schleyer, J. A. Pople, *Ab Initio Molecular Orbital Theory*, Wiley, New York, **1986**.

[5] a) A. E. Reed, L. A. Curtiss, F. Weinhold, *Chem. Rev.* **1988**, *88*, 899–962; b) A. E. Reed, P. von R. Schleyer, *J. Am. Chem. Soc.* **1990**, *112*, 1434–1445.

[6] a) W. Kutzelnigg, *Isr. J. Chem.* **1980**, *19*, 193; b) M. Schindler, W. Kutzelnigg, *J. Chem. Phys.* **1982**, *76*, 1910; c) Review: W. Kutzelnigg, U. Fleischer, M. Schindler, *NMR: Basic Princ. Prog.* **1990**, *23*, 165.

[7] S. Huzinaga, *Gaussian Basis Sets for Molecular Calculations*, Elsevier, Amsterdam, **1984**.
[8] a) R. P. Lutz, *Chem. Rev.* **1984**, *84*, 205–247; b) W. von E. Doering, V. G. Toscano, G. H. Beasley, *Tetrahedron* **1971**, *27*, 5299–5306.
[9] M. J. S. Dewar, C. J. Jie, *J. Am. Chem. Soc.* **1987**, *109*, 5893–5900.
[10] M. Dupuis, C. Murray, E. R. Davidson, *J. Am. Chem. Soc.* **1991**, *113*, 9756–9756.
[11] For example: N. S. Isaacs, *Physical Organic Chemistry*, Wiley, New York, **1987**.
[12] a) Y. C. Wang, H. S. Bauer, *J. Am. Chem. Soc.* **1972**, *94*, 5651–5657; b) H. Quast, J. Carlsen, R. Janiak, E.-M. Peters, K. Peters, H. G. von Schnering, *Chem. Ber.* **1992**, *125*, 955–968.
[13] a) G. A. Olah, G. Asensio, H. Mayer, P. von R. Schleyer, *J. Am. Chem. Soc.* **1978**, *100*, 4347–4352; b) P. von R. Schleyer, *ibid.* **1985**, *107*, 4793–4794; c) P. von R. Schleyer, T. W. Bentley, W. Koch, A. J. Kos, H. Schwarz, *ibid.* **1987**, *109*, 6953–6957; d) P. Buzek, P. von R. Schleyer, S. Sieber, *Chem. Unserer Zeit* **1992**, *24*, 116–128.
[14] This means that there is only one set of vibrational states for the double-well potential, and that the lowest state is energetically above the barrier. We thank a referee for this clarification.
[15] L. A. Paquette, W. Bauer, M. R. Sivik, M. Bühl, M. Feigel, P. von R. Schleyer, *J. Am. Chem. Soc.* **1990**, *112*, 8776–8789, and references therein.

A Detailed Theoretical Analysis of the 1,7-Sigmatropic Hydrogen Shift: The Möbius Character of the Eight-Electron Transition Structure**

By *Haijun Jiao* and *Paul von Ragué Schleyer**

While the [1,5] sigmatropic hydrogen shift in a polyene is, according to the Woodward–Hoffmann rules, a thermally favored suprafacial isomerization involving six electrons, the eight-electron [1,7] hydrogen shift is an antarafacial sigmatropic rearrangement with a Möbius topology.[1] The first observed [1,7] H shift was the rearrangement of calciferol to precalciferol.[2] Theoretical studies of the [1,7] H shift[1b,3] have been less detailed than those for the [1,5] H shift.[1b,4,5] The first ab initio calculation of the [1,7] H shift was carried out by B. Hess et al.[3] with the 3-21G basis set. The transision state was found to have C_2 symmetry, but the computed activation energy of 44 kcal mol^{-1} was much higher than the experimentally observed values (ca. 15–20 kcal mol^{-1}).[6]

A direct kinetic investigation of the [1,7] H shift in the parent 1,3,5-heptatriene **1** was reported only recently by Y. N. Bubnov et al.[7] As the process is too slow to be measured by NMR line shape analysis, the rates of site exchange in a deuterium-labeled compound were determined by ^{2}H NMR spectroscopy over a temperature range of 75–116 °C. The rate constant was described by the Arrhenius equation: $k_H = 1.6 \times 10^8 \exp[-(20.8 \pm 0.7)\,\text{kcal mol}^{-1}/RT]\,\text{s}^{-1}$. The Russian group noted that both the activation energy and the frequency factor were lower than those measured for [1,5] H shifts ($E_a = 24.3 \pm 0.5$ kcal mol^{-1} and $A = 1.3 \times 10^{12}$ s^{-1} for cyclopentadiene; $E_a = 35.6 \pm 0.5$ kcal mol^{-1} and $A = 2.8 \times 10^{11}$ for 1,3-pentadiene).[8]

We now provide a detailed theoretical analysis of the [1,7] H shift prototype in 1,3,5-heptatriene **1**. Ground and transition state geometries of 1,3,5-heptatriene, **1** and **2**, respectively (Fig. 1), were fully optimized first at the RHF/6-31G* and then at the correlated RMP2(full)/6-31G* levels employing the Gaussian 92 program package.[9] RHF/6-31G*

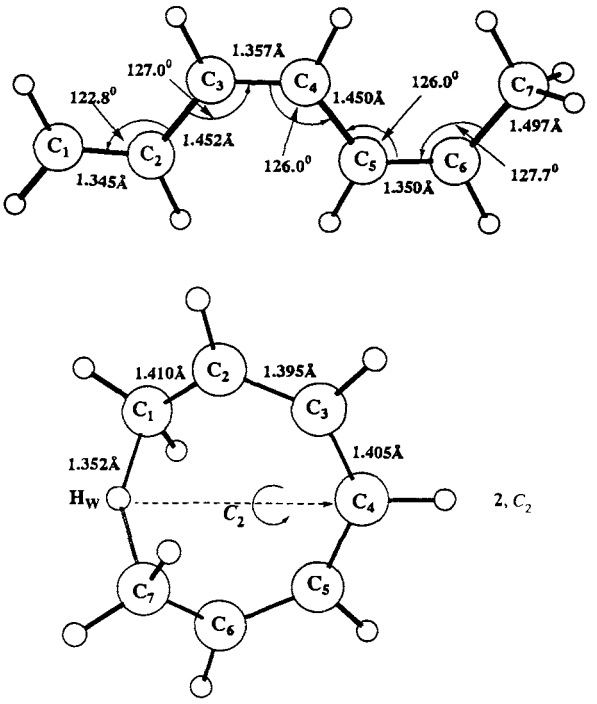

Fig. 1. The RMP2(full)/6-31G* optimized ground state structure of (*Z*,*Z*)-1,3,5-heptatriene (**1**, top) and the 1,7 H shift transition structure **2** (bottom).

frequency calculations established the nature of each stationary point and provided the thermochemical data, for example, the thermal energies E_{Th} (including zero-point energy, vibrational, transitional, and rotational energies) and entropies. The final activation enthalpy ($\Delta H^{\neq}$) and the activation energy ($E_a = \Delta H^{\neq} + RT$)[10] were computed at the RMP2(full)/6-31G* level by addition of ΔE_{Th} (RHF/6-31G*) scaled by 0.89 at 400 K[11] (Table 1).

Table 1. Experimental [7] and calculated [a] activation parameters for the [1,7] H shift in (*Z*,*Z*)-1,3-5-heptatriene (**1**) at 400 K, and for the [1,5] H shift in cyclopentadiene (CPD) and 1,3-pentadiene (PD) (measured values in parentheses).

	E_a [kcal mol^{-1}] [b]	A [c]	$\Delta S^{\neq}$ [d]
1,7 shift in **1**	19.7 (20.8 ± 0.7)	97.7×10^8 (1.6×10^8)	−13.4 (−21.6)
1,5 shift in CPD [e]	25.2 (24.3 ± 0.5)	7.9×10^{12} (1.3×10^{12})	−0.2 (−3.3)
1,5 shift in PD [e]	35.4 (36.3 ± 10^{11})	1.6×10^{11} (2.8×10^{11})	−8.4 (−7.1)

[a] Total energies [a.u.] for the ground state (**1**), −271.76233; the transition state (**2**), −271.72672, and for the isomer with two *trans* double bonds, −271.76775 RMP2(full)/6-31G*). These values were adjusted by the RHF/6-31G* zero-point energies, scaled by 0.89 (88.4 and 86.5 kcal mol^{-1} for **1** and **2**, respectively), and by thermal energies at 400 K [10]. [b] $E_a = \Delta H^{\neq} + RT$. [c] Frequency factor [s^{-1}]. [d] The computed absolute entropies [cal mol^{-1} K^{-1}] are 97.3 for **1** and 83.9 for **2** at 400 K. [e] See ref. [5] (at the same level of theory) and ref. [8].

The optimized (RMP2(full)/6-31G*) transition structure **2** (one imaginary frequency, −2200 cm^{-1}) is helical (C_2 symmetry, Fig. 1 bottom).[3] The C_2 axis is defined by the migrating hydrogen atom, H_w, and the C4 carbon atom. The C1–C7 distance is 2.600 Å, and the W_w–C1 and H_w–C7 bond lengths are 1.352 Å. In accord with Woodward–Hoffmann rules for such an allowed process, the transition structure

[*] Prof. Dr. P. von R. Schleyer, Dipl.-Chem. H. Jiao
Institut für Organische Chemie
der Universität Erlangen-Nürnberg
Henkestrasse 42, D-91054 Erlangen (FRG)
Telefax: Int. code + (9131)85-9132

[**] This work was supported by the Fonds der Deutschen Industrie, the Deutsche Forschungsgemeinschaft, and the Convex Computer Corporation. We also thank Prof. Dr. W. Kutzelnigg, and Dr. U. Fleischer, Bochum (FRG), and Dr. A. Dorigo, Erlangen, for suggestions and helpful discussions. H. J. thanks the Shanxi Normal University (People's Republic of China) for a scholarship.

can be termed aromatic, since the C–C bond lengths (ca. 1.40 Å) are nearly equal and comparable to that in benzene (1.395 Å, also at RMP2(full)/6-31G*). Thus, the geometric criterion of aromaticity[12] is fulfilled.

The magnetic criterion of aromaticity[12] is based on ring current effects, in other words, on the downfield shifts of the outer protons produced by a diamagnetic ring current in a planar $(4n + 2)$ π electron annulene. While *eight* delocalized electrons are involved in **2**, this transition structure has a Möbius, rather than a Hückel topology.[12] What is to be expected in such an unusual case?

Although NMR chemical shifts of transition states cannot be measured, they can be computed easily by the IGLO[14] (Individual Gauge for Localized Orbitals) method. The vinylic hydrogens H1–6 in the ground state structure **1** have IGLO shifts δ (^{1}H) in the range $\delta = 5.0$–6.4 (Table 2). But in the transition structure **2** the calculated δ(^{1}H) values for H2–6 are shifted by $\Delta\delta \approx 1$ to $\delta = 6.3$–6.9 which is very close to the calculated value in benzene (δ (^{1}H) = 7.0; 7.1 is the experimental value in the gas phase). The migrating H_w atom is computed to have a shift of $\delta = 1.9$. The shifts of the two protons at C1 and C7 are revealing. The equatorial protons H1 and H7 are computed to have a chemical shift of $\delta = 5.6$, while the axial protons H1 and H7 have a strong upfield shift of $\delta = -4.6$. The axial protons in **2** (H1 and H7) point toward the center of the carbon skeleton (Fig. 1) and experience a strong ring current (Table 2).

Pauling[15a] noted in 1936 that aromatic compounds exhibit enhanced magnetic susceptibility. This criterion of aromaticity,[15b–e] attributed to the presence of a diamagnetic ring current, applies well to transition structure **2**. The calculated isotropic susceptibility is -71.7 ppm cgs for **1** and -95.1 ppm cgs for **2**. Most of the difference (23.4 ppm cgs) results from the change in the diamagnetic contribution (17.1 ppm cgs). The paramagnetic (1.3 ppm cgs) and nonlocal contributions (3.8 ppm cgs) change little. The calculated diamagnetic exaltation of 17.1 ppm cgs also points to the considerable aromaticity in **2**. For benzene a value of 13.7 ppm cgs is derived from experimental data[15b] and 15.4 ppm cgs from IGLO calculations.[15e] In agreement with this interpretation, the change in the calculated out-of-plane component of χ from **1** to **2** (-65.9 ppm cgs) is much larger than the change in the in-plane component (-2.2 ppm cgs).

The differences in the ^{1}H chemical shifts are not caused by differences in the charges on the hydrogen atoms. According to natural population analysis (NPA),[13] the charges of *all* hydrogen in the transition structure **2** are nearly the same (0.22–0.24) and differ very little form those in the ground state structure **1**. The migrating H_w atom (+0.24) in **2** has almost the same charge as that of the corresponding hydrogen in **1** (+0.22). In comparison, the charge on H_w is +0.36 in the transition structure and +0.23 in the ground state structure.[5] Thus, H_w is more proton-like in the [1,5] H shift transition structure but resembles a "normal" hydrogen atom in the [1,7] H shift transition structure in (*Z*,*Z*)-1,3-5-heptatriene.

Since transition structure for the [1,7] H shift is helix-shaped and chiral, the corresponding ground state structure also might be helical. For this reason we chose a starting geometry for 1,3,5-heptatriene that resembled **2**, but the optimization led to the planar C_s (*Z*,*Z*) isomer **1**. This configuration agrees with that deduced from the ^{1}H NMR spectrum.[7] While (*Z*,*Z*)-1,3,5-heptatriene (**1**) is a minimum on the potential energy surface, the most stable 1,3,5-heptatriene isomer has two *trans* double bonds and is 3.4 kcal mol^{-1} (RMP2(full)/6-31G*) more stable than **1**. But this planar (*E*,*E*) isomer would not lead directly to the transition structure **2**.

The calculated activation energy (E_a) [RMP2(full)/6-31G* energy + 0.89 × E_{Th} (RHF/6-31G*) + RT (400 K)] is 19.7 kcal mol^{-1} (Table 1) and agrees well with the measured value of 20.8 ± 0.7 kcal mol^{-1}.[7] Thus, the barrier for the [1,7] H shift is lower than that for the [1,5] H shifts in cyclopentadiene (25.2 kcal mol^{-1})[5] and in 1,3-pentadiene (35.4 kcal mol^{-1}),[1b,4] although the ground state structure **1** is not helix-shaped and the migrating hydrogen atom H_w at C7 is very far from C1. The barrier for the [1,7] H shift is lower on account of the greater flexibility of 1,3,5-heptatriene, which permits the transition state to have better orbital overlap and to be reached with less distortion energy that in the [1,5] H shift systems.[1b] The experimental frequency factor of **1** (1.6×10^8 s^{-1}) is much lower than those for the [1,5] H shifts in cyclopentadiene (1.3×10^{12} s^{-1}) and 1,3-pentadiene (2.8×10^{11} s^{-1}), which can be explained by the loss of more degrees of freedom during cyclization of larger acyclic systems. For example, the entropy loss on cyclization of 1-pentene to give cyclopentane ($\Delta S = -12.7$ cal mol^{-1} K^{-1}) is smaller than that for cyclization of 1-heptene to give cyclopheptane ($\Delta S = -19.4$ cal mol^{-1} K^{-1}).[16] The calculated frequency factor for the [1,7] H shift (97.7×10^8 s^{-1}) is 61-fold greater than that measured, whereas the calculated frequency factors for the [1,5] H shifts in cyclopentadiene (7.9×10^{12} s^{-1}) and in 1,3-pentadiene (1.6×10^{11} s^{-1}) are very close to the measured values (Table 1). Considering the uncertainties inherent in rate measurements and in the determination of activation parameters, our computed values are in reasonable agreement. It should also be noted that our theoretical level, dictated by the size of the system, is not particularly high.

Our computed results for the [1,7] H shift confirm the predictions of Woodward and Hoffmann and are in agreement with the experimental results. The allowed antarafacial [1,7] H shift has an exceptionally large energy of concert (ca. 60.0 kcal mol^{-1}) relative to the alternative, stepwise, diradical mechanism.[17] The eight-electron Möbius transition

Table 2. IGLO calculated ^{1}H NMR chemical shifts for the ground state structure of (*Z*,*Z*)-1,3,5-heptatriene (**1**) and for the [1,7] H shift transition structure **2** (IGLO/BII//RMP2(full)/6-31G*; IGLO/DZ values given in parentheses) [14].

	δ(^{1}H)							
	C1-H	C2-H	C3-H	C4-H	C5-H	C6-H	C7-H	H_w
1	5.1, 5.0	6.4	5.6	5.9	5.8	5.3	0.9, 1.6	
	(6.5, 6.9)	(7.3)	(6.6)	(6.8)	(6.9)	(6.9)	(0.7, 1.2)	
exp. [a]	5.2, 5.1	6.9	6.0	6.3	6.5	5.5	1.7 [d]	
2	5.6 [b]	6.3	6.6	6.9	6.6	6.3	5.6 [b]	1.9 [d]
	(6.2)	(8.8)	(8.1)	(9.0)	(8.1)	(8.8)	(6.2)	(−2.5)
	−4.6 (−5.5) [c]						−4.6 (−5.5) [c]	

[a] See ref. [7]. [b] Equatorial H1 and H7. [c] Axial H1 and H7. [d] Average value.

structure **2** manifests diamagnetic ring current effects: the outer protons are deshielded and the inner shielded. According to the energetic geometrical, and magnetic criteria, the [1,7] H shift transition structure has pronounced aromatic character.

Received: June 15, 1993 [Z 6142 IE]
German version: *Angew. Chem.* **1993**, *105*, 1833

[1] a) R. B. Woodward, R. Hoffmann, *Angew. Chem.* **1969**, *81*, 797–870; *Angew. Chem. Int. Ed. Engl.* **1969**, *8*, 781–860; b) K. N. Houk, Y. Li, J. D. Evanseck, *ibid.* **1992**, *104*, 711–739 and **1992**, *31*, 682–708.
[2] E. Havinga, J. L. M. A. Schlachtmann, *Tetrahedron* **1961**, *16*, 146–152.
[3] B. A. Hess, L. J. Schaad, J. Pancir, *J. Am. Chem. Soc.* **1985**, *107*, 149–154.
[4] a) N. G. Rondan, K. N. Houk, *Tetrahedron Lett.* **1984**, *24*, 2519–2522; b) F. Jensen, K. N. Houk, *J. Am. Chem. Soc.* **1987**, *109*, 3139–3140.
[5] H. Jiao, P. von R. Schleyer, unpublished.
[6] C. W. Spangler, *Chem. Rev.* **1976**, *76*, 187–217.
[7] M. E. Gurskii, I. D. Gridnev, Y. V. Il'ichev, A. V. Ignatenko, Y. N. Bubnov, *Angew. Chem.* **1992**, *104*, 762–764; *Angew. Chem. Int. Ed. Engl.* **1992**, *31*, 781–783.
[8] a) W. R. Roth, *Tetrahedron Lett.* **1964**, 1009–1013; b) W. R. Roth, J. König, *Justus Liebigs Ann. Chem.* **1966**, *699*, 24–32.
[9] GAUSSIAN 92, Revision B, M. J. Frisch, G. W. Trucks, M. Head-Gordon, P. M. W. Gill, M. W. Wong, J. B. Foresman, B. G. Johnson, H. B. Schlegel, M. A. Robb, E. S. Replogle, R. Gomperts, J. L. Andres, K. Raghavachari, J. S. Binkley, C. Gonzalez, R. L. Martin, D. J. Fox, D. J. Defrees, J. Baker, J. J. P. Stewart, J. A. Pople, Gaussian Inc., Pittsburgh, PA, USA, **1992**.
[10] N. S. Isaacs, *Physical Organic Chemistry*, Wiley, New York, **1987**.
[11] W. J. Hehre, L. Radom, P. von R. Schleyer, J. A. Pople, *Ab Initio Molecular Orbital Theory*, Wiley, New York, **1986**.
[12] P. J. Garratt, *Aromaticity*, Wiley, New York, **1986**, Chapter 11, p. 52.
[13] a) A. E. Reed, L. A. Curtiss, F. Weinhold, *Chem. Rev.* **1988**, *88*, 899–962; b) A. E. Reed, P. von R. Schleyer, *J. Am. Chem. Soc.* **1990**, *122*, 1434–1445.
[14] For the IGLO method and its applications, see: W. Kutzelnigg, M. Schindler, U. Fleischer, *NMR, Basic Princ. Prog.* **1990**, *23*, p. 165.
[15] a) L. Pauling, *J. Chem. Phys.* **1936**, *4*, 763; b) H. J. Dauben, Jr., J. D. Wilson, J. L. Laity, *J. Am. Chem. Soc.* **1968**, *90*, 811–813; *ibid.* **1969**, *91*, 1991–1998; c) J.-F. Labarre, F. Crasnier, *Top. Curr. Chem.* **1971**, *24*, 37–38; d) R. C. Haddon, V. R. Haddon, L. M. Jackman, *ibid.* **1971**, *16*, 122–123; e) U. Fleischer, W. Kutzelnigg, unpublished.
[16] D. R. Stull, E. F. Westrum, Jr., G. C. Sinke, *The Chemical Thermodynamics of Organic Compounds*, Wiley, New York, **1969**.
[17] The C1–H bond dissociation energy in **1** can be estimated from data given by Doering to be around 81 kcal mol^{-1}, see a) W. von E. Doering, K. Sorma, *J. Am. Chem. Soc.* **1992**, *114*, 6037–6043; b) W. von E. Doering, T. Kitagawa, *ibid.* **1991**, *113*, 4288–4297 and ref. [1b].

(*R*)- and (*S*)-4-Alkoxy-2-*tert*-butyl-2,5-dihydroimidazole-1-carboxylates—New Chiral Glycine Derivatives for Amino Acid Synthesis**

By *Stefan Blank* and *Dieter Seebach**

For the synthesis of nonproteinogenic α-amino acids there are several chiral glycine derivatives available having electrophilic, radical, or nucleophilic reactivity. Nearly all of them contain a chiral building block, an auxiliary incorporated in the synthesis that must be removed and recycled, discarded, or destroyed after use.[1] Schöllkopf's "bis-lactim ether" **A**, which is obtained from valine, is an example of these chiral glycine derivatives.[1,2] A different approach is chosen in the synthesis of the heterocyclic glycine derivatives **B**:[1,3] the enantiomers are separated by formation of diastereoisomeric salts or on chiral columns, and the undesired enantiomer is recycled.[4] A disadvantage in this case is the harsh conditions necessary for the hydrolysis, in particular of imidazolidinones (from **B**, X = NMe), to provide the free amino acids.[3,4]

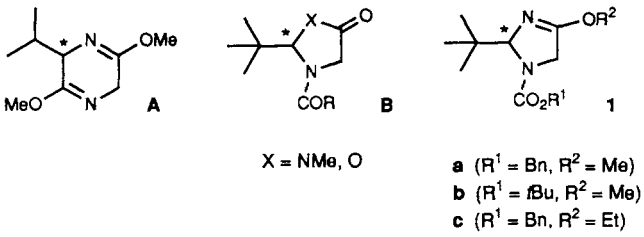

The (*R*)- and (*S*)-alkoxydihydroimidazolecarboxylates **1** we are now introducing combine all the advantages of previously employed reagents regarding accessibility of starting material, stability, reactivity, and selectivity of the Li derivative, as well as ease of hydrolysis. All preliminary experiments were performed on racemic materials.

The synthesis of the dihydroimidazoles is outlined in Scheme 1. Imidazolidinone **2** is prepared from commercial glycine amide hydrochloride following standard procedures.[4] The protective group is introduced, and the amide group is O-alkylated with Me_3OBF_4.

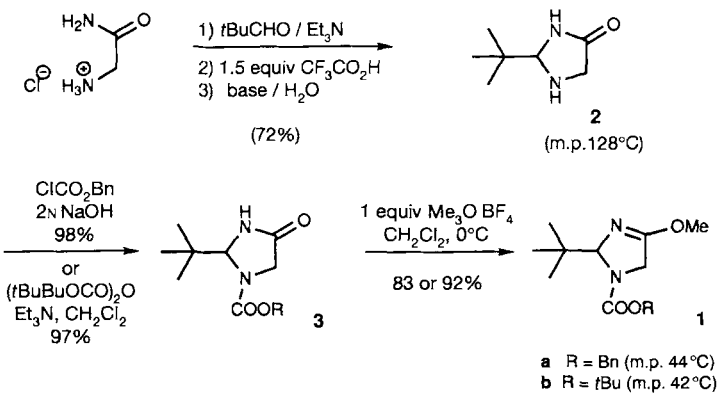

Scheme 1. Synthesis of benzyl and *tert*-butyl 2-*tert*-butyl-2,5-dihydro-4-methoxyimidazole-1-carboxylates (**1a**, **1b**).

The reactions carried out so far with Boc-protected dihydroimidazole **1b** are summarized in Scheme 2 and Table 1. Treatment of **1b** with lithium diisopropylamide (LDA) in THF at −78 °C provides enaminate **C** of the cyclic imidate, which reacts with alkyl halides in good yields (Table 1) and with such high selectivity (> 99:1) that a second diastereoisomer is not evident in the 300 MHz ^{1}H NMR spectrum of the crude product. The *trans* configuration of the products was proved by NOE (nuclear Overhauser effect) measurements and X-ray analysis (for **4f**). The reactions of lithium derivative **C** with isopropyl iodide (92%, **4d**) and *p*-nitrobenzyl bromide (30%, **4f**) are remarkable demonstrations of its high nucleophilicity. Second alkylations also proceed smoothly (→ **5**, **6**), as shown by the reaction of ethylated compound **4b** with isopropyl iodide (62% yield).[6] Finally Li-dihydroimidazole **C** adds to benzaldehyde (→ **7a**) and acetaldehyde (→ **7b**) giving mainly one out of four pos-

[*] Prof. Dr. D. Seebach, Dr. S. Blank
Laboratorium für Organische Chemie
der Eidgenössischen Technischen Hochschule
ETH-Zentrum, Universitätstrasse 16
CH-8092 Zürich (Switzerland)

[**] Part of the Ph.D. thesis of S. Blank, Dissertation No. 10193, ETH Zürich 1993. We gratefully acknowledge the German Fonds der Chemischen Industrie for a doctoral stipend for S. B.

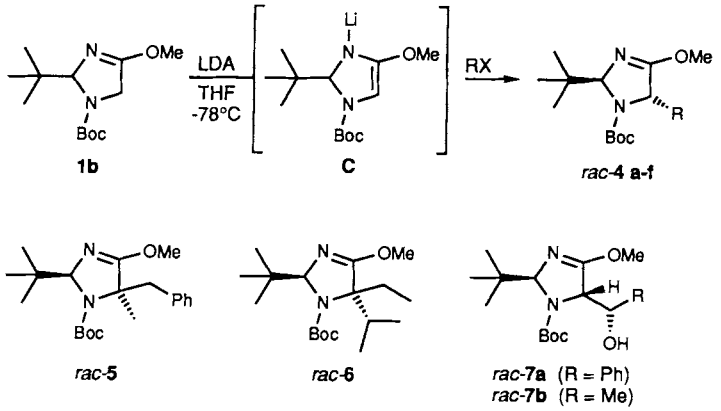

Scheme 2. Reactions of the glycine derivative **1b** with electrophiles (only one enantiomer shown). After addition of one equivalent of the electrophile the yellow solution of the Li compound C decolorizes. Boc = *tert*-butyloxycarbonyl. Compounds **4** are specified in Table 1.

sible stereoisomers (35:1 and 7.6:1, respectively, according to NMR analysis). Again the depicted products having *trans* configuration are formed; the hydrolysis product of **7b** correlates to *allo*-threonine. Similar results are obtained when Z-protected alkoxydihydroimidazoles **1a** and **1c** are used (Z = benzyloxycarbonyl).

Table 1. Alkylation of **1b** with alkyl halides. Only one diastereomer is formed according to analysis by NMR spectroscopy. The yields given refer to chromatographically purified (SiO_2, pentane/ether) samples

Prod.	RX	Yield [%]	Prod.	RX	Yield [%]
4a	CH_3I	99	**4e**	$PhCH_2Br$	81
4b	CH_3CH_2I	92	**4f**	O_2N-$C_6H_4CH_2Br$	30
4c	$H_2C{=}CHCH_2Br$	93	**5** [a]	CH_3I	98
4d	$(CH_3)_2CHI$	92	**6** [b]	$(CH_3)_2CHI$	62

[a] Prepared from **4e**. [b] Prepared from **4b**.

As expected, hydrolysis of the dihydroimidazoles to give α-amino acid methyl esters is very easy (Scheme 3) and provides pure products directly, as evidenced by NMR spectroscopy. The mild hydrolysis conditions employed should allow for the synthesis of many sensitive amino acid derivatives previously not accessible to us,[3,4] for example those containing double bonds, three-membered rings, and other acid-labile groups in the side chain, as well as racemization-prone aryl glycines.

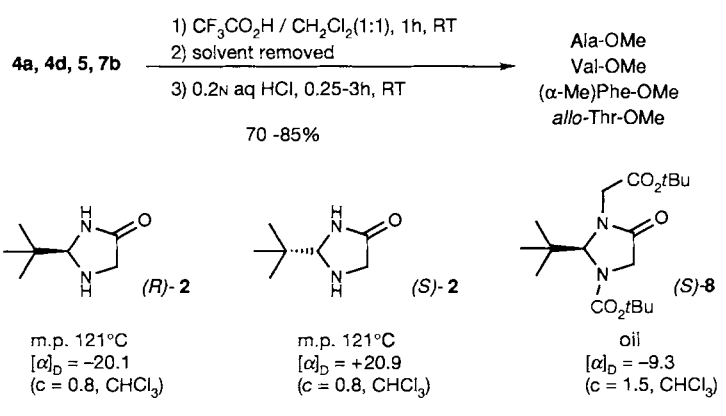

Scheme 3. Transformation of dihydroimidazoles **4a,d**, **5**, and **7b** to provide α-amino acid methyl esters.

For the preparation of enantiomerically pure alkoxydihydroimidazoles **1a** and **1b**, the enantiomers of the stable imidazolidinone **2** were separated by crystallization of their diastereoisomeric salts. Camphorsulfonic acid (CSA), available in both enantiomeric forms,[7a] turns out so far to be best suited for this.[7b] A preliminary experiment using enantiomerically enriched (*S*)-**1b**[7c] (87% *ee*) gave the L-valine methyl ester after isopropylation and hydrolysis with 81% *ee*. Further investigations with enantiomerically pure material are currently in progress.

Since the imidazolidinones **2** and **3** are readily available, we now have a route to the glycyl glycine building block **8** in enantiomerically pure form.[8a] Previous work has demonstrated the utility of racemic **8**.[8b]

Received: June 24, 1993 [Z6166IE]
German version: *Angew. Chem.* **1993**, *105*, 1780

[1] For an overview that is still up to date see: R. M. Williams, *Synthesis of Optically Active α-Amino Acids*, Pergamon, Oxford, **1989**.
[2] U. Schöllkopf, *Asymmetric syntheses via heterocyclic intermediates*, in: *Organic Synthesis, an Interdisciplinary Challenge*; 5th IUPAC Symposium on Organic Synthesis, Freiburg i. Br., **1984**; J. Streith, H. Prinzbach, G. Schill, Blackwell, Oxford, **1985**, pp. 101-112; K. Busch, U. M. Groth, W. Kühnle, U. Schöllkopf, *Tetrahedron* **1992**, *48*, 5607-5618.
[3] For more recent discussions and comparison of different heterocycles **B** see: K. Suzuki, D. Seebach, *Liebigs Ann. Chem.* **1992**, 51-61; D. Seebach, T. Gees, F. Schuler, *ibid.* **1993**, 785.
[4] The noncovalently bound chiral "auxiliary" in this case is a commercial carboxylic acid or the stationary phase used for chromatography. R. Fitzi, D. Seebach, *Tetrahedron* **1988**, *44*, 5277-5292 (there refs. [16,17,25]); D. Seebach, S. G. Müller, U. Gysel, J. Zimmermann, *Helv. Chim. Acta* **1988**, *71*, 1303-1318; D. Blaser, D. Seebach, *Liebigs Ann. Chem.* **1991**, 1067-1078; W. Müller, D. A. Lowe, H. Neijt, S. Urwyler, P. L. Herrling, D. Blaser, D. Seebach, *Helv. Chim. Acta* **1992**, *75*, 855-864.
[5] Pivalaldehyde now is available from the Shell Chemical Corporation.
[6] The *cis* configuration of the benzyl and the *tert*-butyl groups in **5** has been established by X-ray analysis.
[7] a) (1*S*)-CSA purchased commercially costs about $40 per mol, the (1*R*) isomer about $100 per mol. b) The *ul* salt is less soluble in acetone/methanol; we obtained ≥ 98% enantiomerically pure (*S*)- and (*R*)-**2** (each in 20% yield) from the crystalline solid and the mother liquor after two recrystallizations. c) An X-ray analysis of (*R*)-**2**·(*S*)-CSA was obtained.
[8] a) Reaction of **3** with bromoacetic acid esters gives **8** quantitatively. b) R. Polt, D. Seebach, *Helv. Chim. Acta* **1987**, *70*, 1930-1936; R. Polt, D. Seebach, *J. Am. Chem. Soc.* **1989**, *111*, 2622-2632.

Self-Assembly Through Hydrogen Bonding: Preparation of a Supramolecular Aggregate Composed of Ten Molecules**

By *John P. Mathias, Eric E. Simanek, Christopher T. Seto*, and *George M. Whitesides**

Learning how to control the association of many molecules into single, highly-structured supramolecular aggregates is a current objective in molecular self-assembly.[1-5] In this communication we report the self-assembly of a supramolecular aggregate based on a compound containing

[*] Prof. G. M. Whitesides, Dr. J. P. Mathias, E. E. Simanek, Dr. C. T. Seto
Department of Chemistry, Harvard University
12 Oxford Street, Cambridge, MA 02138 (USA)
Telefax: Int. code + (617)495-9857

[**] This work was supported by the National Science Foundation (Grants CHE-91-22331 to G.M.W. and DMR-89-20490 to the Harvard University Materials Research Laboratory). NMR instrumentation was supported by the National Science Foundation Grant CHE-88-14019 and the National Institutes of Health Grant 1 S10 RR 4870. Mass spectrometry was performed by Dr. A. Tyler. The Harvard University Mass Spectrometry Facility was supported by The National Science Foundation Grant CHE-90-20043 and The National Institutes of Health Grant 1 S10 RR 06716-01. J. P. M. was an SERC/NATO Postdoctoral Fellow, 1991-1993.

nine melamine rings (M) that we have called Hub(MMM)$_3$ (**2**). This molecule associates with nine equivalents of neohexylisocyanurate (neohex(CA) **3**) to form a hydrogen-bonded supramolecular aggregate of composition Hub-(MMM)$_3$ · 9neohex(CA) (**4**). This aggregate is composed of ten molecules in three parallel $CA_3 \cdot M_3$ "rosettes",[6] and is stabilized by 54 hydrogen bonds.

The nonamelamine derivative **2** was synthesized by using the procedure shown in Scheme 1. This synthesis extends a strategy we have described previously.[2, 7] The *m*-xylyl spacers between adjacent melamine rings in each arm of **2** match those we have used in aggregates based on two parallel $CA_3 \cdot M_3$ rosettes.[3, 8]

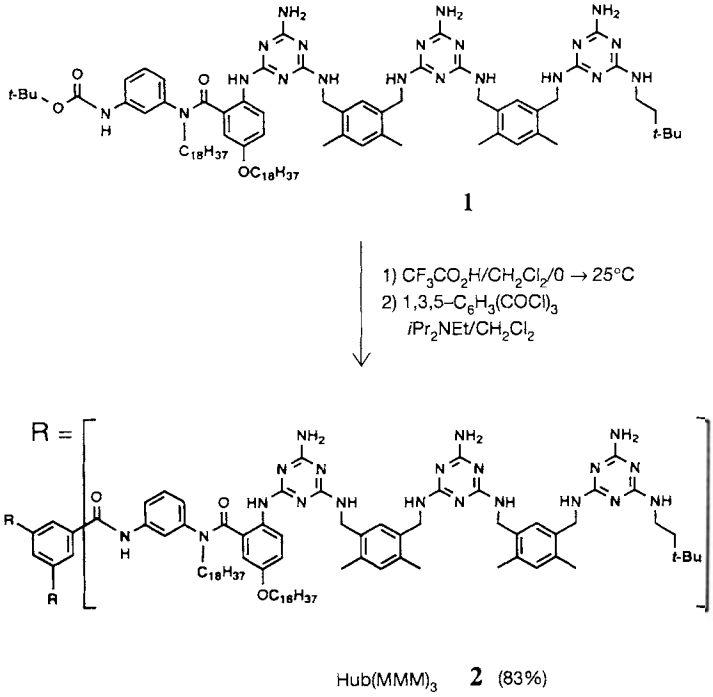

Scheme 1. Synthesis of Hub(MMM)$_3$ (**2**).

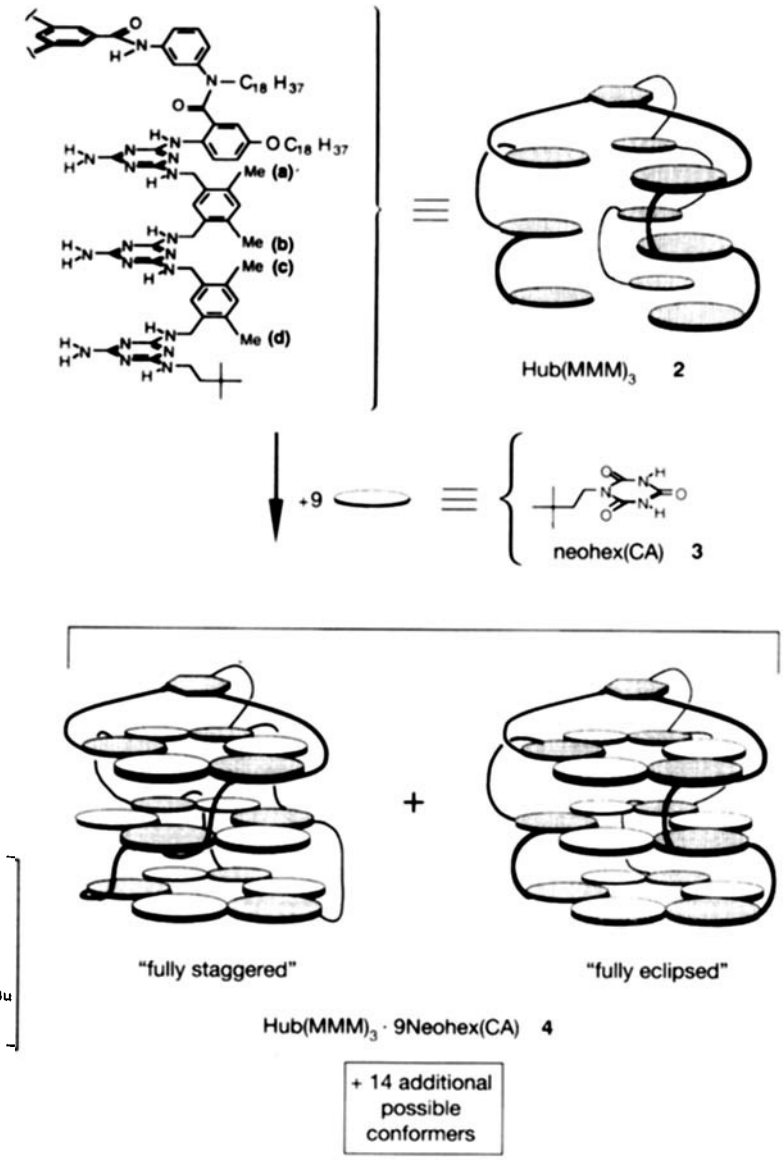

Scheme 2. Self-assembly of Hub(MMM)$_3$ · 9neohex(CA) (**4**). The conformational isomers shown are just two of at least 16 possibilities.

A homogeneous solution of Hub(MMM)$_3$ · 9neohex(CA) (**4**) was prepared by mixing one equivalent of **2** and nine equivalents of **3** in chloroform (Scheme 2). We have ennumerated at least 16 different geometrical conformers as being possibilities for **4**.[9] We believe that the aggregate exists initially as a mixture of the many available conformers on mixing the two different components. The conversion of this mixture to a single supramolecular aggregate of composition **4** occurs over about 48 h at room temperature (or 1 min at reflux) in chloroform, as judged by ^{1}H NMR spectroscopy.

The supramolecular aggregate **4** was characterized by ^{1}H NMR spectroscopy (COSY, NOE, and NOESY experiments), gel permeation chromatography (GPC), and vapor pressure osmometry (VPO). The ^{1}H NMR spectrum of **4** (Fig. 1a) shows a sharp set of resonances that can be assigned to a single conformer of the supramolecular aggregate. These sharp resonances contrast with the broad, poorly-defined resonances observed in the spectrum obtained from uncomplexed **2** in $CDCl_3$ (Fig. 1c); the broadening of the resonances in this spectrum may reflect hindered rotation about amide bonds in **2** and/or self-association of **2**. Even in a strong hydrogen-bonding solvent such as dimethylsulfoxide (DMSO), however, there is little detail in the ^{1}H NMR spectrum of **2**. The spectrum in Figure 1b shows the aggregate immediately after mixing the components **2** and **3**. The progression from a mixture of conformers of **4** (Fig. 1b) to a single conformer (Fig. 1a) is clear in these ^{1}H NMR spectra. The observation of discrete resonances for the different conformers confirms that exchange between them is slow on the NMR time scale. The six resonances with equal intensities (●, in Fig. 1a) between $\delta = 14$ and 16 correspond to three sets of the two unsymmetrical hydrogen-bonded isocyanurate protons seen in each $CA_3 \cdot M_3$ rosette in **4**. The observation of four discrete singlets (▽, Fig. 1a) between $\delta = 1.8$ and 2.1 for the four methyl substituents [(a)–(d), Scheme 2] provides further support for the proposed structure of **4**. Cooling the sample has no effect on the signals observed in the ^{1}H NMR spectrum. This feature strengthens the inference that the resonances observed at 298 K in Figure 1a belong to a single conformer and not to a rapidly-equilibrating mixture of conformations.[10] Nuclear Overhauser effects between the imide protons on the isocyanurate molecules (**3**) and those of the melamine rings in **2** confirm the geometry of the hydrogen-bonded regions, and are

consistent with the structure that we propose for **4**. We do not see NOE interactions between protons in adjacent $CA_3 \cdot M_3$ rosettes. This feature means that we cannot deduce, unambiguously, which of the possible conformational isomers is the thermodynamically preferred (observed) one.

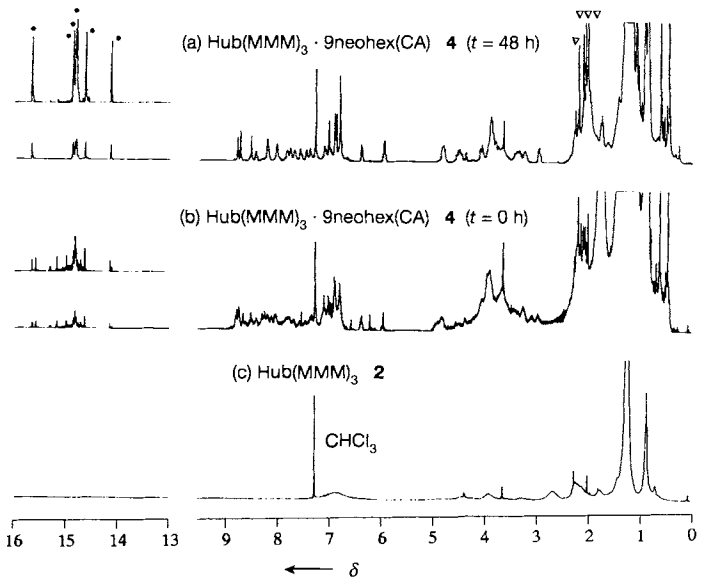

Fig. 1. ^{1}H NMR spectra (500 MHz, $CDCl_3$) of **4** (a) after equilibration and (b) on initial mixing of the components. The spectrum of uncomplexed **2** is shown in (c).

Retention times and shapes of the peaks for **4** (hatched) in $CHCl_3$ and CH_2Cl_2 as the eluent are consistent with observations from other self-assembled aggregates (Fig. 2). In each trace, *p*-xylene (shaded peak) was used as an internal standard. The trace in CH_2Cl_2 shows a single peak for the aggregate. The trace in $CHCl_3$ shows a much broader peak for the aggregate with a larger degree of "tailing" toward longer retention time. In each case, the peaks for the aggregate have sharp leading edges. This feature indicates that the solutions do not contain stable self-assembled or associated supramolecular aggregates that are *larger* than **4**. The tailing in these traces is a consequence of dissociation of the aggregate that occurs during the analysis by GPC, and more tailing is seen in $CHCl_3$ than in CH_2Cl_2. This difference indicates that the stability of **4** is lower in $CHCl_3$, the stronger hydrogen-bonding solvent, than it is in CH_2Cl_2.[11] Although dissociation occurs during analysis of **4**, the GPC results establish that the dissociation is slow and indicate, therefore, that **4** is surprisingly stable.

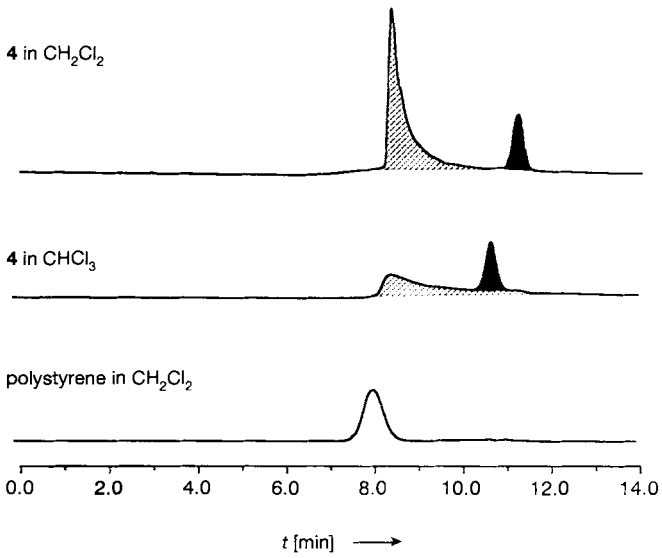

Fig. 2. Top and middle: Gel permeation chromatograms of **4** (hatched peaks). The shaded peaks are *p*-xylene, which is used as an internal standard. Bottom: Gel permeation chromatogram of polystyrene (PS) (F.W. 5050).

The molecular weight *m* for **4** has been obtained by VPO in chloroform, using four different molecular weight standards.[12] Each standard gives an observed *m* that is within 15% of the calculated value of **4** (6.435 kDa). Observed molecular weights of **4** are 5.6 kDa (standard: *N,N'*-bis-*tert*-butoxycarbonyl-gramicidin S), 6.4 kDa (sucrose octaacetate), 6.5 kDa (polystyrene), 7.5 kDa (perbenzoyl-β-cyclodextrin).

Addition of only three equivalents of **3** to one equivalent of **2** leads to formation of only fully assembled **4**; excess **2** remains uncomplexed. We do not observe any intermediates (such as Hub(MMM)$_3$ · 3neohex(CA)—the single layer aggregate **5**—or Hub(MMM)$_3$ · 6neohex(CA)—the double layer aggregate **6**) on the pathway between **2** and **4**. This observation indicates that the self-assembly of **4** displays positive cooperativity.

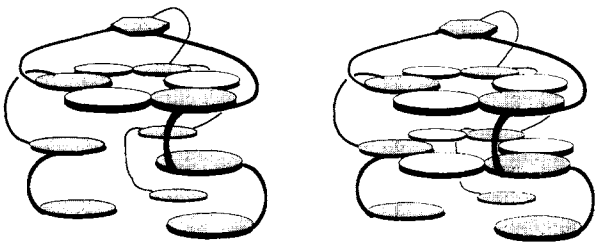

5 **6**

The self-assembly of *ten* molecules into a single *supramolecular aggregate* (**4**) that is stabilized by *fifty four* hydrogen bonds demonstrates further the potential of molecular self-assembly as a stategy for the preparation of well-defined chemical nanostructures. In particular, these results illustrate that parallel hydrogen-bonded $CA_3 \cdot M_3$ rosettes are a structural motif that is well-suited to the preparation of large, structurally complex supramolecular aggregates.

Experimental Procedure

Hub(MMM)$_3$ (**2**): Trifluoroacetic acid (2.5 mL) was added dropwise to a solution of **1** (451 mg, 0.29 mmol) in CH_2Cl_2 (10 mL) at 0 °C. The reaction mixture was warmed to 25 °C and stirred for 2 h. This solution was diluted with toluene (20 mL) and concentrated in vacuo. The residue was partitioned between EtOAc (50 mL) and aqueous Na_2CO_3 (5% solution, 25 mL). The organic extract was washed with aqueous Na_2CO_3 (5% solution, 25 mL), brine (2 × 25 mL), dried over $MgSO_4$, filtered, and concentrated in vacuo to give 402 mg (0.276 mmol, 95%) of the deprotected amine as a white foam [high-resolution FAB-MS: *m/z* calcd for $C_{84}H_{133}N_{20}O_2$: ($[M + H]^+$) 1454.0920, found: 1454.0959]. This amine (399 mg, 0.274 mmol) was dissolved in CH_2Cl_2 (10 mL) and di-isopropylethylamine (DIPEA) (0.19 mL) and the solution was cooled to 0 °C. 1,3,5-Benzene tricarbonyl chloride (24.2 mg, 0.0913 mmol) was added and the solution was allowed to warm to 25 °C. After 90 mins, the reaction mixture was diluted with CH_2Cl_2 (25 mL) and washed with aqueous Na_2CO_3 (5% solution, 20 mL), brine (2 × 35 mL), dried over $MgSO_4$, filtered, and concentrated in vacuo. The residue was purified by column chromatography (eluted with a solution of 7.5% NH_4OH/MeOH in CH_2Cl_2 [7.5:92.5 v:v]) to give 342 mg (0.0757 mmol, 83%, two steps) of the product (**2**) as a white solid; correct elemental analysis.

Received: July 12, 1993 [Z 6207 IE]
German version: *Angew. Chem.* **1993**, *105*, 1848

[1] G. M. Whitesides, J. P. Mathias, C. T. Seto, *Science* **1991**, *254*, 1312–1319.
[2] C. T. Seto, G. M. Whitesides, *J. Am. Chem. Soc.* **1993**, *115*, 905–916.
[3] C. T. Seto, J. P. Mathias, G. M. Whitesides, *J. Am. Chem. Soc.* **1993**, *115*, 1321–1329.
[4] C. T. Seto, G. M. Whitesides, *J. Am. Chem. Soc.* **1993**, *115*, 1330–1340.
[5] a) P. Baxter, J.-M. Lehn, A. DeCian, J. Fischer, *Angew. Chem.* **1993**, *105*, 92–96; *Angew. Chem. Int. Ed. Engl.* **1993**, *32*, 69–72; b) S. Bonazzi, M. M. DeMorais, G. Gottarelli, P. Mariani, G. P. Spada, *ibid.* **1993**, *105*, 251–253 bzw. **1993**, *32*, 240–250; c) S. J. Geib, C. Vicent, E. Fan, A. D. Hamilton, *ibid.* **1993**, *105*, 83–85 and **1993**, *32*, 119–121; d) S. C. Zimmerman, B. F. Duerr, *J. Org. Chem.* **1992**, *57*, 2215–2217; e) J. F. Stoddart et al. *Synlett.* **1992**, 914–918, 919–922, 923–926; f) E. C. Constable, *Tetrahedron* **1992**, *48*, 10013–10059.
[6] J. A. Zerkowski, C. T. Seto, G. M. Whitesides, *J. Am. Chem. Soc.* **1992**, *114*, 5473–5475.
[7] C. T. Seto, G. M. Whitesides, *J. Am. Chem. Soc.* **1990**, *112*, 6409–6411.
[8] C. T. Seto, G. M. Whitesides, *J. Am. Chem. Soc.* **1991**, *113*, 712–713.
[9] In principle, there are least four conformations in which the linker arm can join the uppermost melamine ring in **4** to the central benzene "hub" [2]. Additionally, adjacent melamine rings in each arm of the Hub(MMM)$_3$ unit can lie in eclipsed or staggered conformations, resulting in a total of at least 16 discrete conformers.
[10] Supramolecular aggregates based on a single $CA_3 \cdot M_3$ rosette often exist as mixtures of different geometrical isomers. The exchange between these structures can be slowed to reveal the separate isomers by ^{1}H NMR at temperatures below ambient; M. Wazeer, J. P. Mathias, E. E. Simanek, G. M. Whitesides, unpublished results.
[11] The traces from **4** in the GPC are significantly broader than those of previously reported double-layer aggregates, such as that between the hexamelamine derivative Hub(MM)$_3$ and six equivalent of neohexylisocyanurate, Hub(MM)$_3$ · 6*neo*hex(CA). The reduction in stability for **4** suggested by this observation places this aggregate close to the lower limit of stability that can be observed successfully by GPC.
[12] Chloroform was Aldrich HPLC grade. No attempt was made to monitor its moisture content during analysis by VPO.

The First Structure of a Lithiated Cyanamide; Synthesis of (PhNCNLi · HMPA)$_n$ by Extrusion of N_2 and S from 5-Phenylamino-1,2,3,4-thiatriazole with Li Reagents and HMPA**

By *David R. Armstrong, F. Adele Banbury, Ian Cragg-Hine, Matthew G. Davidson, Francis S. Mair, Ehmke Pohl, Paul R. Raithby*, and *Ronald Snaith**

We described recently the product resulting from the reaction of solid $Ba(OH)_2$ with aminothiatriazole (**AH**; R = naphthyl) and HMPA [O=P(NMe$_2$)$_3$] dissolved in toluene.[1] Instead of the expected aqua complex, (**A**)$_2$Ba · 2H$_2$O · *x* HMPA,[2] a rearrangement occurs to give the thioxotetrazole derivative, (**B**)$_2$Ba · 3HMPA, in 60% yield. This rearrangement has been known for a long time[3] as has the fact that compounds of the type **AH** react with excess aqueous NaOH along two different paths: the first path involves the degradation of the heterocycle **AH** to give RNCS and azide; the RNCS is subsequently hydrolyzed to the corresponding amine. The second path involves the isomerization of the thiatriazole **AH** to the thioxotetrazolyl anion (**B**$^-$). Path 1 is favored when an excess of OH^- ions and H_2O is used. In contrast, our recent study[1] showed that in the presence of HMPA ligands, the use of stoichiometric amounts of solid $Ba(OH)_2$ and **AH** prevent the hydrolysis step in path 1, and indeed, constructively favor path 2: the rearrangement increases the distance of the R group (naphthyl) from the $(N\cdots C\cdots S)^-$ unit which chelates the large $Ba(HMPA)_3^{2+}$ fragment.

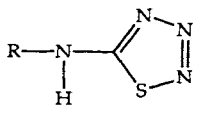

AH

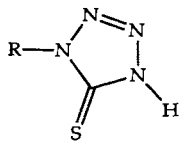

BH

Here we report a third, and rather more spectacular, pathway for the deprotonation of aminothiatriazoles **AH**: extrusion of N_2 and S at ambient temperature lead to metal complexes of the anion of R–N(H)–C≡N. Thus, in this way complex **1**, whose solid-state structure—the first of a lithiated cyanamide—was determined, was formed from **AH** (R = phenyl). Deprotonations of 5-(phenylamino)-1,2,3,4-thiatriazole (**AH**; R = Ph) were performed with a range of lithium bases. In general, equimolar amounts of **AH** and HMPA are dissolved in toluene at −78 °C, and then one equivalent of the chosen base (LiOH, MeOLi, $LiNH_2$, *i*Pr$_2$NLi as solids; *n*BuLi as a solution in hexane; see the Experimental Procedure for specific details) is added. Warming the mixture to room temperature causes dissolution of any solid, usually accompanied by visible gas evolution. Refrigeration of the resulting solution gives crystals of **1** (20–60% yield) except when the base used for the reaction is solid LiOH. In this case crystals of (**B**)Li · H_2O · HMPA are isolated initially; that is those containing the rearranged, rather than the extruded, anion. However, subsequent treatment of these crystals with additional LiOH/HMPA, or with *n*BuLi/HMPA, affords **1**. Interestingly, the reaction of **BH** with *n*BuLi/HMPA affords (**B**)Li · HMPA rather than **1**. The most immediate evidence for an extrusion product [$(RNCN)_x \cdot M^{x+} \cdot y$ ligand] is the appearance of a strong $\nu(N\cdots C\equiv N)^-$ stretch in the IR spectrum; for **1**, this band appears at 2147 cm^{-1}. The products of the reactions of **AH** (R = naphthyl) with HMPA and all the above-mentioned lithium bases show a similar absorption. However, treatment of HMPA and **AH** (R = Ph) in toluene with the highly reactive system Ba/Ba(NH$_2$)$_2$ (obtained by evaporating a solution of metallic Ba in liquid NH_3) affords a product having no such band. In this case the rearrangement product (**B**)$_2$Ba · 3HMPA (R = Ph) is formed. This product is akin to that [R = naphthyl in **B**] obtained from a similar reaction in which rather unreactive solid $Ba(OH)_2$ is used.[1] Thus it seems that formation of extrusion products is dependent on the metal atom attached to the base (switch from Ba to Li) rather than on the R group (switch from R = naphthyl to R = Ph in **AH**), or on a change in the general reactivity of the metalating reagent used.

[*] Dr. R. Snaith, F. A. Banbury, I. Cragg-Hine, M. G. Davidson, Dr. F. S. Mair, Dr. P. R. Raithby
University Chemical Laboratory
Lensfield Road, GB-Cambridge, CB2 1EW (UK)
Telefax: Int. code + (223) 336-362.
Dr. D. R. Armstrong
Department of Pure and Applied Chemistry
University of Strathclyde, GB-Glasgow, G1 1XL (UK)
E. Pohl
Institut für Anorganische Chemie der Universität
Tammanstrasse 4, D-37077 Göttingen (FRG)

[**] This work was supported by the Science and Engineering Research Council (SERC) (quota award, F.A.B.), the SERC and Associated Octel (CASE awards, I. C-H., M.G.D.), Queens' College, Cambridge and Associated Octel (Research Fellowship, F.S.M.), and St. John's College, Cambridge (Research Fellowship, M.G.D.). We thank Professor G. M. Sheldrick (University of Göttingen) for providing access to crystallographic facilities.

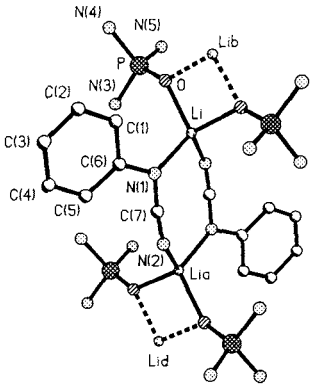

Fig. 1. The molecular structure of **1**, showing the central $(LiNCN)_2$ ring and adjacent $(LiO)_2$ rings.

The solid-state structure of **1** has been resolved by X-ray crystallography.[4] The most important structural feature (Fig. 1) is a $(LiNCN)_2$ ring [distances: Li–N1 2.061(4) Å; Lia–N2 1.984(4) Å]. The distances along the near-linear N1-C7-N2 portion of the anion are N1–C7 1.303(3) and C7–N2 1.157(3) Å, suggesting that the anion is best considered as $[Ph\text{-}N\cdots C\equiv\!\!=N]^-$. The eight-membered ring itself is slightly chair-shaped [internal angles: 106.4(2) at Li, 111.3(2) at N1, 175.7(2) at C7, and 142.8(2)° at N2; Li and Lia are 0.311 Å above and below the mean plane defined by N1-C7-N2].

Each Li is also coordinated to two HMPA molecules [Li–O 1.958(4) Å, Lib–O 1.973(4) Å] which in turn bridge to a Li atom in a neighboring $(LiNCN)_2$ ring. This leads to the formation of polymeric strands (Fig. 2) consisting of alternating and orthogonal eight-membered $(LiNCN)_2$ and four-membered $(LiO)_2$ rings.

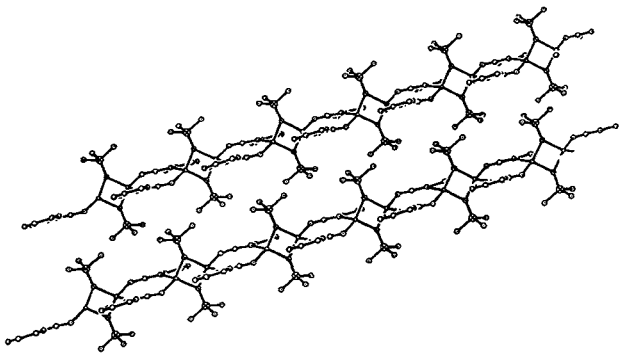

Fig. 2. Two polymeric strands of **1** showing alternating and orthogonal eight- and four-membered rings.

The structure of **1** is the first for a lithium cyanamide and as such it is unique, although certain of its features have analogies. For example, eight-membered rings of type $(LiXYZ)_2$ are well known in dimeric systems such as the lithium thiobenzoate $[PhC(=O)SLi \cdot TMEDA]_2$ with a $(LiOCS)_2$ ring[5] and the lithiosulfones $[PhSO_2CH(R)Li \cdot TMEDA]_2$ (R = H,[6] R = Ph[7, 8]) with $(LiOSO)_2$ rings. However, in comparison with the near-linear NCN^- unit in **1**, in all these structures an acute angle is found at atom Y. More akin to cyanamides, lithiated nitriles might be expected to contain eight-membered $(LiCCN)_2$ rings. MNDO calculations predict such a feature for uncomplexed $(LiCH_2CN)_2$.[9] However, on complexation a ketenimine structure $(H_2C\cdots C\equiv\!\!=NLi \cdot OH_2)_2$ with a four-membered $(NLi)_2$ ring is favored; such was indeed found for the first structurally characterized lithionitrile $[PhC(H)\cdots C\equiv\!\!=NLi \cdot TMEDA]_2$ (**C**).[8, 10] An example of the eight-membered $(LiCCN)_2$ unit is found in the structure of the 1-cyano-2,2-dimethylcyclopropyllithium complex (**D**).[8, 11] Here, the anionic α-C atom of the cyclopropyl unit is coordinated to the Li center so that an eight-membered $(LiCCN)_2$ ring results. The N atoms of each such ring bridge to the lithium atoms of neighboring eight-membered rings, resulting in alternating eight- and four-membered rings sharing a common LiN edge. In contrast, in **1**, the alternating rings share merely a common Li atom.

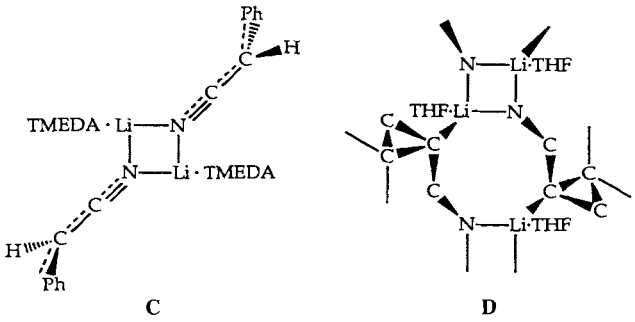

C **D**

It has not yet been possible to explain the rather dramatic extrusion reactions that occur when thiatriazoles **AH** are treated with HMPA and lithium bases. An earlier report[3] noted that a mercaptotetrazole **BH** (R = Ph) degraded violently at its melting point (147 °C), evolving N_2 and forming sulfur and unidentified organic product(s). It was suggested that isomerization to the thiatriazole **AH** occurs first, followed by bond cleavage and an "explosive internal oxidition–reduction" between the thiol and azido groups (Scheme 1).

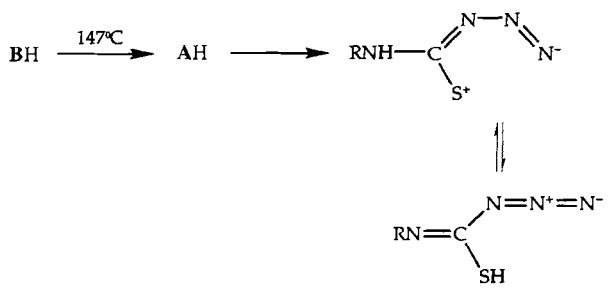

Scheme 1.

Our results here imply that the unidentified organic product of the earlier study was PhNHC≡N. However, a striking difference between the two studies is that all the reactions we describe occur at or below room temperature. Furthermore, it is clear that the metal cation and the added ligand play crucial roles. The different reactions of **AH** and HMPA with lithium (extrusion) and with barium (rearrangement) reagents have been noted; however, **AH**, $LiNH_2$, and the ligand PMDETA $[(Me_2NCH_2CH_2)_2NMe]$ react to give a rearrangement product containing $\mathbf{B}^-$. In addition, some of the reactions of **AH** and HMPA with lithium bases (e.g., with $LiNH_2$, *n*BuLi) proceed through numerous color changes, but others (e.g., with MeOLi, iPr_2NLi) do not. Further experiments are planned in the hope of elucidating the mechanisms of these unusual reactions.

Experimental Procedure

Typical syntheses of **1**: 1) With *n*BuLi. Solid **AH** (R = Ph; 0.89 g, 5 mmol) was dissolved under nitrogen in a mixture of HMPA (0.89 g, 5 mmol) and toluene (10 mL). The solution was cooled to −78 °C in an acetone/dry ice bath, and

*n*BuLi solution (5 mmol; in hexane) added. On warming to room temperature the original yellow solution changed color from green to reddish-brown, and gas evolution was observed. After the mixture had been stirred at room temperature for 30 min the resulting clear yellow solution was refrigerated overnight. This afforded very pale yellow crystals of **1** [first batch yield, 0.76 g, 50%; m.p. 132–135 C; correct analysis for $C_{13}H_{23}LiN_5OP$; ^1H NMR (CD_3CN, 250 MHz, 25 C): $\delta = 7.03$ (m_c, 2H), 6.78 (m, 2H), 6.53 (m, 1H), 2.58 (d, 18H, HMPA)]. – 2) With $LiNH_2$. To a chilled solution of **AH** and HMPA in toluene [as in 1)] was added solid $LiNH_2$ (0.12 g, 5 mmol). On warming to room temperature with stirring the yellow solution became first green and then blue, with gradual dissolution of the white solid. Stirring the blue solution at room temperature for a further 45 min gave, after a green color, a yellow solution. Storage at 25 C over 2 days afforded yellow crystals of **1** (first batch yield, 0.30 g, 20%).

Received: May 25, 1993 [Z 6105 IE]
German version: *Angew. Chem.* **1993**, *105*, 1801

[1] F. A. Banbury, M. G. Davidson, A. Martin, P. R. Raithby, R. Snaith, K. L. Verhorevoort, D. S. Wright, *J. Chem. Soc. Chem. Commun.* **1992**, 1152–1154.
[2] P. Mikulcik, P. R. Raithby, R. Snaith, D. S. Wright, *Angew. Chem.* **1991**, *103*, 452–454; *Angew. Chem. Int. Ed. Engl.* **1991**, *30*, 428–430.
[3] E. Lieber, C. N. Pillai, R. D. Hites, *Can. J. Chem.* **1957**, *35*, 832–842.
[4] X-ray crystal data for $(C_6H_5NCNLi \cdot HMPA)_n$ (**1**): $C_{13}H_{23}N_5OPLi$, $M = 303.27$, triclinic, space group $P\bar{1}$, $a = 7.3531(12)$, $b = 10.6051(15)$, $c = 11.462(3)$ Å, $\alpha = 82.210(12)$, $\beta = 79.700(12)$, $\gamma = 72.610(9)°$, $V = 836.0(3)$ Å^3, $Z = 2$, $\varrho_{calcd} = 1.205$ Mgm^{-3}, $F(000) = 324$, $\lambda(Mo_{K\alpha}) = 0.71073$ Å, $\mu(Mo_{K\alpha}) = 0.169$ mm^{-1}, $T = 193.0(20)$ K. Data were collected on a Stoe-Siemens diffractometer in the range $8° \leq 2\theta \leq 52°$, 2625 unique reflections measured. The structure was solved by direct methods and refined by full-matrix least-squares techniques (SHELX 92, G. M. Sheldrick, Universität Göttingen; all non-hydrogen atoms were refined anisotropically and hydrogen atoms were included in calculated positions) to $R_1 = 0.0414$, $wR_2 = 0.0905$, 2025 observed reflections, $[F > 4\sigma(F)]$. Further details of the crystal structure investigation are available on request from the Director of the Cambridge Crystallographic Data Centre, 12 Union Road, GB-Cambridge, CB2 1EZ (UK), on quoting the full journal citation.
[5] D. R. Armstrong, A. J. Banister, W. Clegg, W. R. Gill, *J. Chem. Soc. Chem. Commun.* **1986**, 1672–1673.
[6] H.-J. Gais, H. J. Lindner, J. Vollhardt, *Angew. Chem.* **1985**, *97*, 865; *Angew. Chem. Int. Ed. Engl.* **1985**, *24*, 859–860.
[7] G. Boche, M. Marsch, K. Harms, G. M. Sheldrick, *Angew. Chem.* **1985**, *97*, 577–578; *Angew. Chem. Int. Ed. Engl.* **1985**, *24*, 573–575.
[8] Review: G. Boche, *Angew. Chem.* **1989**, *101*, 286–306; *Angew. Chem. Int. Ed. Engl.* **1989**, *28*, 277–297.
[9] J. Kaneti, P. von R. Schleyer, T. Clark, A. J. Kos, G. W. Spitznagel, J. G. Andrade, J. B. Moffat, *J. Am. Chem. Soc.* **1986**, *108*, 1481–1492.
[10] G. Boche, M. Marsch, K. Harms, *Angew. Chem.* **1986**, *98*, 373–374; *Angew. Chem. Int. Ed. Engl.* **1986**, *25*, 373–374.
[11] G. Boche, K. Harms, M. Marsch, *J. Am. Chem. Soc.* **1988**, *110*, 6925–6926.

Synthesis and Reactivity of α,α-Dichloroglycyl Peptides**

By *Stefan Jaroch, Thomas Schwarz, Wolfgang Steglich,** and *Peter Zistler*

Dedicated to Professor Heinrich Nöth on the occasion of his 65th birthday

We recently introduced a new method for the synthesis of α-chloroglycyl peptides which makes it possible to prepare interesting peptide modifications.[1, 2] We now describe for the first time an approach to peptide derivatives that contain the α,α-dichloroglycine residue.

[*] Prof. Dr. W. Steglich, Dr. S. Jaroch, Dipl.-Chem. T. Schwarz, Dipl.-Chem. P. Zistler
Institut für Organische Chemie der Universität
Karlstrasse 23, D-80333 München (FRG)
Telefax: Int. code + (89)5902-604

[**] S. J. would like to thank the Fonds der Chemischen Industrie for a predoctoral fellowship.

The synthesis of these peptide derivatives begins with 2-phenyl-5(4*H*)-oxazolone (**1**),[3] which reacts readily with *N*-sulfenylsuccinimides such as **2**[4] to give 4,4-di(isopropylthio)oxazolones **3**.[5] If this reaction is conducted with the azlactone of Boc-Val-Gly-OH,[6] the doubly sulfurated peptide azlactone **3b**[5] is obtained in 37% yield. The oxazolones **3** can be stored at approximately −20 °C for several days without decomposition. We found that the five-membered ring of 4,4-disubstituted oxazolones **3** opens to give *N*-acyl peptides **4** containing an α,α-di(isopropylthio)glycine residue (see Table 1) when amino acid esters are added in the presence of catalytic quantities of 4-dimethylaminopyridine (DMAP). Reaction of a peptide azlactone such as **3b** provides peptide derivatives of type **4c**, in which the α,α-di(isopropylthio)glycine residue is not located terminally but within the peptide chain. These compounds are generally obtained as stable solids that can be purified by chromatography or recrystallization.

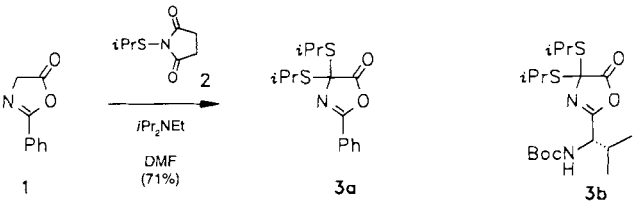

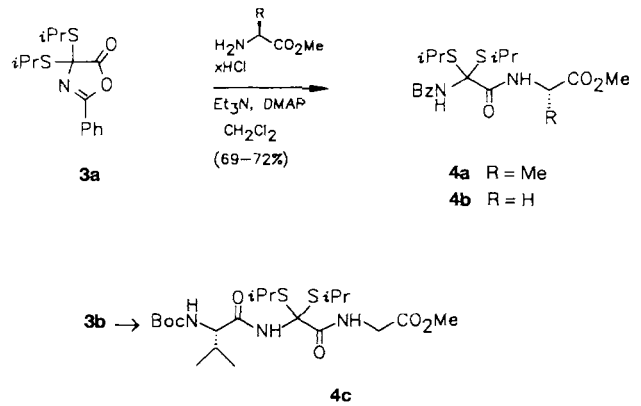

In analogy to the mono(alkylthio)glycine derivatives,[1, 2] when **4** is treated with sulfuryl chloride the alkylthio residues are readily exchanged for chlorine substituents. In this way

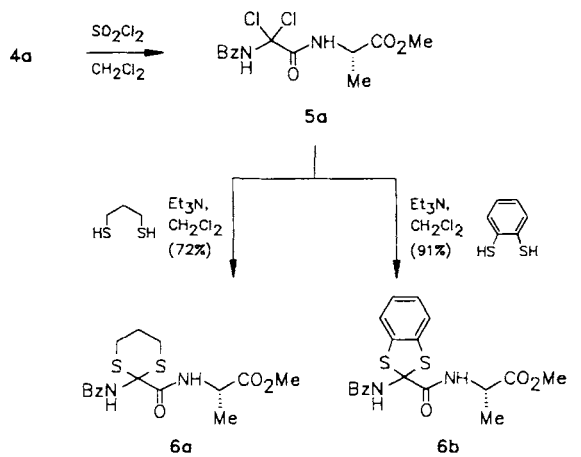

the reactive α,α-dichloroglycyl peptides **5** are obtained, which in turn react with nucleophiles in a double elimination–addition reaction to give the peptide derivatives **6**. Reaction of the dichloro compound **5a**, for example, with propane-1,3-dithiol produces the dithiane derivative **6a**, whereas benzodithiolane **6b** is formed with 1,2-dithiophenol (Table 1). As a result of conformational restrictions, the melting points of these dipeptides are approximately 50 °C higher than the melting point of the open-chain compound **4a**.

Table 1. Selected physical and spectroscopic properties of compounds **4** and **6**.

4a: M.p. 107–108 °C; $[\alpha]_D^{25} = -26.1$ ($c = 1.53$ in $CHCl_3$); ^1H NMR ($CDCl_3$, 80 MHz): $\delta = 1.25$ (d, $J = 7$ Hz, 12H), 1.55 (d, $J = 7$ Hz, 3H), 2.80–3.30 (m, 2H), 3.78 (s, 3H), 4.60 (quint, $J = 7$ Hz, 1H), 7.30–7.55 (m, 3H), 7.60–8.00 (m, 3H), 8.35 (br. S, 1H); FAB-MS: $m/z = 413$ [MH^+].

4b: M.p. 130–132 °C; ^1H NMR ($CDCl_3$, 400 MHz): $\delta = 1.23$ (d, $J = 6.9$ Hz, 12H), 3.09 (sept. $J = 6.9$ Hz, 2H), 3.80 (s, 3H), 4.18 (d, $J = 5.6$ Hz, 2H), 7.44–7.56 (m, 3H), 7.78 (m, 1H), 7.86–7.91 (m, 2H), 8.35 (br. s, 1H); FAB-MS: $m/z = 399$ [MH^+].

4c: M.p. 113–114 °C; $[\alpha]_D^{25} = -40.3$ ($c = 1.1$ in MeOH); ^1H NMR ($CDCl_3$, 400 MHz): $\delta = 0.94$ (d, $J = 7$ Hz, 3H), 1.01 (d, $J = 7$ Hz, 3H), 1.18 (d, $J = 7$ Hz, 3H), 1.19 (d, $J = 7$ Hz, 3H), 1.22 (d, $J = 7$ Hz, 3H), 1.24 (d, $J = 7$ Hz, 3H), 1.44 (s, 9H), 2.24 (m, 1H), 3.04 (sept, $J = 7$ Hz, 1H), 3.10 (sept, $J = 7$ Hz, 1H), 3.79 (s, 3H), 4.00 (dd, $J = 8$, 6 Hz, 1H), 4.11 (dd, $J = 18$, 6 Hz, 1H), 4.14 (dd, $J = 18$, 6 Hz, 1H), 5.03 (d, $J = 8$ Hz, 1H), 7.66 (t, $J = 6$ Hz, 1H), 7.92 (s, 1H); FAB-MS: $m/z = 494$ [MH^+].

6a: M.p. 156–157 °C; $[\alpha]_D^{25} = +26.0$ ($c = 0.53$ in $CHCl_3$); ^1H NMR ($CDCl_3$, 400 MHz): $\delta = 1.55$ (d, $J = 7$ Hz, 3H), 2.10–2.22 (m, 2H), 2.88–3.03 (m, 2H), 3.24–3.42 (m, 2H), 3.78 (s, 3H), 4.64 (quint, $J = 7$ Hz, 1H), 7.40–7.55 (m, 3H), 7.57 (br. s, 1H), 7.80–7.85 (m, 2H), 7.89 (br. d, $J = 7$ Hz, 1H); FAB-MS: $m/z = 369$ [MH^+].

6b: M.p. 162–163 °C; $[\alpha]_D^{25} = +40.4$ ($c = 1.24$ in $CHCl_3$); ^1H NMR ($CDCl_3$, 80 MHz): $\delta = 1.50$ (d, $J = 7$ Hz, 3H), 3.75 (s, 3H), 4.55 (quint, $J = 7$ Hz, 1H), 7.00–7.90 (m, 10H), 8.00 (br. s, 1H); FAB-MS: $m/z = 403$ [MH^+].

6c: M.p. 56–58 °C; $[\alpha]_D^{25} = -13.9$ ($c = 1.0$ in $CHCl_3$); ^1H NMR ($CDCl_3$, 400 MHz): $\delta = 1.36$ (s, 9H), 1.41 (s, 9H), 2.95–3.30 (m, 4H), 3.64 (s, 3H), 3.73 (s, 3H), 3.80 (s, 3H), 4.17 (t, $J = 6$ Hz, 2H), 4.53 (m, 2H), 5.44 (br. d, $J = 8$ Hz, 1H), 5.68 (br. d, $J = 8$ Hz, 1H), 7.44–7.55 (m, 3H), 7.73 (t, $J = 6$ Hz, 1H), 7.85–7.96 (m, 2H), 8.50 (br. s, 1H); FAB-MS: $m/z = 717$ [MH^+].

Reaction of *N*-benzoyl-α,α-dichloroglycyl glycine methyl ester **5b** with *N*-Boc-L-cysteine methyl ester leads to the interesting pseudotetrapeptide **6c**. This synthesis demonstrates that it is possible to connect three peptide chains by means of cysteine residues.

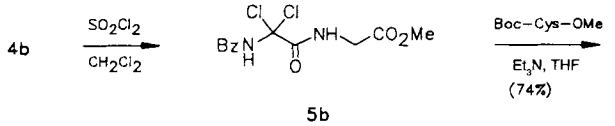

5b

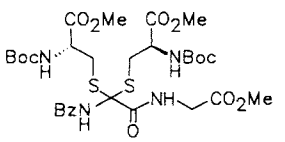

6c

Treatment of di(isopropylthio)glycyl peptide **4b** with *N*-bromosuccinimide (NBS) results in cleavage of an isopropylthio residue to give the *N*-acylthioimino ether **7**. The reaction of **7** with sodium borohydride leads to the α-(isopropylthio)glycyl glycine methyl ester **8**. We are currently trying this same approach with chiral hydride donors to develop a route to homochiral α-(alkylthio)glycine derivatives.

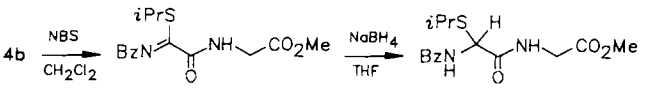

7 **8**

Experimental Procedure

3a: Oxazolone **1** (2.32 g, 14.4 mmol) and **2** (5.00 g, 28.9 mmol) were added under Ar to dry dimethylformamide (DMF) in a flame-dried Schlenk flask. Diisopropylethylamine (5.06 mL, 29 mmol) added slowly through a septum, and the mixture was allowed to stir for 15 h at room temperature. The reaction was quenched with water and extracted twice with diethyl ether. The combined organic extracts were washed with 20% citric acid solution and saturated $NaHCO_3$ solution and were then dried over $MgSO_4$. The solvent was evaporated in vacuo and the residue purified by flash chromatography (SiO_2, petroleum ether/ethyl acetate) to give 3.20 g of product (71% yield).

4a: Oxazolone **3a** (1.15 g, 3.7 mmol), Ala-OMe × HCl (0.56 g, 4 mmol), and DMAP (10 mg) were dissolved under Ar in 10 mL of dry methylene chloride. Triethylamine (0.6 mL, 4.3 mmol) was slowly added while stirring. After 48 h the reaction was diluted with diethyl ether and washed twice with each of three aqueous solutions: 20% citric acid, saturated $NaHCO_3$ and saturated NaCl. After the collected extracts were dried over $MgSO_4$, the solvent was removed in vacuo and the residue recrystallized from ethyl acetate/petroleum ether to give 1.05 g (69%) of product.

Received: July 3, 1993 [Z 6187 IE]
German version: *Angew. Chem.* **1993**, *105*, 1803

[1] G. Apitz, W. Steglich, *Tetrahedron Lett.* **1991**, *32*, 3163.
[2] G. Apitz, M. Jäger, S. Jaroch, M. Kratzel, L. Schäffeler, W. Steglich, *Tetrahedron*, **1993**, *49*, 8223.
[3] G. E. VandenBerg, J. B. Harrison, H. E. Carter, B. J. Magerlein, *Org. Synth.* **1967**, *47*, 101.
[4] Y. Abe, T. Nakabayashi, J. Tsurugi, *Bull. Chem. Soc. Jpn.* **1973**, *46*, 1898.
[5] The compounds were characterized by ^1H NMR and IR spectroscopy. **3a**: Oil; ^1H NMR ($CDCl_3$, 400 MHz): $\delta = 1.34$ (d, $J = 6.3$ Hz, 12H), 3.36 (sept, $J = 6.3$ Hz, 2H), 7.49–7.64 (m, 3H), 8.04–8.07 (m, 2H); IR (KBr): $\tilde{\nu} = 2963$, 2928, 1839, 1816, 1636, 1451 cm^{-1}; FAB-MS: m/z (%) = 310 (24) [MH^+], 105 (100); **3b**: Oil; ^1H NMR ($CDCl_3$, 400 MHz): $\delta = 0.98$ (d, $J = 7$ Hz, 3H), 1.04 (d, $J = 7$ Hz, 3H), 1.30 (d, $J = 7$ Hz, 3H), 1.31 (d, $J = 7$ Hz, 3H), 1.32 (d, $J = 7$ Hz, 3H), 1.33 (d, $J = 7$ Hz, 3H), 1.45 (s, 9H), 2.17 (m, 1H), 3.29 (sept, $J = 7$ Hz, 1H), 3.36 (sept, $J = 7$ Hz, 1H), 4.48 (dd, $J = 9$, 5 Hz, 1H), 4.98 (d, $J = 9$ Hz, 1H); IR (KBr): $\tilde{\nu} = 2960$, 1825, 1680, 1650 cm^{-1}; FAB-MS: m/z (%) = 405 (4) [MH^+].
[6] G. Schulz, W. Steglich, *Chem. Ber.* **1980**, *113*, 787.

[(CO)$_5$Cr=Tl=Cr(CO)$_5$]$^-$, the First Complex Containing Linear Twofold-Coordinated Thallium**

By *Berthold Schiemenz* and *Gottfried Huttner**

Dedicated to Professor Hans Bock on the occasion of his 65 birthday

The compounds [Cp′(CO)$_2$Mn=Ge=Mn(CO)$_2$Cp′][1] (Cp′ = C_5H_4Me) and [Cp(CO)$_2$Mn=Pb=Mn(CO)$_2$Cp][2] are of particular interest as cumulene analogues[3] containing linear-coordinated germanium and lead, respectively.[4] In these complexes all four electrons of the bridging atoms Ge^0 and Pb^0, respectively, participate in the bonding to the 16-electron complex fragments L_nM [Cp′(CO)$_2$Mn and Cp(CO)$_2$Mn, respectively]. The remaining coordination sites on the bridging building blocks are saturated by back bonding from donor orbitals of the metal complex fragments. The

[*] Prof. Dr. G. Huttner, Dipl.-Chem. B. Schiemenz
Anorganisch-chemisches Institut der Universität
Im Neuenheimer Feld 270, D-69120 Heidelberg (FRG)
Telefax: Int. code + (6221)564-197

[**] This work was supported by the Deutsche Forschungsgemeinschaft (SFB 247) and the Fonds der Chemischen Industrie.

short Ge=Mn and Pb=Mn bonds and the linear coordination of the main group elements in these compounds are in agreement with this description, which should also be applicable to other four-electron building blocks. For As^{I}[5] and Sb^{I},[6] this expectation has been confirmed by structure analyses. Access to isoelectronic complexes containing Tl^{-I}[7] as a four-electron building block from group 13 has now been achieved.

$TlCl_3$ reacts with three equivalents of $K_2[Cr(CO)_5]$[8] to give the anionic trimetallacumulene complex **1**. After the addition of [2,2,2]cryptand,[9] [K^+-[2,2,2]cryptand]·**1**·0.6 THF was obtained as a crystalline salt.

$$3\ K_2[Cr(CO)_5] \xrightarrow[\text{[2,2,2] cryptand}]{TlCl_3\ /\ THF} \underset{\mathbf{1}}{\left[(CO)_5Cr{=}Tl{=}{=}Cr(CO)_5\right]^-}$$

The X-ray structure analysis of **1** (Fig. 1)[10] shows that the Tl center in **1** bridges two $Cr(CO)_5$ units in a linear fashion.[11]

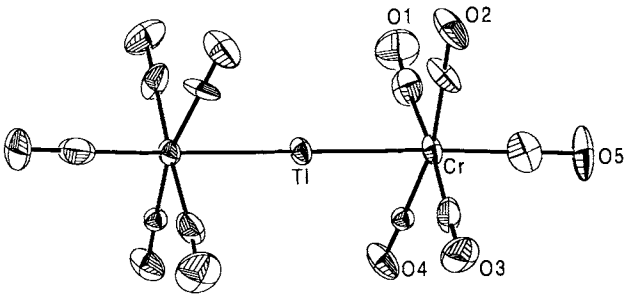

Fig. 1. Crystal structure of the anion $[(CO)_5Cr{=}Tl{=}Cr(CO)_5]^-$ (**1**). The relevant geometric data for the crystallographically independent halves of the two C_2 symmetric anions **1** in the crystal of [K^+-[2,2,2]cryptand]·**1**·0.6 THF are given, separated by a slash: Cr–Tl 264.9(3)/262.9(4) pm; Cr–Tl–Cr' 180.0(2)/177.0(1).

Two crystallographically independent anions **1** occur in the crystal of [K^+-[2,2,2]cryptand]·**1**·0.6 THF; each has crystallographically imposed C_2 symmetry. Since the equatorial carbonyl groups of the $Cr(CO)_5$ groups are almost superimposable, the effective symmetry of **1** is almost D_{4h}.

The Tl centers are each bound only to the Cr atoms; all contacts between the Tl centers and the oxygen atoms of the carbonyl groups of the neighboring complex ions in the crystal are longer than 310 pm.[11] The Tl–Cr distance in **1** (264 pm, Fig. 1) is thus very much shorter than that in **2** (287 pm),[12] which can be considered as a measure for a Tl–Cr single bond. This observation supports the classification of **1** as a member of the isoelectronic series of "cumulene" complexes $[L_nM{=}E{=}ML_n]^m$ (E = Ge, Pb: $m = 0$;[1,2] E = As, Sb: $m = 1$ +[5,6]). A similarly short Tl–Cr distance to that in **1** is only found in **3** (269 pm),[13] which belongs to the isoelectronic series of "inidene" complexes[14] $[L_nM{\cdots}E(R){\cdots}ML_n]^{m-1}$.[15] As expected, in cases when the structure of the "cumulene" complexes $[L_nM{=}E{=}ML_n]^m$ and those of the "inidene" complexes $[L_nM{\cdots}E(R){\cdots}ML_n]^{m-1}$ (E = Ge,[1,16] Pb,[2,17] As,[4,18] Sb,[5,19]) derived from them is known, slightly shorter M–E bonds (7–11 pm) are found for the "cumulene" complexes than for the corresponding "inidene" compounds. Correspondingly, the Tl–Cr distance in "cumulene" complex **1** is about 4 pm shorter than the Tl–Cr distance in the related "inidene" complex **3**.[13] The "cumulene" complex **4**, isoelectronic to **1**, is stabilized by dimerization to give **5** which contains a three-coordinate Tl

$$\underset{\mathbf{2}}{[Tl\{Cr(CO)_3Cp\}_3]} \qquad \underset{\mathbf{3}}{[(CO)_5Cr{\cdots}Tl(Cl){\cdots}Cr(CO)_5]^{2-}}$$

$$\underset{\mathbf{4}}{[(CO)_4Fe{=}Tl{=}Fe(CO)_4]^-} \qquad \underset{\mathbf{5}}{[\{(CO)_4Fe{-}Tl{-}Fe(CO)_4\}_2]^{2-}}$$

center.[20] The "cumulene" complex **1** can only be isolated because the bulky and rigid $Cr(CO)_5$ groups effectively shield the linear-coordinated thallium.

Experimental Procedure

All operations were carried out with freshly dried, and distilled solvents under argon. IR spectra: Bruker IFS 66, NMR spectra: Bruker AC 200.

To a suspension of KC_8 (568 mg, 4.2 mmol) in THF (15 mL) at −70 °C was added $Cr(CO)_6$ (440 mg, 2 mmol) in one batch. The dirty green suspension of the resulting $K_2[Cr(CO)_5]$ [8] was treated with $TlCl_3$ (218 mg, 0.7 mmol) at −70 °C. The mixture was allowed to warm to 20 °C with stirring over 5h; during this time the suspension turned orange. It was then treated with [2,2,2]cryptand (263 mg, 0.7 mmol) and stirred for an additional 5 min. The solvent was then decanted and filtered through 2 cm Celite/THF. The black residue (graphite) was washed twice, each time with THF (10 mL), and the solvent was distilled from the combined orange filtrates under vacuum at 20 °C. The residue was washed twice with deoxygenated H_2O (5 mL). After the washings were decanted off, an orange residue remained which was dried under vacuum for 3 h at 20 °C and then dissolved again in THF (5 mL). The resulting solution was divided equally into three test tubes (∅ = 1 cm), which were then placed in a Schlenk tube (250 mL). The Schlenk tube was filled with diethyl ether (50 mL) and left to stand for 3 h at 20 °C. During this time about 0.5 mL diethyl ether diffused into the THF solutions in the three test tubes. The diethyl ether was removed from the Schlenk tube and the solution in each of the test tubes was layered with 2 mL petroleum ether 40/60. The compound [K^+-[2,2,2]cryptand·1·0.6 THF] crystallized out at 20 °C over three days in the form of orange needles. $M = 1004.07\ g\,mol^{-1}$, $C_{28}H_{36}Cr_2KN_2O_{16}Tl{\cdot}0.6C_4H_8O$, yield: 700 mg (40% based on Tl), correct C, H, N analysis, IR (THF): $\tilde{\nu}$ = 2030 vw, 1982 w, 1939 vs, 1906 s, 1878 m cm^{-1} (CO). The number of bands and the similarity of the band shapes with the absorption pattern observed for the "inidene" complex **3** [13] indicates that in THF solution the Tl center of **1** is additionally coordinated by the solvent. ^1H NMR (200 MHz, [D_6]acetone, 193 K): δ = 3.77 (m, 12H), 3.64 (m, 24H), 3.62 (m, THF), 2.61 (t, THF).

Received: July 8, 1993 [Z6199IE]
German version: *Angew. Chem.* **1993**, *105*, 1840

[1] W. Gäde, E. Weiss, *J. Organomet. Chem.* **1981**, *213*, 451.
[2] W. A. Herrmann, H.-J. Kneuper, E. Herdtweck, *Angew. Chem.* **1985**, *97*, 1060; *Angew. Chem. Int. Ed. Engl.* **1985**, *24*, 1062; *Chem. Ber.* **1989**, *122*, 445.
[3] See also: N. M. Kostić, R. F. Fenske, *J. Organomet. Chem.* **1982**, *233*, 337.
[4] Review: N. A. Compton, R. J. Errington, N. C. Norman, *Adv. Organomet. Chem.* **1990**, *31*, 91; W. A. Herrmann, *Angew. Chem.* **1986**, *98*, 57; *Angew. Chem. Int. Ed. Engl.* **1986**, *25*, 56.
[5] A. Strube, G. Huttner, L. Zsolnai, *Angew. Chem.* **1988**, *100*, 1586; *Angew. Chem. Int. Ed. Engl.* **1988**, *27*, 1529; *Z. Anorg. Allg. Chem.* **1989**, *577*, 263; *J. Organomet. Chem.* **1990**, *399*, 267.
[6] F. Bringewski, G. Huttner, W. Imhof, *J. Organomet. Chem.* **1993**, *448*, C3.
[7] The assignment of the oxidation number Tl^{-I}, which subsumes the coordination to neutral $Cr(CO)_5$ building blocks, is in line with convention; it proves useful for the comparison with the isoelectronic building blocks of group 14 and 15 which usually are considered as neutral Ge^0 [1] and Pb^0 [2] or cationic As^I [4] and Sb^I [5], respectively.
[8] M. A. Schwindt, T. Lejon, L. S. Hegedus, *Organometallics* **1990**, *9*, 2814.
[9] [2,2,2]cryptand = 4,7,13,16,21,24,-hexaoxa-1,10-diazabicyclo[8.8.8]hexacosane, $N(C_2H_4OC_2H_4OC_2H_4)_3N$.
[10] The K^+ ions are each coordinated by a [2,2,2]cryptand; statistically distributed, an additional coordination by one THF molecule is found for 60% of the cations. The THF ligand and parts of the cryptand are disordered. [K^+-[2,2,2]cryptand]·1·0.6 THF: a = 3059(2), b = 1029.0(5), c = 2937(2) pm, β = 113.68(5)°, space group $C2/c$, $Z = 8$, $R_1 = 0.057$, $R_2 = 0.053$. Measurement on a Siemens(Nicolet Syntex)-R3m/V diffractometer, ($Mo_{K\alpha}$ radiation, graphite monochromator, ω scan, $2° \le 2\theta \le 42°$), 3443 independent reflections with ($I \ge 2\sigma(I)$). Refinement: All non-hydrogen atoms except the disordered ones are anisotropic; used program: SHELX76 (G. Sheldrick, University of Cambridge 1976) and SHELXTL PLUS (G. Sheldrick, Universität Göttingen 1988). Further details of the crystal structure investigation may be obtained from the Fachinformationszentrum Karlsruhe, Gesellschaft für wissenschaftlich-technische In-

formation mbH, D-76344 Eggenstein-Leopoldshafen (FRG) on quoting the depository number CSD-57479, the names of the authors, and the journal citation.
[11] The "linear" coordination of thallium in the Tl^{III} compounds R_2TlHal is in reality—as a result of the formation of Tl-Hal-Tl bridges—a sixfold coordination with *trans* R groups: H.-D. Hausen, E. Veigel, H.-J. Guder, *Z. Naturforsch.* **1974**, *29b*, 269; Y. M. Chow, D. Britton, *Acta Crystallogr. Sect. B* **1975**, *31*, 1922. See also the analogous situation in R_2PbHal_2: M. Mammi, V. Busetti, A. Del Pra, *Inorg. Chim. Acta* **1967**, *1*, 419. Twofold coordination of Tl is rare. It is only observed when the occupation of additional coordination sites is prevented by steric shielding; the arrangement is then bent: H. W. Roesky, M. Scholz, M. Noltemeyer, F. T. Edelmann, *Inorg. Chem.* **1989**, *28*, 3829; C. Bianchini, D. Masi, K. Linn, C. Mealli, M. Peruzzini, F. Zanobini, *ibid.* **1992**, *31*, 4036.
[12] L. M. Clarkson, W. Clegg, D. C. R. Hockless, N. C. Norman, T. B. Marder, *J. Chem. Soc. Dalton Trans.* **1991**, 2229.
[13] O. J. Curnow, B. Schiemenz, G. Huttner, L. Zsolnai, *J. Organomet. Chem.*, **1993**, *459*, 17.
[14] The term "-inidene" is be used in the following instead of the IUPAC classification "-andiyl".
[15] G. Huttner, *Pure Appl. Chem.* **1986**, *58*, 585; G. Huttner, K. Evertz, *Acc. Chem. Res.* **1986**, *19*, 406.
[16] B. Schiemenz, G. Huttner, unpublished results.
[17] F. Ettel, G. Huttner, L. Zsolnai, *Angew. Chem.* **1989**, *101*, 1525; *Angew. Chem. Int. Ed. Engl.* **1989**, *28*, 1496.
[18] J. von Seyerl, U. Moering, A. Wagner, A. Frank, G. Huttner, *Angew. Chem.* **1978**, *90*, 911; *Angew. Chem. Int. Ed. Engl.* **1978**, *17*, 843.
[19] F. Bringewski, G. Huttner, W. Imhof, L. Zsolnai, *J. Organomet. Chem.* **1992**, *439*, 33.
[20] J. M. Cassidy, K. H. Whitmire, *Inorg. Chem.* **1989**, *28*, 1432, 1435; K. H. Whitmire, J. M. Cassidy, A. L. Rheingold, R. R. Ryan, *ibid.* **1988**, *27*, 1347; K. H. Whitmire, R. R. Ryan, H. J. Wasserman, T. A. Albright, S.-K. Kang, *J. Am. Chem. Soc.* **1986**, *108*, 6831.

The Bis(cyclopentadienyl)thallate(I) Anion Isoelectronic with Stannocene**

By *David R. Armstrong, Regine Herbst-Irmer, Annja Kuhn, David Moncrieff, Michael A. Paver, Christopher A. Russell, Dietmar Stalke,* Alexander Steiner,* and *Dominic S. Wright**

We have recently shown that a range of tri(cyclopentadienyl)stannate and -plumbate complexes consisting of discrete, "ion-separated" ion pairs and bridged, "contacted" ion pairs can be prepared by nucleophilic addition reactions of [Cp_2Mg] and [CpNa] to [Cp_2E] (Cp = C_5H_5; E = Sn, Pb).[1-3] In all these derivatives the heavy p block metals behave as acceptors rather than donating their electron pairs. In the Pb complexes[3] [$(\eta^5\text{-Cp})_2Pb(\mu\text{-}\eta^5\text{-Cp})Na\cdot PMDETA$] [PMDETA = $(Me_2NCH_2CH_2)_2NMe$] and [$\{(\eta^3\text{-Cp})Pb^-\}_2\cdot Mg(THF)_6^{2+}$], the $[Cp_3Pb]^-$ ions can be seen as extruded fragments of the polymeric zig-zag chain structure of orthorhombic $[Cp_2Pb]_x$.[4] With this in mind, we have turned our attention to cyclopentadienyl complexes with elements of Group 13 (E=Ga, In, Tl). The solid-state structures of [CpIn] and [CpTl] are both known and display polymeric zig-zag chains, $[(\mu\text{-}\eta^5\text{-Cp})E]_x$, in which the metal centers again behave as acceptors to the bridging Cp ligands.[5] We wondered whether complexes containing $[Cp_2E]^-$ units could be prepared by addition of Cp^- to Group 13 metallocenes.

We report the syntheses and structures of the ion-separated complex **1** and of the contacted complex **2**.[6] Both com-

$[(\eta^5\text{-Cp})_2Tl(\eta^5\text{-Cp})Mg\cdot PMDETA]$ **1**
$[(\eta^5\text{-Cp})Tl(\mu\text{-}\eta^5\text{-Cp})Li\cdot PMDETA]$ **2**

plexes contain bent $[(\eta^5\text{-Cp})_2Tl]^-$ ions which are isoelectronic and isostructural with the 14-electron complex stannocene.

Complex **1** is prepared by stirring a mixture of [CpTl] and [Cp_2Mg] (1:1 mol ratio) in THF. Addition of PMDETA (1 mol equiv) produces a colorless precipitate of **1** which is recrystallized from THF. Similar reaction of [CpTl] and [CpLi] (1:2 mol ratio) in THF, followed by addition of PMDETA (1 mol equiv), produces **2** (see Experimental Procedure).

An X-ray crystallographic study on complex **1**[6] shows a structure with discrete ion pairs (Fig. 1). The unit cell con-

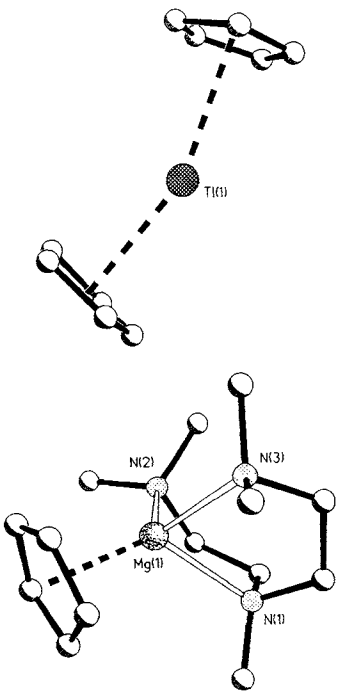

Fig. 1. Molecular structure of **1**. Hydrogen atoms have been omitted for clarity. Selected distances [Å]: Anion 1: Tl(1)-C(1) 2.86(3), Tl(1)-C(2) 2.91(3), Tl(1)-C(3) 2.99(3), Tl(1)-C(4) 3.07(4), Tl(1)-C(5) 2.85(3), Tl(1)-C(6) 3.05(3), Tl(1)-C(7) 3.04(3), Tl(1)-C(8) 2.94(2). Tl(1)-C(9) 2.93(3), Tl(1)-C(10) 2.88(3). Anion 2: Tl(2)-C(11) 3.02(3), Tl(2)-C(12) 2.94(3), Tl(2)-C(13) 2.93(3). Tl(2)-C(14) 2.98(3), Tl(2)-C(15) 3.09(3), Tl(2)-C(16) 2.93(3), Tl(2)-C(17) 2.87(3), Tl(2)-C(18) 2.92(3), Tl(2)-C(19) 3.03(3), Tl(2)-C(20) 3.03(3). Averages over all molecules in the unit cell: Tl-Cp (centroid) 2.72, Mg-N 2.20, Mg-Cp (centroid) 2.08, Cp (centroid)-Tl-Cp (centroid) 156.7°.

[*] Dr. D. S. Wright, M. A. Paver, C. A. Russell
University Chemical Laboratory
Lensfield Road, GB-Cambridge CB21EW (UK)
Telefax: Int. code + (223)3363-62
Priv.-Doz. Dr. D. Stalke, Dr. R. Herbst-Irmer, A. Kuhn, A. Steiner
Institut für Anorganische Chemie
Tammannstrasse 4, D-37077 Göttingen (FRG)
Telefax: Int. code + (551)39-2582
Dr. D. Moncrieff
Supercomputer Computations Research Institute B-186
Florida State University
Tallahasee, FL 32306-4052 (USA)
Dr. D. Armstrong
Department of Pure and Applied Chemistry
Thomas Graham Building
295 Cathedral Street, GB-Glasgow G11XL (UK)

[**] We thank the British Science and Engineering Research Council (M.A.P., C.A.R., D.S.W.), the Royal Society (D.S.W.), the Nuffield Foundation (D.S.W.), the Associated Octel Co. Ltd. (M.A.P., D.S.W.), the Deutsche Forschungsgemeinschaft and the Fonds der Chemischen Industrie (A.S., D.S.; fellowship for A.K.), and the U.S. Department of Energy (no. DE-FC05-85ER 2500000) (D.M.). We also thank SciAm for the use of their graphics package and software and Riedel-de Häen for providing the perfluorinated polyether used in mounting the crystal for the structure determination.

sists of two independent $[(\eta^5\text{-Cp})_2\text{Tl}]^-$ ions and two independent $[(\eta^5\text{-Cp})\text{Mg}\cdot\text{PMDETA}^+]$ ions. The structure of **2** contains two independent contacted ion pairs in the solid state (Fig. 2), in which one Cp ligand bound to Tl is additionally involved with a Lewis base solvated Li^+ ion (av $Li-Cp(b)_{centroid}$ 2.25 Å) as a (μ–Cp) bridge.[6] All the independent $[(\eta^5\text{-Cp})_2\text{Tl}]^-$ units of **1** and **2** are bent, with a mean Cp-Tl-Cp angle (from the centroids of the Cp ligands) of 156.7° in **1** and 153.3° in **2**. These angles can be compared to the average centroid Cp-E-Cp angle of 146° for the two independent bent molecules of $[Cp_2Sn]$ in the solid state[10] and approximately 135° for $[Cp_2Pb]$ in the gas phase,[11] with which the 14-electron thallate ions in **1** and **2** are isostructural and isoelectronic. The Cp-Tl-Cp angle in polymeric $[(\eta^5\text{-Cp})\text{Tl}]_\infty$ is significantly more acute (ca. 137°) than those observed in the $[(\eta^5\text{-Cp})_2\text{Tl}]^-$ ions of both complexes.[5]

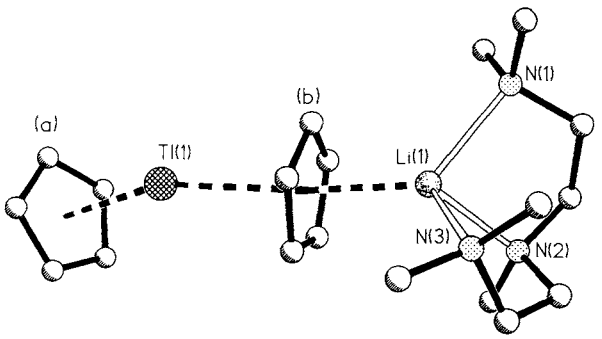

Fig. 2. Molecular structure of **2**. Hydrogen atoms have been omitted for clarity. Selected distances [Å]: Molecule 1: Tl(1)-C(11) 3.02(1), Tl(1)-C(12) 3.07(1), Tl(1)-C(13) 3.20(1), Tl(1)-C(14) 3.19(1), Tl(1)-C(15) 3.10(1), Tl(1)-C(16) 2.81(1), Tl(1)-C(17) 2.86(1), Tl(1)-C(18) 2.89(1), Tl(1)-C(19) 2.89(1), Tl(1)-C(12) 2.82(1), Li(1)-C(11) 2.69(2), Li(1)-C(12) 2.53(2), Li(1)-C(13) 2.34(2), Li(1)-C(14) 2.42(2), Li(1)-C(15) 2.62(2). Molecule 2: Tl(2)-C(21) 3.00(1), Tl(2)-C(22) 3.04(1), Tl(2)-C(23) 3.13(1), Tl(2)-C(24) 3.10(1), Tl(2)-C(25) 3.03(1), Tl(2)-C(26) 2.82(1), Tl(2)-C(27) 2.86(1), Tl(2)-C(28) 2.91(1), Tl(2)-C(29) 2.90(1), Tl(2)-C(30) 2.86(1), Li(2)-C(21) 2.68(2), Li(2)-C(22) 2.61(2), Li(2)-C(23) 2.45(2), Li(2)-C(24) 2.46(2), Li(2)-C(25) 2.59(2). Averages over all molecules in the unit cell: Tl-Cp(a) (centroid) 2.61, Tl-Cp(b) (centroid) 2.85, Li-Cp(b) (centroid) 2.25, Li-N 2.23, Cp(a) (centroid)-Tl-Cp(b) (centroid) 153.3, Cp(a) (centroid)-Li-Cp(b) (centroid) 175.7.

While the Tl center of the discrete $[(\eta^5\text{-Cp})_2\text{Tl}]^-$ ion in **1** is attached almost equivalently to the two η^5-Cp ligands (av $Tl-Cp_{centroid}$ 2.72 Å), in **2** the terminal η^5-Cp contact (av $Tl-Cp(a)_{centroid}$ 2.60 Å) is significantly shorter than that made with the Li^+-bridging μ-Cp ligand (av $Tl-Cp(b)_{centroid}$ 2.85 Å). In **2**, the Li^+ ion competes with Tl for the electron density on the bridging Cp ligand. The Cp ligand is "dragged" away from the Tl center, and there is a compensatory enhancement in the interaction between the terminal η^5–Cp ligand and Tl; the $Tl-Cp(a)_{centroid}$ distance approaches that found in the gas-phase structure of monomeric $[(\eta^5\text{-Cp})\text{Tl}]$ (ca. 2.41 Å).[12] Similarly to the bridging μ–η^5-Cp ligand found in $[(\eta^5\text{-Cp})_2\text{E}(\mu\text{–}\eta^5\text{-Cp})\text{Na}\cdot\text{PMDETA}]$ (E = Sn, Pb), the μ-Cp bridge of **2** is bent (av $Tl-Cp(b)_{centroid}$-Li 175.2°, cf. ca. 172° in $[(\eta^5\text{-Cp})_2\text{E}(\mu\text{-}\eta^5\text{-Cp})\text{Na}\cdot\text{PMDETA}]$).[1–3]

Complexes **1** and **2** are only the second examples of monomeric Cp thallium(I) species characterized in the solid state; the only other known monomeric complex is $[TlC_5(CH_2Ph)_5]$.[13] Almost all structurally characterized Cp-based derivatives of thallium so far have had polymeric structures akin to that of $[(\eta^5\text{-Cp})\text{Tl}]_\infty$.[5] Additionally, **1** and **2** are the only structurally characterized unsubstituted Cp derivatives apart from $[(\eta^5\text{-Cp})\text{Tl}]_\infty$. The closest structural analogue to **1** and **2** is the dimeric ring complex $[\{\text{TlAu}(C_5H_4PPh_2)_2\}_2]$, in which essentially linear $[C_5H_4PPh_2\text{–Au–}C_5H_4PPh_2]$ units are linked together through η^5-Cp contacts to Tl^I ($Cp_{centroid}$-Tl-$Cp_{centroid}$ ca. 135°).[14] In view of our results this complex can be reinterpreted as an ion-contacted gold thallate complex rather than the implied Tl-contacted gold diphosphide, although there is some ambiguity as to the charge distribution in the ligand.

To our knowledge, $[(\eta^5\text{-Cp})\text{Mg}\cdot\text{PMDETA}]^+$ of **1** is the first example of a mononuclear cationic fragment derived from $[Cp_2Mg]$.[15] It is interesting to note that, although its bonding is largely ionic, the cation is formally isoelectronic with the 12-electron compound $[Cp_2Mg]$.

Ab initio MO calculations were performed on various isomers of the discrete $[Cp_2Tl]^-$ ion in **1** at the Hartree–Fock level and with electron correlation.[16, 17] Initially minimum basis set (MBS) calculations were performed on different Cp ring conformations, to assess the relative stabilities of the "linear" and "bent" models. The most stable bent C_s conformer (**I**), the same as that observed for the $[Cp_2Tl]^-$ ion in **1** in the solid state, and the most stable linear D_{5d} conformer (**II**) were then optimized using the ECP-DZ basis set. Their geometries and that of [CpTl] (**III**) are shown in Figure 3. The

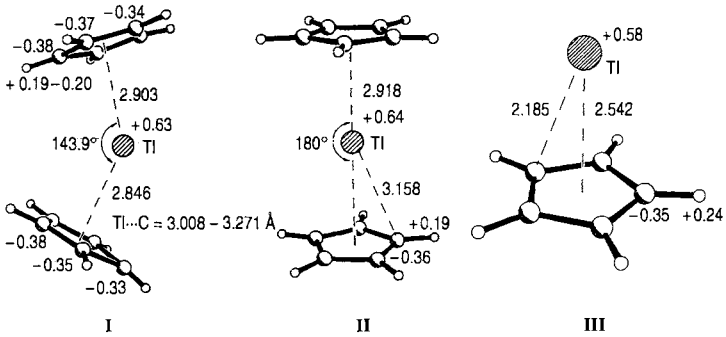

Fig. 3. Optimized geometries (DZ basis set) of the $[Cp_2Tl]^-$ ion—the bent structure with C_s symmetry (**I**) and the linear structure with D_{5d} symmetry (**II**)—and that of monomeric [CpTl] (**III**).

energy for the association of Cp^- and [CpTl] is reasonably favorable (– 6.38 kcal mol^{-1} to give the most stable bent structure **I**).[17] Although the Cp–Tl contacts are significantly elongated in **I** and **II** compared to the Cp–Tl distance in **III**, there is little difference either in the charge carried by the Cp ring atoms or in the charge on the Tl center. Bending of the linear structure **II** producing **I** slightly enhances the Cp–Tl interactions but has only a marginal effect on the charge distribution within the molecule. However, whereas in **II** the Cp ligands are symmetrically attached to Tl ($Cp_{centroid}$–Tl 2.918 Å), in **I** one of the Cp ligands is closer to the metal than the other is ($Cp_{centroid}$–Tl) 2.846 and 2.903 Å).

The optimized geometries (DZ basis set) of the linear and bent isomers of $[Cp_2Tl]^-$ were employed in a series of calculations with electron correlation. The results (MP2, MP3, MP4) confirm that the bent geometry is only slightly more stable than its linear counterpart; at the MP4 level the difference in energy is 0.82 kcal mol^{-1}.[17] This finding is contrary

to that calculated for the 14-electron complex $[Cp_2Ge]$ and to the general concensus concerning $[Cp_2Sn]$,[18–20] which proposes that bent structures are preferred on electronic grounds since bending presumably stabilizes the lone pair in the antibonding a_{1g}^* molecular orbital as a consequence of the admixing of this orbital with the metal p_x atomic orbital. Overall, the calculations on $[Cp_2Tl]^-$ indicate that the geometry of the thallocene anion is highly flexible. Orbital admixing appears to be ineffective here and a largely spherical lone pair orbital is present. This feature is illustrated in Figure 4 where, in addition, it can be seen that there is a constriction in the electron density between Tl and the more weakly attached Cp ligand.

Fig. 4. One of the isosurfaces of electron density for the bent structure of $[Cp_2Tl]^-$ having C_s symmetry (geometry optimization with the DZ basis set).

Experimental Procedure

1: [CpTl] (0.538 g, 2.0 mmol) was stirred with $[Cp_2Mg]$ (0.308 g, 2 mmol) in 10 mL THF. The reactants dissolved giving a golden brown solution. On addition of PMDETA (0.42 mL, 2 mmol) a pink solid precipitated, which dissolved on heating the reaction mixture to reflux. The reaction mixture was filtered and cooled slowly (12 h at 20 °C) to give air-sensitive, light-pink crystals of **1**. Yield 0.360 g (30%) over two batches; decomp 120 °C to black solid; IR (Nujol) $\tilde{\nu}$=3059 cm^{-1} (Cp-H); ^1H NMR (+25 °C, 400 MHz, $[D_8]$ THF): δ=5.66 (s, 15 H; CpH), 2.41 (s, 3H; CH_3N), 2.34 (s, 12H; $(CH_3)_2N$), 2.11 (s, 8 H; $(CH_2)_2$); ^{13}C NMR (+25 °C, 100.6 MHz, $[D_8]$ THF): δ=107.0 (C_5H_5), 55.0–59.0 (CH_3N and $(CH_3)_2N$), 46.0–49.0 ($(CH_2)_2$; correct C, H, N analysis.

2: [CpTl] (0.538 g, 2.0 mmol) was stirred with [CpLi] (0.288 g, 4 mmol) in 10 mL THF. The solid dissolved giving a yellow solution which was filtered before PMDETA (0.42 mL, 2 mmol) was added. Cooling of the resulting solution (2 d at −35 °C) gave air-sensitive, colorless crystals of **2**. The crystals melt and/or redissolve below 0 °C, and all attempts to isolate them were unsuccessful. **2** could only be characterized by low-temperature X-ray crystallography [7].

Received: June 11, 1993 [Z 6134 IE]
German version: *Angew. Chem. 1993, 105*, 1807

[1] M. G. Davidson, D. Stalke, D. S. Wright, *Angew. Chem.* **1992**, *104*, 1265–1266; *Angew. Chem. Int. Ed. Engl.* **1992**, *31*, 1226–1227.
[2] A. J. Edwards, M. A. Paver, P. R. Raithby, C. A. Russell, D. Stalke, D. S. Wright, *J. Chem. Soc. Dalton Trans.* **1993**, 1465–1466.
[3] D. R. Armstrong, M. G. Davidson, D. Moncrieff, C. A. Russell, D. Stalke, A. Steiner, D. S. Wright, *J. Am. Chem. Soc.*, submitted.
[4] C. Panattoni, G. Bombieri, U. Croato, *Acta Crystallogr. Sect. A* **1966**, *21*, 823–826.
[5] C. Panattoni, E. Frasson, F. Menegus, *Nature* **1963**, *199*, 1087–1089.
[6] Crystal data for **1**: $C_{24}H_{38}N_3MgTl$, M = 597.3, monoclinic, space group $P2_1/c$, a = 15.129(3), b = 15.483(4), c = 21.090(4) Å, $\alpha = \gamma = 90°$, β = 90.02(3), V = 4.940 nm^{-3}, Z = 8, ρ_{calcd} = 1.606 $Mg\,m^{-3}$, λ = 0.71073 Å, T = −120 °C, $\mu(Mo_{K\alpha})$ = 6.578 mm^{-1}. Data were collected on a Siemens-Stoe AED diffractometer using an oil-coated, rapidly cooled crystal of dimensions 0.2 × 0.2 × 0.2 mm in an oil drop [7] by the $2\theta/\omega$ method ($8° \le 2\theta \le 45°$). Of a total of 13787 collected reflections, 6434 were independent. The data were corrected for absorption by a semiempirical method based on Ψ scans. The structure was solved by Patterson methods (SHELXS-90)[8] and refined by full-matrix least-squares on F^2 [9] to final values of $R1$ ($F > 4\sigma(F)$) = 0.083 and $wR2$ = 0.193 (all data) [$R1 = \sum|F_o - F_c|/\sum F_o$ and $wR2 = (\sum w(F_o^2 - F_c^2)^2/\sum w(F_o^2)^2)^{0.5}$]; largest peak and hole in the final difference Fourier map were 4.152 and −2.218eÅ^{-3}. The structure was successfully refined as a twin, in which the monoclinic angle, very close to 90°, shows orthorhombic symmetry to be emulated. The twinning factor B refines to 0.488 (C. S. Pratt, B. A. Coyle, J. A. Ibers, *J. Chem. Soc. A.* **1971**, 2146–2152). Crystal data for **2**: $C_{19}H_{33}LiN_3Tl$, M = 514.79, monoclinic, space group $P2_1/c$, a = 13.390(3), b = 25.604(6), c = 13.390(3) Å, $\alpha = \gamma = 90°$, β = 112.39(3)°, V = 4245(2)Å^{-3}, Z = 8, ρ_{calcd} = 1.611 $Mg\,m^{-3}$, λ = 0.71073 Å, T = −120 °C, $\mu(Mo_{K\alpha})$ = 7.615 mm^{-1}. Data were collected on a Siemens-Stoe AED diffractometer using an oil-coated, rapidly-cooled crystal of dimensions 0.2 × 0.1 × 0.1 mm in an oil drop [7] by the $2\theta/\omega$ method ($8° \le 2\theta \le 45°$). Of a total of 17661 collected reflections, 5644 were independent. The data were corrected for absorption by a semiempirical method based on Ψ scans. The structure was solved by Patterson methods (SHELXS-90)[8] and refined by full-matrix least-squares on F^2 [9] to final values of $R1$ ($F > 4\sigma(F)$) = 0.043 and $wR2$ = 0.112 (all data) [$R1 = \sum|F_o - F_c|/\sum F_o$ and $wR2 = (\sum w(F_o^2 - F_c^2)^2/\sum w(F_o^2)^2)^{0.5}$]; largest peak and hole in the final difference Fourier map were 2.117 and −1.887 eÅ. The structure was successfully refined as a twin. Since a and c are the same length orthorhombic symmetry is shown to be emulated. The twinning factor B refines to 0.474(1) (C. S. Pratt, B. A. Coyle, J. A. Ibers, *J. Chem. Soc. A.* **1971**, 2146–2152). Further details of the crystal structure investigations are available on request from the Director of the Cambridge Crystallographic Data Centre, 12 Union Road, GB-Cambridge, CB2 1EZ, on quoting the full journal citation.
[7] T. Kottke, D. Stalke, *J. Appl. Crystallogr.* **1993**, *26*, 615–619.
[8] G. M. Sheldrick, *Acta Crystallogr. Sect. A* **1990**, *46*, 467–473.
[9] G. M. Sheldrick, SHELXL-93, Göttingen, **1992**.
[10] a) First synthesis: E. O. Fischer, H. Grüber, *Z. Naturforsch. B*, **1956**, *11*, 1182; b) Structure analysis: J. L. Atwood, W. E. Hunter, A. H. Cowley, R. A. Jones, C. A. Stewart, *J. Chem. Soc. Chem. Commun.* **1981**, 925–927.
[11] A. Almenningen, A. Haaland, T. Motzfeld, *J. Organomet. Chem.* **1967**, *7*, 97–104.
[12] J. K. Tyler, A. P. Cox, J. Sheridan, *Nature* **1959**, *183*, 1182.
[13] H. Schumann, C. Janiak, M. A. Khan, J. J. Zuckermann, *J. Organomet. Chem.* **1988**, *354*, 7–13.
[14] G. K. Anderson, N. P. Rath, *J. Organomet. Chem.* **1991**, *414*, 129–135.
[15] W. Bünder, E. Weiss, *J. Organomet. Chem.* **1975**, *92*, 1–6.
[16] M. J. Frisch, G. W. Trucks, P. M. Head-Gordon, P. M. W. Gill, M. W. Wong, J. B. Forseman, B. G. Johnson, H. B. Schleger, M. A. Robb, E. S. Replogle, R. Gomperts, J. L. Andres, K. Raghavachari, J. S. Binkley, C. Gonzalez, R. L. Martin, D. Fox, D. J. Defrees, J. Baker, J. J. P. Stewart, J. A. Pople, Gaussian 92, Gaussian Inc., Pittsburgh, PA, **1992**.
[17] Calculational data for $[Cp_2Tl]^-$: An Effective Core Potential (ECP) basis set was used for Tl in all calculations (P. J. Hay and W. R. Wadte, *J. Chem. Phys.* **1985**, *82*, 270, 284, and 299). Absolute energies E in atomic units and relative energies [kcal mol^{-1}] in parentheses: MBS, bent C_{2v} (α) ("toe-to-toe" Cp arrangement) E = −429.834961 (0.25), bent C_s (model **I**) E = −429.835351 (0.0), bent $C_{2v}(\beta)$ ("heel-to-heel" Cp arrangement) E = −429.835305 (0.0), linear D_{5h} E = −429.827620 (4.85), linear D_{5d} (model **II**) E = −429.827622 (4.85). DZ, model **II** E = −434.530730 (0.70), model **I** E = −434.531859 (0.0), CpTl E = −242.341708, Cp^- E = −192.145581. MP2, model **II** E = −435.483388(0.73), model **I** E = −435.484498 (0.0). MP3, Model **II** E = −435.532835 (0.37), model **I** E = −435.533421 (0.0). MP4, model **II** E = −435.5881261 (0.82), model **I** E = −435.589433 (0.0).
[18] C. Elschenbroich, A. Salzer, *Organometallchemie*, 2nd ed., Teubner, Stuttgart, **1988**; *Organometallics*, 1st ed., VCH, Weinheim, **1988**, p. 134.
[19] P. Jutzi, *Adv. Organomet. Chem.* **1986**, *26*, 217–285.
[20] J. Almlöf, L. Fernholt, K. Faegri, Jr., A. Haaland, B. E. R. Schilling, R. Seip, K. Taugløl, *Acta Chem. Scand. Ser. A* **1983**, *37*, 131–140.

Conformational Analysis of Model Complexes for Methyl-Coenzyme-M Reductase from Methanogenic Bacteria: A Comparison of Crystal and Solution Structures**

By *Albrecht Berkessel,* Michael Bolte, Christian Griesinger,* Gottfried Huttner, Thomas Neumann, Berthold Schiemenz, Harald Schwalbe,* and *Thomas Schwenkreis*

In the last step of the archaebacterial methanogenesis, the methylthioether methyl-coenzyme-M **1** reacts with the thiol *N*-7-mercaptoheptanoyl-*O*-phospho-*L*-threonine ("HS-HTP", **2**) to yield methane and the mixed disulfide **3**.[1] This unusual reaction is brought about by the enzyme methyl-coenzyme-M reductase, which contains the nickel tetrahydrocorphinoid "factor 430" (F_{430}) as cofactor.[2] In general, metalloenzyme-mediated catalysis depends on the specific interaction between substrate(s) and metal ion(s). Also in the case of methyl-coenzyme-M reductase it is assumed that the nickel ion of F_{430} participates in the catalytic process.[3]

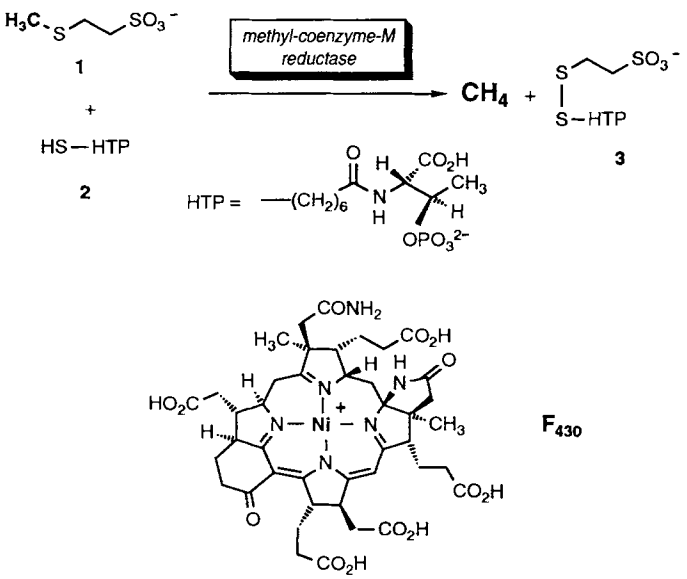

Transition metal complexes of multidentate ligands have been used successfully as models for the study of metal–substrate interactions in metalloenzymes.[4] For methyl-coenzyme-M reductase, nickel chelates such as *rac*-**4** have been used to simulate the interaction of the organosulfur substrates **1** and **2** with cofactor F_{430}: the comparison of the redox properties of model complexes made it possible to develop a mechanistic hypothesis for the catalytic cycle of methyl-coenzyme-M reductase.[5] The Ni^{II} complexes *rac*-**4**–**6** are derivatives of Ni^{II}-salen, in the sense that one C–N double bond has been modified into a C–N single bond.[7, 10] The corresponding carbon atom now bears a thioether-containing side chain; the nitrogen atom is bound to a hydrogen atom in *rac*-**4** and to a methyl group in *rac*-**5**, **6**. The flexibility of the side chain enables the coordination of its heteroatom to the metal ion. Through rotation around the C–C single bond marked by an arrow, however, other local conformations are possible, in which the sulfur atom is turned away from the metal ion. Figure 1 shows the Newman projections of the three staggered conformations about this C–C single bond.

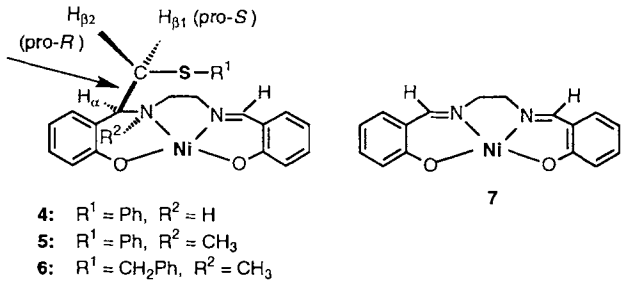

4: $R^1 = Ph$, $R^2 = H$
5: $R^1 = Ph$, $R^2 = CH_3$
6: $R^1 = CH_2Ph$, $R^2 = CH_3$

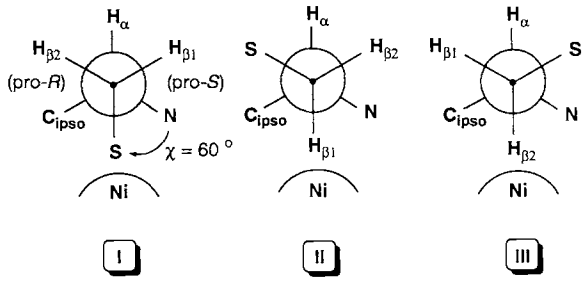

Fig. 1. Newman projections for the staggered conformations of the side chains of the nickel chelates *rac*-**4**–**6**; antiperiplanar arrangement of H_α and S, H_α-$H_{\beta 1}$, and H_α-$H_{\beta 2}$.

In order to find out whether model complexes of the type *rac*-**4**–**6** can be used to demonstrate an attractive interaction between the sulfur atom in the side chain (representing the sulfur-containing substrates of methyl-coenyzme-M reductase) and the nickel ion (representing the nickel ion in F_{430}), it appeared promising to determine the preferred conformation of the thioether side chain in *rac*-**4**–**6**. Herein we report the conformational analysis of the nickel complexes *rac*-**4**–**6** in solution by NMR spectroscopy and compare the preferred conformations thus found with the side chain conformations in the crystals of the respective compounds.

The thioether side chain in the crystal structure of the Ni^{II} complex *rac*-**4** has the local conformation I; the sulfur atom is coordinated to the nickel ion, the dihedral angles H_α-C-C-$H_{\beta 1}$ and H_α-C-C-$H_{\beta 2}$ are $-59.2°$ and $59.7°$, respectively (Fig. 1, conformation I and Fig. 2a). A centrosymmetric dimer is formed from one molecule each of **4** and *ent*-**4**. This dimer is stabilized by two NH···O hydrogen bonds. In this arrangement the sixth coordination site of the nickel ion of one molecule is filled by the phenolate oxygen atom of the other molecule in the dimer, resulting in a distorted octahedral coordination geometry at Ni. The distances from the nickel ions in *rac*-**4**, **5**, and **6** to the N, O, and S atoms of the ligands are listed in Table 1.

[*] Prof. Dr. A. Berkessel, Dipl.-Chem. T. Schwenkreis
Organisch-chemisches Institut der Universität
Im Neuenheimer Feld 270, D-69120 Heidelberg (FRG)
Telefax: Int. code +(6221)56-4205
Prof. Dr. C. Griesinger, Dr. M. Bolte, Dipl.-Chem. H. Schwalbe
Institut für Organische Chemie der Universität
Marie-Curie-Strasse 11, D-60439 Frankfurt am Main
Prof. Dr. G. Huttner, Dipl.-Chem. B. Schiemenz
Anorganisch-chemisches Institut der Universität Heidelberg
Dipl.-Chem. T. Neumann
Institut für Organische Chemie der Universität Göttingen

[**] This work was supported by the Bundesministerium für Forschung und Technologie (Projekt 0318801), the Deutsche Forschungsgemeinschaft (Projekt Be 998/2-1,2), and the Fonds der Chemischen Industrie.

Table 1. Distances [Å] between the nickel ion and the heteroatoms in the ligands in complexes *rac*-**4**[7], *rac*-**5**[9], and **6**[11,12] (from crystal structures).

Complex	Ni-S	Ni-O1	Ni-O2	Ni-O1*	Ni-N1	Ni-N2
rac-**4**	2.575(5)	2.026(4)	1.981(4)	2.109(4)	2.060(5)	1.989(5)
rac-**5**	4.826(3)	1.834(3)	1.864(3)	–	1.846(3)	1.922(4)
6	4.751(3)	1.841(3)	1.847(5)	–	1.843(7)	1.926(4)

Table 2. Vicinal coupling constants[a] and distances determined by NOE experiments[a] on the nickel chelates *rac*-**4**–**6**.

No.	Vicinal coupling constants, distance	Nickel chelate *rac*-**4**	*rac*-**5**	*rac*-**6**
1	$^3J(H_x,H_{\beta 1})$ [Hz]	2.9	2.5	3.4
2	$\delta(H_{\beta 1})$	4.45	5.24	4.29
3	$^3J(H_x,H_{\beta 2})$ [Hz]	9.5	8.0	7.9
4	$\delta(H_{\beta 2})$	4.54	4.82	4.52
5	NOE(H_x-$H_{\beta 1}$) [b] [pm]	278	269	278
6	NOE(H_x-$H_{\beta 2}$) [b] [pm]	250	250	250
7	NOE($H_{\beta 1}$-$H_{ethylene}$) [b, c] [pm]	237	213	213
8	NOE($H_{\beta 2}$-$H_{ethylene}$) [b, c] [pm]	344	272	286

[a] For experimental details see ref.[13]. [b] Calibrations based on NOE cross peak intensities of the two geminal protons $H_{\beta 1}$, $H_{\beta 2}$; $d(H_{\beta 1}\cdots H_{\beta 2}) = 178$ pm (standard bond lengths and angles; error ± 10 pm). [c] pro-*S*-H of the methylene group adjacent to the amine nitrogen atom, labeled H_e ("$H_{ethylene}$") in Figures 2a–c.

The crystal structure of the nickel complex *rac*-**5** shows it to be monomeric, and the sulfur atom of the thioether side chain is *not* bound to the Ni^{II} ion (Fig. 2b).[7,9] Instead, the side chain exhibits conformation II (Fig. 1). Hence, the Ni^{II} ion in *rac*-**5** is four-coordinate with a square-planar coordination geometry. The exchange of the phenylthio moiety in the side chain with a benzylthio group led to the Ni^{II} complex *rac*-**6**, which formed high-quality crystals readily. Its crystal structure[7,11,12] shows that **6** is monomeric in the crystalline state and is present in conformation II (Fig. 1).

The three Ni^{II} chelates *rac*-**4**–**6** are diamagnetic in solution (^{1}H NMR); for *rac*-**4** in $CDCl_3$, however, slightly broadened signals were observed for $H_{x,\beta 1,\beta 2}$. The addition of [D_6]dimethylsulfoxide ([D_6]DMSO) led to "normal" line widths. In spite of the completely different side chain conformations found in the crystal structures, *rac*-**4**–**6** exhibit similar vicinal coupling constants $^3J_{Hx-H\beta 1}$, $^3J_{Hx-H\beta 2}$ (Table 2). These NMR data can be interpreted with three models: 1) *one* staggered conformation (I *or* II *or* III in Fig. 1), 2) *one* nonstaggered conformation ($\varkappa \neq 60, 180, -60°$), and 3) a Pachler equilibrium[14] of the three staggered conformations I–III (Fig. 1). Model 1: The "large–small" coupling pattern observed for all three complexes cannot be explained by the exclusive presence of the staggered conformation I, which was found in the crystal structure of *rac*-**4** (Fig. 2a). The approximately equal dihedral angles H_x-C-C-$H_{\beta 1}$ and H_x-C-C-$H_{\beta 2}$ ($\varkappa \approx \pm 60°$) should lead to roughly equal coupling constants $^3J_{Hx-H\beta 1}$ and $^3J_{Hx-H\beta 2}$. The presence of *exclusively* conformations II and III is contradicted by the value of $^3J_{Hx-H\beta 2}$ (Table 2, line 3), which is too small for a purely *trans* coupling. Model 2: The attempt to interpret the experimental data with a nonstaggered conformation leads to high standard deviations and incompatible results from the ^3J and NOE analyses. Model 3: Table 3 lists the results of the Pachler analysis[14] for the complexes *rac*-**4**–**6**. For all three complexes an approximately 1:1 distribution of a *trans–gauche* (II or III, Fig. 1) and the *gauche–gauche* conforma-

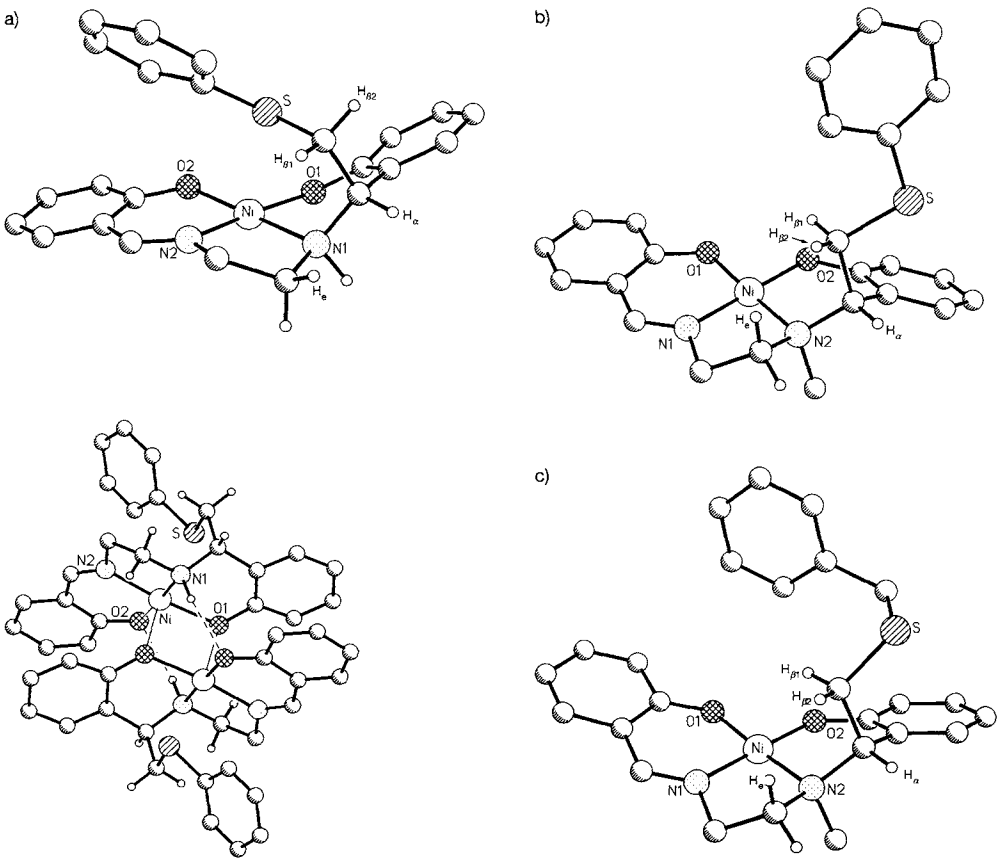

Fig. 2. a) Crystal structure of *rac*-**4**. Top: only **4** is shown; bottom: centrosymmetric dimer of **4** and *ent*-**4**. The hydrogen bonds between N1 and O2* as well as between N1* and O2 are depicted by dashed lines, the intermolecular Ni–O coordination is indicated by thin lines. b) Crystal structure of *rac*-**5** (only one enantiomer is shown). c) Crystal structure of **6**.

Table 3. Model 3: Calculated conformer populations (I, II, III) for the complexes *rac*-**4**–**6** (in %).

Conformation	*rac*-**4**		*rac*-**5**		*rac*-**6**	
	J [a]	NOE [b]	*J* [a]	NOE [b]	*J* [a]	NOE [b]
I	63	60	50	56	49	60
II	6(31) [c]	2(38) [c]	2(48) [c]	1(43) [c]	10(41) [c]	2(38) [c]
III	31(6) [c]	38(2) [c]	48(2) [c]	43(1) [c]	41(10) [c]	38(2) [c]

[a] The Karplus equation was parameterized according to McLaughlin et al. [15c], $^3J(H\alpha,H\beta)(\theta) = 12.1\cos^2\theta - 1.6\cos\theta$. [b] The conformer distribution was calculated assuming an r^{-6} averaging of the NOE. [c] Based on the homonuclear $^3J(H\alpha,H\beta)$ coupling data and the NOEs between these nuclei, it is impossible to distinguish between equilibria of II and I, and III and I.

tion (I, Fig. 1) is found. The determination of the preferred *trans–gauche* conformation and the assignment of the diastereotopic protons $H_{\beta1}$ and $H_{\beta2}$ was possible by measuring the NOE between the pro-*S* methylene proton adjacent to N2 in *rac*-**6** (labeled H_e, "$H_{ethylene}$" in Fig. 2a–c) and $H_{\beta1}$ and $H_{\beta2}$, respectively. If one assumes the conformation for the ethylene group that was found in the crystal structure,[16] the local conformations I, II, and III of the thioether side chain lead to the distances between $H_{\beta1}$, $H_{\beta2}$, and $H_{ethylene}$ that are summarized in Figure 3. By using the Pachler equi-

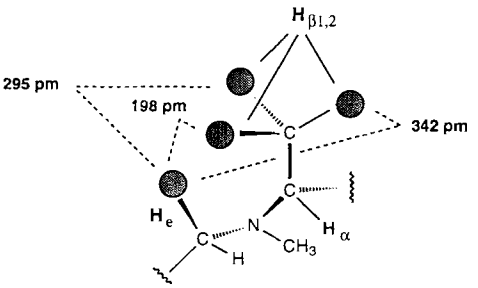

Fig. 3. Distances from the H_e atom ("$H_{ethylene}$", pro-*S*-H) to the three possible positions of $H_{\beta1}$ and $H_{\beta2}$.

librium, (derived from analysis of the coupling constants) for complex *rac*-**6** (conformation I, 49%; II, 10%; III, 41%) (Table 3), the protons $H_{\beta1}$ and $H_{\beta2}$ are calculated to be on average 227 and 269 pm from $H_{ethylene}$. This is in agreement with the experimentally found data (Table 2, lines 7,8). The stereochemical assignment of $H_{\beta1}$ and $H_{\beta2}$ follows from this equilibrium to be pro-*S* and pro-*R*, respectively. The reverse population of conformers II and III (I, 49%; II, 41%; III, 10%) leads to roughly equal average distances between $H_{\beta1,2}$ and $H_{ethylene}$ (225 and 221 pm), which is in contrast to the NOE-derived distances of 213 and 286 pm (Table 2, lines 7,8) and is therefore ruled out. In all three complexes (*rac*-**4**–**6**) one observes average distances between $H_{\beta1,2}$ and $H_{ethylene}$ that are different in magnitude. Hence, it appears justified to assume an approximately 1:1 equilibrium of the conformers I and III for all three complexes in solution. The equilibria found for the three complexes are in agreement with the nearly equal average coupling constants $^3J_{N-H\beta1}$ and $^3J_{N-H\beta2}$ for *rac*-**5** of 1.4 and 1.8 Hz, respectively. These couplings were determined according to the method of Keeler and Neuhaus[18] from a 2D heteronuclear multiple bond correlation (HMBC) NMR spectrum of the complex which was ^{15}N labeled at N2 (Fig. 4).

In summary, the following conclusions appear justified: 1) There is no dominant, attractive Ni–S interaction in the monomeric, neutral Ni^{II}-dihydrosalen complexes *rac*-**4**–**6** in

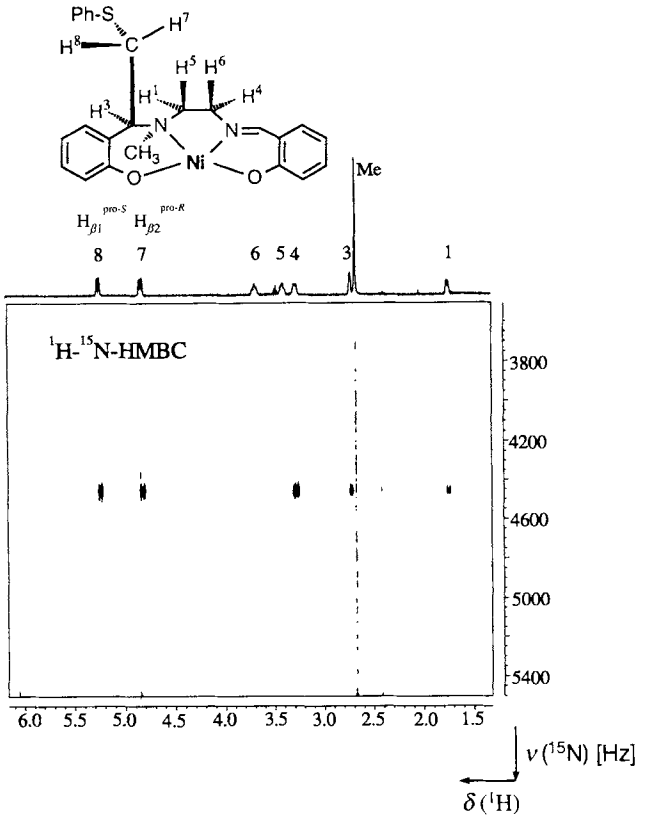

Fig. 4. ^1H-^{15}N HMBC NMR spectrum of the complex *rac*-**5**.

solution. Presumably the conformer equilibrium is regulated in all three cases to about the same extent by nonbonding, intramolecular interactions. 2) The formation of two NH···O hydrogen bonds favors the dimerization of complex *rac*-**4** in the crystal[19] and leads to a higher coordination number for the nickel ion, initially by the axial coordination of a phenolate oxygen atom. The coordination of the thioether sulfur atom then completes the pseudooctahedral ligand sphere.

The study of the complexes *rac*-**4**–**6** by NMR spectroscopy and X-ray crystal structure analysis shows once again[20] that the conformation that is "frozen out" in the crystal is not necessarily the preferred conformation in solution and that the support or hindrance (in the crystal or by the solvent) of hydrogen-bond- induced self-association can result in dramatic changes in the conformer distribution. For the substrate–cofactor interaction in methyl-coenzyme-M reductase, this leads to the interesting possibility that the strength of the binding could be regulated by the absence or presence of a sixth ligand on the nickel ion of F_{430}.

Received: June 24, 1993 [Z 6167 IE]
German version: *Angew. Chem.* **1993**, *105*, 1776

[1] J. Ellermann, R. Hedderich, R. Böcher, R. K. Thauer, *Eur. J. Biochem.* **1988**, *172*, 669–677.
[2] a) G. Färber, W. Keller, C. Kratky, B. Jaun, A. Pfaltz, C. Spinner, A. Kobelt, A. Eschenmoser, *Helv. Chim. Acta* **1991**, *74*, 697–716; b) A. Fässler, A. Kobelt, A. Pfaltz, A. Eschenmoser, C. Bladon, A. R. Battersby, R. K. Thauer, *ibid.* **1985**, *68*, 2287–2298.
[3] a) S. Rospert, M. Voges, A. Berkessel, S. P. J. Albracht, R. K. Thauer, *Eur. J. Biochem.* **1992**, *210*, 101–107; b) S. Rospert, R. Böcher, S. P. J. Albracht, R. K. Thauer, *FEBS Lett.* **1991**, *291*, 371–375.
[4] a) H. Dugas, *Bioorganic Chemistry*, 2nd ed., Springer, Heidelberg, **1989**; b) W. Kaim, B. Schwederski, *Bioanorganische Chemie*, Teubner, Stuttgart, **1991**.
[5] A. Berkessel, *Bioorg. Chem.* **1991**, *19*, 101–115.
[6] a) M. D. Hobday, T. D. Smith, *Coord. Chem. Rev.* **1972/1973**, *9*, 311–337;

b) A. G. Manfredotti, C. Guastini, *Acta Crystallogr. Sect. C* **1983**, *39*, 863–865.

[7] The preparation of complex *rac*-**4** and its crystal structure analysis have both been reported [5,8]. The synthesis of the N-methylated nickel chelates *rac*-**5**,**6** will be reported at a later date. In contrast to *rac*-**4** [8], *rac*-**5**,**6** are *not* oxygen-sensitive.

[8] A. Berkessel, J. W. Bats, C. Schwarz, *Angew. Chem.* **1990**, *102*, 81–84; *Angew. Chem. Int. Ed. Engl.* **1990**, *29*, 106–108.

[9] Crystals of *rac*-**5** suitable for structure determination were obtained from a solution of the complex in methanol by slow evaporation of the solvent at room temperature. *rac*-**5**: $C_{24}H_{24}N_2O_2SNi$, monoclinic, space group $P2_1/n$, $a = 8.577(8)$, $b = 9.936(8)$, $c = 24.66(3)$ Å, $\beta = 99.53(6)^\circ$, $V = 2073(4)$ Å^3, $Z = 4$, $\rho_{calc} = 1.484$ g cm^{-3}; Siemens (Nicolet-Syntex) R3m/V diffractometer, $Mo_{K\alpha}$ radiation, 2θ range = 2–50°, 5119 total measured reflections, 3655 symmetry-independent reflections; no absorption correction; 2880 reflections with $I > 2\sigma(I)$ were used for the structure solution and refinement [SHELX 76 (G. Sheldrick, Cambridge University, **1976**), SHELXTL-PLUS (G. Sheldrick, University of Göttingen, **1988**)]; $R = 0.038$, $R_w = 0.034$; data/parameter ratio = 11.9:1, maximum residual electron density 0.46 eÅ^{-3}. All non-hydrogen atoms were refined anisotropically. The imine H atom was located and refined isotropically. The positions of all other H atoms were calculated and the temperature factors were refined. Ref. [12b].

[10] Examples for Ni^{II}-dihydrosalen complexes without side chains: A. Böttcher, H. Elias, L. Müller, H. Paulus, *Angew. Chem.* **1992**, *104*, 635–637; *Angew. Chem. Int. Ed. Engl.* **1992**, *31*, 623–625.

[11] *rac*-**6** crystallizes as a conglomerate of **6** and *ent*-**6**.

[12] a) Crystals of **6** suitable for structural determination were obtained by slowly cooling a solution of the complex *rac*-**6** in ethyl acetate. **6**: $C_{25}H_{26}N_2O_2SNi$, hexagonal, space group $P6_5$, $a = 21.351(2)$, $c = 10.124(1)$ Å, $V = 3996.9(7)$ Å^3, $Z = 6$, $\mu = 1.91$ mm^{-1}, $\rho_{calc} = 1.190$ g cm^{-3}; Enraf-Nonius CAD4 diffractometer, $Cu_{K\alpha}$ radiation, 2θ range = 2–120°, 3138 total measured reflections, 2802 symmetry-independent reflections; empirical absorption correction based on ψ scans of nine reflections with relative transmissions of 0.78–1.00; 2621 reflections with $F > 3\sigma(F)$ were used for the structure solution (Patterson method) and refinement (SHELXTL-PLUS program package), nonhydrogen atoms were refined anisotropically, H atoms were located using difference electron density maps and refined using a "riding" model. The absolute configuration was determined ($\eta = 1.1(1)$). $R = 0.051$ ($R_w = 0.065$, $w = \sigma^2(F) + 0.0008F^2$); data/parameter ratio = 9.4:1, maximum residual electron density 0.77 eÅ^{-3}. b) Further details of the crystal structure investigations of *rac*-**5** and **6** may be obtained from the Fachinformationszentrum Karlsruhe, Gesellschaft für wissenschaftlich-technische Information mbH, D-76344 Eggenstein-Leopoldshafen, (FRG) on quoting the depository numbers CSD-57467 or CSD-56660, respectively, the names of the authors, and the journal citation.

[13] Experimental details: ROESY of *rac*-**4**: delay 150 ms, spin lock 3 kHz, 1 kHz off resonance, operating frequency 600 MHz. NOESY of *rac*-**5**,**6**: operating frequeny 400 and 600 MHz, delay 150 ms, 200 ms, integration over the entire negative and positive region; 512 experiments with 16 scans per increment and 1024 complex points in t_2, zero filling in both dimensions, apodization using $\cos^2$. An off-resonance correction was performed for the integration of the ROE spectra. The HMBC spectrum was obtained at 600 MHz with 128 experiments and 8 scans. The $^3J(H\alpha\text{-}H\beta 1,2)$ coupling constants were determined using resolution-enhanced 1D spectra. All measurements were conducted at 300 K, *rac*-**4** in $CDCl_3$, *rac*-**5**,**6** in [D$_6$]DMSO. Solutions of *rac*-**4** were prepared under the exclusion of oxygen.

[14] a) K. G. R. Pachler, *Spectrochim. Acta* **1963**, *19*, 2085–2092; b) *ibid.* **1964**, *20*, 581–587.

[15] a) M. Karplus, *J. Am. Chem. Soc.* **1963**, *85*, 2870–2871; b) V. F. Bystrov, *Prog. NMR Spectrosc.* **1976**, *10*, 41–81; c) R. J. Abraham, K. A. McLauchlan, *J. Mol. Phys.* **1962**, *5*, 513–523.

[16] In the case of *rac*-**4**, the crystal structure indicated the "inverted" conformation for the ethylene bridge with a pseudoequatorial $H_{ethylene}$ (pro-*S*-H) (Fig. 2a). The assumption of this conformation for the ethylene bridge leads unambiguously to the same results with quantitatively slightly differing distance data.

[17] A. DeMarco, M. Llinas, K. Wüthrich, *Biopolymers* **1978**, *17*, 2727–2742.

[18] J. Keeler, D. Neuhaus, J. Titman, *Chem. Phys. Lett.* **1988**, *146*, 545–548.

[19] The line broadening observed in the ^{1}H NMR spectrum of the Ni^{II} complex *rac*-**4** in $CDCl_3$ indicates the onset of association/octahedral coordination even in this low-polarity solvent.

[20] a) H. Kessler, G. Zimmermann, H. Förster, J. Engel, G. Oepen, W. S. Sheldrick, *Angew. Chem.* **1981**, *93*, 1085–1086; *Angew. Chem. Int. Ed. Engl.* **1981**, *20*, 1053–1054; b) H. Kessler, J. W. Bats, J. Lautz, A. Müller, *Liebigs Ann. Chem.* **1989**, 913–928; c) N. B. Perry, J. W. Blunt, M. H. G. Munro, *Magn. Reson. Chem.* **1989**, *27*, 624–627; d) M. Billeter, A. D. Kline, W. Braun, R. Huber, K. Wüthrich, *J. Mol. Biol.* **1989**, *206*, 677–687; e) E. T. Baldwin, I. T. Weber, R. S. Charles, J.-C. Xuan, E. Appella, M. Yamada, K. Matsushima, B. F. P. Edwards, G. M. Clore, A. M. Gronenborn, A. Wlodawer, *Proc. Natl. Acad. Sci. USA* **1991**, *88*, 502–506.

Cation Inclusion within the Mixed-Valence Polyanion Cluster $[(Mo^{VI}O_3)_4Mo^{V}_{12}O_{28}(OH)_{12}]^{8-}$: Syntheses and Structures of $(NH_4)_7[NaMo_{16}(OH)_{12}O_{40}]\cdot 4H_2O$ and $(Me_2NH_2)_6[H_2Mo_{16}(OH)_{12}O_{40}]$**

By *M. Ishaque Khan, Achim Müller,* Stephan Dillinger, Hartmut Bögge, Qin Chen,* and *Jon Zubieta**

The understanding of the driving force for the formation of high-nuclearity clusters is still a challenge. This is especially valid for polyoxometalates having a tremendous variety of quasi-spherical structures with highly symmetrical core assemblies of MO_x units.[1] Though the famous α-Keggin anion $[Mo_{12}O_{40}P]^{3-}$,[2] which has an extremely high formation tendency, was isolated nearly 200 years ago and numerous compounds based on this isomer have been reported, the ε isomer (formally obtained by rotation of all four Mo_3O_{13} groups by 60°) seems to be rather unstable. *No pure Mo/O or W/O compound with ε-Keggin structure has yet been isolated.* The reason seems to be that the density of packing of the oxygen atoms decreases gradually from the α to the ε isomer,[3] whereby 12-membered ring systems result. This class of compounds is also of interest with regard to the new area of inorganic host–guest chemistry.[4–7] The polyvanadates, for instance, adopt basket, bowl, belt, barrel, and spherical structures which can encapsulate neutral, anionic, and cationic species, and even cation–anion aggregates.[8–16] Likewise, cyclic arsenic(III) polytungstates and phosphorus (V) polytungstates have been shown to encapsulate a variety of cations.[17, 18] In contrast, oxomolybdate cages or clusters accommodating guest species remain relatively rare, with the notable exception of the recently described cluster species $[Na(H_2O)_3Mo_{42}H_{15}O_{109}\{(OCH_2)_3CCH_2OH\}_7]^{7-}$.[19] We report here on the synthesis of a mixed-valence Mo^V/Mo^{VI} polyanion cluster which exhibits a central ε-Keggin unit and a cavity capable of accommodating protons or metal cations, as demonstrated by clusters **1** and **2**.

$(Me_2NH_2)_6[H_2Mo_{16}(OH)_{12}O_{40}]$ **1**

$(NH_4)_7[NaMo_{16}(OH)_{12}O_{40}]\cdot 4H_2O$ **2**

Both **1** and **2** were isolated in 20% yield from aqueous solutions containing molybdate and both organic and inorganic templates. The red needles of **1** and red-orange cubes of **2** are water soluble, and the latter rapidly become opaque when removed from the mother liquor. X-ray structural analyses[20] of **1** and **2** reveal the presence of discrete, ordered $[Mo_{16}(OH)_{12}O_{40}]^{8-}$ anions (Fig. 1) that have a central cavity encapsulating protons or a Na^+ ion. Both anions contain four Mo^{VI} centers, twelve Mo^V centers, forty oxo groups, and twelve hydroxy groups in full tetrahedral T_d symmetry.

The twelve Mo^V centers in **1** and **2** form six binuclear units with an Mo–Mo distance of 2.62(1) Å (single bond). The

[*] Prof. Dr. A. Müller, Dipl.-Chem. S. Dillinger, Dr. H. Bögge
Fakultät für Chemie der Universität
Postfach 100131, D-33501 Bielefeld 1 (FRG)
Telefax: Int. code + (521) 106-6003
Prof. Dr. J. Zubieta, Dr. M. I. Khan, Dr. Q. Chen
Department of Chemistry
Syracuse University
Syracuse, NY 13244 (USA)
Telefax: Int. code + (315) 443-4070

[**] This work was supported by the National Science Foundation, Grant No. CHE 9119910, and the Fonds der Chemischen Industrie. S. D., H. B., and A. M. thank Frau A. Armatage for her assistance in the X-ray structure analysis of **1**.

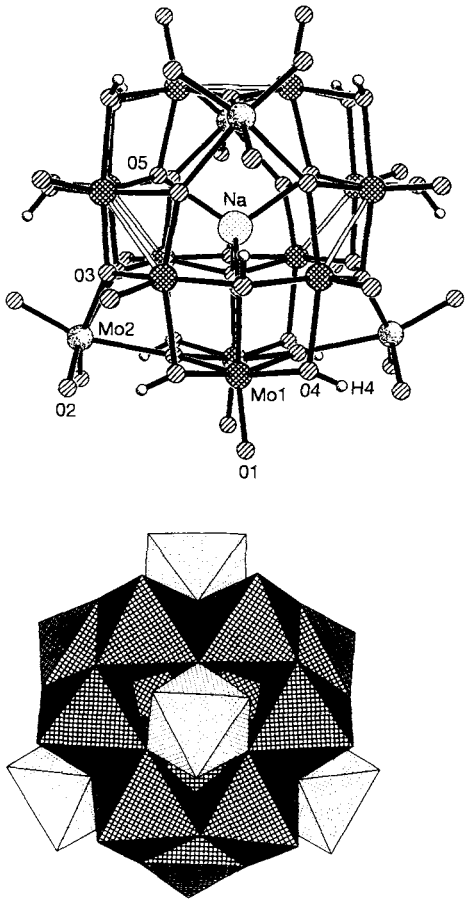

Fig. 1. Top: The structure of the cluster anion of **2**, $[Na(Mo^{VI}O_3)_4Mo^{V}_{12}(OH)_{12}O_{28}]^{7-}$, which possesses a $(H_{12}Mo_{16}O_{52})$ core essentially identical to that of **1**. Bottom: A polyhedral representation of the sturcture of the anion of **2** along the crystallographic threefold axis showing the location of the trioxomolybdenum(VI) units on the hexagonal faces of the $(Mo_{12}O_{40})$ core (see text).

four facial ($Mo^{VI}O_3$) "anti-Lipscomb" units[21] cap four faces of a Mo/O framework based upon the Mo^{V}_{12} truncated tetrahedron, whereby the four Mo^{VI} sites form an expanded Mo_4 tetrahedron. The high degree of reduction of the central core ($Mo_{12}O_{40}$) significantly increases the basicity of the oxygen atoms on the surface, which allows aggregation of the electrophilic (MoO_3) units.

The 52 oxygen atoms of the cluster anion are of five distinct types. The twelve O1 oxygen atoms are each terminally bonded to a Mo^{V} atom of the ($Mo_{12}O_{40}$) core at a distance of 1.69(2) Å. The twelve O2 oxygen atoms are associated with the four facial trioxomolybdenum ($Mo^{VI}O_3$) capping units as strongly bonded terminal oxo groups with an Mo2–O2 separation of 1.74(3) Å. Each of the twelve O3 oxygen atoms binds in an μ_3 fashion to Mo^{V} centers of the binuclear units and an Mo2 site; the bridging to the Mo1 sites is unsymmetrical with Mo1–O3 distances of 1.89(3) Å and 2.08(3) Å, while the Mo2–O3 distance is 2.22(3) Å. The Mo1–O4 bond lengths of 2.14(4) and 2.09(3) Å and valence sum calculations[24] identify the twelve O4 bridging functions as μ_2-hydroxy groups. Although the protons could not be unambiguously located from the X-ray analysis,[25] they most likely form intramolecular hydrogen bonds with the O2 centers, as shown in Figure 1, with O2···O4 and O2···H4 distances of 2.82 Å and 1.89 Å, respectively. The four O5 oxygen atoms define the perimeter of the cavity formed by the molybdenum–oxygen cage. Each O5 atom coordinates in an μ_4 fashion to three Mo^{V} sites and to the encapsulated and tetrahedrally coordinated Na^+ ion in the case of **2**. The Mo1–O5 and Na–O5 distances are 2.10(1) Å and 2.18(3) Å, respectively. The relatively short Na–O distances are consistent with those previously reported in hexanuclear molybdophosphate and molybdophenylphosphonate units in cluster anions such as $[(H_3O)_2NaMo_6P_4O_{24}(OH)_7]^{2-}$[26] and $[Na\{Mo_6O_{15}(O_3PC_6H_5)_4\}_2]^{15-}$.[27, 28] While the low coordination number for Na^+ is unusual, it is not without precedent,[29] and a similar tetrahedral environment has been described for the encapsulated ion of $[Na(i\text{PrSn})_{12}O_4(OH)_{24}]^{5+}$.[30] These results suggest that the geometric requirements of the metal–oxygen cage dictate the size of the cavity. The four oxygen atoms that define the cavity perimeter for **1** exhibit valence sums of 1.19 to 1.35, which suggests that these sites are partially protonated. In view of the total charge of the $[Mo_{16}(OH)_{12}O_{40}]^{8-}$ host and the cation accomodated in the cluster core of **2**, two protons appear to occupy the cavity of **1**, in analogy to the situation in $[H_2W_{12}O_{40}]^{6-}$.[31]

The central ($Mo_{12}O_{40}$) core of the polyanion clusters of **1** and **2** has a type of metal–oxygen framework which has been previously observed only for the cluster species $[Al_{13}O_4(OH)_{24}(H_2O)_{12}]^{7+}$,[32] $[Al_{13}O_4(OH)_{25}(H_2O)_{11}]^{6+}$,[33] $[H_3Mn_3V_{12}O_{40}]^{5-}$[34] and the recently described $[(C_5Me_5Rh)_8(Mo^{V}_{12}O_{36})(Mo^{VI}O_4)]^{2+}$.[35] It is instructive to compare the structure of the central ($Mo_{13}O_{40}$) core of this last cationic cluster to the ($H_2Mo_{12}O_{40}$) and ($NaMo_{12}O_{40}$) cores of **1** and **2**, respectively. All adopt the ε-Keggin structure[36] in which the octahedral Mo^{V} centers form binuclear units with short localized Mo–Mo bonds, a characteristic feature of Mo^{V} compounds encountered both for isolated binuclear species and for reduced polyanions.[37–40] In a very formal consideration the cavity of $[(C_5Me_5Rh)_8(Mo^{V}_{12}O_{36})(Mo^{VI}O_4)]^{2+}$ is occupied by a tetrahedrally coordinated Mo^{VI} center with short Mo–O distances of 1.75(1) Å as expected. In **2** the relevant Na–O distances are 2.18(3) Å. The cavity diameters in both **1** and **2** are defined by O5···O5 distances of 3.3 Å.[40a] The remarkable flexibility of the host ε-$\{Mo^{V}_{12}O_{40}\}$ cage is demonstrated by the existence of clusters encapsulating cationic guests with such diverse coordination requirements as protons and Na^+ ions.

It is noteworthy that encapsulation of a Na^+ ion has also been observed for a supramolecular species of tin, $[Na(i\text{PrSn})_{12}O_4(OH)_{24}]^{5+}$, in which the tin–oxygen frame-

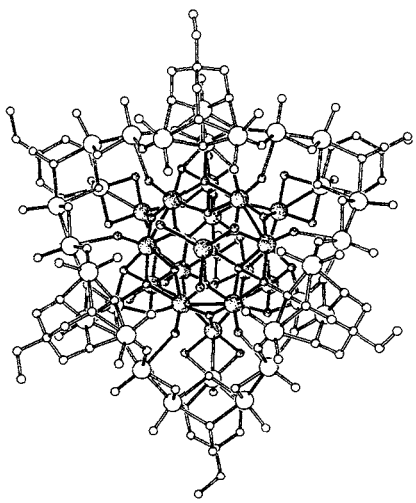

Fig. 2. A view of the structure of $[Mo_{43}H_{15}O_{112}\{(OCH_2)_3CCH_3\}_7]^{8-}$; the ($Mo_{16}O_{52}$) core is highlighted.

work adopts the γ-Keggin core.[30] The structures of this latter cluster cation and of the cluster anions of **1** and **2** most likely reflect the construction of the host framework about the guest in condensation reactions in solution, employing the template effect.[6] It is also significant that **2** is isolated from the same reaction mixtures as the cluster anions $[Na(H_2O)_3Mo_{42}H_{15}O_{109}\{(OCH_2)_3CCH_2OH\}_7]^{7-}$[19] and $[Mo_{43}H_{15}O_{112}\{(OCH_2)_3CCH_3\}_7]^{8-}$.[41] Thus, the structure of $[Mo_{43}H_{15}O_{112}\{(OCH_2)_3CCH_3\}_7]^{8-}$ (Fig. 2) is derived formally from the $(Mo_{16}O_{52})$ core by adding a $[(CH_2)_3CCH_3]^{3+}$ unit to one face of the $(Mo_{16}O_{52})$ cage, condensing three of the (MoO_3) units of the core with three $[Mo_5O_{14}\{(OCH_2)_3CCH_3\}]$ units, and connecting the central core and these latter units through three $[Mo_4O_7\{(OCH_2)_3CCH_3\}]$ moieties.[42] This observation suggests that the $(Mo_{16}O_{52})$ core of **1** and **2** itself could mediate the template-directed synthesis of more complex clusters from simple soluble precursors.

Experimental Procedure

1: $(NH_4)_6[Mo_7O_{24}]\cdot 4H_2O$ (3.18 g, 2.57 mmol) and phenylphosphonic acid (0.6 g, 3.80 mmol) were dissolved in 100 mL of H_2O at 85 °C. Upon addition of hydrazinium dichloride (0.3 g, 2.86 g), the color of the solution turned rapidly from yellow to green to dark blue. After stirring for 15 min at 85 °C, the resultant red solution was treated with a solution of dimethylammonium chloride (1.65 g, 20.23 mmol) in *N*,*N*-dimethylformamide/H_2O (50 mL/10 mL). The volume of the reaction mixture was reduced to 70 mL by heating at 75 °C. After standing at 20 °C for 12 h, red crystals of **1** were collected and air dried. Correct C, H, N, Mo analysis for $C_{12}H_{62}N_6O_{52}Mo_{16}$; IR (KBr): $\tilde{\nu}$ = 963(s), 841(sh), 779(sh), 738(vs), 533(s) cm^{-1}. UV/VIS (solid-state reflectance spectrum with cellulose as reference): λ = 320, 380 nm. Magnetic susceptibility at room temperature: μ_{eff}=1.1 μ_B (0.32 μ_B per Mo^V center).

2: The reaction of MoO_3, $Na_2MoO_4\cdot 2H_2O$, $C(CH_2OH)_4$, $(Et_4N)Cl$, Me_3NH, and H_2O in the mol ratio 6:6:10:10:10:300 at 160 °C for 3 d gave a mixture of red-brown crystals of $(Me_3NH)_2(Et_4N)Na_4[Na(H_2O)_3H_{15}Mo_{42}O_{109}\{(OCH_2)_3CCH_2OH\}_7]\cdot 15H_2O$ and a red-brown solution. After the solid was collected, the filtrate was allowed to stand at room temperature for 10 d, whereupon orange-red cubes of **2** were isolated in 20% yield.

Attempts to prepare **2** in the absence of organic cations and the pentaerythritol template resulted in improved yields of **2** but in microcrystalline precipitates unsuitable for X-ray analysis. In a representative synthesis a mixture of $Na_2MoO_4\cdot 2H_2O$, MoO_3, molybdenum metal (− 325 mesh), NH_4Cl, and water in the mol ratio 6:6:4:20:300 was heated at 160 °C for 3 d to give **2** in 65% yield. Correct H,N,Na, Mo analysis for $N_7H_{48}NaO_{56}Mo_{16}$; Thermogravimetric analysis of **2** exhibited a 3% weight loss at 110–120 °C consistent with the loss of four water molecules of crystallization (2.77% theoretical loss). IR (KBr): $\tilde{\nu}$ = 1407(s), 984(m), 946(vs), 842(m), 786(sh), 732(vs), 535(s), 488(m) cm^{-1}. UV/VIS (solid-state reflectance spectrum), λ = 325, 380 nm. Magnetic susceptibility at room temperature: μ_{eff} = 1.2 μ_B (0.35 μ_B per Mo^V center).

The similar magnetic properties of **1** and **2** suggest that the moments are a consequence of incomplete spin–spin coupling of the metal–metal bonded binuclear units rather than of impurities. Variable-temperature studies are currently in progress; the $M(H)$ isotherms indicate that the contributions of impurities are negligible.

Received: June 25, 1993 [Z 6168IE]
German version: *Angew. Chem.* **1993**, *105*, 1811

[1] M. T. Pope, A. Müller, *Angew. Chem.* **1991**, *103*, 56; *Angew. Chem. Int. Ed. Engl.* **1991**, *30*, 34.
[2] J. J. Berzelius, *Poggendorfs Ann. Phys. Chem.* **1826**, *6*, 369, 380.
[3] A. Müller, M. Penk, J. Döring, *Inorg. Chem.* **1991**, *30*, 4935.
[4] P. C. H. Mitchell, *Nature* **1990**, *348*, 15.
[5] V. W. Day, W. G. Klemperer, O. M. Yaghi, *Nature* **1991**, *352*, 115; A. Müller, *ibid.* **1991**, *352*, 115; M. T. Pope, *ibid.* **1992**, *355*, 27.
[6] H. Reuter, *Angew. Chem.* **1992**, *104*, 1210; *Angew. Chem. Int. Ed. Engl.* **1992**, *31*, 1185.
[7] W. G. Klemperer, T. A. Marquart, O. M. Yaghi, *Angew. Chem.* **1992**, *104*, 51; *Angew. Chem. Int. Ed. Engl.* **1992**, *31*, 49.
[8] Q. Chen, S. Liu, J. Zubieta, *Inorg. Chem.* **1989**, *28*, 4433.
[9] V. W. Day, W. G. Klemperer, O. M. Yaghi, *J. Am. Chem. Soc.* **1989**, *111*, 5959.
[10] D. D. Heinrich, K. Folting, W. E. Streib, J. C. Huffman, G. Christou, *J. Chem. Soc. Chem. Commun.* **1989**, 1411.
[11] W. Priebsch, D. Rehder, M. von Oeynhausen, *Chem. Ber.* **1991**, *124*, 761.
[12] G. Huan, A. J. Jacobson, V. W. Day, *Angew. Chem.* **1991**, *103*, 426; *Angew. Chem. Int. Ed. Engl.* **1991**, *30*, 422; G. Huan, V. W. Day, A. J. Jacobson, D. P. Goshorn, *J. Am. Chem. Soc.* **1991**, *113*, 3188.
[13] A. Müller, R. Rohlfing, J. Döring, M. Penk, *Angew. Chem.* **1991**, *103*, 575; *Angew. Chem. Int. Ed. Engl.* **1991**, *30*, 588.
[14] A. Müller, E. Krickemeyer, M. Penk, R. Rohlfing, A. Armatage, H. Bögge, *Angew. Chem.* **1991**, *103*, 1720; *Angew. Chem. Int. Ed. Engl.* **1991**, *30*, 1674.
[15] A. Müller, M. Penk, R. Rohlfing, E. Krickemeyer, J. Döring, *Angew. Chem.* **1990**, *102*, 927; *Angew. Chem. Int. Ed. Engl.* **1990**, *29*, 926.
[16] A. Müller, K. Hovemeier, R. Rohlfing, *Angew. Chem.* **1992**, *104*, 1214; *Angew. Chem. Int. Ed. Engl.* **1992**, *31*, 1192.
[17] F. Robert, M. Leyrie, G. Hervé, A. Tézé, Y. Jeannin, *Inorg. Chem.* **1980**, *19*, 1746.
[18] M. H. Alizadeh, S. P. Harmalker, Y. Jeannin, J. Martin-Frère, M. T. Pope, *J. Am. Chem. Soc.* **1985**, *107*, 2662.
[19] M. I. Khan, J. Zubieta, *J. Am. Chem. Soc.* **1992**, *114*, 10058.
[20] Crystal data for monoclinic space group $C2/c$, a = 23.851(14), b = 15.167(8), c = 20.496(13) Å, β = 113.59(4); V = 6795(7) $Å^3$, Z = **4**, $\mu(Mo_{K\alpha})$ = 28.76 cm^{-1}; structure solution and refinement based on 3830 independent reflections with $F_o \geq 4.0\sigma(F_o)$; the refinement converged at R = 0.083. Crystal data for **2**: cubic space group $F\bar{4}32$, a = 26.978(3) Å, V = 19539(10) $Å^3$, Z = 8 = 1.768 $g\,cm^{-3}$, $\mu(Mo_{K\alpha})$ = 20.5 cm^{-1}; structure solution and refinement was based on 660 independent reflections with $I_o \geq 3\sigma(I_o)$ to give a final discrepancy factor of 0.076. Further details of the crystal structure investigations may be obtained from the Fachinformationszentrum Karlsruhe, Gesellschaft für wissenschaftlich-technische Information mbH, D-76344 Eggenstein-Leopoldshafen (FRG) on quoting the depository number CSD-57755, the names of the authors, and the journal citation.
[21] The *fac* $[MO_3]$ unit is predicted to be unstable in polyanion frameworks as a consequence of the strong *trans* influence of the M–O(terminal) groups. This results in weakly bonded *fac* $[MO_3]$ groups and consequent dissociation: Lipscomb, W. N. *Inorg. Chem.* **1965**, *4*, 132. However, the *fac* $[MoO_3]$ unit has been observed in the derivatized polyoxomolybdate species $[Mo_3O_7\{(OCH_2)_3CCH_3\}_2]^{2-}$ [22] and $K_{10}[H_6As_8^{III}Mo_8^{V}Mo_{16}^{VI}O_{88}]\cdot 12H_2O$ [23].
[22] L. Ma, S. Liu, J. Zubieta, *Inorg. Chem.* **1989**, *28*, 175.
[23] A. Müller, E. Krickemeyer, H. Bögge, in preparation.
[24] I. D. Brown in *Structure and Bonding in Crystals, Vol. II* (Eds.: M. O'Keefe, A. Navrotsky), Academic Press, New York, **1981**, p. 1.
[25] The final Fourier difference map exhibits an electron density maximum of about 0.7 $eÅ^{-3}$ at a distance of 0.80 Å from O4 and close to the calculated position of H4. However, the positional coordinates could not be refined, and the calculated hydrogen atom position has been used in the discussion.
[26] R. C. Haushalter, F. W. Lei, *Inorg. Chem.* **1989**, *28*, 2904.
[27] G. Cao, R. C. Haushalter, K. G. Strohmaier, *Inorg. Chem.* **1993**, *32*, 127.
[28] M. I. Khan, Q. Chen, J. Zubieta, *Inorg. Chim. Acta*, **1993**, *206*, 131.
[29] R. D. Shannon, *Acta Crystallogr. Sect. A* **1976**, *32*, 751.
[30] H. Reuter, *Angew. Chem.* **1991**, *103*, 1487; *Angew. Chem. Int. Ed. Engl.* **1991**, *30*, 1482.
[31] M. T. Pope, G. M. Varga, Jr., *J. Chem. Soc. Chem. Commun.* **1966**, 653.
[32] G. Johansson, *Ark. Kemi* **1963**, *20*, 305.
[33] G. Johansson, *Ark. Kemi* **1963**, *20*, 321.
[34] H. Ichida, K. Nagai, Y. Sasaki, M. T. Pope, *J. Am. Chem. Soc.* **1989**, *111*, 586.
[35] H. K. Chae, W. G. Klemperer, D. E. Páez Loyo, V. W. Day, T. A. Eberspacher, *Inorg. Chem.* **1992**, *31*, 3187.
[36] L. C. W. Baker, J. S. Figgis, *J. Am. Chem. Soc.* **1970**, *92*, 3794; M. T. Pope, *Heteropoly and Isopoly Oxometalates*, Springer, Berlin, **1983**.
[37] E. I. Stiefel, *Prog. Inorg. Chem.* **1977**, *22*, 1.
[38] A. G. Sykes in *Comprehensive Coordination Chemistry, Vol. 3* (Eds.: G. Wilkinson, R. D. Gillard, J. A. McCleverty), Pergamon, Oxford, **1987**, p. 1229.
[39] M. T. Pope, *Prog. Inorg. Chem.* **1991**, *39*, 181.
[40] a) The small edge lengths of the central O_4 tetrahedron correspond to the small size of the cavity, which allows the incorporation of Na^+. The corresponding distances are, of course, significantly smaller in the case of a central MO_4 entity with covalent M—O bonds, and therefore it makes no sense to define a cavity from a physical point of view. Q. Chen, J. Zubieta, *Coord. Chem. Rev.* **1992**, *114*, 107.
[41] M. I. Khan, Q. Chen, J. Zubieta, unpublished.
[42] We thank Prof. W. G. Klemperer for first drawing our attention to the presence of such structural cores in large polyanions.

New Books

Micromechanics of Concrete and Cementitious Composites. Edited by **C. Huet.** Presses Polytechniques et Universitaires Romandes, Lausanne, **1993.** 252 pp., paperback, SF 78.–.—ISBN 2-88074-260-9

The Measurement of Grain Boundary Geometry. (Electron Microscopy in Materials Science Series). Edited by **V. Randle.** Institute of Physics Publishing, Bristol, **1993.** 169 pp., hardcover, £ 60.–. –ISBN 0-7503-0235-6

Laser Chemistry of Organometallics. (ACS Symposium Series 530). Edited by **J. Chaiken.** American Chemical Society, Washington, **1993.** 313 pp., hardcover, $ 74.95.—ISBN 0-8412-2667-3

Photochemistry of Lignocellulosic Materials. (ACS Symposium Series 531). Edited by **C. Heitner, J. C. Scaiano.** American Chemical Society, Washington, **1993.** 228 pp., hardcover, $ 64.95.—ISBN 0-8412-2692-X

Semiconductor Interfaces, Microstructures and Devices. Properties and Applications. Edited by **Z. C. Feng.** Institute of Physics Publishing, Bristol, **1993.** 293 pp., hardcover, £ 67.50.—ISBN 0-7503-0180-5

Structure and Properties of Polymers. (Materials Science and Technology, Vol. 12). Edited by **E. L. Thomas.** VCH, Weinheim/New York, **1993.** 785 pp., hardcover, DM 430.–/$ 295.–.—ISBN 3-527-26825-1/0-89573-700-0

Scanning Tunneling Microscopy III. (Springer Series in Surface Sciences, Vol. 29). Edited by **R. Wiesendanger, H.-J. Güntherodt.** Springer, Heidelberg, **1993.** 375 pp., hardcover, DM 118.–.—ISBN 3-540-56317-2

Colloid-Polymer Interactions. Particulate, Amphiphilic, and Biological Surfaces. (ACS Symposium Series 532). Edited by **P. L. Dublin, P. Tong.** American Chemical Society, Washington, **1993.** 300 pp., hardcover, $ 74.95.—ISBN 0-8412-2696-2

B-Glucosidases: Biochemistry and Molecular Biology. (ACS Symposium Series 533). Edited by **A. Esen.** American Chemical Society, Washington, **1993.** 249 pp., hardcover, $ 74.95.—ISBN 0-8412-2697-0

Human Medicinal Agents from Plants. (ACS Symposium Series 534). Edited by **A. Douglas, M. F. Balandrin.** American Chemical Society, Washington, **1993.** 359 pp., hardcover, $ 89.95.—ISBN 0-8412-2705-5

Handbook of Affinity Chromatography. (Chromatographic Science Series/63). Edited by **T. Kline.** Marcel Dekker, New York, **1993.** 344 pp., hardcover, $ 135.–.—ISBN 0-8247-8939-3

Materials Thermo-Chemistry 6th Edition. By **O. Kubaschweski, C. B. Alcock, P. J. Spencer.** Pergamon Press, Oxford, **1993.** 363 pp., paperback, £ 47.–. —ISBN 0-08-041888-0

Optical Characterization of Semiconductors. Infrared, Raman, and Photoluminescence Spectroscopy. By **S. Perkowitz.** Academic Press, London, **1993.** 220 pp., hardcover, £ 40.–.—ISBN 0-12-550770-4

Protein Folding. (EPO Applied Technology Series, Vol. 12). By **R. Hermann.** European Patent Office, Patentlaan 2, The Netherlands, **1993.** 122 pp., hardcover, $ 50.–.—ISBN 90-9006173-8

Rechentafeln für die Chemische Analytik. 104. Auflage. By **A. Ruland.** de Gruyter, Berlin, **1993.** 385 pp., paperback, DM 54.–.—ISBN 3-11-012131-X

Progress in Heterocyclic Chemistry, Vol. 5. Edited by **H. Suschitzky, E. F. V. Scriven.** Pergamon Press, Oxford, **1993.** 341 pp., paperback, £ 14.–.—ISBN 0-08-042075-3

Dimensional Scaling in Chemical Physics. Edited by **D. R. Herschbach.** Kluwer, Dordrecht, The Netherlands, **1993.** 519 pp., hardcover, Dfl 260.–.—ISBN 0-7923-2036-0

Handbook of Enantioselective Catalysis. Transition Metal Compounds. Products and Catalysts, Vol. I/ Ligands-References, Vol II. By **H. Brunner, W. Zettelmeier.** VCH, Weinheim/New York, **1993.** 558 pp./359 pp., hardcover, DM 598.–/$ 385.– (subscription price: DM 498.–/$ 320.–).—ISBN 3-527-29068-0/1-56081-811-5

Food Proteins. Structure and Functionality. Edited by **K. D. Schwenke, R. Mothes.** VCH, Weinheim/ New York, **1993.** 363 pp., hardcover, DM 158.–/ $ 100.–.—ISBN 3-527-30037-6/1-56081-769-0

MAK- und BAT-Werte-Liste 1993. Edited by **Deutsche Forschungsgemeinschaft.** VCH, Weinheim, **1993.** 153 pp., paperback, DM 28.–.—ISBN 3-527-27561-4

Spices and Seasonings. By **D. R. Tainter, A. T. Gremis.** VCH, Weinheim/New York, **1993.** 226 pp., hardcover, DM 158.–/$ 95.–.—ISBN 3-527-89572-8/ 1-56081-572-8

Introduction to Molecular Cloning Techniques. By **G. Lucotte, F. Baneyx.** VCH, Weinheim/New York, **1993.** 298 pp., hardcover, DM 79.–/$ 49.–.—ISBN 3-527-89613-9/1-56081-613-9

Unraveling DNA. By **M. D. Frank-Kamenetski.** VCH, Weinheim/New York, **1993.** 205 pp., hardcover, DM 49.–/$25.95.–.—ISBN 3-527-89617-1/1-56081-617-1

Fusion Technologies to Imaging Techniques, Biomedical. (Encyclopedia of Applied Physics, Vol. 7). Edited by **G. L. Trigg.** VCH, Weinheim/New York, **1993.** 611 pp., hardcover, DM 350.–/$ 295.–.— ISBN 3-527-28129-0/1-56081-066-1

NMR of Macromolecules. A Practical Approach. Edited by **G. C. K. Roberts.** Oxford University Press, Oxford, **1993.** 399 pp., paperback, £ 27.50.—ISBN 0-19-963224-3

Genetic Engineering of Animals. Edited by **A. Pühler.** VCH, Weinheim, New York, **1993.** 177 pp., paperback, DM 38.–/$ 25.–.—ISBN 3-527-30041-4/ 1-56081-828-X

Science and Technology of Photography. Edited by **K. Keller.** VCH, Weinheim/New York, **1993.** 260 pp., hardcover, DM 220.–/$ 140.–.—ISBN 3-527-28611-X/1-56081-800-X

Cells and Tissues. (Methods of Immunological Analysis, Vol. 3). Edited by **R. F. Masseyeff, W. H. Albert, N. A. Staines.** VCH, Weinheim, New York, **1993.** 603 pp., hardcover, DM 410.–/$ 265.– (subscription price: DM 330.–/$215.–).—ISBN 3-527-27908-3/0-89573-904-6

Structure and Properties of Composites. (Materials Science and Technology, Vol. 13). Edited by **R. W. Cahn, P. Haasen, E. J. Kramer.** VCH, Weinheim/ New York, **1993.** 625 pp., hardcover, DM 403.–/ $ 295.– (Subscription price: DM 360.–/$ 235.–).— ISBN 3-527-26826-X/0-89573-800-7

Betäubungsmittelrecht Suchtbekämpfung. By **Lundt, Schiwy.** R. S. Schulz, Starnberg, **1993.** 208 pp., paperback, DM 98.–.—ISBN 3-7962-0361-2

Dünnschicht-Chromatographie: Reagenzien und Nachweismethoden, Bd. 1b. By **H. Jork, W. Funk, W. Fischer, H. Wimmer.** VCH, Weinheim, **1993.** 499 pp., paperback, DM 198.–.—ISBN 3-527-26976-2

Deutsche Einheitsverfahren zur Wasser-, Abwasser- und Schlamm-Untersuchung. By **Gesellschaft Deutscher Chemiker.** VCH, Weinheim/ Beuth, Berlin. paperback, DM 158.– (subscription price: DM 126,40).—ISBN 3-527-28563-6/3-410-13028-4

Registered names, trademarks, etc. used in this journal, even when not marked as such, are not to be considered unprotected by law.

© VCH Verlagsgesellschaft mbH, D-69451 Weinheim, 1993. – Printed in the Federal Republic of Germany by Konrad Triltsch Druck- und Verlagsanstalt Würzburg.

All rights reserved (including those of translation into foreign languages). No part of this issue may be reproduced in any form — by photoprint, microfilm, or any other means — nor transmitted or translated into a machine language without written permission from the publishers. Only single copies of contributions, or parts thereof, may be made for personal use. This journal was carefully produced in all its parts. Nevertheless, authors, editors, and publisher do not warrant the information contained therein to be free of errors. Readers are advised to keep in mind that statements, data, illustrations, procedural details, or other items may inadvertently be inaccurate.

Valid for users in the USA: The appearance of the code at the bottom of the first page of an article (serial) indicates the copyright owner's consent that copies of the article may be made for personal or internal use, or for the personal or internal use of specific clients. This consent is given on the condition, however, that the copier pay stated per-copy fee through the Copyright Clearance Center, Inc. (CCC), for copying beyond that permitted by Sections 107 or 108 of the U.S. Copyright Law. This consent does not extend to other kinds of copying, such as copying, for general distribution, for advertising or promotional purposes, for creating new collective works, or for resale. For copying from back volumes of this journal see 'Permissions to Photo-Copy: Publisher's Fee List' of the CCC.

Editorial office: Postfach 10 11 61, D-69451 Weinheim, Federal Republic of Germany, Telephone (06201) 606 315, Telex 465 516 vchwh d, Telefax (06201) 606 328, E-Mail Z16@ DHDURZ2 in Earn Bitnet.

Editor: *Peter Gölitz*

Associate editors: *N. A. Compton, R. H. Schmidt-Radde, K. J. Schneider.* **Book editor:** *G. Karger.* **Editorial assistants:** *J. Göhrig, E. Schweikart*

Publishers: *VCH Verlagsgesellschaft mbH.* (Managing Directors: *Hans Dirk Köhler, Dr. Karlheinz Köpfer*), Pappelallee 3, D-69451 Weinheim, Federal Republic of Germany.

Advertising office (Advertising Manager: *N. Schippel*): Postfach 10 11 61, D-69451 Weinheim, Federal Republic of Germany, Telephone (0 62 01) 606 312, Telefax (0 62 01) 606 328.

Ab initio calculations
- A Detailed Theoretical Analysis of the 1,7-Sigmatropic Hydrogen Shift: The Möbius Character of the Eight-Electron Transition Structure (C) 1763
- $[Al\textit{t}Bu]_6^-$: EPR Spectroscopic Evidence and Ab Initio Calculations (C) 1428
- An Ab Initio MO Study on Stabilizing Interactions in Dinuclear Zr/Al Complexes with a Planar Tetracoordinate Carbon Center (C) 754
- Aza- versus Phospha-Substitution in Cyclobutadiene: A Theoretical Evaluation of Bonding Properties (C) 617
- Contrasting Structures of Pyramidal Carbocations and Their Silicon Analogues (C) 865
- Elimination of the Barrier to Cope Rearrangement in Semibullvalene by Li^+ Complexation (C) 1760
- Gaseous Mercury(IV) Fluoride, HgF_4: An Ab Initio Study (C) 861
- $[Ni(P\textit{t}Bu)_6]$ and $[Ni(SiH_2)_6]$ Are Isolobal, Related to $[In\{Mn(CO)_4\}_5]^{2-}$, and Have 16-Electron Counts (C) 1616
- On the BO Bond Length in Oxadiboriranes (C) 1154
- The Classical 2-Norbornyl Cation Rigorously Defined Ab Initio (C) 1606
- The Nature of the 7-Norbornyl Cation and its Rearrangement into the 2-Norbornyl Cation (C) 1604
- The Search for an Isolable Silyl Cation Must Continue (C) 1471

Acetals
- A Diastereoselective Synthesis of β-(*N*-Acylamino)aldehydes by Rearrangement of *O*-Vinyl-*N*,*O*-Acetals (C) 83

ACRL Toxin III B
- Linear Total Synthesis of (−)-ACRL Toxin III B (C) 1452

Activation of oxygen
- The Coupled Activation of Molecular Oxygen and C–H and C–C Bonds in Gas-Phase Reactions of $[M(C_2H_4)]^+$ (M = Sc–Zn) with O_2 (C) 1420

Adamantanes
- Carbenes in Constrained Systems I: 1,3 C–H Insertion Reaction of Adamantylidene within the β-Cyclodextrin Cavity (C) 1344
- Dilithiation of Two Diphenyl Ethers Each Containing Two $NHCH_2CH_2Y$ (Y = OMe, NMe_2) Side Arms in *ortho* Positions: Assembly of "Adamantanoid" $Li_4O_2N_4$ Cores (C) 1182
- The First Neutral Adamantanoid Iron(III)–chelate Complex: Spontaneous Formation, Structure, and Electrochemistry (C) 1179

Adsorption
- Adsorption of Molecules at Metal Electrodes (B) 1107

AIDS
- Diastereo- and Enantioselective Synthesis of C_2-Symmetrical HIV-1 Protease Inhibitors (C) 423
- Phosphinic Acid-Based C_2-Symmetrical Inhibitors of HIV-Protease (C) 1720
- Selective Cleavage of a 35-mer Single-Stranded DNA Containing the Initiation Codon of the TAT Gene of HIV-1 by a Tailored Cationic Manganese Porphyrin (C) 557
- The Absolute Configuration of Michellamine B, a "Dimeric", Anti-HIV-Active Naphthylisoquinoline Alkaloid (C) 1190

Alcohols
- Enantioselective Catalytic Addition of Functionalized Dialkylzinc Compounds to β-Stannylated Aldehydes: A Convenient Preparation of Chiral β- and γ-Functionalized Secondary Alcohols (C) 582

Aldol reactions
- Computer-Assisted Design of Chiral Boron Enolates: A Novel, Highly Enantioselective Aldol Reaction for Thioacetates and Thiopropionates (C) 1618
- Enantioselective Aldol Reactions with a Phosphoenolpyruvate Equivalent: Asymmetric Synthesis of 4-Hydroxy-2-oxocarboxylic Acid Esters (C) 421

Alkali metal compounds
- A Molecular Heterometal Amide with High Molecular Dynamics: Does the Lithium Atom Orbit? (C) 1731
- [*tert*-Butylcyanide · Lithium Bis(trimethylsilyl)amide]$_2$, a Model of the Intermediate RCN · MR′ Complex Formed in Reactions of Cyanides RCN with Organometallic Compounds R′M (C) 1171
- 1-Chloro-2,2-bis(4-chlorophenyl)-1-lithioethene · TMEDA · 2THF: Structure of a Li-Cl Carbenoid (C) 1032
- Crystal Structure of [(α-Cyanoisopropylsodium · Tetramethylenediamine)$_4$]: How Coordination Expansion from Li to Na Centers can Increase the Aggregation State of an α-Nitrile "Carbanion" (C) 1366
- Cs_3AuO, the First Ternary Oxide with Anionic Gold (C) 1049
- Dilithiation of Two Diphenyl Ethers Each Containing Two $NHCH_2CH_2Y$ (Y = OMe, NMe_2) Side Arms in *ortho* Positions: Assembly of "Adamantanoid" $Li_4O_2N_4$ Cores (C) 1182
- Effects of Ion Pair Separation on Inversion and Rotation of Sulfur-, Selenium-, and Silicon-Stabilized Organolithium Reagents (C) 1469
- Elimination of the Barrier to Cope Rearrangement in Semibullvalene by Li^+ Complexation (C) 1760
- First Structure of a Mixed Organosodium/Lithium Alkoxide Compound: Model for a Superbase (C) 1066
- High-Pressure Synthesis of LiSi: Three-Dimensional Network of Three-Bonded Si^- Ions (C) 1442
- Lithium Di-*tert*-butylmethylsilylhydrazide, a Hexamer with Li^+ Ions Bound Side-on and End-on (C) 1625
- β-Na_3Hg: A Solid with a Quasi-Fluid Sodium Substructure between 36 and 60 °C (C) 1494
- Novel Alkynylcopper(I) Complexes and Lithium Alkynyl Cuprates (C) 1077
- One-Flask Synthesis of Propargylic Alcohols from Organolithium Reagents, *N*,*N*-Disubstituted Amides, and Acetylenes (C) 608
- Reduction of Geminal Dihalocyclopropanes with Lithium 4,4′-Di-*tert*-butylbiphenyl; Cyclopropyl Derivatives of Dilithiomethane and 1,2-Dilithioethane; Inferences Regarding the Intermediate Carbenoids (C) 574
- Rotation about the C–Se Bond as the Rate-Determining Step in the Racemization of α-Selenium-Substituted Alkyllithium Compounds (C) 1467
- Structures of Classical Reagents in Chemical Synthesis: $(n\text{BuLi})_6$, $(t\text{BuLi})_4$, and the Metastable $(t\text{BuLi} \cdot Et_2O)_2$ (C) 580
- Structures of Organo Alkali Metal Complexes and Related Compounds (R) 1501
- Successful X-Ray Structure Analysis of an Alkylidene Carbenoid—A Milestone in Carbenoid Research (H) 1023
- The Dimeric Tris(lithioarsino)germane tBuGe[As(Si*i*Pr$_3$)Li]$_3$: A Self-Assembled, Solvent-Free Lithium–Main Group Element Aggregate with a $Ge_2As_6Li_6$ Rhombododecahedral Framework (C) 1439
- The First Structure of a Lithiated Cyanamide; Synthesis of (PhNCNLi · HMPA)$_n$ by Extrusion of N_2 and S from 5-Phenylamino-1,2,3,4-thiatriazole with Li Reagents and HMPA (C) 1769
- The First Trigonal-Bipyramidal Cluster with an Interstitial C_2 Unit: $[Rb\{Pr_5(C_2)\}Cl_{10}]$ (C) 1318
- (Trimethylstannyl)methyllithium as a Source of a Methylene Bridge Connecting Two Acyl Groups: A Potential Route to D-Mycaroside (C) 105

Alkaline earth metal compounds
- *ansa*-Metallocenes of Calcium and Strontium: One-Pot Synthesis of Organometallic Complexes of the Heavier Alkaline Earth Metals (C) 1079
- The First Unsolvated Chelate and Cubane-Type Barium Complexes: Effective Compounds for the Sol–Gel Process (C) 596

Alkaloids
- The Absolute Configuration of Michellamine B, a "Dimeric", Anti-HIV-Active Naphthylisoquinoline Alkaloid (C) 1190

Alkanes
- Amination of Methane and Ethane by Mercury Photosensitization in the Presence of Ammonia (C) 1491

Alkenes
- Bi[1,3-bis(dicyanomethylene)indan-2-ylidene]—An Ethylene Derivative with Extremely Pronounced Twisting of the C=C Bond (C) 1352
- Non-Twisted Tetrakis(organosilyl)-ethene (C) 1473

Alkoxycarbonylation
- Palladium-Catalyzed Enantioselective Bis-alkoxycarbonylation of Olefins (C) 1719

Alkyne complexes
- Transformation of the First Zirconocene Alkyne Complex without an Additional Phosphane Ligand into a Dinuclear σ-Alkenyl Complex by Hydrogen Transfer from η^5-C_5H_5 to the Alkyne Ligand (C) 1193

Alkynes
- Metal-Initiated Coupling of C_2 Units to Enynes and Butatrienes: Two Different Routes for the Dimerization of 1-Alkynes (C) 1315

- Protonation of Phenyl(trimethylsilyl)-acetylene: A Surprisingly Weak Stabilization of a Carbocation by a β-Trimethylsilyl Group (C) 721
- Rapid Carboalumination of Alkynes in the Presence of Water (C) 1068
- The First Complex with a Tetraethynylcyclobutadiene Ligand (C) 1653

Aluminum compounds
- A Simple Synthesis of $[(Cp^*Al)_4]$ and Its Conversion to the Heterocubanes $[(Cp^*AlSe)_4]$ and $[(Cp^*AlTe)_4]$ ($Cp^* = \eta^5$-$C_5(CH_3)_5$) (C) 1729
- $[AlrBu]_6^-$: EPR Spectroscopic Evidence and Ab Initio Calculations (C) 1428
- An Al–Al One-Electron π Bond (C) 388
- Decamethylaluminocenium, a π-Stabilized R_2Al^+ Cation (C) 1655
- Dimeric and Trimeric Aminoalanes with Inverse Bridging Functions (C) 886
- Organoelement Compounds with Al–Al, Ga–Ga, and In–In Bonds (R) 1386
- Synthesis and Structure of a Sixteen-Membered $(AlNCO)_4$ Ring (C) 1483
- Transition-Metal-Substituted Volatile Alanes, Gallanes, and Indanes: Synthesis and Structure (C) 746

Amides
- Structure and Reactivity of a Highly Twisted Amide (C) 1083

Amination
- Amination of Methane and Ethane by Mercury Photosensitization in the Presence of Ammonia (C) 1491

Amines
- Monoclinic and Triclinic Tetraisopropyl-*p*-phenylenediamine: To what Extent do n_N/π Interactions Determine Structures? (C) 1755
- Tris(chlorodimethylstannyl)amine, a Molecule with a Planar Sn_3N Skeleton Stabilized by Intramolecular Sn-Cl-Sn Bridges (C) 1608

Amino acids
- (*R*)- and (*S*)-4-Alkoxy-2-*tert*-butyl-2,5-dihydroimidazole-1-carboxylates—New Chiral Glycine Derivatives for Amino Acid Synthesis (C) 1765
- Asymmetric Synthesis of α-Amino Acids and N-Protected α-Amino Aldehydes by Addition of Chiral Vinyl Anions to Sulfonylimines (C) 578
- Enantioselective Synthesis of α-Amino Acetals and α-Amino Acids by Nucleophilic 1,2-Addition to Diethoxyacetaldehyde SAMP Hydrazone (C) 418
- New Chiral Porphyrins—Syntheses and Molecular Recognition of Amino Acid Esters (C) 723
- Selective Pd^0-Mediated C–C Bond Constructions on the Imidazole Ring of L-Histidine: A Practical Approach to the Synthesis of Diphthamide and Related Histidine Analogues (C) 1326
- Synthesis of 4-Oxo-L-proline and *cis*-4-Hydroxy-L-proline Derivatives from L-Aspartic Acid (C) 285

Aminoacyl-tRNA synthetases
- Aminoacyl-tRNA Synthetases: The Division into Two Classes was Predicted by the Chemistry of Substrates and Enzymes (R) 190

Amphiphiles
- Can Single-Chain Perfluoroalkylated Amphiphiles Alone Form Vesicles and Other Organized Supramolecular Systems? (C) 741

Analytical methods
- Accurate Molecular Structures. Their Determination and Importance (B) 1668
- Adsorption of Molecules at Metal Electrodes (B) 1107
- Capillary Electrophoresis: Methods and Scope (R) 629
- Capillary Electrophoresis. Principles, Practice and Applications (B) 1372
- Optical Spectroscopy of Single Impurity Molecules in Solids (R) 457
- Rapid Reactions in Solution (B) 624
- Spectrochemical Analysis by Atomic Absorption and Emission (B) 627
- Spectroscopy of Polymers (B) 1109

Annulenes
- A Novel 1,6-Methano[10]annulene Derivative with Bisnorcaradiene Structure—Syntheses with Transition Metal Complexes (C) 1324
- Porphyrin-Like [22]Annulenoquinones (C) 1333
- Stable [12]- and [18]Annulenes Derived from Tetraethynylethene (C) 406

Anthracyclines
- Synthesis of 4-Deoxyaklanonic acid and its Microbial Conversion into Anthracyclinones (C) 1151

Antibiotics
- Posttranslational Backbone Modifications in the Ribosomal Biosynthesis of the Glycine-Rich Antibiotic Microcin B17 (C) 1336
- The Use of Radical Cyclization in the Preparation of Substituted Methyl Carbapenem Antibiotic Precursors (C) 867

Antibodies
- New Developments in the Chemistry of Catalytic Antibodies (H) 1291
- Tautomer-Specific Anti-(N-3-Substituted)-Adenine Antibodies: New Tools in Molecular Dosimetry and Epidemiology (C) 1640

Antimony compounds
- Electrochemical Synthesis of New Sb–Te Zintl Anions by Cathodic Dissolution of Sb_2Te_3 Electrodes: Structures of $[Sb_4Te_4]^{4-}$ and $[Sb_9Te_6]^{3-}$ (C) 1646

Antisense systems
- A Sulfide-Linked Oligonucleotide Analogue with Selective Hybridization Properties (C) 729

Antitumor agents
- The Battle of calicheamicin γ_1^1 (R) 1377
- The Role of Chemistry in the Development of Baron Neutron Capture Therapy of Cancer (R) 950
- Total Synthesis of (−)-Pyrimidoblamic Acid and Deglycobleomycin A_2 (C) 273

Arachidonic acid
- Biologically Active Linear Metabolites of Arachidonic Acid—The First Endogenous Ligand of the Cannabinoid Receptor (H) 1027

Arene complexes
- A Nickel–Anthracene Complex Having η^3 and η^4 Coordination in One Crystal (C) 1475
- A Novel Complex with Boat-Shaped, Synfacially Bound η^3:η^3-Benzene Bridges and the First μ_3-η^2:η^2:η^2-Arenetrirhodium Complex (C) 1697
- η^6-(1,2-Dioxocyclobutabenzene)-tricarbonylchromium(0): Starting Material for Double Anionic Oxy-Cope Rearrangements under Very Mild Conditions (C) 267
- The First Complex with a Tetraethynylcyclobutadiene Ligand (C) 1653
- (η^1-tpMn, η^5-tpCr) → (η^1-tpCr, η^5-tpMn) Thiophene (tp) Conversion due to Bimetallic Activation: A Novel Metal-Exchange Reaction (C) 710
- Two Modifications of a Cyclopentadienylthallium(I) Complex Linking the Chemistry of the Cp and Arene Complexes of Main Group Elements (C) 90

Arenes
- Arene–Arene Interactions: Electrostatic or Charge Transfer? (H) 1584
- Liquid-Crystalline Perylene Derivatives as "Discotic Pigments" (C) 1660
- Trimeric Ketenylidene(triphenyl)-phosphorane: A Hybrid between an Arene and an Ylide (C) 1747

Aromaticity
- Porphyrin-Like [22]Annulenoquinones (C) 1333
- Porphyrins with Aromatic 26π-Electron Systems (C) 1148
- Structural Evidence of the Aromaticity of Borepins: A Comparison of 1-Chloroborepin and Tricarbonyl(1-chloroborepin)molybdenum (C) 1065

Arsaalkenes
- Novel Arsaalkenes from an Arsasilene Derivative and Isocyanides (C) 283

Arsenic compounds
- New As–S Cage Structures with Organometallic Components Formed by Complex-Induced Realgar Fragmentation (C) 1627
- Synthesis and Structure of the Arsaalkyne Tetramer $(AsCtBu)_4$ and its $Fe(CO)_4$ Derivative (C) 103
- The First Heteroallyl Metal Complexes of Arsenic with the Coordination Number 2 (C) 1628

Asymmetric syntheses
- (*R*)- and (*S*)-4-Alkoxy-2-*tert*-butyl-2,5-dihydroimidazole-1-carboxylates—New Chiral Glycine Derivatives for Amino Acid Synthesis (C) 1765
- A Catalytic Enantioselective Michael Addition of a Simple Malonate to Prochiral α,β-Unsaturated Ketones and Aldehydes (C) 1176
- A Diastereoselective Synthesis of β-(*N*-Acylamino)aldehydes by Rearrangement of *O*-Vinyl-*N*,*O*-Acetals (C) 83
- Absolute Asymmetric Synthesis by Irradiation of Chiral Crystals (H) 694
- Asymmetric Synthesis and Highly Diastereoselective *ortho*-Lithiation of Ferrocenyl Sulfoxides. Application to the Synthesis of Ferrocenyl Derivatives with Planar Chirality (C) 568
- Asymmetric Synthesis of α-Amino Acids and N-Protected α-Amino Aldehydes by Addition of Chiral Vinyl Anions to Sulfonylimines (C) 578
- Carbohydrates as Chiral Auxiliaries in Stereoselective Synthesis (R) 336
- Chiral 2-Amino-1,3-butadienes: New Reagents for Asymmetric Cycloadditions (H) 1582
- Chiral Phosphinoaryldihydrooxazoles as Ligands in Asymmetric Catalysis: Pd-Catalyzed Allylic Substitution (C) 566
- Computer-Assisted Design of Chiral Boron Enolates: A Novel, Highly Enantioselective Aldol Reaction for Thioacetates and Thiopropionates (C) 1618
- Diastereo- and Enantioselective Synthesis of 2-Substituted 3-Trialkylstannylcyclohexanones by Michael Addition of Trialkylstannyllithium to Cyclohexenone SAMP Hydrazone (C) 598
- Diastereo- and Enantioselective Synthesis of C_2-Symmetrical HIV-1 Protease Inhibitors (C) 423
- Enantioselective Addition of Aromatic Thiols to a Ketene (C) 1044
- Enantioselective Aldol Reactions with a Phosphoenolpyruvate Equivalent: Asymmetric Synthesis of 4-Hydroxy-2-oxocarboxylic Acid Esters (C) 421
- Enantioselective Catalytic Addition of Functionalized Dialkylzinc Compounds to β-Stannylated Aldehydes: A Conve-

nient Preparation of Chiral β- and γ-Functionalized Secondary Alcohols (C) 582
- Enantioselective Synthesis. Natural Products from Chiral Terpenes (B) 1216
- Enantioselective Synthesis of α-Amino Acetals and α-Amino Acids by Nucleophilic 1,2-Addition to Diethoxyacetaldehyde SAMP Hydrazone (C) 418
- Enantioselective Transition Metal-Catalyzed Hydrogenation for the Asymmetric Synthesis of Amines (H) 232
- Enzyme-Catalyzed Asymmetric Synthesis: Kinetic Resolution of Chiral Hydroperoxides by Enantioselective Reduction to Alcohols with Horseradish Peroxidase (C) 1737
- Highly Enantioselective Protonation of Thiol Ester Enolates (C) 1042
- Linear Total Synthesis of (−)-ACRL Toxin III B (C) 1452
- Palladium-Catalyzed, Enantioselective Allylic Substitutions (H) 547
- Palladium-Catalyzed Enantioselective Bis-alkoxycarbonylation of Olefins (C) 1719
- Stereodivergent Enantioselective Synthesis by Exploiting Unusually Large Kinetic H/D Isotope Effects on Deprotonation (C) 394
- Stereoselective Synthesis of C-Glycosides with a Glycosyl Dianion (C) 1091
- Temperature Effects in Asymmetric Dihydroxylation: Evidence for a Stepwise Mechanism (C) 1329
- The First Example of an Increase in the Enantioselectivity of a Chemical Reaction in the Presence of a Chiral Lewis Acid under High Pressure (C) 1485
- Titanated Methoxyallene as Novel Homoaldol Equivalent for Diasteroselective Additions to Chiral Amino Aldehydes (C) 1449
- Titanium-Catalyzed Epoxy-Hydroxylation of Allylic Alcohols: A Convenient Diastereoselective Synthesis of Epoxy Diols (C) 733
- Vitamin D_3 Synthetic Studies: Enantiospecific Synthesis of the CD Ring Fragment (C) 1444

Atomic absorption spectroscopy
- Spectrochemical Analysis by Atomic Absorption and Emission (B) 627

Atomic force microscopy
- Gas/Solid Reactions of Aliphatic Amines with Thiohydantoins: Atomic Force Microscopy and New Mechanisms (C) 1587

Atropo-diastereomers
- The Absolute Configuration of Michellamine B, a "Dimeric", Anti-HIV-Active Naphthylisoquinoline Alkaloid (C) 1190

Atropo-enantiomers
- Separation of the Enantiomers of 2,2′-Dihydroxy-1,1′-binaphthyl and 10,10′-Dihydroxy-9,9′-biphenanthryl by Complexation with *N*-Alkylcinchonidinium Halides (C) 1147

Atropo-enantioselectivity
- A New Atropisomeric Molecular Structure for Efficient Enantiodifferentiation (C) 606

Autobiographies
- A Semiempirical Life (B) 1102
- A Wandering Natural Products Chemist (B) 311
- Following the Trail of Light. A Scientific Odyssey (B) 444
- Seventy Years in Organic Chemistry (B) 311

Azides
- Cycloalkano-2*H*-pyrrole as a Stable Intermediate in the Conversion of β-Cycloalkenyl-α-azidoacrylates to Cycloalkano-1*H*-pyrroles (C) 1051
- Iodine Azide (C) 275

Basicity
- How Strong and How Hindered Can Uncharged Phosphazene Bases Be? (C) 1361

Benzene cation
- Structure and Symmetry of the Benzene Cation (C) 603
- The Dynamic Jahn–Teller Effect in the Benzene Cation: Rotationally Resolved ZEKE Photoelectron Spectra of the $v_6(e_{2g})$ Mode (C) 1364

Benzofurans
- Epoxidation of 2-Methyl-3-phenylbenzofurans with Dimethyldioxirane: A Novel Reversible Valence Isomerization between Labile Benzofuran Epoxides and Quinone Methides, their Rearrangement, Methanolysis, and Cycloaddition Chemistry (C) 735

Biindanylidene
- Bi[1,3-bis(dicyanomethylene)indan-2-ylidene]—An Ethylene Derivative with Extremely Pronounced Twisting of the C=C Bond (C) 1352

Biochemistry
- Aminoacyl-tRNA Synthetases: The Division into Two Classes was Predicted by the Chemistry of Substrates and Enzymes (R) 190
- Biosynthesis of Tetrapyrroles (B) 448
- How Nature Synthesizes Vitamin B_{12}—A Survey of the Last Four Billion Years (R) 1223
- Hydrogen Bonding in Biological Structures (B) 623
- Metals in Biological Systems (B) 1105
- Nitric Oxide, NO, an Intercellular Messenger (H) 378
- Parallels and Decisive Differences in Vitamin B_{12} Biosyntheses (C) 1651
- Protein Phosphorylation and Cellular Regulation I (Nobel Lecture) (R) 1122
- Protein Phosphorylation and Cellular Regulation II (Nobel Lecture) (R) 1130

Biodegradation
- Bacteria and the Biodegradation of Chemicals Achieved Naturally, by Combination, or by Construction (R) 1398

Biographies
- Michael Faraday and the Royal Institution: The Genius of Man and Place (B) 1371

Bioinorganic chemistry
- A Hemerythrin Model Complex with Catalase Activity (C) 289
- Bioanorganische Chemie (B) 299
- Bioinorganic Chemistry (B) 300
- Conformational Analysis of Model Complexes for Methyl-Coenzyme-M Reductase of *Methanogenic Bacteria*: A Comparison of Crystal and Solution Structures (C) 1777
- How "Innocent" Are Pentane-2,4-dione-bis(*S*-alkylisothiosemicarbazonate) Ligands in Biomimetic Fe^{II} and Fe^{IV} Complexes? (C) 1635
- Perspectives on Bioinorganic Chemistry, Volume 1 (B) 301
- The Biological Chemistry of the Elements. The Inorganic Chemistry of Life (B) 300

Biomembranes
- Transmembrane Signaling of T Lymphocytes by Ligand-Induced Receptor Complex Assembly (R) 54

Biopolymers
- Poly(hydroxyalkanoates): A Fifth Class of Physiologically Important Organic Biopolymers? (R) 477

Biotin
- Propionyl-Aza(dethia)coenzyme A as Pseudosubstrate of the Biotin-Containing Transcarboxylase (C) 278

Bis(furanoside)s
- Domino Reactions of 4-Ene-1,2,3-triol Derivatives (C) 1173

Bismuth compounds
- Structural Variations Observed in the $[Bi(O_2CCF_3)_4Ph]^{2-}$ Anion: Selective Cation–Anion Interactions through Hydrogen Bonds (C) 589

Bleomycins
- Total Synthesis of (−)-Pyrimidoblamic Acid and Deglycobleomycin A_2 (C) 273

Blood coagulation
- A Short Synthetic Route towards a Biologically Active Heparin-like Pentasaccharide with a Pseudo-Alternating Sequence (C) 434

Borates
- The Synthesis and Ab Initio Structure Determination of $Zn_4O(BO_3)_2$, a Microporous Zincoborate Constructed of "Fused" Subunits of Three- and Five-Membered Rings (C) 724

Boron compounds
- BNC Isosteres of Cyclopropane and a Borylated Diazoester from Diazo Compounds and (Dimethylamino)bis(trifluoromethyl)borane (C) 384
- Carbonyl–Metal Complexes of Diphosphadiboretane (mesB–P*t*Bu)$_2$ and of Triphosphatriborinanes (mesB–P*t*Bu)$_3$ (C) 1446
- Carboranes, Anti-Crowns, and Big Wheels (H) 1289
- (1,7-$C_2B_{10}H_{10}$-1′,3′-C_6H_4)$_3$, a Cyclic Trimer from *meta*-Carboranediyl and *meta*-Phenylene Units: A New Category of Macrocycle (C) 1328
- C–H-Activation by Reaction of (Butadiene)zirconocenes and -hafnocenes with 9-BBN (C) 1213
- Classical and Nonclassical Methyleneboranes (R) 985
- Computer-Assisted Design of Chiral Boron Enolates: A Novel, Highly Enantioselective Aldol Reaction for Thioacetates and Thiopropionates (C) 1618
- 1-Hetero-3,4-diborolanes and Two New Routes to 1,2-Diboretanes (C) 295
- "Noncoordinating" Anions, II (H) 1025
- On the BO Bond Length in Oxadiboriranes (C) 1154
- Regiospecific Conversion of 3,4-Bis(trimethylsilyl)furan to 3,4-Disubstituted Furans: A Novel Suzuki-Type Cross-Coupling of Boroxines (C) 432
- Structural Evidence of the Aromaticity of Borepins: A Comparison of 1-Chloroborepin and Tricarbonyl(1-chloroborepin)molybdenum (C) 1065
- The Role of Chemistry in the Development of Baron Neutron Capture Therapy of Cancer (R) 950

BPTI
- The Importance of the Rigidity of the Peptide Backbone for the Inhibitory Properties of BPTI Demonstrated by Semisynthetic Structural Variants (C) 898

Bridging ligands
- A Novel Complex with Boat-Shaped, Synfacially Bound $\eta^3:\eta^3$-Benzene Bridges and the First μ_3-$\eta^2:\eta^2:\eta^2$-Arenetrirhodium Complex (C) 1697
- Methods for the Synthesis of μ-Hydrocarbon Transition Metal Complexes without Metal–Metal Bonds (R) 923

- Ti^{IV} Complexes with Bridging Ylide Ligands: Double Oxophiles in Reactions with Aldehydes (C) 554

Bromine azide
- Bromine Azide—Determination of the Molecular Structure by Electron Diffraction in the Gas Phase (C) 759

Bromine bromate
- Bromine Bromate Br_2O_3 (C) 1632

Butadiynes
- 1,3-Bis(triphenylphosphoranylidene)-allene and Tribenzyl(4-methyldiphenylphosphoniobutadiynyl)borate, Stabilized C_3 and C_4: Confirmation of a Hypothesis (C) 1205

C_1 building blocks
- (Trimethylstannyl)methyllithium as a Source of a Methylene Bridge Connecting Two Acyl Groups: A Potential Route to D-Mycaroside (C) 105

Cadmium compounds
- Synthesis, Structure, and Optical Properties of Cd_4S^{6+} Clusters Encapsulated in an Aluminate Cage (C) 1663

Cage compounds
- Carbocyclic Cage Compounds: Chemistry and Applications (B) 625
- Golcondane: A Novel, Caged, Nonacyclic $C_{20}H_{24}$-Hydrocarbon of D_{2d} Symmetry (C) 1160
- *p*-[$3^2.5^6$]Octahedrane, the $(CH)_{12}$ Hydrocarbon with D_{3d} Symmetry (C) 559
- The Dimeric Tris(lithioarsino)germane *t*BuGe[As(Si*i*Pr$_3$)Li]$_3$: A Self-Assembled, Solvent-Free Lithium–Main Group Element Aggregate with a $Ge_2As_6Li_6$ Rhombododecahedral Framework (C) 1439
- The Pagodane Route to Dodecahedranes: An Improved Approach to the $C_{20}H_{20}$ Parent Framework; Partial and Total Functionalizations—Does C_{20}-Fullerene Exist? (C) 1722

Calicheamicins
- The Battle of calicheamicin γ_1^I (R) 1377

Calixarenes
- Host–Guest Complexes between Calix[4]arenes Derived from Resorcinol and Alkylammonium Ions (C) 1195
- Supramolecular Complexes of Flexible, Extended Cavity Calix[4]arenes—Structural Characterization of a Molecular Venus Flytrap (C) 1093

Calvin, M.
- Following the Trail of Light. A Scientific Odyssey (B) 444

Cannabinoid receptor
- Biologically Active Linear Metabolites of Arachidonic Acid—The First Endogenous Ligand of the Cannabinoid Receptor (H) 1027

Capillary electrophoresis
- Capillary Electrophoresis: Methods and Scope (R) 629
- Capillary Electrophoresis. Principles, Practice and Applications (B) 1372

Carbene complexes
- Carbenerhodium Complexes with Diaryl- and Aryl(alkyl)carbenes as Ligands: The Missing Link in the Series of the Double Bond Systems *trans*-[RhCl{=C(=C)$_n$RR'}(L)$_2$] Where $n = 0$, 1, and 2 (C) 1480
- Competing M=$C_{carbonyl}$ and M=$C_{carbene}$ Bonds: Cycloaddition to the Metal–$C_{carbonyl}$ Bond in η^2-Thiocarbene Complexes (C) 1152
- On the Mechanism of the TCPC^{HFB}-Catalyzed Metathesis of 1,6-Enyne: Evidence for Alkylidenepalladium Intermediates (C) 1085

Carbenes
- A Branched-Chain Nonacarbene with a Nonadecet Ground State: A Step Nearer to Superparamagnetic Polycarbenes (C) 872
- Carbenes in Constrained Systems I: 1,3 C–H Insertion Reaction of Adamantylidene within the β-Cyclodextrin Cavity (C) 1344
- Triplet States in Organic Chemistry (H) 1409

Carbenoids
- 1-Chloro-2,2-bis(4-chlorophenyl)-1-lithioethene · TMEDA · 2THF: Structure of a Li-Cl Carbenoid (C) 1032
- Reduction of Geminal Dihalocyclopropanes with Lithium 4,4'-Di-*tert*-butylbiphenyl; Cyclopropyl Derivatives of Dilithiomethane and 1,2-Dilithioethane; Inferences Regarding the Intermediate Carbenoids (C) 574
- Successful X-Ray Structure Analysis of an Alkylidene Carbenoid—A Milestone in Carbenoid Research (H) 1023

Carboalumination
- Rapid Carboalumination of Alkynes in the Presence of Water (C) 1068

Carbocations
- Comparison of the Electrophilicities of Cationic Metal π Complexes and of Ordinary Carbenium Ions (C) 1630
- Contrasting Structures of Pyramidal Carbocations and Their Silicon Analogues (C) 865
- Protonation of Phenyl(trimethylsilyl)-acetylene: A Surprisingly Weak Stabilization of a Carbocation by a β-Trimethylsilyl Group (C) 721

Carbohydrates
- A Short Synthetic Route towards a Biologically Active Heparin-like Pentasaccharide with a Pseudo-Alternating Sequence (C) 434
- Carbohydrates as Chiral Auxiliaries in Stereoselective Synthesis (R) 336
- Continuous Catalytic Synthesis of *N*-Acetyllactosamine (C) 1342
- Cycloaddition Reactions in Carbohydrate Chemistry (B) 1666
- Got the Flu? Try a Designer Agent Derived from a Sugar (H) 1691
- Selective Dehydrogenation of Aldonic and Aldaric Acid with an *R*-Configurated α Carbon Atom to 2-Oxocarboxylic Acids, and Reduction of the Oxo Group of *N*-Acetylneuraminic Acid with *Proteus mirabilis* (C) 1197
- Sequential Analysis of Oligosaccharide Structures in a Few Minutes (C) 1349
- Stereoselective Synthesis of C-Glycosides with a Glycosyl Dianion (C) 1091
- The Unique Antithrombin III Binding Domain of Heparin: A Lead to New Synthetic Antithrombotics (R) 1671

Carbon modifications
- Hypothetical Carbon Modifications Derived from Zeolite Frameworks (C) 701

Carbon nitride
- Carbon(IV) Nitride C_3N_4—A New Material Harder Than Diamond? (H) 1580

Carbon–carbon linkage
- Benzoannulated Phosphorus–Carbon Four-Membered Rings (C) 1359
- [*tert*-Butylcyanide · Lithium Bis(trimethylsilyl)amide]$_2$, a Model of the Intermediate RCN · MR' Complex Formed in Reactions of Cyanides RCN with Organometallic Compounds R'M (C) 1171
- Formation of Alkynyltrithiocarbonato Ligands from Alkylidyne Ligands and Carbon Disulfide (C) 1726
- 1-Iodoalkynes Can Also Be Dimerized: A New Head-to-Tail Coupling (C) 893
- Metal-Initiated Coupling of C_2 Units to Enynes and Butatrienes: Two Different Routes for the Dimerization of 1-Alkynes (C) 1315
- Palladium-Catalyzed Arylation of Tetrasubstituted Double Bonds: A Simple Synthesis of Annelated Propellanes (C) 1733
- Regiospecific Conversion of 3,4-Bis(trimethylsilyl)furan to 3,4-Disubstituted Furans: A Novel Suzuki-Type Cross-Coupling of Boroxines (C) 432
- Selective Pd^0-Mediated C–C Bond Constructions on the Imidazole Ring of L-Histidine: A Practical Approach to the Synthesis of Diphthamide and Related Histidine Analogues (C) 1326
- The Seven-Component Reaction (C) 563 (916)
- Ti^{IV} Complexes with Bridging Ylide Ligands: Double Oxophiles in Reactions with Aldehydes (C) 554

Carbon–oxygen linkage
- Metal-Mediated Oxyfunctionalization of Organic Substrates by Organometallic Intermediates—More Recent Developments and Perspectives (H) 1144

Carboranes
- Carboranes, Anti-Crowns, and Big Wheels (H) 1289
- (1,7-$C_2B_{10}H_{10}$-1',3'-C_6H_4)$_3$, a Cyclic Trimer from *meta*-Carboranediyl and *meta*-Phenylene Units: A New Category of Macrocycle (C) 1328

Carboxylases
- Propionyl-Aza(dethia)coenzyme A as Pseudosubstrate of the Biotin-Containing Transcarboxylase (C) 278

Carboxylic acids
- Separation of Diastereomers by Distillation—A New Procedure for the Synthesis of Optically Active Heterocyclic Carboxylic Acids (C) 753

Carbyne complexes
- Investigations of the Structure and Kinetics of Intermediates in Proton-Induced Alkylidyne–Isocyanide Ligand Coupling Reactions (C) 743
- [W(CH)(dmpe)$_2$(*n*Bu)], a Complex with a Bent Methylidyne Ligand (C) 858

Carcinogenicity
- Activation of the C2 Position of Purine by the Trifluoromethanesulfonate Group: Synthesis of N^2-Alkylated Deoxyguanosines (C) 404

Catalysis
- Catalytic Chemistry (B) 1667
- Chiral Phosphinoaryldihydrooxazoles as Ligands in Asymmetric Catalysis: Pd-Catalyzed Allylic Substitution (C) 566
- Cobalt Tetra(hydroquinone)porphyrin: An Efficient Electron Transfer Reagent in Aerobic Pd-Catalyzed 1,4-Diacetoxylation of 1,3-Cyclohexadiene (C) 263
- Enantioselective Catalytic Addition of Functionalized Dialkylzinc Compounds to β-Stannylated Aldehydes: A Convenient Preparation of Chiral β- and γ-Functionalized Secondary Alcohols (C) 582
- Extending the Metal Cluster–Metal Surface Analogy (H) 228
- Heterogeneous Catalysis—Still Magic or Already Science? (H) 381
- Homogeneous Catalysis. The Applications and Chemistry of Catalysis by Soluble Transition Metal Complexes (B) 1666
- Methyltrioxorhenium(VII) as Catalyst for Epoxidations: Structure of the Active Species and Mechanism of Catalysis (C) 1157

- New Developments in the Chemistry of Catalytic Antibodies (H) 1291
- Palladium-Catalyzed, Enantioselective Allylic Substitutions (H) 547
- Reaction Tuning in Zeolites: An in situ MAS NMR Study of Acetaldehyde on HZSM-5 (C) 615
- Substrate-Specific Catalysis by Ion Pairs (C) 1648
- Water-Soluble Ligands, Metal Complexes, and Catalysts: Synergism of Homogeneous and Heterogeneous Catalysis (R) 1524

Catenanes
- Isomeric Self-Assembling [2]Catenanes (C) 1297
- Multiring Catenanes with a Macrobicyclic Core (C) 1434
- Photoswitchable Catenanes (C) 1295
- The Self-Assembly of Catenated Cyclodextrins (C) 854

Cations
- Octaethyltetraoxaporphyrin Dication—Counterpart of Octaethylporphyrin in the Tetraoxaporphyrin Series (C) 1597
- Superelectrophiles (R) 767

Cellular regulation
- Protein Phosphorylation and Cellular Regulation I (Nobel Lecture) (R) 1122
- Protein Phosphorylation and Cellular Regulation II (Nobel Lecture) (R) 1130

Cerium compounds
- $CeCl_3$-Mediated Addition of Grignard Reagents to 1,3-Diketones (C) 1061

C-H activation
- C–H Bond Addition to a V=NR Bond: Hydrocarbon Activation by a Sterically Crowded Vanadium System (C) 903
- C–H-Activation by Reaction of (Butadiene)zirconocenes and -hafnocenes with 9-BBN (C) 1213
- Transition Metal Complexation of σ Bonds (R) 789

Chalcogen compounds
- $[Tc_6X_8]$ Clusters in ternary Technetium Chalcogenides (C) 576

Chelate ligands
- Axial Ligation of Diazacyclooctanenickel and -Zinc Complexes (C) 116
- Dilithiation of Two Diphenyl Ethers Each Containing Two $NHCH_2CH_2Y$ (Y = OMe, NMe_2) Side Arms in *ortho* Positions: Assembly of "Adamantanoid" $Li_4O_2N_4$ Cores (C) 1182
- Highly Coordinated Lanthanoid–Phosphane Complexes (C) 1739
- Monomeric Tris(η^2-pyrazolato)lanthanoid Complexes with the Bulky 3,5-Di(*tert*-butyl)pyrazolato Ligand (C) 874
- The Coordination Chemistry of Multidentate Isocyanide Ligands (R) 650
- The First Neutral Adamantanoid Iron(III)–chelate Complex: Spontaneous Formation, Structure, and Electrochemistry (C) 1179

Chemical equilibria
- Chemical Equilibria in Solution. Dependence of Rate and Equilibrium Constants on Temperature and Pressure (B) 308

Chemical sensors
- Organic Clathrate-Forming Compounds as Highly Selective Sensor Coatings for the Gravimetric Detection of Solvent Vapors (C) 110

Chiral auxiliaries
- (*R*)- and (*S*)-4-Alkoxy-2-*tert*-butyl-2,5-dihydroimidazole-1-carboxylates—New Chiral Glycine Derivatives for Amino Acid Synthesis (C) 1765
- A New Atropisomeric Molecular Structure for Efficient Enantiodifferentiation (C) 606
- Carbohydrates as Chiral Auxiliaries in Stereoselective Synthesis (R) 336
- Chiral Phosphinoaryldihydrooxazoles as Ligands in Asymmetric Catalysis: Pd-Catalyzed Allylic Substitution (C) 566

Chirality
- Asymmetric Synthesis and Highly Diastereoselective *ortho*-Lithiation of Ferrocenyl Sulfoxides. Application to the Synthesis of Ferrocenyl Derivatives with Planar Chirality (C) 568

Chlorofluorocarbons
- Complexation of Methane and Chlorofluorocarbons by Cryptophane-A in Organic Solution (C) 1169

Chloroglycyl peptides
- Synthesis and Reactivity of α,α-Dichloroglycyl Peptides (C) 1771

Chromatography
- Chromatographic Separation of the Four Possible Structural Isomers of a Tetrasubstituted Phthalocyanine: Tetrakis(2-ethylhexyloxy)phthalocyaninatonickel(II) (C) 1422
- HPLC of Proteins, Peptides and Polynucleotides. Contemporary Topics and Applications (B) 305
- Ion-Spray Mass Spectrometry and High-Performance Liquid Chromatography—Mass Spectrometry of Synthetic Peptide Libraries (C) 894
- Preparative Enantiomer Separation of the Anesthetic Enflurane by Gas Inclusion Chromatography (C) 1662

Chromium compounds
- Carbonyl–Metal Complexes of Diphosphadiboretane (mesB–P*t*Bu)$_2$ and of Triphosphatriborinanes (mesB–P*t*Bu)$_3$ (C) 1446
- $[(CO)_5Cr=Tl=Cr(CO)_5]^-$, the First Complex Containing Linear Twofold-Coordinated Thallium (C) 1772
- $[Cr(CO)_5PCl_3]$—A P_1 Building Block for the Formation of Complexes with *cyclo*-P_x Ligands (x = 3, 5) (C) 593
- η^6-(1,2-Dioxocyclobutabenzene)-tricarbonylchromium(0): Starting Material for Double Anionic Oxy-Cope Rearrangements under Very Mild Conditions (C) 267
- Synthesis and Reactivity of Hexafluoro-1,2-diisocyanocyclobutanechromium Complexes (C) 1456
- Synthesis of the First Stable 2-Chromaoxetane and its Homologues via α-Phosphonio(methylidene) Complexes of Hexavalent Chromium, Molybdenum, and Tungsten (C) 731
- (η^1-tpMn, η^5-tpCr) → (η^1-tpCr, η^5-tpMn) Thiophene (tp) Conversion due to Bimetallic Activation: A Novel Metal-Exchange Reaction (C) 710
- Unprecedented Cage-Opening of P_4S_3 Initiated by an Organometallic Radical: Synthesis and Structure of $[Cp_4Cr_4(CO)_9(P_4S_3)]$ (C) 1728

Circular dichroism
- CD Exciton Chirality Method: New Chromophores for Primary Amino Groups (C) 888

Clathrates
- Organic Clathrate-Forming Compounds as Highly Selective Sensor Coatings for the Gravimetric Detection of Solvent Vapors (C) 110

Clusters
- A Hexanuclear Organogallium Fluoride Oxide (C) 1701
- A New Copper Selenide Cluster with PPh_3 Ligands: $[Cu_{146}Se_{73}(PPh_3)_{30}]$ (C) 1303
- A New Type of Hexanuclear Iron(III) Hydroxo(oxo) Cluster (C) 570
- Cage Extension to Clusters with Co_2/Co_3MoAs_6 Polyhedron Frameworks (C) 914
- Cation Inclusion within the Mixed-Valence Polyanion Cluster $[(Mo^{VI}O_3)_4Mo^V_{12}O_{28}(OH)_{12}]^{8-}$: Syntheses and Structures of $(NH_4)_7[NaMo_{16}(OH)_{12}O_{40}]\cdot 4H_2O$ and $(Me_2NH_2)_6[H_2Mo_{16}(OH)_{12}O_{40}]$ (C) 1780
- Compounds Containing Silicon, Germanium, and Tin Polyhedra: The First Octahedral Tin Cluster (H) 545
- Control of the Linkage of Inorganic Fragments of V–O Compounds: From Cluster Shells as Carcerands via Cluster Aggregates to Solid-State Structures (C) 909
- $[Cp^*TaS_3\{Rh(cod)\}_2]$ and $[Cp^*TaS_3\{RuH(PPh_3)_2\}_2]$: A New Class of Heterometallic TaM_2 Clusters (C) 763
- Extending the Metal Cluster–Metal Surface Analogy (H) 228
- Mercury, a Structural Building Block and Source of Localized Reactivity in Extended Metal–Metal Bonded Systems (R) 24
- New Cu–Te Clusters (C) 238
- New Phosphido-Bridging Copper Clusters (C) 242
- Structure and Electrochemical Behavior of the Paramagnetic Anion $[Ir_{14}(CO)_{27}]^-$, Possessing a Trigonal Bipyramidal Arrangement of Metal Atoms (C) 1347
- $[Tc_6X_8]$ Clusters in ternary Technetium Chalcogenides (C) 576
- Tetranuclear Cuboidal and Hexanuclear Prismatic Iron–Sulfur–Nitrosyl Clusters (C) 564
- The Application of Au_{55} Clusters as Quantum Dots (C) 250
- The First Trigonal-Bipyramidal Cluster with an Interstitial C_2 Unit: $[Rb\{Pr_5(C_2)\}Cl_{10}]$ (C) 1318

CO dehydrogenases
- Functional Modeling of CO Dehydrogenase: Catalytic Reduction of Methylviologen by CO/H_2O with an N,O,S-Ligated Nickel Catalyst (C) 92

Cobalt compounds
- Cage Extension to Clusters with Co_2/Co_3MoAs_6 Polyhedron Frameworks (C) 914
- Controlling Valence Tautomerism of Cobalt Complexes Containing the Benzosemiquinone Anion as Ligand (C) 880
- Formation and Complex Stabilization of a New Chainlike Phosphazene Anion by Co^{II}-Assisted Oxidative Scrambling of $[N(PPh_2)_2]^-$ (C) 700
- Molecular Recognition within a Rigid Host: Structural Changes Induced in μ-Carboxylato Dimetal(II) Complexes by Replacing Steric Repulsions with Hydrogen Bonds (C) 1321
- Regiospecific Alkylation of 6-Chloropurine and 2,6-Dichloropurine at N7 by Transient Protection of N3/N9 by Methylcobaloxime (C) 1696
- The First Structurally Characterized Heterodinuclear Double-Helicate Complex (C) 1465

Coenzyme A
- Propionyl-Aza(dethia)coenzyme A as Pseudosubstrate of the Biotin-Containing Transcarboxylase (C) 278

Colloids
- Colloidal Semiconductor Q-Particles: Chemistry in the Transition Region Between Solid State and Molecules (R) 41
- Electrochemistry in Colloids and Dispersions (B) 1373

Complexes with arsenic ligands
- Cage Extension to Clusters with Co_2/Co_3MoAs_6 Polyhedron Frameworks (C) 914
Complexes with carbon ligands
- A New Form of Coordinated Carbon: A C_3 Chain That Is Anchored by a Transition Metal on Each End and Spanned by a Third (C) 891
- The First Trigonal-Bipyramidal Cluster with an Interstitial C_2 Unit: $[Rb\{Pr_5(C_2)\}Cl_{10}]$ (C) 1318
Complexes with chalcogen ligands
- Formation of Monomeric Terminal Chalcogenides by Template-Induced Disilylchalcogenide Elimination; the Crystal Structures of $[ETa\{(Me_3SiNCH_2CH_2)_3N\}]$ (E = Se,Te) (C) 1450
Complexes with halogen ligands
- The Behavior of Cp^*MoBr/Br_2 Redox Systems: The Unusual Structure of $[(Cp^*_2Mo_2Br_4)_2(Cp^*MoBr_4)_3]$, a Compound Containing Mo^{III}, Mo^{IV}, and Mo^V (C) 1486
Complexes with hydrido ligands
- Structure and Reactivity of $[HFe(CO)_3(\eta^3\text{-}C_3H_5)]$ (C) 1073
Complexes with nitrogen ligands
- Cavities for Binding Two Metal Atoms: A Novel Pentanuclear Copper(I) Complex with an Anionic, Pentadentate Aryl Ligand with Two *ortho*-Chelating Diamine Substituents (C) 72
- C–H Bond Addition to a V=NR Bond: Hydrocarbon Activation by a Sterically Crowded Vanadium System (C) 903
- Hexakis(benzotriazolato)tetrakis(2,4-pentanedionato)pentacopper(II): A Model for Corrosion Inhibition (C) 1036
- How "Innocent" Are Pentane-2,4-dione-bis(*S*-alkylisothiosemicarbazonate) Ligands in Biomimetic Fe^{II} and Fe^{IV} Complexes? (C) 1635
- Monomeric Tris(η^2-pyrazolato)lanthanoid Complexes with the Bulky 3,5-Di(*tert*-butyl)pyrazolato Ligand (C) 874
- Multicomponent Self-Assembly: Spontaneous Formation of a Cylindrical Complex from Five Ligands and Six Metal Ions (C) 69
- Nucleophilic Substitution of Bis(cyclopentadienyl)tin(II); Synthesis, Structure, and Solution Dynamics of *trans*-$[(\eta^3\text{-}Cp)Sn\{\mu_2\text{-}N=C(NMe_2)_2\}]_2$ (C) 428
- Rigid Rodlike Metal Complexes of Nanometric Dimension: Synthesis, Luminescence Properties, and Long-Range Energy Transfer (C) 1643
- Self-Assembly of a New Class of Tetranuclear Copper(I) and Silver(I) Complexes (C) 877
- Self-Assembly, Structure, and Spontaneous Resolution of a Trinuclear Triple Helix from an Oligobipyridine Ligand and Ni^{II} Ions (C) 703
- Structure of a One-Dimensional Infinite Double-Helical Copper(I) Complex (C) 1463
- Synthesis and Structure of the First Homoleptic Imidotechnetium Complex: $[Tc_2(NAr)_6]$ (Ar = 2,6-diisopropylphenyl) (C) 94
- The First Heteroallyl Metal Complexes of Arsenic with the Coordination Number 2 (C) 1628
- The First Structurally Characterized Heterodinuclear Double-Helicate Complex (C) 1465
- The First Unsolvated Chelate and Cubane-Type Barium Complexes: Effective Compounds for the Sol–Gel Process (C) 596
Complexes with oxygen ligands
- A New Type of Hexanuclear Iron(III) Hydroxo(oxo) Cluster (C) 570
- A Two-Dimensional Ice with the Topography of Edge-Sharing Hexagons Intercalated between $CdNi(CN)_4$ Layers (C) 884
- Alternating Ferro- and Antiferromagnetic Interactions in a Chainlike Cu^{II} Coordination Polymer (C) 1046
- Catalysis of the Hydrolysis of Phosphoric Acid Diesters by Lanthanide Ions and the Influence of Ligands (C) 1716
- Hydrolysis to a Complex with a Central, Octahedral $(\mu_6\text{-}O)In_6$ Unit (C) 1426
- Metal-Mediated Oxyfunctionalization of Organic Substrates by Organometallic Intermediates—More Recent Developments and Perspectives (H) 1144
- Molecular Recognition of Hexaaqua Transition Metal(II) Ions (C) 714
- Structural Variations Observed in the $[Bi(O_2CCF_3)_4Ph]^{2-}$ Anion: Selective Cation–Anion Interactions through Hydrogen Bonds (C) 589
Complexes with phosphorus ligands
- A Highly Electrophilic Unsaturated Ditungsten Dication (C) 1156
- Catalytic Hydrogenation with Rhodium Complexes Containing dipamp-pyrphos Hybrid Ligands (C) 1052
- $[Cr(CO)_5PCl_3]$—A P_1 Building Block for the Formation of Complexes with *cyclo*-P_x Ligands (x = 3, 5) (C) 593
- Formation and Complex Stabilization of a New Chainlike Phosphazene Anion by Co^{II}-Assisted Oxidative Scrambling of $[N(PPh_2)_2]^-$ (C) 700
- Highly Coordinated Lanthanoid–Phosphane Complexes (C) 1739
- New Phosphido-Bridging Copper Clusters (C) 242
- Palladium-Catalyzed Enantioselective Bis-alkoxycarbonylation of Olefins (C) 1719
- Phosphinidenetantalum(V) Complexes of the Type $[(N_3N)Ta{=}PR]$ as Phospha-Wittig Reagents (R = Ph, Cy, *t*Bu; $N_3N = (Me_3SiNCH_2CH_2)_3N$) (C) 756
- Photochemical 1,2 Shift of the Phosphane Ligands in the Silanediyl Complex $[(2\text{-}Ph_2PCH_2C_6H_4)_2Si{=}Cr(CO)_5]$ (C) 1313
- $[(\widehat{PP})_2RhH]$ and $[(\widehat{PP})_2Rh][O_2CH]$ Complexes as Models for the Catalytically Active Intermediates in the Rh-Catalyzed Hydrogenation of CO_2 to HCOOH (C) 739
- Tantalum(V) Phosphinidene Complexes as Phospha-Wittig Reagents (H) 850
- Unprecedented Cage-Opening of P_4S_3 Initiated by an Organometallic Radical: Synthesis and Structure of $[Cp_4Cr_4(CO)_9(P_4S_3)]$ (C) 1728
Complexes with sulfur ligands
- Competing $M{=}C_{carbonyl}$ and $M{=}C_{carbene}$ Bonds: Cycloaddition to the Metal–$C_{carbonyl}$ Bond in η^2-Thiocarbene Complexes (C) 1152
- $[Cp^*TaS_3\{Rh(cod)\}_2]$ and $[Cp^*TaS_3\{RuH(PPh_3)_2\}_2]$: A New Class of Heterometallic TaM_2 Clusters (C) 763
- Formation of Alkynyltrithiocarbonato Ligands from Alkylidyne Ligands and Carbon Disulfide (C) 1726
- $[Mo_2(S)_2(\mu\text{-}S)(syn\text{-}Me_8[16]aneS_4)_2]^{2+}$, a Novel Sulfidomolybdenum Complex Containing a Linear S=Mo–S–Mo=S Linkage (C) 1621
- New Half-Sandwich Polysulfidorhenium Complexes (C) 85
- Novel V^{III} Complexes with a Central $[V_3(\mu_3\text{-}S)(\mu\text{-}S_2)_3]^+$ or $[V_2(\mu\text{-}O)(\mu\text{-}SPh)_2]^{2+}$ Unit (C) 594
- Reduced $[Fe_8S_6]$ Clusters: Binding Links between FeS and Active Centers of Iron-Sulfur Proteins (C) 863
Complexes with tellurium ligands
- Tellurium—An Interesting Bonding Partner for Transition Metals: New Results from Molecular Chemistry (H) 67
Computer
- Graphics and Animation in Surface Science (B) 453
Computer chemistry
- Computer-Assisted Solution of Chemical Problems—The Historical Development and the Present State of the Art of a New Discipline of Chemistry (R) 201
- Neural Networks in Chemistry (R) 503
Condensed matter
- Simple Views on Condensed Matter (B) 917
Conformation
- Bi[1,3-bis(dicyanomethylene)indan-2-ylidene]—An Ethylene Derivative with Extremely Pronounced Twisting of the C=C Bond (C) 1352
- $[(\eta^5\text{-}CH_3C_5H_4)Mn(CO)(dppfe)]$: Two Isomers Distinguished by their Characteristic CO Stretching Frequencies, which Differ Only in Rotation of the Methylcyclopentadienyl Ligand: Evidence for an Intramolecular M–CO···H–C Interaction (C) 87
- Non-Twisted Tetrakis(organosilyl)-ethene (C) 1473
- On the Strength of the C–H···O Hydrogen Bond and the Eclipsed Arrangement of the Methyl Group in a Tricyclic Orthoamide Trihydrate (C) 588
- Silylamines with Pyramidal Coordination at Nitrogen (C) 425
- Structure and Reactivity of a Highly Twisted Amide (C) 1083
Conjugation
- 1,3-Bis(triphenylphosphoranylidene)-allene and Tribenzyl(4-methyldiphenylphosphoniobutadiynyl)borate, Stabilized C_3 and C_4: Confirmation of a Hypothesis (C) 1205
- Synthesis of the Tris(9-fluorenylidene)cyclopropane Dianion and Related Dianions: [3]Radialenes with Novel Electronic Properties (C) 89
- Tetrakis(trialkylsilylethynyl)butatriene and 1,1,4,4-Tetrakis(trialkylsilylethynyl)-1,3-butadiene: Novel Cross-Conjugated Chromophors (C) 1187
Coordination
- A Molecular Heterometal Amide with High Molecular Dynamics: Does the Lithium Atom Orbit? (C) 1731
- A Nickel–Anthracene Complex Having η^3 and η^4 Coordination in One Crystal (C) 1475
- A Two-Dimensional Ice with the Topography of Edge-Sharing Hexagons Intercalated between $CdNi(CN)_4$ Layers (C) 884
- An Al–Al One-Electron π Bond (C) 388
- Axial Ligation of Diazacyclooctane-nickel and -Zinc Complexes (C) 116
- $Ba[Si(OCH_2CH_2O)_3]$, a Hexaalkoxysilicate Synthesized from SiO_2 (C) 287
- Bis(*P*,*P*-di-*tert*-butyl-*N*-cyclohexylphosphinicamidato-*N*,*O*)nickel(II): Whether Planar or Tetrahedral—Both Isomers are Paramagnetic (C) 907
- $[(CO)_5Cr{=}Tl{=}Cr(CO)_5]^-$, the First Complex Containing Linear Twofold-Coordinated Thallium (C) 1772

- [Cp*Ru(acac)] Is Not a Coordinatively Unsaturated, Stable 16-Valence-Electron Complex (C) 1294
- Crystal Structure of [(α-Cyanoisopropylsodium · Tetramethylenediamine)$_4$]: How Coordination Expansion from Li to Na Centers can Increase the Aggregation State of an α-Nitrile "Carbanion" (C) 1366
- [{Et_2O)$_2$ClGa}Ga{$GaCl_2(Et_2O)$}$_3$]: A Molecular Compound with a Tetrahedral Ga_5 unit (C) 1059
- Insertion of a Cp Unit into a Metal–Metal Bond: [$Ru_3(CO)_{10}(C_5H_4)$] and its PPh_3 Derivative (C) 1048
- Intramolecular Base Stabilization of Silicenium Ions: A New Route to Siliconium Ions (C) 1311
- Lithium Di-*tert*-butylmethylsilylhydrazide, a Hexamer with Li^+ Ions Bound Side-on and End-on (C) 1625
- Marine Metabolites and Metal Ion Chelation: The Facts and the Fantasies (R) 1
- "Noncoordinating" Anions, II (H) 1025
- Structure and Reactivity of [$HFe(CO)_3(\eta^3\text{-}C_3H_5)$] (C) 1073
- Synthesis and Structure of a Trimeric Cyclometalated Coordination Compound with a Hydrophobic Cavity (C) 392
- Tetranuclear Silver(I) Clusters Linked by Bridging Succinate Anions in a Three-Dimensional Network: Crystal Structure of Succinatodisilver(I) (C) 1495
- The Coordination Chemistry of Multidentate Isocyanide Ligands (R) 650
- The Energetic Stabilization Caused by a Planar-Tetracoordinate Carbon Atom: A Dynamic NMR Spectroscopic Study of the Dimetallabicycle [$(Cp_2Zr)_2(\mu\text{-}C{\equiv}CCH_3)(\mu\text{-}H_3CCCCH_3)$]$BPh_4$ (C) 1623
- The First Heteroallyl Metal Complexes of Arsenic with the Coordination Number 2 (C) 1628
- The Structures of Tris(8-dimethylamino-1-naphthyl)phosphane and Tris-[2-(dimethylaminomethyl)phenyl]phosphane: Crystallographic Evidence of Seven-Coordinate Phosphorus (C) 1430
- (η^1-tpMn, η^5-tpCr) → (η^1-tpCr, η^5-tpMn) Thiophene (tp) Conversion due to Bimetallic Activation: A Novel Metal-Exchange Reaction (C) 710
- Transition Metal Complexation of σ Bonds (R) 789
- Tris(chlorodimethylstannyl)amine, a Molecule with a Planar Sn_3N Skeleton Stabilized by Intramolecular Sn-Cl-Sn Bridges (C) 1608

Coordination chemistry
- Perspectives in Coordination Chemistry (B) 916

Copper compounds
- A New Copper Selenide Cluster with PPh_3 Ligands: [$Cu_{146}Se_{73}(PPh_3)_{30}$] (C) 1303
- A New Layered Ternary Sulfide: Formation of Cu_2WS_4 by Reaction of WS_4^{2-} and Cu^+ Ions (C) 256
- Alternating Ferro- and Antiferromagnetic Interactions in a Chainlike Cu^{II} Coordination Polymer (C) 1046
- 2,2'-Bipyrimidineoxalatocopper(II) Complexes: From the Mononuclear Complex to the 2D Sheetlike Polymer (C) 613
- Cavities for Binding Two Metal Atoms: A Novel Pentanuclear Copper(I) Complex with an Anionic, Pentadentate Aryl Ligand with Two *ortho*-Chelating Diamine Substituents (C) 72
- Double Lewis Acid Activation in Phosphate Diester Cleavage (C) 1633
- Hexakis(benzotriazolato)tetrakis(2,4-pentanedionato)pentacopper(II): A Model for Corrosion Inhibition (C) 1036
- Multicomponent Self-Assembly: Spontaneous Formation of a Cylindrical Complex from Five Ligands and Six Metal Ions (C) 69
- Multinuclear Sandwich-type Complexes of Deprotonated β-Cyclodextrin and Copper(II) Ions (C) 852
- New Cu–Te Clusters (C) 238
- New Phosphido-Bridging Copper Clusters (C) 242
- Novel Alkynylcopper(I) Complexes and Lithium Alkynyl Cuprates (C) 1077
- Preparation and Structure of Two Highly Reactive Intermediates: [$Li(thf)_4$][$Cu_5Cl_4R_2$] and [$Li(thf)_4$][$AlCl_3R$], R = $Si(SiMe_3)_3$ (C) 121
- Self-Assembly of a New Class of Tetranuclear Copper(I) and Silver(I) Complexes (C) 877
- Structure of a One-Dimensional Infinite Double-Helical Copper(I) Complex (C) 1463
- Synthesis and Structure of Surprisingly Stable Tetrakis(trifluoromethyl)-cuprate(III) Salts (C) 1482

Correspondence
- Concerning "An Evaluation of the Peer Review Process at *Angewandte Chemie*" (C) 1030
- Concerning "An Opinion on the Heterogeneous Photoreduction of N_2 with H_2O" (C) 550
- [Cp*Ru(acac)] Is Not a Coordinatively Unsaturated, Stable 16-Valence-Electron Complex (C) 1294
- Reply: Standards of Demonstration for the Heterogeneous Photoreactions of N_2 with H_2O (C) 552

Corrigendum 916

Corrosion
- Hexakis(benzotriazolato)tetrakis(2,4-pentanedionato)pentacopper(II): A Model for Corrosion Inhibition (C) 1036

Crown ethers
- A Simple One-Step Synthesis of Symmetrical Thiocrown Ethers and the Molecular Structure of an Unusual Sandwich-like Tetrametallic Silver Thiocrown Ether Complex (C) 436

Cryptophanes
- Complexation of Methane and Chlorofluorocarbons by Cryptophane-A in Organic Solution (C) 1169

Crystallography
- Fundamentals of Crystallography (B) 1104

Cubanes
- Photochemical Carboxylation of Cubanes (C) 612
- Synthesis and Structure of the Arsaalkyne Tetramer ($AsCtBu)_4$ and its $Fe(CO)_4$ Derivative (C) 103

Cumulenes
- 1,3-Bis(triphenylphosphoranylidene)-allene and Tribenzyl(4-methyldiphenylphosphoniobutadiynyl)borate, Stabilized C_3 and C_4: Confirmation of a Hypothesis (C) 1205
- Surprising Differences in the Cycloaddition Reactions of Cumulenes and Heterocumulenes to Vinylidenetitanocene: Formation of Four- or Five-Membered Titanacycles (C) 264

Cuprates
- Novel Alkynylcopper(I) Complexes and Lithium Alkynyl Cuprates (C) 1077

Cyanamides
- The First Structure of a Lithiated Cyanamide; Synthesis of (PhNCNLi · $HMPA)_n$ by Extrusion of N_2 and S from 5-Phenylamino-1,2,3,4-thiatriazole with Li Reagents and HMPA (C) 1769

Cyanides
- [*tert*-Butylcyanide · Lithium Bis(trimethylsilyl)amide]$_2$, a Model of the Intermediate RCN · MR' Complex Formed in Reactions of Cyanides RCN with Organometallic Compounds R'M (C) 1171

Cyanosulfines
- Cyanosulfines: An Unexpected Reaction of *N*,*N*-bis(trimethylsilyl)ynamines (C) 258

Cyanuric acid
- Self-Assembly Through Hydrogen Bonding: Preparation of a Supramolecular Aggregate Composed of Ten Molecules (C) 1766

Cyclic peptides
- *S*-Glycosylated Cyclic Peptides (C) 269

Cyclizations
- The Use of Radical Cyclization in the Preparation of Substituted Methyl Carbapenem Antibiotic Precursors (C) 867
- Why is Porphobilinogen the Biological Substrate for the Formation of Porphyrins? Calculations on the Conformation of Acyclic Tetrapyrroles and the Acid-Catalyzed Cyclization of Hydroxymethylpyrroles (C) 1038

Cycloadditions
- A Versatile and Efficient Synthesis of Annulated Cyclopentanes by Stereoselective [3+2] Cycloaddition of Allylsilanes and Cycloalkenyl Methyl Ketones (C) 1081
- Absolute Asymmetric Synthesis by Irradiation of Chiral Crystals (H) 694
- Competing $M{=}C_{carbonyl}$ and $M{=}C_{carbene}$ Bonds: Cycloaddition to the Metal–$C_{carbonyl}$ Bond in η^2-Thiocarbene Complexes (C) 1152
- Cycloaddition Reactions in Carbohydrate Chemistry (B) 1666

Cyclobutadienes
- Structures and Reactions of the Oxidation Products of Dimeric Ketenylidene-(triphenyl)phosphorane (C) 1746

Cyclodextrins
- Aminocyclodextrins as Selective Hosts with Several Binding Sites for Nucleotides (C) 1331
- Carbenes in Constrained Systems I: 1,3 C–H Insertion Reaction of Adamantylidene within the β-Cyclodextrin Cavity (C) 1344
- Multinuclear Sandwich-type Complexes of Deprotonated β-Cyclodextrin and Copper(II) Ions (C) 852
- The Self-Assembly of Catenated Cyclodextrins (C) 854

Cyclohexanones
- Diastereo- and Enantioselective Synthesis of 2-Substituted 3-Trialkylstannylcyclohexanones by Michael Addition of Trialkylstannyllithium to Cyclohexenone SAMP Hydrazone (C) 598

Cyclopentanes
- Substituent Effects on the Zero-Field Splitting Parameters of Localized Triplet 1,3-Cyclopentanediyl Biradicals (C) 1339

Cyclopentenonorbornadiene
- 1,7-Cyclopentenonorbornadiene: Synthesis and Crystal Structure (C) 97

Cyclophanes
- Molecular Tweezers with a Hydrocarbon Skeleton and Convergent Carboxyl Groups (C) 601

- Phenothiazine–Bipyridinium Oligooxacyclophanes (C) 1711
- Synthesis of the Mono(Dewar Benzene) Isomer of [1.1]Metacyclophane (C) 726

Data fitting
- Data Fitting in the Chemical Sciences (B) 626

Defect chemistry
- Defect Chemistry: Composition, Transport, and Reactions in the Solid State; Part I: Thermodynamics (R) 313
- Defect Chemistry: Composition, Transport, and Reactions in the Solid State; Part II: Kinetics (R) 528
- Optical Spectroscopy of Single Impurity Molecules in Solids (R) 457

Dendrimers
- Organometallic Molecular Trees as Multielectron and Multiproton Reservoirs: $CpFe^+$-Induced Nonaallylation of Mesitylene and Phase-Transfer-Catalyzed Synthesis of a Redox-Active Nonairon Complex (C) 1075
- Polynitrile- and Polyamine-Functional Poly(trimethylene imine) Dendrimers (C) 1306
- Poly(propylene imine) Dendrimers: Large-Scale Synthesis by Heterogeneously Catalyzed Hydrogenations (C) 1308
- Rapid Construction of Large-Size Phenylacetylene Dendrimers up to 12.5 Nanometers in Molecular Diameter (C) 1354
- Synthesis and Characterization of a High Molecular Weight Stiff Dendrimer (C) 246

Deoxyaklanonic acid
- Synthesis of 4-Deoxyaklanonic acid and its Microbial Conversion into Anthracyclinones (C) 1151

Deprotonations
- Stereodivergent Enantioselective Synthesis by Exploiting Unusually Large Kinetic H/D Isotope Effects on Deprotonation (C) 394

Dewar benzene
- Synthesis of the Mono(Dewar Benzene) Isomer of [1.1]Metacyclophane (C) 726

Dewar, M. J. S.
- A Semiempirical Life (B) 1102

Diastereomeric resolution
- Separation of Diastereomers by Distillation—A New Procedure for the Synthesis of Optically Active Heterocyclic Carboxylic Acids (C) 753

Diazo compounds
- BNC Isosteres of Cyclopropane and a Borylated Diazoester from Diazo Compounds and (Dimethylamino)bis(trifluoromethyl)borane (C) 384

Dicyanononasulfane
- Dicyanononasulfane $S_9(CN)_2$—An Unbranched Chain of Thirteen Atoms (C) 1702

Diels–Alder reactions
- Chiral 2-Amino-1,3-butadienes: New Reagents for Asymmetric Cycloadditions (H) 1582
- Electron Transfer-Catalyzed Diels–Alder Reactions with 2-Vinylindoles (C) 901
- On the Shape of a Diels–Alder Ladder Polymer (C) 123
- Photo-induced *exo*-Selective Diels–Alder Reactions (C) 1612
- Reaction of Buckminsterfullerene with *ortho*-Quinodimethane: a New Access to Stable C_{60} Derivatives (C) 78
- The First Example of an Increase in the Enantioselectivity of a Chemical Reaction in the Presence of a Chiral Lewis Acid under High Pressure (C) 1485

(9*S*)-Dihydroerythronolide A
- A Short, Linear Synthesis of (9*S*)-Dihydroerythronolide A (C) 101

Diketones
- $CeCl_3$-Mediated Addition of Grignard Reagents to 1,3-Diketones (C) 1061

Dioxetanes
- Photosensitized Oxygenation of an Acyl Furan: Isolation of the First Furan Dioxetane by Rearrangement of its Endoperoxide and Selected Chemical Transformations (C) 80

Dioxiranes
- Difluorodioxirane (C) 905
- Epoxidation of 2-Methyl-3-phenylbenzofurans with Dimethyldioxirane: A Novel Reversible Valence Isomerization between Labile Benzofuran Epoxides and Quinone Methides, their Rearrangement, Methanolysis, and Cycloaddition Chemistry (C) 735
- S_N2 Reaction versus Electron Transfer in the Oxygen Transfer by Dimethyldioxirane to Nitrogen Heteroarenes (C) 737

Diphosphanes
- Reverse Hydrozirconation Reaction: A Regio- and Diastereospecific Route to New Diphosphanes (C) 1735

DNA
- DNA Supercoiling Imaged in Three Dimensions by Scanning Force Microscopy (C) 1461
- Sequence-Specific Recognition and Modification of Double-Helical DNA by Oligonucleotides (R) 666

DNA cleavage
- Nickel(III)-Promoted DNA Cleavage with Ambient Dioxygen (C) 277
- Selective Cleavage of a 35-mer Single-Stranded DNA Containing the Initiation Codon of the TAT Gene of HIV-1 by a Tailored Cationic Manganese Porphyrin (C) 557
- Synthesis of a Nine-Membered Cyclic Analogue of the Neocarzinostatin Chromophore and Its DNA-Cleaving Activity (C) 1657
- The Mechanism of Anaerobic, Radical-Induced DNA Strand Scission (C) 1742

Dodecahedranes
- Delocalization of Electrons in the Dodecahedrane Cage—A D_{2h}-Symmetrical 4c–3e Radical Cation as a Structural Borderline Case (C) 875
- The Pagodane Route to Dodecahedranes: An Improved Approach to the $C_{20}H_{20}$ Parent Framework; Partial and Total Functionalizations—Does C_{20}-Fullerene Exist? (C) 1722

Domino reactions
- Domino Reactions of 4-Ene-1,2,3-triol Derivatives (C) 1173

Dyes
- 5-Dimethylamino-5′-nitro-2,2′-bithiophene—a New Dye with Pronounced Positive Solvatochromism (C) 719

Ecology
- Bacteria and the Biodegradation of Chemicals Achieved Naturally, by Combination, or by Construction (R) 1398
- Chemistry of the Solid-Water Interface. Processes at the Mineral-Water and Particle-Water Interface in Natural Systems (B) 1105
- Organic Clathrate-Forming Compounds as Highly Selective Sensor Coatings for the Gravimetric Detection of Solvent Vapors (C) 110
- Phosphane (PH_3) in the Biosphere (C) 761

Electrochemistry
- Electrochemical Production of Zintl Anions: Renaissance of a Synthesis Route (H) 1693
- Electrochemical Synthesis of New Sb–Te Zintl Anions by Cathodic Dissolution of Sb_2Te_3 Electrodes: Structures of $[Sb_4Te_4]^{4-}$ and $[Sb_9Te_6]^{3-}$ (C) 1646
- Electrochemistry in Colloids and Dispersions (B) 1373
- Novel Synthesis of Tetrasubstituted β-Lactones: The Use of Indium in the Electrochemically Supported Reformatsky Reaction (C) 1191
- Organometallic Ferrocenyl Polymers Displaying Tunable Cooperative Interactions between Transition Metal Centers (C) 1709
- Ultramicroelectrodes in Electrochemistry (R) 1268

Electrode surfaces
- Molecular Design of Electrode Surfaces (B) 919

Electrodes
- Adsorption of Molecules at Metal Electrodes (B) 1107

Electron diffraction
- Bromine Azide—Determination of the Molecular Structure by Electron Diffraction in the Gas Phase (C) 759

Electron transfer
- Electron and Proton Transfer in Chemistry and Biology (B) 1218
- Electron Transfer-Catalyzed Diels–Alder Reactions with 2-Vinylindoles (C) 901

Electronic structure
- A Branched-Chain Nonacarbene with a Nonadecet Ground State: A Step Nearer to Superparamagnetic Polycarbenes (C) 872
- Structure of Diamagnetic $[W(O\text{-}4\text{-}MeC_6H_4)_2Cl_2(PMePh_2)_2]$ and Comparison with Related Paramagnetic 2,6-Diphenylphenoxido Complexes: A Steric Effect on π-Bonding and Electronic Structure (C) 439
- The Triplet Biradical Tris(3,5-di-*tert*-butyl-4-oxophenylene)methane: Crystal Structure, and Spin and Charge Distribution (C) 416
- Transition Metal Oxides. An Introduction to their Electronic Structure and Properties (B) 304

Electron-transfer reactions
- Dynamic Solvent Effects on Electron-Transfer Reactions (R) 359
- Electron Transfer Reactions in Chemistry: Theory and Experiment (Nobel Lecture) (R) 1111
- The Marcus Inverted Region from Theory to Experiment (H) 691

Electrophiles
- Superelectrophiles (R) 767

Electrophilicity
- Comparison of the Electrophilicities of Cationic Metal π Complexes and of Ordinary Carbenium Ions (C) 1630

Electrophoresis
- Capillary Electrophoresis: Methods and Scope (R) 629

Enantiomeric resolution
- Preparative Enantiomer Separation of the Anesthetic Enflurane by Gas Inclusion Chromatography (C) 1662
- Separation of the Enantiomers of 2,2′-Dihydroxy-1,1′-binaphthyl and 10,10′-Dihydroxy-9,9′-biphenanthryl by Complexation with *N*-Alkylcinchonidinium Halides (C) 1147

Encyclopedia
- Kirk/Othmer Encyclopedia of Chemical Techonolgy. Vol. 1: A to Alkaloids. Vol. 2: Alkanolamines to Antibiotics (Glycopeptides) (B) 619

- McGraw-Hill Encyclopedia of Science and Technology. 7th Edition (B) 1217

Enediynes
- Conjugated Enediynes—An Old Topic in a Different Light (H) 842
- Synthesis of a Nine-Membered Cyclic Analogue of the Neocarzinostatin Chromophore and Its DNA-Cleaving Activity (C) 1657
- The Battle of calicheamicin γ_1^I (R) 1377

Energy conversion
- Molecular Machines: How Motion and Other Functions of Living Organisms Can Result from Reversible Chemical Changes (R) 819

Enflurane
- Preparative Enantiomer Separation of the Anesthetic Enflurane by Gas Inclusion Chromatography (C) 1662

Enolates
- Highly Enantioselective Protonation of Thiol Ester Enolates (C) 1042
- Stereoselective Protonation of Boron Enolates (C) 398

Enones
- Copper-Catalyzed 1,4-Additions of Trialkylaluminum Compounds to Enones (C) 1368

Entropy
- Entropy Analysis. An Introduction to Chemical Thermodynamics (B) 621

Enynes
- On the Mechanism of the $TCPC^{HFB}$-Catalyzed Metathesis of 1,6-Enyne: Evidence for Alkylidenepalladium Intermediates (C) 1085

Enzymatic catalysis
- *E*/*Z* Diastereoselective Enzymatic Hydrolysis of Esters and Diesters (C) 572
- Biotransformations in Organic Chemistry (B) 920
- Continuous Catalytic Synthesis of *N*-Acetyllactosamine (C) 1342
- Enzyme-Catalyzed Asymmetric Synthesis: Kinetic Resolution of Chiral Hydroperoxides by Enantioselective Reduction to Alcohols with Horseradish Peroxidase (C) 1737
- Selective Biocatalysis (B) 920
- Selective Dehydrogenation of Aldonic and Aldaric Acid with an *R*-Configurated α Carbon Atom to 2-Oxocarboxylic Acids, and Reduction of the Oxo Group of *N*-Acetylneuraminic Acid with *Proteus mirabilis* (C) 1197

Enzyme inhibitors
- Diastereo- and Enantioselective Synthesis of C_2-Symmetrical HIV-1 Protease Inhibitors (C) 423
- Lipophilic 5′,5′-*O*-Dinucleoside-α-hydroxybenzylphosphonic Acid Esters as Potential Prodrugs of 2′,3′-Dideoxythymidine (ddT) (C) 1704
- Phosphinic Acid-Based C_2-Symmetrical Inhibitors of HIV-Protease (C) 1720
- Synthesis and Pairing Properties of Decanucleotides from (3′*S*,5′*R*)-2′-Deoxy-3′,5′-ethano-β-D-ribofuranosyladenine and -thymine (C) 1432
- The Importance of the Rigidity of the Peptide Backbone for the Inhibitory Properties of BPTI Demonstrated by Semisynthetic Structural Variants (C) 898

Enzymes
- Aminoacyl-tRNA Synthetases: The Division into Two Classes was Predicted by the Chemistry of Substrates and Enzymes (R) 190
- Hydrophobic Effects. Opinions and Facts (R) 1545
- Manganese Redox Enzymes (B) 129
- Organic Synthesis with Oxidative Enzymes (B) 622

Epoxidations
- Epoxidation of 2-Methyl-3-phenylbenzofurans with Dimethyldioxirane: A Novel Reversible Valence Isomerization between Labile Benzofuran Epoxides and Quinone Methides, their Rearrangement, Methanolysis, and Cycloaddition Chemistry (C) 735
- Methyltrioxorhenium(VII) as Catalyst for Epoxidations: Structure of the Active Species and Mechanism of Catalysis (C) 1157
- Titanium-Catalyzed Epoxy-Hydroxylation of Allylic Alcohols: A Convenient Diastereoselective Synthesis of Epoxy Diols (C) 733

Epoxides
- A Simple Route from Glucal to Cerny Epoxides (C) 272

Erythronolides
- A Short, Linear Synthesis of (9*S*)-Dihydroerythronolide A (C) 101

ESR spectroscopy
- $[Al\mathit{t}Bu]_6^-$: EPR Spectroscopic Evidence and Ab Initio Calculations (C) 1428
- Substituent Effects on the Zero-Field Splitting Parameters of Localized Triplet 1,3-Cyclopentanediyl Biradicals (C) 1339

Esters
- *E*/*Z* Diastereoselective Enzymatic Hydrolysis of Esters and Diesters (C) 572

Faraday, M.
- Michael Faraday and the Royal Institution: The Genius of Man and Place (B) 1371

Ferroelectrics
- Improved Properties of Ferroelectric Liquid Crystals from Palladium β-Diketone Complexes (C) 1203

Ferrous chloride
- $[Fe_2Cl_6]^{2-}$: A Discrete Form of Ferrous Chloride (C) 293

Fluorine compounds
- A Hexanuclear Organogallium Fluoride Oxide (C) 1701
- Can Single-Chain Perfluoroalkylated Amphiphiles Alone Form Vesicles and Other Organized Supramolecular Systems? (C) 741
- Difluorodioxirane (C) 905
- Gaseous Mercury(IV) Fluoride, HgF_4: An Ab Initio Study (C) 861
- Organometallic Titanium Complexes with Unpaired Electrons: Syntheses and Structures of $[\{(\eta^5\text{-Cp})_2TiF_2\}_3Ti]$ and $[\{(\eta^5\text{-Cp}')_2TiF_2\}_3Al]$ (C) 442
- Synthesis and Reactivity of Hexafluoro-1,2-diisocyanocyclobutanechromium Complexes (C) 1456
- Synthesis and Structure of Surprisingly Stable Tetrakis(trifluoromethyl)-cuprate(III) Salts (C) 1482
- Synthetic Fluorine Chemistry (B) 1107

Folic acid
- Self-Assembly and Liquid Crystal Formation of Folic Acid Salts (C) 248

Force microscopy
- DNA Supercoiling Imaged in Three Dimensions by Scanning Force Microscopy (C) 1461

Fullerenes
- Bonding in Endohedral Metal–Fullerene Complexes: f-Orbital Covalency in Ce@C_{28} (C) 108
- Diamino and Tetraamino Derivatives of Buckminsterfullerene C_{60} (C) 1174
- Dicyanopolyynes: Formation of New Rod-Shaped Molecules in a Carbon Plasma (C) 1340
- Reaction of Buckminsterfullerene with *ortho*-Quinodimethane: a New Access to Stable C_{60} Derivatives (C) 78
- The Chemistry of the Fullerenes: An Overview (H) 1138
- The Incorporation of C_{60} in Molecular Sieves (C) 556
- The Mechanism of Fullerene Formation (H) 1412
- The Pagodane Route to Dodecahedranes: An Improved Approach to the $C_{20}H_{20}$ Parent Framework; Partial and Total Functionalizations—Does C_{20}-Fullerene Exist? (C) 1722
- Transfer Hydrogenation and Deuteration of Buckminsterfullerene C_{60} by 9,10-Dihydroanthracene and 9,9′,10,10′[D_4]Dihydroanthracene (C) 584

Furans
- Regiospecific Conversion of 3,4-Bis(trimethylsilyl)furan to 3,4-Disubstituted Furans: A Novel Suzuki-Type Cross-Coupling of Boroxines (C) 432

Gallium compounds
- A Hexanuclear Organogallium Fluoride Oxide (C) 1701
- $(C_6F_5NGaMe)_4$ and $(C_6F_5NInMe)_4$: The First Gallium–Nitrogen and Indium–Nitrogen Compounds with Cubane Structures (C) 1056
- β-CoGa and ε-NiIn Films form Organometallic Single-Source Precursors: Ligand-Control of the Film Composition (C) 748
- $[\{Et_2O)_2ClGa\}Ga\{GaCl_2(Et_2O)\}_3]$: A Molecular Compound with a Tetrahedral Ga_5 unit (C) 1059
- Organoelement Compounds with Al–Al, Ga–Ga, and In–In Bonds (R) 1386
- Reduction of a Tetraaryldigallane to Afford a Radical Anion with Ga–Ga Multiple Bonding Character (C) 717
- Superexchange through Orthogonal Magnetic Orbitals in π-Type Organic Triradicals: Quartet Ground State in Ga(3,5-dtbsq)$_3$ (C) 391
- Transition-Metal-Substituted Volatile Alanes, Gallanes, and Indanes: Synthesis and Structure (C) 746

Gas/solid reactions
- Gas/Solid Reactions of Aliphatic Amines with Thiohydantoins: Atomic Force Microscopy and New Mechanisms (C) 1587

Germanium compounds
- A Stable η^5-Germacyclopentadienyl Complex: $[(\eta^5\text{-}C_5Me_5)Ru\{\eta^5\text{-}C_4Me_4\text{-}GeSi(SiMe_3)_3\}]$ (C) 1744
- Novel Insertions of Carbene Homologues into Metal-η^5–Cp Bonds: Sandwich Complexes with Ge_2Ni and Sn_2Ni Cores (C) 106
- Polymeric Hemiporphyrazines, a New Class of Rodlike Macromolecules Suitable for the Langmuir–Blodgett Technique (C) 1184
- Synthesis and Structure of Tetrasilylgermane, $Ge(SiH_3)_4$, and Other Silylgermanes (C) 586
- The Dimeric Tris(lithioarsino)germane tBuGe[As(SiiPr$_3$)Li]$_3$: A Self-Assembled, Solvent-Free Lithium–Main Group Element Aggregate with a $Ge_2As_6Li_6$ Rhombododecahedral Framework (C) 1439

Glycine derivatives
- Synthesis and Reactivity of α,α-Dichloroglycyl Peptides (C) 1771

Glycosides
- Stereoselective Synthesis of C-Glycosides with a Glycosyl Dianion (C) 1091

Gold compounds
- Ca_3AuN: A Calcium Auride Subnitride (C) 709

- Cs_3AuO, the First Ternary Oxide with Anionic Gold (C) 1049
- The Application of Au_{55} Clusters as Quantum Dots (C) 250

Grignard reactions
- $CeCl_3$-Mediated Addition of Grignard Reagents to 1,3-Diketones (C) 1061

Haematopodin
- Haematopodin, an Unusual Pyrroloquinoline Derivative Isolated from the Fungus *Mycena haematopus*, Agaricales (C) 1087

Halogen compounds
- Bromine Bromate Br_2O_3 (C) 1632
- $[(I_6Te_2)Nb(Te_2)_2Nb(Te_2I_6)]$, a Metal Complex with Halochalcogenate Ligands (C) 1751

Helices
- Self-Assembly, Structure, and Spontaneous Resolution of a Trinuclear Triple Helix from an Oligobipyridine Ligand and Ni^{II} Ions (C) 703
- Structure of a One-Dimensional Infinite Double-Helical Copper(I) Complex (C) 1463
- The First Structurally Characterized Heterodinuclear Double-Helicate Complex (C) 1465

Hemerythrin
- A Hemerythrin Model Complex with Catalase Activity (C) 289

Heparin
- A Short Synthetic Route towards a Biologically Active Heparin-like Pentasaccharide with a Pseudo-Alternating Sequence (C) 434
- The Unique Antithrombin III Binding Domain of Heparin: A Lead to New Synthetic Antithrombotics (R) 1671

Hereditary diseases
- The Solution of the Sherman Paradox or the Successful Search for the Huntington Gene (H) 1415

Heteroarenes
- S_N2 Reaction versus Electron Transfer in the Oxygen Transfer by Dimethyldioxirane to Nitrogen Heteroarenes (C) 737

Heterocubanes
- A Simple Synthesis of $[(Cp^*Al)_4]$ and Its Conversion to the Heterocubanes $[(Cp^*AlSe)_4]$ and $[(Cp^*AlTe)_4]$ ($Cp^* = \eta^5$-$C_5(CH_3)_5$) (C) 1729
- $(C_6F_5NGaMe)_4$ and $(C_6F_5NInMe)_4$: The First Gallium–Nitrogen and Indium–Nitrogen Compounds with Cubane Structures (C) 1056

Heterocycles
- (*R*)- and (*S*)-4-Alkoxy-2-*tert*-butyl-2,5-dihydroimidazole-1-carboxylates—New Chiral Glycine Derivatives for Amino Acid Synthesis (C) 1765
- Haematopodin, an Unusual Pyrroloquinoline Derivative Isolated from the Fungus *Mycena haematopus*, Agaricales (C) 1087
- Reverse Hydrozirconation Reaction: A Regio- and Diastereospecific Route to New Diphosphanes (C) 1735
- Self-Assembly Through Hydrogen Bonding: Preparation of a Supramolecular Aggregate Composed of Ten Molecules (C) 1766
- Synthesis, Structure, and Reactivity of Stable PN Heterocycles with Two and Six Methyleneamine Units: $[H_2C{=}N{-}N(Me)]_2P(S)(Ph)$ and $[H_2C{=}N{-}N(Me)]_6P_3N_3$ (C) 1477
- Synthesis, Structure, and Thermolysis of a 3-Methoxycarbonyl-1,2λ^5-oxaphosphetane (C) 869
- The First Structure of a Lithiated Cyanamide; Synthesis of (PhNCNLi · HMPA)$_n$ by Extrusion of N_2 and S from 5-Phenylamino-1,2,3,4-thiatriazole with Li Reagents and HMPA (C) 1769

Hexaalkoxysilicates
- $Ba[Si(OCH_2CH_2O)_3]$, a Hexaalkoxysilicate Synthesized from SiO_2 (C) 287

Hexaaqua complexes
- Molecular Recognition of Hexaaqua Transition Metal(II) Ions (C) 714

High-pressure chemistry
- The First Example of an Increase in the Enantioselectivity of a Chemical Reaction in the Presence of a Chiral Lewis Acid under High Pressure (C) 1485
- Two New High-Pressure Modifications of NaOH (C) 271

Histidines
- Selective Pd^0-Mediated C–C Bond Constructions on the Imidazole Ring of L-Histidine: A Practical Approach to the Synthesis of Diphthamide and Related Histidine Analogues (C) 1326

History of chemistry
- Geschichte der deutschen Großchemie. Entwicklung und Einfluss in Staat und Gesellschaft (B) 918
- Pulsed Magnetic Resonance: NMR, ESR, and Optics. A Recognition of E. L. Hahn (B) 451
- The Historical Development of Chemical Concepts (B) 127
- Transuranium Elements: A Half Century (B) 454

Homoconjugation
- 1,7-Cyclopentenonorbornadiene: Synthesis and Crystal Structure (C) 97

Host–guest chemistry
- A Self-Assembling, Hydrogen-Bonded Helix (C) 119
- Aminocyclodextrins as Selective Hosts with Several Binding Sites for Nucleotides (C) 1331
- Cation Inclusion within the Mixed-Valence Polyanion Cluster $[(Mo^{VI}O_3)_4Mo^{V}_{12}O_{28}(OH)_{12}]^{8-}$: Syntheses and Structures of $(NH_4)_7[NaMo_{16}(OH)_{12}O_{40}] \cdot 4H_2O$ and $(Me_2NH_2)_6[H_2Mo_{16}(OH)_{12}O_{40}]$ (C) 1780
- Complexation of Methane and Chlorofluorocarbons by Cryptophane-A in Organic Solution (C) 1169
- Host–Guest Complexes between Calix[4]arenes Derived from Resorcinol and Alkylammonium Ions (C) 1195
- Molecular Recognition of Hexaaqua Transition Metal(II) Ions (C) 714
- Molecular Tweezers with a Hydrocarbon Skeleton and Convergent Carboxyl Groups (C) 601
- Phenothiazine–Bipyridinium Oligooxacyclophanes (C) 1711
- Separation of the Enantiomers of 2,2′-Dihydroxy-1,1′-binaphthyl and 10,10′-Dihydroxy-9,9′-biphenanthryl by Complexation with *N*-Alkylcinchonidinium Halides (C) 1147
- Supramolecular Complexes of Flexible, Extended Cavity Calix[4]arenes—Structural Characterization of a Molecular Venus Flytrap (C) 1093
- Synthesis and Complexation Studies of Neutral Anion Receptors (C) 900
- Synthesis and Structure of a Trimeric Cyclometalated Coordination Compound with a Hydrophobic Cavity (C) 392

Hybridization
- A Sulfide-Linked Oligonucleotide Analogue with Selective Hybridization Properties (C) 729

Hydrocarbons
- Golcondane: A Novel, Caged, Nonacyclic $C_{20}H_{24}$-Hydrocarbon of D_{2d} Symmetry (C) 1160
- Synthesis and Characterization of a High Molecular Weight Stiff Dendrimer (C) 246

Hydroformylation
- A New Route to Water-Soluble Phosphanes with *para*-Sulfonated Phenyl Substituents. Crystal Structure of $P(C_6H_4$-*p*-$SO_3K)_3 \cdot KCl \cdot 0.5H_2O$ (C) 1058

Hydrogen bonds
- A Self-Assembling, Hydrogen-Bonded Helix (C) 119
- A Synthetic Cavity Assembles Through Self-Complementary Hydrogen Bonds (C) 1699
- $[(\eta^5$-$CH_3C_5H_4)Mn(CO)(dppfe)]$: Two Isomers Distinguished by their Characteristic CO Stretching Frequencies, which Differ Only in Rotation of the Methylcyclopentadienyl Ligand: Evidence for an Intramolecular M–CO···H–C Interaction (C) 87
- Dimeric and Trimeric Aminoalanes with Inverse Bridging Functions (C) 886
- Formation of Molecular Strands by Hydrogen Bonds at the Gas–Water Interface: Molecular Recognition and Quantitative Hydrolysis of Barbituric Acid Lipids (C) 1033
- Hydrogen Bonding in Biological Structures (B) 623
- Hydrogen Bonds as a Crystal Design Element for Organic Molecular Solids with Intermolecular Ferromagnetic Interactions (C) 882
- Molecular Recognition of Hexaaqua Transition Metal(II) Ions (C) 714
- Molecular Recognition within a Rigid Host: Structural Changes Induced in μ-Carboxylato Dimetal(II) Complexes by Replacing Steric Repulsions with Hydrogen Bonds (C) 1321
- Molecular Self-Organization of Amphotropic Cyanobiphenyl Mesogens (C) 1165
- *aci*-Nitrodiphenylmethane: A Hydrogen-Bonded Dimer (C) 1758
- On the Strength of the C–H···O Hydrogen Bond and the Eclipsed Arrangement of the Methyl Group in a Tricyclic Orthoamide Trihydrate (C) 588
- Self-Assembly Through Hydrogen Bonding: Preparation of a Supramolecular Aggregate Composed of Ten Molecules (C) 1766
- Structural Variations Observed in the $[Bi(O_2CCF_3)_4Ph]^{2-}$ Anion: Selective Cation–Anion Interactions through Hydrogen Bonds (C) 589
- Synthesis and Complexation Studies of Neutral Anion Receptors (C) 900
- Tetracyanohydroquinone and its Dimorpholinium Salt: Hydrogen Bonds O–H···N or $O^{\ominus}$···H–$^{\oplus}$N to Nitrogen Bases of Different Strengths (C) 411

Hydrogen migration
- A Detailed Theoretical Analysis of the 1,7-Sigmatropic Hydrogen Shift: The Möbius Character of the Eight-Electron Transition Structure (C) 1763
- Transformation of the First Zirconocene Alkyne Complex without an Additional Phosphane Ligand into a Dinuclear σ-Alkenyl Complex by Hydrogen Transfer from η^5-C_5H_5 to the Alkyne Ligand (C) 1193

Hydrogenation
- Catalytic Hydrogenation with Rhodium Complexes Containing dipamp-pyrphos Hybrid Ligands (C) 1052
- Enantioselective Transition Metal-Catalyzed Hydrogenation for the Asymmetric Synthesis of Amines (H) 232

- $[(\widehat{PP})_2RhH]$ and $[(\widehat{PP})_2Rh][O_2CH]$ Complexes as Models for the Catalytically Active Intermediates in the Rh-Catalyzed Hydrogenation of CO_2 to HCOOH (C) 739
- Transfer Hydrogenation and Deuteration of Buckminsterfullerene C_{60} by 9,10-Dihydroanthracene and 9,9',10,10'[D_4]Dihydroanthracene (C) 584

Hydroperoxides
- Enzyme-Catalyzed Asymmetric Synthesis: Kinetic Resolution of Chiral Hydroperoxides by Enantioselective Reduction to Alcohols with Horseradish Peroxidase (C) 1737

Hydrophobic interactions
- Hydrophobic Effects. Opinions and Facts (R) 1545
- Relative Significance of Electrostatic- and Hydrophobic-Induced pK_a Shifts in a Model Protein: The Aspartic Acid Residue (C) 1440

Hydroquinones
- Tetracyanohydroquinone and its Dimorpholinium Salt: Hydrogen Bonds O–H···N or $O^{\ominus}\cdots H-{}^{\oplus}N$ to Nitrogen Bases of Different Strengths (C) 411

Iminophosphides
- Synthesis and Reactivity of $Me_2P(ZrCp_2Cl)=NAr$, the First Iminozirconiophosphorane, a Masked Iminophosphide (C) 95

Immunology
- Transmembrane Signaling of T Lymphocytes by Ligand-Induced Receptor Complex Assembly (R) 54

Indium compounds
- A Molecular Heterometal Amide with High Molecular Dynamics: Does the Lithium Atom Orbit? (C) 1731
- $(C_6F_5NGaMe)_4$ and $(C_6F_5NInMe)_4$: The First Gallium–Nitrogen and Indium–Nitrogen Compounds with Cubane Structures (C) 1056
- β-CoGa and ε-NiIn Films form Organometallic Single-Source Precursors: Ligand-Control of the Film Composition (C) 748
- Hydrolysis to a Complex with a Central, Octahedral (μ_6-O)In_6 Unit (C) 1426
- Transition-Metal-Substituted Volatile Alanes, Gallanes, and Indanes: Synthesis and Structure (C) 746

Indoles
- Electron Transfer-Catalyzed Diels–Alder Reactions with 2-Vinylindoles (C) 901

Industrial chemistry
- Survey of Industrial Chemistry. 2nd Revised Edition (B) 1095

Influenza
- Got the Flu? Try a Designer Agent Derived from a Sugar (H) 1691

Information management
- Chemical Information Management (B) 452

Inorganic glasses
- Inorganic Polymeric Glasses (B) 1375

Inositol phosphates
- The Inositol Phosphates. Chemical Synthesis and Biological Significance (B) 1103

Interfaces
- Chemistry of the Solid-Water Interface. Processes at the Mineral-Water and Particle-Water Interface in Natural Systems (B) 1105
- Formation of Molecular Strands by Hydrogen Bonds at the Gas–Water Interface: Molecular Recognition and Quantitative Hydrolysis of Barbituric Acid Lipids (C) 1033

Iodine azide
- Iodine Azide (C) 275

Iodine compounds
- The Organic Chemistry of Polycoordinated Iodine (B) 1665

Iodoalkynes
- 1-Iodoalkynes Can Also Be Dimerized: A New Head-to-Tail Coupling (C) 893

Ion conductors
- Proton Conductors. Solids, Membranes and Gels—Materials and Devices (B) 1373

Ion pair catalysis
- Substrate-Specific Catalysis by Ion Pairs (C) 1648

Ion–molecule reactions
- State Selected and State-to-State Ion–Molecule Reaction Dynamics. Part 1: Experiment, Part 2: Theory (B) 447

Ionomycin
- Reductive Ring-Opening of Oxabicyclic Compounds with Diisobutylaluminum Hydride. Application to the Synthesis of the C_{17}–C_{23} Subunit of Ionomycin (C) 281

Iridium compounds
- Structure and Electrochemical Behavior of the Paramagnetic Anion $[Ir_{14}(CO)_{27}]^-$, Possessing a Trigonal Bipyramidal Arrangement of Metal Atoms (C) 1347

Iridodials
- Biosynthesis of Iridodials in the Defense Glands of Beetle Larvae (Chrysomelinae) (C) 912

Iron compounds
- A Hemerythrin Model Complex with Catalase Activity (C) 289
- A New Type of Hexanuclear Iron(III) Hydroxo(oxo) Cluster (C) 570
- Comparison of the Electrophilicities of Cationic Metal π Complexes and of Ordinary Carbenium Ions (C) 1630
- $[Fe_2Cl_6]^{2-}$: A Discrete Form of Ferrous Chloride (C) 293
- Giant Organometallic Networks Derived from Ferrocenepolysulfides (C) 1319
- How "Innocent" Are Pentane-2,4-dione-bis(*S*-alkylisothiosemicarbazonate) Ligands in Biomimetic Fe^{II} and Fe^{IV} Complexes? (C) 1635
- Molecular Recognition within a Rigid Host: Structural Changes Induced in μ-Carboxylato Dimetal(II) Complexes by Replacing Steric Repulsions with Hydrogen Bonds (C) 1321
- Organometallic Ferrocenyl Polymers Displaying Tunable Cooperative Interactions between Transition Metal Centers (C) 1709
- Organometallic Molecular Trees as Multielectron and Multiproton Reservoirs: $CpFe^+$-Induced Nonaallylation of Mesitylene and Phase-Transfer-Catalyzed Synthesis of a Redox-Active Nonairon Complex (C) 1075
- Oxoferryl π-Cation Radical of β-Pyrrole Octachlorinated *meso*-Tetramesitylporphyrin: Electronic and Structural Properties (C) 1437
- Reduced $[Fe_8S_6]$ Clusters: Binding Links between FeS and Active Centers of Iron-Sulfur Proteins (C) 863
- Refinement of a Model for the Nitrogenase Mo–Fe Cluster Using Single-Crystal Mo and Fe EXAFS (C) 1592
- Structure and Reactivity of $[HFe(CO)_3(\eta^3\text{-}C_3H_5)]$ (C) 1073
- Synthesis and Structure of the Arsaalkyne Tetramer $(AsCtBu)_4$ and its $Fe(CO)_4$ Derivative (C) 103
- Tetranuclear Cuboidal and Hexanuclear Prismatic Iron–Sulfur–Nitrosyl Clusters (C) 564
- The Coupled Activation of Molecular Oxygen and C–H and C–C Bonds in Gas-Phase Reactions of $[M(C_2H_4)]^+$ (M = Sc–Zn) with O_2 (C) 1420
- The First Complex with a Tetraethynylcyclobutadiene Ligand (C) 1653
- The First Neutral Adamantanoid Iron(III)–chelate Complex: Spontaneous Formation, Structure, and Electrochemistry (C) 1179

Isocyanates
- Metallacyclic Interconversions in the Chemistry of Palladium with Phenyl Isocyanate (C) 1638
- $[P(MeNCH_2CH_2)_3N]$ as a Superior Catalyst for the Conversion of Isocyanates to Isocyanurates (C) 896

Isocyanides
- Investigations of the Structure and Kinetics of Intermediates in Proton-Induced Alkylidyne–Isocyanide Ligand Coupling Reactions (C) 743
- Synthesis and Reactivity of Hexafluoro-1,2-diisocyanocyclobutanechromium Complexes (C) 1456
- The Coordination Chemistry of Multidentate Isocyanide Ligands (R) 650

Isolobal relationship
- $[Ni(PtBu)_6]$ and $[Ni(SiH_2)_6]$ Arc Isolobal, Related to $[In\{Mn(CO)_4\}_5]^{2-}$, and Have 16-Electron Counts (C) 1616

Isomerization
- Bi[1,3-bis(dicyanomethylene)indan-2-ylidene]—An Ethylene Derivative with Extremely Pronounced Twisting of the C=C Bond (C) 1352
- Effects of Ion Pair Separation on Inversion and Rotation of Sulfur-, Selenium-, and Silicon-Stabilized Organolithium Reagents (C) 1469
- Photoswitchable Catenanes (C) 1295
- Rotation about the C–Se Bond as the Rate-Determining Step in the Racemization of α-Selenium-Substituted Alkyllithium Compounds (C) 1467

Isotope effect
- Stereodivergent Enantioselective Synthesis by Exploiting Unusually Large Kinetic H/D Isotope Effects on Deprotonation (C) 394

Jahn–Teller effect
- The Dynamic Jahn–Teller Effect in the Benzene Cation: Rotationally Resolved ZEKE Photoelectron Spectra of the $\nu_6(e_{2g})$ Mode (C) 1364

Ketenes
- Structures and Reactions of the Oxidation Products of Dimeric Ketenylidene(triphenyl)phosphorane (C) 1746
- Trimeric Ketenylidene(triphenyl)phosphorane: A Hybrid between an Arene and an Ylide (C) 1747

Kinetics
- Rapid Reactions in Solution (B) 624

Kirk/Othmer
- Kirk/Othmer Encyclopedia of Chemical Techonolgy. Vol. 1: A to Alkaloids. Vol. 2: Alkanolamines to Antibiotics (Glycopeptides) (B) 619

β-Lactams
- *E*/*Z* Diastereoselective Enzymatic Hydrolysis of Esters and Diesters (C) 572

β-Lactones
- Novel Synthesis of Tetrasubstituted β-Lactones: The Use of Indium in the Electrochemically Supported Reformatsky Reaction (C) 1191

Lactones
- Titanated Methoxyallene as Novel Homoaldol Equivalent for Diastereoselective Additions to Chiral Amino Aldehydes (C) 1449
Lactosamine
- Continuous Catalytic Synthesis of *N*-Acetyllactosamine (C) 1342
Ladder polymers
- On the Shape of a Diels–Alder Ladder Polymer (C) 123
Lanthanoid compounds
- Catalysis of the Hydrolysis of Phosphoric Acid Diesters by Lanthanide Ions and the Influence of Ligands (C) 1716
- Highly Coordinated Lanthanoid–Phosphane Complexes (C) 1739
- $[\{Me_3Si)_2N\}_2Sm\{\mu\text{-}(\eta^8\text{:}\eta^8\text{-}C_8H_8)\}Sm\{N(SiMe_3)_2\}_2]$: An Inverse Organolanthanoid Sandwich Complex (C) 1208
- Monomeric Tris(η^2-pyrazolato)lanthanoid Complexes with the Bulky 3,5-Di(*tert*-butyl)pyrazolato Ligand (C) 874
- The First Trigonal-Bipyramidal Cluster with an Interstitial C_2 Unit: $[Rb\{Pr_5(C_2)\}Cl_{10}]$ (C) 1318
Liquid crystals
- Conjugated, Liquid Crystalline Polymers (C) 1345
- Highly Branched Liquid Crystalline Polymers with Chiral Terminal Groups (C) 1589
- Improved Properties of Ferroelectric Liquid Crystals from Palladium β-Diketone Complexes (C) 1203
- Liquid-Crystalline Perylene Derivatives as "Discotic Pigments" (C) 1660
- Metallomesogens with a Cholesteric Mesophase (C) 1201
- Molecular Self-Organization of Amphotropic Cyanobiphenyl Mesogens (C) 1165
- Self-Assembly and Liquid Crystal Formation of Folic Acid Salts (C) 248
Liquid–liquid extraction
- Science and Practice of Liquid–Liquid Extraction. Vols. 1 and 2 (B) 919
Low-valent compounds
- Organoelement Compounds with Al–Al, Ga–Ga, and In–In Bonds (R) 1386
Luminescence
- Light from Silicon–Renaissance of Siloxene and Polysilane? (H) 845
- Rigid Rodlike Metal Complexes of Nanometric Dimension: Synthesis, Luminescence Properties, and Long-Range Energy Transfer (C) 1643
Lymphocytes
- Transmembrane Signaling of T Lymphocytes by Ligand-Induced Receptor Complex Assembly (R) 54

Macrocycles
- Marine Metabolites and Metal Ion Chelation: The Facts and the Fantasies (R) 1
- Phenothiazine–Bipyridinium Oligooxacyclophanes (C) 1711
- Synthesis and Structure of a Sixteen-Membered $(AlNCO)_4$ Ring (C) 1483
Macrolides
- Poly(hydroxyalkanoates): A Fifth Class of Physiologically Important Organic Biopolymers? (R) 477
Magnetic properties
- Alternating Ferro- and Antiferromagnetic Interactions in a Chainlike Cu^{II} Coordination Polymer (C) 1046
- 2,2′-Bipyrimidineoxalatocopper(II) Complexes: From the Mononuclear Complex to the 2D Sheetlike Polymer (C) 613
- Bis(*P*,*P*-di-*tert*-butyl-*N*-cyclohexylphosphinicamidato-*N*,*O*)nickel(II): Whether Planar or Tetrahedral—Both Isomers are Paramagnetic (C) 907
- Controlling Valence Tautomerism of Cobalt Complexes Containing the Benzosemiquinone Anion as Ligand (C) 880
- Hydrogen Bonds as a Crystal Design Element for Organic Molecular Solids with Intermolecular Ferromagnetic Interactions (C) 882
- $[MnM(egta)] \cdot 8H_2O$ (M = Mn, Cd): A Novel Type of Two-Dimensional Magnetic Lattice (C) 561
- Structure and Electrochemical Behavior of the Paramagnetic Anion $[Ir_{14}(CO)_{27}]^-$, Possessing a Trigonal Bipyramidal Arrangement of Metal Atoms (C) 1347
- Structure of Diamagnetic $[W(O\text{-}4\text{-}MeC_6H_4)_2Cl_2(PMePh_2)_2]$ and Comparison with Related Paramagnetic 2,6-Diphenylphenoxido Complexes: A Steric Effect on π-Bonding and Electronic Structure (C) 439
- Superexchange through Orthogonal Magnetic Orbitals in π-Type Organic Triradicals: Quartet Ground State in $Ga(3,5\text{-}dtbsq)_3$ (C) 391
Magnetic resonance
- Pulsed Magnetic Resonance: NMR, ESR, and Optics. A Recognition of E. L. Hahn (B) 451
Manganese compounds
- $[(\eta^5\text{-}CH_3C_5H_4)Mn(CO)(dppfe)]$: Two Isomers Distinguished by their Characteristic CO Stretching Frequencies, which Differ Only in Rotation of the Methylcyclopentadienyl Ligand: Evidence for an Intramolecular M–CO···H–C Interaction (C) 87
- Formation of Interwoven 2-D Networks by the Spontaneous Strict Self-Assembly of $[\{M(CO)_3(\mu_3\text{-}OH)\}_4]$ (M = Mn, Re) and Complementary Angular Spacer Molecules (C) 706
- $[MnM(egta)] \cdot 8H_2O$ (M = Mn, Cd): A Novel Type of Two-Dimensional Magnetic Lattice (C) 561
- $(\eta^1\text{-}tpMn,\ \eta^5\text{-}tpCr) \rightarrow (\eta^1\text{-}tpCr,\ \eta^5\text{-}tpMn)$ Thiophene (tp) Conversion due to Bimetallic Activation: A Novel Metal-Exchange Reaction (C) 710
Manganese enzymes
- Manganese Redox Enzymes (B) 129
Marcus theory
- Electron Transfer Reactions in Chemistry: Theory and Experiment (Nobel Lecture) (R) 1111
- The Marcus Inverted Region from Theory to Experiment (H) 691
Mass spectrometry
- Ion-Spray Mass Spectrometry and High-Performance Liquid Chromatography–Mass Spectrometry of Synthetic Peptide Libraries (C) 894
- The Coupled Activation of Molecular Oxygen and C–H and C–C Bonds in Gas-Phase Reactions of $[M(C_2H_4)]^+$ (M = Sc–Zn) with O_2 (C) 1420
Materials science
- Materials Science and Technology. A Comprehensive Treatment—Volume 3A, 4, 7, 15 (B) 309
Melamine
- Self-Assembly Through Hydrogen Bonding: Preparation of a Supramolecular Aggregate Composed of Ten Molecules (C) 1766
Membrane technology
- Basic Principles of Membrane Technology (B) 128
Membranes
- Selective Photolabeling near the Middle of Bilayers with a Photosensitive Transmembrane Probe (C) 259
Mercury compounds
- Decamercuration of Ruthenocene (C) 1161
- Gaseous Mercury(IV) Fluoride, HgF_4: An Ab Initio Study (C) 861
- Mercury, a Structural Building Block and Source of Localized Reactivity in Extended Metal–Metal Bonded Systems (R) 24
- β-Na_3Hg: A Solid with a Quasi-Fluid Sodium Substructure between 36 and 60 °C (C) 1494
Mesoporous materials
- Ordered Molecular Arrays as Templates: A New Approach to the Synthesis of Mesoporous Materials (H) 696
Metabolites
- Marine Metabolites and Metal Ion Chelation: The Facts and the Fantasies (R) 1
Metal activation
- Chemistry of and with Highly Reactive Metals (R) 164
Metallacycles
- A Stable η^5-Germacyclopentadienyl Complex: $[(\eta^5\text{-}C_5Me_5)Ru\{\eta^5\text{-}C_4Me_4GeSi(SiMe_3)_3\}]$ (C) 1744
- Metallacyclic Interconversions in the Chemistry of Palladium with Phenyl Isocyanate (C) 1638
- Surprising Differences in the Cycloaddition Reactions of Cumulenes and Heterocumulenes to Vinylidenetitanocene: Formation of Four- or Five-Membered Titanacycles (C) 264
- Synthesis of the First Stable 2-Chromaoxetane and its Homologues via α-Phosphonio(methylidene) Complexes of Hexavalent Chromium, Molybdenum, and Tungsten (C) 731
- Synthesis, Properties, and Structure of $[L_xLi_2Pt(CH_2CH_2CH_2CH_2)_2]$—A New Type of Pt^{II} Metallacyclopentane Complexes (C) 387
Metallomesogens
- Improved Properties of Ferroelectric Liquid Crystals from Palladium β-Diketone Complexes (C) 1203
- Metallomesogens with a Cholesteric Mesophase (C) 1201
Metalloproteins
- De Novo Design of a Novel Heterodinuclear Three-Helix Bundle Metalloprotein (C) 1594
Metallothioneins
- Metallothioneins. Synthesis, Structure and Properties of Metallothioneins, Phytochelatins and Metal–Thiolate Complexes (B) 1374
Metathesis
- Metathesis of Sulfur-Containing Olefins with a Metallacyclic Aryloxo(chloro)neopentylidenetungsten Complex (C) 112
- On the Mechanism of the $TCPC^{HFB}$-Catalyzed Metathesis of 1,6-Enyne: Evidence for Alkylidenepalladium Intermediates (C) 1085
Methacrylate
- The P4-Phosphazene Base as Part of a New Metal-Free Initiator System for the Anionic Polymerization of Methyl Methacrylate (C) 716
Methyl-Coenzyme-M reductase
- Conformational Analysis of Model Complexes for Methyl-Coenzyme-M Reductase of Methanogenic Bacteria: A Comparison of Crystal and Solution Structures (C) 1777

Methyleneboranes
- Classical and Nonclassical Methyleneboranes (R) 985
Methyltrioxorhenium
- Methyltrioxorhenium(VII) as Catalyst for Epoxidations: Structure of the Active Species and Mechanism of Catalysis (C) 1157
Michael additions
- A Catalytic Enantioselective Michael Addition of a Simple Malonate to Prochiral α,β-Unsaturated Ketones and Aldehydes (C) 1176
- Copper-Catalyzed 1,4-Additions of Trialkylaluminum Compounds to Enones (C) 1368
- Diastereo- and Enantioselective Synthesis of 2-Substituted 3-Trialkylstannylcyclohexanones by Michael Addition of Trialkylstannyllithium to Cyclohexenone SAMP Hydrazone (C) 598
- Syntheses of Polycyclic Natural Products Employing the Intramolecular Double Michael Reaction (R) 1010
Michellamine B
- The Absolute Configuration of Michellamine B, a "Dimeric", Anti-HIV-Active Naphthylisoquinoline Alkaloid (C) 1190
Microbial degradation
- Microbial Degradation of Natural Products (B) 303
Microcin B17
- Posttranslational Backbone Modifications in the Ribosomal Biosynthesis of the Glycine-Rich Antibiotic Microcin B17 (C) 1336
Microwaves
- Fast Solid-State Chemistry: Reactions under the Influence of Microwaves (H) 1411
Mixed-valent compounds
- A Novel Mixed-Valence Tetranuclear V^{II}/V^{III} Complex Isolated from 3,5-Di-*tert*-Butylcatechol/Vanadium(II)/Sodium Methoxide System for Dinitrogen Reduction (C) 1178
- The Behavior of Cp*MoBr/Br_2 Redox Systems: The Unusual Structure of $[(Cp^*_2Mo_2Br_4)_2(Cp^*MoBr_4)_3]$, a Compound Containing Mo^{III}, Mo^{IV}, and Mo^{V} (C) 1486
Modeling living systems
- Artificial Life II. A Proceedings Volume in the Santa Fe Institute Studies on the Sciences of Complexity (B) 1372
Molecular biology
- The Solution of the Sherman Paradox or the Successful Search for the Huntington Gene (H) 1415
Molecular design
- Molecular Design: Chemical Structure Generation from the Properties of Pure Organic Compounds (B) 450
Molecular dynamics
- Molecular Dynamics Simulation. Elementary Methods (B) 765
Molecular machines
- Molecular Machines: How Motion and Other Functions of Living Organisms Can Result from Reversible Chemical Changes (R) 819
Molecular recognition
- Formation of Molecular Strands by Hydrogen Bonds at the Gas–Water Interface: Molecular Recognition and Quantitative Hydrolysis of Barbituric Acid Lipids (C) 1033
- Models for Peptide Receptors (H) 848
- New Chiral Porphyrins—Syntheses and Molecular Recognition of Amino Acid Esters (C) 723
Molybdenum compounds
- Cation Inclusion within the Mixed-Valence Polyanion Cluster $[(Mo^{VI}O_3)_4\text{-}Mo^{V}_{12}O_{28}(OH)_{12}]^{8-}$: Syntheses and Structures of $(NH_4)_7[NaMo_{16}\text{-}(OH)_{12}O_{40}]\cdot 4H_2O$ and $(Me_2NH_2)_6\text{-}[H_2Mo_{16}(OH)_{12}O_{40}]$ (C) 1780
- $[(Me_3Sn^{IV})_2Mo^{VI}O_4]$: An Organometallic Quasi-AB_2 System with a Layered Structure (C) 82
- $[Mo_2(CCH)_4(PMe_3)_4]$, the Parent Dimetallapolyyne (C) 409
- $[Mo_2(S)_2(\mu\text{-}S)(syn\text{-}Me_8[16]aneS_4)_2]^{2+}$, a Novel Sulfidomolybdenum Complex Containing a Linear S=Mo–S–Mo=S Linkage (C) 1621
- Refinement of a Model for the Nitrogenase Mo–Fe Cluster Using Single-Crystal Mo and Fe EXAFS (C) 1592
- The Behavior of Cp*MoBr/Br_2 Redox Systems: The Unusual Structure of $[(Cp^*_2Mo_2Br_4)_2(Cp^*MoBr_4)_3]$, a Compound Containing Mo^{III}, Mo^{IV}, and Mo^{V} (C) 1486
Mössbauer spectroscopy
- How "Innocent" Are Pentane-2,4-dione-bis(*S*-alkylisothiosemicarbazonate) Ligands in Biomimetic Fe^{II} and Fe^{IV} Complexes? (C) 1635
Multicomponent reactions
- The Seven-Component Reaction (C) 563 (916)
Multiple bonds
- A Highly Electrophilic Unsaturated Ditungsten Dication (C) 1156
- Carbenerhodium Complexes with Diaryl- and Aryl(alkyl)carbenes as Ligands: The Missing Link in the Series of the Double Bond Systems *trans*-$[RhCl\{=C(=C)_nRR'\}(L)_2]$ Where $n = 0$, 1, and 2 (C) 1480
- $[(CO)_5Cr{=}Tl{=}Cr(CO)_5]^-$, the First Complex Containing Linear Twofold-Coordinated Thallium (C) 1772
- $[Mo_2(CCH)_4(PMe_3)_4]$, the Parent Dimetallapolyyne (C) 409
- Reduction of a Tetraaryldigallane to Afford a Radical Anion with Ga–Ga Multiple Bonding Character (C) 717

Nakanishi, K.
- A Wandering Natural Products Chemist (B) 311
Natural products
- A Short, Linear Synthesis of (9*S*)-Dihydroerythronolide A (C) 101
- Biologically Active Linear Metabolites of Arachidonic Acid—The First Endogenous Ligand of the Cannabinoid Receptor (H) 1027
- Biosynthesis of Iridodials in the Defense Glands of Beetle Larvae (Chrysomelinae) (C) 912
- Enantioselective Synthesis. Natural Products from Chiral Terpenes (B) 1216
- Haematopodin, an Unusual Pyrroloquinoline Derivative Isolated from the Fungus *Mycena haematopus*, Agaricales (C) 1087
- How Nature Synthesizes Vitamin B_{12}—A Survey of the Last Four Billion Years (R) 1223
- Linear Total Synthesis of (−)-ACRL Toxin IIIB (C) 1452
- Marine Metabolites and Metal Ion Chelation: The Facts and the Fantasies (R) 1
- Metals in Biological Systems (B) 1105
- Microbial Degradation of Natural Products (B) 303
- Natural Products. A Laboratory Guide (B) 302
- Parallels and Decisive Differences in Vitamin B_{12} Biosyntheses (C) 1651
- Reductive Ring-Opening of Oxabicyclic Compounds with Diisobutylaluminum Hydride. Application to the Synthesis of the C_{17}–C_{23} Subunit of Ionomycin (C) 281
- Syntheses of Polycyclic Natural Products Employing the Intramolecular Double Michael Reaction (R) 1010
- The Inositol Phosphates. Chemical Synthesis and Biological Significance (B) 1103
- The Synthesis of Insect Pheromones, 1979–1989 (B) 626
- Vitamin D_3 Synthetic Studies: Enantiospecific Synthesis of the CD Ring Fragment (C) 1444
Neocarzinostatin
- Synthesis of a Nine-Membered Cyclic Analogue of the Neocarzinostatin Chromophore and Its DNA-Cleaving Activity (C) 1657
Neural networks
- Neural Networks in Chemistry (R) 503
- Prediction of the Secondary Structure of Proteins from the Amino Acid Sequence with Artificial Neural Networks (H) 1141
Nickel compounds
- A Nickel–Anthracene Complex Having η^3 and η^4 Coordination in One Crystal (C) 1475
- Axial Ligation of Diazacyclooctanenickel and -Zinc Complexes (C) 116
- Bis(*P,P*-di-*tert*-butyl-*N*-cyclohexylphosphinicamidato-*N,O*)nickel(II): Whether Planar or Tetrahedral—Both Isomers are Paramagnetic (C) 907
- Chromatographic Separation of the Four Possible Structural Isomers of a Tetrasubstituted Phthalocyanine: Tetrakis(2-ethylhexyloxy)phthalocyaninatonickel(II) (C) 1422
- Conformational Analysis of Model Complexes for Methyl-Coenzyme-M Reductase of Methanogenic Bacteria: A Comparison of Crystal and Solution Structures (C) 1777
- Facile Formation of Hexahydroporphyrin Complexes by Reduction of Octaethylisobacteriochlorinnickel(II) (C) 429
- Functional Modeling of CO Dehydrogenase: Catalytic Reduction of Methylviologen by CO/H_2O with an N,O,S-Ligated Nickel Catalyst (C) 92
- $[Ni(PtBu)_6]$ and $[Ni(SiH_2)_6]$ Are Isolobal, Related to $[In\{Mn(CO)_4\}_5]^{2-}$, and Have 16-Electron Counts (C) 1616
- Self-Assembly, Structure, and Spontaneous Resolution of a Trinuclear Triple Helix from an Oligobipyridine Ligand and Ni^{II} Ions (C) 703
Niobium compounds
- $[(I_6Te_2)Nb(Te_2)_2Nb(Te_2I_6)]$, a Metal Complex with Halochalcogenate Ligands (C) 1751
- Superconductivity and Phase Separation in Na_xNbO_2 ($x < 1$) (C) 254
Nitric oxide
- Nitric Oxide, NO, an Intercellular Messenger (H) 378
Nitrides
- Ca_3AuN: A Calcium Auride Subnitride (C) 709
- Solid-State Chemistry with Nonmetal Nitrides (R) 806
Nitridometalates
- $Ba_9N[N_3][TaN_4]_2$: A Nitridotantalate(V) with Nitride and Azide Ions (C) 1350
Nitroarenes
- Nucleophilic Aromatic Displacement. The Influence of the Nitro Group (B) 302

aci-Nitrodiphenylmethane
- *aci*-Nitrodiphenylmethane: A Hydrogen-Bonded Dimer (C) 1758
Nitrogen compounds
- Aza- versus Phospha-Substitution in Cyclobutadiene: A Theoretical Evaluation of Bonding Properties (C) 617
- $Ba_9N[N_3][TaN_4]_2$: A Nitridotantalate(v) with Nitride and Azide Ions (C) 1350
- Lithium Di-*tert*-butylmethylsilylhydrazide, a Hexamer with Li^+ Ions Bound Side-on and End-on (C) 1625
- Nitrosyl Azide, N_4O, an Intrinsically Unstable Oxide of Nitrogen (C) 1610
- Pentazole and Other Nitrogen Rings (H) 230
- Silylamines with Pyramidal Coordination at Nitrogen (C) 425
- Synthesis and Structure of a Sixteen-Membered $(AlNCO)_4$ Ring (C) 1483
- Synthesis, Structure, and Reactivity of Stable PN Heterocycles with Two and Six Methyleneamine Units: $[H_2C=N-N(Me)]_2P(S)(Ph)$ and $[H_2C=N-N(Me)]_6P_3N_3$ (C) 1477
Nitrogen fixation
- A Novel Mixed-Valence Tetranuclear V^{II}/V^{III} Complex Isolated from 3,5-Di-*tert*-Butylcatechol/Vanadium(II)/Sodium Methoxide System for Dinitrogen Reduction (C) 1178
- Concerning "An Opinion on the Heterogeneous Photoreduction of N_2 with H_2O" (C) 550
- Fixation and Reduction of Dinitrogen by Vanadium(II) and Vanadium(III): Synthesis and Structure of Dinitrogen-mesitylvanadium Complexes (C) 396
- How N_2 Might Be Activated by the FeMo-Cofactor in Nitrogenase (C) 1062
- Refinement of a Model for the Nitrogenase Mo–Fe Cluster Using Single-Crystal Mo and Fe EXAFS (C) 1592
- Reply: Standards of Demonstration for the Heterogeneous Photoreactions of N_2 with H_2O (C) 552
- X-ray Structure Analysis of FeMo Nitrogenase—Is the Problem of N_2 Fixation Solved? (H) 64
Nitrogenase
- How N_2 Might Be Activated by the FeMo-Cofactor in Nitrogenase (C) 1062
- X-ray Structure Analysis of FeMo Nitrogenase—Is the Problem of N_2 Fixation Solved? (H) 64
Nitrosyl azide
- Nitrosyl Azide, N_4O, an Intrinsically Unstable Oxide of Nitrogen (C) 1610
NMR spectroscopy
- Coherence Selection by Gradients without Signal Attenuation: Application to the Three-Dimensional HNCO Experiment (C) 1489
- Conformational Analysis of Model Complexes for Methyl-Coenzyme-M Reductase of Methanogenic Bacteria: A Comparison of Crystal and Solution Structures (C) 1777
- Phenothiazine–Bipyridinium Oligooxacyclophanes (C) 1711
- Posttranslational Backbone Modifications in the Ribosomal Biosynthesis of the Glycine-Rich Antibiotic Microcin B17 (C) 1336
- Pulsed Magnetic Resonance: NMR, ESR, and Optics. A Recognition of E. L. Hahn (B) 451
- Reaction Tuning in Zeolites: An in situ MAS NMR Study of Acetaldehyde on HZSM-5 (C) 615
- Sequential Analysis of Oligosaccharide Structures in a Few Minutes (C) 1349
- The Energetic Stabilization Caused by a Planar-Tetracoordinate Carbon Atom: A Dynamic NMR Spectroscopic Study of the Dimetallabicycle $[(Cp_2Zr)_2(\mu\text{-}C\equiv CCH_3)(\mu\text{-}H_3CCCCH_3)]BPh_4$ (C) 1623
Nobel lecture
- Electron Transfer Reactions in Chemistry: Theory and Experiment (Nobel Lecture) (R) 1111
- Protein Phosphorylation and Cellular Regulation I (Nobel Lecture) (R) 1122
- Protein Phosphorylation and Cellular Regulation II (Nobel Lecture) (R) 1130
Nobel-gas compounds
- Pentafluorophenylxenon(II) Pentafluorobenzoate: the First Preparative Synthesis and Structural Characterization of an Acyloxy Compound of Xenon(II) (C) 99
Nomenclature
- Inorganic Chemical Nomenclature (B) 126
Noncovalent interactions
- Arene–Arene Interactions: Electrostatic or Charge Transfer? (H) 1584
Norbornadienes
- 1,7-Cyclopentenonorbornadiene: Synthesis and Crystal Structure (C) 97
Norbornane
- Stereochemistry of Norbornyl → Norpinyl Rearrangements (C) 385
Norbornyl cations
- The Classical 2-Norbornyl Cation Rigorously Defined Ab Initio (C) 1606
- The Nature of the 7-Norbornyl Cation and its Rearrangement into the 2-Norbornyl Cation (C) 1604
Norcaradienes
- A Novel 1,6-Methano[10]annulene Derivative with Bisnorcaradiene Structure—Syntheses with Transition Metal Complexes (C) 1324
N-oxides
- S_N2 Reaction versus Electron Transfer in the Oxygen Transfer by Dimethyldioxirane to Nitrogen Heteroarenes (C) 737
Nozoe, T.
- Seventy Years in Organic Chemistry (B) 311
Nucleobases
- Activation of the C2 Position of Purine by the Trifluoromethanesulfonate Group: Synthesis of N^2-Alkylated Deoxyguanosines (C) 404
- Regiospecific Alkylation of 6-Chloropurine and 2,6-Dichloropurine at N7 by Transient Protection of N3/N9 by Methylcobaloxime (C) 1696
- Tautomer-Specific Anti-(N-3-Substituted)-Adenine Antibodies: New Tools in Molecular Dosimetry and Epidemiology (C) 1640
Nucleophilic substitution
- Nucleophilic Aromatic Displacement. The Influence of the Nitro Group (B) 302
Nucleosides
- Lipophilic 5′,5′-*O*-Dinucleoside-α-hydroxybenzylphosphonic Acid Esters as Potential Prodrugs of 2′,3′-Dideoxythymidine (ddT) (C) 1704
Nucleotides
- A Self-Replicating System from *Three* Starting Materials (C) 1198
- Aminocyclodextrins as Selective Hosts with Several Binding Sites for Nucleotides (C) 1331
- HPLC of Proteins, Peptides and Polynucleotides. Contemporary Topics and Applications (B) 305
- Synthesis and Pairing Properties of Decanucleotides from (3′*S*,5′*R*)-2′-Deoxy-3′,5′-ethano-β-D-ribofuranosyladenine and -thymine (C) 1432

Octahedrane
- *p*-[3^2.5^6]Octahedrane, the $(CH)_{12}$ Hydrocarbon with D_{3d} Symmetry (C) 559
Oligonucleotides
- A Sulfide-Linked Oligonucleotide Analogue with Selective Hybridization Properties (C) 729
- Sequence-Specific Recognition and Modification of Double-Helical DNA by Oligonucleotides (R) 666
- UO_2^{2+}-Catalyzed Oligothioadenylate Synthesis with High Regio- and Stereoselectivity (C) 870
Oligothiophenes
- Didodecylsexithiophene—A Model Compound for the Formation and Characterization of Charge Carriers in Conjugated Chains (C) 76
Orbital symmetry
- Orbital Symmetry and Reaction Mechanisms. The OCAMS View (B) 1220
Organic chemistry
- Fascinating Molecules in Organic Chemistry (B) 306
Organic chemistry in Japan
- Organic Synthesis in Japan. Past, Present, and Future. In Commemoration of the 50th Anniversary of the Society of Synthetic Organic Chemistry, Japan (B) 1219
Organic conductors
- Didodecylsexithiophene—A Model Compound for the Formation and Characterization of Charge Carriers in Conjugated Chains (C) 76
Orthoamides
- On the Strength of the C–H···O Hydrogen Bond and the Eclipsed Arrangement of the Methyl Group in a Tricyclic Orthoamide Trihydrate (C) 588
Oxacyclophanes
- Phenothiazine–Bipyridinium Oligooxacyclophanes (C) 1711
Oxadiboriranes
- On the BO Bond Length in Oxadiboriranes (C) 1154
Oxidations
- Cobalt Tetra(hydroquinone)porphyrin: An Efficient Electron Transfer Reagent in Aerobic Pd-Catalyzed 1,4-Diacetoxylation of 1,3-Cyclohexadiene (C) 263
- Temperature Effects in Asymmetric Dihydroxylation: Evidence for a Stepwise Mechanism (C) 1329
Oxiranes
- A Simple Route from Glucal to Cerny Epoxides (C) 272
2-Oxocarboxylic acids
- Enantioselective Aldol Reactions with a Phosphoenolpyruvate Equivalent: Asymmetric Synthesis of 4-Hydroxy-2-oxocarboxylic Acid Esters (C) 421
- Selective Dehydrogenation of Aldonic and Aldaric Acid with an *R*-Configurated α Carbon Atom to 2-Oxocarboxylic Acids, and Reduction of the Oxo Group of *N*-Acetylneuraminic Acid with *Proteus mirabilis* (C) 1197
Oxocuprates
- $Ba_{44}Cu_{48}(CO_3)_6O_{87.9}$: The Structure of "$BaCuO_2$" from Simultaneous X-ray and Neutron Powder Diffraction (C) 1454
Oxygen
- Oxygen Chemistry (B) 304

Palladium compounds
- Improved Properties of Ferroelectric Liquid Crystals from Palladium β-Diketone Complexes (C) 1203

- Metallacyclic Interconversions in the Chemistry of Palladium with Phenyl Isocyanate (C) 1638
- Metallomesogens with a Cholesteric Mesophase (C) 1201
- On the Mechanism of the TCPC^{HFB}-Catalyzed Metathesis of 1,6-Enyne: Evidence for Alkylidenepalladium Intermediates (C) 1085
- Synthesis and Structure of a Trimeric Cyclometalated Coordination Compound with a Hydrophobic Cavity (C) 392
- Tetrahedral Coordination of Palladium in $Ta_2Pd_3Te_5$: A Compound with a "Stuffed" Ta_2NiSe_5 Structure (C) 1752

Peer review process
- An Evaluation of the Peer Review Process at *Angewandte Chemie* (C) 234
- Concerning "An Evaluation of the Peer Review Process at *Angewandte Chemie*" (C) 1030

Pentazoles
- Pentazole and Other Nitrogen Rings (H) 230

Peptides
- Ion-Spray Mass Spectrometry and High-Performance Liquid Chromatography—Mass Spectrometry of Synthetic Peptide Libraries (C) 894
- Synthesis and Reactivity of α,α-Dichloroglycyl Peptides (C) 1771

Peptidomimetics
- Peptidomimetics for Receptor Ligands—Discovery, Development, and Medical Perspectives (R) 1244

Peptoids
- Peptoids—A New Approach to the Development of Pharmaceuticals (H) 543

Peroxides
- Organic Peroxides (B) 1498

Perylenes
- Liquid-Crystalline Perylene Derivatives as "Discotic Pigments" (C) 1660

Pharmaceuticals
- Diastereo- and Enantioselective Synthesis of C_2-Symmetrical HIV-1 Protease Inhibitors (C) 423
- Got the Flu? Try a Designer Agent Derived from a Sugar (H) 1691
- Lipophilic 5′,5′-*O*-Dinucleoside-α-hydroxybenzylphosphonic Acid Esters as Potential Prodrugs of 2′,3′-Dideoxythymidine (ddT) (C) 1704
- Peptidomimetics for Receptor Ligands—Discovery, Development, and Medical Perspectives (R) 1244
- Peptoids—A New Approach to the Development of Pharmaceuticals (H) 543
- The Unique Antithrombin III Binding Domain of Heparin: A Lead to New Synthetic Antithrombotics (R) 1671

Phase diagrams
- Phase Diagrams of the Elements (B) 305

Pheromones
- The Synthesis of Insect Pheromones, 1979–1989 (B) 626

Phosphaallenes
- The "Phosphonioyl(phosphoranediyl)-carbene" $[(i\mathrm{Pr}_2\mathrm{N})_2\mathrm{P(H)CP(N}i\mathrm{Pr}_2)_2]^+$ as a Source of New 1,3-Diphosphaallene Ylides: The First Carbodiphosphoranes with P–H Bonds (C) 1167

Phosphane
- Phosphane (PH_3) in the Biosphere (C) 761

Phosphanes
- A New Route to Water-Soluble Phosphanes with *para*-Sulfonated Phenyl Substituents. Crystal Structure of $P(C_6H_4\text{-}p\text{-}SO_3K)_3 \cdot KCl \cdot 0.5H_2O$ (C) 1058

Phosphate diesters
- Catalysis of the Hydrolysis of Phosphoric Acid Diesters by Lanthanide Ions and the Influence of Ligands (C) 1716
- Double Lewis Acid Activation in Phosphate Diester Cleavage (C) 1633

Phospha-Wittig reagents
- Phosphinidenetantalum(v) Complexes of the Type $[(N_3N)Ta{=}PR]$ as Phospha-Wittig Reagents (R = Ph, Cy, *t*Bu; $N_3N = (Me_3SiNCH_2CH_2)_3N$) (C) 756
- Tantalum(v) Phosphinidene Complexes as Phospha-Wittig Reagents (H) 850

Phosphazenes
- Formation and Complex Stabilization of a New Chainlike Phosphazene Anion by Co^{II}-Assisted Oxidative Scrambling of $[N(PPh_2)_2]^-$ (C) 700
- How Strong and How Hindered Can Uncharged Phosphazene Bases Be? (C) 1361
- The P4-Phosphazene Base as Part of a New Metal-Free Initiator System for the Anionic Polymerization of Methyl Methacrylate (C) 716

Phosphinic acids
- Phosphinic Acid-Based C_2-Symmetrical Inhibitors of HIV-Protease (C) 1720

Phospholipids
- Selective Photolabeling near the Middle of Bilayers with a Photosensitive Transmembrane Probe (C) 259

Phosphorthioates
- UO_2^{2+}-Catalyzed Oligothioadenylate Synthesis with High Regio- and Stereoselectivity (C) 870

Phosphorus compounds
- Aza- versus Phospha-Substitution in Cyclobutadiene: A Theoretical Evaluation of Bonding Properties (C) 617
- Benzoannulated Phosphorus–Carbon Four-Membered Rings (C) 1359
- 1,3-Bis(triphenylphosphoranylidene)-allene and Tribenzyl(4-methyldiphenylphosphoniobutadiynyl)borate, Stabilized C_3 and C_4: Confirmation of a Hypothesis (C) 1205
- Carbonyl–Metal Complexes of Diphosphadiboretane (mesB–P*t*Bu)$_2$ and of Triphosphatriborinanes (mesB–P*t*Bu)$_3$ (C) 1446
- DBU and DBN are Strong Nucleophiles: X-Ray Crystal Structures of Onio- and Dionio-Substituted Phosphanes (C) 399
- Lipophilic 5′,5′-*O*-Dinucleoside-α-hydroxybenzylphosphonic Acid Esters as Potential Prodrugs of 2′,3′-Dideoxythymidine (ddT) (C) 1704
- Phosphinic Acid-Based C_2-Symmetrical Inhibitors of HIV-Protease (C) 1720
- $[P(MeNCH_2CH_2)_3N]$ as a Superior Catalyst for the Conversion of Isocyanates to Isocyanurates (C) 896
- Reverse Hydrozirconation Reaction: A Regio- and Diastereospecific Route to New Diphosphanes (C) 1735
- Sterically Controlled, Metal-Induced Synthesis of a 1-Thia-2,4-diphosphole (C) 1424
- Structures and Reactions of the Oxidation Products of Dimeric Ketenylidene-(triphenyl)phosphorane (C) 1746
- Synthesis and Structure of a Diphospha[4]radialene (C) 1163
- Synthesis and Structure of Bis(tri-*tert*-butylphenyl)iminohalogenphosphoranes $X{-}P(=N\text{-}t\mathrm{Bu}_3C_6H_2)_2$ (C) 1419
- Synthesis, Structure, and Reactivity of Stable PN Heterocycles with Two and Six Methyleneamine Units: $[H_2C{=}N{-}N(Me)]_2P(S)(Ph)$ and $[H_2C{=}N{-}N(Me)]_6P_3N_3$ (C) 1477
- Synthesis, Structure, and Thermolysis of a 3-Methoxycarbonyl-1,2λ^5-oxaphosphetane (C) 869
- The Chemistry of Organophosphorus Compounds. Vol. 2: Phosphine Oxides, Sulphides, Selenides and Tellurides (B) 1215
- The Structures of Tris(8-dimethylamino-1-naphthyl)phosphane and Tris-[2-(dimethylaminomethyl)phenyl]phosphane: Crystallographic Evidence of Seven-Coordinate Phosphorus (C) 1430
- Trimeric Ketenylidene(triphenyl)-phosphorane: A Hybrid between an Arene and an Ylide (C) 1747
- Unprecedented Cage-Opening of P_4S_3 Initiated by an Organometallic Radical: Synthesis and Structure of $[Cp_4Cr_4(CO)_9(P_4S_3)]$ (C) 1728
- Ylide-Substituted Thioxophosphanes and Dithioxophosphoranes (C) 1089
- Zirconium Phosphite (3,3′,5,5′-Tetramethylbiphenyl)diphosphonate, a Microporous, Layered, Inorganic–Organic Polymer (C) 1357

Phosphorus nitrides
- Ca_2PN_3: A new Phosphorus(v) Nitride with One-Dimensional Infinite Chains of Corner-Sharing PN_4 Tetrahedra (C) 280

Photochemistry
- A Light-Induced Molecular Shuttle Based on a [2]Rotaxane-Derived Triad (C) 1459
- A New Photoreaction of γ,δ-Unsaturated Ketones: The Oxadi-π-ethane (ODPE) Rearrangement (C) 441
- A Photochemically Driven Molecular Machine (C) 1301
- Amination of Methane and Ethane by Mercury Photosensitization in the Presence of Ammonia (C) 1491
- Concerning "An Opinion on the Heterogeneous Photoreduction of N_2 with H_2O" (C) 550
- Crystallographic Study of a Single Crystal to Single Crystal Photodimerization and Its Thermal Reverse Reaction (C) 1614
- Detection of Trimethylenemethane by IR Spectroscopy: The Result of an Unexpected Photoisomerization of Methylenecyclopropane in a Halogen-Doped Xe Matrix (C) 74
- Organic Photochemistry. A Comprehensive Treatment (B) 1219
- Photochemical 1,2 Shift of the Phosphane Ligands in the Silanediyl Complex $[(2\text{-}Ph_2PCH_2C_6H_4)_2Si{=}Cr(CO)_5]$ (C) 1313
- Photochemical Carboxylation of Cubanes (C) 612
- Photochemistry in Organized and Constrained Media (B) 446
- Photo-induced *exo*-Selective Diels–Alder Reactions (C) 1612
- Photosensitized Oxygenation of an Acyl Furan: Isolation of the First Furan Dioxetane by Rearrangement of its Endoperoxide and Selected Chemical Transformations (C) 80
- Photoswitchable Catenanes (C) 1295
- Reply: Standards of Demonstration for the Heterogeneous Photoreactions of N_2 with H_2O (C) 552
- Titanium-Catalyzed Epoxy-Hydroxylation of Allylic Alcohols: A Convenient Diastereoselective Synthesis of Epoxy Diols (C) 733

Photodissociation
- Photodissociation of Simple Molecules in the Gas Phase (B) 621

Photoelectron spectroscopy
- Structure and Symmetry of the Benzene Cation (C) 603
- The Dynamic Jahn–Teller Effect in the Benzene Cation: Rotationally Resolved ZEKE Photoelectron Spectra of the $\nu_6(e_{2g})$ Mode (C) 1364
Phthalocyanines
- Chromatographic Separation of the Four Possible Structural Isomers of a Tetrasubstituted Phthalocyanine: Tetrakis(2-ethylhexyloxy)phthalocyaninatonickel(II) (C) 1422
Physical chemistry
- Chemical Equilibria in Solution. Dependence of Rate and Equilibrium Constants on Temperature and Pressure (B) 308
- Dynamic Solvent Effects on Electron-Transfer Reactions (R) 359
- Entropy Analysis. An Introduction to Chemical Thermodynamics (B) 621
- Physical Chemistry (B) 449
Planar methane
- An Ab Initio MO Study on Stabilizing Interactions in Dinuclear Zr/Al Complexes with a Planar Tetracoordinate Carbon Center (C) 754
Platinum compounds
- Synthesis, Properties, and Structure of $[L_xLi_2Pt(CH_2CH_2CH_2CH_2)_2]$—A New Type of Pt^{II} Metallacyclopentane Complexes (C) 387
Polycycles
- A Synthetic Cavity Assembles Through Self-Complementary Hydrogen Bonds (C) 1699
- Syntheses of Polycyclic Natural Products Employing the Intramolecular Double Michael Reaction (R) 1010
Polyenes
- Tetrakis(trialkylsilylethynyl)butatriene and 1,1,4,4-Tetrakis(trialkylsilylethynyl)-1,3-butadiene: Novel Cross-Conjugated Chromophors (C) 1187
- Tricyclo[6.2.0.$9^{3,6}$]deca-1,3,6,8-tetraene: A Remarkably Stable *para*-Quinodimethane from a Novel Rearrangement Reaction (C) 1706
Poly(hydroxyalkanoate)s
- Poly(hydroxyalkanoates): A Fifth Class of Physiologically Important Organic Biopolymers? (R) 477
Polyketides
- Synthesis of 4-Deoxyaklanonic acid and its Microbial Conversion into Anthracyclinones (C) 1151
Polymerizations
- $[P(MeNCH_2CH_2)_3N]$ as a Superior Catalyst for the Conversion of Isocyanates to Isocyanurates (C) 896
- The P4-Phosphazene Base as Part of a New Metal-Free Initiator System for the Anionic Polymerization of Methyl Methacrylate (C) 716
Polymers
- Conjugated, Liquid Crystalline Polymers (C) 1345
- Giant Organometallic Networks Derived from Ferrocenepolysulfides (C) 1319
- Highly Branched Liquid Crystalline Polymers with Chiral Terminal Groups (C) 1589
- Spectroscopy of Polymers (B) 1109
Polyoxometalates
- A New Type of Paratungstate (C) 1492
- Cation Inclusion within the Mixed-Valence Polyanion Cluster $[(Mo^{VI}O_3)_4\text{-}Mo^{V}_{12}O_{28}(OH)_{12}]^{8-}$: Syntheses and Structures of $(NH_4)_7[NaMo_{16}(OH)_{12}O_{40}]\cdot 4H_2O$ and $(Me_2NH_2)_6[H_2Mo_{16}(OH)_{12}O_{40}]$ (C) 1780
- Control of the Linkage of Inorganic Fragments of V–O Compounds: From Cluster Shells as Carcerands via Cluster Aggregates to Solid-State Structures (C) 909
- Organometallic Oxides: Lacunary Lindqvist-Type Polyanion-Supported Cyclopentadienylrhodium Complex Fragments (C) 115
- Polyoxovanadium–Organophosphonates—Properties and Structure of an Unusual Pentavanadate Species with a V=O Group Directed Toward the Interior of the Molecular Cavity (C) 261
- Vanadium Phosphate Framework Solid Constructed of Octahedra, Square Pyramids, and Tetrahedra with a Cavity Diameter of 18.4 Å (C) 610
Polysulfides
- Giant Organometallic Networks Derived from Ferrocenepolysulfides (C) 1319
Polyynes
- Dicyanopolyynes: Formation of New Rod-Shaped Molecules in a Carbon Plasma (C) 1340
- $[Mo_2(CCH)_4(PMe_3)_4]$, the Parent Dimetallapolyyne (C) 409
- Rapid Construction of Large-Size Phenylacetylene Dendrimers up to 12.5 Nanometers in Molecular Diameter (C) 1354
- Stable [12]- and [18]Annulenes Derived from Tetraethynylethene (C) 406
- Tetrakis(trialkylsilylethynyl)butatriene and 1,1,4,4-Tetrakis(trialkylsilylethynyl)-1,3-butadiene: Novel Cross-Conjugated Chromophors (C) 1187
Porphobilinogen
- Investigations in the Biosynthesis of the Pigments of Life: Calculations on the Formation of Uroporphyrinogen III from Hydroxymethylbilan and Description of a New Mechanism for the D-Ring Inversion (C) 1040
- Why is Porphobilinogen the Biological Substrate for the Formation of Porphyrins? Calculations on the Conformation of Acyclic Tetrapyrroles and the Acid-Catalyzed Cyclization of Hydroxymethylpyrroles (C) 1038
Porphycenes
- New Porphycene Ligands: Octaethyl- and Etioporphycene (OEPc and EtioPc)—Tetra- and Pentacoordinated Zinc Complexes of OEPc (C) 1600
Porphyrazines
- Polymeric Hemiporphyrazines, a New Class of Rodlike Macromolecules Suitable for the Langmuir–Blodgett Technique (C) 1184
Porphyrinoids
- Biosynthesis of Tetrapyrroles (B) 448
- Cobalt Tetra(hydroquinone)porphyrin: An Efficient Electron Transfer Reagent in Aerobic Pd-Catalyzed 1,4-Diacetoxylation of 1,3-Cyclohexadiene (C) 263
- Conformational Analysis of Model Complexes for Methyl-Coenzyme-M Reductase of Methanogenic Bacteria: A Comparison of Crystal and Solution Structures (C) 1777
- Facile Formation of Hexahydroporphyrin Complexes by Reduction of Octaethylisobacteriochlorinnickel(II) (C) 429
- Investigations in the Biosynthesis of the Pigments of Life: Calculations on the Formation of Uroporphyrinogen III from Hydroxymethylbilan and Description of a New Mechanism for the D-Ring Inversion (C) 1040
- Models for the Photosynthetic Reaction Center—Synthesis and Structure of Porphyrin Dimers with *cis*- and *trans*-Ethene and Skewed Hydroxymethylene Bridges (C) 750
- New Chiral Porphyrins—Syntheses and Molecular Recognition of Amino Acid Esters (C) 723
- Octaethyltetraoxaporphyrin Dication—Counterpart of Octaethylporphyrin in the Tetraoxaporphyrin Series (C) 1597
- 2,3,7,8,12,13,17,18-Octamethoxyporphyrin (C) 291
- Oxoferryl π-Cation Radical of β-Pyrrole Octachlorinated *meso*-Tetramesitylporphyrin: Electronic and Structural Properties (C) 1437
- Porphyrin-Like [22]Annulenoquinones (C) 1333
- Porphyrins with Aromatic 26π-Electron Systems (C) 1148
- Selective Cleavage of a 35-mer Single-Stranded DNA Containing the Initiation Codon of the TAT Gene of HIV-1 by a Tailored Cationic Manganese Porphyrin (C) 557
- Why is Porphobilinogen the Biological Substrate for the Formation of Porphyrins? Calculations on the Conformation of Acyclic Tetrapyrroles and the Acid-Catalyzed Cyclization of Hydroxymethylpyrroles (C) 1038
Potential energy surfaces
- Properties of Chemically Interesting Potential Energy Surfaces (B) 307
Propargylic alcohols
- One-Flask Synthesis of Propargylic Alcohols from Organolithium Reagents, *N,N*-Disubstituted Amides, and Acetylenes (C) 608
Propellanes
- Palladium-Catalyzed Arylation of Tetrasubstituted Double Bonds: A Simple Synthesis of Annelated Propellanes (C) 1733
Protecting groups
- Synthesis of 4-Oxo-L-proline and *cis*-4-Hydroxy-L-proline Derivatives from L-Aspartic Acid (C) 285
Protein folding
- Molecular Machines: How Motion and Other Functions of Living Organisms Can Result from Reversible Chemical Changes (R) 819
Protein phosphorylation
- Protein Phosphorylation and Cellular Regulation I (Nobel Lecture) (R) 1122
- Protein Phosphorylation and Cellular Regulation II (Nobel Lecture) (R) 1130
Protein structures
- Prediction of the Secondary Structure of Proteins from the Amino Acid Sequence with Artificial Neural Networks (H) 1141
- The Importance of the Rigidity of the Peptide Backbone for the Inhibitory Properties of BPTI Demonstrated by Semisynthetic Structural Variants (C) 898
Proteins
- De Novo Design of a Novel Heterodinuclear Three-Helix Bundle Metalloprotein (C) 1594
- HPLC of Proteins, Peptides and Polynucleotides. Contemporary Topics and Applications (B) 305
- Human Protein Data. 1st Instalment (B) 1497
- Relative Significance of Electrostatic- and Hydrophobic-Induced pK_a Shifts in a Model Protein: The Aspartic Acid Residue (C) 1440
Proton conductors
- Proton Conductors. Solids, Membranes and Gels—Materials and Devices (B) 1373

Proton transfer
- Electron and Proton Transfer in Chemistry and Biology (B) 1218
Protonations
- Enantioselective Addition of Aromatic Thiols to a Ketene (C) 1044
- Highly Enantioselective Protonation of Thiol Ester Enolates (C) 1042
- Stereoselective Protonation of Boron Enolates (C) 398
Pyranoses
- A Simple Route from Glucal to Cerny Epoxides (C) 272
Pyrrole-2-carboxylic acids
- A Novel Synthesis of Pyrrole-2-carboxylic Acid Derivatives by Ring Transformation of 1,2-Thiazolium Salts through Sulfur Extrusion (C) 712
Pyrroles
- Cycloalkano-2*H*-pyrrole as a Stable Intermediate in the Conversion of β-Cycloalkenyl-α-azidoacrylates to Cycloalkano-1*H*-pyrroles (C) 1051

Q-particles
- Colloidal Semiconductor Q-Particles: Chemistry in the Transition Region Between Solid State and Molecules (R) 41
Quantum dots
- The Application of Au_{55} Clusters as Quantum Dots (C) 250
Quinodimethanes
- Tricyclo[6.2.0.$9^{3,6}$]deca-1,3,6,8-tetraene: A Remarkably Stable *para*-Quinodimethane from a Novel Rearrangement Reaction (C) 1706

Radialenes
- Synthesis and Structure of a Diphospha[4]radialene (C) 1163
- Synthesis of the Tris(9-fluorenylidene)cyclopropane Dianion and Related Dianions: [3]Radialenes with Novel Electronic Properties (C) 89
Radical anions
- Reduction of a Tetraaryldigallane to Afford a Radical Anion with Ga–Ga Multiple Bonding Character (C) 717
Radical cations
- Delocalization of Electrons in the Dodecahedrane Cage—A D_{2h}-Symmetrical 4c–3e Radical Cation as a Structural Borderline Case (C) 875
- Oxoferryl π-Cation Radical of β-Pyrrole Octachlorinated *meso*-Tetramesitylporphyrin: Electronic and Structural Properties (C) 1437
- Stereochemistry of the C–S Bond Cleavage in 1-Phenylethyl Phenyl Sulfide Radical Cation: Evidence for a Unimolecular Pathway (C) 1071
Radical ions
- An Al–Al One-Electron π Bond (C) 388
- "Supersilyl" Compounds $(R_3Si)_3SiSi(SiR_3)_3$ and $(R_3Si)_3SiC_6H_4Si(SiR_3)_3$: Structures and Properties (C) 414
Radicals
- Detection of Trimethylenemethane by IR Spectroscopy: The Result of an Unexpected Photoisomerization of Methylenecyclopropane in a Halogen-Doped Xe Matrix (C) 74
- Substituent Effects on the Zero-Field Splitting Parameters of Localized Triplet 1,3-Cyclopentanediyl Biradicals (C) 1339
- Superexchange through Orthogonal Magnetic Orbitals in π-Type Organic Triradicals: Quartet Ground State in Ga(3,5-dtbsq)$_3$ (C) 391
- The Mechanism of Anaerobic, Radical-Induced DNA Strand Scission (C) 1742
- The Triplet Biradical Tris(3,5-di-*tert*-butyl-4-oxophenylene)methane: Crystal Structure, and Spin and Charge Distribution (C) 416
- Triplet States in Organic Chemistry (H) 1409
- Unprecedented Cage-Opening of P_4S_3 Initiated by an Organometallic Radical: Synthesis and Structure of $[Cp_4Cr_4(CO)_9(P_4S_3)]$ (C) 1728
Reaction mechanisms
- Electron Transfer Reactions in Chemistry: Theory and Experiment (Nobel Lecture) (R) 1111
- Kinetics and Mechanism of Reactions of Transition Metal Complexes (B) 311
- Orbital Symmetry and Reaction Mechanisms. The OCAMS View (B) 1220
- S_N2 Reaction versus Electron Transfer in the Oxygen Transfer by Dimethyldioxirane to Nitrogen Heteroarenes (C) 737
- The Marcus Inverted Region from Theory to Experiment (H) 691
- Theoretical Aspects of Physical Organic Chemistry. The S_N2 Mechanism (B) 1106
- Writing Reaction Mechanisms in Organic Chemistry (*B*) 1498
Reactive intermediates
- Preparation and Structure of Two Highly Reactive Intermediates: $[Li(thf)_4][Cu_5Cl_4R_2]$ and $[Li(thf)_4][AlCl_3R]$, R = $Si(SiMe_3)_3$ (C) 121
Reagents
- Chemistry of and with Highly Reactive Metals (R) 164
- Chiral 2-Amino-1,3-butadienes: New Reagents for Asymmetric Cycloadditions (H) 1582
- DBU and DBN are Strong Nucleophiles: X-Ray Crystal Structures of Onio- and Dionio-Substituted Phosphanes (C) 399
- Diastereo- and Enantioselective Synthesis of 2-Substituted 3-Trialkylstannylcyclohexanones by Michael Addition of Trialkylstannyllithium to Cyclohexenone SAMP Hydrazone (C) 598
- Effects of Ion Pair Separation on Inversion and Rotation of Sulfur-, Selenium-, and Silicon-Stabilized Organolithium Reagents (C) 1469
- Rotation about the C–Se Bond as the Rate-Determining Step in the Racemization of α-Selenium-Substituted Alkyllithium Compounds (C) 1467
- Structures of Classical Reagents in Chemical Synthesis: $(n\text{BuLi})_6$, $(t\text{BuLi})_4$, and the Metastable $(t\text{BuLi} \cdot Et_2O)_2$ (C) 580
- Structures of Organo Alkali Metal Complexes and Related Compounds (R) 1501
- Titanated Methoxyallene as Novel Homoaldol Equivalent for Diastereoselective Additions to Chiral Amino Aldehydes (C) 1449
- Transition Metal Organometallics for Organic Synthesis (B) 307
Realgar
- New As–S Cage Structures with Organometallic Components Formed by Complex-Induced Realgar Fragmentation (C) 1627
Rearrangements
- A Detailed Theoretical Analysis of the 1,7-Sigmatropic Hydrogen Shift: The Möbius Character of the Eight-Electron Transition Structure (C) 1763
- A Diastereoselective Synthesis of β-(*N*-Acylamino)aldehydes by Rearrangement of *O*-Vinyl-*N*,*O*-Acetals (C) 83
- A New Photoreaction of γ,δ-Unsaturated Ketones: The Oxadi-π-ethane (ODPE) Rearrangement (C) 441
- Cycloalkano-2*H*-pyrrole as a Stable Intermediate in the Conversion of β-Cycloalkenyl-α-azidoacrylates to Cycloalkano-1*H*-pyrroles (C) 1051
- η^6-(1,2-Dioxocyclobutabenzene)-tricarbonylchromium(0): Starting Material for Double Anionic Oxy-Cope Rearrangements under Very Mild Conditions (C) 267
- Elimination of the Barrier to Cope Rearrangement in Semibullvalene by Li^+ Complexation (C) 1760
- Photosensitized Oxygenation of an Acyl Furan: Isolation of the First Furan Dioxetane by Rearrangement of its Endoperoxide and Selected Chemical Transformations (C) 80
- Reductive Ring-Opening of Oxabicyclic Compounds with Diisobutylaluminum Hydride. Application to the Synthesis of the C_{17}–C_{23} Subunit of Ionomycin (C) 281
- Stereochemistry of Norbornyl → Norpinyl Rearrangements (C) 385
- The Nature of the 7-Norbornyl Cation and its Rearrangement into the 2-Norbornyl Cation (C) 1604
Receptors
- Models for Peptide Receptors (H) 848
Reductions
- Functional Modeling of CO Dehydrogenase: Catalytic Reduction of Methylviologen by CO/H_2O with an N,O,S-Ligated Nickel Catalyst (C) 92
- Reduction of Geminal Dihalocyclopropanes with Lithium 4,4'-Di-*tert*-butylbiphenyl; Cyclopropyl Derivatives of Dilithiomethane and 1,2-Dilithioethane; Inferences Regarding the Intermediate Carbenoids (C) 574
Referee reports
- An Evaluation of the Peer Review Process at *Angewandte Chemie* (C) 234
- Concerning "An Evaluation of the Peer Review Process at *Angewandte Chemie*" (C) 1030
Reformatsky reactions
- Novel Synthesis of Tetrasubstituted β-Lactones: The Use of Indium in the Electrochemically Supported Reformatsky Reaction (C) 1191
Rhenium compounds
- A New Form of Coordinated Carbon: A C_3 Chain That Is Anchored by a Transition Metal on Each End and Spanned by a Third (C) 891
- Formation of Interwoven 2-D Networks by the Spontaneous Strict Self-Assembly of $[\{M(CO)_3(\mu_3\text{-}OH)\}_4]$ (M = Mn, Re) and Complementary Angular Spacer Molecules (C) 706
- Heterolysis of Re_2O_7: Generation and Stabilization of the Cation $[ReO_3]^+$ (C) 1714
- Methyltrioxorhenium(VII) as Catalyst for Epoxidations: Structure of the Active Species and Mechanism of Catalysis (C) 1157
- New Half-Sandwich Polysulfidorhenium Complexes (C) 85
Rhodium compounds
- A Novel Complex with Boat-Shaped, Synfacially Bound η^3:η^3-Benzene Bridges and the First μ_3-η^2:η^2:η^2-Arenetrirhodium Complex (C) 1697
- Carbenerhodium Complexes with Diaryl- and Aryl(alkyl)carbenes as Ligands: The Missing Link in the Series of the Double Bond Systems *trans*-$[RhCl\{=C(=C)_nRR'\}(L)_2]$ Where $n = 0$, 1, and 2 (C) 1480

- Catalytic Hydrogenation with Rhodium Complexes Containing dipamp-pyrphos Hybrid Ligands (C) 1052
- Metal-Initiated Coupling of C_2 Units to Enynes and Butatrienes: Two Different Routes for the Dimerization of 1-Alkynes (C) 1315
- Organometallic Oxides: Lacunary Lindqvist-Type Polyanion-Supported Cyclopentadienylrhodium Complex Fragments (C) 115
- $[(\widehat{PP})_2RhH]$ and $[(\widehat{PP})_2Rh][O_2CH]$ Complexes as Models for the Catalytically Active Intermediates in the Rh-Catalyzed Hydrogenation of CO_2 to HCOOH (C) 739
- Water-Soluble Ligands, Metal Complexes, and Catalysts: Synergism of Homogeneous and Heterogeneous Catalysis (R) 1524

Rotanes
- Perspirocyclopropanated [3]Rotane—A Section of a Carbon Network Containing Spirocyclopropane Units? (C) 401

Rotaxanes
- A Light-Induced Molecular Shuttle Based on a [2]Rotaxane-Derived Triad (C) 1459
- A Photochemically Driven Molecular Machine (C) 1301

Ruthenium compounds
- A Stable η^5-Germacyclopentadienyl Complex: $[(\eta^5\text{-}C_5Me_5)Ru\{\eta^5\text{-}C_4Me_4GeSi(SiMe_3)_3\}]$ (C) 1744
- [Cp*Ru(acac)] Is Not a Coordinatively Unsaturated, Stable 16-Valence-Electron Complex (C) 1294
- Decamercuration of Ruthenocene (C) 1161
- Insertion of a Cp Unit into a Metal–Metal Bond: $[Ru_3(CO)_{10}(C_5H_4)]$ and its PPh_3 Derivative (C) 1048
- Rigid Rodlike Metal Complexes of Nanometric Dimension: Synthesis, Luminescence Properties, and Long-Range Energy Transfer (C) 1643

Salt effects
- Salt Effects in Organic and Organometallic Chemistry (B) 623

Sandwich complexes
- Asymmetric Synthesis and Highly Diastereoselective *ortho*-Lithiation of Ferrocenyl Sulfoxides. Application to the Synthesis of Ferrocenyl Derivatives with Planar Chirality (C) 568
- C–H-Activation by Reaction of (Butadiene)zirconocenes and -hafnocenes with 9-BBN (C) 1213
- Decamercuration of Ruthenocene (C) 1161
- Decamethylaluminocenium, a π-Stabilized R_2Al^+ Cation (C) 1655
- Giant Organometallic Networks Derived from Ferrocenepolysulfides (C) 1319
- $[\{Me_3Si)_2N\}_2Sm\{\mu\text{-}(\eta^8\text{:}\eta^8\text{-}C_8H_8)\}Sm\{N(SiMe_3)_2\}_2]$: An Inverse Organolanthanoid Sandwich Complex (C) 1208
- *ansa*-Metallocenes of Calcium and Strontium: One-Pot Synthesis of Organometallic Complexes of the Heavier Alkaline Earth Metals (C) 1079
- Multinuclear Sandwich-type Complexes of Deprotonated β-Cyclodextrin and Copper(II) Ions (C) 852
- Novel Insertions of Carbene Homologues into Metal-η^5–Cp Bonds: Sandwich Complexes with Ge_2Ni and Sn_2Ni Cores (C) 106
- Organometallic Ferrocenyl Polymers Displaying Tunable Cooperative Interactions between Transition Metal Centers (C) 1709
- Organometallic Molecular Trees as Multielectron and Multiproton Reservoirs: $CpFe^+$-Induced Nonaallylation of Mesitylene and Phase-Transfer-Catalyzed Synthesis of a Redox-Active Nonairon Complex (C) 1075
- The Bis(cyclopentadienyl)thallate(I) Anion Isoelectronic with Stannocene (C) 1774

Selenium compounds
- A New Copper Selenide Cluster with PPh_3 Ligands: $[Cu_{146}Se_{73}(PPh_3)_{30}]$ (C) 1303
- Novel Triselenidotantalum Halfsandwich Complexes (C) 591
- Rotation about the C–Se Bond as the Rate-Determining Step in the Racemization of α-Selenium-Substituted Alkyllithium Compounds (C) 1467

Self-assembly
- A Self-Assembling, Hydrogen-Bonded Helix (C) 119
- A Synthetic Cavity Assembles Through Self-Complementary Hydrogen Bonds (C) 1699
- Can Single-Chain Perfluoroalkylated Amphiphiles Alone Form Vesicles and Other Organized Supramolecular Systems? (C) 741
- De Novo Design of a Novel Heterodinuclear Three-Helix Bundle Metalloprotein (C) 1594
- Formation of Interwoven 2-D Networks by the Spontaneous Strict Self-Assembly of $[\{M(CO)_3(\mu_3\text{-}OH)\}_4]$ (M = Mn, Re) and Complementary Angular Spacer Molecules (C) 706
- Isomeric Self-Assembling [2]Catenanes (C) 1297
- Molecular Self-Organization of Amphotropic Cyanobiphenyl Mesogens (C) 1165
- Multicomponent Self-Assembly: Spontaneous Formation of a Cylindrical Complex from Five Ligands and Six Metal Ions (C) 69
- Self-Assembly and Liquid Crystal Formation of Folic Acid Salts (C) 248
- Self-Assembly of a New Class of Tetranuclear Copper(I) and Silver(I) Complexes (C) 877
- Self-Assembly, Structure, and Spontaneous Resolution of a Trinuclear Triple Helix from an Oligobipyridine Ligand and Ni^{II} Ions (C) 703
- Self-Assembly Through Hydrogen Bonding: Preparation of a Supramolecular Aggregate Composed of Ten Molecules (C) 1766
- The Self-Assembly of Catenated Cyclodextrins (C) 854

Self-replication
- A Self-Replicating System from *Three* Starting Materials (C) 1198

Semibullvalenes
- Elimination of the Barrier to Cope Rearrangement in Semibullvalene by Li^+ Complexation (C) 1760

Semiconductors
- β-CoGa and ε-NiIn Films form Organometallic Single-Source Precursors: Ligand-Control of the Film Composition (C) 748
- Colloidal Semiconductor Q-Particles: Chemistry in the Transition Region Between Solid State and Molecules (R) 41
- Synthesis, Structure, and Optical Properties of Cd_4S^{6+} Clusters Encapsulated in an Aluminate Cage (C) 1663

Semiempirical calculations
- How N_2 Might Be Activated by the FeMo-Cofactor in Nitrogenase (C) 1062
- Investigations in the Biosynthesis of the Pigments of Life: Calculations on the Formation of Uroporphyrinogen III from Hydroxymethylbilan and Description of a New Mechanism for the D-Ring Inversion (C) 1040
- Why is Porphobilinogen the Biological Substrate for the Formation of Porphyrins? Calculations on the Conformation of Acyclic Tetrapyrroles and the Acid-Catalyzed Cyclization of Hydroxymethylpyrroles (C) 1038

Sequential transformations
- Sequential Transformations in Organic Chemistry: A Synthetic Strategy with a Future (R) 131

Sharpless oxidation
- Temperature Effects in Asymmetric Dihydroxylation: Evidence for a Stepwise Mechanism (C) 1329

Sherman paradox
- The Solution of the Sherman Paradox or the Successful Search for the Huntington Gene (H) 1415

Silicon compounds
- $Ba[Si(OCH_2CH_2O)_3]$, a Hexaalkoxysilicate Synthesized from SiO_2 (C) 287
- Contrasting Structures of Pyramidal Carbocations and Their Silicon Analogues (C) 865
- High-Pressure Synthesis of LiSi: Three-Dimensional Network of Three-Bonded Si^- Ions (C) 1442
- Intramolecular Base Stabilization of Silicenium Ions: A New Route to Siliconium Ions (C) 1311
- Light from Silicon—Renaissance of Siloxene and Polysilane? (H) 845
- $[Ni(PtBu)_6]$ and $[Ni(SiH_2)_6]$ Are Isolobal, Related to $[In\{Mn(CO)_4\}_5]^{2-}$, and Have 16-Electron Counts (C) 1616
- Photochemical 1,2 Shift of the Phosphane Ligands in the Silanediyl Complex $[(2\text{-}Ph_2PCH_2C_6H_4)_2Si{=}Cr(CO)_5]$ (C) 1313
- Polymeric Hemiporphyrazines, a New Class of Rodlike Macromolecules Suitable for the Langmuir–Blodgett Technique (C) 1184
- Preparation and Structure of Two Highly Reactive Intermediates: $[Li(thf)_4][Cu_5Cl_4R_2]$ and $[Li(thf)_4][AlCl_3R]$, R = $Si(SiMe_3)_3$ (C) 121
- Silylamines with Pyramidal Coordination at Nitrogen (C) 425
- "Supersilyl" Compounds $(R_3Si)_3SiSi(SiR_3)_3$ and $(R_3Si)_3SiC_6H_4Si(SiR_3)_3$: Structures and Properties (C) 414
- Synthesis and Structure of Tetrasilylgermane, $Ge(SiH_3)_4$, and Other Silylgermanes (C) 586
- Tetrakis(tri-*tert*-butylsilyl)-*tetrahedro*-tetrasilane $(tBu_3Si)_4Si_4$: The First Molecular Silicon Compound with a Si_4 Tetrahedron (C) 1054

Silver compounds
- A Simple One-Step Synthesis of Symmetrical Thiocrown Ethers and the Molecular Structure of an Unusual Sandwich-like Tetrametallic Silver Thiocrown Ether Complex (C) 436
- Tetranuclear Silver(I) Clusters Linked by Bridging Succinate Anions in a Three-Dimensional Network: Crystal Structure of Succinatodisilver(I) (C) 1495
- The First Structurally Characterized Heterodinuclear Double-Helicate Complex (C) 1465

Silyl cations
- Intramolecular Base Stabilization of Silicenium Ions: A New Route to Siliconium Ions (C) 1311
- The Search for an Isolable Silyl Cation Must Continue (C) 1471
Sodalite
- Synthesis, Structure, and Optical Properties of Cd_4S^{6+} Clusters Encapsulated in an Aluminate Cage (C) 1663
Sodium hydroxide
- Two New High-Pressure Modifications of NaOH (C) 271
Solid-state chemistry
- A New Layered Ternary Sulfide: Formation of Cu_2WS_4 by Reaction of WS_4^{2-} and Cu^+ Ions (C) 256
- Absolute Asymmetric Synthesis by Irradiation of Chiral Crystals (H) 694
- Ca_2PN_3: A new Phosphorus(v) Nitride with One-Dimensional Infinite Chains of Corner-Sharing PN_4 Tetrahedra (C) 280
- Crystallographic Study of a Single Crystal to Single Crystal Photodimerization and Its Thermal Reverse Reaction (C) 1614
- Defect Chemistry: Composition, Transport, and Reactions in the Solid State; Part I: Thermodynamics (R) 313
- *Defect Chemistry: Composition, Transport, and Reactions in the Solid State; Part II: Kinetics* (R) 528
- Fast Solid-State Chemistry: Reactions under the Influence of Microwaves (H) 1411
- $[(Me_3Sn^{IV})_2Mo^{VI}O_4]$: An Organometallic Quasi-AB_2 System with a Layered Structure (C) 82
- Phase Diagrams of the Elements (B) 305
- Proton Conductors. Solids, Membranes and Gels—Materials and Devices (B) 1373
- Superconductivity and Phase Separation in Na_xNbO_2 ($x < 1$) (C) 254
- $[Tc_6X_8]$ Clusters in ternary Technetium Chalcogenides (C) 576
- Transition Metal Oxides. An Introduction to their Electronic Structure and Properties (B) 304
- Two New High-Pressure Modifications of NaOH (C) 271
- Vanadium Phosphate Framework Solid Constructed of Octahedra, Square Pyramids, and Tetrahedra with a Cavity Diameter of 18.4 Å (C) 610
Solid-state structures
- A Two-Dimensional Ice with the Topography of Edge-Sharing Hexagons Intercalated between $CdNi(CN)_4$ Layers (C) 884
- Accurate Molecular Structures. Their Determination and Importance (B) 1668
- $Ba_{44}Cu_{48}(CO_3)_6O_{87.9}$: The Structure of "$BaCuO_2$" from Simultaneous X-ray and Neutron Powder Diffraction (C) 1454
- Ca_3AuN: A Calcium Auride Subnitride (C) 709
- Carbon(IV) Nitride C_3N_4—A New Material Harder Than Diamond? (H) 1580
- Cs_3AuO, the First Ternary Oxide with Anionic Gold (C) 1049
- Formation of Interwoven 2-D Networks by the Spontaneous Strict Self-Assembly of $[\{M(CO)_3(\mu_3\text{-}OH)\}_4]$ (M = Mn, Re) and Complementary Angular Spacer Molecules (C) 706
- High-Pressure Synthesis of LiSi: Three-Dimensional Network of Three-Bonded Si^- Ions (C) 1442
- Hydrogen Bonds as a Crystal Design Element for Organic Molecular Solids with Intermolecular Ferromagnetic Interactions (C) 882
- $[(I_6Te_2)Nb(Te_2)_2Nb(Te_2I_6)]$, a Metal Complex with Halochalcogenate Ligands (C) 1751
- β-Na_3Hg: A Solid with a Quasi-Fluid Sodium Substructure between 36 and 60 °C (C) 1494
- Solid-State Chemistry with Nonmetal Nitrides (R) 806
- Tetrahedral Coordination of Palladium in $Ta_2Pd_3Te_5$: A Compound with a "Stuffed" Ta_2NiSe_5 Structure (C) 1752
- Tetranuclear Silver(I) Clusters Linked by Bridging Succinate Anions in a Three-Dimensional Network: Crystal Structure of Succinatodisilver(I) (C) 1495
- The Synthesis and Ab Initio Structure Determination of $Zn_4O(BO_3)_2$, a Microporous Zincoborate Constructed of "Fused" Subunits of Three- and Five-Membered Rings (C) 724
- Zirconium Phosphite (3,3′,5,5′-Tetramethylbiphenyl)diphosphonate, a Microporous, Layered, Inorganic–Organic Polymer (C) 1357
Solvatochromism
- 5-Dimethylamino-5′-nitro-2,2′-bithiophene—a New Dye with Pronounced Positive Solvatochromism (C) 719
Solvent effects
- Dynamic Solvent Effects on Electron-Transfer Reactions (R) 359
Spectroscopy
- Optical Spectroscopy of Single Impurity Molecules in Solids (R) 457
Spiro compounds
- Perspirocyclopropanated [3]Rotane—A Section of a Carbon Network Containing Spirocyclopropane Units? (C) 401
Strained rings
- A New Photoreaction of γ,δ-Unsaturated Ketones: The Oxadi-π-ethane (ODPE) Rearrangement (C) 441
- Aza- versus Phospha-Substitution in Cyclobutadiene: A Theoretical Evaluation of Bonding Properties (C) 617
- BNC Isosteres of Cyclopropane and a Borylated Diazoester from Diazo Compounds and (Dimethylamino)bis(trifluoromethyl)borane (C) 384
- 1-Hetero-3,4-diborolanes and Two New Routes to 1,2-Diboretanes (C) 295
- *p*-$[3^2.5^6]$Octahedrane, the $(CH)_{12}$ Hydrocarbon with D_{3d} Symmetry (C) 559
- Perspirocyclopropanated [3]Rotane—A Section of a Carbon Network Containing Spirocyclopropane Units? (C) 401
- Synthesis of the Mono(Dewar Benzene) Isomer of [1.1]Metacyclophane (C) 726
- Tetrakis(tri-*tert*-butylsilyl)-*tetrahedro*-tetrasilane $(tBu_3Si)_4Si_4$: The First Molecular Silicon Compound with a Si_4 Tetrahedron (C) 1054
- Tricyclo[6.2.0.$9^{3,6}$]deca-1,3,6,8-tetraene: A Remarkably Stable *para*-Quinodimethane from a Novel Rearrangement Reaction (C) 1706
Structure elucidation
- Accurate Molecular Structures. Their Determination and Importance (B) 1668
- Bromine Azide—Determination of the Molecular Structure by Electron Diffraction in the Gas Phase (C) 759
- CD Exciton Chirality Method: New Chromophores for Primary Amino Groups (C) 888
- 1-Chloro-2,2-bis(4-chlorophenyl)-1-lithioethene · TMEDA · 2THF: Structure of a Li-Cl Carbenoid (C) 1032
- Monoclinic and Triclinic Tetraisopropyl-*p*-phenylenediamine: To what Extent do n_N/π Interactions Determine Structures? (C) 1755
- Posttranslational Backbone Modifications in the Ribosomal Biosynthesis of the Glycine-Rich Antibiotic Microcin B17 (C) 1336
- Sequential Analysis of Oligosaccharide Structures in a Few Minutes (C) 1349
- Successful X-Ray Structure Analysis of an Alkylidene Carbenoid—A Milestone in Carbenoid Research (H) 1023
Structure–activity relationships
- Relative Significance of Electrostatic- and Hydrophobic-Induced pK_a Shifts in a Model Protein: The Aspartic Acid Residue (C) 1440
- The Unique Antithrombin III Binding Domain of Heparin: A Lead to New Synthetic Antithrombotics (R) 1671
Style guide
- Science as Writing (B) 1221
Substituent effects
- Protonation of Phenyl(trimethylsilyl)-acetylene: A Surprisingly Weak Stabilization of a Carbocation by a β-Trimethylsilyl Group (C) 721
Sulfur compounds
- A New Layered Ternary Sulfide: Formation of Cu_2WS_4 by Reaction of WS_4^{2-} and Cu^+ Ions (C) 256
- A Simple One-Step Synthesis of Symmetrical Thiocrown Ethers and the Molecular Structure of an Unusual Sandwich-like Tetrametallic Silver Thiocrown Ether Complex (C) 436
- Cyanosulfines: An Unexpected Reaction of *N,N*-bis(trimethylsilyl)*ynamines* (C) 258
- Dicyanononasulfane $S_9(CN)_2$—An Unbranched Chain of Thirteen Atoms (C) 1702
- Didodecylsexithiophene—A Model Compound for the Formation and Characterization of Charge Carriers in Conjugated Chains (C) 76
- *S*-Glycosylated Cyclic Peptides (C) 269
- Metathesis of Sulfur-Containing Olefins with a Metallacyclic Aryloxo(chloro)neopentylidenetungsten Complex (C) 112
- New As–S Cage Structures with Organometallic Components Formed by Complex-Induced Realgar Fragmentation (C) 1627
- Stereochemistry of the C–S Bond Cleavage in 1-Phenylethyl Phenyl Sulfide Radical Cation: Evidence for a Unimolecular Pathway (C) 1071
- Synthesis, Structure, and Optical Properties of Cd_4S^{6+} Clusters Encapsulated in an Aluminate Cage (C) 1663
- Tetranuclear Cuboidal and Hexanuclear Prismatic Iron–Sulfur–Nitrosyl Clusters (C) 564
- Unprecedented Cage-Opening of P_4S_3 Initiated by an Organometallic Radical: Synthesis and Structure of $[Cp_4Cr_4(CO)_9(P_4S_3)]$ (C) 1728
- Ylide-Substituted Thioxophosphanes and Dithioxophosphoranes (C) 1089
Superbases
- First Structure of a Mixed Organosodium/Lithium Alkoxide Compound: Model for a Superbase (C) 1066
Superconductors
- $Ba_{44}Cu_{48}(CO_3)_6O_{87.9}$: The Structure of "$BaCuO_2$" from Simultaneous X-ray and Neutron Powder Diffraction (C) 1454
- Superconductivity and Phase Separation in Na_xNbO_2 ($x < 1$) (C) 254
Superelectrophiles (R) 767

Supramolecular chemistry
- A Light-Induced Molecular Shuttle Based on a [2]Rotaxane-Derived Triad (C) 1459
- A Photochemically Driven Molecular Machine (C) 1301
- Isomeric Self-Assembling [2]Catenanes (C) 1297
- Multiring Catenanes with a Macrobicyclic Core (C) 1434
- Photoswitchable Catenanes (C) 1295
Surfaces
- Extending the Metal Cluster–Metal Surface Analogy (H) 228
- Gas/Solid Reactions of Aliphatic Amines with Thiohydantoins: Atomic Force Microscopy and New Mechanisms (C) 1587
- Graphics and Animation in Surface Science (B) 453
- Investigation of the Surface Structure of the Zeolites FAU and EMT by High-Resolution Transmission Electron Microscopy (C) 1210
- Molecular Design of Electrode Surfaces (B) 919
- Optical Spectroscopy of Single Impurity Molecules in Solids (R) 457
Suzuki reactions
- Regiospecific Conversion of 3,4-Bis(trimethylsilyl)furan to 3,4-Disubstituted Furans: A Novel Suzuki-Type Cross-Coupling of Boroxines (C) 432
Symmetry in chemistry
- Reflections on Symmetry in Chemistry ... and Elsewhere (B) 129
Synthesis design
- Computer-Assisted Solution of Chemical Problems—The Historical Development and the Present State of the Art of a New Discipline of Chemistry (R) 201
Synthetic methods
- A Novel Synthesis of Pyrrole-2-carboxylic Acid Derivatives by Ring Transformation of 1,2-Thiazolium Salts through Sulfur Extrusion (C) 712
- A Versatile and Efficient Synthesis of Annulated Cyclopentanes by Stereoselective [3+2] Cycloaddition of Allylsilanes and Cycloalkenyl Methyl Ketones (C) 1081
- Carbohydrates as Chiral Auxiliaries in Stereoselective Synthesis (R) 336
- Chemistry of and with Highly Reactive Metals (R) 164
- Comprehensive Organic Synthesis. Selectivity, Strategy and Efficiency in Modern Organic Chemistry. Volumes 1–9 (B) 1095
- Domino Reactions of 4-Ene-1,2,3-triol Derivatives (C) 1173
- Organic Synthesis with Oxidative Enzymes (B) 622
- Poly(hydroxyalkanoates): A Fifth Class of Physiologically Important Organic Biopolymers? (R) 477
- Rapid Carboalumination of Alkynes in the Presence of Water (C) 1068
- Salt Effects in Organic and Organometallic Chemistry (B) 623
- Sequential Transformations in Organic Chemistry: A Synthetic Strategy with a Future (R) 131
- Syntheses of Polycyclic Natural Products Employing the Intramolecular Double Michael Reaction (R) 1010
- Transition Metal Organometallics for Organic Synthesis (B) 307

Tandem reactions
- Tandem Organic Reactions (B) 1108
Tantalum compounds
- $Ba_9N[N_3][TaN_4]_2$: A Nitridotantalate(v) with Nitride and Azide Ions (C) 1350
- $[Cp^*TaS_3\{Rh(cod)\}_2]$ and $[Cp^*TaS_3\{RuH(PPh_3)_2\}_2]$: A New Class of Heterometallic TaM_2 Clusters (C) 763
- Formation of Monomeric Terminal Chalcogenides by Template-Induced Disilylchalcogenide Elimination; the Crystal Structures of $[ETa\{(Me_3SiNCH_2CH_2)_3N\}]$ (E = Se,Te) (C) 1450
- Novel Triselenidotantalum Halfsandwich Complexes (C) 591
- Phosphinidenetantalum(v) Complexes of the Type $[(N_3N)Ta{=}PR]$ as Phospha-Wittig Reagents (R = Ph, Cy, *t*Bu; $N_3N = (Me_3SiNCH_2CH_2)_3N$) (C) 756
- Tantalum(v) Phosphinidene Complexes as Phospha-Wittig Reagents (H) 850
Tautomerism
- *aci*-Nitrodiphenylmethane: A Hydrogen-Bonded Dimer (C) 1758
Technetium compounds
- Synthesis and Structure of the First Homoleptic Imidotechnetium Complex: $[Tc_2(NAr)_6]$ (Ar = 2,6-diisopropylphenyl) (C) 94
- $[Tc_6X_8]$ Clusters in ternary Technetium Chalcogenides (C) 576
Tellurium compounds
- Electrochemical Synthesis of New Sb–Te Zintl Anions by Cathodic Dissolution of Sb_2Te_3 Electrodes: Structures of $[Sb_4Te_4]^{4-}$ and $[Sb_9Te_6]^{3-}$ (C) 1646
- $[(I_6Te_2)Nb(Te_2)_2Nb(Te_2I_6)]$, a Metal Complex with Halochalcogenate Ligands (C) 1751
- New Cu–Te Clusters (C) 238
- "Noncoordinating" Anions, II (H) 1025
- Tellurium—An Interesting Bonding Partner for Transition Metals: New Results from Molecular Chemistry (H) 67
- Tetrahedral Coordination of Palladium in $Ta_2Pd_3Te_5$: A Compound with a "Stuffed" Ta_2NiSe_5 Structure (C) 1752
Tetraisopropyl-*p*-phenylenediamine
- Monoclinic and Triclinic Tetraisopropyl-*p*-phenylenediamine: To what Extent do n_N/π Interactions Determine Structures? (C) 1755
tetrahedro-Tetrasilane
- Tetrakis(tri-*tert*-butylsilyl)-*tetrahedro*-tetrasilane $(tBu_3Si)_4Si_4$: The First Molecular Silicon Compound with a Si_4 Tetrahedron (C) 1054
Textbooks
- Chemistry. The Central Science (B) 917
- Entropy Analysis. An Introduction to Chemical Thermodynamics (B) 621
- Metals in Biological Systems (B) 1105
- Physical Chemistry (B) 449
- Survey of Industrial Chemistry. 2nd Revised Edition (B) 1095
- Writing Reaction Mechanisms in Organic Chemistry (B) 1498
Thallium compounds
- $[(CO)_5Cr{=}Tl{=}Cr(CO)_5]^-$, the First Complex Containing Linear Twofold-Coordinated Thallium (C) 1772
- The Bis(cyclopentadienyl)thallate(I) Anion Isoelectronic with Stannocene (C) 1774
- Two Modifications of a Cyclopentadienylthallium(I) Complex Linking the Chemistry of the Cp and Arene Complexes of Main Group Elements (C) 90
Theoretical chemistry
- A Semiempirical Life (B) 1102
- Atoms in Molecules. A Quantum Theory (B) 128
- Bonding in Endohedral Metal–Fullerene Complexes: f-Orbital Covalency in Ce@C_{28} (C) 108
- Computational Chemistry. Structure, Interactions and Reactivity (B) 620
- Computer-Assisted Solution of Chemical Problems—The Historical Development and the Present State of the Art of a New Discipline of Chemistry (R) 201
- Hypothetical Carbon Modifications Derived from Zeolite Frameworks (C) 701
- Pentazole and Other Nitrogen Rings (H) 230
- Properties of Chemically Interesting Potential Energy Surfaces (B) 307
- Semiclassical Mechanics with Molecular Applications (B) 445
- The Meaning of Quantum Theory (B) 454
- Theoretical Aspects of Physical Organic Chemistry. The S_N2 Mechanism (B) 1106
Thiadiphospholes
- Sterically Controlled, Metal-Induced Synthesis of a 1-Thia-2,4-diphosphole (C) 1424
Thiazoles
- A Novel Synthesis of Pyrrole-2-carboxylic Acid Derivatives by Ring Transformation of 1,2-Thiazolium Salts through Sulfur Extrusion (C) 712
- The Seven-Component Reaction (C) 563 (916)
Thin films
- β-CoGa and ε-NiIn Films form Organometallic Single-Source Precursors: Ligand-Control of the Film Composition (C) 748
- Polymeric Hemiporphyrazines, a New Class of Rodlike Macromolecules Suitable for the Langmuir–Blodgett Technique (C) 1184
Thiols
- Enantioselective Addition of Aromatic Thiols to a Ketene (C) 1044
Thiophenes
- 5-Dimethylamino-5′-nitro-2,2′-bithiophene—a New Dye with Pronounced Positive Solvatochromism (C) 719
Tin compounds
- Compounds Containing Silicon, Germanium, and Tin Polyhedra: The First Octahedral Tin Cluster (H) 545
- $[(Me_3Sn^{IV})_2Mo^{VI}O_4]$: An Organometallic Quasi-AB_2 System with a Layered Structure (C) 82
- Novel Insertions of Carbene Homologues into Metal-η^5-Cp Bonds: Sandwich Complexes with Ge_2Ni and Sn_2Ni Cores (C) 106
- Nucleophilic Substitution of Bis(cyclopentadienyl)tin(II); Synthesis, Structure, and Solution Dynamics of *trans*-$[(\eta^3\text{-}Cp)Sn\{\mu_2\text{-}N{=}C(NMe_2)_2\}]_2$ (C) 428
- The First Octahedral Zintl Ion: Sn_6^{2-} as a Ligand in $[Sn_6\{Cr(CO)_5\}_6]^{2-}$ (C) 297
- Tris(chlorodimethylstannyl)amine, a Molecule with a Planar Sn_3N Skeleton Stabilized by Intramolecular Sn-Cl-Sn Bridges (C) 1608
Titanium compounds
- Organometallic Titanium Complexes with Unpaired Electrons: Syntheses and Structures of $[\{(\eta^5\text{-}Cp)_2TiF_2\}_3Ti]$ and $[\{(\eta^5\text{-}Cp')_2TiF_2\}_3Al]$ (C) 442
- Surprising Differences in the Cycloaddition Reactions of Cumulenes and Heterocumulenes to Vinylidenetitanocene: Formation of Four- or Five-Membered Titanacycles (C) 264
- Ti^{IV} Complexes with Bridging Ylide Ligands: Double Oxophiles in Reactions with Aldehydes (C) 554
Total syntheses
- The Synthesis of Insect Pheromones, 1979–1989 (B) 626

- Total Synthesis of (−)-Pyrimidoblamic Acid and Deglycobleomycin A_2 (C) 273

Transition metal complexes
- Kinetics and Mechanism of Reactions of Transition Metal Complexes (B) 311
- Methods for the Synthesis of μ-Hydrocarbon Transition Metal Complexes without Metal–Metal Bonds (R) 923
- Transition Metal Complexation of σ Bonds (R) 789

Transition metal oxides
- Transition Metal Oxides. An Introduction to their Electronic Structure and Properties (B) 304

Transmission electron microscopy
- Investigation of the Surface Structure of the Zeolites FAU and EMT by High-Resolution Transmission Electron Microscopy (C) 1210

Transuranium elements
- Transuranium Elements: A Half Century (B) 454

Trimethylenemethane
- Detection of Trimethylenemethane by IR Spectroscopy: The Result of an Unexpected Photoisomerization of Methylenecyclopropane in a Halogen-Doped Xe Matrix (C) 74

Triple-helix formation
- Sequence-Specific Recognition and Modification of Double-Helical DNA by Oligonucleotides (R) 666

Tungsten compounds
- A Highly Electrophilic Unsaturated Ditungsten Dication (C) 1156
- A New Layered Ternary Sulfide: Formation of Cu_2WS_4 by Reaction of WS_4^{2-} and Cu^+ Ions (C) 256
- A New Type of Paratungstate (C) 1492
- Competing $M=C_{carbonyl}$ and $M=C_{carbene}$ Bonds: Cycloaddition to the Metal–$C_{carbonyl}$ Bond in η^2-Thiocarbene Complexes (C) 1152
- Formation of Alkynyltrithiocarbonato Ligands from Alkylidyne Ligands and Carbon Disulfide (C) 1726
- Investigations of the Structure and Kinetics of Intermediates in Proton-Induced Alkylidyne–Isocyanide Ligand Coupling Reactions (C) 743
- Metathesis of Sulfur-Containing Olefins with a Metallacyclic Aryloxo(chloro)neopentylidenetungsten Complex (C) 112
- Structure of Diamagnetic $[W(O\text{-}4\text{-}MeC_6H_4)_2Cl_2(PMePh_2)_2]$ and Comparison with Related Paramagnetic 2,6-Diphenylphenoxido Complexes: A Steric Effect on π-Bonding and Electronic Structure (C) 439
- [W(CH)(dmpe)$_2$(*n*Bu)], a Complex with a Bent Methylidyne Ligand (C) 858

Ultramicroelectrodes
- Ultramicroelectrodes in Electrochemistry (R) 1268

UV spectroscopy
- UV-VIS Atlas of Organic Compounds. Part 1: Spectra A1/1-C9/13. Part 2: Spectra D1/1-M19 (B) 1370

Valence isomerization
- Epoxidation of 2-Methyl-3-phenylbenzofurans with Dimethyldioxirane: A Novel Reversible Valence Isomerization between Labile Benzofuran Epoxides and Quinone Methides, their Rearrangement, Methanolysis, and Cycloaddition Chemistry (C) 735

Valence tautomerism
- Controlling Valence Tautomerism of Cobalt Complexes Containing the Benzosemiquinone Anion as Ligand (C) 880

Vanadium compounds
- A Novel Mixed-Valence Tetranuclear V^{II}/V^{III} Complex Isolated from 3,5-Di-*tert*-Butylcatechol/Vanadium(II)/Sodium Methoxide System for Dinitrogen Reduction (C) 1178
- C–H Bond Addition to a V=NR Bond: Hydrocarbon Activation by a Sterically Crowded Vanadium System (C) 903
- Control of the Linkage of Inorganic Fragments of V–O Compounds: From Cluster Shells as Carcerands via Cluster Aggregates to Solid-State Structures (C) 909
- Fixation and Reduction of Dinitrogen by Vanadium(II) and Vanadium(III): Synthesis and Structure of Dinitrogen-mesitylvanadium Complexes (C) 396
- Novel V^{III} Complexes with a Central $[V_3(\mu_3\text{-}S)(\mu\text{-}S_2)_3]^+$ or $[V_2(\mu\text{-}O)(\mu\text{-}SPh)_2]^{2+}$ Unit (C) 594
- Polyoxovanadium–Organophosphonates—Properties and Structure of an Unusual Pentavanadate Species with a V=O Group Directed Toward the Interior of the Molecular Cavity (C) 261
- Vanadium Phosphate Framework Solid Constructed of Octahedra, Square Pyramids, and Tetrahedra with a Cavity Diameter of 18.4 Å (C) 610

Vitamin B_{12}
- How Nature Synthesizes Vitamin B_{12}—A Survey of the Last Four Billion Years (R) 1223
- Parallels and Decisive Differences in Vitamin B_{12} Biosyntheses (C) 1651

Vitamin D_3
- Vitamin D_3 Synthetic Studies: Enantiospecific Synthesis of the CD Ring Fragment (C) 1444

Water research
- Chemistry of the Solid-Water Interface. Processes at the Mineral-Water and Particle-Water Interface in Natural Systems (B) 1105

Water-soluble catalysts
- Homogeneous Catalysis. The Applications and Chemistry of Catalysis by Soluble Transition Metal Complexes (B) 1666
- Water-Soluble Ligands, Metal Complexes, and Catalysts: Synergism of Homogeneous and Heterogeneous Catalysis (R) 1524

Ylides
- Structures and Reactions of the Oxidation Products of Dimeric Ketenylidene(triphenyl)phosphorane (C) 1746
- Synthesis of the First Stable 2-Chromaoxetane and its Homologues via α-Phosphonio(methylidene) Complexes of Hexavalent Chromium, Molybdenum, and Tungsten (C) 731
- The "Phosphonioyl(phosphoranediyl)carbene" $[(iPr_2N)_2P(H)CP(NiPr_2)_2]^+$ as a Source of New 1,3-Diphosphaallene Ylides: The First Carbodiphosphoranes with P–H Bonds (C) 1167
- Ti^{IV} Complexes with Bridging Ylide Ligands: Double Oxophiles in Reactions with Aldehydes (C) 554
- Trimeric Ketenylidene(triphenyl)phosphorane: A Hybrid between an Arene and an Ylide (C) 1747
- Ylide-Substituted Thioxophosphanes and Dithioxophosphoranes (C) 1089

Zeolites
- Investigation of the Surface Structure of the Zeolites FAU and EMT by High-Resolution Transmission Electron Microscopy (C) 1210
- Ordered Molecular Arrays as Templates: A New Approach to the Synthesis of Mesoporous Materials (H) 696
- Reaction Tuning in Zeolites: An in situ MAS NMR Study of Acetaldehyde on HZSM-5 (C) 615
- The Incorporation of C_{60} in Molecular Sieves (C) 556

Zinc compounds
- Enantioselective Catalytic Addition of Functionalized Dialkylzinc Compounds to β-Stannylated Aldehydes: A Convenient Preparation of Chiral β- and γ-Functionalized Secondary Alcohols (C) 582
- New Porphycene Ligands: Octaethyl- and Etioporphycene (OEPc and EtioPc)—Tetra- and Pentacoordinated Zinc Complexes of OEPc (C) 1600
- The Synthesis and Ab Initio Structure Determination of $Zn_4O(BO_3)_2$, a Microporous Zincoborate Constructed of "Fused" Subunits of Three- and Five-Membered Rings (C) 724

Zintl compounds
- Electrochemical Production of Zintl Anions: Renaissance of a Synthesis Route (H) 1693
- Electrochemical Synthesis of New Sb–Te Zintl Anions by Cathodic Dissolution of Sb_2Te_3 Electrodes: Structures of $[Sb_4Te_4]^{4-}$ and $[Sb_9Te_6]^{3-}$ (C) 1646
- The First Octahedral Zintl Ion: Sn_6^{2-} as a Ligand in $[Sn_6\{Cr(CO)_5\}_6]^{2-}$ (C) 297

Zirconium compounds
- An Ab Initio MO Study on Stabilizing Interactions in Dinuclear Zr/Al Complexes with a Planar Tetracoordinate Carbon Center (C) 754
- Reverse Hydrozirconation Reaction: A Regio- and Diastereospecific Route to New Diphosphanes (C) 1735
- Synthesis and Reactivity of $Me_2P(ZrCp_2Cl)=NAr$, the First Iminozirconiophosphorane, a Masked Iminophosphide (C) 95
- The Energetic Stabilization Caused by a Planar-Tetracoordinate Carbon Atom: A Dynamic NMR Spectroscopic Study of the Dimetallabicycle $[(Cp_2Zr)_2(\mu\text{-}C\equiv CCH_3)(\mu\text{-}H_3CCCCH_3)]BPh_4$ (C) 1623
- Transformation of the First Zirconocene Alkyne Complex without an Additional Phosphane Ligand into a Dinuclear σ-Alkenyl Complex by Hydrogen Transfer from η^5-C_5H_5 to the Alkyne Ligand (C) 1193
- Zirconium Phosphite (3,3′,5,5′-Tetramethylbiphenyl)diphosphonate, a Microporous, Layered, Inorganic–Organic Polymer (C) 1357